California Environmental Protection Agency
Air Resources Board

California Greenhouse Gas Inventory for 2000-2012 — by Category as Defined in the 2008 Scoping Plan

million tonnes of CO2 equivalent - (based upon IPCC Fourth Assessement Report's Global Warming Potentials)

	2000	2001	2002	2003	2004	2005	2006	2007	2008	2009	2010	2011	2012
Transportation	**176.21**	**176.62**	**183.80**	**183.52**	**186.88**	**189.08**	**189.18**	**189.27**	**178.02**	**171.47**	**170.46**	**168.13**	**167.38**
On Road	***162.88***	***163.46***	***169.64***	***168.81***	***171.48***	***172.68***	***172.37***	***172.41***	***163.00***	***158.46***	***157.38***	***154.91***	***154.06***
Passenger Vehicles	130.10	129.97	134.46	132.91	133.34	132.75	131.79	130.80	124.27	122.41	121.39	118.85	118.28
Heavy Duty Trucks	32.78	33.50	35.19	35.90	38.13	39.92	40.58	41.61	38.73	36.04	36.00	36.06	35.78
Ships & Commercial Boats	***3.39***	***3.21***	***3.56***	***3.78***	***3.84***	***4.12***	***4.20***	***4.31***	***4.04***	***3.68***	***3.71***	***3.72***	***3.83***
Aviation (Intrastate)	***4.15***	***4.07***	***4.12***	***4.25***	***4.50***	***4.50***	***4.57***	***4.98***	***4.51***	***4.04***	***3.85***	***3.75***	***3.72***
Rail	***1.88***	***1.89***	***2.50***	***2.70***	***2.91***	***3.34***	***3.53***	***3.17***	***2.38***	***1.94***	***2.33***	***2.49***	***2.48***
Off Road [1]	***2.63***	***2.79***	***2.77***	***2.84***	***3.03***	***3.22***	***3.32***	***3.18***	***2.82***	***2.25***	***2.03***	***2.13***	***2.23***
Unspecified	***1.28***	***1.19***	***1.21***	***1.13***	***1.13***	***1.22***	***1.20***	***1.22***	***1.27***	***1.10***	***1.16***	***1.14***	***1.06***
Electric Power	**104.86**	**122.01**	**108.65**	**112.62**	**115.20**	**107.86**	**104.54**	**113.94**	**120.15**	**101.32**	**90.30**	**88.04**	**95.09**
In-State Generation	***58.96***	***62.99***	***49.69***	***48.06***	***49.16***	***45.06***	***49.86***	***54.13***	***54.32***	***53.28***	***46.71***	***41.18***	***51.02***
Natural Gas	50.92	55.46	42.17	40.92	42.40	38.11	43.07	47.12	48.02	46.08	40.59	35.92	45.77
Other Fuels	6.85	6.36	6.37	5.99	5.60	5.78	5.64	5.86	5.16	5.85	5.02	4.01	4.44
Fugitive and Process Emissions	1.18	1.16	1.15	1.15	1.16	1.16	1.15	1.16	1.14	1.34	1.10	1.25	0.82
Imported Electricity	***45.90***	***59.02***	***58.96***	***64.56***	***66.04***	***62.80***	***54.68***	***59.81***	***65.82***	***48.04***	***43.59***	***46.86***	***44.07***
Unspecified Imports	14.27	25.42	26.92	32.05	32.92	30.01	27.95	32.73	37.92	14.99	13.45	15.52	17.48
Specified Imports	31.64	33.59	32.04	32.51	33.13	32.79	26.73	27.08	27.90	33.05	30.14	31.34	26.59
Commercial and Residential	**42.33**	**41.20**	**43.17**	**41.54**	**42.90**	**41.24**	**41.89**	**42.11**	**42.44**	**42.65**	**43.82**	**44.32**	**42.28**
Residential Fuel Use	***29.70***	***28.77***	***28.93***	***28.47***	***29.51***	***28.22***	***28.58***	***28.73***	***29.07***	***28.69***	***29.42***	***29.89***	***28.09***
Natural Gas	28.03	27.43	27.54	26.67	27.38	25.98	26.60	26.73	26.67	26.31	27.04	27.51	25.76
Other Fuels	1.67	1.34	1.39	1.80	2.12	2.25	1.98	2.01	2.40	2.38	2.39	2.38	2.33
Commercial Fuel Use	***11.54***	***11.37***	***13.18***	***12.82***	***12.77***	***12.61***	***12.89***	***12.88***	***13.00***	***13.04***	***13.48***	***13.65***	***13.44***
Natural Gas	10.07	10.10	11.90	11.38	11.16	10.94	11.62	11.49	11.16	11.02	11.19	11.33	11.24
Other Fuels	1.47	1.27	1.28	1.43	1.61	1.67	1.27	1.40	1.83	2.02	2.29	2.32	2.19
Commercial Cogeneration Heat Output	***1.09***	***1.05***	***1.06***	***0.26***	***0.62***	***0.40***	***0.42***	***0.49***	***0.37***	***0.92***	***0.92***	***0.78***	***0.76***
Industrial	**95.01**	**93.16**	**93.14**	**92.47**	**94.48**	**92.29**	**90.28**	**87.10**	**87.54**	**84.95**	**88.51**	**88.34**	**89.16**
Refineries	***28.47***	***29.04***	***29.20***	***29.83***	***29.08***	***29.75***	***29.65***	***29.21***	***28.42***	***28.34***	***30.39***	***30.12***	***29.88***
General Fuel Use	***20.20***	***19.04***	***20.28***	***16.49***	***17.03***	***16.01***	***15.96***	***14.77***	***16.00***	***15.56***	***17.98***	***19.14***	***18.87***
Natural Gas	16.82	14.62	15.18	11.97	12.80	12.72	12.38	11.56	12.37	11.46	13.46	14.48	14.30
Other Fuels	3.38	4.42	5.09	4.52	4.23	3.28	3.58	3.20	3.63	4.10	4.52	4.66	4.56
Oil & Gas Extraction [2]	***18.71***	***19.08***	***17.65***	***20.21***	***19.90***	***18.59***	***16.94***	***17.00***	***18.22***	***17.12***	***16.18***	***16.22***	***16.86***
Fuel Use	17.53	17.76	16.51	19.03	19.20	17.91	15.75	15.78	17.03	15.92	15.01	14.91	15.50
Fugitive Emissions	1.18	1.32	1.14	1.17	0.71	0.69	1.19	1.21	1.20	1.20	1.17	1.31	1.36
Cement Plants	***9.41***	***9.52***	***9.62***	***9.71***	***9.81***	***9.91***	***9.74***	***9.14***	***8.63***	***5.72***	***5.56***	***6.14***	***6.92***
Clinker Production	5.43	5.52	5.60	5.68	5.77	5.85	5.80	5.55	5.28	3.60	3.46	4.08	4.65
Fuel Use	3.98	4.00	4.01	4.03	4.05	4.06	3.95	3.59	3.34	2.12	2.10	2.06	2.26
Cogeneration Heat Output	***11.73***	***10.48***	***10.65***	***10.60***	***12.92***	***12.41***	***12.17***	***11.16***	***10.40***	***12.55***	***12.60***	***11.14***	***10.82***
Other Fugitive and Process Emissions	***6.49***	***6.00***	***5.74***	***5.62***	***5.74***	***5.62***	***5.83***	***5.83***	***5.87***	***5.65***	***5.80***	***5.59***	***5.82***

California Environmental Protection Agency
Air Resources Board

California Greenhouse Gas Inventory for 2000-2012 — by Category as Defined in the 2008 Scoping Plan

million tonnes of CO2 equivalent - (based upon IPCC Fourth Assessement Report's Global Warming Potentials)

	2000	2001	2002	2003	2004	2005	2006	2007	2008	2009	2010	2011	2012
Recycling and Waste	**7.35**	**7.49**	**7.43**	**7.57**	**7.57**	**7.75**	**7.80**	**7.93**	**8.09**	**8.23**	**8.34**	**8.42**	**8.49**
Landfills [3]	***7.11***	***7.23***	***7.14***	***7.26***	***7.24***	***7.40***	***7.42***	***7.53***	***7.66***	***7.78***	***7.86***	***7.92***	***7.97***
Composting	***0.24***	***0.26***	***0.29***	***0.31***	***0.33***	***0.36***	***0.38***	***0.40***	***0.43***	***0.45***	***0.47***	***0.50***	***0.52***
High GWP	**8.03**	**7.99**	**8.14**	**8.83**	**9.56**	**10.36**	**11.08**	**11.78**	**12.87**	**13.99**	**15.89**	**17.35**	**18.41**
Ozone Depleting Substance (ODS) Substitutes	***7.00***	***7.17***	***7.37***	***8.06***	***8.87***	***9.71***	***10.41***	***11.16***	***12.24***	***13.49***	***15.36***	***16.58***	***17.73***
Electricity Grid SF6 Losses [4]	***0.33***	***0.32***	***0.30***	***0.29***	***0.30***	***0.29***	***0.28***	***0.26***	***0.27***	***0.26***	***0.24***	***0.24***	***0.23***
Semiconductor Manufacturing [3]	***0.70***	***0.50***	***0.47***	***0.48***	***0.40***	***0.36***	***0.39***	***0.36***	***0.36***	***0.23***	***0.29***	***0.53***	***0.45***
Agriculture	**32.52**	**32.75**	**35.99**	**36.50**	**36.26**	**36.54**	**37.75**	**37.03**	**37.99**	**35.84**	**35.73**	**36.34**	**37.86**
Livestock	***19.66***	***20.44***	***21.06***	***21.63***	***21.06***	***21.81***	***22.22***	***23.73***	***24.09***	***23.88***	***23.35***	***23.38***	***23.92***
Enteric Fermentation (Digestive Process)	10.26	10.45	10.74	10.89	10.78	11.14	11.24	11.93	11.89	11.71	11.51	11.49	11.78
Manure Management	9.40	10.00	10.32	10.75	10.28	10.67	10.98	11.80	12.20	12.17	11.84	11.89	12.14
Crop Growing & Harvesting	***9.05***	***8.48***	***10.54***	***10.49***	***10.67***	***10.11***	***10.20***	***9.50***	***9.98***	***9.31***	***9.57***	***9.30***	***10.22***
Fertilizers	7.01	6.73	8.56	8.57	8.49	8.09	8.01	7.49	8.04	7.32	7.58	7.25	8.16
Soil Preparation and Disturbances	1.96	1.69	1.91	1.86	2.11	1.95	2.12	1.94	1.87	1.92	1.91	1.98	1.98
Crop Residue Burning	0.08	0.06	0.06	0.07	0.07	0.07	0.07	0.07	0.07	0.07	0.08	0.08	0.08
General Fuel Use	***3.82***	***3.83***	***4.39***	***4.38***	***4.53***	***4.63***	***5.33***	***3.80***	***3.92***	***2.65***	***2.81***	***3.66***	***3.72***
Diesel	2.52	2.70	3.05	3.11	3.18	3.41	3.87	2.68	3.00	1.79	1.99	2.37	2.47
Natural Gas	0.98	0.75	0.94	0.85	0.82	0.70	0.88	0.79	0.75	0.69	0.65	0.66	0.70
Gasoline	0.31	0.38	0.41	0.41	0.52	0.52	0.57	0.32	0.17	0.17	0.17	0.63	0.55
Other Fuels	0.01	0.00	0.00	0.00	0.00	0.00	0.01	0.00	0.00	0.00	0.00	0.00	0.00
Total Emissions	***466.32***	***481.23***	***480.32***	***483.05***	***492.86***	***485.13***	***482.52***	***489.16***	***487.10***	***458.44***	***453.06***	***450.94***	***458.68***

[1] Includes equipment used in construction, mining, oil drilling, industrial and airport ground operations
[2] Reflects emissions from combustion of natural gas, diesel, and lease fuel plus fugitive emissions
[3] These categories are listed in the Industrial sector of ARB's GHG Emission Inventory sectors
[4] This category is listed in the Electric Power sector of ARB's GHG Emission Inventory sectors

California Environmental Protection Agency
Air Resources Board

Last reviewed on January 30, 2015

2020 Business-as-Usual (BAU) Emissions Projection
2014 Edition

Overview

An emission projection estimates future emissions based on current emissions, expected regulatory implementation, and other technological, social, economic, and behavioral patterns. The projected 2020 emissions provided here represent a Business-as-Usual (BAU) scenario assuming none of the Scoping Plan measures are implemented. The 2020 BAU emissions estimate assists the Air Resources Board (ARB) in demonstrating progress toward meeting the 2020 goal of 431 MMTCO2e (the revised target using Global Warming Potentials (GWP) from the IPCC Forth Assessment Report (AR4)).

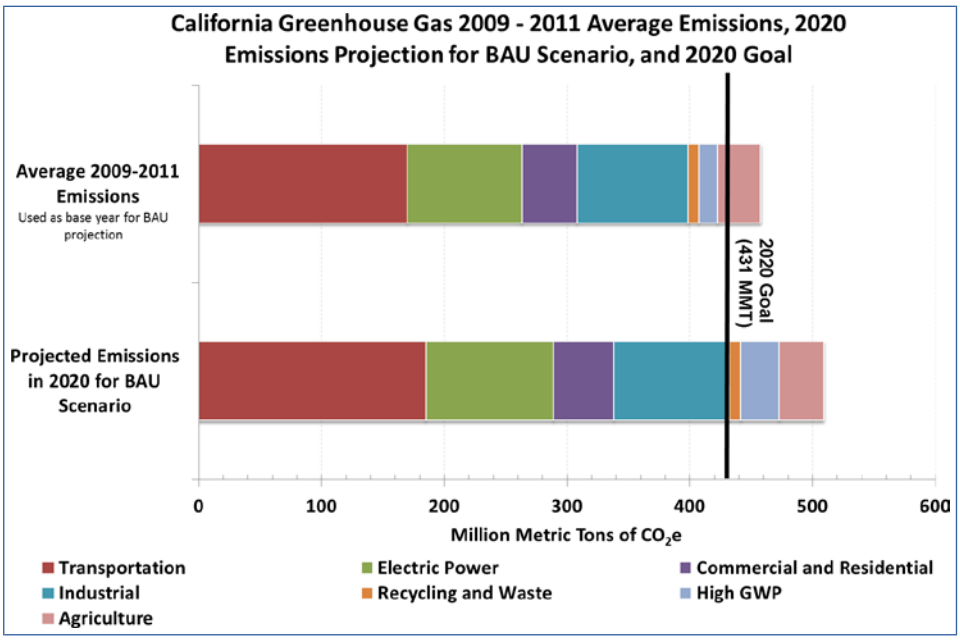
The ARB prepared the first version of 2020 GHG emissions projection in 2008 for the original AB32 Scoping Plan and a second version in 2010 to support Cap & Trade. Previous versions of the 2020 projection are still available on the archived BAU page. The 2020 BAU emissions projection has been revisited in support of the First Update to the Scoping Plan (2014). This projection accounts for updates to the economic forecasts of fuel and energy demand as well as other factors. It also accounts for the effects of the recent economic recession and the projected recovery. Data sources, methods and assumptions are available in the links section below.

The 2020 BAU emissions projection uses the average statewide GHG emissions for 2009-2011 as the base year. Using a three year average dampens variations that may make a given year unsuitable as the basis for projection analysis. For example, using a hot and dry year, with higher power consumption and less hydroelectric power generation as the base year would skew the projected emissions associated with power generation. The current 2020 BAU emissions projection uses GWP values from IPCC AR4, while the previous versions used IPCC Second Assessment Report (SAR) GWPs. The total emissions expected in the 2020 BAU scenario includes reductions anticipated from Pavley I and the Renewable Electricity Standard (30 MMTCO2e total). With these reductions in the baseline, estimated 2020 statewide BAU emissions are 509 $MMTCO_2e$.

2020 BAU Emissions

The bar graph below shows the 2020 BAU emissions relative to the base year average of 2009-2011 by sector. Half the BAU growth in 2020 comes from the Transportation and Electric Power sectors, while another third comes from the High GWP sector alone. Energy use (as seen in the transportation and electricity use emissions) is a driving force leading to emissions increases in the future. Fortunately, these emissions are regulated under Cap & Trade so actual 2020 emissions will be lower than the BAU scenario.

Below the chart are links to materials and methods related to the 2020 BAU emissions projection. These include a summary of 2020 BAU emissions by sector, emissions reduction contribution from each complementary measure, documentation of data sources and methods, time series of projected BAU emissions, and links to previous projections created in support of the AB32 Scoping Plan (2008) and the Cap & Trade Regulation (2010).



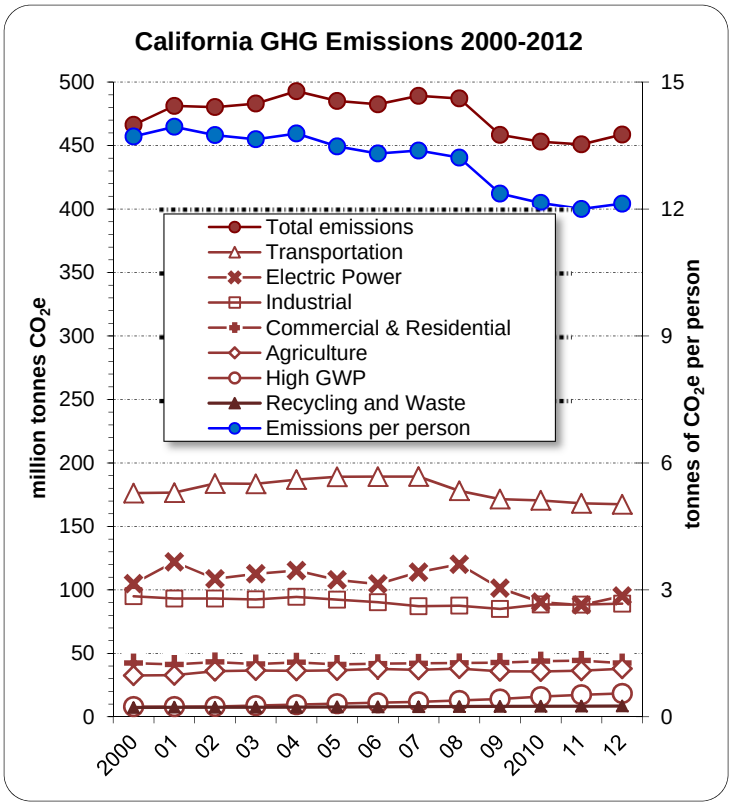
Links:

- 2020 BAU Emissions by Scoping Plan Categories [PDF-18.3 KB]
- Data Sources, Methods, and Assumptions [PDF-41 KB]
- Emissions Reductions from Scoping Plan Measures [PDF-194 KB]
- 2020 BAU Projection Time Series 2009-2020 [PDF-11 KB]
- Archive of Previous 2020 BAU Emissions Projections
- AB 32 Scoping Plan

California Greenhouse Gas Emissions for 2000 to 2012 – Trends of Emissions and Other Indicators

Overview

The Global Warming Solutions Act of 2006 (AB 32) set a goal to reduce California's greenhouse gas (GHG) emissions to 1990 levels by 2020. Annual statewide GHG emission inventories provide an important tool for establishing historical emission trends and tracking California's progress towards the 2020 goal. Over the period of 2000-2012, GHG emissions have decreased by 1.6%.



The 2012 inventory demonstrates that as the state's gross domestic product continues to rise –by 5 percent since 2009 – the carbon intensity, which is the amount of carbon pollution related to the state's overall economy, has fallen steadily over the same time period. This demonstrates that California is getting more economic development for each ton of greenhouse gases emitted overall.

Emissions from the transportation sector –still California's largest single source of greenhouse gases, contributing 36 percent of total emissions– declined marginally compared to 2011, even while the economy continued to grow. The long term direction of transportation-related GHG emissions is another clear trend, with a 12-percent drop over the past seven years.

In 2012, total GHG and per capita emissions increased for the first time, albeit only by a single percentage point, in the last five years. This increase was driven primarily by strong economic growth in the state, the unexpected closure of the San Onofre Nuclear Generating Station (SONGS), and drought conditions that limited in-state hydropower.

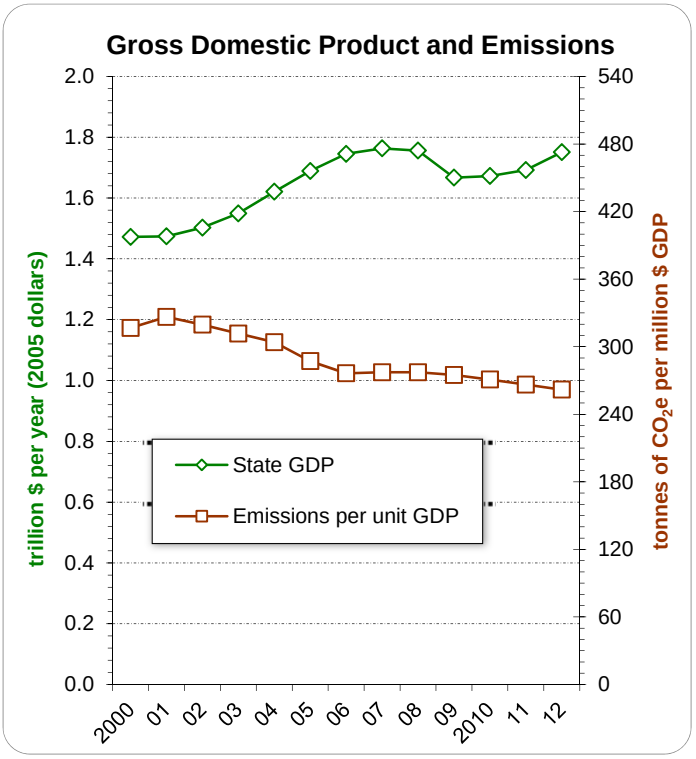
Emissions from sectors other than electricity remained relatively constant from 2011, and the GHG carbon intensity of California's economy continued to decline in 2012.

Beginning in 2013, California's Cap-and-Trade program will ensure that emissions continually decline, even alongside stronger economic growth and potentially drier hydrological conditions, and in the event of any additional unforeseen circumstances.

The 2014 edition GHG inventory represents a transition to global warming potentials (GWPs) from the Intergovernmental Panel on Climate Change (IPCC) 4th Assessment Report[1] (AR4). Previous GHG inventories relied on GWPs from IPCC's Second Assessment Report (SAR).

Introduction

California's gross emissions of greenhouse gases decreased by 1.6 percent from 466.3 million metric tons (or tonnes) of CO_2e (equivalents of CO_2) in 2000 to 458.7 million in 2012, with a maximum of 492.7 million tonnes in 2004. During the same period, California's population grew by 11 percent from 34 to 37.8 million people[2]. As a result, California's per capita GHG emissions have generally decreased over the last 12 years from 13.7 in 2000 to 12.1 tonnes of CO_2e per person in 2012.

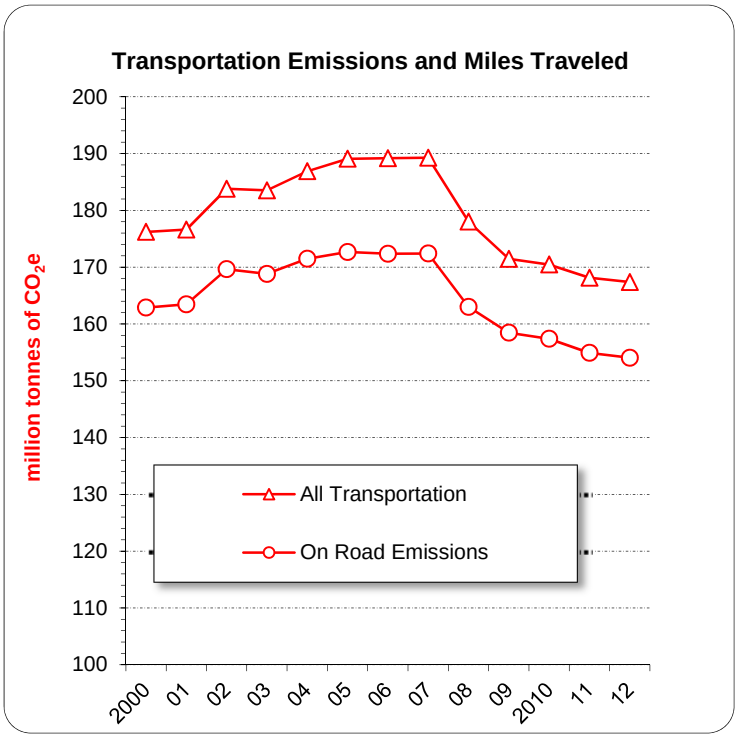


California's Gross Domestic Product (GDP) increased from $1.47 trillion in 2000 to $1.75 trillion in 2012 (in 2005 dollars)[3]. While California's economy has continued to grow, the "carbon intensity" of the economy (tonnes CO_2/ GDP$) has continually declined since 2001, and has decreased from 316.6 tonnes CO_2e per million dollars in 2000 to 261.9 tonnes per million dollars in 2012.

In the IPCC's 4th assessment report[1] (AR4), the GWPs for several GHGs were updated based on the latest science. As a result, the GWP of methane changed from 21 to 25, the GWP for nitrous oxide (N_2O) decreased, and the GWPs for hydrofluorocarbons (HFCs) and perfluorocarbons (PFCs) were updated. For comparability between years, the emissions in all of the 2000 – 2012 years have been updated using AR4 GWPs.

A summary of emission trends for each major sector of the statewide greenhouse gas inventory is provided below. Emissions data is organized by categories in the 2008 Scoping Plan.

Transportation



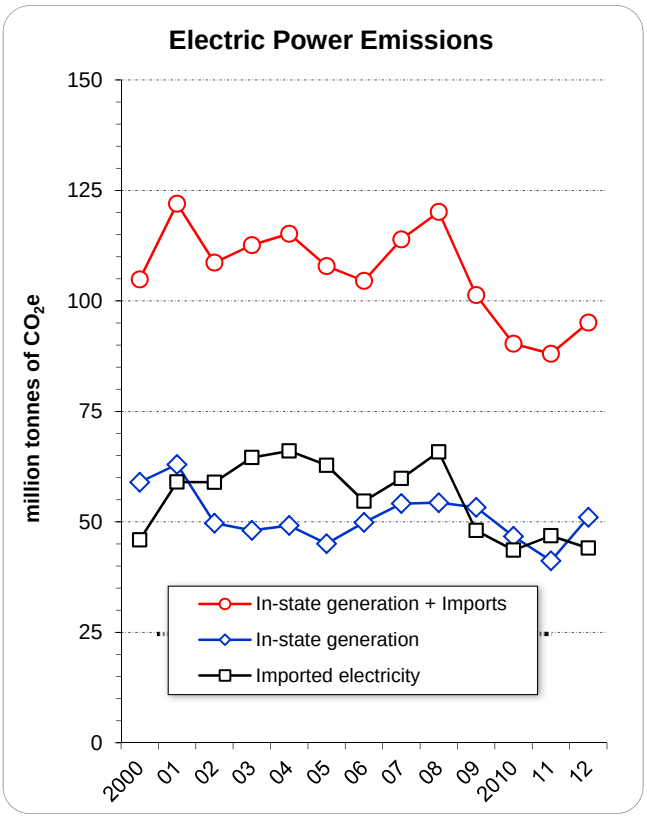
The transportation sector remains the largest source of GHG emissions in 2012, accounting for 36 percent of California's GHG emission inventory. Contributions from the transportation sector include emissions from on-road and off-road vehicles, aviation, rail and water-borne vehicles, and some other minor sources. Transportation-related GHG emissions have dropped 12 percent since reaching a maximum in 2007. In 2012, emissions from the on-road category decreased by 0.5 percent from the previous year.

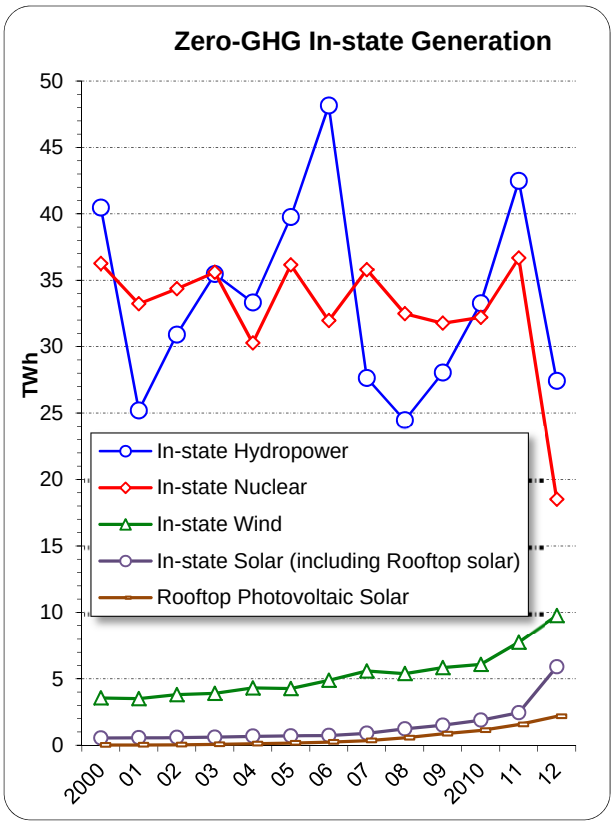
Emissions from on-road sources, which consist of light-duty vehicles (cars, motorcycles, and light-duty trucks), heavy-duty trucks, and buses, accounted for over 92 percent of transportation sector GHG emissions in 2012. Of the on-road vehicles, light duty vehicles accounted for approximately 69 percent of emissions in 2012. On-road emissions have declined each year since 2006. Total transportation sector emissions have continued to decrease since 2007. Emissions from military transportation activities are not included in the inventory total for the State, and would represent less than 1 percent of total statewide emissions.

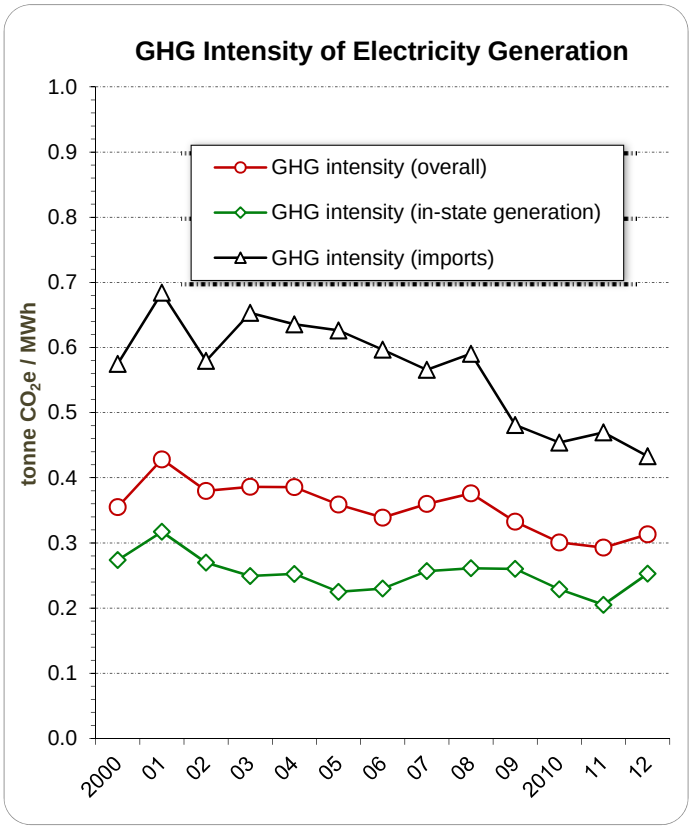
Electric Power

The GHG emission inventory divides the electric power sector into two broad categories, emissions from in-state power generation and emissions from imported electricity.

Total GHG emissions from electric power increased in 2012 for the first time since 2008, driven by greater reliance on natural gas electricity generation sources. This increase in reliance on in-state natural gas generation resulted from the loss of generation due to the closure of the San Onofre Nuclear Generating Station (SONGS) as well as the drought in 2012, causing a drop in the in-state hydropower generation. As these two major electricity generation sources dropped (33 TWh from 2011 to 2012), in-state generation by natural gas needed to increase to meet the electricity demand. Beginning in 2013, California's Cap-and-Trade program will ensure that any unexpected event, such as the SONGS closure, does not increase statewide emissions.







Year 2012 also saw a marked increase in in-state solar generation. Total solar generation in 2012 increased by more than 140 percent from 2011 and rooftop photovoltaic solar generation increased by 40 percent in the same period. In-state generation from wind energy also increased by 26 percent from the previous year.

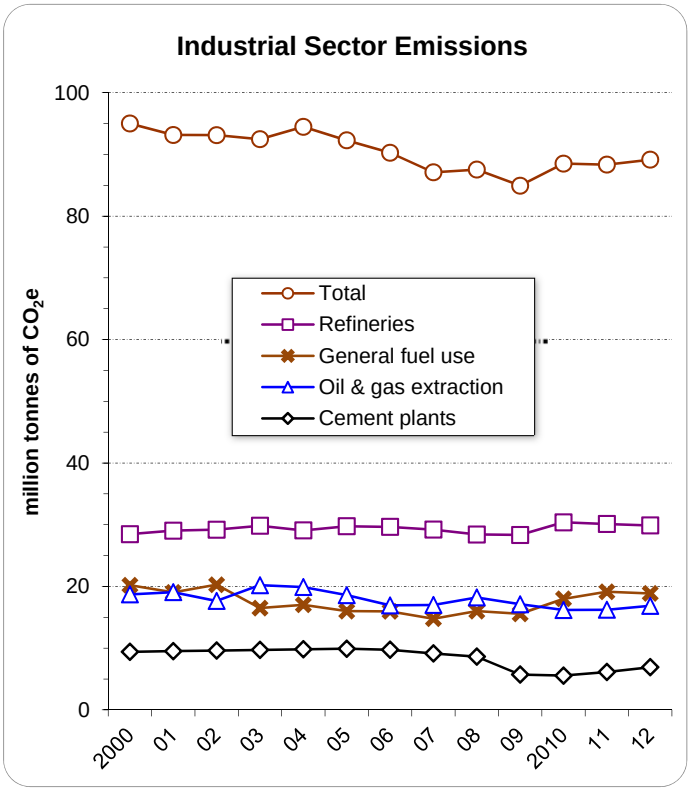
The 12-year trend shows a drop from 104.9 million tonnes CO_2e in 2000 to 95.1 million tonnes in 2012, reaching a high of 122.0 million tonnes in 2001 and a low of 88.0 million tonnes in 2011. During that same period, electricity consumption saw steady growth from 250 terawatt hours (TWh) in 2001 to 288 TWh in 2008, followed by a steady decline to 274.2 TWh in 2011 with a slight rise to 282.1 TWh in 2012[4].

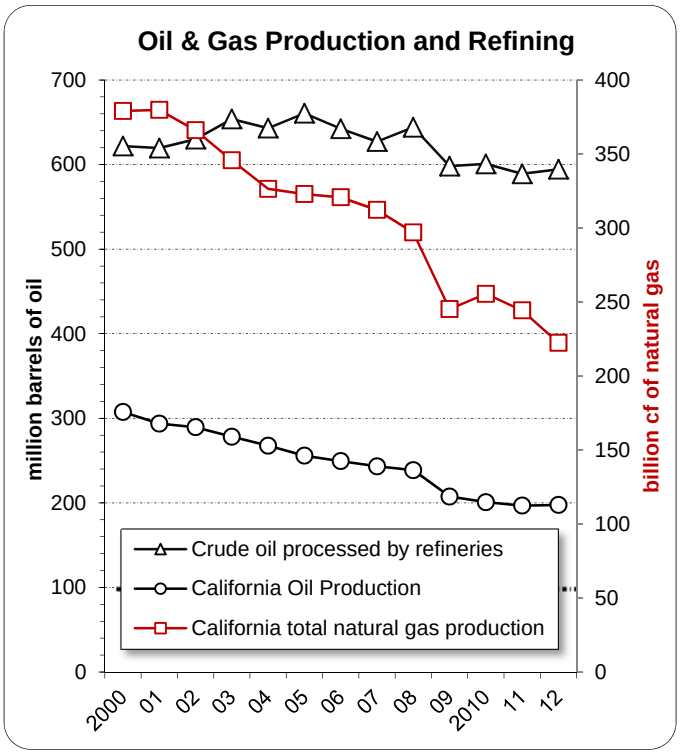
In general, California generates approximately 70 percent of its electricity from power plants located within the state and imports the rest[5]. The GHG intensity of electricity imports declined to its lowest point in 2012, as coal imports continued to decline and greater amounts of renewable imports took their place. Over the last thirteen years, hydropower provided an average of 17 percent of California's in-state power generation. Hydrologic conditions produced two major wet years between 2000 and 2012 — 2006 and 2011. In 2006, hydropower accounted for over 22 percent of in-state power generation and in 2011, it was approximately 21 percent. However, 2012 was a dry year and the hydropower share was only 13.6 percent. The GHG intensity of California electricity peaked in 2001, a year marked by drought and electricity market manipulation. It reached a low point in 2011, a particularly wet year and increased again in 2012, due both to the drought and the closure of SONGS.

Industrial

Industrial emission sources include refineries, oil & gas extraction, cement plants, and other stationary sources that primarily consume fuel. The GHG emissions from industrial sources increased approximately 1 percent between 2011 and 2012. Emissions from this sector have been increasing since 2009.

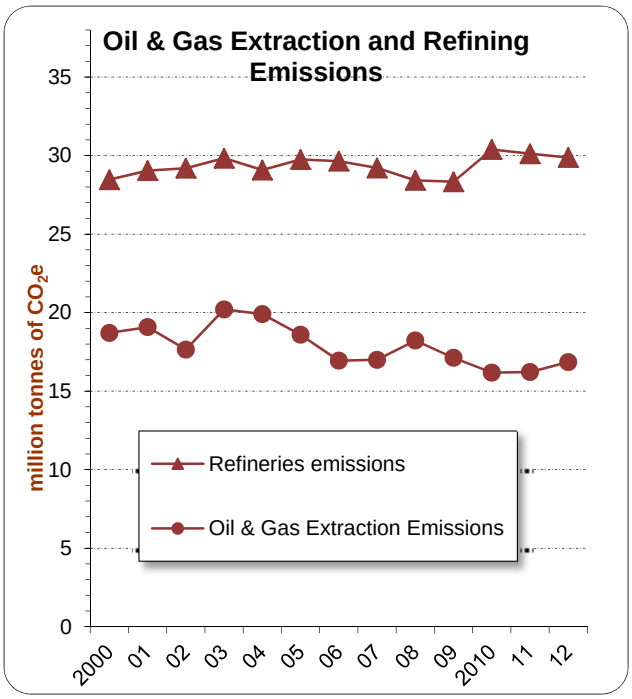
Among the industrial emissions categories, refineries represent about 33 percent of the sector's total emissions. Emissions from refineries remained relatively constant for most of the last thirteen years, with small year-to-year changes. Most recently, refinery emissions increased markedly in 2010 and then declined steadily, to 29.9 million tonnes of CO_2e in 2012. The total net crude oil processed by refineries was 622 million barrels in 2000 and peaked at 661 million in 2005; it dipped to 594 million barrels in 2012[6].

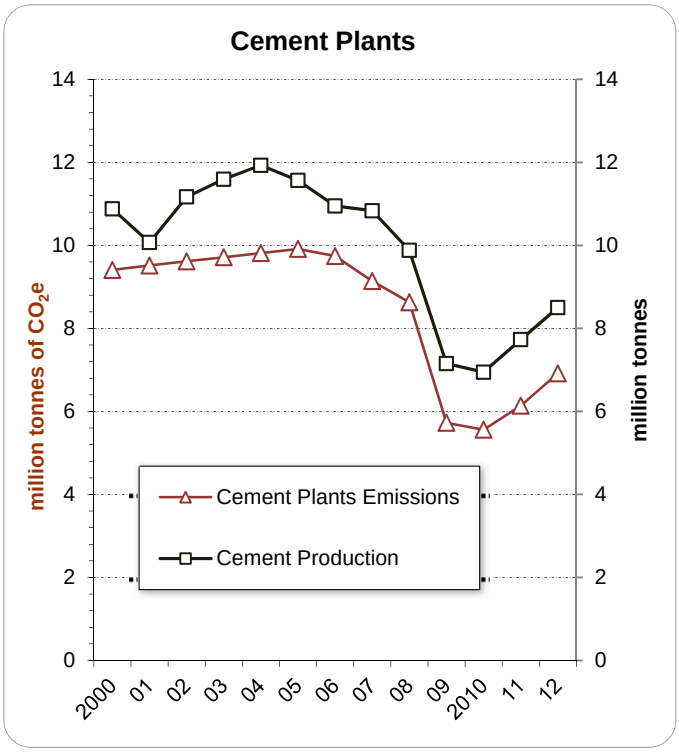




Emissions from oil and gas extraction, another major industrial category, have fluctuated over the last decade from a high of 20.2 million tonnes in 2003 to a low of 16.2 million tonnes in 2010. Emissions increased between 2011 and 2012 by about four percent. Oil and gas production in California declined substantially since 2000: from 307 to 197 million barrels of oil and from 379 billion cubic feet of natural gas to 222 billion in 2012[7]. Declining production from oil wells requires significant fuel use for steam generation which is forced into the wells to stimulate lagging oil production. Although oil production drops, more energy is utilized to extract oil from wells and emissions remain relatively constant.

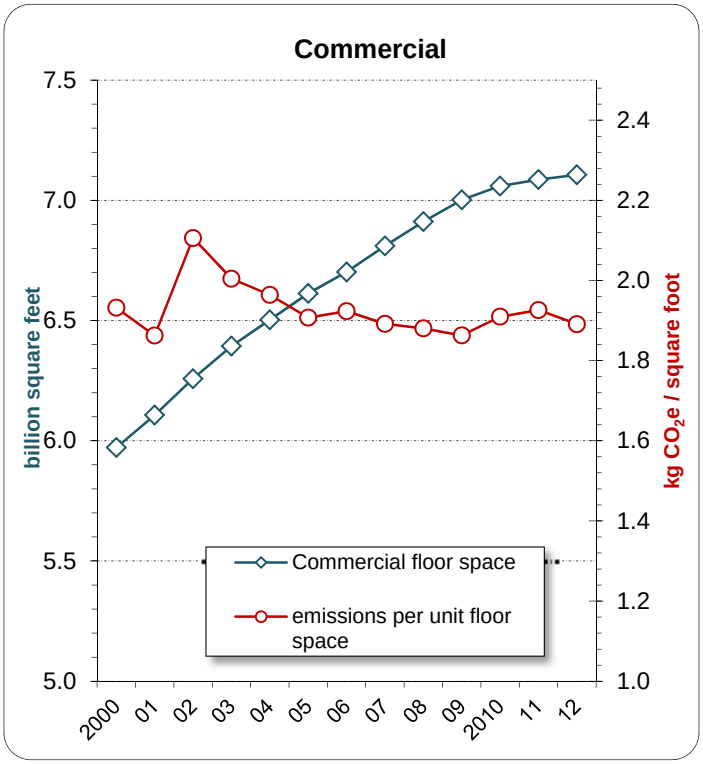
Emissions from cement plants, made up of fuel combustion and clinker process emissions, grew 10 percent in 2012, correlating with the growth in the economy. After 2010, cement production and GHG emissions have grown steadily again since the recession. Longer term trends show that emissions peaked in 2005 with a decrease beginning in 2006 and continuing through 2010. Between 2006 and 2010, cement plant emissions declined 44 percent, reflecting both a large decrease in demand and the closure of three cement plants over the period[8]. This decline continued in 2010 with California cement plants operating at 51 percent capacity[9].



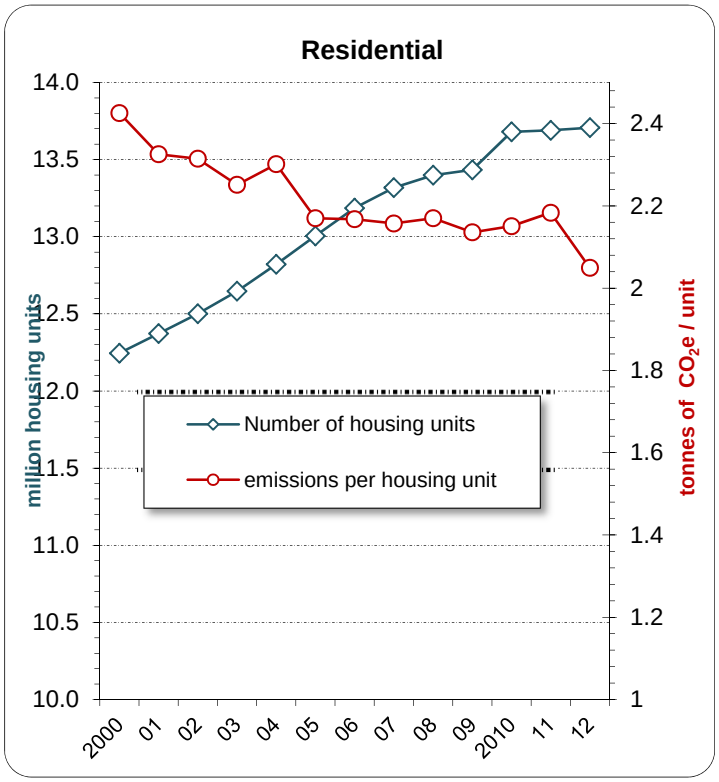


Commercial and Residential

Emissions from the commercial and residential sectors are driven by the combustion of natural gas and other fuels for household use and for providing energy for commercial businesses. In 2012, emissions declined 5 percent from the previous year. While combined emissions from the commercial sector and residential sector have exhibited limited year-to-year variation, individually the sectors exhibit different trends.



The majority of emissions from the residential sector are from natural gas combustion. Although the number of housing units grew steadily from 12.2 million units in 2000 to slightly over 13.7 million housing units in 2012, emissions and fuel consumption per housing unit have generally followed a declining trend during this period[10]. Total emissions from residential fuel combustion show little variation over the last thirteen years ranging from a low in 2005 of 28.1 million tonnes to a high in 2011 of 29.9 million tonnes. The major cause of fuel use fluctuations is annual temperature levels, with colder years resulting in greater fuel use for heating.



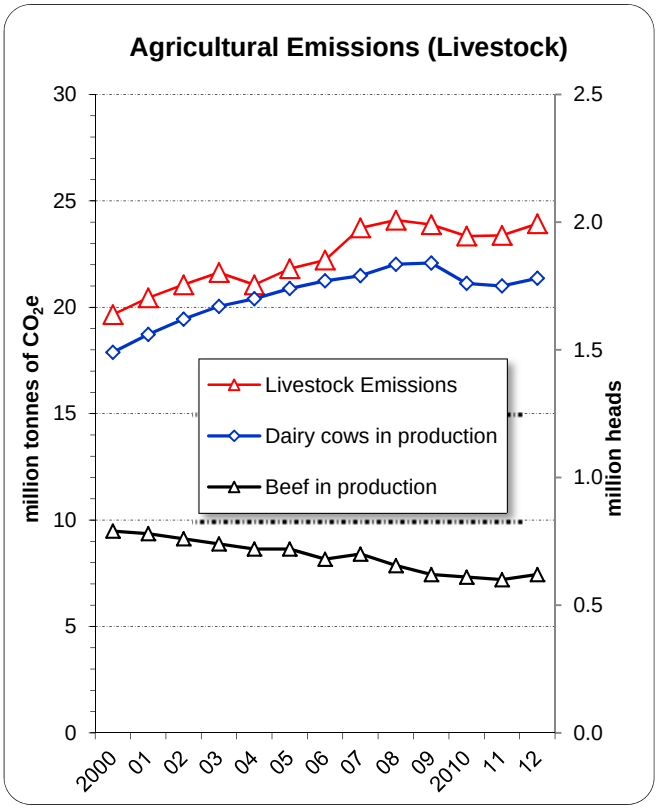
Emissions from commercial fuel use have grown over the period of 2000 and 2012, ranging between 11.5 million tonnes in 2002 to 13.4 million tonnes in 2012. Commercial floor space grew steadily in California from 6.0 billion square feet to 7.1 billion square feet between 2000 and 2012[11]. Like the residential sector, the commercial sector exhibits a slight decline in fuel use per unit of space.

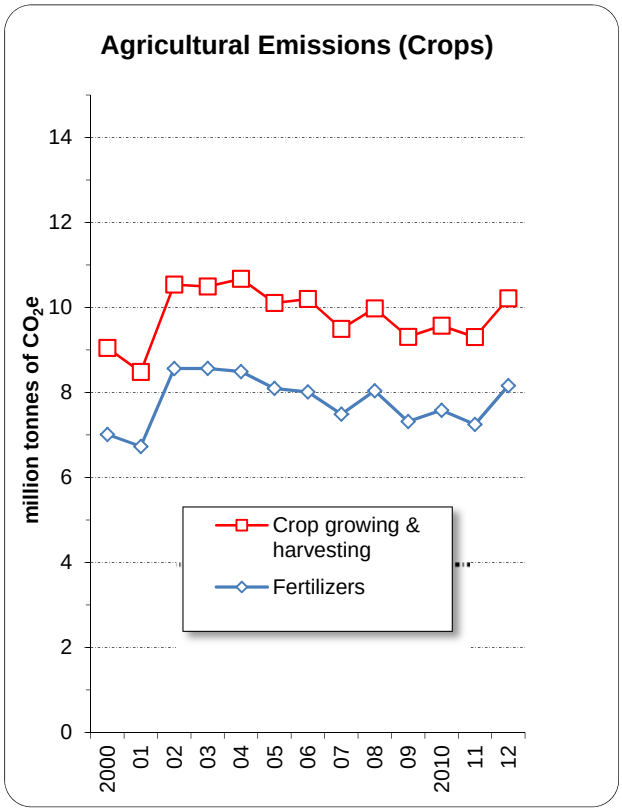
Agriculture

The agricultural sector contributed to more than 8 percent to the total statewide GHG emissions in 2012, mainly from CH_4 and N_2O sources. Livestock account for 63 percent of the total agricultural emissions. Dairy cows are the primary source of these livestock emissions. The enteric fermentation process as well as the manure management practices in dairies give rise to methane emissions, making dairies the major emissions source in the agricultural sector.

California dairies increased their herds from 1.5 million cows in 2000 to 1.8 million in 2012, and their total milk production from 32 to 42 billion pounds[12]. The GHG emissions from livestock manure management and enteric fermentation increased by 22 percent during the same time. Emissions from the agriculture sector grew from 32.5 million tonnes of CO_2e in 2000 to 37.9 million tonnes in 2012.

Emissions from crop growing and harvesting (primarily N_2O emissions from fertilizer use) varied from 9.0 million tonnes of CO_2e in 2000 to approximately 10.2 million tonnes in 2012. About 80 percent of crop related GHG emissions are from the use of fertilizers.



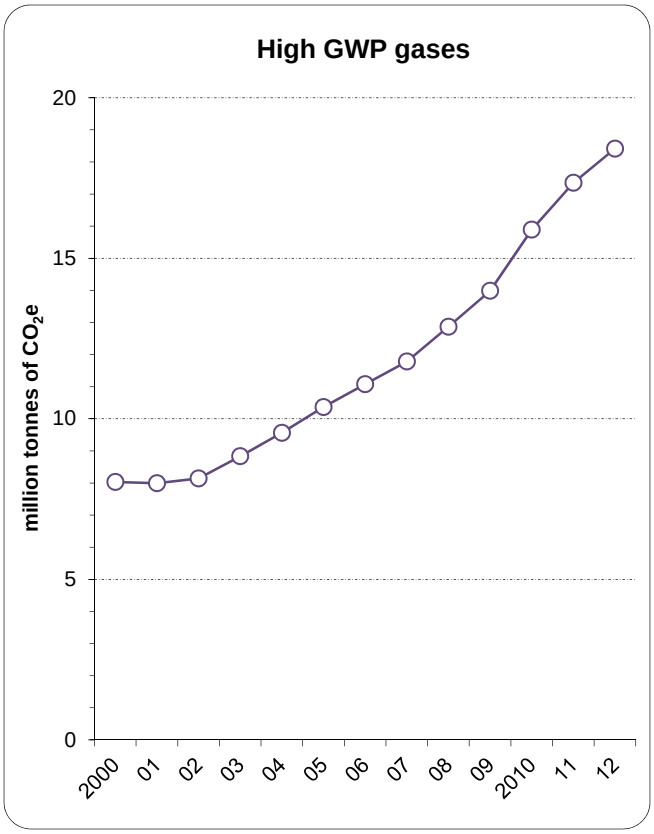


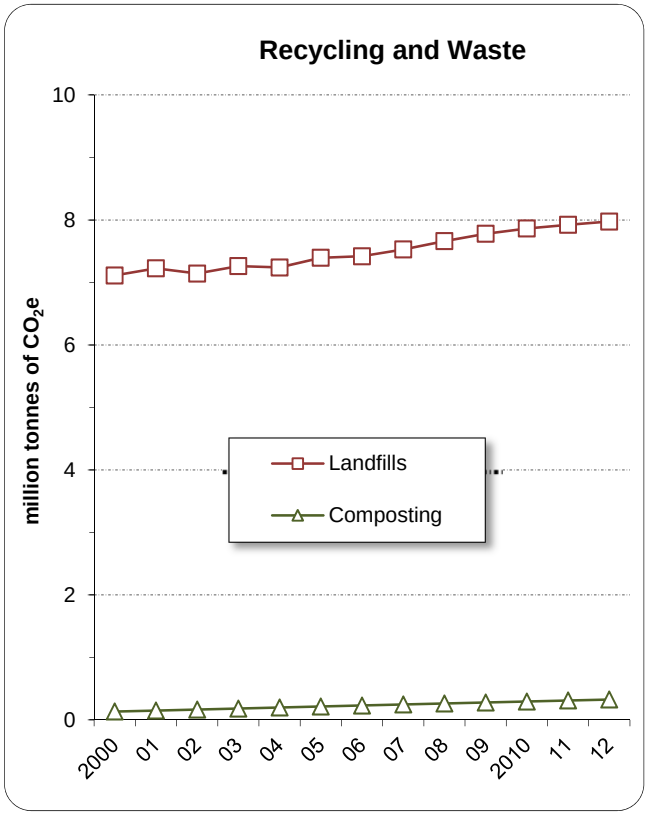
High Global Warming Potential Gases

High Global Warming Potential (high-GWP) gases included in the inventory consist primarily of substitutes for ozone depleting substances (ODS)—primarily HFCs and PFCs—that are used in a variety of applications, including refrigeration and air conditioning equipment, solvent cleaning, foam production, sterilization, fire extinguishing, and aerosols. Since the 1990's, use of ozone depleting substance (ODS) substitutes has grown progressively as they are phased in as replacements for CFCs and HCFCs.

Emissions of all high-GWP gases make up about 4 percent of total statewide GHG emissions in the 2012 inventory. High GWP gas emissions have grown steadily from 8.0 million tonnes of CO_2e in 2000 to 18.4 million tonnes in 2012. This increase is driven both by the increased use of associated applications as well as the displacement of existing ODS gases by these substitutes.

While emissions from most sectors are increasing, some sectors are showing reductions in emissions. Overall, fugitive emissions of SF_6 from electrical switchgears have decreased over the time period 2000 to 2012 by about 29 percent, while high-GWP gases from semiconductor manufacturing have decreased between 2000 and 2012 by about 35 percent. This decrease is believed to have two causes: a sharp increase in the price of SF_6 during the 1990s and a growing awareness of the environmental impact of SF_6 emissions through programs such as EPA's SF_6 Emission Reduction Partnership for Electric Power Systems.





Recycling and Waste

Emissions from the recycling and waste sector consist of methane and nitrous oxide emissions from landfills and from commercial-scale composting. Emissions from recycling and

waste grew from 7.3 million tonnes of CO_2e in 2000 to 8.5 million tonnes in 2012.

Emissions from landfills account for more than 94 percent of the total sector emissions. In 2000, 37 million tons of solid waste was deposited in California's landfills; this amount grew to 42 million tons by 2005, followed by a steady decline to 29 million tons in 2012[13]. The decrease in annual landfill deposits does not produce immediate corresponding declines in landfill GHG emissions since it is the momentum of the total waste-in-place accumulated in the past that also influences the amount of landfill gas generated. GHG emissions from composting have remained relatively small over the last thirteen years, accounting for 6 percent of total sector GHG emissions in 2012.

References

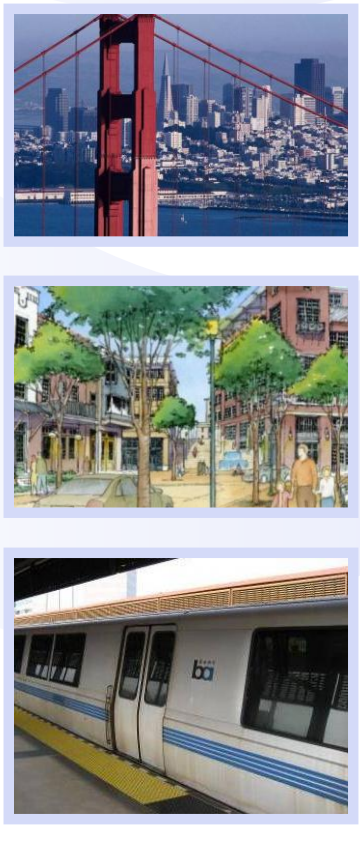
1 – Intergovernmental Panel for Climate Change (IPCC) 4th Assessment Report – Climate Change 2007 (AR4).
2 – California Department of Finance – California Statistical Abstract (including 2010 census data)
3 – California Department of Finance – California State Gross Domestic Product (GDP) 1963 – 2012.
4 – California Energy Commission – California Energy Consumption Database, 2012.
5 – Based on California Energy Commission and U.S. Energy Information Administration data, Electricity Data Browser for 2012.
6 – California Energy Commission – Weekly Fuels Watch Report, 2012.
7 – California Department of Conservation – Annual Reports of the State Oil & Gas Supervisor, 2000-2012.
8 – U.S. Geological Survey – 2012 Mineral Yearbook
9 – U.S. Geological Survey – 2011 Mineral Yearbook
10 – U.S. Census Bureau – State Housing Units Estimates, 2012.
11 – California Energy Commission – Demand forecasting estimates, 2012.
12 – U.S. Department of Agriculture – National Agricultural Statistics Service, Report for 2012.
13 – CalRecycle - Solid Waste Disposal Tonnage Summary Data, 2000-2012.

BAY AREA AIR QUALITY MANAGEMENT DISTRICT

California Environmental Quality Act

Air Quality Guidelines





Updated May 2011

BAY AREA AIR QUALITY MANAGEMENT DISTRICT

California Environmental Quality Act

Air Quality Guidelines

Jack P. Broadbent
Executive Officer/Air Pollution Control Officer

Jean Roggenkamp
Deputy Air Pollution Control Officer

Jeffrey McKay
Deputy Air Pollution Control Officer

Brian Bunger
District Counsel

PRINCIPAL CONTRIBUTORS:

Henry Hilken
Director of Planning, Rules and Research

Dave Vintze
Planning Manager

Greg Tholen
Principal Environmental Planner, Project Manager

Phil Martien
Senior Advanced Project Advisor

Virginia Lau
Advanced Project Advisor

Abby Young
Principal Environmental Planner

Alison Kirk
Senior Environmental Planner

Sigalle Michael
Senior Environmental Planner

BAY AREA AIR QUALITY MANAGEMENT DISTRICT
939 Ellis Street
San Francisco, CA 94109
415-749-5000

UPDATED MAY 2011

The following updates were made in May 2011 to the June 2010 CEQA Guidelines:

2: Thresholds of Significance

- In table 2-1, updated the effective date for the risk and hazards threshold for new receptors.
- In section 2.2, clarified that GHG threshold is based on carbon dioxide equivalent emissions and not just CO2.

3: Screening Criteria

- In section 3.2, clarified that the screening values in Table 3-1 may not be applied as screening level sizes for risk and hazard impacts.
- In section 3.3, clarified that the carbon monoxide screening criteria do not apply to stationary source projects.
- In section 3.5.1, clarified that projects with demolition activities that are inconsistent with BAAQMD's Regulation 11, rule: Asbestos Demolition, Renovation, and Manufacturing cannot be screened using the screening level in Table 3-1.

4: Operational-Related Impacts

- In section 4.2.1, page 4-5, clarified that the GHG threshold is based on carbon dioxide equivalent emissions; and clarified use of BGM as preferred model for estimating greenhouse gas emissions from a proposed land use project

5: Local Community Risk and Hazard Impacts

- Updated sections 5.2.6 and 5.2.7 to reflect the updated stationary source, highway, and roadway screening tools made available in May 2011.

6: Local Carbon Monoxide Impacts

- In section 6.1, clarified that the carbon monoxide screening criteria do not apply to stationary source projects and that potential carbon monoxide impacts from stationary sources should be modeled using AERMOD.

8: Assessing and Mitigation Construction-Related Impacts

- In section 8.1.1, removed Table 8-1.

Appendix B: Air Quality Modeling Instructions and Project Examples

- Pages B-11 to B-13, clarified the percent reductions that apply to construction mitigation measures and corrected references to tables and sections in the CEQA Guidelines.

Other minor editorial edits were made throughout the CEQA Guidelines as needed.

BAY AREA AIR QUALITY MANAGEMENT DISTRICT

TABLE OF CONTENTS

ACRONYMS AND ABBREVIATIONS v

1. INTRODUCTION 1-1
1.1. Purpose of Guidelines 1-1
1.2. Guideline Components 1-3

PART I: THRESHOLDS OF SIGNIFICANCE & PROJECT SCREENING 1-1

2. THRESHOLDS OF SIGNIFICANCE 2-1
2.1. Criteria Air Pollutants and Precursors – Project Level 2-3
2.2. Greenhouse Gases – Project Level 2-4
2.3. Local Community Risk and Hazard Impacts – Project Level 2-4
2.4. Local Carbon Monoxide Impacts – Project level 2-5
2.5. Odor Impacts – Project Level 2-5
2.6. Construction-related Impacts – Project Level 2-6
2.7. Thresholds Of Significance for Plan-Level Impacts 2-7

3. SCREENING CRITERIA 3-1
3.1. Operational-Related Impacts 3-1
3.2. Community Risk and Hazard Impacts 3-3
3.3. Carbon Monoxide Impacts 3-3
3.4. Odor Impacts 3-4
3.5. Construction-Related Impacts 3-5

PART II: ASSESSING & MITIGATING PROJECT LEVEL IMPACTS 3-1

4. OPERATIONAL-RELATED IMPACTS 4-1
4.1. Criteria Air Pollutant and Precursor Emissions 4-1
4.2. Greenhouse Gas Impacts 4-4
4.3. Greenhouse Gas Reduction Strategies 4-7
4.4. Mitigating Operational-Related Impacts 4-11

5. LOCAL COMMUNITY RISK AND HAZARD IMPACTS 5-1
5.1. Toxic Air Contaminants 5-1
5.2. Single Source Impacts 5-3
5.3. Cumulative Impacts 5-15
5.4. Community Risk Reduction Plans 5-16
5.5. Mitigating Local Community Risk and Hazard Impacts 5-17

6. LOCAL CARBON MONOXIDE IMPACTS 6-1
6.1. Significance Determination 6-1
6.2. Mitigating Local Carbon Monoxide Impacts 6-4

7. ODOR IMPACTS 7-1
7.1. Significance Determination 7-2
7.2. Mitigating Odor Impacts 7-3

8. CONSTRUCTION-RELATED IMPACTS 8-1
8.1. Criteria Air Pollutants and Precursors 8-1
8.2. Greenhouse Gases 8-6
8.3. Toxic Air Contaminants 8-6

PART III: ASSESSING & MITIGATING PLAN LEVEL IMPACTS 8-1

9. PLAN-LEVEL IMPACTS 9-1
9.1. Criteria Air Pollutants and Precursor Emissions 9-2

9.2. Greenhouse Gases 9-3
9.3. Local Community Risk and Hazard Impacts 9-6
9.4. Odor Impacts 9-7
9.5. Regional Plans 9-8
9.6. Mitigating Plan-level Impacts 9-8

Appendices

A Construction Assessment Tools
B Air Quality Modeling Instructions and Project Examples
C Sample Air Quality Setting
D Threshold of Significance Justification
E Glossary

List of Figures

1-1 Bay Area Air Quality Management District Jurisdictional Boundaries 1-2

1-2 General Steps for Determining Significance of Air Quality Impacts 1-4

5-1 Impacted Communities 5-4

5-2 Phased Approach for Estimating Community Risks and Hazards – Sources 5-6

5-3 Phased Approach for Estimating Community Risks and Hazards – Receptors 5-9

List of Tables

Table 2-1 Air Quality CEQA Thresholds of Significance* 2-1

Table 2-2 Thresholds of Significance for Operational-Related Criteria Air Pollutants and Precursors 2-4

Table 2-3 Thresholds of Significance for Local Carbon Monoxide Emissions 2-5

Table 2-4 Thresholds of Significance for Construction-Related Criteria Air Pollutants and Precursors 2-6

Table 2-5 Thresholds of Significance for Plans 2-7

Table 3-1 Criteria Air Pollutants and Precursors and GHG Screening Level Sizes 3-2

Table 3-3 Odor Screening Distances 3-4

Table 4-1 Example Operational Criteria Air Pollutant and Precursor Emissions Analysis 4-4

Table 4-2 Guidance for Estimating a Project's Operations GHG Emissions 4-6

Table 4-3 Example of Operational Greenhouse Gas Emissions Analysis 4-7

Table 5-1 Screening Data for Existing Permitted Stationary Sources* (within 1,000 feet of the Proposed Project) 5-11

Table 8-1 Basic Construction Mitigation Measures Recommended for ALL Proposed Projects .. 8-3

Table 8-2 Additional Construction Mitigation Measures Recommended for Projects with Construction Emissions Above the Threshold 8-4

Table 8-3 URBEMIS Guidance for Assessing Construction-Related Impacts 8-5

Table 9-1 Example Plan-level Greenhouse Gas Emissions Analysis 9-6

Table B-1 URBEMIS Input Parameters for Operation Emissions B-1

Table B-1 Roadway Construction Emissions Model Cell Reference for Unmitigated Off-Road Equipment Emissions B-12

Table C.1 Ambient Air Quality Standards and Designations C-13

Table C.2 Common Sources of Health Effects for Criteria Air Pollutants C-15

Table C.3 Examples of Greenhouse Gases C-18

Table 1 – Air Quality CEQA Thresholds of Significance D-7

Table 2 – California 1990, 2002-2004, and 2020 Land Use Sector GHG[1] D-17

Table 3 – 2020 Land Use Sector GHG Emission Reductions from State Regulations and AB 32 Measures D-18

Table 4 – SFBAAB 1990, 2007, and 2020 Land Use Sector GHG Emissions Inventories and Projections (MMT CO_2e/yr) D-19

Table 5 – Operational GHG Threshold Sensitivity Analysis D-21

Table 6 – California 2020 GHG Emissions, Population Projections and GHG Efficiency Thresholds - Land Use Inventory Sectors D-22

Table 7 – California 2020 GHG Emissions, Population Projections and GHG Efficiency Thresholds - All Inventory Sectors D-24

Table 8 – Statistical Summary of Estimated Population-Weighted Ambient Cancer Risk in 2005 ..... D-30

Table 9 – Screening Distances for Potential Odor Sources D-50

ACRONYMS AND ABBREVIATIONS

$\mu g/m^3$	micrograms per cubic meter
AB	Assembly Bill
AB 1807	Tanner Air Toxics Act
AB 2588	Air Toxics Hot Spots Information and Assessment Act of 1987
ABAG	Association of Bay Area Governments
AMS	American Meteorological Society
APS	Alternative Planning Strategy
AQP	Air Quality Plan
ARB	California Air Resources Board
ATCM	air toxics control measures
BAAQMD	Bay Area Quality Management District
BACT	Best Available Control Technology
BMPs	Best Management Practices
CCA	Community Choice Aggregation
CAAQS	California Ambient Air Quality Standards
CALINE4	California Line Source Dispersion Model
CAP	criteria air pollutants
CARE	Community Air Risk Evaluation
CAPCOA	California Air Pollution Control Officers Association
CCAA	California Clean Air Act
CCAR	California Climate Action Registry
CCR	California Code of Regulations
CEC	California Energy Commission
CEQA	California Environmental Quality Act
CalRecycle	The California Department of Resources Recycling and Recovery (formally the California Integrated Waste Management Board)
CFC	Chlorofluorocarbon
CH_4	methane
CHAPIS	Community Health Air Pollution Information System
CO	carbon monoxide
CO Protocol	Carbon Monoxide Protocol
CO_2	Carbon dioxide
CO_2e	carbon dioxide equivalent
CRA	California Resources Agency

DOE	Department of Energy
du	dwelling units
EIR	Environmental Impact Report
EMFAC	On-Road Mobile-Source Emission Factors
EPA	U.S. Environmental Protection Agency
FAR	Floor Area Ratio
FCAA	Federal Clean Air Act
FCAAA	Federal Clean Air Act Amendments of 1990
GHG	greenhouse gas(es)
GRP	General Reporting Protocol
GVW	gross vehicle weight
GWP	global warming potential
H_2S	hydrogen sulfide
HEPA	High Efficiency Particulate Arresting (filter)
HI	Hazard Index
HRA	health risk assessment
HVAC	Heating, Ventilation, and Air Conditioning System
IPCC	Intergovernmental Panel on Climate Change
ISR	Indirect Source Review
ksf	thousand square feet
kwh	Kilowatt hour
lb/acre-day	pound per disturbed acre per day
lb/day	pounds per day
lb/kwh	pounds per kilowatt hour
LCFS	Low-Carbon Fuel Standard
LVW	loaded vehicle weight
MACT	maximum available control technology
mg	million gallons
MMT	million metric tons
mph	miles per hour
MPO	Metropolitan Planning Organizations
MT	metric tons
MTC	Metropolitan Transportation Commission
N_2O	nitrous oxide
NAAQS	National Ambient Air Quality Standards

NESHAP	national emissions standards for hazardous air pollutants
NH_3	mercaptan, ammonia
NOA	Naturally Occurring Asbestos
NOP	Notice of Preparation
NO_X	oxides of nitrogen
OEHHA	Office of Environmental Health Hazard Assessment
OPR	Governor's Office of Planning and Research
PM	particulate matter
PM_{10}	respirable particulate matter with an aerodynamic resistance diameter of 10 micrometers or less
$PM_{2.5}$	fine particulate matter with an aerodynamic resistance diameter of 2.5 micrometers or less
ppm	parts per million
PUC	Public Utilities Commission
RoadMod	Roadway Construction Emissions Model
ROG	reactive organic gases
RTP	Regional Transportation Plan
SB	Senate Bill
SCS	Sustainable Communities Strategy
SF_6	sulfur hexafluoride
SFBAAB	San Francisco Bay Area Air Basin
SIP	State Implementation Plan
SMAQMD	Sacramento Metropolitan Air Quality Management District
SO_2	sulfur dioxide
SP	Service Population
SSIM	Sustainable Systems Integration Model
TAC	toxic air contaminant
T-BACT	Toxic Best Available Control Technology
TBPs	Toxic Best Practices
tpy	tons per year
UC	University of California
URBEMIS	Urban Land Use Emissions Model
VMT	vehicle miles traveled
VT	vehicle trips
yd^3	cubic yards
yr	year

1. INTRODUCTION

1.1. PURPOSE OF GUIDELINES

The purpose of the Bay Area Air Quality Management District (BAAQMD or District) California Environmental Quality Act (CEQA) Guidelines is to assist lead agencies in evaluating air quality impacts of projects and plans proposed in the San Francisco Bay Area Air Basin (SFBAAB). The Guidelines provides BAAQMD-recommended procedures for evaluating potential air quality impacts during the environmental review process consistent with CEQA requirements. These revised Guidelines supersede the BAAQMD's previous CEQA guidance titled *BAAQMD CEQA Guidelines: Assessing the Air Quality Impacts of Projects and Plans* (BAAQMD 1999).

Land development plans and projects have the potential to generate harmful air pollutants that degrade air quality and increase local exposure. The Guidelines contain instructions on how to evaluate, measure, and mitigate air quality impacts generated from land development construction and operation activities. The Guidelines focus on criteria air pollutant, greenhouse gas (GHG), toxic air contaminant, and odor emissions generated from plans or projects.

The Guidelines are intended to help lead agencies navigate through the CEQA process. The Guidelines offer step-by-step procedures for a thorough environmental impact analysis of adverse air emissions due to land development in the Bay Area.

1.1.1. BAAQMD's Role in Air Quality

BAAQMD is the primary agency responsible for assuring that the National and California Ambient Air Quality Standards (NAAQS and CAAQS, respectively) are attained and maintained in the Bay Area. BAAQMD's jurisdiction includes all of Alameda, Contra Costa, Marin, Napa, San Francisco, San Mateo and Santa Clara counties, and the southern portions of Solano and Sonoma counties, as shown in Figure 1-1. The Air District's responsibilities in improving air quality in the region include: preparing plans for attaining and maintaining air quality standards; adopting and enforcing rules and regulations; issuing permits for stationary sources of air pollutants; inspecting stationary sources and responding to citizen complaints; monitoring air quality and meteorological conditions; awarding grants to reduce mobile emissions; implementing public outreach campaigns; and assisting local governments in addressing climate change.

BAAQMD takes on various roles in the CEQA process, depending on the nature of the proposed project, including:

Lead Agency – BAAQMD acts as a lead agency when it has the primary authority to implement or approve a project, such as when it adopts air quality plans for the region, issues stationary source permits, or adopts rules and regulations.

Responsible Agency – BAAQMD acts as a Responsible Agency when it has limited discretionary authority over a portion of a project, but does not have the primary discretionary authority of a lead agency. As a Responsible Agency, BAAQMD may coordinate the environmental review process with the lead agency regarding BAAQMD's permitting process, provide comments to the lead agency regarding potential impacts, and recommend mitigation measures.



Source: ESRI Satellite 2009

Bay Area Air Quality Management District Jurisdictional Boundaries **Figure 1-1**

Commenting Agency – BAAQMD may act as a Commenting Agency when it is not a Lead or Responsible Agency (i.e., it does not have discretionary authority over a project), but when it may have concerns about the air quality impacts of a proposed project or plan. As a Commenting Agency, BAAQMD may review environmental documents prepared for development proposals and plans in the region, such as local general plans, and provide comments to the lead agency regarding the adequacy of the air quality impact analysis, determination of significance, and mitigation measures proposed.

BAAQMD prepared the CEQA Guidelines to assist lead agencies in air quality analysis, as well as to promote sustainable development in the region. The CEQA Guidelines support lead agencies in analyzing air quality impacts and offers numerous mitigation measures and general plan policies to implement smart growth and transit oriented development, minimize construction emissions, and reduce population exposure to air pollution risks.

1.2. GUIDELINE COMPONENTS

The recommendations in the CEQA Guidelines should be viewed as minimum considerations for analyzing air quality impacts. Lead agencies are encouraged to tailor the air quality impact analysis to meet the needs of the local community and may conduct refined analysis that utilize more sophisticated models, more precise input data, innovative mitigation measures, and/or other features. The Guidelines contain the following sections:

Introduction – Chapter 1 provides a summary of the purpose of the Guide, and an overview of BAAQMD responsibilities.

Thresholds of Significance – Chapter 2 outlines the current thresholds or significance for determining the significance of air quality impacts.

Screening Criteria – Chapter 3 provides easy reference tables to determine if your project may have potentially significant impacts requiring a detailed analysis.

Assessing and Mitigating Impacts – Chapters 4 through 9 describe assessment methods and mitigation measures for operational-related, local community risk and hazards, local carbon monoxide (CO), odors, construction-related, and plan-level impacts.

Appendix A – Provides construction assessment tools.

Appendix B – Provides detailed air quality modeling instructions.

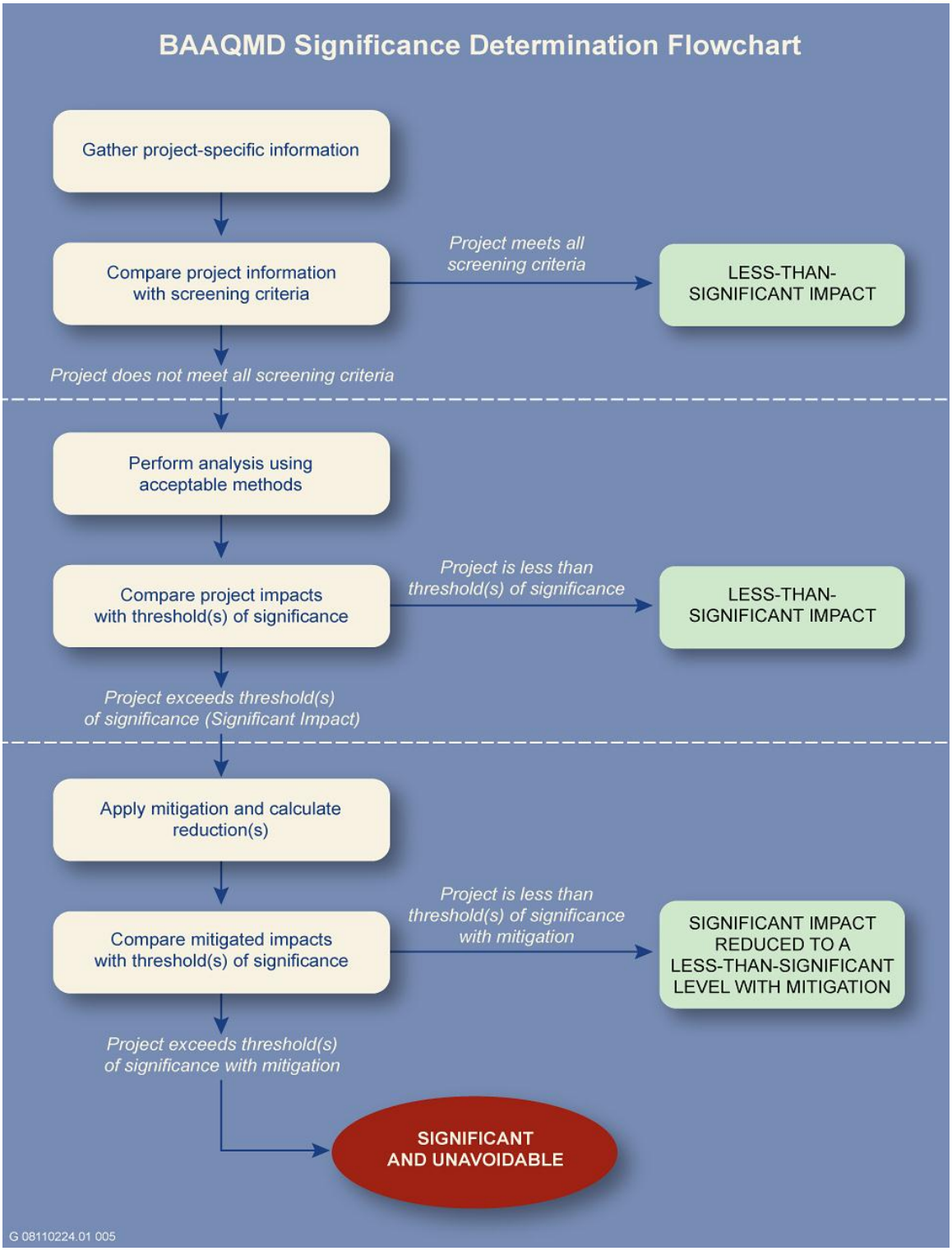
Appendix C – Outlines sample environmental setting information.

Appendix D – Contains justification statements for BAAQMD-adopted thresholds of significance.

Appendix E – Provides a glossary of terms used throughout this guide.

1.2.1. How To Use The Guidelines

Figure 2-1 illustrates general steps for evaluating a project or plan's air quality impacts. The first step is to determine whether the air quality evaluation is for a project or plan. Once identified, the project should be compared with the appropriate construction and operational screening criteria listed in Chapter 2. There are no screening criteria for plans.



General Steps for Determining Significance of Air Quality Impacts **Figure 1-2**



If the project meets the screening criteria and is consistent with the methodology used to develop the screening criteria, then its air quality impacts may be considered less than significant. Otherwise, lead agencies should evaluate potential air quality impacts of projects (and plans) as explained in Chapters 4 through 9. These Chapters describe how to analyze air quality impacts from criteria air pollutants, GHGs, local community risk and hazards, and odors associated with construction activity and operations of a project or plan.

If, after proper analysis, the project or plan's air quality impacts are found to be below the significance thresholds, then the air quality impacts may be considered less than significant. If not, the lead agency should implement appropriate mitigation measures to reduce associated air quality impacts. Lead agencies are responsible for evaluating and implementing all feasible mitigation measures in their CEQA document.

The mitigated project or plan's impacts are then compared again to the significance thresholds. If a project succeeded in mitigating its adverse air quality impacts below the corresponding thresholds, air quality impacts may be considered less than significant. If a project still exceeds the thresholds, the Air District strongly encourages the lead agency to consider project alternatives that could lessen any identified significant impact, including a no project alternative in accordance with CEQA Guidelines section 15126.6(e).

1.2.2. Early Consultation

BAAQMD encourages local jurisdictions and project applicants to address air quality issues as early as possible in the project planning stage. Addressing land use and site design issues while a proposed project is still in the conceptual stage increases opportunities to incorporate project design features to minimize land use compatibility issues and air quality impacts. By the time a project enters the CEQA process, it is usually more costly and time-consuming to redesign the project to incorporate mitigation measures. Early consultation may be achieved by including a formal step in the jurisdiction's development review procedures or simply by discussing air quality concerns at the planning counter when a project proponent makes an initial contact regarding a proposed development. Regardless of the specific procedures a local jurisdiction employs, the objective should be to incorporate features into a project that minimize air quality impacts before significant resources (public and private) have been devoted to the project.

The following air quality considerations warrant particular attention during early consultation between Lead Agencies and project proponents:

1. land use and design measures to encourage alternatives to the automobile, conserve energy and reduce project emissions;
2. land use conflicts and exposure of sensitive receptors to odors, toxics and criteria pollutants; and,
3. applicable District rules, regulations and permit requirements.

[This Page Intentionally Left Blank]

PART I: THRESHOLDS OF SIGNIFICANCE & PROJECT SCREENING

2. THRESHOLDS OF SIGNIFICANCE

The SFBAAB is currently designated as a nonattainment area for state and national ozone standards and national particulate matter ambient air quality standards. SFBAAB's nonattainment status is attributed to the region's development history. Past, present and future development projects contribute to the region's adverse air quality impacts on a cumulative basis. By its very nature, air pollution is largely a cumulative impact. No single project is sufficient in size to, by itself, result in nonattainment of ambient air quality standards. Instead, a project's individual emissions contribute to existing cumulatively significant adverse air quality impacts. If a project's contribution to the cumulative impact is considerable, then the project's impact on air quality would be considered significant.

In developing thresholds of significance for air pollutants, BAAQMD considered the emission levels for which a project's individual emissions would be cumulatively considerable. If a project exceeds the identified significance thresholds, its emissions would be cumulatively considerable, resulting in significant adverse air quality impacts to the region's existing air quality conditions. Therefore, additional analysis to assess cumulative impacts is unnecessary. The analysis to assess project-level air quality impacts should be as comprehensive and rigorous as possible.

Similar to regulated air pollutants, GHG emissions and global climate change also represent cumulative impacts. GHG emissions contribute, on a cumulative basis, to the significant adverse environmental impacts of global climate change. Climate change impacts may include an increase in extreme heat days, higher concentrations of air pollutants, sea level rise, impacts to water supply and water quality, public health impacts, impacts to ecosystems, impacts to agriculture, and other environmental impacts. No single project could generate enough GHG emissions to noticeably change the global average temperature. The combination of GHG emissions from past, present, and future projects contribute substantially to the phenomenon of global climate change and its associated environmental impacts.



© 2009 Jupiterimages Corporation

BAAQMD's approach to developing a *Threshold of Significance* for GHG emissions is to identify the emissions level for which a project would not be expected to substantially conflict with existing California legislation adopted to reduce statewide GHG emissions needed to move us towards climate stabilization. If a project would generate GHG emissions above the threshold level, it would be considered to contribute substantially to a cumulative impact, and would be considered significant. Refer to Table 2-1 for a summary of Air Quality CEQA Thresholds and to Appendix D for *Thresholds of Significance* documentation.

Table 2-1
Air Quality CEQA Thresholds of Significance*

Pollutant	Construction-Related	Operational-Related	
Project-Level			
Criteria Air Pollutants and Precursors (Regional)	**Average Daily Emissions (lb/day)**	**Average Daily Emissions (lb/day)**	**Maximum Annual Emissions (tpy)**
ROG	54	54	10
NO_X	54	54	10
PM_{10}	82 (exhaust)	82	15
$PM_{2.5}$	54 (exhaust)	54	10
$PM_{10}/PM_{2.5}$ (fugitive dust)	Best Management Practices	None	
Local CO	None	9.0 ppm (8-hour average), 20.0 ppm (1-hour average)	
GHGs – Projects other than Stationary Sources	None	Compliance with Qualified GHG Reduction Strategy OR 1,100 MT of CO_2e/yr OR 4.6 MT CO_2e/SP/yr (residents+employees)	
GHGs –Stationary Sources	None	10,000 MT of CO_2e/yr	
Risk and Hazards for new sources and receptors (Individual Project)	Same as Operational Thresholds**	Compliance with Qualified Community Risk Reduction Plan OR Increased cancer risk of >10.0 in a million Increased non-cancer risk of > 1.0 Hazard Index (Chronic or Acute) Ambient $PM_{2.5}$ increase: > 0.3 µg/m^3 annual average Zone of Influence: 1,000-foot radius from property line of source or receptor	
Risk and Hazards for new sources and receptors (Cumulative Threshold)	Same as Operational Thresholds**	Compliance with Qualified Community Risk Reduction Plan OR Cancer: > 100 in a million (from all local sources) Non-cancer: > 10.0 Hazard Index (from all local sources) (Chronic) $PM_{2.5}$: > 0.8 µg/m^3 annual average (from all local sources) Zone of Influence: 1,000-foot radius from property line of source or receptor	
Accidental Release of Acutely Hazardous Air Pollutants	None	Storage or use of acutely hazardous materials locating near receptors or new receptors locating near stored or used acutely hazardous materials considered significant	
Odors	None	5 confirmed complaints per year averaged over three years	
Plan-Level			
Criteria Air Pollutants and Precursors	None	1. Consistency with Current Air Quality Plan control measures, and 2. Projected VMT or vehicle trip increase is less than or equal to projected population increase	
GHGs	None	Compliance with Qualified GHG Reduction Strategy OR 6.6 MT CO_2e/SP/yr (residents + employees)	

Table 2-1 Air Quality CEQA Thresholds of Significance*		
Pollutant	**Construction-Related**	**Operational-Related**
Risks and Hazards	None	1. Overlay zones around existing and planned sources of TACs (including adopted Risk Reduction Plan areas) and 2. Overlay zones of at least 500 feet from all freeways and high volume roadways
Accidental Release of Acutely Hazardous Air Pollutants	None	None
Odors	None	Identify the location, and include policies to reduce the impacts, of existing or planned sources of odors
Regional Plans (Transportation and Air Quality Plans)		
GHGs, Criteria Air Pollutants and Precursors, and Toxic Air Contaminants	None	No net increase in emissions

CEQA = California Environmental Quality Act; CO = carbon monoxide; CO_2e = carbon dioxide equivalent; GHGs = greenhouse gases; lb/day = pounds per day; MT = metric tons; NO_X = oxides of nitrogen; $PM_{2.5}$= fine particulate matter with an aerodynamic resistance diameter of 2.5 micrometers or less; PM_{10} = respirable particulate matter with an aerodynamic resistance diameter of 10 micrometers or less; ppm = parts per million; ROG = reactive organic gases; SO_2 = sulfur dioxide; SP = service population; TACs = toxic air contaminants; TBP = toxic best practices; tons/day = tons per day; tpy = tons per year; yr= year; TBD= to be determined.

*It is the Air District's policy that the adopted thresholds apply to projects for which a Notice of Preparation is published, or environmental analysis begins, on or after the applicable effective date. The adopted CEQA thresholds – *except for the risk and hazards thresholds for new receptors* – are effective June 2, 2010. The risk and hazards thresholds for new receptors are effective May 1, 2011.

** The Air District recommends that for construction projects that are less than one year duration, Lead Agencies should annualize impacts over the scope of actual days that peak impacts are to occur, rather than the full year.

2.1. CRITERIA AIR POLLUTANTS AND PRECURSORS – PROJECT LEVEL

Table 2-2 presents the *Thresholds of Significance* for operational-related criteria air pollutant and precursor emissions. These represent the levels at which a project's individual emissions of criteria air pollutants or precursors would result in a cumulatively considerable contribution to the SFBAAB's existing air quality conditions. If daily average or annual emissions of operational-related criteria air pollutants or precursors would exceed any applicable threshold listed in Table 2-2, the proposed project would result in a cumulatively significant impact.

Table 2-2 Thresholds of Significance for Operational-Related Criteria Air Pollutants and Precursors		
Pollutant/Precursor	**Maximum Annual Emissions (tpy)**	**Average Daily Emissions (lb/day)**
ROG	10	54
NO_X	10	54
PM_{10}	15	82
$PM_{2.5}$	10	54
Notes: tpy = tons per year; lb/day = pounds per day; NO_X = oxides of nitrogen; $PM_{2.5}$ = fine particulate matter with an aerodynamic resistance diameter of 2.5 micrometers or lCOess; PM_{10} = respirable particulate matter with an aerodynamic resistance diameter of 10 micrometers or less; ROG = reactive organic gases; tpy = tons per year. Refer to Appendix D for support documentation.		

2.2. GREENHOUSE GASES – PROJECT LEVEL

The *Thresholds of Significance* for operational-related GHG emissions are:

- For land use development projects, the threshold is compliance with a qualified GHG Reduction Strategy (see Section 4.3); or annual emissions less than 1,100 metric tons per year (MT/yr) of CO_2e; or 4.6 MT CO_2e/SP/yr (residents + employees). Land use development projects include residential, commercial, industrial, and public land uses and facilities.

- For stationary-source projects, the threshold is 10,000 metric tons per year (MT/yr) of CO_2e. Stationary-source projects include land uses that would accommodate processes and equipment that emit GHG emissions and would require an Air District permit to operate.

BAAQMD's GHG threshold is defined in terms of carbon dioxide equivalent (CO_2e), a metric that accounts for the emissions from various greenhouse gases based on their global warming potential.

If annual emissions of operational-related GHGs exceed these threshold levels, the proposed project would result in a cumulatively considerable contribution of GHG emissions and a cumulatively significant impact to global climate change.

2.3. LOCAL COMMUNITY RISK AND HAZARD IMPACTS – PROJECT LEVEL

The *Thresholds of Significance* for local community risk and hazard impacts are identified below, which apply to both the siting of a new source and to the siting of a new receptor. Local community risk and hazard impacts are associated with TACs and $PM_{2.5}$ because emissions of these pollutants can have significant health impacts at the local level. If emissions of TACs or $PM_{2.5}$ exceed



any of the threshold listed below, the proposed project would result in a significant impact.

- Non-compliance with a qualified Community Risk Reduction Plan;
- An excess cancer risk level of more than 10 in one million, or a non-cancer (i.e., chronic or acute) hazard index greater than 1.0 would be a significant cumulatively considerable contribution;
- An incremental increase of greater than 0.3 micrograms per cubic meter ($\mu g/m^3$) annual average $PM_{2.5}$ from a single source would be a significant cumulatively considerable contribution.

Cumulative Impacts

A project would have a cumulative considerable impact if the aggregate total of all past, present, and foreseeable future sources within a 1,000 foot radius from the fence line of a source, or from the location of a receptor, plus the contribution from the project, exceeds the following:

- Non-compliance with a qualified Community Risk Reduction Plan; or
- An excess cancer risk levels of more than 100 in one million or a chronic non-cancer hazard index (from all local sources) greater than 10.0; or
- 0.8 $\mu g/m^3$ annual average $PM_{2.5}$.

A lead agency should enlarge the 1,000-foot radius on a case-by-case basis if an unusually large source or sources of risk or hazard emissions that may affect a proposed project is beyond the recommended radius.

2.4. LOCAL CARBON MONOXIDE IMPACTS – PROJECT LEVEL

Table 2-3 presents the *Thresholds of Significance* for local CO emissions, the 1- and 8-hour California Ambient Air Quality Standards (CAAQS) of 20.0 parts per million (ppm) and 9.0 ppm, respectively. By definition, these represent levels that are protective of public health. If a project would cause local emissions of CO to exceed any of the thresholds listed below, the proposed project would result in a significant impact to air quality.

Table 2-3
Thresholds of Significance for Local Carbon Monoxide Emissions

CAAQS Averaging Time	Concentration (ppm)
1-Hour	20.0
8-Hour	9.0
Refer to Appendix D for support documentation.	

2.5. ODOR IMPACTS – PROJECT LEVEL

The *Thresholds of Significance* for odor impacts are qualitative in nature. A project that would result in the siting of a new source or the exposure of a new receptor to existing or planned odor sources should consider the screening level distances and the complaint history of the odor sources:

- Projects that would site a new odor source or a new receptor farther than the applicable screening distance shown in Table 3-3 from an existing receptor or odor source, respectively, would not likely result in a significant odor impact.

- An odor source with five (5) or more confirmed complaints per year averaged over three years is considered to have a significant impact on receptors within the screening distance shown in Table 3-3.

Facilities that are regulated by the CalRecycle agency (e.g. landfill, composting, etc) are required to have Odor Impact Minimization Plans (OIMP) in place and have procedures that establish fence line odor detection thresholds. The Air District recognizes a lead agency's discretion under CEQA to use established odor detection thresholds as thresholds of significance for CEQA review for CalRecycle regulated facilities with an adopted OIMP. Refer to *Chapter 7 Assessing and Mitigating Odor Impacts* for further discussion of odor analysis.

2.6. CONSTRUCTION-RELATED IMPACTS – PROJECT LEVEL

2.6.1. Criteria Air Pollutants and Precursors

Table 2-4 presents the *Thresholds of Significance* for construction-related criteria air pollutant and precursor emissions. If daily average emissions of construction-related criteria air pollutants or precursors would exceed any applicable threshold listed in Table 2-4, the project would result in a significant cumulative impact.



© 2009 Jupiterimages Corporation

Table 2-4
Thresholds of Significance for Construction-Related Criteria Air Pollutants and Precursors

Pollutant/Precursor	Daily Average Emissions (lb/day)
ROG	54
NO_X	54
PM_{10}	82*
$PM_{2.5}$	54*
PM_{10}/ $PM_{2.5}$Fugitive Dust	Best Management Practices

* Applies to construction exhaust emissions only.

Notes: CO = carbon monoxide; lb/day = pounds per day; NO_X = oxides of nitrogen; $PM_{2.5}$ = fine particulate matter with an aerodynamic resistance diameter of 2.5 micrometers or less; PM_{10} = respirable particulate matter with an aerodynamic resistance diameter of 10 micrometers or less; ROG = reactive organic gases; SO_2 = sulfur dioxide. Refer to Appendix D for support documentation.

2.6.2. Greenhouse Gases

BAAQMD does not have an adopted *Threshold of Significance* for construction-related GHG emissions. However, the Lead Agency should quantify and disclose GHG emissions that would occur during construction, and make a determination on the significance of these construction-generated GHG emission impacts in relation to meeting AB 32 GHG reduction goals, as required by the Public Resources Code, Section 21082.2. The lead agency is encouraged to incorporate

best management practices to reduce GHG emissions during construction, as feasible and applicable.

2.6.3. Local Community Risk and Hazards

The *Threshold of Significance* for construction-related local community risk and hazard impacts is the same as that for project operations. Construction-related TAC and PM impacts should be addressed on a case-by-case basis, taking into consideration the specific construction-related characteristics of each project and proximity to off-site receptors, as applicable. The Air District recommends that for construction projects that are less than one year duration, Lead Agencies should annualize impacts over the scope of actual days that peak impacts are to occur, rather than the full year.

2.7. THRESHOLDS OF SIGNIFICANCE FOR PLAN-LEVEL IMPACTS

The *Thresholds of Significance* for plans (e.g., general plans, community plans, specific plans, regional plans, congestion management plans, etc.) within the SFBAAB are summarized in Table 2-5 and discussed separately below.

Table 2-5
Thresholds of Significance for Plans

Criteria Air Pollutants and Precursors	Construction: none Operational: Consistency with Current AQP and projected VMT or vehicle trip increase is less than or equal to projected population increase.
GHGs	Construction: none Operational: 6.6 MT CO_2e/SP/yr (residents & employees) or a Qualified GHG Reduction Strategy. This threshold should only be applied to general plans. Other plans, e.g. specific plans, congestion management plans, etc., should use the project-level threshold of 4.6 CO_2e/SP/yr.
Local Community Risk and Hazards	Land use diagram identifies special overlay zones around existing and planned sources of TACs and $PM_{2.5}$, including special overlay zones of at least 500 feet (or Air District-approved modeled distance) on each side of all freeways and high-volume roadways, and plan identifies goals, policies, and objectives to minimize potentially adverse impacts.
Odors	Identify locations of odor sources in plan; identify goals, policies, and objectives to minimize potentially adverse impacts.
Regional Plans (transportation and air quality plans)	No net increase in emissions of GHGs, Criteria Air Pollutants and Precursors, and Toxic Air Contaminants. Threshold only applies to regional transportation and air quality plans.

Notes: AQP = Air Quality Plan; CO_2e = carbon dioxide equivalent; GHGs = greenhouse gases; MT = metric tons; SP = service population; TACs = toxic air contaminants; yr = year; $PM_{2.5}$= fine particulate matter
Refer to Appendix D for support documentation.

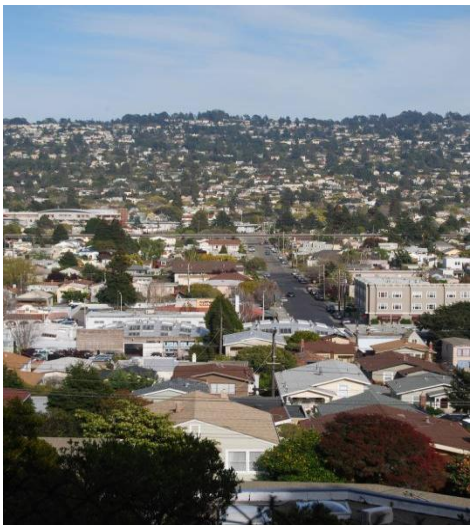
2.7.1. Criteria Air Pollutants and Precursor Emissions

Proposed plans (except regional plans) must show the following over the planning period of the plan to result in a less than significant impact:

- Consistency with current air quality plan control measures.
- A proposed plan's projected VMT or vehicle trips (VT) (either measure may be used) increase is less than or equal to its projected population increase.

2.7.2. Greenhouse Gases

The *Threshold of Significance* for operational-related GHG impacts of plans employs either a GHG efficiency-based metric (per Service Population [SP]), or a GHG Reduction Strategy option, described in Section 4.3.



The *Thresholds of Significance* options for plan level GHG emissions are:

- A GHG efficiency metric of 6.6 MT per SP per year of carbon dioxide equivalent (CO_2e). If annual maximum emissions of operational-related GHGs exceed this level, the proposed plan would result in a significant impact to global climate change.
- Consistency with an adopted GHG Reduction Strategy. If a proposed plan is consistent with an adopted GHG Reduction Strategy that meets the standards described in Section 4.3, the plan would be considered to have a less than significant impact. This approach is consistent with the plan elements described in the State CEQA Guidelines, Section 15183.5.

2.7.3. Local Community Risk and Hazards

The *Thresholds of Significance* for plans with regard to community risk and hazard impacts are:

1. The land use diagram must identify:
    a. Special overlay zones around existing and planned sources of TACs and PM (including adopted risk reduction plan areas); and
    b. Special overlay zones of at least 500 feet (or Air District-approved modeled distance) on each side of all freeways and high-volume roadways.
2. The plan must also identify goals, policies, and objectives to minimize potential impacts and create overlay zones around sources of TACs, PM, and hazards.

2.7.4. Odors

The *Thresholds of Significance* for plans with regard to odor impacts are to identify locations of odor sources in a plan and the plan must also identify goals, policies, and objectives to minimize potentially adverse impacts.

2.7.5. Regional Plans

The *Thresholds of Significance* for regional plans is to achieve a no net increase in emissions of criteria pollutants and precursors, GHG, and toxic air contaminants. This threshold applies only to regional transportation and air quality plans.

3. SCREENING CRITERIA

The screening criteria identified in this section are **not thresholds of significance**. The Air District developed screening criteria to provide lead agencies and project applicants with a conservative indication of whether the proposed project could result in potentially significant air quality impacts. If all of the screening criteria are met by a proposed project, then the lead agency or applicant would not need to perform a detailed air quality assessment of their project's air pollutant emissions. These screening levels are generally representative of new development on greenfield sites without any form of mitigation measures taken into consideration. In addition, the screening criteria in this section do not account for project design features, attributes, or local development requirements that could also result in lower emissions. For projects that are mixed-use, infill, and/or proximate to transit service and local services, emissions would be less than the greenfield type project that these screening criteria are based on.

If a project includes emissions from stationary source engines (e.g., back-up generators) and industrial sources subject to Air District Rules and Regulations, the screening criteria should not be used. The project's stationary source emissions should be analyzed separately from the land use-related indirect mobile- and area-source emissions. Stationary-source emissions are not included in the screening estimates given below and, for criteria pollutants, must be added to the indirect mobile- and area-source emissions generated by the land use development and compared to the appropriate threshold. Greenhouse gas emissions from permitted stationary sources should not be combined with operational emissions, but compared to a separate stationary source greenhouse gas threshold.

3.1. OPERATIONAL-RELATED IMPACTS

3.1.1. Criteria Air Pollutants and Precursors

The screening criteria developed for criteria pollutants and precursors were derived using the default assumptions used by the Urban Land Use Emissions Model (URBEMIS). If the project has sources of emissions not evaluated in the URBEMIS program the screening criteria should not be used. If the project meets the screening criteria in Table 3-1, the project would not result in the generation of operational-related criteria air pollutants and/or precursors that exceed the *Thresholds of Significance* shown in Table 2-2. Operation of the proposed project would result in a less-than-significant cumulative impact to air quality from criteria air pollutant and precursor emissions.

3.1.2. Greenhouse Gases

The screening criteria developed for greenhouse gases were derived using the default emission assumptions in URBEMIS and using off-model GHG estimates for indirect emissions from electrical generation, solid waste and water conveyance. If the project has other significant sources of GHG emissions not accounted for in the methodology described above, then the screening criteria should not be used. Projects below the applicable screening criteria shown in Table 3-1 would not exceed the 1,100 MT of CO_2e/yr GHG threshold of significance for projects other than permitted stationary sources.

If a project, including stationary sources, is located in a community with an adopted qualified GHG Reduction Strategy (see Section 4.3), the project may be considered less than significant if it is consistent with the GHG Reduction Strategy. A project must demonstrate its consistency by identifying and implementing all applicable feasible measures and policies from the GHG Reduction Strategy into the project.

Table 3-1
Criteria Air Pollutants and Precursors and GHG Screening Level Sizes

Land Use Type	Operational Criteria Pollutant Screening Size	Operational GHG Screening Size	Construction Criteria Pollutant Screening Size
Single-family	325 du (NOX)	56 du	114 du (ROG)
Apartment, low-rise	451 du (ROG)	78 du	240 du (ROG)
Apartment, mid-rise	494 du (ROG)	87 du	240 du (ROG)
Apartment, high-rise	510 du (ROG)	91 du	249 du (ROG)
Condo/townhouse, general	451 du (ROG)	78 du	240 du (ROG)
Condo/townhouse, high-rise	511 du (ROG)	92 du	252 du (ROG)
Mobile home park	450 du (ROG)	82 du	114 du (ROG)
Retirement community	487 du (ROG)	94 du	114 du (ROG)
Congregate care facility	657 du (ROG)	143 du	240 du (ROG)
Day-care center	53 ksf (NOX)	11 ksf	277 ksf (ROG)
Elementary school	271 ksf (NOX)	44 ksf	277 ksf (ROG)
Elementary school	2747 students (ROG)	-	3904 students (ROG)
Junior high school	285 ksf (NOX)	-	277 ksf (ROG)
Junior high school	2460 students (NOX)	46 ksf	3261 students (ROG)
High school	311 ksf (NOX)	49 ksf	277 ksf (ROG)
High school	2390 students (NOX)	-	3012 students (ROG)
Junior college (2 years)	152 ksf (NOX)	28 ksf	277 ksf (ROG)
Junior college (2 years)	2865 students (ROG)	-	3012 students (ROG)
University/college (4 years)	1760 students (NOX)	320 students	3012 students (ROG)
Library	78 ksf (NOX)	15 ksf	277 ksf (ROG)
Place of worship	439 ksf (NOX)	61 ksf	277 ksf (ROG)
City park	2613 acres (ROG)	600 acres	67 acres (PM10)
Racquet club	291 ksf (NOX)	46 ksf	277 ksf (ROG)
Racquetball/health	128 ksf (NOX)	24 ksf	277 ksf (ROG)
Quality restaurant	47 ksf (NOX)	9 ksf	277 ksf (ROG)
High turnover restaurant	33 ksf (NOX)	7 ksf	277 ksf (ROG)
Fast food rest. w/ drive thru	6 ksf (NOX)	1 ksf	277 ksf (ROG)
Fast food rest. w/o drive thru	8 ksf (NOX)	1 ksf	277 ksf (ROG)
Hotel	489 rooms (NOX)	83 rooms	554 rooms (ROG)
Motel	688 rooms (NOX)	106 rooms	554 rooms (ROG)
Free-standing discount store	76 ksf (NOX)	15 ksf	277 ksf (ROG)
Free-standing discount superstore	87 ksf (NOX)	17 ksf	277 ksf (ROG)
Discount club	102 ksf (NOX)	20 ksf	277 ksf (ROG)
Regional shopping center	99 ksf (NOX)	19 ksf	277 ksf (ROG)
Electronic Superstore	95 ksf (NOX)	18 ksf	277 ksf (ROG)
Home improvement superstore	142 ksf (NOX)	26 ksf	277 ksf (ROG)
Strip mall	99 ksf (NOX)	19 ksf	277 ksf (ROG)
Hardware/paint store	83 ksf (NOX)	16 ksf	277 ksf (ROG)
Supermarket	42 ksf (NOX)	8 ksf	277 ksf (ROG)
Convenience market (24 hour)	5 ksf (NOX)	1 ksf	277 ksf (ROG)
Convenience market with gas pumps	4 ksf (NOX)	1 ksf	277 ksf (ROG)
Bank (with drive-through)	17 ksf (NOX)	3 ksf	277 ksf (ROG)
General office building	346 ksf (NOX)	53 ksf	277 ksf (ROG)

Table 3-1
Criteria Air Pollutants and Precursors and GHG Screening Level Sizes

Land Use Type	Operational Criteria Pollutant Screening Size	Operational GHG Screening Size	Construction Criteria Pollutant Screening Size
Office park	323 ksf (NOX)	50 ksf	277 ksf (ROG)
Government office building	61 ksf (NOX)	12 ksf	277 ksf (ROG)
Government (civic center)	149 ksf (NOX)	27 ksf	277 ksf (ROG)
Pharmacy/drugstore w/ drive through	49 ksf (NOX)	10 ksf	277 ksf (ROG)
Pharmacy/drugstore w/o drive through	48 ksf (NOX)	10 ksf	277 ksf (ROG)
Medical office building	117 ksf (NOX)	22 ksf	277 ksf (ROG)
Hospital	226 ksf (NOX)	39 ksf	277 ksf (ROG)
Hospital	334 beds (NOX)	84 ksf	337 beds (ROG)
Warehouse	864 ksf (NOX)	64 ksf	259 ksf (NOX)
General light industry	541 ksf (NOX)	121 ksf	259 ksf (NOX)
General light industry	72 acres (NOX)	-	11 acres (NOX)
General light industry	1249 employees (NOX)	-	540 employees (NOX)
General heavy industry	1899 ksf (ROG)	-	259 ksf (NOX)
General heavy industry	281 acres (ROG)	-	11 acres (NOX)
Industrial park	553 ksf (NOX)	65 ksf	259 ksf (NOX)
Industrial park	61 acres (NOX)	-	11 acres (NOX)
Industrial park	1154 employees (NOX)	-	577 employees (NOX)
Manufacturing	992 ksf (NOX)	89 ksf	259 ksf (NOX)

THE SCREENING VALUES IN THIS TABLE CANNOT BE USED AS SCREENING FOR RISK AND HAZARD IMPACTS

Notes: du = dwelling units; ksf = thousand square feet; NO_X = oxides of nitrogen; ROG = reactive organic gases. Screening levels include indirect and area source emissions. Emissions from engines (e.g., back-up generators) and industrial sources subject to Air District Rules and Regulations embedded in the land uses are not included in the screening estimates and must be added to the above land uses.

Refer to Appendix D for support documentation.

Source: Modeled by EDAW 2009.

3.2. COMMUNITY RISK AND HAZARD IMPACTS

Please refer to Chapter 5 for discussion of screening criteria for local community risk and hazard impacts. The screening values in Table 3-1 may not be applied as screening for risk and hazard impacts.

3.3. CARBON MONOXIDE IMPACTS

This preliminary screening methodology provides a conservative indication of whether the implementation of the proposed project would result in CO emissions that exceed the *Thresholds of Significance* shown in Table 2-3. The screening criteria do not apply to proposed stationary source projects.

The proposed project would result in a less-than-significant impact to localized CO concentrations if the following screening criteria is met:

1. Project is consistent with an applicable congestion management program established by the county congestion management agency for designated roads or highways, regional transportation plan, and local congestion management agency plans.
2. The project traffic would not increase traffic volumes at affected intersections to more than 44,000 vehicles per hour.
3. The project traffic would not increase traffic volumes at affected intersections to more than 24,000 vehicles per hour where vertical and/or horizontal mixing is substantially limited (e.g., tunnel, parking garage, bridge underpass, natural or urban street canyon, below-grade roadway).

3.4. ODOR IMPACTS

Table 3-3 presents odor screening distances recommended by BAAQMD for a variety of land uses. Projects that would site a new odor source or a new receptor farther than the applicable screening distance shown in Table 3-3 from an existing receptor or odor source, respectively, would not likely result in a significant odor impact. The odor screening distances in Table 3-3 should not be used as absolute screening criteria, rather as information to consider along with the odor parameters and complaint history. Refer to *Chapter 7 Assessing and Mitigating Odor Impacts* for comprehensive guidance on significance determination.

Table 3-3
Odor Screening Distances

Land Use/Type of Operation	Project Screening Distance
Wastewater Treatment Plant	2 miles
Wastewater Pumping Facilities	1 mile
Sanitary Landfill	2 miles
Transfer Station	1 mile
Composting Facility	1 mile
Petroleum Refinery	2 miles
Asphalt Batch Plant	2 miles
Chemical Manufacturing	2 miles
Fiberglass Manufacturing	1 mile
Painting/Coating Operations	1 mile
Rendering Plant	2 miles
Coffee Roaster	1 mile
Food Processing Facility	1 mile
Confined Animal Facility/Feed Lot/Dairy	1 mile
Green Waste and Recycling Operations	1 mile
Metal Smelting Plants	2 miles
Refer to Appendix D for support documentation.	

Facilities that are regulated by CalRecycle (e.g. landfill, composting, etc.) are required to have Odor Impact Minimization Plans (OIMP) in place and have procedures that establish fence line odor detection thresholds. The Air District recognizes a lead agency's discretion under CEQA to

use established odor detection thresholds as thresholds of significance for CEQA review for CalRecycle regulated facilities with an adopted OIMP.

3.5. CONSTRUCTION-RELATED IMPACTS

3.5.1. Criteria Air Pollutants and Precursors

This preliminary screening provides the lead agency with a conservative indication of whether the proposed project would result in the generation of construction-related criteria air pollutants and/or precursors that exceed the *Thresholds of Significance* shown in Table 2-4.

If all of the following *Screening Criteria* are met, the construction of the proposed project would result in a less-than-significant impact from criteria air pollutant and precursor emissions.

1. The project is below the applicable screening level size shown in Table 3-1; and
2. All *Basic Construction Mitigation Measures* would be included in the project design and implemented during construction; and
3. Construction-related activities would not include any of the following:
    a. Demolition activities inconsistent with District Regulation 11, Rule 2: Asbestos Demolition, Renovation and Manufacturing;
    b. Simultaneous occurrence of more than two construction phases (e.g., paving and building construction would occur simultaneously);
    c. Simultaneous construction of more than one land use type (e.g., project would develop residential and commercial uses on the same site) (not applicable to high density infill development);
    d. Extensive site preparation (i.e., greater than default assumptions used by the Urban Land Use Emissions Model [URBEMIS] for grading, cut/fill, or earth movement); or
    e. Extensive material transport (e.g., greater than 10,000 cubic yards of soil import/export) requiring a considerable amount of haul truck activity.

3.5.2. Community Risk and Hazards

Chapter 5, *Assessing and Mitigating Local Community Risk and Hazard Impacts*, contains information on screening criteria for local risk and hazards.

[This Page Intentionally Left Blank]

PART II: ASSESSING & MITIGATING PROJECT LEVEL IMPACTS

4. OPERATIONAL-RELATED IMPACTS

Operational emissions typically represent the majority of a project's air quality impacts. After a project is built, operational emissions including mobile and area sources, are anticipated to occur continuously throughout the project's lifetime. Operational-related activities, such as driving, use of landscape equipment, and wood burning, could generate emissions of criteria air pollutants, GHG, TACs, and PM. Area sources generally include fuel combustion from space and water heating, landscape maintenance equipment, and fireplaces/stoves, evaporative emissions from architectural coatings and consumer products and unpermitted emissions from stationary sources. This chapter provides recommendations for assessing and mitigating operational-related impacts for individual projects. Recommendations for assessing and mitigating operational-related impacts at the plan-level are discussed in Chapter 9. Chapter 9 also contains guidance for assessing a project's consistency with applicable air quality plans.

When calculating project emissions to compare to the thresholds of significance, lead agencies should account for reductions that would result from state, regional, and local rules and regulations. The Air District also recommends for lead agencies to consider project design features, attributes, or local development requirements as part of the project as proposed and not as mitigation measures. For example, projects that are mixed-use, infill, and/or proximate to transit service and local services, or that provide neighborhood serving commercial and retail services would have substantially lower vehicle trip rates and associated criteria pollutant and GHG emissions than what would be reflected in standard, basin-wide average URBEMIS default trip rates and emission estimates. A project specific transportation study should identify the reductions that can be claimed by projects with the above described attributes. Lead agencies may refer to the California Air Pollution Control Officers Association (CAPCOA) recently released report, *Quantifying Greenhouse Gas Mitigation Measures* for guidance in estimating reductions in standard vehicle trip rates and vehicle miles traveled (VMT) that can be claimed for these land use types when no project specific transportation studies are prepared.

To estimate a project's carbon dioxide equivalent (CO_2e) emissions from direct and indirect emission sources, BAAQMD recommends using the BAAQMD GHG Model (BGM). The Air District developed this model to calculate GHG emissions not included in URBEMIS such as indirect emissions from electricity use and waste and direct fugitive emissions of refrigerants. The BGM is discussed in more detail in Section 4.2 below.

4.1. CRITERIA AIR POLLUTANT AND PRECURSOR EMISSIONS

4.1.1. Significance Determination

Step 1: Comparison of Project Attributes with Screening Criteria

The first step in determining the significance of operational-related criteria air pollutants and precursors is to compare the attributes of the proposed project with the applicable screening criteria listed in Chapter 3. This preliminary screening provides a conservative indication of whether operation of the proposed project would result in the generation of criteria air pollutants and/or precursors that exceed the *Thresholds of Significance* listed in Chapter 2. If all of the screening criteria are met, the operation of the proposed project would result in a less than significant impact to air quality. If the proposed project does not meet all the screening criteria, then project emissions need to be quantified.

Step 2: Emissions Quantification

If a proposed project involves the removal of existing emission sources, BAAQMD recommends subtracting the existing emissions levels from the emissions levels estimated for the new proposed land use. This net calculation is permissible only if the existing emission sources were operational at the time that the Notice of Preparation (NOP) for the CEQA project was circulated or in the absence of an NOP when environmental analysis begins, and would continue if the proposed redevelopment project is not approved. This net calculation is not permitted for emission sources that ceased to operate, or the land uses were vacated and/or demolished, prior to circulation of the NOP or the commencement of environmental analysis. This approach is consistent with the definition of baseline conditions pursuant to CEQA.



© 2009 Jupiterimages Corporation

Land Use Development Projects

For proposed land use development projects, BAAQMD recommends using the most current version of URBEMIS (which to date is version 9.2.4) to quantify operational-related criteria air pollutants and precursors. URBEMIS is a modeling tool initially developed by the California Air Resources Board for calculating air pollutant emissions from land use development projects. URBEMIS uses EMFAC emission factors and ITE trip generation rates to calculate ROG, NO_X, carbon monoxide, particulate matter, carbon dioxide, and total vehicle trips. URBEMIS is not equipped for calculating air quality impacts from stationary sources or plans. For land use projects, URBEMIS quantifies emissions from area sources (e.g., natural gas fuel combustion for space and water heating, wood stoves and fireplace combustion, landscape maintenance equipment, consumer products, and architectural coating) and operational-related emissions (mobile sources).

Appendix B contains more detailed instructions for using URBEMIS to model operational emissions.

Stationary-Source Facilities

A stationary source consists of a single emission source with an identified emission point, such as a stack at a facility. Facilities can have multiple emission point sources located on-site and sometimes the facility as a whole is referred to as a stationary source. Major stationary sources are typically associated with industrial processes, such as refineries or power plants. Minor stationary sources are typically land uses that may require air district permits, such as gasoline dispensing stations, and dry cleaning establishments. Examples of other District-permitted stationary sources include back-up diesel generators, boilers, heaters, flares, cement kilns, and other types of combustion equipment, as well as non-combustion sources such as coating or printing operations. BAAQMD is responsible for issuing permits for the construction and operation of stationary sources in order to reduce air pollution, and to attain and maintain the national and California ambient air quality standards in the SFBAAB. Newly modified or constructed stationary sources subject to Air District permitting may be required to implement Best Available Control Technology (BACT), which may include the installation of emissions control equipment or the implementation of administrative practices that would result in the lowest achievable emission rate. Stationary sources may also be required to offset their emissions of criteria air pollutants and precursors to be permitted. This may entail shutting down or augmenting another stationary source at the same facility. Facilities also may purchase an emissions reduction credit to offset their emissions. Any stationary source emissions remaining after the application of BACT and

offsets should be added to the indirect and area source emissions estimated above to arrive at total project emissions.

URBEMIS is not equipped to estimate emissions generated by stationary sources. Instead emissions from stationary sources should be estimated using manual calculation methods in consultation with BAAQMD. When stationary sources will be subject to BAAQMD regulations, the regulation emission limits should be used as emission factors. If BAAQMD emission limits are not applicable, alternative sources of emission factors include: EPA AP-42 emission factors for particular industrial processes, manufacturer specifications for specific equipment, throughput data (e.g., fuel consumption, rate of material feedstock input) and other specifications provided by the project engineer. To the extent possible, BAAQMD recommends that the methodology used to estimate stationary-source emissions be consistent with calculations that would need to be performed to fulfill requirements of the permitting process and provided in the CEQA document.

Step 3: Comparison of Unmitigated Emissions with Thresholds of Significance
Sum the estimated emissions for area, mobile, and stationary sources (if any) for each pollutant as explained above and compare the total average daily and annual emissions of each criteria pollutant and their precursors with the applicable threshold (refer to Table 2-2). If daily average or annual emissions of operational-related criteria air pollutants or precursors do not exceed any of the thresholds, the project would result in a less than significant impact to air quality. If the quantified emissions of operational-related criteria air pollutants or precursors do exceed any applicable threshold, the proposed project would result in a significant impact to air quality and CEQA requires implementation of all feasible mitigation measures.

Step 4: Mitigation Measures and Emission Reductions
Where operational-related emissions exceed applicable threshold, lead agencies are responsible for implementing all feasible mitigation measures to reduce the project's air quality impacts. Section 4.4 contains numerous examples of mitigation measures and associated emission reductions that may be applied to projects. The project's mitigated emission estimates from mitigation measures included in the proposed project or recommended by the lead agency should be quantified and disclosed in the CEQA document.

Step 5: Comparison of Mitigated Emissions with Thresholds of Significance
Compare the total average daily and annual amounts of mitigated criteria air pollutants and precursors with the applicable threshold (refer to Table 4-1). If the implementation of mitigation measures, including off-site mitigation, would reduce all operational-related criteria air pollutants and precursors to levels below the applicable threshold, the impact to air quality would be reduced to a less than significant level. Implementation of mitigation measures means that they are made conditions of project approval and included in a Mitigation Monitoring and Reporting Plan (MMRP). If mitigated levels of any criteria air pollutant or precursor would still exceed the applicable threshold, the impact to air quality would remain significant and unavoidable.

Table 4-1
Example Operational Criteria Air Pollutant and Precursor Emissions Analysis

Step	Emissions Source	Emissions (lb/day or tpy)*			
		ROG	NO_X	PM_{10}	$PM_{2.5}$
2	Area Sources	A	A	A	A
	Mobile Sources	B	B	B	B
	Stationary Sources	C	C	C	C
	Total Unmitigated Emissions	A + B + C = D	A + B + C = D	A + B + C = D	A + B + C = D
	BAAQMD Threshold	54 lb/day or 10 tpy	54 lb/day or 10 tpy	82 lb/day or 15 tpy	54 lb/day or 10 tpy
3	Unmitigated Emissions Exceed BAAQMD Threshold?	Is D > Threshold? (If Yes, significant. Go to step 4. If No, less than significant)			
4	Mitigated Emissions	E	E	E	E
5	Mitigated Emissions Exceed BAAQMD Threshold?	Is E > Threshold? (If Yes, significant and unavoidable. If No, less than significant with mitigation incorporated)			

* Letters "A", "B", and "C" are used to represent numeric values that would be obtained through modeling for area and mobile sources, and by manual calculations for stationary source-emissions. "D" represents the sum of "A", "B", and "C" (i.e., unmitigated emissions). "E" represents mitigated emissions.
Notes: lb/day = pounds per day; NO_X = oxides of nitrogen; $PM_{2.5}$ = fine particulate matter with an aerodynamic resistance diameter of 2.5 micrometers or less; PM_{10} = respirable particulate matter with an aerodynamic resistance diameter of 10 micrometers or less; ROG = reactive organic gases; tpy = tons per year.
Refer to Appendix D for support documentation.

4.2. GREENHOUSE GAS IMPACTS

4.2.1. Significance Determination

Step 1: Comparison of Project Attributes with Screening Criteria
The first step in determining the significance of operational-related GHG emissions is to compare the attributes of the proposed project with the applicable screening criteria (Refer to Chapter 3). If all of the screening criteria are met, the operation of the proposed project would result in a less than significant impact to global climate change. If the proposed project does not meet all the screening criteria, then project emissions need to be quantified.

If a project is located in a community with an adopted qualified GHG Reduction Strategy (described in section 4.3), the project may be considered less than significant if it is consistent with the GHG Reduction Strategy. A project must demonstrate its consistency by identifying and implementing all applicable feasible mandatory and voluntary measures and policies from the GHG Reduction Strategy into the project.

Step 2: Emissions Quantification
For quantifying a project's GHG emissions, BAAQMD recommends that all GHG emissions from a project be estimated, including a project's direct and indirect GHG emissions from operations.

Direct emissions refer to emissions produced from onsite combustion of energy, such as natural gas used in furnaces and boilers, emissions from industrial processes, and fuel combustion from mobile sources. Indirect emissions are emissions produced offsite from energy production and water conveyance due to a project's energy use and water consumption. See Table 4-2 for a list of GHG emission sources and types that should be estimated for projects.



BAAQMD's GHG threshold is defined in terms of carbon dioxide equivalent (CO_2e), a metric that accounts for the emissions from various greenhouse gases based on their global warming potential. For example, one ton of methane has the same contribution to the greenhouse effect as 23 tons of CO_2. Therefore, methane is a much more potent GHG than CO_2. Expressing emissions in CO_2e considers the contributions of all GHG emissions to the greenhouse effect.

Biogenic CO_2 emissions should not be included in the quantification of GHG emissions for a project. Biogenic CO_2 emissions result from materials that are derived from living cells, as opposed to CO_2 emissions derived from fossil fuels, limestone and other materials that have been transformed by geological processes. Biogenic CO_2 contains carbon that is present in organic materials that include, but are not limited to, wood, paper, vegetable oils, animal fat, and food, animal and yard waste.

The GHG emissions from permitted stationary sources should be calculated separately from a project's operational emissions. Permitted stationary sources are subject to a different threshold than land use developments. For example, if a proposed project anticipates having a permitted stationary source on site, such as a back-up generator, the GHG emissions from the generator should not be added to the project's total emissions. The generator's GHG emissions should be calculated separately and compared to the GHG threshold for stationary sources to determine its impact level.

If a proposed project involves the removal of existing emission sources, BAAQMD recommends subtracting the existing emissions levels from the emissions levels estimated for the new proposed land use. This net calculation is permissible only if the existing emission sources were operational at the time that the Notice of Preparation (NOP) for the CEQA project was circulated (or in the absence of an NOP when environmental analysis begins), and would continue if the proposed redevelopment project is not approved. This net calculation is not permitted for emission sources that ceased to operate, or the land uses were vacated and/or demolished, prior to circulation of the NOP or the commencement of environmental analysis. This approach is consistent with the definition of baseline conditions pursuant to CEQA.

BAAQMD Greenhouse Gas Model

BAAQMD's preferred method for quantifying GHG emissions from a project is to use the BAAQMD GHG Model (BGM). The Air District developed this model to calculate GHG emissions not included in URBEMIS such as indirect emissions from electricity use and waste and direct fugitive emissions of refrigerants. BGM quantifies different types of GHG emissions in terms of CO_2e and contains a broad range of GHG reduction strategies that may be applied to projects. BGM also adjusts for state regulations, specifically California's low carbon fuel rules and Pavley regulations.

To use BMG, a project must first be inputted into URBEMIS and then imported into BGM. When using URBEMIS, the same detailed guidance as described for criteria air pollutants should be followed for inputting proposed land use developments. BGM is available for free and

may be downloaded at: http://www.baaqmd.gov/Divisions/Planning-and-Research/CEQA-GUIDELINES.aspx. BGM is run using Microsoft Excel. Refer to the BGM user's manual for detailed instructions on using the model.

Table 4-2 outlines the recommended methodologies for estimating a project's GHG emissions.

Table 4-2
Guidance for Estimating a Project's Operations GHG Emissions

Emission Source	Emission Type	GHG	Methodology
Area Sources (natural gas, hearth, landscape fuel, etc.)	Direct - natural gas and fuel combustion	CO_2, CH_4, N_20	URBEMIS and BGM
Transportation	Direct - fuel combustion	CO_2, CH_4, N_20	URBEMIS and BGM
Electricity consumption	Indirect - electricity	CO_2, CH_4, N_20	BGM
Solid waste landfill (non-biogenic emissions)*	Direct - landfill	CH_4	BGM
Solid waste transport	Indirect - fuel combustion	CO_2, CH_4, N_20	BGM
Water consumption	Indirect - electricity	CO_2, CH_4, N_20	BGM
Wastewater (non-biogenic emissions)*	Indirect - electricity	CO_2, CH_4, N_20	BGM
Industrial process emissions	Direct	CO_2, CH_4, N_20, and refrigerants	BGM and BAAQMD permits**
Fugitive emissions	Direct	CO_2, CH_4, N_20, and refrigerants	BGM
Loss of trees/vegetation	Loss of sequestration	CO_2	BGM

* Biogenic CO_2 emissions should not be included in the quantification of GHG emissions for a project.
** Industrial processes permitted by the Air District must use the methodology provided in BAAQMD rules and regulations. Other industrial process emissions, such as commercial refrigerants, should use the BGM.

CO_2 (carbon dioxide), CH_4 (methane), N_20 (nitrous oxides), and refrigerants (HFCs and PFCs).

In cases where users may need to estimate a project's GHG emissions manually, BAAQMD recommends using ARB's most current Local Government Operations Protocol (LGOP) as appropriate for guidance. The most current LGOP may be downloaded from ARB's website.

Step 3: Comparison of Unmitigated Emissions with Thresholds of Significance
Sum the estimated GHG emissions from area and mobile sources for the build-out year and compare the total annual GHG emissions with the applicable threshold. If annual emissions of operational-related GHGs do not exceed the thresholds, the project would result in a less than significant impact to global climate change. If annual emissions do exceed the thresholds, the proposed project would result in a significant impact to global climate change and will require mitigation measures for emission reductions.

Step 4: Mitigation Measures and Emission Reductions
Where operational-related emissions exceed applicable thresholds, lead agencies are responsible for implementing all feasible mitigation measures to reduce the project's GHG

emissions. Section 4.4 contains recommended mitigation measures. The Air District recommends using the BGM if additional reductions are needed. The air quality analysis should quantify the reduction of emissions associated with any proposed mitigation measures and include this information in the CEQA document.

Step 5: Comparison of Mitigated Emissions with Thresholds of Significance
Compare the total annual amount of mitigated GHGs with the applicable threshold, as demonstrated in Table 4-3. If the implementation of project proposed or required mitigation measures would reduce operational-related GHGs to a level below either the 1,100 MT CO_2e/year or 4.6 MT CO_2e/SP/year threshold, the impact would be reduced to a less than significant level. If mitigated levels still exceed the applicable threshold, the impact to global climate change would be considered significant and unavoidable.

Table 4-3
Example of Operational Greenhouse Gas Emissions Analysis

Step	Emissions Source	Emissions (MT CO_2e/yr)*
2	Area Sources	A
	Mobile Sources	B
	Indirect Sources	C
	Total Unmitigated Emissions	A + B + C = D
	BAAQMD Threshold	1,100 or 4.6 MT CO_2e/yr/SP
3	Unmitigated Emissions Exceed BAAQMD Threshold?	Is D > 1,100/4.6? (If Yes, significant. Go to step 4. If No, less than significant)
4	Mitigated Emissions	E
5	Mitigated Emissions Exceed BAAQMD Threshold?	Is E > 1,100/4.6? (If Yes, significant and unavoidable. If No, less than significant with mitigation incorporated)

* Letters "A", "B", and "C" are used to represent numeric values that would be obtained through modeling for area and mobile sources, and by manual calculations for indirect source-emissions. "D" represents the sum of "A", "B", and "C" (i.e., unmitigated emissions). "E" represents mitigated emissions.
Notes: CO_2e = carbon dioxide equivalent; MT = metric tons; yr = year.
Refer to Appendix D for support documentation.

4.3. GREENHOUSE GAS REDUCTION STRATEGIES

The Air District encourages local governments to adopt a qualified GHG Reduction Strategy that is consistent with AB 32 goals. If a project is consistent with an adopted qualified GHG Reduction Strategy that meets the standards laid out below, it can be presumed that the project will not have significant GHG emission impacts. This approach is consistent with the State CEQA Guidelines, Section 15183.5 (see text in box below).

> *§15183.5. Tiering and Streamlining the Analysis of Greenhouse Gas Emissions.*
>
> *(a) Lead agencies may analyze and mitigate the significant effects of greenhouse gas emissions at a programmatic level, such as in a general plan, a long range development plan, or a separate plan to reduce greenhouse gas emissions. Later project-specific environmental documents may tier from and/or incorporate by reference that existing programmatic review. Project-specific environmental documents may rely on an EIR containing a programmatic analysis of greenhouse gas emissions as provided in section 15152 (tiering), 15167 (staged*

EIRs) 15168 (program EIRs), 15175-15179.5 (Master EIRs), 15182 (EIRs Prepared for Specific Plans), and 15183 (EIRs Prepared for General Plans, Community Plans, or Zoning).

(b) Plans for the Reduction of Greenhouse Gas Emissions. Public agencies may choose to analyze and mitigate significant greenhouse gas emissions in a plan for the reduction of greenhouse gas emissions or similar document. A plan to reduce greenhouse gas emissions may be used in a cumulative impacts analysis as set forth below. Pursuant to sections 15064(h)(3) and 15130(d), a lead agency may determine that a project's incremental contribution to a cumulative effect is not cumulatively considerable if the project complies with the requirements in a previously adopted plan or mitigation program under specified circumstances.

(1) Plan Elements. A plan for the reduction of greenhouse gas emissions should:

(A) Quantify greenhouse gas emissions, both existing and projected over a specified time period, resulting from activities within a defined geographic area;

(B) Establish a level, based on substantial evidence, below which the contribution to greenhouse gas emissions from activities covered by the plan would not be cumulatively considerable;

(C) Identify and analyze the greenhouse gas emissions resulting from specific actions or categories of actions anticipated within the geographic area;

(D) Specify measures or a group of measures, including performance standards, that substantial evidence demonstrates, if implemented on a project-by-project basis, would collectively achieve the specified emissions level;

(E) Establish a mechanism to monitor the plan's progress toward achieving the level and to require amendment if the plan is not achieving specified levels;

(F) Be adopted in a public process following environmental review

(2) Use with Later Activities. A plan for the reduction of greenhouse gas emissions, once adopted following certification of an EIR or adoption of an environmental document, may be used in the cumulative impacts analysis of later projects. An environmental document that relies on a greenhouse gas reduction plan for a cumulative impacts analysis must identify those requirements specified in the plan that apply to the project, and, if those requirements are not otherwise binding and enforceable, incorporate those requirements as mitigation measures applicable to the project. If there is substantial evidence that the effects of a particular project may be cumulatively considerable notwithstanding the project's compliance with the specified requirements in the plan for the reduction of greenhouse gas emissions, an EIR must be prepared for the project.

Standard Elements of a GHG Reduction Strategy

The Air District recommends the Plan Elements in the state CEQA Guidelines as the minimum standard to meet the GHG Reduction Strategy Thresholds of Significance option. A GHG Reduction Strategy may be one single plan, such as a general plan or climate action plan, or could be comprised of a collection of climate action policies, ordinances and programs that have been legislatively adopted by a local jurisdiction. The GHG Reduction Strategy should identify goals, policies and implementation measures that would achieve AB 32 goals for the entire community. Plans with horizon years beyond 2020 should consider continuing the downward reduction path set by AB 32 and move toward climate stabilization goals established in Executive Order S-3-05.

To meet this threshold of significance, a GHG Reduction Strategy must include the following elements (corresponding to the State CEQA Guidelines Plan Elements):

(A) Quantify greenhouse gas emissions, both existing and projected over a specified time period, resulting from activities within a defined geographic area.

A GHG Reduction Strategy must include an emissions inventory that quantifies an existing baseline level of emissions and projected GHG emissions from a business-as-usual, no-plan, forecast scenario of the horizon year. The baseline year is based on the existing growth pattern defined by an existing general plan. The projected GHG emissions are based on the emissions from the existing growth pattern or general plan through to 2020, and if different, the year used for the forecast. If the forecast year is beyond 2020, BAAQMD recommends also doing a forecast for 2020 to establish a trend. The forecast does not include new growth estimates based on a new or draft general plan.

When conducting the baseline emissions inventory and forecast, ARB's business-as-usual 2020 forecasting methodology should be followed to the extent possible, including the following recommended methodology and assumptions:

- The baseline inventory should include one complete calendar year of data for 2008 or earlier. CO_2 must be inventoried across all sectors (residential, commercial, industrial, transportation and waste at a minimum); accounting of CH_4, N_20, SF6, HFC and PFC emission sources can also be included where reliable estimation methodologies and data are available.

- Business-as-usual emissions are projected in the absence of any policies or actions that would reduce emissions. The forecast should include only adopted and funded projects.

- The business-as-usual forecast should project emissions from the baseline year using growth factors specific to each of the different economic sectors.

BAAQMD's *GHG Plan Level Quantification Guidance* contains detailed recommendations for developing GHG emission inventories and projections and for quantifying emission reductions from policies and mitigation measures. This document is available at BAAQMD's website, http://www.baaqmd.gov/Divisions/Planning-and-Research/CEQA-GUIDELINES.aspx.

(B) Establish a level, based on substantial evidence, below which the contribution to GHG emissions from activities covered by the plan would not be cumulatively considerable.

A GHG Reduction Strategy must establish a target that is adopted by legislation that meets or exceeds one of the following options, all based on AB 32 goals:

- Reduce emissions to 1990 level by 2020[1]

- Reduce emissions 15 percent below baseline (2008 or earlier) emission level by 2020[2]

- Meet the plan efficiency threshold of 6.6 MT CO_2e/service population/year

[1] Specified target in AB 32 legislation
[2] From "Climate Change Scoping Plan", Executive Summary page 5

If the target year for a GHG reduction goal exceeds 2020, then the GHG emission reduction target should be in line with the goals outlined in Executive Order S-3-05, and also include an interim goal for 2020.

(C) Identify and analyze the GHG emissions resulting from specific actions or categories of actions anticipated within the geographic area.

A Strategy should identify and analyze GHG reductions from anticipated actions in order to understand the amount of reductions needed to meet its target. Anticipated actions refer to local and state policies and regulations that may be planned or adopted but not implemented. For example, ARB's Scoping Plan contains a number of measures that are planned but not yet implemented. BAAQMD recommends for the Strategy to include an additional forecast analyzing anticipated actions. Element (C), together with (A), is meant to identify the scope of GHG emissions to be reduced through Element (D).

(D) Specify measures or a group of measures, including performance standards that substantial evidence demonstrates, if implemented on a project-by-project basis, would collectively achieve the specified emissions level.

The GHG Reduction Strategy should include mandatory and enforceable measures that impact new development projects, such as mandatory energy efficiency standards, density requirements, transportation demand management policies, etc., as well as existing development. These measures may exist in codes or other policies and may be included in the Strategy by reference.

The GHG Reduction Strategy should include quantification of expected GHG reductions from each identified measure or categories of measures (such as residential energy efficiency measures, bike/pedestrian measures, recycling measures, etc.), including disclosure of calculation methods and assumptions. Quantification should reflect annual GHG reductions and demonstrate how the GHG reduction target will be met. The Strategy should specify which measures apply to new development projects. For assistance in quantifying potential GHG reductions from different mitigation measures, Lead Agencies may refer to CAPCOA's report, *Quantifying Greenhouse Gas Mitigation Measures*.

(E) Monitor the plan's progress

To ensure that all new development projects are incorporating all applicable measures contained within the GHG Reduction Strategy, the Strategy should include an Implementation Plan containing the following:

- Identification of which measures apply to new development projects vs. existing development, discerning between voluntary and mandatory measures.
- Mechanism for reviewing and determining if all applicable mandatory and voluntary measures are being adequately applied to new development projects.
- Identification of implementation steps and parties responsible for ensuring implementation of each action.
- Schedule of implementation identifying near-term and longer-term implementation steps.
- Procedures for monitoring and updating the GHG inventory and reduction measures every 3-5 years before 2020.

- Annual review and reporting to the jurisdiction's governing body on the progress of implementation of individual measures, including assessment of how new development projects have been incorporating Strategy measures. Review should also include an assessment of the implementation of Scoping Plan measures in order to determine if adjustments to local Strategy must be made to account for any shortfalls in Scoping Plan implementation.

(F) Adopt the GHG Reduction Strategy in a public process following environmental review

A GHG Reduction Strategy should undergo an environmental review which may include a negative declaration or EIR.

If the GHG Reduction Strategy consists of a number of different elements, such as a general plan, a climate action plan and/or separate codes, ordinances and policies, each element that is applicable to new development projects would have to complete an environmental review in order to allow tiering for new development projects.

Sustainable Communities Strategy (SCS) or Alternative Planning Strategy

If a project is located within an adopted Sustainable Communities Strategy or Alternative Planning Strategy, the GHG emissions from cars and light duty trucks do not need to be analyzed in the environmental analysis. This approach is consistent with the State CEQA Guidelines, Section 15183.5(c). This approach only applies to certain residential and mixed use projects and transit priority projects as defined in Section 21155 of the State CEQA Guidelines.

Section 15183.5(c): Special Situations. As provided in Public Resources Code sections 21155.2 and 21159.28, environmental documents for certain residential and mixed us projects, and transit priority projects, as defined in section 21155, that are consistent with the general use designation, density, building intensity, and applicable policies specified for the project area in an applicable sustainable communities strategy or alternative planning strategy need not analyze global warming impacts resulting from cars and light duty trucks. A lead agency should consider whether such projects may result in GHG emissions resulting from other source, however, consistent with these Guidelines.

Section 21155: A transit priority project shall (1) contain at least 50 percent residential use, based on total building square footage and, if the project contains between 26 percent and 50 percent nonresidential uses, a floor area ratio of not less than 0.75; (2) provide a minimum net density of at least 20 dwelling units per acre; and (3) be within one-half mile of a major transit stop or high-quality transit corridor included in a regional transportation plan. A major transit stop is as defined in Section 21064.3, except that, for purposes of this section, it also includes major transit stops that are included in the applicable regional transportation plan. For purposes of this section, a high quality transit corridor means a corridor with fixed route bus service with service intervals no longer than 15 minutes during peak commute hours. A project shall be considered to be within on-half mile of a major transit stop or high-quality transit corridor if all parcels within the project have not more than 25 percent of their area farther than one-half mile from the stop or corridor and if not more than 10 percent of the residential units or 100 units, whichever is less, in the project are farther than one-half mile from the stop or corridor.

4.4. MITIGATING OPERATIONAL-RELATED IMPACTS

The following mitigation measures would reduce operational-related emissions of criteria air pollutants, precursors, and GHGs from mobile, area, and stationary sources. Additional mitigation measures may be used, including off-site measures, provided their mitigation efficiency is

justified. Where a range of emission reduction potential is given for a measure, the lead agency should provide justification for the mitigation reduction efficiency assumed for the project. If mitigation does not bring a project back within the threshold requirements, the project could be cumulatively significant and could be approved only with a Statement of Overriding Considerations and a showing that all feasible mitigation measures have been implemented.

Reductions from mitigation measures should be scaled proportionally to their sector of project-generated emissions. For example, if a measure would result in a 50 percent reduction in residential natural gas consumption, but only 20 percent of a project's emissions are associated with natural gas consumption, and only 10 percent of a project's emissions are from residential land uses, then the scaled reduction would equal one percent (50% * 20% * 10% = 1%).

Once all emission reductions are scaled by their applicable sector and land use, they should be added together for the total sum of emission reductions. Once all emission reductions are scaled by their applicable sector and land use, they should be added together for the total sum of emission reductions.

The Air District prefers for project emissions to be reduced to their extent possible onsite. For projects that are not able to mitigate onsite to a level below significance, offsite mitigation measures serve as a feasible alternative. Recent State's CEQA Guidelines amendments allow for offsite measures to mitigate a project's emissions, (Section 15126.4(c)(4)).

In implementing offsite mitigation measures, the lead agency must ensure that emission reductions from identified projects are real, permanent through the duration of the project, enforceable, and are equal to the pollutant type and amount of the project impact being offset. BAAQMD recommends that offsite mitigation projects occur within the nine-county Bay Area in order to reduce localized impacts and capture potential co-benefits. Offsite mitigation for PM and toxics emission reductions should occur within a five mile radius to the project site.

Another feasible mitigation measure the Air District is exploring establishing is an offsite mitigation program to assist lead agencies and project applicants in achieving emission reductions. A project applicant would enter into an agreement with the Air District and pay into an Air District fund. The Air District would commit to reducing the type and amount of emission indentified in the agreement. The Air District would identify, implement, and manage offsite mitigation projects.

The following tables list feasible mitigation measures for consideration in projects. The estimated emission reductions are a work in progress and the Air District will continue to improve guidance on quantifying the mitigation measures.

URBEMIS Mitigation Measures for Operational Mobile Source Emissions

Measure	Sector Reductions	Applicable Pollutants	Sector	Notes	Additional comments
Mix of Uses	-3% to 9%	CAPs, GHGs	Mobile sources	-3 when no housing or employment centers within 1/2 mile	Residential: % reduction is taken from base trips (9.57) and subtracted from ITE trip generation; Nonresidential:
Local serving retail within 1/2 mile of project	2%	CAPs, GHGs	Mobile sources	Uses lower end of reported research to avoid double counting with mix of uses measure	
Transit Service	0% to 15%	CAPs, GHGs	Mobile sources		

URBEMIS Mitigation Measures for Operational Mobile Source Emissions

Measure	Sector Reductions	Applicable Pollutants	Sector	Notes	Additional comments
Bike & Pedestrian	0%–9%	CAPs, GHGs	Mobile sources	Credit is given based on intersection density, sidewalk completeness, and bike network completeness; No reduction if entire area within 1/2 mile is single use	% reduction from ITE trip generation
Affordable Housing	0%–4%	CAPs, GHGs	Mobile sources		
Transportation Demand Management Parking, Transit Passes					
Daily Parking Charge	0%–25%	CAPs, GHGs	Only resident/ employee trips, no visitor/ shopper trips		
Parking Cash-Out	0%–12.5%	CAPs, GHGs		Shoup, Donald. 2005. Parking Cash Out. American Planning Association. Chicago, IL.	
Free Transit Passes	25% of Transit Service Reduction	CAPs, GHGs			
Telecommuting					
Employee Telecommuting Program	1%–100%	CAPs, GHGs	Mobile sources, Worker Trips only		
Compressed Work Schedule 3/36	1%–40%	CAPs, GHGs			
Compressed Work Schedule 4/40	1%–20%	CAPs, GHGs			
Compressed Work Schedule 9/80	1%–10%	CAPs, GHGs			
Other Transportation Demand Measures					
Secure Bike Parking (at least 1 space per 20 vehicle spaces)	At least 3 elements: 1% reduction, plus 5% of the reduction for transit and pedestrian/bike friendliness; At least 5 elements: 2% reduction, plus 10% of the reduction for transit and pedestrian/bike friendliness	CAPs, GHGs	Mobile sources, Worker Trips only		
Showers/Changing Facilities Provided					
Guaranteed Ride Home Program Provided					
Car-Sharing Services Provided					
Information Provided on Transportation Alternatives (Bike Schedules, Maps)					
Dedicated Employee Transportation Coordinator					

URBEMIS Mitigation Measures for Operational Mobile Source Emissions

Measure	Sector Reductions	Applicable Pollutants	Sector	Notes	Additional comments
Carpool Matching Program					
Preferential Carpool/Vanpool Parking					
Parking Supply	0%–50%	CAPs, GHGs	Mobile sources		
On Road Trucks	As input by user in URBEMIS	CAPs, GHGs	Mobile sources		

URBEMIS Mitigation Measures for Operational Area-Source Emissions

Measure	Sector Reductions	Applicable Pollutants	Sector	Notes
Increase Energy Efficiency Beyond Title 24	Same as % improvement over Title 24	CAPs, GHGs	Natural gas sector in URBEMIS for applicable land use only	User should specify baseline year for the Title 24 standards
Electrically powered landscape equipment and outdoor electrical outlets	Same as % of landscape equipment emissions	CAPs, GHGs	Landscape emissions: residential only	
Low VOC architectural coatings	Same as % VOC reduction in applicable coatings (Interior/Exterior)	ROG only	Architectural coating	

NON-URBEMIS Energy Efficiency Mitigation Measures

Measure	Sector Reductions	Applicable Pollutants	Sector	Notes	Additional comments
Plant shade trees within 40 feet of the south side or within 60 feet of the west sides of properties.	30%	GHGs	R,C A/C Electricity	USDA Forest Service, Pacific Northwest Research Station. "California Study Shows Shade Trees Reduce Summertime Electricity Use." Science Daily 7 January 2009. 20 February 2009 <http://www.sciencedaily.com/releases/2009/01/090105150831.htm>.	Electricity-related measures reduce CAPs off-site, but they are not typically quantified as part of a CEQA analysis.
Require cool roof materials (albedo	34%	GHGs	C A/C Electricity	U.S. EPA Cool Roof Product Information,	

NON-URBEMIS Energy Efficiency Mitigation Measures

Measure	Sector Reductions	Applicable Pollutants	Sector	Notes	Additional comments
>= 30)	69%	GHGs	R A/C Electricity	Available: <http://www.epa.gov/heatisland/resources/pdf/CoolRoofsCompendium.pdf>	
Install green roofs	1%	GHGs	R,C A/C Electricity	Reductions are based on the Energy & Atmosphere credits (EA Credit 2) documented in the Leadership in Energy & Environmental Design (LEED), Green Building Rating System for New Constructions and Major Renovations, Version 2.2, October 2005. The reduction assumes that a vegetated roof is installed on a least 50% of the roof area or that a combination high albedo and vegetated roof surface is installed that meets the following standard: (Area of SRI Roof/0.75)+(Area of vegetated roof/0.5) >= Total Roof Area.	
Require smart meters and programmable thermostats	10%	CAPs, GHGs	R, C electricity and natural gas space heating	U. S. Environmental Protection Agency. 2009. Programmable Thermostat. http://www.energystar.gov/ia/new_homes/features/ProgThermostats1-17-01.pdf	
Meet GBC standards in all New construction	17%	GHGs	R electricity	California Energy Commission [CEC] 2007. Impact Analysis 2008 Update to the California Energy Efficiency Standards for Residential and Nonresidential Buildings	
	7%	GHGs	C electricity		
	9%	CAPs, GHGs	R natural gas		
	3%	CAPs, GHGs	C natural gas		
Retrofit existing buildings to meet CA GBC standards	38%	GHGs	R electricity	California Energy Commission [CEC] 2003. Impact Analysis 2005 Update to the California	
	12%	GHGs	C electricity		
	18%	CAPs, GHGs	R natural gas		

NON-URBEMIS Energy Efficiency Mitigation Measures

Measure	Sector Reductions	Applicable Pollutants	Sector	Notes	Additional comments
	12%	CAPs, GHGs	C natural gas	Energy Efficiency Standards for Residential and Nonresidential Buildings; California Energy Commission [CEC] 2007. Impact Analysis 2008 Update to the California Energy Efficiency Standards for Residential and Nonresidential Buildings	
Install solar water heaters	70%	CAPs, GHGs	R natural gas water heating	Energy Star. 2009. Solar Water Heater. http://www.energystar.gov/ia/new_homes/features/WaterHtrs_062906.pdf; Department of Energy. California Energy Commission [CEC] 2007. Impact Analysis 2008 Update to the California Energy Efficiency Standards for Residential and Nonresidential Buildings	Cannot take credit for both solar and tank-less water heater measures
	70%	CAPs, GHGs	C natural gas water heating		
Install tank-less water heaters	35%	CAPs, GHGs	R natural gas water heating	Tankless Water Heater. 2008. Available: <http://www.eere.energy.gov/consumer/your_home/water_heating/index.cfm/mytopic=12820>	
	35%	CAPs, GHGs	C natural gas water heating		
Install solar panels on residential and commercial buildings	100%	GHGs	R, C electricity		

NON-URBEMIS Energy Efficiency Mitigation Measures

Measure	Sector Reductions	Applicable Pollutants	Sector	Notes	Additional comments
100% increase in diversity of land use mix	5%	CAPs, GHGs	Mobile sources	Ewing, Reid, et al. 2001. *Travel and the Built Environment: A Synthesis.* Transportation Research Record 1780. Paper No. 01-3515 as cited in Urban Land Institute. 2008. *Growing Cooler.* ISBN: 978-0-87420-082-2. Washington, DC	
Jobs housing balance	Trip reduction = (1 – (ABS (1.5 * HH – E)/(1.5 * HH + E)) – 0.25) / 0.25 * 0.03; where ABS = absolute value; HH = study area households ; E = study area employment	CAPs, GHGs	Mobile sources	*Nelson/Nygaard Consultants. 2005. Crediting Low-Traffic Developments: Adjusting Site-Level Vehicle Trip Generation Using URBEMIS. Pg 12, (adapted from Criterion and Fehr & Peers, 2001)*	
100% increase in design (i.e., presence of design guidelines for transit oriented development, complete streets standards)	3%	CAPs, GHGs	Mobile sources	Ewing, Reid, et al. 2001. *Travel and the Built Environment: A Synthesis.* Transportation Research Record 1780. Paper No. 01-3515 as cited in Urban Land Institute. 2008. *Growing Cooler.* ISBN: 978-0-87420-082-2. Washington, DC	

NON-URBEMIS Energy Efficiency Mitigation Measures

Measure	Sector Reductions	Applicable Pollutants	Sector	Notes	Additional comments
100% increase in density	5%	CAPs, GHGs	Mobile sources	Ewing, Reid, et al. 2001. *Travel and the Built Environment: A Synthesis.* Transportation Research Record 1780. Paper No. 01-3515 as cited in Urban Land Institute. 2008. *Growing Cooler.* ISBN: 978-0-87420-082-2. Washington, DC	
HVAC duct sealing	30%	GHGs	R,C A/C electricity	Sacramento Metropolitan Utilities District. 2008. Duct Sealing. Available: <http://www.pge.com/myhome/saveenergymoney/rebates/coolheat/duct/index.shtml>.	
Provide necessary infrastructure and treatment to allow use of 50% greywater/ recycled water in residential and commercial uses for outdoor irrigation	SFR: 74%*50% = 37.5% MFR: 58% * 50% = 29% Commercial: 12% * 50% = 6%	GHGs	R electricity (water consumption) C electricity (water consumption)	Department of Water Resources. 2001. Statewide Indoor/Outdoor Split. Accessed December 2, 2008. Available at: <http://www.landwateruse.water.ca.gov/annualdata/urbanwateruse/2001/landuselevels.cfm?use=8>.	
Complete streets (i.e., bike lanes and pedestrian sidewalks on both sides of streets, traffic calming features such as pedestrian bulb-outs, cross-walks, traffic circles, and elimination of physical and psychological barriers (e.g., sound walls and large arterial roadways, respectively).)	1-5%	CAPs, GHGs	Mobile sources	Dierkers, G., E. Silsbe, S. Stott, S. Winkelman, an M. Wubben. 2007. *CCAP Transportation Emissions Guidebook*. Center for Clean Air Policy. Washington, D.C. Available: <http://www.ccap.org/safe/guidebook.php>. as cited in California Air Pollution Control Officers Association (CAPCOA) 2008. *CEQA and Climate Change.*	

NON-URBEMIS Energy Efficiency Mitigation Measures

Measure	Sector Reductions	Applicable Pollutants	Sector	Notes	Additional comments
Maximize interior day light		GHGs	R, C, M		
Increase roof/ceiling insulation		CAPs, GHGs	R, C, M		
Create program to encourage efficiency improvements in rental units		CAPs, GHGs	R		
Install rainwater collection systems in residential and Commercial Buildings		GHGs	R,C,M		
Install low-water use appliances and fixtures		GHGs	R,C,M	California Air Pollution Control Officers Association (CAPCOA) 2008. CEQA and Climate Change.	
Restrict the use of water for cleaning outdoor surfaces/Prohibit systems that apply water to non-vegetated surfaces		GHGs	R,C,M	California Attorney General's Office GHG Reduction Measures	
Implement water-sensitive urban design practices in new construction		GHGs	R,C,M		
NON-URBEMIS Waste Reduction Mitigation Measures					
Provide composting facilities at residential uses		GHGs	R		
Create food waste and green waste curb-side pickup service		GHGs	R,C,M		
Require the provision of storage areas for recyclables and green waste in new construction		GHGs	R,C,M		

Notes: CAPs = Criteria Air Pollutants; GHGs = Greenhouse Gases; ROG = Reactive Organic Gases; R = Residential Development; C = Commercial Development; M = Mixed Use Development; A/C = Air Conditioning; and VOC = Volatile Organic Compounds.

Source: Information compiled by EDAW 2009.

[This Page Intentionally Left Blank]

5. LOCAL COMMUNITY RISK AND HAZARD IMPACTS

The purpose of this Chapter is (1) to recommend methods whereby local community risk and hazard impacts from projects for both new sources and new receptors can be determined based on comparison with applicable thresholds of significance and screening criteria and (2) to recommend mitigation measures for these impacts. This chapter contains the following sections:

Section 5.2 – Presents methods for assessing single-source impacts from either an individual new source or impacts on new receptors from existing individual sources.

Section 5.3 – Discusses methods for assessing cumulative impacts from multiple sources.

Section 5.4 – Discusses methods for mitigating local community risk and hazard impacts.

The recommendations provided in this chapter apply to assessing and mitigating impacts for project-level impacts and related cumulative impacts. Refer to Chapter 9 for recommendations for assessing and mitigating local community risk and hazard impacts at the plan-level.

To assist the lead agency in evaluating air quality impacts at the community scale, *Thresholds of Significance* have been established for local community risks and hazards associated with TACs and $PM_{2.5}$ with respect to siting a new source and/or receptor; as well as for assessing both individual source and cumulative multiple source impacts. These *Thresholds of Significance* focus on $PM_{2.5}$ and TACs because these more so than other emission types pose significant health impacts at the local level as discussed separately below.

5.1. TOXIC AIR CONTAMINANTS

TACs are a defined set of airborne pollutants that may pose a present or potential hazard to human health. A wide range of sources, from industrial plants to motor vehicles, emit TACs. Like $PM_{2.5}$, TAC can be emitted directly and can also be formed in the atmosphere through reactions among different pollutants. The methods presented in this Chapter for assessing local community risk and hazard impacts only include direct TAC emissions, not those formed in the atmosphere.

The health effects associated with TACs are quite diverse and generally are assessed locally, rather than regionally. TACs can cause long-term health effects such as cancer, birth defects, neurological damage, asthma, bronchitis or genetic damage; or short-term acute affects such as eye watering, respiratory irritation (a cough), running nose, throat pain, and headaches. For evaluation purposes, TACs are separated into carcinogens and non-carcinogens based on the nature of the physiological effects associated with exposure to the pollutant. Carcinogens are assumed to have no safe threshold below which health impacts would not occur, and cancer risk is expressed as excess cancer cases per one million exposed individuals, typically over a lifetime of exposure. Non-carcinogenic substances differ in that there is generally assumed to be a safe level of exposure below which no negative health impact is believed to occur. These levels are



© 2009 Jupiterimages Corporation

determined on a pollutant-by-pollutant basis. Acute and chronic exposure to non-carcinogens is expressed as a hazard index (HI), which is the ratio of expected exposure levels to an acceptable reference exposure levels.

TACs are primarily regulated through State and local risk management programs. These programs are designed to eliminate, avoid, or minimize the risk of adverse health effects from exposures to TACs. A chemical becomes a regulated TAC in California based on designation by the California Office of Environmental Health Hazard Assessment (OEHHA). As part of its jurisdiction under Air Toxics Hot Spots Program (Health and Safety Code Section 44360(b)(2)), OEHHA derives cancer potencies and reference exposure levels (RELs) for individual air contaminants based on the current scientific knowledge that includes consideration of possible differential effects on the health of infants, children and other sensitive subpopulations, in accordance with the mandate of the Children's Environmental Health Protection Act (Senate Bill 25, Escutia, Chapter 731, Statutes of 1999, Health and Safety Code Sections 39669.5 et seq.). The methodology in this Chapter reflects the approach adopted by OEHHA in May 2009, which considers age sensitivity factors to account for early life stage exposures. The specific toxicity values of each particular TAC as identified by OEHHA are listed in BAAQMD's Regulation 2, Rule 5: New Source Review of Toxic Air Contaminants.

5.1.1. Fine Particulate Matter

$PM_{2.5}$ is a complex mixture of substances that includes elements such as carbon and metals; compounds such as nitrates, organics, and sulfates; and complex mixtures such as diesel exhaust and wood smoke. $PM_{2.5}$ can be emitted directly and can also be formed in the atmosphere through reactions among different pollutants. The methods presented in this Chapter for assessing local community risk and hazard impacts only include direct $PM_{2.5}$ emissions, not those formed in the atmosphere.

Compelling evidence suggests that $PM_{2.5}$ is by far the most harmful air pollutant in the SFBAAB in terms of the associated impact on public health. A large body of scientific evidence indicates that both long-term and short-term exposure to $PM_{2.5}$ can cause a wide range of health effects (e.g., aggravating asthma and bronchitis, causing visits to the hospital for respiratory and cardio-vascular symptoms, and contributing to heart attacks and deaths). BAAQMD recommends characterizing potential health effects from exposure to directly $PM_{2.5}$ emissions through comparison to the applicable *Thresholds of Significance*.

5.1.2. Common Source Types

Common stationary source types of TAC and $PM_{2.5}$ emissions include gasoline stations, dry cleaners, and diesel backup generators, which are subject to BAAQMD permit requirements. The other, often more significant, common source type is on-road motor vehicles on freeways and roads such as trucks and cars, and off-road sources such as construction equipment, ships and trains. Because these common sources are prevalent in many communities, this Chapter focuses on screening tools for the evaluation of associated cumulative community risk and hazard impacts. However, it is important to note that other influential source types do exist (e.g., ports, railyards, and truck distribution centers), but these are often more complex and require more advanced modeling techniques beyond those discussed herein.

5.1.3. Area of Influence

For assessing community risks and hazards, a 1,000 foot radius is recommended around the project property boundary. BAAQMD recommends that any proposed project that includes the siting of a new source or receptor assess associated impacts within 1,000 feet, taking into account both individual and nearby cumulative sources (i.e., proposed project plus existing and foreseeable future projects). Cumulative sources represent the combined total risk values of each individual source within the 1,000-foot evaluation zone. A lead agency should enlarge the 1,000-

foot radius on a case-by-case basis if an unusually large source or sources of risk or hazard emissions that may affect a proposed project is beyond the recommended radius.

The recommended methodology for assessing community risks and hazards from $PM_{2.5}$ and TACs follows a phased approach. Within this approach, more advanced techniques, for both new sources and receptors, which require additional site specific information are presented for each progressive phase to assess risks and hazards. Each phase provides concentrations and risks that are directly comparable to the applicable *Thresholds of Significance*, although it is important to note that the use of more site specific modeling input data produces more accurate results. Also, progression from one phase to the next in a sequential fashion is not necessary and a refined modeling analysis can be conducted at any time.

5.1.4. Impacted Communities

In the Bay Area, there are a number of urban or industrialized communities where the exposure to TACs is relatively high in comparison to others. These same communities are often faced with other environmental and socio-economic hardships that further stress their residents and result in poor health outcomes. To address community risk from air toxics, the Air District initiated the Community Air Risk Evaluation (CARE) program in 2004 to identify locations with high levels of risk from TACs co-located with sensitive populations and use the information to help focus mitigation measures. Through the CARE program, the Air District developed an inventory of TAC emissions for 2005 and compiled demographic and health indicator data. According to the findings of the CARE Program, diesel PM, mostly from on and off-road mobile sources, accounts for over 80 percent of the inhalation cancer risk from TACs in the Bay Area. Figure 5-1 shows the impacted communities as of November 2009, including: the urban core areas of Concord, eastern San Francisco, western Alameda County, Redwood City/East Palo Alto, Richmond/San Pablo, and San Jose. For more information on, and possible revisions to, impacted communities, go to the CARE Program website.

In many cases, air quality conditions in impacted communities result in part from land use and transportation decisions made over many years. BAAQMD believes comprehensive, community-wide strategies will achieve the greatest reductions in emissions of and exposure to TAC and $PM_{2.5}$. BAAQMD strongly recommends that within these impacted areas local jurisdictions develop and adopt Community Risk Reduction Plans, described in Section 5.4. The goal of the Community Risk Reduction Plan is to encourage local jurisdictions to take a proactive approach to reduce the overall exposure to TAC and $PM_{2.5}$ emissions and concentrations from new and existing sources. Local plans may also be developed in other areas to address air quality impacts related to land use decisions and ensure sufficient health protection in the community.

5.2. SINGLE SOURCE IMPACTS

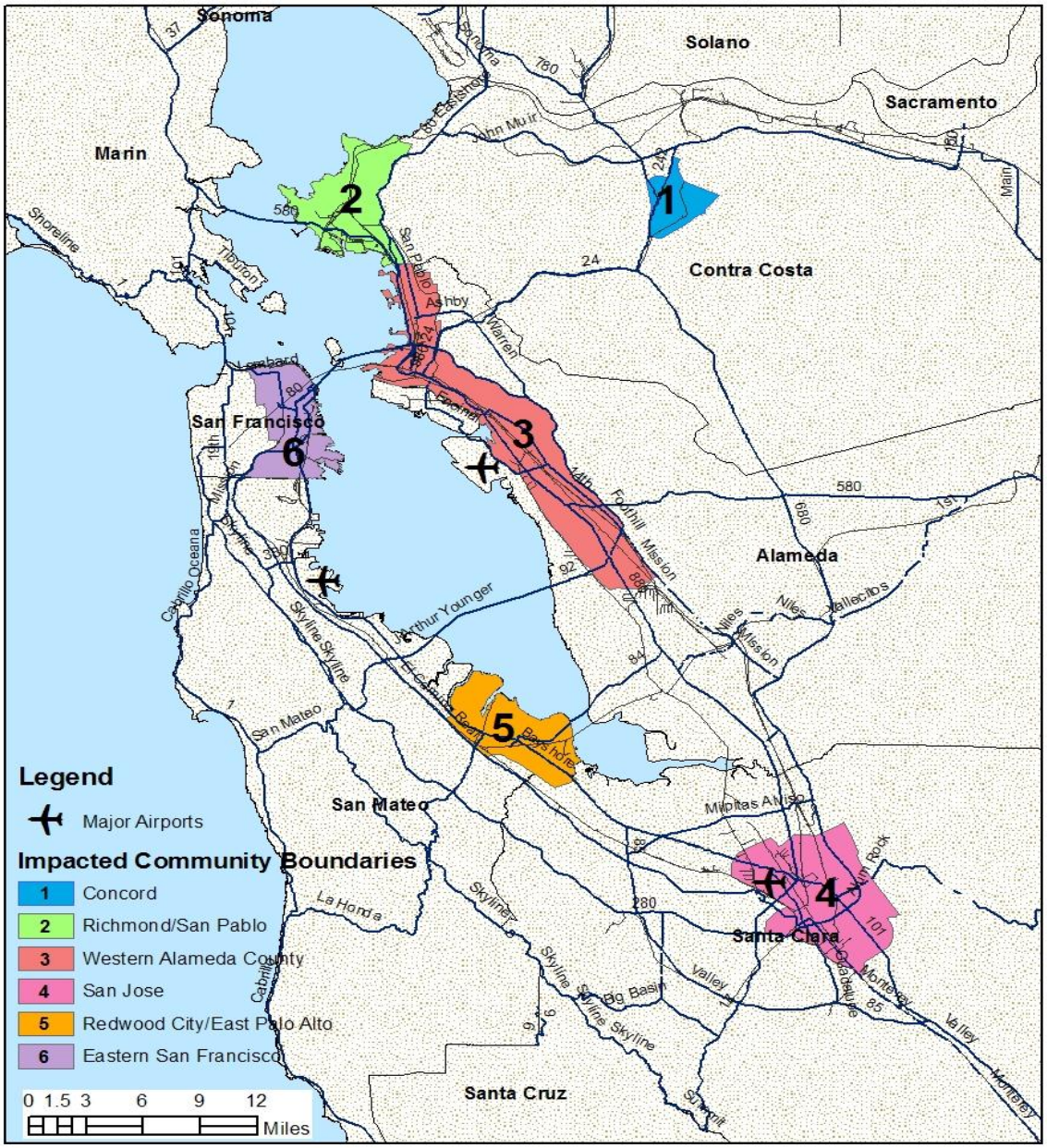
5.2.1. Significance Determination

Lead agencies should determine whether operational-related TAC and $PM_{2.5}$ emissions generated as part of a proposed project would expose existing or new receptors to levels that exceed the following *Thresholds of Significanc*e:

- Non-compliance with a qualified Community Risk Reduction Plan;
- An excess cancer risk level of more than 10 in one million, or a non-cancer (i.e., chronic or acute) risk greater than 1.0 HI from a single source would be a significant cumulatively considerable contribution;
- An incremental increase of greater than 0.3 $\mu g/m^3$ annual average $PM_{2.5}$ from a single source would be a significant cumulatively considerable contribution.

In all areas, but especially within impacted communities identified under BAAQMD's CARE program, the lead agency is encouraged to develop and adopt a Community Risk Reduction Plan. To determine whether an impacted community is located in a jurisdiction, refer to Figure 5-1 and the BAAQMD CARE web page at http://www.baaqmd.gov/CARE/. Please consult with BAAQMD if a more precise map is needed.

Impacted Communities **Figure 5-1**



Source: BAAQMD 2009

Exposure of receptors to substantial concentrations of TACs and $PM_{2.5}$ could occur from the following situations:

1. Siting a new TAC and/or $PM_{2.5}$ source (e.g., diesel generator, truck distribution center, freeway) near existing or planned receptors; and
2. Siting a new receptor near an existing source of TAC and/or $PM_{2.5}$ emissions.

BAAQMD recommendations for evaluating and making a significance determination for each of these situations are discussed separately below.

5.2.2. Siting a New Source

When evaluating whether a new source of TAC and/or $PM_{2.5}$ emissions would adversely affect existing or future proposed receptors, a lead agency should examine:

- the extent to which the new source would increase risk levels, hazard index, and/or $PM_{2.5}$ concentrations at nearby receptors,
- whether the source would be permitted or non-permitted by the BAAQMD, and
- whether the project would implement Best Available Control Technology for Toxics (T-BACT), as determined by BAAQMD.

The incremental increase in cancer and non-cancer (chronic and acute) risk from TACs and $PM_{2.5}$ concentrations at the affected receptors should be assessed. The recommended methodology for assessing community risks and hazards from $PM_{2.5}$ and TACs follows a phased approach, within which progressively more advanced techniques are presented for each phase (Figure 5-2). Each phase provides concentrations and risks that are directly comparable to the applicable threshold, although it is important to note that the use of more site specific modeling input data produces more accurate results. Also, progression from one phase to the next in a sequential fashion is not necessary and a refined modeling analysis can be conducted at any time.

For siting a new source, the first step is to determine the associated emission levels.

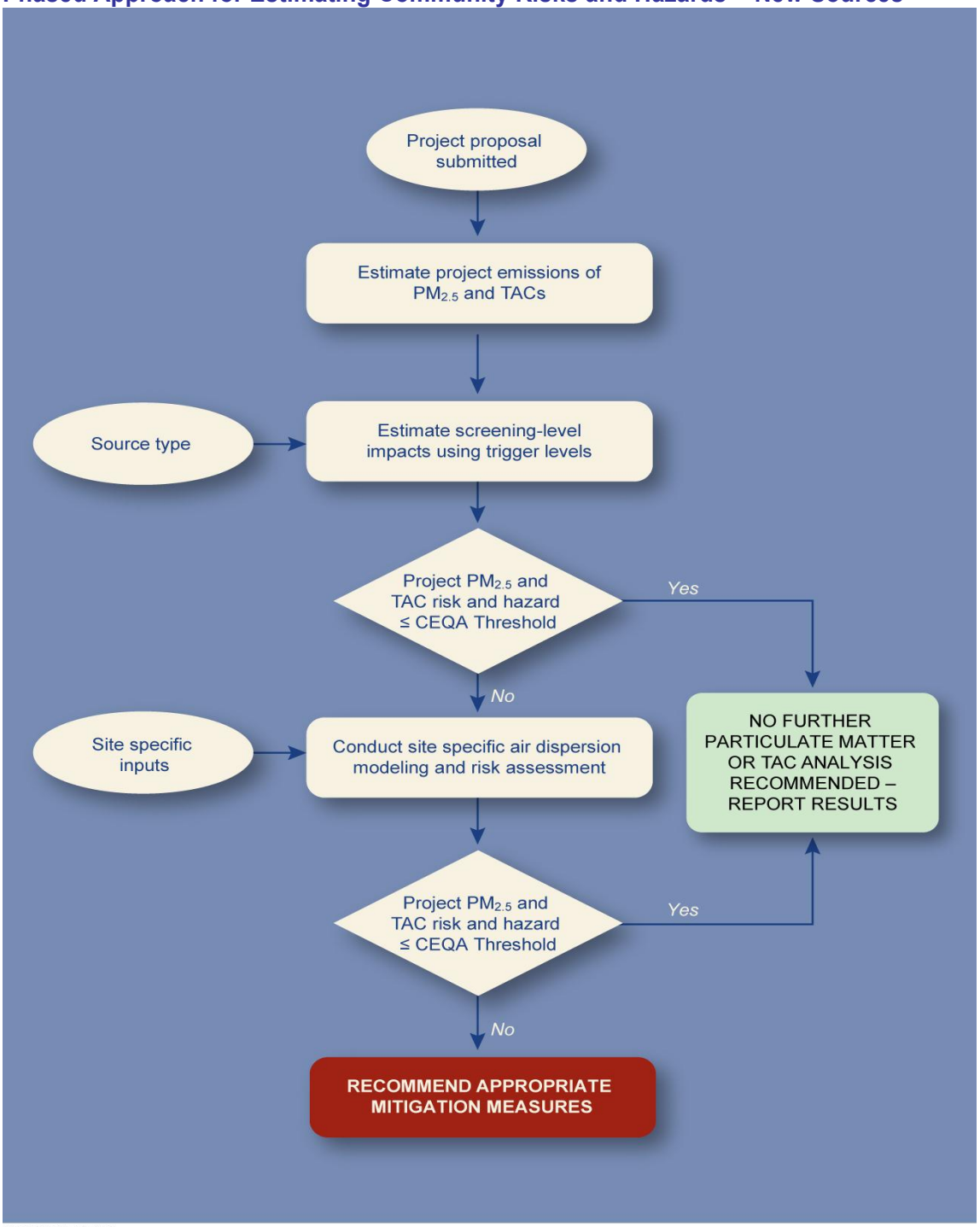
5.2.3. Sources Permitted by BAAQMD

For sources that would be permitted by BAAQMD (e.g., gas stations and back-up diesel generators) the project's type, size, or planned level of use can be used to help estimate $PM_{2.5}$ and TAC emissions. Screening or modeling conducted as part of the permit application can be used to determine cancer and non-cancer risk and $PM_{2.5}$ concentrations for comparing to the applicable threshold. BAAQMD can assist in determining the level of emissions associated with the new source. A lead agency should identify the maximally exposed existing or reasonably foreseeable future receptor.

Requirements of Toxics New Source Review (Regulation 2, Rule 5) will determine whether the project would implement T-BACT.

Figure 5-2

Phased Approach for Estimating Community Risks and Hazards – New Sources



G 08110224.01 007

Concentration estimates of $PM_{2.5}$ from screening or modeling should be compared with the threshold for $PM_{2.5}$. If screening estimates determine $PM_{2.5}$ concentrations from the project would not exceed the thresholds, no further analysis is recommended. If emissions would exceed the thresholds, more refined modeling or mitigation measures to offset emissions should be considered.

5.2.4. Sources Not Requiring a BAAQMD Permit

Some proposed projects would include the operation of non-permitted sources of TAC and/or $PM_{2.5}$ emissions. For instance, projects that would attract high numbers of diesel-powered on-road trucks or use off-road diesel equipment on site, such as a distribution center, a quarry, or a manufacturing facility, would potentially expose existing or future planned receptors to substantial risk levels and/or health hazards.

For sources that would not require permits from BAAQMD (e.g., distribution centers and large retail centers) where emissions are primarily from mobile sources—the number and activity of vehicles and fleet information would be required. The latest version of the State of California's EMFAC model is recommended for estimating emissions from on-road vehicles; the OFFROAD model is recommended for estimating emissions from off-road vehicles. For these types of new sources (not permitted by BAAQMD) screening methods are not currently available and a more refined analysis is necessary.



© 2009 Jupiterimages Corporation

If modeling estimates for community risks and hazards determine that local levels associated with the proposed project meet the applicable thresholds, no further analysis is recommended. More details on project screening and recommended protocols for modeling stationary and mobile sources are presented in *Recommended Methods for Screening and Modeling Local Risks and Hazards*. This online companion describes how to use screening tables to determine whether a site specific modeling analysis and risk assessment may be needed. The document also addresses sources that BAAQMD has determined to have negligible impact on health outcomes. It describes the recommended methodology for performing dispersion modeling and estimating emission factors if the project exceeds the thresholds based on the screening analysis; it describes how to calculate the potential cancer risk using age-sensitivity toxicity factors from the concentrations produced from the air modeling analysis; and it provides a sample calculation and the methodology for estimating short term, acute exposures and long term, chronic health impacts. The recommended protocols are consistent with the most current risk assessment methodology used for the BAAQMD's *New Source Review for Toxic Air Contaminants Regulation 2, Rule 5: Toxics New Source Review* and, with few exceptions, follows the California Air Pollution Control Officers Association's (CAPCOA) *Health Risk Assessments for Proposed Land Use Projects* (July 2009).

BAAQMD recommends that all receptors located within a 1,000 foot radius of the project's fence line be assessed for potentially significant impacts from the incremental increase in risks or hazards from the proposed new source. A lead agency should enlarge the 1,000-foot radius on a case-by-case basis if an unusually large source or sources of risk or hazard emissions that may affect a proposed project is beyond the recommended radius.

For new land uses that would host a high number of non-permitted TAC sources, such as a distribution center, the incremental increase in cancer risk should be determined by an HRA using

an acceptable air dispersion model in accordance with BAAQMD's *Recommended Methods for Screening and Modeling Local Risks and Hazards* and/or CAPCOA's guidance document titled *Health Risk Assessments for Proposed Land Use Projects*. A lead agency may consult HRAs that have previously been conducted for similar land uses to determine whether it assesses the incremental increase in cancer risk qualitatively or by performing an HRA. This analysis should account for all TAC and PM emissions generated on the project site, as well as any TAC emissions that would occur near the site as a result of the implementation of the project (e.g., diesel trucks queuing outside an entrance, a high volume of trucks using a road to access a quarry or landfill).

Some proposed projects would include both permitted and non-permitted TAC sources. For instance, a manufacturing facility may include some permitted stationary sources and also attract a high volume of diesel trucks and/or include a rail yard. All sources should be accounted for in the analysis.

5.2.5. Siting a New Receptor

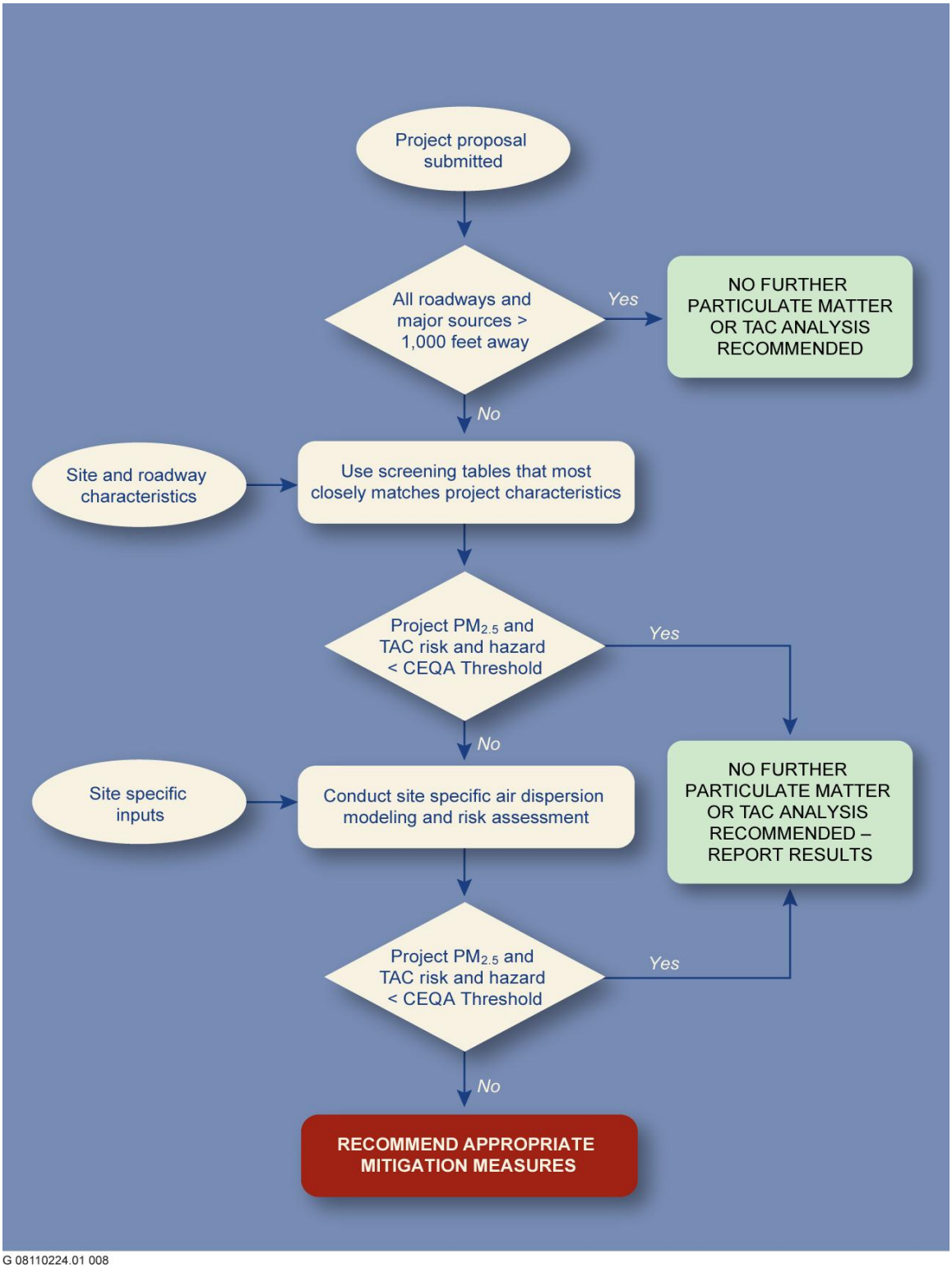
If a project is likely to be a place where people live, play, or convalesce, it should be considered a receptor. It should also be considered a receptor if sensitive individuals are likely to spend a significant amount of time there. Sensitive individuals refer to those segments of the population most susceptible to poor air quality: children, the elderly, and those with pre-existing serious health problems affected by air quality (ARB 2005). Examples of receptors include residences, schools and school yards, parks and play grounds, daycare centers, nursing homes, and medical facilities. Residences can include houses, apartments, and senior living complexes. Medical facilities can include hospitals, convalescent homes, and health clinics. Playgrounds could be play areas associated with parks or community centers.

When siting a new receptor, the existing or future proposed sources of TAC and/or $PM_{2.5}$ emissions that would adversely affect individuals within the planned project should be examined, including:

- the extent to which existing sources would increase risk levels, hazard index, and/or $PM_{2.5}$ concentrations near the planned receptor,
- whether the existing sources are permitted or non-permitted by the BAAQMD, and
- whether there are freeways or major roadways near the planned receptor.

BAAQMD recommends that a lead agency identify all TAC and $PM_{2.5}$ sources located within a 1,000 foot radius of the proposed project site. A lead agency should enlarge the 1,000-foot radius on a case-by-case basis if an unusually large source or sources of risk or hazard emissions that may affect a proposed project is beyond the recommended radius. Permitted sources of TAC and $PM_{2.5}$ should be identified and located as should freeways and major roadways, and other potential sources. To conduct a thorough search, a lead agency should gather all facility data within 1,000 feet of the project site (and beyond where appropriate).

The phased approach for evaluating impacts to new receptors is shown in Figure 5-3.



G 08110224.01 008

Phased Approach for Estimating Community Risks and Hazards – Receptors
Figure 5-3

5.2.6. Stationary Sources Screening Analysis

BAAQMD has developed an online tool containing data for existing permitted, stationary sources of TAC and $PM_{2.5}$ including site locations, UTM coordinates, source type, and screening-level estimates of $PM_{2.5}$ concentrations, cancer risk, and chronic hazard index. The online tool is a Google Earth™ application and may be downloaded for free from the BAAQMD website, http://www.baaqmd.gov/Divisions/Planning-and-Research/CEQA-GUIDELINES/Tools-and-Methodology.aspx. The Google Earth™ files consist of compressed keyhole markup language (kml) files for each of the nine Bay Area counties.

The stationary source screening tool contains all the sources in the Bay Area that have permits to operate and that emit one or more toxic air contaminants. The types of sources include, but are not limited to: refineries, gasoline dispensing facilities, dry cleaners, diesel internal combustion engines, natural gas turbines, crematories, landfills, waste water treatment facilities, hospitals and coffee roasters. The screening tool contains the following information for each source:

- Unique Plant Number for the stationary source used by the District (plant numbers starting with "G" are gasoline dispensing facilities that could be retail or non-retail). Plants are facilities or buildings that require a District permit. Plants are geo-coded and have BAAQMD assigned numbers. Plants can have multiple emission sources.

- The stationary source's plant name.

- Geocoded location for the Plant (Universal Transverse Mercador (UTM) coordinates). Note that the UTM coordinates represent only a single point at a plant, which may not be the point closest to the project. Also, the reference points for the UTM coordinates in the screening table may not be the same for all plants. Potential distance offsets may be as great as 200 meters. To ensure that all relevant plants are included, actual locations of sources should be verified.

- Conservatively estimated $PM_{2.5}$ concentrations, cancer risk, and chronic hazard index due to emissions from a plant are intended for screening purposes only. The screening values do not include acute hazard index since the maximum values for all sources was found to be very minor. Some of the sources may be marked with an asterisk, "*." The estimated risk and hazards for these sources are based on Health Risk Screening Assessments conducted by the District using the most site specific data available. The remaining stationary source risk and hazards impact estimates were derived using conservative modeling parameters and assumptions. The estimated risk and hazard impacts for these sources would be expected to be lower when site-specific Health Risk Screening Assessments are conducted.

The screening-level risk and hazard impacts in the stationary source screening tool do not represent actual impacts. The values are based on worst case assumption scenarios to determine whether or not a refined modeling analysis may be needed. The calculations used in the screening analysis do not include source specific exhaust information such as stack height, exhaust gas exit velocity, exhaust gas temperature, nor do they account for actual distances from receptors. A more refined analysis using source specific exhaust parameters, site specific meteorological data, site specific building dimensions and locations, and actual location of source and receptors is expected to result in lower and more accurate values than those found in the screening tool.

The impacts estimated from a project's screening process and if conducted, modeling analysis, should be summed and compared to the risk and hazards thresholds. If any single project exceeds the single source threshold or the sum of all the sources exceeds the cumulative

thresholds then the lead agency should consider possible mitigations that can reduce potential air quality impacts.

To use the stationary source screening tool, a user would open the county specific kml file, found on BAAQMD's website, where their project is located and identify all the stationary sources within 1,000 feet of the project's boundaries. The Google Earth™ ruler function may be used to measure the distance between stationary sources and the edge of the project boundaries. Users should then select the identified stationary sources to view the estimated $PM_{2.5}$, cancer risk, and chronic hazard index levels estimated for that source.

As an example, Table 5-1 presents a hypothetical location at 19th Avenue and Judah Street in San Francisco and lists the stationary sources within 1,000 feet of the example location. Each row contains entries for a specific existing stationary source and conservative estimates of cancer risk, $PM_{2.5}$ concentration, and chronic hazard index. The risk and hazards for each source should be compared to the appropriate significance thresholds. In Table 5-1 all entries are below the applicable threshold except for the source at 1515 19th Avenue, which has a cancer risk, conservatively estimated at about 58 in a million. In this case, the user may choose to contact BAAQMD staff to learn more about the source and how the risk was estimated and/or opt to conduct site specific modeling for more refined risk and hazard estimates.

Table 5-1
Screening Data for Existing Permitted Stationary Sources*
(within 1,000 feet of the Proposed Project)

EXAMPLE
Proposed Project Location Details:
Address-19th Avenue and Judah Street, San Francisco, CA
Centroid UTMs-E 546090, N 4179460

Plant #	Plant Name	Street Address	City	UTM E	UTM N	Cancer Risk in a million	$PM_{2.5}$ ug/m^3	Chronic Hazard Index	
462	20th Avenue Cleaner	1845 Irving Street	San Francisco	546113	4179490	7.5		0.02	
4672	Sundown Cleaners	1952 Irving Street	San Francisco	546016	4179510	7.5		0.02	
13519	Pacific Bell	1515 19th Avenue	San Francisco	546086	4179240	58.4	0.10	0.10	
2155	Chevron Station #91000	1288 19th Avenue	San Francisco	546052	4179720	5.8		0.03	
8756	ConocoPhillips #251075	1400 19th Avenue	San Francisco	546064	4179490	2.7		0.01	
9266	ConocoPhillips #2611185	1401 19th Avenue	San Francisco	546058	4179500	2.2		0.01	
					Cumulative:	84		0.04	

Source: BAAQMD 2009

*This example provides conservative screening level estimates and does not represent actual risk, hazard index or $PM_{2.5}$ concentrations for the facilities listed.

For detailed information on the methodology and assumptions used in creating the screening tool, and for guidance on conducting site specific modeling see the *Recommended Methods for Screening and Modeling Local Risks and Hazards* report available on the District's website.

5.2.7. On-road Mobile Sources Screening Analysis

BAAQMD developed screening analysis tools for estimating risk and hazard impacts from California highways and surface streets in the Bay Area's nine counties. These tools are available on BAAQMD's website and are discussed individually below.

The highway and roadway screening tools serve as an easy-to-use initial screening process to determine if nearby highway and roadway impacts to a new receptor are below BAAQMD's thresholds of significance. The outcome of the screening may be used to determine whether no further analysis is needed or if a more refined analysis is warranted. BAAQMD recommends the following project screening approach:

1. Determine if the new receptor is at least 1,000 feet from the nearest high volume roadway defined as a freeway or arterial roadway with greater than 10,000 vehicles or 1,000 trucks per day. For new residential developments, the receptor should be placed at the edge of the property boundary. If there are no high volume highway/roadway sources within 1,000 feet of the project, then no further single-source roadway-related air quality evaluation is needed.

2. If the receptor is within the 1,000 foot radius of a nearby highway/roadway that has greater than 10,000 vehicles or 1,000 trucks per day, then the county specific roadway screening tables and the highway screening analysis tool should be used to determine the $PM_{2.5}$ concentrations, cancer risks, and hazards for the project. When two or more highways/roadways are within the1,000 foot radius, sum the contribution from each highway/roadway. If any of the estimates for $PM_{2.5}$ concentration, cancer risk, and hazards exceed the thresholds, then more refined modeling analysis is recommended or the lead agency may choose to implement mitigation measures.

3. For developments that exceed the screening analysis, site specific modeling analysis is recommended following BAAQMD's *Recommended Methods for Screening and Modeling Local Risks and Hazards*.

Highway Screening Analysis

For all state highways in the Bay Area, BAAQMD has developed an online highway screening analysis tool with modeled cancer risk and $PM_{2.5}$ concentrations for each highway link. The online tool consists of Google Earth™ kmz files that may be downloaded from BAAQMD's website, http://www.baaqmd.gov/Divisions/Planning-and-Research/CEQA-GUIDELINES/Tools-and-Methodology.aspx. Estimated risk and hazards impacts are listed for each highway link based on the distance from the edge of a highway's nearest travel lane to the project, AADT count, fleet mix and other modeling parameters specific to that highway link. The estimated risk and hazard impacts are modeled at two different heights, 6 feet and 20 feet. The 6 foot height estimates should be used when receptors are located on the ground floor of a building; and the 20 foot height estimates should be used when receptors are located on the second floor of a building. In each case, the risk and hazard impacts are modeled by distance, from 10 to 1,000 feet on either side of the highway. If a project is located between two highway links or between two distance points, the higher values should be used. If the project is between two distance points in the screening table the cancer risk and $PM_{2.5}$ concentrations may be further refined by linearly interpolating the distance between the project and the highway. See the *Recommended Methods for Screening and Modeling Local Risks and Hazards* report for specific instructions on how to linearly interpolate values. $PM_{2.5}$

As an example, if a proposed project is located 200 feet east of San Pablo Avenue (Highway 123) in Berkeley, and it is known that the ground floor of the project will not house any receptors, the Alameda county ".kmz" file for 20 feet should be downloaded from the BAAQMD website. Once opened in Google Earth™, the closest Highway 123 link to the project should be selected for a summary of the estimated risk and hazard impacts at that highway link. A user would then use the risk and hazard impacts listed at 200 feet east of the freeway in its project analysis. In this case, the highway link table indicates that at 200 feet east of the highway, the PM2.5 concentration is estimated at 0.061 ug/m^3, the cancer risk at 4.524 per million, the chronic hazard index at 0.006, and the acute hazard index at 0.006.

For detailed information on the methodology and assumptions used in creating the screening tool, see the *Recommended Methods for Screening and Modeling Local Risks and Hazards* report available on the District's website.

Roadway Screening Analysis

For major roadways not designated as state highways, BAAQMD developed county-specific screening tables to assess potential impacts for roads with 10,000 to 100,000 annual average daily traffic (AADT). The screening tables present $PM_{2.5}$ concentrations and cancer risk at specific distances away from the edge of the nearest travel lane of a road in relation to the project. These sets of tables correspond to projects located upwind or downwind of the roadway with respect to the prevailing wind direction. Roadways with less than 10,000 vehicles per day are considered minor, low-impact sources and inclusion of these roads in CEQA evaluation is not warranted. In addition, the tables do not include acute or chronic noncancer hazards since the screening values were found to be below the thresholds. The screening tables may be downloaded from the BAAQMD website, http://www.baaqmd.gov/Divisions/Planning-and-Research/CEQA-GUIDELINES/Tools-and-Methodology.aspx. For detailed information on the methodology and assumptions used in creating the screening tables, see the *Recommended Methods for Screening and Modeling Local Risks and Hazards* report available on BAAQMD's website.

When using the roadway screening tables, the lead agency should first gather project information including the county for which the development is proposed and the distance of the project to the nearest roadway. The appropriate cell should be determined by referencing the corresponding county, roadway, and project distance in the tables that most closely matches the project conditions. If the project is predominantly north or south of the roadway, choose the north or south tables. Likewise, if the project is predominantly east or west, choose the east or west tables. If the project is evenly located for example, northeast or southwest of the roadway, select the higher value between either screening tables based on the project distance to the roadway. If the project is between two distances or two AADT values, the cancer risk and $PM_{2.5}$ concentrations may be further refined by linearly interpolating the AADT and distance between the project and the roadway. See *Recommended Methods for Screening and Modeling Local Risks and Hazards* report for specific instructions on how to linearly interpolate values.

Table 5-2 outlines an example using the roadway screening analysis tool. A roadway is located in San Francisco in a north-south direction, has 25,800 vehicles per day, and is approximately 276 feet from the project. To estimate the risks and hazards, the user matches the AADT in the row header with the distance from the project to the roadway in the column header. For cases in which the exact AADT or distances are not estimated in the table, the user should select the higher value between the two estimated values. In Table 5-2, the estimated cancer risk for the example is 2.31 cases per million and the $PM_{2.5}$ concentration is 0.092 ug/m^3.

The values may be further refined to account for the exact roadway AADT and distances by scaling the values in the table. The methodology for scaling values is shown in section 3.1.2 of

the *Recommended Methods for Screening and Modeling Local Risks and Hazards* report available on BAAQMD's website.

Table 5-2. Example Cancer Risk and PM2.5 Estimation for Surface Streets

NORTH-SOUTH DIRECTIONAL ROADWAY							
Annual Average Daily Traffic	Distance East or West of Surface Street - Cancer Risk (per million)						
	10 feet	50 feet	100 feet	200 feet	500 feet	700 feet	1,000 feet
1,000	No analysis required						
5,000							
10,000	2.13	2.10	1.49	0.65	0.36	0.27	0.22
20,000	2.22	2.49	2.22	1.55	0.62	0.51	0.38
30,000	3.37	3.56	3.28	2.31	0.97	0.75	0.55
40,000	4.26	4.46	4.27	3.10	1.33	1.06	0.79
50,000	5.79	6.49	5.78	4.00	1.68	1.33	0.96
60,000	7.81	8.55	7.34	4.76	1.95	1.55	1.15
70,000	9.82	10.60	8.90	5.52	2.22	1.77	1.33
80,000	11.22	12.12	10.17	6.31	2.53	2.02	1.52
90,000	12.63	13.63	11.44	7.10	2.85	2.27	1.71
100,000	14.03	15.15	12.71	7.88	3.17	2.53	1.90

NORTH-SOUTH DIRECTIONAL ROADWAY							
Annual Average Daily Traffic	Distance East or West of Surface Street - PM2.5 Concentration (ug/m^3)						
	10 feet	50 feet	100 feet	200 feet	500 feet	700 feet	1,000 feet
1,000	No analysis required						
5,000							
10,000	0.080	0.063	0.044	0.016	0.012	0.000	0.000
20,000	0.092	0.101	0.092	0.061	0.021	0.016	0.012
30,000	0.129	0.147	0.129	0.092	0.032	0.022	0.017
40,000	0.166	0.193	0.175	0.120	0.051	0.037	0.024
50,000	0.249	0.267	0.239	0.166	0.064	0.050	0.029
60,000	0.341	0.359	0.304	0.198	0.076	0.057	0.039
70,000	0.433	0.451	0.368	0.230	0.087	0.064	0.050
80,000	0.495	0.516	0.421	0.263	0.099	0.074	0.057
90,000	0.557	0.580	0.474	0.296	0.111	0.083	0.064
100,000	0.618	0.645	0.526	0.329	0.124	0.092	0.071

The results of the screening analysis indicate whether new receptors will be exposed to highway/roadway TAC emissions at concentrations exceeding the threshold of significance and whether, a more refined modeling analysis may be needed. If the concentration is less than the thresholds, then no further analysis is required for the single source comparison for roadways. The results of the analysis should be reported in the environmental documentation or staff report that includes a reference to the screening tables used. If the concentrations exceed the thresholds, then the user has the option to conduct a more refined modeling analysis or implement appropriate mitigation measures.

To conduct a more refined modeling analysis, BAAQMD recommends following the methodology in the *Recommended Methods for Screening and Modeling Local Risks and Hazards* report available on BAAQMD's website.

For conducting refined modeling to estimate concentrations from TAC, $PM_{2.5}$, and diesel BAAQMD recommends using the CAL3QHCR model. The CAL3QHCR model can estimate air concentrations at defined receptor locations by processing hourly meteorological data over a year, hourly emissions, and traffic volume. The latest version of the model is available at: http://www.epa.gov/scram001/dispersion_prefrec.htm. For each analysis, the District recommends developing pollutant specific emission factors from EMFAC. As specified in Regulation 2, Rule 5, BAAQMD also recommends that age sensitivity factors be applied to the emissions per year to account for early life-stage exposures. For detailed discussion on this methodology, refer to the *Recommended Methods for Screening and Modeling Local Risks and Hazards* report available on BAAQMD's website.

The risk and hazard levels from the modeling analysis should then be compared with the applicable thresholds. Further assessment may be needed if the thresholds are exceeded, and the lead agency may consider design changes and other mitigation measures as a means of reducing potential risks.

5.3. CUMULATIVE IMPACTS

5.3.1. Significance Determination

A lead agency should examine TAC sources that are located within 1,000 feet of a proposed project site. Sources of TACs include, but are not limited to, land uses such as freeways and high volume roadways, truck distribution centers, ports, rail yards, refineries, chrome plating facilities, dry cleaners using perchloroethylene, and gasoline dispensing facilities. Land uses with permitted sources, such as a landfill or manufacturing plant, may also contain non-permitted TAC and/or $PM_{2.5}$ sources, particularly if they host a high volume of diesel truck activity. A lead agency should determine what the combined risk levels are from all nearby TAC sources in the vicinity of sensitive receptors. Lead agencies should use their judgment to decide if there are large sources outside 1,000 feet that should be included.

A lead agency's analysis should determine whether TAC emissions generated as part of a proposed project would expose off-site receptors to risk levels that exceed BAAQMD's applicable threshold for determining cumulative impacts.

A project would have a significant cumulative impact if the total of all past, present, and foreseeable future sources within a 1,000 foot radius (or beyond where appropriate) from the fence line of a source, or from the location of a receptor, plus the contribution from the project, exceeds the following:

- Non- compliance with a qualified Community Risk Reduction Plan;
- An excess cancer risk levels of more than 100 in one million or a chronic hazard index greater than 10 for TACs; or
- 0.8 $\mu g/m^3$ annual average $PM_{2.5}$.

BAAQMD recommends that cumulative impacts of new sources and new receptors be evaluated as described in Section 5.2, and include the impacts of all individual sources (stationary and on-road mobile) within the 1,000 foot radius. In impacted communities identified under BAAQMD's CARE program, lead agencies are encouraged to develop and adopt a Community Risk Reduction Plan. To determine whether a new source is located in an impacted community, refer to Figure 5-1 and the CARE webpage. See section 5.4 for more information on Community Risk Reduction Plans.

The risk and hazards analysis for assessing potential cumulative impacts should follow the risk screening guidance described in *Recommended Methods for Screening and Modeling Local Risks and Hazards*, which generally follows CAPCOA's guidance document titled *Health Risk Assessments for Proposed Land Use Projects*.

A lead agency should compare the analysis results from TAC emissions with the applicable significance thresholds. BAAQMD's thresholds apply to projects that would site new permitted or non-permitted sources in close proximity to receptors and for projects that would site new sensitive receptors in close proximity to permitted or non-permitted sources of TAC emissions. If a proposed project would not exceed BAAQMD's applicable thresholds then the project would result in a less-than-significant air quality impact. If a project would exceed the applicable thresholds , the proposed project would result in a potentially significant air quality impact and the lead agency should implement all feasible mitigation to reduce the impact (refer to Section 5.5 for mitigating impacts).

If implementation of BAAQMD-recommended mitigation measures for reducing TAC emissions and resultant exposure to health risks would reduce all TAC impacts to levels below the applicable thresholds, TAC impacts would be reduced to a less-than-significant level. If resultant health risk exposure would still exceed the applicable thresholds, the impacts would be considered significant and unavoidable.

5.4. COMMUNITY RISK REDUCTION PLANS

The goal of a Community Risk Reduction Plan is be to bring TAC and $PM_{2.5}$ concentrations for an entire community covered by the Plan down to acceptable levels as identified by the local jurisdiction and approved by the Air District. This approach provides local agencies a proactive alternative to addressing high levels of risk and $PM_{2.5}$ impacts on a project-by-project approach. The Air District has developed detailed guidelines for preparing Community Risk Reduction Plans which can be found BAAQMD's website, http://www.baaqmd.gov/Divisions/Planning-and-Research/CEQA-GUIDELINES.aspx.

Qualified Community Risk Reduction Plans
A qualified Community Risk Reduction Plan adopted by a local jurisdiction should include, at a minimum, the following elements:

(A) Define a planning area;

(B) Include base year and future year emissions inventories of TACs and PM2.5;

(C) Include Air District approved risk modeling of current and future risks;

(D) Establish risk and exposure reduction goals and targets for the community in consultation with Air District staff;

(E) Identify feasible, quantifiable, and verifiable measures to reduce emissions and exposures;

(F) Include procedures for monitoring and updating the inventory, modeling and reduction measures in coordination with Air District staff;

(G) Be adopted in a public process following environmental review.

5.5. MITIGATING LOCAL COMMUNITY RISK AND HAZARD IMPACTS

For stationary sources, please refer to BAAQMD's permit handbook and BACT/T-BACT workbook. For land use projects, BAAQMD is developing community development guidelines to assist lead agencies in identifying mitigation measures to reduce risk and hazard impacts associated with proposed projects. The community development guidelines will contain risk reduction measures with estimated quantified reductions, as well as an analysis worksheet for lead agencies to review as they perform an environmental analysis. The mitigation measures will be helpful in protecting public health for proposed infill and transit-oriented development projects located near TAC sources.

The list below outlines potential mitigation measures for reducing TAC emissions and exposure to sensitive receptors:

1. Increase project distance from freeways and/or major roadways.

2. Redesign the site layout to locate sensitive receptors as far as possible from any freeways, major roadways, or other non-permitted TAC sources (e.g., loading docks, parking lots).

3. Large projects may consider phased development where commercial/retail portions of the project are developed first. This would allow time for CARB's diesel regulations to take effect in reducing diesel emissions along major highways and arterial roadways. Ultimately, lower concentrations would be anticipated along the roads in the near future such that residential development would be impacted by less risk in later phases of development.

4. Projects that propose sensitive receptors adjacent to sources of diesel PM (e.g., freeways, major roadways, rail lines, and rail yards) should consider tiered plantings of trees such as redwood, deodar cedar, live oak and oleander to reduce TAC and PM exposure. This recommendation is based on a laboratory study that measured the removal rates of PM passing through leaves and needles of vegetation. Particles were generated in a wind tunnel and a static chamber and passed through vegetative layers at low wind velocities. Redwood, deodar cedar, live oak, and oleander were tested. The results indicate that all forms of vegetation were able to remove 65–85 percent of very fine particles at wind velocities below 1.5 meters per second, with redwood and deodar cedar being the most effective.

5. Install and maintain air filtration systems of fresh air supply either on an individual unit-by-unit basis, with individual air intake and exhaust ducts ventilating each unit separately, or through a centralized building ventilation system. The ventilation system should be certified to achieve a performance effectiveness, for example, to remove at least 85% of ambient $PM_{2.5}$ concentrations from indoor areas. Air intakes should be located away from emission sources areas, such as major roadways. Users may factor in the amount of time that receptors spend indoors verses out-of-doors to account for air filtration systems in modeling, provided that all assumptions are justified with scientific documentation.

6. Where appropriate, install passive (drop-in) electrostatic filtering systems, especially those with low air velocities (i.e., 1 mph).

7. Require rerouting of nearby heavy-duty truck routes.

8. Enforce illegal parking and/or idling of heavy-duty trucks in vicinity.

6. LOCAL CARBON MONOXIDE IMPACTS



© 2009 Jupiterimages Corporation

Emissions and ambient concentrations of CO have decreased dramatically in the SFBAAB with the introduction of the catalytic converter in 1975. No exceedances of the CAAQS or NAAQS for CO have been recorded at nearby monitoring stations since 1991. SFBAAB is currently designated as an attainment area for the CAAQS and NAAQS for CO; however, elevated localized concentrations of CO still warrant consideration in the environmental review process. Occurrences of localized CO concentrations, known as hotspots, are often associated with heavy traffic congestion, which most frequently occur at signalized intersections of high-volume roadways.

6.1. SIGNIFICANCE DETERMINATION

Step 1: Comparison of Project Attributes with Screening Criteria

The first step in determining the significance of CO emissions is to compare the attributes of the proposed project to the applicable S*creening Criteria* (refer to Chapter 3).

This preliminary screening procedure provides a conservative indication of whether the proposed project would result in the generation of CO concentrations that would substantially contribute to an exceedance of the *Thresholds of Significance*. If all of the screening criteria are met, the proposed project would result in a less-than-significant impact to air quality with respect to concentrations of local CO. If the proposed project does not meet all the screening criteria, then CO emissions should be quantified. The screening criteria do not apply to stationary source projects.

Step 2: Emissions Quantification

This section describes recommended methodologies for quantifying concentrations of local CO for proposed transportation projects that do not meet all of the screening criteria. The recommended methodology is to use both the On-Road Mobile-Source Emission Factors (EMFAC) and the California Line Source Dispersion Model (CALINE4) models in accordance with recommendations in the University of California, Davis, Transportation Project-Level Carbon Monoxide Protocol (*CO Protocol*) (Garza, et al. 1997). Proposed stationary source projects should model their potential CO impacts using AERMOD. For specific guidance on using AERMOD, refer to EPA's website, http://www.epa.gov/ttn/scram/dispersion_prefrec.htm#aermod.

Air Quality Models

BAAQMD recommends using the most current version of the EMFAC model to obtain mobile-source emission factors for CO associated with operating conditions that would be representative of the roadway or facility subject to analysis.

Users should input the emission factors and other input parameters into the CALINE4 model to quantify CO concentrations near roadways.

The *CO Protocol* contains detailed methodology for modeling CO impacts.

Input Parameters

The CALINE4 model contains five screens for input data. CALINE4 input parameters are summarized below. For more detailed descriptions see the CALINE4 Users Guide.

Job Parameters

File Name – Name the file (e.g., data file extension) to create the CALINE4 Input file.

Job Title – Provide a name for the modeling scenario (e.g., existing no project, existing plus project).

Run Type – Select the worst-case wind angle.

Aerodynamic Roughness Coefficient – Choose the characteristic (i.e., rural, suburban, central business district, other) that is most representative of the project site.

Model Information – Indicate the unit of measurement (i.e., meters or feet) and inputs the vertical dimension of the project (i.e., altitude above sea level).

Run – Once data input is completed, return to this screen to run the model. Upon running the model, the output will appear as a text file called C4$.out. Save the output file under an appropriate filename for future reference.

Link Geometry

On this screen, input the dimensions (i.e., coordinates) for the roadway intersection that is the subject of the analysis.

Link Name – Input names for each roadway segment.

Link Type – Indicate the character of the roadway segment (i.e., at-grade, depressed, fill, bridge, parking lot).

Endpoint Coordinates (X_1, X_2, Y_1, Y_2) – Input the dimensions (i.e., coordinates) of the roadway segments as though the intersection were oriented at point of origin X = 0, Y = 0 on a Cartesian coordinate system. Roadway segments approaching the intersection from the west side of the screen (if north is treated as "up", or the top of the screen) would have negative X coordinate endpoints. Similarly, roadway segments approaching the intersection from the south would have negative Y coordinate endpoints.

Link Height – Indicate the vertical dimension of the roadway segment. If the roadway segment is at-grade, should set this parameter to zero. If the roadway segment is depressed, enter a negative value for this parameter.

Mixing Zone Width – The Mixing Zone is defined as the width of the roadway, plus three meters on either side. The minimum allowable value is 10 meters, or 32.81 feet.

Canyon/Bluff (Mix Left/Right) – Set these features to zero.

Link Activity

Traffic Volume – Input hourly traffic volumes applicable to each roadway segment.

Emission Factor – Input the CO emission factor (in units of grams/mile) obtained from EMFAC for the applicable vehicle speed class reflecting operating conditions for the affected intersection.

Run Conditions

Wind Speed – Input 0.5 meters per second to represent worst-case conditions.

Wind Direction – Set parameter to zero. Select "Worst-Case Wind Angle" as the "Run Type" on the "Job Parameters" screen, so this field will be overridden by the model.

Wind Direction Standard Deviation – Use a wind direction standard deviation of 5 degrees to represent worst-case conditions.

Atmospheric Stability Class – Use Stability Class 4 (i.e., class D) to represent average conditions in the SFBAAB.

Mixing Height – Indicate the vertical dimension over which vertical mixing may occur. In most situations, input 300 meters, approximately the height of the atmospheric boundary layer. If the roadway subject to analysis is a bridge underpass, tunnel, or other situation where vertical mixing would be limited, indicates the height of the structure that would hamper vertical mixing (in units of meters).

Ambient Temperature – Indicate the average temperature of the project site during the time of day at which maximum daily traffic volume would occur (in degrees Celsius). A temperature of 7.2 degrees Celsius is recommended.

Ambient Pollutant Concentration – Enter 0 in this field to determine the contribution of CO from the roadway subject to analysis. Add the roadway-related CO concentration to ambient CO levels outside of the CALINE4 model, as discussed later in this section.

Receptor Positions

Receptor Name – Input names for each receptor.

Receptor Coordinates (X, Y, Z) – Input receptor coordinates in a manner similar to the "Link Coordinates" on the "Link Geometry" screen. Locate receptors at three and seven meters from the intersection in all directions from the intersection, in accordance with the recommendations of the *CO Protocol*. The Receptor Coordinates are oriented in the same Cartesian coordinate system as the roadway segment "Link Coordinates." Receptors located to the southwest of the intersection would have negative X and Y coordinates. The Z dimension should be assigned the coordinate of 1.8 meters (5.9 feet); the approximate breathing height of a receptor located adjacent to the roadway.

This screen also contains a window that shows a map of the link and receptor coordinates in the X, Y plane.

Model Output

CALINE4 output includes estimated 1-hour CO concentrations in units of ppm at the receptor locations input into the model. Note the highest concentrations at each of the three meter and seven meter receptor distances from the roadway.

Background Concentrations

Ambient 1-hour CO concentrations can be obtained from ARB air quality monitoring station data and 8-hour concentrations from EPA. Users should obtain the CO monitoring data recorded at the monitoring station nearest the project site. According to the *CO Protocol*, select the second highest concentration recorded during the last two years to represent the ambient CO concentration in the project area.

Estimated Localized CO Concentrations

Users should sum the highest modeled 1-hour CO concentration in units of ppm obtained from CALINE4 to ambient (background) 1-hour CO concentrations in ppm obtained from ARB. This represents the modeled worst-case 1-hour CO concentration near the affected roadway.

Persistence Factor – multiply the highest 1-hour CO concentration estimated by CALINE4 by a persistence factor of 0.7, as recommended in the CO Protocol, to obtain the estimated 8-hour CO concentration.

Add the estimated 8-hour CO concentration (ppm) obtained in the previous step to the ambient 8-hour CO concentration obtained from EPA (ppm). This represents the modeled worst-case 8-hour CO concentration near the affected roadway.

Step 3: Comparison of Unmitigated Emissions with Thresholds of Significance

Following quantification of local CO emissions in accordance with the recommended methods, compare the total modeled worst-case 1-hour and 8-hour CO concentrations with the applicable threshold. If the modeled concentrations do not exceed any of the *Thresholds of Significance*, the project would result in a less-than-significant impact to air quality. If modeled concentrations do exceed any applicable threshold, the proposed project would result in a significant impact to air quality with respect to local CO impacts.

Step 4: Mitigation Measures and Emission Reductions

Where local CO emissions exceed applicable threshold, refer to Section 6.2 for recommended mitigation measures and associated emission reductions. Only reduction measures included in the proposed project or recommended as mitigation in a CEQA-compliant document can be included when quantifying mitigated emission levels.

Step 5: Comparison of Mitigated Emissions with Thresholds of Significance

Following quantification of local CO emissions in accordance with the recommended methods, compare the total modeled worst-case 1-hour and 8-hour CO concentrations with the applicable thresholds. If the implementation of recommended mitigation measures reduces all local CO emissions to levels below the applicable thresholds, the impact to air quality would be reduced to a less-than-significant level. If mitigated levels of local CO emissions still exceed the applicable thresholds, the impact to air quality would remain significant and unavoidable.

6.2. MITIGATING LOCAL CARBON MONOXIDE IMPACTS

The following section describes recommended mitigation measures for reducing local CO impacts to air quality. Consider implementation of the following measures, as feasible, for reducing project-generated traffic volumes and associated CO emissions at affected intersections. Actual emission reductions should be quantified through project-specific transportation modeling.

1. Synchronize traffic signals to improve traffic flow and minimize traffic congestion.

2. Consider additional traffic signals, such as light metering, to relocate congested areas further away from receptors.

3. Improve public transit service to reduce vehicle traffic and increase public transit mode share during peak traffic congestion periods.

4. Improve bicycle and pedestrian infrastructure to reduce vehicle traffic and increase bicycle and pedestrian mode share during peak traffic congestion periods. Improvements may include installing class I or II bike lanes, sidewalks, and traffic calming features.

5. Adjust pedestrian crosswalk signal timing to minimize waiting time for vehicles turning right or otherwise sharing green time with pedestrians. Give pedestrians a head start before traffic signal changes to green.

6. Where pedestrian traffic is high, implement pedestrian crosswalks with multi-directional crossings allowing pedestrians to cross intersections diagonally.

7. Limit heavy-duty truck traffic during peak hours. Designate truck routes that divert truck traffic away from congested intersections.

8. Limit left turns or other maneuvers during peak hours that add to congestion.

9. Limit on-street parking during peak hours to allow for added vehicle capacity.

10. Implement traffic congestion-alleviating mitigation measures as identified by a traffic engineer.

[This Page Intentionally Left Blank]

7. ODOR IMPACTS

Odor impacts could result from siting a new odor source near existing sensitive receptors or siting a new sensitive receptor near an existing odor source. Examples of land uses that have the potential to generate considerable odors include, but are not limited to:

1. Wastewater treatment plants;
2. Landfills;
3. Confined animal facilities;
4. Composting stations;
5. Food manufacturing plants;
6. Refineries; and
7. Chemical plants.

Odors are generally regarded as an annoyance rather than a health hazard. Manifestations of a person's reaction to odors can range from psychological (e.g., irritation, anger, or anxiety) to physiological (e.g., circulatory and respiratory effects, nausea, vomiting, and headache).

The ability to detect odors varies considerably among the population and overall is quite subjective. People may have different reactions to the same odor. An odor that is offensive to one person may be perfectly acceptable to another (e.g., coffee roaster). An unfamiliar odor is more easily detected and is more likely to cause complaints than a familiar one. Known as odor fatigue, a person can become desensitized to almost any odor and recognition only occurs with an alteration in the intensity.

Quality and intensity are two properties present in any odor. The quality of an odor indicates the nature of the smell experience. For instance, if a person describes an odor as flowery or sweet, then the person is describing the quality of the odor. Intensity refers to the strength of the odor. For example, a person may use the word strong to describe the intensity of an odor. Odor intensity depends on the concentration in the air. When an odor sample is progressively diluted, the odor concentration decreases. As this occurs, the odor intensity weakens and eventually becomes so low that the detection or recognition of the odor is quite difficult. At some point during dilution, the concentration of the odor reaches a level that is no longer detectable.

The presence of an odor impact is dependent on a number of variables including:

1. Nature of the odor source (e.g., wastewater treatment plant, food processing plant);
2. Frequency of odor generation (e.g., daily, seasonal, activity-specific);
3. Intensity of odor (e.g., concentration);
4. Distance of odor source to sensitive receptors (e.g., miles);
5. Wind direction (e.g., upwind or downwind); and
6. Sensitivity of the receptor.

The recommendations provided in this chapter only apply to assessing and mitigating odor impacts for individual projects. Please refer to Chapter 9 for recommendations for assessing and mitigating odor impacts at the plan-level.

7.1. SIGNIFICANCE DETERMINATION

Odor impacts could occur from two different situations:

1. Siting a new odor source (e.g., the project includes a proposed odor source near existing sensitive receptors), or
2. Siting a new receptor (e.g., the project includes proposed sensitive receptors near an existing odor source).

Regardless of the situation, BAAQMD recommends completing the following steps to comprehensively analyze the potential for an odor impact.

Step 1: Disclosure of Odor Parameters

The first step in assessing potential odor impacts is to gather and disclose applicable information regarding the characteristics of the buffer zone between the sensitive receptor(s) and the odor source(s), local meteorological conditions, and the nature of the odor source. Consideration of such parameters assists in evaluating the potential for odor impacts as a result of the proposed project. Projects should clearly state the following information in odor analyses, which provide the minimum amount of information required to address potential odor impacts:

1. Type of odor source(s) the project is exposed to or the type of odor source(s) produced by the project (e.g., wastewater treatment plant, landfill, food manufacturing plant);
2. Frequency of odor events generated by odor source(s) (e.g., operating hours, seasonal);
3. Distance and landscape between the odor source(s) and the sensitive receptor(s) (e.g., topography, land features); and
4. Predominant wind direction and speed and whether the sensitive receptor(s) in question are upwind or downwind from the odor source(s).

Step 2: Odor Screening Distances

BAAQMD has developed a list of recommended odor screening distances for specific odor-generating facilities shown in Table 3-3. Projects that would locate sensitive receptor(s) to odor source(s) closer than the screening distances would be considered to result in a potential significant impact. If the proposed project would include the operation of an odor source, the screening distances should also be used to evaluate the potential impact to existing sensitive receptors. Projects that would locate sensitive receptor(s) near odor source(s) further than the screening distances, or vice versa, would be considered to have a sufficient buffer to avoid significant impacts. The odor screening distances in Table 3-3 should not be used as absolute thresholds, rather an indicator to how much further analysis is required. The lead agency should also consider the other parameters listed above in Step 1 and information from Step 3 below to comprehensively evaluate potential odor impacts.

Step 3: Odor Complaint History

The impact of an existing odor source on surrounding sensitive receptors should also be evaluated by identifying the number of confirmed complaints received for that specific odor source.

Facilities that are regulated by CalRecycle (e.g. landfill, composting, etc.) are required to have Odor Impact Minimization Plans (OIMP) in place and have procedures that establish fence line odor detection thresholds. The Air District recognizes a lead agency's discretion under CEQA to use established odor detection thresholds as thresholds of significance for CEQA review for CalRecycle regulated facilities with an adopted OIMP.

If the proposed project would be located near an existing odor source, lead agencies should contact BAAQMD to obtain the odor complaints over the past 3 years for the source in question. Then calculate the annual average confirmed odor complaints filed for the source. BAAQMD considers a source to have a substantial number of odor complaints if the complaint history includes five or more confirmed complaints per year averaged over a 3-year period. Also, disclose the distance at which receptors were affected by the existing odor source. As discussed in Step 1, describe the topography and landscape between the receptors and the odor source. These distances and landscaping should then be compared with the distance and landscape that would separate the proposed project and the odor source.

If the proposed project would locate an odor source, first identify the location of potential sensitive receptors (i.e., distance, upwind/downwind) with respect to the project site. If the proposed odor source does not have any existing or planned sensitive receptors within the screening distances shown in Table 3-3, it may be considered less than significant for odor impacts. To evaluate how implementation of the proposed source project would affect identified sensitive receptors contact BAAQMD to obtain odor complaints in the region for facilities similar in size and type of odor produced in the past 3 years. These surrogate odor complaints should be evaluated for their distance from source to receptor, and then compared with the distance from the proposed project to receptors. Odor complaints from the surrogate odor source are considered substantial if the complaint history includes more than five confirmed complaints per year averaged over a 3-year period.

BAAQMD considers a substantial number of odor complaints, specifically, more than five confirmed complaints per year averaged over the past three years as the indication of an odor impact. As discussed above, the lead agency should compare the odor parameters (i.e., distance and wind direction) associated with the odor complaints that have been filed with those of the proposed project. Similar to the odor screening distances, odor complaints should not be used as an absolute threshold, but evidence to support a significance determination.

Step 4: Significance Determination

An odor source with five or more confirmed complaints per year averaged over three years is considered to have a significant impact. BAAQMD recognizes that there is not one piece of information that can solely be used to determine the significance of an odor impact. The factors (i.e., Step 1 through 3) discussed above could enhance the potential for a significant odor impact or help prevent the potential for a significant odor impact. For example, a project that would be located near an existing odor source may not discover any odor complaints for the existing odor source. It is possible that factors such as a small number of existing nearby receptors, predominate wind direction blowing away from the existing receptors, and/or seasonality of the odor source has prevented any odor complaints from being filed about the existing odor source. The results of each of the steps above should be clearly disclosed in the CEQA document. Projects should use the collective information from Steps 1 through 3 to qualitatively evaluate the potential for a significant odor impact. The lead agency should clearly state the reasoning for the significance determination using information from Steps 1 through 3 to support the determination.

7.2. MITIGATING ODOR IMPACTS

BAAQMD considers appropriate land use planning the primary method to mitigate odor impacts. Providing a sufficient buffer zone between sensitive receptors and odor sources should be considered prior to analyzing implementation of odor mitigation technology. Projects that would include potential sensitive receptors should consider the odor parameters, discussed in Step 1 above, during the planning process to avoid siting receptors near odor sources. Similarly, projects

that would include an odor source should consider the location of nearby existing sensitive receptors that could be affected by the project.

The source types for which mitigation has been provided below have been selected based on the nature of the odors produced as a result of their operational activities. These land use types are those most likely to result in odor impacts if sensitive receptors are located in close proximity. This should not be considered an exhaustive list and due to the subjective nature of odor impacts, there is no formulaic method to assess if odor mitigation is sufficient. In determining whether the implementation of mitigation would reduce the potential odor impact to a less-than-significant level, rely on the information obtained through the steps above.

7.2.1. Wastewater Treatment Plant

Main odor sources for wastewater treatment plants typically are the headworks area where the wastewater enters the facility and large solids and grit are removed, the primary clarifiers where suspended solids are removed, and the aeration basins when poor mixing characteristics lead to inadequate dissolved oxygen levels. Lead agencies should consider applying the following odor mitigation measures to wastewater treatment plants.

1. Activated Carbon Filter/Carbon adsorption
2. Biofiltration/Bio Trickling Filters
3. Fine Bubble Aerator
4. Hooded Enclosures
5. Wet and Dry Scrubbers
6. Caustic and Hypochlorite Chemical Scrubbers
7. Ammonia Scrubber
8. Energy Efficient Blower System
9. Thermal Oxidizer
10. Capping/Covering Storage Basins and Anaerobic Ponds
11. Mixed Flow Exhaust
12. Wastewater circulation technology
13. Exhaust stack and vent location with respect to receptors

7.2.2. Landfill/Recycling/Composting Facilities

Odors generated from landfills and composting facilities are typically associated with methane production from the anaerobic decomposition of waste. Lead agencies should consider applying the mitigation measures below to reduce and treat methane in facilities. Landfill projects should also implement best management practices to avoid and minimize the creation of anaerobic conditions.

1. Passive Gas Collection
2. Active Gas Collection
3. Flaring or energy production/utilization
4. Vegetation Growth on Landfill Cover
5. Cover/Cap Landfill
6. Odor Neutralizing Spray
7. Negative aeration for compost facilities
8. Turning and mixing of compost piles

Facilities that are regulated by CalRecycle (e.g. landfill, composting, etc.) are required to have Odor Impact Minimization Plans (OIMP) in place and have procedures that establish fence line odor detection thresholds. The Air District recognizes a lead agency's discretion under CEQA to use established odor detection thresholds as thresholds of significance for CEQA review for CalRecycle regulated facilities with an adopted OIMP.

7.2.3. Petroleum Refinery

Odors generated from materials and processes associated with petroleum refineries include, but are not limited to, H_2S, SO_2, mercaptan, ammonia (NH_3), and petroleum coke. Installing the following current and feasible odor mitigation measures for petroleum refineries should be considered.

1. Water Injections to Hydrocracking Process
2. Vapor recovery system
3. Injection of masking odorants into process streams
4. Flare meters and controls
5. Wastewater circulation technology for Aerated Ponds
6. Exhaust stack and vent location with respect to receptors
7. Thermal oxidizers
8. Carbon absorption
9. Biofiltration/Bio Trickling Filters

7.2.4. Chemical Plant

Chemical plants can generate a variety of different odors (e.g., acrylates, phenols, and styrene) as a result of process emissions. The range of odor mitigation measures required for chemical plants may vary substantially depending on the type of odors produced. The odor mitigation measures could be applied to chemical plants.

1. Wet scrubbers (50–90 percent efficiency)
2. Catalytic oxidation (99 percent efficiency)
3. Thermal oxidation (90–99 percent efficiency)
4. Carbon adsorption (95 percent efficiency)
5. Exhaust stack and vent location with respect to receptors



© 2009 Jupiterimages Corporation

7.2.5. Food Services

Restaurants, especially fast food restaurants, can generate substantial sources of odors as a result of cooking processes and waste disposal. Char broilers, deep-fryers, and ovens tend to produce food odors that can be considered offensive to some people. The food waste produced by restaurants can putrefy if not properly managed, which can also produce objectionable odors. The follow mitigation measures are management practices and odor technology that can be used to reduce the amount odors generated by food services.

1. Integral grease filtration system or grease removal system
2. Baffle filters
3. Electrostatic precipitator
4. Water cooling/cleaning unit
5. Disposable pleated or bag filters

6. Activated carbon filters
7. Oxidizing pellet beds
8. Incineration
9. Catalytic conversion
10. Proper packaging and frequency of food waste disposal
11. Exhaust stack and vent location with respect to receptors

In conclusion, odor impacts can also be minimized, contained, or prevented by implementing technologies and design measures at the source, or through planning-based measures. Where odor sources and receptors cannot be physically separated to a degree where impacts would be minimized to less-than-significant level, disclosures of odor sources to prospective tenants of sensitive land uses should be used. Mitigation for odors that is both effective and feasible should be selected on a case-by-case basis.

8. CONSTRUCTION-RELATED IMPACTS

Construction-related activities are those associated with the building of a single project or projects that are part of an adopted plan. Construction activities are typically short-term or temporary in duration; however, project-generated emissions could represent a significant impact with respect to air quality and/or global climate change. Construction-related activities generate criteria air pollutants including carbon monoxide (CO), sulfur dioxide (SO_2), particulate matter (PM_{10}, and $PM_{2.5}$); precursor emissions such as, reactive organic gases (ROG) and oxides of nitrogen (NO_X); and GHGs from exhaust, fugitive dust, and off-gas emissions. Sources of exhaust emissions could include on-road haul trucks, delivery trucks, worker commute motor vehicles, and off-road heavy-duty equipment. Sources of fugitive dust emissions could include construction-related activities such as soil disturbance, grading, and material hauling. Sources of off-gas emissions could include asphalt paving and the application of architectural coatings.

The recommendations provided in this chapter only apply to assessing and mitigating construction-related impacts for individual projects. Construction-related assumptions and project-specific information assumed in CEQA analyses should accompany the quantitative analysis described below. Refer to Chapter 9 for recommendations for assessing and mitigating construction-related impacts at the plan level.

8.1. CRITERIA AIR POLLUTANTS AND PRECURSORS

8.1.1. Significance Determination

Step 1: Comparison of Project Attributes with Screening Criteria

The first step in determining the significance of construction-related criteria air pollutants and precursors is to compare the attributes of the proposed project with the applicable screening criteria listed in Chapter 3. If all of the screening criteria are met, construction of the proposed project would result in a less-than-significant impact to air quality (this does not apply to toxic air contaminants). If not, than construction emissions should be quantified.



© 2009 Jupiterimages Corporation

Step 2: Emissions Quantification

BAAQMD recommends using URBEMIS to quantify construction emissions for proposed land use development projects and the Roadway Construction Emissions Model (RoadMod) for proposed linear projects such as, new roadway, roadway widening, or pipeline installation. The most current URBEMIS (currently version 9.2.4) should be used for emission quantification. Table 8-3 outlines summary guidelines for using URBEMIS. Refer to Appendix B for detailed instructions for modeling construction-generated emissions using URBEMIS and RoadMod.

Step 3: Comparison of Unmitigated Emissions with Thresholds of Significance

Following quantification of project-generated construction-related emissions, the total average daily emissions of each criteria pollutant and precursor should be compared with the applicable thresholds. If construction-related emissions have been quantified using multiple models or model runs, sum the criteria air pollutants and precursor levels from each where said activities would

overlap. In cases where the exact timing of construction activities is not known, sum any phases that could overlap to be conservative. For fugitive dust significance, verify that the project incorporates all the *Basic Construction Mitigation Measures* for dust control in Table 8-1.

If daily average emissions of construction-related criteria air pollutants or precursors would not exceed any of the thresholds, the project would result in a less-than-significant impact to air quality. If daily average emissions of construction-related criteria air pollutants or precursors would exceed any applicable thresholds, the proposed project would result in a significant impact to air quality and would require mitigation measures for emission reductions.

Step 4: Mitigation and Emission Reductions

For all proposed projects, BAAQMD recommends the implementation of all *Basic Construction Mitigation Measures* (Table 8.1) whether or not construction-related emissions exceed applicable thresholds. In addition, all projects must implement any applicable air toxic control measures (ATCM). For example, projects that have the potential to disturb asbestos (from soil or building material) must comply with all the requirements of ARB's ATCM for Construction, Grading, Quarrying, and Surface Mining Operations. Only reduction measures included in the proposed project's description or recommended as mitigation in a CEQA-compliant environmental document can be included when quantifying mitigated emission levels. Refer to Appendix B for detailed instructions on how to use URBEMIS to quantify the effects of construction emissions mitigation measures.

Step 5: Comparison of Mitigated (Basic Mitigation) Emissions with Thresholds of Significance

Following quantification of project-generated construction-related emissions, compare the total average daily amount of mitigated (with implementation of *Basic Construction Mitigation Measures)* criteria air pollutants and precursors with the applicable thresholds. If the implementation of BAAQMD-recommended *Basic Construction Mitigation Measures* would reduce all construction-related criteria air pollutants and precursors to levels below the applicable thresholds, the impact to air quality would be less than significant. If emissions of any criteria air pollutant or precursor would exceed the applicable thresholds, the impact to air quality would be significant.

Step 6: Implement Additional Construction Mitigation Measures

BAAQMD recommends that all proposed projects, where construction-related emissions would exceed the applicable thresholds, implement the *Additional Construction Mitigation Measures* (Table 8-2). The methodology for quantifying reductions of fugitive PM dust, exhaust, and off gas emissions associated with the implementation of these mitigation measures is described in Appendix B.

Step 7: Comparison of Mitigated Emissions with Thresholds of Significance

Following quantification of project-generated construction-related emissions in accordance with the BAAQMD-recommended methods, compare the total average daily amount of mitigated (with *Additional Construction Mitigation Measures* implemented) criteria air pollutants and precursors with the applicable thresholds. If the implementation of additional mitigation measures would reduce all construction-related criteria air pollutants and precursors to levels below the applicable thresholds, the impact to air quality would be reduced to a less-than-significant level. If mitigated levels of any criteria air pollutant or precursor still exceed the applicable thresholds, the impact to air quality would remain significant and unavoidable.

8.1.2. Mitigating Criteria Air Pollutants and Precursors

Basic Construction Mitigation Measures

For all proposed projects, BAAQMD recommends implementing all the *Basic Construction Mitigation Measures,* listed in Table 8-1, to meet the best management practices threshold for fugitive dust, and whether or not construction-related emissions exceed applicable thresholds. Appendix B provides guidance on quantifying mitigated emission reductions using URBEMIS and RoadMod.

Table 8-1
Basic Construction Mitigation Measures Recommended for ALL Proposed Projects

1. All exposed surfaces (e.g., parking areas, staging areas, soil piles, graded areas, and unpaved access roads) shall be watered two times per day.
2. All haul trucks transporting soil, sand, or other loose material off-site shall be covered.
3. All visible mud or dirt track-out onto adjacent public roads shall be removed using wet power vacuum street sweepers at least once per day. The use of dry power sweeping is prohibited.
4. All vehicle speeds on unpaved roads shall be limited to 15 mph.
5. All roadways, driveways, and sidewalks to be paved shall be completed as soon as possible. Building pads shall be laid as soon as possible after grading unless seeding or soil binders are used.
6. Idling times shall be minimized either by shutting equipment off when not in use or reducing the maximum idling time to 5 minutes (as required by the California airborne toxics control measure Title 13, Section 2485 of California Code of Regulations [CCR]). Clear signage shall be provided for construction workers at all access points.
7. All construction equipment shall be maintained and properly tuned in accordance with manufacturer's specifications. All equipment shall be checked by a certified visible emissions evaluator.
8. Post a publicly visible sign with the telephone number and person to contact at the lead agency regarding dust complaints. This person shall respond and take corrective action within 48 hours. The Air District's phone number shall also be visible to ensure compliance with applicable regulations.

Additional Construction Mitigation Measures

BAAQMD recommends that all proposed projects, where construction-related emissions would exceed the applicable thresholds, implement the *Additional Construction Mitigation Measures* listed in Table 8-2. Appendix B contains more detailed guidance on emission reductions by source type (i.e., fugitive dust and exhaust) for quantification in URBEMIS and RoadMod.



© 2009 Jupiterimages Corporation

Table 8-2
Additional Construction Mitigation Measures Recommended for Projects with Construction Emissions Above the Threshold

1. All exposed surfaces shall be watered at a frequency adequate to maintain minimum soil moisture of 12 percent. Moisture content can be verified by lab samples or moisture probe.
2. All excavation, grading, and/or demolition activities shall be suspended when average wind speeds exceed 20 mph.
3. Wind breaks (e.g., trees, fences) shall be installed on the windward side(s) of actively disturbed areas of construction. Wind breaks should have at maximum 50 percent air porosity.
4. Vegetative ground cover (e.g., fast-germinating native grass seed) shall be planted in disturbed areas as soon as possible and watered appropriately until vegetation is established.
5. The simultaneous occurrence of excavation, grading, and ground-disturbing construction activities on the same area at any one time shall be limited. Activities shall be phased to reduce the amount of disturbed surfaces at any one time.
6. All trucks and equipment, including their tires, shall be washed off prior to leaving the site.
7. Site accesses to a distance of 100 feet from the paved road shall be treated with a 6 to 12 inch compacted layer of wood chips, mulch, or gravel.
8. Sandbags or other erosion control measures shall be installed to prevent silt runoff to public roadways from sites with a slope greater than one percent.
9. Minimizing the idling time of diesel powered construction equipment to two minutes.
10. The project shall develop a plan demonstrating that the off-road equipment (more than 50 horsepower) to be used in the construction project (i.e., owned, leased, and subcontractor vehicles) would achieve a project wide fleet-average 20 percent NO_X reduction and 45 percent PM reduction compared to the most recent ARB fleet average. Acceptable options for reducing emissions include the use of late model engines, low-emission diesel products, alternative fuels, engine retrofit technology, after-treatment products, add-on devices such as particulate filters, and/or other options as such become available.
11. Use low VOC (i.e., ROG) coatings beyond the local requirements (i.e., Regulation 8, Rule 3: Architectural Coatings).
12. Requiring that all construction equipment, diesel trucks, and generators be equipped with Best Available Control Technology for emission reductions of NOx and PM.
13. Requiring all contractors use equipment that meets CARB's most recent certification standard for off-road heavy duty diesel engines.

Assessing Mitigation Measures

Table 8-3 provides a summary of BAAQMD recommendations for assessing construction-related impacts and mitigation measures using URBEMIS. See Appendix B for additional guidance.

Table 8-3
URBEMIS Guidance for Assessing Construction-Related Impacts

URBEMIS Construction Input Parameter	Guidance Principle
Land Use Type and Size	• Select most applicable land use type. • Use the appropriate land use units.
Construction Schedule	• Use the earliest possible commencement date(s) if project-specific information is unknown. • Overlap phases that will or have the potential to occur simultaneously. • Check the selected number of work days per week to ensure an accurate number of construction work days for each phase.
Demolition Phase	• Use a separate demolition URBEMIS run if the land use size to be developed differs from the land use size to be demolished. • Demolition fugitive dust is based on maximum daily volume of building to be demolished. • Demolition construction equipment is based on acres of land use to be demolished (in *Enter Land Use Data* module).
Site Grading Phase	• Site grading construction equipment is based on maximum daily acres disturbed. • Enter project-specific maximum daily acres disturbed if known, otherwise URBEMIS assumes the maximum daily amount of acres disturbed is 25 percent of total acres disturbed.
Site Grading Fugitive Dust	• Select the appropriate fugitive dust quantification methodology based on the amount and type of project-specific information available. • The more specific grading information available will result in more accurate quantification of PM emissions.
Asphalt Paving Phase	• Acres to be asphalt paved are based on land use type and size (in *Enter Land Use Data* module). • Asphalt paving construction equipment is based on total acres to be paved. • Assumes asphalt paving occurs at equal rate throughout phase. • Account for excess asphalt paving requirements of project beyond default assumptions by adjusting the acres to be paved.
Architectural Coatings	• Assumes architectural coating operations occur at equal rate throughout phase.
Basic Construction Mitigation Measures	• All projects must implement Basic Construction Mitigation Measures, including those below the construction screening levels. • Use surrogate URBEMIS mitigation to account for Basic Construction Mitigation Measures' emission reductions.
Additional Construction Mitigation Measures	• Projects with construction emissions that exceed the thresholds are required to implement Additional Construction Mitigation Measures. • Use surrogate URBEMIS mitigation to account for Additional Construction Mitigation Measures' emission reductions.
Other	• For all construction phases, the more specific information available will result in more accurate emissions quantification. • When a specific construction schedule is unknown, all phases that could potentially overlap should be added to calculate maximum daily emissions.

8.2. GREENHOUSE GASES

BAAQMD does not have an adopted *Threshold of Significance* for construction-related GHG emissions. However, lead agencies should quantify and disclose GHG emissions that would occur during construction, and make a determination on the significance of these construction-generated GHG emission impacts in relation to meeting AB 32 GHG reduction goals. BAAQMD recommends using URBEMIS for proposed land use development projects and RoadMod for proposed projects that are linear in nature. Sources of construction-related GHGs include exhaust, for which the same detailed guidance as described for criteria air pollutants and precursors should be followed.

Lead agencies are encouraged to incorporate best management practices to reduce GHG emissions during construction, as applicable. Best management practices may include, but are not limited to: using alternative fueled (e.g., biodiesel, electric) construction vehicles/equipment of at least 15 percent of the fleet; using local building materials of at least 10 percent; and recycling or reusing at least 50 percent of construction waste or demolition materials.

8.3. TOXIC AIR CONTAMINANTS

BAAQMD recommends that the same community risk and hazard *Threshold of Significance* for project operations be applied to construction. However, BAAQMD suggests associated impacts should be addressed on a case-by-case basis, taking into consideration the specific construction-related characteristics of each project and proximity to off-site receptors, as applicable. BAAQMD recommends that for construction projects that are less than one year duration, lead agencies should annualize impacts over the scope of actual days that peak impacts are to occur, rather than the full year.

BAAQMD has developed guidance for estimating risk and hazards impacts entitled *Recommended Methods for Screening and Modeling Local Risks and Hazards* which also includes recommendations for mitigation of significant risk and hazards impacts. BAAQMD has also developed a Construction Risk Calculator model that provides distances from a construction site, based on user-provided project date, where the risk impacts are estimated to be less than significant; sensitive receptors located within these distances would be considered to have potentially significant risk and hazards impacts from construction. The Construction Risk Calculator will be available on BAAQMD's website, http://www.baaqmd.gov/Divisions/Planning-and-Research/CEQA-GUIDELINES.aspx.

8.3.1. Diesel Particulate Matter

Construction-related activities could result in the generation of TACs, specifically diesel PM, from on-road haul trucks and off-road equipment exhaust emissions. Due to the variable nature of construction activity, the generation of TAC emissions in most cases would be temporary, especially considering the short amount of time such equipment is typically within an influential distance that would result in the exposure of sensitive receptors to substantial concentrations. Concentrations of mobile-source diesel PM emissions are typically reduced by 70 percent at a distance of approximately 500 feet (ARB 2005). In addition, current models and methodologies for conducting health risk assessments are associated with longer-term exposure periods of 9, 40, and 70 years, which do not correlate well with the temporary and highly variable nature of construction activities. This results in difficulties with producing accurate estimates of health risk. Additionally, the implementation of the *Basic Construction Mitigation Measures* (table 8-1), which is recommended for all proposed projects, would also reduce diesel PM exhaust emissions.

However, these variability issues associated with construction do not necessarily minimize the significance of possible impacts.

The analysis should disclose the following about construction-related activities:

1. Types of off-site receptors and their proximity to construction activity within approximately 1,000 feet;
2. Duration of construction period;
3. Quantity and types of diesel-powered equipment;
4. Number of hours equipment would be operated each day;
5. Location(s) of equipment use, distance to nearest off-site sensitive receptors, and orientation with respect to the predominant wind direction;
6. Location of equipment staging area; and
7. Amount of on-site diesel-generated $PM_{2.5}$ exhaust (assuming that all on-site diesel $PM_{2.5}$ exhaust is diesel PM) if mass emission levels from construction activity are estimated.

In cases where construction-generated emissions of diesel PM are anticipated to occur in close proximity to sensitive receptors for extended periods of time, lead agencies are encouraged to consult with BAAQMD.

8.3.2. Demolition and Renovation of Asbestos-Containing Materials

Demolition of existing buildings and structures would be subject to BAAQMD Regulation 11, Rule 2 (Asbestos Demolition, Renovation, and Manufacturing). BAAQMD Regulation 11, Rule 2 is intended to limit asbestos emissions from demolition or renovation of structures and the associated disturbance of asbestos-containing waste material generated or handled during these activities. The rule addresses the national emissions standards for asbestos along with some additional requirements. The rule requires the lead agency and its contractors to notify BAAQMD of any regulated renovation or demolition activity. This notification includes a description of structures and methods utilized to determine whether asbestos-containing materials are potentially present. All asbestos-containing material found on the site must be removed prior to demolition or renovation activity in accordance with BAAQMD Regulation 11, Rule 2, including specific requirements for surveying, notification, removal, and disposal of material containing asbestos. Therefore, projects that comply with Regulation 11, Rule 2 would ensure that asbestos-containing materials would be disposed of appropriately and safely. By complying with BAAQMD Regulation 11, Rule 2, thereby minimizing the release of airborne asbestos emissions, demolition activity would not result in a significant impact to air quality.

Because BAAQMD Regulation 11, Rule 2 is in place, no further analysis about the demolition of asbestos-containing materials is needed in a CEQA document. BAAQMD does recommend that CEQA documents acknowledge and discuss BAAQMD Regulation 11, Rule 2 to support the public's understanding of this issue.

8.3.3. Naturally Occurring Asbestos

Naturally occurring asbestos (NOA) was identified as a TAC in 1986 by ARB. NOA is located in many parts of California and is commonly associated with ultramafic rocks, according to the California Department of Geology's special publication titled Guidelines for Geologic Investigations of Naturally Occurring Asbestos in California. Asbestos is the common name for a group of naturally occurring fibrous silicate minerals that can separate into thin but strong and durable fibers. Ultramafic rocks form in high-temperature environments well below the surface of the earth. By the time they are exposed at the surface by geologic uplift and erosion, ultramafic rocks may be partially to completely altered into a type of metamorphic rock called serpentinite.

Sometimes the metamorphic conditions are right for the formation of chrysotile asbestos or tremolite-actinolite asbestos in the bodies of these rocks, along their boundaries, or in the soil.

For individuals living in areas of NOA, there are many potential pathways for airborne exposure. Exposures to soil dust containing asbestos can occur under a variety of scenarios, including children playing in the dirt; dust raised from unpaved roads and driveways covered with crushed serpentine; grading and earth disturbance associated with construction activity; quarrying; gardening; and other human activities. For homes built on asbestos outcroppings, asbestos can be tracked into the home and can also enter as fibers suspended in the air. Once such fibers are indoors, they can be entrained into the air by normal household activities, such as vacuuming (as many respirable fibers will simply pass through vacuum cleaner bags).

People exposed to low levels of asbestos may be at elevated risk (e.g., above background rates) of lung cancer and mesothelioma. The risk is proportional to the cumulative inhaled dose (quantity of fibers), and also increases with the time since first exposure. Although there are a number of factors that influence the disease-causing potency of any given asbestos (such as fiber length and width, fiber type, and fiber chemistry), all forms are carcinogens.

8.3.4. Mitigating Naturally Occurring Asbestos

BAAQMD enforces CARB's ATCM which regulates NOA emissions from grading, quarrying, and surface mining operations at sites which contain ultramafic rock. The provisions that cover these operations are found specifically in the California Code of Regulations, Section 93105. The ATCM for Construction, Grading, Quarrying and Surface Mining Operations was signed into State law on July 22, 2002, and became effective in the SFBAAB on November 19, 2002. The purpose of this regulation is to reduce public exposure to NOA from construction and mining activities that emit or re-suspend dust which may contain NOA.

The ATCM requires regulated operations engaged in road construction and maintenance activities, construction and grading operations, and quarrying and surface mining operations in areas where NOA is likely to be found, to employ the best available dust mitigation measures to reduce and control dust emissions. Tables 8-1 and 8-2 list a number of dust mitigation measures for construction.

BAAQMD's NOA program requires that the applicable notification forms from the Air District's website be submitted by qualifying operations in accordance with the procedures detailed in the ATCM Inspection Guidelines Policies and Procedures. The lead agency should reference BAAQMD's ATCM Policies and Procedures to determine which NOA Notification Form is applicable to the proposed project (NOA Notification Forms).

Using the geologic map of the SFBAAB (Geologic Map), the lead agency should discuss whether a proposed project would be located in "areas moderately likely to contain NOA." If a project would not involve earth-disturbing construction activity in one of these areas or would not locate receptors in one of these areas then it can be assumed that the project would not have the potential to expose people to airborne asbestos particles.

[This Page Intentionally Left Blank]

PART III: ASSESSING & MITIGATING PLAN LEVEL IMPACTS

9. PLAN-LEVEL IMPACTS



Long range plans (e.g., general plan, redevelopment plans, specific plans, area plans, community plans, regional plans, congestion management plans, etc.) present unique challenges for assessing impacts. These plans often contain development strategies for 20-year, or longer, time horizons. They can also provide for a wide range of potential land uses and densities that accommodate all types of development. General plan updates and large specific plans nearly always require the lead agency to prepare an Environmental Impact Report (EIR). Due to the SFBAAB's nonattainment status for ozone and PM, and the cumulative impacts of growth on air quality, these plans almost always have significant, unavoidable adverse air quality impacts. CEQA requires the lead agency to evaluate individual as well as cumulative impacts of general plans, and all feasible mitigation measures must be incorporated within the proposed plan to reduce significant air quality impacts.

This chapter provides guidance on methods to evaluate air quality and climate change impacts of long-range plans prepared within the SFBAAB pursuant to CEQA. The term *general and area plan* refers broadly to discretionary planning activities which may include, but are not limited to the following: general plans, redevelopment plans, specific plans, area plans, community plans, congestion management plans, and annexations of lands and service areas. General and area plans are often subject to program-level analysis under CEQA, as opposed to project-level analysis. As a general principle, the guidance offered within this chapter should be applied to discretionary, program-level planning activities; whereas the project-level guidance offered in other chapters should be applied to individual project-specific approvals, such as a proposed development project.

Air quality impacts from future development pursuant to general or area plans can be divided into construction-related impacts and operational-related impacts. Construction-related impacts are associated with construction activities likely to occur in conjunction with future development allocated by the plan. Operational-related impacts are associated with continued and future operation of developed land uses, including increased vehicle trips and energy use.

Please note that the plan-level approach described here differs for greenhouse gas (GHG) impact assessments. BAAQMD recommends that when assessing GHG impacts for plans other than regional plans (transportation and air quality plans) and general plans, such as specific plans and area plans, the appropriate thresholds and methodology is the same as project-level GHG impact assessments described in Chapter 4.

Regional plan (transportation and air quality plans) impacts also are assessed differently because of their unique characteristics (regional plans do not establish land use designations) and are subject to a threshold of "no net increase in emissions."

9.1. CRITERIA AIR POLLUTANTS AND PRECURSOR EMISSIONS

To meet the *Threshold of Significance* for operational-related criteria air pollutant and precursor impacts for plans (other than regional plans), a proposed plan must satisfy the following criteria:

- Consistency with current air quality plan (AQP) control measures (this requirement applies to project-level as well as plan-level analyses).
- A proposed plan's projected VMT or vehicle trips (VT) (either measure may be used) increase is less than or equal to its projected population increase.

Air Quality Plan Control Measures

For this threshold, an air quality plan refers to clean air plans, state implementation plans (SIPS), ozone plans, and other potential air quality plans developed by BAAQMD. To date, the Air District's most current plan is the 2010 Clean Air Plan.

The following approach for incorporating current AQP control measures into a plan is also applicable for determining a project's consistency with an air quality plan. CEQA requires lead agencies to determine whether a project is consistent with all applicable air quality plans. In addition, the State CEQA Guidelines sample Environmental Checklist Form (Appendix G), poses the question: "Would the project conflict with or obstruct implementation of the applicable air quality plan?"

BAAQMD recommends that the agency approving a project where an air quality plan consistency determination is required analyze the project with respect to the following questions. If all the questions are concluded in the affirmative, and those conclusions are supported by substantial evidence, BAAQMD considers the project consistent with air quality plans prepared for the Bay Area.

1. Does the project support the primary goals of the AQP?

The primary goals of the 2010 Bay Area Clean Air Plan (CAP), the current AQP to date, are to:

- Attain air quality standards;
- Reduce population exposure and protecting public health in the Bay Area; and
- Reduce greenhouse gas emissions and protect the climate.

Any project (i.e. project or plan) that would not support these goals would not be considered consistent with the 2010 CAP. The recommended measure for determining project support of these goals is consistency with District-approved CEQA thresholds of significance. Therefore, if approval of a project would not result in significant and unavoidable air quality impacts, after the application of all feasible mitigation, the project would be considered consistent with the 2010 CAP.

2. Does the project include applicable control measures from the AQP?

Agencies approving projects should require that they include all air quality plan control measures that can feasibly be incorporated into the project design or applied as mitigation, or justify the reasons, supported by substantial evidence, why a measure or measures are not incorporated into the project. Projects that incorporate all feasible air quality plan control measures are considered consistent with the 2010 CAP.

The 2010 CAP contains 55 control measures aimed at reducing air pollution in the Bay Area. Along with the traditional stationary, area, mobile source and transportation control measures, the 2010 CAP contains a number of new control measures designed to protect the climate and promote mixed use, compact development to reduce vehicle emissions and exposure to pollutants from stationary and mobile sources. BAAQMD encourages project developers and lead agencies to incorporate these Land Use and Local Impact (LUM) measures and Energy and Climate measures (ECM) into proposed project designs and plan elements.

Refer to Volume II of the 2010 CAP Control Measure for a list of all the control measures and implementation guidance.

3. Does the project disrupt or hinder implementation of any AQP control measures?

If approval of a project would not cause the disruption, delay or otherwise hinder the implementation of any air quality plan control measure, it would be considered consistent with the 2010 CAP. Examples of how a project may cause the disruption or delay of control measures include a project that precludes an extension of a transit line or bike path, or proposes excessive parking beyond parking requirements.

Projected VMT and Population Growth

A proposed plan must demonstrate that its projected VMT or vehicle trips (VT) (either measure may be used) is less than or equal to its projected population increase to be considered to have a less than significant impact on criteria air pollutants and precursor emissions.

9.2. GREENHOUSE GASES

California's legislative mandate (AB 32) is to reduce total projected 2020 GHG emissions to 1990 levels, a reduction of approximately 30 percent. To achieve this target, future development must be planned and implemented in the most GHG-efficient manner possible. GHG-efficient development reduces vehicle miles traveled by supporting compact, dense, mixed-use, pedestrian- and bicycle-friendly, transit oriented development. State, regional and local agencies are strongly encouraged to address GHG emissions when updating and/or adopting long-range plans. For local jurisdictions, the general plan is perhaps the best venue for addressing GHG emissions in making meaningful progress toward attaining AB 32 goals while addressing CEQA requirements.



If a long-range plan includes goals, policies, performance standards, and implementation measures achieving GHG emission reductions that can be shown to meet and/or exceed AB 32 mandates, as outlined in Section 4.3, subsequent projects consistent with the plan could be relieved of performing GHG analysis as part of their CEQA compliance.

The threshold for operational-related GHG impacts of plans employs either a GHG efficiency-based metric of 6.6 MT per SP per year of carbon dioxide equivalent (CO_2e), or a GHG Reduction Strategy option. Unlike the other plan-level thresholds that apply to the different plans

mentioned in Section 9 above, the GHG efficiency threshold may only be applied to general plans. A lead agency may also determine that this threshold is appropriate for a GHG Reduction Strategy's 2020 milestone target. GHG Reduction Strategies using this threshold with horizon years beyond 2020 should consider horizon-year goals consistent with climate stabilization predictions identified in the Governor's Executive Order S-03-05, and include an interim goal for 2020..

Step 1. GHG Reduction Strategy Approach

A general plan would be assumed to have a less than significant impact related to GHG emissions if the lead agency has a qualified GHG Reduction Strategy that is referenced and or integrated within the general plan. See Section 4.3 for qualifying criteria for a qualified GHG Reduction Strategy.

If the lead agency does not have a qualified GHG Reduction Strategy meeting established criteria, refer to Step 2.

Step 2. GHG Efficiency Approach – Emissions Quantification



BAAQMD recommends quantifying community-wide GHG emissions from a general plan through development of a GHG emissions inventory and projections report. The emissions inventory should be conducted for a base year at or before the current year of the plan; and should follow published ARB protocols for municipal and community-wide inventories (when available). The base year inventory should be expressed in terms of metric tons CO_2e emissions and account for municipal and community-wide emission sectors applicable in the jurisdiction such as, transportation, commercial, residential, water use and treatment, solid waste, and agriculture. BAAQMD's *GHG Plan Level Quantification Guidance* contains detailed recommendations for developing GHG emission inventories and projections. This document is available at BAAQMD's website, http://www.baaqmd.gov/Divisions/Planning-and-Research/CEQA-GUIDELINES.aspx.

Section 4.3 contains additional guidance on preparing a GHG emissions inventory and projections report for a qualified GHG Reduction Strategy that should be applied to general plans as well. A range of tools and resources are available to assist lead agencies in completing inventories, including the Air District's *GHG Plan Level Quantification Guidance*, Intergovernmental Panel on Climate Change (IPCC) Emissions Inventory Guidelines, the California Climate Action Registry's General Reporting Protocol and ICLEI's Clean Air and Climate Protection (CACP) model. In all instances where regional, statewide or national data sources are available, BAAQMD recommends that local data be used if available and more accurate.

Step 3. Prepare Greenhouse Gas Emissions Projections

BAAQMD recommends preparing a community-wide GHG emission projection to identify the expected levels of GHG emissions for: 1) 2020 (i.e., the AB 32 benchmark year), and 2) the projected year of the plan build out. Two projections should be prepared for each year:

- A projection reflecting existing conditions (e.g., business-as-usual), and

- A projection that accounts for proposed policies, programs, and plans included within the general plan that would reduce GHG emissions from build-out of the plan.

The first projection should be used as the basis for evaluation of the no project alternative in the plan's EIR. The second projection should be used as the basis for evaluation of the proposed project. Additional projections corresponding to plan alternatives considered within the EIR should also be prepared and included within the EIR's alternatives analysis. Examples of policies, performance standards and implementation measures are included in Section 9.6.

Where possible, emission projections should account for population and employment growth rates published by ABAG, VMT growth rates available from MTC, energy consumption growth rates available from California Energy Commission (CEC) planned expansions of municipal infrastructure or services, and anticipated statewide legislative requirements or mandates (e.g., Renewable Energy Portfolio, Green Building Code Standards, on-road vehicle emission regulations).

A range of GIS-based planning models are available that can assist lead agencies in completing projections, including Index, PLACE3S, UPlan, and the Sustainable Systems Integration Model (SSIM). The projection should be expressed in metric tons CO_2e emissions, and include the expected municipal and community-wide emissions across all sectors evaluated in the base year inventory.

BAAQMD encourages lead agencies to prepare similar projections for 2050 (the Executive Order S-03-05 benchmark year). As we approach the 2020 timeframe, BAAQMD will reevaluate this significance threshold to better represent progress toward 2050 goals. The lead agency should use the projected build-out emissions profile of the general or area plan as a benchmark to ensure that adoption of the plan would not preclude attainment of 2050 goals.

Step 4. Determine Planned Population and Employment Levels and Service Population

State law requires that general and area plans identify the planned density and intensity of land uses for all lands within the planning area established by the lead agency. These measures of density (typically dwelling units/acre) and intensity (typically floor-area ratios) are often translated into expected population and employment levels for estimating traffic impacts associated with the proposed plan. Most demand-based transportation models use population and employment to determine trip generation. Measures of population and employment are typically available for general and area plans. In evaluating GHG impacts, estimates of the number of residents and jobs anticipated in the general or area plan are required for 2020, the build-out year of the proposed plan, the no project alternative, and additional alternatives the lead agency is evaluating in the environmental review.

Service population (SP) is an efficiency-based measure used by BAAQMD to estimate the development potential of a general or area plan. SP is determined by adding the number of residents to the number of jobs estimated for a given point in time. For purposes of evaluating GHG impacts, SP estimates are required for 2020 and for the build-out year of the proposed plan.

Step 5. Compare Service Population to 2020 GHG Projections and Thresholds of Significance

The lead agency should divide the 2020 GHG emissions inventory by 2020 SP estimates to determine the per-SP emissions associated with the proposed general or area plan, the no project alternative, and additional alternatives the lead agency is evaluating. The lead agency should then compare these per-SP emissions to the significance thresholds identified in Chapter 2 (refer to Table 9-1).

Table 9-1 Example Plan-level Greenhouse Gas Emissions Analysis			
Step	**Emissions Source**	**Year**	**Emissions (MT CO2e/yr)***
2	GHG Emissions Inventory (Community-wide and municipal)	Base year (e.g., 2007)	A
3	GHG Emissions Projections	2020	B
		GP Buildout (e.g., 2030)	C
4	Projected Service Population (population + employment)	SP	
	GHG/SP (2020)	B/SP (MT CO_2e/SP/yr)	
5	BAAQMD GHG/SP Threshold	6.6 (MT CO_2e/SP/yr)	
	Is B/SP > 6.6? (If Yes, Significant. Proceed to Step 6. If No, less than significant).		
*Letters "A", "B", and "C" are used to represent numeric values that would be obtained through conducting a community-wide emissions inventory and projections. Notes: CO_2e = carbon dioxide equivalent; MT = metric tons; yr = year, P = population, SP = service population. Refer to Appendix D for support documentation.			

If the estimated per-SP emissions exceed identified thresholds, the general or area plan would be considered to have a significant impact with respect to GHG emissions, and mitigation would be required.

Step 6. Mitigation Measures

General or area plans found to have a significant impact should implement all feasible mitigation measures to reduce impacts. Refer to Section 9.5 for examples of appropriate mitigation measures for operational impacts relative to GHG emissions. Mitigation measures identified through the environmental review process must be made into binding and enforceable policies and implementation programs within the long range plan.

9.3. LOCAL COMMUNITY RISK AND HAZARD IMPACTS

For general and area plans to have a less-than-significant impact with respect to potential toxic air contaminants (TACs), special overlay zones need to be established around existing and proposed land uses that emit TACs. Special overlay zones should be included in proposed plan policies, land use maps, and implementing ordinances.



The *Thresholds of Significance* for plans with regard to community risk and hazard impacts are:

1. The land use diagram must identify:

© 2009 Jupiterimages Corporation

a. Special overlay zones around existing and planned sources of TACs;

b. Special overlay zones of at least 500 feet (or Air District-approved modeled distance) on each side of all freeways and high-volume roadways.

2. The plan must also identify goals, policies, and objectives to minimize potential impacts and create overlay zones for sources of TACs and receptors.

ARB's Land Use Handbook offers advisory recommendations for locating sensitive receptors near uses associated with TACs, such as freeways and high-traffic roads, commercial distribution centers, rail yards, ports, refineries, chrome platers, dry cleaners, gasoline stations, and other industrial facilities, to reduce exposure of sensitive populations. The lead agency should refer to this handbook when evaluating whether the proposed general or area plan includes adequate buffer distances between TAC sources and sensitive receptors.

9.3.1. Community Risk Reduction Plans

The goal of a Community Risk Reduction Plan (CRRP) would be to bring TAC and $PM_{2.5}$ concentrations for the entire community covered by the Plan down to acceptable levels as identified by the local jurisdiction and approved by the Air District. This approach provides local agencies a proactive alternative to addressing communities with high levels of risk on a project-by-project approach.

A qualified Community Risk Reduction Plan adopted by a local jurisdiction should include, at a minimum, the following elements:

(A) Define a planning area;

(B) Include base year and future year emissions inventories of TACs and PM2.5;

(C) Include Air District–approved risk modeling of current and future risks;

(D) Establish risk and exposure reduction goals and targets for the community in consultation with BAAQMD staff;

(E) Identify feasible, quantifiable, and verifiable measures to reduce emissions and exposures;

(F) Include procedures for monitoring and updating the inventory, modeling and reduction measures in coordination with Air District staff; and

(G) Be adopted in a public process following environmental review.

Refer to Chapter 5 for additional guidance on preparing a CRRP. BAAQMD has also developed the *Community Risk Reduction Plan Methodology* guidance document, which can found at http://www.baaqmd.gov/Divisions/Planning-and-Research/CEQA-GUIDELINES.aspx.

9.4. ODOR IMPACTS

For plans to have a less-than-significant impact, a plan must identify the location of existing and planned odor sources in the plan area. The plan must also include policies to reduce potential odor impacts in the plan area.

9.5. REGIONAL PLANS

Regional plans must demonstrate a no net increase in emissions to satisfy the *Threshold of Significance* for operational-related criteria air pollutant and precursor impacts, GHGs, and toxic air contaminants.

Regional plans include the Regional Transportation Plan prepared by the Metropolitan Transportation Commission (MTC) and air quality plans prepared by the Air District. In order to meet this threshold, these agencies must compare the regional plan's baseline emissions with its projected future emissions. This approach requires two comparative analyses:

a. Compare existing (base year) emissions with projected future year plus project emissions (base year/project comparison);

b. Compare projected future year emissions without the project with projected future year emissions plus the project (no project/project comparison).

A regional plan is considered less than significant if each scenario demonstrates that no net increase in emissions of criteria air pollutants and precursors, GHGs, and toxic air contaminants will occur.

9.6. MITIGATING PLAN-LEVEL IMPACTS

Plans often have significant, unavoidable adverse air quality impacts due to the SFBAAB's nonattainment status and the cumulative impacts of growth on air quality. In addition, plans generally have long-term planning horizons of twenty years or more. For these reasons, it is essential for plans to incorporate all feasible strategies and measures to reduce air quality impacts. Mitigation measures for plans are often broad in scope due to the long timeframe and comprehensive nature of general and area plan policies and programs.

This section contains mitigation measures recommended for plans prepared within the SFBAAB. Measures are identified by state-required general plan element, planning issue, development phase, and type of air quality impact. Proposed plans should incorporate mitigation measures applicable to their elements and planning issues.



© 2009 Jupiterimages Corporation

Plans are the appropriate place to establish community-wide air quality policies that reinforce regional air quality plans. Plans present opportunities to establish requirements for new construction, future development, and redevelopment projects within a community that will ensure new or revised plans do not inhibit attainment of state and national air quality standards and actually assist in improving local and regional air quality. Binding, enforceable mitigation measures identified through the environmental review process should be incorporated as policies and implementation programs within the plan to the

greatest extent feasible. Ideally, air quality related goals, policies, performance measures and standards should be incorporated within the context of the proposed project itself, rather than introduced as corrective actions within the proposed project's EIR. The list below is not intended to serve as an exhaustive list. The Air District also recommends that Lead Agencies refer to CAPCOA's reports, *Model Policies for Greenhouse Gases in General Plans* (June 2009) for additional guidance (http://www.capcoa.org/modelpolicies/CAPCOA-ModelPolicies-6-12-09-915am.pdf) and *Quantifying GHG Mitigation Measures*.

9.6.1. Land Use Element

Urban Form

Mitigation Measure or General/Area Plan Policy	Construction				Operational			
	CAPs	GHGs	TACs	Odors	CAPs	GHGs	TACs	Odors
Create and enhance landscaped greenway, trail, and sidewalk connections between neighborhoods, commercial areas, activity centers, and parks.					X	X		
Adopt policies supporting infill development					X	X		
Ensure that proposed land uses are supported by a multi-modal transportation system and that the land uses themselves support the development of the transportation system.					X	X		
Designate a central city core for high-density and mixed-use development.					X	X		
Discourage high intensity office and commercial uses from locating outside of designated centers or downtowns, or far from residential areas and transit stations.					X	X		
Provide financial incentives and density bonuses to entice development within the designated central city.					X	X		
Provide public education about benefits of well-designed, higher-density housing and relationships between land use and transportation.					X	X		

Compact Development

Mitigation Measure or General/Area Plan Policy	Construction				Operational			
	CAPs	GHGs	TACs	Odors	CAPs	GHGs	TACs	Odors
Achieve a jobs/housing balance or improve the jobs/housing ratio within the plan area.					X	X		
Create incentives to attract mixed-use projects to older commercial and industrial areas.					X	X		
Adopt incentives for the concurrent development of retail, office, and residential land uses within mixed-use projects or areas. Require mixed-use development to include ground-floor retail.					X	X		
Provide adaptive re-use alternatives to demolition of historic buildings. Provide incentives to prevent demolition of historic buildings.	X	X			X	X		
Facilitate lot consolidation that promotes integrated development with improved pedestrian and vehicular access.					X	X		
Reinvest in existing neighborhoods and promote infill development as a					X	X		

preference over new, greenfield development.								
Ensure that new development finances the full cost of expanding public infrastructure and services to provide an economic incentive for incremental expansion.					X	X		
Require new developments to extend sewer and water lines from existing systems or to be in conformance with a master sewer and water plan.	X	X			X	X		

Transit-oriented Design

Mitigation Measure or General/Area Plan Policy	Construction				Operational			
	CAPs	GHGs	TACs	Odors	CAPs	GHGs	TACs	Odors
Require all development projects proposed within 2,000 feet of an existing or planned light rail transit, commuter rail, express bus, or transit corridor stop, to incorporate site design measures that enhance the efficiency of the transit system.					X	X		
Develop transit/pedestrian-oriented design guidelines. Identify and designate appropriate sites during general plan updates and amendments.					X	X		
Plan areas within ¼-mile of locations identified as transit hubs and commercial centers for higher density development.					X	X		

Sustainable Development

Mitigation Measure or General/Area Plan Policy	Construction				Operational			
	CAPs	GHGs	TACs	Odors	CAPs	GHGs	TACs	Odors
Ensure new construction complies with California Green Building Code Standards and local green building ordinances.					X	X		
Promote re-use of previously developed property, construction materials, and/or vacant sites within a built-up area.					X	X		
Avoid development of isolated residential areas near hillsides or other areas where such development would require significant infrastructure investment or adversely impact biological resources.						X		
Require orientation of buildings to maximize passive solar heating during cool seasons, avoid solar heat gain during hot periods, enhance natural ventilation, and promote effective use of daylight. Orientation should optimize opportunities for on-site solar generation.					X	X		
Provide land area zoned for commercial and industrial uses to support a mix of retail, office, professional, service, and manufacturing businesses.					X	X		
Provide permitting incentives for energy efficient and solar building projects.					X	X		
Develop a joint powers agreement or other legal instrument that provides incentive for counties to discourage urban commercial development in unincorporated areas and promote urban infill and redevelopment projects.					X	X		

Activity Centers

Mitigation Measure or General/Area Plan Policy	Construction				Operational			
	CAPs	GHGs	TACs	Odors	CAPs	GHGs	TACs	Odors
Provide pedestrian amenities, traffic-calming features, plazas and public areas, attractive streetscapes, shade trees, lighting, and retail stores at activity centers.					X	X		
Provide for a mix of complementary retail uses to be located together to create activity centers and commercial districts serving adjacent neighborhoods.					X	X		
Permit upper-story residential and office uses in neighborhood shopping areas.					X	X		
Provide pedestrian links between commercial districts and neighborhoods.					X	X		
Provide benches, streetlights, public art, and other amenities in activity centers to attract pedestrians.					X	X		

Green Economy and Businesses

Mitigation Measure or General/Area Plan Policy	Construction				Operational			
	CAPs	GHGs	TACs	Odors	CAPs	GHGs	TACs	Odors
Work with businesses to encourage employee transit subsidies and shuttles from transit stations.					X	X		
Encourage businesses to participate in local green business programs.					X	X		
Offer incentives to attract businesses to city core and infill areas.					X	X		
Work to attract green businesses and promote local green job training programs.					X	X		
Support regional collaboration to strengthen the green economy.					X	X		
Provide outreach and education to local businesses on energy, waste, and water conservation benefits and cost savings.					X	X		
Support innovative energy technology companies.					X	X		

9.6.2. Circulation Element

Local Circulation

Mitigation Measure or General/Area Plan Policy	Construction				Operational			
	CAPs	GHGs	TACs	Odors	CAPs	GHGs	TACs	Odors
Create or reinforce a grid street pattern with small block sizes and maintain high connectivity within the roadway network.					X	X		
Implement circulation improvements that reduce vehicle idling, such as signal timing systems and controlled intersections.					X	X	X	
Consider alternatives such as increasing public transit or improving bicycle or pedestrian travel routes before funding transportation improvements that increase VMT.					X	X		
Require payment of transportation impact fees and/or roadway and transit improvements as a condition upon new development.					X	X		
Minimize use of cul-de-sacs and incomplete roadway segments.					X	X		
Actively promote walking as a safe mode of local travel, particularly for children attending local schools.					X	X		
Consult with school districts, private schools, and other operators to coordinate local busing, to expand ride-sharing programs, and to replace older diesel buses with low or zero emission vehicles.					X	X	X	
Evaluate all busing options as a preferential strategy to roadway improvements in the vicinity of schools to ease congestion.					X	X		
Establish public/private partnerships to develop satellite and neighborhood work centers for telecommuting.					X	X		
Employ traffic calming methods such as median landscaping and provision of bike or transit lanes to slow traffic, improve roadway capacity, and address safety issues.					X	X		
Support the use of electric vehicles where appropriate. Provide electric recharge facilities.					X	X		

Regional Transportation

Mitigation Measure or General/Area Plan Policy	Construction				Operational			
	CAPs	GHGs	TACs	Odors	CAPs	GHGs	TACs	Odors
Ensure that submittals of transportation improvement projects to be included in regional transportation plans (RTP, RTIP, CMP, etc.) are consistent with the air quality goals and policies of the general plan.					X	X		
Consult with adjacent jurisdictions to address the impacts of regional development patterns on the circulation system.					X	X		
Adopt a (or implement the existing) Transportation Demand Management Ordinance.					X	X		
Create financing programs for the purchase or lease of vehicles used in employer ride sharing programs.					X	X		
Consult with adjacent jurisdictions to maintain adequate service levels at shared intersections and to provide adequate capacity on regional routes for through traffic.					X	X		
Work to provide a strong paratransit system that promotes the mobility of all residents and educate residents about local mobility choices.					X	X		
Designate sites for park-and-ride lots. Consider funding of the park and ride lots as mitigation during CEQA review of residential development projects.					X	X		
Consult with appropriate transportation agencies and major employers to establish express buses and vanpools to increase the patronage of park and ride lots.					X	X		
Allow developers to reach agreements with auto-oriented shopping center owners to use commercial parking lots as park-and-ride lots and multimodal transfer sites.					X	X		

Parking

Mitigation Measure or General/Area Plan Policy	Construction				Operational			
	CAPs	GHGs	TACs	Odors	CAPs	GHGs	TACs	Odors
Reduce parking for private vehicles while increasing options for alternative transportation.					X	X		
Eliminate minimum parking requirements for new development.					X	X		
Establish commercial district parking fees.					X	X		
Require that parking is paid for separately and is not included in rent for residential or commercial space.					X	X		
Encourage parking sharing between different land uses.					X	X		
Encourage businesses to offer parking cash-outs to employees.					X	X		
Encourage parking assessment districts.					X	X		
Encourage car-share and bike-share programs and dedicated parking spaces in new development.					X	X		
Support preferential parking for low emission and carpool vehicles					X	X		

Bicycles and Pedestrians

Mitigation Measure or General/Area Plan Policy	Construction				Operational			
	CAPs	GHGs	TACs	Odors	CAPs	GHGs	TACs	Odors
Provide safe and convenient pedestrian and bicycle connections to and from activity centers, commercial districts, offices, neighborhoods, schools, other major activity centers.					X	X		
Ensure that non-motorized transportation systems are connected and not interrupted by impassable barriers, such as freeways.					X	X		
Provide pedestrian pathways that are well-shaded and pleasantly landscaped to encourage use.					X	X		
Consult with transit providers to increase the number of bicycles that can be accommodated on buses.					X	X		
Provide crosswalks and sidewalks along streets that are accessible for people with disabilities and people who are physically challenged.					X	X		
Prohibit on-street parking to reduce bicycle/automobile conflicts in appropriate target areas.					X	X		
Prohibit projects that impede bicycle and walking access.					X	X		
Retrofit abandoned rail corridors as segments of a bikeway and pedestrian trail system.					X	X		
Require commercial developments and business centers to include bicycle amenities in building such as bicycle racks, showers, and lockers.					X	X		

Regional Rail Transit

Mitigation Measure or General/Area Plan Policy	Construction				Operational			
	CAPs	GHGs	TACs	Odors	CAPs	GHGs	TACs	Odors
Support regional rail service and consult with rail operators to expand services.					X	X		
Create activity centers and transit-oriented development projects near transit stations.					X	X		

Local and Regional Bus Transit

Mitigation Measure or General/Area Plan Policy	Construction				Operational			
	CAPs	GHGs	TACs	Odors	CAPs	GHGs	TACs	Odors
Give funding preference to investment in public transit over investment in infrastructure for private automobile traffic.					X	X		
Establish a local shuttle service to connect neighborhoods, commercial centers, and public facilities to rail transit.					X	X		
Empower seniors and those with physical disabilities who desire maximum personal freedom and independence of lifestyle with unimpeded access to public transportation.					X	X		
Provide transit shelters that are comfortable, attractive, and accommodate transit riders. Ensure that shelters provide shade, route information, benches and lighting.					X	X		
Design all arterial and collector streets planned as transit routes to allow for the efficient operation of public transit.					X	X		
Require transit providers to coordinate intermodal time schedules					X	X		

9.6.3. Conservation Element

Municipal Operations

Mitigation Measure or General/Area Plan Policy	Construction				Operational			
	CAPs	GHGs	TACs	Odors	CAPs	GHGs	TACs	Odors
Replace existing City vehicles with ultra-low or zero emission vehicles and purchase new low emission vehicles.					X	X		
Require that all new government buildings, and all major renovations and additions, meet identified green building standards.					X	X		
Install cost-effective renewable energy systems on all city buildings and purchase remaining electricity from renewable sources.					X	X		
Support the use of teleconferencing in lieu of city/county employee travel to conferences and meetings when feasible.					X	X		
Require city/county departments to set up telecommuting programs as part of their trip reduction strategies.					X	X		
Require environmentally responsible government purchasing. Require or give preference to products that reduce or eliminate indirect GHG emissions.						X		
Investigate the feasibility of using solar (photovoltaic) street lights instead of conventional street lights to conserve energy.					X	X		
Support investment in cost-effective land use and transportation modeling and geographic information system technology.					X	X	X	X
Install LED lighting for all traffic light systems.						X		
Implement a timed traffic light system to reduce idling.					X	X		

Air Quality – Sensitive Receptors

Mitigation Measure or General/Area Plan Policy	Construction				Operational			
	CAPs	GHGs	TACs	Odors	CAPs	GHGs	TACs	Odors
Develop and adopt a comprehensive Community Risk Reduction Plan that includes: baseline inventory of TAC and $PM_{2.5}$ emissions from all sources, emissions reduction targets, and enforceable emission reduction strategies and performance measures. Community Risk Reduction Plan to include enforcement and monitoring tools to ensure regular review of progress toward the emission reduction targets, report progress to the public and responsible agencies, and revise the plan as appropriate.			X				X	
Require residential development projects and projects categorized as sensitive receptors to be located an adequate distance from existing and potential sources of TACs and odors.				X			X	X
Require new air pollution point sources such as, but not limited to, industrial, manufacturing, and processing facilities to be located an adequate distance from residential areas and other sensitive receptors.	X		X	X	X		X	X
Consult with BAAQMD to identify TAC sources and determine the need for and requirements of a health risk assessment for proposed developments.			X	X			X	X
Consult with project proponents during the pre-application review process to avoid inappropriate uses at affected sites and during the environmental review process for general plan amendments and general plan updates.					X		X	X
Require project proponents to prepare health risk assessments in accordance with BAAQMD-recommended procedures as part of environmental review when the proposed project has associated air-toxic emissions.			X				X	
Designate adequate industrial land in areas downwind and well-separated from sensitive uses.							X	X
Designate non-sensitive land uses for areas surrounding industrial sites.					X		X	X
Protect vacant industrial sites from encroachment by residential or other sensitive uses through appropriate zoning.					X		X	X
Require indoor air quality equipment, such as enhanced air filters, to be installed at schools, residences, and other sensitive receptor uses located near pollution sources.							X	X
Quantify the existing and added health risks to new sensitive receptors or for new sources.							X	
Utilize pollution absorbing trees and vegetation in buffer areas.					X	X	X	

Air Quality – PM_{10} and Dust Control

Mitigation Measure or General/Area Plan Policy	Construction				Operational			
	CAPs	GHGs	TACs	Odors	CAPs	GHGs	TACs	Odors
Include PM_{10} control measures as conditions of approval for subdivision maps, site plans, and grading permits.	X				X			
Minimize vegetation removal required for fire prevention.	X				X			
Require alternatives to discing, such as mowing, to the extent feasible. Where vegetation removal is required for aesthetic or property maintenance purposes, encourage or require alternatives to discing.	X	X			X	X		
Require subdivision designs and site planning to minimize grading and use landform grading in hillside areas.	X							
Condition grading permits to require that graded areas be stabilized from the completion of grading to commencement of construction.	X							
Require all access roads, driveways, and parking areas serving new commercial and industrial development to be constructed with materials that minimize particulate emissions and are appropriate to the scale and intensity of use.	X							
Develop a street cleaning program aimed at removing heavy silt loadings from roadways that result from sources such as storm water runoff and construction sites.	X				X			
Pave shoulders and pave or landscape medians. Curb and gutter installation may provide additional benefits where paving is contiguous to the curb.	X	X			X	X		

Water Conservation

Mitigation Measure or General/Area Plan Policy	Construction				Operational			
	CAPs	GHGs	TACs	Odors	CAPs	GHGs	TACs	Odors
Require residential remodels and renovations to improve plumbing fixture and fixture-fitting water efficiency by an established amount above the California Building Standards Code water efficiency standards.		X						
Provide water use audits to identify conservation opportunities and financial incentives for adopting identified efficiency measures.		X						
Require use of native and drought-tolerant plants, proper soil preparation, and efficient irrigation systems for landscaping.		X				X		
Maximize use of native, low-water plants for landscaping of areas adjacent to sidewalks or other impermeable surfaces.		X				X		
Increase use of recycled and reclaimed water for landscaping projects.		X				X		
Adopt a water-efficient landscaping ordinance and implement the Bay-Friendly Landscaping Guidelines established by StopWaste.org.						X		
Provide public water conservation education.						X		
Reduce pollutant runoff from new development through use of Best Management Practices.	X	X	X		X	X	X	
Minimize impervious surfaces and associated urban runoff pollutants in new development and reuse projects.	X	X	X		X	X	X	
Utilize permeable surfaces and green roof technologies where appropriate.					X	X	X	

Energy Conservation

Mitigation Measure or General/Area Plan Policy	Construction				Operational			
	CAPs	GHGs	TACs	Odors	CAPs	GHGs	TACs	Odors
Conduct energy efficiency audits of existing buildings by checking, repairing, and readjusting heating, ventilation, air conditioning, and lighting, water heating equipment, insulation and weatherization. Offer financial incentives for adoption of identified efficiency measures.		X				X		
Require implementation of energy-efficient design features in new development, including appropriate site orientation, exceedance of Title 24, use of light color roofing and building materials, and use of evergreen and wind-break trees to reduce heating and cooling fuel consumption.		X				X		
Adopt residential and commercial energy efficiency retrofit ordinances that require upgrades as a condition of issuing permits for renovations or additions, and on the sale of residences and buildings.		X				X		
Facilitate cooperation between neighboring development projects to use on-site renewable energy supplies or combined heat and power co-generation facilities.		X				X		
Develop a comprehensive renewable energy financing and informational program for residential and commercial uses.		X				X		
Partner with community services agencies to fund energy efficiency projects for low income residents.		X				X		
Encourage the installation of energy efficient fireplaces in lieu of normal open-hearth fireplaces. Prohibit installation of wood burning devices.	X	X			X	X		
Provide natural gas lines or electrical outlets to backyards to encourage the use of natural gas or electric barbecues, and electric gardening equipment.	X				X			
Implement Community Choice Aggregation (CCA) for renewable electricity generation.		X				X		

Solid Waste

Mitigation Measure or General/Area Plan Policy	Construction				Operational			
	CAPs	GHGs	TACs	Odors	CAPs	GHGs	TACs	Odors
Achieve established local and regional waste-reduction and diversion goals. Adopt more stringent waste reduction goals.		X				X		
Establish programs that enable residents to donate or recycle surplus furniture, old electronics, clothing, and other household items.		X				X		
Establish methane recovery in local landfills and wastewater treatment plants to generate electricity.		X				X		
Participate or initiate a composting program for restaurants and residences.						X		
Implement recycling programs for businesses and construction waste.	X	X			X	X		
Prohibit styrofoam containers and plastic bag use by businesses.					X	X		

9.6.4. Open Space Element

Community Forestry

Mitigation Measure or General/Area Plan Policy	Construction				Operational			
	CAPs	GHGs	TACs	Odors	CAPs	GHGs	TACs	Odors
Require inclusion of low VOC-emitting street trees and landscaping for all development projects.		X				X		
Require that trees larger than a specified diameter that are removed to accommodate development must be replaced at a set ratio.		X				X		
Provide adequate funding to manage and maintain the existing community forest, including sufficient funds for tree planting, pest control, scheduled pruning, and removal and replacement of dead trees.		X				X		
Provide public education regarding the benefits of street trees and the community forest.		X				X		

Sustainable Agriculture

Mitigation Measure or General/Area Plan Policy	Construction				Operational			
	CAPs	GHGs	TACs	Odors	CAPs	GHGs	TACs	Odors
Require agricultural practices be conducted in a manner that minimizes harmful effects on soils, air and water quality, and marsh and wildlife habitat. Sustainable agricultural practices should be addressed in the Qualified GHG Reduction Strategy to address climate change effects if relevant.	X	X			X	X		
Preserve forested areas, agricultural lands, wildlife habitat and corridors, wetlands, watersheds, groundwater recharge areas and other open spaces that provide carbon sequestration benefits.	X	X			X	X		
Establish a mitigation program for establishing conservation areas. Impose mitigation fees on development of such lands and use funds generated to protect existing, or create replacement, conservation areas.	X	X			X	X		
Require no-till farming, crop rotation, cover cropping, and residue farming.	X	X			X	X		
Require the use of appropriate vegetation within urban-agricultural buffer areas.		X				X		
Protect grasslands from conversion to non-agricultural uses.	X	X			X	X		
Support energy production activities that are compatible with agriculture, including biogas, wind and solar.		X				X		
Allow alternative energy projects in areas zoned for agriculture or open space where consistent with primary uses.		X				X		
Provide spaces within the community suitable for farmers markets.						X		
Promote local produce and garden programs at schools.						X		

Parks and Recreation

Mitigation Measure or General/Area Plan Policy	Construction				Operational			
	CAPs	GHGs	TACs	Odors	CAPs	GHGs	TACs	Odors
Expand and improve community recreation amenities including parks, pedestrian trails and connections to regional trail facilities.						X		
Require payment of park fees and/or dedication and provision of parkland, recreation facilities and/or multi-use trails as a condition upon new development.		X				X		
Encourage development of pocket parks in neighborhoods. Improve equal accessibility to park space across communities.		X				X		
Encourage joint use of parks with schools and community centers and facilities.		X				X		

9.6.5. Housing Element

Affordable Housing

Mitigation Measure or General/Area Plan Policy	Construction				Operational			
	CAPs	GHGs	TACs	Odors	CAPs	GHGs	TACs	Odors
Ensure a portion of future residential development is affordable to low and very low income households.		X				X		
Target local funds, including redevelopment and Community Development or Energy Efficiency Block Grant resources, to assist affordable housing developers in incorporating energy efficient designs and features.						X		
Adopt minimum residential densities in areas designated for transit-oriented, mixed use development to ensure higher density in these areas.					X	X		
Consult with the Housing Authority, transit providers, and developers to facilitate construction of low-income housing developments that employ transit-oriented and pedestrian-oriented design principles.					X	X		
Offer density-bonus incentives for projects that provide for infill, mixed use, and higher density residential development.					X	X		

9.6.6. Safety Element

Traffic Safety

Mitigation Measure or General/Area Plan Policy	Construction				Operational			
	CAPs	GHGs	TACs	Odors	CAPs	GHGs	TACs	Odors
Facilitate traffic safety for motorists and pedestrians through proper street design and traffic monitoring.					X	X		
Require traffic control devices, crosswalks, and pedestrian-oriented lighting within design of streets, sidewalks, trails, and school routes.					X	X		

A. CONSTRUCTION ASSESSMENT TOOLS

High Level Haulage Input Worksheet
High Level of Detail Fugitive Dust Quantification Method

Instructions: When using the *High Level of Detail* quantificaiton method to calculate fugitive dust emissions from cut/fill activities, BAAQMD recommends using this worksheet to calculate the on- and off-site haulage inputs for URBEMIS. If a project would involve both on-site and off-site cut/fill operations, the user should create two separate High Level Haulage Input Worksheets (i.e., one worksheet calculation for on-site and one for off-site).

Project Name:

Grading Activity/Phase:

User inputs
Input to use in URBEMIS
Calculation (do not change)

Cut/Fill Operations

Description	Amount	Units	Notes
Total Cut/Fill Volume	1,800	cubic yards	Enter information
Months of Activity	2	months	Enter information
Days of Activity	44	days	
Daily Cut/Fill Volume	40.91	cubic yards/day	

Soil Density by Soil Type and Condition

Soil Type	Bulk Density (grams/cubic centimeter)	Density (pounds/cubic yard)	Density (tons/cubic yard)
Sandy	1.69	2,849	1.42
Loamy Coarse-Loamy	1.63	2,747	1.37
Loamy Fine-Loamy	1.60	2,697	1.35
Loamy Coarse-Silty	1.60	2,697	1.35
Loamy Fine-Silty	1.54	2,596	1.30
Clayey 25-25% clay	1.49	2,511	1.26
Clayey >45% clay	1.39	2,343	1.17

Source: U.S. Department of Agriculture, Natural Resources Conservation Service, 2007. National Soil Survey Handbook, title 430-VI. [Online] Available at <http://soils.usda.gov/technical/handbook/>.

URBEMIS 2007 Ton-Mile Calculation

Description	Amount	Units	Notes
Soil Type	Loamy Coarse-Loamy		Use drop-down menu to select soil type. Assume Sandy unless project-specific soil type is known.
Soil Density	1.37	tons/cubic yard	Enter project specific soil density if known
Haul Distance (Round Trip On-Site)	0.04	miles	Enter distance
Ton-Mile per Day	2.25	ton-miles/day	

Notes:
On-site ton-mile assumes cut/fill volume is moved by scrapers.
Off-site ton-mile assumes cut/fill volume is moved by haul trucks.

URBEMIS Construction Modeling Data Needs/Requests

1) Construction Schedule
   Land use type and size to be developed
   Commencement and buildout date
   Duration and start date for each construction phase (e.g., demolition, grading, building construction)
   Identify any potential or planned overlap in phases

   Note: If project will be built out in multiple phases, provide information above for each phase.

2) Demolition
   Commencement date and duration of activities
   Total volume to be demolished
   Maximum daily volume to be demolished
   Haul truck capacity and distance to disposal site (URBEMIS defaults provided)
   Demolition equipment required (URBEMIS defaults provided)

   Note: URBEMIS estimates demolition construction equipment based on the land use being developed.

3) Grading (Mass and Fine)
   Commencement date and duration of activities
   Maximum daily acres disturbed (URBEMIS defaults provided)
   Volume of material to be cut and/or filled (cubic yards)
   Volume of material to be exported and/or exported (cubic yards)
   Construction equipment required

   Note: URBEMIS estimates grading construction equipment based on maximum daily acres disturbed.

4) Fugitive Dust
   A) Method 1 (Default)
      Maximum daily acres disturbed (URBEMIS defaults provided)

   B) Method 2 (Low Level of Detail)
      Duration of cut/fill operations
      Volume of material to be cut and/or filled (cubic yards)
      Origin of soil material (i.e., on-site or off-site)

   C) Method 3 (Medium Level of Detail)
      Duration of cut/fill operations
      Number of scrapers or haul trucks operating per day
      Hours of operation for each scraper or haul truck (scraper hours and haul truck hours)

   D) Method 4 (High Level of Detail)
      Duration of cut/fill operations
      Volume of material to be cut and/or filled (cubic yards)
      Bulk density of material (i.e., tons per cubic yard)
      Round trip distance required to move materials on-site (on-site miles only)

5) Asphalt Paving
   Commencement date and duration of activities
   Total acres to be paved
   Construction equipment required

   Note: URBEMIS estimates asphalt paving construction equipment based on total acres to be paved.

6) Architectural Coatings
   Commencement date and duration of activities

B. AIR QUALITY MODELING INSTRUCTIONS (URBEMIS)

This section provides detailed instructions for and examples of air quality modeling of operational and construction-related emissions pursuant to the methodological recommendations in this guide.

OPERATIONAL-RELATED EMISSIONS

URBEMIS Input Parameters

URBEMIS provides default values for Bay Area specific modeling parameters. Users may use the default values or provide project specific information when possible for more accurate emission quantification. BAAQMD-recommended input parameters and data requirements along with general URBEMIS user information for each operational-related activity are described below. Refer to the URBEMIS User's Guide and the BAAQMD Greenhouse Gas Model User's Manual (referred to collectively as the "User's Guide" below) for more detailed information.

Table B-1
URBEMIS Input Parameters for Operation Emissions

Operational Input Parameters	Guidance Principle
Air District	Bay Area Air District
Analysis Year	Earliest possible year when project would be operational
Land Use Type and Units	Based on project description
Trip Rate	From project traffic study, local trip rates, or ITE Trip Generation Manual
Project Location	Urban
Road Dust	Category should not be turned off but can be modified if project information is known
Pass-by Trips	See User's Guide for further instructions
Double Counting Correction	See User's Guide for further instructions
Percentage of Land Uses using Natural Gas	100 percent for both residential and nonresidential development
Persons per Residential Unit (Consumer Products)	Based on estimated number of residents
All Other URBEMIS Inputs	Use default values, unless project-specific data is available. See User's Guide for further instructions[1]

[1] The rationale for changing default values should be disclosed in the CEQA document

Land Use Type and Size

Choose each individual land use type (e.g., single family housing, apartment high rise, regional shopping center, or office park) that is most applicable to the proposed development project in the *Enter Land Use Data* module and enter the size of the project (e.g., acres, thousand square feet [ksf], students, dwelling units [du], rooms, pumps, rooms, or employees). Ensure that the unit type for the project-specific data is consistent with the unit type selected in URBEMIS. By default, URBEMIS estimates the trip generation rates for each land use type based on equations included in the ITE Trip Generation Manual. The trip rate represents the number of daily trips generated by a particular land use type by size. Override the default trip rate if project-specific data is available from the transportation analysis.

URBEMIS estimates the trip rate differently for residential land use types than for non-residential land use types. For residential land use types, URBEMIS adjusts the default trip rate based on residential density (i.e., dwelling units/residential acre). Overriding the default value for the number of acres for a residential land use type would automatically result in a change in the trip rate value. If both the number of acres and the trip rates for a residential development are known, enter the unit amount for the land use first, then adjust the acreage second, and then adjust the trip rate last. Select the *Submit* button after completing the *Enter Land Use Data* module.

For nonresidential land use types, URBEMIS uses a default trip rate value that is directly based on the unit amount entered into the *Enter Land Use Data* module. URBEMIS also assumes a Floor Area Ratio (FAR) of 0.5 for all nonresidential uses. The FAR is the ratio of the total floor area of a building to the size of the parcel on which it is located. Override the value in the acres data field based on the FAR for the proposed nonresidential land uses. URBEMIS does not adjust the default trip rate if the acre value is adjusted.

The *Enter Land Use Data* module includes a default worker commute trip percentage for all nonresidential land use types, which is used to estimate percentages of other commercial trip types in the *Enter Operational Data* module. The *Enter Land Use Data* module also contains default percentages of primary, diverted, and pass-by trips for all land use types, residential and non-residential. Primary trips are trips made for the specific purpose of visiting the generator and URBEMIS assumes that primary trips travel a full trip length; pass-by trips are trips made as intermediate stops on the way from an origin to another trip destination; and diverted-linked trips are trips attracted from the traffic volume on roadways in the vicinity of the generator but which require a diversion from that roadway to another roadway to gain access to the site. Pass-by and diverted-linked trips are assigned a shorter trip distance than primary trips. URBEMIS assumes that pass-by trips result in virtually no extra travel, with an assumed trip length of 0.1 mile. Diverted-linked trip lengths are assumed to equal 25 percent of the primary trip length. URBEMIS allows users to edit these data fields. URBEMIS incorporates this information for estimation of mobile-source emissions only if the check box for the Pass-by Trips category in the *Enter Operational Data* module is selected. When not selected, URBEMIS assumes all trips are primary trips. BAAQMD recommends reviewing the User's Guide for more information about when to use this feature. Additional discussion about pass-by trips is provided under the *Enter Operational Data* module guidance below.

When estimating emissions for a type of land use that is not listed in URBEMIS, select a similar land use type or add a new land use type on the Blank tab of the *Enter Land Use Data* module. When selecting a similar nonresidential land use type as a proxy, consider the worker commute trip percentage and the primary, diverted, and pass-by trip values. The name of the land use type is unimportant and can be overridden with new text if desired. BAAQMD recommends using one of the types of residential land uses listed in URBEMIS as a proxy when analyzing any type of unique residential project.

For unique nonresidential types of land uses, BAAQMD recommends either using another nonresidential land use type as a proxy or using a Blank land use type. If a new land use type is analyzed using a row on the Blank tab of the *Enter Land Use Data* module, enter a trip rate as URBEMIS does not provide default trip rate on the Blank tab. BAAQMD recommends using a trip rate from the ITE Trip Generation Manual, if an appropriate trip rate is available. If an applicable trip generation rate is not available, the lead agency should make a good faith effort to derive a trip generation rate for the proposed project.

Operational Data

The *Enter Operational Data* module allows users to estimate vehicle exhaust emissions from trips (and associated VMT) generated by a project. The module consists of seven operational

parameter categories including *Year & Vehicle Fleet*, *Trip Characteristics*, *Temperature Data*, *Variable Starts*, *Road Dust*, *Pass-by Trips*, and *Double-Counting Correction*. The first five operational categories are all needed to calculate vehicle exhaust emissions and cannot be turned off. Three of the seven operational categories can be turned off: *Road Dust*, *Pass-by Trips*, and *Double-Counting Correction*.

Guidance regarding each of the operational categories is provided below. In general, most of the default values for these seven source categories do not need to be changed, except where otherwise noted.

Year & Vehicle Fleet

The *Year & Vehicle Fleet* category allows users to specify the operational year for the project. Use the earliest possible year when the project would be operational to estimate worst-case operational emissions. Be aware that changing the project start year also changes the vehicle fleet mix. The default fleet mix values (i.e., *Fleet %, Vehicle Type*, *Non-Catalyst*, *Catalyst*, *Diesel*) are based on values from EMFAC using the year and the location of the project that is specified when users creates a new project in URBEMIS. The fleet mix should be modified only if it is known that the fleet mix for a project would be different from the average vehicle fleet mix in the project area. In that situation, select *Keep Current Fleet Mix When Changing Years*. Changes to the fleet mix data should be based on information provided by the transportation analysis and/or assumptions that are disclosed in the CEQA document. For instance, the fleet mix of motor vehicle trips generated by a school project would likely consist of a higher percentage of school buses and a lower percentage of motor homes and motorcycles than the URBEMIS average.

Trip Characteristics

The *Trip Characteristics* category includes trip data such as average speed, trip percentages, urban and rural trip lengths for different trip types. The trip percentages for home-based trips can be modified; however, it is not possible to modify the same for commercial-based trips, which URBEMIS calculates using the worker commute trip percentage entered in the *Enter Land Use Data* module. URBEMIS uses either the urban or rural trip length values depending on whether *Urban Project* or *Rural Project* is selected on the same screen. In general, the *Urban Project* option should be selected for most land use development projects under BAAQMD's jurisdiction. The trip length values can be changed if supported by information produced in a transportation analysis and/or reasonable assumptions about the project. For instance, the trip length for a proposed school might be adjusted according to the spatial distribution of the households that would be served by that school, particularly if the majority of trip generation would consist of parents driving their children to the school.

In addition to trip rate adjustments based on residential density, URBEMIS allows for modifications to vehicle trips based on other project characteristics. If specific project information is available for any land use type it should be reflected in the URBEMIS inputs. The table "URBEMIS Measures – Operational (Mobile-source) Measures" in Section 4.2 lists available measures to alter the trip rate to better reflect specific conditions. For example, if a project includes access to transit, URBEMIS trip rates can be adjusted between 0% and 15%. A 15% reduction in vehicle trips due to transit access would only be appropriate for a project that offers access to exceptional transit service. See the User's Guide for further instructions on all adjustments. Lead agencies must discuss and justify their reductions with substantial evidence.

Temperature Data

The *Temperature Data* category contains default ambient winter and summer temperature values which are used to estimate winter and summer emissions, respectively. The default temperature values in these data fields are specific to SFBAAB and should only be modified in consultation with BAAQMD.

Variable Starts
The *Variable Starts* parameter category shows the percentage of vehicles in several time classes (minutes since the vehicle engine was turned off) for the six trip types defined in the *Trip Characteristics* parameter category. This information is derived from the applicable EMFAC file and should only be modified in consultation BAAQMD.

Road Dust
The *Road Dust* parameter category allows users to specify the distribution of vehicle travel between paved and unpaved roads. This category is used to calculate entrained road dust emissions due to vehicle travel on paved and unpaved surfaces. Do not turn this category off, and users can adjust the percentage of travel on paved and unpaved roads if detailed project information is known.

Pass-by Trips
The *Pass-by Trips* parameter category can only be turned on or off. When selected, this category divides all the project-generated trips into primary, pass-by, and diverted-linked trips (entered as percentages in *Enter Land Use Data* module). When this category is not selected, URBEMIS assumes 100 percent of the project-generated trips are primary trips. Pass-by trips are trips made as intermediate stops on the way from an origin to a primary trip destination. URBEMIS accounts for these trips by setting the trip length to 0.1 miles for each pass-by trip. These trips are most important for retail and commercial land uses, such as gas stations and fast food restaurants. This option is not applicable to all land use types. For example, most of the trips to and from a *Warehouse* are typically expected to be primary trips and the *Pass-by Trips* option should not be used. This category check box should not be selected unless the percentage of pass-by trips is supported by a transportation analysis or a set of reasonable assumptions discussed in the CEQA document. If the trip length values in the *Trip Characteristics* category or the trip rate values in the Enter Land Use Data module are overwritten using information provided by a transportation analysis, be aware of whether the traffic data incorporated the occurrence of pass-by trips. If the *Pass-By Trips* checkbox is selected then the lead agency should discuss its reasoning for assuming that some of the project-generated vehicle trips would be considered pass-by trips.

Double-Counting Correction
The *Double-Counting Correction* parameter category is designed to account for internal trips between residential and nonresidential land uses. The *Double-Counting Correction* is applicable to mixed-use projects that include both residential and nonresidential land use types in the *Enter Land Use Data* module. For example, a residential trip and a retail trip generated by a mixed-use project may be the same trip. Users have the option of entering the number of internal trips between residential and nonresidential land uses in the *Enter the gross internal trip* as desired. The value entered represents the number of internal trips that would not be included in the emissions estimate. This category should not be used unless the transportation analysis or local transportation studies contain data to support the correction factor. In some cases, the transportation analysis may report project-specific trip generation that is already corrected for internal trips. Consult with a traffic engineer to determine the appropriate method to account for internal trips. The *Double-Counting Correction* checkbox should not be selected if detailed project information is unknown.

Area Source
The *Enter Area Source Data* module allows users to adjust the five area-source emission categories including, natural gas fuel combustion, hearth fuel combustion, landscape fuel combustion, consumer products, and architectural coatings. The natural gas, hearth, and landscape maintenance categories relate to on-site fuel combustion and the consumer products and architectural coatings categories address on-site evaporative emissions.

Guidance regarding each of the area-source categories is provided below. In general, most of the default values for these five source categories do not need to be changed except where otherwise noted in this guide.

Natural Gas Fuel Combustion
Parameters in the *Natural Gas Fuel Combustion* category are used to estimate the natural gas combustion emissions from space and water heating. On the *Natural Gas* tab the default percentage for land uses using natural gas should be changed to 100 percent for both residential and nonresidential land use types, as is representative of most development projects in the SFBAAB, unless project-specific data is available. Similarly, do not override the default natural gas usage values unless project-specific data is available.

Hearth Fuel Combustion
The *Hearth Fuel Combustion* category consists of separate tabs for *Hearth Percentages*, *Wood Stoves*, *Wood Fireplaces*, *Natural Gas Fireplaces*, and *Natural Gas Emission Factors*. Each of the tabs is discussed separately below.

- *Hearth Percentages*
  The parameters on the *Hearth Percentages* tab are applicable only to projects that include residential units. The default percentages should be used for the wood stoves, wood fireplaces, and wood stoves unless project-specific information is available. URBEMIS does not estimate emissions from any hearth types for nonresidential land use types.

- *Wood Stoves*
  On the *Wood Stoves* tab, the default percent values for the types of wood stoves (i.e., *Noncatalytic*, *Catalytic*, *Conventional*, and *Pellet*) should be changed in accordance with District Regulation 6, Rule 3, which allows only EPA-certified wood burning fireplaces and pellet stoves in new construction projects. The values for *Wood Burned*, *Wood Stove Usage*, and *Pounds in a Cord of Wood* should not be changed unless project-specific information is available.

- *Wood Fireplaces*
  The *Wood Fireplaces* tab is similar to the *Wood Stoves* tab. The emission factors on this tab cannot be modified. The values for *Wood Burned*, *Wood Stove Usage*, and *Pounds in a Cord of Wood* should not be changed unless project-specific information is available. District Regulation 6, Rule 3 allows only EPA-certified wood burning fireplaces in new construction projects.

- *Natural Gas Fireplaces*
  The values in the data fields on the *Natural Gas Fireplaces* tab should only be modified in the case that project-specific information is available that supports overriding default values.

- *Natural Gas Emission Factors*
  The emission factors contained in the *Natural Gas Emission Factors* tab cannot be modified. These values are used to estimate emissions from natural gas combustion in fireplaces/stoves and, according to the URBEMIS User's Guide, are based on U.S. Environmental Protection Agency Air Pollutant (AP-42) emission factors.

Landscape Fuel Combustion
The *Landscape Fuel Combustion* source category calculates on-site emissions from landscaping equipment such as lawn mowers, leaf blowers, chain saws, and hedge trimmers that are powered by internal combustion engines. On this tab, only adjust the value for the year being analyzed. The year entered into this field should be the earliest year when the project could become fully

operational. Landscaping emissions are estimated for the summer period only. URBEMIS uses emission rates from ARB's OFFROAD model to estimate of landscape maintenance equipment emissions.

Consumer Products
The *Consumer Products* source category is only relevant to projects that include residential land use types. The *Pounds of ROG (per person)* value should not be adjusted in this category. The persons per residential unit data field should be adjusted based on the estimated number of residents that would be supported by the proposed project, if available. The value should be consistent with the number of residents divided by the number of residential units.

Architectural Coating
Do not make changes to the values in the *Architectural Coating* source category without consulting BAAQMD.

EXAMPLE PROJECT OPERATIONAL-RELATED EMISSIONS CALCULATION

Description
The Example Project would develop a multi-story, mixed-use building that includes 40 units of residential condominium apartments, 50,000 square feet (or "50 thousand square feet" [ksf]) of offices and 35 ksf of retail land uses on an undeveloped 4.0-acre site. All of the residential condominium apartments would have natural gas lines for space heating but half of the units would be referred to as "suites" and include natural gas fireplaces. The regular apartments would not have natural gas fireplaces. Project construction would last two years beginning in 2010 and the project would be fully operational by 2013.

Screening Analysis
In the Land Use Module of URBEMIS (*Enter Land Use Data*) the corresponding Land Use Types of the proposed development would be Apartment High Rise units, General Office Building, and Strip Mall.

When each of the Land Use Types (i.e., Apartment High Rise units, General Office Building, and Strip Mall) is considered individually, their respective sizes would not exceed any of the District's Operational Screening Criteria (Table 3-1). However, because the project would contain more than one land use type, the operational screening levels cannot be used to assess the project's operational emissions, as explained in the discussion about the screening levels earlier in this guidance. The lead agency would be required to perform a detailed estimation of operational emissions using URBEMIS.

Emissions Quantification
When entering the proposed land uses into the Land Use Module, URBEMIS estimates the number of Acres for each Land Use Type assuming that each land use type would be constructed on separate lots. Using default values URBEMIS would assume this Example Project is 4.56 total acres (i.e., 0.65 acres for Apartment High Rise, 2.30 acres for General Office Building, and 1.61 acres for Strip Mall). For mixed-use and/or multi-level developments, the user should adjust the Acres for each of the proposed land uses such that the combined total acreage of all land use types is equal to the actual combined total size of the proposed project site (i.e., 4.0 acres, in this example) prior to running the model.

URBEMIS estimates the Trip Rate differently for residential land use types than for non-residential land use types. For residential land use types, URBEMIS adjusts the default Trip Rate based on residential density (i.e., dwelling units/residential acre). Therefore, overriding the default

value for the number of Acres assumed by URBEMIS for a residential land use type would automatically result in a change to the value assumed in the Trip Rate data field. If both the number of Acres and the Trip Rate for a residential development are known, the user should adjust the Acres field first, then adjust the Trip Rate field, and then click the Submit button. For nonresidential Land Use Types, URBEMIS uses a default value for in the Trip Rate data field that is directly based on the Unit Amt entered into the Land Use Module. The trip rates used by URBEMIS are based on standard rates from the ITE Trip Generation Manual. URBEMIS also assumes a Floor Area Ratio (FAR) of 0.5 for all nonresidential land use types. The FAR is the ratio of the total floor area of a building to the size of the parcel on which it is located. The user should override the value in the Acres data field based on the actual FAR for the development, as appropriate.

In the Area Source Module, Hearth Fuel Combustion category, the user should change the data fields for Wood Stoves, Wood Fireplaces, Natural Gas Fireplaces, and None (% w/o any hearth option) on the Hearth Percentages tab to 0, 0, 50, and 50, respectively to match the project description. In the Landscape Fuel Combustion source category the Year being Analyzed data field should be changed to 2013.

In the Operational Module the year data field in the Year & Vehicle Fleet category page should also be changed to 2013.

Lastly, the estimated daily and annual emissions of criteria air pollutants and precursors should be compared to the District's thresholds of significance (Table 2-2). If the daily or annual emissions would exceed the thresholds of significance, operational emissions would be considered significant and all feasible mitigation measures should be implemented to reduce these emissions.

CONSTRUCTION-RELATED EMISSIONS

Land Use Development Projects

URBEMIS includes a module (*Enter Construction Data*) that quantifies emissions from the following construction-related activity phases: demolition, mass and fine grading ("grading"), trenching, asphalt paving, building construction, and the application of architectural coatings.

URBEMIS Input Parameters

BAAQMD recommends input parameters and data requirements along with general URBEMIS user information for each construction-related activity phase below. Refer to the URBEMIS User's Manual for more detailed information. Appendix A contains a *Construction Data Needs Form* template that can be used to assist with requesting and gathering project-specific information.

Land Use Type and Size

Choose each individual land use type (e.g., single family housing, apartment high rise, regional shopping center, or office park) that is most applicable to the proposed development project in the *Enter Land Use Data* module and enter the size of the project (e.g., acres, thousand square feet [ksf], students, dwelling units [du], rooms, pumps, rooms, or employees). For several of the land use types, various size units are available (e.g., ksf and acres); ensure that the unit type for the project-specific data is consistent with the unit type selected in URBEMIS.

Schedule

The project schedule typically provides the number of months or days required for the completion of each construction-related activity phase (e.g., grading, building construction, asphalt paving), as well as the total duration of project construction. Where project-specific information is

available, modify URBEMIS default assumptions in *Click to Add, Delete, or Modify Phases* under the *Enter Construction Data* module. In this module, add or delete construction activities, add multiple similar construction activities (e.g., three grading phases), as well as overlap any construction activities as necessary. The URBEMIS default assumption for the number of work days per week is five, which inherently assumes that construction-related activities would only occur during weekdays, not on weekends. This can be altered if project-specific data is available in *Click to Add, Delete, or Modify Phases* under the construction phase setting *Work Days/Week.* For projects with specific phasing information (i.e., duration of each construction phase), but no definite construction commencement date, the earliest feasible start date should be used to be conservative. In addition, when project-specific information is not known, assume some overlap of construction phases (e.g., overlap of grading and asphalt paving activities or asphalt paving and building construction activities) to also be conservative. Please note that URBEMIS quantifies annual emissions on a calendar year basis (i.e., January to December) rather than the year-long period (running yearly average from the start date of construction) with the maximum amount of emissions.

Demolition

URBEMIS quantifies exhaust and fugitive PM dust emissions from demolition activities in the *Demolition Phase* within the *Enter Construction Data* module. Information to quantify emissions from this activity phase includes:

1. Duration of demolition (work days/week, phase start and end dates);
2. Total volume of building to be demolished (width, length, and height);
3. Maximum daily volume of building to be demolished (width, length, and height);
4. Haul truck capacity (cubic yards [yd^3]);
5. Haul truck trip length to disposal site (round trip miles); and
6. Off-road equipment requirements (number and type of equipment).

URBEMIS contains default assumptions for haul truck capacity (yd^3 per truck) and round trip distance (miles), if project-specific information is not available. URBEMIS also contains default assumptions for off-road equipment requirements. URBEMIS bases these on the size(s) of the proposed land use type(s) in the *Enter Land Use Data* module to estimate the off-road equipment requirements. In other words, URBEMIS assumes the size of the land use to be demolished is equal to the land use that would be developed. If the size(s) and/or type(s) of the land use(s) to be demolished are different from the land use(s) to be developed, create a separate URBEMIS run to quantify demolition emissions. Input the size and type of land use(s) for the different demolition building space versus the proposed building space in the *Enter Land Use Data* module for the separate URBEMIS run and only include the *Demolition* phase within the *Enter Construction Data* module.

Site Grading (Mass and Fine)

URBEMIS quantifies exhaust and fugitive PM dust emissions from grading activities in the *Site Grading* phase within the *Enter Construction Data* module. Information to quantify emissions from this activity phase includes, where applicable:

1. Duration of grading (work days/week, phase start and end dates);
2. Total acreage to be graded (acres);
3. Maximum daily acreage disturbed (acres per day);
4. Type and amount of cut/fill activities (yd^3 per day on- or off-site);
5. Description of soil hauling (amount of soil import/export [yd^3], haul truck capacity [yd^3 per truck], round trips per day, round trip distance [miles]); and

6. Off-road grading equipment requirements (number and type of equipment).

URBEMIS default assumptions for the total acreage to be graded and the maximum daily acreage disturbed are shown in the *Daily Acreage* tab within the *Site Grading* phase. Under the default settings, URBEMIS assumes that the maximum daily acreage disturbed is equivalent to 25 percent of the total acreage to be graded. Override this default assumption if more specific project information is available. The *Site Grading* phase consists of separate tabs for *Daily Acreage*, as mentioned above, *Fugitive Dust*, *Soil Hauling*, and *Site Grading Equipment*. Due to the differences in methodology and level of information required, each is discussed separately below.

Fugitive Dust
URBEMIS quantifies fugitive PM dust emissions in the *Site Grading* phase under the *Fugitive Dust* tab. URBEMIS provides four different levels of detail from which to select (i.e., default, low, medium, and high), described below.

Default: This method involves the use of the *Default Emission Rate* quantification methodology in the *Fugitive Dust* tab for which fugitive PM dust emissions are based on an emission rate (pound per disturbed acre per day [lb/acre-day]). This method should only be used when no project-specific information is known, or when no cut/fill activities would occur. Use the selection of the worst-case emission rate (i.e., 38.2 lb/acre-day) for extensive site preparation activities (e.g., cut/fill) where the exact type and amount (e.g., yd^3 per day on- or off-site) are not known, and selection of the average emission rate (i.e., 10 lb/acre-day) otherwise. The average emission rate would be used for projects that involve typical site grading activities, but no cut/fill or earthmoving activities.

Low: The *Low Level of Detail* quantification method should be used when cut/fill activities would occur and the amount of on-site and off-site cut/fill is known. Input the type and amount of cut/fill activities (yd^3 per day on- or off-site). On-site cut/fill activities involve soil movement within the boundaries of the project site via scrapers or graders, while off-site cut/fill activities involve soil movement outside of the boundaries of the project site via haul trucks. Projects that require off-site cut/fill should also enter the appropriate amount of soil import/export in the *Soil Hauling* tab, as discussed in more detail below.

Medium: The *Medium Level of Detail* quantification method should be used when cut/fill activities would occur and the required number of activity hours per day for on-site scrapers and off-site haul trucks is known. Input the number of hours per day for on-site scraper and off-site haul trucks conducting cut/fill activities. Input the total number of scraper-hours and/or haul truck-hours that are anticipated to occur per day. For example, if two scrapers would operate for eight hours per day each and three haul trucks would operate for four hours per day each, enter 16 for the *Onsite Scraper* parameter (i.e., 2 scrapers × 8 hours) and 12 for the *Offsite Haul* parameter (i.e., 3 haul trucks × 4 hours). Similar to the *Low Level of Detail* quantification method, on-site cut/fill activities involve soil movement within the boundaries of the project site via scrapers or graders, while off-site cut/fill activities involve soil movement outside of the boundaries of the project site via haul trucks. Projects that require off-site cut/fill should also enter the appropriate amount of soil import/export in the *Soil Hauling* tab, as discussed in more detail below.

High: The *High Level of Detail* quantification method should be used when cut/fill activities would occur and details about soil haulage is known. Input data on the amount of on- and off-site haulage (ton-miles per day) based on the total volume of cut/fill (yd^3), duration of the cut/fill activities (work days), density of soil being moved (tons per yd^3), and the scraper or haul truck round-trip distance (miles). A *High Level Haulage Input* worksheet that can be used to assist with

determining the amount of on- and off-site haulage (ton-miles per day) required for this method is contained in Appendix A.

Soil Hauling
URBEMIS quantifies entrained PM road dust and exhaust emissions from soil hauling in the *Soil Hauling* tab within the *Site Grading* phase. Information requirements include the amount of soil import/export (yd^3), round trips per day, round trip distance (miles), and haul truck capacity (yd^3 per truck). For round trip distance and haul truck capacity, URBEMIS provides default assumptions of 20 yd^3 per truck and 20 miles, respectively. Override the default assumptions if the project specific values are known.

Grading Equipment
URBEMIS quantifies exhaust emissions from on-site heavy-duty equipment in the *Site Grading Equipment* tab within the *Site Grading* phase. Information requirements include the type of equipment and quantity or amount, along with horsepower, load factor, and hours of operation per work day. URBEMIS provides default assumptions for all of these, primarily based on the amount of maximum daily acreage disturbed shown in the *Daily Acreage* tab. If project-specific grading equipment is known, click on the *All Checks Off* button and input the number for each type of equipment to be used for the project. Note that although the *All Checks Off* button will allow users to override the URBEMIS default equipment assumptions in the *Amount Model Uses* column, make sure to delete the previous URBEMIS default equipment selections prior to entering the project-specific equipment information.

Asphalt Paving
URBEMIS quantifies off-gas and exhaust emissions from asphalt paving activities in the *Paving* tab within the *Enter Construction Data* module. Information to quantify emissions from this activity phase includes the duration of asphalt paving (work days/week, phase start and end dates), total acreage to be paved, and off-road equipment requirements. URBEMIS includes default assumptions for the amount of asphalt to be paved based on the size of the proposed land use type(s) in the *Enter Land Use Data* module. Account for the size of project features (e.g., parking structure, roadways, and large hardtop fields) that would require asphalt paving in excess of default assumptions (i.e., standard site access and parking spaces) within the *Total Acreage to be Paved with Asphalt* parameter.

Architectural Coating
URBEMIS quantifies off-gas emissions from the application of architectural coatings in the *Arch Coating* tab within the *Enter Construction Data* module. Information to quantify emissions from this phase include the duration of activities (i.e., work days/week, phase start and end dates). URBEMIS includes default parameters for the volatile organic compound content per liter of coating based on BAAQMD's Regulation 8, Rule 3: Architectural Coating.

Construction Mitigation Measures
BAAQMD recommends that all proposed projects implement the *Basic Construction Mitigation Measures* listed in Table 8-1regardless of the significance determination. Where construction-related emissions would exceed the thresholds, the *Additional Construction Mitigation Measures* in Table 8-2 should be implemented. The methodology for quantifying criteria air pollutant and precursor emission reductions from fugitive PM dust and exhaust emissions are discussed below.

Fugitive Particulate Matter Dust Emissions
For quantification of fugitive PM dust-related *Basic Construction Mitigation Measures* in URBEMIS, select the *Mitigation* option in the *Enter Construction Data* module for the *Site Grading* phase. For *Site Grading Soil Disturbance Mitigation*, select (turn on) the soil stabilizing measure titled *Water exposed surfaces* along with the two times daily option without altering the default

percent reduction. For *Unpaved Roads Mitigation*, select the measure titled *Reduce speed on unpaved roads to less than 15 mph* without altering the default percent reduction. URBEMIS assumes that fugitive PM dust emissions from soil disturbance activities and travel on unpaved roads account for approximately 79 percent and 21 percent of total the fugitive PM dust emissions, respectively. URBEMIS will apply an approximate 53 percent reduction to total fugitive PM dust emissions for implementing the *Basic Construction Mitigation Measures* 1 through 5 in Table 8-1.

To account for the implementation of the *Additional Construction Mitigation Measures* 1 through 8, alter the default percent reduction to 63 percent, which would result in a total reduction of 75 percent in fugitive PM dust emissions. For *Site Grading Soil Disturbance Mitigation* select (turn on) the soil stabilizing measure titled *Equipment loading/unloading*.

In RoadMod, select water trucks to account for the implemented of the Basic Construction Mitigation Measures. Roadmod assumes an inherent 50 percent reduction in fugitive PM dust emissions when water trucks are selected.

Apply an additional 50 percent reduction to the fugitive PM dust emissions contained in the *Emission Estimates* tab of RoadMod to account for the implementation of the *Additional Construction Mitigation Measures* 1 through 8. The resulting total percent reduction from fugitive PM dust emissions would be 75 percent (i.e., 1 – (0.5 × 0.5)). The resultant amount of fugitive PM dust emissions should be added to the average daily mitigated exhaust PM emissions (methodology described below) to calculate the total amount of mitigated PM_{10} and $PM_{2.5}$ emissions.

Exhaust Emissions

A 5 percent reduction could be applied for NO_X, PM_{10}, and $PM_{2.5}$ to account for implementing measures 6 and 7 in the *Basic Construction Mitigation Measures.* For quantification in URBEMIS, select the *Mitigation* option in the *Enter Construction Data* module for the *Site Grading*, *Building Construction,* and *Asphalt Paving* phases, as applicable to the proposed project. Then for the *Off-Road Equipment Mitigation*, select (turn on) the measure titled *Use aqueous diesel fuel* and alter the default percent reduction for each.

To estimate exhaust emission reductions related to measure 10 in the *Additional Construction Mitigation Measures*, turn on the measure titled *Use aqueous diesel fuel* and alter the default percent reduction values to 20 percent for NO_X and 45 percent for PM_{10}, and $PM_{2.5}$. For the *Off-Road Equipment Mitigation* select (turn on) the measure titled *Diesel particulate filter* and alter the default percent reductions as listed in measure 10.

RoadMod does not calculate emission reductions associated with the implementation of the exhaust-related *Basic Construction Mitigation Measures*. To quantify the exhaust-related emission reductions associated with the implementation of the *Basic Construction Mitigation Measures*, rely on the information and data contained in the *Data Entry* and *Emission Estimates* tabs in RoadMod. Reductions in exhaust emissions should be quantified separately for each phase (i.e., Grubbing/Land Clearing, Grading/Excavation, Drainage/Utilities/ Sub-Grade, and Paving). First isolate the exhaust emissions from off-road (e.g., heavy-duty) equipment for each phase. Table B-1 below provides a cell reference for the *Data Entry* tab of RoadMod to assist with the identification and isolation of such emissions.

Once isolated, a 5 percent reduction could be applied to account for implementing measures 6 and 7 in the *Basic Construction Mitigation Measures* for NO_X, PM_{10}, and $PM_{2.5}$.

Emission reductions should be estimated by multiplying the total emissions for each compound by the anticipated emission reduction applicable for that compound to estimate the mitigated amount of emissions reductions.

Apply a 20 percent reduction for NO_X and a 45 percent reduction for PM_{10} and $PM_{2.5}$ to account for implementation of Measure 9 in the *Additional Construction Mitigation Measure*. To quantify the other exhaust-related emission reductions associated with the implementation of the *Additional Construction Mitigation Measures*, follow the same methodology described above for applying the reductions associated with the implementation of the *Basic Construction Mitigation Measures*.

Off-Gas Emissions

For quantification of off-gas-related *Additional Construction Mitigation Measures* (measure 11) first select the *Mitigation* option in the *Enter Construction Data* module for the *Architectural Coating* phase. Then select (turn on) the measures applicable to the proposed project and alter the default percent reduction as appropriate.

Linear Projects

For proposed projects that are linear in nature (e.g., road or levee construction, pipeline installation, transmission lines), use the most current version of Sacramento Metropolitan Air Quality Management District's (SMAQMD) Road Construction Emissions Model (RoadMod) to quantify construction-related criteria air pollutants and precursors. Similar to URBEMIS, RoadMod quantifies fugitive PM dust, exhaust, and off-gas emissions from the following construction-related activity phases: grubbing/land clearing, grading/excavation, drainage/utilities/sub-grade, and paving. Use RoadMod in accordance with the user instructions and default assumptions unless project-specific information is available. The default assumptions are applicable to projects located within the SFBAAB. Also, URBEMIS inherently accounts for the on-site construction of roadways and the installation of project infrastructure. If the proposed project involves off-site improvements that are linear in nature (e.g., roadway widening), use RoadMod in addition to URBEMIS to determine total emissions.

Table B-1
Roadway Construction Emissions Model
Cell Reference for Unmitigated Off-Road Equipment Emissions

Linear Construction Phase	NO_X	PM_{10}	$PM_{2.5}$
Grubbing/Land Clearing	G155	H155	I155
Grading/Excavation	G195	H195	I195
Drainage/Utilities/Sub-Grade	G235	H235	I235
Paving	G275	H275	I275

Notes: NO_X = oxides of nitrogen; $PM_{2.5}$ = fine particulate matter with an aerodynamic resistance diameter of 2.5 micrometers or less; PM_{10} = respirable particulate matter with an aerodynamic resistance diameter of 10 micrometers or less.
Cell references refer to the *Data Entry* tab from the SMAQMD Road Construction Emissions Model.
Source: SMAQMD 2009.

NO_X Emission Reduction
Emissions of NO_X (lb/day) × (1 – [NO_X percent reduction])

PM_{10} Emission Reduction
Emissions of PM_{10} (lb/day) × (1 – [PM_{10} percent reduction])

$PM_{2.5}$ Emission Reduction
Emissions of $PM_{2.5}$ (lb/day) × ([1 – [$PM_{2.5}$ percent reduction])

Users should use the *Emission Estimates* tab to calculate the total mitigated amount of emissions for each phase of construction. The total NO_X, PM_{10}, and $PM_{2.5}$ exhaust emissions for each phase are contained in cells E6 to E9, H6 to H9, and K6 to K9, respectively. To calculate the total amount of mitigated emissions, first subtract the unmitigated off-road equipment exhaust emissions from the total exhaust emissions to calculate total emissions without inclusion of off-road equipment exhaust emissions. Then, add the mitigated off-road exhaust emissions (calculated with the method described above) to the remaining emissions to calculate the total emissions with mitigated off-road construction equipment exhaust emissions. For PM_{10} and $PM_{2.5}$, add the mitigated exhaust emissions with the mitigated fugitive PM dust emissions (calculated by RoadMod) to calculate the total amount of mitigated PM_{10} and $PM_{2.5}$ emissions.

EXAMPLE PROJECT CONSTRUCTION-RELATED EMISSIONS CALCULATION

Description

This Example Project proposes development of 100 single-family residential units over a 2-year period. The project site would be approximately 33 acres (URBEMIS default assumption) and require an undetermined volume of fill materials to be imported to the site. In addition, the project would involve construction of a new access road to serve the development.

Screening Analysis

The project size is less than the construction screening level for single-family residential uses listed in Table 3-4. However, because the project includes the import of fill to the site, the construction screening levels cannot be used to address construction emissions. Therefore, a detailed quantitative analysis of construction-generated NO_X emissions should be performed using URBEMIS to estimate NO_X generated by construction of the residential units and using the RoadMod to estimate NO_X emissions from construction of the new access road.

Emissions Quantification

The size and type of land use proposed (i.e., single family housing) should be entered into the Land Use Module in URBEMIS. In this case, the project's total acres are equal to the default URBEMIS assumption and no override is necessary in the Acres data field. Modeling the construction emissions associated with single-family residential units in URBEMIS requires detailed information about the construction schedule (e.g., commencement date, types of construction activities required, and length of construction activities).

The fugitive PM dust emissions associated with fill activities should be estimated using the Fugitive Dust tab of the Mass Site Grading phase. For use of the Low Level of Detail quantification method, the volume of fill activities should be divided by the number of days that fill activities would occur. For example, if the project would require up to 20,000 yd^3 of fill materials to be imported over a minimum of 40 work days, the user should enter 500 (i.e., 20,000 yd^3 ÷ 40 days) into the Amount of Offsite Cut/Fill (cubic yards/day) data field. In addition, users should also input the total volume of fill materials to be imported into the Total Amount of Soil to Import (cubic yards) data field in the Soil Hauling tab. Off-road construction equipment for grading activities is estimated by URBEMIS based on the Maximum Daily Acreage Disturbed data field.

URBEMIS estimates the types and quantities of construction equipment in the Building Construction phase to develop the proposed project. For the Asphalt Paving phase, URBEMIS assumes the project requires asphalt paving for 25% of the total site. If more specific information can be provided, then user should turn off the Reset acreage with land use changes button in the Off Gas Emissions tab and override the Total Acreage to be Paved with Asphalt data field.

Due to the linear nature of the new access road to the project, daily mass emissions associated with its construction should be quantified using RoadMod. Users should obtain basic project information for the new access road and enter the information into the Data Entry tab of RoadMod. If project-specific information is not available RoadMod estimates the construction schedule for the road and the equipment used in each construction phase.

For analysis of the project's total average daily emissions, users should add emissions of each respective pollutant associated with development of the single-family residential units with the respective emissions associated with construction of the access road where construction activities are anticipated to overlap in the construction schedule. The average daily emissions of each pollutant that would occur throughout the entire construction period should be identified and compared with the District's threshold of significance. If the emissions would exceed the threshold of significance, construction emissions would be considered significant and all feasible mitigation measures to reduce emissions should be implemented.

The user should keep in mind that the District's numeric thresholds for construction emissions apply to exhaust emissions only. BAAQMD recommends implementation *of Basic Construction Mitigation Measures* to reduce fugitive dust emissions for all projects, and *Additional Construction Mitigation Measures* to reduce fugitive dust emissions for significant projects.

C. SAMPLE AIR QUALITY SETTING

The Bay Area Air Quality Management District (BAAQMD) is the regional air quality agency for the San Francisco Bay Area Air Basin (SFBAAB), which comprises all of Alameda, Contra Costa, Marin, Napa, San Francisco, San Mateo, and Santa Clara counties, the southern portion of Sonoma, and the southwestern portion of Solano County. Air quality in this area is determined by such natural factors as topography, meteorology, and climate, in addition to the presence of existing air pollution sources and ambient conditions. These factors along with applicable regulations are discussed below.

C.1.1. Climate, Topography, Air Pollution Potential

The SFBAAB is characterized by complex terrain, consisting of coastal mountain ranges, inland valleys, and bays, which distort normal wind flow patterns. The Coast Range splits resulting in a western coast gap, Golden Gate, and an eastern coast gap, Carquinez Strait, which allow air to flow in and out of the SFBAAB and the Central Valley.

The climate is dominated by the strength and location of a semi-permanent, subtropical high-pressure cell. During the summer, the Pacific high pressure cell is centered over the northeastern Pacific Ocean resulting in stable meteorological conditions and a steady northwesterly wind flow. Upwelling of cold ocean water from below to the surface because of the northwesterly flow produces a band of cold water off the California coast. The cool and moisture-laden air approaching the coast from the Pacific Ocean is further cooled by the presence of the cold water band resulting in condensation and the presence of fog and stratus clouds along the Northern California coast.

In the winter, the Pacific high-pressure cell weakens and shifts southward resulting in wind flow offshore, the absence of upwelling, and the occurrence of storms. Weak inversions coupled with moderate winds result in a low air pollution potential.

High Pressure Cell

During the summer, the large-scale meteorological condition that dominates the West Coast is a semi-permanent high pressure cell centered over the northeastern Pacific Ocean. This high pressure cell keeps storms from affecting the California coast. Hence, the SFBAAB experiences little precipitation in the summer months. Winds tend to blow on shore out of the north/northwest.

The steady northwesterly flow induces upwelling of cold water from below. This upwelling produces a band of cold water off the California coast. When air approaches the California coast, already cool and moisture-laden from its long journey over the Pacific, it is further cooled as it crosses this bank of cold water. This cooling often produces condensation resulting in a high incidence of fog and stratus clouds along the Northern California coast in the summer.

Generally in the winter, the Pacific high weakens and shifts southward, winds tend to flow offshore, upwelling ceases and storms occur. During the winter rainy periods, inversions (layers of warmer air over colder air; see below) are weak or nonexistent, winds are usually moderate and air pollution potential is low. The Pacific high does periodically become dominant, bringing strong inversions, light winds and high pollution potential.

Topography

The topography of the SFBAAB is characterized by complex terrain, consisting of coastal mountain ranges, inland valleys and bays. This complex terrain, especially the higher elevations, distorts the normal wind flow patterns in the SFBAAB. The greatest distortion occur when low-level inversions are present and the air beneath the inversion flows independently of air above the inversion, a condition that is common in the summer time.

The only major break in California's Coast Range occurs in the SFBAAB. Here the Coast Range splits into western and eastern ranges. Between the two ranges lies San Francisco Bay. The gap in the western coast range is known as the Golden Gate, and the gap in the eastern coast range is the Carquinez Strait. These gaps allow air to pass into and out of the SFBAAB and the Central Valley.

Wind Patterns

During the summer, winds flowing from the northwest are drawn inland through the Golden Gate and over the lower portions of the San Francisco Peninsula. Immediately south of Mount Tamalpais, the northwesterly winds accelerate considerably and come more directly from the west as they stream through the Golden Gate. This channeling of wind through the Golden Gate produces a jet that sweeps eastward and splits off to the northwest toward Richmond and to the southwest toward San Jose when it meets the East Bay hills.

Wind speeds may be strong locally in areas where air is channeled through a narrow opening, such as the Carquinez Strait, the Golden Gate or the San Bruno gap. For example, the average wind speed at San Francisco International Airport in July is about 17 knots (from 3 p.m. to 4 p.m.), compared with only 7 knots at San Jose and less than 6 knots at the Farallon Islands.

The air flowing in from the coast to the Central Valley, called the sea breeze, begins developing at or near ground level along the coast in late morning or early afternoon. As the day progresses, the sea breeze layer deepens and increases in velocity while spreading inland. The depth of the sea breeze depends in large part upon the height and strength of the inversion. If the inversion is low and strong, and hence stable, the flow of the sea breeze will be inhibited and stagnant conditions are likely to result.

In the winter, the SFBAAB frequently experiences stormy conditions with moderate to strong winds, as well as periods of stagnation with very light winds. Winter stagnation episodes are characterized by nighttime drainage flows in coastal valleys. Drainage is a reversal of the usual daytime air-flow patterns; air moves from the Central Valley toward the coast and back down toward the Bay from the smaller valleys within the SFBAAB.

Temperature

Summertime temperatures in the SFBAAB are determined in large part by the effect of differential heating between land and water surfaces. Because land tends to heat up and cool off more quickly than water, a large-scale gradient (differential) in temperature is often created between the coast and the Central Valley, and small-scale local gradients are often produced along the shorelines of the ocean and bays. The temperature gradient near the ocean is also exaggerated, especially in summer, because of the upwelling of cold ocean bottom water along the coast. On summer afternoons the temperatures at the coast can be 35°F cooler than temperatures 15 to 20 miles inland. At night this contrast usually decreases to less than 10°.

In the winter, the relationship of minimum and maximum temperatures is reversed. During the daytime the temperature contrast between the coast and inland areas is small, whereas at night the variation in temperature is large.

Precipitation

The SFBAAB is characterized by moderately wet winters and dry summers. Winter rains account for about 75 percent of the average annual rainfall. The amount of annual precipitation can vary greatly from one part of the SFBAAB to another even within short distances. In general, total annual rainfall can reach 40 inches in the mountains, but it is often less than 16 inches in sheltered valleys.

During rainy periods, ventilation (rapid horizontal movement of air and injection of cleaner air) and vertical mixing are usually high, and thus pollution levels tend to be low. However, frequent dry periods do occur during the winter where mixing and ventilation are low and pollutant levels build up.

Air Pollution Potential

The potential for high pollutant concentrations developing at a given location depends upon the quantity of pollutants emitted into the atmosphere in the surrounding area or upwind, and the ability of the atmosphere to disperse the contaminated air. The topographic and climatological factors discussed above influence the atmospheric pollution potential of an area. Atmospheric pollution potential, as the term is used here, is independent of the location of emission sources and is instead a function of factors described below.

Wind Circulation

Low wind speed contributes to the buildup of air pollution because it allows more pollutants to be emitted into the air mass per unit of time. Light winds occur most frequently during periods of low sun (fall and winter, and early morning) and at night. These are also periods when air pollutant emissions from some sources are at their peak, namely, commute traffic (early morning) and wood burning appliances (nighttime). The problem can be compounded in valleys, when weak flows carry the pollutants upvalley during the day, and cold air drainage flows move the air mass downvalley at night. Such restricted movement of trapped air provides little opportunity for ventilation and leads to buildup of pollutants to potentially unhealthful levels.

Wind-roses provide useful information for communities that contain industry, landfills or other potentially odorous or noxious land uses. Each wind-rose diagram provides a general indication of the proportion of time that winds blow from each compass direction. The longer the vector length, the greater the frequency of wind occurring from that direction. Such information may be particularly useful in planning buffer zones. For example, sensitive receptors such as residential developments, schools or hospitals are inappropriate uses immediately downwind from facilities that emit toxic or odorous pollutants, unless adequate separation is provided by a buffer zone. Caution should be taken in using wind-roses in planning and environmental review processes. A site on the opposite side of a hill or tall building, even a short distance from a meteorological monitoring station, may experience a significant difference in wind pattern. Consult BAAQMD meteorologists if more detailed wind circulation information is needed.

Inversions

An inversion is a layer of warmer air over a layer of cooler air. Inversions affect air quality conditions significantly because they influence the mixing depth, i.e., the vertical depth in the atmosphere available for diluting air contaminants near the ground. The highest air pollutant concentrations in the SFBAAB generally occur during inversions.

There are two types of inversions that occur regularly in the SFBAAB. One is more common in the summer and fall, while the other is most common during the winter. The frequent occurrence of elevated temperature inversions in summer and fall months acts to cap the mixing depth, limiting the depth of air available for dilution. Elevated inversions are caused by subsiding air from the subtropical high pressure zone, and from the cool marine air layer that is drawn into the SFBAAB by the heated low pressure region in the Central Valley.

The inversions typical of winter, called radiation inversions, are formed as heat quickly radiates from the earth's surface after sunset, causing the air in contact with it to rapidly cool. Radiation inversions are strongest on clear, low-wind, cold winter nights, allowing the build-up of such pollutants as carbon monoxide and particulate matter. When wind speeds are low, there is little mechanical turbulence to mix the air, resulting in a layer of warm air over a layer of cooler air next

to the ground. Mixing depths under these conditions can be as shallow as 50 to 100 meters, particularly in rural areas. Urban areas usually have deeper minimum mixing layers because of heat island effects and increased surface roughness. During radiation inversions downwind transport is slow, the mixing depths are shallow, and turbulence is minimal, all factors which contribute to ozone formation.

Although each type of inversion is most common during a specific season, either inversion mechanism can occur at any time of the year. Sometimes both occur simultaneously. Moreover, the characteristics of an inversion often change throughout the course of a day. The terrain of the SFBAAB also induces significant variations among subregions.

Solar Radiation

The frequency of hot, sunny days during the summer months in the SFBAAB is another important factor that affects air pollution potential. It is at the higher temperatures that ozone is formed. In the presence of ultraviolet sunlight and warm temperatures, reactive organic gases and oxides of nitrogen react to form secondary photochemical pollutants, including ozone.

Because temperatures in many of the SFBAAB inland valleys are so much higher than near the coast, the inland areas are especially prone to photochemical air pollution.

In late fall and winter, solar angles are low, resulting in insufficient ultraviolet light and warming of the atmosphere to drive the photochemical reactions. Ozone concentrations do not reach significant levels in the SFBAAB during these seasons.

Sheltered Terrain

The hills and mountains in the SFBAAB contribute to the high pollution potential of some areas. During the day, or at night during windy conditions, areas in the lee sides of mountains are sheltered from the prevailing winds, thereby reducing turbulence and downwind transport. At night, when wind speeds are low, the upper atmospheric layers are often decoupled from the surface layers during radiation conditions. If elevated terrain is present, it will tend to block pollutant transport in that direction. Elevated terrain also can create a recirculation pattern by inducing upvalley air flows during the day and reverse downvalley flows during the night, allowing little inflow of fresh air.

The areas having the highest air pollution potential tend to be those that experience the highest temperatures in the summer and the lowest temperatures in the winter. The coastal areas are exposed to the prevailing marine air , creating cooler temperatures in the summer, warmer temperatures in winter, and stratus clouds all year. The inland valleys are sheltered from the marine air and experience hotter summers and colder winters. Thus, the topography of the inland valleys creates conditions conducive to high air pollution potential.

Pollution Potential Related to Emissions

Although air pollution potential is strongly influenced by climate and topography, the air pollution that occurs in a location also depends upon the amount of air pollutant emissions in the surrounding area or transported from more distant places. Air pollutant emissions generally are highest in areas that have high population densities, high motor vehicle use and/or industrialization. These contaminants created by photochemical processes in the atmosphere, such as ozone, may result in high concentrations many miles downwind from the sources of their precursor chemicals.

Climatological Subregions

This section discusses the varying climatological and topographic conditions, and the resulting variations in air pollution potential, within inhabited subregions of the SFBAAB. All urbanized areas of the SFBAAB are included in one of 11 climatological subregions. Sparsely inhabited

areas are excluded from the subregional designations. Some of the climatological subregions discussed in this appendix overlap county boundaries. The Lead Agencies analyzing projects located close to the boundary between subregions may need to examine the characteristics of the neighboring subregions to adequately evaluate potential air quality impacts.

The information about each subregion includes location, topography and climatological factors relevant to air quality. Where relevant to air quality concerns, more localized subareas within a subregion are discussed. Each subregional section concludes with a discussion of pollution potential resulting from climatological and topographic variables and the major types of air pollutant sources in the subregion.

Carquinez Strait Region

The Carquinez Strait runs from Rodeo to Martinez. It is the only sea-level gap between the Bay and the Central Valley. The subregion includes the lowlands bordering the strait to the north and south, and includes the area adjoining Suisun Bay and the western part of the Sacramento-San Joaquin Delta as far east as Bethel Island. The subregion extends from Rodeo in the southwest and Vallejo in the northwest to Fairfield on the northeast and Brentwood on the southeast.

Prevailing winds are from the west in the Carquinez Strait. During the summer and fall months, high pressure offshore coupled with low pressure in the Central Valley causes marine air to flow eastward through the Carquinez Strait. The wind is strongest in the afternoon. Afternoon wind speeds of 15 to 20 mph are common throughout the strait region. Annual average wind speeds are 8 mph in Martinez, and 9 to 10 mph further east. Sometimes atmospheric conditions cause air to flow from the east. East winds usually contain more pollutants than the cleaner marine air from the west. In the summer and fall months, this can cause elevated pollutant levels to move into the central SFBAAB through the strait. These high pressure periods are usually accompanied by low wind speeds, shallow mixing depths, higher temperatures and little or no rainfall.

Summer mean maximum temperatures reach about 90° F. in the subregion. Mean minimum temperatures in the winter are in the high 30's. Temperature extremes are especially pronounced in sheltered areas farther from the moderating effects of the strait itself, e.g. at Fairfield.

Many industrial facilities with significant air pollutant emissions — e.g., chemical plants and refineries — are located within the Carquinez Strait Region. The pollution potential of this area is often moderated by high wind speeds. However, upsets at industrial facilities can lead to short-term pollution episodes, and emissions of unpleasant odors may occur at anytime. Receptors downwind of these facilities could suffer more long-term exposure to air contaminants than individuals elsewhere., It is important that local governments and other Lead Agencies maintain buffers zones around sources of air pollution sufficient to avoid adverse health and nuisance impacts on nearby receptors. Areas of the subregion that are traversed by major roadways, e.g. Interstate 80, may also be subject to higher local concentrations of carbon monoxide and particulate matter, as well as certain toxic air contaminants such as benzene.

Cotati and Petaluma Valleys

The subregion that stretches from Santa Rosa to the San Pablo Bay is often considered as two different valleys: the Cotati Valley in the north and the Petaluma Valley in the south. To the east, the valley is bordered by the Sonoma Mountains, while to the west is a series of low hills, followed by the Estero Lowlands, which open to the Pacific Ocean. The region from the Estero Lowlands to the San Pablo Bay is known as the Petaluma Gap. This low-terrain area allows marine air to travel into the SFBAAB.

Wind patterns in the Petaluma and Cotati Valleys are strongly influenced by the Petaluma Gap, with winds flowing predominantly from the west. As marine air travels through the Petaluma Gap, it splits into northward and southward paths moving into the Cotati and Petaluma valleys. The

southward path crosses San Pablo Bay and moves eastward through the Carquinez Strait. The northward path contributes to Santa Rosa's prevailing winds from the south and southeast. Petaluma's prevailing winds are from the northwest.

When the ocean breeze is weak, strong winds from the east can predominate, carrying pollutants from the Central Valley and the Carquinez Strait. During these periods, upvalley flows can carry the polluted air as far north as Santa Rosa.

Winds are usually stronger in the Petaluma Valley than the Cotati Valley because the former is directly in line with the Petaluma Gap. Petaluma's climate is similar to areas closer to the coast even though Petaluma is 28 miles from the ocean. Average annual wind speed at the Petaluma Airport is seven mph. The Cotati Valley, being slightly north of the Petaluma Gap, experiences lower wind speeds. The annual average wind speed in Santa Rosa is five mph.

Air temperatures are very similar in the two valleys. Summer maximum temperatures for this subregion are in the low-to-mid-80's, while winter maximum temperatures are in the high-50's to low-60's. Summer minimum temperatures are around 50 degrees, and winter minimum temperatures are in the high 30's.

Generally, air pollution potential is low in the Petaluma Valley because of its link to the Petaluma Gap and because of its low population density. There are two scenarios that could produce elevated pollutant levels: 1) stagnant conditions in the morning hours created when a weak ocean breeze meets a weak bay breeze, and 2) an eastern or southeastern wind pattern in the afternoon brings in pollution from the Carquinez Strait Region and the Central Valley.

The Cotati Valley has a higher pollution potential than does the Petaluma Valley. The Cotati Valley lacks a gap to the sea, contains a larger population and has natural barriers at its northern and eastern ends. There are also industrial facilities in and around Santa Rosa. Both valleys of this subregion are also threatened by increased motor vehicle traffic and the associated air contaminants. Population and motor vehicle use are increasing significantly, and housing costs and the suburbanization of employment are leading to more and longer commutes traversing the subregion.

Diablo and San Ramon Valleys

East of the Coast Range lay the Diablo and San Ramon Valleys. The valleys have a northwest to southeast orientation, with the northern portion known as Diablo Valley and the southern portion as San Ramon Valley. The Diablo Valley is bordered in the north by the Carquinez Strait and in the south by the San Ramon Valley. The San Ramon Valley is long and narrow and extends south from Walnut Creek to Dublin. At its southern end it opens onto the Amador Valley.

The mountains on the west side of these valleys block much of the marine air from reaching the valleys. During the daytime, there are two predominant flow patterns: an upvalley flow from the north and a westerly flow (wind from the west) across the lower elevations of the Coast Range. On clear nights, surface inversions separate the flow of air into two layers: the surface flow and the upper layer flow. When this happens, there are often drainage surface winds which flow downvalley toward the Carquinez Strait.

Wind speeds in these valleys generally are low. Monitoring stations in Concord and Danville report annual average wind speeds of 5 mph. Winds can increase in the afternoon near San Ramon because it is located at the eastern edge of the Crow Canyon gap. Through this gap, polluted air from cities near the Bay travels to the valley in the summer months.

Air temperatures in these valleys are cooler in the winter and warmer in the summer than are temperatures further west, as these valleys are far from the moderating effect of the Bay and

ocean. Mean summer maximum temperatures are in the low- to mid-80's. Mean winter minimum temperatures are in the high-30's to low-40's.

Pollution potential is relatively high in these valleys. On winter evenings, light winds combined with surface-based inversions and terrain that restricts air flow can cause pollutant levels to build up. San Ramon Valley can experience high pollution concentrations due to motor vehicle emissions and emissions from fireplaces and wood stoves. In the summer months, ozone and ozone precursors are often transported into the valleys from both the central SFBAAB and the Central Valley.

Livermore Valley

The Livermore Valley is a sheltered inland valley near the eastern border of SFBAAB. The western side of the valley is bordered by 1,000 to 1,500 foot hills with two gaps connecting the valley to the central SFBAAB, the Hayward Pass and Niles Canyon. The eastern side of the valley also is bordered by 1,000 to 1,500 foot hills with one major passage to the San Joaquin Valley called the Altamont Pass and several secondary passages. To the north lie the Black Hills and Mount Diablo. A northwest to southeast channel connects the Diablo Valley to the Livermore Valley. The south side of the Livermore Valley is bordered by mountains approximately 3,000 to 3,500 feet high.

During the summer months, when there is a strong inversion with a low ceiling, air movement is weak and pollutants become trapped and concentrated. Maximum summer temperatures in the Livermore Valley range from the high-80's to the low-90's, with extremes in the 100's. At other times in the summer, a strong Pacific high pressure cell from the west, coupled with hot inland temperatures causes a strong onshore pressure gradient which produces a strong, afternoon wind. With a weak temperature inversion, air moves over the hills with ease, dispersing pollutants.

In the winter, with the exception of an occasional storm moving through the area, air movement is often dictated by local conditions. At night and early morning, especially under clear, calm and cold conditions, gravity drives cold air downward. The cold air drains off the hills and moves into the gaps and passes. On the eastern side of the valley the prevailing winds blow from north, northeast and east out of the Altamont Pass. Winds are light during the late night and early morning hours. Winter daytime winds sometimes flow from the south through the Altamont Pass to the San Joaquin Valley. Average winter maximum temperatures range from the high-50's to the low-60's, while minimum temperatures are from the mid-to-high-30's, with extremes in the high teens and low-20's.

Air pollution potential is high in the Livermore Valley, especially for photochemical pollutants in the summer and fall. High temperatures increase the potential for ozone to build up. The valley not only traps locally generated pollutants but can be the receptor of ozone and ozone precursors from San Francisco, Alameda, Contra Costa and Santa Clara counties. On northeasterly wind flow days, most common in the early fall, ozone may be carried west from the San Joaquin Valley to the Livermore Valley.

During the winter, the sheltering effect of the valley, its distance from moderating water bodies, and the presence of a strong high pressure system contribute to the development of strong, surface-based temperature inversions. Pollutants such as carbon monoxide and particulate matter, generated by motor vehicles, fireplaces and agricultural burning, can become concentrated. Air pollution problems could intensify because of population growth and increased commuting to and through the subregion.

Marin County Basins

Marin County is bounded on the west by the Pacific Ocean, on the east by San Pablo Bay, on the south by the Golden Gate and on the north by the Petaluma Gap. Most of Marin's population lives in the eastern part of the county, in small, sheltered valleys. These valleys act like a series of miniature air basins.

Although there are a few mountains above 1500 feet, most of the terrain is only 800 to 1000 feet high, which usually is not high enough to block the marine layer. Because of the wedge shape of the county, northeast Marin County is further from the ocean than is the southeastern section. This extra distance from the ocean allows the marine air to be moderated by bayside conditions as it travels to northeastern Marin County. In southern Marin the distance from the ocean is short and elevations are lower, resulting in higher incidence of maritime air in that area.

Wind speeds are highest along the west coast of Marin, averaging about 8 to 10 miles per hour. The complex terrain in central Marin creates sufficient friction to slow the air flow. At Hamilton Air Force Base, in Novato, the annual average wind speeds are only 5 mph. The prevailing wind directions throughout Marin County are generally from the northwest.

In the summer months, areas along the coast are usually subject to onshore movement of cool marine air. In the winter, proximity to the ocean keeps the coastal regions relatively warm, with temperatures varying little throughout the year. Coastal temperatures are usually in the high-50's in the winter and the low-60's in the summer. The warmest months are September and October.

The eastern side of Marin County has warmer weather than the western side because of its distance from the ocean and because the hills that separate eastern Marin from western Marin occasionally block the flow of the marine air. The temperatures of cities next to the Bay are moderated by the cooling effect of the Bay in the summer and the warming effect of the Bay in the winter. For example, San Rafael experiences average maximum summer temperatures in the low-80's and average minimum winter temperatures in the low-40’s. Inland towns such as Kentfield experience average maximum temperatures that are two degrees cooler in the winter and two degrees warmer in the summer.

Air pollution potential is highest in eastern Marin County, where most of population is located in semi-sheltered valleys. In the southeast, the influence of marine air keeps pollution levels low. As development moves further north, there is greater potential for air pollution to build up because the valleys are more sheltered from the sea breeze. While Marin County does not have many polluting industries, the air quality on its eastern side — especially along the U.S. 101 corridor — may be affected by emissions from increasing motor vehicle use within and through the county.

Napa Valley

The Napa Valley is bordered by relatively high mountains. With an average ridge line height of about 2000 feet, with some peaks approaching 3000 to 4000 feet, these mountains are effective barriers to the prevailing northwesterly winds. The Napa Valley is widest at its southern end and narrows in the north.

During the day, the prevailing winds flow upvalley from the south about half of the time. A strong upvalley wind frequently develops during warm summer afternoons, drawing air in from the San Pablo Bay. Daytime winds sometimes flow downvalley from the north. During the evening, especially in the winter, downvalley drainage often occurs. Wind speeds are generally low, with almost 50 percent of the winds less than 4 mph. Only 5 percent of the winds are between 16 and 18 mph, representing strong summertime upvalley winds and winter storms.

Summer average maximum temperatures are in the low 80's at the southern end of the valley and in the low 90's at the northern end. Winter average maximum temperatures are in the high-

50's and low-60's, and minimum temperatures are in the high to mid 30's with the slightly cooler temperatures in the northern end.

The air pollution potential in the Napa Valley could be high if there were sufficient sources of air contaminants nearby. Summer and fall prevailing winds can transport ozone precursors northward from the Carquinez Strait Region to the Napa Valley, effectively trapping and concentrating the pollutants when stable conditions are present. The local upslope and downslope flows created by the surrounding mountains may also recirculate pollutants already present, contributing to buildup of air pollution. High ozone concentrations are a potential problem to sensitive crops such as wine grapes, as well as to human health. The high frequency of light winds and stable conditions during the late fall and winter contribute to the buildup of particulate matter from motor vehicles, agriculture and wood burning in fireplaces and stoves.

Northern Alameda and Western Contra Costa Counties

This climatological subregion stretches from Richmond to San Leandro. Its western boundary is defined by the Bay and its eastern boundary by the Oakland-Berkeley Hills. The Oakland-Berkeley Hills have a ridge line height of approximately 1500 feet, a significant barrier to air flow. The most densely populated area of the subregion lies in a strip of land between the Bay and the lower hills.

In this area, marine air traveling through the Golden Gate, as well as across San Francisco and through the San Bruno Gap, is a dominant weather factor. The Oakland-Berkeley Hills cause the westerly flow of air to split off to the north and south of Oakland, which causes diminished wind speeds. The prevailing winds for most of this subregion are from the west. At the northern end, near Richmond, prevailing winds are from the south-southwest.

Temperatures in this subregion have a narrow range due to the proximity of the moderating marine air. Maximum temperatures during summer average in the mid-70's, with minimums in the mid-50's. Winter highs are in the mid- to high-50's, with lows in the low- to mid-40's.

The air pollution potential is lowest for the parts of the subregion that are closest to the bay, due largely to good ventilation and less influx of pollutants from upwind sources. The occurrence of light winds in the evenings and early mornings occasionally causes elevated pollutant levels.

The air pollution potential at the northern (Richmond) and southern (Oakland, San Leandro) parts of this subregion is marginally higher than communities directly east of the Golden Gate, because of the lower frequency of strong winds.

This subregion contains a variety of industrial air pollution sources. Some industries are quite close to residential areas. The subregion is also traversed by frequently congested major freeways. Traffic and congestion, and the motor vehicle emissions they generate, are increasing.

Peninsula

The peninsula region extends from northwest of San Jose to the Golden Gate. The Santa Cruz Mountains run up the center of the peninsula, with elevations exceeding 2000 feet at the southern end, decreasing to 500 feet in South San Francisco. Coastal towns experience a high incidence of cool, foggy weather in the summer. Cities in the southeastern peninsula experience warmer temperatures and fewer foggy days because the marine layer is blocked by the ridgeline to the west. San Francisco lies at the northern end of the peninsula. Because most of San Francisco's topography is below 200 feet, marine air is able to flow easily across most of the city, making its climate cool and windy.

The blocking effect of the Santa Cruz Mountains results in variations in summertime maximum temperatures in different parts of the peninsula. For example, in coastal areas and San Francisco

the mean maximum summer temperatures are in the mid-60's, while in Redwood City the mean maximum summer temperatures are in the low-80's. Mean minimum temperatures during the winter months are in the high-30's to low-40's on the eastern side of the Peninsula and in the low 40's on the coast.

Two important gaps in the Santa Cruz Mountains occur on the peninsula. The larger of the two is the San Bruno Gap, extending from Fort Funston on the ocean to the San Francisco Airport. Because the gap is oriented in the same northwest to southeast direction as the prevailing winds, and because the elevations along the gap are less than 200 feet, marine air is easily able to penetrate into the bay. The other gap is the Crystal Springs Gap, between Half Moon Bay and San Carlos. As the sea breeze strengthens on summer afternoons, the gap permits maritime air to pass across the mountains, and its cooling effect is commonly seen from San Mateo to Redwood City.

Annual average wind speeds range from 5 to 10 mph throughout the peninsula, with higher wind speeds usually found along the coast. Winds on the eastern side of the peninsula are often high in certain areas, such as near the San Bruno Gap and the Crystal Springs Gap.

The prevailing winds along the peninsula's coast are from the west, although individual sites can show significant differences. For example, Fort Funston in western San Francisco shows a southwest wind pattern while Pillar Point in San Mateo County shows a northwest wind pattern. On the east side of the mountains winds are generally from the west, although wind patterns in this area are often influenced greatly by local topographic features.

Air pollution potential is highest along the southeastern portion of the peninsula. This is the area most protected from the high winds and fog of the marine layer. Pollutant transport from upwind sites is common. In the southeastern portion of the peninsula, air pollutant emissions are relatively high due to motor vehicle traffic as well as stationary sources. At the northern end of the peninsula in San Francisco, pollutant emissions are high, especially from motor vehicle congestion. Localized pollutants, such as carbon monoxide, can build up in "urban canyons." Winds are generally fast enough to carry the pollutants away before they can accumulate.

Santa Clara Valley

The Santa Clara Valley is bounded by the Bay to the north and by mountains to the east, south and west. Temperatures are warm on summer days and cool on summer nights, and winter temperatures are fairly mild. At the northern end of the valley, mean maximum temperatures are in the low-80's during the summer and the high-50's during the winter, and mean minimum temperatures range from the high-50's in the summer to the low-40's in the winter. Further inland, where the moderating effect of the Bay is not as strong, temperature extremes are greater. For example, in San Martin, located 27 miles south of the San Jose Airport, temperatures can be more than 10 degrees warmer on summer afternoons and more than 10 degrees cooler on winter nights.

Winds in the valley are greatly influenced by the terrain, resulting in a prevailing flow that roughly parallels the valley's northwest-southeast axis. A north-northwesterly sea breeze flows through the valley during the afternoon and early evening, and a light south-southeasterly drainage flow occurs during the late evening and early morning. In the summer the southern end of the valley sometimes becomes a "convergence zone," when air flowing from the Monterey Bay gets channeled northward into the southern end of the valley and meets with the prevailing north-northwesterly winds.

Wind speeds are greatest in the spring and summer and weakest in the fall and winter. Nighttime and early morning hours frequently have calm winds in all seasons, while summer afternoons and

evenings are quite breezy. Strong winds are rare, associated mostly with the occasional winter storm.

The air pollution potential of the Santa Clara Valley is high. High summer temperatures, stable air and mountains surrounding the valley combine to promote ozone formation. In addition to the many local sources of pollution, ozone precursors from San Francisco, San Mateo and Alameda Counties are carried by prevailing winds to the Santa Clara Valley. The valley tends to channel pollutants to the southeast. In addition, on summer days with low level inversions, ozone can be recirculated by southerly drainage flows in the late evening and early morning and by the prevailing northwesterlies in the afternoon. A similar recirculation pattern occurs in the winter, affecting levels of carbon monoxide and particulate matter. This movement of the air up and down the valley increases the impact of the pollutants significantly.

Pollution sources are plentiful and complex in this subregion. The Santa Clara Valley has a high concentration of industry at the northern end, in the Silicon Valley. Some of these industries are sources of air toxics as well as criteria air pollutants. In addition, Santa Clara Valley's large population and many work-site destinations generate the highest mobile source emissions of any subregion in the SFBAAB.

Sonoma Valley

The Sonoma Valley is west of the Napa Valley. It is separated from the Napa Valley and from the Cotati and Petaluma Valleys by mountains. The Sonoma Valley is long and narrow, approximately 5 miles wide at its southern end and less than a mile wide at the northern end.

The climate is similar to that of the Napa Valley, with the same basic wind characteristics. The strongest upvalley winds occur in the afternoon during the summer and the strongest downvalley winds occur during clear, calm winter nights. Prevailing winds follow the axis of the valley, northwest/southeast, while some upslope flow during the day and downslope flow during the night occurs near the base of the mountains. Summer average maximum temperatures are usually in the high-80's, and summer minimums are around 50 degrees. Winter maximums are in the high-50's to the mid-60's, with minimums ranging from the mid-30's to low-40's.

As in the Napa Valley, the air pollution potential of the Sonoma Valley could be high if there were significant sources of pollution nearby. Prevailing winds can transport local and nonlocally generated pollutants northward into the narrow valley, which often traps and concentrates the pollutants under stable conditions. The local upslope and downslope flows set up by the surrounding mountains may also recirculate pollutants.

However, local sources of air pollution are minor. With the exception of some processing of agricultural goods, such as wine and cheese manufacturing, there is little industry in this valley. Increases in motor vehicle emissions and woodsmoke emissions from stoves and fireplaces may increase pollution as the valley grows in population and as a tourist attraction.

Southwestern Alameda County

This subregion encompasses the southeast side of San Francisco Bay, from Dublin Canyon to north of Milpitas. The subregion is bordered on the east by the East Bay hills and on the west by the bay. Most of the area is flat.

This subregion is indirectly affected by marine air flow. Marine air entering through the Golden Gate is blocked by the East Bay hills, forcing the air to diverge into northerly and southerly paths. The southern flow is directed down the bay, parallel to the hills, where it eventually passes over southwestern Alameda County. These sea breezes are strongest in the afternoon. The further from the ocean the marine air travels, the more the ocean’s effect is diminished. Although the

climate in this region is affected by sea breezes, it is affected less so than the regions closer to the Golden Gate.

The climate of southwestern Alameda County is also affected by its close proximity to San Francisco Bay. The Bay cools the air with which it comes in contact during warm weather, while during cold weather the Bay warms the air. The normal northwest wind pattern carries this air onshore. Bay breezes push cool air onshore during the daytime and draw air from the land offshore at night.

Winds are predominantly out of the northwest during the summer months. In the winter, winds are equally likely to be from the east. Easterly-southeasterly surface flow into southern Alameda County passes through three major gaps: Hayward/Dublin Canyon, Niles Canyon and Mission Pass. Areas north of the gaps experience winds from the southeast, while areas south of the gaps experience winds from the northeast. Wind speeds are moderate in this subregion, with annual average wind speeds close to the Bay at about 7 mph, while further inland they average 6 mph.

Air temperatures are moderated by the subregion's proximity to the Bay and to the sea breeze. Temperatures are slightly cooler in the winter and slightly warmer in the summer than East Bay cities to the north. During the summer months, average maximum temperatures are in the mid-70's. Average maximum winter temperatures are in the high-50's to low-60's. Average minimum temperatures are in the low 40's in winter and mid-50's in the summer.

Pollution potential is relatively high in this subregion during the summer and fall. When high pressure dominates, low mixing depths and Bay and ocean wind patterns can concentrate and carry pollutants from other cities to this area, adding to the locally emitted pollutant mix. The polluted air is then pushed up against the East Bay hills. In the wintertime, the air pollution potential in southwestern Alameda County is moderate. Air pollution sources include light and heavy industry, and motor vehicles. Increasing motor vehicle traffic and congestion in the subregion may increase Southwest Alameda County pollution as well as that of its neighboring subregions.

C.1.2. Existing Ambient Air Quality: Criteria Air Pollutants

The California Air Resources Board (ARB) and the U.S. Environmental Protection Agency (EPA) currently focus on the following air pollutants as indicators of ambient air quality: ozone, particulate matter (PM), nitrogen dioxide (NO_2), CO, sulfur dioxide (SO_2), and lead. Because these are the most prevalent air pollutants known to be deleterious to human health and extensive health-effects criteria documents are available, they are commonly referred to as "criteria air pollutants." Sources and health effects of the criteria air pollutants are summarized in Table C.2. Current state and federal air quality standards are available at http://www.arb.ca.gov/research/aaqs/aaqs2.pdf and designations are available at http://www.arb.ca.gov/desig/desig.htm. See Table C.1 for current attainment status.

Table C.1
Ambient Air Quality Standards and Designations

Pollutant	Averaging Time	California		National Standards[a]		
		Standards[b, c]	Attainment Status[d]	Primary[c,e]	Secondary[c,f]	Attainment Status[g]
Ozone	1-hour	0.09 ppm (180 µg/m^3)	N (Serious)	–[h]	Same as Primary Standard	–[h]
	8-hour	0.070 ppm (137 µg/m^3)	–	0.075 ppm (147 µg/m^3)		N
Carbon Monoxide (CO)	1-hour	20 ppm (23 mg/m^3)	A	35 ppm (40 mg/m^3)	–	U/A
	8-hour	9 ppm (10 mg/m^3)		9 ppm (10 mg/m^3)		
Nitrogen Dioxide (NO_2)	Annual Arithmetic Mean	0.030 ppm (57 µg/m^3)	–	0.053 ppm (100 µg/m^3)	Same as Primary Standard	U/A
	1-hour	0.18 ppm (339 µg/m^3)	A	–		–
Sulfur Dioxide (SO_2)	Annual Arithmetic Mean	–	–	0.030 ppm (80 µg/m^3)	–	A
	24-hour	0.04 ppm (105 µg/m^3)	A	0.14 ppm (365 µg/m^3)	–	
	3-hour	–	–	–	0.5 ppm (1300 µg/m^3)	
	1-hour	0.25 ppm (655 µg/m^3)	A	–	–	–
Respirable Particulate Matter (PM_{10})	Annual Arithmetic Mean	20 µg/m^3	N	–[h]	Same as Primary Standard	U
	24-hour	50 µg/m^3		150 µg/m^3		
Fine Particulate Matter ($PM_{2.5}$)	Annual Arithmetic Mean	12 µg/m^3	N	15 µg/m^3	Same as Primary Standard	N[j]
	24-hour	–	–	35 µg/m^3		
Lead[i]	30-day Average	1.5 µg/m^3	A	–	–	–
	Calendar Quarter	–	–	1.5 µg/m^3	Same as Primary Standard	–

Table C.1
Ambient Air Quality Standards and Designations

Pollutant	Averaging Time	California		National Standards[a]		
		Standards[b, c]	Attainment Status[d]	Primary[c,e]	Secondary[c,f]	Attainment Status[g]
Sulfates	24-hour	25 µg/m^3	A	**No National Standards**		
Hydrogen Sulfide	1-hour	0.03 ppm (42 µg/m^3)	U			
Vinyl Chloride[i]	24-hour	0.01 ppm (26 µg/m^3)	–			
Visibility-Reducing Particle Matter	8-hour	Extinction coefficient of 0.23 per kilometer —visibility of 10 miles or more (0.07—30 miles or more for Lake Tahoe) because of particles when the relative humidity is less than 70%.	U			

[a] National standards (other than ozone, PM, and those based on annual averages or annual arithmetic means) are not to be exceeded more than once a year. The ozone standard is attained when the fourth highest 8-hour concentration in a year, averaged over 3 years, is equal to or less than the standard. The PM_{10} 24-hour standard is attained when 99% of the daily concentrations, averaged over 3 years, are equal to or less than the standard. The $PM_{2.5}$ 24-hour standard is attained when 98% of the daily concentrations, averaged over 3 years, are equal to or less than the standard. Contact the EPA for further clarification and current federal policies.

[b] California standards for ozone, CO (except Lake Tahoe), SO_2 (1- and 24-hour), NO_2, PM, and visibility-reducing particles are values that are not to be exceeded. All others are not to be equaled or exceeded. CAAQS are listed in the Table of Standards in Section 70200 of Title 17 of the California Code of Regulations.

[c] Concentration expressed first in units in which it was promulgated [i.e., parts per million (ppm) or micrograms per cubic meter (µg/m^3)]. Equivalent units given in parentheses are based upon a reference temperature of 25°C and a reference pressure of 760 torr. Most measurements of air quality are to be corrected to a reference temperature of 25°C and a reference pressure of 760 torr; ppm in this table refers to ppm by volume, or micromoles of pollutant per mole of gas.

[d] Unclassified (U): a pollutant is designated unclassified if the data are incomplete and do not support a designation of attainment or nonattainment.
Attainment (A): a pollutant is designated attainment if the state standard for that pollutant was not violated at any site in the area during a 3-year period.
Nonattainment (N): a pollutant is designated nonattainment if there was a least one violation of a state standard for that pollutant in the area.
Nonattainment/Transitional (NT): is a subcategory of the nonattainment designation. An area is designated nonattainment/transitional to signify that the area is close to attaining the standard for that pollutant.

[e] National Primary Standards: The levels of air quality necessary, with an adequate margin of safety, to protect the public health.

[f] National Secondary Standards: The levels of air quality necessary to protect the public welfare from any known or anticipated adverse effects of a pollutant.

[g] Nonattainment (N): any area that does not meet (or that contributes to ambient air quality in a nearby area that does not meet) the national primary or secondary ambient air quality standard for the pollutant.
Attainment (A): any area that meets the national primary or secondary ambient air quality standard for the pollutant.
Unclassifiable (U): any area that cannot be classified on the basis of available information as meeting or not meeting the national primary or secondary ambient air quality standard for the pollutant.

[h] The 1-hour ozone NAAQS was revoked on June 15, 2005 and the annual PM_{10} NAAQS was revoked in 2006.

[i] ARB has identified lead and vinyl chloride as toxic air contaminants with no threshold of exposure for adverse health effects determined. These actions allow for the implementation of control measures at levels below the ambient concentrations specified for this pollutant.

[j] U.S EPA lowered the 24-hour $PM_{2.5}$ standard from 65 µg/m^3 to 35 µg/m^3 in 2006. EPA issued attainment status designations for the 35 µg/m^{3}standard on December 22, 2008. EPA has designated the Bay Area as nonattainment for the 35 µg/m^3 $PM_{2.5}$ standard. The EPA designation will be effective 90 days after publication of the regulation in the Federal Register.

Table C.2
Common Sources of Health Effects for Criteria Air Pollutants

Pollutants	Sources	Health Effects
Ozone	Atmospheric reaction of organic gases with nitrogen oxides in sunlight	Aggravation of respiratory and cardiovascular diseases; reduced lung function; increased cough and chest discomfort
Fine Particulate Matter (PM_{10} and $PM_{2.5}$)	Stationary combustion of solid fuels; construction activities; industrial processes; atmospheric chemical reactions	Reduced lung function; aggravation of respiratory and cardiovascular diseases; increases in mortality rate; reduced lung function growth in children
Nitrogen Dioxide (NO_2)	Motor vehicle exhaust; high temperature stationary combustion; atmospheric reactions	Aggravation of respiratory illness
Carbon Monoxide (CO)	Incomplete combustion of fuels and other carbon-containing substances, such as motor vehicle exhaust; natural events, such as decomposition of organic matter	Aggravation of some heart diseases; reduced tolerance for exercise; impairment of mental function; birth defects; death at high levels of exposure
Sulfur Dioxide (SO_2)	Combination of sulfur-containing fossil fuels; smelting of sulfur-bearing metal ore; industrial processes	Aggravation of respiratory diseases; reduced lung function
Lead	Contaminated soil	Behavioral and hearing disabilities in children; nervous system impairment

Source: South Coast Air Quality Management District 2005; EPA 2009; EDAW 2009

Ozone, or smog, is not emitted directly into the environment, but is formed in the atmosphere by complex chemical reactions between ROG and NO_X in the presence of sunlight. Ozone formation is greatest on warm, windless, sunny days. The main sources of NO_X and ROG, often referred to as ozone precursors, are combustion processes (including motor vehicle engines) the evaporation of solvents, paints, and fuels, and biogenic sources. Automobiles are the single largest source of ozone precursors in the SFBAAB. Tailpipe emissions of ROG are highest during cold starts, hard acceleration, stop-and-go conditions, and slow speeds. They decline as speeds increase up to about 50 mph, then increase again at high speeds and high engine loads. ROG emissions associated with evaporation of unburned fuel depend on vehicle and ambient temperature cycles. Nitrogen oxide emissions exhibit a different curve; emissions decrease as the vehicle approaches 30 mph and then begin to increase with increasing speeds.

Ozone levels usually build up during the day and peak in the afternoon hours. Short-term exposure can irritate the eyes and cause constriction of the airways. Besides causing shortness of breath, it can aggravate existing respiratory diseases such as asthma, bronchitis and emphysema. Chronic exposure to high ozone levels can permanently damage lung tissue. Ozone can also damage plants and trees, and materials such as rubber and fabrics.

Particulate Matter refers to a wide range of solid or liquid particles in the atmosphere, including smoke, dust, aerosols, and metallic oxides. Respirable particulate matter with an aerodynamic diameter of 10 micrometers or less is referred to as PM_{10}. $PM_{2.5}$ includes a subgroup of finer particles that have an aerodynamic diameter of 2.5 micrometers or less. Some particulate matter,

such as pollen, is naturally occurring. In the SFBAAB most particulate matter is caused by combustion, factories, construction, grading, demolition, agricultural activities, and motor vehicles. Extended exposure to particulate matter can increase the risk of chronic respiratory disease. PM_{10} is of concern because it bypasses the body's natural filtration system more easily than larger particles, and can lodge deep in the lungs. The EPA and the state of California revised their PM standards several years ago to apply only to these fine particles. $PM_{2.5}$ poses an increased health risk because the particles can deposit deep in the lungs and contain substances that are particularly harmful to human health. Motor vehicles are currently responsible for about half of particulates in the SFBAAB. Wood burning in fireplaces and stoves is another large source of fine particulates.

Nitrogen Dioxide (NO_2) is a reddish-brown gas that is a by-product of combustion processes. Automobiles and industrial operations are the main sources of NO_2. Aside from its contribution to ozone formation, nitrogen dioxide can increase the risk of acute and chronic respiratory disease and reduce visibility. NO_2 may be visible as a coloring component of a brown cloud on high pollution days, especially in conjunction with high ozone levels.

Carbon Monoxide (CO) is an odorless, colorless gas. It is formed by the incomplete combustion of fuels. The single largest source of CO in the SFBAAB is motor vehicles. Emissions are highest during cold starts, hard acceleration, stop-and-go driving, and when a vehicle is moving at low speeds. New findings indicate that CO emissions per mile are lowest at about 45 mph for the average light-duty motor vehicle and begin to increase again at higher speeds. When inhaled at high concentrations, CO combines with hemoglobin in the blood and reduces the oxygen-carrying capacity of the blood. This results in reduced oxygen reaching the brain, heart and other body tissues. This condition is especially critical for people with cardiovascular diseases, chronic lung disease or anemia, as well as fetuses. Even healthy people exposed to high CO concentrations can experience headaches, dizziness, fatigue, unconsciousness, and even death.

Sulfur Dioxide (SO_2) is a colorless acid gas with a pungent odor. It has potential to damage materials and it can have health effects at high concentrations. It is produced by the combustion of sulfur-containing fuels, such as oil, coal and diesel. SO_2 can irritate lung tissue and increase the risk of acute and chronic respiratory disease.

Lead is a metal found naturally in the environment as well as in manufactured products. The major sources of lead emissions have historically been mobile and industrial sources. As a result of the phase-out of leaded gasoline, metal processing is currently the primary source of lead emissions. The highest levels of lead in air are generally found near lead smelters. Other stationary sources are waste incinerators, utilities, and lead-acid battery manufacturers.

Twenty years ago, mobile sources were the main contributor to ambient lead concentrations in the air. In the early 1970s, the EPA set national regulations to gradually reduce the lead content in gasoline. In 1975, unleaded gasoline was introduced for motor vehicles equipped with catalytic converters. The EPA banned the use of leaded gasoline in highway vehicles in December 1995. As a result of the EPA's regulatory efforts to remove lead from gasoline, emissions of lead from the transportation sector and levels of lead in the air decreased dramatically.

Monitoring Data

The BAAQMD operates a regional air quality monitoring network that regularly measures the concentrations of the five major criteria air pollutants. Air pollutant monitoring data is available at http://www.arb.ca.gov/adam/welcome.html. Air quality conditions in the SFBAAB have improved significantly since the BAAQMD was created in 1955. Ambient concentrations and the number of days on which the region exceeds standards have declined dramatically. Neither State nor

national ambient air quality standards of these chemicals have been violated in recent decades for nitrogen dioxide, sulfur dioxide, sulfates, lead, hydrogen sulfide, and vinyl chloride.

Emissions Inventory

The BAAQMD estimates emissions of criteria air pollutants from approximately nine hundred source categories. The estimates are based on BAAQMD permit information for stationary sources (e.g., manufacturing industries, refineries, dry-cleaning operations), plus more generalized estimates for area sources (e.g., space heating, landscaping activities, use of consumer products) and mobile sources (e.g., trains, ships and planes, as well as on-road and off-road motor vehicles). BAAQMD emissions inventory data is available at http://www.arb.ca.gov/ei/maps/statemap/dismap.htm.

C.1.2. Existing Ambient Air Quality: Toxic Air Contaminants

In addition to the criteria air pollutants listed above, another group of pollutants, commonly referred to as toxic air contaminants (TACs) or hazardous air pollutants can result in health effects that can be quite severe. Many TACs are confirmed or suspected carcinogens, or are known or suspected to cause birth defects or neurological damage. Secondly, many TACs can be toxic at very low concentrations. For some chemicals, such as carcinogens, there are no thresholds below which exposure can be considered risk-free.

Industrial facilities and mobile sources are significant sources of TACs. The electronics industry, including semiconductor manufacturing, has the potential to contaminate both air and water due to the highly toxic chlorinated solvents commonly used in semiconductor production processes. Sources of TACs go beyond industry. Various common urban facilities also produce TAC emissions, such as gasoline stations (benzene), hospitals (ethylene oxide), and dry cleaners (perchloroethylene). Automobile exhaust also contains TACs such as benzene and 1,3-butadiene. Most recently, diesel particulate matter was identified as a TAC by the ARB. Diesel PM differs from other TACs in that it is not a single substance but rather a complex mixture of hundreds of substances. BAAQMD research indicates that mobile-source emissions of diesel PM, benzene, and 1,3-butadiene represent a substantial portion of the ambient background risk from TACs in the SFBAAB.

C.1.3. Greenhouse Gases and Global Climate Change

Unlike emissions of criteria and toxic air pollutants, which have local or regional impacts, emissions of greenhouse gases (GHGs) that contribute to global warming or global climate change have a broader, global impact. Global warming is a process whereby GHGs accumulating in the atmosphere contribute to an increase in the temperature of the earth's atmosphere. The principal GHGs contributing to global warming are carbon dioxide (CO_2), methane (CH_4), nitrous oxide (N_2O), and fluorinated compounds. The primary GHGs of concern are summarized in Table C.3. These gases allow visible and ultraviolet light from the sun to pass through the atmosphere, but they prevent heat from escaping back out into space. Among the potential implications of global warming are rising sea levels, and adverse impacts to water supply, water quality, agriculture, forestry, and habitats. In addition, global warming may increase electricity demand for cooling, decrease the availability of hydroelectric power, and affect regional air quality and public health. Like most criteria and toxic air pollutants, much of the GHG production comes from motor vehicles. GHG emissions can be reduced to some degree by improved coordination of land use and transportation planning on the city, county, and subregional level, and other measures to reduce automobile use. Energy conservation measures also can contribute to reductions in GHG emissions.

Table C.3 Examples of Greenhouse Gases	
Gas	**Sources**
Carbon dioxide (CO_2)	Fossil fuel combustion in stationary and point sources; emission sources includes burning of oil, coal, gas.
Methane (CH_4)	Incomplete combustion in forest fires, landfills, and leaks in natural gas and petroleum systems, agricultural activities, coal mining, wastewater treatment, and certain industrial processes.
Nitrous oxide (N_2O)	Fossil fuel combustion in stationary and point sources; other emission sources include agricultural soil management, animal manure management, sewage treatment, adipic acid production, and nitric acid production.
Chlorofluorocarbon (CFC), and Hydro-chlorofluorocarbon (HCFC)	Agents used in production of foam insulation; other sources include air conditioners, refrigerators, and solvents in cleaners.
Sulfur hexafluoride (SF_6)	Electric insulation in high voltage equipment that transmits and distributes electricity, including circuit breakers, gas-insulated substations, and other switchgear used in the transmission system to manage the high voltages carried between generating stations and customer load centers.
Perfluorocarbons (PFC's)	Primary aluminum production and semiconductor manufacturing.
Source: EPA 2009	

California Greenhouse Gas Emissions Inventory

Emissions of GHGs contributing to global climate change are attributable in large part to human activities associated with the transportation, industrial/manufacturing, utility, residential, commercial and agricultural sectors. In California, the transportation sector is the largest emitter of GHGs, followed by electricity generation. Emissions of CO_2 are byproducts of fossil fuel combustion. CH_4, a highly potent GHG, results from off-gassing (the release of chemicals from nonmetallic substances under ambient or greater pressure conditions) is largely associated with agricultural practices and landfills. N_2O is also largely attributable to agricultural practices and soil management. CO_2 sinks, or reservoirs, include vegetation and the ocean, which absorb CO_2 through sequestration and dissolution, respectively, two of the most common processes of CO_2 sequestration.

California produced 474 million gross metric tons (MMT) of CO_2 equivalent (CO_2e) averaged over the period from 2002-2004. CO_2e is a measurement used to account for the fact that different GHGs have different potential to retain infrared radiation in the atmosphere and contribute to the greenhouse effect. This potential, known as the global warming potential (GWP) of a GHG, is dependent on the lifetime, or persistence, of the gas molecule in the atmosphere. For example, one ton of CH_4 has the same contribution to the greenhouse effect as approximately 23 tons of CO_2. Therefore, CH_4 is a much more potent GHG than CO_2. Expressing emissions in CO_2e takes the contributions of all GHG emissions to the greenhouse effect and converts them to a single unit equivalent to the effect that would occur if only CO_2 were being emitted.

Combustion of fossil fuel in the transportation sector was the single largest source of California's GHG emissions in 2002-2004, accounting for 38 percent of total GHG emissions in the state. This sector was followed by the electric power sector (including both in-state and out-of-state sources) (18 percent) and the industrial sector (21 percent).

California Greenhouse Gas Emissions Projections

The 1990 GHG emissions limit is approximately 430 MMT CO_2e, which must be met in California by 2020 per the requirements of AB 32 (discussed below in the Regulatory Setting). ARB's GHG inventory for all emissions sectors would require an approximate 28 percent reduction in GHG emissions from projected 2020 forecasts to meet the target emissions limit (equivalent to levels in 1990) established in AB 32. The AB 32 Scoping Plan, discussed further below, is ARB's plan for meeting this mandate.

C.1.4. Existing Ambient Air Quality: Odors and Dust

Other air quality issues of concern in the SFBAAB include nuisance impacts of odors and dust. Objectionable odors may be associated with a variety of pollutants. Common sources of odors include wastewater treatment plants, landfills, composting facilities, refineries and chemical plants. Similarly, nuisance dust may be generated by a variety of sources including quarries, agriculture, grading and construction. Odors rarely have direct health impacts, but they can be very unpleasant and can lead to anger and concern over possible health effects among the public. Each year the BAAQMD receives thousands of citizen complaints about objectionable odors. Dust emissions can contribute to increased ambient concentrations of PM_{10}, and can also contribute to reduced visibility and soiling of exposed surfaces.

REGULATORY SETTING

Air quality with respect to criteria air pollutants and TACs within the SFBAAB is regulated by such agencies as the BAAQMD, ARB, and EPA. Each of these agencies develops rules, regulations, policies, and/or goals to attain the goals or directives imposed through legislation. Although the EPA regulations may not be superseded, both state and local regulations may be more stringent.

C.1.5. Criteria Air Pollutants

Federal Air Quality Regulations

U.S. Environmental Protection Agency

At the federal level, EPA has been charged with implementing national air quality programs. EPA's air quality mandates are drawn primarily from the Federal Clean Air Act (FCAA), which was enacted in 1963. The FCAA was amended in 1970, 1977, and 1990.

The FCAA required EPA to establish primary and secondary NAAQS, which are available at http://www.arb.ca.gov/research/aaqs/aaqs2.pdf. The FCAA also required each state to prepare an air quality control plan referred to as a State Implementation Plan (SIP). The Federal Clean Air Act Amendments of 1990 (FCAAA) added requirements for states with nonattainment areas to revise their SIPs to incorporate additional control measures to reduce air pollution. The SIP is periodically modified to reflect the latest emissions inventories, planning documents, and rules and regulations of the air basins as reported by their jurisdictional agencies. EPA has responsibility to review all state SIPs to determine conformation to the mandates of the FCAAA and determine if implementation will achieve air quality goals. If the EPA determines a SIP to be inadequate, a Federal Implementation Plan (FIP) may be prepared for the nonattainment area that imposes additional control measures. Failure to submit an approvable SIP or to implement the plan within the mandated timeframe may result in sanctions being applied to transportation funding and stationary air pollution sources in the air basin.

State Air Quality Regulations

In 1992 and 1993, the California Air Resources Board (CARB) requested delegation of authority for the implementation and enforcement of specified New Source Performance Standards

(NSPS) and National Emission Standards for Hazardous Air Pollutants (NESHAPS) to the following local agencies: Bay Area and South Coast Air Quality Management Districts (AQMDs). EPA's review of the State of California's laws, rules, and regulations showed them to be adequate for the implementation and enforcement of these federal standards, and EPA granted the delegations as requested.

California Air Resources Board

ARB is the agency responsible for coordination and oversight of state and local air pollution control programs in California and for implementing the California Clean Air Act (CCAA), which was adopted in 1988. The CCAA requires that all air districts in the state endeavor to achieve and maintain the CAAQS by the earliest practical date. The act specifies that districts should focus particular attention on reducing the emissions from transportation and area-wide emission sources, and provides districts with the authority to regulate indirect sources.

ARB is primarily responsible for developing and implementing air pollution control plans to achieve and maintain the NAAQS. The ARB is primarily responsibility for statewide pollution sources and produces a major part of the SIP. Local air districts are still relied upon to provide additional strategies for sources under their jurisdiction. The ARB combines this data and submits the completed SIP to EPA.

Other ARB duties include monitoring air quality (in conjunction with air monitoring networks maintained by air pollution control and air quality management districts), establishing CAAQS (which in many cases are more stringent than the NAAQS), determining and updating area designations and maps, and setting emissions standards for new mobile sources, consumer products, small utility engines, and off-road vehicles.

Transport of Pollutants

The California Clean Air Act, Section 39610 (a), directs the ARB to “identify each district in which transported air pollutants from upwind areas outside the district cause or contribute to a violation of the ozone standard and to identify the district of origin of transported pollutants.” The information regarding the transport of air pollutants from one basin to another was to be quantified to assist interrelated basins in the preparation of plans for the attainment of State ambient air quality standards. Numerous studies conducted by the ARB have identified air basins that are impacted by pollutants transported from other air basins (as of 1993). Among the air basins affected by air pollution transport from the SFBAAB are the North Central Coast Air Basin, the Mountain Counties Air Basin, the San Joaquin Valley Air Basin, and the Sacramento Valley Air Basin. The SFBAAB was also identified as an area impacted by the transport of air pollutants from the Sacramento region.

Local Air Quality Regulations

Bay Area Air Quality Management District

The BAAQMD attains and maintains air quality conditions in the SFBAAB through a comprehensive program of planning, regulation, enforcement, technical innovation, and promotion of the understanding of air quality issues. The clean air strategy of the BAAQMD includes the preparation of plans for the attainment of ambient air quality standards, adoption and enforcement of rules and regulations concerning sources of air pollution, and issuance of permits for stationary sources of air pollution. The BAAQMD also inspects stationary sources of air pollution and responds to citizen complaints, monitors ambient air quality and meteorological conditions, and implements programs and regulations required by the FCAA, FCAAA, and the CCAA.

In 2009, the BAAQMD released the update to its CEQA Guidelines. This is an advisory document that provides the lead agency, consultants, and project applicants with uniform procedures for

addressing air quality in environmental documents. The handbook contains the following applicable components:

1. Criteria and thresholds for determining whether a project may have a significant adverse air quality impact;
2. Specific procedures and modeling protocols for quantifying and analyzing air quality impacts;
3. Methods available to mitigate air quality impacts;
4. Information for use in air quality assessments and environmental documents that will be updated more frequently such as air quality data, regulatory setting, climate, topography.

Air Quality Plans

As stated above, the BAAQMD prepares plans to attain ambient air quality standards in the SFBAAB. The BAAQMD prepares ozone attainment plans (OAP) for the national ozone standard and clean air plans (CAP) for the California standard both in coordination with the Metropolitan Transportation Commission and the Association of Bay Area Governments (ABAG).

With respect to applicable air quality plans, the BAAQMD prepared the *2010 Clean Air Plan* to address nonattainment of the national 1-hour ozone standard in the SFBAAB. The purpose of the 2010 Clean Air Plan is to:

1. Update the Bay Area 2005 Ozone Strategy in accordance with the requirements of the California Clean Air Act to implement "all feasible measures" to reduce ozone;
2. Consider the impacts of ozone control measures on particulate matter (PM), air toxics, and greenhouse gases in a single, integrated plan;
3. Review progress in improving air quality in recent years;
4. Establish emission control measures to be adopted or implemented in the 2009-2012 timeframe.

Similarly, the BAAQMD prepared the 2010 Clean Air Plan to address nonattainment of the CAAQS.

C.1.6. Toxic Air Contaminants

TACs, or in federal parlance under the FCAA, HAPs, are pollutants that result in an increase in mortality, a serious illness, or pose a present or potential hazard to human health. Health effects of TACs may include cancer, birth defects, and immune system and neurological damage.

TACs can be separated into carcinogens and noncarcinogens based on the nature of the physiological degradation associated with exposure to the pollutant. For regulatory purposes, carcinogens are assumed to have no safe threshold below which health impacts will not occur. Noncarcinogenic TACs differ in that there is a safe level in which it is generally assumed that no negative health impacts would occur. These levels are determined on a pollutant-by-pollutant basis.

It is important to understand that TACs are not considered criteria air pollutants and thus are not specifically addressed through the setting of ambient air quality standards. Instead, the EPA and ARB regulate HAPs and TACs, respectively, through statutes and regulations that generally require the use of the maximum or best available control technology (MACT and BACT) to limit emissions. These in conjunction with additional rules set forth by the BAAQMD establish the regulatory framework for TACs.

Federal Hazardous Air Pollutant Program

Title III of the FCAAA requires the EPA to promulgate national emissions standards for hazardous air pollutants (NESHAPs). The NESHAP may differ for major sources than for area sources of HAPs (major sources are defined as stationary sources with potential to emit more than 10 tons per year [TPY] of any HAP or more than 25 TPY of any combination of HAPs; all other sources are considered area sources). The emissions standards are to be promulgated in two phases. In the first phase (1992–2000), the EPA developed technology-based emission standards designed to produce the maximum emission reduction achievable. These standards are generally referred to as requiring MACT. These federal rules are also commonly referred to as MACT standards, because they reflect the Maximum Achievable Control Technology. For area sources, the standards may be different, based on generally available control technology. In the second phase (2001–2008), the EPA is required to promulgate health risk–based emissions standards where deemed necessary to address risks remaining after implementation of the technology-based NESHAP standards. The FCAAA required the EPA to promulgate vehicle or fuel standards containing reasonable requirements that control toxic emissions, at a minimum to benzene and formaldehyde. Performance criteria were established to limit mobile-source emissions of toxics, including benzene, formaldehyde, and 1,3-butadiene. In addition, §219 required the use of reformulated gasoline in selected U.S. cities (those with the most severe ozone nonattainment conditions) to further reduce mobile-source emissions.

State Toxic Air Contaminant Programs

California regulates TACs primarily through the Tanner Air Toxics Act (AB 1807) and the Air Toxics Hot Spots Information and Assessment Act of 1987 (AB 2588). The Tanner Act sets forth a formal procedure for ARB to designate substances as TACs. This includes research, public participation, and scientific peer review before ARB can designate a substance as a TAC. To date, ARB has identified over 21 TACs, and adopted the EPA's list of HAPs as TACs. Most recently, diesel exhaust particulate was added to the ARB list of TACs. Once a TAC is identified, ARB's then adopts an Airborne Toxics Control Measure for sources that emit that particular TAC. If there is a safe threshold for a substance at which there is no toxic effect, the control measure must reduce exposure below that threshold. If there is no safe threshold, the measure must incorporate TBACT to minimize emissions. None of the TACs identified by ARB have a safe threshold.

The Hot Spots Act requires that existing facilities that emit toxic substances above specified level:

1. Prepare a toxic emission inventory;
2. Prepare a risk assessment if emissions are significant;
3. Notify the public of significant risk levels;
4. Prepare and implement risk reduction measure.

ARB has adopted diesel exhaust control measures and more stringent emission standards for various on-road mobile sources of emissions, including transit buses, and off-road diesel equipment (e.g., tractors, generators). In February 2000, ARB adopted a new public transit bus fleet rule and emission standards for new urban buses. These new rules and standards provide for 1) more stringent emission standards for some new urban bus engines beginning with 2002 model year engines, 2) zero-emission bus demonstration and purchase requirements applicable to transit agencies, and 3) reporting requirements with which transit agencies must demonstrate compliance with the urban transit bus fleet rule. Upcoming milestones include the low sulfur diesel fuel requirement, and tighter emission standards for heavy-duty diesel trucks (2007) and off-road diesel equipment (2011) nationwide. Over time, the replacement of older vehicles will result in a vehicle fleet that produces substantially less TACs than under current conditions. Mobile-source emissions of TACs (e.g., benzene, 1-3-butadiene, diesel PM) have been reduced

significantly over the last decade, and will be reduced further in California through a progression of regulatory measures [e.g., Low Emission Vehicle/Clean Fuels and Phase II reformulated gasoline regulations) and control technologies. With implementation of ARB's Risk Reduction Plan, it is expected that diesel PM concentrations will be reduced by 75% in 2010 and 85% in 2020 from the estimated year 2000 level. Adopted regulations are also expected to continue to reduce formaldehyde emissions from cars and light-duty trucks. As emissions are reduced, it is expected that risks associated with exposure to the emissions will also be reduced.

Local Air Quality Regulations

Bay Area Air Quality Management District

The BAAQMD has regulated TACs since the 1980s. At the local level, air pollution control or management districts may adopt and enforce ARB's control measures. Under BAAQMD Regulation 2-1 (General Permit Requirements), Regulation 2-2 (New Source Review), and Regulation 2-5 (New Source Review), all nonexempt sources that possess the potential to emit TACs are required to obtain permits from BAAQMD. Permits may be granted to these operations if they are constructed and operated in accordance with applicable regulations, including new source review standards and air toxics control measures. The BAAQMD limits emissions and public exposure to TACs through a number of programs. The BAAQMD prioritizes TAC-emitting stationary sources based on the quantity and toxicity of the TAC emissions and the proximity of the facilities to sensitive receptors. In addition, the BAAQMD has adopted Regulation 11 Rules 2 and 14, which address asbestos demolition renovation, manufacturing, and standards for asbestos containing serpentine.

C.1.7. Greenhouse Gases and Global Climate Change

Federal Greenhouse Gas Regulations

Supreme Court Ruling

The U.S. Environmental Protection Agency (EPA) is the Federal agency responsible for implementing the Clean Air Act (CAA). The U.S. Supreme Court ruled in its decision in *Massachusetts et al. v. Environmental Protection Agency* et al. ([2007] 549 U.S. 05-1120), issued on April 2, 2007, that carbon dioxide (CO_2) is an air pollutant as defined under the CAA, and that EPA has the authority to regulate emissions of GHGs.

EPA Actions

In response to the mounting issue of climate change, EPA has taken actions to regulate, monitor, and potentially reduce GHG emissions.

Mandatory Greenhouse Gas Reporting Rule

On September 22, 2009, EPA issued a final rule for mandatory reporting of GHGs from large GHG emissions sources in the United States. In general, this national reporting requirement will provide EPA with accurate and timely GHG emissions data from facilities that emit 25,000 metric tons or more of CO2 per year. This publically available data will allow the reporters to track their own emissions, compare them to similar facilities, and aid in identifying cost effective opportunities to reduce emissions in the future. Reporting is at the facility level, except that certain suppliers of fossil fuels and industrial greenhouse gases along with vehicle and engine manufacturers will report at the corporate level. An estimated 85% of the total U.S. GHG emissions, from approximately 10,000 facilities, are covered by this final rule.

Proposed Endangerment and Cause or Contribute Findings for Greenhouse Gases under the Clean Air Act

On April 23, 2009, EPA published their Proposed Endangerment and Cause or Contribute Findings for Greenhouse Gases under the CCA (Endangerment Finding) in the Federal Register. The Endangerment Finding is based on Section 202(a) of the CAA, which states that the Administrator (of EPA) should regulate and develop standards for "emission[s] of air pollution from any class of classes of new motor vehicles or new motor vehicle engines, which in [its] judgment cause, or contribute to, air pollution which may reasonably be anticipated to endanger public health or welfare." The proposed rule addresses Section 202(a) in two distinct findings. The first addresses whether or not the concentrations of the six key GHGs (i.e., carbon dioxide [CO_2], methane [CH_4], nitrous oxide [N_2O], hydrofluorocarbons [HFCs], perflurorocarbons [PFCs], and sulfur hexafluoride [SF_6]) in the atmosphere threaten the public health and welfare of current and future generations. The second addresses whether or not the combined emissions of GHGs from new motor vehicles and motor vehicle engines contribute to atmospheric concentrations of GHGs and to the threat of climate change.

The Administrator proposed the finding that atmospheric concentrations of GHGs endanger the public health and welfare within the meaning of Section 202(a) of the CCA. The evidence supporting this finding consists of human activity resulting in "high atmospheric levels" of GHG emissions, which are very likely responsible for increases in average temperatures and other climatic changes. Furthermore, the observed and projected results of climate change (e.g., higher likelihood of heat waves, wild fires, droughts, sea level rise, higher intensity storms) are a threat to the public health and welfare. Therefore, GHGs were found to endanger the public health and welfare of current and future generations.

The Administrator also proposed the finding that GHG emissions from new motor vehicles and motor vehicle engines are contributing to air pollution, which is endangering public health and welfare. The proposed finding cites that in 2006, motor vehicles were the second largest contributor to domestic GHG emissions (24 percent of total) behind electricity generation. Furthermore, in 2005, the U.S. was responsible for 18 percent of global GHG emissions. Therefore, GHG emissions from motor vehicles and motor vehicle engines were found to contribute to air pollution that endangers public health and welfare.

State Greenhouse Gas Regulations

Assembly Bill 1493 (2002)

In 2002, then-Governor Gray Davis signed Assembly Bill (AB) 1493. AB 1493 requires that ARB develop and adopt, by January 1, 2005, regulations that achieve "the maximum feasible reduction of greenhouse gases emitted by passenger vehicles and light-duty trucks and other vehicles determined by ARB to be vehicles whose primary use is noncommercial personal transportation in the state."

To meet the requirements of AB 1493, in 2004 ARB approved amendments to the California Code of Regulations (CCR) adding GHG emissions standards to California's existing standards for motor vehicle emissions. Amendments to CCR Title 13, Sections 1900 and 1961 (13 CCR 1900, 1961), and adoption of Section 1961.1 (13 CCR 1961.1) require automobile manufacturers to meet fleet-average GHG emissions limits for all passenger cars, light-duty trucks within various weight criteria, and medium-duty passenger vehicle weight classes (i.e., any medium-duty vehicle with a gross vehicle weight rating less than 10,000 pounds that is designed primarily for the transportation of persons), beginning with the 2009 model year. For passenger cars and light-duty trucks with a loaded vehicle weight (LVW) of 3,750 pounds or less, the GHG emission limits for the 2016 model year are approximately 37percent lower than the limits for the first year of the regulations, the 2009 model year. For light-duty trucks with LVW of 3,751 pounds to gross vehicle

weight (GVW) of 8,500 pounds, as well as medium-duty passenger vehicles, GHG emissions would be reduced approximately 24 percent between 2009 and 2016.

In December 2004, a group of car dealerships, automobile manufacturers, and trade groups representing automobile manufacturers filed suit against ARB to prevent enforcement of 13 CCR Sections 1900 and 1961 as amended by AB 1493 and 13 CCR 1961.1 (*Central Valley Chrysler-Jeep et al. v. Catherine E. Witherspoon, in Her Official Capacity as Executive Director of the California Air Resources Board, et al.*). The auto-makers' suit in the U.S. District Court for the Eastern District of California, contended California's implementation of regulations that, in effect, regulate vehicle fuel economy violates various federal laws, regulations, and policies.

On December 12, 2007, the Court found that if California receives appropriate authorization from EPA (the last remaining factor in enforcing the standard), these regulations would be consistent with and have the force of federal law, thus, rejecting the automakers' claim. This authorization to implement more stringent standards in California was requested in the form of a CAA Section 209, subsection (b) waiver in 2005. Since that time, EPA failed to act on granting California authorization to implement the standards. Governor Schwarzenegger and Attorney General Edmund G. Brown filed suit against EPA for the delay. In December 2007, EPA Administrator Stephen Johnson denied California's request for the waiver to implement AB 1493. Johnson cited the need for a national approach to reducing GHG emissions, the lack of a "need to meet compelling and extraordinary conditions", and the emissions reductions that would be achieved through the Energy Independence and Security Act of 2007 as the reasoning for the denial.

The state of California filed suit against EPA for its decision to deny the CAA waiver. The recent change in presidential administration directed EPA to reexamine its position for denial of California's CAA waiver and for its past opposition to GHG emissions regulation. California received the waiver, notwithstanding the previous denial by EPA, on June 30, 2009.

Assembly Bill 32 (2006), California Global Warming Solutions Act

In September 2006, the governor of California signed AB 32 (Chapter 488, Statutes of 2006), the California Global Warming Solutions Act of 2006, which enacted Sections 38500–38599 of the California Health and Safety Code. AB 32 requires the reduction of statewide GHG emissions to 1990 levels by 2020. This equates to an approximate 15 percent reduction compared to existing statewide GHG emission levels or a 30 percent reduction from projected 2020 "business as usual" emission levels. The required reduction will be accomplished through an enforceable statewide cap on GHG emissions beginning in 2012.

To effectively implement the statewide cap on GHG emissions, AB 32 directs ARB to develop and implement regulations that reduce statewide GHG emissions generated by stationary sources. Specific actions required of ARB under AB 32 include adoption of a quantified cap on GHG emissions that represent 1990 emissions levels along with disclosing how the cap was quantified, institution of a schedule to meet the emissions cap, and development of tracking, reporting, and enforcement mechanisms to ensure that the state achieves the reductions in GHG emissions needed to meet the cap.

In addition, AB 32 states that if any regulations established under AB 1493 (2002) cannot be implemented then ARB is required to develop additional, new regulations to control GHG emissions from vehicles as part of AB 32.

AB 32 Climate Change Scoping Plan

In December 2008, ARB adopted its *Climate Change Scoping Plan*, which contains the main strategies California will implement to achieve reduction of approximately 169 million metric tons (MMT) of CO_2e, or approximately 30% from the state's projected 2020 emission level of 596 MMT of CO_2e under a business-as-usual scenario (this is a reduction of 42 MMT CO_2e, or almost 10%,

from 2002-2004 average emissions). The *Scoping Plan* also includes ARB-recommended GHG reductions for each emissions sector of the state's GHG inventory. The Scoping Plan calls for the largest reductions in GHG emissions to be achieved by implementing the following measures and standards:

- improved emissions standards for light-duty vehicles (estimated reductions of 31.7 MMT CO_2e);
- the Low-Carbon Fuel Standard (15.0 MMT CO_2e);
- energy efficiency measures in buildings and appliances and the widespread development of combined heat and power systems (26.3 MMT CO_2e); and
- a renewable portfolio standard for electricity production (21.3 MMT CO_2e).

ARB has not yet determined what amount of GHG reductions it recommends from local government operations; however, the *Scoping Plan* does state that land use planning and urban growth decisions will play an important role in the state's GHG reductions because local governments have primary authority to plan, zone, approve, and permit how land is developed to accommodate population growth and the changing needs of their jurisdictions(meanwhile, ARB is also developing an additional protocol for community emissions). ARB further acknowledges that decisions on how land is used will have large impacts on the GHG emissions that will result from the transportation, housing, industry, forestry, water, agriculture, electricity, and natural gas emission sectors. The *Scoping Plan* states that the ultimate GHG reduction assignment to local government operations is to be determined (ARB 2008). With regard to land use planning, the *Scoping Plan* expects approximately 5.0 MMT CO_2e will be achieved associated with implementation of SB 375, which is discussed further below.

Senate Bills 1078 and 107 and Executive Order S-14-08

SB 1078 (Chapter 516, Statutes of 2002) requires retail sellers of electricity, including investor-owned utilities and community choice aggregators, to provide at least 20 percent of their supply from renewable sources by 2017. SB 107 (Chapter 464, Statutes of 2006) changed the target date to 2010. In November 2008 Governor Schwarzenegger signed Executive Order S-14-08, which expands the state's Renewable Energy Standard to 33 percent renewable power by 2020. Governor Schwarzenegger plans to propose legislative language that will codify the new higher standard.

Senate Bill 1368 (2006)

SB 1368 is the companion bill of AB 32 and was signed by Governor Schwarzenegger in September 2006. SB 1368 requires the California Public Utilities Commission (PUC) to establish a greenhouse gas emission performance standard for baseload generation from investor owned utilities by February 1, 2007. The California Energy Commission (CEC) must establish a similar standard for local publicly owned utilities by June 30, 2007. These standards cannot exceed the greenhouse gas emission rate from a baseload combined-cycle natural gas fired plant. The legislation further requires that all electricity provided to California, including imported electricity, must be generated from plants that meet the standards set by the PUC and CEC.

Senate Bill 97 (2007)

SB 97, signed by governor of California in August 2007 (Chapter 185, Statutes of 2007; Public Resources Code, Sections 21083.05 and 21097), acknowledges climate change is a prominent environmental issue that requires analysis under CEQA. This bill directed the Governor's Office of Planning and Research (OPR) to prepare, develop, and transmit to the California Resources Agency by July 1, 2009 guidelines for mitigating GHG emissions or the effects of GHG emissions,

as required by CEQA. The California Resources Agency is required to certify and adopt these guidelines by January 1, 2010.

This bill also removes, both retroactively and prospectively, as legitimate causes of action in litigation any claim of inadequate CEQA analysis of effects of GHG emissions associated with environmental review for projects funded by the Highway Safety, Traffic Reduction, Air Quality and Port Security Bond Act of 2006 (Proposition 1B) or the Disaster Preparedness and Flood Protection Bond Act of 2006 (Proposition 1E). This provision will be repealed by provision of law on January 1, 2010 at that time such projects, if any remain unapproved, will no longer enjoy protection against litigation claims based on failure to adequately address issues related to GHG emissions.

Senate Bill 375 (2008)

SB 375, signed in September 2008, aligns regional transportation planning efforts, regional GHG reduction targets, and land use and housing allocation. As part of the alignment, SB 375 requires Metropolitan Planning Organizations (MPOs) to adopt a Sustainable Communities Strategy (SCS) or Alternative Planning Strategy (APS) which prescribes land use allocation in that MPO's Regional Transportation Plan (RTP). The ARB, in consultation with MPOs, is required to provide each affected region with reduction targets for GHGs emitted by passenger cars and light trucks in the region for the years 2020 and 2035. These reduction targets will be updated every 8 years but can be updated every 4 years if advancements in emissions technologies affect the reduction strategies to achieve the targets. The ARB is also charged with reviewing each MPO's SCS or APS for consistency with its assigned GHG emission reduction targets. If MPOs do not meet the GHG reduction targets, transportation projects located in the MPO boundaries would not be eligible for funding programmed after January 1, 2012.

This bill also extends the minimum time period for the Regional Housing Needs Allocation (RNHA) cycle from 5 years to 8 years for local governments located in an MPO that meets certain requirements. City or County land use policies (e.g., General Plans) are not required to be consistent with the RTP including associated SCSs or APSs. Qualified projects consistent with an approved SCS or APS and categorized as "transit priority projects" would receive incentives under new provisions of CEQA.

Executive Order S-3-05 (2005)

Governor Schwarzenegger signed Executive Order S-3-05 on June 1, 2005 which proclaimed California is vulnerable to the impacts of climate change. The executive order declared increased temperatures could reduce snowpack in the Sierra Nevada Mountains, further exacerbate California's air quality problems, and potentially cause a rise in sea levels. To combat those concerns, the executive order established targets for total GHG emissions which include reducing GHG emissions to the 2000 level by 2010, to the 1990 level by 2020, and to 80 percent below the 1990 level by 2050.

The executive order also directed the secretary of the California Environmental Protection Agency to coordinate a multiagency effort to reduce GHG emissions to the target levels. The secretary will submit biannual reports to the governor and legislature describing progress made toward reaching the emission targets; impacts of global warming on California's resources; and mitigation and adaptation plans to combat impacts of global warming.

To comply with the executive order, the Secretary of the California Environmental Protection Agency created the California Climate Action Team which is made up of members from various state agencies and commissions. The California Climate Action Team released its first report in March 2006 of which proposed achieving the GHG emissions targets by building on voluntary

actions of California businesses and actions by local governments and communities along with continued implementation of state incentive and regulatory programs.

Executive Order S-13-08

Governor Schwarzenegger signed Executive Order S-13-08 on November 14, 2008 which directs California to develop methods for adapting to climate change through preparation of a statewide plan. The executive order directs OPR, in cooperation with the California Resources Agency (CRA), to provide land use planning guidance related to sea level rise and other climate change impacts by May 30, 2009. The order also directs the CRA to develop a state Climate Adaptation Strategy by June 30, 2009 and to convene an independent panel to complete the first California Sea Level Rise Assessment Report. The assessment report is required to be completed by December 1, 2010 and required to include the following four items:

1. Project the relative sea level rise specific to California by taking into account issues such as coastal erosion rates, tidal impacts, El Niño and La Niña events, storm surge, and land subsidence rates;
2. Identify the range of uncertainty in selected sea level rise projections;
3. Synthesize existing information on projected sea level rise impacts to state infrastructure (e.g., roads, public facilities, beaches), natural areas, and coastal and marine ecosystems; and
4. Discuss future research needs relating to sea level rise in California.

Executive Order S-1-07

Governor Schwarzenegger signed Executive Order S-1-07 in 2007 which proclaimed the transportation sector as the main source of GHG emissions in California. The executive order proclaims the transportation sector accounts for over 40 percent of statewide GHG emissions. The executive order also establishes a goal to reduce the carbon intensity of transportation fuels sold in California by a minimum of 10 percent by 2020.

In particular, the executive order established a Low-Carbon Fuel Standard (LCFS) and directed the Secretary for Environmental Protection to coordinate the actions of the CEC, the ARB, the University of California, and other agencies to develop and propose protocols for measuring the "life-cycle carbon intensity" of transportation fuels. This analysis supporting development of the protocols was included in the State Implementation Plan for alternative fuels (*State Alternative Fuels Plan* adopted by CEC on December 24, 2007) and was submitted to ARB for consideration as an "early action" item under AB 32. The ARB adopted the LCFS on April 23, 2009.

Local Greenhouse Gas Regulations

Bay Area Air Quality Management District Climate Protection Program

The BAAQMD established a climate protection program to reduce pollutants that contribute to global climate change and affect air quality in the SFBAAB. The climate protection program includes measures that promote energy efficiency, reduce vehicle miles traveled, and develop alternative sources of energy all of which assist in reducing emissions of GHG and in reducing air pollutants that affect the health of residents. BAAQMD also seeks to support current climate protection programs in the region and to stimulate additional efforts through public education and outreach, technical assistance to local governments and other interested parties, and promotion of collaborative efforts among stakeholders.

D. THRESHOLDS OF SIGNIFICANCE JUSTIFICATION

BAY AREA AIR QUALITY MANAGEMENT DISTRICT

California Environmental Quality Act Guidelines Update

Thresholds of Significance

June 2, 2010

BAY AREA AIR QUALITY MANAGEMENT DISTRICT

Table of Contents

Section **Page**

1 INTRODUCTION D-4
1.1 BAAQMD/CEQA Regulatory Authority D-4
1.2 Justification for Updating CEQA Thresholds D-5

2 GREENHOUSE GAS THRESHOLDS D-10
2.2 Thresholds of Significance D-11
2.3 Justification and Substantial Evidence Supporting Thresholds D-11
2.3.1 Scientific and Regulatory Justification D-12
2.3.2 Project-Level GHG Thresholds D-13
2.3.3 Plan-Level GHG Thresholds D-22
2.3.4 Greenhouse Gas Reduction Strategies D-24
2.3.5 Stationary Source GHG Threshold D-27
2.3.6 Summary of Justification for GHG Thresholds D-27

3 COMMUNITY RISK AND HAZARD THRESHOLDS D-29
3.2 Thresholds of Significance D-31
3.3 Justification and Substantial Evidence Supporting Thresholds D-34
3.3.1 Scientific and Regulatory Justification D-34
3.3.2 Construction, Land Use and Stationary Source Risk and Hazard Thresholds D-39
3.3.3 Cumulative Risk and Hazard Thresholds D-42
3.3.4 Plan-Level Risk and Hazard Thresholds D-44
3.3.5 Community Risk Reduction Plans D-44

4 CRITERIA POLLUTANT THRESHOLDS D-46
4.2 Thresholds of Significance D-46
4.3 Justification and Substantial Evidence Supporting Thresholds D-46
4.3.1 Project Construction Criteria Pollutant Thresholds D-46
4.3.2 Project Operation Criteria Pollutant Thresholds D-47
4.3.3 Local Carbon Monoxide Thresholds D-47
4.3.4 Plan-Level Criteria Pollutant Thresholds D-48
4.3.5 Criteria Pollutant Thresholds for Regional Plans D-48

5 ODOR THRESHOLDS D-49
5.2 Thresholds of Significance D-49
5.3 Justification and Substantial Evidence Supporting Thresholds D-49

REFERENCES D-52

BOARD RESOLUTION D-52

List of Tables

Table 1 – Air Quality CEQA Thresholds of Significance D-7

Table 2 – California 1990, 2002-2004, and 2020 Land Use Sector GHG[1] D-17

Table 3 – 2020 Land Use Sector GHG Emission Reductions from State Regulations and AB 32 Measures D-18

Table 4 – SFBAAB 1990, 2007, and 2020 Land Use Sector GHG Emissions Inventories and Projections (MMT CO_2e/yr) D-19

Table 5 – Operational GHG Threshold Sensitivity Analysis D-21

Table 6 – California 2020 GHG Emissions, Population Projections and GHG Efficiency Thresholds - Land Use Inventory Sectors D-22

Table 7 – California 2020 GHG Emissions, Population Projections and GHG Efficiency Thresholds - All Inventory Sectors D-24

Table 8 – Statistical Summary of Estimated Population-Weighted Ambient Cancer Risk in 2005 ..... D-30

Table 9 – Screening Distances for Potential Odor Sources D-50

Bay Area Air Quality Management District

Air Quality CEQA Thresholds of Significance

1. INTRODUCTION

Bay Area Air Quality Management District (BAAQMD or Air District) staff analyzed various options for California Environmental Quality Act (CEQA) air quality thresholds of significance for use within BAAQMD's jurisdiction. The analysis and evaluation undertaken by Air District staff is documented in the *Revised Draft Options and Justification Report – California Environmental Quality Act Thresholds of Significance* (Draft Options Report) (BAAQMD October 2009).

Air District staff hosted public workshops in February, April, September and October 2009, and April 2010 at several locations around the Bay Area. Air District staff also hosted additional workshops in each of the nine Bay Area counties specifically designed for, and to solicit input from, local agency staff. In addition, Air District staff met with regional stakeholder groups to discuss and receive input on the threshold options being evaluated. Throughout the course of the public workshops and stakeholder meetings Air District staff received many comments on the various options under consideration. Based on comments received and additional staff analysis, the threshold options and staff-recommended thresholds were further refined. The culmination of this nearly year and a half-long effort was presented in the Proposed Thresholds of Significance Report published on November 2, 2009 as the Air District staff's proposed air quality thresholds of significance.

The Air District Board of Directors (Board) held public hearings on November 18 and December 2, 2009 and January 6, 2010, to receive comments on staff's Proposed Thresholds of Significance (November 2, 2009; revised December 7, 2009). After public testimony and Board deliberations, the Board requested staff to present additional options for risk and hazard thresholds for Board consideration. This Report includes risks and hazards threshold options, as requested by the Board, in addition to staff's previously recommended thresholds of significance. The thresholds presented herein, adopted by the Air District Board of Directors, are intended to replace all of the Air District's currently recommended thresholds. The air quality thresholds of significance, and Board-requested risk and hazard threshold options, are provided in Table 1 at the end of this introduction.

1.1. BAAQMD/CEQA REGULATORY AUTHORITY

The BAAQMD has direct and indirect regulatory authority over sources of air pollution in the San Francisco Bay Area Air Basin (SFBAAB). CEQA requires that public agencies consider the potential adverse environmental impacts of any project that a public agency proposes to carry out, fund or approve. CEQA requires that a lead agency prepare an Environmental Impact Report (EIR) whenever it can be fairly argued (the "fair argument" standard), based on substantial evidence,[3] that a project may have a significant effect[4] on the environment, even if there is

[3] "Substantial evidence" includes facts, reasonable assumptions predicated upon facts, or expert opinions supported by facts, but does not include argument, speculation, unsubstantiated opinion or narrative, evidence that is clearly inaccurate

substantial evidence to the contrary (CEQA Guidelines §15064). CEQA requires that the lead agency review not only a project's direct effects on the environment, but also the cumulative impacts of a project and other projects causing related impacts. When the incremental effect of a project is cumulatively considerable, the lead agency must discuss the cumulative impacts in an EIR. (CEQA Guidelines §15064).

The "fair argument" standard refers to whether a fair argument can be made that a project may have a significant effect on the environment (*No Oil, Inc. v. City of Los Angeles* (1974) 13 Cal.3d 68, 84). The fair argument standard is generally considered a low threshold requirement for preparation of an EIR. The legal standards reflect a preference for requiring preparation of an EIR and for "resolving doubts in favor of environmental review." *Meija v. City of Los Angeles* (2005) 130 Cal. App. 4th 322, 332. "The determination of whether a project may have a significant effect on the environment calls for careful judgment on the part of the public agency involved, based to the extent possible on scientific and factual data." (CEQA Guidelines §15064(b).

In determining whether a project may have a significant effect on the environment, CEQA Guidelines Section 15064.7 provides that lead agencies may adopt and/or apply "thresholds of significance." A threshold of significance is "an identifiable quantitative, qualitative or performance level of a particular environmental effect, non-compliance with which means the effect will normally be determined to be significant by the agency and compliance with which means the effect normally will be determined to be less than significant" (CEQA Guidelines §15064.7).

While thresholds of significance give rise to a presumption of insignificance, thresholds are not conclusive, and do not excuse a public agency of the duty to consider evidence that a significant effect may occur under the fair argument standard. *Meija*, 130 Cal. App. 4th at 342. "A public agency cannot apply a threshold of significance or regulatory standard 'in a way that forecloses the consideration of any other substantial evidence showing there may be a significant effect.'" *Id.* This means that if a public agency is presented with factual information or other substantial evidence establishing a fair argument that a project may have a significant effect on the environment, the agency must prepare an EIR to study those impacts even if the project's impacts fall below the applicable threshold of significance.

Thresholds of significance must be supported by substantial evidence. This Report provides the substantial evidence in support of the thresholds of significance developed by the BAAQMD. If adopted by the BAAQMD Board of Directors, the Air District will recommend that lead agencies within the nine counties of the BAAQMD's jurisdiction use the thresholds of significance in this Report when considering the air quality impacts of projects under their consideration.

1.2. JUSTIFICATION FOR UPDATING CEQA THRESHOLDS

Any analysis of environmental impacts under CEQA includes an assessment of the nature and extent of each impact expected to result from the project to determine whether the impact will be treated as significant or less than significant. CEQA gives lead agencies discretion whether to classify a particular environmental impact as significant. Ultimately, formulation of a standard of significance requires the lead agency to make a policy judgment about where the line should be drawn distinguishing adverse impacts it considers significant from those that are not deemed significant. This judgment must, however, be based on scientific information and other factual data to the extent possible (CEQA Guidelines §15064(b)).

or erroneous, or evidence of social or economic impacts that do not contribute to, or are not caused by, physical impacts on the environment. Cal. Pub. Res. C. §21080(c); *see also* CEQA Guidelines §15384.

[4] A "significant effect" on the environment is defined as a "substantial, or potentially substantial, adverse change in the environment." Cal. Pub. Res. C. §21068; *see also* CEQA Guidelines §15382.

In the sense that advances in science provide new or refined factual data, combined with advances in technology and the gradual improvement or degradation of an environmental resource, the point where an environmental effect is considered significant is fluid over time. Other factors influencing this fluidity include new or revised regulations and standards, and emerging, new areas of concern.

In the ten years since BAAQMD last reviewed its recommended CEQA thresholds of significance for air quality, there have been tremendous changes that affect the quality and management of the air resources in the Bay Area. Traditional criteria air pollutant ambient air quality standards, at both the state and federal levels, have become increasingly more stringent. A new criteria air pollutant standard for fine particulate matter less than 2.5 microns in diameter ($PM_{2.5}$) has been added to federal and state ambient air quality standards. We have found, through technical advances in impact assessment, that toxic air contaminants are not only worse than previously thought from a health perspective, but that certain communities experience high levels of toxic air contaminants, giving rise to new regulations and programs to reduce the significantly elevated levels of ambient toxic air contaminant concentrations in the Bay Area.

In response to the elevated levels of toxic air contaminants in some Bay Area communities, the Air District created the Community Air Risk Evaluation (CARE) Program. Phase 1 of the BAAQMD's CARE program compiled and analyzed a regional emissions inventory of toxic air contaminants (TACs), including emissions from stationary sources, area sources, and on-road and off-road mobile sources. Phase 2 of the CARE Program conducted regional computer modeling of selected TAC species, species which collectively posed the greatest risk to Bay Area residents. In both Phases 1 and 2, demographic data were combined with estimates of TAC emissions or concentrations to identify communities that are disproportionally impacted from high concentrations of TACs. Bay Area Public Health Officers, in discussions with Air District staff and in comments to the Air District's Advisory Council (February 11, 2009, Advisory Council Meeting on Air Quality and Public Health), have recommended that $PM_{2.5}$, in addition to TACs, be considered in assessments of community-scale impacts of air pollution.

Another significant issue that affects the quality of life for Bay Area residents is the growing concern with global climate change. In just the past few years, estimates of the global atmospheric temperature and greenhouse gas concentration limits needed to stabilize climate change have been adjusted downward and the impacts of greenhouse gas emissions considered more dire. Previous scientific assessments assumed that limiting global temperature rise to 2-3°C above pre-industrial levels would stabilize greenhouse gas concentrations in the range of 450-550 parts per million (ppm) of carbon dioxide-equivalent (CO_2e). Now the science indicates that a temperature rise of 2°C would not prevent dangerous interference with the climate system. Recent scientific assessments suggest that global temperature rise should be kept below 2°C by stabilizing greenhouse gas concentrations below 350 ppm CO_2e, a significant reduction from the current level of 385 ppm CO_2e.

For the reasons stated above, and to further the goals of other District programs such as encouraging transit-oriented and infill development, BAAQMD has undertaken an effort to review all of its currently-recommended CEQA thresholds, revise them as appropriate, and develop new thresholds where appropriate. The overall goal of this effort is to develop CEQA significance criteria that ensure new development implements appropriate and feasible emission reduction measures to mitigate significant air quality impacts. The Air District's recommended CEQA significance thresholds have been vetted through a public review process and will be presented to the BAAQMD Board of Directors for adoption.

Table 1 – Air Quality CEQA Thresholds of Significance			
Pollutant	**Construction-Related**	**Operational-Related**	
Project-Level			
Criteria Air Pollutants and Precursors (Regional)	**Average Daily Emissions (lb/day)**	**Average Daily Emissions (lb/day)**	**Maximum Annual Emissions (tpy)**
ROG	54	54	10
NO_X	54	54	10
PM_{10}	82 (exhaust only)	82	15
$PM_{2.5}$	54 (exhaust only)	54	10
$PM_{10}/PM_{2.5}$ (fugitive dust)	Best Management Practices	None	
Local CO	None	9.0 ppm (8-hour average), 20.0 ppm (1-hour average)	
GHGs **Projects other than Stationary Sources**	None	Compliance with Qualified Greenhouse Gas Reduction Strategy OR 1,100 MT of CO_2e/yr OR 4.6 MT CO_2e/SP/yr (residents + employees)	
GHGs **Stationary Sources**	None	10,000 MT/yr	
Risks and Hazards – New Source (All Areas) (Individual Project) **Staff Proposal**	Same as Operational Thresholds*	Compliance with Qualified Community Risk Reduction Plan OR Increased cancer risk of >10.0 in a million Increased non-cancer risk of > 1.0 Hazard Index (Chronic or Acute) Ambient $PM_{2.5}$ increase: > 0.3 µg/m^3 annual average Zone of Influence: 1,000-foot radius from fence line of source or receptor	

Table 1 – Air Quality CEQA Thresholds of Significance		
Pollutant	**Construction-Related**	**Operational-Related**
Risks and Hazards – New Receptor (All Areas) (Individual Project) **Staff Proposal**	Same as Operational Thresholds*	Compliance with Qualified Community Risk Reduction Plan OR Increased cancer risk of >10.0 in a million Increased non-cancer risk of > 1.0 Hazard Index (Chronic or Acute) Ambient $PM_{2.5}$ increase: > 0.3 µg/m^3 annual average Zone of Influence: 1,000-foot radius from fence line of source or receptor
Risks and Hazards (Individual Project) **Tiered Thresholds Option**	Same as Operational Thresholds*	**Impacted Communities:** Siting a New Source Compliance with Qualified Community Risk Reduction Plan OR Increased cancer risk of >5.0 in a million Increased non-cancer risk of > 1.0 Hazard Index (Chronic or Acute) Ambient $PM_{2.5}$ increase: > 0.2 µg/m^3 annual average Zone of Influence: 1,000-foot radius from fence line of source or receptor
Risks and Hazards (Individual Project) **Tiered Thresholds Option** (Continued)	Same as Operational Thresholds*	**Impacted Communities:** Siting a New Receptor **All Other Areas:** Siting a New Source or Receptor Compliance with Qualified Community Risk Reduction Plan OR Increased cancer risk of >10.0 in a million Increased non-cancer risk of > 1.0 Hazard Index (Chronic or Acute) Ambient $PM_{2.5}$ increase: > 0.3 µg/m^3 annual average Zone of Influence: 1,000-foot radius from fence line of source or receptor

Table 1 – Air Quality CEQA Thresholds of Significance		
Pollutant	**Construction-Related**	**Operational-Related**
Risks and Hazards – New Source (All Areas) (Cumulative Thresholds)	Same as Operational Thresholds*	Compliance with Qualified Community Risk Reduction Plan OR Cancer: > 100 in a million (from all local sources) Non-cancer: > 10.0 Hazard Index (from all local sources) (Chronic) $PM_{2.5}$: > 0.8 µg/m^3 annual average (from all local sources) Zone of Influence: 1,000-foot radius from fence line of source or receptor
Risks and Hazards – New Receptor (All Areas) (Cumulative Thresholds)	Same as Operational Thresholds*	Compliance with Qualified Community Risk Reduction Plan OR Cancer: > 100 in a million (from all local sources) Non-cancer: > 10.0 Hazard Index (from all local sources) (Chronic) $PM_{2.5}$: > 0.8 µg/m^3 annual average (from all local sources) Zone of Influence: 1,000-foot radius from fence line of source or receptor
Accidental Release of Acutely Hazardous Air Pollutants	None	Storage or use of acutely hazardous materials locating near receptors or receptors locating near stored or used acutely hazardous materials considered significant
Odors	None	Complaint History—Five confirmed complaints per year averaged over three years
Plan-Level		
Criteria Air Pollutants and Precursors	None	1. Consistency with Current Air Quality Plan control measures 2. Projected VMT or vehicle trip increase is less than or equal to projected population increase

Table 1 – Air Quality CEQA Thresholds of Significance		
Pollutant	**Construction-Related**	**Operational-Related**
GHGs	None	Compliance with Qualified Greenhouse Gas Reduction Strategy (or similar criteria included in a General Plan) OR 6.6 MT CO2e/ SP/yr (residents + employees)
Risks and Hazards	None	1. Overlay zones around existing and planned sources of TACs (including adopted Risk Reduction Plan areas) 2. Overlay zones of at least 500 feet (or Air District-approved modeled distance) from all freeways and high volume roadways
Odors	None	Identify the location of existing and planned sources of odors
Accidental Release of Acutely Hazardous Air Pollutants	None	None
Regional Plans (Transportation and Air Quality Plans)		
GHGs, Criteria Air Pollutants and Precursors, and Toxic Air Contaminants	None	No net increase in emissions

Notes: CO = carbon monoxide; CO_2e = carbon dioxide equivalent; GHGs = greenhouse gases; lb/day = pounds per day; MT = metric tons; NO_X = oxides of nitrogen; $PM_{2.5}$= fine particulate matter with an aerodynamic resistance diameter of 2.5 micrometers or less; PM_{10} = respirable particulate matter with an aerodynamic resistance diameter of 10 micrometers or less; ppm = parts per million; ROG = reactive organic gases; SO_2 = sulfur dioxide; SP = service population; TACs = toxic air contaminants; TBP = toxic best practices; tons/day = tons per day; tpy = tons per year; yr= year.

* Note: The Air District recommends that for construction projects that are less than one year duration, Lead Agencies should annualize impacts over the scope of actual days that peak impacts are to occur, rather than the full year.

2. GREENHOUSE GAS THRESHOLDS

BAAQMD does not currently have an adopted threshold of significance for GHG emissions. BAAQMD currently recommends that lead agencies quantify GHG emissions resulting from new development and apply all feasible mitigation measures to lessen the potentially significant adverse impacts. One of the primary objectives in updating the current CEQA Guidelines is to identify a GHG significance threshold, analytical methodologies, and mitigation measures to ensure new land use development meets its fair share of the emission reductions needed to address the cumulative environmental impact from GHG emissions. GHG emissions contribute, on a cumulative basis, to the significant adverse environmental impacts of global climate change. As reviewed herein, climate change impacts include an increase in extreme heat days, higher ambient concentrations of air pollutants, sea level rise, impacts to water supply and water quality, public health impacts, impacts to ecosystems, impacts to agriculture, and other environmental

impacts. No single land use project could generate enough GHG emissions to noticeably change the global average temperature. The combination of GHG emissions from past, present, and future projects contribute substantially to the phenomenon of global climate change and its associated environmental impacts.

2.1. THRESHOLDS OF SIGNIFICANCE

Project Type	Thresholds
Projects other than Stationary Sources	Compliance with Qualified Greenhouse Gas Reduction Strategy OR 1,100 MT of CO_2e/yr OR 4.6 MT CO_2e/SP/yr (residents + employees)
Stationary Sources	10,000 MT of CO_2e/yr
Plans	Compliance with Qualified Greenhouse Gas Reduction Strategy (or similar criteria included in a General Plan) OR 6.6 MT CO_2e/SP/yr (residents + employees)
Regional Plans (Transportation and Air Quality Plans)	No net increase in GHG emissions

2.2. JUSTIFICATION AND SUBSTANTIAL EVIDENCE SUPPORTING THRESHOLDS

BAAQMD's approach to developing a threshold of significance for GHG emissions is to identify the emissions level for which a project would not be expected to substantially conflict with existing California legislation adopted to reduce statewide GHG emissions. If a project would generate GHG emissions above the threshold level, it would be considered to contribute substantially to a cumulative impact, and would be considered significant. If mitigation can be applied to lessen the emissions such that the project meets its share of emission reductions needed to address the cumulative impact, the project would normally be considered less than significant.

As explained in the District's *Revised Draft Options and Justifications Report* (BAAQMD 2009), there are several types of thresholds that may be supported by substantial evidence and be consistent with existing California legislation and policy to reduce statewide GHG emissions. In determining which thresholds to recommend, Staff studied numerous options, relying on reasonable, environmentally conservative assumptions on growth in the land use sector, predicted emissions reductions from statewide regulatory measures and resulting emissions inventories, and the efficacies of GHG mitigation measures. The thresholds recommended herein were chosen based on the substantial evidence that such thresholds represent quantitative and/or qualitative levels of GHG emissions, compliance with which means that the environmental impact of the GHG emissions will normally not be cumulatively considerable under CEQA. Compliance with such thresholds will be part of the solution to the cumulative GHG emissions problem, rather than hinder the state's ability to meet its goals of reduced statewide GHG emissions. Staff notes that it does not believe there is only one threshold for GHG emissions that can be supported by substantial evidence.

GHG CEQA significance thresholds recommended herein are intended to serve as interim levels during the implementation of the AB 32 Scoping Plan and SB 375, which will occur over time. Until AB 32 has been fully implemented in terms of adopted regulations, incentives, and programs and until SB 375 required plans have been fully adopted, or the California Air Resources Board (ARB) adopts a recommended threshold, the BAAQMD recommends that local agencies in the Bay Area apply the GHG thresholds recommended herein.

If left unchecked, GHG emissions from new land use development in California will result in a cumulatively considerable amount of GHG emissions and a substantial conflict with the State's ability to meet the goals within AB 32. Thus, BAAQMD proposes to adopt interim GHG thresholds for CEQA analysis, which can be used by lead agencies within the Bay Area. This would help lead agencies navigate this dynamic regulatory and technological environment where the field of analysis has remained wide open and inconsistent. BAAQMD's framework for developing a GHG threshold for land development projects that is based on policy and substantial evidence follows.

2.2.1. Scientific and Regulatory Justification

Climate Science Overview

Prominent GHGs contributing to the greenhouse effect are carbon dioxide (CO_2), methane (CH_4), nitrous oxide (N_2O), hydrofluorocarbons, chlorofluorocarbons, and sulfur hexafluoride. Human-caused emissions of these GHGs in excess of natural ambient concentrations are responsible for intensifying the greenhouse effect and have led to a trend of unnatural warming of the earth's climate, known as global climate change or global warming. It is *extremely unlikely* that global climate change of the past 50 years can be explained without the contribution from human activities (IPCC 2007a).

According to Article 2 of the United Nations Framework Convention on Climate Change (UNFCCC), "Avoiding Dangerous Climate Change" means: *"stabilization of greenhouse gas concentrations in the atmosphere at a level that would prevent dangerous anthropogenic interference with the climate system."* Dangerous climate change defined in the UNFCCC is based on several key indicators including the potential for severe degradation of coral reef systems, disintegration of the West Antarctic Ice Sheet, and shut down of the large-scale, salinity- and thermally-driven circulation of the oceans. (UNFCCC 2009). The global atmospheric concentration of carbon dioxide has increased from a pre-industrial value of about 280 ppm to 379 ppm in 2005 (IPCC 2007a). "Avoiding dangerous climate change" is generally understood to be achieved by stabilizing global average temperatures between 2 and 2.4°C above pre-industrial levels. In order to limit temperature increases to this level, ambient global CO_2 concentrations must stabilize between 350 and 400 ppm (IPCC 2007b).

Executive Order S-3-05

Executive Order S-3-05, which was signed by Governor Schwarzenegger in 2005, proclaims that California is vulnerable to the impacts of climate change. It declares that increased temperatures could reduce the Sierra's snowpack, further exacerbate California's air quality problems, and potentially cause a rise in sea levels. To combat those concerns, the Executive Order established total GHG emission targets. Specifically, emissions are to be reduced to the 2000 level by 2010, the 1990 level by 2020, and to 80 percent below the 1990 level by 2050.

Assembly Bill 32, the California Global Warming Solutions Act of 2006

In September 2006, Governor Arnold Schwarzenegger signed Assembly Bill 32, the California Global Warming Solutions Act of 2006, which set the 2020 greenhouse gas emissions reduction goal into law. AB 32 finds and declares that "Global warming poses a serious threat to the economic well-being, public health, natural resources, and the environment of California." AB 32 requires that statewide GHG emissions be reduced to 1990 levels by 2020, and establishes

regulatory, reporting, voluntary, and market mechanisms to achieve quantifiable reductions in GHG emissions to meet the statewide goal.

In December of 2008, ARB adopted its *Climate Change Scoping Plan* (*Scoping Plan*), which is the State's plan to achieve GHG reductions in California, as required by AB 32 (ARB 2008). The Scoping Plan contains strategies California will implement to achieve a reduction of 169 MMT CO_2e emissions, or approximately 28 percent from the state's projected 2020 emission level of 596 MMT of CO_2e under a business-as-usual scenario (this is a reduction of 42 MMT of CO_2e, or almost 10 percent, from 2002-2004 average emissions), so that the state can return to 1990 emission levels, as required by AB 32.

While the Scoping Plan establishes the policy intent to control numerous GHG sources through regulatory, incentive, and market means, given the early phase of implementation and the level of control that local CEQA lead agencies have over numerous GHG sources, CEQA is an important and supporting tool in achieving GHG reductions overall in compliance with AB 32. In this spirit, BAAQMD is considering the adoption of thresholds of significance for GHG emissions for stationary source and land use development projects.

Senate Bill 375

Senate Bill (SB) 375, signed in September 2008, aligns regional transportation planning efforts, regional GHG reduction targets, and land use and housing allocation. SB 375 requires Metropolitan Planning Organizations (MPOs) to adopt a Sustainable Communities Strategy (SCS) or Alternative Planning Strategy (APS), which will prescribe land use allocation in that MPO's Regional Transportation Plan (RTP). ARB, in consultation with MPOs, will provide each affected region with reduction targets for GHGs emitted by passenger cars and light trucks in the region for the years 2020 and 2035. These reduction targets will be updated every eight years, but can be updated every four years if advancements in emission technologies affect the reduction strategies to achieve the targets. ARB is also charged with reviewing each MPO's SCS or APS for consistency with its assigned targets. If MPOs do not meet the GHG reduction targets, transportation projects would not be eligible for State funding programmed after January 1, 2012. New provisions of CEQA incentivize qualified projects that are consistent with an approved SCS or APS, categorized as "transit priority projects."

The revised District CEQA Guidelines includes methodology consistent with the recently updated State CEQA Guidelines, which provides that certain residential and mixed use projects, and transit priority projects consistent with an applicable SCS or APS need not analyze GHG impacts from cars and light duty trucks (CEQA Guidelines §15183.5(c)).

2.2.2. Project-Level GHG Thresholds

Staff recommends setting GHG significance thresholds based on AB 32 GHG emission reduction goals while taking into consideration emission reduction strategies outlined in ARB's Scoping Plan. Staff proposes two quantitative thresholds for land use projects: a bright line threshold based on a "gap" analysis and an efficiency threshold based on emission levels required to be met in order to achieve AB 32 goals.

Staff also proposes one qualitative threshold for land use projects: if a project complies with a Qualified Greenhouse Gas Reduction Strategy (as defined in Section 2.3.4 below) that addresses the project it would be considered less than significant. As explained in detail in Section 2.3.4 below, compliance with a Qualified Greenhouse Gas Reduction Strategy (or similar adopted policies, ordinances and programs), would provide the evidentiary basis for making CEQA findings that development consistent with the plan would result in feasible, measureable, and verifiable GHG reductions consistent with broad state goals such that projects approved under

qualified Greenhouse Gas Reduction Strategies or equivalent demonstrations would achieve their fair share of GHG emission reductions.

Land Use Projects "Gap-Based" Threshold

Staff took eight steps in developing this threshold approach, which are summarized here and detailed in the sections that follow. It should be noted that the "gap-based approach" used for threshold development is a conservative approach that focuses on a limited set of state mandates that appear to have the greatest potential to reduce land use development-related GHG emissions at the time of this writing. It is also important to note that over time, as the effectiveness of the State's implementation of AB 32 (and SB 375) progresses, BAAQMD will need to reconsider the extent of GHG reductions needed over and above those from the implementation thereof for the discretionary approval of land use development projects. Although there is an inherent amount of uncertainty in the estimated capture rates (i.e., frequency at which project-generated emissions would exceed a threshold and would be subject to mitigation under CEQA) and the aggregate emission reductions used in the gap analysis, they are based on BAAQMD's expertise, the best available data, and use conservative assumptions for the amount of emission reductions from legislation in derivation of the gap (e.g., only adopted legislation was relied upon). This approach is intended to attribute an appropriate share of GHG emission reductions necessary to reach AB 32 goals to new land use development projects in BAAQMD's jurisdiction that are evaluated pursuant to CEQA.

Step 1 Estimate from ARB's statewide GHG emissions inventory the growth in emissions between 1990 and 2020 attributable to "land use-driven" sectors of the emission inventory as defined by OPR's guidance document (*CEQA and Climate Change*). Land use-driven emission sectors include Transportation (On-Road Passenger Vehicles; On-Road Heavy Duty), Electric Power (Electricity; Cogeneration), Commercial and Residential (Residential Fuel Use; Commercial Fuel Use) and Recycling and Waste (Domestic Waste Water Treatment).

Result:1990 GHG emissions were 295.53 MMT CO_2e/yr and projected 2020 business-as-usual GHG emissions would be 400.22 MMT CO_2e/yr; thus a 26.2 percent reduction from statewide land use-driven GHG emissions would be necessary to meet the AB 32 goal of returning to 1990 emission levels by 2020. (See Table 2)

Step 2 Estimate the anticipated GHG emission reductions affecting the same land use-driven emissions inventory sectors associated with adopted statewide regulations identified in the AB 32 Scoping Plan.

Result: Estimated a 23.9 percent reduction can be expected in the land use-driven GHG emissions inventory from adopted Scoping Plan regulations, including AB 1493 (Pavley), LCFS, Heavy/Medium Duty Efficiency, Passenger Vehicle Efficiency, Energy-Efficiency Measures, Renewable Portfolio Standard, and Solar Roofs. (See Table 3)

Step 3 Determine any short fall or "gap" between the 2020 statewide emission inventory estimates and the anticipated emission reductions from adopted Scoping Plan regulations. This "gap" represents additional GHG emission reductions needed statewide from the land use-driven emissions inventory sectors, which represents new land use development's share of the emission reductions needed to meet statewide GHG emission reduction goals.

Result: With the 23.9 percent reductions from AB 32 Scoping Measures, there is a "gap" of 2.3 percent in necessary additional GHG emissions reductions to meet AB 32

goals of a 26.2 percent reduction from statewide land use-driven GHG emissions to return to 1990 levels in 2020. (See Table 2)

Step 4 Determine the percent reduction this "gap" represents in the "land use-driven" emissions inventory sectors from BAAQMD's 2020 GHG emissions inventory. Identify the mass of emission reductions needed in the SFBAAB from land use-driven emissions inventory sectors.

Result: Estimated that a 2.3 percent reduction in BAAQMD's projected 2020 emissions projections requires emissions reductions of 1.6 MMT CO_2e/yr from the land use-driven sectors. (See Table 4)

Step 5 Assess BAAQMD's historical CEQA database (2001-2008) to determine the frequency distribution trend of project sizes and types that have been subject to CEQA over the past several years.

Result: Determined historical patterns of residential, commercial and industrial development by ranges of average sizes of each development type. Results were used in Step 6 below to distribute anticipated Bay Area growth among different future project types and sizes.

Step 6 Forecast new land use development for the Bay Area using DOF/EDD population and employment projections and distribute the anticipated growth into appropriate land use types and sizes needed to accommodate the anticipated growth (based on the trend analysis in Step 5 above). Translate the land use development projections into land use categories consistent with those contained in the Urban Emissions Model (URBEMIS).

Result: Based on population and employment projections and the trend analysis from Step 5 above, forecasted approximately 4,000 new development projects, averaging about 400 projects per year through 2020 in the Bay Area.

Step 7 Estimate the amount of GHG emissions from each land use development project type and size using URBEMIS and post-model manual calculation methods (for emissions not included in URBEMIS). Determine the amount of GHG emissions that can reasonably and feasibly be reduced through currently available mitigation measures ("mitigation effectiveness") for future land use development projects subject to CEQA (based on land use development projections and frequency distribution from Step 6 above).

Result: Based on the information available and on sample URBEMIS calculations, found that mitigation effectiveness of between 25 and 30 percent is feasible.

Step 8 Conduct a sensitivity analysis of the numeric GHG mass emissions threshold needed to achieve the desired emissions reduction (i.e., "gap") determined in Step 4. This mass emission GHG threshold is that which would be needed to achieve the emission reductions necessary by 2020 to meet the Bay Area's share of the statewide "gap" needed from the land use-driven emissions inventory sectors.

Result: The results of the sensitivity analysis conducted in Step 8 found that reductions between about 125,000 MT/yr (an aggregate of 1.3 MMT in 2020) and over 200,000 MT/yr (an aggregate of over 2.0 MMT in 2020) were achievable and feasible. A mass emissions threshold of 1,100 MT of CO_2e/yr would result in approximately 59 percent of all projects being above the significance threshold (e.g., this is approximately the operational GHG emissions that would be associated with a 60 residential unit

subdivision) and must implement feasible mitigation measures to meet CEQA requirements. With an estimated 26 percent mitigation effectiveness, the 1,100 MT threshold would achieve 1.6 MMT CO_2e/yr in GHG emissions reductions.

Detailed Basis and Analysis

Derivation of Greenhouse Gas Reduction Goal

To meet the target emissions limit established in AB 32 (equivalent to levels in 1990), total GHG emissions would need to be reduced by approximately 28 percent from projected 2020 forecasts (ARB 2009a). The AB 32 Scoping Plan is ARB's plan for meeting this mandate (ARB 2008). While the Scoping Plan does not specifically identify GHG emission reductions from the CEQA process for meeting AB 32 derived emission limits, the scoping plan acknowledges that "other strategies to mitigate climate change . . . should also be explored." The Scoping Plan also acknowledges that "Some of the measures in the plan may deliver more emission reductions than we expect; others less . . . and new ideas and strategies will emerge." In addition, climate change is considered a significant environmental issue and warrants consideration under CEQA. SB 97 represents the State Legislature's confirmation of this fact, and it directed the Governor's Office of Planning and Research (OPR) to develop CEQA Guidelines for evaluation of GHG emissions impacts and recommend mitigation strategies. In response, OPR released the *Technical Advisory: CEQA and Climate Change* (OPR 2008), and proposed revisions to the State CEQA guidelines (April 14, 2009) for consideration of GHG emissions. The California Natural Resources Agency adopted the proposed State CEQA Guidelines revisions on December 30, 2009 and the revisions were effective beginning March 18, 2010. It is known that new land use development must also do its fair share toward achieving AB 32 goals (or, at a minimum, should not hinder the State's progress toward the mandated emission reductions).

Foreseeable Scoping Plan Measures Emission Reductions and Remaining "Gap"

Step 1 of the Gap Analysis entailed estimating from ARB's statewide GHG inventory the growth in emissions between 1990 and 2020 attributable to land use driven sectors of the emissions inventory. As stated above, to meet the requirements set forth in AB 32 (i.e., achieve California's 1990-equivalent GHG emissions levels by 2020) California would need to achieve an approximate 28 percent reduction in emissions across all sectors of the GHG emissions inventory compared with 2020 projections. However, to meet the AB 32 reduction goals in the emissions sectors that are related to land use development (e.g., on-road passenger and heavy-duty motor vehicles, commercial and residential area sources [i.e., natural gas], electricity generation/consumption, wastewater treatment, and water distribution/consumption), staff determined that California would need to achieve an approximate 26 percent reduction in GHG emissions from these land use-driven sectors (ARB 2009a) by 2020 to return to 1990 land use emission levels.

Next, in Step 2 of the Gap Analysis, Staff determined the GHG emission reductions within the land use-driven sectors that are anticipated to occur from implementation of the Scoping Plan measures statewide, which are summarized in Table 2 and described below. Since the GHG emission reductions anticipated with the Scoping Plan were not accounted for in ARB's or BAAQMD's 2020 GHG emissions inventory forecasts (i.e., business as usual), an adjustment was made to include (i.e., give credit for) GHG emission reductions associated with key Scoping Plans measures, such as the Renewable Portfolio Standard, improvements in energy efficiency through periodic updates to Title 24, AB 1493 (Pavley) (which recently received a federal waiver to allow it to be enacted in law), the Low Carbon Fuel Standard (LCFS), and other measures. With reductions from these State regulations (Scoping Plan measures) taken into consideration and accounting for an estimated 23.9 percent reduction in GHG emissions, in Step 3 of the Gap Analysis Staff determined that the Bay Area would still need to achieve an additional 2.3 percent reduction from projected 2020 GHG emissions to meet the 1990 GHG emissions goal from the

land-use driven sectors. This necessary 2.3 percent reduction in projected GHG emissions from the land use sector is the "gap" the Bay Area needs to fill to do its share to meet the AB 32 goals. Refer to the following explanation and Tables 2 through 4 for data used in this analysis.

Because the transportation sector is the largest emissions sector of the state's GHG emissions inventory, it is aggressively targeted in early actions and other priority actions in the Scoping Plan including measures concerning gas mileage (Pavley), fuel carbon intensity (LCFS) and vehicle efficiency measures.

Table 2 – California 1990, 2002-2004, and 2020 Land Use Sector GHG[1] (MMT CO_2e/yr)

Sector	1990 Emissions	2002-2004 Average	2020 BAU Emissions Projections	% of 2020 Total
Transportation	**137.98**	**168.66**	**209.06**	**52%**
On-Road Passenger Vehicles	108.95	133.95	160.78	40%
On-Road Heavy Duty	29.03	34.69	48.28	12%
Electric Power	**110.63**	**110.04**	**140.24**	**35%**
Electricity	95.39	88.97	107.40	27%
Cogeneration[2]	15.24	21.07	32.84	8%
Commercial and Residential	**44.09**	**40.96**	**46.79**	**12%**
Residential Fuel Use	29.66	28.52	32.10	8%
Commercial Fuel Use	14.43	12.45	14.63	4%
Recycling and Waste[1]	**2.83**	**3.39**	**4.19**	**1%**
Domestic Wastewater Treatment	2.83	3.39	4.19	1%
TOTAL GROSS EMISSIONS	**295.53**	**323.05**	**400.22**	
% Reduction Goal from Statewide land use driven sectors (from 2020 levels to reach 1990 levels in these emission inventory sectors)			26.2%	
% Reduction from AB32 Scoping Plan measures applied to land use sectors (see Table 3)			-23.9%	
% Reduction needed statewide beyond Scoping Plan measures (Gap)			2.3%	

Notes: MMT CO_2e /yr = million metric tons of carbon dioxide equivalent emissions per year.

[1] Landfills not included. See text.

[2] Cogeneration included due to many different applications for electricity, in some cases provides substantial power for grid use, and because electricity use served by cogeneration is often amenable to efficiency requirements of local land use authorities.

Sources: Data compiled by EDAW and ICF Jones & Stokes from ARB data.

Pavley Regulations. The AB 32 Scoping Plan assigns an approximate 20 percent reduction in emissions from passenger vehicles associated with the implementation of AB 1493. The AB 32 Scoping Plan also notes that "AB 32 specifically states that if the Pavley regulations do not remain in effect, ARB shall implement alternative regulations to control mobile sources to achieve

equivalent or greater reductions of greenhouse gas emissions (HSC §38590)." Thus, it is reasonable to assume full implementation of AB 1493 standards, or equivalent programs that would be implemented by ARB. Furthermore, on April 1, 2010, U.S. EPA and the Department of Transportation's National Highway Safety Administration (NHTSA) announced a joint final rule establishing a national program that will dramatically reduce greenhouse gas emissions and improve fuel economy for new cars and trucks sold in the United States after 2011. Under this national program, automobile manufacturers will be able to build a single light-duty national fleet that satisfies all requirements under both the national program and the standards of California and other states. Nonetheless, BAAQMD may need to revisit this methodology as the federal standards come on line to ensure that vehicle standards are as aggressive as contemplated in development of this threshold.

Table 3 – 2020 Land Use Sector GHG Emission Reductions from State Regulations and AB 32 Measures

Affected Emissions Source	California Legislation	% Reduction from 2020 GHG inventory	End Use Sector (% of Bay Area LU Inventory)	Scaled % Emissions Reduction (credit)
Mobile	AB 1493 (Pavley)	19.7%	On road passenger/light truck transportation (45%)	8.9%
	LCFS	7.2%	On road passenger/light truck transportation (45%)	3.2%
	LCFS	7.2%	On road Heavy/Medium Duty Transportation (5%)	0.4%
	Heavy/Medium Duty Efficiency	2.9%	On road Heavy/Medium Duty Transportation (5%)	0.2%
	Passenger Vehicle Efficiency	2.8%	On road passenger/light truck transportation (45%)	1.3%
Area	Energy-Efficiency Measures	9.5%	Natural gas (Residential, 10%)	1.0%
			Natural gas (Non-residential, 13%)	1.2%
Indirect	Renewable Portfolio Standard	21.0%	Electricity (excluding cogen) (17%)	3.5%
	Energy-Efficiency Measures	15.7%	Electricity (26%)	4.0%
	Solar Roofs	1.5%	Electricity (excluding cogen) (17%)	0.2%
Total credits given to land use-driven emission inventory sectors from Scoping Plan measures				**23.9%**

Notes: AB = Assembly Bill; LCFS = Low Carbon Fuel Standard; SB = Senate Bill; RPS = Renewable Portfolio Standard
Sources: Data compiled by ICF Jones & Stokes.

LCFS. According to the adopted LCFS rule (CARB, April 2009), the LCFS is expected to result in approximately 10 percent reduction in the carbon intensity of transportation fuels. However, a

portion of the emission reductions required from the LCFS would be achieved over the life cycle of transportation fuel production rather than from mobile-source emission factors. Based on CARB's estimate of nearly 16 MMT reductions in on-road emissions from implementation of the LCFS and comparison to the statewide on-road emissions sector, the LCFS is assumed to result in a 7.2 percent reduction compared to 2020 BAU conditions (CARB 2009e).

Table 4 – SFBAAB 1990, 2007, and 2020 Land Use Sector GHG Emissions Inventories and Projections (MMT CO_2e/yr)

Sector	1990 Emissions	2007 Emissions	2020 Emissions Projections	% of 2020 Total[2]
Transportation	**26.1**	**30.8**	**35.7**	**50%**
On-Road Passenger Vehicles	23.0	27.5	32.0	
On-Road Heavy Duty	3.1	3.3	3.7	
Electric Power	**25.1**	**15.2**	**18.2**	**26%**
Electricity	16.5	9.9	11.8	
Cogeneration	8.6	5.3	6.4	
Commercial and Residential	**8.9**	**15.0**	**16.8**	**24%**
Residential Fuel Use	5.8	7.0	7.5	
Commercial Fuel Use	3.1	8.0	9.3	
Recycling and Waste[1]	**0.2**	**0.4**	**0.4**	**1%**
Domestic Waste Water Treatment	0.2	0.4	0.4	
TOTAL GROSS EMISSIONS	**60.3**	**61.4**	**71.1**	
SFBAAB's "Fair Share" % Reduction (from 2020 levels to reach 1990 levels) with AB-32 Reductions (from Table 3)			2.3%	
SFBAAB's Equivalent Mass Emissions Land Use Reduction Target at 2020 (MMT CO2e/yr)			1.6	

Notes: MMT CO_2e /yr = million metric tons of carbon dioxide equivalent emissions per year; SFBAAB = San Francisco Bay Area Air Basin.

[1] Landfills not included.

[2] Percentages do not sum exactly to 100% in table due to rounding.

Sources: Data compiled by EDAW 2009, ICF Jones & Stokes 2009, BAAQMD 2008.

Renewable Portfolio Standard, Energy Efficiency and Solar Roofs. Energy efficiency and renewable energy measures from the Scoping Plan were also included in the gap analysis. The Renewable Portfolio Standard (rules) will require the renewable energy portion of the retail electricity portfolio to be 33 percent in 2020. For PG&E, the dominant electricity provider in the Basin, approximately 12 percent of their current portfolio qualifies under the RPS rules and thus the gain by 2020 would be approximately 21 percent. The Scoping Plan also estimates that energy efficiency gains with periodic improvement in building and appliance energy standards and incentives will reach 10 to 15 percent for natural gas and electricity respectively. The final state measure included in this gap analysis is the solar roof initiative, which is estimated to result in reduction of the overall electricity inventory of 1.5 percent.

Landfill emissions are excluded from this analysis. While land use development does generate waste related to both construction and operations, the California Integrated Waste Management Board (CIWMB) has mandatory diversion requirements that will, in all probability, increase over time to promote waste reductions, reuse, and recycle. The Bay Area has relatively high levels of waste diversion and extensive recycling efforts. Further, ARB has established and proposes to increase methane capture requirements for all major landfills. Thus, at this time, landfill emissions associated with land use development waste generation is not included in the land use sector inventory used to develop this threshold approach.

Industrial stationary sources thresholds were developed separately from the land use threshold development using a market capture approach as described below. However, mobile source and area source emissions, as well as indirect electricity emissions that derive from industrial use are included in the land use inventory above as these particular activities fall within the influence of local land use authorities in terms of the affect on trip generation and energy efficiency.

AB 32 mandates reduction to 1990-equivalent GHG levels by 2020, with foreseeable emission reductions from State regulations and key Scoping Plan measures taken into account, were applied to the land use-driven emission sectors within the SFBAAB (i.e., those that are included in the quantification of emissions from a land use project pursuant to a CEQA analysis [on-road passenger vehicles, commercial and residential natural gas, commercial and residential electricity consumption, and domestic waste water treatment], as directed by OPR in the Technical Advisory: *Climate Change and CEQA* [OPR 2008]). This translates to a 2.3 percent gap in necessary GHG emission reductions by 2020 from these sectors.

Land Use Projects Bright Line Threshold

In Steps 4 and 5 of the gap analysis, Staff determined that applying a 2.3 percent reduction to these land use emissions sectors in the SFBAAB's GHG emissions inventory would result in an equivalent fair share of 1.6 million metric tons per year (MMT/yr) reductions in GHG emissions from new land use development. As additional regulations and legislation aimed at reducing GHG emissions from land use-related sectors become available in the future, the 1.6 MMT GHG emissions reduction goal may be revisited and recalculated by BAAQMD.

In order to derive the 1.6 MMT "gap," a projected development inventory for the next ten years in the SFBAAB was calculated (see Table 4 and *Revised Draft Options and Justifications Report* (BAAQMD 2009)). CO_2e emissions were modeled for projected development in the SFBAAB and compiled to estimate the associated GHG emissions inventory. The GHG (i.e., CO_2e) CEQA threshold level was adjusted for projected land use development that would occur within BAAQMD's jurisdiction over the period from 2010 through 2020.

Projects with emissions greater than the threshold would be required to mitigate to the threshold level or reduce project emissions by a percentage (mitigation effectiveness) deemed feasible by the lead agency under CEQA compared to a base year condition. The base year condition is defined by an equivalent size and character of project with annual emissions using the defaults in URBEMIS and the California Climate Action Registry's General Reporting Protocol for 2008. By this method, land use project mitigation subject to CEQA would help close the "gap" remaining after application of the key regulations and measures noted above supporting overall AB 32 goals.

This threshold takes into account Steps 1-8 of the gap analysis described above to arrive at a numerical mass emissions threshold. Various mass emissions significance threshold levels (i.e., bright lines) could be chosen based on the mitigation effectiveness and performance anticipated to be achieved per project to meet the aggregate emission reductions of 1.6 MMT needed in the

SFBAAB by 2020(see Table 5 and *Revised Draft Options and Justifications Report* (BAAQMD 2009)). Staff recommends a 1,100 MT CO_2e per year threshold. Choosing a 1,100 MT mass emissions significance threshold level (equivalent to approximately 60 single-family units), would result in about 59 percent of all projects being above the significance threshold and having to implement feasible mitigation measures to meet their CEQA obligations. These projects account for approximately 92 percent of all GHG emissions anticipated to occur between now and 2020 from new land use development in the SFBAAB.

Project applicants and lead agencies could use readily available computer models to estimate a project's GHG emissions, based on project specific attributes, to determine if they are above or below the bright line numeric threshold. With this threshold, projects that are above the threshold level, after consideration of emission-reducing characteristics of the project as proposed, would have to reduce their emissions to below the threshold to be considered less than significant.

Table 5 – Operational GHG Threshold Sensitivity Analysis

Option	Mitigation Effectiveness Assumptions		Mass Emission Threshold Level (MT CO_2e/yr)	% of Projects Captured (>threshold)	% of Emissions Captured (> threshold)	Emissions Reduction per year (MT/yr)	Aggregate Emissions Reduction (MMT) at 2020	Threshold Project Size Equivalent (single family dwelling units)
	Performance Standards Applied to All Projects with Emissions < Threshold Level	Mitigation Effectiveness Applied to Emissions > Threshold Level						
1A	N/A	30%	975	60%	93%	201,664	2.0	53
1A	N/A	25%	110	96%	100%	200,108	2.0	66
1A	N/A	30%	1,225	21%	67%	159,276	1.6	67
1A	N/A	26%	1,100	59%	92%	159,877	1.6	60
1A	N/A	30%	2,000	14%	61%	143,418	1.4	109
1A	N/A	25%	1,200	58%	92%	136,907	1.4	66
1A	N/A	30%	3,000	10%	56%	127,427	1.3	164
1A	N/A	25%	1,500	20%	67%	127,303	1.3	82
1B	26%	N/A	N/A	100%	100%	208,594	2.1	N/A[1]
1C	5%	30%	1,900	15%	62%	160,073	1.6	104
1C	10%	25%	1,250	21%	67%	159,555	1.6	68
1C	5%	30%	3,000	10%	56%	145,261	1.5	164
1C	10%	25%	2,000	4%	61%	151,410	1.5	109
1C	10%	30%	10,000	2%	33%	125,271	1.3	547

MMT = million metric tons per year; MT CO_2e/yr = metric tons of carbon dioxide equivalent emissions per year; MT/yr = metric tons per year; N/A = not applicable.

[1] Any project subject to CEQA would trigger this threshold.

Source: Data modeled by ICF Jones& Stokes

Source: Data modeled by ICF Jones & Stokes.

Establishing a "bright line" to determine the significance of a project's GHG emissions impact provides a level of certainty to lead agencies in determining if a project needs to reduce its GHG emissions through mitigation measures and when an EIR is required.

Land Use Projects Efficiency-Based Threshold

GHG efficiency metrics can also be utilized as thresholds to assess the GHG efficiency of a project on a per capita basis (residential only projects) or on a "service population" basis (the sum of the number of jobs and the number of residents provided by a project) such that the project will allow for consistency with the goals of AB 32 (i.e., 1990 GHG emissions levels by 2020). GHG efficiency thresholds can be determined by dividing the GHG emissions inventory goal (allowable emissions), by the estimated 2020 population and employment. This method allows highly efficient projects with higher mass emissions to meet the overall reduction goals of AB 32. Staff believes it is more appropriate to base the land use efficiency threshold on the service population metric for the land use-driven emission inventory. This approach is appropriate because the threshold can be applied evenly to all project types (residential or commercial/retail only and mixed use) and uses only the land use emissions inventory that is comprised of all land use projects. Staff will provide the methodology to calculate a project's GHG emissions in the revised CEQA Guidelines, such as allowing infill projects up to a 50 percent or more reduction in daily vehicle trips if the reduction can be supported by close proximity to transit and support services, or a traffic study prepared for the project.

Table 6 – California 2020 GHG Emissions, Population Projections and GHG Efficiency Thresholds - Land Use Inventory Sectors

Land Use Sectors Greenhouse Gas Emissions Target	295,530,000
Population	44,135,923
Employment	20,194,661
California Service Population (Population + Employment)	64,330,584
AB 32 Goal GHG emissions (metric tons CO_2e)/SP[1]	**4.6**

Notes: AB = Assembly Bill; CO_2e = carbon dioxide equivalent; GHG = greenhouse gas; SP = service population.
[1] Greenhouse gas efficiency levels were calculated using only the "land use-related" sectors of ARB's emissions inventory.
Sources: Data compiled by EDAW 2009, ARB 2009a, DOF 2009, EDD 2009, ICF Jones & Stokes 2009.

Staff proposes a project-level efficiency threshold of 4.6 MT CO_2e/SP, the derivation of which is shown Table 6. This efficiency-based threshold reflects very GHG-efficient projects. As stated previously and below, staff anticipates that significance thresholds (rebuttable presumptions of significance at the project level) will function on an interim basis only until adequate programmatic approaches are in place at the city, county, and regional level that will allow the CEQA streamlining of individual projects. (See State CEQA Guidelines §15183.5 ["Tiering and Streamlining the Analysis of Greenhouse Gas Emissions"]).

2.2.3. Plan-Level GHG Thresholds

Staff proposes using a two step process for determining the significance of proposed plans and plan amendments for GHG. As a first step in assessing plan-level impacts, Staff is proposing that agencies that have adopted a qualified Greenhouse Gas Reduction Strategy (or have incorporated similar criteria in their general plan) and the general plan is consistent with the Greenhouse Gas Reduction Strategy, the general plan would be considered less than significant. In addition, as discussed above for project-level GHG impacts, Staff is proposing an efficiency

threshold to assess plan-level impacts. Staff believes a programmatic approach to limiting GHG emissions is appropriate at the plan-level. Thus, as projects consistent with the Greenhouse Gas Reduction Strategy are proposed, they may be able to tier off the plan and its environmental analysis.

GHG Efficiency Metrics for Plans

For local land use plans, a GHG-efficiency metric (e.g., GHG emissions per unit) would enable comparison of a proposed general plan to its alternatives and to determine if the proposed general plan meets AB 32 emission reduction goals.

AB 32 identifies local governments as essential partners in achieving California's goal to reduce GHG emissions. Local governments have primary authority to plan, zone, approve, and permit how and where land is developed to accommodate population growth and the changing needs of their jurisdiction. ARB has developed the Local Government Operations Protocol and is developing a protocol to estimate community-wide GHG emissions. ARB encourages local governments to use these protocols to track progress in reducing GHG emissions. ARB encourages local governments to institutionalize the community's strategy for reducing its carbon footprint in its general plan. SB 375 creates a process for regional integration of land development patterns and transportation infrastructure planning with the primary goal of reducing GHG emissions from the largest sector of the GHG emission inventory, light duty vehicles.

If the statewide AB 32 GHG emissions reduction context is established, GHG efficiency can be viewed independently from the jurisdiction in which the plan is located. Expressing projected 2020 mass of emissions from land use-related emissions sectors by comparison to a demographic unit (e.g., population and employment) provides evaluation of the GHG efficiency of a project in terms of what emissions are allowable while meeting AB 32 targets.

Two approaches were considered for efficiency metrics. The "service population" (SP) approach would consider efficiency in terms of the GHG emissions compared to the sum of the number of jobs and the number of residents at a point in time. The per capita option would consider efficiency in terms of GHG emissions per resident only. Staff recommends that the efficiency threshold for plans be based on all emission inventory sectors because, unlike land use projects, general plans comprise more than just land use related emissions (e.g. industrial). Further, Staff recommends that the plan threshold be based on the service population metric as general plans include a mix of residents and employees. The Service Population metric would allow decision makers to compare GHG efficiency of general plan alternatives that vary residential and non-residential development totals, encouraging GHG efficiency through improving jobs/housing balance. This approach would not give preference to communities that accommodate more residential (population-driven) land uses than non-residential (employment driven) land uses which could occur with the per capita approach.

A SP-based GHG efficiency metric (see Table 7) was derived from the emission rates at the State level that would accommodate projected population and employment growth under trend forecast conditions, and the emission rates needed to accommodate growth while allowing for consistency with the goals of AB 32 (i.e., 1990 GHG emissions levels by 2020).

Table 7 – California 2020 GHG Emissions, Population Projections and GHG Efficiency Thresholds - All Inventory Sectors	
All Inventory Sectors Greenhouse Gas Emissions Target	426,500,000
Population	44,135,923
Employment	20,194,661
California Service Population (Population + Employment)	64,330,584
AB 32 Goal GHG emissions (metric tons CO_2e)/SP[1]	**6.6**

Notes: AB = Assembly Bill; CO_2e = carbon dioxide equivalent; GHG = greenhouse gas; SP = service population.
[1] Greenhouse gas efficiency levels were calculated using only the "land use-related" sectors of ARB's emissions inventory.
Sources: Data compiled by EDAW 2009, ARB 2009a, DOF 2009, EDD 2009, ICF Jones & Stokes 2009.

If a general plan demonstrates, through dividing the emissions inventory projections (MT CO_2e) by the amount of growth that would be accommodated in 2020, that it could meet the GHG efficiency metrics in this section (6.6 MT CO_2e/SP from all emission sectors, as noted in Table 7), then the amount of GHG emissions associated with the general plan would be considered less than significant, regardless of its size (and magnitude of GHG emissions). In other words, the general plan would accommodate growth in a manner that would not hinder the State's ability to achieve AB 32 goals, and thus, would be less than significant for GHG emissions and their contribution to climate change. The efficiency metric would not penalize well-planned communities that propose a large amount of development. Instead, the SP-based GHG efficiency metric acts to encourage the types of development that BAAQMD and OPR support (i.e., infill and transit-oriented development) because it tends to reduce GHG and other air pollutant emissions overall, rather than discourage large developments for being accompanied by a large mass of GHG emissions. Plans that are more GHG efficient would have no or limited mitigation requirements to help them complete the CEQA process more readily than plans that promote GHG inefficiencies, which will require detailed design of mitigation during the CEQA process and could subject a plan to potential challenge as to whether all feasible mitigation was identified and adopted. This type of threshold can shed light on a well-planned general plan that accommodates a large amount of growth in a GHG-efficient way.

When analyzing long-range plans, such as general plans, it is important to note that the planning horizon will often surpass the 2020 timeframe for implementation of AB 32. Executive Order S-3-05 establishes a more aggressive emissions reduction goal for the year 2050 of 80 percent below 1990 emissions levels. The year 2020 should be viewed as a milestone year, and the general plan should not preclude the community from a trajectory toward the 2050 goal. However, the 2020 timeframe is examined in this threshold evaluation because doing so for the 2050 timeframe (with respect to population, employment, and GHG emissions projections) would be too speculative. Advances in technology and policy decisions at the state level will be needed to meet the aggressive 2050 goals. It is beyond the scope of the analysis tools available at this time to examine reasonable emissions reductions that can be achieved through CEQA analysis in the year 2050. As the 2020 timeframe draws nearer, BAAQMD will need to reevaluate the threshold to better represent progress toward 2050 goals.

2.2.4. Greenhouse Gas Reduction Strategies

Finally, many local agencies have already undergone or plan to undergo efforts to create general or other plans that are consistent with AB 32 goals. The Air District encourages such planning efforts and recognizes that careful upfront planning by local agencies is invaluable to achieving

the state's GHG reduction goals. If a project is consistent with an adopted Qualified Greenhouse Gas Reduction Strategy that addresses the project's GHG emissions, it can be presumed that the project will not have significant GHG emission impacts. This approach is consistent with CEQA Guidelines Sections 15064(h)(3) and 15183.5(b), which provides that a lead agency may determine that a project's incremental contribution to a cumulative effect is not cumulatively considerable if the project will comply with the requirements in a previously approved plan or mitigation program which provides specific requirements that will avoid or substantially lessen the cumulative problem."

A qualified Greenhouse Gas Reduction Strategy (or similar adopted policies, ordinances and programs) is one that is consistent with all of the AB 32 Scoping Plan measures and goals. The Greenhouse Gas Reduction Strategy should identify a land use design, transportation network, goals, policies and implementation measures that would achieve AB 32 goals. Strategies with horizon years beyond 2020 should consider continuing the downward reduction path set by AB 32 and move toward climate stabilization goals established in Executive Order S-3-05.

Qualified Greenhouse Gas Reduction Strategy

A qualified Greenhouse Gas Reduction Strategy adopted by a local jurisdiction should include the following elements as described in the State CEQA Guidelines Section 15183.5. BAAQMD's revised CEQA Guidelines provides the methodology to determine if a Greenhouse Gas Reduction Strategy meets these requirements.

(A) Quantify greenhouse gas emissions, both existing and projected over a specified time period, resulting from activities within a defined geographic area;

(B) Establish a level, based on substantial evidence, below which the contribution to greenhouse gas emissions from activities covered by the plan would not be cumulatively considerable;

(C) Identify and analyze the greenhouse gas emissions resulting from specific actions or categories of actions anticipated within the geographic area;

(D) Specify measures or a group of measures, including performance standards, that substantial evidence demonstrates, if implemented on a project-by-project basis, would collectively achieve the specified emissions level;

(E) Establish a mechanism to monitor the plan's progress toward achieving the level and to require amendment if the plan is not achieving specified levels;

(F) Be adopted in a public process following environmental review.

Local Climate Action Policies, Ordinances and Programs

Air District staff recognizes that many communities in the Bay Area have been proactive in planning for climate change but have not yet developed a stand-alone Greenhouse Gas Reduction Strategy that meets the above criteria. Many cities and counties have adopted climate action policies, ordinances and program that may in fact achieve the goals of AB 32 and a qualified Greenhouse Gas Reduction Strategy. Staff recommends that if a local jurisdiction can demonstrate that its collective set of climate action policies, ordinances and other programs is consistent with AB 32 and State CEQA Guidelines Section 15183.5, includes requirements or feasible measures to reduce GHG emissions and achieves one of the following GHG emission reduction goals,[5] the AB 32 consistency demonstration should be considered equivalent to a qualified Greenhouse Gas Reduction Strategy:

[5] Lead agencies using consistency with their jurisdiction's climate action policies, ordinances and programs as a measure of significance under CEQA Guidelines section 15064(h)(3) and

- 1990 GHG emission levels,
- 15 percent below 2008 emission levels, or
- Meet the plan efficiency threshold of 6.6 MT CO_2e/service population/year.

Qualified Greenhouse Gas Reduction Strategies that are tied to the AB 32 reduction goals would promote reductions on a plan level without impeding the implementation of GHG-efficient development, and would recognize the initiative of many Bay Area communities who have already developed or are in the process of developing a GHG reduction plan. The details required above for a qualified Greenhouse Gas Reduction Strategy (or similar adopted policies, ordinances and programs) would provide the evidentiary basis for making CEQA findings that development consistent with the plan would result in feasible, measureable, and verifiable GHG reductions consistent with broad state goals such that projects approved under qualified Greenhouse Gas Reduction Strategies or equivalent demonstrations would achieve their fair share of GHG emission reductions.

GHG Thresholds for Regional Plans

Regional plans include the Regional Transportation Plan prepared by the Metropolitan Transportation Commission (MTC) and air quality plans prepared by the Air District.

The Regional Transportation Plan (RTP), also called a Metropolitan Transportation Plan (MTP) or Long-Range Transportation Plan is the mechanism used in California by both Metropolitan Planning Organizations (MPOs) and Regional Transportation Planning Agencies (RTPAs) to conduct long-range (minimum of 20 years) planning in their regions. MTC functions as both the regional transportation planning agency, a state designation, and, for federal purposes, as the region's metropolitan planning organization (MPO). As such, it is responsible for regularly updating the Regional Transportation Plan, a comprehensive blueprint for the development of the Bay Area's transportation system that includes mass transit, highway, airport, seaport, railroad, bicycle and pedestrian facilities. The performance of this system affects such public policy concerns as air quality, environmental resource consumption, social equity, "smart growth," economic development, safety, and security. Transportation planning recognizes the critical links between transportation and other societal goals. The planning process requires developing strategies for operating, managing, maintaining, and financing the area's transportation system in such a way as to advance the area's long-term goals.

The Air District periodically prepares and updates plans to achieve the goal of healthy air. Typically, a plan will analyze emissions inventories (estimates of current and future emissions from industry, motor vehicles, and other sources) and combine that information with air monitoring data (used to assess progress in improving air quality) and computer modeling simulations to test future strategies to reduce emissions in order to achieve air quality standards. Air quality plans usually include measures to reduce air pollutant emissions from industrial facilities, commercial processes, motor vehicles, and other sources. Bay Area air quality plans are prepared with the cooperation of MTC, the Association of Bay Area Governments (ABAG) and the Bay Conservation and Development Commission (BCDC).

The threshold of significance for regional plans is no net increase in emissions including greenhouse gas emissions. This threshold serves to answer the State CEQA Guidelines

15183.5(b) should ensure that the policies, ordinances and programs satisfy all of the requirements of that subsection before relying on them in a CEQA analysis.

Appendix G sample question: "Would the project generate greenhouse gas emissions, either directly or indirectly, that may have a significant impact on the environment?"

2.2.5. Stationary Source GHG Threshold

Staff's recommended threshold for stationary source GHG emissions is based on estimating the GHG emissions from combustion sources for all permit applications submitted to the Air District in 2005, 2006 and 2007. The analysis is based only on CO_2 emissions from stationary sources, as that would cover the vast majority of the GHG emissions due to stationary combustion sources in the SFBAAB. The estimated CO_2 emissions were calculated for the maximum permitted amount, i.e. emissions that would be emitted if the sources applying for a permit application operate at maximum permitted load and for the total permitted hours. All fuel types are included in the estimates. For boilers burning natural gas, diesel fuel is excluded since it is backup fuel and is used only if natural gas is not available. Emission values are estimated before any offsets (i.e., Emission Reduction Credits) are applied. GHG emissions from mobile sources, electricity use and water delivery associated with the operation of the permitted sources are not included in the estimates.

It is projected that a threshold level of 10,000 metric tons of CO_2e per year would capture approximately 95 percent of all GHG emissions from new permit applications from stationary sources in the SFBAAB. That threshold level was calculated as an average of the combined CO_2 emissions from all stationary source permit applications submitted to the Air District during the three year analysis period.

Staff recommends this 10,000 MT of CO_2/yr as it would address a broad range of combustion sources and thus provide for a greater amount of GHG reductions to be captured and mitigated through the CEQA process. As documented in the Scoping Plan, in order to achieve statewide reduction targets, emissions reductions need to be obtained through a broad range of sources throughout the California economy and this threshold would achieve this purpose. While this threshold would capture 95 percent of the GHG emissions from new permit applications, the threshold would do so by capturing only the large, significant projects. Permit applications with emissions above the 10,000 MT of CO_2/yr threshold account for less than 10 percent of stationary source permit applications which represent 95 percent of GHG emissions from new permits analyzed during the three year analysis period.

This threshold would be considered an interim threshold and Air District staff will reevaluate the threshold as AB 32 Scoping Plan measures such as cap and trade are more fully developed and implemented at the state level.

2.2.6. Summary of Justification for GHG Thresholds

The bright-line numeric threshold of 1,100 MT CO_2e/yr is a numeric emissions level below which a project's contribution to global climate change would be less than "cumulatively considerable." This emissions rate is equivalent to a project size of approximately 60 single-family dwelling units, and approximately 59 percent of all future projects and 92 percent of all emissions from future projects would exceed this level. For projects that are above this bright-line cutoff level, emissions from these projects would still be less than cumulatively significant if the project as a whole would result in an efficiency of 4.6 MT CO_2e per service population or better for mixed-use projects. Projects with emissions above 1,100 MT CO_2e/yr would still be less than significant if they achieved project efficiencies below these levels. If projects as proposed exceed these levels, they would be required to implement mitigation measures to bring them back below the 1,100 MT CO_2e/yr bright-line cutoff or within the 4.6 MT CO_2e Service Population efficiency threshold. If mitigation did not bring a project back within the threshold requirements, the project would be cumulatively significant and could be approved only with a Statement of Overriding

Considerations and a showing that all feasible mitigation measures have been implemented. Projects' GHG emissions would also be less than significant if they comply with a Qualified Greenhouse Gas Reduction Strategy.

As explained in the preceding analyses of these thresholds, the greenhouse gas emissions from land use projects expected between now and 2020 built in compliance with these thresholds would be approximately 26 percent below BAU 2020 conditions and thus would be consistent with achieving an AB 32 equivalent reduction. The 26 percent reduction from BAU 2020 from new projects built in conformance with these thresholds would achieve an aggregate reduction of approximately 1.6 MMT CO_2e/yr, which is the level of emission reductions from new Bay Area land use sources needed to meet the AB 32 goals, per ARB's Scoping Plan as discussed above.

Projects with greenhouse gas emissions in conformance with these thresholds would not be considered significant for purposes of CEQA. Although the emissions from such projects would add an incremental amount to the overall greenhouse gas emissions that cause global climate change impacts, emissions from projects consistent with these thresholds would not be a "cumulatively considerable" contribution under CEQA. Such projects would not be "cumulatively considerable" because they would be helping to solve the cumulative problem as a part of the AB 32 process.

California's response to the problem of global climate change is to reduce greenhouse gas emissions to 1990 levels by 2020 under AB 32 as a near-term measure and ultimately to 80 percent below 1990 levels by 2050 as the long-term solution to stabilizing greenhouse gas concentrations in the atmosphere at a level that will not cause unacceptable climate change impacts. To implement this solution, the Air Resources Board has adopted a Scoping Plan and budgeted emissions reductions that will be needed from all sectors of society in order to reach the interim 2020 target.

The land-use sector in the Bay Area needs to achieve aggregate emission reductions of approximately 1.6 MMT CO_2e/yr from new projects between now and 2020 to achieve this goal, as noted above, and each individual new project will need to achieve its own respective portion of this amount in order for the Bay Area land use sector as a whole to achieve its allocated emissions target. Building all of the new projects expected in the Bay Area between now and 2020 in accordance with the thresholds that District staff are proposing will achieve the overall appropriate share for the land use sector, and building each individual project in accordance with the thresholds will achieve that individual project's respective portion of the emission reductions needed to implement the AB 32 solution. For these reasons, projects built in conformance with the thresholds will be part of the solution to the cumulative problem, and not part of the continuing problem. They will allow the Bay Area's land use sector to achieve the emission reductions necessary from that sector for California to implement its solution to the cumulative problem of global climate change. As such, even though such projects will add an incremental amount of greenhouse gas emissions, their incremental contribution will be less than "cumulatively considerable" because they are helping to achieve the cumulative solution, not hindering it. Such projects will not be "significant" for purposes of CEQA (see CEQA Guidelines §15064(h)(1)).

The conclusion that land use projects that comply with these thresholds is also supported by CEQA Guidelines Section 15030(a)(3), which provides that a project's contribution to a cumulative problem can be less that cumulatively considerable "if the project is required to implement or fund its fair share of a mitigation measure or measures designed to alleviate the cumulative impact." In the case of greenhouse gas emissions associated with land use projects, achieving the amount of emission reductions below BAU that will be required to achieve the AB 32 goals is the project's "fair share" of the overall emission reductions needed under ARB's scoping plan to reach the overall statewide AB 32 emissions levels for 2020. If a project is

designed to implement greenhouse gas mitigation measures that achieve a level of reductions consistent with what is required from all new land use projects to achieve the land use sector "budget" – *i.e.*, keeping overall project emissions below 1,100 MT CO_2e/yr or ensuring that project efficiency is better than 4.6 MT CO_2e/service population – then it will be implementing its share of the mitigation measures necessary to alleviate the cumulative impact, as shown in the analyses set forth above.

It is also worth noting that this "fair share" approach is flexible and will allow a project's significance to be determined by how well it is designed from a greenhouse gas efficiency standpoint, and not just by the project's size. For example, a large high-density infill project located in an urban core nearby to public transit and other alternative transportation options, and built using state-of-the-art energy efficiency methods and improvements such as solar panels, as well as all other feasible mitigation measures, would not become significant for greenhouse gas purposes (and thus require a Statement of Overriding Considerations in order to be approved) simply because it happened to be a large project. Projects such as this hypothetical development with low greenhouse gas emissions per service population are what California will need in the future in order to do its part in achieving a solution to the problem of global climate change. The determination of significance under CEQA should take these factors into account, and the significance thresholds would achieve this important policy goal. In all, land use sector projects that comply with the GHG thresholds would not be "cumulatively considerable" because they would be helping to solve the cumulative problem as a part of the AB 32 process.

Likewise, new Air District permit applications for stationary sources that comply with the quantitative threshold of 10,000 MT CO_2e/yr would not be "cumulatively considerable" because they also would not hinder the state's ability to solve the cumulative greenhouse gas emissions problem pursuant to AB 32. Unlike the land use sector, the AB 32 Scoping Plan measures, including the cap-and-trade program, provide for necessary emissions reductions from the stationary source sector to achieve AB 32 2020 goals.

While stationary source projects will need to comply with the cap-and-trade program once it is enacted and reduce their emissions accordingly, the program will be phased in over time starting in 2012 and at first will only apply to the very largest sources of GHG emissions. In the mean time, certain stationary source projects, particularly those with large GHG emissions, still will have a cumulatively considerable impact on climate change. The 10,000 MT CO_2e/yr threshold will capture 95 percent of the stationary source sector GHG emissions in the Bay Area. The five percent of emissions that are from stationary source projects below the 10,000 MT CO_2e/yr threshold account for a small portion of the Bay Area's total GHG emissions from stationary sources and these emissions come from very small projects. Such small stationary source projects will not significantly add to the global problem of climate change, and they will not hinder the Bay Area's ability to reach the AB 32 goal in any significant way, even when considered cumulatively. In Air District's staff's judgment, the potential environmental benefits from requiring EIRs and mitigation for these projects would be insignificant. In all, based on staff's expertise, stationary source projects with emissions below 10,000 MT CO_2e/yr will not provide a cumulatively considerable contribution to the cumulative impact of climate change.

3. COMMUNITY RISK AND HAZARD THRESHOLDS

To address community risk from air toxics, the Air District initiated the Community Air Risk Evaluation (CARE) program in 2004 to identify locations with high levels of risk from ambient toxic air contaminants (TAC) co-located with sensitive populations and use the information to help focus mitigation measures. Through the CARE program, the Air District developed an inventory of

TAC emissions for 2005 and compiled demographic and health indicator data. According to the findings of the CARE Program, diesel PM—mostly from on and off-road mobile sources—accounts for over 80 percent of the inhalation cancer risk from TACs in the Bay Area (BAAQMD 2006).

The Air District applied a regional air quality model using the 2005 emission inventory data to estimate excess cancer risk from ambient concentrations of important TAC species, including diesel PM, 1,3-butadiene, benzene, formaldehyde and acetaldehyde. The highest cancer risk levels from ambient TAC in the Bay Area tend to occur in the core urban areas, along major roadways and adjacent to freeways and port activity. Cancer risks in areas along these major freeways are estimated to range from 200 to over 500 excess cases in a million for a lifetime of exposure. Priority communities within the Bay Area – defined as having higher emitting sources, highest air concentrations, and nearby low income and sensitive populations – include the urban core areas of Concord, eastern San Francisco, western Alameda County, Redwood City/East Palo Alto, Richmond/San Pablo, and San Jose.

Fifty percent of BAAQMD's population was estimated to have an ambient background inhalation cancer risk of less than 500 cases in one million, based on emission levels in 2005. Table 8 presents a summary of percentages of the population exposed to varying levels of cancer risk from ambient TACs. Approximately two percent of the SFBAAB population is exposed to background risk levels of less than 200 excess cases in one million. This is in contrast to the upper percentile ranges where eight percent of the SFBAAB population is exposed to background risk levels of greater than 1,000 excess cases per one million. To identify and reduce risks from TAC, this chapter presents thresholds of significance for both cancer risk and non-cancer health hazards.

Table 8 – Statistical Summary of Estimated Population-Weighted Ambient Cancer Risk in 2005

Percentage of Population (Percent below level of ambient risk)	Ambient Cancer Risk (inhalation cancer cases in one million)
92	1,000
90	900
83	800
77	700
63	600
50	500
32	400
13	300
2	200
<1	100

Source: Data compiled by EDAW 2009.

Many scientific studies have linked fine particulate matter and traffic-related air pollution to respiratory illness (Hiltermann et al. 1997, Schikowski et al 2005, Vineis et al. 2007) and premature mortality (Dockery 1993, Pope et al. 1995, Jerrett et al. 2005). Traffic-related air pollution is a complex mix of chemical compounds (Schauer et al. 2006), often spatially correlated

with other stressors, such as noise and poverty (Wheeler and Ben-Shlomo 2005). While such correlations can be difficult to disentangle, strong evidence for adverse health effects of fine particulate matter ($PM_{2.5}$) has been developed for regulatory applications in a study by the U.S, EPA. This study found that a 10 percent increase in $PM_{2.5}$ concentrations increased the non-injury death rate by 10 percent (U.S. EPA 2006).

Public Health Officers for four counties in the San Francisco Bay Area in 2009 provided testimony to the Air District's Advisory Council (February 11, 2009, Advisory Council Meeting on Air Quality and Public Health). Among the recommendations made, was that $PM_{2.5}$, in addition to TACs, be considered in assessments of community-scale impacts of air pollution. In consideration of the scientific studies and recommendations by the Bay Area Health Directors, it is apparent that, in addition to the significance thresholds for local-scale TAC, thresholds of significance are required for near-source, local-scale concentrations of $PM_{2.5}$.

3.1. THRESHOLDS OF SIGNIFICANCE

The thresholds of significance and Board-requested options are presented in this section:

- The **Staff Proposal** includes thresholds for cancer risk, non-cancer health hazards, and fine particulate matter.
- **Tiered Thresholds Option** includes tiered thresholds for new sources in impacted communities. Thresholds for receptors and cumulative impacts are the same as the Staff Proposal.

Proposal/Option	Construction-Related	Operational-Related
Project-Level – Individual Project		
Risks and Hazards – New Source (All Areas) (Individual Project) **Staff Proposal**	Same as Operational Thresholds*	Compliance with Qualified Community Risk Reduction Plan OR Increased cancer risk of >10.0 in a million Increased non-cancer risk of > 1.0 Hazard Index (Chronic or Acute) Ambient $PM_{2.5}$ increase: > 0.3 µg/m^3 annual average Zone of Influence: 1,000-foot radius from fence line of source or receptor

Proposal/Option	Construction-Related	Operational-Related
Risks and Hazards – New Receptor (All Areas) (Individual Project) **Staff Proposal**	Same as Operational Thresholds*	Compliance with Qualified Community Risk Reduction Plan OR Increased cancer risk of >10.0 in a million Increased non-cancer risk of > 1.0 Hazard Index (Chronic or Acute) Ambient $PM_{2.5}$ increase: > 0.3 µg/m^3 annual average Zone of Influence: 1,000-foot radius from fence line of source or receptor
Risks and Hazards (Individual Project) **Tiered Thresholds Option**	Same as Operational Thresholds*	**Impacted Communities:** Siting a New Source Compliance with Qualified Community Risk Reduction Plan OR Increased cancer risk of >5.0 in a million Increased non-cancer risk of > 1.0 Hazard Index (Chronic or Acute) Ambient $PM_{2.5}$ increase: > 0.2 µg/m^3 annual average Zone of Influence: 1,000-foot radius from fence line of source or receptor
	Same as Operational Thresholds*	**Impacted Communities:** Siting a New Receptor **All Other Areas:** Siting a New Source or Receptor Compliance with Qualified Community Risk Reduction Plan OR Increased cancer risk of >10.0 in a million Increased non-cancer risk of > 1.0 Hazard Index (Chronic or Acute) Ambient $PM_{2.5}$ increase: > 0.3 µg/m^3 annual average Zone of Influence: 1,000-foot radius from fence line of source or receptor
Accidental Release of Acutely Hazardous Air Pollutants	None	Storage or use of acutely hazardous materials locating near receptors or receptors locating near stored or used acutely hazardous materials considered significant
Project-Level – Cumulative		

Proposal/Option	Construction-Related	Operational-Related
Risks and Hazards – New Source (All Areas) (Cumulative Thresholds)	Same as Operational Thresholds*	Compliance with Qualified Community Risk Reduction Plan OR Cancer: > 100 in a million (from all local sources) Non-cancer: > 10.0 Hazard Index (from all local sources) (Chronic) $PM_{2.5}$: > 0.8 µg/m^3 annual average (from all local sources) Zone of Influence: 1,000-foot radius from fence line of source or receptor
Risks and Hazards – New Receptor (All Areas) (Cumulative Thresholds)	Same as Operational Thresholds*	Compliance with Qualified Community Risk Reduction Plan OR Cancer: > 100 in a million (from all local sources) Non-cancer: > 10.0 Hazard Index (from all local sources) (Chronic) $PM_{2.5}$: > 0.8 µg/m^3 annual average (from all local sources) Zone of Influence: 1,000-foot radius from fence line of source or receptor
Plan-Level		
Risks and Hazards	None	1. Overlay zones around existing and planned sources of TACs (including adopted Risk Reduction Plan areas). 2. Overlay zones of at least 500 feet (or Air District-approved modeled distance) from all freeways and high volume roadways.
Accidental Release of Acutely Hazardous Air Pollutants	None	None
Regional Plans (Transportation and Air Quality Plans)		
Risks and Hazards	None	No net increase in toxic air contaminants

* Note: The Air District recommends that for construction projects that are less than one year duration, Lead Agencies should annualize impacts over the scope of actual days that peak impacts are to occur, rather than the full year.

3.2. JUSTIFICATION AND SUBSTANTIAL EVIDENCE SUPPORTING THRESHOLDS

The goal of the thresholds is to ensure that no source creates, or receptor endures, a significant adverse impact from any individual project, and that the total of all nearby directly emitted risk and hazard emissions is also not significantly adverse. The thresholds for local risks and hazards from TAC and $PM_{2.5}$ are intended to apply to all sources of emissions, including both permitted stationary sources and on- and off-road mobile sources, such as sources related to construction, busy roadways, or freight movement.

Thresholds for an individual new source are designed to ensure that the source does not contribute to a cumulatively significant impact. Cumulative thresholds for sources recognize that some areas are already near or at levels of significant impact. If within such an area there are receptors, or it can reasonably be foreseen that there will be receptors, then a cumulative significance threshold sets a level beyond which any additional risk is significant.

For new receptors – sensitive populations or the general public – thresholds of significance are designed to identify levels of contributed risk or hazards from existing local sources that pose a significant risk to the receptors. Single-source thresholds for receptors are provided to recognize that within the area defined there can be variations in risk levels that may be significant. Single-source thresholds assist in the identification of significant risks, hazards, or concentrations in a subarea, within the area defined by the selected radius. Cumulative thresholds for receptors are designed to account for the effects of all sources within the defined area.

Cumulative thresholds, for both sources and receptors, must consider the size of the source area, defined by a radius from the proposed project. To determine cumulative impacts from a prescribed zone of influence requires the use of modeling. The larger the radius, the greater the number of sources considered that may contribute to the modeled risk and, until the radius approaches a regional length scale, the greater the expected modeled risk increment. If the area of impact considered were grown to the scale of a city, the modeled risk increment would approach the risk level present in the ambient air.

3.2.1. Scientific and Regulatory Justification

Regulatory Framework for TACs

Prior to 1990, the Clean Air Act required EPA to list air toxics it deemed hazardous and to establish control standards which would restrict concentrations of hazardous air pollutants (HAP) to a level that would prevent any adverse effects "with an ample margin of safety." By 1990, EPA had regulated only seven such pollutants and it was widely acknowledged by that time that the original Clean Air Act had failed to address toxic air emissions in any meaningful way. As a result, Congress changed the focus of regulation in 1990 from a risk-based approach to technology-based standards. Title III, Section 112(b) of the 1990 Clean Air Act Amendment established this new regulatory approach. Under this framework, prescribed pollution control technologies based upon maximum achievable control technology (MACT) were installed without the a priori estimation of the health or environmental risk associated with each individual source. The law listed 188 HAPs that would be subject to the MACT standards. EPA issued 53 standards for 89 different types of major industrial sources of air toxics and eight categories of smaller sources such as dry cleaners. These requirements took effect between 1996 and 2002. Under the federal Title V Air Operating Permit Program, a facility with the potential to emit 10 tons of any toxic air pollutant, or 25 tons per year of any combination of toxic air pollutants, is defined as a major source HAPs. Title V permits include requirements for these facilities to limit toxic air pollutant emissions.

Several state and local agencies adopted programs to address gaps in EPA's program prior to the overhaul of the national program in 1990. California's program to reduce exposure to air toxics was established in 1983 by the Toxic Air Contaminant Identification and Control Act (AB 1807, Tanner 1983) and the Air Toxics "Hot Spots" Information and Assessment Act (AB 2588, Connelly 1987). Under AB 1807, ARB and the Office of Environmental Health Hazard Assessment (OEHHA) determines if a substance should be formally identified as a toxic air contaminant (TAC) in California. OEHHA also establishes associated risk factors and safe concentrations of exposure.

AB 1807 was amended in 1993 by AB 2728, which required ARB to identify the 189 federal hazardous air pollutants as TACs. AB 2588 (Connelly, 1987) supplements the AB 1807 program, by requiring a statewide air toxics inventory, notification of people exposed to a significant health risk, and facility plans to reduce these risks. In September 1992, the "Hot Spots" Act was amended by Senate Bill 1731 which required facilities that pose a significant health risk to the community to reduce their risk through a risk management plan.

Cancer Risk

Cancer risk from TACs is typically expressed in numbers of excess cancer cases per million persons exposed over a defined period of exposure, for example, over an assumed 70 year lifetime. The Air District is not aware of any agency that has established an acceptable level of cancer risk for TACs. However, a range of what constitutes a significant increment of cancer risk from any compound has been established by the U.S. EPA. EPA's guidance for conducting air toxics analyses and making risk management decisions at the facility- and community-scale level considers a range of acceptable cancer risks from one in a million to one in ten thousand (100 in a million). The guidance considers an acceptable range of cancer risk increments to be from one in a million to one in ten thousand. In protecting public health with an ample margin of safety, EPA strives to provide maximum feasible protection against risks to health from HAPs by limiting additional risk to a level no higher than the one in ten thousand estimated risk that a person living near a source would be exposed to at the maximum pollutant concentrations for 70 years. This goal is described in the preamble to the benzene National Emissions Standards for Hazardous Air Pollutants (NESHAP) rulemaking (54 Federal Register 38044, September 14, 1989) and is incorporated by Congress for EPA's residual risk program under Clean Air Act section 112(f).

Regulation 2, Rule 5 of the Air District specifies permit requirements for new and modified stationary sources of TAC. The Project Risk Requirement (2-5-302.1) states that the Air Pollution Control Officer shall deny an Authority to Construct or Permit to Operate for any new or modified source of TACs if the project cancer risk exceeds 10.0 in one million.

Hazard Index for Non-cancer Health Effects

Non-cancer health hazards for chronic and acute diseases are expressed in terms of a hazard index (HI), a ratio of TAC concentration to a reference exposure level (REL), below which no adverse health effects are expected, even for sensitive individuals. As such, OEHHA has defined acceptable concentration levels, and also significant concentration increments, for compounds that pose non-cancer health hazards. If the HI for a compound is less than one, non-cancer chronic and acute health impacts have been determined to be less than significant.

State and Federal Ambient Air Quality Standards for $PM_{2.5}$

The Children's Environmental Health Protection Act (Senate Bill 25), passed by the California state legislature in 1999, requires ARB, in consultation with OEHHA, to "review all existing health-based ambient air quality standards to determine whether, based on public health, scientific literature and exposure pattern data, these standards adequately protect the public, including infants and children, with an adequate margin of safety." As a result of the review requirement, in 2002 ARB adopted an annual average California Ambient Air Quality Standard (CAAQS) for

$PM_{2.5}$ of 12 ug/m^3 that is not to be exceeded (California Code of Regulations, Title 17 § 70200, Table of Standards). The National Ambient Air Quality Standard (NAAQS) established an annual standard for $PM_{2.5}$ (15 ug/m^3) that is less stringent that the CAAQS, but also set a 24-hour average standard (35 ug/m^3), which is not included in the CAAQS (Code of Federal Regulations, Title 40, Part 50.7).

Significant Impact Levels for $PM_{2.5}$

EPA recently proposed and documented alternative options for $PM_{2.5}$ Significant Impact Levels (SILs) (Federal Register 40 CFR Parts 51 and 52, September 21, 2007). The EPA is proposing to facilitate implementation of a $PM_{2.5}$ Prevention of Significant Deterioration (PSD) program in areas attaining the $PM_{2.5}$ NAAQS by developing $PM_{2.5}$ increments, or SILs. These "increments" are maximum increases in ambient $PM_{2.5}$ concentrations ($PM_{2.5}$ increments) allowed in an area above the baseline concentration.

The SIL is a threshold that would be applied to individual facilities that apply for a permit to emit a regulated pollutant in an area that meets the NAAQS. The State and EPA must determine if emissions from that facility will cause the air quality to worsen. If an individual facility projects an increase in emissions that result in ambient impacts greater than the established SIL, the permit applicant would be required to perform additional analyses to determine if those impacts will be more than the amount of the PSD increment. This analysis would combine the impact of the proposed facility when added to all other sources in the area.

The EPA is proposing such values for $PM_{2.5}$ that will be used as screening tools by a major source subject to PSD to determine the subsequent level of analysis and data gathering required for a PSD permit application for emissions of $PM_{2.5}$. The SIL is one element of the EPA program to prevent deterioration in regional air quality and is utilized in the new source review (NSR) process. New source review is required under Section 165 of the Clean Air Act, whereby a permit applicant must demonstrate that emissions from the proposed construction and operation of a facility "will not cause, or contribute to, air pollution in excess of any maximum allowable increase or maximum allowable concentration for any pollutant." The purpose of the SIL is to provide a screening level that triggers further analysis in the permit application process.

For the purpose of NSR, SILs are set for three types of areas: Class I areas where especially clean air is most desirable, including national parks and wilderness areas; Class II areas where there is not expected to be substantial industrial growth; and Class III areas where the highest relative level of industrial development is expected. In Class II and Class III areas, a $PM_{2.5}$ concentration of 0.3, 0.8, and 1 µg/m^3 has been proposed as a SIL. To arrive at the SIL $PM_{2.5}$ option of 0.8 µg/m^3 , EPA scaled an established PM_{10} SILs of 1.0 µg/m^3 by the ratio of emissions of $PM_{2.5}$ to PM_{10} using the EPA's 1999 National Emissions Inventory. To arrive at the SIL option of 0.3 µg/m^3, EPA scaled the PM_{10} SIL of 1.0 µg/m^3 by the ratio of the current Federal ambient air quality standards for $PM_{2.5}$ and PM_{10} (15/50). These options represent what EPA currently considers as a range of appropriate SIL values.

EPA interprets the SIL to be the level of $PM_{2.5}$ increment that represents a "significant contribution" to regional non-attainment. While SIL options were not designed to be thresholds for assessing community risk and hazards, they are being considered to protect public health at a regional level by helping an area maintain the NAAQS. Furthermore, since it is the goal of the Air District to achieve and maintain the NAAQS and CAAQS at both regional and local scales, the SILs may be reasonably be considered as thresholds of significance under CEQA for local-scale increments of $PM_{2.5}$.

Roadway Proximity Health Studies

Several medical research studies have linked near-road pollution exposure to a variety of adverse health outcomes impacting children and adults. Kleinman et al. (2007) studied the potential of roadway particles to aggravate allergic and immune responses in mice. Using mice that were not inherently susceptible, the researchers placed these mice at various distances downwind of State Road 60 and Interstate 5 freeways in Los Angeles to test the effect these roadway particles have on their immune system. They found that within five meters of the roadway, there was a significant allergic response and elevated production of specific antibodies. At 150 meters (492 feet) and 500 meters (1,640 feet) downwind of the roadway, these effects were not statistically significant.

Another significant study (Ven Hee et al. 2009) conducted a survey involving 3,827 participants that aimed to determine the effect of residential traffic exposure on two preclinical indicators of heart failure; left ventricular mass index (LVMI), measured by the cardiac magnetic resonance imaging (MRI), and ejection fraction. The studies classified participants based on the distance between their residence and the nearest interstate highway, state or local highway, or major arterial road. Four distance groups were defined: less than 50 meters (165 feet), 50-100 meters, 101-150 meters, and greater than 150 meters. After adjusting for demographics, behavioral, and clinical covariates, the study found that living within 50 meters of a major roadway was associated with a 1.4 g/m^2 higher LVMI than living more than 150 meters from one. This suggests an association between traffic-related air pollution and increased prevalence of a preclinical predictor of heart failure among people living near roadways.

To quantify the roadway concentrations of $PM_{2.5}$ that contributed to the health impacts reported by Kleinman et al (2007), the Air District modeled the emissions and associated particulate matter concentrations for the roadways studied. To perform the modeling, emissions were estimated for Los Angeles using the EMFAC model and annual average vehicle traffic data taken from Caltrans was used in the roadway model (CAL3QHCR) to estimate the downwind $PM_{2.5}$ concentrations at 50 meters and 150 meters. Additionally, emissions were assumed to occur from 10:00 a.m. to 2:00 p.m. corresponding to the time in which the mice were exposed during the study. The results of the modeling indicate that at 150 meters, where no significant health effects were found, the downwind concentration of $PM_{2.5}$ was 0.78 $\mu g/m^3$, consistent with the proposed EPA SIL option of 0.8 $\mu g/m^3$.

Concentration-Response Function for $PM_{2.5}$

The U.S. EPA reevaluated the relative risk of premature death associated with $PM_{2.5}$ exposure and developed a new relative risk factor (U.S. EPA 2006). This expert elicitation was prepared in support of the characterization of uncertainty in EPA's benefits analyses associated with reductions in exposure to particulate matter pollution. As recommended by the National Academy of Sciences, EPA used expert judgment to better describe the uncertainties inherent in their benefits analysis. Twelve experts participated in the study and provided not just a point estimate of the health effects of PM2.5, but a probability distribution representing the range where they expected the true effect would be. Among the experts who directly incorporated their views on the likelihood of a causal relationship into their distributions, the central (median) estimates of the percent change in all-cause mortality in the adult U.S. population that would result from a permanent 1 µg/m3 drop in annual average PM2.5 concentrations ranged from 0.7 to 1.6 percent. The median of their estimates was 1.0 (% increase per 1 µg/m3 increase in PM2.5), with a 90% confidence interval of 0.3 to 2.0 (medians of their 5^{th} and 95^{th} percentiles, respectively) (BAAQMD 2010).Subsequent to the EPA elicitation, Schwartz et al. (2008) examined the linearity of the concentration-response function of $PM_{2.5}$-mortality and showed that the response function was linear, with health effects clearly continuing below the current U.S. standard of 15 $\mu g/m^3$, and that the effects of changes in exposure on mortality were seen within two years.

San Francisco Ordinance on Roadway Proximity Health Effects

In 2008, the City and County of San Francisco adopted an ordinance (San Francisco Health Code, Article 38 - Air Quality Assessment and Ventilation Requirement for Urban Infill Residential Development, Ord. 281-08, File No. 080934, December 5, 2008) requiring that public agencies in San Francisco take regulatory action to prevent future air quality health impacts from new sensitive uses proposed near busy roadways (SFDPH 2008). The regulation requires that developers screen sensitive use projects for proximity to traffic and calculate the concentration of $PM_{2.5}$ from traffic sources where traffic volumes suggest a potential hazard. If modeled levels of traffic-attributable $PM_{2.5}$ at a project site exceed an action level (currently set at 0.2 $\mu g/m^3$) developers would be required to incorporate ventilation systems to remove 80 percent of $PM_{2.5}$ from outdoor air. The regulation does not place any requirements on proposed sensitive uses if modeled air pollutant levels fall below the action threshold. This ordinance only considers impacts from on-road motor vehicles, not impacts related to construction equipment or stationary sources.

A report with supporting documentation for the ordinance (SFPHD 2008) provided a threshold to trigger action or mitigation of 0.2 $\mu g/m^3$ of $PM_{2.5}$ annual average exposure from roadway vehicles within a 150 meter (492 feet) maximum radius of a sensitive receptor. The report applied the concentration-response function from Jerrett et al. (2005) that attributed 14 percent increase in mortality to a 10 $\mu g/m^3$ increase in $PM_{2.5}$ to estimate an increase in non-injury mortality in San Francisco of about 21 excess deaths per million population per year from a 0.2 $\mu g/m^3$ increment of annual average $PM_{2.5}$.

Distance for Significant Impact

The distance used for the radius around the project boundary should reflect the zone or area over which sources may have a significant influence. For cumulative thresholds, for both sources and receptors, this distance also determines the size of the source area, defined. To determine cumulative impacts from a prescribed zone of influence requires the use of modeling. The larger the radius, the greater the number of sources considered that may contribute to the risk and the greater the expected modeled risk increment. If the area of impact considered were grown to approach the scale of a city, the modeled risk increment would approach the risk level present in the ambient air.

A summary of research findings in ARB's Land Use Compatibility Handbook (ARB 2005) indicates that traffic-related pollutants were higher than regional levels within approximately 1,000 feet downwind and that differences in health-related effects (such as asthma, bronchitis, reduced lung function, and increased medical visits) could be attributed in part to the proximity to heavy vehicle and truck traffic within 300 to 1,000 feet of receptors. In the same summary report, ARB recommended avoiding siting sensitive land uses within 1,000 feet of a distribution center and major rail yard, which supports the use of a 1,000 feet evaluation distance in case such sources may be relevant to a particular project setting. A 1,000 foot zone of influence is also supported by Health & Safety Code §42301.6 (Notice for Possible Source Near School).

Some studies have shown that the concentrations of particulate matter tend to be reduced substantially or can even be indistinguishable from upwind background concentrations at a distance 1,000 feet downwind from sources such as freeways or large distribution centers. Zhu et al. (2002) conducted a systematic ultrafine particle study near Interstate 710, one of the busiest freeways in the Los Angeles Basin. Particle number concentration and size distribution were measured as a function of distances upwind and downwind of the I-710 freeway. Approximately 25 percent of the 12,180 vehicles per hour are heavy duty diesel trucks based on video counts conducted as part of the research. Measurements were taken at 13 feet, 23 feet, 55 feet, 252 feet, 449 feet, and 941 feet downwind and 613 feet upwind from the edge of the freeway. The particle number and supporting measurements of carbon monoxide and black carbon decreased

exponentially and all constituents simultaneously tracked with each other as one moves away from the freeway. Ultrafine particle size distribution changed markedly and its number concentrations dropped dramatically with increasing distance. The study found that ultrafine particle concentrations measured 941 feet downwind of I-710 were indistinguishable from the upwind background concentration.

Impacted Communities

Starting in 2006, the Air District's CARE program developed gridded TAC emissions inventories and compiled demographic information that were used to identify communities that were particularly impacted by toxic air pollution for the purposes of distributing grant and incentive funding. In 2009, the District completed regional modeling of TAC on a one kilometer by one kilometer grid system. This modeling was used to estimate cancer risk and TAC population exposures for the entire District. The information derived from the modeling was then used to update and refine the identification of impacted communities. One kilometer modeling yielded estimates of annual concentrations of five key compounds – diesel particulate matter, benzene, 1,3-butadiene, formaldehyde, and acetaldehyde – for year 2005. These concentrations were multiplied by their respective unit cancer risk factors, as established by OEHHA, to estimate the expected excess cancer risk per million people from these compounds.

Sensitive populations from the 2000 U.S. Census database were identified as youth (under 18) and seniors (over 64) and mapped to the same one kilometer grid used for the toxics modeling. Excess cancers from TAC exposure were determined by multiplying these sensitive populations by the model-estimated excess risk to establish a data set representing sensitive populations with high TAC exposures. TAC emissions (year 2005) were mapped to the one kilometer grid and also scaled by their unit cancer risk factor to provide a data set representing source regions for TAC emissions. Block-group level household income data from the U.S. Census database were used to identify block groups with family incomes where more than 40 percent of the population was below 185 percent of the federal poverty level (FPL). Poverty-level polygons that intersect high (top 50 percent) exposure cells and are within one grid cell of a high emissions cell (top 25 percent) were used to identify impacted areas. Boundaries were constructed along major roads or highways that encompass nearby high emission cells and low income areas. This method identified the following six areas as priority communities: (1) portions of the City of Concord; (2) Western Contra Costa County (including portions of the Cities of Richmond and San Pablo); (3) Western Alameda County along the Interstate-880 corridor (including portions of the Cities of Berkeley, Oakland, San Leandro, San Lorenzo, Hayward; (4) Portions of the City of San Jose. (5) Eastern San Mateo County (including portions of the Cities of Redwood City and East Palo Alto); and (6) Eastern portions of the City of San Francisco.

3.2.2. Construction, Land Use and Stationary Source Risk and Hazard Thresholds

The options for local risk and hazards thresholds of significance are based on U.S. EPA guidance for conducting air toxics analyses and making risk management decisions at the facility and community-scale level. The thresholds consider reviews of recent health effects studies that link increased concentrations of fine particulate matter to increased mortality. The thresholds would apply to both siting new sources and siting new receptors.

For new sources of TACs, thresholds of significance for a single source are designed to ensure that emissions do not raise the risk of cancer or non-cancer health impacts to cumulatively significant levels. For new sources of $PM_{2.5}$, thresholds are designed to ensure that $PM_{2.5}$ concentrations are maintained below state and federal standards in all areas where sensitive receptors or members of the general public live or may foreseeably live, even if at the local- or community-scale where sources of TACs and PM may be nearby.

Project Radius for Assessing Impacts

For a project proposing a new source or receptor it is recommended to assess impacts within 1,000 feet, taking into account both its individual and nearby cumulative sources (i.e. proposed project plus existing and foreseeable future projects). Cumulative sources are the combined total risk values of each individual source within the 1,000-foot evaluation zone. A lead agency should enlarge the 1,000-foot radius on a case-by-case basis if an unusually large source or sources of risk or hazard emissions that may affect a proposed project is beyond the recommended radius.

The 1,000 foot radius is consistent with findings in ARB's Land Use Compatibility Handbook (ARB 2005), the Health & Safety Code §42301.6 (Notice for Possible Source Near School), and studies such as that of Zhu et al (2002) which found that concentrations of particulate matter tend to be reduced substantially at a distance 1,000 feet downwind from sources such as freeways or large distribution centers.

Qualified Community Risk Reduction Plan

Within the framework of these thresholds, proposed projects would be considered to be less than significant if they are consistent with a qualified Community Risk Reduction Plan (CRRP) adopted by the local jurisdiction with enforceable measures to reduce the community risk.

Project proposed in areas where a CRRP has been adopted that are not consistent with the CRRP would be considered to have a significant impact.

Projects proposed in areas where a CRRP has not been adopted and that have the potential to expose sensitive receptors or the general public to emissions-related risk in excess of the thresholds below from any source would be considered to have a significant air quality impact.

The conclusion that land use projects that comply with qualified Community Risk Reduction Plans are less than significant is supported by CEQA Guidelines Sections 15030(a)(3) and 15064(h)(3), which provides that a project's contribution to a cumulative problem can be less that cumulatively considerable if the project is required to implement or fund its fair share of a mitigation measure or measures designed to alleviate the cumulative impact.

Increased Cancer Risk to Maximally Exposed Individual (MEI)

Emissions from a new source or emissions affecting a new receptor would be considered significant where ground-level concentrations of carcinogenic TACs from any source result in an increased cancer risk greater than 10.0 in one million, assuming a 70 year lifetime exposure. Under Board Option 1, within Impacted Communities as defined through the CARE program, the significance level for cancer would be reduced to 5.0 in one million for new sources.

The 10.0 in one million cancer risk threshold for a single source is supported by EPA's guidance for conducting air toxics analyses and making risk management decisions at the facility and community-scale level. It is also the level set by the Project Risk Requirement in the Air District's Regulation 2, Rule 5 new and modified stationary sources of TAC, which states that the Air Pollution Control Officer shall deny an Authority to Construct or Permit to Operate for any new or modified source of TACs if the project risk exceeds a cancer risk of 10.0 in one million.

This threshold for an individual new source is designed to ensure that the source does not contribute a cumulatively significant impact. The justification for the Tiered Thresholds Option threshold of 5.0 in one million for new sources in an impacted community is that in these areas the cancer risk burden is higher than in other parts of the Bay Area; the threshold at which an individual source becomes significant is lower for an area that is already at or near unhealthy levels. However, even without a tiered approach, the recommended thresholds already address the burden of impacted communities via the cumulative thresholds: specifically, if an area has

many existing TAC sources near receptors, then the cumulative threshold will be reached sooner than it would in another area with fewer TAC sources.

The single-source threshold for receptors is provided to address the possibility that within the area defined by the 1,000 foot radius there can be variations in risk levels that may be significant, below the corresponding cumulative threshold. Single-source thresholds assist in the identification of significant risks, hazards, or concentrations in a subarea, within the 1,000 foot radius.

Increased Non-Cancer Risk to MEI

Emissions from a new source or emissions affecting a new receptor would be considered significant where ground-level concentrations of non-carcinogenic TACs result in an increased chronic or acute Hazard Index (HI) from any source greater than 1.0. This threshold is unchanged under Tiered Thresholds Option.

A HI less than 1.0 represents a TAC concentration, as determined by OEHHA that is at a health protective level. While some TACs pose non-carcinogenic, chronic and acute health hazards, if the TAC concentrations result in a HI less than one, those concentrations have been determined to be less than significant.

Increased Ambient Concentration of $PM_{2.5}$

Emissions from a new source or emissions affecting a new receptor would be considered significant where ground-level concentrations of $PM_{2.5}$ from any source would result in an average annual increase greater than 0.3 $\mu g/m^3$. Under Tiered Thresholds Option, within Impacted Communities as defined through the CARE program, the significance level for a $PM_{2.5}$ increment is 0.2 $\mu g/m^3$.

If one applies the concentration-response of the median of the EPA consensus review (EPA 2005, BAAQMD 2010) and attributes a 1 percent increase in mortality to a 1 $\mu g/m^3$ increase in $PM_{2.5}$, one finds an increase in non-injury mortality in the Bay Area of about 20 excess deaths per million per year from a 0.3 $\mu g/m^3$ increment of $PM_{2.5}$. This is consistent with the impacts reported and considered significant by SFDPH (2008) using an earlier study (Jerrett et al. 2005) to estimate the increase in mortality from a 0.2 $\mu g/m^3$ $PM_{2.5}$ increment.

The SFDPH recommended a lower threshold of significance for multiple sources but only considered roadway emissions within a 492 foot radius. This recommendation applies to a single source but considers all types of emissions within 1,000 feet. On balance, the Air District estimates that the SFDPH threshold and this one, in combination with the cumulative threshold for $PM_{2.5}$, will afford similar levels of health protection.

The $PM_{2.5}$ threshold represents the lower range of an EPA proposed Significant Impact Level (SIL). EPA interprets the SIL to be the level of ambient impact that is considered to represent a "significant contribution" to regional non-attainment. While this threshold was not designed to be a threshold for assessing community risk and hazards, it was designed to protect public health at a regional level by helping an area maintain the NAAQS. Since achieving and maintaining state and federal AAQS is a reasonable goal at the local scale, the SIL provides a useful reference for comparison.

This threshold for an individual new source is designed to ensure that the source does not contribute a cumulatively significant impact. The justification for the Tiered Thresholds Option threshold of 0.2 $\mu g/m^3$ for new sources in an impacted community is that these areas have higher levels of diesel particulate matter than do other parts of the Bay Area; the threshold at which an individual source becomes significant is lower for an area that is already at or near unhealthy

levels. However, even without a tiered approach, the recommended thresholds already address the burden of impacted communities via the cumulative thresholds: specifically, if an area has many existing $PM_{2.5}$ sources near receptors, then the cumulative threshold will be reached sooner than it would in another area with fewer $PM_{2.5}$ sources.

The single-source threshold for receptors is provided to address the possibility that within the area defined by the 1,000 foot radius there can be variations in risk levels that may be significant, below the corresponding cumulative threshold. Single-source thresholds assist in the identification of significant risks, hazards, or concentrations in a subarea, within the 1,000 foot radius.

Accidental Release of Acutely Hazardous Air Emissions

The BAAQMD currently recommends, at a minimum, that the lead agency, in consultation with the administering agency of the Risk Management Prevention Program (RMPP), find that any project resulting in receptors being within the Emergency Response Planning Guidelines (ERPG) exposure level 2 for a facility has a significant air quality impact. ERPG exposure level 2 is defined as "the maximum airborne concentration below which it is believed that nearly all individuals could be exposed for up to one hour without experiencing or developing irreversible or other serious health effects or symptoms which could impair an individual's ability to take protective action."

Staff proposes continuing with the current threshold for the accidental release of hazardous air pollutants. Staff recommends that agencies consult with the California Emergency Management Agency for the most recent guidelines and regulations for the storage of hazardous materials. Staff proposes that projects using or storing acutely hazardous materials locating near existing receptors, and projects resulting in receptors locating near facilities using or storing acutely hazardous materials be considered significant.

The current Accidental Release/Hazardous Air Emissions threshold of significance could affect all projects, regardless of size, and require mitigation for Accidental Release/Hazardous Air Emissions impacts.

3.2.3. Cumulative Risk and Hazard Thresholds

Qualified Community Risk Reduction Plan

Proposed projects would be considered to be less than significant if they are consistent with a qualified Community Risk Reduction Plan (CRRP) adopted by the local jurisdiction with enforceable measures to reduce the community risk.

Project proposed in areas where a CRRP has been adopted that are not consistent with the CRRP would be considered to have a significant impact.

Projects proposed in areas where a CRRP has not been adopted and that have the potential to expose sensitive receptors or the general public to emissions-related risk in excess of the following thresholds from the aggregate of cumulative sources would be considered to have a significant air quality impact.

The conclusion that land use projects that comply with qualified Community Risk Reduction Plans are less than significant is supported by CEQA Guidelines Sections 15030(a)(3) and 15064(h)(3), which provides that a project's contribution to a cumulative problem can be less that cumulatively considerable if the project is required to implement or fund its fair share of a mitigation measure or measures designed to alleviate the cumulative impact.

Increased Cancer Risk to Maximally Exposed Individual (MEI)
Emissions from a new source or emissions affecting a new receptor would be considered significant where ground-level concentrations of carcinogenic TACs from any source result in an increased cancer risk greater than 100.0 in one million.

The significance threshold of 100 in a million increased excess cancer risk would be applied to the cumulative emissions. The 100 in a million threshold is based on EPA guidance for conducting air toxics analyses and making risk management decisions at the facility and community-scale level. In protecting public health with an ample margin of safety, EPA strives to provide maximum feasible protection against risks to health from hazardous air pollutants (HAPs) by limiting risk to a level no higher than the one in ten thousand (100 in a million) estimated risk that a person living near a source would be exposed to at the maximum pollutant concentrations for 70 years (NESHAP 54 Federal Register 38044, September 14, 1989; CAA section 112(f)). One hundred in a million excess cancer cases is also consistent with the ambient cancer risk in the most pristine portions of the Bay Area based on the District's recent regional modeling analysis.

Increased Non-Cancer Risk to MEI
Emissions from a new source or emissions affecting a new receptor would be considered significant where ground-level concentrations of non-carcinogenic TACs result in an increased chronic Hazard Index from any source greater than 10.0.

The Air District has developed an Air Toxics Hot Spots (ATHS) program that provides guidance for implementing the Air Toxics "Hot Spots" Information and Assessment Act (AB 2588, Connelly, 1987: chaptered in the California Health and Safety Code § 44300, et. al.). The ATHS provides that if the health risks resulting from the facility's emissions exceed significance levels established by the air district, the facility is required to conduct an airborne toxic risk reduction audit and develop a plan to implement measures that will reduce emissions from the facility to a level below the significance level. The Air District has established a non-cancer Hazard Index of ten (10.0) as ATHS mandatory risk reduction levels. The cumulative chronic non-cancer Hazard Index threshold is consistent with the Air District's ATHS program.

Increased Ambient Concentration of $PM_{2.5}$
Emissions from a new source or emissions affecting a new receptor would be considered significant where ground-level concentrations of $PM_{2.5}$ from any source would result in an average annual increase greater than 0.8 $\mu g/m^3$.

If one applies the concentration-response function from the U.S, EPA assessment (U.S. EPA 2006) and attributes a 10 percent increase in mortality to a 10 $\mu g/m^3$ increase in $PM_{2.5}$, one finds an increase in non-injury mortality in the Bay Area of about 50 excess deaths per year from a 0.8 $\mu g/m^3$ increment of $PM_{2.5}$. This is greater than the impacts reported and considered significant by SFDPH (2008) using an earlier study (Jerrett et al. 2005) to estimate the increase in mortality from a 0.2 $\mu g/m^3$ $PM_{2.5}$ increment (SFDPH reported 21 excess deaths per year). However, SFDPH only considered roadway emissions within a 492 foot radius. This threshold applies to all types of emissions within 1,000 feet. In modeling applications for proposed projects, a larger radius results in a greater number of sources considered and higher modeled concentrations. On balance, the Air District estimates that the SFDPH threshold and this one, in combination with the individual source threshold for $PM_{2.5}$, will afford similar levels of health protection.

The cumulative $PM_{2.5}$ threshold represents the middle range of an EPA proposed Significant Impact Level (SIL). EPA interprets the SIL to be the level of ambient impact that is considered to represent a "significant contribution" to regional non-attainment. While this threshold was not designed to be a threshold for assessing community risk and hazards, it was designed to protect public health at a regional level by helping an area maintain the NAAQS. Since achieving and

maintaining state and federal AAQS is a reasonable goal at the local scale, the SIL provides a useful reference for comparison. Furthermore, the 0.8 $\mu g/m^3$ threshold is consistent with studies (Kleinman et al 2007) that examined the potential health impacts of roadway particles.

3.2.4. Plan-Level Risk and Hazard Thresholds

Staff proposes plan-level thresholds that will encourage a programmatic approach to addressing the overall adverse conditions resulting from risks and hazards that many Bay Area communities experience. By designating overlay zones in land use plans, local land use jurisdictions can take preemptive action before project-level review to reduce the potential for significant exposures to risk and hazard emissions. While this will require more up-front work at the general plan level, in the long-run this approach is a more feasible approach consistent with Air District and CARB guidance about siting sources and sensitive receptors that is more effective than project by project consideration of effects that often has more limited mitigation opportunities. This approach would also promote more robust cumulative consideration of effects of both existing and future development for the plan-level CEQA analysis as well as subsequent project-level analysis.

For local plans to have a less-than-significant impact with respect to potential risks and hazards, overlay zones would have to be established around existing and proposed land uses that would emit these air pollutants. Overlay zones to avoid risk impacts should be reflected in local plan policies, land use map(s), and implementing ordinances (e.g., zoning ordinance). The overlay zones around existing and future risk sources would be delineated using the quantitative approaches described above for project-level review and the resultant risk buffers would be included in the General Plan (or the EIR for the General Plan) to assist in site planning. BAAQMD will provide guidance as to the methods used to establish the TAC buffers and what standards to be applied for acceptable exposure level in the updated CEQA Guidelines document. Special overlay zones of at least 500 feet (or an appropriate distance determined by modeling and approved by the Air District) on each side of all freeways and high volume roadways would be included in this threshold.

The threshold of significance for plan impacts could affect all plan adoptions and amendments and require mitigation for a plan's air quality impacts. Where sensitive receptors would be exposed above the acceptable exposure level, the plan impacts would be considered significant and mitigation would be required to be imposed either at the plan level (through policy) or at the project level (through project level requirements).

3.2.5. Community Risk Reduction Plans

The goal of a Community Risk Reduction Plan would be to bring TAC and $PM_{2.5}$ concentrations for the entire community covered by the Plan down to acceptable levels as identified by the local jurisdiction and approved by the Air District. This approach provides local agencies a proactive alternative to addressing communities with high levels of risk on a project-by-project approach. This approach is supported by CEQA Guidelines Section 15030(a)(3), which provides that a project's contribution to a cumulative problem can be less than cumulatively considerable "if the project is required to implement or fund its fair share of a mitigation measure or measures designed to alleviate the cumulative impact." This approach is also further supported by CEQA Guidelines Section 15064(h)(3), which provides that a project's contribution to a cumulative effect is not considerable "if the project will comply with the requirements in a previously approved plan or mitigation program which provides specific requirements that will avoid or substantially lessen the cumulative problem."

Qualified Community Risk Reduction Plans

(A) A qualified Community Risk Reduction Plan adopted by a local jurisdiction should include, at a minimum, the following elements. BAAQMD's revised CEQA Guidelines provides the methodology to determine if a Community Risk Reduction Plan meets these requirements. Define a planning area;

(B) Include base year and future year emissions inventories of TACs and PM2.5;

(C) Include Air District–approved risk modeling of current and future risks;

(D) Establish risk and exposure reduction goals and targets for the community in consultation with Air District staff;

(E) Identify feasible, quantifiable, and verifiable measures to reduce emissions and exposures;

(F) Include procedures for monitoring and updating the inventory, modeling and reduction measures in coordination with Air District staff;

(G) Be adopted in a public process following environmental review.

4. CRITERIA POLLUTANT THRESHOLDS

4.1. THRESHOLDS OF SIGNIFICANCE

Project Construction	
Pollutant	**Average Daily (pounds/day)**
ROG (reactive organic gases)	54
NO_X (nitrogen oxides)	54
PM_{10} (exhaust) (particulate matter-10 microns)	82
$PM_{2.5}$ (exhaust) (particulate matter-2.5 microns)	54
$PM_{10}/PM_{2.5}$ (fugitive dust)	Best Management Practices
Local CO (carbon monoxide)	None

Project Operations		
Pollutant	**Average Daily (pounds/day)**	**Maximum Annual (tons/year)**
ROG	54	10
NO_X	54	10
PM_{10}	82	15
$PM_{2.5}$	54	10
Local CO	9.0 ppm (8-hour average), 20.0 ppm (1-hour average)	

Plans
1. Consistency with Current Air Quality Plan control measures 2. Projected VMT or vehicle trip increase is less than or equal to projected population increase

Regional Plans (Transportation and Air Quality Plans)
No net increase in emissions of criteria air pollutants and precursors

4.2. JUSTIFICATION AND SUBSTANTIAL EVIDENCE SUPPORTING THRESHOLDS

4.2.1. Project Construction Criteria Pollutant Thresholds

Staff proposes criteria pollutant construction thresholds that add significance criteria for exhaust emissions to the existing fugitive dust criteria employed by the Air District. While our current Guidelines considered construction exhaust emissions controlled by the overall air quality plan, the implementation of new and more stringent state and federal standards over the past ten years now warrants additional control of this source of emissions.

The average daily criteria air pollutant and precursor emission levels shown above are recommended as the thresholds of significance for construction activity for exhaust emissions. These thresholds represent the levels above which a project's individual emissions would result in a considerable contribution (i.e., significant) to the SFBAAB's existing non-attainment air quality

conditions and thus establish a nexus to regional air quality impacts that satisfies CEQA requirements for evidence-based determinations of significant impacts.

For fugitive dust emissions, staff recommends following the current best management practices approach which has been a pragmatic and effective approach to the control of fugitive dust emissions. Studies have demonstrated (Western Regional Air Partnership, U.S.EPA) that the application of best management practices at construction sites have significantly controlled fugitive dust emissions. Individual measures have been shown to reduce fugitive dust by anywhere from 30 percent to more than 90 percent. In the aggregate best management practices will substantially reduce fugitive dust emissions from construction sites. These studies support staff's recommendation that projects implementing construction best management practices will reduce fugitive dust emissions to a less than significant level.

4.2.2. Project Operation Criteria Pollutant Thresholds

The thresholds for project operations are the average daily and maximum annual criteria air pollutant and precursor levels shown above. These thresholds are based on the federal BAAQMD Offset Requirements to ozone precursors for which the SFBAAB is designated as a non-attainment area which is an appropriate approach to prevent further deterioration of ambient air quality and thus has nexus and proportionality to prevention of a regionally cumulative significant impact (e.g. worsened status of non-attainment). Despite non-attainment area for state PM_{10} and pending nonattainment for federal $PM_{2.5}$, the federal NSR Significant Emission Rate annual limits of 15 and 10 tons per year, respectively, are the thresholds as BAAQMD has not established an Offset Requirement limit for $PM_{2.5}$ and the existing limit of 100 tons per year is much less stringent and would not be appropriate in light of our pending nonattainment designation for the federal 24-hour $PM_{2.5}$ standard. These thresholds represent the emission levels above which a project's individual emissions would result in a cumulatively considerable contribution to the SFBAAB's existing air quality conditions. The thresholds would be an evaluation of the incremental contribution of a project to a significant cumulative impact. These threshold levels are well-established in terms of existing regulations as promoting review of emissions sources to prevent cumulative deterioration of air quality. Using existing environmental standards in this way to establish CEQA thresholds of significance under Guidelines section 15067.4 is an appropriate and effective means of promoting consistency in significance determinations and integrating CEQA environmental review activities with other areas of environmental regulation. (*See Communities for a Better Environment v. California Resources Agency* (2002) 103 Cal. App. 4th 98, 111.[6])

4.2.3. Local Carbon Monoxide Thresholds

The carbon monoxide thresholds are based solely on ambient concentration limits set by the California Clean Air Act for Carbon Monoxide and Appendix G of the State of California CEQA Guidelines.

Since the ambient air quality standards are health-based (i.e., protective of public health), there is substantial evidence (i.e., health studies that the standards are based on) in support of their use

[6] The Court of Appeal in the *Communities for a Better Environment* case held that existing regulatory standards could not be used as a definitive determination of whether a project would be significant under CEQA where there is substantial evidence to the contrary. Staff's thresholds would not do that. The thresholds are levels at which a project's emissions would normally be significant, but would not be binding on a lead agency if there is contrary evidence in the record.

as CEQA significance thresholds. The use of the ambient standard would relate directly to the CEQA checklist question. By not using a proxy standard, there would be a definitive bright line about what is or is not a significant impact and that line would be set using a health-based level.

The CAAQS of 20.0 ppm and 9 ppm for 1-hour and 8-hour CO, respectively, would be used as the thresholds of significance for localized concentrations of CO. Carbon monoxide is a directly emitted pollutant with primarily localized adverse effects when concentrations exceed the health based standards established by the California Air Resources Board (ARB).

In addition, Appendix G of the State of California CEQA Guidelines includes the checklist question: Would the project violate any air quality standard or contribute substantially to an existing or projected air quality violation? Answering yes to this question would indicate that the project would result in a significant impact under CEQA. The use of the ambient standard would relate directly to this checklist question.

4.2.4. Plan-Level Criteria Pollutant Thresholds

This threshold achieves the same goals as the Air District's current approach while alleviating the existing analytical difficulties and the inconsistency of comparing a plan update with AQP growth projections that may be up to several years old. Eliminating the analytical inconsistency provides better nexus and proportionality for evaluating air quality impacts for plans.

Over the years staff has received comments on the difficulties inherent in the current approach regarding the consistency tests for population and VMT growth. First, the population growth estimates used in the most recent AQP can be up to several years older than growth estimates used in a recent plan update, creating an inconsistency in this analysis. Staff recommends that this test of consistency be eliminated because the Air District and local jurisdictions all use regional population growth estimates that are disaggregated to local cities and counties. In addition, the impact to air quality is not necessarily growth but where that growth is located. The second test, rate of increase in vehicle use compared to growth rate, will determine if planned growth will impact air quality. Compact infill development inherently has less vehicle travel and more transit opportunities than suburban sprawl.

Second, the consistency test of comparing the rate of increase in VMT to the rate of increase in population has been problematic at times for practitioners because VMT is not always available with the project analysis. Staff recommends that either the rate of increase in VMT or vehicle trips be compared to the rate of increase in population. Staff also recommends that the growth estimates used in this analysis be for the years covered by the plan. Staff also recommends that the growth estimates be obtained from the Association of Bay Area Governments since the Air District uses ABAG growth estimates for air quality planning purposes.

4.2.5. Criteria Pollutant Thresholds for Regional Plans

Regional plans include the Regional Transportation Plan prepared by the Metropolitan Transportation Commission (MTC) and air quality plans prepared by the Air District.

The Regional Transportation Plan (RTP), also called a Metropolitan Transportation Plan (MTP) or Long-Range Transportation Plan is the mechanism used in California by both Metropolitan Planning Organizations (MPOs) and Regional Transportation Planning Agencies (RTPAs) to conduct long-range (minimum of 20 years) planning in their regions. MTC functions as both the regional transportation planning agency, a state designation, and, for federal purposes, as the region's metropolitan planning organization (MPO). As such, it is responsible for regularly updating the Regional Transportation Plan, a comprehensive blueprint for the development of

comprehensive transportation system that includes mass transit, highway, airport, seaport, railroad, bicycle and pedestrian facilities. The performance of this system affects such public policy concerns as air quality, environmental resource consumption, social equity, "smart growth," economic development, safety, and security. Transportation planning recognizes the critical links between transportation and other societal goals. The planning process requires developing strategies for operating, managing, maintaining, and financing the area's transportation system in such a way as to advance the area's long-term goals.

The Air District periodically prepares and updates plans to achieve the goal of healthy air. Typically, a plan will analyze emissions inventories (estimates of current and future emissions from industry, motor vehicles, and other sources) and combine that information with air monitoring data (used to assess progress in improving air quality) and computer modeling simulations to test future strategies to reduce emissions in order to achieve air quality standards. Air quality plans usually include measures to reduce air pollutant emissions from industrial facilities, commercial processes, motor vehicles, and other sources. Bay Area air quality plans are prepared with the cooperation of MTC and the Association of Bay Area Governments (ABAG).

The threshold of significance for regional plans is no net increase in emissions including criteria pollutant emissions. This threshold serves to answer the State CEQA Guidelines Appendix G sample question: "Would the project Result in a cumulatively considerable net increase of any criteria pollutant for which the project region is non-attainment under an applicable federal or state ambient air quality standard (including releasing emissions which exceed quantitative thresholds for ozone precursors)?"

5. ODOR THRESHOLDS

5.1. THRESHOLDS OF SIGNIFICANCE

Project Operations – Source or Receptor	Plans
Five confirmed complaints per year averaged over three years	Identify the location, and include policies to reduce the impacts, of existing or planned sources of odors

5.2. JUSTIFICATION AND SUBSTANTIAL EVIDENCE SUPPORTING THRESHOLDS

Staff proposes revising the current CEQA significance threshold for odors to be consistent with the Air District's regulation governing odor nuisances (Regulation 7—Odorous Substances). The current approach includes assessing the number of unconfirmed complaints which are not considered indicative of actual odor impacts. Basing the threshold on an average of five confirmed complaints per year over a three year period reflects the most stringent standards derived from the Air District rule and is considered an appropriate approach to a CEQA evaluation of odor impacts.

Odors are generally considered a nuisance, but can result in a public health concern. Some land uses that are needed to provide services to the population of an area can result in offensive odors, such as filling portable propane tanks or recycling center operations. When a proposed project includes the siting of sensitive receptors in proximity to an existing odor source, or when siting a new source of potential odors, the following qualitative evaluation should be performed.

When determining whether potential for odor impacts exists, it is recommended that Lead Agencies consider the following factors and make a determination based on evidence in each qualitative analysis category:

Distance: Use the screening-level distances in Table 9.

Wind Direction: Consider whether sensitive receptors are located upwind or downwind from the source for the most of the year. If odor occurrences associated with the source are seasonal in nature, consider whether sensitive receptors are located downwind during the season in which odor emissions occur.

Complaint History: Consider whether there is a history of complaints associated with the source. If there is no complaint history associated with a particular source (perhaps because sensitive receptors do not already exist in proximity to the source), consider complaint-history associated with other similar sources in BAAQMD's jurisdiction with potential to emit the same or similar types of odorous chemicals or compounds, or that accommodate similar types of processes.

Character of Source: Consider the character of the odor source, for example, the type of odor events according to duration of exposure or averaging time (e.g., continuous release, frequent release events, or infrequent events).

Exposure: Consider whether the project would result in the exposure of a substantial number of people to odorous emissions.

Table 9 – Screening Distances for Potential Odor Sources

Type of Operation Project Screening	Distance
Wastewater Treatment Plant	2 miles
Wastewater Pumping Facilities	1 mile
Sanitary Landfill	2 miles
Transfer Station	1 mile
Composting Facility	1 mile
Petroleum Refinery	2 miles
Asphalt Batch Plant	2 miles
Chemical Manufacturing	2 miles
Fiberglass Manufacturing	1 mile
Painting/Coating Operations	1 mile
Rendering Plant	2 miles
Food Processing Facility	1 mile
Confined Animal Facility/Feed Lot/Dairy	1 mile
Green Waste and Recycling Operations	1 mile
Coffee Roaster	1 mile

California Integrated Waste Management Board (CIWMB). Facilities that are regulated by the CIWMB (e.g. landfill, composting, etc.) are required to have Odor Impact Minimization Plans (OIMP) in place and have procedures that establish fence line odor detection thresholds. The Air District recognizes a lead agency's discretion under CEQA to use established odor detection thresholds as thresholds of significance for CEQA review for CIWMB regulated facilities with an adopted OIMP.

REFERENCES

ARB. *See* California Air Resources Board.

BAAQMD. *See* Bay Area Air Quality Management District.

Bay Area Air Quality Management District. 1999 (December). *BAAQMD CEQA Guidelines*. San Francisco, CA.

_____. 2005. Regulation 2, Rule 2. New Source Review. Available: <http://www.baaqmd.gov/dst/regulations/rg0202.pdf>. Accessed February 2009.

_____. 2006. CARE Phase 1 Findings and Policy Recommendations. Available: <http://baaqmd.gov/CARE/documents/care_p1_findings_recommendations_v2.pdf>. Accessed March 2009.

_____. 2008. Source Inventory of Bay Area Greenhouse Gas Emissions. San Francisco, CA.

_____. 2009. *Revised Draft Options and Justifications Report – California Environmental Quality Act Thresholds of Significance* (http://www.baaqmd.gov/~/media/Files/Planning%20and%20Research/CEQA/Revised%20Draft%20CEQA%20Thresholds%20%20Justification%20Report%20Oct%202009.ashx)

_____. 2010. *Draft 2010 CAP Appendix A – Bay Area Air Pollution Burden: Past & Present* San Francisco, CA

California Air Pollution Control Officers Association. 2008 (January). *CEQA and Climate Change*. Sacramento, CA. Available: <http://www.capcoa.org/CEQA/CAPCOA%20White%20Paper.pdf>. Accessed April 10, 2009.

California Air Resources Board. 2000. Risk Reduction Plan to Reduce Particulate Matter Emissions from Diesel-Fueled Engines and Vehicles. Stationary Source Division. Mobile Source Control Division. October.

_____. 2002. Staff Report: Public Hearing to Consider Amendments to the Ambient Air Quality Standards for Particulate Matter and Sulfates. Available: http://www.arb.ca.gov/research/aaqs/std-rs/pm-final/pm-final.htm.

_____. 2005. *Land Use Compatibility Handbook. A Community Health Perspective.* Sacramento, CA.

_____. 2008a. *Climate Change Proposed Scoping Plan*. Sacramento, CA. Adopted in December 2008Available: <http://www.arb.ca.gov/cc/scopingplan/document/scopingplandocument.htm>. Accessed March 2009.

_____. *Climate Change Proposed Scoping Plan*. Sacramento, CA. Adopted in December 2008 Available:

<http://www.arb.ca.gov/cc/scopingplan/document/scopingplandocument.htm>. Accessed March 2009.

_____. 2009a. Greenhouse Gas Inventory and Forecast. Available: <http://www.arb.ca.gov/cc/inventory/data/tables/arb_ghg_inventory_forecast_2008_06_26.xls>. Accessed March 2009.

_____. 2009b. *Preliminary Draft Staff Proposal: Recommended Approaches for Setting Interim Significance Thresholds for Greenhouse Gases under the California Environmental Quality Act*. Available: <http://www.arb.ca.gov/cc/localgov/ceqa/meetings/10270prelimdraftproposal102408.pdf> . Accessed March 2009.

_____. 2009c. *Area Designations and Maps*. Available: <http://www.arb.ca.gov/desig/desig.htm>, Accessed April 10.

_____. 2009d. Proposed Regulation to Implement the Low Carbon Fuel Standard, Staff Report Initial Statement Reasons. March 5. Available: http://www.arb.ca.gov/fuels/lcfs/lcfs.htm. Accessed, August 20, 2009.

CEC. *See* California Energy Commission.

CEC. 2007. Impact Analysis 2008 Update to the California Energy Efficiency Standards for Residential and Nonresidential Buildings. Available: <http://www.energy.ca.gov/title22008standards/rulemaking/documents/2007-11-07_IMPACT_ANALYSIS.PDF>. Accessed March 2009.

California Department of Finance. 2009. Residential Development Data: E5 – City and County Population Estimates. 2000-2050 - Race and Ethnic Populations Totals. Available: <http://www.labormarketinfo.edd.ca.gov/?pageid=145 >. Accessed February 2009.

California Economic Development Department. 2009. Commercial/Industrial Employment Data: Projections of Employment by Industry and Occupation. Available: <http://www.labormarketinfo.edd.ca.gov/?pageid=145>. Accessed February 2009.

City and County of San Francisco Department of Public Health. 2008. Assessment and Mitigation of Air Pollutant Health Effects from Intra-urban Roadways: Guidance for Land Use Planning and Environmental Review. Program on Health, Equity, & Sustainability. Occupational & Environmental Health Section. Prepared by Rajiv Bhatia and Thomas Rivard. May 6.

Dockery D. 1993. An association between air pollution and mortality in six U.S. cities. N Engl J Med 329:1753–1759.

EPA. *See* U.S. Environmental Protection Agency.

Governor's Office of Planning and Research. 2008 (June 19). *Technical Advisory: CEQA and Climate Change: Addressing Climate Change Through California Environmental Quality Act (CEQA) Review.* Sacramento, CA. Available: <http://opr.ca.gov/ceqa/pdfs/june08-ceqa.pdf>. Accessed February 2009.

Hiltermann T, Bruijne Cd, Stolk J, Zwinderman A, Spieksma F, Roemer W, et al. 1997. Effects of photochemical air pollution and allergen exposure on upper respiratory tract inflammation in asthmatics. Am J Respir Crit Care Med 156(6):1765–1772.

Intergovernmental Panel on Climate Change. 2007a (February). *Climate Change 2007: The Physical Science Basis. Contribution of Working Group I to the Fourth Assessment Report of the IPCC.* Geneva, Switzerland.

_____. 2007a (February). *Climate Change 2007: Climate Change 2007:Synthesis Report*
Summary for Policymakers. Geneva, Switzerland.

IPCC. *See* Intergovernmental Panel on Climate Change.

Jerrett M et al. 2005. Spatial Analysis of Air Pollution and Mortality in Los Angeles. Epidemiology. 16: 727-736

Kleinman, M.T., Sioutas, C., Froines, J.R., Fanning, E., Hamade, A., Mendez, L., Meacher, D., Oldham, M. Inhalation of Concentrated Ambient Particulate Matter Near a Heavily Trafficked Road Simulates Antigen-Induced Airway Responses in Mice; Inhal. Toxicol. 2007, 19 (Supp. 1), 117-126.

Laden, F.; Schwartz, J.; Speizer, F.E.; Dockery, D.W. Reduction in Fine Particulate Air Pollution and Mortality: Extended Follow-Up of the Harvard Six Cities Study. *Am. J. Respir. Crit. Care Med.* (2006), *173,* 667-672.

OPR. *See* Governor's Office of Planning and Research.

Pope C III, Thun M, Namboordiri M, Dockery D, Evans J, Speizer F. 1995. Particulate air pollution as a predictor of mortality in a prospective study of U.S. adults. Am J Respir Crit Care Med 151(3):669–6

Rimpo and Associates. 2009. BAAQMD CEQA Projects Database. Orangevale, CA.

Schauer JJ, Lough GC, Schafer MM, Christensen WF, Arndt MF, DeMinter JT, et al. 2006. Characterization of metals emitted from motor vehicles. Res Rep Health Eff Inst 133:1–7.

Schikowski T, Sugiri D, Ranft U, Gehring U, Heinrich J, Wichmann E, et al. 2005. Long-term air pollution exposure and living close to busy roads are associated with COPD in women. Respir Res 6(1):152.

Schwartz, J.; Coull, B.; Laden, F.; Ryan, L. The Effect of Dose and Timing of Dose on the Association between Airborne Particles and Survival. Env Health Persp (2008) 116, 1: 64-69.

SFDPH. See City and County of San Francisco Department of Public Health.

UNFCCC. *See* United Nations Framework Convention on Climate Change.

United Nations Framework Convention on Climate Change. 2009. *Article 1 of the UNFCCC.* Available: http://unfccc.int/essential_background/convention/background/items/2536.php. Accessed April 8, 2009.

U.S. Environmental Protection Agency. 2008. Federal Register: Implementation of the New Source Review (NSR) Program for Particulate Matter ($PM_{2.5}$) less than 2.5 Micrometers.

Available: <http://www.epa.gov/fedrgstr/EPA-AIR/200May/Day-1a10768.pdf>. Accessed February 2009.

_____. 2009. Monitor Values Report Data. Available: <http://www.epa.gov/air/data/index.html>. Accessed April 8, 2009.

_____. 2006. *Expanded Expert Judgment Assessment of the Concentration-Response Relationship between $PM_{2.5}$ Exposure and Mortality*, prepared for OAQPS-EPA by Industrial Economics Inc., September 21, 2006. A summary of this study is provided in Roman, HA et al., *Environ. Sci. Tech.* 2008, 42, 2268-2274.

_____. 1988. C. Cowherd, et al., *Control of Open Fugitive Dust Sources*, EPA-450/3-88-008, U. S. Environmental Protection Agency, Research Triangle Park, NC, September 1988.

Van Hee, V.C., Adar, S.D., Szpiro, A.A., Barr, R.G., Bluemke, D.A., Diez Roux, A.V., Gill, E.A., Sheppard, L., Kaufman, J.D. Exposure to Traffic and Left Ventricular Mass and Function; Am. J. Respir. Crit. Care Med. 2009, 179 (9), 827-834.

Vineis P, Hoek G, Krzyzanowski M, Vigna-Taglianti F, Veglia F, Airoldi L, et al. 2007. Lung cancers attributable to environmental tobacco smoke and air pollution in non-smokers in different European countries: a prospective study. Environ Health 6:7; doi:10.1186/1476-069X-6-7 [Online 15 February 2007]

Western Regional Air Partnership. 2006. *WRAP Fugitive Dust Handbook.* September 7, 2006. Available: http://www.wrapair.org/forums/dejf/fdh/content/FDHandbook_Rev_06.pdf. Accessed September 2009.

Zhu, Y. Hinds, W.C., Kim S, and Sioutas, C. 2002. Concentration and size distribution of ultrafine particles near a major highway. Journal of Air and Waste Management Association. 2002 Sep; 52 (9): 1032-42.

BAY AREA AIR QUALITY MANAGEMENT DISTRICT

RESOLUTION No. 2010-06

A Resolution of the Board of Directors of the Bay Area Air Quality Management District Adopting Thresholds For Use In Determining the Significance of Projects' Environmental Effects Under the California Environmental Quality Act

WHEREAS, pursuant to Title 14, Chapter 3, Article 5, Section 15064.7 of the California Code of Regulations ("Section 15064.7"), the California Resources Agency encourages public agencies to adopt "Thresholds of Significance" under the California Environmental Quality Act ("CEQA");

WHEREAS, pursuant to Section 15064.7, CEQA Thresholds of Significance are identifiable quantitative, qualitative or performance levels of a particular environmental effect, non-compliance with which means the effect will normally be determined to be "significant" under CEQA, and compliance with which means the effect normally will be determined to be less than significant under CEQA;

WHEREAS, the Board of Directors ("Board") of the Bay Area Air Quality Management District ("District") finds it necessary and appropriate to adopt CEQA Thresholds of Significance as set forth in Attachment A hereto for use by District staff and by other appropriate agencies in determining whether projects may have significant effects on the environment for purposes of CEQA environmental analyses;

WHEREAS, the CEQA Thresholds of Significance as set forth in Attachment A hereto do not alter the existing procedural and substantive requirements of CEQA under California law, but simply clarify the level at which, in the District's considered opinion, an environmental effect should normally be considered "significant" for purposes of existing CEQA law;

WHEREAS, the CEQA Thresholds of Significance set forth in Attachment A hereto were developed through an extensive public review process, which included public workshops, Board meetings and meetings with local government agency and non-government organization staff, including the cities of Berkeley, Colma, Daly City, Dublin, Fremont, Livermore, Oakland, Pleasanton, Richmond, San Leandro, San Mateo, San Francisco and Santa Rosa; the counties of Alameda, Contra Costa, Napa, Santa Clara, and Sonoma; and the CARE Task Force, the Alameda County Planning for Healthy Communities Network and the Governor's Office of Planning and Research Local Government Roundtable;

WHEREAS, District staff held ten public workshops throughout the Bay Area on February 26, 2009, April 27, 29 and 30, 2009, September 8, 9, and 10, 2009, October 2, 2009, and April 15 and 26, 2010; solicited Thresholds of Significance options for consideration; and published for public review and comment the Threshold Options Report on April 24, 2009, the CEQA Thresholds Options and Justification Report on October 8, 2009, and the Proposed Thresholds of Significance Report on November 2, 2009, December 7, 2009 and May 3, 2010;

meetings were held on November 18, 2009, December 2, 2009, January 6, 2010, May 5, 2010 and June 2, 2010;

WHEREAS, at the November 18, 2009, December 2, 2009, January 6, 2010, May 5, 2010 and June 2, 2010 public meetings, the subject matter of the Thresholds of Significance was discussed with interested persons in accordance with all provisions of law;

WHEREAS, the November 18, 2009, December 2, 2009, January 6, 2010, May 5, 2010 and June 2, 2010 public meetings and the other public review opportunities that the District has provided regarding the Thresholds of Significance, constitute a public review process as required by Section 15064.7;

WHEREAS, District staff has prepared and presented to this Board the May 3, 2010, Proposed Thresholds of Significance report, which has been considered by this Board and is incorporated herein by reference;

WHEREAS, the documents and other materials that constitute the record of the public review process under Section 15064.7 on which this Resolution is based are located at the Bay Area Air Quality Management District, 939 Ellis Street, San Francisco, 94109, and the custodian for these documents is Ms. Lisa Harper, Clerk of the Boards;

WHEREAS, District staff recommends adoption of the CEQA Thresholds of Significance set forth in Attachment A hereto;

WHEREAS, the Board of Directors concurs with District staff's recommendations and desires to adopt the CEQA Thresholds of Significance set forth in Attachment A hereto;

NOW, THEREFORE, BE IT RESOLVED that that the Board of Directors of the Bay Area Air Quality Management District does hereby adopt the CEQA Thresholds of Significance, pursuant to the authority granted by law, as set forth in Attachment A hereto, and discussed in the Proposed Thresholds of Significance report dated May 3, 2010, with instructions to staff to correct any typographical or formatting errors before final publication of the CEQA Thresholds of Significance.

BE IT FURTHER RESOLVED that it is the policy of the Bay Area Air Quality Management District that projects that do not comply with the CEQA Thresholds of Significance will normally be determined to have a significant effect on the environment for purposes of CEQA, and projects that comply with the CEQA Thresholds of Significance normally will be determined to have a less-than-significant effect on the environment for purposes of CEQA.

BE IT FURTHER RESOLVED that it is the policy of the Bay Area Air Quality Management District that Lead Agencies in the Bay Area apply the CEQA Thresholds of Significance, except for the Risk and Hazard thresholds for Receptor Projects, for Notices of Preparation issued, and environmental analyses begun, on or after the date of adoption of this Resolution.

BE IT FURTHER RESOLVED that it is the policy of the Bay Area Air Quality Management District that Lead Agencies in the Bay Area apply the CEQA Thresholds of Significance for the

Risk and Hazard thresholds for Receptor Projects for Notices of Preparation issued, and environmental analyses begun, after January 1, 2011.

The foregoing Resolution was duly and regularly introduced, passed and adopted at a regular meeting of the Board of Directors of the Bay Area Air Quality Management District on the Motion of Director KALRA, seconded by Director UILKEMA, on the 2nd day of JUNE, 2010, by the following vote of the Board:

AYES: BATES, GARNER, GIOIA, GROOM, HOSTERMAN, HUDSON, KALRA, MAR, ROSS, SPERING, TORLIATT, UILKEMA, YEAGER, WAGENKNECHT

NOES: NONE

RECUSED: HAGGERTY

ABSENT: BROWN, DALY, DUNNIGAN, KLATT, KNISS, MILEY, ZANE

Brad Wagenknecht
Chairperson of the Board of Directors

ATTEST:

John Gioia
Secretary of the Board of Directors

4

ATTACHMENT A

Proposed Air Quality CEQA Thresholds of Significance (May 3, 2010)

Pollutant	Construction-Related	Operational-Related	
Project-Level			
Criteria Air Pollutants and Precursors (Regional)	**Average Daily Emissions (lb/day)**	**Average Daily Emissions (lb/day)**	**Maximum Annual Emissions (tpy)**
ROG	54	54	10
NO_X	54	54	10
PM_{10} (exhaust)	82	82	15
$PM_{2.5}$ (exhaust)	54	54	10
$PM_{10}/PM_{2.5}$ (fugitive dust)	Best Management Practices	None	
Local CO	None	9.0 ppm (8-hour average), 20.0 ppm (1-hour average)	
GHGs **Projects other than Stationary Sources**	None	Compliance with Qualified Greenhouse Gas Reduction Strategy OR 1,100 MT of CO_2e/yr OR 4.6 MT CO_2e/SP/yr (residents + employees)	
GHGs **Stationary Sources**	None	10,000 MT/yr	
Risks and Hazards – New Source (Individual Project)	Same as Operational Thresholds*	Compliance with Qualified Community Risk Reduction Plan OR Increased cancer risk of >10.0 in a million Increased non-cancer risk of > 1.0 Hazard Index (Chronic or Acute) Ambient $PM_{2.5}$ increase: > 0.3 $\mu g/m^3$ annual average Zone of Influence: 1,000-foot radius from fence line of source or receptor	
Risks and Hazards – New Receptor (Individual Project)	Same as Operational Thresholds*	Compliance with Qualified Community Risk Reduction Plan OR Increased cancer risk of >10.0 in a million Increased non-cancer risk of > 1.0 Hazard Index (Chronic or Acute) Ambient $PM_{2.5}$ increase: > 0.3 $\mu g/m^3$ annual average Zone of Influence: 1,000-foot radius from fence line of source or receptor	
Risks and Hazards – New Source (Cumulative Thresholds)	Same as Operational Thresholds*	Compliance with Qualified Community Risk Reduction Plan OR Cancer: > 100 in a million (from all local sources) Non-cancer: > 10.0 Hazard Index (from all local sources) (Chronic) $PM_{2.5}$: > 0.8 $\mu g/m^3$ annual average (from all local sources) Zone of Influence: 1,000-foot radius from fence line of source or receptor	

Proposed Air Quality CEQA Thresholds of Significance (May 3, 2010)		
Pollutant	**Construction-Related**	**Operational-Related**
Risks and Hazards – New Receptor (Cumulative Thresholds)	Same as Operational Thresholds*	Compliance with Qualified Community Risk Reduction Plan OR Cancer: > 100 in a million (from all local sources) Non-cancer: > 10.0 Hazard Index (from all local sources) (Chronic) $PM_{2.5}$: > 0.8 µg/m^3 annual average (from all local sources) Zone of Influence: 1,000-foot radius from fence line of source or receptor
Accidental Release of Acutely Hazardous Air Pollutants	None	Storage or use of acutely hazardous materials locating near receptors or receptors locating near stored or used acutely hazardous materials considered significant
Odors	None	Complaint History—5 confirmed complaints per year averaged over three years
Plan-Level		
Criteria Air Pollutants and Precursors	None	1. Consistency with Current Air Quality Plan control measures 2. Projected VMT or vehicle trip increase is less than or equal to projected population increase
GHGs	None	Compliance with Qualified Greenhouse Gas Reduction Strategy (or similar criteria included in a General Plan) OR 6.6 MT CO2e/ SP/yr (residents + employees)
Risks and Hazards	None	1. Overlay zones around existing and planned sources of TACs (including adopted Risk Reduction Plan areas) 2. Overlay zones of at least 500 feet (or Air District-approved modeled distance) from all freeways and high volume roadways
Odors	None	Identify locations of odor sources in general plan
Accidental Release of Acutely Hazardous Air Pollutants	None	None
Regional Plans (Transportation and Air Quality Plans)		
GHGs, Criteria Air Pollutants and Precursors, and Toxic Air Contaminants	None	No net increase in emissions

Notes: CO = carbon monoxide; CO_2e = carbon dioxide equivalent; GHGs = greenhouse gases; lb/day = pounds per day; MT = metric tons; NO_X = oxides of nitrogen; $PM_{2.5}$= fine particulate matter with an aerodynamic resistance diameter of 2.5 micrometers or less; PM_{10} = respirable particulate matter with an aerodynamic resistance diameter of 10 micrometers or less; ppm = parts per million; ROG = reactive organic gases; SP = service population; tpy = tons per year; yr= year.

* Note: The Air District recommends that for construction projects that are less than one year duration, Lead Agencies should annualize impacts over the scope of actual days that peak impacts are to occur, rather than the full year.

E. GLOSSARY

Aerosol -- Particle of solid or liquid matter that can remain suspended in the air because of its small size (generally under one micrometer in diameter).

Air Quality Management District (AQMD) -- Local agency charged with controlling air pollution and attaining air quality standards. The Bay Area Air Quality Management District is the regional AQMD that includes Alameda, Contra Costa, Marin, Napa, San Francisco, San Mateo and Santa Clara Counties and the southern halves of Solano and Sonoma Counties.

Air Resources Board (ARB) -- The State of California agency responsible for air pollution control. Responsibilities include: establishing State ambient air quality standards, setting allowable emission levels for motor vehicles in California and oversight of local air quality management districts.

Area Sources -- Sources of air pollutants that individually emit relatively small quantities of air pollutants, but that may emit considerable quantities of emissions when aggregated over a large area. Examples include water heaters, lawn maintenance equipment, and consumer products.

Best Available Control Technology (BACT) -- The most stringent emissions control that has been achieved in practice, identified in a state implementation plan, or found by the District to be technologically feasible and cost-effective for a given class of sources.

California Clean Air Act (CCAA) -- Legislation enacted in 1988 mandating a planning process to attain state ambient air quality standards.

CALINE -- A model developed by the Air Resources Board that calculates carbon monoxide concentrations resulting from motor vehicle use.

Carbon Monoxide (CO) -- A colorless, odorless, toxic gas produced by the incomplete combustion of carbon-containing substances. It is emitted in large quantities by exhaust of gasoline-powered vehicles.

Carbon Dioxide (CO_2) -- A colorless, odorless gas that is an important contributor to Earth's greenhouse effect.

Carbon Dioxide Equivalent (CO_2E) -- A metric measure used to compare the emissions from various greenhouse gases based upon their global warming potential.

Chlorofluorocarbons (CFCs) -- A family of inert, nontoxic, and easily liquefied chemicals used in refrigeration, air conditioning, packaging, insulation, or as solvents and aerosol propellants. CFCs drift into the upper atmosphere where their chlorine components destroy stratospheric ozone.

Clean Air Act (CAA) -- Long-standing federal legislation, last amended in 1990, that is the legal basis for the national clean air programs.

Conformity -- A requirement in federal law and administrative practice that requires that projects will not be approved if they do not conform with the State Implementation Plan by: causing or contributing to an increase in air pollutant emissions, violating an air pollutant standard, or increasing the frequency of violations of an air pollutant standard.

Criteria Air Pollutants -- Air pollutants for which the federal or State government has established ambient air quality standards, or criteria, for outdoor concentration in order to protect public

health. Criteria pollutants include: ozone, carbon monoxide, sulfur dioxide PM10 (previously total suspended particulate), nitrogen oxide, and lead.

EMFAC -- The computer model developed by the California Air Resources Board to estimate composite on-road motor vehicle emission factors by vehicle class.

Emission Factor -- The amount of a specific pollutant emitted from a specified polluting source per unit quantity of material handled, processed, or burned.

Emission Inventory -- A list of air pollutants emitted over a determined area by type of source. Typically expressed in mass per unit time.

Environmental Protection Agency (EPA) -- The federal agency responsible for control of air and water pollution, toxic substances, solid waste, and cleanup of contaminated sites.

Exceedance -- A monitored level of concentration of any air contaminant higher than national or state ambient air quality standards.

Global Warming Potential (GWP) -- The index used to translate the level of emissions of various gases into a common measure in order to compare the relative radiative forcing of different gases without directly calculating the changes in atmospheric concentrations. GWPs are calculated as the ratio of the radiative forcing that would result from the emissions of one kilogram of a greenhouse gas to that from emission of one kilogram of carbon dioxide over a period of time (usually 100 years).

Greenhouse Gas (GHG) -- Any gas that absorbs infrared radiation in the atmosphere. Greenhouse gases include water vapor, carbon dioxide (CO_2), methane (CH_4), nitrous oxide (N_2O), halogenated fluorocarbons (HCFCs), ozone (O_3), perfluorocarbons (PFCs), sulfur hexafluoride (SF_6) and hydrofluorocarbons (HFCs).

Hazardous Air Pollutants – Federal terminology for air pollutants which are not covered by ambient air quality standards but may reasonably be expected to cause or contribute to serious illness or death (see NESHAPs).

Health Risk Assessment -- An analysis where human exposure to toxic substances is estimated, and considered together with information regarding the toxic potency of the substances, to provide quantitative estimates of health risk.

Hot Spot -- A location where emissions from specific sources may expose individuals and population groups to elevated risks of adverse health effects and contribute to the cumulative health risks of emissions from other sources in the area.

Hydrogen Sulfide (H_2S) -- A gas characterized by "rotten egg" smell, found in the vicinity of oil refineries, chemical plants and sewage treatment plants.

Impacted Communities – Also known as priority communities, the Air District defines impacted communities within the Bay Area as having higher emitting sources, highest air concentrations, and nearby low income and sensitive populations. The Air District identified the following impacted communities: the urban core areas of Concord, eastern San Francisco, western Alameda County, Redwood City/East Palo Alto, Richmond/San Pablo, and San Jose.

Indirect Sources – Land uses and facilities that attract or generate motor vehicle trips and thus result in air pollutant emissions, e.g., shopping centers, office buildings, and airports.

Inversion -- The phenomenon of a layer of warm air over cooler air below. This atmospheric condition resists the natural dispersion and dilution of air pollutants.

Level of Service (LOS) -- A transportation planning term for a method of measurement of traffic congestion. The LOS compares actual or projected traffic volume to the maximum capacity of the road under study. LOS ranges from A through F. LOS A describes free flow conditions, while LOS F describes the most congested conditions, up to or over the maximum capacity for which the road was designed.

Mobile Source -- Any motor vehicle that produces air pollution, e.g., cars, trucks, motorcycles (on-road mobile sources) or airplanes, trains and construction equipment (off-road mobile sources).

National Ambient Air Quality Standards (NAAQS) -- Health-based pollutant concentration limits established by EPA that apply to outdoor air (see Criteria Air Pollutants).

National Emissions Standards for Hazardous Air Pollutants (NESHAPs) – Emissions standards set by EPA for air pollutants not covered by NAAQS that may cause an increase in deaths or in serious, irreversible, or incapacitating illness.

Nitrogen Oxides (NO_X) -- Gases formed in great part from atmospheric nitrogen and oxygen when combustion takes place under conditions of high temperature and high pressure; NOX is a precursor to the criteria air pollutant ozone.

Nonattainment Area -- Defined geographic area that does not meet one or more of the

Ambient Air Quality Standards for the criteria pollutants designated in the federal Clean Air Act and/or California Clean Air Act.

Ozone (O_3) -- A pungent, colorless, toxic gas. A product of complex photochemical processes, usually in the presence of sunlight. Tropospheric (lower atmosphere) ozone is a criteria air pollutant.

Particulate -- A particle of solid or liquid matter; soot, dust, aerosols, fumes and mists.

Photochemical Process -- The chemical changes brought about by the radiant energy of the sun acting upon various polluting substances. The products are known as photochemical smog.

$PM_{2.5}$ -- Fine particulate matter (solid or liquid) with an aerodynamic diameter equal to or less than 2.5 micrometers. Individual particles of this size are small enough to be inhaled deeply into the lungs..

PM_{10} -- Fine particulate matter (solid or liquid) with an aerodynamic diameter equal to or less than 10 micrometers. Individual particles of this size are small enough to be inhaled into human lungs; they are not visible to the human eye.

Precursor -- Compounds that change chemically or physically after being emitted into the air and eventually produce air pollutants. For example, organic compounds are precursors to ozone.

Prevention of Significant Deterioration (PSD) -- EPA program in which State and/or federal permits are required that are intended to restrict emissions for new or modified sources in places where air quality is already better than required to meet primary and secondary ambient air quality standards.

Reactive Organic Gases (ROG) -- Classes of organic compounds, especially olefins, substituted aromatics and aldehydes, that react rapidly in the atmosphere to form photochemical smog or ozone.

Sensitive Receptors -- Facilities or land uses that include members of the population that are particularly sensitive to the effects of air pollutants, such as children, the elderly, and people with illnesses. Examples include schools, hospitals and residential areas.

State Implementation Plan (SIP) -- EPA-approved state plans for attaining and maintaining federal air quality standards.

Stationary Source -- A fixed, non-mobile source of air pollution, usually found at industrial or commercial facilities.

Sulfur Oxides (SO_X) -- Pungent, colorless gases formed primarily by the combustion of sulfur-containing fossil fuels, especially coal and oil. Considered a criteria air pollutant, sulfur oxides may damage the respiratory tract as well as vegetation.

Toxic Air Contaminants -- Air pollutants which cause illness or death in relatively small quantities. Non-criteria air contaminants that, upon exposure, ingestion, inhalation, or assimilation into organisms either directly from the environment or indirectly by ingestion through food chains, may cause death, disease, behavioral abnormalities, cancer, genetic mutations, physiological malfunctions, or physical deformations in such organisms or their offspring.

Transportation Control Measures (TCMs) -- Measures to reduce traffic congestion and decrease emissions from motor vehicles by reducing vehicle use.

URBEMIS -- A computer model developed by the California Air Resources Board to estimate air pollutant emissions from motor vehicle trips associated with land use development.

BAY AREA AIR QUALITY MANAGEMENT DISTRICT

Planning, Rules and Research | CEQA Guidelines

CEQA Guidelines

UPDATE: January 16, 2014: On June 2, 2010, the Bay Area Air Quality Management District's Board of Directors unanimously adopted thresholds of significance to assist in the review of projects under the California Environmental Quality Act. These Thresholds are designed to establish the level at which the District believed air pollution emissions would cause significant environmental impacts under CEQA and were posted on the Air District's website and included in the Air District's updated CEQA Guidelines (updated May 2012).

On March 5, 2012 the Alameda County Superior Court issued a judgment finding that the Air District had failed to comply with CEQA when it adopted the Thresholds. The court did not determine whether the Thresholds were valid on the merits, but found that the adoption of the Thresholds was a project under CEQA. The court issued a writ of mandate ordering the District to set aside the Thresholds and cease dissemination of them until the Air District had complied with CEQA. The Air District has appealed the Alameda County Superior Court's decision. The Court of Appeal of the State of California, First Appellate District, reversed the trial court's decision. The Court of Appeal's decision was appealed to the California Supreme Court, which granted limited review, and the matter is currently pending there.

In view of the trial court's order which remains in place pending final resolution of the case, the Air District is no longer recommending that the Thresholds be used as a generally applicable measure of a project's significant air quality impacts. Lead agencies will need to determine appropriate air quality thresholds of significance based on substantial evidence in the record. Although lead agencies may rely on the Air District's updated CEQA Guidelines (updated May 2012) for assistance in calculating air pollution emissions, obtaining information regarding the health impacts of air pollutants, and identifying potential mitigation measures, the Air District has been ordered to set aside the Thresholds and is no longer recommending that these Thresholds be used as a general measure of project's significant air quality impacts. Lead agencies may continue to rely on the Air District's 1999 Thresholds of Significance and they may continue to make determinations regarding the significance of an individual project's air quality impacts based on the substantial evidence in the record for that project.

Various tools and resources are available on this website to assist local jurisdictions in applying the Air District's CEQA Guidelines.

For more information, please contact Alison Kirk, Senior Environmental Planner at akirk@baaqmd.gov or 415-749-5169.

Learn more about the updated CEQA Guidelines.

View the District's 1999 CEQA Guidelines.

To view the State CEQA Guidelines and related materials visit the California Resources Agency.

California Air Districts Launch Greenhouse Gas Exchange

Update: January 2, 2014

The California Air Pollution Control Officers Association (CAPCOA), representing California's 35 local air districts, has launched the CAPCOA *Greenhouse Gas Exchange*. The *Exchange* provides a reliable, low-cost, secure platform to encourage locally generated, high quality GHG emission reduction credits that can be used to meet CEQA or other compliance requirements.

CalEEMod Release

Update: August 5, 2013

On July 31, 2013, the California Air Pollution Control Officers Association (CAPCOA) released CalEEMod 2013.2. This land use model can be downloaded from www.caleemod.com. From this point forward, the BAAQMD will no longer support the use of Urbemis. Please perform all future analyses using CalEEmod. For more information or to ask questions, please contact Alison Kirk, Senior Environmental Planner at akirk@baaqmd.gov or 415-749-5169.

Last Updated: 1/12/2015

Bay Area Air Quality Management District
939 Ellis St. San Francisco, CA 94109
(415) 771-6000 | 1-800-HELP AIR

BAAQMD CEQA GUIDELINES
Assessing the Air Quality Impacts of Projects and Plans

Prepared by the Planning and Research Division of the
Bay Area Air Quality Management District
939 Ellis Street
San Francisco, CA 94109

December, 1999

This document is intended to serve as a guide for those who prepare or evaluate air quality impact analyses for projects and plans in the San Francisco Bay Area. The GUIDELINES include information on legal requirements, BAAQMD rules, plans and procedures, methods of analyzing air quality impacts, thresholds of significance, mitigation measures, and background air quality information. Copies and updates are available from the BAAQMD Public Information Office at (415) 749-4900. Questions on content may be addressed to the BAAQMD's Planning and Transportation Section at (415) 749-4995.

Ellen Garvey - Air Pollution Control Officer
Peter Hess - Deputy Air Pollution Control Officer
Thomas Perardi - Director, Planning & Research Division
Jean Roggenkamp - Manager, Planning and Transportation Section

ACKNOWLEDGMENTS

The principal authors of this document were:

Henry Hilken, Senior Environmental Planner

Irwin Mussen, Principal Environmental Planner

Joseph Steinberger, Environmental Planner

Significant contributions were also made by:

Tom Addison, Environmental Planner

Michael Basso, Senior Air Quality Meteorologist

Dick Duker, Senior Air Quality Meteorologist

Amir Fanai, Senior Air Quality Engineer

Mike Kim, Senior Transportation Engineer

Tirlochan (Toch) Mangat, Special Projects Manager

The authors also wish to thank Lilia Martinez and Judith Williams, who provided the word processing for this document.

TABLE OF CONTENTS

TABLE OF CONTENTS iii
LIST OF TABLES iii
LIST OF FIGURES iii

CHAPTER 1 - INTRODUCTION 1
1.1 Background 1
1.2 How To Use These Guidelines 1
1.3 District Responsibilities 3
1.4 Air Pollutants Of Concern In The Bay Area 5
1.5 Air Quality Conditions In The Bay Area 7

CHAPTER 2 - PRELIMINARY REVIEW AND THRESHOLDS OF SIGNIFICANCE 9
2.1 Early Consultation 9
2.2 Preparation Of The Initial Study 12
2.3 Thresholds Of Significance 13
2.4 Project Screening 24

CHAPTER 3 - ASSESSING AIR QUALITY IMPACTS 26
3.1 Introduction 26
3.2 Environmental Setting 27
3.3 Evaluating Construction Emissions 28
3.4 Calculating Emissions From Project Operations 30
3.5 Evaluating Odor Impacts 49
3.6 Evaluating Impacts Of Toxic Air Contaminants 49
3.7 Evaluating Impacts Of Accidental Releases Of Hazardous Materials 50
3.8 Evaluating Cumulative Impacts 51
3.9 Evaluating Plans 51

CHAPTER 4 - MITIGATING AIR QUALITY IMPACTS 52
4.1 Introduction 52
4.2 Mitigating Construction Impacts 52
4.3 Mitigating Air Quality Impacts Through Land Use And Design Measures 53
4.4 Mitigating Impacts Of Project Operations 56
4.5 Mitigating Odor Impacts 68
4.6 Mitigating Impacts From Toxic Air Contaminants And Accidental Releases Of Hazardous Materials 68
4.7 Mitigation Monitoring And Reporting 69

APPENDIX A - AIR QUALITY LAWS, PROGRAMS AND STANDARDS A-1
APPENDIX B - AIR POLLUTANT SOURCES AND EFFECTS B-1
APPENDIX C - AIR POLLUTION — STATUS, PROBLEMS AND TRENDS C-1
APPENDIX D - CLIMATE, TOPOGRAPHY AND AIR POLLUTION POTENTIAL D-1
APPENDIX E - TOXIC AIR CONTAMINANTS E-1
APPENDIX F - RESOURCE DOCUMENTS F-1
APPENDIX G - GLOSSARY G-1
APPENDIX H - REFERENCES H-1

LIST OF TABLES

TABLE 1 BAY AREA ATTAINMENT STATUS AS OF APRIL 1996 8
TABLE 2 FEASIBLE CONTROL MEASURES FOR CONSTRUCTION EMISSIONS OF PM_{10} 15
TABLE 3 THRESHOLDS OF SIGNIFICANCE FOR PROJECT OPERATIONS 16
TABLE 4 PROJECT SCREENING TRIGGER LEVELS FOR POTENTIAL ODOR SOURCES 18
TABLE 5 CAP TCMS TO BE IMPLEMENTED BY LOCAL GOVERNMENT 23
TABLE 6 PROJECTS WITH POTENTIALLY SIGNIFICANT EMISSIONS 25
TABLE 7 HEAVY AND LIGHT DUTY CONSTRUCTION EQUIPMENT EXHAUST EMISSION FACTORS 29
TABLE 8 AVERAGE TRIP GENERATION RATES FOR SELECTED LAND USES 34
TABLE 9 AVERAGE TRIP LENGTH BY COUNTY AND YEAR 35
TABLE 10 AVERAGE EXHAUST EMISSION RATES 35
TABLE 11 TRIP END EMISSION FACTORS 36
TABLE 12 REFERENCE CARBON MONOXIDE CONCENTRATIONS 39
TABLE 13 FUTURE YEAR CARBON MONOXIDE ROLLBACK FACTORS 42
TABLE 14 GENERALIZED EMISSION FACTORS FOR SELECTED INDUSTRY GROUPS 48
TABLE 15 MITIGATION MEASURES FOR REDUCING MOTOR VEHICLE EMISSIONS FROM COMMERCIAL, INSTITUTIONAL AND INDUSTRIAL PROJECTS 61
TABLE 16 MITIGATION MEASURES FOR REDUCING MOTOR VEHICLE EMISSIONS FROM RESIDENTIAL PROJECTS 65
TABLE 17 LOW EMISSION VEHICLE MITIGATION MEASURES……...67

TABLE A-1 AMBIENT AIR QUALITY STANDARDS A-2
TABLE C-1 EXCEEDANCES OF THE NATIONAL OZONE STANDARD C-3
TABLE C-2 EXCEEDANCES OF THE STATE OZONE STANDARD C-4
TABLE C-3 EXCEEDANCES OF NATIONAL AND STATE CARBON MONOXIDE STANDARD C-5
TABLE C-4 EXCEEDANCES OF THE STATE AND NATIONAL FINE PARTICULATE MATTER STANDARD C-6
TABLE C-5 MOTOR VEHICLE SHARE OF CRITERIA CONTAMINANT EMISSIONS C-8
TABLE E-1 POLLUTANTS THAT TRIGGER DISTRICT RISK SCREENING REQUIREMENTS E-2
TABLE E-2 SUBSTANCES DESIGNATED BY ARB AS TOXIC AIR CONTAMINANTS E-4

LIST OF FIGURES

FIGURE 1 BAAQMD JURISDICTION ..... **Error! Bookmark not defined.**
FIGURE 2 EVALUATING CUMULATIVE IMPACTS 20
FIGURE 3 ONE HOUR CO BACKGROUND CONCENTRATIONS 43
FIGURE 4 EIGHT HOUR CO BACKGROUND CONCENTRATIONS 44
FIGURE 5 DETERMINING CO BACKGROUND CONCENTRATIONS - EXAMPLE **Error! Bookmark not defined.**

FIGURE C-1 BAAQMD AIR QUALITY MONITORING STATIONS ..... C-**Error! Bookmark not defined.**
FIGURE C-2 BAY AREA EMISSION INVENTORY PROJECTIONS 1980-2010 ..... C-10
FIGURE D-1 1992 ANNUAL WIND ROSES ..... D-**Error! Bookmark not defined.**
FIGURE D-2 CLIMATOLOGICAL SUBREGIONS ..... D-**Error! Bookmark not defined.**

CHAPTER 1 - INTRODUCTION

1.1 Background

The purpose of these Guidelines is to assist Lead Agencies, as well as consultants, project proponents and other interested parties, in evaluating potential air quality impacts of projects and plans proposed in the San Francisco Bay Area. Specifically, these Guidelines explain the procedures that the Bay Area Air Quality Management District (BAAQMD or "District") recommends be followed during environmental review processes required by the California Environmental Quality Act (CEQA). The Guidelines provide direction on how to evaluate potential air quality impacts, how to determine whether these impacts are significant, and how to mitigate these impacts. It is hoped that by providing this guidance, the air quality impacts of plans and development proposals will be analyzed accurately and consistently, and adverse impacts will be minimized.

These guidelines do not attempt to address every type of project that may be subject to CEQA analysis. Greatest emphasis is placed on: development proposals, such as commercial or residential projects, that generate significant numbers of vehicle trips (and associated air pollutant emissions); impacts related to nuisances (such as odors and dust), toxic air contaminants and accidental releases of hazardous materials, often resulting from air pollutant sources and members of the public being in close proximity; and preparation or revision of plans, such as general plans or specific plans.

1.2 How to Use These Guidelines

This document replaces the District's previous CEQA guidance document, *Air Quality and Urban Development: Guidelines for Assessing Impacts of Projects and Plans*, published in November 1985 (with revisions through August 1991). This 1996 document has more current information regarding issues including federal and State requirements, regional air quality plans, emission inventories, analytical procedures and mitigation strategies. Some of the more significant additions or revisions in this document include the following:

- Recommendations regarding early consultation procedures between Lead Agencies and project proponents on issues such as land use and design measures to reduce auto use, land use conflicts and sensitive receptors, and District regulatory requirements. (See pages 9-11.)

- Thresholds of significance for impacts associated with construction, project operations, odors, toxics, accidental releases, cumulative impacts, and plans. (See pages 13-25.)

- Calculating mobile source emissions using the URBEMIS model. (See pages 31-33.)

- Determining background carbon monoxide (CO) concentrations for use in microscale CO modeling. (See pages 41-46.)

- Mitigating air quality impacts through land use and design measures. (See pp. 9-11, 53-56.)

The recommendations in these Guidelines should be viewed as minimum considerations for air quality analysis. A Lead Agency or a project proponent may substitute more sophisticated models, more precise input data, innovative mitigation measures and/or other features. The District encourages creative approaches to impact analysis and mitigation in planning for air quality improvement.

Portions of these Guidelines will be revised as new information becomes available on such matters as revised emission factors for the Bay Area motor vehicle fleet or emission inventories. Copies and updates of these Guidelines are available from the District's Public Information Office at (415) 749-4900. Questions on content may be addressed to the District's Planning and Transportation Section at (415) 749-4995.

Organization of the Guidelines

Chapter 1 provides a summary of the purpose of the document, a brief overview of District responsibilities, and summary information regarding air pollution in the Bay Area.

Chapter 2 suggests early consultation procedures and issues for consideration by Lead Agencies, discusses preparation of the Initial Study, and provides thresholds of significance for determining whether an air quality impact is significant.

Chapter 3 describes methods for estimating air quality impacts. The chapter addresses impacts from project construction, project operations, and plans.

Chapter 4 describes methods for mitigating air quality impacts. The chapter discusses mitigation strategies to be considered at the general plan level, and project-specific mitigation measures.

Appendix A discusses laws, regulations, programs and plans related to air quality management.

Appendix B summarizes sources and effects of air pollutants.

Appendix C summarizes the region's attainment status with respect to national and State air quality standards, and discusses air quality problems and trends.

Appendix D discusses how climate and topography influence air quality conditions, and provides a detailed description of climate and topography for various subregions in the Bay Area.

Appendix E summarizes the District's activities with respect to toxic air contaminants.

Appendix F summarizes recommended resources and guidance documents that Lead Agencies may wish to consult when developing mitigation measures.

Appendix G provides a glossary.

Appendix H provides the references used in the preparation of this document.

1.3 District Responsibilities

The District is the agency primarily responsible for assuring that national and State ambient air quality standards are attained and maintained in the San Francisco Bay Area. Among the District's many responsibilities are the following: preparation of plans for attaining and maintaining ambient air quality standards in the region; adoption and enforcement of rules and regulations concerning air pollutant sources; issuing permits for stationary sources of air pollutants; inspecting stationary sources of air pollutants and responding to citizen complaints; monitoring ambient air quality and meteorological conditions; awarding grants to reduce motor vehicle emissions; conducting public education campaigns; and many other activities. The District's jurisdiction includes all of Alameda, Contra Costa, Marin, Napa, San Francisco, San Mateo and Santa Clara Counties, and the southern portions of Solano and Sonoma Counties. Figure 1 shows the boundaries of the District's jurisdiction. Further information about District activities is provided in Appendix A.

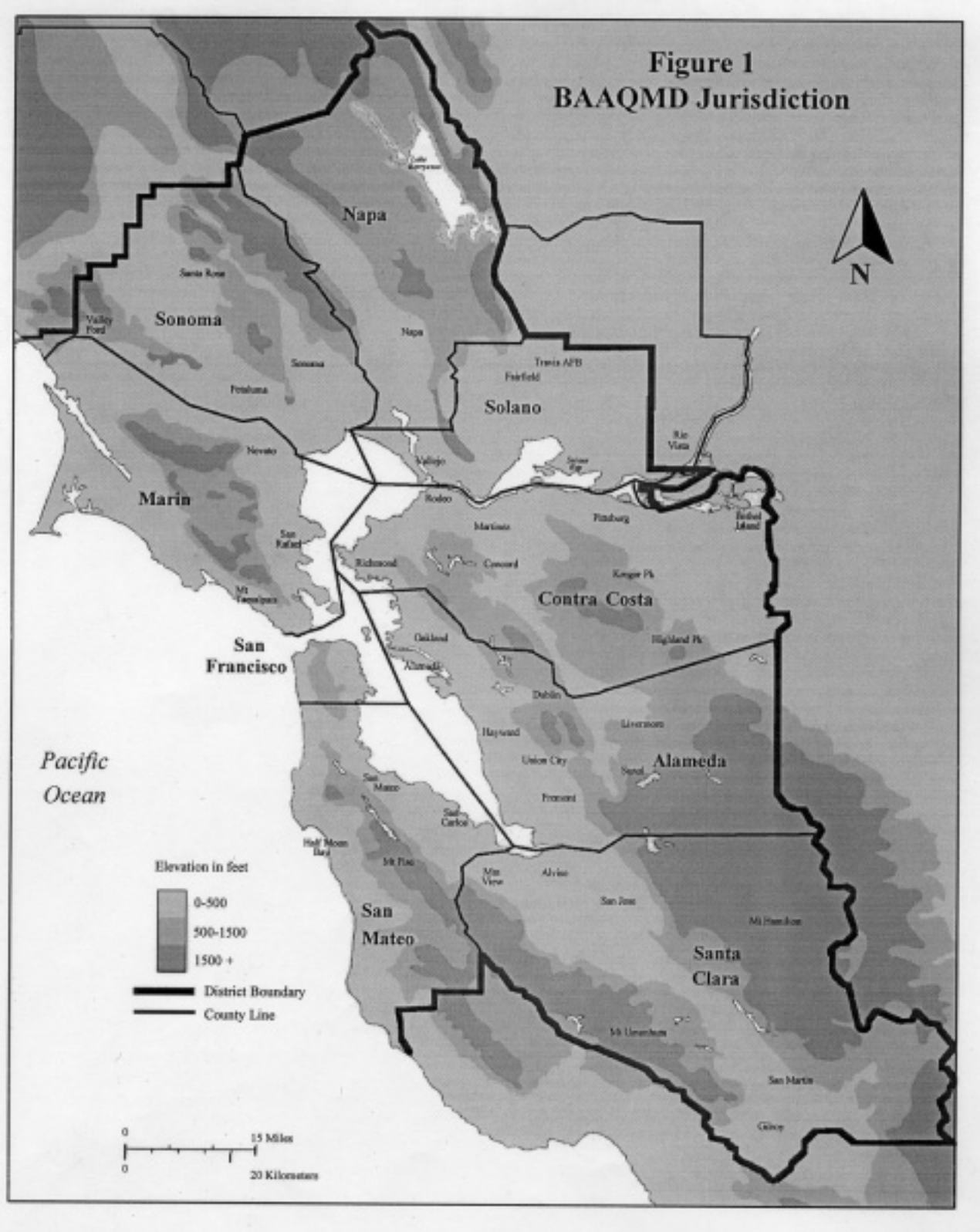
In its efforts to reduce air pollution and achieve ambient air quality standards, the District also works with many other agencies and organizations, including: U.S. Environmental Protection Agency, California Air Resources Board, Metropolitan Transportation Commission, Association of Bay Area Governments, congestion management agencies, cities and counties, and various non-governmental organizations. Appendix A provides further information regarding other agencies with whom the District cooperates. Appendix A also provides an overview of federal and State laws and programs that affect air quality.

The District is involved in the CEQA process in a variety of ways.

Lead Agency - The District acts as a Lead Agency when it has the primary authority to implement or approve a project. The District acts as a Lead Agency when it adopts air quality plans for the region, as well as when it adopts rules and regulations. The District also occasionally acts as a Lead Agency, or prepares supplemental environmental documentation, for projects subject to District permit requirements.

Responsible Agency - The District acts as a Responsible Agency when it has discretionary authority over a project, but does not have the primary discretionary authority of a Lead Agency. As a Responsible Agency, the District may coordinate the environmental review process with the District's permitting process, provide comments to the Lead Agency regarding potential impacts, and recommend mitigation measures.

Commenting Agency - The District acts as a Commenting Agency when it is not a Lead or Responsible Agency (i.e., it does not have discretionary authority over a project), but when it may have concerns about the air quality impacts of a proposed project or plan. As a Commenting Agency, the District reviews environmental documents prepared for development proposals and plans in the Bay Area and provides comments to Lead Agencies regarding air quality impacts and mitigation measures.


Figure 1
BAAQMD Jurisdiction
N
Napa
Sonoma
Solano
Marin
San Francisco
Contra Costa
Alameda
San Mateo
Santa Clara
Pacific Ocean
Elevation in feet
0-500
500-1500
1500 +
District Boundary
County Line
0
15 Miles
0
20 Kilometers

1.4 Air Pollutants of Concern in the Bay Area

State and national ambient air quality standards have been established for the following pollutants: ozone, carbon monoxide, nitrogen dioxide, sulfur dioxide, fine particulate matter (PM_{10}) and lead. For some of these pollutants, notably ozone and PM_{10}, the State standards are more stringent than the national standards. The State has also established ambient air quality standards for sulfates, hydrogen sulfide, vinyl chloride and visibility reducing particles. The above-mentioned pollutants are generally known as "criteria pollutants." Appendix A provides further information on ambient air quality standards.

District regulations and programs seek to minimize emissions of all air pollutants. These Guidelines, however, focus primarily on the criteria pollutants for which the region still periodically exceeds State and national standards (ozone and PM_{10}) or for which the region occasionally exceeded State or national standards in the recent past (carbon monoxide).

Ground level ozone, often referred to as smog, is not emitted directly, but is formed in the atmosphere through complex chemical reactions between nitrogen oxides (NO_x) and reactive organic gases (ROG) in the presence of sunlight. The principal sources of NO_x and ROG, often termed ozone precursors, are combustion processes (including motor vehicle engines) and evaporation of solvents, paints and fuels. Motor vehicles are the single largest source of ozone precursor emissions in the Bay Area. Exposure to ozone can cause eye irritation, aggravate respiratory diseases and damage lung tissue, as well as damage vegetation and reduce visibility.

Fine particulate matter (PM_{10}, or particulate matter less than 10 microns in diameter) includes a wide range of solid or liquid particles, including smoke, dust, aerosols and metallic oxides. There are many sources of PM_{10} emissions, including combustion, industrial processes, grading and construction, and motor vehicles. Of the PM_{10} emissions associated with motor vehicle use, some are tailpipe and tire wear emissions, but greater quantities are generated by resuspended road dust. Consequently, improvements in motor vehicle engines and fuels have not reduced PM_{10} emissions as significantly as they have reduced emissions of other pollutants. Reductions in motor vehicle *use* are needed to significantly reduce PM_{10} emissions from resuspended road dust. District research also has shown that wood burning in fireplaces and stoves is a significant source of PM_{10}, particularly during episodes when PM_{10} levels are at their highest.

Fine particulate matter is of concern because it can bypass the body's natural filtration system more easily than larger particles, and can lodge deep in the lungs. Health effects of PM_{10} vary depending on a variety of factors, including the type and size of particle. Research has demonstrated a correlation between high PM_{10} concentrations and increased mortality rates. Elevated PM_{10} concentrations can also aggravate chronic respiratory illness such as bronchitis and asthma.

U.S. EPA in 1997 announced new ambient air quality standards for ozone and fine particulate matter. The new standards were intended to provide greater protection of public health. EPA proposed to phase out the 1-hour ozone standard and replace it with an 8-hour standard. With respect to fine particulate, EPA proposed a new standard for the smaller particles, $PM_{2.5}$, or particulate matter less than 2.5 microns in diameter. The new $PM_{2.5}$ standards included an

annual standard and a 24-hour standard. Following the announcement of the new national standards, the District began collecting monitoring data to determine the region's attainment status with respect to the new standards. Industry groups challenged the new standards in court, but as of December 1999 the status of the new standards was uncertain.

Carbon monoxide (CO) is an odorless, colorless gas that is formed by the incomplete combustion of fuels. Motor vehicles are by far the single largest source of CO in the Bay Area. At high concentrations, CO reduces the oxygen-carrying capacity of the blood and can cause headaches, dizziness, unconsciousness, and even death. CO also can aggravate cardiovascular disease.

In addition to the criteria pollutants discussed above, toxic air contaminants (TACs) are another group of pollutants of concern in the Bay Area. There are many different types of TACs, with varying degrees of toxicity. Sources of TACs include industrial processes such as petroleum refining and chrome plating operations, commercial operations such as gasoline stations and dry cleaners, and motor vehicle exhaust. Public exposure to TACs can result from emissions from normal operations, as well as accidental releases of hazardous materials during upset conditions. Health effects of TACs include cancer, birth defects, neurological damage and death.

Diesel exhaust is a growing concern in the Bay Area and throughout California. The California Air Resources Board (ARB) in 1998 identified diesel engine particulate matter as a toxic air contaminant. The exhaust from diesel engines includes hundreds of different gaseous and particulate components, many of which are toxic. Many of these toxic compounds adhere to the particles, and because diesel particles are very small, they penetrate deeply into the lungs. Diesel engine particulate matter has been identified as a human carcinogen. Mobile sources – including trucks, buses, automobiles, trains, ships and farm equipment – are by far the largest source of diesel emissions. Studies show that diesel particulate matter concentrations are much higher near heavily traveled highways and intersections. District analysis shows that the cancer risk from exposure to diesel exhaust is much higher than the risk associated with any other toxic air pollutant routinely measured in the region.

Prior to the listing of diesel exhaust as a toxic air contaminant, California had already adopted various regulations that would reduce diesel emissions. These regulations include new standards for diesel fuel, emission standards for new diesel trucks, buses, autos, and utility equipment, and inspection and maintenance requirements for heavy duty vehicles. Following the listing of diesel engine particulate matter as a toxic air contaminant, ARB is currently (as of December 1999) evaluating what additional regulatory action is needed to reduce public exposure. ARB does not plan on banning diesel fuel or engines. ARB may consider additional requirements for diesel fuel and engines, however, as well as other measures to reduce public exposure.

Other air quality issues of concern in the Bay Area include nuisance impacts of odors and dust. Objectionable odors may be associated with a variety of pollutants. Common sources of odors include wastewater treatment plants, landfills, composting facilities, refineries and chemical plants. Similarly, nuisance dust may be generated by a variety of sources including quarries, agriculture, grading and construction. Odors rarely have direct health impacts, but they can be very unpleasant and can lead to anger and concern over possible health effects among the public. Each year the District receives thousands of citizen complaints about objectionable odors. Dust

emissions can contribute to increased ambient concentrations of PM_{10}, particularly when dust settles on roadways where it can be pulverized and resuspended by traffic. Dust emissions also contribute to reduced visibility and soiling of exposed surfaces.

1.5 Air Quality Conditions in the Bay Area

Air quality conditions in the San Francisco Bay Area have improved significantly since the District was created in 1955. Ambient concentrations of air pollutants and the number of days on which the region exceeds air quality standards have fallen dramatically. Public health benefits, improved visibility, and reduced damage to plants and materials are among the benefits of this progress.

Continued progress is necessary, however. Following years of declining emissions and ambient concentrations of ozone, the Bay Area in 1995 was redesignated as an attainment area for the national 1-hour ozone standard. However, unusual heat waves triggered new exceedances of the national ozone standard during the summers of 1995 and 1996. As a result, in 1998 U.S. EPA redesignated the region back into nonattainment status for the national 1-hour ozone standard. The region also periodically exceeds State ambient air quality standards for ozone and particulate matter. The State standards for these pollutants are more stringent than the national standards. Exceedances of air quality standards occur primarily during meteorological conditions conducive to high pollution levels, such as cold, windless winter nights (for particulate matter) or hot, sunny summer afternoons (for ozone). As is true throughout much of the U.S., motor vehicle use is projected to increase substantially in the region. The District, local jurisdictions, and other parties responsible for protecting public health and welfare will need to continue to minimize the air quality impacts of growth and development.

Table 1 provides a summary of the current attainment status for the San Francisco Bay Area with respect to national and State ambient air quality standards. Appendix B provides information regarding sources and effects of air pollutants. Appendix C discusses air pollutant status, problems and trends in the Bay Area and summarizes ambient air quality monitoring data for recent years.

TABLE 1
BAY AREA ATTAINMENT STATUS AS OF DECEMBER 1999

Pollutant	Averaging Time	California Standards [1]		National Standards [2]	
		Concentration	Attainment Status	Concentration	Attainment Status
Ozone	8-hour			0.08 ppm	U[5]
	1-hour	0.09 ppm	N	0.12 ppm	N[3]
Carbon Monoxide	8-hour	9.0 ppm	A	9 ppm	A[4]
	1-hour	20 ppm	A	35 ppm	A
Nitrogen Dioxide	Annual Average			0.053 ppm	A
	1 Hour	0.25 ppm	A		
Sulfur Dioxide	Annual Average			0.03 ppm	A
	24 Hour	0.05 ppm	A	0.14 ppm	A
	1-hour	0.25 ppm	A		
Fine Particulate Matter (PM_{10})	Annual Arithmetic Mean			50 $\mu g/m^3$	A
	Annual Geometric Mean	30 $\mu g/m^3$	N		
	24 Hour	50 $\mu g/m^3$	N	150 $\mu g/m^3$	U
Fine Particulate Matter ($PM_{2.5}$)	Annual Arithmetic Mean			15 $\mu g/m^3$	U[5]
	24 Hour			65 $\mu g/m^3$	U[5]

A=Attainment N=Nonattainment U=Unclassified
ppm=parts per million $\mu g/m^3$=micrograms per cubic meter

1. California standards for ozone, carbon monoxide (except Lake Tahoe), sulfur dioxide (1-hour and 24-hour), nitrogen dioxide, and PM_{10} are values that are not to be exceeded. If the standard is for a 1-hour, 8-hour or 24-hour average, then some measurements may be excluded. In particular, measurements are excluded that ARB determines would occur less than once per year on the average.
2. National standards other than for ozone and those based on annual averages or annual arithmetic means are not to be exceeded more than once a year. For example, the ozone standard is attained if, during the most recent three-year period, the average number of days per year with maximum hourly concentrations above the standard is equal to or less than one.
3. In August 1998 the Bay Area was redesignated to nonattainment for the national 1-hour ozone standard.
4. In June 1998 the Bay Area was redesignated to attainment for the national 8-hour CO standard.
5. In 1997 EPA established an 8-hour standard for ozone, and annual and 24-hour standards for very fine particulate matter (PM2.5). As of December 1999, the District did not have sufficient monitoring data to determine the region's attainment status. The new standards were challenged in court, and as of December 1999 their status was uncertain.

CHAPTER 2 - PRELIMINARY REVIEW AND THRESHOLDS OF SIGNIFICANCE

This chapter of the District's CEQA Guidelines provides guidance regarding early consultation between project proponents and local governments. This chapter also provides thresholds to be used to determine whether a project or plan will have a significant air quality impact.

2.1 Early Consultation

The District encourages local jurisdictions to address air quality issues as early as possible in the development review process. Issues such as potential land use conflicts (e.g., odors) or site design to encourage alternatives to the automobile should be considered. Addressing land use and site design issues while a proposed project is still in the conceptual stage increases opportunities to incorporate mitigation measures and desirable modifications to minimize air quality impacts. By the time a project enters the CEQA process, it is usually more costly and time-consuming to redesign the project to incorporate mitigation measures. Early consultation may be achieved by including a formal step in the jurisdiction's development review procedures or simply by discussing air quality concerns at the planning counter when a project proponent makes an initial contact regarding a proposed development. Regardless of the specific procedures a local jurisdiction employs, the objective should be to incorporate air quality beneficial features into a project before significant resources (public and private) have been devoted to the project.

The following air quality considerations warrant particular attention during early consultation between Lead Agencies and project proponents: 1) land use and design measures to encourage alternatives to the automobile and conserve energy; 2) land use conflicts and exposure of sensitive receptors to odors, toxics and criteria pollutants; and 3) applicable District rules, regulations and permit requirements. Lead Agencies and project proponents also are encouraged to consult with the District on these issues.

Land Use and Design Considerations - Land use decisions are critical to air quality planning because land use patterns greatly influence transportation needs, and motor vehicles are the largest source of air pollution. The location, intensity and design of land use development projects significantly influences how people travel. For example, land use strategies such as locating moderate or high density development near transit stations increases opportunities for residents/employees to use transit rather than drive their cars. Similarly, design considerations such as orienting a building entrance towards a sidewalk and/or transit stop increases the attractiveness of walking and transit as an alternative to driving. Some important land use and design issues to consider include the following:

- Encourage the development of higher density housing and employment centers near transit stations.
- Encourage compact development featuring a mix of uses that locates residences near jobs and services.
- Provide neighborhood retail within or adjacent to large residential developments.

- Provide services, such as restaurants, banks, copy shops, post office, etc., within office parks and other large employment centers.
- Encourage infill development.
- Ensure that the design of streets, sidewalks and bike paths/routes within a development encourages walking and biking.
- Orient building entrances towards sidewalks and transit stops.
- Provide landscaping to reduce energy demand for cooling.
- Orient buildings to minimize energy required for heating and cooling.

Local governments and other Lead Agencies are encouraged to consider land use and design measures to reduce auto use and promote energy conservation early in planning and development review processes. By incorporating such measures in local plans and addressing them during initial contacts with project proponents, Lead Agencies greatly increase the likelihood of their implementation. The environmental impacts of development proposals may be lessened and environmental review processes simplified.

Further information regarding land use and design strategies is provided in Chapter 4 and Appendix F. Also, the District and ABAG have prepared a guidance document on these issues entitled *Improving Air Quality Through Local Plans and Programs*. The document provides guidance to local officials and staff on developing and implementing local policies and programs to improve air quality. Lead Agency staff also may contact District planners for assistance.

Land Use Conflicts and Sensitive Receptors - The location of a development project is a major factor in determining whether it will result in localized air quality impacts. The potential for adverse air quality impacts increases as the distance between the source of emissions and members of the public decreases. Impacts on sensitive receptors are of particular concern. Sensitive receptors are facilities that house or attract children, the elderly, people with illnesses or others who are especially sensitive to the effects of air pollutants. Hospitals, schools, convalescent facilities, and residential areas are examples of sensitive receptors.

For each of the situations discussed below, the impacts generally are not limited only to sensitive receptors. *All* members of the population can be adversely affected by criteria pollutants, toxic air contaminants, odor and dust, and thus any consideration of potential air quality impacts should include all members of the population. This discussion focuses on sensitive receptors, however, because they are the people most vulnerable to the effects of air pollution.

Air quality problems arise when sources of air pollutants and sensitive receptors are located near one another. There are several types of land use conflicts that should be avoided:

- A sensitive receptor is in close proximity to a congested intersection or roadway with high levels of emissions from motor vehicles. High concentrations of carbon monoxide, fine particulate matter or toxic air contaminants are the most common concerns.

- A sensitive receptor is close to a source of toxic air contaminants or a potential source of accidental releases of hazardous materials.

- A sensitive receptor is close to a source of odorous emissions. Although odors generally do not pose a health risk, they can be quite unpleasant and often lead to citizen complaints to the District and to local governments.

- A sensitive receptor is close to a source of high levels of nuisance dust emissions.

Localized impacts to sensitive receptors generally occur in one of two ways:

- A (new) source of air pollutants is proposed to be located close to existing sensitive receptors. For example, an industrial facility is proposed for a site near a school.

- A (new) sensitive receptor is proposed near an existing source of air pollutants. For example, a residential development is proposed near a wastewater treatment plant.

Early consultation between project proponents and Lead Agency staff can avoid or minimize localized impacts to sensitive receptors. When evaluating whether a development proposal has the potential to result in localized impacts, Lead Agency staff need to consider the nature of the air pollutant emissions, the proximity between the emitting facility and sensitive receptors, the direction of prevailing winds, and local topography. Often, the provision of an adequate distance, or buffer zone, between the source of emissions and the receptor(s) is necessary to mitigate the problem. This underscores the importance of addressing these potential land use conflicts during the preparation of the general plan and as early as possible in the development review process for specific projects.

It should be noted that there may be instances when some of the land use considerations discussed above, such as infill development and mixed use projects, could result in localized impacts to sensitive receptors. For example, an infill or mixed use project might result in residences being in close proximity to a source of odors or toxic air contaminants. Or a child care facility might be proposed at a worksite in an area where large quantities of hazardous materials are stored and used. Such situations should be avoided. Lead Agencies should bear in mind that while infill and mixed use development are desirable (to reduce auto trips), such projects should be approved only when they do not subject receptors to health or nuisance impacts.

BAAQMD Rules and Regulations - District regulations and permit requirements apply to most industrial processes (e.g., manufacturing facilities, cement terminals, food processing), many commercial operations (e.g., print shops, drycleaners, gasoline stations), and other miscellaneous activities (e.g., demolition of buildings containing asbestos and aeration of contaminated soils). During early consultation, Lead Agency staff should address air pollution regulations and requirements of other public agencies that may apply to the proposed project. Lead Agency staff are encouraged to coordinate directly with the District during the environmental review process on issues such as regulatory requirements, impact analyses and mitigation measures.

2.2 Preparation of the Initial Study

Projects that are subject to CEQA generally undergo a preliminary evaluation in an Initial Study, which is prepared by the Lead Agency. The Initial Study is used to determine if a project may have a significant effect on the environment. The Initial Study should evaluate the potential impact of a proposed project upon air quality. The air quality impact of a project is determined by examining the types and levels of emissions generated by the project, the existing air quality conditions and neighboring land uses. The Initial Study should analyze all phases of project planning, construction and operation, as well as cumulative impacts. The District recommends that the answers/determinations provided in an Initial Study checklist be explained.[1]

The District has established significance thresholds to assist Lead Agencies in determining whether a project or plan may have a significant air quality impact. The District's thresholds of significance are based on the State Office of Planning and Research definitions of significant environmental effect. Section 15382 of the State CEQA Guidelines defines "significant effect on the environment" as "a substantial, or potentially substantial, adverse change in any of the physical conditions within the area affected by the project including ... air."

Appendix G to the State CEQA Guidelines contains a list of effects that will normally be considered significant. These include:

- A project that will "violate any ambient air quality standard, contribute substantially to an existing or projected air quality violation, or expose sensitive receptors to substantial pollutant concentrations,"
- A project that "conflicts with adopted environmental plans or goals of the community where it is located,"
- A project that would "create a potential public health hazard or involve the use, production or disposal of materials which pose a hazard to people or animal or plant populations in the area affected," or
- A project that would "have a substantial, demonstrable negative aesthetic effect."

Appendix I of the State CEQA Guidelines also indicates that a project could have a significant air quality impact if it would result in:

- "The creation of objectionable odors," or
- "Alteration of air movement, moisture, or temperature, or change in climate, either locally or regionally."

The Lead Agency should determine whether the proposed project or plan would exceed any of the thresholds discussed in this chapter. If any of the thresholds are exceeded, then an EIR should be prepared. The more comprehensive analysis of an EIR will provide a more detailed picture of the project's or plan's impacts and will help identify the most appropriate and effective mitigation measures to minimize the impacts. Where no significant air quality impacts of a

[1] The Initial Study identifies potential effects by use of a checklist, matrix or other method. The process, contents, and use of the Inital Study are contained in Section 15063 and Appendix I of the State CEQA Guidelines.

project or plan can be identified in the Initial Study (i.e., none of the significance thresholds are exceeded), the District recommends the Lead Agency either prepare a Negative Declaration or include in an EIR a statement indicating the reasons why potential air quality impacts were determined not to be significant.

Sources of air pollutant emissions complying with all applicable District regulations generally will not be considered to have a significant air quality impact.[2] Stationary sources that are exempt from District permit requirements because they fall below emission thresholds for permitting will not be considered to have a significant air quality impact (unless it is demonstrated that they may have a significant cumulative impact). The Lead Agency can and should make exception to this determination if special circumstances suggest that the emissions from the permitted or exempt source may cause a significant air quality impact. For example, if a permitted or exempt source may emit objectionable odors, then odor impacts on nearby receptors should be considered a potentially significant air quality impact.

2.3 Thresholds of Significance

This section describes the District's recommended thresholds of significance to be used by a Lead Agency when preparing an Initial Study. If, during the preparation of the Initial Study, the Lead Agency finds that any of the following thresholds may be exceeded, then an EIR should be prepared in order to more accurately evaluate project impacts and identify mitigation measures. These thresholds also may be used when preparing an EIR. If the more detailed analysis in an EIR indicates that any of these thresholds would be exceeded, the document should identify the impact as a significant air quality impact and propose mitigation measures. Chapter 3 explains how to calculate emissions to determine whether the thresholds have been exceeded. The following thresholds address impacts associated with: 1) project construction, 2) project operations, and 3) plans.

Threshold of Significance for Construction Impacts

Construction-related emissions are generally short-term in duration, but may still cause adverse air quality impacts. Fine particulate matter (PM_{10}) is the pollutant of greatest concern with respect to construction activities.[3] PM_{10} emissions can result from a variety of construction activities, including excavation, grading, demolition, vehicle travel on paved and unpaved surfaces, and vehicle and equipment exhaust. Construction-related emissions can cause substantial increases in localized concentrations of PM_{10}. Particulate emissions from construction activities can lead to adverse health effects as well as nuisance concerns such as reduced visibility and soiling of exposed surfaces.

Construction emissions of PM_{10} can vary greatly depending on the level of activity, the specific operations taking place, the equipment being operated, local soils, weather conditions and other factors. Despite this variability in emissions, experience has shown that there are a number of

[2]CEQA Guidelines, Section 15064(i).

[3] Construction equipment emits carbon monoxide and ozone precursors. However, these emissions are included in the emission inventory that is the basis for regional air quality plans, and are not expected to impede attainment or maintenance of ozone and carbon monoxide standards in the Bay Area.

feasible control measures that can be reasonably implemented to significantly reduce PM_{10} emissions from construction. The District's approach to CEQA analyses of construction impacts is to emphasize implementation of effective and comprehensive control measures rather than detailed quantification of emissions.

The District has identified a set of feasible PM_{10} control measures for construction activities. These control measures are listed in Table 2. As noted in the table, some measures ("Basic Measures") should be implemented at all construction sites, regardless of size. Additional measures ("Enhanced Measures") should be implemented at larger construction sites (greater than 4 acres) where PM_{10} emissions generally will be higher. Table 2 also lists other PM_{10} controls ("Optional Measures") that may be implemented if further emission reductions are deemed necessary by the Lead Agency.

The determination of significance with respect to construction emissions should be based on a consideration of the control measures to be implemented. From the District's perspective, quantification of construction emissions is not necessary (although a Lead Agency may elect to do so - see Section 3.3 of these Guidelines, "Calculating Construction Emissions," for guidance). The Lead Agency should review Table 2. If all of the control measures indicated in Table 2 (as appropriate, depending on the size of the project area) will be implemented, then air pollutant emissions from construction activities would be considered a less than significant impact. If all of the appropriate measures in Table 2 will not be implemented, then construction impacts would be considered to be significant (unless the Lead Agency provides a detailed explanation as to why a specific measure is unnecessary or not feasible).

Project construction sometimes requires the demolition of existing buildings at the project site. Buildings constructed prior to 1980 often include building materials containing asbestos. Airborne asbestos fibers pose a serious health threat. The demolition, renovation or removal of asbestos-containing building materials is subject to the limitations of District Regulation 11, Rule 2: Hazardous Materials; Asbestos Demolition, Renovation and Manufacturing. The District's Enforcement Division should be consulted prior to commencing demolition of a building containing asbestos building materials. Any demolition activity subject to but not complying with the requirements of District Regulation 11, Rule 2 would be considered to have a significant impact.

TABLE 2
FEASIBLE CONTROL MEASURES FOR CONSTRUCTION EMISSIONS OF PM_{10}

Basic Control Measures. - The following controls should be implemented at all construction sites.
• Water all active construction areas at least twice daily. • Cover all trucks hauling soil, sand, and other loose materials *or* require all trucks to maintain at least two feet of freeboard. • Pave, apply water three times daily, or apply (non-toxic) soil stabilizers on all unpaved access roads, parking areas and staging areas at construction sites. • Sweep daily (with water sweepers) all paved access roads, parking areas and staging areas at construction sites. • Sweep streets daily (with water sweepers) if visible soil material is carried onto adjacent public streets.
Enhanced Control Measures. - The following measures should be implemented at construction sites greater than four acres in area.
• All "Basic" control measures listed above. • Hydroseed or apply (non-toxic) soil stabilizers to inactive construction areas (previously graded areas inactive for ten days or more). • Enclose, cover, water twice daily or apply (non-toxic) soil binders to exposed stockpiles (dirt, sand, etc.) • Limit traffic speeds on unpaved roads to 15 mph. • Install sandbags or other erosion control measures to prevent silt runoff to public roadways. • Replant vegetation in disturbed areas as quickly as possible.
Optional Control Measures. - The following control measures are strongly encouraged at construction sites that are large in area, located near sensitive receptors or which for any other reason may warrant additional emissions reductions.
• Install wheel washers for all exiting trucks, or wash off the tires or tracks of all trucks and equipment leaving the site. • Install wind breaks, or plant trees/vegetative wind breaks at windward side(s) of construction areas. • Suspend excavation and grading activity when winds (instantaneous gusts) exceed 25 mph. • Limit the area subject to excavation, grading and other construction activity at any one time.

Thresholds of Significance for Impacts From Project Operations

For many types of land use development, such as office parks, shopping centers, residential subdivisions and other "indirect sources", motor vehicles traveling to and from the projects represent the primary source of air pollutant emissions associated with project operations. Significance thresholds discussed below address the impacts of these indirect source emissions on local and regional air quality. Thresholds are also provided for other potential impacts related to project operations, such as odors and toxic air contaminants.

(Lead Agencies may refer to Section 2.4, Project Screening, for guidance on determining whether significance thresholds for project operations may be exceeded, and thus whether more detailed air quality analysis may be needed.)

1. Local Carbon Monoxide Concentrations. Localized carbon monoxide concentrations should be estimated for projects in which: 1) vehicle emissions of CO would exceed 550 lb./day, 2) project traffic would impact intersections or roadway links operating at Level of Service (LOS) D, E or F or would cause LOS to decline to D, E or F, or 3) project traffic would increase traffic volumes on nearby roadways by 10% or more.[4] A project contributing to CO concentrations exceeding the State Ambient Air Quality Standard of 9 parts per million (ppm) averaged over 8 hours and 20 ppm for 1 hour would be considered to have a significant impact.

2. Total Emissions. Total emissions from project operations should be compared to the thresholds provided in Table 3.[5] Total operational emissions evaluated under this threshold should include all emissions from motor vehicle use associated with the project. A project that generates criteria air pollutant emissions in excess of the annual *or* daily thresholds in Table 3 would be considered to have a significant air quality impact.

TABLE 3
THRESHOLDS OF SIGNIFICANCE
FOR PROJECT OPERATIONS

Pollutant	ton/yr	lb/day	kgm/day
ROG	15	80	36
NO_X	15	80	36
PM_{10}	15	80	36

3. Odors. While offensive odors rarely cause any physical harm, they still can be very unpleasant, leading to considerable distress among the public and often generating citizen complaints to local governments and the District. Any project with the potential to frequently expose members of the public to objectionable odors would be deemed to have a significant

[4] Unless the increase in traffic volume is less than 100 vehicles per hour.

[5] The thresholds for ROG and NOx are equivalent to the District offset requirement threshold (15 tons per year) for stationary sources (Regulation 2-2-302). The threshold for PM_{10} is based on the District's definition of a major modification to a major facility (Regulation 2-2-221).

impact. Odor impacts on residential areas and other sensitive receptors warrant the closest scrutiny, but consideration should also be given to other land uses where people may congregate, such as recreational facilities, worksites and commercial areas. Analysis of potential odor impacts should be conducted for both of the following situations: 1) sources of odorous emissions locating near existing receptors, *and* 2) receptors locating near existing odor sources.[6]

Determining the significance of potential odor impacts involves a two-step process. *First*, determine whether the project would result in an odor source and receptors being located within the distances indicated in Table 4. Table 4 lists types of facilities known to emit objectionable odors. The Lead Agency should evaluate facilities not included in Table 4 or projects separated by greater distances than indicated in Table 4 if warranted by local conditions or special circumstances. *Second*, if the proposed project would result in an odor source and receptors being located closer than the screening level distances indicated in Table 4, a more detailed analysis, as described in Chapter 3, should be conducted.

After reviewing District enforcement records as described in Chapter 3, a determination of significance should be made. For a project locating near an existing source of odors, the project should be identified as having a significant odor impact if it is proposed for a site that is closer to an existing odor source than any location where there has been:

a) more than one confirmed complaint per year averaged over a three year period, or
b) three unconfirmed complaints per year averaged over a three year period.

For projects locating near a source of odors where there is currently no nearby development *and* for odor sources locating near existing receptors, the determination of significance should be based on the distance and frequency at which odor complaints from the public have occurred in the vicinity of a similar facility.

If a proposed project is determined to result in potential odor problems, mitigation measures should be identified. For some projects, add-on controls or process changes, such as carbon absorption, incineration or relocation of stacks/vents, can reduce odorous emissions. In many cases, however, the most effective mitigation strategy is the provision of a sufficient distance, or buffer zone, between the source and the receptor(s).

TABLE 4

[6] In a January, 1995 decision (*Baird v. County of Contra Costa*, 32 Cal. App. 4th 1464), a California appellate court held that the effects of a contaminated pre-existing environment upon the residents of a proposed project were beyond the scope of CEQA.

Notwithstanding this decision, the District believes that the Legislature generally did intend that CEQA documents should consider the effects of the pre-existing environment on a proposed project, and that the ruling in the *Baird* case should be limited to the factual particulars of the decision (which involved a neighborhood group's attempt to set aside the approval of an addiction treatment facility).

In the District's view, Lead Agencies therefore should not rely on the *Baird* decision and should analyze the impacts of existing sources of air pollution on occupants or residents of proposed projects. Such impacts include, but are not limited to, those from toxic air contaminants, odors and dust.

PROJECT SCREENING TRIGGER LEVELS FOR POTENTIAL ODOR SOURCES

Type of Operation	Project Screening Distance
Wastewater Treatment Plant	1 mile
Sanitary Landfill	1 mile
Transfer Station	1 mile
Composting Facility	1 mile
Petroleum Refinery	2 miles
Asphalt Batch Plant	1 mile
Chemical Manufacturing	1 mile
Fiberglass Manufacturing	1 mile
Painting/Coating Operations (e.g. auto body shops)	1 mile
Rendering Plant	1 mile
Coffee Roaster	1 mile

4. Toxic Air Contaminants. Any project with the potential to expose sensitive receptors (including residential areas) or the general public to substantial levels of toxic air contaminants would be deemed to have a significant impact. This applies to receptors locating near existing sources of toxic air contaminants, as well as sources of toxic air contaminants locating near existing receptors.

Proposed development projects that have the potential to expose the public to toxic air contaminants in excess of the following thresholds would be considered to have a significant air quality impact. These thresholds are based on the District's Risk Management Policy.

Thresholds of Significance for Toxic Air Contaminants

1. Probability of contracting cancer for the Maximally Exposed Individual (MEI) exceeds 10 in one million.
2. Ground-level concentrations of non-carcinogenic toxic air contaminants would result in a Hazard Index greater than 1 for the MEI.

5. Accidental Releases/Acutely Hazardous Air Emissions. The determination of significance for potential impacts from accidental releases of acutely hazardous materials should be made in consultation with the local administering agency of the Risk Management Prevention Program (RMPP). The county health department is usually the administering agency. A determination of significance regarding accidental releases of acutely hazardous materials (AHMs) should be made for: 1) projects using or storing AHMs locating near existing receptors, and 2) development projects resulting in receptors locating near existing facilities using or storing AHMs.

The District recommends, at a minimum, that the Lead Agency, in consultation with the administering agency of the RMPP, find that any project resulting in receptors being within the Emergency Response Planning Guidelines (ERPG) exposure level 2 for a facility has a significant air quality impact. ERPG exposure level 2 is defined as "the maximum airborne concentration below which it is believed that nearly all individuals could be exposed for up to one hour without experiencing or developing irreversible or other serious health effects or symptoms which could impair an individual's ability to take protective action".[7]

6. Cumulative Impacts. Any proposed project that would individually have a significant air quality impact (see Thresholds of Significance for Impacts from Project Operations, above) would also be considered to have a significant cumulative air quality impact.

For any project that does not individually have significant operational air quality impacts, the determination of significant cumulative impact should be based on an evaluation of the consistency of the project with the local general plan *and* of the general plan with the regional air quality plan. (The appropriate regional air quality plan for the Bay Area is the most recently adopted Clean Air Plan.) See Thresholds of Significance for Plan Impacts, below, for guidance on evaluating the consistency of a local general plan with the Clean Air Plan. Figure 2 provides a flow chart depicting the process for evaluating cumulative impacts.

Projects in Jurisdictions with Local Plans Consistent with the Clean Air Plan

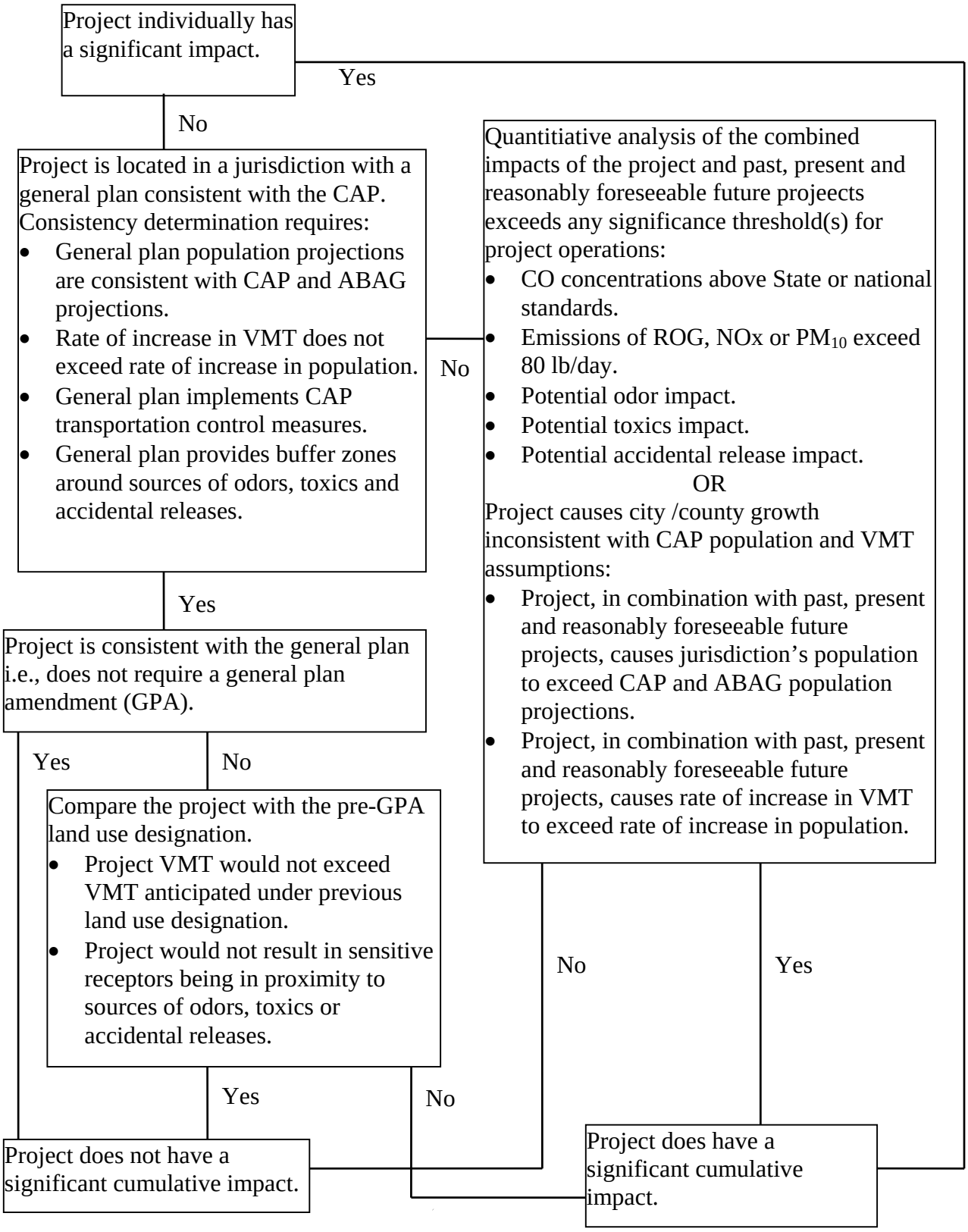
If a project is proposed in a city or county with a general plan that is consistent with the Clean Air Plan (see below) *and* the project is consistent with that general plan (i.e., it does not require a general plan amendment), then the project will not have a significant cumulative impact (provided, of course, the project does not individually have any significant impacts). No further analysis regarding cumulative impacts is necessary.

In a jurisdiction with a general plan consistent with the Clean Air Plan, a project may be proposed that is not consistent with that general plan because it requires a general plan amendment (GPA). In such instances, the cumulative impact analysis should consider the difference(s) between the project and the original (pre-GPA) land use designation for the site with respect to motor vehicle use and potential land use conflicts. A project would not have a significant cumulative impact if: VMT from the project would not be greater than the VMT that would be anticipated under the original land use designation, and 2) the project would not result in sensitive receptors being in close proximity to sources of objectionable odors, toxics or accidental releases of hazardous materials.

[7] State of California Guidance for the Preparation of a Risk Management and Prevention Program, California Office of Emergency Services, November 1989, pg. D-2.

FIGURE 2

EVALUATING CUMULATIVE IMPACTS



Lead Agencies should note that demonstrating general plan consistency with the CAP (and project consistency with the general plan) is the minimum that must be done to support a finding of no significant cumulative impact. Depending on the specific type of project and its setting, there may be additional measures - such as additional measures to reduce auto use, scrappage of high emitting vehicles, conversion to alternative fuels, etc. - that could be implemented to reduce emissions. Even in jurisdictions with a general plan consistent with the CAP, Lead Agencies are encouraged to pursue all feasible measures to minimize cumulative air quality impacts.

Projects in Jurisdictions with Local Plans Not Consistent with the Clean Air Plan

For a project in a city or county with a general plan that is not consistent with the Clean Air Plan, the cumulative impact analysis should consider the combined impacts of the proposed project and past, present and reasonably anticipated future projects. ("Reasonably anticipated future projects" should include, at a minimum, projects of which the Lead Agency is aware based on applications for permits and other land use entitlements, environmental documents, and discussions with probable future developers.) A project would have a significant cumulative impact if these combined impacts would exceed any of the thresholds established above for project operations. A quantitative analysis of past, present and future projects would be required as part of this determination. The analysis should also address how the project and past, present and future projects would influence population and vehicle use projections (see Thresholds of Significance for Plan Impacts, Determining Consistency with Clean Air Plan Population and VMT Assumptions, below).

Thresholds of Significance for Plan Impacts

Regarding plans, the State CEQA Guidelines, Section 15125(b), states that an EIR shall discuss "any inconsistencies between a proposed project and applicable general plans and regional plans. Such regional plans include, but are not limited to, the applicable Air Quality Management Plan (or State Implementation Plan)...". General Plans of cities and counties must show consistency with regional plans and policies affecting air quality to claim a less than significant impact on air quality. General plan amendments, redevelopment plans, specific area plans, annexations of lands and services, and similar planning activities should receive the same scrutiny as general plans with respect to consistency with regional air quality plans.

For a local plan to be consistent with the regional air quality plan it must be consistent with the most recently adopted Clean Air Plan (CAP). (At the time of this writing, December 1999, the most recently adopted CAP is the *Bay Area '97 Clean Air Plan*.) The goal of the CAP is to reduce ground-level ozone and satisfy other California Clean Air Act (CCAA) requirements (e.g., performance objectives related to motor vehicle use). *All of the following criteria must be satisfied for a local plan to be determined to be consistent with the CAP*. Local plans found to be consistent with the CAP would have a less than significant impact on air quality.

1. Determining Local Plan Consistency With Clean Air Plan Population and VMT Assumptions. Plans must show over the planning period of the plan that:

a) population growth for the jurisdiction will not exceed the values included in the current CAP[8], and
b) the rate of increase in VMT for the jurisdiction is equal to or lower than the rate of increase in population.

The first criterion (a) is necessary to establish that population growth in cities and counties will not exceed the growth assumed in the preparation of the CAP emission inventory. Air pollutant emissions are a function of population and human activity. If growth in population is greater than assumed in the CAP emission inventory, then population-based emissions also are likely to be greater than assumed in the CAP. Consequently, attainment of the State air quality standards would be delayed. Therefore, plans showing estimated population greater than that assumed in the *ABAG Projections* would be inconsistent with air quality planning and have a significant air quality impact.

The second plan criterion (b) is derived from the CCAA, Section 40919(d), which requires regions to implement "transportation control measures to substantially reduce the rate of increase in passenger vehicle trips and miles traveled." Plans showing a VMT growth rate higher than the population growth rate would be considered to be hindering progress towards achieving this performance objective, and thus inconsistent with regional air quality planning. This would represent a significant air quality impact.[9]

2. Determining Local Plan Consistency With Clean Air Plan Transportation Control Measures. Determining consistency of local plans with the CAP also involves assessing whether CAP transportation control measures (TCMs) for which local governments are implementing agencies are indeed being implemented. The CAP identifies implementing agencies/entities for each of the TCMs included in the Plan. Cities and counties are identified among the implementing agencies for some of the TCMs. These TCMs are listed in Table 5. Local plans that do not demonstrate reasonable efforts to implement TCMs in the CAP would be considered to be inconsistent with the regional air quality plan and therefore have a significant air quality impact. For further information regarding CAP TCMs, refer to Appendix A of these Guidelines and the *Bay Area '97 Clean Air Plan*.

[8] For the *1997 CAP*, ABAG's *Projections '96* are the appropriate set of population projections.

[9] In some cases, estimating total VMT at the general plan horizon year may be beyond the level of analysis historically conducted in assessing general plan impacts. Lead Agencies may wish to consult with MTC and the county congestion management agency for assistance in developing VMT estimates.

TABLE 5
CAP TCMs TO BE IMPLEMENTED BY LOCAL GOVERNMENT

Transportation Control Measure	Description
1. Support Voluntary Employer-Based Trip Reduction Programs	• Provide assistance to regional and local ridesharing organizations; advocate legislation to maintain and expand incentives (e.g., tax deductions/credits).
9. Improve Bicycle Access and Facilities	• Improve and expand bicycle lane system by providing bicycle access in plans for all new road construction or modifications. • Establish and maintain bicycle advisory committees in all nine Bay Area counties. • Designate a staff person as a Bicycle Program Manager. • Develop and implement comprehensive bicycle plans. • Encourage employers and developers to provide bicycle access and facilities. • Provide bicycle safety education.
12. Improve Arterial Traffic Management	• Study signal preemption for buses on arterials with high volume of bus traffic. • Improve arterials for bus operations and to encourage bicycling and walking. • Continue and expand local signal timing programs, only where air quality benefits can be demonstrated.
15. Local Clean Air Plans, Policies and Programs	• Incorporate air quality beneficial policies and programs into local planning and development activities, with a particular focus on subdivision, zoning and site design measures that reduce the number and length of single-occupant automobile trips.
17. Conduct Demonstration Projects	• Promote demonstration projects to develop new strategies to reduce motor vehicle emissions. Projects include: low emission vehicle fleets and LEV refueling infrastructure.
19. Pedestrian Travel	• Review/revise general/specific plan policies to promote development patterns that encourage walking and circulation policies that emphasize pedestrian travel and modify zoning ordinances to include pedestrian-friendly design standards. • Include pedestrian improvements in capital improvement programs. • Designate a staff person as a Pedestrian Program Manager.
20. Promote Traffic Calming Measures	• Include traffic calming strategies in the transportation and land use elements of general and specific plans. • Include traffic calming strategies in capital improvement programs.

3. Local Plan Impacts Associated with Odors and Toxics. For local plans to have a less than significant impact with respect to potential odors and/or toxic air contaminants, buffer zones should be established around existing and proposed land uses that would emit these air pollutants. Buffer zones to avoid odors and toxics impacts should be reflected in local plan policies, land use map(s), and implementing ordinances (e.g., zoning ordinance). Refer to the discussion regarding project operations impacts related to odors, toxics and accidental releases for guidance in establishing buffer zones in local plans.

2.4 Project Screening

It sometimes may be evident to the Lead Agency that an EIR will be required for a project. In such cases the Lead Agency may forgo preparing an Initial Study and immediately begin preparing an EIR (State CEQA Guidelines, Section 15060(c)). In many cases, however, the Lead Agency will need to prepare an Initial Study to determine whether any of the thresholds of significance discussed in this chapter would be exceeded. Chapter 3 provides guidance on how to assess the air quality impacts of a proposed project.

For one of the thresholds of significance (total emissions from project operations), project screening may provide a simple indication of whether a project may exceed the threshold. The Lead Agency may consult Table 6 for an indication as to whether the threshold for total emissions from project operations might be exceeded. Table 6 provides size or activity levels for various types of land uses which, based on default assumptions, would result in mobile source emissions exceeding the District's threshold of significance for NOx (80 lbs/day). The values provided in Table 6 are based on average, default assumptions for modeling inputs using the URBEMIS7G model (described in Section 3.4).[10] Therefore, the values in Table 6 represent approximate sizes of projects for which total emissions may exceed the threshold. The values should be used only for project screening, and should not be considered absolute thresholds of project significance. Projects approaching or exceeding the levels indicated in Table 6 should undergo a more detailed analysis, as described in Chapter 3. The District recommends that a more detailed analysis be conducted for any project whose size is within 20% of the values indicated in Table 6. The District generally does not recommend a detailed air quality analysis for projects generating less than 2,000 vehicle trips per day, unless warranted by the specific nature of the project or project setting.

[10] The values were calculated using the URBEMIS7G model based on default assumptions for the SF Bay Area:

- Emission factors based on EMFAC7G.
- Average speed of 30 mph and URBEMIS7G default trip lengths.
- Analysis year of 2000.
- Trip generation rates as indicated in table.

The total number of trips for projects with potentially significant impacts varies somewhat between land uses. This is primarily because different land uses generate different distributions of trip type (e.g., home to work, home to shop, etc.) with varying percentages of cold and hot starts.

The Lead Agency should note that Table 6 only addresses one threshold of significance. There are other air quality issues, such as high CO concentrations, odors, toxics and cumulative impacts, that must be considered when evaluating a project's potential for causing adverse air quality impacts. Depending on the nature of the project and local conditions, a project below the values in Table 6 could still cause an adverse air quality impact.

TABLE 6
PROJECTS WITH POTENTIALLY SIGNIFICANT EMISSIONS

Land Use Category	Trip Generation Rate*	Size of Project Likely to Generate 80 lb/day NOx
Housing		
Single Family	9.4/d.u.	320 units
Apartments	5.9/d.u.	510 units
Retail		
Discount Store	48.3/1000 sq.ft.	87,000 sq.ft.
Regional Shopping Center	96.2/1000 sq.ft.	44,000 sq.ft.
Supermarket	178/1000 sq.ft.	24,000 sq.ft.
Office		
General Office	10.9/1000 sq.ft.	280,000 sq.ft.
Government Office	68.9/1000 sq.ft.	55,000 sq.ft.
Office Park	12.8/1000 sq.ft.	210,000 sq.ft.
Medical Office	37.1/1000 sq.ft.	110,000 sq.ft.
Other		
Hospital	13.8/1000 sq.ft.	240,000 sq.ft.
Hotel	8.7/room	460 rooms

* Trip rates for many land uses will vary depending upon size of project. See latest edition of Trip Generation, Institute of Transportation Engineers.

CHAPTER 3 - ASSESSING AIR QUALITY IMPACTS

3.1 Introduction

This chapter provides guidance on how to evaluate the impact(s) of a proposed project or plan[11] on local and regional air quality. The impact assessment portion of an environmental document should evaluate all stages of a project. This chapter addresses the following issues:

- Information that should be discussed in the description of the project's environmental setting
- Evaluating emissions from project construction
- Calculating emissions from project operations, including:
  - mobile source (or "indirect") emissions
  - localized carbon monoxide concentrations
  - stationary source emissions
  - odor impacts
  - toxic air contaminants
- Cumulative impacts

The basic method for calculating project emissions is to apply specific emission factors to sources of air pollutants whose magnitude and characteristics are either known or estimated. Emission factors may be defined as standardized relationships between particular sources of air pollution, such as motor vehicles or pieces of industrial equipment, and their air pollutant emissions. For example, emission factors for motor vehicles generally specify the amount (in grams) of certain air pollutants emitted, per mile traveled. This chapter provides emission factors and quantification procedures for construction activities, motor vehicles, and stationary sources. This chapter also describes methods for evaluating air quality impacts that are not easily quantified, such as impacts associated with objectionable odors.

Once the impacts of a proposed project have been identified, a determination must be made as to whether the project would have a significant adverse impact on the environment. Significance criteria discussed in Chapter 2 of these Guidelines should be used in making this determination. For any potentially significant impacts, mitigation measures should be incorporated into the project to reduce the impact(s) to a level of insignificance. Chapter 4 provides guidance on mitigation measures.

CEQA requires that the project description include a list of agencies that are expected to use the EIR in their decision-making, and a list of the approvals for which the EIR will be used (State CEQA Guidelines Section 15124(d)). If the project will require a permit from the District, all applicable District regulations should be cited in the project description section of the EIR.

[11] This chapter discusses how to evaluate the air quality impacts of development projects and plans. For the sake of brevity, this chapter generally refers only to "project(s)". The reader should note, however, that unless specifically noted otherwise, the discussion also addresses plans.

3.2 Environmental Setting

In order to assess whether a proposed project would have a significant air quality impact, it is necessary to prepare a detailed description of the environmental setting in which the project would be located. Developing the environmental setting, or baseline, is necessary for establishing a basis for comparing the project's subsequent air quality impacts. The environmental setting should also discuss the adverse health effects of air pollutants. With respect to air quality impacts, the description of the project's environmental setting should include the following components:

- Climate and topography influencing the project's impacts on local and regional air quality should be described. Appendix D provides an overview of how climate and topography affect air quality conditions. Appendix D also provides more detailed information on climate, topography and pollution potential for various climatological subregions in the Bay Area.

- Existing air quality conditions should be described. A discussion of trends and expected future conditions (without the project) also should be included. Data from the air quality monitoring station(s) closest to the project site should be included. Appendix C provides ambient air quality monitoring data. Appendix C also provides projections of expected emissions for future years.

- Any sensitive receptors located near the project site should be identified. Areas that are currently undeveloped but that may include sensitive receptors in the future, for example a future school site or residential area, also should be identified.

- Sources of air pollutants located near the project site (including existing sources *at* the project site, if applicable) should be identified. The description of existing air pollution sources should include criteria pollutants, toxic air contaminants and nuisance emissions such as odors and dust. More detailed information regarding existing emissions, including emissions of odors and toxic air contaminants, may be obtained by contacting the District.

- The transportation system serving the project site should be described. Describe traffic conditions, including traffic volumes and levels of service; transit service; and other relevant transportation facilities such as bicycle facilities, shuttle services, telecommuting centers, etc. The discussion of the existing transportation system should describe both current conditions and future conditions without the project.

- Any special circumstances, such as sources of odors, toxic air contaminants or accidental releases of hazardous materials located near the project site, should be described.

- Provide a discussion of why air pollution is a concern, including adverse health effects of criteria and toxic pollutants, nuisance impacts such as odors and dust, and other effects such as reduced visibility and plant damage. Appendix B provides information on effects of air pollution.

Special emphasis should be placed on air quality resources that are rare or unique to the region and would be affected by the project (State CEQA Guidelines Section 15125 (a)). Regulatory requirements identify areas which are pristine and classified as Class I airsheds. These airsheds are subject to specific standards (Prevention of Significant Deterioration requirements). Within the Bay Area, the Point Reyes National Seashore is designated as a Class I area. Projects proposed in the vicinity of that area should note the project's proximity to a Class I area in the description of the project setting.

3.3 Evaluating Construction Emissions

Construction activities result in air pollutant emissions and should be addressed in environmental documents. Although construction-related emissions are generally temporary in duration, they can be substantial and can represent a significant impact on air quality. This is particularly true with respect to emissions of PM_{10}. Construction-related emissions come from a variety of activities including: 1) grading, excavation, roadbuilding and other earthmoving activities, 2) travel by construction equipment, especially on unpaved surfaces, and 3) exhaust from construction equipment. Demolition of buildings also generates PM_{10} emissions, and is of particular concern if the building(s) contain any asbestos-bearing materials.

PM_{10} emissions from construction activity can vary considerably depending on factors such as the level of activity, the specific operations taking place, and weather and soil conditions. As noted in Section 2.3, the District emphasizes implementation of effective and comprehensive control measures rather than detailed quantification of construction emissions. The District urges Lead Agencies to consider the size of the construction area and the nature of the activities that will occur, and require the implementation of all feasible control measures (indicated in Table 2).

If a Lead Agency wants to quantify construction emission, however, generalized emission factors are available. U.S. EPA has developed an approximate emission factor for construction-related emissions of total suspended particulate of 1.2 tons per acre per month of activity. This factor assumes a moderate activity level, moderate silt content in soils being disturbed, and a semi-arid climate. ARB estimates that 64% of construction-related total suspended particulate emissions is PM_{10}.[12] This yields the following **emission factors for uncontrolled construction-related PM_{10} emissions:**

- 0.77 tons per acre per month of PM_{10}, or
- 51 lbs. per acre per day of PM_{10}.[13]

The emission factors provided above are approximate values and do not reflect site-specific conditions and operations. EPA recommends that if construction emissions from a specific site are to be quantified, the construction process should be divided into component operations (e.g., bulldozing, loading of excavated materials, vehicular traffic, etc.) and more specific emission factors should be used. See Section 13.2.3, Heavy Construction Operations, and related sections

[12] California Air Resources Board, Methods for Assessing Area Source Emissions in California, September 1991.

[13] EPA's emission factor was derived based on the assumption that construction activity occurs 30 days per month. See Section 13.2.3, Heavy Construction Operations, U.S. EPA, Compilation of Air Pollutant Emission Factors, Volume I: Stationary, Point and Area Sources, AP-42, 5th Edition, January 1995.

of U.S. EPA, Compilation of Air Pollutant Emission Factors, Volume I: Stationary, Point and Area Sources, AP-42, 5th Edition, January 1995 for further information.

In addition to particulate emissions from earthmoving, air pollutants also are emitted in the exhaust of construction equipment. Table 7 presents emission factors for estimating construction equipment emissions (assuming an average of 0.27 gallons of fuel burned per cubic yard of earth moved). These emission factors represent a composite fleet of heavy and light duty construction equipment in the Bay Area. Emissions from construction equipment during building construction, as differentiated from earthmoving in site preparation, vary greatly from project to project. Table 7 can be used to estimate construction exhaust emissions based on gallons of fuel consumed or cubic yards of material moved. Lead Agencies also may consult the most recent edition of U.S. EPA's AP-42 for emission factors for specific types of construction equipment.

TABLE 7
HEAVY AND LIGHT DUTY CONSTRUCTION EQUIPMENT
EXHAUST EMISSION FACTORS

Contaminant	gm/yd^3*	gm/gallon**
PM_{10}	2.2	8.0
CO	138.0	511.0
ROG	9.2	34.0
NO_x	42.4	157.0
SO_x	4.6	17.0

* Grams per cubic yard of earth moved. ** Grams per gallon of fuel burned.

Project construction sometimes involves the demolition of existing buildings. Demolition also produces PM_{10} emissions. PM_{10} emissions from demolition activities may be estimated using the following emission factor: 0.00042 lbs PM_{10} per cubic feet of building volume.[14] Buildings constructed prior to 1980 often include building materials containing asbestos. As noted in Section 2.3, Thresholds of Significance, the demolition, renovation or removal of asbestos-containing building materials is subject to District Regulations. The District's Enforcement Division should be consulted prior to commencing demolition of a building containing asbestos building materials.

The emission factors provided above represent uncontrolled emissions. Section 2.3, Thresholds of Significance, and Section 4.2, Mitigating Construction Impacts, provide information on mitigating construction-related emissions. If an environmental document will include quantification of construction emissions, the Lead Agency should be sure to apply the estimated control effectiveness to the appropriate emission source. For example, watering a construction site can reduce PM_{10} emissions from earthmoving activities, but will not reduce equipment exhaust emissions.

[14] South Coast Air Quality Management District, CEQA Air Quality Handbook, April 1993.

3.4 Calculating Emissions from Project Operations

Introduction

Several types of emissions should be considered when evaluating the impacts of a project's operations. For many types of land use development projects, the principal sources of air pollutant emissions are the motor vehicle trips generated by the project. These are often referred to as "indirect sources" and include projects such as shopping centers, office buildings, arenas and residential developments. The evaluation of an indirect source's impact should consider localized pollutants such as carbon monoxide and PM_{10}, as well as regional pollutants such as ozone. This section describes methods for estimating total project emissions from motor vehicles (see "Calculating Mobile Source Emissions"), as well as methods for estimating localized CO concentrations (see "Calculating Carbon Monoxide Concentrations").

Most land use projects also generate "area source" emissions. Area sources are sources that individually emit fairly small quantities of air pollutants, but which cumulatively may represent significant quantities of emissions. Water heaters, fireplaces, lawn maintenance equipment, and application of paints and lacquers are examples of area source emissions.

Certain projects also may generate stationary, or "point", source emissions. Although most area sources discussed above are usually stationary, the terms stationary or point source usually refer to equipment or devices operating at industrial and commercial facilities. Examples of facilities with stationary sources include manufacturing plants, quarries, print shops and gasoline stations.

Depending on the nature of the proposed project and/or the land uses near the project site, other air quality impacts associated with project operation may arise. These impacts include odor problems, emissions of toxic air contaminants and accidental releases of hazardous/toxic materials. Most of this chapter addresses the evaluation of the impacts a project would have on the surrounding environment. However, with respect to potential impacts related to odors, toxics, and accidental releases it is equally important to also consider the impact of the surrounding environment on the proposed project. For example, if a residential development were proposed for a site near an existing wastewater treatment plant, exposure of the new residents to objectionable odors would be a significant air quality impact associated with the project.

Calculating Mobile Source Emissions

As noted above, virtually all land use development projects result in indirect source emissions due to the motor vehicle trips generated by the project. The following discussion describes how to calculate these emissions.

Whenever possible, the air quality impact analysis for a project should be based on the results of a traffic study conducted specifically for the project. The number of vehicle trips that a project will generate, and the average speed and length of the trips, will vary depending on a variety of factors such as the specific nature of the project and its location. If project-specific data are not available, then the default values provided in this chapter may be used. The most recently

published set of trip generation rates from the Institute of Transportation Engineers (ITE) also may be used.

Transportation analyses for projects consisting of two or more land uses often adjust the number of anticipated new vehicle trips to account for internal trips. These adjustments (or "capture rates") reflect the fact that some trips at multi-use projects will occur internally to the project. As a result, the total number of new vehicle trips associated with the project would be less than the sum of the trips expected from all of the individual land uses. Traffic studies for such projects should include a clear explanation of all capture rate assumptions. Internal trips should be excluded from the air quality analysis only if they are expected to occur by walking, bicycling or other nonpolluting mode.

Traffic studies for commercial projects often distinguish between primary trips and pass-by and diverted linked trips.[15] The air quality analysis for such projects should include emissions from pass-by and diverted linked trips. While the emissions from these trips will be lower than for primary trips (due to shorter trip lengths), they still do produce emissions (trip end emissions and some running emissions). Adjustments can be made to trip length and cold start/hot start assumptions for pass-by and diverted linked trips. Assumptions regarding pass-by and diverted linked trips should be clearly identified and the underlying rationale explained.

ARB calculates motor vehicle emissions using computer models. Currently, ARB is using the Motor Vehicle Emissions Inventory model (MVEI). Motor vehicle emission factors are calculated with the EMFAC model, which is a component of MVEI. ARB periodically revises emission factors. At the time of this writing (December 1999), the most current set of motor vehicle emission factors is MVEI7G, Version 1.0c. The emission factors provided in these Guidelines (Table 10) are based on MVEI7G,1.0c. The differences between successive versions of the model can lead to significant variation in estimates of mobile source emissions calculated using these emission factors. As of December 1999, ARB was preparing updated emission factors ("EMFAC2000"), but it is uncertain when the new emission factors will be released. As future revisions to the model are approved by ARB, the District will revise the emission factors in Table 10. Lead Agencies should always use the most recent emission factors prepared by the District.

URBEMIS7G

The Air Resources Board developed the URBEMIS model to calculate mobile source emissions associated with various types of land use projects, using EMFAC emission factors and ITE trip generation rates. URBEMIS calculates emissions of ROG, NO_x, CO and PM_{10}, as well as total vehicle trips. ARB's last update of the model was URBEMIS5, released in 1995. In 1998, the San Joaquin Valley Unified Air Pollution Control District coordinated an update of the URBEMIS model, released as URBEMIS7G. The new version is different from previous versions in several ways. URBEMIS7G uses more recent motor vehicle emission factors, EMFAC7G, as well as updated ITE trip generation rates. It can calculate construction emissions

[15] Primary trips are trips made specifically to visit a particular facility. Pass-by trips are trips made as intermediate stops on the way to a primary trip destination. Diverted linked trips are trips attracted from roadways near a facility, but which require a diversion from the roadway to another roadway to access the facility.

and area source emissions, and also can estimate emission reductions from construction and area source mitigation measures. URBEMIS7G also can calculate air quality benefits of mitigation measures to reduce motor vehicles emissions. The model includes options to minimize "double-counting" of trips in mixed use projects and to account for "pass-by" trips.

URBEMIS7G is a sketch planning tool for calculating criteria air pollutant emissions from land use development projects. URBEMIS7G is not appropriate for calculating air pollutant emissions associated with plans. Other models, such as the Direct Travel Impact Model (DTIM), may be used to quantify (mobile source) air pollutant emissions associated with plans.

The program provides default values for all modeling parameters for several regions within California, including the San Francisco Bay Area. The user may use the default values or may provide project-specific values for parameters including trip generation, trip length, trip speed, vehicle fleet mix, percentage of cold starts, and temperature. The District recommends that the following input assumptions be used for projects in the San Francisco Bay Area. If project-specific travel data are available, that data should be used. The source(s) of any project-specific data should be described.

Recommended URBEMIS7G Inputs for the San Francisco Bay Area

Trip Generation - Use the default values for the San Francisco Bay Area or the most recent version of ITE's *Trip Generation* manual if project-specific data are not available.

Fleet Mix – Generally, use the default values for the San Francisco Bay Area. If evaluating a project that is likely to have a different fleet mix, e.g., an industrial project with many heavy duty vehicle trips, make the necessary adjustments.

Temperature - Meteorological conditions in the Bay Area vary considerably between climatological subregions. Refer to Appendix D for subregional information. Use mean summer maximum temperatures for all pollutants except CO. Use mean winter minimum temperatures for CO.

Trip Length - Use the data in Table 9 or the most recent edition of MTC's *Bay Area Travel Forecasts* if project-specific data are not available.

Variable Starts - Use the default values for the San Francisco Bay Area if project-specific data are not available.

Trip Speed - Use 25 mph for San Francisco and 30 mph for all other Bay Area counties if project-specific data are not available.

Percent Trip - Use the default values for the San Francisco Bay Area if project-specific data are not available.

The URBEMIS7G program and Users'Guide is available free of charge on the ARB's website, at www.arb.ca.gov/urbemis7/urbemis7.htm. Because of URBEMIS7G's many enhancements, its

ease of use, and its ready availability, the District strongly encourages Lead Agencies to use the model to estimate motor vehicle emissions from development proposals. Because URBEMIS7G includes the most current emission factors (EMFAC7G), as well as other improvements, older versions of URBEMIS should not be used.

Manual Calculation

The District has developed a methodology for manually calculating mobile source emissions associated with land use development. The manual method may be useful for project screening purposes or for quickly generating rough estimates of project impacts. For this calculation it is necessary to provide the following inputs: trip generation rate, average trip length, exhaust emission factors (varying by analysis year), and trip end emission factors.

As previously noted, project-specific traffic data should be used in the air quality analysis whenever it is available. If project-specific data are not available, the default values provided in these Guidelines may be used. Table 8 provides trip generation rates for various types of land uses. The trip generation rates provided in Table 8 are based on data in the Institute of Transportation Engineers (ITE) *Trip Generation*, 6th Edition, 1997. For land use projects not included in Table 8 and for which project-specific data are not available, consult the most recent edition of ITE's *Trip Generation* manual.

Table 9 provides average trip lengths for each of the nine Bay Area counties. These trip lengths were derived from MTC travel data used by the District in the preparation of the Bay Area mobile source emission inventory.

Table 10 provides emission factors, based on MVEI7G,1.0c. The emission factors in Table 10 are representative of Bay Area driving conditions and the District's emission inventory. They reflect the mix of vehicles typical of Bay Area roadways, as well as climatic conditions assumed in the emission inventory. The emission factors also include the benefits of the 1995 motor vehicle Inspection and Maintenance program and reformulated fuels requirements.

Table 11 provides trip end emission factors. These include start emissions for ROG, NO_x and CO (reflecting cold and hot start emissions consistent with Bay Area driving conditions) and “hot soak” emissions for ROG. The total mobile source emissions from a project are the sum of trip end emissions and “running” emissions.

TABLE 8
AVERAGE TRIP GENERATION RATES FOR SELECTED LAND USES

LAND USE	UNIT OF MEASURE	TRIP RATE	LAND USE	UNIT OF MEASURE	TRIP RATE
RESIDENTIAL			***INDUSTRIAL***		
Single Family Housing	D.U.	9.6	Light Industrial	1000 GSF	7.0
Apartment	D.U.	6.6	Industrial Park	1000 GSF	7.0
Resid. Condominium	D.U.	5.9	Manufacturing	1000 GSF	3.8
Mobile Home Park	D.U.	4.8	Warehousing	1000 GSF	5.0
RETAIL			Mini Warehouse	1000 GSF	2.5
Discount Store (Saturday)	1000 GFA	72.0	***OFFICE***		
Factory Outlet Center (Saturday)	1000 GFA	41.0	General Office Building	1000 GSF	11.0
Shopping Center (Saturday)	1000 GLA	50.0	Corp. Headquarters Building	1000 GSF	7.7
Supermarket (Saturday)	1000 GSF	177.6	Gov't Office Building	1000 GSF	68.9
Convenience Market (24 hour) (Saturday)	1000 GSF	863.1	Medical/Dental Office Building	1000 GSF	36.1
INSTITUTIONAL			Office Park	1000 GSF	11.4
High School	1000 GSF	13.3	Business Park	1000 GSF	12.8
Community College	1000 GSF	18.4	Research and Development Center	1000 GSF	8.1
Church (Sunday)	1000 GSF	36.6	***RECREATIONAL***		
Hospital	1000 GSF	16.8	Movie Theater (w/Matinee) (Saturday)	screen	529.5
Library	1000 GSF	54.0	Racquet Club (Saturday)	1000 GSF	24.5
Post Office	1000 GSF	108.2	Golf Course (Saturday)	Acre	5.8
LODGING					
Hotel	Room	8.2			
Motel	Room	5.6			

GSF = Gross Square Feet; GLA = Gross Leasable Area; GFA = Gross Floor Area; D.U. = Dwelling Unit

All rates are for weekdays unless otherwise noted.

For some land uses, trip rates will vary depending upon size of project. See the most recent edition of *Trip Generation*, Institute of Transportation Engineers.

Source: Institute of Transportation Engineers, *Trip Generation*, 6th Ed. 1997.

TABLE 9
AVERAGE TRIP LENGTH (in miles)
BY COUNTY AND YEAR

County	1995	2000	2005	2010	2015
Alameda	7.7	7.7	7.7	7.3	7.0
Contra Costa	7.5	7.5	7.5	7.2	6.9
Marin	8.0	8.0	8.2	7.7	7.2
Napa	6.5	6.5	6.5	6.2	5.9
San Francisco	6.5	6.5	6.2	6.0	5.9
San Mateo	8.0	7.8	7.7	7.5	7.2
Santa Clara	6.9	6.9	6.9	6.9	6.9
Solano	10.4	10.1	9.8	8.8	8.2
Sonoma	7.2	7.0	6.9	6.5	6.2
District Average	7.5	7.4	7.3	7.6	6.9

Average trip lengths are based on MTC data used in preparation of Bay Area mobile source emission inventory.

TABLE 10
AVERAGE EXHAUST EMISSION RATES

	Emissions (grams per mile)				
Year	**ROG**	**NO_x**	**CO**	**SO_x**	**PM_{10}**
1995	1.08	2.04	13.45	0.06	0.47
2000	0.62	1.42	7.27	0.03	0.45
2005	0.36	0.97	4.63	0.03	0.44
2010	0.22	0.76	3.66	0.03	0.44
2015	0.15	0.66	3.07	0.03	0.44

Notes:
1) Emission rates from CARB's MVEI7G,1.0c (5/97).
2) Fleet mix as per CARB's MVEI7G,1.0c (5/97).
3) Inspection and Maintenance Program effectiveness included.
4) Ambient temperatures consistent with District Planning Inventory (varies throughout region).
5) ROG emission rates include evaporative running loss emissions.
6) Particulate matter emission rates include exhaust, tire wear, and entrained road dust emissions.
7) Trip end emissions are not included and must be calculated separately as described in the text.

Mobile source emissions from land use projects may be calculated using the equation provided below. A separate calculation must be made for each pollutant.

$$E = (U \times T) \times [(L \times R) + S]$$

Where:

E equals total emissions (of each pollutant), in grams per day;

U equals number of units in the project, e.g. number of dwelling units or thousands of square feet in shopping center buildings (see units in Table 8);

T equals trip generation rate, or average trips per day generated per unit of land use (Table 8);

L equals average trip length, in miles per trip (Table 9);

R equals motor vehicle emission rate, or emission factor, for each pollutant, by analysis year (Table 10);

S equals trip end emissions, comprised of start emissions for ROG, NO_x and CO, and "hot soak" emissions for ROG (Table 11).

To convert grams per day to pounds per day, divide the total by 454. To convert grams per day to tons per day, divide the total by 908,000.

TABLE 11
TRIP END EMISSION FACTORS
(grams per trip)

Year	ROG	NO_x	CO
1995	3.44	1.89	49.89
2000	2.20	1.35	35.53
2005	1.36	1.08	21.07
2010	0.79	0.89	12.85
2015	0.50	0.78	8.33

Calculating Carbon Monoxide Concentrations

Emissions and ambient concentrations of carbon monoxide have decreased greatly in recent years. These improvements are due largely to the introduction of cleaner burning motor vehicles and motor vehicle fuels. No exceedances of the State or national CO standard have been recorded at any of the region's monitoring stations since 1991. The Bay Area has attained the State and national CO standard.

Despite this progress, however, localized CO concentration still warrant concern in the Bay Area and should be addressed in environmental documents. The reasons for this are twofold. First, State and federal laws require the region to attain *and maintain* ambient air quality standards. The region must ensure that increased motor vehicle use and congestion do not nullify the great strides that have been made with respect to ambient concentrations of CO. Secondly, the region must safeguard against localized high concentrations of CO that may not be recorded at monitoring sites. Because elevated CO concentrations are generally fairly localized, heavy traffic volumes and congestion can lead to high levels of CO, or "hotspots," while concentrations at the closest air quality monitoring station may be below State and national standards.

A variety of computer models have been developed to estimate local CO concentrations resulting from motor vehicle emissions. One of the most common models is CALINE4, developed by and available from the California Department of Transportation. The District has developed a simplified screening method, which is based on CALINE4 and takes into account CO field studies conducted by the District in the Bay Area. The screening method enables the user to manually calculate local CO concentrations resulting from motor vehicles. Except for very large projects, the District recommends that the manual method be used to estimate CO concentrations. The resulting estimated CO concentrations should be compared to State and national CO standards to determine whether the project would have a significant air quality impact. If the results of the manual method indicate CO concentrations below the standards, then no further CO analysis is required. If the manual method predicts concentrations above the standards, the Lead Agency may either: make a finding of a significant impact and identify mitigation measures, or conduct a more detailed analysis using the CALINE4 model. Similarly, if the results of a CALINE4 analysis indicate a significant impact, mitigation measures should be identified. The effectiveness of any proposed mitigation measure(s) should be quantified by estimating the effects of the measure(s) on traffic volumes and/or speeds, and CO concentrations.

Manual Calculation of CO Concentrations

The following procedure is designed to provide a reasonable estimate of carbon monoxide concentrations near roads under worst case conditions. It is a simplified version of CALINE4. The District suggests that the full CALINE4 model be used, instead of this simplified formula, for any projects or plans that will generate 10,000 or more motor vehicle trips per day. The full CALINE4 model also may be used for smaller projects if the simplified screening method indicates that an air quality standard may be exceeded.

In the Bay Area, the highest CO concentrations usually occur in winter, on cold, clear days and nights with little or no wind. Low wind speeds inhibit horizontal dispersion and radiation inversions inhibit vertical mixing. Worst case conditions are built into the simplified model formula. Default conditions are as follows:

1. wind direction parallel to the primary roadway, 90^o angle to secondary road;
2. wind speed less than 1 meter per second;
3. extreme atmospheric stability (class F);
4. receptor at edge of the roadway.

The carbon monoxide concentration, C, is the sum of a background value, C_o, and the total contribution from local traffic C_t,

$$C = C_o + C_t$$

The total contribution from local traffic, C_t, is the sum of the contributions from each contributing local road, C_i,

$$C_t = C_{i1} + C_{i2}$$

The contribution from one road, C_i, can be computed by the formula:

$$C_i = C_{ri} \times \frac{V_i \times EF_i}{V_r \times EF_r}$$

where:

C_{ri} is a reference case concentration for the i-th roadway,

V_r is the traffic volume for the reference case,

V_i is the traffic volume for the i-th roadway,

EF_r is the emission factor for the reference case,

EF_i is the emission factor for the i-th roadway,

Table 12 gives reference case concentrations for various road configurations with traffic volumes of 1000 vehicles per hour and emission factors of 100 grams per mile. The concentration relative to this reference case is then computed in parts per million (ppm), by the formula:

$$C_i = \frac{C_{ri} \times V_i \times EF_i}{100{,}000}$$

where Cr_i is taken from Table 12, V_i is the estimated traffic volume in vehicles per hour, and EF_i is the emission factor taken from Table 10 for the appropriate year of analysis.

The following discussion provides guidance on how to use the formulas provided above, and describes in detail each step of the manual method for calculating CO concentrations.

TABLE 12
REFERENCE CARBON MONOXIDE CONCENTRATIONS (ppm)

Roadway Type	Primary Road (Highest Volume Road)						Secondary Road (Intersecting Road)					
	(receptor distance from edge--in feet)											
At Grade	**At Edge**	**25'**	**50'**	**100'**	**300'**	**500'**	**At Edge**	**25'**	**50'**	**100'**	**300'**	**500'**
2 lane	14.0	7.6	5.7	4.0	1.7	0.9	3.7	2.7	2.2	1.7	1.0	0.8
4 lane	11.9	7.0	5.4	3.8	1.6	0.9	3.3	2.6	2.2	1.7	1.1	0.8
6 lane	9.5	6.1	4.9	3.5	1.6	0.8	2.8	2.3	2.0	1.7	1.1	0.9
8 lane	8.5	5.7	4.6	3.4	1.5	0.8	2.6	2.2	1.9	1.6	1.1	0.9
Depressed 15 feet												
2 lane	20.9	8.2	4.7	3.3	1.5	0.8	4.8	2.4	1.4	1.1	0.8	0.5
8 lane	15.4	6.3	3.6	2.7	1.3	0.7	3.7	1.9	1.1	1.0	0.7	0.6
Depressed 30 feet												
2 lane	26.8	7.9	3.4	1.7	0.8	0.3	5.2	3.2	2.0	0.8	0.4	0.3
8 lane	21.3	6.0	2.3	1.1	0.6	0.2	4.1	2.7	1.7	0.7	0.5	0.4
Elevated 15 feet												
2 lane	14.0	7.3	5.7	4.0	1.7	0.9	3.7	2.6	2.2	1.7	1.0	0.8
8 lane	8.5	5.4	4.6	3.4	1.5	0.8	2.6	2.1	1.9	1.6	1.1	0.9
Elevated 30 feet												
2 lane	14.0	7.3	5.4	4.0	1.7	0.9	3.6	2.6	2.2	1.7	1.0	0.8
8 lane	8.5	5.4	4.3	3.4	1.5	0.8	2.5	2.1	1.9	1.6	1.1	0.9

Notes: Normalized CO concentration is calculated based on the following assumptions: wind direction parallel to the highest volume roadway; wind speed less than 1 meter per second; extreme atmospheric stability (class F); receptor at edge of roadway; emission rate = 100 gm/mi.; vehicles per hour = 1,000; surface roughness = 100 cm; mixing cell width = roadway width (2 lane = 40 ft; 4 lane = 64 ft; 6 lane = 88 ft; 8 lane = 112 ft).

This simplified model was adapted from CALINE3 and CALINE4 (California Department of Transportation) by Mike Kim, Senior Transportation Engineer, BAAQMD.

Step by Step Procedure for CO Analysis

Make separate computations for current conditions, future no-project conditions (including cumulative), and future conditions with the project. For future year project and no-project conditions, select an analysis year corresponding to the estimated year of project completion. Also use the procedure to show the effects of mitigation measures, where such effects are quantifiable.

1. Identify intersections and/or roadway links that will be most impacted by the proposed project, according to the traffic impact analysis. An analysis should be made for each such intersection and link. (Include a map showing these points.)

2. Obtain peak-hour traffic volumes in both directions on each roadway considered for each year of consideration. If only average daily traffic is known, assume 10% for peak hour volumes. Use actual traffic counts, if available, for current year. Traffic levels for future years should include traffic generated by the proposed project plus other estimated growth distributed among roadway links.

3. Obtain the CO emission factor for each roadway, for each relevant year from Table 10. (Interpolate if necessary.)

4. Determine the number of lanes and type of each roadway. (Do not count turning or parking lanes.) If the road is to be altered, use the appropriate width for the year being analyzed.

5. Based on the number of lanes, obtain the reference one hour concentration for each roadway from Table 12. The road with the most traffic should be considered the "Primary Road". Be careful to use the proper reference factor in the table if the receptor is not at the edge of the road or if one or both of the roadways is elevated or depressed.

6. Compute each roadway's contribution to the total concentration by using the equation above. If modeling an intersection, add the concentrations of all roadways.

7. Add the total roadway (local) contribution to the one hour background value from the background map (Figure 3) to obtain the estimated worst case concentration. Interpolate between isopleth lines and apply rollback factors for future years (Table 13) to determine the appropriate background value. Refer to the discussion below for guidance on determining background values.

8. To obtain the worst case eight hour concentration, multiply the one hour value for the local contribution by 0.7 (persistence factor). Add this derived eight hour local contribution to the eight hour background level (Figure 4). Interpolate between isopleth lines and apply rollback factors (Table 13) to determine the appropriate background value. Refer to the discussion below for guidance on determining background values.

Determining Background CO Concentrations

As noted above, estimating a project's impact on ambient CO concentrations involves adding the contribution from the project to existing background levels. Background carbon monoxide is defined as that part of the ambient CO concentration that is not attributable to traffic sources from a nearby street or intersection. Thus, during stagnant conditions, the background conditions at a site may include carbon monoxide emitted from outside the modeling area, as well as carbon monoxide emitted within the modeling area during the previous time periods.

In order to determine a reasonable background CO concentration, refer to Figures 3, 4 and 5 and Table 13. Figures 3 and 4 are isopleth maps of the Bay Area Air Basin showing estimated one hour and eight hour background CO values, respectively, in parts per million (ppm) for 1992. The maps are based on 1990 to 1992 CO concentration data from multiple monitoring sites of various types located throughout the region. Table 13 provides rollback factors to be used in conjunction with the isopleth maps when determining CO background concentrations for years beyond 1992. 1992 background values may be derived from the maps according to the following procedures, after first locating the project on the map.

If the project site happens to fall on an isopleth (contour) line, use the value marked for that line. If the project is determined to be between two different isopleth lines (i.e., between 3.0 and 6.0 or between 6.0 and 9.0 ppm), interpolate to select the appropriate intermediate value. Calculate the shortest distance to the lower and higher isopleths. Call these distances X and Y, respectively. Divide X by the sum of X + Y. Multiply this quotient by 3.0 ppm, and add this product to the lower isopleth value, I. This methodology is illustrated in Figure 5 and is represented by the following formula:

$\{[X / (X+Y)] \times 3.0 \text{ ppm}\} + I_L$ = CO background concentration in ppm, where

I_L = the lower isopleth concentration
X = shortest distance to lower isopleth
Y = shortest distance to higher isopleth

TABLE 13
FUTURE YEAR CARBON MONOXIDE
ROLLBACK FACTORS

*Rollback Factors to be used in conjunction with Figures 3 and 4 to determine one hour and eight hour average carbon monoxide background concentrations from 1993 to 2010**

Year	Rollback Factor
1992	1.0
1993	.97
1994	.94
1995	.90
1996	.87
1997	.84
1998	.81
1999	.78
2000	.75
2001	.73
2002	.70
2003	.67
2004	.65
2005	.63
2006	.62
2007	.60
2008	.59
2009	.59
2010	.58

*After the 1992 carbon monoxide background concentration has been determined, estimates of any year through 2010 can be made using the factors above. For the year desired, multiply the 1992 concentration times the appropriate factor. For example, if the 1992 concentration is 6.0 ppm, the 1999 concentration is calculated to be (6.0 ppm) x (.78) = 4.7 ppm.

Note: Ambient concentrations of carbon monoxide are expected to decline, *on average*, in future years. This will occur because emission controls on new vehicles will reduce CO emission rates faster than vehicle travel increases. (*Local* CO emissions and concentrations might increase under conditions of intense development and increasing travel. These procedures are intended to assess such situations.)

FIGURE 3

ONE HOUR CO BACKGROUND CONCENTRATIONS

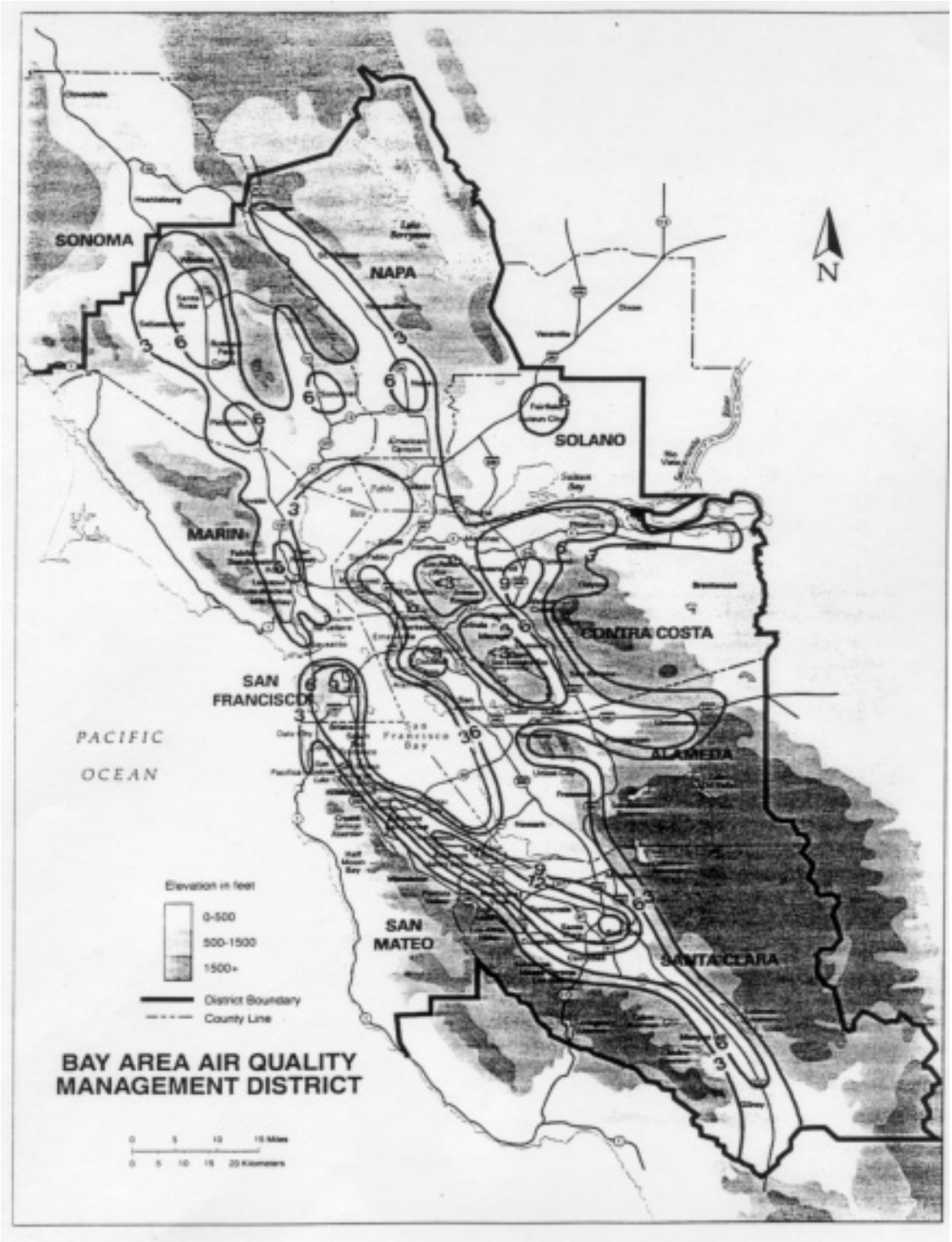


FIGURE 4

EIGHT HOUR CO BACKGROUND CONCENTRATIONS

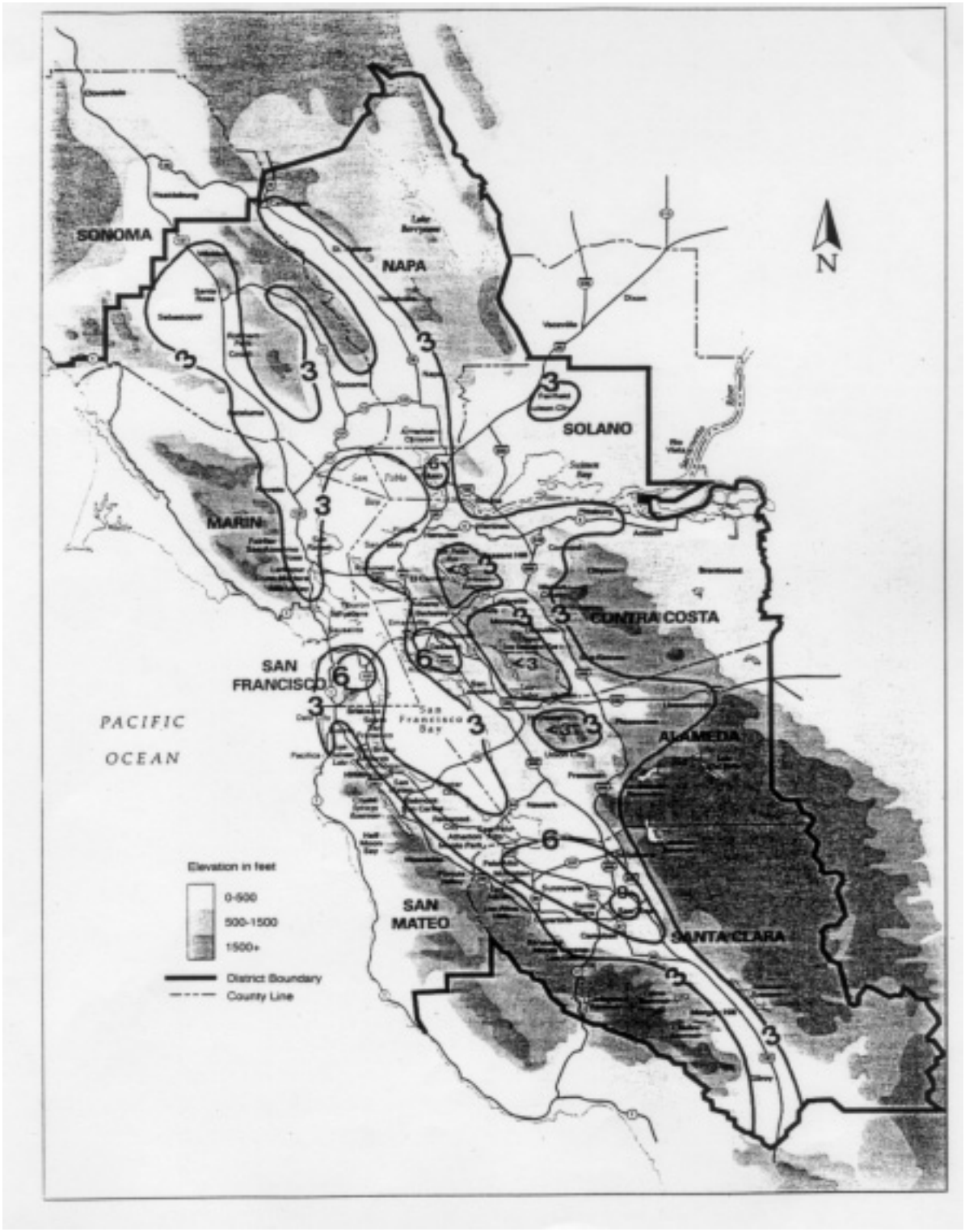


FIGURE 5

DETERMINING CO BACKGROUND CONCENTRATIONS EXAMPLE

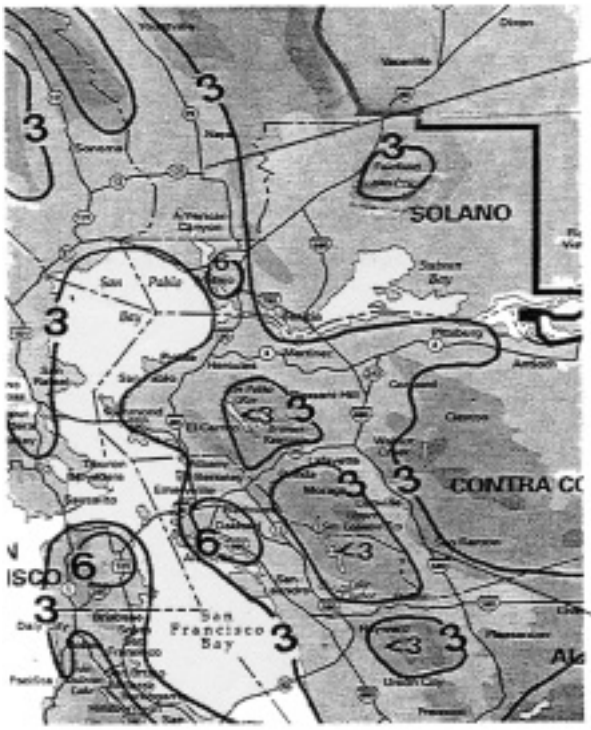




Figure 1A:

Intersection of Rtes. 29 and 121 in Napa County:
An intersection project at this location would be between the 3.0 and 6.0 isopleths. The shortest distance to the 3.0 isopleth is represented by line segment X, and measures 5mm. The shortest distance to the 6.0 isopleth is represented by line segment Y, and measures 13mm. The background concentration for the project would thus be found as follows:

(5mm)/(5mm + 13mm) = 5/18 = .28

(.28)(3.0 ppm) + 3.0 ppm = the background concentration = 3.83 ppm



Figure 1B:

Project on I-680 in San Ramon:
A project on this section of interstate would be between the 3.0 and 6.0 isopleths. The shortest distance to the 3.0 isopleth is represented by line segment X, and measures 2mm. (Note that the project is roughly equidistant from 2 distinct 3.0 isopleths. One is due east, and one is due west.) The shortest distance to the 6.0 isopleth is 23mm. The background concentration for the project would thus be found as follows:

(2mm)/(2mm + 23mm) = 2/25 = .08

(.08)(3.0 ppm) + 3.0 ppm = the background concentration = 3.24 ppm



Figure 1C:

Project on I-980 in Oakland roughly intermediate between I-580 and I-880:
Such a project is located within a peak on the map. The shortest distance to the 6.0 isopleth forming the boundary of the peak is 2mm, and is represented by the line segment X. The distance to the centroid is also 2mm, and is represented by line segment Z. The background concentration for the project would be calculated as follows:

(2mm)/(2mm + 2mm) = 2/4 = .5

(.5)(2.9 ppm) + 6.0 ppm = the background concentration = 7.5 ppm

If the project is located within a "peak" on the map (i.e., within an enclosed area free of a higher isopleth), use the following procedure. (Such a peak could be above a 3.0, 6.0 or 9.0 ppm isopleth.) Measure the shortest distance to the isopleth forming the boundary of the peak. Call this distance X. Measure the distance to the centroid of the enclosure. Call this distance Z. Divide X by the sum of X + Z. Multiply this quotient by 2.9 ppm, and add this product to the boundary isopleth value, I_B. This methodology is illustrated in Figure 5 and is represented by the following formula:

$$\{[X / (X + Z)] \times 2.9 \text{ ppm}\} + I_B = \text{CO background concentration in ppm, where}$$

I_B = boundary isopleth concentration
X = shortest distance to boundary isopleth
Y = distance to centroid

For projects located in areas of the map below the 3.0 isopleth, a background concentration of 2.5 ppm should be assumed.

Example Calculation

Situation: Analysis year: 2000

Intersection of 6-lane highway and a 4-lane road at grade level.

Receptor point at edge of roadway.

Background one hour CO concentration is 9.0 ppm.

Background eight hour CO concentration is 6.0 ppm.

	Primary Road	Secondary Road
Hourly Traffic Volume	3400	2700
Equation	$\frac{(9.5)(3400)(7.27)}{100,000}$	$\frac{(3.3)(2700)(7.27)}{100,000}$

1-Hr Local Concentration: 2.4 + 0.7 = 3.1 ppm

1-Hr Total Concentration: 3.1 (intersection) + 9.0 (1-hr background) = 12.1 ppm

8-Hr Local Concentration: (3.1) x (.7) = 2.2 ppm

8-Hr Total Concentration: 2.2 (intersection) + 6.0 (8-hr background) = 8.2 ppm

Evaluating Diesel Engine Exhaust Emissions

As noted in Section 1.4, ARB in 1998 identified diesel engine particulate matter as a toxic air contaminant, and is evaluating what regulatory action may be needed to reduce public exposure. ARB and the District do not currently have recommended methodologies for Lead Agencies to use in quantifying impacts from diesel exhaust emissions. Because of the potential public health impacts, however, the District strongly encourages Lead Agencies to consider the issue and address potential impacts based on the best information available at the time the analysis is prepared. Particular attention should be paid to projects that might result in sensitive receptors being exposed to high levels of diesel exhaust. This applies both to situations where a new or modified source of emissions is proposed near existing receptors and to new receptors locating near an existing source. Facilities that may have substantial diesel exhaust emissions include the following.

- Truck stop
- Warehouse/distribution center
- Large retail or industrial facility
- High volume transit center
- School with high volume of bus traffic
- High volume highway
- High volume arterial/roadway with high level of diesel traffic

The most current information regarding ARB programs to reduce emissions from diesel engines is available at ARB's website at http://www.arb.ca.gov/toxics/diesel/diesel.htm.

Estimating Stationary Source Emissions

Environmental documents for proposed stationary sources of air pollutants should include a detailed analysis of the project's emissions of criteria pollutants and toxic air contaminants. The document also should describe District regulations applicable to the project and summarize how project design and operations will comply with applicable regulations. Lead Agencies should consult the District's Permit Services Division for guidance on calculating emissions from stationary sources of air pollutants.

For stationary sources being evaluated at an early planning stage, only a general planning or zoning classification may be available, e.g. "research and development" or "light industry". Use of specific emission factors may be difficult. In such cases, the best estimate of future uses should be made. Where an industry designation like "electronic components" or "food processing" is known or assumed, generalized emission factors may be used. Table 14 provides generalized estimates of air contaminant emissions for various categories of industrial land uses in the region. These generalized emission factors were derived from information in the District's emission inventory. Caution should be exercised in using these figures because of the wide range of facilities under each of the categories. However, they may be useful as first estimates of contaminant levels to be expected when only the general category of development is known.

These estimates do not include emissions that can be expected from motor vehicles attracted to these facilities. The indirect source emissions should be calculated separately, as explained earlier in this chapter. Total emissions generated by a proposed project would be the sum of the direct and indirect emissions calculated.

TABLE 14
GENERALIZED EMISSION FACTORS
FOR SELECTED INDUSTRY GROUPS*

Industry Group (Sub-groups)	Average Emissions per Facility (lbs/acre/day)				
	Part.	Org.**	NO_x	SO_2	CO
Manufacturing					
Food Canning (2032, 2033)	0.3	0.5	19.0	22.0	2.2
Paper Prod.(2643, 2647, 2649, 2653, 2654)	0.2	4.4	2.8	0.01	0.6
Printing & Publishing (2700-2771)	3.5	31.0	42.0	0.2	6.0
Inorganic Chemicals (2812, 2813, 2816, 2819)	1.6	0.6	4.9	2.6	5.9
Paints, Varnishes, etc. (2851)	0.2	20.0	0.5	0.0	0.1
Organic Chemicals (2861, 2865, 2869)	1.4	8.5	3.0	0.5	1.6
Petroleum Refining (2911)	1.4	18.0	26.0	16.0	1.3
Paving & Roofing (2951, 2952)	17.0	1.9	11.0	0.7	5.3
Plastic Products, Misc. (3079)	1.1	51.0	0.6	0.0	0.1
Stone, Clay, Glass & Concrete Prod. (3200-3299)	14.0	2.4	17.0	4.6	3.0
Iron & Steel Foundries (3321, 3324, 3325)	11.0	44.0	5.0	2.8	23.0
Metal Containers (3411, 3412)	0.5	90.0	5.5	0.03	0.8
Heating Equipment (3433)	0.1	2.7	0.2	0.00	0.03
Metal Work (3443, 3444, 3448, 3449)	5.3	11.0	1.3	0.01	0.2
Metal Coating (3471, 3479)	0.3	13.0	0.8	0.00	0.1
Machinery, except electrical (3500-3599)	72.0	23.0	0.5	0.02	0.1
Semiconductors, etc. (3674)	0.1	32.0	0.3	0.01	0.1
Electronic Components (3679)	0.1	5.6	0.1	0.00	0.02
Instruments (3800-3873)	0.3	23.0	1.4	0.01	0.2
Other					
Electric Utility plus Other Services (4931)	17.0	12.0	410.0	78.0	32.0
Petroleum Bulk Stations & Terminals (5171)	0.01	150.0	0.1	0.02	0.01
Dry Cleaning Plants (7216)	0.00	6.6	0.1	0.00	0.01
General Hospitals (8062)	2.9	2.3	30.0	0.2	6.0
National Security (9711)	2.8	2.5	22.0	0.01	5.5

* Based on U.S. Standard Industrial Classification (S.I.C.) Code groupings. As compiled by the Statistical Policy Division, Office of Management and Budget.

** Table lists total organic gases (TOG). Reactive organic gases (ROG) is virtually the same for the industrial categories.

3.5 Evaluating Odor Impacts

As noted in Chapter 2, an analysis of potential odor impacts should be conducted for both of the following situations: 1) a potential source of objectionable odors is proposed for a location near existing sensitive receptors, *and* 2) sensitive receptors are proposed to be located near an existing source of objectionable odors. Section 2.3 discusses thresholds of significance for odor impacts.

Odor problems vary greatly. The occurrence and severity of odor impacts depends on numerous factors, including: the nature, frequency and intensity of the source; wind speed and direction; and the sensitivity of the receptor(s). Therefore, to the extent feasible, the analysis of potential odor impacts should be based on District experience and data regarding similar facilities in similar settings. Lead Agencies should consult the District's Enforcement Division for information regarding specific facilities and categories of facilities, and associated odor complaint records.

Any project that would result in an odor source and sensitive receptors being located closer to one another than the distances indicated in Table 4 should be subjected to a more detailed analysis. (Table 4 lists types of facilities that commonly emit objectionable odors.) For any projects triggering the screening level distances in Table 4, the District's Enforcement Division should be contacted for information regarding odor complaints. For projects involving a new receptor being located near an existing odor source(s), the District's inventory of odor complaints for the nearest odor emitting facility(ies) should be reviewed for the previous three years. Odor complaints should be mapped in relation to the odor source to establish a general boundary of any existing impacts.[16] The location of the proposed project should be identified.

For projects involving new receptors locating near an existing odor source where there is currently no nearby development, and for new odor sources locating near existing receptors, the analysis should be based on a review of odor complaints for similar facilities.

In assessing potential odor impacts, consideration also should be given to local meteorological conditions, particularly the intensity and direction of prevailing winds. Refer to Appendix D or contact the District for local meteorological data.

3.6 Evaluating Impacts of Toxic Air Contaminants

The District limits emissions of and public exposure to toxic air contaminants (TACs) through a number of programs. TAC emissions from new and modified stationary sources are limited through an air toxics new source review program, which implements the District's Risk Management Policy via the District's permitting process for stationary sources. TAC emissions from existing sources are limited by: 1) District adoption and enforcement of rules aimed at specific types of sources known to emit high levels of TACs (e.g., chrome plating operations), and 2) implementation of the Air Toxics "Hot Spots" (AB 2588) Program. Appendix E provides more detailed information on District air toxics programs.

---

[16] Due to confidentiality requirements regarding odor complaints, only the block number will be provided for mapping. The name of the complainant, date of complaint, and specific address of the complainant will not be provided.

When considering potential impacts related to TACs, Lead Agencies should consider both of the following situations: 1) a new or modified source of TACs is proposed for a location near an existing residential area or other sensitive receptor, and 2) a residential development or other sensitive receptor is proposed for a site near an existing source of TACs.

For the first scenario, a source of TACs proposed near sensitive receptors, the Lead Agency should consult with the District's Toxics Evaluation Section for information regarding anticipated TAC emissions, potential health impacts and control measures. Preparation of the environmental document should be closely coordinated with the District review of the facility's permit application.

For the second scenario, sensitive receptors locating near sources of TACs, the Lead Agency should consult the District's Toxics Evaluation Section to review information gathered pursuant to the AB 2588 Program. AB 2588 requires plants emitting TACs to prepare inventories of TAC emissions from the facility. The District has prioritized these facilities based on the quantity and toxicity of the emissions, and their proximity to areas where the public may be exposed. Facilities put in a "high priority" category were required to prepare a comprehensive, facility-wide health risk assessment. The Lead Agency should review the health risk assessments for facilities subject to AB 2588 on file at the District offices. For facilities for which risk assessments have been conducted, these assessments may be used to identify an area around the facility within which individuals would be exposed to cancer or noncancer risks that would be identified as significant impacts. For facilities for which risk assessments have not been conducted, the District's Toxics Evaluation Section should be consulted to determine whether location of nearby sensitive receptors would expose individuals to cancer or noncancer risks that would be considered significant.

3.7 Evaluating Impacts of Accidental Releases of Hazardous Materials

Health and safety impacts associated with accidental releases of acutely hazardous materials (AHMs) should be evaluated when: 1) a facility storing or using AHMs is proposed near an existing residential area or other sensitive receptor, and 2) a proposed project would result in new receptors locating near an existing facility storing or using AHMs. As noted in Section 2.3, this evaluation should be based on the analyses conducted pursuant to the Risk Management Prevention Program (RMPP) process. Lead Agencies should consult with the local administering agency of the RMPP process (usually the county health department) for guidance in evaluating impacts from accidental releases.

3.8 Evaluating Cumulative Impacts

The evaluation of a project's cumulative impacts should be based on an analysis of the consistency of the project with the local general plan and the local general plan with the regional air quality plan. Refer to the discussion in Section 2.3 of these Guidelines regarding Cumulative Impacts and Plan Impacts for guidance on evaluating cumulative impacts.

3.9 Evaluating Plans

Planning documents such as city and county general plans, specific area plans and redevelopment plans should be evaluated for their potential air quality impacts. The evaluation of a plan's air quality impacts should focus on an analysis of the plan's consistency with the most recently adopted regional air quality plan. At the time of this writing, the most recently adopted regional air quality plan is the *Bay Area 1997 Clean Air Plan* (CAP). (As the CAP is updated in future years, the analysis should evaluate consistency with the updated CAP.)

To evaluate local plan consistency with the CAP, the Lead Agency should consider the following: the local plan's consistency with CAP population and vehicle use projections, the extent to which the plan implements CAP transportation control measures, and whether the plan provides buffer zones around sources of odors and toxics. Refer to Section 2.3, Thresholds of Significance, for guidance on how to determine whether a local plan is consistent with the CAP.

In most cases, quantification of future air pollutant emissions is not necessary as part of this analysis. If a Lead Agency does quantify emissions, note that the URBEMIS7G model discussed previously should not be used to analyze plan impacts. Other models, such as DTIM or BURDEN, may be more appropriate. There may be some instances where quantification of a plan's air quality impacts is appropriate. For example, a specific plan or a redevelopment plan might lead to increased traffic congestion (and possibly cause high CO concentrations) or result in substantial growth in stationary sources of air pollutants. Lead Agencies should consider including a quantitative assessment of a plan's impacts if warranted by special circumstances.

CHAPTER 4 - MITIGATING AIR QUALITY IMPACTS

4.1 Introduction

CEQA requires Lead Agencies to eliminate or minimize significant environmental impacts associated with projects subject to their (discretionary) approval. If an environmental document indicates that a proposed project will have any significant environmental impacts, the document should identify feasible mitigation measures to reduce the impacts below a level of significance. If, after the identification of all feasible mitigation measures, a project is still deemed to have significant environmental impacts, the Lead Agency must adopt a Statement of Overriding Considerations to explain why further mitigation measures are not feasible and why approval of a project with significant unavoidable impacts is warranted.

The District considers a project's air quality impacts to be reduced below a level of significance if the impacts are mitigated to levels below the thresholds discussed in Chapter 2 of these Guidelines. CEQA documents should identify all significant air quality impacts that may result from a project, propose mitigation measures to reduce those impacts, and evaluate the effectiveness of the mitigation measures. To the extent feasible, the effectiveness of mitigation measures should be quantified. The analysis of mitigation measures' effectiveness should be based on reasonable assumptions, and the analysis and underlying assumptions should be clearly explained. The estimation of the effectiveness of mitigation measures is discussed further below.

This chapter provides guidance on mitigation measures that may be implemented to reduce air quality impacts from project construction and operations. The chapter also provides guidance regarding evaluating mitigation measure effectiveness, addresses mitigation monitoring and reporting requirements, and identifies other useful resources and guidance documents. The lists of mitigation measures included in this chapter are not considered to be exhaustive, and Lead Agencies and project proponents are encouraged to think creatively in devising measures to mitigate air quality impacts.

4.2 Mitigating Construction Impacts

Although the impacts from construction related air pollutant emissions are temporary in duration, such emissions can still represent a significant air quality impact. In some cases, construction impacts may represent the largest air quality impact associated with a proposed project. Construction activities such as grading, excavation and travel on unpaved surfaces can generate substantial amounts of dust, and can lead to elevated concentrations of PM_{10}. Emissions from construction equipment engines also can contribute to high localized concentrations of PM_{10}, as well as increased emissions of ozone precursors and carbon monoxide.

Control measures for construction emissions of PM_{10} are discussed in Section 2.3, Thresholds of Significance. Table 2 describes a variety of measures to mitigate construction-related emissions of PM_{10}. Some control measures, e.g., watering the site twice daily and sweeping roadways, should be implemented at all construction sites, regardless of size. Additional measures are recommended for larger sites (over four acres) where emissions will usually be greater.

As noted previously in these Guidelines, the District does not expect Lead Agencies to provide detailed quantification of construction emissions. Similarly, Lead Agencies need not quantify emission reductions from construction-related mitigation measures. The District's recommended approach to mitigating construction emissions focuses on a consideration of whether all feasible control measures are being implemented. (See Section 2.3 for further information.) If a Lead Agency chooses to quantify the effect of construction-related mitigation measures, the Lead Agency should consult Section 13.2.3, Heavy Construction Operations, and related sections of the most recent edition of U.S. EPA's Compilation of Air Pollutant Emission Factors, Volume I: Stationary, Point and Area Sources, AP-42. (When quantifying the effectiveness of construction mitigation measures, the estimated effectiveness of each mitigation measure should be applied only to the corresponding source of emissions. For example, paving or sweeping access roads will reduce emissions of entrained dust from travel on the roadways, but will not reduce emissions from grading and earth moving.)

The discussion of construction impacts and mitigation measures in these Guidelines focuses primarily on PM_{10} emissions from fugitive dust sources. Lead Agencies seeking to reduce emissions from construction equipment exhaust should consider the following mitigation measures:

- Use alternative fueled construction equipment.
- Minimize idling time (e.g., 5 minute maximum).
- Maintain properly tuned equipment.
- Limit the hours of operation of heavy duty equipment and/or the amount of equipment in use.

4.3 Mitigating Air Quality Impacts Through Land Use and Design Measures

There is a growing recognition among air quality professionals that the location, intensity, configuration and design of land use development greatly influences travel behavior and air quality. Land use patterns typical of post-World War II development have contributed greatly to increases in motor vehicle use and emissions. Characteristics that contribute to automobile dependency include low residential and commercial densities, segregated land uses, and street and site design guided solely by the needs of the automobile. Air quality and transportation planners are concluding that we must reexamine the way we build our communities in order to reduce reliance on the automobile. There are myriad ways in which land use influences travel behavior. Examples of such considerations include the following:

- Are residential and commercial developments of sufficient density to support transit service?

- Are neighborhoods sufficiently "compact" to encourage walking and biking for errands, socializing, etc.?

- Are houses, jobs and services located close enough together to allow walking and biking for at least some trips?
- Does the circulation network and the design of individual streets provide a safe and attractive environment for bicyclists and pedestrians?

- Do the designs of individual development projects provide direct, safe and attractive pedestrian access to transit stops and nearby development?

- Does the community have a rough balance between the number of jobs and the number of employed residents?

Solutions do not necessarily have to occur on a grand scale. Incremental improvements can be made by actions as simple as including a neighborhood commercial center within a residential development, locating a child care center near a transit station, placing parking in the rear of a commercial building, or providing sidewalks and benches in new subdivisions or commercial development. The District strongly encourages Lead Agencies and project proponents to take advantage of every opportunity to make development projects more pedestrian-, bicycle- and transit-friendly.

In recent years, increased attention is also being paid to more ambitious solutions, such as "Transit-Oriented Development". Transit-Oriented Development (TOD) is a land use strategy which is intended to reduce the automobile dependence of typical suburban growth. TOD designs specifically emphasize the needs of pedestrians and transit users. TOD designs include features such as clustering of public and commercial uses around a "town center", a range of residential densities, narrower street widths, and a gridded street pattern. TODs can be defined as follows:

> (TODs) are mixed-use neighborhoods, up to 160 acres in size, which are developed around a transit stop and core commercial area. The entire TOD site must be within an average 2,000 foot walking distance of a transit stop. Secondary areas of lower density housing, schools, parks, and commercial and employment uses surround TODs for up to one mile.[17]

TODs may come in various shapes and sizes, depending on the surrounding built environment. "Urban TODs" are oriented toward rail stations and express bus stops, and are characterized by a greater proportion of employment-generating land uses and higher commercial and residential densities. "Neighborhood TODs" are more appropriate for high frequency bus routes and feeder routes, and place greater emphasis on housing and local-serving shopping and services.

Improved coordination of land use and transportation planning and greater emphasis on making communities more transit-, bicycle- and pedestrian-friendly can reduce reliance on the automobile for all kinds of trips: trips to work, shopping, school, recreation, personal business. Such strategies can result in many other benefits to the community as well, such as reduced traffic congestion, energy conservation, preservation of open space, improved water quality (fewer contaminants in urban run-off), and more attractive, cohesive communities.

Land use considerations also can reduce air quality problems not related to motor vehicle use. By separating residential areas and other sensitive receptors from sources of odors, dust and

[17] Calthorpe Associates, "Transit-Oriented Development Design Guidelines," prepared for the City of San Diego, 1992.

toxic air contaminants, health and nuisance impacts can be minimized. Buffer zones should *always* be provided between sensitive receptors and sources of odors, dust, toxics and accidental releases of hazardous materials. (As noted in Section 2.1, Early Consultation, some infill and mixed use projects occasionally may result in sensitive receptors and sources of odors or toxics being in close proximity. Lead Agencies are encouraged to promote infill and mixed use development, but should avoid locations that would lead to health or nuisance impacts to sensitive receptors.)

Many land use and design measures can be implemented on a project-by-project level. For instance, the site plan for a commercial development can promote pedestrian access by locating parking lots in the rear of the building and placing building entrances near transit stops and sidewalks. Or the circulation plan for a residential subdivision can provide dedicated bicycle routes and direct pedestrian access to transit stops and adjacent development. (As noted in Section 2.1, Early Consultation, land use and design measures targeted at individual projects should be addressed as early in the development review process as possible so as to minimize costs to developers and local government and increase the likelihood of implementation.)

Many land use and design measures, however, are most effective if implemented community-wide, or even at the subregional level. Issues such as allowable land use densities, mixing of land uses, street standards, parking requirements, etc. are most appropriately addressed throughout the entire community or subregion. Policy documents such as general plans and specific area plans, as well as implementing mechanisms such as zoning ordinances, parking standards and design guidelines, may need to be revised. Ad hoc implementation of these strategies to individual projects can still be beneficial, even absent a community-wide strategy, but the benefits will be greater if implemented broadly. For example, a 1993 study by U.C. Berkeley researchers examined the effects of (rail) transit-based development on transit ridership.[18] The study found that residents of higher density housing located near rail transit stations commuted by rail at much higher rates than did residents living further away from transit stations. The study concluded, however, that the increases in transit ridership were much more pronounced if the worksite also was located near a transit station and if the worksite charged for parking. In other words, concentrating housing near transit helps, but the location and parking policies of the destinations are also critical factors.

Therefore, the District strongly encourages local governments to examine local plans and implementing programs to look for opportunities to better coordinate land use, transportation and air quality planning. To the extent that cities and counties can make their communities more transit-, bicycle- and pedestrian-friendly, and minimize land use conflicts that lead to toxics and nuisance problems, the need to mitigate significant air quality impacts of individual development proposals will be minimized. The District and ABAG have jointly prepared a guidance document to assist local governments in developing these strategies, *Improving Air Quality Through Local Plans and Programs, A Guidebook for City and County Governments*. Copies are available from ABAG. Appendix F of these Guidelines lists additional resources that may be useful.

---

[18] Cervero, Robert, "Ridership Impacts of Transit-Focused Development in California", for the National Transit Access Center, November 1993.

A study released by the ARB in June 1995 may be especially useful to Lead Agencies considering land use strategies to reduce air pollutant emissions. The report, prepared by JHK & Associates, is titled *Transportation-Related Land Use Strategies to Minimize Motor Vehicle Emissions: An Indirect Source Research Study*. The report discusses a number of land use strategies that can reduce motor vehicle use and emissions:

- Provide pedestrian facilities.
- Increase density near transit corridors.
- Increase density near transit stations.
- Encourage mixed-use development.
- Encourage infill and densification.
- Develop concentrated activity centers.
- Strengthen downtowns.
- Develop interconnected street network.
- Provide strategic parking facilities.

The report provides estimates of the measures' effectiveness in reducing vehicle use and emissions in various types of communities (urban, suburban and exurban). The estimated ranges of effectiveness are based on quantitative data from existing California communities. It is hoped that by identifying ranges of effectiveness for the land use measures, local officials will be able to set performance goals (e.g., vehicle trips or emissions per household) for their communities. The report recommends combinations of strategies to achieve the performance goals, and provides guidance on implementation mechanisms. One of the study's findings is that although it is difficult to quantify reductions in vehicle use and emissions from individual strategies applied at individual sites, combinations of strategies implemented community-wide can achieve significant reductions in vehicle use and emissions. The report is available from ARB's Transportation Strategies Group.

4.4 Mitigating Impacts of Project Operations

Introduction

In many cases, motor vehicles traveling to and from a facility represent the principal source of air pollutants associated with the project. Therefore, this section focuses primarily on measures to reduce mobile source emissions by reducing motor vehicle trips and vehicle miles traveled. If the procedures outlined in Chapters 2 and 3 of these Guidelines indicate that a project's motor vehicle emissions would be a significant impact, mitigation measures should be identified to reduce the impact to a level of insignificance.

A wide variety of measures may be implemented to reduce air pollutant emissions resulting from land use development. The appropriateness of a given mitigation measure depends on a number of factors, such as the type and size of project being proposed, the location and characteristics of the community in which the project will be located, neighboring land uses, availability of transit, etc. For example, consider the provision of bicycle racks and showers and lockers at a worksite in order to encourage commuters to bike to work. Such measures will be more effective in a

community with a comprehensive network of bicycle routes and fairly flat terrain than in a community with poor bicycle access and hilly terrain. Lead Agencies and project proponents should carefully consider the specific nature of the project and its setting when developing mitigation measures.

Estimating the Effectiveness of Mitigation Measures for Project Operations

To the extent feasible, the effectiveness of proposed mitigation measures should be quantified. Because the measures' effectiveness will depend greatly on the specific characteristics of the project and its setting, this quantification should be based on a project-specific analysis whenever possible. For mitigation measures to reduce vehicle use, this means conducting a travel analysis for the project using appropriate local modeling inputs.

Tables 15 and 16 identify mitigation measures that may be used to reduce motor vehicle emissions from commercial and residential projects, respectively. The tables provide estimates of each measure's effectiveness in reducing vehicle trips. In cases where a range of estimated effectiveness is provided, the low end of the range should be used unless local conditions warrant a higher figure. The column of supporting factors should be consulted to see if a higher figure is justified. The effectiveness estimates are based on a review of published literature and represent what the District believes to be reasonable expectations regarding effectiveness. However, the percentages in Tables 15 and 16 are default values, and should be used only in the absence of project-specific analysis.

Several cautionary notes regarding estimating the effectiveness of mitigation measures are warranted.

Clearly explain the assumptions underlying the environmental document's analysis of mitigation measures' effectiveness. The analysis should specifically describe the mitigation measure, identify the source(s) of air pollutants that are expected to be affected by the measure, clearly explain how and to what extent the measure will affect the source(s), and identify the basis for the estimate (empirical observations, computer modeling, case studies, etc.). Critical assumptions should be linked to the mitigation monitoring and reporting program. For example, if the environmental analysis for a commercial development assumes that 20% of employees will carpool to work, then such an objective should be included in the mitigation monitoring and reporting program as a test of whether the measure is being implemented.

Be specific regarding implementation of mitigation measures. The environmental document should describe each mitigation measure in detail, identify who is responsible for implementing the measure, and clearly explain how and when the measure will be implemented. Methods for assessing the measure's effectiveness once it is in place, and possible triggers for additional mitigation if necessary, are also desirable. This level of detail regarding mitigation measure implementation frequently is not addressed until the preparation of the mitigation monitoring and reporting program, which often takes place very late in the environmental review process. In order to reliably assess the effectiveness and feasibility of mitigation measures, however, the District believes it is necessary to

consider the specifics of mitigation measure implementation as early in the environmental review process as possible.

Be sure not to double count the effect of proposed mitigation measures. The project description and assumptions underlying the analysis of project impacts should be carefully considered when estimating the effect of mitigation measures. If certain conditions or behavior are assumed in the impact analysis, then credit may not be claimed when proposing mitigation measures. For example, if the traffic and air quality analyses for a proposed project assume that a certain percentage of people will access the project by transit or bicycle, then any credit claimed for transit- or bicycle-related mitigation must clearly demonstrate effectiveness above and beyond the mode split assumed in the impact analysis.

In some cases it simply may not be possible to quantify the effect of proposed mitigation measures. It may be that the specific conditions surrounding a particular project are so unique as to render extrapolation from other examples unreliable. A proposed measure may be innovative, with little precedent. The combined effects of a package of measures may be too difficult to quantify. While a certain degree of professional judgment is usually involved in estimating the effectiveness of mitigation measures, overly speculative estimates should be avoided. If the Lead Agency cannot quantify mitigation effectiveness with a reasonable degree of certainty, the environmental document should at least address effectiveness qualitatively. If the Lead Agency makes a finding that non-quantified mitigation measures reduce an impact to a level of insignificance, the document should provide a detailed justification of that conclusion.

Mitigating Impacts from Motor Vehicles

Several general approaches can be taken to reduce emissions from motor vehicles:

- Reduce vehicle trips. These measures reduce air pollutant emissions by eliminating entirely some of the vehicle trips associated with a project. An example would be the provision of bicycle facilities to encourage bicycle use instead of driving.

- Reduce vehicle miles traveled. These measures reduce emissions by reducing the length of vehicle trips associated with a project. An example would be the provision of satellite offices/telecommuting centers to reduce the distance of employee commute trips.

- Use of low emission vehicles. These measures do not aim to reduce trips or VMT, but rather promote the use of fuels that are less polluting than gasoline or diesel. An example would be the conversion of a vehicle fleet to operate on compressed natural gas.

- Improve traffic flows/reduce congestion. These measures reduce emissions by reducing traffic congestion and/or reducing stops and starts. This allows vehicles to operate at steady and moderate speeds, and thus lowers pollution per mile traveled. An example would be timing the traffic signals on an arterial to facilitate uninterrupted travel.

- Support measures. These measures may not directly reduce emissions, but rather support and facilitate other emission reduction strategies. An example would be a guaranteed ride home program implemented at a worksite in order to encourage employees to use commute alternatives by allaying concerns over being without a vehicle in case of emergency.

Emission reduction measures from each of the above categories can be implemented in combination with one another. (Support measures, by definition, are implemented to reinforce other emission reduction strategies.) In general, the District prefers measures that reduce vehicle trips entirely, as they achieve the greatest emission reductions. (This is because vehicle emissions are highest during the first several miles of a trip.) Strategies to reduce VMT should also be pursued, however. Reducing VMT has a greater impact on PM_{10} emission than other pollutants, because PM_{10} emission (due to entrained road dust) are more directly correlated to VMT. Measures to encourage low emission vehicles are also desirable, especially for projects that include a sizable fleet of vehicles (delivery services, taxis, airport shuttles, airport ground support equipment, etc.). Traffic flow improvements may be beneficial if congestion is a major factor in the air quality impact, but particular caution is warranted to avoid traffic-inducing effects of increased roadway capacity.

There is an increasing range of alternatively-fueled, low emission vehicles and equipment available on the market. Examples include light and medium duty automobiles and vans, heavy duty trucks and buses, and specialty equipment such as forklifts, construction equipment, parking enforcement vehicles, and airport ground support equipment. Compressed natural gas-powered vehicles and electric vehicles (EVs) are probably the most common in the Bay Area, but other fuels such as liquefied natural gas and propane are also in use. Emerging technologies such as hybrid electric vehicles and fuel cells also are promising.

While the District urges Lead Agencies to emphasize measures to reduce trips and VMT, careful consideration should always be given to opportunities to promote use of low emission fuels. Low emission vehicles and equipment are particularly well suited in situations where there is a large fleet of vehicles, at large facilities (either a single facility or a conglomeration of multiple facilities in proximity) where there may be the critical mass to justify a fueling facility, and at projects where trip reduction strategies are less promising due to specific circumstances (e.g., little or no transit service, poor bike/ped access, etc.). Low emission vehicles and equipment also are a good complement to trip reduction strategies. For trips that can't or won't be eliminated, low emission vehicles reduce emissions with little or no change in behavior. Use of low emission vehicles and equipment will help implement mobile source control measures in the *1997 CAP* that aim to increase the use of this equipment.

Table 17 provides examples of low emission vehicle projects that may be appropriate at a variety of land uses. Lead Agencies and project proponents should always consider such opportunities when devising mitigation strategies. More information on low emission vehicles and equipment is available at the websites listed below.

The District administers several programs that provide funding assistance for low emission vehicles and infrastructure. Information on these programs, as well as information on low emission vehicle technology in general, is available on the District's website at

www.baaqmd.gov/planning/plntrns/tfcapage.htm. ARB and the U.S. Department of Energy also provide extensive information on low emission vehicles at www.arb.ca.gov/altfuels/altfuels.htm and www.afdc.nrel.gov, respectively.

If a project may result in public exposure to high levels of diesel exhaust, the Lead Agency should propose mitigation measures to reduce this impact. Although the District does not currently (as of December 1999) provide a methodology for quantifying the effectiveness of these measures, they should be given careful consideration. In addition to reducing toxic diesel exhaust emissions, these measures also will reduce emissions of NO_x and PM_{10}. Possible mitigation measures include the following.

Heavy Duty Truck Emissions

- Truck stop electrification – minimize truck idling for heating, air conditioning and refrigeration units
- Conversion to cleaner engines
- Use of cleaner (reduced sulfur) fuel
- Regular maintenance – keep equipment well tuned
- Add-on control devices, e.g., particulate traps, catalytic oxidizers
- Buffer zone between facility and sensitive receptors

Heavy Duty Bus Emissions

- Conversion to cleaner engines
- Use of cleaner (reduced sulfur) fuel
- Regular maintenance – keep equipment well tuned
- Reduce idling
- Add-on control devices, e.g., particulate traps, catalytic oxidizers
- Buffer zone between facility and sensitive receptors

Other Mobile Equipment Emissions (construction equipment, locomotives, marine vessels)

- Conversion to cleaner engines
- Use of cleaner (reduced sulfur) fuel
- Regular maintenance – keep equipment well tuned
- Add-on control devices, e.g., particulate traps, catalytic oxidizers
- Buffer zone between facility and sensitive receptors

TABLE 15
MITIGATION MEASURES FOR REDUCING MOTOR VEHICLE EMISSIONS FROM COMMERCIAL, INSTITUTIONAL AND INDUSTRIAL PROJECTS

Mitigation Measure	Supporting Factors to Enhance Effectiveness	Effectiveness
Rideshare Measures		
Implement carpool/vanpool program e.g., carpool ridematching for employees, assistance with vanpool formation, provision of vanpool vehicles, etc.	• Employer provides support measures such as carpool/vanpool subsidies, preferential parking, guaranteed ride home program, etc. • Coordinate with regional ridesharing organization, e.g., RIDES for Bay Area Commuters. • Multiple smaller worksites coordinate programs. • Limited parking supply and/or implementation of parking fees or parking cash-out.	1% - 4% (work trips)
Transit Measures		
Construct transit facilities such as bus turnouts/bus bulbs, benches, shelters, etc.	• Transit service with frequent headways available at project or on roadways adjacent to project. • Transit use incentives for employees, e.g., on-site distribution of passes, subsidized transit passes, etc. • Transit route maps and schedules posted at stops. • Shade trees/landscaping planted at transit stops.	0.5% - 2% (all trips)
Design and locate buildings to facilitate transit access, e.g., locate building entrances near transit stops, eliminate building setbacks, etc.	• Jurisdiction provides design guidelines addressing transit accessibility. • Consultation with transit provider during project design, review.	0.1% - 0.5% (all trips)
Services Measures		
Provide on-site shops and services for employees, such as cafeteria, bank/ATM, dry cleaners, convenience market, etc.	• Sufficient number of employees at worksite, or cooperation among multiple worksites. • Safe, direct pedestrian access between employment and retail areas. • Jurisdiction provides density bonuses, other incentives to encourage mixed land uses.	0.5% - 5% (work trips)
Provide on-site child care, or contribute to off-site child care within walking distance.	• Sufficient number of employees at worksite, or cooperation among multiple worksites.	0.1% - 1% (work trips)

Shuttle Measures		
Establish mid-day shuttle service from worksite to food service establishments/commercial areas.	• Sufficient number of employees at worksite, or cooperation among multiple worksites. • Commercial area located within 3 miles. • Frequent, scheduled service during lunch hours. • Coordination among multiple employers, e.g., at business parks. • Provide commute shuttle to transit station, use same vehicle for mid-day shuttle.	0.5% - 1.5% (work trips)
Provide shuttle service to transit stations/multimodal centers.	• Major transit facility/multimodal center located within 3 miles of project. • Transit use incentives for employees, e.g., on-site distribution of passes, subsidized transit passes, etc. • Frequent, scheduled service during peak commute periods. • Coordination among multiple employers, e.g., at business parks. • Free or subsidized service. • Provide mid-day shuttle to commercial areas, use same vehicle for commute shuttle.	1% - 2% (work trips)
Parking Measures		
Provide preferential parking (e.g., near building entrance, sheltered area, etc.) for carpool and vanpool vehicles.	• Most effective if parking supply is limited and/or located far from building entrance.	0.5% - 1.5% (work trips)
Implement parking fees for single occupancy vehicle commuters.	• Reduced or waived fees for carpools and vanpools. • Complemented by transit, ridesharing programs, other commute alternatives. • Revenues used to support commute alternatives. • Provisions in place to avoid offsite parking spillover.	2% - 20% (work trips)

Implement parking cash-out program for employees (i.e., non-driving employees receive transportation allowance equivalent to value of subsidized parking).	• Complemented by transit, ridesharing programs, other commute alternatives. • Implement at worksites not subject to State parking cash-out requirements. • Tax benefits if travel allowance offered as transit/ridesharing subsidy. • Provisions in place to avoid offsite parking spillover.	2% - 20% (work trips)
Bicycle and Pedestrian Measures		
Provide secure, weather-protected bicycle parking for employees.	• Bicycle parking location is more convenient than auto parking. • Project located adjacent to, or within 1/4 mile of, Class I bicycle path or Class II bicycle lane. • Significant number of employees live within 5 miles of worksite. • Employer provides bicycle support measures, e.g., bicycle route maps, tools for emergency repairs, etc.	0.5% - 2% (work trips)
Provide safe, direct access for bicyclists to adjacent bicycle routes.	• Local jurisdiction has adopted comprehensive bicycle plan. • Significant number of employees live within 5 miles of worksite. • Employer provides bicycle support measures, e.g., bicycle route maps, tools for emergency repairs, etc. • Provide push buttons or sensors to activate traffic signals.	0.5% - 2% (work trips)

Provide showers and lockers for employees bicycling or walking to work.	• Significant number of employees live within 5 miles (bicycling)/2 miles (walking). • Project located adjacent to, or within 1/4 mile of, Class I bicycle path or Class II bicycle lane. • Employer provides bicycle support measures, e.g., bicycle route maps, tools for emergency repairs, etc.	0.5% - 2% (work trips)
Provide secure short-term bicycle parking for retail customers and other non-commute trips.	• Bicycle parking location is more convenient than auto parking. • Project located adjacent to, or within 1/4 mile of, Class I bicycle path or Class II bicycle route.	1% - 2% (non-work trips)
Provide direct, safe, attractive pedestrian access from project to transit stops and adjacent development.	• Jurisdiction provides design guidelines addressing pedestrian accessibility. • Pedestrians separated from traffic, parking areas. • Shade trees/landscaping planted at pedestrian areas. • Benches, fountains, other amenities provided to enhance pedestrian environment.	0.5% - 1.5% (all trips)
Other Measures		
Implement compressed work week schedule (e.g., 4/40, 9/80).	• Consult with employees prior to program implementation.	2% - 10% (work trips)
Implement home-based telecommuting program.	• Participation increased if employer provides/assists with provision of equipment (modem, computer, etc.). • Especially effective if employee commute trips are long.	0.5% - 1.5% (work trips)

TABLE 16
MITIGATION MEASURES FOR REDUCING MOTOR VEHICLE EMISSIONS FROM RESIDENTIAL PROJECTS

Mitigation Measure	Supporting Factors to Enhance Effectiveness	Effectiveness
Provide neighborhood-serving shops and services within or adjacent to (1/4-1/2 mile) residential project.	• Direct pedestrian/bicycle access is available. • Medium or high residential densities located closer to commercial areas. • Jurisdiction has design guidelines addressing issues such as pedestrian access, parking, compatibility with neighboring land uses, etc.	1% - 4% (all trips)
Provide transit facilities, e.g., bus bulbs/turnouts, benches, shelters, etc.	• Transit service is available in or adjacent to project. • Project is of sufficient density to support transit service. • Transit service with frequent headways. • Consultation with transit provider during project design, review	0.2% - 2% (all trips)
Provide shuttle service to regional transit system or multimodal center.	• Transit station or multimodal center located within 5 miles of project. • Medium to high residential densities.	0.1% - 0.5% (all trips)
Provide shuttle service to major destinations such as employment centers, shopping centers, schools.	• Destinations located within 5 miles of project. • Medium to high residential densities.	0.1% - 0.3% (all trips)
Provide bicycle lanes and/or paths, connected to community-wide network.	• Local jurisdiction has adopted comprehensive bicycle plan. • Project is located adjacent to, or within 1/4 mile of, Class I bicycle path or Class II bicycle lane. • Routes are direct and convenient, not curving recreational paths.	0.1% - 2% (all trips)

Provide sidewalks and/or paths, connected to adjacent land uses, transit stops, and/or community-wide network.	• Destinations such as commercial areas, schools, parks, community centers, etc. are located nearby. • Cul-de-sacs are discouraged, or easements are provided for pedestrian access. • Shade trees/landscaping provided.	0.1% - 1% (all trips)
Provide satellite telecommute centers in large residential developments.	• Most effective if residential area is located far from employment centers	0.1% - 1.5% (work trips)
Provide interconnected street network, with a regular grid or similar interconnected street pattern.	• Multiple ingress/egress points are available. • Large, multi-lane arterials are discouraged. • Reduced street widths and curb radii. • Cul-de-sacs are discouraged. • Street trees required.	1% - 5% (all trips)

TABLE 17
LOW EMISSION VEHICLE MITIGATION MEASURES

	Office (office building, office park)	Retail (large retail building, shopping center, mall)	Institutional (airport, university, hospital, etc.)	Residential
Electric Vehicles/Equipment				
Install EV charging facility	X	X	X	
Provide EVs in vehicle fleet	X	X	X	
Preferential parking location for EVs	X	X	X	
Reduced/no parking fee for EVs	X	X	X	
Use electric lawn & garden equipment	X	X	X	
Use electrically powered specialty equipment, e.g., utility carts, airport ground support equipment, etc.	X	X	X	
Require/provide incentives for airport tenants to use electrically powered shuttles, GSE, rental cars, etc.			X	
Provide electrical power in garage/driveway for EV charging				X
Provide electrical power outdoors to allow use of electric lawn & garden equipment				X
At multifamily residential projects, provide EV charging facilities and/or preferential parking for EVs				X
Compressed Natural Gas Vehicles/Equipment				
Provide CNG vehicles in vehicle fleet	X	X	X	
Preferential parking location for CNG vehicles	X	X	X	
Reduced/no parking fee for CNG vehicles	X	X	X	
Install CNG fueling facility	X	X	X	
Use CNG specialty equipment, e.g., utility carts, airport ground support equipment, etc.	X	X	X	
Require/provide incentives for airport tenants to use CNG powered shuttles, GSE, rental cars, etc.			X	
Other Vehicles/Equipment				
Use propane powered specialty equipment, e.g., forklifts, utility carts, airport GSE, etc.		X	X	

4.5 Mitigating Odor Impacts

Projects that have a significant odor impact because they place sources of odors and members of the public near each other should establish a buffer zone to reduce odor impacts to a less than significant level. The dimensions of the buffer zone must ensure that the encroaching project does not expose the public to nuisance levels of odorous emissions. In establishing the appropriate dimensions of the buffer zone, the Lead Agency should consider actions currently being taken at the facility to control odors, as well as any future actions to which the facility is firmly committed. A safety margin also should be considered in establishing a buffer zone to allow for future expansion of operations at the source of the odors.

In order to reduce the dimensions of the buffer zone, add-on control devices (e.g., filters or incinerators) and/or process modifications implemented at the source of the odors may be feasible, depending on the specific nature of the facility. Lead Agencies should consult the District's Enforcement Division for further information regarding add-on controls and process modifications to control odors. Odor mitigation measures that are targeted at the *receptors* (e.g., residential areas) that rely on sealing buildings, filtering air or disclosure statements are not appropriate mitigation measures to be used in lieu of buffer zones or technical controls.

4.6 Mitigating Impacts from Toxic Air Contaminants and Accidental Releases of Hazardous Materials

A project would have a significant impact if it resulted in members of the public being close enough to either 1) a source of toxic air contaminants (TACs) or 2) a potential source of accidental releases of hazardous materials, such that the thresholds described in Section 2.3 would be exceeded. To mitigate such impacts, a buffer zone should be provided between the source and the receptors. The appropriate dimensions of the buffer zone will depend on a variety of factors, including the nature of the activities occurring at the source, the types and quantities of materials being stored or used at the facility, and local topography and meteorology.

As discussed in Section 2.3, the determination of significant impact with respect to accidental releases should be based on analyses prepared pursuant to the Risk Management Prevention Program (RMPP). RMPP analyses will be key inputs in establishing the appropriate dimensions of buffer zones around potential sources of accidental releases. Lead Agencies should consult with the local administering agency of the RMPP process (usually the county health department) when establishing buffer zones around sources of accidental releases to assure that the thresholds described in Section 2.3 are not exceeded.

The determination of significance with respect to TAC emissions will generally be based on analyses conducted as part of the District’s permitting process and/or implementation of the Air Toxics “Hot Spots” (AB 2588) program. Section 3.6 describes processes for evaluating

potential TAC impacts. These analyses will assist Lead Agencies in establishing buffer zones and, if necessary, identifying other mitigation measures to reduce TAC impacts.

In most cases, control devices and/or changes in industrial processes may be implemented at the source(s) in order to reduce the risk from TAC emissions or accidental releases. All feasible measures to reduce risks from TAC emissions and accidental releases should be implemented. While such measures may reduce the necessary dimensions of a buffer zone, they do not obviate the need to maintain buffer zones to protect public health and safety. This is particularly true in situations where residential development (or any other sensitive receptor) is encroaching on an existing source of TACs or accidental releases. Also, as noted above regarding odor impacts, mitigation measures for TACs or accidental releases (such as disclosure statements, sealing of buildings, community alert procedures, etc.) that are targeted at potential *receptors* are not appropriate mitigations to be used in lieu of buffer zones or technical controls.

4.7 Mitigation Monitoring and Reporting

State law requires that when a public agency makes findings based on an EIR that mitigation measures are required to avoid or lessen significant environmental effects identified in the EIR, the public agency must adopt a reporting or monitoring program for those mitigation measures (California Public Resources Code, Section 21086.6). This requirement is intended to assure that mitigation measures included in a certified EIR are indeed implemented. A mitigation monitoring and reporting program should include the following components:

- A description of each mitigation measure adopted by the Lead Agency.
- The party responsible for implementing each mitigation measure.
- A schedule for the implementation of each mitigation measure.
- The agency or entity responsible for monitoring mitigation measure implementation.
- Criteria for assessing whether each measure has been implemented.
- Enforcement mechanism(s).

Although the mitigation monitoring and reporting program is not required to be included in the EIR, the District recommends that the Lead Agency do so. This will encourage the Lead Agency and other entities to specifically consider the feasibility and effectiveness of each mitigation measure while the environmental analysis is still underway.

If a responsible agency or any agency having jurisdiction over natural resources affected by the project proposes mitigation measures, the Lead Agency may require that agency to prepare a monitoring and reporting program for those mitigation measures.

APPENDIX A - AIR QUALITY LAWS, PROGRAMS AND STANDARDS

This appendix summarizes the major federal and State laws, regulations and programs that establish the legal framework for protecting and improving air quality in the Bay Area. Some of these regulations have air quality improvement as their primary purpose. Others deal with air quality within the context of other public objectives. Table A-1 summarizes national and State ambient air quality standards — the quantitative air quality objectives that the Bay Area is required to attain.

FEDERAL PROGRAMS

Federal Clean Air Act and 1990 Clean Air Act Amendments. National ambient air quality standards (NAAQS) were established in 1970 by the federal Clean Air Act for six pollutants: carbon monoxide, ozone, particulate, nitrogen dioxide, sulfur dioxide and lead. These pollutants are commonly referred to as "criteria" pollutants because they are considered the most prevalent air pollutants that are known to be hazardous to human health and because criteria documents, including ambient air quality standards, have been prepared for each of these contaminants.

The Act required states exceeding the NAAQS to prepare air quality plans showing how the standards were to be met by December 1987. The Act was amended in 1977, and again in 1990, to extend the deadline for compliance and require that revised State Implementation Plans (SIP) be prepared. Failure to submit and implement an acceptable plan meant a state could be denied federal highway funding and/or be required to increase emission offsets for industrial expansion. The 1990 Clean Air Act Amendments established categories of air pollution severity for nonattainment areas ("marginal" to "extreme"). SIP requirements varied, depending on degree of severity. (For a discussion of the Bay Area's portion of the California SIP, see "Bay Area Regional Agencies and their Programs" below.)

The conformity provisions of the Act are essentially designed to ensure that federal agencies contribute to, instead of jeopardizing, efforts to achieve the NAAQS. In November of 1993, U.S. EPA issued two regulations implementing these provisions. The transportation conformity regulation deals with transportation projects. The general conformity regulation addresses actions of federal agencies other than the Federal Highway Administration and the Federal Transit Administration.

The primary requirements of transportation conformity of note to Lead Agencies are that transportation plans and programs cannot produce more emissions than were budgeted for in the latest SIP. Projects receiving federal funds or approvals also must undergo localized air quality modeling. Finally, emissions from local projects with no federal funding must be included in regional plans and programs, if the sponsoring agency receives any federal funds.

TABLE A-1 AMBIENT AIR QUALITY STANDARDS

Pollutant	Averaging Time	California Standards[1, 3]	National Standards[2, 3]
Ozone[4]	1 Hour	0.09 ppm	0.12 ppm
	8 Hour		0.08 ppm
Carbon Monoxide	8 Hour	9.0 ppm	9 ppm
	1 Hour	20 ppm	35 ppm
Nitrogen Dioxide	Annual Average		0.053 ppm
	1 Hour	0.25 ppm	
Sulfur Dioxide	Annual Average		80 $\mu g/m^3$
	24 Hour	0.04 ppm	365 $\mu g/m^3$
	1 Hour	0.25 ppm	
Fine Particulate Matter (PM_{10})	Annual Arithmetic Mean		50 $\mu g/m^3$
	Annual Geometric Mean	30 $\mu g/m^3$	
	24 Hour	50 $\mu g/m^3$	150 $\mu g/m^3$
Fine Particulate Matter ($PM_{2.5}$)[4]	Annual Arithmetic Mean		15 $\mu g/m^3$
	24 Hour		65 $\mu g/m^3$
Sulfates	24 Hour	25 $\mu g/m^3$	
Lead	Calendar Quarter		1.5 $\mu g/m^3$
	30 Day Average	1.5 $\mu g/m^3$	
Hydrogen Sulfide	1 Hour	0.03 ppm	
Vinyl Chloride (chloroethene)	24 Hour	0.010 ppm	
Visibility Reducing Particles[5]	8 Hour (10 am to 6 pm PST)	10-mile visual range when relative humidity is less than 70%	

ppm = parts per million. $\mu g/m^3$ = micrograms per cubic meter.

FOOTNOTES

1. California standards for ozone, carbon monoxide (except Lake Tahoe), sulfur dioxide (1-hour and 24-hour), nitrogen dioxide, fine particulate matter, and visibility reducing particles are values that are not to be exceeded. The standards for sulfates, lead, hydrogen sulfide, and vinyl chloride are not to be equaled or exceeded. If the standard is for a 1-hour, 8-hour or 24-hour average (i.e., all standards except for lead and the PM_{10} annual standard), then some measurements may be excluded. In particular, measurements are excluded that ARB determines would occur less than once per year on the average.
2. National standards other than for ozone and those based on annual averages or arithmetic means are not to be exceeded more than once a year. The ozone standard is attained if, during the most recent 3-year period, the average number of days per year with maximum hourly concentrations above the standard is one or less.
3. National air quality standards are set at levels determined, by the U.S. Environmental Protection Agency, to be protective of public health with an adequate margin of safety. The State of California has set more stringent standards for a number of contaminants, based on independent medical judgment.
4. In 1997 EPA established an 8-hour standard for ozone, and annual and 24-hour standards for very fine particulate matter (PM2.5). The new standards were challenged in court, and as of December 1999 their status was uncertain.
5. This standard is intended to limit the frequency and severity of visibility impairment due to regional haze and is equivalent to a 10-mile nominal visual range when relative humidity is less than 70 percent.

General conformity applies to a wide range of actions or approvals by federal agencies. Potentially covered by the regulation are actions of concern to local governments such as decisions on wastewater treatment facilities and airport expansions. Essentially, projects are subject to general conformity if they generate more emissions than minimum thresholds set in the rule (currently 100 tons per year of ROG, NO_x, or CO in the Bay Area), and that are not specifically exempted by the regulation. Such projects are required to fully offset or mitigate the emissions caused by the action. This includes both direct emissions and indirect emissions over which the federal agency has some control.

The U.S. EPA also has programs for identifying and regulating toxic air pollutants (air toxics). The Clean Air Act Amendments of 1990 directed EPA to set standards for air toxics and to require facilities to sharply reduce emissions of controlled chemicals. The 1990 Amendments specified 174 industrial sources that are to be regulated. An industry is classified as a major source — and must be regulated — if it emits ten tons per year of any of the listed air toxics, or a combination of 25 tons or more of all listed air toxics.

National Environmental Policy Act (NEPA). NEPA requires that major projects to be conducted or approved by the federal government be subject to environmental assessments. If the potential for significant adverse environmental impacts exists, an Environmental Impact Statement (EIS) must be prepared and circulated to affected jurisdictions and the interested public.

Intermodal Surface Transportation Efficiency Act, 1991 (ISTEA). This law requires a regional transportation planning process that includes consideration of 15 factors, two of which address consistency with adopted land use plans and potential environmental effects. ISTEA also provides funds for transportation projects and activities that contribute to meeting air quality standards, including transit, pedestrian, and bicycle-oriented projects. The Congestion Management and Air Quality Improvement Program (CMAQ) directs funds toward transportation projects that will contribute to the attainment of NAAQS for ozone and carbon monoxide. The funds are distributed based on population size and severity of a region's air pollution problem.

CALIFORNIA PROGRAMS

California Clean Air Act, 1988. The 1988 California Clean Air Act (CCAA), amended in 1992, requires regions to develop and implement strategies to attain California's ambient air quality standards. For some pollutants, the California standards are more stringent than the national standards. In addition to the six criteria pollutants regulated by the federal Clean Air Act, California has established standards for three other pollutants: hydrogen sulfide, sulfates, and vinyl chloride. In general, the CCAA requires regions like the Bay Area, which exceed certain State air quality standards for criteria pollutants, to reduce emissions of harmful pollutants by five percent or more per year or implement all feasible measures to meet the state air quality standards as expeditiously as possible. Regional air quality management districts like the BAAQMD must prepare air quality plans specifying how State

standards would be met. State agencies are required to implement a number of statewide automobile emission control regulations, including the "Smog Check" program.

State Motor Vehicle Emission Control Program. The California Air Resources Board (ARB) regulates the amount of pollutants that can be emitted by new motor vehicles sold in California. California motor vehicle emission standards are more stringent than the federal standards and have become increasingly more stringent since they were first imposed in 1961 by the State Motor Vehicle Pollution Control Board (the predecessor to the ARB). To help meet the State ambient air quality standards, the ARB has instituted regulations that will require manufacturers selling vehicles in California to manufacture and phase-in a proportion of motor vehicles in the following categories: Transitional Low Emission Vehicles, Low Emission Vehicles, Ultra-Low Emission Vehicles, and Zero Emission Vehicles (e.g., electric vehicles — 10% of California-sold vehicles by 2003). These requirements apply to passenger vehicles and are intended to reduce emissions of carbon monoxide, reactive hydrocarbons, and nitrogen oxides. The ARB has also set requirements for the distribution of alternative fuels.

ARB also has implemented a heavy duty vehicle inspection program, which applies to diesel-powered trucks and buses. The ARB is also working on fuel requirements that would reduce toxic emissions from motor vehicles. The California Bureau of Automotive Repair continues to administer the vehicle inspection and maintenance program (I/M or "Smog Check" Program).

Air Toxics "Hot Spots" Information and Assessment Act, 1987. The Air Toxic "Hot Spots" Information and Assessment Act was enacted by the California Legislature to identify toxic air contaminant hot spots where emissions from specific sources may expose individuals to elevated risk of adverse health effects. The State Department of Health Services and the Air Resources Board work together to administer the provisions of this Act statewide, but its implementation and enforcement are the responsibility of local/regional air districts. The Act requires that a business or other establishment, identified as a significant source of toxic emissions, notify the affected population and provide them with information about health risks posed by the emissions. (While not part of the Hot Spots program, the State of California Health and Safety Code, Section 25534 allows "Administering Agencies" — usually county health departments — to require "Risk Management and Prevention Plans" of facilities which handle hazardous materials.) Appendix E provides further information on the Air Toxics "Hot Spots" program.

California Planning Law and Guidelines. The State of California does not require air quality elements for general plans. Seven elements are mandated by the California Government Code. Air quality is mentioned as an optional issue in the "Conservation" element. Nonetheless, the District has been urging all cities and counties in the Bay Area to include an air quality element or section in their general plans since 1986.

One of the most important features of California general plans is that even though air quality elements are not mandated, general plans are required by law to be consistent with any air

quality policies and programs that exist within local jurisdiction. Local plans must also be consistent with regional air quality plans such as the Bay Area Clean Air Plan.

California Transportation Plan. The most recent State transportation plan prepared by Caltrans addresses air quality, and cites the funding of transportation control measures (TCMs) as a high priority. In addition, telecommuting is promoted as well as other "nonstructural" transportation solutions such as: reducing demand, increasing transit service, and implementing market-based measures (e.g., a demonstration project of congestion pricing on the San Francisco-Oakland Bay Bridge).

BAY AREA REGIONAL AGENCIES AND THEIR PROGRAMS

Bay Area Air Quality Plan, 1979 and 1982. The *Bay Area Air Quality Plan* is a regional plan required by the federal government. It is prepared jointly by the District, the Metropolitan Transportation Commission (MTC), and the Association of Bay Area Governments (ABAG) to address how the Bay Area will attain the NAAQS. The plan contains stationary source controls, motor vehicle emission controls, and transportation system improvement measures that would reduce the amount of air pollutants released into the atmosphere. These measures are implemented primarily by the District, ARB and MTC, respectively.

The federal Clean Air Act (1970, 1977) required the District, MTC and ABAG to prepare the first Bay Area Air Quality Plan in 1979 and then amend it in 1982. Its primary objective was to attain NAAQS by 1987. The 1982 Air Quality Plan required that: (1) major stationary sources install emission control devices, (2) new sources apply for air quality permits, (3) registered Bay Area vehicles pass a vehicle inspection and maintenance program (e.g., "Smog Check") every two years, (4) transportation control measures be implemented, and (5) MTC assess the conformity of regional transportation plans, programs and projects to air quality objectives.

Although these requirements resulted in significant air quality improvement, the Bay Area failed to attain NAAQS for carbon monoxide and ozone by 1987. In 1989, in response to a court order, MTC implemented contingency measures to assure that the Bay Area was making all reasonable further progress toward attaining NAAQS. These measures included additional transportation control measures and a revised conformity assessment procedure.

Ozone Maintenance Plan, 1993. Through 1989, the Bay Area air basin had continued to violate the national ozone standard. Under the 1990 federal Clean Air Act amendments, the Bay Area was classified as a “moderate” nonattainment area for the national ozone standard. But because of significant improvements in Bay Area air quality over the last couple of decades, the number of exceedances of the national ozone standard declined greatly. Air quality monitoring data from 1990 to 1994 indicated that the region had attained the national ozone standard. Based on monitoring data collected from 1990 to 1992, the District, MTC and ABAG requested in 1993 that the U.S. EPA redesignate the Bay Area as an attainment area and approve the Ozone Maintenance Plan. In June, 1995 U.S. EPA approved the

request and the Bay Area was redesignated an attainment area with respect to the national ozone standard. EPA also approved the Ozone Maintenance Plan.

Ozone Attainment Plan, 1999. Hot stagnant weather in the summers of 1995 and 1996 led to exceedances of the national 1-hour ozone standard, leading U.S. EPA in 1998 to redesignate the region back into nonattainment status for the national 1-hour ozone standard. EPA's redesignation required the region to prepare a plan with three principal elements: 1) a 1995 emission inventory for ROG and NO_x, 2) an assessment of the reductions in these precursor pollutants needed to attain the national standard by 2000 ("attainment assessment"), and 3) a control strategy of adopted regulations and/or control measures sufficient to meet reasonable further progress and attain the 1-hour standard no later than November 15, 2000. The attainment assessment estimates the amount by which ROG and NO_x emissions must be reduced between 1995 and 2000 in order to meet the national 1-hour ozone standard of 0.12 parts per million, and the control strategy describes how these reductions will be achieved.

The *San Francisco Bay Area Ozone Attainment Plan* was prepared by the three co-lead agencies: the District, MTC and ABAG. The Plan includes control measures to reduce emissions from stationary, area and mobile sources sufficient to achieve the necessary emission reductions by June 2000. The Plan also includes contingency measures in case the control measures do not result in attainment by the deadline. The Plan was adopted by the co-lead agencies in June 1999. The Plan was approved by ARB in July 1999 and transmitted to U.S. EPA.

Carbon Monoxide Maintenance Plan, 1994. From 1992 to 1998, no District monitor has registered an exceedance of the national carbon monoxide standard. A *San Francisco Bay Area Redesignation Request and Maintenance Plan for the National Carbon Monoxide Standard* was adopted in 1994 by the three regional agencies. In 1998, U.S. EPA redesignated the Bay Area as an attainment area for the national CO standard.

Bay Area Clean Air Plan, 1997. The *Bay Area 1997 Clean Air Plan* (CAP) was prepared pursuant to the 1988 California Clean Air Act. Prepared by the District in cooperation with MTC and ABAG, its main objective is to attain the State air quality standards for ozone. The CAP presents a comprehensive strategy to reduce emissions from stationary, area and mobile sources. The CAP includes a specific measure which encourages cities and counties to develop and implement local plans, policies and programs to reduce auto use and improve air quality. The California Clean Air Act requires regions to update their (State) air quality plans every three years. The CAP will be updated in 2000.

Under the California Clean Air Act nonattainment classifications, the Bay Area is classified as a "serious" air basin for ozone. (The state classification system for nonattainment areas uses the designations "Moderate," "Serious," "Severe," and "Extreme.") The region had been classified a "moderate" air basin for CO, but the region was redesignated an attainment area

for the State CO standard in 1994 and thus the Act's planning requirements for CO nonattainment areas no longer apply to the Bay Area. The CAP must indicate how the District will attain the State ozone standard by the earliest practicable date, including: (1) additional control measures for existing stationary sources, (2) a permitting program that will result in no net increase in emissions from new stationary sources, (3) provisions for indirect source controls, and (4) transportation control measures.

The prime objective of transportation control measures (TCMs) is to reduce vehicle trips and vehicle miles traveled within the region. These measures are geared toward the following: (1) trip reduction, (2) mobility improvements, (3) implementation support, (4) traffic operation management, (5) user incentives, and (6) pricing strategies.

The CAP also strives to reduce emissions by implementing additional and more stringent stationary source control measures. These include measures to control emissions from surface coating and solvent use, fuels/organic liquids storage and distribution, refinery and chemical processes, combustion of fuels, and other industrial/commercial processes.

The California Clean Air Act expanded the scope and accelerated the pace of air pollution control efforts in California. If possible, air quality plans should achieve a reduction in district-wide emissions of 5% per year for each nonattainment pollutant or its precursors. As an alternative strategy (employed in the Bay Area CAP), the adoption of all feasible measures on an expeditious schedule is acceptable, even if a district is unable to achieve 5% annual reduction.

Other legal requirements applicable to the Bay Area include the following:

- Indirect source and area source control programs.
- A regional public education program.
- Transportation controls to achieve a 1.4 average vehicle ridership during weekday commute hours by 1999, substantial reduction in the rate of increase of vehicle trips and vehicle miles traveled and no net increase in motor vehicle emissions after 1997.
- An assessment of cost-effectiveness of proposed control measures.
- Transport mitigation requirements.

Toxic Air Contaminant Control Program. The Toxic Air Contaminant Control Program is a regional program administered by the District. Its main objective is to reduce public exposure to toxic air contaminants. Appendix E provides further information on the District's Air Toxics program.

Odorous Substances Regulation. The District has enacted an odorous substance control program as part of its effort to control the use and emission of odorous substances within the Bay Area. This program places general limitations on odorous substances and provides the

District with authority to respond to public complaints about offensive odors. The regulation is intended to help the public identify and control offensive odors that are not otherwise controlled by other federal or State air quality laws.

Regional Transportation Plan, 1994. The Metropolitan Transportation Commission's Regional Transportation Plan (RTP) guides Bay Area transportation system improvement projects and shows how they will help attain regional air quality objectives. The plan promotes projects that will provide reasonable and predictable mobility within the region, ensure that all people have equitable access to transportation, support a healthy environment and mitigate any adverse impacts, and promote economic vitality within the region. The plan identifies and evaluates the Bay Area Metropolitan Transportation System, a network of regionally significant streets and highways, transit systems and intermodal transfer facilities, and recommends projects that will improve its performance. Many of these recommendations implement federal (1982 Bay Area Air Quality Plan and contingencies) and state ('94 CAP) TCMs.

Congestion Management Program. Each county in the state is required to establish a Congestion Management Agency (CMA) and prepare a Congestion Management Program (CMP). The main goals of the CMP are to establish a political process through which countywide roadway congestion can be controlled or relieved, and to develop a comprehensive strategy to respond to countywide transportation needs. State law requires that each CMA prepare, implement and biennially update the CMP. The CMP consists of the following basic elements: (1) a transportation network that includes State highways and principal arterials, (2) traffic level of service (LOS) standards for the CMP network, (3) performance measures to evaluate current and future multimodal system performance for the movement of people and goods, (4) a travel demand program to promote travel by alternative transportation modes (non-single-occupancy vehicle), (5) a land use impact analysis program to evaluate land use development impacts on the CMP network, and (6) a multi-year capital improvement program (CIP) to fund transportation projects that support CMP goals. The CMP must be updated biennially to reflect changing transportation needs and conditions within the county. The CMP CIP must be submitted to MTC every two years to be incorporated into the Bay Area Regional Transportation Improvement Program.

If traffic conditions on a roadway segment or intersection fall below the LOS standard, the local jurisdiction is required to develop a Deficiency Plan. In some instances, cities and counties may be monitoring LOS based upon transportation models, attempting to predict conditions in the future. The intent is to develop plans for deficient segments prior to the actual occurrence of a deficiency. The CMP statutes direct the District to establish and periodically update a list of improvements, programs and actions which can be used by local governments in developing Deficiency Plans. The list should include items that "...measurably improve multimodal performance, and contribute to significant improvements in air quality, such as improved public transit service and facilities, improved non-motorized transportation facilities, high occupancy vehicle facilities, parking cash out programs, and transportation control measures." The statutes also state that "if an improvement, program, or action is not on the approved list, it shall not be implemented unless approved by the local

air quality management district." In 1992, the District prepared the *Deficiency List: Programs, Actions and Improvements for Inclusion in Congestion Management Program Deficiency Plans.* Subsequent consultation with Bay Area CMAs has not indicated a need to revise the deficiency list.

Transportation Fund for Clean Air (AB 434). Assembly Bill 434 (Sher, 1991) established a vehicle registration surcharge to fund specified TCMs. This bill gave the District the authority to impose a $4 surcharge on motor vehicle registrations within the Bay Area to pay for programs that reduce mobile source emissions. These fees generate approximately $17 million per year. The District directly allocates 40 percent of the funds to county program managers who then distribute the funds to agencies sponsoring eligible projects. The District allocates the remaining 60 percent regionwide to public agencies sponsoring the most cost-effective projects.

The projects and programs eligible for AB 434 funds are: (1) ridesharing and trip reduction programs, (2) clean fuel buses for schools and transit operators; (3) feeder bus/shuttle service to rail and ferry stations and airports; (4) local arterial traffic management; (5) rail-bus integration and regional transit information; (6) congestion pricing and low emission vehicle demonstration projects; (7) vehicle buy back; (8) a smoking vehicle program (citizen reports to the District about vehicles with visible exhaust); and (9) bicycle facility improvements.

APPENDIX B - AIR POLLUTANT SOURCES AND EFFECTS

This appendix discusses the harmful effects of air contaminants on health and other qualities of life and the environment. Sources of air pollution are described. Appendix C provides more detailed information on air pollutant emissions in the Bay Area.

CRITERIA CONTAMINANTS — HEALTH EFFECTS AND SOURCES

Criteria contaminants are those air pollutants for which ambient air quality standards have been set by the United States Environmental Protection Agency or the California Air Resources Board. Most of the criteria contaminants are generated to a large degree by motor vehicles, as well as by industry and other stationary sources. Appendix C provides further detail regarding the sources of each criteria contaminant in each county of the Bay Area.

Carbon Monoxide (CO) is an odorless, colorless gas. It is formed by the incomplete combustion of fuels. The single largest source of CO is the motor vehicle. Emissions are highest during cold starts, hard acceleration, stop-and-go driving, and when a vehicle is moving at low speeds. New findings indicate that CO emissions per mile are lowest at about 45 mph for the average light-duty motor vehicle and begin to increase again at higher speeds.

When inhaled at high concentrations, CO combines with hemoglobin in the blood and reduces the oxygen-carrying capacity of the blood. This results in reduced oxygen reaching the brain, heart and other body tissues. This condition is especially critical for people with cardiovascular diseases, chronic lung disease or anemia, as well as fetuses. Even healthy people exposed to high CO concentrations can experience headaches, dizziness, fatigue, unconsciousness, and even death.

Ozone (O_3), or smog, is not emitted directly into the environment, but is formed in the atmosphere by complex chemical reactions between oxides of nitrogen and reactive organic gases (ROG) in the presence of sunlight. Ozone formation is greatest on warm, windless, sunny days. The main sources of nitrogen oxides (NO_X) and ROG, often referred to as ozone precursors, are combustion processes (including motor vehicle engines) and the evaporation of solvents, paints and fuels. As with CO, automobiles are the single largest source of ozone precursors in the Bay Area. Tailpipe emissions of ROG follow CO. They are highest during cold starts, hard acceleration, stop-and-go conditions, and slow speeds. They decline as speeds increase up to about 50 mph, then increase again at high speeds and high engine loads. ROG emissions associated with evaporation of unburned fuel depends on vehicle and ambient temperature cycles. Nitrogen oxide emissions exhibit a different curve; emissions decrease as the vehicle approaches 30 mph and then begin to increase with increasing speeds.

Ozone levels usually build up during the day and peak in the afternoon hours. Short-term exposure can irritate the eyes and cause constriction of the airways. Besides causing shortness of breath, it can aggravate existing respiratory diseases such as asthma, bronchitis and emphysema. Chronic exposure to high ozone levels can permanently damage lung tissue. Ozone can also damage plants and trees, and materials such as rubber and fabrics (see Non-Health Effects, below).

Nitrogen dioxide (NO_2) is a reddish brown gas that is a by-product of combustion processes. Automobiles and industrial operations are the main sources of NO_2. Aside from its contribution to ozone formation, nitrogen dioxide can increase the risk of acute and chronic respiratory disease and reduce visibility. NO_2 may be visible as a coloring component of a brown cloud on high pollution days, especially in conjunction with high ozone levels.

Sulfur dioxide (SO_2) is a colorless acid gas with a strong odor. It has potential to damage materials and it can have health effects at high concentrations. It is produced by the combustion of sulfur-containing fuels, such as oil, coal and diesel. Sulfur dioxide can irritate lung tissue and increase the risk of acute and chronic respiratory disease.

PM_{10} (Particulate matter 10 microns or less in diameter) refers to a wide range of solid or liquid particles in the atmosphere, including smoke, dust, aerosols, and metallic oxides. Some particulate matter, such as pollen, is naturally occurring. However, in the Bay Area most particulate matter is caused by combustion, factories, construction, grading, demolition, agricultural activities and motor vehicles. Extended exposure to particulate matter can increase the risk of chronic respiratory disease. PM_{10} is of concern because it bypasses the body's natural filtration system more easily than larger particles, and can lodge deep in the lungs. Thus, the U.S. EPA and the state of California revised their PM standards several years ago to apply only to these fine particles.

As with CO and ozone precursors, motor vehicles constitute the single largest source of PM_{10} in the Bay Area, based on the best available data. Motor vehicles produce particulates through direct tailpipe emissions of particulate matter; direct emissions of nitrogen oxides, which become particulate ammonium nitrate in the atmosphere; and the kicking up of road dust by tires. Vehicles also produce PM_{10} from brake pad and tirewear. Motor vehicles are currently responsible for about half of Bay Area particulates.

Fine particulate pollution is an example of a problem that is projected to increase in the Bay Area as motor vehicle use increases, though there may be short-term decreases. For instance, when construction activity is reduced during a recession, direct construction dust is reduced. Therefore there is less dirt spilled on roads via trucks and other mobile equipment, reducing the amount of dust that can be resuspended by the tires of passing motor vehicles. But, as seen in the graph of Bay Area Emissions Inventory Projections (in Appendix C), total PM_{10} emissions are expected to increase, and the proportion attributable to motor vehicles will also increase. Resuspended road dust has not been reduced by improvements in motor vehicle air pollution controls. In fact, road dust is expected to continue to increase unless there is a reduction in motor vehicle use and adoption of dust control measures. Dust control measures may be needed at construction sites, unpaved roads and parking lots, agricultural and other area sources that emit dust directly into the ambient air and/or convey mud and dirt to roadways.

Wood burning in fireplaces and stoves is another large source of fine particulates. The District and consultants have recently analyzed the results of a study of the sources of particulates at two monitoring sites in San Jose. In and near downtown San Jose — and

perhaps in many other parts of the Bay Area — wood smoke can contribute up to 40% of the particulate mix during the winter months. Wood burning alone may cause exceedances of California's particulate standard.[19]

Among the criteria pollutants that the District regulates, particulates appear to represent the most serious overall health hazard. Studies in a number of cities have demonstrated statistically significant correlations between daily and average annual particulate levels and mortality. According to one estimate, elevated particulate levels contribute to the death of approximately 200 people annually for the Bay Area.[20] Other studies, which include findings from the Bay Area, yield higher estimates of mortality — 300 to 500 deaths per year in the Bay Area — based on a one percent increase in mortality per 10 micrograms per cubic meter increase in PM_{10} levels.[21][22] High levels of particulates have also been known to exacerbate chronic respiratory ailments, such as bronchitis and asthma, and have been associated with increased emergency room visits and hospital admissions.

TOXIC AIR CONTAMINANTS

In addition to the *criteria pollutants* listed above, another group of pollutants, commonly referred to as toxic air contaminants (TACs) or hazardous air pollutants, has received increasing scrutiny in recent years and warrant concern for several reasons. First, the health effects can be quite severe. Many hazardous air pollutants are confirmed or suspected carcinogens, or are known or suspected to cause birth defects or neurological damage. Secondly, many hazardous air pollutants can be toxic at very low concentrations. For some chemicals, such as carcinogens, there are no thresholds below which exposure can be considered risk-free.

Industrial facilities are significant sources of toxic air contaminants. Rather than coming out of a smokestack, however, toxic contaminants often result from "fugitive emissions," such as leaking valves and pipes. The electronics industry, including semiconductor manufacturing, has the potential to contaminate both air and water due to the highly toxic chlorinated solvents commonly used in semiconductor production processes. Sources of air toxics go beyond industry, however. Various common urban facilities also produce hazardous pollutants, such as gasoline stations (benzene), hospitals (ethylene oxide), and dry cleaners (perchloroethylene). Automobile exhaust also contains toxic air pollutants such as benzene and 1,3-butadiene. (Lead as a gasoline additive has been phased out in California). District research indicates that mobile source emissions of benzene and 1,3-butadiene represent a substantial portion of the ambient background risk from toxic air contaminants in the Bay

[19]Chow, Judith, and David Fairley et al., "Source Apportionment of Wintertime PM_{10} at San Jose, California," Journal of Environmental Engineering, May 1995.

[20]Fairley, David, "The Relationship of Daily Mortality to Suspended Particulates in Santa Clara County, 1980-1986," Environmental Health Perspectives, Vol. 89, 1990.

[21]Ostro, Bart, "The Association of Air Pollution and Mortality: Examining the Case for Inference," Archives of Environmental Health, September/October 1993.

[22]Dockery, Douglas and C.A. Pope III, "Acute Respiratory Effects of Particlate Air Pollution," Annual Review of Public Health, 1994.

Area. Reformulated fuel requirements that have already been adopted are expected to reduce, but not eliminate, mobile source TAC emissions.

NON-HEALTH EFFECTS OF AIR POLLUTION

Visibility Reduction

Visibility reduction and discoloration of the sky are obvious effects of air pollution. Reduced visibility may be caused by the brownish haze of nitrogen dioxide or by the accumulation of particulate matter in the atmosphere. When particles are present in sufficient quantities, distant objects become obscured. Visibility reduction is primarily caused by emissions from the following sources:

- Construction and demolition.
- Auto exhaust, diesel soot, and resuspended road dust.
- Wood burning, incineration, and other combustion activities.
- Particles or aerosols formed by photochemical reactions occurring in the atmosphere.
- Agricultural and mining activities.
- Stationary sources such as cement kilns and refineries.
- Naturally occurring particles from salt water, vegetation, soil, and wind erosion processes.
- Atmospheric particles, normally too small to affect visibility, which grow to visibility-reducing size through the process of agglomeration (clustering) or through condensation, where moisture condenses on small particles causing them to grow to visibility-reducing size.

Visibility in the Bay Area can vary dramatically, depending on meteorological conditions. The major factors causing these fluctuations are the amount of moisture in the air, the strength of the air currents, and the volume of air available for dilution and dispersion of visibility-reducing particles. Under adverse weather conditions, particularly high heat and intense sunlight, some or all of the factors discussed above cause visibility to become very restricted. These conditions are especially common in summer and early fall.

During the winter months, visibility-reducing particles from photochemical activity are greatly diminished due to colder temperatures and the decreased intensity of ultraviolet light. Thus, when restricted visibility occurs during this period, it is often caused by smoke and dust particles and the growth of particles through agglomeration and condensation.

Effects on Materials

Air pollution effects on materials vary widely in type and severity among the different contaminants. For example, ozone, the primary constituent of photochemical smog, can

harden and crack rubber materials, causing them to lose their flexibility. It also affects other types of synthetic materials. For example, it can weaken nylon, and can cause fabric dye fading and paint damage.

Other pollutants in combination produce synergistic effects, causing greater damage than each could cause alone. The interaction of sulfur dioxide and particulate matter has a greatly enhanced ability to corrode materials such as steel, iron, copper, zinc, tin, and stone. In some industries, extensive measures must be taken to protect equipment from polluted air. In the aerospace industry, for example, where silver and other metals used in sensitive electronic equipment are particularly vulnerable to corrosion, great care must be taken to protect components.

Particles settling on buildings, automobiles, outdoor furniture, and other surfaces are usually considered to be nuisances causing soiling, even when they do not produce damage to health or materials.

Plant Damage

The effects of air pollution on plants, crops, and forests depend both on plant susceptibility and the types of pollutants involved. Plant damage is difficult to assess because damage is often manifested as stunted growth or diminished yields, rather than the death of the plant.

Among the recorded effects of air pollution on plants are flower and foliage discoloration; bloom failure; plant malformation; leaf, needle, and fruit drop; and failure of fruit to ripen. Particularly vulnerable to ozone damage are grapes, lettuce, spinach and many garden flowers and shrubs. Additionally, some greenhouse crops, including flowers and some herbs, suffer damage when certain hydrocarbon levels are elevated.

Localized plant damage has been noted in the Bay Area from other gases, including nitric oxide, hydrogen chloride, formaldehyde, sulfur dioxide, and fluorides. Sulfur dioxide, for example, is particularly damaging to pasture crops and leafy vegetables. And although a highly localized problem, fluoride threatens both plants and animals. The susceptibility of plants to fluoride damage varies greatly; apricots, grapes, strawberries, bulb crops, and conifers have low resistance. The more serious effect is seen in animals, who may consume fodder that offers no detectable signs of damage but in fact contains relatively high concentrations of fluorides. Over a period of time, animals build up a concentration of fluorides in their tissues, which eventually leads to fluorosis, a bone disease.

APPENDIX C - AIR POLLUTION — STATUS, PROBLEMS AND TRENDS

Monitoring Data and Attainment Status

The District operates a regional air quality monitoring network that regularly measures the concentrations of the five major criteria air pollutants. Figure C-1 indicates the location of the District's permanent monitoring stations and lists the pollutants monitored at each station. Tables C-1, C-2, C-3 and C-4 summarize the exceedance records for the last decade for ozone, CO and PM_{10}.

Air quality conditions in the San Francisco Bay Area have improved significantly since the District was created in 1955. Ambient concentrations and the number of days on which the region exceeds standards have declined dramatically. Following years of declining emissions and ambient concentrations, the Bay Area in 1995 was redesignated as an attainment area for the national 1-hour ozone standard. However, hot stagnant weather led to new exceedances of the national ozone standard in the summers of 1995 and 1996. As a result, U.S. EPA in 1998 redesignated the region back as a nonattainment area for the national 1-hour ozone standard. Table C-1 summarizes recent monitoring data with respect to the national 1-hour ozone standard.

The Bay Area also violates the State ozone standard. The State 1-hour ozone standard, 9 parts per hundred million (9 pphm), is considerably more stringent than the national standard of 12 pphm. Table C-2 indicates the number of days the State ozone standard has been exceeded in recent years.

The region has made significant progress in reducing carbon monoxide levels in the Bay Area. The District's air monitoring records of 1992 through 1998 demonstrate attainment of the national and State 8-hour standard, and neither the national 1-hour standard nor the State 1-hour standard has been exceeded since the 1980s. The Bay Area is now an attainment area for the State and national CO standard. Table C-3 summarizes recent monitoring data for the State and national CO standard.

With regard to fine particulate matter (PM_{10}), the State standard has been exceeded fairly frequently in recent years. The national standard was exceeded a few times in 1990 and 1991, but has not been exceeded since then. Table C-4 summarizes recent monitoring data for the State and national PM_{10} standards.

Additional criteria pollutants include nitrogen dioxide, sulfur dioxide, sulfates, lead, hydrogen sulfide, and vinyl chloride (chloroethane). Neither State nor national ambient air quality standards of these chemicals have been violated in recent decades. Table 1 (in Chapter 1 of these Guidelines) summarizes the Bay Area's attainment status for the State and national ambient air quality standards.

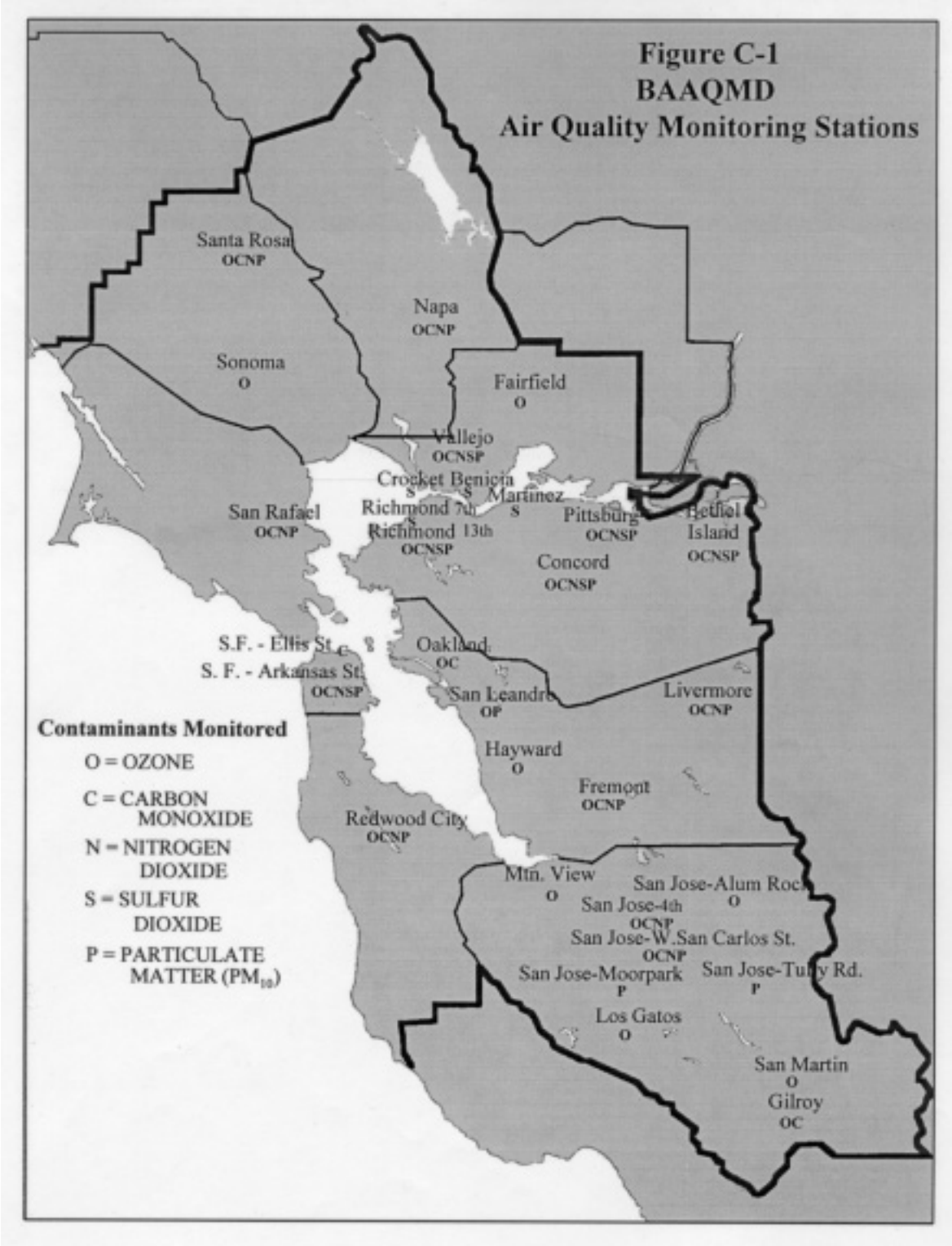

Figure C-1
BAAQMD
Air Quality Monitoring Stations
Santa Rosa
OCNP
Napa
OCNP
Sonoma
O
Fairfield
O
Vallejo
OCNSP
Crocket
S
Benicia
S
Martinez
S
San Rafael
OCNP
Richmond 7th
S
Richmond 13th
OCNSP
Pittsburg
OCNSP
Bethel Island
OCNSP
Concord
OCNSP
S.F. - Ellis St.
C
S. F. - Arkansas St.
OCNSP
Oakland
OC
San Leandro
OP
Livermore
OCNP
Hayward
O
Fremont
OCNP
Redwood City
OCNP
Mtn. View
O
San Jose-Alum Rock
O
San Jose-4th
OCNP
San Jose-W.San Carlos St.
OCNP
San Jose-Moorpark
P
San Jose-Tully Rd.
P
Los Gatos
O
San Martin
O
Gilroy
OC
Contaminants Monitored
O = OZONE
C = CARBON MONOXIDE
N = NITROGEN DIOXIDE
S = SULFUR DIOXIDE
P = PARTICULATE MATTER (PM_{10})

TABLE C-1
EXCEEDANCES OF THE NATIONAL OZONE STANDARD
Number Of Days With Maximum One-Hour Concentration Exceeding 12 Parts Per Hundred Million (pphm)
1988 - 1998

County	Site	1988	1989	1990	1991	1992	1993	1994	1995	1996	1997	1998
Alameda County	Fremont	1	0	1	0	0	1	0	2	0	0	0
	Hayward	0	0	0	0	1	0	0	2	0	0	0
	Livermore	4	2	1	1	0	1	2	7	8	0	6
	Oakland	0	0	0	0	0	0	0	0	0	0	0
	San Leandro	0	0	0	0	0	0	0	3	0	0	0
Contra Costa County	Concord	1	0	0	0	0	2	0	3	1	0	2
	Pittsburg	0	0	0	0	0	1	0	0	0	0	0
	Richmond	0	0	0	0	0	0	0	0	0	-	-
	Bethel Island	0	0	0	0	0	0	0	1	1	0	0
Marin County	San Rafael	0	0	0	0	0	0	0	0	0	0	0
Napa County	Napa	0	0	0	0	0	0	0	1	0	0	1
San Francisco	San Francisco	0	0	0	0	0	0	0	0	0	0	0
San Mateo County	Redwood City	0	0	0	0	0	0	0	1	0	0	0
Santa Clara County	Mountain View	0	0	0	0	0	0	0	0	0	0	0
	San Martin	-	-	-	-	-	-	1	1	0	0	3
	Gilroy	1	2	0	1	0	0	0	1	0	0	2
	Los Gatos	1	0	0	0	1	1	0	4	1	0	1
	San Jose-4th Street	0	1	0	0	0	0	0	1	0	0	1
	San Carlos St./ Burbank	-	-	1	0	0	1	0	-	-	-	-
	Alum Rock	0	0	0	0	1	0	0	3	-	-	-
Solano County	Fairfield	1	0	0	0	0	1	0	1	0	0	0
	Vallejo	0	0	0	0	0	0	0	1	0	0	0
Sonoma County	Santa Rosa	0	0	0	0	0	0	0	0	0	0	0
	Sonoma	0	0	0	0	0	0	0	0	0	-	-
AIR DISTRICT DAYS		5	4	2	2	2	3	2	11	8	0	8

"*AIR DISTRICT DAYS*" are the number of days in a year that one or more monitoring stations recorded an exceedance. Air District Days are not usually the sums of the numbers above them in the column because two or more monitoring stations often record exceedances during the same day. More than three exceedances in three years, at any one monitoring station, rates a federal classification of "nonattainment" for ozone for the entire air basin.

- = Monitor not operational.

TABLE C-2
EXCEEDANCES OF THE STATE OZONE STANDARD
Number Of Days With Maximum One-Hour Concentration Exceeding 9 Parts Per Hundred Million (pphm)
1988-1998

County	Site	1988	1989	1990	1991	1992	1993	1994	1995	1996	1997	1998
Alameda County	Fremont	7	11	3	6	5	5	4	10	2	2	7
	Hayward	9	1	0	2	1	0	1	7	2	2	4
	Livermore	21	9	8	17	14	7	5	20	22	3	21
	Oakland	1	0	0	0	0	1	0	0	0	0	0
	San Leandro	0	0	0	2	2	3	0	6	2	3	2
Contra Costa County	Concord	10	6	3	4	3	7	4	9	11	2	13
	Pittsburg	8	5	4	0	3	4	3	8	5	0	4
	Richmond	2	1	0	0	0	2	0	0	0	-	-
	Bethel Island	7	11	5	3	7	3	5	6	6	1	10
Marin County	San Rafael	1	0	0	0	0	0	0	0	2	1	0
Napa County	Napa	1	2	0	3	0	2	0	4	0	0	3
San Francisco	San Francisco	0	0	0	0	0	0	0	0	0	0	0
San Mateo County	Redwood City	2	1	0	0	0	1	0	5	1	0	0
Santa Clara County	Mountain View	13	6	1	3	1	2	0	2	3	1	2
	San Martin	-	-	-	-	-	-	5	14	18	0	15
	Gilroy	23	10	5	5	12	6	3	10	15	1	10
	Los Gatos	12	1	5	7	3	8	2	13	10	1	5
	San Jose-4th St.	12	10	4	6	3	3	2	14	5	0	4
	San Carlos St./ Burbank	-	-	5	0	1	4	1	-	-	-	-
	Alum Rock	13	9	1		5	5	3	15	-	-	-
Solano County	Fairfield	3	4	1	3	3	3	2	10	5	0	9
	Vallejo	5	2	2	2	1	3	2	6	5	1	3
Sonoma County	Santa Rosa	0	0	0	0	0	0	0	1	0	0	0
	Sonoma	2	3	0	3	0	0	0	0	0	-	-
AIR DISTRICT DAYS		41	22	14	23	23	19	13	28	34	8	29

"*AIR DISTRICT DAYS*" are the number of days in a year that one or more monitoring stations recorded an exceedance. Air District Days are not usually the sums of the numbers above them in the column because two or more monitoring stations often record exceedances during the same day.

- = Monitor not operational.

TABLE C-3
EXCEEDANCES OF NATIONAL AND STATE* CARBON MONOXIDE STANDARD
Number Of Days With Maximum 8-Hour Concentration Exceeding 9 Parts Per Million (ppm)
1988-1998

County	Site	1988	1989	1990	1991	1992	1993	1994	1995	1996	1997	1998
Alameda County	Fremont	0	0	0	0	0	0	0	0	0	0	0
	Livermore	0	0	0	0	0	0	0	0	0	0	0
	Oakland	0	0	0	0	0	0	0	0	0	0	0
Contra Costa County	Concord	0	0	0	0	0	0	0	0	0	0	0
	Pittsburg	0	0	0	0	0	0	0	0	0	0	0
	Richmond	0	0	0	0	0	0	0	0	0	-	-
	Bethel Island	0	0	0	0	0	0	0	0	0	0	0
Marin County	San Rafael	0	0	0	0	0	0	0	0	0	0	0
Napa County	Napa	0	0	0	0	0	0	0	0	0	0	0
San Francisco	Arkansas St./ Potrero	0	0	0	0	0	0	0	0	0	0	0
	Ellis Street	1	0	0	0	0	0	0	0	0	0	0
San Mateo County	Redwood City	0	0	0	0	0	0	0	0	0	0	0
Santa Clara County	Gilroy	0	0	0	0	0	0	0	-	-	-	-
	San Jose-4th St.	2 (3)	6	2 (5)	4	0	0	0	0	0	0	0
	San Carlos St./ Burbank	-	-	0	0	0	0	0	-	-	-	-
Solano County	Vallejo	1	2	0	0 (1)	0	0	0	0	0	0	0
Sonoma County	Santa Rosa	0	0	0	0	0	0	0	0	0	0	0
AIR DISTRICT DAYS		3 (4)	8	2 (5)	4 (5)	0	0	0	0	0	0	0

*The recorded number of exceedances of the State — as differentiated from the National — Carbon Monoxide 8-Hour Ambient Air Quality Standard is sometimes slightly higher due to prescribed procedures for calculating each. The State Standard is given as 9.0 ppm and is considered to be exceeded when a monitor records a CO 8-hour average level of 9.1 or higher. The National Standard is given as 9 ppm and is considered to be exceeded at a level of 9.5 ppm or higher. In the table above, when the number of days of exceedance in a year differed among the two, the number of days exceeding the State Standard is given in parentheses.

"AIR DISTRICT DAYS" are the number of days in a year that one or more monitoring stations recorded an exceedance of the ambient air quality standard for CO. Air District Days are not usually the sums of the numbers above them in the column because two or more monitoring stations often record exceedances during the same day. More than one exceedance per year, at any one monitoring station, rates a federal classification of "nonattainment" for CO.

- = Monitor not operational.

TABLE C-4
EXCEEDANCES OF THE STATE AND NATIONAL* FINE PARTICULATE MATTER STANDARD
Number Of Days With Maximum 24-Hour Concentration Exceeding 50 micrograms per cubic meter ($\mu g/m^3$)
1988 - 1998

County	Site	1988	1989	1990	1991	1992	1993	1994	1995	1996	1997	1998
Alameda County	Fremont	-	5	10	14	4	3	3	1	1	1	1
	Livermore	7	13	10	12 (1)	5	3	4	1	1	2	2
	San Leandro	-	-	-	10	2	1	1	0	1	1	0
Contra Costa County	Concord	10	9	6	13	8	2	4	1	1	2	1
	Richmond	-	5	5	9	3	3	3	1	0	-	-
	Bethel Island	14	7	7	10	4	6	3	3	1	2	2
Marin County	San Rafael	2	8	4	10	5	1	4	1	0	2	1
Napa County	Napa	8	9	8	11	5	3	2	1	1	3	1
San Francisco	San Francisco	7	13	12 (1)	15	9	5	6	0	2	0	1
San Mateo County	Redwood City	5	10	8	12	7	5	6	0	0	2	0
Santa Clara County	San Jose-4th St.	14	15	9 (1)	10	13	10	7	4	2	3	3
	Moorpark	8	13	11	13	8	3	4	1	1	3	-
	San Carlos St./ Burbank	-	7	9	14	9	5	6	-	-	-	-
	Tully Road	-	-	11 (1)	11	11	7	7	0	1	3	1
Solano County	Vallejo	-	-	-	-	-	-	1	1	0	3	1
Sonoma County	Santa Rosa	-	-	-	-	-	-	1	0	0	2	1
AIR DISTRICT DAYS		24	21	15 (3)	18 (1)	18	10	9	7	3	4	5

*In instances when the National PM_{10} 24-Hour Standard (150 $\mu g/m^3$) has been exceeded, the number of days of exceedance of the National Standard is given in parentheses.

"AIR DISTRICT DAYS" are the number of days in a year that one or more monitoring stations recorded an exceedance. Air District Days are not usually the sums of the numbers above them in the column because two or more monitoring stations often record exceedances during the same day. PM_{10} is only sampled every sixth day. Actual days over standards can be estimated as six times the number shown.

- = Monitor not operational.

Problems and Trends

Throughout the Bay Area, automobile ownership and use is increasing at a faster rate than population growth. Countering this trend is the move toward cleaner, newer vehicles with fleet turnover and the introduction of cleaner fuels. Overall, projections indicate a net reduction in the emissions of ozone precursors and carbon monoxide, while fine particulate emissions are expected to increase with total miles traveled.

Table C-5 shows projected future emissions of criteria pollutants for the Bay Area for the years 1995, 2000, 2005 and 2010 in terms of total emissions and motor vehicle emissions. Total emissions and the amount and proportion attributable to motor vehicles are expected to decline, especially for reactive organic gases (ROG), nitrogen oxides (NO_x) and carbon monoxide. A small increase is predicted for SO_2 emissions. Most significant is the predicted increase in PM_{10} emissions.

Regionally, the most complex air quality problem has been ozone. Ozone is formed in the atmosphere through a complex series of photochemical reactions involving ROG and NO_x. Because it takes some time for the photochemical reactions to occur, emissions of ROG and NO_x are transported away from their sources and affect ozone concentrations in downwind areas. Motor vehicles account for the majority of the ROG and NO_x emissions. Although the Bay Area's highest ozone levels can fluctuate from year to year depending on weather conditions, ambient ozone standards are exceeded most often in the Santa Clara, Livermore and Diablo valleys.

In contrast to ozone, carbon monoxide (CO) is a more localized concern in the Bay Area, because CO is a nonreactive pollutant with one major source — motor vehicles. Approximately 70 percent of CO in the Bay Area is generated by motor vehicles. The areas with the highest CO levels typically have been those with high levels of vehicular traffic. CO levels are strongly influenced by meteorological factors such as wind speed and atmospheric stability. High concentrations of CO build up on cold, clear winter nights with no wind. The eight-hour CO standards historically were occasionally exceeded in those parts of the Bay Area subject to a combination of high traffic density and susceptibility to the occurrence of surface-based radiation inversions, during the winter months. The CO standards were last exceeded prior to 1992 in San Francisco, San Jose and Vallejo.

Air pollution problems related to particulate matter also occur during winter months, usually under the same weather conditions that foster CO buildup. Particulate levels in the Bay Area are typically low near the coast and higher inland, with the highest levels in dry, sheltered valleys, such as the Santa Clara, Livermore and Diablo valleys. The major human-generated (anthropogenic) sources in the Bay Area include motor vehicle travel over paved and unpaved roads, demolition and construction activity and woodburning in fireplaces and stoves. Agricultural operations and burning also contribute significantly to particulate concentrations in rural areas. PM_{10} emissions are expected to increase in future years.

TABLE C-5
MOTOR VEHICLE SHARE OF CRITERIA CONTAMINANT EMISSIONS

Total Emissions and On-Road Motor Vehicle Emissions in the Bay Area Air Basin

Tons/Day (Annual Average)

Year	CO	ROG*	NOx	SO_2	PM_{10}**
1995					
Total Emissions	3705	550	624	91	200
Motor Vehicle (MV) Emissions	2952	294	351	8	106
MV as % of Total	80%	54%	56%	9%	53%
2000					
Total Emissions	2615	435	508	99	218
Motor Vehicle Emissions	1853	189	265	4	111
MV as % of Total	71%	44%	52%	4%	51%
2005					
Total Emissions	2051	372	419	103	231
Motor Vehicle Emissions	1265	120	198	4	117
MV as % of Total	62%	32%	47%	4%	51%
2010					
Total Emissions	1763	335	394	107	241
Motor Vehicle Emissions	960	76	163	4	122
MV as % of Total	55%	23%	41%	4%	51%

* Reactive organic gases (anthropogenic — i.e. excluding emissions from natural vegetation).

** Including entrained road dust.

Projections are based on the District *Base Year 1996 Emission Inventory*, using ARB's EMFAC7G.

The major sources of nitrogen oxides (NO_X) are vehicular, residential and industrial fuel combustion. Concentrations of nitrogen dioxide, the most abundant form of ambient NO_X, are highest in the South Bay, where the standard was last exceeded in 1980.

Major sources of ambient sulfur dioxide (SO_2) include activities such as electricity generation, petroleum refining and shipping. The highest levels of SO_2 are recorded by monitoring stations located in northern Contra Costa County, where most of the major sources of SO_2 are located. The SO_2 standard is currently being met throughout the Bay Area, with seasonal maximums rarely exceeding 50 percent of the standard. SO_2 levels at most Bay Area monitoring stations are less than 10 percent of the standard.

Emissions Inventory

The District estimates emissions of criteria pollutants from approximately nine hundred source categories. The estimates are based on District permit information for "point sources" (e.g. manufacturing industries, refineries, dry-cleaning plants) plus more generalized estimates for "area sources" (e.g. house heating, use of consumer products) and "mobile sources" (trains, ships and planes, as well as on-road and off-road motor vehicles). Figure C-2 and Table C-5 indicate future projections of emissions for the region. The significant role of mobile sources is highlighted in these charts. More detailed information on individual point sources may be obtained by contacting the District.

The emission inventories and projections assume that the Bay Area will continue to grow as forecast and that all currently adopted control measures will continue. Assumptions underlying the projections include the following:

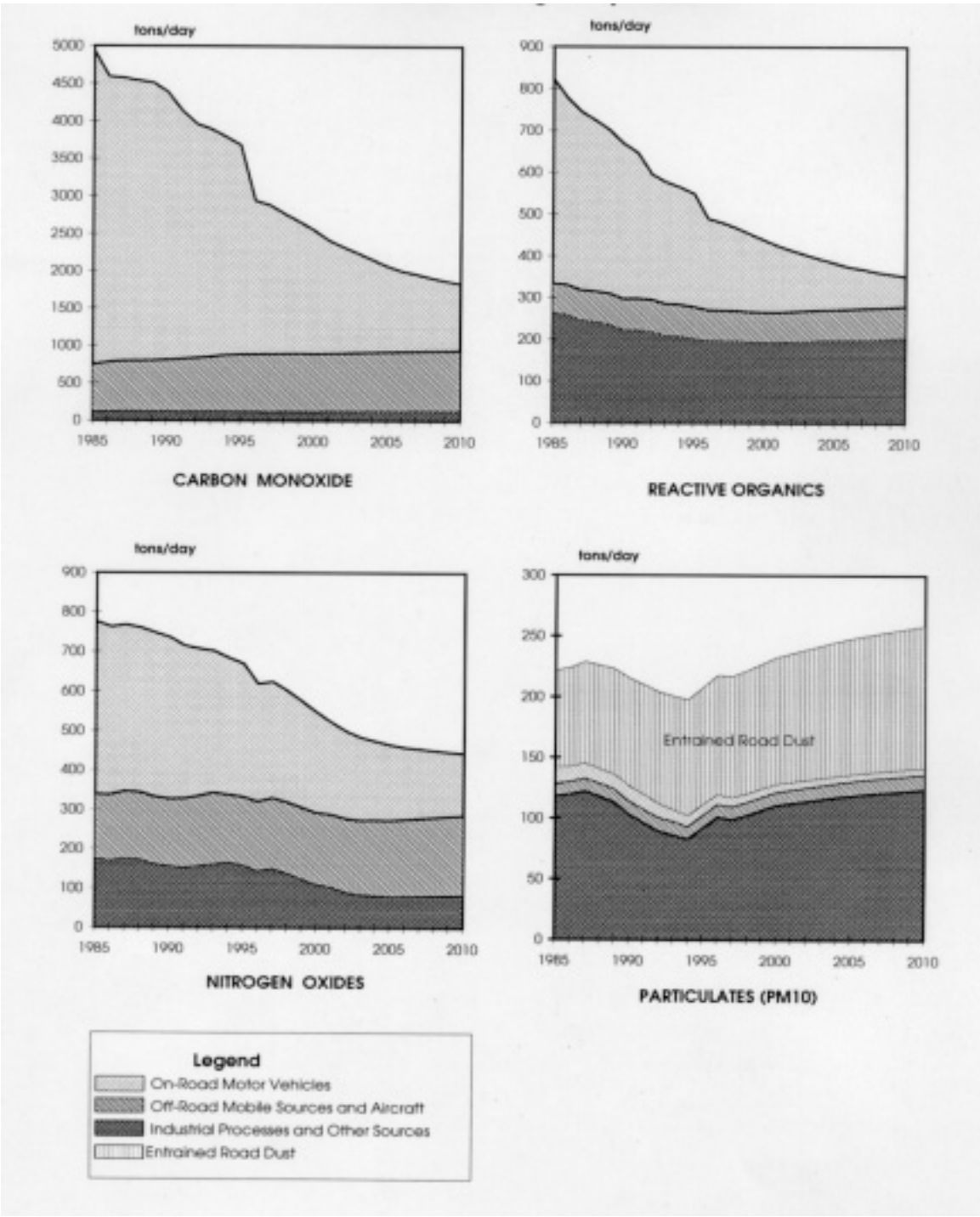
- Population, housing, employment, economic growth and land use development will increase as regionally forecast (ABAG, *Projections '96*).
- New cars will be cleaner than older model vehicles, as required by California regulations.
- The recently improved "Smog Check" program will continue.
- Controls on industry and business will continue.
- Currently implemented transportation control measures will continue.

Lead agencies should be aware that actions which alter these assumptions may also affect progress toward attainment and maintenance of ambient air quality standards.

FIGURE C-2

BAY AREA EMISSION INVENTORY PROJECTIONS 1985-2010
(Base Year 1996)

Annual Average Daily Emissions



Transport of Pollutants

The California Clean Air Act, Section 39610 (a), directs the ARB to "identify each district in which transported air pollutants from upwind areas outside the district cause or contribute to a violation of the ozone standard and to identify the district of origin of transported pollutants." The information regarding the transport of air pollutants from one basin to another was to be quantified to assist interrelated basins in the preparation of plans for the attainment of State ambient air quality standards.

Numerous studies conducted by the ARB have identified air basins that are impacted by pollutants transported from other air basins (as of 1993). Among the air basins affected by air pollution transport from the Bay Area are the North Central Coast Air Basin, the Mountain Counties Air Basin, the San Joaquin Valley Air Basin, and the broader Sacramento Area. The Bay Area was also identified as an area impacted by the transport of air pollutants from the Sacramento area.

Other possible transport corridors being studied by the District and the ARB are from the Bay Area to the Upper Sacramento Valley and from the San Joaquin Valley Air Basin to the Bay Area.

Toxic Air Contaminants

The District has established a number of monitoring stations to track ambient levels of 11 toxic air pollutants: benzene, 1,1,1-trichloroethane (TCA), trichloroethylene (TCE), chloroform (TCM), 1,2-dichloroethane (EDC), 1,2-dibromoethane (EDB), methylene dichloride (DCM), carbon tetrachloride, tetrachloroethylene (perc), vinyl chloride, and toluene. The District is also in the process of establishing a monitoring network to trace 1,3-butadiene. Of the toxics monitored by the District, State ambient air quality standards have been set only for vinyl chloride. (Other toxic substances are regulated or controlled through risk assessment and risk management programs. See Appendix E.)

Because the District's air toxics monitoring program is relatively new, little trend information is available. Based on ARB information, it is expected that benzene and 1,3-butadiene — both generated largely by motor vehicles — will be reduced substantially when reformulated fuels are introduced. These two toxic compounds together account for more than half the background health risk from identified air toxics.

Global Warming and Stratospheric Ozone Depletion

Global warming and stratospheric ozone depletion are issues which have gained increased public attention over the last decade. Unlike emissions of criteria and toxic air pollutants, which have local or regional impacts, emissions contributing to global warming and ozone depletion have a broader, global impact.

Global warming is a process whereby "greenhouse gases" accumulating in the atmosphere contribute to an increase in the temperature of the earth's atmosphere. The principal compounds contributing to global warming are carbon dioxide (CO_2), methane, nitrous oxide, ozone and water vapor. These gases allow visible and ultraviolet light from the sun to pass through the atmosphere, but they prevent heat from escaping back out into space. Among the potential implications of global warming are rising sea levels, climate changes and adverse impacts to agriculture, forestry and natural habitats. In addition, global warming may increase electricity demand for cooling, decrease the availability of hydroelectric power, and affect regional air quality and human health. Like most criteria and toxic pollutants, much of the greenhouse gas production comes from motor vehicles. Greenhouse gas emissions can be reduced to some degree by improved coordination of land use and transportation planning on the city, county and subregional level and other measures to reduce auto use. Energy conservation measures also can contribute to reductions in greenhouse gas emissions.

One group of greenhouse gases, chlorinated fluorocarbons (CFCs) also depletes stratospheric ozone in addition to causing global warming. Ozone in the stratosphere, unlike ground-level ozone, is beneficial. It acts as a solar radiation “screen” reducing the amount of short-wave ultraviolet radiation which can cause skin cancer, damage agricultural crops and increase photochemical smog. By depleting ozone in the upper atmosphere, CFCs not only allow more short-wave ultraviolet radiation to enter the earth's atmosphere, but they are several thousand times more effective than CO_2 in trapping infrared radiation. Since the mid-1930s, CFCs have been used as refrigerants, solvents, and in the production of foam materials. Moreover, CFCs survive in the atmosphere for decades.

National and international agreements have been made to control CFCs and to study air quality problems related to ozone depletion. Recent laws and practices governing repair and recharging of air conditioners and refrigerators have served to reduce CFC emissions. Although local governments alone cannot solve these global problems, some cities in the Bay Area have already demonstrated that local and regional efforts can make a contribution, e.g., banning the sale and commercial use of plastics made with CFCs.

APPENDIX D - CLIMATE, TOPOGRAPHY AND AIR POLLUTION POTENTIAL

Appendix D provides climatological and topographic information about the Bay Area, and explains how these natural factors influence air quality conditions. The first two sections address region-wide conditions relevant to all cities and counties in the Bay Area. The final sections discuss climatological subregions in the Bay Area.

BAY AREA CLIMATE AND TOPOGRAPHY

High Pressure Cell

During the summer, the large-scale meteorological condition that dominates the West Coast is a semipermanent high pressure cell centered over the northeastern Pacific Ocean. This high pressure cell keeps storms from affecting the California coast. Hence, the Bay Area experiences little precipitation in the summer months. Winds tend to blow on shore out of the north/northwest.

The steady northwesterly flow induces upwelling of cold water from below. This upwelling produces a band of cold water off the California coast. When air approaches the California coast, already cool and moisture-laden from its long journey over the Pacific, it is further cooled as it crosses this bank of cold water. This cooling often produces condensation resulting in a high incidence of fog and stratus clouds along the Northern California coast in the summer.

Generally in the winter, the Pacific high weakens and shifts southward, winds tend to flow offshore, upwelling ceases and storms occur. During the winter rainy periods, inversions (layers of warmer air over colder air; see below) are weak or nonexistent, winds are usually moderate and air pollution potential is low. The Pacific high does periodically become dominant however, bringing strong inversions, light winds and high pollution potential.

Topography

Bay Area topography is characterized by complex terrain, consisting of coastal mountain ranges, inland valleys and bays. This complex terrain, especially the higher elevations, distorts the normal wind flow patterns in the Bay Area. The greatest distortion occurs when low-level inversions are present and the air beneath the inversion flows independently of air above the inversion, a condition that is common in the summer time.

The only major break in California's Coast Range occurs in the Bay Area. Here the Coast Range splits into western and eastern ranges. Between the two ranges lies San Francisco Bay. The gap in the western coast range is known as the Golden Gate, and the gap in the eastern coast range is the Carquinez Strait. These gaps allow air to pass into and out of the Bay Area and the Central Valley.

Wind Patterns

During the summer, winds flowing from the northwest are drawn inland through the Golden Gate and over the lower portions of the San Francisco Peninsula. Immediately south of Mount Tamalpais, the northwesterly winds accelerate considerably and come more directly from the west as they stream through the Golden Gate. This channeling of wind through the Golden Gate produces a jet that sweeps eastward and splits off to the northwest toward Richmond and to the southwest toward San Jose when it meets the East Bay hills.

Wind speeds may be strong locally in areas where air is channeled through a narrow opening, such as the Carquinez Strait, the Golden Gate or the San Bruno gap. For example, the average wind speed at San Francisco International Airport in July is about 17 knots (from 3 p.m. to 4 p.m.), compared with only 7 knots at San Jose and less than 6 knots at the Farallon Islands.

The air flowing in from the coast to the Central Valley, called the sea breeze, begins developing at or near ground level along the coast in late morning or early afternoon. As the day progresses, the sea breeze layer deepens and increases in velocity while spreading inland. The depth of the sea breeze depends in large part upon the height and strength of the inversion. If the inversion is low and strong, and hence stable, the flow of the sea breeze will be inhibited and stagnant conditions are likely to result.

In the winter, the Bay Area frequently experiences stormy conditions with moderate to strong winds, as well as periods of stagnation with very light winds. Winter stagnation episodes are characterized by nighttime drainage flows in coastal valleys. Drainage is a reversal of the usual daytime air-flow patterns; air moves from the Central Valley toward the coast and back down toward the Bay from the smaller valleys within the Bay Area.

Temperature

Summertime temperatures in the Bay Area are determined in large part by the effect of differential heating between land and water surfaces. Because land tends to heat up and cool off more quickly than water, a large-scale gradient (differential) in temperature is often created between the coast and the Central Valley, and small-scale local gradients are often produced along the shorelines of the ocean and bays. The temperature gradient near the ocean is also exaggerated, especially in summer, because of the upwelling of cold ocean bottom water along the coast. Thus, on summer afternoons the temperatures at the coast can be 35°F cooler than temperatures 15 to 20 miles inland. At night this contrast usually decreases to less than 10°.

In the winter, the relationship of minimum and maximum temperatures is reversed. During the daytime the temperature contrast between the coast and inland areas is small, whereas at night the variation in temperature is large.

Precipitation

The Bay Area is characterized by moderately wet winters and dry summers. Winter rains account for about 75 percent of the average annual rainfall. The amount of annual precipitation can vary greatly from one part of the Bay Area to another even within short distances. In general, total annual rainfall can reach 40 inches in the mountains, but it is often less than 16 inches in sheltered valleys.

During rainy periods, ventilation (rapid horizontal movement of air and injection of cleaner air) and vertical mixing are usually high, and thus pollution levels tend to be low. However, frequent dry periods do occur during the winter where mixing and ventilation are low and pollutant levels build up.

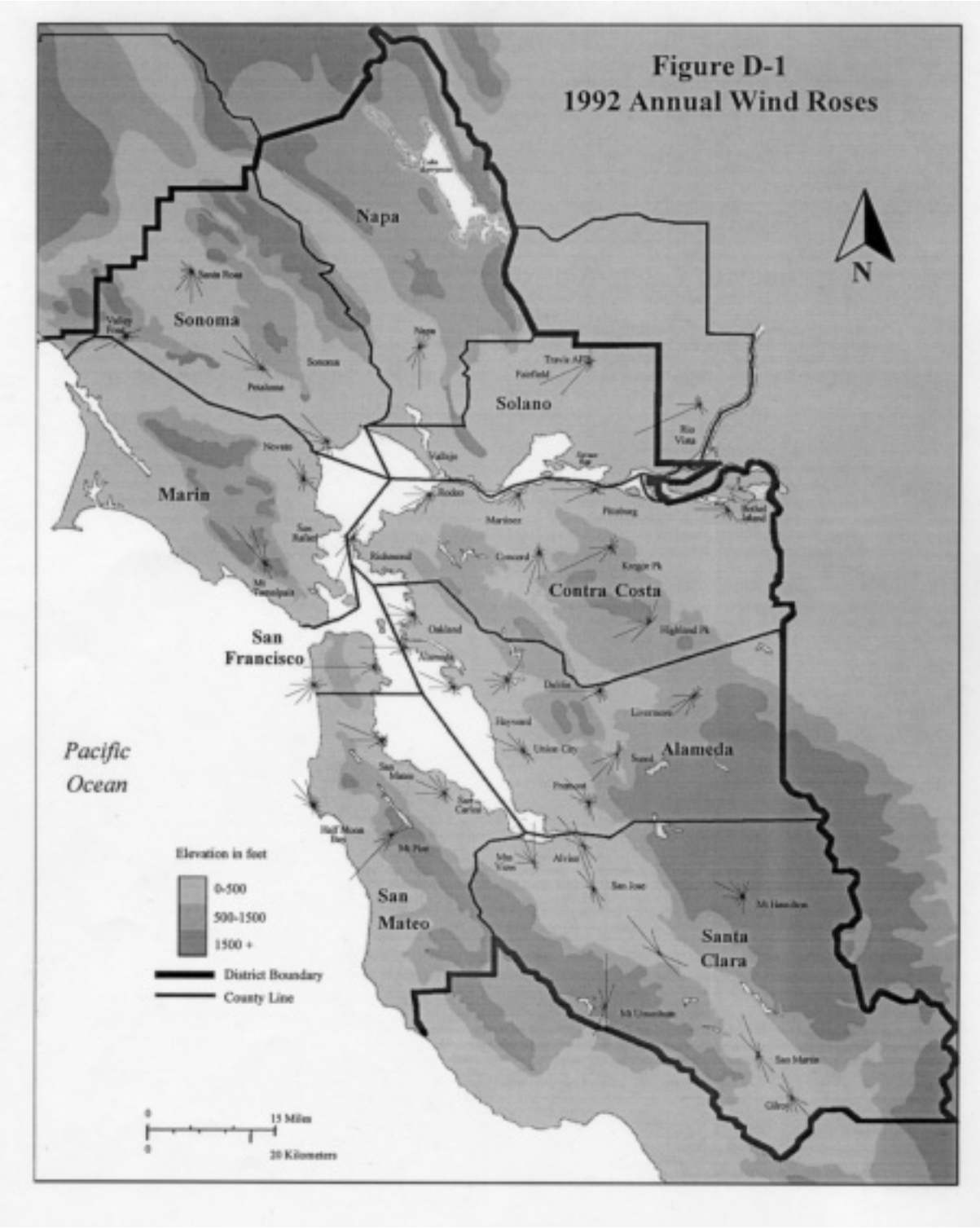
AIR POLLUTION POTENTIAL

The potential for high pollutant concentrations developing at a given location depends upon the quantity of pollutants emitted into the atmosphere in the surrounding area or upwind, and the ability of the atmosphere to disperse the contaminated air. The topographic and climatological factors discussed above influence the atmospheric pollution potential of an area. Atmospheric pollution potential, as the term is used here, is independent of the location of emission sources and is instead a function of factors described below.

Wind Circulation

Low wind speed contributes to the buildup of air pollution because it allows more pollutants to be emitted into the air mass per unit of time. Light winds occur most frequently during periods of low sun (fall and winter, and early morning) and at night. These are also periods when air pollutant emissions from some sources are at their peak, namely, commute traffic (early morning) and wood burning appliances (nighttime). The problem can be compounded in valleys, when weak flows carry the pollutants upvalley during the day, and cold air drainage flows move the air mass downvalley at night. Such restricted movement of trapped air provides little opportunity for ventilation and leads to buildup of pollutants to potentially unhealthful levels.

Wind-roses (Figure D-1) provide useful information for communities that contain industry, landfills or other potentially odorous or noxious land uses. Each wind-rose diagram provides a general indication of the proportion of time that winds blow from each compass direction. The longer the vector length, the greater the frequency of wind occurring from that direction. Such information may be particularly useful in planning buffer zones. For example, sensitive receptors such as residential developments, schools or hospitals are inappropriate uses immediately downwind from facilities that emit toxic or odorous pollutants, unless adequate separation is provided by a buffer zone. Caution should be taken, however, in using wind-roses in planning and environmental review processes. A site on the opposite side of a hill or tall building, even a short distance from a meteorological monitoring station, may experience a significant difference in wind pattern. Figure D-1 is a map of simplified wind roses, composed of data from a number of Bay Area meteorological stations. Lead agencies should consult District meteorologists if more detailed information is needed.


Figure D-1
1992 Annual Wind Roses
N
Napa
Sonoma
Solano
Marin
Contra Costa
San Francisco
Alameda
San Mateo
Santa Clara
Pacific Ocean
Elevation in feet
0-500
500-1500
1500 +
District Boundary
County Line
15 Miles
20 Kilometers

Inversions

An inversion is a layer of warmer air over a layer of cooler air. Inversions affect air quality conditions significantly because they influence the mixing depth, i.e., the vertical depth in the atmosphere available for diluting air contaminants near the ground. The highest air pollutant concentrations in the Bay Area generally occur during inversions.

There are two types of inversions that occur regularly in the Bay Area. One is more common in the summer and fall, while the other is most common during the winter. The frequent occurrence of elevated temperature inversions in summer and fall months acts to cap the mixing depth and consequently limit the depth of air available for dilution. Elevated inversions are caused by subsiding air from the subtropical high pressure zone, and from the cool marine air layer that is drawn into the Bay Area by the heated low pressure region in the Central Valley.

The inversions typical of winter, called radiation inversions, are formed as heat quickly radiates from the earth's surface after sunset, causing the air in contact with it to rapidly cool. Radiation inversions are strongest on clear, low-wind, cold winter nights, allowing the build-up of such pollutants as carbon monoxide and particulate matter. When wind speeds are low, there is little mechanical turbulence to mix the air, resulting in a layer of warm air over a layer of cooler air next to the ground. Mixing depths under these conditions can be as shallow as 50 to 100 meters, particularly in rural areas. Urban areas usually have deeper minimum mixing layers because of heat island effects and increased surface roughness. During radiation inversions downwind transport is slow, the mixing depths are shallow, and turbulence is minimal. All of these factors contribute to increased pollution levels near the ground.

Although each type of inversion is most common during a specific season, either inversion mechanism can occur at any time of the year. Sometimes both occur simultaneously. Moreover, the characteristics of an inversion often change throughout the course of a day. The terrain of the Bay Area also induces significant variations among subregions.

Stability

Stability is defined as the atmosphere's resistance to vertical motions. The more stable the air, the slower the mixing, resulting in increased probability for air pollutants to build up and exceed ambient air quality standards.

The stability of the atmosphere is highly dependent upon the vertical distribution of temperature with height. When the temperature decreases vertically ("lapse rate") at 10 degrees Celsius per 1000 meters, the atmosphere is classified as "neutral stability". When the lapse rate is greater than 10 degrees C per 100 meters, the atmosphere is "unstable". If the lapse rate is less than 10 degrees per 1000 meters, or the temperature increases with height, the atmosphere is "stable". These stabilities have been categorized for use in dispersion models. Stability categories range from "Extremely Unstable" (Stability Class A), through "Neutral" (D), to "Stable" (F).

Unstable conditions can only occur during daytime hours when solar heating warms the lower layers sufficiently. Under A stability conditions, large horizontal wind direction fluctuations occur, along with large vertical mixing. These motions usually only occur midday during

summer months on cloudless days with light winds. Under B stability conditions, wind direction fluctuations and vertical mixing are less pronounced, because the heating is less strong. The fluctuations found during both A and B stability conditions are mostly due to thermal turbulence. Under C stability conditions, the solar insulation is weaker, or the wind speeds are stronger, so that the surface heating is weaker. The horizontal and vertical fluctuations are weaker yet, and are caused by a combination of thermal and mechanical turbulence.

D stability can occur either during the day or at night. Under D stability conditions, the wind speeds are usually strong — greater than 5 meters per second — or the sky is obscured by clouds. Wind direction fluctuations are small, while vertical motions are primarily generated by mechanical turbulence.

Stabilities E and F can only occur at night. The necessary conditions can only occur in the absence of sunlight, and with light to moderate winds. Under these conditions, there is little turbulence because of the atmosphere's resistance to vertical motion. Pollutants emitted into a stable air mass will travel downwind with little dispersion.

Solar Radiation

The frequency of hot, sunny days during the summer months in the Bay Area is another important factor that affects air pollution potential. It is at the higher temperatures that ozone is formed. In the presence of ultraviolet sunlight and warm temperatures, reactive organic gases and oxides of nitrogen react to form secondary photochemical pollutants, including ozone. Because temperatures in many of the Bay Area inland valleys are so much higher than near the coast, the inland areas are especially prone to photochemical air pollution.

In late fall and winter, solar angles are low, resulting in insufficient ultraviolet light and warming of the atmosphere to drive the photochemical reactions. Consequently, ozone concentrations do not reach significant levels in the Bay Area during these seasons.

Sheltered Terrain

The hills and mountains in the Bay Area contribute to the high pollution potential of some areas. During the day, or at night during windy conditions, areas in the lee sides of mountains are sheltered from the prevailing winds, thereby reducing turbulence and downwind transport. At night, when wind speeds are low, the upper atmospheric layers are often decoupled from the surface layers during radiation conditions. If elevated terrain is present, it will tend to block pollutant transport in that direction. Elevated terrain also can create a recirculation pattern by inducing upvalley air flows during the day and reverse downvalley flows during the night, allowing little inflow of fresh air.

The areas having the highest air pollution potential tend to be those that experience the highest temperatures in the summer and the lowest temperatures in the winter. Bay Area coastal areas are exposed to the prevailing marine air and consequently have cooler temperatures in the summer, warmer temperatures in winter, and experience stratus clouds all year. The inland valleys are sheltered from the marine air and consequently experience hotter summers and colder

winters. Thus, the topography of the inland valleys creates conditions conducive to high air pollution potential.

Pollution Potential Related to Emissions

Although air pollution potential is strongly influenced by climate and topography, the air pollution that occurs in a location also depends upon the amount of air pollutant emissions in the surrounding area or transported from more distant places. Air pollutant emissions generally are highest in areas that have high population densities, high motor vehicle use and/or industrialization. However, contaminants created by photochemical processes in the atmosphere, such as ozone, may result in high concentrations many miles downwind from the sources of their precursor chemicals.

CLIMATOLOGICAL SUBREGIONS

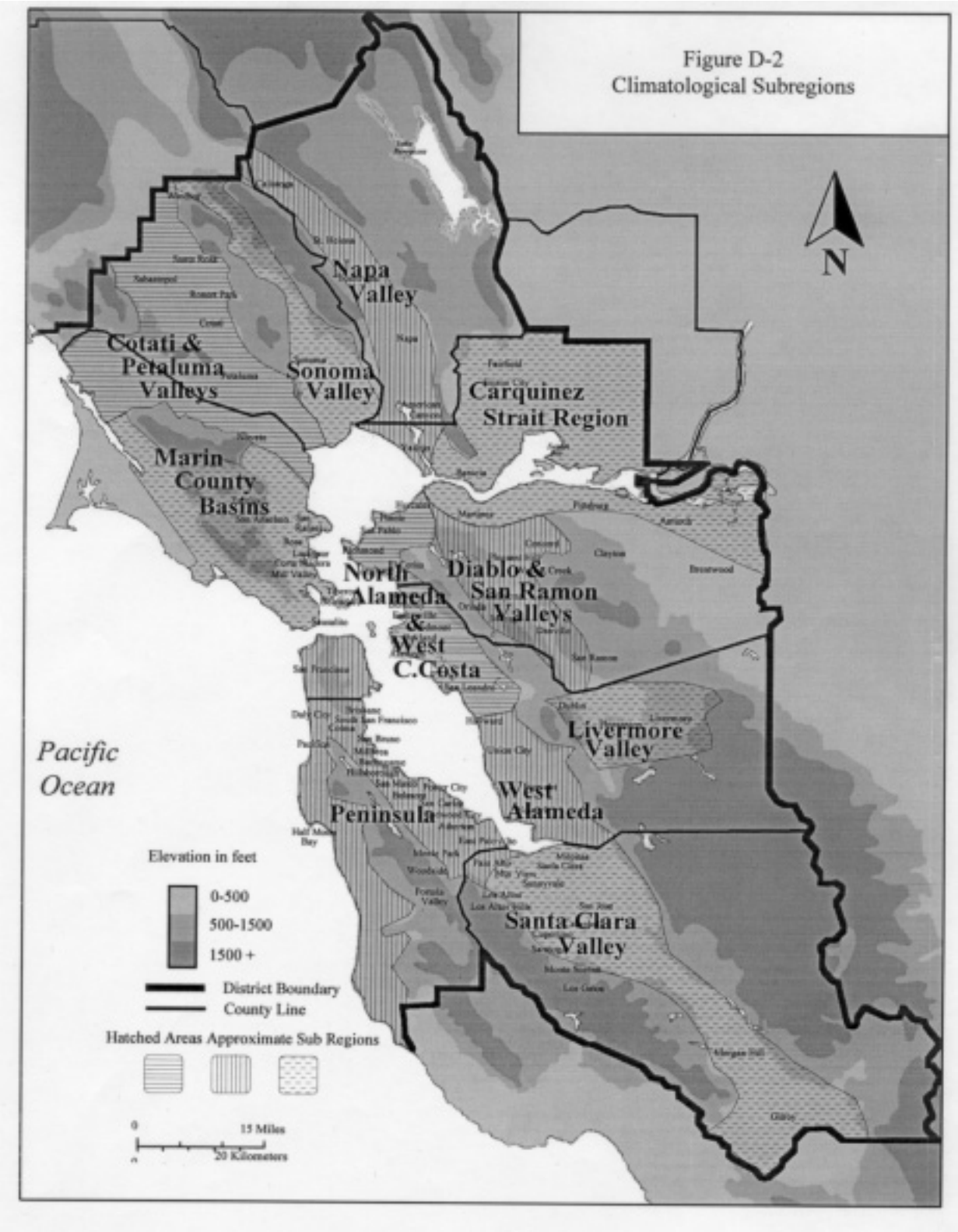
This section discusses the varying climatological and topographic conditions, and the resulting variations in air pollution potential, within inhabited subregions of the Bay Area Air Basin. All urbanized areas of the Bay Area are included in one of 11 climatological subregions. Sparsely inhabited areas are excluded from the subregional designations. Some of the climatological subregions discussed in this appendix overlap county boundaries. Lead Agencies analyzing projects located close to the boundary between subregions may need to examine the characteristics of the neighboring subregions in order to adequately evaluate potential air quality impacts. The 11 subregions are portrayed in Figure D-2.

The information about each subregion includes location, topography and climatological factors relevant to air quality. Where relevant to air quality concerns, more localized subareas within a subregion are discussed. Each subregional section concludes with a discussion of pollution potential resulting from climatological and topographic variables and the major types of air pollutant sources in the subregion.

Carquinez Strait Region

The Carquinez Strait runs from Rodeo to Martinez. It is the only sea-level gap between San Francisco Bay and the Central Valley. The subregion includes the lowlands bordering the strait to the north and south, and includes the area adjoining Suisun Bay and the western part of the Sacramento-San Joaquin Delta as far east as Bethel Island. The subregion extends from Rodeo in the southwest and Vallejo in the northwest to Fairfield on the northeast and Brentwood on the southeast.

Prevailing winds are from the west in the Carquinez Strait. During the summer and fall months, high pressure offshore coupled with low pressure in the Central Valley causes marine air to flow eastward through the Carquinez Strait. The wind is strongest in the afternoon. Afternoon wind speeds of 15 to 20 mph are common throughout the strait region. Annual average wind speeds


Figure D-2
Climatological Subregions
N
Napa Valley
Cotati & Petaluma Valleys
Sonoma Valley
Carquinez Strait Region
Marin County Basins
North Alameda & West C.Costa
Diablo & San Ramon Valleys
Livermore Valley
West Alameda
Peninsula
Santa Clara Valley
Pacific Ocean
Elevation in feet
0-500
500-1500
1500 +
District Boundary
County Line
Hatched Areas Approximate Sub Regions
0
15 Miles
20 Kilometers

are 8 mph in Martinez, and 9 to 10 mph further east. Sometimes atmospheric conditions cause air to flow from the east. East winds usually contain more pollutants than the cleaner marine air from the west. In the summer and fall months, this can cause elevated pollutant levels to move into the central Bay Area through the strait. These high pressure periods are usually accompanied by low wind speeds, shallow mixing depths, higher temperatures and little or no rainfall.

Summer mean maximum temperatures reach about 90° F. in the subregion. Mean minimum temperatures in the winter are in the high 30's. Temperature extremes are especially pronounced in sheltered areas farther from the moderating effects of the strait itself, e.g. at Fairfield.

Many industrial facilities with significant air pollutant emissions — e.g., chemical plants and refineries — are located within the Carquinez Strait Region. The pollution potential of this area is often moderated by high wind speeds. However, upsets at industrial facilities can lead to short-term pollution episodes, and emissions of unpleasant odors may occur at anytime. Receptors downwind of these facilities could suffer more long-term exposure to air contaminants than individuals elsewhere. Consequently, it is important that local governments and other Lead Agencies maintain buffers zones around sources of air pollution sufficient to avoid adverse health and nuisance impacts on nearby receptors. Areas of the subregion that are traversed by major roadways, e.g. Interstate 80, may also be subject to higher local concentrations of carbon monoxide and particulate matter, as well as certain toxic air contaminants such as benzene.

Cotati and Petaluma Valleys

The subregion that stretches from Santa Rosa to the San Pablo Bay is often considered as two different valleys: the Cotati Valley in the north and the Petaluma Valley in the south. To the east, the valley is bordered by the Sonoma Mountains, while to the west is a series of low hills, followed by the Estero Lowlands, which open to the Pacific Ocean. The region from the Estero Lowlands to the San Pablo Bay is known as the Petaluma Gap. This low-terrain area allows marine air to travel into the Bay Area.

Wind patterns in the Petaluma and Cotati Valleys are strongly influenced by the Petaluma Gap, with winds flowing predominantly from the west. As marine air travels through the Petaluma Gap, it splits into northward and southward paths moving into the Cotati and Petaluma valleys. The southward path crosses San Pablo Bay and moves eastward through the Carquinez Strait. The northward path contributes to Santa Rosa's prevailing winds from the south and southeast. Petaluma's prevailing winds are from the northwest.

When the ocean breeze is weak, strong winds from the east can predominate, carrying pollutants from the Central Valley and the Carquinez Strait. During these periods, upvalley flows can carry the polluted air as far north as Santa Rosa.

Winds are usually stronger in the Petaluma Valley than the Cotati Valley because the former is directly in line with the Petaluma Gap. Consequently, Petaluma's climate is similar to areas closer to the coast even though Petaluma is 28 miles from the ocean. Average annual wind speed at the Petaluma Airport is seven mph. The Cotati Valley, being slightly north of the

Petaluma Gap, experiences lower wind speeds. The annual average wind speed in Santa Rosa is five mph.

Air temperatures are very similar in the two valleys. Summer maximum temperatures for this subregion are in the low-to-mid-80's, while winter maximum temperatures are in the high-50's to low-60's. Summer minimum temperatures are around 50 degrees, and winter minimum temperatures are in the high 30's.

Generally, air pollution potential is low in the Petaluma Valley because of its link to the Petaluma Gap and because of its low population density. However, there are two scenarios that could produce elevated pollutant levels: 1) stagnant conditions in the morning hours created when a weak ocean breeze meets a weak bay breeze, and 2) an eastern or southeastern wind pattern in the afternoon brings in pollution from the Carquinez Strait Region and the Central Valley.

The Cotati Valley has a higher pollution potential than does the Petaluma Valley. The Cotati Valley lacks a gap to the sea, contains a larger population and has natural barriers at its northern and eastern ends. There are also industrial facilities in and around Santa Rosa. Both valleys of this subregion are also threatened by increased motor vehicle traffic and the associated air contaminants. Population and motor vehicle use are increasing significantly, and housing costs and the suburbanization of employment are leading to more and longer commutes traversing the subregion.

Diablo and San Ramon Valleys

East of the Coast Range lie the Diablo and San Ramon Valleys. The valleys have a northwest to southeast orientation, with the northern portion known as Diablo Valley and the southern portion as San Ramon Valley. The Diablo Valley is bordered in the north by the Carquinez Strait and in the south by the San Ramon Valley. The San Ramon Valley is long and narrow and extends south from Walnut Creek to Dublin. At its southern end it opens onto the Amador Valley.

The mountains on the west side of these valleys block much of the marine air from reaching the valleys. During the daytime, there are two predominant flow patterns: an upvalley flow from the north and a westerly flow (wind from the west) across the lower elevations of the Coast Range. On clear nights, surface inversions separate the flow of air into two layers: the surface flow and the upper layer flow. When this happens, there are often drainage surface winds which flow downvalley toward the Carquinez Strait.

Wind speeds in these valleys generally are low. Monitoring stations in Concord and Danville report annual average wind speeds of 5 mph. However, winds can increase in the afternoon near San Ramon because it is located at the eastern edge of the Crow Canyon gap. Through this gap, polluted air from cities near the bay travels to the valley in the summer months.

Air temperatures in these valleys are cooler in the winter and warmer in the summer than are temperatures further west, as these valleys are far from the moderating effect of the bay and ocean. Mean summer maximum temperatures are in the low- to mid-80’s. Mean winter minimum temperatures are in the high-30’s to low-40’s.

Pollution potential is relatively high in these valleys. On winter evenings, light winds combined with surface-based inversions and terrain that restricts air flow can cause pollutant levels to build up. San Ramon Valley can experience high pollution concentrations due to motor vehicle emissions and emissions from fireplaces and wood stoves. In the summer months, ozone and ozone precursors are often transported into the valleys from both the central Bay Area and the Central Valley.

Livermore Valley

The Livermore Valley is a sheltered inland valley near the eastern border of the District. The western side of the valley is bordered by 1,000 to 1,500 foot hills with two gaps connecting the valley to the central Bay Area, the Hayward Pass and Niles Canyon. The eastern side of the valley also is bordered by 1,000 to 1,500 foot hills with one major passage to the San Joaquin Valley called the Altamont Pass and several secondary passages. To the north lie the Black Hills and Mount Diablo. A northwest to southeast channel connects the Diablo Valley to the Livermore Valley. The south side of the Livermore Valley is bordered by mountains approximately 3,000 to 3,500 feet high.

During the summer months, when there is a strong inversion with a low ceiling, air movement is weak and pollutants become trapped and concentrated. Maximum summer temperatures in the Livermore Valley range from the high-80's to the low-90's, with extremes in the 100's. At other times in the summer, a strong Pacific high pressure cell from the west, coupled with hot inland temperatures causes a strong onshore pressure gradient which produces a strong, afternoon wind. With a weak temperature inversion, air moves over the hills with ease, dispersing pollutants.

In the winter, with the exception of an occasional storm moving through the area, air movement is often dictated by local conditions. At night and early morning, especially under clear, calm and cold conditions, gravity drives cold air downward. The cold air drains off the hills and moves into the gaps and passes. On the eastern side of the valley the prevailing winds blow from north, northeast and east out of the Altamont Pass. Winds are light during the late night and early morning hours. Winter daytime winds sometimes flow from the south through the Altamont Pass to the San Joaquin Valley. Average winter maximum temperatures range from the high-50's to the low-60's, while minimum temperatures are from the mid-to-high-30's, with extremes in the high teens and low-20's.

Air pollution potential is high in the Livermore Valley, especially for photochemical pollutants in the summer and fall. High temperatures increase the potential for ozone to build up. The valley not only traps locally generated pollutants but can be the receptor of ozone and ozone precursors from San Francisco, Alameda, Contra Costa and Santa Clara counties. On northeasterly wind flow days, most common in the early fall, ozone may be carried west from the San Joaquin Valley to the Livermore Valley.

During the winter, the sheltering effect of the valley, its distance from moderating water bodies, and the presence of a strong high pressure system contribute to the development of strong, surface-based temperature inversions. Pollutants such as carbon monoxide and particulate matter, generated by motor vehicles, fireplaces and agricultural burning, can become

concentrated. Air pollution problems could intensify because of population growth and increased commuting to and through the subregion.

Marin County Basins

Marin County is bounded on the west by the Pacific Ocean, on the east by San Pablo Bay, on the south by the Golden Gate and on the north by the Petaluma Gap. Most of Marin's population lives in the eastern part of the county, in small, sheltered valleys. These valleys act like a series of miniature air basins.

Although there are a few mountains above 1500 feet, most of the terrain is only 800 to 1000 feet high, which usually is not high enough to block the marine layer. Because of the wedge shape of the county, northeast Marin County is further from the ocean than is the southeastern section. This extra distance from the ocean allows the marine air to be moderated by bayside conditions as it travels to northeastern Marin County. In southern Marin the distance from the ocean is short and elevations are lower, resulting in higher incidence of maritime air in that area.

Wind speeds are highest along the west coast of Marin, averaging about 8 to 10 miles per hour. The complex terrain in central Marin creates sufficient friction to slow the air flow. At Hamilton Air Force Base, in Novato, the annual average wind speeds are only 5 mph. The prevailing wind directions throughout Marin County are generally from the northwest.

In the summer months, areas along the coast are usually subject to onshore movement of cool marine air. In the winter, proximity to the ocean keeps the coastal regions relatively warm, with temperatures varying little throughout the year. Coastal temperatures are usually in the high-50's in the winter and the low-60's in the summer. The warmest months are September and October.

The eastern side of Marin County has warmer weather than the western side because of its distance from the ocean and because the hills that separate eastern Marin from western Marin occasionally block the flow of the marine air. The temperatures of cities next to the bay are moderated by the cooling effect of the bay in the summer and the warming effect of the bay in the winter. For example, San Rafael experiences average maximum summer temperatures in the low-80's and average minimum winter temperatures in the low-40’s. Inland towns such as Kentfield experience average maximum temperatures that are two degrees cooler in the winter and two degrees warmer in the summer.

Air pollution potential is highest in eastern Marin County, where most of population is located in semi-sheltered valleys. In the southeast, the influence of marine air keeps pollution levels low. However, as development moves further north, there is greater potential for air pollution to build up because the valleys are more sheltered from the sea breeze. While Marin County does not have many polluting industries, the air quality on its eastern side — especially along the U.S. 101 corridor — may be affected by emissions from increasing motor vehicle use within and through the county.

Napa Valley

The Napa Valley is bordered by relatively high mountains. With an average ridge line height of about 2000 feet, with some peaks approaching 3000 to 4000 feet, these mountains are effective barriers to the prevailing northwesterly winds. The Napa Valley is widest at its southern end and narrows in the north.
During the day, the prevailing winds flow upvalley from the south about half of the time. A strong upvalley wind frequently develops during warm summer afternoons, drawing air in from the San Pablo Bay. Daytime winds sometimes flow downvalley from the north. During the evening, especially in the winter, downvalley drainage often occurs. Wind speeds are generally low, with almost 50 percent of the winds less than 4 mph. Only 5 percent of the winds are between 16 and 18 mph, representing strong summertime upvalley winds and winter storms.

Summer average maximum temperatures are in the low 80's at the southern end of the valley and in the low 90's at the northern end. Winter average maximum temperatures are in the high-50's and low-60's, and minimum temperatures are in the high to mid 30's with the slightly cooler temperatures in the northern end.

The air pollution potential in the Napa Valley could be high if there were sufficient sources of air contaminants nearby. Summer and fall prevailing winds can transport ozone precursors northward from the Carquinez Strait Region to the Napa Valley, effectively trapping and concentrating the pollutants when stable conditions are present. The local upslope and downslope flows created by the surrounding mountains may also recirculate pollutants already present, contributing to buildup of air pollution. High ozone concentrations are a potential problem to sensitive crops such as wine grapes, as well as to human health. The high frequency of light winds and stable conditions during the late fall and winter contribute to the buildup of particulate matter from motor vehicles, agriculture and woodburning in fireplaces and stoves.

Northern Alameda and Western Contra Costa Counties

This climatological subregion stretches from Richmond to San Leandro. Its western boundary is defined by San Francisco Bay and its eastern boundary by the Oakland-Berkeley Hills. The Oakland-Berkeley Hills have a ridge line height of approximately 1500 feet, a significant barrier to air flow. The most densely populated area of the subregion lies in a strip of land between the bay and the lower hills.

In this area, marine air traveling through the Golden Gate, as well as across San Francisco and through the San Bruno Gap, is a dominant weather factor. The Oakland-Berkeley Hills cause the westerly flow of air to split off to the north and south of Oakland, which causes diminished wind speeds. The prevailing winds for most of this subregion are from the west. At the northern end, near Richmond, prevailing winds are from the south-southwest.

Temperatures in this subregion have a narrow range due to the proximity of the moderating marine air. Maximum temperatures in summer average in the mid-70's, with minimums in the mid-50's. Winter highs are in the mid- to high-50's, with lows in the low- to mid-40's.

The air pollution potential is lowest for the parts of the subregion that are closest to the bay, due largely to good ventilation and less influx of pollutants from upwind sources. The occurrence of light winds in the evenings and early mornings occasionally causes elevated pollutant levels.

The air pollution potential at the northern (Richmond) and southern (Oakland, San Leandro) parts of this subregion is marginally higher than communities directly east of the Golden Gate, because of the lower frequency of strong winds.

This subregion contains a variety of industrial air pollution sources. Some industries are quite close to residential areas. The subregion is also traversed by frequently congested major freeways. Traffic and congestion, and the motor vehicle emissions they generate, are increasing.

Peninsula

The peninsula region extends from northwest of San Jose to the Golden Gate. The Santa Cruz Mountains run up the center of the peninsula, with elevations exceeding 2000 feet at the southern end, decreasing to 500 feet in South San Francisco. Coastal towns experience a high incidence of cool, foggy weather in the summer. Cities in the southeastern peninsula experience warmer temperatures and fewer foggy days because the marine layer is blocked by the ridgeline to the west. San Francisco lies at the northern end of the peninsula. Because most of San Francisco's topography is below 200 feet, marine air is able to flow easily across most of the city, making its climate cool and windy.

The blocking effect of the Santa Cruz Mountains results in variations in summertime maximum temperatures in different parts of the peninsula. For example, in coastal areas and San Francisco the mean maximum summer temperatures are in the mid-60's, while in Redwood City the mean maximum summer temperatures are in the low-80's. Mean minimum temperatures during the winter months are in the high-30’s to low-40’s on the eastern side of the Peninsula and in the low 40’s on the coast..

Two important gaps in the Santa Cruz Mountains occur on the peninsula. The larger of the two is the San Bruno Gap, extending from Fort Funston on the ocean to the San Francisco Airport. Because the gap is oriented in the same northwest to southeast direction as the prevailing winds, and because the elevations along the gap are under 200 feet, marine air is easily able to penetrate into the bay. The other gap is the Crystal Springs Gap, between Half Moon Bay and San Carlos. As the sea breeze strengthens on summer afternoons, the gap permits maritime air to pass across the mountains, and its cooling effect is commonly seen from San Mateo to Redwood City.

Annual average wind speeds range from 5 to 10 mph throughout the peninsula, with higher wind speeds usually found along the coast. However, winds on the eastern side of the peninsula are often high in certain areas, such as near the San Bruno Gap and the Crystal Springs Gap.

The prevailing winds along the peninsula's coast are from the west, although individual sites can show significant differences. For example, Fort Funston in western San Francisco shows a southwest wind pattern while Pillar Point in San Mateo County shows a northwest wind pattern. On the east side of the mountains winds are generally from the west, although wind patterns in this area are often influenced greatly by local topographic features.

Air pollution potential is highest along the southeastern portion of the peninsula. This is the area most protected from the high winds and fog of the marine layer. Pollutant transport from upwind sites is common. In the southeastern portion of the peninsula, air pollutant emissions are

relatively high due to motor vehicle traffic as well as stationary sources. At the northern end of the peninsula in San Francisco, pollutant emissions are high, especially from motor vehicle congestion. Localized pollutants, such as carbon monoxide, can build up in "urban canyons". However, winds are generally fast enough to carry the pollutants away before they can accumulate.

Santa Clara Valley

The Santa Clara Valley is bounded by the San Francisco Bay to the north and by mountains to the east, south and west. Temperatures are warm on summer days and cool on summer nights, and winter temperatures are fairly mild. At the northern end of the valley, mean maximum temperatures are in the low-80's during the summer and the high-50's during the winter, and mean minimum temperatures range from the high-50's in the summer to the low-40's in the winter. Further inland, where the moderating effect of the bay is not as strong, temperature extremes are greater. For example, in San Martin, located 27 miles south of the San Jose Airport, temperatures can be more than 10 degrees warmer on summer afternoons and more than 10 degrees cooler on winter nights.

Winds in the valley are greatly influenced by the terrain, resulting in a prevailing flow that roughly parallels the valley's northwest-southeast axis. A north-northwesterly sea breeze flows through the valley during the afternoon and early evening, and a light south-southeasterly drainage flow occurs during the late evening and early morning. In the summer the southern end of the valley sometimes becomes a "convergence zone," when air flowing from the Monterey Bay gets channeled northward into the southern end of the valley and meets with the prevailing north-northwesterly winds.

Wind speeds are greatest in the spring and summer and weakest in the fall and winter. Nighttime and early morning hours frequently have calm winds in all seasons, while summer afternoons and evenings are quite breezy. Strong winds are rare, associated mostly with the occasional winter storm.

The air pollution potential of the Santa Clara Valley is high. High summer temperatures, stable air and mountains surrounding the valley combine to promote ozone formation. In addition to the many local sources of pollution, ozone precursors from San Francisco, San Mateo and Alameda Counties are carried by prevailing winds to the Santa Clara Valley. The valley tends to channel pollutants to the southeast. In addition, on summer days with low level inversions, ozone can be recirculated by southerly drainage flows in the late evening and early morning and by the prevailing northwesterlies in the afternoon. A similar recirculation pattern occurs in the winter, affecting levels of carbon monoxide and particulate matter. This movement of the air up and down the valley increases the impact of the pollutants significantly.

Pollution sources are plentiful and complex in this subregion. The Santa Clara Valley has a high concentration of industry at the northern end, in the Silicon Valley. Some of these industries are sources of air toxics as well as criteria pollutants. In addition, Santa Clara Valley's large population and many work-site destinations generate the highest mobile source emissions of any subregion in the Bay Area.

Sonoma Valley

The Sonoma Valley is west of the Napa Valley. It is separated from the Napa Valley and from the Cotati and Petaluma Valleys by mountains. The Sonoma Valley is long and narrow, approximately 5 miles wide at its southern end and less than a mile wide at the northern end.

The climate is similar to that of the Napa Valley, with the same basic wind characteristics. The strongest upvalley winds occur in the afternoon during the summer and the strongest downvalley winds occur during clear, calm winter nights. Prevailing winds follow the axis of the valley, northwest/southeast, while some upslope flow during the day and downslope flow during the night occurs near the base of the mountains. Summer average maximum temperatures are usually in the high-80's, and summer minimums are around 50 degrees. Winter maximums are in the high-50's to the mid-60's, with minimums ranging from the mid-30's to low-40's.

As in the Napa Valley, the air pollution potential of the Sonoma Valley could be high if there were significant sources of pollution nearby. Prevailing winds can transport locally and non-locally generated pollutants northward into the narrow valley, which often traps and concentrates the pollutants under stable conditions. The local upslope and downslope flows set up by the surrounding mountains may also recirculate pollutants.

However, local sources of air pollution are minor. With the exception of some processing of agricultural goods, such as wine and cheese manufacturing, there is little industry in this valley. Increases in motor vehicle emissions and woodsmoke emissions from stoves and fireplaces may increase pollution as the valley grows in population and as a tourist attraction.

Southwestern Alameda County

This subregion encompasses the southeast side of San Francisco Bay, from Dublin Canyon to north of Milpitas. The subregion is bordered on the east by the East Bay hills and on the west by the bay. Most of the area is flat.

This subregion is indirectly affected by marine air flow. Marine air entering through the Golden Gate is blocked by the East Bay hills, forcing the air to diverge into northerly and southerly paths. The southern flow is directed down the bay, parallel to the hills, where it eventually passes over southwestern Alameda County. These sea breezes are strongest in the afternoon. The further from the ocean the marine air travels, however, the ocean’s effect is diminished. Thus, although the climate in this region is affected by sea breezes, it is affected less so than the regions closer to the Golden Gate.

The climate of southwestern Alameda County is also affected by its close proximity to San Francisco Bay. The bay cools the air with which it comes in contact during warm weather, while during cold weather the bay warms the air. The normal northwest wind pattern carries this air onshore. Bay breezes push cool air onshore during the daytime and draw air from the land offshore at night.

Winds are predominantly out of the northwest during the summer months. In the winter, winds are equally likely to be from the east. Easterly-southeasterly surface flow into southern Alameda

County passes through three major gaps: Hayward/Dublin Canyon, Niles Canyon and Mission Pass. Areas north of the gaps experience winds from the southeast, while areas south of the gaps experience winds from the northeast. Wind speeds are moderate in this subregion, with annual average wind speeds close to the bay at about 7 mph, while further inland they average 6 mph.

Air temperatures are moderated by the subregion's proximity to the bay and to the sea breeze. Temperatures are slightly cooler in the winter and slightly warmer in the summer than East Bay cities to the north. During the summer months, average maximum temperatures are in the mid-70’s. Average maximum winter temperatures are in the high-50's to low-60's. Average minimum temperatures are in the low 40's in winter and mid-50's in the summer.

Pollution potential is relatively high in this subregion during the summer and fall. When high pressure dominates, low mixing depths and bay and ocean wind patterns can concentrate and carry pollutants from other cities to this area, adding to the locally emitted pollutant mix. The polluted air is then pushed up against the East Bay hills. In the wintertime, the air pollution potential in southwestern Alameda county is moderate. Air pollution sources include light and heavy industry, and motor vehicles. Increasing motor vehicle traffic and congestion in the subregion may increase Southwest Alameda County pollution as well as that of its neighboring subregions.

APPENDIX E - TOXIC AIR CONTAMINANTS

Introduction

Toxic air contaminants (TACs) are air pollutants which may lead to serious illness or increased mortality, even when present in relatively low concentrations. Potential human health effects of TACs include birth defects, neurological damage, cancer and death. There are hundreds of different types of TACs, with varying degrees of toxicity. TACs may be produced by a variety of sources, including industrial facilities such as refineries, chemical plants and chrome platers, commercial facilities such as dry cleaners and gasoline stations, and motor vehicles.

District Programs

The District has regulated TACs since the 1980's as a complement to the traditional efforts to reduce emissions of criteria air pollutants. To date, the District's air toxics program has been a risk-based approach, meaning that the decisions over what sources and pollutants to control and the degree to which to control them have been based on the results of health risk assessment. A health risk assessment is an analysis where human health exposure to toxic substances is estimated, and then considered together with information regarding the toxic potency of the substances, to provide quantitative estimates of health risks. (The risk assessments used by the District do not address the possibility of, or adverse health effects resulting from, accidental releases of toxic materials such as a fire or major spill. Review of industry's preparation for, and protection from, accidental releases is performed by emergency response agencies, such as local fire and health departments.) The District's air toxics program consists of three major elements: a program to control emissions from new and modified sources; and two programs directed at existing sources - one with retrofit requirements for categories of sources, and another which is based on facility-specific analyses.

Air Toxics New Source Review

The District reviews new and modified source permit applications in accordance with the District's Risk Management Policy (adopted by the District Board of Directors in 1987). The goal of the program is to prevent any proposed stationary sources from creating new air toxics problems. In addition, benefits are realized when older, more highly polluting sources are replaced with new sources that must meet more stringent control requirements.

The need for, and degree of, emissions control required in toxics new source review is based on the results of health risk screening analysis or health risk assessment. All new/modified permit applications are reviewed for potential health impacts. If any TACs are emitted in amounts that exceed de minimus levels, a risk screening analysis, using computer-modeled estimates of atmospheric dispersion, is completed by District staff. Table E-1 lists the pollutants that trigger the District's risk screening requirements. A project that passes this risk screen is judged to have an insignificant impact on public health. A project that fails the screen does not necessarily have a significant impact, but requires further review. Further review usually consists of more detailed dispersion modeling (including the use of actual meteorological data when applicable), and consideration of other site-specific factors.

TABLE E-1
POLLUTANTS THAT TRIGGER
DISTRICT RISK SCREENING REQUIREMENTS

Carcinogenic Compounds

- Acetaldehyde
- Acrylamide
- Acrylonitrile
- Arsenic and arsenic compounds
- Asbestos
- Benzene
- Benzidine and salts
- Beryllium
- Bis(chloromethyl)ether
- Butadiene, 1,3-
- Cadmium and cadmium compounds
- Carbon tetrachloride
- Chlorinated dibenzodioxins and dibenzofurans (TCDD and TCDF)
- Chloroform
- Chromium (hexavalent)
- Dichlorobenzene, 1,4-
- Dichlorobenzidine, 3,3'-
- Diethylhexylphthalate (DEHP)
- Dioxane, 1,4-
- Epichlorohydrin
- Ethylene dibromide (1,2-dibromoethane)
- Ethylene dichloride (1,2-dichloroethane)
- Ethylene oxide
- Formaldehyde
- Hexachlorobenzene
- Hexachlorocyclohexanes
- Hydrazine
- Methylene chloride
- Methylene dianiline & chloride, 4,4'-
- Nickel and nickel compounds
- Nickel subsulfide
- N-Nitrosodiethylamine
- N-Nitrosodimethylamine
- N-Nitrosodiphenylamine
- N-Nitrosodi-n-butylamine
- N-Nitrosomethylethylamine
- N-Nitrosodi-n-propylamine
- N-Nitrosopyrrolidine
- PCBs
- PAHs (including but not limited to):
  - Benz(a)anthracene
  - Benzo(b)fluoroanthene
  - Benzo(k)fluoroanthene
  - Benzo(a)pyrene
  - Dibenz(a,h)anthracene
  - Ideno(1,2,3-cd)pyrene
- Perchloroethylene (tretrachloroethylene)
- Propylene oxide
- Trichloroethylene
- Trichlorophenol, 2,4,6-
- Urethane
- Vinyl chloride

Noncarcinogenic Compounds

- Acetone
- Acrolein
- Ammonia
- Benzyl chloride
- Bromine and compounds
- Butyl alcohol, tert-
- Carbon disulfide
- Chlorine
- Chlorobenzene
- Chlorofluorocarbons
- Chloropicrin
- Chloroprene
- Chlorotoluene
- Cresol
- Diethylaminoethanol
- Dimethylamine
- Dimethyl phthalate
- Dioctyl phthalate
- Ethyl alcohol (ethanol)
- Ethyl acetate
- Ethyl benzene
- Ethyl chloride
- Freons; (see Chlorofluorocarbons)
- Glycol ethers:
  - 2-ethoxyethanol (Cellosolve)
  - 2-methoxymethanol (Methylcellosolve)
  - 2-butoxyethanol (Butylcellosolve)
- Hexachlorocyclopentadiene
- Hexane, n-
- Hydrogen chloride
- Hydrogen cyanide
- Hydrogen fluoride
- Hydrogen sulfide
- Isocyanates:
  - methylene-bis-phenyliso-cyanate
  - methyl isocyanate
  - toluene diisocyanate
- Isophorone
- Isopropyl alcohol
- Lead, inorganic, and compounds
- Maleic anhydride
- Manganese and compounds
- Mercury and compounds
- Methyl alcohol (methanol)
- Methyl bromide
- Methyl chloroform (TCA)
- Methylethylketone (MEK)
- Methyl mercury
- Methyl methacrylate
- N-Methylpyrrolidone
- Naphthalene
- Nitrobenzene
- Phenol
- Phosgene
- Phosphine
- Phosphorus (white)
- Phthalic anhydride
- Selenium and compounds
- Sodium Hydroxide
- Styrene monomer
- Tetrahydrofuran
- Toluene
- Trichlorobenzene, 1,2,4-
- Tricholorethane, 1,1,1-; (see Methyl cloroform)
- Vapam (Na diethyldithio-carbamate)
- Xylene
- Zinc and compounds

Where risks cannot be reduced below specified health-based significance levels, sources must use the Best Available Control Technology for Toxics, or "T-BACT". The significance level for T-BACT is an individual cancer risk of 1-in-one million, or an ambient concentration above a non-cancer reference exposure level. If the residual health risks, after controls are applied, result in risks that exceed higher significance levels established for the overall acceptability of a project, then other risk reduction measures may be required, or the permits for the proposed source(s) may be denied.

The program has resulted in T-BACT being implemented on a variety of the most significant sources of TACs in the Bay Area. The program also encourages sound land use planning in that, through the risk assessment process, control requirements for sources increase in relation to their proximity to downwind sources.

Retrofit Requirements for Categories of Existing Sources

The primary mechanism for the development of retrofit air toxics control measures in California has been through the Toxic Air Contaminant Act, also referred to as the Tanner Act, adopted by the State legislature in 1983. The Tanner Act establishes a process for the identification of TACs, and for the preparation of retrofit toxic control measures on a Statewide basis. TACs are identified in a scientific review process involving the Air Resources Board (ARB), the Office of Environmental Health Hazard Assessment, and an independent scientific review panel. Once a contaminant is identified as a TAC, control measures, called Airborne Toxic Control Measures (ATCMs), are developed by the ARB. The measures are implemented and enforced by the local air districts, which may adopt the ATCMs as established by ARB, or set more stringent standards.

As of February 1996, 19 compounds have been identified as TACs through the State's scientific review process, and eight statewide ATCMs have been adopted. The first six adopted ATCMs have been adopted into District Rules and have been fully implemented in the Bay Area. These include measures for chrome plating, cooling towers, commercial and hospital sterilizers, medical waste incinerators, paving operations that use serpentine materials, and gasoline stations. The two most recently adopted ATCMs have been adopted as District rules, but final compliance dates have not yet been reached (as of February 1996). These rules address secondary metal melting operations and perchloroethylene dry cleaners.

The District has accelerated the control of air toxics for existing air toxics by supplementing the ATCMs with rules developed locally. Examples of these rules include those covering aeration of contaminated soil and water, marine vessel loading and unloading, and the addition of more stringent requirements for gasoline stations.

In 1990, the federal Clean Air Act was amended creating an ambitious federal air toxics program. In 1992, the State legislature adopted AB 2728 to provide a legal framework for the integration of the existing air toxics programs in California with the new federal program. This legislation required ARB to designate the 189 substances that were listed as Hazardous Air Pollutants in the federal Clean Air Act as TACs without going through the scientific review process. The list of substances designated by the ARB as TACs (as of August 1995) is given in Table E-2.

TABLE E-2
SUBSTANCES DESIGNATED BY ARB AS TOXIC AIR CONTAMINANTS

Chemical Name	CAS No.	Chemical Name	CAS No.
Acetaldehyde	75070	Cresol(o)	95487
Acetamide	60355	Cresol(p)	106445
Acetonitrile	75058	Cresols/Cresylic acid	1319773
Acetophenone	98862	Cumene (Isopropylbenzene)	98828
Acetylaminofluorene(2)	53963	Cyanide Compounds[23]	----
Acrolein	107028	D(2,4), salts and esters	94757
Acrylamide	79061	DDE	3547044
Acrylic acid	79107	Diazomethane	334883
Acrylonitrile	107131	Dibenzofurans	132649
Allylchloride	107051	Dibromo-3-chloropropane(1,2)	96128
Aminobiphenyl(4)	92671	Dibutylphthalate	84742
Aniline	62533	Dichlorobenzene(1,4)(p)	106467
Anisidine(o)	90040	Dichlorobenzidene(3,3)	91941
Antimony Compounds	----	Dichloroethyl ether	
Arsenic Compounds		(Bis(2-chloroethyl)ether)	111444
(inorganic including arsine)	----	Dichloropropene(1,3)	542756
Asbestos	1332214	Dichlorvos	62737
Benzene	71432	Diethanolamine	111422
Benzidine	92875	Diethylaniline(N,N)	
Benzotrichloride	98077	(Dimethylaniline(N,N)	121697
Benzyl chloride	100447	Diethyl sulfate	64675
Beryllium Compounds	----	Dimethoxybenzidine(3,3')	1119904
Biphenyl	192524	Dimethyl aminoazobenzene	60117
Bis(2-ethylhexyl)phthalate (DEHP)	117817	Dimethyl Benzidine(3,3')	119937
Bis(chloromethyl)ether	542881	Dimethyl carbamoyl chloride	79447
Bromoform	75252	Dimethyl formamide	68122
Butadiene(1,3)	106990	Dimethyl hydrazine(1,1)	57147
Cadmium Compounds	----	Dimethyl phthalate	131113
Calcium cyanamide	156627	Dimethyl sulfate	77781
Caprolactam	105602	Dinitro-o-cresol(4,6), and salts	534521
Captan	133062	Dinitrophenol(2,4)	51285
Carbaryl	63252	Dintrotoluene(2,4)	121142
Carbon disulfide	75150	Dioxane(1,4)(1,4-Diethyleneoxide)	123911
Carbon tetrachloride	56235	Diphenylhydrazine(1,2)	122667
Carbonyl sulfide	463581	Epichlorohydrin	
Catechol	120809	(Chloro-2,3-epoxypropane(1))	106898
Chloramben	133904	Epoxybutane(1,2)(1,2-Butylene oxide)	106887
Chlordane	57749	Ethyl acrylate	140885
Chlorine	7782505	Ethyl benzene	100414
Chloroacetic acid	79118	Ethyl carbamate (Urethane)	51796
Chloroacetophenone(2)	532274	Ethyl chloride (Chloroethane)	75003
Chlorobenzene	108907	Ethylene dibromide (1,2-Dibromoethane)	106934
Chlorobenzilate	510156	Ethylene dichloride (1,2-Dichloroethane)	107062
Chloroform	67663	Ethylene glycol	107211
Chloromethyl methyl ether	107302	Ethylene imine (Aziridine)	151564
Chloroprene		Ethylene oxide	75218
(Neoprene; 2-chloro-1,3-butadiene)	126998	Ethylene thiourea	96457
Chromium Compounds	----	Ethylidene dichloride	
Cobalt Compounds	----	(1,1-Dichloroethane)	75343 Coke Oven Emissions
----	Formaldehyde	50000	
Cresol(m)	108394	Glycol ethers[24]	----

[23] X'CN where X = H' or any other group where a formal dissociation may occur, for example KCN or $Ca(CN)_2$.

[24] Includes mono- and di-ethers of ethylene glycol, diethylene glycol and triethylene glycol $R-(OCH_2CH_2)_n-OR'$ where: n = 1,2,or 3 - R = alkyl or aryl groups - R' = R, H, or group which, when removed, yield glycol ethers with the structure: $R-(OCH_2CH)_n-OH$. Polymers are excluded from the glycol category.

TABLE E-2 (CONTINUED)
SUBSTANCES DESIGNATED BY ARB AS TOXIC AIR CONTAMINANTS

Chemical Name	CAS No.	Chemical Name	CAS No.
Heptachlor	76448	Phenylenediamine(p)	106503
Hexachlorobenzene	118741	Phosgene	75445
Hexachlorobutadiene	87683	Phosphine	7803512
Hexachlorocyclopentadiene	77474	Phosphorus	7723140
Hexachloroethane	67721	Pthalic anhydride	85449
Hexamethylene-1,6-disocyanate	822060	Polychlorinated biphenyls (Arochlors)	1336363
Hexamethylphosphoramide	680319	Polycylic Organic Matter[25]	----
Hexane	110543	Propane sultone(1,3)	1120714
Hydrazine	302012	Propiolactone(beta)	57578
Hydrochloric acid	7647010	Propionaldehyde	123386
Hydrogen fluoride (Hydrofluoric acid)	7664393	Propoxur (Baygon)	114261
Hydroquinone	123319	Propylene dichloride	
Isophorone	78591	(1,2-Dichloropropane)	78875
Lead Compounds	----	Propylene oxide	75569
Lindane (all isomers)	58899	Propylenimine(1,2) (2-Methyl aziridine)	75558
Maleic anhydride	108316	Quinoline	91225
Manganese Compounds	----	Quinone (1,4-Cyclohexadienedione)	106514
Mercury Compounds	----	Radionuclides (including radon)[26]	----
Methanol	67561	Selenium Compounds	----
Methoxychlor	72435	Styrene	100425
Methyl bromide (Bromomethane)	74839	Styrene oxide	96093
Methyl chloride (Chloromethane)	74873	Tetrachlorodibenzo-p-dioxin(2,3,7,8)	1746016
Methyl chloroform (1,1,1-Trichloroethane)	71556	Tetrachloroethane(1,1,2,2)	79345
Methyl ethyl ketone (2-Butanone)	78933	Tetrachloroethylene (Perchloroethylene)	127184
Methyl hydrazine	03464	Titanium tetrachloride	7550450
Methyl iodide (Iodomethane)	74884	Toluene	108883
Methyl isobutyl ketone (Hexone)	108101	Toluene diamine(2,4)	
Methyl isocyanate	624839	(2,4-Diaminotoluene)	95807
Methyl methacrylate	80626	Toluene diisocyanate(2,4)	584849
Methyl tert butyl ether	1634044	Toluidine(o)	95534
Methylene bis(2-chloroaniline)(4,4)	101144	Toxaphene (Chlorinated camphene)	8001352
Methylene chloride (Dichloromethane)	75092	Trichlorobenzene(1,2,4)	120821
Methylene diphenyl diisocynate (MDI)	101688	Trichloroethane(1,1,2,)	79005
Methylenedianiline(4,4')	101779	Trichloroethylene	79016
Mineral fibers[27]	----	Trichlorophenol(2,4,5)	95954
Naphthalene	91203	Trichlorophenol(2,4,6)	88062
Nickel Compounds	----	Triethylamine	121448
Nitrobenzene	98953	Trifluralin	1582098
Nitrobiphenyl(4)	92933	Trimethylpentane(2,2,4)	540841
Nitrophenol(4)	100027	Vinyl acetate	108054
Nitropropane(2)	79469	Vinyl bromide	593602
Nitroso-N-methylurea(N)	684935	Vinyl chloride	75014
Nitrosodimethylamine(N)	62759	Vinylidene chloride	
Nitrosomorpholine(N)	59892	(1,1-Dichloroethylene)	75354
Parathion	56382	Xylene(m)	108383
Pentachloronitrobenzene(Quintobenzene)	82688	Xylene(o)	95476
Pentachlorophenol	87865	Xylene(p)	106423
Phenol	108952	Xylenes(mixed)	1330207

[25] Include organic compounds with more than one benzene ring, and which have a boiling point greater than or equal to 100°C.

[26] A type of atom which spontaneously undergoes radioactive decay.

[27] Includes glass microfibers, glass wool fibers, rock wool fibers, and slag wool fibers, each characterized as "respirable" (fiber diameter less than 3.5 micrometers and possessing an aspect ratio (fiber length divided by fiber diameter) greater than 3.

Because of the federal program, the primary source of new air toxics rules in the Bay Area has shifted from the ATCMs developed by ARB to the National Emission Standards for Hazardous Air Pollutants (NESHAPs), developed by the U.S. EPA. (These federal rules are also commonly referred to as MACT standards, because they reflect the Maximum Achievable Control Technology.) A large number of MACT standards are due to be promulgated on a schedule extending through the year 2000. AB 2728 requires the District to implement and enforce all MACT standards, or rules that are at least as stringent.

Air Toxics "Hot Spots" Program

Assembly Bill 2588, the Air Toxics "Hot Spots" Information and Assessment Act, was enacted by the State legislature in 1987. AB 2588 requires plants emitting TACs to prepare inventories of the toxic air emissions from their entire facility. Air districts are then required to prioritize these facilities based on the quantity and toxicity of these emissions, and their proximity to areas where the public may be exposed.

Each facility that is put into a "high priority" category as a result of this review is required to prepare a comprehensive facility-wide health risk assessment. AB 2588 requires that exposed individuals then be notified of any "significant health risks" identified in the health risk assessment. The health risk levels used for public notification in the "hot spots" program are set by each individual air district. In the Bay Area, the District used a maximum individual cancer risk of 10 in one million, or an ambient concentration above a non-cancer reference exposure level, as the threshold of notification.

The first cycle of the District's "hot spots" program was completed in 1991. Out of the 129 "high priority" facilities preparing risk assessments, 30 had risk levels that required public notification. The number of facilities with risks over the notification levels was reduced to 16 in 1992. As of 1995, the number of facilities requiring public notification was 5. These reductions were attributable to efforts to further reduce emissions and to further refine risk assessments. Through 1995, no new high priority facilities had been identified since the original prioritization.

As part of the "hot spots" program, the District also is focusing on "industry-wide" risk assessments, which AB 2588 provides for small businesses that operate in a similar manner. Under the industry-wide program, the District is responsible for the preparation of risk assessments and for performing public notification. Industry-wide studies for gasoline stations and dry cleaners are scheduled for completion in 1996.

In 1992, the State "hot spots" program was amended with the passage of SB 1731. This legislation requires facilities to implement measures to reduce risks below levels determined by the District to be significant within a certain time frame. In 1994, the District took its first regulatory action under SB 1731 with the adoption of a more stringent rule for perchloroethylene dry cleaners. The risk reduction requirements of SB 1731 were incorporated into this rule because many dry cleaners (and in particular those that are located in residential buildings) have been identified with lifetime cancer risks that exceed 100-in-one-million.

APPENDIX F - RESOURCE DOCUMENTS

There is a growing body of research concerning land use and design strategies to reduce automobile use. This appendix identifies selected resources that may be useful to Lead Agencies and other parties interested in pursuing such strategies. This is not intended to be a comprehensive list, but rather a good starting point for those interested in land use-related measures to reduce auto use. Interested parties are encouraged in particular to refer to the report prepared by JHK & Associates for the California Air Resources Board indicated below (Transportation-Related Land Use Strategies to Minimize Motor Vehicle Emission: An Indirect Source Research Study). The report includes an annotated bibliography listing over 150 documents.

Association of Bay Area Governments and Bay Area Air Quality Management District, Improving Air Quality Through Local Plans and Programs, A Guidebook for City and County Governments, April 1994.

California Air Resources Board, The Land Use - Air Quality Linkage, 1994.

California Resources Agency, Bank of America, Greenbelt Alliance and Low Income Housing Fund, Beyond Sprawl: New Patterns of Growth to Fit the New California, February 1995.

California Energy Commission, Energy Aware Planning Guide, January 1993.

Calthorpe, Peter, The Next American Metropolis: Ecology, Community and the American Dream, 1993.

Calthorpe Associates, Transit-Oriented Development Design Guidelines, prepared for the City of San Diego, August 1992.

Calthorpe Associates, Transit-Oriented Development Design Guidelines (final public review draft), prepared for Sacramento County Planning and Community Development Department, September 1990.

Cambridge Systematics Inc., Calthorpe Associates with Parsons Brinkerhoff Quade & Douglas Inc., The LUTRAQ Alternative Interim Report, 1992

Cervero, Robert, Suburban Gridlock, 1986.

Cervero, Robert, America's Suburban Centers: The Land Use-Transportation Link, 1989.

Citizens Advocating Responsible Transportation, Traffic Calming: The Solution to Urban Traffic and a New Vision for Neighborhood Livibility, 1989.

Handy, Susan, How Land Use Patterns Affect Travel Patterns: A Bibliography, 1992.

Holtzclaw, John, Using Residential Patterns and Transit to Decrease Auto Dependence and Cost, Natural Resources Defense Council, June 1994.

JHK & Associates, Inc., Analysis of Indirect Source Trip Activity at Regional Shopping Centers, 1993.

JHK & Associates, Inc., Transportation-Related Land Use Strategies to Minimize Motor Vehicle Emissions: An Indirect Source Research Study, prepared for the California Air Resources Board, June 1995.

Kelbaugh, Doug, et al., The Pedestrian Pocket Book: A New Suburban Design Strategy, 1989.

Local Government Commission, Land Use Strategies for More Livable Places, June 1992.

Local Government Commission, Participation Tools for Better Land Use Planning, May 1995.

Local Government Commission, Building Livable Communities: A Policymaker's Guide to Infill Development, August 1995.

Metropolitan Transportation Commission, Moving Towards More Community-Oriented Transportation Strategies in the Bay Area: A Guide to Getting the Information (Draft), May 1996.

New Jersey Transit, Planning for Transit-Friendly Land Use: A Handbook for New Jersey Communities, June 1994.

Newman, Peter and Kenworthy, Jefferey, Cities and Automobile Dependence: An International Sourcebook, 1989.

Oregon Chapter American Planning Association, Transportation Rule Working Group, "Recommendations for Pedestrian, Bicycle and Transit Friendly Development Ordinances" (working draft), February 1993.

Oregon Department of Transportation, Transportation Development Branch, "Best Management Practices for Transportation/Land Use Planning" (working draft), August 1993.

Pivo, Gary, et al., A Summary of Guidelines for Coordinated Urban Design, Transportation and Land Use Planning, with an Emphasis on Encouraging Alternatives to Driving Alone, 1992.

The Planning Center, Land Use, Transportation and Air Quality: A Manual for Planning Practitioners, prepared for San Bernardino County, March 1993.

Pushkarev, Boris S. and Zuppan, Jefferey M., Public Transportation and Land Use Policy, 1977.

Snohomish County Transportation Authority, A Guide to Land Use and Public Transportation for Snohomish County, Washington, Volume I, December 1989.

Snohomish County Transportation Authority, A Guide to Land Use and Public Transportation, Volume II: Applying the Concepts, December 1993.

TriCounty Metropolitan Transportation District of Oregon, Planning and Design for Transit, March 1993.

Untermann, Richard, Linking Land Use and Transportation: Design Strategies to Serve HOVs and Pedestrians, 1991.

U.S. Department of Transportation, Guidelines for Transit-Sensitive Suburban Land Use Design, July 1991.

APPENDIX G - GLOSSARY

Acid Deposition -- Conversion of sulfur oxide and nitrogen oxide emissions into acidic compounds which precipitate in rain, snow, fog, or dry particles.

Aerosol -- Particle of solid or liquid matter that can remain suspended in the air because of its small size (generally under one micron).

Air Quality Management District (AQMD) -- Local agency charged with controlling air pollution and attaining air quality standards. The Bay Area Air Quality Management District is the regional AQMD that includes Alameda, Contra Costa, Marin, Napa, San Francisco, San Mateo and Santa Clara Counties and the southern halves of Solano and Sonoma Counties.

Air Resources Board (ARB) -- The State of California agency responsible for air pollution control. Responsibilities include: establishing State ambient air quality standards, setting allowable emission levels for motor vehicles in California and oversight of local air quality management districts.

Area Sources -- Sources of air pollutants that individually emit relatively small quantities of air pollutants, but which cumulatively may emit large quantities of emissions. Examples include water heaters, lawn maintenance equipment and consumer products.

Authority to Construct (A/C) -- A preconstruction permit issued by the District. An A/C typically includes conditions which the applicant must incorporate into facility design, operations, etc. in order to comply with District regulations.

Best Available Control Technology (BACT) -- The most stringent emissions control that has been achieved in practice, identified in a state implementation plan, or found by the District to be technologically feasible and cost-effective for a given class of sources.

California Clean Air Act (CCAA) -- Legislation enacted in 1988 mandating a planning process to attain state ambient air quality standards.

CALINE -- A model developed by the Air Resources Board that calculates carbon monoxide concentrations resulting from motor vehicle use.

Carbon Monoxide (CO) -- A colorless, odorless, toxic gas produced by the incomplete combustion of carbon-containing substances. It is emitted in large quantities by exhaust of gasoline-powered vehicles.

Catalytic Converter -- An air pollution abatement device used primarily on motor vehicles. It removes organic contaminants by oxidizing them into carbon dioxide and water through chemical reaction. May convert nitrogen dioxide to nitrogen and oxygen, as well as promoting other similar reactions.

Chlorofluorocarbons (CFCs) -- A family of inert, nontoxic, and easily liquefied chemicals used in refrigeration, air conditioning, packaging, insulation, or as solvents and aerosol propellants. CFCs drift into the upper atmosphere where their chlorine components destroy stratospheric ozone.

Clean Air Act (CAA) -- Long-standing federal legislation, last amended in 1990, that is the legal basis for the national clean air programs.

Cold Start -- Starting a motor vehicle after the engine has cooled. The duration of time after engine shut-off needed to produce a cold start is typically about an hour for a catalyst equipped vehicle and about four hours for a non-catalyst equipped vehicle.

Conformity -- A requirement in federal law and administrative practice that requires that projects will not be approved if they do not conform with the State Implementation Plan by: causing or contributing to an increase in air pollutant emissions, violating an air pollutant standard, or increasing the frequency of violations of an air pollutant standard.

Criteria Air Pollutants -- Air pollutants for which the federal or State government has established ambient air quality standards, or criteria, for outdoor concentration in order to protect public health. Criteria pollutants include: ozone, carbon monoxide, sulfur dioxide PM_{10} (previously total suspended particulate), nitrogen oxide, and lead.

EMFAC - The computer model developed by the California Air Resources Board to estimate composite on-road motor vehicle emission factors by vehicle class.

Emission Factor -- The amount of a specific pollutant emitted from a specified polluting source per unit quantity of material handled, processed, or burned.

Emission lnventory -- A list of air pollutants emitted into an area's atmosphere, in amounts (commonly tons) per day or year, by type of source.

Environmental Protection Agency (EPA) -- The federal agency responsible for control of air and water pollution, toxic substances, solid waste, and cleanup of contaminated sites.

Exceedance -- A monitored level of concentration of any air contaminant higher than national or state ambient air quality standards.

Hazardous Air Pollutants -- Air pollutants which are not covered by ambient air quality standards but which may reasonably be expected to cause or contribute to serious illness or death (see NESHAPs).

Health Risk Assessment -- An analysis where human exposure to toxic substances is estimated, and considered together with information regarding the toxic potency of the substances, to provide quantitative estimates of health risk.

Hot Spot -- A location where emissions from specific sources may expose individuals and population groups to elevated risks of adverse health effects and contribute to the cumulative health risks of emissions from other sources in the area.

Hot Start - Starting a motor vehicle while the engine is still fully warmed up.

Hydrocarbon -- Any of a vast family of compounds containing carbon and hydrogen in various combinations; found especially in fossil fuels. Some of the hydrocarbon compounds are major air pollutants; they may be active participants in the photochemical process or affect health.

Hydrogen Sulfide (H_2S) -- A gas characterized by "rotten egg" smell, found in the vicinity of oil refineries, chemical plants and sewage treatment plants.

Indirect Sources -- Land-uses and facilities which attract or generate motor vehicle trips and thus result in air pollutant emissions, e.g., shopping centers, office buildings, and airports.

Inversion -- The phenomenon of a layer of warm air over cooler air below. A special problem in polluted areas because this atmospheric structure resists the natural dispersion and dilution of air contaminants.

Level of Service (LOS) -- A transportation planning term for a method of measurement of congestion. The LOS compares actual or projected traffic volume to the maximum capacity of the road under study. LOS ranges from A through F. LOS A describes free flow conditions, while LOS F describes the most congested conditions, up to or over the maximum capacity for which the road was designed.

Mixing Depth -- The expanse in which air rises from the earth and mixes with the air above it until it meets air equal or warmer in temperature -- the inversion cap.

Mobile Source -- Any vehicle that produces air pollution, such as cars, trucks and motorcycles (on road mobile sources) or airplanes, trains and construction equipment (off-road mobile sources).

National Ambient Air Quality Standards (NAAQS) -- Health-based pollutant concentration limits established by EPA that apply to outside air (see Criteria Air Pollutants).

National Emissions Standards for Hazardous Air Pollutants (NESHAPs) -- Emissions standards set by EPA for air pollutants not covered by NAAQS that may cause an increase in deaths or in serious, irreversible, or incapacitating illness.

Nitrogen Oxides (NOx) -- Gases formed in great part from atmospheric nitrogen and oxygen when combustion takes place under conditions of high temperature and high pressure; NOx is a criteria air pollutant.

Non-Attainment Area -- Defined geographic area that does not meet one or more of the Ambient Air Quality Standards for the criteria pollutants designated in the federal Clean Air Act and/or California Clean Air Act.

Organic Compounds -- Large group of chemical compounds that contain carbon. Some types of organic gases, including olefins, aromatics and aldehydes, are highly reactive -- that is, participate in photochemical reactions in the atmosphere to form oxidant.

Ozone (0_3) -- A pungent, colorless, toxic gas. A product of complex photochemical processes, usually in the presence of sunlight. Tropospheric (lower atmosphere) ozone is a criteria air pollutant.

Ozone Depletion -- Destruction of the stratospheric ozone layer (10 to 20 miles above the earth) which shields the earth from ultraviolet radiation. This destruction is caused by the breakdown of certain chlorine and/or bromine-containing compounds (chlorofluorocarbons or halons).

Particulate -- A particle of solid or liquid matter; soot, dust, aerosols, fumes and mists.

Permit to Operate (P/O) -- An operational permit issued yearly by the Air District to industrial sources which emit air contaminants..

Photochemical Process -- The chemical changes brought about by the radiant energy of the sun acting upon various polluting substances. The products are known as photochemical smog.

Pollution Standards Index (PSI) -- A national, standardized system of reporting air pollution levels to the public by assigning them a numerical value.

PM_{10} -- Fine particulate matter (solid or liquid) with an aerodynamic diameter equal to or less than 10 microns. Individual particles of this size are small enough to be inhaled into human lungs; they are not visible to the human eye.

Precursor -- Compounds that change chemically or physically after being emitted into the air and eventually produce air pollutants. For example, organic compounds are precursors for ozone.

Prevention of Significant Deterioration (PSD) -- EPA program in which state and/or federal permits are required that are intended to restrict emissions for new or modified sources in places where air quality is already better than required to meet primary and secondary ambient air quality standards.

Reactive Organic Gases (ROG) -- Classes of organic compounds, especially olefins, substituted aromatics and aldehydes, that react more rapidly in the atmosphere to form photochemical smog or ozone.

Risk Management and Prevention Program (RMPP) -- A program enacted by the State Legislature in 1986 in order to reduce the risk of public exposure to acutely hazardous materials resulting from upsets at industrial and commercial facilities. RMPP analyses identify possible hazards at a facility, estimate potential consequences of an upset to public health and safety, address measures to reduce the chances of an upset, and identify measures for responding to accidents that may occur. The program is usually administered by the county health department or the local fire department.

Sensitive Receptors -- Facilities or land uses that include members of the population that are particularly sensitive to the effects of air pollutants, such as children, the elderly and people with illnesses. Examples include schools, hospitals and residential areas.

State Implementation Plan (SIP) -- EPA-approved state plans for attaining and maintaining federal air quality standards.

Stationary Source -- A fixed, non-mobile source of air pollution, usually at industrial or commercial facilities.

Sulfur Oxides (SO_X) -- Pungent, colorless gases formed primarily by the combustion of sulfur-containing fossil fuels, especially coal and oil. Considered a criteria air pollutant, sulfur oxides may damage the respiratory tract as well as vegetation.

Total Suspended Particulate Matter (TSP) -- Particles of solid or liquid matter -- soot, dust, aerosols, fumes and mist -- up to approximately 30 microns in size. As a criteria pollutant TSP has been replaced by PM_{10}.

Toxic Air Pollutants -- Air pollutants which cause illness or death in relatively small quantities. Non-criteria air contaminants that, upon exposure, ingestion, inhalation, or assimilation into organisms either directly from the environment or indirectly by ingestion through food chains, will cause death, disease, behavioral abnormalities, cancer, genetic mutations, physiological malfunctions, or physical deformations in such organisms or their offspring.

Transportation Control Measures (**TCM**s) -- Measures to reduce congestion and decrease emissions from motor vehicles by reducing vehicle use.

URBEMIS - A computer model developed by the California Air Resources Board to estimate air pollutant emissions from motor vehicle trips associated with land use development.

Volatile Organic Compound (VOC) -- An organic compound that evaporates readily at normal temperatures; a precursor to ozone.

APPENDIX H - REFERENCES

Association of Bay Area Governments and Bay Area Air Quality Management District, Improving Air Quality Through Local Plans and Programs, October 1994.

Bay Area Air Quality Management District, Air Quality and Urban Development: Guidelines for Assessing Impacts of Projects and Plans, November 1985.

_____, Bay Area '91 Clean Air Plan, Volumes 1-4, October 1991.

_____, Base Year 1990 Emission Inventory: Summary Report, October 1993.

_____, Bay Area '94 Clean Air Plan and Triennial Progress Report, Volume 1-4, December 1994.

California Air Resources Board, Methods for Assessing Area Source Emissions in California, September 1991.

_____, Air Pollution Mitigation Measures for Airports and Associated Activity, May 1994.

_____, The Land Use-Air Quality Linkage, 1994.

California Energy Commission, Energy-Aware Planning Guide, 1993.

Cervero, Robert, Ridership Impacts of Transit-Focused Development in California, for the National Transit Access Center, November 1993.

Harvey, Greig, et al, Transportation Control Measures for the San Francisco Bay Area: Analysis of Effectiveness and Costs, October 1991.

Holtzclaw, John, Using Residential Patterns and Transit to Decrease Auto Dependence and Cost, Natural Resources Defense Council, June 1994.

Institute of Transportation Engineers, Trip Generation, Fifth Edition, 1991.

_____, Trip Generation, February 1995 Update to the 5th Edition, 1995.

JHK & Associates, Transportation-Related Land Use Strategies to Minimize Motor Vehicle Emissions: An Indirect Source Research Study, Final Report, prepared for the California Air Resources Board, June 1995.

Metropolitan Transportation Commission, Bay Area Travel Forecasts: Congestion Management Program Databook #1, Regional Summary, March 1991.

_____, Bay Area Travel Forecasts for Years 1990, 1996 and 2010, Technical Summary, September 1993.

_____, 1994 Regional Transportation Plan for the San Francisco Bay Area, June 1994.

_____, Transportation Improvement Program for the Nine-County San Francisco Bay Area, 1995, Volume 3, Air Quality Assessment, October 1994.

Monterey Bay Unified Air Pollution Control District, CEQA Air Quality Guidelines, October 1995.

Sacramento Metropolitan Air Quality Management District, Mitigation Resource Handbook, First Edition, 1995.

_____, Air Quality Thresholds of Significance, First Edition, 1994.

South Coast Air Quality Management District, CEQA Air Quality Handbook, April 1993.

State of California Governor's Office of Planning and Research, CEQA: California Environmental Quality Act, Statute and Guidelines, 1992, June 1992.

Taback, H.J., et al, KVB Inc., Inventory of Emissions From Non-Automotive Vehicular Sources, Final Report, February 1980.

U.S. Environmental Protection Agency, Compilation of Air Pollutant Emission Factors, Volume I: Stationary, Point and Area Sources, AP-42, 5th Edition, January 1995.

Source Inventory of Bay Area Greenhouse Gas Emissions



Updated: February 2010

BAY AREA AIR QUALITY MANAGEMENT DISTRICT

939 Ellis Street
San Francisco, California 94109

SOURCE INVENTORY OF BAY AREA

GREENHOUSE GAS EMISSIONS

Base Year 2007

BAY AREA AIR QUALITY MANAGEMENT DISTRICT

February 2010

Prepared by
Emission Inventory Section
Tirlochan S. Mangat, Manager

Sukarn J. Claire
Tan M. Dinh
Amir K. Fanai
Michael H. Nguyen
Stuart A. Schultz

Approved by
Henry D. Hilken, Director of Planning, Rules & Research

TABLE OF CONTENTS

Page

Introduction ……..……...…. 1

Greenhouse Gas (GHG) Emissions Inventory …….…… 4

Summary of Bay Area GHG Emissions ……. 7

GHG Emissions Trends for Bay Area ……..……...…. 16

List of Figures and Tables

Table A: Global Warming Potentials (GWPs) ……...…. 4

Table B: Emission Factors ……. ……..……..….. 5

Table C: General Statistics …….……...…….…. 6

Figure 1, Table D: Bay Area Emissions Summary …….…… 8

Figure 2, Table E: Emissions by Sector …….…….…… 10

Figure 3, Table F: Industrial/Commercial Sector Emissions Breakdown.. 12

Figure 4, Table G: Transportation Sector Emissions Breakdown ……..… 13

Figure 5, Table H: Emissions by County ……..……. 14

Figure 6, Table I: County Emissions Breakdown by Sector ……..…….. 15

Figure 7, Table J: Emissions Trends by Sector …….…….. 16

Figure 8: Bay Area Emissions Trends …….……..…...…….. 17

Table K: Bay Area Emissions by Major Category ….....…….. 19

Table L-T: County Emissions by Major Category 20-28

Table U: Bay Area GHG Emissions Projections by Major Category ….. 29-30

Table V: Bay Area Major GHG Emitting Facilities …….....…..…… 31-37

Bay Area Greenhouse Gas Emissions Inventory: 2007

Introduction

The Bay Area Air Quality Management District (Air District or BAAQMD) is the regional public agency responsible for the protection of the public's health and welfare from airborne pollutants, primarily by promulgating and enforcing regulations to reduce air pollution as provided by the Federal Clean Air Act, California Clean Air Act and State legislative mandates. The District's jurisdiction encompasses all of seven counties- Alameda, Contra Costa, Marin, San Francisco, San Mateo, Santa Clara, Napa- and the southern portions of Solano and Sonoma counties. The Air District is governed by a 23-member Board of Directors composed of locally elected officials from each of the nine Bay Area counties. In addition to its regulatory program, the Air District issues permits, operates an extensive incentives program, and conducts public outreach and education.

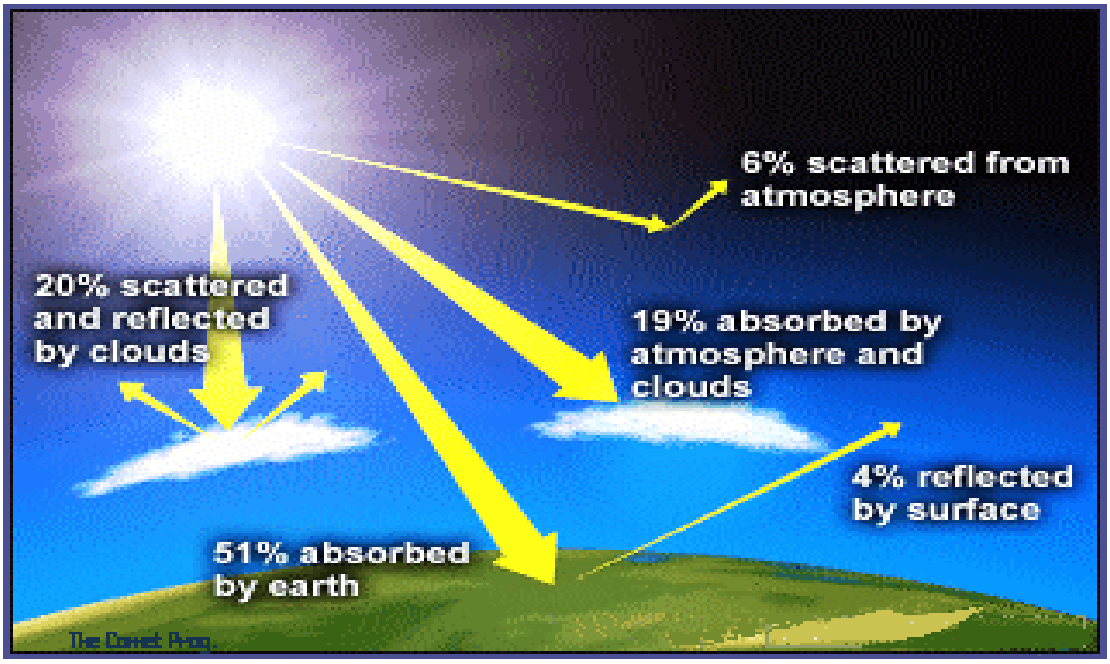
The Air District established a climate protection program in 2005 to explicitly acknowledge the link between climate change and air quality. Rising temperatures as a result of climate change threaten to undermine years of progress in improving air quality in the San Francisco Bay Area. At the same time, many longstanding air quality strategies such as programs to promote alternatives to the automobile, improve energy efficiency and encourage cleaner technologies also reduce greenhouse gases. The Air District regularly prepares inventories of criteria and toxic air pollutants to support planning, regulatory and other programs. This greenhouse gas inventory is based on the standards for criteria pollutant inventories and is intended to support the Air District's climate protection activities.

Climate Change and Greenhouse Gas Emissions

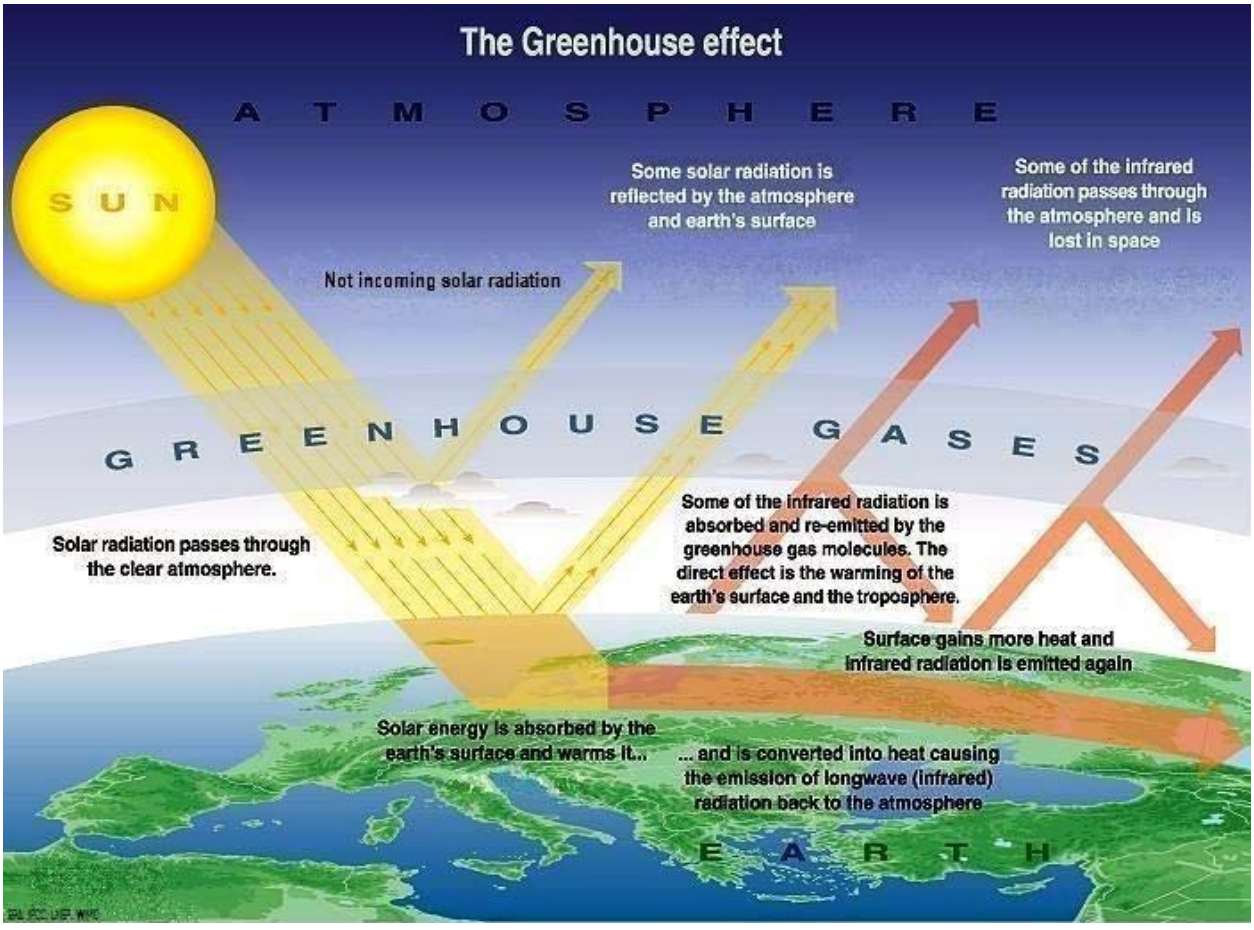
The greenhouse effect is a natural process by which some of the radiant heat from the Sun is captured in the lower atmosphere of the Earth, thus maintaining the temperature and making Earth habitable. The gases that help capture the heat are called greenhouse gases (GHG). All of these gases have been identified as forcing the earth's atmosphere and oceans to warm above naturally occurring temperatures.

Once, all climate changes on Earth occurred naturally. However, during the Industrial Revolution, we began altering our climate and environment through changing agricultural and industrial practices. Before the Industrial Revolution, human activity released very few gases into the atmosphere, but now through fossil fuel burning, deforestation and growing population (e.g. waste disposal), we are affecting the natural mixture of gases in the Earth's atmosphere. Increased concentration of these gases is upsetting the natural balance of incoming and outgoing solar energy. Emissions of carbon dioxide are the leading cause of global warming, with other pollutants also contributing. Carbon dioxide

concentrations, which ranged from 265 ppm to 280 ppm over the last 10,000 years, only began rising in the last two hundred years to current levels of 365 ppm, a 30% increase.



The natural balance of solar energy received by Earth



Some greenhouse gases occur naturally in the atmosphere, while others result from human activities. Naturally occurring greenhouse gases include water vapor, carbon dioxide, methane, nitrous oxide, and ozone. Certain human activities, however, add to the levels of most of these naturally occurring gases. The most common greenhouse gases, and those which are identified in AB32, the Global Warming Solutions Act of 2006 and are discussed in this report, are carbon dioxide, methane, nitrous oxide, hydrofluorocarbons, perfluorocarbons, and sulfur hexafluoride.

Carbon Dioxide (CO_2) is released to the atmosphere when solid waste, fossil fuels (oil, natural gas, and coal), and wood and wood products are burned.

Biogenic Carbon Dioxide (Bio-CO_2) emissions are a subset of total CO_2 emissions which are emitted from materials that are derived from living cells, excluding fossil fuels, limestone and other materials that have been transformed by geological processes. Bio-CO_2 originates from carbon that is present in materials such as wood, paper, vegetable oils and food, animal, and yard waste.

Methane (CH_4) is emitted during the production and transport of coal, natural gas, and oil. Methane emissions also result from the decomposition of organic waste in municipal solid waste landfills and the raising of livestock.

Nitrous oxide (N_2O) is emitted from agricultural and industrial activities, as well as during combustion of solid waste and fossil fuels and during production of adipic acid, and nitric acid.

Very powerful greenhouse gases, also known as *high global warming potential* (GWP) *gases* that are not naturally occurring, include hydrofluorocarbons (HFCs), perfluorocarbons (PFCs), and sulfur hexafluoride (SF_6). These gases are emitted from industrial processes such as semiconductor manufacturing, use as refrigerants and other products, and electric power transmission and distribution.

Each greenhouse gas differs in its ability to absorb heat in the atmosphere. High GWP gases such as HFCs, PFCs, and SF_6 are the most heat-absorbent. Methane traps over 21 times more heat per molecule than carbon dioxide, and nitrous oxide absorbs 310 times more heat per molecule than carbon dioxide. Often, estimates of greenhouse gas emissions are presented in carbon dioxide equivalents, which weight each gas by its global warning potential. Table A shows the global warming potentials for different greenhouse gases for a 100 year time horizon. The global warming potentials used in this report are in accordance with the Second Assessment Report (SAR) of the Intergovernmental Panel on Climate Change (IPCC).

Table A: Global Warming Potentials (GWPs) for Greenhouse Gases

Gas	GWP
CO_2	1
CH_4	21
N_2O	310
HFCs/PFCs	90- 11,700
SF_6	23,900

Greenhouse Gas Emissions Inventory

An emissions inventory is a detailed estimate of the amount of air pollutants discharged into the atmosphere of a given area by various emission sources during a specific time period. This GHG emissions inventory builds on the Air District's many years of experience preparing inventories of criteria and toxic air pollutants.

This emission inventory includes direct and indirect GHG emissions due to human activities. The emissions are estimated for industrial, commercial, transportation, residential, forestry, and agriculture activities in the San Francisco Bay Area region of California. Both direct greenhouse gas emissions from locally generated electricity in the Bay Area and indirect emissions from out-of-region generated electricity for consumption in the region are reported.

Emissions of CO_2, Bio-CO_2, CH_4, N_2O, HFCs, PFCs, and SF_6 are estimated using the most current activity (e.g., cubic feet of natural gas burned or vehicle miles traveled) and emission factor data from various sources. Activity data used in preparing this GHG inventory is the same as is used in preparing the Air District's criteria and toxic inventories. Emission factor data was obtained from the U.S. Department of Energy's (DOE's) Energy Information Administration (EIA), the California Energy Commission (CEC), and the California Air Resources Board (CARB).

Methodology

Emission sources can be broadly divided between stationary and mobile sources. Stationary sources can be further divided between point and area sources. Stationary emission sources identified on an individual basis or as a single source are called point sources. Electric power generating plants and oil refineries are examples of point sources. Based on Air District permits for stationary sources, the Air District maintains a computer database with detailed information on operations and emission characteristics for nearly 4,000 facilities, which include roughly 25,000 different sources, throughout the Bay Area. Activity data on the sources are collected at the process level from each facility and are updated regularly as part of permit renewal. The greenhouse gas emissions from these sources are calculated by multiplying activity data by standardized

emission factors for each greenhouse gas. These emission factors take into account fuel-specific carbon content and the percent of carbon that oxidizes to convert to carbon dioxide emissions. Some of the combustion emission factors for various fuels used for this emissions inventory are shown in Table B. Examples of activity data used to develop the inventory are shown in Table C.

Stationary emission sources that are not identified individually are called area sources. Area sources are groups of numerous small emission sources, which individually do not emit significant amounts of pollutants but together make an appreciable contribution to the emission inventory. Many area sources do not require permits from the Air District, such as residential heating, restaurants, and the wide range of consumer products such as paints, solvents, and cleaners. Some facilities considered as area sources do require permits from the Air District, such as gas stations and dry cleaners. Emissions estimates for area sources are developed based on estimated activities and emission factors for various categories.

Mobile sources consist of on-road motor vehicles and other mobile sources. Examples of on-road motor vehicles are cars, trucks, buses and motorcycles. Other mobile sources include boats, ships, trains, aircraft, and garden, farm and construction equipment. Greenhouse gas emissions for on-road motor vehicles were calculated using CARB's EMFAC2007 model together with vehicle miles travelled (VMT) and other activity data by county from the Metropolitan Transportation Commission's (MTC) Regional Transportation Plan (RTP2030). Other off- and on- road mobile source emissions were calculated based on estimated fuel used and emission factors in Table B. GHG emissions for ships are calculated for ship travel within 100 miles of the San Francisco coastline. Aircraft emissions are calculated for air travel within the Air District boundaries.

Table B: Generalized GHG Emission Factors (Lbs. /Usage Unit)

Fuel	CO_2	CH_4	N_2O	Unit
Liquid Fuels				
Distillate Fuel (Fuel Oil, Diesel)	22.4	0.00053	0.00019	Gallon
Jet Fuel	21.1	0.00052	0.00019	Gallon
Kerosene/Naphtha	21.5	0.00050	0.00018	Gallon
Liquified Petroleum Gases (LPG)	12.8	0.00025	0.00002	Gallon
Motor Gasoline	19.6	0.00055	0.00020	Gallon
Residual Fuel (Bunker C Fuel Oil)	26.0	0.00022	0.00021	Gallon
Aviation Gasoline	18.4	0.00052	0.00019	Gallon
Bio-diesel	20.7	0.00049	0.00018	Gallon
Propane	12.7	0.000003	2.3E-07	Gallon
Butane	14.7	0.000003	2.3E-07	Gallon

Table B (continued)

Fuel	CO_2	CH_4	N_2O	Unit
Gaseous Fuels				
Natural Gas	120.6	0.00020	0.00020	1000 ft^3
Landfill Gas	110.5	0.21050	0.00024	1000 ft^3
Digester Gas	104.7	0.02997	0.00030	1000 ft^3
Carbon Monoxide	116.1	0.00270	0.00019	1000 ft^3
Refinery Waste Gases	139.0	0.00320	0.00022	1000 ft^3
Solids				
Refuse/Waste	2,000	0.29790	0.08980	Ton
Wood and Other	3,814	0.29790	0.08980	Ton
Agriculture Waste Burning	174	0.14000	0.35000	Ton
Petroleum Coke	6,769	0.44920	0.10630	Ton

Table C: 2007 General Statistics

County	Population (1000's)	Daily Electricity Usage (Megawatt hours)	Daily Natural Gas Usage (Million cu.ft.)	Daily Gasoline Sales (1000's gal.)	Daily Vehicle Miles Traveled (Millions)
Alameda	1,532	31,395	150	1,759	38.0
Contra Costa	1,039	23,204	636	1,150	25.7
Marin	255	4,033	24	337	6.2
Napa	136	2,679	13	169	4.5
San Francisco	801	17,720	118	961	12.4
San Mateo	729	12,909	71	947	19.4
Santa Clara	1,805	44,114	212	2,160	40.1
Solano*	308	6,443	44	353	7.2
Sonoma*	431	6,977	31	489	10.6
Total	**7,036**	**149,474**	**1,300**	**8,327**	**164.1**

* Portion within Bay Area Air Quality Management District

Revisions to the Previous GHG Inventory

This emissions inventory estimates greenhouse gas emissions produced by the San Francisco Bay Area in 2007. This inventory updates the Air District's previous GHG emission inventory for base year 2002 (published November 2006). All activity data has been updated to reflect more current industrial activity, motor vehicle travel, and economic and population growth. Most of the methodologies for calculating emissions remain the same, with certain exceptions: 1) emissions from electricity consumed in the Bay Area but generated outside the region are now included; 2) emissions of ozone depleting substance (ODS) substitutes such as hydrofluorocarbons and perfluorocarbons used as refrigerants etc. are now included; 3) more complete oil refinery process emissions are included in this inventory; 4) certain off-road equipment (e.g., construction and industrial) previously was included in the transportation sector and is now reported separately; 5) ship emissions are now calculated for travel within 100 nautical mile of the California coastline rather than 3 nautical miles to be consistent with the Air District's criteria pollutant inventory and; 6) biogenic CO_2 emissions are calculated but not included in the total CO_2 equivalent estimates for the region.

Because of these revisions, caution should be used in comparing this 2007 GHG emission inventory to the previous 2002 inventory. These revisions have resulted in different estimates of Bay Area greenhouse gas emissions. Consequently, the percentage contributions from individual sectors may be affected. For example, estimates of transportation emissions have not changed significantly between the two inventories, but the percentage from the transportation sector has changed because the estimated total emissions are greater in this inventory (due mainly to increased estimated emissions resulting from the revisions summarized above). Such ongoing updates are typical of emission inventories. Examining emissions forecasts and backcasts in a single emission inventory is more useful in determining trends than comparing one inventory against another.

Summary of Bay Area GHG Emissions

In 2007, 95.8 million metric tons of CO_2-equivalent ($MMTCO_2E$) greenhouse gases were emitted by the San Francisco Bay Area (88.7 $MMTCO_2E$ were emitted within the Bay Area Air District and 7.1 $MMTCO_2E$ were indirect emissions from imported electricity). A breakdown of Bay Area greenhouse gas emissions by pollutant is shown in Figure 1 and Table D.

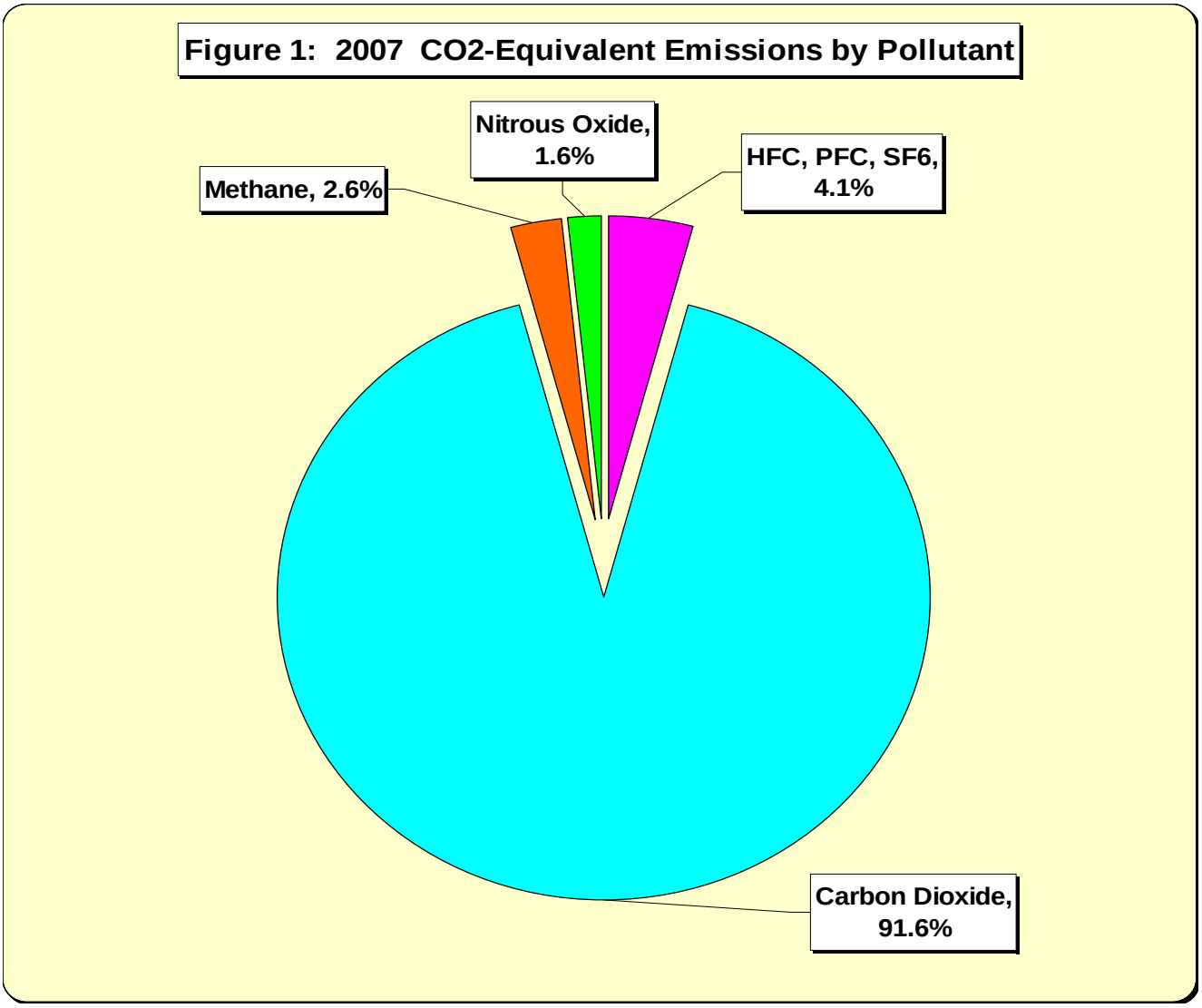


Table D: 2007 CO2- Equivalent Emissions by Pollutant

Pollutant	Percentage	CO2-Equivalent (Million Metric Tons / Year)
Carbon Dioxide	91.6%	87.8
Methane	2.6%	2.5
Nitrous Oxide	1.6%	1.5
HFC, PFC, SF6	4.1%	4.0
Total	**100%**	**95.8**

The greenhouse gas with the greatest emissions is carbon dioxide (CO_2). Carbon dioxide emissions from various activities in the Bay Area represented about 91.6 percent of total greenhouse gas emissions in 2007. Carbon dioxide emissions are mainly associated with combustion of carbon-bearing fossil fuels such as gasoline, diesel, and natural gas used in mobile sources and energy-generation-related activities. Other activities that produce CO_2 emissions include oil refining processes, cement manufacturing, waste combustion, and waste and forest management.

Bio-CO_2 emissions are from materials that were grown through the process of photosynthesis and thus the carbon they contain was relatively recently in the atmosphere. Burning of these materials does not add any net CO_2 to the atmosphere. Bio-CO_2 emissions are tracked and shown separately in Tables K through T and Table V and are not counted in the anthropogenic emissions inventory directly. This is consistent with CARB's methodology for GHG inventories. Landfills, fireplaces, and wastewater treatment plants are the largest sources of Bio-CO_2 emissions.

Methane (CH_4) emissions from various sources represent 2.6 percent of Bay Area's total CO_2-equivalent GHG emissions. Landfills, natural gas distribution systems, agricultural activities, stationary and mobile fuel combustion, and gas and oil production fields categories are the major sources of these emissions.

Nitrous oxide (N_2O) emissions represent 1.6 percent of the overall greenhouse gas emissions inventory. Municipal wastewater treatment facilities, fuel combustion, and agricultural soil and manure management are the major contributors of nitrous oxide emissions in the Bay Area.

Emissions from high GWP gases such as hydrofluorocarbons (HFCs), perfluorocarbons (PFCs), and sulfur hexafluoride (SF_6) make up about 4.1 percent of the total CO_2-equivalent emissions. Industrial processes such as semiconductor manufacturing, use as refrigerants and other products, and electric power transmission and distribution systems are the major sources of HFCs, PFCs and SF_6 emissions in the Bay Area.

GHG Emissions by Sector

Greenhouse gas emissions by end-use sectors are shown in Figure 2 and Table E. Fossil fuel consumption in the transportation sector was the single largest source of the San Francisco Bay Area's greenhouse gas emissions in 2007. The transportation sector contributed about 36.41 percent of greenhouse gas emissions in the Bay Area. Categories included in this sector are on-road motor vehicles, locomotives, ships and boats, and aircraft.

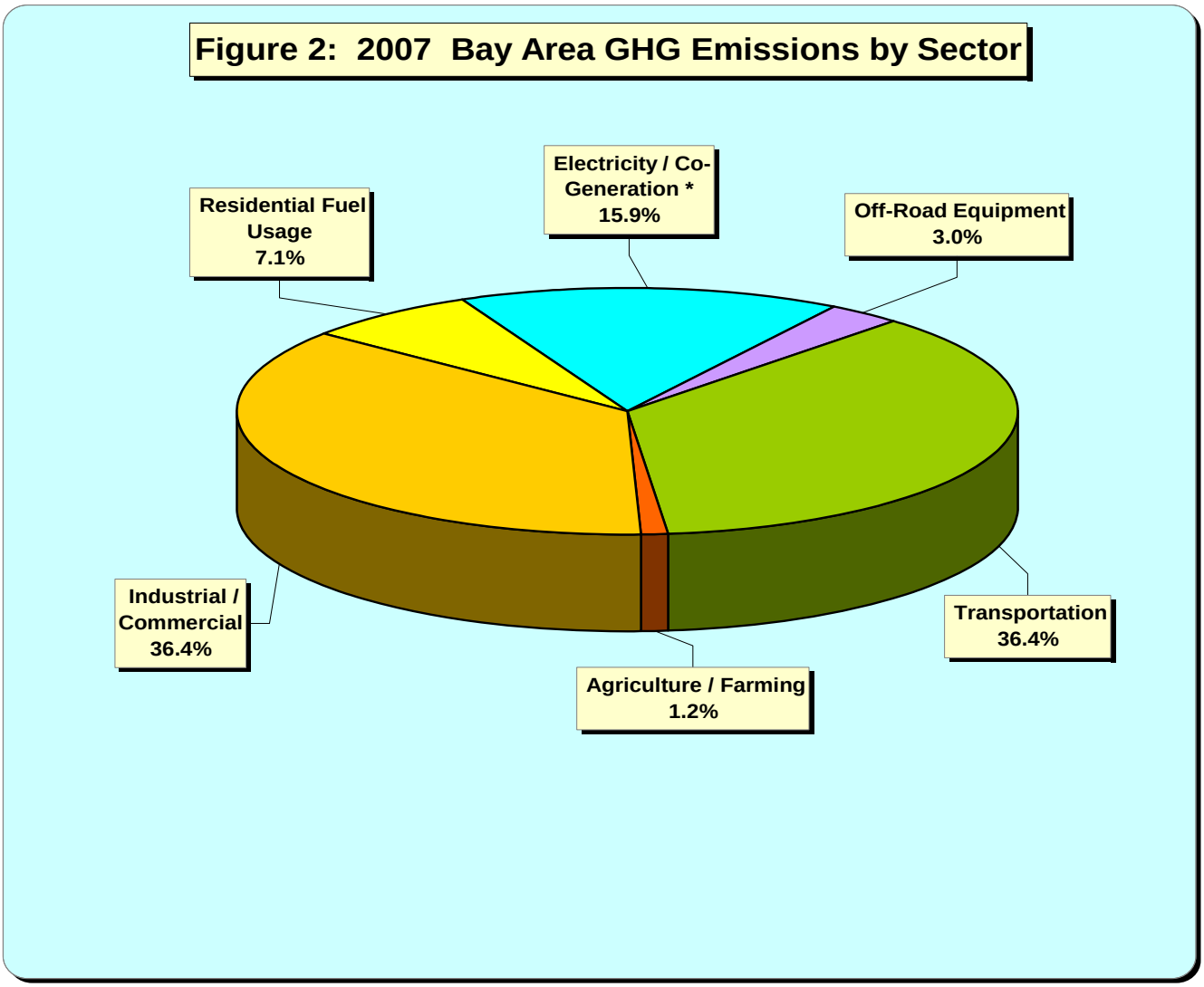


Table E: 2007 Bay Area GHG Emissions by Sector

End-Use Sector	% of Total Emissions	CO2- Equivalent (Million Metric Tons / Year)
Industrial / Commercial	36.40%	34.86
Residential Fuel Usage	7.12%	6.82
Electricity / Co-Generation *	15.87%	15.20
Off-Road Equipment	3.05%	2.92
Transportation	36.41%	34.87
Agriculture / Farming	1.16%	1.11
Total	**100%**	**95.8**

* Includes Imported Electricity emissions of 7.1 $MMTCO_2E$

The industrial and commercial sector (excluding electricity/co-generation and agriculture/farming, which are reported separately) was the second largest contributor, closely following the transportation sector, with 36.4 percent of total GHG emissions. Industrial and commercial sources include industrial processes such as oil refining, natural gas and other fuel combustion, waste management, cement manufacturing, fuel distribution, refrigerant usage, and some other small sources.

Energy production activities such as electricity generation and co-generation were the third largest contributor with 15.9 percent of the total GHG emissions (including imported electricity emissions). California imports about one-fifth to one-third of its total electricity usage, mainly from the northwestern and southwestern states. The Bay Area used about 54.6 million megawatt hours of electricity in 2007, about one-third of it was generated outside of the Bay Area. Electricity and co-generation facilities within the Bay Area Air District emitted about 8.1 million metric tons of CO_2-equivalent ($MMTCO_2E$) emissions in 2007 and emissions from electricity imports were estimated to be 7.1 $MMTCO_2E$. While imported electricity is a relatively small share of the Bay Area's electricity mix, out-of-region electricity generation sources contribute a larger share of GHG emissions. This is due to the fact that electricity generation in the Bay Area is mainly from natural gas-fired and other cleaner burning power plants. Out-of-state electricity generation is also from coal-fired power plants which have higher carbon intensity.

The contribution from residential fuel combustion was the fourth largest with 7.1 percent of the total GHG emissions. Residential fuel combustion emissions are primarily from space heating, cooking and water heating.

Off-road equipment such as construction, industrial, commercial, and lawn and garden equipment contributed 3.0 percent of GHG emissions.

Agriculture and farming was the smallest sector with 1.2 percent of the total greenhouse emissions in the Bay Area.

More detailed information on greenhouse gas emissions by source category, for the region and for each county, is provided in Tables K through U. Table V contains the list of the 200 largest greenhouse gas emission point sources/facilities in the San Francisco Bay Area.

An emissions breakdown for the two largest greenhouse gas emitting sectors in the Bay Area, industrial/commercial and transportation, is shown in Figure 3, Table F and Figure 4, Table G respectively.

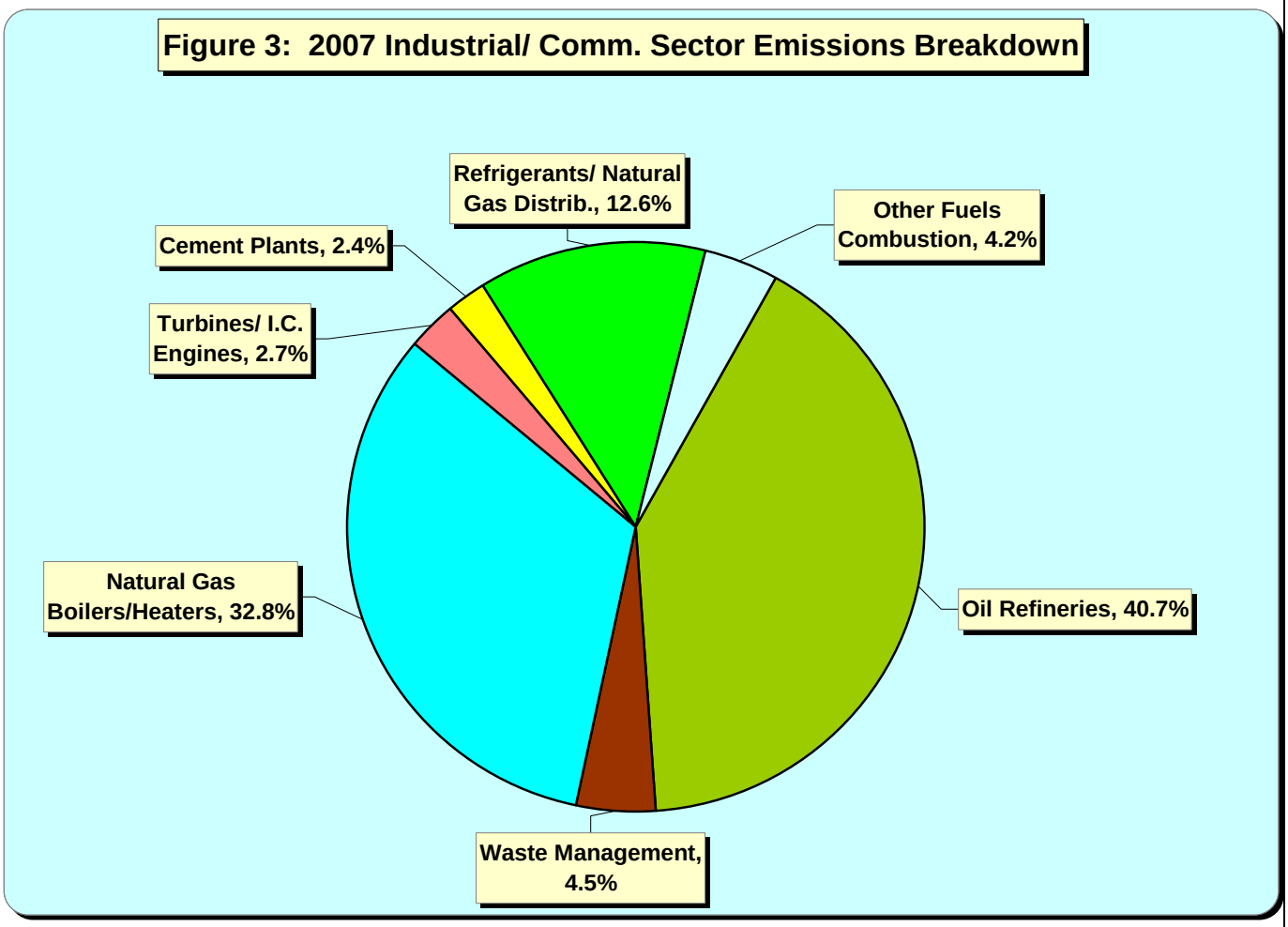


Table F: 2007 Industrial/ Commercial Sector Emissions Breakdown

Source Category	% of Total Emissions	CO2-Equivalent (Million Metric Tons / Year)
Oil Refineries	40.7%	14.2
Waste Management	4.5%	1.6
Natural Gas Boilers/Heaters	32.8%	11.4
Turbines/ I.C. Engines	2.7%	1.0
Cement Plants	2.4%	0.8
Refrigerants/ Natural Gas Distrib.	12.6%	4.4
Other Fuels Combustion	4.2%	1.5
Total	**100%**	**34.9**

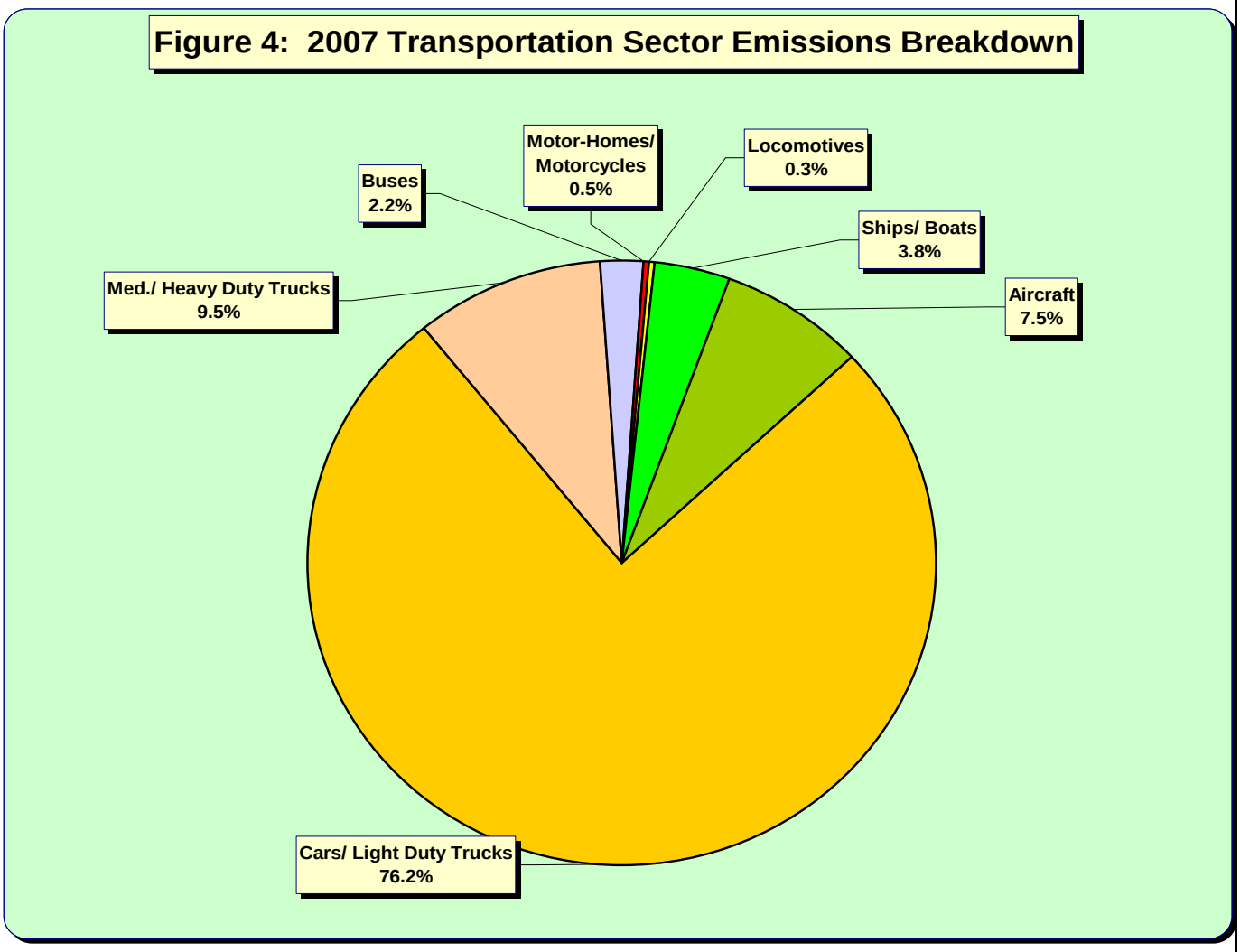


Table G: 2007 Transportation Sector Emissions Breakdown

Source Category	% of Total Emissions	CO2-Equivalent (Million Metric Tons / Year)
Cars/ Light Duty Trucks	76.2%	26.6
Med./ Heavy Duty Trucks	9.5%	3.3
Buses	2.2%	0.8
Motor-Homes/ Motorcycles	0.5%	0.2
Locomotives	0.3%	0.1
Ships/ Boats	3.8%	1.3
Aircraft	7.5%	2.6
Total	**100%**	**34.9**

GHG Emissions by County

GHG emissions for the nine Bay Area counties under the Air District's jurisdiction are summarized in Figure 5 and Table H. See Tables K-T for detailed emissions information.

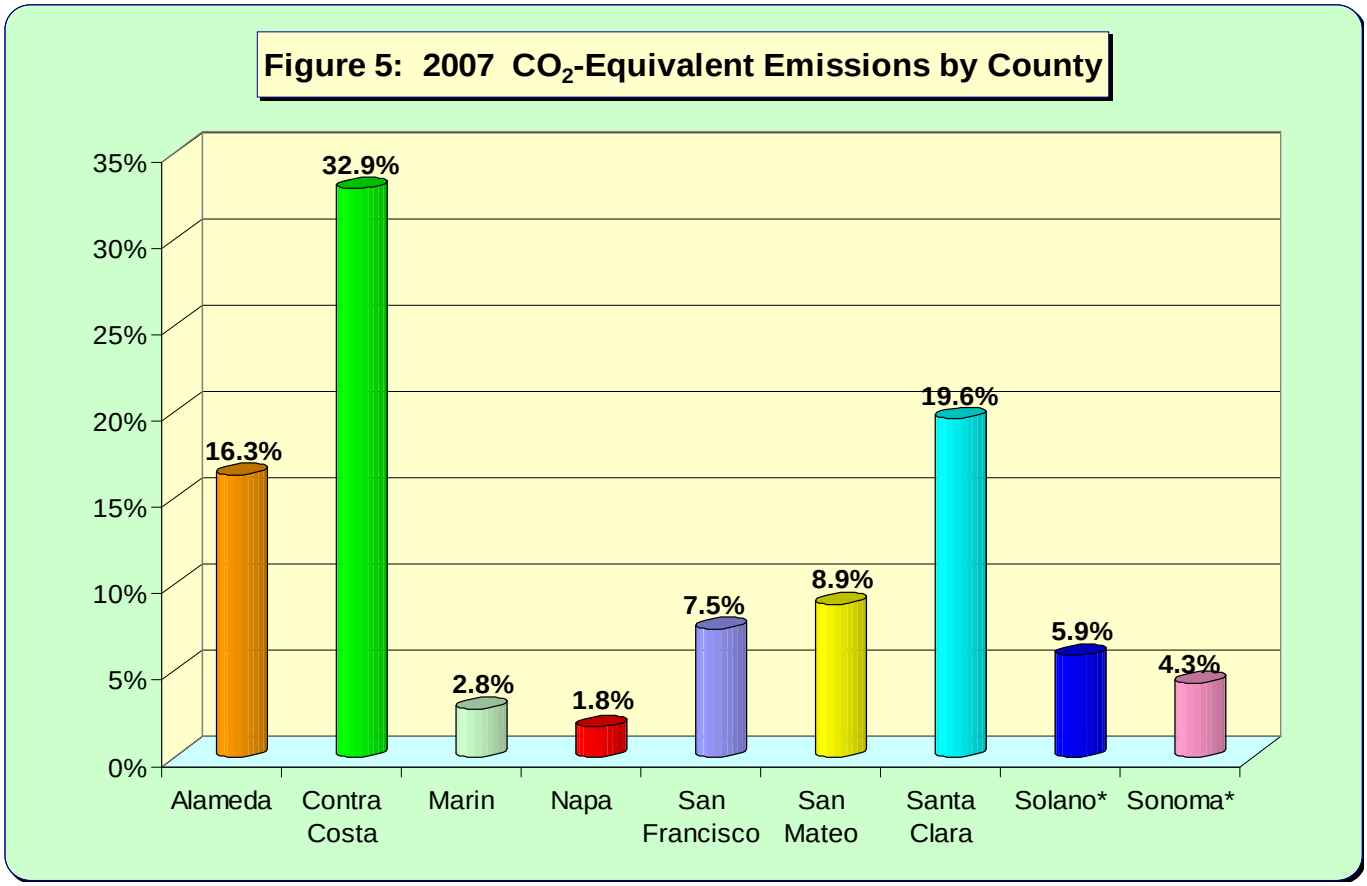


Table H: 2007 CO2- Equivalent Emissions by County

County	% of Total Emissions	CO2- Equivalent (Million Metric Tons / Year)
Alameda	16.3%	15.7
Contra Costa	32.9%	31.5
Marin	2.8%	2.7
Napa	1.8%	1.7
San Francisco	7.5%	7.1
San Mateo	8.9%	8.5
Santa Clara	19.6%	18.8
Solano*	5.9%	5.7
Sonoma*	4.3%	4.1
Total	**100%**	**95.8**

* Portion within BAAQMD

A breakdown of emissions by end-use sectors for each county is shown in Figure 6 and Table I. This figure and table show relatively higher industrial/commercial sector

emissions in Contra Costa and Solano Counties due to the oil refining industry. All other counties show the largest contribution from the transportation sector.

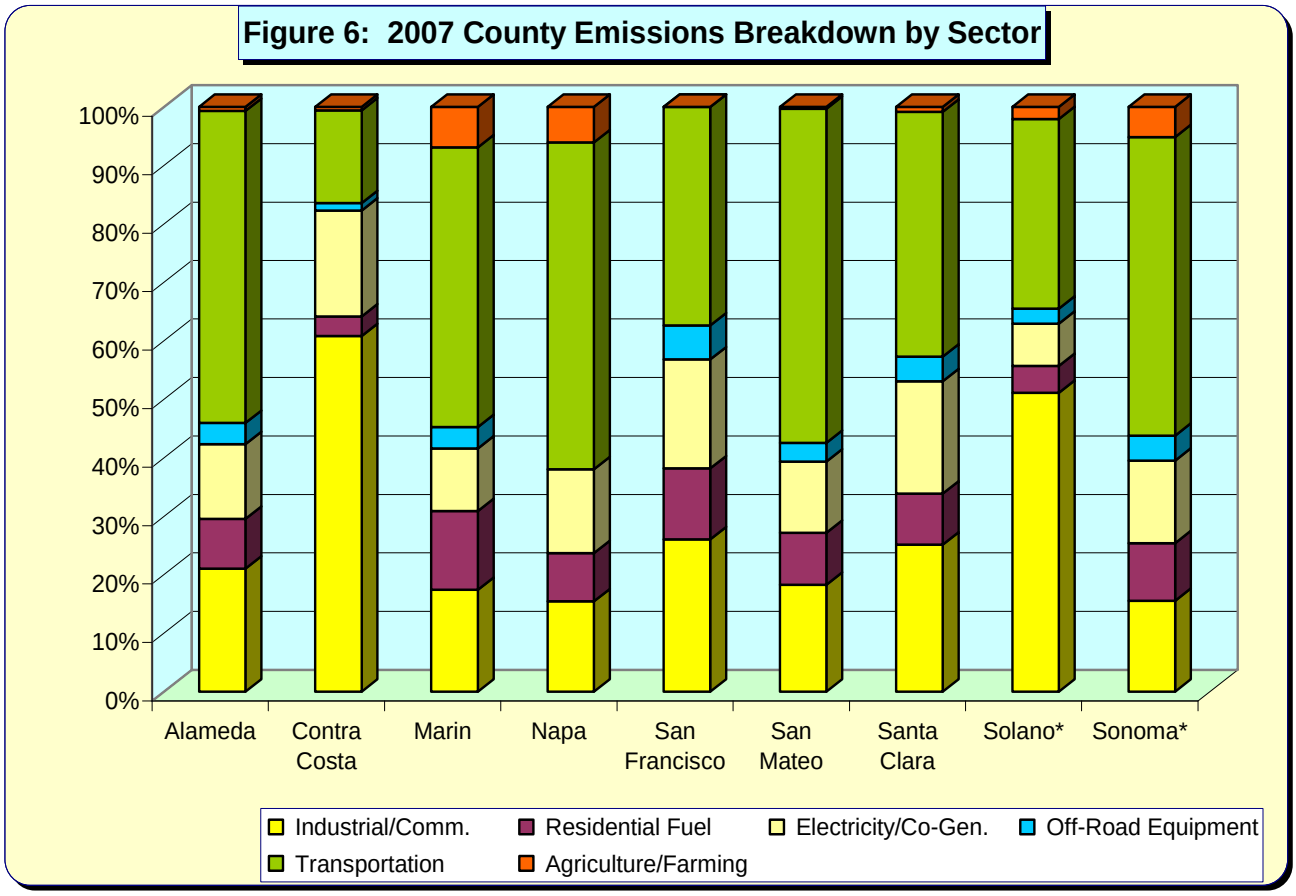


Table I: 2007 County Emissions Breakdown by Sector (Million Metric Tons CO2-Equiv./Yr.)

Sector	Alameda	Contra Costa	Marin	Napa	San Francisco	San Mateo	Santa Clara	Solano*	Sonoma*
Industrial/Comm.	3.3	19.2	0.5	0.3	1.9	1.6	4.7	2.9	0.6
Residential Fuel	1.3	1.1	0.4	0.1	0.9	0.8	1.6	0.3	0.4
Electricity/Co-Gen.	2.0	5.7	0.3	0.2	1.3	1.0	3.6	0.4	0.6
Off-Road Equipment	0.6	0.4	0.1	0.0	0.4	0.3	0.8	0.1	0.2
Transportation	8.4	5.0	1.3	0.9	2.7	4.8	7.9	1.8	2.1
Agriculture/Farming	0.1	0.2	0.2	0.1	0.0	0.0	0.2	0.1	0.2
Total	15.7	31.5	2.7	1.6	7.1	8.5	18.8	5.7	4.1

* Portion within BAAQMD

GHG Emission Trends for Bay Area

Under "business as usual" conditions, greenhouse gas emissions are expected to grow in the future due to population growth and economic expansion. Figure 7 and Tables J and U show emissions trends by sectors for the period 1990 to 2029.

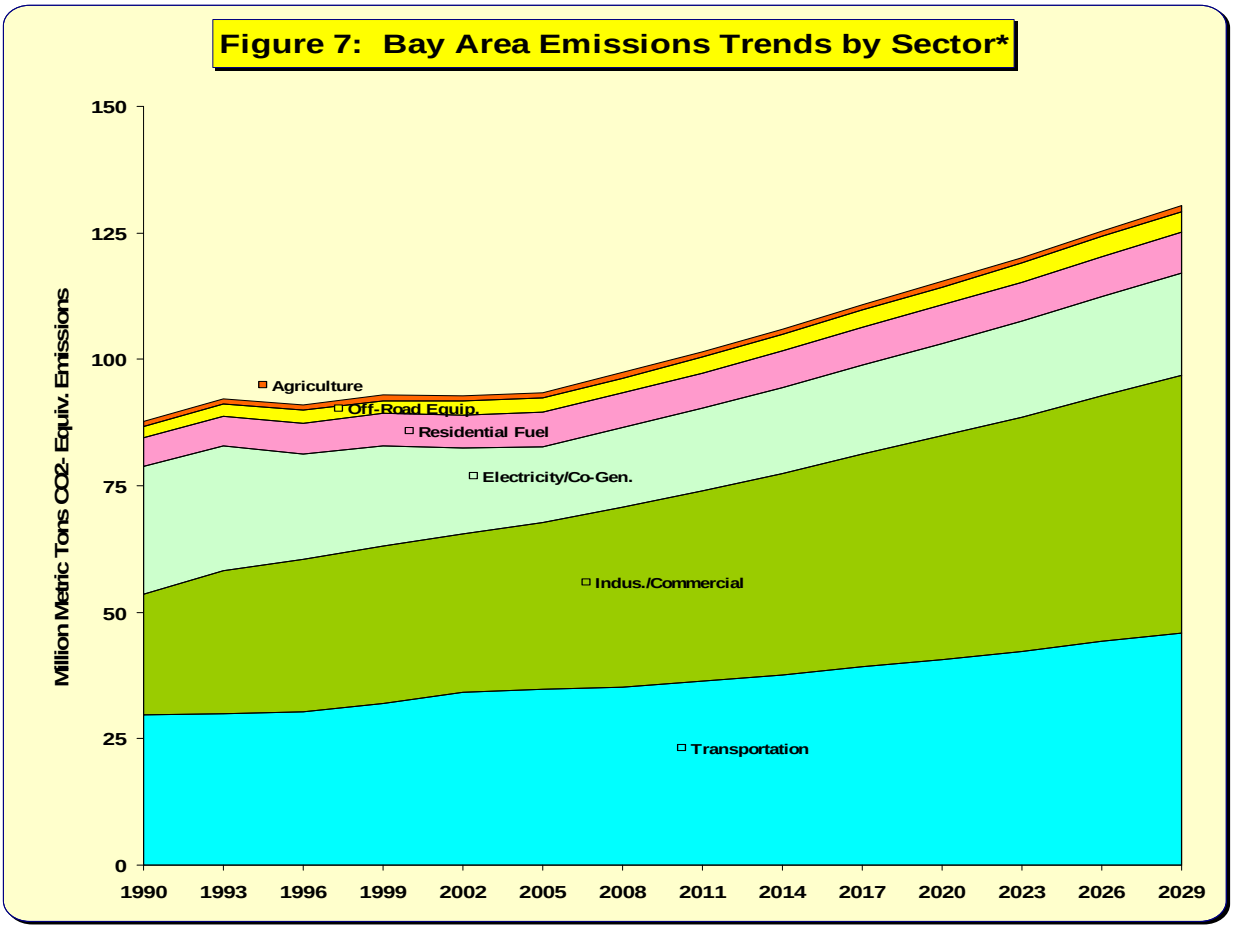


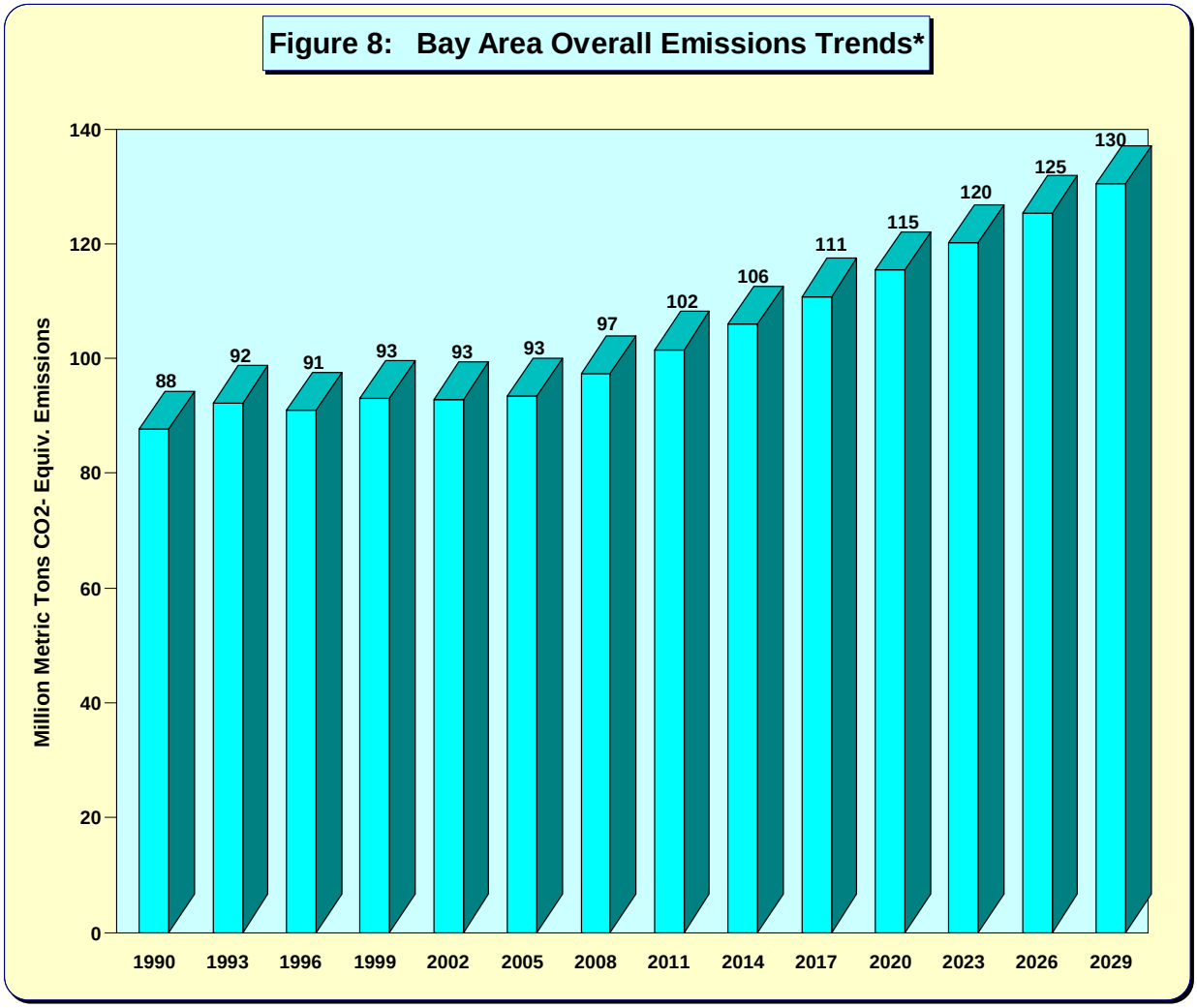
Table J: Bay Area Emissions Trends by Sector (Million Metric Tons CO_2-Equiv.)*

Category	1990	1993	1996	1999	2002	2005	2008	2011	2014	2017	2020	2023	2026	2029
Transportation	29.8	29.8	30.4	32.0	34.1	34.8	35.3	36.3	37.6	39.3	40.7	42.2	44.2	46.0
Indus./Commercial	23.9	28.5	29.9	31.1	31.4	32.8	35.6	37.7	39.9	42.0	44.2	46.4	48.6	50.8
Electricity/Co-Gen.	25.1	24.6	20.9	19.8	17.0	15.1	15.6	16.3	16.9	17.6	18.3	18.9	19.6	20.4
Residential Fuel	5.8	6.0	6.2	6.4	6.6	6.7	6.9	7.0	7.2	7.4	7.5	7.7	7.9	8.0
Off-Road Equip.	2.2	2.3	2.5	2.6	2.7	2.8	3.0	3.1	3.3	3.4	3.6	3.8	3.9	4.1
Agriculture	1.0	1.1	1.1	1.1	1.1	1.1	1.1	1.1	1.1	1.1	1.1	1.1	1.1	1.1
Total	87.7	92.2	91.0	93.0	92.8	93.4	97.4	101.5	106.0	110.8	115.4	120.2	125.3	130.4

* "Business as usual" projection

Figure 8 shows the San Francisco Bay Area region's overall greenhouse gas emissions trends. More details on emissions trends are provided in Table U.

Figure 8: Bay Area Overall Emissions Trends*



* "Business as usual" projection

These projections reflect regulatory programs in place as of 2007 (benefits of CARB GHG regulations for motor vehicles adopted in 2004, the Pavley regulations, are not included in this inventory, pending U.S. EPA approval of a waiver under the Clean Air Act to implement the regulations). If current trends continue, Bay Area GHG emissions are expected to increase at an average rate of approximately 1.4 percent per year. The long term GHG emissions trends are expected to go upwards *absent policy changes*. Year-to-year fluctuation in emissions trends is due to variation in economic activity and the fraction of electric power generation in this region. Power generation in the Bay Area varies year-to-year depending on various factors including the availability of hydroelectric and other imported power.

Greenhouse gas emissions are projected based on estimated growth in various source categories. For example, CARB's EMFAC2007 computer model was utilized to project GHG emissions from transportation sources. In these models, fuel consumption estimates were based on the anticipated change of fleet mix and the growth of various types of on-road and off-road vehicles. Growth in VMT is based on the MTC's Regional Transportation Plan (RTP2030). For aircraft categories, the fleet mix and the growth data from the MTC's Regional Airport System Plan were incorporated into the GHG projection models.

The projected GHG emissions from power plants operating in the Bay Area were based on the California Energy Commission's 2003 Fuel Usage Forecasts for the Bay Area.

Emission projections for the oil refineries were based on the California Energy Commission's report on California's Petroleum Infrastructure (2007).

The GHG projections from other major sources such as landfills, natural gas fuel distribution, and cement manufacturing were estimated by using Association of Bay Area Government's employment and population data. California Integrated Waste Management data were also considered in the landfill projection process.

Climate protection activities in California are occurring at the state, regional and local level. CARB and other state agencies are identifying measures to achieve the AB32 emission reduction goal of meeting statewide 1990 GHG emissions levels by 2020. Specifically, in December 2008 CARB adopted the AB32 Scoping Plan which outlines a strategy to achieve AB32 goals. The Scoping Plan does not set emission reduction goals for regions within the state, but it is expected that all California communities will need to contribute to statewide reductions. The Air District and our regional agency partners are implementing climate protection programs. Bay Area cities and counties are preparing local climate action plans. These efforts are expected to reduce future Bay Area GHG Emissions below the projections presented here.

This GHG emissions inventory will be updated as climate protection programs are implemented and as additional information about activity data, emission factors and other inputs becomes available.

Table K:
Annual GHG Emissions: Bay Area Year 2007 (Metric Tons / Year)

SOURCE CATEGORY	CO_2	CH_4	N_2O	PFC/HFC	SF_6	Total GHG CO_2-Equivalent	Biogenic CO_2
INDUSTRIAL/ COMMERCIAL							
Oil Refineries							
Refining Processes	3,445,064	79	--	--	--	3,446,782	--
Refinery Make Gas Combustion	4,772,971	97	6	--	--	4,776,959	--
Natural Gas and Other Gases Combustion	4,860,268	267	18	--	--	4,871,495	--
Liquid Fuel Combustion	89,450	1	1	--	--	89,760	--
Solid Fuel Combustion	1,000,216	29	6	--	--	1,002,637	--
Waste Management							
Landfill Combustion Sources	--	1,241	1	--	--	26,455	584,565
Landfill Fugitive Sources	--	56,747	3	--	--	1,192,596	154,411
Composting/POTWs	--	2,773	965	--	--	357,224	--
Other Industrial/ Commercial							
Cement Plants	841,350	13	3	--	--	842,475	--
Commercial Cooking	134,612	--	--	--	--	134,612	--
ODS Substitutes/Nat. Gas Distrib./Other	--	16,356	--	2,184	0.13	4,390,999	21
Reciprocating Engines	550,270	1,989	1	--	--	593,584	234,013
Turbines	354,697	78	1	--	--	356,663	66,141
Natural Gas- Major Combustion Sources	2,400,044	51	3	--	--	2,402,179	--
Natural Gas- Minor Combustion Sources	8,979,100	172	165	--	--	9,033,745	--
Coke Coal	989,442	28	6	--	--	991,823	--
Other Fuels Combustion	349,171	132	2	--	--	352,485	85,346
Subtotal	28,766,652	80,052	1,181	2,184	0.13	34,862,465	1,124,497
RESIDENTIAL FUEL USAGE							
Natural Gas	6,456,173	124	118	--	--	6,495,464	--
LPgas/Liquid Fuel	166,508	3	11	--	--	169,911	--
Solid Fuel	--	6,242	67	--	--	151,742	628,550
Subtotal	6,622,682	6,369	196	--	--	6,817,118	628,550
ELECTRICITY/ CO-GENERATION							
Co-Generation	5,292,826	1,261	4	--	--	5,320,398	89,512
Electricity Generation	2,730,973	163	1	--	1.18	2,762,968	3,525
Electricity Imports	7,102,311	59	33	--	--	7,113,680	--
Subtotal	15,126,111	1,483	37	--	1.18	15,197,047	93,037
OFF-ROAD EQUIPMENT							
Lawn and Garden Equipment	105,742	192	77	--	--	133,803	--
Construction Equipment	1,785,078	289	11	--	--	1,794,433	--
Industrial Equipment	729,035	433	41	--	--	750,852	--
Light Commercial Equipment	226,118	111	42	--	--	241,375	--
Subtotal	2,845,974	1,025	171	--	--	2,920,462	--
TRANSPORTATION							
Off-Road							
Locomotives	88,092	5	35	--	--	99,152	--
Ships	731,679	74	28	--	--	742,064	--
Boats	509,165	252	168	--	--	566,451	--
Commercial Aircraft	1,877,665	91	68	--	--	1,900,661	--
General Aviation	231,066	46	8	--	--	234,642	--
Military Aircraft	478,178	31	15	--	--	483,454	--
On-Road							
Passenger Cars/Trucks up to 10,000 lbs	26,070,815	2,783	1,480	--	--	26,587,907	--
Medium/Heavy Duty Trucks > 10,000 lbs	3,232,949	181	208	--	--	3,301,335	--
Urban,School and Other Buses	722,698	21	192	--	--	782,755	--
Motor-Homes and Motorcycles	156,636	147	42	--	--	172,846	--
Subtotal	34,098,941	3,629	2,246	--	--	34,871,276	--
AGRICULTURE/ FARMING							
Agricultural Equipment	183,929	34	2	--	--	185,364	--
Animal Waste	--	25,860	254	--	--	621,761	--
Soil Management	15,954	--	899	--	--	294,758	43,110
Biomass Burning	--	97	8	--	--	4,363	3,145
Subtotal	199,883	25,991	1,163	--	--	1,106,246	46,255
GRAND TOTAL EMISSIONS	**87,660,281**	**118,549**	**4,993**	**2,184**	**1.3**	**95,774,635**	**1,892,340**

Table L:

Annual GHG Emissions: ALAMEDA Year 2007 (Metric Tons / Year)

SOURCE CATEGORY	CO_2	CH_4	N_2O	PFC/HFC	SF_6	Total GHG CO_2-Equivalent	Biogenic CO_2
INDUSTRIAL/ COMMERCIAL							
Oil Refineries							
Refining Processes	--	--	--	--	--	--	--
Refinery Make Gas Combustion	--	--	--	--	--	--	--
Natural Gas and Other Gases Combustion	--	--	--	--	--	--	--
Liquid Fuel Combustion	--	--	--	--	--	--	--
Solid Fuel Combustion	--	--	--	--	--	--	--
Waste Management							
Landfill Combustion Sources	--	304	--	--	--	6,475	143,077
Landfill Fugitive Sources	--	17,818	1	--	--	374,448	48,018
Composting/POTWs	--	280	196	--	--	66,683	--
Other Industrial/ Commercial							
Cement Plants	--	--	--	--	--	--	--
Commercial Cooking	26,922	--	--	--	--	26,922	--
ODS Substitutes/Nat. Gas Distrib./Other	--	1,659	--	479	0.13	945,746	--
Reciprocating Engines	73,600	129	--	--	--	76,331	16,585
Turbines	31,710	71	--	--	--	33,325	66,141
Natural Gas- Major Combustion Sources	497,257	18	1	--	--	497,927	--
Natural Gas- Minor Combustion Sources	1,141,243	22	21	--	--	1,148,189	--
Coke Coal	25,266	--	--	--	--	25,313	--
Other Fuels Combustion	88,518	25	--	--	--	89,133	9,320
Subtotal	1,884,516	20,325	220	479	0.13	3,290,493	283,142
RESIDENTIAL FUEL USAGE							
Natural Gas	1,286,715	25	24	--	--	1,294,546	--
LPgas/Liquid Fuel	24,050	--	2	--	--	24,543	--
Solid Fuel	--	710	8	--	--	17,255	71,930
Subtotal	1,310,766	735	33	--	--	1,336,344	71,930
ELECTRICITY/ CO-GENERATION							
Co-Generation	111,703	394	--	--	--	120,085	55,974
Electricity Generation	26,465	1	--	--	0.26	32,715	396
Electricity Imports	1,846,601	15	8	--	--	1,849,556	--
Subtotal	1,984,769	411	9	--	0.26	2,002,356	56,370
OFF-ROAD EQUIPMENT							
Lawn and Garden Equipment	23,536	43	17	--	--	29,781	--
Construction Equipment	360,793	58	2	--	--	362,691	--
Industrial Equipment	122,557	75	7	--	--	126,281	--
Light Commercial Equipment	46,774	23	9	--	--	49,913	--
Subtotal	553,660	199	35	--	--	568,666	--
TRANSPORTATION							
Off-Road							
Locomotives	24,977	1	10	--	--	28,113	--
Ships	108,727	6	2	--	--	109,479	--
Boats	293,593	35	106	--	--	327,032	--
Commercial Aircraft	482,494	20	17	--	--	488,135	--
General Aviation	64,925	11	2	--	--	65,881	--
Military Aircraft	3,677	--	--	--	--	3,694	--
On-Road							
Passenger Cars/Trucks up to 10,000 lbs	5,744,125	621	336	--	--	5,861,250	--
Medium/Heavy Duty Trucks > 10,000 lbs	1,209,381	54	60	--	--	1,229,050	--
Urban,School and Other Buses	186,711	4	57	--	--	204,517	--
Motor-Homes and Motorcycles	30,728	29	9	--	--	34,017	--
Subtotal	8,149,332	782	598	--	--	8,351,165	--
AGRICULTURE/ FARMING							
Agricultural Equipment	15,487	3	--	--	--	15,607	--
Animal Waste	--	2,814	52	--	--	75,340	--
Soil Management	954	--	40	--	--	13,305	1,146
Biomass Burning	--	58	3	--	--	2,269	1,199
Subtotal	16,441	2,875	96	--	--	106,522	2,345
GRAND TOTAL EMISSIONS	**13,899,491**	**25,326**	**991**	**479**	**0.4**	**15,655,546**	**413,788**

Table M:

Annual GHG Emissions: CONTRA COSTA Year 2007 (Metric Tons / Year)

SOURCE CATEGORY	CO_2	CH_4	N_2O	PFC/HFC	SF_6	Total GHG CO_2-Equivalent	Biogenic CO_2
INDUSTRIAL/ COMMERCIAL							
Oil Refineries							
Refining Processes	2,910,760	71	--	--	--	2,912,287	--
Refinery Make Gas Combustion	3,455,837	70	5	--	--	3,458,717	--
Natural Gas and Other Gases Combustion	4,773,383	258	18	--	--	4,784,246	--
Liquid Fuel Combustion	89,450	1	1	--	--	89,760	--
Solid Fuel Combustion	1,000,216	29	6	--	--	1,002,637	--
Waste Management							
Landfill Combustion Sources	--	83	--	--	--	1,761	38,904
Landfill Fugitive Sources	--	6,168	--	--	--	129,622	17,044
Composting/POTWs	--	65	87	--	--	28,228	--
Other Industrial/ Commercial							
Cement Plants	--	--	--	--	--	--	--
Commercial Cooking	13,461	--	--	--	--	13,461	--
ODS Substitutes/Nat. Gas Distrib./Other	--	8,604	--	282	--	686,738	--
Reciprocating Engines	81,825	391	--	--	--	90,082	18,464
Turbines	3,781	--	--	--	--	3,788	--
Natural Gas- Major Combustion Sources	633,351	7	1	--	--	633,758	--
Natural Gas- Minor Combustion Sources	4,137,569	79	76	--	--	4,162,750	--
Coke Coal	964,175	28	6	--	--	966,509	--
Other Fuels Combustion	213,592	26	1	--	--	214,332	34,769
Subtotal	18,277,402	15,880	199	282	--	19,178,675	109,181
RESIDENTIAL FUEL USAGE							
Natural Gas	994,896	19	18	--	--	1,000,951	--
LPgas/Liquid Fuel	18,887	--	1	--	--	19,288	--
Solid Fuel	--	1,666	18	--	--	40,504	167,246
Subtotal	1,013,783	1,686	37	--	--	1,060,743	167,246
ELECTRICITY/ CO-GENERATION							
Co-Generation	4,245,060	372	2	--	--	4,253,633	--
Electricity Generation	1,449,714	73	--	--	0.17	1,455,466	1,620
Electricity Imports	--	--	--	--	--	--	--
Subtotal	5,694,774	444	3	--	0.17	5,709,099	1,620
OFF-ROAD EQUIPMENT							
Lawn and Garden Equipment	16,040	29	12	--	--	20,296	--
Construction Equipment	303,191	49	2	--	--	304,760	--
Industrial Equipment	52,636	29	2	--	--	53,996	--
Light Commercial Equipment	25,132	12	5	--	--	26,861	--
Subtotal	397,000	120	21	--	--	405,913	--
TRANSPORTATION							
Off-Road							
Locomotives	24,562	1	10	--	--	27,646	--
Ships	63,340	3	1	--	--	63,758	--
Boats	69,323	44	21	--	--	76,609	--
Commercial Aircraft	--	--	--	--	--	--	--
General Aviation	19,607	11	1	--	--	20,037	--
Military Aircraft	--	--	--	--	--	--	--
On-Road	--	--	--	--	--	--	
Passenger Cars/Trucks up to 10,000 lbs	4,178,993	432	234	--	--	4,260,682	--
Medium/Heavy Duty Trucks > 10,000 lbs	401,364	23	27	--	--	410,348	--
Urban,School and Other Buses	102,211	2	15	--	--	106,770	--
Motor-Homes and Motorcycles	29,368	27	8	--	--	32,309	--
Subtotal	4,888,771	543	316	--	--	4,998,160	--
AGRICULTURE/ FARMING							
Agricultural Equipment	19,349	4	--	--	--	19,500	--
Animal Waste	--	4,440	44	--	--	106,901	--
Soil Management	913	--	204	--	--	64,034	589
Biomass Burning	--	10	1	--	--	431	274
Subtotal	20,262	4,454	249	--	--	190,867	863
GRAND TOTAL EMISSIONS	**30,291,977**	**23,126**	**825**	**282**	**0.17**	**31,543,450**	**278,910**

Table N:

Annual GHG Emissions: MARIN Year 2007 (Metric Tons / Year)

SOURCE CATEGORY	CO_2	CH_4	N_2O	PFC/HFC	SF_6	Total GHG CO_2-Equivalent	Biogenic CO_2
INDUSTRIAL/ COMMERCIAL							
Oil Refineries							
Refining Processes	--	--	--	--	--	--	--
Refinery Make Gas Combustion	--	--	--	--	--	--	--
Natural Gas and Other Gases Combustion	--	--	--	--	--	--	--
Liquid Fuel Combustion	--	--	--	--	--	--	--
Solid Fuel Combustion	--	--	--	--	--	--	--
Waste Management							
Landfill Combustion Sources	--	131	--	--	--	2,788	61,597
Landfill Fugitive Sources	--	5,278	--	--	--	110,927	14,093
Composting/POTWs	--	39	37	--	--	12,390	--
Other Industrial/ Commercial							
Cement Plants	--	--	--	--	--	--	--
Commercial Cooking	4,038	--	--	--	--	4,038	--
ODS Substitutes/Nat. Gas Distrib./Other	--	273	--	87	--	161,358	--
Reciprocating Engines	16,158	4	--	--	--	16,237	401
Turbines	1	--	--	--	--	1	--
Natural Gas- Major Combustion Sources	22,929	--	--	--	--	22,950	--
Natural Gas- Minor Combustion Sources	132,891	3	2	--	--	133,699	--
Coke Coal	--	--	--	--	--	--	--
Other Fuels Combustion	4,472	6	--	--	--	4,602	1,173
Subtotal	180,489	5,733	40	87	--	468,992	77,263
RESIDENTIAL FUEL USAGE							
Natural Gas	331,202	6	6	--	--	333,217	--
LPgas/Liquid Fuel	14,330	--	1	--	--	14,630	--
Solid Fuel	--	587	6	--	--	14,264	58,869
Subtotal	345,532	593	13	--	--	362,111	58,869
ELECTRICITY/ CO-GENERATION							
Co-Generation	2,581	31	--	--	--	3,224	1,776
Electricity Generation	--	--	--	--	0.04	1,022	--
Electricity Imports	284,092	2	1	--	--	284,547	--
Subtotal	286,673	33	1	--	0.04	288,793	1,776
OFF-ROAD EQUIPMENT							
Lawn and Garden Equipment	6,259	11	5	--	--	7,920	--
Construction Equipment	66,234	11	--	--	--	66,583	--
Industrial Equipment	11,942	6	1	--	--	12,230	--
Light Commercial Equipment	11,588	6	2	--	--	12,345	--
Subtotal	96,023	34	8	--	--	99,079	--
TRANSPORTATION							
Off-Road							
Locomotives	725	--	--	--	--	817	--
Ships	53,605	6	2	--	--	54,497	--
Boats	20,077	48	6	--	--	22,818	--
Commercial Aircraft	--	--	--	--	--	--	--
General Aviation	17,302	3	1	--	--	17,559	--
Military Aircraft	--	--	--	--	--	--	--
On-Road							
Passenger Cars/Trucks up to 10,000 lbs	1,008,598	108	59	--	--	1,029,239	--
Medium/Heavy Duty Trucks > 10,000 lbs	80,905	6	8	--	--	83,376	--
Urban,School and Other Buses	64,651	1	20	--	--	71,011	--
Motor-Homes and Motorcycles	5,642	6	2	--	--	6,283	--
Subtotal	1,251,506	177	98	--	--	1,285,600	--
AGRICULTURE/ FARMING							
Agricultural Equipment	7,486	1	--	--	--	7,544	--
Animal Waste	--	7,352	44	--	--	168,172	--
Soil Management	695	--	34	--	--	11,178	--
Biomass Burning	--	3	--	--	--	120	104
Subtotal	8,181	7,356	79	--	--	187,014	104
GRAND TOTAL EMISSIONS	**2,168,404**	**13,927**	**239**	**87**	**0.04**	**2,691,589**	**138,012**

Table O:

Annual GHG Emissions: NAPA Year 2007 (Metric Tons / Year)

SOURCE CATEGORY	CO_2	CH_4	N_2O	PFC/HFC	SF_6	Total GHG CO_2-Equivalent	Biogenic CO_2
INDUSTRIAL/ COMMERCIAL							
Oil Refineries							
Refining Processes	--	--	--	--	--	--	--
Refinery Make Gas Combustion	--	--	--	--	--	--	--
Natural Gas and Other Gases Combustion	--	--	--	--	--	--	--
Liquid Fuel Combustion	--	--	--	--	--	--	--
Solid Fuel Combustion	--	--	--	--	--	--	--
Waste Management							
Landfill Combustion Sources	--	31	--	--	--	651	14,380
Landfill Fugitive Sources	--	535	--	--	--	11,245	1,669
Composting/POTWs	--	149	43	--	--	16,359	--
Other Industrial/ Commercial							
Cement Plants	--	--	--	--	--	--	--
Commercial Cooking	2,692	--	--	--	--	2,692	--
ODS Substitutes/Nat. Gas Distrib./Other	--	128	--	40	--	74,966	--
Reciprocating Engines	17,563	106	--	--	--	19,801	15,424
Turbines	6	--	--	--	--	6	--
Natural Gas- Major Combustion Sources	32,505	1	--	--	--	32,534	--
Natural Gas- Minor Combustion Sources	94,281	2	2	--	--	94,854	--
Coke Coal	--	--	--	--	--	--	--
Other Fuels Combustion	460	2	--	--	--	511	1,106
Subtotal	147,506	953	45	40	--	253,621	32,580
RESIDENTIAL FUEL USAGE							
Natural Gas	121,376	2	2	--	--	122,115	--
LPgas/Liquid Fuel	6,334	--	--	--	--	6,468	--
Solid Fuel	--	275	3	--	--	6,688	27,600
Subtotal	127,710	278	6	--	--	135,271	27,600
ELECTRICITY/ CO-GENERATION							
Co-Generation	12,847	1	--	--	--	12,874	--
Electricity Generation	7,917	1	--	--	0.02	8,474	--
Electricity Imports	213,069	2	1	--	--	213,410	--
Subtotal	233,833	3	1	--	0.02	234,758	--
OFF-ROAD EQUIPMENT							
Lawn and Garden Equipment	2,252	4	2	--	--	2,850	--
Construction Equipment	31,597	5	--	--	--	31,763	--
Industrial Equipment	10,994	6	--	--	--	11,267	--
Light Commercial Equipment	4,050	2	1	--	--	4,340	--
Subtotal	48,893	17	3	--	--	50,220	--
TRANSPORTATION							
Off-Road							
Locomotives	4,353	--	2	--	--	4,899	--
Ships	--	--	--	--	--	--	--
Boats	24,628	29	6	--	--	27,189	--
Commercial Aircraft	--	--	--	--	--	--	--
General Aviation	16,274	3	1	--	--	16,517	--
Military Aircraft	--	--	--	--	--	--	--
On-Road							
Passenger Cars/Trucks up to 10,000 lbs	747,955	89	50	--	--	765,209	--
Medium/Heavy Duty Trucks > 10,000 lbs	83,920	6	6	--	--	85,933	--
Urban,School and Other Buses	9,640	--	2	--	--	10,289	--
Motor-Homes and Motorcycles	6,650	4	2	--	--	7,213	--
Subtotal	893,420	131	68	--	--	917,248	--
AGRICULTURE/ FARMING							
Agricultural Equipment	32,463	6	--	--	--	32,716	--
Animal Waste	--	1,131	21	--	--	30,180	--
Soil Management	7,431	--	93	--	--	36,148	35
Biomass Burning	--	2	1	--	--	423	596
Subtotal	39,894	1,139	115	--	--	99,467	631
GRAND TOTAL EMISSIONS	**1,491,256**	**2,522**	**237**	**40**	**0.02**	**1,690,586**	**60,810**

Table P:

Annual GHG Emissions: SAN FRANCISCO Year 2007 (Metric Tons / Year)

SOURCE CATEGORY	CO_2	CH_4	N_2O	PFC/HFC	SF_6	Total GHG CO_2-Equivalent	Biogenic CO_2
INDUSTRIAL/ COMMERCIAL							
Oil Refineries							
Refining Processes	--	--	--	--	--	--	--
Refinery Make Gas Combustion	--	--	--	--	--	--	--
Natural Gas and Other Gases Combustion	--	--	--	--	--	--	--
Liquid Fuel Combustion	--	--	--	--	--	--	--
Solid Fuel Combustion	--	--	--	--	--	--	--
Waste Management							
Landfill Combustion Sources	--	--	--	--	--	--	--
Landfill Fugitive Sources	--	--	--	--	--	--	--
Composting/POTWs	--	8	74	--	--	23,029	--
Other Industrial/ Commercial							
Cement Plants	--	--	--	--	--	--	--
Commercial Cooking	25,576	--	--	--	--	25,576	--
ODS Substitutes/Nat. Gas Distrib./Other	--	1,595	--	279	--	534,013	1
Reciprocating Engines	68,970	56	--	--	--	71,300	--
Turbines	45,071	1	--	--	--	45,197	--
Natural Gas- Major Combustion Sources	674,021	5	1	--	--	674,276	--
Natural Gas- Minor Combustion Sources	470,505	9	9	--	--	473,368	--
Coke Coal	--	--	--	--	--	--	--
Other Fuels Combustion	11,686	43	--	--	--	12,653	16,498
Subtotal	1,295,829	1,716	84	279	--	1,859,413	16,499
RESIDENTIAL FUEL USAGE							
Natural Gas	838,011	16	15	--	--	843,111	--
LPgas/Liquid Fuel	23,226	--	1	--	--	23,647	--
Solid Fuel	--	104	1	--	--	2,525	10,988
Subtotal	861,237	120	18	--	--	869,283	10,988
ELECTRICITY/ CO-GENERATION							
Co-Generation	178,970	89	--	--	--	180,863	100
Electricity Generation	7,504	--	--	--	0.14	10,753	--
Electricity Imports	1,136,370	9	5	--	--	1,138,188	--
Subtotal	1,322,843	99	5	--	0.14	1,329,804	100
OFF-ROAD EQUIPMENT							
Lawn and Garden Equipment	11,250	20	8	--	--	14,235	--
Construction Equipment	292,545	47	2	--	--	294,071	--
Industrial Equipment	60,802	38	4	--	--	62,697	--
Light Commercial Equipment	41,246	20	7	--	--	43,884	--
Subtotal	405,842	125	21	--	--	414,888	--
TRANSPORTATION							
Off-Road							
Locomotives	2,176	--	1	--	--	2,450	--
Ships	146,036	17	6	--	--	148,381	--
Boats	38,535	25	12	--	--	42,843	--
Commercial Aircraft	--	--	--	--	--	--	--
General Aviation	--	--	--	--	--	--	--
Military Aircraft	--	--	--	--	--	--	--
On-Road							
Passenger Cars/Trucks up to 10,000 lbs	2,059,302	221	106	--	--	2,096,833	--
Medium/Heavy Duty Trucks > 10,000 lbs	212,244	14	19	--	--	218,391	--
Urban,School and Other Buses	140,574	4	48	--	--	155,441	--
Motor-Homes and Motorcycles	7,248	12	3	--	--	8,344	--
Subtotal	2,606,117	292	195	--	--	2,672,683	--
AGRICULTURE/ FARMING							
Agricultural Equipment	110	--	--	--	--	111	--
Animal Waste	--	--	--	--	--	--	--
Soil Management	4	--	--	--	--	4	1,007
Biomass Burning	--	--	--	--	--	--	--
Subtotal	115	--	--	--	--	116	1,007
GRAND TOTAL EMISSIONS	**6,491,990**	**2,352**	**322**	**279**	**0.14**	**7,146,187**	**28,594**

Table Q:

Annual GHG Emissions: SAN MATEO Year 2007 (Metric Tons / Year)

SOURCE CATEGORY	CO_2	CH_4	N_2O	PFC/HFC	SF_6	Total GHG CO_2-Equivalent	Biogenic CO_2
INDUSTRIAL/ COMMERCIAL							
Oil Refineries							
Refining Processes	--	--	--	--	--	--	--
Refinery Make Gas Combustion	--	--	--	--	--	--	--
Natural Gas and Other Gases Combustion	--	--	--	--	--	--	--
Liquid Fuel Combustion	--	--	--	--	--	--	--
Solid Fuel Combustion	--	--	--	--	--	--	--
Waste Management							
Landfill Combustion Sources	--	245	--	--	--	5,234	115,658
Landfill Fugitive Sources	--	8,537	--	--	--	179,414	22,593
Composting/POTWs	--	60	86	--	--	27,932	--
Other Industrial/ Commercial							
Cement Plants	--	--	--	--	--	--	--
Commercial Cooking	13,461	--	--	--	--	13,461	--
ODS Substitutes/Nat. Gas Distrib./Other	--	835	--	236	--	442,682	20
Reciprocating Engines	46,803	112	--	--	--	49,172	18,613
Turbines	18	--	--	--	--	18	--
Natural Gas- Major Combustion Sources	76,685	1	--	--	--	76,754	--
Natural Gas- Minor Combustion Sources	747,061	14	14	--	--	751,608	--
Coke Coal	--	--	--	--	--	--	--
Other Fuels Combustion	5,274	16	--	--	--	5,632	4,455
Subtotal	889,303	9,821	101	236	--	1,551,908	161,338
RESIDENTIAL FUEL USAGE							
Natural Gas	719,218	14	13	--	--	723,595	--
LPgas/Liquid Fuel	19,086	--	1	--	--	19,481	--
Solid Fuel	--	379	4	--	--	9,203	38,326
Subtotal	738,303	393	18	--	--	752,278	38,326
ELECTRICITY/ CO-GENERATION							
Co-Generation	36,874	24	--	--	--	37,399	1,344
Electricity Generation	--	--	--	--	0.12	2,939	--
Electricity Imports	994,323	8	5	--	--	995,915	--
Subtotal	1,031,197	32	5	--	0.12	1,036,254	1,344
OFF-ROAD EQUIPMENT							
Lawn and Garden Equipment	11,208	20	8	--	--	14,182	--
Construction Equipment	173,531	28	1	--	--	174,445	--
Industrial Equipment	52,204	32	3	--	--	53,797	--
Light Commercial Equipment	25,539	12	5	--	--	27,226	--
Subtotal	262,482	93	17	--	--	269,650	--
TRANSPORTATION							
Off-Road							
Locomotives	4,353	--	2	--	--	4,899	--
Ships	347,697	41	16	--	--	353,471	--
Boats	17,157	19	6	--	--	19,293	--
Commercial Aircraft	1,076,869	61	39	--	--	1,090,389	--
General Aviation	25,284	4	1	--	--	25,664	--
Military Aircraft	4,449	--	--	--	--	4,470	--
On-Road							
Passenger Cars/Trucks up to 10,000 lbs	2,972,646	281	154	--	--	3,026,154	--
Medium/Heavy Duty Trucks > 10,000 lbs	224,315	14	21	--	--	230,958	--
Urban,School and Other Buses	74,368	2	19	--	--	80,264	--
Motor-Homes and Motorcycles	12,494	16	4	--	--	14,098	--
Subtotal	4,759,634	437	261	--	--	4,849,664	--
AGRICULTURE/ FARMING							
Agricultural Equipment	9,233	2	--	--	--	9,305	--
Animal Waste	--	257	9	--	--	8,101	--
Soil Management	348	--	30	--	--	9,520	139
Biomass Burning	--	3	--	--	--	136	98
Subtotal	9,581	262	39	--	--	27,062	237
GRAND TOTAL EMISSIONS	**7,690,500**	**11,037**	**440**	**236**	**0.12**	**8,486,808**	**201,245**

Table R:

Annual GHG Emissions: SANTA CLARA Year 2007 (Metric Tons / Year)

SOURCE CATEGORY	CO_2	CH_4	N_2O	PFC/HFC	SF_6	Total GHG CO_2-Equivalent	Biogenic CO_2
INDUSTRIAL/ COMMERCIAL							
Oil Refineries							
Refining Processes	--	--	--	--	--	--	--
Refinery Make Gas Combustion	--	--	--	--	--	--	--
Natural Gas and Other Gases Combustion	--	--	--	--	--	--	--
Liquid Fuel Combustion	--	--	--	--	--	--	--
Solid Fuel Combustion	--	--	--	--	--	--	--
Waste Management							
Landfill Combustion Sources	--	440	--	--	--	9,374	207,134
Landfill Fugitive Sources	--	12,444	1	--	--	261,566	35,205
Composting/POTWs	--	1,382	309	--	--	124,918	--
Other Industrial/ Commercial							
Cement Plants	841,350	13	3	--	--	842,475	--
Commercial Cooking	30,961	--	--	--	--	30,961	--
ODS Substitutes/Nat. Gas Distrib./Other	--	2,426	--	582	--	1,167,459	--
Reciprocating Engines	193,233	742	1	--	--	209,049	104,164
Turbines	349	--	--	--	--	350	--
Natural Gas- Major Combustion Sources	361,211	5	1	--	--	361,532	--
Natural Gas- Minor Combustion Sources	1,691,662	32	31	--	--	1,701,957	--
Coke Coal	--	--	--	--	--	--	--
Other Fuels Combustion	15,307	5	--	--	--	15,554	15,266
Subtotal	3,134,075	17,489	346	582	--	4,725,195	361,770
RESIDENTIAL FUEL USAGE							
Natural Gas	1,555,938	30	29	--	--	1,565,407	--
LPgas/Liquid Fuel	40,631	1	3	--	--	41,464	--
Solid Fuel	--	1,238	13	--	--	30,092	124,813
Subtotal	1,596,569	1,268	44	--	--	1,636,963	124,813
ELECTRICITY/ CO-GENERATION							
Co-Generation	322,599	242	--	--	--	327,843	24,023
Electricity Generation	1,207,022	88	--	--	0.30	1,216,062	1,510
Electricity Imports	2,059,670	17	9	--	--	2,062,967	--
Subtotal	3,589,291	347	10	--	0.30	3,606,872	25,533
OFF-ROAD EQUIPMENT							
Lawn and Garden Equipment	26,010	47	19	--	--	32,912	--
Construction Equipment	370,445	60	2	--	--	372,396	--
Industrial Equipment	316,775	216	22	--	--	328,058	--
Light Commercial Equipment	52,797	26	10	--	--	56,451	--
Subtotal	766,027	349	53	--	--	789,817	--
TRANSPORTATION							
Off-Road							
Locomotives	16,064	1	6	--	--	18,081	--
Ships	--	--	--	--	--	--	--
Boats	17,199	10	4	--	--	18,721	--
Commercial Aircraft	318,300	9	12	--	--	322,137	--
General Aviation	63,542	10	2	--	--	64,493	--
Military Aircraft	46,921	9	2	--	--	47,627	--
On-Road							
Passenger Cars/Trucks up to 10,000 lbs	6,428,736	704	363	--	--	6,555,920	--
Medium/Heavy Duty Trucks > 10,000 lbs	678,747	40	45	--	--	693,658	--
Urban,School and Other Buses	88,596	3	22	--	--	95,407	--
Motor-Homes and Motorcycles	39,091	32	10	--	--	42,785	--
Subtotal	7,697,197	818	466	--	--	7,858,834	--
AGRICULTURE/ FARMING							
Agricultural Equipment	35,719	7	--	--	--	35,997	--
Animal Waste	--	2,095	44	--	--	57,557	--
Soil Management	1,034	--	225	--	--	70,707	318
Biomass Burning	--	2	--	--	--	139	141
Subtotal	36,753	2,104	269	--	--	164,401	459
GRAND TOTAL EMISSIONS	**16,819,916**	**22,376**	**1,189**	**582**	**0.30**	**18,782,077**	**512,575**

Table S:

Annual GHG Emissions: SOLANO* Year 2007 (Metric Tons / Year)

SOURCE CATEGORY	CO_2	CH_4	N_2O	PFC/HFC	SF_6	Total GHG CO_2-Equivalent	Biogenic CO_2
INDUSTRIAL/ COMMERCIAL							
Oil Refineries							
Refining Processes	534,305	9	--	--	--	534,495	--
Refinery Make Gas Combustion	1,317,135	27	2	--	--	1,318,241	--
Natural Gas and Other Gases Combustion	86,885	9	1	--	--	87,249	--
Liquid Fuel Combustion	--	--	--	--	--	--	--
Solid Fuel Combustion	--	--	--	--	--	--	--
Waste Management							
Landfill Combustion Sources	--	8	--	--	--	172	3,803
Landfill Fugitive Sources	--	1,550	--	--	--	32,564	4,120
Composting/POTWs	--	218	44	--	--	18,110	--
Other Industrial/ Commercial							
Cement Plants	--	--	--	--	--	--	--
Commercial Cooking	8,077	--	--	--	--	8,077	--
ODS Substitutes/Nat. Gas Distrib./Other	--	498	--	84	--	160,727	--
Reciprocating Engines	27,294	71	--	--	--	28,792	1,775
Turbines	273,754	6	--	--	--	273,970	--
Natural Gas- Major Combustion Sources	76,427	14	--	--	--	76,769	--
Natural Gas- Minor Combustion Sources	348,389	7	6	--	--	350,509	--
Coke Coal	--	--	--	--	--	--	--
Other Fuels Combustion	3,506	6	--	--	--	3,635	2,344
Subtotal	2,675,772	2,421	53	84	--	2,893,310	12,042
RESIDENTIAL FUEL USAGE							
Natural Gas	245,980	5	5	--	--	247,477	--
LPgas/Liquid Fuel	3,763	--	--	--	--	3,843	--
Solid Fuel	--	264	3	--	--	6,426	26,568
Subtotal	249,744	269	8	--	--	257,747	26,568
ELECTRICITY/ CO-GENERATION							
Co-Generation	375,712	12	--	--	--	375,968	--
Electricity Generation	32,350	1	--	--	0.05	33,595	--
Electricity Imports	--	--	--	--	--	--	--
Subtotal	408,063	12	--	--	0.05	409,563	--
OFF-ROAD EQUIPMENT							
Lawn and Garden Equipment	3,045	6	2	--	--	3,853	--
Construction Equipment	68,732	11	--	--	--	69,093	--
Industrial Equipment	66,709	12	1	--	--	67,152	--
Light Commercial Equipment	6,391	3	1	--	--	6,848	--
Subtotal	144,876	32	5	--	--	146,946	--
TRANSPORTATION							
Off-Road							
Locomotives	5,804	--	2	--	--	6,532	--
Ships	12,274	2	1	--	--	12,478	--
Boats	11,276	25	3	--	--	12,732	--
Commercial Aircraft	--	--	--	--	--	--	--
General Aviation	--	--	--	--	--	--	--
Military Aircraft	423,131	21	13	--	--	427,663	--
On-Road							
Passenger Cars/Trucks up to 10,000 lbs	1,139,899	114	63	--	--	1,161,801	--
Medium/Heavy Duty Trucks > 10,000 lbs	168,039	9	9	--	--	170,918	--
Urban,School and Other Buses	30,727	--	5	--	--	32,268	--
Motor-Homes and Motorcycles	9,193	8	2	--	--	10,048	--
Subtotal	1,800,342	178	98	--	--	1,834,440	--
AGRICULTURE/ FARMING							
Agricultural Equipment	32,041	6	--	--	--	32,291	--
Animal Waste	--	1,037	3	--	--	22,727	--
Soil Management	871	--	197	--	--	62,013	39,600
Biomass Burning	--	2	--	--	--	95	76
Subtotal	32,912	1,045	201	--	--	117,126	39,676
GRAND TOTAL EMISSIONS	**5,311,708**	**3,957**	**364**	**84**	**0.05**	**5,659,130**	**78,287**

*** BAAQMD Jurisdiction only**

Table T:

Annual GHG Emissions: SONOMA* Year 2007 (Metric Tons / Year)

SOURCE CATEGORY	CO_2	CH_4	N_2O	PFC/HFC	SF_6	Total GHG CO_2-Equivalent	Biogenic CO_2
INDUSTRIAL/ COMMERCIAL							
Oil Refineries							
Refining Processes	--	--	--	--	--	--	--
Refinery Make Gas Combustion	--	--	--	--	--	--	--
Natural Gas and Other Gases Combustion	--	--	--	--	--	--	--
Liquid Fuel Combustion	--	--	--	--	--	--	--
Solid Fuel Combustion	--	--	--	--	--	--	--
Waste Management							
Landfill Combustion Sources	--	--	--	--	--	1	13
Landfill Fugitive Sources	--	4,416	--	--	--	92,809	11,669
Composting/POTWs	--	573	89	--	--	39,574	--
Other Industrial/ Commercial							
Cement Plants	--	--	--	--	--	--	--
Commercial Cooking	9,423	--	--	--	--	9,423	--
ODS Substitutes/Nat. Gas Distrib./Other	--	337	--	117	--	217,310	--
Reciprocating Engines	24,824	379	--	--	--	32,820	58,586
Turbines	7	--	--	--	--	7	--
Natural Gas- Major Combustion Sources	25,653	--	--	--	--	25,676	--
Natural Gas- Minor Combustion Sources	215,498	4	4	--	--	216,810	--
Coke Coal	--	--	--	--	--	--	--
Other Fuels Combustion	6,357	3	--	--	--	6,433	415
Subtotal	281,761	5,713	93	117	--	640,862	70,682
RESIDENTIAL FUEL USAGE							
Natural Gas	362,837	7	7	--	--	365,045	--
LPgas/Liquid Fuel	16,199	--	1	--	--	16,546	--
Solid Fuel	--	1,020	11	--	--	24,786	102,209
Subtotal	379,036	1,027	19	--	--	406,377	102,209
ELECTRICITY/ CO-GENERATION							
Co-Generation	6,478	96	--	--	--	8,506	6,294
Electricity Generation	--	--	--	--	0.08	1,940	--
Electricity Imports	568,185	5	3	--	--	569,094	--
Subtotal	574,663	101	3	--	0.08	579,541	6,294
OFF-ROAD EQUIPMENT							
Lawn and Garden Equipment	6,143	11	5	--	--	7,773	--
Construction Equipment	118,009	19	1	--	--	118,631	--
Industrial Equipment	34,416	20	2	--	--	35,374	--
Light Commercial Equipment	12,601	6	2	--	--	13,506	--
Subtotal	171,169	56	9	--	--	175,285	--
TRANSPORTATION							
Off-Road							
Locomotives	5,078	--	2	--	--	5,716	--
Ships	--	--	--	--	--	--	--
Boats	17,376	19	5	--	--	19,213	--
Commercial Aircraft	--	--	--	--	--	--	--
General Aviation	24,133	4	1	--	--	24,492	--
Military Aircraft	--	--	--	--	--	--	--
On-Road							
Passenger Cars/Trucks up to 10,000 lbs	1,790,567	211	115	--	--	1,830,792	--
Medium/Heavy Duty Trucks > 10,000 lbs	174,035	12	14	--	--	178,612	--
Urban,School and Other Buses	25,221	1	5	--	--	26,677	--
Motor-Homes and Motorcycles	16,221	13	4	--	--	17,730	--
Subtotal	2,052,632	260	146	--	--	2,103,232	--
AGRICULTURE/ FARMING							
Agricultural Equipment	32,040	6	--	--	--	32,290	--
Animal Waste	--	6,735	37	--	--	152,783	--
Soil Management	3,703	--	78	--	--	27,848	277
Biomass Burning	--	16	1	--	--	750	657
Subtotal	35,744	6,757	116	--	--	213,671	934
GRAND TOTAL EMISSIONS	**3,495,004**	**13,914**	**386**	**117**	**0.08**	**4,118,968**	**180,119**

*** BAAQMD Jurisdiction only**

Table U: Bay Area Greenhouse Gas Emission Inventory Projections : 1990 - 2029

(Million Metric Tons CO_2- Equivalent)

SOURCE CATEGORY	Year 1990	1993	1996	1999	2002	2005	2008	2011	2014	2017	2020	2023	2026	2029
INDUSTRIAL/ COMMERCIAL														
Oil Refineries														
Refining Processes	3.3	3.5	3.6	3.7	3.5	3.4	3.5	3.6	3.7	3.8	3.9	4.0	4.2	4.3
Refinery Make Gas Combustion	3.8	4.0	3.7	4.4	4.5	4.7	4.8	5.0	5.1	5.3	5.4	5.6	5.8	5.9
Natural Gas and Other Gases Combustion	4.5	4.3	4.5	4.5	4.6	4.8	4.9	5.1	5.2	5.4	5.5	5.7	5.9	6.1
Liquid Fuel Combustion	0.1	0.1	0.1	0.1	0.1	0.1	0.1	0.1	0.1	0.1	0.1	0.1	0.1	0.1
Solid Fuel Combustion	0.8	0.9	0.9	0.9	1.0	1.0	1.0	1.0	1.1	1.1	1.1	1.2	1.2	1.2
Waste Management														
Landfill Combustion Sources	0.0	0.0	0.0	0.0	0.0	0.0	0.0	0.0	0.0	0.0	0.0	0.0	0.0	0.0
Landfill Fugitive Sources	1.7	1.4	1.1	1.1	1.1	1.2	1.2	1.2	1.2	1.2	1.2	1.2	1.1	1.1
Composting/POTWs	0.2	0.3	0.3	0.4	0.3	0.4	0.4	0.4	0.4	0.4	0.4	0.4	0.4	0.4
Other Industrial/ Commercial														
Cement Plants	0.9	0.9	0.9	1.0	0.8	0.9	0.9	0.9	0.9	1.0	1.0	1.0	1.1	1.1
Commercial Cooking	0.1	0.1	0.1	0.1	0.1	0.1	0.1	0.1	0.1	0.1	0.2	0.2	0.2	0.2
ODS Substitutes/Nat. Gas Distrib./Other	1.1	1.3	1.8	2.4	2.9	3.6	4.8	5.9	7.1	8.3	9.4	10.6	11.7	12.8
Reciprocating Engines	0.5	0.5	0.6	0.5	0.5	0.6	0.6	0.6	0.6	0.7	0.7	0.7	0.8	0.8
Turbines	0.4	0.4	0.4	0.4	0.4	0.4	0.4	0.4	0.4	0.4	0.4	0.4	0.4	0.5
Natural Gas- Major Combustion Sources	1.9	1.8	1.6	1.8	1.5	1.6	2.4	2.5	2.6	2.7	2.8	3.0	3.1	3.2
Natural Gas- Minor Combustion Sources	2.3	7.2	8.5	8.5	8.5	8.8	9.1	9.4	9.7	10.1	10.4	10.7	11.0	11.3
Coke Coal	1.7	1.5	1.5	1.0	1.0	1.0	1.0	1.0	1.1	1.1	1.2	1.2	1.2	1.3
Other Fuels Combustion	0.4	0.4	0.4	0.3	0.3	0.3	0.4	0.4	0.4	0.4	0.4	0.4	0.4	0.5
Subtotal	23.9	28.5	29.9	31.1	31.4	32.8	35.6	37.7	39.9	42.0	44.2	46.4	48.6	50.8
RESIDENTIAL FUEL USAGE														
Natural Gas	5.4	5.6	5.9	6.1	6.2	6.4	6.5	6.7	6.9	7.0	7.2	7.4	7.5	7.7
LPgas/Liquid Fuel	0.2	0.2	0.2	0.2	0.2	0.2	0.2	0.2	0.2	0.2	0.2	0.2	0.2	0.2
Solid Fuel	0.1	0.2	0.2	0.1	0.1	0.1	0.2	0.2	0.2	0.2	0.2	0.2	0.2	0.2
Subtotal	5.8	6.0	6.2	6.4	6.6	6.7	6.9	7.0	7.2	7.4	7.5	7.7	7.9	8.0
ELECTRICITY/ CO-GENERATION														
Co-Generation	8.6	7.2	6.7	5.2	5.4	5.5	5.4	5.6	5.9	6.1	6.4	6.7	6.9	7.2
Electricity Generation	7.6	8.5	4.0	4.6	4.7	2.8	3.0	3.1	3.3	3.4	3.5	3.7	3.8	4.0
Electricity Imports	8.9	8.8	10.3	10.1	6.9	6.8	7.2	7.5	7.8	8.1	8.3	8.6	8.9	9.1
Subtotal	25.1	24.6	20.9	19.8	17.0	15.1	15.6	16.3	16.9	17.6	18.3	18.9	19.6	20.4

Table U: Bay Area Greenhouse Gas Emission Inventory Projections : 1990 - 2029

(Million Metric Tons CO_2- Equivalent)

SOURCE CATEGORY	Year 1990	1993	1996	1999	2002	2005	2008	2011	2014	2017	2020	2023	2026	2029
OFF-ROAD EQUIPMENT														
Lawn and Garden Equipment	0.1	0.1	0.1	0.1	0.1	0.1	0.1	0.1	0.1	0.1	0.1	0.1	0.1	0.1
Construction Equipment	1.3	1.4	1.5	1.6	1.6	1.7	1.8	1.9	2.0	2.1	2.2	2.3	2.3	2.4
Industrial Equipment	0.6	0.6	0.6	0.7	0.7	0.7	0.8	0.8	0.9	0.9	1.0	1.1	1.1	1.2
Light Commercial Equipment	0.2	0.2	0.2	0.2	0.2	0.2	0.2	0.3	0.3	0.3	0.3	0.3	0.3	0.3
Subtotal	2.2	2.3	2.5	2.6	2.7	2.8	3.0	3.1	3.3	3.4	3.6	3.8	3.9	4.1
TRANSPORTATION														
Off-Road														
Locomotives	0.1	0.1	0.1	0.1	0.1	0.1	0.1	0.1	0.1	0.1	0.1	0.1	0.1	0.1
Ships	0.6	0.6	0.6	0.6	0.7	0.7	0.8	0.8	0.8	0.9	1.0	1.1	1.2	1.3
Boats	0.5	0.5	0.5	0.5	0.6	0.6	0.6	0.6	0.5	0.5	0.6	0.6	0.6	0.7
Commercial Aircraft	1.6	1.7	1.8	1.9	1.7	1.8	1.9	2.1	2.2	2.4	2.6	2.7	2.9	3.2
General Aviation	0.3	0.3	0.3	0.3	0.2	0.2	0.2	0.2	0.3	0.3	0.3	0.3	0.3	0.3
Military Aircraft	0.6	0.5	0.5	0.5	0.5	0.5	0.5	0.5	0.5	0.5	0.5	0.5	0.5	0.5
On-Road														
Passenger Cars/Trucks up to 10,000 lbs	22.3	22.6	23.1	24.3	26.4	26.6	26.9	27.6	28.6	29.9	30.9	31.9	33.5	34.7
Medium/Heavy Duty Trucks > 10,000 lbs	3.1	2.8	2.8	2.9	3.0	3.3	3.3	3.4	3.5	3.6	3.7	3.8	3.9	4.0
Urban,School and Other Buses	0.5	0.6	0.6	0.7	0.8	0.8	0.8	0.8	0.8	0.8	0.9	0.9	0.9	0.9
Motor-Homes and Motorcycles	0.2	0.2	0.2	0.2	0.2	0.2	0.2	0.2	0.2	0.2	0.2	0.3	0.3	0.3
Subtotal	29.8	29.8	30.4	32.0	34.1	34.8	35.3	36.3	37.6	39.3	40.7	42.2	44.2	46.0
AGRICULTURE/ FARMING														
Agricultural Equipment	0.2	0.2	0.2	0.2	0.2	0.2	0.2	0.2	0.2	0.2	0.2	0.2	0.2	0.2
Animal Waste	0.5	0.6	0.6	0.6	0.6	0.6	0.6	0.6	0.6	0.6	0.6	0.6	0.6	0.6
Soil Management	0.3	0.3	0.3	0.3	0.3	0.3	0.3	0.3	0.3	0.3	0.3	0.3	0.3	0.3
Biomass Burning	0.0	0.0	0.0	0.0	0.0	0.0	0.0	0.0	0.0	0.0	0.0	0.0	0.0	0.0
Subtotal	1.0	1.1	1.1	1.1	1.1	1.1	1.1	1.1	1.1	1.1	1.1	1.1	1.1	1.1
GRAND TOTAL EMISSIONS	**87.7**	**92.2**	**91.0**	**93.0**	**92.8**	**93.4**	**97.4**	**101.5**	**106.0**	**110.8**	**115.4**	**120.2**	**125.3**	**130.4**

Table V: 2007 BAY AREA MAJOR (TOP 200) GHG EMITTING FACILITIES

						CO2 Equivalent Emissions (Metric Tons per year)		
No.	Plant #	Plant Name	Plant Address	City	Zipcode	Biogenic	Non-Biogenic	Total
1	11	Shell Martinez Refinery	3485 Pacheco Blvd	Martinez	94553	-	4,976,544	4,976,544
2	10	Chevron Products Company	841 Chevron Way	Richmond	94802	-	4,303,800	4,303,800
3	14628	Tesoro Refining and Marketing Company	150 Solano Way, Avon Refinery	Martinez	94553	-	2,804,678	2,804,678
4	12626	Valero Refining Company - California	3400 E 2nd Street	Benicia	94510	-	2,568,988	2,568,988
5	12095	Delta Energy Center	Arcy Lane	Pittsburg	94565	-	1,895,320	1,895,320
6	16	ConocoPhillips - San Francisco Refinery	1380 San Pablo Ave	Rodeo	94572	-	1,577,872	1,577,872
7	11866	Los Medanos Energy Center	750 E 3rd Street	Pittsburg	94565	-	1,368,588	1,368,588
8	12183	Metcalf Energy Center	One Blanchard Road	Coyote	95013	-	1,120,115	1,120,115
9	17	Lehigh Southwest Cement Company	24001 Stevens Creek Blvd	Cupertino	95014	-	842,475	842,475
10	26	Mirant Potrero, LLC	1201 Illinois Street	San Francisco	94107	-	462,505	462,505
11	8664	Crockett Cogeneration, A Cal Ltd Partnership	550 Loring Avenue	Crockett	94525	-	427,300	427,300
12	1820	Martinez Cogen Limited Partnership	550 Solano Way, Avon Refinery	Martinez	94553	-	410,970	410,970
13	10295	Air Products & Chemicals, Inc	Tesoro, Avon Refinery	Martinez	94553	-	361,179	361,179
14	2066	Waste Management of Alameda County	10840 Altamont Pass Rd	Livermore	94551	121,019	143,881	264,900
15	2266	Browning-Ferris Industries of CA, Inc	12310 San Mateo Road	Half Moon Bay	94019	109,503	130,538	240,041
16	3981	GWF Power Systems,LP (Site 4)	3400 Wilbur Avenue	Antioch	94509	-	201,672	201,672
17	3243	GWF Power Systems,LP (Site 1)	895 E 3rd Street	Pittsburg	94565	-	200,700	200,700
18	3244	GWF Power Systems,LP (Site 2)	1600 Loveridge Road	Pittsburg	94565	-	196,800	196,800
19	3245	GWF Power Systems,LP (Site 3)	1900 Wilbur Avenue	Antioch	94509	-	184,660	184,660
20	3246	GWF Power Systems,LP (Site 5)	555 Nichols Road	Pittsburg	94565	-	183,237	183,237
21	1812	Kirby Canyon Landfill	910 Coyote Creek Glf Dr	San Jose	95198	120,641	50,361	171,002
22	1179	Redwood Landfill Inc	8950 Redwood Hwy	Novato	94948	72,532	93,942	166,474
23	2254	Sonoma County Department of Public Works	500 Mecham Road	Petaluma	94952	68,119	87,311	155,430
24	732	Bluegrass Mills Holding Co	2600 De La Cruz Blvd	Santa Clara	95050	-	128,963	128,963
25	11326	PE Berkeley, Inc	Univ of Calif, Berkeley Campus	Berkeley	94720	-	126,541	126,541
26	51	United Airlines, SF Maintenance Center	SF Int'l Airport	San Francisco	94128	-	123,861	123,861
27	12	Mirant Delta, LLC	696 W 10th Street	Pittsburg	94565	-	121,624	121,624
28	2246	Tri-Cities Recycling	7010 Auto Mall Pkwy	Fremont	94538	54,680	65,197	119,877
29	11928	Calpine Pittsburg LLC	Loveridge Road	Pittsburg	94565	-	116,440	116,440

Table V: 2007 BAY AREA MAJOR (TOP 200) GHG EMITTING FACILITIES

No.	Plant #	Plant Name	Plant Address	City	Zipcode	CO2 Equivalent Emissions (Metric Tons per year)		
						Biogenic	Non-Biogenic	Total
30	5095	Republic Services Vasco Road, LLC	4001 N Vasco Road	Livermore	94550	**48,063**	**57,316**	**105,378**
31	6044	O L S Energy-Agnews	3530 Zanker Road	San Jose	95134	**-**	**104,777**	**104,777**
32	2740	City of Mountain View (Shoreline)	2600 Shoreline Boulevard	Mountain View	94043	**53,132**	**48,687**	**101,819**
33	11180	LLC	1400 Pacheco Pass Hwy	Gilroy	95020	**-**	**94,712**	**94,712**
34	10978	Seagate Technology	311 Turquoise Street	Milpitas	95035	**-**	**86,229**	**86,229**
35	151	Hexion Specialty Chemicals, Inc	41100 Boyce Road	Fremont	94538	**-**	**80,865**	**80,865**
36	18	Mirant Delta, LLC	3201 Wilbur Avenue	Antioch	94509	**-**	**80,803**	**80,803**
37	606	Anheuser-Busch, Inc	3101 Busch Drive	Fairfield	94533	**38,630**	**37,409**	**76,039**
38	778	San Jose/Santa Clara Water Pollution Control	700 Los Esteros Road	San Jose	95134	**47,537**	**26,689**	**74,226**
39	2371	USS-POSCO Industries	900 Loveridge Road	Pittsburg	94565	**-**	**68,215**	**68,215**
40	3921	Seagate Technology, LLC	47010 Kato Road	Fremont	94538	**-**	**68,048**	**68,048**
41	2478	UCSF/Parnassus	3rd Avenue & Parnassus	San Francisco	94122	**-**	**64,882**	**64,882**
42	16151	NRG Energy Center LLC	465 Stevenson Street	San Francisco	94103	**-**	**64,559**	**64,559**
43	1840	West Contra Costa County Landfill	Foot of Parr Blvd	Richmond	94801	**28,773**	**34,212**	**62,984**
44	907	Central Contra Costa Sanitary District	5019 Imhoff Place	Martinez	94553	**33,215**	**29,239**	**62,454**
45	4618	Keller Canyon Landfill Company	901 Bailey Road	Pittsburg	94565	**26,956**	**32,134**	**59,089**
46	30	Owens-Brockway Glass Container Inc	3600 Alameda Avenue	Oakland	94601	**-**	**53,055**	**53,055**
47	14483	California Water Service Company	1720 N 1st Street	San Jose	95112	**-**	**50,164**	**50,164**
48	591	East Bay Municipal Utility District	2020 Wake Avenue	Oakland	94607	**42,742**	**6,212**	**48,954**
49	14017	American Lithographers & Business Forms	21062 Forbes Street	Hayward	94545	**-**	**45,790**	**45,790**
50	621	City of Santa Clara, Silicon Valley Power	560 Robert Avenue	Santa Clara	95050	**-**	**45,288**	**45,288**
51	1364	Cypress Amloc Land Co , Inc	1 Sand Hill Road	Colma	94014	**19,074**	**22,738**	**41,812**
52	11670	Gas Recovery Systems, Inc	1804 Dixon Landing Rd	San Jose	95134	**36,129**	**4,913**	**41,042**
53	1438	New United Motor Manufacturing, Inc	45500 Fremont Blvd	Fremont	94538	**-**	**39,344**	**39,344**
54	2039	Potrero Hills Landfill, Inc	3675 Potrero Hills Lane	Suisun City	94585	**7,064**	**29,268**	**36,332**
55	13289	Los Esteros Critical Energy Facility	800 Thomas Foon Chew Way	San Jose	95134	**-**	**35,555**	**35,555**
56	83	United States Pipe & Foundry Company, LLC	1295 Whipple Road	Union City	94587	**-**	**34,560**	**34,560**
57	173	Georgia Pacific Gypsum LLC	801 Minaker Street	Antioch	94509	**-**	**34,348**	**34,348**
58	3464	City of Santa Clara	5401 Lafayette	Santa Clara	95050	**15,098**	**17,998**	**33,096**

Table V: 2007 BAY AREA MAJOR (TOP 200) GHG EMITTING FACILITIES

No.	Plant #	Plant Name	Plant Address	City	Zipcode	CO2 Equivalent Emissions (Metric Tons per year)		
						Biogenic	Non-Biogenic	Total
59	12728	Waste Management Inc	2615 Davis Street	San Leandro	94577	**14,847**	**17,734**	**32,581**
60	153	PABCO Gypsum	37851 Cherry Street	Newark	94560	**-**	**32,171**	**32,171**
61	1201	Rolls-Royce Engine Services - Oakland, Inc	6711 Lockheed Street	Oakland	94621	**-**	**31,795**	**31,795**
62	15128	Cardinal Cogen Inc	Campus & Jordan Way	Palo Alto	94305	**-**	**30,626**	**30,626**
63	7265	San Jose State University (Cogen Plant)	San Carlos Street	San Jose	95192	**-**	**30,390**	**30,390**
64	706	New NGC, Inc	1040 Canal Boulevard	Richmond	94804	**-**	**29,252**	**29,252**
65	3011	IPT SRI Cogeneration Inc	333 Ravenswood Drive	Menlo Park	94025	**-**	**28,540**	**28,540**
66	13566	Norcal Waste Systems Pacheco Pass Landfill, Inc	Bloomfield Rd & Highway 152	Gilroy	95021	**12,486**	**14,884**	**27,370**
67	85	Hitachi Global Storage Technologies Inc	5600 Cottle Road	San Jose	95193	**-**	**26,909**	**26,909**
68	1257	Genentech, Inc	460 Point San Bruno Boulevard	Francisco	94080	**-**	**26,324**	**26,324**
69	41	Owens Corning Insulating Systems, LLC	960 Central Expressway	Santa Clara	95050	**-**	**25,432**	**25,432**
70	13193	Valero Benicia Asphalt Plant	3001 Park Road	Benicia	94510	**-**	**24,851**	**24,851**
71	11669	Gas Recovery Systems, Inc	15999 Guadalupe Mines Rd	San Jose	95120	**21,411**	**2,912**	**24,323**
72	11327	ConAgra Foods, Gilroy Foods	1350 Pacheco Pass Hwy	Gilroy	95020	**-**	**23,928**	**23,928**
73	1464	Acme Fill Corporation	950 Waterbird Way	Martinez	94553	**2,953**	**20,968**	**23,920**
74	1784	San Francisco International Airport	SF Int'l Airport	San Francisco	94128	**321**	**23,490**	**23,811**
75	698	Georgia-Pacific Gypsum LLC	1988 Marina Boulevard	San Leandro	94577	**-**	**23,535**	**23,535**
76	31	Dow Chemical Company	901 Loveridge Road	Pittsburg	94565	**-**	**22,900**	**22,900**
77	11887	Dynegy Oakland LLC	50 Martin Luthr Kng, Jr Way	Oakland	94607	**-**	**22,764**	**22,764**
78	3294	Guadalupe Rubbish Disposal	15999 Guadalupe Mines Rd	San Jose	95120	**11,947**	**10,813**	**22,759**
79	568	San Francisco South East Treatment Plant	1700 Jerrold Avenue	San Francisco	94124	**13,360**	**9,176**	**22,535**
80	617	Palo Alto Regional Water Quality Control Plant	2501 Embarcadero Way	Palo Alto	94303	**15,163**	**6,407**	**21,570**
81	3974	San Francisco General Hospital	1118	San Francisco	94110	**-**	**21,370**	**21,370**
82	1190	Evergreen Oil, Inc	6880 Smith Avenue	Newark	94560	**-**	**21,055**	**21,055**
83	13160	University of California SF	600 16th Street	San Francisco	94107	**-**	**19,847**	**19,847**
84	55	Lockheed Martin Corporation	1111 Lockheed Martin Way	Sunnyvale	94089	**-**	**18,632**	**18,632**
85	1634	Napa State Hospital	2100 Napa Vallejo Hwy	Napa	94558	**-**	**18,048**	**18,048**
86	11247	Clover Flat Landfill Inc	4380 Silverado Trail	Calistoga	94515	**13,181**	**3,769**	**16,951**
87	22	Conoco Phillips Refining Company	2101 Franklin Canyon Rd	Rodeo	94572	**-**	**16,697**	**16,697**

Table V: 2007 BAY AREA MAJOR (TOP 200) GHG EMITTING FACILITIES

						CO2 Equivalent Emissions (Metric Tons per year)		
No.	Plant #	Plant Name	Plant Address	City	Zipcode	Biogenic	Non-Biogenic	Total
88	12071	Bayer Healthcare LLC	800 Dwight Way	Berkeley	94710	-	16,609	16,609
89	11668	Gas Recovery Systems, Inc	Marsh Road	Menlo Park	94025	14,574	1,982	16,556
90	3256	Turk Island Solid Waste Disposal Site	Union City Boulevard	Union City	94587	7,527	8,973	16,500
91	11671	Gas Recovery Systems, Inc	Landfill	Canyon	94558	14,231	1,935	16,167
92	94	Cargill Salt	7220 Central Ave	Newark	94560	-	16,147	16,147
93	13631	Morgan Advanced Ceramics	2425 Whipple Road	Hayward	94544	-	16,071	16,071
94	5905	City of Sunnyvale/Public Works Dept	301 Carl Road	Sunnyvale	94088	1,799	14,204	16,003
95	12967	TRC	James Donlon Blvd	Antioch	94509	7,188	8,569	15,758
96	733	City of Sunnyvale Water Pollution Control	1440 Borregas Avenue	Sunnyvale	94089	13,277	2,345	15,622
97	9029	Kie-Con	3551 Wilbur Avenue	Antioch	94509	-	15,494	15,494
98	4272	El Camino Hospital	2500 Grant Road	Mountain View	94040	-	15,403	15,403
99	2721	City of Palo Alto Landfill	Byxbee Park	Palo Alto	94301	4,722	10,665	15,387
100	9010	California Paperboard Corporation	525 Mathew Street	Santa Clara	95050	-	14,247	14,247
101	14512	Gilroy Energy Center,LLC for Riverview Energy Ctr	801 Minaker Road	Antioch	94509	-	14,035	14,035
102	1403	City of Santa Rosa Wastewater Treatment	4300 Llano Road	Santa Rosa	95407	6,302	7,534	13,836
103	3590	City of Berkeley/Engr Div/Public Works	Cesar Chavez Prk	Berkeley	94704	6,195	7,385	13,581
104	7264	California Pacific Medical Center	3700 California Street	San Francisco	94118	-	13,399	13,399
105	11661	Rhodia Inc	100 Mococo Road	Martinez	94553	-	13,294	13,294
106	227	Criterion Catalysts Company LP	2840 Willow Pass Road	Pittsburg	94565	-	12,953	12,953
107	79	Morton International Inc	7380 Morton Avenue	Newark	94560	-	12,135	12,135
108	1371	TP	7399 Johnson Drive	Pleasanton	94588	5,959.6	5,830.9	11,790.5
109	18198	New WinCup Holdings, Inc	195 Tamal Vista Boulevard	Corte Madera	94925	-	11,563	11,563
110	1579	Granite Rock Company	1321 Lowrie Avenue	Francisco	94080	-	11,397	11,397
111	5081	ALZA Corporation	1015 Joaquin Road	Mountain View	94043	9,680	1,549	11,229
112	475	Santa Clara Valley Health & Hospital System	751 So Bascom Avenue	San Jose	95128	-	10,969	10,969
113	11374	WD Media, Inc	1710 Automation Pkwy	San Jose	95131	-	10,965	10,965
114	1605	Services	2003 Diamond Blvd	Concord	94520	-	10,920	10,920
115	632	Intel Corporation	2150 Mission College Blvd	Santa Clara	95054	-	10,759	10,759
116	14511	Gilroy Energy Center, LLC (Wolfskill Energy Ctr)	2425 Cordelia Road	Fairfield	94534	-	10,660	10,660

Table V: 2007 BAY AREA MAJOR (TOP 200) GHG EMITTING FACILITIES

No.	Plant #	Plant Name	Plant Address	City	Zipcode	CO2 Equivalent Emissions (Metric Tons per year)		
						Biogenic	Non-Biogenic	Total
117	1004	SFSU Housing Facilities (Cogeneration Plant)	1600 Holloway Avenue	San Francisco	94132	-	10,192	10,192
118	2025	University of San Francisco	2130 Fulton Street	San Francisco	94117	-	10,070	10,070
119	450	Veterans Administration Medical Center	3801 Miranda Avenue	Palo Alto	94304	-	9,783	9,783
120	3312	Zanker Road Resource Management,Ltd	705 Los Esteros Road	San Jose	95134	1,250	8,243	9,493
121	550	NASA-AMES Research Center	Moffett Field NS	Mountain View	94035	-	9,347	9,347
122	3273	Pacific Union College	1 Angwin Avenue	Angwin	94508	-	9,217	9,217
123	1209	Union Sanitary District	5072 Benson Road	Union City	94587	8,069	889	8,958
124	10271	Darling International	429 Amador Street	San Francisco	94124	-	8,883.9	8,883.9
125	541	Pacific Gas & Electric Co	4690 Evora Road	Concord	94520	-	8,828	8,828
126	927	California Oils Corporation	1145 Harbour Way, South	Richmond	94804	-	8,797	8,797
127	10583	Monterey Mushrooms Inc	642 Hale Avenue	Morgan Hill	95038	-	8,482	8,482
128	705	Vulcan Materials Company Western Division	52 El Charro Road	Pleasanton	94566	-	8,215	8,215
129	12870	Shell Chemical LP	10 Mococo Road	Martinez	94553	-	8,092	8,092
130	9455	American Licorice Company	2477 Liston Way	Union City	94587	-	8,061	8,061
131	9573	Diageo North America, Inc	151 Commonwealth Drive	Menlo Park	94025	-	7,987	7,987
132	1995	Solano County Facilities Operations	501 Delaware Street	Fairfield	94533	-	7,864	7,864
133	459	Veterans Administration Medical Center	4150 Clement Street	San Francisco	94121	-	7,847	7,847
134	8025	Novartis Vaccines and Diagn	4560 Horton Street	Emeryville	94608	-	7,821	7,821
135	12557	AMCAN Beverages, Inc	1201 Commerce Boulevard	Canyon	94503	-	7,715	7,715
136	14415	Center	5975 Lambie Road	Suisun City	94585	-	7,695	7,695
137	10437	Byron Power Company,c/o Ridgewood Power Mgnt	4901 Bruns Road	Byron	94514	-	7,650	7,650
138	3194	City of Alameda, Maint Serv Center	Doolittle Drive	Alameda	94501	3,413	4,068	7,481
139	17559	Pacific Atlantic Terminals LLC	2801 Waterfront Road	Martinez	94553	-	7,467	7,467
140	10861	Northrop Grumman Systems Corporation	401 E Hendy Ave, 62/1	Sunnyvale	94088	-	7,351	7,351
141	14416	Goose Haven Energy Center	3853 Goose Haven Road	Suisun City	94585	-	7,146	7,146
142	13683	Dey L P	2751 Napa Valley Corp Dr	Napa	94558	-	7,002	7,002
143	4175	City of San Jose (Singleton Road Landfill)	885 Singleton Road	San Jose	95111	3,187	3,799	6,986
144	14414	Creed Energy Center LLC	6150 Creed Road	Suisun City	94585	-	6,867	6,867
145	17925	Transamerica Pyramid Properties, LLC	600 Montgomery Street	San Francisco	94111	-	6,860	6,860

Table V: 2007 BAY AREA MAJOR (TOP 200) GHG EMITTING FACILITIES

						CO2 Equivalent Emissions (Metric Tons per year)		
No.	Plant #	Plant Name	Plant Address	City	Zipcode	Biogenic	Non-Biogenic	Total
146	148	Ball Metal Beverage Container Corp	2400 Huntington Drive	Fairfield	94533	-	6,795	6,795
147	2531	Santa Rosa Memorial Hospital	1165 Montgomery Drive	Santa Rosa	95402	-	6,772	6,772
148	16855	Kaiser Antioch Deer Valley	4501 Sand Creek Rd	Antioch	94509	-	6,594	6,594
149	4446	Veterans' Home of California	100 California Dr, Administration	Yountville	94599	-	6,483	6,483
150	3024	Isola USA Corp	401 Whitney Place	Fremont	94539	-	6,362	6,362
151	556	Stanford Linear Accelerator	2575 Sand Hill Road	Menlo Park	94025	-	6,274.2	6,274.2
152	3613	St Mary's Medical Center	450 Stanyan Street	San Francisco	94117	-	6,228	6,228
153	255	Lawrence Livermore National Laboratory	7000 East Avenue	Livermore	94550	-	6,218	6,218
154	4116	San Francisco, City & County, PUC	3500 Great Highway	San Francisco	94132	2,780	3,428	6,208
155	849	Roche Palo Alto LLC	3431 Hillview Avenue	Palo Alto	94304	-	5,885	5,885
156	110	Burke Industries, Inc	2250 So 10th Street	San Jose	95112	-	5,849	5,849
157	12965	John Zink Company	2150 Kruse Drive	San Jose	95131	-	5,777	5,777
158	11924	California Pacific Medical Center	Castro & Duboce Street	San Francisco	94114	-	5,767	5,767
159	15816	Cal-Pox, Inc	103 Shoreline Parkway	San Rafael	94901	786	4,926	5,713
160	2035	PEPSICO Beverages and Foods	1175 57th Avenue	Oakland	94621	-	5,700	5,700
161	167	Maxwell House, Div of Kraft Foods	100 Halcyon Drive	San Leandro	94578	-	5,609	5,609
162	9339	San Jose State University	One Washington Square	San Jose	95192	-	5,540	5,540
163	1067	Oro Loma Sanitary District	2600 Grant Avenue	San Lorenzo	94580	4,315	1,203	5,519
164	16930	San Mateo County Youth Services Center	70 Loop Road	San Mateo	94402	-	5,369	5,369
165	8287	Coca-Cola	5800 3rd Street	San Francisco	94124	-	5,263	5,263
166	15117	Bay Sheets	6791 Alexander St	Gilroy	95020	-	5,204	5,204
167	1472	Unimin Corporation	Camino Diablo Rd	Byron	94514	-	5,093	5,093
168	16023	Georgia-Pacific Corrugated LLC	2800 Alvarado Street	San Leandro	94577	-	5,014	5,014
169	18447	PPF OFF One Market Plaza LLC	Tow	San Francisco	94105	-	4,979	4,979
170	2168	Jelly Belly Candy Company	One Jelly Belly Lane	Fairfield	94533	-	4,858	4,858
171	17315	C & H Sugar Company, Inc	830 Loring Avenue	Crockett	94525	-	4,817	4,817
172	10408	County Asphalt	5501 Imhoff Drive	Martinez	94553	-	4,807	4,807
173	2561	Shoreline Amphitheatre	One Amphitheatre Parkway	Mountain View	94043	2,171	2,592	4,763
174	1860	Laguna Honda Hospital	375 Laguna Honda Boulevard	San Francisco	94116	-	4,686	4,686

Table V: 2007 BAY AREA MAJOR (TOP 200) GHG EMITTING FACILITIES

						CO2 Equivalent Emissions (Metric Tons per year)		
No.	**Plant #**	**Plant Name**	**Plant Address**	**City**	**Zipcode**	**Biogenic**	**Non-Biogenic**	**Total**
175	14327	Silgan Containers Mfg Corp	2200 Wilbur Avenue	Antioch	94509	-	4,632	4,632
176	2451	Pleasanton Garbage Service, Inc	2512 Vineyard Avenue	Pleasanton	94566	1,301	3,298	4,599
177	17560	Mission Foods	23423 Cabot Blvd	Hayward	94545	-	4,594	4,594
178	1700	California Pacific Med Ctr, Pacific Campus	2333 Buchanan Street	San Francisco	94115	-	4,593	4,593
179	15501	Spansion LLC	915 De Guigne Drive	Sunnyvale	94086	-	4,557	4,557
180	3919	Kaiser Permanente San Jose Medical Center	250 Hospital Parkway	San Jose	95119	-	4,546	4,546
181	3885	Highland General Hospital	1411 E 31st Street	Oakland	94602	-	4,517	4,517
182	1258	Delta Diablo Sanitation District	2500 Pittsburg & Antioch Hwy	Antioch	94509	2,049	2,400	4,449
183	653	Central Marin Sanitation Agency	Andersen Drive, East end	San Rafael	94901	1,776	2,542	4,318
184	73	Gallagher & Burk, Inc	344 High Street	Oakland	94601	-	4,301.4	4,301.4
185	128	Syar Industries, Inc	Lake Herman Road	Vallejo	94591	-	4,182	4,182
186	1351	City of Burlingame, Waste Water Treatment Plant	1103 Airport Boulevard	Burlingame	94010	1,937	2,220	4,157
187	1009	Hayward Waste Water Treatment Plant	3700 Enterprise Ave	Hayward	94545	3,563	491	4,053
188	453	Good Samaritan Hospital	2425 Samaritan Drive	San Jose	95124	-	4,034	4,034
189	460	Alta Bates Hospital	2450 Ashby Avenue	Berkeley	94705	-	4,004	4,004
190	12001	Quikrete Northern California	6950 Stevenson Blvd	Fremont	94538	-	3,866	3,866
191	16888	Ingersoll-Rand Energy Systems	5858 Horton Street	Emeryville	94608	-	3,864	3,864
192	92	Antioch Building Materials Company	1375 California Ave	Pittsburg	94565	-	3,839	3,839
193	1404	Fairfield-Suisun Sewer District	1010 Chadbourne Road	Fairfield	94534	1,775	2,061	3,836
194	13617	Delta Air Lines Inc	SJ Int'l Airport	San Jose	95120	-	3,805.7	3,805.7
195	5691	Sunquest Properties Inc	Landfill, Brisbane	Brisbane	94005	1,711	2,040	3,750
196	2957	Super Store Industries/Fairfield Dairy Division	199 Red Top Road	Fairfield	94533	-	3,689	3,689
197	10162	EXAR Corporation	48760 Kato Road	Fremont	94538	-	3,688	3,688
198	1534	South Bayside System Authority	Radio Road, End of	Redwood City	94065	3,356	233	3,589
199	232	Onizuka Air Force Base	1080 Innovation Way	Sunnyvale	94089	-	3,568	3,568
200	3893	Sonoma Valley Hospital District	347 Andrieux Street	Sonoma	95476	-	3,550	3,550
Total (Metric Tons per year)						**1,183,471**	**28,052,724**	**29,236,195**











Our Changing Climate

Assessing the Risks to California

A Summary Report from
the California Climate Change Center

Because most global warming emissions remain in the atmosphere for decades or centuries, the choices we make today greatly influence the climate our children and grandchildren inherit. The quality of life they experience will depend on if and how rapidly California and the rest of the world reduce these emissions.

In California and throughout western North America, signs of a changing climate are evident. During the last 50 years, winter and spring temperatures have been warmer, spring snow levels in lower- and mid-elevation mountains have dropped, snowpack has been melting one to four weeks earlier, and flowers are blooming one to two weeks earlier.



These regional changes are consistent with global trends. During the past 100 years, average temperatures have risen more than one degree Fahrenheit worldwide. Research indicates that much of this warming is due to human activities, primarily burning fossil fuels and clearing forests, that release carbon dioxide (CO_2) and other gases into the atmosphere, trapping in heat that would otherwise escape into space. Once in the atmosphere, these heat-trapping emissions remain there for many years—CO_2, for example, lasts about 100 years. As a result, atmospheric concentration of CO_2 has increased more than 30 percent above pre-industrial levels. If left unchecked, by the end of the century CO_2 concentrations could reach levels three times higher than pre-industrial times, leading to dangerous global warming that threatens our public health, economy, and environment.

The latest projections, based on state-of-the art climate models, indicate that if global heat-trapping emissions proceed at a medium to high rate, temperatures in California are expected to rise 4.7 to 10.5°F by the end of the century. In contrast, a lower emissions rate would keep the projected warming to 3 to 5.6°F. These temperature increases would have widespread consequences including substantial loss of snowpack, increased risk of large wildfires, and reductions in the quality and quantity of certain agricultural products. The state's vital resources and natural landscapes are already under increasing stress due to California's rapidly growing population, which is expected to grow from 35 million today to 55 million by 2050.

This document summarizes the recent findings of the California Climate Change Center's "Climate Scenarios" project, which analyzed a range of impacts that projected rising temperatures would likely have on California. The growing severity of the consequences as temperature rises underscores the importance of reducing emissions to minimize further warming. At the same time, it is essential to identify those consequences that may be unavoidable, for which we will need to develop coping and adaptation strategies.

In 2003, the California Energy Commission's Public Interest Energy Research (PIER) program established the California Climate Change Center to conduct climate change research relevant to the state. This Center is a virtual organization with core research activities at Scripps Institution of Oceanography and the University of California, Berkeley, complemented by efforts at other research institutions. Priority research areas defined in PIER's five-year Climate Change Research Plan are: monitoring, analysis, and modeling of climate; analysis of options to reduce greenhouse gas emissions; assessment of physical impacts and of adaptation strategies; and analysis of the economic consequences of both climate change impacts as well as the efforts designed to reduce emissions.

Executive Order #S-3-05, signed by Governor Arnold Schwarzenegger on June 1, 2005, called for the California Environmental Protection Agency (CalEPA) to prepare biennial science reports on the potential impact of continued global warming on certain sectors of the California economy. CalEPA entrusted PIER and its California Climate Change Center to lead this effort. The "Climate Scenarios" analysis summarized here is the first of these biennial science reports, and is the product of a multi-institution collaboration among the California Air Resources Board, California Department of Water Resources, California Energy Commission, CalEPA, and the Union of Concerned Scientists.

Cover photos: (sunset) Photos.com; (from top to bottom) AP Photo/Paul Sakuma, iStockphoto, IndexStock, Picturequest, iStockphoto. Above: Bureau of Land Management. Background: IndexStock

California's Future Climate

California's climate is expected to become considerably warmer during this century. How much warmer depends on the rate at which human activities, such as the burning of fossil fuels, continue. The projections presented here illustrate the climatic changes that are likely from three different heat-trapping emissions scenarios (see figure below).

Projected Warming

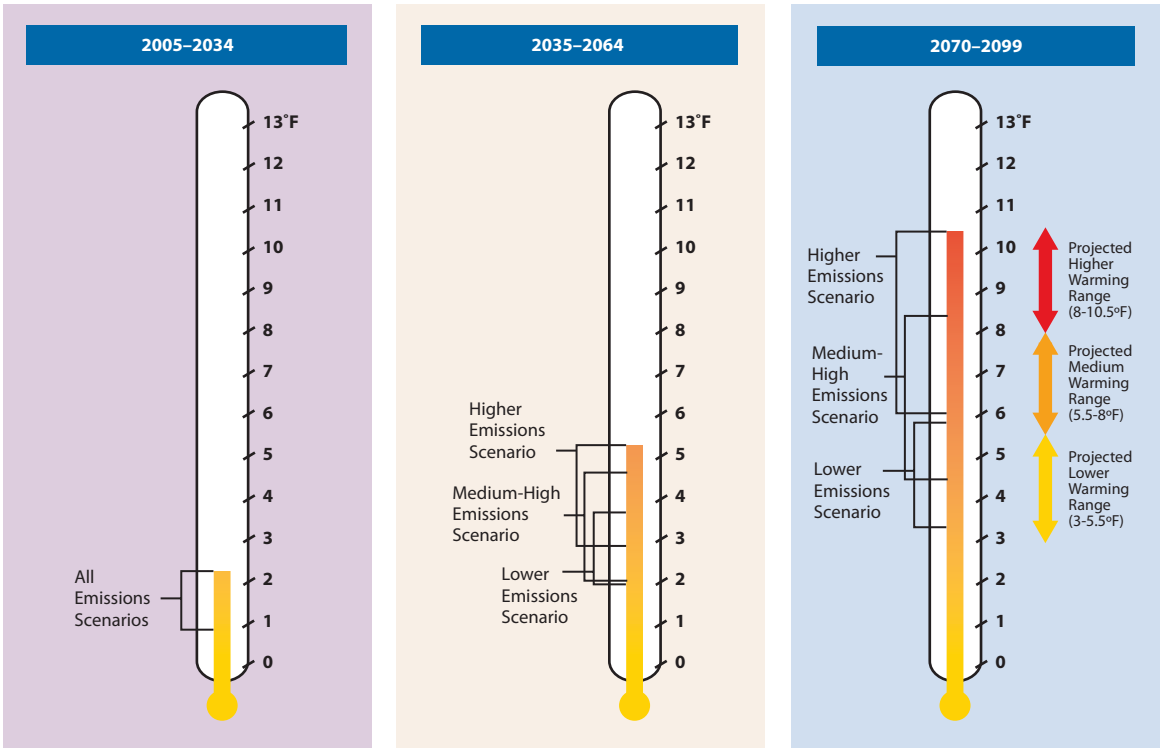
Temperatures are expected to rise substantially in all three emissions scenarios. During the next few decades, the three scenarios project average temperatures to rise between 1 and 2.3°F; however, the projected temperature increases begin to diverge at mid-century so that, by the end of the century, the temperature increases projected in the higher emissions scenario are approximately twice as high as those projected in the lower emissions scenario. Some climate models indicate that warming would be greater in summer than in winter, which would have widespread effects on ecosystem health, agricultural production, water use and availability, and energy demand.

Toward the end of the century, depending on future heat-trapping emissions, statewide average temperatures are expected to rise between 3 and 10.5°F. The analysis presented here examines the future climate under three projected warming ranges:[1]

- **Lower warming range:** projected temperature rises between 3 and 5.5°F
- **Medium warming range:** projected temperature rises between 5.5 and 8°F
- **Higher warming range:** projected temperature rises between 8 and 10.5°F

Precipitation

On average, the projections show little change in total annual precipitation in California. Furthermore, among several models, precipitation projections do not show a consistent trend during the next century. The Mediterranean seasonal precipitation pattern is expected to continue, with most precipitation falling during winter from North Pacific storms. One of the three climate models projects slightly wetter winters, and another projects slightly drier winters with a 10 to 20 percent decrease in total annual precipitation. However, even modest changes would have a significant impact because California ecosystems are conditioned to historical precipitation levels and water resources are nearly fully utilized.



California is expected to experience dramatically warmer temperatures during the 21st century. This figure shows projected increases in statewide annual temperatures for three 30-year periods. Ranges for each emissions scenario represent results from state-of-the-art climate models.

1 These warming ranges are for illustrative purposes only. These ranges were defined in the original Climate Scenarios analysis to capture the full range of projected temperature rise. The exact values for the warming ranges as presented in the original summary report are: lower warming range (3 to 5.4°F); medium warming range (5.5 to 7.9°F); and higher warming range (8 to 10.4°F).

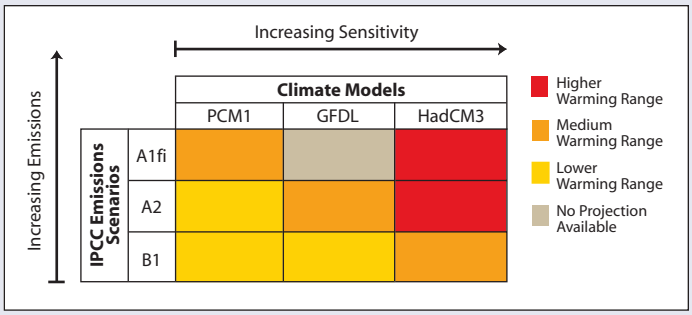
Projecting Future Climate

How much temperatures rise depends in large part on how much and how quickly heat-trapping emissions accumulate in the atmosphere and how the climate responds to these emissions. The projections presented in this report are based on three different heat-trapping emissions scenarios and three climate models.

Emissions Scenarios

The three global emissions scenarios used in this analysis were selected from a set of scenarios developed by the Intergovernmental Panel on Climate Change's (IPCC) *Special Report on Emissions Scenarios*, based on different assumptions about population growth and economic development (measured in gross domestic product).

- The **lower emissions scenario (B1)** characterizes a world with high economic growth and a global population that peaks by mid-century and then declines. There is a rapid shift toward less fossil fuel-intensive industries and introduction of clean and resource-efficient technologies. Heat-trapping emissions peak about mid-century and then decline; CO_2 concentration approximately doubles, relative to pre-industrial levels, by 2100.
- The **medium-high emissions scenario (A2)** projects continuous population growth and uneven economic and technological growth. The income gap between now-industrialized and developing parts of the world does not narrow. Heat-trapping emissions increase through the 21st century; atmospheric CO_2 concentration approximately triples, relative to pre-industrial levels, by 2100.
- The **higher emissions scenario (A1fi)** represents a world with high fossil fuel-intensive economic growth, and a global population that peaks mid-century then declines. New and more efficient technologies are introduced toward the end of the century. Heat-trapping emissions increase through the 21st century; CO_2 concentration more than triples, relative to pre-industrial levels, by 2100.



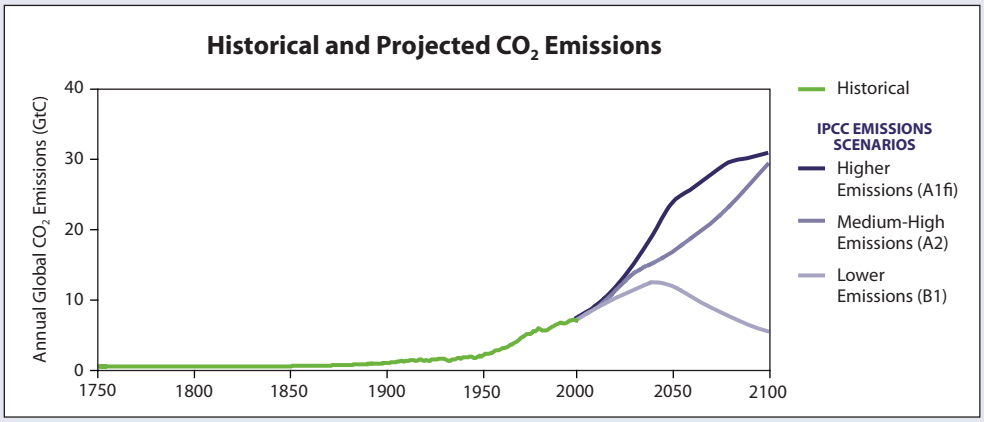
This matrix shows the temperature increases that result from the three climate models, assuming emission inputs indicated in the IPCC emissions scenarios. The resulting temperatures are grouped into three warming ranges defined in the "Climate Scenarios" analysis.

Climate Sensitivity

The three models used in this analysis represent different climate sensitivities, or the extent to which temperatures will rise as a result of increasing atmospheric concentrations of heat-trapping gases. Climate sensitivity depends on Earth's response to certain physical processes, including a number of "feedbacks" that might amplify or lessen warming. For example, as heat-trapping emissions cause temperatures to rise, the atmosphere can hold more water vapor, which traps heat and raises temperatures further—a positive feedback. Clouds created by this water vapor could absorb and re-radiate outgoing infrared radiation from Earth's surface (another positive feedback) or reflect more incoming shortwave radiation from the sun before it reaches Earth's surface (a negative feedback).

Because many of these processes and their feedbacks are not yet fully understood, they are represented somewhat differently in different global climate models. The three global climate models used in this analysis are:

- **National Center for Atmospheric Research Parallel Climate Model (PCM1):** low climate sensitivity
- **Geophysical Fluids Dynamic Laboratory (GFDL) CM2.1:** medium climate sensitivity
- **United Kingdom Met Office Hadley Centre Climate Model, version 3 (HadCM3):** medium-high climate sensitivity



As this figure shows, CO_2 emissions from human activities (such as the burning of fossil fuels) were negligible until around the so-called industrial age starting in the 1850s.



Public Health

Continued global warming will affect Californians' health by exacerbating air pollution, intensifying heat waves, and expanding the range of infectious diseases. The primary concern is not so much the change in *average* climate but the projected increase in *extreme* conditions, which pose the most serious health risks.

Poor Air Quality Made Worse

Californians currently experience the worst air quality in the nation, with more than 90 percent of the population living in areas that violate the state's air quality standard for either ground-level ozone or airborne particulate matter. These pollutants can cause or aggravate a wide range of health problems including asthma and other acute respiratory and cardiovascular diseases, and can decrease lung function in children. Combined, ozone and particulate matter contribute to 8,800 deaths and $71 billion in healthcare costs every year. If global background ozone levels increase as projected in some scenarios, it may become impossible to meet local air quality standards.

Higher temperatures are expected to increase the frequency, duration, and intensity of conditions conducive to air pollution formation. For example, if temperatures rise to the medium warming range, there will be 75 to 85 percent more days with weather conducive to ozone formation in Los Angeles and the San Joaquin Valley, relative to today's conditions. This is more than twice the increase expected if temperature rises are kept in the lower warming range.

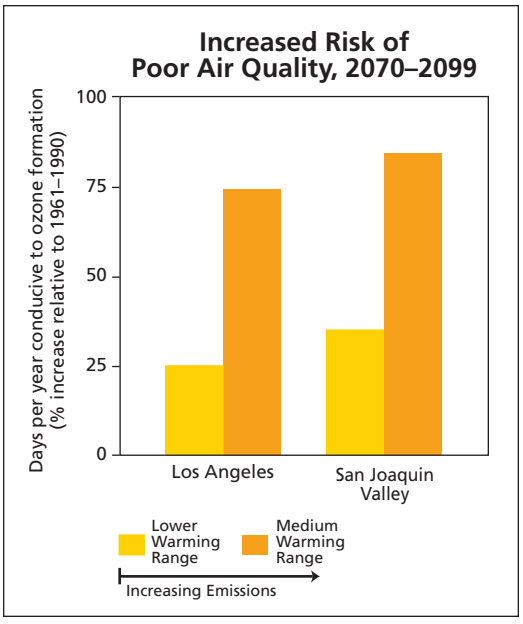
Air quality could be further compromised by increases in wildfires, which emit fine particulate matter that can travel long distances depending on wind conditions. The most recent analysis suggests that if heat-trapping gas emissions are not significantly reduced, large wildfires could become up to 55 percent more frequent toward the end of the century.

More Severe Heat

By 2100, if temperatures rise to the higher warming range, there could be up to 100 more days per year with temperatures above 90°F in Los Angeles and above 95°F in Sacramento. This is a striking increase over historical patterns (see chart on p. 6), and almost twice the increase projected if temperatures remain within or below the lower warming range.

As temperatures rise, Californians will face greater risk of death from dehydration, heat stroke/exhaustion, heart attack, stroke, and respiratory distress caused by extreme heat. By mid century, extreme heat events in urban centers such as Sacramento, Los Angeles, and San Bernardino could cause two to three times more heat-related deaths than occur today. The members of the population most vulnerable to the effects of extreme heat include people who are already ill; children; the elderly;

As temperatures rise, Californians will face greater risk of death from dehydration, heat stroke, heart attack, and other heat-related illnesses.

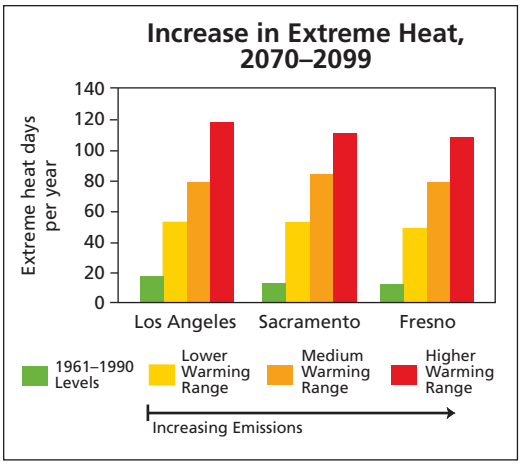




Cars and power plants emit pollutants that contribute to global warming and poor air quality. As temperatures increase, it will be increasingly difficult to meet air quality standards throughout the state.

and the poor, who may lack access to air conditioning and medical assistance.

More research is needed to better understand the potential effects of higher temperatures and the role that adaptation can play in minimizing these effects. For example, expanding air conditioner use can help people cope with extreme heat; however, it also increases energy consumption, which, using today's fossil fuel-heavy energy sources, would contribute to further global warming and air pollution.





iStockphoto



Water Resources



If global warming emissions continue unabated, Sierra Nevada snowpack could decline 70 to 90 percent, with cascading effects on winter recreation, water supply, and natural ecosystems.

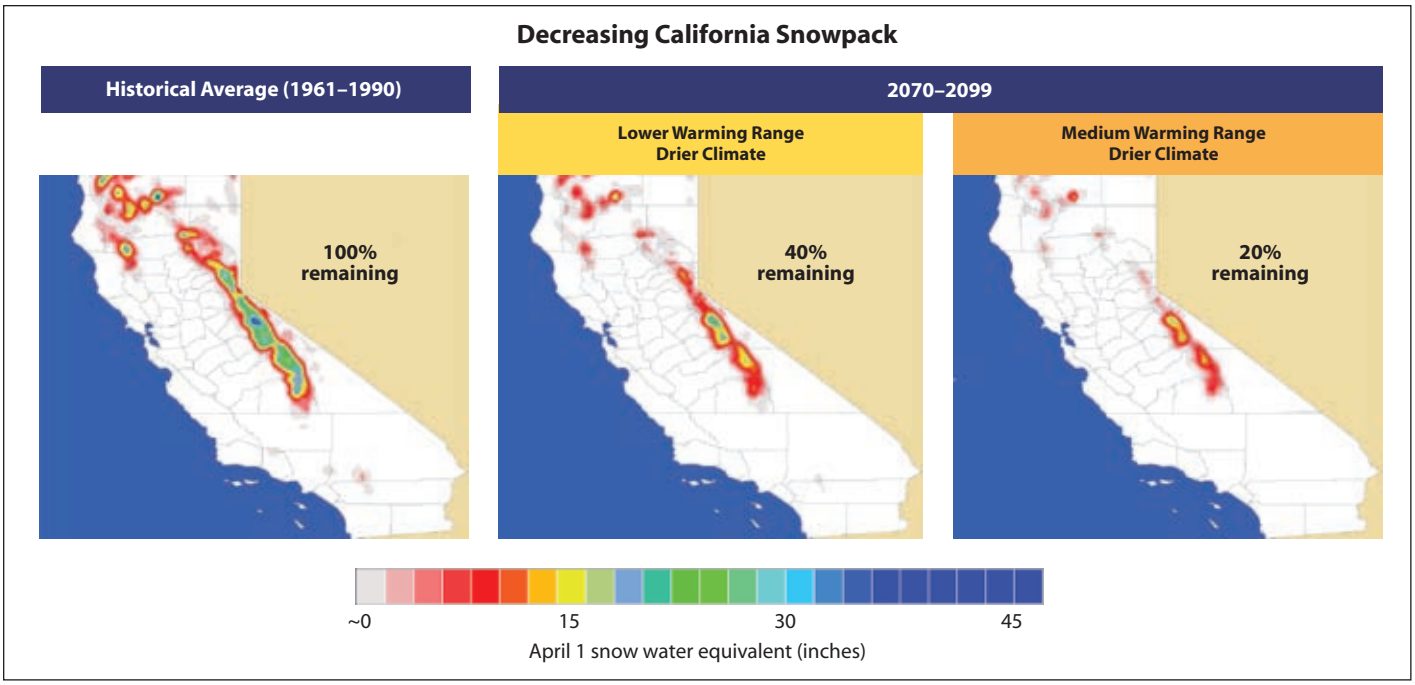
Most of California's precipitation falls in the northern part of the state during the winter while the greatest demand for water comes from users in the southern part of the state during the spring and summer. A vast network of man-made reservoirs and aqueducts capture and transport water throughout the state from northern California rivers and the Colorado River. The current distribution system relies on Sierra Nevada mountain snowpack to supply water during the dry spring and summer months. Rising temperatures, potentially compounded by decreases in precipitation, could severely reduce spring snowpack, increasing the risk of summer water shortages.

Decreasing Sierra Nevada Snowpack

If heat-trapping emissions continue unabated, more precipitation will fall as rain instead of snow, and the snow that does fall will melt earlier, reducing the Sierra Nevada spring snowpack by as much as 70 to 90 percent. How much snowpack will be lost depends in part on future precipitation patterns, the projections for which remain uncertain. However, even under wetter climate projections, the loss of snowpack would pose challenges to water managers, hamper hydropower generation, and nearly eliminate skiing and other snow-related recreational activities. If global warming emissions are significantly curbed and temperature increases are kept in the lower warming range, snowpack losses are expected to be only half as large as those expected if temperatures were to rise to the higher warming range.

Challenges in Securing Adequate Water Supplies

Continued global warming will increase pressure on California's water resources, which are already over-stretched by the demands of a growing



economy and population. Decreasing snowmelt and spring stream flows coupled with increasing demand for water resulting from both a growing population and hotter climate could lead to increasing water shortages. By the end of the century, if temperatures rise to the medium warming range and precipitation decreases, late spring stream flow could decline by up to 30 percent. Agricultural areas could be hard hit, with California farmers losing as much as 25 percent of the water supply they need.

Water supplies are also at risk from rising sea levels. An influx of saltwater would degrade California's estuaries, wetlands, and groundwater aquifers. In particular, saltwater intrusion would threaten the quality and reliability of the major state fresh water supply that is pumped from the southern edge of the Sacramento/San Joaquin River Delta.

Coping with the most severe consequences of global warming would require major changes in water management and allocation systems. As more winter precipitation falls as rain instead of snow, water managers will have to balance the need to fill constructed reservoirs for water supply and the need to maintain reservoir space for winter flood control. Some additional storage could be developed; however, the economic and environmental costs would be high.



Left: Photodisc. Right: Corbis

Rising temperatures, potentially exacerbated by decreasing precipitation, could increase the risk of water shortages in urban and agricultural sectors.

Potential Reduction in Hydropower

Higher temperatures will likely increase electricity demand due to higher air conditioning use. Even if the population remained unchanged, toward the end of the century annual electricity demand could increase by as much as 20 percent if temperatures rise into the higher warming range. (Implementing aggressive efficiency measures could lower this estimate.)

At the same time, diminished snow melt flowing through dams will decrease the potential for hydropower production, which now comprises about 15 percent of California's in-state electricity production. If temperatures rise to the medium warming range and precipitation decreases by 10 to 20 percent, hydropower production may be reduced by up to 30 percent. However, future precipitation projections are quite uncertain so it is possible that precipitation may increase and expand hydropower generation.

Loss of Winter Recreation

Continued global warming will have widespread implications for winter tourism. Declines in Sierra Nevada snowpack would lead to later starting and earlier closing dates of the ski season. Toward the end of the century, if temperatures rise to the lower warming range, the ski season at lower and middle elevations could shorten by as much as a month. If temperatures reach the higher warming range and precipitation declines, there might be many years with insufficient snow for skiing and snowboarding.



Stephen McMillan

Agriculture

California is home to a $30 billion agriculture industry that employs more than one million workers. It is the largest and most diverse agriculture industry in the nation, producing more than 300 commodities including half the country's fruits and vegetables. Increased heat-trapping emissions are expected to cause widespread changes to this industry, reducing the quantity and quality of agricultural products statewide.

Although higher carbon dioxide levels can stimulate plant production and increase plant water-use efficiency, California farmers will face greater water demand for crops and a less reliable water supply as temperatures rise. Crop growth and development will change, as will the intensity and frequency of pest and disease outbreaks. Rising temperatures will likely aggravate ozone pollution, which makes plants more susceptible to disease and pests and interferes with plant growth.

To prepare for these changes, and to adapt to changes already under way, major efforts will be needed to move crops to new locations, respond to climate variability, and develop new cultivars and agricultural technologies. With adequate research and advance preparation, some of the consequences could be reduced.

Increasing Temperature

Plant growth tends to be slow at low temperatures, increasing with rising temperatures up to a threshold. However, faster growth can result in less-than-optimal development for many crops, so rising temperatures are likely to worsen the quantity and quality of yield for a number of California's agricultural products. Crops that are likely to be hard hit include:

Wine Grapes

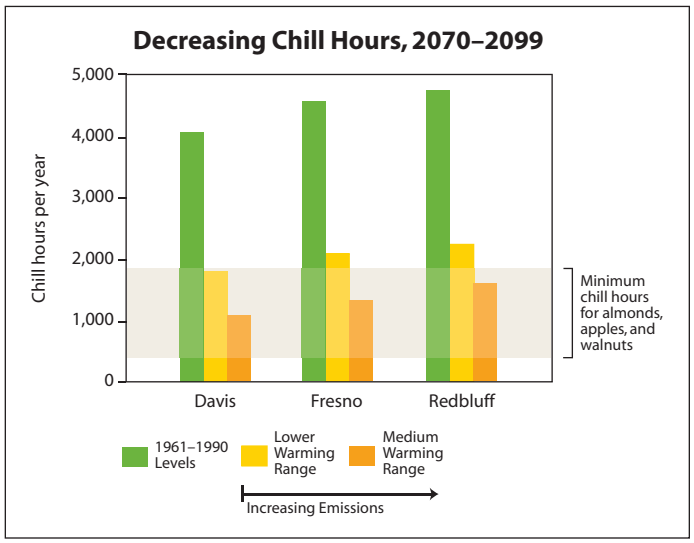
California is the nation's largest wine producer and the fourth-largest wine producer worldwide. High-quality wines produced throughout the Napa and Sonoma Valleys and along the northern and central coasts generate $3.2 billion in revenue each year. High temperatures during the growing season can cause premature ripening and reduce grape quality. Temperature increases are expected to have only modest effect on grape quality in most regions over the next few decades. However, toward the end of the century, wine grapes could ripen as much as one to two months earlier, which will affect grape quality in all but the coolest coastal locations (Mendocino and Monterey Counties).



IndexOpen

Fruits and Nuts

Many fruit and nut trees are particularly sensitive to temperature changes because of heat-accumulation limits and chill-hour requirements. Heat accumulation, which refers to the total hours during which temperatures reach between 45 and 95°F, is critical for fruit development. Rising temperatures could increase fruit development rates and decrease fruit size.



For example, peaches and nectarines developed and were harvested early in 2004 because of warm spring temperatures. The fruits were smaller than normal, which placed them in a lower quality category.

A minimum number of chill hours (hours during which temperatures drop below 45°F) is required for proper bud setting; too few hours can cause late or irregular bloom, decreasing fruit quality and subsequent marketable yield. California is currently classified as a moderate to high chill-hour region, but chill hours are diminishing in many areas of the state. If temperatures rise to the medium warming range, the number of chill hours in the entire Central Valley is expected to approach a critical threshold for some fruit trees.

Milk

California's $3 billion dairy industry supplies nearly one-fifth of the nation's milk products. High temperatures can stress dairy cows, reducing milk production. Production begins to decline at temperatures as low as 77°F and can drop substantially as temperatures climb above 90°F. Toward the end of the century, if temperatures rise to the higher warming range, milk production is expected to decrease by up to 20 percent. This is more

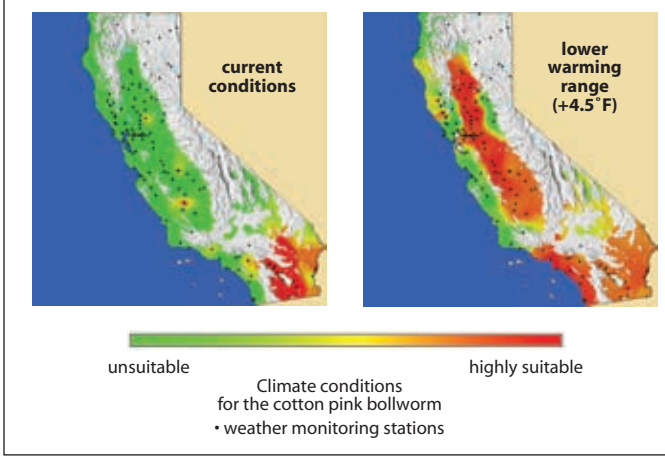


Increasing temperatures will likely decrease the quantity and quality of some agricultural commodities, such as certain varieties of fruit trees, wine grapes, and dairy products.

than twice the reduction expected if temperatures stay within or below the lower warming range.

Expanding Ranges of Agricultural Weeds

Noxious and invasive weeds currently infest more than 20 million acres of California farmland, costing hundreds of millions of dollars annually in control measures and lost productivity. Continued climate change will likely shift the ranges of existing invasive plants and weeds and alter competition patterns with native plants. Range expansion is expected in many species while range contractions are less likely in rapidly evolving species with significant populations already established. Should range contractions occur, it is likely that new or different weed species will fill the emerging gaps.



Increasing Threats from Pests and Pathogens

California farmers contend with a wide range of crop-damaging pests and pathogens. Continued climate change is likely to alter the abundance and types of many pests, lengthen pests' breeding season, and increase pathogen growth rates. For example, the pink bollworm, a common pest of cotton crops, is currently a problem only in southern desert valleys because it cannot survive winter frosts elsewhere in the state. However, if winter temperatures rise 3 to 4.5°F, the pink bollworm's range would likely expand northward, which could lead to substantial economic and ecological consequences for the state.

Temperature is not the only climatic influence on pests. For example, some insects are unable to cope in extreme drought, while others cannot survive in extremely wet conditions. Furthermore, while warming speeds up the lifecycles of many insects, suggesting that pest problems could increase, some insects may grow more slowly as elevated CO_2 levels decrease the protein content of the leaves on which they feed.

Multiple and Interacting Stresses

Although the effects on specific crops of individual factors (e.g., temperatures, pests, water supply) are increasingly well understood, trying to quantify interactions among these and other environmental factors is challenging. For example, the quality of certain grape varieties is expected to decline as temperatures rise. But the wine-grape industry also faces increasing risks from pests such as the glassy-winged sharpshooter, which transmits Pierce's disease. In 2002, this bacterial disease caused damage worth $13 million in Riverside County alone. The optimum temperature for growth of Pierce's disease is 82°F, so this disease is currently uncommon in the cooler northern and coastal regions of the state. However, with continued warming, these regions may face increased risk of the glassy-winged sharpshooter feeding on leaves and transmitting Pierce's disease.



U.S. Dept. of Agriculture

As temperatures rise, the climate is expected to become more favorable for the pink bollworm (above), a major cotton pest in southern California. The pink bollworm's geographic range is limited by winter frosts that kill over-wintering dormant larvae. As temperatures rise, winter frosts will decrease, greatly increasing the winter survival and subsequent spread of the pest throughout the state.



Forests and Landscapes

California is one of the most climatically and biologically diverse areas in the world, supporting thousands of plant and animal species. The state's burgeoning population and consequent impact on local landscapes is threatening much of this biological wealth. Global warming is expected to intensify this threat by increasing the risk of wildfire and altering the distribution and character of natural vegetation.

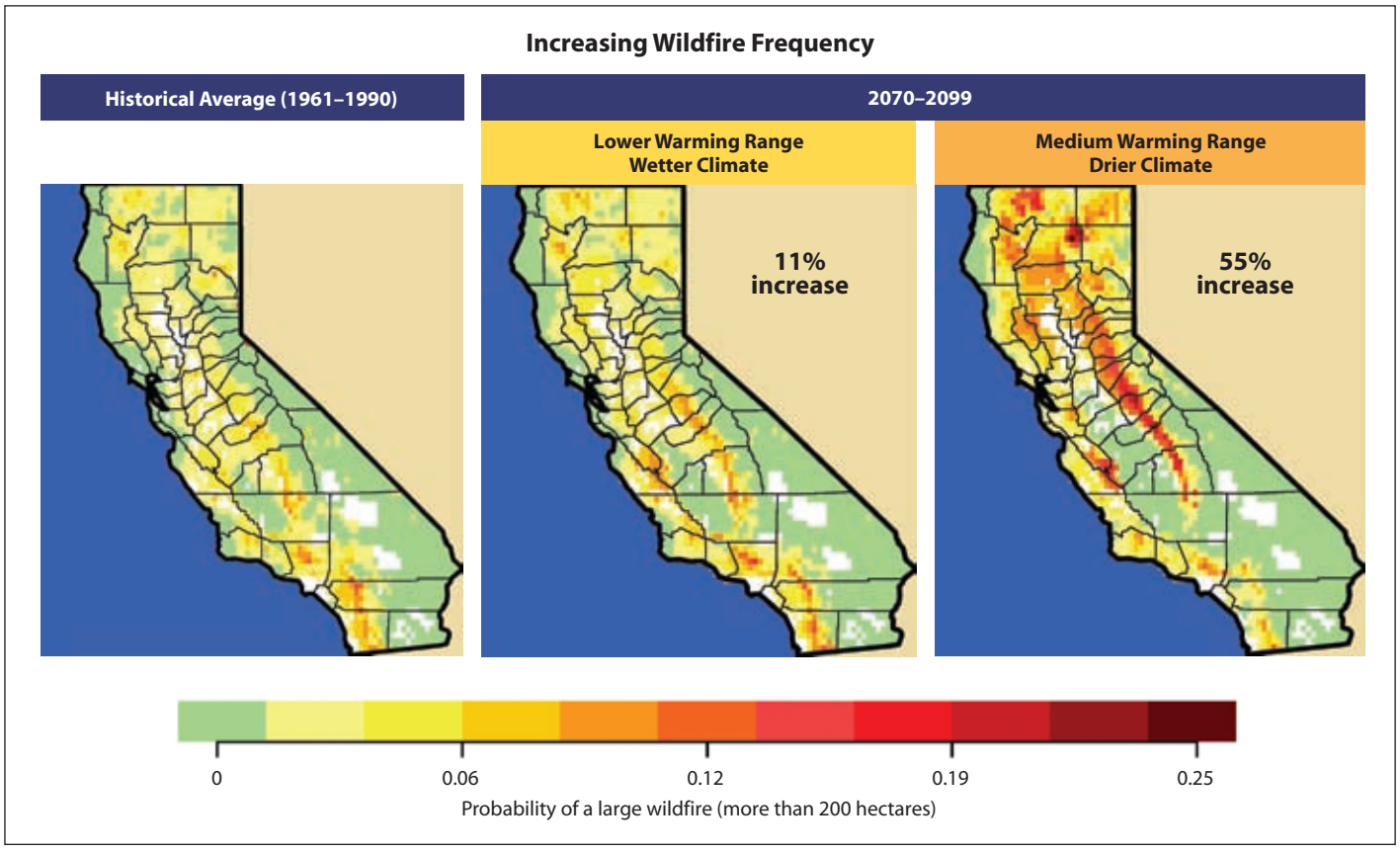
Increasing Wildfires

Fire is an important ecosystem disturbance. It promotes vegetation and wildlife diversity, releases nutrients into the soil, and eliminates heavy accumulation of underbrush that can fuel catastrophic fires. However, if temperatures rise into the medium warming range, the risk of large wildfires in California could increase by as much as 55 percent, which is almost twice the increase expected if temperatures stay in the lower warming range.

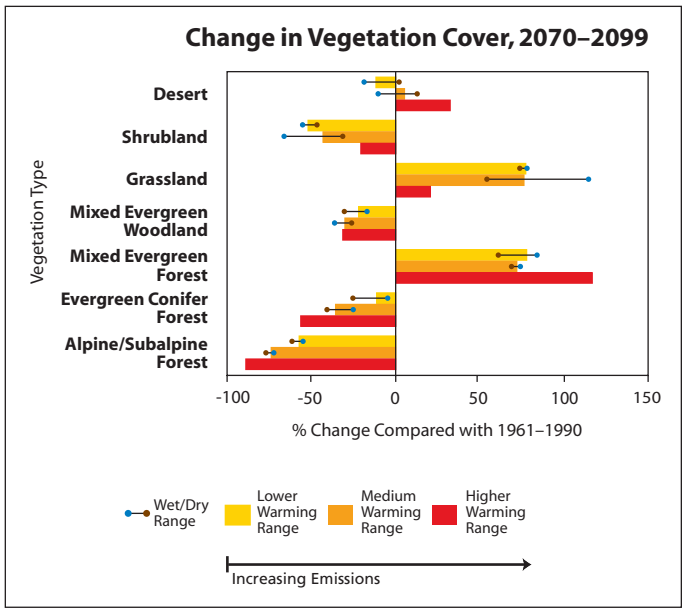
Because wildfire risk is determined by a combination of factors including precipitation, winds, temperature, and landscape and vegetation conditions, future risks will not be uniform throughout the state. In many regions, wildfire activity will depend critically on future precipitation patterns. For

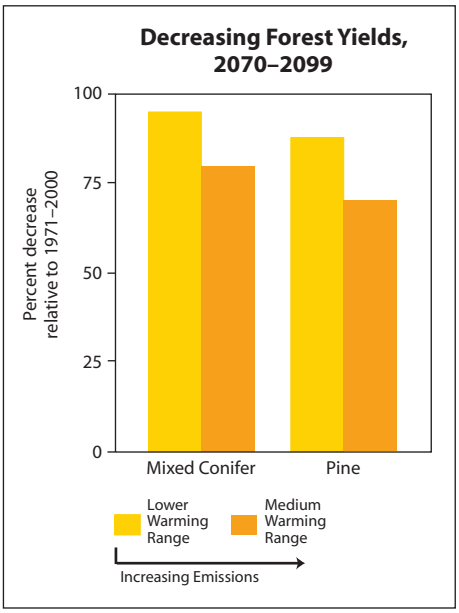


Global warming threatens alpine and subalpine ecosystems, which have no place to move as temperatures rise.



Vegetation cover over the 21st century will depend on both temperature and precipitation. The lower and medium warming range bars reflect vegetation cover under a wetter climate (blue) and a drier climate (brown) projected in the different climate models. For the higher warming range, only a drier climate was considered.





example, if precipitation increases as temperatures rise, wildfires in the grasslands and chaparral ecosystems of southern California are expected to increase by approximately 30 percent toward the end of the century because more winter rain will stimulate the growth of more plant "fuel" available to burn in the fall. In contrast, a hotter, drier climate could promote up to 90 percent more northern California fires by the end of the century by drying out and increasing the flammability of forest vegetation.

Shifting Vegetation

Land use and other changes resulting from economic development are altering natural habitats throughout the state. Continued global warming will intensify these pressures on the state's natural ecosystems and biological diversity. For example, in northern California, warmer temperatures are expected to shift dominant forest species from Douglas and White Fir to madrone and oaks. In inland regions, increases in fire frequency are expected to promote expansion of grasslands into current shrub and woodland areas. Alpine and subalpine ecosystems are among the most threatened in the state; plants suited to these regions have limited opportunity to migrate "up slope" and are expected to decline by as much as 60 to 80 percent by the end of the century as a result of increasing temperatures.

Declining Forest Productivity

Forestlands cover 45 percent of the state; 35 percent of this is commercial forests such as pine plantations. Recent projections suggest that continued global warming could adversely affect the health and productivity of California's forests. If average statewide temperatures rise to the medium warming range, the productivity of mixed conifer forests is expected to diminish by as much as 18 percent by the end of the century. Yield reductions from pine plantations are expected to be even more severe, with up to a 30 percent decrease by the end of the century.

The risk of large wildfires in California could increase by as much as 55 percent.



iStockphoto

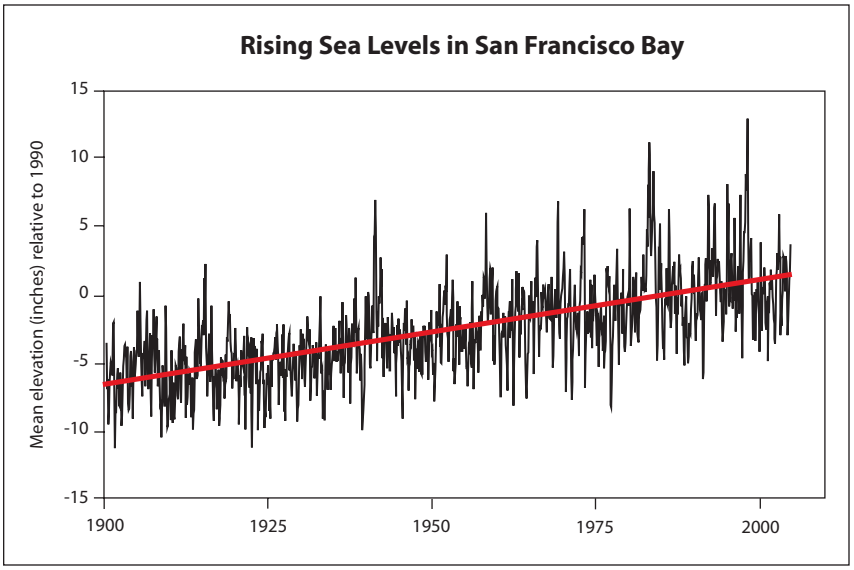
iStockphoto



Rising Sea Levels

California's 1,100 miles of coastline are a major attraction for tourism, recreation, and other economic activity. The coast is also home to unique ecosystems that are among the world's most imperiled. As global warming continues, California's coastal regions will be increasingly threatened by rising sea levels, more intense coastal storms, and warmer water temperatures.

During the past century, sea levels along California's coast have risen about seven inches. If heat-trapping emissions continue unabated and temperatures rise into the higher warming range, sea level is expected to rise an additional 22 to 35 inches by the end of the century. Elevations of this magnitude would inundate coastal areas with salt water, accelerate coastal erosion, threaten vital levees and inland water systems, and disrupt wetlands and natural habitats.



Increasing Coastal Floods

The combination of increasingly severe winter storms, rising mean sea levels, and high tides is expected to cause more frequent and severe flooding, erosion, and damage to coastal structures. Many California coastal areas are at significant risk for flood damage. For example, the city of Santa Cruz is built on the 100-year floodplain and is only 20 feet above sea level. Although levees have been built to contain the 100-year flood, a 12-inch increase in sea levels (projected for the medium warming range of temperatures) would mean storm-surge-induced flood events at the 100-year level would likely occur once every 10 years.

Flooding can create significant damage and enormous financial losses. Despite extensive engineering efforts, major floods have repeatedly breached levees that protect freshwater supplies and islands in the San Francisco Bay Delta as well as fragile marine estuaries and wetlands throughout the



Robert A. Eplett/CA Governor's Office of Emergency Services

Rising sea levels and more intense storm surges could increase the risk for coastal flooding.

Sea levels could rise up to three feet by the end of the century, accelerating coastal erosion, threating vital levees, and disrupting wetlands.

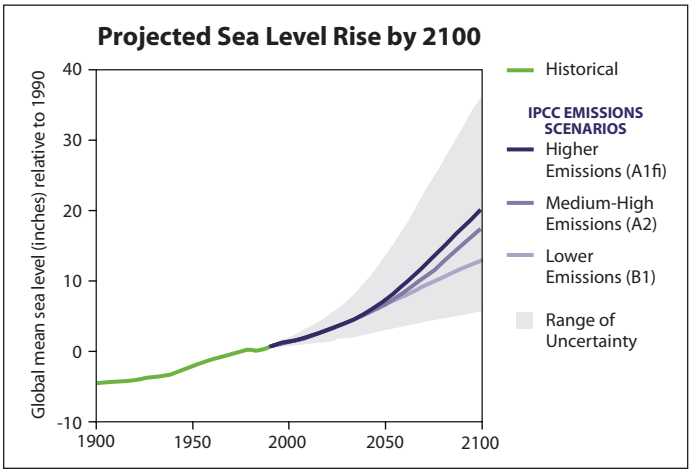
iStockphoto



Many California beaches are threatened from rising sea levels and increased erosion, an expected consequence of continued global warming.

state. Continued sea level rise will further increase vulnerability to levee failures. Some of the most extreme flooding during the past few decades has occurred during El Niño winters, when warmer waters fuel more intense storms. During the winters of 1982–1983 and 1997–1998, for example, abnormally high seas and storm surges caused millions of dollars' worth of damage in the San Francisco Bay area. Highways were flooded as six-foot waves crashed over waterfront bulkheads, and valuable coastal real estate was destroyed.

Continued global warming will require major changes in flood management. In many regions such as the Central Valley, where urbanization and limited river channel capacity already exacerbate rising flood risks, flood damage and flood control costs could amount to several billion dollars.



Shrinking Beaches

Many of California's beaches may shrink in the future because of rising seas and increased erosion from winter storms. Currently, many beaches are protected from erosion through manmade sand replenishment (or "nourishment") programs, which bring in sand from outside sources to replace the diminishing supply of natural sand. In fact, many of the wide sandy beaches in southern California around Santa Monica, Venice, and Newport Beach were created and are maintained entirely by sand nourishment programs. As sea levels rise, increasing volumes of replacement sand will be needed to maintain current beach width and quality. California beach nourishment programs currently cost millions of dollars each year. As global warming continues, the costs of beach nourishment programs will rise, and in some regions beach replenishment may no longer be viable.

Multiple Causes of Coastal Flooding

Several factors play a role in sea level and coastal flooding, including tides, waves temperature, and storm activity. Sea levels fluctuate daily, monthly, and seasonally; the highest tides occur in winter and in summer, during new and full moons. Sea levels often rise even higher during El Niño winters, when the Eastern Pacific Ocean is warmer than usual and westerly wind patterns are strengthened.

Coastal flooding usually occurs during winter storms, which bring strong winds and high waves. Storm winds tend to raise water levels along the coast and produce high waves at the same time, compounding the risk of damaging waves—a doubling of wave height is equivalent to a four-fold increase in wave energy. When these factors coincide with high tides, the chances for coastal damage are greatly heightened.

As sea levels rise, flood stages in the Sacramento/San Joaquin Delta of the San Francisco Bay estuary may also rise, putting increasing pressure on Delta levees. This threat may be particularly significant because recent estimates indicate the additional force exerted upon the levees is equivalent to the square of the water level rise. Estimates using historical observations and climate model projections suggest that extreme high water levels in the Bay and Delta will increase markedly if sea level rises above its historical rate. These extremes are most likely to occur during storm events, leading to more severe damage from waves and floods.

Top left & right: Photos.com. Bottom: CA Fuel Cell Partnership







Cleaner energy and vehicle technologies can help California reduce global warming emissions, improve air quality, and protect public health.

Managing Global Warming

Continued global warming will have widespread and significant impacts on the Golden State. Solutions are available today to reduce emissions and minimize these impacts.

The projections presented in this analysis suggest that many of the most severe consequences that are expected from the medium and higher warming ranges could be avoided if heat-trapping emissions can be reduced to levels that will hold temperature increases at or below the lower warming range (i.e., an increase of no more than 5.5°F). However, even if emissions are substantially reduced, research indicates that some climatic changes are unavoidable. Although not the solution to global warming, plans to cope with these changes are essential.

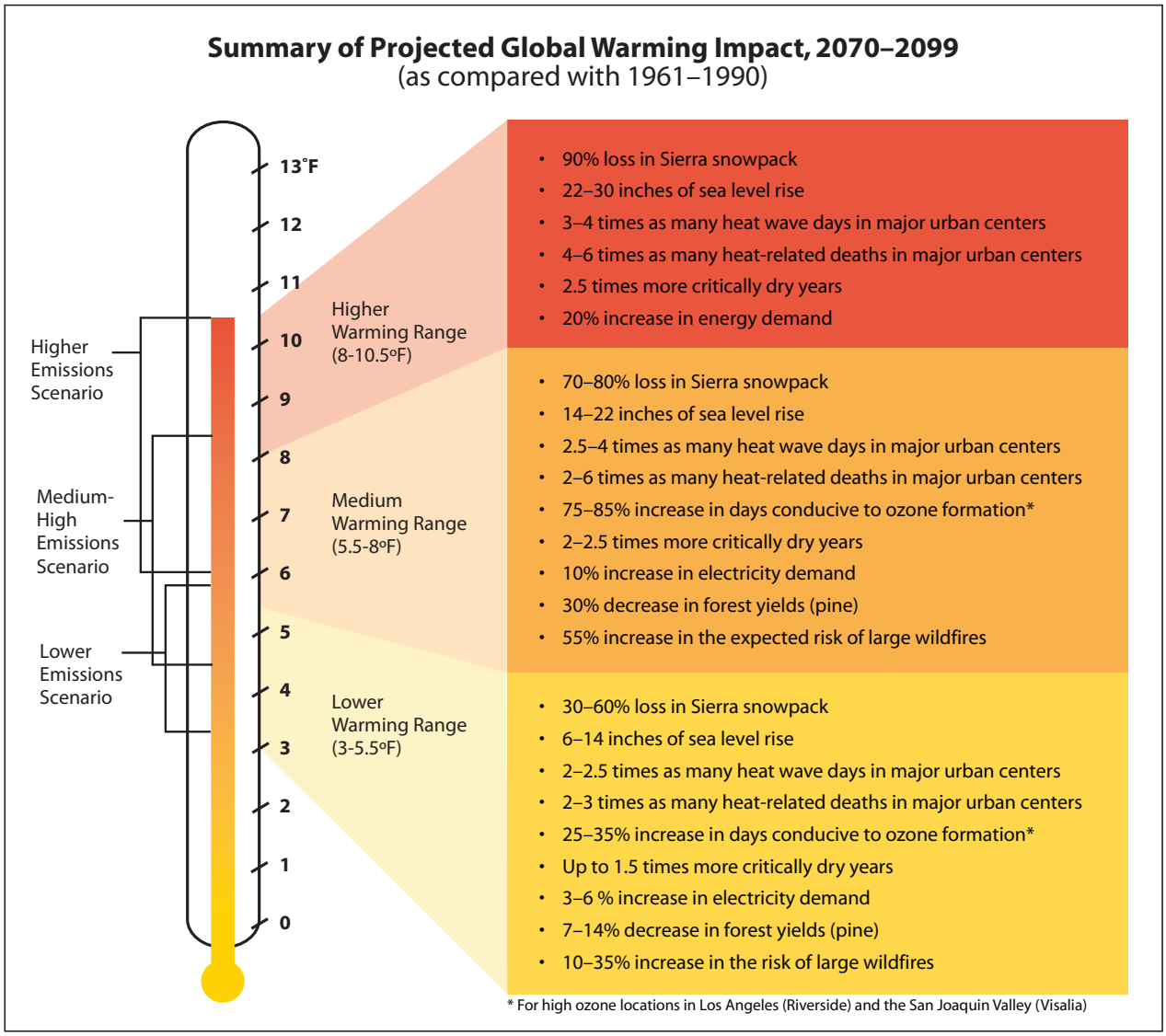
California's actions can drive global progress to address global warming.

Reducing Heat-Trapping Emissions

Reducing heat-trapping emissions is the most important way to slow the rate of global warming. On June 1, 2005, Governor Arnold Schwarzenegger signed an executive order (#S-3-05) that sets goals for significantly lowering the state's share of global warming pollution. The executive order calls for a reduction in heat-trapping emissions to 1990 levels by 2020 and for an 80 percent emissions reduction below 1990 levels by 2050. These emission reduction targets will help stimulate technological innovation needed to help transition to more efficient and renewable transportation and energy systems.

Coping with Unavoidable Climatic Changes

Because global warming is already upon us, and some amount of additional warming is inevitable, we must prepare for the changes that are already under way.



Preparing for these unavoidable changes will require minimizing further stresses on sensitive ecosystems and implementing management practices that integrate climate risks into long-term planning strategies.

California's Leadership

California has been a leader in both the science of climate change and in identifying solutions. The California Climate Change Center is one of the first—and perhaps the only—state-sponsored research institution in the nation dedicated to climate change research, and other state agencies such as the Air Resources Board support similar research. Continuing this strong research agenda is critical for developing effective strategies for addressing global warming in California.

The state has also been at the forefront of efforts to reduce heat-trapping emissions, passing precedent-setting policies such as aggressive standards for tailpipe emissions, renewable energy, and energy efficiency. However, existing policies are not likely to be sufficient to meet the ambitious emission reduction goals set by the governor. To meet these ambitious goals California will need to build on its legacy of environmental leadership and develop new strategies and technologies to reduce emissions.

By reducing heat-trapping emissions, severe consequences can be avoided.

California alone cannot stabilize the climate. However, the state's actions can drive global progress. If the industrialized world were to follow the emission reduction targets established in California's executive order, and industrializing nations reduced emissions according to the lower emissions path (B1) presented in this analysis, we would be on track to keep temperatures from rising to the medium or higher (and possibly even the lower) warming ranges and thus avoid the most severe consequences of global warming.

The full text of the Climate Scenarios analysis overview report, and the core scientific papers that comprise this analysis, are online at *www.climatechange.ca.gov*. The scientists that participated in this effort are:

Jamie Anderson
Department of Water Resources
Michael Anderson
Department of Water Resources
Dominique Bachelet
Oregon State University
Dennis Baldocchi
University of California, Berkeley
John Battles
University of California, Berkeley
Gregory Biging
University of California, Berkeley
Celine Bonfils
University of California, Merced
Peter Bromirski
Scripps Institution of Oceanography
Benjamin Bryant
Scripps Institution of Oceanography
Timothy Cavagnaro
University of California, Davis
Daniel R. Cayan
Scripps Institution of Oceanography
Francis Chung
Department of Water Resources
Bart Croes
California Air Resources Board
Larry Dale
Lawrence Berkeley National Laboratory
Adrian Das
University of California, Berkeley
Michael Dettinger
Scripps Institution of Oceanography
Thibaud d'Ouitremont
University of California, Berkeley
John Dracup
University of California, Berkeley
Raymond Drapek
Oregon State University
Deborah Drechsler
California Air Resources Board
Philip B. Duffy
Lawrence Livermore National Laboratory
Daniel Easton
Department of Water Resources
C.K. Ellis
University of California, Berkeley
Reinhard Flick
Department of Boating and Waterways
Michael Floyd
Department of Water Resources
Guido Franco
California Energy Commission
Jeremy Fried
USDA Forest Service
J. Keith Gilless
University of California, Berkeley
Andrew Paul Gutierrez
University of California, Berkeley
Michael Hanemann
University of California, Berkeley
Julien Harou
University of California, Davis
Katharine Hayhoe
ATMOS Research and Consulting
Richard Howitt
University of California, Davis
Louise Jackson
University of California, Davis
Marion Jenkins
University of California, Davis
Jiming Jin
Lawrence Berkeley National Laboratory
Brian Joyce
Natural Heritage Institute
Laurence Kalkstein
University of Delaware
Michael Kleeman
University of California, Davis
John LeBlanc
University of California, Berkeley
James Lenihan
USDA Forest Service
Rebecca Leonardson
University of California, Berkeley
Amy Lynd Luers
Union of Concerned Scientists
Jay Lund
University of California, Davis
Kaveh Madani
University of California, Davis
Edwin Maurer
Santa Clara University
Josue Medellin
University of California, Davis
Norman Miller
Lawrence Berkeley National Laboratory
Tadashi Moody
University of California, Berkeley
Max Moritz
University of California, Berkeley
Susanne Moser
National Center for Atmospheric Research
Nehzat Motallebi
California Air Resources Board
Ronald Neilson
USDA Forest Service
Marcelo Olivares
University of California, Davis
Roy Peterson
Department of Water Resources
Luigi Ponti
University of California, Berkeley
David Purkey
Natural Heritage Institute
William J. Riley
Lawrence Berkeley National Laboratory
Timothy Robards
California Department of Forestry and Fire Protection
University of California, Berkeley
Alan Sanstad
Lawrence Berkeley National Laboratory
Benjamin D. Santer
Lawrence Livermore National Laboratory
Nicole Schlegel
University of California, Berkeley
Frieder Schurr
University of California, Berkeley
Kate Scow
University of California, Davis
Scott Sheridan
Kent State University
Clara Simón de Blas
Universidad Rey Juan Carlos (Spain)
Scott Stephens
University of California, Berkeley
Stacy Tanaka
University of California, Davis
Margaret Torn
Lawrence Berkeley National Laboratory
Mary Tyree
Scripps Institution of Oceanography
R.A. VanCuren
California Air Resources Board
Sebastian Vicuna
University of California, Berkeley
Kristen Waring
University of California, Berkeley
Anthony Westerling
Scripps Institution of Oceanography
Simon Wong
University of California, Berkeley
David Yates
National Center for Atmospheric Research
Tingju Zhu
International Food Policy Research Institute

July 2006
CEC-500-2006-077

This summary was prepared by **Amy Lynd Luers** (Union of Concerned Scientists), **Daniel R. Cayan** (Scripps Institution of Oceanography), **Guido Franco** (California Energy Commission), **Michael Hanemann** (University of California, Berkeley), and **Bart Croes** (California Air Resources Board).

For more information, please contact:

Guido Franco
California Energy Commission
gfranco@energy.state.ca.us
http://www.climatechange.ca.gov

Daniel R. Cayan
Scripps Institution of Oceanography
dcayan@ucsd.edu
http://meteora.ucsd.edu/cap

Amy Lynd Luers
Union of Concerned Scientists
aluers@ucsusa.org
http://www.climatechoices.org

Support was provided in part by the California Energy Commission and the California Environmental Protection Agency.
The material contained in this document does not necessarily represent the views of the funding agencies or the State of California.

Design & Production: David Gerratt/NonprofitDesign.com. Printed on recycled paper using soy-based inks.

Arnold Schwarzenegger
Governor

THE FUTURE IS NOW: AN UPDATE ON CLIMATE CHANGE SCIENCE IMPACTS AND RESPONSE OPTIONS FOR CALIFORNIA

SPECIAL REPORT
CALIFORNIA CLIMATE CHANGE CENTER

Prepared For:
California Energy Commission
Public Interest Energy Research Program

Prepared By:
Susan Moser, Guido Franco, Sarah Pittiglio, Wendy Chou, Dan Cayan

May 2009
CEC-500-2008-071

Prepared By:
Susan Moser
Susanne Moser Research & Consulting

Guido Franco
Sarah Pittiglio
California Energy Commission

Wendy Chou
Consultant

Dan Cayan
Scripps Institute of Oceanography

Prepared For:
Public Interest Energy Research (PIER)
California Energy Commission

Guido Franco
Contract Manager

Linda Spiegel
Program Area Lead
Energy-Related Environmental Research

Kenneth Koyama
Office Manager
Energy Generation Research

Martha Krebs, Ph.D.
PIER Director

Thom Kelly, Ph.D.
Deputy Director
ENERGY RESEARCH & DEVELOPMENT DIVISION

Melissa Jones
Executive Director

DISCLAIMER

This report was prepared as the result of work sponsored by the California Energy Commission. It does not necessarily represent the views of the Energy Commission, its employees or the State of California. The Energy Commission, the State of California, its employees, contractors and subcontractors make no warrant, express or implied, and assume no legal liability for the information in this report; nor does any party represent that the uses of this information will not infringe upon privately owned rights. This report has not been approved or disapproved by the California Energy Commission nor has the California Energy Commission passed upon the accuracy or adequacy of the information in this report.

Acknowledgments

The authors thank the student interns Daniel Mourad, Molly O'Hagan, and Trina Filan for their invaluable research assistance and the peer-reviewers for their insightful comments. Finally, the authors appreciate the overall guidance provided by Tony Brunello, Deputy Secretary on Climate Change and Energy, from the Resources Agency.

Please cite this report as follows:

Moser, Susie, Guido Franco, Sarah Pittiglio, Wendy Chou, Dan Cayan. 2009. *The Future Is Now: An Update on Climate Change Science Impacts and Response Options for California.* California Energy Commission, PIER Energy-Related Environmental Research Program. CEC-500-2008-071.

Preface

The California Energy Commission's Public Interest Energy Research (PIER) Program supports public interest energy research and development that will help improve the quality of life in California by bringing environmentally safe, affordable, and reliable energy services and products to the marketplace.

The PIER Program conducts public interest research, development, and demonstration (RD&D) projects to benefit California's electricity and natural gas ratepayers.

The PIER Program strives to conduct the most promising public interest energy research by partnering with RD&D entities, including individuals, businesses, utilities, and public or private research institutions.

PIER funding efforts focus on the following RD&D program areas:

- Buildings End-Use Energy Efficiency
- Energy Innovations Small Grants
- Energy-Related Environmental Research
- Energy Systems Integration
- Environmentally Preferred Advanced Generation
- Industrial/Agricultural/Water End-Use Energy Efficiency
- Renewable Energy Technologies
- Transportation

The Future Is Now: An Update on Climate Change Science Impacts and Response Options for California is a special report conducted by the California Energy Commission's California Climate Change Center. The information from this project contributes to PIER's Energy-Related Environmental Research Program.

For more information about the PIER Program, please visit the Energy Commission's website at www.energy.ca.gov/pier or contact the Energy Commission at 916-654-5164.

Table of Contents

Preface iii

Abstract ix

Executive Summary 1

1.0 Introduction and Purpose of This Report 5

1.1. Guide to the Report 7

2.0 Climate Change Is Here, Now: Already Observed Changes and Accelerating Trends 9

2.1. California's Temperatures Are Already Changing 9

2.2. Adverse Effects of Climate Change on Public Health 12

2.3. The Changing Water Cycle 15

2.4. Growing Stresses in Agriculture 17

2.5. Decreasing Chill Hours 18

2.6. The Disassembly of California's Ecosystems 19

2.7. Shifts and Disturbances in Forests and Other Managed Landscapes 20

2.8. Increasing Wildfire Frequency 23

2.9. The Warming of Lake Tahoe 23

2.10. Increasing Rate of Sea-Level Rise 24

2.11. Conclusions 25

3.0 Detecting the Human Fingerprint on Our Changing Climate: The Scientific Verdict Is In 27

3.1. Human Attribution Studies: How IS IT Known? 28

3.2. Detection 28

3.3. Attribution 28

3.4. Evidence of Human Influence on Global and Continental Climate 30

3.5. Evidence of Human Influence on Western United States and California's Climate 35

3.6. Detection Study 1: Warming Over the Sierra Nevada and Retreat of the Ponderosa Pine Forest 36

3.7. Detection Study 2: Migratory Songbirds in California 36

3.8. Attribution Study 1: Human-Caused Warming Over California 37

3.9. Attribution Study 2: Changes in the Hydrological Cycle in the Western United States 37

3.10. Conclusions 38

4.0 Projected Impacts of Climate Change in California Updating "Our Changing Climate": What More Have Californians Learned? 39
4.1. California's Warmer Future: Temperature Projections 41
4.2. Public Health: Stark Challenges for Vulnerable Populations 43
4.3. Water Resources: Summertime Scarcity and Changes in Snowfall 44
4.4. Increased Risks and Costs for Agriculture 45
4.5. Changing Landscapes: Forests and Aquatic Ecosystems 47
4.6. Sea-Level Rise: Greater Than Previously Thought? 49
4.7. Growing Energy Demands 53
4.8. Climate Change in a Multi-Stressor World 54
4.9. Growing Water and Energy Management Challenges in Southern California 54
4.10. Growing Wildfire Risk 55
4.11. Growing Vulnerability of the Sacramento-San Joaquin Delta 56
4.12. Keeping the Eye on the Ball: A Global Perspective 56
4.13. Global Teleconnections of Air Quality 57
4.14. Inter- and Intrastate Water Movement 57
4.15. Conclusions 58
5.0 Managing California's Climate Risks: Need for a Two-Pronged Strategy 59
5.1. A Compelling Case: Why California—and the World—Must Mitigate Climate Change and Adapt to Its Impacts 59
5.2. The Two-Pronged Approach to Reduce Climate Risks: Mitigation and Adaptation 62
5.3. California's Emerging Efforts in Adaptation Planning 64
5.4. Adaptation, Coping Range, and Climate Extremes 64
5.5. The Goal of Adaptation: Not "Free From Risk" but "Well-Managed Risk" 66
5.6. Adaptation Needs Assessments 66
5.7. Adaptation Planning in California 69
5.7.1. Research in Support of Adaptation Planning 70
5.8. Adaptation Studies Supported by Local, State, and Federal Agencies 71
5.9. PIER-Supported Studies 71
5.10. Development of Climate Projections for California 72
5.11. Development of Tools for Impacts and Adaptation Studies 73
5.12. Effect of Aerosols on Precipitation Levels and Regional Climate 73
5.13. Adaptation to Present Climate Variability as a Parallel for Climate Change 73
5.14. Vulnerability-Based Adaptation 75

6.0 References....77

Appendix 1: Detection of Climatic and Related Environmental Changes and Attribution to Anthropogenic Causes....1

Growing Scientific Confidence over Time....1

Human Attribution Studies: How Do We Know?....2

Detection....2

Attribution....3

Detection and Attribution of Environmental and Societal Impacts of Climate Change....4

Changes in Physical Systems....5

Changes in Biological Systems....6

Changes in Managed and Human Systems....7

List of Figures

Figure 1. Co-evolution of climate change science and policy in California....6

Figure 2. Historical annual average temperature for California......10

Figure 3. Minimum (a) and maximum (b) daily summer temperature trends at 52 weather stations in California (1920-2003)....11

Figure 4. Historical differences in maximum temperature (between irrigated lands and non-irrigated areas, red line) and concurrent changes in irrigated land area in the same region (blue line)....12

Figure 5a. Ninety-ninth percentile metric comparisons at Firebaugh, California, Climate Station......14

Figure 5b. Overall magnitude of the major heat waves in California and Nevada (°F) from 1948 to 2006......14

Figure 6. April 1st snow level trends 1950-1997. The red points indicate percentage decrease in April 1st snow levels and blue points indicate percent increase....16

Figure 7. Sacramento River runoff (April – July) as a percentage of annual runoff....17

Figure 8. Map of the trends in the change in winter chill hours since 1950. 18

Figure 9. Upslope retraction of ponderosa pine-dominated woodlands between 1930s and 1996....21

Figure 10. Change in nighttime frozen areas during the winter quarter from 1920 to 1993.....22

Figure 11. Historical sea-level rise for San Francisco and San Diego. 25

Figure 12. Growing scientific confidence regarding human contribution to climate change.. 27

Figure 13: Global and continental temperature change.. 31

Figure 14: Selected detected climate changes attributable to human forcing likelihood of occurrence or outcome of each of the identified changes is given in standard IPCC language and probabilities. 32

Figure 15. CO_2 emissions under three IPCC scenarios. 40

Figure 16. Historical and projected annual average temperatures for California. 42

Figure 17. Global average temperature projections for 2100 for the B1 and "policy" scenarios at the end of this century 43

Figure 18. Historical data (black) and projected decrease in annual accumulated chill hours for the city of Davis, California. Future projections used scenarios B1 (magenta squares) and A2 (open blue triangles). 46

Figure 19. Observed sea levels in San Francisco and projected global levels for the B1 and "Policy" scenario. 50

Figure 20: Projected exceedence hours per year at Fort Point, San Francisco (SFO), over the next century. The GFDL model (A2 emissions scenario) was used. 51

Figure 21. Areas inundated or at risk of inundation by average yearly Bay high-water levels, for both present-day (blue) and projected 2100 (red) conditions.. 52

Figure 22. SLR, La Jolla "Regions of inundation at La Jolla Shores for sea level rise and various wave event scenarios in 2050. 53

Figure 23. Temperature distribution for California from a global climate model and downscaled results for California.. 72

List of Tables

Table 1: Observed changes in physical, biological and managed or human systems in response to anthropogenic climate warming 34

Table 2: Comparison of hazards- and vulnerability-based approaches to adaptation 68

Abstract

This report presents an interim summary of the latest in climate change science and outlines recommended response options for decision makers in California. This document contains four key messages:

- Observed changes in temperature, sea level, precipitation regime, fire frequency, and agricultural and ecological systems reveal that California is already experiencing the measurable effects of climate change.
- Scientific confidence in attributing climate change to human activities has increased since the Fourth Assessment Report (AR4), which was recently made available by the Intergovernmental Panel on Climate Change.
- New scientific studies suggest that the climatic and hydrologic changes already experienced in California are due to human activity.
- Unmitigated climate change will lead to grave consequences for California's economy and ecosystems. Furthermore, it appears that even a scenario that drastically curtails emissions of greenhouse gases may still lead to undesirable trends in warming and sea-level rise.

A rapid two-pronged response to climate that which encompasses both mitigation and adaptation has the potential to promote innovative investment by businesses and protect environmental quality while increasing community preparedness and capacity to cope with change. Conversely, a path of inaction exposes a community's vulnerability to climate variability and is ultimately costly.

Keywords: Climate change, scenario, warming, temperature, precipitation, adaptation, mitigation, sea level, greenhouse gas, vulnerability

Executive Summary

Introduction

Climate change is a critical issue facing California's citizens, ecosystems, and economic vitality. In June 2005, Governor's Schwarzenegger's Executive Order S-3-05 initiated a process that requires biennial updates on the state of climate change science, the expected impacts on the state under different climate change scenarios, and an assessment of whether state efforts to address these impacts are adequate. The biennial reports mainly focus on impacts while this report demonstrates that climate is already changing in California in a way that is consistent with what is expected from climate change. In addition, this report makes a strong case about the need to consider adaptation to deal with the impacts that are already underway and can no longer be avoided. A full-color summary of this document's highlights is also available.

Purpose

Coordination is needed between climate science practitioners and those individuals helping to develop and implement a statewide climate change response strategy. This document, intended for use by the state agencies and Legislature, seeks to:

- Synthesize the most recent findings on climate change science.
- Outline a response strategy that encompasses both mitigation and adaptation.

Project Objectives

- Document how climate change in California is now occurring, has already affected public health, the economy, and natural ecosystems, and is likely to accelerate in the future. (Chapter 2)
- Explain the evidence attributing past and current observations of climate change to direct human causes such as emissions of greenhouse gases. (Chapter 3)
- Examine what would happen to California's climate under hypothetical emissions scenarios, including a scenario of drastically reduced emissions more stringent than any studied previously. (Chapter 4)
- Summarize the most up-to-date scientific understanding of how future climate change will affect California's economy and ecosystems. (Chapter 4)
- Describe the necessity of a two-pronged response strategy that includes both mitigation of emissions and adaptation to that climate change that is already underway. (Chapter 5)

Project Outcomes

The following are some of the most important recent findings taken from the published literature and summarized here:

- The American West is heating faster than the United States taken as a whole.
- Warming and precipitation changes are not occurring uniformly throughout the state. Two examples relating to temperature are the effect of intensive crop irrigation in the Central Valley, which has historically decreased the amount of warming in this region, and the increased warming effect observed in urban areas. For precipitation, changes in snowpack and the timing of spring runoff have already been observed in the Sierra Nevada Mountains over the past century.
- Agricultural productivity, forest composition, timing of ecological events (for example, migration), and wildfire frequency are all arenas that have experienced measurable changes resulting from a changing climate.
- Observed global and regional changes are largely due to human activity.
- A "Policy" scenario was modeled to simulate a drastic reduction in emissions and the stabilization of atmospheric carbon dioxide levels by 2100. Importantly, though it is more stringent than scenarios previously analyzed (such as B1) under the Scenarios Project, the Policy scenario still yields forecasts for detrimental warming and rising sea levels.
- Factors that can aggravate problems caused by climate change include population growth, the presence of poor or vulnerable social groups, and seismic risks in the San Joaquin Delta. In addition, some climate change impacts will overlap and combine in challenging ways.
- A mitigation approach aims to reduce emissions without barring economic progress. An adaptation approach accommodates the unpredictable nature of climate variability and attempts to minimize societal risk to an acceptable level. Both of these approaches are deemed necessary to address climate change. The state is implementing several adaptation programs described in Chapter 5.

Conclusions

Abundant evidence now shows that climate change is not just a future problem, but is already observable now, with measurable impacts for the state's citizens, natural resources, and economic sectors. California's position as a national leader of state-sponsored climate change research provides us a unique perspective on how best to manage for the effects of climate change. Future management decisions should recognize that current emissions have committed the state to some amount of ongoing and irreversible climate change. The consequences of taking no action on adaptation and mitigation would be costly for California and the world.

Recommendations

In 2006, California elected to take decisive action on mitigation via Assembly Bill 32, the Global Warming Solutions Act of 2006 (Núñez, Chapter 488, Statutes of 2006; AB 32), a comprehensive cap on greenhouse emissions. A complementary pathway of adaptation measures is also needed to ensure that potential harm and burden to the economy and environment of California is minimized. The Resources Agency, under the leadership of Secretary Mike Chrisman, has started a new initiative to develop a statewide adaptation strategy that will be updated every other year.

Additional recommendations include:

- Preparing for change via forward-looking, well-designed adaptation plans.
- Understanding connections between climate change and land use decisions, and understanding how climate change affects multiple sectors of the economy.
- Understanding accelerating climate change trends and examining the risks of abrupt climate change.
- Managing climate change efforts via private and public sector channels and promoting cooperation among local and regional stakeholders.

Benefits to California

- California's landmark AB 32 legislation and history of technological innovation make it a current leader in climate change science and action. With planning and foresight, both mitigation and adaptation may offer important opportunities for California businesses.
- Decreasing the human footprint on the environment, reducing vulnerability to climate variability and change, and planning ahead can improve environmental conditions and economic welfare, enhance social justice, and ensure people's quality of life.

1.0 Introduction and Purpose of This Report

California is exemplary in the nation for its commitment to state-funded climate change research, its efforts to understand the climate risks it faces, and its wide range of efforts to confront the challenge. In 1988, the Legislature mandated the preparation of the first state-focused climate change impacts assessment (leading to two high-profile reports, *The Impacts of Global Warming on California* (Energy Commission 1989) and *Climate Change Potential Impacts and Policy Recommendations* (Energy Commission 1991). Other state-focused impacts assessments, initiated and conducted by researchers outside state government, were presented in 1999 (Field et al., 1999), 2002 (USGCRP, 2002), 2003 (Wilson et al., 2003), and 2004 (Hayhoe et al., 2004). In 2003, the state also founded the California Climate Change Center to coordinate climate change research. Together these efforts are steadily building up the necessary knowledge base to inform California state policies on energy, land use, and climate change (see Franco et al., 2008a, for an extended history of the science-policy interaction around climate change in California).

With Governor's Schwarzenegger's June 2005 Executive Order S-3-05, a process was initiated that requires biannual updates on the state of climate change science, expected impacts on the state using several climate change scenarios, and an assessment whether state efforts to minimize and adapt to these impacts are adequate. The first of these "Scenarios Reports" was produced in 2006 (*Our Changing Climate*; CCCC, 2006), and work is underway to develop the scientific basis for the 2008 and future scenarios reports. Figure 1 presents a side-by-side illustration of how science and policy co-evolved in the state.

The present report discusses how climate is already changing in California and makes a strong case about the need to consider adaptation to deal with the impacts that are already underway and can no longer be avoided. It has three main goals:

- To synthesize existing knowledge with new scientific findings in order to keep policy-makers, resource managers, and the public abreast of the rapidly evolving climate change science.
- To dispel any lingering doubts about the human influence on the observed changes in the climate and the natural environment on which Californians depend.
- To underscore the increasingly urgent need for a dual approach to managing California's climate change risks:
    - To reduce greenhouse gas emissions to minimize and slow down global warming.
    - To prepare adaptation plans to deal with the impacts that are already underway and cannot be avoided.
- To minimize harm and take advantage of any opportunities that may arise from climate change.

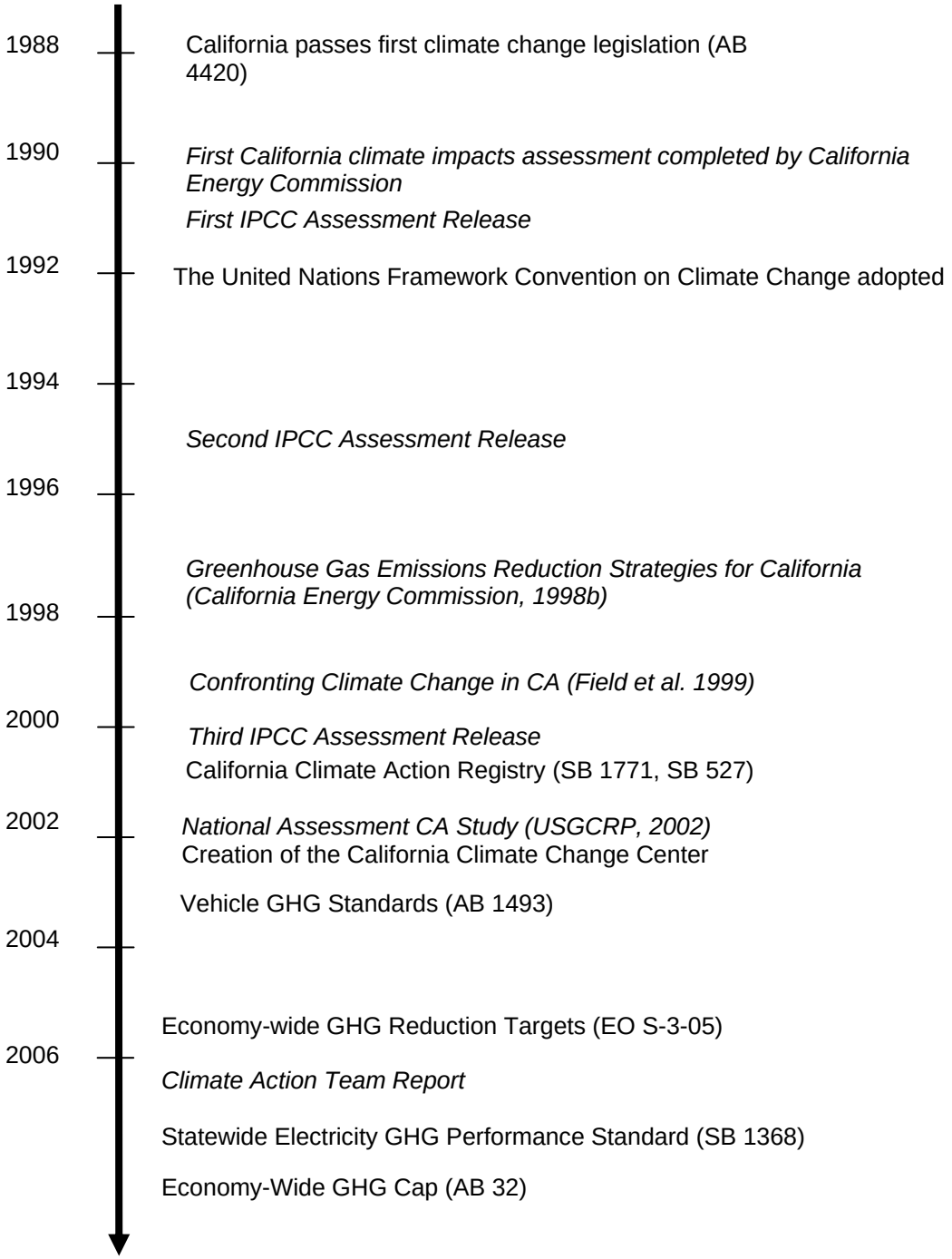


Figure 1. Co-evolution of climate change science and policy in California. Major scientific reports are italicized.

Source: Franco et al. 2008a

1.1. Guide to the Report

Chapter 2 uses primarily local examples of already observed trends in physical parameters and biological changes to illustrate that climate change is not a problem of the future but happening already, here and now, and that many of the observed trends are accelerating. Chapter 3 turns to the question of causality: What is causing these changes? It uses primarily consensus science to illustrate that the majority of climate changes witnessed over the past 50 years can be attributed to human alterations of the atmosphere and land. It also includes, to the extent possible, regional climate change detection and attribution studies of high relevance for California. Chapter 4 then updates previously published projections of climate change and related impacts with new scientific insights that have become available since *Our Changing Climate* in 2006. It focuses on all sectors relevant in California and highlights interconnections between what may happen in California and elsewhere in the nation and world. Finally, C lays the foundation for why mitigation is essential but no longer sufficient to manage the climate change risks California is already and will be facing in the future. It highlights efforts to reduce emissions and of the emerging adaptation planning efforts at the state level.

2.0 Climate Change Is Here, Now: Already Observed Changes and Accelerating Trends

2.1. California's Temperatures Are Already Changing

There is now irrefutable scientific evidence that increasing emissions of greenhouse gases are changing the Earth's climate. The most recent report by the Intergovernmental Panel on Climate Change (IPCC), released in February 2007, states, "Warming of the climate system is unequivocal, as is now evident from observation of increases in average air and ocean temperatures, widespread melting of snow and ice, and rising global average sea level" (Le Treut et al., 2007).

Review of Temperature Impacts
• Overwhelming scientific consensus that greenhouse gas emissions are changing our climate • The western United States is warming faster than the rest of the United States • California's annual nighttime temperatures have increased 0.33 °F per decade since 1920 • California's annual daytime temperatures have increased 0.1 °F per decade • In the Central Valley, irrigation has reduced the expected warming from climate change

The current post-industrial warming trend differs alarmingly from past changes in the Earth's climate because greenhouse gas emissions are higher and warming is occurring faster than at any other time on record within the past 650,000 years. Historical long-term as well as decadal and inter-annual fluctuations in the Earth's climate resulted from natural processes such as plate tectonics, the Earth's rotational orbit in space, solar radiation variability, and volcanism. The current trend derives from an added factor: human activities (see this section). Worldwide, eleven of the last 12 years (1995-2006) rank among the 12 warmest years in the instrumental record of global surface temperature since 1850 (Le Treut et al., 2007).

The American West is heating up faster than any other region of the United States (reference from a report from the U.S. Climate Change Science Program, 2008, Saunders et al., 2008). For the last five years, from 2003 through 2007, the global temperature averaged 1°F warmer than its 20th-century average. During the same period, 11 western states averaged 1.7 degrees warmer, 70% more than the world average. This is primarily due to the fact that arid land areas prevalent in American West heat more easily in contrast to the slow-warming oceans. A second explanation may be that atmospheric conditions in the East have produced cloudier and wetter weather, cooling the region relative to the West. Regardless, scientists have shown that the warming trend is more than 99% likely to be outside the normal bounds of climate variation.

In California, average annual temperature has been increasing since 1920 (Figure 2).

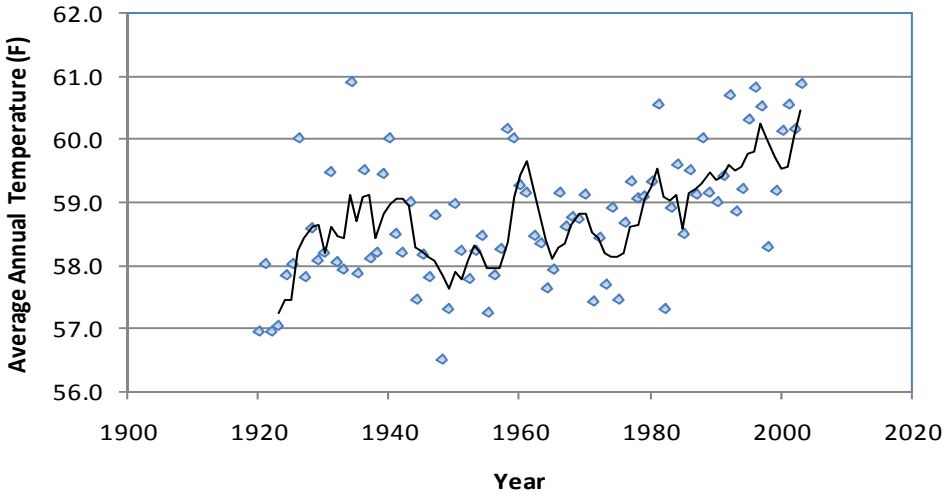


Figure 2. Historical annual average temperature for California. The solid line shows the five-year running average trending upwards. Warming trends due to urbanization have been removed from these long-term climate data.

Source: The National Climatic Data Center, available at http://cdiac.ornl.gov/epubs/ndp/ushcn/state_CA_mon.html.

The warming of California is not geographically uniform. Minimum temperatures (typically nighttime) are increasing almost everywhere in California (Figure 3a) during the summer. On the other hand, maximum daily temperatures are increasing at a slower rate, with some locations (for example, the Central Valley), experiencing a cooling trend (Figure 3b, blue circles). The annual minimum temperature averaged over all of California has increased 0.33°F per decade during the period 1920 to 2003, while the average annual maximum temperature has increased 0.1°F per decade. Measurements taken from other stations in the United States show a similar pattern of stronger nighttime warming (Easterling et al., 1997). The heat wave that affected California in July 2006 was the largest heat wave on record since 1948. This heat wave has been linked to a warming of the ocean especially west of Baja California, which seems to be part of a global pattern of warming of the ocean waters during the last six decades (Gershunov and Cayan, 2008). As explained in the next section, the gradual warming of the oceans is now clearly attributed to increased concentrations of greenhouse gases in the atmosphere.

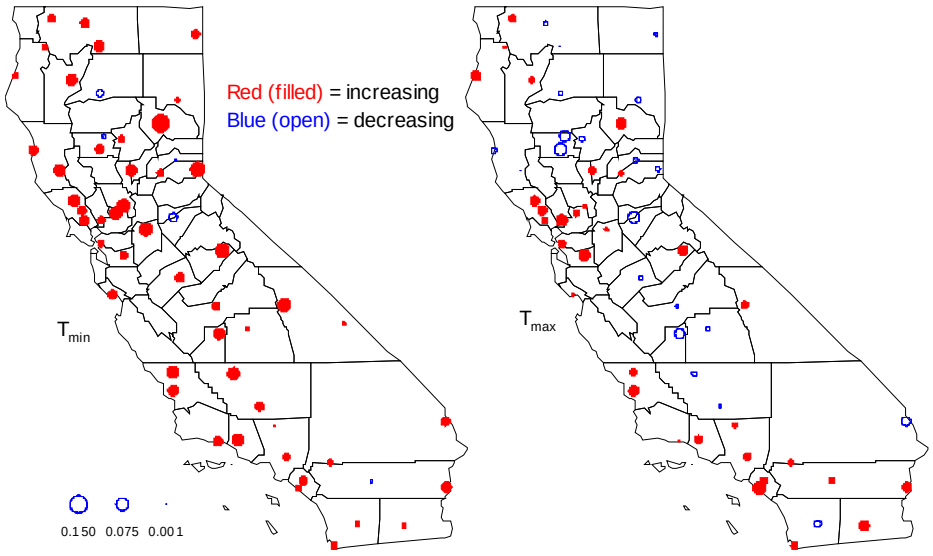


Figure 3. Minimum (a) and maximum (b) daily summer temperature trends at 52 different weather stations in California (1920-2003). Red points indicate warming; blue points indicate cooling. The size of the points is proportional to the rate of change.

Source: California Energy Commission, CEC-500-2005-103-SD.

It appears that intensive irrigated agriculture explains why summer maximum temperatures in the Central Valley have either cooled or have warmed less than other areas of California[1] (Bonfils and Lobell, 2007). Irrigated agriculture in the Central Valley increased between 1920 and 2000, doubling in area by 1979 and eventually stabilizing in the 1980s. During this period of expanding irrigation practices, a large cooling effect of -1.8°F to -3.2°F (relative to non-irrigated areas) has been observed for summertime average daily daytime temperatures in the Valley. The difference in daytime temperatures between irrigated and non-irrigated lands is strongly related to the trend in the amount of irrigated area since 1920 (Figure 4).

[1] Simulations using regional climate models have also suggested that agricultural irrigation in California has dampened the expected increase of daytime temperatures in the Central Valley (Snyder et al., 2006). The study by Bonfils and Lobell (2008) was the first to experimentally confirm this effect.

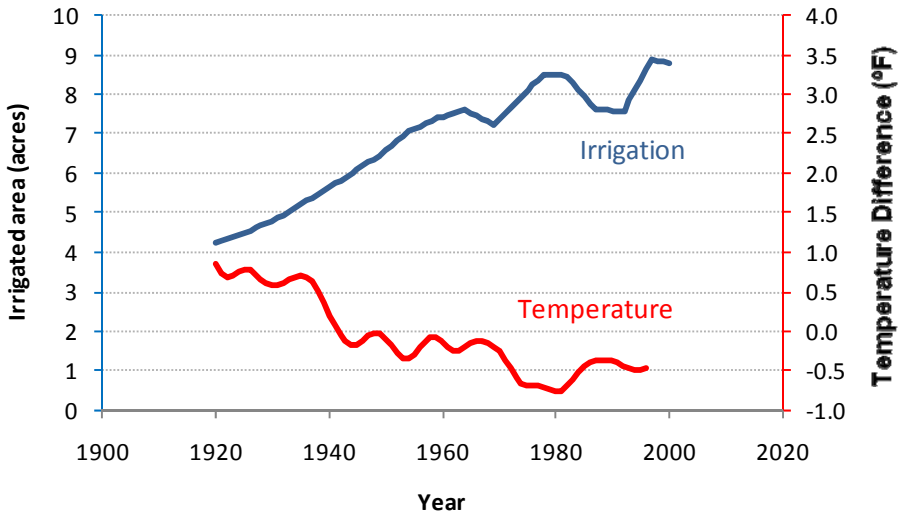


Figure 4. Historical differences in maximum temperature (between irrigated lands and non-irrigated areas, red line) and concurrent changes in irrigated land area in the same region (blue line). Temperature data are June to August months. All data were located in the Central Valley, California.

Source: Adapted from Bonfils and Lobell, 2007.

The empirical evidence from Figure 4 indicates that an increase in agricultural irrigation in the Central Valley has progressively cooled this region, partially masking the warming trend observed in non-irrigated regions. Moist irrigated soil allows for evaporative cooling of the air above, much the same way an evaporative cooler can be used to cool our homes in the dry summer months. A serious concern is that the amount of water available for irrigation is leveling off and is expected to decline in the future, which could prompt an acceleration of warming in the Central Valley.

2.2. Adverse Effects of Climate Change on Public Health

Warming temperatures in the U.S. have given rise to increasingly frequent heat stress events over the last fifty years (NOAA 1999). The largest and most statistically significant trends occurred in some of the most populated areas, in the eastern and western thirds of the United States (Gaffen and Ross, 1998).

Review of Public Health Impacts
• Higher temperatures are correlated with increased heat-related mortality • Increasing nighttime temperatures make it difficult for the body to cool overnight, increasing the risk of heat related illness • Persons in socioeconomically depressed areas are at a greater risk for heat-related mortality due to lack of access to in-home air conditioning or neighborhood cooling places, social isolation, and lack of social networks and support systems • Increased frequency in heat stress events over last fifty years

With climate change, nighttime minimum temperatures have increased significantly (Easterling, 1997; Bonfils et al., 2008), which limits the body's ability to cool overnight during heat waves (English et. al., 2007). Urban areas tend to have higher nighttime temperatures than less developed rural areas since buildings and pavement reemit the heat that they absorbed during the day. In addition, waste heat from vehicles, industry and air conditioners contribute to warmer temperatures in urban areas, exacerbating heat-related illness and mortality and increasing the heat stress vulnerability of millions of Californians living in urban areas (e.g., English et al., 2007; Hayhoe et al., 2004). While the July 2006 heat wave in California did not raise daytime temperatures beyond those of heat waves from the last six decades, the nighttime temperatures experienced during this event were truly unprecedented. Although the authors cannot directly attribute the July 2006 heat wave to climate change, abundant evidence suggests a causal link between climate warming and extreme events. A recent study analyzing this heat wave from a historical perspective concluded that "Generally, there is positive trend in heat wave activity over the entire region that is expressed more strongly and clearly in nighttime rather than daytime temperature extremes. Daytime heat wave activity has been intensifying more rapidly over the elevated interior compared to the lowland valleys." (Gershunov and Cayan, 2008).

There is no uniform definition of a "heat wave"; for example, temperatures that might be considered "normal" in Fresno would constitute an extreme heat event in San Francisco, based on historical precedent. What is considered a "heat wave" locally is the important metric regarding human health, however, because of the temperatures to which the local population is acclimatized. A useful metric at a given climate station is the number of degrees Fahrenheit warmer than 99 percent of the historically recorded temperatures (the 99th percentile). For example, Figure 5a represents this 99th percentile metric at the Firebaugh, California, climate station in the heart of the San Joaquin Valley. To capture the geographical coverage of the heat wave, the authors could add up these hours for all the stations in a given region to generate a composite metric. Figure 5b presents the cumulative degrees for meteorological stations in California and Nevada for the major regional historical heat waves from 1948 to 2006. For the last six major daytime (blue plus-signs) and nighttime (red boxes) heat waves that occurred in "California region," the magnitude of nighttime heat waves has substantially increased over time (Figure 5b).

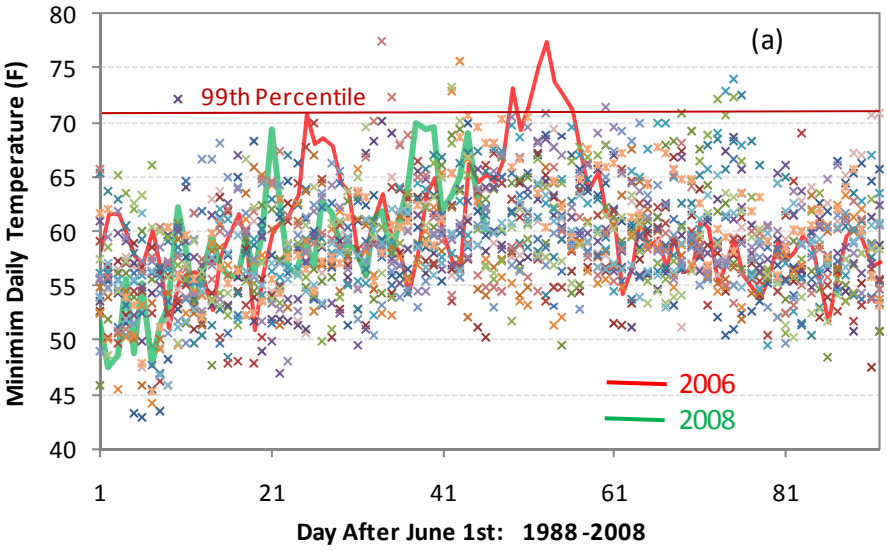


Figure 5a. Ninety-ninth percentile metric comparisons at Firebaugh, California, Climate Station. Red and green lines represent minimum daily summer temperatures each day from June 1 to August 31 (day 1 to day 92) during 2006 and 2008, respectively. The 99th percentile line indicates nights during which the minimum temperature exceeded 99 percent of historically recorded temperatures for that climate station.

Adapted from Gershunov and Cayan, 2008.

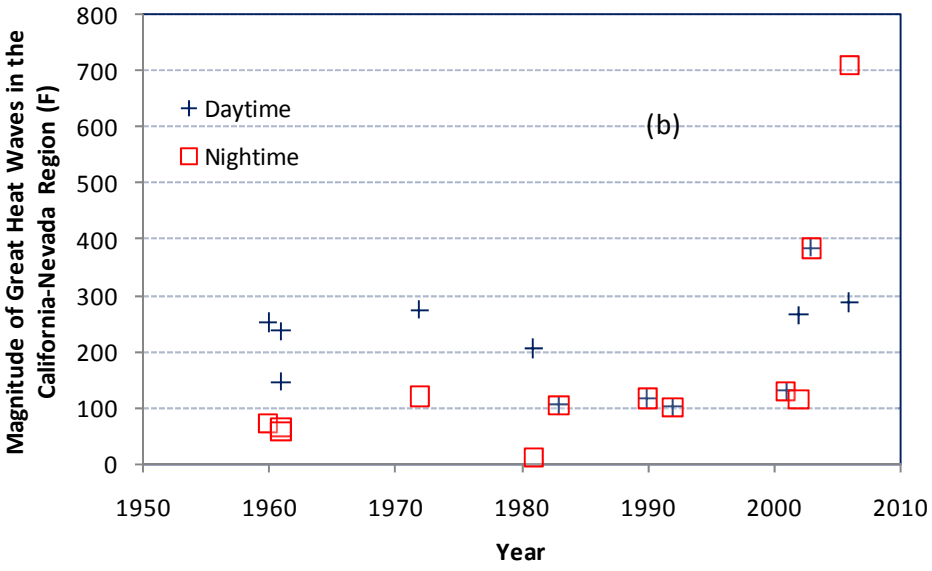


Figure 5b. Overall magnitude of the major heat waves in California and Nevada (˚F) from 1948 to 2006. Blue plus-signs and red boxes represent events dominated by temperatures during the day or night, respectively. The vertical scale represents the summation of degrees F above the 99 percentile for all the stations included in the analysis.

Adapted from Gershunov and Cayan, 2008.

Increases in mortality are commonly observed during heat waves (Basu and Samet, 2002). Heat especially increases the vulnerability of the elderly and of infants as well as persons with cardiovascular, respirator and/or cerebrovascular diseases (English et al., 2007). An analysis of temperatures during summers in several counties in California with no heat waves from 1999 to 2003 found a 3% increase in deaths on any given day for a 10°F increase in the heat index, which is a measure of combined temperature and humidity (Basu et al., 2008).

In the summer of 2006, a heat wave of unusually long duration led to 140 heat-related deaths in California (CDHS, 2007), which excludes potentially heat-related deaths not seen by coroners or medical examiners, who do not typically investigate deaths of persons currently under a doctor's care. During this two-week heat wave, 80% of the reported deaths occurred in seven inland, low-lying areas, such as the Imperial Valley, San Bernardino and the San Joaquin Valley. Sixty-four percent of the heat-related death cases occurred in socioeconomically depressed areas (zip codes where more than 20% of the residents earn less than the Federal Poverty Threshold). A preliminary epidemiological analysis of the July 2006 heat wave and other similar extreme events in California suggest mortality rates higher than the reported 3% increase per 10°F discussed above (Ostro, 2008, personal communication).

The ability to use cooling mechanisms such as air conditioning is one way to combat the negative health effects of rising temperatures. Statewide, older homes (built before 1975), coastal properties, and low-income households are less likely to have air conditioning in the home. The victims of the 2006 heat wave were predominately male (66%), older adults (median age of 66 years), and had a history of chronic disease (73%) (English et al., 2007). Indoor temperatures (only noted in 36 of the recorded 140 cases) averaged 103.5°F, with a range of 85-140°F. None of the decedents was known to have visited a cooling center, and only one individual had an air conditioner running in her home at the time of death.

2.3. The Changing Water Cycle

Declining Snowpack and Earlier Spring Runoff

Review of Water Resources Impacts
• Recorded reductions in the Sierra snowpack
• The Sierra snowpack is melting earlier in the spring season
• A decrease in spring runoff is creating deficits in reservoir storage during the dry season

Most of California's precipitation falls in the winter as snow in the Sierra Nevada mountain range. Sierra snowpack is extremely important because it acts as a large natural reservoir and provides water for the summer and fall when rainfall is scarce. Over the past century, rising temperatures over the Sierra Nevada have had two major implications: first, more precipitation is falling as rain and less as snow (Mote et al., 2005; Knowles, 2006); and second, snowmelt is occurring earlier in the spring (Hamlet et al., 2007), leading to a shortened winter recreation season and earlier low-flow conditions, with potentially severe implications for fish and other aquatic life and California's all-important water supplies.

One important trend is the decline of total snow accumulation (and water content in the snow) on April 1st (Mote et al., 2005). April 1 is an important date for water managers because it is when they estimate the amount of water stored in the snow and determine how much water will be available to satisfy water demands in the spring and summer.

The amount of water contained in the accumulated snow on April 1 has been declining in low-elevation areas (Figure 6) while snowfall in higher elevations of the southern portion of the Sierra Nevada has been increasing. Lower elevations are more vulnerable to the effects of warming since a small rise in average temperature will create an earlier snowmelt or a shift from snow to precipitation. At high elevations, cooler temperatures provide a buffer that can maintain the snowpack until spring, but this "safety" factor is being eroded by observed warming of the Sierra Nevada. As more snow falls as rain during the winter, and spring snow melt occurs sooner, the risk of flooding increases and water shortages may occur in the summer.

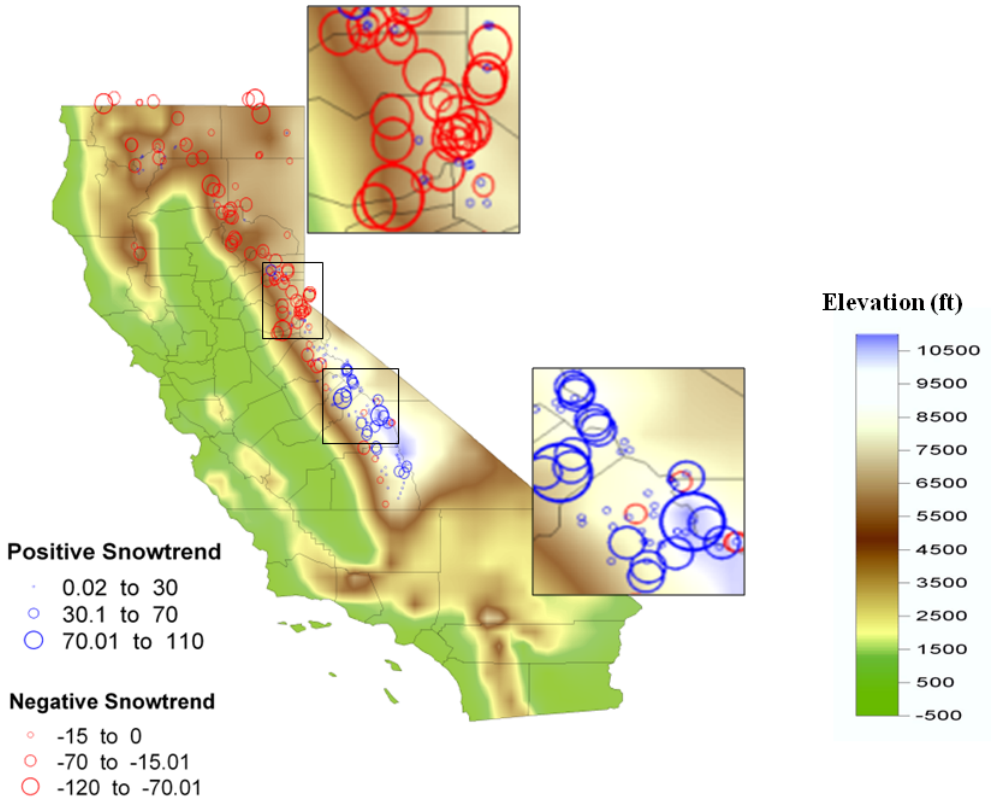


Figure 6. April 1 snow level trends 1950-1997. The red points indicate percent decrease in April 1 snow levels and blue points indicate percentage increase.
Source: Adapted from Mote et al. (2005).

Consistent with the decreasing spring snow levels, California, as well as most of the western United States, is experiencing a related decrease in the fraction of total runoff occurring in the spring (Figure 7). Spring runoff provides a significant portion of the water supply for dry

summers and falls in California. Over the past 100 years, the fraction of the annual runoff that occurs during April–July has decreased by 23% for the Sacramento basin and 19% for the San Joaquin basin. This indicates that a greater percentage of the annual runoff is occurring outside the traditional snowmelt season possibly as a result of an earlier onset of snowpack melting. If, as expected, the snowmelt season were to migrate to earlier times in the year as a result of global warming, it would reduce the amount of runoff that could be stored in man-made reservoirs for later use, because runoff would occur during times when flood control requirements mandate release of water from reservoirs to take into account the possibility of strong precipitation events late in the winter (wet) season.

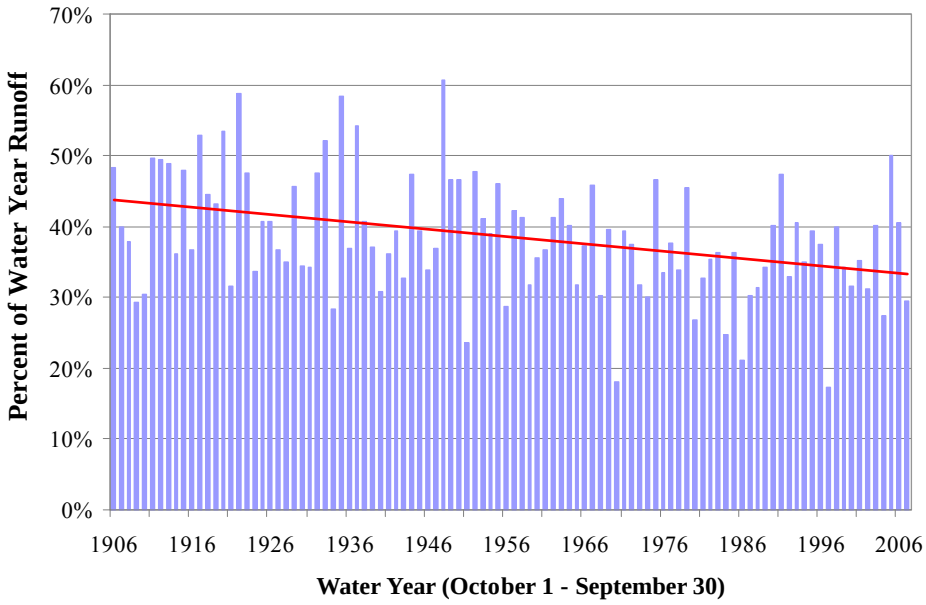


Figure 7. Sacramento River Runoff (April – July) as a percentage of annual runoff. The red linear regression line shows the decreasing historical trend in river runoff.

Source: California Department of Water Resources.

2.4. Growing Stresses in Agriculture

Agriculture is a major sector of California's economy. Statewide agricultural income from sales in 2003 was $27.8 billion, or 13% of the U.S. total (2004). As the nation's leading producer of 74 different crops, California supplies more than half of all domestic fruit and vegetables (CASS, 2004). California is also responsible for more than 90 percent of the nation's production of almonds, apricots, raisin grapes, olives, pistachios, and walnuts (Baldocchi and Wong, 2008; Cavagnaro et al., 2006). Many of these crops are sensitive to multiple facets of climate change, but here the authors focus solely on changes in temperature.

2.5. Decreasing Chill Hours

Review of Agriculture Impacts
• The decreasing trend in wintertime and nighttime chill hours threatens the fruit and nut industry • Recent climatic trends have had mixed effects on crop yields, with orange, lettuce, grape, and walnut yields aided, avocado yields hurt, and most crops little affected by recent climatic trends

Temperature plays a critical role in determining the yield and quality of several economically important crops. Fruit and nut crops, for example, are especially climate-sensitive and require a certain number of hours of cool temperatures (200 to 1200 hours, depending on the crop) during the winter months to properly set fruit. The number of chill hours (time during which temperature drops below 45°F in California's major fruit growing region), however, has been decreasing since 1950 (Baldocchi and Wong, 2008). Failure to meet the minimum requirement of chill hours can cause late or irregular blooming, which decreases fruit quality and reduces economic yield.

The greatest rates of change in chill hours are occurring in the Bay Delta region and the mid-Sacramento Valley (Figure 8).

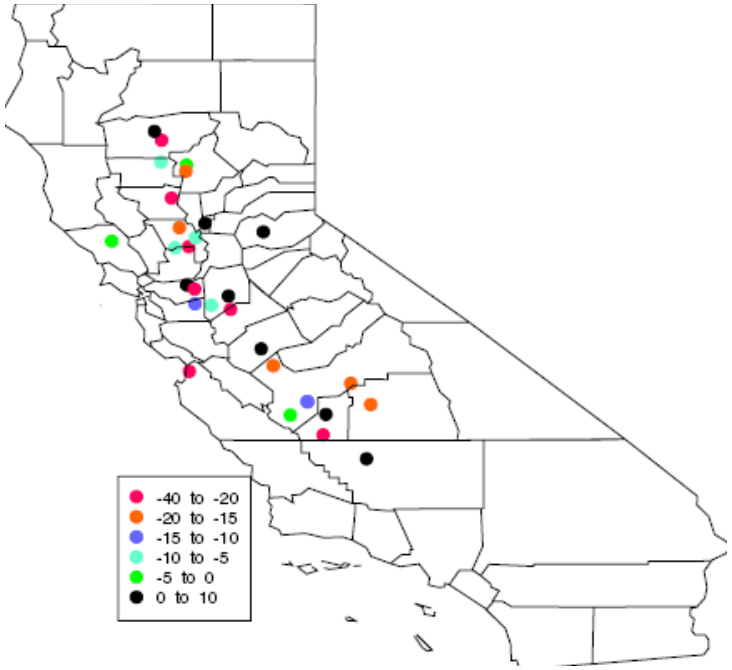


Figure 8. Map of the trends in the change in winter chill hours (hours per year) since 1950.

Source: Baldocchi and Wong, 2008 (data are derived from the California Climate Archive).

Grapes and almonds represent the two of the most valuable food crops in the state. Chill-hour requirements for grapes (depending on variety) are between 100-500 and 400-700 for almonds. If chill hours dropped below the threshold for grapes and almonds it would represent a $3.3 billion dollar loss (2003 value).

While warmer nights have negative impacts on many fruits, nuts, avocados and cotton, it has actually enhanced the production of high-quality wine grapes (Nemani et al., 2001) and oranges (Lobell et al., 2006). Since the early 1950s, winegrape growers in California have seen dramatic increases in premium wine quality and grape yield associated with climate change (Nemani 2001). In the Napa and Sonoma valleys, warmer winter and spring temperatures have resulted in a longer growing season and more favorable growing conditions. However, with the continuation of these warming trends, conditions will be too warm and no longer favorable for the production of certain grape varieties. This creates large financial risks for grape growers who must make significant upfront investments in crops which generally take many years to provide financial paybacks.

2.6. The Disassembly of California's Ecosystems

Review of Ecosystem Impacts

- The early arrival of spring and delay of fall has had numerous ecological impacts on species that rely on temperatures to dictate migration and reproduction
- The ecological ranges of Sierra Nevada flora and fauna are shifting north and higher in elevation
- Wildfires have increased in frequency, duration and size due to a longer dry season
- The water of Lake Tahoe is warming in accordance with increasing nighttime temperatures.

A number of ecological changes have already occurred in the United States over the past century in concert with increases in average temperature and changes in precipitation patterns (Peñuelas and Filella, 2001; Fields, 2007), Walther et al., 2002; Parmesan and Yohe, 2003, Root et al., 2003, 2005; Parmesan, 2006). Currently, spring is beginning earlier, while the arrival of autumn is being delayed (Menzel et al., 2006). Change in seasonal timing has serious implications for the life cycles and competitive abilities of numerous species (Walther et al., 2002; Visser and Both, 2005; Parmesan, 2006). Examples of different ecological effects in Europe and North America include shifts in phenological spring events such as budburst, egg laying, bird migration and the hatching of caterpillars occurring earlier over the course of the last 30 years (Menzel et al., 2006; Schwartz et al., 2006; van Asch and Visser, 2007). In California, 70% of 23 butterfly species advanced the date of first spring flights by an average 24 days over the period from 1972 to 2002 (Forister and Shapiro, 2003). Climate warming during spring is the only factor that was able to explain this shift in the date of the butterfly's first flight.

2.7. Shifts and Disturbances in Forests and Other Managed Landscapes

Many ecosystems in California, including managed ecosystems such as rangelands, timberlands and agricultural lands, are highly sensitive to the influence of temperature and water availability. Increasing temperatures, changing precipitation patterns, and declining soil moisture trends have shifted the suitable range for many species typically to the north or to higher elevations (Parmesan and Yohe, 2003).

In the 1930s, a U.S. Forest Service team led by A. E. Wieslander surveyed California's vegetation over roughly one-third of the state, producing a rich data set including vegetation type maps, thousands of photographs, and 25,000 herbarium specimens. This historical data has enabled researchers today to assess vegetation changes over the interim (Thorne et al., 2006). In a study of ponderosa pine forest changes between 1934 and 1996 on the western edge of the Sierra Nevada (Placerville Quadrangle), researchers found that the western edge of the forest moved an average of 4.4 miles (7.1 km) eastward and shifted upward by about 637 feet (193 meters), with the previously ponderosa-dominant areas being replaced by non-conifer species (e.g., oaks). Thorne et al. (2006) hypothesized that these changes were at least partially due to anthropogenic climate change. Figure 9 presents more recent results from ongoing research on this topic (Thorne, 2008).

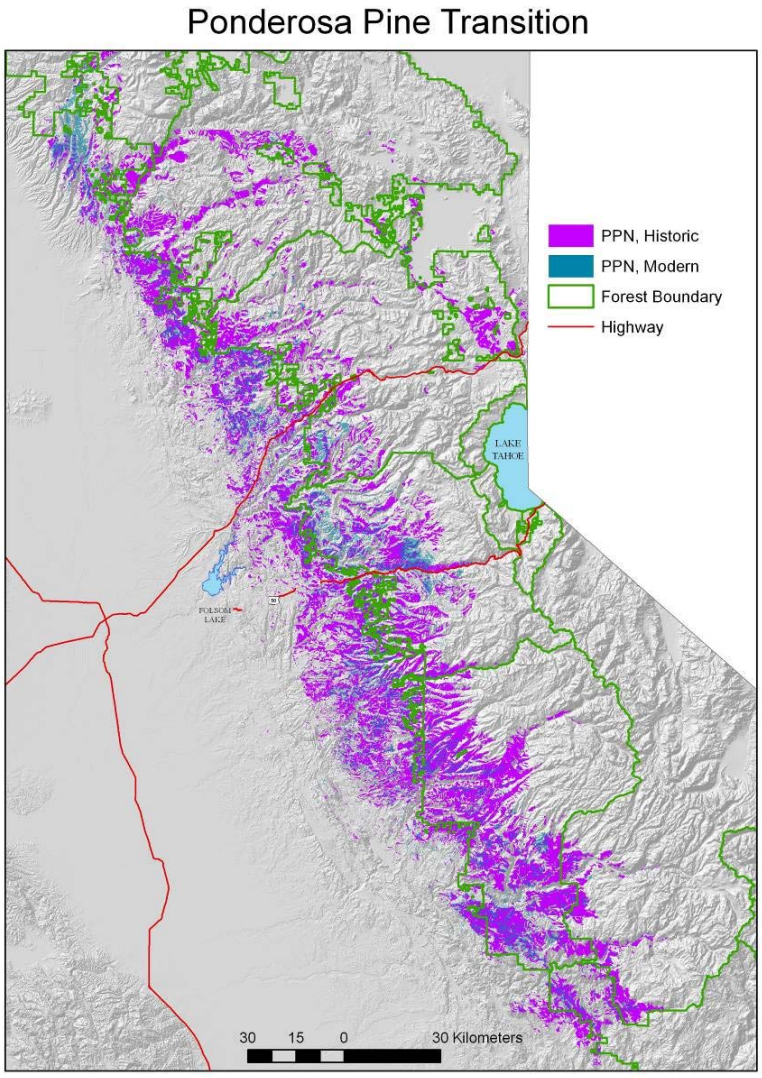


Figure 9. Upslope retraction of ponderosa pine-dominated woodlands between 1930s and 1996.Note also the downslope retraction of the upper edge, related to fire suppression which provides competitive advantage to Douglas fir and white fir over ponderosa.

PPN Source: Thorne, 2008.

Sierra Nevada warming had already been documented by other scientists and was confirmed by Thorne et al. (2006), who found an increase in monthly minimum temperatures in the middle-elevation Sierra Nevada Mountains over the past 100 years by about 5.4 ºF. In the 1930s, the coldest months still registered with their minimum temperatures below freezing (Figure 10). While unlikely to be responsible for the death of mature pines, which were harvested, the higher temperatures correlate with longer summer drought conditions, which in turn increase drought stress on seedlings. "Drought stress–driven mortality of seedlings following stand removal is the suspected driver of the diminishing range of the Ponderosa Pine Forest" (Thorne

et al., 2006, p.3). Corroborating evidence came from the fact that areas potentially affected by other factors such as fire, urbanization, and areas that had converted to grassland with competitive nonnative grasses and pressure from cattle grazing, were removed from the analysis. About 58% of the area had not been affected by these confounding factors, thus suggesting strongly that anthropogenic climate was the key driver behind the observed eastern and upward retreat of ponderosa pine.

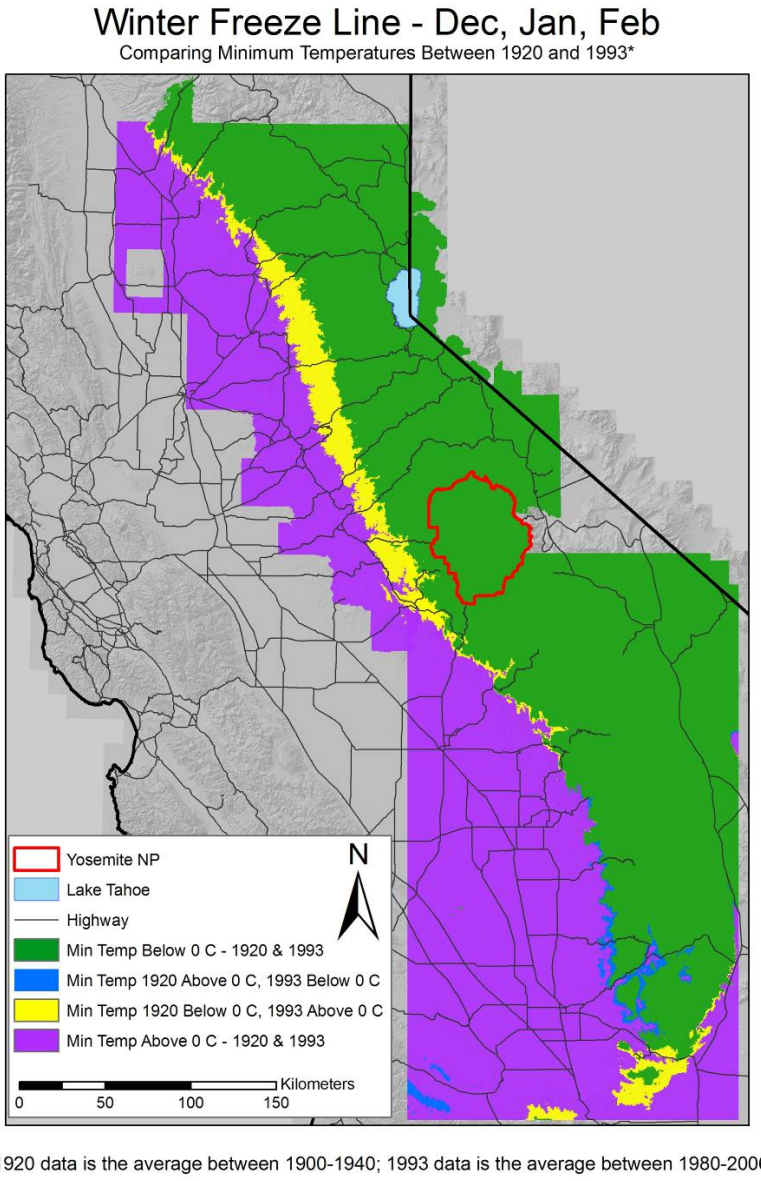


Figure 10. Change in nighttime frozen areas during the winter quarter, from 1920 to 1993. The yellow sections of the map represent areas that are now no longer frozen at night.
Source: Thorne, 2008.

2.8. Increasing Wildfire Frequency

In recent years, wildfires have increased in frequency, duration and size. The forested area burned in the western United States from 1987 to 2003 is 6.7 times the area burned from 1970 to 1986 (Westerling et al., 2006). Land management is often blamed for the increase in wildfire frequency. A century of fire suppression has lead to increased forest densities and accumulation of fuel wood that can result in more severe fires when this excess buildup of fuel is ignited. Yet climate also plays an important role: Warmer temperatures and longer dry seasons are the main reasons for the increasing trend in forest wildfire risk (Westerling et al., 2006). Reduced winter precipitation and early spring snowmelt deplete the moisture in soils and vegetation, leading to longer growing seasons and drought. These increasingly dry conditions provide more favorable conditions for ignition. In addition, higher temperatures increase evaporative water loss from vegetation, increasing the risk of rapidly spreading and large fires. In the last three decades the wildfire season in the western United States has increased by 78 days, and burn durations of fires >1000 ha in area have increased from 7.5 to 37.1 days, in response to a spring-summer warming of 33.6°F (Westerling 2006). Forests at mid-elevations are at a greater risk for wildfire than lower or higher elevational bands. At high elevations the conditions are less favorable for wildfires because even if the dry season is longer, it is still relatively short and is more protected from the drying effects of the higher temperatures.

2.9. The Warming of Lake Tahoe

The waters of Lake Tahoe are warming at almost twice the rate of the world's oceans (Coats et al., 2006). Analysis of a 33-year data set of more than 7,300 measurements of lake-water temperature collected found that from 1969 to 2002, Lake Tahoe's water temperature increased, on average, 0.027°F per year. Over the 33-year period, the temperature increased about 0.88°F. This is similar to warming reported in other big lakes around the world, including the Great Lakes of North America; Lake Zurich, Switzerland; and Lake Tanganyika, Africa. Tahoe water temperature records are comparable to Tahoe air-temperature records. Nighttime air temperatures rose 3.6°F over the period 1914–2002. The warming of air temperatures is sufficient to account for most of the increase in water temperature.

The lake water warming rate varies with depth. The warming rate is highest at 0 and 38 feet, decreases at depths of 65.6 and 98.4 feet, and increases again at 164 feet. The upward trend in lake temperature is modifying the thermal structure of the lake, and increasing its resistance to stratification and remixing. The continual mixing of lake water is an essential phenomenon that provides oxygen to the deep waters. The most significant effects on the lake ecosystem with continued warming trends will most likely be associated with the increased thermal stability and resistance to mixing (Coats et al., 2006).

2.10. Increasing Rate of Sea-Level Rise

Review of Sea-Level Changes
• Global average sea level rose at an average rate of 0.07 inches per year from 1961 to 2003 • The rate of sea-level rise has accelerated to an average rate of 0.12 inches per year over the decade from 1993-2003 • The combination of higher sea levels and larger precipitation events has increased the frequency of extreme tidal events in the San Joaquin Delta

Sea level has been rising globally since the end of the last glaciation more than 10,000 years ago. Global average sea level rose at an average rate of 0.07 inches per year from 1961 to 2003 and at an accelerated average rate of about 0.12 inches per year during the last decade of this period (1993 to 2003) (IPCC 2007).

Global sea-level rise is primarily the result of thermal expansion of the ocean water (water expands as it heats up) and the melting of land-based ice (which adds water to the ocean basins). These two contributors account for most, but not all of, the observed sea-level rise. For the recent period 1993 to 2003 the small discrepancy between observed sea level rise and the sum of known contributions might be due to as-yet-unquantified human induced processes (for example, groundwater extraction, impoundment in reservoirs, wetland drainage and deforestation) (Bindoff et al., 2007).

Sea-level rise is already affecting much of California's coastal region, including the Southern California coast, the Central California open coast, and the San Francisco Bay and upper estuary. Figure 11 shows relative sea-level height for a north and a south coast tide gauge station in California. During the past century, sea levels along California's coast have risen about seven inches. The rate of sea-level rise observed at the gauges along the California coast is similar to the estimate for global mean sea level.

Bromirski and Flick (submitted) demonstrated that extreme sea-level events in the ocean near San Francisco propagate to the Sacramento/San Joaquin Delta. For this reason, extreme sea-level events (also known as "surge events") observed at San Francisco are associated with extremes within the Delta. According to these authors, since the 1950s, extreme sea water level events have become more frequent in the ocean close to San Francisco. This upward trend in extreme sea-level events "underscores the potential impact of sea level rise on the Delta levees and Bay/Delta ecosystem, and also suggests an increased risk of saltwater intrusion into coastal aquifers." (Bromirski and Flick, submitted). In addition, in the historical record, extremes in storm surge and floods due to high runoff levels in California rivers coincide very frequently. During such instances, the risk of levee failure is enhanced (Bromirski and Flick, submitted).

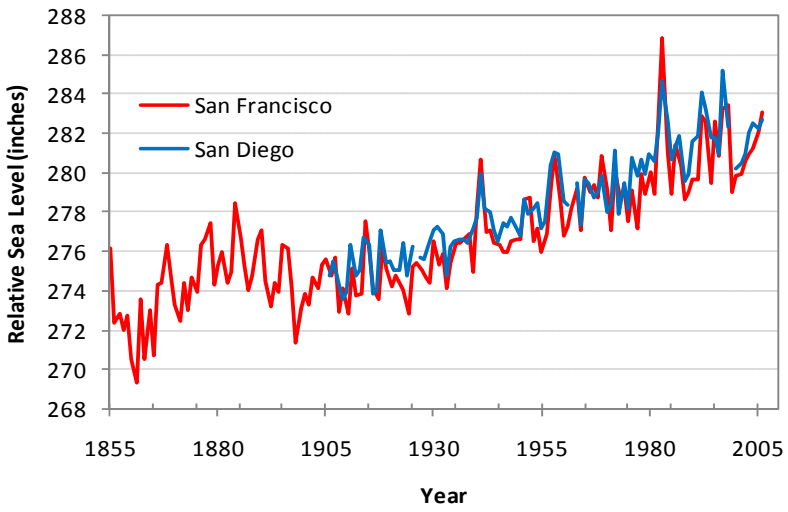


Figure 11. Historical sea-level rise for San Francisco and San Diego.
Data Source: NOAA, 2008[2].

2.11. Conclusions

In this section, the authors have provided examples of recent research that documents observed changes in California's regional climate, as well as climate-driven changes in physical and biological, both natural and managed, systems. Two conclusions emerge from these studies: first, the impacts of climate change, often still perceived as problems that might manifest in the distant future and in distant places, are actually evident in California at this time. Second, with only a relatively small temperature increase over the past few decades, the magnitude of impacts on physical and ecological systems is surprisingly large, especially for essential resources such as snowpack and water supplies. Moreover, in the last few decades, these changes have begun to accelerate. As the next section will document, there is now overwhelming evidence that the observed climate changes are driven by human activities. Even if these activities could be curtailed dramatically, climatic and related environmental changes would continue to impact California for the foreseeable future. This conclusion alone suggests that California will need to pursue a two-pronged approach to managing its climate change risks—the ones already evident and those coming in the future, and the authors will return to this issue in Section 4. Below, the authors provide evidence for the clear human influence on changes in the global and regional climate.

[2] http://tidesandcurrents.noaa.gov/sltrends/sltrends.html

3.0 Detecting the Human Fingerprint on Our Changing Climate: The Scientific Verdict Is In

Over the course of four IPCC assessment reports from 1990 to 2007, the conclusions regarding whether human activities can be held responsible for the changes observed in global and regional climates have become stronger. While the IPCC's first assessment could only state that the observational evidence was insufficient to either clearly detect or deny a human influence on the global climate (IPCC, 1990), in its most recent assessment, the IPCC essentially eradicated any remaining doubt over human responsibility for the observed impacts over the last half of the 20th century (Figure 12; Solomon et al., 2007).

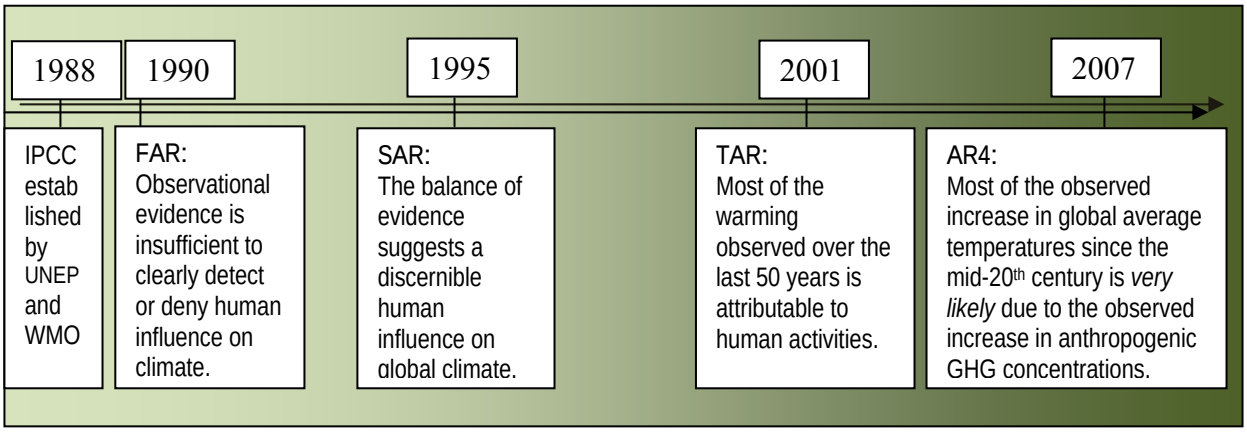


Figure 12. Growing scientific confidence regarding human contribution to climate change. Since the founding of the Intergovernmental Panel on Climate Change in 1988, the scientific community has conducted four global climate change assessments. Each time, the conclusions regarding human attribution became stronger. In its latest assessment, the IPCC concluded with a greater than 90% likelihood that human use of fossil fuels, land use changes, and agriculture have caused most of the changes observed since the middle of the 20th century.

It clearly showed that the steep increase over the past 250 years in emissions and atmospheric concentrations of carbon dioxide, methane, and nitrous oxide, along with several other powerful heat-trapping gases, was primarily due to fossil fuel use, land use changes and agriculture (see also Appendix 1). Moreover, considering all types of emissions (gases and aerosols) and activities, the IPCC stated with very high confidence[3] that "the global average net effect of human activities since 1750 has been one of warming" (IPCC, 2007, p.3). Greenhouse gas concentrations alone would have warmed temperatures even more were it not for the cooling effect of certain natural and anthropogenic (that is, from human sources, such as aerosols) that reflect solar radiation back to space. Agricultural irrigation in different parts of the world may have also reduced some regional warming (Lobell, 2006). Based on longer and

[3] "Very high confidence" means that there is a 9 out of 10 chance that the scientific judgment is correct.

improved data records, an expanded range of observations, improved simulations of many aspects of the climate and new attribution studies, the IPCC arrived at its strongest conclusion yet regarding the "human fingerprint" on the global climate when it stated,

"Most of the observed increase in global average temperatures since the mid-20th century is very likely[4] due to the observed increase in anthropogenic greenhouse gas concentrations. […] Discernible human influences now extend to other aspects of climate, including ocean warming, continental-average temperatures, temperature extremes and wind patterns." (IPCC, 2007, 10)

How have scientists come to such a strong conclusion about human causation, that is, how can observed changes be attributed to human as opposed to natural causes? This section provides evidence from studies of global and—to the extent possible—regional (including Californian) climate and other environmental variables that show a clear human influence.

3.1. Human Attribution Studies: How IS IT Known?

The process of understanding the causes and impacts of climate variability and change involves, first, the detection of change, and second, the attribution of that change to a particular cause or set of causes. Both are challenging, and a variety of methods and data sets are typically used to determine connections between cause and effect (Appendix 1).

3.2. Detection

The task of detection is to discern a real trend in any climatic variable away from a long-term average that is, showing with statistical significance that the observed change is indeed a notable deviation from the long-term average (Houghton et al., 1996, pp.4-5). Given the "noise" of natural variability in climate observations (or computer simulations), detecting a real change often requires longer data records[5], and confidence grows typically with the length of the records. If an observed change or trend is larger than internal variability alone is likely to produce by chance, that change is said to be "detected" (Hegerl et al., 2007, p.667).

3.3. Attribution

By contrast, the task of attribution is to establish the most likely cause(s) of the observed change or trend, typically by testing alternative explanations for example, the observed trend is due to

[4] "Very likely" indicates a greater than 90% likelihood of an outcome or result occurring, based on expert judgment.

[5] In modern climate studies, it is common to use a baseline of 30 years, for example, 1961-1990 or 1971-2000, and determine the average value of the variable of interest.

natural vs. anthropogenic forcings[6], or drivers of climate change). Unequivocal attribution to a cause would only be possible in a completely controlled experiment. Since this is impossible, scientists instead use model-based climate simulations as "laboratories" to test alternative explanations. Attribution then, in practical terms, means that scientists test two principal hypotheses:

- An observed change is consistent with the estimated or expected response of the climate system to the actual combination of natural and anthropogenic forcing.
- An observed change is inconsistent with an alternative, physically plausible (but not actually realized) climate change as a result of a different set of forcings.

If an observed change meets both criteria, and especially if multiple observed changes withstand this type of testing, confidence in the causal linkage between a forcing or combination of forcings increases (Hegerl et al., 2007, p.668). In some cases (such as global temperature change), such attribution studies can be done quantitatively, using computer simulations and illustrating statistical significance. In other cases, the human fingerprint on observed trends is not yet apparent, that is, statistically significant, and scientific confidence lower, though the observed change may still be physically consistent with expected change and therefore important (see Appendix 1 for more detail).

[6] "Forcing" is formally defined as the change in net (downward minus upward) irradiance (in W/m^2) at the tropopause due to an external driver of climate change such as carbon dioxide concentration (Forster et al., 2007: p.133).

3.4. Evidence of Human Influence on Global and Continental Climate

In general, scientific confidence in detection and attribution is higher the more closely causally linked a climate variable is to radiative forcing, that is, temperature changes are more directly linked than precipitation changes to radiative changes, although latitudinal changes in average precipitation have now also been detected and attributed to human causation (Zhang et al., 2007)). Confidence also tends to be stronger for larger (global and continental) than for smaller (regional and local) scales, because more sampling data available over large regions raises the signal-to-noise ratio, that is, improves our ability to detect a trend ("signal") out from natural variability ("noise").

The strong overall conclusion of human contribution to climatic changes observed since the middle of the 20th century thus rests predominantly on global and continental fingerprints, with smaller-scale changes (such as those found for the western United States or California, see below) confirming and adding weight to the overall findings, but being associated with somewhat greater uncertainty.

Extreme Events: Acts of God or …?

One question many people have is whether any given individual extreme event such as a heat wave, a drought, a hurricane, or a record-breaking flood is the result of global warming. Differently put: are extreme events still purely "natural" (or, as some would have it, "acts of God") or are they caused by anthropogenic climate change, that is, by human emissions of greenhouse gases?

Stanford University scientist Stephen H. Schneider perhaps best captured the answer in this very complex area of research by saying, "Humans are loading the die." Human emissions of heat-trapping gases change the composition of the atmosphere, which increases average temperatures and affects temperature extremes. Climate models project—in general—more frequent abnormally hot days and nights and more heat waves with global warming. They also project that cold days and nights are very likely to become much less frequent, as will the number of days with below-zero temperatures. Sea surface temperatures will also increase, which are correlated with more intense hurricanes. Furthermore, "droughts are likely to become more frequent and severe in some regions as higher air temperatures increase the potential for evaporation. Over most regions, precipitation is likely to be less frequent but more intense, and precipitation extremes are very likely to increase," thereby increasing the risk of flooding (CCSP, 2008, p.81). In short, anthropogenic forcing is changing the climate such that the risk of many extreme events is increasing. But is it possible to say that any *single* extreme event is due to human influence on the climate? The simple answer at this time is: No.

One of the principal reasons is that extreme events have always occurred on Earth. They are part of any region's typical climate. While there is often a seasonality to when they happen, their exact timing, occurrence, and magnitude is very difficult to predict, and typically only on very short notice, for example, in snow-dominated regions, spring meltwater runoff combined with rainfall makes flooding more likely in later winter and spring; tropical storms are most common to affect the North American continent from June to November). Typically the more "extreme" an event is, the less common or frequent it is, hence even with a relatively long historical record, there may only be a relatively small number of events in the data base that researchers can use to understand and predict them. Extreme events, however, are typically caused by a combination of factors—some of which may be influenced by human forcings on the climate, others not. This is the second principal reason why it is impossible to say whether any individual event was caused by humans.

Figure 13 shows temperature changes over the last 100 years at global and continental scales, both as model-reproduced actual trends and modeled trends with and without human forcing. It is the signature illustration of how observed changes over the past 50-60 years cannot be explained without accounting for the human contribution to radiative forcing. This has led the IPCC to conclude that it is *extremely likely* (>95%) that anthropogenic temperature change has been detected and that it is *extremely unlikely* (<5%) that natural forces alone could have produced these changes.

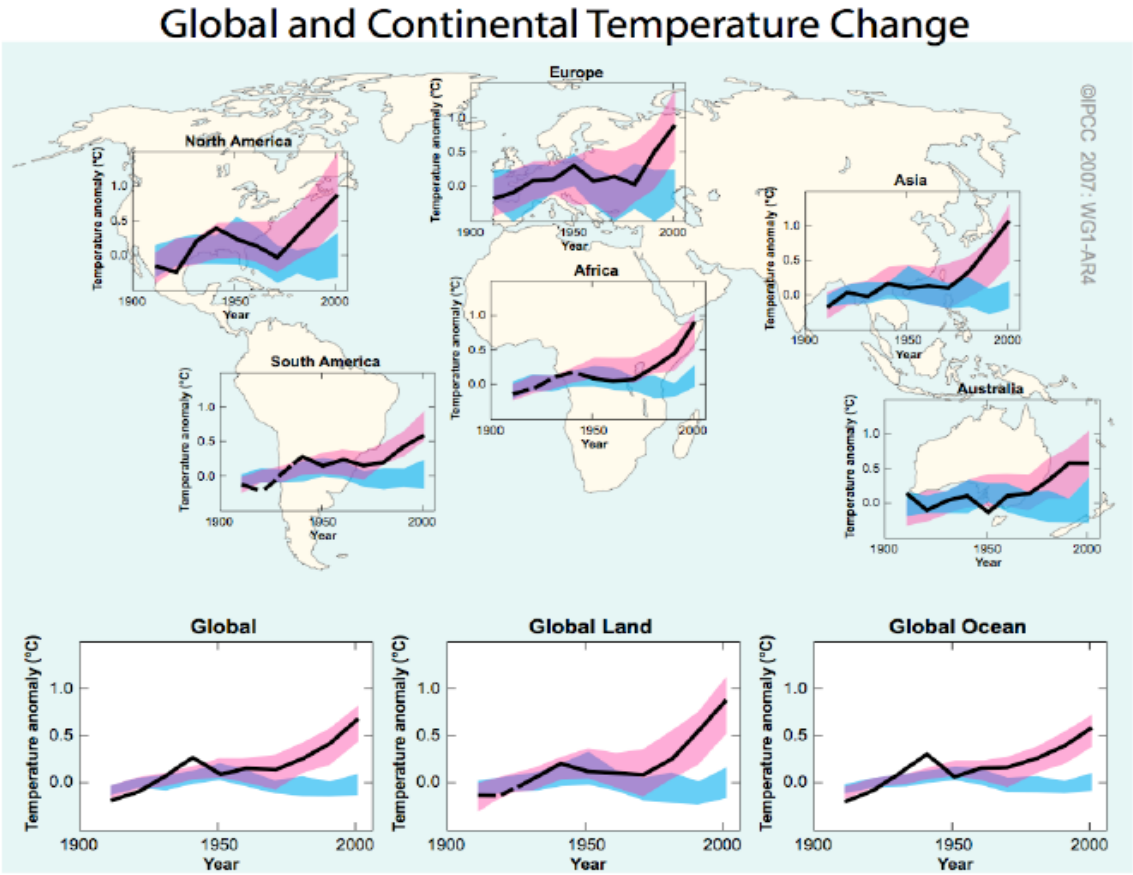


Figure 13: Global and continental temperature change. For each continent, simulated reproduction of observed temperatures are shown in black, modeled temperatures driven only by natural forcings in blue, and modeled temperatures driven by both natural and anthropogenic forcings in pink. For all but Antarctica (where the observational basis is too small), natural and anthropogenic forcings are needed to reproduce observed temperature changes over the past 100 years. The fit of modeled (pink) and observed (black) temperatures on global and continental scales increases over time as the anthropogenic forcing becomes ever more dominant.

Source: Solomon et al., 2007, p.11.

Figure 14 provides a simplified overview of additional observed climatic changes; the length of each bar corresponds to the estimated likelihood that the observed changes have been caused by human forcing (Hegerl et al., 2007, pp.729-732).

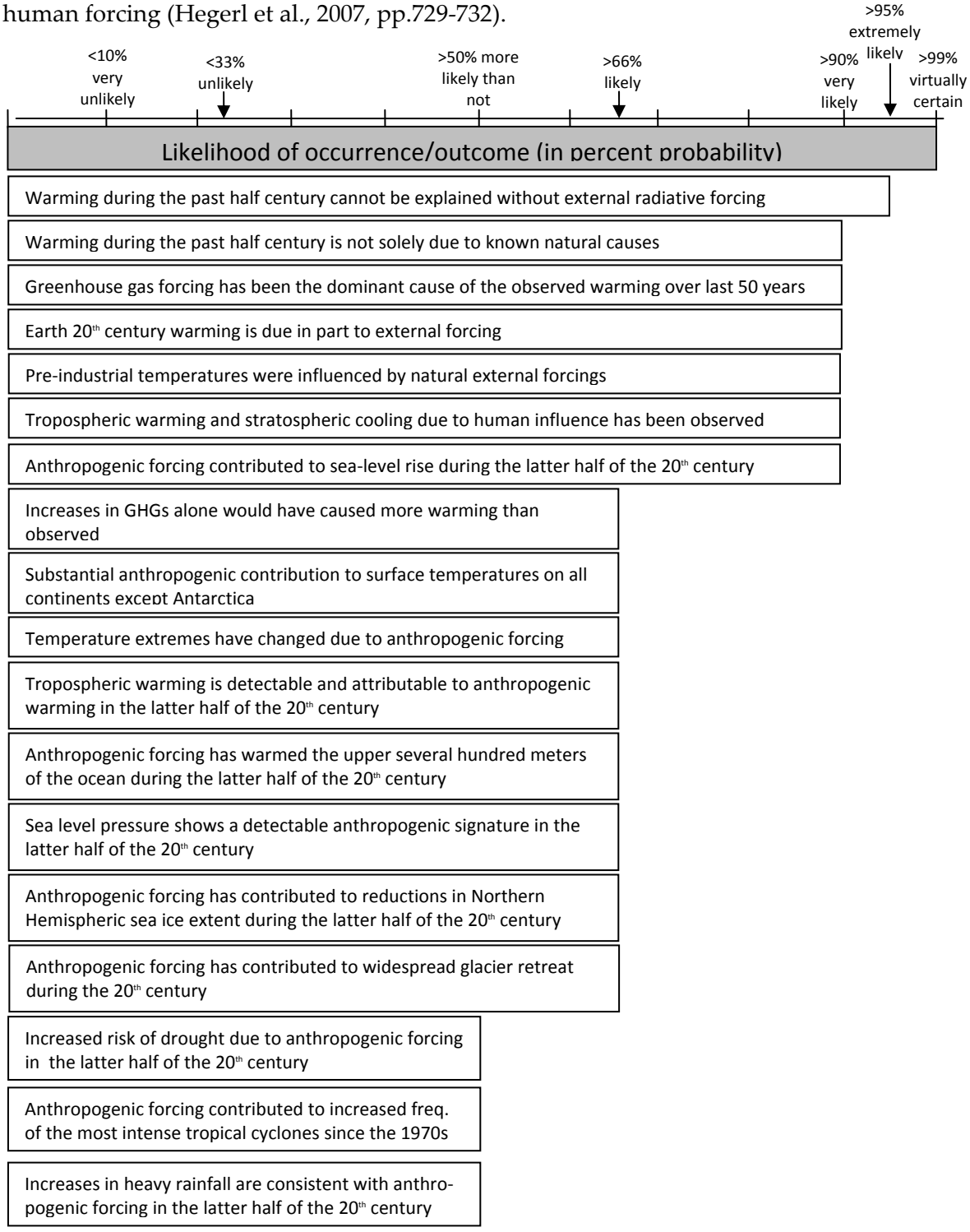


Figure 14: Selected detected climate changes attributable to human forcing likelihood of occurrence or outcome of each of the identified changes is given in standard IPCC language and probabilities. Some changes are detected at global scales, others at continental scales.

Source: Based on information provided by Hegerl et al., 2007, pp.729-732.

The scale at which these changes have been detected range from global to hemispheric to continental. Many additional ones, such as the declining number of frost days, increasing temperatures of extreme hot nights, cold nights and cold days, the increased risk of heat waves, wind pattern changes that affect extratropical storm tracks and temperature patterns in both hemispheres, shifts in precipitation patterns over land, and changes in the extent and quality of snow have been observed and are consistent with the changes noted in Figure 12.

In addition to the geophysical changes in climate discussed above, the IPCC's Working Group II also assessed climate change-driven ecological and societal impacts. It concluded that

> "A global assessment of data since 1970 has shown it is likely [66-90% probability] that anthropogenic warming has had a discernible influence on many physical and biological systems." (Parry et al., 2007, p.9)

Limited data sets from relatively few systems and locations are an important reason for the more tentative tone in this conclusion. Attribution studies of impacts observed in physical and biological systems also have to contend with relatively greater climate variability at regional and local scales, and the concurrent non-climatic influences such as land use change, pollution, and invasive species. Until recently, scientists expressed nonetheless high confidence that anthropogenic warming of the last few decades has discernibly influenced a wide range of systems (Rosenzweig et al., 2007). More recently, a global study explicitly tested for the first time whether observed physical and ecological changes can be attributed to human forcing. It came to a stronger conclusion, stating that "anthropogenic climate change is having a significant impact on physical and biological systems globally and in some continents" (Rosenzweig et al., 2008, p.353, emphasis added).

Scientists have detected changes in numerous physical and ecological systems and are beginning to identify impacts in human systems as well. These higher order impacts are more difficult to detect and attribute to anthropogenic climate change. In particular in systems managed by humans (such as agriculture, water resources, forestry) or directly impacting humans (such as human health, tourism and recreation), efforts undertaken to cope with extremes and variability or adapt to longer-term change may mask the direct impact that climate change and related physical and ecological responses may have. Table 1 (based on Rosenzweig et al., 2007) lists the most important observed changes that are largely driven by anthropogenic climate change (see Appendix 1 for more detail on each of these observed changes).

Table 1: Observed changes in physical, biological and managed or human systems in response to anthropogenic climate warming

Changes in Physical Systems	• *Arctic sea ice* extent is continuing to decline • *Mountain glaciers* are receding on all continents, at high and low latitudes • *Land-based ice caps* are melting at increasing rates • *Northern Hemisphere permafrost* is thawing • Extent of *snow cover in the Northern Hemisphere* is decreasing, especially at lower elevations • Annual duration of *lake and river ice cover* in the mid- and high latitudes of the Northern Hemisphere has been shortened and become more variable • Changes in *surface and groundwater* in many systems, but uniform global trends are not detectable due to complex influences on water systems • In snow-driven catchments, *earlier peak runoff* in spring • Some evidence of *the most catastrophic floods increasing in frequency* • In some regions *more severe droughts and more heavy rainfall events* • *Increased rate of global sea-level rise*, greater rates and extent of coastal erosion, wetland loss, and increases in wave height, storm surges, and inland flooding extent. • Overall, *extension of the growing season* by up to two weeks in the latter half of the 20th century
Changes in Biological Systems	• *Terrestrial plant and animal ranges* are shifting poleward and to higher elevations • Similar observations in *marine ecosystems* in response to warmer water and sea surface temperatures, stratification, changes in salinity and upwelling • Within the ranges of some terrestrial and marine species, *populations* are increasing in some areas and declining in others • Many *phenological life cycle events* (e.g., blooming, migration, insect emergence, leaf unfolding, coloring and fall, fruit ripening, breeding) are occurring earlier in spring and/or later in fall • *Species interactions* are becoming decoupled from each other as individual species react differently to warming • *Productivity (or biomass) increases* due to warmer temperatures, a longer growing season, and higher CO_2 levels • Climate change driven range contraction, loss of suitable habitat, favorable conditions for invasive competitors, or spread of deadly diseases has contributed to *local extirpation and global extinction of some species.*
Changes in Managed and Human Systems	• Changing *energy demand* for cooling and heating, with summer increases in peak demand typically more pronounced • Some evidence for *shifts in skiing and winter recreation*; otherwise still difficult to detect the impact of climate change in tourism and outdoor recreation • *Widespread adaptive responses in agriculture* such as crop switching, later sowing dates, diversification of livelihoods, tree planting, cooling and irrigation technology changes • *Northward shift of some disease vectors* and *changes in the seasonal pattern of allergens*, but no documented increase in incidence of climate-driven human health problems, except for *excess heat-related mortality* • When normalized by population and growth in overall wealth, *no significant upward trend* had been identified *in economic losses from floods and storms*.[7]

[7] Normalization by population and economic growth does not account for all changes that have occurred over time in risk-prone areas. Other changes, for example, in building codes, emergency response, warning systems, land use and so on also affect what is at risk and how much. Currently there is no universally accepted approach to normalization (see discussion in CCSP (2008).

Considering the available global data base of all the physical and biological changes observed, Rosenzweig et al. (2007) found that 94% of statistically significant observed changes in physical systems, and 90% of significant observed changes in biological systems are consistent with the warming trend observed in the regions in which they occurred.

3.5. Evidence of Human Influence on Western United States and California's Climate

It is more difficult at smaller-than-continental scales and for observational records of less than 50 years to reliably simulate and attribute observed temperature changes and related impacts. At these smaller scales, climate variability is relatively larger and the distinction of natural and anthropogenic forcing of climate is more challenging. Non-climatic processes such as land-use change, human management practices, pollution, population growth and urbanization, and other anthropogenic factors interact with climatic changes to produce the observed changes. The added complexity at these smaller scales, however, helps improve our understanding of causal links, and climatic and ecological changes observed locally add to the overall global picture described above. And as Rosenzweig et al. (2007, p.115) observe, "[T]hese [human] factors are very unlikely to explain the coherent response that has been found across the diverse range of systems and across the broad geographical regions considered."

Observed temperature extremes over North America., including in the Western United States, have clearly been attributed to human influence, as have been the increases in extreme precipitation events (via the greenhouse gas-induced increases in atmospheric water content) (CCSP, 2008, pp.81-116; Burkholder and Karoly, 2007). More specifically, there are a number of new regional climate change detection and attribution studies (beyond those previously cited in *Our Changing Climate* (California Climate Change Center, 2006) that are of high relevance for the Western United States and California. These illustrate—even at the regional and local level—the overall consistency with the global picture: temperature increases and related climate changes are affecting natural systems in the expected direction.

As described above, it is essential both for a reliable projection of future climate and for the design of appropriate response options to accurately characterize (detection) current climate trends above and beyond natural variability (caused, for example, by El Niño or the Pacific Decadal Oscillation), and to understand what forces caused these changes (attribution). Below the authors highlight several studies that are relevant to California, the first two of which are considered detection studies, while the latter two constitute attribution studies.

3.6. Detection Study 1: Warming Over the Sierra Nevada and Retreat of the Ponderosa Pine Forest

The Wieslander data set spanning the period 1934 to 1996 has provided critical documentation of vegetation-range changes in the Sierra Nevada Mountains. Sierra Nevada warming had already been documented by other scientists and was confirmed by Thorne et al. (2006), who found an increase in monthly minimum temperatures in the middle-elevation Sierra Nevada over the past 100 years by about 3°C (5.4°F). In the 1930s, the coldest months still registered with their minimum temperatures below freezing. While unlikely to be responsible for the death of mature pines, which were harvested, the higher temperatures correlate with longer summer drought conditions, which in turn increase drought stress on seedlings. "Drought stress–driven mortality of seedlings following stand removal is the suspected driver of the diminishing range of the Ponderosa Pine Forest" (Thorne et al., 2006, p.3). Corroborating evidence came from the fact that areas potentially affected by other factors such as fire, urbanization, and areas that had converted to grassland with competitive non-native grasses and pressure from cattle grazing, were removed from the analysis. About 58% of the area had not been affected by these confounding factors, suggesting strongly that anthropogenic climate was the key driver behind the observed eastern and upward retreat of ponderosa pine.

3.7. Detection Study 2: Migratory Songbirds in California

California is home to dozens of migratory bird species and throughway for millions of birds along the Pacific Flyway. For these birds, "Time is of the essence […]: it is critical for departures with favorable weather conditions, intersecting adequate resources to fuel further flight, and for spring migrants, ensuring that arrival on the breeding grounds is coincident with the flush of spring insects to feed offspring" (MacMynowsky and Root, 2007, p. 1). Importantly, to obtain a comprehensive picture of the vulnerability of migratory birds to climate change, species responses to shifts in climate should be studied in all destination regions that the birds cover over the course of an annual migratory cycle. However, even significant changes in any of the critical habitats along the migratory route can disrupt the life cycle of the species and affect its reproductive success.

In a study analyzing spring and fall phenology of migratory songbirds moving through Central and Northern California, MacMynowski and Root (2007) found that all those species that are sensitive to changes in climate (so-called"climate associates") changed their migratory arrival in spring (most of them now come earlier), whereas none of the species that are insensitive to changes in climate shifted their arrival dates. They found that climate-sensitive migratory birds tend to arrive earlier in spring in association with warmer local temperatures, positive NAO indices, and stronger ENSO indices. Fall phenological changes were also apparent, with a majority of climate associates arriving earlier, but a statistically significant correlation with

regional climate warming was not detected. The analysis of data from multiple sites, correlated with climate data from multiple scales, and using multiple indices of migratory behavior, however, adds more "evidence that changes in western North American land ecosystems are already detectable with warming of less than a degree Celsius over the past century" (MacMynowski and Root, 2007, p.2).

3.8. Attribution Study 1: Human-Caused Warming Over California

A number of external factors influence California's climate including solar variability, volcanic eruptions, aerosols, greenhouse gases released from human activities, and land-use changes (especially urbanization and irrigation). Bonfils and colleagues (2007,2008) used eight observational data sets to estimate temperature trends during the last five decades of the 20th century (1950–1999) and over a longer period (1914–1999).

Bonfils et al. (2007, 2008) noted, first of all, that trends among these different datasets were quite consistent, giving confidence that the trends are not simply artifacts of location or measurement. The researchers then compared these observed data trends to trends from a suite of control simulations of natural climate variability alone (without additional external forcing). These comparisons showed for most data sets that the observed increases in annual mean surface temperature were outside the "noise" of natural variability. "The most robust results are large positive trends in mean and maximum daily temperatures in late winter/early spring, as well as increases in minimum daily temperatures from January to September. These trends are inconsistent with model-based estimates of natural internal climate variability, and thus cannot be explained without invoking one or more external forcing agents" (Bonfils et al., 2007, p.2). In particular, warming of California's winters over the second half of the 20th century is associated with human-induced changes in large-scale atmospheric circulation, whereas the lack of a detectable increase in summertime maximum temperature arises from a cooling associated with large-scale irrigation, particularly in the Central Valley (Bonfils et al., 2008). This cooling may have counteracted the warming induced by increasing greenhouse gases and urbanization effects lowering summertime average daily daytime temperatures by as much as –0.14°C to –0.25°C (-.252 to -.45°F) per decade for an estimated total of –1.8°C to –3.2°C (-3.24 to -5.76°F) cooling since the introduction of widespread irrigation (Bonfils and Lobell, 2007). To the extent irrigated areas are not further expanded or may shrink in the future, this cooling effect may be increasingly overpowered by global warming (Bonfils and Lobell, 2007; see also Kueppers et al., 2007; Weare and Du, 2007).

3.9. Attribution Study 2: Changes in the Hydrological Cycle in the Western United States

Previous studies already documented significant shifts in the hydrological cycle over the Western United States, including more winter precipitation falling as rain rather than as snow, the snow line retreating upward, earlier snow melt and associated increases in spring and

decreases in summer river flow. One recent study went beyond these well established findings to demonstrate with statistical significance, "that the majority of the observed low-frequency changes in the hydrological cycle (river flow, temperature, and snow pack) over the western United States from 1950 to 1999 are due to human caused climate changes from greenhouse gases and aerosols" (Barnett et al., 2008, p.1080). Using a high-resolution hydrologic model with climate inputs derived from several global climate models, the researchers showed that "up to 60% using the model with the best ability to reproduce regional climate of the climate-related trends of river flow, winter air temperature, and snow pack between 1950 and 1999 are human-induced" (ibid.). These results were robust across climate models and using different hydrological variables and methods.

3.10. Conclusions

Evidence for long-term climatic changes and related responses in physical and ecological systems above and beyond the "noise" of natural variability is now available from every continent. Scientists' ability to attribute these observed changes to anthropogenic forcing by greenhouse gas emissions and aerosols is increasing steadily. While end-to-end models that relate ecological changes directly to human causes are not yet available (Zwiers and Hegerl, 2008), the indirect attribution of ecological changes to climatic changes and these, in turn, to greenhouse gas emissions has led to the strong conclusion that most of the climatic changes observed over the latter half of the 20th century are due to human activities and that many related physical and ecological responses bear clear evidence of human influence—at local to global scales.

This conclusion challenges the fundamental belief held still by many that human actions are too small to exert a global influence on the Earth's life support systems. While adjusting basic assumptions to the facts of the matter, and recognizing that many of the observed changes are predominantly negative for the systems involved, Californians must realize what the world might look like if the human imprint on its climate and natural and managed ecosystems were not rapidly minimized. The potential impacts of climate change without concerted efforts to reduce anthropogenic emissions and land use changes are discussed in the next section.

4.0 Projected Impacts of Climate Change in California Updating "Our Changing Climate": What More Have Californian's Learned?

In July 2006, the California Climate Change Center (CCCC) published a non-technical document called *Our Changing Climate: Assessing the Risks to California*, (California Climate Change Center, 2006) representing the culmination of a major research effort by the CCCC[8] (Cayan et al., 2008a). This outreach publication summarized the latest "state of the science" on the climate change impacts facing California over the next century. Today, as climate change research continues to move forward, new details can be added toward understanding how California's environment, economy, and societal well-being will be affected by climate change. The following section provides, sector by sector, a brief encapsulated review of the existing knowledge on future impacts, taken largely from *Our Changing Climate*, then presents and interprets research findings that have emerged since 2006. The newest findings reinforce the idea that climate change will have significant impacts for both the natural and managed systems on which California depends.

[8] The "2006 Scenarios Report" involved a series of assessments conducted over the course of two years. According to Executive Order S-E-05, such assessments are to be produced every two years. *Our Changing Climate* was preceded by another technical document comprehensively assessing climate change impacts on California (Hayhoe et al., 2004), which has been widely cited in the scientific community.

"Scenarios" Terminology

The Special Report on Emissions Scenarios (SRES) approach used by the Intergovernmental Panel on Climate Change (IPCC) acknowledges that future levels of carbon dioxide (CO_2) in the atmosphere will depend upon human activities. Policy and development outcomes will affect emissions from carbon-based fossil fuel burning and other human activities driving climate change. Importantly, the SRES scenarios do not assume *explicit* climate change or emission-reducing policies. Three scenarios are referenced in this section. One **lower-emissions scenario (called "B1")** projects future decreases in CO_2 concentrations following significant "decarbonization" of the economy. If CO_2 emissions continue unabated, **high emissions** ensue, under a scenario called "**A1fi**" (for fossil fuel-intensive). The **"A2"** scenario describes a **medium-high emissions** scenario (Figure 15). The impacts discussed below include some of these scenarios to frame the range of plausible futures. Three caveats should be noted. First, it is important to recognize differences between weather and climate; while weather occurs at a point in time, climate represents a longer time period. Even with sophisticated computer modeling, then, scenarios-based climate models are not intended to provide specific or detailed forecasts as one might request for tomorrow's temperature. Rather, they usually present a range of plausible futures and the impacts associated with each, based on our best available knowledge. Second, because of limitations in our scientific understanding and our imperfect ability to reproduce these complex interactions in computer models, the projections produced by the IPCC do not fully account for potential reinforcing feedbacks (e.g., the loss of sea ice over Greenland or Antarctica, and some unaccounted-for changes in the carbon cycle) as warming increases (IPCC 2007a). Third, when assessing future impacts resulting from climate change, modeling to date does not account for other societal pressures that may increase or decrease the ultimate severity of impacts. Multiple stressors including demographic changes, pollution, land use changes, political discord, and economic factors, are not included in these projections, but nevertheless will influence impacts. The descriptions of impacts below, then, must be considered an incomplete picture of the future, but one that emphasizes the climatic stresses different regions and economic sectors may experience under different emissions scenarios.

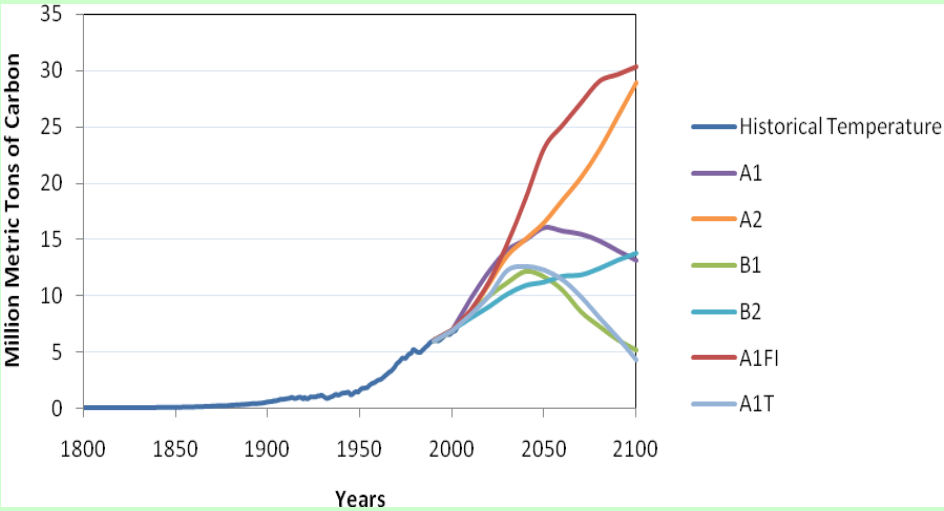


Figure 15. CO_2 emissions under three IPCC scenarios.

Data Source: Marland et al. 2008 and IPCC

In addition to the IPCC SRES scenarios, the authors present preliminary estimates for changes in temperature and sea-level rise over this century under a scenario that assumes the implementation of policies to limit global average temperature increase to less than 2°C (3.6°F) above pre-industrial temperatures (referred to as the "policy scenario" in this document). Since the atmosphere has already warmed by about 1.4 ºF, this scenario assumes that the additional warming in this century will not surpass 2.2 º F. The policy scenario is characterized by emission reductions in the industrialized nations of about 30 percent below 1990 levels by 2020, about 80 percent by 2050, and extremely low emissions by the end of this century[9] The policy scenario also assumes eventual reductions from the developing world so that overall global emissions by 2050 are reduced by 50 percent with more drastic reductions after 2050. This scenario is presented and discussed in a report prepared by the United Nations Development Programme (UNDP, 2008).

4.1. California's Warmer Future: Temperature Projections

Review of Temperature Impacts
• Increasing temperatures (between 3 and 5.5°F for B1, and between 8 and 10.5°F for A1fi)
• Some models predict more warming in the summer and less in the winter
• Warmer nights

As outlined in *Our Changing Climate*, hotter temperatures are expected throughout the state, with an increase of 3-5.5°F under the lower emissions scenario (B1) and 8-10.5°F under the higher emissions scenario (A1fi), and intermediate temperature increases under the A2 emissions scenario by the end of the century (average for the period 2070-2099) (Hayhoe et al., 2004).

Within the past year, carbon emissions accounting has revealed that emissions are rising more rapidly than those predicted by even the most "aggressive" scenario (A1fi) (Raupach et al., 2007). In future IPCC reports, scenarios such as A2 and A1fi will represent "middle-of-the-road" scenarios and new higher emissions scenarios will be used (Moss et al., 2007). Thus, future projections of temperature increases for the state are likely to increase (IPCC 2007a) if no global actions are adopted to reduce emissions.

Temperatures will vary locally and by the time of day. Urban areas can exacerbate the "heat island" effect, especially by raising nighttime temperatures. In areas like the Central Valley, for instance, future warming will be governed in part by future rates of irrigation (known to mask warming effects, see Chapter 2) (LaDochy, Medina, and Patzert, 2007). The Hadley Centre (U.K.) model (HadCM3) predicts greater summertime warming relative to wintertime warming, whereas one of the U.S. National Center for Atmospheric Research models (Parallel Climate Model) shows less seasonality of temperature increases (Hayhoe et al., 2004). Researchers report

[9] This document, titled *Human Development Report 2007/2008. Fighting Climate Change: Human Solidarity in a Divided World*, can be accessed at http://hdr.undp.org/en/reports/global/hdr2007-2008/

that, under climate change, nights (typically representing minimum temperatures) are projected to warm slightly more relative to daytime temperatures (Lobell et al., 2007).

Figure 16 presents preliminary projections of annual average temperature for California for the A2 and B1 global emission scenarios. The left portion of the graph also shows the observed temperatures in the last several decades as reported in Chapter 2. The main message from this figure is that lower emissions (B1) results in less warming at the end of this century than higher emissions would. Each global emission scenario is represented by a solid color line, which is the smoothed average of outputs from different climate models, all using the same emissions scenario (represented by the similarly colored lines underlying each of the ensemble averages). While, of course, there is only one realization of past temperatures (temperatures in the historical record), there are three estimated sets of temperatures each for the A2 and B1 scenarios. This is due to the fact that different climate models produce alternative views on how temperatures would evolve in the future.

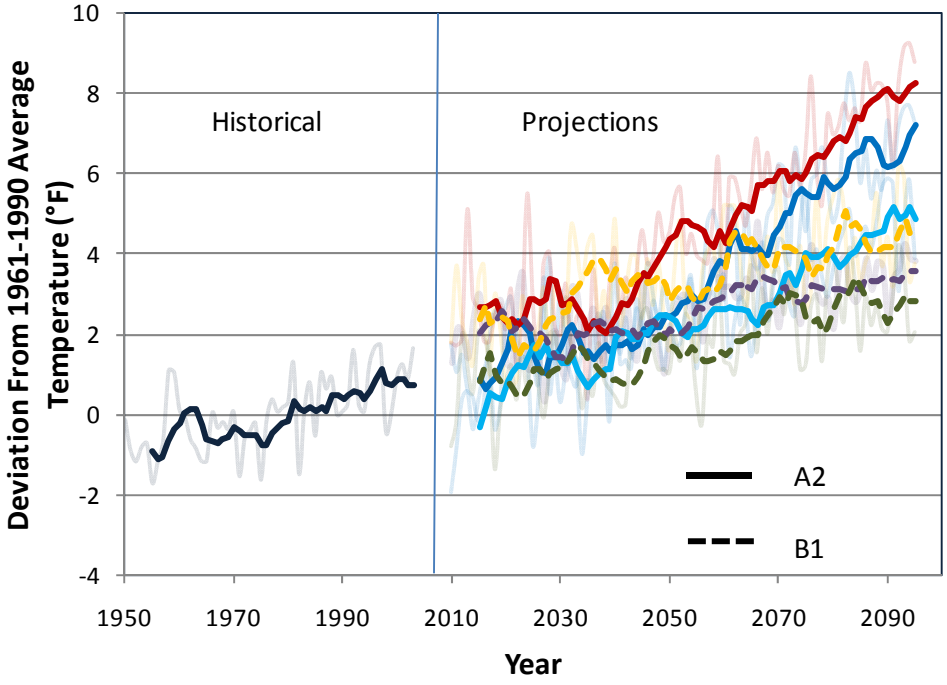


Figure 16. Historical and projected annual average temperatures for California. The soft lines represent annual average temperatures while the thick lines are the smoothed time series of annual average temperatures using 6-year running averages to more clearly detect overall trends. The projections for the A2 and B1 global emission scenarios are represented with solid and dashed lines, respectively.

Figure 17 shows changes in global average temperature around 2100 under the B1 and the "policy" scenarios. It is clear from this figure that even with a strong policy scenario, with global emissions lower than in the B1 scenario, temperatures might still rise dangerously high.

However, the risk of crossing dangerous temperature thresholds is lower in the policy case than in the B1 case.

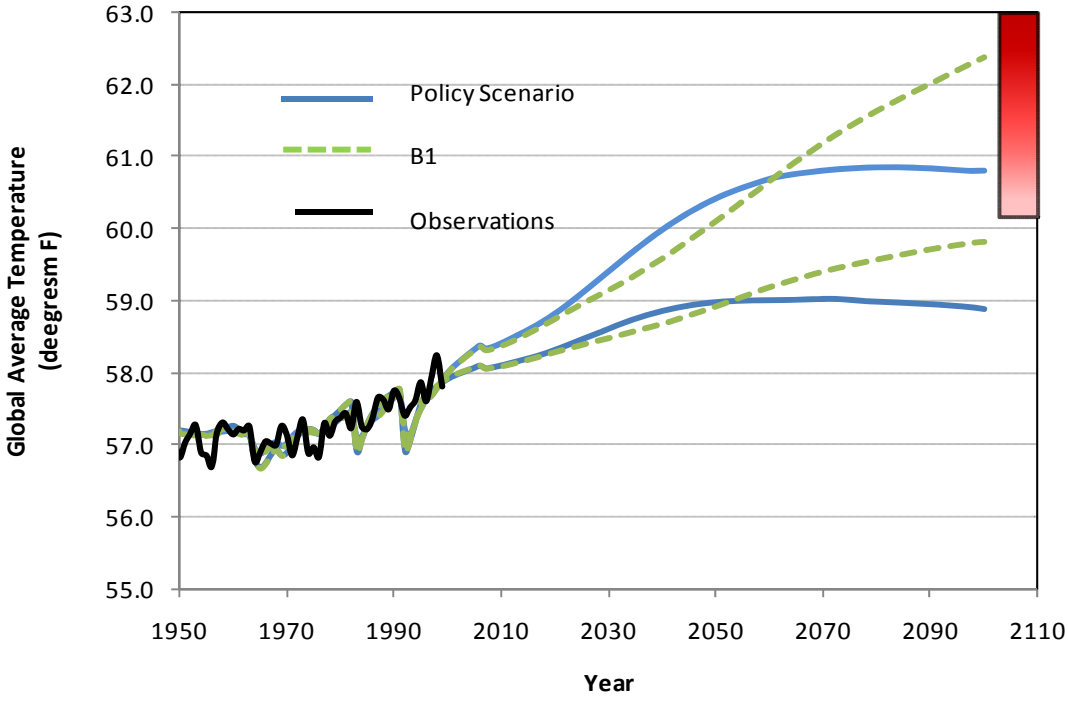


Figure 17. Global average temperature projections for 2100 for the B1 and "policy" scenarios at the end of this century.

Data Source: (Meinshausen et al., 2008 and personal communication)

4.2. Public Health: Stark Challenges for Vulnerable Populations

Review of Public Health Impacts
• Demographic shifts may lead to increased social vulnerability to stresses and shocks, including worsening climate extremes • Disproportionate suffering by the aged, the infirm, the socially isolated, racial minorities, low-income residents, and outdoor laborers • Increased transmission of mosquito-borne diseases such as West Nile Virus and encephalitis

As *Our Changing Climate* reported, the degree to which climate change impacts public health depends strongly on the groups experiencing the climate-related stress (English et al., 2007). One recent finding is that "social vulnerability"—a measure of how exposed to hazards and how well equipped society is to handle stresses and shocks—in California is predicted to increase in future decades due simply to demographic shifts (Cutter and Finch, 2008). A recent study of all counties in the United States concluded that counties in California's Central Valley, Orange County, and San Francisco were either currently rated (in 2000), or predicted to be (by 2010), among the highest in the country in social vulnerability, as measured by demographic factors such as socio-economic status, race, age, and gender. Social

vulnerability suggests the potential for greater harm to the affected public in the event of natural disasters, although the metric is used only comparatively (across localities) rather than in an absolute sense (Cutter and Finch, 2008). For the noted communities that are more vulnerable to natural hazards, the impacts of climate variability and extremes (e.g., droughts, heat events) will involve added societal burdens. Residents in the communities of concern may find it increasingly difficult to cope with climate-related stresses and may well require additional public resources or actions to prevent or alleviate potential harm.

4.3. Water Resources: Summertime Scarcity and Changes in Snowfall

Review of Water Resources Impacts
• Decreased snowpack by the end of the century (20 to 40% under different emissions scenarios) • Increased risk of winter flooding • Earlier timing of meltwater runoff and greater vulnerability to summer shortfalls • Decreased hydropower generation (under dry warming) • Decreased quality of winter recreation

Water resource management under a changing climate could emerge as California's greatest future challenge. Satisfying the water needs for the state's industrial, urban, agricultural, energy, and environmental uses will be harder for two reasons: the decreasing reliability of surface water storage (Jain et al., 2005, Medellín-Azuara et al., 2008, Vicuna et al., 2007) and anticipated population growth (PPIC, 2006). Ongoing modeling efforts are attempting to understand how the state can best manage flows under climate change (Anderson et al., 2008). A dry warming scenario, by a recent estimate, would raise statewide water scarcity and total operation costs by at least $500 million per year by 2085 (Medellín-Azuara et al., 2008). The actual costs may be two to three times higher because these authors assume perfect water markets and do not consider all the potential costs associated with climate change, such as flood protection or recovery costs in the event of floods.

California's management of groundwater will be critical in the next century because surface water supplies appear to be less able to accommodate the water needs of the state's growing population and economy. Currently about half of California's water supply for human consumption or use comes from groundwater (Franco, 2005). Questions researchers hope to answer in the near future include whether Central Valley growers can safely pump groundwater from aquifers to irrigate their crops (Purkey et al., 2004). Additionally, more information is needed regarding the reliability and management of groundwater recharge, i.e., the natural penetration of surface water to deeper storage layers underground. Groundwater recharge would be especially valuable if the greater winter flows expected under climate change could essentially be "banked" underground for later use (i.e., in times of water shortage) (Earman and Dettinger, 2008). Researchers at U.C. Davis and U.S. Geological Survey (USGS) are modeling groundwater behavior and dynamics under climate change (LaBolle et al., 2003,

Niswonger and Fogg, 2008). Ensuring proper protection of groundwater quality is also a high priority for future research.

California's prominent Sierra Nevada range controls some precipitation patterns such as higher rain totals on the windward side. In mountainous areas, certain rain effects, such as the quantity of aerosols in the air, are not yet well understood. Aerosols (e.g., soot and dust) are tiny airborne particles that travel in the air for days to weeks. Recent research has shown that these particles can inhibit cloud formation which typically occurs when air rises over mountains. In the presence of aerosols, fewer clouds form and less rain falls on the windward side of the Sierra, compared to pristine conditions (Rosenfeld and Gavati, 2006; Givati and Rosenfeld, 2004). Motivating this research is the idea that decreasing the pollution that produces aerosols might help mitigate the problem of reduced precipitation over the Sierra.

4.4. Increased Risks and Costs for Agriculture

Review of Agriculture Impacts
• Decreased productivity of almonds, cotton, and dairy products • Increased pest range and viability • Crop stress due to high temperatures, decreased chill hours reduces quality of cherries, almonds, apples, and walnuts • Irrigation water shortages; Greater evaporative demand by crops

California's agricultural yields are sensitive to climate and management practices. In addition, management practices are also likely to be influenced by changes in climate. Changes are expected for maximum and minimum temperatures, growing season length, chill hour accumulation for fruits and nuts (see Chapter 2), precipitation regime, and atmospheric CO_2 levels (CO_2 serves as a fertilizer to fuel growth). A recent study modeled one consequence of warmer temperatures, namely the projected decline in accumulated chill hours that leads to decreased fruit and nut quality[10] (Figure 18) (Baldocchi and Wong, 2008).

[10] This study used the National Oceanic and Atmospheric Administration (NOAA) Geophysical Fluid Dynamic Laboratory (GFDL) model (Stouffer, 2006) and the A2 scenario.

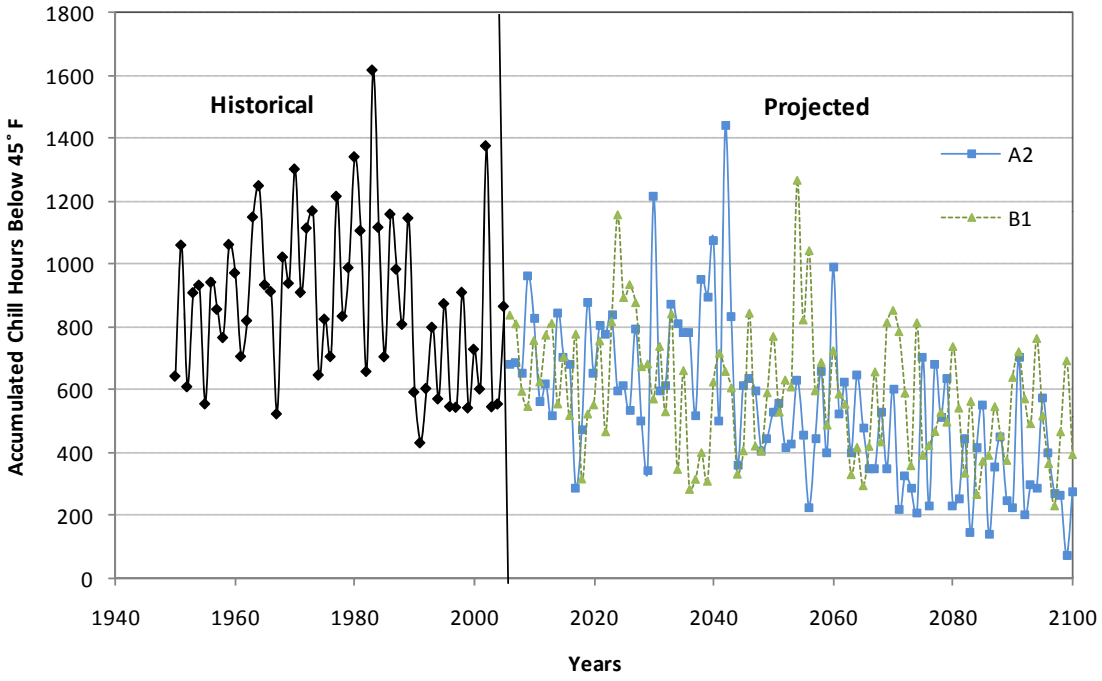


Figure 18. Historical data (black) and projected decrease in annual accumulated chill hours for the city of Davis, California. Future projections utilized scenarios B1 (green diamonds) and A2 (blue squares).

Source: Adapted from Baldocchi and Wong (2008).

Recent research has revealed serious vulnerabilities of growers in the Sacramento-San Joaquin Delta to negative impacts from climate change. The Delta contains an array of carbon-rich peat soils and marshlands which have supported high agricultural productivity (including crops such as corn, grain and hay, alfalfa, tomatoes, asparagus, fruit, safflower, pears, and wine grapes) for over a century following the establishment of levees separating the water from the land. However, cutting off the land from flood waters has barred replacement of sediments, leading to dramatic land subsidence as previously flooded, low-oxygen soils have been drained and aerated, losing significant amounts of organic carbon in the process. Certain parts of the central and western Delta currently sit more than 10 feet below sea level (Lund et al., 2007). As steady sea-rise (a major consequence of climate change) is projected to increase flood elevations, the aging levees are slowly but surely losing their protective function. Together, land subsidence and rising sea levels have rendered the region behind the levees increasingly vulnerable to flooding (Zhu et al., 2007), with particular susceptibility noted for the western and central Delta (Lund et al., 2007). And, as soils become more saline, especially in the western, central and southern areas of the Delta, economic impacts would be felt by growers, bringing into question the future ability of those regions to sustain irrigated agriculture (Mount et al., 2006, Schoups et al., 2005).

The snowmelt that passes through the Delta supplies water to farms throughout the Central Valley. In fact, it is estimated that 3.6 million acres of farmland depend on water from the Delta

(Vicuna, Hanemann and Dale, 2006). A recent study analyzed costs to farmers south of the Delta stemming from a hypothetical breaching of the Delta levees assuming that such an event would affect water supplies (Vicuna, Hanemann, and Dale, 2006). In effect, they found that different climatic conditions affected the size of the economic burden from the levee breach. Three hypothetical scenarios[11] were treated in this economic analysis. In the first scenario, a time of drought preceded the levee failure, which led to $2 billion in net farm revenue losses. In the second scenario, a period of high rainfall preceded the levee failure, resulting in net revenue losses of $0.7 billion. Finally, a levee failure followed by drought was found to place the greatest squeeze on water supplies, inflicting more strain on growers and increasing farm revenue losses to $2.6 billion due to limited water supplies (Vicuna, Hanemann, and Dale, 2006). Such an analysis illustrates how economic impacts are highly sensitive to the specific climatic conditions (including the frequency and specific sequence of changes and extreme events) that California might encounter in the future. Advances in technology, such as irrigation efficiency, can lessen the severity of impacts to agriculture (Purkey et al., 2008).

4.5. Changing Landscapes: Forests and Aquatic Ecosystems

In addition to providing recreational opportunities and economic revenue, the state's forests and aquatic ecosystems harbor wildlife, help sustain biodiversity, promote clean water, and sequester carbon. The species that inhabit these ecosystems represent a cultural and ecological heritage for California. Under pressure from climate change, however, these ecosystems, including the distinctive species associated with these places, will necessarily respond and change.

Review of Ecosystem Impacts

- Coverage of certain tree species, especially pines, will shrink and/or relocate, including high-altitude alpine and sub-alpine forests
- Key changes in competition are likely to occur among species, such as a gain in broad-leaved species at the expense of needle-leaved species
- Number of large wildfires increase by 12–53% statewide depending on emissions scenario, with larger increases in Northern California

While *Our Changing Climate* highlighted the relocation of certain high-altitude evergreen species further upslope in response to warming, additional research in the interim has indicated that pines might feature a much wider array of responses, including changes in stand density, decreased growth, increased mortality, susceptibility to disease, and complex interactions with other species (Millar, Westfall, and Delany, 2007).

California possesses tremendous biodiversity, including approximately 1300 "endemic" species—native species that occur nowhere else in the world. Conserving this biodiversity is an important goal. An ongoing project based at U.C. Santa Barbara is developing a species-specific demographic computer model called "BioMove" to determine how climate change will affect the geographic ranges of some 300 California plant species, including 89 endemics. Users of the

[11] Note that for all three hypothetical scenarios, the Geophysical Fluid Dynamics Laboratory (GFDL) model was applied, using the A2 emissions scenario.

model can select a species for which historical data exist, then vary factors such as dispersal (i.e., the distance that seeds can travel), competition against other plants (e.g., those already occupying territory, or new invaders), and disturbance (e.g., wildfire frequency). By adjusting these values, users can estimate the relative importance of these factors in assessing the eventual range of the target species under different climate change scenarios. At this stage of development, BioMove's target species include the iconic Joshua tree (Mojave Desert), the valuable sugar pine (Sierra Nevada), and the endemic blue oak (Central Valley). Animal species will be added in the future. As the model is finalized, it will help managers prioritize research areas that can best assess extinction threats and protect biodiversity. For example, understanding dispersal patterns of the Joshua tree may be critical, as model simulations suggest that long-range dispersal could offset negative impacts from a warmer climate, increased competition from invasive grasses, and increased fire disturbance (Conservation International et al., 2008).

Oak woodlands are a distinctive and visually evocative landscape in the state. Earlier work suggested that climate change, including changes in temperature and precipitation, would shift the area suitable for oaks (their so-called "climate envelope") northward. A new study modeled the controls on California oak regeneration as affected by climate change. Successful regeneration of oaks was linked to whether the area had "reserved" status, suggesting that species dispersal is an important determinant of regenerative ability (Zavaleta, Hulvey, and Fulfrost, 2007). The critical role of dispersal was similarly highlighted in a much broader study that modeled ranges for over 500 endemic plant species 80 years from the present. These researchers observed decreases in biodiversity under a higher-emissions scenario (a loss of about 1 species per acre), but found that increasing the species' dispersal ability buffered against species losses. At a lower emissions scenario (B1) and high dispersal capability, biodiversity actually increased in many areas of the state[12] (Loarie et al., 2008).

Salmon, spawning along the Sacramento, American, and Feather Rivers, are an important part of Northern California's economy and a cultural icon to fishermen and naturalists. In 2008, unusually low populations of California's wild salmon forced a curtailment of the entire fishing season, resulting in estimated losses of $255 million and 2,263 jobs, according to the Department of Fish and Game (Weiser, 2008). The complex reasons for these unusual low salmon runs are not yet fully understood, although in the Sacramento basin, temperature change or water withdrawals could have played a role.

Although more locally specific research on the impacts of climate change on salmon is still needed for California, research conducted in the Puget Sound area of Washington state shows that the modeled population of salmon will be negatively impacted by climate change, largely due to the reduction in snowpack and hence runoff during important stages in the salmon's life cycle, as well as to increases in water temperature (Battin et al., 2007). In a relevant study, two global climate models (both using the "A2" emissions scenario) were used to test how future

[12] Note that differences in model results stemmed from the different ways these models forecast future precipitation patterns, an area which deserves future research emphasis.

climate would affect in-stream habitat for spawning salmon with a separate modeling component that addressed salmon population dynamics. Both models produced a strong negative effect of climate change on salmon population: a 40% decline by 2050 (Geophysical Fluid Dynamics Laboratory model, based in Princeton, New Jersey), versus a 20% decline (Hadley Center model). The two primary reasons for this substantial decline were the climate change-induced reduction in suitable cold-water habitat and reduced stream flows for salmon spawning, incubation, and rearing, plus the increased damage to salmon eggs from increased winter runoff scouring streambeds (Battin et al., 2007). These findings suggest that climate change impacts to California salmon should be a high priority for future research.

4.6. Sea-Level Rise: Greater Than Previously Thought?

Review of Sea Level Impacts
• Sea level likely to increase by up to 35 inches by 2100, depending on the magnitude of climate warming • Most severe impacts result from the coincidence of sea-level rise with storm surge, tides, and other climatic fluctuations (like El Niño)

California is vulnerable to significant economic costs resulting from loss of, or damage to, coastal property and infrastructure as sea levels rise. Additional impacts include erosion of recreational area (such as beaches), inundation of wildlife habitat, and salinization of inland water supplies. Estimates of future global sea-level rise have recently been revised upwards. Estimates by Rahmstorf (2007) suggest global sea-level rise could increase by over 4 feet by 2100, depending on the warming scenario employed (Figure 19), as opposed to the very modest 0.6 to 1.9 feet (7.12 to 23.4 inches) projected in the most recent assessment of the IPCC (2007). However, a recent paper in the journal *Science* asserts that artificial water reservoirs (dams) around the world have had a significant impact on sea-level rise, reducing the magnitude of global sea level rise by about 30 millimeters (1.2 inches) during the last half of the 20th century (Chao, Wu and Li, 2008). In other words, if there had been no dams retaining water on land, global sea level rise would have been 30 mm (1.18 inches) higher than they actually are, suggesting that warming of the oceans and/or water additions to the oceans from land-based ice must have been greater than previously assumed.

Figure 19 shows global average sea level changes over the 21st century for the B1 and "Policy" scenarios. The projected increases are larger than previously reported due to recent improvements in sea-level rise science, though still not accounting for the possibility of rapid ice loss from Greenland and Antarctica. There is almost no difference in the expected range of increase in sea level (about 8 inches higher by 2050 and about 18 inches higher by 2100 above the 1961–1990 average) between the two scenarios. This suggests that even stringent emissions reductions and resulting lower temperature increases—while critically important in limiting other dangers to human health, water resources, food supplies and ecosystems—cannot prevent substantial sea-level rise because ocean waters store heat effectively and will expand for

centuries, long after air temperatures have been stabilized. Adaptation is the only way to deal with the long-lasting threat of sea-level rise to coastal areas.

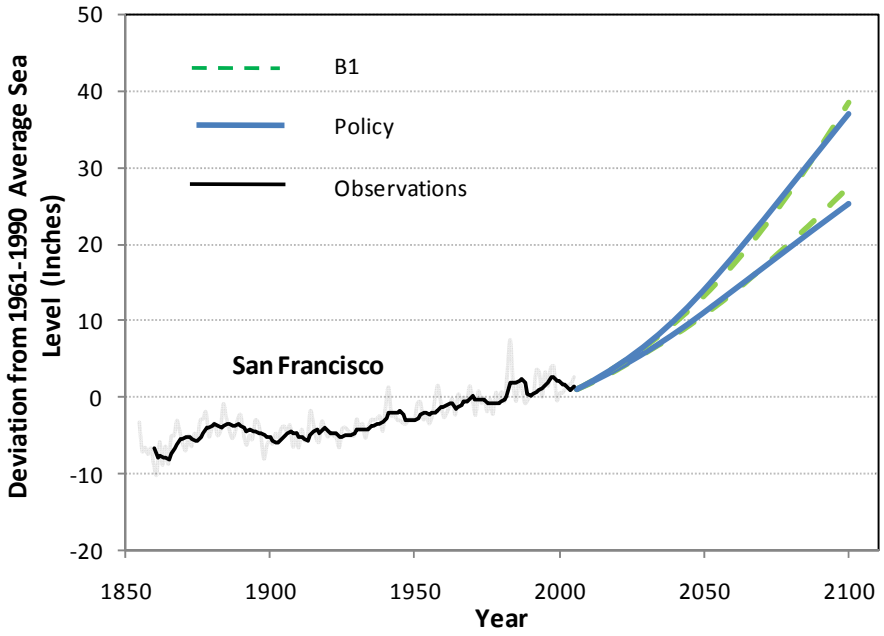


Figure 19. Observed sea levels in San Francisco and projected global levels for the B1 and "Policy" scenario.
Source: Dan Cayan (forthcoming PIER report)

A striking feature of Figure 19 is the amount of sea level rise even for the policy scenario. This again emphasizes the need for the development of adaptation strategies. Another consideration is the fact that given the residence time of carbon dioxide and other long-lived greenhouse gases, sea level rise will continue for many centuries and, for this reason, only planning for expected sea levels expected by 2100,which would be a good start, may not be enough in the long run. Recently a group of researchers from France has estimated non-linear melting behaviors of Greenland. According to the researchers, the ice sheets in Greenland could completely melt in an irreversible way if a cumulative amount of 2,480 gigatonnes of carbon dioxide (GtC) are released to the atmosphere, which is a plausible scenario if California continues to follow or exceed the emissions under the A1Fi emission scenarios (Charbit et al., 2008). A melting of Greenland ice would result in a catastrophic rise of sea level in the order of 23 feet (7 meters). Cumulative total emissions of 2,150 GtC, on the other hand, would result in only partial melting of the Greenland ice sheet, causing significantly less impacts and damages in coastal regions around the world. The question of what level of emissions would allow a crossing of the warming threshold that would lead to irreversible melting is not yet scientifically settled and requires further attention.

Future changes in storminess (frequency, intensity and paths) strength are of particular concern because storms can generate extreme sea levels (short-term) increases in that can cause rapid shifts and economic damage. These extreme events are defined operationally as those where water levels exceed a given threshold. The climate models project two important trends: higher

sea level extremes resulting from increasing storm intensity and more frequent extreme events. As shown in Figure 20, a sea-level threshold that was previously crossed only once out of 10,000 measurements at Fort Point, California historical record is projected to be exceeded for more than 20 hours per year by the end of the century (Cayan et al., 2008b). Researchers also are projecting a trend of longer-lasting extreme events (Bromirski and Flick, submitted). One mechanism behind these trends relates to changes in the water cycle discussed above: increased winter rainfall (tied to warmer temperatures and decreased snowfall) and earlier spring runoff creates more discharge into San Francisco Bay from storm water, also elevating water levels (Bromirski and Flick, submitted).

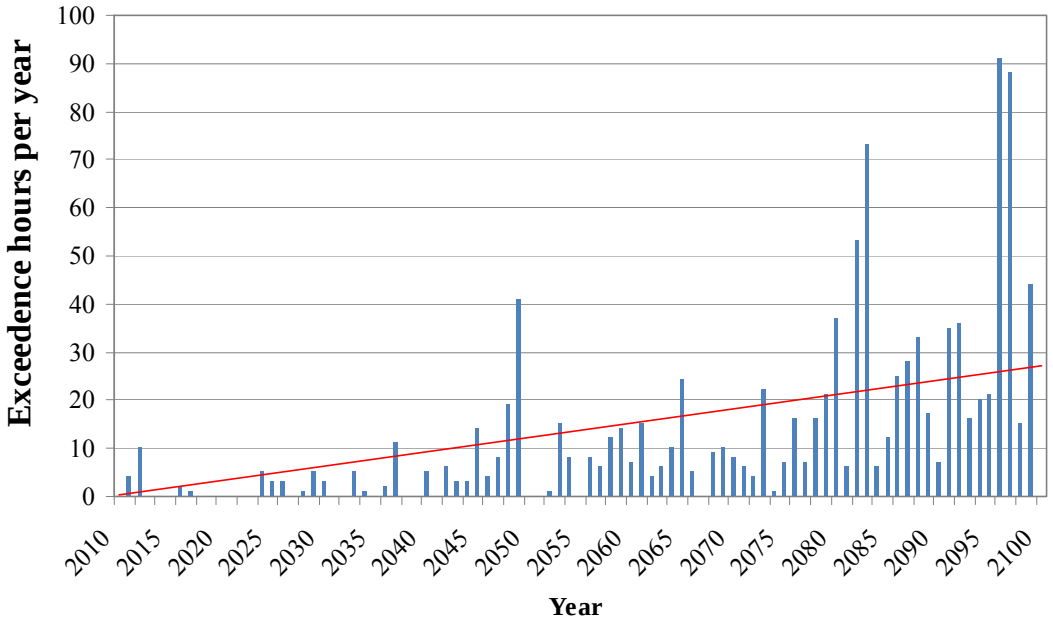


Figure 20: Projected sea level exceedence hours per year at Fort Point, San Francisco (SFO), over the next century. The GFDL model (A2 emissions scenario) was used. The figure illustrates the hours per year when sea level will exceed the threshold of 56.4 inches (historical 99.99th percentile). The red line indicates the increasing linear trend.

Source: Adapted from Cayan et al. (2008b).

Under the former projections for sea-level rise, experts calculated that California needed to invest hundreds of millions of dollars to protect vulnerable coastal areas against damage. For instance, an analysis by Neumann and others from 2003 extrapolated from a subset of seven locations throughout the state to conclude that a sea-level rise of 39 inches would cost the state an estimated $0.4 to $0.6 billion for coastal protection (beach nourishment and armoring of our coasts) state-wide as measured in year 2000 dollars (Neumann et al., 2003). Consistent with the old predictions, the San Francisco Bay Conservation and Development Commission (http://www.bcdc.ca.gov/) assembled maps of areas which would be inundated by the encroaching sea. However, economic impact assessments conducted using past projections now

are seen as under-estimates of the magnitude of both costs and adaptive actions needed by state and local decision makers.

How do the new sea-level rise figures translate to economic impacts for California coastal communities? The state can focus on certain urban locales as indicators of coastal regions: San Francisco Bay Area and San Diego are economically important, low-elevation locales that are vulnerable to flooding and coastal erosion. Newer maps are now available for San Francisco Bay (Figure 21).

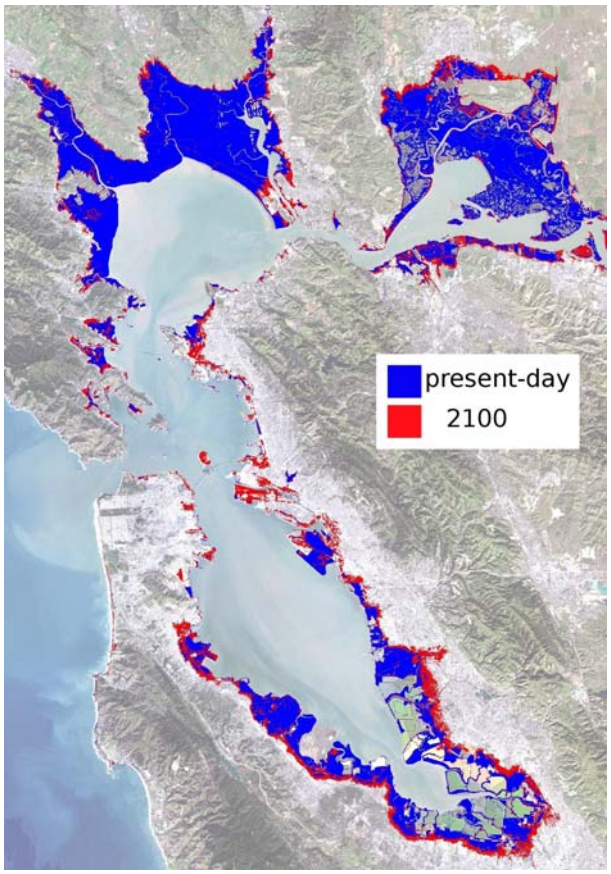


Figure 21. Areas inundated or at risk of inundation by average yearly Bay high-water levels, for both present-day (blue) and projected 2100 (red) conditions. The projected sea level rise by 2100 used in this analysis is 140cm (55 inches).

Source: Bay Conservation and Development Commission

A recent county-level analysis for San Diego and La Jolla estimates a one-time cost of protecting San Diego's coastline ranging from $24 million to $47.5 million for activities such as sea wall construction, beach nourishment and halting new building in heavily disturbed areas (San Diego Foundation, 2008). Figure 22 shows updated inundation maps for La Jolla.

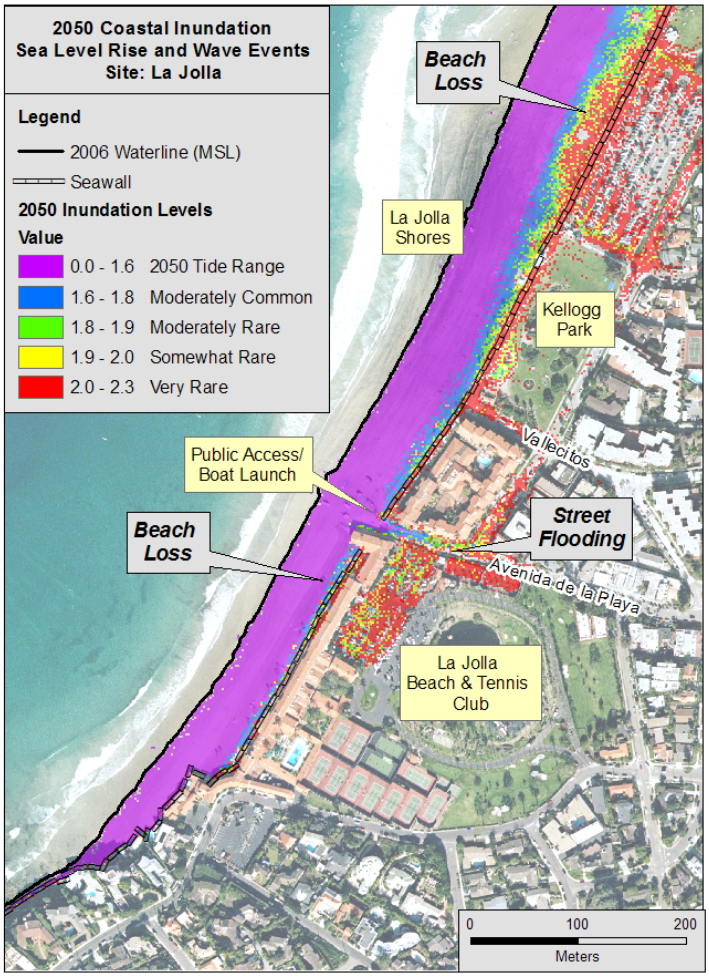


Figure 22. SLR, La Jolla "Regions of inundation at La Jolla Shores for sea level rise and various wave event scenarios in year 2050. Tidal fluctuations alone (purple) appear to inundate sandy beach and access road. Adding run-up from moderately common wave events (blue) floods majority of sandy beach. Very rare wave events (red) flood sandy beach, some surface streets, the heavily-used Kellogg Park, and parts of the La Jolla Beach and Tennis Club."
(Source: San Diego Foundation, 2008)

4.7. Growing Energy Demands

Under climate warming, higher costs from increased demand for cooling in the summer are expected to outweigh the decreases in heating costs in the cooler seasons (Franco and Sanstad, 2008b). Hotter temperatures in California will mean more energy (typically measured in "cooling-degree days") needed to cool homes and businesses both during heat waves and on a daily basis, during the daytime peak of the diurnal temperature cycle (Franco and Sanstad, 2008b). A high-emissions warming scenario such as A1fi results in a tripling, and the B1 scenario results in a doubling, in the statewide number of cooling degree days compared to

historical values (Miller et al., 2008). During future heat waves, historically cooler coastal cities (e.g., San Francisco and Los Angeles) are projected to experience greater relative increases in temperature, such that areas that never before relied air conditioning will experience new cooling demands (Miller et al., 2008). A confounding concern is that similar to other western states, California expects to see extensive population growth, especially in the southern and central part of the state, where the climate is already hot enough to require air conditioning. Will California have enough electricity reserves to prevent shortages and blackouts? Unfortunately, decreased hydropower supplies are a likely consequence of climate change if precipitation decreases, although uncertainties in the precipitation projections hinder more precise predictions for hydropower (Vicuna and Dracup, 2007). The state's electrical capacity, while growing, is unlikely to be able to accommodate the dual pressures of increased cooling demand and increased population. The work by Miller and others (2008) suggests that summer electricity shortages may occur as early as 2020, with particular shortage vulnerabilities noted for Southern California.

4.8. Climate Change in a Multi-Stressor World

Climate change will impact many sectors simultaneously, yet different systems will vary in both their sensitivities and their responses to the coming changes. Moreover, any climate-related impacts will interact with non-climatic stresses. The resulting combined effects could be larger or smaller than any single projected impact occurring in isolation. One example may be a multi-year drought, followed by wildfire, followed by flooding. Another may be a number of severe coastal storms during an El Niño occurring at a time of economic recession. If compounding impacts lead to increased vulnerability to future climate change, there will be a growing need for broad-based management and adaptation plans. Cooperation and collaborative management among multiple agencies will be required to develop appropriate response strategies. Example cases where critical climate change impacts interact with non-climatic stressors and affect multiple sectors simultaneously are discussed below.

4.9. Growing Water and Energy Management Challenges in Southern California

Population growth promises to compound water management challenges under climate change. By 2030, the population of California is expected to grow by 14 million overall (California Department of Finance; Public Policy Institute of California, 2006). Most of this growth will occur in Southern California, resulting in a geographic disconnect between demand and supply. Dry Southern California imports water from the wetter north, yet the population in Southern California is growing faster than elsewhere in the state (PPIC, 2006). In addition,

energy demand for cooling in Southern California is also expected to outpace that of Northern California due to both higher temperatures and intense development pressures in the southern half of the state. Finally, an aging and increasingly immigrant population in the southern part of the state is contributing to growing social vulnerability there compared to other regions of the state (Cutter and Finch, 2008).

4.10. Growing Wildfire Risk

Climate change can increase wildfire risks by elevating temperatures (a noted corollary) and by either increasing the vegetative fuel load (in wetter years) or drying out vegetation (in drier years). It is important to highlight that the existing projection is for 12-53 %[13] increases in the frequency of large wildfires in California by the end of the century, using the B1 and A2 scenarios, respectively. Under a higher-emissions scenario like A2, the value of structures lost to fire is projected to increase by 32-36 %, or by 6-11 % under the B1 scenario (Westerling and Bryant, 2008). Recent work has focused heavily on fire patterns within the wildland-urban interface, where more development and urbanization in fire-prone areas add to the climate-related increase in fire risk. Researchers are addressing issues such as land use planning measures (e.g., building density, buffers) that can minimize fire spread (Spyratos, Bourgeron, and Ghil, 2007) as well as the effect of increased urbanization in Southern California on both future vegetation distribution and urban fire risk (Syphard, Clarke, and Franklin, 2007). Future research will continue to probe the possible ways human activities can mediate California's vulnerability to wildfire and which actions can be taken to mitigate those risks.

Wildfire affects a host of economic and environmental issues, including air pollution, visibility, and human health (from smoke and aerosols), ecosystem dynamics, wildlife habitat, timber production, hydrologic cycling, and flooding and soil erosion risks (from loss of forest cover). This range of impacts illustrates how climate change and non-climatic stressors interact to create impacts that span multiple sectors. The resulting economic damages and costs are enormous (e.g., private property damages, tourism and recreation, evacuation, and fire suppression). By a 1996 state estimate, air quality degradation alone adds up to $15,000 per acre burned to economic costs of wildfire, depending on the type of area burned and the location of the air basin (Department of Forestry and Fire Protection, 1996). California's Department of Forestry and Fire Protection also reported that during the 2007 wildfire season, fire suppression costs totaled nearly $300 million, over 3,000 structures were destroyed, and damages totaled roughly $250 million. To minimize negative economic impacts, further studies are needed to analyze both costs and benefits of long-term investments to reduce the severity of fire, such as the use of prescribed fire treatments or strategies to reduce fuel loads.

[13] These estimates are supplied by the Department of Forestry and Fire Protection (2007), available on-line at http://www.fire.ca.gov/communications/downloads/fact_sheets/2007Summary.pdf

4.11. Growing Vulnerability of the Sacramento-San Joaquin Delta

The confluence of the Sacramento and San Joaquin rivers that forms the Delta also represents an amalgamation of many issues impacted by climate change. The Delta provides local services for users from diverse sectors: agriculture, recreation, urban land use, and wildlife habitat, all of which depend upon water. As much of the land is below sea level, increased flood risk and salt water intrusion are both serious concerns; these can stem from sea level rise, an earthquake, levee failure from structural weakness with increasing age, or some combination of these processes. At least a portion of the drinking water supply for two-thirds of California's population passes through the Delta on its way to other areas. Thus, if the Delta's water system is compromised, this will affect potable water supplies for Central Valley users, customers in the Bay Area (in Silicon Valley and counties such as Contra Costa, Napa, and Solano), as well as the Metropolitan Water District of Southern California via the California Aqueduct. Research has shown that the impacts of climate change combined with a levee failure increases costs for the agricultural sector (Vicuna, Hanemann, and Dale, 2006). Meanwhile, the mountain snowmelt that supplies water to the area is expected to decrease with warming. The likelihood of decreased flows during the summertime, when demand is high, also creates problems concerning water quality standards for human uses and wildlife.

The Delta region currently accommodates considerable power and fuel infrastructure (e.g., electricity transmission lines, gas lines) plus corridors for transportation and shipping. If levees are compromised by flooding or seismic activity, the resulting consequences could be costly (Mount, Twiss, and Adams, 2006), reaching up to $40 billion cumulatively by one estimate (Lund et al., 2007). Such costs are expected to increase as urbanization of the Delta, especially in the periphery, is a major driver of change and is expected to accelerate in coming decades. As more land is converted from agricultural use to urban uses, more pressure will be focused to meet increasing demands for transportation and other urban infrastructure.

4.12. Keeping the Eye on the Ball: A Global Perspective

California clearly does not operate in isolation from the global community. For example, California's CO_2 emissions, while sizeable, are only a part of the whole. Thus, California has an important responsibility to reduce its own carbon footprint as well as to engage with partners elsewhere to support their carbon emission reduction efforts. This approach is critical because the global total of greenhouse gas emissions will ultimately affect California. Just a couple of examples are given here to illustrate the climate connectivity shared among different regions of the world.

4.13. Global Teleconnections of Air Quality

More than at any previous time in our history, human-generated air-quality problems have not just local or regional, but global reach. The atmosphere is capable of moving pollutants relatively rapidly—in a matter of days—in the west-east direction. Pollution arising from areas at a similar latitude to (west of) California are therefore able to affect California's air quality. Specifically, particulate pollutants from combustion known as black carbon are increasingly being transported across the Pacific Ocean, from Asia to California. In fact, the majority of black carbon passing over the West Coast of North America (measured in a spring month) originates on the Asian continent (Hadley et al., 2007), adding to the locally generated black carbon. Black carbon absorbs sunlight, which affects the rate of snowmelt (by darkening otherwise highly reflective snow), and contributes to climatic warming of the atmosphere (Reddy and Boucher, 2007). In addition to these important effects, an increase in black carbon pollution from combustion, whether locally or remotely sourced, causes health concerns, including respiratory symptoms as well as cardiovascular effects (Jansen et al., 2005).

4.14. Inter- and Intrastate Water Movement

Natural precipitation varies throughout California, and the state has engineered a massive system of infrastructure, such as aqueducts, to move water from areas of abundance to places of relative scarcity. Flexibility is also an important feature in allocating water supply regionally among western states. In future decades, some areas in the western United States, especially the southwest, may experience greater drought, necessitating more interaction in regional water markets (Seager et al., 2007). In the southern part of the state, water supplies from the Colorado River may decrease in the future. A recent comprehensive modeling study projected an 8-11 % decrease in runoff by 2100 for the Colorado River Basin depending on the emissions scenario. This study also found that water shortages for the basin became more frequent (Christensen and Lettenmaier, 2007). This reduction in water availability will require that all states within the Colorado River watershed collaborate to share the diminishing water resources fairly. Much of the West, like California, is considering some use of groundwater sources to supplement shrinking water supplies. However, groundwater access and rights among multiple regional players is subject to debate, as is currently playing out in the area surrounding Las Vegas, which is experiencing tremendous population and development growth (Deacon et al., 2007). Both the physical and social trends require a better understanding of the full implications for resource management at the regional scale.

4.15. Conclusions

The emerging projections of climate change impacts offer several sobering conclusions. In areas such as sea-level rise and carbon emissions, recent scientific progress suggests that impacts are likely be more severe than previously anticipated. Moreover, climate change impacts will not occur in isolation from other global environmental and societal changes, but will compound underlying environmental and economic stresses that are already occurring in California from development and urbanization. In addition, impacts that may occur in distant places can impact California through physical teleconnections (e.g., in the case of air pollution) or via societal and economic interactions (e.g., market interactions in an increasingly globalized world).

This section has focused on the ways in which changes in climate are projected to affect the environment and society over the 21st century. However, what will actually occur depends greatly on efforts to reduce emissions and to minimize future negative impacts. In short, human decisions are key to determining the true severity of future impacts. As will be discussed in the following section, California has already demonstrated, through legislative and other civic action, the enormous potential for positive change. Mitigation of emissions to slow down climate change and efforts in adaptation to deal with the impacts of change will help minimize the harmful impacts of climate change and provide valuable co-benefits. Efforts in both arenas currently underway in the state are discussed in the next section.

5.0 Managing California's Climate Risks: Need for a Two-Pronged Strategy

5.1. A Compelling Case: Why California—and the World—Must Mitigate Climate Change and Adapt to Its Impacts

Climate change risks are no longer a matter of the future or of places far away. As a growing number of studies of changes already observed in California's climate and ecosystems makes clear: climate change is already evident in the state, and it is happening now (see Chapter 2). Science is able to show that these local changes are consistent with a collective picture of physical and biological changes across the globe, which—in the vast majority of cases—are driven by anthropogenic climate warming and cannot be explained by natural changes alone (see Chapter 3). While modified by local climate variability and other human impacts such as pollution and land use change, the irrefutable conclusion is that humans affect the global environment in ways never thought possible before. If heat-trapping greenhouse gases are not curtailed and the related impacts are not reduced, the state faces tremendous impacts on its natural resource base, its ecological treasures, and the lives, livelihoods, and well-being of its citizens (see Chapter 4).

10 Reasons Why California Must Adapt

1— California's climate and ecosystems are already changing, demanding management changes.
2— Observed global and regional changes are largely due to human activity.
3— Without swift and concerted action, climate change will produce severe and costly consequences for California and the world.
4— Current greenhouse gas emissions commit the state for decades to centuries to further warming and climate change impacts that must be managed.
5 — While mitigation is critical for long-term reduction of global warming, it will not help manage the impacts to which past emissions have committed California.
6— Land use changes are equally long-lasting and interact with climate change and response options.
7— Changes in the atmosphere, climate and other natural systems are accelerating, increasing the risk of abrupt and dramatic changes for which society is currently entirely unprepared.
8— Adaptation may offer important opportunities for California businesses.
9— Decreasing the human footprint on the environment, reducing vulnerability to climate variability and change, and planning ahead can improve environmental conditions and economic welfare, enhance social justice, and ensure people's quality of life.
10 — Well thought out adaptation plans, implemented over time, are less risky, less costly, and allow Californians to *create* their future, rather than being compelled later to just *cope* with it.

These three arguments—each detailed in the previous three sections—serve as a strong basis for action. Clearly they have motivated the mitigation efforts already underway in the state (see further discussion below, especially of the implementation of AB32). Yet there are several other reasons why California must complement its mitigation efforts with planning for adaptation to ongoing and future impacts of climate change. These reasons add urgency to the need for

stepped up mitigation efforts and for adaptation to the problem while also pointing to the opportunities involved (see Textbox "10 Reasons to Mitigate and Adapt").

Dealing with the emissions that are the principal causes of global warming is different than dealing with other types of pollution. Many of the already emitted greenhouse gases—primarily carbon dioxide (CO_2), methane (CH_4), and nitrous oxide (N_2O), but also halocarbons—are so-called "long-lived" greenhouse gases because they remain in the atmosphere for decades to centuries. To illustrate this point, consider the fact that about half of all the CO_2 added to the atmosphere today will still reside in the atmosphere 50 years from now, about a third will remain after 100 years, and about a fifth will still be there 1000 years hence (Hansen et al., 2007; Archer, Kheshgi and Maier-Reimer, 1997). Related studies show that if CO_2 emissions had been completely stopped in 2000, 25 years later the atmospheric concentration would only be reduced by 25 parts per million (ppm) and only by 40 ppm by 2100, i.e., getting back to 1975 levels (Friedlingstein and Solomon, 2005, p.10834).

This means that the warming experienced to date is mostly due to emissions released into the atmosphere decades ago, while more is yet to come. Current emissions are committing California and the world to decades if not hundreds of years of further warming, and some changes—such as sea-level rise—will go on for millennia because the oceans store heat even more effectively than the air (Meehl et al., 2005; Wigley, 2005; Friendlichstein and Solomon, 2005). So even if no more emissions were released from now on (which is practically impossible), warming would still continue because plants and oceans can absorb carbon dioxide only slowly, and their capacity to do so appears to be slowing (Canadell et al., 2007; Raupach et al., 2007). In short, the longer the reduction of emissions is delayed, the longer the world commits itself to additional warming and more changes in the environment. Moreover, the faster our climate changes, the more difficult and costly adaptation will be.

Similarly, land use changes (e.g., converting forests to grasslands, agricultural areas to urban areas) are long-term commitments, which change the reflectivity of the surface, and diminish the ability of ecosystems to absorb carbon dioxide, adapt effectively to climatic changes or maintain local climate conditions. Such land use changes are responsible for about one quarter of the anthropogenic forcing, and present similarly long-term commitments to additional impacts.

Furthermore, it is unlikely that future impacts are simply linear extensions of past trends. Emissions, greenhouse gas concentrations in the atmosphere, global temperature increases, sea ice losses, sea-level rise and other changes all are accelerating (Solomon et al., 2007). Evidence from the geologic past suggests that very abrupt climatic and environmental changes can happen (dramatic shifts far outside interdecadal variability over the course of just a few years) (Steffensen et al., 2008), and that these abrupt changes are more likely the more a system is pushed out of its dynamic equilibrium (as reflected in the range of natural variability). This is currently occurring with the climate as a result of anthropogenic forcing and there is considerable concern in the scientific community that abrupt changes—imaginable, but not predictable at present—may occur again (e.g., NRC, 2002; Schellenhuber et al., 2006; Lenton et al., 2008; McCracken, Moore and Topping, 2008). The social and economic costs of such abrupt changes have not been assessed but may be beyond the capacity of many countries and communities to absorb without major suffering (Schellenhuber et al., 2006; Holdren, 2008).

Reducing greenhouse gas emissions, on the other hand, by launching already existing and developing additional new technologies offers significant economic opportunities. Achieving the level of emission reductions recommended by many scientists and discussed in various policy circles (e.g., 80% reduction below 2000 emissions levels by 2050 as, for example, targeted in AB32) requires an almost complete "retooling" of society. Priority areas will include:

- Novel ways to meet our mobility needs through new modes of transportation using alternative, low- to zero-emission fuels.
- Alternative energy production systems involving virtually no net emissions of heat-trapping gases over the entire life cycle of the system.
- Significant reductions in energy demand/consumption through a mix of technological and behavioral changes.
- Denser and mixed, integrated land use, renewal of the existing building stock and a widespread, green revolution in building design.
- Changes in agricultural production technologies and the food distribution system.
- Changes in the design, production and consumption of other materials and appliances across all sectors of society.

Beyond these high-priority changes, every sector of society will need to be involved and contribute to the overall goal of climate stabilization. If climatic changes unfolded even more rapidly than currently observed or anticipated, such social and technological changes would need to be implemented very quickly, incurring dramatic economic costs. If, on the other hand, technological and policy changes were set in motion and pursued persistently over the course of several decades, innovation and stock turn-over could instead be a driver of a worldwide "sustainability revolution." Estimated impacts on the global economy over the next 50 years range from a few percentage points reduction in global GDP to several percentage points growth over what would be expected otherwise, without consideration of mitigation actions (IPCC, 2007c). Clearly, policy proposals must also consider equity, justice, and many other welfare concerns. But as national and international climate change policy will be put in place

over the coming years, the global market for energy efficiency and zero-emission technologies will grow exponentially, and California's industry and overall economy could benefit tremendously.

In fact, California, a proving ground for technological and policy innovation, has benefited from similar pioneering thinking in the IT sector in the past. From appliance efficiency improvements to air quality regulations, to vehicle emission standards, the state has proven again and again that when California leads, other states follow (Rabe, in press; Kosloff, Trexler and Nelson, 2004; McKinstry, 2004). The resulting policy patchwork across the nation has repeatedly been an important driver of federal environmental and public health policies. Given the size of the California economy and market, technological and policy changes also have global ramifications. This puts a great responsibility and opportunity to act before California's political and business leaders.

In addition to the opportunities emerging with technological innovation and the remaking of the infrastructure and functioning of society, the larger sustainability challenge also beckons. In fact, it is the integrated approach of decreasing the total human impact on the environment, reducing social vulnerability to climate variability and change, and planning ahead for the unavoidable impacts of climate change that can improve environmental conditions and economic welfare, enhance social justice, and ensure quality of life (e.g., Holdren, 2008; Bizikova, Robinson, and Cohen, 2007; Eriksen and O'Brien, 2007; Yohe et al., 2007). As many of the changes observed in ecological and social systems to date are the result of both anthropogenic climate change and other human impacts on the environment, reducing any additional stressors will give these natural systems the best chance at adapting to additional climate changes expected in the future.

Finally, if California acts now together with other states and nations to reduce climate change risks through stringent mitigation and adaptation to the impacts that cannot be avoided, the world community has a chance to create its future, rather than being compelled later to just cope with it. While generations of humans before could not imagine affecting a system as large as the entire planet, the collective and cumulative impact of the human species has become that powerful. The challenge now is to redirect that powerful impact toward reducing and managing climate change risks and steer the world toward sustainability.

5.2. The Two-Pronged Approach to Reduce Climate Risks: Mitigation and Adaptation

Until fairly recently, the almost exclusive focus in climate policy has been on reducing greenhouse gas emissions from energy use and other forcings (such as large-scale deforestation) that cause global warming. Together, these efforts are commonly known as "mitigation." More recently, the climate policy discussion—internationally, at the federal level, and in California—has been expanded to now also include a concern with adaptation (e.g., Pielke et al., 2007), i.e.,

with the wide range of efforts needed to plan for and deal with the impacts of climate change to avoid or minimize harm and take advantage of any potential opportunities climate change may involve.

According to Moser and Luers (2008, pp. S309-S310),

> "Society's and the environment's ability to cope with climate impacts depends in important ways on the pace and magnitude of global climate change, thus continuing to require substantial mitigation efforts. However, because society is already facing risks associated with climate variability at present, the first signs of change are already being observed, and further impacts over the next 30 years are unavoidable due to the emissions already released into the atmosphere, adaptation is increasingly recognized as a complementary necessity to mitigation."

Managing California's climate risks then means reducing the drivers of change on the front end of the problem and minimizing the impacts on the back end, with the overall goal of ensuring public safety and welfare, continued economic vitality of the state's climate-sensitive sectors, and a rich and functional natural environment on which people and the economy depend.

California's ability to manage climate risks with such a dual approach, i.e., its response capacity, depends on a set of factors that apply to both mitigation and adaptation (e.g., Yohe and Tol, 2002; Smith, Klein and Huq, 2003; Brooks, Adger and Kelly, 2005; Pelling and High, 2005; Gallopín, 2006; Smit and Wandel, 2006; Adger et al., 2007):

- A strong economic resource base.
- Appropriate technologies.
- Adequate infrastructure.
- Institutional support and strong governance mechanisms.
- Highly educated and skilled workforce.
- Widespread public awareness and adequate information/knowledge to support decisions.
- Natural resources and functioning ecosystems.
- Equity in access to the above resources and institutions.

In fact, these factors have helped California invest in technological innovation, become a world leader in various technologies and market sectors, and create the image of a forward-thinking culture. They have also helped Californians cope with the challenges associated with historical climate variability.

In the future, as California increases its efforts in mitigation and adaptation (see below), it can bank on the existing strengths that increase the state's response capacity but must also strengthen that capacity where it may be insufficient, especially in light of rapidly unfolding climate impacts in the state. Moreover, the capacity to act does not automatically translate into action. Preliminary studies for California (e.g., Moser and Luers, 2008; Moser and Tribbia, 2006/2007; Tribbia and Moser, 2008) and elsewhere (e.g., Adger and Vincent, 2005; O'Brien et al.,

2006) suggest that communities, businesses and local and state agencies face considerable challenges and barriers in beginning to plan for climate change. Thus, there is a significant need for the state to not just build capacity but also help remove the barriers in the way of using it and implementing mitigation and adaptation plans.

5.3. California's Emerging Efforts in Adaptation Planning

As argued above, to minimize the potential harm from climate change and take advantage of potential opportunities, California must pursue a two-pronged strategy, where one is not exclusive of, but complementary to, the other. Importantly, mitigation and adaptation should be considered in concert as sometimes they can be mutually reinforcing (e.g., increasing or maintaining tree cover in urban areas to provide shade and to capture carbon), and other times undermine each other (e.g., more air conditioning to provide cooling against increased heat will consume more energy and increase CO_2 emissions) (Klein et al., 2007; Füssel, 2007). Here the authors focus on the meaning of adaptation and the emerging efforts at the state level to plan and prepare for adaptation to climate change impacts.

5.4. Adaptation, Coping Range, and Climate Extremes

Because adaptation is a relatively new concept in California state policy, it is helpful to first clarify what is meant by this term and what it involves. At the most general level, "Adaptation […] usually refers to a process, action or outcome in a system (household, community, group, sector, region, country) in order for the system to better cope with, manage or adjust to some changing condition, stress, hazard, risk or opportunity" (Smit and Wandel, 2006, p.282).

It is difficult to state in general what adaptation involves in any one situation because it is highly context specific. There are key dimensions, however, that apply to all contexts (adapted from Füssel, 2007, pp.266-267):

- *Climate sensitivity*—Adaptation is only relevant if the system or decision at hand is sensitive to climate and changes in it.
- *Climate hazards*—Adaptation can be to changes in average climate conditions, climate variability, or climatic extremes.
- *Predictability vs. uncertainty of climatic changes*—Adaptation is generally easier, all else being equal, if the climatic change is well understood and can be predicted with considerable confidence than if there is significant uncertainty associated with climate change projections.

- *Non-climatic context of adaptation*—Adaptation does not occur in a vacuum, but in a context of multiple stresses and place-specific environmental, socioeconomic, political, institutional, and cultural conditions that deeply affect what types of adaptation measures are relevant, effective and feasible.
- *Purposefulness*—Adaptation can be autonomous (happening spontaneously, without concerted effort) or planned (occurring with the express purpose of addressing climate change risks).
- *Timing*—Planned adaptation can be reactive (i.e., after some impacts have occurred) or proactive or anticipatory (i.e., before some impacts have occurred).
- *Planning horizon*—planned adaptation may aim to affect systems over the next few months or for many decades to come.
- *Measures*—Adaptation can involve technological, economic, organizational, legal/policy/regulatory, informational, educational, behavioral, or research measures.
- *Actors involved*—Typically, a wide range of actors should be involved in adaptation planning and policy development and implementation, from several levels of governance and from the public and private sectors.

Societies are already adapted to some range of variability in the local climate. For example, in California, state agencies—and in some instances private sector parties—built reservoirs and levees to protect against common winter and springtime floods and periods of summer drought; snowmaking equipment was put in place in part to compensate for insufficient snowfall in winter tourism locations in the Sierra; emergency warning and response systems as well as building codes were established for coastal storms, floods and other hazards; insurance mechanisms were established to deal with wildfires and agricultural losses from frost. Together, such structural, technological, monetary, institutional and other mechanisms have helped individuals and the state's economy deal with the vagaries of nature; they have built its "coping capacity" (e.g., Adger, 2003; Brooks et al., 2005; Pelling and High, 2005; Tompkins and Adger, 2005).

As climate change accelerates against a backdrop of other changes in society and the environment, three possible conditions would require additional adaptation efforts beyond those already in place:

Case 1: Along with average changes in climate, climate variability increases (e.g., more frequent and/or more intense extreme events) but society's coping capacity remains unchanged; consequently, more and more extreme events will fall outside the normal coping range and cause damages to people, property, infrastructure and ecosystems.

Case 2: Even if climate variability were not to change markedly with average changes in climate, societal coping capacity might decline for unrelated reasons; this means that even historically common extreme events can cause more damage because society is less well-prepared, protected, or able to recover.

Case 3: Average climate and climate variability change rather dramatically, and some efforts are made to increase society's coping capacity, but they are incommensurate with the shifts in climate; this means that society is drastically underprepared to deal with the major climatic changes unfolding.

Many researchers have observed that, "Climate extremes expose existing human and natural system vulnerabilities" (CCSP, 2008, p.28). In fact, "[c]hanges in extreme events are one of the most significant ways socioeconomic and natural systems are likely to experience climate change" (ibid). While such extremes may have positive or negative impacts, the most severe of these extreme events are outside society's coping range and hence produce negative impacts.

5.5. The Goal of Adaptation: Not "Free from Risk" but "Well-Managed Risk"

Adaptation to climate change does not mean preventing all adverse impacts. Since neither the climate nor society is entirely predictable or controllable, "perfect" adaptation with no adverse consequences of climate variability ever is impossible. Rather, the goal of adaptation is to create the conditions in which society and managed ecosystems are largely able to absorb the impacts from climate variability and change, such that any residual impacts beyond their coping capacity remains within (socially defined) acceptable limits of risk. For example, when people build in a floodplain, they are typically made aware of the fact that in their desired location they face a given flooding risk (e.g., in any given year there is a 1 in 100 chance to be flooded). Since this is a high level of risk, people are typically required to purchase flood insurance and make various structural changes to their homes. As climate changes and increases the frequency or magnitude of flooding and people experience floods repeatedly, they may choose or be required to relocate out of the floodplain. Insurance, elevation of homes, and relocation are all forms of adaptive adjustments to live with climate variability and change.

Ultimately, then, the goal of adaptation is to enhance the long-term resilience of society and of socio-ecological systems, i.e., their capacity to withstand and bounce back from disturbances and impacts, and—if necessary—to learn and transform themselves while continuing or regaining the ability to provide essential functions, services, amenities, or qualities (e.g., Walker and Salt, 2006). Importantly, "the resilience perspective shifts policies from those that aspire to control change in systems assumed to be stable, to managing the capacity of social–ecological systems to cope with, adapt to, and shape change" (Folke 2006, p. 254).

5.6. Adaptation Needs Assessments

How then can communities, industries, business sectors, and resource managers assess how much adaptation is needed to attain resilience in the face of change? Researchers have

approached this question from the two obvious sides of the problem: the amount of climate change that may occur and the system's ability to cope, adapt, and change. For several decades, the scientific traditions using either of these approaches have been working quite separately; in recent years, the two approaches are increasingly viewed as complementary, and both are necessary (Burton et al., 2005; Füssel, 2007).

The first, sometimes called the *hazards-based approach*, begins with the change in climate (typically, model-based climate change projections), and aims to ascertain the incremental impacts of climate change. Any impacts beyond the historical norm would require adaptation, and their magnitude suggests how much. Consideration of non-climatic factors is typically limited. This approach—traditionally, the approach used in California's climate change (impacts) research—is critical for identifying climate change risks, but is limited for the development or assessment of different adaptation options. From this perspective, adaptation depends primarily on the magnitude of the expected change in climate. Consequently, if somewhat simplified, the most important information needed to guide adaptation actions are projections of climate change. More specifically, and pointing to future research needs (see below), the projected changes in climate, including in extremes, must be translated into changes in risk to inform adaptation planning decisions (CCSP 2008, p.29).

The *vulnerability-based approach*, on the other hand, is strongly focused on the socioeconomic factors that determine a system's ability to cope with climate change. Typically, such an assessment explicitly examines past experience with climatic variability and extremes and considers non-climatic factors and changes that affect a system's vulnerability and coping range. Vulnerability is the starting point, i.e., the initial context in which climate along with multiple other stressors combine to influence which impacts a system or community might experience. The key factors affecting vulnerability are:

- The geographic or functional *exposure* to a risk (e.g., projected temperature extremes, sea-level rise, or reduction in water supply for a specified sector; one's location vis-à-vis a specified climate hazard; one's dependence on a particular resource; the number of people at risk of experiencing a particular hazard).
- The degree of *sensitivity* to that risk (e.g., older people are more susceptible than younger people to extreme heat; coastal communities with seawalls may be less sensitive to sea-level rise than those without).
- The *ability to respond* (coping and adaptive capacity) (e.g., the availability of insurance; tight social networks; strong emergency response capacity; flexible institutions; economic resources).

Combining these three factors, it becomes apparent then why "a system can be sensitive to change but not be vulnerable, such as some aspects of agriculture in North America, because of the rich adaptive capacity; or relatively insensitive but highly vulnerable" (CCSP, 2008, p.21).

The vulnerability-based approach is most useful for identifying priority areas for action, and for assessing adaptation options and their relative effectiveness in the practical context of other stresses and demands on resources. Importantly, "[i]n practice, adaptations tend to be on-going

processes, reflecting many factors or stresses, rather than discrete measures to address climate change specifically" or exclusively (Adger et al., 2007, p.720). Adaptation planning, from this perspective then, does require more than climate change information; substantial input from the social, economic, engineering, and ecological sciences on all factors affecting vulnerability and response options is needed. Table 2 places the characteristics and pros and cons of these two approaches to assessing adaptation needs side by side.

Table 2: Comparison of hazards- and vulnerability-based approaches to adaptation

Hazards-based approach	Vulnerability-based approach
Focus: • Incremental impacts of climate change	Focus: • Social factors determining the exposure, sensitivity and ability to cope with climate hazards
Starting point: • Model-based climate change projections	Starting point: • Experience with managing climate risks in the past
Benefits: • Critical for identifying climate change risks and raising awareness of climate change problems • Useful for identifying research priorities • Useful in long-term decisions, especially where projections are quite reliable already • Particularly useful if sufficient data and resources are available to develop high-resolution projections	Benefits: • Involve stakeholders often from the start to link climate and adaptation to their activities • Can produce useful results even in the absence of useful climate change projections or where climatic and other stressors are deeply intertwined • Useful for identifying priority areas for action • Useful for assessing the relative effectiveness of different interventions
Drawbacks: • Consideration of non-climatic factors is limited, especially the non-technical aspects and policy context of adaptation • Strong reliance on model-based climate and impacts projections (possibly not available at relevant spatial scales) • Long timeframe of projections are of little relevance to management today • Insufficient consideration of current climate risks • Insufficient consideration of key uncertainties and their implications for designing robust adaptation options	Drawbacks: • Greater reliance on expert judgment • Limited comparability across regions, sectors, contexts • Wide range of methodologies produce different results • Requires non-climatic data which are also often unavailable, unreliable, or difficult to integrate
Common in: • IPCC impacts assessment guidelines; • UNEP adaptation assessment handbook; • California climate (impacts) research to date*	Common in: • UNDP-GEF Adaptation Policy Framework • Many local vulnerability and adaptation assessments

Source: Information compiled and adapted from Füssel (2007).

*** The California Energy Commission's California Climate Change Center has begun studies using the vulnerability-based approach, and this effort will be enhanced in the future.**

Ideally then, California's adaptation planning will draw on both approaches to chart the way forward (Smit et al., 1999; McCarthy et al., 2001):

- Model-driven climate projections to better understand what risks the state must adapt to ("adapt to what?").
- On-the-ground social scientific assessments of vulnerability ("who/what must adapt?").
- Assessments of adaptive capacities, adaptation options, costs, ancillary positive and negative consequences, and barriers to action ("how to adapt?").
- Over time, assessments of the selected adaptive actions' outcomes ("how good is it?").

It is quite possible that many measures employed to adapt to climate change will have ancillary benefits, e.g., because they aim at reducing vulnerability to climate variability and extremes or because they improve environmental or social conditions more generally. On the other hand, policy- and decision-makers must be careful to avoid negative consequences of adaptation, e.g., in terms of social justice, unintended environmental consequences, or other impacts on sectors and communities (see examples discussed in Moser et al., 2008). Moreover, "actions that lessen the risk from small or moderate events in the short-term, such as construction of levees, can lead to increases in vulnerability to larger extremes in the long-term, because perceived safety induces increased development" (CCSP, 2008, p.28).

Another important inference of the projected increase in the frequency of extreme events is that there is less time between events available for recovery. This, in turn, increases the risk of such maladaptations—i.e., actions that may meet an immediate need but may have negative social and environmental consequences and increase vulnerability in the long-term, rather than reduce it. The higher frequency of extreme events will also alter "the feasibility and effectiveness of adaptation measures" (CCSP, 2008, p.29).

5.7. Adaptation Planning in California

Climate change impacts will need to be managed by involving both private and public sector decision-makers, climate science experts, vulnerability and adaptation analysts, and all affected stakeholders. Actions will need to be coordinated across relevant sectors and levels of government, as climate change impacts and many response efforts are not neatly confined in space (see Chapter 4). Clearly, because climate change impacts will manifest in specific ways at the local level, local governments, businesses and individuals will play a prominent part in minimizing risks and taking advantage – where possible – of potential opportunities. In many instances, however, it is unrealistic to assume local decision-makers can manage all the impacts by themselves. Often, state- and federal-level leadership and guidance will be needed, as will financial and technical resources (Tribbia and Moser, 2008). In addition, many impacts occurring in different places or having cross-regional and cross-sectoral linkages will best be managed through a coordinated effort at a higher level.

The State of California has recognized the need for adaptation and in early 2008 began coordinated efforts to develop adaptation plans and strategies across state agencies. This effort is linked institutionally to California's mitigation efforts through a subcommittee of the Climate

Action Team, which coordinates the implementation of AB 32 and the strategic planning of deeper emissions cuts. The goal is to establish an adaptation planning process in each of the relevant state agencies (see textbox for more information) and to develop an initial state adaptation plan by the first or second quarter of 2009. This plan is only the first step in the state's ongoing adaptation efforts, which will need to be maintained for as long as climate change impacts are felt in the state.

The California Adaptation Strategy (CAS), with the help of sector-focused working groups and in coordination with key state agency stakeholders, will

- Synthesize information on anticipated climate change impacts for California policy-makers and resource managers.
- Provide strategies to promote resiliency to these impacts.
- Develop implementation plans for short and long term actions.

The CAS process will be guided by peer-reviewed scientific information gathered from scientists, agencies, cities, states, and countries around the world.

For more information on California's Adaptation Strategy (CAS):

http://www.climatechange.ca.gov/adaptation

5.7.1. Research in Support of Adaptation Planning

California is strongly committed to climate change research that will support the state's adaptation efforts. Since 2001 the California Energy Commission's Public Interest Energy Research (PIER) Program has been funding research climate change research. With the adoption of a long-term PIER climate change research plan in 2003, this effort has been substantially enhanced. Since 2003 PIER has been funding research on 1) climate monitoring, analysis, and modeling; 2) improving greenhouse gas inventory methods; 3) identifying options to reduce emissions, and 4) impacts and adaptation studies. In this document the authors discuss only the fourth area of research but more information about the other areas can be found in numerous other sources, including: Franco et al, 2008a; the California Climate Change Center (Center) website, at http://calclimate.berkeley.edu/; and a brochure describing the activities of the center (Energy Comission, in preparation).

The rest of this section briefly describes several PIER studies designed to support adaptation in California and concludes with a brief description of other relevant research and decision support efforts currently underway.

5.8. Adaptation Studies Supported by Local, State, and Federal Agencies

Federal agencies such as National Oceanic and Atmospheric Administration, the U.S. Environmental Protection Agency (EPA), the U.S. Department of Energy (DOE), and the National Science Foundation (NSF) are funding studies on adaptation for the water sector. For example, NOAA will continue to fund the follow-up phase of the INFORM project that is described below. Both NOAA and US EPA have contracts with the Stockholm Environmental Institute (SEI) to apply the Water Evaluation and Planning (WEAP) model – a water resources planning tool with a GIS-based interface that allows supply, demand, water quality, and ecological issues to be integrated into analyses of water allocations – for adaptation studies at the water district level. NSF funded RAND Corporation for a study of adaptation in the water sector in Southern California (Groves et al, 2008). US DOE has an on-going project with The Nature Conservancy and others for a study on potential ecological effects from climate change in a region in the Sierra Nevada, including a preliminary identification of adaptation strategies (Gonzalez et al., 2007).

At the state level, several agencies have in-house efforts, such as the San Francisco Bay Conservation and Development Commission (BCDC), which is also working with PIER and the Pacific Institute to estimate potential impacts to the San Francisco Bay and the identification of adaptation measures. DWR is preparing an update of its State Water Plan with a substantial amount of work being done by DWR staff and a team formed by SEI and RAND on impacts and adaptation issues. The California Department of Public Health has released its first report on impacts and adaptation options titled *Public Health Impacts of Climate Change in California: Community Vulnerability Assessments and Adaptation Strategies – Report No. 1: Heat-Related Illness and Mortality Information for the Public Health Network in California*.

At the local level, counties and cities such as the county of San Diego have prepared preliminary impacts and adaptation plans (San Diego Foundation, 2008), but they are requesting additional scientific information to refine these plans.

5.9. PIER-Supported Studies

The majority of PIER-supported research in the past falls within the hazards-based approach to assess adaptation needs. Here the authors highlight several relevant efforts before turning to the emerging efforts in vulnerability-based adaptation research.

5.10. Development of Climate Projections for California

Substantial effort has been invested to develop methods to focus the output from global climate models specifically to the California region. The grid cells of global climate models (typically from 150 kilometers (90 miles) to 300 kilometers) are too coarse to properly capture the diverse climatic conditions in California (see Figure 23). California impacts and adaptation studies require a much finer geographical resolution. A number of models are being developed that can simulate climate at grid resolutions of approximately 12 km (7.5 miles) (Kanamaru and Kanamitsu, 2007), which are better able to model ambient ground-level temperatures and precipitation. The statistical techniques used to generate these projections, however, cannot provide complex meteorological and hydrological information such as three-dimensional temperature and wind fields that would be needed for more detailed impacts and adaptation studies. For this reason, enhancements to and validation of regional climate models (similar to the sophisticated models used for weather forecasting) are underway or have been completed. These models are now ready for the creation of probabilistic climate projections for California at a resolution that will be adequate for local and regional impacts and adaptation studies. These scenarios will be ready in the third or last quarter of 2009.

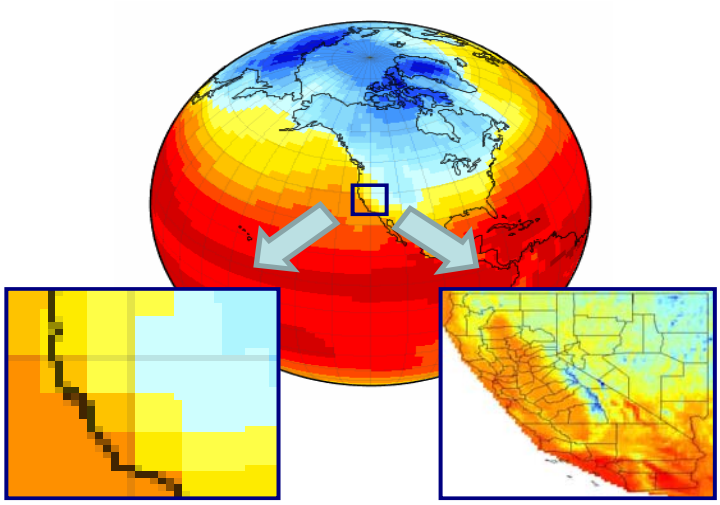


Figure 23. Temperature distribution for California from a global climate model and downscaled results for California. The global temperature distribution is an example for a given month in a given year for a typical global climate model. The map on the left shows how downscaling provides fine-scale (about 7.5 miles) resolution.[14]

Source: Authors

[14] Mary Tyree from Scripps Institution of Oceanography provided the data, and Franco and Pittiglio (Energy Commission) generated the maps.

5.11. Development of Tools for Impacts and Adaptation Studies

An ongoing and acute need for improved tools and models to understand the effects of climate change on California's resources has led to the continued support of development of several new predictive and analytical tools and the preparation and refinement of several others. For example, researchers at UC Davis enhanced its California Value Integrated Network (CALVIN) model to improve the representation of groundwater resources after a preliminary study suggested that water storage in underground aquifers could ameliorate some of the negative impacts of climate change on water availability (Lund, 2003). Researchers at UC Santa Barbara, Stanford, UC Davis, and Conservation International have developed a new dynamic ecological model for California that addresses some limitations of existing ecological models such as incomplete assessment of barriers (e.g., urban areas) to the dispersal of fauna and flora (Conservation International et al., 2008). A coastal evolution model is under development at the University of Florida and Scripps Institute of Oceanography to improve estimations of coastal responses to accelerating sea-level rise.

5.12. Effect of Aerosols on Precipitation Levels and Regional Climate

Aerosols (fine particles suspended in air) may be reducing precipitation levels over the Sierra Nevada mountains (Lynn et al., 2007; Rosenfeld and Gavati, 2006) and affecting the regional climate (Jacobson, 2004). The reported precipitation reductions are on the order of 15 percent, representing a substantial loss of water resources that otherwise could have been used for environmental purposes, to provide water to cities and farms, and to produce hydroelectricity. Several studies using numerical models, satellite data, and field measurements using research aircraft have facilitated the accumulation of evidence that appears to confirm the negative role of aerosols on the amount of precipitation in the Sierra Nevada (Rosenfeld et al., 2007), with similar findings reported in other parts of the world where the topography influences the generation of rain and snow (Woodley, 2008). Further studies are being planned to identify the types of sources (e.g., cars, natural gas combustion) responsible for generating the detrimental aerosols. If climate change results in a drying of the West, including California, actions to reduce the aerosols that are affecting precipitation levels in California could become an extremely important adaptation tool.

5.13. Adaptation to Present Climate Variability as a Parallel for Climate Change

As discussed earlier, climate change not only will result in changes in average climate conditions but will also increase climate variability (deviations from "normal" conditions). For

example, more frequent heat waves, flooding events, and forest fires are expected for California in this century. Common sense suggests that improving the ability to manage current climate variability may also be useful in a changing climate. The following example details a strategy for water management that provides an example for this type of adaptation.

Researchers associated with the Hydrologic Research Center (HRC) published a paper in 2001 (Yao and Georgakakos, 2001) that demonstrated that probabilistic climate forecasts in combination with a modern decision support system could substantially improve the management of the Shasta Reservoir. According to the study, this new management system would be more efficient, resulting in more water available for consumptive use and electric power generation while still providing other needed services such as recreation and flood protection (Carpenter and Georgakakos 2001). This new management system would replace the existing operating rules, which are very conservative and are based on historical hydrological conditions.

A second paper by HRC researchers suggested that negative impacts from climate change on the services provided by the Shasta Reservoir could also be substantially ameliorated (Yao and Georgakakos 2001). Given the importance of these findings, the National Oceanic Atmospheric Administration (NOAA), CALFED (a consortium of state and federal agencies), and the PIER Program together funded a demonstration project known as the Integrated Forecast and Management (INFORM) system for the coordinated management of five major reservoirs in Northern California, including Shasta. After system development, INFORM entered a demonstration phase involving participation by all the agencies responsible for the operation of these reservoirs (e.g., California Department of Water Resources, U.S. Bureau of Reclamation). INFORM system was run on a near-real-time basis during this phase, during which appropriate management decisions were suggested by the system while the water managers continued to operate the reservoirs using existing operating rules. A retrospective evaluation conducted months after the management decisions were made indicated that the INFORM system was superior to the traditional operating rules (i.e., it would have been superior to follow the forecasting information and decision support provided by INFORM). Given the success of the INFORM study, the participating agencies, along with DWR, plan to fund further enhancements to INFORM to extend the geographical coverage area and carry out additional demonstrations to capture different hydrologic conditions (O'Hagan, Personal communication). DWR and other agencies are seriously considering using INFORM to "re-operate" the five reservoirs included in INFORM.

The existing INFORM system is in the process of being evaluated using one or two climate scenarios to estimate how and if the system might alleviate some of the expected negative impacts of climate change and increased climate variability on water resources.

5.14. Vulnerability-Based Adaptation

To complement the state's existing strengths in the hazards-based approach to assessing adaptation needs, the state has recognized the need to foster a greater focus on vulnerability-based adaptation studies. Only one such study on the barriers to adaptation faced in California's coastal sector has been funded to date (Moser and Tribbia, 2006/07; Tribbia and Moser, 2008), but several proposals are under review for future funding. Moreover, this type of research will be emphasized increasingly in the future along with a stepped-up effort to build California's decision support capacity for climate change adaptation decisions, as will be evident in the Energy Commission's revised strategic research plan available later in 2008. Social science studies designed to identify barriers for adaptation have also started. Barriers include any regulatory, legal, socio-economic, cultural, and economic barriers for the implementation of adaptation measures.

6.0 References

Adger, W.N. (2003). "Social Capital, Collective Action and Adaptation to Climate Change." *Econ Geogr* 79: 387–404.

Adger, W.N. and K. Vincent (2005). "Uncertainty in adaptive capacity." *Comptes Rendus Geoscience* 337:399-410.

Adger, W.N. et al. (2007). "Assessment of Adaptation Practices, Options, Constraints and Capacity." In: *Climate Change 2007: Impacts, Adaptation and Vulnerability.* Contribution of Working Group II to the Fourth Assessment Report of the Intergovernmental Panel on Climate Change, Cambridge University Press, Cambridge, UK, 717-743.

Anderson, J. et al. (2008). "Progress on Incorporating Climate Change Into Management of California's water resources." *Climatic Change* 87(Suppl 1): 91-108.

Archer, D. H. Kheshgi, and E. Maier-Reimer (1997). "Multiple Timescales for Neutralization of Fossil-Fuel CO_2." *Geophysical Research Letters* 24: 405-408.

Baldocchi, D. and S. Wong (2008). "Accumulated Winter Chill is Decreasing in the Fruit Growing Regions of California." *Climatic Change* 87(Suppl 1): 153-166.

Barnett, T. et al. (2008). "Human-Induced Changes in the Hydrology of the Western United States." *Science* 319: 1080-1083.

Barry, J.P., C.H. Baxter, R.D. Sgarin, and S.E. Gilman (1995). "Climate-Related Long-Term Faunal Changes in a California Rocky Intertidal Community." *Science* 267: 672-678.

Basu, R. and J.M. Samet (2002). Relation Between Elevated Ambient Temperature and Mortality: A Review of the Epidemiologic Evidence. *Epidemiologic Reviews* 24(2): 190-202.

Basu, R., W.Y. Feng, and B.D. Ostro (2008). "Characterizing Temperature and Mortality in Nine California Counties." *Epidemiology* 19(1): 138-145.

Basu, R., F. Dominici, and J.M. Samet (2005). "Temperature and Mortality Among the Elderly in the United States: A Comparison of Epidemiologic Methods." *Epidemiology* 19(1): 138-145.

Battin, J., et al. (2007). "Projected Impacts of Climate Change on Salmon Habitat Restoration." *PNAS* 104(16): 6720-6725.

Battles, J.J., T. Robards, A. Das, K. Waring, J.K. Gilless, F. Schurr, J. LeBlanc, G. Biging and C. Simon. (2006) "Climate Change Impacts on Forest Resources." California Energy Commission White Paper CEC-500-2005-193-SF. 45p.

Bizikova, L., J. Robinson, and S. Cohen (2007). "Linking Climate Change and Sustainable Development at the Local Level." *Climate Policy* 7: 271-277.

Bonfils, C. et al. (2008). "Identification of External Influences on Temperatures in California." *Climatic Change* 87 (Suppl 1): S43–S55.

Bonfils, C. and D. Lobell (2007a). "Empirical Evidence for a Recent Slowdown in Irrigation-Induced Cooling." *PNAS* 104(34): 13582-13587.

Bonfils, C. et al. (2007b). *Identification of External Influences on Temperatures in California.* California Energy Commission, PIER Energy-Related Environmental Research. CEC-500-2007-047.

Bromirski, P.D. and R.E. Flick (submitted). "Storm Surge in the San Francisco Bay/Delta and Nearby Coastal Locations." *Shore and Beach*, submitted, 2008.

Bromirski, P.D., R.E. Flick and D.R. Cayan (2003). "Storminess variability along the California coast: 1858-2000." *Journal of Climate* vol?: 1-12.

Brooks, N., Adger, W.N., and M.P. Kelly (2005). "The Determinants of Vulnerability and Adaptive Capacity at the National Level and the Implications for Adaptation." *Global Environmental Change* 15(2): 151-163.

Burkholder, B.A. and D.J. Karoly (2007). "An Assessment of US Climate Variability Using the Climate Extremes Index." In: Nineteenth Conference on Climate Variability and Change, 15-18 January, 2007, San Antonio, TX. American Meteorological Society, Boston, Paper 2B.9. Extended abstract available at http://ams.confex.com/ams/pdfpapers/117942.pdf.

Burton, I., E. Malone, S. Huq, B. Lim, E. Spanger-Siegfried. (2005). *Adaptation Policy Frameworks for Climate Change: Developing Strategies, Policies and Measures*. Cambridge University Press.

Cahill, K.N. et al. (2007). "Modeling Climate and Climate Change Impacts on Winegrape Yields in California." *American Journal of Enology and Viticulture* 58(3): 414A-414A.

California Climate Change Center (2006). *Our Changing Climate: Assessing the Risks to California. California Energy Commission*. CEC-500-2006-077.

California Energy Commission (1989). *The impacts of global warming in California*. (P500-89-004)

California Energy Commission (1991). *Global Climate Change: Potential Impacts and Policy Recommendations* [P500-91-007, Sacramento, California]

California Energy Commission. (2005). *Climate Change Impacts and Adaptation in California*. Pages 1-41. California Energy Commission, Sacramento. CEC-500-2005-103-SD.

Canadell, J. et al. (2007). "Contributions to Accelerating Atmospheric CO_2 Growth From Economic Activity, Carbon Intensity, and Efficiency of Natural Sinks." *PNAS* 104: 18866-18870.

Carpenter, T. M. and K. P. Georgakakos (2001). "Assessment of Folsom Lake Response to Historical and Potential Future Climate Scenarios: 1. Forecasting." *Journal of Hydrology* 249(1-4): 148-175.

Cavagnaro, T., L. Jackson, and K. Scow (2006). *Climate Change: Challenges and Solutions for California Agricultural Landscapes*. California Climate Change Center.

Cayan, D., et al. (2008a). "Overview of the California Climate Change Scenarios Project." *Climatic Change* 87(Suppl 1): 1-6.

Cayan, D., et al. (2008b). "Climate Change Projections of Sea Level Extremes Along the California Coast." *Climatic Change* 87(Suppl 1): S57-S73.

Cayan, D., et al. (2008c). "Climate Change Scenarios for the California Region." *Climatic Change* 87: S21-S42.

Cayan, D. R., S. A. Kammerdiener, et al. (2001). "Changes in the onset of spring in the western United States." *Bulletin of the American Meteorological Society* 82(3): 399-415.

CCSP (2008). *Weather and Climate Extremes in a Changing Climate. Regions of Focus: North America, Hawaii, Caribbean, and U.S. Pacific Islands*. A Report by the U.S. Climate Change Science Program and the Subcommittee on Global Change Research, SAP 3.3. T.R. Karl et al., eds., Department of Commerce, NOAA's National Climatic Data Center, Washington, D.C., USA, 164 pp.

Cavagnaro, T., L. Jackson, and K. Scow. (2006). *Climate Change: Challenges and Solutions for California Agricultural Landscapes*. California Climate Change Center. CEC-500-2005-189-SF.

Charbit, S., D. Paillard, and G. Ramstein. (2008). "Amount of CO_2 Emissions Irreversibly Leading to the Total Melting of Greenland." *Geophysical Research Letters* 35: L12503, doi:10.1029/2008GL033472.

Choa, B. F., Y.H. Wu, and Y.S. Li. (2008) "Impact of Artificial Reservoir Water Impoundment on Global Sea Level." *Science* 320(5873): 212-214.

Christensen, N.S. and D.P. Lettenmaier (2007). "A Multimodel Ensemble Approach to Assessment of Climate Change Impacts on the Hydrology and Water Resources of the Colorado River Basin." *Hydrology and Earth System Sciences* 11(4): 1417-1434.

City of San Diego. (2005). *City of San Diego Climate Protection Action Plan*. July 22, 2008. http://www.sandiego.gov/environmental-services/sustainable/pdf/action_plan_07_05.pdf

Coats, R., J. Perez-Losada, G. Schladow, R. Richards and C. Goldman (2006). "The Warming of Lake Tahoe." *Climatic Change* 76(1-2): 121-148.

Conservation International, B. Ellis, L. Hannah, G. Midgley, I. Davies, F. Davis, L. Ries, W. Thuiller, J. Thorne, C. Seo, D. Stoms, and N. Snider (2008). *BioMove—Improvement and Parameterization of a Hybrid Model for the Assessment of Climate Change Impacts on the Vegetation of California: PIER Final Project Report*. 96 pp. Public Interest Energy Research Program.CEC-500-04-2008

Cutter, S.L. and C. Finch (2008). "Temporal and spatial changes in social vulnerability to natural hazards." *PNAS* 105(7): 2301-2306.

Deacon, J. E., A. E. Williams, C. D. Williams, and J. E. Williams (2007). "Fueling Population Growth in Las Vegas: How Large-Scale Groundwater Withdrawal Could Burn Regional" *Biodiversity*. BioScience 57: 688-698.

Dettinger, M.D. and S. Culberson (2008). "Internalizing Climate Change—Scientific Resource Management and the Climate Change Challenges." *San Francisco Estuary and Watershed Science* 6(2): [Article 5]; available on-line at: http://repositories.cdlib.org/jmie/sfews/vol6/iss2/art5/.

Diffenbaugh, N.S., M.A. Snyder, and L.C. Sloan (2004). "Could CO_2-Induced Land-Cover Feedbacks Alter Near-Shore Upwelling Regimes?" *PNAS* 101(1): 27-32.

Earman, S., and M. Dettinger (2008). *Monitoring Networks for Long-Term Recharge Change in The Mountains of California and Nevada: A Meeting Report*. Pages 1-32. California Energy Commission.CEC-500-2008-006

Easterling, D.R., B. Horton, P.D. Jones, T.C. Peterson, T.R. Karl, D.E. Parker, M.J. Salinger, V. Razuvayev, N. Plummer, P. Jamason, C.K. Folland (1997). "Maximum and Minimum Temperature Trends for the Globe." *Science* 277: 364-367.

English, P., K. Fitzsimmons, S. Hoshiko, T. Kim, H.G. Margolis, T.E. McKone, M. Rotkin-Ellman, G. Solomon, R. Trent, and Z. Ross. (2007). *Public Health Impacts of Climate Change in California: Community Vulnerability Assessments and Adaptation Strategies*. Climate Change Public Health Impacts Assessment and Response Collaborative, Sacramento, CA.

Eriksen, S.H. and K. O'Brien (2007). "Vulnerability, Poverty and the Need for Sustainable Adaptation Measures." *Climate Policy* 7: 337–352.

Friedlingstein, P. and S. Solomon (2005). "Contributions of Past and Present Human Generations to Committed Warming Caused by Carbon Dioxide." *PNAS* 102(31): 10832–10836.

Field, C. et al. (1999). *Confronting climate change in California ecological impacts on the Golden State.* The Union of Concerned Scientists, Cambridge, MA, and The Ecological Society of America, Washington, DC.

Feng, S., and Q. Hu. (2004). "Changes in Agro-Meteorological Indicators in the Contiguous United States: 1951-2000." *Theoretical and Applied Climatology* 78: 247-264.

Forister, M.L., A.M. Shapiro. (2003). "Climatic Trends and Advancing Spring Flight of Butterflies in Lowland California." *Global Change Biology* 9(7): 1130-1135.

Forster, R. et al. (2007). "Changes in Atmospheric Constituents and in Radiative Forcing." In: *Climate Change* 2007: The Physical Science Basis. Contribution of Working Group I to the Fourth Assessment Report of the IPCC, Solomon, S. et al., eds., Cambridge University Press: Cambridge, UK, pp.129-234.

Franco, G., D. Cayan, A. Luers, M. Hanemann, B. Croes (2008a). "Linking Climate Change Science With Policy in California." *Climatic Change* 87(Supple 1): S7-S20.

Franco, G. and A. Sanstad (2008b). "Climate Change and Electricity Demand in California." *Climatic Change* 87(Suppl 1): S139-S151.

Frumkin, H., et al. (2008). "Climate Change: The Public Health Response." *American Journal of Public Health* 983(3): 435-445.

Füssel, H.-M. (2007). "Adaptation Planning for Climate Change: Concepts, Assessment Approaches, and Key Lessons." *Sustainability Science* 2: 265-275.

Gallopín, G.C. (2006). "Linkages Between Vulnerability, Resilience, and Adaptive Capacity." *Global Environmental Change* 16: 293–303.

Georgakakos, K. et al. (2005). "Integrating Climate-Hydrology Forecasts and Multi-Objective Reservoir Management for Northern California." *EOS* 86(12): 122, 127.

Gershunov, A., D., and D.R. Cayan. (2008). "Recent Increase in California Heat Waves: July 2006 and the Last Six Decades." PIER report to be released by September 15, 2008.

Givati, A. and D. Rosenfeld (2004). "Quantifying precipitation suppression due to air pollution." *Journal of Applied Meteorology* 43: 1038-1056.

Glynn, P.W. (1988). "El Niño-Southern Oscillation 1982-1983: Nearshore Population, Community and Ecosystem Responses." *Annual Review of Ecology and Systematics* 19: 309-345.

Gonzalez, P., G.P. Asner, J.J. Battles, M.A. Lefsky, K.M. Waring. (2007). "Monitoring Forest Carbon in Sierra Nevada and North Coast Forests With Field Inventories, LIDAR, and QuickBird." Presentation at Fourth Annual California Climate Change Conference, Sacramento, CA.

Gordo, Oscar. (2007) "Why are Bird Migration Dates Shifting? A Review of Weather and Climate Effects on Avian Migratory Phenology." *Climate Research* 35: 37-58.

Groves, D.G., D. Knopman, R. J. Lempert, S. H. Berry, L. Wainfan (2008). *Presenting Uncertainty About Climate Change to Water-Resource Managers: A Summary of Workshops with the Inland Empire Utilities Agency*. RAND Corporation National Science Foundation Technical Report. 80 pages.

Gutierrez, A., et al. (2008). "Climate Change Effects on Poikilotherm Tritrophic Interactions." *Climatic Change* 87(Suppl 1): S167-S192.

Gutierrez, A.P., C.K. Ellis, and R. Ghezelbash (2006). "Climatic Limits of Pink Bollworm in Arizona and California: Effects of Climate warming." *Acta Oecologica* 30(3): 353-364.

Hadley, O.L., et al. (2007). "Trans-Pacific transport of black carbon and fine aerosols (D < 2.5 μm) into North America." *Journal of Geophysical Research* 112: [page] doi:10.1029/2006JD007632.

Hanemann, M. and L. Dale (2006). *Economic Damages from Climate Change: An Assessment of Market Impacts.* Department of Agricultural and Resource Economics and Policy, Division of Agriculture and Natural Resources, University of California at Berkeley.

Hansen, J. et al. (2007). Dangerous human-made interference with climate: a GISS modelE study. Atmos. Chem. Phys. 7, 2287-2312. Available at: http://www.atmos-chem-phys.org/7/2287/2007/acp-7-2287-2007.html

Hayhoe, K., et al. (2004). Emissions pathways, climate change, and impacts on California. PNAS 101(34): 12422-12427.

Hegerl, G. et al. (2007). Understanding and attributing climate change. In: Climate Change 2007: The Physical Science Basis. Contribution of Working Group I to the Fourth Assessment Report of the Intergovernmental Panel on Climate Change, S. Solomon et al., eds., Cambridge University Press: Cambridge, UK, 663-745.

Holdren, J.P. (2008). Science and Technology for Sustainable Well-Being. Science 319: 424-434

Human Development Report 2007/2008. Fighting climate change: Human solidarity in a divided world," can be accessed at http://hdr.undp.org/en/reports/global/hdr2007-2008/ Accessed in august 2008.

IPCC (2007). Fourth Assessment Report. Cambridge, Cambridge University Press.[Sarah]

IPCC (2007a). Summary for Policymakers. In: Climate Change 2007: The Physical Science Basis. Contribution of Working Group I to the Fourth Assessment Report of the Intergovernmental Panel on Climate Change, S. Solomon et al., eds., Cambridge University Press: Cambridge, UK, 1-18.

IPCC (2007b). Summary for Policymakers. In: Climate Change 2007: Impacts, Adaptation and Vulnerability. Contribution of Working Group II to the Fourth Assessment Report of the Intergovernmental Panel on Climate Change, M.L. Parry et al., eds., Cambridge University Press: Cambridge, UK, 7-22.

IPCC (2007c). Summary for Policymakers. In: Climate Change 2007: Mitigation. Contribution of Working Group III to the Fourth Assessment Report of the Intergovernmental Panel on Climate Change, Betz, B. et al., eds., Cambridge University Press: Cambridge, UK, 1-23.

IPCC (2001). Summary for Policymakers. In: Climate Change 2001: The Science of Climate Change. Contribution of Working Group I to the Third Assessment Report of the Intergovernmental Panel on Climate Change, J.T. Houghton et al., eds., Cambridge University Press, Cambridge, UK, 20 pp.

IPCC (1996). Summary for Policymakers. In: Climate Change 1995: The Science of Climate Change. Contribution of Working Group I to the Second Assessment Report of the Intergovernmental Panel on Climate Change, J.T. Houghton et al., eds., Cambridge University Press, Cambridge, UK, 1-7.

IPCC (1990). Scientific Assessment of Climate Change. Contribution of Working Group I to the First Assessment Report of the Intergovernmental Panel on Climate Change, J.T. Houghton et al., eds., Cambridge University Press, Cambridge, UK.

Jacobson, Mark Z. 2004. *Effects of Anthropogenic Aerosol Particles and their Precursor Gases on California and South Coast Climate.* California Energy Commission, PIER Energy-Related Environmental Research. CEC-500-2005-003.

Jain, S., M. Hoerling, and J. Eischeid (2005). "Decreasing Reliability and Increasing Synchroneity of Western North American Streamflow." *Journal of Climate* 18: 613-618.

Jansen, K.L., et al. (2005). "Associations Between Health Effects and Particulate Matter and Black Carbon in Subjects With Respiratory Disease." *Environmental Health Perspectives* 113(12): 1741–1746.

Kalkstein, L.S. and J.S. Greene (1997). "An Evaluation of Climate/Mortality Relationships in Large US Cities and the Possible Impacts of a Climate Change." *Environmental Health Perspective*s 105(1): 84-93.

Kanamaru, H and M. Kanamitsu., (2006). *Fifty-Seven Year California Reanalysis Downscaling at 10 Kilometers* (CaRD10). CEC-500-2006-071.

Kinney, P.L., et al. (2008). "Approaches for Estimating Effects of Climate Change on Heat-Related Deaths: Challenges and Opportunities." *Environmental Science & Policy* 11(1): 87-96.

Klein, R.J.T. et al. (2007). "Inter-relationships between adaptation and mitigation." *Climate Change 2007: Impacts, Adaptation and Vulnerability.* Contribution of Working Group II to the Fourth Assessment Report of the Intergovernmental Panel on Climate Change, M.L. Parry et al., eds., Cambridge University Press, Cambridge, UK, 745-777.

Knowles, N., M. Dettinger, and D. Cayan. 2007. *Trends in Snowfall Versus Rainfall for the Western United States, 1949–2001.* California Energy Commission, PIER Energy-Related Environmental Research Program. CEC-500-2007-032

Kosloff, L. H., Trexler, M. C., and Nelson, H. (2004)." Outcome-Oriented Leadership: How State and Local Climate Change Strategies can Most Effectively Contribute to Global Warming Mitigation." *Widener Law Journal* 14: 173-204.

Kueppers, L.M., M.A. Snyder, and L.C. Sloan (2007). "Irrigation Cooling Effect: Regional Climate Forcing by Land-Use Change." *Geophys. Res. Lett*. 34: L03703.

Kueppers, L.M., et al. (2005). "Modeled Regional Climate Change and California Endemic Oak Ranges." *PNAS* 102(45): 16281-16286.

LaBolle, E.M., A.A. Ahmed, and G.E. Fogg (2003). "Review of the Integrated Groundwater and Surface-Water Model (IGSM)." *Ground Water* 41: 238-246.

LaDochy, S. R. Medina, W. Patzert. (2007). "Recent California Climate Variability: Spatial and Temporal Patterns in Temperature Trends." *Climate Research* 33 (2): 159-169.

Landis, J.D. and M. Reilly. (2003). "How We Will Grow: Baseline Projections of California's Urban Footprint Through 2100." Appendix III in Wilson, T. et al., *Global Climate Change and California: Potential Implications for Ecosystems, Health, and the Economy.* California Energy Commission: Sacramento. 87pp.

Lebel, L., J. M. Anderies, B. Campbell, C. Folke, S. Hatfield-Dodds, T. P. Hughes. and J. Wilson (2006). "Governance and the Capacity to Manage Resilience in Regional Social-Ecological Systems." *Ecology and Society* 11(1): 19; available online at: http://www.ecologyandsociety.org/vol11/iss1/art19/.

Lenton, T.M., Held, H., Kriegler, E., Hall, J.W., Lucht, W., Rahmstorf, S. and Schellnhuber, H.-J. (2008). "Tipping Elements in the Earth's Climate System." *PNAS* 105(6): 1786–1793.

Lobell, D.B., G. Bala, and P.B. Duffy. (2006). "Biogeophysical Impacts of Cropland Management Changes on Climate." *Geophysical Research Letters* Vol 33, doi:10.1029/2005GL025492.

Lobell, D. B., G. Bala, C. Bonfils, and P.B. Duffy. (2006). "Potential Bias of Model Projected Greenhouse Warming in Irrigated Regions." *Geophysical Research Letters* 33.

Lobell, D.B., C. Bonfils, and P.B. Duffy (2007). "Climate Change Uncertainty for Daily Minimum and Maximum Temperatures: A Model Inter-Comparison." *Geophysical Research Letters* Vol 34, doi:10.1029/2006GL028726.

Loarie, S.R., B.E. Carter, K. Hayhoe, S. McMahon, R. Moe, C.A. Knight, D.D. Ackerly. (2008). "Climate Change and the Future of California's Endemic Flora." *PLoS ONE* 3(6): e2502. doi:10.1371/journal.pone.0002502.

Luers, A.L. and S. Moser (2005). *Preparing for the Impacts of Climate Change in California: Opportunities and constraints for adaptation*. California Climate Change Center.

Lund, J., et al. (2007). *Envisioning Futures for the Sacramento-San Joaquin Delta*. Public Policy Institute of California, San Francisco, CA.

MacCracken, M.C., F. Moore, and J.C. Topping Jr. (2008). "Sudden and Disruptive Climate Change: Explroing the Real Risks and How We Can Avoid Them." *Earthscan*: London, UK.

MacMynowski, D. P., and T. L. Root. 2007. *Climatic Change and the Timing of Songbird Migration in California: Focus on Coastal Central and Northern Regions.* California Energy Commission, PIER Energy-Related Environmental Research. CEC-500-2007-010.

Marland, G., T.A. Boden, and R.J. Andres. 2008. "Global, Regional, and National Fossil Fuel CO2 Emissions." In *Trends: A Compendium of Data on Global Change*. Carbon Dioxide Information Analysis Center, Oak Ridge National Laboratory, U.S. Department of Energy, Oak Ridge, Tenn., U.S.A.

Maurer, E.P., et al. (2007). "Detection, Attribution, and Sensitivity of Trends Toward Earlier Streamflow in the Sierra Nevada." *Journal of Geophysical Research* 112(D11).

McCarthy, J. et al. (2001). *Climate Change 2001. Impacts, Adaptation and Vulnerability*. Contribution of Working Group II to the Third Assessment of the IPCC. Cambridge University Press, Cambridge, UK.

McKinstry Jr., R. B. (2004). "Laboratories for Local Solutions for Global Problems: State, Local and Private Leadership in Developing Strategies to Mitigate the Causes and Effects of Climate Change." *Penn State Environmental Law Review* 12(1): 15-82.

McGeehin, M.A. and M. Mirabelli (2001). "The Potential Impacts of Climate Variability and Change on Temperature-Related Morbidity and Mortality in the United States." *Environmental Health Perspectives* 109: 185-189.

Medellín-Azuara, J. et al. (2008). "Adaptability and Adaptations of California's Water Supply System to Dry Climate Warming." *Climatic Change* 87(Suppl 1): S75-S90.

Meehl, G.A. et al. (2005). How much more global warming and sea level rise? Science 307: 1769-1772.

Mendelsohn, R. (2003). "The Impact of Climate Change on Energy Expenditures in California," Appendix XI in Wilson, T. et al., *Global Climate Change and California: Potential Implications for Ecosystems, Health, and the Economy*, California Energy Commission: Sacramento. 43 pp.

Menzel, A. et al. (2006) "European Phenological Response to Climate Change Matches the Warming Pattern." *Global Change Biology* 12: 1969–1976.

Millar, C.I., R.D. Westfall, and D.L. Delany (2007). "Response of High-Elevation Limber Pine (Pinus flexilis) to Multi-Year Droughts and 20th-Century Warming; Sierra Nevada, California, USA." Sierra Nevada Research Center. Pp.1-48.

Miller, N., K. Hayhoe, J. Jin, and M. Auffhammer. 2008. "Climate, Extreme Heat, and Electricity Demand in California." *Journal of Applied Meteorology and Climatology*: doi: 10.1175/JAM2597.1.

Mount, J., R. Twiss, and R. Adams (2006). *The Role of Science in the Delta Visioning Process: A report of the Delta Science Panel of the CALFED Science Program*. Complete ref?

Morton, D.C., et al. (2003). Assessing the Environmental, Social, and Economic Impacts of Wildfire. Global Institute of Sustainable Forestry, Yale University.

Moser, S.C. and A.L. Luers (2008). "Managing Climate Risks in California: The Need to Engage Resource Managers for Successful Adaptation to Change." *Climatic Change* 87(Suppl 1): S309-S322.

Moser, S.C. and J. Tribbia (2006/2007). "Vulnerability to Inundation and Climate Change Impacts in California: Coastal Managers' Attitudes and Perceptions." *Mar Technol Soc* J 40(4): 35–44.

Moser, S.C. et al. (2008). "Adaptation to Climate Change in the Northeast United States: Opportunities, Processes, Constraints." *Mitigation and Adaptation Strategies for Global Change* 13(5-6): 643-659.

Moss, R. et al. (2007). Towards New Scenarios for Analysis of Emissions, Climate Change, Impacts, and Response Strategies. IPCC Expert Meeting Report. Intergovernmental Panel on Climate Change, Geneva, 132 pp.

Mote, P.W. et al. (2005). "Declining Mountain Snowpack in Western North America." *Bulletin of the American Meteorological Society* 86: 39-49.

Mueller, J., J. Loomis, and A. González-Cabán (2007). "Do Repeated Wildfires Change Homebuyers' Demand for Homes in High-Risk Areas? A Hedonic Analysis of the Short and Long-Term Effects of Repeated Wildfires on House Prices in Southern California." *The Journal of Real Estate Finance and Economics*. DOI 10.1007/s11146-007-9083-1.

National Research Council (2002). *Abrupt Climate Change: Inevitable Surprises*. National Academies Press: Washington, DC.

Nemani, R.R. et al. (2001) "Asymmetric Warming Over Coastal California and its Impact on the Premium Wine Industry." *Climate Research* 19(1): 25-34.

Neumann, J.E. et al. (2003). "Market Impacts of Sea Level Rise on California Coasts," Appendix XIII in Wilson, T., L. Williams, J. Smith, and R Mendelsohn, *Global Climate Change and California: Potential Implications for Ecosystems, Health, and the Economy*, California Energy Commission, Sacramento, CA, 23 pp.

Niswonger, R. G., and G. E. Fogg (2008). "Influence of Perched Groundwater on Base Flow." *Water Resources Research* 44: doi:10.1029/2007WR006160.

O'Brien, K. et al. (2006). "Questioning Complacency: Climate Change Impacts, Vulnerability, and Adaptation in Norway." *Ambio* 35: 50–56.

O'Hagan, Joe. (2008). Personal communication.

Ostro, Bart. (2008). Personal communication.

Parmesan, C. (1996). Climate and species' range. Nature 382: 765-766.

Parmesan, C. et al. (1999). "Poleward Shirts in Geographical Ranges of Butterfly Species Associated with Regional Warming." *Nature* 399: 579-583.

Parmesan, C. (2006). "Ecological and Evolutionary Responses to Recent Climate Change." *Annu Rev Ecol Evol Syst* 37: 637–669.

Parmesan, C. and G. Yohe (2003). "A Globally Coherent Fingerprint of Climate Change Impacts Across Natural Systems." *Nature* 421: 37–42.

Parry, M. et al. (eds., 2007). *Climate Change 2007: Impacts, Adaptation and Vulnerability*. Contribution of Working Group II to the Fourth Assessment Report of the Intergovernmental Panel on Climate Change. Cambridge University Press: Cambridge, UK.

Pelling, M. and C. High (2005). "Understanding Adaptation: What can Social Capital Offer Assessments of Adaptive Capacity?" *Global Environmental Change* 15: 308–319.

Penuelas, J. and I. Filella (2003). "Phenology—Responses to a Warming World." *Science* 294: 793.

Pielke, R.A. Jr. et al. (2007). "Lifting the Taboo on Adaptation." *Nature* 445: 597-598.

Public Policy Institute of California (2006). "California's Future Population" (Factsheet). URL: http://www.ppic.org/content/pubs/jtf/JTF_FuturePopulationJTF.pdf. Accessed on June 23, 2008.

Purkey, D., et al. (2008). "Robust Analysis of Future Climate Change Impacts on Water for Agriculture and Other Sectors: A Case Study in the Sacramento Valley." *Climatic Change* 87(Suppl 1): S109-S122.

Purkey, D.R., W.W. Wallender, G.E. Fogg, and B. Sivakumar (2004). "Describing Near Surface, Transient Flow Processes in Unconfined Aquifers Below Irrigated Lands: Model Application in the Western San Joaquin Valley, California." *Journal of Irrigation and Drainage Engineering-Asce* 130: 451-459.

Rabe, B.G. (in press). "Second Generation Climate Policies in the States: Proliferation, Diffusion, and Regionalization." In: *Changing Climates in North American Politics: Institutions, Policymaking and Multilevel Governance*, The MIT Press, Cambridge, MA, pp 88-117.

Rahmstorf, S. (2007). "A Semi-Empirical Approach to Projecting Future Sea-Level Rise." *Science* 315(5810): 368-370.

Raupach, M.R., et al. (2007). "Global and Regional Drivers of Accelerating CO_2 Emissions." *PNAS* 104: 10288-10293.

Reddy, M.S. and O. Boucher (2007). "Climate Impact of Black Carbon Emitted From Energy Consumption in the World's Regions." Geophysical Research Letters 34: 1-5.

Root, T.L., Price, J.T., Hall, K.R., Schneider, S.H., Rosenzweig, C., and Pounds, J.A. (2003). "Fingerprints of Global Warming on Wild Animals and Plants." *Nature* 421: 57–60.

Root, T.L., MacMynowski, D.P., Mastrandrea, M.D., and Schneider, S.H. (2005) "Human-Modified Temperatures Induce Species Changes: Joint attribution." *PNAS* 102: 7465–7469.

Rosenfeld, D. and A. Gavati (2006). "Evidence of Orographic Precipitation Suppression by Air Pollution–Induced Aerosols in the Western United States." *Journal of Applied Meteorology and Climatology* 45(7): 893–911.

Rosenzweig, C. et al. (2008). "Attributing Physical and Biological Impacts to Anthropogenic Climate Change." *Nature* 453: 353-357.

Rosenzweig, C. et al. (2007). "Assessment of Observed Changes and Responses in Natural and Managed Systems." In: *Climate Change 2007: Impacts, Adaptation and Vulnerability*. Contribution of Working Group II to the Fourth Assessment Report of the Intergovernmental Panel on Climate Change, M.L. Parry et al., eds, Cambridge University Press: Cambridge, UK, 79-131.

Rykaczewski, R.R. and D.M. Checkley, Jr. (2008). "Influence of Ocean Winds on the Pelagic Ecosystem in Upwelling Regions." *PNAS* 105(6): 1965-1970.

San Diego Foundation, 2008 in press. "San Diego 2050," Report.

Schellenhuber, H.-J. et al. (eds., 2006). *Avoiding Dangerous Climate Change*. Cambridge University Press; Cambridge, UK.

Schoups, G., et al. (2005). "Sustainability of Irrigated Agriculture in the San Joaquin Valley, California." *PNAS* 102(43): 15352-15356.

Schwartz MD, Ahas R, Aasa A (2006) Onset of spring starting earlier across the Northern Hemisphere. Global Change Biology 12: 343–351.

Seager, R., M. F. Ting, I. Held, Y. Kushnir, J. Lu, G. Vecchi, H. P. Huang, N. Harnik, A. Leetmaa, N. C. Lau, C. H. Li, J. Velez, and N. Naik (2007). "Model Projections of an Imminent Transition to a More Arid Climate in Southwestern North America." *Science* 316: 1181-1184.

Smit, B. and J. Wandel (2006). "Adaptation, Adaptive Capacity and Vulnerability." *Global Environmental Change* 16(3): 282-292.

Smit, B. et al. (1999). "The Science of Adaptation: A Framework for Assessment." *Mitigation and Adaptation Strategies for Global Change* 4: 199-213.

Smith, J., Klein, R. and Huq, S. (2003). *Climate Change, Adaptive Capacity and Development*. London: Imperial College Press.

Solomon, S. et al. (eds., 2007). *Climate Change 2007: The Physical Science Basis*. Contribution of Working Group I to the Fourth Assessment Report of the Intergovernmental Panel on Climate Change. Cambridge University Press: Cambridge, UK.

Snyder, M.A., et al. (2003). "Future climate change and upwelling in the California Current." *Geophysical Research Letters* 30(15): [1823].

Snyder, M. A., L. M. Kueppers, L. C. Sloan, D. Cayan, J. Jin, H. Kanamaru, M. Kanamitsu, N. L. Miller, M. Tyree, H. Du, and B. Weare. 2006. *Regional Climate Effects of Irrigation and*

Urbanization in the Western United States: A Model Intercomparison. California Energy Commission, PIER Energy-Related Environmental Research. CEC-500-2006-031.

Spyratos, V., P.S. Bourgeron, and M. Ghil (2007). "Development at the Wildland - Urban Interface and the Mitigation of Forest-Fire Risk." *PNAS* 104(36): 14272-14276.

Syphard, A.D., et al. (2007). "Human Influence on California Fire Regimes." *Ecological Applications* 17(5): 1388-1402.

Syphard, A.D., K.C. Clarke, and J. Franklin (2007). "Simulating Fire Frequency and Urban Growth in Southern California Coastal Shrublands, USA." *Landscape Ecology* 22(3): 431-445.

Steffensen, J.P. et al. (2008). "High-Resolution Greenland Ice Core Data Show Abrupt Climate Change Happens in Few Years." *Science Express,* 19 June 2008, DOI 10.1126/science.1157707.

Stewart, I.T., D.R. Cayan, and M.D. Dettinger (2005). "Changes Towards Earlier Streamflow Timing Across North America." *Journal of Climate*18: 1136-1155.

Stouffer, R.J., et al., 2006: "GFDL's CM2 Global Coupled Climate Models. Part IV: Idealized Climate Response." *J. Clim*., 19, 723–740.

Tanaka, S.K., et al. (2006). "Climate Warming and Water Management Adaptation for California." *Climatic Change* 76(3-4): 361-387.

Thorne, J.H. et al. (2006). *The Development of 70-Year-Old Wieslander Vegetation Type Maps and an Assessment of Landscape Change in the Central Sierra Nevada.* California Energy Commission, PIER Energy-Related Environmental Program. CEC 500-2006-107.

Thorne, J.H. (2008). Quarterly PIER Report. *Dynamics of Sierra Nevada Conifer Loss Under Climate Change.* Contract 500-07-004.

Tompkins, E.L. and W.N. Adger (2005). "Defining Response Capacity to Enhance Elimate Change Policy." *Environmental Science & Policy* 8: 562–571.

Tribbia, J. and S.C. Moser (2008). "More than Information: What Coastal Managers Need to Prepare for Climate Change." *Environmental Science & Policy* 11: 315-328.

USGCRP (2002). *The Potential Consequences of Climate Variability and Change for California. The California Regional Assessment*. http://www.usgcrp.gov/usgcrp/nacc/california.htm

van Asch, M. and M.E. Visser (2007). "Phenology of Forest Caterpillars and Their Host Trees: the Importance of Synchrony." *Annu Rev Entomol* 52: 37–55.

Vicuna, S. and J.A. Dracup (2007). "The Evolution of Cimate Change Impact Studies on Hydrology and Water Resources in California." *Climatic Change* 82(3-4): 327-350.

Vicuna, S., M. Hanemann, and L. Dale (2006). *Economic Impacts of Delta Levee Failure Due to Climate Change: A scenario analysis.* PIER CEC-500-2006-004

Visser, M.E. and L.J.M. Holleman (2001). "Warmer Springs Disrupt the Synchrony of Oak and Winter Moth Phenology." Proceedings of the Royal Society of London B 268: 289–294.

Visser, M.E. and C. Both (2005). "Shifts in Phenology Due to Global Climate Change: The Need for a Yardstick." Proceedings of the Royal Society of London B Bio 272: 2561–2569.

Walker, B. and D. Salt (2006). *Resilience Thinking: Sustaining Ecosystems and People in a Changing World.* Washington, DC: Island Press.

Walther, B.A. and C. Rahbek (2002). "Where do Paleoarctic migratory birds overwinter in Africa?" *Danks Orn Foren Tidsskr* 96: 4–8.

Walther, G.R., et al. (2002). "Ecological Response to Recent Climate Change." *Nature* 416: 389–395.

Weare B.C. and H. Du (2007). "Modeling Regional Climate Changes: Influences of Recent Global Warming and Irrigation in California." *International Journal of Climatology* (DOI: 10.1002/joc.1622).

Weiser, M. (2008). "California Bans Salmon Fishing in Coastal Waters." *The Sacramento Bee*, April 16, 2008, p.A1, Sacramento.

Westerling, A.L., H.G. Hidalgo, D.R. Cayan, and T.W. Swetnam (2006). "Warming and Earlier Spring Increase Western U.S. Forest Wildfire Activity." *Science* 313: 940-943.

Westerling, A.L., and B.P. Bryant. (2008). "Climate Change and Wildfire in California." *Climatic Change* 87(Suppl 1): S231-S249.

Wigley, T. (2005). "The Climate Change Commitment." *Science* 307: 1766-1769.

Wilson, T., et al. (2003). *Global Climate Change and California: Potential Implications for Ecosystems, Health, and the Economy*. California Energy Commission: Sacramento, 138 pp., Report 500-03-058CF, http://www.energy.ca.gov/pier/final_project_reports/500-03-058cf.html.

Woodley, William L., Daniel Rosenfeld, Duncan Axisa, Eyal Freud, and James G. Hudson. 2008. *Aircraft Measurements of the Impacts of Pollution Aerosols on Clouds and Precipitation Over the Sierra Nevada*. California Energy Commission, PIER Energy-Related Environmental Research. CEC- 500-2008-015.

Yao, H. and A. Georgakakos (2001). "Assessment of Folsom Lake Response to Historical and Potential Future Climate Scenarios 2. Reservoir management." *Journal of Hydrology* 249(1-4): 176-196.

Yohe, G. and R.S.J. Tol. (2002). "Indicators for Social and Economic Coping Capacity: Moving Toward a Working Definition of Adaptive Capacity." *Global Environmental Change* 12(1): 25-40.

Yohe, G. et al. (2007). "Perspectives on Climate Change and Sustainability." In*: Climate Change 2007: Impacts, Adaptation and Vulnerability.* Contribution of Working Group II to the Fourth Assessment Report of the Intergovernmental Panel on Climate Change, Parry, M.L. et al., eds., Cambridge University Press, Cambridge, UK, 811-841.

Zavaleta, E.S., K.B. Hulvey, and B. Fulfrost (2007). "Regional Patterns of Recruitment Success and Failure in Two Endemic California Oaks." *Diversity and Distributions* 13(6): 735-745.

Zhang, X. et al. (2007). "Detection of Human Influence on Twentieth-Century Precipitation Trends." *Nature* 448: 461-465.

Zhu, T., et al. (2007). "Climate Change, Urbanization, and Optimal Long-Term Floodplain Protection." *Water Resources Research* 43: 1-11.

Appendix 1: Detection of Climatic and Related Environmental Changes and Attribution to Anthropogenic Causes

Growing Scientific Confidence over Time

In 1990, at the time of the IPCC's first assessment, scientists concluded that the observational evidence was insufficient to either clearly detect or deny a human influence on the global climate (IPCC, 1990). By the time of the second IPCC assessment report in 1995, the consensus view had strengthened, but many uncertainties remained when scientists carefully stated that, "The balance of evidence suggests a discernible human influence on global climate" (IPCC, 1996, p.4). In 2001, at the time of the Third Assessment Report, the scientific community had advanced significantly concluding that, "There is new and stronger evidence that most of the warming observed over the last 50 years is attributable to human activities" (IPCC, 2001, p.10). Finally, in its most recent assessment in 2007, the IPCC essentially eradicated any remaining doubt over human responsibility for the observed impacts over the last half of the 20th century.

Regarding the emissions of heat-trapping greenhouse gases in the atmosphere, the IPCC observed,

> "Global atmospheric concentrations of carbon dioxide, methane, and nitrous oxide have increased markedly as a result of human activities since 1750 and now far exceed pre-industrial values determined from ice cores spanning many thousands of years. The global increases in carbon dioxide concentrations are due primarily to fossil fuel use and land use change, while those of methane and nitrous oxide are primarily due to agriculture." (Solomon et al., 2007, p.2)

Moreover, considering all types of emissions (gases and aerosols) and activities, the IPCC stated with *very high confidence*[15] that "the global average net effect of human activities since 1750 has been one of warming" (IPCC, 2007, p.3) and that greenhouse gas concentrations alone would have warmed temperatures even more were it not for the cooling effect of natural and anthropogenic aerosols. Based on longer and improved data records, an expanded range of observations, improved simulations of many aspects of the climate and new attribution studies, the IPCC arrived at its strongest conclusion yet regarding the "human fingerprint" on the global climate when it stated,

> "Most of the observed increase in global average temperatures since the mid-20th century is *very likely* due to the observed increase in anthropogenic greenhouse gas concentrations.[16] […] Discernible human influences now extend to other aspects of climate, including ocean warming, continental-average temperatures, temperature extremes and wind patterns." (IPCC, 2007, 10)

---

[15] "Very high confidence" means that there is a 9 out of 10 chance that the scientific judgment is correct.

[16] "Very likely" indicates a greater than 90% likelihood of an outcome or result occurring, based on expert judgment.

How have scientists come to such a strong conclusion about human causation, i.e., how can observed changes be attributed to human as opposed to natural causes. This section provides evidence from studies of global and – to the extent possible – regional climate variables that show a clear human influence.

Human Attribution Studies: How Do We Know?

The process of understanding the causes and impacts of climate variability and change involves, first, the *detection* of change, and second, the *attribution* of that change to a particular cause or set of causes. Both are challenging, and a variety of methods and data sets are typically used to determine connections between cause and effect.

One fundamental challenge lies in the fact that the climate system is inherently variable, i.e., dynamic processes in the atmosphere cause temperatures, atmospheric pressure, precipitation patterns, sea levels and so on to vary from place to place and from month to month, year to year, decade to decade, and even over much longer timeframes. In addition, there are external "forcings," i.e. perturbation in the radiative energy budget of the Earth's climate system, which also lead to changes in climate variables such as temperature or precipitation. Such perturbations or forcings may be natural or human in source, including variations in solar radiation, aerosols from volcanic eruptions, or greenhouse gases and aerosols produced from human activities. In an effort to detect and explain observed changes, it is essential then to understand three critical components:

- The natural dynamics and resulting internal variability of the climate system
- The magnitude of any external forcings, both natural and anthropogenic
- The response or sensitivity of the climate system to that forcing

Scientific understanding of each of these components has improved significantly over the past 20 years, leading to the growing confidence in human causation mentioned above. Clearly, additional uncertainties remain and knowledge is likely to improve further by the time of the next IPCC assessment.

Detection

The task of *detection* is to discern a real trend in any climatic variable away from a long-term average, i.e., showing with statistical significance that the observed change is indeed a notable deviation from the long-term average (Houghton et al., 1996, pp.4-5).[17] Given the "noise" of natural variability in climate observations (or computer simulations), detecting a real change often requires longer data records, and confidence grows typically with the length of the records. If an observed change or trend is larger than internal variability alone is likely to produce by chance, that change is said to be 'detected' (Hegerl et al., 2007, p.667).

[17] In modern climate studies, it is common to use a baseline of 30 years (e.g., 1961-1990 or 1971-2000) and determine the average value of the variable of interest.

Detection can be difficult when the observational record is too short to conclude anything with statistical significance, when the climate system's response to a forcing is small relative to natural variability, or when the climate system responds in some areas in one direction (e.g., precipitation increases in one region) but in the opposite direction elsewhere (precipitation decreases in another region), thus canceling each other out on a global average. It is therefore important to carefully analyze climate records at those spatio-temporal scales at which the climate system is expected to respond, filter out, as much as possible, internal variability, use the longest possible data records, look for patterns of variation in time and space (so-called 'fingerprints') that are consistent with physical understanding of the climate system, and identify changes in several indicators so as to combine various lines of corroborating evidence into a consistent and physically plausible picture (Hegerl et al., 2007, pp.667-668).

Attribution

By contrast, the task of *attribution* is to establish the most likely cause(s) of the observed change or trend, typically by testing alternative explanations (e.g., the observed trend is due to natural forcing vs. anthropogenic forcing). Unequivocal attribution to a cause would only be possible in a completely controlled experiment. Given that there is only one Earth, however, and no alternative planet with similar baseline conditions but without humans, a "natural" comparison between changes observed on Earth and elsewhere is impossible. Differently put, the Earth is undergoing at present a global experiment as a result of human activities without a "control run."

In the absence of a second Earth, scientists instead use model-based climate simulations as "laboratories" to test alternative explanations. Attribution then, in practical terms, means that scientists combine their best current understanding of the climate system and of natural and anthropogenic forcings, with their by now quite sophisticated ability to reproduce these dynamics in powerful super-computer models to test two principal hypotheses:

- An observed change is consistent with the estimated or expected response of the climate system to the actual combination of natural and anthropogenic forcing; and
- An observed change is inconsistent with an alternative, physically plausible (but not actually realized) climate change as a result of a different set of forcings.

If an observed change meets both criteria, and especially if multiple observed changes withstand this type of testing, confidence in the causal linkage between a forcing or combination of forcings increases (Hegerl et al., 2007, p.668). In some cases (such as global temperature change), such attribution studies can be done quantitatively, using computer simulations and illustrating statistical significance. In other cases, the human fingerprint on observed trends is not yet apparent (i.e., statistically significant) and scientific confidence lower, though the observed change may still be physically consistent with expected change and therefore important.

Attribution studies, like detection studies, are constrained by our knowledge of internal climate variability over the course of decades or longer, uncertainties in models, uncertainties in climate forcings and in our understanding of the responses to a given level of forcing. Multiple simulations (ensembles) from a single model, systematic comparison between simulations of the same observed modes of variability from different models, comparisons of simulated and observed variability, and comparisons of proxy records with simulations of climate variability over the last millennium have all helped to increase confidence in our ability to attribute changes to specific (combinations of) causes. Moreover, the improved observational basis (longer data records, more records, different kinds of indicators of change), more insights from paleoclimatological studies, increased modeling capacity (using different models, faster computers enabling work at higher temporal and spatial resolution), better theoretical understanding, and the use of different analytical techniques, have allowed scientists to repeatedly test their detection and attribution claims. In fact, "detection of an anthropogenic contribution to the observed warming [in the 20th century] is a result that is robust to a wide range of model uncertainty, forcing uncertainties, and analysis techniques" (Hegerl et al., 2007, p.687).

Uncertainties remain in the estimates of radiative forcing of some substances (e.g., aerosols) and in the magnitude of interdecadal variability of solar forcing, in the understanding of forcing at smaller space and time-scales, and in the attribution of surface pressure, precipitation changes, and higher-order impacts (such as some observed ecological responses).

Detection and Attribution of Environmental and Societal Impacts of Climate Change

The IPCC assessed more than the climatic changes discussed so far. Working Group II in its assessment of ecological and societal impacts, similarly concluded that,

> "A global assessment of data since 1970 has shown it is likely [66-90% probability] that anthropogenic warming has had a discernible influence on many physical and biological systems." (Parry et al., 2007, p.9)

This conclusion is based on four sets of evidence:

- The IPCC Working Group I conclusion – based on its extensive detection and attribution work – that most of the observed increase in globally averaged temperature since the middle of the 20th century is very likely due to observed increases in anthropogenic forcing.
- Based on 75 studies providing more than 29,000 data series, 89% of those that show any change exhibit responses from physical and biological systems that are consistent with the expected response to warming.
- There is strong spatial agreement between regions of significant warming and the locations where significant physical or biological response has been observed. Natural variability of the climate or the observed system is very unlikely to have solely caused the observed changes.

- Several modeling efforts were undertaken, akin to those in physical climate attribution studies, that linked physical and biological system responses to anthropogenic warming and then compared system response driven solely by climatic changes due to natural forcing."Models with combined natural and anthropogenic forcings simulate observed responses significantly better than models with natural forcing only" (Parry et al., 2007: p.9)

Limited data sets from relatively few systems and locations are an important reason for the more tentative tone in these conclusions. Attribution studies of impacts observed in physical and biological systems also have to contend with relatively greater climate variability at regional and local scales, and the concurrent non-climatic influences such as land use change, pollution, and invasive species. Until recently, scientists expressed nonetheless high confidence that anthropogenic warming of the last few decades has *discernibly* influenced a wide range of systems (Rosenzweig et al., 2007, emphasis added, from which the following summary points about observed changes is extracted). More recently, a global study explicitly tested for the first time whether observed physical and ecological changes can be attributed to human forcing. It came to a stronger conclusion, stating that, "anthropogenic climate change is having a *significant* impact on physical and biological systems globally and in some continents" (Rosenzweig et al., 2008, p.353, emphasis added).

Changes in Physical Systems

- *Arctic sea ice* extent is continuing to decline, and at increasing rates especially in the last few years; impacts on ice-dependent species (e.g., nutritional stress) and human activities (e.g., travel on ice; navigation of increasingly open Arctic waters) are already documented
- *Mountain glaciers* are receding on all continents, at high and low latitudes, leading to changing runoff, and hazard conditions (e.g., debris flows, rock fall, glacial lake outbursts, crustal uplift); *land-based ice caps* are also melting, causing freshening on ocean waters (and related ecological changes in the marine food web), and increased iceberg calving.
- *Northern Hemisphere permafrost* is thawing, leading to temporary lake expansion, eventual surface water drainage and disappearance, weakening of the mechanical stability of the ground, formation of thermokarst, ground subsidence, slope instability, increased coastal erosion, and subsequent structural impacts on buildings and infrastructure
- The extent of *snow cover in the Northern Hemisphere* is decreasing, especially at lower elevations; spring peak flows of meltwater are occurring earlier
- The annual duration of *lake and river ice cover* in the mid- and high latitudes of the Northern Hemisphere has been shortened and become more variable; some evidence for a reduction in ice-jam floods exists from Europe; other chemical and ecological changes are only beginning to be documented.

- Changes in *surface and groundwater* have been observed in many systems, and some have been linked with statistical significance to trends in temperature and precipitation, but because of different trends in regional climate change, climate variability, and the complexity of non-climatic influences on surface and groundwater, uniform global trends have not been identified. One globally coherent, if not uniform, picture is emerging regarding changes in river runoff, with increases in higher latitudes and decreases in some lower, drier latitudes. Moreover, in snow-driven catchments, there is a consistent finding of earlier peak runoff in spring
- Documented trends in floods are ambiguous with some basins showing increases, others decreases, and yet others no statistically significant trends. There is some evidence of the most catastrophic floods to increase in frequency in recent years. There is also a documented trend in some regions toward more severe droughts and more heavy rainfall events, indicating an intensification of the hydrological cycle.
- Changes in coastal processes and systems are widely evident. While clearly influenced by human activities along the coast and upstream in coastal catchments (destruction of mangroves, corals, pavement, hard protection measures, etc.), coastal erosion is occurring and possibly increasing along most of the world's coasts. Similarly, coastal wetland losses are increasing particularly where other human influences do not allow for wetlands to migrate inland and upland. Regionally, there have also been documented increases in wave height increases, coastal storm surges, flood heights and inland flooding extent, partly driven by sea-level rise and changes in storm climatology, but also land subsidence and other influences on coastal hydrology.

Changes in Biological Systems

- *Terrestrial plant and animal ranges* are shifting poleward and to higher elevations; areas where snow and ice have recently receded are quickly being colonized by plants and animals. Similar observations are made in *marine ecosystems*, where plankton, pelagic organisms, and populations of higher organisms are responding to warmer water and sea surface temperatures, stratification, changes in salinity and upwelling.
- Within the ranges of some terrestrial and marine species, *populations* are increasing in some areas and declining in others. Warm-water species, for example, are becoming more prevalent in their habitat and increasing their range.
- The timing of many *phenological life cycle events* (e.g., blooming, migration, insect emergence, leaf unfolding, coloring and fall, fruit ripening, breeding) is shifting earlier in spring and/or later in fall.
- *Species interactions* are becoming decoupled from each other as individual species react more readily than others to warming or respond in different directions. Some are changing their migratory patterns; in other cases trophic relationships and interactions are changing. Where species lose their habitat (e.g., ice), new interactions are established in alternative habitat, if available and suitable in principle.

- There are also documented *productivity (or biomass) increases* due to warmer temperatures, a longer growing season, and higher CO_2 levels (and where other factors, such as nutrient availability, were not restrictive).
- While the causes of extinctions/extirpations are typically multifactorial, climate change can play a significant part in the process, e.g., through range contraction and loss of sufficient suitable habitat, warmer temperatures and higher CO2 concentrations creating more favorable conditions for invasive competitors, or climate-driven spread of deadly diseases.

While differences among individual regions and species are apparent, the mid- and high Northern Hemisphere latitudes show a clear trend toward extension of the growing season by up to two weeks in the latter half of the 20th century, driving many of the changes observed in biological systems. A more complete assessment of these changes, i.e., higher-order impacts of the primary, climate-driven responses mentioned above, is constrained by lack of data, lack of understanding of functional interactions, and the interactive nature of many of the observed changes. For example, changes in population size of one species interact with phenological changes among species in a particular region, together producing shifts in species interactions, yet they themselves may also be directly affected by climatic changes. Moreover, "non-climate synergistic factors can significantly limit migration and acclimatization capacities" of individual species (Rosenzweig et al., 2007, p.104).

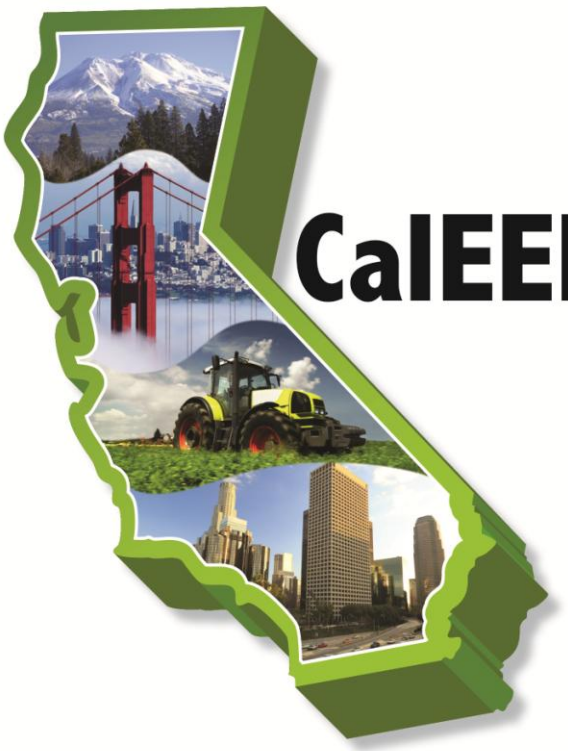
Changes in Managed and Human Systems

In general then, higher order impacts are difficult to detect and attribute to anthropogenic climate change. In particular in systems managed by humans (such as agriculture, water resources, forestry) or directly impacting humans (such as human health, tourism and recreation), efforts undertaken to cope with extremes and variability or adapt to longer-term change may mask the direct impact climate change and related physical and ecological responses may have.

- Extreme heat periods and milder winters have affected *energy demand* for cooling and heating, with summer increases in peak demand typically more pronounced.
- While it has been shown that people's destination choices regarding *tourism and outdoor recreation* are highly climate sensitive, it is difficult to isolate the role climate changes to date have played in vacation or recreation behavior, although some evidence for shifts in skiing and winter recreation has been documented.
- In *agriculture* – a sector already sensitive to climate variability – switching crops, later sowing dates, diversification of livelihoods, tree planting, cooling and irrigation technology employment or changes have all been observed as adaptive responses to observed climate changes.
- The northward shift of some disease vectors and changes in the seasonal pattern of allergens is well documented but a greater incidence of related *human health* problems is

not, due to the complexity of the disease and health care systems. Excess mortality due to extreme heat events, however, is documented on several continents.

- While statistically significant upward trends in extreme floods or storms are not yet available, *economic and insurance losses* from such events have grown tremendously. The dominant reason for these growing losses is the increase of insured and uninsured property, structures, and value in high-risk areas. When normalized by population and growth in overall wealth, no significant upward trend has been identified – at least not prior to the hurricane seasons of 2004 and 2005 in the US. Significant adaptations (e.g., early warning systems, building code and land use changes, various protection measures) have been observed in many countries.



California Emissions Estimator Model®

User's Guide

Version 2013.2

Prepared for:
California Air Pollution Control Officers Association (CAPCOA)

Prepared by:
ENVIRON International Corporation and the California Air Districts

Date:
July 2013

Acknowledgements

This program has been developed by ENVIRON International Corporation (ENVIRON) in collaboration with South Coast Air Quality Management District (SCAQMD) and California air districts. The following individuals should be recognized for their contributions to this program

California Air Districts' Development Staff

Michael Krause	South Coast AQMD
Ian MacMillan	South Coast AQMD
Steve Smith	South Coast AQMD
James Koizumi	South Coast AQMD
Jeffrey Inabinet	South Coast AQMD
Barbara Radlein	South Coast AQMD
Karen Huss	Sacramento Metropolitan AQMD
Alison Kirk	Bay Area AQMD
Ian Peterson	Bay Area AQMD
Molly Pearson	Santa Barbara County APCD
Carly Wilburton	Santa Barbara County APCD
Eric Gage	Santa Barbara County APCD
Patia Siong	San Joaquin Valley APCD
Mark Montelongo	San Joaquin Valley APCD
Jessica Willis	San Joaquin Valley APCD
Andy Mutziger	SLO County APCD

Additional Beta Testers/Contributors

Karina O'Connor	U.S. EPA
Jamesine Rogers	California Air Resources Board
Nicole Dolney	California Air Resources Board
Todd Sax	California Air Resources Board
Kathy Jaw	California Air Resources Board
Dave Vintze	Bay Area AQMD
Monica Soucier	Imperial County APCD
Sam Longmire	Northern Sierra AQMD
Jean Getchell	Monterey Bay Unified APCD
David Craft	Monterey Bay Unified APCD
Angel Green	Placer County APCD
Larry Robinson	Sacramento Metropolitan AQMD
Joseph Carle	Sacramento Metropolitan AQMD
Arnaud Marjollet	San Joaquin Valley APCD
Dan Barber	San Joaquin Valley APCD
Leland Villalvazo	San Joaquin Valley APCD
Dan Garcia	South Coast AQMD
Aeron Arlin Genet	San Luis Obispo County APCD
Melissa Guise	San Luis Obispo County APCD
Chuck Thomas	Ventura County APCD

Elaine Searcy	Ventura County APCD
Alicia Stratton	Ventura County APCD
Lauren Hocker	Sacramento County
Cindy Thielman-Braun	County of Riverside Planning Department
Jessica Range	City of San Francisco Planning Department
Patrick Griffith	Los Angeles County Sanitation Districts
Vicki Fry	Sacramento Regional County Sanitation Districts
Eliza Laws	Albert A. Webb Associates
Brad Perrine	Albert A. Webb Associates
Michael Hendrix	Atkins
Cori Wilson	Michael Brandman Associates
Katie Wilson	Michael Brandman Associates
Vince Mirabella	Consultant *(previously with Michael Brandman)*
Dave Deckman	Dudek
Debbie Bright-Stevens	Environmental Audit, Inc
Marcia Baverman	Environmental Audit, Inc
Michael Choi	Environmental Audit, Inc
Joe O'Bannon	OB-1 Air Analyses *(previously with Chambers Group)*
Nicole Vermilion	The Planning Center
John Vang	The Planning Center
Scott Gallic	RECON Environmental, Inc.
Jennifer Schulte	URS *(previously with ENVIRON)*
Tin Cheung	URS *(previously with The Planning Center)*

ENVIRON Staff

Shari Libicki	Principal and Air Quality Practice Leader
Greg Yarwood	Principal
Lit Chan	Senior Manager
Michael Masonjones	Senior Manager
David Kim	Manager
Kai Zhao	Senior Associate
Jennifer Schulte	Senior Associate *(now with URS)*
Tejas Shah	Associate
Piti Piyachaturawat	Associate

Traffic Technical Consultants

Jerry Walters	Fehr & Peers
Meghan Mitman	Fehr & Peers
Tien-Tien Chan	Fehr & Peers

Copyright

California Emission Estimator Model (CalEEMod)®
Version 2013.2
® 2013 All Rights Reserved by the California Air Pollution Control Officers Association (CAPCOA)
Developed by ENVIRON International Corporation in collaboration with the California air districts

Contents

		Page
Acknowledgements		**i**
Copyright		**iii**
1	**Introduction**	**2**
1.1	Purpose of Model	2
2	**Program Installation**	**4**
2.1	Operating System Requirements	4
2.2	Installation Procedures	4
2.3	Starting CalEEMod	6
3	**Using CalEEMod**	**6**
3.1	Home	9
3.2	Defining a Project	9
3.3	Altering Default Data	9
3.4	Mitigation	10
3.5	Reporting	10
4	**Detailed Program Screens**	**10**
4.1	Project Characteristics	10
4.2	Land Use	14
4.3	Construction	24
4.3.1	Construction Phase	24
4.3.2	Off-Road Equipment	25
4.3.3	Dust from Material Movement	26
4.3.4	Demolition	26
4.3.5	Trip and VMT	26
4.3.6	On-Road Fugitive Dust	27
4.3.7	Architectural Coatings	27
4.4	Mobile	27
4.4.1	Vehicle Trips	28
4.4.2	Vehicle Emissions	29
4.4.3	Road Dust	30
4.5	Area	30
4.5.1	Hearths and Woodstoves	31
4.5.2	Consumer Products	32
4.5.3	Area Architectural Coating	32
4.5.4	Landscape Equipment	32
4.6	Energy Use	33
4.7	Water and Wastewater Use	34

4.8 Solid Waste 36
4.9 Off -Road Equipment 35
4.10 Vegetation 38
4.10.1 Sequestration 38
4.11 Mitigation 38
4.11.1 Construction Mitigation 39
4.11.2 Traffic Mitigation 40
4.11.3 Area Mitigation 42
4.11.4 Energy Mitigation 42
4.11.5 Water Mitigation 43
4.11.6 Solid Waste Mitigation 43
4.12 Reporting 44

List of Appendices

Appendix A: Calculation Details
Appendix B: Glossary
Appendix C: Acronym List
Appendix D: Default Data Tables
Appendix E: Technical Source Documentation
Appendix F: Climate Zone Lookup

1 Introduction

This User's Guide (Guide) to the California Emission Estimator Model (CalEEMod)® is meant to give the user an introduction on how to use the program as well as document the detailed calculations and default assumptions made in associated appendices. The purpose of CalEEMod is to provide a uniform platform for government agencies, land use planners, and environmental professionals to estimate potential emissions associated with both construction and operational use of land use projects. It is intended that these emission estimates are suitable for use in California Environmental Quality Act (CEQA) compliant documents for air quality and climate change impacts. In addition individual districts may develop additional uses for the model's emission estimates to show compliance with local agency rules.

CalEEMod utilizes widely accepted models for emission estimates combined with appropriate default data that can be used if site-specific information is not available. These models and default estimates use sources such as the United States Environmental Protection Agency (USEPA) AP-42 emission factors, California Air Resources Board (ARB) vehicle emission models, studies commissioned by California agencies such as the California Energy commission (CEC) and CalRecycle. In addition, local air districts were given the opportunity to provide default values and existing regulation methodologies to use in their specific regions. If no information was provided by local air districts, appropriate state-wide values were utilized if regional differences could not otherwise be defined. Since new information and regulations are always changing, local agencies should be consulted to determine any recommended values to use that may differ from the defaults currently used in CalEEMod. User's of CalEEMod should keep in mind the assumptions and limitations of the default data in CalEEMod. A large majority of the default data associated with locations and land use is based on surveys of existing land uses. Caution should be taken if the project deviates significantly from the types and features included in the survey that forms the substantial evidence supporting the default data. In these situations site specific data that is supported by substantial evidence should be used if available.

The model provides a number of opportunities for the user to change the defaults in the model, however, users are recommended to provide justification for changing the defaults (e.g., reference more appropriate data) in the "Remarks" box provided at the bottom of the screen. Further, the user is reminded that CalEEMod is an emissions model and not an enforcement mechanism, thus, the user should ensure correct data is inputted, including the choice and percent reduction of mitigation most applicable to the land use project being evaluated.

1.1 Purpose of Model

CalEEMod provides a simple platform to calculate both construction emissions and operational emissions from a land use project. It calculates both the daily max and annual average for criteria pollutants as well as total or annual greenhouse gas (GHG) emissions which can be used in support of analyses in CEQA documents such as Environmental Impact Reports (EIRs) and Negative Declarations. In addition, default values for water and energy use are quantified which may be useful for other sections in an EIR or represent opportunities to incorporate the

rigorous site-specific information from the other EIR sections. Specifically the model aids the user in the following calculations:

- Short term construction emissions associated with demolition, site preparation, grading, building, coating, and paving from the following sources
  - Off-road construction equipment
  - On-road mobile equipment associated with workers, vendors, and hauling
  - Fugitive dust associated with grading, demolition, truck loading, and roads (Fugitive dust from wind blown sources such as storage piles are not quantified in CalEEMod which is consistent with approaches taken in other comprehensive models.)
  - Volatile emissions of reactive organic gasses (ROG) from architectural coating *(including painting on parking lots)* and paving.
- Operational emissions associated with the fully built out land use development
  - On-road mobile vehicle traffic generated by the land uses
  - Fugitive dust associated with roads
  - Volatile emissions of ROG from architectural coating
  - Emissions from off-road equipment (e.g., forklifts, cranes) used during operation
  - Off-road emissions from landscaping equipment
  - Volatile emissions of ROG from consumer products and cleaning supplies
  - Wood stoves and hearth usage
  - Natural gas usage in the buildings
  - Electricity usage in the buildings (GHG only)
  - Electricity usage from lighting in parking lots and lighting, ventilation and elevators in parking structures
  - Water usage by the land uses (GHG only)
  - Solid waste disposal by the land uses (GHG only)
- One-time vegetation sequestration changes
  - Permanent vegetation land use changes
  - New tree plantings
- Mitigation impacts to both short-term construction and operational emissions
- Several of the mitigation measures described in CAPCOA's Quantifying Greenhouse Gas Mitigation Measures[1] have been incorporated into CalEEMod.

[1] Available at : http://www.capcoa.org/wp-content/uploads/2010/11/CAPCOA-Quantification-Report-9-14-Final.pdf

2 Program Installation

The program is distributed and maintained by the California Air Pollution Control Officers Association[2]. The most recent version can be downloaded from www.caleemod.com.

2.1 Operating System Requirements

CalEEMod was programmed by ENVIRON using Microsoft SQL Compact Edition in conjunction with a Visual Basic Graphical User Interface (GUI). CalEEMod requires the following system requirements:

- Microsoft Windows XP, Vista, or 7 Operating System
- Microsoft .Net Framework 4 or higher
- 90 Mb hard drive space available

2.2 Installation Procedures

To install

1. Be sure to uninstall any previous versions of CalEEMod before installing a new version as some file names will be the same potentially confusing the computer. To uninstall for most computers, under Settings, Control Panel. Programs and Features, highlight CalEEMod .msi and .exe files and then click 'uninstall.'

2. Ensure you have the required Microsoft .Net framework 4 or higher installed on your machine. If not install this first. It is available free from Microsoft at http://www.microsoft.com/net/download.aspx

3. Download the installation files (setup.exe and CalEEMod_2013.2.msi).

4. Click the setup.exe file that you downloaded. This should walk you through the rest of the installation.

5. The default directory for CalEEMod is C:\CalEEMod\. The user may select alternative locations for installation[3]. The user will also be prompted to select to install CalEEMod for everyone who uses the computer or just the current user.

6. Click "Next" until the installation has completed. Then click close to exit the installer.

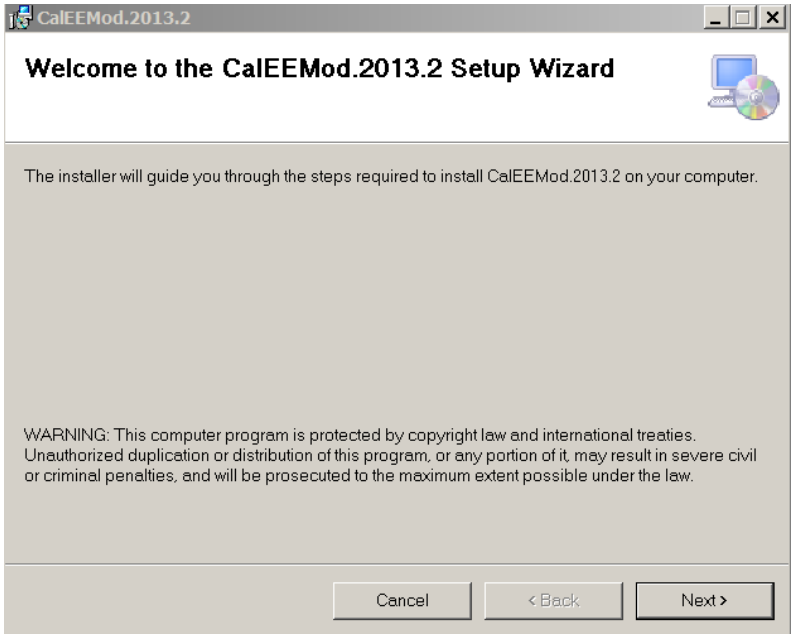
7. Click the link below to install SQL Server Compact 3.5 SP2

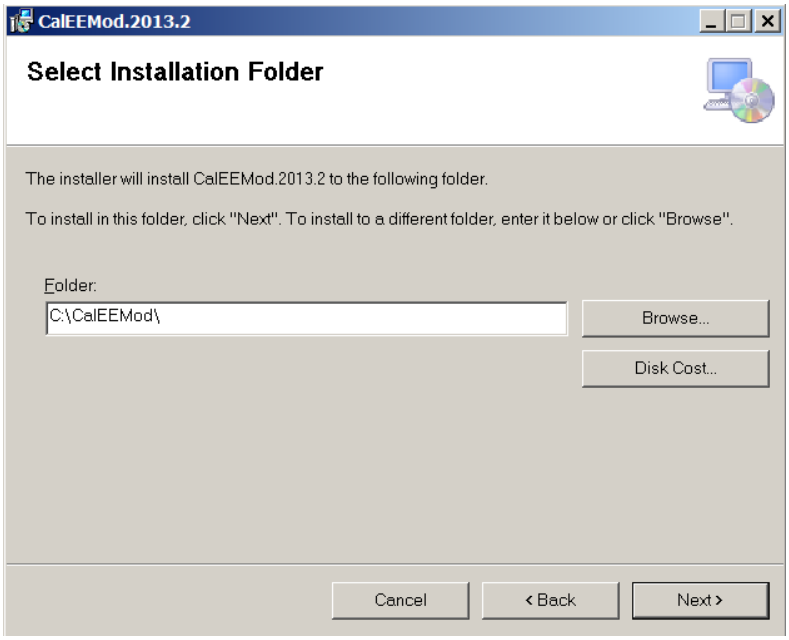
   http://www.microsoft.com/downloads/details.aspx?familyid=E497988A-C93A-404C-B161-3A0B323DCE24&displaylang=en

2 CalEEMod® 2012 All Rights Reserved by California Air Pollution Control Officers Association.
3 If you use windows Vista or 7, please be aware of file privileges which may not allow access rights to some folders during program operations such as C:\Program Files\

Once this file is downloaded, unzip the file anywhere on your computer and run the installation file (setup.exe). Be sure to follow the instructions on Microsoft's website and locate the appropriate .msi file. For 32-bit computers, one needs SSCERuntime_x86-ENU.msi and on a 64-bit computer, install both the 32-bit and the 64-bit version of the SQL Server Compact 3.5 SP2 MSI files. Existing SQL Server Compact 3.5 applications may fail if only the 32-bit version of the MSI file is installed on the 64-bit computer.

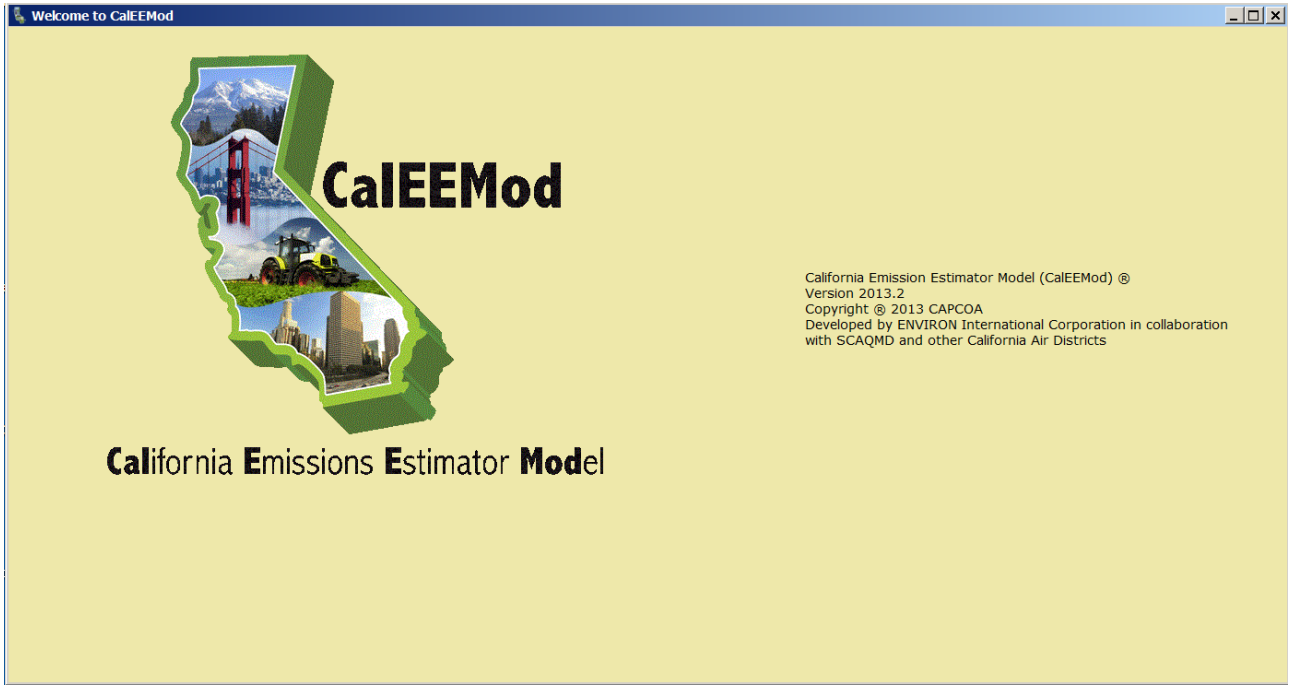
8. If you have any further trouble installing CalEEMod, make sure you have appropriate user privileges and the system requirements.





2.3 Starting CalEEMod

The installation will create a short cut icon on the desktop as well as add CalEEMod to the Programs available from the Start Button. Select CalEEMod from the program files or double click on the CalEEMod short cut. This will open CalEEMod.



3 Using CalEEMod

CalEEMod is designed as a linear series of screens with an individual purpose such as project characteristics, construction schedule and equipment, operational activity, mitigation measures, etc. The user is expected to input basic information about the project such as location, land use type (e.g., residential, commercial, retail, etc.) and its size. The functionality of the model is to populate later screens with pre-determined defaults based on basic project and location information provided by the user. However, if more accurate information is known, the user has the ability to override the defaults provided.

The figure on page 7 identifies some key features of CalEEMod which are described below.

1. Menu Bar: A drop down menu found on all screens. The "Home" menu controls file features such as New Project, Open Project, Save Project, and Save As Project. The "Help" will link to appropriate information for the relevant screen from this User's Guide. All other menus will allow navigation between screens in any order.

2. Screen Name: Identifies the name of the current screen.

3. Default Button: This button allows the restoration of program defaults if the user has changed any values on the screen. User entered values will be highlighted yellow to clearly indicate that they have been changed from the defaults. The user will be prompted if they would like to restore default for the current or last cell or the whole page. "Import CSV" will allow a user to load in a csv file for a specific data grid. "Cancel" cancels the previous action.

4. Remarks: This section at the bottom of each screen allows the user to enter comments regarding any user defined values entered on this screen. This is meant to assist reviewers of the program in determining justification for values selected.

5. Next Button: This button when clicked will take the user to the next sequential step. Later modules will also have a "Previous" button that will take the user back to the previous sequential step.

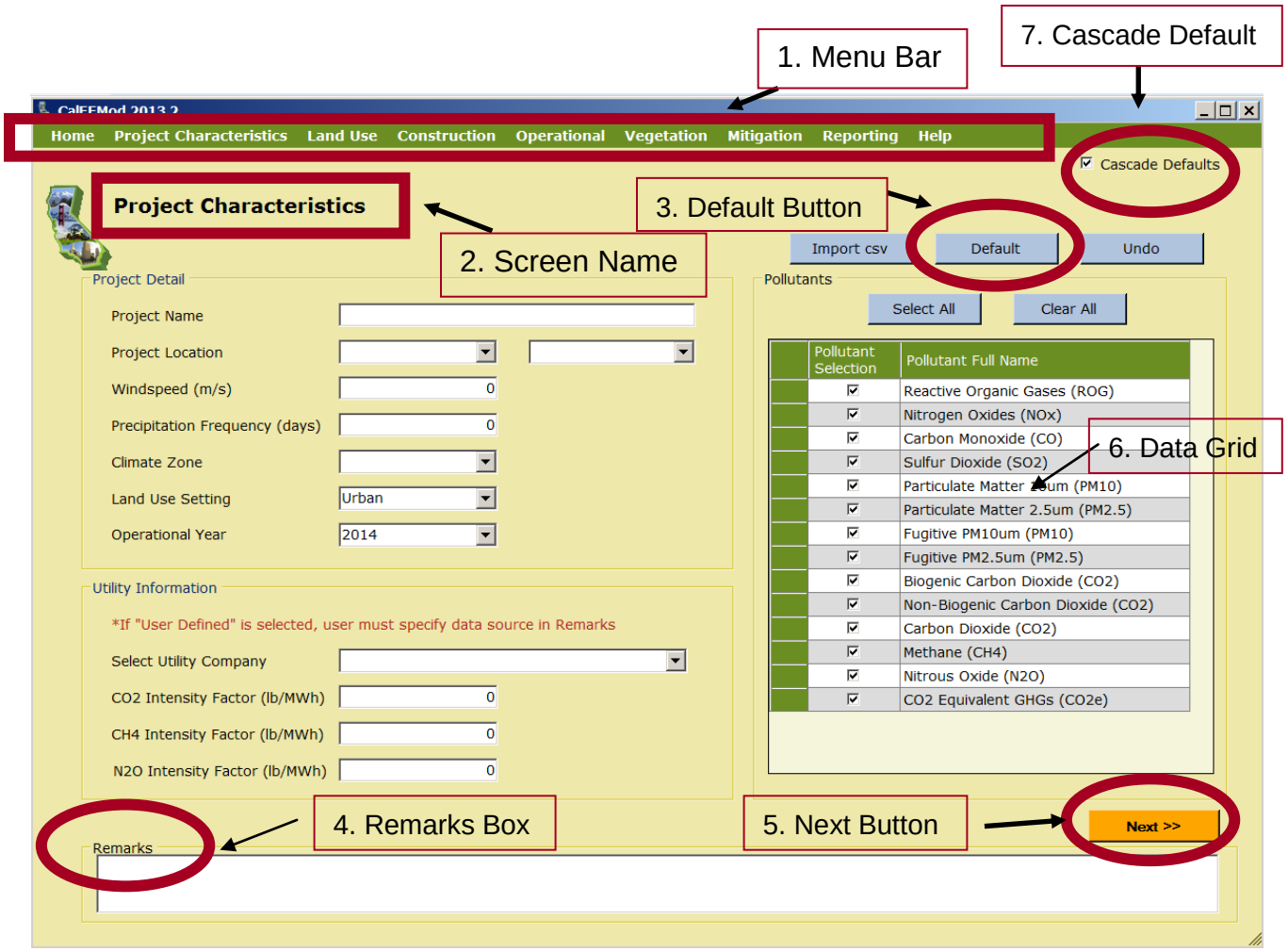
6. Data Grid: This is a common box where values for the variables defined across the top to be filled in. The number of rows will automatically be adjusted based on the number of rows of information required to define the information. The last row is indicated with an asterisk (*) and once information is started to be added to this row a new row will be added at the end. To delete a row select the desired row to delete, and hit the delete button on your keyboard (This is allowed unless the data grid is a fixed list such as the Pollutant selection list.). Scroll bars (both horizontal and vertical) will occur automatically if necessary.

7. Cascade Default: CalEEMod version 2013.2 introduces a new feature freezing the downloading of programmed defaults. Each input screen displays a box called "cascade default" automatically checked to populate defaults in future screens. However, if the "cascade default" box is unchecked, no defaults will be populated in subsequent screens. Unless all the necessary input parameters required for a proper analysis are known, it is recommended the user runs the model at least once with "cascade default" clicked on to allow the defaults to be populated. Then, if the user would like to change project parameters (e.g., number of dwelling units, building square footage, etc) without cascading new defaults in later screens, then uncheck the "cascade default" box when in the land use screen. This feature will prove useful for those users who override the defaults with specific project information (e.g., construction schedule, construction equipment, water use, energy use, etc.) and would like to evaluate different project scenarios with the same basic project information (i.e., land use type, location). If unchecking the "cascade default" box, the user should also be aware of the following:

    - *All* subsequent screens will freeze defaults
    - Changes to screens after land use (e.g., adding a new construction phase) will not cascade defaults relating to that change or add new tabs (e.g., trips and VMT, dust material movement) so any necessary input information will have to be added manual or impact will not be calculated
    - If changing or adding a land use type (e.g., from single family housing to a hospital), the future screens will not reflect the new land use type so some calculations (e.g., impacts from energy and water use) will not be properly performed

If a land use type is changed or added, it is recommended to click on the "cascade default" so the future screens can be populated with appropriate defaults and included in the analysis.

The next sections will give you some quick details on how to get started with a project in CalEEMod. Section 4 gives more specific details about each individual screen the user can encounter in CalEEMod.



3.1 Home

This is the part of the file menu bar that controls the file saving and opening features. The available options are:

- New Project
- Open Project
- Save
- Save As
- Exit

The user should select Open Project if they wish to load in a project that has been previously saved. Note that this will remove any information that has been entered into the GUI unless it has been saved to a file. Save will save the currently loaded project database as a Microsoft Excel file that can be used to open this project again into CalEEMod. Save As will allow the user to change the name of the saved project file. Exit will close CalEEMod. The Microsoft Excel file can be edited following the format of the save file to quickly make edits outside of the Graphical User Interface (GUI). The user will still need to use the GUI for reporting of results. This can be most useful in making changes to construction lists. Individual tabs can be loaded in as a .csv file in various places in CalEEMod to minimize the data entry.

3.2 Defining a Project

In order to define a project, the user will have to enter information on both the Project Characteristics screen and land use screen. After entering information on these two screens, CalEEMod will populate all of the other information required to calculate unmitigated construction (unless there is demolition, grading, or site preparation) and operation emissions using default data. Demolition, grading, and site preparation requires additional information regarding the amount of material to be demolished and material (debris, soil, etc) transported to or from the site that is entered on the appropriate construction screens. If site specific information will not be used, the user can jump to entering mitigation measures followed by reporting. If the user has any site-specific information that will replace the default information, this should be entered on the appropriate screens and provide justification for the change in the "Remarks" section at the bottom of each screen before moving on to mitigation and reporting. This justification for the default override will be printed in the report so the user is encouraged to provide a robust reasoning to allow for seamless review of the analysis.

3.3 Altering Default Data

CalEEMod was designed to allow for ease in changing default assumptions. Site-specific information that is supported with substantial evidence required by CEQA, is preferred when it is available. However, it is often the case that site-specific information is not available. CalEEMod was designed to assume reasonable default assumptions supported by substantial evidence to

the degree available at the time of programming. CalEEMod is based on fully adopted methods and data. Therefore, draft methods and data are not used as defaults.

3.4 Mitigation

Common construction mitigation measures that impact the calculations in CalEEMod have been incorporated as options for the user to select. At this time, required mitigation measures to comply with individual fugitive dust rules have not been incorporated in unmitigated calculations due to different interpretations of CEQA guidance regarding required mitigation.

Several mitigation measures from CAPCOA's Quantifying Greenhouse Mitigation Measures have been incorporated including combinations and caps when using multiple mitigation measures. Some mitigation measures are not as amenable to simple input information or are less common in their use and therefore not included at this time. CalEEMod was designed to include typical mitigation measures that are some of the more effective measures available to development projects. If mitigation measures are not available as options in CalEEMod, the user can likely alter values in the program that will allow for adjustment of hand calculated reductions due to mitigation that may be less common. This will require separate runs of CalEEMod files in order to properly account for unmitigated and mitigated scenarios.

3.5 Reporting

This is the part of the program that allows the user to select predefined reports that will display the emission calculation results. The user will be able to view these on a screen and save as either a Microsoft Excel file or a pdf file.

4 Detailed Program Screens

4.1 Project Characteristics

The project characteristics screen is where the user enters key location, electricity company information and pollutants they want to analyze. The information on this screen needs to be entered before proper default information can be used in subsequent screens. Changes on this screen will result in over riding user defined data with defaults in subsequent screens where this information is used. Under the Project Detail section the user enters the Project Name which will appear in the reports. The user then selects information from drop down boxes or overrides the default values in the text boxes. Each of the information categories on this screen are described in more detail below.

Project Location

The user selects the region in which the project is located. The user first selects if they want to choose an Air District, Air Basin, County, or State-wide. The second drop down box will give the list of specific locations based on the first drop down box which the user selects. For counties

that are divided between air districts, air basins or district requested subregions; the county is followed by the sub-county area which can influence some of the default values selected by modules. Consult your lead agency on their preference for location. This primarily influences on-road vehicle emissions, trip lengths, water supply and treatment electricity use, solid waste disposal rates, amount of paved roads, days of landscaping equipment use, architectural coating emissions, and hearth usage.

Wind Speed and Precipitation Frequency

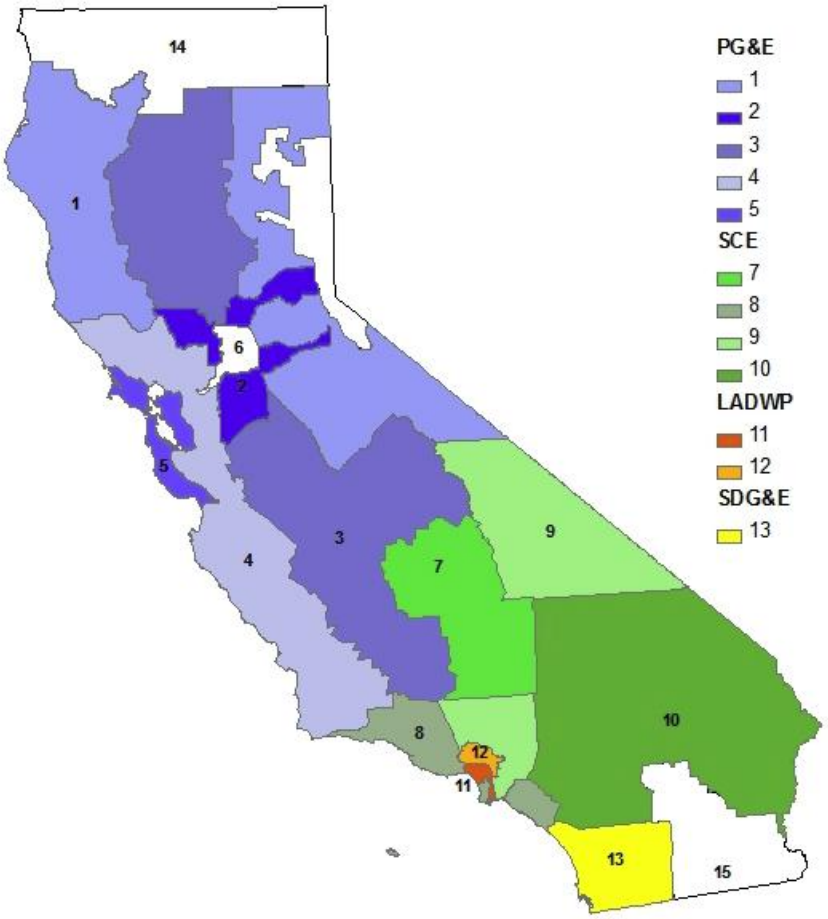
Selection of project location will fill in the default wind speed and precipitation frequency. The user can choose to override this information and type in a different value. The wind speed is in units of meters per second and is used in some fugitive dust calculations. Precipitation frequency is the number of days in a year that has precipitation greater than 0.01 inches in a day and is used in fugitive dust calculations.

Climate Zone

Selection of project location will restrict the climate zones available for the user to choose from based on the climate zones in the project location. The climate zones used are based on CEC forecasting climate zones (different than Title-24 building climate zones) as used in the California Commercial End Use Survey (CEUS) and Residential Appliance Saturation Survey (RASS)[4.] The figure below indicates these climate zones. A spreadsheet is available in Appendix F, which allows the user to look up climate zones based on city or zipcodes if a user needs further assistance in selecting the appropriate climate zone.

4 CalEEMod v. 2013.2 has been updated to incorporate the October 2010 version of RASS.

CEC Forecast Climate Zones[5,6]



Land Use Setting

This is where the user indicates if the project is located in a rural or urban setting. The user should contact their local air districts for guidance on the appropriate land use setting to select as the definition used may differ based on the definitions used to support the urban and rural trip lengths in the relevant air basin.

5 Adapted from Figure ES-2 of CEC. 2010. Residential Appliance Saturation Survey. Available online at: http://www.energy.ca.gov/2010publications/CEC-200-2010-004/CEC-200-2010-004-ES.PDF

6 White spaces represent areas served by other electric utilities not included in survey.

Operational Year

The user should indicate the first year the project will be fully operational that they wish to use as a basis for determining emission factors for all operational modules. CalEEMod can handle the following years: 1990, 2000, 2005, 2010-2025, 2030, 2035, and 2040. This was done to limit the file size associated with vehicle emission factors. CalEEMod is currently designed for one year that initiates the beginning of the full operation of the project. However, it is recognized that some projects could be phased so the operation of the project begins over more than one year. In that case, it is recommended the user run the model multiple times for the various input parameters for each operational year.

Utility Information

The user should select the appropriate electricity utility provider from the list or select "user defined". If a specific utility is entered, the default GHG intensity factors will be filled in. The user will need to enter values if "user defined" is selected. These values are used to determine the GHG emissions associated with electricity use in various modules. The default values are based on ARB's Local Government Operations Protocol (LGO)[7](CO_2), updated public utility protocols (CO_2), and E-Grid values (CH_4 and N_2O). The CO_2 intensity factor used as defaults in CalEEMod are based on the latest reporting year available for each of the different utilities. Table 1.2 in Appendix D provides the default CO_2 intensity factor used and reporting year from which the factor was identified for each of the utilities. As with other defaults in the model, if a new value is identified before the defaults are updated, the user has the ability to override the default and provide justification for the change in the "Remarks" section at the bottom of the "Project Characteristics" screen.

Pollutants

The list of pollutants to the right of the screen automatically has all boxes checked. Uncheck any pollutants you don't want reported. Some of the pollutants are a combination of other identified pollutants such as Carbon dioxide (CO_2) is made up of biogenic and non-biogenic carbon dioxide. CO_2 Equivalent GHGs is the Global Warming Potential (GWP) weighted value of all GHGs. GWPs are based on the IPCC's Second Assessment Report[8].

Remarks

The user can enter any remarks to describe the reasonable explanation and justification of non-default values or to add additional detail regarding the basis for information used such as relevant EIR sections. These remarks are included in the report and will assist a reviewer in understanding the reasons for a change in the default value (e.g., new trip rate based on a project specific traffic study conducted by (*reputable traffic engineers*)).

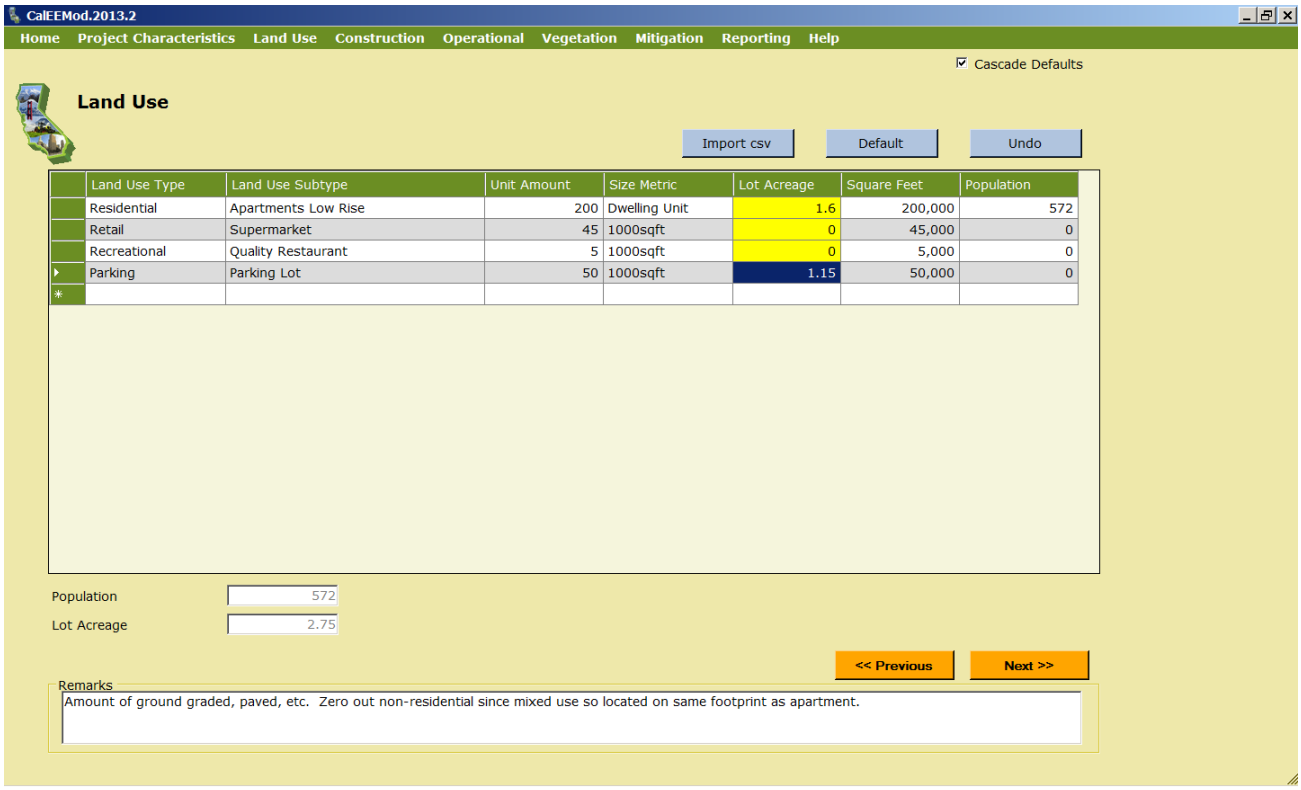
---

7 Available at: http://www.arb.ca.gov/cc/protocols/localgov/localgov.htm

8 Available at: http://www.ipcc.ch/pdf/climate-changes-1995/ipcc-2nd-assessment/2nd-assessment-en.pdf

4.2 Land Use

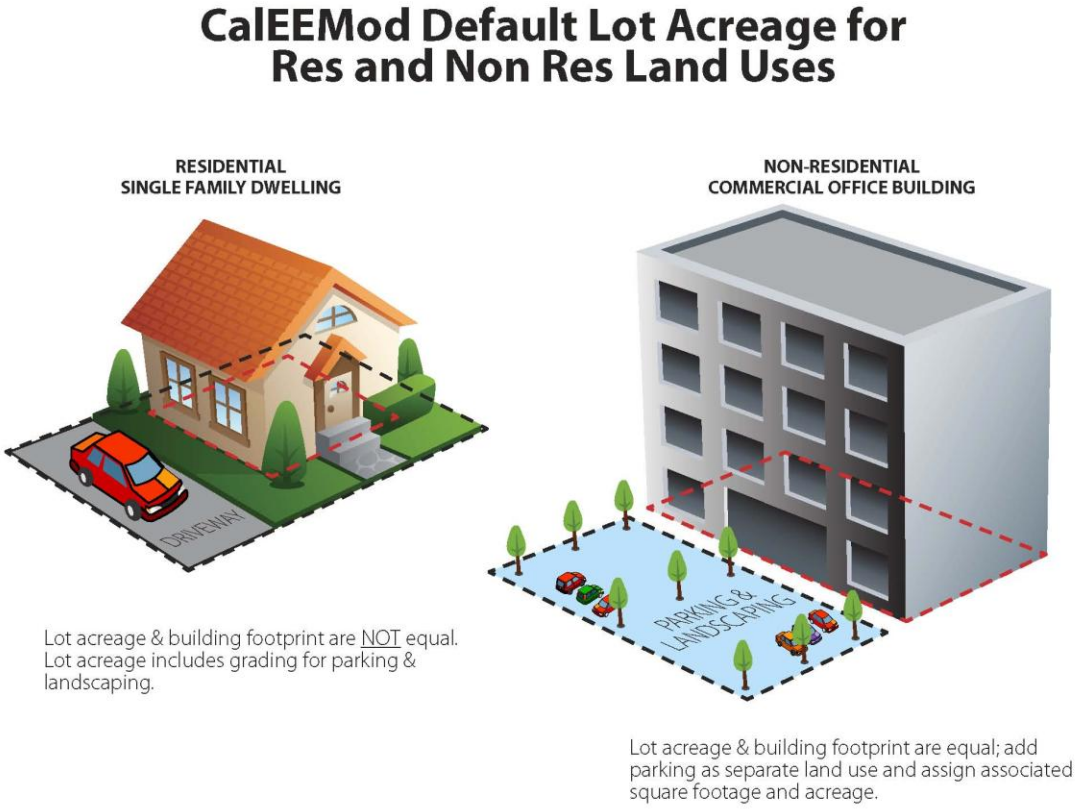
This screen is used to define the specific land uses that will occur at the project site. The land uses, size features and population are used throughout CalEEMod in determining default variables and calculations.



Land Use Type

The user selects from the drop down list of the primary land use types: Commercial, Educational, Industrial, Residential, Retail, Recreational, and ***Parking***. The 63 different land uses types were chosen for inclusion in CalEEMod because each has an established trip rate critical for mobile source calculations.

This program specifically designates parking areas as a separate land use rather than as a part of an associated non-residential land use (e.g., commercial buildings, retail facilities, etc.). Due to the nature of the available data, parking (i.e., driveway) for residential land uses have been incorporated (see discussion under Lot Acreage) so no separate parking land use needs to be identified. For a better understanding of how CalEEMod treats parking based on the footprint and lot acreage of residential and non-residential land uses, please refer to the following figure. As depicted, the lot acreage of a residential land use includes the parking and building footprint. For non-residential land uses, the lot acreage is the same as the building footprint so parking needs to be added as a separate land use.



For the parking land use, two primary options are available: parking lots or parking structure (e.g.,garages). There are four types of parking structures for the user to choose – enclosed, enclosed with an elevator, unenclosed, or unenclosed with an elevator. The reason for the specific description is to properly calculate energy impacts from ventilation and elevator operation. Parking as a separate land use made the estimate of default acreage and paving area easier.

For those land uses not listed (e.g., roads, underground parking, pipelines, etc.) each land use type has a "User Defined" land use subtype associated with it that the user can select if the other land use subtypes do not describe or reflect the project being analyzed. It is critical to understand that there is no default data (including size metric) associated with the "User Defined" land uses and all information that is based on these land uses will need to be entered by the user otherwise no emissions will be calculated. Also, whatever size metric (e.g., per acre, per 1000 square foot, etc.) the user chooses for the "User Defined" land use needs to be applied to all subsequent default values (e.g., gallons of water used *per acre* or *per 1000 square foot*) associated with that "User Defined" land use. An alternative approach would be to choose a land use that most closely fits the proposed project and allow the model to populate with pre-

determined defaults. Then, go back through the model and modify the defaults with any known specific project information.

Land Use Subtype

Tabbing over to the next column in a row, the user selects from a drop down list of available land use subtypes based on the primary land use type selected. The user also has the option to select a "User Defined" land use subtype, however, as discussed above, no default data will be available and the user will have to enter in subsequent screens the appropriate values. Land use subtypes are based primarily on the ITE land use definitions used for (mobile source) trip generation rate information. In some cases similar generalized land uses or surrogate data was mapped to some land use subtypes in order to generate the default data needed for various modules.

Table 1: Land Use Sub Type Descriptions

Land UseSubType	Description[1]	ITE Number
RESIDENTIAL		
Apartments High Rise	High-rise apartments are units located in rental buildings that have more than 10 levels and most likely have one or more elevators.	222
Apartments Low Rise	Low-rise apartments are units located in rental buildings that have 1-2 levels.	221
Apartments Mid Rise	Mid-rise apartments in rental buildings that have between 3 and 10 levels.	223
Condo/Townhouse	These are ownership units that have at least one other owned unit within the same building structure.	230
Condo/Townhouse High Rise	These are ownership units that have three or more levels.	232
Congregate Care (Assisted Living)	These facilities are independent living developments that provide centralized amenities such as dining, housekeeping, transportation and organized social/recreational activities. Limited medical services may or may not be provided.	253
Mobile Home Park	Mobile home parks consist of manufactured homes that are sited and installed on permanent foundations and typically have community facilities such as recreation rooms, swimming pools and laundry facilities.	240
Retirement Community	These communities provide multiple elements of senior adult living. Housing options may include various combinations of senior adult housing, congregate care, assisted living, and skilled nursing care aimed at allowing the residents to live in one community as their medical needs change.	255
Single Family Housing	All single-family detached homes on individual lots typical of a suburban subdivision	210

Table 1: Land Use Sub Type Descriptions

Land UseSubType	Description[1]	ITE Number
EDUCATIONAL		
Day-Care Center	A day care center is a facility where care for pre-school age children is provided, normally during the daytime hours. Day care facilities generally include classrooms, offices, eating areas and playgrounds.	565
Elementary School	Elementary schools typically serve students attending kindergarten through the fifth or sixth grade. They are usually centrally located in residential communities in order to facilitate student access and have no student drivers.	520
High School	High schools serve students who have completed middle or junior high school.	530
Junior College (2Yr)	This land use includes two-year junior, community, or technical colleges.	540
Junior High School	Junior High schools serve students who have completed elementary school and have not yet entered high school.	522
Library	A library is a facility that consists of shelved books; reading rooms or areas; and sometimes meeting rooms.	590
Place Of Worship	A church is a building in which public worship services are held. A church houses an assembly hall or sanctuary; it may also house meeting rooms, classrooms and occasionally dining catering or party facilities.	560
University/College (4Yr)	This land use includes four-year universities or colleges that may or may not offer graduate programs.	550
RECREATIONAL		
Arena	Arenas are large indoor structures in which spectator events are held. These events vary from professional ice hockey and basketball to non-sporting events such as concerts, shows, or religious services. Arenas generally have large parking facilities, except when located in or around the downtown of a large city.	460
City Park	City parks are owned and operated by a city.	411
Fast Food Restaurant W/O Drive Thru	This land use includes fast-food restaurants without drive-through windows. Patrons generally order at a cash register and pay before they eat.	933
Fast Food Restaurant With Drive Thru	This category includes fast-food restaurants with drive-through windows.	934
Golf Course	Golf courses include 9, 18, 27 and 36 hole courses. Some sites may also have driving ranges and clubhouses with a pro shop, restaurant, lounge and banquet facilities.	430
Health Club	These are privately-owned facilities that primarily focus on individual fitness or training. Typically they provide exercise classes; weightlifting, fitness and gymnastics equipment; spas; locker rooms; and small restaurants or snack bars.	492

Table 1: Land Use Sub Type Descriptions

Land UseSubType	Description[1]	ITE Number
High Turnover (Sit Down Restaurant)	This land use consists of sit-down, full-service eating establishments with turnover rates of approximately one hour or less. This type of restaurant is usually moderately priced and frequently belongs to a restaurant chain.	932
Hotel	Hotels are places of lodging that provide sleeping accommodations and supporting facilities such as restaurants; cocktail lounges; meeting and banquet rooms or convention facilities; limited recreational facilities and other retail and service shops.	310
Motel	Motels are places of lodging that provide sleeping accommodations and often a restaurant. Motels generally offer free on-site parking and provide little or no meeting space and few supporting facilities.	320
Movie Theater (No Matinee)	Movie theaters consist of audience seating, single or multiple screens and auditoriums, a lobby and a refreshment stand. Movie theaters without matinees show movies on weekday evenings and weekends only; there are no weekday daytime showings.	443
Quality Restaurant	This land use consists of high quality, full-service eating establishments with typical turnover rates of at least one hour or longer. Quality restaurants generally do not serve breakfast, some do not serve lunch; all serve dinner. This type of restaurant usually requires reservations and is generally not part of a chain. Patrons commonly wait to be seated, are served by a waiter, order from menus and pay for meals after they eat.	931
Racquet Club	These are privately-owned facilities that primarily cater to racquet sports.	491
Recreational Swimming Pool	This is a typical recreational swimming pool that may be associated with community centers, parks, swim clubs, etc.	
PARKING		
Enclosed Parking Structure	This is an enclosed parking structure that may be above or below ground. It is not covered in asphalt. This land use will require lighting and ventilation, and will be more than one floor with no elevator.	
Enclosed Parking with Elevator	This is an enclosed parking structure that may be above or below ground. It is not covered in asphalt. This land use will require lighting and ventilation, and will be more than one floor with an elevator.	
Other Asphalt Surfaces	This is an asphalt area not used as a parking lot (e.g., long driveway, basketball court, etc.)	
Other Non-Asphalt Surfaces	This is a non-asphalt area (e.g., equipment foundation, loading dock area, etc.).	
Parking Lot	This is a typical single surface parking lot typically covered with asphalt. This land use will require lighting.	
Unenclosed Parking Structure	This is an unenclosed parking structure that may be above or below ground. It is not covered in asphalt. This land use will require lighting but not ventilation. It will be more than one floor with no elevator.	
Unenclosed Parking with Elevator	This is a unenclosed parking structure that may be above or below ground. It is not covered in asphalt. This land use will require lighting but not ventilation. It will be more than one floor with an elevator.	

Table 1: Land Use Sub Type Descriptions

Land UseSubType	Description[1]	ITE Number
RETAIL		
Automobile Care Center	An automobile care center houses numerous businesses that provide automobile-related services, such as repair and servicing; stereo installation; and seat cover upholstering.	942
Convenience Market (24 Hour)	These markets sell convenience foods, newspapers, magazines and often beer and wine. They do not have gasoline pumps.	851
Convenience Market With Gas Pumps	These markets sell gasoline, convenience foods, newspapers, magazines and often beer and wine. This includes convenience markets with gasoline pumps where the primary business is the selling of convenience items, not the fueling of motor vehicles.	853
Discount Club	A discount club is a discount store or warehouse where shoppers pay a membership fee in order to take advantage of discounted prices on a wide variety of items such as food, clothing, tires and appliances. Many items are sold in large quantities or in bulk.	857
Electronic Superstore	These are free-standing facilities that specialize in the sale of electronic merchandise.	863
Free-Standing Discount Store	Discount stores offer centralized cashiering and sell products that are advertised at discount prices. These stores offer a variety of customer services and maintain long store hours seven days a week.	815
Free-Standing Discount Superstore	The discount superstore is similar to the free-standing discount stores with the addition that they also contain a full-service grocery department under the same roof that shares entrances and exits with the discount store area.	813
Gasoline/Service Station	This land use includes gasoline/service stations where the primary business is the fueling of motor vehicles. They may also have ancillary facilities for servicing and repairing motor vehicles.	944
Hardware/Paint Store	These stores sell hardware and paint supplies and are generally free-standing buildings.	816
Home Improvement Superstore	These are free-standing facilities that specialize in the sale of home improvement merchandise.	862
Regional Shopping Center	A shopping center is an integrated group of commercial establishments that is planned, developed, owned and managed as a unit. A shopping center's composition is related to its market area in terms of size, location and type of store.	820
Strip Mall	Small strip shopping centers contain a variety of retail shops and specialize in quality apparel, hard goods and services such as real estate offices, dance studios, florists and small restaurants.	814

Table 1: Land Use Sub Type Descriptions

Land UseSubType	Description[1]	ITE Number
Supermarket	Supermarkets are free-standing retail stores selling a complete assortment of food: food preparation and wrapping materials; and household, cleaning items. Supermarkets may also contain the following products and services: ATMs, automobile supplies, bakeries, books and magazines, dry cleaning, floral arrangements, greeting cards, limited-service banks, photo centers, pharmacies and video rental areas.	850
COMMERCIAL		
Bank (With Drive-Through)	Drive-in banks provide banking facilities for motorists who conduct financial transactions from their vehicles; many also serve patrons who walk into the building.	912
General Office Building	A general office building houses multiple tenants where affairs of businesses commercial or industrial organizations or professional persons or firms are conducted. If information is known about individual buildings, it is suggested that this land use be used instead of the more generic office park.	710
Government (Civic Center)	A group of government buildings that are interconnected by pedestrian walkways.	733
Government Office Building	This is an individual building containing either the entire function or simply one agency of a city, county, state, federal, or other governmental unit.	730
Hospital	A hospital is any institution where medical or surgical care and overnight accommodations are provided to non-ambulatory and ambulatory patients. However, it does not refer to medical clinics or nursing homes.	610
Medical Office Building	This is a facility that provides diagnoses and outpatient care on a routine basis but is unable to provide prolonged in-house medical and surgical care. One or more private physicians or dentists generally operate this type of facility.	720
Office Park	Office parks are usually suburban subdivisions or planned unit developments containing general office buildings and support services, such as banks, restaurants and service stations, arranged in a park-or campus-like atmosphere. This should be used if details on individual buildings are not available.	750
Pharmacy/Drugstore W/O Drive Thru	These are retail facilities that primarily sell prescription and non-prescription drugs. These facilities may also sell cosmetics, toiletries, medications, stationery, personal care products, limited food products and general merchandise. The drug stores in this category do not contain drive-through windows.	880

Table 1: Land Use Sub Type Descriptions

Land UseSubType	Description[1]	ITE Number
Pharmacy/Drugstore With Drive Thru	These are retail facilities that primarily sell prescription and non-prescription drugs. These facilities may also sell cosmetics, toiletries, medications, stationery, personal care products, limited food products and general merchandise. The drug stores in this category contain drive-through windows.	881
Research & Development	R&D centers are facilities devoted almost exclusively to R&D activities. The range of specific types of businesses contained in this land use category varies significantly. R&D centers may contain offices and light fabrication areas.	760
INDUSTRIAL		
General Heavy Industry	Heavy industrial facilities usually have a high number of employees per industrial plant and are generally limited to the manufacturing of large items.	120
General Light Industry	Light industrial facilities are free-standing facilities devoted to a single use. The facilities have an emphasis on activities other than manufacturing and typically have minimal office space. Typical light industrial activities include printing, material testing and assembly of data processing equipment.	110
Industrial Park	Industrial parks contain a number of industrial or related facilities. They are characterized by a mix of manufacturing, service and warehouse facilities with a wide variation in the proportion of each type of use from one location to another. Many industrial parks contain highly diversified facilities.	130
Manufacturing	Manufacturing facilities are areas where the primary activity is the conversion of raw materials or parts into finished products. It generally also has office, warehouse, R&D functions at the site.	140
Refrigerated Warehouse-No Rail	This is a warehouse that has refrigeration but no rail spur.	150
Refrigerated Warehouse-Rail	This is a warehouse that has refrigeration and a rail spur.	150
Unrefrigerated Warehouse-No Rail	This is a warehouse that does not have refrigeration and no rail spur.	150
Unrefrigerated Warehouse-Rail	This is a warehouse that does not have refrigeration but has a rail spur.	150

1. Based on land use descriptions in ITE Trip Generation 8th Edition. In September 2012, ITE published the 9th edition that updated some of the trip rates from the 8th edition. The updates are not yet incorporated into CalEEMod. However, the user has the ability to override the trip rate default but is expected to justify the change in the "Remarks" section at the bottom of the Operational -Mobile screen.

Unit Amount

Tabbing over to the next column, the user enters the appropriate size of the land use in terms of the size metric selected. This will be used to calculate the rest of the columns in this datagrid.

Size Metric

Tabbing over to the next column in the land use identification row, the user can select another size metric unit if it is available for that land use subtype. For example, a school land use allows the user to define its size by the number of students, building square footage, or number of employees. Please note that the square footage, which is used for calculating such impacts as architectural coatings and energy use, relates to the total building square footage and not the building footprint or lot acreage (which is used for housing density as well as grading and site preparation calculations).

Lot Acreage (datagrid)

The user should override the default value if known. For multi-use, multistory building, the square footage should be preserved for each individual land use and the acreage assigned to the residential portion or split between non-residential land uses if there is no residential. The figure below provides an example of a mixed use project and how to apply the appropriate square footage and acreage for an accurate calculation of air quality impacts.

Acreage is used to estimate housing density as needed for calculations (see Table 2) and total acreage for the project is used in assigning construction default data (e.g., grading, site preparation, etc.). Based on ITE data, CalEEMod is able to estimate the acres per dwelling unit (DU) for residential land use. For example, 10 apartments in a low rise will need a 0.625 acre lot (10 DU divided by 16 acres/DU). According to the California Energy Commission's Residential Appliance Saturation Survey (RASS), low rise apartments are 1000 square foot per DU (see Table 2.1) so the building footprint is 0.23 acres (10 DU x 1000 sq ft/DU divided by 43,560 sq ft per acre). Thus, the lot space beyond the residential footprint accounts for driveway and landscaping.

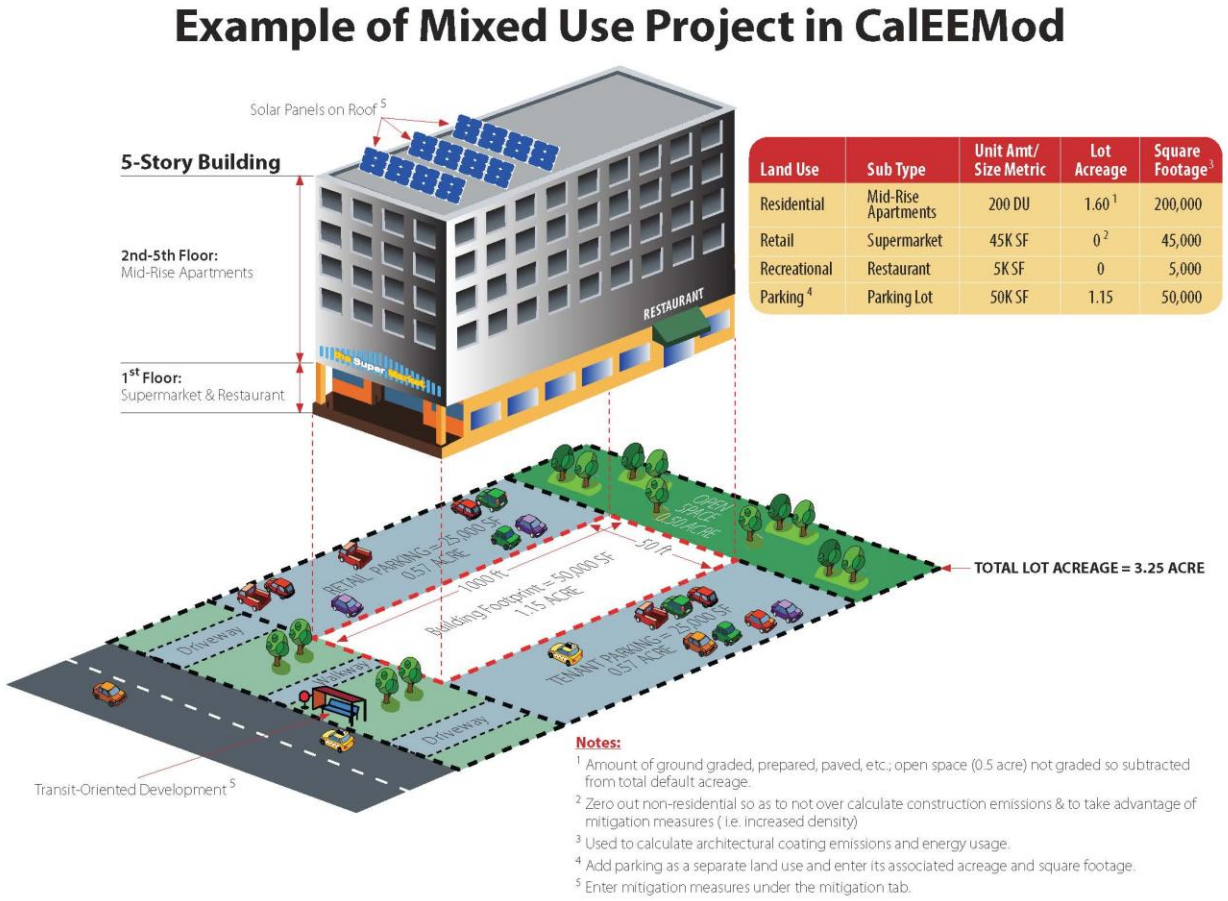


Table 2: Default Housing Density

Land Use Sub Type	Density (Dwelling Units/Acre)
Single Family Housing	3
Apartments low rise	16
Apartments mid rise	38
Apartments high rise	62
Condo/townhouse	16
Condo/townhouse high rise	64
Mobile Home Park	8
Retirement Community	5
Congregate care (Assisted Living)	16

1. Based on the density assumed in ITE Trip Generation 8th Edition

Square Footage

The user should override the default value if known. This is the total building square footage.

Population (datagrid)

This is the population estimated for the land use identified. The user should override the default value if known.

Population and Lot Acreage (text box)

This is the total population and acreage of all land uses entered in the data grid. This is for informational purposes of values that will be used by the program and can't be changed by the user.

4.3 Construction

The construction screen introduces the first of a tabbed structure subscreens. There are seven subscreens for construction with each one listed in the grey area under the screen name. To jump to different subscreens: the user can use the next and previous buttons, click on the grey tab name, or use the menu bar. Default information is based on a survey of construction sites grouped by construction phase and lot acreage performed by SCAQMD which can be found in Appendix E. The default construction equipment list and phase length are most appropriate for the size and types surveyed while the survey has been extrapolated to indicate default values, more detailed site specific equipment and phases are highly suggested in these cases for the most accurate results.

4.3.1 Construction Phase

This is the screen where the user enters the type of each construction phase and the date range of these phases. The date of the construction phase is critical in determining the correct emission factor for the off-road equipment since CARB's factors change each year. Default phases are based on the total lot acreage of the project. Depending on the project being modeled, not all phases will be necessary (e.g., not all projects require demolition). In addition multiple phases of similar types may be used for large projects with build out in stages. If the project has demolition, grading, and site preparation phases, additional project specific data will need to be entered on Demolition subscreen and Dust from Material Movement subscreen.

Phase Name

The user should enter a unique name for the phase in the text box.

Phase Type

The user selects from the drop down list the type of construction phase: Site preparation, demolition, grading, building construction, paving, and architectural coating. This influences the types of calculations and default assumptions for on-road vehicle trips and fugitive emissions that occur in subsequent construction subscreens. The definitions of the default data phases are as follows:

- *Demolition* involves tearing down of buildings or structures.
- *Site Preparation* involves clearing vegetation (grubbing and tree/stump removal) and stones prior to grading.
- *Grading* involves the cut and fill of land to ensure the proper base and slope for the construction foundation.
- *Building Construction* involves the construction of structures and buildings.
- *Architectural Coating* involves the application of coatings to both the interior and exterior of buildings or structures and includes parking lot striping as well as painting of the walls of parking structures.
- *Paving* involves the laying of concrete or asphalt such as in parking lots or roads.

Start Date and End Date

The user can enter with the aid of a calendar, the start and end dates. The default start date is 1/1/2014 starting with demolition with subsequent phases starting the next day after the previous phase's end date. Changes to these cells will alter the total days estimated for the phase.

Days per Week

The user can select from a drop down box the number of days per week (5, 6, or 7) the project will operate. Five days per week is assumed to be Monday through Friday, and six days per week is Monday through Saturday.

Total Days

The total number of days in the construction phase is indicated. If the end date or the days per week are changed, clicking in this cell will recalculate the number of days. If the total number of days for a phase is changed, then once leaving this cell, the program will adjust the end date based on the start date for that phase.

4.3.2 Off-Road Equipment

This subscreen shows the off-road equipment usage for each phase. Since equipment lists can be lengthy, the user must go through a different subscreen for each phase. This is done by selecting the appropriate phase name from the drop down list or the Previous or Next buttons located next to the phase name. The emission calculations associated with this screen are from off-road equipment engine use based on the equipment list and phase length. The fugitive emissions from off-road equipment performing work are associated with additional information in other construction screens.

The user enters in the datagrid each piece of equipment in the phase in a new row. The user enters the unit amount and hours per day of equipment usage. Horsepower and load factors are loaded with the default average values of the mode tier according to population based on OFFROAD2011, but the user can override these values. Since CalEEMod is restricted in the

years of OFFROAD emission factors, CalEEMod will use the lower end year if a construction year is in between a year of OFFROAD values in the database. For example if a construction phase is in 2027, CalEEMod will use OFFROAD emission factors from 2025.

For site specific construction equipment lists including equipment not specifically listed can be added under the Other Equipment categories or Off-Highway Trucks listed in CalEEMod matching the closest in horsepower to the missing equipment for each phase the construction equipment is operating. For inclusion of water trucks and cement trucks specifically can be considered in two ways although both of those trucks were part of the SMAQMD vendor trip survey during construction. The first is to use the Off-Highway Trucks category in this screen. The second is to add these as additional vendor trips in the Trips and VMT screen.

4.3.3 Dust from Material Movement

This subscreen is used to enter the information necessary to calculate the fugitive dust emissions associated with grading phases. Three distinct fugitive dust calculations are performed as described in Appendix A: dust from dozers moving dirt around, dust from graders or scrapers leveling the land, and loading or unloading the dirt into haul trucks. These methods have been adapted from USEPA's AP-42 method for Western Coal Mining. The user needs to enter the amount of material imported and exported to the site in order for CalEEMod to estimate hauling trips correctly from material transport. There is an option to select either ton of debris or cubic yards. The user also selects if the import and export of material are phased. If they are phased a truck comes in with material and leaves with another load of material to export. Non-phased trips have one-way of the haul trip performed with an empty truck. Phasing material import and export reduces the number of haul trips. The number of acres that are displayed represent the total acres traversed by grading equipment assuming a blade width of 12 feet. In order to properly grade a piece of land multiple passes with equipment may be required. The acres is based on the equipment list and days in grading or site preparation phase according to the anticipated maximum number of acres a given piece of equipment can pass over in an 8-hour workday. See Appendix A for the equipment specific grading rates.

4.3.4 Demolition

This subscreen is used to enter the amount of material that is demolished if demolition phases are selected. The user can enter either the ton of material or the building square footage. Fugitive dust emissions from the demolition are then calculated. Demolition fugitive dust emissions are based on the methodology described in the report prepared for the USEPA by Midwest Research Institute, Gap Filling PM_{10} Emission Factors for Selected Open Area Dust Sources.

4.3.5 Trip and VMT

This subscreen is used to provide the number and length of on-road vehicle trips for workers, vendors, and hauling. It also allows the user to select different weightings of vehicle fleet mixes and is either the EMFAC mix for the region, or an mix of the vehicle classes listed. HHDT,MHDT is a 50/50 percent mix of heavy-heavy duty trucks and medium-heavy duty trucks. LDA,LDT1,

LDT2 is 50/25/25 percent mix of light duty autos, light duty truck class 1 and light duty truck class 2. Since CalEEMod is restricted in the years of EMFAC emission factors, CalEEMod will use the lower end year if a construction year is in between a year of EMFAC values in the database. For example if a construction phase is in 2027, CalEEMod will use EMFAC emission factors from 2025.

The number of workers is 1.25 times the number of pieces of equipment for all phases except building construction and architectural coating. Building construction estimates the number of workers based on the types of land use and their size based on an analysis of a study conducted by SMAQMD. This study and its analysis are included in Appendix E. The number of workers for architectural coating is based on 20% of the building construction workers.

The number of vendor trips for building construction phase is based on a study performed by SMAQMD based on land use types and their size. As noted earlier, the SMAQMD trip survey during construction counted cement and water trucks as vendor trips. These values were placed under the "building construction" phase in CalEEMod. If the "building construction" phase is being eliminated and there are known water (and/or cement) trucks, it is recommended to consider those vendor trips under another phase or accounted for as OFFROAD equipment. Hauling trips are based on the assumption that a truck can handle 20 tons (or 16 cubic yards) of material per load. Assuming one load of material, CalEEMod considers a haul truck importing material will have a return trip with an empty truck (2 trips). Similarly, the haul truck to take material away will have an arrival trip in an empty truck (2 trips). Thus, each trip to import and export material is considered as two separate round trips (4 trips) unless the "phase" box is clicked. Then, a haul truck trip to import material will be the same haul truck to export material (2 trips).

4.3.6 On-Road Fugitive Dust

This subscreen defines the variables that will be used to determine the fugitive dust emissions from construction on-road vehicles over paved and unpaved roads. The emission calculations are based on USEPA's AP-42 Janaury 2011 paved road and November 2006 unpaved roads emission factors. The variables in this datagrid are the same as those defined in the appropriate AP-42 sections.

4.3.7 Architectural Coatings

This subscreen allows the user to override any of the default interior and exterior surface area estimated for residential and non-residential buildings. In addition, each of these surface types has a different emission factor indicating the VOC content of the paint in grams per liter. See Appendix A for the method of estimating surface areas to be coated from building square footage.

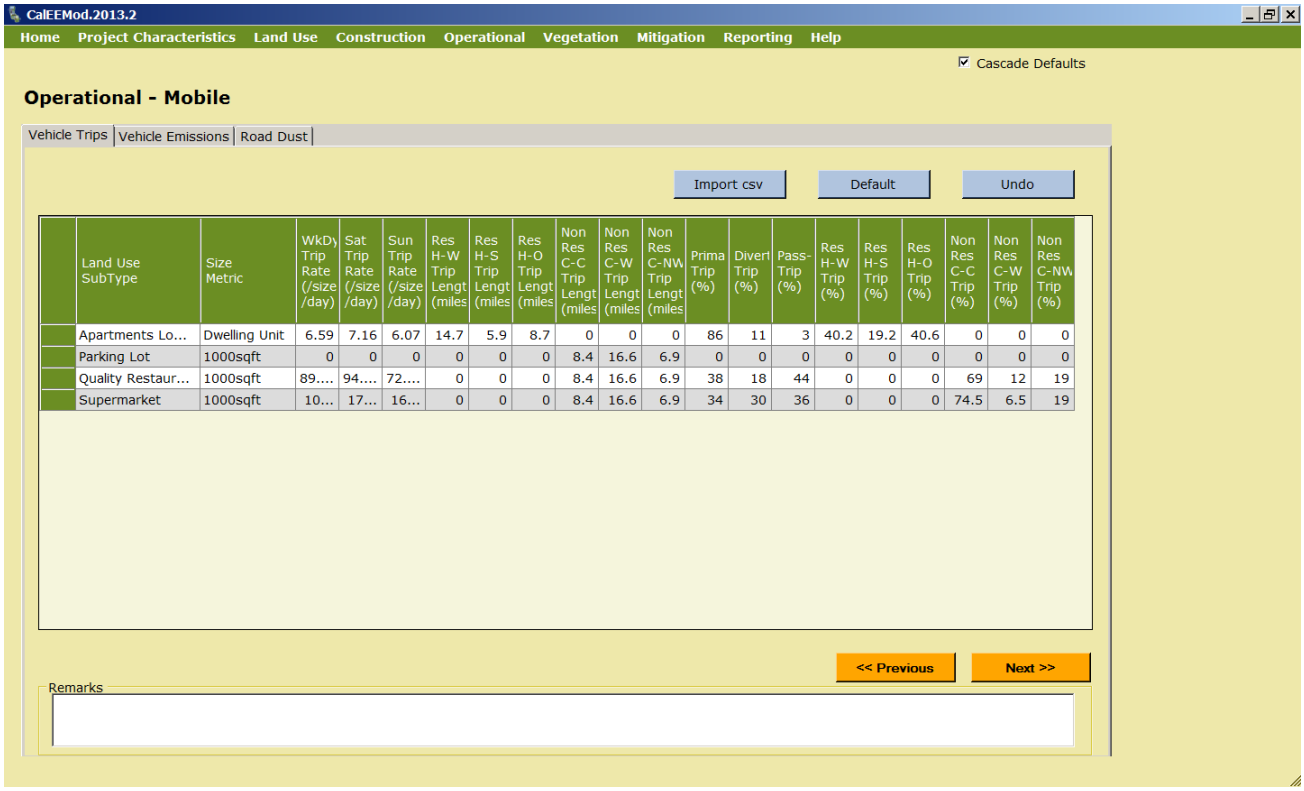
4.4 Operational Mobile

The operational mobile screen is made up of 3 subscreens: Vehicle Trips, Vehicle Emissions, and Road Dust. These screens are used in defining the information necessary to calculate the emissions associated with operational on-road vehicles.

4.4.1 Vehicle Trips

This subscreen's datagrid lists the trip rate, trip lengths, trip purpose, and trip type percentages for each land use subtype in the project. The user can edit any of this information by entering a new value in the appropriate cell. Trip rates are in terms of the size metric (square footage or dwelling unit) defined on the land use screen and are listed for weekday, Saturday and Sunday if available. Trip lengths are for primary trips. Trip purposes are primary, diverted, or pass-by trips. Diverted trips are assumed to take a slightly different pass than a primary trip and are assumed to be 25% of the primary trip lengths. Pass-by trips are assumed to be 0.1 miles in length and are a result of no diversion from the primary route. Residential trip types are defined as home-work (H-W), home-shop (H-S), and home-other (H-O). Non-residential trip types are defined as commercial –customer (C-C), commercial-work (C-W), and commercial-nonwork (C-NW) such as delivery trips. See Appendix A for the equations and methodology used to calculate motor vehicle emissions from the operation of a project.

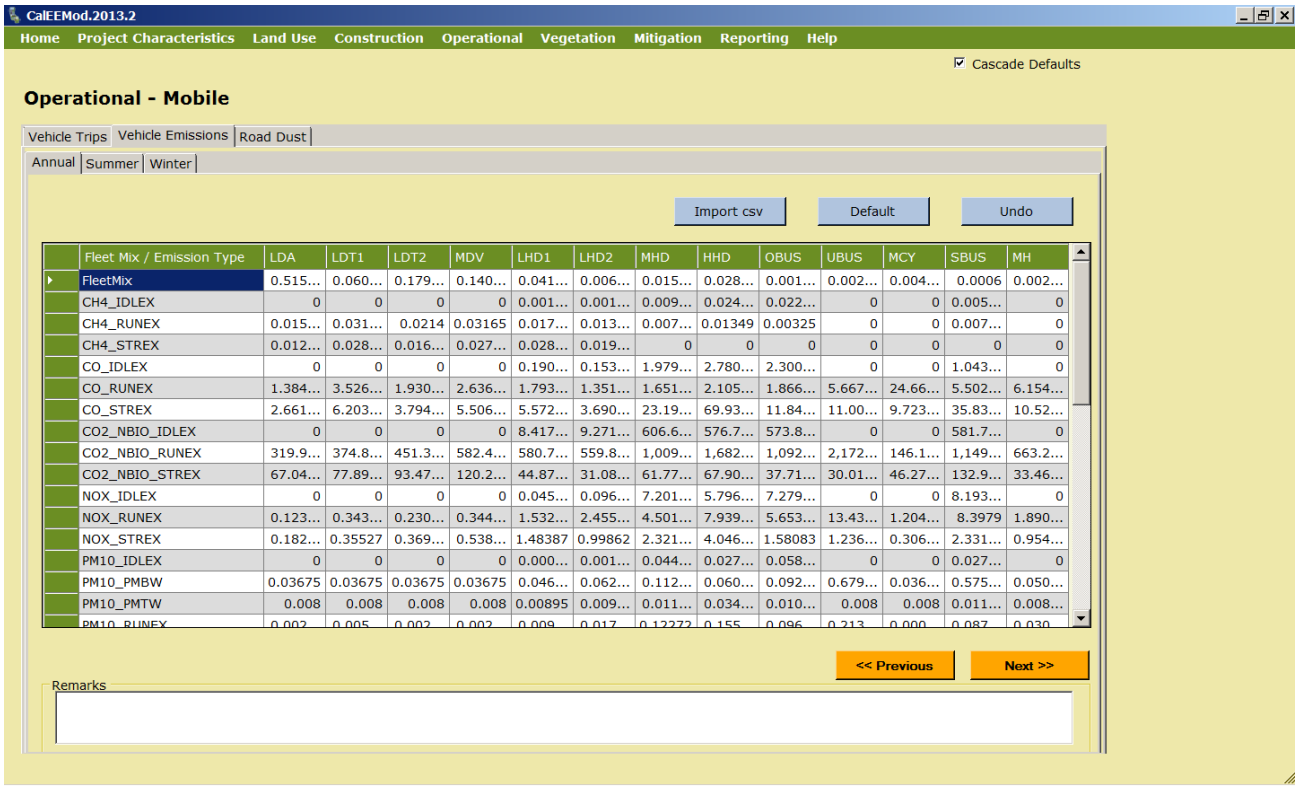
In most cases the trip rate is based on ITE's average trip rate for the respective land use category. For warehouses, SCAQMD evaluated the primary data from ITE along with other recent studies regarding warehouses and concluded that it was more appropriate to break out the warehouses based on access to a rail spur and refrigeration. In addition, they concluded that it was more appropriate to use the maximum values from the studies. A detail memorandum describing the justification for these values is contained in Appendix E.



4.4.2 Vehicle Emissions

This subscreen is a large datagrid containing the detailed vehicle emission factors and fleet mix based on EMFAC2011. See Appendix A for information on how these emission factors were developed based on burden mode EMFAC runs including effects from Pavley (Clean Car Standards) and Low Carbon Fuel Standards. Pavley and Low Carbon Fuel Standards are applicable for future years and do not impact EMFAC values prior to these regulations implementations (i.e, 1990, 2000, 2005, etc). It is anticipated that most users will not edit data in this subscreen. There is a separate tab for annual, summer, and winter emission values. If the user wants to alter the breakdown of fuel types (catalytic, non-catalytic, other) within a vehicle class, they will have to provide their own data as this will likely be an infrequent change due to CEQA enforceability requirements. For details on how EMFAC data was processed see Appendix A.

This screen along with the previous screen (Vehicle Trips) will calculate the emissions associated with on-road motor vehicle use. It does not include the fugitive dust emissions from travel over roads as these are associated with the next screen (Road Dust).



4.4.3 Road Dust

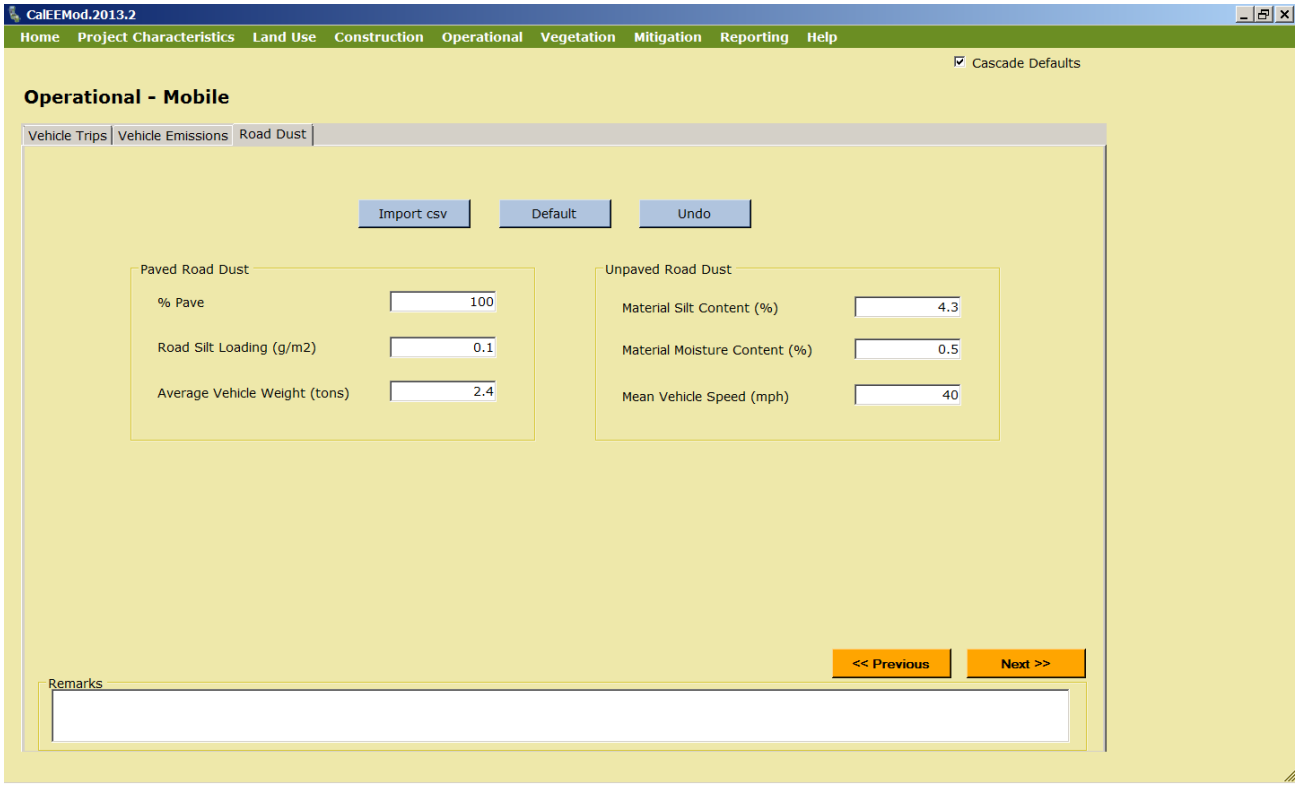
This subscreen is used to change any of the default values that are used in the USEPA's AP-42 methods for calculating fugitive emissions from paved and unpaved roads. The defaults for the road dust (e.g., material silt content, material moisture content,) are statewide averages, but the user has the ability to override the defaults if data specific to the project is known. Local jurisdictions can also provide guidance to users as to what default properly reflects known regional road dust parameters.

For the San Luis Obispo region, users are recommended to provide the following road dust parameters overriding the statewide defaults:

9.3 for "Material Silt Content (%)" *(instead of 4.3 statewide default)*

0.1 for "Material Moisture Content (%)" *(instead of 0.5 statewide default)*

32.4 for "Mean Vehicle Speed (mph)" *(instead of 40 statewide default)*

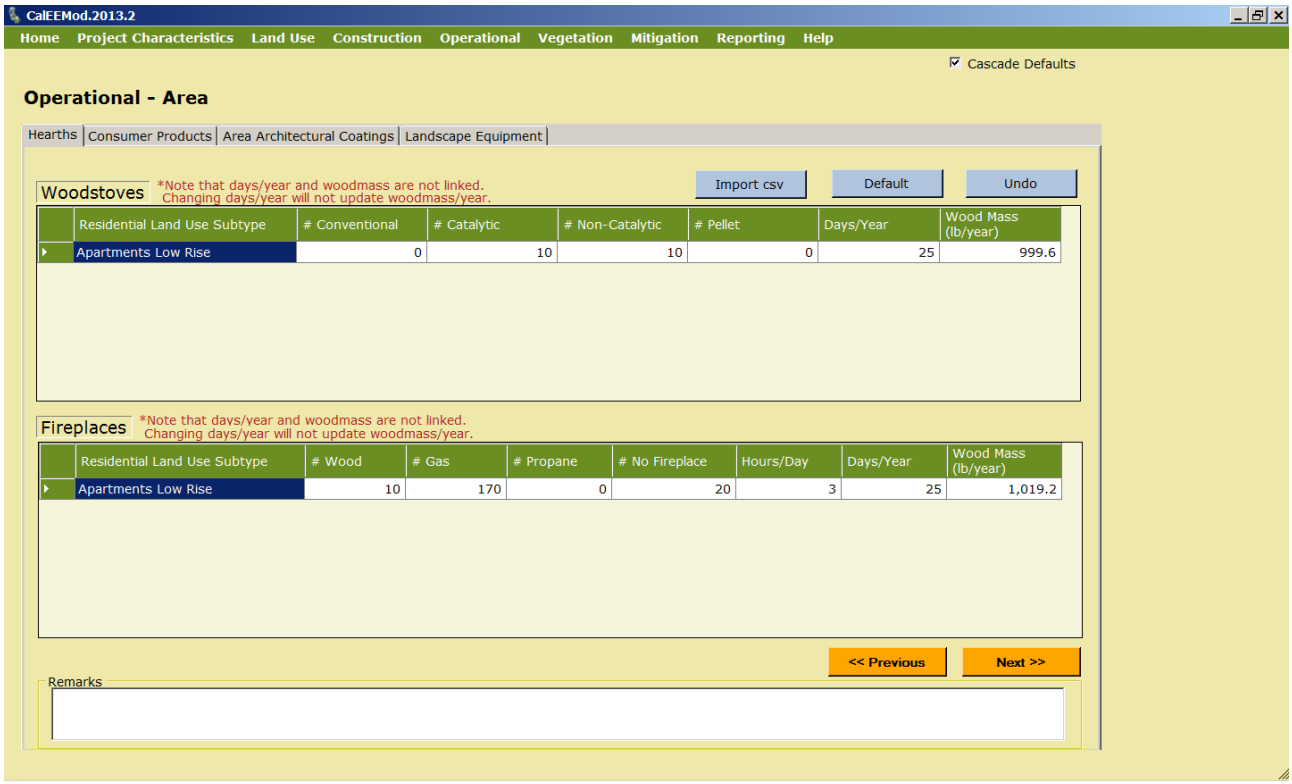


4.5 Area

The area source screen consists of four subscreens: Hearths, Consumer Products, Area Architectural Coatings, and Landscaping Equipment. Natural gas emission variables from all uses except hearths are included in the energy use screen.

4.5.1 Hearths and Woodstoves

This subscreen allows the user to enter the number of woodstoves and hearths of various types as well as the usage of these devices. Woodstoves are separate from fireplaces since a home may have both and these devices may have different use patterns. The number of devices that is entered for each device type represents the total number of devices installed in the dwelling units for a particular land use. See Appendix A for emissions calculation methodology and details of variables that the user can not override. Some of these emissions may be classified as biogenic and are therefore reported as CO_2-Biogenic. For most locations a default percent of hearths and stoves was provided by districts and is multiplied through. The number was chosen for CalEEMod instead of a percentage to allow for incorporation of various districts rules regarding hearths and woodstoves in new residences without having specialized screens. Commercial land uses by default do not have any hearths or woodstoves in CalEEMod. These are included for those cases where they may occur such as in restaurants or hotels.



The San Joaquin Valley jurisdiction has a regulatory limit on the number of hearths depending upon the type and number of residential development. The regulatory limit is generated by CalEEMod but all the input parameters (e.g., unit density, etc.) are necessary to determine the value. Thus, the regulatory limit is disclosed during the reporting stage under the "Default Value" box in the report. The model, however, calculates emission impacts from the number of hearths inputted on the Area source screen (listed under the "New Value" column in the report). Therefore, if the user wants to calculate emissions from regulatory limit, the report needs to be run to determine the regulatory limit and the user needs to go back to the Area source screen to

input that value and re-run the report. If the user chooses to calculate emissions from a different number of hearths (e.g, a number of hearths less than the regulatory limit), then that number needs to be inputted on the Area source screen to properly calculate emissions. Again, the report will provide the regulatory limit under the "Default Value" column and the user input value under "New Value" column.

4.5.2 Consumer Products

Consumer products are various solvents used in non-industrial applications which emit VOCs during their product use. These typically include cleaning supplies, kitchen aerosols, cosmetics and toiletries. SCAQMD has developed an emission factor based on the total of all building square footage for both residential and non-residential buildings. Details of how this emission factor was developed can be found in Appendix E. The user can change this emission factor if they have more relevant data.

4.5.3 Area Architectural Coating

This subscreen has text boxes for the reapplication rate and paint VOC content for each building surface type. The reapplication rate is the frequency at which surfaces get repainted every year. A default of 10% is used which means that 10% of the surface area is repainted each year so all surfaces are completely repainted once every 10 years. Daily emissions divide the annual rate by 365 days per year. This is based on assumptions used by SCAQMD in their district rules regarding architectural coatings. Some districts provided details on their coating regulations that phase in over time which have been incorporated to the extent feasible given the general classifications of paint (interior or exterior for residential and non-residential). As not all districts submitted their architectural coating regulations, consult your local agency for any suggested values that may be lower than the state regulations.

If changing the operational architectural coating VOC content (e.g., lower VOC content limit), the User is advised to change the architectural coating VOC content under the Area Mitigation screen where the operational coating VOC content defaults will not change unless prompted. If not, the model assumes the value on the mitigation screen is the "New Value" (as listed in report). In the case of applying a lower VOC content limit on the operational architectural coating screen, the unchanged mitigation value ("New Value") will be higher. However, unless the box is checked on the Area Mitigation screen next to the coating type, the model will not calculate a mitigated emissions value.

4.5.4 Landscape Equipment

This subscreen has two text boxes to show the number of snow days or summer days. In addition, the defaults consider a realistic number of days which the landscaping equipment would be operated. For example, landscaping at commercial facilities typically do not take place during a weekend or during the summer at educational facilities that are not open. The number of days are applied to the appropriate landscape equipment types available in OFFROAD2011 using the average horsepower and load factors of the population mode. The

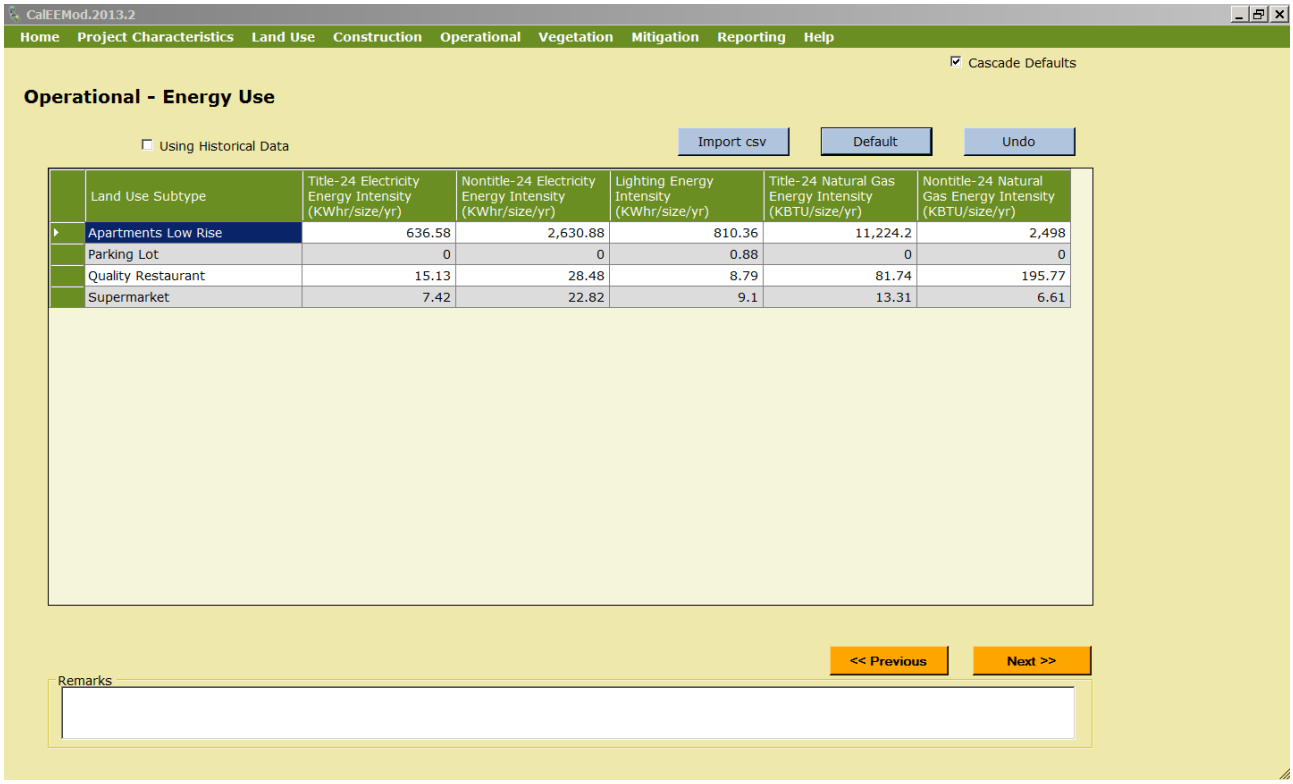
derivation of emission factors used for each equipment type from OFFROAD2011 is described in Appendix A.

4.6 Energy Use

The energy use screen is used to gather the information necessary to estimate the emissions associated with building electricity and natural gas usage (non-hearth). The electricity energy use is in kilowatt hours per size metric for each land use subtype and natural gas use is in kiloBritish Thermal Units (kBTU) per size metric for each land use subtype. The California Energy Code contains energy conservation standards applicable to all residential and non-residential buildings throughout California, including schools. The electricity use is split into three areas: Title-24, non-Title 24, and lighting. The Title 24 of the California Code of Regulations, known as the California Building Standards Code (or "Title 24"), uses are defined as the major building envelope systems covered by Part 6 (California Energy Code) of Title 24 such as space heating, space cooling, water heating, and ventilation. Lighting was separated out since it can be both part and not part of Title-24. Since lighting is not considered as part of the building envelope energy budget, CalEEMod does not consider lighting to have any further association with Title 24 references in the program. Non-Title 24 is everything else such as appliances and electronics. Natural gas is just distinguished as Title 24 or Non-Title 24. The default values are based on the CEC sponsored California Commercial End Use Survey (CEUS) and Residential Appliance Saturation Survey (RASS) studies[9]. For climate zones not included in these surveys a data from the closest climate zone was used as a surrogate. Since these studies are based on older buildings, adjustments have been made to account for changes to Title 24 building codes as described in Appendix A. A user should select the use historical box if they only want an adjustment to the 2005 standards which were in effect when ARB developed its Scoping Plan 2020 No Action Taken predictions. After selecting the historical button, the user must also click the default button to load the historical default values.

9 CEC. October 2010. Residential Appliance Saturation Survey. Available online at: http://www.energy.ca.gov/appliances/rass

CEC. 2006. Commercial End-Use Survey. Available online at: http://www.energy.ca.gov/ceus/



4.7 Water and Wastewater Use

This module only estimates the land uses contribution of GHG emissions associated with supplying and treating the water and wastewater. This screen is used to enter the amount of water in gallons used indoors and outdoors for each land use subtype[10]. The indoor water is also used to estimate the amount of wastewater. The electricity intensity for various phases of providing water is broken out. Depending on the specific water supply used or treatment method used these numbers can vary over a wide range. Supplying water is bringing the water from its primary source such as the ground, river, or snowpack to the treatment plant. Distributing the water is bringing the water from the treatment plant to the end users. The electricity intensities are multiplied by the utility intensity factors for the GHGs and are classified as indirect emissions. The default electricity intensity is from the CEC's 2006 Refining Estimates of Water-Related Energy Use in California using the average values for Northern and

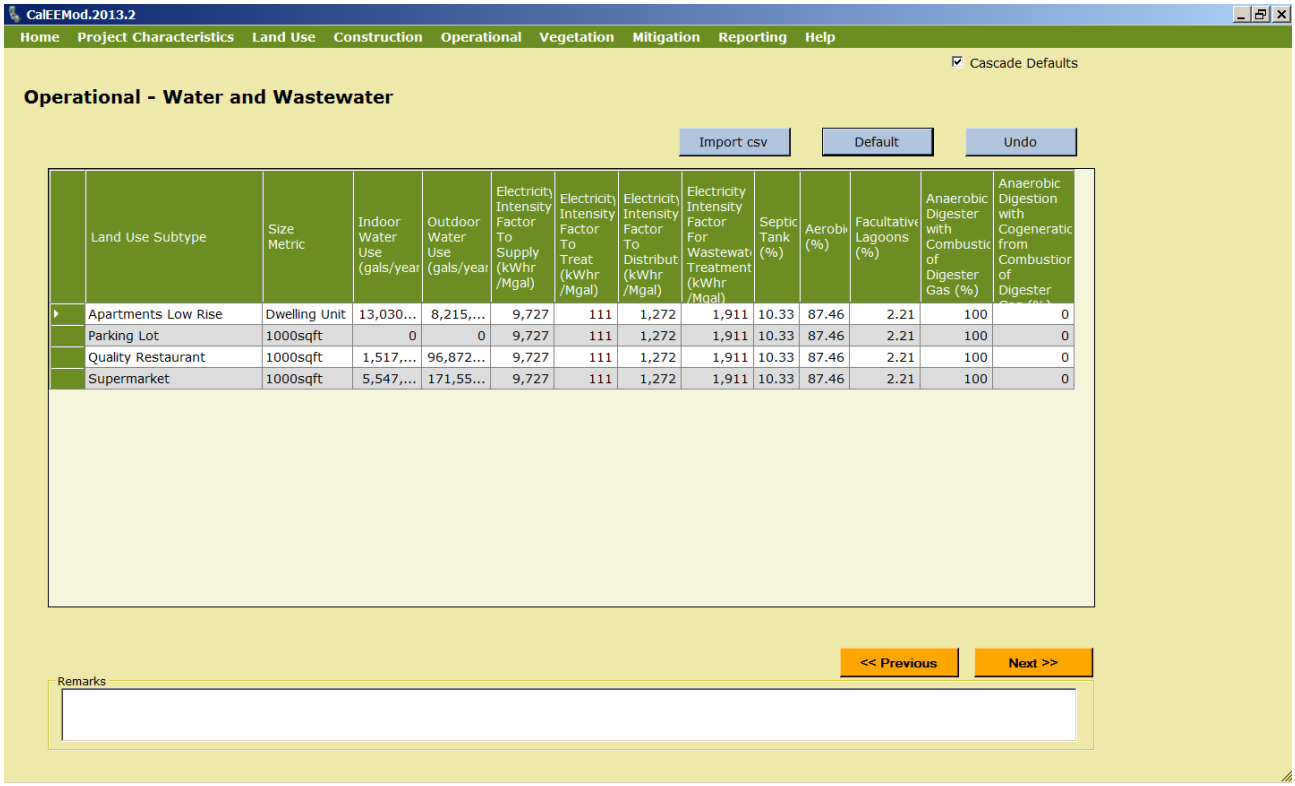
10 Gleick, P.H.; Haasz, D.; Henges-Jeck, C.; Srinivasan, V.; Cushing, K.K.; Mann, A. 2003. Waste Not, Want Not: The Potential for Urban Water Conservation in California. Published by the Pacific Institute for Studies in Development, Environment, and Security. Full report available online at: http://www.pacinst.org/reports/urban_usage/waste_not_want_not_full_report.pdf. Appendices available online at: http://www.pacinst.org/reports/urban_usage/appendices.htm

Dziegielewski; B.; Kiefer, J.C.; Optiz, E.M.; Porter, G.A.; Lantz, G.L.; DeOreo, W.B.; Mayer, P.W.; Nelson, J.O. 2000. Commercial and Institutional End Uses of Water. Published by the American Water Works Association Research Foundation.

Northern California Golf Association. Improving California Golf Course Water Efficiency. http://www.owue.water.ca.gov/docs/2004Apps/2004-079.pdf

Southern California[11]. The location will automatically select the appropriate values if using these defaults. Since the electricity can vary greatly based on locations, the user should override these values if they have more specific information regarding their specific water supply and treatment.

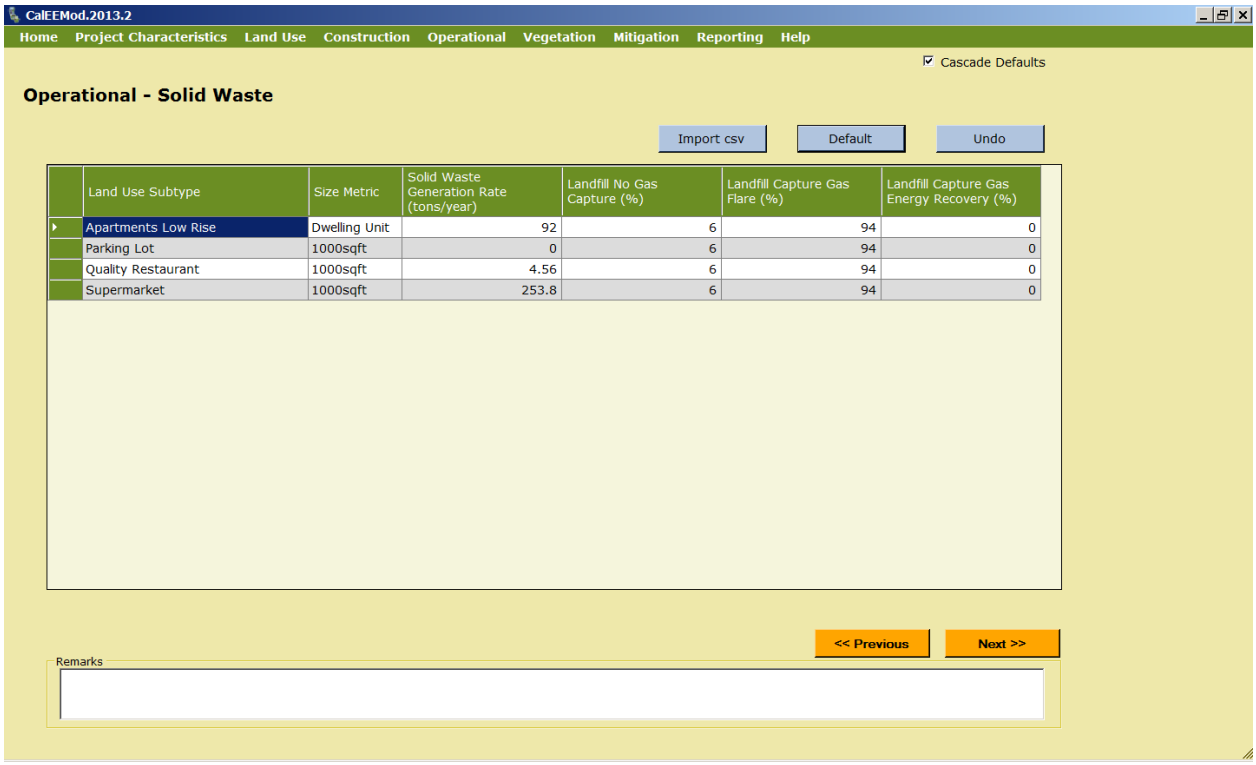
Wastewater may also have direct emissions of GHGs. These depend on the type of wastewater treatment system (e.g., septic, aerobic or lagoons) used and therefore the wastewater treatment type percentages are variables. In addition, the model calculates impacts if the solids are digested either through an anaerobic digester or with co-generation from combustion of digester gas. Each type has associated GHG emission factors. Some of these may be classified as biogenic. Not all of the biogenic emissions are accounted for since there are not adequate emissions factors at this time. Refer to Appendix A on how to properly change the defaults, if necessary, and the methodology used to calculate impacts from wastewater treatment.



[11] CEC-500-2006-118.

4.8 Solid Waste

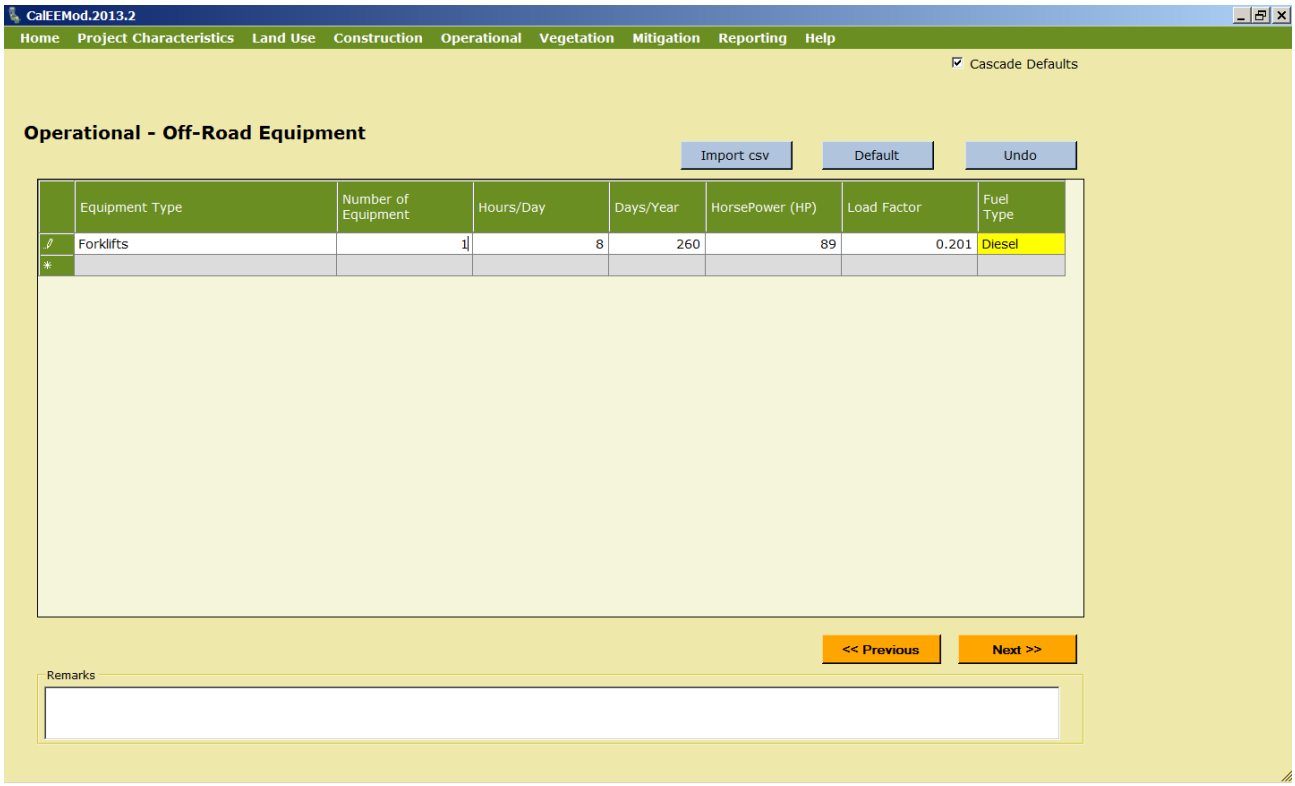
The solid waste module determines the GHG emissions associated with disposal of solid waste into landfills. In order to estimate the eventual contribution of GHG emissions from solid waste for the waste disposed by a land use annually, the total amount of carbon dioxide and methane that would be evolved over the span of many years is calculated. This is based on the IPCC's methods for quantifying GHG emissions from solid waste using the degradable organic content of waste[12]. Waste disposal rates by land use and overall composition of municipal solid waste in California was primarily based on Calrecycle data. The amount of methane emitted depends on characteristics of the landfill, and therefore the default percentage is based on the types of landfills assumed by ARB in their GHG emission inventories. Portions of these emissions are biogenic. The defaults for the gas capture (e.g., no capture, flaring, energy recovery) are statewide averages, but the user has the ability to override the defaults if the gas capture is known. Local jurisdictions can also provide guidance to users as to what default properly reflects known regional solid waste gas capture. Users in the Santa Barbara region are recommended to apply 100% landfill capture gas flare overriding the statewide default to reflect a more accurate regional solid waste activity.



12 IPCC. 2006. 2006 IPCC Guidelines for National Greenhouse Gas Inventories. Volume 5 Waste.

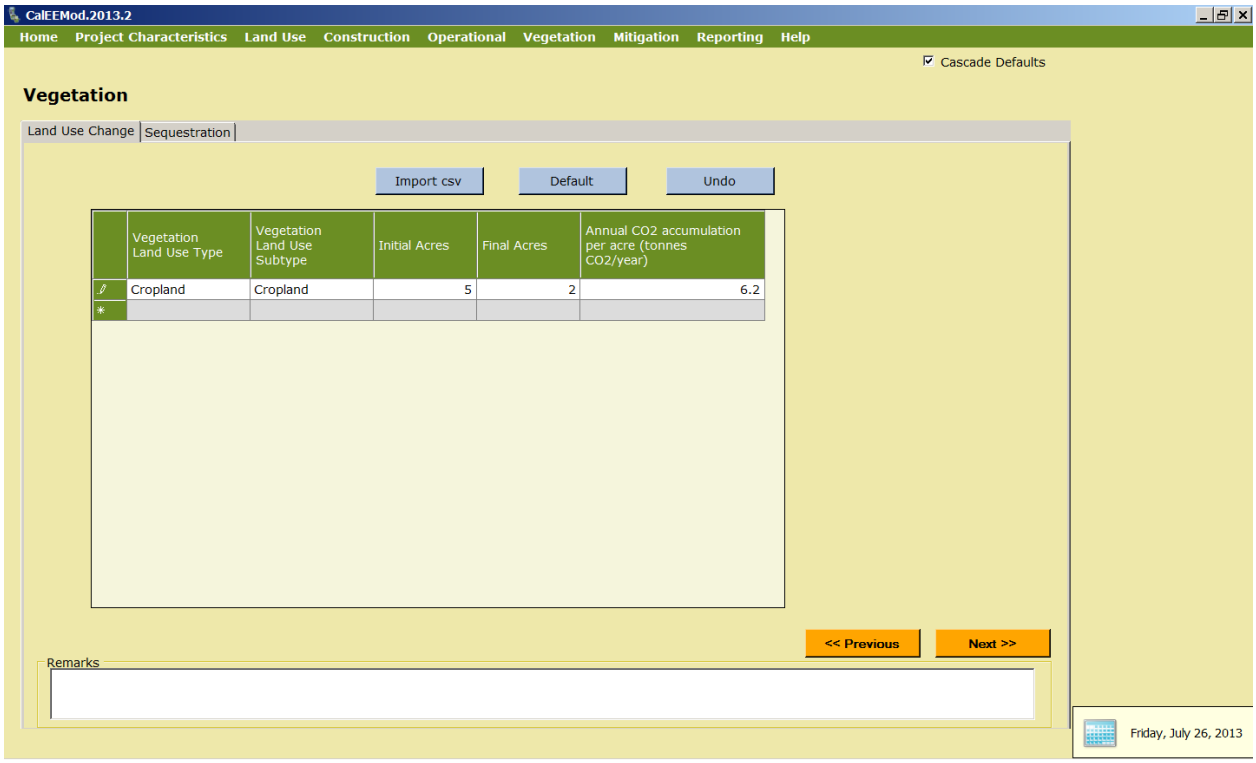
4.9 Off-Road Equipment

A new sub-screen under Operational allows the user to identify any off-road equipment used during operational activities (e.g., forklifts, cranes, loaders, generator sets, pumps, pressure washers, etc.) at the project site. Because such equipment cannot be assumed to be needed for a particular land use project, a user needs to provide the input in order for CalEEMod to calculate the resulting emissions from equipment operation. A dropdown list of off-road equipment is provided for the user to identify each piece of equipment. The model requires the following specific information per equipment type. The user would need to provide the number of pieces for each equipment type. The model assumes an operation activity of 8 hours per day and 260 days per year, as well as the horsepower and load factor of the equipment type, but the user has the ability to override the default assumptions with project specific information. Finally, the model assumes diesel fuel, but a dropdown menu is provided to allow the user to choose bio-diesel or compressed natural gas (CNG) if known to power the equipment.



4.10 Vegetation

The vegetation module is used to estimate the one-time change in carbon sequestration capacity of a vegetation land use type. The methods used are based on IPCC[13]. The user enters the vegetation land use type, the initial and final acreage of the vegetation land use type, and the annual carbon dioxide equivalent accumulation per acre if the user chooses to over ride the default value. Settlement land use acreage is not considered since it is a net zero at steady state unless trees are added.



4.10.1 Sequestration

This subscreen to vegetation is used to estimate the GHG emissions associated with the sequestration of net new trees added to the project site. Consistent with IPCC recommendations a 20 year active growth period is assumed. The user enters the tree type or miscellaneous if it is not known, and the total number of trees. The user can override the default carbon sequestration rate.

4.11 Mitigation

The mitigation module screen consists of six subscreens that the user can indicate and supply the necessary information to estimate the emissions after mitigation measures have been implemented. The mitigation measures included in CalEEMod are largely based on the recent

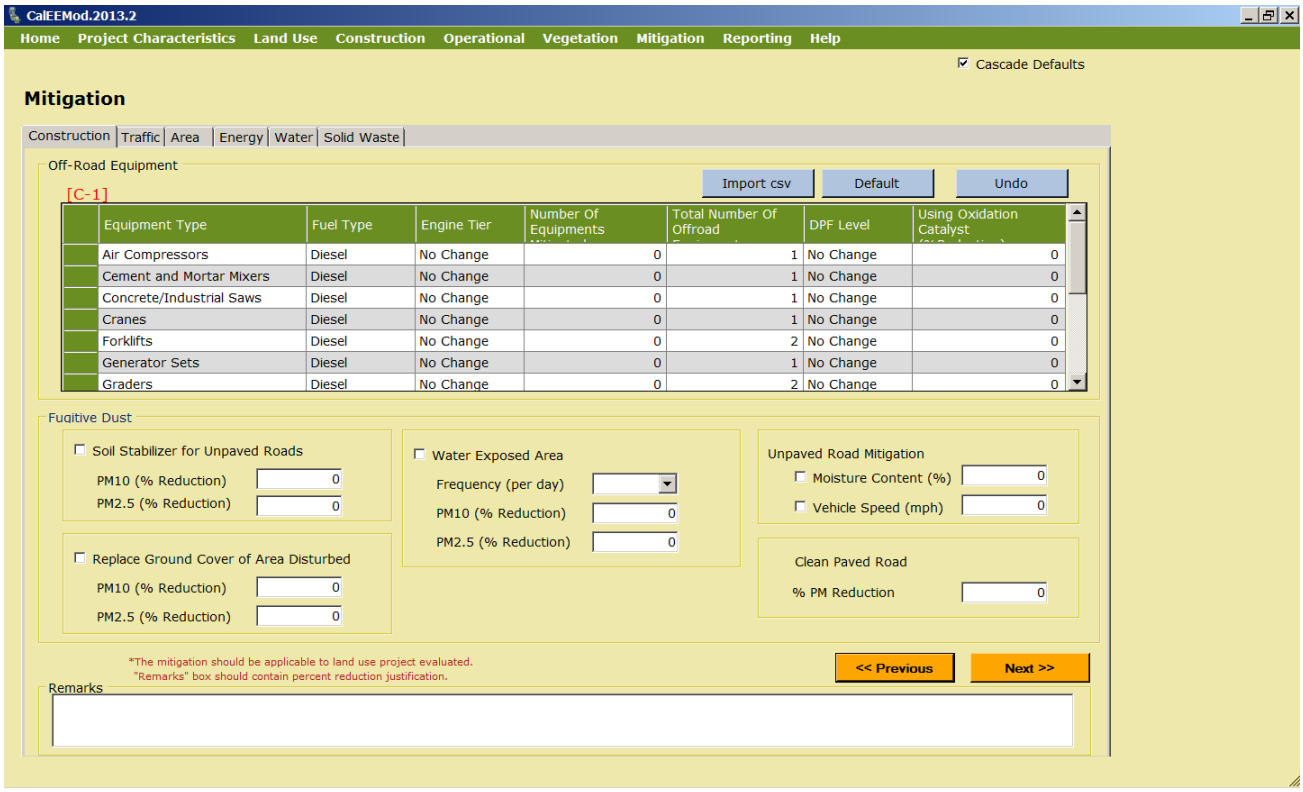
13 IPCC. 2006. 2006 IPCC Guidelines for National Greenhouse Gas Inventories Volume 4.

CAPCOA Quantifying Greenhouse Gas Mitigation Measures (http://www.capcoa.org/wp-content/uploads/downloads/2010/09/CAPCOA-Quantification-Report-9-14-Final.pdf) document. To assist the user in understanding each measure by referencing back to the CAPCOA document, the CAPCOA measure numbers are provided next to the listed measures in CalEEMod. Therefore, this user's guide focuses on key aspects of the program screens that user's should pay attention to.

4.11.1 Construction Mitigation

This screen consists of a datagrid to apply mitigation to off-road construction equipment and check boxes with supplemental information for fugitive dust emissions.

To apply mitigation to construction equipment, the user selects the equipment type the number of equipment noting the total number displayed based on construction equipment lists, and type of mitigation to apply. If substantial evidence supporting reductions was available at the time of development, options include fuel type (diesel, CNG, electric, hybrid, biodiesel), engine tier (typically will select Tier 4), diesel particulate filter tiers (Tier 3 being the best), and oxidative catalyst reduction. The program estimates how much if any increase or decrease in emissions to apply for each pollutant. Some mitigation measures have trade-offs in pollutant reductions and therefore may result in increases of some pollutants.



To apply mitigation to fugitive dust from construction, the user selects the check box in front of the mitigation measure name, and enters in the appropriate information in the drop down or text

boxes. Some fugitive dust mitigation required by some districts do not appear here since the fugitive dust source they mitigate is not quantified by CalEEMod in particular this includes fugitive dust generated by wind over land and storage piles. Since they are not quantified it is not appropriate to apply the reduction. The construction mitigation to use alternative fuel for construction equipment is consistent with the mitigation number C-1 in the CAPCOA Quantifying GHG Mitigation document.

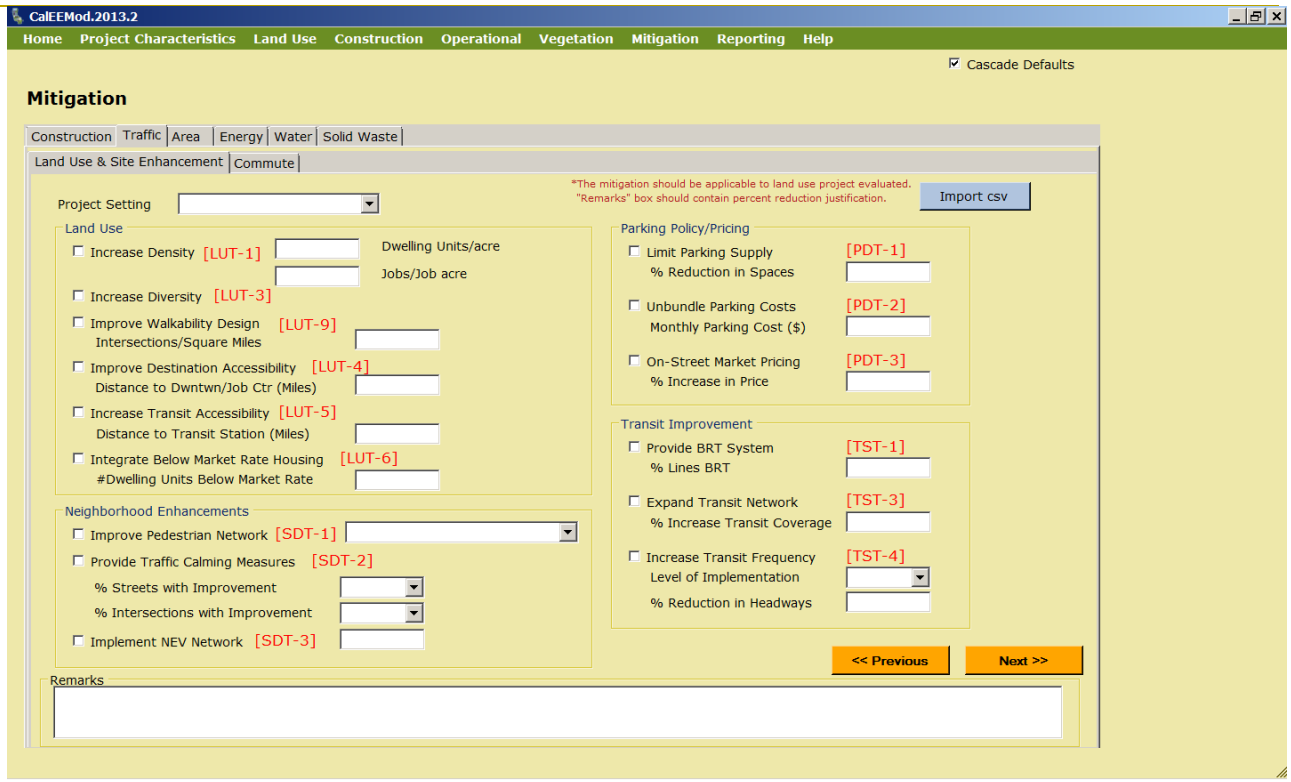
4.11.2 Traffic Mitigation

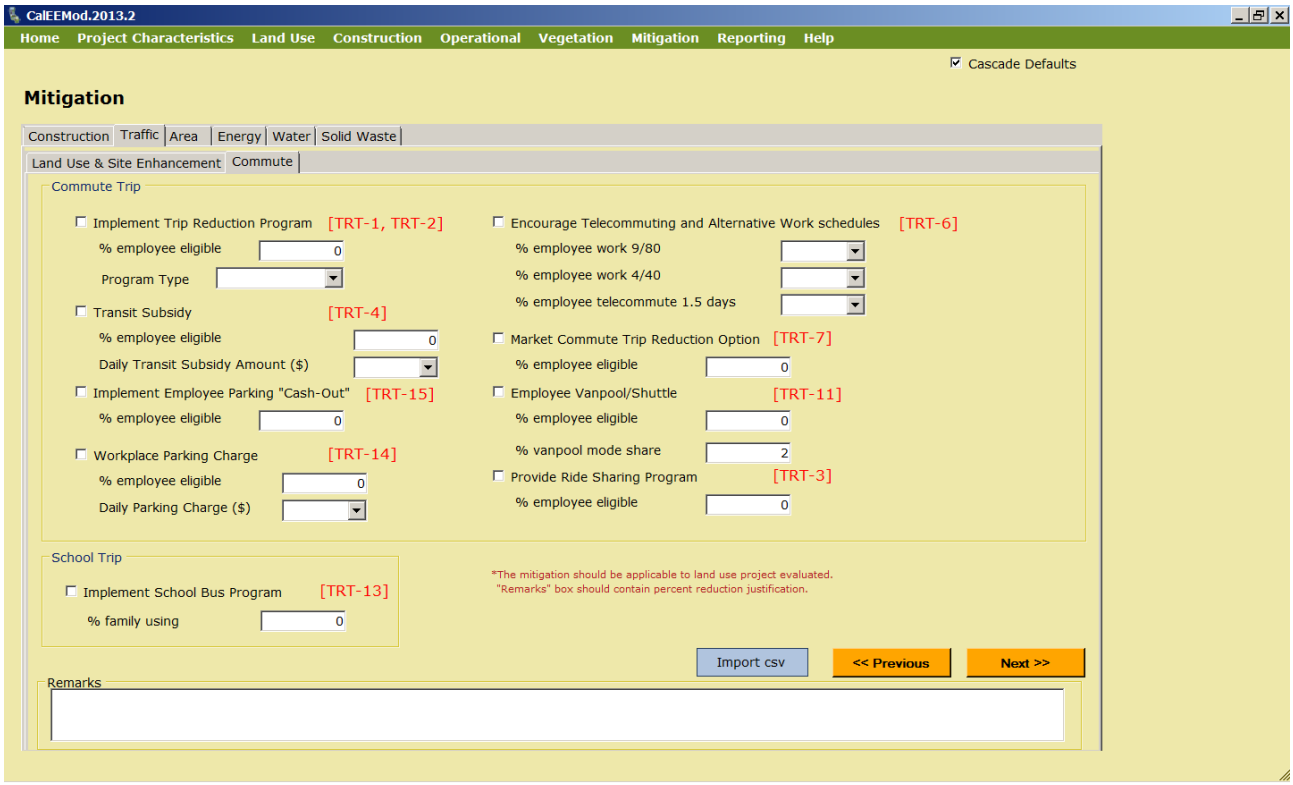
There are two traffic mitigation subscreens that the user can select from. First the user must select the Project Setting as defined in the CAPCOA document (pages 59-60).

- Low Density Suburban: An area characterized by dispersed, low-density, single-use, automobile dependent land use patterns, usually outside of the central city (a suburb).
- Suburban Center: serves the population of the suburb with office, retail and housing which is denser than the surrounding suburb.
- Urban: an area which is located within the central city with higher density of land uses than you would find in the suburbs. It may be characterized by multi-family housing and located near office and retail.
- Urban Center *(known as "Compact Infill" in CAPCOA document)* : A project which is located within or contiguous with the central city. Examples may include redevelopment areas, abandoned sites, or underutilized older buildings/sites.

If the CAPCOA measure did not distinguish between suburban center and low density suburban, values for low density suburban were used. Similarly, if urban center and urban values were not distinguished urban values were used.

The user checks the box next to each mitigation measure and fills in the appropriate information as required. The maximum reduction caps defined in the CAPCOA Quantifying GHG Mitigation document are integrated into these calculations. The CAPCOA traffic mitigation measure numbers included in CalEEMod are the following: LUT-1, LUT-3, LUT-9, LUT-4, LUT-5, LUT-6, SDT-1, SDT-2, SDT-3, PDT-1, PDT-2, PDT-3, TST-1, TST-3, TST-4, TRT-1, TRT-2, TRT-4, TRT-15, TRT-14, TRT-6, TRT-7, TRT-11,TRT-3, and TRT-13. The NEV network mitigation measure assumes the low end of the CAPCOA recommendations.


CalEEMod.2013.2
Home Project Characteristics Land Use Construction Operational Vegetation Mitigation Reporting Help
Cascade Defaults
Mitigation
Construction Traffic Area Energy Water Solid Waste
Land Use & Site Enhancement Commute
*The mitigation should be applicable to land use project evaluated.
"Remarks" box should contain percent reduction justification.
Import csv
Project Setting
Land Use
Increase Density [LUT-1]
Dwelling Units/acre
Jobs/Job acre
Increase Diversity [LUT-3]
Improve Walkability Design [LUT-9]
Intersections/Square Miles
Improve Destination Accessibility [LUT-4]
Distance to Dwntwn/Job Ctr (Miles)
Increase Transit Accessibility [LUT-5]
Distance to Transit Station (Miles)
Integrate Below Market Rate Housing [LUT-6]
#Dwelling Units Below Market Rate
Neighborhood Enhancements
Improve Pedestrian Network [SDT-1]
Provide Traffic Calming Measures [SDT-2]
% Streets with Improvement
% Intersections with Improvement
Implement NEV Network [SDT-3]
Parking Policy/Pricing
Limit Parking Supply [PDT-1]
% Reduction in Spaces
Unbundle Parking Costs [PDT-2]
Monthly Parking Cost ($)
On-Street Market Pricing [PDT-3]
% Increase in Price
Transit Improvement
Provide BRT System [TST-1]
% Lines BRT
Expand Transit Network [TST-3]
% Increase Transit Coverage
Increase Transit Frequency [TST-4]
Level of Implementation
% Reduction in Headways
<< Previous
Next >>
Remarks

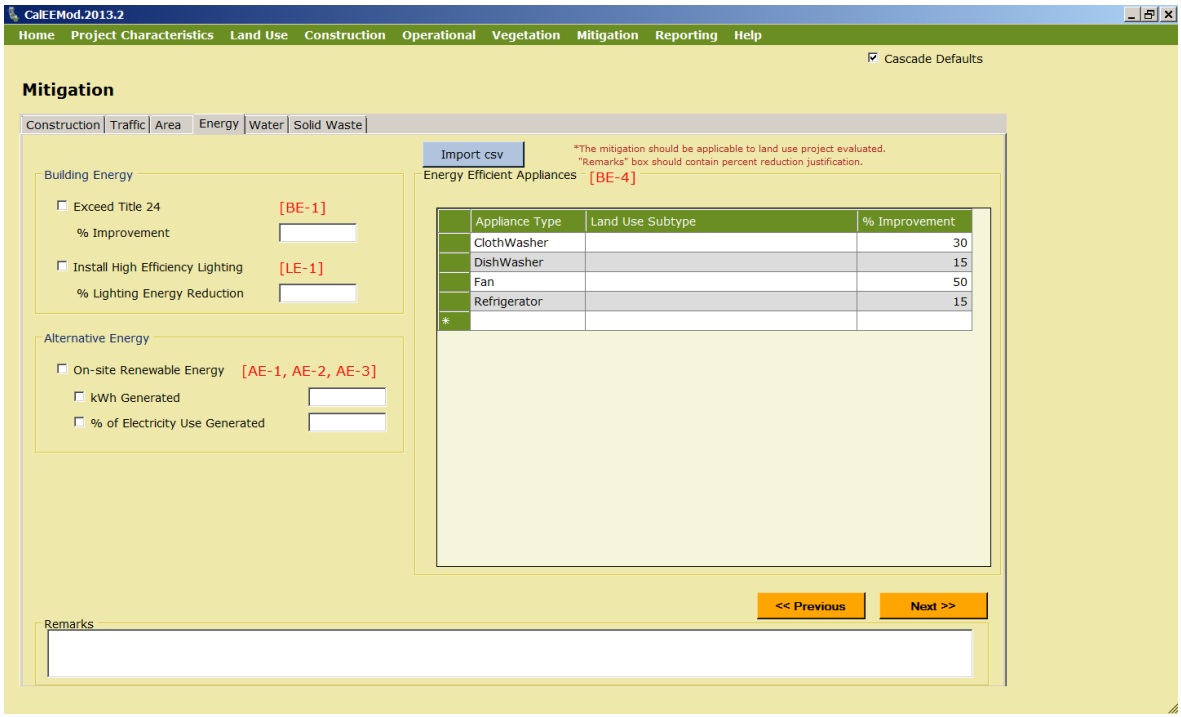

CalEEMod.2013.2
Home Project Characteristics Land Use Construction Operational Vegetation Mitigation Reporting Help
Cascade Defaults
Mitigation
Construction Traffic Area Energy Water Solid Waste
Land Use & Site Enhancement Commute
Commute Trip
Implement Trip Reduction Program [TRT-1, TRT-2]
% employee eligible
Program Type
Transit Subsidy [TRT-4]
% employee eligible
Daily Transit Subsidy Amount ($)
Implement Employee Parking "Cash-Out" [TRT-15]
% employee eligible
Workplace Parking Charge [TRT-14]
% employee eligible
Daily Parking Charge ($)
Encourage Telecommuting and Alternative Work schedules [TRT-6]
% employee work 9/80
% employee work 4/40
% employee telecommute 1.5 days
Market Commute Trip Reduction Option [TRT-7]
% employee eligible
Employee Vanpool/Shuttle [TRT-11]
% employee eligible
% vanpool mode share
Provide Ride Sharing Program [TRT-3]
% employee eligible
School Trip
Implement School Bus Program [TRT-13]
% family using
*The mitigation should be applicable to land use project evaluated.
"Remarks" box should contain percent reduction justification.
Import csv
<< Previous
Next >>
Remarks

4.11.3 Area Mitigation

The user can select from a few area source mitigation measures by checking the appropriate box and supplying any additional information in the text boxes. These measures include all natural gas hearths, no hearths, electric landscaping equipment use, reduced VOC coatings, and reduced consumer product VOC content. The area landscaping mitigation to prohibit gas powered landscape equipment is consistent with the mitigation number A-1 in the CAPCOA Quantifying GHG Mitigation document.

4.11.4 Energy Mitigation

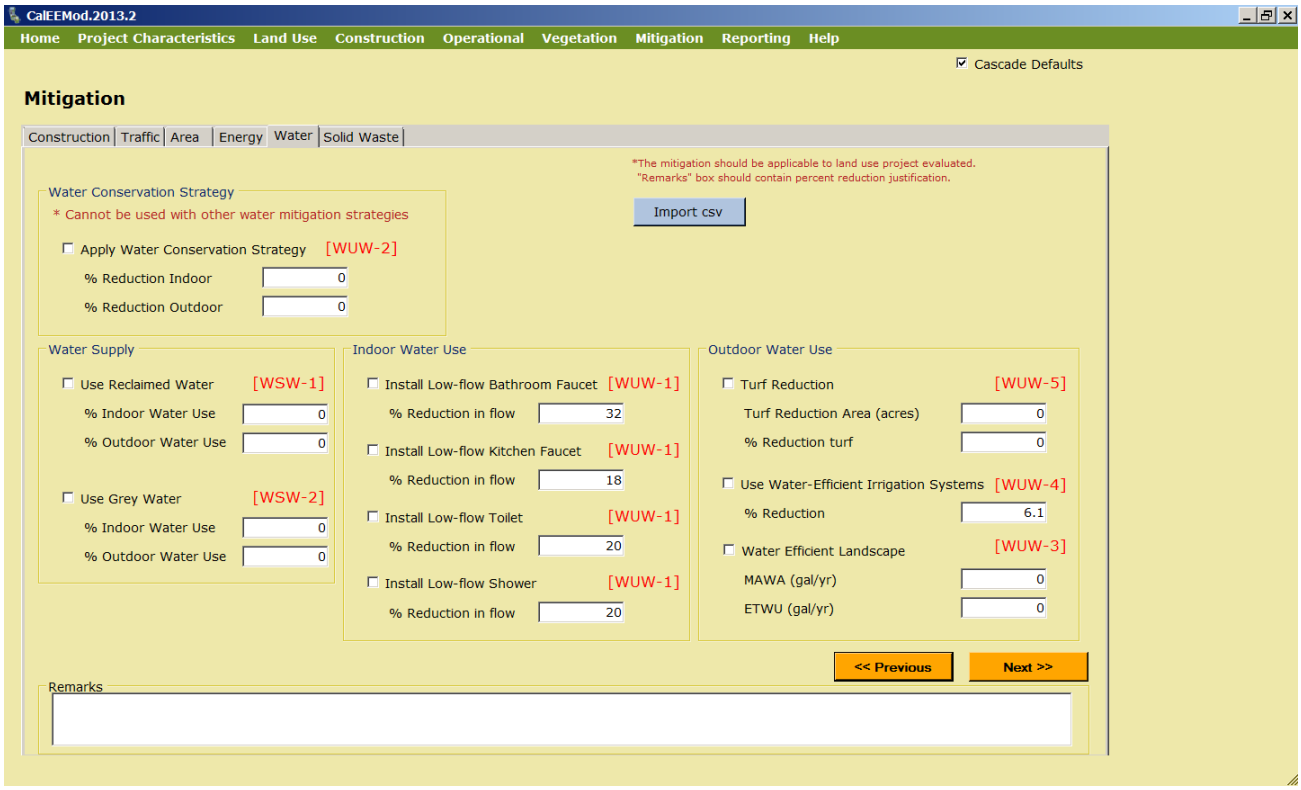
The user selects energy mitigation measures by using check boxes or a datagrid. These correspond to CAPCOA Mitigation Measures LE-1, BE-1, AE-1, AE-2, AE-3 and BE-4 as listed in the CAPCOA Quantifying GHG Mitigation document. The lighting is a percentage reduction in lighting as supplied by the user. The datagrid is used to enter the land use subtypes that will use energy efficient appliances. The percent improvement is the typical percent improvement above standard appliances according to the 2008 Energy Star Annual Report[14]. Alternative Energy has two methods to enter the amount of alternative energy. The first is the amount of kWhr generated. The second is the percentage of the total electricity use by buildings that is generated. At this time alternative energy methods that are not carbon neutral are not quantified. To apply the amount of alternative energy only one of the two methods (kWhr or percentage) needs to be entered for CalEEMod to calculate emission reductions.



14 Available at http://www.epa.gov/cpd/annualreports/annualreports.htm

4.11.5 Water Mitigation

Water mitigation can either be estimated as the percent reduction based on a water conservation strategy or the other individual mitigation measures. The CAPCOA Quantifying GHG Mitigation document includes water supply and use measures WSW-1 & 2, WUW-1 through 5. For CAPCOA Mitigation Measure WSW- 3 (Use Locally Sourced Water Supply), using locally-sourced water or water from less energy-intensive sources reduces the electricity and indirect CO_2 emissions associated with water supply and transport because water from local or nearby groundwater basins, nearby surface water and gravity-dominated systems have smaller energy-intensity factors. Therefore, for WSW-3, the user should alter the energy intensity values in water and run a separate CalEEMod run to accommodate these values.



4.11.6 Solid Waste Mitigation

The user can get a reduction for recycling waste. This mitigation measure corresponds to CAPCOA Mitigation Measure: SW-1.

4.12 Reporting

The user initiates final calculations by selecting the report and clicking on the button. The available reports include: Annual, Summer (peak) Daily, Winter (peak) Daily and Mitigation. A separate report viewer will come up. From this report viewer, the user can view their report on-screen, print reports, save as Microsoft excel file or save as a pdf file, or in the case of the Mitigation report, a Microsoft doc file. The data in the excel file has already been calculated and placed in the grids as text, thus, for example, one cannot change an emission value and expect the report to change the summed total value. These values, however, can be copied to new excel spreadsheet for any further desired calculation with the data.



CALIFORNIA ENERGY COMMISSION

California's Water – Energy Relationship

Prepared in Support of the 2005 Integrated Energy Policy Report Proceeding (04-IEPR-01E)

FINAL STAFF REPORT

NOVEMBER 2005
CEC-700-2005-011-SF

Arnold Schwarzenegger, *Governor*

CALIFORNIA ENERGY COMMISSION

Primary Author
Gary Klein
California Energy Commission

Martha Krebs
Deputy Director
Energy Research and Development Division

Valerie Hall
Deputy Director
Energy Efficiency & Demand Analysis Division

Terry O'Brien
Deputy Director
Systems Assessment & Facilities Siting Division

B. B. Blevins
Executive Director

DISCLAIMER

This paper was prepared as the result of work by one or more members of the staff of the California Energy Commission. It does not necessarily represent the views of the Energy Commission, its employees, or the State of California. The Energy Commission, the State of California, its employees, contractors and subcontractors make no warrant, express or implied, and assume no legal liability for the information in this paper; nor does any party represent that the uses of this information will not infringe upon privately owned rights. This paper has not been approved or disapproved by the California Energy Commission nor has the California Energy Commission passed upon the accuracy or adequacy of the information in this paper.

ACKNOWLEDGEMENTS

The *California's Water-Energy Relationship* report is the product of contributions by many California Energy Commission staff and consultants, including Ricardo Amon, Shahid Chaudhry, Thomas S. Crooks, Marilyn Davin, Joe O'Hagan, Pramod Kulkarni, Kae Lewis, Laurie Park, Paul Roggensack, Monica Rudman, Matt Trask, Lorraine White and Zhiqin Zhang.

Staff would also like to thank the members of the Water-Energy Working Group who so graciously gave of their time and expertise to inform this report.

TABLE OF CONTENTS

ACKNOWLEDGEMENTS ..... **I**

TABLE OF CONTENTS ..... **II**

EXECUTIVE SUMMARY **1**

INTRODUCTION **3**

CHAPTER 1 - WHAT IS THE WATER-ENERGY RELATIONSHIP? **6**

THE WATER USE CYCLE 6
WATER-RELATED ENERGY USE 7
THE ENERGY INTENSITY OF THE WATER USE CYCLE 9
ENERGY INTENSITY IN NORTHERN AND SOUTHERN CALIFORNIA 11
WATER END USE ENERGY 12
Agriculture *12*
Residential, Commercial and Industrial *15*
HYDROPOWER PRODUCTION, ENERGY RECOVERY, AND RENEWABLE RESOURCES 16
Hydropower *16*
Energy Recovery from the Water Use Cycle *17*
In-Conduit Hydropower 17
Biogas 17
Other Renewable Energy Resources *17*
A Loading Order for Water Resources *18*

CHAPTER 2 – WATER SUPPLY AND CONVEYANCE **21**

PRIMARY SOURCES OF CALIFORNIA WATER 21
The Energy Intensity of Water Supplies *22*
Surface Water *23*
Groundwater Sources *26*
Ocean and Brackish Water *27*
Recycled Water *28*
The Energy Intensity of the Water Resource Portfolio *30*

CHAPTER 3 – WATER AND WASTEWATER TREATMENT AND DISTRIBUTION **31**

WATER TREATMENT 33
Desalination *36*
WATER DISTRIBUTION 37
WASTEWATER TREATMENT 38
CONCLUSIONS 41

CHAPTER 4 – WATER RELATED END-USE EFFICIENCY **42**

THE ENERGY IMPACT OF WATER USE EFFICIENCY 42
AGRICULTURAL WATER USE EFFICIENCY 44
ENERGY EFFICIENCY AND CONSERVATION MEASURES 44

ADOPTION OF TIME OF USE (TOU) AGRICULTURAL ELECTRIC RATES 45
OTHER FACTORS AFFECTING AGRICULTURAL WATER ENERGY USE IN CALIFORNIA 46
URBAN WATER USE EFFICIENCY 48
TOU WATER TARIFFS AND METERS 50
Water Storage for Peak Electric Load Shifting *51*
Investing in Water and Energy Efficiency *51*
CONCLUSIONS 52

CHAPTER 5 – RENEWABLE ENERGY GENERATION POTENTIAL 53

DISTRIBUTED GENERATION 54
In-Conduit Hydropower *54*
Biogas *55*
OTHER DISTRIBUTED GENERATION OPTIONS 56
Utility Scale Generation *57*
Large-Scale Hydropower *57*
Pumped Storage *58*
Retrofit *60*
Other Renewable Resources *61*
Barriers to Energy Production *62*
CONCLUSIONS 63

CHAPTER 6 – POTENTIAL EFFECTS OF FUTURE CHANGES 64

INCREASED WATER DEMAND 64
CHANGES IN WATER END USE 68
Changes in Agricultural Water Use *68*
CHANGES IN REGULATION AND LEGISLATION 69
Water Quality Regulations *69*
Changes in Water and Energy Markets *72*
Water Markets 72
Energy Markets 73
Hydrology *73*
Drought 73
Climate Change 74
TECHNOLOGY 75
POLICIES 76
CONCLUSIONS 76

CHAPTER 7 – STAFF RECOMMENDATIONS 77

FINDINGS 77
STAFF RECOMMENDATIONS 79
Save energy by saving water *79*
Reduce water system net power requirements *81*
RECOMMENDED JOINT ACTIONS 82
CONCLUSION 83

APPENDICES 85

APPENDIX A: EXISTING ORGANIZATIONS, PROGRAMS, AND RESEARCH 86

THE CALIFORNIA WATER PLAN 86
ENERGY USE IN THE WATER CYCLE 86
THE U.S. DEPARTMENT OF ENERGY'S ENERGY-WATER NEXUS TEAM 87
WATER AND WASTEWATER FACILITIES 88
AGRICULTURAL WATER 92
WATER SUPPLY 94
WATER TREATMENT 97
WASTEWATER TREATMENT 98
WATER-RELATED END USES 98
WATER FOR ELECTRICITY GENERATION 101

APPENDIX B: 2001 CALIFORNIA ENERGY CONSUMPTION BY END USE 104

APPENDIX C: ENERGY IMPACT ANALYSIS OF EXISTING WATER MANAGEMENT PRACTICES 107

INTRODUCTION 107
THE WATER USE CYCLE 107
WATER USE CYCLE ENERGY REQUIREMENTS 108
REGIONAL WATER-ENERGY CHARACTERISTICS 109
WATER USE CYCLE ENERGY INTENSITY 110
WATER CONVEYANCE 111
WATER TREATMENT 113
WATER DISTRIBUTION 116
WASTEWATER TREATMENT 116
SUMMARY OF WATER ENERGY INTENSITY FOR NORTHERN AND SOUTHERN CALIFORNIA 117
THE ENERGY EFFICIENCY OF WATER USE EFFICIENCY 118
COST-EFFECTIVENESS ASSUMPTIONS 119
ENERGY VALUE OF 2004 BEST (WATER) MANAGEMENT PRACTICES 120
STATEWIDE WATER USE EFFICIENCY (WUE) POTENTIAL 125
COMPARING WATER AND ENERGY EFFICIENCY PROGRAMS 129
PROGRAM OVERSIGHT AND COMPLIANCE 129
PROGRAM FUNDING 132
CURRENT ENERGY EFFICIENCY PROGRAM FUNDING 133
CURRENT WATER EFFICIENCY PROGRAM FUNDING 133
INTEGRATED RESOURCE PLANNING 134
SUGGESTED RESEARCH TOPICS 135

APPENDIX D: EXCERPT FROM CALIFORNIA WATER PLAN UPDATE 2005 138

VOLUME 1, STRATEGIC PLAN, CHAPTER 2, A FRAMEWORK FOR ACTION 138
Sustaining Our Water Resources *138*
Fundamental Lessons 138
Foundational Actions 139
Use Water Efficiently 139
Protect Water Quality 139
Support Environmental Stewardship 140
RECOMMENDATIONS 140

APPENDIX E: A WATER-ENERGY ROADMAP 142

RECOMMENDATIONS OF THE WATER-ENERGY RELATIONSHIP WORKING GROUP 142
GLOSSARY 168

EXECUTIVE SUMMARY

As California continues to struggle with its many critical energy supply and infrastructure challenges, the state must identify and address the points of highest stress. At the top of this list is California's water-energy relationship: water-related energy use consumes 19 percent of the state's electricity, 30 percent of its natural gas, and 88 billion gallons of diesel fuel every year – and this demand is growing.

As water demand grows, so grows energy demand. Since population growth drives demand for both resources, water and energy demand are growing at about the same rates and, importantly, in many of the same geographic areas. This dynamic is exacerbated by the fact that Northern California has two-thirds of the state's precipitation while two-thirds of the population resides in Southern California. Water demand and electricity demand are growing rapidly in many of the same parts of the state stressing already constrained electricity delivery systems. When electric infrastructure fails, water system reliability quickly plummets and threatens the public health and safety.

The state water plan concludes that the largest single new supply available for meeting this expected growth in water demand over the next 25 years is water use efficiency. The remainder must be provided by the development of new water supplies including water recycling, and desalination of both brackish and seawater[1], all of which will increase energy demand over current levels.

Worse, the times when the highest energy intensity water supply options will be most needed are most likely to occur during multi-year drought periods when surface water supplies are low and groundwater levels drop, requiring even more energy for pumping each gallon of water. To compound the problem, reduced surface water supplies and snowpack in high elevations are likely to reduce the availability of valuable hydroelectric supplies. Yet, these are also the times when the most aggressive water conservation efforts are implemented, reducing overall water use, which helps reduce the total impact on energy demand. Although the net effects of this dynamic are not fully understood, this report presents current knowledge to assist with further analysis.

This is an urgent time of both challenge and opportunity. The primary finding of this paper is that a major portion of the solution is closer coordination between the water and energy sectors. A meaningful solution cannot be reached in the current regulatory environment where water utilities value only the cost of acquisition, conveyance, treatment, and delivery; wastewater utilities value only the cost of collection, treatment, and disposal; electric utilities value only saved electricity; and natural gas utilities value only saved natural gas. The state must both develop and expand best practices and existing programs to realize the substantial incremental benefits of joint water and energy resources and infrastructure management.

1 State Water Plan, B160-05.

While many nuances of this complex statewide problem are still unclear, staff's analysis shows that significant energy benefits can be reaped through the twin goals of the efficient use of water by end users and the efficient use of energy by water systems. It is also clear that not nearly enough has been done to ensure that California's water supply strategies are synchronized, hand-in-hand, with its energy strategies. Nor has enough been done to forge partnerships between the water and energy sectors so that their natural synergies, joint resources, and assets can be effectively leveraged for the benefit of all Californians.

The state has the opportunity now to reap near-term energy benefits by helping California's water and wastewater utilities become more energy self-sufficient, which will ease pressures on California's already stressed electric system. By adjusting existing policies, programs, and resources, water and wastewater utilities could be converted from high energy users to net renewable energy producers.

California's water and energy policymakers need to commit today to the joint planning and management of these critical resources. The state's water plan and resource strategies are being reviewed with all key stakeholders, and implementation plans are already on the drawing table. At the same time, the California Public Utilities Commission has approved substantial utility ratepayer expenditures in energy efficiency programs for the 2006-2008 program cycle. The state must waste no time in taking advantage of these rapidly evolving events.

The state can meet energy and demand-reduction goals comparable to those already planned by the state's investor-owned energy utilities for the 2006-2008 program period by simply recognizing the value of the energy saved for each unit of water saved. If allowed to invest in these cold water energy savings, energy utilities could co-invest in water use efficiency programs, which would in turn supplement water utilities' efforts to meet as much load growth as possible through water efficiency. Remarkably, staff's initial assessment indicates that this benefit could be realized at less than half the cost to electric ratepayers of traditional energy efficiency measures.

This staff report examines how energy is used – and how it can be saved – in the water use cycle. The strategies and goals for a comprehensive statewide water-energy program would achieve incremental energy benefits for water and energy utilities. The overarching goal of establishing a comprehensive statewide water-energy program would create a dynamic, living process where key stakeholders have incentives to continuously identify and implement strategies optimizing the state's water and energy resources and assets on an integrated, coordinated, and collaborative basis. This opportunity must not be lost since the need is so great. Because of all these factors, staff recommends that an action-oriented approach structured to achieve near-term results be developed immediately.

INTRODUCTION

The California Energy Commission's (Energy Commission) *California's Water Energy Relationship* staff report is part of the *Integrated Energy Policy Report* (*Energy Report*) proceeding. It was prepared to promote greater understanding of the critical symbiotic relationship between the water and energy sectors, especially electricity. In its scoping order, the Energy Commission stated that:

- "(f)or 2005, the Committee will continue the emphasis from the *2003 Energy Report* on increasing the level of energy efficiency and diversity in the state's energy systems and understanding the limitations of the state's electricity, natural gas, and transportation fuel infrastructure." [2]
- "The need for new water supplies in California and the West due to population growth and potential changes in the state's hydrological cycle has important implications for the state's energy system that are not yet fully understood. The *2005 Energy Report* will need to evaluate this issue as part of pursuing the broader goal of sustainability.[3]
- "To meet the challenge of sustainability, California's energy and environmental agencies, along with key private and public stakeholders, must work together to address critical issues that include:

  > Impacts of water demand and supply strategies, including the need for increased pumping to provide reliable water supplies, increased need for water treatment, and possible development of desalination facilities..."[4]

This report examines the dynamic give-and-take relationship between California's water and energy resources. Among many other issues, this staff report examines the state's water sector and its energy use, along with changes likely to occur in the future. The staff considered various components of the system and the energy implications, or characteristics of these components, for both energy use and generation. With the participation of a broad base of key stakeholders, the staff evaluated actions and methods that can boost the synergistic efficiencies of both the energy and water sectors. This report is meant to inform and provide technical support for decision makers, water and energy industry professionals, and the general public about critical energy supply and demand issues plaguing the state's water sector today.

[2] California Energy Commission, Integrated Energy Policy Report Committee Scoping Order, dated September 3, 2004, p. 2.
[3] Ibid.
[4] Ibid, p.7.

This study presents the best, most updated available information on linkages between California's energy and water sectors. The process to develop this report included two public workshops, several meetings of an ad hoc working group[5] formed for the study, and interviews with scores of water professionals. This outreach included two meetings with members of the Association of California Water Agencies, which represents about 90 percent of the state's water agencies (many of which also operate wastewater treatment facilities), members of the California Municipal Utilities Association, and participation in the annual plenary of the California Urban Water Conservation Council.

The following key concepts form the basis of the analysis in this paper:

- ***Water and energy relationship:*** Refers to the types and magnitude of water and energy interdependencies requiring documentation and evaluation for various types of water resources, end uses, systems, and processes in order to fully understand the water-energy tradeoffs under different resource planning scenarios. In this report staff uses ***water and energy utilities*** when encompassing all water, wastewater, electricity, natural gas, and diesel fuel suppliers, utilities, and districts, both public and private.

- ***Water use cycle:*** Refers to the overall process of collecting, developing, conveying, treating, and delivering water to end users; using the water; and collecting, treating, and disposing of wastewater.

- ***Energy intensity:*** Energy intensity is defined as the amount of energy consumed per unit of water to perform water management-related actions such as desalting, pumping, pressurizing, groundwater extraction, conveyance, and treatment - for example, the number of kilowatt-hours consumed per million gallons (kWh/MG) of water. This concept is applied to water supplies, to components of the water use cycle, and to the total energy intensity of a unit of water throughout the entire water use cycle.

- ***Energy self-sufficiency:*** Refers to an entity that supplies its own energy requirements. This would typically be done through a combination of energy efficiency and self-provision of power, whether purchased or produced.

- ***Integrated water and energy resource management:*** Refers to the comprehensive body of policies, practices, methods, tools, and procedures

[5] The Water-Energy Relationship Working Group consists of representatives from state water and energy-related government agencies, local and regional water agencies, industry organizations, environmental and citizen groups, and other key water professionals. It was established to help guide and critique this Staff Paper, but its life is expected to extend beyond the WER study process to work on other planning efforts, such as DWR's Water Plan process, and perhaps a planning effort related to optimization of pumped-storage opportunities in the state. The transcripts of all Water-Energy Relationship Working Group meetings on pumped-storage will be made available to the public and will become part of the record of evidence for the 2005 Energy Report.

that collectively comprise “statewide integrated water and energy resource planning and management.” Appendix A summarizes most of the existing organizations, programs, and research. Optimal integration is presently beyond the reach of both water and energy resource management best practices.

Chapter 1 describes California’s water-energy relationship – what it is and what it means within the context of California’s current energy circumstances. Chapters 2, 3, and 4 examine the primary components of the entire water cycle and address their energy intensity. Chapter 5 discusses the potential development of new renewable energy resources by water and wastewater utilities. Chapter 6 explores different types of future changes likely to affect the energy intensity of water supplies; water treatment and distribution; water end use; and wastewater treatment and disposal. Findings and recommendations are contained in Chapter 7. Appendices appearing at the end of the report provide additional detail, and a glossary of terms is included.

CHAPTER 1 - WHAT IS THE WATER-ENERGY RELATIONSHIP?

The nation's water and energy resources are inextricably entwined. Energy is needed to pump, treat, transport, heat, cool, and recycle water. On the flip side, the force of falling water turns the turbines that generate hydroelectric electricity, and most thermal power plants are dependent on water for cooling. In California, an elaborate system of manmade storage, treatment and conveyance structures exist to augment natural hydrologic features. This system not only helps produce needed electricity supplies but requires large amounts of energy to deliver quality water where Californians need and want it.

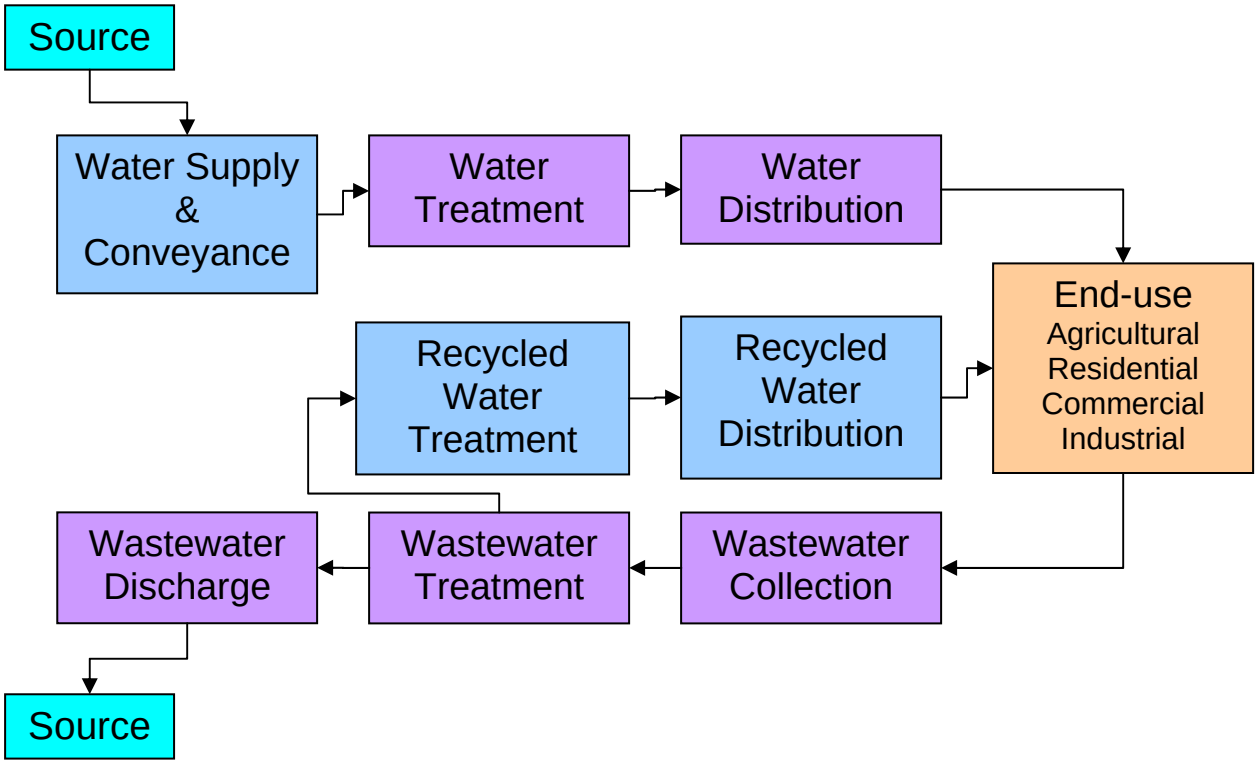
This chapter describes the overall water use cycle and introduces the concept of energy intensity. The energy intensity framework in the water use cycle helps identify opportunities for changing the pattern and magnitude of water-related energy consumption in California.

The Water Use Cycle

The Water-Energy Relationship Working Group discussed the state's water use cycle at length. While there are exceptions, Figure 1-1 illustrates the state's typical cycle.[6] Turquoise blue represents sources of water, water supplies are shown in light blue, water and wastewater treatment are shown in purple, and end use is shown in beige.

[6] This schematic is based on work by Dr. Robert Wilkinson (Wilkinson, Robert C., 2000. *Methodology For Analysis of The Energy Intensity of California's Water Systems, and an Assessment of Multiple Potential Benefits Through Integrated Water-Energy Efficiency Measures*, Exploratory Research Project, Ernest Orlando Lawrence Berkeley Laboratory, California Institute for Energy Efficiency) and on Wilkinson and Gary Wolff in current work on the energy intensity of water in California with additions by Energy Commission staff.

Figure 1-1: California's Water Use Cycle



Water is first diverted, collected, or extracted from a source. It is then transported to water treatment facilities and distributed to end users. What happens during end use depends primarily on whether the water is for agricultural or urban use. Wastewater from urban uses is collected, treated, and discharged back to the environment, where it becomes a source for someone else. In general, wastewater from agricultural uses does not get treated (except for holding periods to degrade chemical contaminants) before being discharged directly back to the environment, either as runoff to natural waterways or into groundwater basins. There is a growing trend to recycle some portion of the wastewater stream – recycled water – and redistributing it for non-potable end uses like landscape irrigation or industrial process cooling.

Water-Related Energy Use

Energy is required at all stages of the water use cycle. It is difficult to measure the amount of water-related energy that is actually consumed. Better information is available about energy consumption by water and wastewater utilities. However,

energy consumption by water users is harder to determine since electric and gas meters do not separately measure water-related uses.[7]

The data presented in Table 1-1, with supporting details in Appendix B: 2001 California Energy Consumption by End Use, are based on information provided by the state's energy utilities to the Energy Commission for use in demand forecasting.[8] The Water-Energy Relationship Working Group and other stakeholders participated in extensive discussions to help staff estimate the magnitude of water-related energy consumption by water and wastewater utilities, and agricultural and urban water end users. As shown in Table 1-1, these estimates indicate that total water-related consumption is large – 19 percent of all electricity used in California, approximately 30 percent of all natural gas, and more than 80 million gallons of diesel fuel. The Energy Commission is funding a research project to refine the numbers, and results are expected in early 2006.

Table 1-1: Water-Related Energy Use in California in 2001

	Electricity (GWh)	Natural Gas (Million Therms)	Diesel (Million Gallons)
Water Supply and Treatment			
Urban	7,554	19	?
Agricultural	3,188		
End Uses			
Agricultural	7,372	18	88
Residential	27,887	4,220	?
Commercial			
Industrial			
Wastewater Treatment	2,012	27	?
Total Water Related Energy Use	**48,012**	**4,284**	**88**
Total California Energy Use	**250,494**	**13,571**	?
Percent	**19%**	**32%**	?

Source: California Energy Commission

The data in this table have been organized to align with the water use cycle in Figure 1-1. Water supply and treatment corresponds to the part of the water use

[7] Meters are typically installed to record all the electricity or natural gas use by an entire household, building or other type of facility.
[8] Agricultural data in this table is taken from Tables 1-4 and 1-5 in this chapter.

cycle between the source and end-user. Water supply and treatment account for 22 percent of water-related electricity consumption; 70 percent is required by urban water users and 30 percent by agriculture. On-farm agricultural water use consumes additional energy, estimated at 15 percent of water-related electricity demand. Residential, commercial, and industrial end uses combined represent 58 percent of the electricity consumed. Wastewater treatment accounts for 4 percent. The vast majority of water-related natural gas consumption is by residential, commercial, and industrial customers, primarily for heating water. Natural gas consumption in the agricultural sector is primarily for irrigation pumping. Agriculture is the only sector where diesel fuel consumption, which is also used for water pumping, is quantified. Question marks in the table indicate areas where additional information is needed.

The Energy Intensity of the Water Use Cycle

Each element of the water use cycle has unique energy intensities (kilowatt hours/million gallons (kWh/MG)). Table 1-2 illustrates the considerable variability in both the range of intensities for each segment and the components of the water use cycle. End use energy demand was excluded since the focus is on the energy requirements in the remaining conveyance, treatment, distribution, and wastewater treatment processes. Details supporting this table are in Appendix C: Energy Impact Analysis of Existing Water Management Practices.

Table 1-2: Range of Energy Intensities for Water Use Cycle Segments

	Range of Energy Intensity kWh/MG	
Water-Use Cycle Segments	**Low**	**High**
Water Supply and Conveyance	0	14,000
Water Treatment	100	16,000
Water Distribution	700	1,200
Wastewater Collection and Treatment	1,100	4,600
Wastewater Discharge	0	400
Recycled Water Treatment and Distribution	400	1,200

Water Supply and Conveyance

Energy intensity for this portion of the water use cycle is determined primarily by the volume of water that is transported, the distance, and the changes in topography along its route. California's water supply varies significantly with annual and seasonal hydrologic conditions, and with climate, geography, and topography. Nearly 70 percent of the state's total stream runoff is north of Sacramento, but 80

percent of the water demand is south of Sacramento. This creates challenges that policymakers have struggled to resolve for nearly a century.

The energy intensity of collection, extraction, and conveyance of raw water supplies can be near zero for gravity-fed systems from the Sierra to both urban areas in Northern California and agricultural districts in the Central Valley. However, other systems use very large pumps to transport large volumes of water hundreds of miles from points of collection to points of need. As a consequence, the energy intensity of water supplies in Central and Southern California is typically much higher than in Northern California, with Southern California the highest due to the need to transport water more than 3,000 feet up over the Tehachapi Mountains.

Water Treatment

Some sources of water need very little treatment, so their energy intensity is low. Other sources, such as brackish groundwater or seawater desalination, require much more treatment so their energy intensity is significantly higher. The energy intensity also varies depending on the intended end user. For example, most agricultural and some industrial end users can use water that requires little or no treatment, while most residential and commercial users need water treated to potable standards.

Energy use for water treatment will increase as more stringent water quality rules are implemented under the Safe Drinking Water Act and the Clean Water Act. These new rules require multi-stage disinfection - including treating potable water more than once to ensure the removal of harmful organisms that may grow during storage and transport - and improved disinfection technologies that reduce risk of carcinogens and other potentially harmful disinfection by-products. These improved disinfection technologies – principally, ultraviolet treatment and ozonation – are much more energy intensive than prior chemical methods.[9]

Water Distribution

Some fresh water distribution systems are gravity fed, but most require some pumping. The primary driver of increased energy for water distribution is urban growth.

Wastewater Collection

Some wastewater collection systems use gravity to bring the wastewater to a treatment plant. Others need energy to lift or transfer the wastewater.

Wastewater Treatment

All wastewater treatment systems require energy, though some require more than others depending on the quality of the waste stream, the level of treatment required, and the treatment technologies used. Energy use for wastewater treatment is expected to increase with adoption of more stringent water quality rules under the

[9] There may be some energy savings that are not considered here due to the reduction in needed chemicals for treatment.

Clean Water Act. However, by increasing the quality of wastewater effluent, more recycled water can be added to the state's water supply portfolio.

Wastewater Discharge
Some wastewater discharge systems use gravity to return wastewater to the environment. Others need energy to lift or transfer the wastewater.

Recycled Water and Distribution
Depending upon the level of wastewater treatment in existing facilities, the effluent may be recyclable without requiring additional treatment to displace potable water sources used for non-potable applications. More energy is needed if additional treatment is required. Most recycled water distribution systems require additional energy to pump water uphill to intended users.

As noted previously, since there are so few options to make new water, the increased use of recycled water is a major strategy in the state's water plan.

Energy Intensity in Northern and Southern California

Due to significant variations in energy used to convey bulk water supplies from one place to another, the average energy intensity of the water use cycle in Southern California is much higher than in Northern California. This is due to the fact that Southern California imports about 50 percent of its water supplies from the Colorado River and from the State Water Project (SWP) – each of which is more energy intensive than any single source of water supply used in Northern California.

Table 1-3 shows the combined energy intensity of the water use cycle for typical urban communities in Northern and Southern California. Details supporting this table can be found in Appendix C.

Table 1-3: Electricity Use in Typical Urban Water Systems

	Northern California kWh/MG	Southern California kWh/MG
Water Supply and Conveyance	150	8,900
Water Treatment	100	100
Water Distribution	1,200	1,200
Wastewater Treatment	2,500	2,500
Total	3,950	12,700
Values used in this report	4,000	12,700

Staff recognizes that no two water treatment, distribution, or wastewater treatment systems are identical, so the relative energy intensities reflected above are prototypical. However, within these processes, variability is lower in magnitude than with conveyance and is not linked to a north/south differentiation. The primary north/south regional variation that causes the state's unique and important water energy dynamic is linked to the magnitude of energy required to convey Northern California water supplies to Southern California.

On average, water conveyance requires more than 50 times the energy for Southern California than it does for Northern California. This is also five times the national average. Southern California depends heavily on water imports from the Colorado River and from Northern California. This water travels hundreds of miles through pipelines and aqueducts and, in some places, must be pumped over mountain ranges before reaching its destination. Conversely, 40 percent of Northern California's population is served by gravity-fed systems, with the balance supplied by surface supplies or relatively shallow wells. Recognizing that the actual energy intensity in each component of the water use cycle will vary by utility, the energy values reflected above appear to be reasonable and conservative. This paper assumes that 4,000 and 12,700 kWh per million gallons are consumed for water that is supplied, treated, consumed, treated again, and disposed of in Northern and Southern California, respectively.

Water End Use Energy

California uses about 14 trillion gallons of water in a normal year, with about 79 percent used for agriculture and the remainder in the urban sector. Once water is delivered, customers use it in a variety of applications. Combined agricultural, residential, commercial, and industrial water-related end uses account for 58 percent of all water-related electricity and 99 percent of water-related natural gas use.

Agriculture

Agricultural water use can be both energy intensive, requiring extensive pumping and, in some cases, treatment; but it can also be essentially energy-free, using gravity alone to flow raw surface water onto fields. Each year, California's agricultural sector uses roughly 34 million acre-feet of water to grow food and fiber commodities. It takes more than 10,000 GWh of electrical power to pump and move this water. The energy is used by large state and federal water projects, by irrigation districts, and by on-farm requirements, as outlined in Table1- 4 below.

Table 1-4: Energy Consumed in Agriculture for Water

Category	Energy Consumption (GWh)[1]
Conveyance to Irrigation Districts by the State and Federal water projects[2]	1,720
Conveyance to Irrigation Districts by the Western Area Power Administration	400
Irrigation District surface water pumping	822
Irrigation District ground water pumping	246
On-farm ground water pumping	4,499
On-farm booster pumping[3]	2,873
Subtotal	10,560
Electric equivalent for diesel and natural gas engine driven water pumping[4]	1,231
Total	11,791

[1]Values shown in this table only include agricultural water pumping to meet crop applied water demands. Other agricultural water uses not included in this table include water used for livestock and food processing that is not considered to be commercial. Source: California Agricultural Water Electrical Energy Requirements, ITRC Report No. R 03-006, Irrigation Training and Research Center, 2003
http://www.itrc.org/reports/cec/energyreq.html
[2] Energy used to pump surface water through state and federal water projects to supply irrigation and water districts.
[3]This includes groundwater and surface water pumping to supply pressurized irrigation systems such as sprinkler, drip, and micro spray.
[4]Diesel and natural gas are the second and third most prevalent energy sources used to pump agricultural water. These sources are used to run engines that directly run the water pumps, typically for on-farm groundwater and booster pumping. Emissions requirements typically prevent the use of diesel for pumping in irrigation districts.

The numbers in Table 1-4 represent energy consumption for a typical weather or water year. These numbers will change with different water year scenarios. For example, during a wetter-than-average year with larger surface water deliveries, the energy used for groundwater pumping will decrease. During a period of several back-to-back dry years, a significant amount of additional energy will be used because of increased on-farm groundwater pumping.

In general terms, the electricity used for water represents more than 90 percent of the total electricity used for crop production in the agricultural sector. This applies mostly to field crops, but also to the state's fruit and nut trees and vineyards.

Dairy farms use electricity and other fuels for pumping water for crops, heating water for cleaning and disinfecting barns, and transporting wastewater for lagoon disposal and aerators. Most of the remaining electricity is used for milking equipment and refrigeration. Fans are also used for animal cooling. Greenhouses and nurseries use electricity and other fuels for watering crops, ventilation, and heating. Other agricultural on-farm electricity use goes to food processing including washing, packaging, and refrigeration. However the majority of food processing is in large-scale processing facilities typically classified as industrial. Their energy requirements are discussed in the section describing industrial water users.

Although most agricultural electricity use is during the summer months, there are many year-round operations including dairies, nurseries and greenhouses, feedlots, and other animal production farms.

As shown in the previous table, diesel and natural gas are also used to pump water. Table 1-5 provides an estimate of the breakdown between diesel and natural gas used for agricultural water use in California (Cal Poly 2003).

Table 1-5: Estimates for Diesel and Natural Gas Engine Driven Water Pumping in California Agriculture

Type	Number of Engines[1]	Fuel Required	Conversion to kWh[2]	Equivalent Electricity (GWh)
Natural Gas	1,932	17.5 Million Therms	6.76 kWh/Therm	118
Diesel	12,535	88 Million Gallons	12.8 kWh/gallon	1,113
Totals	14,467			1,231

[1] These data were generated by Cal Poly ITRC during the analysis for the *California Agricultural Water Electrical Energy Requirements Report* (2003). However, it was not published in that report (Cal Poly ITRC unpublished data, 2005). It was subsequently submitted as testimony in the June 21, 2005, IEPR workshop.

[2] The total number of diesel-and natural gas-engine-driven water pumps was obtained from the 2003 USDA Farm and Ranch Irrigation Survey. In comparison, the estimate used for the 2005, AG-ICE proceeding with the CPUC (A.04-11-007/008) provided by the California Air Resources Board (CARB) reported about 8200 diesel driven irrigation pumps. The estimate from CARB is low compared to the USDA survey. We chose the USDA data because they survey more farms throughout California [http://www.nass.usda.gov/census/census02/fris/tables/fris03_20.pdf].

[3] The conversion from kWh to therms and gallons of diesel is based on the Nebraska Performance Standards for Irrigation Energy Sources (Source: Dorn, T.W., P.E. Fishbach, D.F. Eisenhauer, J.R. Gilley, and L.E. Stateson, *It Pays to Test Your Irrigation Pumping Plant*. Publication EC-713. Lincoln: University of Nebraska, Cooperative Extension Service).

Changes to air quality regulations in agricultural regions will likely lead to conversion of many of these pumps, primarily the diesel-powered ones, to electric pumps. If they were all converted to electric, this would increase the electric requirements of

the agricultural sector by more than 10 percent. Although the total number of potential conversions is limited by regulation and available program incentives, the state's planners and electric utilities will need to account for and supply the additional peaking capacity and electricity needed for these pumps. This is discussed in more detail in Chapter 4.

Residential, Commercial and Industrial

Staff has only recently focused on water-related energy consumption in the residential, commercial, and industrial sectors, collectively referred to as urban water users. Table 1-6 presents the aggregated data for each sector. Detailed information can be found in Appendix B.

Table 1-6: End-Use Energy Associated with Urban Water Users

Sector	Electricity (GWh)	Natural Gas (Million Therms)
Residential	13,528	2,055
Commercial	8,341	250
Industrial	6,017	1,914
Total	**27,887**	**4,220**

Source: California Energy Commission

The residential sector accounts for 48 percent of both the electricity and natural gas consumption associated with urban water use. Residential water uses include personal hygiene (shower, bath, sink), dish and clothes washing, toilets, landscape irrigation, chilled water and ice in refrigerators, and swimming pools and spas. Residential energy uses related to these activities include water treatment (filtering and softening), heating (natural gas or electric water heaters), hot water circulation loops, cooling (icemakers and chilled water systems for HVAC and chilled drinking water), circulation (spa pumps, as one example), and, in some cases, the groundwater pumping of private wells.

Commercial water-related energy use represents 30 percent of the electricity and 6 percent of the natural gas use. Industrial water-related energy use represents 22 percent of the electricity and 45 percent of the natural gas. Commercial and industrial water uses include all those found in residences, plus hundreds more. Some of the more energy-intensive applications related to commercial or industrial water use include high-rise supplemental pressurization to serve upper floors, steam ovens and tables, car and truck washes, process hot water and steam, process chilling, equipment cooling (x-ray machines, for example), and cooling towers. In the commercial sector, the major water-related end uses that use electricity are cooling and water heating. Cooling towers for air conditioning are large water users. In the industrial sector, water-related energy use is very dependent upon specific processes. Except for oil and gas extraction, no single industrial category stands out

as a major user of electricity or natural gas. Water heating and process heating are the largest users of natural gas.

In general, urban water use in California is more energy intensive than agricultural water use. This is because every urban water system requires energy for water and wastewater treatment, both of which are not generally required for agriculture. The vast majority of urban water systems also require energy for distribution.

Hydropower Production, Energy Recovery, and Renewable Resources

Hydropower

The most widely recognized aspect of the water-energy relationship is hydropower production. As discussed in Chapter 2, California is served by a vast system of reservoirs and dams, pumped storage, and run-of-river facilities. These facilities are operated by investor-owned utilities (IOU), publicly owned utilities (POU), state and federal agencies, irrigation districts, and other entities, mostly to serve multiple purposes including power generation, water supply, recreation, and flood control. California's hydropower system provides valuable peaking reserve capacity, spinning reserve capacity, load following capacity, and transmission support, all at low production costs.[10] California's combined total hydroelectric capacity is more than 14,000 megawatts (MW)[11] or about one-quarter of the in-state generation capacity. Hydro-generated energy was about 29,000 GWh, or 13 percent of the in-state generation in 2004.[12] The state has conducted extensive studies on traditional hydropower, both in the contexts of its value to the California electric system and issues relating to environmental impacts. Staff refers the reader to these existing reports reference herein, all of which are available on the Energy Commission's Web site.

[10] California Energy Commission Staff Report, *California Hydropower System: Energy and Environment*, Appendix D, *2003 Environmental Performance Report*; prepared in support of the Electricity and Natural Gas Report under the Integrated Energy Policy Report Proceeding (02-IEP-01), October 2003 [Publication 100-03-018].
[11] California Energy Commission, *2003 Environmental Performance Report*. Appendix D, *California Hydropower System: Energy and Environment*, Sacramento, CA. 100-03-018, March 2003, p. D-6.
[12] California Energy Commission, *Potential Changes in Hydropower Production from Global Climate Change in California and the Western United States*, June 2005, consultant report, Prepared in support of the *2005 Integrated Energy Policy Report*, Publication No. CEC 700-2005-010.

Energy Recovery from the Water Use Cycle

In-Conduit Hydropower

The state's large water conveyance projects already take advantage of the energy in the water flowing through their pipelines. Wherever there is flowing water, there exist both energy and the potential to capture and utilize that energy. Pipelines that convey water supplies by gravity have energy that could be captured, but care must be taken to make sure that sufficient 'head', or force, remains to carry the water to its final destination. Wherever pressure-reducing valves or stations are used to reduce the energy in moving water, there is an opportunity for energy production. At any point in a water or wastewater system where influent is delivered for treatment or wastewater effluent is discharged, there may be further opportunities for power production. Barriers and challenges to additional development of in-conduit hydropower that recovers energy from the water delivery and conveyance process are discussed in more detail in Chapter 5.

Biogas

Another option for developing generation in the water sector is to increase beneficial use of digester gas produced by the sewage wastewater, dairy manure, and food processing wastes/wastewater. Biogas, composed primarily of methane, can be used for combined heat and power (CHP) production.

California has 311 sewage wastewater treatment facilities, 2,300 dairy operations, and 3,000 food processing establishments. Currently, about 50 percent of sewage sludge, 2 percent of dairy manure, and less then 1 percent of food processing wastes/wastewater generated in the state are used to produce biogas. Converting these wastes into energy can help operating facilities offset the purchase of electricity and provide environmental benefits by reducing discharged air and ground water pollutants.

The Energy Commission is working with Commerce Energy Inc. and Inland Empire Utility Agency (IEUA) to develop technologies that will address the lack of knowledge of the relationship between various co-digestion feedstocks (sewage sludge, food processing wastes, and dairy manure) and gas production.

Other Renewable Energy Resources

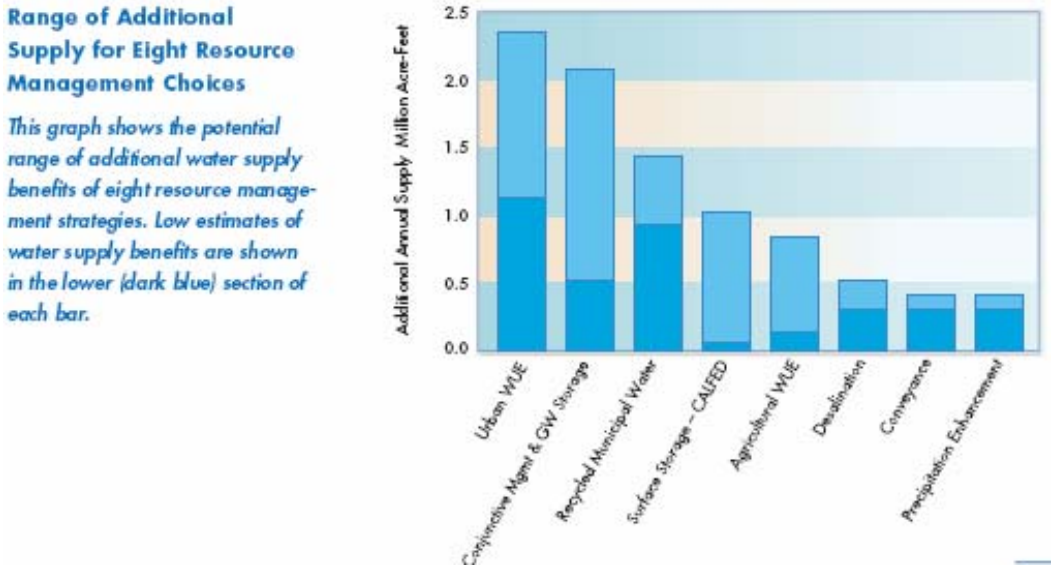
Water and wastewater agencies typically have very large landholdings with characteristics that readily lend themselves to the development of renewable resources, especially wind and solar. These resources could be used to help California meet its aggressive Renewable Portfolio Standard (RPS) goals. For example, regional water and wastewater agencies have hundreds of miles of rights-

of-way, often in areas suitable for solar production. These agencies also have watershed lands that collect water for end-use applications, either potable or for agricultural or industrial use. In order to protect the water quality, large portions of these watershed lands are inaccessible to public recreational use. Many are remotely located, which make their visual impact of little public concern. Watershed lands are also at higher elevations, where wind resources are typically of fairly good quality. Some wastewater utilities also have extensive lands, which are used to dispose of treated effluent and are inaccessible to the public. Municipal or governmental control over these lands could accelerate their use as sites for renewable energy generation

A Loading Order for Water Resources

The *California Water Plan Update 2005,* prepared by the Department of Water Resources (DWR), established a strategic plan that prioritized resource measures to meet new load growth and other water supply challenges. As shown in Figure 1-2, first among the strategies is increased urban water efficiency. Appendix D provides an excerpt of the plan from the Water Plan Update. Thereafter, the plan depends upon increased reliance on conjunctive management and groundwater, followed by recycled water. Agricultural water use efficiency is also an important strategy.

Figure 1-2: New Water Supplies for California



Source: *2005 State Water Plan Update*, DWR.

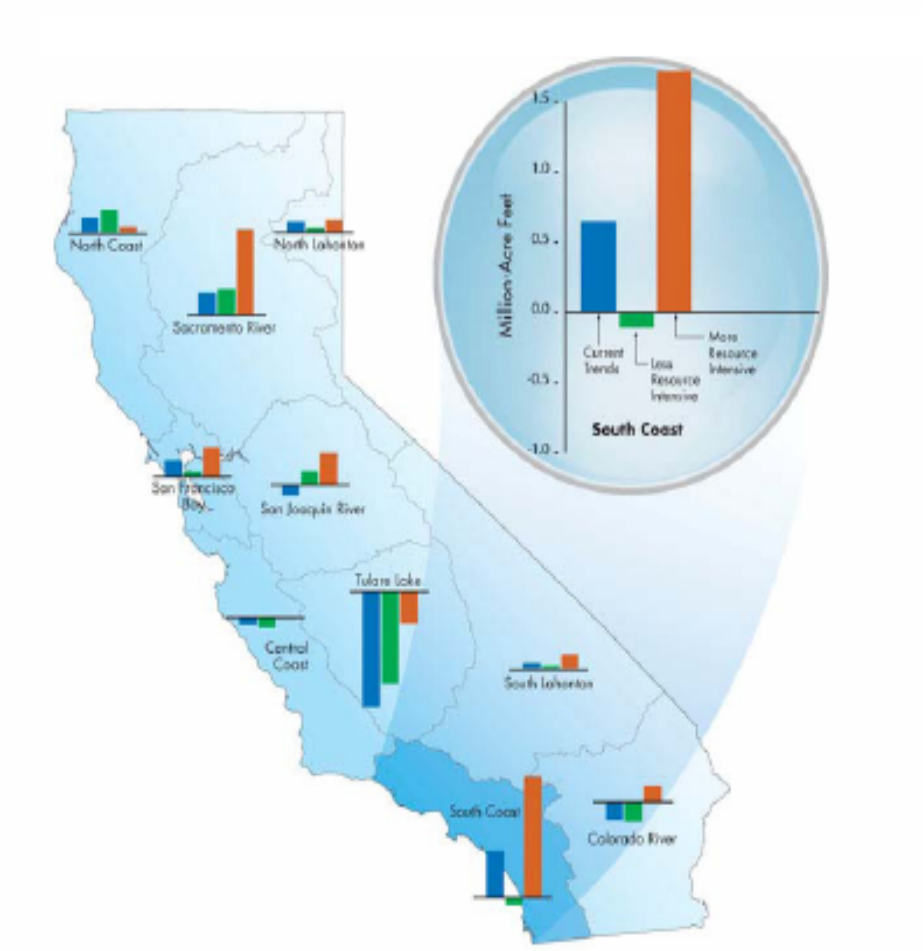
In many respects, the *2005 Water Plan Update* mirrors the state's adopted loading order for electricity resources described in the Energy Commission's *Integrated Energy Policy Report 2005* and the multi-agency *Energy Action Plan*. The first three

strategies all concern the efficient use of existing resources. These strategies encompass efficient use, efficient operations and management, and efficient reuse. Including agricultural water use efficiency, the state's water resources strategy targets will meet 70 percent of future growth in water demand through efficiency measures.

This is a very important concept. Specifically, like energy utilities, water utilities already apply integrated resource planning tools and techniques in their future plans. Similar to energy utilities, they also already apply strategies of "least-cost, best-fit." Thus, in order to optimize the state's water and energy resources on an integrated basis, the primary concept that needs to be integrated into California's water planning on the supply side is the energy intensity of various water supply options. On the demand side, the primary concept is recognition of the energy embedded in various types of water end use throughout the entire water use cycle. Just as energy efficiency increases available supplies and avoids incremental infrastructure costs and environmental impacts, every unit of water not consumed can displace a more energy-intensive water source.

In many cases, the areas of the state that are most stressed with respect to water supplies are also areas with transmission congestion and shortages of local energy supplies. Not surprisingly, since load growth is largely driven by population growth, the geographic areas most resource constrained are the same for both water and for energy. Figure 1-3 shows the projected water demand as estimated by DWR for three different future scenarios and demonstrates the sizable gap between the less and more water-resource-intensive projections. This makes a compelling case for close coordination between water and energy planning and synchronization of both resources and infrastructure goals.

Figure 1-3: Net Change in Average-Year Water Demand for 3 Scenarios by Region, 2000-2030

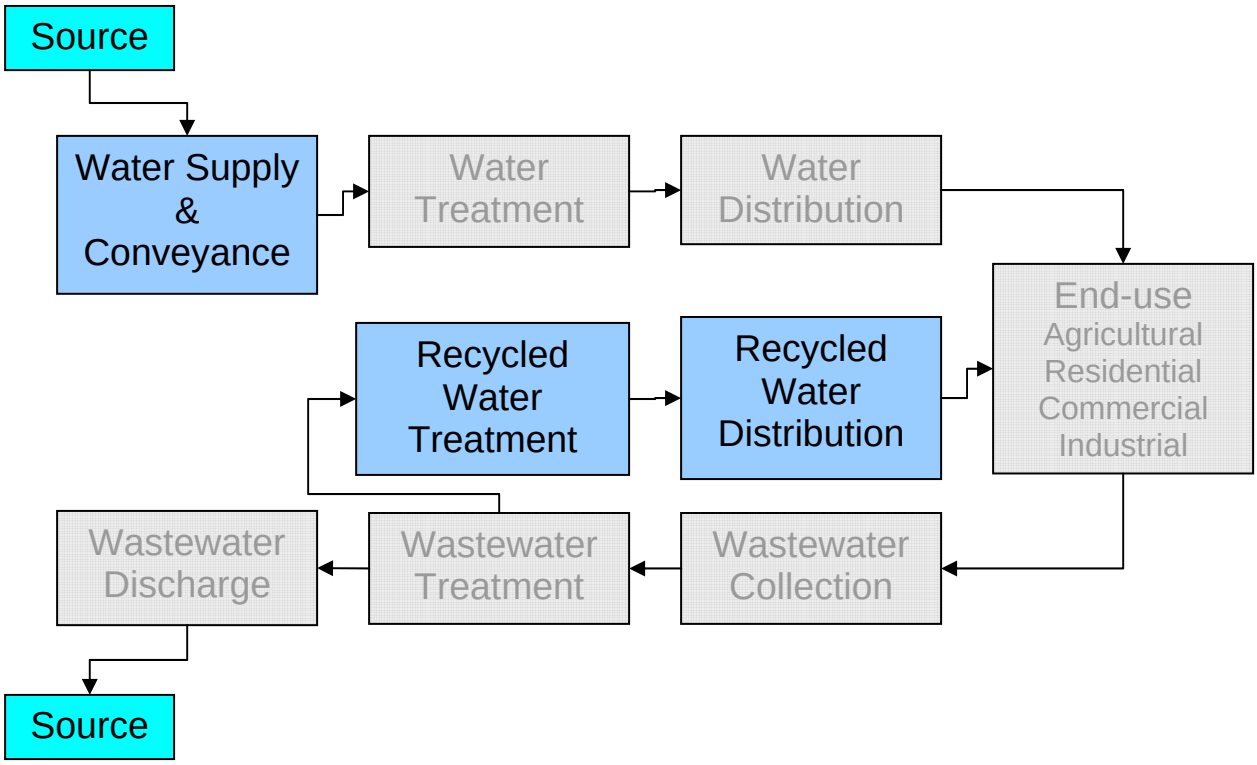


Source: *2005 State Water Plan Update*, DWR.

CHAPTER 2 – WATER SUPPLY AND CONVEYANCE

This section discusses the energy intensity of different water supply sources, all the way through the cycle to conveyance for water treatment. Recycled water, a by-product of wastewater treatment, is also discussed here as an additional source of supply.

Figure 2-1: Water Use Cycle - Supply Source



Primary Sources of California Water

Californians collectively use about 43 million acre-feet (about 14 trillion gallons) of developed water for urban and agricultural use in a normal year. Of this total, 34 million acre-feet go to agriculture (about 11 trillion gallons and 79 percent) and 9 million acre-feet (about 3 trillion gallons and 21 percent) go to the urban sector.[13]

Understanding the energy implications of water use in California requires a basic knowledge of the various water systems that collect, store, and transport water

[13] DWR *2005 Water Plan Update* Volume 1, Table 3-1.

supplies. These supplies can be roughly categorized as surface water, groundwater, desalted water, and recycled water.

- Surface water comes from precipitation, rain and snow, captured and stored in natural lakes and streams, and manmade reservoirs, canals or aqueducts. Most surface water storage is fed from runoff coming from the state's large mountain ranges. The greatest source of surface water supplies is the Sierra snowpack, which holds more water than all of the state's lakes and reservoirs put together, and conveniently melts during the warmer and drier months when California most needs water.

- Groundwater is precisely that – water stored in the ground. Rain directly irrigates farms and gardens but also feeds groundwater basins and aquifers.[14]

- Recycled water, also known as "reclaimed" water or "reuse", is water produced from wastewater effluent. Water quality regulations specify approved uses for recycled water. The level of use depends upon the level of wastewater treatment applied.

- Ocean or brackish water is used for some industrial purposes but must be treated to remove salts and dissolved solids (desalted) for agricultural and urban purposes.

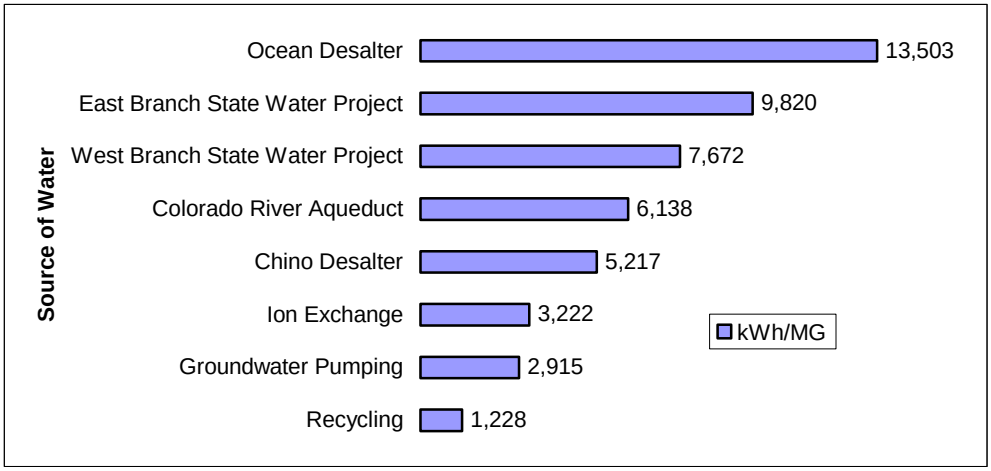
According to DWR's *2005 Water Plan Update*, surface water accounts for more than 60 percent of the state's water use in a typical hydrology year. Groundwater accounts for about 30 percent, although this is highly variable since groundwater makes up most of the state's water supply shortages in dry years. Use of desalted and recycled water, while still a very small percentage of California's total water supply portfolio, is increasing -- both as a means to supplement limited water supplies and provide a hedge against drought risk.

The Energy Intensity of Water Supplies

Every source of water has a different energy intensity. Figure 2-2 shows the relative energy intensity of water supply options for one Southern California regional water and wastewater utility, the Inland Empire Utilities Agency (IEUA).

[14] An aquifer is a body of permeable rock that can contain or transmit water.

Figure 2-2 Energy Intensity of IEUA Water Supply Options



Source: Dr. Robert Wilkinson, Environmental Studies Program, University of California, Santa Barbara, and Martha Davis, IEUA.

Of the above IEUA options, the East Branch State Water Project source is second only to ocean desalination in energy intensity. Recycled water is the least energy-intensive supply option. The relative energy intensity of supply options varies for each water utility, depending upon the nature and characteristics of its water supplies.

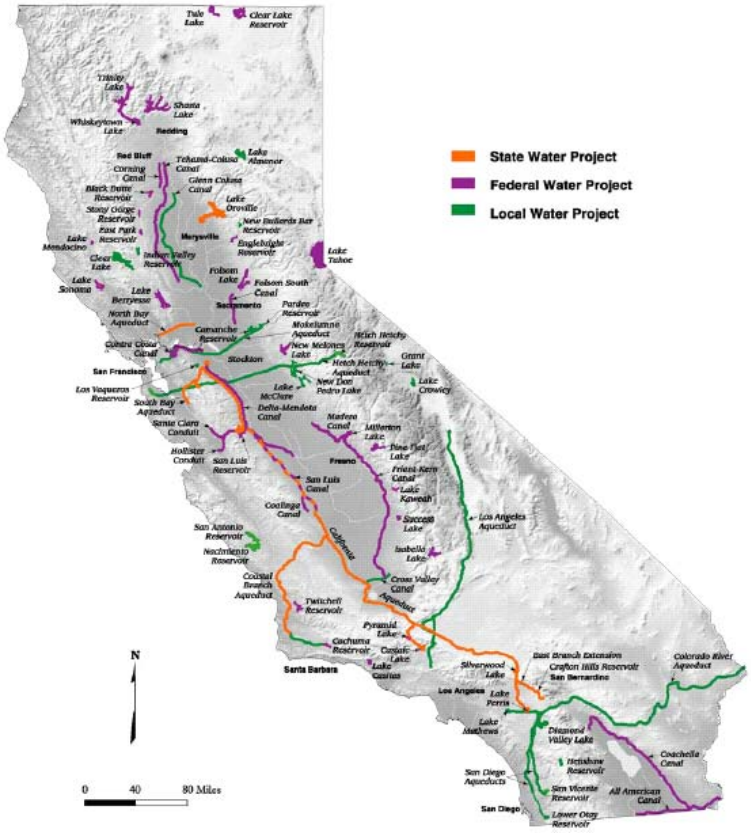
The sections below describe the relative energy intensities of various water supply sources. This concept is important to the discussions in the following chapters since the energy intensity of supply is the most significant sector in which near-term action can positively affect the state's energy circumstances.

Surface Water

The energy intensity of surface water supplies is mainly in the conveyance of raw water for either agricultural and some industrial uses or to treatment facilities for potable urban water use.

California's water supply varies significantly with annual and seasonal hydrological conditions, as well as geography and topography. The major water sources are in Northern California, while the major urban centers and agricultural lands are in the Northern Bay Area, Central Valley, and Southern California. Surface water conveyance systems were built to balance statewide water supplies with demands. These conveyance systems were designed to move water to areas of need outside the basin in which water is collected. This process – known as "interbasin transfers" – accounts for most of the energy embedded in California's surface water supplies. The energy intensity of various interbasin transfers depends on the distance and elevation over which the water must travel. The map in Figure 2-3 shows the state's interbasin transfer systems.

Figure 2-3 Interbasin Transfer Systems in California



Source: *2005 State Water Plan Update*, DWR.

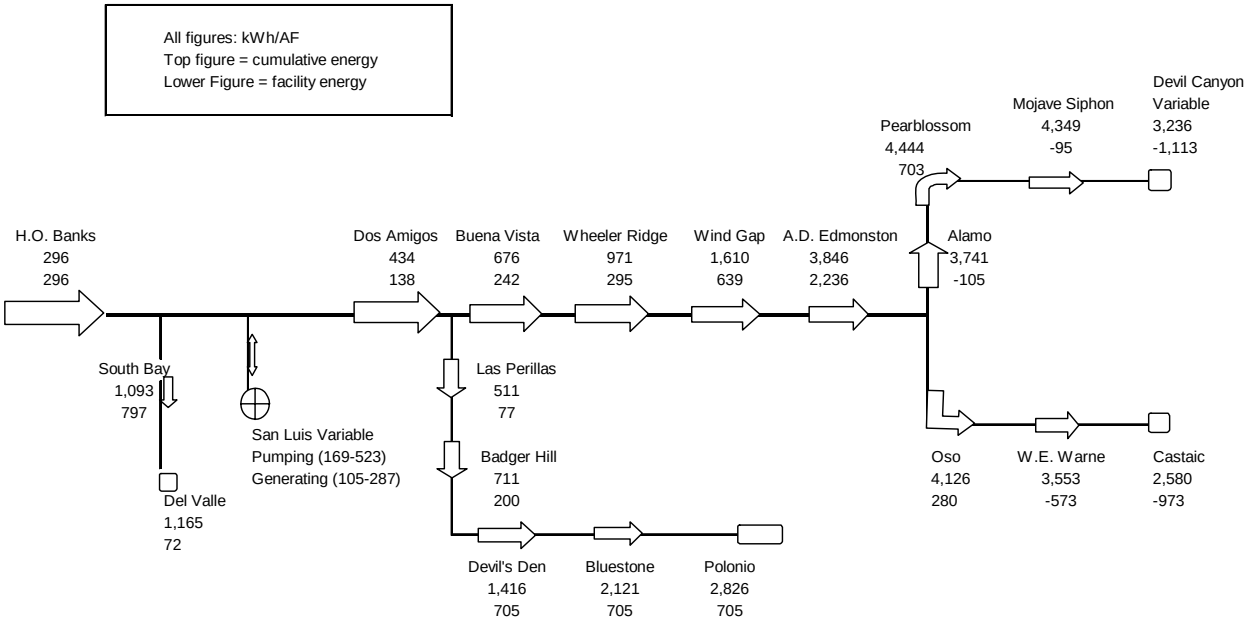
It is the pumping of this water that accounts for the relative energy intensities of different surface water sources. Note that some systems originate in mountain ranges and use gravity to naturally deliver water to points of need. These systems use very little energy. Other systems must transport water long distances on relatively flat valley floors. The State Water Project must also pump water more than 3,000 feet over the Tehachapi range to reach end users in Southern California.

SWP, the largest state-built multipurpose water project in the U.S., was planned, designed, built, and is now operated and maintained by the DWR. The SWP was constructed for the primary purpose of transporting water from Northern California to arid areas, both agricultural and urban, in Central and Southern California. The SWP delivers water to 29 water agencies and irrigation districts, which then distribute the

water to 20 million people and 900,000 acres of crops. SWP water is distributed about 50/50 to agricultural and urban water uses.[15]

The elevation diagram below (Figure 2-4) illustrates the relative energy intensity of delivered SWP water at various points along the California aqueduct. The numbers are shown in kilowatt-hours per acre-foot (kWh/AF). They include transmission losses and, where applicable, energy recovery.

Figure 2-4: State Water Project Pumping Energy



Source: Dr. Robert Wilkinson, PhD, University of California, Santa Barbara, based on DWR data.

Depending on the point at which SWP water is delivered, the embedded energy may range from a low of 676 kWh/AF (676 x 1,000,000 gallons/325,851 gallons/AF = 1,330 kWh/MG) at Dos Amigos, to a high of 3,236kwh/AF (9,930 kWh/MG) at Devil Canyon.

Many of the state's interbasin transfer systems also have significant hydroelectric generation. The Central Valley Project, the East Bay Municipal Utility District's (EBMUD) Mokelumne Aqueduct, and San Francisco's Hetch Hetchy Regional Water System, are all net energy producers. Despite its significant hydroelectric capacity, the State Water Project is a net energy consumer. The Colorado River Aqueduct is also a net energy consumer in California, although the project itself includes significant federal hydroelectric projects on the Colorado River.

[15] Presentation by Bill Forsythe, DWR, to Committee Workshop January 14, 2005.

Groundwater Sources

Groundwater supplies about 30 percent of the state's water needs on average but as much as 60 percent during times of severe drought.

Several hundred million acre-feet of water are stored in 450 groundwater aquifers in the state, compared with approximately 45 million acre-feet in California's 1,200 surface water reservoirs.[16] These aquifers are recharged either naturally or artificially. Natural recharge generally consists of runoff that percolates into the soil, or migration of surface water through a lake or streambed. Almost all of the 450 groundwater aquifers in the state are in decline or overdrafted, forcing users of that water to pump from greater and greater depths, requiring greater amounts of energy in the process.

The process of artificially storing groundwater for future withdrawal is known as aquifer storage and recovery (ASR). Closely related to ASR are "conjunctive use" and "artificial recharge," terms that are often used interchangeably. Water agencies around the state store water in aquifers for both daily and seasonal use and for emergency drought supplies. In general, surplus water is pumped into wells or allowed to percolate into aquifers from ponds and lakes, then pumped from wells when needed.[17]

Less is known about groundwater than about any other water source. This is because each groundwater basin is unique and production characteristics of wells are often interlinked. Since groundwater use is largely unregulated, the actual quantity of energy used for groundwater pumping statewide is also not readily determinable.[18]

In a 2003 study, the Electric Power Research Institute (EPRI) estimated national averages ranging from 700 to 1,800 kWh/MG, depending on use and customer sector.[19] Dr. Robert Wilkinson, director of Water Policy Program at the Bren School of Environmental Science and Management, University of California, Santa Barbara, estimated 2,915 kWh/MG, for groundwater pumping in the Chino Basin.[20] This number reflects the fact that the groundwater aquifers in Southern California, where the Chino Basin is located, are relatively deep compared to those in the northern and central part of the state.

---

[16] ACWA Water Facts website.
[17] USGS 2005, Introduction to Aquifer Storage and Recovery, [http://ca.water.usgs.gov/issues/6.html].
[18] Hundreds of thousands of groundwater wells are privately owned, and serve residences, farms, businesses, and small water systems. The electricity used for pumping from private wells is often not separately metered and is not captured in the Energy Commission's and electric utilities' energy use data.
[19] "Water & Sustainability (Volume 4): U.S. Electricity Consumption for Water Supply & Treatment – The Next Half Century", EPRI Topical Report, March 2002.
[20] Dr. Robert Wilkinson's presentation to the January 14, 2005 *Energy Report* Committee workshop.

It is reasonable to expect wide variability in the energy intensity of different groundwater sources, depending upon both the depth at which the groundwater resides and the efficiency of the pumps and motors used to pump it. In the context of energy intensity and benefits to the state, the primary benefit of groundwater is its ability to offset the high energy intensity of SWP deliveries in the fall. In Southern California, some water agencies already pump groundwater during the summer and recharge aquifers with SWP imports during the non-summer months. Even at the upper end of energy intensity, using local groundwater supplies to defer summer deliveries of SWP water to Southern California results in significant energy and reliability impacts for the state overall.

Ocean and Brackish Water

Treating ocean or brackish water -- desalination -- began in California in 1965. In 1999, there were 30 desalting plants operating in California for municipal purposes, with total capacity of 80,000 acre-feet per year. Table 2-1 illustrates the expected growth in desalination in California.[21] If all of the planned new capacity is built, total production of desalination will increase from about 80,000 acre-feet per year to nearly 600,000 acre-feet.

Table 2-1: Desalting in California for New Water Supply

	Plants in Operation		Plants in Design & Construction		Plants Planned or Projected	
Feedwater Source	No. Of Plants	Annual Capacity	No. Of Plants	Annual Capacity	No. Of Plants	Annual Capacity
Groundwater	16	79,100	6	29,500	6	61,700
Seawater	7	1,500	1	300	13	415,100
Total	23	80,600	7	29,800	19	476,800
Cumulative			30	110,400	49	587,200

1. Capacity in Acre-feet per year. No. of Plants is the number of new plants.
2. Design & Construction – Construction underway or preparation of plans and specifications has begun for new plants or plant expansions.
3. Planned – Planning studies underway for new plants or plant expansions.
4. Projected – Projected new plants or plant expansions.
5. Sources: "Water Desalination Report" and Worldwide Desalting Plants Inventory series by International Desalination Association as cited in the DWR Bulleting 160-05.

Source: 2005 State Water Plan Update, DWR

[21] *California Water Plan Update 2005* Volume 2, Resource Management Strategies, Chapter 6 Desalination.

Recycled Water

The fastest growing new source of water in the state is not a new source at all; it's recycled water from wastewater systems, commonly referred to as reclaimed water or reuse. Californians have used recycled water since the late 1800s. Faced with increasingly stringent requirements governing disposal of wastewater and limited water supplies, many agencies are installing additional treatment facilities that can purify wastewater to the point where it can be substituted for fresh water in many applications, including power plant cooling and landscape irrigation.

The primary benefit of increasing the use of recycled water, from an energy perspective, is the displacement of other, more energy-intensive water supplies.

- By using local recycled water to recharge depleted groundwater aquifers in Southern California, the amounts of energy-intensive seawater desalination and SWP imports could be reduced.

- When recycled water is distributed to local end users for landscape irrigation, significant energy savings accrue:

    - First, from displacing the energy intensity of the highest marginal water source.

    - Second, from avoiding the energy used to treat the water unnecessarily to potable water standards.

Since recycled water is often a by-product of existing secondary and tertiary wastewater treatment processes, it is the least energy-intensive source in the state's water supply. While incremental energy is typically required to pump recycled water uphill to redistribute it to end users, this incremental energy is offset in part or in whole by displacing higher energy intensity water supplies, as well as reducing potable water treatment and distribution.

The actual net energy benefit of any proposed project also needs to consider the incremental energy that might be needed to treat the wastewater to higher standards than normal, such as targeted end use water quality requirements. Table 2-2 describes the level of treatment needed for different types of reuse.

Table 2-2: Demand Sectors and Minimum Treatment Levels

Demand Sectors and Examples of Minimum Treatment Levels for Specific Uses to Protect Public Health

Types of Use	*Treatment Level*		
	Disinfected Tertiary	*Disinfected Secondary*	*Undisinfected Secondary*
Urban Uses and Landscape Irrigation			
Fire protection	☑		
Toilet & urinal flushing	☑		
Irrigation of parks, schoolyards, residential landscaping	☑		
Irrigation of cemeteries, highway landscaping		☑	
Irrigation of nurseries		☑	
Landscape impoundment	☑	☑*	
Agricultural Irrigation			
Pasture for milk animals		☑	
Fodder and fiber crops			☑
Orchards (no contact between fruit and recycled water)			☑
Vineyards (no contact between fruit and recycled water)			☑
Non-food bearing trees			☑
Food crops eaten after processing		☑	
Food crops eaten raw	☑		
Commercial/Industrial			
Cooling & air conditioning - w/cooling towers	☑	☑*	
Structural fire fighting	☑		
Commercial car washes	☑		
Commercial laundries	☑		
Artificial snow making	☑		
Soil compaction, concrete mixing		☑	
Environmental and Other Uses			
Recreational ponds with body contact (swimming)	☑		
Wildlife habitat/wetland		☑	
Aquaculture	☑	☑*	
Groundwater Recharge			
Seawater intrusion barrier	☑*		
Replenishment of potable aquifers	☑*		

**Restrictions may apply*

Source: DWR's Water Facts 23 issued October 2004.

In most circumstances, from an energy perspective, recycled water made as a by-product of the wastewater treatment process is the most preferred option. Primary barriers to increasing the use of recycled water include the incremental cost of dual piping systems to deliver this source of non-potable but usable water and public apprehension about using water recovered from the sewage treatment process.

The Energy Intensity of the Water Resource Portfolio

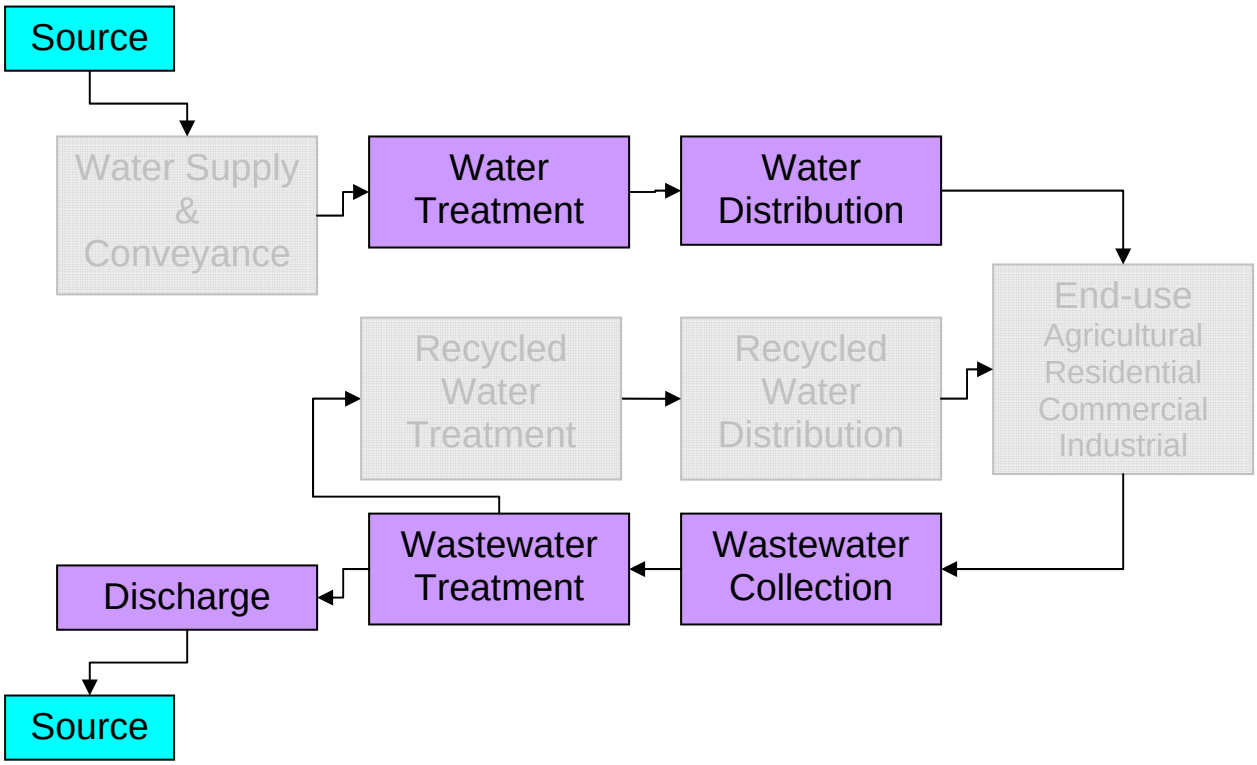
Ultimately, all of these resource choices come together in a water utility's water resource portfolio. Similar to energy utilities, water utilities conduct integrated resource planning (IRP) on a "least cost/best fit" basis. Since energy is typically the highest cost of water supply resources, embedded energy in delivered water supplies is generally reflected in the preferred loading order of water resources in the state's *2005 Water Plan Update.* Using water more efficiently frees up current resources to meet some of the future demand growth.

This is particularly critical in Southern California, where its water mix is roughly half from local sources, and half from imported sources. While water utilities are working hard to develop more local supplies and improve water use efficiency, there are not many options to develop new water sources. Presently, the primary available options are recycled water and seawater desalination.

CHAPTER 3 – WATER AND WASTEWATER TREATMENT AND DISTRIBUTION

This section will discuss, due to their similarities, both the energy intensity of potable and waste water treatment and distribution and the distribution of recycled water.

Figure 3-1: Water Use Cycle – Treatment and Distribution



Energy use for water distribution loads is primarily for pumping water and maintaining sufficient pipe pressure to assure that flows can be made at scheduled rates while maintaining sufficient pressure for fire service.

Water and wastewater treatment processes also use large quantities of energy. In water treatment, energy requirements depend primarily on the characteristics of the raw water, plant size, treatment process, and the distance and elevation of the treatment plant in relation to water sources and water distribution systems. In wastewater treatment, the characteristics of the influent and the level of treatment (primary, secondary or tertiary) are principal drivers of energy consumption.

Electric loads at water and wastewater treatment plants consist primarily of pump motors but also include air blowers, injection equipment, controls, lighting, and, in

some cases, ultraviolet light disinfection and ozonation. Wastewater treatment plants also require activated sludge and sludge handling systems that consume large quantities of energy. The Energy Commission Demand Office estimates that a total of about 9,000 GWh of electricity is used annually by both water and wastewater facilities. This is based on both electric and water meter data and assumptions from engineering handbooks and other sources about the electricity use of certain equipment. Because the meter data is not reported in separate categories it cannot be disaggregated to separate water from wastewater treatment.

The Association of California Water Agencies (ACWA) estimates that the state's water and wastewater treatment facilities collectively draw about 3,000 MW at peak, with 1,800 MW occurring in Southern California Edison's (SCE) service territory, with the rest geographically distributed throughout the state more or less in proportion with population.

Both water and wastewater treatment processes require pumps and motors to transport water before, during, and after treatment. Pumping is not as significant a portion of the load for wastewater as for water because wastewater treatment processes are significantly more energy intensive, and both wastewater collection and disposal typically rely heavily upon gravity. Thereafter, the treatment processes and their relative energy intensities vary considerably.

Water treatment has historically been a comparatively modest user of energy, relying primarily upon settlement and passive filtration to remove particles from water, and chemical treatment (chlorination or chloramination) for disinfection. As new water quality regulations are implemented, energy-intensive technologies such as membranes, UV and ozonation will require large quantities of energy. Wastewater treatment requires much more energy, with each progressive level of treatment requiring still more. In secondary treatment, most of the energy is used for biological treatment; pumping of wastewater, liquid sludge, biosolids and process water; and processing, dewatering, and drying of solids and biosolids. Tertiary treatment requires additional energy for aeration, pumping, and solids processing. All of these processes present opportunities for energy reduction.

To reduce energy costs, many utilities have already replaced pumps and motors with newer, more efficient equipment. The addition of variable frequency drives and customized pumping algorithms provide the capability to further reduce energy requirements by more closely matching pumping capacity with loads. In addition, both water and wastewater utilities have recently demonstrated that significant reductions in energy consumption could be achieved by employing interim storage to shift processing to off-peak periods and balance processing loads among multiple plants to optimize plant efficiencies.

In the mid-1990s, EPRI and HDR Engineering, Inc. conducted an audit of the energy savings potential for water and wastewater facilities in California. At that time, they estimated that more than 880 million kWhs could be saved by implementing several measures: load shifting, variable frequency drives, high-efficiency motors and

pumps, equipment modifications, and process optimization with and without Supervisory Control and Data Acquisition (SCADA) systems. These estimates did not include incorporating interim storage to shift loads and optimize plant efficiencies. Industry experts estimate that untapped energy efficiency opportunities through the optimization of water and wastewater treatment processes could be as high as 30 percent of existing processes.

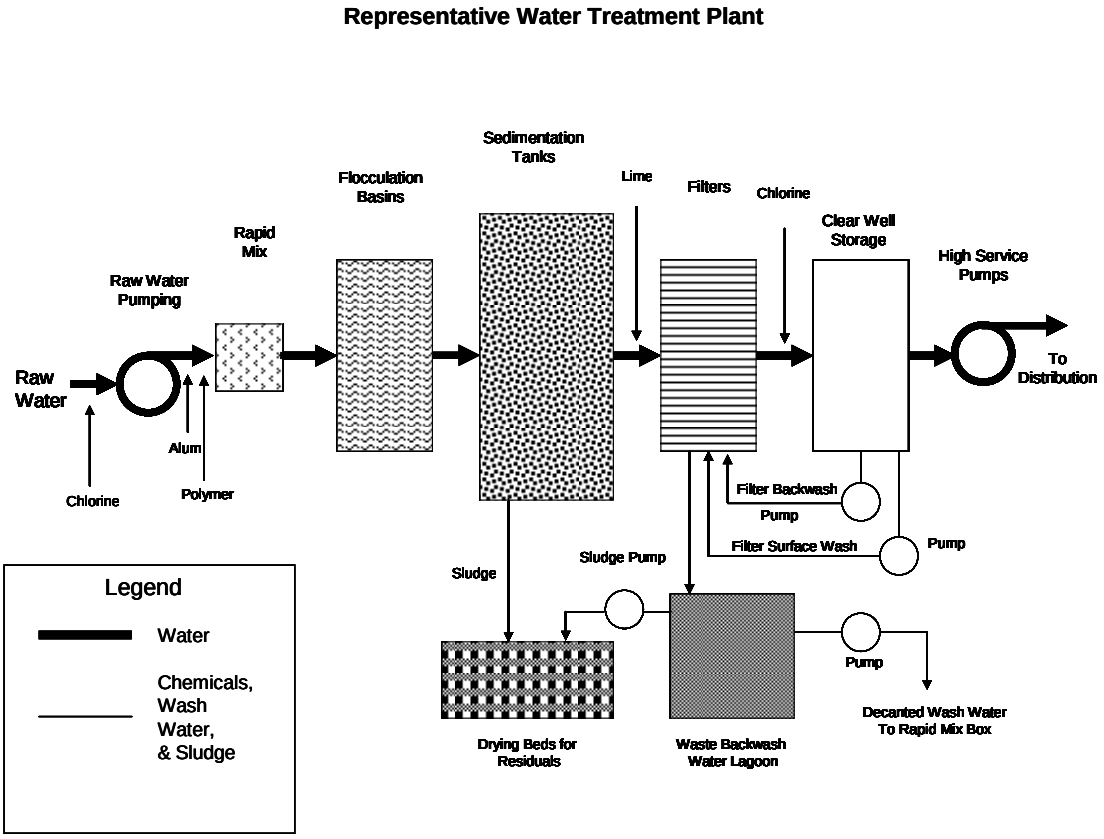
The sections below will describe energy uses for water treatment and distribution, and for wastewater treatment.

Water Treatment

Source water quality and the end use of the water dictate the level of treatment required. For potable uses, a typical sequence of operations for surface water treatment is described in the following steps (refer to Figure 3-2).

- Raw water is first screened, pre-oxidized using chlorine or ozone to kill organisms.
- Alum and/or polymeric materials are added to the water.
- Flocculation and sedimentation remove finer particles.
- A second disinfection step kills remaining organisms.
- The clear tank allows contact time for disinfection.
- Treated water is distributed to consumers by high-pressure pumps (disinfectant residue is carried into the distribution system to prevent organism growth). Sludges and other impurities removed from water are concentrated and disposed of.

Figure 3-2: Sequence of Operations in Surface Water Treatment



Source: Electric Power Research Institute

As shown in Table 3-1, although no two treatment facilities are identical, the following survey of more than 30,000 public supply systems in the United States[22] indicates little variation in water treatment energy intensity for plant capacities of at least 1 million gallons per day[23].

[22] Inventory of public water supply systems maintained by the U.S. Environmental Protection Agency in the Safe Drinking Water Information System.
[23] *Water & Sustainability* (Volume 4): *U.S. Electricity Consumption for Water Supply & Treatment*, EPRI March 2002, Figure 2-1, page 2-2,

Table 3-1 Energy Use by Surface Water Treatment Plants

Plant Size (Million Gallons per Day)	Energy Intensity (kWh/MG)
1	1,483
5	1,418
10	1,406
20	1,409
50	1,408
100	1,407
Average	**1,422**

Source: Electric Power Research Institute

Water treatment energy requirements are driven principally by the characteristics of incoming raw water and by the distance and elevation of the treatment plant in relation to water sources and the distribution system. Actual energy demand is highly variable by water utility. Lowest is pristine Hetch Hetchy water, which is exempted from filtration by the U.S. Environmental Protection Agency (US EPA)[24]. However, most surface and groundwater sources require treatment to meet regulatory standards and the taste and odor preferences of the public. Some treatment plants also have unique requirements, such as the removal of industrial chemicals from well water that require more energy. Net energy demand is expected to change as more energy-intensive disinfection processes are used to address water quality concerns and meet increasingly stringent potable water rules under the federal Safe Drinking Water Act (see discussion in Chapter 6).

Despite extensive data searches, staff found only a few studies that attempted to determine the exact electricity use for water treatment facilities. One of the most comprehensive and innovative studies came from an effort in Sonoma County to address greenhouse gas emissions. This study included energy use by municipal facilities, including the county's wholesale water agency, the Sonoma County Water Agency, and all of its municipal system water customers.

The Sonoma County Water Agency provides domestic water to 540,000 domestic water users in Sonoma, Marin, and Mendocino counties. Its only source of water is the highly variable flow of the Russian River and storage in two reservoirs on tributaries of the Russian, Lake Sonoma, near Healdsburg, and Lake Mendocino, near Ukiah. The EPA has listed the Russian River as impaired because of dissolved solids and nutrients. To both avoid these impairment issues and comply with federal

[24] The high quality Hetch Hetchy's water supply, produced by Sierra snowmelt in a protected watershed, has been granted a filtration exemption from the U.S. Environmental Protection Agency (U.S. EPA) and the California Department of Health Services (DHS).

Endangered Species Act limitations on stream withdrawals, many of the county water agency's municipal customers mix the river water with about equal amounts of groundwater, which is generally less costly.

The Sonoma County Water Agency required nearly 2,600 kWh/million gallons to pump and treat water from the river over the period of April 2000 to September 2002. Pumping costs were essentially linear throughout the year (that is, the electricity use per million gallon rate was essentially constant) except for spikes in January and February, when large amounts of surplus water were transferred to storage in reservoirs, especially in Marin County (Rosenblum 2003). Data are insufficient to determine the amount of energy used for pumping the water (which corresponds to the "Collection, Extraction and Conveyance" portion of the water use cycle described in Chapter 2) as opposed to energy used solely for water treatment.

In addition to Hetch Hetchy, EBMUD is an example of an agency with energy intensity of water treatment on the lower end of the spectrum. EBMUD gets 95 percent of its water from the Mokelumne River, delivered by gravity through the Mokelumne Aqueduct. The Mokelumne water is relatively high quality at its source, requiring little treatment; and the EBMUD's treatment facilities are located high in the East Bay Hills, using elevation to help pressurize its distribution system. Because of these factors, EBMUD's electricity use is a low 150 kWh/million gallons for conveyance, and 275 kWh/million gallons for treatment (EBMUD 2000 and Navigant Consulting 2004).

Desalination

Desalination involves removal of salts and dissolved solids from seawater or brackish water. Most desalination processes are based on either thermal distillation or membrane filtration technologies, both of which are very energy intensive.

The primary benefit of desalination is its ability to increase potable water supply by reclaiming water of poor quality. The most significant challenge of desalination is that it is a very energy-intensive source of water, and its highest use will likely coincide with extended drought periods when hydropower production is lowest.

Unlike every other type of water facility, where staffing edges out energy use as the main expense, desalination's primary operating cost is for energy, with seawater desalination being considerably more energy intensive (9,780-16,500 kWh/million gallons) than brackish groundwater desalination (3,900–9,750 kWh/million gallons).[25] The difference between seawater and brackish desalination ranges is due primarily to the difference in the initial water quality, and within each range the variance is due primarily to the plant design and technology employed. Most desalination plants operate continuously, so this electricity is used during all seasons and at all times of

[25] California Department of Water Resources Desalination Task Force Final Report 2003.

the day. Current plants are operating 90 percent of the time, with downtimes only for maintenance (DWR, 2005).

According to the *2005 Water Plan Update*, a 50 MGD seawater plant (approximately 50,000 acre-feet per year, or 16.25 billion gallons, assuming operations 90 percent of the time) would require about 33 MW of power.[26] This translates to about 5,200 kWh per acre-foot, or 16,000 kWh per million gallons, which is the upper-end of California's energy intensity of water supplies. Multiple efforts are underway to increase the energy efficiency of desalination through improved membranes, dual pass processes, and additional energy recovery systems.

Present estimates indicate that existing desalination facilities use 370-890 GWh per year. As stated in Chapter 2, if all of the planned new capacity is built, total production of desalination will increase from about 70,000 acre-feet per year to nearly 300,000 acre-feet. Assuming an average of 3,900 kWh/acre-foot (about 12,000 kWh per million gallons),[27] an incremental 230,000 acre-feet would require about 897 GWh. In the IEUA example, desalination of local brackish groundwater supplies can produce a net energy benefit when displacing higher energy intensity desalted seawater or SWP imports.

Desalination of seawater has the highest energy intensity of all water treatment options.

Water Distribution

Once treated to potable standards, the water must be distributed to customers, generally through a network of storage tanks, pipes, and pumps. During distribution, water must be kept moving and under pressure to minimize corrosion and biological contamination. Storage tanks and water mainlines must be flushed periodically to prevent oxidation and control biofilms (AWAARF 2000). Even the farthest reaches of the network must be kept under adequate pressure and constantly flushed since low pressure and low flow allow microbes to flourish (ACWA workshop April 14, 2005).

On average, staff estimates that city water agencies use about 1,150 kWh/million gallons of electricity just to deliver water from the treatment plant to their customers. The energy required for distribution pumping is mainly driven by the distribution system configuration, its relative size, elevations, and system age.

The water supply diagram and the results of the EPRI survey in Table 3.1, above, reflect little variation in the amount of energy required to treat and distribute a unit of water for systems requiring at least 1 million gallons per day. For this large survey

[26] *California Water Plan Update 2005* Volume 2, Resource Management Strategies, Chapter 6 – Desalination.
[27] The average of the Chino desalter and seawater desalination in IEUA's water supply options.

size of approximately 30,000 public water supply systems, distribution pumping of treated water remained fairly constant at between 80 to 85 percent of total energy requirements when treatment and distribution energy loads are combined. For purposes of this paper, staff adopted this ratio and assumed prototypical water distribution energy intensity to be about 1,200 kWh/MG.

Cities with hilly terrains can use hilltop tanks both as storage and to provide pressure into the distribution system; San Francisco is perhaps the best example of this, serving virtually all of its customers from hilltop tanks. But the water must first be pumped up to the tank, often several hundred feet in elevation. In addition, though water agencies loathe wasting water and energy, they often must flush water from the tanks to prevent microbial contamination and then fill them up once again through the pumping station. In fact, this flushing accounts for the bulk of electricity used in EBMUD's distribution system.

Wastewater Treatment

Other than water devoted to landscape irrigation, or lost through evaporation (such as in cooling towers and other processes), almost all the water entering homes and businesses in California eventually leaves as wastewater. Wastewater treatment is similar to freshwater treatment. But most wastewater treatment systems have the additional step of using biological reactors that use bacteria to break down waste. Wastewater pumps are inherently more inefficient because they must pump both liquids and solids, and must have greater clearances between the pump impeller and the casing, allowing much of the pumped water to return to the intake plenum. Energy use in a wastewater system is primarily from use of very large electric pumps and blowers and use of natural gas to heat the anaerobic digesters.

Digester biogas (approximately 60 percent methane and 40 percent CO_2) is produced by anaerobic bacteria. The gas can be collected and used to generate electricity, usually powered by an internal combustion engine and used to run the facility itself. Waste heat recovered from the engine can be used to heat the digesters and displace natural gas use.

The number of water and wastewater treatment techniques and the combinations of techniques are expected to increase over time as more complex contaminants are discovered and regulated.

Wastewater consumes electricity in three stages: transport to the facility, treatment, and disposal/recycle. The first stage, transporting from the customer to the wastewater treatment facility, requires about 150 kWh/million gallons of electricity on average to pump the water, depending on topography, system size, and age. When they have a choice, agencies prefer to place water treatment facilities above their customers and the wastewater treatment facilities below, to harness the pull of

gravity where possible, and to place water intakes above wastewater outfalls on rivers.

There are levels of treatment, and each progressively requires higher levels of energy use. These steps may consist of physical processes, biological processes, or chemical processes.

Physical Processes
The initial steps involved in the sewage wastewater treatment are physical processes, which separate larger solids from liquid using screening or grit removal. Steps that remove larger solids are termed preliminary treatment. The solids separated from the preliminary processes are usually disposed of in a landfill. After removal of larger solids, primary treatment follows to separate the smaller solids. Some chemicals may be added to assist with solids removal.

Biological Processes
The physical processes are followed by biological aerobic treatment in which extended aeration (oxygen) and environmental conditions are provided for microbes to break down organic material into carbon dioxide and water. Equipment used for the aerobic treatment includes tricking filter, aeration basin, and others. This biological aerobic treatment is commonly called secondary treatment.

After the aerobic treatment, the wastewater is separated with a sedimentation tank to separate the sludge and the clear effluent. The sludge is then sent to an anaerobic digester where the organic material is broken down into biogas, which is primarily methane and carbon dioxide.

Chemical Processes
The clear effluent, after the secondary treatment is further treated with physical filtration, chemical, or ultraviolet disinfections. This further treatment is commonly called tertiary treatment. The tertiary effluent can be used for beneficial reuse or discharged to surface water.

The progressive levels of treatment are commonly referred to as “primary”, “secondary” and “tertiary”, with primary being the lowest level, and tertiary the highest. Effluent from both secondary and tertiary treated water can be reused. The levels of treatment required for types of reuse (i.e., recycled water) are described in Table 2-2 in Chapter 2.

The major driver of unit energy consumption is the degree of treatment required. As noted above, there has been a trend toward more thorough treatment, with upgrades or replacements of older systems that could not provide this higher level of treatment. This trend is seen in comparing the estimated unit electricity consumption in 1988 with consumption in 2000: the baseline unit energy consumption was

estimated to increase at an average compound rate of about .08 percent per year. This upward trend in unit electricity consumption is expected to continue as more thorough treatment is required.

Unlike water treatment and distribution systems, unit volume energy requirements for wastewater treatment plants vary greatly depending upon plant size. Energy intensity for a 1 MGD wastewater treatment plant can be approximately three times that of a 100 MGD wastewater treatment plant[28]. As expected, unit electricity consumption rises as the degree of treatment and complexity of the process increases. For example, advanced wastewater treatment with nitrification is three times as energy intensive (due to additional pumping requirements) than that of a relatively simple trickling filter plant.[29] Further complicating the assessment of prototypical unit volume energy intensity are unique operational environments, discharge limitations, influent characteristics, permitted effluent limitations, and variations in plant permitting cycles.

Table 3-2 Energy Intensity of Wastewater Treatment Facilities

Source of Data	kWh/MG
Inland Empire Utilities Agency	2,971
City of Santa Rosa	2,920
East Bay Municipal Utilities District	2,001
Metropolitan Water District	2,655
Methodology for Analysis of Energy Intensity in California's Water Systems	1,911
Energy Down The Drain, The Hidden Costs of California's Water Supply	2,302
Energy Benchmarking Secondary Wastewater Treatment	2,625

Source: Multiple, see Appendix C

Table 3-2 shows wastewater treatment plant energy intensities reflecting a range of energy intensity for facilities operating in California and cited in studies. Based on this range, 2,500 kWh/ MG has been adopted as the prototypical wastewater treatment energy intensity (for more detailed discussion and references see Appendix C).

One of the most interesting opportunities for reducing energy use for wastewater treatment is to improve storm water management. During rainy weather, a considerable amount of runoff ends up in wastewater systems, greatly increasing treatment costs. Even communities that do their best to keep stormwater out of their sewer systems see nearly double the flow during a winter storm than during the dry summer months. This “infiltration/inflow” of stormwater into the sewer system has on

[28] *Water & Sustainability* (Volume 4) *U.S. Electricity Consumption for Water Supply & Treatment – The Next Half Century*, EPRI 2002, Pages 3-4 & 5 and Table 3-1.
[29] *Water & Sustainability* (Volume 4) *U.S. Electricity Consumption for Water Supply & Treatment – The Next Half Century*, EPRI 2002, Pages 3-4 & 5 and Table 3-1.

occasion forced many communities to discharge raw or minimally treated wastewater directly into local waters.

For example, Sonoma County's largest wastewater facility, the Laguna Wastewater Treatment Plant, operated by the City of Santa Rosa, experienced a peak inflow of nearly a billion gallons per month in January and February of 2000 and 2002, while average inflow in the summer months was just over half that amount (Rosenblum 2003, Figure 7). Its wastewater treatment electricity use is proportionate to these flows, and therefore nearly twice as high in winter than in summer.

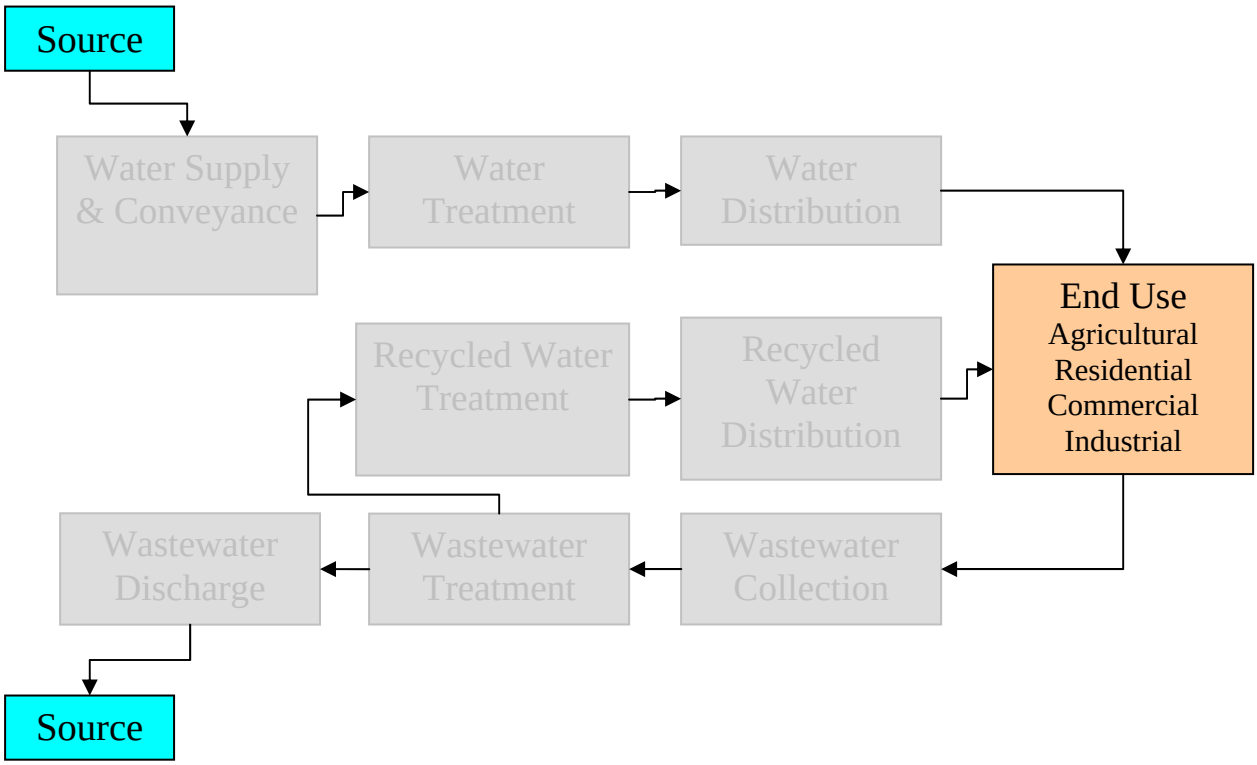
Conclusions

In this chapter, staff has generally described water energy intensity for water treatment, wastewater treatment, and water distribution. Staff has also identified areas that will require additional information and analysis to better understand these systems and how modifications or improvements could benefit the energy sector. Future regulatory changes made in response to health and water quality concerns will affect the overall energy demand of these systems.

CHAPTER 4 – WATER RELATED END-USE EFFICIENCY

This chapter addresses opportunities to increase water and energy end-use efficiency.

Figure 4-1: Water Use Cycle – End Use



The Energy Impact of Water Use Efficiency

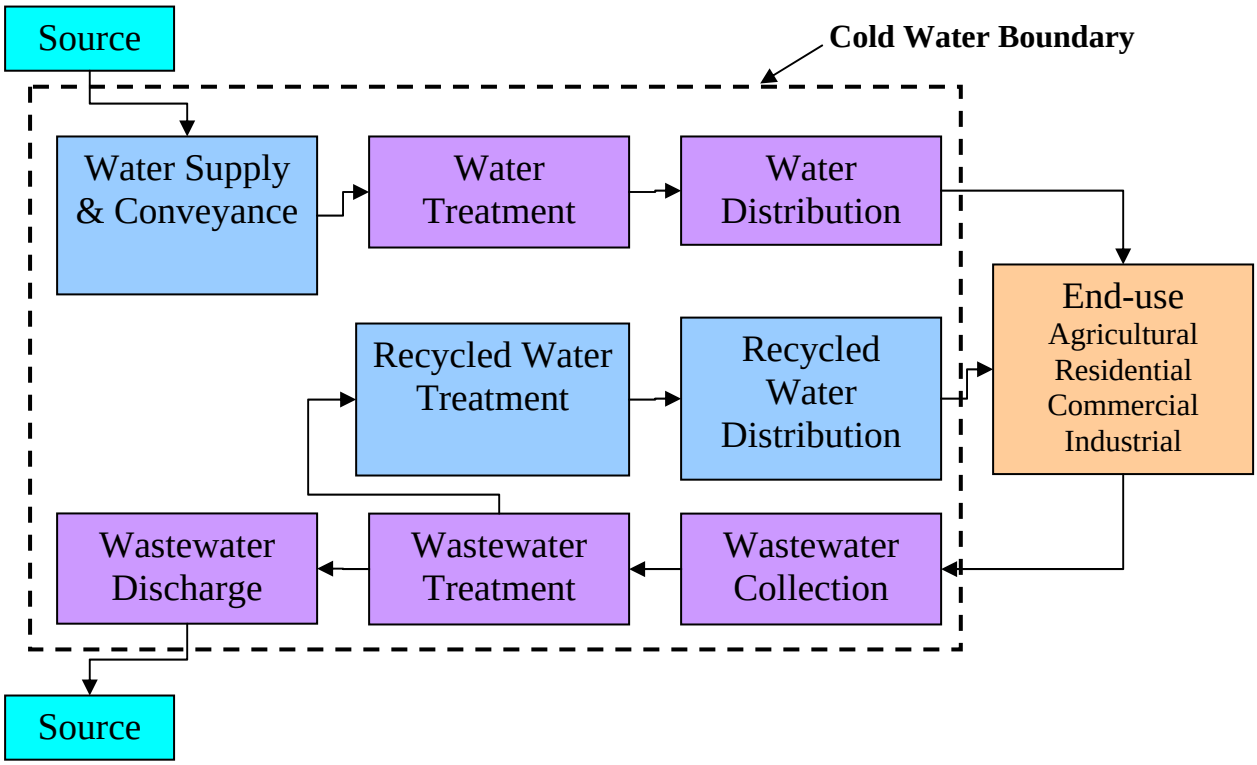
Water end-use applications in California use more energy than any other part of the state's water use cycle. Energy efficiency water programs have traditionally focused on either saving energy in water and wastewater treatment facilities or saving energy in end-use applications including water heating, clothes washing and drying or process heating. Water use efficiency programs have similarly focused on saving water in end-use applications. In both cases, end-use efficiency measures are beneficial, to both utilities and end users, when the value of the saved energy or water exceeds the cost of the measure.

For the most part, these efficiency improvements have been pursued separately by water and energy utilities, although there are some examples of close coordination, including the effort to introduce high-energy-efficiency and low-water-factor clothes washers to the consumer market. What appears to be missing is the recognition that saving water also saves energy throughout the conveyance, treatment, distribution and wastewater treatment processes of the water use cycle.

The energy intensity of water use varies depending on its end use and location in the state. For example “statewide average,” agricultural end uses are less energy-intensive than either “statewide average” urban end uses or agricultural end uses in Southern California that rely upon SWP or Colorado River Aqueduct water deliveries. All are more energy-intensive than those in Northern California. On average, urban water uses in Southern California are more than three times as energy-intensive as those in Northern California.

While these relationships are useful for policy development and planning, it is important to recognize that the actual energy intensity of the water use cycle is very location- and application-dependent; this information is important as specific projects are considered. Figure 4-2 shows the overall cold water boundary. To apply the concept of energy intensity, the cold water boundary must be identified for specific locations and applications. Further details are in Appendix C.

Figure 4-2 Cold Water Boundary in the Water Use Cycle



Conserving a unit of cold water avoids using the energy that would have been needed to supply, treat, deliver, consume, collect, treat, and dispose of it as wastewater. The actual amount of energy saved depends upon the type and source of water supply, the distance the water has to travel, the nature and extent of its treatment, and the type of end use.

In California, saving cold water, both indoors and outdoors, saves energy. The energy saved is primarily electricity. Saving outdoor water saves the energy it takes to extract, convey, treat, and distribute water to customers. Saving indoor water saves the additional energy, again mostly electricity, used to collect, treat and dispose of the waste water. Saving indoor hot water saves the additional energy needed to heat this water. In California, this additional energy is mostly in the form of natural gas.

From an energy perspective, saving cold outdoor water is good. Saving cold indoor water is better. Saving hot indoor water is better still.

Saving end-use energy can also save water and the energy associated with the applicable portion of the water use cycle. For example, when air conditioning is reduced in large buildings that use cooling towers to remove the heat, every unit of energy that does not need to be removed means that less water is needed in the process. Also, saving electricity in any fashion saves water at power plants that use cooling water.

Agricultural Water Use Efficiency

About 79 percent of the state's water is used by the agricultural industry to grow more than 200 crops that generate more than $29 billion dollars a year for the state's economy (CDFA, 2003). Because water conveyance and pumping are very costly, efficient irrigation technologies and farming practices hold promise for reducing both the amount of water needed and the energy intensity of crop production.

While a unit of agricultural water is not as energy intensive as a unit of urban water, the agricultural industry strives to meet water conservation objectives, save money, and preserve water resources. Many times the adoption of natural resource conservation practices creates new energy expenditures. The industry can reduce these costs by participating in energy efficiency and demand response programs through the public goods charge funds administered by their investor-owned utilities (IOU).

Energy Efficiency and Conservation Measures

Since the mid-1990s, the agricultural industry has adopted multiple water conservation practices, among which are installation of drip- and micro-irrigation

technologies. The use of on-farm pressurized irrigation methods has increased from about 1.4 million acres in the early 1980s to more than 4.2 million acres today.[30] These changes can result in better crops, reduced water use, and the reduced use of fertilizers and chemicals, all of which result in greater productivity and energy efficiency.[31]

To be more productive, farms must also improve the efficiency of their water pumping systems. Since the 2000-2001 energy crisis, thousands of farmers and irrigation districts have used state- and ratepayer-funded pump test and repair program incentives. Many of the pumps were repaired to boost their pumping plant efficiencies.[32] When pump tests are performed and cost-effective pump repairs are completed, pump efficiencies can increase by 5 to 15 percentage points. This improved efficiency provides increased pumping capacity. Where previously a farmer might have used seven days to water his fields, it might now instead take five or six days to do the same work. Most farmers will adjust their irrigation set times to reflect the new water output and reduce the total number of hours of operation, saving both water and energy.

These measures can more than offset the new energy requirements that most often accompany drip system installations. Although there will be a higher demand for connected load from the installation of booster pumps, the total hours of operation will depend on the source of water and the irrigation system that is being converted to drip. Most often farms are required to pump from groundwater sources to satisfy the on-demand, clean, and flexible water delivery needs of the drip systems, possibly increasing their energy costs. Studies have shown that the conversion from surface irrigation to drip/micro- and sprinkler-irrigation technologies has lead to increased on-farm groundwater pumping on the east side of the San Joaquin Valley.[33]

Adoption of Time of Use (TOU) Agricultural Electric Rates

Large numbers of both Pacific Gas and Electric (PG&E) and SCE agricultural customers have signed on to TOU electric rate schedules. In the PG&E service area 81 percent of agricultural revenues and 89 percent of agricultural kWh sales are on TOU rates, representing 40,000 accounts of the total 80,000 agricultural accounts[34]. In the SCE service area, 71 percent of agricultural kWh sales are on TOU rates, generated by 18 percent of the utility's customer accounts[35].

[30] CalPoly ITRC, Memorandum, 2005
[31] CalPoly San Luis Obispo University, ITRC Report No. R 96-001, Row Crop Drip Irrigation on Peppers Study - High Rise Farms, 2006
[32] Nexant, M&V report from the California Energy Commission Agricultural Peak Load Reduction Program, 2003
[33] CalPoly ITRC, California Agricultural Water Electrical Energy Requirements, 2003
[34] Personal communication with Keith Coyne, PGE, 8 4 2005
[35] Personal communication with Cyrus Sorooshian, SCE, 8 11 2005

Although there are many accounts on TOU rates, farmers still use energy during peak-period hours. If crop water needs require irrigating during peak periods, the farmer will exercise the option to use on-peak power and pay the penalties, leading to higher average energy costs. The farmer's goal is to provide water to crops when it's needed, in the proper amount, using high distribution uniformity for optimal crop growth. It is not always possible to meet all of these requirements and take maximum advantage of TOU rates.

Staff recognizes that, to pump water during off-peak hours, farms will require larger pumping plants with properly designed irrigation systems, improved control systems, and flexible working hours. To take full advantage of these changes farmers will have to maintain high efficiencies in their pumping and irrigation systems in addition to adopting scientific irrigation scheduling management practices.

Agricultural electricity end users would benefit from energy policies that allow end users to choose the demand response practice that best meets the requirements of their business. The industry will also be more inclined to invest in peak load reduction measures with both flexibility and strong stable price signals.

Other Factors Affecting Agricultural Water Energy Use in California

There are several trends to watch that affect the future use of energy to provide water to agriculture, including:

- Sustained adoption of drip and micro irrigation technologies. Although there are more than 4 million acres under drip irrigation, from a total of less than 9 million acres of irrigated land reported for the state, it is reasonable to assume that, over time, another 3 million acres could be converted to drip irrigation. The agriculture industry will make the conversion partly to meet water conservation goals but mostly by recognizing the production benefits from the technology. CalPoly ITRC forecasted an increase of 2.9 million kWh from the doubling of drip irrigation acreage.[36]

- Continued reliance on ground water, with reductions in surface water. There is a high probability that farmers will continue to pump from wells to supply groundwater to drip systems until irrigation districts provide surface supplies with flexible schedules.

- An increase in agricultural water conjunctive use programs with transfers to urban regions. There are many water transfer agreements already in place, with more to come as the urban sector finds that the agricultural industry can provide storage services as well as new water transfers from achieved

[36] CalPoly ITRC, California Agricultural Water Electrical Energy Requirements, 2003.

conservation measures. There are significant energy expenditures to accomplish the process of banking the water, pumping it for extraction and delivering it to the water account owner[37].

- Conversion from diesel-powered pumping systems to electric motors. On August 1, 2005, a new rate schedule (AG-ICE) became available for current agricultural diesel-driven irrigation pumps in both PG&E's and SCE's service territories. The rate encourages the switch from engines to electric motor-driven systems for agricultural customers with diesel engines of greater than 50 horsepower for irrigation pumping before September 1, 2004. In the PG&E territory it is possible that 200 to 300 MW of new coincident peak load could be added to its system during the course of the two-year open enrollment period.[38]

The Energy Commission's *2005 California Energy Demand Forecast* shows that agricultural electricity consumption is expected to increase by 1.4 percent a year through 2016.[39] The actual amount will fluctuate depending upon the total number of irrigated acres, the crop patterns, the source of water and, obviously, the price of electricity.

From a state energy policy perspective, the agricultural industry's effort to achieve electricity use efficiency and demand response savings would satisfy the first target in the state's loading order. The agricultural industry also has the opportunity to adopt the second item in the loading order with installation of renewable energy systems.

The agriculture industry does have great potential to develop renewable energy sources. However, investment recovery will require the aggregation of electricity account meters so that the generated power can be applied to all existing accounts. Today, these accounts can only apply the power produced to the single connection attached to the power system. Therefore only a limited amount of power can be sold at the retail price, with the remainder sold at wholesale prices. This situation is similar to that faced by water and wastewater utilities. These issues affect many customers in the state and are being considered by the CPUC as it attempts to balance a wide variety of factors related to distributed generation in California.

The agricultural industry's economic sustainability greatly depends upon nature's water cycle. During dry years, the amount of energy used to deliver water increases. In drought years, groundwater sources are used extensively to supplement lower surface water deliveries. Several consecutive dry years can also lower the groundwater subsurface level of the water table, requiring more energy to overcome the lift needed to pump the water up to the surface. Typical groundwater lifts vary by

[37] CalPoly ITRC, California Agricultural Water Electrical Energy Requirements, 2003) [http://itrc.org/reports/energyreq/energyreq.pdf].
[38] Personal communication with Keith Coyne, PG&E August 4, 2005.
[39] *California Energy Demand 2006-2016, June 2005*

region throughout the state, which influence both motor size and power usage. The state has been fortunate in that there has not been a continuous series of dry years since the 1988-1992 drought. Since then, new groundwater recharge basins have been developed to serve as infrastructure for water transfer transactions. These measures are important both for water management flexibility and energy efficiency.

Additional small-scale water storage systems located in irrigation districts and on farms could help increase the flexibility of water deliveries. Surface and tank storage facilities can store water during off-peak periods and reduce the need for on-peak electricity consumption.

Urban Water Use Efficiency

Approximately 21 percent of the state's water is for urban uses. Urban water use efficiency includes improvements in the residential, commercial and industrial sectors. It includes opportunities to increase the efficiency of water-related end uses that use either electricity or natural gas.

In November 2003, the Pacific Institute published a study[40] that estimated the minimum cost effective urban water conservation at around 2 million acre-feet (651 billion gallons) per year, about 22 percent of all urban water use -- without technological change. The California Urban Water Conservation Council (CUWCC) recently posted the results from 32 percent of the agencies that signed on to their memorandum of understanding to institute best management practices (BMPs) in their water agencies. Taking only those BMPs for which water savings could be quantified, the reporting agencies saved more than 27 billion gallons of water in 2004, resulting in significant electricity energy savings, as shown in Table 4-1. The water savings from the BMPs, reported in 2004, are roughly 4 percent of the potential described by the Pacific Institute.

[40] *Waste Not, Want Not: The Potential for Urban Water Conservation in California,* The Pacific Institute, November 2003.

Table 4-1: Energy Value of Saved Water Due to Implementation of 2004 BMP Measures

	Annual Savings		Useful	Life-Cycle Electricity	NPV Electric
Statewide	**Water (MG)**	**Electricity (kWh)**	**Life (Years)**	**Savings (kWh)**	**Avoided Cost ($)**
BMP 1 Water Survey Programs MF/SF	1,897	17,114,500	5	85,572,500	6,220,866
BMP 2 Residential Plumbing Retrofit	311	2,814,000	5	14,070,000	1,022,865
BMP 4 Metering & Commodity Rates	1,587	14,317,200	11	157,489,200	9,472,790
BMP 5 Large Landscape Conservation Programs	5,320	34,595,450	10	345,954,500	21,149,701
BMP 6 High-Efficiency Washing Machine Rebate	317	2,860,100	15	42,901,500	2,346,888
BMP 9 Conservation Programs CII	4,814	43,433,300	12	521,199,600	30,567,522
BMP 9a CII ULFT	258	2,328,300	25	58,207,500	2,522,363
BMP 14 Residential ULFT	12,987	117,184,600	25	2,929,615,000	126,950,010
Statewide Total	27,492	234,647,450		4,155,009,800	200,253,005

Source: California Urban Water Conservation Council (CUWCC) Reporting Database, April 2005 with 86 of 269 Reporting Units (32%) reporting BMP expenditures in 2004. Reporting Units include: water utility districts, water agencies, irrigation districts, city and county water departments and water service companies implementing BMPs.

Saving this water also saved more than 234 million kWh of electricity. Taken over the lifetime of each measure, the net present value of the energy for this saved water is more than $200 million. The saved energy was computed using the urban use energy intensity of 4,000 kWh/MG in Northern California and 12,700 kWh/MG in Southern California. These values assume that all water delivered to these uses is also treated as wastewater and applies to all of the BMPs (except the landscape conservation programs, which used a lower number to account only for the water delivery portion of the water use cycle). The computations were done separately for Northern and Southern California and aggregated to arrive at the statewide totals shown in the table. Details of this analysis can be found in Appendix C.

The energy saved from the saved water was passed on to the California water and wastewater treatment utilities that participated in implementing the BMPs. It also showed up as reduced electricity sales and some peak demand reduction. However, energy savings from savings in the water use cycle were not recognized by either the CPUC or by the energy utilities as fundable energy conservation measures.

Members of the Water-Energy Relationship Working Group presented testimony on this topic, suggesting it would be valuable to assess how large the energy value of the conservation potential identified by the Pacific Institute might be in comparison with energy efficiency programs currently approved by the CPUC. Table 4-2 presents the comparison of programs funded in 2004-2005 with those planned for 2006-2008. The water use efficiency (WUE) program is based on the Pacific Institute's expressed water saving potential.

Table 4-2: Comparison of Energy Efficiency Programs Resource Value to Water Use Efficiency

	Energy Efficiency Programs		
	2004-2005	2006-2008	WUE
GWh (Annualized)	2,745	6,812	6,500
MW	690	1,417	850
Funding ($ million)	$762	$1,500	$826
$/Annual kWh	$0.28	$0.22	$0.13
WUE Relative Cost	46%	58%	

Source: California Public Utilities Commission, with WUE estimates from Appendix C

The numbers for the energy programs are from CPUC documents.[41] The numbers for the WUE program are discussed in detail in Appendix C. The energy savings were assigned to Northern and Southern California based upon their respective populations. The cost of water efficiency measures assumes an average of $384 per acre-foot, based on a range of $58-$710.

There is clearly significant untapped energy savings potential in programs focused on water use efficiency. If all of the identified urban water savings could be achieved, the energy savings would achieve 95 percent of the savings expected from the 2006-2008 energy efficiency programs, at 58 percent of the cost. Peak savings could account for 60 percent of the utilities' expected demand reductions.

TOU Water Tariffs and Meters

The idea of TOU water tariffs and meters was suggested several times during the proceedings as a means to give customers a more accurate assessment of the value of the water they use. Historically, water agencies have treated their product as a commodity; water flows and people use it. Before the 2000-2001 energy crisis, even though water agencies were on standard TOU and demand rates, the incremental costs between on and off peak were not large enough to affect their decision making. They did not attach time value to water until SWP and the state water contractors became sensitized to hourly energy costs in the highly volatile bulk power market. At the retail level, it is important to recognize that many water customers in the state do not even have water meters, although legislation is changing that. Currently, TOU water meters do not exist. Water agencies are also grappling with how to develop tariffs and rate schedules that both properly reflect the value of water at different times during the day and account for delays between

[41] 2004-2005, CPUC Rulemaking R.01-08-028, Decision D.03-12-060, 2005-2006, CPUC Rulemaking R.-01-08-0228, Decision D.04-09-060.

energy consumption and water use. The Energy Commission is funding a project to look at the feasibility of these meters and associated tariffs.

Because the vast majority of the financial benefits of water use efficiency go to customers instead of water, wastewater, or energy utilities, informing customers of the financial upside of more efficient appliances and practices could be very effective. The new "Flex Your Power at the Tap" campaign is one example. In the longer term, water and energy bills could also serve as informational pathways leading customers to efficiency investments and choices that are best for both them and the greater society.

Water Storage for Peak Electric Load Shifting

Water and wastewater treatment require approximately 3,000 MW of peak load. There is a minimum level of electrical consumption needed to operate their systems during peak periods. Beyond that, virtually all of the on peak energy use is discretionary - if there is sufficient storage. For example, the El Dorado Irrigation District reduced its on-peak electric usage by more than 60 percent by allowing their tanks to drop to a lower minimum level and installing an additional 5-million-gallon storage tank. An estimated 250 MW of peak demand could be saved if water agencies statewide viewed their storage as an energy asset as well as a water asset. Another 1,000 MW of peak demand could be saved from increased treated water storage in urban areas. In total this represents more than one-third of the water use cycle load.

Investing in Water and Energy Efficiency

California has water-related energy programs to increase the energy efficiency of existing water and wastewater utility operations; increase the energy efficiency of the appliances that move water; and increase generation from renewable resources. These programs include building and appliance standards, technical support and loan programs, and incentive programs funded through the state’s energy utilities. The state also conducts research to modify existing treatment processes; develop more efficient water and wastewater treatment and water supply technologies; increase the efficiency of heating, cooling, and moving water for end users; and improve the effectiveness of renewable energy sources.

However, since the state’s largest energy utilities have no authority to invest in programs that save cold water to capture the upstream energy benefits, these benefits are not realized. If the CPUC authorizes investment in cold water savings, the state will have a new source of energy savings.

Because of the interconnectedness of water and energy resources in California, the fact that cost-effectiveness is determined solely from a single utility and single

resource perspective is a glaring problem. Water utilities value only the cost of treating and delivering water. Wastewater utilities value only the cost of collection, treatment and disposal. Electric utilities value only saved electricity. Natural gas utilities value only saved natural gas. This causes underinvestment in programs that would increase the energy efficiency of the water use cycle and increase agricultural and urban water use efficiency.

By valuing a unit of water on its total value – the water resource itself, plus its energy intensity and externalities throughout the entire water cycle -- many water and energy programs and measures that could not meet the earlier cost-effectiveness threshold are now possible. California could reap large energy benefits by encouraging greater collaboration between energy, water, and wastewater utilities.

Conclusions

In this chapter, staff has generally described the water energy intensity for agricultural and urban end uses. Staff recommends additional research to provide needed information to better understand these systems and how modifications or improvements could benefit the energy sector. Future regulatory change will also affect the overall energy demand of these systems. To ensure high-quality water supplies for the state, energy and water utilities should collaborate to efficiently operate water and wastewater treatment facilities. Water and wastewater utilities can take advantage of current energy efficiency programs for near-term retrofits and design modifications to increase efficiency now, with existing technology. Additional research is needed on technologies and system designs.

CHAPTER 5 – RENEWABLE ENERGY GENERATION POTENTIAL

The most widely recognized aspect of the water-energy relationship is power production in large scale hydroelectric dams. However, water and wastewater utilities have other opportunities to develop energy supplies. These include biogas cogeneration at wastewater treatment plants and development of local renewable resources on water and wastewater utilities' extensive watersheds and rights-of-way. For purposes of this paper, we will address the potential for new renewable generation by water and wastewater utilities for two distinctly different types of opportunities:

- Distributed generation
- Utility scale generation

These energy generation opportunities require different types of permits, approvals, metering, and interconnections, and have different production characteristics, economics, and operating and financial risks. Detailed aspects of distributed generation and large-scale hydroelectric generation are addressed separately in the *Energy Report*. [42]

Table 5-1 illustrates the range of renewable power production opportunities for water and wastewater utilities.

Table 5-1: Renewable Power Production Opportunities

Energy Resource	Distributed Generation	Utility Scale Generation
Hydropower	Energy Recovery through In-Conduit Hydropower	▪ Relicensing ▪ Pumped Storage ▪ Repowering
Biogas	Biogas Co-Generation	Biosolids Waste-to-Energy plants that utilize methane from sewage digesters, dairy manure, agricultural and food processing wastes, and other organic materials
Solar	Photovoltaics for irrigation pumps & motors	Central concentrating solar power plants (solar thermal and photovoltaics)
Wind	Modest site specific applications	Wind farms on watershed lands
Advanced Generation, including Fuel Cells and MicroTurbines	Potential applications for small pumping loads	n/a

[42] For a complete listing of all documents and reports associated with the IEPR proceeding, including distributed generation, please see [http://www.energy.ca.gov/2005_energypolicy/documents/index.html].

The potential, issues, and challenges of these opportunities are discussed below.

Distributed Generation

The term distributed generation is used to describe both customer-side and utility-scale generation. For purposes of this staff report, distributed generation refers to generation facilities sited on the customer side of the meter that are used primarily to serve a customer's own energy requirements, specifically a water or wastewater utility. This discussion is limited to opportunities for water and wastewater utilities to self-generate power, and the barriers and hurdles that prevent them from generating more. These facilities include in-conduit hydropower, biogas combustion, and other small-scale distributed generation facilities.

In-Conduit Hydropower

Wherever there is flowing water, there is both energy and the potential to capture and utilize that energy. In-conduit hydropower captures the energy from flowing water in a pipeline with a turbine or generating device installed directly in the conduit. Most of the state's large water conveyance projects already take advantage of the energy in water flowing through their pipelines, canals, and aqueducts. Additional opportunities remain to develop new or retrofitted generation in the state's water systems, if costs and risk can be minimized. These are environmentally attractive because they are built in existing water and wastewater systems.

In most cases, in-conduit hydropower potential ranges from very small – 1 or 2 kW to a high of about 1 MW. Often, the hydropower site is not near loads, requiring construction of expensive transmission or distribution lines to interconnect to the electric system. Even in cases where it may be cost-effective to construct such lines, existing rules do not allow the produced power to be credited against the water or wastewater utility's total energy bills. Instead, wherever such self-produced power cannot be directly connected to an existing load, it must be sold into the wholesale bulk power market. The costs and complexities of participating in the wholesale bulk power and transmission markets are daunting, even for large generators. They are prohibitive for very small generators.

A recent Energy Commission Public Interest Energy Research (PIER) study estimated the statewide developable potential of hydropower capacity in manmade conduits (including pipelines, irrigation ditches, canals and aqueducts) at about 255 MW - 231 MW at coincident peak - with annual production of approximately 1,100 GWh. The potential was about evenly split between municipal and irrigation district systems.[43]

[43] *California Small Hydropower and Ocean Wave Energy Resources*, Mike Kane, Energy Commission PIER, April 2005.

The PIER study focused on identifying the statewide potential for RPS-eligible small hydropower (less than 30 MW). Under SB1078, RPS-eligible hydropower must be constructed on or after September 12, 2002, and must not require a new diversion or a new appropriation of a water right.[44] Consequently, staff determined that the most likely class of hydropower to be developed under the present RPS is small hydropower within conduits. The PIER study only considered sites with potential of at least 100 kW since projects of lesser size tend to be uneconomic.

Changes in technology may reduce the economic threshold of in-conduit hydropower to less than 100 kW. New packaged systems are being developed that could be dropped into pipelines and other types of conduits – like canals and aqueducts - without expensive civil works or permitting costs. However, the challenge of siting in-conduit hydropower close to local loads remains.

Another way to look at in-conduit hydropower is to view it as an increase in the energy efficiency of the water delivery system. Without water agency investment in the water delivery system in the first place, this resource would not be available. Currently in-conduit hydropower is treated like any conventional energy generation resource owned and operated by a non-utility generator. This classification seems inappropriate since there is no prime mover and no new natural resource is used to generate the electricity.

Existing energy efficiency programs can be tailored for special circumstances, using customized incentives and standard performance contracting. Water agencies have taken advantage of these incentives for energy efficiency improvements, including increasing pipe diameter to reduce friction losses and the requisite pumping requirements; installing a parallel pipe system; and changing pump impellers and lining pipes to reduce friction losses. In-conduit hydropower could be looked at in a similar fashion and be included as an element of these tailored programs. Again, the issues of interconnection and the sale or application of the power to multiple accounts will still need to be addressed.

Biogas

Another option for developing generation in the water sector is to increase beneficial use of digester gas produced by the sewage wastewater, dairy manure, and food processing wastes/wastewater. Biogas, primarily composed of methane, can be used for a combined heat and power production.

California has 311 sewage wastewater treatment facilities, 2300 dairy operations, and 3000 food processing establishments. Currently, about 50 percent of sewage sludge, 2 percent of dairy manure, and less then 1 percent of food processing wastes/wastewater generated in the state are utilized to produce biogas. Converting

[44] *Renewables Portfolio Standard Eligibility Guidebook*, Energy Commission Publication Number 500-04-002F1, adopted August 11, 2004.

these wastes into energy can help operating facilities offset the purchase of electricity and provide environmental benefits by reducing air and groundwater pollutants discharged.

Unused biogas is typically flared to the atmosphere. Not only is this a waste of a renewable resource – flared biogas creates odors and air emissions.

Biogas producing facilities can be near significant loads, for example the wastewater treatment plant itself. However, this load may be on multiple meters and current rules discourage full use of the available biogas for maximum generation for onsite or offsite loads. Currently, there are provisions under regulated tariffs that enable dairy operations to produce electricity from biogas resources at one location and use it to offset electricity use at multiple locations, under multiple accounts, for one customer. This same approach would significantly increase opportunities for biogas-fired (and other renewable) generation in water and wastewater agencies.

The Inland Empire Utilities Agency (IEUA) is a leader among regional wastewater treatment agencies for innovative and proactive energy management. IEUA's facilities process 65 million gallons of wastewater into high-quality recycled water. IEUA's wastewater treatment system has three anaerobic digesters. Dairy manure is collected from seven nearby dairies and processed through two of IEUA's digesters. At one facility, biosolids from the sewage treatment process are combined with dairy manure. At another facility, dairy manure alone is used to produce the methane that is piped to the Chino Basin desalter, where it is used to produce electricity for desalination of groundwater.

IEUA believes there is significant potential for increasing biogas production by combining different types of biosolids. For example, by blending dairy manure with food waste, IEUA expects this year to double its amount of biogas production (from 0.5 MW to the total load of the Chino desalter of 1 MW).

IEUA's biogas power production is expected to continue to grow as it adds another 15 MGD wastewater treatment plant next year, and it plans to develop another 10 MW in renewable biogas generating capacity with a centralized biodigester that will take dairy waste, green and food residuals (generally used to make compost) and biosolids to produce biogas for power generation and compost. IEUA is also considering using its excess biogas to heat water and sell a new product, hot process water, to industrial customers.

While IEUA has been much more successful than other wastewater utilities in the innovative development of biogas power production, it has not been simple.

Other Distributed Generation Options

Other distributed generation options include solar thermal, photovoltaics, small wind power, and advanced generation technologies including fuel cells and advanced

microturbines. These distributed generation opportunities are discussed at length in the *Energy Report* proceeding.

Utility Scale Generation

Many water and wastewater utilities have the opportunity to develop utility-scale power production facilities that produce more power than utilities need for their own processes. With technical and funding support and removal of major barriers, water and wastewater utilities could become net exporters of power. Whether conventional hydropower facilities developed in conjunction with large water conveyance systems - like the Oroville Hydroelectric Facility, owned and operated by DWR on behalf of the State Water Project, or wind farms constructed on watershed lands – substantial untapped renewable resource potential resides with water and wastewater utilities that have little incentive, and, in fact, many barriers and disincentives, to develop these resources.

Large-Scale Hydropower

In addition to the in-conduit hydropower opportunities described above, utility scale generation consists of conventional hydropower (less than 30 MW) produced by water releases from natural or manmade impoundments like reservoirs and dams.

Opportunities for new hydropower dam and storage projects are extremely limited in California for a variety of reasons. Most economically viable sites have already been developed; but even where suitable sites exist, development is limited by lack of availability of unallocated water rights, environmental protection measures (such as Wild and Scenic Rivers, Endangered Species, and Wilderness Area designations), and strong opposition from environmental advocates.

Staff has investigated ways to balance the electric system benefits offered by hydropower with their significant adverse environmental impacts. Both the Energy Commission's *2003 IEPR*[45] and staff's *California Hydropower System: Energy and*

---

[45] *2003 Energy Report*. California Energy Commission, *2003 Integrated Energy Policy Report*, December 2003, Docket No. 02-IEP-1, Publication No. 100-03-019, page 43.

> "Hydroelectricity has historically played an important role in meeting California's electricity needs. Its low production costs and unique ability to meet critical peak demand have long benefited the state's ratepayers. Some hydroelectric projects unfortunately have serious environmental consequences, such as significant, ongoing impacts to many California rivers and streams, native salmon and trout populations, and the water quality needed to support sustainable riverine ecosystems.
>
> The restoration of imperiled salmon and trout fisheries is one of California's environmental policy objectives. ... [D]ecommissioning of high environmental impacts hydroelectric facilities that supply little power is a possible method of restoring important aquatic habitat."

Environment[46] provide key findings with respect to hydropower's value and impacts. Staff provides recommendations to minimize the adverse environmental impacts of these facilities.

At this time, only two utilities are expected to develop hydroelectric resources. [47] The Sacramento Municipal Utility District (SMUD) proposes the Iowa Hill Project to add 400 MW of pumped-storage capacity to its Upper South Fork American River Project. This may be especially helpful for integrating wind energy produced in the Delta, since the Delta breeze on a hot summer day usually begins a few hours after the daily load peak, which is driven by air conditioning. For San Diego Gas and Electric (SDG&E), about 40 MW of new hydro are planned, beginning in 2008, from San Diego County Water Authority projects.

Long lead times are needed to plan new hydro projects, prepare appropriate environmental documents, obtain a license from the Federal Energy Regulatory Commission (FERC), and build the project. However, opportunities for incremental development, such as adding or improving generation facilities attached to existing dams, water conveyance facilities, and powerhouses, remain an option for increasing California's hydropower production.[48] These opportunities include pumped storage and retrofit.

Pumped Storage

Pumped storage typically involves pumping water from a water source into a reservoir or tank, to be held for later scheduled hydropower production. Water is pumped uphill during off-peak hours and provides peaking capacity during on-peak hours. Pumped storage has high energy value since it is virtually the only viable means to store energy. There are several significant pumped storage projects currently under development:

- The proposed 500 MW Lake Elsinore Advanced Pumped Storage Project (LEAPS)[49].

---

[46] California Energy Commission, *California Hydropower System; Energy and Environment*, Appendix D to the *2003 Environmental Performance Report*, prepared in support of the *2003 Integrated Energy Policy Report*, October 2003, Publication No. 100-03-018. Prepared in support of the *Electricity and Natural Gas Report* under the Integrated Energy Policy Report proceeding (02-IEP-01), October 2003, Publication 100-03-018.

[47] *California and Western Electricity Supply Outlook Report* Draft, California Energy Commission, July 15, 2005, pages 74-76, posted on the website of the California Energy Commission.

[48] Excerpt from the *California and Western Electricity Supply Outlook Report* Draft pages 74-76, in progress for posting to the website of the California Energy Commission, July 15, 2005. For information about California's overall hydropower outlook, please refer to the Energy Commission's 2005 report, *Potential Changes in Hydropower Production from Global Climate Change in California and the Western United States*, prepared in support of the *2005 Integrated Energy Policy Report* proceeding (Docket # 04-IEPR-01G).

[49] EVMWD Web site (www.evmwd.com).

- SMUD's proposed 400 MW Iowa Hill Pumped Storage Development.

- The US Bureau of Reclamation is also exploring several pumped-storage options in the Upper San Joaquin River Basin.[50]

As with any dam or reservoir, development of new pumped-storage facilities faces major challenges. Some of the issues associated with conventional hydroelectric power generation and typical on-stream pumped hydroelectric storage facilities include:

- Water resources impacts - hydroelectric facilities may change stream flows, reservoir surface area, the amount of groundwater recharge, and water temperature, turbidity, and oxygen content.

- Biological impacts, including the possible displacement of terrestrial habitat with a new lake environment, alteration of fish migration patterns, and other impacts on aquatic life due to changes in water quality and quantity.

- Possible damage to, or inundation of, archaeological, cultural, or historic sites (primarily if a reservoir is created).

- Changes in visual quality.

- Possible loss of scenic or wilderness resources.

- Increase in potential for landslides and erosion.

- Recreational resource impacts/benefits.

Another possibility for developing new pumped-storage projects is to connect two or more existing reservoirs or lakes with new pipelines or penstocks for water pumping and power generation. A U.S. Department of Energy (DOE) study identified dozens of such potential reservoir pairs in California, requiring construction of an average of about 10 miles of pipeline to connect each pair. (Lamont 2004). Though this type of development would increase operating flexibility and peaking capacity without need to construct new reservoirs, it would still involve construction of large pipelines through difficult terrain on protected lands, which could require significant expense for environmental mitigations and permitting.

Because of the costs associated with new pumped-storage facilities using existing or new reservoirs, development of modular pumped storage (MPS) may have greater potential in the near future. MPS systems are not dependent upon

[50] USBOR website 2005a.

natural waterways and watersheds and can be sited in areas that avoid many of the issues described above. In fact, they are generally purposely sited away from sensitive areas to avoid the regulatory and operational complexity often associated with conventional pumped hydroelectric storage facilities. MPS systems can also be added to existing water systems wherever the necessary elevation difference exists. They could also be developed in places like abandoned mines, taking advantage of elevation differences and storage created by mine shafts and open pits. If their capacity was less than 30 MW, these pumped-storage facilities could also qualify for supplemental energy payments under the RPS.[51]

Retrofit[52]

Retrofitting existing hydroelectric facilities, specifically replacing turbine runners and generators with new, more efficient equipment, may increase the capacity of these facilities. To the extent that retrofit does not result in changed flows, no permits may be needed. Hetch Hetchy Water and Power increased the capacity of its system 48 MW by replacing turbine runners and generators with newer, more efficient equipment – at a capital cost of $8 million, less than 17 percent of the cost of installing a new unit of comparable capacity. Since the purpose of these retrofits was to increase the efficiency of hydropower production using the same amount of flows, no permits or approvals were required.

Existing hydropower facilities can be upgraded to increase both capacity and output without changing flows. Below are the primary means for attaining such efficiency gains:

- Tunnels. Most power tunnels in California were built using drill and shot methods for rock excavation. The resulting rough rock linings have high friction losses and capacity issues. Existing unlined tunnels could be lined to decrease friction losses and produce more power with the same amount of water. Existing lined tunnels can be made smoother by relining or coating abraded surfaces. Some tunnels can be enlarged or made smoother by selectively trimming tunnel walls. The longer the distance of the tunnel and the greater the friction, the greater the opportunity for incremental gains in power production. Some tunnel lining projects have increased hydropower production up to as much as 7 percent.

- Penstocks and Pipelines. Similarly, penstocks and pipelines could be relined or replaced to reduce friction losses during times of high flows. The decision to reline or replace is an economic one that depends in large part upon the remaining useful life of the hydropower facility itself. The potential benefit also

[51] Aspen 2004
[52] Matthew Gass, Engineering Manager, Hetch Hetchy Water and Power, San Francisco Public Utilities Commission.

depends upon the length of the penstock or pipeline, and the amount of friction losses. Here, again, benefits of up to 7 percent have been documented.

- Turbines. The easiest and frequently most economical improvement could be to replace a turbine's runner. Computerized design, manufacture, and improved testing and modeling methods have increased the efficiency of turbine runners. Minimum efficiency gains for replacements of turbine runners installed in the 1970s and 1980s have been reported at 1 percent. When older designs are replaced by customized efficiency designs, increased output as high as 30 percent has been reported.

Other types of hydropower efficiency gains are attainable through improved planning, controls, and management. Most large hydropower plants in California are multi-unit facilities. In many cases, there are opportunities to optimize operations by balancing the loads of individual units. Specialized computer selection software has helped attain performance improvements of 1-3 percent. In addition, improved controls and monitoring systems allow more efficient operations and reduce downtime from unplanned outages. All of these things have potential to increase net power production. Applied to the state's hydropower inventory, these minor tweaks could cost-effectively increase the state's total hydropower production by at least 3 percent within just a few years.[53] However, FERC rules regarding system modifications and upgrades will need to be reviewed to confirm the trigger points that could reopen a license to scrutiny.

There is constant tension among competing interests for water supply, water quality, hydropower production, and flood control. A better understanding of opportunities for optimizing the state's hydropower supplies and the key stakeholders needed to attain those incremental benefits would provide a useful framework for identifying feasible options and resolving points of conflict.

Other Renewable Resources

Both water and wastewater utilities have extensive watershed lands and rights-of-way with potential for wind and solar development.

- In spring 2005, the Semitropic Water Storage District completed installation of a 1 MW solar facility that provides peaking power for local pump loads.[54]

- At the Solar Power 2004 Conference and Exposition, San Francisco announced that it will soon build a 225 kW solar facility covering 20,000 square feet at its Southeast Water Pollution Control Plant.

[53] Matthew E. Gass, P.E., Engineering Manager Hetch-Hetchy Water and Power.
[54] Boschman 2005..

- IEUA will install solar panels on its new LEED Platinum headquarters, which was designed to reduce energy use by 90 percent and water use by 70 percent compared with its previous building. IEUA expects its headquarters to be completely energy independent by next year.[55]

- Hetch Hetchy conducted a wind resource assessment of its Calaveras watershed that indicated a potential of more than 30 MW.

The developable renewable energy potential owned by water and wastewater utilities is not yet known. It would be beneficial to identify, assess and prioritize these resources, and provide technical and financial assistance to help develop renewable energy for the benefit of all California ratepayers.

Barriers to Energy Production

Even when transmission is available to move the power out of a water agency's conduit hydropower, biogas, or solar facility, the water professionals interviewed for this paper expressed frustration with their limited ability to deliver self-generated power to their various facilities. Water and wastewater facilities are often dispersed over large distances. These facilities typically take electric service at multiple points and are metered separately at each point.

During public workshops and working group meetings, water and wastewater utilities cited the following primary barriers to self-generation:

- Complex, costly and long lead time interconnections.
- Prohibitive stand-by costs.
- Disincentives to fully utilize available renewable or distributed resources.

Issues of interconnections are being addressed by both the CPUC and the Energy Commission with respect to Rule 21.

Present regulations do not allow aggregation of a customer's electric metered loads within a single facility, much less with metered loads at their other facilities. Therefore, the only means for a water or wastewater utility to deliver self-generated power to itself anywhere on its system is to own and operate its own transmission and distribution systems -- essentially, to operate its own electric utility contiguous with its water service territory boundaries. Of course, this would be cost prohibitive.

At the April 8, 2005, *Energy Report* Committee workshop, IEUA identified the following barriers to its efforts to become energy self-sufficient and possible solutions to these barriers (Table 5-2).

[55] Davis 2005.

Table 5-2: Barriers to Energy Self Sufficiency

Barrier	Solution
Presently, IEUA is metered at multiple points, making it difficult to understand, plan and manage its total energy requirements.	The ability to aggregate all of IEUA's electric loads into a single consolidated load would enhance IEUA's ability to self supply its loads. In addition, it would enhance IEUA's ability to develop creative approaches, whether through modified system design and/or operations, to further reducing peak period consumption.
CPUC "single premise rules" discourage building generation greater than connected load.	IEUA would increase the size of its generation facilities if it had ability to wheel self generated power to itself.
Energy utility programs often fail to capture opportunities to encourage energy efficient design principles in water agencies' facilities.	IEUA and other water agencies have substantial continuous capital programs and, thus, opportunities to incorporate non-conventional energy efficient design principles into large facilities. For example, most of the cost of a new or replaced pipeline is in the trenching. The incremental cost of oversizing a pipeline is fairly modest and should be encouraged wherever cost-effective in reducing energy consumption. Some Energy Performance Contracting programs can be accessed for these types of projects; but applying for and collecting incentives are often difficult.
IEUA and other water agencies have unique opportunities for renewable energy development (e.g., biogas; pipeline conduit hydro; extensive rights of way and watershed lands); but the development costs and risks are often daunting for an entity for which energy is not its primary business.	IEUA is hosting various pilot programs that test and refine renewable energy technologies. Energy utilities could partner with water agencies to optimize development of their renewable energy potential, first to offset their own loads, and then potentially to also become net exporters of renewables and help energy utilities meet RPS and achieve other environmental benefits, including greenhouse gas reductions. Incentive programs are key to testing new technologies at scale. Net metering program (SB 728) will be essential to capturing value of renewable energy.

Source: IEUA testimony

Conclusions

Given the state's energy and capacity shortages, it would be beneficial to help water and wastewater utilities develop all potential renewable and distributed resources. This can be facilitated by allowing these utilities to aggregate their metered load and remove net metering caps. Excess power could then be sold to the energy utilities. Ultimately, the tension between energy utilities and their customers needs to be resolved through policy. The fundamental issue is whether customer-sited distributed generation provides an energy system benefit that reduces total societal costs.

CHAPTER 6 – POTENTIAL EFFECTS OF FUTURE CHANGES

Several factors are causing changes to California's water supply portfolio; legislative, regulatory, market, and technological changes will affect both water-related energy consumption and energy production.

The following discussion addresses a variety of known and anticipated energy impacts, the primary drivers of these impacts, and the extent to which the magnitude and timing of these impacts can be predicted. The primary drivers to be discussed are:

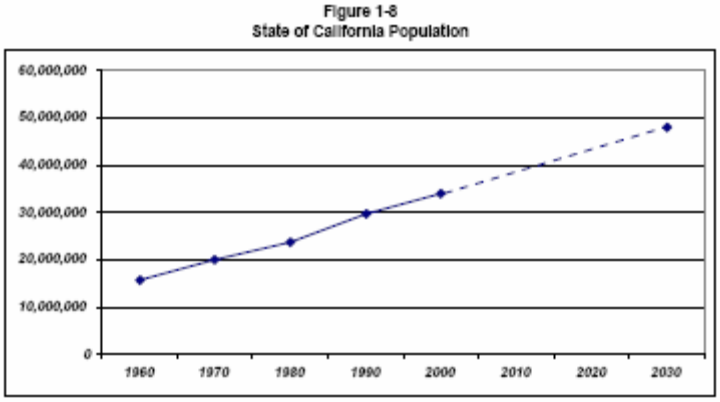
- Increased water demand
- Changes in water end use
- Changes in regulation and legislation
- Changes in water and energy markets
- Hydrology
- Technology
- Policy

Where reasonable bases exist for estimating these impacts, they will be described. If their impacts cannot be reasonably projected, staff identifies needed additional information.

Increased Water Demand

DWR, in the *2005 Water Plan Update,* based its estimates for water demand growth on data from the Department of Finance (DOF) that estimates California's population will increase more than 40 percent by 2030 - from about 34 million in 2000 to 48 million in 2030 (Figure 6-1). Absent mitigation, water-related energy consumption attributable to urban water use is expected to match this growth. The plan projects that, without mitigation, urban water use will increase substantially - as much as 6 million acre-feet, or 67 percent, by 2030.

Figure 6-1: Projected Population Growth in California



The actual impact of water demand growth on energy is difficult to predict for the following reasons:

1. The water supply portfolio planned to meet water demand growth is significantly different from the state's existing portfolio. Consequently, a simple extrapolation of the current average energy intensity of water supplies makes no sense.

2. The state water plan indicates that the largest new supply available to provide for the expected growth in water demand over the next 25 years is water use efficiency. To the extent that the state may not attain its targeted level of efficiency, any shortfalls in water supplies will need to be made up from other sources, most likely recycled water and desalination. Both of these options require new infrastructure that will need to be developed years before it is actually needed. If these are not in place in time, forced conservation, such as the shortage allocations during the 1987-1992 drought, may need to be implemented.

3. Industry experts predict there will be an increase in water market transactions. Some broad generalizations about water market transactions can be made. For example, to the extent that these transfers result in a net increase in physical deliveries of Northern California water supplies to Southern California or agricultural water use is converted to urban water use, energy consumption for water conveyance will increase. However, the net energy impact of increased water transactions cannot be determined. There are many variations in the types of transactions that could occur and no certainty as to which will or will not occur.

4. The recent Colorado River Quantification Settlement Agreement (QSA) requires that California beneficiaries of Colorado River water reduce their use over the next 14 years to California's basic annual allocation of 4.4 million acre-feet. A number of specific actions are being taken by Southern California water utilities to implement the QSA and make up for reductions in Colorado River imports.

> Strategies include increased water use efficiency, increased imports from the State Water Project, development of 126,000 acre-feet of desalinated ocean water, managing the San Bernardino Basin as a groundwater facility, increased use of recycled water, and paying farmers to fallow their land. It seems likely that these strategies will have significant impacts on energy use. However, the net impacts of all of the combined strategies and any offsets, such as reduced energy due to lower Colorado River imports, are not yet known.

In order to assess its range of potential impacts, staff estimated the energy implications of the water supply portfolio strategy illustrated by DWR for low and high growth scenarios. Table 6-1 shows that energy associated with the water plan strategy will increase water sector energy use by 12.3 percent in the low-growth scenario, to as much as 25.8 percent in the high-growth scenario, over the period 2000 to 2030. The energy impacts were derived by multiplying the energy intensity numbers for each type of incremental water source from Figure 2-2 in Chapter 2, by DWR's projections.

Table 6-1: Estimated Energy Impacts of Proposed Incremental Water Supplies[56]

Resource	Low Growth Projection				High Growth Projection			
	Water		Energy		Water		Energy	
	MAF	%	GWh	%	MAF	%	GWh	%
Conjunctive Management	0.5	21.3%	475	19.2%	2.1	36%	1,995	40%
Recycled	0.9	38.3%	352	14.2%	1.4	24.1%	547	11%
Surface Storage	0.05	2.1%			1.0	17.2%		
Inland - Desalter	0.2	8.5%	340	13.7%	0.3	5.8%	570	11%
Ocean - Desalter	0.1	4.3%	440	17.8%	0.2	2.8%	726	15%
Conveyance	0.3	12.8%	870	35.1%	0.4	6.9%	1,160	23%
Precipitation Enhancemer	0.3	12.8%			0.4	6.9%		
	2.35	100.0%	2,477	100.0%	5.8	100.0%	4,998	100.0%
Current - Base	43		19,345		43		19,345	
Total Projected	45.35	5.5% Growth	21,822	12.8% Growth	49	13.5% Growth	24,343	25.8% Growth
Water Use Efficiency								
Urban	1.1				2.3			
Agriculture	0.2				0.9			
Total	1.3				3.2			

Source: 2005 State Water Plan Update, DWR for water projections. Appendix C for energy calculations

DWR's plan calls for urban and agricultural water use efficiency to make the largest contribution to the state's water supplies. However, conserved water will be redistributed to new users as the population increases. Recycled water, planned to provide almost 40 percent of incremental water supplies in the low-growth projection, will contribute 14 percent to incremental energy use. At the other extreme, ocean desalting is planned to provide only 4 percent of the incremental water, but will require almost 18 percent of the energy. These estimates are indicative of the need to better understand the energy implications when developing the state's future water supply portfolio.

[56] Low-growth projections reflect a 2030 water demand scenario where current trends continue, resulting in reduced agricultural irrigated crop area and reduced agricultural production. Urban water demand increases are linked to population increases and corollary increases in employment sectors. Under this scenario, per-household as well as per-employee water demand decreases slightly. Environmental water demand increases, and naturally occurring conservation decreases slightly. Population growth is based on Department of Finance (DOF) 2004 projections for growth and density.

High-growth projections reflect a 2030 water demand scenario where agricultural irrigated crop areas hold constant with year 2000; urban related water demand grows significantly, linked to population growth exceeding DOF projections by 12 percent, and lower overall population density and greater population growth occurs in inland and in southern hydrologic regions. Per-household and per-employee demand is elevated, and naturally occurring conservation decreases slightly. Urban water prices continue current trends.

Changes in Water End Use

A number of factors are driving changes in water end use. Changes impact both the urban and agricultural sectors. There are many types of changes – some that may increase energy consumption and some that may decrease energy consumption. Net impacts are difficult to predict. The discussion below about changes in agricultural water use illustrates the complexity of evaluating the net energy impacts of changed water use patterns.

Changes in Agricultural Water Use

As discussed in Chapter 4, changes in crops and irrigation methods affect overall energy demand. In the future, staff expects that periodic changes in crops will occur. Staff cannot predict what those changes will be. Consequently, only general statements can be made about the energy impacts of different trends. The *California Water Plan* projects that the agricultural sector will reduce overall water demand, predominantly through conservation. Any saved agricultural water will likely be applied to higher energy intensity urban uses.

Other signs point to decreased energy use in the agriculture sector, including efforts to conserve water and energy, following the example of urban agencies that universally follow a set of BMPs in managing their systems. For example, some irrigation districts have signed on to a program sponsored by DWR that requires implementation of Efficient Water Management Practices (EWMPs) that address energy management (Efficient Water Management Practices by Agricultural Water Suppliers in California, Memorandum of Understanding, January 1, 1999). That effort was prompted by the Agricultural Water Suppliers Efficient Water Management Practices Act of 1990. However, unlike urban water systems where water conservation also brings energy conservation, agricultural water conservation can often lead to increased energy demand. Reuse of tailwater, for example, requires installation of additional pumps, and drip and microspray irrigation need more electricity than other irrigation methods. Some of these uses, however, such as reuse of tailwater, could have the benefit of avoiding long-distance conveyance energy use.

Utilities and agencies are also addressing agricultural energy use through several energy efficiency programs. A good example is the Agricultural Pumping Efficiency Program (APEP), run by the Center for Irrigation Technology, which is part of the California Agricultural Technology Institute at the College of Agricultural Sciences and Technology, California State University, Fresno. The program receives funding from the Public Goods Charge on utility bills and provides free pump efficiency evaluations for farmers and irrigation districts served by the state's three large investor-owned utilities. Since 2002, the program has resulted in at least 15 GWh of savings from approximately 350 pump retrofit/repair projects.[57]

[57] Canessa 2005

Taken together, no definite conclusion can be drawn concerning the future trend of energy use in the agricultural sector. It is necessary to look at all applicable portions of the water use cycle when assessing the net energy impacts. More work is needed.

Changes in Regulation and Legislation

There are a number of regulatory and legislative actions that will impact both energy consumption and energy production by the water sector.

Water Quality Regulations

Energy use for water treatment will increase as more stringent water quality rules are implemented under the federal Safe Drinking Water Act. These new rules require multi-stage disinfection including treating potable water more than once, which ensures removal of harmful organisms that may grow during storage and transport, and improved disinfection technologies that reduce the risk of carcinogens and other potentially harmful disinfection by-products. These improved disinfection technologies – principally, ultraviolet treatment and ozonation[58] – are much more energy intensive than prior chemical methods.

Energy use for wastewater treatment is also expected to increase because of new requirements under the Clean Water Act for treating effluent before discharging it into natural waterways. However, by increasing the quality of wastewater effluent, more recyclable water can be added to the water supply portfolio. Therefore, any increased energy use for wastewater treatment may be accompanied by a decrease from increased use of low energy intensity recycled water that can be used to displace higher energy intensity water supplies.

The actual impact of these new regulations is not yet known, and water agencies are still making decisions as to which treatment processes and technologies to adopt. In addition, the net impacts need to be better understood. However, a 2002 EPRI study estimated that these new water quality rules could increase energy consumption by wastewater treatment facilities by 20 percent between 2000-2005 and another 20 percent between 2006 and 2050.[59]

FERC Relicensing

FERC licenses 119 hydropower projects in California representing 11,930 MW, or 85 percent of the state's hydroelectric capacity. Thirty-seven percent of the state's entire hydropower system, totaling 5,000 MW, will be relicensed by 2015.

[58] Ozonation requires about twice the amount of electricity used by chloramination to disinfect the same quantity of water. In addition, the requirement for multi-stage disinfection increases the number of processes and overall electricity use.

[59] *Water & Sustainability* (Volume 4): *U.S. Electricity Consumption for Water Supply & Treatment – The Next Half Century*, EPRI, March 2002.

Typically, the FERC relicensing process results in increased requirements for in-stream flows. This has the result of decreasing overall hydroelectric generation. The National Hydropower Association reported a decrease of about 8 percent on average for the nation as a whole. The California experience has been less – a loss of about 2 percent in in-state hydroelectric energy production to date. An odd twist is that hydroelectric capacity actually tends to increase during FERC relicensing, as old units are either repowered or replaced.

In its *2003 Integrated Energy Policy Report*, the Energy Commission reported findings from analyses of six projects being relicensed. The analyses included studies of changes in energy capacity and production from the perspective of statewide and regional electricity supply adequacy and the reliability and cost of replacement power that would result if the proposals were implemented. The study concluded that combined annual energy production losses from relicensing would represent approximately 1 percent of the state's total annual hydroelectric production. The study concludes that "Specific decommissioning proposals would need to be fully evaluated on a case-by-case basis to identify potential local area reliability effects."[60]

Both the Energy Commission's *2003 IEPR* and staff's *California Hydropower System*: *Energy and Environment* provide key findings, as of October 2003, with respect to the potential energy and environmental impacts of FERC hydroelectric relicensing.

[60] California Energy Commission, *2003 Environmental Performance Report*. Appendix D, *California Hydropower System: Energy and Environment*, Sacramento, CA. 100-03-018, March 2003, p. D-4.

2005 Energy Policy Act

The 2005 Energy Policy Act (EPAct) recently signed into law by President Bush contains significant provisions that could affect both water-related energy use and production.

Water-Energy Relationship

- Funding for research, development, demonstration, and commercial applications to address water-energy issues including energy-related issues in optimal management and efficient use of water, and water-related issues in optimal management and efficient use of energy [Section 979].

Hydropower Incentives

- Ten-year production incentive payments for hydroelectric power from generation additions to existing dams or conduits completed within the next 10 years, limited to $750,000/year per facility [Section 242].

- Incentive payments for up to 10 percent of capital improvement costs for hydroelectric facilities that increase efficiency by more than 3 percent, not to exceed $750,000 per facility [Section 243].

- Inclusion of qualifying hydropower production (due to efficiency gains or capacity expansions placed in service after the date of the Act and before 2008) for Section 45 tax credits [Section 1301].

Other Renewable Energy Technology Development & Incentives

- Funding of more than $2.2 billion for fiscal years 2007-2009 for research, development, demonstration, and commercial application on renewable energy issues, including efficiency, cost and diversity, addressing a variety of renewable energy technologies (solar, wind, geothermal, hydropower, and other technologies) [Section 931].

- Funding of more than $750 million for fiscal years 2007-2009 to support a program of research, development, demonstration, and commercial applications for distributed energy resources and systems reliability and efficiency [Section 921].

- Funding for a State Technologies Advancement Collaborative (STAC) to research, develop, demonstrate, and deploy technologies where there is a common federal and state renewable energy interest [Section 127].

- Extension of in-service date deadlines to October 1, 2016, for facilities to receive renewable production incentive payments for solar, wind, biomass,

geothermal, plus the addition of landfill gas, livestock methane, and ocean-related energy resources [Section 202].

- Extension of in-service date deadlines for two years, to December 31, 2007, for renewable energy production tax credits under Section 45 of the Internal Revenue Code of 1986 for qualifying facilities: wind, closed and open-loop biomass, geothermal, small irrigation power, landfill gas, and trash combustion [Section 1301].

- An increase in the Business Solar Investment Tax Credit, from 10 percent to 30 percent [Section 1337].

- Amendment of the Public Utilities Regulatory Policy Act (PURPA) of 1978 to add the requirement that each electric utility shall make available to any electric consumer a net-metering service relative to an eligible on-site generating facility [Section 1251].

Where significant tax incentives exist, there is the opportunity to develop public-private partnerships that bring private investment to help develop renewable energy resources. The impacts of the 2005 EPAct on renewable energy development of water and wastewater utilities' resources and assets cannot be determined.

Changes in Water and Energy Markets

Changes in both water and energy markets have potential to impact energy consumption and production by the water sector. For both, the primary driver of change is economics.

Water Markets

California's water markets are changing. The ability to sell water under some circumstances without losing water rights will likely increase transactions. The provisions of the Colorado River Quantification Settlement Agreement are driving Southern California water utilities to make changes in their water supply portfolios. Further, changes in the mix of crops being planted in California and economic pressures to convert agricultural land to urban use will affect water-related energy consumption.

As discussed previously, because the wide variety of potential transactions, it is difficult to project the net impacts of water market transactions on future energy use. Not all water transactions result in more transported water. Transactions often involve exchanges of water rights among multiple interconnected parties that merely allow the downstream purchaser to take more water from existing sources for a price that compensates each party involved in the transaction. The transaction can sometimes result in a net energy benefit, especially when reducing SWP or other energy intensive imports.

Energy Markets

The 2005 Energy Policy Act will certainly have an impact on the pace and types of renewable energy development. In addition, other impacts - natural gas and diesel price volatility, the impact of competition for renewables to meet RPS goals, and the cost of bundled versus unbundled delivered energy to various load centers - will all affect how agriculture and water and wastewater utilities use energy.

One example is the agricultural pumping switch from diesel to electric. Thousands of diesel-powered pumps are now operating in the Central Valley. With diesel prices soaring and air quality rules tightening, farmers are being encouraged to consider switching back to electric motors. ITRC estimates that converting all of those diesel engine pumps back to electric would increase energy consumption by 1,131 GWh (ITRC 2003). On August 1, 2005, both PG&E and SCE's "AGICE" (Agricultural Internal Combustion Engine) incentive programs went into effect. They are available to owners of pumps of 50 horsepower and above, provide a 20 percent discount over other agriculture rates, increase at 1.5 percent per year until eliminated, and offer an environmental adder that will reduce the costs to the customer of extending distribution lines to the pump. PG&E's program is capped at $27.5 million per year in total incentives, including discounts and environmental adders.[61] SCE's program is capped at $9.2 million. In the PG&E territory, it is possible that 200-300 MW of new coincident peak will be added to its system during the course of the two-year open enrollment period.[62].

Hydrology

There are two primary types of hydrological conditions that could affect both energy consumption and energy production by water and wastewater utilities: drought and climate change.

Drought

Changes in hydrology significantly affect the availability of water supplies and water use from year to year. The worst case scenario, from both a water supply and energy perspective, is a multi-year drought. During past droughts, surface water deliveries dropped in some places to less than half of average year deliveries, forcing water users to rely much more on groundwater pumping and emergency conservation measures.

During prolonged droughts, certain types of electricity use increase. For example, when surface water supplies are low, more groundwater is pumped. During

[61] Mayers, 2005
[62] Keith Coyne, PG&E, August 4, 2005

sequential dry years, water must be pumped from even greater depths as aquifer levels fall. Periods of drought also significantly increase pumping from existing and future conjunctive use field, as agencies tap emergency water supplies. An extended multi-year drought could also spark the rapid development of additional desalination facilities.

Estimating the water-related energy impact of a multi-year drought, however, is more complicated than simply adding up projected increases of energy consumption. During droughts, water shortage policies and plans place limits on water use by various market sectors and customer groups to allocate limited supplies. In addition, SWP and other large water systems will not have as much water to pump. The combination of these impacts would need to be netted out against incremental energy consumption for water supplies - like groundwater pumping and desalination - to understand the true energy impacts.

In evaluating water-related energy consumption from prior years, staff has been unable to find data that definitively support the premise that water-related energy consumption increases during dry years. In general, staff can say that an increase in water-related consumption and a decrease in energy supply are likely during a dry year. However, water industry experts are divided as to whether there is a net positive or net negative impact in energy consumption during a prolonged multi-year drought where serious reductions in water storage could trigger mandatory water use reductions.

Climate Change

A change in the patterns of rain and snow could have significant effects on both electricity production and consumption. Climate change scenarios show that global warming trends may result in more rain, but less snow. As a result, even when total precipitation is near normal levels, spring runoff will likely occur earlier in the year, resulting in early "spills"[63].

The Energy Commission has already conducted substantial research into the effects of climate change and is taking a lead role for the state in developing strategies to reduce greenhouse gas emissions. These efforts, as well as other statewide studies, were summarized in two recent Energy Commission reports prepared in support of the *2005 Integrated Energy Policy Report*. The first report, *Climate Change Impacts and Adaptation in California,* summarizes available scientific literature and provides a brief overview of the research agenda. The second report, *Global Climate Change*, provides background and context to guide the formulation of policy options for reducing greenhouse gas emissions in California.

[63] Overfilling of reservoirs in spring months, with spills bypassing turbines and reducing energy production and sometimes, also reducing summer peaking capacity.

A third report, *Potential Changes in Hydropower Production from Global Climate Change in California and the Western United States,* evaluated the potential effects of climate change on hydropower operations and production. This study included the following findings and recommendations:

- Climate change studies to date have depended upon broad trend analyses and are not yet useful in predicting impacts at the local watershed level.

- California is experiencing a warming trend. This could precipitate earlier snowmelts, reduce summer hydropower production and capacity, and increase summer air-conditioning loads.

- Although more work is needed to predict local impacts, warmer temperatures could cause earlier snowmelts, reducing stored water supplies.

Reduction of stored water has several potentially adverse impacts:

- Less availability of surface water supplies (which could lead to increased use of more energy intensive supplies).

- Less hydropower peaking capacity.

- Lower head (reducing hydropower energy production as well).

Clearly, climate change impacts will need to be studied over many years before the true net impacts on both energy consumption and energy production can be accurately measured.

Technology

Changes in technology could change energy consumption and energy production, though the net impact of such changes is undeterminable. Below are some examples of potential changes in technologies that could affect water-related energy consumption or energy production:

- In addition to continually seeking more efficient water and energy systems and processes (e.g., desalination and disinfection technologies), research continues into streamlining system processes and plant designs.

- In addition, research continues into improving the efficiency of pumps, motors, and equipment to reduce energy consumption and increase operating flexibility to shift loads off-peak.

- Specific research into modifying the reverse osmosis process used in desalination to reduce energy requirements is occurring in multiple forums.

- New technologies are improving the design of turbine runners, making it possible to increase both capacity and output of existing hydropower systems through retrofits. In addition, research continues into developing packaged systems that can be dropped into existing pipelines without need for costly civil works and low head turbine technologies.

- Automated controls technologies also optimize water releases to better balance hydropower production with water supplies and electric loads, and allow more efficient pumping in water and wastewater treatment plants.

The American Water Works Association Research Foundation (Awwa-RF) and PIER are already collaborating on a portfolio of research and development projects related to the interdependencies of water and power.

Policies

Several policies have been adopted for both the water and energy sectors. Policies to reduce water and energy consumption will certainly impact both the water and energy sectors, but the net energy benefits may differ. Energy demand could go up as a result of water decisions. Ultimately, it matters tremendously what policy options are implemented and how well these policies are coordinated for mutual water and energy benefits. Thoughtful policies can mitigate the potential adverse impacts of water decisions on energy resources and infrastructure.

Conclusions

The common theme of all of these potential changes is that there are both threats and opportunities. In order to better understand these and develop plans and measures that leverage opportunities and mitigate threats, more information is needed by water and energy policymakers and implementing entities. Ultimately, the *net* energy impacts of various water policies and strategies need to be well understood in order to tailor effective mitigation measures.

CHAPTER 7 – STAFF RECOMMENDATIONS

Findings

During these proceedings, state and federal agencies, water and energy utilities, industry associations, research organizations, and a wide variety of other stakeholders came together to consider the state's water-energy relationship and what it means to the state's energy resources and infrastructure. While acknowledging there is much yet to be learned about the nature and extent of the state's water-energy relationships, some things are clear.

- The relationship between the water sector and the energy sector is complex and highly interdependent.

  - ✓ In-state hydroelectric power generation in 2004 accounted for approximately 11 percent of the state's in-state energy resources. When hydropower imports from the Pacific Northwest and the Desert Southwest are included, hydropower accounted for as much as 15 percent of the state's energy in 2004.

  - ✓ The water sector is the largest consumer of energy in California, estimated to account for 19 percent of total electricity and 32 percent of total natural gas consumed in the state.

- Saving a unit of water reduces the amount of energy used to collect, treat, deliver it, consume it, treat it, and dispose of it as wastewater. If used elsewhere, this saved water may displace the need to develop new, more costly water sources.

  - ✓ With few exceptions, the avoided energy value embedded in a unit of water throughout the applicable portion of the water use cycle is not accounted for by either water or energy utilities.

  - ✓ Presently, the magnitude of this total energy savings cannot be fully calculated, though sufficient information exists to compute a proxy to support near-term programs.

  - ✓ The state's current energy programs (codes and standards, incentives, and rebates) focus on energy saved at a single location from increasing water and process heating efficiency – not on energy that can be saved from reductions in water use. Not including cold water savings misses significant energy savings opportunities upstream in the water use cycle.

  - ✓ There are significant differences in the energy intensity of the water use cycle between Northern and Southern California because of differences in the energy intensity of water supply portfolios that are heavily dependent on imported resources.

- ✓ Options for new water resources in the future are limited. The least energy intensive option for future supplies is water use efficiency. The most energy intensive option is ocean water desalination.

- ✓ Water that is not consumed generally becomes available to offset highest marginal cost supplies.

- Modifications to the operations or design of the water system infrastructure present opportunities to reduce water system peak electric demand.

  - ✓ Some existing surface storage facilities can be modified to maximize generation opportunities and increase operational (peaking, load following) flexibility.

  - ✓ Many existing and most new water and wastewater treatment plants can be designed to detain water for treatment during off-peak hours.

  - ✓ Increased conjunctive use programs may allow for greater ability to shift energy demand seasonally.

- Currently, most water and energy systems are internally optimized on a single utility basis. Systems are rarely optimized in coordination with other systems (water, wastewater, electric and natural gas) or with their customers, missing opportunities to reduce total energy consumption, shift loads off-peak, or maximize energy generation.

- Opportunities within a utility system to develop additional generation resources (in-conduit hydroelectric generation, biogas combustion, and other renewable development) exist. However, significant barriers frustrate development of these resources.

- Energy demand in the water sector will likely increase over time due to a number of factors, including population and urban load growth, increased water and wastewater treatment because of more stringent water quality regulations to protect water quality, and market, economic, regulatory, and legislative changes.

- Several actions can be taken now to significantly reduce energy demand throughout the water use cycle and slow its future growth. This is particularly true in areas, like Southern California, which have tight energy supplies and constrained transmission systems.

The state's water and energy utilities separately seek to optimize their respective water and energy resources within their own portfolios. There are strong similarities between their IRP goals, methods and techniques. However, in developing its water resource strategy, DWR did not synchronize its water resource planning goals and

objectives with those of the Energy Commission to assure, for example, that local energy supplies and infrastructure can support greater desalination production. Where seawater desalination plants may be planned at points downstream of electric transmission congestion zones, the energy solution may be to build new generation in combination with the desalination plant. Another solution may be joint water and energy investments in recycled water infrastructure processing that could displace the need to build desalination facilities in the first place. This is one example of the types of water and energy tradeoffs that should be examined.

The most significant finding of this paper is that the greatest potential for positively impacting the state's energy circumstance is beyond current water and energy best practices. The opportunity is fortuitous, and the need is great. To accomplish mutually beneficial results will require increased coordination between programs and agencies, as well as a more complete understanding of the needs of both systems and customers. At a minimum, the state's future water plans should be coordinated with the state's energy management plans to both identify and reconcile potential areas of conflict and take advantage of points of synergy. Optimizing the systems and operations of both water and energy utilities throughout the state on a holistic societal value basis will provide the greatest net benefits.

Staff Recommendations

Based on the findings in this analysis, staff recommends an action-oriented approach that is structured to attain near- and long-term results. This approach should include policy integration that seeks to optimize the mutual and synergistic benefits of the water and energy systems and resources. A key aspect of this approach is the development and implementation of a comprehensive, statewide water-energy program that integrates water and energy resource planning and management. The following essential elements have been identified for a successful program.

1. Save energy by saving water.
2. Reduce water system net power requirements.

Importantly, while this is a significant undertaking, near-term benefits could be attained while longer-term plans and studies begin at the same time.

Save energy by saving water

Even though water efficiency programs and conservation efforts exist in the state, there are many missed opportunities to save energy and manage load. These include energy savings throughout the water use cycle through water use efficiency; changes in systems and operations to reduce peak time-of-use and seasonal demands; and changes in water management to reduce use of the highest energy intensive supplies. This is particularly unfortunate in areas where energy resources

are tight or peak energy demand is a problem. In fact, since load growth is the primary stressor of both water and energy resources, those areas that are shortest in water supplies are also energy constrained, making it even more crucial that the state's water and energy resources be managed on an integrated basis.

Staff concludes that the state could achieve nearly all of its energy and demand reduction goals for the 2006-2008 program period by simply allowing energy utilities to realize the value of energy saved for each unit of water saved. In that manner, energy utilities can co-invest in water use reduction programs, supplementing water utilities' efforts to meet as much load growth as possible through water efficiency. Remarkably, staff's initial assessment indicates that this benefit could be attained at less than half the cost to electric ratepayers for traditional energy efficiency measures. Staff should work with the CPUC and the energy and water utilities to evaluate the achievable savings and implementation strategies.

Staff therefore recommends that the state pursue policy options that achieve greater energy efficiency and saving through a more aggressive and comprehensive statewide water efficiency program. This program should target both site-specific efficiencies and actions that will result in net system energy savings. These actions could be a key part of the utility energy efficiency portfolios that accomplish savings needed to meet the CPUC's goals. Key elements of such a program include:

- Allowing energy utilities to count energy savings related not only to those achieved on site, but, where appropriate, those that can be identified throughout applicable portions of the water use cycle.

- Working with the Task Force, CPUC, DWR, and other stakeholders, refine data related to energy use and generation associated with the various parts of the water use cycle for use in accounting for the net energy impacts of this system and in calculating the effects of various programs designed to attain synergistic benefits.

- Target end user water efficiency measures that result in net energy savings – both on premises and in the water use cycle. For example, in addition to programs that save hot water, include programs that seek to maximize cold water savings in homes and businesses and count the net energy benefits attributable to a unit of avoided water consumption embedded in the entire water use cycle.

- Establish a collaborative with DWR, the CPUC, and the Energy Commission to achieve the state's least energy resource intensive water future by 2030. Align programs and policies to complement one another and remove barriers to mutually beneficial results.

- Invest in research that develops more water and energy efficient appliances, processes, designs, demand side management methods and technologies, and treatment systems.

- Establish a water resource loading order that incorporates the societal value of an avoided unit of water consumption that mirrors the preferred energy resource loading order in the *2005 Energy Report* and the Joint Agency *Energy Action Plan*.

- Establish a public goods charge equivalent for public purpose water conservation and efficiency programs that attain targeted net energy benefits.

- Require the state's energy and water planners to collaborate on plans and strategies to reduce net water sector energy consumption while meeting projected water and energy load growth with environmentally preferred resources and strategies.

- Commit public goods charge funds for expanded water efficiency programs and innovative technology development to reduce the net energy demand of the water use cycle in current 2006-2008 IOU energy efficiency portfolios.

Reduce water system net power requirements

The state should adopt a comprehensive policy to facilitate water and wastewater utility energy self-sufficiency by reducing water system net power requirements. This policy should include reducing operational energy requirements, shifting loads off-peak, and increasing energy generation from water- and wastewater-related resources and renewable opportunities. Implementing this policy is consistent with the objectives of the *2005 Energy Report* and the *Energy Action Plan* loading order and helps achieve the state's RPS goals.

- Develop cost-effective, environmentally preferred in-conduit, biogas and other renewable options for water and wastewater systems. To accomplish this, the Energy Commission should facilitate greater participation of water utilities in its loan and rebate programs by targeting planned retrofits at existing facilities and providing design assistance for planned facilities.

- Remove barriers to energy self-sufficiency by allowing water and wastewater utilities to self-generate power and provide this power to themselves anywhere on their systems; expedite and reduce costs of interconnections; eliminate economic penalties such as prohibitive standby charges; and remove caps on size of facilities eligible for net metering.

- Identify and implement retrofits in the water system that attain energy benefits, including but not limited to treatment system upgrades, turbine and pump replacements, and delivery system modifications.

- Require water and wastewater utilities to assess the energy impacts attributable to new or changed infrastructure and operations and evaluate feasible alternatives to reduce overall energy demand associated with these decisions.

- Provide incentives for incremental and/or joint infrastructure improvements that reduce total and peak energy requirements for water and wastewater conveyance and treatment.

- Facilitate collaboration among water and energy utilities and other local and state entities for the joint development of resources and infrastructure to further leverage benefits of their combined assets.

- Provide incentives for water, wastewater and energy utilities to optimize their joint resources beyond traditional discrete single utility service boundaries - water, wastewater, electricity, and natural gas.

In developing this report, Energy Commission staff established the Water Energy Relationship Working Group, which helped identify issues, evaluate possible resolution of those issues, and provide input on future policy options. This group demonstrated the need for the committed involvement of key stakeholders and an ongoing dialogue about the water-energy relationship. This cooperation and communication are vital to achieving the mutually synergistic benefits of water and energy systems.

Recommended Joint Actions

The Energy Commission, the DWR, the CPUC, the Air Resources Board, the State Water Resources Control Board, and the California Department of Health Services, should:

- Establish a valuation methodology for the water use cycle that accounts for embedded energy and externalities. This methodology is needed to capture these diversities in a manner that would assist planners in prioritizing their investments.

  - ✓ Incorporate a societal valuation approach in both water and energy utilities' resource pricing methodologies, water and energy efficiency program portfolios, and investment criteria.

  - ✓ To facilitate early results, establish a proxy for the societal value while a detailed methodology is being developed.

- Seek opportunities for joint investment that could produce incremental energy benefits but are not deemed cost-effective on a single-utility resource cost test.

- Leverage work already in progress by others, including the U.S. Department of Energy National Laboratories' Water-Energy Nexus Program, Pacific Institute, California Urban Water Conservation Council, and the Irrigation Training and Research Center. Work closely with these (and other) entities to:

  - ✓ Inventory, characterize, and measure California's water and energy interdependencies.

  - ✓ Develop pilot programs to test tools and methodologies for evaluating tradeoffs among these interdependencies.

  - ✓ Develop analytical models and tools for policymakers, regulators, utilities and other key stakeholders to use in developing cost-effective joint water and energy programs.

  - ✓ Research opportunities and technologies that improve the energy performance of the water use cycle and increase the generation capabilities of the water system.

Conclusion

While all of the nuances are not yet understood, it is clear that significant energy benefits are attainable through water use-efficiency and through increased energy efficiency in the water use-cycle. It is also clear that not nearly enough has been done to make sure that California's water supply strategies are synchronized with its energy strategies. Nor has enough been done to forge partnerships between the water and energy sectors and leverage the natural synergies of their joint resources and assets for the benefit of all Californians.

The state has the timely opportunity to reap near-term energy savings benefits by helping California's agricultural industry and water and wastewater utilities become more energy efficient. The CPUC could direct IOUs to invest current PGC funds for 2006-2008 energy efficiency programs in existing water infrastructure to improve operations, switch operations off-peak, and partially fund retrofits of equipment such as pumps and treatment equipment. These funds could also be used in conjunction with water conservation dollars to leverage greater water end use efficiency to realize net energy savings in the water use cycle. In addition, near-term actions could include minor adjustments to existing policies, programs, and market rules, to facilitate renewable and distributed generation development at water and wastewater facilities as well as agricultural resources to convert them from high energy users to net renewable energy producers.

For the long-term, California's water and energy policymakers need to commit today to joint planning and management of these critical resources. Conflicting policies and objectives need to be identified and conflicts resolved. Water resource plans need to include an accounting of energy impacts and evaluate alternatives to decrease

overall energy demand of water systems. The state's energy resource portfolio needs to consider and facilitate the development of all cost-effective and environmentally preferred water system related options. Water and energy agencies and utilities need to work together to identify mutually beneficial research and develop opportunities that the state can pursue to improve both systems, followed with market transformation strategies to accelerate adoption of resource efficient behavior. To achieve mutually synergistic benefits in the water and energy sector, policymakers, agencies, and utilities will need to work together and make long-term commitments of funds and programs.

APPENDICES

APPENDIX A: EXISTING ORGANIZATIONS, PROGRAMS, AND RESEARCH

The California Water Plan

The Department of Water Resources (DWR) is responsible for updating the *California Water Plan (Plan)*, which provides a framework for water managers, legislators, and the public to consider options and make decisions regarding California's water future. The *Plan*, which is updated every five years, presents basic data and information on California's water resources, including water supply evaluations and assessments of agricultural, urban, and environmental water uses to quantify the gap between water supplies and uses. The *Plan* also identifies and evaluates existing and proposed statewide demand management and water supply augmentation programs and projects to address the state's water needs. Often referred to as Bulletin 160, the most recent version is scheduled to be published in late 2005.

DWR is also responsible for managing the State Water Project, including the California Aqueduct, and managing the contracts for electricity created following the 2000-2001 energy crisis. The department also provides dam safety and flood control services, assists local water districts in water management, conservation, recycling and desalination activities, and promotes recreational opportunities.

Energy Use in the Water Cycle

Energy is used in every phase of water use within the state, from extraction through conveyance, treatment, use, and disposal. The Energy Commission has funded several projects to define this interaction between water and energy.

Electricity and Water Flows with California
The purpose of this project, conducted by the University of California, Santa Barbara and the Pacific Institute, is to identify the flows of both water and energy within California. This includes water for electricity generation (hydropower) and all of the electricity used for water – from initial diversion or extraction through conveyance, treatment, use, and disposal. This project will increase understanding of the electricity demand for different water uses within the residential, commercial, and industrial sectors. It will also further understanding of the energy intensity of the water cycle. The results of this study will help focus future water conservation programs where they will make the greatest impact on energy (PIER Environmental[64]).

[64] The names in parentheses at the end of the paragraphs identify the group within the Energy Commission that is responsible for the activity described in the paragraph.

Groundwater and Surface Water Management and Electricity Demand
Conjunctive use of surface and groundwater supplies is increasingly relied upon as a water management tool. Concern about a significant increase in conjunctive use and its associated electricity demand, particularly under drought conditions, is a major concern. Conducted by Lawrence Berkeley National Laboratory (LBNL), the aim of this project is to see how surface and groundwater supplies will be managed under different climatic conditions, and what the consequences would be for electricity demand and prices. It is important to consider not only the likely impact of new conjunctive use programs on regional electricity demands, but also how reservoir management will affect water supply for agriculture and municipal uses and electricity generation and demand. (PIER Environmental).

The U.S. Department of Energy's Energy-Water Nexus Team

In partial response to an identified gap in federal jurisdiction at the nexus of energy and water, the Energy Policy Act of 2003[65] directed the U.S. DOE to:

- Assess future water needs for energy, future energy for water purification and treatment, use of impaired water by energy, and technology for water use efficiency.

- Develop a program plan that incorporates scientific and technology requirements, decision tools, demonstration projects, and information transfer.

Eleven national laboratories and EPRI came together to form the federal Energy-Water Nexus Team (Team), which is charged with developing technology products that will help increase the nation's energy security. The scope of the Team's investigations is very broad:

- Energy versus water tradeoffs in optimizing hydropower and the implications of those tradeoffs on energy supply risk.

- Energy usage by water-related systems and processes (including municipal water, wastewater, and industry).

- Water used to produce energy, such as hydropower and water for cooling.

[65] Section 961, Subtitle (f) *Water and Energy Sustainability Program*.

- Development of tools, including benchmarking, and opportunities to improve efficiency both through more efficient energy consumption and redesigning processes, systems, and operations.

- Financial and economic analyses of markets and participants, including impacts on equipment manufacturers and utilities.

- Environmental impacts, including the economic impacts of hydrology and climate factors, relationships, impacts, and interdependencies.

Presently, the Team is undertaking a road-mapping process for the US DOE, viewed primarily from the perspective of water used for energy and energy used for water - particularly with respect to the research and development of new technologies to improve water and/or energy use and efficiency.

The Ernest Orlando Lawrence Berkeley National Laboratory and the Lawrence Livermore National Laboratory are participating in the Energy Commission's Water Energy Relationship Working Group and can help merge efforts undertaken by the state and the federal government.

The ***2005 Energy Policy Act*** (EPAct) expanded the scope of US DOE's studies on the water-energy nexus.

Water and Wastewater Facilities

Energy consumption is a significant cost component of providing water and wastewater services to the public. The Energy Commission is dedicated to providing resources to help water professionals reduce these costs through implementation of energy efficiency measures at their facilities.

AB 970 – Peak Load Reduction at Water and Wastewater Facilities
At the peak of the 2000-2001 energy crisis, AB 970 provided $4.5 million in grant funding to reduce 52.1 MW of peak electrical load at water and wastewater facilities in four categories: curtailment, efficiency, generation, and load shifting. The grants ranged from $9,000 to $486,000, with an average amount of roughly $110,000 per project, at a rate of $300 per peak kW reduction. This program has been completed (Energy Efficiency Division).

SB 5X – Water Agency Generation Retrofit Program
The program started in May 2001 and was completed in December 2003. Projects were funded in two categories - distributed generation and energy efficiency - with a total on-peak load reduction capacity of 17.7 MW. Of this capacity, distributed generation retrofits provided up to 9.2 MW of on-peak load reduction, while energy efficiency projects provided up to 8.5 MW of load reduction. Twenty-eight qualified applicants received $4.35 million from this

program. The program paid distributed generation participants an average of $259/kW for projects with a combined construction cost of $7,205,488. Energy efficiency participants received an average of $230/kW for their projects, which cost $6,598,108 to install. Overall, the program averaged $245/kW of electrical load reduction (Energy Efficiency Division).

Flex-Your-Power's Water and Wastewater Guide: Reduce Energy Use in Water and Wastewater Facilities Through Conservation and Efficiency Measures

In response to the 2000-2001 energy crisis, the state's Flex-Your-Power program worked with hundreds of California water and wastewater agencies to develop measures to reduce energy consumption by 15 percent within their systems and facilities, for the purpose of both reducing power costs and alleviating the risk of rotating outages. A four-step process was developed to increase energy self-sufficiency through a combination of on-site power production, total energy consumption reductions through energy efficiency measures and retrofits, and peak shifting to partial- and off-peak periods wherever possible.

Energy Partnership Program

This program provides customized technical assistance to water and wastewater facilities to identify energy efficiency projects, project costs, and associated savings. Consultants are paid up to $20,000 for a detailed study of the facilities. Approximately $260,000 have been paid so far to consultants for feasibility studies, comprehensive energy audits, reviews of energy projects proposals, identifying cost-effective energy-saving measures, review of specifications for energy efficient equipment, and assistance in selecting contractors and design professionals for the water and wastewater facilities that have participated in this program (Energy Efficiency Division).

Energy Efficiency Financing Program

Energy Efficiency Financing Program: The Energy Commission provides low-interest rate loans to fund up to 100 percent of the cost of energy efficiency and self-generation projects. Loans are provided on a first-come, first-served basis. Eligible projects must have an average simple payback of less than 9.8 years. If projects have a greater simple payback, the Energy Commission can provide a loan equal to 9.8 times the annual energy cost savings. Eligible projects include pumps and motors, variable frequency drives, lighting, building insulation, HVAC modifications, automated energy management systems, automated energy management controls, energy generation, streetlights and light emitting diode (LED) signals. The Energy Commission has provided more than $11.2 million in loans for projects associated with both improving the energy efficiency of water and wastewater facilities and reducing the energy costs of these facilities. These projects have saved public facilities about $1.9 million annually in lower energy bills. This is

equivalent to saving 23 million kWh annually, with billing demand savings of about 2.3 MW (Energy Efficiency Division).

Development of a Water and Wastewater Industry Energy Efficiency Roadmap

The Energy Commission collaborated with the American Water Works Association Research Foundation (AwwaRF) {Note: Thought I'd flag this since lower-case letters are so rare in acronyms – is this correct?] to develop a roadmap to fund the highest priority research and development energy needs of California's water and wastewater utilities. To achieve this, the Commission and AwwaRF in February 2003 conducted a workshop that was attended by water experts from water and wastewater facilities, electric utilities, academia, researchers, and consultants. More than 44 projects in eight research areas were developed and ranked according to their savings potential (in either kilowatts or dollars), likelihood of success, and timeliness. The Energy Commission and AwwaRF committed to more than $2 million in funding for the five highest-ranked projects. These projects are:

Development of a Utility Energy Index to Assist in Benchmarking of Energy Management for Water and Wastewater Utilities

The objective of this project is to produce industrywide energy performance metrics to describe the performance of water and wastewater utilities that will subsequently be incorporated within a comparison framework (benchmarking tool) to facilitate internal and external comparisons within and between utilities. The approach will be similar to the US EPA's **Energy Star®** program, which makes energy performance comparisons in commercial buildings (PIER Industry, Agriculture and Water).

Zero Liquid Discharge and Volume Minimization for Inland Desalination

This project is discussed in the section on desalination (PIER Industry, Agriculture and Water).

Assessing Risks and Benefits of Drinking Water Utility Energy Management Practices

The project will develop a decision framework based on risk management principles for water utilities implementing energy management strategies. The risks and benefits of a broad array of both supply-side and demand-side energy management options will be assessed. The decision framework will provide a management tool for water utilities to mitigate possible downsides to water quality and reliability when implementing energy management practices or technologies (PIER Industry, Agriculture and Water).

Water Consumption Forecasting to Improve Energy Efficiency of Pumping Operations

The purpose of this project is to provide the best options for short-term water consumption forecasting for water utilities. Short-term consumption forecasting (SCTF) is required for water utilities to proactively optimize both their pumping and treatment operations and water supply and treatment costs while maintaining a reliable and high-quality product for their customers. The project will provide information on various techniques, performance data, benchmarks, selection criteria, and functional requirements to help utilities evaluate and select the best forecasting techniques. The project will examine different forecasting methods currently used at public utilities. These forecasting methods will be tested at utilities that are not currently forecasting their water consumption, and the results will be documented. The SCTF performance data will be analyzed for all seasons of the year to provide peak, off-peak, and average-day consumption data (PIER Industry, Agriculture and Water).

Evaluation of the Dynamic Energy Consumption of Advanced Water and Wastewater Treatment Technologies

The objectives of this project are to quantify the actual and theoretical energy consumption of selected water and wastewater advanced treatment unit operations, evaluate the factors that affect energy consumption, and identify energy optimization opportunities while still maintaining treatment performance (PIER Industry, Agriculture and Water).

Future Projects in Collaboration with AwwaRF

Five more projects from the roadmap are being considered for future funding by the Energy Commission and AwwaRF.

1. Review of international desalination research. The product would be a searchable CD ROM database similar to Desal Net, owned by AWWA (not AwwaRF). Desal Net is a searchable CD ROM database for the U.S.
2. Energy consumption of ultraviolet and chlorine/hypochlorite disinfection.
3. UV disinfection: Develop next generation of energy efficient UV disinfection systems for water and wastewater treatment.
4. Development of a guidance manual to design and operate desalination facilities for maximum energy efficiency.
5. Identification and evaluation of innovative water treatment processes.

Agricultural Water

Energy consumption is a significant cost component of providing water to the agricultural industry. State and IOU ratepayer funds, administered by the Energy Commission, CalPoly San Luis Obispo, and Fresno State University have delivered energy efficiency and water conservation programs aimed at conservation and peak load reduction in agriculture. Programs include:

SB 5X –Agricultural Peak Load Reduction Program

- The program started on June 1, 2001, and was completed on December 31, 2004. The program components related to electricity used for water purposes, include:
- 1. The development and implementation of a pump test and repair program to improve pumping plant efficiencies.
- 2. Funding projects with irrigation districts and large farming companies to participate in demand response and TOU schedules. Over 60 MW of on-peak load reduction was achieved. Thousands of pump tests were performed and many of the tested pumps were repaired to achieve even higher efficiencies (Nexant, M&V report for California Energy Commission Agricultural Peak Load Reduction Program, 2003). More than $7 million were dedicated to water-related energy projects.

CPUC- Public Goods Charge (PGC)-Third-Party Administrator for Pump Test and Repair Program

The program, administered by the Fresno State University Center for Irrigation Technology, delivers pump test services to customers in the PG&E and SDG&E service territories. The pump tests are conducted by private sector providers that have enhanced the quality and standards of properly conducted pump test results for several years. The program also provides pump repair incentive payments. The educational component is a valuable tool for communicating efficiency principles and water conservation practices to farmers. A $5 million annual appropriation from the CPUC has funded this effort to date.

Development of an Agricultural Water Energy Efficiency Roadmap

The Energy Commission's PIER Agricultural Program Technology Roadmap was accomplished in collaboration with CalPoly San Luis Obispo, Fresno State University, the University of California Cooperative Extension Program, industry associations, farmers, and irrigation district managers. The roadmap document calls for research and development efforts that improve irrigation efficiency, create flexible water delivery systems, and achieve peak load reduction. Possible research, development, and demonstration projects include reducing the total pressure required to operate drip irrigation technologies (including the filter system as well as the pipe and micro-sprayer

technologies), advancing the use of longer-lasting materials for pump components, and working with the State Water Project, the Central Valley Project, and the irrigation districts to increase the flexibility of water deliveries to farms. Additional information is available at: [http://energy.ca.gov/2005publications/CEC-400-2005-002/CEC-400-2005-002.PDF].

PIER Agriculture Energy End Use Efficiency

The purpose of this contract is to improve the energy efficiency in the transportation, delivery, and utilization of agricultural water provided by irrigation districts. Proposed outcomes include:

1. Documenting the implementation of new technologies.
2. Developing a simple procedure for tuning controller constants for automatic upstream control of canal check structures.
3. Developing new devices resistant to plugging or tangling moss for volumetric metering of delivered water - trash shedding propeller meters.
4. Testing and evaluating new electronic technologies for the volumetric metering of delivered water such as magnetic meters, ultrasonic meters (Doppler), vortex shedding meters, and ultrasonic flow-measurement meters.
5. Developing strategies for energy-efficient transition from low-pressure non-reinforced concrete pipe.
6. Verifying power quality measurement and conditioning methods.
7. Assessing use of variable frequency drives on agricultural pumps.

National Programs

Development of a National Water-Wastewater Industry Energy Roadmap
In order to bring together the energy efficiency and water/wastewater communities to define avenues for increasing energy efficiency in the water and wastewater sectors, the American Council for an Energy Efficient Economy (ACEEE) organized a national road mapping workshop to further explore and plan next steps for greater energy efficiency in the water/wastewater sectors. A workshop was held in Washington, D.C., in July 2004, and a final report is being refined for publication. The Energy Commission was a member of the advisory committee. The advisory committee defined the scope of this effort, developed a mission statement for the project, and established a set of goals. It also assisted ACEEE staff in identifying key issues relating to energy use in the water and wastewater industries. These issues formed the basis for design of a survey instrument that was used to collect impressions of key issues from a wider group of

stakeholders identified by the advisory committee. Based on this research and the goals of the workshop, ACEEE staff and the advisory committee developed an agenda that addressed key topics (Energy Efficiency Division).

National Municipal Water and Wastewater Facility Initiative
In 2002, the Consortium for Energy Efficiency (CEE) formed the Water and Wastewater Exploratory Committee to:

- Serve as a platform for members to exchange program information and resources.
- Better understand the water and wastewater industry - its structure, energy use, decision-making, and regulatory environment.
- Begin outreach efforts to the water and wastewater industry and other industry stakeholders.
- Explore the merits of a national program initiative to improve the effectiveness of local programs serving this sector. This initiative is intended to maintain a sustained focus on facility energy-efficiency at the national and local levels by increasing demand for energy-efficiency products and services within the municipal water and wastewater sector, and by transforming the delivery of products and services to the municipal water and wastewater sector by encouraging industry stakeholders to incorporate energy-efficiency as a standard business practice. The Energy Commission is a founding member of this initiative (Energy Efficiency Division).

US EPA's ENERGY STAR Water and Wastewater Facilities Initiative
ENERGY STAR is a voluntary program that helps organizations, businesses, and individuals protect the environment through superior energy performance. The ENERGY STAR Water and Wastewater Facilities Initiative helps improve energy performance by creating momentum for the continued improvement of energy efficiency by identifying and tackling barriers to energy efficiency in the water and wastewater industry, providing tools and resources to enhance energy performance, uncovering new energy-saving opportunities, and encouraging information-sharing on efficiency in the water and wastewater industry. The Energy Commission is one of the founding members of this initiative. The first Web conference on the Energy Star Water and Wastewater Facilities Initiative was on May 12, 2005 (Energy Efficiency Division).

Water Supply

Desalination
Desalination is one of the sources of new water identified by the Department of Water Resources in the ***2005 Water Plan Update***. It is also the most energy intensive of these new sources. There are several efforts underway to assist in the

development of low-cost, energy-efficient desalination technologies for various source waters using membrane and thermal processes.

Improving Energy Usage, Water Supply Reliability and Water Quality Using Advanced Water Treatment Processes

The Energy Commission and the Metropolitan Water District of Southern California are jointly funding the full-scale demonstration and refinement of newly developed electro-technologies for producing potable and non-potable water. These technologies remove salts and disinfect various source waters, including Colorado River water, brackish groundwater, municipal wastewater, and agricultural drainage water. There are 18 individual projects and eight research partners involved in this research program (PIER Industry, Agriculture and Water).

Zero Liquid Discharge (ZLD) Desalination of Inland Waters

At coastal facilities, concentrate is typically discharged to the ocean. This option is not available at inland facilities, and the need to protect surface water and groundwater sources may preclude disposal into the environment. The alternative is ZLD, in which the concentrate is further treated to produce desalinated water and essentially dry salts. In collaboration with AwwaRF, this research project will develop technologies that reduce the cost and energy consumption for inland desalination (PIER Industry, Agriculture and Water).

West Basin Municipal Water District – Demonstration of a Low Energy Sea Water Reverse Osmosis (SWRO) Desalination

Energy is the single largest cost component of operating seawater desalination systems. The purpose of this project is to demonstrate that SWRO desalination can be performed at 1.6 kWh/m^3 of permeate produced. The project will also establish the relationships between reverse osmosis recovery rate, membrane salt rejection, permeate quality, boron levels, feed pressure, and energy consumption. These relationships will help the SWRO desalination industry establish optimum recovery, flux, and salt rejection rates using today's best-available technologies. This research is being conducted by the West Basin Municipal Water District, in collaboration with the DWR, several local water agencies, and the industry, in collaboration with the Naval Facilities Engineering Service Center's Seawater Desalination Test Facility at Port Hueneme, California (PIER Industry, Agriculture and Water).

California Desalination Task Force

In September 2002, AB 2717 (Hertzberg) was signed into law, directing the DWR to convene a Desalination Task Force (Task Force) to "make recommendations related to potential opportunities for the use of seawater and brackish water desalination." The work of the Task Force and its subsequent findings and recommendations provided a useful background to DWR in developing Proposition 50 guidelines for funding desalination

projects and for estimating the future potential and prospects of desalination in the ***2005 California Water Plan Update***. The Energy Commission served as one of the four co-chairs of the Task Force along with California Coastal Commission, State Water Resources Control Board, and State Department of Health Services (Energy Efficiency Division).

Salton Sea Desalination Demonstration Project Using Geothermal Heat
Energy Commission staff is serving on the advisory panel for U.S. Bureau of Reclamation's geothermal-driven vertical tube evaporation (VTE) desalination test project at the Salton Sea, to be conducted by Sephton Water Technology (SWT). The purpose of this project is to demonstrate the feasibility of controlling the salinity, nutrient, selenium, and other contaminant content of seawater by using geothermal waste steam to drive a VTE desalting system. The project satisfies one of the principal goals of the California Desalination Task Force, which is to identify potential opportunities for brackish water desalination, as well as the Energy Commission's need to improve the energy efficiency of water and wastewater treatment facilities in California. The project also addresses the problem of concentrate disposal. In this case, the plan calls for the concentrate to be pumped "down hole" to help recharge the geothermal aquifer, resulting in zero liquid discharge from the desalting plant (Energy Efficiency Division).

National Programs

Implementation of the U.S. Bureau of Reclamation's Desalination Roadmap
In 2001, Congress directed the Bureau of Reclamation to work with Sandia National Laboratories (SNL) to develop a desalination technology research plan for the United States. With the help of a multidisciplinary committee of representatives from academia and the public, private, and non-profit sectors***, The Desalination and Water Purification Technology Roadmap: A Report of the Executive Committee (Roadmap)*** was published in January 2003. The ***Roadmap*** presents a summary of water supply challenges facing our nation through 2020 and suggests areas of research that could lead to technological solutions for these challenges. The ***Roadmap*** may be used as a planning tool to facilitate science and technology investment decisions or as a management tool to help coordinate research efforts. To develop a mechanism to implement the recommendations of the Desalination Roadmap, the Joint Water Reuse and Desalination Task Force (JWR&DTF) was formed and is conducting workshops to establish a desalination research funding process. The Energy Commission was a member of the JWR&DTF planning committee that organized these workshops, and will participate in these workshops in the near future (Energy Efficiency Division).

Working Group on Concentrate Management Guidelines for Desalination and Water Reuse
Both the U.S. Bureau of Reclamation's ***Desalination and Water Purification Technology Roadmap,*** published in 2003*,* and the California Desalination Task Force identified concentrate management as a major area where research is needed to create next-generation desalination technologies. To help address the identified technical and environmental concerns associated with desalination and water reuse concentrate, Sandia National Laboratories initiated an effort, in cooperation with the Bureau of Reclamation, the American Water Works Association, the American Society of Civil Engineers, and the Water Reuse Foundation, to jointly develop guidelines for concentrate management. Energy Commission staff actively participate in the Concentrate Management Working Group, which is working on these guidelines (Energy Efficiency Division).

National Salinity Management Conference
This high-profile annual national conference is jointly sponsored by Multi-State Salinity Coalition, the US Desalination Coalition, the Northern California Salinity Coalition, the Water Reuse Association, the Southern California Salinity Coalition, and others in conjunction with the Nevada Water Reuse Association. It includes invaluable presentations, industry tours, and roundtable discussions on technical, policy, and program issues concerning energy issues in desalination. Energy Commission staff are regular members of the planning committee for this conference (Energy Efficiency Division).

Water Treatment

Developing and Validating an Energy Efficient Arsenic Removal Process
The current EPA standard for arsenic, a naturally occurring contaminant in groundwater, is 50 parts per billion (ppb). Effective January 2006, federal standard for arsenic in drinking water will be lowered to 10 ppb. The new arsenic standard will leave many public drinking water supply systems out of compliance, including several hundred systems in California. California has set a long-term public health goal for arsenic in drinking water at 4 parts per trillion (ppt) -- 2,500 times lower than the new federal standard of 10 ppb.

To attain this standard, the water systems in California will have to first meet the EPA standards in a cost-effective manner. Currently, the average cost of lowering arsenic from 50 ppb to 10 ppb from drinking water is in the range of $58 to $237 per household per year. Lawrence Berkeley National Laboratory is conducting research on an innovative medium, which, if successful, will lower the arsenic removal cost to $1 per household per year and have little or no incremental energy costs over current practices (PIER Industry, Agriculture and Water).

Wastewater Treatment

Development and Demonstration of a Digital System for Control and Mentoring of Oxygen Transfer Efficiency (OTE) Measurements
The majority of wastewater treatment plants nationwide uses an activated sludge secondary treatment process. Blowing air into the activated sludge aeration tanks accounts for 50 to 80 percent of a wastewater treatment plant's entire energy consumption. Over time, the diffusers through which this air blows become fouled by bacterial slime growth and scale buildup from hard water. One of the challenges of the wastewater industry is to monitor in real time the performance of wastewater treatment and how well aeration systems function.

Aeration system performance can be correlated with power consumption and calculated from material balances, but these results are not obtained in real time and can take weeks or months to obtain. A much better method is to measure OTE directly, using data collected from an instrument that measures oxygen in the gas released from the surface of the aeration basin. Currently, commercially available OTE instruments are large, heavy, and fragile, and require a crew of several people to operate. The purpose of this project is to design and demonstrate a new digital, fully-automated off-gas testing technology for purposes of evaluating and optimizing oxygen transfer efficiency, which would reduce energy demand (PIER Industry, Agriculture and Water).

Water-Related End Uses

Several projects underway are looking at ways to reduce the energy consumption of water-related end uses. Other efforts are focusing on increasing water use efficiency.

Waste Not, Want Not: The Potential for Urban Water Conservation in California
In 2003, the Pacific Institute published a report that quantified the unrealized potential for cost-effective water conservation in California. The report estimated that nearly 30 percent of potable water consumed in California – as much as 2 million acre-feet per year – could be cost-effectively conserved. In the context of the Pacific Institute's report, cost-effective is defined as "… the point where the marginal cost of the efficiency improvements is less than or equal to the marginal cost of developing new supplies."

Energy Down the Drain -The Hidden Costs of California's Water Supply
In the western United States there is a close connection between water and power resources. Water utilities use large amounts of energy to treat and deliver water, and even after utilities deliver water, consumers use even more

energy to heat, cool, and use it. This August 2004 report from the National Resources Defense Council (NRDC) and the Pacific Institute shows how water planners in California have largely failed to consider the energy implications of their decisions, and suggests a model for policymakers to calculate the amount of energy consumed during water use. Integrating energy use into water planning can save money, reduce waste, protect the environment, and strengthen the economy.

Water for Growth: California's New Frontier

According to the Public Policy Institute of California, which issued this report in July 2005, California's population grew by over 10 million between 1980 and 2000. It is expected to increase by another 14 million by 2030, reaching a total of 48 million by that date. One of the most serious concerns of policymakers is whether the state will be able to supply enough water to support a population of this size. If per capita urban water use remains at its 2000 levels of 232 gallons per person per day, California will face an expansion of water demand of 40 percent, or 3.6 million acre-feet, by 2030. Policymakers and water planners have begun to consider several ways to bring supply and demand into balance over the years ahead. Options include expansion of nontraditional sources of supply (for example, underground storage, recycling, and desalination), reallocation through water marketing and conservation incentives and regulations.

California Water 2030: An Efficient Future

On September 13, 2005, the Pacific Institute released its newest report on the potential for saving water in California by 20 percent over the next 25 years while satisfying a growing population, maintaining a healthy agricultural sector, and supporting a vibrant economy. The report discusses how smart technology, strong management, and appropriate rates and incentives can allow the state to meet its needs well into the future, using less water.

The Irrigation Training and Research Center (ITRC)

The Irrigation Training and Research Center (ITRC) was established in 1989 at California Polytechnic State University, San Luis Obispo, as a center of excellence built upon a history of contributions to agriculture. The ITRC has a number of ongoing programs to develop and promulgate irrigation best practices in California. While ITRC's research focuses on irrigation for agriculture, the tools, technologies, and techniques are often applicable to landscape irrigation as well (PIER Industry, Agriculture and Water).

California Urban Water Conservation Council (CUWCC)

The CUWCC is a non-profit organization created to increase efficient water use statewide through partnerships among urban water agencies, public interest organizations, and private entities. The Council's goal is to integrate urban water conservation BMPs into the planning and management of California's water resources. Presently, more than 300 urban water agencies

and environmental groups are signatories to a historic memorandum of understanding pledging to develop and implement 14 comprehensive water conservation BMPs. To the extent that the state adopts a policy allowing energy utilities to invest in water savings for their energy and environmental benefits, CUWCC's goals and activities are certainly in direct alignment.

Residential Hot Water Distribution System Research Project
The purpose of this project was to conduct a scoping study to establish the first-order estimate for the water and energy wasted in hot water distribution systems in California and the United States. This study found that the losses in residential hot water distribution systems total more than $1 billion per year in California and $10 billion per year in the United States, including the cost of energy, water, and wastewater treatment. A roadmap to identify future activities was part of the original project but has not been completed (PIER Buildings).

Testing of Hot Water Distribution Systems
The purpose of this project was to systematically test the performance of hot water distribution systems. Field work assessing the types of distribution systems in current construction practice was combined with laboratory testing. Test procedures were developed and used on ½- and ¾-inch copper piping and ¾-inch PEX-Aluminum-PEX piping. Tests were conducted in air on both uninsulated and insulated pipe. The results of this project will be combined with additional testing to support the 2008 Title 24 Residential Building Energy Efficiency Standards proceeding (PIER Buildings).

Water Heating R&D for the 2008 Residential Building Energy Efficiency Standards
This research will provide hot water distribution system data, analysis, and recommendations to the 2008 Title 24 Residential Building Energy Efficiency Standards proceedings. Specific efforts will inform the building standards proceeding in the areas of multi-family water heating, hot water pipe losses, single family water heating construction practices, and hot water distribution system modeling. This project will also study California housing's current hot water performance issues and cost-effective retrofit opportunities, and identify future research priorities for hot water distribution systems (PIER Buildings).

Super Efficient Gas Water Heating Appliance Initiative
This research will develop the foundation for a multi-year initiative to determine the best approach for achieving a 30 percent efficiency improvement in gas water heaters. Technical and market analysis will be conducted, along with stakeholder involvement, to implement a product development competition that develops and tests prototypes for safe, reliable, and cost-effective replacements for natural gas water heaters (PIER Buildings).

Market and Technical Considerations for a Next Generation Instantaneous Water Heater

Gas-fired instantaneous water heaters are highly efficient and can play an important role in reducing energy consumption. The barriers to the current generation of instantaneous water heaters include higher initial cost, installation cost adders, water waste associated with start-up, the inability to adjust to low flow rates or relatively warm incoming cold water, and the inability to meet large household or simultaneous demands. The goal of this research is to determine if current state-of-the art instantaneous water heaters can meet both current and projected California domestic hot water needs and to identify technology(ies) that can be incorporated into instantaneous water heaters to overcome current market and technical barriers (PIER Buildings).

Energy Efficiency Potential of Gas-Fired Commercial Water Heating Equipment

The goal of this research is to establish representative gas loads for both the installed base and higher-efficiency hot water systems in commercial kitchens, based upon a review of current literature monitoring data for three commercial food service sites (a quick-service, full-service, and institutional facility). This field experience will form the basis for a design guide for hot water systems in commercial food service (PIER Buildings).

Water for Electricity Generation

Water is used to generate electricity, both directly in hydropower plants and indirectly as part of cooling systems in thermal electric facilities. The Energy Commission has funded several projects to evaluate ways to reduce the effects of electricity generation on California's freshwater supplies and on aquatic species and habitats.

The Ecological Effects of Pulsed Flows from Hydropower Plants

The Center for Aquatic Biology at the University of California, Davis, is conducting research addressing the ecological effects of ramping and other pulsed flows from hydropower plants. These discharges are results of load following, sediment and vegetation management, and recreational requirements. Seven different projects are evaluating a wide range of issues, from the effects of these flows on invertebrates residing in stream and river bed sediment to the effects on the potentially threatened foothill yellow-legged frog. The purpose of this research is to provide information that will prompt regulatory decision making that would not otherwise be accomplished within the regulatory process. The information from this research will be used by regulators to establish information needs for impact assessment, set impact thresholds, and establish suitable mitigation measures. Research partners include the State Department of Water Resources, California Department of Fish & Game, PG&E, EBMUD, and NOAA Fisheries (PIER Environmental).

Development of Bioassessment Criteria for Hydropower Operation
The California Department of Fish and Game is conducting research to develop environmental indicators, using benthic macroinvertebrates, to assess and monitor the effects of hydropower operation on rivers and streams. The purpose of this project is to establish a low-cost assessment and monitoring tool that will provide a direct indication of ecosystem health, as opposed to relying upon indirect factors such as water temperature or flow. Research partners include the California Department of Fish and Game, California State Water Resources Control Board and California State University, Chico (PIER Environmental).

Integrated Forecast and Reservoir Management Project
Runoff and stream flow forecasting has historically relied upon limited hydrologic records. With the development and refinement of global circulation models and an improved understanding of climate conditions and their ramifications for California, future runoff probabilities can be more accurately predicted. Using these forecasts on an hourly to seasonal basis can result in better planning and optimization of California's water resources. The Energy Commission is funding a demonstration of this approach for four Northern California reservoirs: Shasta, Trinity, Oroville, and Folsom. This effort uses global circulation model scenarios, downscaled to hydrologic models, that encompass the catchments of each of these reservoirs, as well as the entire Sacramento River. This information is used to create probabilistic forecasts on an hourly to month-long basis. Since these major reservoirs are all multi-purpose, the project includes the development of decision support models that will allow reservoir operators to make better decisions about the balance between flood control, water supply, hydropower generation, and instream flow requirements. Based upon a retrospective analysis of Folsom Reservoir using this methodology, the researchers showed that there could be a15 percent increase in hydropower generation. Research partners include the National Oceanic and Atmospheric Administration, CalFed, the Department of Water Resources, Sacramento Area Flood Control District, the U.S. Bureau of Reclamation and the Army Corps of Engineers (PIER Environmental).

Development of Seasonal Forecast of Hydropower Generation
Scripps Institute is developing seasonal forecasts of hydropower production in the Pacific Northwest and California. Since the amount of hydropower production in these two regions has a significant effect on the cost and availability of electricity within California, providing forecasts on a seasonal basis will improve energy planning, especially natural gas demand. Another aspect of this project is to develop seasonal temperature predictions for California based upon global circulation model simulations. This information will allow planners to predict whether an upcoming summer will be exceptionally severe and plan accordingly. Research Partners include the Western Electricity Coordinating Council (WECC), Pacific Northwest National Laboratory and the University of Washington (PIER Environmental).

Advanced Cooling Strategies and Technologies
This program is being managed by EPRI and addresses approaches for reducing freshwater consumption in the thermal generating sector. Specifically, the program addresses both the barriers to wider adoption of water conserving cooling technologies and alternative cooling technologies. These approaches, such as the use of air-cooled condensers, can substantially reduce the amount of water used within a power plant. There are, however, economic and performance issues to overcome before industry will adopt these approaches. Research partners include NETL, Reliant, AES and Crockett Cogeneration (PIER Environmental).

Ecological Effects of Cooling Water Intake Structures
Within California, a significant portion of in-state thermal electric generation is from coastal power plants that use once-through cooling, which uses millions of gallons of water per day. The intake of these vast amounts of cooling water, which is not evaporated, means that millions of the eggs, larvae, and other early life stages of fish, clams, and other aquatic species are destroyed by the heat transferred to the cooling water. The ecological effects of this once-through cooling are not known. In addition, there is a need to develop new assessment techniques and establish the suitability of innovative technology to reduce this impact. The Moss Landing Marine Laboratory, a part of California State University, San Jose, is managing the research program on this topic. Research partners include the California Costal Commission, the California Department of Fish and Game, NOAA Fisheries and the University of California, Santa Cruz (PIER Environmental).

RPS-Eligible Small Hydropower Resource Assessment
The purpose of this project is to assess the magnitude of in-conduit resources potentially available for greater small hydropower development in California. Specifically, the study focuses on irrigation and municipal water systems where no new appropriation or diversion is required, which retains RPS eligibility under the conditions of SB1078. This study does not cover new or incremental power at existing dams or other potential in-conduit resources such as industrial process water and municipal wastewater (PIER Renewables).

Use of a Down-Hole Pump as a Turbine-Generator
The purpose of this project is to demonstrate and assess the performance of a reverse operated down-hole pump commonly used in the oil and gas industry as a turbine-generator for power production. The unit will be demonstrated in a Northern California Power Agency injection well at the Geysers, where the feedstock will be treated wastewater used to replenish and extend the life of the region’s underground steam fields. If successful, this would provide a means of partially offsetting the cost of pumping wastewater to the injection site (PIER Renewables and GRDA).

APPENDIX B: 2001 CALIFORNIA ENERGY CONSUMPTION BY END USE

2001 California Energy Consumption by End Use

Sector	Description	Electricity (GWh)	Percent Related to Water	Natural Gas (million therms)	Percent Related to Water	Adjusted Electricity (GWh)	Adjusted Natural Gas (million therms)
AG & WP	Domestic Water Pumping	11,953	1.00	19	1.00	11,953	19
AG & WP	Crops	3,284	1.00	103	0.05	3,284	5
AG & WP	Irrigation Water Pumping	2,269	1.00	5	1.00	2,269	5
AG & WP	Livestock	1,216	0.50	15	0.50	608	8
RESIDENTIAL	Clothes Drying	5,769	1.00	145	1.00	5,769	145
RESIDENTIAL	Water Heating	2,352	1.00	1,079	1.00	2,352	1,079
RESIDENTIAL	Indirect Hot Water Heating for Clothes Washing	1,053	1.00	486	1.00	1,053	486
RESIDENTIAL	Washing Machine	726	1.00	0		726	0
RESIDENTIAL	Indirect Hot Water Heating for Dish Washing	686	1.00	316	1.00	686	316
COMMERCIAL	Water Heating	549	1.00	174	1.00	549	174
RESIDENTIAL	Evaporative Cooling	519	1.00	0		519	0
RESIDENTIAL	Solar Water Heating	18	1.00	7	1.00	18	7
COMMERCIAL	Cooling	12,916	0.50	66	0.50	6,458	33
MINING & CON	Oil and Gas Extraction	3,958	0.50	2,775	0.50	1,979	1,388
RESIDENTIAL	Dish Washing	2,008	0.50	0		1,004	0
INDUSTRY	Publishing and Broadcasting Industries	955	0.50	9		478	0
INDUSTRY	Printing and Related Support Activities	773	0.50	19		386	0
INDUSTRY	Nonmetallic Mineral Product Manufacturing	710	0.50	116		355	0
TCU	National Security and International Affairs	2,649	0.20	60	0.30	530	18
RESIDENTIAL	Residential Miscellaneous	24,419	0.05	168	0.05	1,221	8
COMMERCIAL	Commercial Miscellaneous	19,156	0.05	722	0.05	958	36
INDUSTRY	Petroleum Refining and Related Industries	7,194	0.05	1,464	0.05	360	73
COMMERCIAL	Refrigeration	6,771	0.05	5	0.05	339	0
INDUSTRY	Food Manufacturing, Beverage and Tobacco	4,939	0.05	390	0.50	247	195
INDUSTRY	Chemicals	3,674	0.05	226	0.05	184	11
RESIDENTIAL	Cooking	3,595	0.05	286	0.05	180	14
INDUSTRY	Electronic Components	3,261	0.05	39		163	0
INDUSTRY	Computer and Electronic Product Manufacturing	2,988	0.05	37	0.05	149	2
INDUSTRY	Plastics and Rubber Products Manufacturing	2,886	0.05	40		144	0
TCU	Telephone	2,289	0.05	3		114	0
INDUSTRY	Fabricated Metals	2,045	0.05	122	0.05	102	6
INDUSTRY	Transportation Equipment	1,960	0.05	84		98	0
INDUSTRY	Machinery Manufacturing	1,777	0.05	24		89	0
INDUSTRY	Miscellaneous Assembly Industry	1,300	0.05	14		65	0
INDUSTRY	Sugar and Canned, Dried, and Frozen Food	1,283	0.05	299	0.50	64	149
MINING & CON	Construction	1,213	0.05	22	0.05	61	1
INDUSTRY	Primary Metals	1,192	0.05	133	0.05	60	7
INDUSTRY	Pulp, Paper, and Paperboard Mills	1,149	0.05	110	0.50	57	55
TCU	Electric and Gas Services, Steam Supply	1,006	0.05	25	0.05	50	1
INDUSTRY	Lumber	951	0.05	56		48	0
INDUSTRY	Paper Products; Excludes SIC 261,262,263,266	895	0.05	51		45	0
INDUSTRY	Furniture and Fixtures	793	0.05	9		40	0

Sector	Description	Electricity (GWh)	Percent Related to Water	Natural Gas (million therms)	Percent Related to Water	Adjusted Electricity (GWh)	Adjusted Natural Gas (million therms)
TCU	Airports, Flying Field and Airport Terminal Service	771	0.05	5	0.05	39	0
COMMERCIAL	Cooking	758	0.05	141	0.05	38	7
INDUSTRY	Electrical Equipment, Appliance, and Component Manufacturing	646	0.05	7		32	0
MINING & CON	Mining (except Oil and Gas)	615	0.05	58	0.05	31	3
INDUSTRY	Textile Products	397	0.05	8	0.05	20	0
INDUSTRY	Textiles	386	0.05	65	0.05	19	3
INDUSTRY	Textile Products	183	0.05	14	0.05	9	1
RESIDENTIAL	Pool Heating	60		100		0	0
RESIDENTIAL	Hot Tub Fuel	168		93		0	0
RESIDENTIAL	Water Bed	2,150		0		0	0
INDUSTRY	Glass manufacturing	877		128		0	0
INDUSTRY	Cement, Hydraulic	1,636		38		0	0
RESIDENTIAL	Pool Pump	3,024		0		0	0
RESIDENTIAL	Solar Pool Heating	0		64		0	0
RESIDENTIAL	Refrigeration	13,282		0		0	0
RESIDENTIAL	Solar Heater Pump	97		0		0	0
RESIDENTIAL	Hot Tub Pump	901		0		0	0
TCU	Water Transportation	48		0		0	0
TCU	Pipeline	935		16		0	0
COMMERCIAL	Heating	2,625		670		0	0
COMMERCIAL	Indoor Lighting	31,568		0		0	0
COMMERCIAL	Office Equipment	1,405		0		0	0
COMMERCIAL	Outdoor Lighting	5,332		0		0	0
COMMERCIAL	Ventilation	9,325		0		0	0
STLT	Street lighting and Traffic Control	1,713		0		0	0
RESIDENTIAL	Central Air Conditioning	4,199		45		0	0
RESIDENTIAL	Color Television	3,425		0		0	0
RESIDENTIAL	Freezer	2,461		0		0	0
RESIDENTIAL	Furnace Fan	1,273		0		0	0
RESIDENTIAL	Room Air Conditioner	486		0		0	0
RESIDENTIAL	Central Space Heating	3,245		2,339		0	0
TCU	Other Local Transportation, Parking Garages	212		5		0	0
TCU	Trucking and Warehousing	545		2		0	0
TCU	Post Office	528		3		0	0
TCU	Shipping Terminals	262		1		0	0
TCU	Air Transportation, Carrier	121		2		0	0
TCU	Transportation Service	201		2		0	0
TCU	Telegraph Communication	6		0		0	0
TCU	Radio and Television	461		1		0	0
TCU	Cable TV	514		1		0	0
TCU	Railroad Transportation	143		3		0	0
TCU	Rapid Transit	400		5		0	0
TCU	Sanitary Service	2,012	1.00	27	1.00	2,012	27
	Totals	**250,494**		**13,571**		**48,012**	**4,284**
	Percent					**19%**	**32%**

This table comes from the California Energy Commission's Demand Analysis Office. The data are for 2001 and are based on energy utility reporting for that year. They also include self generation above 1 MW. The percent of the energy related to water was discussed by the WER Working Group on July 29, 2005. If we agreed that most of the energy was water related, we assigned it a 1. If we knew there was a relationship but didn't understand enough to know how big, we assigned it 0.05. If there was some intermediate relationship, we assigned it 0.5, except for National Security and International Affairs which we felt was typical of the overall energy relationship to water. We assigned zero to those categories where there did appear to be a relationship.

APPENDIX C: ENERGY IMPACT ANALYSIS OF EXISTING WATER MANAGEMENT PRACTICES

Introduction

This appendix examines various water management practices focused on water conservation and efficiency and estimates the effects of water efficiency activities on energy savings. The analysis in this appendix is intended to:

- ✓ Quantify energy requirements in water use cycle processes.
- ✓ Determine current water efficiency measure energy impacts.
- ✓ Compare water and energy efficiency program characteristics.
- ✓ Recommend policy changes to incorporate water efficiency in the energy efficiency portfolio.
- ✓ Identify areas of research to better understand water-energy interdependencies.

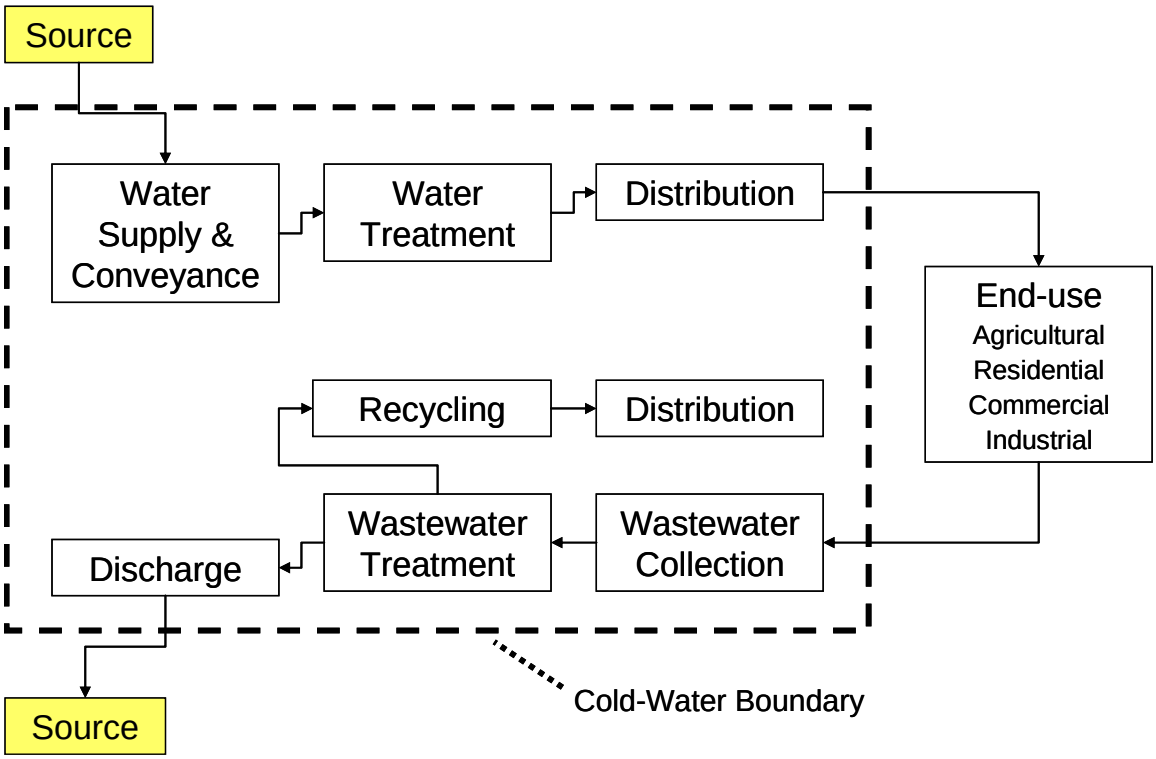
The Water Use Cycle

Electric and natural gas energy efficiency programs focus primarily on the application of energy consuming end-use technologies at utility customer facilities. In contrast to conservation, where usage is reduced through end-user behavioral changes, energy efficiency program planners target more permanent efficiency gains through known end-use technology or design applications. Likewise water use efficiency is achieved by implementing measures that result in reduced water consumption without customer behavioral changes.

In water systems, energy utilities target efficiency gains primarily by improving heating and pressurizing processes. For example, a low-flow showerhead saves energy because less hot water is used, thereby reducing the amount of energy needed to heat water. This is the case for water efficiency measures included in past energy efficiency programs such as faucet aerators, high-efficiency washing machines, and restaurant pre-rinse valves. Energy efficiency programs target efficiency gains in pressurizing applications by improving electric motor and/or pump efficiencies often at water and wastewater utility facilities. In each case the application is an end-use energy consuming technology located behind a customer meter.

When a unit of water is saved, so too is the energy required to convey, treat, deliver, perform wastewater treatment, and safely dispose of that unit of water. The energy intensity of the water use cycle must be examined on a systemic basis and varies widely by delivery location. Figure C-1 identifies the boundary of the water use cycle, showing the water processes that require energy, defined as cold water energy.

Figure C-1 Water Use Cycle



Significant customer-end use energy and water efficiencies have been, and are yet to be, achieved in the water sector[66]. These customer end-use efficiencies, while important, are excluded from this analysis to bring visibility to incremental cold-water energy savings.

When a water efficiency measure is implemented, the cold-water energy savings are achieved at multiple locations often transcending utility, city, and county jurisdictional boundaries. This analysis addresses the integration of water and energy demand-side management to increase cold water energy efficiency gains.

Water Use Cycle Energy Requirements

Electricity used to move or process water supplies (described above as cold water related energy) is quantified below in four primary stages or processes: conveyance, treatment, distribution, and wastewater treatment. The following table documents

[66] Even after accounting for expectations from existing efforts in this area, an additional 30-50 percent urban water (and associated energy) savings are possible with cost-effective existing technologies. (Waste Not, Want Not: The Potential for Urban Water Conservation in California, Pacific Institute, 2004.)

ranges of energy intensity for each process in terms of kilowatt-hours (kWh) per million gallons (MG):

Table C-1 Range of Energy Intensities for Water Use Cycle Processes (kWh/MG)

Water Cycle Segments	Low	High	Assumptions (Numbers in parentheses refer to sources listed below in this table)	
1. Water Supply & Conveyance	0	14,000	0: 14,000:	(1) Assume total gravity feed; (2) pg. 27 - SWP @ Pearblossom 4,444 kWh/AF or 13,638 kWh/MG (14,000 kWh/MG)
2. Water Treatment	100	16,000	100: 16,000:	(3) Water treatment without raw water pumping (max. gravity feed) and distribution pumping (accounted for under Distribution) = 99.7 kWh/MG Table 2-1, page 2-3 (7) Sea Water Desalination
3. Water Distribution	700	1,200	700: 1,200:	(6) (3) High Service Pumps To Distribution - 12,055 kWh/day for a Typical 10 MGD Surface Water Treatment Plant - figure 2-1, page 2-2 equivalent to 1,205.5 kWh/MG
4. Waste Water Collection	-	-		This category has been incorporated into the next category.
5. Waste Water Collection & Treatment	1,100	4,600	1,100: 4,630:	(4) Electric Use of Total Plant Operations Exec-1 and pg. 5, Table 3 - Range from 1,073 kWh/MG to 4,630 kWh/MG (3) Influent wastewater pumping is included in wastewater treatment process; figures 3-2 and 3-3, pages 3-3 and 3-4, respectively
6. Waste Water Discharge	0	400	0: 400:	(1) assumes gravity ocean outfall; 400 ground water recharge (3) pg. 3-7
7. Recycled Water Treatment	-	-		(4)(5) Tertiary/Advanced Waste Water Treatment Included under range of Waste Water Collection & Treatment
8. Recycled Water Distribution	400	1,200	Range:	(5) Municipal Recycled Water Use in California 2002: 46% Ag. Irrigation; 21 % landscape irrigation; 10% ground water recharge; Industrial 5%. This accounts for 82% of all recycled water. Energy needed for these applications fall within the ranges of the energy needed for typical water distribution and ground water recharge 400 - 1200 kWh/MG.

Sources:
(1) - Water Energy Working Group Assumption
(2) - Methodology for Analysis of the Energy Intensity of California's Water Systems; LBL January 2000
(3) - Water & Sustainability (Volume 4): U.S. Electricity Consumption for Water Supply & Treatment, EPRI March 2002
(4) - Energy Benchmarking Secondary Wastewater Treatment and Ultraviolet Disinfection Processes at Various Municipal Wastewater Treatment Facilities, PG&E February 2002
(5) - DWR Water Facts No. 23
(6) - EBMUD 2003 Load Study by Navigant Consulting
(7) - California Water Plan Update 2005 Volume 2, Resource Management Strategies, Chapter 6 – Desalination. A 50 mgd seawater plant (approximately 50,000 acre-feet per year, or 16.25 billion gallons, assuming operations 90% of the time) would require about 33 MW of power. California Water Plan Update 2005 Volume 2, Resource Management Strategies, Chapter 6 – Desalination. This translates to about 5,200 kWh per acre-foot, or 16,000 kWh per million gallons

Regional Water-Energy Characteristics

The ranges of water use cycle energy requirements identified above vary significantly because of regional water system operating requirements. To project energy savings associated with unit volume reductions in water requires adoption of prototypical energy needs, incorporating the variability inherent in regional resource alternatives. Analysis in this appendix separates water energy regions broadly into the Northern and Southern California regions, but additional research to assess regional water-energy characteristics is needed (see Suggested Research Topics, below).

The Northern California Region: Contains the North Coast, San Francisco, Sacramento River, San Joaquin River, Tulare Lake and Central Coast[67] Hydrologic Regions as defined by the California Department of Water Resources. The Northern California region contains 42 percent of the state's population and 42 percent of urban residential and non-residential applied water[68]. The region is characterized overall by relatively higher annual precipitation than in Southern California and significant native ground and surface water resources.

The Southern California Region: Contains the South Coast Hydrologic Region; 53 percent of the state's population and 48 percent of urban residential and non-residential applied water[69]. The region is characterized by relatively low annual precipitation and limited native surface water resources and has historically relied heavily on groundwater and imported water to meet water demand.

Other Hydrologic Regions: Hydrologic regions not included in this analysis are the North Lahontan, South Lahontan and Colorado River Hydrologic Regions[70]. Future studies will need to refine analyses addressed herein and incorporate these regions.

For purposes of this analysis, the Northern and Southern California regions, as referred to in this appendix, include 95 percent of the state's population and 90 percent of urban residential and non-residential applied water.

Water Use Cycle Energy Intensity

Table C-2 reflects the variability between water use cycle energy requirements between Northern and Southern California.

[67] The Central Coast hydrologic region includes Santa Barbara and San Luis Obispo Counties that are served by the SWP Coastal Branch with transport energy intensity on-par with the SWP West Branch (water must be lifted over the coastal mountain range). For the purposes of this analysis, the Central Coast is included in the Northern California region because 80 percent of the population within the Central Coast Hydrologic region resides north and east of the mountain range in communities such as Salinas, Santa Maria, Santa Cruz, Lompoc, and Monterey.

[68] Department of Water Resources 2005 Water Plan Update, Volume 3, Chapter 1 Table 1-4. Year 2000 is referenced for all regional characteristics and is described (same reference Table 1-1, page 1-10) as the "Average Year" within the context of precipitation and Wet versus Dry Years.

[69] Ibid

[70] North Lahanton is the extreme northeast of the state; South Lahanton is the region east of the Sierra Nevada Mountains including Mono Lake, Owens Valley and Death Valley; Colorado River Hydrologic Region include eastern San Bernardino, Riverside and Imperial Counties.

Table C-2 Percent Electricity Use for Water System Components[71]

	Northern California	Southern California
Imported Water Supply	-	71%
Local Ground/Surface Water Supply	17%	6%
Local Distribution	26%	9%
Wastewater Treatment	56%	14%

As reflected in Table C-2, the majority of the water use cycle energy required for Southern California, due to imported water, is not present in Northern California. To define process energy savings from water unit volume reductions, representative applications have been adopted for each primary process type: conveyance, treatment, distribution, and wastewater treatment. Energy use scenarios adopted and supported here are based on prototypical values for each process type. For purposes of this analysis, north/south water conveyance energy requirements are addressed separately and water treatment, distribution, and wastewater treatment assumptions are constant.

Water Conveyance

Northern California: As described in Table C-1, the range of water energy intensity for supply and conveyance ranges from 0 to 14,000 kWh/MG. Zero is assumed for gravity-fed systems. Water supplies from native surface water and groundwater sources require much less energy per unit conveyed than in Southern California. Approximately 60 percent of Northern California's urban water requirements are met with surface water and 40 percent is met with groundwater[72]. Additionally, roughly 40 percent of the region's population is located in the San Francisco Hydrological Region, where much of the water is conveyed by gravity from higher elevation reservoirs.

In this analysis, a prototypical value for water conveyance for Northern California is taken from the raw water pumping requirements of surface water treatment, based

[71] Methodology for Analysis of Energy Intensity of California's Water Systems and An Assessment of Multiple Potentials Benefits through Integrated Water-Energy Efficiency Measures; Exploratory Research Project Supported by: Ernest Orlando Lawrence Berkeley Laboratory, California Institute for Energy Efficiency; Principle Investigator Robert Wilkinson, PhD. January 2000, pg-7.

[72] Surface water and groundwater supply percentages are calculated using Water Supply and Use information provided in the California Water Plan Update 2005, Volume 3 for the California Department of Water Resources' North Coast, San Francisco, Sacramento River, San Joaquin River, Tulare Lake, and Central Cost Hydrological Regions.

upon a survey of approximately 30,000 public water supply systems in the United States[73] (see Water Treatment, below) and is estimated at 150 kWh/MG[74].

Southern California: Groundwater meets 23 and 29 percent of Southern California's water demand in normal and dry years, respectively[75]. The Metropolitan Water District (MWD) of Southern California provides 85 percent of the region's water supply to 26 cities and water districts serving 18 million people[76]. MWD's *Integrated Resource Plan* cites goals to mitigate heavy dependence on imported water by balancing its supply portfolio between imports; storage and transfers; recycling; groundwater recovery; conservation; brackish and seawater desalination; and exchanges[77]. While the region's water agencies have compiled a wide array of water management tools and planning practices to bring local water resources on a more equal footing, the region remains dependent on imported water for at least 50 percent of its water supplies[78].

As water agencies develop and employ least-cost resources to meet regional water demands, imported water serves as the primary baseline or "marginal resource." The 2003 *Qualifying Settlement Agreement* enabled implementation of the "4.4 Plan," where California will reduce its use of Colorado River water from a high of 5.3 million acre-feet to its 4.4 million acre-feet annual apportionment, by year 2016[79]. For Southern California, State Water Project (SWP) water supplies from Northern California are treated as the marginal water resource. A brief description of SWP water delivery to Southern California follows:

> As the California Aqueduct moves water south along the west side of the San Joaquin Valley, four pumping plants raise it more than 1,000 feet before reaching the Tehachapi Mountains. Pumps situated at the foot of the mountains pump the water up 1,926 feet through tunnels, which take the water into the Antelope Valley. In the Antelope Valley, the aqueduct divides into two branches: the East Branch and the West Branch.

---

[73] Water & Sustainability (Volume 4) U.S. Electricity Consumption for Water Supply & Treatment – The Next Half Century, EPRI 2002, Page 2-3

[74] Ibid, Figure 2-1, page 2-2, Raw Water Pumping 1,205 kWh per day for a treatment plant with 10 MGD capacity; equivalent to 120.5 per MG; assumption is raised to 150 kWh/MG as a minimum prototypical energy requirement.

[75] Ibid, Chapter 5, page 5-3

[76] Ibid, pages 5-2 and 3.

[77] MWD presentation to the Water Energy Working Group April 8, 2005.

[78] Ibid, page 5-5

[79] Department of Water Resources 2005 Water Plan Update, Volume 3, Chapter 5, page 5-8

The East branch carries water through the Antelope Valley into Silverwood Lake in the San Bernardino Mountains. From Silverwood Lake, the water flows through the San Bernardino Tunnel, through the Devil Canyon Power Plant before continuing on to the southernmost SWP reservoir, Lake Perris. East Branch water energy intensity, net of any SWP system generation, is 3,236 kWh per acre-foot, or 9,931 kWh per MG. Water in the West Branch flows through the Warne Power Plant into Pyramid Lake in Los Angeles County. From there it flows through the Angeles Tunnel and Castaic Power Plant into Castaic Lake, terminus of the West Branch. West Branch water energy intensity, net of any SWP system generation, is 2,580 kWh per acre-foot, or 7,918 kWh per MG[80].

For purposes of this analysis, the energy intensity of Southern California's dominant and marginal water source, averaged between the SWP East and West Branch, is 8,924 kWh/MG (rounded off to 8,900 kWh/MG).

Water Treatment

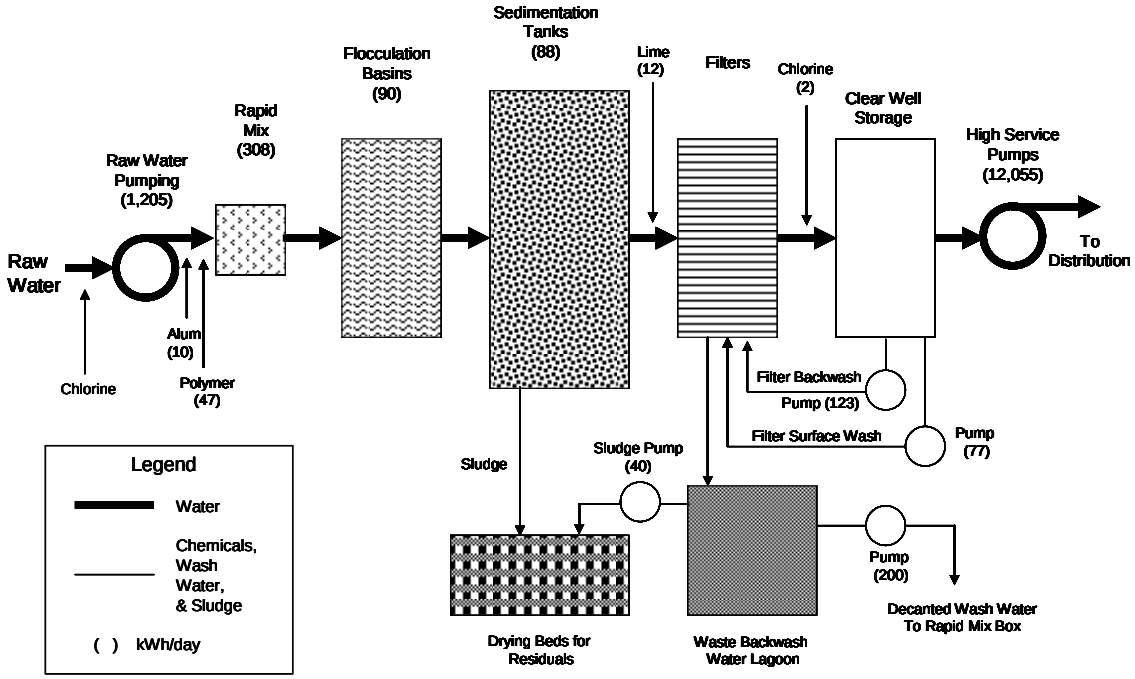
As explained above, for purposes of this analysis, water supply and conveyance energy requirements were addressed separately for Northern and Southern California. The remaining processes, water treatment, distribution, and wastewater treatment are considered similar enough between the two regions to assign the same prototypical water energy intensity. Due to the relative reliance on surface water supply in California, surface water treatment energy intensity has been adopted as prototypical.

In a typical sequence of operations for surface water treatment, the following steps are followed (see Figure C-2): Raw water is first screened and pre-oxidized, using chlorine or ozone to kill organisms; alum and/or polymeric materials are added to the water; flocculation and sedimentation remove finer particles; a second disinfection step kills remaining organisms with disinfectant residue carried into the distribution system to prevent organism growth; the clear well storage tank allows contact time for disinfection; and treated water is distributed to consumers by high-pressure pumps. Sludge and other impurities removed from the water are concentrated and disposed of.

[80] Methodology for Analysis of Energy Intensity of California's Water Systems and An Assessment of Multiple Potentials Benefits through Integrated Water-Energy Efficiency Measures; Exploratory Research Project Supported by: Ernest Orlando Lawrence Berkeley Laboratory, California Institute for Energy Efficiency; Principle Investigator Robert Wilkinson, PhD. January 2000, pages 24 through 27.

Figure C-2 Water Treatment Process Energy Requirements[81]

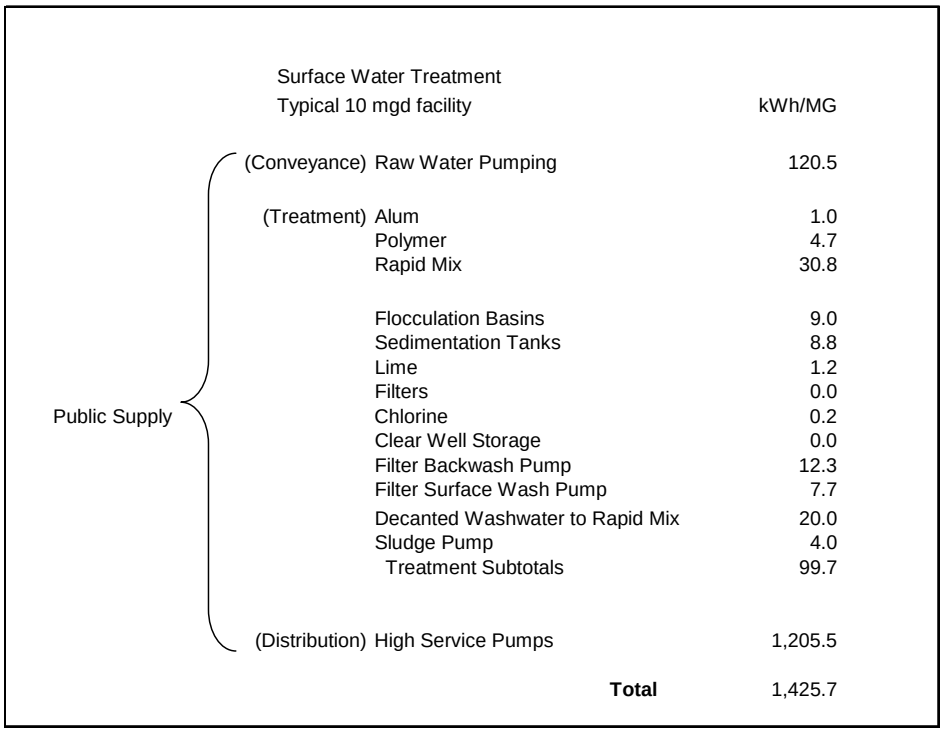
Representative Water Treatment Plant
Typical Daily Electricity Consumption for a 10 Million Gallon/Day Facility



Source: Electric Power Research Institute

[81] Water & Sustainability (Volume 4) U.S. Electricity Consumption for Water Supply & Treatment – The Next Half Century, EPRI 2002, Page 2-2, Figure 2-1.

Table C-3 Water Treatment Energy Intensity *(based on Figure C-2)*



	Surface Water Treatment		
	Typical 10 mgd facility		kWh/MG
Public Supply	(Conveyance)	Raw Water Pumping	120.5
	(Treatment)	Alum	1.0
		Polymer	4.7
		Rapid Mix	30.8
		Flocculation Basins	9.0
		Sedimentation Tanks	8.8
		Lime	1.2
		Filters	0.0
		Chlorine	0.2
		Clear Well Storage	0.0
		Filter Backwash Pump	12.3
		Filter Surface Wash Pump	7.7
		Decanted Washwater to Rapid Mix	20.0
		Sludge Pump	4.0
		Treatment Subtotals	99.7
	(Distribution)	High Service Pumps	1,205.5
		Total	1,425.7

There is little variation in water energy intensity between plant sizes (shown in million gallons per day (MGD), as reflected in the following table:

Table C-4 Unit Electricity Consumption for Surface Water Treatment Plants[82]

Plant Size	kWh/MG
1 MGD	1,483
5 MGD	1,418
10 MGD	1,406
20 MGD	1,409
50 MGD	1,408
100 MGD	1,407

Referring back to Table C-3, in order to isolate the energy requirements for water treatment, the energy needed for raw water pumping and high service pumps to distribution have been removed. The remaining treatment processes total 997 kWh

[82] ibid, Page 2-3, Table 2-1. However, this study omitted the decanted wash water to rapid mix box pump rated at 20 kWh/MG from its totals. This amount was included in the numbers in the table.

per day for a typical 10 MGD capacity treatment plant or 99.7 kWh/MG. Actual energy requirements are driven by the site-specific characteristics of incoming raw water and water quality mandates. Industry standard practice, as well as process load metering, often doesn't differentiate raw water pumping, water treatment and distribution pumping loads adequately. Information provided in Table C-3 is drawn from large treatment plant populations and demonstrates this practice. Operational reporting of water treatment energy intensity is often driven more by the distance and elevation of the treatment plant in relation to water sources and the water distribution system than by the characteristics of raw water due to these vagaries. Typical water treatment processes are estimated at between 100 and 250 kWh/MG, and can be as high as 500 kWh/MG. In this analysis, 100 kWh/MG has been adopted as the prototypical and conservative water treatment energy intensity.

Water Distribution

Table C-4 shows there is little variation in the amount of energy required to treat and distribute a unit of water, regardless of plant size. As described above, Service Pumps to Distribution (for a typical 10 MGD water treatment plant) consume 12,055 kWh per day or 1,205.5 kWh per MG, or roughly 85 percent of total energy requirements (1,205 kWh/MG/1425 kWh/MG). For purposes of this analysis, a prototypical water distribution system energy intensity of 1,200 kWh/MG was adopted.

Wastewater Treatment

Unlike the water treatment and distribution systems, unit volume energy requirements for wastewater treatment plants vary greatly depending upon plant size. As would be expected, unit electricity consumption rises as the degree of treatment and complexity of the process increases. For example, advanced wastewater treatment with nitrification is three times as energy intensive (due to additional pumping requirements) as the relatively simple trickling filter plant[83]. Further complicating the assessment of prototypical wastewater treatment energy intensity are unique operational environments, discharge limitations, influent characteristics, and permitted effluent limitations as well as variations in plant permitting cycles. Table C-5 shows wastewater treatment plant energy intensities reflecting a range of energy intensity for facilities operating in California and cited in studies. Based on this range, 2,500 kWh per MG has been adopted as the prototypical wastewater treatment energy intensity.

[83] ibid, Pages 3-4 & 5 and Table 3-1.

Table C-5 Wastewater Treatment Energy Intensity

	kWh/MG
Inland Empire Utilities Agency [A]	2,971
City of Santa Rosa [B]	2,920
East Bay Municipal Utilities District [C]	2,001
Metropolitan Water District [D]	2655
Methodology for Analysis of Energy Intensity in California's Water Systems [E]	1,911
Energy Down The Drain, The Hidden Costs of California's Water Supply [F]	2,302
Energy Benchmarking Secondary Wastewater Treatment [G]	2,625

[A] Average of Five Wastewater Treatment Plants, CALeep Program Analysis May 2005
Program 1241-04, Conducted under the Auspices of the California Public Utilities Commission

[B] Laguna Wastewater Treatment
Sonoma County August 2002 Greenhouse Gas Emission Analysis, Page B-7

[C] EBMUD Load Studies Prepared by Navigant Consulting, December 2004

[D] The Metropolitan Water District of Southern California estimates that the wastewater facilities in its service territory consume between 1,470 to 3,840 kWh/MG

[E] Methodology for Analysis of Energy Intensity in California's Water Systems, January 2000, P. 43
Wastewater Treatment Plants with Nitrification
Ernest Orlando Lawrence Berkeley Laboratory
Principal Investigator: Robert Wilkinson, Ph.D.
Ref.: Burton, Franklin L. (Burton Engineering) , 1996 Water and Wastewater Industries
Electric Power Research Institute Report CR-106941, p. 2-45

[F] Wastewater Treatment with Nitrification (average 1-100 mgd plant capacities)
Energy Down The Drain, p. 26

[G] Energy Benchmarking Secondary Wastewater Treatment and Ultraviolet Disinfection Processes at Various (nine) Municipal Wastewater Treatment Facilities, PG&E February 2002
Electric Use of Total Plant Operations Exec-1 and pg. 5, Table 3 - 1,073 kWh/MG
Electric Use of Total Plant Operations Exec-1 and pg. 5, Table 3 - 4,630 kWh/MG

Summary of Water Energy Intensity for Northern and Southern California

The rest of this analysis is based on the following estimated energy intensities per million gallons of water (kWh/MG) delivered, treated, distributed, and disposed of in Northern and Southern California:[84]

[84] ibid (In this example NorCal system-wide Supply is estimated at 30 percent).

Table C-6 Prototypical Water Use Cycle Process Energy Intensity

	Northern California kWh/MG	Southern California kWh/MG
Water Supply and Conveyance	150	8,900
Water Treatment	100	100
Water Distribution	1,200	1,200
Wastewater Treatment	2,500	2,500
Total	3,950	12,700
Adopted	4,000	12,700

The Energy Efficiency of Water Use Efficiency

Energy savings associated with water savings provided in Table C-7 support the inclusion of water efficiency measures in energy efficiency program portfolios because of their relative low cost, long service life, and high resource value in terms of the avoided cost of energy. The following table reflects traditional water efficiency measures and their associated cold water energy savings resource values.

Table C-7 Water Efficiency Measure Cold Water Energy Savings

			Northern California			Southern California		
	Annual Savings Gallons/Year	Service Life	Annual kWh	Life-Cycle kWh	Resource Value	Annual kWh	Life-Cycle kWh	Resource Value
Residential								
Toilet Replacement 1.6 gpf (pre-1992)	2,250	25	9	225.0	$9	29	714	$32
Ultra Low-Flow Toilets	11,340	25	45	1,134.0	$44	144	3,600	$159
Energy Star Washing Machine	7,866	15	31	471.9	$27	100	1,498	$81
Commercial								
Ultra Low Flush Urinals	13,323	25	53	1,332	$52	169	4,230	$187
Waterless Urinals	25,568	25	102	2,557	$101	325	8,118	$359
Cooling Tower Condition Meter	729,906	10	2,920	29,196	$1,961	9,270	92,698	$5,609
Pre-Rinse Spray Head Installation	87,120	5	348	1,742	$136	1,106	5,532	$395
X-Ray Processor	1,042,723	5	4,171	20,854	$1,627	13,243	66,213	$4,733

Cost-effectiveness Assumptions

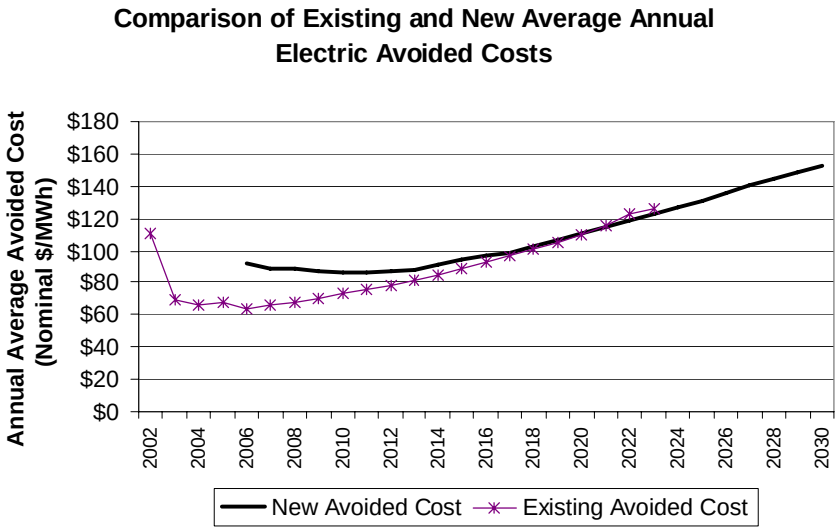
Resource values in this appendix were developed using the E3 Avoided Cost Methodology adopted by the California Public Utilities Commission (CPUC) in the April 7, 2005, Decision 05-04-024, Rulemaking (R.) 04-04-025. The CPUC adopted the E3 methodology for purposes of evaluating energy efficiency programs in R.01-08-028 and related energy efficiency proceedings.

The E3 model incorporates market price effects; the value of reliability through ancillary services; and the disaggregation of the avoided costs to time (hour, month, or time-of-use period) and to California climate zones. The E3 model forecasts the avoided costs of electric generation, transmission, and distribution that vary by hour, and the avoided costs of natural gas procurement, transportation, and delivery, which vary by month. Transmission and distribution (T&D) costs vary by utility service territory, planning division, and by the 16 Title-24 climate zones. Externality adders report environmental externalities: a T&D adder, which captures incremental demand-related capital expenditures, line losses and maintenance costs associated with increased energy use; a system reliability adder, which includes the cost of maintaining a reserve margin; and a price elasticity of demand adder, which recognizes that reduced demand results in a decrease in market-clearing price for electricity and therefore an increase in consumer surplus. The price elasticity of demand estimate varies by time-of-use period and month.

As currently utilized by the CPUC and energy utilities, the avoided cost projections in the E3 methodology extend to 2025. The calculations in this appendix include water use efficiency measures with 25-year service lives requiring that avoided cost projections be extended to 2030. The energy utilities submitted advice letter filings to the CPUC in April 2005 for purposes of updating their avoided cost projections. These filings projected utility avoided costs through 2030 for incorporation into the E3 methodology for valuing their energy efficiency resources. Figure C-3[85] compares the average utility avoided cost in place before and after the advice letter filings.

[85] Figure comes from E-3 published analysis of new and existing utility avoided costs.

Figure C-3



Source: E3

To calculate the resource value associated with the water use efficiency measures, the E3 methodology was modified to extend avoided cost projections to 2030. The adjustment from a 20-year to a 25-year measure results in less than a 7 percent change in the stated energy resource values. This means that the significant resource value potentials identified later in this appendix are not contingent upon modifying the avoided cost projections. E3 reviewed the adjustments and agreed the calculations were performed correctly.

Cold water energy savings are realized when one or more elements of the water use cycle - water conveyance, water treatment, water distribution systems and wastewater treatment facilities - process less water. They are also realized by avoiding incremental growth and requirements for plant expansions. In both cases the energy savings in the water use cycle result from the water use efficiency measures that were implemented. In this analysis water use cycle processes are assumed to operate 24 hours per day with an 85 percent load factor.

Energy Value of 2004 Best (Water) Management Practices

At a programmatic level, the California Urban Water Conservation Council (CUWCC) was created through the *Memorandum of Understanding (MOU) Regarding Urban Water Conservation in California* in 1991 to manage the process of implementing and updating the list of Best [water] Management Practices (BMP). To date 189 water agencies have pledged to implement the BMPs. CUWCC BMPs serve as a framework to quantify the energy resource value associated with water efficiency. The current lists of BMPs developed by the CUWCC follow.

Table C-8 CUWCC Best Management Practices[86]

BMP	Quantifiable Results
BMP 01: Water Survey Programs for Residential Customers	X
BMP 02: Residential Plumbing Retrofit	X
BMP 03: System Water Audits, Leak Detection and Repair	
BMP 04: Metering with Commodity Rates for all New Connections and Retrofit of Existing	X
BMP 05: Large Landscape Conservation Programs and Incentives	X
BMP 06: High-Efficiency Washing Machine Rebate Programs	X
BMP 07: Public Information Programs	
BMP 08: School Education Programs	
BMP 09: Conservation Programs for CII Accounts	X
BMP 09a: CII ULFT Water Savings	X
BMP 10: Wholesale Agency Assistance Programs	
BMP 11: Conservation Pricing	
BMP 12: Conservation Coordinator	
BMP 13: Water Waste Prohibition	
BMP 14: Residential ULFT Replacement Programs	X

Source: California Urban Water Conservation Council

[86] Quantifiable means annual reported BMP water use efficiency savings in acre feet per year, net of plumbing code compliance savings, reported pursuant to the 1991 Memorandum of Understanding Regarding Urban Water Conservation in California under protocol set forth by CUWCC. References: CUWCC (2005) *BMP Costs and Savings Study - A guide to Data and Methods for Cost-Effectiveness Analysis of Urban Water Conservation Best Management Practices* and (2003) *First Partial Revision*; M. Cubed (2003) *BMP Reporting Database Water Savings Calculations*; M. Cubed (1997) *California Urban water Agencies BMP Performance Evaluation, Final Report*; A&N Services (1996) *Guidelines to Conduct Cost-Effectiveness Analysis of Urban Water Conservation Best Management Practices*; U.S. EPA (1994) *Customer Incentives for Water Conservation, A Guide,* EPA/X820683-01-1, U.S. Environmental Protection Agency, Washington, DC. Measurement and evaluation is addressed by the CUWCC Measurement & Evaluation Committee.

To provide visibility to the potential impacts of integrated resource planning for water and energy efficiency programs, 2004 water sector BMP achievements were examined using the adopted energy efficiency avoided cost valuation methodology[87]. This analysis combines known planning criteria from each industry to assess the efficiency gain potential though programmatic integration.

Quantifiable water savings are available for eight of the BMPs, as shown in Table C-8. Each BMP includes several related water use efficiency measures. Assumptions for the water savings of each measure in gallons per day (GPD) and measure service life are reflected below in Table C-9.

[87] Resource values are produced using the E3 Avoided Cost Methodology adopted by the CPUC in the April 7, 2005 Decision 05-04-024, Rulemaking (R.) 04-04-025. The Commission adopted the E3 Methodology for the purposes of evaluating energy efficiency programs in R.01-08-028 and related energy efficiency proceedings. Avoided cost bases are maintained at the website http://www.ethree.com/CPUC/cpucAvoided26.xls

Southern California Resource Values: The E3 calculator utilized is version "SCE Tool 1q" and incorporates SCE's update to the E3 Methodology as described in SCE Advice 1187-E (U-338-E) of April 25, 2005 specifically "extending the avoided cost forecast to 25 years from the base year of 2006" and applying "a linear trend based on the last five years of data contained in the E3 Methodology" as described in the referenced Advice Letter, page 3, Section A.

Northern California Resource Values; The E3 calculator utilized is version "CEE_Calc_Tool_Commercial_1d" and incorporates PG&E's update to the E3 Methodology as described in PG&E Advice 2626-G/2654-E (U-39-M) of April 25, 2205 and reflect ATTACHMENT A, Table 4: Adjustments Made to Extend Forecast through 2030.

Table C-9 BMP Water Use Efficiency Measure Service Life and Savings

	Service Life	Savings gpd	Reference
BMP 01:	4.5	26.6	Residential Surveys: BMP Costs & Savings Study, Draft Revision March 2005, page 1-10 & 11, Table 1-3 (average of range)
	5	21.0	Residential Surveys, Single Family: Metropolitan Water District of Southern California (MWD) program planning assumptions
	4	8.8	Residential Surveys, Multi-Family: MWD program planning assumptions
BMP 02:	5.1		Residential Plumbing Retrofits: BMP Costs & Savings Study (July 2000 ed.), page 2-13, mid-point range, equivalent useful life five years April 28 2003 M. Cubed Technical Memorandum to M&E Committee re; BMP Reporting Database Water Savings Calculations - Page 4 of 15
	5	5.5	Low Flow Showerheads: BMP Costs & Savings Study, First Partial Revision December 2003, page 2-38, Table 1 Method 1 average
	3.5	4.2	Toilet Displacement Devices: BMP Costs & Savings Study, First Partial Revision December 2003, page 2-38, Table 1 Method 1 average
	2	1.5	Faucet Aerators: BMP Costs & Savings Study, First Partial Revision December 2003, page 2-38, Table 1 Method 1 average
	8.5	0.64	Toilet Leak Detection: BMP Costs & Savings Study, First Partial Revision December 2003, page 2-38, Table 1 Method 1 average
	8.5	0.5	Other Household Leak Detection: BMP Costs & Savings Study, First Partial Revision December 2003, page 2-38, Table 1 Method 1 average
	4	12.2	Turf Audit: BMP Costs & Savings Study, First Partial Revision December 2003, page 2-38, Table 1 Method 1 average
	4	25.9	Turf Audit With Timer: BMP Costs & Savings Study, First Partial Revision December 2003, page 2-38, Table 1 Method 1 average
	25	24.2	Ultra Low-Flow Toilets (ULFT): BMP Costs & Savings Study, Draft Revision March 2005, page 1-10 & 11, Table 1-3 (average of range)
	17.5		Hot Water on Demand: BMP Costs & Savings Study, Draft Revision March 2005, page 1-10 & 11, Table 1-3 (average of range)
BMP 04:	10.5	Reported	Metering With Commodity Rates: BMP Costs & Savings Study, Draft Revision March 2005, page 2-29 (though should probable be 20+, as if and when a meter fails, it would be replaced see Section 2.5
BMP 05:	10	Reported	Large Landscape: Budgets and Surveys: MWD Planning Practices; BMP Costs & Savings Study, Draft Revision March 2005, page 1-10 & 11, Table 1-3 (average of range) see Section 2.16
			Evapotranspiration (Eto)-based budgets: BMP Costs & Savings Study (July 2000 ed.), Table 1, page 53
			Large Landscape Surveys: Urban Water Conservation Potential (August 2001)
BMP 06:	14	21.6	H/E Washing Machines: BMP Costs & Savings Study, Draft Revision March 2005, page 1-10 & 11, Table 1-3 (average of range)
	15	21.6	BMP Costs & Savings Study, First Partial Revision December 2003, page A-6
		13.8	BMP Costs & Savings Study, First Partial Revision December 2003, page A-8 range average
BMP 09:	12.4		CII Conservation Programs: Urban Water Conservation Potential (August 2001) (decay rate 10%)
		527.5	CII Surveys: BMP Costs & Savings Study, Draft Revision March 2005, page 1-10 & 11, Table 1-3 (average of range)
	5	2,856.8	X-Ray Processor: MWD Program Planning assumptions
	3	136.6	Water Broom: MWD Program Planning assumptions
	5	300.0	Pre-Rinse Spray Head: BMP Costs & Savings Study, Draft Revision March 2005, page 1-10 & 11, Table 1-3 (average of range 100-500 gpd); expected life span see page 2-80
	3	200.0	MWD program planning assumptions
	5	240.0	PG&E Non-Residential Work Papers Supporting Application For Approval of 2006-2008 Energy Efficiency Programs and Budgets filed June 20 2005, R.01-08-028, pages 40 - 43 (electric) and 57 - 59 (gas) of 279, Non-Res Deemed Savings pages 14 or 20
	5	892.7	Industrial Process Improvement: MWD program planning assumptions
	8	103.6	High-Efficiency Washers: MWD program planning assumptions
	5	22.3	Flush Valve Kit: MWD program planning assumptions
	10	1,999.7	Cooling Tower Conditioning Meter: MWD program planning assumptions
BMP 09a:	25	36.5	CII ULFT Replacement: M. Cubed (2003) Technical Memorandum to the CUWCC M&E Committee re; BMP Reporting Database Water Savings Calculations - Page 10 of 15; BMP Costs & Savings Study, Draft Revision March 2005, page 1-10 & 11, Table 1-3 (average of range); BMP Costs & Savings Study, First Partial Revision December 2003, page A-12, Example 2A
	25	30.4	CII Dual Flush CII ULFT: MWD program planning assumptions
	30	30.1	Ultra Low-Flow Urinals: BMP Costs & Savings Study, Draft Revision March 2005, page 1-10 & 11, Table 1-3 (average of range)
	25	70.1	Waterless Urinals: BMP Costs & Savings Study, Draft Revision March 2005, page 1-10 & 11, Table 1-3 (average of range)
BMP 14:	25	31.1	Res - ULFT: BMP Costs & Savings Study, First Partial Revision December 2003, page A-12, Example 2A; MWD program planning assumptions; BMP Costs & Savings Study (July 2000 ed.), page 2-29; April 2003 Technical Memorandum, page 15 of 15

Source: California Urban Water Conservation Council

The CUWCC reporting system for reductions in water used by member agencies reflects 2004 BMP achievements for BMPs with quantifiable results.[88] The energy savings for these measures, both annual and life cycle, are shown for each of these measures in Table C-10.

[88] Data was obtained from public access CUWCC website http://bmp.cuwcc.org/bmp/summaries/public/bmpsavings.lasso

Table C-10 Energy Resource Value in Water Use Efficiency (2006-2008 (E3) Avoided Cost)[89]

Northern California (PG&E/SMUD)	MG	Annual Savings kWh	Useful Life	Life-Cycle kWh Savings	NPV Electric Avoided Cost
BMP 1 Water Survey Programs MF/SF	802	3,208,000	5	16,040,000	1,251,113
BMP 2 Residential Plumbing Retrofit	132	528,000	5	2,640,000	205,919
BMP 4 Metering & Commodity Rates	671	2,684,000	11	29,524,000	1,929,737
BMP 5 Large Landscape Conservation Programs	2,249	3,261,050	10	32,610,500	2,190,009
BMP 6 High-Efficiency Washing Machine Rebate	134	536,000	15	8,040,000	474,057
BMP 9 Conservation Programs CII	2,035	8,140,000	12	97,680,000	6,217,380
BMP 9a CII ULFT	109	436,000	25	10,900,000	430,340
BMP 14 Residential ULFT	5,490	21,960,000	25	549,000,000	21,674,941
Total Northern California	11,621	40,753,050			$34,373,496
Southern California (SCE/LADWP/SDG&E)					
BMP 1 Water Survey Programs MF/SF	1,095	13,906,500	5	69,532,500	4,969,753
BMP 2 Residential Plumbing Retrofit	180	2,286,000	5	11,430,000	816,946
BMP 4 Metering & Commodity Rates	916	11,633,200	11	127,965,200	7,543,053
BMP 5 Large Landscape Conservation Programs	3,072	31,334,400	10	313,344,000	18,959,692
BMP 6 High-Efficiency Washing Machine Rebate Program	183	2,324,100	15	34,861,500	1,872,831
BMP 9 Conservation Programs CII	2,779	35,293,300	12	423,519,600	24,350,142
BMP 9a CII ULFT	149	1,892,300	25	47,307,500	2,092,023
BMP 14 Residential ULFT	7,498	95,224,600	25	2,380,615,000	105,275,069
Total Southern California	15,871	193,894,400			$165,879,509
Total Statewide Impacts	27,492	234,647,450			$200,253,005

Source: CUWCC Reporting Database, April 2005 with 86 of 269 Reporting Units (32%) reporting BMP expenditures in 2004 Reporting Units include: Water utility districts, water agencies, irrigation districts, city and county water departments and, water service companies implementing BMPs.

The numbers shown in Table C-10 reflect the variability in water conservation impacts on water related energy requirements, depending upon measure location.[90] The energy values have been obtained based on the multipliers for Northern and Southern California. The landscape numbers assume that the applied water is not treated as wastewater. In addition to the more than 27 million gallons saved from the 2004 BMPs, 234 million kWh were also saved that year, worth more than $200 million over their useful lives.

At this time it is reasonable to use the energy intensity values contained in this appendix as proxy values to support program planning. Future analyses of water energy intensity should be refined geographically by applying characteristics of hydrologic regions, planning areas or detailed analysis units as required, and finally

[89] See footnote 83.

[90] Water conservation activity is reported by CUWCC aggregated; to support disaggregating between SoCal and NorCal, electric service customer populations were used to establish approximately 60 percent - 40 percent shares for SoCal and NorCal, respectively.

applied to a structure that will align with energy efficiency planning climate zones[91] (See Suggested Research Topics).

The need to measure location-specific water-energy efficiency impact does not constitute a programmatic barrier for energy efficiency planners. This treatment is consistent with current energy efficiency program planning practices. For example, all current weather-dependent energy efficiency measure savings reflect location-specific savings across 16 climate zones - for example heating; ventilation and air-conditioning as well as building envelope measures; insulation; window glazing; and infiltration. Therefore, adopting savings for water-energy efficiency reflecting regional water energy intensity could be readily incorporated into current energy efficiency program planning protocols. The key point is that regional variability in water energy intensity should not defeat integrated planning. Energy efficiency planning already addresses many efficiency measures with varying degrees of savings in 16 geographic climate zones.

Statewide Water Use Efficiency (WUE) Potential

While the energy saving potential of 2004 BMP results are significant, they in no way indicate statewide potential. As related above, this appendix relied on the CUWCC's reporting database and used CUWCC's BMP reporting structure to provide visibility for associated energy benefits. CUWCC stresses that the reported savings are conservative and "the database does not include water efficiency for a whole series of BMPs for which CUWCC did not have a method to calculate water savings"[92].

The Pacific Institute, in its November 2003 report *Waste Not, Want Not: The Potential for Urban Water Conservation in California*, cites water savings potential, reflected in Table C-11. The 2004 BMP reported results in Table C-10 that represent approximately 4 percent of the minimum potential cost-effective savings identified here.

[91] The California Department of Water Resources subdivides the state into 10 hydrological regions, 56 planning areas plus a more detailed breakdown into 278 detailed analysis units. Existing spatial analysis (GIS) readily supports integration of water measures into energy-efficiency program planning climate zones to ensure regional values align with energy-efficiency program planning protocols.

[92] Comments of Mary Ann Dickinson, Executive Director of the California Urban Water Conservation Council at the California Energy Commission Energy-Water Relationship Comment Workshop, Docket No. 04-IEP-01-H, June 21, 2005; Proceeding Minutes page 22.

Table C-11 California Urban Water Use in 2000

Potential to Improve Water Use Efficiency and Conservation

California Urban Water Use by Sector	Current (2000) Water Use (AF/year)	Best Estimate of Conservation (AF/year)	Potential to Reduce Use (%)	Minimum Cost-Effective Conservation (AF/year)
Residential Indoor	2,300,000	893,000	39	893,000
Residential Outdoor	983,000 to 1,900,000 (b)	360,000 to 580,000 (c)	25 to 40	470,000
Commercial/ Institutional	1,850,000	714,000	39	Combined CII: 658,000
Industrial	665,000	260,000	39	(e)
Unaccounted-for Water	695,000	(d)	(d)	(d)
Total	**6,960,000** (+/- 10%)	2,337,000	34	2,020,000

Source: The Pacific Institute

The question is really how much energy savings can actually be achieved through this much water use efficiency. The following calculations were performed to make this determination:

1. The average of *Best Estimate of [Water] Conservation* and *Minimum Cost-Effective Conservation* (Table C-11 above) is 2,178,500 acre feet per year, rounded to 2,150,000.
2. As shown in Table C-6 (and applied in Table C-11), the average energy intensity for Northern and Southern California is 4,000 and 12,700 kWh/MG, respectively; the weighted average based on customer populations is 9,220 kWh per MG[93].
3. 2,150,000 AF or 700,580 MG of California's achievable water conservation, multiplied by the 9,220 kWh per MG (the state's weight average water use cycle energy intensity), yields equivalent energy savings of 6,450 GWh, rounded to 6,500 GWh.

[93] The weight average of water use cycle energy intensity is based on year 2000 customer populations for Northern California of 5.167 million customers (PG&E and SMUD) and for Southern California of 7.057 million customers (SCE, LADWP and SDG&E) representing 92 percent of California's electric customers. This yields a customer allocation of 42.3 percent for Northern and 57.7 percent for Southern California. Applying the rounded allocation of 40 percent and 60 percent to respective energy intensities of 4,000 and 12,700 kWh per MG yields a population based weighted average of 9,220 kWh per MG.

4. 6,500 GWh and an 85 percent load factor yield a demand reduction of 873 MW, rounded to 850 MW.

   In Summary:

   - ✓ Annual water use efficiency water savings:
     - 700,580 MG
   - ✓ Water use cycle energy requirements:
     - 9,220 kWh/MG
   - ✓ Water use efficiency energy savings:
     700,580 (MG) X 9,220 (kWh/MG) = 6,459,344,373 kWh or 6,459 GWh
     Assumed Water Use Cycle Energy Savings = 6,500 GWh
   - ✓ Water use efficiency demand reduction:
     Peak Load (kW) = kWh / (Load Factor * 8760)
     Peak Load (kW) = 6,500,000,000 / (.85 * 8760) =
     873,000 kW or 873 MW
     Assumed Peak Load Reduction = 850 MW

5. Information from multiple sources shows that the cost of most water use efficiency measures ranges from about $58 to $710 per acre-foot or $178 to $2,179 per MG, depending upon the program. These costs include the full cost to manage the programs, capital investments, and required staffing[94]. Assuming an average of this range, or $384 per acre-foot ($1,178 per MG), the approximate cost in terms of energy efficiency is $0.13 per annualized kWh (700,580 MG X $1,178/MG = $825.6 million / 6,500,000,000 kWh = $0.127/kWh, rounded to $0.13/kWh).

Table C-12 presents the results of these calculations and compares them to the California's energy efficiency programs for 2004-2005 and those planned for 2006-2008.

[94] Department of Water Resources 2005 Water Plan Update, Volume 2, page 22-2, Potential Benefits of Urban Water Use Efficiency, and; Potential Costs of Urban Water Use Efficiency

Table C-12 Comparison of Water Use Efficiency to Energy Efficiency Resource Value

	2004-2005 [1]	2006-2008 [2]	WUE [3]
GWh (Annualized)	2,745	6,812	6,500
MW	690	1,417	850
Funding ($ million)	$762	$1,500	$826
Cost per Annual kWh	$0.28	$0.22	$0.13
WUE Relative Cost	46%	58%	

[1] CPUC Rulemaking R.01-08-028, Decision D.03-12-060
[2] CPUC Rulemaking R.-01-08-0228, Decision D.04-09-060
[3] California Water Plan Update 2005, Bulletin 160-05 California Department of Water Resources, page 22-2

The table shows that the estimated energy savings from statewide water use efficiency is more than double the energy savings from the 2004-2005 energy efficiency programs and almost as large as those planned for 2006-2008. The estimated peak reduction from water use efficiency falls between the values for these years. From a program cost standpoint, water use efficiency is roughly one-half the cost of energy efficiency programs.

These estimates are reasonably robust. If the energy savings were only half as much or if the costs were twice as much, water use efficiency would be as cost-effective as current and planned energy efficiency programs.

One of the questions that came up during the California Energy Commission's (Energy Commission) *Integrated Energy Policy Report (Energy Report)* proceedings was concerned with the different ways that water and energy programs address the useful life of the same measures. To evaluate the potential impact of this difference, Table C-13 compares several measures that are common to both energy efficiency and water use efficiency programs. The Estimated Useful Life (EUL) and energy savings from water heating and from savings in the water use cycle (cold water savings) are presented for four common measures:

Table C-13 Energy Efficiency – Water Use Efficiency Common Measures

	Energy - EUL	Water – EUL	Heating Annual Savings (kWh)	Cold Water Savings (kWh)
Low-Flow Showerhead[1]	10	5	202	16
Faucet Aerator[2]	10	2	78	4
Clothes Washer[3]	15	15	644	100
Pre-Rinse Spray Valve[4]	5	5	12,310	1,106

[1] Measure #504 California Statewide Residential Sector Energy Efficiency Potential Study #SW063
[2] Measure #506 ibid
[3] Measure #601 ibid
[4] PG&E CPUC Application for Approval of 2006-2008 Energy Efficiency Programs and Budget (U 39 M), Advice Letter 05-06-004 ATTACHMENT 4, ERRATA FOR PROGRAM DESCRIPTIONS, Workpapers

As shown above, water use efficiency planners apply estimated useful lives to the same measures that are either equal to or lower than those applied by energy efficiency planners. For purposes of consistency with the energy savings calculations shown later in this appendix, the EULs used by the energy planners were adopted.

Another concern was that these four measures represent the full potential for additional water use efficiency gains. However, the small set of overlapping measures represents less than 2 percent of the *known* energy savings and resource value that can be created through cold water savings. These additional savings – 98 percent - will come from measures that have been generally overlooked by energy efficiency planners.

At one time water use efficiency was narrowly viewed as a temporary source of water supply in response to drought or emergency water shortage situations. However, this analysis shows that water use efficiency is a viable long-term water and energy resource supply option. In short, significant, attainable energy savings can be realized in the form of water use efficiency.

Comparing Water and Energy Efficiency Programs

Comparing water and energy efficiency programs reveals differences in treatment in the following areas: program oversight, resource valuation, technical potential, budgets (trends), planning, implementation and evaluation, measurement, and verification. This section examines how both programs address these areas.

Program Oversight and Compliance

There is significant variability between water and energy efficiency program targets, regulatory oversight, and compliance. Targets for water conservation are referenced

to a 10-year reporting period. Performance requirements for the BMPs with quantifiable results follow in Table C-14:

Table C-14 Best Management Practices

BMP	Requirements
BMP 01: Water Survey Programs for Single-Family and Multi-Family Residential Customers	Survey 15 percent of residential customers within 10 years
BMP 02: Residential Plumbing Retrofit	Retrofit 75 percent of residential housing constructed prior to 1992 with low-flow showerheads, toilet displacement devices, toilet flappers and faucet aerators
BMP 04: Metering with Commodity Rates for all New Connections and Retrofit of Existing	Install meters in 100 percent of existing un-metered accounts within 10 years; bill by volume of water use; assess feasibility of installing dedicated landscape meters
BMP 05: Large Landscape Conservation Programs and Incentives	Prepare water budgets for 90 percent of commercial and industrial accounts with dedicated meters; provide irrigation surveys to 15 percent of mixed-metered customers
BMP 06: High-Efficiency Washing Machine Rebate Programs	Provide cost-effective customer incentives, such as rebates, to encourage purchase of machines that use 40 percent less water per load
BMP 09: Conservation Programs for CII Accounts	Provide a water survey of 10 percent of these customers within 10 years and identify retrofitting options; OR reduce water use by an amount equal to 10 percent of the baseline use within 10 years
BMP 14: Residential ULFT Replacement Programs	Replace older toilets for residential customers at a rate equal to that of an ordinance requiring retrofit upon resale

Source: California Urban Water Conservation Council

A consistent and broadly acceptable method to evaluate (water use efficiency) cost-effectiveness and water savings is needed[95]. Documentation and evaluation of the achievements attributable to water use efficiency projects and programs, vital elements of successful water use efficiency efforts, need to be improved. The quantification of benefits for many projects lacks a necessary level of scientific

[95] Ibid

rigor[96]. Implementation of the BMPs by the water agencies is voluntary, and water efficiency program performance is self-reported, monitored by the CUWCC[97]. CUWCC is a non-profit agency with its governance administered by a committee comprising six representatives: three representatives from member water agencies and three representatives from public advocacy organizations[98]. Not all water agencies have signed onto the MOU agreement, and not all signatories are fully implementing the BMPs[99].

In contrast, the state's investor-owned utilities (IOU) energy efficiency programs are regulated by the CPUC[100]. The requirements include:

- ✓ Administrative structure for efficiency programs
- ✓ Program evaluation, measurement, and verification (EM&V)
- ✓ Separation between "those who do" and "those who evaluate" programs
- ✓ Protocols for measuring efficiency programs are defined in the *Protocols and Procedures for the Verification of Costs, Benefits, and Shareholder Earnings from Demand-Side Management Programs* [101]
- ✓ EM&V integration into the program planning process
- ✓ EM&V funding guidelines
- ✓ The type and frequency of EM&V studies conducted for each program and the major study parameters utilized for each study, including sample design, monitoring duration and schedule, and approaches undertaken to evaluate and minimize bias
- ✓ Cost-effectiveness tests used to evaluate program performance and proposed programs including:

[96] Department of Water Resources 2005 Water Plan Update, Volume 2, page 22-4, WUE Challenges – Data Collection.

[97] CUWCC Governance Policies Section 10. Access to BMP Reporting Data: 10.1a.: "The Council will regard any data stored in the Council BMP Reporting Database that has been formally 'submitted as final" as public information', and; Section 10.1c.: "All publicly-released reports shall carry a disclaimer indicating that reports are based on self-reported data that has not been 100% validated by the Council."

[98] CUWCC Governance Policies Section 6.1, "The Council's Governance Committee shall be responsible for initiating the Executive Director's Annual Performance Review. The committee shall be responsible for oversight of Council governance, including review of bylaws, policies, membership development and training, communication (internal and external), strategic planning and meeting protocol." "The Governance Committee shall be composed of three Group 1 representatives (urban water supplier representatives) and three Group 2 representatives (public advocacy organizations) from the Steering Committee.

[99] Department of Water Resources 2005 Water Plan Update, Volume 2, page 22-3

[100] See CPUC Rulemaking 01-08-028, Decision 05-04-051 April 21, 2005

[101] As adopted by California Public Utilities Commission Decision 93-05-063 Revised March 1998 Pursuant to Decisions 94-05-063, 94-10-059, 94-12-021,95-12-054, 96-12-079, D.98-03-063, and D.99-06-052.

- program costs and participation levels
- number and type of measures
- environmental adders informed by and coordinated with the Climate Change Action Registry
- continuity of the input assumptions and calculations for the tests of cost-effectiveness (California Standard Practice Manual[102])
- *ex post* (after-installation) measurement of lifecycle savings inform and update *ex ante* (pre-installation) assumptions for future programs
- values for the weighted cost of capital (instead of using different values for each implementer). The current authorized cost of capital for the IOUs ranges between 7.6 percent and 8.7 percent, depending upon the IOU.

Program Funding

Variations in program oversight and compliance might reflect, in part, energy efficiency program ratepayer funding and funding levels. California electric industry deregulation legislation and other regulation established minimum levels of energy efficiency funding from 1998 through 2001, and are currently used by both IOUs and local publicly owned electric utilities[103].

Additionally, in 2003 the CPUC ordered IOUs to file plans to include energy efficiency as part of their long-term procurement supply portfolios for the first year, five years, and twenty years[104].

[102]http://www.cpuc.ca.gov/static/industry/electric/energy+efficiency/rulemaking/03eeproposalinfo.htm

[103] Electric Industry restructuring legislation Assembly Bill 1890 (Brulte, 1996) codified in Public Utilities Code (PU Code) under Division 1, Part 1, Chapter 2.3. Electrical Restructuring. Under Article 7 Research, Environmental, and Low-Income Funds, Section 381 directed the CPUC to require each IOU to identify a separate rate component to collect revenues used to fund cost-effective energy efficiency and conservation activities. Herein the IOUs were directed to fund not less than the following levels commencing January 1998 through 2001 ($ million dollars):

	1998	1999	2000	2001	Total
SDG&E	$32	$32	$32	$32	$128
SCE	$90	$90	$90	$50	$320
PG&E	$106	$106	$106	$106	$424
Total	$228	$228	$228	$188	$872

Article 8, Section 385 (a) directs each local publicly owned electric utility to establish a non-bypassable, usage based charge on local distribution service of not less than the lowest expenditure level of the three largest IOUs on a percent of revenue basis, calculated using the utility's total revenue requirement for the year ended December 31, 1994, and IOU total annual expenditures described above under section 381 (approximately 3 percent).

[104] CPUC Decision D.0312062 directs IOUs recover authorized procurement-related energy efficiency [costs] through its existing non-bypassable Public Purpose Programs Charge (PPPC), which applies to all IOU retail customers. Additionally, CPUC D.03-12-062 directs that incremental procurement

Table C-15 shows projected procurement costs for utility energy efficiency programs for the years 2004 through 2008 ($ millions):

Table C-15 IOU Supply Portfolio of Electric Energy Efficiency Procurement

Utility	2004	2005	2006	2007	2008	Total
PG&E	25	50	50	75	100	300
SCE	60	60	60	60	60	300
SDG&E	25	25	25	25	25	125
Total	**110**	**135**	**135**	**160**	**185**	**725**

Table C-16 shows the effect of combining the procurement budget with the budget for electric energy efficiency programs directed under the Public Goods Charge (PGC) funds for 2004 and 2005 ($ millions). This increases the total electric energy efficiency budget for 2004-2005 by $245 million, bringing the total to more than $760 million.

Table C-16 IOU Combined Electric Energy Efficiency Budgets 2004-2005

	PGC Budget	Procurement Budget	Total Budget
PG&E	258	75	333
SCE	183	120	303
SDG&E	77	50	127
Total	**518**	**245**	**763**

Current Energy Efficiency Program Funding

- $763 million was allocated to 2004-2005 electric energy efficiency programs, an increase of $245 million (43 percent) over statutory levels
- The 2006 – 2008 funding cycle was approved at just under $2 billion, of which approximately $1.5 billion is for electric energy efficiency, with the balance for natural gas.

Current Water Efficiency Program Funding

- In 2002 voters approved Proposition 50, which provides $180 million for water use efficiency programs in the years 2003 – 2007[105]. Proposition 50 annual

---

energy efficiency costs be subject to recovery though a non-bypassable charge to all customers and orders IOUs to establish the Procurement Energy Efficiency and Balancing Account (PEEBA) to track costs and revenues.

[105] Proposition 50 Chapter 7 provides $180 million for water use efficiency programs per year as follows: Urban water use efficiency $60 million; Agricultural water use efficiency $60 million; Water

funding for water efficiency is estimated at $36 million (actual program funds provided water agencies is reported to be an average of approximately $30 million per year[106]).

- Funding for water efficiency programs also comes from several other sources, including the implementing water agency, the state's General Fund, federal funds, and general obligation bonds. While these sources add to the available funds, the total is significantly less than that committed to energy efficiency programs.
- Funding has fallen below commitments made in 2000 through the CALFED Record of Decisions, Stage 1 2000-2007. By 2003 investments lagged by $235 million[107].

Integrated Resource Planning

Currently, water efficiency programs receive no credit for, and planners do not quantify, the large energy savings associated with water saving measures that are implemented. Additionally, until energy efficiency regulation and policy are changed, energy utilities cannot include or target these significant energy-efficiency gains. Neither water nor energy efficiency program planners address or target these potential efficiency gains, and a significant gap exists in statewide water and energy resource planning.

Water, wastewater, and energy efficiency program planners acknowledge the importance of comprehensive resource management. Water efficiency programs are based on the same cost-benefit methodology as energy efficiency programs and reference the Standard Practice Manual.[108] This common methodology recognizes the importance of clearly understanding the following four cost-effectiveness perspectives:

1. Water, wastewater or energy program participants
2. The water, wastewater or energy utility
3. The water, wastewater or energy supply system
4. Society

---

recycling $60,000. The Bond law was passed in November 2002, and the funding will be allocated through 2007 (five years). Proposition 13 also had funding for water use efficiency but in form of loan. DWR Water Use Efficiency Office is funded partially through the general fund; annual budget less than $1 million. In addition to Statewide funding, local agencies also budget for water use efficiency programs.

[106] See footnote 72, Proceeding Minutes page 23.

[107] Department of Water Resources 2005 Water Plan Update, Volume 2, page 22-2.

[108] "A Guide to Customer Incentives for Water Conservation" Prepared by Barakat and Chamberlain for CUWA, CUWCC, and US EPA, February 1994 (EPA # 230R94001).

However, water, wastewater, and energy efficiency cost-benefit valuation is performed from the utility and, in the best cases, the electric supply system ***or*** the water supply system ***or*** the wastewater collection system perspective (See 2 or 3 above). Ultimately the suboptimal affects of this discrete or isolated water, wastewater, and energy resource management is borne by the consumer who must pay the water, the wastewater, and the energy utility bills.

Under the broader societal perspective, transfer payments between the water utility and participating customers are canceled out; also eliminated are transfer payments among the water utility and other utilities. The costs that are avoided by the electric, gas, water, or wastewater utilities are viewed as societal benefits, and any additional costs that are incurred by these utilities as a result of a water efficiency program are societal costs. Drawing the boundary around the entire water use cycle and including all end users and affected utilities facilitates this societal valuation.

Analysis contained in this appendix has demonstrated that the state's water, wastewater and energy resources are inextricably entwined. Incomplete accounting understates the resource value of water use efficiency. Integrated resource planning of water, wastewater and energy must be performed from *society's* perspective and answer the question, "What mix of water and energy efficiency measures will create the greatest return on the combined ratepayer investment?"

An integrated water-energy societal total resource cost valuation would include the avoided marginal cost of water and wastewater treatment, related environmental externalities, and the associated marginal cost of energy (kWh), capacity (kW), transmission, distribution (including line losses), and environmental externalities. Environmental externalities related to avoiding water and energy use need to be itemized (to remove potential double-counting) and combined to reflect composite environmental impacts.

With a more complete avoided cost-based justification, improved cost-benefit ratios and corollary increased program funding, water-efficiency program market penetration could significantly increase. Integrated water and energy demand-side management would increase both water and energy efficiency program impacts.

Suggested Research Topics

1. Regional Cold Water Energy Intensity (near-term):

    a. Research and develop regional cold water energy intensities. Adopt proxy values and establish linkage to forecasting climate zones. The information being developed by the University of California, Santa Barbara and the Pacific Institute will help develop a proxy that can be relied upon to develop pilot water-energy programs while more detailed studies are being conducted. In particular, while studies of urban water

uses indicate that significant energy can be saved by reducing water consumption, the drivers for these opportunities are not well understood. A comprehensive inventory, characterization, and assessment of the primary types of water-related energy consumption by type of water source, system, function, and end use will eventually be needed to develop the detailed methodologies upon which cost-effective programs can be based. Water-related energy consumption can then be mapped from its source through various categories of end use to develop a comprehensive understanding of the points and relative magnitudes of energy consumption along the water supply chain, and the types of systems, processes, equipment, and measures that could reduce water and energy consumption at these points.

b. For existing cold ,water measures develop base case unit energy consumption (UEC), high-efficiency (HE) UEC, Base and HE Peak watt and demand savings, volume sensitive installed measure costs, and expected useful life values.
c. Identify opportunities for participating in demand response programs.
d. Identify and evaluate new cold water measures targeted to create resource value specifically suited to integrated water-energy resource planning not previously addressed under the discrete/isolated water/energy resource management regime.
e. For cold water measures found to be viable under item d., above, develop planning data identified for existing cold water measures.
f. Incorporate research elements (steps a. through d., above) into the Database for Energy Efficiency Resources (DEER) for use by energy efficiency program planners consistent with program planning protocols enunciated in CPUC Rulemaking 01-08-028, Decision 05-04-051.

2. Pilot Projects that Document and Quantify the State's Primary Water-Energy Interdependencies (longer-term):

    a. Select water utilities that collectively represent most of the primary types of water-energy interdependencies in California to include in the pilot. Several water utilities have already indicated interest in participating in such a pilot. These include the Metropolitan Water District (MWD), Inland Empire Utilities Agency (IEUA), the Los Angeles Department of Water and Power (LADWP), Palo Alto Utilities, and Sonoma County Water Agency.
    b. Conduct pilot projects to document the specific relationships.
    c. Inform and adjust proxy values developed above.

3. Seasonal Demand Shifting

    a. In Southern California, groundwater pumping uses approximately 30 percent of the energy required to import water from Northern

California. Groundwater aquifer source production and recharge requirements are fixed and finite. During periods of seasonal peak energy demand water agencies might rely on groundwater sources and recharge the aquifers using imported water months later in the off-peak season. In this manner ground water storage capacities could be used to encourage large-scale and long-term seasonal peak demand shifting.

b. Identify groundwater aquifers where groundwater pumping and recharge is being performed by water agencies.
c. Identify groundwater aquifers that are not currently being tapped for groundwater pumping.
d. Assess the operational feasibility and associated costs and benefits to encourage the seasonal demand shifting described above (item a.).

4. Conveyance-Related Peak Demand Reduction (State Water Project and other systems)

    a. Water agencies undertake projects to increase pumping and storage capacities based upon the given agency's operational cost-benefit perspective. Assess and report incremental cost-effective measures that can be implemented to increase pumping capacities and storage to reduce peak energy demands that are cost-effective, based upon a more comprehensive societal cost-benefit evaluation.
    b. Evaluate opportunities to reduce peak demand through the coordinated operation of federal and state water projects.

APPENDIX D: EXCERPT FROM CALIFORNIA WATER PLAN UPDATE 2005

VOLUME 1, STRATEGIC PLAN, CHAPTER 2, A FRAMEWORK FOR ACTION

Sustaining Our Water Resources

Fundamental Lessons

The Framework for Action embodies the following fundamental lessons, learned by California's water community through the experience of recent decades.

- The practice of water conservation and recycling in California has grown dramatically and must continue as a fundamental strategy for all regions and individual water users in California. The cumulative effect of each decision to use water more efficiently has an enormous impact on future water supplies and water quality.
- California must protect the quality of its water and use available supplies with great efficiency because water will always be a precious resource.
- Science and technology are providing new insights into threats to our watersheds, including our waterways and groundwater basins. California must use this knowledge to take protective actions and manage water in ways that protect and restore the environment.
- Sustainable development and water use foster a strong economy, protect public health and the environment, and enhance our quality of life. Sustainable development relies on the full consideration of social, economic, and environmental issues in policy- and decision-making. Sustainable water use assures that we develop and manage our water and related resources in a way that meets the needs of the present while protecting our environment and assuring the ability to meet the needs of the future.
- Solutions to California's water management issues are best planned and carried out on a regional basis. Hydrological, demographic, geopolitical, socioeconomic, and other differences among California's regions demand that the mix of water management strategies be suited to meet each region's needs for the long term.
- California needs additional groundwater and surface water storage capacity. Storage gives water managers tremendous flexibility to meet multiple needs and provide vital reserves in drier years.

Foundational Actions

To ensure that our water resource use is sustainable, water management at all levels – State, federal, regional, and local - must achieve these three foundational actions:

1. Use water efficiently.
2. Protect water quality.
3. Support environmental stewardship.

A number of resource management strategies that can be used to accomplish the foundational actions are listed in the following sections and described in more detail in Volume 2 Resource Management Strategies.

Use Water Efficiently

To minimize the impacts of water management on California's natural environment and ensure that our state continues to have the water supplies it needs, Californians must use water efficiently to get maximum utility from existing supplies. Californians are already leaders in water use efficiency measures such as conservation and recycling. Because competition for California's limited water resources is growing, we must continue these efforts and be innovative in our pursuit of efficiency. Water use efficiency will continue to be a primary way that we meet increased demand. In the future, we must broaden our definition of efficient water use to include other ways of getting the most utility out of our groundwater and surface water resources and water management systems:

- Increase levels of urban and agricultural water use efficiency.
- Increase recycled municipal water and expand its uses.
- Reoperate water facilities to improve their operation and efficiency.
- Facilitate environmentally, economically, and socially sound transfers.
- Reduce and eliminate groundwater overdraft.

As California's population grows from 36.5 million to a projected 48 million in 2030, there is bound to be an effect on California's environment. By wringing every bit of utility from every drop of water, Californians can stretch water supplies and help ensure continued economic and environmental health.

Protect Water Quality

California must also protect and improve water quality to safeguard public and environmental health and secure the state's water supplies for their intended uses. Water supply and water quality are inseparable in water management. While implementing projects to reduce water demand or to augment supply, water managers must employ methods and strategies that protect and improve water quality:

- Protect surface waters and aquifers from contamination.
- Explore new treatment technologies for drinking water and groundwater remediation.

- Match water quality to its intended uses.
- Improve management of urban and agricultural runoff.
- Improve watershed management.

Support Environmental Stewardship

To ensure sustainability, California must also manage water in ways that protect and restore the environment. Water is a vital natural resource for people and the environment, so water management activities must occur in the context of resource management and environmental protection. Water development in California has a rich history of conflict, at times pitting water supply projects against ecosystem protection. Water supplies and the environment must both be considered together. Water managers must support environmental stewardship as part of their management responsibilities. As managers develop and deliver reliable water supplies, environmental stewardship can be incorporated in many ways:

- Integrate ecosystem restoration with water planning and land use planning.
- Restore and maintain the structure and function of aquatic ecosystems.
- Minimize the alteration of ecosystems by water management actions.
- Improve watershed management.
- Protect public trust resources.
- Integrate flood management with water supply management.

Recommendations

California Water Plan Update 2005 provides recommendations for the next 25 years. These recommendations are directed at decision-makers throughout the state (referred to as California), the executive and legislative branches of State government, and DWR and other State agencies. (See Chapter 5 Implementation Plan for details.)

1. California needs to invest in reliable, high quality, sustainable, and affordable water conservation, efficient water management, and development of water supplies to protect public health, and to maintain and improve California's economy, environment, and standard of living.

2. State government must provide incentives and assist regional and local agencies and governments and private utilities to prepare integrated resource and drought contingency plans on a watershed basis; to diversify their regional resource management strategies; and to empower them to implement their plans.

3. State government must lead an effort with local agencies and governments to inventory, evaluate, and propose management strategies to remediate the causes and effects of contaminants on surface and groundwater quality.

4. California needs to rehabilitate and maintain its aging water infrastructure, especially drinking water and sewage treatment facilities, operated by State, federal, and local entities.

5. State government must continue to provide leadership for the CALFED Bay-Delta Program to ensure continued and balanced progress on greater water supply reliability, water quality, ecosystem restoration, and levee system integrity.

6. State government needs to take the lead in water planning and management activities that: (a) regions cannot accomplish on their own, (b) the State can do more efficiently, (c) involve interregional, interstate, or international issues, or (d) have broad public benefits.

7. California needs to define and articulate the respective roles, authorities, and responsibilities of State, federal, and local agencies and governments responsible for water.

8. California needs to develop broad and realistic funding strategies that define the role of public investments for water and other water-related resource needs over the next quarter century.

9. State government should invest in research and development to help local agencies and governments implement promising water technologies more cost effectively.

APPENDIX E: A WATER-ENERGY ROADMAP

Recommendations of the Water-Energy Relationship Working Group

Presently, water and energy utilities seek to separately optimize their respective resource portfolios. Since energy is typically their second largest cost,[109] water utilities already proactively seek opportunities to reduce energy consumption and increase energy production to reduce the net cost of their water supplies. However, the search for opportunities typically does not extend beyond their own systems and facilities. This is more a significant opportunity than a problem.

Stakeholder input for this staff paper indicates that the greatest potential for positively affecting the state's energy circumstance is beyond current best practices. Specifically, the primary opportunity is in the integrated value of water, energy, and externalities - like societal value - embedded in a unit of saved water. The incremental benefit of these integrated values can be realized by arranging the systems and operations of both the state's water and energy utilities around this holistic valuation approach.

For example, the state's single largest consumer of energy, the State Water Project (SWP), already strives to maximize off-peak and minimize on-peak pumping. However, if the goal were instead to minimize total and peak water-related energy consumption throughout the state, what options might be considered that would otherwise remain unconsidered? Below is a sample of the types of opportunities that could be possible if the planning perspective were broadened to include the optimization of water and energy resources statewide.

- Shift water pumping to off- and partial-peak time periods. Both DWR and the State Water Contractors (SWC) – 29 water agencies that purchase water from the SWP -- note that the SWP is designed to deliver water 24 hours a day, 365 days a year. Purchasers of SWP water need to take delivery when it comes down the aqueduct. Additional storage at strategic points along the aqueduct, whether owned by SWP or any of its customers, could increase operating flexibility and allow additional shifting of both SWP and SWC pumping loads to partial-and off-peak periods.[110]

- Shift water pumping to non-summer periods. Some water agencies in Southern California already rely heavily on groundwater pumping during the

[109] Salaries are usually first.

[110] Any increase in storage increases operational flexibility. This can be accomplished by oversizing aqueducts and canals, off-stream storage, and pipelines. SWP agricultural customers' systems are presently optimized for 24-hour deliveries. With proper incentives, it may be possible to modify these agricultural customers' systems to increase flexibility in SWP deliveries.

summer, and recharge their wells with imported SWP water during other times of the year. This groundwater production and recharge could be coordinated to create seasonal load-shifting.[111]

- Increase use of recycled water. While use of recycled water has nearly tripled since 1970, it still accounts for a very small percentage of the state's water supplies.[112] At a minimum, recycled water should be used wherever possible for landscape irrigation, though the high cost of dual distribution networks has been a major barrier.[113] When viewed from a societal perspective, significant investment in programs to reduce landscape irrigation is warranted on the basis of their energy benefits alone.

- Capture energy in water systems. Water utilities purchase significant amounts of energy to transport water though their systems. There are opportunities to recapture some of this energy through in-conduit turbines. The effect of this in-conduit hydropower production would be to decrease a water utility's net energy requirements. While opportunities exist to capture this energy, there are few incentives (and many disincentives) for development. Viewed on a holistic basis, the efficient utilization of energy within an existing pipeline or conduit would be viewed as an efficiency retrofit that qualifies for funding support by energy utilities.[114]

- Reduce energy for water pumping. Oversizing and/or lining pipelines can reduce friction and the amount of energy needed to transport water.

- Reduce energy for treatment. Both potable and wastewater systems could be reconfigured to incorporate storage, allowing treatment to be deferred to off-peak periods.

In addition to opportunities for reducing and shifting water utilities' energy consumption, stakeholders identified an important new opportunity – saving energy by saving water. When a unit of water is saved, so too is the energy required to convey, treat, deliver, and safely dispose of that unit of water.

In order to employ this value in designing cost-effective programs, this water ***energy intensity*** must take into account all of the steps in the water cycle. The energy

[111] The state's highest electric demand is on hot summer days. If significant water activities could be shifted to other months, the state may need to build less generation and transmission capacity. In addition, electric reliability would be increased, and the adverse public health, safety, and economic impacts of rotating outages avoided.
[112] *California Water Plan Update* 2005, public review draft, April 2005.
[113] During summer months, as much as 50-70 percent of residential water use in Central and Southern California is for landscape irrigation.
[114] In-conduit hydropower does not presently qualify as an energy efficiency retrofit for purposes of energy utilities' programs. While in-conduit hydropower is RPS-eligible and could qualify for supplemental energy payments (SEPs), it would not be feasible to develop mini- and micro-hydro under the same rules as utility-scale generation.

intensity of cold-water energy savings is presently not considered in water or energy efficiency program planning. When a saved unit of water is valued from a societal cost perspective, significant energy-efficiency, embedded in water efficiency, is clear. The following example shows the electric energy resource value of just one water efficiency measure, BMP14[115]:

> An ultra-low-flow toilet saves 11,340 gallons of water per year and has a service life of 25 years. This results in potable cold-water energy savings of 91 kilowatt hours (kWh) per year, or 2,275 kWh over its useful life. The present value of electricity's avoided cost is $141. In 2004, water utility programs installed 1.8 million ultra-low-flow toilets in California residences, resulting in cold water savings of 60 million kWh per year, or 1.5 billion kWh over the program's life. The present avoided cost value through this single BMP is $119 million[116].

This simple analysis shows how energy can be saved by saving water. However, energy utilities are not currently authorized to invest in cold water savings. This raises some important questions:

- How much water or energy could be saved with existing technology, without basing their cost-effectiveness upon a single resource like the avoided cost of water or electricity, natural gas, or diesel?

- What incremental energy benefits would be realized if saved water were valued on a societal basis, and energy utilities were allowed to participate in programs that save energy by saving water?

Regarding a comprehensive statewide water and energy program:

- How can programs and incentives be structured to both encourage collaboration across utility systems and boundaries and allow energy utilities to share the costs of water conservation and efficiency programs (to access water savings not deemed cost-effective on a single utility resource cost test)?

The following table describes some actions that could facilitate a statewide shift toward integrating the water and energy resource planning and management needed to achieve incremental societal benefits.

[115] See discussion of water conservation and efficiency "best management practices" (BMPs) in Appendix C.
[116] See Appendix C for full discussion of this issue and information source references.

ENERGY OBJECTIVE	APPROACH	OPTIONS
Optimize the state's water and energy resources & assets on an integrated basis	Build policy framework & infrastructure	1. Identify synergistic benefits that make business sense to both water & energy stakeholders. 2. Revise both water & energy utilities' investment criteria to incorporate a societal perspective. 3. Adjust resource pricing methodologies to reflect total societal values. 4. Authorize energy utilities to invest in programs for cold water savings. 5. Structure funding & incentives to attain targeted responses. 6. Provide low-interest loans & grants for incremental water infrastructure that produce benefits to the electric grid. 7. Create a joint agency task force to establish protocols for sharing costs, benefits and responsibilities among multiple stakeholders subject to different jurisdictional rules and regulations. 8. Coordinate water and energy capital programs to maximize infrastructure investments for benefit of both resources.
Increase energy supplies	Support development of additional hydropower capacity	1. Resolve conflicts with FERC relicensing process. 2. Modify Renewable Portfolio Standards to include all new and increased hydropower capacity. 3. Provide access to Supplemental Energy Payments. 4. Establish incentives for re-powering for incremental pumped storage capacity.[117] 5. Allow in-conduit hydropower to qualify for funding as an energy recovery facility, qualified as an energy efficiency retrofit.
	Remove disincentives to energy self-sufficiency	1. Allow water utilities to wheel self-produced power to themselves, anywhere on their systems. 2. Streamline the interconnection process and reduce costs. 3. Remove net metering caps.
	Encourage production of excess power	1. Provide technical & funding support for development of renewable resources & distributed generation. 2. Encourage partnering between water & energy utilities in power development. 3. Establish long-term power purchase agreement for such excess production that exceeds bulk wholesale markets and

[117] Hetch Hetchy implemented system improvements that increased peak hydropower capacity by 48 MW at a capital cost of $8 million, 83 percent less than the cost of installing a new unit of comparable capacity.

ENERGY OBJECTIVE	APPROACH	OPTIONS
		assures payments that support project financing. 4. Provide a ready market for purchasing any over-production of power (e.g., require investor-owned utilities to include in their energy supply portfolios).
Increase energy efficiency and demand side management	Help water utilities develop & implement comprehensive energy management	Provide technical, funding & other support.
	Reduce peak energy consumption (seasonal & time-of-use)	Increase system & operating flexibility (e.g., increase capacity for pumping groundwater during summer, deferring water imports to fall and winter).
	Establish incentives for shifting seasonal use	Compensate water utilities for deferring water imports from summer to fall.[118]
Increase operating flexibility	Maximize ancillary services benefits of the state's hydropower resources	1. Increase pump storage capacity. 2. Use hydro to shape wind & other intermittent resources (e.g., solar).
	Increase storage	Support development of new and incremental storage wherever possible.[119]
Increase water conservation & efficiency	Increase investments that attain statewide energy benefits	1. Incorporate a societal perspective into water utilities' investment criteria. 2. Allow energy utilities to invest in water system improvements that attain benefits for energy ratepayers. 3 Create a Public Goods Charge equivalent for water utilities.

A Conceptual Road Map

Following is a conceptual road map for a five-year program structured to achieve the above objectives. The plan considers a three-phase approach:

Phase 1 – Policy Framework and Infrastructure
Phase 2 – Pilot Programs
Phase 3 – Implementation

The process of building the policy framework and infrastructure needed to support a major policy shift of this kind would begin in *Phase 1*. *Phase 2* would be triggered by adoption of interim policies and pilot programs by energy utilities, and their regulator(s), in recognition of the energy value of saved water. *Phase 3* would begin with adoption of permanent policies and programs by energy utilities and their regulator(s) that will invest in saving water to save energy.

[118] Incentives already exist to encourage shifting loads from on-peak to partial- and off-peak periods.
[119] Water remains the most effective means of storing energy.

The work in each phase is generally described below.

Phase 1 – Policy Framework and Infrastructure [8-12 months]

During the initial phase, three distinct activities would proceed concurrently:

- Task 1: Increase access to existing energy programs and resources by water and wastewater utilities.

- Task 2: Develop a policy roadmap for statewide integrated water and energy planning and management.

- Task 3: Conduct studies of California's water-energy relationships.

Activities included in each task could include, but are not limited to, the following:

Task 1: Increase access by water and wastewater utilities to existing energy programs and resources. Energy utilities already offer programs where water utilities can participate. These include traditional energy efficiency programs such as retrofits of lighting and HVAC and programs for increasing the efficiency of pumps and motors. In addition, the state's investor-owned utilities (IOU) offer energy-performance contracts (EPCs) that provide customized cash incentives for projects that demonstrate real energy savings.

The following tasks are designed to increase access to existing programs and resources, identify additional resources, and facilitate identification of opportunities for attaining incremental benefits through increased collaboration, and, potentially, the joint operation of multi-utilities' systems, resources, and assets.

1.1 Develop a clearinghouse of water-related energy information for water professionals and others concerned about energy and water use in California. The clearinghouse should include the leading references and studies that highlight energy best practices for water utilities; creative approaches to system design and operations that provide operating flexibility to moderate peak energy consumption; opportunities to become energy self-sufficient; and sources of technical, funding and other types of support.

1.2 Develop a pilot assistance program for water utilities to help individual water agencies integrate comprehensive energy planning and management into their activities.

1.2.1 Establish the baseline of current practices. Provide direct and active technical assistance for best practices for reducing energy consumption by water systems and processes. Encode these best practices into benchmarking tools and make them available to practitioners, enabling them to compare their current practices with what is possible. Develop a clearinghouse of information on a range

from current to best practices. Establish measurement and evaluation protocols to verify savings and share lessons learned.

1.2.2 Provide incentives for incremental and/or joint infrastructure improvements that reduce total and peak energy requirements for water transport and processing. These incremental facilities would likely include storage (reservoirs, groundwater wells, and oversized pipelines) that both increases system flexibility and facilitates time-of-use (TOU) and/or seasonal load shifting.

1.2.3 Identify long-term funding opportunities for both ongoing existing programs and for funding retrofits that exceed single utility resource cost-effectiveness tests.[120]

1.2.4 Assist in identifying opportunities for peak-load reductions and seasonal load shifting.

1.2.5 Provide technical and funding assistance in identifying and implementing self-generation opportunities, especially renewable resources and emerging technologies.

1.2.6 Facilitate opportunities for collaborating with local energy distribution companies on all aspects of energy management and energy self-sufficiency, including strategies to meet projected load growth.

Depending upon the results of the pilot, successful programs could be quickly ramped up to provide assistance to water agencies statewide.

Task 2: Develop a policy roadmap for statewide integrated water and energy planning and management. A policy shift of this magnitude requires thoughtful consideration of the barriers and hurdles that need to be overcome before successful implementation. A policy roadmap identifying key changes to laws and regulations that would help facilitate the shift would be very beneficial when embarking upon this effort. The types of activities within this task could include:

2.1 Establish a statewide multi-agency Water-Energy Task Force. This task force would provide consistent, long-term leadership, policy direction, and technical and resource support for a comprehensive statewide water-energy program. The Water-Energy Task Force would include staff from the Energy Commission, Department of Water Resources, California Public Utilities Commission, Air Resources Board, State Water Resources Control Board, and the California Department of Health Services.

The goal of the task force would be to achieve the benefits of *statewide integrated planning and management of the state's water and energy resources*. Specific tasks include the following:

[120] Long-term funding was identified as an important factor in gaining support from water utilities.

- Collaboratively build a knowledge base of water and energy interdependencies. Investigate beneficial statewide integrated water and energy planning and management practices and recommend policies, programs, and funding for successful programs.

- Expand the Water-Energy Relationship (WER) Working Group created through this process to include strong participation by all key stakeholder groups needed for successful implementation of the program. The WER Working Group will provide technical advice to the Water-Energy Task Force.

- Designate a Water-Energy Liaison at the Energy Commission. This person or group would be responsible for coordinating policy, research, and programmatic efforts within the Energy Commission and act as liaison to the Water-Energy Task Force, other state agencies, local jurisdictions, and water, wastewater, and energy utilities. Similar people or groups should be identified at other agencies on the Task Force.

- Collaborate with other parties and entities with compatible goals. These include DWR's Office of Water Use Efficiency, the Recycling Task Force, and the Desalination Task Force.

- Develop a roadmap that establishes goals for increasing water efficiency and demand-side management. Among other things, the roadmap should prioritize investments in programs and measures that have the highest resource value and impact. In recognizing that every unit of water saved allows displacement of higher-energy intensity water supplies, high priority should be assigned to reductions in agricultural water use and urban landscape irrigation, both residential and commercial.

- Charge the Water-Energy Task Force with monitoring technology changes that affect the energy intensity of the water cycle, and identify potentially feasible and cost-effective applications.[121] A mechanism should be established to continually identify and incorporate new technologies wherever beneficial and feasible.

2.2 *Build the policy framework and infrastructure.* The concept that there are statewide benefits from "saving water to save energy" needs to be emphasized and regularly underscored*. Energy Report* findings and recommendations should be presented to the CPUC, water and energy utilities, key water and energy

[121] For example, new tunneling equipment and techniques may one day make it possible to drill through mountains instead of transporting water over mountains, significantly reducing energy used for water pumping. In addition, improvements in desalination and other water supply development techniques may become more cost-effective than transporting water from Northern California to Southern California. Further, technologies such as cloud seeding may become more successful in producing local supplies that could reduce Southern California's need for water imports.

policymakers, and other key stakeholders. The bases for computing potential benefits needs to be widely and clearly understood.

Policies, procedures, business processes, analytical methods, investment criteria, and decision making tools all need to be adjusted to support a policy and planning shift of this magnitude. To support this shift, the importance of the state's water-energy relationship needs to be better understood. Preliminary studies show the complexities of the water supply balance and cycle, and geographic, source, end user and other diversities – all of which must be documented, quantified, and modeled to assure that programs and strategies achieve their intended results. Thereafter, policies, rules, regulations, protocols, methodologies, programs, and funding need to be brought into alignment.

- Establish a valuation methodology for the societal value of water. We are just beginning to understand the water-energy relationship. Preliminary studies of the water supply-use-disposal cycle and overall water supply balance show distinctly different energy intensities of water in various regions of the state, depending upon climate, topography, and water storage/recovery/delivery options and methods. In addition, different uses have different energy intensities. A valuation methodology is needed to capture these diversities in a manner that will help planners prioritize their investments.[122]

- Leverage developmental work already in progress by others, including the U.S. Department of Energy National Laboratories' Water-Energy Nexus Program, Pacific Institute, California Urban Water Conservation Council, and the Irrigation Training and Research Center. Collaborate with these (and other) entities, to:

    - Inventory, characterize, and measure California's types of water and energy interdependencies.

    - Develop pilot programs to test tools and methodologies for evaluating tradeoffs among these interdependencies.

    - Develop analytical models for policymakers, regulators, utilities, and other key stakeholders in developing cost effective joint water and energy programs.

- Facilitate joint investment to attain societal benefits. As opportunities are identified that could produce incremental energy benefits but are not deemed

[122] For example, while it may be possible to increase total groundwater capacity in Southern California, unique geological characteristics create uncertainties as to both ultimate capacity (groundwater doesn't behave predictably) and impacts on production capacity of other wells in the vicinity. Similarly, displacing SWP imports with increased seawater desalination in Southern California may not produce a net benefit; nor would over-pumping of groundwater supplies and reducing drought reserves be desirable. All of the interdependencies – water to energy, energy to water, and water to water -- need to be evaluated to determine how best to attain positive net benefits.

cost-effective on a single utility resource cost test, mechanisms are needed that facilitate joint investment to attain those incremental benefits.

- Incorporate a societal valuation approach in both water and energy utilities' resource pricing methodologies, water and energy efficiency program portfolios, and investment criteria.

- To facilitate early results, establish a proxy for the societal value while a detailed methodology is developed.

- Establish a water resource loading order that incorporates the societal value of an avoided unit of water consumption and that mirrors the preferred energy resource loading order in the Joint Agency Energy Action Plan for energy.[123]

- Establish a public goods charge equivalent for public purpose water conservation and efficiency programs.

- Provide incentives for water, wastewater, and energy utilities to optimize their joint resources beyond traditional discrete single utility service boundaries (water or energy).[124]

- Require the state's energy and water planners to collaborate on plans and strategies to reduce net water sector energy consumption and to meet projected energy load growth.

2.3 Identify changes to existing laws and regulations. Examples of some proposed changes are provided in the table of potential actions on pp. 4-5.

2.4 Request that DWR provide input to the IEPR with respect to projected energy load growth in the water sector and potential energy impacts of drought risk mitigation measures. Similarly, request Energy Commission's participation in DWR's Water Plan Update process to provide assumptions as to energy supply availability and price forecasts.[125] Energy Commission and DWR should also synchronize planning assumptions for dry, wet and average hydrology years, as well as

[123] The California Water Plan Update 2005 already identifies a prioritized resource strategy. In order to attain results that optimize the state's water and energy resources on a joint basis, societal values should also be considered in the resource loading order. For example, least-cost water supply options at low electricity prices (e.g., desalination and water transfers) may become expensive when electricity prices are high. Since high electricity prices typically coincide with electricity supply shortages, water resource planning that does not consider energy impacts during times of shortage can create electric reliability risks that affect all California ratepayers. Integrated planning of water and energy resources provides the policy perspective needed to develop contingency plans and strategies for mitigating these types of risks.

[124] For example, the SWP could work with the water agencies that take water from the aqueduct to identify incremental infrastructure and changes to operations that can shift more water pumping to off-peak periods and/or non-summer months.

[125] This could result in a water supply equivalent of the state Energy Action Plan's resource load order.

assumptions as to the duration and magnitude of a multi-year drought for contingency planning purposes.

2.5 Expand the 14 water conservation best management practices (BMPs) to include new measures that meet the broader goals of statewide integrated water and energy planning and management.[126] Prioritize investments in BMPs in accordance with cost-effectiveness from a societal perspective.

2.6 Resurrect long-term purchase commitments (e.g., "standard offer contracts") that provide a ready market for excess power produced by water agencies after meeting all of their own energy requirements. One option might be to merely include such default purchase mechanisms in investor-owned utilities' procurement baselines.

2.7 Increase collaboration among state agencies to assure a consistent policy perspective. Unintended consequences result when multiple regulators seek to discharge their separate responsibilities in absence of a consistent policy framework. For example, while the state is encouraging increased energy production, the Department of Fish and Game restricted operational flows at Silverwood, a man-made reservoir, to protect non-native fish. The WER Working Group identified a need for consistent policy in which state agencies collaborate regularly to assure that energy, water and environmental benefits are continually balanced.

Task 3: Conduct studies of California's water-energy relationships. There is a near-term opportunity to access California ratepayer funds to support the policy shift to statewide integrated water and energy planning and management. Specifically, the state's investor-owned utilities are challenged to attain the targeted energy efficiency goals established by the CPUC for the 2006-2008 round of ratepayer investments. The opportunity to save water to save energy has significant promise to deliver, and potentially to exceed, system benefits targeted by the CPUC. In fact, water-energy programs may well represent the most promising opportunity for "second generation" energy efficiency measures.

The purpose of this task is to establish the foundation for an interim water-energy program that will demonstrate the expected benefits of statewide integrated water and energy resource management, prior to establishing permanent programs. The following work will need to be accomplished to support design of one or more interim programs.

3.1 Establish an interim methodology and proxy for the societal value of a unit of water saved. Design of cost effective programs requires computation of the societal value of a saved unit of water. The computation needs to be performed over the

[126] See Appendix C for a discussion about water conservation BMPs.

entire water use cycle (i.e., the total costs of water, externalities and energy incurred during the entire life of a unit of water[127]).

Ultimately, a comprehensive methodology is needed that recognizes the diversity of water supplies, treatment processes, types of end use, and other factors. The number and complexity of variables will need to be analyzed to determine which are most significant in computing the societal value. In the meantime, a proxy can be employed to allow interim water-energy programs to go forward while detailed studies of the water-energy relationship continue in parallel. There is precedent at the CPUC for utilizing proxies while formal methodologies are being debated and refined.[128]

[Note: The "triple bottom line" concept captures the full spectrum of economic and societal values that today's organizations must address. In developing the proxy, it may be desirable to consider aligning the components of the societal value of water with this evolving concept that is gaining increased acceptance.]

3.2 Inventory needs. Prior to designing the studies, a needs assessment should be conducted to inventory the spectrum of primary water-energy relationships in California, and the current body of data, models, tools, policies, programs, practices, funding, legislation and regulations. Water-related energy consumption will be benchmarked by type of water system, function, and end use. Water-related energy consumption will then be mapped from source through various categories of end use to develop a comprehensive understanding of the points and relative magnitudes of energy consumption along the supply chain, and the types of systems, processes, equipment and measures that could reduce energy consumption at these points.

3.3 Conduct detailed studies. The final task under Phase 1 is to conduct detailed studies of California's water-energy interdependencies and to integrate these data into analytical models and tools that can help both water and energy utilities develop cost-effective joint water-energy programs. The scope of these studies will include establishing baseline water use by all sectors and then linking this to the energy baseline. In addition, technologies will be researched for their water and energy savings potential, and the associated environmental benefits.

Studies will proceed in parallel with commencement of Phase 2 – Pilot Programs. The Pilot Programs will employ a proxy until more detailed data and methods become available to support adoption of a formal methodology for valuing the energy and societal value of an avoided unit of water. The types of studies needed are described more fully at the end of this appendix.

[127] Water collection, transmission, treatment, distribution, wastewater treatment, and ultimate disposal or recycling.
[128] In recent years, for example, proxies were established and relied upon by the CPUC for both the market price referent and avoided costs of energy.

Phase 2 – Pilot Programs [12-24 months]

During Phase 2, a proxy will be adopted and applied to develop pilot water-energy programs in which the projected incremental benefits of joint water and energy planning and management can be verified. Concurrently, Phase 1 studies to perfect the data, methods, and tools needed to establish a reliable methodology for supporting development of cost effective programs on an ongoing basis will continue in parallel.

Several water-energy pilot programs are recommended:

- A pilot for investor-owned and municipal utilities that targets specific types of water use reduction to demonstrate and measure the expected economic and reliability benefits to energy ratepayers and the California electric grid. The pilot would employ a proxy for the societal value of each type of water use reduction based on a preliminary methodology, pending completion of further studies and analyses. The scope of such a pilot could include:

    - Direct co-investment by energy utilities in water conservation and efficiency programs with high potential for energy savings. (The Pacific Institute, in its November 2003 study "Waste Not, Want Not: The Potential for Urban Water Conservation in California", estimated a remaining annual potential for cost effective urban water conservation as high as 2 million acre feet (651.7 billion gallons). Assuming a conservative estimate of 5,000 kWhrs/mg[129], this quantity of saved water could reduce energy consumption by 3,258 Gwh per year. This is about 1.8% of the state's total energy consumption.)

[129] Refer Appendix C, Energy Impact Analysis of Existing Water Management Practices. For the sole purpose of illustrating the potential magnitude of impacts, we have assumed a statewide average value of 5,000 kWhrs/mg.

California Urban Water Use in 2000
and the Potential to Improve Efficiency and Conservation

California Urban Water Use by Sector	Current (2000) Water Use (AF/year)	Best Estimate of Conservation (AF/year)	Potential to Reduce Use (%)	Minimum Cost-Effective Conservation (AF/year)
Residential Indoor	2,300,000	893,000	39	893,000
Residential Outdoor	983,000 to 1,900,000 (b)	360,000 to 580,000 (c)	25 to 40	470,000
Commercial/ Institutional	1,850,000	714,000	39	Combined CII: 658,000
Industrial	665,000	260,000	39	(e)
Unaccounted-for Water	695,000	(d)	(d)	(d)
Total	**6,960,000** (+/- 10%)	2,337,000	34	2,020,000

Source: "Waste Not, Want Not: The Potential for Urban Water Conservation in California", The Pacific Institute, November 2003.

  - Subsidized investments in incremental water infrastructure that are expected to attain significant energy benefits (e.g., increasing capacity of, or adding new reservoirs, pipelines, and groundwater wells).

- A pilot that investigates the potential incremental benefits attainable by optimizing joint water and energy resource management of the state's largest water utilities on a combined basis. For example, the pilot could investigate incremental water and/or energy infrastructure (water storage, delivery, power production, etc.) that could increase the operating flexibility of combined large water systems (SWP, SWC, CVP and/or the Colorado River System, as well as other large water systems that are now or could become interconnected).

<u>Phase 3 – Implementation</u>
Phase 3 will be defined by completion of most of the detailed studies of the state's water-energy interdependencies, and of the analytical models and tools that employ these data to design cost effective joint water-energy efficiency programs. During Phase 3, proxies for the societal value of saved water will be replaced with permanent methodologies, and long-lived (5-10 years) water-energy programs will be established and funded.

Implementation Challenges

While some opportunities could be accessed now for early results, there are some challenges to implementation of joint investments that attain the incremental energy resource and reliability benefits of fully integrated water and energy resource planning and management.

1. Water and energy utilities are regulated, operated and managed separately. Short of a few programs in which end users can earn energy incentives for reducing consumption of hot water, there presently is little incentive for water, wastewater, and energy utilities to even coordinate their resource planning activities and much less to share investments in programs and infrastructure.

2. Program goals and incentives will need to be aligned. Societal values are derived from reducing or avoiding the buildup of costs along the water cycle. In this case, water and wastewater utilities and their ratepayers will need to make the investments that attain energy resource and reliability values that benefit other ratepayers and the state overall. This presents challenges with respect to equitable sharing of joint program costs. For example:

    - Increasing use of recycled water in Southern California to reduce high-energy water imports from Northern California may well provide a benefit to all water and energy ratepayers.[130] However, the incremental investment in recycled water distribution facilities needs to be made by a local government or wastewater utility that must then seek recovery of its investment. If the costs of such incremental facilities are allocated only to users of that recycled water, the cost of recycled water may far exceed the cost of potable water.

    - During summer months, as much as 50 to 70 percent of residential water use in central and Southern California is for landscape irrigation. When viewed from a societal perspective, significant investments in programs to reduce landscape irrigation are warranted on the basis of the energy benefits alone. However, water utilities' investments are limited to those that benefit their own ratepayers (i.e., not on the basis of benefits that may accrue to the entire water supply chain or to other stakeholders). Further, there presently is no mechanism that allows energy utilities to invest in programs that reduce water use to save energy.

Allocating incentives to the stakeholder(s) who need to make the investment on behalf of all California ratepayers, both water and energy, is not a trivial task.

[130]Water ratepayers benefit by avoiding investments in higher cost water supplies and increasing water supply reliability. Energy ratepayers benefit from associated reductions in energy procurement, as well as by avoiding investments in additional electric infrastructure and by increased electric system reliability.

Additional Needs for Research and Assistance

Integrating water and energy resource management will require additional knowledge in a number of key areas to develop the analytical methods, tools, and data needed to develop and implement cost effective water-energy projects and programs.

Building on Present Knowledge

Considerable work is already being performed in this area. Some current efforts are described in Appendix A.

Additional information is needed to facilitate a statewide policy shift to comprehensive planning and management of the state's water and energy resources. In particular, more accurate information about the nature and magnitude of the state's water and energy relationships -- including the spectrum of opportunities for realizing the synergies of integrated water and energy resource management, the amount of needed investments, and the relative costs vs. benefits of each type of measure – is needed to prioritize investments and develop methods, models, and tools that support cost-effective program design.

The following ***conceptual*** research and development plan describes the primary research activities needed to support the program objectives identified in the table in the first section of this appendix. The plan is structured to allow near- and long-term initiatives to proceed in parallel to provide opportunities for early benefits.

CONCEPTUAL Research and Development Plan

R+D Program Objectives	Near-Term Strategies	Long-Term Strategies
1. Proactively manage water-related energy consumption	Synchronize the state's water & energy planning assumptions and strategies to meet projected energy load growth	Develop comprehensive programs for technical & resource assistance that attain water utilities' energy management best practices
2. Increase understanding of the state's water-energy relationship	Demonstrate primary water-energy interdependencies; develop prototypical values by Forecasting Climate Zones	Inventory, document & quantify the state's primary water-energy interdependencies for input to detailed models & tools
3. Implement statewide integrated water and energy resource management	Develop proxy for interim societal valuation methodology for cold water savings for discussion with CPUC[131], policymakers, other interested stakeholders	Develop data, analytical tools and methodology for computing the societal value of saved water for different water sources, end uses, climate zones, etc. for valuation of societal costs in long-term cold water savings programs
4. Increase water utilities' energy self-sufficiency	Investigate potential for revising existing programs, policies, methods & practices to reduce water utilities' net energy consumption ('net' of power production)	Develop studies, methods, tools & techniques to assist water utilities in becoming energy self-sufficient, and potentially becoming net exporters of power
5. Increase water efficiency and demand-side management	Develop preliminary valuation of existing cold-water efficiency measures	Identify & evaluate new cold-water measures; develop cost-effective programs

Primary research and assistance needs identified to-date are described in more detail below by program objective.

.

Objective 1: Proactively manage water-related energy consumption.

1. Establish baseline of current practices. Research "best practices" for reducing energy consumption by water systems and processes. Encode "best practices" into benchmarking tools and make them available to practitioners, enabling them to compare their current practices to what is possible. Populate the "Clearinghouse" with information on the range from current to best practices. Establish measurement and evaluation protocols to verify savings and provide lessons learned.

2. Conduct an assessment of the penetration and adoption of "best energy practices" by water and wastewater utilities, and barriers and hurdles that prevent or restrict adoption, to support development of targeted assistance programs that incorporate workarounds to identified barriers and hurdles.

3. Track and evaluate energy use by function to enable development of targeted measures and retrofits with high benefit potential. For example, a better

[131] CPUC could adopt a proxy for the societal value of cold water savings that would allow pilot programs to go forward in the 2006-2008 energy efficiency funding cycle.

understanding is needed as to how recycled water fits into the water supply portfolio and water balance. While increasingly stringent federal discharge rules are pressing water utilities to upgrade secondary treatment to higher energy intensive tertiary treatment, incremental energy consumption attributable to the higher level of treatment should be offset (at least in part) by using recycled water to displace higher energy intensity water supplies.

4. Continue to monitor and plan for projected changes in energy usage by water systems and treatment processes. Continue to study the projected energy requirements of changed federal water treatment and discharge regulations as these evolve, and develop approaches to help energy and water utilities manage the energy impacts of these changes.

5. Continue to identify and evaluate opportunities to reduce energy consumption in targeted high-use sectors, such as agriculture. Work with interested stakeholders to identify and evaluate opportunities to reduce energy use by the agricultural sector and to conduct various studies. Potential projects might, for example, include tracking energy-use trends associated with changes in crop-planting and harvesting patterns; evaluating impacts of pressurized irrigation systems (drip and spray) on fields now irrigated by gravity; and converting diesel-engine pumps to motor-driven pumps.

6. Evaluate the potential energy impacts of increased water transfer transactions. Little is known about whether changes in conveyance patterns will have a noticeable impact on water-related energy consumption. The Energy Commission could work with water utilities involved in contracting for or providing conveyance services, to first determine the likely extent of such transactions, and make a rough estimate of the magnitude of change in electricity use patterns. If warranted, staff could recommend further study of methods to track such transactions, and determine and prepare for their expected energy impact.

7. Continue studies with AwwaRF and others to reduce energy consumption by desalination technologies, and to coordinate water and energy planning for dry years. Though the WER Staff Paper identified only fairly modest impacts on the electric system from known planned desalination plant development, the number of planned facilities could increase quickly if one or both of two things occur: an extended drought or other scenario that significantly curtails surface water deliveries, and/or a significant decrease in the cost of operating such facilities.

8. Develop a comprehensive program to study groundwater-related energy use. Groundwater is a particularly significant area of study, since use of groundwater storage has potentially significant impacts, both positive and negative, on water-related energy consumption. On one hand, increased groundwater storage provides significant operating flexibility that could allow

more SWP water deliveries to be shifted from summer to fall. On the other hand, over-pumping groundwater basins could increase energy consumption at undesirable times and also reduce critical drought supplies.

Less is known about groundwater than any other water source. This is due to the fact that each groundwater basin is unique, and production characteristics of wells are often interlinked. Further, since use of groundwater is largely unregulated, the actual quantity of energy used for groundwater pumping statewide is undeterminable. The complexities of groundwater warrants a comprehensive monitoring approach that tracks groundwater levels, pump production, electricity use, and other data over multiple years.[132]

9. Assist water utilities in developing less energy intensive water supplies. For example, increased reliance on recycled water to displace need for desalted water.

10. Continue to build on PIER/AwwaRF's Water and Wastewater Technology Roadmap.

Objective 2: Increase understanding of the state's water-energy relationship.

1. Conduct pilots and studies that document and quantify the state's primary water-energy interdependencies. The information being developed by UCSB and Pacific Institute will help develop a proxy that can be relied upon to develop pilot water-energy programs while more detailed studies are being conducted. In particular, while studies of urban water uses indicate significant energy can be saved by reducing water consumption, the drivers for such opportunities are not well understood. A comprehensive inventory, characterization, and assessment of the primary types of water-related energy consumption by type of water

[132] The Irrigation Training and Research Center (ITRC) study on agricultural energy requirements perhaps goes farther than any other, and bases much of its information on real-world geographical information system (GIS) data; but it must make many assumptions concerning average pump lift (groundwater levels), distribution uniformity, surface water availability (timing factor), irrigation type, average drawdown, discharge pressure, and so forth. It uses the real-world results of the pump efficiency tests conducted for the Agricultural Peak Load Reduction Program by the Center for Irrigation Technology, but those data did not include static or pumping water levels and primarily covered only wells in PG&E's territory.

Considerable additional study is needed in order to facilitate detailed modeling of groundwater supplies. The ITRC study also is the result of at least two levels of computer modeling: that by Department of Water Resources to estimate groundwater levels in Northern California and ITRC's own crop water model, which produced the energy use estimates in its groundbreaking study. Much of ITRC's results are based on what can only be described as rough calculated estimates by DWR for Central and Southern California groundwater volumes, which is especially critical in the Kings and Kern River Basins, where more than 50 percent of the energy used for agriculture-related groundwater pumping occurs. (A detailed discussion of ITRC's model can be found in their report No. 02-001, available on their Web site at www.itrc.org)

source, system, function, and end use will eventually be needed to develop the detailed methodologies on which cost-effective programs can be based.

Water-related energy consumption can then be mapped from the source through various categories of end use to develop a comprehensive understanding of the points and relative magnitudes of energy consumption along the water supply chain, and the types of systems, processes, equipment, and measures that could reduce water and energy consumption at these points. Ideally, a sampling of water utilities that collectively represent most of the primary types of water-energy interdependencies in California would be included in such a pilot. Several water utilities have already indicated interest in participating in such a pilot. These include MWD, IEUA, LADWP, Palo Alto Utilities, Sonoma County Water Agency, and Semitropic Water District.

2. Construct a valuation methodology that accounts for the societal cost (water, energy and externalities) of avoided water consumption for various types of water sources and end uses. Relying upon the data and knowledge gained from detailed studies, quantify the water-energy tradeoffs of various resource decisions through computation of the "Regional Cold-Water Energy Intensity".

    - Research and develop regional cold-water energy intensities (or co-opt existing research), adopt prototypical values, and establish linkage to Forecasting Climate Zones;

    - For existing "cold-water measures" develop base case Unit Energy Consumption (UEC), High-Efficiency (HE) UEC, Base and HE Peak watt and demand savings, volume-sensitive installed measure costs and expected useful life values;

    - Identify and evaluate new cold-water measures targeted to create resource value specifically suited to integrated water/energy resource planning not previously addressed under the discrete/isolated water/energy resource management regime;

    - For new cold-water measures deemed viable, develop planning data identified for existing cold-water measures, and;

    - Incorporate research elements into the Database for Energy Efficiency Resources (DEER) for use by energy-efficiency program planners consistent with program planning protocols enunciated in CPUC Rulemaking 01-08-028, Decision 05-04-051.

The above described methodology is consistent with that employed by the CPUC in its regulation of investor-owned utilities' energy efficiency programs, thus allowing proposed investments in water saving measures to be considered on an equivalent basis.

Objective 3: Implement statewide integrated water and energy resource management.

1. Develop tools and techniques for identifying potential infrastructure upgrades that extend beyond a single utility's service boundaries. The goal of implementing statewide integrated water and energy resource planning and management opens up new opportunities that heretofore have not been considered. Specifically, water and energy utilities presently attempt to optimize their separate resources and systems. Many of these utilities have calibrated their models and tools to simulate their own systems' operations. New analytical models, tools, and methods will be needed to help water and energy utilities look beyond their system boundaries, looking for opportunities to optimize their systems and resources on a joint basis with other water and energy utilities with which they may now be interconnected (or potentially could be interconnected). The underlying premise of joint optimization is that it is at this level of fully integrated planning – i.e., the "nexus" – that the most beneficial incremental benefits will be found.

   Potential opportunities include optimizing the systems and operations of the SWP and the 29 member agencies that comprise its sole customer, the SWC, as well as the CVP, the Colorado River system, and any other points of interconnection along the way.

2. Develop analytical models and tools that:

   - Assist both water and energy utilities in developing joint programs that are cost-effective from a societal point of view;
   - Assist wholesale water utilities in evaluating the net benefits of system reconfigurations or retrofits that exceed their own boundaries[133];
   - Assist both water and energy utilities in assessing the net water supply and associated energy and externalities benefits of proposed measures and retrofits (e.g., assessing the net impact on the water supply balance);l
   - Other analytical models and tools needed to support development and implementation of cost-effective joint water-energy programs.

[133] These may include those that assist the State Water Project operator in making determinations as to how to optimize energy consumption for itself and its customer, the SWC, (and potentially other interconnected systems such as CVP and the Colorado River system) on a combined basis.

Objective 4: Increase water utilities' energy self-sufficiency.

Reduce Energy Consumption:

1. Identify opportunities to reduce conveyance-related peak demand reduction (State Water Project and other large water systems). The State Water Contractors and DWR observed that it might be possible to increase off-peak pumping at Edmonston Pumping Station; however, additional pumping capacity would be needed. In addition, they noted that while there may be opportunities to further increase operational flexibility, additional storage would be needed at points along the aqueduct.[134] In order to assess the statewide opportunity to support such incremental capital expenditures that may be beneficial to the state overall, but are not deemed cost-effective from the perspective of a single entity, the Energy Commission could:

    - Assess and report incremental cost-effective measures that can be implemented to increase pumping capacities and storage to reduce peak energy demands that are cost effective based upon a more comprehensive societal cost-benefit evaluation.

    - Evaluate opportunities to reduce peak demands through coordinated operation of federal and state water projects.

2. Assist water utilities in identifying methods to increase operational flexibility such that energy intensive pumping and water treatment processes could be shifted from on-peak periods, to partial- and off-peak periods.

    - According to ACWA, installation of sensors and other equipment could substantially increase water utilities' flexibility in operating their systems. This flexibility could allow water utilities to maintain minimal pumping loads during peak periods, either by delaying such use into the evening hours or at least by cycling such loads sequentially to minimize peak use.

[134] Reservoirs, depending on location and size, including intake and discharge capacities, provide opportunities for pumping load and generation time-shifting -- hourly/daily shifts for small reservoirs, and sometimes monthly/seasonal shifts for larger reservoirs. For large river reservoirs, like Lake Mead, a downstream re-regulation reservoir such as Lake Mojave could support optimum water deliveries and peak generation. However, Lakes Mead and Mojave increase evaporative losses and incur greater costs and environmental concerns.

Urban hillside tank storage reservoirs that provide system pressure for urban retail water users can be oversized to emphasize off-peak pumping to fill the reservoirs if the pumping capacity in the supply system (say, groundwater wells) is simultaneously increased to produce needed water yield in the less-than-24-hours window. (Note: the pumps can wear out sooner and incur increased operations and maintenance costs if the frequency stop/starts increase to match daily Flex-Your-Power objectives.)

- IEUA has designed its systems to allow water to be "detained" during critical peak periods and held for processing during partial- and off-peak periods.

3. Explore increased use of groundwater storage to allow shifting of summer SWP deliveries to fall. In Southern California, groundwater pumping uses approximately 30 percent of the energy required to import water from Northern California. Groundwater aquifer source production and recharge requirements are fixed and finite. During periods of seasonal peak energy demand, water agencies might rely on groundwater sources and recharge the aquifers using imported water months later in the off-peak season. As noted previously, some Southern California water utilities already choose to pump groundwater during summer and recharge groundwater wells during fall. In this manner groundwater storage capacities could be employed to affect large-scale and long-term seasonal peak demand shifting.

   The potential of increasing groundwater storage capacity to further defer seasonal deliveries should be studied. These studies are complicated, due to unique hydrogeology of groundwater basins and potential linkages among wells. The scope would include:

   - Identification of groundwater aquifers where groundwater pumping and recharge is being performed by water utilities;

   - Identification of groundwater aquifers that are not currently being tapped for groundwater pumping that could be used to affect the aforementioned, and;

   - Assessment of the operational feasibility and associated costs and benefits of potential incremental seasonal demand shifting.

   Analytical tools and techniques will be needed to help determine the efficacy and relative costs vs. benefits of this approach. The study should include consideration of who should develop, fund, own, and operate such assets, which potentially may be constructed primarily for energy benefits (i.e., the value of shifting summer demand to other months).

Increase Power Production:

1. Conduct studies of potential for incremental power production through in-conduit hydropower, pumped storage, and repowering. In-conduit hydropower is a very attractive option since it produces energy as a by-product of water operations. Pumped storage has unique capabilities to produce power during peak periods. The Hetchy Hetchy example illustrated a potential for increasing the state's hydropower capacity by as much as 10 percent at a fraction of the cost of installing new units and much more quickly.

There are multiple barriers to water utilities' energy self-sufficiency. The statewide potential for increased hydropower and pumped storage capacity should be assessed, and a roadmap developed for attaining this potential that includes potential work-arounds to the policy, regulatory, economic, technical, and other barriers that will need to be overcome.

2. Develop mitigation strategies to reduce lost hydropower capacity during FERC relicensing. As discussed previously, the National Hydropower Association reported that an average of 8 percent of the nation's total hydropower capacity is being lost through relicensing. The Energy Commission could evaluate causes and identify potential mitigation strategies that consider the societal value of associated hydropower capacity.

3. Develop models and tools to evaluate the energy water tradeoff for reservoir storage. Detailed modeling studies of reservoir operations should be performed to evaluate the additional hydropower generated by changing average year reservoir releases. Similarly, conduct studies detailing the decrease in groundwater pump electricity demand associated with a change in average and dry-year reservoir releases.

4. Develop analytical models and tools that assist both water and energy utilities in assessing power production potential by water utilities including, but not limited to:

    - Self-generation utilizing local renewable resources (digester gas[135], agricultural wastes and other biomass, solar,[136] and hydropower).

    - Renewable resource potential for utility scale generation facilities on watershed lands and rights-of-way.[137]

5. Conduct demonstration projects that allow testing of workarounds to barriers and hurdles and verification of net energy and other benefits of water projects that produce energy. In particular, demonstrate means for water utilities to produce energy as a by-product of water delivery and treatment processes (e.g., in-line conduit applications for water and wastewater utilities), and extrapolate statewide potential for these types of opportunities.

[135] Biogas potential need not be restricted to that produced by sewage digesters. Studies are underway to test the energy potential of blending sewage sludge with other biosolids, such as dairy animal waste and food refuse. In addition to increasing power production, this process provides an attractive means for disposing of other types of waste products. In addition, some parties are investigating development of a sludge-derived solid fuel that could be burned in power plants.

[136] Solar power is well suited to meeting small pumping loads in water distribution systems.

[137] Water utilities' extensive watershed land holdings could provide good opportunities for utility-scale wind and concentrating solar power development.

6. Conduct a comprehensive resource assessment of the renewable resource potential of watershed lands and rights-of-way and determine the barriers and hurdles that would need to be overcome.

Objective 5: Increase water efficiency and demand-side management.

1. Develop a pilot program that evaluates societal benefits of water conservation and efficiency programs presently deemed non-cost-effective under traditional water utility planning criteria. Potential items include: new balanced irrigation systems, weather based-irrigation systems, drought tolerant plant/low runoff landscape retrofits, synthetic turf retrofits, free water brooms for every school, connectionless water steamers, digital x-ray machines or x-ray water recirculation systems for doctors and hospitals, free cooling tower conductivity controllers for all public schools and buildings (may be commercial uses too), small scale water recycling projects for communities and golf courses, incentives for new home owners to buy water/energy efficient new homes, large-scale irrigation controllers and landscape retrofits for parks and greenbelts, water softeners[138], etc.

2. Expand the 14 BMPs to include other water conservation measures that meet the more comprehensive "societal" resource test. Building on the important work by CUWCC and its members, Pacific Institute, and other key stakeholders, identify and value incremental measures that can help meet the goals for a comprehensive statewide water-energy program. These measures should then be ranked alongside other feasible water and energy efficiency options on the basis of highest benefit:cost ratio, and then incorporated into joint water-energy programs.

3. Continually improve agricultural water use efficiency.
   - Continue to implement the PIER Agricultural Irrigation Technology Roadmap calling for research and development efforts improve irrigation efficiency. Possible studies include:

     - Reduce the total pressure required to operate drip irrigation technologies; this includes the filter system as well as the pipe and micro-sprayer technologies.

     - Advance the use of longer lasting materials for pump components.

     - Work with the SWP, the CVP and the irrigation districts to increase the flexibility of water deliveries to farms.

[138] One California water agency performed an analysis of retrofits of water softeners. The program did not meet the cost-effectiveness threshold on water alone, but the societal benefits are potentially large.

- Learn more about the increasing trend to adopt drip/micro systems, the implications to energy consumption, and the energy management benefits the systems provide.

- Work with irrigation districts to understand the ramifications increased reliance on groundwater.

- Work with the CPUC to ensure appropriate implementation of Critical Peak Pricing and other TOU rates.

- Work with the CPUC, the utilities, the irrigation districts, and the farmers to ensure widespread use of available energy efficiency programs.

4. Reduce outdoor water consumption. In the context of greatest near-term benefit, there is no dispute among stakeholders: The single largest opportunity for saving a lot of water quickly is through reductions of outdoor water use, both in agricultural and landscape irrigation.

    - Pacific Institute stated that more than 75 percent of the state's total water consumption is used by agriculture.

    - IEUA stated that during summer, outdoor water use for landscape irrigation accounts for 50 to 70 percent of all water consumed by the residential sector. Regions along the coast tend to use less; hotter interior uses more. Seasonal factor translates into even bigger impacts. Overall, reducing residential usage from 200 gal per capita daily down to 80 gal per capita daily (SF/LA numbers).

    - MWD stated that the biggest opportunity for outdoor water savings is in landscape replacement with native plants and synthetic turf.

5. Reduce industrial water use. Pacific Institute estimates that as much as 658,000 AF/year could be saved by the commercial and industrial sectors. Opportunities include joint investment in existing water savings programs, as well as potential joint investment in new technologies. MWD, for example, suggests joint investigation of innovative conservation program investments in industrial process water improvements, such as optimal approaches to industrial recirculation. In addition, this program could include investigation of new water efficiency technologies for various types of industrial processes.

6. Explore a "Golden Carrot" equivalent for water conservation programs. Develop joint investment opportunities in use funds to conduct innovative conservation program investigations into new technology and to kick start methods of obtaining water customer responses to these opportunities. One or more cash and other prizes could be awarded through a competitive innovation program that includes, for example, a call for water and energy-efficient home water heating systems and improvements.

Glossary

acre-foot (AF) - a quantity or volume of water covering one acre to a depth of one foot; equal to 43,560 cubic feet or 325,851 gallons.

active storage capacity - the total usable reservoir capacity available for seasonal or cyclic water storage. It is gross reservoir capacity minus inactive storage capacity.

adjudication - the act of judging or deciding by law. In the context of an adjudicated groundwater basin, landowners or other parties have turned to the courts to settle disputes over how much groundwater can be extracted by each party to the decision.

afterbay - a reservoir that regulates fluctuating discharges from a hydroelectric power plant or a pumping plant.

alluvium - a stratified bed of sand, gravel, silt, and clay deposited by flowing water.

aquifer - a geologic formation that stores and transmits water and yields significant quantities of water to wells and springs.

artificial recharge - the addition of water to a groundwater reservoir by human activity, such as putting surface water into dug or constructed spreading basins or injecting water through wells.

average annual runoff - the average value of annual runoff amounts for a specified area calculated for a selected period of record that represents average hydrologic conditions.

brackish water - water containing dissolved minerals in amounts that exceed normally acceptable standards for municipal, domestic, and irrigation uses. Considerably less saline than sea water.

conjunctive use - the coordinated and planned management of both surface and groundwater resources in order to maximize the efficient use of the resource; that is, the planned and managed operation of a groundwater basin and a surface water storage system combined through a coordinated conveyance infrastructure. Water is stored in the groundwater basin for later and planned use by intentionally recharging the basin during years of above-average surface water supply.

contaminant - any substance or property preventing the use or reducing the usability of the water for ordinary purposes such as drinking, preparing food, bathing washing, recreation, and cooling. Any solute or cause of change in physical properties that renders water unfit for a given use. (Generally considered synonymous with pollutant.)

conveyance - provides for the movement of water and includes the use of natural and constructed facilities including open channels, pipelines, diversions, fish screens distribution systems, and pumplifts.

cost-effective - means that the benefit-to-cost ratio of a proposed program or measure exceeds 1.0. As applied to this test, both costs and benefits are measured either over the life of the program or in terms of societal cost. Water and energy utilities currently include only costs and benefits that affect their respective ratepayers in their cost-effectiveness computations. The conclusion of this staff paper is that a cost-effectiveness test should expand to include all economic, environmental, and societal costs and benefits over the entire water use cycle - even those extending beyond the boundaries of a utility's service territory, resources, and assets - in order to identify opportunities to benefit the state as a whole.[139]

desalination - water treatment process for the removal of salt from water for beneficial use. Source water can be brackish (low salinity) or seawater.

drainage basin - the area of land from which water drains into a river; for example, the Sacramento River Basin, in which all land area drains into the Sacramento River. Also called, "catchment area," "watershed," or "river basin."

drip irrigation - a method of microirrigation wherein water is applied to the soil surface as drops or small streams through emitters. Discharge rates are generally less than 8 L/h (2 gal/h) for a single outlet emitters and 12 L/h (3 gal/h) per meter for line-source emitters.

drought - the magnitude and probability of economic, social or environmental consequences that would occur as a result of a sustained drought under a given study plan. Measures the "drought tolerance" of study plans.

energy consumption - the energy consumption required to facilitate water management-related actions such as desalting, pump-storage, groundwater extraction, conveyance, or treatment. This criterion pertains to the economic feasibility of a proposed action in terms of O&M costs.

energy costs - refers to the cost of energy use related to producing, conveying and applying water. It also refers to the cost of energy use for processes and inputs not directly related to water, but which can affect the demand for water (e.g., the cost of nitrogen fertilizer, tractor manufacturing, etc.).

energy production - both instantaneous capacity (megawatt) and energy produced (kilowatt hours).

[139] Eventually, the issue as to who pays for such incremental statewide benefits will also need to be addressed.

energy self-sufficiency – Refers to an entity that self-supplies its own energy requirements. This would typically be done through a combination of energy efficiency and self-provision of power, whether purchased or produced. Current regulatory barriers prevent water and wastewater utilities from becoming energy self-sufficient.[140]

effluent - wastewater or other liquid, partially or completely treated or in its natural state, flowing from a treatment plant.

end use – the use of energy or water for specific activities such as heating, cooling, toilets, or irrigation.

end users – the consumers of energy or water.

estuary - the lower course of a river entering the sea influenced by tidal action where the tide meets the river current.

evapotranspiration (ET) - the quantity of water transpired (given off), retained in plant tissues, and evaporated from plant tissues and surrounding soil surfaces. Quantitatively, it is usually expressed in terms of depth of water per unit area during a specified period of time.

forebay - a reservoir or pond situated at the intake of a pumping plant or power plant to stabilize water levels; also a storage basin for regulating water for percolation into ground water basins.

gigawatt (GW) - one thousand megawatts (1,000 MW) or one million kilowatts (1,000,000 kW) or one billion watts (1,000,000,000 watts) of electricity. One gigawatt is enough to supply the electric demand of about one million average California homes.

gigawatt-hour (GWh) - one million kilowatt-hours of electric power. California's electric utilities generated a total of about 250,000 gigawatt-hours in 2001.

gross reservoir capacity - the total storage capacity available in a reservoir for all purposes, from the streambed to the normal maximum operating level. Includes

[140] Barriers to energy self-sufficiency include:
(a) Long lead-time, complicated and costly interconnections;
(b) Prohibitive stand-by charges for grid-connected self-generation facilities:
(c) Net metering caps that discourage self-production of power at any site in an amount greater than 1MW (or the then current cap);
(d) Inability to “wheel” self-produced and/or purchased power to themselves anywhere on their own system (causing excess power to be either “lost” or sold at uneconomic wholesale prices that do not recover costs;
(e) Lack of standardized contracts, rates and terms for purchasing self-produced power that exceeds water and wastewater utilities’ needs at prices that at least recover costs; and
(f) Prohibitive exit fees assessed to entities departing from bundled electric utility service.

dead (or inactive) storage, but excludes surcharge (water temporarily stored above the elevation of the top of the spillway).

groundwater - water that occurs beneath the land surface and completely fills all pore spaces of the alluvium, soil or rock formation in which it is situated. It excludes soil moisture, which refers to water held by capillary action in the upper unsaturated zones of soil or rock.

groundwater basin - a groundwater reservoir, defined by an overlying land surface and the underlying aquifers that contain water stored in the reservoir.

groundwater overdraft - the condition of a groundwater basin in which the amount of water withdrawn by pumping exceeds the amount of water that recharges the basin over a period of years during which water supply conditions approximate average.

groundwater recharge - increases in groundwater storage by natural conditions or by human activity.

groundwater table - the upper surface of the zone of saturation, except where the surface is formed by an impermeable body.

hydraulic barrier - a barrier developed in the estuary by release of fresh water from upstream reservoirs to prevent intrusion of sea water into the body of fresh water.

hydrologic balance - an accounting of all water inflow to, water outflow from, and changes in water storage within a hydrologic unit over a specified period of time.

hydrologic basin - the complete drainage area upstream from a given point on a stream.

hydrologic region - a study area, consisting of one or more planning subareas.

infiltration - the flow of water downward from the land surface into and through the upper soil layers.

irrigation efficiency (IE) - the efficiency of water application and use, calculated by dividing a portion of applied water that is beneficially used by the total applied water, expressed as a percentage The two main beneficial uses are crop water use (evapotranspiration, etc.) and leaching to maintain a salt balance.

kilovolt (kV) - one-thousand volts (1,000). Distribution lines in residential areas usually are 12 kv (12,000 volts).

kilowatt (kW) - one thousand (1,000) watts. A unit of measure of the amount of electricity needed to operate given equipment. On a hot summer afternoon a typical

home, with central air conditioning and other equipment in use, might have a demand of 4 kW each hour.

kilowatt-hour (kWh) - the most commonly-used unit of measure telling the amount of electricity consumed over time. It means one kilowatt of electricity supplied for one hour. In 1989, a typical California household consumes 534 kWh in an average month.

land subsidence - the lowering of the natural land surface due to groundwater (or oil and gas) extraction.

maximum contaminant level (MCL) - the highest drinking water contaminant concentration allowed under federal and State Safe Drinking Water Act regulations.

megawatt (MW) - one thousand kilowatts (1,000 kW) or one million (1,000,000) watts. One megawatt is enough energy to power 1,000 average California homes.

methane (CH_4) - the simplest of hydrocarbons and the principal constituent of natural gas. Pure methane has a heating value of 1,1012 Btu per standard cubic foot.

methanol (also known as Methyl Alcohol, Wood Alcohol, CH_3OH) - a liquid formed by catalytically combining carbon monoxide (CO) with hydrogen (H_2) in a 1:2 ratio, under high temperature and pressure. Commercially it is typically made by steam reforming natural gas. Also formed in the destructive distillation of wood.

microirrigation - the frequent application of small quantities of water as drops, tiny streams, or miniature spray through emitters or applicators placed along a water delivery line. Microirrigation encompasses a number of methods or concepts such as bubbler, drip, trickle, mist, or spray.

minimum pool - the reservoir or lake level at which water can no longer flow into any conveyance system connected to it.

natural recharge - natural replenishment of an aquifer generally from snowmelt and runoff; through seepage from the surface.

percolation - process in which water moves through a porous material, usually surface water migrating through soil toward a groundwater aquifer.

photovoltaic cell - a semiconductor that converts light directly into electricity.

public water system - a system for the provision of water for human consumption through pipes or other constructed conveyances that has 15 or more service connections or regularly serves at least 25 individuals daily at least 60 days out of the year.

recharge - water added to an aquifer or the process of adding water to an aquifer. Groundwater recharge occurs either naturally as the net gain from precipitation or artificially as the result of human influence.

recycled water - the process of treating municipal, industrial, and agricultural wastewater to produce water that can be productively reused.

riparian right - a right to use surface water, such right derived from the fact that the land in question abuts the banks of streams.

runoff - the volume of surface flow from an area.

salinity - generally, the concentration of mineral salts dissolved in water. Salinity may be expressed in terms of a concentration or as electrical conductivity. When describing salinity influenced by seawater, salinity often refers to the concentration of chlorides in the water.

seawater intrusion barrier - a system designed to retard, cease or repel the advancement of seawater intrusion into potable groundwater supplies along coastal portions of California. The system may be a series of specifically placed injection wells where water is injected to form a hydraulic barrier.

single utility resource cost test - refers to resource optimization from the perspective of a single utility - for example, a water utility already seeking optimization of its own water resources. Energy costs embedded in delivered wholesale water are included when considering cost-effectiveness. However, the single utility resource cost test does not evaluate the impact of these water resource decisions on either water or energy utilities, or on statewide water and energy resources and infrastructure. Similarly, neither water nor energy utilities consider the energy intensity embedded in a unit of avoided water over the entire water use cycle.

societal cost or societal value - refers to the total resource cost, including water and energy and externalities, embedded in a unit of water. For purposes of this staff paper, this term is consistent with that used by the California Public Utilities Commission when determining the cost-effectiveness of energy efficiency programs and measures, and by water utilities when determining the cost-effectiveness of their water conservation incentive programs.[141]

---

[141] The CPUC's Energy Efficiency Policy Manual, Chapter 4 Cost-Effectiveness Methodology, relies upon a "Total Resource Cost (TRC) test - Societal Version" as "articulated [in] the California Standard Practices Manual: Economic Analysis of Demand-Side Management Programs." The California Standard Practices Manual states that "The Total Resource Cost Test measures the net costs of a demand-side management program as a resource option based on the total cost of the program, including both the participant's and the utility's costs." "A variant on the TRC test is the Societal Test. The Societal Test differs from the TRC test in that it includes the effects of externalities, excludes tax credit benefits, and uses a different (societal) discount rate." Water conservation incentives are typically valued in accordance with the February 1994 EPA manual, "A Guide to Customer Incentives

surface supply - water supply obtained from streams, lakes, and reservoirs.

surplus water - water that is not being used directly or indirectly to benefit the environmental, agricultural or urban use sectors.

tailwater – the excess water that was applied for agricultural irrigation water. This water is either returned to the environment or reused for irrigation.

transpiration - an essential physiological process in which plant tissues give off water vapor to the atmosphere.

Urban Water Management Planning Act – Sections 10610 through 10657 of the California Water Code. The Act requires urban water suppliers to prepare urban water management plans which describe and evaluate sources of water supplies, efficient uses of water, demand management measures, implementation strategies and schedules, and other relevant information and programs within their water service areas. Urban water suppliers (CWC Section 10617) are either publicly or privately owned and provide water for municipal purposes, either directly or indirectly, to more than 3,000 customers or supply more than 3,000 acre-feet of water annually.

volt - a unit of electromotive force. It is the amount of force required to drive a steady current of one ampere through a resistance of one ohm. Electrical systems of most homes and office have 120 volts.

water balance - an analysis of the total developed/dedicated supplies, uses, and operational characteristics for a region.

water quality - description of the chemical, physical, and biological characteristics of water, usually in regard to its suitability for a particular purpose or use.

watershed - the land area from which water drains into a stream, river, or reservoir.

---

for Water Conservation" which incorporates by reference the societal valuation approach adopted in the California Standard Practice Manual.

2015
California Environmental Quality Act (CEQA)
Statute and Guidelines

This book is an unofficial copy of CEQA (Public Resources Code 21000–21189) and the CEQA Guidelines (California Code of Regulations, Title 14, Division 6, Chapter 3, Sections 15000–15387) available from http://leginfo.ca.gov/ and http://ccr.oal.ca.gov/, respectively, as of January 1, 2015. While AEP has made every effort to see that this book is accurate, and that no changes have been made to the content of these state documents as a result of reformatting and reprinting, readers should reference official state versions to verify accuracy. Readers should also be aware that some changes in statutes, guidelines, or case law may have gone into effect since the date of publication. This book does not attempt to offer legal advice and readers should consult their own attorney.



40747 Baranda Court
Palm Desert, CA 92260
(760) 340-4499
www.califaep.org

Guidelines for Implementation of the California Environmental Quality Act have been reproduced with the permission of the California Resources Agency, all rights reserved. AEP thanks the California Resources Agency for its support and cooperation in bringing this resource to the environmental community.



Contents

OVERVIEW OF THE ASSOCIATION OF ENVIRONMENTAL PROFESSIONALS XVII
SUMMARY OF KEY 2014 CEQA COURT CASES XXII
SUMMARY OF KEY 2014 CEQA LEGISLATION XXXIV
STATUTE, AS AMENDED IN 2014 1
Chapter 1: Policy 1
§ 21000. Legislative intent 1
§ 21001. Additional legislative intent 2
§ 21001.1. Review of public agency projects 2
§ 21002. Approval of projects; feasible alternative or mitigation measures 2
§ 21002.1. Use of environmental impact reports; policy 2
§ 21003. Planning and environmental review procedures; documents; reports; data base; administration of process 3
§ 21003.1. Environmental effects of projects; comments from public and public agencies to lead agencies; availability of information 3
§ 21004. Mitigating or avoiding a significant effect; powers of public agency 4
§ 21005. Information disclosure provisions; noncompliance; presumption; findings 4
§ 21006. Issuance of permits, licenses, certificates or other entitlements; waivers of sovereign 4
Chapter 2: Short Title 4
§ 21050. Citation 4
Chapter 2.5: Definitions 5
§ 21060. Application of Definitions 5
§ 21060.1. Agricultural land 5
§ 21060.3. Emergency 5
§ 21060.5. Environment 5
§ 21061. Environmental impact report 5
§ 21061.1. Feasible 5
§ 21061.2. Land evaluation and site assessment 6
§ 21061.3. Infill Site 6
§ 21062. Local agency 6
§ 21063. Public agency 6
§ 21064. Negative declaration 6

§ 21064.3. Major transit stop 6
§ 21064.5. Mitigated negative declaration 6
§ 21065. Project 6
§ 21065.3. Project-specific effect 7
§ 21065.5. Geothermal exploratory project 7
§ 21066. Person 7
§ 21067. Lead agency 7
§ 21068. Significant effect on the environment 7
§ 21068.5. Tiering or tier 7
§ 21069. Responsible agency 7
§ 21070. Trustee Agency 7
§ 21071. Urbanized area; definition 7
§ 21072. Qualified urban use; definition 8
§ 21073. 8
§ 21074. 8
Chapter 2.6: General 9
§ 21080. Division application to discretionary projects; nonapplication; negative declarations; environmental impact report preparation 9
§ 21080.01. California Men's Colony West Facility in San Luis Obispo County; inapplicability of division to reopening and operation 11
§ 21080.02. Kings County; vicinity of Corcoran; new prison facilities; application of division 11
§ 21080.03. Kings and Amador (Ione) Counties; prisons; application of division 12
§ 21080.04. Rocktram-Krug passenger rail service project; application of division; lead agency; legislative intent 12
§ 21080.05. San Francisco Peninsula commute service project between San Francisco and San Jose; application of division 12
§ 21080.07. Riverside and Del Norte Counties; planning and construction of new prison facilities; application of division 12
§ 21080.09. Public higher education; campus location; long-range development plans 12
§ 21080.1. Environmental impact report or negative declaration; determination by lead agency; finality; consultation 13
§ 21080.2. Issuance of lease, permit, license, certificate or other entitlement; determination by lead agency; time 13
§ 21080.3. Consultation with responsible agencies; assistance by office of planning and research 13
§ 21080.3.1. 13
§ 21080.3.2. 14
§ 21080.4. Environmental impact report; requirement determined by lead agency; duties of responsible agencies and certain public agencies; consultation; assistance by office of planning and research 15
§ 21080.5. Plan or other written documentation; submission in lieu of impact report; regulatory programs; criteria; certification; proposed changes; review; commencement of actions; state agencies 15
§ 21080.8. Application of division; conversion of existing rental mobilehome park to resident initiated subdivision, cooperative, condominium for mobilehomes 18

§ 21080.9. Local coastal programs or long-range land use development; university or governmental activities and approvals; application of division 18
§ 21080.10. Application of division; general plans; low- or moderate- income or residential housing; agricultural employee housing 18
§ 21080.11. Application of division; settlements by state lands commission 18
§ 21080.12. Application of Division; repair of Critical Levees 19
§ 21080.13. Railroad grade separation projects; application of division 19
§ 21080.14. 19
§ 21080.14. [DELETED] 19
§ 21080.16. [REPEALED] 19
§ 21080.17. Application of division to ordinances implementing law relating to construction of dwelling units and second units 20
§ 21080.18. Application of division to closing of public school maintaining kindergarten or any of grades 1 through 12 20
§ 21080.19. Restriping of streets or highways; application of division 20
§ 21080.20 Bicycle Transportation Plans 20
§ 21080.20.5 Restriping for bicycle lanes in urbanized areas 20
§ 21080.21. Application of division to public right-of-way pipeline projects less than one mile in length 21
§ 21080.21. 22
§ 21080.22. Local governments; preparation of general plan amendments; application of division 22
§ 21080.23. Pipeline projects; application of division 22
§ 21080.23.5. Pipeline; biogas; application of division 23
§ 21080.24. Permits; issuance, modification, amendment, or renewal; application of law 23
§ 21080.25. LA-RICS; application of division 24
§ 21080.26. Fluoridation; application of division; minor alterations 25
§ 21080.29. La Playa Project; Application of Division 25
§ 21080.32. Exemption of specified actions by publicly owned transit agencies; implementation of budget reductions 26
§ 21080.33. Emergency projects to maintain, repair or restore existing highways; application of division; exceptions 27
§ 21080.35. Carrying out or approving a project; definition 27
§ 21080.35. 27
§ 21080.37. alteration of existing roadway; application of division 28
§ 21080.42. 29
§ 21081. Necessary findings where environmental impact report identifies effects 30
§ 21081.2 Exception to Findings for Infill Residential Projects 30
§ 21081.5. Feasibility of mitigation measures or project alternatives; basis for findings 31
§ 21081.6. Findings or negative declarations; reporting or monitoring project changes; effect on environment; conditions 31
§ 21081.7. Transportation information; submission of report to transportation planning agency 32
§ 21082. Public agencies; adoption of objectives, criteria and procedures; consistency with guidelines 32

§ 21082.1. Draft environmental impact report, environmental impact report, or negative declaration; preparation by public agency....32
§ 21082.2. Significant effect on environment; determination; environmental impact report preparation....33
§ 21082.3....33
§ 21083. Office of planning and research; preparation and development of guidelines; conditions....35
§ 21083.01. guidelines amendments; fire hazard....36
§ 21083.05....36
§ 21083.09....36
§ 21083.1. Legislative intent; interpretation by courts....37
§ 21083.2. Archaeological resources; determination of effect of project; EIR or negative declaration; mitigation measures....37
§ 21083.3. Application of division to approval of subdivision map or other project; limitation; mitigation measures under prior environmental impact report; public hearing; finding....39
§ 21083.4. Counties; Conversion of Oak Woodlands; Mitigation Alternatives; Oak Woodlands Conservation Act Grant Use; Exemptions....40
§ 21083.5. Environmental impact statement or report; submission in lieu of impact report; compliance by adoption of Tahoe regional plan; public review and notice requirements....41
§ 21083.6. Combined environmental impact report and statement; time limits....41
§ 21083.7. Use of impact statement as the impact report; consultations....42
§ 21083.8.1. Reuse plans....42
§ 21083.9. Scoping meetings....43
§ 21084. List of exempt classes of projects; projects damaging scenic resources....44
§ 21084.1. Historical resource; substantial adverse change....45
§ 21084.2....45
§ 21084.3....45
§ 21085.7. [DELETED]....45
§ 21086. Addition or deletion of exempt classes of projects; procedure....45
§ 21088. Distribution of guidelines, amendments and changes; notice....46
§ 21089. Fees....46
§ 21090. Redevelopment plan deemed single project....46
§ 21090.1. Geothermal exploratory project deemed separate and distinct from field development project....47
§ 21091. Draft environmental impact reports and negative declarations; review periods....47
§ 21091.5. Public review period for draft environmental impact report; publicly owned airports....48
§ 21092. Public notice of preparation of environmental impact report or negative declaration; publication....48
§ 21092.1. Addition of new information; notice and consultation....49
§ 21092.2. Requests for certain notices....50
§ 21092.3. Posting of certain notices....50
§ 21092.4. Consultation with transportation planning agencies and public agencies....50
§ 21092.5. Proposed response to public agency comments received by lead agency; notice to agency commenting on negative declaration; untimely comments....50

§ 21092.6. Application of Govt. C. § 65962.5; duties of lead agency; notice by environmental protection agency of failure to specify 51
§ 21093. Legislative findings and declaration; public agencies may tier environmental impact reports....51
§ 21094. Later projects; tiered environmental impact reports; initial study; use of prior reports....51
§ 21094. [Not currently in effect]....53
§ 21094.5....54
§ 21094.5.5....55
§ 21095. Amendment to state guidelines to provide optional methodology to evaluate environmental effects of agricultural land conversions....56
§ 21096. Airport-related safety hazards and noise problems; projects within airport comprehensive land use plan boundaries or within two nautical miles of airport; preparation of environmental impact reports....56
§ 21097. [DELETED]....57
§ 21098. Low-level flight path; military impact zone; special use airspace....57
Chapter 2.7: Modernization of Transportation Analysis for Transit-Oriented Infill Projects....58
§ 21099....58
Chapter 3: State Agencies, Boards and Commissions....59
§ 21100. Environmental impact report on proposed state projects; significant effect; cumulative impact analysis....59
§ 21100.1. Information required in certain environmental impact reports....60
§ 21100.2. Leases, permits, licenses, certificates and other entitlements; establishment of time limits for impact reports and negative declarations....60
§ 21100.2. [not currently in effect]....61
§ 21101. Environmental impact report on proposed federal projects....61
§ 21102. Request for or authorization of expenditure of funds; statement of effect on environment....61
§ 21104. State lead agency; consultations prior to completion of impact report....62
§ 21104.2. Consultation and findings; effect of projects on threatened or endangered species....62
§ 21105. Environmental impact report and comments as part of regular project report; availability to legislature and general public....62
§ 21106. Request of funds to protect environment....62
§ 21108. State agency, board or commission; approval of determination to carry out project; notice; contents; public inspection; posting....62
Chapter 4: Local Agencies....63
§ 21150. Environmental impact report required before allocation of state or federal funds....63
§ 21151. Local agencies; preparation and completion of impact report; submission as part of general plan report; significant effect....63
§ 21151.1. Waste-burning projects; land disposal facilities, and offsite large treatment facilities; environmental impact reports; application of section; exemptions; offsite facility defined....64
§ 21151.2. School site proposed acquisition or addition; notice to planning commission; investigation; report....66
§ 21151.4. Construction or alteration of facility Within One-Fourth of a mile of school; reasonable anticipation of air emission or handling of hazardous or acutely hazardous material; approval of environmental impact report or negative declaration....66
§ 21151.5. Time limits for preparation of environmental impact reports and negative declarations....66

§ 21151.7. Preparation and certification of completion of environmental impact report for open-pit mining operation by lead agency....67
§ 21151.8. Schoolsite acquisition or construction; approval of environmental impact report or negative declaration; conditions....67
§ 21151.9. Projects subject to this division; compliance requirement....69
§ 21151.10. [DELETED]....69
§ 21152. Local agency; approval or determination to carry out project; notice; contents; public inspection; posting....69
§ 21152.1. Local Agency; Exempt Housing Projects; Notice Filing and Posting....70
§ 21153. Local lead agency; consultations prior to completion of impact report....70
§ 21154. Issuance of project order by state; effect on impact report of local agency....71
Chapter 4.2: Implementation of the Sustainable Communities Strategy....71
§ 21155....71
§ 21155. 1....71
§ 21155.2....74
§ 21155.3....75
§ 21155.4....76
Chapter 4.5: Streamlined Environmental Review....76
Article 1: Findings....76
§ 21156. Legislative intent....76
Article 2: Master Environmental Impact Report....76
§ 21157. Preparation; content; fee program....76
§ 21157.1. Review of subsequent projects described in report; requirements....77
§ 21157.5. Mitigated negative declarations; preparation; conditions; alternative....78
§ 21157.6. Limitation period on use of environmental impact report....78
§ 21157.7. Improvements to Roadway Segments of Highway 99; Use of Master Environmental Impact Report....79
Article 3: Focused Environmental Impact Report....80
§ 21158. Purpose; content; additional significant effect on the environment....80
§ 21158.1. Regulatory programs certified under Public Resources Code § 21080.5; certain master and focused environmental impact reports....81
§ 21158.5. Multiple-family residential development of not more than 100 units; residential and commercial or retail mixed-use development of not more than 100,000 square feet; preparation of report; limitations....81
Article 4: Expedited Environmental Review for Environmentally Mandated Projects....81
§ 21159. Rule or regulation adoption; environmental analysis; content....81
§ 21159.1. Utilization of focused environmental impact report; requirements; limitations....82
§ 21159.2. Negative declaration; mitigated negative declaration; environmental impact report on compliance project; project-specific issued; contents....83
§ 21159.3. Deadlines for preparation of report....83
§ 21159.4. Agencies; article application....83
Article 5: Public Assistance Program....84
§ 21159.9. Implementation of program....84

Article 6: Special Review of Housing Projects 84
§ 21159.20. Definitions 84
§ 21159.21. Criteria to qualify for housing project exemptions 85
§ 21159.22. Agricultural employee housing exemption 86
§ 21159.23. Low-income housing exemption 87
§ 21159.24. Infill housing exemption 88
§ 21159.25. [DELETED] 89
§ 21159.26. Reductions in housing units as mitigation discouraged 89
§ 21159.27. Prohibition against piecemealing to qualify for exemptions 89
§ 21159.28. 89
Chapter 5: Submission of Information 90
§ 21160. Application for lease, permit, license, etc.; data and information; purpose; trade secrets 90
§ 21161. Completion of impact report; notice; validity of project 90
§ 21162. [DELETED] 90
Chapter 6: Limitations 90
§ 21165. Lead agency; preparation of impact report 90
§ 21166. Subsequent or supplemental impact report; conditions 91
§ 21166.1. Effect of preparation of impact report by lead agency 91
§ 21167. Commencement of actions or proceedings; time 91
§ 21167.1. Preferential hearing or other civil actions; designation of judges to develop expertise 92
§ 21167.2. Failure to commence action or proceeding within time limits; presumption that impact report complies with division 92
§ 21167.3. Assumption that impact report or negative declaration complies with division; conditional approval or disapproval 92
§ 21167.4. Mandate proceeding alleging noncompliance with division; hearing request; dismissal; briefing schedules and hearing dates 93
§ 21167.4. [Not Currently in Effect] 93
§ 21167.5. Proof of service; filing with initial pleading 94
§ 21167.6. Record of proceedings; clerk's transcript on appeal; filing briefs on appeal; date of appeal for hearing 94
§ 21167.6.5. Service of real party in interest; listing and notice to responsible and trustee agencies; failure to name potential parties 96
§ 21167.7. Copy of pleadings to attorney general; granting of relief 96
§ 21167.8. Settlement meeting; presettlement and settlement statements; further settlement conference; failure to participate 96
§ 21167.8. [Not currently in effect] 97
§ 21167.9. 98
§ 21167.10. 98
§ 21168. Review of determination; finding or decision of public agency; law governing; scope 98
§ 21168.5. Abuse of discretion 98
§ 21168.6. Mandate to public utilities commission; supreme court jurisdiction 99
§ 21168.6.5. 99
§ 21168.6.6 105

§ 21168.7. Declaration of existing law....109
§ 21168.9. Public agency actions; noncompliance with division; court order; content; restrictions....109
§ 21169. Validation of projects....110
§ 21169.11....110
§ 21170. Judicial proceedings in progress; effect....111
§ 21171. Moratorium provision for certain projects....111
§ 21172. [DELETED]....111
§ 21172.5. [DELETED]....111
§ 21173. Severability....111
§ 21174. Construction of division; enforcement of other provisions; coastal act....111
§ 21175. [DELETED]....112
§ 21176. [DELETED]....112
§ 21177. Presentation of grounds for noncompliance; objections to approval of project....112
§ 21177. [Not currently in effect]....112
Chapter 6.5: Jobs and Economic Improvement through Environmental Leadership Act of 2011....113
§ 21178....113
§ 21180....113
§ 21181....114
§ 21182....114
§ 21183....114
§ 21184....115
§ 21185....115
§ 21186....115
§ 21187....116
§ 21188....116
§ 21189....116
§ 21189.1....117
§ 21189.2....117
§ 21189.3....117
TITLE 14. NATURAL RESOURCES....118
DIVISION 6. RESOURCES AGENCY....118
CHAPTER 3: GUIDELINES FOR IMPLEMENTATION OF THE CALIFORNIA ENVIRONMENTAL QUALITY ACT....118
Article 1. General....118
15000. Authority....118
15001. Short Title....119
15002. General Concepts....119
15003. Policies....121
15004. Time of Preparation....121
15005. Terminology....122
15006. Reducing Delay and Paperwork....122
15007. Amendments....123

Article 2. General Responsibilities 124
15020. General 124
15021. Duty to Minimize Environmental Damage and Balance Competing Public Objectives 124
15022. Public Agency Implementing Procedures 125
15023. Office of Planning and Research (OPR) 126
15024. Secretary for Resources 126
15025. Delegation of Responsibilities 126
Article 3. Authorities Granted to Public Agencies by CEQA 127
15040. Authority Provided by CEQA 127
15041. Authority to Mitigate 127
15042. Authority to Disapprove Projects 128
15043. Authority to Approve Projects Despite Significant Effects 128
15044. Authority to Comment 128
15045. Fees 128
Article 4. Lead Agency 129
15050. Lead Agency Concept 129
15051. Criteria for Identifying the Lead Agency 129
15052. Shift in Lead Agency Designation 130
15053. Designation of Lead Agency by the Office of Planning and Research 130
Article 5. Preliminary Review of Projects and Conduct of Initial Study 131
15060. Preliminary Review 131
15060.5. Preapplication Consultation 131
15061. Review for Exemption 131
15062. Notice of Exemption 132
15063. Initial Study 133
15064. Determining the Significance of the Environmental Effects Caused by a Project 135
15064.4. Determining the Significance of Impacts from Greenhouse Gas Emissions 138
15064.5. Determining the Significance of Impacts to Archaeological and Historical Resources 139
15064.7. Thresholds of Significance. 141
15065. Mandatory Findings of Significance 142
Article 6. Negative Declaration Process 143
15070. Decision to Prepare a Negative or Mitigated Negative Declaration 143
15071. Contents 143
15072. Notice of Intent to Adopt a Negative Declaration or Mitigated Negative Declaration 144
15073. Public Review of a Proposed Negative Declaration or Mitigated Negative Declaration 145
15073.5. Recirculation of a Negative Declaration Prior to Adoption. 146
15074. Consideration and Adoption of a Negative Declaration or Mitigated Negative Declaration. 146
15074.1. Substitution of Mitigation Measures in a Proposed Mitigated Negative Declaration. 147
15075. Notice of Determination on a Project for which a Proposed Negative or Mitigated Negative Declaration has been Approved. 148
Article 7. EIR Process 149
15080. General 149
15081. Decision to Prepare an EIR 149

15081.5. EIRs Required by Statute 149
15082. Notice of preparation and Determination of Scope of EIR 150
15083. Early Public Consultation 152
15083.5. [DELETED] 152
15084. Preparing the Draft EIR 152
15085. Notice of Completion 153
15086. Consultation Concerning Draft EIR 153
15087. Public Review of Draft EIR 154
15088. Evaluation of and Response to Comments 156
15088.5. Recirculation of an EIR Prior to Certification 156
15089. Preparation of Final EIR 158
15090. Certification of the Final EIR 158
15091. Findings 158
15092. Approval 159
15093. Statement of Overriding Considerations 159
15094. Notice of Determination 160
15095. Disposition of a Final EIR 161
15096. Process for a Responsible Agency 161
15097. Mitigation Monitoring or Reporting. 163
Article 8. Time Limits 164
15100. General 164
15101. Review of Application for Completeness 164
15102. Initial Study 164
15103. Response to Notice of Preparation 165
15104. Convening of Meetings 165
15105. Public Review Period for a Draft EIR or a Proposed Negative Declaration or Mitigated Negative Declaration 165
15106. [DELETED] 166
15107. Completion of Negative Declaration 166
15108. Completion and Certification of EIR 166
15109. Suspension of Time Periods 166
15110. Projects with Federal Involvement 166
15111. Projects with Short Time Periods for Approval 167
15112. Statutes of Limitations 167
Article 9. Contents of Environmental Impact Reports 168
15120. General 168
15121. Informational Document 168
15122. Table of Contents or Index 169
15123. Summary 169
15124. Project Description 169
15125. Environmental Setting 170
15126. Consideration and Discussion of Environmental Impacts 170
15126.2 Consideration and Discussion of Significant Environmental Impacts. 171

15126.4 Consideration and Discussion of Mitigation Measures Proposed to Minimize Significant Effects. 172
15126.6. Consideration and Discussion of Alternatives to the Proposed Project. 174
15127. Limitations on Discussion of Environmental Impact 177
15128. Effects Not Found to be Significant 177
15129. Organizations and Persons Consulted 177
15130. Discussion of Cumulative Impacts 177
15131. Economic and Social Effects 179
15132. Contents of Final Environmental Impact Report 179
Article 10. Considerations in Preparing EIRs and Negative Declarations 180
15140. Writing 180
15141. Page Limits 180
15142. Interdisciplinary Approach 180
15143. Emphasis 180
15144. Forecasting 180
15145. Speculation 181
15146. Degree of Specificity 181
15147. Technical Detail 181
15148. Citation 181
15149. Use of Registered Professionals in Preparing EIRs 181
15150. Incorporation by Reference 182
15151. Standards for Adequacy of an EIR 182
15152. Tiering 183
15153. Use of an EIR from an Earlier Project 184
15154. Projects Near Airports 185
15155. City or County Consultation with Water Agencies. 185
Article 11. Types of EIRs 188
15160. General 188
15161. Project EIR 188
15162. Subsequent EIRs and Negative Declarations 188
15163. Supplement to an EIR 189
15164. Addendum to an EIR or Negative Declaration 189
15165. Multiple and Phased Projects 190
15166. EIR as Part of a General Plan 190
15167. Staged EIR 190
15168. Program EIR 191
15169. Master Environmental Assessment 192
15170. Joint EIR-EIS 193
Article 11.5 Master Environmental Impact Report 193
15175. Master EIR 193
15176. Contents of a Master EIR 194
15177. Subsequent Projects Within the Scope of the MEIR 195
15178. Subsequent Projects Identified in the MEIR 195

15179. Limitations on the Use of the Master EIR 197
15179.5. Focused EIRs and Small Projects 197
Article 12. Special Situations 198
15180. Redevelopment Projects 198
15181. [DELETED] 198
15182. Residential Projects Pursuant to a Specific Plan 198
15183. Projects Consistent with a Community Plan or Zoning 199
15183.3 Streamlining for infill projects 201
15183.5. Tiering and Streamlining the Analysis of Greenhouse Gas Emissions 205
15184. State Mandated Local Projects 206
15185. Administrative Appeals 207
15186. School Facilities 207
15187. Environmental Review of New Rules and Regulations 209
15188. Focused EIR for Pollution Control Equipment 210
15189. Compliance with Performance Standard or Treatment Requirement Rule or Regulation 210
15190. Deadlines for Compliance with Sections 15188 and 15189 211
15190.5. Department Of Defense Notification Requirement 211
Article 12.5 Exemptions for Agricultural Housing, Affordable Housing, and Residential Infill Projects 212
15191. Definitions 212
15192. Threshold Requirements for Exemptions for Agricultural Housing, Affordable Housing, and Residential Infill Projects 215
15193. Agricultural Housing Exemption 217
15194. Affordable Housing Exemption 218
15195. Residential Infill Exemption 219
15196. Notice of Exemption for Agricultural Housing, Affordable Housing, and Residential Infill Projects 220
Article 13. Review and Evaluation of EIRs and Negative Declarations 220
15200. Purposes of Review 220
15201. Public Participation 221
15202. Public Hearings 221
15203. Adequate Time for Review and Comment 221
15204. Focus of Review 222
15205. Review by State Agencies 222
15206. Projects of Statewide, Regional, or Areawide Significance 223
15207. Failure to Comment 225
15208. Retention and Availability of Comments 225
15209. Comments on Initiative of Public Agencies 225
Article 14. Projects Also Subject to the National Environmental Policy Act (NEPA) 225
15220. General 225
15221. NEPA Document Ready Before CEQA Document 226
15222. Preparation of Joint Documents 226
15223. Consultation With Federal Agencies 226

15224. Time Limits 226
15225. Circulation of Documents 226
15226. Joint Activities 227
15227. State Comments on a Federal Project 227
15228. Where Federal Agency Will Not Cooperate 227
15229. Baseline Analysis for Military Base Reuse Plan EIRs 228
Article 15. Litigation 229
15230. Time Limits and Criteria 229
15231. Adequacy of EIR or Negative Declaration for Use By Responsible Agencies 230
15232. Request for Hearing 230
15233. Conditional Permits 230
Article 16. EIR Monitor 230
15240. EIR Monitor 230
Article 17. Exemption for Certified State Regulatory Programs 231
15250. General 231
15251. List of Certified Programs 231
15252. Substitute Document 232
15253. Use of an EIR Substitute by a Responsible Agency 233
Article 18. Statutory Exemptions 234
15260. General 234
15261. Ongoing Project 234
15262. Feasibility and Planning Studies 234
15263. Discharge Requirements 235
15264. Timberland Preserves 235
15265. Adoption of Coastal Plans and Programs 235
15266. General Plan Time Extension 235
15267. Financial Assistance to Low or Moderate Income Housing 235
15268. Ministerial Projects 236
15269. Emergency Projects 236
15270. Projects Which are Disapproved 237
15271. Early Activities Related to Thermal Power Plants 237
15272. Olympic Games 237
15273. Rates, Tolls, Fares, and Charges 238
15274. Family Day Care Homes 238
15275. Specified Mass Transit Projects 238
15276. Transportation Improvement and Congestion Management Programs 238
15277. Projects Located Outside California 239
15278. Application of Coatings 239
15279. [DELETED] 240
15280. [DELETED] 240
15281. Air Quality Permits 240
15282. Other Statutory Exemptions 240

15283. Housing Needs Allocation 241
15284. Pipelines 241
15285. Transit Agency Responses to Revenue Shortfalls 243
Article 19. Categorical Exemptions 244
15300. Categorical Exemptions 244
15300.1. Relation to Ministerial Projects 244
15300.2. Exceptions 244
15300.3. Revisions to List of Categorical Exemptions 245
15300.4. Application By Public Agencies 245
15301. Existing Facilities 245
15302. Replacement or Reconstruction 246
15303. New Construction or Conversion of Small Structures 247
15304. Minor Alterations to Land 247
15305. Minor Alterations in Land Use Limitations 248
15306. Information Collection 248
15307. Actions by Regulatory Agencies for Protection of Natural Resources 248
15308. Actions by Regulatory Agencies for Protection of the Environment 249
15309. Inspections 249
15310. Loans 249
15311. Accessory Structures 249
15312. Surplus Government Property Sales 249
15313. Acquisition of Lands for Wildlife Conservation Purposes 250
15314. Minor Additions to Schools 250
15315. Minor Land Divisions 250
15316. Transfer of Ownership of Land in Order to Create Parks 250
15317. Open Space Contracts or Easements 250
15318. Designation of Wilderness Areas 251
15319. Annexations of Existing Facilities and Lots for Exempt Facilities 251
15320. Changes in Organization of Local Agencies 251
15321. Enforcement Actions by Regulatory Agencies 251
15322. Educational or Training Programs Involving No Physical Changes 252
15323. Normal Operations of Facilities for Public Gatherings 252
15324. Regulations of Working Conditions 252
15325. Transfers of Ownership of Interest In Land to Preserve Existing Natural Conditions and Historical Resources 252
15326. Acquisition of Housing for Housing Assistance Programs 253
15327. Leasing New Facilities 253
15328. Small Hydroelectric Projects at Existing Facilities 253
15329. Cogeneration Projects at Existing Facilities 254
15330. Minor Actions to Prevent, Minimize, Stabilize, Mitigate or Eliminate the Release or Threat of Release of Hazardous Waste or Hazardous Substances 254
15331. Historical Resource Restoration/Rehabilitation 255
15332. In-Fill Development Projects 255

15333. Small Habitat Restoration Projects. 255
Article 20. Definitions 256
15350. General 256
15351. Applicant 256
15352. Approval 256
15353. CEQA 256
15354. Categorical Exemption 257
15355. Cumulative Impacts 257
15356. Decision-Making Body 257
15357. Discretionary Project 257
15358. Effects 257
15359. Emergency 258
15360. Environment 258
15361. Environmental Documents 258
15362. EIR - Environmental Impact Report 258
15363. EIS - Environmental Impact Statement 259
15364. Feasible 259
15364.5. Greenhouse Gas 259
15365. Initial Study 259
15366. Jurisdiction by Law 259
15367. Lead Agency 260
15368. Local Agency 260
15369. Ministerial 260
15369.5. Mitigated Negative Declaration 260
15370. Mitigation 260
15371. Negative Declaration 261
15372. Notice of Completion 261
15373. Notice of Determination 261
15374. Notice of Exemption 261
15375. Notice of Preparation 261
15376. Person 262
15377. Private Project 262
15378. Project 262
15379. Public Agency 263
15380. Endangered, Rare or Threatened Species 263
15381. Responsible Agency 264
15382. Significant Effect on the Environment 264
15383. State Agency 264
15384. Substantial Evidence 264
15385. Tiering 264
15386. Trustee Agency 265
15387. Urbanized Area 265

CEQA GUIDELINES APPENDICES 266
Appendix A: CEQA Process Flow Chart 267
Appendix B: Statutory Authority of State Departments 268
Appendix C: Notice of Completion & Environmental Document Transmittal 271
Appendix D: Notice of Determination 273
Appendix E: Notice of Exemption 274
Appendix F: Energy Conservation 275
Appendix G: Environmental Checklist form 277
Appendix H: Environmental Information Form 292
Appendix I: Notice of Preparation 294
Appendix J: Examples of Tiering EIRs 295
Appendix K: Criteria for shortened clearinghouse review 298
Appendix L: Notice of Completion of Draft EIR 299
Appendix M: Performance Standards for Infill Projects Eligible for Streamlined Review 300
Appendix N: Infill Environmental Checklist form 304
INDEX 320
CEQA GUIDELINES TOPICS INDEX 327

Overview of the Association of Environmental Professionals

AEP is a non-profit organization of professionals working to improve their skills as environmental and resource managers. Since its formation in 1974, AEP has grown to over 1,700 members: planners, environmental scientists, biologists, lawyers, noise specialists, transportation planners, paralegals, archeologists, geologists, engineers, visual analysts, and other professionals in numerous disciplines. There are nine regional AEP chapters covering the following regions:

- Central
- Channel Counties
- Inland Empire
- Los Angeles County
- Monterey Bay Area
- Orange County
- San Diego
- San Francisco Bay
- Superior California

AEP is dedicated to the enhancement, maintenance and protection of the natural and human environment, as well as the continued improvement of the environmental profession and its members.

AEP's Mission is to:

- Enhance, maintain and protect the quality of the natural and human environment.
- Encourage and carry out research and education, including regular meetings for the benefit of AEP members, the public and concerned professionals in all fields related to environmental planning and analysis.
- Improve public awareness and involvement in the environmental planning, analysis and review process.
- Improve communication and advance the state of the art among people who deal with the environmental planning, analysis and evaluation.

NAEP AFFILIATION

California AEP is affiliated with the National Association of Environmental Professionals and serves as the California Chapter for NAEP. California AEP members are not obligated to join NAEP but may do so to receive the additional benefits of NAEP. California AEP's affiliation with NAEP provides additional benefits to members of both organizations by fostering networking and educational opportunities between the two organizations. For additional information about NAEP, please visit www.naep.org.

AEP MEMBERSHIP CATEGORIES

Full (Individual) Membership

A full (individual) membership includes all of the many services, benefits and discounts of membership. Depending on your location, you will become a member of the local chapter nearest

you and will start to receive the newsletter for that Chapter, which will list AEP activities in your area. The AEP State Board also provides outlying area support through the Directors at Large, to keep members in touch with items of interest and to facilitate establishment of new Chapters.

Agency/Corporate Membership

Agency or Corporate Members are provided two or one "floating" membership, respectively. Corporate Members also receive special recognition at the annual State Conference, a 10 percent discount on advertising, and a highlighted listing in AEP's statewide magazine the *Environmental Monitor*. Each Chapter may provide additional recognition for Corporate Members. The floating memberships entitle individuals to attend local chapter activities, regional workshops and the State Conference at the discounted member rate. NOTE: The agency or company takes responsibility to notify the appropriate AEP officer regarding which employee will attend a given AEP activity on behalf of the company.

Emeritus Membership

Emeritus Members are provided full membership benefits at a reduced rate if they have just retired and have been full AEP members for the past five years.

Young Professionals Membership

Students who have graduated from college within the past two years with a degree in and/or beginning a career in the environmental field can have the benefits of full membership at this reduced rate. To qualify, a person must have been a registered student member with AEP the year before graduation and must supply proof of graduation upon request. This reduced membership rate can be claimed for up to two years past graduation.

Student Membership

The student membership includes all of the individual membership services and eligibility for the annual AEP Student Awards Program. Student members must be currently enrolled in 12 units or more at an accredited school. The State Conference Committee typically offers students reduced registration rates to the State Conference. In addition, AEP is an excellent resource for internship opportunities and networking with environmental professionals while seeking employment opportunities. Contact the local chapter for more information on student benefits and activities.

AEP MEMBERSHIP BENEFITS AND SERVICES

Web Site

AEP's website is a great resource for members, providing information about upcoming events, pending legislation and membership information. AEP's website address is www.califaep.org.

Environmental Monitor

The Environmental Monitor is a quarterly statewide magazine with information on top leaders in the profession, articles of interest, job opportunities and summaries of state and local chapter activities. The magazine is recognized throughout the environmental planning profession as an important source of information.

Environmental Assessor

The Environmental Assessor is a pull-out of environmental legislative activities for your personal library. The Environmental Assessor includes information describing the latest environmental legislation working through the State Senate and Assembly, the status of such legislation, and the position of AEP on such legislation. It also provides an update from AEP's State Legislative Committee and its interaction with and recommendations to the State Legislature.

Local Chapter Activities

Local chapters are governed by the local members with guidance and assistance, as needed, from the State Board. The local chapters offer a wide range of services and activities, typically consisting of a regular newsletter, membership meetings featuring top environmental professionals discussing current environmental topics, and a chance to network with local environmental professionals from diverse backgrounds and environmental fields. Some chapters engage in educational activities based upon topical environmental issues and trends.

Environmental Services Bulletin

The Environmental Services Bulletin announces statewide job opportunities. This service also allows for private consultants to bid on new project contracts.

Annual State Conference

California AEP holds an annual Conference at various locations throughout the state, providing members with an opportunity to hear leading speakers in the environmental field, improve their skills, network with people from around the state, and discuss major environmental issues with experts in the field.

Professional Practice Insurance Discounts

AEP members can receive a discount on general liability and professional liability insurance through AEP's partnership with Hilb Rogal & Hobbs PPIB.

Biannual CEQA Workshops

Annual CEQA workshops provide updates of existing and recently adopted CEQA laws and current court actions. AEP members receive a discount when attending the annual CEQA workshops at locations throughout the state. The format of the workshops has proven successful, providing both basic and advanced information.

Membership Certificate

A membership certificate, suitable for framing, is sent to each new AEP member.

Annual CEQA Handbook

AEP annually publishes a CEQA Handbook, including the up to date text of the Statute and Guidelines, an update of CEQA Legislation and Court Cases, and a comprehensive index. Members receive a free copy of the CEQA Handbook. Additional copies in hardcopy and electronic (CD) format are available.

Legislative Activities

AEP has an active Legislative Committee which closely tracks and responds to proposed CEQA legislation in order to influence the pending legislation in a positive and meaningful manner. Current summaries and analysis of the bills are published regularly in the *Environmental Assessor* and on AEP's website.

Regional Area Support

Regional area support ensures representation no matter where you live. Directors-at-Large and state-sponsored events provide service to all areas within California.

Professional Award Program

The Professional Award Program provides an excellent opportunity for professional recognition of outstanding achievements and document preparation. AEP offers an awards program, the results of which are presented at the State Conference.

Association of Environmental Professionals Continuing Education Credit

Members who attend AEP workshops and other events earn special credit. CEQA Workshop participants are able to count attendance toward continuing education credit requirements under AICP and MCLE.

Member Services

To contact the AEP Membership Hotline, call (760) 340-4499.

Special Committees

The AEP Board appoints special committees to address issues of concern to its membership. Committees include the Legislative Committee, the Emerging Issues Committee, and the Climate Change Committee.

Professional Discounts

AEP is continuously negotiating professional discounts for AEP members to attend U.C. Extension courses and to obtain professional guidebooks of interest to members. The discounts vary depending on the event and/or the publisher.

Membership application forms are also available from your local AEP Chapter or at www.califaep.org.

NEW/RENEWAL MEMBERSHIP APPLICATION

Association of Environmental Professionals

www.CalifAEP.org

Please mail this portion along with your check made payable to AEP: c/o Lynne C. Bynder, CMP, Meetings Xceptional, 40747 Baranda Court, Palm Desert, CA 92260
AEP can not invoice for new memberships. Questions: 760.340.4499, fax: 760.674.2479.
Online application available at http://www.califaep.org/index.php?option=com_osemsc&view=register

GENERAL INFORMATION

First _____ Last _____ Certification _____ Firm/Agency _____

Address _____

City _____ State _____ Zip _____ Email _____

Daytime Phone No. _____ Ext. _____ Fax _____

☐ Check to be OMITTED from the AEP *Web Site Directory*. Employment type: ☐ Non-Profit ☐ Private ☐ Public ☐ Other _____

☐ Please send me a National Association of Environmental Professionals (NAEP) membership application.

TO PAY BY CREDIT CARD (PLEASE FILL OUT BELOW)

Card Holder Name _____ Signature _____

Billing Address _____ City _____ State _____ Zip _____

Card type ☐ Visa ☐ Mastercard ☐ Discover Card No. _____ CVC# _____ Exp. Date _____

AREAS OF INTEREST (SELECT 3)

- ☐ 1. CEQA/NEPA Compliance
- ☐ 2. Environmental Impact Analysis
- ☐ 3. Resource Management
- ☐ 4. Solid/Hazardous Waste
- ☐ 5. Air Quality
- ☐ 6. Noise
- ☐ 7. Transportation
- ☐ 8. Hydrology/Water
- ☐ 9. Endangered Species/Biology
- ☐ 10. Geology/Seismic
- ☐ 11. Cultural Resources
- ☐ 12. Growth Management/ Regional Planning
- ☐ 13. Environmental Law/Policy
- ☐ 14. Land Use/Site Planning
- ☐ 15. Geographic Information Systems
- ☐ 16. Environmental Justice
- ☐ 17. Environmental Engineering
- ☐ 18. Other _____

CHAPTER REGIONS AND MEMBERSHIP

AEP CODE OF ETHICS

1. I will conduct myself and my work in a manner that will uphold the values, integrity, and respect of the profession.
2. I will uphold the stated intent as well as the letter of environmental policies, laws, and regulations which are adopted by governmental bodies or agencies.
3. I will not engage in, encourage, or condone dishonesty, fraud, deceit, discrimination, or misrepresentation in the solicitation, preparation, or use of work prepared by me or under my direction.
4. I will fully disclose to my employers and my prospective clients any economic or ethical interests which could reasonably be interpreted as a conflict of interest by them or by other affected parties with regard to my professional work.
5. I will ensure a good faith effort at full disclosure, technical accuracy, sound methodology, clarity, and objectivity in the collection, analysis, interpretation, and presentation of environmental information by me or under my direction.
6. I will achieve and maintain the highest level of professional competency, for myself and require the same for those I supervise.

Signature acknowledges full understanding & acceptance of the AEP Code of Ethics & Professional Conduct Guidelines.

OFFICE USE ONLY Co. _____ P. _____ Date _____ Amount _____ Check # _____

Contributions or gifts to AEP are not tax deductible as charitable contributions for income tax purposes. However, they may be tax deductible as ordinary and necessary business expenses subject to restrictions imposed as a result of association lobbying activities. AEP estimates that the nondeductible portion of your dues allocable to lobbying is 5%.

Status	Please Check
New Member Application	☐
Renewal Membership	☐
Change of Address, Etc.	☐

Membership Category	Annual Dues	Please Check
Full AEP Member	$150.00	☐
AEP Sponsor Member *Government/Corporate Sponsors are provided one Full Membership which can "float" within the sponsor company.*	$250.00	☐
Young Professionals Member *Must have graduated in 2011 or 2012.*	$70.00	☐
Emeritus Member *Must have been a full member within the last 5 years.*	$70.00	☐
AEP Full Time Student Member *Please include current student schedule showing 12 units or more with application.*	$35.00	☐

Note: See full category descriptions on line at CalifAEP.org

AEP Chapter Areas (check one chapter only)

- ☐ 1. Channel Counties
- ☐ 2. Inland Empire
- ☐ 3. Los Angeles
- ☐ 4. Monterey Bay
- ☐ 5. Superior California
- ☐ 6. Orange County
- ☐ 7. San Diego
- ☐ 8. San Francisco Bay Area
- ☐ 9. Central

Summary of Key 2014 CEQA Court Cases

By Terry Rivasplata of ICF International

The following discussions of California court decisions are very brief summaries of CEQA cases from 2014 and are certainly no substitute for legal advice. For more detail and interpretation, please consult your legal counsel.

California Clean Energy Committee v. City of Woodland **(April 1, 2014) __ Cal.App.4th __**

The project at issue (known as Gateway II) began as a 154-acre regional commercial center with approximately 808,000 square feet of retail space, three hotels, restaurants, an auto mall, and 100,000 square feet of office space on agricultural land at the edge of existing urbanization. The Woodland City Council significantly scaled back the size of Gateway II with its approval.

The EIR prepared for Gateway II concluded that it would result in "urban decay" in both the downtown and the city's existing regional mall, and identified five mitigation measures to reduce, but not fully avoid, that impact. The draft EIR considered a mixed-use alternative consisting of a smaller site with a local-serving commercial "town center," a 100-unit multi-family residential component, 200,000 square feet of commercial space, and two auto dealerships. This alternative was rejected as economically infeasible. The EIR addressed the energy impact of the proposed project, noted that the project would be consistent with California Building Standards and Green Building Standards, and concluded that it would have a less than significant impact regarding the "wasteful, inefficient, or unnecessary consumption of energy."

The California Clean Energy Committee (CCEC) challenged the EIR and the trial court decided in favor of the City. The Court of Appeal reversed that decision in the published portion of its decision. CCEC successfully argued that the City's mitigation measures are insufficient to reduce the urban decay that will be caused by the project, the City failed to give meaningful consideration to feasible project alternatives such as the mixed-use alternative, and the final EIR did not properly identify and analyze potentially significant energy impacts generated by the project.

Center for Biological Diversity v. Department of Fish and Wildlife **(March 20, 2014) __ Cal.App.4th __**
[Accepted for review by California Supreme Court, not citable.]

CBD challenged the EIR certified by CDFW for approval of the Newhall Ranch Resource Management and Development Plan, Spineflower Conservation Plan, Master Streambed Alteration Agreement, and two related incidental take permits. One of the incidental take permits was for the spineflower, the other was a multi-species permit that included incidental take of several bird species. The Spineflower Conservation Plan, which extended beyond the boundaries of the specific plan, required the establishment of spineflower preserves and buffer areas, to be maintained in perpetuity. The resource management plan included specific provisions that were intended to avoid impacts on the unarmored three-spine stickleback, a native fish.

These approvals relate to development of the Newhall Ranch in Los Angeles County under the previously adopted specific plan for this new community. Build-out of the specific plan will eventually result in a mixed-use community with a population of approximately 58,000. An EIR was certified for the specific plan and the present EIR relied to some degree on the studies and analyses prepared for that earlier document.

The trial court set aside the EIR; the Court of Appeal emphatically reversed that decision. The Court's decision emphasizes the importance of documentation of impacts and mitigation, and points out the deference given to agencies when an EIR has been prepared in cases where there are differences between experts.

***Citizens Against Airport Pollution v. City of San Jose* (July 2, 2014) 227 Cal.App.4th 788**

The City amended its international airport's Airport Master Plan (AMP) to change the size and location of future air cargo facilities, replace air cargo facilities with general aviation facilities, and modify two taxiways to provide better access for corporate jets. These amendments were prompted by reductions in the projected level of air passenger, air cargo, and general aviation, as well as an actual decrease in the annual number of passengers served. To comply with CEQA, the City adopted the eighth addendum to the 1997 EIR certified for the AMP. A supplemental EIR for the airport was certified in 2003.

CAAP sued, alleging that as a matter of law the amendments to the AMP constitute a new project and therefore an addendum cannot be used. They further alleged that the amendments required preparation of an EIR to address the amendments' noise, greenhouse gas emissions, toxic air contaminants, and burrowing owl habitat impacts. The Court of Appeal decided in favor of the City.

***Citizens for a Sustainable Treasure Island v. City and County of San Francisco* (July 7, 2014) 227 Cal.App.4th 1036**

The City approved plans and ordinances for the conversion of the former naval station on Treasure Island to a mixed-use community, including up to 8,000 residences; commercial/retail space; offices; hotels; public utilities; parks, playgrounds, and public open spaces; a new ferry terminal and intermodal transportation hub; and a K-8 school. The project will also restore and reuse historic buildings on the island. The City certified an EIR for the project.

CSTI sued, claiming that the EIR should have been a program EIR rather than a project EIR, that the project description was insufficiently accurate and stable, and that significant new information received during the draft EIR review period necessitated recirculation of the EIR. The trial court denied CSTI's writ. This appeal followed. The Court of Appeal decided in favor of the City.

***Citizens for Environmental Responsibility v. State of California ex rel. 14th District Agricultural Association* (March 26, 2014) __ Cal.App.4th __**
[Accepted for review by California Supreme Court, not citable.]

At issue in this case was a proposal by the Santa Cruz County Sheriff's Association to hold a three-day rodeo at the Santa Cruz County fairgrounds to benefit children's programs. The application included improvements to the fairgrounds and contemplated future rodeos. The fair board (i.e., the 14th District Agricultural Association) approved the project in 2010, finding that it was exempt from CEQA under the Class 23 categorical exemption. That exemption applies to normal operations of existing facilities for public gatherings "where there is a past history of the facility being used for the same or similar kind of purpose." After a disagreement with the sponsors, the board later rescinded its approval. It ultimately approved a two-day rodeo in 2011, with no proposed changes to the fairgrounds.

The proposed two-day event was expected to attract 1,500 spectators. Up to 500 horses would be involved, with about 100 on the grounds at any given time, and up to 250 cattle, with about 50 on the grounds at any time. The second approval included an analysis supporting the applicability of the Class 23 exemption. The second approval is the subject of this lawsuit.

Separate from the rodeo proposal, in 2009 the Central Coast Regional Water Quality Control Board (CCRWQB) found that Salsipuedes and Corralitos Creeks, to which the fairgrounds drain, are impaired water bodies as a result of human and animal coliform bacteria discharged to those creeks. The CCRWQB imposed requirements to use management practices to control discharges and to monitor and report progress on implementing those practices. In 2010, the Fairground formalized

its prior manure manage practices in a written Manure Management Plan (MMP) to satisfy the CCRWQCB's requirements.

Citizens for Environmental Responsibility argued that the MMP constituted a mitigation measure for the rodeo project and that the "unusual circumstances" exception applied in this situation, both of which precluded the use of a categorical exemption. The trial court decided in favor of the Agricultural Association. The Court of Appeal upheld that decision.

Citizens for Green San Mateo v. San Mateo County Community College District **(June 17, 2014) 226 Cal.App.4th 1572**

In 2006, the District adopted a comprehensive Facilities Master Plan setting out renovations, demolitions, and construction of buildings, parking, roads, and outdoor spaces on the College of San Mateo campus. The District adopted a mitigated negative declaration (MND), disclosing the potential impacts of these activities. The MND noted that the project would include the removal of trees, but that this impact would be compensated for by the planting of replacement trees and vegetation around the new and renovated buildings and elsewhere on campus. The MND concluded that this impact would be less than significant.

In late 2010 and early 2011, after a public hearing awarding a contract for a portion of the Master Plan construction work (including tree removal), the District's contractor removed and trimmed numerous trees in the campus' North Gateway Area. After expressing concern over the tree cutting in January, Citizens filed suit in July 2011, challenging the tree removal. The trial court held in favor of Citizens and this appeal followed.

The Court of Appeal found in favor of the District. The District had argued in trial court that Citizens' challenge was time-barred by virtue of being filed long after the notice of determination (NOD) for the Master Plan was filed in 2007. Under CEQA, a lawsuit must be filed within 30 days of the filing of an NOD or, if no NOD was filed, within 180 days of the project decision.

Citizens challenged the tree removal and not the original approval of the Facilities Master Plan, on the theory that the tree removal was not contemplated in the original MND. Under this line of reasoning, the NOD filed in 2007 did not establish CEQA's 30-day statute of limitations. Instead, Citizens claimed that the actual observation of tree removal in January 2011 started a 180-day statute of limitations. The Court disagreed.

Citizens for the Restoration of L Street v. City of Fresno **(August 29, 2014) 229 Cal.App.4th 340**

The City approved a residential infill project consisting of 28 two-story townhomes on a site containing two homes built in the early twentieth century. One of the homes had previously been designated as a "Heritage Property" by the city's Historic Preservation Commission; the other had no historical listing because of its prior loss of integrity as a historical building. The designated home was vacant and in an advanced state of disrepair. The project site is within an area that had been studied as a possible historic district, but had never been formally designated as such. The City considered the potential historic significance of the two homes, concluded that they were not significant, and prepared a Mitigated Negative Declaration (MND) for the project.

The Historic Preservation Commission held a public meeting on the project and adopted the MND along with findings regarding the lack of historic resources. The City Council subsequently upheld the Commission's findings regarding the historic significance of the homes and approval of the MND. Citizens sued, alleging that there was a fair argument that the project may have a significant effect on historical resources and that an EIR should be prepared. The trial court held that the Preservation Commission was not authorized to approve the MND and that the Council's decision did not cure this defect. The trial court ordered the demolition permit vacated and directed the

Council to conduct a new hearing on the MND. It did not mandate preparation of an EIR. In the meantime, both homes were demolished.

The City appealed the holding that it could not delegate CEQA authority to the Preservation Commission; Citizens cross-appealed to challenge the trial court's decision not to require an EIR. The Court of Appeal decided against the City in the first instance, and in the City's favor on the second. On the issue of whether there was a fair argument sufficient to require preparation of an EIR, the Court held that CEQA did not intend the fair argument to apply to the lead agency's initial determination of the historic significance of a resource.

Citizens Opposing a Dangerous Environment v. County of Kern **(July 25, 2014) 228 Cal.App.4th 360**

The County prepared an EIR for a proposed rezoning and use permit to authorize a wind farm and associated concrete batch plant in the Tehachapi area. The proposed wind turbines would be 500 feet tall. Potential safety hazards related to existing aircraft and glider use at the nearby Kelso Valley airport were identified in the EIR and Mitigation Measure (MM) 4.8-8 required the windfarm developer to obtain prior to the issuance of building permits a "Determination of No Hazard to Air Navigation" from the Federal Aviation Administration (FAA), including written concurrence from the military, for each wind turbine to be installed. The County concluded that the measure reduced this impact to a less than significant level. The EIR also examined three alternatives: no project, relocation to the San Gorgonio Pass area, and reduced number of turbines.

During public review, the owner of the Kelso Valley airport (KVA) submitted comments regarding the windfarm's hazards for gliders using the airport. Locating the towers on ridges that are used for lift by glider pilots, combined with gliders' shallow descent ratio, would effectively block safe access to the airport. The County responded that this would be avoided by the FAA review of each turbine (noting that the FAA's review process was outside the County's control), certified the EIR, and approved the project. Additionally, the applicant submitted expert testimony asserting that FAA had already issued preliminary no hazard determinations after review of the airport and that the project complied with FAA regulations.

CODE sued, alleging that the EIR was inadequate. The trial court decided in the County's favor. The Court of Appeal upheld the adequacy of the EIR.

On appeal, CODE carried forward the following claims: (1) federal aviation law did not preempt the County from identifying and imposing feasible alternatives and/or mitigation measures on the Project to *avoid* or *eliminate* the Project's admitted potentially hazardous impacts on KVA; (2) the County's responses to CODE's comments on the EIR and the Project didn't comply with CEQA and the Guidelines; (3) the County's finding that MM 4.8-8 reduces the Project's admitted potentially hazardous aviation impacts on KVA to a level of insignificance was unsupported by substantial evidence; (4) the County improperly rejected CODE's suggested feasible alternatives and mitigation measures to eliminate the Project's potential impact on aviation; and (5) no substantial evidence in the administrative record supports the County's rejection of the EIR's environmentally superior alternative.

Cleveland National Forest Foundation v. San Diego Association of Governments **(Nov. 24, 2014) __ Cal.App.4th __**

This case concerns a challenge to adequacy of the program EIR (PEIR) certified for SANDAG's 2011 Regional Transportation Plan/Sustainable Communities Strategy (RTP/SCS). SANDAG was the first regional government to adopt an SCS after the passage of the Sustainable Communities and Climate Protection Act (SB 375) in 2008. An SCS is intended to establish land use policies complementary to regional housing needs and transportation investments that will help reduce

regional greenhouse gas (GHG) emissions from autos and light trucks. The California Air Resources Board (CARB) is responsible for setting regional the GHG reduction target to be met by the SCS. SANDAG's GHG emissions reduction target is 7% by the year 2020.

SANDAG's RTP/SCS is fundamentally a plan for long-term transportation investments within the San Diego region, identifying transportation projects that will receive a share of an estimated $214 billion in financing that will be available over the next several decades. Under SB 375, the RTP/SCS must also identify a land use pattern that in conjunction with transportation investments and local planning decisions will meet the region's GHG emissions reduction target.

The RTP/SCS EIR was invalidated by the trial court, largely on the issue of GHG emissions reduction. The Court of Appeal upheld that decision in a 2-1 opinion, along with a number of cross-appeals. This case is marked by a lengthy, stinging dissent that characterizes the majority opinion as "judicial interference."

Coalition of Adequate Review v. City and County of San Francisco **(Sept. 15, 2014) __ Cal.App.4th __**

This case is about the recovery of costs for the record of proceedings. CEQA cases are based on the administrative record that was before the public agency at the time it made its decision on the project. The plaintiff in a CEQA lawsuit may elect to prepare the administrative record, using the information available in the records of the public agency, that is to be used by the Court in its deliberations.

The City won a CEQA case brought by the Coalition and filed a claim of $64,144, primarily to cover its costs for preparing a supplemental record of the proceedings. The trial court denied the City's claim for costs on two grounds: first, because the Coalition had elected to prepare the record themselves, as allowed by CEQA's record preparation statute (Public Resources Code Section 21167.6(b)(2)), and second, because the court feared a sizeable cost award to the defendant would have a chilling effect on lawsuits challenging important public projects. The Court of Appeal found that "[n]either rationale is a legally permissible basis for denying record preparation costs to the City." The Court granted the City its costs for preparing the supplemental record, denied claimed costs for responding to petitioners' document requests, and sent the case back to the trial court for final disposition of copying, postage, and express delivery costs.

Foothill Communities Coalition v. County of Orange **(January 13, 2014) 222 Cal.App.4th 1302**

This case arose over the County's establishment of a new zoning definition for senior residential housing, which it applied to the project site. Foothill claimed that applying this to a site while other surrounding sites did not have the same allowed uses amounted to illegal "spot zoning." Coalition also challenged the EIR for the project. The trial court decided in favor of Foothill, but declined to act on the CEQA challenge because it had overturned the project. The Court of Appeal reversed the judgment, finding in favor of the County.

Friends of the Eel River v. North Coast Railroad Authority **(Sept. 29, 2014) 277 Cal.App.4th 832 [Accepted for review by California Supreme Court, not citable.]**

The North Coast Railroad Authority (NCRA) entered into a contract with the Northwestern Pacific Railroad Company (NWPRC) that allows NWPRC to provide freight service on tracks controlled by NCRA. NCRA is a public agency established under state law (Government Code section 93000 et seq.). Its enabling statute identifies Humboldt, Mendocino, Sonoma, and Trinity Counties as NCRA's service area. It authorizes NCRA "to provide rail passenger and freight service within those counties." NCRA certified an EIR in conjunction with its approval of the NWPRC contract.

Friends of the Eel River and Californians for Alternatives to Toxics (together, FOER) brought suit to challenge NCRA's certification of the EIR and approval of NWPRC's freight operations. The trial court denied the petitions for writ, concluding that CEQA review is actually preempted by the Interstate Commerce Commission Termination Act (ICCTA). The ICCTA grants the federal Surface Transportation Board (STB) exclusive jurisdiction over rail operations. STB must give its permission before a rail carrier can operate. This exclusive federal jurisdiction preempts CEQA. Subsequently, NCRA rescinded its EIR certification.

On appeal, FOER argued that the ICCTA preempts only the "regulation" of rail transportation, not CEQA's applicability. They further claimed that NCRA was required to prepare a CEQA analysis of the rail operations and related repair/maintenance activities as part of an agreement to receive Transportation Congestion Relief Program funds and as part of a settlement of an earlier lawsuit over the rail line and could not later claim federal preemption. FOER also claimed that the EIR improperly "segmented" the project, given that additional rail operations were contemplated on other sections of the line. The Court of Appeal rejected all of these claims.

Lotus v. Department of Transportation (Jan. 30, 2014) 223 Cal.App.4th 625

Caltrans prepared an EIR for its proposed project to "adjust" the alignment of Highway 101 through Richardson Grove State Park to accommodate trucks of federal standard length. The road adjustments included realignment, curve corrections, shoulder widening, culvert replacement, and repaving. The state park is centered on a grove of old growth redwoods, and a major concern about the project was its potential to remove or damage redwoods along the Highway 101 alignment. Although no old growth redwoods were proposed to be removed, the EIR found that six smaller redwoods would be taken out and that scores of old growth and smaller redwoods would be affected by excavation and fill activities occurring within their root zones. In keeping with Caltrans' usual practice, the EIR described "avoidance, minimization, and/or mitigation measures" that had been incorporated into the project to mitigate its impacts on redwoods. The EIR identified nine such measures addressing the methods of excavation in root zones, watering regimes, plant care, fill management, and replanting methods. The EIR concluded that the project would not result in significant effects on redwoods.

Lotus sued Caltrans, alleging that the department had failed to comply with CEQA. The trial court decided in Caltrans' favor, but noted that Caltrans may not have fully complied with CEQA in using avoidance, minimization, and/or mitigation measures in place of standard mitigation measures. The Court of Appeal rejected most of Lotus' challenge, but in the published portion of its opinion, held that the EIR had failed to properly evaluate the project's impacts on the roots of old growth redwoods along the highway alignment. It sent the case back to the trial court for further consideration.

North Coast Rivers Alliance v. Westlands Water District (July 3, 2014) __ Cal.App.4th __

The Westlands Water District contracts with the Bureau of Reclamation for delivery of agricultural water from the Central Valley Project. In 2012, Westlands entered into a two-year interim renewal contract with Reclamation that continued the existing water delivery contracts in advance of expected new 25-year renewal contracts. Westlands had previously entered into a three-year interim renewal contract in 2007 and a two-year interim contract in 2010.

The Bureau is required, upon request, to renew existing long-term water service contracts for up to 25 years under the provisions of the 1992 Central Valley Project Improvement Act (CVPIA). However, no renewal can be approved until the Bureau has prepared a programmatic Environmental Impact Statement (PEIS) examining the impacts of implementing the CVPIA, including renewal of water service contracts. The CVPIA provides that until the PEIS is completed, the Bureau is authorized to enter into serial interim renewal contracts with its contractors.

Westlands entered into the 2012 interim contract because the Bureau had not yet completed the PEIS that is a prerequisite to enter into a new long-term contract. Westlands found that the interim contract was exempt from CEQA under the statutory exemptions for ongoing activities that were approved before CEQA was enacted on November 23, 1970 (CEQA Guidelines Section 15261) and rate-setting (Section 15273), and the categorical exemption for existing facilities (Section 15301).

North Coast brought suit, alleging that Westlands had failed to comply with CEQA because there is no CEQA exemption that applies to the interim contract. The Court of Appeal ruled in favor of Westlands, upholding the exemptions.

***Paulek v. California Department of Water Resources* (Oct. 31, 2014) __ Cal.App.4th __**

The DWR certified an EIR for its approval of the Perris Dam Remediation Project. Perris Dam was found to be structurally deficient in a 2005 report and the project constituted the improvements needed in order that it could withstand future seismic events. The Draft EIR addressed three activities: (1) remediating structural deficiencies in the dam, (2) replacing the dam's outlet tower, and (3) creating a new "Emergency Outlet Extension." The first two were recommended in the 2005 report; consideration of replacing the existing emergency outlet came up when it was found that although the spill area had been empty of structures when the dam was built, it was now covered by houses. In response to comments on the DEIR, DWR decided to undertake a separate CEQA process for the emergency outlet extension and the Final EIR considered only the first two activities.

Paulek participated at the public workshop on the DEIR held by DWR; he also signed a letter from a conservation group raising issues about the Draft EIR's adequacy. He brought suit against DWR after approval of the revised project. The trial court held that Paulek had standing to bring suit, but dismissed his claims on their merits. The Court of Appeal upheld this decision.

***Picayune Rancheria of Chukchansi Indians v. Brown (Sept. 24, 2014)* __ Cal.App.4th __**

Under the federal Indian Gaming Regulatory Act, the Secretary of the Interior may determine that the establishment of tribal gaming on newly acquired lands would be in the best interest of the tribe and not detrimental to the surrounding community. The Governor must concur in this determination for it take effect.

The Department of the Interior notified Governor Brown in 2011 that it had reached such a determination for lands to be acquired by the North Fork Tribe and asked the Governor for his concurrence. Despite the request of the Picayune Tribe and others that he prepare an EIR before acting, the Governor issued a concurrence and executed a tribal-state gaming compact with the North Fork Tribe.

The Picayune Tribe sued, alleging that the Governor is a "public agency" for CEQA purposes and that his action in concurring with the Secretary of the Interior's determination is a project subject to CEQA review. The Court of Appeal found that, as a matter of law, the Governor is not a public agency for CEQA purposes.

***Property Reserve v. Superior Court of San Joaquin County* (March 13, 2014) __ Cal.App.4th __**

This case does not directly involve CEQA. However, it addresses the ability of a public agency to access property for environmental surveys. The extent to which this decision may restrict typical environmental surveys is unclear, given that it involves surveys being undertaken pre-condemnation and with rather extensive work periods.

The Department of Water Resources (DWR) proposed to conduct geotechnical studies of the potential tunnel alignment, as well as environmental surveys. The environmental surveys were "to

determine and document each parcel's botany and hydrology; the existence of sensitive plant and animal species; the existence of vernal pools, wetlands, and other animal habitat; the existence of cultural resources and utilities; and the parcel's recreational uses. Personnel would also map the properties using aerial photography and large targets secured by stakes. Personnel would take minor soil samples, and they would observe and trap certain animal species. They would access the properties by motor vehicle, on foot, and by boat when necessary."

DWR filed a master petition pursuant to Code of Civil Procedure Section 1245.010 et seq. (the pre-condemnation entry statutes of Eminent Domain Law) to obtain the rights of entry to conduct the surveys. The petitions affect more than 150 owners of more than 240 parcels in San Joaquin, Contra Costa, Solano, Yolo, and Sacramento Counties. The plaintiff sued to stop entry to these parcels. The entry orders allowed surveys taking up to 66 days, over a one-year period, by as many as eight people at a time per owner. Biological surveys could also involve trapping, with traps being left on the subject property during the survey.

The trial court authorized entry for purposes of environmental studies, but not for geotechnical surveys (which involve boring and then plugging bores with grout). It ruled that "the activities constituted a taking or damaging, and the entry statutes were unconstitutional if used to take or damage property. The court stated the State had conceded its geological borings would result in a taking or damaging of property, and the court so found. It further found that the entry statutes did not comply with article I, section 19, subdivision (a), of the California Constitution (Section 19(a)), the state constitutional provision limiting the use of eminent domain, and thus they could not be used to authorize the State's proposed taking or damaging of property. The entry statutes failed to satisfy Section 19(a) because the court proceeding they authorized was not an 'eminent domain proceeding' as referenced in Section 19(a) that provided the affected landowners with all of their constitutional rights against the State's exercise of eminent domain authority, including the right to a jury determination of just compensation."

In a split decision, the Court of Appeal concluded that in the situation before them, that both types of studies constituted takings.

***Protect Agricultural Land v. Stanislaus County Local Agency Formation Commission* (January 29, 2014) 223 Cal.App.4th 550**

The City of Ceres (City) approved the West Landing Specific Plan and certified an EIR for the project prior to applying for approval of a sphere of influence amendment and related annexation of the 960-acre site to the City. The project's EIR identified significant environmental impacts that could not be mitigated to a level of insignificance, including impacts on agricultural land. The City adopted the required findings and statement of overriding considerations. The City then applied to the LAFCO, which approved its applications based on the City's EIR.

After the LAFCO approved the City's applications, Protect Agricultural Land (PAL) sued the LAFCO, alleging that the approval of modifications to the City's sphere of influence and the annexation violated CEQA and the Cortese-Knox-Hertzberg Local Government Reorganization Act of 2000, which governs annexations and sphere of influence modifications. In response, the LAFCO and City filed a demurrer, contending that Government Code section 56103 requires challenges to a LAFCO's approval of an annexation and a change in a sphere of influence be brought as a "reverse validation action" and that PAL failed to comply with the summons and publication procedures required by the statutes governing validation actions (Code of Civil Procedure section 860 et seq.). The trial court treated the demurrer as a motion for judgment on the pleadings and granted the motion without leave to amend. PAL appealed.

The Court of Appeal interpreted section 56103 to mean that lawsuits seeking to set aside a LAFCO approval of this type, whether brought under CEQA, the Cortese-Knox-Hertzberg Act, or both, are

subject to the procedural requirements applicable to reverse validation actions. The Court found that PAL failed to comply with those procedural requirements. Therefore, pursuant to Code of Civil Procedure section 863, dismissal of PAL's action was required "unless good cause for such failure [wa]s shown." The Court's review of the appellate record satisfied it that the trial court's express and implied findings regarding good cause were supported by substantial evidence.

Regarding the CEQA claim, the Court found that in making that claim, PAL was attempting to invalidate the LAFCO's action. As such: "Section 56103 applies to CEQA claims that seek to invalidate a LAFCO's approval of an annexation or a modification of a sphere of influence and, therefore, the procedures applicable to a reverse validation action apply to those particular types of CEQA claims against a LAFCO." The Court affirmed the judgment of the trial court.

Roberson v. City of Rialto **(June 17, 2014) __ Cal.App.4th __**

Rialto approved general plan and specific plan amendments to allow construction of a large commercial retail center on the basis of an EIR. Roberson sued the City, alleging that the notice of the project's initial hearing before the City Council was flawed (it allegedly failed to note the Planning Commission's recommendation for approval) and therefore the approvals were invalid. The trial court denied Roberson's claim and this appeal followed.

The City argued to the Court of Appeal that the defective notice claim is barred by the doctrine of "res judicata," because the same claim had been litigated on its merits and a final decision rendered in the previous case of *Rialto Citizens for Responsible Growth v. City of Rialto* (2012) 208 Cal.App.4th 899, 916-921, where Roberson had a relationship with the plaintiff in that action, Rialto Citizens for Responsible Growth. The City also asked for sanctions. The Court agreed on the first point.

Rominger v. County of Colusa **(Sept. 9, 2014) __ Cal.App.4th __**

The County approved a 16-parcel tentative tract map (TTM) on a 159-acre site zoned for industrial use located in an agricultural area. The County believed that the TTM was not subject to CEQA on the theory that approval would not actually be approving any specific development. Nonetheless, the County adopted an MND, claiming it was for informational purposes only, not because the project was subject to CEQA.

Rominger sued, alleging that the TTM was subject to CEQA, the MND review period was too short, the MND was flawed for failure to examine reasonably foreseeable future development, and an EIR should be prepared. The Court of Appeal held that, pursuant to Public Resources Code Section 21080, which identifies "the approval of tentative subdivision maps" as a CEQA project, a TTM is a CEQA project as a matter of law. The Court rejected the County's claim that the "common sense" exemption should apply. With approval of a subdivision map allowing the independent sale of the 16 parcels, development is a reasonable probability and therefore the County cannot "see with certainty" that the project would have no possibility of resulting in an environmental impact. The Court also invalidated the MND on fair argument grounds and required the County to prepare an EIR.

Saltonstall v. City of Sacramento **(Nov. 20, 2014) __ Cal.App.4th __**

Saltonstall is an opponent of the City's efforts to build a new downtown arena (the Entertainment and Sports Complex or "ESC") for the Sacramento Kings basketball team. In 2013, as part of the push to keep the Kings from moving to Seattle, the Legislature passed SB 743, which, among other things, created special provisions for CEQA litigation that might arise over the proposed ESC (Public Resources Code Section 21168.6.6).

This decision upheld the special provisions. Saltonstall argued that the shortened schedule for judicial review created by Section 21168.6.6 was unconstitutional interference by the Legislature in the operations of the Judicial Branch, and therefore in violation of the separation of powers. The Court dismissed this line of argument.

San Francisco Beautiful v. City and County of San Francisco **(May 30, 2014) __ Cal.App.4th __**

San Francisco approved AT&T's proposal to install 726 telecommunications utility boxes on city sidewalks to serve its expanded fiber optic network. In its application, AT&T avoided placing boxes in historic districts, promised to work with the City to screen the boxes, proposed a graffiti hotline that would alert AT&T personnel to remove graffiti, proposed setbacks from corners and pedestrian access, and promised to site boxes so as not to obstruct views of traffic signs and signals. The City's approval was based on a Class 3 CEQA exemption (15303—new construction of small structures).

San Francisco Beautiful brought suit, alleging that the City's use of the Class 3 exemption was wrong as a matter of law. In relevant part, Section 15303 establishes an exemption for: "limited numbers of new, small facilities or structures; installation of small new equipment and facilities in small structures." They argued that this exemption could not apply in this case because (1) 726 boxes is not "limited numbers," and (2) "small structures" is intended to apply only to existing small structures. The Court of Appeal decided in favor of the City.

Save the Plastic Bag Coalition v. City and County of San Francisco **(Jan. 3, 2014) 222 Cal.App.4th 863**

The City enacted the state's first municipal ban on the use of plastic grocery bags in 2007. In 2012, the City amended its ban to cover a wider range of retail stores, finding that this action was exempt from CEQA under the Class 7 and 8 categorical exemptions (regulatory actions for the protection of the environment). During deliberations on the ordinance, the City amended the proposed charge on single-use check-out bags from 25 cents to 10 cents. The Save the Plastic Bag Coalition sued, alleging that the California Supreme Court's decision in *Save the Plastic Bag Coalition v. City of Manhattan Beach* (2011) 52 Cal.4th 155 (negative declaration for city's plastic grocery bag ban upheld) precluded any city larger than Manhattan Beach from relying on a categorical exemption for an ordinance restricting the use of plastic bags. The Coalition argued that the Class 7 and 8 exemptions could not be applied in this instance because they apply only to regulatory actions, not legislative actions (i.e., adoption of an ordinance). The Coalition claimed that there was a fair argument that "unusual circumstances" exist that require preparation of an EIR. The City prevailed in the trial court. The Court of Appeal affirmed the decision of the lower court.

Sierra Club v. County of Fresno **(May 27, 2014)**
[Accepted for review by California Supreme Court, not citable.]

Fresno County approved "Friant Ranch," a proposed master-planned, age-restricted community located on 942 acres of grazing land near the unincorporated community of Friant. The approval included a General Plan amendment to expand the boundaries of the Friant Community Plan to include the project site. The EIR certified for the project also analyzed the impacts of the related wastewater treatment plant and disposal facilities. The treatment plant and disposal/storage area for treated wastewater would be located adjacent to the San Joaquin River.

The Sierra Club's lawsuit claimed that the project is inconsistent with the County General Plan's policies and therefore should not have been approved, and that the EIR's analysis of wastewater disposal and air quality were inadequate. The Court of Appeal found that the County had properly interpreted its General Plan policies, but set aside the project approval and ordered that the County prepare a revised EIR before proceeding with reconsideration of the project.

Sierra Club v. County of San Diego **(Nov. 25, 2014) __ Cal.App.4th __**

San Diego County adopted a new General Plan in 2011. Mitigation Measure CC-1.2 in the General Plan's EIR committed the County to preparing a climate action plan (CAP). On the basis of that mitigation measure and its prospective compliance with reduction goals of Assembly Bill 32 and the "Executive Order S-3-05 trajectory," the EIR concluded that the General Plan's impact would be less than significant. The CAP was to include detailed GHG reduction targets, deadlines for achievement, and "comprehensive and enforceable GHG emissions reductions measures" that would provide a 17% reduction in GHG emissions from County operations and a 9% reduction in community GHG emissions by 2020.

The County proceeded to draft the CAP and adopted it in 2012 on the basis of an addendum to the General Plan EIR. The CAP included thresholds for determining the significance of individual projects' GHG emissions. The Sierra Club challenged the adequacy of the CAP and thresholds in meeting the requirements of Mitigation Measure CC-1.2, and the adoption of an addendum rather than a more intensive CEQA analysis. The trial court decided in favor of the Sierra Club that adoption of a CAP that did not meet the requirements of Mitigation Measure CC-1.2. The Court of Appeal upheld the lower court's decision.

Town of Atherton v. California High-Speed Rail Authority **(July 24, 2014) 228 Cal.App.4th 314**

The Town successfully challenged the adequacy of the 2008 Program EIR/EIS (PEIR/EIS) prepared for the High Speed Rail (HSR) San Francisco Bay Area to Central Valley segment. Consistent with the writ of mandate in that case, the Authority prepared a revised PEIR/EIS and certified it as a final document for that segment of the HSR. This case is the Town's challenge to the adequacy of the revised PEIR/EIS.

The Town alleged that the revised PEIR/EIS: (1) provides an inadequate analysis of where to elevate the HSR track along the San Francisco Peninsula; (2) uses a flawed revenue and ridership model; and (3) has an inadequate range of alternatives, specifically because it rejects an alternative proposed by an expert consulting company (Setec) hired by project opponents. The Authority requested that the court dismiss the case on the theory that the project is subject to the jurisdiction of the federal Surface Transportation Board (STB) and that CEQA is preempted by this federal jurisdiction. The Court held that CEQA is not preempted by the jurisdiction of the STB. The Court of Appeal then upheld the PEIR/EIS.

Tuolumne Jobs and Small Business Alliance v. Superior Court of Tuolumne County **(Aug. 7, 2014) 59 Cal.4th 1029**

The City of Sonora approved the expansion of its existing Walmart to a Walmart Supercenter in a rather novel way. Rather than pursuing a development permit to conclusion, Walmart collected sufficient voter signatures (over 15% of the city's registered voters) to qualify an initiative ordinance for the City ballot. The ordinance proposed to establish a specific plan applicable to the Walmart site enacting the necessary zoning regulations to allow the expansion. The City Council (Council) held a public hearing on the qualified initiative and, as provided under Elections Code Section 9214 (requiring the City to either [1] adopt the ordinance, [2] place it on the ballot at a special election, or [3] order a report on the proposal prior to either adopting it or placing it on the ballot), chose to adopt the initiative ordinance. This effectively approved the Walmart project without completing the EIR or hearing process that had been started prior to the submittal of the voter signatures.

The Alliance brought suit alleging that: the Council's action violated CEQA because it was distinguishable from the situation where a voter initiative goes to election (voter initiatives taken to election are not subject to CEQA); the initiative was inconsistent with the Sonora General Plan; and the initiative would both improperly limit the power of future city councils and enact an

administrative rather than legislative act (the initiative power extends only to legislative actions, not administrative ones). The Court of Appeal held in favor of the Alliance, expressing its concern that "[d]evelopers' strategy of obtaining project approvals without environmental review *and* without elections threatens both to defeat CEQA's important statutory objectives and to subvert the constitutional goals of the initiative process." (emphasis in original)

The California Supreme Court reversed this decision, holding that the clear language of Section 9214 precludes the application of CEQA to a voter-qualified initiative submitted to the City Council for action.

Summary of Key 2014 CEQA Legislation

By Terry Rivasplata of ICF International

The following are summaries of the CEQA-related bills that were signed into law in 2014. All the signed legislation will take effect January 1, 2015, unless otherwise noted. The texts of these bills and any Legislative committee analyses can be found at http://www.leginfo.ca.gov/bilinfo.html. The acronym "PRC" is used for references to the Public Resources Code.

AB 52 (Gatto). AB 52 creates a formal role for California Native American tribes in the CEQA process by creating a formal consultation process and establishing significant impacts on "tribal cultural resources" as significant environmental impacts. New PRC Section 21084.2 states that: "[a] project with an effect that may cause a substantial adverse change in the significance of a tribal cultural resource is a project that may have a significant effect on the environment." It only applies to projects that have a notice of preparation or notice of negative declaration/mitigated negative declaration filed on or after January 1, 2015. AB 52's statement of legislative intent states that tribes may have expertise in tribal history and knowledge, and "tribal knowledge about land and tribal cultural resources at issue should be included in environmental assessments for projects that may have a significant impact on those resources." The legislative intent makes clear that CEQA analyses must consider tribal cultural resources, including "the tribal cultural values in addition to the scientific and archaeological values when determining impacts and mitigation."

(Chapter 532, Statutes of 2014)

AB 1104 (Salas). This bill adds PRC Section 21080.23.5, effectively reinstating the statutory exemption for maintenance, repair, etc. of existing pipelines for the transport of biogas, which expired January 1, 2013.

(Chapter 534, Statutes of 2014)

AB 1739 (Dickinson). This bill is part of the 2014 groundwater management legislation package (other bills are SB 1168 and SB 1319) and addresses the formation and responsibility of "groundwater sustainability agencies." Water Code Section 10736.2 establishes a new statutory exemption for "any action or failure to act" by the State Water Resources Control Board under its authority to review proposed groundwater sustainability plans and to designate a basin as a probationary basin. CEQA would still apply to the adoption or amendment of an interim plan pursuant to Section 10735.8.

(Chapter 347, Statutes of 2014)

SB 674 (Corbett). This bill amends PRC 21159.24 to specify that the exemption for residential infill projects where a community-level environmental review has been adopted or certified within 5 years of the date that the application for the project is deemed complete applies to "residential" projects consisting of residential units and primarily neighborhood-serving goods, services, or retail uses that do not exceed 25% of the total building square footage of the project. Under current law, such projects cannot include a commercial component exceeding 15% of the total building square footage.

(Chapter 549, Statutes of 2014)

Changes made to CEQA in 2014

Section	Effect	Bill	Chapter	Effective
21073	Add	AB 52	532	January 1, 2015
21074	Add			
21080.3.1	Add			
21080.3.2	Add			
21082.3	Add			
21083.09	Add			
21084.2	Add			
21084.3	Add			
21080.23.5	Add	AB 1104	534	
21159.24	Amend	SB 674	549	

Changes made to CEQA Guidelines in 2014

None				

California Environmental Quality Act
California Public Resources Code
Division 13. Environmental Quality

Statute, as amended in 2014

[The 2014 revisions are shown as follows: new additions are underlined and deletions are indicated by ~~strikeout~~.]

Chapter 1: Policy

§ 21000. LEGISLATIVE INTENT

The Legislature finds and declares as follows:

(a) The maintenance of a quality environment for the people of this state now and in the future is a matter of statewide concern.

(b) It is necessary to provide a high-quality environment that at all times is healthful and pleasing to the senses and intellect of man.

(c) There is a need to understand the relationship between the maintenance of high-quality ecological systems and the general welfare of the people of the state, including their enjoyment of the natural resources of the state.

(d) The capacity of the environment is limited, and it is the intent of the Legislature that the government of the state take immediate steps to identify any critical thresholds for the health and safety of the people of the state and take all coordinated actions necessary to prevent such thresholds being reached.

(e) Every citizen has a responsibility to contribute to the preservation and enhancement of the environment.

(f) The interrelationship of policies and practices in the management of natural resources and waste disposal requires systematic and concerted efforts by public and private interests to enhance environmental quality and to control environmental pollution.

(g) It is the intent of the Legislature that all agencies of the state government which regulate activities of private individuals, corporations, and public agencies which are found to affect the quality of the environment, shall regulate such activities so that major consideration is given to preventing environmental damage, while providing a decent home and satisfying living environment for every Californian.

§ 21001. ADDITIONAL LEGISLATIVE INTENT

The Legislature further finds and declares that it is the policy of the state to:

(a) Develop and maintain a high-quality environment now and in the future, and take all action necessary to protect, rehabilitate, and enhance the environmental quality of the state.

(b) Take all action necessary to provide the people of this state with clean air and water, enjoyment of aesthetic, natural, scenic, and historic environmental qualities, and freedom from excessive noise.

(c) Prevent the elimination of fish or wildlife species due to man's activities, insure that fish and wildlife populations do not drop below self-perpetuating levels, and preserve for future generations representations of all plant and animal communities and examples of the major periods of California history.

(d) Ensure that the long-term protection of the environment, consistent with the provision of a decent home and suitable living environment for every Californian, shall be the guiding criterion in public decisions.

(e) Create and maintain conditions under which man and nature can exist in productive harmony to fulfill the social and economic requirements of present and future generations.

(f) Require governmental agencies at all levels to develop standards and procedures necessary to protect environmental quality.

(g) Require governmental agencies at all levels to consider qualitative factors as well as economic and technical factors and long-term benefits and costs, in addition to short-term benefits and costs and to consider alternatives to proposed actions affecting the environment.

§ 21001.1. REVIEW OF PUBLIC AGENCY PROJECTS

The Legislature further finds and declares that it is the policy of the state that projects to be carried out by public agencies be subject to the same level of review and consideration under this division as that of private projects required to be approved by public agencies.

§ 21002. APPROVAL OF PROJECTS; FEASIBLE ALTERNATIVE OR MITIGATION MEASURES

The Legislature finds and declares that it is the policy of the state that public agencies should not approve projects as proposed if there are feasible alternatives or feasible mitigation measures available which would substantially lessen the significant environmental effects of such projects, and that the procedures required by this division are intended to assist public agencies in systematically identifying both the significant effects of proposed projects and the feasible alternatives or feasible mitigation measures which will avoid or substantially lessen such significant effects. The Legislature further finds and declares that in the event specific economic, social, or other conditions make infeasible such project alternatives or such mitigation measures, individual projects may be approved in spite of one or more significant effects thereof.

§ 21002.1. USE OF ENVIRONMENTAL IMPACT REPORTS; POLICY

In order to achieve the objectives set forth in Section 21002, the Legislature hereby finds and declares that the following policy shall apply to the use of environmental impact reports prepared pursuant to this division:

(a) The purpose of an environmental impact report is to identify the significant effects on the environment of a project, to identify alternatives to the project, and to indicate the manner in which those significant effects can be mitigated or avoided.

(b) Each public agency shall mitigate or avoid the significant effects on the environment of projects that it carries out or approves whenever it is feasible to do so.

(c) If economic, social, or other conditions make it infeasible to mitigate one or more significant effects on the environment of a project, the project may nonetheless be carried out or approved at the discretion of a public agency if the project is otherwise permissible under applicable laws and regulations.

(d) In applying the policies of subdivisions (b) and (c) to individual projects, the responsibility of the lead agency shall differ from that of a responsible agency. The lead agency shall be responsible for considering the effects, both individual and collective, of all activities involved in a project. A responsible agency shall be responsible for considering only the effects of those activities involved in a project which it is required by law to carry out or approve. This subdivision applies only to decisions by a public agency to carry out or approve a project and does not otherwise affect the scope of the comments that the public agency may wish to make pursuant to Section 21104 or 21153.

(e) To provide more meaningful public disclosure, reduce the time and cost required to prepare an environmental impact report, and focus on potentially significant effects on the environment of a proposed project, lead agencies shall, in accordance with Section 21100, focus the discussion in the environmental impact report on those potential effects on the environment of a proposed project which the lead agency has determined are or may be significant. Lead agencies may limit discussion on other effects to a brief explanation as to why those effects are not potentially significant.

§ 21003. PLANNING AND ENVIRONMENTAL REVIEW PROCEDURES; DOCUMENTS; REPORTS; DATA BASE; ADMINISTRATION OF PROCESS

The Legislature further finds and declares that it is the policy of the state that:

(a) Local agencies integrate the requirements of this division with planning and environmental review procedures otherwise required by law or by local practice so that all those procedures, to the maximum feasible extent, run concurrently, rather than consecutively.

(b) Documents prepared pursuant to this division be organized and written in a manner that will be meaningful and useful to decision makers and to the public.

(c) Environmental impact reports omit unnecessary descriptions of projects and emphasize feasible mitigation measures and feasible alternatives to projects.

(d) Information developed in individual environmental impact reports be incorporated into a data base which can be used to reduce delay and duplication in preparation of subsequent environmental impact reports.

(e) Information developed in environmental impact reports and negative declarations be incorporated into a data base which may be used to make subsequent or supplemental environmental determinations.

(f) All persons and public agencies involved in the environmental review process be responsible for carrying out the process in the most efficient, expeditious manner in order to conserve the available financial, governmental, physical, and social resources with the objective that those resources may be better applied toward the mitigation of actual significant effects on the environment.

§ 21003.1. ENVIRONMENTAL EFFECTS OF PROJECTS; COMMENTS FROM PUBLIC AND PUBLIC AGENCIES TO LEAD AGENCIES; AVAILABILITY OF INFORMATION

The Legislature further finds and declares it is the policy of the state that:

(a) Comments from the public and public agencies on the environmental effects of a project shall be made to lead agencies as soon as possible in the review of environmental documents, including, but not limited to, draft environmental impact reports and negative declarations, in order to allow the lead agencies to identify, at the earliest possible time in the environmental

review process, potential significant effects of a project, alternatives, and mitigation measures which would substantially reduce the effects.

(b) Information relevant to the significant effects of a project, alternatives, and mitigation measures which substantially reduce the effects shall be made available as soon as possible by lead agencies, other public agencies, and interested persons and organizations.

(c) Nothing in subdivisions (a) or (b) reduces or otherwise limits public review or comment periods currently prescribed either by statute or in guidelines prepared and adopted pursuant to Section 21083 for environmental documents, including, but not limited to, draft environmental impact reports and negative declarations.

§ 21004. MITIGATING OR AVOIDING A SIGNIFICANT EFFECT; POWERS OF PUBLIC AGENCY

In mitigating or avoiding a significant effect of a project on the environment, a public agency may exercise only those express or implied powers provided by law other than this division. However, a public agency may use discretionary powers provided by such other law for the purpose of mitigating or avoiding a significant effect on the environment subject to the express or implied constraints or limitations that may be provided by law.

§ 21005. INFORMATION DISCLOSURE PROVISIONS; NONCOMPLIANCE; PRESUMPTION; FINDINGS

(a) The Legislature finds and declares that it is the policy of the state that noncompliance with the information disclosure provisions of this division which precludes relevant information from being presented to the public agency, or noncompliance with substantive requirements of this division, may constitute a prejudicial abuse of discretion within the meaning of Sections 21168 and 21168.5, regardless of whether a different outcome would have resulted if the public agency had complied with those provisions.

(b) It is the intent of the Legislature that, in undertaking judicial review pursuant to Sections 21168 and 21168.5, courts shall continue to follow the established principle that there is no presumption that error is prejudicial.

(c) It is further the intent of the Legislature that any court, which finds, or, in the process of reviewing a previous court finding, finds, that a public agency has taken an action without compliance with this division, shall specifically address each of the alleged grounds for noncompliance.

§ 21006. ISSUANCE OF PERMITS, LICENSES, CERTIFICATES OR OTHER ENTITLEMENTS; WAIVERS OF SOVEREIGN

The Legislature finds and declares that this division is an integral part of any public agency's decisionmaking process, including, but not limited to, the issuance of permits, licenses, certificates, or other entitlements required for activities undertaken pursuant to federal statutes containing specific waivers of sovereign immunity.

Chapter 2: Short Title

§ 21050. CITATION

This division shall be known and may be cited as the California Environmental Quality Act.

Chapter 2.5: Definitions

§ 21060. APPLICATION OF DEFINITIONS

Unless the context otherwise requires, the definitions in this chapter govern the construction of this division.

§ 21060.1. AGRICULTURAL LAND

(a) "Agricultural land" means prime farmland, farmland of statewide importance, or unique farmland, as defined by the United States Department of Agriculture land inventory and monitoring criteria, as modified for California.

(b) In those areas of the state where lands have not been surveyed for the classifications specified in subdivision (a), "agricultural land" means land that meets the requirements of "prime agricultural land" as defined in paragraph (1), (2), (3), or (4) of subdivision (c) of Section 51201 of the Government Code.

§ 21060.3. EMERGENCY

"Emergency" means a sudden, unexpected occurrence, involving a clear and imminent danger, demanding immediate action to prevent or mitigate loss of, or damage to, life, health, property, or essential public services. "Emergency" includes such occurrences as fire, flood, earthquake, or other soil or geologic movements, as well as such occurrences as riot, accident, or sabotage.

§ 21060.5. ENVIRONMENT

"Environment" means the physical conditions that exist within the area which will be affected by a proposed project, including land, air, water, minerals, flora, fauna, noise, or objects of historic or aesthetic significance.

§ 21061. ENVIRONMENTAL IMPACT REPORT

"Environmental impact report" means a detailed statement setting forth the matters specified in Sections 21100 and 21100.1; provided that information or data which is relevant to such a statement and is a matter of public record or is generally available to the public need not be repeated in its entirety in such statement, but may be specifically cited as the source for conclusions stated therein; and provided further that such information or data shall be briefly described, that its relationship to the environmental impact report shall be indicated, and that the source thereof shall be reasonably available for inspection at a public place or public building. An environmental impact report also includes any comments which are obtained pursuant to Section 21104 or 21153, or which are required to be obtained pursuant to this division.

An environmental impact report is an informational document which, when its preparation is required by this division, shall be considered by every public agency prior to its approval or disapproval of a project. The purpose of an environmental impact report is to provide public agencies and the public in general with detailed information about the effect which a proposed project is likely to have on the environment; to list ways in which the significant effects of such a project might be minimized; and to indicate alternatives to such a project.

In order to facilitate the use of environmental impact reports, public agencies shall require that such reports contain an index or table of contents and a summary. Failure to include such index, table of contents, or summary shall not constitute a cause of action pursuant to Section 21167.

§ 21061.1. FEASIBLE

"Feasible" means capable of being accomplished in a successful manner within a reasonable period of time, taking into account economic, environmental, social, and technological factors.

§ 21061.2. LAND EVALUATION AND SITE ASSESSMENT

"Land evaluation and site assessment" means a decision-making methodology for assessing the potential environmental impact of state and local projects on agricultural land.

§ 21061.3. INFILL SITE

"Infill site" means a site in an urbanized area that meets either of the following criteria:

(a) The site has not been previously developed for urban uses and both of the following apply:

  (1) The site is immediately adjacent to parcels that are developed with qualified urban uses, or at least 75 percent of the perimeter of the site adjoins parcels that are developed with qualified urban uses and the remaining 25 percent of the site adjoins parcels that have previously been developed for qualified urban uses.

  (2) No parcel within the site has been created within the past 10 years unless the parcel was created as a result of the plan of a redevelopment agency.

(b) The site has been previously developed for qualified urban uses.

§ 21062. LOCAL AGENCY

"Local agency" means any public agency other than a state agency, board, or commission. For purposes of this division a redevelopment agency and a local agency formation commission are local agencies, and neither is a state agency, board, or commission.

§ 21063. PUBLIC AGENCY

"Public agency" includes any state agency, board, or commission, any county, city and county, city, regional agency, public district, redevelopment agency, or other political subdivision.

§ 21064. NEGATIVE DECLARATION

"Negative declaration" means a written statement briefly describing the reasons that a proposed project will not have a significant effect on the environment and does not require the preparation of an environmental impact report.

§ 21064.3. MAJOR TRANSIT STOP

"Major transit stop" means a site containing an existing rail transit station, a ferry terminal served by either a bus or rail transit service, or the intersection of two or more major bus routes with a frequency of service interval of 15 minutes or less during the morning and afternoon peak commute periods.

§ 21064.5. MITIGATED NEGATIVE DECLARATION

"Mitigated negative declaration" means a negative declaration prepared for a project when the initial study has identified potentially significant effects on the environment, but (1) revisions in the project plans or proposals made by, or agreed to by, the applicant before the proposed negative declaration and initial study are released for public review would avoid the effects or mitigate the effects to a point where clearly no significant effect on the environment would occur, and (2) there is no substantial evidence in light of the whole record before the public agency that the project, as revised, may have a significant effect on the environment.

§ 21065. PROJECT

"Project" means an activity which may cause either a direct physical change in the environment, or a reasonably foreseeable indirect physical change in the environment, and which is any of the following:

(a) An activity directly undertaken by any public agency.

(b) An activity undertaken by a person which is supported, in whole or in part, through contracts, grants, subsidies, loans, or other forms of assistance from one or more public agencies.

(c) An activity that involves the issuance to a person of a lease, permit, license, certificate, or other entitlement for use by one or more public agencies.

§ 21065.3. PROJECT-SPECIFIC EFFECT

"Project-specific effect" means all the direct or indirect environmental effects of a project other than cumulative effects and growth-inducing effects.

§ 21065.5. GEOTHERMAL EXPLORATORY PROJECT

"Geothermal exploratory project" means a project as defined in Section 21065 composed of not more than six wells and associated drilling and testing equipment, whose chief and original purpose is to evaluate the presence and characteristics of geothermal resources prior to commencement of a geothermal field development project as defined in Section 65928.5 of the Government Code. Wells included within a geothermal exploratory project must be located at least one-half mile from geothermal development wells which are capable of producing geothermal resources in commercial quantities.

§ 21066. PERSON

"Person" includes any person, firm, association, organization, partnership, business, trust, corporation, limited liability company, company, district, county, city and county, city, town, the state, and any of the agencies and political subdivisions of those entities, and, to the extent permitted by federal law, the United States, or any of its agencies or political subdivisions.

§ 21067. LEAD AGENCY

"Lead agency" means the public agency which has the principal responsibility for carrying out or approving a project which may have a significant effect upon the environment.

§ 21068. SIGNIFICANT EFFECT ON THE ENVIRONMENT

"Significant effect on the environment" means a substantial, or potentially substantial, adverse change in the environment.

§ 21068.5. TIERING OR TIER

"Tiering" or "tier" means the coverage of general matters and environmental effects in an environmental impact report prepared for a policy, plan, program or ordinance followed by narrower or site-specific environmental impact reports which incorporate by reference the discussion in any prior environmental impact report and which concentrate on the environmental effects which (a) are capable of being mitigated, or (b) were not analyzed as significant effects on the environment in the prior environmental impact report.

§ 21069. RESPONSIBLE AGENCY

"Responsible agency" means a public agency, other than the lead agency, which has responsibility for carrying out or approving a project.

§ 21070. TRUSTEE AGENCY

"Trustee agency" means a state agency that has jurisdiction by law over natural resources affected by a project, that are held in trust for the people of the State of California.

§ 21071. URBANIZED AREA; DEFINITION

"Urbanized area" means either of the following:

(a) An incorporated city that meets either of the following criteria:

(1) Has a population of at least 100,000 persons.

(2) Has a population of less than 100,000 persons if the population of that city and not more than two contiguous incorporated cities combined equals at least 100,000 persons.

(b) An unincorporated area that satisfies the criteria in both paragraph (1) and (2) of the following criteria:

(1) Is either of the following:

(A) Completely surrounded by one or more incorporated cities, and both of the following criteria are met:

(i) The population of the unincorporated area and the population of the surrounding incorporated city or cities equals not less than 100,000 persons.

(ii) The population density of the unincorporated area at least equals the population density of the surrounding city or cities.

(B) Located within an urban growth boundary and has an existing residential population of at least 5,000 persons per square mile. For purposes of this subparagraph, an "urban growth boundary" means a provision of a locally adopted general plan that allows urban uses on one side of the boundary and prohibits urban uses on the other side.

(2) The board of supervisors with jurisdiction over the unincorporated area has previously taken both of the following actions:

(A) Issued a finding that the general plan, zoning ordinance, and related policies and programs applicable to the unincorporated area are consistent with principles that encourage compact development in a manner that does both of the following:

(i) Promotes efficient transportation systems, economic growth, affordable housing, energy efficiency, and an appropriate balance of jobs and housing.

(ii) Protects the environment, open space, and agricultural areas.

(B) Submitted a draft finding to the Office of Planning and Research at least 30 days prior to issuing a final finding, and allowed the office 30 days to submit comments on the draft findings to the board of supervisors.

§ 21072. QUALIFIED URBAN USE; DEFINITION

"Qualified urban use" means any residential, commercial, public institutional, transit or transportation passenger facility, or retail use, or any combination of those uses.

§ 21073.

"California Native American tribe" means a Native American tribe located in California that is on the contact list maintained by the Native American Heritage Commission for the purposes of Chapter 905 of the Statutes of 2004.

§ 21074.

(a) "Tribal cultural resources" are either of the following:

(1) Sites, features, places, cultural landscapes, sacred places, and objects with cultural value to a California Native American tribe that are either of the following:

(A) Included or determined to be eligible for inclusion in the California Register of Historical Resources.

(B) Included in a local register of historical resources as defined in subdivision (k) of Section 5020.1.

(2) A resource determined by the lead agency, in its discretion and supported by substantial evidence, to be significant pursuant to criteria set forth in subdivision (c) of Section 5024.1.

In applying the criteria set forth in subdivision (c) of Section 5024.1 for the purposes of this paragraph, the lead agency shall consider the significance of the resource to a California Native American tribe.

(b) A cultural landscape that meets the criteria of subdivision (a) is a tribal cultural resource to the extent that the landscape is geographically defined in terms of the size and scope of the landscape.

(c) A historical resource described in Section 21084.1, a unique archaeological resource as defined in subdivision (g) of Section 21083.2, or a "nonunique archaeological resource" as defined in subdivision (h) of Section 21083.2 may also be a tribal cultural resource if it conforms with the criteria of subdivision (a).

Chapter 2.6: General

§ 21080. DIVISION APPLICATION TO DISCRETIONARY PROJECTS; NONAPPLICATION; NEGATIVE DECLARATIONS; ENVIRONMENTAL IMPACT REPORT PREPARATION

(a) Except as otherwise provided in this division, this division shall apply to discretionary projects proposed to be carried out or approved by public agencies, including, but not limited to, the enactment and amendment of zoning ordinances, the issuance of zoning variances, the issuance of conditional use permits, and the approval of tentative subdivision maps unless the project is exempt from this division.

(b) This division does not apply to any of the following activities:

(1) Ministerial projects proposed to be carried out or approved by public agencies.

(2) Emergency repairs to public service facilities necessary to maintain service.

(3) Projects undertaken, carried out, or approved by a public agency to maintain, repair, restore, demolish, or replace property or facilities damaged or destroyed as a result of a disaster in a disaster-stricken area in which a state of emergency has been proclaimed by the Governor pursuant to Chapter 7 (commencing with Section 8550) of Division 1 of Title 2 of the Government Code.

(4) Specific actions necessary to prevent or mitigate an emergency.

(5) Projects which a public agency rejects or disapproves.

(6) Actions undertaken by a public agency relating to any thermal powerplant site or facility, including the expenditure, obligation, or encumbrance of funds by a public agency for planning, engineering, or design purposes, or for the conditional sale or purchase of equipment, fuel, water (except groundwater), steam, or power for a thermal powerplant, if the powerplant site and related facility will be the subject of an environmental impact report, negative declaration, or other document, prepared pursuant to a regulatory program certified pursuant to Section 21080.5, which will be prepared by the State Energy Resources Conservation and Development Commission, by the Public Utilities Commission, or by the city or county in which the powerplant and related facility would be located if the environmental impact report, negative declaration, or document includes the environmental impact, if any, of the action described in this paragraph.

(7) Activities or approvals necessary to the bidding for, hosting or staging of, and funding or carrying out of, an Olympic games under the authority of the International Olympic Committee, except for the construction of facilities necessary for the Olympic games.

(8) The establishment, modification, structuring, restructuring, or approval of rates, tolls, fares, or other charges by public agencies which the public agency finds are for the purpose of (A) meeting operating expenses, including employee wage rates and fringe benefits, (B) purchasing or leasing supplies, equipment, or materials, (C) meeting financial reserve needs

and requirements, (D) obtaining funds for capital projects necessary to maintain service within existing service areas, or (E) obtaining funds necessary to maintain those intracity transfers as are authorized by city charter. The public agency shall incorporate written findings in the record of any proceeding in which an exemption under this paragraph is claimed setting forth with specificity the basis for the claim of exemption.

(9) All classes of projects designated pursuant to Section 21084.

(10) A project for the institution or increase of passenger or commuter services on rail or highway rights-of-way already in use, including modernization of existing stations and parking facilities. For purposes of this paragraph, "highway" shall have the same meaning as defined in Section 360 of the Vehicle Code.

(11) A project for the institution or increase of passenger or commuter service on high-occupancy vehicle lanes already in use, including the modernization of existing stations and parking facilities.

(12) Facility extensions not to exceed four miles in length which are required for the transfer of passengers from or to exclusive public mass transit guideway or busway public transit services.

(13) A project for the development of a regional transportation improvement program, the state transportation improvement program, or a congestion management program prepared pursuant to Section 65089 of the Government Code.

(14) Any project or portion thereof located in another state which will be subject to environmental impact review pursuant to the National Environmental Policy Act of 1969 (42 U.S.C. Sec. 4321 et seq.) or similar state laws of that state. Any emissions or discharges that would have a significant effect on the environment in this state are subject to this division.

(15) Projects undertaken by a local agency to implement a rule or regulation imposed by a state agency, board, or commission under a certified regulatory program pursuant to Section 21080.5. Any site-specific effect of the project which was not analyzed as a significant effect on the environment in the plan or other written documentation required by Section 21080.5 is subject to this division.

(16) The selection, credit, and transfer of emission credits by the South Coast Air Quality Management District pursuant to Section 40440.14 of the Health and Safety Code, until the repeal of that section of January 1, 2012, or a later date. (c) If a lead agency determines that a proposed project, not otherwise exempt from this division, would not have a significant effect on the environment, the lead agency shall adopt a negative declaration to that effect. The negative declaration shall be prepared for the proposed project in either of the following circumstances:

(1) There is no substantial evidence, in light of the whole record before the lead agency, that the project may have a significant effect on the environment.

(2) An initial study identifies potentially significant effects on the environment, but (A) revisions in the project plans or proposals made by, or agreed to by, the applicant before the proposed negative declaration and initial study are released for public review would avoid the effects or mitigate the effects to a point where clearly no significant effect on the environment would occur, and (B) there is no substantial evidence, in light of the whole record before the lead agency, that the project, as revised, may have a significant effect on the environment.

(c) If a lead agency determines that a proposed project, not otherwise exempt from this division, would not have a significant effect on the environment, the lead agency shall adopt a negative declaration to that effect. The negative declaration shall be prepared for the proposed project in either of the following circumstances:

(1) There is no substantial evidence, in light of the whole record before the lead agency, that the project may have a significant effect on the environment.

(2) An initial study identifies potentially significant effects on the environment, but (A) revisions in the project plans or proposals made by, or agreed to by, the applicant before the proposed negative declaration and initial study are released for public review would avoid the effects or mitigate the effects to a point where clearly no significant effect on the environment would occur, and (B) there is no substantial evidence, in light of the whole record before the lead agency, that the project, as revised, may have a significant effect on the environment.

(d) If there is substantial evidence, in light of the whole record before the lead agency, that the project may have a significant effect on the environment, an environmental impact report shall be prepared.

(e) (1) For the purposes of this section and this division, substantial evidence includes fact, a reasonable assumption predicated upon fact, or expert opinion supported by fact.

(2) Substantial evidence is not argument, speculation, unsubstantiated opinion or narrative, evidence that is clearly inaccurate or erroneous, or evidence of social or economic impacts that do not contribute to, or are not caused by, physical impacts on the environment.

(f) As a result of the public review process for a mitigated negative declaration, including administrative decisions and public hearings, the lead agency may conclude that certain mitigation measures identified pursuant to paragraph (2) of subdivision (c) are infeasible or otherwise undesirable. In those circumstances, the lead agency, prior to approving the project, may delete those mitigation measures and substitute for them other mitigation measures that the lead agency finds, after holding a public hearing on the matter, are equivalent or more effective in mitigating significant effects on the environment to a less than significant level and that do not cause any potentially significant effect on the environment. If those new mitigation measures are made conditions of project approval or are otherwise made part of the project approval, the deletion of the former measures and the substitution of the new mitigation measures shall not constitute an action or circumstance requiring recirculation of the mitigated negative declaration.

(g) Nothing in this section shall preclude a project applicant or any other person from challenging, in an administrative or judicial proceeding, the legality of a condition of project approval imposed by the lead agency. If, however, any condition of project approval set aside by either an administrative body or court was necessary to avoid or lessen the likelihood of the occurrence of a significant effect on the environment, the lead agency's approval of the negative declaration and project shall be invalid and a new environmental review process shall be conducted before the project can be reapproved, unless the lead agency substitutes a new condition that the lead agency finds, after holding a public hearing on the matter, is equivalent to, or more effective in, lessening or avoiding significant effects on the environment and that does not cause any potentially significant effect on the environment.

§ 21080.01. CALIFORNIA MEN'S COLONY WEST FACILITY IN SAN LUIS OBISPO COUNTY; INAPPLICABILITY OF DIVISION TO REOPENING AND OPERATION

This division shall not apply to any activity or approval necessary for the reopening and operation of the California Men's Colony West Facility in San Luis Obispo County.

§ 21080.02. KINGS COUNTY; VICINITY OF CORCORAN; NEW PRISON FACILITIES; APPLICATION OF DIVISION

This division shall not apply to any activity or approval necessary for or incidental to planning, design, site acquisition, construction, operation, or maintenance of the new prison facility at or in the vicinity of Corcoran in Kings County as authorized by the act that enacted this section.

§ 21080.03. KINGS AND AMADOR (IONE) COUNTIES; PRISONS; APPLICATION OF DIVISION

This division shall not apply to any activity or approval necessary for or incidental to the location, development, construction, operation, or maintenance of the prison in the County of Kings, authorized by Section 9 of Chapter 958 of the Statutes of 1983, as amended, and of the prison in the County of Amador (Ione), authorized by Chapter 957 of the Statutes of 1983, as amended.

§ 21080.04. ROCKTRAM-KRUG PASSENGER RAIL SERVICE PROJECT; APPLICATION OF DIVISION; LEAD AGENCY; LEGISLATIVE INTENT

(a) Notwithstanding paragraph (10) of subdivision (b) of Section 21080, this division applies to a project for the institution of passenger rail service on a line paralleling State Highway 29 and running from Rocktram to Krug in the Napa Valley. With respect to that project, and for the purposes of this division, the Public Utilities Commission is the lead agency.

(b) It is the intent of the Legislature in enacting this section to abrogate the decision of the California Supreme Court "that Section 21080, subdivision (b)(11), exempts Wine Train's institution of passenger service on the Rocktram-Krug line from the requirements of CEQA" in *Napa Valley Wine Train, Inc. v. Public Utilities Com.*, 50 Cal. 3d 370.

(c) Nothing in this section is intended to affect or apply to, or to confer jurisdiction upon the Public Utilities Commission with respect to, any other project involving rail service.

§ 21080.05. SAN FRANCISCO PENINSULA COMMUTE SERVICE PROJECT BETWEEN SAN FRANCISCO AND SAN JOSE; APPLICATION OF DIVISION

This division does not apply to a project by a public agency to lease or purchase the rail right-of-way used for the San Francisco Peninsula commute service between San Francisco and San Jose, together with all branch and spur lines, including the Dumbarton and Vasona lines.

§ 21080.07. RIVERSIDE AND DEL NORTE COUNTIES; PLANNING AND CONSTRUCTION OF NEW PRISON FACILITIES; APPLICATION OF DIVISION

This division shall not apply to any activity or approval necessary for or incidental to planning, design, site acquisition, construction, operation, or maintenance of the new prison facilities located in any of the following places:

(a) The County of Riverside.

(b) The County of Del Norte.

§ 21080.09. PUBLIC HIGHER EDUCATION; CAMPUS LOCATION; LONG-RANGE DEVELOPMENT PLANS

(a) For purposes of this section, the following definitions apply:

  (1) "Public higher education" has the same meaning as specified in Section 66010 of the Education Code.

  (2) "Long range development plan" means a physical development and land use plan to meet the academic and institutional objectives for a particular campus or medical center of public higher education.

(b) The selection of a location for a particular campus and the approval of a long range development plan are subject to this division and require the preparation of an environmental impact report. Environmental effects relating to changes in enrollment levels shall be considered for each campus or medical center of public higher education in the environmental impact report prepared for the long range development plan for the campus or medical center.

(c) The approval of a project on a particular campus or medical center of public higher education is subject to this division and may be addressed, subject to the other provisions of this division, in

a tiered environmental analysis based upon a long range development plan environmental impact report.

(d) Compliance with this section satisfies the obligations of public higher education pursuant to this division to consider the environmental impact of academic and enrollment plans as they affect campuses or medical centers, provided that any such plans shall become effective for a campus or medical center only after the environmental effects of those plans have been analyzed as required by this division in a long range development plan environmental impact report or tiered analysis based upon that environmental impact report for that campus or medical center, and addressed as required by this division.

§ 21080.1. ENVIRONMENTAL IMPACT REPORT OR NEGATIVE DECLARATION; DETERMINATION BY LEAD AGENCY; FINALITY; CONSULTATION

(a) The lead agency shall be responsible for determining whether an environmental impact report, a negative declaration, or a mitigated negative declaration shall be required for any project which is subject to this division. That determination shall be final and conclusive on all persons, including responsible agencies, unless challenged as provided in Section 21167.

(b) In the case of a project described in subdivision (c) of Section 21065, the lead agency shall, upon the request of a potential applicant, provide for consultation prior to the filing of the application regarding the range of actions, potential alternatives, mitigation measures, and any potential and significant effects on the environment of the project.

§ 21080.2. ISSUANCE OF LEASE, PERMIT, LICENSE, CERTIFICATE OR OTHER ENTITLEMENT; DETERMINATION BY LEAD AGENCY; TIME

In the case of a project described in subdivision (c) of Section 21065, the determination required by Section 21080.1 shall be made within 30 days from the date on which an application for a project has been received and accepted as complete by the lead agency. This period may be extended 15 days upon the consent of the lead agency and the project applicant.

§ 21080.3. CONSULTATION WITH RESPONSIBLE AGENCIES; ASSISTANCE BY OFFICE OF PLANNING AND RESEARCH

(a) Prior to determining whether a negative declaration or environmental impact report is required for a project, the lead agency shall consult with all responsible agencies and trustee agencies. Prior to that required consultation, the lead agency may informally contact any of those agencies.

(b) In order to expedite the requirements of subdivision (a), the Office of Planning and Research, upon request of a lead agency, shall assist the lead agency in determining the various responsible agencies and trustee agencies, for a proposed project. In the case of a project described in subdivision (c) of Section 21065, the request may also be made by the project applicant.

§ 21080.3.1.

(a) The Legislature finds and declares that California Native American tribes traditionally and culturally affiliated with a geographic area may have expertise concerning their tribal cultural resources.

(b) Prior to the release of a negative declaration, mitigated negative declaration, or environmental impact report for a project, the lead agency shall begin consultation with a California Native American tribe that is traditionally and culturally affiliated with the geographic area of the proposed project if: (1) the California Native American tribe requested to the lead agency, in writing, to be informed by the lead agency through formal notification of proposed projects in the geographic area that is traditionally and culturally affiliated with the tribe, and (2) the

California Native American tribe responds, in writing, within 30 days of receipt of the formal notification, and requests the consultation. When responding to the lead agency, the California Native American tribe shall designate a lead contact person. If the California Native American tribe does not designate a lead contact person, or designates multiple lead contact people, the lead agency shall defer to the individual listed on the contact list maintained by the Native American Heritage Commission for the purposes of Chapter 905 of the Statutes of 2004. For purposes of this section and Section 21080.3.2, "consultation" shall have the same meaning as provided in Section 65352.4 of the Government Code.

(c) To expedite the requirements of this section, the Native American Heritage Commission shall assist the lead agency in identifying the California Native American tribes that are traditionally and culturally affiliated with the project area.

(d) Within 14 days of determining that an application for a project is complete or a decision by a public agency to undertake a project, the lead agency shall provide formal notification to the designated contact of, or a tribal representative of, traditionally and culturally affiliated California Native American tribes that have requested notice, which shall be accomplished by means of at least one written notification that includes a brief description of the proposed project and its location, the lead agency contact information, and a notification that the California Native American tribe has 30 days to request consultation pursuant to this section.

(e) The lead agency shall begin the consultation process within 30 days of receiving a California Native American tribe's request for consultation.

§ 21080.3.2.

(a) As a part of the consultation pursuant to Section 21080.3.1, the parties may propose mitigation measures, including, but not limited to, those recommended in Section 21084.3, capable of avoiding or substantially lessening potential significant impacts to a tribal cultural resource or alternatives that would avoid significant impacts to a tribal cultural resource. If the California Native American tribe requests consultation regarding alternatives to the project, recommended mitigation measures, or significant effects, the consultation shall include those topics. The consultation may include discussion concerning the type of environmental review necessary, the significance of tribal cultural resources, the significance of the project's impacts on the tribal cultural resources, and, if necessary, project alternatives or the appropriate measures for preservation or mitigation that the California Native American tribe may recommended to the lead agency.

(b) The consultation shall be considered concluded when either of the following occurs:

(1) The parties agree to measures to mitigate or avoid a significant effect, if a significant effect exists, on a tribal cultural resource.

(2) A party, acting in good faith and after reasonable effort, concludes that mutual agreement cannot be reached.

(c) (1) This section does not limit the ability of a California Native American tribe or the public to submit information to the lead agency regarding the significance of the tribal cultural resources, the significance of the project's impact on tribal cultural resources, or any appropriate measures to mitigate the impact.

(2) This section does not limit the ability of the lead agency or project proponent to incorporate changes and additions to the project as a result of the consultation, even if not legally required.

(d) If the project proponent or its consultants participate in the consultation, those parties shall respect the principles set forth in this section.

§ 21080.4. ENVIRONMENTAL IMPACT REPORT; REQUIREMENT DETERMINED BY LEAD AGENCY; DUTIES OF RESPONSIBLE AGENCIES AND CERTAIN PUBLIC AGENCIES; CONSULTATION; ASSISTANCE BY OFFICE OF PLANNING AND RESEARCH

(a) If a lead agency determines that an environmental impact report is required for a project, the lead agency shall immediately send notice of that determination by certified mail or an equivalent procedure to each responsible agency, the Office of Planning and Research, and those public agencies having jurisdiction by law over natural resources affected by the project that are held in trust for the people of the State of California. Upon receipt of the notice, each responsible agency, the office, and each public agency having jurisdiction by law over natural resources affected by the project that are held in trust for the people of the State of California shall specify to the lead agency the scope and content of the environmental information that is germane to the statutory responsibilities of that responsible agency, the office, or the public agency in connection with the proposed project and which, pursuant to the requirements of this division, shall be included in the environmental impact report. The information shall be specified in writing and shall be communicated to the lead agency by certified mail or equivalent procedure not later than 30 days after the date of receipt of the notice of the lead agency's determination. The lead agency shall request similar guidance from appropriate federal agencies.

(b) To expedite the requirements of subdivision (a), the lead agency, any responsible agency, the Office of Planning and Research, or a public agency having jurisdiction by law over natural resources affected by the project that are held in trust for the people of the State of California, may request one or more meetings between representatives of those agencies and the office for the purpose of assisting the lead agency to determine the scope and content of the environmental information that any of those responsible agencies, the office, or the public agencies may require. In the case of a project described in subdivision (c) of Section 21065, the request may also be made by the project applicant. The meetings shall be convened by the lead agency as soon as possible, but not later than 30 days after the date that the meeting was requested.

(c) To expedite the requirements of subdivision (a), the Office of Planning and Research, upon request of a lead agency, shall assist the lead agency in determining the various responsible agencies, public agencies having jurisdiction by law over natural resources affected by the project that are held in trust for the people of the State of California, and any federal agencies that have responsibility for carrying out or approving a proposed project. In the case of a project described in subdivision (c) of Section 21065, that request may also be made by the project applicant.

(d) With respect to the Department of Transportation, and with respect to any state agency that is a responsible agency or a public agency having jurisdiction by law over natural resources affected by the project that are held in trust for the people of the State of California, subject to the requirements of subdivision (a), the Office of Planning and Research shall ensure that the information required by subdivision (a) is transmitted to the lead agency, and that affected agencies are notified regarding meetings to be held upon request pursuant to subdivision (b), within the required time period.

§ 21080.5. PLAN OR OTHER WRITTEN DOCUMENTATION; SUBMISSION IN LIEU OF IMPACT REPORT; REGULATORY PROGRAMS; CRITERIA; CERTIFICATION; PROPOSED CHANGES; REVIEW; COMMENCEMENT OF ACTIONS; STATE AGENCIES

(a) Except as provided in Section 21158.1, when the regulatory program of a state agency requires a plan or other written documentation containing environmental information and complying with paragraph (3) of subdivision (d) to be submitted in support of an activity listed in subdivision (b), the plan or other written documentation may be submitted in lieu of the

environmental impact report required by this division if the Secretary of the Resources Agency has certified the regulatory program pursuant to this section.

(b) This section applies only to regulatory programs or portions thereof that involve either of the following:

(1) The issuance to a person of a lease, permit, license, certificate, or other entitlement for use.

(2) The adoption or approval of standards, rules, regulations, or plans for use in the regulatory program.

(c) A regulatory program certified pursuant to this section is exempt from Chapter 3 (commencing with Section 21100), Chapter 4 (commencing with Section 21150), and Section 21167, except as provided in Article 2 (commencing with Section 21157) of Chapter 4.5.

(d) To qualify for certification pursuant to this section, a regulatory program shall require the utilization of an interdisciplinary approach that will ensure the integrated use of the natural and social sciences in decision-making and that shall meet all of the following criteria:

(1) The enabling legislation of the regulatory program does both of the following:

(A) Includes protection of the environment among its principal purposes.

(B) Contains authority for the administering agency to adopt rules and regulations for the protection of the environment, guided by standards set forth in the enabling legislation.

(2) The rules and regulations adopted by the administering agency for the regulatory program do all of the following:

(A) Require that an activity will not be approved or adopted as proposed if there are feasible alternatives or feasible mitigation measures available that would substantially lessen a significant adverse effect that the activity may have on the environment.

(B) Include guidelines for the orderly evaluation of proposed activities and the preparation of the plan or other written documentation in a manner consistent with the environmental protection purposes of the regulatory program.

(C) Require the administering agency to consult with all public agencies that have jurisdiction, by law, with respect to the proposed activity.

(D) Require that final action on the proposed activity include the written responses of the issuing authority to significant environmental points raised during the evaluation process.

(E) Require the filing of a notice of the decision by the administering agency on the proposed activity with the Secretary of the Resources Agency. Those notices shall be available for public inspection, and a list of the notices shall be posted on a weekly basis in the Office of the Resources Agency. Each list shall remain posted for a period of 30 days.

(F) Require notice of the filing of the plan or other written documentation to be made to the public and to a person who requests, in writing, notification. The notification shall be made in a manner that will provide the public or a person requesting notification with sufficient time to review and comment on the filing.

(3) The plan or other written documentation required by the regulatory program does both of the following:

(A) Includes a description of the proposed activity with alternatives to the activity, and mitigation measures to minimize any significant adverse effect on the environment of the activity.

(B) Is available for a reasonable time for review and comment by other public agencies and the general public.

(e) (1) The Secretary of the Resources Agency shall certify a regulatory program that the secretary determines meets all the qualifications for certification set forth in this section, and withdraw certification on determination that the regulatory program has been altered so that it no longer meets those qualifications. Certification and withdrawal of certification shall occur only after compliance with Chapter 3.5 (commencing with Section 11340) of Part 1 of Division 3 of Title 2 of the Government Code.

(2) In determining whether or not a regulatory program meets the qualifications for certification set forth in this section, the inquiry of the secretary shall extend only to the question of whether the regulatory program meets the generic requirements of subdivision (d). The inquiry may not extend to individual decisions to be reached under the regulatory program, including the nature of specific alternatives or mitigation measures that might be proposed to lessen any significant adverse effect on the environment of the activity.

(3) If the secretary determines that the regulatory program submitted for certification does not meet the qualifications for certification set forth in this section, the secretary shall adopt findings setting forth the reasons for the determination.

(f) After a regulatory program has been certified pursuant to this section, a proposed change in the program that could affect compliance with the qualifications for certification specified in subdivision (d) may be submitted to the Secretary of the Resources Agency for review and comment. The scope of the secretary's review shall extend only to the question of whether the regulatory program meets the generic requirements of subdivision (d). The review may not extend to individual decisions to be reached under the regulatory program, including specific alternatives or mitigation measures that might be proposed to lessen any significant adverse effect on the environment of the activity. The secretary shall have 30 days from the date of receipt of the proposed change to notify the state agency whether the proposed change will alter the regulatory program so that it no longer meets the qualification for certification established in this section and will result in a withdrawal of certification as provided in this section.

(g) An action or proceeding to attack, review, set aside, void, or annul a determination or decision of a state agency approving or adopting a proposed activity under a regulatory program that has been certified pursuant to this section on the basis that the plan or other written documentation prepared pursuant to paragraph (3) of subdivision (d) does not comply with this section shall be commenced not later than 30 days from the date of the filing of notice of the approval or adoption of the activity.

(h) (1) An action or proceeding to attack, review, set aside, void, or annul a determination of the Secretary of the Resources Agency to certify a regulatory program pursuant to this section on the basis that the regulatory program does not comply with this section shall be commenced within 30 days from the date of certification by the secretary.

(2) In an action brought pursuant to paragraph (1), the inquiry shall extend only to whether there was a prejudicial abuse of discretion by the secretary. Abuse of discretion is established if the secretary has not proceeded in a manner required by law or if the determination is not supported by substantial evidence.

(i) For purposes of this section, a county agricultural commissioner is a state agency.

(j) For purposes of this section, an air quality management district or air pollution control district is a state agency, except that the approval, if any, by a district of a nonattainment area plan is subject to this section only if, and to the extent that, the approval adopts or amends rules or regulations.

(k) (1) The secretary, by July 1, 2004, shall develop a protocol for reviewing the prospective application of certified regulatory programs to evaluate the consistency of those programs with the requirements of this division. Following the completion of the development of the protocol, the secretary shall provide a report to the Senate Committee on Environmental

Quality and the Assembly Committee on Natural Resources regarding the need for a grant of additional statutory authority authorizing the secretary to undertake a review of the certified regulatory programs.

(2) The secretary may update the protocol, and may update the report provided to the legislative committees pursuant to paragraph (1) and provide, in compliance with Section 9795 of the Government Code, the updated report to those committees if additional statutory authority is needed.

(3) The secretary shall provide a significant opportunity for public participation in developing or updating the protocol described in paragraph (1) or (2) including, but not limited to, at least two public meetings with interested parties. A notice of each meeting shall be provided at least 10 days prior to the meeting to a person who files a written request for a notice with the agency and to the Senate Committee on Environmental Quality and the Assembly Committee on Natural Resources.

§ 21080.8. APPLICATION OF DIVISION; CONVERSION OF EXISTING RENTAL MOBILEHOME PARK TO RESIDENT INITIATED SUBDIVISION, COOPERATIVE, CONDOMINIUM FOR MOBILEHOMES

This division does not apply to the conversion of an existing rental mobilehome park to a resident initiated subdivision, cooperative, or condominium for mobilehomes if the conversion will not result in an expansion of or change in existing use of the property.

§ 21080.9. LOCAL COASTAL PROGRAMS OR LONG-RANGE LAND USE DEVELOPMENT; UNIVERSITY OR GOVERNMENTAL ACTIVITIES AND APPROVALS; APPLICATION OF DIVISION

This division shall not apply to activities and approvals by any local government, as defined in Section 30109, or any state university or college, as defined in Section 30119, as necessary for the preparation and adoption of a local coastal program or long-range land use development plan pursuant to Division 20 (commencing with Section 30000); provided, however, that certification of a local coastal program or long-range land use development plan by the California Coastal Commission pursuant to Chapter 6 (commencing with Section 30500) of Division 20 shall be subject to the requirements of this division. For the purpose of Section 21080.5, a certified local coastal program or long-range land use development plan constitutes a plan for use in the California Coastal Commission's regulatory program.

§ 21080.10. APPLICATION OF DIVISION; GENERAL PLANS; LOW- OR MODERATE- INCOME OR RESIDENTIAL HOUSING; AGRICULTURAL EMPLOYEE HOUSING

This division does not apply to any of the following:

(a) An extension of time, granted pursuant to Section 65361 of the Government Code, for the preparation and adoption of one or more elements of a city or county general plan.

(b) Actions taken by the Department of Housing and Community Development or the California Housing Finance Agency to provide financial assistance or insurance for the development and construction of residential housing for persons and families of low or moderate income, as defined in Section 50093 of the Health and Safety Code, if the project that is the subject of the application for financial assistance or insurance will be reviewed pursuant to this division by another public agency.

§ 21080.11. APPLICATION OF DIVISION; SETTLEMENTS BY STATE LANDS COMMISSION

This division shall not apply to settlements of title and boundary problems by the State Lands Commission and to exchanges or leases in connection with those settlements.

§ 21080.12. APPLICATION OF DIVISION; REPAIR OF CRITICAL LEVEES

(a) This division does not apply to the repair of critical levees of the State Plan for Flood Control specified pursuant to Section 8361 of the Water Code within an existing levee footprint to meet standards of public health and safety funded pursuant to Section 5096.821, except as otherwise provided in Section 15300.2 of Title 14 of the California Code of Regulations.

(b) For purposes of undertaking urgent levee repairs, the lead agency shall do all of the following:

(1) Conduct outreach efforts in the vicinity of the project to ensure public awareness of the proposed repair work prior to approval of the project.

(2) To the extent feasible, comply with standard construction practices, including, but not limited to, any rules, guidelines, or regulations adopted by the applicable air district for construction equipment and for control of particulate matter emissions.

(3) To the extent feasible, use equipment powered by emulsified diesel fuel, electricity, natural gas, or ultralow sulfur diesel as an alternative to conventional diesel-powered construction equipment.

(c) This section shall remain in effect only until July 1, 2016, and as of that date is repealed, unless a later enacted statute, that is enacted before July 1, 2016, deletes or extends that date.

§ 21080.13. RAILROAD GRADE SEPARATION PROJECTS; APPLICATION OF DIVISION

This division shall not apply to any railroad grade separation project which eliminates an existing grade crossing or which reconstructs an existing grade separation.

§ 21080.14.

(a) This division does not apply to the closure of a railroad grade crossing by order of the Public Utilities Commission, pursuant to the commission's authority under Chapter 6 (commencing with Section 1201) of Part 1 of Division 1 of the Public Utilities Code, if the commission finds the crossing to present a threat to public safety.

(b) This section shall not apply to any crossing for high-speed rail, as defined in subdivision (c) of Section 185012 of the Public Utilities Code, or any crossing for any project carried out by the High-Speed Rail Authority, as described in Section 185020 of the Public Utilities Code, or a successor agency.

(c) (1) Whenever a state agency determines that a project is not subject to this division pursuant to this section, and it approves or determines to carry out the project, the state agency shall file a notice with the Office of Planning and Research in the manner specified in subdivisions (b) and (c) of Section 21108.

(2) Whenever a local agency determines that a project is not subject to this division pursuant to this section, and it approves or determines to carry out the project, the local agency shall file a notice with the Office of Planning and Research and with the county clerk in each county in which the project will be located in the manner specified in subdivisions (b) and (c) of Section 21152.

(d) This section shall remain in effect only until January 1, 2016, and as of that date is repealed, unless a later enacted statute, that is enacted before January 1, 2016, deletes or extends that date.

§ 21080.14. [DELETED]

§ 21080.16. [REPEALED]

§ 21080.17. APPLICATION OF DIVISION TO ORDINANCES IMPLEMENTING LAW RELATING TO CONSTRUCTION OF DWELLING UNITS AND SECOND UNITS

This division does not apply to the adoption of an ordinance by a city or county to implement the provisions of Section 65852.1 or Section 65852.2 of the Government Code.

§ 21080.18. APPLICATION OF DIVISION TO CLOSING OF PUBLIC SCHOOL MAINTAINING KINDERGARTEN OR ANY OF GRADES 1 THROUGH 12

This division does not apply to the closing of any public school in which kindergarten or any of grades 1 through 12 is maintained or the transfer of students from that public school to another school if the only physical changes involved are categorically exempt under Chapter 3 (commencing with Section 15000) of Division 6 of Title 14 of the California Administrative Code.

§ 21080.19. RESTRIPING OF STREETS OR HIGHWAYS; APPLICATION OF DIVISION

This division does not apply to a project for restriping of streets or highways to relieve traffic congestion.

§ 21080.20 BICYCLE TRANSPORTATION PLANS

(a) This division does not apply to a bicycle transportation plan prepared pursuant to Section 891.2 of the Streets and Highways Code for an urbanized area for restriping of streets and highways, bicycle parking and storage, signal timing to improve street and highway intersection operations, and related signage for bicycles, pedestrians, and vehicles.

(b) Prior to determining that a project is exempt pursuant to this section, the lead agency shall do both of the following:

  (1) Hold noticed public hearings in areas affected by the bicycle transportation plan to hear and respond to public comments. Publication of the notice shall be no fewer times than required by Section 6061 of the Government Code, by the public agency in a newspaper of general circulation in the area affected by the proposed project. If more than one area will be affected, the notice shall be published in the newspaper of largest circulation from among the newspapers of general circulation in those areas.

  (2) Prepare an assessment of any traffic and safety impacts of the project and include measures in the bicycle transportation plan to mitigate potential vehicular traffic impacts and bicycle and pedestrian safety impacts.

(c) If a local agency determines that a project is not subject to this division pursuant to this section, and it determines to approve or carry out that project, the notice shall be filed with the Office of Planning and Research and the county clerk in the county in which the project is located in the manner specified in subdivisions (b) and (c) of Section 21152.

(d) This section shall remain in effect only until January 1, 2018, and as of that date is repealed, unless a later enacted statute, that is enacted before January 1, 2018, deletes or extends that date.

§ 21080.20.5 RESTRIPING FOR BICYCLE LANES IN URBANIZED AREAS

(a) This division does not apply to a project that consists of the restriping of streets and highways for bicycle lanes in an urbanized area that is consistent with a bicycle transportation plan prepared pursuant to Section 891.2 of the Streets and Highways Code.

(b) Prior to determining that a project is exempt pursuant to this section, the lead agency shall do both of the following:

  (1) (A) Prepare an assessment of any traffic and safety impacts of the project and include measures in the project to mitigate potential vehicular traffic impacts and bicycle and pedestrian safety impacts.

(B) The requirement to prepare an assessment pursuant to subparagraph (A) shall not apply if either of the following conditions is met:

(i) Measures to mitigate these impacts are identified in an environmental impact report, negative declaration, or mitigated negative declaration prepared pursuant to this division for the bicycle transportation plan, certified or approved no more than five years prior to making the determination, the measures are included in the plan, and those measures are incorporated into the project.

(ii) An assessment was prepared pursuant to paragraph (2) of subdivision (b) of Section 21080.20 no more than five years prior to making the determination, the measures to mitigate these impacts are included in the plan, and those measures are incorporated into the project.

(2) Hold noticed public hearings in areas affected by the project to hear and respond to public comments. Publication of the notice shall be no fewer times than required by Section 6061 of the Government Code, by the public agency in a newspaper of general circulation in the area affected by the proposed project. If more than one area will be affected, the notice shall be published in the newspaper of largest circulation from among the newspapers of general circulation in those areas.

(c) (1) If a state agency determines that a project is not subject to this division pursuant to this section, and it determines to approve or carry out that project, the notice shall be filed with the Office of Planning and Research in the manner specified in subdivisions (b) and (c) of Section 21108.

(2) If a local agency determines that a project is not subject to this division pursuant to this section, and it determines to approve or carry out that project, the notice shall be filed with the Office of Planning and Research, and filed with the county clerk in the county in which the project is located in the manner specified in subdivisions (b) and (c) of Section 21152.

(d) This section shall remain in effect only until January 1, 2018, and as of that date is repealed, unless a later enacted statute, that is enacted before January 1, 2018, deletes or extends that date.

§ 21080.21. APPLICATION OF DIVISION TO PUBLIC RIGHT-OF-WAY PIPELINE PROJECTS LESS THAN ONE MILE IN LENGTH

(a) This division does not apply to any project of less than one mile in length within a public street or highway or any other public right-of-way for the installation of a new pipeline or the maintenance, repair, restoration, reconditioning, relocation, replacement, removal, or demolition of an existing pipeline.

(b) For purposes of this section, "pipeline" means subsurface pipelines and subsurface or surface accessories or appurtenances to a pipeline, such as mains, traps, vents, cables, conduits, vaults, valves, flanges, manholes, and meters.

(c) In determining the applicability of the exemption provided by this section to a natural gas pipeline safety enhancement activity under review by a resource agency, the resource agency shall consider only the length of pipeline that is within its legal jurisdiction.

(d) For purposes of this section, the following definitions shall apply:

(1) "Natural gas pipeline safety enhancement activity" means an activity undertaken by a public utility as part of a program to enhance the safety of intrastate natural gas pipelines in accordance with a decision, rule, or regulation adopted by the Public Utilities Commission.

(2) "Resource agency" means the State Lands Commission, the California Coastal Commission, the Department of Fish and Game, or the State Water Resources Control Board, and local or regional agencies with permitting authority under the California Coastal

Act of 1976 (Division 20 (commencing with Section 30000)) or Chapter 4 (commencing with Section 13200) of Division 7 of the Water Code.

(e) This section shall remain in effect only until January 1, 2018, and as of that date is repealed, unless a later enacted statute, that is enacted before January 1, 2018, deletes or extends that date.

§ 21080.21.

(a) This division does not apply to any project of less than one mile in length within a public street or highway or any other public right-of-way for the installation of a new pipeline or the maintenance, repair, restoration, reconditioning, relocation, replacement, removal, or demolition of an existing pipeline. For purposes of this section, "pipeline" includes subsurface facilities but does not include any surface facility related to the operation of the underground facility.

(b) This section shall become operative January 1, 2018.

§ 21080.22. LOCAL GOVERNMENTS; PREPARATION OF GENERAL PLAN AMENDMENTS; APPLICATION OF DIVISION

(a) This division does not apply to activities and approvals by a local government necessary for the preparation of general plan amendments pursuant to Section 29763, except that the approval of general plan amendments by the Delta Protection Commission is subject to the requirements of this division.

(b) For purposes of Section 21080.5, a general plan amendment is a plan required by the regulatory program of the Delta Protection Commission.

§ 21080.23. PIPELINE PROJECTS; APPLICATION OF DIVISION

(a) This division does not apply to any project which consists of the inspection, maintenance, repair, restoration, reconditioning, relocation, replacement, or removal of an existing pipeline, as defined in subdivision (a) of Section 51010.5 of the Government Code, or any valve, flange, meter, or other piece of equipment that is directly attached to the pipeline, if the project meets all of the following conditions:

(1) (A) The project is less than eight miles in length.

(B) Notwithstanding subparagraph (A), actual construction and excavation activities undertaken to achieve the maintenance, repair, restoration, reconditioning, relocation, replacement, or removal of an existing pipeline are not undertaken over a length of more than one-half mile at any one time.

(2) The project consists of a section of pipeline that is not less than eight miles from any section of pipeline that has been subject to an exemption pursuant to this section in the past 12 months.

(3) The project is not solely for the purpose of excavating soil that is contaminated by hazardous materials, and, to the extent not otherwise expressly required by law, the party undertaking the project immediately informs the lead agency of the discovery of contaminated soil.

(4) To the extent not otherwise expressly required by law, the person undertaking the project has, in advance of undertaking the project, prepared a plan that will result in notification of the appropriate agencies so that they may take action, if determined to be necessary, to provide for the emergency evacuation of members of the public who may be located in close proximity to the project.

(5) Project activities are undertaken within an existing right-of-way and the right-of-way is restored to its condition prior to the project.

(6) The project applicant agrees to comply with all conditions otherwise authorized by law, imposed by the city or county planning department as part of any local agency permit process, that are required to mitigate potential impacts of the proposed project, and to otherwise comply with the Keene-Nejedly California Wetlands Preservation Act (Chapter 7 (commencing with Section 5810) of Division 5), the California Endangered Species Act (Chapter 1.5 (commencing with Section 2050) of Division 3 of the Fish and Game Code), and other applicable state laws, and with all applicable federal laws.

(b) If a project meets all of the requirements of subdivision (a), the person undertaking the project shall do all of the following:

(1) Notify, in writing, any affected public agency, including, but not limited to, any public agency having permit, land use, environmental, public health protection, or emergency response authority of the exemption of the project from this division by subdivision (a).

(2) Provide notice to the public in the affected area in a manner consistent with paragraph (3) of subdivision (b) of Section 21092.

(3) In the case of private rights-of-way over private property, receive from the underlying property owner permission for access to the property.

(4) Comply with all conditions otherwise authorized by law, imposed by the city or county planning department as part of any local agency permit process, that are required to mitigate potential impacts of the proposed project, and otherwise comply with the Keene-Nejedly California Wetlands Preservation Act (Chapter 7 (commencing with Section 5810) of Division 5), the California Endangered Species Act (Chapter 1.5 (commencing with Section 2050) of Division 3 of the Fish and Game Code), and other applicable state laws, and with all applicable federal laws.

(c) This section does not apply to either of the following:

(1) A project in which the diameter of the pipeline is increased.

(2) A project undertaken within the boundaries of an oil refinery.

§ 21080.23.5. PIPELINE; BIOGAS; APPLICATION OF DIVISION

(a) For purposes of Section 21080.23, "pipeline" also means a pipeline located in Fresno, Kern, Kings, or Tulare County, that is used to transport biogas, and meeting the requirements of Section 21080.23 and all local, state, and federal laws.

(b) For purposes of this section, "biogas" means natural gas that meets the requirements of Section 2292.5 of Title 13 of the California Code of Regulations and is derived from anaerobic digestion of dairy animal waste.

(c) This section shall remain in effect only until January 1, 2018, and as of that date is repealed, unless a later enacted statute, that is enacted before January 1, 2018, deletes or extends that date.

§ 21080.24. PERMITS; ISSUANCE, MODIFICATION, AMENDMENT, OR RENEWAL; APPLICATION OF LAW

This division does not apply to the issuance, modification, amendment, or renewal of a permit by an air pollution control district or air quality management district pursuant to Title V, as defined in Section 39053.3 of the Health and Safety Code, or pursuant to a district Title V program established pursuant to Sections 42301.10, 42301.11, and 42301.12 of the Health and Safety Code, unless the issuance, modification, amendment, or renewal authorizes a physical or operational change to a source or facility.

§ 21080.25. LA-RICS; APPLICATION OF DIVISION

(a) For purposes of this section, the following definitions shall apply:

(1) "Antenna support structures" means lattice towers, monopoles, and roof-mounts.

(2) "Habitat of significant value" includes all of the following:

(A) Wildlife habitat of national, statewide, or regional importance.

(B) Habitat identified as candidate, fully protected, sensitive, or species of special status by a state or federal agency.

(C) Habitat essential to the movement of resident or migratory wildlife.

(3) "LA-RICS" means the Los Angeles Regional Interoperable Communications System, consisting of a long-term evolution broadband mobile data system, a land mobile radio system, or both.

(4) "LMR" means a land mobile radio system.

(5) "LTE" means a long-term evolution broadband mobile data system.

(6) "Riparian area" means an area that is transitional between terrestrial and aquatic ecosystems, that is distinguished by gradients in biophysical conditions, ecological processes, and biota, and that meets the following criteria:

(A) Is an area through which surface and subsurface hydrology connect waterbodies with their adjacent uplands.

(B) Is adjacent to perennial, intermittent, and ephemeral streams, lakes, or estuarine or marine shorelines.

(C) Includes those portions of terrestrial ecosystems that significantly influence exchanges of energy and matter with aquatic ecosystems.

(7) "Wetlands" has the same meaning as defined in the United States Fish and Wildlife Service Manual, Part 660 FW 2 (June 21, 1993).

(8) "Wildlife habitat" means the ecological communities upon which wild animals, birds, plants, fish, amphibians, and invertebrates depend for their conservation and protection.

(b) If all the criteria specified in subdivision (c) are met at the individual project site, this division does not apply to the design, site acquisition, construction, operation, or maintenance of the following elements of the LA-RICS:

(1) Antennas, including microwave dishes and arrays.

(2) Antenna support structures.

(3) Equipment enclosures.

(4) Central system switch facilities.

(5) Associated foundations and equipment.

(c) As a condition of the exemption specified in subdivision (b), all of the following criteria shall be met at the individual project site:

(1) The project site is publicly owned and already contains one or both of the following:

(A) An antenna support structure and one or both of the following components:

(i) Antennas.

(ii) Equipment enclosures.

(B) A police, sheriff, or fire station, or other public facility that transmits or receives public safety radio signals.

(2) Construction and implementation at the project site would not have a substantial adverse impact on wetlands, riparian areas, or habitat of significant value, and would not harm any species protected by the federal Endangered Species Act of 1973 (16 U.S.C. Sec. 1531 et seq.), the Native Plant Protection Act (Chapter 10 (commencing with Section 1900) of the Fish and Game Code), or the California Endangered Species Act (Chapter 1.5 (commencing with Section 2050) of Division 3 of the Fish and Game Code), or the habitat of those species.

(3) Construction and implementation of the project at the site would not have a substantial adverse impact on historical resources pursuant to Section 21084.1.

(4) Operation of the project at the site would not exceed the maximum permissible exposure standards established by the Federal Communications Commission, as set forth in Sections 1.1307 and 1.1310 of Title 47 of the Code of Federal Regulations.

(5) Any new LTE antenna support structures or LMR antenna support structures would comply with applicable state and federal height restrictions, and any height restrictions mandated by an applicable comprehensive land use plan adopted by an airport land use commission. The new monopoles shall not exceed 70 feet in height without appurtenances and attachments, and new lattice towers shall not exceed 180 feet in height without appurtenances and attachments.

(6) Each new central system switch is located within an existing enclosed structure at a publicly owned project site, or is housed at an existing private communications facility.

(d) This section shall remain in effect only until January 1, 2017, and as of that date is repealed, unless a later enacted statute, that is enacted before January 1, 2017, deletes or extends that date.

§ 21080.26. FLUORIDATION; APPLICATION OF DIVISION; MINOR ALTERATIONS

This division does not apply to minor alterations to utilities made for the purposes of complying with Sections 4026.7 and 4026.8 of the Health and Safety Code or regulations adopted thereunder.

§ 21080.29. LA PLAYA PROJECT; APPLICATION OF DIVISION

(a) A project located in Los Angeles County that is approved by a public agency before the effective date of the act adding this section is not in violation of any requirement of this division by reason of the failure to construct a roadway across the property transferred to the state pursuant to subdivision (c) and to construct a bridge over the adjacent Ballona Channel in Los Angeles County, otherwise required as a mitigation measure pursuant to this division, if all of the following conditions apply:

(1) The improvements specified in this subdivision are not constructed, due in whole or in part, to the project owner's or developer's relinquishment of easement rights to construct those improvements.

(2) The easement rights in paragraph (1) are relinquished in connection with the State of California, acting by and through the Wildlife Conservation Board of the Department of Fish and Game, acquiring a wetlands project that is a minimum of 400 acres in size and located within the coastal zone.

(b) Where those easement rights have been relinquished, any municipal ordinance or regulation adopted by a charter city or a general law city shall be inapplicable to the extent that the ordinance or regulation requires construction of the transportation improvements specified in subdivision (a), or would otherwise require reprocessing or resubmittal of a permit or approval, including, but not limited to, a final recorded map, a vesting tentative map, or a tentative map, as a result of the transportation improvements specified in subdivision (a) not being constructed.

(c) (1) If the Wildlife Conservation Board of the Department of Fish and Game acquires property within the coastal zone that is a minimum of 400 acres in size pursuant to a purchase and sale agreement with Playa Capital Company, LLC, the Controller shall direct the trustee under the Amendment to Declaration of Trust entered into on or about December 11, 1984, by First Nationwide Savings, as trustee, Summa Corporation, as trustor, and the Controller, as beneficiary, known as the HRH Inheritance Tax Security Trust, to convey title to the trust estate of the trust, including real property commonly known as Playa Vista Area C, to the State of California acting by and through the Wildlife Conservation Board of the Department of Fish and Game for conservation, restoration, or recreation purposes only, with the right to transfer the property for those uses to any other agency of the State of California.

(2) This subdivision shall constitute the enabling legislation required by the Amendment to Declaration of Trust to empower the Controller to direct the trustee to convey title to the trust estate under the HRH Inheritance Tax Security Trust to the State of California or an agency thereof.

(3) The conveyance of the trust estate to the Wildlife Conservation Board pursuant to this subdivision shall supersede any duty or obligation imposed upon the Controller under the Probate Code or the Revenue and Taxation Code with respect to the disposition or application of the net proceeds of the trust estate.

§ 21080.32. EXEMPTION OF SPECIFIED ACTIONS BY PUBLICLY OWNED TRANSIT AGENCIES; IMPLEMENTATION OF BUDGET REDUCTIONS

(a) This section shall only apply to publicly owned transit agencies, but shall not apply to any publicly owned transit agency created pursuant to Section 130050.2 of the Public Utilities Code.

(b) Except as provided in subdivision (c), and in accordance with subdivision (d), this division does not apply to actions taken on or after July 1, 1995, by a publicly owned transit agency to implement budget reductions caused by the failure of agency revenues to adequately fund agency programs and facilities.

(c) This section does not apply to any action to reduce or eliminate a transit service, facility, program, or activity that was approved or adopted as a mitigation measure in any environmental document authorized by this division or the National Environmental Policy Act (42 U.S.C. Sec. 4321 et seq.) or to any state or federal requirement that is imposed for the protection of the environment.

(d) (1) This section applies only to actions taken after the publicly owned transit agency has made a finding that there is a fiscal emergency caused by the failure of agency revenues to adequately fund agency programs and facilities, and after the publicly owned transit agency has held a public hearing to consider those actions. A publicly owned transit agency that has held such a hearing shall respond within 30 days at a regular public meeting to suggestions made by the public at the initial public hearing. Those actions shall be limited to projects defined in subdivision (a) or (b) of Section 21065 which initiate or increase fees, rates, or charges charged for any existing public service, program, or activity; or reduce or eliminate the availability of an existing publicly owned transit service, facility, program, or activity.

(2) For purposes of this subdivision, “fiscal emergency,” when applied to a publicly owned transit agency, means that the agency is projected to have negative working capital within one year from the date that the agency makes the finding that there is a fiscal emergency pursuant to this section. Working capital shall be determined by adding together all unrestricted cash, unrestricted short-term investments, and unrestricted short-term accounts receivable and then subtracting unrestricted accounts payable. Employee retirement funds,

including Internal Revenue Code Section 457 deferred compensation plans and Section 401(k) plans, health insurance reserves, bond payment reserves, workers' compensation reserves, and insurance reserves, shall not be factored into the formula for working capital.

§ 21080.33. EMERGENCY PROJECTS TO MAINTAIN, REPAIR OR RESTORE EXISTING HIGHWAYS; APPLICATION OF DIVISION; EXCEPTIONS

This division does not apply to any emergency project undertaken, carried out, or approved by a public agency to maintain, repair, or restore an existing highway, as defined in Section 360 of the Vehicle Code, except for a highway designated as an official state scenic highway pursuant to Section 262 of the Streets and Highways Code, within the existing right-of-way of the highway, damaged as a result of fire, flood, storm, earthquake, land subsidence, gradual earth movement, or landslide, within one year of the damage. This section does not exempt from this division any project undertaken, carried out, or approved by a public agency to expand or widen a highway damaged by fire, flood, storm, earthquake, land subsidence, gradual earth movement, or landslide.

§ 21080.35. CARRYING OUT OR APPROVING A PROJECT; DEFINITION

For the purposes of Section 21069, the phrase "carrying out or approving a project" shall include the carrying out or approval of a plan for a project that expands or enlarges an existing publicly owned airport by any political subdivision, as described in Section 21661.6 of the Public Utilities Code.

§ 21080.35.[1]

(a) Except as provided in subdivision (d), this division does not apply to the installation of a solar energy system on the roof of an existing building or at an existing parking lot.

(b) For the purposes of this section, the following terms mean the following:

(1) "Existing parking lot" means an area designated and used for parking of vehicles as of the time of the application for the solar energy system and for at least the previous two years.

(2) "Solar energy system" includes all associated equipment. Associated equipment consists of parts and materials that enable the generation and use of solar electricity or solar-heated water, including any monitoring and control, safety, conversion, and emergency responder equipment necessary to connect to the customer's electrical service or plumbing and any equipment, as well as any equipment necessary to connect the energy generated to the electrical grid, whether that connection is onsite or on an adjacent parcel of the building and separated only by an improved right-of-way. "Associated equipment" does not include a substation.

(c) (1) Associated equipment shall be located on the same parcel of the building, except that associated equipment necessary to connect the energy generated to the electrical grid may be located immediately adjacent to the parcel of the building or immediately adjacent to the parcel of the building and separated only by an improved right-of-way.

(2) Associated equipment shall not occupy more than 500 square feet of ground surface and the site of the associated equipment shall not contain plants protected by the Native Plant Protection Act (Chapter 10 (commencing with Section 1900) of Division 2 of the Fish and Game Code).

(d) This section does not apply if the associated equipment would otherwise require one of the following:

[1] Section 21080.35, as added by SB 226, was mislabeled and codified under the same number as an existing code section with unrelated content. AB 226 does not amend the existing language of Section 21080.35.

(1) An individual federal permit pursuant to Section 401 or 404 of the federal Clean Water Act (33 U.S.C. Sec. 1341 or 1344) or waste discharge requirements pursuant to the Porter-Cologne Water Quality Control Act (Division 7 (commencing with Section 13000) of the Water Code).

(2) An individual take permit for species protected under the federal Endangered Species Act of 1973 (16 U.S.C. Sec. 1531 et seq.) or the California Endangered Species Act (Chapter 1.5 (commencing with Section 2050) of Division 3 of the Fish and Game Code).

(3) A streambed alteration permit pursuant to Chapter 6 (commencing with Section 1600) of Division 2 of the Fish and Game Code.

(e) This section does not apply if the installation of a solar energy system at an existing parking lot involves either of the following:

(1) The removal of a tree required to be planted, maintained, or protected pursuant to local, state, or federal requirements, unless the tree dies and there is no requirement to replace the tree.

(2) The removal of a native tree over 25 years old.

(f) This section does not apply to any transmission or distribution facility or connection.

§ 21080.37. ALTERATION OF EXISTING ROADWAY; APPLICATION OF DIVISION

(a) This division does not apply to a project or an activity to repair, maintain, or make minor alterations to an existing roadway if all of the following conditions are met:

(1) The project is carried out by a city or county with a population of less than 100,000 persons to improve public safety.

(2) (A) The project does not cross a waterway.

(B) For purposes of the paragraph, "waterway" means a bay, estuary, lake, pond, river, slough, or a perennial, intermittent, or ephemeral stream, lake, or estuarine-marine shoreline.

(3) The project involves negligible or no expansion of an existing use beyond that existing at the time of the lead agency's determination.

(4) The roadway is not a state roadway.

(5) (A) The site of the project does not contain wetlands or riparian areas and does not have significant value as a wildlife habitat, and the project does not harm any species protected by the federal Endangered Species Act of 1973 (16 U.S.C. Sec. 1531 et seq.), the Native Plant Protection Act (Chapter 10 (commencing with Section 1900) of Division 2 of the Fish and Game Code), or the California Endangered Species Act (Chapter 1.5 (commencing with Section 2050) of Division 3 of the Fish and Game Code), and the project does not cause the destruction or removal of any species protected by a local ordinance.

(B) For the purposes of this paragraph:

(i) "Riparian areas" mean those areas transitional between terrestrial and aquatic ecosystems and that are distinguished by gradients in biophysical conditions, ecological processes, and biota. A riparian area is an area through which surface and subsurface hydrology connect waterbodies with their adjacent uplands. A riparian area includes those portions of terrestrial ecosystems that significantly influence exchanges of energy and matter with aquatic ecosystems. A riparian area is adjacent to perennial, intermittent, and ephemeral streams, lakes, and estuarine-marine shorelines.

(ii) "Significant value as a wildlife habitat" includes wildlife habitat of national, statewide, regional, or local importance; habitat for species protected by the federal Endangered Species Act of 1973 (16 U.S.C. Sec. 1531, et seq.), the California Endangered Species Act (Chapter 1.5 (commencing with Section 2050) of Division 3 of the Fish and Game Code), or the Native Plant Protection Act (Chapter 10 (commencing with Section 1900) of Division 2 of the Fish and Game Code); habitat identified as candidate, fully protected, sensitive, or species of special status by local, state, or federal agencies; or habitat essential to the movement of resident or migratory wildlife.

(iii) "Wetlands" has the same meaning as in the United States Fish and Wildlife Service Manual, Part 660 FW 2 (June 21, 1993).

(iv) "Wildlife habitat" means the ecological communities upon which wild animals, birds, plants, fish, amphibians, and invertebrates depend for their conservation and protection.

(6) The project does not impact cultural resources.

(7) The roadway does not affect scenic resources, as provided pursuant to subdivision (c) of Section 21084.

(b) Prior to determining that a project is exempt pursuant to this section, the lead agency shall do both of the following:

(1) Include measures in the project to mitigate potential vehicular traffic and safety impacts and bicycle and pedestrian safety impacts.

(2) Hold a noticed public hearing on the project to hear and respond to public comments. The hearing on the project may be conducted with another noticed lead agency public hearing. Publication of the notice shall be no fewer times than required by Section 6061 of the Government Code, by the public agency in a newspaper of general circulation in the area.

(c) For purposes of this section, "roadway" means a roadway as defined pursuant to Section 530 of the Vehicle Code and the previously graded and maintained shoulder that is within a roadway right-of-way of no more than five feet from the edge of the roadway.

(d) Whenever a local agency determines that a project is not subject to this division pursuant to this notice with the Office of Planning and Research, and with the county clerk in the county in which the project will be located in the manner specified in subdivisions (b) and (c) of Section 21152.

(e) This section shall remain in effect only until January 1, 2016, and as of that date is repealed, unless a later enacted statute, that is enacted before January 1, 2016, deletes or extends that date.

§ 21080.42.

(a) The following transportation projects are exempt from this division:

(1) U.S. Highway 101 interchange modification, adding southbound auxiliary lane and southbound mixed flow lane, from Interstate 280 to Yerba Buena Road, in Santa Clara County.

(2) Construct north and southbound high-occupancy vehicle lanes on I-805 from I-5 to Carroll Canyon Road, including construction of north-facing direct access ramps in San Diego County.

(3) State Route 99, Los Molinas rehabilitation and traffic calming, from Orange Street to Tehama Vine Road, in Tehama County.

(4) State Route 99, Island Park widening project, adding one mixed flow lane in each direction, from Ashlan Avenue to Grantlund Avenue, in Fresno County.

(5) State Route 99 median widening, adding one mixed flow lane in each direction, from State Route 120 west to 0.4 miles north of Arch Road, in Manteca in San Joaquin County.

(6) State Route 12 pavement rehabilitation and shoulder widening in San Joaquin County on Bouldin Island.

(7) State Route 91 widening, adding one mixed flow lane in each direction, from State Route 55 to Weir Canyon Road in Orange County.

(8) U.S. Highway 101 pavement rehabilitation and shoulder widening in San Luis Obispo County.

(b) An exemption provided pursuant to subdivision (a) shall not apply to a transportation project if, on or after February 1, 2009, a lead agency changes the scope of that project from the manner in which the project is described in subdivision (a).

§ 21081. NECESSARY FINDINGS WHERE ENVIRONMENTAL IMPACT REPORT IDENTIFIES EFFECTS

Pursuant to the policy stated in Sections 21002 and 21002.1, no public agency shall approve or carry out a project for which an environmental impact report has been certified which identifies one or more significant effects on the environment that would occur if the project is approved or carried out unless both of the following occur:

(a) The public agency makes one or more of the following findings with respect to each significant effect:

(1) Changes or alterations have been required in, or incorporated into, the project which mitigate or avoid the significant effects on the environment.

(2) Those changes or alterations are within the responsibility and jurisdiction of another public agency and have been, or can and should be, adopted by that other agency.

(3) Specific economic, legal, social, technological, or other considerations, including considerations for the provision of employment opportunities for highly trained workers, make infeasible the mitigation measures or alternatives identified in the environmental impact report.

(b) With respect to significant effects which were subject to a finding under paragraph (3) of subdivision (a), the public agency finds that specific overriding economic, legal, social, technological, or other benefits of the project outweigh the significant effects on the environment.

§ 21081.2 EXCEPTION TO FINDINGS FOR INFILL RESIDENTIAL PROJECTS

(a) Except as provided in subdivision (c), if a residential project, not exceeding 100 units, with a minimum residential density of 20 units per acre and within one-half mile of a transit stop, on an infill site in an urbanized area is in compliance with the traffic, circulation, and transportation policies of the general plan, applicable community plan, applicable specific plan, and applicable ordinances of the city or county with jurisdiction over the area where the project is located, and the city or county requires that the mitigation measures approved in a previously certified project area environmental impact report applicable to the project be incorporated into the project, the city or county is not required to comply with subdivision (a) of Section 21081 with respect to the making of any findings regarding the impacts of the project on traffic at intersections, or on streets, highways, or freeways.

(b) Nothing in subdivision (a) restricts the authority of a city or county to adopt feasible mitigation measures with respect to the impacts of a project on pedestrian and bicycle safety.

(c) Subdivision (a) does not apply in any of the following circumstances:

(1) The application for a proposed project is made more than five years after certification of the project area environmental impact report applicable to the project.

(2) A major change has occurred within the project area after certification of the project area environmental impact report applicable to the project.

(3) The project area environmental impact report applicable to the project was certified with overriding considerations pursuant to subdivision (b) of Section 21081 to the significant impacts on the environment with respect to traffic or transportation.

(4) The proposed project covers more than four acres.

(d) A project shall not be divided into smaller projects in order to qualify pursuant to this section.

(e) Nothing in this section relieves a city or county from the requirement to analyze the project's effects on traffic at intersections, or on streets, highways, or freeways, or from making a determination that the project may have a significant effect on traffic.

(f) For the purposes of this section, "project area environmental impact report" means an environmental impact report certified on any of the following:

(1) A general plan.

(2) A revision or update to the general plan that includes at least the land use and circulation elements.

(3) An applicable community plan.

(4) An applicable specific plan.

(5) A housing element of the general plan, if the environmental impact report analyzed the environmental effects of the density of the proposed project.

(6) A zoning ordinance.

§ 21081.5. FEASIBILITY OF MITIGATION MEASURES OR PROJECT ALTERNATIVES; BASIS FOR FINDINGS

In making the findings required by paragraph (3) of subdivision (a) of Section 21081, the public agency shall base its findings on substantial evidence in the record.

§ 21081.6. FINDINGS OR NEGATIVE DECLARATIONS; REPORTING OR MONITORING PROJECT CHANGES; EFFECT ON ENVIRONMENT; CONDITIONS

(a) When making the findings required by paragraph (1) of subdivision (a) of Section 21081 or when adopting a mitigated negative declaration pursuant to paragraph (2) of subdivision (c) of Section 21080, the following requirements shall apply:

(1) The public agency shall adopt a reporting or monitoring program for the changes made to the project or conditions of project approval, adopted in order to mitigate or avoid significant effects on the environment. The reporting or monitoring program shall be designed to ensure compliance during project implementation. For those changes which have been required or incorporated into the project at the request of a responsible agency or a public agency having jurisdiction by law over natural resources affected by the project, that agency shall, if so requested by the lead agency or a responsible agency, prepare and submit a proposed reporting or monitoring program.

(2) The lead agency shall specify the location and custodian of the documents or other material which constitute the record of proceedings upon which its decision is based.

(b) A public agency shall provide that measures to mitigate or avoid significant effects on the environment are fully enforceable through permit conditions, agreements, or other measures. Conditions of project approval may be set forth in referenced documents which address

required mitigation measures or, in the case of the adoption of a plan, policy, regulation, or other public project, by incorporating the mitigation measures into the plan, policy, regulation, or project design.

(c) Prior to the close of the public review period for a draft environmental impact report or mitigated negative declaration, a responsible agency, or a public agency having jurisdiction over natural resources affected by the project, shall either submit to the lead agency complete and detailed performance objectives for mitigation measures which would address the significant effects on the environment identified by the responsible agency or agency having jurisdiction over natural resources affected by the project, or refer the lead agency to appropriate, readily available guidelines or reference documents. Any mitigation measures submitted to a lead agency by a responsible agency or an agency having jurisdiction over natural resources affected by the project shall be limited to measures which mitigate impacts to resources which are subject to the statutory authority of, and definitions applicable to, that agency. Compliance or noncompliance by a responsible agency or agency having jurisdiction over natural resources affected by a project with that requirement shall not limit the authority of the responsible agency or agency having jurisdiction over natural resources affected by a project, or the authority of the lead agency, to approve, condition, or deny projects as provided by this division or any other provision of law.

§ 21081.7. TRANSPORTATION INFORMATION; SUBMISSION OF REPORT TO TRANSPORTATION PLANNING AGENCY

Transportation information resulting from the reporting or monitoring program required to be adopted by a public agency pursuant to Section 21081.6 shall be submitted to the transportation planning agency in the region where the project is located and to the Department of Transportation for a project of statewide, regional, or areawide significance according to criteria developed pursuant to Section 21083. The transportation planning agency and the Department of Transportation shall adopt guidelines for the submittal of those reporting or monitoring programs.

§ 21082. PUBLIC AGENCIES; ADOPTION OF OBJECTIVES, CRITERIA AND PROCEDURES; CONSISTENCY WITH GUIDELINES

All public agencies shall adopt by ordinance, resolution, rule, or regulation, objectives, criteria, and procedures for the evaluation of projects and the preparation of environmental impact reports and negative declarations pursuant to this division. A school district, or any other district, whose boundaries are coterminous with a city, county, or city and county, may utilize the objectives, criteria, and procedures of the city, county, or city and county, as may be applicable, in which case, the school district or other district need not adopt objectives, criteria, and procedures of its own. The objectives, criteria, and procedures shall be consistent with the provisions of this division and with the guidelines adopted by the Secretary of the Resources Agency pursuant to Section 21083. Such objectives, criteria, and procedures shall be adopted by each public agency no later than 60 days after the Secretary of the Resources Agency has adopted guidelines pursuant to Section 21083.

§ 21082.1. DRAFT ENVIRONMENTAL IMPACT REPORT, ENVIRONMENTAL IMPACT REPORT, OR NEGATIVE DECLARATION; PREPARATION BY PUBLIC AGENCY

(a) Any draft environmental impact report, environmental impact report, negative declaration, or mitigated negative declaration prepared pursuant to the requirements of this division shall be prepared directly by, or under contract to, a public agency.

(b) This section is not intended to prohibit, and shall not be construed as prohibiting, any person from submitting information or other comments to the public agency responsible for preparing an environmental impact report, draft environmental impact report, negative declaration, or mitigated negative declaration. The information or other comments may be submitted in any

format, shall be considered by the public agency, and may be included, in whole or in part, in any report or declaration.

(c) The lead agency shall do all of the following:

(1) Independently review and analyze any report or declaration required by this division.

(2) Circulate draft documents that reflect its independent judgment.

(3) As part of the adoption of a negative declaration or a mitigated negative declaration, or certification of an environmental impact report, find that the report or declaration reflects the independent judgment of the lead agency.

(4) Submit a sufficient number of copies of the draft environmental impact report, proposed negative declaration, or proposed mitigated negative declaration, and a copy of the report or declaration in an electronic form as required by the guidelines adopted pursuant to Section 21083, to the State Clearinghouse for review and comment by state agencies, if any of the following apply:

(A) A state agency is any of the following:

(i) The lead agency.

(ii) A responsible agency.

(iii) A trustee agency.

(B) A state agency otherwise has jurisdiction by law with respect to the project.

(C) The proposed project is of sufficient statewide, regional, or areawide environmental significance as determined pursuant to the guidelines certified and adopted pursuant to Section 21083.

§ 21082.2. SIGNIFICANT EFFECT ON ENVIRONMENT; DETERMINATION; ENVIRONMENTAL IMPACT REPORT PREPARATION

(a) The lead agency shall determine whether a project may have a significant effect on the environment based on substantial evidence in light of the whole record.

(b) The existence of public controversy over the environmental effects of a project shall not require preparation of an environmental impact report if there is no substantial evidence in light of the whole record before the lead agency that the project may have a significant effect on the environment.

(c) Argument, speculation, unsubstantiated opinion or narrative, evidence which is clearly inaccurate or erroneous, or evidence of social or economic impacts which do not contribute to, or are not caused by, physical impacts on the environment, is not substantial evidence. Substantial evidence shall include facts, reasonable assumptions predicated upon facts, and expert opinion supported by facts.

(d) If there is substantial evidence, in light of the whole record before the lead agency, that a project may have a significant effect on the environment, an environmental impact report shall be prepared.

(e) Statements in an environmental impact report and comments with respect to an environmental impact report shall not be deemed determinative of whether the project may have a significant effect on the environment.

§ 21082.3.

(a) Any mitigation measures agreed upon in the consultation conducted pursuant to Section 21080.3.2 shall be recommended for inclusion in the environmental document and in an adopted mitigation monitoring and reporting program, if determined to avoid or lessen the impact pursuant to paragraph (2) of subdivision (b), and shall be fully enforceable.

(b) If a project may have a significant impact on a tribal cultural resource, the lead agency's environmental document shall discuss both of the following:

(1) Whether the proposed project has a significant impact on an identified tribal cultural resource.

(2) Whether feasible alternatives or mitigation measures, including those measures that may be agreed to pursuant to subdivision (a), avoid or substantially lessen the impact on the identified tribal cultural resource.

(c) (1) Any information, including, but not limited to, the location, description, and use of the tribal cultural resources, that is submitted by a California Native American tribe during the environmental review process shall not be included in the environmental document or otherwise disclosed by the lead agency or any other public agency to the public, consistent with subdivision (r) of Section 6254 of, and Section 6254.10 of, the Government Code, and subdivision (d) of Section 15120 of Title 14 of the California Code of Regulations, without the prior consent of the tribe that provided the information. If the lead agency publishes any information submitted by a California Native American tribe during the consultation or environmental review process, that information shall be published in a confidential appendix to the environmental document unless the tribe that provided the information consents, in writing, to the disclosure of some or all of the information to the public. This subdivision does not prohibit the confidential exchange of the submitted information between public agencies that have lawful jurisdiction over the preparation of the environmental document.

(2) (A) This subdivision does not prohibit the confidential exchange of information regarding tribal cultural resources submitted by a California Native American tribe during the consultation or environmental review process among the lead agency, the California Native American tribe, the project applicant, or the project applicant's agent. Except as provided in subparagraph (B) or unless the California Native American tribe providing the information consents, in writing, to public disclosure, the project applicant or the project applicant's legal advisers, using a reasonable degree of care, shall maintain the confidentiality of the information exchanged for the purposes of preventing looting, vandalism, or damage to a tribal cultural resource and shall not disclose to a third party confidential information regarding tribal cultural resources.

(B) This paragraph does not apply to data or information that are or become publicly available, are already in the lawful possession of the project applicant before the provision of the information by the California Native American tribe, are independently developed by the project applicant or the project applicant's agents, or are lawfully obtained by the project applicant from a third party that is not the lead agency, a California Native American tribe, or another public agency.

(3) This subdivision does not affect or alter the application of subdivision (r) of Section 6254 of the Government Code, Section 6254.10 of the Government Code, or subdivision (d) of Section 15120 of Title 14 of the California Code of Regulations.

(4) This subdivision does not prevent a lead agency or other public agency from describing the information in general terms in the environmental document so as to inform the public of the basis of the lead agency's or other public agency's decision without breaching the confidentiality required by this subdivision.

(d) In addition to other provisions of this division, the lead agency may certify an environmental impact report or adopt a mitigated negative declaration for a project with a significant impact on an identified tribal cultural resource only if one of the following occurs:

(1) The consultation process between the California Native American tribe and the lead agency has occurred as provided in Sections 21080.3.1 and 21080.3.2 and concluded pursuant to subdivision (b) of Section 21080.3.2.

(2) The California Native American tribe has requested consultation pursuant to Section 21080.3.1 and has failed to provide comments to the lead agency, or otherwise failed to engage, in the consultation process.

(3) The lead agency has complied with subdivision (d) of Section 21080.3.1 and the California Native American tribe has failed to request consultation within 30 days.

(e) If the mitigation measures recommended by the staff of the lead agency as a result of the consultation process are not included in the environmental document or if there are no agreed upon mitigation measures at the conclusion of the consultation or if consultation does not occur, and if substantial evidence demonstrates that a project will cause a significant effect to a tribal cultural resources, the lead agency shall consider feasible mitigation pursuant to subdivision (b) of Section 21084.3.

(f) Consistent with subdivision (c), the lead agency shall publish confidential information obtained from a California Native American tribe during the consultation process in a confidential appendix to the environmental document and shall include a general description of the information, as provided in paragraph (4) of subdivision (c) in the environmental document for public review during the public comment period provided pursuant to this division.

(g) This section is not intended, and may not be construed, to limit consultation between the state and tribal governments, existing confidentiality provisions, or the protection of religious exercise to the fullest extent permitted under state and federal law.

§ 21083. OFFICE OF PLANNING AND RESEARCH; PREPARATION AND DEVELOPMENT OF GUIDELINES; CONDITIONS

(a) The Office of Planning and Research shall prepare and develop proposed guidelines for the implementation of this division by public agencies. The guidelines shall include objectives and criteria for the orderly evaluation of projects and the preparation of environmental impact reports and negative declarations in a manner consistent with this division.

(b) The guidelines shall specifically include criteria for public agencies to follow in determining whether or not a proposed project may have a "significant effect on the environment." The criteria shall require a finding that a project may have a "significant effect on the environment" if one or more of the following conditions exist:

(1) A proposed project has the potential to degrade the quality of the environment, curtail the range of the environment, or to achieve short-term, to the disadvantage of long-term, environmental goals.

(2) The possible effects of a project are individually limited but cumulatively considerable. As used in this paragraph, "cumulatively considerable" means that the incremental effects of an individual project are considerable when viewed in connection with the effects of past projects, the effects of other current projects, and the effects of probable future projects.

(3) The environmental effects of a project will cause substantial adverse effects on human beings, either directly or indirectly.

(c) The guidelines shall include procedures for determining the lead agency pursuant to Section 21165.

(d) The guidelines shall include criteria for public agencies to use in determining when a proposed project is of sufficient statewide, regional, or areawide environmental significance that a draft environmental impact report, a proposed negative declaration, or a proposed mitigated negative declaration shall be submitted to appropriate state agencies, through the State Clearinghouse,

for review and comment prior to completion of the environmental impact report, negative declaration, or mitigated negative declaration.

(e) The Office of Planning and Research shall develop and prepare the proposed guidelines as soon as possible and shall transmit them immediately to the Secretary of the Resources Agency. The Secretary of the Resources Agency shall certify and adopt the guidelines pursuant to Chapter 3.5 (commencing with Section 11340) of Part 1 of Division 3 of Title 2 of the Government Code, which shall become effective upon the filing thereof. However, the guidelines shall not be adopted without compliance with Sections 11346.4, 11346.5, and 11346.8 of the Government Code.

(f) The Office of Planning and Research shall, at least once every two years, review the guidelines adopted pursuant to this section and shall recommend proposed changes or amendments to the Secretary of the Resources Agency. The Secretary of the Resources Agency shall certify and adopt guidelines, and any amendments thereto, at least once every two years, pursuant to Chapter 3.5 (commencing with Section 11340) of Part 1 of Division 3 of Title 2 of the Government Code, which shall become effective upon the filing thereof. However, guidelines may not be adopted or amended without compliance with Sections 11346.4, 11346.5, and 11346.8 of the Government Code.

§ 21083.01. GUIDELINES AMENDMENTS; FIRE HAZARD

(a) On or after January 1, 2013, at the time of the next review of the guidelines prepared and developed to implement this division pursuant to subdivision (f) of Section 21083, the Office of Planning and Research, in cooperation with the Department of Forestry and Fire Protection, shall prepare, develop, and transmit to the Secretary of the Natural Resources Agency recommended proposed changes or amendments to the initial study checklist of the guidelines implementing this division for the inclusion of questions related to fire hazard impacts for projects located on lands classified as state responsibility areas, as defined in Section 4102, and on lands classified as very high fire hazard severity zones, as defined in subdivision (i) of Section 51177 of the Government Code.

(b) Upon receipt and review, the Secretary of the Natural Resources Agency shall certify and adopt the recommended proposed changes or amendments prepared and developed by the Office of Planning and Research pursuant to subdivision (a).

§ 21083.05.

The Office of Planning and Research shall periodically update the guidelines for the mitigation of greenhouse gas emissions or the effects of greenhouse gas emissions as required by this division, including, but not limited to, effects associated with transportation or energy consumption to incorporate new information or criteria established by the State Air Resources Board pursuant to Division 25.5 (commencing with Section 38500) of the Health and Safety Code.

§ 21083.09.

On or before July 1, 2016, the Office of Planning and Research shall prepare and develop, and the Secretary of the Natural Resources Agency shall certify and adopt, revisions to the guidelines that update Appendix G of Chapter 3 (commencing with Section 15000) of Division 6 of Title 4 of the California Code of Regulations to do both of the following:

(a) Separate the consideration of paleontological resources from tribal cultural resources and update the relevant sample questions.

(b) Add consideration of tribal cultural resources with relevant sample questions.

§ 21083.1. LEGISLATIVE INTENT; INTERPRETATION BY COURTS

It is the intent of the Legislature that courts, consistent with generally accepted rules of statutory interpretation, shall not interpret this division or the state guidelines adopted pursuant to Section 21083 in a manner which imposes procedural or substantive requirements beyond those explicitly stated in this division or in the state guidelines.

§ 21083.2. ARCHAEOLOGICAL RESOURCES; DETERMINATION OF EFFECT OF PROJECT; EIR OR NEGATIVE DECLARATION; MITIGATION MEASURES

(a) As part of the determination made pursuant to Section 21080.1, the lead agency shall determine whether the project may have a significant effect on archaeological resources. If the lead agency determines that the project may have a significant effect on unique archaeological resources, the environmental impact report shall address the issue of those resources. An environmental impact report, if otherwise necessary, shall not address the issue of nonunique archaeological resources. A negative declaration shall be issued with respect to a project if, but for the issue of nonunique archaeological resources, the negative declaration would be otherwise issued.

(b) If it can be demonstrated that a project will cause damage to a unique archaeological resource, the lead agency may require reasonable efforts to be made to permit any or all of these resources to be preserved in place or left in an undisturbed state. Examples of that treatment, in no order of preference, may include, but are not limited to, any of the following:

(1) Planning construction to avoid archaeological sites.

(2) Deeding archaeological sites into permanent conservation easements.

(3) Capping or covering archaeological sites with a layer of soil before building on the sites.

(4) Planning parks, greenspace, or other open space to incorporate archaeological sites.

(c) To the extent that unique archaeological resources are not preserved in place or not left in an undisturbed state, mitigation measures shall be required as provided in this subdivision. The project applicant shall provide a guarantee to the lead agency to pay one-half the estimated cost of mitigating the significant effects of the project on unique archaeological resources. In determining payment, the lead agency shall give due consideration to the in-kind value of project design or expenditures that are intended to permit any or all archaeological resources or California Native American culturally significant sites to be preserved in place or left in an undisturbed state. When a final decision is made to carry out or approve the project, the lead agency shall, if necessary, reduce the specified mitigation measures to those which can be funded with the money guaranteed by the project applicant plus the money voluntarily guaranteed by any other person or persons for those mitigation purposes. In order to allow time for interested persons to provide the funding guarantee referred to in this subdivision, a final decision to carry out or approve a project shall not occur sooner than 60 days after completion of the recommended special environmental impact report required by this section.

(d) Excavation as mitigation shall be restricted to those parts of the unique archaeological resource that would be damaged or destroyed by the project. Excavation as mitigation shall not be required for a unique archaeological resource if the lead agency determines that testing or studies already completed have adequately recovered the scientifically consequential information from and about the resource, if this determination is documented in the environmental impact report.

(e) In no event shall the amount paid by a project applicant for mitigation measures required pursuant to subdivision (c) exceed the following amounts:

(1) An amount equal to one-half of 1 percent of the projected cost of the project for mitigation measures undertaken within the site boundaries of a commercial or industrial project.

(2) An amount equal to three-fourths of 1 percent of the projected cost of the project for mitigation measures undertaken within the site boundaries of a housing project consisting of a single unit.

(3) If a housing project consists of more than a single unit, an amount equal to three-fourths of 1 percent of the projected cost of the project for mitigation measures undertaken within the site boundaries of the project for the first unit plus the sum of the following:

(A) Two hundred dollars ($200) per unit for any of the next 99 units.

(B) One hundred fifty dollars ($150) per unit for any of the next 400 units.

(C) One hundred dollars ($100) per unit in excess of 500 units.

(f) Unless special or unusual circumstances warrant an exception, the field excavation phase of an approved mitigation plan shall be completed within 90 days after final approval necessary to implement the physical development of the project or, if a phased project, in connection with the phased portion to which the specific mitigation measures are applicable. However, the project applicant may extend that period if he or she so elects. Nothing in this section shall nullify protections for Indian cemeteries under any other provision of law.

(g) As used in this section, "unique archaeological resource" means an archaeological artifact, object, or site about which it can be clearly demonstrated that, without merely adding to the current body of knowledge, there is a high probability that it meets any of the following criteria:

(1) Contains information needed to answer important scientific research questions and that there is a demonstrable public interest in that information.

(2) Has a special and particular quality such as being the oldest of its type or the best available example of its type.

(3) Is directly associated with a scientifically recognized important prehistoric or historic event or person.

(h) As used in this section, "nonunique archaeological resource" means an archaeological artifact, object, or site which does not meet the criteria in subdivision (g). A nonunique archaeological resource need be given no further consideration, other than the simple recording of its existence by the lead agency if it so elects.

(i) As part of the objectives, criteria, and procedures required by Section 21082 or as part of conditions imposed for mitigation, a lead agency may make provisions for archaeological sites accidentally discovered during construction. These provisions may include an immediate evaluation of the find. If the find is determined to be a unique archaeological resource, contingency funding and a time allotment sufficient to allow recovering an archaeological sample or to employ one of the avoidance measures may be required under the provisions set forth in this section. Construction work may continue on other parts of the building site while archaeological mitigation takes place.

(j) This section does not apply to any project described in subdivision (a) or (b) of Section 21065 if the lead agency elects to comply with all other applicable provisions of this division. This section does not apply to any project described in subdivision (c) of Section 21065 if the applicant and the lead agency jointly elect to comply with all other applicable provisions of this division.

(k) Any additional costs to any local agency as a result of complying with this section with respect to a project of other than a public agency shall be borne by the project applicant.

(l) Nothing in this section is intended to affect or modify the requirements of Section 21084 or 21084.1.

§ 21083.3. APPLICATION OF DIVISION TO APPROVAL OF SUBDIVISION MAP OR OTHER PROJECT; LIMITATION; MITIGATION MEASURES UNDER PRIOR ENVIRONMENTAL IMPACT REPORT; PUBLIC HEARING; FINDING

(a) If a parcel has been zoned to accommodate a particular density of development or has been designated in a community plan to accommodate a particular density of development and an environmental impact report was certified for that zoning or planning action, the application of this division to the approval of any subdivision map or other project that is consistent with the zoning or community plan shall be limited to effects upon the environment which are peculiar to the parcel or to the project and which were not addressed as significant effects in the prior environmental impact report, or which substantial new information shows will be more significant than described in the prior environmental impact report.

(b) If a development project is consistent with the general plan of a local agency and an environmental impact report was certified with respect to that general plan, the application of this division to the approval of that development project shall be limited to effects on the environment which are peculiar to the parcel or to the project and which were not addressed as significant effects in the prior environmental impact report, or which substantial new information shows will be more significant than described in the prior environmental impact report.

(c) Nothing in this section affects any requirement to analyze potentially significant offsite impacts and cumulative impacts of the project not discussed in the prior environmental impact report with respect to the general plan. However, all public agencies with authority to mitigate the significant effects shall undertake or require the undertaking of any feasible mitigation measures specified in the prior environmental impact report relevant to a significant effect which the project will have on the environment or, if not, then the provisions of this section shall have no application to that effect. The lead agency shall make a finding, at a public hearing, as to whether those mitigation measures will be undertaken.

(d) An effect of a project upon the environment shall not be considered peculiar to the parcel or to the project, for purposes of this section, if uniformly applied development policies or standards have been previously adopted by the city or county, with a finding based upon substantial evidence, which need not include an environmental impact report, that the development policies or standards will substantially mitigate that environmental effect when applied to future projects, unless substantial new information shows that the policies or standards will not substantially mitigate the environmental effect.

(e) Where a community plan is the basis for application of this section, any rezoning action consistent with the community plan shall be a project subject to exemption from this division in accordance with this section. As used in this section, "community plan" means a part of the general plan of a city or county which (1) applies to a defined geographic portion of the total area included in the general plan, (2) complies with Article 5 (commencing with Section 65300) of Chapter 3 of Division 1 of Title 7 of the Government Code by including or referencing each of the mandatory elements specified in Section 65302 of the Government Code, and (3) contains specific development policies adopted for the area included in the community plan and identifies measures to implement those policies, so that the policies which will apply to each parcel can be determined.

(f) No person shall have standing to bring an action or proceeding to attack, review, set aside, void, or annul a finding of a public agency made at a public hearing pursuant to subdivision (a) with respect to the conformity of the project to the mitigation measures identified in the prior environmental impact report for the zoning or planning action, unless he or she has participated in that public hearing. However, this subdivision shall not be applicable if the local agency failed to give public notice of the hearing as required by law. For purposes of this subdivision, a person has participated in the public hearing if he or she has either submitted oral or written

testimony regarding the proposed determination, finding, or decision prior to the close of the hearing.

(g) Any community plan adopted prior to January 1, 1982, which does not comply with the definitional criteria specified in subdivision (e) may be amended to comply with that criteria, in which case the plan shall be deemed a "community plan" within the meaning of subdivision (e) if (1) an environmental impact report was certified for adoption of the plan, and (2) at the time of the conforming amendment, the environmental impact report has not been held inadequate by a court of this state and is not the subject of pending litigation challenging its adequacy.

§ 21083.4. COUNTIES; CONVERSION OF OAK WOODLANDS; MITIGATION ALTERNATIVES; OAK WOODLANDS CONSERVATION ACT GRANT USE; EXEMPTIONS

(a) For purposes of this section, "oak" means a native tree species in the genus Quercus, not designated as Group A or Group B commercial species pursuant to regulations adopted by the State Board of Forestry and Fire Protection pursuant to Section 4526, and that is 5 inches or more in diameter at breast height.

(b) As part of the determination made pursuant to Section 21080.1, a county shall determine whether a project within its jurisdiction may result in a conversion of oak woodlands that will have a significant effect on the environment. If a county determines that there may be a significant effect to oak woodlands, the county shall require one or more of the following oak woodlands mitigation alternatives to mitigate the significant effect of the conversion of oak woodlands:

(1) Conserve oak woodlands, through the use of conservation easements.

(2) (A) Plant an appropriate number of trees, including maintaining plantings and replacing dead or diseased trees.

(B) The requirement to maintain trees pursuant to this paragraph terminates seven years after the trees are planted.

(C) Mitigation pursuant to this paragraph shall not fulfill more than one-half of the mitigation requirement for the project.

(D) The requirements imposed pursuant to this paragraph also may be used to restore former oak woodlands.

(3) Contribute funds to the Oak Woodlands Conservation Fund, as established under subdivision (a) of Section 1363 of the Fish and Game Code, for the purpose of purchasing oak woodlands conservation easements, as specified under paragraph (1) of subdivision (d) of that section and the guidelines and criteria of the Wildlife Conservation Board. A project applicant that contributes funds under this paragraph shall not receive a grant from the Oak Woodlands Conservation Fund as part of the mitigation for the project.

(4) Other mitigation measures developed by the county.

(c) Notwithstanding subdivision (d) of Section 1363 of the Fish and Game Code, a county may use a grant awarded pursuant to the Oak Woodlands Conservation Act (Article 3.5 (commencing with Section 1360) of Chapter 4 of Division 2 of the Fish and Game Code) to prepare an oak conservation element for a general plan, an oak protection ordinance, or an oak woodlands management plan, or amendments thereto, that meets the requirements of this section.

(d) The following are exempt from this section:

(1) Projects undertaken pursuant to an approved Natural Community Conservation Plan or approved subarea plan within an approved Natural Community Conservation Plan that includes oaks as a covered species or that conserves oak habitat through natural community conservation preserve designation and implementation and mitigation measures that are consistent with this section.

(2) Affordable housing projects for lower income households, as defined pursuant to Section 50079.5 of the Health and Safety Code, that are located within an urbanized area, or within a sphere of influence as defined pursuant to Section 56076 of the Government Code.

(3) Conversion of oak woodlands on agricultural land that includes land that is used to produce or process plant and animal products for commercial purposes.

(4) Projects undertaken pursuant to Section 21080.5 of the Public Resources Code.

(e) (1) A lead agency that adopts, and a project that incorporates, one or more of the measures specified in this section to mitigate the significant effects to oaks and oak woodlands shall be deemed to be in compliance with this division only as it applies to effects on oaks and oak woodlands.

(2) The Legislature does not intend this section to modify requirements of this division, other than with regard to effects on oaks and oak woodlands.

(f) This section does not preclude the application of Section 21081 to a project.

(g) This section, and the regulations adopted pursuant to this section, shall not be construed as a limitation on the power of a public agency to comply with this division or any other provision of law.

§ 21083.5. ENVIRONMENTAL IMPACT STATEMENT OR REPORT; SUBMISSION IN LIEU OF IMPACT REPORT; COMPLIANCE BY ADOPTION OF TAHOE REGIONAL PLAN; PUBLIC REVIEW AND NOTICE REQUIREMENTS

(a) The guidelines prepared and adopted pursuant to Section 21083 shall provide that, when an environmental impact statement has been, or will be, prepared for the same project pursuant to the requirements of the National Environmental Policy Act of 1969 (42 U.S.C. Sec. 4321 et seq.) and implementing regulations, or an environmental impact report has been, or will be, prepared for the same project pursuant to the requirements of the Tahoe Regional Planning Compact (Section 66801 of the Government Code) and implementing regulations, all or any part of that statement or report may be submitted in lieu of all or any part of an environmental impact report required by this division, if that statement or report, or the part which is used, complies with the requirements of this division and the guidelines adopted pursuant thereto.

(b) Notwithstanding subdivision (a), compliance with this division may be achieved for the adoption in a city or county general plan, without any additions or change, of all or any part of the regional plan prepared pursuant to the Tahoe Regional Planning Compact and implementing regulations by reviewing environmental documents prepared by the Tahoe Regional Planning Agency addressing the plan, providing an analysis pursuant to this division of any significant effect on the environment not addressed in the environmental documents, and proceeding in accordance with Section 21081. This subdivision does not exempt a city or county from complying with the public review and notice requirements of this division.

§ 21083.6. COMBINED ENVIRONMENTAL IMPACT REPORT AND STATEMENT; TIME LIMITS

In the event that a project requires both an environmental impact report prepared pursuant to the requirements of this division and an environmental impact statement prepared pursuant to the requirements of the National Environmental Policy Act of 1969, an applicant may request and the lead agency may waive the time limits established pursuant to Section 21100.2 or 21151.5 if it finds that additional time is required to prepare a combined environmental impact report-environmental impact statement and that the time required to prepare such a combined document would be shorter than that required to prepare each document separately.

§ 21083.7. USE OF IMPACT STATEMENT AS THE IMPACT REPORT; CONSULTATIONS

(a) In the event that a project requires both an environmental impact report prepared pursuant to the requirements of this division and an environmental impact statement prepared pursuant to the requirements of the National Environmental Policy Act of 1969, the lead agency shall, whenever possible, use the environmental impact statement as such environmental impact report as provided in Section 21083.5.

(b) In order to implement this section, each lead agency to which this section is applicable shall do both of the following, as soon as possible:

(1) Consult with the federal agency required to prepare such environmental impact statement.

(2) Notify the federal agency required to prepare the environmental impact statement regarding any scoping meeting for the proposed project.

§ 21083.8.1. REUSE PLANS

(a) (1) For purposes of this section, "reuse plan" for a military base means an initial plan for the reuse of a military base adopted by a local government or a redevelopment agency in the form of a general plan, general plan amendment, specific plan, redevelopment plan, or other planning document, except that the reuse plan shall also consist of a statement of development policies, include a diagram or diagrams illustrating its provisions, and make the designation required in paragraph (2). "Military base" or "base" means a military base or reservation either closed or realigned by, or scheduled for closure or realignment by, the federal government.

(2) The reuse plan shall designate the proposed general distribution and general location of development intensity for housing, business, industry, open space, recreation, natural resources, public buildings and grounds, roads and other transportation facilities, infrastructure, and other categories of public and private uses of land.

(b) (1) When preparing and certifying an environmental impact report for a reuse plan, including when utilizing an environmental impact statement pursuant to Section 21083.5, the determination of whether the reuse plan may have a significant effect on the environment may be made in the context of the physical conditions that were present at the time that the federal decision became final for the closure or realignment of the base. The no project alternative analyzed in the environmental impact report shall discuss the existing conditions on the base, as they exist at the time that the environmental impact report is prepared, as well as what could be reasonably expected to occur in the foreseeable future if the reuse plan were not approved, based on current plans and consistent with available infrastructure and services.

(2) For purposes of this division, all public and private activities taken pursuant to, or in furtherance of, a reuse plan shall be deemed to be a single project. However, further environmental review of any such public or private activity shall be conducted if any of the events specified in Section 21166 have occurred.

(c) Prior to preparing an environmental impact report for which a lead agency chooses to utilize the provisions of this section, the lead agency shall do all of the following:

(A) Hold a public hearing at which is discussed the federal environmental impact statement prepared for, or in the process of being prepared for, the closure of the military base. The discussion shall include the significant effects on the environment examined in the environmental impact statement, potential methods of mitigating those effects, including feasible alternatives, and the mitigative effects of federal, state, and local laws applicable to future nonmilitary activities. Prior to the close of the hearing, the lead agency may specify the baseline conditions for the reuse plan environmental impact report prepared, or in the process of being prepared, for the closure of the base. The lead agency may specify

particular physical conditions that it will examine in greater detail than were examined in the environmental impact statement. Notice of the hearing shall be given as provided in Section 21092. The hearing may be continued from time to time.

(B) Identify pertinent responsible agencies and trustee agencies and consult with those agencies prior to the public hearing as to the application of their regulatory policies and permitting standards to the proposed baseline for environmental analysis, as well as to the reuse plan and planned future nonmilitary land uses of the base. The affected agencies shall have not less than 30 days prior to the public hearing to review the proposed reuse plan and to submit their comments to the lead agency.

(C) At the close of the hearing, the lead agency shall state in writing how the lead agency intends to integrate the baseline for analysis with the reuse planning and environmental review process, taking into account the adopted environmental standards of the community, including, but not limited to, the applicable general plan, specific plan, and redevelopment plan, and including other applicable provisions of adopted congestion management plans, habitat conservation or natural communities conservation plans, integrated waste management plans, and county hazardous waste management plans.

(D) At the close of the hearing, the lead agency shall state, in writing, the specific economic or social reasons, including, but not limited to, new job creation, opportunities for employment of skilled workers, availability of low- and moderate-income housing, and economic continuity, which support the selection of the baseline.

(d) (1) Nothing in this section shall in any way limit the scope of a review or determination of significance of the presence of hazardous or toxic wastes, substances, or materials including, but not limited to, contaminated soils and groundwater, nor shall the regulation of hazardous or toxic wastes, substances, or materials be constrained by prior levels of activity that existed at the time that the federal agency decision to close the military base became final.

(2) This section does not apply to any project undertaken pursuant to Chapter 6.5 (commencing with Section 25100) of, or Chapter 6.8 (commencing with Section 25300) of, Division 20 of the Health and Safety Code, or pursuant to the Porter-Cologne Water Quality Control Act (Division 7 (commencing with Section 13000) of the Water Code).

(3) This section may apply to any reuse plan environmental impact report for which a notice of preparation pursuant to subdivision (a) of Section 21092 is issued within one year from the date that the federal record of decision was rendered for the military base closure or realignment and reuse, or prior to January 1, 1997, whichever is later, if the environmental impact report is completed and certified within five years from the date that the federal record of decision was rendered.

(e) All subsequent development at the military base shall be subject to all applicable federal, state, or local laws, including, but not limited to, those relating to air quality, water quality, traffic, threatened and endangered species, noise, and hazardous or toxic wastes, substances, or materials.

§ 21083.9. SCOPING MEETINGS

(a) Notwithstanding Section 21080.4, 21104, or 21153, a lead agency shall call at least one scoping meeting for either of the following:

(1) A proposed project that may affect highways or other facilities under the jurisdiction of the Department of Transportation if the meeting is requested by the department. The lead agency shall call the scoping meeting as soon as possible, but not later than 30 days after receiving the request from the Department of Transportation.

(2) A project of statewide, regional, or areawide significance.

(b) The lead agency shall provide notice of at least one scoping meeting held pursuant to paragraph (2) of subdivision (a) to all of the following:

(1) A county or city that borders on a county or city within which the project is located, unless otherwise designated annually by agreement between the lead agency and the county or city.

(2) A responsible agency.

(3) A public agency that has jurisdiction by law with respect to the project.

(4) A transportation planning agency or public agency required to be consulted pursuant to Section 21092.4.

(5) A public agency, organization or individual who has filed a written request for the notice.

(c) For a public agency, organization, or individual that is required to be provided notice of a lead agency public meeting, the requirement for notice of a scoping meeting pursuant to subdivision (b) may be met by including the notice of a scoping meeting in the public meeting notice.

(d) A scoping meeting that is held in the city or county within which the project is located pursuant to the National Environmental Policy Act (42 U.S.C. Sec. 4321 et seq.) and the regulations adopted pursuant to that act shall be deemed to satisfy the requirement that a scoping meeting be held for a project subject to paragraph (2) of subdivision (a) if the lead agency meets the notice requirements of subdivision (b) or subdivision (c).

(e) The referral of a proposed action to adopt or substantially amend a general plan to a city or county pursuant to paragraph (1) of subdivision (a) of Section 65352 of the Government Code may be conducted concurrently with the scoping meeting required pursuant to this section, and the city or county may submit its comments as provided pursuant to subdivision (b) of that section at the scoping meeting.

§ 21084. LIST OF EXEMPT CLASSES OF PROJECTS; PROJECTS DAMAGING SCENIC RESOURCES

(a) The guidelines prepared and adopted pursuant to Section 21083 shall include a list of classes of projects that have been determined not to have a significant effect on the environment and that shall be exempt from this division. In adopting the guidelines, the Secretary of the Natural Resources Agency shall make a finding that the listed classes of projects referred to in this section do not have a significant effect on the environment.

(b) A project's greenhouse gas emissions shall not, in and of themselves, be deemed to cause an exemption adopted pursuant to subdivision (a) to be inapplicable if the project complies with all applicable regulations or requirements adopted to implement statewide, regional, or local plans consistent with Section 15183.5 of Title 14 of the California Code of Regulations.

c) A project that may result in damage to scenic resources, including, but not limited to, trees, historic buildings, rock outcroppings, or similar resources, within a highway designated as an official state scenic highway, pursuant to Article 2.5 (commencing with Section 260) of Chapter 2 of Division 1 of the Streets and Highways Code, shall be exempted from this division pursuant to subdivision (a). This subdivision does not apply to improvements as mitigation for a project for which a negative declaration has been approved or an environmental impact report has been certified.

(d) A project located on a site that is included on any list compiled pursuant to Section 65962.5 of the Government Code shall not be exempted from this division pursuant to subdivision (a).

(e) A project that may cause a substantial adverse change in the significance of a historical resource, as specified in Section 21084.1, shall not be exempted from this division pursuant to subdivision (a).

§ 21084.1. HISTORICAL RESOURCE; SUBSTANTIAL ADVERSE CHANGE

A project that may cause a substantial adverse change in the significance of an historical resource is a project that may have a significant effect on the environment. For purposes of this section, an historical resource is a resource listed in, or determined to be eligible for listing in, the California Register of Historical Resources. Historical resources included in a local register of historical resources, as defined in subdivision (k) of Section 5020.1, or deemed significant pursuant to criteria set forth in subdivision (g) of Section 5024.1, are presumed to be historically or culturally significant for purposes of this section, unless the preponderance of the evidence demonstrates that the resource is not historically or culturally significant. The fact that a resource is not listed in, or determined to be eligible for listing in, the California Register of Historical Resources, not included in a local register of historical resources, or not deemed significant pursuant to criteria set forth in subdivision (g) of Section 5024.1 shall not preclude a lead agency from determining whether the resource may be an historical resource for purposes of this section.

§ 21084.2.

A project with an effect that may cause a substantial adverse change in the significance of a tribal cultural resource is a project that may have a significant effect on the environment.

§ 21084.3.

(a) Public agencies shall, when feasible, avoid damaging effects to any tribal cultural resource.

(b) If the lead agency determines that a project may cause a substantial adverse change to a tribal cultural resource, and measures are not otherwise identified in the consultation process provided in Section 21080.3.2, the following are examples of mitigation measures that, if feasible, may be considered to avoid or minimize the significant adverse impacts:

  (1) Avoidance and preservation of the resources in place, including, but not limited to, planning and construction to avoid the resources and protect the cultural and natural context, or planning greenspace, parks, or other open space, to incorporate the resources with culturally appropriate protection and management criteria.

  (2) Treating the resource with culturally appropriate dignity taking into account the tribal cultural values and meaning of the resource, including, but not limited to, the following:

    (A) Protecting the cultural character and integrity of the resource.

    (B) Protecting the traditional use of the resource.

    (C) Protecting the confidentiality of the resource.

  (3) Permanent conservation easements or other interests in real property, with culturally appropriate management criteria for the purposes of preserving or utilizing the resources or places.

  (4) Protecting the resource.

§ 21085.7. [DELETED]

§ 21086. ADDITION OR DELETION OF EXEMPT CLASSES OF PROJECTS; PROCEDURE

(a) A public agency may, at any time, request the addition or deletion of a class of projects, to the list designated pursuant to Section 21084. That request shall be made in writing to the Office of Planning and Research and shall include information supporting the public agency's position that the class of projects does, or does not, have a significant effect on the environment.

(b) The Office of Planning and Research shall review each request and, as soon as possible, shall submit its recommendation to the Secretary of the Resources Agency. Following the receipt of that recommendation, the Secretary of the Resources Agency may add or delete the class of

projects to the list of classes of projects designated pursuant to Section 21084 that are exempt from the requirements of this division.

(c) The addition or deletion of a class of projects, as provided in this section, to the list specified in Section 21084 shall constitute an amendment to the guidelines adopted pursuant to Section 21083 and shall be adopted in the manner prescribed in Sections 21083 and 21084.

§ 21088. DISTRIBUTION OF GUIDELINES, AMENDMENTS AND CHANGES; NOTICE

The Secretary of the Resources Agency shall provide for the timely distribution to all public agencies of the guidelines and any amendments or changes thereto. In addition, the Secretary of the Resources Agency may provide for publication of a bulletin to provide public notice of the guidelines, or any amendments or changes thereto, and of the completion of environmental impact reports prepared in compliance with this division.

§ 21089. FEES

(a) A lead agency may charge and collect a reasonable fee from a person proposing a project subject to this division in order to recover the estimated costs incurred by the lead agency in preparing a negative declaration or an environmental impact report for the project and for procedures necessary to comply with this division on the project. Litigation expenses, costs, and fees incurred in actions alleging noncompliance with this division under Section 21167 are not recoverable under this section.

(b) The Department of Fish and Game may charge and collect filing fees, as provided in Section 711.4 of the Fish and Game Code. Notwithstanding Section 21080.1, a finding required under Section 21081, or a project approved under a certified regulatory program authorized pursuant to Section 21080.5 is not operative, vested, or final until the filing fees required pursuant to Section 711.4 of the Fish and Game Code are paid.

(c) (1) A public agency may charge and collect a reasonable fee from members of the public for a copy of an environmental document not to exceed the cost of reproducing the environmental document. A public agency may provide the environmental document in an electronic format as provided pursuant to Section 6253.9 of the Government Code.

(2) For purposes of this subdivision, "environmental document" means an initial study, negative declaration, mitigated negative declaration, draft and final environmental impact report, a document prepared as a substitute for an environmental impact report, negative declaration, or mitigated negative declaration under a program certified pursuant to Section 21080.5, and a document prepared under the federal National Environmental Policy Act of 1969 (42 U.S.C. Sec. 4321 et seq.) and used by a state or local agency in the place of the initial study, negative declaration, mitigated negative declaration, or an environmental impact report.

§ 21090. REDEVELOPMENT PLAN DEEMED SINGLE PROJECT

(a) An environmental impact report for a redevelopment plan may be a master environmental impact report, program environmental impact report, or a project environmental impact report. Any environmental impact report for a redevelopment plan shall specify the type of environmental impact report that is prepared for the redevelopment plan.

(b) If the environmental impact report for a redevelopment plan is a project environmental impact report, all public and private activities or undertakings pursuant to, or in furtherance of, a redevelopment plan shall be deemed to be a single project. However, further environmental review of any public or private activity or undertaking pursuant to, or in furtherance of, a redevelopment plan for which a project environmental impact report has been certified shall be conducted if any of the events specified in Section 21166 have occurred.

§ 21090.1. GEOTHERMAL EXPLORATORY PROJECT DEEMED SEPARATE AND DISTINCT FROM FIELD DEVELOPMENT PROJECT

For all purposes of this division, a geothermal exploratory project shall be deemed to be separate and distinct from any subsequent geothermal field development project as defined in Section 65928.5 of the Government Code.

§ 21091. DRAFT ENVIRONMENTAL IMPACT REPORTS AND NEGATIVE DECLARATIONS; REVIEW PERIODS

(a) The public review period for a draft environmental impact report may not be less than 30 days. If the draft environmental impact report is submitted to the State Clearinghouse for review, the review period shall be at least 45 days, and the lead agency shall provide a sufficient number of copies of the document to the State Clearinghouse for review and comment by state agencies.

(b) The public review period for a proposed negative declaration or proposed mitigated negative declaration may not be less than 20 days. If the proposed negative declaration or proposed mitigated negative declaration is submitted to the State Clearinghouse for review, the review period shall be at least 30 days, and the lead agency shall provide a sufficient number of copies of the document to the State Clearinghouse for review and comment by state agencies.

(c) (1) Notwithstanding subdivisions (a) and (b), if a draft environmental impact report, proposed negative declaration, or proposed mitigated negative declaration is submitted to the State Clearinghouse for review and the period of review by the State Clearinghouse is longer than the public review period established pursuant to subdivision (a) or (b), whichever is applicable, the public review period shall be at least as long as the period of review and comment by state agencies as established by the State Clearinghouse.

(2) The public review period and the state agency review period may, but are not required to, begin and end at the same time. Day one of the state agency review period shall be the date that the State Clearinghouse distributes the CEQA document to state agencies.

(3) If the submittal of a CEQA document is determined by the State Clearinghouse to be complete, the State Clearinghouse shall distribute the document within three working days from the date of receipt. The State Clearinghouse shall specify the information that will be required in order to determine the completeness of the submittal of a CEQA document.

(d) (1) The lead agency shall consider comments it receives on a draft environmental impact report, proposed negative declaration, or proposed mitigated negative declaration if those comments are received within the public review period.

(2) (A) With respect to the consideration of comments received on a draft environmental impact report, the lead agency shall evaluate comments on environmental issues that are received from persons who have reviewed the draft and shall prepare a written response pursuant to subparagraph (B). The lead agency may also respond to comments that are received after the close of the public review period.

(B) The written response shall describe the disposition of each significant environmental issue that is raised by commenters. The responses shall be prepared consistent with Section 15088 of Title 14 of the California Code of Regulations.

(3) (A) With respect to the consideration of comments received on a draft environmental impact report, proposed negative declaration, proposed mitigated negative declaration, or notice pursuant to Section 21080.4, the lead agency shall accept comments via e-mail and shall treat e-mail comments as equivalent to written comments.

(B) Any law or regulation relating to written comments received on a draft environmental impact report, proposed negative declaration, proposed mitigated negative declaration,

or notice received pursuant to Section 21080.4, shall also apply to e-mail comments received for those reasons.

(e) (1) Criteria for shorter review periods by the State Clearinghouse for documents that must be submitted to the State Clearinghouse shall be set forth in the written guidelines issued by the Office of Planning and Research and made available to the public.

(2) Those shortened review periods may not be less than 30 days for a draft environmental impact report and 20 days for a negative declaration.

(3) A request for a shortened review period shall only be made in writing by the decision-making body of the lead agency to the Office of Planning and Research. The decision-making body may designate by resolution or ordinance a person authorized to request a shortened review period. A designated person shall notify the decision-making body of this request.

(4) A request approved by the State Clearinghouse shall be consistent with the criteria set forth in the written guidelines of the Office of Planning and Research .

(5) A shortened review period may not be approved by the Office of Planning and Research for a proposed project of statewide, regional, or areawide environmental significance as determined pursuant to Section 21083.

(6) An approval of a shortened review period shall be given prior to, and reflected in, the public notice required pursuant to Section 21092.

(f) Prior to carrying out or approving a project for which a negative declaration has been adopted, the lead agency shall consider the negative declaration together with comments that were received and considered pursuant to paragraph (1) of subdivision (d).

§ 21091.5. PUBLIC REVIEW PERIOD FOR DRAFT ENVIRONMENTAL IMPACT REPORT; PUBLICLY OWNED AIRPORTS

Notwithstanding subdivision (a) of Section 21091, or any other provision of this division, the public review period for a draft environmental impact report prepared for a proposed project involving the expansion or enlargement of a publicly owned airport requiring the acquisition of any tide and submerged lands or other lands subject to the public trust for commerce, navigation, or fisheries, or any interest therein, shall be not less than 120 days.

§ 21092. PUBLIC NOTICE OF PREPARATION OF ENVIRONMENTAL IMPACT REPORT OR NEGATIVE DECLARATION; PUBLICATION

(a) A lead agency that is preparing an environmental impact report or a negative declaration or making a determination pursuant to subdivision (c) of Section 21157.1 shall provide public notice of that fact within a reasonable period of time prior to certification of the environmental impact report, adoption of the negative declaration, or making the determination pursuant to subdivision (c) of Section 21157.1.

(b) (1) The notice shall specify the period during which comments will be received on the draft environmental impact report or negative declaration, and shall include the date, time, and place of any public meetings or hearings on the proposed project, a brief description of the proposed project and its location, the significant effects on the environment, if any, anticipated as a result of the project, the address where copies of the draft environmental impact report or negative declaration, and all documents referenced in the draft environmental impact report or negative declaration, are available for review, and a description of how the draft environmental impact report or negative declaration can be provided in an electronic format.

(2) This section shall not be construed in any manner that results in the invalidation of an action because of the alleged inadequacy of the notice content if there has been substantial compliance with the notice content requirements of this section.

(3) The notice required by this section shall be given to the last known name and address of all organizations and individuals who have previously requested notice and shall also be given by at least one of the following procedures:

(A) Publication, no fewer times than required by Section 6061 of the Government Code, by the public agency in a newspaper of general circulation in the area affected by the proposed project. If more than one area will be affected, the notice shall be published in the newspaper of largest circulation from among the newspapers of general circulation in those areas.

(B) Posting of notice by the lead agency on- and off-site in the area where the project is to be located.

(C) Direct mailing to the owners and occupants of contiguous property shown on the latest equalized assessment roll.

(c) For a project involving the burning of municipal wastes, hazardous waste, or refuse-derived fuel, including, but not limited to, tires, meeting the qualifications of subdivision (d), notice shall be given to all organizations and individuals who have previously requested notice and shall also be given by at least the procedures specified in subparagraphs (A), (B), and (C) of paragraph (3) of subdivision (b). In addition, notification shall be given by direct mailing to the owners and occupants of property within one-fourth of a mile of any parcel or parcels on which is located a project subject to this subdivision.

(d) The notice requirements of subdivision (c) apply to both of the following:

(1) The construction of a new facility.

(2) The expansion of an existing facility that burns hazardous waste which would increase its permitted capacity by more than 10 percent. For purposes of this paragraph, the amount of expansion of an existing facility shall be calculated by comparing the proposed facility capacity with whichever of the following is applicable:

(A) The facility capacity approved in the facility's hazardous waste facilities permit pursuant to Section 25200 of the Health and Safety Code or its grant of interim status pursuant to Section 25200.5 of the Health and Safety Code, or the facility capacity authorized in any state or local agency permit allowing the construction or operation of a facility for the burning of hazardous waste, granted before January 1, 1990.

(B) The facility capacity authorized in the facility's original hazardous waste facilities permit, grant of interim status, or any state or local agency permit allowing the construction or operation of a facility for the burning of hazardous waste, granted on or after January 1, 1990.

(e) The notice requirements specified in subdivision (b) or (c) shall not preclude a public agency from providing additional notice by other means if the agency so desires, or from providing the public notice required by this section at the same time and in the same manner as public notice otherwise required by law for the project.

§ 21092.1. ADDITION OF NEW INFORMATION; NOTICE AND CONSULTATION

When significant new information is added to an environmental impact report after notice has been given pursuant to Section 21092 and consultation has occurred pursuant to Sections 21104 and 21153, but prior to certification, the public agency shall give notice again pursuant to Section 21092, and consult again pursuant to Sections 21104 and 21153 before certifying the environmental impact report.

§ 21092.2. REQUESTS FOR CERTAIN NOTICES

(a) The notices required pursuant to Sections 21080.4, 21083.9, 21092, 21108, 21152 and 21161 shall be mailed to every person who has filed a written request for notices with either the clerk of the governing body or, if there is no governing body, the director of the agency. If the agency offers to provide the notices by e-mail, upon filing a written request for notices, a person may request that the notices be provided to him or her by e-mail. The request may also be filed with any other person designated by the governing body or director to receive these requests. The agency may require requests for notices to be annually renewed. The public agency may charge a fee, except to other public agencies, that is reasonably related to the costs of providing this service.

(b) Subdivision (a) shall not be construed in any manner that results in the invalidation of an action because of the failure of a person to receive a requested notice, if there has been substantial compliance with the requirements of this section.

(c) The notices required pursuant to Sections 21080.4 and 21161 shall be provided by the State Clearinghouse to any legislator in whose district the project has an environmental impact, if the legislator requests the notice and the State Clearinghouse has received it.

§ 21092.3. POSTING OF CERTAIN NOTICES

The notices required pursuant to Sections 21080.4 and 21092 for an environmental impact report shall be posted in the office of the county clerk of each county in which the project will be located and shall remain posted for a period of 30 days. The notice required pursuant to Section 21092 for a negative declaration shall be so posted for a period of 20 days, unless otherwise required by law to be posted for 30 days. The county clerk shall post the notices within 24 hours of receipt.

§ 21092.4. CONSULTATION WITH TRANSPORTATION PLANNING AGENCIES AND PUBLIC AGENCIES

(a) For a project of statewide, regional, or areawide significance, the lead agency shall consult with transportation planning agencies and public agencies that have transportation facilities within their jurisdictions that could be affected by the project. Consultation shall be conducted in the same manner as for responsible agencies pursuant to this division, and shall be for the purpose of the lead agency obtaining information concerning the project's effect on major local arterials, public transit, freeways, highways, overpasses, on-ramps, off-ramps, and rail transit service within the jurisdiction of a transportation planning agency or a public agency that is consulted by the lead agency. A transportation planning agency or public agency that provides information to the lead agency shall be notified of, and provided with copies of, environmental documents pertaining to the project.

(b) As used in this section, "transportation facilities" includes major local arterials and public transit within five miles of the project site and freeways, highways, overpasses, on-ramps, off-ramps, and rail transit service within 10 miles of the project site.

§ 21092.5. PROPOSED RESPONSE TO PUBLIC AGENCY COMMENTS RECEIVED BY LEAD AGENCY; NOTICE TO AGENCY COMMENTING ON NEGATIVE DECLARATION; UNTIMELY COMMENTS

(a) At least 10 days prior to certifying an environmental impact report, the lead agency shall provide a written proposed response to a public agency on comments made by that agency which conform with the requirements of this division. Proposed responses shall conform with the legal standards established for responses to comments on draft environmental impact reports. Copies of responses or the environmental document in which they are contained, prepared in conformance with other requirements of this division and the guidelines adopted pursuant to Section 21083, may be used to meet the requirements imposed by this section.

(b) The lead agency shall notify any public agency which comments on a negative declaration, of the public hearing or hearings, if any, on the project for which the negative declaration was prepared. If notice to the commenting public agency is provided pursuant to Section 21092, the notice shall satisfy the requirement of this subdivision.

(c) Nothing in this section requires the lead agency to respond to comments not received within the comment periods specified in this division, to reopen comment periods, or to delay acting on a negative declaration or environmental impact report.

§ 21092.6. APPLICATION OF GOVT. C. § 65962.5; DUTIES OF LEAD AGENCY; NOTICE BY ENVIRONMENTAL PROTECTION AGENCY OF FAILURE TO SPECIFY

(a) The lead agency shall consult the lists compiled pursuant to Section 65962.5 of the Government Code to determine whether the project and any alternatives are located on a site which is included on any list. The lead agency shall indicate whether a site is on any list not already identified by the applicant. The lead agency shall specify the list and include the information in the statement required pursuant to subdivision (f) of Section 65962.5 of the Government Code, in the notice required pursuant to Section 21080.4, a negative declaration, and a draft environmental impact report. The requirement in this section to specify any list shall not be construed to limit compliance with this division.

(b) If a project or any alternatives are located on a site which is included on any of the lists compiled pursuant to Section 65962.5 of the Government Code and the lead agency did not accurately specify or did not specify any list pursuant to subdivision (a), the California Environmental Protection Agency shall notify the lead agency specifying any list with the site when it receives notice pursuant to Section 21080.4, a negative declaration, and a draft environmental impact report. The California Environmental Protection Agency shall not be liable for failure to notify the lead agency pursuant to this subdivision.

§ 21093. LEGISLATIVE FINDINGS AND DECLARATION; PUBLIC AGENCIES MAY TIER ENVIRONMENTAL IMPACT REPORTS

(a) The Legislature finds and declares that tiering of environmental impact reports will promote construction of needed housing and other development projects by (1) streamlining regulatory procedures, (2) avoiding repetitive discussions of the same issues in successive environmental impact reports, and (3) ensuring that environmental impact reports prepared for later projects which are consistent with a previously approved policy, plan, program, or ordinance concentrate upon environmental effects which may be mitigated or avoided in connection with the decision on each later project. The Legislature further finds and declares that tiering is appropriate when it helps a public agency to focus upon the issues ripe for decision at each level of environmental review and in order to exclude duplicative analysis of environmental effects examined in previous environmental impact reports.

(b) To achieve this purpose, environmental impact reports shall be tiered whenever feasible, as determined by the lead agency.

§ 21094. LATER PROJECTS; TIERED ENVIRONMENTAL IMPACT REPORTS; INITIAL STUDY; USE OF PRIOR REPORTS

(a) (1) If a prior environmental impact report has been prepared and certified for a program, plan, policy, or ordinance, the lead agency for a later project that meets the requirements of this section shall examine significant effects of the later project upon the environment by using a tiered environmental impact report, except that the report on the later project is not required to examine those effects that the lead agency determines were either of the following:

(A) Mitigated or avoided pursuant to paragraph (1) of subdivision (a) of Section 21081 as a result of the prior environmental impact report.

(B) Examined at a sufficient level of detail in the prior environmental impact report to enable those effects to be mitigated or avoided by site specific revisions, the imposition of conditions, or by other means in connection with the approval of the later project.

(2) If a prior environmental impact report has been prepared and certified for a program, plan, policy, or ordinance, and the lead agency makes a finding of overriding consideration pursuant to subdivision (b) of Section 21081, the lead agency for a later project that uses a tiered environmental impact report from that program, plan, policy, or ordinance may incorporate by reference that finding of overriding consideration if all of the following conditions are met:

(A) The lead agency determines that the project's significant impacts on the environment are not greater than or different from those identified in the prior environmental impact report.

(B) The lead agency incorporates into the later project all the applicable mitigation measures identified by the prior environmental impact report.

(C) The prior finding of overriding considerations was not based on a determination that mitigation measures should be identified and approved in a subsequent environmental review.

(D) The prior environmental impact report was certified not more than three years before the date findings are made pursuant to Section 21081 for the later project.

(E) The lead agency has determined that the mitigation measures or alternatives found to be infeasible in the prior environmental impact report pursuant to paragraph (3) of subdivision (a) of Section 21081 remain infeasible based on the criteria set forth in that section.

(b) This section applies only to a later project that the lead agency determines is all of the following:

(1) Consistent with the program, plan, policy, or ordinance for which an environmental impact report has been prepared and certified.

(2) Consistent with applicable local land use plans and zoning of the city, county, or city and county in which the later project would be located.

(3) Not subject to Section 21166.

(c) For purposes of compliance with this section, an initial study shall be prepared to assist the lead agency in making the determinations required by this section. The initial study shall analyze whether the later project may cause significant effects on the environment that were not examined in the prior environmental impact report.

(d) All public agencies that propose to carry out or approve the later project may utilize the prior environmental impact report and the environmental impact report on the later project to fulfill the requirements of Section 21081.

(e) (1) If a lead agency determines pursuant to this subdivision that a cumulative effect has been adequately addressed in a prior environmental impact report, that cumulative effect is not required to be examined in a later environmental impact report, mitigated negative declaration, or negative declaration for purposes of subparagraph (B) of paragraph (1) of subdivision (a).

(2) When assessing whether there is a new significant cumulative effect, the lead agency shall consider whether the incremental effects of the project are cumulatively considerable.

(3) (A) For purposes of paragraph (2), if the lead agency determines the incremental effects of the project are significant when viewed in connection with the effects of past, present,

and probable future projects, the incremental effects of a project are cumulatively considerable.

(B) If the lead agency determines incremental effects of a project are cumulatively considerable, the later environmental impact report, mitigated negative declaration, or negative declaration shall examine those effects.

(4) If the lead agency makes one of the following determinations, the cumulative effects of a project are adequately addressed for purposes of paragraph (1):

(A) The cumulative effect has been mitigated or avoided as a result of the prior environmental impact report and findings adopted pursuant to paragraph (1) of subdivision (a) of Section 21081 as a result of the prior environmental impact report.

(B) The cumulative effect has been examined at a sufficient level of detail in the prior environmental impact report to enable the effect to be mitigated or avoided by site-specific revisions, the imposition of conditions, or by other means in connection with the approval of the later project.

(f) If tiering is used pursuant to this section, an environmental impact report prepared for a later project shall refer to the prior environmental impact report and state where a copy of the prior environmental impact report may be examined.

(g) This section shall remain in effect only until January 1, 2016, and as of that date is repealed, unless a later enacted statute, that is enacted before January 1, 2016, deletes or extends that date.

§ 21094. [NOT CURRENTLY IN EFFECT]

(a) Where a prior environmental impact report has been prepared and certified for a program, plan, policy, or ordinance, the lead agency for a later project that meets the requirements of this section shall examine significant effects of the later project upon the environment by using a tiered environmental impact report, except that the report on the later project is not required to examine those effects that the lead agency determines were either of the following:

(1) Mitigated or avoided pursuant to paragraph (1) of subdivision (a) of Section 21081 as a result of the prior environmental impact report.

(2) Examined at a sufficient level of detail in the prior environmental impact report to enable those effects to be mitigated or avoided by site-specific revisions, the imposition of conditions, or by other means in connection with the approval of the later project.

(b) This section applies only to a later project that the lead agency determines is all of the following:

(1) Consistent with the program, plan, policy, or ordinance for which an environmental impact report has been prepared and certified.

(2) Consistent with applicable local land use plans and zoning of the city, county, or city and county in which the later project would be located.

(3) Not subject to Section 21166.

(c) For purposes of compliance with this section, an initial study shall be prepared to assist the lead agency in making the determinations required by this section. The initial study shall analyze whether the later project may cause significant effects on the environment that were not examined in the prior environmental impact report.

(d) All public agencies that propose to carry out or approve the later project may utilize the prior environmental impact report and the environmental impact report on the later project to fulfill the requirements of Section 21081.

(e) When tiering is used pursuant to this section, an environmental impact report prepared for a later project shall refer to the prior environmental impact report and state where a copy of the prior environmental impact report may be examined.

(f) This section shall become operative on January 1, 2016.

§ 21094.5.

(a) (1) If an environmental impact report was certified for a planning level decision of a city or county, the application of this division to the approval of an infill project shall be limited to the effects on the environment that (A) are specific to the project or to the project site and were not addressed as significant effects in the prior environmental impact report or (B) substantial new information shows the effects will be more significant than described in the prior environmental impact report. A lead agency's determination pursuant to this section shall be supported by substantial evidence.

(2) An effect of a project upon the environment shall not be considered a specific effect of the project or a significant effect that was not considered significant in a prior environmental impact report, or an effect that is more significant than was described in the prior environmental impact report if uniformly applicable development policies or standards adopted by the city, county, or the lead agency, would apply to the project and the lead agency makes a finding, based upon substantial evidence, that the development policies or standards will substantially mitigate that effect.

(b) If an infill project would result in significant effects that are specific to the project or the project site, or if the significant effects of the infill project were not addressed in the prior environmental impact report, or are more significant than the effects addressed in the prior environmental impact report, and if a mitigated negative declaration or a sustainable communities environmental assessment could not be otherwise adopted, an environmental impact report prepared for the project analyzing those effects shall be limited as follows:

(1) Alternative locations, densities, and building intensities to the project need not be considered.

(2) Growth inducing impacts of the project need not be considered.

(c) This section applies to an infill project that satisfies both of the following:

(1) The project satisfies any of the following:

(A) Is consistent with the general use designation, density, building intensity, and applicable policies specified for the project area in either a sustainable communities strategy or an alternative planning strategy for which the State Air Resources Board, pursuant to subparagraph (H) of paragraph (2) of subdivision (b) of Section 65080 of the Government Code, has accepted a metropolitan planning organization's determination that the sustainable communities strategy or the alternative planning strategy would, if implemented, achieve the greenhouse gas emission reduction targets.

(B) Consists of a small walkable community project located in an area designated by a city for that purpose.

(C) Is located within the boundaries of a metropolitan planning organization that has not yet adopted a sustainable communities strategy or alternative planning strategy, and the project has a residential density of at least 20 units per acre or a floor area ratio of at least 0.75.

(2) Satisfies all applicable statewide performance standards contained in the guidelines adopted pursuant to Section 21094.5.5.

(d) This section applies after the Secretary of the Natural Resources Agency adopts and certifies the guidelines establishing statewide standards pursuant to Section 21094.5.5.

(e) For the purposes of this section, the following terms mean the following:

(1) "Infill project" means a project that meets the following conditions:

(A) Consists of any one, or combination, of the following uses:

(i) Residential.

(ii) Retail or commercial, where no more than one-half of the project area is used for parking.

(iii) A transit station.

(iv) A school.

(v) A public office building.

(B) Is located within an urban area on a site that has been previously developed, or on a vacant site where at least 75 percent of the perimeter of the site adjoins, or is separated only by an improved public right-of-way from, parcels that are developed with qualified urban uses.

(2) "Planning level decision" means the enactment or amendment of a general plan, community plan, specific plan, or zoning code.

(3) "Prior environmental impact report" means the environmental impact report certified for a planning level decision, as supplemented by any subsequent or supplemental environmental impact reports, negative declarations, or addenda to those documents.

(4) "Small walkable community project" means a project that is in an incorporated city, which is not within the boundary of a metropolitan planning organization and that satisfies the following requirements:

(A) Has a project area of approximately one-quarter mile diameter of contiguous land completely within the existing incorporated boundaries of the city.

(B) Has a project area that includes a residential area adjacent to a retail downtown area.

(C) The project has a density of at least eight dwelling units per acre or a floor area ratio for retail or commercial use of not less than 0.50.

(5) "Urban area" includes either an incorporated city or an unincorporated area that is completely surrounded by one or more incorporated cities that meets both of the following criteria:

(A) The population of the unincorporated area and the population of the surrounding incorporated cities equal a population of 100,000 or more.

(B) The population density of the unincorporated area is equal to, or greater than, the population density of the surrounding cities.

§ 21094.5.5.

(a) On or before July 1, 2012, the Office of Planning and Research shall prepare, develop, and transmit to the Natural Resources Agency for certification and adoption guidelines for the implementation of Section 21094.5 and the Secretary of the Natural Resources Agency, on or before January 1, 2013, shall certify and adopt the guidelines.

(b) The guidelines prepared pursuant to this section shall include statewide standards for infill projects that may be amended from time to time and promote all of the following:

(1) The implementation of the land use and transportation policies in the Sustainable Communities and Climate Protection Act of 2008 (Chapter 728 of the Statutes of 2008).

(2) The state planning priorities specified in Section 65041.1 of the Government Code and in the most recently adopted Environmental Goals and Policy Report issued by the Office of Planning and Research supporting infill development.

(3) The reduction of greenhouse gas emissions under the California Global Warming Solutions Act of 2006 (Division 25.5 (commencing with Section 38500) of the Health and Safety Code).

(4) The reduction in per capita water use pursuant to Section 10608.16 of the Water Code.

(5) The creation of a transit village development district consistent with Section 65460.1 of the Government Code.

(6) Substantial energy efficiency improvements, including improvements to projects related to transportation energy.

(7) Protection of public health, including the health of vulnerable populations from air or water pollution, or soil contamination.

(c) The standards for projects on infill sites shall be updated as frequently as necessary to ensure the protection of the environment.

§ 21095. AMENDMENT TO STATE GUIDELINES TO PROVIDE OPTIONAL METHODOLOGY TO EVALUATE ENVIRONMENTAL EFFECTS OF AGRICULTURAL LAND CONVERSIONS

(a) The Resources Agency, in consultation with the Office of Planning and Research, shall develop an amendment to Appendix G of the state guidelines, for adoption pursuant to Section 21083, to provide lead agencies an optional methodology to ensure that significant effects on the environment of agricultural land conversions are quantitatively and consistently considered in the environmental review process.

(b) The Department of Conservation, in consultation with the United States Department of Agriculture pursuant to Section 658.6 of Title 7 of the Code of Federal Regulations, and in consultation with the Resources Agency and the Office of Planning and Research, shall develop a state model land evaluation and site assessment system, contingent upon the availability of funding from non-General Fund sources. The department shall seek funding for that purpose from non-General Fund sources, including, but not limited to, the United States Department of Agriculture.

(c) In lieu of developing an amendment to Appendix G of the state guidelines pursuant to subdivision (a), the Resources Agency may adopt the state model land evaluation and site assessment system developed pursuant to subdivision (b) as that amendment to Appendix G.

§ 21096. AIRPORT-RELATED SAFETY HAZARDS AND NOISE PROBLEMS; PROJECTS WITHIN AIRPORT COMPREHENSIVE LAND USE PLAN BOUNDARIES OR WITHIN TWO NAUTICAL MILES OF AIRPORT; PREPARATION OF ENVIRONMENTAL IMPACT REPORTS

(a) If a lead agency prepares an environmental impact report for a project situated within airport land use compatibility plan boundaries, or, if an airport land use compatibility plan has not been adopted, for a project within two nautical miles of a public airport or public use airport, the Airport Land Use Planning Handbook published by the Division of Aeronautics of the Department of Transportation, in compliance with Section 21674.5 of the Public Utilities Code and other documents, shall be utilized as technical resources to assist in the preparation of the environmental impact report as the report relates to airport-related safety hazards and noise problems.

(b) A lead agency shall not adopt a negative declaration for a project described in subdivision (a) unless the lead agency considers whether the project will result in a safety hazard or noise problem for persons using the airport or for persons residing or working in the project area.

§ 21097. [DELETED]

§ 21098. LOW-LEVEL FLIGHT PATH; MILITARY IMPACT ZONE; SPECIAL USE AIRSPACE

(a) For the purposes of this section, the following terms have the following meanings:

(1) "Low-level flight path" includes any flight path for any aircraft owned, maintained, or that is under the jurisdiction of the United States Department of Defense that flies lower than 1,500 feet above ground level, as indicated in the United States Department of Defense Flight Information Publication, "Area Planning Military Training Routes: North and South America (AP/1B)" published by the United States National Imagery and Mapping Agency.

(2) "Military impact zone" includes any area, including airspace, that meets both of the following criteria:

(A) Is within two miles of a military installation, including, but not limited to, any base, military airport, camp, post, station, yard, center, homeport facility for a ship, or any other military activity center that is under the jurisdiction of the United States Department of Defense.

(B) Covers greater than 500 acres of unincorporated land, or greater than 100 acres of city incorporated land.

(3) "Military service" means any branch of the United States Armed Forces.

(4) "Special use airspace" means the land area underlying the airspace that is designated for training, research, development, or evaluation for a military service, as that land area is established by the United States Department of Defense Flight Information Publication, "Area Planning: Special Use Airspace: North and South America (AP/1A)" published by the United States National Imagery and Mapping Agency.

(b) If the United States Department of Defense or a military service notifies a lead agency of the contact office and address for the military service and the specific boundaries of a low-level flight path, military impact zone, or special use airspace, the lead agency shall submit notices, as required pursuant to Sections 21080.4 and 21092, to the military service if the project is within those boundaries and any of the following apply:

(1) The project includes a general plan amendment.

(2) The project is of statewide, regional, or areawide significance.

(3) The project is required to be referred to the airport land use commission, or appropriately designated body, pursuant to Article 3.5 (commencing with Section 21670) of Chapter 4 of Part 1 of Division 9 of the Public Utilities Code.

(c) The requirement to submit notices imposed by this section does not apply to any of the following:

(1) Response actions taken pursuant to Chapter 6.8 (commencing with Section 25300) of Division 20 of the Health and Safety Code.

(2) Response actions taken pursuant to Chapter 6.85 (commencing with Section 25396) of Division 20 of the Health and Safety Code.

(3) Sites subject to corrective action orders issued pursuant to Section 25187 of the Health and Safety Code.

(d) (1) The effect or potential effect that a project may have on military activities does not itself constitute an adverse effect on the environment for the purposes of this division.

(2) Notwithstanding paragraph (1), a project's impact on military activities may cause, or be associated with, adverse effects on the environment that are subject to the requirements of this division, including, but not limited to, Section 21081.

Chapter 2.7: Modernization of Transportation Analysis for Transit-Oriented Infill Projects

§ 21099.

(a) For purposes of this section, the following terms mean the following:

(1) "Employment center project" means a project located on property zoned for commercial uses with a floor area ratio of no less than 0.75 and that is located within a transit priority area.

(2) "Floor area ratio" means the ratio of gross building area of the development, excluding structured parking areas, proposed for the project divided by the net lot area.

(3) "Gross building area" means the sum of all finished areas of all floors of a building included within the outside faces of its exterior walls.

(4) "Infill site" means a lot located within an urban area that has been previously developed, or on a vacant site where at least 75 percent of the perimeter of the site adjoins, or is separated only by an improved public right-of-way from, parcels that are developed with qualified urban uses.

(5) "Lot" means all parcels utilized by the project.

(6) "Net lot area" means the area of a lot, excluding publicly dedicated land and private streets that meet local standards, and other public use areas as determined by the local land use authority.

(7) "Transit priority area" means an area within one-half mile of a major transit stop that is existing or planned, if the planned stop is scheduled to be completed within the planning horizon included in a Transportation Improvement Program adopted pursuant to Section 450.216 or 450.322 of Title 23 of the Code of Federal Regulations.

(b) (1) The Office of Planning and Research shall prepare, develop, and transmit to the Secretary of the Natural Resources Agency for certification and adoption proposed revisions to the guidelines adopted pursuant to Section 21083 establishing criteria for determining the significance of transportation impacts of projects within transit priority areas. Those criteria shall promote the reduction of greenhouse gas emissions, the development of multimodal transportation networks, and a diversity of land uses. In developing the criteria, the office shall recommend potential metrics to measure transportation impacts that may include, but are not limited to, vehicle miles traveled, vehicle miles traveled per capita, automobile trip generation rates, or automobile trips generated. The office may also establish criteria for models used to analyze transportation impacts to ensure the models are accurate, reliable, and consistent with the intent of this section.

(2) Upon certification of the guidelines by the Secretary of the Natural Resources Agency pursuant to this section, automobile delay, as described solely by level of service or similar measures of vehicular capacity or traffic congestion shall not be considered a significant impact on the environment pursuant to this division, except in locations specifically identified in the guidelines, if any.

(3) This subdivision does not relieve a public agency of the requirement to analyze a project's potentially significant transportation impacts related to air quality, noise, safety, or any other impact associated with transportation. The methodology established by these guidelines shall not create a presumption that a project will not result in significant impacts related to air quality, noise, safety, or any other impact associated with transportation. Notwithstanding the foregoing, the adequacy of parking for a project shall not support a finding of significance pursuant to this section.

(4) This subdivision does not preclude the application of local general plan policies, zoning codes, conditions of approval, thresholds, or any other planning requirements pursuant to the police power or any other authority.

(5) On or before July 1, 2014, the Office of Planning and Research shall circulate a draft revision prepared pursuant to paragraph (1).

(c) (1) The Office of Planning and Research may adopt guidelines pursuant to Section 21083 establishing alternative metrics to the metrics used for traffic levels of service for transportation impacts outside transit priority areas. The alternative metrics may include the retention of traffic levels of service, where appropriate and as determined by the office.

(2) This subdivision shall not affect the standard of review that would apply to the new guidelines adopted pursuant to this section.

(d) (1) Aesthetic and parking impacts of a residential, mixed-use residential, or employment center project on an infill site within a transit priority area shall not be considered significant impacts on the environment.

(2) (A) This subdivision does not affect, change, or modify the authority of a lead agency to consider aesthetic impacts pursuant to local design review ordinances or other discretionary powers provided by other laws or policies.

(B) For the purposes of this subdivision, aesthetic impacts do not include impacts on historical or cultural resources.

(e) This section does not affect the authority of a public agency to establish or adopt thresholds of significance that are more protective of the environment.

Chapter 3: State Agencies, Boards and Commissions

§ 21100. ENVIRONMENTAL IMPACT REPORT ON PROPOSED STATE PROJECTS; SIGNIFICANT EFFECT; CUMULATIVE IMPACT ANALYSIS

(a) All lead agencies shall prepare, or cause to be prepared by contract, and certify the completion of, an environmental impact report on any project which they propose to carry out or approve that may have a significant effect on the environment. Whenever feasible, a standard format shall be used for environmental impact reports.

(b) The environmental impact report shall include a detailed statement setting forth all of the following:

(1) All significant effects on the environment of the proposed project.

(2) In a separate section:

(A) Any significant effect on the environment that cannot be avoided if the project is implemented.

(B) Any significant effect on the environment that would be irreversible if the project is implemented.

(3) Mitigation measures proposed to minimize significant effects on the environment, including, but not limited to, measures to reduce the wasteful, inefficient, and unnecessary consumption of energy.

(4) Alternatives to the proposed project.

(5) The growth-inducing impact of the proposed project.

(c) The report shall also contain a statement briefly indicating the reasons for determining that various effects on the environment of a project are not significant and consequently have not been discussed in detail in the environmental impact report.

(d) For purposes of this section, any significant effect on the environment shall be limited to substantial, or potentially substantial, adverse changes in physical conditions which exist within the area as defined in Section 21060.5.

(e) Previously approved land use documents, including, but not limited to, general plans, specific plans, and local coastal plans, may be used in cumulative impact analysis.

§ 21100.1. INFORMATION REQUIRED IN CERTAIN ENVIRONMENTAL IMPACT REPORTS

The information described in subparagraph (B) of paragraph (2) of subdivision (b) of Section 21100 shall be required only in environmental impact reports prepared in connection with the following:

(a) The adoption, amendment, or enactment of a plan, policy, or ordinance of a public agency.

(b) The adoption by a local agency formation commission of a resolution making determinations.

(c) A project which will be subject to the requirement for preparing an environmental impact statement pursuant to the requirements of the National Environmental Policy Act of 1969.

§ 21100.2. LEASES, PERMITS, LICENSES, CERTIFICATES AND OTHER ENTITLEMENTS; ESTABLISHMENT OF TIME LIMITS FOR IMPACT REPORTS AND NEGATIVE DECLARATIONS

(a) (1) For projects described in subdivision (c) of Section 21065, each state agency shall establish, by resolution or order, time limits that do not exceed the following:

(A) One year for completing and certifying environmental impact reports.

(B) One hundred eighty days for completing and adopting negative declarations.

(2) The time limits specified in paragraph (1) shall apply only to those circumstances in which the state agency is the lead agency for a project. These resolutions or orders may establish different time limits for different types or classes of projects, but all limits shall be measured from the date on which an application requesting approval of the project is received and accepted as complete by the state agency.

(3) No application for a project may be deemed incomplete for lack of a waiver of time periods prescribed in state regulations.

(4) The resolutions or orders required by this section may provide for a reasonable extension of the time period in the event that compelling circumstances justify additional time and the project applicant consents thereto.

(b) If a draft environmental impact report, environmental impact report, or focused environmental impact report is prepared under a contract to a state agency, the contract shall be executed within 45 days from the date on which the state agency sends a notice of preparation pursuant to Section 21080.4. The state agency may take longer to execute the contract if the project applicant and the state agency mutually agree to an extension of the time limit provided by this subdivision.

(c) (1) A public agency may establish a process that would allow an applicant for a natural gas pipeline safety enhancement activity to elect to pay additional fees to be used by the public agency in determining whether to approve a natural gas pipeline safety enhancement activity by entering into a contract with one or more third parties to assist the public agency to perform the analysis, consistent with Article VII of the California Constitution and Section 19130 of the Government Code and the charter of a chartered city or county, as applicable. The public agency may, but is not required to, offer an applicant the option to pay those fees and subject a project to this process.

(2) All fees paid by a natural gas pipeline safety enhancement activity applicant shall be used exclusively for analysis of that applicant's application for certification.

(3) For purposes of this section, "natural gas pipeline safety enhancement activity" has the same meaning as defined in paragraph (1) of subdivision (d) of Section 21080.21.

(d) This section shall remain in effect only until January 1, 2018, and as of that date is repealed, unless a later enacted statute, that is enacted before January 1, 2018, deletes or extends that date.

§ 21100.2. [NOT CURRENTLY IN EFFECT]

(a) (1) For projects described in subdivision (c) of Section 21065, each state agency shall establish, by resolution or order, time limits that do not exceed the following:

(A) One year for completing and certifying environmental impact reports.

(B) One hundred eighty days for completing and adopting negative declarations.

(2) The time limits specified in paragraph (1) shall apply only to those circumstances in which the state agency is the lead agency for a project. These resolutions or orders may establish different time limits for different types or classes of projects, but all limits shall be measured from the date on which an application requesting approval of the project is received and accepted as complete by the state agency.

(3) No application for a project may be deemed incomplete for lack of a waiver of time periods prescribed in state regulations.

(4) The resolutions or orders required by this section may provide for a reasonable extension of the time period in the event that compelling circumstances justify additional time and the project applicant consents thereto.

(b) If a draft environmental impact report, environmental impact report, or focused environmental impact report is prepared under a contract to a state agency, the contract shall be executed within 45 days from the date on which the state agency sends a notice of preparation pursuant to Section 21080.4. The state agency may take longer to execute the contract if the project applicant and the state agency mutually agree to an extension of the time limit provided by this subdivision.

(c) This section shall become operative January 1, 2018.

§ 21101. ENVIRONMENTAL IMPACT REPORT ON PROPOSED FEDERAL PROJECTS

In regard to any proposed federal project in this state which may have a significant effect on the environment and on which the state officially comments, the state officials responsible for such comments shall include in their report a detailed statement setting forth the matters specified in Section 21100 prior to transmitting the comments of the state to the federal government. No report shall be transmitted to the federal government unless it includes such a detailed statement as to the matters specified in Section 21100.

§ 21102. REQUEST FOR OR AUTHORIZATION OF EXPENDITURE OF FUNDS; STATEMENT OF EFFECT ON ENVIRONMENT

No state agency, board, or commission shall request funds, nor shall any state agency, board, or commission which authorizes expenditures of funds, other than funds appropriated in the Budget Act, authorize funds for expenditure for any project, other than a project involving only feasibility or planning studies for possible future actions which the agency, board, or commission has not approved, adopted or funded, which may have a significant effect on the environment unless such request or authorization is accompanied by an environmental impact report. Feasibility and planning studies exempted by this section from the preparation of an environmental impact report shall nevertheless include consideration of environmental factors.

§ 21104. STATE LEAD AGENCY; CONSULTATIONS PRIOR TO COMPLETION OF IMPACT REPORT

(a) Prior to completing an environmental impact report, the state lead agency shall consult with, and obtain comments from, each responsible agency, trustee agency, any public agency that has jurisdiction by law with respect to the project, and any city or county that borders on a city or county within which the project is located unless otherwise designated annually by agreement between the state lead agency and the city or county, and may consult with any person who has special expertise with respect to any environmental impact involved. In the case of a project described in subdivision (c) of Section 21065, the state lead agency shall, upon the request of the applicant, provide for early consultation to identify the range of actions, alternatives, mitigation measures, and significant effects to be analyzed in depth in the environmental impact report. The state lead agency may consult with persons identified by the applicant who the applicant believes will be concerned with the environmental effects of the project and may consult with members of the public who have made a written request to be consulted on the project. A request by the applicant for early consultation shall be made not later than 30 days after the determination required by Section 21080.1 with respect to the project.

(b) The state lead agency shall consult with, and obtain comments from, the State Air Resources Board in preparing an environmental impact report on a highway or freeway project, as to the air pollution impact of the potential vehicular use of the highway or freeway.

(c) A responsible agency or other public agency shall only make substantive comments regarding those activities involved in a project that are within an area of expertise of the agency or that are required to be carried out or approved by the agency. Those comments shall be supported by specific documentation.

§ 21104.2. CONSULTATION AND FINDINGS; EFFECT OF PROJECTS ON THREATENED OR ENDANGERED SPECIES

The state lead agency shall consult with, and obtain written findings from, the Department of Fish and Game in preparing an environmental impact report on a project, as to the impact of the project on the continued existence of any endangered species or threatened species pursuant to Article 4 (commencing with Section 2090) of Chapter 1.5 of Division 3 of the Fish and Game Code.

§ 21105. ENVIRONMENTAL IMPACT REPORT AND COMMENTS AS PART OF REGULAR PROJECT REPORT; AVAILABILITY TO LEGISLATURE AND GENERAL PUBLIC

The state lead agency shall include the environmental impact report as a part of the regular project report used in the existing review and budgetary process. It shall be available to the Legislature. It shall also be available for inspection by any member of the general public, who may secure a copy thereof by paying for the actual cost of such a copy. It shall be filed by the state lead agency with the appropriate local planning agency of any city, county, or city and county which will be affected by the project.

§ 21106. REQUEST OF FUNDS TO PROTECT ENVIRONMENT

All state agencies, boards, and commissions shall request in their budgets the funds necessary to protect the environment in relation to problems caused by their activities.

§ 21108. STATE AGENCY, BOARD OR COMMISSION; APPROVAL OF DETERMINATION TO CARRY OUT PROJECT; NOTICE; CONTENTS; PUBLIC INSPECTION; POSTING

(a) If a state agency approves or determines to carry out a project that is subject to this division, the state agency shall file notice of that approval or that determination with the Office of Planning and Research. The notice shall identify the person or persons in subdivision (b) or (c) of Section 21065, as reflected in the agency's record of proceedings, and indicate the

determination of the state agency whether the project will, or will not, have a significant effect on the environment and shall indicate whether an environmental impact report has been prepared pursuant to this division.

(b) If a state agency determines that a project is not subject to this division pursuant to subdivision (b) of Section 21080 or Section 21172, and the state agency approves or determines to carry out the project, the state agency or the person specified in subdivision (b) or (c) of Section 21065 may file notice of the determination with the Office of Planning and Research. A notice filed pursuant to this subdivision shall identify the person or persons in subdivision (b) or (c) of Section 21065, as reflected in the agency's record of proceedings. A notice filed pursuant to this subdivision by a person specified in subdivision (b) or (c) of Section 21065 shall have a certificate of determination attached to it issued by the state agency responsible for making the determination that the project is not subject to this division pursuant to subdivision (b) of Section 21080 or pursuant to Section 21172. The certificate of determination may be in the form of a certified copy of an existing document or record of the state agency.

(c) A notice filed pursuant to this section shall be available for public inspection, and a list of these notices shall be posted on a weekly basis in the Office of Planning and Research. Each list shall remain posted for a period of 30 days. The Office of Planning and Research shall retain each notice for not less than 12 months.

Chapter 4: Local Agencies

§ 21150. ENVIRONMENTAL IMPACT REPORT REQUIRED BEFORE ALLOCATION OF STATE OR FEDERAL FUNDS

State agencies, boards, and commissions, responsible for allocating state or federal funds on a project-by-project basis to local agencies for any project which may have a significant effect on the environment, shall require from the responsible local governmental agency a detailed statement setting forth the matters specified in Section 21100 prior to the allocation of any funds other than funds solely for projects involving only feasibility or planning studies for possible future actions which the agency, board, or commission has not approved, adopted, or funded.

§ 21151. LOCAL AGENCIES; PREPARATION AND COMPLETION OF IMPACT REPORT; SUBMISSION AS PART OF GENERAL PLAN REPORT; SIGNIFICANT EFFECT

(a) All local agencies shall prepare, or cause to be prepared by contract, and certify the completion of, an environmental impact report on any project that they intend to carry out or approve which may have a significant effect on the environment. When a report is required by Section 65402 of the Government Code, the environmental impact report may be submitted as a part of that report.

(b) For purposes of this section, any significant effect on the environment shall be limited to substantial, or potentially substantial, adverse changes in physical conditions which exist within the area as defined in Section 21060.5.

(c) If a nonelected decision-making body of a local lead agency certifies an environmental impact report, approves a negative declaration or mitigated negative declaration, or determines that a project is not subject to this division, that certification, approval, or determination may be appealed to the agency's elected decision-making body, if any.

§ 21151.1. WASTE-BURNING PROJECTS; LAND DISPOSAL FACILITIES, AND OFFSITE LARGE TREATMENT FACILITIES; ENVIRONMENTAL IMPACT REPORTS; APPLICATION OF SECTION; EXEMPTIONS; OFFSITE FACILITY DEFINED

(a) Notwithstanding paragraph (6) of subdivision (b) of Section 21080, or Section 21080.5 or 21084, or any other provision of law, except as provided in this section, a lead agency shall prepare or cause to be prepared by contract, and certify the completion of, an environmental impact report or, if appropriate, a modification, addendum, or supplement to an existing environmental impact report, for a project involving any of the following:

(1) The burning of municipal wastes, hazardous waste, or refuse-derived fuel, including, but not limited to, tires, if the project is either of the following:

(A) The construction of a new facility.

(B) The expansion of an existing facility that burns hazardous waste that would increase its permitted capacity by more than 10 percent.

(2) The initial issuance of a hazardous waste facilities permit to a land disposal facility, as defined in subdivision (d) of Section 25199.1 of the Health and Safety Code.

(3) The initial issuance of a hazardous waste facilities permit pursuant to Section 25200 of the Health and Safety Code to an offsite large treatment facility, as defined pursuant to subdivision (d) of Section 25205.1 of the Health and Safety Code.

(4) A base reuse plan as defined in Section 21083.8.1. The Legislature hereby finds that no reimbursement is required pursuant to Section 6 of Article XIII_B of the California Constitution for an environmental impact report for a base reuse plan if an environmental impact report is otherwise required for that base reuse plan pursuant to any other provision of this division.

(b) For purposes of clause (ii) of subparagraph (A) of paragraph (1) of subdivision (a), the amount of expansion of an existing facility shall be calculated by comparing the proposed facility capacity with whichever of the following is applicable:

(1) The facility capacity authorized in the facility's hazardous waste facilities permit pursuant to Section 25200 of the Health and Safety Code or its grant of interim status pursuant to Section 25200.5 of the Health and Safety Code, or the facility capacity authorized in a state or local agency permit allowing the construction or operation of a facility for the burning of hazardous waste, granted before January 1, 1990.

(2) The facility capacity authorized in the facility's original hazardous waste facilities permit, grant of interim status, or a state or local agency permit allowing the construction or operation of a facility for the burning of hazardous waste, granted on or after January 1, 1990.

(c) For purposes of paragraphs (2) and (3) of subdivision (a), the initial issuance of a hazardous waste facilities permit does not include the issuance of a closure or postclosure permit pursuant to Chapter 6.5 (commencing with Section 25100) of Division 20 of the Health and Safety Code.

(d) Paragraph (1) of subdivision (a) does not apply to a project that does any of the following:

(1) Exclusively burns digester gas produced from manure or any other solid or semisolid animal waste.

(2) Exclusively burns methane gas produced from a disposal site, as defined in Section 40122, that is used only for the disposal of solid waste, as defined in Section 40191.

(3) Exclusively burns forest, agricultural, wood, or other biomass wastes.

(4) Exclusively burns hazardous waste in an incineration unit that is transportable and that is either at a site for not longer than three years or is part of a remedial or removal action. For purposes of this paragraph, "transportable" means any equipment that performs a

"treatment" as defined in Section 66216 of Title 22 of the California Code of Regulations, and that is transported on a vehicle as defined in Section 66230 of Title 22 of the California Code of Regulations, as those sections read on June 1, 1991.

(5) Exclusively burns refinery waste in a flare on the site of generation.

(6) Exclusively burns in a flare methane gas produced at a municipal sewage treatment plant.

(7) Exclusively burns hazardous waste, or exclusively burns hazardous waste as a supplemental fuel, as part of a research, development, or demonstration project that, consistent with federal regulations implementing the Resource Conservation and Recovery Act of 1976, as amended (42 U.S.C. Sec. 6901 et seq.), has been determined to be innovative and experimental by the Department of Toxic Substances Control and that is limited in type and quantity of waste to that necessary to determine the efficacy and performance capabilities of the technology or process. However, a facility that operated as a research, development, or demonstration project and for which an application is thereafter submitted for a hazardous waste facility permit for operation other than as a research, development, or demonstration project shall be considered a new facility for the burning of hazardous waste and shall be subject to subdivision (a) of Section 21151.1.

(8) Exclusively burns soils contaminated only with petroleum fuels or the vapors from these soils.

(9) Exclusively treats less than 3,000 pounds of hazardous waste per day in a thermal processing unit operated in the absence of open flame, and submits a worst-case health risk assessment of the technology to the Department of Toxic Substances Control for review and distribution to the interested public. This assessment shall be prepared in accordance with guidelines set forth in the Air Toxics Assessment Manual of the California Air Pollution Control Officers Association.

(10) Exclusively burns less than 1,200 pounds per day of medical waste, as defined in Section 117690 of the Health and Safety Code, on hospital sites.

(11) Exclusively burns chemicals and fuels as part of firefighter training.

(12) Exclusively conducts open burns of explosives subject to the requirements of the air pollution control district or air quality management district and in compliance with OSHA and Cal-OSHA regulations.

(13) Exclusively conducts onsite burning of less than 3,000 pounds per day of fumes directly from a manufacturing or commercial process.

(14) Exclusively conducts onsite burning of hazardous waste in an industrial furnace that recovers hydrogen chloride from the flue gas if the hydrogen chloride is subsequently sold, distributed in commerce, or used in a manufacturing process at the site where the hydrogen chloride is recovered, and the burning is in compliance with the requirements of the air pollution control district or air quality management district and the Department of Toxic Substances Control.

(e) Paragraph (1) of subdivision (a) does not apply to a project for which the State Energy Resources Conservation and Development Commission has assumed jurisdiction under Chapter 6 (commencing with Section 25500) of Division 15.

(f) Paragraphs (2) and (3) of subdivision (a) do not apply if the facility only manages hazardous waste that is identified or listed pursuant to Section 25140 or 25141 of the Health and Safety Code on or after January 1, 1992, but not before that date, or only conducts activities that are regulated pursuant to Chapter 6.5 (commencing with Section 25100) of Division 20 of the Health and Safety Code on or after January 1, 1992, but not before that date.

(g) This section does not exempt a project from any other requirement of this division.

(h) For purposes of this section, offsite facility means a facility that serves more than one generator of hazardous waste.

§ 21151.2. SCHOOL SITE PROPOSED ACQUISITION OR ADDITION; NOTICE TO PLANNING COMMISSION; INVESTIGATION; REPORT

To promote the safety of pupils and comprehensive community planning the governing board of each school district before acquiring title to property for a new school site or for an addition to a present school site, shall give the planning commission having jurisdiction notice in writing of the proposed acquisition. The planning commission shall investigate the proposed site and within 30 days after receipt of the notice shall submit to the governing board a written report of the investigation and its recommendations concerning acquisition of the site.

The governing board shall not acquire title to the property until the report of the planning commission has been received. If the report does not favor the acquisition of the property for a school site, or for an addition to a present school site, the governing board of the school district shall not acquire title to the property until 30 days after the commission's report is received.

§ 21151.4. CONSTRUCTION OR ALTERATION OF FACILITY WITHIN ONE-FOURTH OF A MILE OF SCHOOL; REASONABLE ANTICIPATION OF AIR EMISSION OR HANDLING OF HAZARDOUS OR ACUTELY HAZARDOUS MATERIAL; APPROVAL OF ENVIRONMENTAL IMPACT REPORT OR NEGATIVE DECLARATION

(a) An environmental impact report shall not be certified or a negative declaration shall not be approved for any project involving the construction or alteration of a facility within one-fourth of a mile of a school that might reasonably be anticipated to emit hazardous air emissions, or that would handle an extremely hazardous substance or a mixture containing extremely hazardous substances in a quantity equal to or greater than the state threshold quantity specified pursuant to subdivision (j) of Section 25532 of the Health and Safety Code, that may pose a health or safety hazard to persons who would attend or would be employed at the school, unless both of the following occur:

  (1) The lead agency preparing the environmental impact report or negative declaration has consulted with the school district having jurisdiction regarding the potential impact of the project on the school.

  (2) The school district has been given written notification of the project not less than 30 days prior to the proposed certification of the environmental impact report or approval of the negative declaration.

(b) As used in this section, the following definitions apply:

  (1) "Extremely hazardous substance" means an extremely hazardous substance as defined pursuant to paragraph (2) of subdivision (g) of Section 25532 of the Health and Safety Code.

  (2) "Hazardous air emissions" means emissions into the ambient air of air contaminants that have been identified as a toxic air contaminant by the State Air Resources Board or by the air pollution control officer for the jurisdiction in which the project is located. As determined by the air pollution control officer, hazardous air emissions also means emissions into the ambient air of a substance identified in subdivisions (a) to (f), inclusive, of Section 44321 of the Health and Safety Code.

§ 21151.5. TIME LIMITS FOR PREPARATION OF ENVIRONMENTAL IMPACT REPORTS AND NEGATIVE DECLARATIONS

(a) (1) For projects described in subdivision (c) of Section 21065, each local agency shall establish, by ordinance or resolution, time limits that do not exceed the following:

(A) One year for completing and certifying environmental impact reports.

(B) One hundred eighty days for completing and adopting negative declarations.

(2) The time limits specified in paragraph (1) shall apply only to those circumstances in which the local agency is the lead agency for a project. These ordinances or resolutions may establish different time limits for different types or classes of projects and different types of environmental impact reports, but all limits shall be measured from the date on which an application requesting approval of the project is received and accepted as complete by the local agency.

(3) No application for a project may be deemed incomplete for lack of a waiver of time periods prescribed by local ordinance or resolution.

(4) The ordinances or resolutions required by this section may provide for a reasonable extension of the time period in the event that compelling circumstances justify additional time and the project applicant consents thereto.

(b) If a draft environmental impact report, environmental impact report, or focused environmental impact report is prepared under a contract to a local agency, the contract shall be executed within 45 days from the date on which the local agency sends a notice of preparation pursuant to Section 21080.4. The local agency may take longer to execute the contract if the project applicant and the local agency mutually agree to an extension of the time limit provided by this subdivision.

§ 21151.7. PREPARATION AND CERTIFICATION OF COMPLETION OF ENVIRONMENTAL IMPACT REPORT FOR OPEN-PIT MINING OPERATION BY LEAD AGENCY

Notwithstanding any other provision of law, a lead agency shall prepare or cause to be prepared by contract, and certify the completion of, an environmental impact report for any open-pit mining operation which is subject to the permit requirements of the Surface Mining and Reclamation Act of 1975 (Chapter 9 (commencing with Section 2710) of Division 2) and utilizes a cyanide heap-leaching process for the purpose of producing gold or other precious metals.

§ 21151.8. SCHOOLSITE ACQUISITION OR CONSTRUCTION; APPROVAL OF ENVIRONMENTAL IMPACT REPORT OR NEGATIVE DECLARATION; CONDITIONS

(a) An environmental impact report shall not be certified or a negative declaration shall not be approved for a project involving the purchase of a schoolsite or the construction of a new elementary or secondary school by a school district unless all of the following occur:

(1) The environmental impact report or negative declaration includes information that is needed to determine if the property proposed to be purchased, or to be constructed upon, is any of the following:

(A) The site of a current or former hazardous waste disposal site or solid waste disposal site and, if so, whether the wastes have been removed.

(B) A hazardous substance release site identified by the Department of Toxic Substances Control in a current list adopted pursuant to Section 25356 of the Health and Safety Code for removal or remedial action pursuant to Chapter 6.8 (commencing with Section 25300) of Division 20 of the Health and Safety Code.

(C) A site that contains one or more pipelines, situated underground or aboveground, that carries hazardous substances, extremely hazardous substances, or hazardous wastes, unless the pipeline is a natural gas line that is used only to supply natural gas to that school or neighborhood, or other nearby schools.

(D) A site that is within 500 feet of the edge of the closest traffic lane of a freeway or other busy traffic corridor.

(2) (A) The school district, as the lead agency, in preparing the environmental impact report or negative declaration has notified in writing and consulted with the administering agency in which the proposed schoolsite is located, pursuant to Section 2735.3 of Title 19 of the California Code of Regulations, and with any air pollution control district or air quality management district having jurisdiction in the area, to identify both permitted and nonpermitted facilities within that district's authority, including, but not limited to, freeways and busy traffic corridors, large agricultural operations, and railyards, within one-fourth of a mile of the proposed schoolsite, that might reasonably be anticipated to emit hazardous emissions or handle hazardous or extremely hazardous substances or waste. The notification by the school district, as the lead agency, shall include a list of the locations for which information is sought.

(B) Each administering agency, air pollution control district, or air quality management district receiving written notification from a lead agency to identify facilities pursuant to subparagraph (A) shall provide the requested information and provide a written response to the lead agency within 30 days of receiving the notification. The environmental impact report or negative declaration shall be conclusively presumed to comply with subparagraph (A) as to the area of responsibility of an agency that does not respond within 30 days.

(C) If the school district, as a lead agency, has carried out the consultation required by subparagraph (A), the environmental impact report or the negative declaration shall be conclusively presumed to comply with subparagraph (A), notwithstanding any failure of the consultation to identify an existing facility or other pollution source specified in subparagraph (A).

(3) The governing board of the school district makes one of the following written findings:

(A) Consultation identified no facilities of this type or other significant pollution sources specified in paragraph (2).

(B) The facilities or other pollution sources specified in paragraph (2) exist, but one of the following conditions applies:

(i) The health risks from the facilities or other pollution sources do not and will not constitute an actual or potential endangerment of public health to persons who would attend or be employed at the proposed school.

(ii) Corrective measures required under an existing order by another agency having jurisdiction over the facilities or other pollution sources will, before the school is occupied, result in the mitigation of all chronic or accidental hazardous air emissions to levels that do not constitute an actual or potential endangerment of public health to persons who would attend or be employed at the proposed school. If the governing board makes a finding pursuant to this clause, it shall also make a subsequent finding, prior to occupancy of the school, that the emissions have been so mitigated.

(iii) For a schoolsite with a boundary that is within 500 feet of the edge of the closest traffic lane of a freeway or other busy traffic corridor, the governing board of the school district determines, through analysis pursuant to paragraph (2) of subdivision (b) of Section 44360 of the Health and Safety Code, based on appropriate air dispersion modeling, and after considering any potential mitigation measures, that the air quality at the proposed site is such that neither short-term nor long-term exposure poses significant health risks to pupils.

(C) The facilities or other pollution sources specified in paragraph (2) exist, but conditions in clause (i), (ii) or (iii) of subparagraph (B) cannot be met, and the school district is unable to locate an alternative site that is suitable due to a severe shortage of sites that meet the

requirements in subdivision (a) of Section 17213 of the Education Code. If the governing board makes this finding, the governing board shall adopt a statement of Overriding Considerations pursuant to Section 15093 of Title 14 of the California Code of Regulations.

(b) As used in this section, the following definitions shall apply:

(1) "Hazardous substance" means any substance defined in Section 25316 of the Health and Safety Code.

(2) "Extremely hazardous substances" means an extremely hazardous substance as defined pursuant to paragraph (2) of subdivision (a) of Section 25532 of the Health and Safety Code.

(3) "Hazardous waste" means any waste defined in Section 25117 of the Health and Safety Code.

(4) "Hazardous waste disposal site" means any site defined in Section 25114 of the Health and Safety Code.

(5) "Hazardous air emissions" means emissions into the ambient air of air contaminants that have been identified as a toxic air contaminant by the State Air Resources Board or by the air pollution control officer for the jurisdiction in which the project is located. As determined by the air pollution control officer, hazardous air emissions also means emissions into the ambient air from any substances identified in subdivisions (a) to (f), inclusive, of Section 44321 of the Health and Safety Code.

(6) "Administering agency" means an agency designated pursuant to Section 25502 of the Health and Safety Code to implement and enforce Chapter 6.95 (commencing with Section 25500) of Division 20 of the Health and Safety Code.

(7) "Handle" means handle as defined in Article 1 (commencing with Section 25500) of Chapter 6.95 of Division 20 of the Health and Safety Code.

(8) "Facilities" means any source with a potential to use, generate, emit or discharge hazardous air pollutants, including, but not limited to, pollutants that meet the definition of a hazardous substance, and whose process or operation is identified as an emission source pursuant to the most recent list of source categories published by the California Air Resources Board.

(9) "Freeway or other busy traffic corridors" means those roadways that, on an average day, have traffic in excess of 50,000 vehicles in a rural area, as defined in Section 50101 of the Health and Safety Code, and 100,000 vehicles in an urban area, as defined in Section 50104.7 of the Health and Safety Code.

§ 21151.9. PROJECTS SUBJECT TO THIS DIVISION; COMPLIANCE REQUIREMENT

Whenever a city or county determines that a project, as defined in Section 10912 of the Water Code, is subject to this division, it shall comply with Part 2.10 (commencing with Section 10910) of Division 6 of the Water Code.

§ 21151.10. [DELETED]

§ 21152. LOCAL AGENCY; APPROVAL OR DETERMINATION TO CARRY OUT PROJECT; NOTICE; CONTENTS; PUBLIC INSPECTION; POSTING

(a) If a local agency approves or determines to carry out a project that is subject to this division, the local agency shall file notice of the approval or the determination within five working days after the approval or determination becomes final, with the county clerk of each county in which the project will be located. The notice shall identify the person or persons in subdivision (b) or (c) of Section 21065, as reflected in the agency's record of proceedings, and indicate the determination of the local agency whether the project will, or will not, have a significant effect

on the environment and shall indicate whether an environmental impact report has been prepared pursuant to this division. The notice shall also include certification that the final environmental impact report, if one was prepared, together with comments and responses, is available to the general public.

(b) If a local agency determines that a project is not subject to this division pursuant to subdivision (b) of Section 21080 or pursuant to Section 21172, and the local agency approves or determines to carry out the project, the local agency or the person specified in subdivision (b) or (c) of Section 21065 may file a notice of the determination with the county clerk of each county in which the project will be located. A notice filed pursuant to this subdivision shall identify the person or persons in subdivision (b) or (c) of Section 21065, as reflected in the agency's record of proceedings. A notice filed pursuant to this subdivision by a person specified in subdivision (b) or (c) of Section 21065 shall have a certificate of determination attached to it issued by the local agency responsible for making the determination that the project is not subject to this division pursuant to subdivision (b) of Section 21080 or Section 21172. The certificate of determination may be in the form of a certified copy of an existing document or record of the local agency.

(c) A notice filed pursuant to this section shall be available for public inspection, and shall be posted within 24 hours of receipt in the office of the county clerk. A notice shall remain posted for a period of 30 days. Thereafter, the clerk shall return the notice to the local agency with a notation of the period it was posted. The local agency shall retain the notice for not less than 12 months.

§ 21152.1. LOCAL AGENCY; EXEMPT HOUSING PROJECTS; NOTICE FILING AND POSTING

(a) When a local agency determines that a project is not subject to this division pursuant to Section 21159.22, 21159.23, or 21159.24, and it approves or determines to carry out that project, the local agency or the person specified in subdivision (b) or (c) of Section 21065, shall file notice of the determination with the Office of Planning and Research.

(b) All notices filed pursuant to this section shall be available for public inspection, and a list of these notices shall be posted on a weekly basis in the Office of Planning and Research. Each list shall remain posted for a period of 30 days.

(c) Failure to file the notice required by this section does not affect the validity of a project.

(d) Nothing in this section affects the time limitations contained in Section 21167.

§ 21153. LOCAL LEAD AGENCY; CONSULTATIONS PRIOR TO COMPLETION OF IMPACT REPORT

(a) Prior to completing an environmental impact report, every local lead agency shall consult with, and obtain comments from, each responsible agency, trustee agency, any public agency that has jurisdiction by law with respect to the project, and any city or county that borders on a city or county within which the project is located unless otherwise designated annually by agreement between the local lead agency and the city or county, and may consult with any person who has special expertise with respect to any environmental impact involved. In the case of a project described in subdivision (c) of Section 21065, the local lead agency shall, upon the request of the project applicant, provide for early consultation to identify the range of actions, alternatives, mitigation measures, and significant effects to be analyzed in depth in the environmental impact report. The local lead agency may consult with persons identified by the project applicant who the applicant believes will be concerned with the environmental effects of the project and may consult with members of the public who have made written request to be consulted on the project. A request by the project applicant for early consultation shall be made not later than 30 days after the date that the determination required by Section 21080.1 was

made with respect to the project. The local lead agency may charge and collect a fee from the project applicant in an amount that does not exceed the actual costs of the consultations.

(b) In the case of a project described in subdivision (a) of Section 21065, the lead agency may provide for early consultation to identify the range of actions, alternatives, mitigation measures, and significant effects to be analyzed in depth in the environmental impact report. At the request of the lead agency, the Office of Planning and Research shall ensure that each responsible agency, and any public agency that has jurisdiction by law with respect to the project, is notified regarding any early consultation.

(c) A responsible agency or other public agency shall only make substantive comments regarding those activities involved in a project that are within an area of expertise of the agency or that are required to be carried out or approved by the agency. Those comments shall be supported by specific documentation.

§ 21154. ISSUANCE OF PROJECT ORDER BY STATE; EFFECT ON IMPACT REPORT OF LOCAL AGENCY

Whenever any state agency, board, or commission issues an order which requires a local agency to carry out a project which may have a significant effect on the environment, any environmental impact report which the local agency may prepare shall be limited to consideration of those factors and alternatives which will not conflict with such order.

Chapter 4.2: Implementation of the Sustainable Communities Strategy

§ 21155.

(a) This chapter applies only to a transit priority project that is consistent with the general use designation, density, building intensity, and applicable policies specified for the project area in either a sustainable communities strategy or an alternative planning strategy, for which the State Air Resources Board, pursuant to subparagraph (H) of paragraph (2) of subdivision (b) of Section 65080 of the Government Code, has accepted a metropolitan planning organization's determination that the sustainable communities strategy or the alternative planning strategy would, if implemented, achieve the greenhouse gas emission reduction targets.

(b) For purposes of this chapter, a transit priority project shall (1) contain at least 50 percent residential use, based on total building square footage and, if the project contains between 26 percent and 50 percent nonresidential uses, a floor area ratio of not less than 0.75; (2) provide a minimum net density of at least 20 dwelling units per acre; and (3) be within one-half mile of a major transit stop or high-quality transit corridor included in a regional transportation plan. A major transit stop is as defined in Section 21064.3, except that, for purposes of this section, it also includes major transit stops that are included in the applicable regional transportation plan. For purposes of this section, a high-quality transit corridor means a corridor with fixed route bus service with service intervals no longer than 15 minutes during peak commute hours. A project shall be considered to be within one-half mile of a major transit stop or high-quality transit corridor if all parcels within the project have no more than 25 percent of their area farther than one-half mile from the stop or corridor and if not more than 10 percent of the residential units or 100 units, whichever is less, in the project are farther than one-half mile from the stop or corridor.

§ 21155. 1.

If the legislative body finds, after conducting a public hearing, that a transit priority project meets all of the requirements of subdivisions (a) and (b) and one of the requirements of subdivision (c), the

transit priority project is declared to be a sustainable communities project and shall be exempt from this division.

(a) The transit priority project complies with all of the following environmental criteria:

(1) The transit priority project and other projects approved prior to the approval of the transit priority project but not yet built can be adequately served by existing utilities, and the transit priority project applicant has paid, or has committed to pay, all applicable in-lieu or development fees.

(2) (A) The site of the transit priority project does not contain wetlands or riparian areas and does not have significant value as a wildlife habitat, and the transit priority project does not harm any species protected by the federal Endangered Species Act of 1973 (16 U.S.C. Sec. 1531 et seq.), the Native Plant Protection Act (Chapter 10 (commencing with Section 1900) of Division 2 of the Fish and Game Code), or the California Endangered Species Act (Chapter 1.5 (commencing with Section 2050) of Division 3 of the Fish and Game Code), and the project does not cause the destruction or removal of any species protected by a local ordinance in effect at the time the application for the project was deemed complete.

(B) For the purposes of this paragraph, "wetlands" has the same meaning as in the United States Fish and Wildlife Service Manual, Part 660 FW 2 (June 21, 1993).

(C) For the purposes of this paragraph:

(i) "Riparian areas" means those areas transitional between terrestrial and aquatic ecosystems and that are distinguished by gradients in biophysical conditions, ecological processes, and biota. A riparian area is an area through which surface and subsurface hydrology connect waterbodies with their adjacent uplands. A riparian area includes those portions of terrestrial ecosystems that significantly influence exchanges of energy and matter with aquatic ecosystems. A riparian area is adjacent to perennial, intermittent, and ephemeral streams, lakes, and estuarine-marine shorelines.

(ii) "Wildlife habitat" means the ecological communities upon which wild animals, birds, plants, fish, amphibians, and invertebrates depend for their conservation and protection.

(iii) Habitat of "significant value" includes wildlife habitat of national, statewide, regional, or local importance; habitat for species protected by the federal Endangered Species Act of 1973 (16 U.S.C. Sec. 1531, et seq.), the California Endangered Species Act (Chapter 1.5 (commencing with Section 2050) of Division 3 of the Fish and Game Code), or the Native Plant Protection Act (Chapter 10 (commencing with Section 1900) of Division 2 of the Fish and Game Code); habitat identified as candidate, fully protected, sensitive, or species of special status by local, state, or federal agencies; or habitat essential to the movement of resident or migratory wildlife.

(3) The site of the transit priority project is not included on any list of facilities and sites compiled pursuant to Section 65962.5 of the Government Code.

(4) The site of the transit priority project is subject to a preliminary endangerment assessment prepared by a registered environmental assessor to determine the existence of any release of a hazardous substance on the site and to determine the potential for exposure of future occupants to significant health hazards from any nearby property or activity.

(A) If a release of a hazardous substance is found to exist on the site, the release shall be removed or any significant effects of the release shall be mitigated to a level of insignificance in compliance with state and federal requirements.

(B) If a potential for exposure to significant hazards from surrounding properties or activities is found to exist, the effects of the potential exposure shall be mitigated to a level of insignificance in compliance with state and federal requirements.

(5) The transit priority project does not have a significant effect on historical resources pursuant to Section 21084.1.

(6) The transit priority project site is not subject to any of the following:

(A) A wildland fire hazard, as determined by the Department of Forestry and Fire Protection, unless the applicable general plan or zoning ordinance contains provisions to mitigate the risk of a wildland fire hazard.

(B) An unusually high risk of fire or explosion from materials stored or used on nearby properties.

(C) Risk of a public health exposure at a level that would exceed the standards established by any state or federal agency.

(D) Seismic risk as a result of being within a delineated earthquake fault zone, as determined pursuant to Section 2622, or a seismic hazard zone, as determined pursuant to Section 2696, unless the applicable general plan or zoning ordinance contains provisions to mitigate the risk of an earthquake fault or seismic hazard zone.

(E) Landslide hazard, flood plain, flood way, or restriction zone, unless the applicable general plan or zoning ordinance contains provisions to mitigate the risk of a landslide or flood.

(7) The transit priority project site is not located on developed open space.

(A) For the purposes of this paragraph, "developed open space" means land that meets all of the following criteria:

(i) Is publicly owned, or financed in whole or in part by public funds.

(ii) Is generally open to, and available for use by, the public.

(iii) Is predominantly lacking in structural development other than structures associated with open spaces, including, but not limited to, playgrounds, swimming pools, ballfields, enclosed child play areas, and picnic facilities.

(B) For the purposes of this paragraph, "developed open space" includes land that has been designated for acquisition by a public agency for developed open space, but does not include lands acquired with public funds dedicated to the acquisition of land for housing purposes.

(8) The buildings in the transit priority project are 15 percent more energy efficient than required by Chapter 6 of Title 24 of the California Code of Regulations and the buildings and landscaping are designed to achieve 25 percent less water usage than the average household use in the region.

(b) The transit priority project meets all of the following land use criteria:

(1) The site of the transit priority project is not more than eight acres in total area.

(2) The transit priority project does not contain more than 200 residential units.

(3) The transit priority project does not result in any net loss in the number of affordable housing units within the project area.

(4) The transit priority project does not include any single level building that exceeds 75,000 square feet.

(5) Any applicable mitigation measures or performance standards or criteria set forth in the prior environmental impact reports, and adopted in findings, have been or will be incorporated into the transit priority project.

(6) The transit priority project is determined not to conflict with nearby operating industrial uses.

(7) The transit priority project is located within one-half mile of a rail transit station or a ferry terminal included in a regional transportation plan or within one-quarter mile of a high-quality transit corridor included in a regional transportation plan.

(c) The transit priority project meets at least one of the following three criteria:

(1) The transit priority project meets both of the following:

(A) At least 20 percent of the housing will be sold to families of moderate income, or not less than 10 percent of the housing will be rented to families of low income, or not less than 5 percent of the housing is rented to families of very low income.

(B) The transit priority project developer provides sufficient legal commitments to the appropriate local agency to ensure the continued availability and use of the housing units for very low, low-, and moderate-income households at monthly housing costs with an affordable housing cost or affordable rent, as defined in Section 50052.5 or 50053 of the Health and Safety Code, respectively, for the period required by the applicable financing. Rental units shall be affordable for at least 55 years. Ownership units shall be subject to resale restrictions or equity sharing requirements for at least 30 years.

(2) The transit priority project developer has paid or will pay in-lieu fees pursuant to a local ordinance in an amount sufficient to result in the development of an equivalent number of units that would otherwise be required pursuant to paragraph (1).

(3) The transit priority project provides public open space equal to or greater than five acres per 1,000 residents of the project.

§ 21155.2.

(a) A transit priority project that has incorporated all feasible mitigation measures, performance standards, or criteria set forth in the prior applicable environmental impact reports and adopted in findings made pursuant to Section 21081, shall be eligible for either the provisions of subdivision (b) or (c).

(b) A transit priority project that satisfies the requirements of subdivision (a) may be reviewed through a sustainable communities environmental assessment as follows:

(1) An initial study shall be prepared to identify all significant or potentially significant impacts of the transit priority project, other than those which do not need to be reviewed pursuant to Section 21159.28 based on substantial evidence in light of the whole record. The initial study shall identify any cumulative effects that have been adequately addressed and mitigated pursuant to the requirements of this division in prior applicable certified environmental impact reports. Where the lead agency determines that a cumulative effect has been adequately addressed and mitigated, that cumulative effect shall not be treated as cumulatively considerable for the purposes of this subdivision.

(2) The sustainable communities environmental assessment shall contain measures that either avoid or mitigate to a level of insignificance all potentially significant or significant effects of the project required to be identified in the initial study.

(3) A draft of the sustainable communities environmental assessment shall be circulated for public comment for a period of not less than 30 days. Notice shall be provided in the same manner as required for an environmental impact report pursuant to Section 21092.

(4) Prior to acting on the sustainable communities environmental assessment, the lead agency shall consider all comments received.

(5) A sustainable communities environmental assessment may be approved by the lead agency after conducting a public hearing, reviewing the comments received, and finding that:

(A) All potentially significant or significant effects required to be identified in the initial study have been identified and analyzed.

(B) With respect to each significant effect on the environment required to be identified in the initial study, either of the following apply:

(i) Changes or alterations have been required in or incorporated into the project that avoid or mitigate the significant effects to a level of insignificance.

(ii) Those changes or alterations are within the responsibility and jurisdiction of another public agency and have been, or can and should be, adopted by that other agency.

(6) The legislative body of the lead agency shall conduct the public hearing or a planning commission may conduct the public hearing if local ordinances allow a direct appeal of approval of a document prepared pursuant to this division to the legislative body subject to a fee not to exceed five hundred dollars ($500).

(7) The lead agency's decision to review and approve a transit priority project with a sustainable communities environmental assessment shall be reviewed under the substantial evidence standard.

(c) A transit priority project that satisfies the requirements of subdivision (a) may be reviewed by an environmental impact report that complies with all of the following:

(1) An initial study shall be prepared to identify all significant or potentially significant effects of the transit priority project other than those that do not need to be reviewed pursuant to Section 21159.28 based upon substantial evidence in light of the whole record. The initial study shall identify any cumulative effects that have been adequately addressed and mitigated pursuant to the requirements of this division in prior applicable certified environmental impact reports. Where the lead agency determines that a cumulative effect has been adequately addressed and mitigated, that cumulative effect shall not be treated as cumulatively considerable for the purposes of this subdivision.

(2) An environmental impact report prepared pursuant to this subdivision need only address the significant or potentially significant effects of the transit priority project on the environment identified pursuant to paragraph (1). It is not required to analyze off-site alternatives to the transit priority project. It shall otherwise comply with the requirements of this division.

§ 21155.3

(a) The legislative body of a local jurisdiction may adopt traffic mitigation measures that would apply to transit priority projects. These measures shall be adopted or amended after a public hearing and may include requirements for the installation of traffic control improvements, street or road improvements, and contributions to road improvement or transit funds, transit passes for future residents, or other measures that will avoid or mitigate the traffic impacts of those transit priority projects.

(b) (1) A transit priority project that is seeking a discretionary approval is not required to comply with any additional mitigation measures required by paragraph (1) or (2) of subdivision (a) of Section 21081, for the traffic impacts of that project on intersections, streets, highways, freeways, or mass transit, if the local jurisdiction issuing that discretionary approval has adopted traffic mitigation measures in accordance with this section.

(2) Paragraph (1) does not restrict the authority of a local jurisdiction to adopt feasible mitigation measures with respect to the effects of a project on public health or on pedestrian or bicycle safety.

(c) The legislative body shall review its traffic mitigation measures and update them as needed at least every five years.

§ 21155.4

(a) Except as provided in subdivision (b), a residential, employment center, as defined in paragraph (1) of subdivision (a) of Section 21099, or mixed-use development project, including any subdivision, or any zoning, change that meets all of the following criteria is exempt from the requirements of this division:

(1) The project is proposed within a transit priority area, as defined in subdivision (a) of Section 21099.

(2) The project is undertaken to implement and is consistent with a specific plan for which an environmental impact report has been certified.

(3) The project is consistent with the general use designation, density, building intensity, and applicable policies specified for the project area in either a sustainable communities strategy or an alternative planning strategy for which the State Air Resources Board, pursuant to subparagraph (H) of paragraph (2) of subdivision (b) of Section 65080 of the Government Code, has accepted a metropolitan planning organization's determination that the sustainable communities strategy or the alternative planning strategy would, if implemented, achieve the greenhouse gas emissions reduction targets.

(b) Further environmental review shall be conducted only if any of the events specified in Section 21166 have occurred.

Chapter 4.5: Streamlined Environmental Review

Article 1: Findings

§ 21156. LEGISLATIVE INTENT

It is the intent of the Legislature in enacting this chapter that a master environmental impact report shall evaluate the cumulative impacts, growth inducing impacts, and irreversible significant effects on the environment of subsequent projects to the greatest extent feasible. The Legislature further intends that the environmental review of subsequent projects be substantially reduced to the extent that the project impacts have been reviewed and appropriate mitigation measures are set forth in a certified master environmental impact report.

Article 2: Master Environmental Impact Report

§ 21157. PREPARATION; CONTENT; FEE PROGRAM

(a) A master environmental impact report may be prepared for any one of the following projects:

(1) A general plan, element, general plan amendment, or specific plan.

(2) A project that consists of smaller individual projects that will be carried out in phases.

(3) A rule or regulation that will be implemented by subsequent projects.

(4) A project that will be carried out or approved pursuant to a development agreement.

(5) A public or private project that will be carried out or approved pursuant to, or in furtherance of, a redevelopment plan.

(6) A state highway project or mass transit project that will be subject to multiple stages of review or approval.

(7) A regional transportation plan or congestion management plan.

(8) A plan proposed by a local agency for the reuse of a federal military base or reservation that has been closed or that is proposed for closure.

(9) Regulations adopted by the Fish and Game Commission for the regulation of hunting and fishing.

(10) A plan for district projects to be undertaken by a school district, that also complies with applicable school facilities requirements, including, but not limited to, the requirements of Chapter 12.5 (commencing with Section 17070.10) of Part 10 of, and Article 1 (commencing with Section 17210) of Chapter 1 of Part 10.5 of, Division 1 of Title 1 of the Education Code.

(b) When a lead agency prepares a master environmental impact report, the document shall include all of the following:

(1) A detailed statement as required by Section 21100.

(2) A description of anticipated subsequent projects that would be within the scope of the master environmental impact report, that contains sufficient information with regard to the kind, size, intensity, and location of the subsequent projects, including, but not limited to, all of the following:

(A) The specific type of project anticipated to be undertaken.

(B) The maximum and minimum intensity of any anticipated subsequent project, such as the number of residences in a residential development, and, with regard to a public works facility, its anticipated capacity and service area.

(C) The anticipated location and alternative locations for any development projects.

(D) A capital outlay or capital improvement program, or other scheduling or implementing device that governs the submission and approval of subsequent projects.

(3) A description of potential impacts of anticipated subsequent projects for which there is not sufficient information reasonably available to support a full assessment of potential impacts in the master environmental impact report. This description shall not be construed as a limitation on the impacts which may be considered in a focused environmental impact report.

(c) Lead agencies may develop and implement a fee program in accordance with applicable provisions of law to generate the revenue necessary to prepare a master environmental impact report.

§ 21157.1. REVIEW OF SUBSEQUENT PROJECTS DESCRIBED IN REPORT; REQUIREMENTS

The preparation and certification of a master environmental impact report, if prepared and certified consistent with this division, may allow for the limited review of subsequent projects that were described in the master environmental impact report as being within the scope of the report, in accordance with the following requirements:

(a) The lead agency for a subsequent project shall be the lead agency or any responsible agency identified in the master environmental impact report.

(b) The lead agency shall prepare an initial study on any proposed subsequent project. This initial study shall analyze whether the subsequent project may cause any significant effect on the environment that was not examined in the master environmental impact report and whether the subsequent project was described in the master environmental impact report as being within the scope of the report.

(c) If the lead agency, based on the initial study, determines that a proposed subsequent project will have no additional significant effect on the environment, as defined in subdivision (d) of Section 21158, that was not identified in the master environmental impact report and that no new or additional mitigation measures or alternatives may be required, the lead agency shall make a written finding based upon the information contained in the initial study that the subsequent project is within the scope of the project covered by the master environmental impact report. No new environmental document nor findings pursuant to Section 21081 shall be required by this division. Prior to approving or carrying out the proposed subsequent project, the lead agency shall provide notice of this fact pursuant to Section 21092 and incorporate all feasible mitigation measures or feasible alternatives set forth in the master environmental impact report which are appropriate to the project. Whenever a lead agency approves or determines to carry out any subsequent project pursuant to this section, it shall file a notice pursuant to Section 21108 or 21152.

(d) Where a lead agency cannot make the findings required in subdivision (c), the lead agency shall prepare, pursuant to Section 21157.7, either a mitigated negative declaration or environmental impact report.

§ 21157.5. MITIGATED NEGATIVE DECLARATIONS; PREPARATION; CONDITIONS; ALTERNATIVE

(a) A proposed mitigated negative declaration shall be prepared for any proposed subsequent project if both of the following occur:

(1) An initial study has identified potentially new or additional significant effects on the environment that were not analyzed in the master environmental impact report.

(2) Feasible mitigation measures or alternatives will be incorporated to revise the proposed subsequent project, before the negative declaration is released for public review, in order to avoid the effects or mitigate the effects to a point where clearly no significant effect on the environment will occur.

(b) If there is substantial evidence in light of the whole record before the lead agency that the proposed subsequent project may have a significant effect on the environment and a mitigated negative declaration is not prepared, the lead agency shall prepare an environmental impact report or a focused environmental impact report pursuant to Section 21158.

§ 21157.6. LIMITATION PERIOD ON USE OF ENVIRONMENTAL IMPACT REPORT

(a) The master environmental impact report shall not be used for the purposes of this chapter if either of the following has occurred:

(1) The certification of the master environmental impact report occurred more than five years prior to the filing of an application for the subsequent project.

(2) The filing of an application for the subsequent project occurs following the certification of the master environmental impact report, and the approval of a project that was not described in the master environmental impact report, may affect the adequacy of the environmental review in the master environmental impact report for any subsequent project.

(b) A master environmental impact report that was certified more than five years prior to the filing of an application for the subsequent project may be used for purposes of this chapter to review a subsequent project that was described in the master environmental impact report if the lead agency reviews the adequacy of the master environmental impact report and does either of the following:

(1) Finds that no substantial changes have occurred with respect to the circumstances under which the master environmental impact report was certified or that no new information,

which was not known and could not have been known at the time that the master environmental impact report was certified as complete, has become available.

(2) Prepares an initial study and, pursuant to the findings of the initial study, does either of the following:

(A) Certifies a subsequent or supplemental environmental impact report that has been either incorporated into the previously certified master environmental impact report or references any deletions, additions, or any other modifications to the previously certified master environmental impact report.

(B) Approves a mitigated negative declaration that addresses substantial changes that have occurred with respect to the circumstances under which the master environmental impact report was certified or the new information that was not known and could not have been known at the time the master environmental impact report was certified.

§ 21157.7. IMPROVEMENTS TO ROADWAY SEGMENTS OF HIGHWAY 99; USE OF MASTER ENVIRONMENTAL IMPACT REPORT

(a) For purposes of this section, a master environmental impact report is a document prepared in accordance with subdivision (c) for the projects described in subdivision (b) that, upon certification, is followed by review of subsequent projects as provided in Sections 21157.1 and 21157.5.

(b) A master environmental impact report may be prepared for a plan adopted by the Department of Transportation for improvements to regional segments of Highway 99 funded pursuant to subdivision (b) of Section 8879.23 of the Government Code, to streamline, coordinate, and improve environmental review.

(c) The report shall include all of the following:

(1) A detailed statement as required by Section 21100.

(2) A description of the anticipated highway improvements along Highway 99 that would be within the scope of the master environmental impact report, that contains sufficient information about all phases of the Highway 99 construction activities, including, but not limited to, all of the following:

(A) The specific types of improvements that will be undertaken.

(B) The anticipated location and alternative locations for any of the Highway 99 improvements, including overpasses, bridges, railroad crossings, and interchanges.

(C) A capital outlay or capital improvement program, or other scheduling or implementing device that governs the construction activities associated with the Highway 99 improvements.

(d) The Department of Transportation may communicate, coordinate, and consult with the Resources Agency, Wildlife Conservation Board, Department of Fish and Game, Department of Conservation, and other appropriate federal, state, or local governments, including interested stakeholders, to consider and implement mitigation requirements on a regional basis for the projects described in subdivision (b). This may include both of the following:

(1) Identification of priority areas for mitigation, using information from these agencies and departments as well as from other sources.

(2) Utilization of existing conservation programs of the agencies or departments identified in this subdivision, if mitigation under those programs for improvements under this section does not supplant mitigation for a project.

(e) The Department of Transportation may execute an agreement, memorandum of understanding, or other similar instrument to memorialize its understanding of any communication,

coordination, or implementation activities with other state agencies for the purposes of meeting mitigation requirements on a regional basis.

(f) Notwithstanding any other provision of law, nothing in this section is intended to interfere with or prevent the existing authority of an agency or department to carry out its programs, projects, or responsibilities to identify, review, approve, deny, or implement any mitigation requirements, and nothing in this section shall be construed as a limitation on mitigation requirements for the project, or a limitation on compliance with requirements under this division or any other provision of law.

(g) Notwithstanding Section 21157.6, the master environmental impact report shall not be used for the purposes of this section, if the certification of the master environmental impact report occurred more than seven years prior to the filing of an application for the subsequent project.

Article 3: Focused Environmental Impact Report

§ 21158. PURPOSE; CONTENT; ADDITIONAL SIGNIFICANT EFFECT ON THE ENVIRONMENT

(a) A focused environmental impact report is an environmental impact report on a subsequent project identified in a master environmental impact report. A focused environmental impact report may be utilized only if the lead agency finds that the analysis in the master environmental impact report of cumulative impacts, growth inducing impacts, and irreversible significant effects on the environment is adequate for the subsequent project.

The focused environmental impact report shall incorporate, by reference, the master environmental impact report and analyze only the subsequent project's additional significant effects on the environment, as defined in subdivision (d), and any new or additional mitigation measures or alternatives that were not identified and analyzed by the master environmental impact report.

(b) The focused environmental impact report need not examine those effects which the lead agency finds were one of the following:

(1) Mitigated or avoided pursuant to paragraph (1) of subdivision (a) of Section 21081 as a result of mitigation measures identified in the master environmental impact report which will be required as part of the approval of the subsequent project.

(2) Examined at a sufficient level of detail in the master environmental impact report to enable those significant environmental effects to be mitigated or avoided by specific revisions to the project, the imposition of conditions, or by other means in connection with the approval of the subsequent project.

(3) Subject to a finding pursuant to paragraph (2) of subdivision (a) of Section 21081.

(c) A focused environmental impact report on any subsequent project shall analyze any significant effects on the environment where substantial new or additional information shows that the adverse environmental impact may be more significant than was described in the master environmental impact report. The substantial new or additional information may also show that mitigation measures or alternatives identified in the master environmental impact report, which were previously determined to be infeasible, are feasible and will avoid or reduce the significant effects on the environment of the subsequent project to a level of insignificance.

(d) For purposes of this chapter, "additional significant effects on the environment" are those project specific effects on the environment which were not addressed as significant effects on the environment in the master environmental impact report.

(e) Nothing in this chapter is intended to limit or abridge the ability of a lead agency to focus upon the issues that are ripe for decision at each level of environmental review, or to exclude

duplicative analysis of environmental effects examined in previous environmental impact reports pursuant to Section 21093.

§ 21158.1. REGULATORY PROGRAMS CERTIFIED UNDER PUBLIC RESOURCES CODE § 21080.5; CERTAIN MASTER AND FOCUSED ENVIRONMENTAL IMPACT REPORTS

When a lead agency is required to prepare an environmental impact report pursuant to subdivision (d) of Section 21157.1 or is authorized to prepare a focused environmental impact report pursuant to Section 21158, the lead agency may not rely on subdivision (a) of Section 21080.5 for that purpose even though the lead agency's regulatory program is otherwise certified in accordance with Section 21080.5.

§ 21158.5. MULTIPLE-FAMILY RESIDENTIAL DEVELOPMENT OF NOT MORE THAN 100 UNITS; RESIDENTIAL AND COMMERCIAL OR RETAIL MIXED-USE DEVELOPMENT OF NOT MORE THAN 100,000 SQUARE FEET; PREPARATION OF REPORT; LIMITATIONS

(a) Where a project consists of multiple-family residential development of not more than 100 units or a residential and commercial or retail mixed-use development of not more than 100,000 square feet which complies with all of the following, a focused environmental impact report shall be prepared, notwithstanding that the project was not identified in a master environmental impact report:

  (1) Is consistent with a general plan, specific plan, community plan, or zoning ordinance for which an environmental impact report was prepared within five years of the certification of the focused environmental impact report.

  (2) The lead agency cannot make the finding described in subdivision (c) of Section 21157.1, a negative declaration or mitigated negative declaration cannot be prepared pursuant to Section 21080, 21157.5, or 21158, and Section 21166 does not apply.

  (3) Meets one or more of the following conditions:

    (A) The parcel on which the project is to be developed is surrounded by immediately contiguous urban development.

    (B) The parcel on which the project is to be developed has been previously developed with urban uses.

    (C) The parcel on which the project is to be developed is within one-half mile of an existing rail transit station.

(b) A focused environmental impact report prepared pursuant to this section shall be limited to a discussion of potentially significant effects on the environment specific to the project, or which substantial new information shows will be more significant than described in the prior environmental impact report. No discussion shall be required of alternatives to the project, cumulative impacts of the project, or the growth inducing impacts of the project.

Article 4: Expedited Environmental Review for Environmentally Mandated Projects

§ 21159. RULE OR REGULATION ADOPTION; ENVIRONMENTAL ANALYSIS; CONTENT

(a) An agency listed in Section 21159.4 shall perform, at the time of the adoption of a rule or regulation requiring the installation of pollution control equipment, or a performance standard or treatment requirement, including a rule or regulation that requires the installation of pollution control equipment or a performance standard or treatment requirement pursuant to the California Global Warming Solutions Act of 2006 (Division 25.5 (commencing with Section 38500) of the Health and Safety Code), an environmental analysis of the reasonably foreseeable

methods of compliance. In the preparation of this analysis, the agency may utilize numerical ranges or averages where specific data is not available; however, the agency shall not be required to engage in speculation or conjecture. The environmental analysis shall, at minimum, include all of the following:

(1) An analysis of the reasonably foreseeable environmental impacts of the methods of compliance.

(2) An analysis of reasonably foreseeable feasible mitigation measures.

(3) An analysis of reasonably foreseeable alternative means of compliance with the rule or regulation.

(4) For a rule or regulation that requires the installation of pollution control equipment adopted pursuant to the California Global Warming Solutions Act of 2006 (Division 25.5 (commencing with Section 38500) of the Health and Safety Code), the analysis shall also include reasonably foreseeable greenhouse gas emission impacts of compliance with the rule or regulation.

(b) The preparation of an environmental impact report at the time of adopting a rule or regulation pursuant to this division shall be deemed to satisfy the requirements of this section.

(c) The environmental analysis shall take into account a reasonable range of environmental, economic, and technical factors, population and geographic areas, and specific sites.

(d) This section does not require the agency to conduct a project-level analysis.

(e) For purposes of this article, the term "performance standard" includes process or raw material changes or product reformulation.

(f) This section is not intended, and may not be used, to delay the adoption of any rule or regulation for which an analysis is required to be performed pursuant to this section.

§ 21159.1. UTILIZATION OF FOCUSED ENVIRONMENTAL IMPACT REPORT; REQUIREMENTS; LIMITATIONS

(a) A focused environmental impact report may be utilized if a project meets all of the following requirements:

(1) The project consists solely of the installation of either of the following:

(A) Pollution control equipment required by a rule or regulation of an agency listed in subdivision (a) of Section 21159.4 and other components necessary to complete the installation of that equipment.

(B) Pollution control equipment and other components necessary to complete the installation of that equipment that reduces greenhouse gases required by a rule or regulation of an agency listed in Section 21159.4 pursuant to the California Global Warming Solutions Act of 2006 (Division 25.5 (commencing with Section 38500) of the Health and Safety Code).

(2) The agency certified an environmental impact report on the rule or regulation or reviewed it pursuant to a certified regulatory program, and, in either case, the review included an assessment of growth inducing impacts and cumulative impacts of, and alternatives to, the project.

(3) The environmental review required by paragraph (2) was completed within five years of certification of the focused environmental impact report.

(4) An environmental impact report is not required pursuant to Section 21166.

(b) The discussion of significant effects on the environment in the focused environmental impact report shall be limited to project-specific potentially significant effects on the environment of the project that were not discussed in the environmental analysis of the rule or regulation

required pursuant to subdivision (a) of Section 21159. A discussion of growth-inducing impacts or cumulative impacts shall not be required in the focused environmental impact report, and the discussion of alternatives shall be limited to a discussion of alternative means of compliance, if any, with the rule or regulation.

§ 21159.2. NEGATIVE DECLARATION; MITIGATED NEGATIVE DECLARATION; ENVIRONMENTAL IMPACT REPORT ON COMPLIANCE PROJECT; PROJECT-SPECIFIC ISSUED; CONTENTS

(a) If a project consists solely of compliance with a performance standard or treatment requirement imposed by an agency listed in Section 21159.4, the lead agency for the compliance project shall, to the greatest extent feasible, utilize the environmental analysis required pursuant to subdivision (a) of Section 21159 in the preparation of a negative declaration, mitigated negative declaration, or environmental impact report on the compliance project or in otherwise fulfilling its responsibilities under this division. The use of numerical averages or ranges in an environmental analysis shall not relieve a lead agency of its obligations under this division to identify and evaluate the environmental effects of a compliance project.

(b) If the lead agency determines that an environmental impact report on the compliance project is required, the lead agency shall prepare an environmental impact report which addresses only the project-specific issues related to the compliance project or other issues that were not discussed in sufficient detail in the environmental analysis to enable the lead agency to fulfill its responsibilities under Section 21100 or 21151, as applicable. The mitigation measures imposed by the lead agency for the project shall relate only to the significant effects on the environment to be mitigated. The discussion of alternatives shall be limited to a discussion of alternative means of compliance, if any, with the rule or regulation.

§ 21159.3. DEADLINES FOR PREPARATION OF REPORT

In the preparation of any environmental impact report pursuant to Section 21159.1 or 21159.2, the following deadlines shall apply:

(a) A lead agency shall determine whether an environmental impact report should be prepared within 30 days of its determination that the application for the project is complete.

(b) If the environmental impact report will be prepared under contract to the lead agency pursuant to Section 21082.1, the lead agency shall issue a request for proposals for preparation of the environmental impact report as soon as it has enough information to prepare a request for proposals, and in any event, not later than 30 days after the time for response to the notice of preparation has expired. The contract shall be awarded within 30 days of the response date for the request for proposals.

§ 21159.4. AGENCIES; ARTICLE APPLICATION

(a) This article shall apply to all of the following agencies:

(1) The State Air Resources Board.

(2) A district as defined in Section 39025 of the Health and Safety Code.

(3) The State Water Resources Control Board.

(4) A California regional water quality control board.

(5) The Department of Toxic Substances Control.

(6) The Department of Resources Recycling and Recovery.

(b) This article shall apply to the State Energy Resources Conservation and Development Commission and the California Public Utilities Commission for rules and regulations requiring the installation of pollution control equipment adopted pursuant to the California Global

Warming Solutions Act of 2006 (Division 25.5 (commencing with Section 38500) of the Health and Safety Code).

Article 5: Public Assistance Program

§ 21159.9. IMPLEMENTATION OF PROGRAM

The Office of Planning and Research shall implement, utilizing existing resources, a public assistance and information program, to ensure efficient and effective implementation of this division, to do all of the following:

(a) Establish a public education and training program for planners, developers, and other interested parties to assist them in implementing this division.

(b) Establish and maintain a data-base to assist in the preparation of environmental documents.

(c) Establish and maintain a central repository for the collection, storage, retrieval, and dissemination of notices of exemption, notices of preparation, notices of determination, and notices of completion provided to the office, and make the notices available through the Internet. The office may coordinate with another state agency for that agency to make the notices available through the Internet.

(d) Provide to the California State Library copies of documents submitted in electronic format to the Office of Planning and Research pursuant to this division. The California State Library shall be the repository for those electronic documents, which shall be made available for viewing by the general public upon request.

Article 6: Special Review of Housing Projects

§ 21159.20. DEFINITIONS

For the purposes of this article, the following terms have the following meanings:

(a) "Census-defined place" means a specific unincorporated land area within boundaries determined by the United States Census Bureau in the most recent decennial census.

(b) "Community-level environmental review" means either of the following:

  (1) An environmental impact report certified on any of the following:

    (A) A general plan.

    (B) A revision or update to the general plan that includes at least the land use and circulation elements.

    (C) An applicable community plan.

    (D) An applicable specific plan.

    (E) A housing element of the general plan, if the environmental impact report analyzed the environmental effects of the density of the proposed project.

  (2) Pursuant to this division and the implementing guidelines adopted pursuant to this division that govern subsequent review following a program environmental impact report, or pursuant to Section 21157.1, 21157.5, or 21166, a negative declaration or mitigated negative declaration was adopted as a subsequent environmental review document, following and based upon an environmental impact report on any of the projects listed in subparagraphs (A), (C), or (D) of paragraph (1).

(c) "Low-income households" means households of persons and families of very low and low income, as defined in Sections 50093 and 50105 of the Health and Safety Code.

(d) "Low- and moderate-income households" means households of persons and families of low or moderate income, as defined in Section 50093 of the Health and Safety Code.

§ 21159.21. CRITERIA TO QUALIFY FOR HOUSING PROJECT EXEMPTIONS

A housing project qualifies for an exemption from this division pursuant to Section 21159.22, 21159.23, or 21159.24 if it meets the criteria in the applicable section and all of the following criteria:

(a) The project is consistent with any applicable general plan, specific plan, and local coastal program, including any mitigation measures required by a plan or program, as that plan or program existed on the date that the application was deemed complete and with any applicable zoning ordinance, as that zoning ordinance existed on the date that the application was deemed complete, except that a project shall not be deemed to be inconsistent with the zoning designation for the site if that zoning designation is inconsistent with the general plan only because the project site has not been rezoned to conform with a more recently adopted general plan.

(b) Community-level environmental review has been adopted or certified.

(c) The project and other projects approved prior to the approval of the project can be adequately served by existing utilities, and the project applicant has paid, or has committed to pay, all applicable in-lieu or development fees.

(d) The site of the project does not contain wetlands, does not have any value as a wildlife habitat, and the project does not harm any species protected by the federal Endangered Species Act of 1973 (16 U.S.C. Sec. 1531 et seq.) or by the Native Plant Protection Act (Chapter 10 (commencing with Section 1900) of Division 2 of the Fish and Game Code), the California Endangered Species Act (Chapter 1.5 (commencing with Section 2050), of Division 3 of the Fish and Game Code), and the project does not cause the destruction or removal of any species protected by a local ordinance in effect at the time the application for the project was deemed complete. For the purposes of this subdivision, "wetlands" has the same meaning as in Section 328.3 of Title 33 of the Code of Federal Regulations and "wildlife habitat" means the ecological communities upon which wild animals, birds, plants, fish, amphibians, and invertebrates depend for their conservation and protection.

(e) The site of the project is not included on any list of facilities and sites compiled pursuant to Section 65962.5 of the Government Code.

(f) The site of the project is subject to a preliminary endangerment assessment prepared by an environmental assessor to determine the existence of any release of a hazardous substance on the site and to determine the potential for exposure of future occupants to significant health hazards from any nearby property or activity.

  (1) If a release of a hazardous substance is found to exist on the site, the release shall be removed, or any significant effects of the release shall be mitigated to a level of insignificance in compliance with state and federal requirements.

  (2) If a potential for exposure to significant hazards from surrounding properties or activities is found to exist, the effects of the potential exposure shall be mitigated to a level of insignificance in compliance with state and federal requirements.

(g) The project does not have a significant effect on historical resources pursuant to Section 21084.1.

(h) The project site is not subject to any of the following:

  (1) A wildland fire hazard, as determined by the Department of Forestry and Fire Protection, unless the applicable general plan or zoning ordinance contains provisions to mitigate the risk of a wildland fire hazard.

(2) An unusually high risk of fire or explosion from materials stored or used on nearby properties.

(3) Risk of a public health exposure at a level that would exceed the standards established by any state or federal agency.

(4) Within a delineated earthquake fault zone, as determined pursuant to Section 2622, or a seismic hazard zone, as determined pursuant to Section 2696, unless the applicable general plan or zoning ordinance contains provisions to mitigate the risk of an earthquake fault or seismic hazard zone.

(5) Landslide hazard, flood plain, flood way, or restriction zone, unless the applicable general plan or zoning ordinance contains provisions to mitigate the risk of a landslide or flood.

(i) (1) The project site is not located on developed open space.

(2) For the purposes of this subdivision, "developed open space" means land that meets all of the following criteria:

(A) Is publicly owned, or financed in whole or in part by public funds.

(B) Is generally open to, and available for use by, the public.

(C) Is predominantly lacking in structural development other than structures associated with open spaces, including, but not limited to, playgrounds, swimming pools, ballfields, enclosed child play areas, and picnic facilities.

(3) For the purposes of this subdivision, "developed open space" includes land that has been designated for acquisition by a public agency for developed open space, but does not include lands acquired by public funds dedicated to the acquisition of land for housing purposes.

(j) The project site is not located within the boundaries of a state conservancy.

§ 21159.22. AGRICULTURAL EMPLOYEE HOUSING EXEMPTION

(a) This division does not apply to any development project that meets the requirements of subdivision (b), and meets either of the following criteria:

(1) Consists of the construction, conversion, or use of residential housing for agricultural employees, and meets all of the following criteria:

(A) Is affordable to lower income households, as defined in Section 50079.5 of the Health and Safety Code.

(B) Lacks public financial assistance.

(C) The developer of the development project provides sufficient legal commitments to the appropriate local agency to ensure the continued availability and use of the housing units for lower income households for a period of at least 15 years.

(2) Consists of the construction, conversion, or use of residential housing for agricultural employees and meets all of the following criteria:

(A) Is housing for very low, low-, or moderate-income households as defined in paragraph (2) of subdivision (h) of Section 65589.5 of the Government Code.

(B) Public financial assistance exists for the development project.

(C) The developer of the development project provides sufficient legal commitments to the appropriate local agency to ensure the continued availability and use of the housing units for low- and moderate-income households for a period of at least 15 years.

(b) (1) If the development project is proposed within incorporated city limits or within a census defined place with a minimum population density of at least 5,000 persons per square mile, it is located on a project site that is adjacent, on at least two sides, to land that has been

developed, and consists of not more than 45 units, or is housing for a total of 45 or fewer agricultural employees if the housing consists of dormitories, barracks, or other group living facilities.

(2) If the development project is located on a project site zoned for general agricultural use, and consists of not more than 20 units, or is housing for a total of 20 or fewer agricultural employees if the housing consists of dormitories, barracks, or other group living facilities.

(3) The project satisfies the criteria in Section 21159.21.

(4) The development project is not more than five acres in area, except that a project site located in an area with a population density of at least 1,000 persons per square mile shall not be more than two acres in area.

(c) Notwithstanding subdivision (a), if a project satisfies the criteria described in subdivisions (a) and (b), but does not satisfy the criteria described in paragraph (1) of subdivision (b), this division does not apply to the project if the project meets all of the following criteria:

(1) Is located within either an incorporated city or a census-defined place.

(2) The population density of the incorporated city or census-defined place has a population density of at least 1,000 persons per square mile.

(3) The project site is adjacent on at least two sides to land that has been developed and the project consists of not more than 45 units, or the project consist of dormitories, barracks, or other group housing facilities for a total of 45 or fewer agricultural employees.

(d) Notwithstanding subdivision (c), this division shall apply to a project that meets the criteria described in subdivision (c) if a public agency that is carrying out or approving the project determines that there is a reasonable possibility that the project, if completed, would have a significant effect on the environment due to unusual circumstances or that the cumulative impacts of successive projects of the same type in the same area, over time, would be significant.

For the purposes of this section, "agricultural employee" has the same meaning as defined by subdivision (b) of Section 1140.4 of the Labor Code.

§ 21159.23. LOW-INCOME HOUSING EXEMPTION

(a) This division does not apply to any development project that consists of the construction, conversion, or use of residential housing consisting of 100 or fewer that is affordable to low-income households if both of the following criteria are met:

(1) The developer of the development project provides sufficient legal commitments to the appropriate local agency to ensure the continued availability and use of the housing units for lower income households, as defined in Section 50079.5 of the Health and Safety Code, for a period of at least 30 years, at monthly housing costs, as determined pursuant to Section 50053 of the Health and Safety Code.

(2) The development project meets all of the following requirements:

(A) The project satisfies the criteria described in Section 21159.21.

(B) The project site meets one of the following conditions:

(i) Has been previously developed for qualified urban uses.

(ii) The parcels immediately adjacent to the site are developed with qualified urban uses, or at least 75 percent of the perimeter of the site adjoins parcels that are developed with qualified urban uses and the remaining 25 percent of the perimeter of the site adjoins parcels that have previously been developed for qualified urban uses, and the site has not been developed for urban uses and no parcel within the site has been created within 10 years prior to the proposed development of the site.

(C) The project site is not more than five acres in area.

(D) The project site is located within an urbanized area or within a census-defined place with a population density of at least 5,000 persons per square mile or, if the project consists of 50 or fewer units, within an incorporated city with a population density of at least 2,500 persons per square mile and a total population of at least 25,000 persons.

(b) Notwithstanding subdivision (a), if a project satisfies all of the criteria described in subdivision (a) except subparagraph (D) of paragraph (2) of that subdivision, this division does not apply to the project if the project is located within either an incorporated city or a census defined place with a population density of at least 1,000 persons per square mile.

(c) Notwithstanding subdivision (b), this division applies to a project that meets the criteria of subdivision (b), if there is a reasonable possibility that the project would have a significant effect on the environment or the residents of the project due to unusual circumstances or due to the related or cumulative impacts of reasonably foreseeable projects in the vicinity of the project.

(d) For the purposes of this section, "residential" means a use consisting of either of the following:

(1) Residential units only.

(2) Residential units and primarily neighborhood-serving goods, services, or retail uses that do not exceed 15 percent of the total floor area of the project.

§ 21159.24. INFILL HOUSING EXEMPTION

(a) Except as provided in subdivision (b), this division does not apply to a project if all of the following criteria are met:

(1) The project is a residential project on an infill site.

(2) The project is located within an urbanized area.

(3) The project satisfies the criteria of Section 21159.21.

(4) Within five years of the date that the application for the project is deemed complete pursuant to Section 65943 of the Government Code, community-level environmental review was certified or adopted.

(5) The site of the project is not more than four acres in total area.

(6) The project does not contain more than 100 residential units.

(7) Either of the following criteria are met:

(A) (i) At least 10 percent of the housing is sold to families of moderate income, or not less than 10 percent of the housing is rented to families of low income, or not less than 5 percent of the housing is rented to families of very low income.

(ii) The project developer provides sufficient legal commitments to the appropriate local agency to ensure the continued availability and use of the housing units for very low, low-, and moderate-income households at monthly housing costs determined pursuant to paragraph (3) of subdivision (h) of Section 65589.5 of the Government Code.

(B) The project developer has paid or will pay in-lieu fees pursuant to a local ordinance in an amount sufficient to result in the development of an equivalent number of units that would otherwise be required pursuant to subparagraph (A).

(8) The project is within one-half mile of a major transit stop.

(9) The project does not include any single level building that exceeds 100,000 square feet.

(10) The project promotes higher density infill housing. A project with a density of at least 20 units per acre shall be conclusively presumed to promote higher density infill housing. A project with a density of at least 10 units per acre and a density greater than the average

density of the residential properties within 1,500 feet shall be presumed to promote higher density housing unless the preponderance of the evidence demonstrates otherwise.

(b) Notwithstanding subdivision (a), this division shall apply to a development project that meets the criteria described in subdivision (a), if any of the following occur:

(1) There is a reasonable possibility that the project will have a project-specific, significant effect on the environment due to unusual circumstances.

(2) Substantial changes with respect to the circumstances under which the project is being undertaken that are related to the project have occurred since community-level environmental review was certified or adopted.

(3) New information becomes available regarding the circumstances under which the project is being undertaken and that is related to the project, that was not known, and could not have been known, at the time that community-level environmental review was certified or adopted.

(c) If a project satisfies the criteria described in subdivision (a), but is not exempt from this division as result of satisfying the criteria described in subdivision (b), the analysis of the environmental effects of the project in the environmental impact report or the negative declaration shall be limited to an analysis of the project-specific effect of the projects and any effects identified pursuant to paragraph (2) or (3) of subdivision (b).

(d) For the purposes of this section, "residential" means a use consisting of either of the following:

(1) Residential units only.

(2) Residential units and primarily neighborhood-serving goods, services, or retail uses that do not exceed 25 percent of the total building square footage of the project ~~15 percent of the total floor area of the project~~.

§ 21159.25. [DELETED]

§ 21159.26. REDUCTIONS IN HOUSING UNITS AS MITIGATION DISCOURAGED

With respect to a project that includes a housing development, a public agency may not reduce the proposed number of housing units as a mitigation measure or project alternative for a particular significant effect on the environment if it determines that there is another feasible specific mitigation measure or project alternative that would provide a comparable level of mitigation. This section does not affect any other requirement regarding the residential density of that project.

§ 21159.27. PROHIBITION AGAINST PIECEMEALING TO QUALIFY FOR EXEMPTIONS

A project may not be divided into smaller projects to qualify for one or more exemptions pursuant to this article.

§ 21159.28.

(a) If a residential or mixed-use residential project is consistent with the use designation, density, building intensity, and applicable policies specified for the project area in either a sustainable communities strategy or an alternative planning strategy, for which the State Air Resources Board pursuant to subparagraph (I) of paragraph (2) of subdivision (b) of Section 65080 of the Government Code has accepted the metropolitan planning organization's determination that the sustainable communities strategy or the alternative planning strategy would, if implemented, achieve the greenhouse gas emission reduction targets and if the project incorporates the mitigation measures required by an applicable prior environmental document, then any findings or other determinations for an exemption, a negative declaration, a mitigated negative declaration, a sustainable communities environmental assessment, an environmental impact report, or addenda prepared or adopted for the project pursuant to this division shall not be required to reference, describe, or discuss (1) growth inducing impacts; or (2) any project

specific or cumulative impacts from cars and light-duty truck trips generated by the project on global warming or the regional transportation network.

(b) Any environmental impact report prepared for a project described in subdivision (a) shall not be required to reference, describe, or discuss a reduced residential density alternative to address the effects of car and light-duty truck trips generated by the project.

(c) "Regional transportation network," for purposes of this section, means all existing and proposed transportation system improvements, including the state transportation system, that were included in the transportation and air quality conformity modeling, including congestion modeling, for the final regional transportation plan adopted by the metropolitan planning organization, but shall not include local streets and roads. Nothing in the foregoing relieves any project from a requirement to comply with any conditions, exactions, or fees for the mitigation of the project's impacts on the structure, safety, or operations of the regional transportation network or local streets and roads.

(d) A residential or mixed-use residential project is a project where at least 75 percent of the total building square footage of the project consists of residential use or a project that is a transit priority project as defined in Section 21155.

Chapter 5: Submission of Information

§ 21160. APPLICATION FOR LEASE, PERMIT, LICENSE, ETC.; DATA AND INFORMATION; PURPOSE; TRADE SECRETS

Whenever any person applies to any public agency for a lease, permit, license, certificate, or other entitlement for use, the public agency may require that person to submit data and information which may be necessary to enable the public agency to determine whether the proposed project may have a significant effect on the environment or to prepare an environmental impact report.

If any or all of the information so submitted is a "trade secret" as defined in Section 6254.7 of the Government Code by those submitting that information, it shall not be included in the impact report or otherwise disclosed by any public agency. This section shall not be construed to prohibit the exchange of properly designated trade secrets between public agencies who have lawful jurisdiction over the preparation of the impact report.

§ 21161. COMPLETION OF IMPACT REPORT; NOTICE; VALIDITY OF PROJECT

Whenever a public agency has completed an environmental impact report, it shall cause a notice of completion of that report to be filed with the Office of Planning and Research. The notice of completion shall briefly identify the project and shall indicate that an environmental impact report has been prepared. The notice of completion shall identify the project location by latitude and longitude. Failure to file the notice required by this section shall not affect the validity of a project.

§ 21162. [DELETED]

Chapter 6: Limitations

§ 21165. LEAD AGENCY; PREPARATION OF IMPACT REPORT

(a) When a project is to be carried out or approved by two or more public agencies, the determination of whether the project may have a significant effect on the environment shall be made by the lead agency, and that agency shall prepare, or cause to be prepared by contract, the environmental impact report for the project, if a report is required by this division. In the event that a dispute arises as to which is the lead agency, any of the disputing public agencies, or in the case of a project described in subdivision (c) of Section 21065 the applicant for such project,

may submit the question to the Office of Planning and Research, and the Office of Planning and Research shall designate, within 21 days of receiving the request, the lead agency, giving due consideration to the capacity of that agency to adequately fulfill the requirements of this division.

(b) For the purposes of this section, a "dispute" means a contested, active difference of opinion between two or more public agencies as to which of those agencies shall prepare any necessary environmental document. A dispute exists where each of those agencies claims that it either has or does not have the obligation to prepare that environmental document. The Office of Planning and Research shall not designate a lead agency in the absence of such a dispute.

§ 21166. SUBSEQUENT OR SUPPLEMENTAL IMPACT REPORT; CONDITIONS

When an environmental impact report has been prepared for a project pursuant to this division, no subsequent or supplemental environmental impact report shall be required by the lead agency or by any responsible agency, unless one or more of the following events occurs:

(a) Substantial changes are proposed in the project which will require major revisions of the environmental impact report.

(b) Substantial changes occur with respect to the circumstances under which the project is being undertaken which will require major revisions in the environmental impact report.

(c) New information, which was not known and could not have been known at the time the environmental impact report was certified as complete, becomes available.

§ 21166.1. EFFECT OF PREPARATION OF IMPACT REPORT BY LEAD AGENCY

The decision of a lead agency to prepare an environmental impact report with respect to environmental impacts within a geographic area or for a group of projects shall not be a basis for determining that an environmental document prepared for an individual project within that area or group is inadequate.

§ 21167. COMMENCEMENT OF ACTIONS OR PROCEEDINGS; TIME

An action or proceeding to attack, review, set aside, void, or annul the following acts or decisions of a public agency on the grounds of noncompliance with this division shall be commenced as follows:

(a) An action or proceeding alleging that a public agency is carrying out or has approved a project that may have a significant effect on the environment without having determined whether the project may have a significant effect on the environment shall be commenced within 180 days from the date of the public agency's decision to carry out or approve the project, or, if a project is undertaken without a formal decision by the public agency, within 180 days from the date of commencement of the project.

(b) An action or proceeding alleging that a public agency has improperly determined whether a project may have a significant effect on the environment shall be commenced within 30 days from the date of the filing of the notice required by subdivision (a) of Section 21108 or subdivision (a) of Section 21152.

(c) An action or proceeding alleging that an environmental impact report does not comply with this division shall be commenced within 30 days from the date of the filing of the notice required by subdivision (a) of Section 21108 or subdivision (a) of Section 21152 by the lead agency.

(d) An action or proceeding alleging that a public agency has improperly determined that a project is not subject to this division pursuant to subdivision (b) of Section 21080 or Section 21172 shall be commenced within 35 days from the date of the filing by the public agency, or person specified in subdivision (b) or (c) of Section 21065, of the notice authorized by subdivision (b) of Section 21108 or subdivision (b) of Section 21152. If the notice has not been filed, the action or

proceeding shall be commenced within 180 days from the date of the public agency's decision to carry out or approve the project, or, if a project is undertaken without a formal decision by the public agency, within 180 days from the date of commencement of the project.

(e) An action or proceeding alleging that another act or omission of a public agency does not comply with this division shall be commenced within 30 days from the date of the filing of the notice required by subdivision (a) of Section 21108 or subdivision (a) of Section 21152.

(f) If a person has made a written request to the public agency for a copy of the notice specified in Section 21108 or 21152 prior to the date on which the agency approves or determines to carry out the project, then not later than five days from the date of the agency's action, the public agency shall deposit a written copy of the notice addressed to that person in the United States mail, first class postage prepaid. The date upon which this notice is mailed shall not affect the time periods specified in subdivisions (b), (c), (d), and (e).

§ 21167.1. PREFERENTIAL HEARING OR OTHER CIVIL ACTIONS; DESIGNATION OF JUDGES TO DEVELOP EXPERTISE

(a) In all actions or proceedings brought pursuant to Sections 21167, 21168, and 21168.5, including the hearing of an action or proceeding on appeal from a decision of a lower court, all courts in which the action or proceeding is pending shall give the action or proceeding preference over all other civil actions, in the matter of setting the action or proceeding for hearing or trial, and in hearing or trying the action or proceeding, so that the action or proceeding shall be quickly heard and determined. The court shall regulate the briefing schedule so that, to the extent feasible, the court shall commence hearings on an appeal within one year of the date of the filing of the appeal.

(b) To ensure that actions or proceedings brought pursuant to Sections 21167, 21168, and 21168.5 may be quickly heard and determined in the lower courts, the superior courts in all counties with a population of more than 200,000 shall designate one or more judges to develop expertise in this division and related land use and environmental laws, so that those judges will be available to hear, and quickly resolve, actions or proceedings brought pursuant to Sections 21167, 21168, and 21168.5.

(c) In an action or proceeding filed pursuant to this chapter that is joined with any other cause of action, the court, upon a motion by any party, may grant severance of the actions. In determining whether to grant severance, the court shall consider such as matters judicial economy, administrative economy, and prejudice to any party.

§ 21167.2. FAILURE TO COMMENCE ACTION OR PROCEEDING WITHIN TIME LIMITS; PRESUMPTION THAT IMPACT REPORT COMPLIES WITH DIVISION

If no action or proceeding alleging that an environmental impact report does not comply with the provisions of this division is commenced during the period prescribed in subdivision (c) of Section 21167, the environmental impact report shall be conclusively presumed to comply with the provisions of this division for purposes of its use by responsible agencies, unless the provisions of Section 21166 are applicable.

§ 21167.3. ASSUMPTION THAT IMPACT REPORT OR NEGATIVE DECLARATION COMPLIES WITH DIVISION; CONDITIONAL APPROVAL OR DISAPPROVAL

(a) If an action or proceeding alleging that an environmental impact report or a negative declaration does not comply with the provisions of this division is commenced during the period described in subdivision (b) or (c) of Section 21167, and if an injunction or stay is issued prohibiting the project from being carried out or approved pending final determination of the issue of such compliance, responsible agencies shall assume that the environmental impact report or the negative declaration for the project does comply with the provisions of this

division and shall issue a conditional approval or disapproval of such project according to the timetable for agency action in Article 5 (commencing with Section 65950) of Chapter 4.5 of Division 1 of Title 7 of the Government Code. A conditional approval shall constitute permission to proceed with a project when and only when such action or proceeding results in a final determination that the environmental impact report or negative declaration does comply with the provisions of this division.

(b) In the event that an action or proceeding is commenced as described in subdivision (a) but no injunction or similar relief is sought and granted, responsible agencies shall assume that the environmental impact report or negative declaration for the project does comply with the provisions of this division and shall approve or disapprove the project according to the timetable for agency action in Article 5 (commencing with Section 65950) of Chapter 4.5 of Division 1 of Title 7 of the Government Code. Such approval shall constitute permission to proceed with the project at the applicant's risk pending final determination of such action or proceeding.

§ 21167.4. MANDATE PROCEEDING ALLEGING NONCOMPLIANCE WITH DIVISION; HEARING REQUEST; DISMISSAL; BRIEFING SCHEDULES AND HEARING DATES

(a) In any action or proceeding alleging noncompliance with this division, the petitioner shall request a hearing within 90 days from the date of filing the petition or shall be subject to dismissal on the court's own motion or on the motion of any party interested in the action or proceeding.

(b) The petitioner shall serve a notice of the request for a hearing on all parties at the time that the petitioner files the request for a hearing.

(c) Upon the filing of a request by the petitioner for a hearing and upon application by any party, the court shall establish a briefing schedule and a hearing date. In the absence of good cause, briefing shall be completed within 90 days from the date that the request for a hearing is filed, and the hearing, to the extent feasible, shall be held within 30 days thereafter. Good cause may include, but shall not be limited to, the conduct of discovery, determination of the completeness of the record of proceedings, the complexity of the issues, and the length of the record of proceedings and the timeliness of its production. The parties may stipulate to a briefing schedule or hearing date that differs from the schedule set forth in this subdivision if the stipulation is approved by the court.

(d) In an action or proceeding alleging noncompliance with this division, the Attorney General may file a motion with the court seeking an expedited schedule for resolution of the case upon the grounds that it would be in the public interest to do so. This subdivision does not affect the rights of any party under existing law to seek an expedited schedule for resolution of the case.

(e) This section shall remain in effect only until January 1, 2016, and as of that date is repealed, unless a later enacted statute, that is enacted before January 1, 2016, deletes or extends that date.

§ 21167.4. [NOT CURRENTLY IN EFFECT]

(a) In any action or proceeding alleging noncompliance with this division, the petitioner shall request a hearing within 90 days from the date of filing the petition or shall be subject to dismissal on the court's own motion or on the motion of any party interested in the action or proceeding.

(b) The petitioner shall serve a notice of the request for a hearing on all parties at the time that the petitioner files the request for a hearing.

(c) Upon the filing of a request by the petitioner for a hearing and upon application by any party, the court shall establish a briefing schedule and a hearing date. In the absence of good cause, briefing shall be completed within 90 days from the date that the request for a hearing is filed,

and the hearing, to the extent feasible, shall be held within 30 days thereafter. Good cause may include, but shall not be limited to, the conduct of discovery, determination of the completeness of the record of proceedings, the complexity of the issues, and the length of the record of proceedings and the timeliness of its production. The parties may stipulate to a briefing schedule or hearing date that differs from the schedule set forth in this subdivision if the stipulation is approved by the court.

(d) This section shall become operative on January 1, 2016.

§ 21167.5. PROOF OF SERVICE; FILING WITH INITIAL PLEADING

Proof of prior service by mail upon the public agency carrying out or approving the project of a written notice of the commencement of any action or proceeding described in Section 21167 identifying the project shall be filed concurrently with the initial pleading in such action or proceeding.

§ 21167.6. RECORD OF PROCEEDINGS; CLERK'S TRANSCRIPT ON APPEAL; FILING BRIEFS ON APPEAL; DATE OF APPEAL FOR HEARING

Notwithstanding any other provision of law, in all actions or proceedings brought pursuant to Section 21167, except those involving the Public Utilities Commission, all of the following shall apply:

(a) At the time that the action or proceeding is filed, the plaintiff or petitioner shall file a request that the respondent public agency prepare the record of proceedings relating to the subject of the action or proceeding. The request, together with the complaint or petition, shall be served personally upon the public agency not later than 10 business days from the date that the action or proceeding was filed.

(b) (1) The public agency shall prepare and certify the record of proceedings not later than 60 days from the date that the request specified in subdivision (a) was served upon the public agency. Upon certification, the public agency shall lodge a copy of the record of proceedings with the court and shall serve on the parties notice that the record of proceedings has been certified and lodged with the court. The parties shall pay any reasonable costs or fees imposed for the preparation of the record of proceedings in conformance with any law or rule of court.

(2) The plaintiff or petitioner may elect to prepare the record of proceedings or the parties may agree to an alternative method of preparation of the record of proceedings, subject to certification of its accuracy by the public agency, within the time limit specified in this subdivision.

(c) The time limit established by subdivision (b) may be extended only upon the stipulation of all parties who have been properly served in the action or proceeding or upon order of the court. Extensions shall be liberally granted by the court when the size of the record of proceedings renders infeasible compliance with that time limit. There is no limit on the number of extensions that may be granted by the court, but no single extension shall exceed 60 days unless the court determines that a longer extension is in the public interest.

(d) If the public agency fails to prepare and certify the record within the time limit established in paragraph (1) of subdivision (b), or any continuances of that time limit, the plaintiff or petitioner may move for sanctions, and the court may, upon that motion, grant appropriate sanctions.

(e) The record of proceedings shall include, but is not limited to, all of the following items:

(1) All project application materials.

(2) All staff reports and related documents prepared by the respondent public agency with respect to its compliance with the substantive and procedural requirements of this division and with respect to the action on the project.

(3) All staff reports and related documents prepared by the respondent public agency and written testimony or documents submitted by any person relevant to any findings or statement of overriding considerations adopted by the respondent agency pursuant to this division.

(4) Any transcript or minutes of the proceedings at which the decision-making body of the respondent public agency heard testimony on, or considered any environmental document on, the project, and any transcript or minutes of proceedings before any advisory body to the respondent public agency that were presented to the decisionmaking body prior to action on the environmental documents or on the project.

(5) All notices issued by the respondent public agency to comply with this division or with any other law governing the processing and approval of the project.

(6) All written comments received in response to, or in connection with, environmental documents prepared for the project, including responses to the notice of preparation.

(7) All written evidence or correspondence submitted to, or transferred from, the respondent public agency with respect to compliance with this division or with respect to the project.

(8) Any proposed decisions or findings submitted to the decisionmaking body of the respondent public agency by its staff, or the project proponent, project opponents, or other persons.

(9) The documentation of the final public agency decision, including the final environmental impact report, mitigated negative declaration, or negative declaration, and all documents, in addition to those referenced in paragraph (3), cited or relied on in the findings or in a statement of overriding considerations adopted pursuant to this division.

(10) Any other written materials relevant to the respondent public agency's compliance with this division or to its decision on the merits of the project, including the initial study, any drafts of any environmental document, or portions thereof, that have been released for public review, and copies of studies or other documents relied upon in any environmental document prepared for the project and either made available to the public during the public review period or included in the respondent public agency's files on the project, and all internal agency communications, including staff notes and memoranda related to the project or to compliance with this division.

(11) The full written record before any inferior administrative decision-making body whose decision was appealed to a superior administrative decision-making body prior to the filing of litigation.

(f) In preparing the record of proceedings, the party preparing the record shall strive to do so at reasonable cost in light of the scope of the record.

(g) The clerk of the superior court shall prepare and certify the clerk's transcript on appeal not later than 60 days from the date that the notice designating the papers or records to be included in the clerk's transcript was filed with the superior court, if the party or parties pay any costs or fees for the preparation of the clerk's transcript imposed in conformance with any law or rules of court. Nothing in this subdivision precludes an election to proceed by appendix, as provided in Rule 8.124 of the California Rules of Court.

(h) Extensions of the period for the filing of any brief on appeal may be allowed only by stipulation of the parties or by order of the court for good cause shown. Extensions for the filing of a brief on appeal shall be limited to one 30-day extension for the preparation of an opening brief, and one 30-day extension for the preparation of a responding brief, except that the court may grant a longer extension or additional extensions if it determines that there is a substantial likelihood of settlement that would avoid the necessity of completing the appeal.

(i) At the completion of the filing of briefs on appeal, the appellant shall notify the court of the completion of the filing of briefs, whereupon the clerk of the reviewing court shall set the appeal for hearing on the first available calendar date.

§ 21167.6.5. SERVICE OF REAL PARTY IN INTEREST; LISTING AND NOTICE TO RESPONSIBLE AND TRUSTEE AGENCIES; FAILURE TO NAME POTENTIAL PARTIES

(a) The petitioner or plaintiff shall name, as a real party in interest, the person or persons identified by the public agency in its notice filed pursuant to subdivision (a) or (b) of Section 21108 or Section 21152 or, if no notice is filed, the person or persons in subdivision (b) or (c) of Section 21065, as reflected in the agency's record of proceedings for the project that is the subject of an action or proceeding brought pursuant to Section 21167, 21168, or 21168.5, and shall serve the petition or complaint on that real party in interest, by personal service, mail facsimile, or any other method permitted by law not later than 20 business days following service of the petition or complaint on the public agency.

(b) The public agency shall provide the petitioner or plaintiff, not later than 10 business days following service of the petition or complaint on the public agency, with a list of responsible agencies and a public agency having jurisdiction over a natural resource affected by the project.

(c) The petitioner or plaintiff shall provide the responsible agencies, and a public agency having jurisdiction over a natural resource affected by the project, with notice of the action or proceeding within 15 days of receipt of the list described in subdivision (b).

(d) Failure to name potential persons, other than those real parties in interest described in subdivision (a), is not grounds for dismissal pursuant to Section 389 of the Code of Civil Procedure.

(e) This section is not intended to affect an existing right of a party to intervene in the action.

§ 21167.7. COPY OF PLEADINGS TO ATTORNEY GENERAL; GRANTING OF RELIEF

Every person who brings an action pursuant to Section 21167 shall comply with the requirements of Section 388 of the Code of Civil Procedure. Every such person shall also furnish pursuant to Section 388 of the Code of Civil Procedure a copy of any amended or supplemental pleading filed by such person in such action to the Attorney General. No relief, temporary or permanent, shall be granted until a copy of the pleading has been furnished to the Attorney General in accordance with such requirements.

§ 21167.8. SETTLEMENT MEETING; PRESETTLEMENT AND SETTLEMENT STATEMENTS; FURTHER SETTLEMENT CONFERENCE; FAILURE TO PARTICIPATE

(a) Not later than 20 days from the date of service upon a public agency of a petition or complaint brought pursuant to Section 21167, the public agency shall file with the court a notice setting forth the time and place at which all parties shall meet and attempt to settle the litigation. The meeting shall be scheduled and held not later than 45 days from the date of service of the petition or complaint upon the public agency. The notice of the settlement meeting shall be served by mail upon the counsel for each party. If the public agency does not know the identity of counsel for a party, the notice shall be served by mail upon the party for whom counsel is not known.

(b) At the time and place specified in the notice filed with the court, the parties shall meet and confer regarding anticipated issues to be raised in the litigation and shall attempt in good faith to settle the litigation and the dispute which forms the basis of the litigation. The settlement meeting discussions shall be comprehensive in nature and shall focus on the legal issues raised by the parties concerning the project that is the subject of the litigation.

(c) The settlement meeting may be continued from time to time without postponing or otherwise delaying other applicable time limits in the litigation. The settlement meeting, or a mediation

proceeding that is conducted pursuant to Chapter 9.3 (commencing with Section 66030) of Division 1 of Title 7 of the Government Code, is intended to be conducted concurrently with any judicial proceedings.

(d) If the litigation is not settled, the court, in its discretion, may, or at the request of any party, shall, schedule a further settlement conference before a judge of the superior court. If the petition or complaint is later heard on its merits, the judge hearing the matter shall not be the same judge conducting the settlement conference, except in counties that have only one judge of the superior court.

(e) The failure of any party, who was notified pursuant to subdivision (a), to participate in the litigation settlement process, without good cause, may result in an imposition of sanctions by the court.

(f) Not later than 30 days from the date that notice of certification of the record of proceedings was filed and served in accordance with Section 21167.6, the petitioner or plaintiff shall file and serve on all other parties a statement of issues which the petitioner or plaintiff intends to raise in any brief or at any hearing or trial. Not later than 10 days from the date on which the respondent or real party in interest has been served with the statement of issues from the petitioner or plaintiff, each respondent and real party in interest shall file and serve on all other parties a statement of issues which that party intends to raise in any brief or at any hearing or trial.

(g) This section shall remain in effect only until January 1, 2016, and as of that date is repealed, unless a later enacted statute, that is enacted before January 1, 2016, deletes or extends that date.

§ 21167.8. [NOT CURRENTLY IN EFFECT]

(a) Not later than 20 days from the date of service upon a public agency of a petition or complaint brought pursuant to Section 21167, the public agency shall file with the court a notice setting forth the time and place at which all parties shall meet and attempt to settle the litigation. The meeting shall be scheduled and held not later than 45 days from the date of service of the petition or complaint upon the public agency. The notice of the settlement meeting shall be served by mail upon the counsel for each party. If the public agency does not know the identity of counsel for any party, the notice shall be served by mail upon the party for whom counsel is not known.

(b) At the time and place specified in the notice filed with the court, the parties shall meet and confer regarding anticipated issues to be raised in the litigation and shall attempt in good faith to settle the litigation and the dispute which forms the basis of the litigation. The settlement meeting discussions shall be comprehensive in nature and shall focus on the legal issues raised by the parties concerning the project that is the subject of the litigation.

(c) The settlement meeting may be continued from time to time without postponing or otherwise delaying other applicable time limits in the litigation. The settlement meeting is intended to be conducted concurrently with any judicial proceedings.

(d) If the litigation is not settled, the court, in its discretion, may, or at the request of any party, shall, schedule a further settlement conference before a judge of the superior court. If the petition or complaint is later heard on its merits, the judge hearing the matter shall not be the same judge conducting the settlement conference, except in counties that have only one judge of the superior court.

(e) The failure of any party, who was notified pursuant to subdivision (a), to participate in the litigation settlement process, without good cause, may result in an imposition of sanctions by the court.

(f) Not later than 30 days from the date that notice of certification of the record of proceedings was filed and served in accordance with Section 21167.6, the petitioner or plaintiff shall file and serve on all other parties a statement of issues which the petitioner or plaintiff intends to raise

in any brief or at any hearing or trial. Not later than 10 days from the date on which the respondent or real party in interest has been served with the statement of issues from the petitioner or plaintiff, each respondent and real party in interest shall file and serve on all other parties a statement of issues which that party intends to raise in any brief or at any hearing or trial.

(g) This section shall become operative on January 1, 2016.

§ 21167.9.

Any action brought in the superior court relating to this division may be subject to a mediation proceeding conducted pursuant to Chapter 9.3 (commencing with Section 66030) of Division 1 of Title 7 of the Government Code.

§ 21167.10.

(a) Within five business days of the filing of a notice required by subdivision (a) or (b) of Section 21108, or subdivision (a) or (b) of Section 21152 by the lead agency, a person wishing to bring an action or a proceeding pursuant to Section 21167, 21168, or 21168.5 may file with the lead agency and the real party in interest a notice requesting mediation.

(b) Within five business days of the receipt of the notice requesting mediation, a lead agency may respond to the person by accepting the request for mediation and proceed with mediation.

(c) The request for mediation is deemed denied if the lead agency fails to respond within five business days of receiving the request for mediation.

(d) The limitation periods provided pursuant to this chapter shall be tolled until the completion of the mediation conducted pursuant to this section.

(e) This section does not apply in cases where the lead agency has not filed the notice required by subdivision (a) or (b) of Section 21108, or subdivision (a) or (b) of Section 21152.

(f) (1) Except as set forth in paragraph (2), this section shall remain in effect only until January 1, 2016, and as of that date is repealed, unless a later enacted statute, that is enacted before January 1, 2016, deletes or extends that date.

(2) Notwithstanding paragraph (1), the tolling of the limitation periods provided pursuant to subdivision (d) shall apply if a mediation conducted pursuant to this section is completed on or after January 1, 2016.

§ 21168. REVIEW OF DETERMINATION; FINDING OR DECISION OF PUBLIC AGENCY; LAW GOVERNING; SCOPE

Any action or proceeding to attack, review, set aside, void or annul a determination, finding, or decision of a public agency, made as a result of a proceeding in which by law a hearing is required to be given, evidence is required to be taken and discretion in the determination of facts is vested in a public agency, on the grounds of noncompliance with the provisions of this division shall be in accordance with the provisions of Section 1094.5 of the Code of Civil Procedure.

In any such action, the court shall not exercise its independent judgment on the evidence but shall only determine whether the act or decision is supported by substantial evidence in the light of the whole record.

§ 21168.5. ABUSE OF DISCRETION

In any action or proceeding, other than an action or proceeding under Section 21168, to attack, review, set aside, void or annul a determination, finding, or decision of a public agency on the grounds of noncompliance with this division, the inquiry shall extend only to whether there was a prejudicial abuse of discretion. Abuse of discretion is established if the agency has not proceeded in

a manner required by law or if the determination or decision is not supported by substantial evidence.

§ 21168.6. MANDATE TO PUBLIC UTILITIES COMMISSION; SUPREME COURT JURISDICTION

In any action or proceeding under Sections 21168 or 21168.5 against the Public Utilities Commission the writ of mandate shall lie only from the Supreme Court to such commission.

§ 21168.6.5.

(a) For the purposes of this section, the following definitions shall apply:

(1) "Applicant" means a private entity or its affiliates that proposes the project and its successors, heirs, and assignees.

(2) "Initial project approval" means any actions, activities, ordinances, resolutions, agreements, approvals, determinations, findings, or decisions taken, adopted, or approved by the lead agency required to allow the applicant to commence the construction of the project, as determined by the lead agency.

(3) "Project" means a project that substantially conforms to the project description for the Convention Center Modernization and Farmers Field Project set forth in the notice of preparation released by the City of Los Angeles on March 17, 2011.

(4) "Stadium" means, except as the context indicates otherwise, the stadium built pursuant to the project for football and other spectator events.

(5) "Subsequent project approval" means any actions, activities, ordinances, resolutions, agreements, approvals, determinations, findings, or decisions by the lead agency required for, or in furtherance of, the project that are taken, adopted, or approved following the initial project approvals until the project obtains certificates of occupancy.

(6) "Trip ratio" means the total annual number of private automobiles arriving at the stadium for spectator events divided by the total annual number of spectators at the events.

(b) (1) This section does not apply to the project and shall become inoperative on the date of the release of the draft environmental impact report and is repealed on January 1 of the following year, if the applicant fails to notify the lead agency prior to the release of the draft environmental impact report for public comment that the applicant is electing to proceed pursuant to this section.

(2) The lead agency shall notify the Secretary of State if the applicant fails to notify the lead agency of its election to proceed pursuant to this section.

(c) (1) (A) Notwithstanding any other law, the procedures set forth in subdivision (d) shall apply to any action or proceeding brought to attack, review, set aside, void, or annul the certification of the environmental impact report for the project or the granting of any initial project approvals.

(B) Notwithstanding any other law, the procedures set forth in subdivision (j) shall apply to any action or proceeding brought to attack, review, set aside, void, or annul any subsequent project approvals.

(2) Notwithstanding any other law, the procedure set forth in subdivision (f) shall apply to the certification of the environmental impact report for the project and to any initial project approvals.

(d) (1) An action or proceeding to attack, set aside, void, or annul a determination, finding, or decision of the lead agency certifying the environmental impact report or granting one or more initial project approvals shall be commenced by filing a petition for a writ of mandate with the Second District Court of Appeal and shall be served on the respondent and the real

party in interest within 30 days of the filing by the lead agency of the notice required by subdivision (a) of Section 21152.

(2) The petitioner shall file and serve the opening brief in support of the petition for writ of mandate within 40 days of the filing of the petition for a writ of mandate.

(3) The respondent and real party in interest shall file and serve any brief in opposition to the petition for writ of mandate within 25 days of the filing of the opening brief.

(4) The petitioner shall file and serve the reply brief within 20 days of the filing of the last opposition brief to the petitioner's opening brief.

(5) Except as provided in paragraph (6), parties to the action shall comply with all applicable California Rules of Court in the filing of the petition for writ of mandate and the briefs.

(6) (A) Rule 8.220 of the California Rules of Court shall not apply to the time periods set forth in paragraphs (2) to (4), inclusive.

(B) If a petitioner fails to file the opening brief pursuant to paragraph (2), the Court of Appeal shall dismiss the petition.

(C) If the respondents and real party in interest fail to file the brief in opposition pursuant to paragraph (3), the Court of Appeal shall decide the petition for writ of mandate based on the record, the opening brief, and any oral argument by the petitioner.

(7) Except upon a showing of extraordinary good cause, the Court of Appeal shall not grant any extensions of time to the deadlines specified in this subdivision. Any extension shall be limited to the minimum amount the Court of Appeal deems to be necessary.

(8) The Court of Appeal may, on its motion or upon request from a party, appoint a special master to assist the Court of Appeal in conducting the expedited judicial review required pursuant to this subdivision. If the Court of Appeal appoints a special master, the applicant shall pay all reasonable costs for the special master, not to exceed one hundred fifty thousand dollars ($150,000). If the Court of Appeal determines that the cost of the special master may exceed one hundred fifty thousand dollars ($150,000), it may request that additional funds be provided by the applicant and, if the applicant agrees to provide the funding, shall use the funds to pay the additional costs of the special master.

(9) The Court of Appeal shall hold a hearing and issue a decision on all petitions for writ of mandate filed pursuant to this subdivision within 60 days of the filing of the last timely reply brief.

(10) (A) A petition for review of the decision rendered by the Court of Appeal shall be filed with the Supreme Court and served on all parties to the petition for writ of mandate within 15 days of the decision.

(B) Any opposition to the petition for review shall be filed and served within 15 days of the filing of the petition for review.

(C) The Supreme Court shall render a decision on the petition for review within 30 days after the filing of the petition for review or within 15 days after the filing of the opposition to the petition for review, whichever is earlier.

(11) All briefs and notices filed pursuant to this subdivision shall be electronically served on parties pursuant to Rule 8.71 of the California Rules of Court. Each party to the petition shall provide an electronic service address at which the party agrees to accept the service.

(12) (A) No provision of law that is inconsistent or conflicts with this subdivision shall apply to a petition for a writ of mandate subject to this subdivision, including, but not limited to, any of the following:

(i) Section 21167.4.

(ii) Subdivisions (a) through (d), inclusive, and (g) through (i), inclusive, of Section 21167.6.

(iii) Subdivision (f) of Section 21167.8.

(iv) Section 21167.6.5.

(v) Sections 66031 through 66035, inclusive, of the Government Code.

(B) Except as provided in this section, including subparagraph (A), the requirements of this division are fully applicable to the project.

(e) (1) The draft and final environmental impact report shall include a notice in not less than 12-point type stating the following:

THIS EIR IS SUBJECT TO SECTION 21168.6.5 OF THE PUBLIC RESOURCES CODE, WHICH PROVIDES, AMONG OTHER THINGS, THAT THE LEAD AGENCY NEED NOT CONSIDER CERTAIN COMMENTS FILED AFTER THE CLOSE OF THE PUBLIC COMMENT PERIOD FOR THE DRAFT EIR. ANY JUDICIAL ACTION CHALLENGING THE CERTIFICATION OF THE EIR OR THE APPROVAL OF THE PROJECT DESCRIBED IN THE EIR IS SUBJECT TO THE PROCEDURES SET FORTH IN SECTION 21168.6.5 OF THE PUBLIC RESOURCES CODE AND MUST BE FILED WITH THE SECOND DISTRICT COURT OF APPEAL. A COPY OF SECTION 21168.6.5 OF THE PUBLIC RESOURCES CODE IS INCLUDED IN THE APPENDIX TO THIS EIR.

(2) The draft environmental impact report and final environmental impact report shall contain, as an appendix, the full text of this section.

(f) (1) Within 10 days after the release of the draft environmental impact report, the lead agency shall conduct an informational workshop to inform the public of the key analyses and conclusions of that report.

(2) Within 10 days before the close of the public comment period, the lead agency shall hold a public hearing to receive testimony on the draft environmental impact report. A transcript of the hearing shall be included as an appendix to the final environmental impact report.

(3) (A) Within five days following the close of the public comment period, a commenter on the draft environmental impact report may submit to the lead agency a written request for nonbinding mediation. The lead agency and applicant shall participate in nonbinding mediation with all commenters who submitted timely comments on the draft environmental impact report and who requested the mediation. Mediation conducted pursuant to this paragraph shall end no later than 35 days after the close of the public comment period.

(B) A request for mediation shall identify all areas of dispute raised in the comment submitted by the commenter that are to be mediated.

(C) The lead agency shall select one or more mediators who shall be retired judges or recognized experts with at least five years experience in land use and environmental law or science, or mediation. The applicant shall bear the costs of mediation.

(D) A mediation session shall be conducted on each area of dispute with the parties requesting mediation on that area of dispute.

(E) The lead agency shall adopt, as a condition of approval, any measures agreed upon by the lead agency, the applicant, and any commenter who requested mediation. A commenter who agrees to a measure pursuant to this subparagraph shall not raise the issue addressed by that measure as a basis for a petition for writ of mandate challenging the lead agency's decision to certify the environmental impact report or to grant one or more initial project approvals.

(4) The lead agency need not consider written comments submitted after the close of the public comment period, unless those comments address any of the following:

(A) New issues raised in the response to comments by the lead agency.

(B) New information released by the public agency subsequent to the release of the draft environmental impact report, such as new information set forth or embodied in a staff report, proposed permit, proposed resolution, ordinance, or similar documents.

(C) Changes made to the project after the close of the public comment period.

(D) Proposed conditions for approval, mitigation measures, or proposed findings required by Section 21081 or a proposed reporting and monitoring program required by paragraph (1) of subdivision (a) of Section 21081.6, where the lead agency releases those documents subsequent to the release of the draft environmental impact report.

(E) New information that was not reasonably known and could not have been reasonably known during the public comment period.

(5) (A) The lead agency shall file the notice required by subdivision (a) of Section 21152 within five days after the last initial project approval.

(B) If the notice required by subdivision (a) of Section 21152 is filed after June 1, 2013, this section shall become inoperative as of June 1, 2013, and is repealed as of January 1, 2014.

(C) In the event this section is repealed pursuant to subparagraph (B), the lead agency shall notify the Secretary of State.

(g) (1) For a petition for writ of mandate filed pursuant to this section, the lead agency shall prepare and certify the record of the proceedings in accordance with this subdivision and in accordance with Rule 3.1365 of the California Rules of Court. The applicant shall pay the lead agency for all costs of preparing and certifying the record of proceedings.

(2) No later than the date of the release of the draft environmental impact report, the lead agency shall make available to the public in a readily accessible electronic format the draft environmental impact report and all other documents submitted to or relied on by the lead agency in the preparation of the draft environmental impact report. A document prepared by the lead agency or submitted by the applicant after the date of the release of the draft environmental impact report that is a part of the record of the proceedings shall be made available to the public in a readily accessible electronic format within five business days after the document is prepared or received by the lead agency.

(3) The lead agency shall encourage written comments on the project to be submitted in a readily accessible electronic format, and shall make any such comment available to the public in a readily accessible electronic format within five days of its receipt.

(4) Within seven business days after the receipt of any comment that is not in an electronic format, the lead agency shall convert that comment into a readily accessible electronic format and make it available to the public in that format.

(5) The lead agency shall indicate in the record of the proceedings comments received that were not considered by the lead agency pursuant to paragraph (4) of subdivision (f) and need not include the content of the comments as a part of the record.

(6) Within five days after the filing of the notice required by subdivision (a) of Section 21152, the lead agency shall certify the record of the proceedings for the approval or determination and shall provide an electronic copy of the record to a party that has submitted a written request for a copy. The lead agency may charge and collect a reasonable fee for the electronic copy, which shall not exceed the reasonable cost of reproducing that copy.

(7) Within 10 days after being served with a petition for a writ of mandate pursuant to paragraph (1) of subdivision (d), the lead agency shall lodge a copy of the certified record of proceedings with the Court of Appeal.

(8) Any dispute over the content of the record of the proceedings shall be resolved by the Court of Appeal. Unless the Court of Appeal directs otherwise, a party disputing the content of the record shall file a motion to augment the record at the time it files its initial brief.

(9) The contents of the record of proceedings shall be as set forth in subdivision (e) of Section 21167.6.

(h) It is the intent of the Legislature that the project minimize traffic congestion and air quality impacts that may result from private automobile trips to the stadium through the requirements of this division as supplemented, pursuant to subdivision (i), by the implementation of measures that will do both of the following:

(1) Achieve and maintain carbon neutrality by reducing to zero the net emissions of greenhouse gases, as defined in subdivision (g) of Section 38505 of the Health and Safety Code, from private automobile trips to the stadium.

(2) Achieve and maintain a trip ratio that is no more than 90 percent of the trip ratio at any other stadium serving a team in the National Football League.

(i) (1) As a condition of approval of the project subject to this section, the lead agency shall require the applicant to implement measures that will meet the requirements of this division and paragraph (1) of subdivision (h) by the end of the first season during which a National Football League team has played at the stadium. To maximize public health, environmental, and employment benefits, the lead agency shall place the highest priority on feasible measures that will reduce greenhouse gas emissions on the stadium site and in the neighboring communities of the stadium. Offset credits shall be employed by the applicant only after feasible local emission reduction measures have been implemented. The applicant shall, to the extent feasible, place the highest priority on the purchase of offset credits that produce emission reductions within the city or the boundaries of the South Coast Air Quality Management District.

(2) To ensure that the stadium achieves a trip ratio that is no more than 90 percent of the trip ratio at any other stadium serving a team in the National Football League, the applicant shall implement the necessary measures as follows:

(A) Not later than the date of the certification of the environmental impact report for the project, the lead agency shall develop and adopt a protocol to implement this subdivision pursuant to this division and subdivision (h), including, but not limited to, criteria and guidelines that will be used to determine the trip ratio.

(B) Following the conclusion of the second, third, fourth, and fifth seasons during which a National Football League team has played at the stadium, the applicant shall prepare a report to the lead agency that describes the measures it has undertaken to reduce trips based on the protocol developed and adopted pursuant to subparagraph (A), the trip ratio at the stadium, and the results of those measures. The report shall also include a summary of publicly available data and other data gathered by the applicant regarding average vehicle ridership, nonpassenger automobile modes of arrival, and trip reduction measures undertaken at other stadiums serving a team in the National Football League.

(C) Following the lead agency's review of the report submitted allowing the fourth season, the lead agency shall determine whether adequate data is available to determine whether the trip ratio at stadium events is more than 90 percent of the trip ratio at any other stadiums serving a National Football League team. If the lead agency concludes that adequate data does not exist, the lead agency shall take necessary steps to collect, or cause to be collected, the data reasonably necessary to make the determination. The

applicant shall pay the reasonable costs of collecting the data pursuant to subdivision (a) of Section 21089.

(D) Following the lead agency's review of the report submitted following the fifth season, the lead agency shall determine the trip ratio at stadium events and the lowest trip ratio at any other stadium serving a National Football League team. If the trip ratio at the stadium is more than 90 percent of the trip ratio at the other stadium with the lowest trip ratio, the lead agency shall, within six months following the receipt of the report, require the applicant to implement additional feasible measures that the lead agency determines pursuant to subparagraph (E) will be sufficient for the stadium to achieve the target specified in paragraph (2) of subdivision (h).

(E) Any trip reduction measure used at other stadiums serving a National Football League team shall be presumed to be feasible unless a preponderance of the evidence demonstrates that the measure is infeasible. The lead agency's decision whether to adopt any mitigation measures pursuant to subparagraph (D) other than those used at another stadium serving a National Football League team shall be governed by the substantial evidence test. This subparagraph does not require the applicant to bear the cost of improving the capacity or performance of transit facilities other than the following:

(i) Temporarily expanding the capacity of a public transit line, as needed, to serve stadium events.

(ii) Providing private charter buses or other similar services, as needed, to serve stadium events.

(iii) Paying its fair share of the cost of measures that expand the capacity of a public fixed or light rail station that is used by spectators attending stadium events.

(F) Any action or proceeding to attack, review, set aside, void, or annul a determination, finding, or decision of the lead agency regarding the additional mitigation measures pursuant to subparagraph (D) shall be commenced within 30 days following the lead agency's filing of the notice required by subdivision (a) of Section 21152 and shall be governed by this division. The procedures set forth in subdivision (d) shall not apply to that action or proceeding. Notwithstanding any other law, compliance or noncompliance with this paragraph shall not result in the stadium being required to cease or limit operations.

(G) If the lead agency requires the applicant to implement additional measures pursuant to subparagraph (D), the applicant shall submit the report described in subparagraph (B) to the lead agency following the conclusion of each subsequent season until the lead agency determines that the applicant has achieved a trip ratio at the stadium that is not more than 90 percent of the trip ratio at any other stadium serving a National Football League team for two consecutive seasons or until the applicant submits the required report following the conclusion of the 10th season, whichever occurs earlier. Nothing in this subparagraph affects the ongoing obligations of the applicant pursuant to subdivision (h) and this subdivision.

(H) All obligations of the applicant set forth in this subdivision or imposed upon the applicant by the lead agency pursuant to this subdivision shall run with the land.

(3) This subdivision and subdivision (h) shall not serve as a basis for any action or proceeding to attack, set aside, void, or annul a determination, finding, or decision of the lead agency in certifying the environmental impact report for the project or in granting the initial or subsequent project approvals.

(4) The obligations imposed pursuant to this subdivision and subdivision (h) supplement, and do not replace, mitigation measures otherwise imposed on the project pursuant to this division.

(j) (1) An action or proceeding to attack, set aside, void, or annul a determination, finding, or decision of the lead agency granting a subsequent project approval shall be subject to the requirements of Chapter 6 (commencing with Section 21165).

(2) (A) In granting relief in an action or proceeding brought pursuant to this subdivision, the court shall not stay or enjoin the construction or operation of the project unless the court finds either of the following:

(i) The continued construction or operation of the project presents an imminent threat to the public health and safety.

(ii) The project site contains unforeseen important Native American artifacts or unforeseen important historical, archaeological, or ecological values that would be materially, permanently, and adversely affected by the continued construction or operation of the project.

(B) If the court finds that clause (i) or (ii) is satisfied, the court shall only enjoin those specific project activities that present an imminent threat to public health and safety or that materially, permanently, and adversely affect unforeseen important Native American artifacts or unforeseen important historical, archaeological, or ecological values.

(k) The provisions of this section are severable. If any provision of this section or its application is held invalid, that invalidity shall not affect other provisions or applications that can be given effect without the invalid provision or application.

§ 21168.6.6

(a) For the purposes of this section, the following definitions shall have the following meanings:

(1) "Applicant" means a private entity or its affiliates that proposes the project and its successors, heirs, and assignees.

(2) "City" means the City of Sacramento.

(3) "Downtown arena" means the following components of the entertainment and sports center project from demolition and site preparation through operation:

(A) An arena facility that will become the new home to the City of Sacramento's National Basketball Association (NBA) team that does both of the following:

(i) Receives Leadership in Energy and Environmental Design (LEED) gold certification for new construction within one year of completion of the first NBA season.

(ii) Minimizes operational traffic congestion and air quality impacts through either or both project design and the implementation of feasible mitigation measures that will do all of the following:

(I) Achieve and maintain carbon neutrality or better by reducing to at least zero the net emissions of greenhouse gases, as defined in subdivision (g) of Section 38505 of the Health and Safety Code, from private automobile trips to the downtown arena as compared to the baseline as verified by the Sacramento Metropolitan Air Quality Management District.

(II) Achieve a per attendee reduction in greenhouse gas emissions from automobiles and light trucks compared to per attendee greenhouse gas emissions associated with the existing arena during the 2012-13 NBA season that will exceed the carbon reduction targets for 2020 and 2035 achieved in the

sustainable communities strategy prepared by the Sacramento Area Council of Governments for the Sacramento region pursuant to Chapter 728 of the Statutes of 2008.

(III) Achieve and maintain vehicle-miles-traveled per attendee for NBA events at the downtown arena that is no more than 85 percent of the baseline.

(B) Associated public spaces.

(C) Facilities and infrastructure for ingress, egress, and use of the arena facility.

(4) "Entertainment and sports center project" or "project" means a project that substantially conforms to the project description for the entertainment and sports center project set forth in the notice of preparation released by the City of Sacramento on April 12, 2013.

(b) (1) The city may prosecute an eminent domain action for 545 and 600 K Street, Sacramento, California, and surrounding publicly accessible areas and rights-of-way within 200 feet of 600 K Street, Sacramento, California, through order of possession pursuant to the Eminent Domain Law (Title 7 (commencing with Section 1230.010) of Part 3 of the Code of Civil Procedure) prior to completing the environmental review under this division.

(2) Paragraph (1) shall not apply to any other eminent domain actions prosecuted by the City of Sacramento or to eminent domain actions based on a finding of blight.

(c) Notwithstanding any other law, the procedures established pursuant to subdivision (d) shall apply to an action or proceeding brought to attack, review, set aside, void, or annul the certification of the environmental impact report for the project or the granting of any project approvals.

(d) On or before July 1, 2014, the Judicial Council shall adopt a rule of court to establish procedures applicable to actions or proceedings brought to attack, review, set aside, void, or annul the certification of the environmental impact report for the project or the granting of any project approvals that require the actions or proceedings, including any potential appeals therefrom, be resolved, to the extent feasible, within 270 days of certification of the record of proceedings pursuant to subdivision (f).

(e) (1) The draft and final environmental impact report shall include a notice in not less than 12-point type stating the following:

THIS EIR IS SUBJECT TO SECTION 21168.6.6 OF THE PUBLIC RESOURCES CODE, WHICH PROVIDES, AMONG OTHER THINGS, THAT THE LEAD AGENCY NEED NOT CONSIDER CERTAIN COMMENTS FILED AFTER THE CLOSE OF THE PUBLIC COMMENT PERIOD FOR THE DRAFT EIR. ANY JUDICIAL ACTION CHALLENGING THE CERTIFICATION OF THE EIR OR THE APPROVAL OF THE PROJECT DESCRIBED IN THE EIR IS SUBJECT TO THE PROCEDURES SET FORTH IN SECTION 21168.6.6 OF THE PUBLIC RESOURCES CODE. A COPY OF SECTION 21168.6.6 OF THE PUBLIC RESOURCES CODE IS INCLUDED IN THE APPENDIX TO THIS EIR.

(2) The draft environmental impact report and final environmental impact report shall contain, as an appendix, the full text of this section.

(3) Within 10 days after the release of the draft environmental impact report, the lead agency shall conduct an informational workshop to inform the public of the key analyses and conclusions of that report.

(4) Within 10 days before the close of the public comment period, the lead agency shall hold a public hearing to receive testimony on the draft environmental impact report. A transcript of the hearing shall be included as an appendix to the final environmental impact report.

(5) (A) Within five days following the close of the public comment period, a commenter on the draft environmental impact report may submit to the lead agency a written request for

nonbinding mediation. The lead agency and applicant shall participate in nonbinding mediation with all commenters who submitted timely comments on the draft environmental impact report and who requested the mediation. Mediation conducted pursuant to this paragraph shall end no later than 35 days after the close of the public comment period.

(B) A request for mediation shall identify all areas of dispute raised in the comment submitted by the commenter that are to be mediated.

(C) The lead agency shall select one or more mediators who shall be retired judges or recognized experts with at least five years experience in land use and environmental law or science, or mediation. The applicant shall bear the costs of mediation.

(D) A mediation session shall be conducted on each area of dispute with the parties requesting mediation on that area of dispute.

(E) The lead agency shall adopt, as a condition of approval, any measures agreed upon by the lead agency, the applicant, and any commenter who requested mediation. A commenter who agrees to a measure pursuant to this subparagraph shall not raise the issue addressed by that measure as a basis for an action or proceeding challenging the lead agency's decision to certify the environmental impact report or to grant one or more initial project approvals.

(6) The lead agency need not consider written comments submitted after the close of the public comment period, unless those comments address any of the following:

(A) New issues raised in the response to comments by the lead agency.

(B) New information released by the public agency subsequent to the release of the draft environmental impact report, such as new information set forth or embodied in a staff report, proposed permit, proposed resolution, ordinance, or similar documents.

(C) Changes made to the project after the close of the public comment period.

(D) Proposed conditions for approval, mitigation measures, or proposed findings required by Section 21081 or a proposed reporting and monitoring program required by paragraph (1) of subdivision (a) of Section 21081.6, where the lead agency releases those documents subsequent to the release of the draft environmental impact report.

(E) New information that was not reasonably known and could not have been reasonably known during the public comment period.

(7) The lead agency shall file the notice required by subdivision (a) of Section 21152 within five days after the last initial project approval.

(f) (1) The lead agency shall prepare and certify the record of the proceedings in accordance with this subdivision and in accordance with Rule 3.1365 of the California Rules of Court. The applicant shall pay the lead agency for all costs of preparing and certifying the record of proceedings.

(2) No later than three business days following the date of the release of the draft environmental impact report, the lead agency shall make available to the public in a readily accessible electronic format the draft environmental impact report and all other documents submitted to or relied on by the lead agency in the preparation of the draft environmental impact report. A document prepared by the lead agency or submitted by the applicant after the date of the release of the draft environmental impact report that is a part of the record of the proceedings shall be made available to the public in a readily accessible electronic format within five business days after the document is prepared or received by the lead agency.

(3) Notwithstanding paragraph (2), documents submitted to or relied on by the lead agency that were not prepared specifically for the project and are copyright protected are not required to

be made readily accessible in an electronic format. For those copyright protected documents, the lead agency shall make an index of these documents available in an electronic format no later than the date of the release of the draft environmental impact report, or within five business days if the document is received or relied on by the lead agency after the release of the draft environmental impact report. The index must specify the libraries or lead agency offices in which hardcopies of the copyrighted materials are available for public review.

(4) The lead agency shall encourage written comments on the project to be submitted in a readily accessible electronic format, and shall make any such comment available to the public in a readily accessible electronic format within five days of its receipt.

(5) Within seven business days after the receipt of any comment that is not in an electronic format, the lead agency shall convert that comment into a readily accessible electronic format and make it available to the public in that format.

(6) The lead agency shall indicate in the record of the proceedings comments received that were not considered by the lead agency pursuant to paragraph (6) of subdivision (e) and need not include the content of the comments as a part of the record.

(7) Within five days after the filing of the notice required by subdivision (a) of Section 21152, the lead agency shall certify the record of the proceedings for the approval or determination and shall provide an electronic copy of the record to a party that has submitted a written request for a copy. The lead agency may charge and collect a reasonable fee from a party requesting a copy of the record for the electronic copy, which shall not exceed the reasonable cost of reproducing that copy.

(8) Within 10 days after being served with a complaint or a petition for a writ of mandate, the lead agency shall lodge a copy of the certified record of proceedings with the superior court.

(9) Any dispute over the content of the record of the proceedings shall be resolved by the superior court. Unless the superior court directs otherwise, a party disputing the content of the record shall file a motion to augment the record at the time it files its initial brief.

(10) The contents of the record of proceedings shall be as set forth in subdivision (e) of Section 21167.6.

(g) (1) As a condition of approval of the project subject to this section, the lead agency shall require the applicant, with respect to any measures specific to the operation of the downtown arena, to implement those measures that will meet the requirements of this division by the end of the first NBA regular season or June of the first NBA regular season, whichever is later, during which an NBA team has played at the downtown arena.

(2) To maximize public health, environmental, and employment benefits, the lead agency shall place the highest priority on feasible measures that will reduce greenhouse gas emissions on the downtown arena site and in the neighboring communities of the downtown arena. Mitigation measures that shall be considered and implemented, if feasible and necessary, to achieve the standards set forth in subclauses (I) to (III), inclusive, of clause (ii) of subparagraph (A) of paragraph (3) of subdivision (a), including, but not limited to:

(A) Temporarily expanding the capacity of a public transit line, as needed, to serve downtown arena events.

(B) Providing private charter buses or other similar services, as needed, to serve downtown arena events.

(C) Paying its fair share of the cost of measures that expand the capacity of a public fixed or light rail station that is used by spectators attending downtown arena events.

(3) Offset credits shall be employed by the applicant only after feasible local emission reduction measures have been implemented. The applicant shall, to the extent feasible, place the highest priority on the purchase of offset credits that produce emission reductions within the city or the boundaries of the Sacramento Metropolitan Air Quality Management District.

(h) (1) (A) In granting relief in an action or proceeding brought pursuant to this section, the court shall not stay or enjoin the construction or operation of the downtown arena unless the court finds either of the following:

(i) The continued construction or operation of the downtown arena presents an imminent threat to the public health and safety.

(ii) The downtown arena site contains unforeseen important Native American artifacts or unforeseen important historical, archaeological, or ecological values that would be materially, permanently, and adversely affected by the continued construction or operation of the downtown arena unless the court stays or enjoins the construction or operation of the downtown arena.

(B) If the court finds that clause (i) or (ii) is satisfied, the court shall only enjoin those specific activities associated with the downtown arena that present an imminent threat to public health and safety or that materially, permanently, and adversely affect unforeseen important Native American artifacts or unforeseen important historical, archaeological, or ecological values.

(2) An action or proceeding to attack, set aside, void, or annul a determination, finding, or decision of the lead agency granting a subsequent project approval shall be subject to the requirements of Chapter 6 (commencing with Section 21165).

(3) Where an action or proceeding brought pursuant to this section challenges aspects of the project other than the downtown arena and those portions or specific project activities are severable from the downtown arena, the court may enter an order as to aspects of the project other than the downtown arena that includes one or more of the remedies set forth in Section 21168.9.

(i) The provisions of this section are severable. If any provision of this section or its application is held invalid, that invalidity shall not affect other provisions or applications that can be given effect without the invalid provision or application.

(j) (1) This section does not apply to the project and shall become inoperative on the date of the release of the draft environmental impact report and is repealed on January 1 of the following year, if the applicant fails to notify the lead agency prior to the release of the draft environmental impact report for public comment that the applicant is electing to proceed pursuant to this section.

(2) The lead agency shall notify the Secretary of State if the applicant fails to notify the lead agency of its election to proceed pursuant to this section.

§ 21168.7. DECLARATION OF EXISTING LAW

Sections 21168 and 21168.5 are declaratory of existing law with respect to the judicial review of determinations or decisions of public agencies made pursuant to this division.

§ 21168.9. PUBLIC AGENCY ACTIONS; NONCOMPLIANCE WITH DIVISION; COURT ORDER; CONTENT; RESTRICTIONS

(a) If a court finds, as a result of a trial, hearing, or remand from an appellate court, that any determination, finding, or decision of a public agency has been made without compliance with this division, the court shall enter an order that includes one or more of the following:

(1) A mandate that the determination, finding, or decision be voided by the public agency, in whole or in part.

(2) If the court finds that a specific project activity or activities will prejudice the consideration or implementation of particular mitigation measures or alternatives to the project, a mandate that the public agency and any real parties in interest suspend any or all specific project activity or activities, pursuant to the determination, finding, or decision, that could result in an adverse change or alteration to the physical environment, until the public agency has taken any actions that may be necessary to bring the determination, finding, or decision into compliance with this division.

(3) A mandate that the public agency take specific action as may be necessary to bring the determination, finding, or decision into compliance with this division.

(b) Any order pursuant to subdivision (a) shall include only those mandates which are necessary to achieve compliance with this division and only those specific project activities in noncompliance with this division. The order shall be made by the issuance of a peremptory writ of mandate specifying what action by the public agency is necessary to comply with this division. However, the order shall be limited to that portion of a determination, finding, or decision or the specific project activity or activities found to be in noncompliance only if a court finds that (1) the portion or specific project activity or activities are severable, (2) severance will not prejudice complete and full compliance with this division, and (3) the court has not found the remainder of the project to be in noncompliance with this division. The trial court shall retain jurisdiction over the public agency's proceedings by way of a return to the peremptory writ until the court has determined that the public agency has complied with this division.

(c) Nothing in this section authorizes a court to direct any public agency to exercise its discretion in any particular way. Except as expressly provided in this section, nothing in this Section is intended to limit the equitable powers of the court.

§ 21169. VALIDATION OF PROJECTS.

Any project defined in subdivision (c) of Section 21065 undertaken, carried out or approved on or before the effective date of this section and the issuance by any public agency of any lease, permit, license, certificate or other entitlement for use executed or issued on or before the effective date of this section notwithstanding a failure to comply with this division, if otherwise legal and valid, is hereby confirmed, validated and declared legally effective. Any project undertaken by a person which was supported in whole or part through contracts with one or more public agencies on or before the effective date of this section, notwithstanding a failure to comply with this division, if otherwise legal and valid, is hereby confirmed, validated and declared legally effective.

§ 21169.11.

(a) At any time after a petition has been filed pursuant to this division[4], but at least 30 days before the hearing on the merits, a party may file a motion requesting the court to impose a sanction for a frivolous claim made in the course of an action brought pursuant to this division.

(b) If the court determines that a claim is frivolous, the court may impose an appropriate sanction, in an amount up to ten thousand dollars ($10,000), upon the attorneys, law firms, or parties responsible for the violation.

(c) For purposes of this section, "frivolous" means totally and completely without merit.

(d) (1) This section shall remain in effect only until January 1, 2016, and as of that date is repealed, unless a later enacted statute, that is enacted before January 1, 2016, deletes or extends that date.

(2) Notwithstanding paragraph (1), the sanction provided pursuant to this section shall apply to an action filed on or before December 31, 2015.

§ 21170. JUDICIAL PROCEEDINGS IN PROGRESS; EFFECT

(a) Section 21169 shall not operate to confirm, validate or give legal effect to any project the legality of which was being contested in a judicial proceeding in which proceeding the pleadings, prior to the effective date of this section, alleged facts constituting a cause of action for, or raised the issue of, a violation of this division and which was pending and undetermined on the effective date of this section; provided, however, that Section 21169 shall operate to confirm, validate or give legal effect to any project to which this subdivision applies if, prior to the commencement of judicial proceedings and in good faith and in reliance upon the issuance by a public agency of any lease, permit, license, certificate or other entitlement for use, substantial construction has been performed and substantial liabilities for construction and necessary materials have been incurred.

(b) Section 21169 shall not operate to confirm, validate or give legal effect to any project which had been determined in any judicial proceeding, on or before the effective date of this section to be illegal, void or ineffective because of noncompliance with this division.

§ 21171. MORATORIUM PROVISION FOR CERTAIN PROJECTS

This division, except for Section 21169, shall not apply to the issuance of any lease, permit, license, certificate or other entitlement for use for any project defined in subdivision (c) of Section 21065 or to any project undertaken by a person which is supported in whole or in part through contracts with one or more public agencies until the 121st day after the effective date of this section. This section shall not apply to any project to which Section 21170 is applicable or to any successor project which is the same as, or substantially identical to, such a project.

This section shall not prohibit or prevent a public agency, prior to the 121st day after the effective date of this section, from considering environmental factors in connection with the approval or disapproval of a project and from imposing reasonable fees in connection therewith.

§ 21172. [DELETED]

§ 21172.5. [DELETED]

§ 21173. SEVERABILITY

If any provision of this division or the application thereof to any person or circumstances is held invalid, such invalidity shall not affect other provisions or applications of this division which can be given effect without the invalid provision or application thereof, and to this end the provisions of this division are severable.

§ 21174. CONSTRUCTION OF DIVISION; ENFORCEMENT OF OTHER PROVISIONS; COASTAL ACT

No provision of this division is a limitation or restriction on the power or authority of any public agency in the enforcement or administration of any provision of law which it is specifically permitted or required to enforce or administer, including, but not limited to, the powers and authority granted to the California Coastal Commission pursuant to Division 20 (commencing with Section 30000). To the extent of any inconsistency or conflict between the provisions of the California Coastal Act of 1976 (Division 20 (commencing with Section 30000)) and the provisions of this division, the provisions of Division 20 (commencing with Section 30000) shall control.

§ 21175. [DELETED]

§ 21176. [DELETED]

§ 21177. PRESENTATION OF GROUNDS FOR NONCOMPLIANCE; OBJECTIONS TO APPROVAL OF PROJECT

(a) An action or proceeding shall not be brought pursuant to Section 21167 unless the alleged grounds for noncompliance with this division were presented to the public agency orally or in writing by any person during the public comment period provided by this division or prior to the close of the public hearing on the project before the issuance of the notice of determination.

(b) A person shall not maintain an action or proceeding unless that person objected to the approval of the project orally or in writing during the public comment period provided by this division or prior to the close of the public hearing on the project before the filing of the notice of determination pursuant to Sections 21108 and 21152.

(c) This section does not preclude any organization formed after the approval of a project from maintaining an action pursuant to Section 21167 if a member of that organization has complied with subdivision (a) and (b) The grounds for noncompliance may have been presented directly by a member or by a member agreeing with or supporting the comments of another person.

(d) This section does not apply to the Attorney General.

(e) This section does not apply to any alleged grounds for noncompliance with this division for which there was no public hearing or other opportunity for members of the public to raise those objections orally or in writing prior to the approval of the project, or if the public agency failed to give the notice required by law.

(f) This section shall remain in effect only until January 1, 2016, and as of that date is repealed, unless a later enacted statute, that is enacted before January 1, 2016, deletes or extends that date.

§ 21177. [NOT CURRENTLY IN EFFECT]

(a) An action or proceeding shall not be brought pursuant to Section 21167 unless the alleged grounds for noncompliance with this division were presented to the public agency orally or in writing by any person during the public comment period provided by this division or prior to the close of the public hearing on the project before the issuance of the notice of determination.

(b) A person shall not maintain an action or proceeding unless that person objected to the approval of the project orally or in writing during the public comment period provided by this division or prior to the close of the public hearing on the project before the filing of notice of determination pursuant to Sections 21108 and 21152.

(c) This section does not preclude any organization formed after the approval of a project from maintaining an action pursuant to Section 21167 if a member of that organization has complied with subdivision (b).

(d) This section does not apply to the Attorney General.

(e) This section does not apply to any alleged grounds for noncompliance with this division for which there was no public hearing or other opportunity for members of the public to raise those objections orally or in writing prior to the approval of the project, or if the public agency failed to give the notice required by law.

(f) This section shall become operative on January 1, 2016.

Chapter 6.5: Jobs and Economic Improvement through Environmental Leadership Act of 2011

§ 21178.

The Legislature finds and declares all of the following:

(a) The overall unemployment rate in California is 12 percent, and in certain regions of the state that rate exceeds 13 percent.

(b) The California Environmental Quality Act (Division 13 (commencing with Section 21000) of the Public Resources Code) requires that the environmental impacts of development projects be identified and mitigated.

(c) The act also guarantees the public an opportunity to review and comment on the environmental impacts of a project and to participate meaningfully in the development of mitigation measures for potentially significant environmental impacts.

(d) There are large projects under consideration in various regions of the state that would replace old and outmoded facilities with new job-creating facilities to meet those regions' needs while also establishing new, cutting-edge environmental benefits to those regions.

(e) These projects are privately financed or financed from revenues generated from the projects themselves and do not require taxpayer financing.

(f) These projects further will generate thousands of full-time jobs during construction and thousands of additional permanent jobs once they are constructed and operating.

(g) These projects also present an unprecedented opportunity to implement nation-leading innovative measures that will significantly reduce traffic, air quality, and other significant environmental impacts, and fully mitigate the greenhouse gas emissions resulting from passenger vehicle trips attributed to the project.

(h) These pollution reductions will be the best in the nation compared to other comparable projects in the United States.

(i) The purpose of this act is to provide unique and unprecedented streamlining benefits under the California Environmental Quality Act for projects that provide the benefits described above for a limited period of time to put people to work as soon as possible.

§ 21180.

For the purposes of this chapter, the following terms shall have the following meanings:

(a) "Applicant" means a public or private entity or its affiliates, or a person or entity that undertakes a public works project, that proposes a project and its successors, heirs, and assignees.

(b) "Environmental leadership development project," "leadership project," or "project" means a project as described in Section 21065 that is one the following:

(1) A residential, retail, commercial, sports, cultural, entertainment, or recreational use project that is certified as LEED silver or better by the United States Green Building Council and, where applicable, that achieves a 10-percent greater standard for transportation efficiency than for comparable projects. These projects must be located on an infill site. For a project that is within a metropolitan planning organization for which a sustainable communities strategy or alternative planning strategy is in effect, the infill project shall be consistent with the general use designation, density, building intensity, and applicable policies specified for the project area in either a sustainable communities strategy or an alternative planning strategy, for which the State Air Resources Board, pursuant to subparagraph (H) of paragraph (2) of subdivision (b) of Section 65080 of the Government Code, has accepted a

metropolitan planning organization's determination that the sustainable communities strategy or the alternative planning strategy would, if implemented, achieve the greenhouse gas emission reduction targets.

(2) A clean renewable energy project that generates electricity exclusively through wind or solar, but not including waste incineration or conversion.

(3) A clean energy manufacturing project that manufactures products, equipment, or components used for renewable energy generation, energy efficiency, or for the production of clean alternative fuel vehicles.

(c) "Transportation efficiency" means the number of vehicle trips by employees, visitors, or customers of the residential, retail, commercial, sports, cultural, entertainment, or recreational use project divided by the total number of employees, visitors, and customers.

§ 21181.

This chapter does not apply to a project if the Governor does not certify a project as an environmental leadership development project eligible for streamlining provided pursuant to this chapter prior to January 1, 2016.

§ 21182.

A person proposing to construct a leadership project may apply to the Governor for certification that the leadership project is eligible for streamlining provided by this chapter. The person shall supply evidence and materials that the Governor deems necessary to make a decision on the application. Any evidence or materials shall be made available to the public at least 15 days before the Governor certifies a project pursuant to this chapter.

§ 21183.

The Governor may certify a leadership project for streamlining pursuant to this chapter if all the following conditions are met:

(a) The project will result in a minimum investment of one hundred million dollars ($100,000,000) in California upon completion of construction.

(b) The project creates high-wage, highly skilled jobs that pay prevailing wages and living wages and provide construction jobs and permanent jobs for Californians, and helps reduce unemployment. For purposes of this subdivision, "jobs that pay prevailing wages" means that all construction workers employed in the execution of the project will receive at least the general prevailing rate of per diem wages for the type of work and geographic area, as determined by the Director of Industrial Relations pursuant to Sections 1773 and 1773.9 of the Labor Code. If the project is certified for streamlining, the project applicant shall include this requirement in all contracts for the performance of the work.

(c) The project does not result in any net additional emission of greenhouse gases, including greenhouse gas emissions from employee transportation, as determined by the State Air Resources Board pursuant to Division 25.5 (commencing with Section 38500) of the Health and Safety Code.

(d) The project applicant has entered into a binding and enforceable agreement that all mitigation measures required pursuant to this division to certify the project under this chapter shall be conditions of approval of the project, and those conditions will be fully enforceable by the lead agency or another agency designated by the lead agency. In the case of environmental mitigation measures, the applicant agrees, as an ongoing obligation, that those measures will be monitored and enforced by the lead agency for the life of the obligation.

(e) The project applicant agrees to pay the costs of the Court of Appeal in hearing and deciding any case, including payment of the costs for the appointment of a special master if deemed

appropriate by the court, in a form and manner specified by the Judicial Council, as provided in the Rules of Court adopted by the Judicial Council pursuant to subdivision (f) of Section 21185.

(f) The project applicant agrees to pay the costs of preparing the administrative record for the project concurrent with review and consideration of the project pursuant to this division, in a form and manner specified by the lead agency for the project.

§ 21184.

(a) The Governor may certify a project for streamlining pursuant to this chapter if it complies with the conditions specified in Section 21183.

(b) (1) Prior to certifying a project, the Governor shall make a determination that each of the conditions specified in Section 21183 has been met. These findings are not subject to judicial review.

(2) (A) If the Governor determines that a leadership project is eligible for streamlining pursuant to this chapter, he or she shall submit that determination, and any supporting information, to the Joint Legislative Budget Committee for review and concurrence or nonconcurrence.

(B) Within 30 days of receiving the determination, the Joint Legislative Budget Committee shall concur or nonconcur in writing on the determination.

(C) If the Joint Legislative Budget Committee fails to concur or nonconcur on a determination by the Governor within 30 days of the submittal, the leadership project is deemed to be certified.

(c) The Governor may issue guidelines regarding application and certification of projects pursuant to this chapter. Any guidelines issued pursuant to this subdivision are not subject to the rulemaking provisions of the Administrative Procedure Act (Chapter 3.5 (commencing with Section 11340) of Part 1 of Division 3 of Title 2 of the Government Code).

§ 21185.

On or before July 1, 2014, the Judicial Council shall adopt a rule of court to establish procedures applicable to actions or proceedings brought to attack, review, set aside, void, or annul the certification of the environmental impact report for an environmental leadership development project certified by the Governor pursuant to this chapter or the granting of any project approvals that require the actions or proceedings, including any potential appeals therefrom, be resolved, within 270 days of certification of the record of proceedings pursuant to Section 21186.

§ 21186.

Notwithstanding any other law, the preparation and certification of the administrative record for a leadership project certified by the Governor shall be performed in the following manner:

(a) The lead agency for the project shall prepare the administrative record pursuant to this division concurrently with the administrative process.

(b) All documents and other materials placed in the administrative record shall be posted on, and be downloadable from, an Internet Web site maintained by the lead agency commencing with the date of the release of the draft environmental impact report.

(c) The lead agency shall make available to the public in a readily accessible electronic format the draft environmental impact report and all other documents submitted to, or relied on by, the lead agency in the preparation of the draft environmental impact report.

(d) A document prepared by the lead agency or submitted by the applicant after the date of the release of the draft environmental impact report that is a part of the record of the proceedings

shall be made available to the public in a readily accessible electronic format within five business days after the document is released or received by the lead agency.

(e) The lead agency shall encourage written comments on the project to be submitted in a readily accessible electronic format, and shall make any comment available to the public in a readily accessible electronic format within five days of its receipt.

(f) Within seven business days after the receipt of any comment that is not in an electronic format, the lead agency shall convert that comment into a readily accessible electronic format and make it available to the public in that format.

(g) Notwithstanding paragraphs (b) to (f), inclusive, documents submitted to or relied on by the lead agency that were not prepared specifically for the project and are copyright protected are not required to be made readily accessible in an electronic format. For those copyright-protected documents, the lead agency shall make an index of these documents available in an electronic format no later than the date of the release of the draft environmental impact report, or within five business days if the document is received or relied on by the lead agency after the release of the draft environmental impact report. The index must specify the libraries or lead agency offices in which hardcopies of the copyrighted materials are available for public review.

(h) The lead agency shall certify the final administrative record within five days of its approval of the project.

(i) Any dispute arising from the administrative record shall be resolved by the superior court. Unless the superior court directs otherwise, a party disputing the content of the record shall file a motion to augment the record at the time it files its initial brief.

(j) The contents of the record of proceedings shall be as set forth in subdivision (e) of Section 21167.6.

§ 21187.

Within 10 days of the Governor certifying an environmental leadership development project pursuant to this section, the lead agency shall, at the applicant's expense, issue a public notice in no less than 12-point type stating the following:

"THE APPLICANT HAS ELECTED TO PROCEED UNDER CHAPTER 6.5 (COMMENCING WITH SECTION 21178) OF THE PUBLIC RESOURCES CODE, WHICH PROVIDES, AMONG OTHER THINGS, THAT ANY JUDICIAL ACTION CHALLENGING THE CERTIFICATION OF THE EIR OR THE APPROVAL OF THE PROJECT DESCRIBED IN THE EIR IS SUBJECT TO THE PROCEDURES SET FORTH IN SECTIONS 21185 TO 21186, INCLUSIVE, OF THE PUBLIC RESOURCES CODE. A COPY OF CHAPTER 6.5 (COMMENCING WITH SECTION 21178) OF THE PUBLIC RESOURCES CODE IS INCLUDED BELOW."

The public notice shall be distributed by the lead agency as required for public notices issued pursuant to paragraph (3) of subdivision (b) of Section 21092.

§ 21188.

The provisions of this chapter are severable. If any provision of this chapter or its application is held to be invalid, that invalidity shall not affect any other provision or application that can be given effect without the invalid provision or application.

§ 21189.

Except as otherwise provided expressly in this chapter, nothing in this chapter affects the duty of any party to comply with this division.

§ 21189.1.

If, prior to January 1, 2016, a lead agency fails to approve a project certified by the Governor pursuant to this chapter, then the certification expires and is no longer valid.

§ 21189.2.

The Judicial Council shall report to the Legislature on or before January 1, 2017, on the effects of this chapter on the administration of justice.

§ 21189.3

This chapter shall remain in effect until January 1, 2017, and as of that date is repealed unless a later enacted statute extends or repeals that date.

California Code of Regulations

Title 14. Natural Resources
Division 6. Resources Agency
Chapter 3: Guidelines for Implementation of the California Environmental Quality Act

As amended January 4, 2013

In January 4, 2013, changes to the CEQA Guidelines were adopted by the Secretary for the California Natural Resources Agency to implement Public Resources Code section 21094.5, setting out a streamlined environmental review process for qualifying infill projects. These changes included adding Section 15183.3, Appendix M, and Appendix N. No amendments to the CEQA Guidelines have been made since this date but several amendments are in process to update the Guidelines and to address SB 743 and AB 52. Visit http://www.opr.ca.gov/m_ceqa.php for more information.

Note: The numbered sections have been adopted by the Secretary of Resources as part of the California Code of Regulations.

Reproduced with the permission of the California Resources Agency; all rights reserved.

Article 1. General

SECTIONS 15000 TO 15007

15000. AUTHORITY

The regulations contained in this chapter are prescribed by the Secretary for Resources to be followed by all state and local agencies in California in the implementation of the California Environmental Quality Act. These Guidelines have been developed by the Office of Planning and Research for adoption by the Secretary for Resources in accordance with Section 21083. Additional information may be obtained by writing:

Secretary for Resources
1416 Ninth Street, Room 1311
Sacramento, CA 95814

These Guidelines are binding on all public agencies in California.

Note: Authority cited: Section 21083, Public Resources Code; Reference: Sections 21082 and 21083, Public Resources Code; *City of Santa Ana v. City of Garden Grove*, (1979) 100 Cal. App. 3d 521.

15001. SHORT TITLE

These Guidelines may be cited as the "State CEQA Guidelines." Existing references to the "State EIR Guidelines" shall be construed to be references to the State CEQA Guidelines.

Note: Authority cited: Sections 21083, Public Resources Code; Reference: Section 21083, Public Resources Code.

15002. GENERAL CONCEPTS

(a) Basic Purposes of CEQA. The basic purposes of CEQA are to:

(1) Inform governmental decision makers and the public about the potential, significant environmental effects of proposed activities.

(2) Identify the ways that environmental damage can be avoided or significantly reduced.

(3) Prevent significant, avoidable damage to the environment by requiring changes in projects through the use of alternatives or mitigation measures when the governmental agency finds the changes to be feasible.

(4) Disclose to the public the reasons why a governmental agency approved the project in the manner the agency chose if significant environmental effects are involved.

(b) Governmental Action. CEQA applies to governmental action. This action may involve:

(1) Activities directly undertaken by a governmental agency,

(2) Activities financed in whole or in part by a governmental agency, or

(3) Private activities which require approval from a governmental agency.

(c) Private Action. Private action is not subject to CEQA unless the action involves governmental participation, financing, or approval.

(d) Project. A "project" is an activity subject to CEQA. The term "project" has been interpreted to mean far more than the ordinary dictionary definition of the term. (See: Section 15378.)

(e) Time for Compliance. A governmental agency is required to comply with CEQA procedures when the agency proposes to carry out or approve the activity. (See: Section 15004.)

(f) Environmental Impact Reports and Negative Declarations. An Environmental Impact Report (EIR) is the public document used by the governmental agency to analyze the significant environmental effects of a proposed project, to identify alternatives, and to disclose possible ways to reduce or avoid the possible environmental damage.

(1) An EIR is prepared when the public agency finds substantial evidence that the project may have a significant effect on the environment. (See: Section 15064(a)(1).)

(2) When the agency finds that there is no substantial evidence that a project may have a significant environmental effect, the agency will prepare a "Negative Declaration" instead of an EIR. (See: Section 15070.)

(g) Significant Effect on the Environment. A significant effect on the environment is defined as a substantial adverse change in the physical conditions which exist in the area affected by the proposed project. (See: Section 15382.) Further, when an EIR identifies a significant effect, the government agency approving the project must make findings on whether the adverse environmental effects have been substantially reduced or if not, why not. (See: Section 15091.)

(h) Methods for Protecting the Environment. CEQA requires more than merely preparing environmental documents. The EIR by itself does not control the way in which a project can be built or carried out. Rather, when an EIR shows that a project would cause substantial adverse changes in the environment, the governmental agency must respond to the information by one or more of the following methods:

(1) Changing a proposed project

(2) Imposing conditions on the approval of the project;

(3) Adopting plans or ordinances to control a broader class of projects to avoid the adverse changes;

(4) Choosing an alternative way of meeting the same need;

(5) Disapproving the project;

(6) Finding that changing or altering the project is not feasible;

(7) Finding that the unavoidable significant environmental damage is acceptable as provided in Section 15093.

(i) Discretionary Action. CEQA applies in situations where a governmental agency can use its judgment in deciding whether and how to carry out or approve a project. A project subject to such judgmental controls is called a "discretionary project." (See: Section 15357.)

(1) Where the law requires a governmental agency to act on a project in a set way without allowing the agency to use its own judgment, the project is called "ministerial," and CEQA does not apply. (See: Section 15369.)

(2) Whether an agency has discretionary or ministerial controls over a project depends on the authority granted by the law providing the controls over the activity. Similar projects may be subject to discretionary controls in one city or county and only ministerial controls in another. (See: Section 15268.)

(j) Public Involvement. Under CEQA, an agency must solicit and respond to comments from the public and other agencies concerned with the project. (See: Sections 15073, 15086, 15087, and 15088.)

(k) Three Step Process. An agency will normally take up to three separate steps in deciding which document to prepare for a project subject to CEQA.

(1) In the first step the Lead Agency examines the project to determine whether the project is subject to CEQA at all. If the project is exempt, the process does not need to proceed any farther. The agency may prepare a Notice of Exemption. (See: Sections 15061 and 15062.)

(2) If the project is not exempt, the Lead Agency takes the second step and conducts an Initial Study (Section 15063) to determine whether the project may have a significant effect on the environment. If the Initial Study shows that there is no substantial evidence that the project may have a significant effect, the Lead Agency prepares a Negative Declaration. (See: Sections 15070 et seq.)

(3) If the Initial Study shows that the project may have a significant effect, the Lead Agency takes the third step and prepares an EIR. (See: Sections 15080 et seq.)

(l) Certified Equivalent Programs. A number of environmental regulatory programs have been certified by the Secretary of the Resources Agency as involving essentially the same consideration of environmental issues as is provided by use of EIRs and Negative Declarations. Certified programs are exempt from preparing EIRs and Negative Declarations but use other documents instead. Certified programs are discussed in Article 17 and are listed in Section 15251.

(m) This section is intended to present the general concepts of CEQA in a simplified and introductory manner. If there are any conflicts between the short statement of a concept in this section and the provisions of other sections of these Guidelines, the other sections shall prevail.

Note: Authority cited: Section 21083, Public Resources Code; Reference: Sections 21000–21176, Public Resources Code; *No Oil, Inc. v. City of Los Angeles*, 13 Cal. 3d 68 (1974); *Running Fence Corp. v. Superior Court*, 51 Cal. App. 3d 400 (1975).

15003. POLICIES

In addition to the policies declared by the Legislature concerning environmental protection and administration of CEQA in Sections 21000, 21001, 21002, and 21002.1 of the Public Resources Code, the courts of this state have declared the following policies to be implicit in CEQA:

(a) The EIR requirement is the heart of CEQA. (*County of Inyo v. Yorty*, 32 Cal. App. 3d 795.)

(b) The EIR serves not only to protect the environment but also to demonstrate to the public that it is being protected. (*County of Inyo v. Yorty*, 32 Cal. App. 3d 795.)

(c) The EIR is to inform other governmental agencies and the public generally of the environmental impact of a proposed project. (*No Oil, Inc. v. City of Los Angeles*, 13 Cal. 3d 68.)

(d) The EIR is to demonstrate to an apprehensive citizenry that the agency has, in fact, analyzed and considered the ecological implications of its action. (*People ex rel. Department of Public Works v. Bosio*, 47 Cal. App. 3d 495.)

(e) The EIR process will enable the public to determine the environmental and economic values of their elected and appointed officials thus allowing for appropriate action come election day should a majority of the voters disagree. (*People v. County of Kern*, 39 Cal. App. 3d 830.)

(f) CEQA was intended to be interpreted in such a manner as to afford the fullest possible protection to the environment within the reasonable scope of the statutory language. (*Friends of Mammoth v. Board of Supervisors*, 8 Cal. 3d 247.)

(g) The purpose of CEQA is not to generate paper, but to compel government at all levels to make decisions with environmental consequences in mind. (*Bozung v. LAFCO* (1975) 13 Cal.3d 263)

(h) The lead agency must consider the whole of an action, not simply its constituent parts, when determining whether it will have a significant environmental effect. (*Citizens Assoc. For Sensible Development of Bishop Area v. County of Inyo* (1985) 172 Cal.App.3d 151)

(i) CEQA does not require technical perfection in an EIR, but rather adequacy, completeness, and a good-faith effort at full disclosure. A court does not pass upon the correctness of an EIR's environmental conclusions, but only determines if the EIR is sufficient as an informational document. (*Kings County Farm Bureau v. City of Hanford* (1990) 221 Cal.App.3d 692)

(j) CEQA requires that decisions be informed and balanced. It must not be subverted into an instrument for the oppression and delay of social, economic, or recreational development or advancement. (*Laurel Heights Improvement Assoc. v. Regents of U.C.* (1993) 6 Cal.4th 1112 and *Citizens of Goleta Valley v. Board of Supervisors* (1990) 52 Cal.3d 553)

Note: Authority cited: Section 21083, Public Resources Code; Reference: Sections 21000–21176, Public Resources Code.

15004. TIME OF PREPARATION

(a) Before granting any approval of a project subject to CEQA, every Lead Agency or Responsible Agency shall consider a final EIR or Negative Declaration or another document authorized by these Guidelines to be used in the place of an EIR or Negative Declaration. (See: The definition of "approval" in Section 15352.)

(b) Choosing the precise time for CEQA compliance involves a balancing of competing factors. EIRs and negative declarations should be prepared as early as feasible in the planning process to enable environmental considerations to influence project program and design and yet late enough to provide meaningful information for environmental assessment.

(1) With public projects, at the earliest feasible time, project sponsors shall incorporate environmental considerations into project conceptualization, design, and planning. CEQA compliance should be completed prior to acquisition of a site for a public project.

(2) To implement the above principles, public agencies shall not undertake actions concerning the proposed public project that would have a significant adverse effect or limit the choice of alternatives or mitigation measures, before completion of CEQA compliance. For example, agencies shall not:

(A) Formally make a decision to proceed with the use of a site for facilities which would require CEQA review, regardless of whether the agency has made any final purchase of the site for these facilities, except that agencies may designate a preferred site for CEQA review and may enter into land acquisition agreements when the agency has conditioned the agency's future use of the site on CEQA compliance.

(B) Otherwise take any action which gives impetus to a planned or foreseeable project in a manner that forecloses alternatives or mitigation measures that would ordinarily be part of CEQA review of that public project.

(3) With private projects, the lead agency shall encourage the project proponent to incorporate environmental considerations into project conceptualization, design, and planning at the earliest feasible time.

(c) The environmental document preparation and review should be coordinated in a timely fashion with the existing planning, review, and project approval processes being used by each public agency. These procedures, to the maximum extent feasible, are to run concurrently, not consecutively. When the lead agency is a state agency, the environmental document shall be included as part of the regular project report if such a report is used in its existing review and budgetary process.

Note: Authority cited: Section 21083, Public Resources Code; Reference: Sections 21003, 21061 and 21105, Public Resources Code; *Friends of Mammoth v. Board of Supervisors*, (1972) 8 Cal.3d 247; *Mount Sutro Defense Committee v. Regents of the University of California*, (1978) 77 Cal.App.3d 20.

15005. TERMINOLOGY

The following words are used to indicate whether a particular subject in the Guidelines is mandatory, advisory, or permissive:

(a) "Must" or "shall" identifies a mandatory element which all public agencies are required to follow.

(b) "Should" identifies guidance provided by the Secretary for Resources based on policy considerations contained in CEQA, in the legislative history of the statute, or in federal court decisions which California courts can be expected to follow. Public agencies are advised to follow this guidance in the absence of compelling, countervailing considerations.

(c) "May" identifies a permissive element which is left fully to the discretion of the public agencies involved.

Note: Authority cited: Section 21083, Public Resources Code; Reference: Sections 21082 and 21083, Public Resources Code.

15006. REDUCING DELAY AND PAPERWORK

Public agencies should reduce delay and paperwork by:

(a) Integrating the CEQA process into early planning. (15004(c))

(b) Ensuring the swift and fair resolution of Lead Agency disputes. (15053)

(c) Identifying projects which fit within categorical exemptions and are therefore exempt from CEQA processing. (15300.4)

(d) Using Initial Studies to identify significant environmental issues and to narrow the scope of EIRs. (15063)

(e) Using a Negative Declaration when a project not otherwise exempt will not have a significant effect on the environment. (15070)

(f) Using a previously prepared EIR when it adequately addresses the proposed project. (15153)

(g) Consulting with state and local Responsible Agencies before and during preparation of an Environmental Impact Report so that the document will meet the needs of all the agencies which will use it. (15083)

(h) Urging applicants, either before or after the filing of an application, to revise projects to eliminate possible significant effects on the environment, thereby enabling the project to qualify for a Negative Declaration rather than an Environmental Impact Report. (15063(c)(2))

(i) Integrating CEQA requirements with other environmental review and consulting requirements. (Public Resources Code Section 21080.5)

(j) Eliminating duplication with federal procedures by providing for joint preparation of environmental documents with federal agencies and by adopting completed federal NEPA documents. (15227)

(k) Emphasizing consultation before an Environmental Impact Report is prepared, rather than submitting adversary comments on a completed document. (15082(b))

(l) Combining environmental documents with other documents such as general plans. (15166)

(m) Eliminating repetitive discussions of the same issues by using Environmental Impact Reports on programs, policies, or plans and tiering from reports of broad scope to those of narrower scope. (15152)

(n) Reducing the length of Environmental Impact Reports by means such as setting appropriate page limits. (15141)

(o) Preparing analytic rather than encyclopedic Environmental Impact Reports. (15142)

(p) Mentioning only briefly issues other than significant ones in EIRs. (15143)

(q) Writing Environmental Impact Reports in plain language. (15140)

(r) Following a clear format for Environmental Impact Reports. (15120)

(s) Emphasizing the portions of the Environmental Impact Report that are useful to decision makers and the public and reducing emphasis on background material. (15143)

(t) Using incorporation by reference. (15150)

(u) Making comments on Environmental Impact Reports as specific as possible. (15204)

Note: Authority cited: Section 21083, Public Resources Code; Reference: Sections 21003 and 21083, Public Resources Code.

15007. AMENDMENTS

(a) These Guidelines will be amended from time to time to match new developments relating to CEQA.

(b) Amendments to the Guidelines apply prospectively only. New requirements in amendments will apply to steps in the CEQA process not yet undertaken by the date when agencies must comply with the amendments.

(c) If a document meets the content requirements in effect when the document is sent out for public review, the document shall not need to be revised to conform to any new content requirements in Guideline amendments taking effect before the document is finally approved.

(d) Public agencies shall comply with new requirements in amendments to the Guidelines beginning with the earlier of the following two dates:

(1) The effective date of the agency's procedures amended to conform to the new Guideline amendments; or

(2) The 120th day after the effective date of the Guideline amendments.

(e) Public agencies may implement any permissive or advisory elements of the Guidelines beginning with the effective date of the Guideline amendments.

Note: Authority cited: Section 21083, Public Resources Code; Reference: Sections 21082–21086, Public Resources Code; *Stevens v. City of Glendale*, 125 Cal. App. 3d 986.

Article 2. General Responsibilities

SECTIONS 15020 TO 15025

15020. GENERAL

Each public agency is responsible for complying with CEQA and these Guidelines. A public agency must meet its own responsibilities under CEQA and shall not rely on comments from other public agencies or private citizens as a substitute for work CEQA requires the Lead Agency to accomplish. For example, a Lead Agency is responsible for the adequacy of its environmental documents. The Lead Agency shall not knowingly release a deficient document hoping that public comments will correct defects in the document.

Note: Authority cited: Section 21083, Public Resources Code; Reference: Sections 21082 and 21082.1, Public Resources Code; *Russian Hill Improvement Association v. Board of Permit Appeals*, 44 Cal. App. 3d 158 (1975).

15021. DUTY TO MINIMIZE ENVIRONMENTAL DAMAGE AND BALANCE COMPETING PUBLIC OBJECTIVES

(a) CEQA establishes a duty for public agencies to avoid or minimize environmental damage where feasible.

(1) In regulating public or private activities, agencies are required to give major consideration to preventing environmental damage.

(2) A public agency should not approve a project as proposed if there are feasible alternatives or mitigation measures available that would substantially lessen any significant effects that the project would have on the environment.

(b) In deciding whether changes in a project are feasible, an agency may consider specific economic, environmental, legal, social, and technological factors.

(c) The duty to prevent or minimize environmental damage is implemented through the findings required by Section 15091.

(d) CEQA recognizes that in determining whether and how a project should be approved, a public agency has an obligation to balance a variety of public objectives, including economic, environmental, and social factors and in particular the goal of providing a decent home and satisfying living environment for every Californian. An agency shall prepare a statement of overriding considerations as described in Section 15093 to reflect the ultimate balancing of competing public objectives when the agency decides to approve a project that will cause one or more significant effects on the environment.

Note: Authority cited: Section 21083, Public Resources Code; Reference: Public Resources Code Sections 21000, 21001, 21002, 21002.1, and 21081; *San Francisco Ecology Center v. City and County of San Francisco*, (1975) 48 Cal. App. 3d 584; *Laurel Hills Homeowners Association v. City Council*, (1978) 83 Cal. App. 3d 515.

15022. PUBLIC AGENCY IMPLEMENTING PROCEDURES

(a) Each public agency shall adopt objectives, criteria, and specific procedures consistent with CEQA and these Guidelines for administering its responsibilities under CEQA, including the orderly evaluation of projects and preparation of environmental documents. The implementing procedures should contain at least provisions for:

(1) Identifying the activities that are exempt from CEQA. These procedures should contain:

(A) Provisions for evaluating a proposed activity to determine if there is no possibility that the activity may have a significant effect on the environment.

(B) A list of projects or permits over which the public agency has only ministerial authority.

(C) A list of specific activities which the public agency has found to be within the categorical exemptions established by these Guidelines.

(2) Conducting Initial Studies.

(3) Preparing Negative Declarations.

(4) Preparing draft and final EIRs.

(5) Consulting with and obtaining comments from other public agencies and members of the public with regard to the environmental effects of projects.

(6) Assuring adequate opportunity and time for public review and comment on the Draft EIR or Negative Declaration.

(7) Evaluating and responding to comments received on environmental documents.

(8) Assigning responsibility for determining the adequacy of an EIR or Negative Declaration.

(9) Reviewing and considering environmental documents by the person or decision-making body who will approve or disapprove a project.

(10) Filing documents required or authorized by CEQA and these Guidelines.

(11) Providing adequate comments on environmental documents which are submitted to the public agency for review.

(12) Assigning responsibility for specific functions to particular units of the public agency.

(13) Providing time periods for performing functions under CEQA.

(b) Any district, including a school district, need not adopt objectives, criteria, and procedures of its own if it uses the objectives, criteria, and procedures of another public agency whose boundaries are coterminous with or entirely encompass the district.

(c) Public agencies should revise their implementing procedures to conform to amendments to these Guidelines within 120 days after the effective date of the amendments. During the period while the public agency is revising its procedures, the agency must conform to any statutory changes in the California Environmental Quality Act that have become effective regardless of whether the public agency has revised its formally adopted procedures to conform to the statutory changes.

(d) In adopting procedures to implement CEQA, a public agency may adopt the State CEQA Guidelines through incorporation by reference. The agency may then adopt only those specific procedures or provisions described in subsection (a) which are necessary to tailor the general provisions of the Guidelines to the specific operations of the agency. A public agency may also choose to adopt a complete set of procedures identifying in one document all the necessary requirements.

Note: Authority cited: Section 21083, Public Resources Code; Reference: Sections 21082, 21100.2 and 21151.5, Public Resources Code.

15023. OFFICE OF PLANNING AND RESEARCH (OPR)

(a) From time to time OPR shall review the State CEQA Guidelines and shall make recommendations for amendments to the Secretary for Resources.

(b) OPR shall receive and evaluate proposals for adoption, amendment, or repeal of categorical exemptions and shall make recommendations on the proposals to the Secretary for Resources. People making suggestions concerning categorical exemptions shall submit their recommendations to OPR with supporting information to show that the class of projects in the proposal either will or will not have a significant effect on the environment.

(c) The State Clearinghouse in the Office of Planning and Research shall be responsible for distributing environmental documents to state agencies, departments, boards, and commissions for review and comment.

(d) Upon request of a Lead Agency or a project applicant, OPR shall provide assistance in identifying the various responsible agencies and any federal agencies which have responsibility for carrying out or approving a proposed project.

(e) OPR shall ensure that state Responsible Agencies provide the necessary information to Lead Agencies in response to Notices of Preparation within, at most, 30 days after receiving a Notice of Preparation.

(f) OPR shall resolve disputes as to which agency is the Lead Agency for a project.

(g) OPR shall receive and file all notices of completion, determination, and exemption.

(h) OPR shall establish and maintain a database for the collection, storage, retrieval, and dissemination of notices of exemption, notices of preparation, notices of determination, and notices of completion provided to the office. This database of notice information shall be available through the Internet.

Note: Authority cited: Section 21083, Public Resources Code. Reference: Sections 21080.4, 21083, 21086, 21087, 21108, 21159.9 and 21161, Public Resources Code.

15024. SECRETARY FOR RESOURCES

(a) The Guidelines shall be adopted by the Secretary for Resources. The Secretary shall make a finding that each class of projects given a categorical exemption will not have a significant effect on the environment.

(b) The Secretary may issue amendments to these Guidelines.

(c) The Secretary shall certify state environmental regulatory programs which meet the standards for certification in Section 21080.5, Public Resources Code.

(d) The Secretary shall receive and file notices required by certified state environmental regulatory programs.

Note: Authority cited: Section 21083, Public Resources Code; Reference: Sections 21080.5, 21083, 21084, 21086, 21088, and 21152, Public Resources Code.

15025. DELEGATION OF RESPONSIBILITIES

(a) A public agency may assign specific functions to its staff to assist in administering CEQA. Functions which may be delegated include but are not limited to:

(1) Determining whether a project is exempt.

(2) Conducting an Initial Study and deciding whether to prepare a draft EIR or Negative Declaration.

(3) Preparing a Negative Declaration or EIR.

(4) Determining that a Negative Declaration has been completed within a period of 180 days.

(5) Preparing responses to comments on environmental documents.

(6) Filing of notices.

(b) The decision-making body of a public agency shall not delegate the following functions:

(1) Reviewing and considering a final EIR or approving a Negative Declaration prior to approving a project.

(2) The making of findings as required by Sections 15091 and 15093.

(c) Where an advisory body such as a planning commission is required to make a recommendation on a project to the decision-making body, the advisory body shall also review and consider the EIR or Negative Declaration in draft or final form.

Note: Authority cited: Sections 21083 and 21087, Public Resources Code; Reference: Section 21082, 21100.2 and 21151.5, Public Resources Code; *Kleist v. City of Glendale*, (1976) 56 Cal. App. 3d 770.

Article 3. Authorities Granted to Public Agencies by CEQA

SECTIONS 15040 TO 15045

15040. AUTHORITY PROVIDED BY CEQA

(a) CEQA is intended to be used in conjunction with discretionary powers granted to public agencies by other laws.

(b) CEQA does not grant an agency new powers independent of the powers granted to the agency by other laws.

(c) Where another law grants an agency discretionary powers, CEQA supplements those discretionary powers by authorizing the agency to use the discretionary powers to mitigate or avoid significant effects on the environment when it is feasible to do so with respect to projects subject to the powers of the agency. Prior to January 1, 1983, CEQA provided implied authority for an agency to use its discretionary powers to mitigate or avoid significant effects on the environment. Effective January 1, 1983, CEQA provides express authority to do so.

(d) The exercise of the discretionary powers may take forms that had not been expected before the enactment of CEQA, but the exercise must be within the scope of the power.

(e) The exercise of discretionary powers for environmental protection shall be consistent with express or implied limitations provided by other laws.

Note: Authority cited: Section 21083, Public Resources Code; Reference: Sections 21000, 21001, 21002, 21002.1, and 21004, Public Resources Code; Section 4, Chapter 1438, Statutes of 1982; *Golden Gate Bridge, etc., District v. Muzzi*, (1978) 83 Cal. App. 3d 707; *E.D.F. v. Mathews*, 410 F. Supp. 336, 339 (D.D.C., 1976); *Friends of Mammoth v. Board of Supervisors*, (1972) 8 Cal. 3d 247; *Pinewood Investors v. City of Oxnard*, (1982) 133 Cal. App. 3d 1030.

15041. AUTHORITY TO MITIGATE

Within the limitations described in Section 15040:

(a) A lead agency for a project has authority to require feasible changes in any or all activities involved in the project in order to substantially lessen or avoid significant effects on the environment, consistent with applicable constitutional requirements such as the "nexus" and "rough proportionality" standards established by case law (*Nollan v. California Coastal Commission* (1987) 483 U.S. 825, *Dolan v. City of Tigard*, (1994) 512 U.S. 374, *Ehrlich v. City of Culver City*, (1996) 12 Cal. 4th 854.).

(b) When a public agency acts as a Responsible Agency for a project, the agency shall have more limited authority than a Lead Agency. The Responsible Agency may require changes in a project to lessen or avoid only the effects, either direct or indirect, of that part of the project which the agency will be called on to carry out or approve.

(c) With respect to a project which includes housing development, a Lead or Responsible Agency shall not reduce the proposed number of housing units as a mitigation measure or alternative to lessen a particular significant effect on the environment if that agency determines that there is another feasible, specific mitigation measure or alternative that would provide a comparable lessening of the significant effect.

Note: Authority cited: Section 21083, Public Resources Code; Reference: Sections 21002, 21002.1, and 21159.26, Public Resources Code; *Golden Gate Bridge, etc., District v. Muzzi*, (1978) 83 Cal. App. 3d 707; and *Laurel Hills Homeowners Assn. v. City Council of City of Los Angeles* (1978) 83 Cal.App.3d 515.

15042. AUTHORITY TO DISAPPROVE PROJECTS

A public agency may disapprove a project if necessary in order to avoid one or more significant effects on the environment that would occur if the project were approved as proposed. A Lead Agency has broader authority to disapprove a project than does a Responsible Agency. A Responsible Agency may refuse to approve a project in order to avoid direct or indirect environmental effects of that part of the project which the Responsible Agency would be called on to carry out or approve. For example, an air quality management district acting as a Responsible Agency would not have authority to disapprove a project for water pollution effects that were unrelated to the air quality aspects of the project regulated by the district.

Note: Authority cited: Section 21083, Public Resources Code; Reference: Sections 21002 and 21002.1, Public Resources Code; *Friends of Mammoth v. Mono County*, 8 Cal. App. 3d 247; *San Diego Trust and Savings Bank v. Friends of Gill*, 121 Cal. App. 3d 203.

15043. AUTHORITY TO APPROVE PROJECTS DESPITE SIGNIFICANT EFFECTS

A public agency may approve a project even though the project would cause a significant effect on the environment if the agency makes a fully informed and publicly disclosed decision that:

(a) There is no feasible way to lessen or avoid the significant effect (see Section 15091); and

(b) Specifically identified expected benefits from the project outweigh the policy of reducing or avoiding significant environmental impacts of the project. (See: Section 15093.)

Note: Authority cited: Section 21083, Public Resources Code; Reference: Sections 21002 and 21002.1, Public Resources Code; *San Francisco Ecology Center v. City and County of San Francisco*, (1975) 48 Cal. App. 3d 584; *San Diego Trust & Savings Bank v. Friends of Gill*, (1981) 121 Cal. App. 3d 203.

15044. AUTHORITY TO COMMENT

Any person or entity other than a Responsible Agency may submit comments to a Lead Agency concerning any environmental effects of a project being considered by the Lead Agency.

Note: Authority cited: Section 21083, Public Resources Code; Reference: Sections 21000, 21001, 21002.1, 21104, and 21153, Public Resources Code.

15045. FEES

(a) For a project to be carried out by any person or entity other than the lead agency, the lead agency may charge and collect a reasonable fee from the person or entity proposing the project in order to recover the estimated costs incurred in preparing environmental documents and for procedures necessary to comply with CEQA on the project. Litigation expenses, costs and fees incurred in actions alleging noncompliance with CEQA are not recoverable under this section.

(b) Public agencies may charge and collect a reasonable fee from members of the public for a copy of an environmental document not to exceed the actual cost of reproducing a copy.

Note: Authority: Section 21083, Public Resources Code. Reference: Section 21089 and 21105, Public Resources Code.

Article 4. Lead Agency

SECTIONS 15050 TO 15053

15050. LEAD AGENCY CONCEPT

(a) Where a project is to be carried out or approved by more than one public agency, one public agency shall be responsible for preparing an EIR or Negative Declaration for the project. This agency shall be called the Lead Agency.

(b) Except as provided in subdivision (c), the decision-making body of each Responsible Agency shall consider the Lead Agency's EIR or Negative Declaration prior to acting upon or approving the project. Each Responsible Agency shall certify that its decision-making body reviewed and considered the information contained in the EIR or Negative Declaration on the project.

(c) The determination of the Lead Agency of whether to prepare an EIR or a Negative Declaration shall be final and conclusive for all persons, including Responsible Agencies, unless:

(1) The decision is successfully challenged as provided in Section 21167 of the Public Resources Code,

(2) Circumstances or conditions changed as provided in Section 15162, or

(3) A Responsible Agency becomes a Lead Agency under Section 15052.

Note: Authority cited: Section 21083, Public Resources Code; Reference: Sections 21080.1, 21165, and 21167.2, Public Resources Code.

15051. CRITERIA FOR IDENTIFYING THE LEAD AGENCY

Where two or more public agencies will be involved with a project, the determination of which agency will be the Lead Agency shall be governed by the following criteria:

(a) If the project will be carried out by a public agency, that agency shall be the Lead Agency even if the project would be located within the jurisdiction of another public agency.

(b) If the project is to be carried out by a nongovernmental person or entity, the Lead Agency shall be the public agency with the greatest responsibility for supervising or approving the project as a whole.

(1) The Lead Agency will normally be the agency with general governmental powers, such as a city or county, rather than an agency with a single or limited purpose such as an air pollution control district or a district which will provide a public service or public utility to the project.

(2) Where a city prezones an area, the city will be the appropriate Lead Agency for any subsequent annexation of the area and should prepare the appropriate environmental document at the time of the prezoning. The Local Agency Formation Commission shall act as a Responsible Agency.

(c) Where more than one public agency equally meet the criteria in subdivision (b), the agency which will act first on the project in question shall be the Lead Agency.

(d) Where the provisions of subdivision (a), (b), and (c) leave two or more public agencies with a substantial claim to be the Lead Agency, the public agencies may by agreement designate an

agency as the Lead Agency. An agreement may also provide for cooperative efforts by two or more agencies by contract, joint exercise of powers, or similar devices.

Note: Authority cited: Section 21083, Public Resources Code; Reference: Section 21165, Public Resources Code.

15052. SHIFT IN LEAD AGENCY DESIGNATION

(a) Where a Responsible Agency is called on to grant an approval for a project subject to CEQA for which another public agency was the appropriate Lead Agency, the Responsible Agency shall assume the role of the Lead Agency when any of the following conditions occur:

  (1) The Lead Agency did not prepare any environmental documents for the project, and the statute of limitations has expired for a challenge to the action of the appropriate Lead Agency.

  (2) The Lead Agency prepared environmental documents for the project, but the following conditions occur:

    (A) A subsequent EIR is required pursuant to Section 15162,

    (B) The Lead Agency has granted a final approval for the project, and

    (C) The statute of limitations for challenging the Lead Agency‘s action under CEQA has expired.

  (3) The Lead Agency prepared inadequate environmental documents without consulting with the Responsible Agency as required by Sections 15072 or 15082, and the statute of limitations has expired for a challenge to the action of the appropriate Lead Agency.

(b) When a Responsible Agency assumes the duties of a Lead Agency under this section, the time limits applicable to a Lead Agency shall apply to the actions of the agency assuming the Lead Agency duties.

Note: Authority cited: Section 21083, Public Resources Code; Reference: Section 21165, Public Resources Code.

15053. DESIGNATION OF LEAD AGENCY BY THE OFFICE OF PLANNING AND RESEARCH

(a) If there is a dispute over which of several agencies should be the Lead Agency for a project, the disputing agencies should consult with each other in an effort to resolve the dispute prior to submitting it to the Office of Planning and Research. If an agreement cannot be reached, any of the disputing public agencies, or the applicant if a private project is involved, may submit the dispute to the Office of Planning and Research for resolution.

(b) For purposes of this section, a “dispute” means a contested, active difference of opinion between two or more public agencies as to which of those agencies shall prepare any necessary environmental document. A dispute exists where each of those agencies claims that it either has or does not have the obligation to prepare that environmental document.

(c) The Office of Planning and Research shall designate a Lead Agency within 21 days after receiving a completed request to resolve a dispute. The Office of Planning and Research shall not designate a lead agency in the absence of a dispute.

(d) Regulations adopted by the Office of Planning and Research for resolving Lead Agency disputes may be found in Title 14, California Code of Regulations, Sections 16000 et seq.

(e) Designation of a Lead Agency by the Office of Planning and Research shall be based on consideration of the criteria in Section 15051 as well as the capacity of the agency to adequately fulfill the requirements of CEQA.

Note: Authority cited: Section 21083, Public Resources Code; Reference: Section 21165, Public Resources Code; California Code of Regulations, Title 14, Sections 16000–16041.

Article 5. Preliminary Review of Projects and Conduct of Initial Study

SECTIONS 15060 TO 15065

15060. PRELIMINARY REVIEW

(a) A lead agency is allowed 30 days to review for completeness applications for permits or other entitlements for use. While conducting this review for completeness, the agency should be alert for environmental issues that might require preparation of an EIR or that may require additional explanation by the applicant. Accepting an application as complete does not limit the authority of the lead agency to require the applicant to submit additional information needed for environmental evaluation of the project. Requiring such additional information after the application is complete does not change the status of the application.

(b) Except as provided in Section 15111, the lead agency shall begin the formal environmental evaluation of the project after accepting an application as complete and determining that the project is subject to CEQA.

(c) Once an application is deemed complete, a lead agency must first determine whether an activity is subject to CEQA before conducting an initial study. An activity is not subject to CEQA if:

(1) The activity does not involve the exercise of discretionary powers by a public agency;

(2) The activity will not result in a direct or reasonably foreseeable indirect physical change in the environment; or

(3) The activity is not a project as defined in Section 15378.

(d) If the lead agency can determine that an EIR will be clearly required for a project, the agency may skip further initial review of the project and begin work directly on the EIR process described in Article 9, commencing with Section 15080. In the absence of an initial study, the lead agency shall still focus the EIR on the significant effects of the project and indicate briefly its reasons for determining that other effects would not be significant or potentially significant.

Authority: Sections 21083, Public Resources Code; Reference: Sections 21080(b), 21080.2 and 21160, Public Resources Code.

Note: Authority cited: Sections 21083 and 21087, Public Resources Code; Reference: Section 65944, Government Code; Section 21080.2, Public Resources Code.

15060.5. PREAPPLICATION CONSULTATION

(a) For a potential project involving the issuance of a lease, permit, license, certificate, or other entitlement for use by one or more public agencies, the lead agency shall, upon the request of a potential applicant and prior to the filing of a formal application, provide for consultation with the potential applicant to consider the range of actions, potential alternatives, mitigation measures, and any potential significant effects on the environment of the potential project.

(b) The lead agency may include in the consultation one or more responsible agencies, trustee agencies, and other public agencies who in the opinion of the lead agency may have an interest in the proposed project. The lead agency may consult the Office of Permit Assistance in the Trade and Commerce Agency for help in identifying interested agencies.

Note: Authority cited: Section 21083, Public Resources Code; Reference: Section 21080.1, Public Resources Code.

15061. REVIEW FOR EXEMPTION

(a) Once a lead agency has determined that an activity is a project subject to CEQA, a lead agency shall determine whether the project is exempt from CEQA.

(b) A project is exempt from CEQA if:

(1) The project is exempt by statute (see, e.g. Article 18, commencing with Section 15260).

(2) The project is exempt pursuant to a categorical exemption (see Article 19, commencing with Section 15300) and the application of that categorical exemption is not barred by one of the exceptions set forth in Section 15300.2.

(3) The activity is covered by the general rule that CEQA applies only to projects which have the potential for causing a significant effect on the environment. Where it can be seen with certainty that there is no possibility that the activity in question may have a significant effect on the environment, the activity is not subject to CEQA.

(4) The project will be rejected or disapproved by a public agency. (See Section 15270(b)).

(5) The project is exempt pursuant to the provisions of Article 12.5 of this Chapter.

(c) Each public agency should include in its implementing procedures a listing of the projects often handled by the agency that the agency has determined to be exempt. This listing should be used in preliminary review.

(d) After determining that a project is exempt, the agency may prepare a Notice of Exemption as provided in Section 15062. Although the notice may be kept with the project application at this time, the notice shall not be filed with the Office of Planning and Research or the county clerk until the project has been approved.

(e) When a non-elected official or decisionmaking body of a local lead agency decides that a project is exempt from CEQA, and the public agency approves or determines to carry out the project, the decision that the project is exempt may be appealed to the local lead agency's elected decisionmaking body, if one exists. A local lead agency may establish procedures governing such appeals.

Note: Authority cited: Section 21083, Public Resources Code; Reference: Sections 21080(b), 21080.9, 21080.10, 21084, 21108(b), 21151, 21152(b), and 21159.21, Public Resources Code; *No Oil, Inc. v. City of Los Angeles* (1974) 13 Cal. 3d 68.

15062. NOTICE OF EXEMPTION

(a) When a public agency decides that a project is exempt from CEQA pursuant to Section 15061, and the public agency approves or determines to carry out the project, the agency may file a Notice of Exemption. The notice shall be filed, if at all, after approval of the project. Such a notice shall include:

(1) A brief description of the project,

(2) The location of the project (either by street address and cross street for a project in an urbanized area or by attaching a specific map, preferably a copy of a U.S.G.S. 15' or 7-1/2' topographical map identified by quadrangle name).

(3) A finding that the project is exempt from CEQA, including a citation to the State Guidelines section or statute under which it is found to be exempt, and

(4) A brief statement of reasons to support the finding, and

(5) The applicant's name, if any.

(b) A Notice of Exemption may be filled out and may accompany the project application through the approval process. The notice shall not be filed with the county clerk or the OPR until the project has been approved.

(c) When a public agency approves an applicant's project, either the agency or the applicant may file a Notice of Exemption.

(1) When a state agency files this notice, the notice of exemption shall be filed with the Office of Planning and Research. A form for this notice is provided in Appendix E. A list of all

such notices shall be posted on a weekly basis at the Office of Planning and Research, 1400 Tenth Street, Sacramento, California. The list shall remain posted for at least 30 days. The Office of Planning and Research shall retain each notice for not less than 12 months.

(2) When a local agency files this notice, the notice of exemption shall be filed with the county clerk of each county in which the project will be located. Copies of all such notices shall be available for public inspection and such notices shall be posted within 24 hours of receipt in the office of the county clerk. Each notice shall remain posted for a period of 30 days. Thereafter, the clerk shall return the notice to the local agency with a notation of the period it was posted. The local agency shall retain the notice for not less than 12 months

(3) All public agencies are encouraged to make postings pursuant to this section available in electronic format on the Internet. Such electronic postings are in addition to the procedures required by these guidelines and the Public Resources Code.

(4) When an applicant files this notice, special rules apply.

(A) The notice filed by an applicant is filed in the same place as if it were filed by the agency granting the permit. If the permit was granted by a state agency, the notice is filed with the Office of Planning and Research. If the permit was granted by a local agency, the notice is filed with the county clerk of the county or counties in which the project will be located.

(B) The Notice of Exemption filed by an applicant shall contain the information required in subdivision (a) together with a certified document issued by the public agency stating that the agency has found the project to be exempt. The certified document may be a certified copy of an existing document or record of the public agency.

(C) A notice filed by an applicant is subject to the same posting and time requirements as a notice filed by a public agency.

(d) The filing of a Notice of Exemption and the posting on the list of notices start a 35 day statute of limitations period on legal challenges to the agency's decision that the project is exempt from CEQA. If a Notice of Exemption is not filed, a 180 day statute of limitations will apply.

(e) When a local agency determines that a project is not subject to CEQA under sections 15193, 15194, or 15195, and it approves or determines to carry out that project, the local agency or person seeking project approval shall file a notice with OPR identifying the section under which the exemption is claimed.

Note: Authority cited: Section 21083, Public Resources Code; Reference: Sections 21108, 21152, and 21152.1, Public Resources Code.

15063. INITIAL STUDY

(a) Following preliminary review, the Lead Agency shall conduct an Initial Study to determine if the project may have a significant effect on the environment. If the Lead Agency can determine that an EIR will clearly be required for the project, an Initial Study is not required but may still be desirable.

(1) All phases of project planning, implementation, and operation must be considered in the Initial Study of the project.

(2) To meet the requirements of this section, the lead agency may use an environmental assessment or a similar analysis prepared pursuant to the National Environmental Policy Act.

(3) An initial study may rely upon expert opinion supported by facts, technical studies or other substantial evidence to document its findings. However, an initial study is neither intended nor required to include the level of detail included in an EIR.

(b) Results.

(1) If the agency determines that there is substantial evidence that any aspect of the project, either individually or cumulatively, may cause a significant effect on the environment, regardless of whether the overall effect of the project is adverse or beneficial, the Lead Agency shall do one of the following:

(A) Prepare an EIR, or

(B) Use a previously prepared EIR which the Lead Agency determines would adequately analyze the project at hand, or

(C) Determine, pursuant to a program EIR, tiering, or another appropriate process, which of a project's effects were adequately examined by an earlier EIR or negative declaration. Another appropriate process may include, for example, a master EIR, a master environmental assessment, approval of housing and neighborhood commercial facilities in urban areas, approval of residential projects pursuant to a specific plans described in section 15182, approval of residential projects consistent with a community plan, general plan or zoning as described in section 15183, or an environmental document prepared under a State certified regulatory program. The lead agency shall then ascertain which effects, if any, should be analyzed in a later EIR or negative declaration.

(2) The Lead Agency shall prepare a Negative Declaration if there is no substantial evidence that the project or any of its aspects may cause a significant effect on the environment.

(c) Purposes. The purposes of an Initial Study are to:

(1) Provide the Lead Agency with information to use as the basis for deciding whether to prepare an EIR or a Negative Declaration.

(2) Enable an applicant or Lead Agency to modify a project, mitigating adverse impacts before an EIR is prepared, thereby enabling the project to qualify for a Negative Declaration.

(3) Assist in the preparation of an EIR, if one is required, by:

(A) Focusing the EIR on the effects determined to be significant,

(B) Identifying the effects determined not to be significant,

(C) Explaining the reasons for determining that potentially significant effects would not be significant, and

(D) Identifying whether a program EIR, tiering, or another appropriate process can be used for analysis of the project's environmental effects.

(4) Facilitate environmental assessment early in the design of a project;

(5) Provide documentation of the factual basis for the finding in a Negative Declaration that a project will not have a significant effect on the environment;

(6) Eliminate unnecessary EIRs;

(7) Determine whether a previously prepared EIR could be used with the project.

(d) Contents. An Initial Study shall contain in brief form:

(1) A description of the project including the location of the project;

(2) An identification of the environmental setting;

(3) An identification of environmental effects by use of a checklist, matrix, or other method, provided that entries on a checklist or other form are briefly explained to indicate that there is some evidence to support the entries. The brief explanation may be either through a narrative or a reference to another information source such as an attached map, photographs, or an earlier EIR or negative declaration. A reference to another document should include, where appropriate, a citation to the page or pages where the information is found.

(4) A discussion of the ways to mitigate the significant effects identified, if any;

(5) An examination of whether the project would be consistent with existing zoning, plans, and other applicable land use controls;

(6) The name of the person or persons who prepared or participated in the Initial Study.

(e) Submission of Data. If the project is to be carried out by a private person or private organization, the Lead Agency may require such person or organization to submit data and information which will enable the Lead Agency to prepare the Initial Study. Any person may submit any information in any form to assist a Lead Agency in preparing an Initial Study.

(f) Format. Sample forms for an applicant's project description and a review form for use by the lead agency are contained in Appendices G and H. When used together, these forms would meet the requirements for an initial study, provided that the entries on the checklist are briefly explained pursuant to subdivision (d)(3). These forms are only suggested, and public agencies are free to devise their own format for an initial study. A previously prepared EIR may also be used as the initial study for a later project.

(g) Consultation. As soon as a Lead Agency has determined that an Initial Study will be required for the project, the Lead Agency shall consult informally with all Responsible Agencies and all Trustee Agencies responsible for resources affected by the project to obtain the recommendations of those agencies as to whether an EIR or a Negative Declaration should be prepared. During or immediately after preparation of an Initial Study for a private project, the Lead Agency may consult with the applicant to determine if the applicant is willing to modify the project to reduce or avoid the significant effects identified in the Initial Study.

Note: Authority cited: Section 21083, Public Resources Code; Reference: Sections 21080(c), 21080.1, 21080.3, 21082.1, 21100 and 21151, Public Resources Code; *Gentry v. City of Murrieta* (1995) 36 Cal.App.4th 1359, *San Joaquin Raptor/Wildlife Rescue Center v. County of Stanislaus* (1994) 27 Cal.App.4th 713, *Leonoff v. Monterey County Board of Supervisors* (1990) 222 Cal.App.3d 1337.

15064. DETERMINING THE SIGNIFICANCE OF THE ENVIRONMENTAL EFFECTS CAUSED BY A PROJECT

(a) Determining whether a project may have a significant effect plays a critical role in the CEQA process.

(1) If there is substantial evidence, in light of the whole record before a lead agency, that a project may have a significant effect on the environment, the agency shall prepare a draft EIR.

(2) When a final EIR identifies one or more significant effects, the Lead Agency and each Responsible Agency shall make a finding under Section 15091 for each significant effect and may need to make a statement of overriding considerations under Section 15093 for the project.

(b) The determination of whether a project may have a significant effect on the environment calls for careful judgment on the part of the public agency involved, based to the extent possible on scientific and factual data. An ironclad definition of significant effect is not always possible because the significance of an activity may vary with the setting. For example, an activity which may not be significant in an urban area may be significant in a rural area.

(c) In determining whether an effect will be adverse or beneficial, the Lead Agency shall consider the views held by members of the public in all areas affected as expressed in the whole record before the lead agency. Before requiring the preparation of an EIR, the Lead Agency must still determine whether environmental change itself might be substantial.

(d) In evaluating the significance of the environmental effect of a project, the Lead Agency shall consider direct physical changes in the environment which may be caused by the project and reasonably foreseeable indirect physical changes in the environment which may be caused by the project.

(1) A direct physical change in the environment is a physical change in the environment which is caused by and immediately related to the project. Examples of direct physical changes in the environment are the dust, noise, and traffic of heavy equipment that would result from construction of a sewage treatment plant and possible odors from operation of the plant.

(2) An indirect physical change in the environment is a physical change in the environment which is not immediately related to the project, but which is caused indirectly by the project. If a direct physical change in the environment in turn causes another change in the environment, then the other change is an indirect physical change in the environment. For example, the construction of a new sewage treatment plant may facilitate population growth in the service area due to the increase in sewage treatment capacity and may lead to an increase in air pollution.

(3) An indirect physical change is to be considered only if that change is a reasonably foreseeable impact which may be caused by the project. A change which is speculative or unlikely to occur is not reasonably foreseeable.

(e) Economic and social changes resulting from a project shall not be treated as significant effects on the environment. Economic or social changes may be used, however, to determine that a physical change shall be regarded as a significant effect on the environment. Where a physical change is caused by economic or social effects of a project, the physical change may be regarded as a significant effect in the same manner as any other physical change resulting from the project. Alternatively, economic and social effects of a physical change may be used to determine that the physical change is a significant effect on the environment. If the physical change causes adverse economic or social effects on people, those adverse effects may be used as a factor in determining whether the physical change is significant. For example, if a project would cause overcrowding of a public facility and the overcrowding causes an adverse effect on people, the overcrowding would be regarded as a significant effect.

(f) The decision as to whether a project may have one or more significant effects shall be based on substantial evidence in the record of the lead agency.

(1) If the lead agency determines there is substantial evidence in the record that the project may have a significant effect on the environment, the lead agency shall prepare an EIR (*Friends of B Street v. City of Hayward* (1980) 106 Cal.App.3d 988). Said another way, if a lead agency is presented with a fair argument that a project may have a significant effect on the environment, the lead agency shall prepare an EIR even though it may also be presented with other substantial evidence that the project will not have a significant effect (*No Oil, Inc. v. City of Los Angeles* (1974) 13 Cal.3d 68).

(2) If the lead agency determines there is substantial evidence in the record that the project may have a significant effect on the environment but the lead agency determines that revisions in the project plans or proposals made by, or agreed to by, the applicant would avoid the effects or mitigate the effects to a point where clearly no significant effect on the environment would occur and there is no substantial evidence in light of the whole record before the public agency that the project, as revised, may have a significant effect on the environment then a mitigated negative declaration shall be prepared.

(3) If the lead agency determines there is no substantial evidence that the project may have a significant effect on the environment, the lead agency shall prepare a negative declaration (*Friends of B Street v. City of Hayward* (1980) 106 Cal.App. 3d 988).

(4) The existence of public controversy over the environmental effects of a project will not require preparation of an EIR if there is no substantial evidence before the agency that the project may have a significant effect on the environment.

(5) Argument, speculation, unsubstantiated opinion or narrative, or evidence that is clearly inaccurate or erroneous, or evidence that is not credible, shall not constitute substantial evidence. Substantial evidence shall include facts, reasonable assumptions predicated upon facts, and expert opinion support by facts.

(6) Evidence of economic and social impacts that do not contribute to or are not caused by physical changes in the environment is not substantial evidence that the project may have a significant effect on the environment.

(7) The provisions of sections 15162, 15163, and 15164 apply when the project being analyzed is a change to, or further approval for, a project for which an EIR or negative declaration was previously certified or adopted (e.g. a tentative subdivision, conditional use permit). Under case law, the fair argument standard does not apply to determinations of significance pursuant to sections 15162, 15163, and 15164.

(g) After application of the principles set forth above in Section 15064(f)(g), and in marginal cases where it is not clear whether there is substantial evidence that a project may have a significant effect on the environment, the lead agency shall be guided by the following principle: If there is disagreement among expert opinion supported by facts over the significance of an effect on the environment, the Lead Agency shall treat the effect as significant and shall prepare an EIR.

(h) (1) When assessing whether a cumulative effect requires an EIR, the lead agency shall consider whether the cumulative impact is significant and whether the effects of the project are cumulatively considerable. An EIR must be prepared if the cumulative impact may be significant and the project's incremental effect, though individually limited, is cumulatively considerable. "Cumulatively considerable" means that the incremental effects of an individual project are significant when viewed in connection with the effects of past projects, the effects of other current projects, and the effects of probable future projects.

(2) A lead agency may determine in an initial study that a project's contribution to a significant cumulative impact will be rendered less than cumulatively considerable and thus is not significant. When a project might contribute to a significant cumulative impact, but the contribution will be rendered less than cumulatively considerable through mitigation measures set forth in a mitigated negative declaration, the initial study shall briefly indicate and explain how the contribution has been rendered less than cumulatively considerable.

(3) A lead agency may determine that a project's incremental contribution to a cumulative effect is not cumulatively considerable if the project will comply with the requirements in a previously approved plan or mitigation program (including, but not limited to, water quality control plan, air quality attainment or maintenance plan, integrated waste management plan, habitat conservation plan, natural community conservation plan, plans or regulations for the reduction of greenhouse gas emissions) that provides specific requirements that will avoid or substantially lessen the cumulative problem within the geographic area in which the project is located. Such plans or programs must be specified in law or adopted by the public agency with jurisdiction over the affected resources through a public review process to implement, interpret, or make specific the law enforced or administered by the public agency. When relying on a plan, regulation or program, the lead agency should explain how implementing the particular requirements in the plan, regulation or program ensure that the project's incremental contribution to the cumulative effect is not cumulatively considerable. If there is substantial evidence that the possible effects of a particular project are still cumulatively considerable notwithstanding that the project complies with the specified plan or mitigation program addressing the cumulative problem, an EIR must be prepared for the project.

(4) The mere existence of significant cumulative impacts caused by other projects alone shall not constitute substantial evidence that the proposed project's incremental effects are cumulatively considerable.

Note: Authority cited: Sections 21083, 21083.05, Public Resources Code. Reference: Sections 21003, 21065, 21068, 21080, 21082, 21082.1, 21082.2, 21083, 21083.05, and 21100, Public Resources Code; *No Oil, Inc. v. City of Los Angeles* (1974) 13 Cal.3d 68; *San Joaquin Raptor/Wildlife Center v. County of Stanislaus* (1996) 42 Cal.App.4th 608; *Gentry v. City of Murrieta* (1995) 36 Cal.App.4th 1359; *Laurel Heights Improvement Assn. v. Regents of the University of California* (1993) 6 Cal.4th 1112; and *Communities for a Better Environment v. California Resources Agency* (2002) 103 Cal.App.4th 98.

15064.4. DETERMINING THE SIGNIFICANCE OF IMPACTS FROM GREENHOUSE GAS EMISSIONS

(a) The determination of the significance of greenhouse gas emissions calls for a careful judgment by the lead agency consistent with the provisions in section 15064. A lead agency should make a good-faith effort, based to the extent possible on scientific and factual data, to describe, calculate or estimate the amount of greenhouse gas emissions resulting from a project. A lead agency shall have discretion to determine, in the context of a particular project, whether to:

(1) Use a model or methodology to quantify greenhouse gas emissions resulting from a project, and which model or methodology to use. The lead agency has discretion to select the model or methodology it considers most appropriate provided it supports its decision with substantial evidence. The lead agency should explain the limitations of the particular model or methodology selected for use; and/or

(2) Rely on a qualitative analysis or performance based standards.

(b) A lead agency should consider the following factors, among others, when assessing the significance of impacts from greenhouse gas emissions on the environment:

(1) The extent to which the project may increase or reduce greenhouse gas emissions as compared to the existing environmental setting;

(2) Whether the project emissions exceed a threshold of significance that the lead agency determines applies to the project.

(3) The extent to which the project complies with regulations or requirements adopted to implement a statewide, regional, or local plan for the reduction or mitigation of greenhouse gas emissions. Such requirements must be adopted by the relevant public agency through a public review process and must reduce or mitigate the project's incremental contribution of greenhouse gas emissions. If there is substantial evidence that the possible effects of a particular project are still cumulatively considerable notwithstanding compliance with the adopted regulations or requirements, an EIR must be prepared for the project.

Note: Authority cited: Sections 21083, 21083.05, Public Resources Code. Reference: Sections 21001, 21002, 21003, 21065, 21068, 21080, 21082, 21082.1, 21082.2, 21083.05, 21100, Pub. Resources Code; *Eureka Citizens for Responsible Govt. v. City of Eureka* (2007) 147 Cal.App.4th 357; *Mejia v. City of Los Angeles* (2005) 130 Cal.App.4th 322; *Protect the Historic Amador Waterways v. Amador Water Agency* (2004) 116 Cal.App.4th 1099; *Communities for a Better Environment v. California Resources Agency* (2002) 103 Cal.App.4th 98; *Berkeley Keep Jets Over the Bay Com. v. Board of Port Comm.* (2001) 91 Cal.App.4th 1344; and *City of Irvine v. Irvine Citizens Against Overdevelopment* (1994) 25 Cal.App.4th 868.

15064.5. DETERMINING THE SIGNIFICANCE OF IMPACTS TO ARCHAEOLOGICAL AND HISTORICAL RESOURCES

(a) For purposes of this section, the term "historical resources" shall include the following:

(1) A resource listed in, or determined to be eligible by the State Historical Resources Commission, for listing in the California Register of Historical Resources (Pub. Res. Code § 5024.1, Title 14 CCR, Section 4850 et seq.).

(2) A resource included in a local register of historical resources, as defined in section 5020.1(k) of the Public Resources Code or identified as significant in an historical resource survey meeting the requirements section 5024.1(g) of the Public Resources Code, shall be presumed to be historically or culturally significant. Public agencies must treat any such resource as significant unless the preponderance of evidence demonstrates that it is not historically or culturally significant.

(3) Any object, building, structure, site, area, place, record, or manuscript which a lead agency determines to be historically significant or significant in the architectural, engineering, scientific, economic, agricultural, educational, social, political, military, or cultural annals of California may be considered to be an historical resource, provided the lead agency's determination is supported by substantial evidence in light of the whole record. Generally, a resource shall be considered by the lead agency to be "historically significant" if the resource meets the criteria for listing on the California Register of Historical Resources (Pub. Res. Code § 5024.1, Title 14 CCR, Section 4852) including the following:

(A) Is associated with events that have made a significant contribution to the broad patterns of California's history and cultural heritage;

(B) Is associated with the lives of persons important in our past;

(C) Embodies the distinctive characteristics of a type, period, region, or method of construction, or represents the work of an important creative individual, or possesses high artistic values; or

(D) Has yielded, or may be likely to yield, information important in prehistory or history.

(4) The fact that a resource is not listed in, or determined to be eligible for listing in the California Register of Historical Resources, not included in a local register of historical resources (pursuant to section 5020.1(k) of the Public Resources Code), or identified in an historical resources survey (meeting the criteria in section 5024.1(g) of the Public Resources Code) does not preclude a lead agency from determining that the resource may be an historical resource as defined in Public Resources Code sections 5020.1(j) or 5024.1.

(b) A project with an effect that may cause a substantial adverse change in the significance of an historical resource is a project that may have a significant effect on the environment.

(1) Substantial adverse change in the significance of an historical resource means physical demolition, destruction, relocation, or alteration of the resource or its immediate surroundings such that the significance of an historical resource would be materially impaired.

(2) The significance of an historical resource is materially impaired when a project:

(A) Demolishes or materially alters in an adverse manner those physical characteristics of an historical resource that convey its historical significance and that justify its inclusion in, or eligibility for, inclusion in the California Register of Historical Resources; or

(B) Demolishes or materially alters in an adverse manner those physical characteristics that account for its inclusion in a local register of historical resources pursuant to section 5020.1(k) of the Public Resources Code or its identification in an historical resources survey meeting the requirements of section 5024.1(g) of the Public Resources Code,

unless the public agency reviewing the effects of the project establishes by a preponderance of evidence that the resource is not historically or culturally significant; or

(C) Demolishes or materially alters in an adverse manner those physical characteristics of a historical resource that convey its historical significance and that justify its eligibility for inclusion in the California Register of Historical Resources as determined by a lead agency for purposes of CEQA.

(3) Generally, a project that follows the Secretary of the Interior's Standards for the Treatment of Historic Properties with Guidelines for Preserving, Rehabilitating, Restoring, and Reconstructing Historic Buildings or the Secretary of the Interior's Standards for Rehabilitation and Guidelines for Rehabilitating Historic Buildings (1995), Weeks and Grimmer, shall be considered as mitigated to a level of less than a significant impact on the historical resource.

(4) A lead agency shall identify potentially feasible measures to mitigate significant adverse changes in the significance of an historical resource. The lead agency shall ensure that any adopted measures to mitigate or avoid significant adverse changes are fully enforceable through permit conditions, agreements, or other measures.

(5) When a project will affect state-owned historical resources, as described in Public Resources Code Section 5024, and the lead agency is a state agency, the lead agency shall consult with the State Historic Preservation Officer as provided in Public Resources Code Section 5024.5. Consultation should be coordinated in a timely fashion with the preparation of environmental documents.

(c) CEQA applies to effects on archaeological sites.

(1) When a project will impact an archaeological site, a lead agency shall first determine whether the site is an historical resource, as defined in subdivision (a).

(2) If a lead agency determines that the archaeological site is an historical resource, it shall refer to the provisions of Section 21084.1 of the Public Resources Code, and this section, Section 15126.4 of the Guidelines, and the limits contained in Section 21083.2 of the Public Resources Code do not apply.

(3) If an archaeological site does not meet the criteria defined in subdivision (a), but does meet the definition of a unique archeological resource in Section 21083.2 of the Public Resources Code, the site shall be treated in accordance with the provisions of section 21083.2. The time and cost limitations described in Public Resources Code Section 21083.2 (c–f) do not apply to surveys and site evaluation activities intended to determine whether the project location contains unique archaeological resources.

(4) If an archaeological resource is neither a unique archaeological nor an historical resource, the effects of the project on those resources shall not be considered a significant effect on the environment. It shall be sufficient that both the resource and the effect on it are noted in the Initial Study or EIR, if one is prepared to address impacts on other resources, but they need not be considered further in the CEQA process.

(d) When an initial study identifies the existence of, or the probable likelihood, of Native American human remains within the project, a lead agency shall work with the appropriate Native Americans as identified by the Native American Heritage Commission as provided in Public Resources Code Section 5097.98. The applicant may develop an agreement for treating or disposing of, with appropriate dignity, the human remains and any items associated with Native American burials with the appropriate Native Americans as identified by the Native American Heritage Commission. Action implementing such an agreement is exempt from:

(1) The general prohibition on disinterring, disturbing, or removing human remains from any location other than a dedicated cemetery (Health and Safety Code Section 7050.5).

(2) The requirements of CEQA and the Coastal Act.

(e) In the event of the accidental discovery or recognition of any human remains in any location other than a dedicated cemetery, the following steps should be taken:

(1) There shall be no further excavation or disturbance of the site or any nearby area reasonably suspected to overlie adjacent human remains until:

(A) The coroner of the county in which the remains are discovered must be contacted to determine that no investigation of the cause of death is required, and

(B) If the coroner determines the remains to be Native American:

1. The coroner shall contact the Native American Heritage Commission within 24 hours.

2. The Native American Heritage Commission shall identify the person or persons it believes to be the most likely descended from the deceased Native American.

3. The most likely descendent may make recommendations to the landowner or the person responsible for the excavation work, for means of treating or disposing of, with appropriate dignity, the human remains and any associated grave goods as provided in Public Resources Code Section 5097.98, or

(2) Where the following conditions occur, the landowner or his authorized representative shall rebury the Native American human remains and associated grave goods with appropriate dignity on the property in a location not subject to further subsurface disturbance.

(A) The Native American Heritage Commission is unable to identify a most likely descendent or the most likely descendent failed to make a recommendation within 24 hours after being notified by the commission.

(B) The descendant identified fails to make a recommendation; or

(C) The landowner or his authorized representative rejects the recommendation of the descendant, and the mediation by the Native American Heritage Commission fails to provide measures acceptable to the landowner.

(f) As part of the objectives, criteria, and procedures required by Section 21082 of the Public Resources Code, a lead agency should make provisions for historical or unique archaeological resources accidentally discovered during construction. These provisions should include an immediate evaluation of the find by a qualified archaeologist. If the find is determined to be an historical or unique archaeological resource, contingency funding and a time allotment sufficient to allow for implementation of avoidance measures or appropriate mitigation should be available. Work could continue on other parts of the building site while historical or unique archaeological resource mitigation takes place.

Note: Authority: Section 21083, Public Resources Code. Reference: Sections 21083.2, 21084, and 21084.1, Public Resources Code; *Citizens for Responsible Development in West Hollywood v. City of West Hollywood* (1995) 39 Cal.App.4th 490.

15064.7. THRESHOLDS OF SIGNIFICANCE.

(a) Each public agency is encouraged to develop and publish thresholds of significance that the agency uses in the determination of the significance of environmental effects. A threshold of significance is an identifiable quantitative, qualitative or performance level of a particular environmental effect, non-compliance with which means the effect will normally be determined to be significant by the agency and compliance with which means the effect normally will be determined to be less than significant.

(b) Thresholds of significance to be adopted for general use as part of the lead agency's environmental review process must be adopted by ordinance, resolution, rule, or regulation, and developed through a public review process and be supported by substantial evidence.

(c) When adopting thresholds of significance, a lead agency may consider thresholds of significance previously adopted or recommended by other public agencies or recommended by experts, provided the decision of the lead agency to adopt such thresholds is supported by substantial evidence.

Note: Authority cited: Section 21083, Public Resources Code. Reference: Sections 21000, 21082 and 21083, Public Resources Code.

15065. MANDATORY FINDINGS OF SIGNIFICANCE

(a) A lead agency shall find that a project may have a significant effect on the environment and thereby require an EIR to be prepared for the project where there is substantial evidence, in light of the whole record, that any of the following conditions may occur:

(1) The project has the potential to*:* substantially degrade the quality of the environment*;* substantially reduce the habitat of a fish or wildlife species*;* cause a fish or wildlife population to drop below self-sustaining levels*;* threaten to eliminate a plant or animal community*;* substantially reduce the number or restrict the range of an endangered, rare or threatened species*;* or eliminate important examples of the major periods of California history or prehistory.

(2) The project has the potential to achieve short-term environmental goals to the disadvantage of long-term environmental goals.

(3) The project has possible environmental effects that are individually limited but cumulatively considerable. "Cumulatively considerable" means that the incremental effects of an individual project are significant when viewed in connection with the effects of past projects, the effects of other current projects, and the effects of probable future projects.

(4) The environmental effects of a project will cause substantial adverse effects on human beings, either directly or indirectly.

(b) (1) Where, prior to the commencement of public review of an environmental document, a project proponent agrees to mitigation measures or project modifications that would avoid any significant effect on the environment specified by subdivision (a) or would mitigate the significant effect to a point where clearly no significant effect on the environment would occur, a lead agency need not prepare an environmental impact report solely because, without mitigation, the environmental effects at issue would have been significant.

(2) Furthermore, where a proposed project has the potential to substantially reduce the number or restrict the range of an endangered, rare or threatened species, the lead agency need not prepare an EIR solely because of such an effect, if:

(A) the project proponent is bound to implement mitigation requirements relating to such species and habitat pursuant to an approved habitat conservation plan or natural community conservation plan;

(B) the state or federal agency approved the habitat conservation plan or natural community conservation plan in reliance on an environmental impact report or environmental impact statement; and

(C) 1. such requirements avoid any net loss of habitat and net reduction in number of the affected species, or

2. such requirements preserve, restore, or enhance sufficient habitat to mitigate the reduction in habitat and number of the affected species to below a level of significance.

(c) Following the decision to prepare an EIR, if a lead agency determines that any of the conditions specified by subdivision (a) will occur, such a determination shall apply to:

(1) the identification of effects to be analyzed in depth in the environmental impact report or the functional equivalent thereof,

(2) the requirement to make detailed findings on the feasibility of alternatives or mitigation measures to substantially lessen or avoid the significant effects on the environment,

(3) when found to be feasible, the making of changes in the project to substantially lessen or avoid the significant effects on the environment, and

(4) where necessary, the requirement to adopt a statement of overriding considerations.

Note: Authority cited: Section 21083, Public Resources Code. Reference: Sections 21001(c), *21082.2*, and 21083, Public Resources Code; *San Joaquin Raptor/Wildlife Center v. County of Stanislaus* (1996) 42 Cal.App.4th *608; Los Angeles Unified School District v. City of Los Angeles* (1997) 58 Cal.App.4th 1019, 1024; and *Communities for a Better Environment v. California Resources Agency* (2002) 103 Cal.App.4th 98.

Article 6. Negative Declaration Process

SECTIONS 15070 TO 15075

15070. DECISION TO PREPARE A NEGATIVE OR MITIGATED NEGATIVE DECLARATION

A public agency shall prepare or have prepared a proposed negative declaration or mitigated negative declaration for a project subject to CEQA when:

(a) The initial study shows that there is no substantial evidence, in light of the whole record before the agency, that the project may have a significant effect on the environment, or

(b) The initial study identifies potentially significant effects, but:

(1) Revisions in the project plans or proposals made by, or agreed to by the applicant before a proposed mitigated negative declaration and initial study are released for public review would avoid the effects or mitigate the effects to a point where clearly no significant effects would occur, and

(2) There is no substantial evidence, in light of the whole record before the agency, that the project as revised may have a significant effect on the environment.

Note: Authority cited: Section 21083, Public Resources Code; Reference: Sections 21064, 21064.5, 21080(c), and 21082.1, Public Resources Code; *Friends of B Street v. City of Hayward* (1980) 106 Cal.App.3d 988; *Running Fence Corp. v. Superior Court* (1975) 51 Cal.App.3d 400.

15071. CONTENTS

A Negative Declaration circulated for public review shall include:

(a) A brief description of the project, including a commonly used name for the project, if any;

(b) The location of the project, preferably shown on a map, and the name of the project proponent;

(c) A proposed finding that the project will not have a significant effect on the environment;

(d) An attached copy of the Initial Study documenting reasons to support the finding; and

(e) Mitigation measures, if any, included in the project to avoid potentially significant effects.

Note: Authority cited: Section 21083, Public Resources Code. Reference: Section 21080(c), Public Resources Code.

15072. NOTICE OF INTENT TO ADOPT A NEGATIVE DECLARATION OR MITIGATED NEGATIVE DECLARATION

(a) A lead agency shall provide a notice of intent to adopt a negative declaration or mitigated negative declaration to the public, responsible agencies, trustee agencies, and the county clerk of each county within which the proposed project is located, sufficiently prior to adoption by the lead agency of the negative declaration or mitigated negative declaration to allow the public and agencies the review period provided under Section 15105.

(b) The lead agency shall mail a notice of intent to adopt a negative declaration or mitigated negative declaration to the last known name and address of all organizations and individuals who have previously requested such notice in writing and shall also give notice of intent to adopt a negative declaration or mitigated negative declaration by at least one of the following procedures to allow the public the review period provided under Section 15105:

(1) Publication at least one time by the lead agency in a newspaper of general circulation in the area affected by the proposed project. If more than one area is affected, the notice shall be published in the newspaper of largest circulation from among the newspapers of general circulation in those areas.

(2) Posting of notice by the lead agency on and off site in the area where the project is to be located.

(3) Direct mailing to the owners and occupants of property contiguous to the project. Owners of such property shall be identified as shown on the latest equalized assessment roll.

(c) The alternatives for providing notice specified in subdivision (b) shall not preclude a lead agency from providing additional notice by other means if the agency so desires, nor shall the requirements of this section preclude a lead agency from providing the public notice at the same time and in the same manner as public notice required by any other laws for the project.

(d) The county clerk of each county within which the proposed project is located shall post such notices in the office of the county clerk within 24 hours of receipt for a period of at least 20 days.

(e) For a project of statewide, regional, or areawide significance, the lead agency shall also provide notice to transportation planning agencies and public agencies which have transportation facilities within their jurisdictions which could be affected by the project as specified in Section 21092.4(a) of the Public Resources Code. "Transportation facilities" includes: major local arterials and public transit within five miles of the project site and freeways, highways and rail transit service within 10 miles of the project site.

(f) If the United States Department of Defense or any branch of the United States Armed Forces has given a lead agency written notification of the specific boundaries of a low-level flight path, military impact zone, or special use airspace and provided the lead agency with written notification of the military contact office and address for the military service pursuant to subdivision (b) of Section 15190.5, then the lead agency shall include the specified military contact office in the list of organizations and individuals receiving a notice of intent to adopt a negative declaration or a mitigated negative declaration pursuant to this section for projects that meet the criteria set forth in subdivision (c) of Section 15190.5. The lead agency shall send the specified military contact office such notice of intent sufficiently prior to adoption by the lead agency of the negative declaration or mitigated negative declaration to allow the military service the review period provided under Section 15105.

(g) A notice of intent to adopt a negative declaration or mitigated negative declaration shall specify the following:

(1) A brief description of the proposed project and its location.

(2) The starting and ending dates for the review period during which the lead agency will receive comments on the proposed negative declaration or mitigated negative declaration. This shall include starting and ending dates for the review period. If the review period has been is shortened pursuant to Section 15105, the notice shall include a statement to that effect.

(3) The date, time, and place of any scheduled public meetings or hearings to be held by the lead agency on the proposed project, when known to the lead agency at the time of notice.

(4) The address or addresses where copies of the proposed negative declaration or mitigated negative declaration including the revisions developed under Section 15070(b) and all documents referenced in the proposed negative declaration or mitigated negative declaration are available for review. This location or locations shall be readily accessible to the public during the lead agency's normal working hours.

(5) The presence of the site on any of the lists enumerated under Section 65962.5 of the Government Code including, but not limited to lists of hazardous waste facilities, land designated as hazardous waste property, and hazardous waste disposal sites, and the information in the Hazardous Waste and Substances Statement required under subdivision (f) of that section.

(6) Other information specifically required by statute or regulation for a particular project or type of project.

Note: Authority cited: Section 21083, Public Resources Code; Reference: Sections 21091, 21092, 21092.2, 21092.4, 21092.3, 21092.6, 21098 and 21151.8, Public Resources Code.

15073. PUBLIC REVIEW OF A PROPOSED NEGATIVE DECLARATION OR MITIGATED NEGATIVE DECLARATION

(a) The lead agency shall provide a public review period pursuant to Section 15105 of not less than 20 days. When a proposed negative declaration or mitigated negative declaration and initial study are submitted to the State Clearinghouse for review by state agencies, the public review period shall not be less than 30 days, unless a shorter period is approved by the State Clearinghouse under Section 15105(d).

(b) When a proposed negative declaration or mitigated negative declaration and initial study have been submitted to the State Clearinghouse for review by state agencies, the public review period shall be at least as long as the review period established by the State Clearinghouse. The public review period and the state agency review period may, but are not required to, begin and end at the same time. Day one of the state review period shall be the date that the State Clearinghouse distributes the document to state agencies.

(c) A copy of the proposed negative declaration or mitigated negative declaration and the initial study shall be attached to the notice of intent to adopt the proposed declaration that is sent to every responsible agency and trustee agency concerned with the project and every other public agency with jurisdiction by law over resources affected by the project.

(d) Where one or more state agencies will be a responsible agency or a trustee agency or will exercise jurisdiction by law over natural resources affected by the project, or where the project is of statewide, regional, or areawide environmental significance, the lead agency shall send copies of the proposed negative declaration or mitigated negative declaration to the State Clearinghouse for distribution to state agencies.

(e) The lead agency shall notify in writing any public agency which comments on a proposed negative declaration or mitigated negative declaration of any public hearing to be held for the project for which the document was prepared. A notice provided to a public agency pursuant to Section 15072 satisfies this requirement.

Note: Authority cited: Section 21083, Public Resources Code; References: Sections 21000(e), 21003(b), 21080(c), 21081.6, 21091, and 21092.5, Public Resources Code; *Plaggmier v. City of San Jose* (1980) 101 Cal.App.3d 842.

15073.5. RECIRCULATION OF A NEGATIVE DECLARATION PRIOR TO ADOPTION.

(a) A lead agency is required to recirculate a negative declaration when the document must be substantially revised after public notice of its availability has previously been given pursuant to Section 15072, but prior to its adoption. Notice of recirculation shall comply with Sections 15072 and 15073.

(b) A "substantial revision" of the negative declaration shall mean:

(1) A new, avoidable significant effect is identified and mitigation measures or project revisions must be added in order to reduce the effect to insignificance, or

(2) The lead agency determines that the proposed mitigation measures or project revisions will not reduce potential effects to less than significance and new measures or revisions must be required.

(c) Recirculation is not required under the following circumstances:

(1) Mitigation measures are replaced with equal or more effective measures pursuant to Section 15074.1.

(2) New project revisions are added in response to written or verbal comments on the project's effects identified in the proposed negative declaration which are not new avoidable significant effects.

(3) Measures or conditions of project approval are added after circulation of the negative declaration which are not required by CEQA, which do not create new significant environmental effects and are not necessary to mitigate an avoidable significant effect.

(4) New information is added to the negative declaration which merely clarifies, amplifies, or makes insignificant modifications to the negative declaration.

(d) If during the negative declaration process there is substantial evidence in light of the whole record, before the lead agency that the project, as revised, may have a significant effect on the environment which cannot be mitigated or avoided, the lead agency shall prepare a draft EIR and certify a final EIR prior to approving the project. It shall circulate the draft EIR for consultation and review pursuant to Sections 15086 and 15087, and advise reviewers in writing that a proposed negative declaration had previously been circulated for the project.

Note: Authority cited: Section 21083, Public Resources Code. Reference: Section 21080, Public Resources Code; *Gentry v. City of Murrieta* (1995) 36 Cal.App.4th 1359; *Leonoff v. Monterey County Board of Supervisors* (1990) 222 Cal.App.3d 1337; *Long Beach Savings and Loan Assn. v. Long Beach Redevelopment Agency* (1986) 188 Cal.App.3d 249.

15074. CONSIDERATION AND ADOPTION OF A NEGATIVE DECLARATION OR MITIGATED NEGATIVE DECLARATION.

(a) Any advisory body of a public agency making a recommendation to the decision-making body shall consider the proposed negative declaration or mitigated negative declaration before making its recommendation.

(b) Prior to approving a project, the decision-making body of the lead agency shall consider the proposed negative declaration or mitigated negative declaration together with any comments received during the public review process. The decision-making body shall adopt the proposed negative declaration or mitigated negative declaration only if it finds on the basis of the whole record before it (including the initial study and any comments received), that there is no substantial evidence that the project will have a significant effect on the environment and that

the negative declaration or mitigated negative declaration reflects the lead agency's independent judgment and analysis.

(c) When adopting a negative declaration or mitigated negative declaration, the lead agency shall specify the location and custodian of the documents or other material which constitute the record of proceedings upon which its decision is based.

(d) When adopting a mitigated negative declaration, the lead agency shall also adopt a program for reporting on or monitoring the changes which it has either required in the project or made a condition of approval to mitigate or avoid significant environmental effects.

(e) A lead agency shall not adopt a negative declaration or mitigated negative declaration for a project within the boundaries of a comprehensive airport land use plan or, if a comprehensive airport land use plan has not been adopted, for a project within two nautical miles of a public airport or public use airport, without first considering whether the project will result in a safety hazard or noise problem for persons using the airport or for persons residing or working in the project area.

(f) When a non-elected official or decisionmaking body of a local lead agency adopts a negative declaration or mitigated negative declaration, that adoption may be appealed to the agency's elected decisionmaking body, if one exists. For example, adoption of a negative declaration for a project by a city's planning commission may be appealed to the city council. A local lead agency may establish procedures governing such appeals.

Note: Authority cited: Section 21083, Public Resources Code; Reference: Sections 21080(c), 21081.6, 21082.1, 21096, and 21151, Public Resources Code; *Friends of B Street v. City of Hayward* (1980) 106 Cal.App.3d 988.

15074.1. SUBSTITUTION OF MITIGATION MEASURES IN A PROPOSED MITIGATED NEGATIVE DECLARATION.

(a) As a result of the public review process for a proposed mitigated negative declaration, including any administrative decisions or public hearings conducted on the project prior to its approval, the lead agency may conclude that certain mitigation measures identified in the mitigated negative declaration are infeasible or otherwise undesirable. Prior to approving the project, the lead agency may, in accordance with this section, delete those mitigation measures and substitute for them other measures which the lead agency determines are equivalent or more effective.

(b) Prior to deleting and substituting for a mitigation measure, the lead agency shall do both of the following:

(1) Hold a public hearing on the matter. Where a public hearing is to be held in order to consider the project, the public hearing required by this section may be combined with that hearing. Where no public hearing would otherwise be held to consider the project, then a public hearing shall be required before a mitigation measure may be deleted and a new measure adopted in its place.

(2) Adopt a written finding that the new measure is equivalent or more effective in mitigating or avoiding potential significant effects and that it in itself will not cause any potentially significant effect on the environment.

(c) No recirculation of the proposed mitigated negative declaration pursuant to Section 15072 is required where the new mitigation measures are made conditions of, or are otherwise incorporated into, project approval in accordance with this section.

(d) "Equivalent or more effective" means that the new measure will avoid or reduce the significant effect to at least the same degree as, or to a greater degree than, the original measure and will create no more adverse effect of its own than would have the original measure.

Note: Authority cited: Section 21083, Public Resources Code; Reference: Section 21080(f), Public Resources Code.

15075. NOTICE OF DETERMINATION ON A PROJECT FOR WHICH A PROPOSED NEGATIVE OR MITIGATED NEGATIVE DECLARATION HAS BEEN APPROVED.

(a) The lead agency shall file a notice of determination within five working days after deciding to carry out or approve the project. For projects with more than one phase, the lead agency shall file a notice of determination for each phase requiring a discretionary approval.

(b) The notice of determination shall include:

(1) An identification of the project including the project title as identified on the proposed negative declaration, its location, and the State Clearinghouse identification number for the proposed negative declaration if the notice of determination is filed with the State Clearinghouse.

(2) A brief description of the project.

(3) The agency's name, the applicant's name, if any, and the date on which the agency approved the project.

(4) The determination of the agency that the project will not have a significant effect on the environment.

(5) A statement that a negative declaration or a mitigated negative declaration was adopted pursuant to the provisions of CEQA.

(6) A statement indicating whether mitigation measures were made a condition of the approval of the project, and whether a mitigation monitoring plan/program was adopted.

(7) The address where a copy of the negative declaration or mitigated negative declaration may be examined.

(c) If the lead agency is a state agency, the lead agency shall file the notice of determination with the Office of Planning and Research within five working days after approval of the project by the lead agency.

(d) If the lead agency is a local agency, the local lead agency shall file the notice of determination with the county clerk of the county or counties in which the project will be located, within five working days after approval of the project by the lead agency. If the project requires discretionary approval from any state agency, the local lead agency shall also, within five working days of this approval, file a copy of the notice of determination with the Office of Planning and Research.

(e) A notice of determination filed with the county clerk shall be available for public inspection and shall be posted by the county clerk within 24 hours of receipt for a period of at least 30 days. Thereafter, the clerk shall return the notice to the local lead agency with a notation of the period during which it was posted. The local lead agency shall retain the notice for not less than 12 months.

(f) A notice of determination filed with the Office of Planning and Research shall be available for public inspection and shall be posted for a period of at least 30 days. The Office of Planning and Research shall retain each notice for not less than 12 months.

(g) The filing of the notice of determination pursuant to subdivision (c) above for state agencies and the filing and posting of the notice of determination pursuant to subdivisions (d) and (e) above for local agencies, start a 30-day statute of limitations on court challenges to the approval under CEQA.

(h) A sample notice of determination is provided in Appendix D. Each public agency may devise its own form, but the minimum content requirements of subdivision (b) above shall be met.

Public agencies are encouraged to make copies of all notices filed pursuant to this section available in electronic format on the Internet. Such electronic notices are in addition to the posting requirements of these guidelines and the Public Resources Code.

Note: Authority cited: Section 21083 and 21152, Public Resources Code. Reference: Sections 21080(c), 21108(a) and (c), 21152 and 21167(b), Public Resources Code; *Citizens of Lake Murray Area Association* v. *City Council* (1982) 129 Cal. App. 3d 436.

Article 7. EIR Process

SECTIONS 15080 TO 15097

15080. GENERAL

To the extent possible, the EIR process should be combined with the existing planning, review, and project approval process used by each public agency.

Note: Authority cited: Section 21083, Public Resources Code; Reference: Sections 21003, 21061, 21100, and 21151, Public Resources Code.

15081. DECISION TO PREPARE AN EIR

The EIR process starts with the decision to prepare an EIR. This decision will be made either during preliminary review under Section 15060 or at the conclusion of an Initial Study after applying the standards described in Section 15064.

Note: Authority cited: Section 21083, Public Resources Code; Reference: Section 21100, Public Resources Code; *No Oil, Inc. v. City of Los Angeles*, (1974) 13 Cal. 3d 68; *Friends of B Street v. City of Hayward*, (1980) 106 Cal. App. 3d 988.

15081.5. EIRS REQUIRED BY STATUTE

(a) A lead agency shall prepare or have prepared an EIR for the following types of projects. An initial study may be prepared to help identify the significant effects of the project.

(1) The burning of municipal wastes, hazardous wastes, or refuse-derived fuel, including but not limited to tires, if the project is either:

(A) The construction of a new facility; or

(B) The expansion of an existing facility that burns hazardous waste that would increase its permitted capacity by more than 10 percent. This does not apply to any project exclusively burning hazardous waste for which a determination to prepare a negative declaration, or mitigated negative declaration or environmental impact report was made prior to July 14, 1989. The amount of expansion of an existing facility is calculated pursuant to subdivision (b) of Section 21151.1 of the Public Resources Code.

(C) Subdivision (1) of the subdivision does not apply to:

1. Projects for which the State Energy Resources Conservation and Development Commission has assumed jurisdiction pursuant to Chapter 6 (commencing with Section 25500) of Division 15 of the Public Resources Code.

2. Any of the types of burn or thermal processing projects listed in subdivision (d) of Section 21151.1 of the Public Resources Code.

(2) The initial issuance of a hazardous waste facilities permit to a land disposal facility, as defined in subdivision (d) of Section 25199.1 of the Health and Safety Code. Preparation of an EIR is not mandatory if the facility only manages hazardous waste which is identified or listed pursuant to Section 25140 or Section 25141 of the Health and Safety Code on or after January 1, 1992; or only conducts activities which are regulated pursuant to Chapter 6.5

(commencing with Section 25100) of Division 20 of the Health and Safety Code on or after January 1, 1992. "Initial issuance" does not include the issuance of a closure or postclosure permit pursuant to Chapter 6.5 (commencing with Section 25100) of Division 20 of the Health and Safety Code.

(3) The initial issuance of a hazardous waste facility permit pursuant to Section 25200 of the Health and Safety Code to an off-site large treatment facility, as defined pursuant to subdivision (d) of Section 25205.1 of that code. Preparation of an EIR is not mandatory if the facility only manages hazardous waste which is identified or listed pursuant to Section 25140 or Section 25141 of the Health and Safety Code on or after January 1, 1992; or only conducts activities which are regulated pursuant to Chapter 6.5 (commencing with Section 25100) of Division 20 of the Health and Safety Code on or after January 1, 1992. "Initial issuance" does not include the issuance of a closure or postclosure permit pursuant to Chapter 6.5 (commencing with Section 25100) of Division 20 of the Health and Safety Code.

(4) Any open pit mining operation which is subject to the permit requirements of the Surface Mining and Reclamation Act (beginning at Section 2710 of the Public Resources Code) and which utilizes a cyanide heap-leaching process for the purpose of extracting gold or other precious metals.

(5) An initial base reuse plan as defined in Section 15229.

(b) A lead agency shall prepare or have prepared an EIR for the selection of a California Community College, California State University, University of California, or California Maritime Academy campus location and approval of a long range development plan for that campus.

(1) The EIR for a long range development plan for a campus shall include an analysis of, among other significant impacts, those environmental effects relating to changes in enrollment levels.

(2) Subsequent projects within the campus may be addressed in environmental analyses tiered on the EIR prepared for the long range development plan.

Note: Authority cited: Section 21083, Public Resources Code; References: Sections 21080.09, 21083.8.1, 21151.1, and 21151.7, Public Resources Code.

15082. NOTICE OF PREPARATION AND DETERMINATION OF SCOPE OF EIR

(a) Notice of Preparation. Immediately after deciding that an environmental impact report is required for a project, the lead agency shall send to the Office of Planning and Research and each responsible and trustee agency a notice of preparation stating that an environmental impact report will be prepared. This notice shall also be sent to every federal agency involved in approving or funding the project. If the United States Department of Defense or any branch of the United States Armed Forces has given the lead agency written notification of the specific boundaries of a low-level flight path, military impact zone, or special use airspace and provided the lead agency with written notification of the military contact office and address for the military service pursuant to subdivision (b) of Section 15190.5, then the lead agency shall include the specified military contact office in the list of organizations and individuals receiving a notice of preparation of an EIR pursuant to this section for projects that meet the criteria set forth in subdivision (c) of Section 15190.5.

(1) The notice of preparation shall provide the responsible and trustee agencies and the Office of Planning and Research with sufficient information describing the project and the potential environmental effects to enable the responsible agencies to make a meaningful response. At a minimum, the information shall include:

(A) Description of the project,

(B) Location of the project (either by street address and cross street, for a project in an urbanized area, or by attaching a specific map, preferably a copy of a U.S.G.S. 15' or 7-1/2' topographical map identified by quadrangle name), and

(C) Probable environmental effects of the project.

(2) A sample notice of preparation is shown in Appendix I. Public agencies are free to devise their own formats for this notice. A copy of the initial study may be sent with the notice to supply the necessary information.

(3) To send copies of the notice of preparation, the lead agency shall use either certified mail or any other method of transmittal that provides it with a record that the notice was received.

(4) The lead agency may begin work on the draft EIR immediately without awaiting responses to the notice of preparation. The draft EIR in preparation may need to be revised or expanded to conform to responses to the notice of preparation. A lead agency shall not circulate a draft EIR for public review before the time period for responses to the notice of preparation has expired.

(b) Response to Notice of Preparation. Within 30 days after receiving the notice of preparation under subdivision (a), each responsible and trustee agency and the Office of Planning and Research shall provide the lead agency with specific detail about the scope and content of the environmental information related to the responsible or trustee agency's area of statutory responsibility that must be included in the draft EIR.

(1) The response at a minimum shall identify:

(A) The significant environmental issues and reasonable alternatives and mitigation measures that the responsible or trustee agency, or the Office of Planning and Research, will need to have explored in the draft EIR; and

(B) Whether the agency will be a responsible agency or trustee agency for the project.

(2) If a responsible or trustee agency or the Office of Planning and Research fails by the end of the 30-day period to provide the lead agency with either a response to the notice or a well-justified request for additional time, the lead agency may presume that none of those entities have a response to make.

(3) A generalized list of concerns not related to the specific project shall not meet the requirements of this section for a response.

(c) Meetings. In order to expedite the consultation, the lead agency, a responsible agency, a trustee agency, the Office of Planning and Research or a project applicant may request one or more meetings between representatives of the agencies involved to assist the lead agency in determining the scope and content of the environmental information that the responsible or trustee agency may require. Such meetings shall be convened by the lead agency as soon as possible, but no later than 30 days after the meetings were requested. On request, the Office of Planning and Research will assist in convening meetings that involve state agencies.

(1) For projects of statewide, regional or areawide significance pursuant to Section 15206, the lead agency shall conduct at least one scoping meeting. A scoping meeting held pursuant to the National Environmental Policy Act, 42 USC 4321 et seq. (NEPA) in the city or county within which the project is located satisfies this requirement if the lead agency meets the notice requirements of subsection (c)(2) below.

(2) The lead agency shall provide notice of the scoping meeting to all of the following:

(A) any county or city that borders on a county or city within which the project is located, unless otherwise designated annually by agreement between the lead agency and the county or city;

(B) any responsible agency

(C) any public agency that has jurisdiction by law with respect to the project;

(D) any organization or individual who has filed a written request for the notice.

(3) A lead agency shall call at least one scoping meeting for a proposed project that may affect highways or other facilities under the jurisdiction of the Department of Transportation if the meeting is requested by the Department. The lead agency shall call the scoping meeting as soon as possible but not later than 30 days after receiving the request from the Department of Transportation.

(d) The Office of Planning and Research. The Office of Planning and Research will ensure that the state responsible and trustee agencies reply to the lead agency within 30 days of receipt of the notice of preparation by the state responsible and trustee agencies.

(e) Identification Number. When the notice of preparation is submitted to the State Clearinghouse, the state identification number issued by the Clearinghouse shall be the identification number for all subsequent environmental documents on the project. The identification number should be referenced on all subsequent correspondence regarding the project, specifically on the title page of the draft and final EIR and on the notice of determination.

Note: Authority cited: Section 21083, Public Resources Code. Reference: Sections 21083.9, 21080.4, and 21098, Public Resources Code.

15083. EARLY PUBLIC CONSULTATION

Prior to completing the draft EIR, the Lead Agency may also consult directly with any person or organization it believes will be concerned with the environmental effects of the project. Many public agencies have found that early consultation solves many potential problems that would arise in more serious forms later in the review process. This early consultation may be called scoping. Scoping will be necessary when preparing an EIR/EIS jointly with a federal agency.

(a) Scoping has been helpful to agencies in identifying the range of actions, alternatives, mitigation measures, and significant effects to be analyzed in depth in an EIR and in eliminating from detailed study issues found not to be important.

(b) Scoping has been found to be an effective way to bring together and resolve the concerns of affected federal, state, and local agencies, the proponent of the action, and other interested persons including those who might not be in accord with the action on environmental grounds.

(c) Where scoping is used, it should be combined to the extent possible with consultation under Section 15082.

Note: Authority cited: Section 21083, Public Resources Code; Reference: Section 21082.1, Public Resources Code; Section 4, Chapter 480 of the Statutes of 1981; 40 Code of Federal Regulations, Part 1501.7.

15083.5. [DELETED]

15084. PREPARING THE DRAFT EIR

(a) The draft EIR shall be prepared directly by or under contract to the Lead Agency. The required contents of a draft EIR are discussed in Article 9 beginning with Section 15120.

(b) The Lead Agency may require the project applicant to supply data and information both to determine whether the project may have a significant effect on the environment and to assist the Lead Agency in preparing the draft EIR. The requested information should include an identification of other public agencies which will have jurisdiction by law over the project.

(c) Any person, including the applicant, may submit information or comments to the Lead Agency to assist in the preparation of the draft EIR. The submittal may be presented in any format, including the form of a draft EIR. The Lead Agency must consider all information and

comments received. The information or comments may be included in the draft EIR in whole or in part.

(d) The Lead Agency may choose one of the following arrangements or a combination of them for preparing a draft EIR.

(1) Preparing the draft EIR directly with its own staff.

(2) Contracting with another entity, public or private, to prepare the draft EIR.

(3) Accepting a draft prepared by the applicant, a consultant retained by the applicant, or any other person.

(4) Executing a third party contract or Memorandum of Understanding with the applicant to govern the preparation of a draft EIR by an independent contractor.

(5) Using a previously prepared EIR.

(e) Before using a draft prepared by another person, the Lead Agency shall subject the draft to the agency's own review and analysis. The draft EIR which is sent out for public review must reflect the independent judgment of the Lead Agency. The Lead Agency is responsible for the adequacy and objectivity of the draft EIR.

Note: Authority cited: Section 21083, Public Resources Code; Reference: Section 21082.1, Public Resources Code.

15085. NOTICE OF COMPLETION

(a) As soon as the draft EIR is completed, a notice of completion must be filed with the Office of Planning and Research in a printed hard copy or in electronic form on a diskette or by electronic mail transmission.

(b) The notice of completion shall include:

(1) A brief description of the project,

(2) The proposed location of the project (either by street address and cross street, for a project in an urbanized area, or by attaching a specific map, preferably a copy of a U.S.G.S. 15' or 7-1/2' topographical map identified by quadrangle name).

(3) An address where copies of the draft EIR are available, and

(4) The review period during which comments will be received on the draft EIR.

(c) A sample form for the notice of completion is included in Appendix L

(d) Where the EIR will be reviewed through the state review process handled by the State Clearinghouse, the notice of completion cover form required by the State Clearinghouse will serve as the notice of completion (see Appendix C).

(e) Public agencies are encouraged to make copies of notices of completion filed pursuant to this section available in electronic format on the Internet.

Note: Authority cited: Section 21083, Public Resources Code. Reference: Section 21161, Public Resources Code.

15086. CONSULTATION CONCERNING DRAFT EIR

(a) The Lead Agency shall consult with and request comments on the draft EIR from:

(1) Responsible Agencies,

(2) Trustee agencies with resources affected by the project, and

(3) Any other state, federal, and local agencies which have jurisdiction by law with respect to the project or which exercise authority over resources which may be affected by the project, including water agencies consulted pursuant to section 15083.5.

(4) Any city or county which borders on a city or county within which the project is located.

(5) For a project of statewide, regional, or areawide significance, the transportation planning agencies and public agencies which have transportation facilities within their jurisdictions which could be affected by the project. "Transportation facilities" includes: major local arterials and public transit within five miles of the project site, and freeways, highways and rail transit service within 10 miles of the project site.

(6) For a state lead agency when the EIR is being prepared for a highway or freeway project, the California Air Resources Board as to the air pollution impact of the potential vehicular use of the highway or freeway and if a non-attainment area, the local air quality management district for a determination of conformity with the air quality management plan.

(7) For a subdivision project located within one mile of a facility of the State Water Resources Development System, the California Department of Water Resources.

(b) The lead agency may consult directly with:

(1) Any person who has special expertise with respect to any environmental impact involved,

(2) Any member of the public who has filed a written request for notice with the lead agency or the clerk of the governing body.

(3) Any person identified by the applicant whom the applicant believes will be concerned with the environmental effects of the project.

(c) A responsible agency or other public agency shall only make substantive comments regarding those activities involved in the project that are within an area of expertise of the agency or which are required to be carried out or approved by the responsible agency. Those comments shall be supported by specific documentation.

(d) Prior to the close of the public review period, a responsible agency or trustee agency which has identified what that agency considers to be significant environmental effects shall advise the lead agency of those effects. As to those effects relevant to its decision, if any, on the project, the responsible or trustee agency shall either submit to the lead agency complete and detailed performance objectives for mitigation measures addressing those effects or refer the lead agency to appropriate, readily available guidelines or reference documents concerning mitigation measures. If the responsible or trustee agency is not aware of mitigation measures that address identified effects, the responsible or trustee agency shall so state.

Note: Authority cited: Section 21083, Public Resources Code; Reference: Sections 21081.6, 21092.4, 21092.5, 21104 and 21153, Public Resources Code.

15087. PUBLIC REVIEW OF DRAFT EIR

(a) The lead agency shall provide public notice of the availability of a draft EIR at the same time as it sends a notice of completion to the Office of Planning and Research. If the United States Department of Defense or any branch of the United States Armed Forces has given the lead agency written notification of the specific boundaries of a low-level flight path, military impact zone, or special use airspace and provided the lead agency with written notification of the contact office and address for the military service pursuant to subdivision (b) of Section 15190.5, then the lead agency shall include the specified military contact office in the list of organizations and individuals receiving a notice of availability of a draft EIR pursuant to this section for projects that meet the criteria set forth in subdivision (c) of Section 15190.5. The public notice shall be given as provided under Section 15105 (a sample form is provided in Appendix L). Notice shall be mailed to the last known name and address of all organizations and individuals who have previously requested such notice in writing, and shall also be given by at least one of the following procedures:

(1) Publication at least one time by the public agency in a newspaper of general circulation in the area affected by the proposed project. If more than one area is affected, the notice shall be published in the newspaper of largest circulation from among the newspapers of general circulation in those areas.

(2) Posting of notice by the public agency on and off the site in the area where the project is to be located.

(3) Direct mailing to the owners and occupants of property contiguous to the parcel or parcels on which the project is located. Owners of such property shall be identified as shown on the latest equalized assessment roll.

(b) The alternatives for providing notice specified in subdivision (a) shall not preclude a public agency from providing additional notice by other means if such agency so desires, nor shall the requirements of this section preclude a public agency from providing the public notice required by this section at the same time and in the same manner as public notice otherwise required by law for the project.

(c) The notice shall disclose the following:

(1) A brief description of the proposed project and its location.

(2) The starting and ending dates for the review period during which the lead agency will receive comments. If the review period is shortened, the notice shall disclose that fact.

(3) The date, time, and place of any scheduled public meetings or hearings to be held by the lead agency on the proposed project when known to the lead agency at the time of notice.

(4) A list of the significant environmental effects anticipated as a result of the project, to the extent which such effects are known to the lead agency at the time of the notice.

(5) The address where copies of the EIR and all documents referenced in the EIR will be available for public review. This location shall be readily accessible to the public during the lead agency‘s normal working hours.

(6) The presence of the site on any of the lists of sites enumerated under Section 65962.5 of the Government Code including, but not limited to, lists of hazardous waste facilities, land designated as hazardous waste property, hazardous waste disposal sites and others, and the information in the Hazardous Waste and Substances Statement required under subdivision (f) of that Section.

(d) The notice required under this section shall be posted in the office of the county clerk of each county in which the project will be located for a period of at least 30 days. The county clerk shall post such notices within 24 hours of receipt.

(e) In order to provide sufficient time for public review, the review period for a draft EIR shall be as provided in Section 15105. The review period shall be combined with the consultation required under Section 15086. When a draft EIR has been submitted to the State Clearinghouse, the public review period shall be at least as long as the review period established by the State Clearinghouse. The public review period and the state agency review period may, but are not required to, begin and end at the same time. Day one of the state review period shall be the date that the State Clearinghouse distributes the document to state agencies.

(f) Public agencies shall use the State Clearinghouse to distribute draft EIRs to state agencies for review and should use areawide clearinghouses to distribute the documents to regional and local agencies.

(g) To make copies of EIRs available to the public, Lead Agencies should furnish copies of draft EIRs to public library systems serving the area involved. Copies should also be available in offices of the Lead Agency.

(h) Public agencies should compile listings of other agencies, particularly local agencies, which have jurisdiction by law and/or special expertise with respect to various projects and project locations. Such listings should be a guide in determining which agencies should be consulted with regard to a particular project.

(i) Public hearings may be conducted on the environmental documents, either in separate proceedings or in conjunction with other proceedings of the public agency. Public hearings are encouraged, but not required as an element of the CEQA process.

Note: Authority cited: Section 21083, Public Resources Code. Reference: Sections 21091, 21092, 21092.2, 21092.3, 21092.6, 21098, 21104, 21152, 21153 and 21161, Public Resources Code.

15088. EVALUATION OF AND RESPONSE TO COMMENTS

(a) The lead agency shall evaluate comments on environmental issues received from persons who reviewed the draft EIR and shall prepare a written response. The Lead Agency shall respond to comments received during the noticed comment period and any extensions and may respond to late comments.

(b) The lead agency shall provide a written proposed response to a public agency on comments made by that public agency at least 10 days prior to certifying an environmental impact report.

(c) The written response shall describe the disposition of significant environmental issues raised (e.g., revisions to the proposed project to mitigate anticipated impacts or objections). In particular, the major environmental issues raised when the Lead Agency‘s position is at variance with recommendations and objections raised in the comments must be addressed in detail giving reasons why specific comments and suggestions were not accepted. There must be good faith, reasoned analysis in response. Conclusory statements unsupported by factual information will not suffice.

(d) The response to comments may take the form of a revision to the draft EIR or may be a separate section in the final EIR. Where the response to comments makes important changes in the information contained in the text of the draft EIR, the Lead Agency should either:

  (1) Revise the text in the body of the EIR, or

  (2) Include marginal notes showing that the information is revised in the response to comments.

Note: Authority cited: Section 21083, Public Resources Code. Reference: Sections 21092.5, 21104, and 21153, Public Resources Code; *People* v. *County of Kern* (1974) 39 Cal. App. 3d 830; *Cleary v. County of Stanislaus* (1981) 118 Cal. App. 3d 348.

15088.5. RECIRCULATION OF AN EIR PRIOR TO CERTIFICATION

(a) A lead agency is required to recirculate an EIR when significant new information is added to the EIR after public notice is given of the availability of the draft EIR for public review under Section 15087 but before certification. As used in this section, the term “information” can include changes in the project or environmental setting as well as additional data or other information. New information added to an EIR is not “significant” unless the EIR is changed in a way that deprives the public of a meaningful opportunity to comment upon a substantial adverse environmental effect of the project or a feasible way to mitigate or avoid such an effect (including a feasible project alternative) that the project’s proponents have declined to implement. “Significant new information” requiring recirculation include, for example, a disclosure showing that:

  (1) A new significant environmental impact would result from the project or from a new mitigation measure proposed to be implemented.

  (2) A substantial increase in the severity of an environmental impact would result unless mitigation measures are adopted that reduce the impact to a level of insignificance.

(3) A feasible project alternative or mitigation measure considerably different from others previously analyzed would clearly lessen the environmental impacts of the project, but the project's proponents decline to adopt it.

(4) The draft EIR was so fundamentally and basically inadequate and conclusory in nature that meaningful public review and comment were precluded. (*Mountain Lion Coalition v. Fish and Game Com.* (1989) 214 Cal.App.3d 1043)

(b) Recirculation is not required where the new information added to the EIR merely clarifies or amplifies or makes insignificant modifications in an adequate EIR.

(c) If the revision is limited to a few chapters or portions of the EIR, the lead agency need only recirculate the chapters or portions that have been modified.

(d) Recirculation of an EIR requires notice pursuant to Section 15087, and consultation pursuant to Section 15086.

(e) A decision not to recirculate an EIR must be supported by substantial evidence in the administrative record.

(f) The lead agency shall evaluate and respond to comments as provided in Section 15088. Recirculating an EIR can result in the lead agency receiving more than one set of comments from reviewers. The following are two ways in which the lead agency may identify the set of comments to which it will respond. This dual approach avoids confusion over whether the lead agency must respond to comments which are duplicates or which are no longer pertinent due to revisions to the EIR. In no case shall the lead agency fail to respond to pertinent comments on significant environmental issues.

(1) When an EIR is substantially revised and the entire document is recirculated, the lead agency may require reviewers to submit new comments and**,** in such cases, need not respond to those comments received during the earlier circulation period. The lead agency shall advise reviewers, either in the text of the revised EIR or by an attachment to the revised EIR, that although part of the administrative record, the previous comments do not require a written response in the final EIR, and that new comments must be submitted for the revised EIR. The lead agency need only respond to those comments submitted in response to the recirculated revised EIR.

(2) When the EIR is revised only in part and the lead agency is recirculating only the revised chapters or portions of the EIR, the lead agency may request that reviewers limit their comments to the revised chapters or portions of the recirculated EIR. The lead agency need only respond to (i) comments received during the initial circulation period that relate to chapters or portions of the document that were not revised and recirculated, and (ii) comments received during the recirculation period that relate to the chapters or portions of the earlier EIR that were revised and recirculated. The lead agency's request that reviewers limit the scope of their comments shall be included either within the text of the revised EIR or by an attachment to the revised EIR.

(3) As part of providing notice of recirculation as required by Public Resources Code Section 21092.1, the lead agency shall send a notice of recirculation to every agency, person, or organization that commented on the prior EIR. The notice shall indicate, at a minimum, whether new comments may be submitted only on the recirculated portions of the EIR or on the entire EIR in order to be considered by the agency.

(g) When recirculating a revised EIR, either in whole or in part, the lead agency shall, in the revised EIR or by an attachment to the revised EIR, summarize the revisions made to the previously circulated draft EIR.

Note: Authority cited: Section 21083, Public Resources Code. Reference: Section 21092.1, Public Resources Code; *Laurel Heights Improvement Association v. Regents of the University of California* (1993) 6 Cal. 4th 1112.

15089. PREPARATION OF FINAL EIR

(a) The Lead Agency shall prepare a final EIR before approving the project. The contents of a final EIR are specified in Section 15132 of these Guidelines.

(b) Lead Agencies may provide an opportunity for review of the final EIR by the public or by commenting agencies before approving the project. The review of a final EIR should focus on the responses to comments on the draft EIR.

Note: Authority cited: Section 21083, Public Resources Code; Reference: Sections 21100, 21105, and 21151, Public Resources Code; *City of Carmel-by-the-Sea v. Board of Supervisors*, (1977) 71 Cal. App. 3d 84; State Administrative Manual, Section 1060.

15090. CERTIFICATION OF THE FINAL EIR

(a) Prior to approving a project the lead agency shall certify that:

(1) The final EIR has been completed in compliance with CEQA;

(2) The final EIR was presented to the decision-making body of the lead agency, and that the decision-making body reviewed and considered the information contained in the final EIR prior to approving the project; and

(3) The final EIR reflects the lead agency's independent judgment and analysis.

(b) When an EIR is certified by a non-elected decision-making body within a local lead agency, that certification may be appealed to the local lead agency's elected decision-making body, if one exists. For example, certification of an EIR for a tentative subdivision map by a city's planning commission may be appealed to the city council. Each local lead agency shall provide for such appeals.

Note: Authority cited: Section 21083, Public Resources Code; Reference: Sections 21082.1, 21100,and 21151, Public Resources Code; *City of Carmel-by-the-Sea v. Board of Supervisors* (1977) 71 Cal.App.3d 84; *Kleist v. City of Glendale* (1976) 56 Cal.App.3d 770.

15091. FINDINGS

(a) No public agency shall approve or carry out a project for which an EIR has been certified which identifies one or more significant environmental effects of the project unless the public agency makes one or more written findings for each of those significant effects, accompanied by a brief explanation of the rationale for each finding. The possible findings are:

(1) Changes or alterations have been required in, or incorporated into, the project which avoid or substantially lessen the significant environmental effect as identified in the final EIR.

(2) Such changes or alterations are within the responsibility and jurisdiction of another public agency and not the agency making the finding. Such changes have been adopted by such other agency or can and should be adopted by such other agency.

(3) Specific economic, legal, social, technological, or other considerations, including provision of employment opportunities for highly trained workers, make infeasible the mitigation measures or project alternatives identified in the final EIR.

(b) The findings required by subdivision (a) shall be supported by substantial evidence in the record.

(c) The finding in subdivision (a)(2) shall not be made if the agency making the finding has concurrent jurisdiction with another agency to deal with identified feasible mitigation measures or alternatives. The finding in subdivision (a)(3) shall describe the specific reasons for rejecting identified mitigation measures and project alternatives.

(d) When making the findings required in subdivision (a)(1), the agency shall also adopt a program for reporting on or monitoring the changes which it has either required in the project or made a

condition of approval to avoid or substantially lessen significant environmental effects. These measures must be fully enforceable through permit conditions, agreements, or other measures.

(e) The public agency shall specify the location and custodian of the documents or other material which constitute the record of the proceedings upon which its decision is based.

(f) A statement made pursuant to Section 15093 does not substitute for the findings required by this section.

Note: Authority cited: Section 21083, Public Resources Code; Reference: Sections 21002, 21002.1, 21081, and 21081.6, Public Resources Code; *Laurel Hills Homeowners Association v. City Council* (1978) 83 Cal.App.3d 515; *Cleary v. County of Stanislaus* (1981) 118 Cal.App.3d 348; *Sierra Club v. Contra Costa County* (1992) 10 Cal.App.4th 1212; *Citizens for Quality Growth v. City of Mount Shasta* (1988) 198 Cal.App.3d 433.

15092. APPROVAL

(a) After considering the final EIR and in conjunction with making findings under Section 15091, the Lead Agency may decide whether or how to approve or carry out the project.

(b) A public agency shall not decide to approve or carry out a project for which an EIR was prepared unless either:

(1) The project as approved will not have a significant effect on the environment, or

(2) The agency has:

(A) Eliminated or substantially lessened all significant effects on the environment where feasible as shown in findings under Section 15091, and

(B) Determined that any remaining significant effects on the environment found to be unavoidable under Section 15091 are acceptable due to overriding concerns as described in Section 15093.

(c) With respect to a project which includes housing development, the public agency shall not reduce the proposed number of housing units as a mitigation measure if it determines that there is another feasible specific mitigation measure available that will provide a comparable level of mitigation.

Note: Authority cited: Section 21083, Public Resources Code. Reference: Sections 21002, 21002.1, 21081 and 21159.26, Public Resources Code; *Friends of Mammoth v. Board of Supervisors*, (1972) 8 Cal. App. 3d 247; *San Francisco Ecology Center v. City and County of San Francisco*, (1975) 48 Cal. App. 3d 584; *City of Carmel-by-the-Sea v. Board of Supervisors*, (1977) 71 Cal. App. 3d 84; *Laurel Hills Homeowners Association v. City Council*, (1978) 83 Cal. App. 3d 515.

15093. STATEMENT OF OVERRIDING CONSIDERATIONS

(a) CEQA requires the decision-making agency to balance, as applicable, the economic, legal, social, technological, or other benefits, including region-wide or statewide environmental benefits, of a proposed project against its unavoidable environmental risks when determining whether to approve the project. If the specific economic, legal, social, technological, or other benefits, including region-wide or statewide environmental benefits, of a proposed project outweigh the unavoidable adverse environmental effects, the adverse environmental effects may be considered "acceptable."

(b) When the lead agency approves a project which will result in the occurrence of significant effects which are identified in the final EIR but are not avoided or substantially lessened, the agency shall state in writing the specific reasons to support its action based on the final EIR and/or other information in the record. The statement of overriding considerations shall be supported by substantial evidence in the record.

(c) If an agency makes a statement of overriding considerations, the statement should be included in the record of the project approval and should be mentioned in the notice of determination. This statement does not substitute for, and shall be in addition to, findings required pursuant to Section 15091.

Note: Authority cited: Sections 21083 and 21083.05, Public Resources Code; Reference: Sections 21002 and 21081, Public Resources Code; *San Francisco Ecology Center v. City and County of San Francisco* (1975) 48 Cal.App.3d 584; *City of Carmel-by-the-Sea v. Board of Supervisors* (1977) 71 Cal.App.3d 84; *Sierra Club v. Contra Costa County* (1992) 10 Cal.App.4th 1212; *Citizens for Quality Growth v. City of Mount Shasta* (1988) 198 Cal.App.3d 433; *City of Marina v. Board of Trustees of Cal. State Univ.* (2006) 39 Cal.4th 341.

15094. NOTICE OF DETERMINATION

(a) The lead agency shall file a notice of determination within five working days after deciding to carry out or approve the project.

(b) The notice of determination shall include:

(1) An identification of the project including the project title as identified on the draft EIR, and the location of the project (either by street address and cross street for a project in an urbanized area or by attaching a specific map, preferably a copy of a U.S.G.S. 15' or 7-1/2' topographical map identified by quadrangle name). If the notice of determination is filed with the State Clearinghouse, the State Clearinghouse identification number for the draft EIR shall be provided.

(2) A brief description of the project.

(3) The lead agency‘s name, the applicant’s name, if any, and the date on which the agency approved the project. If a responsible agency files the notice of determination pursuant to Section 15096(i), the responsible agency’s name, the applicant name, if any, and date of approval shall also be identified.

(4) The determination of the agency whether the project in its approved form will have a significant effect on the environment.

(5) A statement that an EIR was prepared and certified pursuant to the provisions of CEQA.

(6) Whether mitigation measures were made a condition of the approval of the project, and whether a mitigation monitoring plan/program was adopted.

(7) Whether findings were made pursuant to Section 15091.

(8) Whether a statement of overriding considerations was adopted for the project.

(9) The address where a copy of the final EIR and the record of project approval may be examined.

(c) If the lead agency is a state agency, the lead agency shall file the notice of determination with the Office of Planning and Research within five working days after approval of the project by the lead agency.

(d) If the lead agency is a local agency, the local lead agency shall file the notice of determination with the county clerk of the county or counties in which the project will be located, within five working days after approval of the project by the lead agency. If the project requires discretionary approval from any state agency, the local lead agency shall also, within five working days of this approval, file a copy of the notice of determination with the Office of Planning and Research.

(e) A notice of determination filed with the county clerk shall be available for public inspection and shall be posted within 24 hours of receipt for a period of at least 30 days. Thereafter, the clerk shall return the notice to the local lead agency with a notation of the period during which it was posted. The local lead agency shall retain the notice for not less than 12 months.

(f) A notice of determination filed with the Office of Planning and Research shall be available for public inspection and shall be posted for a period of at least 30 days. The Office of Planning and Research shall retain each notice for not less than 12 months.

(g) The filing of the notice of determination pursuant to subdivision (c) above for state agencies and the filing and posting of the notice of determination pursuant to subdivisions (d) and (e) above for local agencies, start a 30-day statute of limitations on court challenges to the approval under CEQA.

(h) A sample notice of determination is provided in Appendix D. Each public agency may devise its own form, but any such form shall include, at a minimum, the information required by subdivision (b). Public agencies are encouraged to make copies of all notices filed pursuant to this section available in electronic format on the Internet. Such electronic notices are in addition to the posting requirements of the Guidelines and the Public Resources Code.

Note: Authority cited: Section 21083 and 21152, Public Resources Code. Reference: Sections 21108, 21152 and 21167, Public Resources Code; *Citizens of Lake Murray Area Association v. City Council* (1982) 129 Cal. App. 3d 436.

15095. DISPOSITION OF A FINAL EIR

The lead agency shall:

(a) File a copy of the final EIR with the appropriate planning agency of any city, county, or city and county where significant effects on the environment may occur.

(b) Include the final EIR as part of the regular project report which is used in the existing project review and budgetary process if such a report is used.

(c) Retain one or more copies of the final EIR as public records for a reasonable period of time.

(d) Require the applicant to provide a copy of the certified, final EIR to each responsible agency.

Note: Authority cited: Section 21083, Public Resources Code. Reference: Sections 21105, 21151 and 21165, Public Resources Code; County of Inyo v. Yorty, (1973) 32 Cal. App. 3d 795.

15096. PROCESS FOR A RESPONSIBLE AGENCY

(a) General. A Responsible Agency complies with CEQA by considering the EIR or Negative Declaration prepared by the Lead Agency and by reaching its own conclusions on whether and how to approve the project involved. This section identifies the special duties a public agency will have when acting as a Responsible Agency.

(b) Response to Consultation. A Responsible Agency shall respond to consultation by the Lead Agency in order to assist the Lead Agency in preparing adequate environmental documents for the project. By this means, the Responsible Agency will ensure that the documents it will use will comply with CEQA.

  (1) In response to consultation, a Responsible Agency shall explain its reasons for recommending whether the Lead Agency should prepare an EIR or Negative Declaration for a project. Where the Responsible Agency disagrees with the Lead Agency's proposal to prepare a Negative Declaration for a project, the Responsible Agency should identify the significant environmental effects which it believes could result from the project and recommend either that an EIR be prepared or that the project be modified to eliminate the significant effects.

  (2) As soon as possible, but not longer than 30 days after receiving a Notice of Preparation from the Lead Agency, the Responsible Agency shall send a written reply by certified mail or any other method which provides the agency with a record showing that the notice was received. The reply shall specify the scope and content of the environmental information which would be germane to the Responsible Agency's statutory responsibilities in

connection with the proposed project. The Lead Agency shall include this information in the EIR.

(c) Meetings. The Responsible Agency shall designate employees or representatives to attend meetings requested by the Lead Agency to discuss the scope and content of the EIR.

(d) Comments on Draft EIRs and Negative Declarations. A Responsible Agency should review and comment on draft EIRs and Negative Declarations for projects which the Responsible Agency would later be asked to approve. Comments should focus on any shortcomings in the EIR, the appropriateness of using a Negative Declaration, or on additional alternatives or mitigation measures which the EIR should include. The comments shall be limited to those project activities which are within the agency's area of expertise or which are required to be carried out or approved by the agency or which will be subject to the exercise of powers by the agency. Comments shall be as specific as possible and supported by either oral or written documentation.

(e) Decision on Adequacy of EIR or Negative Declaration. If a Responsible Agency believes that the final EIR or Negative Declaration prepared by the Lead Agency is not adequate for use by the Responsible Agency, the Responsible Agency must either:

(1) Take the issue to court within 30 days after the Lead Agency files a Notice of Determination;

(2) Be deemed to have waived any objection to the adequacy of the EIR or Negative Declaration;

(3) Prepare a subsequent EIR if permissible under Section 15162; or

(4) Assume the Lead Agency role as provided in Section 15052(a)(3).

(f) Consider the EIR or Negative Declaration. Prior to reaching a decision on the project, the Responsible Agency must consider the environmental effects of the project as shown in the EIR or Negative Declaration. A subsequent or supplemental EIR can be prepared only as provided in Sections 15162 or 15163.

(g) Adoption of Alternatives or Mitigation Measures.

(1) When considering alternatives and mitigation measures, a Responsible Agency is more limited than a Lead Agency. A Responsible Agency has responsibility for mitigating or avoiding only the direct or indirect environmental effects of those parts of the project which it decides to carry out, finance, or approve.

(2) When an EIR has been prepared for a project, the Responsible Agency shall not approve the project as proposed if the agency finds any feasible alternative or feasible mitigation measures within its powers that would substantially lessen or avoid any significant effect the project would have on the environment. With respect to a project which includes housing development, the Responsible Agency shall not reduce the proposed number of housing units as a mitigation measure if it determines that there is another feasible specific mitigation measure available that will provide a comparable level of mitigation.

(h) Findings. The Responsible Agency shall make the findings required by Section 15091 for each significant effect of the project and shall make the findings in Section 15093 if necessary.

(i) Notice of Determination. The Responsible Agency should file a Notice of Determination in the same manner as a Lead Agency under Section 15075 or 15094 except that the Responsible Agency does not need to state that the EIR or Negative Declaration complies with CEQA. The Responsible Agency should state that it considered the EIR or Negative Declaration as prepared by a Lead Agency.

Note: Authority cited: Section 21083, Public Resources Code; Reference: Sections 21165, 21080.1, 21080.3, 21080.4, 21082.1, and 21002.1(b) and (d), Public Resources Code.

15097. MITIGATION MONITORING OR REPORTING.

(a) This section applies when a public agency has made the findings required under paragraph (1) of subdivision (a) of Section 15091 relative to an EIR or adopted a mitigated negative declaration in conjunction with approving a project. In order to ensure that the mitigation measures and project revisions identified in the EIR or negative declaration are implemented, the public agency shall adopt a program for monitoring or reporting on the revisions which it has required in the project and the measures it has imposed to mitigate or avoid significant environmental effects. A public agency may delegate reporting or monitoring responsibilities to another public agency or to a private entity which accepts the delegation; however, until mitigation measures have been completed the lead agency remains responsible for ensuring that implementation of the mitigation measures occurs in accordance with the program.

(b) Where the project at issue is the adoption of a general plan, specific plan, community plan or other plan-level document (zoning, ordinance, regulation, policy), the monitoring plan shall apply to policies and any other portion of the plan that is a mitigation measure or adopted alternative. The monitoring plan may consist of policies included in plan-level documents. The annual report on general plan status required pursuant to the Government Code is one example of a reporting program for adoption of a city or county general plan.

(c) The public agency may choose whether its program will monitor mitigation, report on mitigation, or both. "Reporting" generally consists of a written compliance review that is presented to the decision making body or authorized staff person. A report may be required at various stages during project implementation or upon completion of the mitigation measure. "Monitoring" is generally an ongoing or periodic process of project oversight. There is often no clear distinction between monitoring and reporting and the program best suited to ensuring compliance in any given instance will usually involve elements of both. The choice of program may be guided by the following:

  (1) Reporting is suited to projects which have readily measurable or quantitative mitigation measures or which already involve regular review. For example, a report may be required upon issuance of final occupancy to a project whose mitigation measures were confirmed by building inspection.

  (2) Monitoring is suited to projects with complex mitigation measures, such as wetlands restoration or archeological protection, which may exceed the expertise of the local agency to oversee, are expected to be implemented over a period of time, or require careful implementation to assure compliance.

  (3) Reporting and monitoring are suited to all but the most simple projects. Monitoring ensures that project compliance is checked on a regular basis during and, if necessary after, implementation. Reporting ensures that the approving agency is informed of compliance with mitigation requirements.

(d) Lead and responsible agencies should coordinate their mitigation monitoring or reporting programs where possible. Generally, lead and responsible agencies for a given project will adopt separate and different monitoring or reporting programs. This occurs because of any of the following reasons: the agencies have adopted and are responsible for reporting on or monitoring different mitigation measures; the agencies are deciding on the project at different times; each agency has the discretion to choose its own approach to monitoring or reporting; and each agency has its own special expertise.

(e) At its discretion, an agency may adopt standardized policies and requirements to guide individually adopted monitoring or reporting programs. Standardized policies and requirements may describe, but are not limited to:

(1) The relative responsibilities of various departments within the agency for various aspects of monitoring or reporting, including lead responsibility for administering typical programs and support responsibilities.

(2) The responsibilities of the project proponent.

(3) Agency guidelines for preparing monitoring or reporting programs.

(4) General standards for determining project compliance with the mitigation measures or revisions and related conditions of approval.

(5) Enforcement procedures for noncompliance, including provisions for administrative appeal.

(6) Process for informing staff and decision makers of the relative success of mitigation measures and using those results to improve future mitigation measures.

(f) Where a trustee agency, in timely commenting upon a draft EIR or a proposed mitigated negative declaration, proposes mitigation measures or project revisions for incorporation into a project, that agency, at the same time, shall prepare and submit to the lead or responsible agency a draft monitoring or reporting program for those measures or revisions. The lead or responsible agency may use this information in preparing its monitoring or reporting program.

(g) When a project is of statewide, regional, or areawide importance, any transportation information generated by a required monitoring or reporting program shall be submitted to the transportation planning agency in the region where the project is located and to the California Department of Transportation. Each transportation planning agency and the California Department of Transportation shall adopt guidelines for the submittal of such information.

Note: Authority cited: Section 21083, Public Resources Code. References: Sections 21081.6 and 21081.7, Public Resources Code.

Article 8. Time Limits

SECTIONS 15100 TO 15112

15100. GENERAL

(a) Public agencies shall adopt time limits to govern their implementation of CEQA consistent with this article.

(b) Public agencies should carry out their responsibilities for preparing and reviewing EIRs within a reasonable period of time. The requirement for the preparation of an EIR should not cause undue delays in the processing of applications for permits or other entitlements to use.

Note: Authority cited: Section 21083, Public Resources Code; Reference: Sections 21000–21176, Public Resources Code.

15101. REVIEW OF APPLICATION FOR COMPLETENESS

A Lead Agency or Responsible Agency shall determine whether an application for a permit or other entitlement for use is complete within 30 days from the receipt of the application except as provided in Section 15111. If no written determination of the completeness of the application is made within that period, the application will be deemed complete on the 30th day.

Note: Authority cited: Section 21083, Public Resources Code; Reference: Section 21083, Public Resources Code; Section 65943, Government Code.

15102. INITIAL STUDY

The Lead Agency shall determine within 30 days after accepting an application as complete whether it intends to prepare an EIR or a Negative Declaration or use a previously prepared EIR or

Negative Declaration except as provided in Section 15111. The 30 day period may be extended 15 days upon the consent of the lead agency and the project applicant.

Note: Authority cited: Section 21083, Public Resources Code; Reference: Section 21080.2, Public Resources Code.

15103. RESPONSE TO NOTICE OF PREPARATION

Responsible and Trustee Agencies, and the Office of Planning and Research shall provide a response to a Notice of Preparation to the Lead Agency within 30 days after receipt of the notice. If they fail to reply within the 30 days with either a response or a well justified request for additional time, the Lead Agency may assume that none of those entitles have a response to make and may ignore a late response.

Note: Authority cited: Section 21083, Public Resources Code; Reference: Sections 21080.4, Public Resources Code.

15104. CONVENING OF MEETINGS

The Lead Agency shall convene a meeting with agency representatives to discuss the scope and content of the environmental information a Responsible Agency will need in the EIR as soon as possible but no later than 30 days after receiving a request for the meeting. The meeting may be requested by the Lead Agency, a Responsible Agency, a Trustee Agency, the Office of Planning and Research, or by the project applicant.

Note: Authority cited: Section 21083, Public Resources Code; Reference: Section 21080.4, Public Resources Code.

15105. PUBLIC REVIEW PERIOD FOR A DRAFT EIR OR A PROPOSED NEGATIVE DECLARATION OR MITIGATED NEGATIVE DECLARATION

(a) The public review period for a draft EIR shall not be less than 30 days nor should it be longer than 60 days except under unusual circumstances. When a draft EIR is submitted to the State Clearinghouse for review by state agencies, the public review period shall not be less than 45 days, unless a shorter period, not less than 30 days, is approved by the State Clearinghouse.

(b) The public review period for a proposed negative declaration or mitigated negative declaration shall be not less than 20 days. When a proposed negative declaration or mitigated negative declaration is submitted to the State Clearinghouse for review by state agencies, the public review period shall not be less than 30 days, unless a shorter period, not less than 20 days, is approved by the State Clearinghouse.

(c) If a draft EIR or proposed negative declaration or mitigated negative declaration has been submitted to the State Clearinghouse for review by state agencies, the public review period shall be at least as long as the review period established by the State Clearinghouse. The public review period and the state agency review period may, but are not required to, begin and end at the same time. Day one of the state review period shall be the date that the State Clearinghouse distributes the document to state agencies.

(d) A shortened Clearinghouse review period may be granted in accordance with the provisions of Appendix K and the following principles:

  (1) A shortened review shall not be granted for any proposed project of statewide, areawide, or regional environmental significance.

  (2) Requests for shortened review periods shall be submitted to the Clearinghouse in writing by the decision-making body of the lead agency, or a representative authorized by ordinance, resolution, or delegation of the decision-making body.

  (3) The lead agency has contacted responsible and trustee agencies and they have agreed to the shortened review period.

(e) The State Clearinghouse shall distribute a draft EIR or proposed negative declaration or mitigated negative declaration within three working days after the date of receipt if the submittal is determined by the State Clearinghouse to be complete.

Note: Authority cited: Section 21083, Public Resources Code; Reference: Sections 21091 and 21092, Public Resources Code; *People v. County of Kern* (1974) 39 Cal.App.3d 830.

15106. [DELETED]

15107. COMPLETION OF NEGATIVE DECLARATION

With private projects involving the issuance of a lease, permit, license, certificate, or other entitlement for use by one or more public agencies, the negative declaration must be completed and approved within 180 days from the date when the lead agency accepted the application as complete.

Note: Authority cited: Section 21083, Public Resources Code; Reference: Sections 21100.2 and 21151.5, Public Resources Code.

15108. COMPLETION AND CERTIFICATION OF EIR

With a private project, the Lead Agency shall complete and certify the final EIR as provided in Section 15090 within one year after the date when the Lead Agency accepted the application as complete. Lead Agency procedures may provide that the one-year time limit may be extended once for a period of not more than 90 days upon consent of the Lead Agency and the applicant.

Note: Authority cited: Section 21083, Public Resources Code; Reference: Sections 21100.2 and 21151.5, Public Resources Code; Government Code Section 65950.

15109. SUSPENSION OF TIME PERIODS

An unreasonable delay by an applicant in meeting requests by the Lead Agency necessary for the preparation of a Negative Declaration or an EIR shall suspend the running of the time periods described in Sections 15107 and 15108 for the period of the unreasonable delay. Alternatively, an agency may disapprove a project application where there is unreasonable delay in meeting requests. The agency may allow a renewed application to start at the same point in the process where the application was when it was disapproved.

Note: Authority cited: Section 21083, Public Resources Code; Reference: Sections 21100.2 and 21151.5, Public Resources Code; *Carmel Valley View, Ltd. v. Maggini*, 91 Cal. App. 3d 318.

15110. PROJECTS WITH FEDERAL INVOLVEMENT

(a) At the request of an applicant, the Lead Agency may waive the one-year time limit for completing and certifying a final EIR or the 105-day period for completing a Negative Declaration if:

  (1) The project will be subject to CEQA and to the National Environmental Policy Act,

  (2) Additional time will be required to prepare a combined EIR-EIS or combined Negative Declaration-Finding of No Significant Impact as provided in Section 15221, and

  (3) The time required to prepare the combined document will be shorter than the time required to prepare the documents separately.

(b) The time limits for taking final action on a permit for a development project may also be waived where a combined EIR-EIS will be prepared.

(c) The time limits for processing permits for development projects under Government Code Sections 65950–65960 shall not apply if federal statutes or regulations require time schedules which exceed the state time limits. In this event, any state agencies involved shall make a final decision on the project within the federal time limits.

Note: Authority cited: Section 21083, Public Resources Code; Reference: Sections 21083.6 and 21083.7, Public Resources Code; Sections 65951 and 65954, Government Code; Public Law 91–190 as amended, 42 U.S.C.A. 4321–4347.

15111. PROJECTS WITH SHORT TIME PERIODS FOR APPROVAL

(a) A few statutes or ordinances require agencies to make decisions on permits within time limits that are so short that review of the project under CEQA would be difficult. To enable the Lead Agency to comply with both the permit statute and CEQA, the Lead Agency shall deem an application for a project not received for filing under the permit statute or ordinance until such time as progress toward completing the environmental documentation required by CEQA is sufficient to enable the Lead Agency to finish the CEQA process within the short permit time limit. This section will apply where all of the following conditions are met:

(1) The enabling legislation for a program, other than Chapter 4.5 (commencing with Section 65920) of Division 1 of Title 7 of the Government Code, requires the Lead Agency to take action on an application within a specified period of time that is six months or less, and

(2) The enabling legislation provides that the project will become approved by operation of law if the Lead Agency fails to take any action within such specified time period, and

(3) The project involves the issuance of a lease, permit, license, certificate, or other entitlement for use.

(b) Examples of time periods subject to this section include, but are not limited to:

(1) Action on a timber harvesting plan by the Director of Forestry within 15 days pursuant to Section 4582.7 of the Public Resources Code,

(2) Action on a permit by the San Francisco Bay Conservation and Development Commission within 90 days pursuant to Section 66632(f) of the Government Code, and

(3) Action on an oil and gas permit by the Division of Oil and Gas within 10 days pursuant to Sections 3203 or 3724 of the Public Resources Code.

(c) In any case described in this section, the environmental document shall be completed or certified and the decision on the project shall be made within the period established under the Permit Streamlining Act (Government Code Sections 65920, et seq.).

Note: Authority cited: Section 21083, Public Resources Code; Reference: Sections 21100.2 and 21151.5, Public Resources Code; *N.R.D.C. v. Arcata National Corp.* (1976) 59 Cal.App.3d 959.

15112. STATUTES OF LIMITATIONS

(a) CEQA provides unusually short statutes of limitations on filing court challenges to the approval of projects under the Act.

(b) The statute of limitations periods are not public review periods or waiting periods for the person whose project has been approved. The project sponsor may proceed to carry out the project as soon as the necessary permits have been granted. The statute of limitations cuts off the right of another person to file a court action challenging approval of the project after the specified time period has expired.

(c) The statute of limitations periods under CEQA are as follows:

(1) Where the public agency filed a Notice of Determination in compliance with Sections 15075 or 15094, 30 days after the filing of the notice and the posting on a list of such notices.

(2) Where the public agency filed a Notice of Exemption in compliance with Section 15062, 35 days after the filing of the notice and the posting on a list of such notices.

(3) Where a certified state regulatory agency files a Notice of Decision in compliance with Public Resources Code Section 21080.5(d)(2)(E), 30 days after the filing of the notice.

(4) Where the Secretary for Resources certifies a state environmental regulatory agency under Public Resources Code Section 21080.5, the certification may be challenged only during the 30 days following the certification decision.

(5) Where none of the other statute of limitations periods in this section apply, 180 days after either:

(A) The public agency's decision to carry out or approve the project, or

(B) Commencement of the project if the project is undertaken without a formal decision by the public agency.

Note: Authority cited: Section 21083, Public Resources Code; Reference: Sections 21167, 21167.3, and 21080.5, Public Resources Code; *Kriebel v. City Council*, 112 Cal. App. 3d 693; *Citizens of Lake Murray Area Association v. City Council*, (1982) 129 Cal. App. 3d 436.

Article 9. Contents of Environmental Impact Reports

SECTIONS 15120 TO 15132

15120. GENERAL

(a) Environmental Impact Reports shall contain the information outlined in this article, but the format of the document may be varied. Each element must be covered, and when these elements are not separated into distinct sections, the document shall state where in the document each element is discussed.

(b) The EIR may be prepared as a separate document, as part of a general plan, or as part of a project report. If prepared as a part of the project report, it must still contain one separate and distinguishable section providing either analysis of all the subjects required in an EIR or, as a minimum, a table showing where each of the subjects is discussed. When the Lead Agency is a state agency, the EIR shall be included as part of the regular project report if such a report is used in the agency's existing review and budgetary process.

(c) Draft EIRs shall contain the information required by Sections 15122 through 15131. Final EIRs shall contain the same information and the subjects described in Section 15132.

(d) No document prepared pursuant to this article that is available for public examination shall include a "trade secret" as defined in Section 6254.7 of the Government Code, information about the location of archaeological sites and sacred lands, or any other information that is subject to the disclosure restrictions of Section 6254 of the Government Code.

Note: Authority cited: Section 21083, Public Resources Code; Reference: Sections 21100, 21105 and 21160, Public Resources Code.

15121. INFORMATIONAL DOCUMENT

(a) An EIR is an informational document which will inform public agency decision makers and the public generally of the significant environmental effect of a project, identify possible ways to minimize the significant effects, and describe reasonable alternatives to the project. The public agency shall consider the information in the EIR along with other information which may be presented to the agency.

(b) While the information in the EIR does not control the agency's ultimate discretion on the project, the agency must respond to each significant effect identified in the EIR by making findings under Section 15091 and if necessary by making a statement of overriding consideration under Section 15093.

(c) The information in an EIR may constitute substantial evidence in the record to support the agency's action on the project if its decision is later challenged in court.

Note: Authority cited: Section 21083, Public Resources Code; Reference: Section 21061, Public Resources Code; *Carmel Valley View, Ltd. v. Board of Supervisors*, (1976) 58 Cal. App. 3d 817.

15122. TABLE OF CONTENTS OR INDEX

An EIR shall contain at least a table of contents or an index to assist readers in finding the analysis of different subjects and issues.

Note: Authority cited: Section 21083, Public Resources Code; Reference: Section 21061, Public Resources Code.

15123. SUMMARY

(a) An EIR shall contain a brief summary of the proposed actions and its consequences. The language of the summary should be as clear and simple as reasonably practical.

(b) The summary shall identify:

(1) Each significant effect with proposed mitigation measures and alternatives that would reduce or avoid that effect;

(2) Areas of controversy known to the Lead Agency including issues raised by agencies and the public; and

(3) Issues to be resolved including the choice among alternatives and whether or how to mitigate the significant effects.

(c) The summary should normally not exceed 15 pages.

Note: Authority cited: Section 21083, Public Resources Code; Reference: Section 21061, Public Resources Code.

15124. PROJECT DESCRIPTION

The description of the project shall contain the following information but should not supply extensive detail beyond that needed for evaluation and review of the environmental impact.

(a) The precise location and boundaries of the proposed project shall be shown on a detailed map, preferably topographic. The location of the project shall also appear on a regional map.

(b) A statement of the objectives sought by the proposed project. A clearly written statement of objectives will help the lead agency develop a reasonable range of alternatives to evaluate in the EIR and will aid the decision makers in preparing findings or a statement of overriding considerations, if necessary. The statement of objectives should include the underlying purpose of the project.

(c) A general description of the project's technical, economic, and environmental characteristics, considering the principal engineering proposals if any and supporting public service facilities.

(d) A statement briefly describing the intended uses of the EIR.

(1) This statement shall include, to the extent that the information is known to the Lead Agency,

(A) A list of the agencies that are expected to use the EIR in their decision making, and

(B) A list of permits and other approvals required to implement the project.

(C) A list of related environmental review and consultation requirements required by federal, state, or local laws, regulations, or policies. To the fullest extent possible, the lead agency should integrate CEQA review with these related environmental review and consultation requirements.

(2) If a public agency must make more than one decision on a project, all its decisions subject to CEQA should be listed, preferably in the order in which they will occur. On request, the

Office of Planning and Research will provide assistance in identifying state permits for a project.

Note: Authority cited: Section 21083, Public Resources Code; Reference: Sections 21080.3, 21080.4, 21165, 21166, and 21167.2, Public Resources Code; *County of Inyo v. City of Los Angeles* (1977) 71 Cal.App.3d 185.

15125. ENVIRONMENTAL SETTING

(a) An EIR must include a description of the physical environmental conditions in the vicinity of the project, as they exist at the time the notice of preparation is published, or if no notice of preparation is published, at the time environmental analysis is commenced, from both a local and regional perspective. This environmental setting will normally constitute the baseline physical conditions by which a lead agency determines whether an impact is significant. The description of the environmental setting shall be no longer than is necessary to an understanding of the significant effects of the proposed project and its alternatives.

(b) When preparing an EIR for a plan for the reuse of a military base, lead agencies should refer to the special application of the principle of baseline conditions for determining significant impacts contained in Section 15229.

(c) Knowledge of the regional setting is critical to the assessment of environmental impacts. Special emphasis should be placed on environmental resources that are rare or unique to that region and would be affected by the project. The EIR must demonstrate that the significant environmental impacts of the proposed project were adequately investigated and discussed and it must permit the significant effects of the project to be considered in the full environmental context.

(d) The EIR shall discuss any inconsistencies between the proposed project and applicable general plans, specific plans, and regional plans. Such regional plans include, but are not limited to, the applicable air quality attainment or maintenance plan or State Implementation Plan, area-wide waste treatment and water quality control plans, regional transportation plans, regional housing allocation plans, regional blueprint plans, plans for the reduction of greenhouse gas emissions, habitat conservation plans, natural community conservation plans and regional land use plans for the protection of the Coastal Zone, Lake Tahoe Basin, San Francisco Bay, and Santa Monica Mountains.

(e) Where a proposed project is compared with an adopted plan, the analysis shall examine the existing physical conditions at the time the notice of preparation is published, or if no notice of preparation is published, at the time environmental analysis is commenced as well as the potential future conditions discussed in the plan.

Note: Authority cited: Sections 21083, 21083.05, Public Resources Code; Reference: Sections 21060.5, 21061, and 21100, Public Resources Code; *E.P.I.C. v. County of El Dorado* (1982) 131 Cal.App.3d 350; *San Joaquin Raptor/Wildlife Rescue Center v. County of Stanislaus* (1994) 27 Cal.App.4th 713; *Bloom v. McGurk* (1994) 26 Cal.App.4th 1307.

15126. CONSIDERATION AND DISCUSSION OF ENVIRONMENTAL IMPACTS

All phases of a project must be considered when evaluating its impact on the environment: planning, acquisition, development, and operation. The subjects listed below shall be discussed as directed in Sections 15126.2, 15126.4 and 15126.6, preferably in separate sections or paragraphs of the EIR. If they are not discussed separately, the EIR shall include a table showing where each of the subjects is discussed.

(a) Significant Environmental Effects of the Proposed Project.

(b) Significant Environmental Effects Which Cannot be Avoided if the Proposed Project is Implemented.

(c) Significant Irreversible Environmental Changes Which Would be Involved in the Proposed Project Should it be Implemented.

(d) Growth-Inducing Impact of the Proposed Project.

(e) The Mitigation Measures Proposed to Minimize the Significant Effects.

(f) Alternatives to the Proposed Project.

Note: Authority cited: Section 21083, Public Resources Code; Reference: Sections 21002, 21003, 21100, and 21081.6, Public Resources Code; *Citizens of Goleta Valley v. Board of Supervisors* (1990) 52 Cal.3d 553; *Laurel Heights Improvement Association v. Regents of the University of California* (1988) 47 Cal.3d 376; *Gentry v. City of Murrieta* (1995) 36 Cal.App.4th 1359; and *Laurel Heights Improvement Association v. Regents of the University of California* (1993) 6 Cal.4th 1112.

15126.2 CONSIDERATION AND DISCUSSION OF SIGNIFICANT ENVIRONMENTAL IMPACTS.

(a) The Significant Environmental Effects of the Proposed Project. An EIR shall identify and focus on the significant environmental effects of the proposed project. In assessing the impact of a proposed project on the environment, the lead agency should normally limit its examination to changes in the existing physical conditions in the affected area as they exist at the time the notice of preparation is published, or where no notice of preparation is published, at the time environmental analysis is commenced. Direct and indirect significant effects of the project on the environment shall be clearly identified and described, giving due consideration to both the short-term and long-term effects. The discussion should include relevant specifics of the area, the resources involved, physical changes, alterations to ecological systems, and changes induced in population distribution, population concentration, the human use of the land (including commercial and residential development), health and safety problems caused by the physical changes, and other aspects of the resource base such as water, historical resources, scenic quality, and public services. The EIR shall also analyze any significant environmental effects the project might cause by bringing development and people into the area affected. For example, an EIR on a subdivision astride an active fault line should identify as a significant effect the seismic hazard to future occupants of the subdivision. The subdivision would have the effect of attracting people to the location and exposing them to the hazards found there. Similarly, the EIR should evaluate any potentially significant impacts of locating development in other areas susceptible to hazardous conditions (e.g., floodplains, coastlines, wildfire risk areas) as identified in authoritative hazard maps, risk assessments or in land use plans addressing such hazards areas.

(b) Significant Environmental Effects Which Cannot be Avoided if the Proposed Project is Implemented. Describe any significant impacts, including those which can be mitigated but not reduced to a level of insignificance. Where there are impacts that cannot be alleviated without imposing an alternative design, their implications and the reasons why the project is being proposed, notwithstanding their effect, should be described.

(c) Significant Irreversible Environmental Changes Which Would be Caused by the Proposed Project Should it be Implemented. Uses of nonrenewable resources during the initial and continued phases of the project may be irreversible since a large commitment of such resources makes removal or nonuse thereafter unlikely. Primary impacts and, particularly, secondary impacts (such as highway improvement which provides access to a previously inaccessible area) generally commit future generations to similar uses. Also irreversible damage can result from environmental accidents associated with the project. Irretrievable commitments of resources should be evaluated to assure that such current consumption is justified. (See Public Resources Code section 21100.1 and Title 14, California Code of Regulations, section 15127 for limitations to applicability of this requirement.)

(d) Growth-Inducing Impact of the Proposed Project. Discuss the ways in which the proposed project could foster economic or population growth, or the construction of additional housing, either directly or indirectly, in the surrounding environment. Included in this are projects which would remove obstacles to population growth (a major expansion of a waste water treatment plant might, for example, allow for more construction in service areas). Increases in the population may tax existing community service facilities, requiring construction of new facilities that could cause significant environmental effects. Also discuss the characteristic of some projects which may encourage and facilitate other activities that could significantly affect the environment, either individually or cumulatively. It must not be assumed that growth in any area is necessarily beneficial, detrimental, or of little significance to the environment.

Note: Authority cited: Sections 21083, 21083.05, Public Resources Code. Reference: Sections 21002, 21003, and 21100, Public Resources Code; *Citizens of Goleta Valley v. Board of Supervisors*, (1990) 52 Cal.3d 553; *Laurel Heights Improvement Association v. Regents of the University of California*, (1988) 47 Cal.3d 376; *Gentry v. City of Murrieta* (1995) 36 Cal.App.4th 1359; and *Laurel Heights Improvement Association v. Regents of the University of California* (1993) 6 Cal.4th 1112; *Goleta Union School Dist. v. Regents of the Univ. of Calif* (1995) 37 Cal. App.4th 1025.

15126.4 CONSIDERATION AND DISCUSSION OF MITIGATION MEASURES PROPOSED TO MINIMIZE SIGNIFICANT EFFECTS.

(a) Mitigation Measures in General.

(1) An EIR shall describe feasible measures which could minimize significant adverse impacts, including where relevant, inefficient and unnecessary consumption of energy.

(A) The discussion of mitigation measures shall distinguish between the measures which are proposed by project proponents to be included in the project and other measures proposed by the lead, responsible or trustee agency or other persons which are not included but the lead agency determines could reasonably be expected to reduce adverse impacts if required as conditions of approving the project. This discussion shall identify mitigation measures for each significant environmental effect identified in the EIR.

(B) Where several measures are available to mitigate an impact, each should be discussed and the basis for selecting a particular measure should be identified. Formulation of mitigation measures should not be deferred until some future time. However, measures may specify performance standards which would mitigate the significant effect of the project and which may be accomplished in more than one specified way.

(C) Energy conservation measures, as well as other appropriate mitigation measures, shall be discussed when relevant. Examples of energy conservation measures are provided in Appendix F.

(D) If a mitigation measure would cause one or more significant effects in addition to those that would be caused by the project as proposed, the effects of the mitigation measure shall be discussed but in less detail than the significant effects of the project as proposed. (*Stevens v. City of Glendale* (1981) 125 Cal.App.3d 986.)

(2) Mitigation measures must be fully enforceable through permit conditions, agreements, or other legally binding instruments. In the case of the adoption of a plan, policy, regulation, or other public project, mitigation measures can be incorporated into the plan, policy, regulation, or project design.

(3) Mitigation measures are not required for effects which are not found to be significant.

(4) Mitigation measures must be consistent with all applicable constitutional requirements, including the following:

(A) There must be an essential nexus (i.e. connection) between the mitigation measure and a legitimate governmental interest. *Nollan v. California Coastal Commission*, 483 U.S. 825 (1987); and

(B) The mitigation measure must be "roughly proportional" to the impacts of the project. *Dolan v. City of Tigard*, 512 U.S. 374 (1994). Where the mitigation measure is an *ad hoc* exaction, it must be "roughly proportional" to the impacts of the project. *Ehrlich v. City of Culver City* (1996) 12 Cal.4th 854.

(5) If the lead agency determines that a mitigation measure cannot be legally imposed, the measure need not be proposed or analyzed. Instead, the EIR may simply reference that fact and briefly explain the reasons underlying the lead agency's determination.

(b) Mitigation Measures Related to Impacts on Historical Resources.

(1) Where maintenance, repair, stabilization, rehabilitation, restoration, preservation, conservation or reconstruction of the historical resource will be conducted in a manner consistent with the Secretary of the Interior's Standards for the Treatment of Historic Properties with Guidelines for Preserving, Rehabilitating, Restoring, and Reconstructing Historic Buildings (1995), Weeks and Grimmer, the project's impact on the historical resource shall generally be considered mitigated below a level of significance and thus is not significant.

(2) In some circumstances, documentation of an historical resource, by way of historic narrative, photographs or architectural drawings, as mitigation for the effects of demolition of the resource will not mitigate the effects to a point where clearly no significant effect on the environment would occur.

(3) Public agencies should, whenever feasible, seek to avoid damaging effects on any historical resource of an archaeological nature. The following factors shall be considered and discussed in an EIR for a project involving such an archaeological site:

(A) Preservation in place is the preferred manner of mitigating impacts to archaeological sites. Preservation in place maintains the relationship between artifacts and the archaeological context. Preservation may also avoid conflict with religious or cultural values of groups associated with the site.

(B) Preservation in place may be accomplished by, but is not limited to, the following:

1. Planning construction to avoid archaeological sites;
2. Incorporation of sites within parks, greenspace, or other open space;
3. Covering the archaeological sites with a layer of chemically stable soil before building tennis courts, parking lots, or similar facilities on the site.
4. Deeding the site into a permanent conservation easement.

(C) When data recovery through excavation is the only feasible mitigation, a data recovery plan, which makes provisions for adequately recovering the scientifically consequential information from and about the historical resource, shall be prepared and adopted prior to any excavation being undertaken. Such studies shall be deposited with the California Historical Resources Regional Information Center. Archeological sites known to contain human remains shall be treated in accordance with the provisions of Section 7050.5 Health and Safety Code. If an artifact must be removed during project excavation or testing, curation may be an appropriate mitigation.

(D) Data recovery shall not be required for an historical resource if the lead agency determines that testing or studies already completed have adequately recovered the scientifically consequential information from and about the archaeological or historical resource, provided that the determination is documented in the EIR and that the studies are deposited with the California Historical Resources Regional Information Center.

(c) Mitigation Measures Related to Greenhouse Gas Emissions.

Consistent with section 15126.4(a), lead agencies shall consider feasible means, supported by substantial evidence and subject to monitoring or reporting, of mitigating the significant effects of greenhouse gas emissions. Measures to mitigate the significant effects of greenhouse gas emissions may include, among others:

(1) Measures in an existing plan or mitigation program for the reduction of emissions that are required as part of the lead agency's decision;

(2) Reductions in emissions resulting from a project through implementation of project features, project design, or other measures, such as those described in Appendix F;

(3) Off-site measures, including offsets that are not otherwise required, to mitigate a project's emissions;

(4) Measures that sequester greenhouse gases;

(5) In the case of the adoption of a plan, such as a general plan, long range development plan, or plans for the reduction of greenhouse gas emissions, mitigation may include the identification of specific measures that may be implemented on a project-by-project basis. Mitigation may also include the incorporation of specific measures or policies found in an adopted ordinance or regulation that reduces the cumulative effect of emissions.

Note: Authority cited: Sections 21083, 21083.05, Public Resources Code. Reference: Sections 5020.5, 21002, 21003, 21083.05, 21100 and 21084.1, Public Resources Code; *Citizens of Goleta Valley v. Board of Supervisors* (1990) 52 Cal.3d 553; *Laurel Heights Improvement Association v. Regents of the University of California* (1988) 47 Cal.3d 376; *Gentry v. City of Murrieta* (1995) 36 Cal.App.4th 1359; *Laurel Heights Improvement Association v. Regents of the University of California* (1993) 6 Cal.4th 1112; *Sacramento Old City Assn. v. City Council of Sacramento* (1991) 229 Cal.App.3d 1011; *San Franciscans Upholding the Downtown Plan v. City & Co. of San Francisco* (2002) 102 Cal.App.4th 656; *Ass'n of Irritated Residents v. County of Madera* (2003) 107 Cal.App.4th 1383; *Environmental Council of Sacramento v. City of Sacramento* (2006) 142 Cal.App.4th 1018.

15126.6. CONSIDERATION AND DISCUSSION OF ALTERNATIVES TO THE PROPOSED PROJECT.

(a) Alternatives to the Proposed Project. An EIR shall describe a range of reasonable alternatives to the project, or to the location of the project, which would feasibly attain most of the basic objectives of the project but would avoid or substantially lessen any of the significant effects of the project, and evaluate the comparative merits of the alternatives. An EIR need not consider every conceivable alternative to a project. Rather it must consider a reasonable range of potentially feasible alternatives that will foster informed decision making and public participation. An EIR is not required to consider alternatives which are infeasible. The lead agency is responsible for selecting a range of project alternatives for examination and must publicly disclose its reasoning for selecting those alternatives. There is no ironclad rule governing the nature or scope of the alternatives to be discussed other than the rule of reason. (*Citizens of Goleta Valley v. Board of Supervisors* (1990) 52 Cal.3d 553 and *Laurel Heights Improvement Association v. Regents of the University of California* (1988) 47 Cal.3d 376).

(b) Purpose. Because an EIR must identify ways to mitigate or avoid the significant effects that a project may have on the environment (Public Resources Code Section 21002.1), the discussion of alternatives shall focus on alternatives to the project or its location which are capable of avoiding or substantially lessening any significant effects of the project, even if these alternatives would impede to some degree the attainment of the project objectives, or would be more costly.

(c) Selection of a range of reasonable alternatives. The range of potential alternatives to the proposed project shall include those that could feasibly accomplish most of the basic objectives of the project and could avoid or substantially lessen one or more of the significant effects. The EIR should briefly describe the rationale for selecting the alternatives to be discussed. The EIR should also identify any alternatives that were considered by the lead agency but were rejected as infeasible during the scoping process and briefly explain the reasons underlying the lead agency's determination. Additional information explaining the choice of alternatives may be included in the administrative record. Among the factors that may be used to eliminate alternatives from detailed consideration in an EIR are:(i) failure to meet most of the basic project objectives, (ii) infeasibility, or (iii) inability to avoid significant environmental impacts.

(d) Evaluation of alternatives. The EIR shall include sufficient information about each alternative to allow meaningful evaluation, analysis, and comparison with the proposed project. A matrix displaying the major characteristics and significant environmental effects of each alternative may be used to summarize the comparison. If an alternative would cause one or more significant effects in addition to those that would be caused by the project as proposed, the significant effects of the alternative shall be discussed, but in less detail than the significant effects of the project as proposed. (*County of Inyo v. City of Los Angeles* (1981) 124 Cal.App.3d 1).

(e) "No project" alternative.

(1) The specific alternative of "no project" shall also be evaluated along with its impact. The purpose of describing and analyzing a no project alternative is to allow decision makers to compare the impacts of approving the proposed project with the impacts of not approving the proposed project. The no project alternative analysis is not the baseline for determining whether the proposed project's environmental impacts may be significant, unless it is identical to the existing environmental setting analysis which does establish that baseline (see Section 15125).

(2) The "no project" analysis shall discuss the existing conditions at the time the notice of preparation is published, or if no notice of preparation is published, at the time environmental analysis is commenced, as well as what would be reasonably expected to occur in the foreseeable future if the project were not approved, based on current plans and consistent with available infrastructure and community services. If the environmentally superior alternative is the "no project" alternative, the EIR shall also identify an environmentally superior alternative among the other alternatives.

(3) A discussion of the "no project" alternative will usually proceed along one of two lines:

(A) When the project is the revision of an existing land use or regulatory plan, policy or ongoing operation, the "no project" alternative will be the continuation of the existing plan, policy or operation into the future. Typically this is a situation where other projects initiated under the existing plan will continue while the new plan is developed. Thus, the projected impacts of the proposed plan or alternative plans would be compared to the impacts that would occur under the existing plan.

(B) If the project is other than a land use or regulatory plan, for example a development project on identifiable property, the "no project" alternative is the circumstance under which the project does not proceed. Here the discussion would compare the environmental effects of the property remaining in its existing state against environmental effects which would occur if the project is approved. If disapproval of the project under consideration would result in predictable actions by others, such as the proposal of some other project, this "no project" consequence should be discussed. In certain instances, the no project alternative means "no build" wherein the existing environmental setting is maintained. However, where failure to proceed with the project will not result in preservation of existing environmental conditions, the analysis

should identify the practical result of the project's non-approval and not create and analyze a set of artificial assumptions that would be required to preserve the existing physical environment.

(C) After defining the no project alternative using one of these approaches, the lead agency should proceed to analyze the impacts of the no project alternative by projecting what would reasonably be expected to occur in the foreseeable future if the project were not approved, based on current plans and consistent with available infrastructure and community services.

(f) Rule of reason. The range of alternatives required in an EIR is governed by a "rule of reason" that requires the EIR to set forth only those alternatives necessary to permit a reasoned choice. The alternatives shall be limited to ones that would avoid or substantially lessen any of the significant effects of the project. Of those alternatives, the EIR need examine in detail only the ones that the lead agency determines could feasibly attain most of the basic objectives of the project. The range of feasible alternatives shall be selected and discussed in a manner to foster meaningful public participation and informed decision making.

(1) Feasibility. Among the factors that may be taken into account when addressing the feasibility of alternatives are site suitability, economic viability, availability of infrastructure, general plan consistency, other plans or regulatory limitations, jurisdictional boundaries (projects with a regionally significant impact should consider the regional context), and whether the proponent can reasonably acquire, control or otherwise have access to the alternative site (or the site is already owned by the proponent). No one of these factors establishes a fixed limit on the scope of reasonable alternatives. (*Citizens of Goleta Valley v. Board of Supervisors* (1990) 52 Cal.3d 553; see *Save Our Residential Environment v. City of West Hollywood* (1992) 9 Cal.App.4th 1745, 1753, fn. 1).

(2) Alternative locations.

(A) Key question. The key question and first step in analysis is whether any of the significant effects of the project would be avoided or substantially lessened by putting the project in another location. Only locations that would avoid or substantially lessen any of the significant effects of the project need be considered for inclusion in the EIR.

(B) None feasible. If the lead agency concludes that no feasible alternative locations exist, it must disclose the reasons for this conclusion, and should include the reasons in the EIR. For example, in some cases there may be no feasible alternative locations for a geothermal plant or mining project which must be in close proximity to natural resources at a given location.

(C) Limited new analysis required. Where a previous document has sufficiently analyzed a range of reasonable alternative locations and environmental impacts for projects with the same basic purpose, the lead agency should review the previous document. The EIR may rely on the previous document to help it assess the feasibility of potential project alternatives to the extent the circumstances remain substantially the same as they relate to the alternative. (*Citizens of Goleta Valley v. Board of Supervisors* (1990) 52 Cal.3d 553, 573).

(3) An EIR need not consider an alternative whose effect cannot be reasonably ascertained and whose implementation is remote and speculative. (*Residents Ad Hoc Stadium Committee v. Board of Trustees* (1979) 89 Cal. App.3d 274).

Note: Authority cited: Section 21083, Public Resources Code. Reference: Sections 21002, 21002.1, 21003, and 21100, Public Resources Code; *Citizens of Goleta Valley v. Board of Supervisors*, (1990) 52 Cal.3d 553; *Laurel Heights Improvement Association v. Regents of the University of California*, (1988) 47 Cal.3d 376; *Gentry v. City of Murrieta* (1995) 36 Cal.App.4th 1359; and

Laurel Heights Improvement Association v. Regents of the University of California (1993) 6 Cal.4th 1112.

15127. LIMITATIONS ON DISCUSSION OF ENVIRONMENTAL IMPACT

The information required by Section 15126.2(c) concerning irreversible changes, need be included only in EIRs prepared in connection with any of the following activities:

(a) The adoption, amendment, or enactment of a plan, policy, or ordinance of a public agency;

(b) The adoption by a Local Agency Formation Commission of a resolution making determinations; or

(c) A project which will be subject to the requirement for preparing an environmental impact statement pursuant to the requirements of the National Environmental Policy Act of 1969, 42 U.S.C. 4321–4347.

Note: Authority cited: Section 21083, Public Resources Code; Reference: Section 21100.1, Public Resources Code.

15128. EFFECTS NOT FOUND TO BE SIGNIFICANT

An EIR shall contain a statement briefly indicating the reasons that various possible significant effects of a project were determined not to be significant and were therefore not discussed in detail in the EIR. Such a statement may be contained in an attached copy of an Initial Study.

Note: Authority cited: Section 21083, Public Resources Code; Reference: Section 21100, Public Resources Code.

15129. ORGANIZATIONS AND PERSONS CONSULTED

The EIR shall identify all federal, state, or local agencies, other organizations, and private individuals consulted in preparing the draft EIR, and the persons, firm, or agency preparing the draft EIR, by contract or other authorization.

Note: Authority cited: Section 21083, Public Resources Code; Reference: Sections 21104 and 21153, Public Resources Code.

15130. DISCUSSION OF CUMULATIVE IMPACTS

(a) An EIR shall discuss cumulative impacts of a project when the project's incremental effect is cumulatively considerable, as defined in section 15065 (a)(3). Where a lead agency is examining a project with an incremental effect that is not "cumulatively considerable," a lead agency need not consider that effect significant, but shall briefly describe its basis for concluding that the incremental effect is not cumulatively considerable.

  (1) As defined in Section 15355, a cumulative impact consists of an impact which is created as a result of the combination of the project evaluated in the EIR together with other projects causing related impacts. An EIR should not discuss impacts which do not result in part from the project evaluated in the EIR.

  (2) When the combined cumulative impact associated with the project's incremental effect and the effects of other projects is not significant, the EIR shall briefly indicate why the cumulative impact is not significant and is not discussed in further detail in the EIR. A lead agency shall identify facts and analysis supporting the lead agency's conclusion that the cumulative impact is less than significant.

  (3) An EIR may determine that a project's contribution to a significant cumulative impact will be rendered less than cumulatively considerable and thus is not significant. A project's contribution is less than cumulatively considerable if the project is required to implement or fund its fair share of a mitigation measure or measures designed to alleviate the

cumulative impact. The lead agency shall identify facts and analysis supporting its conclusion that the contribution will be rendered less than cumulatively considerable.

(b) The discussion of cumulative impacts shall reflect the severity of the impacts and their likelihood of occurrence, but the discussion need not provide as great detail as is provided for the effects attributable to the project alone. The discussion should be guided by the standards of practicality and reasonableness, and should focus on the cumulative impact to which the identified other projects contribute rather than the attributes of other projects which do not contribute to the cumulative impact. The following elements are necessary to an adequate discussion of significant cumulative impacts:

(1) Either:

(A) A list of past, present, and probable future projects producing related or cumulative impacts, including, if necessary, those projects outside the control of the agency, or

(B) A summary of projections contained in an adopted local, regional or statewide plan, or related planning document, that describes or evaluates conditions contributing to the cumulative effect. Such plans may include: a general plan, regional transportation plan, or plans for the reduction of greenhouse gas emissions. A summary of projections may also be contained in an adopted or certified prior environmental document for such a plan. Such projections may be supplemented with additional information such as a regional modeling program. Any such document shall be referenced and made available to the public at a location specified by the lead agency.

(2) When utilizing a list, as suggested in paragraph (1) of subdivision (b), factors to consider when determining whether to include a related project should include the nature of each environmental resource being examined, the location of the project and its type. Location may be important, for example, when water quality impacts are at issue since projects outside the watershed would probably not contribute to a cumulative effect. Project type may be important, for example, when the impact is specialized, such as a particular air pollutant or mode of traffic.

(3) Lead agencies should define the geographic scope of the area affected by the cumulative effect and provide a reasonable explanation for the geographic limitation used.

(4) A summary of the expected environmental effects to be produced by those projects with specific reference to additional information stating where that information is available; and

(5) A reasonable analysis of the cumulative impacts of the relevant projects. An EIR shall examine reasonable, feasible options for mitigating or avoiding the project's contribution to any significant cumulative effects.

(c) With some projects, the only feasible mitigation for cumulative impacts may involve the adoption of ordinances or regulations rather than the imposition of conditions on a project-by-project basis.

(d) Previously approved land use documents , including, but not limited to, general plans, specific plans, regional transportation plans, plans for the reduction of greenhouse gas emissions, and local coastal plans may be used in cumulative impact analysis. A pertinent discussion of cumulative impacts contained in one or more previously certified EIRs may be incorporated by reference pursuant to the provisions for tiering and program EIRs. No further cumulative impacts analysis is required when a project is consistent with a general, specific, master or comparable programmatic plan where the lead agency determines that the regional or areawide cumulative impacts of the proposed project have already been adequately addressed, as defined in section 15152(f), in a certified EIR for that plan.

(e) If a cumulative impact was adequately addressed in a prior EIR for a community plan, zoning action, or general plan, and the project is consistent with that plan or action, then an EIR for such a project should not further analyze that cumulative impact, as provided in Section 15183(j).

Note: Authority cited: Sections 21083, 21083.05, Public Resources Code. Reference: Sections 21003(d), 21083(b), 21093, 21094 and 21100, Public Resources Code; *Whitman v. Board of Supervisors*, (1979) 88 Cal. App. 3d 397; *San Franciscans for Reasonable Growth v. City and County of San Francisco* (1984) 151 Cal.App.3d 61; *Kings County Farm Bureau v. City of Hanford* (1990) 221 Cal.App.3d 692; *Laurel Heights Homeowners Association v. Regents of the University of California* (1988) 47 Cal.3d 376; *Sierra Club v. Gilroy* (1990) 220 Cal.App.3d 30; *Citizens to Preserve the Ojai v. County of Ventura* (1985) 176 Cal.App.3d 421; *Concerned Citizens of South Cent. Los Angeles v. Los Angeles Unified Sch. Dist.* (1994) 24 Cal.App.4th 826; *Las Virgenes Homeowners Fed'n v. County of Los Angeles* (1986) 177 Cal.App.3d 300; *San Joaquin Raptor/Wildlife Rescue Ctr v. County of Stanislaus* (1994) 27 Cal.App.4th 713; *Fort Mojave Indian Tribe v. Cal. Dept. Of Health Services* (1995) 38 Cal.App.4th 1574; *Santa Monica Chamber of Commerce v. City of Santa Monica* (2002) 101 Cal.App.4th 786; *Communities for a Better Environment v. California Resources Agency* (2002) 103 Cal.App.4th 98; and *Ass'n of Irritated Residents v. County of Madera* (2003) 107 Cal.App.4th 1383.

15131. ECONOMIC AND SOCIAL EFFECTS

Economic or social information may be included in an EIR or may be presented in whatever form the agency desires.

(a) Economic or social effects of a project shall not be treated as significant effects on the environment. An EIR may trace a chain of cause and effect from a proposed decision on a project through anticipated economic or social changes resulting from the project to physical changes caused in turn by the economic or social changes. The intermediate economic or social changes need not be analyzed in any detail greater than necessary to trace the chain of cause and effect. The focus of the analysis shall be on the physical changes.

(b) Economic or social effects of a project may be used to determine the significance of physical changes caused by the project. For example, if the construction of a new freeway or rail line divides an existing community, the construction would be the physical change, but the social effect on the community would be the basis for determining that the effect would be significant. As an additional example, if the construction of a road and the resulting increase in noise in an area disturbed existing religious practices in the area, the disturbance of the religious practices could be used to determine that the construction and use of the road and the resulting noise would be significant effects on the environment. The religious practices would need to be analyzed only to the extent to show that the increase in traffic and noise would conflict with the religious practices. Where an EIR uses economic or social effects to determine that a physical change is significant, the EIR shall explain the reason for determining that the effect is significant.

(c) Economic, social, and particularly housing factors shall be considered by public agencies together with technological and environmental factors in deciding whether changes in a project are feasible to reduce or avoid the significant effects on the environment identified in the EIR. If information on these factors is not contained in the EIR, the information must be added to the record in some other manner to allow the agency to consider the factors in reaching a decision on the project.

Note: Authority cited: Section 21083, Public Resources Code; Reference: Sections 21001(e) and (g), 21002, 21002.1, 21060.5, 21080.1, 21083(c), and 21100, Public Resources Code.

15132. CONTENTS OF FINAL ENVIRONMENTAL IMPACT REPORT

The Final EIR shall consist of:

(a) The draft EIR or a revision of the draft.

(b) Comments and recommendations received on the draft EIR either verbatim or in summary.

(c) A list of persons, organizations, and public agencies commenting on the draft EIR.

(d) The responses of the Lead Agency to significant environmental points raised in the review and consultation process.

(e) Any other information added by the Lead Agency.

Note: Authority cited: Section 21083, Public Resources Code; Reference: Section 21100, Public Resources Code.

Article 10. Considerations in Preparing EIRs and Negative Declarations

SECTIONS 15140 TO 15155

15140. WRITING

EIRs shall be written in plain language and may use appropriate graphics so that decision makers and the public can rapidly understand the documents.

Note: Authority cited: Section 21083, Public Resources Code; Reference: Sections 21003 and 21100, Public Resources Code.

15141. PAGE LIMITS

The text of draft EIRs should normally be less than 150 pages and for proposals of unusual scope or complexity should normally be less than 300 pages.

Note: Authority cited: Section 21083, Public Resources Code; Reference: Section 21100, Public Resources Code.

15142. INTERDISCIPLINARY APPROACH

An EIR shall be prepared using an interdisciplinary approach which will ensure the integrated use of the natural and social sciences and the consideration of qualitative as well as quantitative factors. The interdisciplinary analysis shall be conducted by competent individuals, but no single discipline shall be designated or required to undertake this evaluation.

Note: Authority cited: Section 21083, Public Resources Code; Reference Sections 21000, 21001, and 21100, Public Resources Code.

15143. EMPHASIS

The EIR shall focus on the significant effects on the environment. The significant effects should be discussed with emphasis in proportion to their severity and probability of occurrence. Effects dismissed in an Initial Study as clearly insignificant and unlikely to occur need not be discussed further in the EIR unless the Lead Agency subsequently receives information inconsistent with the finding in the Initial Study. A copy of the Initial Study may be attached to the EIR to provide the basis for limiting the impacts discussed.

Note: Authority cited: Section 21083, Public Resources Code; Reference: Sections 21003, 21061, and 21100, Public Resources Code.

15144. FORECASTING

Drafting an EIR or preparing a Negative Declaration necessarily involves some degree of forecasting. While foreseeing the unforeseeable is not possible, an agency must use its best efforts to find out and disclose all that it reasonably can.

Note: Authority cited: Section 21083, Public Resources Code; Reference: Sections 21003, 21061, and 21100, Public Resources Code.

15145. SPECULATION

If, after thorough investigation, a Lead Agency finds that a particular impact is too speculative for evaluation, the agency should note its conclusion and terminate discussion of the impact.

Note: Authority cited: Section 21083, Public Resources Code; Reference: Sections 21003, 21061, and 21100, Public Resources Code; *Topanga Beach Renters Association v. Department of General Services*, (1976) 58 Cal. App. 3d 712.

15146. DEGREE OF SPECIFICITY

The degree of specificity required in an EIR will correspond to the degree of specificity involved in the underlying activity which is described in the EIR.

(a) An EIR on a construction project will necessarily be more detailed in the specific effects of the project than will be an EIR on the adoption of a local general plan or comprehensive zoning ordinance because the effects of the construction can be predicted with greater accuracy.

(b) An EIR on a project such as the adoption or amendment of a comprehensive zoning ordinance or a local general plan should focus on the secondary effects that can be expected to follow from the adoption or amendment, but the EIR need not be as detailed as an EIR on the specific construction projects that might follow.

Note: Authority cited: Section 21083, Public Resources Code; Reference: Sections 21003, 21061, and 21100, Public Resources Code. Formerly Section 15147.

15147. TECHNICAL DETAIL

The information contained in an EIR shall include summarized technical data, maps, plot plans, diagrams, and similar relevant information sufficient to permit full assessment of significant environmental impacts by reviewing agencies and members of the public. Placement of highly technical and specialized analysis and data in the body of an EIR should be avoided through inclusion of supporting information and analyses as appendices to the main body of the EIR. Appendices to the EIR may be prepared in volumes separate from the basic EIR document, but shall be readily available for public examination and shall be submitted to all clearinghouses which assist in public review.

Note: Authority cited: Section 21083, Public Resources Code; Reference: Sections 21003, 21061, and 21100, Public Resources Code.

15148. CITATION

Preparation of EIRs is dependent upon information from many sources, including engineering project reports and many scientific documents relating to environmental features. These documents should be cited but not included in the EIR. The EIR shall cite all documents used in its preparation including, where possible, the page and section number of any technical reports which were used as the basis for any statements in the EIR.

Note: Authority cited: Section 21083, Public Resources Code; Reference: Sections 21003, 21061, and 21100, Public Resources Code.

15149. USE OF REGISTERED PROFESSIONALS IN PREPARING EIRS

(a) A number of statutes provide that certain professional services can be provided to the public only by individuals who have been registered by a registration board established under California law. Such statutory restrictions apply to a number of professions including but not limited to engineering, land surveying, forestry, geology, and geophysics.

(b) In its intended usage, an EIR is not a technical document that can be prepared only by a registered professional. The EIR serves as a public disclosure document explaining the effects of the proposed project on the environment, alternatives to the project, and ways to minimize

adverse effects and to increase beneficial effects. As a result of information in the EIR, the Lead Agency should establish requirements or conditions on project design, construction, or operation in order to protect or enhance the environment. State statutes may provide that only registered professionals can prepare technical studies which will be used in or which will control the detailed design, construction, or operation of the proposed project and which will be prepared in support of an EIR.

Note: Authority cited: Section 21083, Public Resources Code; Reference: Sections 21003, 21061, and 21100, Public Resources Code.

15150. INCORPORATION BY REFERENCE

(a) An EIR or Negative Declaration may incorporate by reference all or portions of another document which is a matter of public record or is generally available to the public. Where all or part of another document is incorporated by reference, the incorporated language shall be considered to be set forth in full as part of the text of the EIR or Negative Declaration.

(b) Where part of another document is incorporated by reference, such other document shall be made available to the public for inspection at a public place or public building. The EIR or Negative Declaration shall state where the incorporated documents will be available for inspection. At a minimum, the incorporated document shall be made available to the public in an office of the Lead Agency in the county where the project would be carried out or in one or more public buildings such as county offices or public libraries if the Lead Agency does not have an office in the county.

(c) Where an EIR or Negative Declaration uses incorporation by reference, the incorporated part of the referenced document shall be briefly summarized where possible or briefly described if the data or information cannot be summarized. The relationship between the incorporated part of the referenced document and the EIR shall be described.

(d) Where an agency incorporates information from an EIR that has previously been reviewed through the state review system, the state identification number of the incorporated document should be included in the summary or designation described in subdivision (c).

(e) Examples of materials that may be incorporated by reference include but are not limited to:

(1) A description of the environmental setting from another EIR.

(2) A description of the air pollution problems prepared by an air pollution control agency concerning a process involved in the project.

(3) A description of the city or county general plan that applies to the location of the project.

(4) A description of the effects of greenhouse gas emissions on the environment.

(f) Incorporation by reference is most appropriate for including long, descriptive, or technical materials that provide general background but do not contribute directly to the analysis of the problem at hand.

Note: Authority cited: Sections 21083, 21083.05, Public Resources Code; Reference Sections 21003, 21061, 21083.05, and 21100, Public Resources Code.

15151. STANDARDS FOR ADEQUACY OF AN EIR

An EIR should be prepared with a sufficient degree of analysis to provide decision makers with information which enables them to make a decision which intelligently takes account of environmental consequences. An evaluation of the environmental effects of a proposed project need not be exhaustive, but the sufficiency of an EIR is to be reviewed in the light of what is reasonably feasible. Disagreement among experts does not make an EIR inadequate, but the EIR should summarize the main points of disagreement among the experts. The courts have looked not for perfection but for adequacy, completeness, and a good faith effort at full disclosure.

Note: Authority cited: Section 21083, Public Resources Code; Reference: Sections 21061 and 21100, Public Resources Code; *San Francisco Ecology Center v. City and County of San Francisco*, (1975) 48 Cal. App. 3d 584.

15152. TIERING

(a) "Tiering" refers to using the analysis of general matters contained in a broader EIR (such as one prepared for a general plan or policy statement) with later EIRs and negative declarations on narrower projects; incorporating by reference the general discussions from the broader EIR; and concentrating the later EIR or negative declaration solely on the issues specific to the later project.

(b) Agencies are encouraged to tier the environmental analyses which they prepare for separate but related projects including general plans, zoning changes, and development projects. This approach can eliminate repetitive discussions of the same issues and focus the later EIR or negative declaration on the actual issues ripe for decision at each level of environmental review. Tiering is appropriate when the sequence of analysis is from an EIR prepared for a general plan, policy, or program to an EIR or negative declaration for another plan, policy, or program of lesser scope, or to a site-specific EIR or negative declaration. Tiering does not excuse the lead agency from adequately analyzing reasonably foreseeable significant environmental effects of the project and does not justify deferring such analysis to a later tier EIR or negative declaration. However, the level of detail contained in a first tier EIR need not be greater than that of the program, plan, policy, or ordinance being analyzed.

(c) Where a lead agency is using the tiering process in connection with an EIR for a large-scale planning approval, such as a general plan or component thereof (e.g., an area plan or community plan), the development of detailed, site-specific information may not be feasible but can be deferred, in many instances, until such time as the lead agency prepares a future environmental document in connection with a project of a more limited geographical scale, as long as deferral does not prevent adequate identification of significant effects of the planning approval at hand.

(d) Where an EIR has been prepared and certified for a program, plan, policy, or ordinance consistent with the requirements of this section, any lead agency for a later project pursuant to or consistent with the program, plan, policy, or ordinance should limit the EIR or negative declaration on the later project to effects which:

  (1) Were not examined as significant effects on the environment in the prior EIR; or

  (2) Are susceptible to substantial reduction or avoidance by the choice of specific revisions in the project, by the imposition of conditions, or other means.

(e) Tiering under this section shall be limited to situations where the project is consistent with the general plan and zoning of the city or county in which the project is located, except that a project requiring a rezone to achieve or maintain conformity with a general plan may be subject to tiering.

(f) A later EIR shall be required when the initial study or other analysis finds that the later project may cause significant effects on the environment that were not adequately addressed in the prior EIR. A negative declaration shall be required when the provisions of Section 15070 are met.

  (1) Where a lead agency determines that a cumulative effect has been adequately addressed in the prior EIR, that effect is not treated as significant for purposes of the later EIR or negative declaration, and need not be discussed in detail.

  (2) When assessing whether there is a new significant cumulative effect, the lead agency shall consider whether the incremental effects of the project would be considerable when viewed in the context of past, present, and probable future projects. At this point, the question is

not whether there is a significant cumulative impact, but whether the effects of the project are cumulatively considerable. For a discussion on how to assess whether project impacts are cumulatively considerable, see Section 15064(i).

(3) Significant environmental effects have been "adequately addressed" if the lead agency determines that:

(A) they have been mitigated or avoided as a result of the prior environmental impact report and findings adopted in connection with that prior environmental report; or

(B) they have been examined at a sufficient level of detail in the prior environmental impact report to enable those effects to be mitigated or avoided by site specific revisions, the imposition of conditions, or by other means in connection with the approval of the later project.

(g) When tiering is used, the later EIRs or negative declarations shall refer to the prior EIR and state where a copy of the prior EIR may be examined. The later EIR or negative declaration should state that the lead agency is using the tiering concept and that it is being tiered with the earlier EIR.

(h) There are various types of EIRs that may be used in a tiering situation. These include, but are not limited to, the following:

(1) General plan EIR (Section 15166).

(2) Staged EIR (Section 15167).

(3) Program EIR (Section 15168).

(4) Master EIR (Section 15175).

(5) Multiple-family residential development / residential and commercial or retail mixed-use development (Section 15179.5).

(6) Redevelopment project (Section 15180).

(7) Projects consistent with community plan, general plan, or zoning (Section 15183).

Note: Authority: Section 21083, Public Resources Code. Reference: Sections 21003, 21061, 21093, 21094, 21100, and 21151, Public Resources Code; *Stanislaus Natural Heritage Project, Sierra Club v. County of Stanislaus* (1996) 48 Cal.App.4th 182; *Al Larson Boat Shop, Inc. v. Board of Harbor Commissioners* (1993) 18 Cal.App. 4th 729; and *Sierra Club v. County of Sonoma* (1992) 6 Cal.App. 4th 1307.

15153. USE OF AN EIR FROM AN EARLIER PROJECT

(a) The Lead Agency may employ a single EIR to describe more than one project, if such projects are essentially the same in terms of environmental impact. Further, the Lead Agency may use an earlier EIR prepared in connection with an earlier project to apply to a later project, if the circumstances of the projects are essentially the same.

(b) When a Lead Agency proposes to use an EIR from an earlier project as the EIR for a separate, later project, the Lead Agency shall use the following procedures:

(1) The Lead Agency shall review the proposed project with an Initial Study, using incorporation by reference if necessary, to determine whether the EIR would adequately describe:

(A) The general environmental setting of the project,

(B) The significant environmental impacts of the project, and

(C) Alternatives and mitigation measures related to each significant effect.

(2) If the Lead Agency believes that the EIR would meet the requirements of subdivision (1), it shall provide public review as provided in Section 15087 stating that it plans to use the

previously prepared EIR as the draft EIR for this project. The notice shall include as a minimum:

(A) An identification of the project with a brief description;

(B) A statement that the agency plans to use a certain EIR prepared for a previous project as the EIR for this project;

(C) A listing of places where copies of the EIR may be examined; and

(D) A statement that the key issues involving the EIR are whether the EIR should be used for this project and whether there are any additional, reasonable alternatives or mitigation measures that should be considered as ways of avoiding or reducing the significant effects of the project.

(3) The Lead Agency shall prepare responses to comments received during the review period.

(4) Before approving the project, the decision maker in the Lead Agency shall:

(A) Consider the information in the EIR including comments received during the review period and responses to those comments,

(B) Decide either on its own or on a staff recommendation whether the EIR is adequate for the project at hand, and

(C) Make or require certification to be made as described in Section 15090.

(D) Make findings as provided in Sections 15091 and 15093 as necessary.

(5) After making a decision on the project, the Lead Agency shall file a Notice of Determination.

(c) An EIR prepared for an earlier project may also be used as part of an Initial Study to document a finding that a later project will not have a significant effect. In this situation a Negative Declaration will be prepared.

(d) An EIR prepared for an earlier project shall not be used as the EIR for a later project if any of the conditions described in Section 15162 would require preparation of a subsequent or supplemental EIR.

Note: Authority cited: Section 21083, Public Resources Code; Reference: Sections 21100, 21151, and 21166, Public Resources Code.

15154. PROJECTS NEAR AIRPORTS

(a) When a lead agency prepares an EIR for a project within the boundaries of a comprehensive airport land use plan or, if a comprehensive airport land use plan has not been adopted for a project within two nautical miles of a public airport or public use airport, the agency shall utilize the Airport Land Use Planning Handbook published by Caltrans' Division of Aeronautics to assist in the preparation of the EIR relative to potential airport-related safety hazards and noise problems.

(b) A lead agency shall not adopt a negative declaration or mitigated negative declaration for a project described in subdivision (a) unless the lead agency considers whether the project will result in a safety hazard or noise problem for persons using the airport or for persons residing or working in the project area.

Note: Authority cited: Section 21083, Public Resources Code; Reference: Section 21096, Public Resources Code.

15155. CITY OR COUNTY CONSULTATION WITH WATER AGENCIES.

(a) The following definitions are applicable to this section.

(1) A "water-demand project" means:

(A) A residential development of more than 500 dwelling units.

(B) A shopping center or business establishment employing more than 1,000 persons or having more than 500,000 square feet of floor space.

(C) A commercial office building employing more than 1,000 persons or having more than 250,000 square feet of floor space.

(D) A hotel or motel, or both, having more than 500 rooms.

(E) An industrial, manufacturing, or processing plant, or industrial park planned to house more than 1,000 persons, occupying more than 40 acres of land, or having more than 650,000 square feet of floor area.

(F) A mixed-use project that includes one or more of the projects specified in subdivisions (a)(1)(A), (a)(1)(B), (a)(1)(C), (a)(1)(D), (a)(1)(E), and (a)(1)(G) of this section.

(G) A project that would demand an amount of water equivalent to, or greater than, the amount of water required by a 500 dwelling unit project.

(H) For public water systems with fewer than 5,000 service connections, a project that meets the following criteria:

1. A proposed residential, business, commercial, hotel or motel, or industrial development that would account for an increase of 10 percent or more in the number of a public water system's existing service connections; or

2. A mixed-use project that would demand an amount of water equivalent to, or greater than, the amount of water required by residential development that would represent an increase of 10 percent or more in the number of the public water system's existing service connections.

(2) "Public water system" means a system for the provision of piped water to the public for human consumption that has 3000 or more service connections. A public water system includes all of the following:

(A) Any collection, treatment, storage, and distribution facility under control of the operator of the system which is used primarily in connection with the system.

(B) Any collection or pretreatment storage facility not under the control of the operator that is used primarily in connection with the system.

(C) Any person who treats water on behalf of one or more public water systems for the purpose of rendering it safe for human consumption.

(3) "Water acquisition plans" means any plans for acquiring additional water supplies prepared by the public water system or a city or county lead agency pursuant to subdivision (a) of section 10911 of the Water Code.

(4) "Water assessment" means the water supply assessment that must be prepared by the governing body of a public water system, or the city or county lead agency, pursuant to and in compliance with sections 10910 to 10915 of the Water Code, and that includes, without limitation, the elements of the assessment required to comply with subdivisions (d), (e), (f), and (g) of section 10910 of the Water Code.

(5) "City or county lead agency" means a city or county, acting as lead agency, for purposes of certifying or approving an environmental impact report, a negative declaration, or a mitigated negative declaration for a water-demand project.

(b) Subject to section 15155, subdivision (d) below, at the time a city or county lead agency determines whether an environmental impact report, a negative declaration, or a mitigated negative declaration, or any supplement thereto, is required for the water-demand project, the city or county lead agency shall take the following steps:

(1) The city or county lead agency shall identify any water system that either: (A) is a public water system that may supply water to the water-demand project, or (B) that may become such a public water system as a result of supplying water to the water-demand project. The city or county lead agency shall request the governing body of each such public water system to determine whether the projected water demand associated with a water-demand project was included in the most recently adopted urban water management plan adopted pursuant to Part 2.6 (commencing with section 10610) of the Water Code, and to prepare a water assessment approved at a regular or special meeting of that governing body.

(2) If the city or county lead agency is not able to identify any public water system that may supply water for the water-demand project, the city or county lead agency shall prepare a water assessment after consulting with any entity serving domestic water supplies whose service area includes the site of the water-demand project, the local agency formation commission, and the governing body of any public water system adjacent to the site of the water-demand project. The governing body of the city or county lead agency must approve the water assessment prepared pursuant to this section at a regular or special meeting.

(c) The city or county lead agency shall grant any reasonable request for an extension of time that is made by the governing body of a public water system preparing the water assessment, provided that the request for an extension of time is made within 90 days after the date on which the governing body of the public water system received the request to prepare a water assessment. If the governing body of the public water system fails to request and receive an extension of time, or fails to submit the water assessment notwithstanding the 30-day extension, the city or county lead agency may seek a writ of mandamus to compel the governing body of the public water system to comply with the requirements of Part 2.10 of Division 6 (commencing with section 10910) of the Water Code relating to the submission of the water assessment.

(d) If a water-demand project has been the subject of a water assessment, no additional water assessment shall be required for subsequent water-demand projects that were included in such larger water-demand project if all of the following criteria are met:

(1) The entity completing the water assessment had concluded that its water supplies are sufficient to meet the projected water demand associated with the larger water-demand project, in addition to the existing and planned future uses, including, but not limited to, agricultural and industrial uses; and

(2) None of the following changes has occurred since the completion of the water assessment for the larger water-demand project:

(A) Changes in the larger water-demand project that result in a substantial increase in water demand for the water-demand project.

(B) Changes in the circumstances or conditions substantially affecting the ability of the public water system or the water supplying city or county identified in the water assessment to provide a sufficient supply of water for the water demand project.

(C) Significant new information becomes available which was not known and could not have been known at the time when the entity had reached the conclusion in subdivision (d)(1).

(e) The city or county lead agency shall include the water assessment, and any water acquisition plan in the EIR, negative declaration, or mitigated negative declaration, or any supplement thereto, prepared for the water-demand project, and may include an evaluation of the water assessment and water acquisition plan information within such environmental document. The city or county lead agency shall determine, based on the entire record, whether projected water supplies will be sufficient to satisfy the demands of the project, in addition to existing and planned future uses. If a city or county lead agency determines that water supplies will not be

sufficient, the city or county lead agency shall include that determination in its findings for the water-demand project.

Note: Authority Cited: Section 21083, Public Resources Code. Reference: Section 21151.9, Public Resources Code, Sections 10910–10915 of the Water Code.

Article 11. Types of EIRs

SECTIONS 15160 TO 15170

15160. GENERAL

This article describes a number of examples of variations in EIRs as the documents are tailored to different situations and intended uses. These variations are not exclusive. Lead Agencies may use other variations consistent with the Guidelines to meet the needs of other circumstances. All EIRs must meet the content requirements discussed in Article 9 beginning with Section 15120.

Note: Authority cited: Section 21083, Public Resources Code; Reference: Sections 21061, 21100, and 21151, Public Resources Code.

15161. PROJECT EIR

The most common type of EIR examines the environmental impacts of a specific development project. This type of EIR should focus primarily on the changes in the environment that would result from the development project. The EIR shall examine all phases of the project including planning, construction, and operation.

Note: Authority cited: Section 21083, Public Resources Code; Reference: Sections 21061, 21100, and 21151, Public Resources Code.

15162. SUBSEQUENT EIRS AND NEGATIVE DECLARATIONS

(a) When an EIR has been certified or a negative declaration adopted for a project, no subsequent EIR shall be prepared for that project unless the lead agency determines, on the basis of substantial evidence in the light of the whole record, one or more of the following:

(1) Substantial changes are proposed in the project which will require major revisions of the previous EIR or negative declaration due to the involvement of new significant environmental effects or a substantial increase in the severity of previously identified significant effects;

(2) Substantial changes occur with respect to the circumstances under which the project is undertaken which will require major revisions of the previous EIR or Negative Declaration due to the involvement of new significant environmental effects or a substantial increase in the severity of previously identified significant effects; or

(3) New information of substantial importance, which was not known and could not have been known with the exercise of reasonable diligence at the time the previous EIR was certified as complete or the Negative Declaration was adopted, shows any of the following:

(A) The project will have one or more significant effects not discussed in the previous EIR or negative declaration;

(B) Significant effects previously examined will be substantially more severe than shown in the previous EIR;

(C) Mitigation measures or alternatives previously found not to be feasible would in fact be feasible, and would substantially reduce one or more significant effects of the project, but the project proponents decline to adopt the mitigation measure or alternative; or

(D) Mitigation measures or alternatives which are considerably different from those analyzed in the previous EIR would substantially reduce one or more significant effects on the environment, but the project proponents decline to adopt the mitigation measure or alternative.

(b) If changes to a project or its circumstances occur or new information becomes available after adoption of a negative declaration, the lead agency shall prepare a subsequent EIR if required under subdivision (a). Otherwise the lead agency shall determine whether to prepare a subsequent negative declaration, an addendum, or no further documentation.

(c) Once a project has been approved, the lead agency's role in project approval is completed, unless further discretionary approval on that project is required. Information appearing after an approval does not require reopening of that approval. If after the project is approved, any of the conditions described in subdivision (a) occurs, a subsequent EIR or negative declaration shall only be prepared by the public agency which grants the next discretionary approval for the project, if any. In this situation no other responsible agency shall grant an approval for the project until the subsequent EIR has been certified or subsequent negative declaration adopted.

(d) A subsequent EIR or subsequent negative declaration shall be given the same notice and public review as required under Section 15087 or Section 15072. A subsequent EIR or negative declaration shall state where the previous document is available and can be reviewed.

Note: Authority cited: Section 21083, Public Resources Code; Reference: Section 21166, Public Resources Code; *Bowman v. City of Petaluma* (1986) 185 Cal.App.3d 1065; *Benton v. Board of Supervisors* (1991) 226 Cal.App.3d 1467; and *Fort Mojave Indian Tribe v. California Department of Health Services et al.* (1995) 38 Cal.App.4th 1574.

15163. SUPPLEMENT TO AN EIR

(a) The Lead or Responsible Agency may choose to prepare a supplement to an EIR rather than a subsequent EIR if:

(1) Any of the conditions described in Section 15162 would require the preparation of a subsequent EIR, and

(2) Only minor additions or changes would be necessary to make the previous EIR adequately apply to the project in the changed situation.

(b) The supplement to the EIR need contain only the information necessary to make the previous EIR adequate for the project as revised.

(c) A supplement to an EIR shall be given the same kind of notice and public review as is given to a draft EIR under Section 15087.

(d) A supplement to an EIR may be circulated by itself without recirculating the previous draft or final EIR.

(e) When the agency decides whether to approve the project, the decision-making body shall consider the previous EIR as revised by the supplemental EIR. A finding under Section 15091 shall be made for each significant effect shown in the previous EIR as revised.

Note: Authority cited: Section 21083, Public Resources Code; Reference: Section 21166, Public Resources Code.

15164. ADDENDUM TO AN EIR OR NEGATIVE DECLARATION

(a) The lead agency or responsible agency shall prepare an addendum to a previously certified EIR if some changes or additions are necessary but none of the conditions described in Section 15162 calling for preparation of a subsequent EIR have occurred.

(b) An addendum to an adopted negative declaration may be prepared if only minor technical changes or additions are necessary or none of the conditions described in Section 15162 calling for the preparation of a subsequent EIR or negative declaration have occurred.

(c) An addendum need not be circulated for public review but can be included in or attached to the final EIR or adopted negative declaration.

(d) The decision making body shall consider the addendum with the final EIR or adopted negative declaration prior to making a decision on the project.

(e) A brief explanation of the decision not to prepare a subsequent EIR pursuant to Section 15162 should be included in an addendum to an EIR, the lead agency's findings on the project, or elsewhere in the record. The explanation must be supported by substantial evidence.

Note: Authority cited: Section 21083, Public Resources Code; Reference: Section 21166, Public Resources Code; *Bowman v. City of Petaluma* (1986) 185 Cal.App.3d 1065; and *Benton v. Board of Supervisors* (1991) 226 Cal.App.3d 1467.

15165. MULTIPLE AND PHASED PROJECTS

Where individual projects are, or a phased project is, to be undertaken and where the total undertaking comprises a project with significant environmental effect, the Lead Agency shall prepare a single program EIR for the ultimate project as described in Section 15168. Where an individual project is a necessary precedent for action on a larger project, or commits the Lead Agency to a larger project, with significant environmental effect, an EIR must address itself to the scope of the larger project. Where one project is one of several similar projects of a public agency, but is not deemed a part of a larger undertaking or a larger project, the agency may prepare one EIR for all projects, or one for each project, but shall in either case comment upon the cumulative effect.

Note: Authority cited: Section 21083, Public Resources Code; Reference: Sections 21061, 21100, and 21151, Public Resources Code; *Whitman v. Board of Supervisors*, (1979) 88 Cal. App. 3d 397.

15166. EIR AS PART OF A GENERAL PLAN

(a) The requirements for preparing an EIR on a local general plan, element, or amendment thereof will be satisfied by using the general plan, or element document, as the EIR and no separate EIR will be required, if:

  (1) The general plan addresses all the points required to be in an EIR by Article 9 of these Guidelines, and

  (2) The document contains a special section or a cover sheet identifying where the general plan document addresses each of the points required.

(b) Where an EIR rather than a Negative Declaration has been prepared for a general plan, element, or amendment thereto, the EIR shall be forwarded to the State Clearinghouse for review. The requirement shall apply regardless of whether the EIR is prepared as a separate document or as a part of the general plan or element document.

Note: Authority cited: Section 21083, Public Resources Code; Reference: Sections 21003, 21061, 21083, 21100, 21104, 21151, and 21152, Public Resources Code.

15167. STAGED EIR

(a) Where a large capital project will require a number of discretionary approvals from government agencies and one of the approvals will occur more than two years before construction will begin, a staged EIR may be prepared covering the entire project in a general form. The staged EIR shall evaluate the proposal in light of current and contemplated plans and produce an informed estimate of the environmental consequences of the entire project. The aspect of the project before the public agency for approval shall be discussed with a greater degree of specificity.

(b) When a staged EIR has been prepared, a supplement to the EIR shall be prepared when a later approval is required for the project, and the information available at the time of the later approval would permit consideration of additional environmental impacts, mitigation measures, or reasonable alternatives to the project.

(c) Where a statute such as the Warren-Alquist Energy Resources Conservation and Development Act provides that a specific agency shall be the Lead Agency for a project and requires the Lead Agency to prepare an EIR, a Responsible Agency which must grant an approval for the project before the Lead Agency has completed the EIR may prepare and consider a staged EIR.

(d) An agency requested to prepare a staged EIR may decline to act as the Lead Agency if it determines, among other factors, that:

(1) Another agency would be the appropriate Lead Agency; and

(2) There is no compelling need to prepare a staged EIR and grant an approval for the project before the appropriate Lead Agency will take its action on the project.

Note: Authority cited: Section 21083, Public Resources Code; Reference: Section 21003, Public Resources Code.

15168. PROGRAM EIR

(a) General. A program EIR is an EIR which may be prepared on a series of actions that can be characterized as one large project and are related either:

(1) Geographically,

(2) A logical parts in the chain of contemplated actions,

(3) In connection with issuance of rules, regulations, plans, or other general criteria to govern the conduct of a continuing program, or

(4) As individual activities carried out under the same authorizing statutory or regulatory authority and having generally similar environmental effects which can be mitigated in similar ways.

(b) Advantages. Use of a program EIR can provide the following advantages. The program EIR can:

(1) Provide an occasion for a more exhaustive consideration of effects and alternatives than would be practical in an EIR on an individual action,

(2) Ensure consideration of cumulative impacts that might be slighted in a case-by-case analysis,

(3) Avoid duplicative reconsideration of basic policy considerations,

(4) Allow the Lead Agency to consider broad policy alternatives and programwide mitigation measures at an early time when the agency has greater flexibility to deal with basic problems or cumulative impacts, and

(5) Allow reduction in paperwork.

(c) Use with Later Activities. Subsequent activities in the program must be examined in the light of the program EIR to determine whether an additional environmental document must be prepared.

(1) If a later activity would have effects that were not examined in the program EIR, a new Initial Study would need to be prepared leading to either an EIR or a Negative Declaration.

(2) If the agency finds that pursuant to Section 15162, no new effects could occur or no new mitigation measures would be required, the agency can approve the activity as being within the scope of the project covered by the program EIR, and no new environmental document would be required.

(3) An agency shall incorporate feasible mitigation measures and alternatives developed in the program EIR into subsequent actions in the program.

(4) Where the subsequent activities involve site specific operations, the agency should use a written checklist or similar device to document the evaluation of the site and the activity to determine whether the environmental effects of the operation were covered in the program EIR.

(5) A program EIR will be most helpful in dealing with subsequent activities if it deals with the effects of the program as specifically and comprehensively as possible. With a good and detailed analysis of the program, many subsequent activities could be found to be within the scope of the project described in the program EIR, and no further environmental documents would be required.

(d) Use with Subsequent EIRs and Negative Declarations. A program EIR can be used to simplify the task of preparing environmental documents on later parts of the program. The program EIR can:

(1) Provide the basis in an Initial Study for determining whether the later activity may have any significant effects.

(2) Be incorporated by reference to deal with regional influences, secondary effects, cumulative impacts, broad alternatives, and other factors that apply to the program as a whole.

(3) Focus an EIR on a subsequent project to permit discussion solely of new effects which had not been considered before.

(e) Notice with Later Activities. When a law other than CEQA requires public notice when the agency later proposes to carry out or approve an activity within the program and to rely on the program EIR for CEQA compliance, the notice for the activity shall include a statement that:

(1) This activity is within the scope of the program approved earlier, and

(2) The program EIR adequately describes the activity for the purposes of CEQA.

Note: Authority cited: Section 21083, Public Resources Code; Reference: Section 21003, Public Resources Code; *County of Inyo v. Yorty*, (1973) 32 Cal. App. 3d 795.

15169. MASTER ENVIRONMENTAL ASSESSMENT

(a) General. A public agency may prepare a Master Environmental Assessment, inventory, or data base for all, or a portion of, the territory subject to its control in order to provide information which may be used or referenced in EIRs or Negative Declarations. Neither the content, the format, nor the procedures to be used to develop a Master Environmental Assessment are prescribed by these Guidelines. The descriptions contained in this section are advisory. A Master Environmental Assessment is suggested solely as an approach to identify and organize environmental information for a region or area of the state.

(b) Contents. A Master Environmental Assessment may contain an inventory of the physical and biological characteristics of the area for which it is prepared and may contain such additional data and information as the public agency determines is useful or necessary to describe environmental characteristics of the area. It may include identification of existing levels of quality and supply of air and water, capacities and levels of use of existing services and facilities, and generalized incremental effects of different categories of development projects by type, scale, and location.

(c) Preparation.

(1) A Master Environmental Assessment or inventory may be prepared in many possible ways. For example, a Master Environmental Assessment may be prepared as a special, comprehensive study of the area involved, as part of the EIR on a general plan, or as a data

base accumulated by indexing EIRs prepared for individual projects or programs in the area involved.

(2) The information contained in a Master Environmental Assessment should be reviewed periodically and revised as needed so that it is accurate and current.

(3) When advantageous to do so, Master Environmental Assessments may be prepared through a joint exercise of powers agreement with neighboring local agencies or with the assistance of the appropriate Council of Governments.

(d) Uses.

(1) A Master Environmental Assessment can identify the environmental characteristics and constraints of an area. This information can be used to influence the design and location of individual projects.

(2) A Master Environmental Assessment may provide information agencies can use in initial studies to decide whether certain environmental effects are likely to occur and whether certain effects will be significant.

(3) A Master Environmental Assessment can provide a central source of current information for use in preparing individual EIRs and Negative Declarations.

(4) Relevant portions of a Master Environmental Assessment can be referenced and summarized in EIRs and Negative Declarations.

(5) A Master Environmental Assessment can assist in identifying long range, areawide, and cumulative impacts of individual projects proposed in the area covered by the assessment.

(6) A Master Environmental Assessment can assist a city or county in formulating a general plan or any element of such a plan by identifying environmental characteristics and constraints that need to be addressed in the general plan.

(7) A Master Environmental Assessment can serve as a reference document to assist public agencies which review other environmental documents dealing with activities in the area covered by the assessment. The public agency preparing the assessment should forward a completed copy to each agency which will review projects in the area.

Note: Authority cited: Section 21083, Public Resources Code; Reference: Section 21003, Public Resources Code.

15170. JOINT EIR-EIS

A Lead Agency under CEQA may work with a federal agency to prepare a joint document which will meet the requirements of both CEQA and NEPA. Use of such a joint document is described in Article 14, beginning with Section 15220.

Note: Authority cited: Section 21083, Public Resources Code; Reference: Sections 21083.5 and 21083.7, Public Resources Code.

Article 11.5 Master Environmental Impact Report

SECTIONS 15175 TO 15179.5

15175. MASTER EIR

(a) The Master EIR procedure is an alternative to preparing a project EIR, staged EIR, or program EIR for certain projects which will form the basis for later decision making. It is intended to streamline the later environmental review of projects or approval included within the project, plan or program analyzed in the Master EIR. Accordingly, a Master EIR shall, to the greatest

extent feasible, evaluate the cumulative impacts, growth inducing impacts, and irreversible significant effects on the environment of subsequent projects.

(b) A lead agency may prepare a Master EIR for any of the following classes of projects:

(1) A general plan, general plan update, general plan element, general plan amendment, or specific plan.

(2) Public or private projects that will be carried out or approved pursuant to, or in furtherance of, a redevelopment plan.

(3) A project that consists of smaller individual projects which will be carried out in phases.

(4) A rule or regulation which will be implemented by later projects.

(5) Projects that will be carried out or approved pursuant to a development agreement.

(6) A state highway project or mass transit project which will be subject to multiple stages of review or approval.

(7) A plan proposed by a local agency, including a joint powers authority, for the reuse of a federal military base or reservation that has been closed or is proposed for closure by the federal government.

(8) A regional transportation plan or congestion management plan.

(9) Regulations adopted by the California Department of Fish and Game for the regulation of hunting and fishing.

(c) A lead agency may develop and implement a fee program in accordance with applicable provisions of law to generate the revenue necessary to prepare a Master EIR.

Note: Authority cited: Section 21083, Public Resources Code; Reference: Sections 21156, 21157, and 21089, Public Resources Code.

15176. CONTENTS OF A MASTER EIR

A lead agency shall include in a Master EIR all of the following:

(a) A detailed discussion as required by Section 15126.

(b) A description of anticipated subsequent projects that are within the scope of the Master EIR, including information with regard to the kind, size, intensity, and location of the subsequent projects, including, but not limited to all of the following:

(1) The specific type of project anticipated to be undertaken such as a single family development, office-commercial development, sewer line installation or other activities.

(2) The maximum and minimum intensity of any anticipated subsequent project, such as the number of residences in a residential development, and with regard to a public works facility, its anticipated capacity and service area.

(3) The anticipated location for any subsequent development projects, and, consistent with the rule of reason set forth in Section 15126.6(f), alternative locations for any such projects.

(4) A capital outlay or capital improvement program, or other scheduling or implementing device that governs the submission and approval of subsequent projects, or an explanation as to why practical planning considerations render it impractical to identify any such program or scheduling or other device at the time of preparing the Master EIR.

(c) A description of potential impacts of anticipated projects for which there is not sufficient information reasonably available to support a full assessment of potential impacts in the Master EIR. This description shall not be construed as a limitation on the impacts which may be considered in a focused EIR.

(d) Where a Master EIR is prepared in connection with a project identified in subdivision (b)(1) of section 15175, the anticipated subsequent projects included within a Master EIR may consist of

later planning approvals, including parcel-specific approvals, consistent with the overall planning decision (e.g., general plan, or specific plan, or redevelopment plan) for which the Master EIR has been prepared. Such subsequent projects shall be adequately described for purposes of subdivision (b) or of this section (15176) if the Master EIR and any other documents embodying or relating to the overall planning decision identify the land use designations and the permissible densities and intensities of use for the affected parcel(s). The proponents of such subsequent projects shall not be precluded from relying on the Master EIR solely because that document did not specifically identify or list, by name, the subsequent project as ultimately proposed for approval.

Note: Authority cited: Section 21083, Public Resources Code; Reference: Section 21157, Public Resources Code.

15177. SUBSEQUENT PROJECTS WITHIN THE SCOPE OF THE MEIR

(a) After a Master EIR has been prepared and certified, subsequent projects which the lead agency determines as being within the scope of the Master EIR will be subject to only limited environmental review.

(b) Except as provided in subdivision (2) of this subdivision, neither a new environmental document nor the preparation of findings pursuant to section 15091 shall be required of a subsequent project when all of the following requirements are met:

(1) The lead agency for the subsequent project is the lead agency or any responsible agency identified in the Master EIR.

(2) The lead agency for the subsequent project prepares an initial study on the proposal. The initial study shall analyze whether the subsequent project was described in the Master EIR and whether the subsequent project may cause any additional significant effect on the environment which was not previously examined in the Master EIR.

(3) The lead agency for the subsequent project determines, on the basis of written findings, that no additional significant environmental effect will result from the proposal, no new additional mitigation measures or alternatives may be required, and that the project is within the scope of the Master EIR. “Additional significant environmental effect” means any project-specific effect which was not addressed as a significant effect in the Master EIR.

(c) Whether a subsequent project is within the scope of the Master EIR is a question of fact to be determined by the lead agency based upon a review of the initial study to determine whether there are additional significant effects or new additional mitigation measures or alternatives required for the subsequent project that are not already discussed in the Master EIR.

(d) Prior to approval of the proposed subsequent project, the lead agency shall incorporate all feasible mitigation measures or feasible alternatives appropriate to the project as set forth in the Master EIR and provide notice in the manner required by Section 15087.

(e) When the lead agency approves a project pursuant to this section, the lead agency shall file a notice in the manner required by Section 15075.

Note: Authority cited: Section 21083, Public Resources Code; References: Sections 21157, 21157.6 and 21158, Public Resources Code.

15178. SUBSEQUENT PROJECTS IDENTIFIED IN THE MEIR

(a) When a proposed subsequent project is identified in the Master EIR, but the lead agency cannot make a determination pursuant to Section 15177 that the subsequent project is within the scope of the Master EIR, and the lead agency determines that the cumulative impacts, growth inducing impacts and irreversible significant effects analysis in the Master EIR is adequate for the subsequent project, the lead agency shall prepare a mitigated negative declaration or a

focused EIR if, after preparing an initial study, the lead agency determines that the project may result in new or additional significant effects. Whether the cumulative impacts, growth inducing impacts and irreversible significant effects analyses are adequate is a question of fact to be determined by the lead agency based upon a review of the proposed subsequent project in light of the Master EIR.

(b) A lead agency shall prepare a mitigated negative declaration for any proposed subsequent project if both of the following occur:

(1) The initial study prepared pursuant to Section 15177 has identified potentially new or additional significant environmental effects that were not analyzed in the Master EIR; and

(2) Feasible mitigation measures or alternatives will be incorporated to revise the subsequent project before the negative declaration is released for public review pursuant to Section 15073 in order to avoid or mitigate the identified effects to a level of insignificance.

(c) A lead agency shall prepare a focused EIR if the subsequent project may have a significant effect on the environment and a mitigated negative declaration pursuant to subdivision (b) of this section cannot be prepared.

(1) The focused EIR shall incorporate by reference the Master EIR and analyze only the subsequent project's additional significant environmental effects and any new or additional mitigation measures or alternatives that were not identified and analyzed by the Master EIR. "Additional significant environmental effects" are those project-specific effects on the environment which were not addressed as significant in the Master EIR.

(2) A focused EIR need not examine those effects which the lead agency, prior to public release of the focused EIR, finds, on the basis of the initial study, related documents, and commitments from the proponent of a subsequent project, have been mitigated in one of the following manners:

(A) Mitigated or avoided as a result of mitigation measures identified in the Master EIR which the lead agency will require as part of the approval of the subsequent project;

(B) Examined at a sufficient level of detail in the Master EIR to enable those significant effects to be mitigated or avoided by specific revisions to the project, the imposition of conditions of approval, or by other means in connection with approval of the subsequent project; or

(C) The mitigation or avoidance of which is the responsibility of and within the jurisdiction of another public agency and is, or can and should be, undertaken by that agency.

(3) The lead agency's findings pursuant to subdivision (2) shall be included in the focused EIR prior to public release pursuant to Section 15087.

(4) A focused EIR prepared pursuant to this section shall analyze any significant environmental effects when:

(A) Substantial new or additional information shows that the adverse environmental effect may be more significant than was described in the Master EIR; or

(B) Substantial new or additional information shows that mitigation measures or alternatives which were previously determined to be infeasible are feasible and will avoid or reduce the significant effects of the subsequent project to a level of insignificance.

(d) A lead agency shall file a notice of determination shall be filed pursuant to Section 15075 if a project has been approved for which a mitigated negative declaration has been prepared pursuant to this section and a notice of determination shall be filed pursuant to Section 15094 if a project has been approved for which a focused EIR has been prepared pursuant to this section.

(e) When a lead agency determines that the cumulative impacts, growth inducing impacts and irreversible significant effects analysis in the Master EIR is inadequate for the subsequent project, the subsequent project is no longer eligible for the limited environmental review available under the Master EIR process and shall be reviewed according to Article 7 (commencing with Section 15080) of these guidelines. The lead agency shall tier the project specific EIR upon the Master EIR to the extent feasible under Section 15152.

Note: Authority cited: Section 21083, Public Resources Code; References: Sections 21081(a)(2), 21157.5 and 21158, Public Resources Code.

15179. LIMITATIONS ON THE USE OF THE MASTER EIR

(a) The certified Master EIR shall not be used for a subsequent project described in the Master EIR in accordance with this article if either:

(1) The Master EIR was certified more than five years prior to the filing of an application for a subsequent project except as set forth in subsection (b) below, or

(2) After the certification of the Master EIR, a project not described in the certified Master EIR as an anticipated subsequent project is approved and the approved project may affect the adequacy of the Master EIR for any subsequent project that was described in the Master EIR.

(b) A Master EIR that was certified more than five years prior to the filing of an application for a subsequent project described in the Master EIR may be used in accordance with this article to review such a subsequent project if the lead agency reviews the adequacy of the Master EIR and takes either of the following steps:

(1) Finds that no substantial changes have occurred with respect to the circumstances under which the Master EIR was certified, or that there is no new available information which was not known and could not have been known at the time the Master EIR was certified; or

(2) Prepares an initial study, and, pursuant to the findings of the initial study, does either (A) or (B) below:

(A) certifies a subsequent or supplemental EIR that updates or revises the Master EIR and which either:

1. is incorporated into the previously certified Master EIR, or
2. references any deletions, additions or other modifications to the previously certified Master EIR.;

(B) approves a mitigated negative declaration that addresses substantial changes that have occurred with respect to the circumstances under which the Master EIR was certified or the new information that was not known and could not have been known at the time the Master EIR was certified.

Note: Authority cited: Section 21083, Public Resources Code; Reference: Section 21157.6, Public Resources Code.

15179.5. FOCUSED EIRS AND SMALL PROJECTS

(a) When a project is a multiple family residential development of 100 units or less or is a residential and commercial or retail mixed-use commercial development of not more then 100,000 square feet, whether or not the project is identified in the Master EIR, a focused EIR shall be prepared pursuant to this section when the following conditions are met:

(1) The project is consistent with a general plan, specific plan, community plan, or zoning ordinance for which an EIR was prepared within five years of certification of the focused EIR; and

(2) The parcel on which the project is to be developed is either:

(A) Surrounded by immediately contiguous urban development;

(B) Previously developed with urban uses; or

(C) Within one-half mile of an existing rail transit station.

(b) A focused environmental impact report prepared pursuant to this section shall be limited to a discussion of potentially significant effects on the environment specific to the project, or which substantial new information shows will be more significant than described in the prior environmental impact report. No discussion shall be required of alternatives to the project, cumulative impacts of the project, or the growth inducing impacts of the project.

(c) This section does not apply where the lead agency can make a finding pursuant to Section 15177 that the subsequent project is within the scope of the Master EIR, where the lead agency can prepare a mitigated negative declaration or focused EIR pursuant to Section 15178, or where, pursuant to Section 15162 or Section 15163, the environmental impact report referenced in subdivision (a)(1) of this section must be updated through the preparation of a subsequent environmental impact report or a supplemental environmental impact report.

Note: Authority cited: Section 21083, Public Resources Code; Reference: Section 21158.5, Public Resources Code.

Article 12. Special Situations

SECTIONS 15180 TO 15190

15180. REDEVELOPMENT PROJECTS

(a) An EIR for a redevelopment plan may be a Master EIR, a program EIR, or a project EIR. An EIR for a redevelopment plan must specify whether it is a Master EIR, a program EIR, or a project EIR.

(b) If the EIR for a redevelopment plan is a project EIR, all public and private activities or undertakings pursuant to or in furtherance of the redevelopment plan shall constitute a single project, which shall be deemed approved at the time of adoption of the redevelopment plan by the legislative body. The EIR in connection with the redevelopment plan shall be submitted in accordance with Section 33352 of the Health and Safety Code.

If a project EIR has been certified for the redevelopment plan, no subsequent EIRs are required for individual components of the redevelopment plan unless a subsequent EIR or a supplement to an EIR would be required by Section 15162 or 15163.

(c) If the EIR for a redevelopment plan is a Master EIR, subsequent projects which the lead agency determines as being within the scope of the Master EIR will be subject to the review required by Section 15177. If the EIR for a redevelopment plan is a program EIR, subsequent activities in the program will be subject to the review required by Section 15168.

Note: Authority cited: Section 21083, Public Resources Code; Reference: Sections 21090 and 21166, Public Resources Code.

15181. [DELETED]

15182. RESIDENTIAL PROJECTS PURSUANT TO A SPECIFIC PLAN

(a) Exemption. Where a public agency has prepared an EIR on a specific plan after January 1, 1980, no EIR or negative declaration need be prepared for a residential project undertaken pursuant to and in conformity to that specific plan if the project meets the requirements of this section.

(b) Scope. Residential projects covered by this section include but are not limited to land subdivisions, zoning changes, and residential planned unit developments.

(c) Limitation. This section is subject to the limitation that if after the adoption of the specific plan, an event described in Section 15162 should occur, this exemption shall not apply until the city or county which adopted the specific plan completes a subsequent EIR or a supplement to an EIR on the specific plan. The exemption provided by this section shall again be available to residential projects after the Lead Agency has filed a Notice of Determination on the specific plan as reconsidered by the subsequent EIR or supplement to the EIR.

(d) Fees. The Lead Agency has authority to charge fees to applicants for projects which benefit from this section. The fees shall be calculated in the aggregate to defray but not to exceed the cost of developing and adopting the specific plan including the cost of preparing the EIR.

(e) Statute of Limitations. A court action challenging the approval of a project under this section for failure to prepare a supplemental EIR shall be commenced within 30 days after the Lead Agency's decision to carry out or approve the project in accordance with the specific plan.

Note: Authority cited: Section 21083, Public Resources Code; Reference: Section 65453, Government Code.

15183. PROJECTS CONSISTENT WITH A COMMUNITY PLAN OR ZONING

(a) CEQA mandates that projects which are consistent with the development density established by existing zoning, community plan, or general plan policies for which an EIR was certified shall not require additional environmental review, except as might be necessary to examine whether there are project-specific significant effects which are peculiar to the project or its site. This streamlines the review of such projects and reduces the need to prepare repetitive environmental studies.

(b) In approving a project meeting the requirements of this section, a public agency shall limit its examination of environmental effects to those which the agency determines, in an initial study or other analysis:

(1) Are peculiar to the project or the parcel on which the project would be located,

(2) Were not analyzed as significant effects in a prior EIR on the zoning action, general plan, or community plan, with which the project is consistent,

(3) Are potentially significant off-site impacts and cumulative impacts which were not discussed in the prior EIR prepared for the general plan, community plan or zoning action, or

(4) Are previously identified significant effects which, as a result of substantial new information which was not known at the time the EIR was certified, are determined to have a more severe adverse impact than discussed in the prior EIR.

(c) If an impact is not peculiar to the parcel or to the project, has been addressed as a significant effect in the prior EIR, or can be substantially mitigated by the imposition of uniformly applied development policies or standards, as contemplated by subdivision (e) below, then an additional EIR need not be prepared for the project solely on the basis of that impact.

(d) This section shall apply only to projects which meet the following conditions:

(1) The project is consistent with:

(A) A community plan adopted as part of a general plan,

(B) A zoning action which zoned or designated the parcel on which the project would be located to accommodate a particular density of development, or

(C) A general plan of a local agency, and

(2) An EIR was certified by the lead agency for the zoning action, the community plan, or the general plan.

(e) This section shall limit the analysis of only those significant environmental effects for which:

(1) Each public agency with authority to mitigate any of the significant effects on the environment identified in the EIR on the planning or zoning action undertakes or requires others to undertake mitigation measures specified in the EIR which the lead agency found to be feasible, and

(2) The lead agency makes a finding at a public hearing as to whether the feasible mitigation measures will be undertaken.

(f) An effect of a project on the environment shall not be considered peculiar to the project or the parcel for the purposes of this section if uniformly applied development policies or standards have been previously adopted by the city or county with a finding that the development policies or standards will substantially mitigate that environmental effect when applied to future projects, unless substantial new information shows that the policies or standards will not substantially mitigate the environmental effect. The finding shall be based on substantial evidence which need not include an EIR. Such development policies or standards need not apply throughout the entire city or county, but can apply only within the zoning district in which the project is located, or within the area subject to the community plan on which the lead agency is relying. Moreover, such policies or standards need not be part of the general plan or any community plan, but can be found within another pertinent planning document such as a zoning ordinance. Where a city or county, in previously adopting uniformly applied development policies or standards for imposition on future projects, failed to make a finding as to whether such policies or standards would substantially mitigate the effects of future projects, the decision-making body of the city or county, prior to approving such a future project pursuant to this section, may hold a public hearing for the purpose of considering whether, as applied to the project, such standards or policies would substantially mitigate the effects of the project. Such a public hearing need only be held if the city or county decides to apply the standards or policies as permitted in this section.

(g) Examples of uniformly applied development policies or standards include, but are not limited to:

(1) Parking ordinances.

(2) Public access requirements.

(3) Grading ordinances.

(4) Hillside development ordinances.

(5) Flood plain ordinances.

(6) Habitat protection or conservation ordinances.

(7) View protection ordinances.

(8) Requirements for reducing greenhouse gas emissions, as set forth in adopted land use plans, policies, or regulations.

(h) An environmental effect shall not be considered peculiar to the project or parcel solely because no uniformly applied development policy or standard is applicable to it.

(i) Where the prior EIR relied upon by the lead agency was prepared for a general plan or community plan that meets the requirements of this section, any rezoning action consistent with the general plan or community plan shall be treated as a project subject to this section.

(1) "Community plan" is defined as a part of the general plan of a city or county which applies to a defined geographic portion of the total area included in the general plan, includes or references each of the mandatory elements specified in Section 65302 of the Government

Code, and contains specific development policies and implementation measures which will apply those policies to each involved parcel.

(2) For purposes of this section, "consistent" means that the density of the proposed project is the same or less than the standard expressed for the involved parcel in the general plan, community plan or zoning action for which an EIR has been certified, and that the project complies with the density-related standards contained in that plan or zoning. Where the zoning ordinance refers to the general plan or community plan for its density standard, the project shall be consistent with the applicable plan.

(j) This section does not affect any requirement to analyze potentially significant offsite or cumulative impacts if those impacts were not adequately discussed in the prior EIR. If a significant offsite or cumulative impact was adequately discussed in the prior EIR, then this section may be used as a basis for excluding further analysis of that offsite or cumulative impact.

Note: Authority cited: Sections 21083 and 21083.05, Public Resources Code; Reference: Section 21083.3, 21083.05, Public Resources Code.

15183.3 STREAMLINING FOR INFILL PROJECTS

(a) Purpose. The purpose of this section is to streamline the environmental review process for eligible infill projects by limiting the topics subject to review at the project level where the effects of infill development have been addressed in a planning level decision or by uniformly applicable development policies.

(b) Eligibility. To be eligible for the streamlining procedures prescribed in this section, an infill project must:

(1) Be located in an urban area on a site that either has been previously developed or that adjoins existing qualified urban uses on at least seventy-five percent of the site's perimeter. For the purpose of this subdivision "adjoin" means the infill project is immediately adjacent to qualified urban uses, or is only separated from such uses by an improved public right-of-way;

(2) Satisfy the performance standards provided in Appendix M; and

(3) Be consistent with the general use designation, density, building intensity, and applicable policies specified for the project area in either a sustainable communities strategy or an alternative planning strategy, except as provided in subdivisions (b)(3)(A) or (b)(3)(B) below.

(A) Only where an infill project is proposed within the boundaries of a metropolitan planning organization for which a sustainable communities strategy or an alternative planning strategy will be, but is not yet, in effect, a residential infill project must have a density of at least 20 units per acre, and a retail or commercial infill project must have a floor area ratio of at least 0.75.

(B) Where an infill project is proposed outside of the boundaries of a metropolitan planning organization, the infill project must meet the definition of a small walkable community project in subdivision (f)(5), below.

(c) Streamlined Review. CEQA does not apply to the effects of an eligible infill project under two circumstances. First, if an effect was addressed as a significant effect in a prior EIR for a planning level decision, then, with some exceptions, that effect need not be analyzed again for an individual infill project even when that effect was not reduced to a less than significant level in the prior EIR. Second, an effect need not be analyzed, even if it was not analyzed in a prior EIR or is more significant than previously analyzed, if the lead agency makes a finding that uniformly applicable development policies or standards, adopted by the lead agency or a city or county, apply to the infill project and would substantially mitigate that effect. Depending on the effects addressed in the prior EIR and the availability of uniformly applicable development

policies or standards that apply to the eligible infill project, streamlining under this section will range from a complete exemption to an obligation to prepare a narrowed, project-specific environmental document. A prior EIR will be most helpful in dealing with later infill projects if it deals with the effects of infill development as specifically and comprehensively as possible. With a good and detailed analysis of such development, the effects of many infill projects could be found to have been addressed in the prior EIR, and no further environmental documents would be required.

(d) Procedure. Following preliminary review of an infill project pursuant to Section 15060, the lead agency must examine an eligible infill project in light of the prior EIR to determine whether the infill project will cause any effects that require additional review under CEQA. Determinations pursuant to this section are questions of fact to be resolved by the lead agency. Such determinations must be supported with enough relevant information and reasonable inferences from this information to support a conclusion, even though other conclusions might also be reached. (See Section 15384.)

(1) Evaluation of the lnfill Project. A lead agency should prepare a written checklist or similar device to document the infill project's eligibility for streamlining and to assist in making the determinations required by this section. The sample written checklist provided in Appendix N may be used for this purpose. A written checklist prepared pursuant to this section should do all of the following:

(A) Document whether the infill project satisfies the applicable performance standards in Appendix M.

(B) Explain whether the effects of the infill project were analyzed in a prior EIR. The written checklist should cite the specific portions of the prior EIR, including page and section references, containing the analysis of the infill project's significant effects. The written checklist should also indicate whether the infill project incorporates all applicable mitigation measures from the prior EIR.

(C) Explain whether the infill project will cause new specific effects. For the purposes of this section, a new specific effect is an effect that was not addressed in the prior EIR and that is specific to the infill project or the infill project site. A new specific effect may result if, for example, the prior EIR stated that sufficient site-specific information was not available to analyze the significance of that effect. Substantial changes in circumstances following certification of a prior EIR may also result in a new specific effect.

(D) Explain whether substantial new information shows that the adverse environmental effects of the infill project are more significant than described in the prior EIR. For the purpose of this section, "more significant" means an effect will be substantially more severe than described in the prior EIR. More significant effects include those that result from changes in circumstances or changes in the development assumptions underlying the prior EIR's analysis. An effect is also more significant if substantial new information shows that: (1) mitigation measures that were previously rejected as infeasible are in fact feasible, and such measures are not included in the project; (2) feasible mitigation measures considerably different than those previously analyzed could substantially reduce a significant effect described in the prior EIR, but such measures are not included in the project; or (3) an applicable mitigation measure was adopted in connection with a planning level decision, but the lead agency determines that it is not feasible for the infill project to implement that measure.

(E) If the infill project will cause new specific effects or more significant effects, the written checklist should indicate whether uniformly applicable development policies or standards will substantially mitigate those effects. For the purpose of this section, "substantially mitigate" means that the policy or standard will substantially lessen the

effect, but not necessarily below the level of significance. The written checklist should specifically identify the uniformly applicable development policy or standard and explain how it will substantially mitigate the effects of the infill project. The explanation in the written checklist may be used to support the finding required in subdivision (d)(2)(D) below.

(2) Environmental Document. After examining the effects of the infill project in light of the analysis in any prior EIR and uniformly applicable development policies or standards, the lead agency shall determine what type of environmental document shall be prepared for the infill project.

(A) No Further Review. No additional environmental review is required if the infill project would not cause any new specific effects or more significant effects, or if uniformly applicable development policies or standards would substantially mitigate such effects. Where the lead agency determines that no additional environmental review of the effects of the infill project is required, the lead agency shall file a Notice of Determination as provided in Section 15094. Where the lead agency finds that uniformly applicable development policies substantially mitigate a significant effect of an infill project, the lead agency shall make the finding described in subdivision (d)(2)(D).

(B) Negative Declaration, Mitigated Negative Declaration or Sustainable Communities Environmental Assessment. If the infill project would result in new specific effects or more significant effects, and uniformly applicable development policies or standards would not substantially mitigate such effects, those effects shall be subject to CEQA. If a new specific effect is less than significant, the lead agency may prepare a negative declaration. If new specific effects or more significant effects can be mitigated to a less than significant level through project changes agreed to prior to circulation of the written checklist, the lead agency may prepare a mitigated negative declaration. In these circumstances, the lead agency shall follow the procedure set forth in Sections 15072 to 15075. Alternatively, if the infill project is a transit priority project, the lead agency may follow the procedures in Section 21155.2 of the Public Resources Code. In either instance, the written checklist should clearly state which effects are new or more significant, and are subject to CEQA, and which effects have been previously analyzed and are not subject to further environmental review. Where the lead agency finds that uniformly applicable development policies or standards substantially mitigate a significant effect of an infill project, the lead agency shall make the finding described in subdivision (d)(2)(D).

(C) Infill EIR. If the infill project would result in new specific effects or more significant effects, and uniformly applicable development policies or standards would not substantially mitigate such effects, those effects are subject to CEQA. With respect to those effects that are subject to CEQA, the lead agency shall prepare an infill EIR if the written checklist shows that the effects of the infill project would be potentially significant. In this circumstance, the lead agency shall prepare an infill EIR as provided in subdivision (e) and, except as otherwise provided in this section, shall follow the procedures in Article 7. Where the lead agency finds that uniformly applicable development policies or standards substantially mitigate a significant effect of an infill project, the lead agency shall make the finding described in subdivision (d)(2)(D).

(D) Findings. Any findings or statement of overriding considerations required by Sections 15091 or 15093 shall be limited to those effects analyzed in an infill EIR. Findings for such effects should incorporate by reference any such findings made in connection with a planning level decision. Where uniformly applicable development policies or standards substantially mitigate the significant effects of an infill project, the lead

agency shall also make a written finding, supported with substantial evidence, providing a brief explanation of the rationale for the finding.

(e) Infill EIR Contents. An infill EIR shall analyze only those significant effects that uniformly applicable development policies or standards do not substantially mitigate, and that are either new specific effects or are more significant than a prior EIR analyzed. All other effects of the infill project should be described in the written checklist as provided in subdivision (d)(1), and that written checklist should be circulated for public review along with the infill EIR. The written checklist should clearly set forth those effects that are new specific effects, and are subject to CEQA, and those effects which have been previously analyzed and are not subject to further environmental review. The analysis of alternatives in an infill EIR need not address alternative locations, densities, or building intensities. An infill EIR need not analyze growth inducing impacts. Except as provided in this subdivision, an infill EIR shall contain all elements described in Article 9.

(f) Terminology. The following definitions apply to this section:

(1) "lnfill project" includes the whole of an action consisting of residential, commercial, retail, transit station, school, or public office building uses, or any combination of such uses that meet the eligibility requirements set forth in subdivision (b). For retail and commercial projects, no more than one half of the project area may be used for parking. "Transit station" means a rail or light-rail station, ferry terminal, bus hub, bus transfer station, or bus stop, and includes all streetscape improvements constructed in the public right-of-way within one-quarter mile of such facility to improve multi-modal access to the facility, such as pedestrian and bicycle safety improvements and traffic-calming design changes that support pedestrian and bicycle access.

(2) "Planning level decision" means the enactment or amendment of a general plan or any general plan element, community plan, specific plan, or zoning code.

(3) "Prior EIR" means the environmental impact report certified for a planning level decision, as supplemented by any subsequent or supplemental environmental impact reports, negative declarations, or addenda to those documents.

(4) "Qualified urban use" is defined in Public Resources Code Section 21072.

(5) "Small walkable community project" means a project that is all of the following:

(A) In an incorporated city that is not within the boundary of metropolitan planning organization;

(B) Within an area of approximately one-quarter mile diameter of contiguous land that includes a residential area adjacent to a retail downtown area and that is designated by the city for infill development consisting of residential and commercial uses. A city may designate such an area within its general plan, zoning code, or by any legislative act creating such a designation, and may make such designation concurrently with project approval; and

(C) Either a residential project that has a density of at least eight units to the acre or a commercial project with a floor area ratio of at least 0.5, or both.

(6) The terms "sustainable communities strategy" and "alternative planning strategy" refer to a strategy for which the State Air Resources Board, pursuant to subparagraph (H) of paragraph (2) of subdivision (b) of Section 65080 of the Government Code, has accepted a metropolitan planning organization's determination that the sustainable communities strategy or the alternative planning strategy would, if implemented, achieve its greenhouse gas emission reduction targets.

(7) "Uniformly applicable development policies or standards" are policies or standards adopted or enacted by a city or county, or by a lead agency, that reduce one or more adverse

environmental effects. Examples of uniformly applicable development policies or standards include, but are not limited to:

(A) Regulations governing construction activities, including noise regulations, dust control, provisions for discovery of archeological and paleontological resources, stormwater runoff treatment and containment, protection against the release of hazardous materials, recycling of construction and demolition waste, temporary street closure and traffic rerouting, and similar regulations.

(B) Requirements in locally adopted building, grading and stormwater codes.

(C) Design guidelines.

(D) Requirements for protecting residents from sources of air pollution including high volume roadways and stationary sources.

(E) Impact fee programs to provide public improvements, police, fire, parks and other open space, libraries and other public services and infrastructure, including transit, bicycle and pedestrian infrastructure and traffic calming devices.

(F) Traffic impact fees.

(G) Requirements for reducing greenhouse gas emissions, as set forth in adopted land use plans, policies, or regulations.

(H) Ordinances addressing protection of urban trees and historic resources.

(8) "Urban area" is defined in Public Resources Code Section 21094.5(e)(5).

Note: Authority cited: Sections 21083, 21094.5.5, Public Resources Code. Reference: Sections 21094.5 and 21094.5.5, Public Resources Code.

15183.5. TIERING AND STREAMLINING THE ANALYSIS OF GREENHOUSE GAS EMISSIONS

(a) Lead agencies may analyze and mitigate the significant effects of greenhouse gas emissions at a programmatic level, such as in a general plan, a long range development plan, or a separate plan to reduce greenhouse gas emissions. Later project-specific environmental documents may tier from and/or incorporate by reference that existing programmatic review. Project-specific environmental documents may rely on an EIR containing a programmatic analysis of greenhouse gas emissions as provided in section 15152 (tiering), 15167 (staged EIRs) 15168 (program EIRs), 15175–15179.5 (Master EIRs), 15182 (EIRs Prepared for Specific Plans), and 15183 (EIRs Prepared for General Plans, Community Plans, or Zoning).

(b) Plans for the Reduction of Greenhouse Gas Emissions. Public agencies may choose to analyze and mitigate significant greenhouse gas emissions in a plan for the reduction of greenhouse gas emissions or similar document. A plan to reduce greenhouse gas emissions may be used in a cumulative impacts analysis as set forth below. Pursuant to sections 15064(h)(3) and 15130(d), a lead agency may determine that a project's incremental contribution to a cumulative effect is not cumulatively considerable if the project complies with the requirements in a previously adopted plan or mitigation program under specified circumstances.

(1) Plan Elements. A plan for the reduction of greenhouse gas emissions should:

(A) Quantify greenhouse gas emissions, both existing and projected over a specified time period, resulting from activities within a defined geographic area;

(B) Establish a level, based on substantial evidence, below which the contribution to greenhouse gas emissions from activities covered by the plan would not be cumulatively considerable;

(C) Identify and analyze the greenhouse gas emissions resulting from specific actions or categories of actions anticipated within the geographic area;

(D) Specify measures or a group of measures, including performance standards, that substantial evidence demonstrates, if implemented on a project-by-project basis, would collectively achieve the specified emissions level;

(E) Establish a mechanism to monitor the plan's progress toward achieving the level and to require amendment if the plan is not achieving specified levels;

(F) Be adopted in a public process following environmental review.

(2) Use with Later Activities. A plan for the reduction of greenhouse gas emissions, once adopted following certification of an EIR or adoption of an environmental document, may be used in the cumulative impacts analysis of later projects. An environmental document that relies on a greenhouse gas reduction plan for a cumulative impacts analysis must identify those requirements specified in the plan that apply to the project, and, if those requirements are not otherwise binding and enforceable, incorporate those requirements as mitigation measures applicable to the project. If there is substantial evidence that the effects of a particular project may be cumulatively considerable, notwithstanding the project's compliance with the specified requirements in the plan for the reduction of greenhouse gas emissions, an EIR must be prepared for the project.

(c) Special Situations. As provided in Public Resources Code sections 21155.2 and 21159.28, environmental documents for certain residential and mixed use projects, and transit priority projects, as defined in section 21155, that are consistent with the general use designation, density, building intensity, and applicable policies specified for the project area in an applicable sustainable communities strategy or alternative planning strategy need not analyze global warming impacts resulting from cars and light duty trucks. A lead agency should consider whether such projects may result in greenhouse gas emissions resulting from other sources, however, consistent with these Guidelines.

Note: Authority cited: Sections 21083, 21083.05, Public Resources Code. Reference: Section 65457, Gov. Code; Sections 21003, 21061, 21068.5, 21081(a)(2), 21083.05, 21083.3, 21081.6, 21093, 21094, 21100, 21151, 21155, 21155.2, 21156, 21157, 21157.1, 21157.5, 21157.6, 21158, 21158.5, 21159.28, Pub. Resources Code; *California Native Plant Society v. County of El Dorado* (2009) 170 Cal.App.4th 1026; *Protect the Historic Amador Waterways v. Amador Water Agency* (2004) 116 Cal.App.4th 1099.

15184. STATE MANDATED LOCAL PROJECTS

Whenever a state agency issues an order which requires a local agency to carry out a project subject to CEQA, the following rules apply:

(a) If an EIR is prepared for the project, the local agency shall limit the EIR to considering those factors and alternatives which will not conflict with the order.

(b) If a local agency undertakes a project to implement a rule or regulation imposed by a certified state environmental regulatory program listed in Section 15251, the project shall be exempt from CEQA with regard to the significant effects analyzed in the document prepared by the state agency as a substitute for an EIR. The local agency shall comply with CEQA with regard to any site-specific effect of the project which was not analyzed by the certified state agency as a significant effect on the environment. The local agency need not re-examine the general environmental effects of the state rule or regulation.

Note: Authority cited: Section 21083, Public Resources Code; Reference: Sections 21080, 21080.5, and 21154, Public Resources Code.

15185. ADMINISTRATIVE APPEALS

(a) Where an agency allows administrative appeals upon the adequacy of an environmental document, an appeal shall be handled according to the procedures of that agency. Public notice shall be handled in accordance with individual agency requirements and Section 15202(e).

(b) The decision-making body to which an appeal has been made shall consider the environmental document and make findings under Sections 15091 and 15093 if appropriate.

Note: Authority cited: Section 21083, Public Resources Code; Reference: Sections 21082 and 21083, Public Resources Code.

15186. SCHOOL FACILITIES

(a) CEQA establishes a special requirement for certain school projects, as well as certain projects near schools, to ensure that potential health impacts resulting from exposure to hazardous materials, wastes, and substances will be carefully examined and disclosed in a negative declaration or EIR, and that the lead agency will consult with other agencies in this regard.

(b) Before certifying an EIR or adopting a negative declaration for a project located within one-fourth mile of a school that involves the construction or alteration of a facility that might reasonably be anticipated to emit hazardous air emissions, or that would handle an extremely hazardous substance or a mixture containing extremely hazardous substances in a quantity equal to or greater than the state threshold quantity specified in subdivision (j) of Section 25532 of the Health and Safety code, that may impose a health or safety hazard to persons who would attend or would be employed at the school, the lead agency must do both of the following:

(1) Consult with the affected school district or districts regarding the potential impact of the project on the school; and

(2) Notify the affected school district or districts of the project, in writing, not less than 30 days prior to approval or certification of the negative declaration or EIR.

(c) When the project involves the purchase of a school site or the construction of a secondary or elementary school by a school district, the negative declaration or EIR prepared for the project shall not be adopted or certified unless:

(1) The negative declaration, mitigated negative declaration, or EIR contains sufficient information to determine whether the property is:

(A) The site of a current or former hazardous waste or solid waste disposal facility and, if so, whether wastes have been removed.

(B) A hazardous substance release site identified by the Department of Toxic Substances Control in a current list adopted pursuant to Section 25356 of the Health and Safety Code for removal or remedial action pursuant to Chapter 6.8 (commencing with Section 25300) of Division 20 of the Health and Safety Code.

(C) The site of one or more buried or above ground pipelines which carry hazardous substances, acutely hazardous materials, or hazardous wastes, as defined in Division 20 of the Health and Safety Code. This does not include a natural gas pipeline used only to supply the school or neighborhood.

(D) Within 500 feet of the edge of the closest traffic lane of a freeway or other busy traffic corridor.

(2) The lead agency has notified in writing and consulted with the county or city administering agency (as designated pursuant to Section 25502 of the Health and Safety Code) and with any air pollution control district or air quality management district having jurisdiction, to identify facilities within one-fourth mile of the proposed school site which might reasonably be anticipated to emit hazardous emissions or handle hazardous or acutely hazardous material, substances, or waste. The notice shall include a list of the school sites

for which information is sought. Each agency or district receiving notice shall provide the requested information and provide a written response to the lead agency within 30 days of receiving the notification. If any such agency or district fails to respond within that time, the negative declaration or EIR shall be conclusively presumed to comply with this section as to the area of responsibility of that agency.

(3) The school district makes, on the basis of substantial evidence, one of the following written findings:

(A) Consultation identified none of the facilities specified in paragraph (2).

(B) The facilities specified in paragraph (2) exist, but one of the following conditions applies:

1. The health risks from the facilities do not and will not constitute an actual or potential endangerment of public health to persons who would attend or be employed at the proposed school.

2. Corrective measures required under an existing order by another agency having jurisdiction over the facilities will, before the school is occupied, mitigate all chronic or accidental hazardous air emissions to levels that do not constitute any actual or potential public health danger to persons who would attend or be employed at the proposed school. When the school district board makes such a finding, it shall also make a subsequent finding, prior to occupancy of the school, that the emissions have been so mitigated.

3. For a school site with boundary that is within 500 feet of the edge of the closest traffic lane of a freeway or other busy traffic corridor, the school district determines, through a health risk assessment pursuant to subdivision (b)(2) of Section 44360 of the Health and Safety Code, based on appropriate air dispersion modeling, and after considering any potential mitigation measures, that the air quality at the proposed site is such that neither short-term nor long-term exposure poses significant health risks to pupils.

(C) The facilities or other pollution sources specified in subsection (c)(2) exist, but conditions in subdivisions (c)(3)(B)(1), (2) or (3) cannot be met, and the school district is unable to locate an alternative site that is suitable due to a severe shortage of sites that meet the requirements in subdivision (a) of Section 17213 of the Education Code. If the school district makes this finding, the school board shall prepare an EIR and adopt a statement of overriding considerations.

This finding shall be in addition to any findings which may be required pursuant to Sections 15074, 15091 or 15093.

(d) When the lead agency has carried out the consultation required by paragraph (2) of subdivision (b), the negative declaration or EIR shall be conclusively presumed to comply with this section, notwithstanding any failure of the consultation to identify an existing facility.

(e) The following definitions shall apply for the purposes of this section:

(1) "Acutely hazardous material," is as defined in 22 C.C.R. § 66260.10.

(2) "Administering agency," is as defined in Section 25501 of the Health and Safety Code.

(3) "Extremely hazardous substance," is as defined in subdivision (g)(2)(B) of Section 25532 of the Health and Safety Code and listed in Section 2770.5, Table 3, of Title 19 of the California Code of Regulations.

(4) "Facilities" means any source with a potential to use, generate, emit or discharge hazardous air pollutants, including, but not limited to, pollutants that meet the definition of a hazardous substance, and whose process or operation is identified as an emission source

pursuant to the most recent list of source categories published by the California Air Resources Board.

(5) "Freeway or other busy traffic corridors" means those roadways that, on an average day, have traffic in excess of 50,000 vehicles in a rural area, as defined in Section 50101 of the Health and Safety Code, and 100,000 vehicles in an urban area, as defined in Section 50104.7 of the Health and Safety Code.

(6) "Handle" means to use, generate, process, produce, package, treat, store, emit, discharge, or dispose of a hazardous material in any fashion.

(7) "Hazardous air emissions," is as defined in subdivisions (a) to (f), inclusive, of Section 44321 of the Health and Safety Code.

(8) "Hazardous substance," is as defined in Section 25316 of the Health and Safety Code.

(9) "Hazardous waste," is as defined in Section 25117 of the Health and Safety Code.

(10) "Hazardous waste disposal site," is as defined in Section 25114 of the Health and Safety Code.

Note: Authority cited: Sections Section 21083, Public Resources Code. References: Sections 21151.4 and 21151.8, Public Resources Code.

15187. ENVIRONMENTAL REVIEW OF NEW RULES AND REGULATIONS

(a) At the time of the adoption of a rule or regulation requiring the installation of pollution control equipment, establishing a performance standard, or establishing a treatment requirement, the California Air Resources Board, Department of Toxic Substances Control, Integrated Waste Management Board, State Water Resources Control Board, all regional water quality control boards, and all air pollution control districts and air quality management districts, as defined in Section 39025 of the Health and Safety Code, must perform an environmental analysis of the reasonably foreseeable methods by which compliance with that rule or regulation will be achieved.

(b) If an EIR is prepared by the agency at the time of adoption of a rule or regulation, it satisfies the requirements of this section provided that the document contains the information specified in subdivision (c) below. Similarly, for those State agencies whose regulatory programs have been certified by the Resources Agency pursuant to Section 21080.5 of the Public Resources Code, an environmental document prepared pursuant to such programs satisfies the requirements of this section, provided that the document contains the information specified in subdivision (c) below.

(c) The environmental analysis shall include at least the following:

(1) An analysis of reasonably foreseeable environmental impacts of the methods of compliance;

(2) An analysis of reasonably foreseeable feasible mitigation measures relating to those impacts; and

(3) An analysis of reasonably foreseeable alternative means of compliance with the rule or regulation, which would avoid or eliminate the identified impacts.

(d) The environmental analysis shall take into account a reasonable range of environmental, economic, and technical factors, population and geographic areas, and specific sites. The agency may utilize numerical ranges and averages where specific data is not available, but is not required to, nor should it, engage in speculation or conjecture.

(e) Nothing in this section shall require the agency to conduct a project level analysis.

(f) Nothing in this section is intended, or may be used, to delay the adoption of any rule or regulation for which this section requires an environmental analysis.

Note: Authority cited: Section 21083, Public Resources Code; References: Sections 21159 and 21159.4, Public Resources Code.

15188. FOCUSED EIR FOR POLLUTION CONTROL EQUIPMENT

This section applies to projects consisting solely of the installation of pollution control equipment and other components necessary to the installation of that equipment which are undertaken for the purpose of complying with a rule or regulation which was the subject of an environmental analysis as described in Section 15187.

(a) The lead agency for the compliance project may prepare a focused EIR to analyze the effects of that project when the following occur:

  (1) the agency which promulgated the rule or regulation certified an EIR on that rule or regulation, or reviewed it pursuant to an environmental analysis prepared under a certified regulatory program and, in either case, the review included an assessment of growth inducing impacts and cumulative impacts of, and alternatives to, the project;

  (2) the focused EIR for the compliance project is certified within five years of the certified EIR or environmental analysis required by subdivision (a)(1); and

  (3) the EIR prepared in connection with the adoption of the rule or regulation need not be updated through the preparation of a subsequent EIR or supplemental EIR pursuant to section 15162 or section 15163.

(b) The discussion of significant environmental effects in the focused EIR shall be limited to project-specific, potentially significant effects which were not discussed in the environmental analysis required under Section 15187. No discussion of growth-inducing or cumulative impacts is required. Discussion of alternatives shall be limited to alternative means of compliance, if any, with the rule or regulation.

Note: Authority: Section 21083, Public Resources Code; Reference: Section 21159.1, Public Resources Code.

15189. COMPLIANCE WITH PERFORMANCE STANDARD OR TREATMENT REQUIREMENT RULE OR REGULATION

This section applies to projects consisting solely of compliance with a performance standard or treatment requirement which was the subject of an environmental analysis as described in Section 15187.

(a) If preparing a negative declaration, mitigated negative declaration or EIR on the compliance project the lead agency for the compliance project shall, to the greatest extent feasible, use the environmental analysis prepared pursuant to Section 15187. The use of numerical averages or ranges in the environmental analysis prepared under Section 15187 does not relieve the lead agency on the compliance project from its obligation to identify and evaluate the environmental effects of the project.

(b) Where the lead agency determines that an EIR is required for the compliance project, the EIR need address only the project-specific issues or other issues that were not discussed in sufficient detail in the environmental analysis prepared under Section 15187. The mitigation measures imposed by the lead agency shall be limited to addressing the significant effects on the environment of the compliance project. The discussion of alternatives shall be limited to a discussion of alternative means of compliance, if any, with the rule or regulation.

Note: Authority cited: Section 21083, Public Resources Code; Reference: Section 21159.2, Public Resources Code.

15190. DEADLINES FOR COMPLIANCE WITH SECTIONS 15188 AND 15189

(a) The lead agency for a compliance project under either Section 15188 or Section 15189 shall determine whether an EIR or negative declaration should be prepared within 30 days of its determination that the application for the project is complete.

(b) Where the EIR will be prepared under contract to the lead agency for the compliance project, the agency shall issue a request for proposal for preparation of the EIR not later than 30 days after the deadline for response to the notice of preparation has expired. The contract shall be awarded within 30 days of the response date on the request for proposals.

Note: Authority cited: Section 21083, Public Resources Code; Reference: Section 21159.3, Public Resources Code.

15190.5. DEPARTMENT OF DEFENSE NOTIFICATION REQUIREMENT

(a) For purposes of this section, the following definitions are applicable.

(1) "Low-level flight path" means any flight path for any aircraft owned, maintained, or that is under the jurisdiction of the United States Department of Defense that flies lower than 1,500 feet above ground level, as indicated in the United States Department of Defense Flight Information Publication, "Area Planning Military Training Routes: North and South America (AP/1B)" published by the United States National Imagery and Mapping Agency, or its successor, as of the date the military service gives written notification to a lead agency pursuant to subdivision (b).

(2) "Military impact zone" means any area, including airspace, that meets both of the following criteria:

(A) Is within two miles of a military installation, including, but not limited to, any base, military airport, camp, post, station, yard, center, homeport facility for a ship, or any other military activity center that is under the jurisdiction of the United States Department of Defense; and

(B) Covers greater than 500 acres of unincorporated land, or greater than 100 acres of city incorporated land.

(3) "Military service" means the United States Department of Defense or any branch of the United States Armed Forces.

(4) "Special use airspace" means the land area underlying the airspace that is designated for training, research, development, or evaluation for a military service, as that land area is established by the United States Department of Defense Flight Information Publication, "Area Planning: Special Use Airspace: North and South America (AP/1A)" published by the United States National Imagery and Mapping Agency, or its successor, as of the date the military service gives written notification to a lead agency pursuant to subdivision (b).

(b) A military service may give written notification to a lead agency of the specific boundaries of a low-level flight path, military impact zone, or special use airspace, and provide the lead agency, in writing, the military contact office and address for the military service. If the notice references the specific boundaries of a low-level flight path, such notification must include a copy of the applicable United States Department of Defense Flight Information Publication, "Area Planning Military Training Routes: North and South America (AP/1B)." If the notice references the specific boundaries of a special use airspace, such notification must include a copy of the applicable United States Department of Defense Flight Information Publication, "Area Planning: Special Use Airspace: North and South America (AP/1A)."

(c) If a military service provides the written notification specified in subdivision (b) of this section, a lead agency must include the specified military contact office in the list of organizations and individuals receiving a notice of intent to adopt a negative declaration or a mitigated negative

declaration pursuant to Section 15072, in the list of organizations and individuals receiving a notice of preparation of an EIR pursuant to Section 15082, and in the list of organizations and individuals receiving a notice of availability of a draft EIR pursuant to Section 15087 for any project that meets all of the criteria specified below:

(1) The project to be carried out or approved by the lead agency is within the boundaries specified in subdivision (b).

(2) The project is one of the following:

(A) a project that includes a general plan amendment; or

(B) a project that is of statewide, regional, or areawide significance; or

(C) a project that relates to a public use airport and the area surrounding such airport which is required to be referred to the airport land use commission, or appropriately designated body, pursuant to Sections 21670–21679.5 of the Public Utilities Code.

(3) The project is not one of the actions described below. A lead agency does not need to send to the specified military contact office a notice of intent to adopt a negative declaration or a mitigated negative declaration, a notice of preparation of an EIR, or a notice of availability of a draft EIR for such actions.

(A) a response action taken pursuant to Chapter 6.8 (commencing with Section 25300) of Division 20 of the Health and Safety Code.

(B) a response action taken pursuant to Chapter 6.85 (commencing with Section 25396) of Division 20 of the Health and Safety Code.

(C) a project undertaken at a site in response to a corrective action order issued pursuant to Section 25187 of the Health and Safety Code.

The lead agency shall send the specified military contact office a notice of intent or a notice of availability sufficiently prior to adoption or certification of the environmental documents by the lead agency to allow the military service the review period provided under Section 15105.

(d) The effect or potential effect that a project may have on military activities does not itself constitute an adverse effect on the environment for the purposes of CEQA.

Note: Authority cited: Section 21083, Public Resources Code. Reference: Section 21098, Public Resources Code. § 15190.5.

Article 12.5 Exemptions for Agricultural Housing, Affordable Housing, and Residential Infill Projects

SECTIONS 15191 TO 15196

15191. DEFINITIONS

For purposes of this Article 12.5 only, the following words shall have the following meanings:

(a) "Agricultural employee" means a person engaged in agriculture, including: farming in all its branches, and, among other things, includes: (1) the cultivation and tillage of the soil, (2) dairying, (3) the production, cultivation, growing, and harvesting of any agricultural or horticultural commodities (including commodities defined as agricultural commodities in Section 1141j(g) of Title 12 of the United States Code), (4) the raising of livestock, bees, furbearing animals, or poultry, and (5) any practices (including any forestry or lumbering operations) performed by a farmer or on a farm as an incident to or in conjunction with such farming operations, including preparation for market and delivery to storage or to market or to carriers for transportation to market. This definition is subject to the following limitations:

This definition shall not be construed to include any person other than those employees excluded from the coverage of the National Labor Relations Act, as amended, as agricultural employees, pursuant to Section 2(3) of the Labor Management Relations Act (Section 152(3), Title 29, United States Code), and Section 3(f) of the Fair Labor Standards Act (Section 203(f), Title 29, United States Code).

This definition shall not apply, or be construed to apply, to any employee who performs work to be done at the site of the construction, alteration, painting, or repair of a building, structure, or other work (as these terms have been construed under Section 8(e) of the Labor Management Relations Act, 29 U.S.C. Sec. 158(e)) or logging or timber-clearing operations in initial preparation of land for farming, or who does land leveling or only land surveying for any of the above. As used in this definition, "land leveling" shall include only major land moving operations changing the contour of the land, but shall not include annual or seasonal tillage or preparation of land for cultivation.

(b) "Census-defined place" means a specific unincorporated land area within boundaries determined by the United States Census Bureau in the most recent decennial census.

(c) "Community-level environmental review" means either of the following:

(1) An EIR certified on any of the following:

(A) A general plan.

(B) A revision or update to the general plan that includes at least the land use and circulation elements.

(C) An applicable community plan.

(D) An applicable specific plan.

(E) A housing element of the general plan, if the environmental impact report analyzed the environmental effects of the density of the proposed project.

(2) A negative declaration or mitigated negative declaration adopted as a subsequent environmental review document, following and based upon an EIR on a general plan, an applicable community plan, or an applicable specific plan, provided that the subsequent environmental review document is allowed by CEQA following a master EIR or a program EIR, or is required pursuant to Section 21166.

(d) "Developed open space" means land that meets all of the following criteria:

(1) land that is publicly owned, or financed in whole or in part by public funds,

(2) is generally open to, and available for use by, the public, and

(3) is predominantly lacking in structural development other than structures associated with open spaces, including, but not limited to, playgrounds, swimming pools, ball fields, enclosed child play areas, and picnic facilities.

Developed open space may include land that has been designated for acquisition by a public agency for developed open space but does not include lands acquired by public funds dedicated to the acquisition of land for housing purposes.

(e) "Infill site" means a site in an urbanized area that meets one of the following criteria:

(1) The site has been previously developed for qualified urban uses; or

(2) The site has not been developed for qualified urban uses but all immediately adjacent parcels are developed with existing qualified urban uses; or

(3) The site has not been developed for qualified urban uses, no parcel within the site has been created within the past 10 years, and the site is situated so that:

(A) at least 75 percent of the perimeter of the site is adjacent to parcels that are developed with existing qualified urban uses at the time the lead agency receives an application for an approval; and

(B) the remaining 25 percent of the perimeter of the site adjoins parcels that had been previously developed for qualified urban uses.

(f) "Low- and moderate-income households" means "persons and families of low or moderate income" as defined in Section 50093 of the Health and Safety Code to mean persons and families whose income does not exceed 120 percent of area median income, adjusted for family size by the Department of Housing and Community Development, in accordance with adjustment factors adopted and amended from time to time by the United States Department of Housing and Urban Development pursuant to Section 8 of the United States Housing Act of 1937.

(g) "Low-income households" means households of persons and families of very low and low income, which are defined in Sections 50093 and 50105 of the Health and Safety Code as follows:

(1) "Persons and families of low income" or "persons of low income" is defined in Section 50093 of the Health & Safety Code to mean persons or families who are eligible for financial assistance specifically provided by a governmental agency for the benefit of occupants of housing financed pursuant to this division.

(2) "Very low income households" is defined in Section 50105 of the Health & Safety Code to mean persons and families whose incomes do not exceed the qualifying limits for very low income families as established and amended from time to time pursuant to Section 8 of the United States Housing Act of 1937. "Very low income households" includes extremely low income households, as defined in Section 50106 of the Health & Safety Code.

(h) "Lower income households" is defined in Section 50079.5 of the Health and Safety Code to mean any of the following:

(1) "Lower income households," which means persons and families whose income does not exceed the qualifying limits for lower income families as established and amended from time to time pursuant to Section 8 of the United States Housing Act of 1937.

(2) "Very low income households," which means persons and families whose incomes do not exceed the qualifying limits for very low income families as established and amended from time to time pursuant to Section 8 of the United States Housing Act of 1937.

(3) "Extremely low income households," which means persons and families whose incomes do not exceed the qualifying limits for extremely low income families as established and amended from time to time by the Secretary of Housing and Urban Development and defined in Section 5.603(b) of Title 24 of the Code of Federal Regulations.

(i) "Major transit stop" means a site containing an existing rail transit station, a ferry terminal served by either a bus or rail transit service, or the intersection of two or more major bus routes with a frequency of service interval of 15 minutes or less during the morning and afternoon peak commute periods.

(j) "Project-specific effect" means all the direct or indirect environmental effects of a project other than cumulative effects and growth-inducing effects.

(k) "Qualified urban use" means any residential, commercial, public institutional, transit or transportation passenger facility, or retail use, or any combination of those uses.

(l) "Residential" means a use consisting of either of the following:

(1) Residential units only.

(2) Residential units and primarily neighborhood-serving goods, services, or retail uses that do not exceed 15 percent of the total floor area of the project.

(m) "Urbanized area" means either of the following:

(1) An incorporated city that either by itself or in combination with two contiguous incorporated cities has a population of at least 100,000 persons; or

(2) An unincorporated area that meets the requirements set forth in subdivision (m)(2)(A) and subdivision (m)(2)(B) below.

(A) The unincorporated area must meet one of the following location or density requirements:

1. The unincorporated area must be: (i) completely surrounded by one or more incorporated cities, (ii) have a population of at least 100,000 persons either by itself or in combination with the surrounding incorporated city or cities, and (iii) have a population density that at least equals the population density of the surrounding city or cities; or

2. The unincorporated area must be located within an urban growth boundary and have an existing residential population of at least 5,000 persons per square mile. For purposes of this subparagraph, an "urban growth boundary" means a provision of a locally adopted general plan that allows urban uses on one side of the boundary and prohibits urban uses on the other side.

(B) The board of supervisors with jurisdiction over the unincorporated area must have taken the following steps:

1. The board has prepared a draft document by which the board would find that the general plan, zoning ordinance, and related policies and programs applicable to the unincorporated area are consistent with principles that: (i) encourage compact development in a manner that promotes efficient transportation systems, economic growth, affordable housing, energy efficiency, and an appropriate balance of jobs and housing, and (ii) protects the environment, open space, and agricultural areas.

2. The board has submitted the draft document to OPR and allowed OPR thirty days to submit comments on the draft findings to the board.

3. No earlier than thirty days after submitting the draft document to OPR, the board has adopted a final finding in substantial conformity with the draft finding described in the draft document referenced in subdivision (m)(2)(B)(1) above.

Note: Authority cited: Section 21083, Public Resources Code. Reference: Sections 21159.20, 21159.21, 21159.22, 21159.23, 21159.24, Public Resources Code.

15192. THRESHOLD REQUIREMENTS FOR EXEMPTIONS FOR AGRICULTURAL HOUSING, AFFORDABLE HOUSING, AND RESIDENTIAL INFILL PROJECTS

In order to qualify for an exemption set forth in sections 15193, 15194 or 15195, a housing project must meet all of the threshold criteria set forth below.

(a) The project must be consistent with:

(1) Any applicable general plan, specific plan, or local coastal program, including any mitigation measures required by such plan or program, as that plan or program existed on the date that the application for the project pursuant to Section 65943 of the Government Code was deemed complete; and

(2) Any applicable zoning ordinance, as that zoning ordinance existed on the date that the application for the project pursuant to Section 65943 of the Government Code was deemed

complete, unless the zoning of project property is inconsistent with the general plan because the project property has not been rezoned to conform to the general plan.

(b) Community-level environmental review has been adopted or certified.

(c) The project and other projects approved prior to the approval of the project can be adequately served by existing utilities, and the project applicant has paid, or has committed to pay, all applicable in-lieu or development fees.

(d) The site of the project:

(1) Does not contain wetlands, as defined in Section 328.3 of Title 33 of the Code of Federal Regulations.

(2) Does not have any value as an ecological community upon which wild animals, birds, plants, fish, amphibians, and invertebrates depend for their conservation and protection.

(3) Does not harm any species protected by the federal Endangered Species Act of 1973 (16 U.S.C. Sec. 1531 et seq.) or by the Native Plant Protection Act (Chapter 10 (commencing with Section 1900) of Division 2 of the Fish and Game Code), the California Endangered Species Act (Chapter 1.5 (commencing with Section 2050) of Division 3 of the Fish and Game Code.

(4) Does not cause the destruction or removal of any species protected by a local ordinance in effect at the time the application for the project was deemed complete.

(e) The site of the project is not included on any list of facilities and sites compiled pursuant to Section 65962.5 of the Government Code.

(f) The site of the project is subject to a preliminary endangerment assessment prepared by a registered environmental assessor to determine the existence of any release of a hazardous substance on the site and to determine the potential for exposure of future occupants to significant health hazards from any nearby property or activity. In addition, the following steps have been taken in response to the results of this assessment:

(1) If a release of a hazardous substance is found to exist on the site, the release shall be removed, or any significant effects of the release shall be mitigated to a level of insignificance in compliance with state and federal requirements.

(2) If a potential for exposure to significant hazards from surrounding properties or activities is found to exist, the effects of the potential exposure shall be mitigated to a level of insignificance in compliance with state and federal requirements.

(g) The project does not have a significant effect on historical resources pursuant to Section 21084.1 of the Public Resources Code.

(h) The project site is not subject to wildland fire hazard, as determined by the Department of Forestry and Fire Protection, unless the applicable general plan or zoning ordinance contains provisions to mitigate the risk of a wildland fire hazard.

(i) The project site does not have an unusually high risk of fire or explosion from materials stored or used on nearby properties.

(j) The project site does not present a risk of a public health exposure at a level that would exceed the standards established by any state or federal agency.

(k) Either the project site is not within a delineated earthquake fault zone or a seismic hazard zone, as determined pursuant to Section 2622 and 2696 of the Public Resources Code respectively, or the applicable general plan or zoning ordinance contains provisions to mitigate the risk of an earthquake or seismic hazard.

(l) Either the project site does not present a landslide hazard, flood plain, flood way, or restriction zone, or the applicable general plan or zoning ordinance contains provisions to mitigate the risk of a landslide or flood.

(m) The project site is not located on developed open space.

(n) The project site is not located within the boundaries of a state conservancy.

(o) The project has not been divided into smaller projects to qualify for one or more of the exemptions set forth in sections 15193 to 15195.

Note: Authority cited: Section 21083, Public Resources Code. Reference: Section 21159.21, 21159.27, Public Resources Code.

15193. AGRICULTURAL HOUSING EXEMPTION

CEQA does not apply to any development project that meets the following criteria.

(a) The project meets the threshold criteria set forth in section 15192.

(b) The project site meets the following size criteria:

(1) The project site is located in an area with a population density of at least 1,000 persons per square mile and is two acres or less in area; or

(2) The project site is located in an area with a population density of less than 1,000 persons per square mile and is five acres or less in area.

(c) The project meets the following requirements regarding location and number of units.

(1) If the proposed development project is located on a project site within city limits or in a census-defined place, it must meet the following requirements:

(A) The proposed project location must be within one of the following:

1. Incorporated city limits; or
2. A census defined place with a minimum population density of at least 5,000 persons per square mile; or
3. A census-defined place with a minimum population density of at least 1,000 persons per square mile, unless a public agency that is carrying out or approving the project determines that there is a reasonable possibility that the project, if completed, would have a significant effect on the environment due to unusual circumstances or that the cumulative impacts of successive projects of the same type in the same area, over time, would be significant.

(B) The proposed development project must be located on a project site that is adjacent, on at least two sides, to land that has been developed.

(C) The proposed development project must meet either of the following requirements:

1. Consist of not more than 45 units, or
2. Consist of housing for a total of 45 or fewer agricultural employees if the housing consists of dormitories, barracks, or other group living facilities.

(2) If the proposed development project is located on a project site zoned for general agricultural use, it must meet either of the following requirements:

(A) Consist of not more than 20 units, or

(B) Consist of housing for a total of 20 or fewer agricultural employees if the housing consists of dormitories, barracks, or other group living facilities.

(d) The project meets the following requirements regarding provision of housing for agricultural employees:

(1) The project must consist of the construction, conversion, or use of residential housing for agricultural employees.

(2) If the project lacks public financial assistance, then:

(A) The project must be affordable to lower income households; and

(B) The developer of the development project must provide sufficient legal commitments to the appropriate local agency to ensure the continued availability and use of the housing units for lower income households for a period of at least 15 years.

(3) If public financial assistance exists for the project, then:

(A) The project must be housing for very low, low-, or moderate-income households; and

(B) The developer of the development project must provide sufficient legal commitments to the appropriate local agency to ensure the continued availability and use of the housing units for low- and moderate-income households for a period of at least 15 years.

Note: Authority cited: Section 21083, Public Resources Code. Reference: Section 21159.22, Public Resources Code.

15194. AFFORDABLE HOUSING EXEMPTION

CEQA does not apply to any development project that meets the following criteria:

(a) The project meets the threshold criteria set forth in section 15192.

(b) The project meets the following size criteria: the project site is not more than five acres in area.

(c) The project meets both of the following requirements regarding location:

(1) The project meets one of the following location requirements relating to population density:

(A) The project site is located within an urbanized area or within a census-defined place with a population density of at least 5,000 persons per square mile.

(B) If the project consists of 50 or fewer units, the project site is located within an incorporated city with a population density of at least 2,500 persons per square mile and a total population of at least 25,000 persons.

(C) The project is located within either an incorporated city or a census defined place with a population density of at least 1,000 persons per square mile and there is no reasonable possibility that the project would have a significant effect on the environment or the residents of the project due to unusual circumstances or due to the related or cumulative impacts of reasonably foreseeable projects in the vicinity of the project.

(2) The project meets one of the following site-specific location requirements:

(A) The project site has been previously developed for qualified urban uses; or

(B) The parcels immediately adjacent to the project site are developed with qualified urban uses.

(C) The project site has not been developed for urban uses and all of the following conditions are met:

1. No parcel within the site has been created within 10 years prior to the proposed development of the site.
2. At least 75 percent of the perimeter of the site adjoins parcels that are developed with qualified urban uses.
3. The existing remaining 25 percent of the perimeter of the site adjoins parcels that have previously been developed for qualified urban uses.

(d) The project meets both of the following requirements regarding provision of affordable housing.

(1) The project consists of the construction, conversion, or use of residential housing consisting of 100 or fewer units that are affordable to low-income households.

(2) The developer of the project provides sufficient legal commitments to the appropriate local agency to ensure the continued availability and use of the housing units for lower income households for a period of at least 30 years, at monthly housing costs deemed to be

"affordable rent" for lower income, very low income, and extremely low income households, as determined pursuant to Section 50053 of the Health and Safety Code.

Note: Authority cited: Section 21083, Public Resources Code. Reference: Section 21159.23, Public Resources Code.

15195. RESIDENTIAL INFILL EXEMPTION

(a) Except as set forth in subdivision (b), CEQA does not apply to any development project that meets the following criteria:

(1) The project meets the threshold criteria set forth in section 15192; provided that with respect to the requirement in section 15192(b) regarding community-level environmental review, such review must be certified or adopted within five years of the date that the lead agency deems the application for the project to be complete pursuant to Section 65943 of the Government Code.

(2) The project meets both of the following size criteria:

(A) The site of the project is not more than four acres in total area.

(B) The project does not include any single level building that exceeds 100,000 square feet.

(3) The project meets both of the following requirements regarding location:

(A) The project is a residential project on an infill site.

(B) The project is within one-half mile of a major transit stop.

(4) The project meets both of the following requirements regarding number of units:

(A) The project does not contain more than 100 residential units.

(B) The project promotes higher density infill housing. The lead agency may establish its own criteria for determining whether the project promotes higher density infill housing except in either of the following two circumstances:

1. A project with a density of at least 20 units per acre is conclusively presumed to promote higher density infill housing.

2. A project with a density of at least 10 units per acre and a density greater than the average density of the residential properties within 1,500 feet shall be presumed to promote higher density infill housing unless the preponderance of the evidence demonstrates otherwise.

(5) The project meets the following requirements regarding availability of affordable housing: The project would result in housing units being made available to moderate, low or very low income families as set forth in either A or B below:

(A) The project meets one of the following criteria, and the project developer provides sufficient legal commitments to the appropriate local agency to ensure the continued availability and use of the housing units as set forth below at monthly housing costs determined pursuant to paragraph (3) of subdivision (h) of Section 65589.5 of the Government Code.

1. At least 10 percent of the housing is sold to families of moderate income, or

2. Not less than 10 percent of the housing is rented to families of low income, or

3. Not less than 5 percent of the housing is rented to families of very low income.

(B) If the project does not result in housing units being available as set forth in subdivision (A) above, then the project developer has paid or will pay in-lieu fees pursuant to a local ordinance in an amount sufficient to result in the development of an equivalent number of units that would otherwise be required pursuant to subparagraph (A).

(b) A project that otherwise meets the criteria set forth in subdivision (a) is not exempt from CEQA if any of the following occur:

(1) There is a reasonable possibility that the project will have a project-specific, significant effect on the environment due to unusual circumstances.

(2) Substantial changes with respect to the circumstances under which the project is being undertaken that are related to the project have occurred since community-level environmental review was certified or adopted.

(3) New information becomes available regarding the circumstances under which the project is being undertaken and that is related to the project that was not known, and could not have been known at the time that community-level environmental review was certified or adopted.

If a project is not exempt from CEQA due to subdivision (b), the analysis of the environmental effects of the project covered in the EIR or the negative declaration shall be limited to an analysis of the project-specific effect of the projects and any effects identified pursuant to subdivisions (b)(2) and (3).

Note: Authority cited: Section 21083, Public Resources Code. Reference: Section 21159.24, Public Resources Code.

15196. NOTICE OF EXEMPTION FOR AGRICULTURAL HOUSING, AFFORDABLE HOUSING, AND RESIDENTIAL INFILL PROJECTS

(a) When a local agency determines that a project is not subject to CEQA under Section 15193, 15194, or 15195, and it approves or determines to carry out that project, the local agency or person seeking project approval shall file the notice required by Section 21152.1 of the Public Resources Code, pursuant to Section 15062.

(b) Failure to file the notice required by this section does not affect the validity of a project.

(c) Nothing in this section affects the time limitations contained in Section 21167.

Note: Authority cited: Section 21083, Public Resources Code. Reference: 21152.1, Public Resources Code.

Article 13. Review and Evaluation of EIRs and Negative Declarations

SECTIONS 15200 TO 15209

15200. PURPOSES OF REVIEW

The purposes of review of EIRs and Negative Declarations include:

(a) Sharing expertise,

(b) Disclosing agency analyses,

(c) Checking for accuracy,

(d) Detecting omissions,

(e) Discovering public concerns, and

(f) Soliciting counter proposals.

Note: Authority cited: Section 21083, Public Resources Code; Reference: Sections 21000, 21108, and 21152, Public Resources Code; *Environmental Defense Fund v. Coastside County Water District*, (1972) 27 Cal. App. 3d 695; *County of Inyo v. City of Los Angeles*, (1977) 71 Cal. App. 3d 185.

15201. PUBLIC PARTICIPATION

Public participation is an essential part of the CEQA process. Each public agency should include provisions in its CEQA procedures for wide public involvement, formal and informal, consistent with its existing activities and procedures, in order to receive and evaluate public reactions to environmental issues related to the agency's activities. Such procedures should include, whenever possible, making environmental information available in electronic format on the Internet, on a web site maintained or utilized by the public agency.

Note: Authority cited: Section 21083, Public Resources Code; Reference: Sections 21000, 21082, 21108, and 21152, Public Resources Code; *Environmental Defense Fund v. Coastside County Water District*, (1972) 27 Cal. App. 3d 695; *People v. County of Kern*, (1974) 39 Cal. App. 3d 830; *County of Inyo v. City of Los Angeles*, (1977) 71 Cal. App. 3d 185.

15202. PUBLIC HEARINGS

(a) CEQA does not require formal hearings at any stage of the environmental review process. Public comments may be restricted to written communication.

(b) If an agency provides a public hearing on its decision to carry out or approve a project, the agency should include environmental review as one of the subjects for the hearing.

(c) A public hearing on the environmental impact of a project should usually be held when the Lead Agency determines it would facilitate the purposes and goals of CEQA to do so. The hearing may be held in conjunction with and as a part of normal planning activities.

(d) A draft EIR or Negative Declaration should be used as a basis for discussion at a public hearing. The hearing may be held at a place where public hearings are regularly conducted by the Lead Agency or at another location expected to be convenient to the public.

(e) Notice of all public hearings shall be given in a timely manner. This notice may be given in the same form and time as notice for other regularly conducted public hearings of the public agency. To the extent that the public agency maintains an Internet web site, notice of all public hearings should be made available in electronic format on that site.

(f) A public agency may include, in its implementing procedures, procedures for the conducting of public hearings pursuant to this section. The procedures may adopt existing notice and hearing requirements of the public agency for regularly conducted legislative, planning, and other activities.

(g) There is no requirement for a public agency to conduct a public hearing in connection with its review of an EIR prepared by another public agency.

Note: Authority cited: Section 21083, Public Resources Code; Reference: Sections 21000, 21082, 21108, and 21152, Public Resources Code; *Concerned Citizens of Palm Desert, Inc. v. Board of Supervisors*, (1974) 38 Cal. App. 3d 272.

15203. ADEQUATE TIME FOR REVIEW AND COMMENT

The Lead Agency shall provide adequate time for other public agencies and members of the public to review and comment on a draft EIR or Negative Declaration that it has prepared.

(a) Public agencies may establish time periods for review in their implementing procedures and shall notify the public and reviewing agencies of the time for receipt of comments on EIRs. These time periods shall be consistent with applicable statutes, the State CEQA Guidelines, and applicable Clearinghouse review periods.

(b) A review period for an EIR does not require a halt in other planning or evaluation activities related to a project. Planning should continue in conjunction with environmental evaluation.

Note: Authority cited: Section 21083, Public Resources Code; Reference: Sections 21082, 21108 and 21152, Public Resources Code. Formerly Sections 15160(a) and (e).

15204. FOCUS OF REVIEW

(a) In reviewing draft EIRs, persons and public agencies should focus on the sufficiency of the document in identifying and analyzing the possible impacts on the environment and ways in which the significant effects of the project might be avoided or mitigated. Comments are most helpful when they suggest additional specific alternatives or mitigation measures that would provide better ways to avoid or mitigate the significant environmental effects. At the same time, reviewers should be aware that the adequacy of an EIR is determined in terms of what is reasonably feasible, in light of factors such as the magnitude of the project at issue, the severity of its likely environmental impacts, and the geographic scope of the project. CEQA does not require a lead agency to conduct every test or perform all research, study, and experimentation recommended or demanded by commentors. When responding to comments, lead agencies need only respond to significant environmental issues and do not need to provide all information requested by reviewers, as long as a good faith effort at full disclosure is made in the EIR.

(b) In reviewing negative declarations, persons and public agencies should focus on the proposed finding that the project will not have a significant effect on the environment. If persons and public agencies believe that the project may have a significant effect, they should:

  (1) Identify the specific effect,

  (2) Explain why they believe the effect would occur, and

  (3) Explain why they believe the effect would be significant.

(c) Reviewers should explain the basis for their comments, and should submit data or references offering facts, reasonable assumptions based on facts, or expert opinion supported by facts in support of the comments. Pursuant to Section 15064, an effect shall not be considered significant in the absence of substantial evidence.

(d) Reviewing agencies or organizations should include with their comments the name of a contact person who would be available for later consultation if necessary. Each responsible agency and trustee agency shall focus its comments on environmental information germane to that agency's statutory responsibility.

(e) This section shall not be used to restrict the ability of reviewers to comment on the general adequacy of a document or of the lead agency to reject comments not focused as recommended by this section.

(f) Prior to the close of the public review period for an EIR or mitigated negative declaration, a responsible or trustee agency which has identified significant effects on the environment may submit to the lead agency proposed mitigation measures which would address those significant effects. Any such measures shall be limited to impacts affecting those resources which are subject to the statutory authority of that agency. If mitigation measures are submitted, the responsible or trustee agency shall either submit to the lead agency complete and detailed performance objectives for the mitigation measures, or shall refer the lead agency to appropriate, readily available guidelines or reference documents which meet the same purpose.

Note: Authority cited: Section 21083, Public Resources Code. Reference: Sections 21080, 21081.6, and 21080.4, 21104 and 21153, Public Resources Code, Formerly Section 15161; *San Joaquin Raptor/Wildlife Rescue Center v. County of Stanislaus* (1996) 42 Cal.App.4th 608; and *Leonoff v. Monterey County Board of Supervisors* (1990) 222 Cal.App.3d 1337.

15205. REVIEW BY STATE AGENCIES

(a) Draft EIRs and negative declarations to be reviewed by state agencies shall be submitted to the State Clearinghouse, 1400 Tenth Street, Sacramento, California 95814. For U.S. Mail, submit to P.O. Box 3044, Sacramento, California 95812-3044. When submitting such documents to

the State Clearinghouse, the public agency shall include, in addition to the printed copy, a copy of the document in electronic form on a diskette or by electronic mail transmission, if available.

(b) The following environmental documents shall be submitted to the State Clearinghouse for review by state agencies:

(1) Draft EIRs and Negative Declarations prepared by a state agency where such agency is a Lead Agency.

(2) Draft EIRs and Negative Declarations prepared by a public agency where a state agency is a Responsible Agency, Trustee Agency, or otherwise has jurisdiction by law with respect to the project.

(3) Draft EIRs and Negative Declarations on projects identified in Section 15206 as being of statewide, regional, or areawide significance.

(4) Draft EISs, environmental assessments, and findings of no significant impact prepared pursuant to NEPA, the Federal Guidelines (Title 40 CFR, Part 1500, commencing with Section 1500.1).

(c) Public agencies may send environmental documents to the State Clearinghouse for review where a state agency has special expertise with regard to the environmental impacts involved. The areas of statutory authorities of state agencies are identified in Appendix B. Any such environmental documents submitted to the State Clearinghouse shall include, in addition to the printed copy, a copy of the document in electronic format, on a diskette or by electronic mail transmission, if available.

(d) When an EIR or Negative Declaration is submitted to the State Clearinghouse for review, the review period set by the Lead Agency shall be at least as long as the period provided in the state review system operated by the State Clearinghouse. In the state review system, the normal review period is 45 days for EIRs and 30 days for Negative Declarations. In exceptional circumstances, the State Clearinghouse may set shorter review periods when requested by the Lead Agency.

(e) A sufficient number of copies of an EIR, negative declaration, or mitigated negative declaration, shall be submitted to the State Clearinghouse for review and comment by state agencies. The notice of completion form required by the State Clearinghouse must be submitted together with the copies of the EIR and may be submitted together with the copies of the negative declaration or mitigated negative declaration. The notice of completion form required by the State Clearinghouse is included in Appendix C. If the lead agency uses the on-line process for submittal of the notice of completion form to the State Clearinghouse, the form generated from the Internet shall satisfy this requirement (refer to www.ceqanet.ca.gov.).

(f) While the Lead Agency is encouraged to contact the regional and district offices of state Responsible Agencies, the Lead Agency must, in all cases, submit documents to the State Clearinghouse for distribution in order to comply with the review requirements of this section.

Note: Authority cited: Section 21083, Public Resources Code. Reference: Section 21083, 21091, 21104, and 21153, Public Resources Code.

15206. PROJECTS OF STATEWIDE, REGIONAL, OR AREAWIDE SIGNIFICANCE

(a) Projects meeting the criteria in this section shall be deemed to be of statewide, regional, or areawide significance.

(1) A draft EIR or negative declaration prepared by any public agency on a project described in this section shall be submitted to the State Clearinghouse and should be submitted also to the appropriate metropolitan area council of governments for review and comment. The notice of completion form required by the State Clearinghouse must be submitted together with the copies of the EIR and may be submitted together with the copies of the negative declaration. The notice of completion form required by the State Clearinghouse is included

in Appendix C. If the lead agency uses the on-line process for submittal of the notice of completion form to the State Clearinghouse, the form generated from the Internet shall satisfy this requirement (refer to www.ceqanet.ca.gov).

(2) When such documents are submitted to the State Clearinghouse, the public agency shall include, in addition to the printed copy, a copy of the document in electronic format on a diskette or by electronic mail transmission, if available.

(b) The Lead Agency shall determine that a proposed project is of statewide, regional, or areawide significance if the project meets any of the following criteria:

(1) A proposed local general plan, element, or amendment thereof for which an EIR was prepared. If a Negative Declaration was prepared for the plan, element, or amendment, the document need not be submitted for review.

(2) A project has the potential for causing significant effects on the environment extending beyond the city or county in which the project would be located. Examples of the effects include generating significant amounts of traffic or interfering with the attainment or maintenance of state or national air quality standards. Projects subject to this subdivision include:

(A) A proposed residential development of more than 500 dwelling units.

(B) A proposed shopping center or business establishment employing more than 1,000 persons or encompassing more than 500,000 square feet of floor space.

(C) A proposed commercial office building employing more than 1,000 persons or encompassing more than 250,000 square feet of floor space.

(D) A proposed hotel/motel development of more than 500 rooms.

(E) A proposed industrial, manufacturing, or processing plant, or industrial park planned to house more than 1,000 persons, occupying more than 40 acres of land, or encompassing more than 650,000 square feet of floor area.

(3) A project which would result in the cancellation of an open space contract made pursuant to the California Land Conservation Act of 1965 (Williamson Act) for any parcel of 100 or more acres.

(4) A project for which an EIR and not a Negative Declaration was prepared which would be located in and would substantially impact the following areas of critical environmental sensitivity:

(A) The Lake Tahoe Basin.

(B) The Santa Monica Mountains Zone as defined by Section 33105 of the Public Resources Code.

(C) The California Coastal Zone as defined in, and mapped pursuant to, Section 30103 of the Public Resources Code.

(D) An area within 1/4 mile of a wild and scenic river as defined by Section 5093.5 of the Public Resources Code.

(E) The Sacramento-San Joaquin Delta, as defined in Water Code Section 12220.

(F) The Suisun Marsh as defined in Public Resources Code Section 29101.

(G) The jurisdiction of the San Francisco Bay Conservation and Development Commission as defined in Government Code Section 66610.

(5) A project which would substantially affect sensitive wildlife habitats including but not limited to riparian lands, wetlands, bays, estuaries, marshes, and habitats for endangered, rare and threatened species as defined by Section 15380 of this Chapter.

(6) A project which would interfere with attainment of regional water quality standards as stated in the approved areawide waste treatment management plan.

(7) A project which would provide housing, jobs, or occupancy for 500 or more people within 10 miles of a nuclear power plant.

Note: Authority cited: Section 21083, Public Resources Code. Reference: Section 21083, Public Resources Code.

15207. FAILURE TO COMMENT

If any public agency or person who is consulted with regard to an EIR or Negative Declaration fails to comment within a reasonable time as specified by the Lead Agency, it shall be assumed, without a request for a specific extension of time, that such agency or person has no comment to make. Although the Lead Agency need not respond to late comments, the Lead Agency may choose to respond to them.

Note: Authority cited: Section 21083, Public Resources Code; Reference: Sections 21104 and 21153, Public Resources Code; *Cleary v. County of Stanislaus*, (1981) 118 Cal. App. 3d 348. Formerly Section 15162.

15208. RETENTION AND AVAILABILITY OF COMMENTS

Comments received through the consultation process shall be retained for a reasonable period and available for public inspection at an address given in the final EIR. Comments which may be received on a draft EIR or Negative Declaration under preparation shall also be considered and kept on file.

Note: Authority cited: Section 21083, Public Resources Code; Reference: Sections 21104, 21082.1 and 21153, Public Resources Code; Section 4, Chapter 480, Statutes of 1981; *People v. County of Kern*, (1974) 39 Cal. App. 3d 830. Formerly Section 15166.

15209. COMMENTS ON INITIATIVE OF PUBLIC AGENCIES

Every public agency may comment on environmental documents dealing with projects which affect resources with which the agency has special expertise regardless of whether its comments were solicited or whether the effects fall within the legal jurisdiction of the agency.

Note: Authority cited: Section 21083, Public Resources Code; Reference: Sections 21002, 21104, and 21153, Public Resources Code.

Article 14. Projects Also Subject to the National Environmental Policy Act (NEPA)

SECTIONS 15220 TO 15229

15220. GENERAL

This article applies to projects that are subject to both CEQA and NEPA. NEPA applies to projects which are carried out, financed, or approved in whole or in part by federal agencies. Accordingly, this article applies to projects which involve one or more state or local agencies and one or more federal agencies.

Note: Authority cited: Section 21083, Public Resources Code; Reference: Sections 21083.5, 21083.6, and 21083.7, Public Resources Code; National Environmental Policy Act of 1969, Public Law 91–190 as amended, 42 U.S.C.A. 4321–4347; NEPA Regulations, 40 Code of Federal Regulations (C.F.R.) Parts 1500–1508.

15221. NEPA DOCUMENT READY BEFORE CEQA DOCUMENT

(a) When a project will require compliance with both CEQA and NEPA, state or local agencies should use the EIS or Finding of No Significant Impact rather than preparing an EIR or Negative Declaration if the following two conditions occur:

(1) An EIS or Finding of No Significant Impact will be prepared before an EIR or Negative Declaration would otherwise be completed for the project; and

(2) The EIS or Finding of No Significant Impact complies with the provisions of these Guidelines.

(b) Because NEPA does not require separate discussion of mitigation measures or growth inducing impacts, these points of analysis will need to be added, supplemented, or identified before the EIS can be used as an EIR.

Note: Authority cited: Section 21083, Public Resources Code; Reference: Sections 21083.5 and 21083.7, Public Resources Code; Section 102(2)(C) of NEPA, 43 U.S.C.A. 4322(2)(C).

15222. PREPARATION OF JOINT DOCUMENTS

If a Lead Agency finds that an EIS or Finding of No Significant Impact for a project would not be prepared by the federal agency by the time when the Lead Agency will need to consider an EIR or Negative Declaration, the Lead Agency should try to prepare a combined EIR-EIS or Negative Declaration-Finding of No Significant Impact. To avoid the need for the federal agency to prepare a separate document for the same project, the Lead Agency must involve the federal agency in the preparation of the joint document.

This involvement is necessary because federal law generally prohibits a federal agency from using an EIR prepared by a state agency unless the federal agency was involved in the preparation of the document.

Note: Authority cited: Section 21083, Public Resources Code; Reference: Sections 21083.5 and 21083.7, Public Resources Code; Section 102(2)(D) of NEPA, 43 U.S.C.A. 4322(2)(D); 40 C.F.R. Part 1506.2.

15223. CONSULTATION WITH FEDERAL AGENCIES

When it plans to use an EIS or Finding of No Significant Impact or to prepare such a document jointly with a federal agency, the Lead Agency shall consult as soon as possible with the federal agency.

Note: Authority cited: Section 21083, Public Resources Code; Reference: Sections 21083.5 and 21083.7, Public Resources Code.

15224. TIME LIMITS

Where a project will be subject to both CEQA and the National Environmental Policy Act, the one year time limit and the 105-day time limit may be waived pursuant to Section 15110.

Note: Authority cited: Section 21083, Public Resources Code; Reference: Section 21083.6, Public Resources Code.

15225. CIRCULATION OF DOCUMENTS

(a) Where the federal agency circulated the EIS or Finding of No Significant Impact for public review as broadly as state or local law may require and gave notice meeting the standards in Section 15072(a) or 15087(a), the Lead Agency under CEQA may use the federal document in the place of an EIR or Negative Declaration without recirculating the federal document for public review. One review and comment period is enough. Prior to using the federal document in this situation, the Lead Agency shall give notice that it will use the federal document in the place of an EIR or Negative Declaration and that it believes that the federal document meets the

requirements of CEQA. The notice shall be given in the same manner as a notice of the public availability of a draft EIR under Section 15087.

(b) If an EIS has been prepared and filed pursuant to NEPA on the closure and reuse of a military base and the Lead Agency decides that the EIS does not fully meet the requirements of CEQA or has not been circulated for public review as state and local law may require, the Lead Agency responsible for preparation of an EIR for a reuse plan for the same base may proceed in the following manner:

(1) Prepare and circulate a notice of preparation pursuant to Section 15082. The notice shall include a description of the reuse plan, a copy of the EIS, an address to which to send comments, and the deadline for submitting comments. The notice shall state that the lead agency intends to utilize the EIS as a draft EIR and requests comments on whether the EIS provides adequate information to serve as a draft EIR and what specific additional information, if any, is necessary.

(2) Upon the close of the comment period, the lead agency may proceed with preparation and circulation for comment of the draft EIR for the reuse plan. To the greatest extent feasible, the lead agency shall avoid duplication and utilize the EIS or information in the EIS as all or part of the draft EIR. The EIR shall be completed in compliance with the provisions of CEQA.

Note: Authority cited: Section 21083, Public Resources Code; References: Sections 21083.5 and 21092, Public Resources Code.

15226. JOINT ACTIVITIES

State and local agencies should cooperate with federal agencies to the fullest extent possible to reduce duplication between the California Environmental Quality Act and the National Environmental Policy Act. Such cooperation should, to the fullest extent possible, include:

(a) Joint planning processes,

(b) Joint environmental research and studies,

(c) Joint public hearings,

(d) Joint environmental documents.

Note: Authority cited: Section 21083, Public Resources Code; Reference: Sections 21083.5 and 21083.7, Public Resources Code; 40 C.F.R. Part 1506.2. Formerly Section 15063(h).

15227. STATE COMMENTS ON A FEDERAL PROJECT

When a state agency officially comments on a proposed federal project which may have a significant effect on the environment, the comments shall include or reference a discussion of the material specified in Section 15126. An EIS on the federal project may be referenced to meet the requirements of this section.

Note: Authority cited: Section 21083, Public Resources Code; Reference: Section 21101, Public Resources Code.

15228. WHERE FEDERAL AGENCY WILL NOT COOPERATE

Where a federal agency will not cooperate in the preparation of joint document and will require separate NEPA compliance for the project at a later time, the state or local agency should persist in efforts to cooperate with the federal agency. Because NEPA expressly allows federal agencies to use environmental documents prepared by an agency of statewide jurisdiction, a local agency should try to involve a state agency in helping prepare an EIR or Negative Declaration for the project. In this way there will be a greater chance that the federal agency may later use the CEQA document and not require the applicant to pay for preparation of a second document to meet NEPA requirements at a later time.

Note: Authority cited: Section 21083, Public Resources Code; Reference: Section 21083.5, Public Resources Code; Section 102(2)(D) of NEPA, 42 U.S.C.A. 4322(2)(D).

15229. BASELINE ANALYSIS FOR MILITARY BASE REUSE PLAN EIRS

When preparing and certifying an EIR for a plan for the reuse of a military base, including when utilizing an Environmental Impact Statement pursuant to Section 21083.5 of the Public Resources Code, the determination of whether the reuse plan may have a significant effect on the environment may, at the discretion of the lead agency, be based upon the physical conditions which were present at the time that the federal decision for the closure or realignment of the base or reservation became final. These conditions shall be referred to as the "baseline physical conditions." Impacts which do not exceed the baseline physical conditions shall not be considered significant.

(a) Prior to circulating a draft EIR pursuant to the provisions of this Section, the lead agency shall do all of the following, in order:

(1) Prepare proposed baseline physical conditions, identify pertinent responsible and trustee agencies and consult with those agencies prior to the public hearing required by subdivision (a)(2) as to the application of their regulatory authority and permitting standards to the proposed baseline physical conditions, the proposed reuse plan, and specific, planned future nonmilitary land uses of the base or reservation. The affected agencies shall have not less than 30 days prior to the public hearing to review the proposed baseline physical conditions and the proposed reuse plan and to submit their comments to the lead agency.

(2) Hold a public hearing at which is discussed the federal EIS prepared for, or being prepared for, the closure or realignment of the military base or reservation. The discussion shall include the significant effects on the environment, if any, examined in the EIS, potential methods of mitigating those effects, including feasible alternatives, and the mitigative effects of federal, state, and local laws applicable to future nonmilitary activities. Prior to the close of the hearing, the lead agency shall specify whether it will adopt any of the baseline physical conditions for the reuse plan EIR and identify those conditions. The lead agency shall specify particular baseline physical conditions, if any, which it will examine in greater detail than they were examined in the EIS. Notice of the hearing shall be given pursuant to Section 15087. The hearing may be continued from time to time.

(3) Prior to the close of the hearing, the lead agency shall do all of the following:

(A) Specify the baseline physical conditions which it intends to adopt for the reuse plan EIR, and specify particular physical conditions, if any, which it will examine in greater detail than were examined in the EIS.

(B) State specifically how it intends to integrate its discussion of the baseline physical conditions in the EIR with the reuse planning process, taking into account the adopted environmental standards of the community, including but not limited to, the adopted general plan, specific plan or redevelopment plan, and including other applicable provisions of adopted congestion management plans, habitat conservation or natural communities conservation plans, air quality management plans, integrated waste management plans, and county hazardous waste management plans.

(C) State the specific economic or social reasons, including but not limited to, new job creation, opportunities for employment of skilled workers, availability of low and moderate-income housing, and economic continuity which support selection of the baseline physical conditions.

(b) An EIR prepared under this section should identify any adopted baseline physical conditions in the environmental setting section. The baseline physical conditions should be cited in discussions of effects. The no-project alternative analyzed in an EIR prepared under this section shall discuss the conditions on the base as they exist at the time of preparation, as well as what

could be reasonably expected to occur in the foreseeable future if the reuse plan were not approved, based on current plans and consistent with available infrastructure and services.

(c) All public and private activities taken pursuant to or in furtherance of a reuse plan for which an EIR was prepared and certified pursuant to this section shall be deemed to be a single project. A subsequent or supplemental EIR shall be required only if the lead agency determines that any of the circumstances described in Section 15162 or 15163 exist.

(d) Limitations:

(1) Nothing in this section shall in any way limit the scope of review or determination of significance of the presence of hazardous or toxic wastes, substances, and materials, including but not limited to, contaminated soils and groundwater. The regulation of hazardous or toxic wastes, substances, and materials shall not be constrained by this section.

(2) This section does not apply to hazardous waste regulation and remediation projects undertaken pursuant to Chapter 6.5 (commencing with Section 25100) or Chapter 6.8 (commencing with Section 25300) of Division 20 of the Health and Safety Code or pursuant to the Porter-Cologne Water Quality Control Act (Water Code Section 13000, et seq.)

(3) All subsequent development at the military base or reservation shall be subject to all applicable federal, state, or local laws, including but not limited to, those relating to air quality, water quality, traffic, threatened and endangered species, noise, and hazardous or toxic wastes, substances, or materials.

(e) "Reuse plan" means the initial plan for the reuse of military base adopted by a local government, including a redevelopment agency or joint powers authority, in the form of a general plan, general plan amendment, specific plan, redevelopment plan, or other planning document. For purposes of this section, a reuse plan also shall include a statement of development policies, a diagram or diagrams illustrating its provisions, including a designation of the proposed general distribution, location, and development intensity for housing, business, industry, open space, recreation, natural resources, public buildings and grounds, roads, and other transportation facilities, infrastructure, and other categories of proposed uses, whether public or private.

(f) This section may be applied to any reuse plan EIR for which a notice of preparation is issued within one year from the date that the federal record of decision was rendered for the military base or reservation closure or realignment and reuse, or prior to January 1, 1997, whichever is later, but only if the EIR is completed and certified within five years from the date that the federal record of decision was rendered.

Note: Authority cited: Section 21083, Public Resources Code; Reference: Section 21083.1, Public Resources Code.

Article 15. Litigation

SECTIONS 15230 TO 15233

15230. TIME LIMITS AND CRITERIA

Litigation under CEQA must be handled under the time limits and criteria described in Sections 21167 et seq. of the Public Resources Code and Section 15112 of these Guidelines in addition to provisions in this article.

Note: Authority cited: Section 21083, Public Resources Code; Reference: Sections 21167 et seq., Public Resources Code.

15231. ADEQUACY OF EIR OR NEGATIVE DECLARATION FOR USE BY RESPONSIBLE AGENCIES

A final EIR prepared by a Lead Agency or a Negative Declaration adopted by a Lead Agency shall be conclusively presumed to comply with CEQA for purposes of use by Responsible Agencies which were consulted pursuant to sections 15072 or 15082 unless one of the following conditions occurs:

(a) The EIR or Negative Declaration is finally adjudged in a legal proceeding not to comply with the requirements of CEQA, or

(b) A subsequent EIR is made necessary by Section 15162 of these Guidelines.

Note: Authority cited: Section 21083, Public Resources Code; Reference: Sections 21080.1, 21166, 21167.2, and 21167.3, Public Resources Code.

15232. REQUEST FOR HEARING

In a writ of mandate proceeding challenging approval of a project under CEQA, the petitioner shall, within 90 days of filing the petition, request a hearing or otherwise be subject to dismissal on the court's own motion or on the motion of any party to the suit.

Note: Authority cited: Section 21083, Public Resources Code; Reference: Section 21167.4, Public Resources Code.

15233. CONDITIONAL PERMITS

If a lawsuit is filed challenging an EIR or Negative Declaration for noncompliance with CEQA, Responsible Agencies shall act as if the EIR or Negative Declaration complies with CEQA and continue to process the application for the project according to the time limits for Responsible Agency action contained in Government Code Section 65952.

(a) If an injunction or a stay has been granted in the lawsuit prohibiting the project from being carried out, the Responsible Agency shall have authority only to disapprove the project or to grant a conditional approval of the project. A conditional approval shall constitute permission to proceed with a project only when the court action results in a final determination that the EIR or Negative Declaration does comply with the provisions of CEQA (Public Resources Code Section 21167.3(a)).

(b) If no injunction or stay is granted in the lawsuit, the Responsible Agency shall assume that the EIR or Negative Declaration fully meets the requirements of CEQA. The Responsible Agency shall approve or disapprove the project within the time limits described in Article 8, commencing with Section 15100, of these Guidelines and described in Government Code Section 65952. An approval granted by a Responsible Agency in this situation provides only permission to proceed with the project at the applicant's risk prior to a final decision in the lawsuit (Public Resources Code Section 21167.3(b)).

Note: Authority cited: Section 21083, Public Resources Code; Reference: Section 21167.3, Public Resources Code; *Kriebel v. City Council* (1980) 112 Cal. App. 3d 693.

Article 16. EIR Monitor

SECTION 15240

15240. EIR MONITOR

The Secretary for Resources may provide for publication of a bulletin entitled "California EIR Monitor" on a subscription basis to provide public notice of amendments to the Guidelines, the

completion of draft EIRs, and other matters as deemed appropriate. Inquiries and subscription requests should be sent to the following address:

Secretary for Resources Attention: California EIR Monitor 1416 Ninth Street, Room 1311 Sacramento, California 95814

Note: Authority cited: Section 21083, Public Resources Code; Reference: Section 21088, Public Resources Code.

Article 17. Exemption for Certified State Regulatory Programs

SECTIONS 15250 TO 15253

15250. GENERAL

Section 21080.5 of the Public Resources Code provides that a regulatory program of a state agency shall be certified by the Secretary for Resources as being exempt from the requirements for preparing EIRs, Negative Declarations, and Initial Studies if the Secretary finds that the program meets the criteria contained in that code section. A certified program remains subject to other provisions in CEQA such as the policy of avoiding significant adverse effects on the environment where feasible. This article provides information concerning certified programs.

Note: Authority cited: Section 21083, Public Resources Code; Reference: Section 21080.5, Public Resources Code.

15251. LIST OF CERTIFIED PROGRAMS

The following programs of state regulatory agencies have been certified by the Secretary for Resources as meeting the requirements of Section 21080.5:

(a) The regulation of timber harvesting operations by the California Department of Forestry and the State Board of Forestry pursuant to Chapter 8, commencing with Section 4511 of Part 2 of Division 4 of the Public Resources Code.

(b) The regulatory program of the Fish and Game Commission pursuant to the Fish and Game Code.

(c) The regulatory program of the California Coastal Commission and the regional coastal commissions dealing with the consideration and granting of coastal development permits under the California Coastal Act of 1976, Division 20 (commencing with Section 30000) of the Public Resources Code.

(d) That portion of the regulatory program of the Air Resources Board which involves the adoption, approval, amendment, or repeal of standards, rules, regulations, or plans to be used in the regulatory program for the protection and enhancement of ambient air quality in California.

(e) The regulatory program of the State Board of Forestry in adopting, amending, or repealing standards, rules, regulations, or plans under the Z'berg-Nejedly Forest Practice Act, Chapter 8 (commencing with Section 4511) of Part 2 of Division 4 of the Public Resources Code.

(f) The program of the California Coastal Commission involving the preparation, approval, and certification of local coastal programs as provided in Sections 30500 through 30522 of the Public Resources Code.

(g) The Water Quality Control (Basin)/208 Planning Program of the State Water Resources Control Board and the Regional Water Quality Control Boards.

(h) The permit and planning programs of the San Francisco Bay Conservation and Development Commission under the McAteer-Petris Act, Title 7.2 (commencing with Section 66600) of the Government Code; and the planning program of the San Francisco Bay Conservation and

Development Commission under the Suisun Marsh Preservation Act, Division 19 (commencing with Section 29000) of the Public Resources Code.

(i) The pesticide regulatory program administered by the Department of Pesticide Regulation and the county agricultural commissioners insofar as the program consists of:

(1) The registration, evaluation, and classification of pesticides.

(2) The adoption, amendment, or repeal of regulations and standards for the licensing and regulation of pesticide dealers and pest control operators and advisors.

(3) The adoption, amendment, or repeal of regulations for standards dealing with the monitoring of pesticides and of the human health and environmental effects of pesticides.

(4) The regulation of the use of pesticides in agricultural and urban areas of the state through the permit system administered by the county agricultural commissioners.

(j) The power plant site certification program of the State Energy Resources Conservation and Development Commission under Chapter 6 of the Warren-Alquist Act, commencing with Public Resources Code Section 25500.

(k) The regulatory program of the State Water Resources Control Board to establish instream beneficial use protection programs.

(l) That portion of the regulatory program of the South Coast Air Quality Management District which involves the adoption, amendment, and repeal of regulations pursuant to the provisions of the Health and Safety Code.

(m) The Program of the Delta Protection Commission involving the preparation and adoption of a Resources Management Plan for the Sacramento-San Joaquin Delta (Pub. Resources Code § 29760 ff.), and the Commission's review and action on general plan amendments proposed by local governments to make their plans consistent with the provisions of the Commission's Resource Management Plan (Pub. Resources Code § 29763.5).

(n) The program of the Department of Fish and Game for the adoption of regulations under the Fish and Game Code.

(o) The program of the Department of Fish and Game implementing the incidental take permit application process under the California Endangered Species Act ("CESA"), Fish and Game Code sections 2080 and 2081, and specifically the regulation governing the Department of Fish and Game's role as a "lead agency" when issuing incidental take permits, found at California Code of Regulations, Title 14, section 783.5(d).

(p) The regulatory program of the Department of Fish and Game for review and approval of voluntary local programs for routine and ongoing agricultural activities, as authorized by the California Endangered Species Act, Fish and Game Code section 2086.

Note: Authority cited: Sections 21083 and 21080.5, Public Resources Code; Reference: Section 21080.5, Public Resources Code.

15252. SUBSTITUTE DOCUMENT

(a) The document used as a substitute for an EIR or Negative Declaration in a certified program shall include at least the following items:

(1) A description of the proposed activity, and

(2) Either:

(A) Alternatives to the activity and mitigation measures to avoid or reduce any significant or potentially significant effects that the project might have on the environment, or

(B) A statement that the agency's review of the project showed that the project would not have any significant or potentially significant effects on the environment and therefore no alternatives or mitigation measures are proposed to avoid or reduce any significant

effects on the environment. This statement shall be supported by a checklist or other documentation to show the possible effects that the agency examined in reaching this conclusion.

(b) The notice of the decision on the proposed activity shall be filed with the Secretary for Resources.

Note: Authority cited: Section 21083, Public Resources Code; Reference: Section 21080.5, Public Resources Code.

15253. USE OF AN EIR SUBSTITUTE BY A RESPONSIBLE AGENCY

(a) An environmental analysis document prepared for a project under a certified program listed in Section 15251 shall be used by another agency granting an approval for the same project where the conditions in subdivision (b) have been met. In this situation, the certified agency shall act as Lead Agency, and the other permitting agencies shall act as Responsible Agencies using the certified agency's document.

(b) The conditions under which a public agency shall act as a Responsible Agency when approving a project using an environmental analysis document prepared under a certified program in the place of an EIR or Negative Declaration are as follows:

(1) The certified agency is the first agency to grant a discretionary approval for the project.

(2) The certified agency consults with the Responsible Agencies, but the consultation need not include the exchange of written notices.

(3) The environmental analysis document identifies:

(A) The significant environmental effects within the jurisdiction or special expertise of the Responsible Agency.

(B) Alternatives or mitigation measures that could avoid or reduce the severity of the significant environmental effects.

(4) Where written notices were not exchanged in the consultation process, the Responsible Agency was afforded the opportunity to participate in the review of the property by the certified agency in a regular manner designed to inform the certified agency of the concerns of the Responsible Agency before release of the EIR substitute for public review.

(5) The certified agency established a consultation period between the certified agency and the Responsible Agency that was at least as long as the period allowed for public review of the EIR substitute document.

(6) The certified agency exercised the powers of a Lead Agency by considering all the significant environmental effects of the project and making a finding under Section 15091 for each significant effect.

(c) Certified agencies are not required to adjust their activities to meet the criteria in subdivision (b). Where a certified agency does not meet the criteria in subdivision (b):

(1) The substitute document prepared by the agency shall not be used by other permitting agencies in the place of an EIR or Negative Declaration, and

(2) Any other agencies granting approvals for the project shall comply with CEQA in the normal manner. A permitting agency shall act as a Lead Agency and prepare an EIR or a Negative Declaration. Other permitting agencies, if any, shall act as Responsible Agencies and use the EIR or Negative Declaration prepared by the Lead Agency.

Note: Authority cited: Section 21083, Public Resources Code; Reference: Sections 21002.1(d), 21080.5, and 21165, Public Resources Code.

Article 18. Statutory Exemptions

SECTIONS 15260 TO 15285

15260. GENERAL

This article describes the exemptions from CEQA granted by the Legislature. The exemptions take several forms. Some exemptions are complete exemptions from CEQA. Other exemptions apply to only part of the requirements of CEQA, and still other exemptions apply only to the timing of CEQA compliance.

Note: Authority cited: Section 21083, Public Resources Code; Reference: Section 21080(b), Public Resources Code.

15261. ONGOING PROJECT

(a) If a project being carried out by a public agency was approved prior to November 23, 1970, the project shall be exempt from CEQA unless either of the following conditions exist:

(1) A substantial portion of public funds allocated for the project have not been spent, and it is still feasible to modify the project to mitigate potentially adverse environmental effects, or to choose feasible alternatives to the project, including the alternative of "no project" or halting the project; provided that a project subject to the National Environmental Policy Act (NEPA) shall be exempt from CEQA as an on-going project if, under regulations promulgated under NEPA, the project would be too far advanced as of January 1, 1970, to require preparation of an EIS.

(2) A public agency proposes to modify the project in such a way that the project might have a new significant effect on the environment.

(b) A private project shall be exempt from CEQA if the project received approval of a lease, license, certificate, permit, or other entitlement for use from a public agency prior to April 5, 1973, subject to the following provisions:

(1) CEQA does not prohibit a public agency from considering environmental factors in connection with the approval or disapproval of a project, or from imposing reasonable fees on the appropriate private person or entity for preparing an environmental report under authority other than CEQA. Local agencies may require environmental reports for projects covered by this paragraph pursuant to local ordinances during this interim period.

(2) Where a project was approved prior to December 5, 1972, and prior to that date the project was legally challenged for noncompliance with CEQA, the project shall be bound by special rules set forth in Section 21170 of CEQA.

(3) Where a private project has been granted a discretionary governmental approval for part of the project before April 5, 1973, and another or additional discretionary governmental approvals after April 5, 1973, the project shall be subject to CEQA only if the approval or approvals after April 5, 1973, involve a greater degree of responsibility or control over the project as a whole than did the approval or approvals prior to that date.

Note: Authority cited: Section 21083, Public Resources Code; Reference: Sections 21169, 21170, and 21171, Public Resources Code; *County of Inyo v. Yorty*, 32 Cal. App. 3d 795.

15262. FEASIBILITY AND PLANNING STUDIES

A project involving only feasibility or planning studies for possible future actions which the agency, board, or commission has not approved, adopted, or funded does not require the preparation of an EIR or Negative Declaration but does require consideration of environmental factors. This section does not apply to the adoption of a plan that will have a legally binding effect on later activities.

Note: Authority cited: Section 21083, Public Resources Code; Reference: Sections 21102 and 21150, Public Resources Code.

15263. DISCHARGE REQUIREMENTS

The State Water Resources Control Board and the regional boards are exempt from the requirement to prepare an EIR or a Negative Declaration prior to the adoption of waste discharge requirements, except requirements for new sources as defined in the Federal Water Pollution Control Act or in other acts which amend or supplement the Federal Water Pollution Control Act. The term "waste discharge requirements" as used in this section is the equivalent of the term "permits" as used in the Federal Water Pollution Control Act.

Note: Authority cited: Section 21083, Public Resources Code; Reference: Section 13389, Water Code.

15264. TIMBERLAND PRESERVES

Local agencies are exempt from the requirement to prepare an EIR or Negative Declaration on the adoption of timberland preserve zones under Government Code Sections 51100 et seq. (Gov. Code, Sec. 51119).

Note: Authority cited: Section 21083, Public Resources Code; Reference: Government Code Section 51119, Government Code.

15265. ADOPTION OF COASTAL PLANS AND PROGRAMS

(a) CEQA does not apply to activities and approvals pursuant to the California Coastal Act (commencing with Section 30000 of the Public Resources Code) by:

  (1) Any local government, as defined in Section 30109 of the Public Resources Code, necessary for the preparation and adoption of a local coastal program, or

  (2) Any state university or college, as defined in Section 30119, as necessary for the preparation and adoption of a long-range land use development plan.

(b) CEQA shall apply to the certification of a local coastal program or long-range land use development plan by the California Coastal Commission.

(c) This section shifts the burden of CEQA compliance from the local agency or the state university or college to the California Coastal Commission. The Coastal Commission's program of certifying local coastal programs and long-range land use development plans has been certified under Section 21080.5, Public Resources Code. See: Section 15192.

Note: Authority cited: Section 21083, Public Resources Code; Reference: Sections 21080.9, Public Resources Code.

15266. GENERAL PLAN TIME EXTENSION

CEQA shall not apply to the granting of an extension of time by the Office of Planning and Research to a city or county for the preparation and adoption of one or more elements of a city or county general plan.

Note: Authority cited: Section 21083, Public Resources Code; Reference: Section 21080.10(a), Public Resources Code.

15267. FINANCIAL ASSISTANCE TO LOW OR MODERATE INCOME HOUSING

CEQA does not apply to actions taken by the Department of Housing and Community Development to provide financial assistance for the development and construction of residential housing for persons and families of low or moderate income, as defined in Section 50093 of the Health and Safety Code. The residential project which is the subject of the application for financial assistance will be subject to CEQA when approvals are granted by another agency.

Note: Authority cited: Section 21083, Public Resources Code; Reference: Section 21080.10(b), Public Resources Code.

15268. MINISTERIAL PROJECTS

(a) Ministerial projects are exempt from the requirements of CEQA. The determination of what is "ministerial" can most appropriately be made by the particular public agency involved based upon its analysis of its own laws, and each public agency should make such determination either as a part of its implementing regulations or on a case-by-case basis.

(b) In the absence of any discretionary provision contained in the local ordinance or other law establishing the requirements for the permit, license, or other entitlement for use, the following actions shall be presumed to be ministerial:

(1) Issuance of building permits.

(2) Issuance of business licenses.

(3) Approval of final subdivision maps.

(4) Approval of individual utility service connections and disconnections.

(c) Each public agency should, in its implementing regulations or ordinances, provide an identification or itemization of its projects and actions which are deemed ministerial under the applicable laws and ordinances.

(d) Where a project involves an approval that contains elements of both a ministerial action and a discretionary action, the project will be deemed to be discretionary and will be subject to the requirements of CEQA.

Note: Authority cited: Section 21083, Public Resources Code; Reference: Section 21080(b)(1), Public Resources Code; *Day v. City of Glendale*, 51 Cal. App. 3d 817.

15269. EMERGENCY PROJECTS

The following emergency projects are exempt from the requirements of CEQA.

(a) Projects to maintain, repair, restore, demolish, or replace property or facilities damaged or destroyed as a result of a disaster in a disaster stricken area in which a state of emergency has been proclaimed by the Governor pursuant to the California Emergency Services Act, commencing with Section 8550 of the Government Code. This includes projects that will remove, destroy, or significantly alter an historical resource when that resource represents an imminent threat to the public of bodily harm or of damage to adjacent property or when the project has received a determination by the State Office of Historic Preservation pursuant to Section 5028(b) of Public Resources Code.

(b) Emergency repairs to publicly or privately owned service facilities necessary to maintain service essential to the public health, safety or welfare.

(c) Specific actions necessary to prevent or mitigate an emergency. This does not include long-term projects undertaken for the purpose of preventing or mitigating a situation that has a low probability of occurrence in the short-term.

(d) Projects undertaken, carried out, or approved by a public agency to maintain, repair, or restore an existing highway damaged by fire, flood, storm, earthquake, land subsidence, gradual earth movement, or landslide, provided that the project is within the existing right of way of that highway and is initiated within one year of the damage occurring. This exemption does not apply to highways designated as official state scenic highways, nor any project undertaken, carried out, or approved by a public agency to expand or widen a highway damaged by fire, flood, storm, earthquake, land subsidence, gradual earth movement, or landslide.

(e) Seismic work on highways and bridges pursuant to Section 180.2 of the Streets and Highways Code, Section 180 et seq.

Note: Authority: Section 21083, Public Resources Code; Reference: Sections 21080(b)(2), (3), and (4), 21080.33 and 21172, Public Resources Code; *Castaic Lake Water Agency v. City of Santa Clarita* (1995) 41 Cal.App.4th 1257; and *Western Municipal Water District of Riverside County v. Superior Court of San Bernardino County* (1987) 187 Cal.App.3d 1104.

15270. PROJECTS WHICH ARE DISAPPROVED

(a) CEQA does not apply to projects which a public agency rejects or disapproves.

(b) This section is intended to allow an initial screening of projects on the merits for quick disapprovals prior to the initiation of the CEQA process where the agency can determine that the project cannot be approved.

(c) This section shall not relieve an applicant from paying the costs for an EIR or Negative Declaration prepared for his project prior to the Lead Agency's disapproval of the project after normal evaluation and processing.

Note: Authority cited: Section 21083, Public Resources Code; Reference: Section 21080(b)(5), Public Resources Code.

15271. EARLY ACTIVITIES RELATED TO THERMAL POWER PLANTS

(a) CEQA does not apply to actions undertaken by a public agency relating to any thermal power plant site or facility including the expenditure, obligation, or encumbrance of funds by a public agency for planning, engineering, or design purposes, or for the conditional sale or purchase of equipment, fuel, water (except groundwater), steam, or power for such a thermal power plant, if the thermal power plant site and related facility will be the subject of an EIR or Negative Declaration or other document or documents prepared pursuant to a regulatory program certified pursuant to Public Resources Code Section 21080.5, which will be prepared by:

(1) The State Energy Resources Conservation and Development Commission,

(2) The Public Utilities Commission, or

(3) The city or county in which the power plant and related facility would be located.

(b) The EIR, Negative Declaration, or other document prepared for the thermal power plant site or facility, shall include the environmental impact, if any, of the early activities described in this section.

(c) This section acts to delay the timing of CEQA compliance from the early activities of a utility to the time when a regulatory agency is requested to approve the thermal power plant and shifts the responsibility for preparing the document to the regulatory agency.

Note: Authority cited: Section 21083, Public Resources Code; Reference: Section 15080(b)(6), Public Resources Code.

15272. OLYMPIC GAMES

CEQA does not apply to activities or approvals necessary to the bidding for, hosting or staging of, and funding or carrying out of, Olympic Games under the authority of the International Olympic Committee, except for the construction of facilities necessary for such Olympic Games. If the facilities are required by the International Olympic Committee as a condition of being awarded the Olympic Games, the Lead Agency need not discuss the "no project" alternative in an EIR with respect to those facilities.

Note: Authority cited: Section 21083, Public Resources Code; Reference: Section 21080(b)(7), Public Resources Code.

15273. RATES, TOLLS, FARES, AND CHARGES

(a) CEQA does not apply to the establishment, modification, structuring, restructuring, or approval of rates, tolls, fares, or other charges by public agencies which the public agency finds are for the purpose of:

(1) Meeting operating expenses, including employee wage rates and fringe benefits,

(2) Purchasing or leasing supplies, equipment, or materials,

(3) Meeting financial reserve needs and requirements,

(4) Obtaining funds for capital projects, necessary to maintain service within existing service areas, or

(5) Obtaining funds necessary to maintain such intra-city transfers as are authorized by city charter.

(b) Rate increases to fund capital projects for the expansion of a system remain subject to CEQA. The agency granting the rate increase shall act either as the Lead Agency if no other agency has prepared environmental documents for the capital project or as a Responsible Agency if another agency has already complied with CEQA as the Lead Agency.

(c) The public agency shall incorporate written findings in the record of any proceeding in which an exemption under this section is claimed setting forth with specificity the basis for the claim of exemption.

Note: Authority cited: Section 21083, Public Resources Code; Reference: Section 21080(b)(8), Public Resources Code.

15274. FAMILY DAY CARE HOMES

(a) CEQA does not apply to establishment or operation of a large family day care home, which provides in-home care for up to fourteen children, as defined in Section 1596.78 of the Health and Safety Code.

(b) Under the Health and Safety Code, local agencies cannot require use permits for the establishment or operation of a small family day care home, which provides in-home care for up to eight children, and the establishment or operation of a small family day care home is a ministerial action which is not subject to CEQA.

Note: Authority cited: Section 21083, Public Resources Code; Reference: Section 21083, Public Resources Code.

15275. SPECIFIED MASS TRANSIT PROJECTS

CEQA does not apply to the following mass transit projects:

(a) The institution or increase of passenger or commuter service on rail lines or high-occupancy vehicle lanes already in use, including the modernization of existing stations and parking facilities;

(b) Facility extensions not to exceed four miles in length which are required for transfer of passengers from or to exclusive public mass transit guideway or busway public transit services.

Note: Authority cited: Section 21083, Public Resources Code; Reference: Section 21080(b)(11), (12), and (13), Public Resources Code.

15276. TRANSPORTATION IMPROVEMENT AND CONGESTION MANAGEMENT PROGRAMS

(a) CEQA does not apply to the development or adoption of a regional transportation improvement program or the state transportation improvement program. Individual projects developed pursuant to these programs shall remain subject to CEQA.

(b) CEQA does not apply to preparation and adoption of a congestion management program by a county congestion management agency pursuant to Government Code Section 65089, et seq.

Note: Authority cited: Section 21083, Public Resources Code; Reference: Section 21080(b)(13), Public Resources Code.

15277. PROJECTS LOCATED OUTSIDE CALIFORNIA

CEQA does not apply to any project or portion thereof located outside of California which will be subject to environmental impact review pursuant to the National Environmental Policy Act of 1969 or pursuant to a law of that state requiring preparation of a document containing essentially the same points of analysis as in an Environmental Impact Statement prepared under the National Environmental Policy Act of 1969. Any emissions or discharges that would have a significant effect on the environment in the State of California are subject to CEQA where a California public agency has authority over the emissions or discharges.

Note: Authority cited: Section 21083, Public Resources Code; Reference: Section 21080(b)(15), Public Resources Code; 58 Opinions of the California Attorney General 614 (S.O. 75/50).

15278. APPLICATION OF COATINGS

(a) CEQA does not apply to a discretionary decision by an air quality management district for a project consisting of the application of coatings within an existing facility at an automotive manufacturing plant if the district finds all of the following:

(1) The project will not cause a net increase in any emissions of any pollutant for which a national or state ambient air quality standard has been established after the internal emission accounting for previous emission reductions achieved at the facility and recognized by the district.

(2) The project will not cause a net increase in adverse impacts of toxic air contaminants as determined by a health risk assessment. The term "net increase in adverse impacts of toxic air contaminants as determined by a health risk assessment" shall be determined in accordance with the rules and regulations of the district.

(3) The project will not cause any other adverse effect on the environment.

(b) The district shall provide a 10-day notice, at the time of the issuance of the permit, of any such exemption. Notice shall be published in two newspapers of general circulation in the area of the project and shall be mailed to any person who makes a written request for such a notice. The notice shall state that the complete file on the project and the basis for the district's findings of exemption are available for inspection and copying at the office of the district.

(c) Any person may appeal the issuance of a permit based on an exemption under subdivision (a) to the hearing board as provided in Section 42302.1 of the Health and Safety Code. The permit shall be revoked by the hearing board if there is substantial evidence in light of the whole record before the board that the project may not satisfy one or more of the criteria established pursuant to subdivision (a). If there is no such substantial evidence, the exemption shall be upheld. Any appeal under this subdivision shall be scheduled for hearing on the calendar of the hearing board within 10 working days of the appeal being filed. The hearing board shall give the appeal priority on its calendar and shall render a decision on the appeal within 21 working days of the appeal being filed. The hearing board may delegate the authority to hear and decide such an appeal to a subcommittee of its body.

Note: Authority cited: Section 21083, Public Resources Code; Reference: Chapter 1131, Statutes of 1993, Section 1.

15279. [DELETED]

15280. [DELETED]

15281. AIR QUALITY PERMITS

CEQA does not apply to the issuance, modification, amendment, or renewal of any permit by an air pollution control district or air quality management district pursuant to Title V, as defined in Section 39053.3 of the Health and Safety Code, or pursuant to an air district Title V program established under Sections 42301.10, 42301.11, and 42301.12 of the Health and Safety Code, unless the issuance, modification, amendment, or renewal authorizes a physical or operational change to a source or facility.

Note: Authority cited: Section 21083, Public Resources Code; Reference: Section 21080.24, Public Resources Code.

15282. OTHER STATUTORY EXEMPTIONS

The following is a list of existing statutory exemptions. Each subdivision summarizes statutory exemptions found in the California Code. Lead agencies are not to rely on the language contained in the summaries below but must rely on the actual statutory language that creates the exemption. This list is intended to assist lead agencies in finding them, but not as a substitute for them. This section is merely a reference tool.

(a) The notification of discovery of Native American burial sites as set forth in Section 5097.98(c) of the Public Resources Code.

(b) Specified prison facilities as set forth in Sections 21080.01, 21080.02, 21080.03 and 21080.07 of the Public Resources Code.

(c) The lease or purchase of the rail right-of-way used for the San Francisco Peninsula commute service between San Francisco and San Jose as set forth in Section 21080.05 of the Public Resources Code.

(d) Any activity or approval necessary for or incidental to project funding or authorization for the expenditure of funds for the project, by the Rural Economic Development Infrastructure Panel as set forth in Section 21080.08 of the Public Resources Code.

(e) The conversion of an existing rental mobilehome park to a resident initiated subdivision, cooperative, or condominium for mobilehomes as set forth in Section 21080.8 of the Public Resources Code.

(f) Settlements of title and boundary problems by the State Lands Commission and to exchanges or leases in connection with those settlements as set forth in Section 21080.11 of the Public Resources Code.

(g) Any railroad grade separation project which eliminates an existing grade crossing or which reconstructs an existing grade separation as set forth in Section 21080.13 of the Public Resources Code.

(h) The adoption of an ordinance regarding second units in a single-family or multifamily residential zone by a city or county to implement the provisions of Sections 65852.1 and 65852.2 of the Government Code as set forth in Section 21080.17 of the Public Resources Code.

(i) The closing of any public school or the transfer of students from that public school to another school in which kindergarten or any grades 1 through 12 is maintained as set forth in 21080.18 of the Public Resources Code.

(j) A project for restriping streets or highways to relieve traffic congestion as set forth in Section 21080.19 of the Public Resources Code.

(k) The installation of new pipeline or maintenance, repair, restoration, removal, or demolition of an existing pipeline as set forth in Section 21080.21 of the Public Resources Code, as long as the project does not exceed one mile in length.

(l) The activities and approvals by a local government necessary for the preparation of general plan amendments pursuant to Public Resources Code § 29763 as set forth in Section 21080.22 of the Public Resources Code. Section 29763 of the Public Resources Code refers to local government amendments made for consistency with the Delta Protection Commission's regional plan.

(m) Minor alterations to utilities made for the purposes of complying with Sections 116410 and 116415 of the Health and Safety Code as set forth in Section 21080.26 of the Public Resources Code.

(n) The adoption of an ordinance exempting a city or county from the provisions of the Solar Shade Control Act as set forth in Section 25985 of the Public Resources Code.

(o) The acquisition of land by the Department of Transportation if received or acquired within a statewide or regional priority corridor designated pursuant to Section 65081.3 of the Government Code as set forth in Section 33911 of the Public Resources Code.

(p) The adoption or amendment of a nondisposal facility element as set forth in Section 41735 of the Public Resources Code.

(q) Cooperative agreements for the development of Solid Waste Management Facilities on Indian country as set forth in Section 44203(g) of the Public Resources Code.

(r) Determinations made regarding a city or county's regional housing needs as set forth in Section 65584 of the Government Code.

(s) Any action necessary to bring a general plan or relevant mandatory element of the general plan into compliance pursuant to a court order as set forth in Section 65759 of the Government Code.

(t) Industrial Development Authority activities as set forth in Section 91543 of the Government Code.

(u) Temporary changes in the point of diversion, place of use, of purpose of use due to a transfer or exchange of water or water rights as set forth in Section 1729 of the Water Code.

(v) The preparation and adoption of Urban Water Management Plans pursuant to the provisions of Section 10652 of the Water Code.

Note: Authority cited: Section 21083, Public Resources Code; References: Sections 5097.98(c), 21080.01, 21080.02, 21080.03, 21080.05, 21080.07, 21080.08, 21080.8, 21080.11, 21080.13, 21080.17, 21080.18, 21080.19, 21080.21, 21080.22, 21080.26, 25985, 33911, 41735, and 44203(g), Public Resources Code.

15283. HOUSING NEEDS ALLOCATION

CEQA does not apply to regional housing needs determinations made by the Department of Housing and Community Development, a council of governments, or a city or county pursuant to Section 65584 of the Government Code.

Note: Authority cited: Section 21083, Public Resources Code; Reference: Section 65584, Government Code.

15284. PIPELINES

(a) CEQA does not apply to any project consisting of the inspection, maintenance, repair, restoration, reconditioning, relocation, replacement, or removal of an existing hazardous or volatile liquid pipeline or any valve, flange, meter, or other piece of equipment that is directly attached to the pipeline.

(b) To qualify for this exemption, the diameter of the affected pipeline must not be increased and the project must be located outside the boundaries of an oil refinery. The project must also meet all of the following criteria:

(1) The affected section of pipeline is less than eight miles in length and actual construction and excavation activities are not undertaken over a length of more than one-half mile at a time.

(2) The affected section of pipeline is not less than eight miles distance from any section of pipeline that had been subject to this exemption in the previous 12 months.

(3) The project is not solely for the purpose of excavating soil that is contaminated by hazardous materials.

(4) To the extent not otherwise required by law, the person undertaking the project has, in advance of undertaking the project, prepared a plan that will result in notification of the appropriate agencies so that they may take action, if necessary, to provide for the emergency evacuation of members of the public who may be located in close proximity to the project, and those agencies, including but not limited to the local fire department, police, sheriff, and California Highway Patrol as appropriate, have reviewed and agreed to that plan.

(5) Project activities take place within an existing right-of-way and that right-of-way will be restored to its pre-project condition upon completion of the project.

(6) The project applicant will comply with all conditions otherwise authorized by law, imposed by the city or county as part of any local agency permit process, and to comply with the Keene-Nejedly California Wetlands Preservation Act (Public Resources Code Section 5810, et seq.), the California Endangered Species Act (Fish and Game Code Section 2050, et seq.), other applicable state laws, and all applicable federal laws.

(c) When the lead agency determines that a project meets all of the criteria of subdivisions (a) and (b), the party undertaking the project shall do all of the following:

(1) Notify in writing all responsible and trustee agencies, as well as any public agency with environmental, public health protection, or emergency response authority, of the lead agency‘s invocation of this exemption.

(2) Mail notice of the project to the last known name and address of all organizations and individuals who have previously requested such notice and notify the public in the affected area by at least one of the following procedures:

(A) Publication at least one time in a newspaper of general circulation in the area affected by the proposed project. If more than one area is affected, the notice shall be published in the newspaper of largest circulation from among the newspapers of general circulation in those areas.

(B) Posting of notice on and off site in the area where the project is to be located.

(C) Direct mailing to the owners and occupants of contiguous property shown on the latest equalized assessment roll.

The notice shall include a brief description of the proposed project and its location, and the date, time, and place of any public meetings or hearings on the proposed project. This notice may be combined with the public notice required under other law, as applicable, but shall meet the preceding minimum requirements.

(3) In the case of private rights-of-way over private property, receive from the underlying property owner permission for access to the property.

(4) Immediately inform the lead agency if any soil contaminated with hazardous materials is discovered.

(5) Comply with all conditions otherwise authorized by law, imposed by the city or county as part of any local agency permit process, and to comply with the Keene-Nejedly California Wetlands Preservation Act (Public Resources Code Section 5810, et seq.), the California Endangered Species Act (Fish and Game Code Section 2050, et seq.), other applicable state laws, and all applicable federal laws.

(d) For purposes of this section, "pipeline" is used as defined in subdivision (a) of Government Code Section 51010.5. This definition includes every intrastate pipeline used for the transportation of hazardous liquid substances or highly volatile liquid substances, including a common carrier pipeline, and all piping containing those substances located within a refined products bulk loading facility which is owned by a common carrier and is served by a pipeline of that common carrier, and the common carrier owns and serves by pipeline at least five such facilities in California.

Note: Authority cited: Section 21083, Public Resources Code; Reference: Section 21080.23, Public Resources Code.

15285. TRANSIT AGENCY RESPONSES TO REVENUE SHORTFALLS

(a) CEQA does not apply to actions taken on or after July 1, 1995 to implement budget reductions made by a publicly owned transit agency as a result of a fiscal emergency caused by the failure of agency revenues to adequately fund agency programs and facilities. Actions shall be limited to those directly undertaken by or financially supported in whole or in part by the transit agency pursuant to Section 15378(a)(1) or (2), including actions which reduce or eliminate the availability of an existing publicly owned transit service, facility, program, or activity.

(b) When invoking this exemption, the transit agency shall make a specific finding that there is a fiscal emergency. Before taking its proposed budgetary actions and making the finding of fiscal emergency, the transit agency shall hold a public hearing. After this public hearing, the transit agency shall respond within 30 days at a regular public meeting to suggestions made by the public at that initial hearing. The transit agency may make the finding of fiscal emergency only after it has responded to public suggestions.

(c) For purposes of this subdivision, "fiscal emergency" means that the transit agency is projected to have negative working capital within one year from the date that the agency finds that a fiscal emergency exists. "Working capital" is defined as the sum of all unrestricted cash, unrestricted short-term investments, and unrestricted short-term accounts receivable, minus unrestricted accounts payable. Employee retirements funds, including deferred compensation plans and Section 401(k) plans, health insurance reserves, bond payment reserves, workers' compensation reserves, and insurance reserves shall not be included as working capital.

(d) This exemption does not apply to the action of any publicly owned transit agency to reduce or eliminate a transit service, facility, program, or activity that was approved or adopted as a mitigation measure in any environmental document certified or adopted by any public agency under either CEQA or NEPA. Further, it does not apply to actions of the Los Angeles County Metropolitan Transportation Authority.

Note: Authority cited: Sections Section 21083, Public Resources Code; References: Sections 21080 and 21080.32, Public Resources Code.

Article 19. Categorical Exemptions

SECTIONS 15300 TO 15332

15300. CATEGORICAL EXEMPTIONS

Section 21084 of the Public Resources Code requires these Guidelines to include a list of classes of projects which have been determined not to have a significant effect on the environment and which shall, therefore, be exempt from the provisions of CEQA.

In response to that mandate, the Secretary for Resources has found that the following classes of projects listed in this article do not have a significant effect on the environment, and they are declared to be categorically exempt from the requirement for the preparation of environmental documents.

Note: Authority cited: Section 21083, Public Resources Code; Reference: Section 21084, Public Resources Code.

15300.1. RELATION TO MINISTERIAL PROJECTS

Section 21080 of the Public Resources Code exempts from the application of CEQA those projects over which public agencies exercise only ministerial authority. Since ministerial projects are already exempt, categorical exemptions should be applied only where a project is not ministerial under a public agency's statutes and ordinances. The inclusion of activities which may be ministerial within the classes and examples contained in this article shall not be construed as a finding by the Secretary for Resources that such an activity is discretionary.

Note: Authority cited: Section 21083, Public Resources Code; Reference: Section 21084, Public Resources Code.

15300.2. EXCEPTIONS

(a) Location. Classes 3, 4, 5, 6, and 11 are qualified by consideration of where the project is to be located – a project that is ordinarily insignificant in its impact on the environment may in a particularly sensitive environment be significant. Therefore, these classes are considered to apply all instances, except where the project may impact on an environmental resource of hazardous or critical concern where designated, precisely mapped, and officially adopted pursuant to law by federal, state, or local agencies.

(b) Cumulative Impact. All exemptions for these classes are inapplicable when the cumulative impact of successive projects of the same type in the same place, over time is significant.

(c) Significant Effect. A categorical exemption shall not be used for an activity where there is a reasonable possibility that the activity will have a significant effect on the environment due to unusual circumstances.

(d) Scenic Highways. A categorical exemption shall not be used for a project which may result in damage to scenic resources, including but not limited to, trees, historic buildings, rock outcroppings, or similar resources, within a highway officially designated as a state scenic highway. This does not apply to improvements which are required as mitigation by an adopted negative declaration or certified EIR.

(e) Hazardous Waste Sites. A categorical exemption shall not be used for a project located on a site which is included on any list compiled pursuant to Section 65962.5 of the Government Code.

(f) Historical Resources. A categorical exemption shall not be used for a project which may cause a substantial adverse change in the significance of a historical resource.

Note: Authority cited: Section 21083, Public Resources Code; References: Sections 21084 and 21084.1, Public Resources Code; *Wildlife Alive v. Chickering* (1977) 18 Cal.3d 190; *League for*

Protection of Oakland's Architectural and Historic Resources v. City of Oakland (1997) 52 Cal.App.4th 896; *Citizens for Responsible Development in West Hollywood v. City of West Hollywood* (1995) 39 Cal.App.4th 925; *City of Pasadena v. State of California* (1993) 14 Cal.App.4th 810; *Association for the Protection etc. Values v. City of Ukiah* (1991) 2 Cal.App.4th 720; and *Baird v. County of Contra Costa* (1995) 32 Cal.App.4th 1464

15300.3. REVISIONS TO LIST OF CATEGORICAL EXEMPTIONS

A public agency may, at any time, request that a new class of categorical exemptions be added, or an existing one amended or deleted. This request must be made in writing to the Office of Planning and Research and shall contain detailed information to support the request. The granting of such request shall be by amendment to these Guidelines.

Note: Authority cited: Section 21083, Public Resources Code; Reference: Section 21084, Public Resources Code.

15300.4. APPLICATION BY PUBLIC AGENCIES

Each public agency shall, in the course of establishing its own procedures, list those specific activities which fall within each of the exempt classes, subject to the qualification that these lists must be consistent with both the letter and the intent expressed in the classes. Public agencies may omit from their implementing procedures classes and examples that do not apply to their activities, but they may not require EIRs for projects described in the classes and examples in this article except under the provisions of Section 15300.2.

Note: Authority cited: Section 21083, Public Resources Code; Reference: Section 21084, Public Resources Code.

15301. EXISTING FACILITIES

Class 1 consists of the operation, repair, maintenance, permitting, leasing, licensing, or minor alteration of existing public or private structures, facilities, mechanical equipment, or topographical features, involving negligible or no expansion of use beyond that existing at the time of the lead agency's determination. The types of "existing facilities" itemized below are not intended to be all-inclusive of the types of projects which might fall within Class 1. The key consideration is whether the project involves negligible or no expansion of an existing use. Examples include but are not limited to:

(a) Interior or exterior alterations involving such things as interior partitions, plumbing, and electrical conveyances;

(b) Existing facilities of both investor and publicly owned utilities used to provide electric power, natural gas, sewerage, or other public utility services;

(c) Existing highways and streets, sidewalks, gutters, bicycle and pedestrian trails, and similar facilities (this includes road grading for the purpose of public safety).

(d) Restoration or rehabilitation of deteriorated or damaged structures, facilities, or mechanical equipment to meet current standards of public health and safety, unless it is determined that the damage was substantial and resulted from an environmental hazard such as earthquake, landslide, or flood;

(e) Additions to existing structures provided that the addition will not result in an increase of more than:

  (1) 50 percent of the floor area of the structures before the addition, or 2,500 square feet, whichever is less; or

  (2) 10,000 square feet if:

    (A) The project is in an area where all public services and facilities are available to allow for maximum development permissible in the General Plan and

(B) The area in which the project is located is not environmentally sensitive.

(f) Addition of safety or health protection devices for use during construction of or in conjunction with existing structures, facilities, or mechanical equipment, or topographical features including navigational devices;

(g) New copy on existing on and off-premise signs;

(h) Maintenance of existing landscaping, native growth, and water supply reservoirs (excluding the use of pesticides, as defined in Section 12753, Division 7, Chapter 2, Food and Agricultural Code);

(i) Maintenance of fish screens, fish ladders, wildlife habitat areas, artificial wildlife waterway devices, streamflows, springs and waterholes, and stream channels (clearing of debris) to protect fish and wildlife resources;

(j) Fish stocking by the California Department of Fish and Game;

(k) Division of existing multiple family or single-family residences into common-interest ownership and subdivision of existing commercial or industrial buildings, where no physical changes occur which are not otherwise exempt;

(l) Demolition and removal of individual small structures listed in this subdivision:

(1) One single-family residence. In urbanized areas, up to three single-family residences may be demolished under this exemption.

(2) A duplex or similar multifamily residential structure. In urbanized areas, this exemption applies to duplexes and similar structures where not more than six dwelling units will be demolished.

(3) A store, motel, office, restaurant, or similar small commercial structure if designed for an occupant load of 30 persons or less. In urbanized areas, the exemption also applies to the demolition of up to three such commercial buildings on sites zoned for such use.

(4) Accessory (appurtenant) structures including garages, carports, patios, swimming pools, and fences.

(m) Minor repairs and alterations to existing dams and appurtenant structures under the supervision of the Department of Water Resources.

(n) Conversion of a single family residence to office use.

(o) Installation, in an existing facility occupied by a medical waste generator, of a steam sterilization unit for the treatment of medical waste generated by that facility provided that the unit is installed and operated in accordance with the Medical Waste Management Act (Section 117600, et seq., of the Health and Safety Code) and accepts no offsite waste.

(p) Use of a single-family residence as a small family day care home, as defined in Section 1596.78 of the Health and Safety Code.

Note: Authority cited: Section 21083, Public Resources Code; References: Sections 21084, Public Resources Code; *Bloom v. McGurk* (1994) 26 Cal.App.4th 1307.

15302. REPLACEMENT OR RECONSTRUCTION

Class 2 consists of replacement or reconstruction of existing structures and facilities where the new structure will be located on the same site as the structure replaced and will have substantially the same purpose and capacity as the structure replaced, including but not limited to:

(a) Replacement or reconstruction of existing schools and hospitals to provide earthquake resistant structures which do not increase capacity more than 50 percent.

(b) Replacement of a commercial structure with a new structure of substantially the same size, purpose, and capacity.

(c) Replacement or reconstruction of existing utility systems and/or facilities involving negligible or no expansion of capacity.

(d) Conversion of overhead electric utility distribution system facilities to underground including connection to existing overhead electric utility distribution lines where the surface is restored to the condition existing prior to the undergrounding.

Note: Authority cited: Section 21083, Public Resources Code; Reference: Section 21084, Public Resources Code.

15303. NEW CONSTRUCTION OR CONVERSION OF SMALL STRUCTURES

Class 3 consists of construction and location of limited numbers of new, small facilities or structures; installation of small new equipment and facilities in small structures; and the conversion of existing small structures from one use to another where only minor modifications are made in the exterior of the structure. The numbers of structures described in this section are the maximum allowable on any legal parcel. Examples of this exemption include, but are not limited to:

(a) One single-family residence, or a second dwelling unit in a residential zone. In urbanized areas, up to three single-family residences may be constructed or converted under this exemption.

(b) A duplex or similar multi-family residential structure, totaling no more than four dwelling units. In urbanized areas, this exemption applies to apartments, duplexes and similar structures designed for not more than six dwelling units.

(c) A store, motel, office, restaurant or similar structure not involving the use of significant amounts of hazardous substances, and not exceeding 2500 square feet in floor area. In urbanized areas, the exemption also applies to up to four such commercial buildings not exceeding 10,000 square feet in floor area on sites zoned for such use if not involving the use of significant amounts of hazardous substances where all necessary public services and facilities are available and the surrounding area is not environmentally sensitive.

(d) Water main, sewage, electrical, gas, and other utility extensions, including street improvements, of reasonable length to serve such construction.

(e) Accessory (appurtenant) structures including garages, carports, patios, swimming pools, and fences.

(f) An accessory steam sterilization unit for the treatment of medical waste at a facility occupied by a medical waste generator, provided that the unit is installed and operated in accordance with the Medical Waste Management Act (Section 117600, et seq., of the Health and Safety Code) and accepts no offsite waste.

Note: Authority cited: Section 21083, Public Resources Code; Reference: Sections 21084, Public Resources Code.

15304. MINOR ALTERATIONS TO LAND

Class 4 consists of minor public or private alterations in the condition of land, water, and/or vegetation which do not involve removal of healthy, mature, scenic trees except for forestry or agricultural purposes. Examples include, but are not limited to:

(a) Grading on land with a slope of less than 10 percent, except that grading shall not be exempt in a waterway, in any wetland, in an officially designated (by federal, state, or local government action) scenic area, or in officially mapped areas of severe geologic hazard such as an Alquist-Priolo Earthquake Fault Zone or within an official Seismic Hazard Zone, as delineated by the State Geologist.

(b) New gardening or landscaping, including the replacement of existing conventional landscaping with water efficient or fire resistant landscaping.

(c) Filling of earth into previously excavated land with material compatible with the natural features of the site;

(d) Minor alterations in land, water, and vegetation on existing officially designated wildlife management areas or fish production facilities which result in improvement of habitat for fish and wildlife resources or greater fish production;

(e) Minor temporary use of land having negligible or no permanent effects on the environment, including carnivals, sales of Christmas trees, etc;

(f) Minor trenching and backfilling where the surface is restored;

(g) Maintenance dredging where the spoil is deposited in a spoil area authorized by all applicable state and federal regulatory agencies;

(h) The creation of bicycle lanes on existing rights-of-way.

(i) Fuel management activities within 30 feet of structures to reduce the volume of flammable vegetation, provided that the activities will not result in the taking of endangered, rare, or threatened plant or animal species or significant erosion and sedimentation of surface waters. This exemption shall apply to fuel management activities within 100 feet of a structure if the public agency having fire protection responsibility for the area has determined that 100 feet of fuel clearance is required due to extra hazardous fire conditions.

Note: Authority cited: Section 21083, Public Resources Code; Reference: Section 21084, Public Resources Code.

15305. MINOR ALTERATIONS IN LAND USE LIMITATIONS

Class 5 consists of minor alterations in land use limitations in areas with an average slope of less than 20%, which do not result in any changes in land use or density, including but not limited to:

(a) Minor lot line adjustments, side yard, and set back variances not resulting in the creation of any new parcel;

(b) Issuance of minor encroachment permits;

(c) Reversion to acreage in accordance with the Subdivision Map Act.

Note: Authority cited: Section 21083, Public Resources Code; Reference: Section 21084, Public Resources Code.

15306. INFORMATION COLLECTION

Class 6 consists of basic data collection, research, experimental management, and resource evaluation activities which do not result in a serious or major disturbance to an environmental resource. These may be strictly for information gathering purposes, or as part of a study leading to an action which a public agency has not yet approved, adopted, or funded.

Note: Authority cited: Section 21083, Public Resources Code; Reference: Section 21084, Public Resources Code.

15307. ACTIONS BY REGULATORY AGENCIES FOR PROTECTION OF NATURAL RESOURCES

Class 7 consists of actions taken by regulatory agencies as authorized by state law or local ordinance to assure the maintenance, restoration, or enhancement of a natural resource where the regulatory process involves procedures for protection of the environment. Examples include but are not limited to wildlife preservation activities of the State Department of Fish and Game. Construction activities are not included in this exemption.

Note: Authority cited: Section 21083, Public Resources Codee; Reference: Section 21084, Public Resources Code.

15308. ACTIONS BY REGULATORY AGENCIES FOR PROTECTION OF THE ENVIRONMENT

Class 8 consists of actions taken by regulatory agencies, as authorized by state or local ordinance, to assure the maintenance, restoration, enhancement, or protection of the environment where the regulatory process involves procedures for protection of the environment. Construction activities and relaxation of standards allowing environmental degradation are not included in this exemption.

Note: Authority cited: Section 21083, Public Resources Code; Reference: Section 21084, Public Resources Code; *International Longshoremen's and Warehousemen's Union v. Board of Supervisors*, (1981) 116 Cal. App. 3d 265.

15309. INSPECTIONS

Class 9 consists of activities limited entirely to inspections, to check for performance of an operation, or quality, health, or safety of a project, including related activities such as inspection for possible mislabeling, misrepresentation, or adulteration of products.

Note: Authority cited: Section 21083, Public Resources Code; Reference: Section 21084, Public Resources Code.

15310. LOANS

Class 10 consists of loans made by the Department of Veterans Affairs under the Veterans Farm and Home Purchase Act of 1943, mortgages for the purchase of existing structures where the loan will not be used for new construction and the purchase of such mortgages by financial institutions. Class 10 includes but is not limited to the following examples:

(a) Loans made by the Department of Veterans Affairs under the Veterans Farm and Home Purchase Act of 1943.

(b) Purchases of mortgages from banks and mortgage companies by the Public Employees Retirement System and by the State Teachers Retirement System.

Note: Authority cited: Section 21083, Public Resources Code; Reference: Section 21084, Public Resources Code.

15311. ACCESSORY STRUCTURES

Class 11 consists of construction, or placement of minor structures accessory to (appurtenant to) existing commercial, industrial, or institutional facilities, including but not limited to:

(a) On-premise signs;

(b) Small parking lots;

(c) Placement of seasonal or temporary use items such as lifeguard towers, mobile food units, portable restrooms, or similar items in generally the same locations from time to time in publicly owned parks, stadiums, or other facilities designed for public use.

Note: Authority cited: Section 21083, Public Resources Code; Reference: Section 21084, Public Resources Code.

15312. SURPLUS GOVERNMENT PROPERTY SALES

Class 12 consists of sales of surplus government property except for parcels of land located in an area of statewide, regional, or areawide concern identified in Section 15206(b)(4). However, even if the surplus property to be sold is located in any of those areas, its sale is exempt if:

(a) The property does not have significant values for wildlife habitat or other environmental purposes, and

(b) Any of the following conditions exist:

  (1) The property is of such size, shape, or inaccessibility that it is incapable of independent development or use; or

(2) The property to be sold would qualify for an exemption under any other class of categorical exemption in these Guidelines; or

(3) The use of the property and adjacent property has not changed since the time of purchase by the public agency.

Note: Authority cited: Section 21083, Public Resources Code; Reference: Section 21084, Public Resources Code.

15313. ACQUISITION OF LANDS FOR WILDLIFE CONSERVATION PURPOSES

Class 13 consists of the acquisition of lands for fish and wildlife conservation purposes including (a) preservation of fish and wildlife habitat, (b) establishing ecological reserves under Fish and Game Code Section 1580, and (c) preserving access to public lands and waters where the purpose of the acquisition is to preserve the land in its natural condition.

Note: Authority cited: Sections 21083 and 21087, Public Resources Code; Reference: Section 21084, Public Resources Code.

15314. MINOR ADDITIONS TO SCHOOLS

Class 14 consists of minor additions to existing schools within existing school grounds where the addition does not increase original student capacity by more than 25% or ten classrooms, whichever is less. The addition of portable classrooms is included in this exemption.

Note: Authority cited: Section 21083, Public Resources Code; Reference: Section 21084, Public Resources Code.

15315. MINOR LAND DIVISIONS

Class 15 consists of the division of property in urbanized areas zoned for residential, commercial, or industrial use into four or fewer parcels when the division is in conformance with the General Plan and zoning, no variances or exceptions are required, all services and access to the proposed parcels to local standards are available, the parcel was not involved in a division of a larger parcel within the previous 2 years, and the parcel does not have an average slope greater than 20 percent.

Note: Authority cited: Sections Section 21083, Public Resources Code; Reference: Section 21084, Public Resources Code.

15316. TRANSFER OF OWNERSHIP OF LAND IN ORDER TO CREATE PARKS

Class 16 consists of the acquisition, sale, or other transfer of land in order to establish a park where the land is in a natural condition or contains historical or archaeological resources and either:

(a) The management plan for the park has not been prepared, or

(b) The management plan proposes to keep the area in a natural condition or preserve the historic or archaeological resources. CEQA will apply when a management plan is proposed that will change the area from its natural condition or cause substantial adverse change in the significance of the historic or archaeological resource.

Note: Authority cited: Section 21083, Public Resources Code; Reference: Sections 21084, 21083.2, and 21084.1, Public Resources Code.

15317. OPEN SPACE CONTRACTS OR EASEMENTS

Class 17 consists of the establishment of agricultural preserves, the making and renewing of open space contracts under the Williamson Act, or the acceptance of easements or fee interests in order to maintain the open space character of the area. The cancellation of such preserves, contracts, interests, or easements is not included and will normally be an action subject to the CEQA process.

Note: Authority cited: Section 21083, Public Resources Code; Reference: Section 21084, Public Resources Code.

15318. DESIGNATION OF WILDERNESS AREAS

Class 18 consists of the designation of wilderness areas under the California Wilderness System.

Note: Authority cited: Section 21083, Public Resources Code; Reference: Section 21084, Public Resources Code.

15319. ANNEXATIONS OF EXISTING FACILITIES AND LOTS FOR EXEMPT FACILITIES

Class 19 consists of only the following annexations:

(a) Annexations to a city or special district of areas containing existing public or private structures developed to the density allowed by the current zoning or pre-zoning of either the gaining or losing governmental agency whichever is more restrictive, provided, however, that the extension of utility services to the existing facilities would have a capacity to serve only the existing facilities.

(b) Annexations of individual small parcels of the minimum size for facilities exempted by Section 15303, New Construction or Conversion of Small Structures.

Note: Authority cited: Section 21083, Public Resources Code; Reference: Section 21084, Public Resources Code.

15320. CHANGES IN ORGANIZATION OF LOCAL AGENCIES

Class 20 consists of changes in the organization or reorganization of local governmental agencies where the changes do not change the geographical area in which previously existing powers are exercised. Examples include but are not limited to:

(a) Establishment of a subsidiary district;

(b) Consolidation of two or more districts having identical powers;

(c) Merger with a city of a district lying entirely within the boundaries of the city.

Note: Authority cited: Section 21083, Public Resources Code; Reference: Section 21084, Public Resources Code.

15321. ENFORCEMENT ACTIONS BY REGULATORY AGENCIES

Class 21 consists of:

(a) Actions by regulatory agencies to enforce or revoke a lease, permit, license, certificate, or other entitlement for use issued, adopted, or prescribed by the regulatory agency or enforcement of a law, general rule, standard, or objective, administered or adopted by the regulatory agency. Such actions include, but are not limited to, the following:

  (1) The direct referral of a violation of lease, permit, license, certificate, or entitlement for use or of a general rule, standard, or objective to the Attorney General, District Attorney, or City Attorney as appropriate, for judicial enforcement;

  (2) The adoption of an administrative decision or order enforcing or revoking the lease, permit, license, certificate, or entitlement for use or enforcing the general rule, standard, or objective.

(b) Law enforcement activities by peace officers acting under any law that provides a criminal sanction;

(c) Construction activities undertaken by the public agency taking the enforcement or revocation action are not included in this exemption.

Note: Authority cited: Section 21083, Public Resources Code; Reference: Section 21084, Public Resources Code.

15322. EDUCATIONAL OR TRAINING PROGRAMS INVOLVING NO PHYSICAL CHANGES

Class 22 consists of the adoption, alteration, or termination of educational or training programs which involve no physical alteration in the area affected or which involve physical changes only in the interior of existing school or training structures. Examples include but are not limited to:

(a) Development of or changes in curriculum or training methods.

(b) Changes in the grade structure in a school which do not result in changes in student transportation.

Note: Authority cited: Section 21083, Public Resources Code; Reference: Section 21084, Public Resources Code.

15323. NORMAL OPERATIONS OF FACILITIES FOR PUBLIC GATHERINGS

Class 23 consists of the normal operations of existing facilities for public gatherings for which the facilities were designed, where there is a past history of the facility being used for the same or similar kind of purpose. For the purposes of this section, "past history" shall mean that the same or similar kind of activity has been occurring for at least three years and that there is a reasonable expectation that the future occurrence of the activity would not represent a change in the operation of the facility. Facilities included within this exemption include, but are not limited to, racetracks, stadiums, convention centers, auditoriums, amphitheaters, planetariums, swimming pools, and amusement parks.

Note: Authority cited: Section 21083, Public Resources Code; Reference: Section 21084, Public Resources Code.

15324. REGULATIONS OF WORKING CONDITIONS

Class 24 consists of actions taken by regulatory agencies, including the Industrial Welfare Commission as authorized by statute, to regulate any of the following:

(a) Employee wages,

(b) Hours of work, or

(c) Working conditions where there will be no demonstrable physical changes outside the place of work.

Note: Authority cited: Section 21083, Public Resources Code; Reference: Section 21084, Public Resources Code.

15325. TRANSFERS OF OWNERSHIP OF INTEREST IN LAND TO PRESERVE EXISTING NATURAL CONDITIONS AND HISTORICAL RESOURCES

Class 25 consists of the transfers of ownership of interests in land in order to preserve open space, habitat, or historical resources. Examples include but are not limited to:

(a) Acquisition, sale, or other transfer of areas to preserve the existing natural conditions, including plant or animal habitats.

(b) Acquisition, sale, or other transfer of areas to allow continued agricultural use of the areas.

(c) Acquisition, sale, or other transfer to allow restoration of natural conditions, including plant or animal habitats.

(d) Acquisition, sale, or other transfer to prevent encroachment of development into flood plains.

(e) Acquisition, sale, or other transfer to preserve historical resources.

(f) Acquisition, sale, or other transfer to preserve open space or lands for park purposes.

Note: Authority cited: Section 21083, Public Resources Code; Reference: Section 21084, Public Resources Code.

15326. ACQUISITION OF HOUSING FOR HOUSING ASSISTANCE PROGRAMS

Class 26 consists of actions by a redevelopment agency, housing authority, or other public agency to implement an adopted Housing Assistance Plan by acquiring an interest in housing units. The housing units may be either in existence or possessing all required permits for construction when the agency makes its final decision to acquire the units.

Note: Authority cited: Section 21083, Public Resources Code; Reference: Section 21084, Public Resources Code.

15327. LEASING NEW FACILITIES

(a) Class 27 consists of the leasing of a newly constructed or previously unoccupied privately owned facility by a local or state agency where the local governing authority determined that the building was exempt from CEQA. To be exempt under this section, the proposed use of the facility:

  (1) Shall be in conformance with existing state plans and policies and with general, community, and specific plans for which an EIR or Negative Declaration has been prepared;

  (2) Shall be substantially the same as that originally proposed at the time the building permit was issued;

  (3) Shall not result in a traffic increase of greater than 10% of front access road capacity; and

  (4) Shall include the provision of adequate employee and visitor parking facilities.

(b) Examples of Class 27 include, but are not limited to:

  (1) Leasing of administrative offices in newly constructed office space;

  (2) Leasing of client service offices in newly constructed retail space;

  (3) Leasing of administrative and/or client service offices in newly constructed industrial parks.

Note: Authority cited: Section 21083, Public Resources Code; Reference: Section 21084, Public Resources Code.

15328. SMALL HYDROELECTRIC PROJECTS AT EXISTING FACILITIES

Class 28 consists of the installation of hydroelectric generating facilities in connection with existing dams, canals, and pipelines where:

(a) The capacity of the generating facilities is 5 megawatts or less;

(b) Operation of the generating facilities will not change the flow regime in the affected stream, canal, or pipeline including but not limited to:

  (1) Rate and volume of flow;

  (2) Temperature;

  (3) Amounts of dissolved oxygen to a degree that could adversely affect aquatic life; and

  (4) Timing of release.

(c) New power lines to connect the generating facilities to existing power lines will not exceed one mile in length if located on a new right of way and will not be located adjacent to a wild or scenic river;

(d) Repair or reconstruction of the diversion structure will not raise the normal maximum surface elevation of the impoundment;

(e) There will be no significant upstream or downstream passage of fish affected by the project;

(f) The discharge from the power house will not be located more than 300 feet from the toe of the diversion structure;

(g) The project will not cause violations of applicable state or federal water quality standards;

(h) The project will not entail any construction on or alteration of a site included in or eligible for inclusion in the National Register of Historic Places; and

(i) Construction will not occur in the vicinity of any endangered, rare, or threatened species.

Note: Authority cited: Section 21083, Public Resources Code; Reference: Section 21084, Public Resources Code.

15329. COGENERATION PROJECTS AT EXISTING FACILITIES

Class 29 consists of the installation of cogeneration equipment with a capacity of 50 megawatts or less at existing facilities meeting the conditions described in this section.

(a) At existing industrial facilities, the installation of cogeneration facilities will be exempt where it will:

  (1) Result in no net increases in air emissions from the industrial facility, or will produce emissions lower than the amount that would require review under the new source review rules applicable in the county, and

  (2) Comply with all applicable state, federal, and local air quality laws.

(b) At commercial and institutional facilities, the installation of cogeneration facilities will be exempt if the installation will:

  (1) Meet all the criteria described in subdivision (a);

  (2) Result in no noticeable increase in noise to nearby residential structures;

  (3) Be contiguous to other commercial or institutional structures.

Note: Authority cited: Section 21083, Public Resources Code; Reference: Section 21084, Public Resources Code.

15330. MINOR ACTIONS TO PREVENT, MINIMIZE, STABILIZE, MITIGATE OR ELIMINATE THE RELEASE OR THREAT OF RELEASE OF HAZARDOUS WASTE OR HAZARDOUS SUBSTANCES

Class 30 consists of any minor cleanup actions taken to prevent, minimize, stabilize, mitigate, or eliminate the release or threat of release of a hazardous waste or substance which are small or medium removal actions costing $1 million or less.

(a) No cleanup action shall be subject to this Class 30 exemption if the action requires the onsite use of a hazardous waste incinerator or thermal treatment unit or the relocation of residences or businesses, or the action involves the potential release into the air of volatile organic compounds as defined in Health and Safety Code Section 25123.6, except for small scale in situ soil vapor extraction and treatment systems which have been permitted by the local Air Pollution Control District or Air Quality Management District. All actions must be consistent with applicable state and local environmental permitting requirements including, but not limited to, off-site disposal, air quality rules such as those governing volatile organic compounds and water quality standards, and approved by the regulatory body with jurisdiction over the site.

(b) Examples of such minor cleanup actions include but are not limited to:

  (1) Removal of sealed, non-leaking drums or barrels of hazardous waste or substances that have been stabilized, containerized and are designated for a lawfully permitted destination;

  (2) Maintenance or stabilization of berms, dikes, or surface impoundments;

(3) Construction or maintenance or interim of temporary surface caps;

(4) Onsite treatment of contaminated soils or sludges provided treatment system meets Title 22 requirements and local air district requirements;

(5) Excavation and/or offsite disposal of contaminated soils or sludges in regulated units;

(6) Application of dust suppressants or dust binders to surface soils;

(7) Controls for surface water run-on and run-off that meets seismic safety standards;

(8) Pumping of leaking ponds into an enclosed container;

(9) Construction of interim or emergency ground water treatment systems;

(10) Posting of warning signs and fencing for a hazardous waste or substance site that meets legal requirements for protection of wildlife.

Note: Authority cited: Section 21083, Public Resources Code; Reference: Section 21084, Public Resources Code.

15331. HISTORICAL RESOURCE RESTORATION/REHABILITATION

Class 31 consists of projects limited to maintenance, repair, stabilization, rehabilitation, restoration, preservation, conservation or reconstruction of historical resources in a manner consistent with the Secretary of the Interior's Standards for the Treatment of Historic Properties with Guidelines for Preserving, Rehabilitating, Restoring, and Reconstructing Historic Buildings (1995), Weeks and Grimmer.

Note: Authority cited: Section 21083, Public Resources Code; Reference: Section 21084, Public Resources Code.

15332. IN-FILL DEVELOPMENT PROJECTS

Class 32 consists of projects characterized as in-fill development meeting the conditions described in this section.

(a) The project is consistent with the applicable general plan designation and all applicable general plan policies as well as with applicable zoning designation and regulations.

(b) The proposed development occurs within city limits on a project site of no more than five acres substantially surrounded by urban uses.

(c) The project site has no value as habitat for endangered, rare or threatened species.

(d) Approval of the project would not result in any significant effects relating to traffic, noise, air quality, or water quality.

(e) The site can be adequately served by all required utilities and public services.

Note: Authority cited: Section 21083, Public Resources Code. Reference: Section 21084, Public Resources Code.

15333. SMALL HABITAT RESTORATION PROJECTS.

Class 33 consists of projects not to exceed five acres in size to assure the maintenance, restoration, enhancement, or protection of habitat for fish, plants, or wildlife provided that:

(a) There would be no significant adverse impact on endangered, rare or threatened species or their habitat pursuant to section 15065,

(b) There are no hazardous materials at or around the project site that may be disturbed or removed, and

(c) The project will not result in impacts that are significant when viewed in connection with the effects of past projects, the effects of other current projects, and the effects of probable future projects.

(d) Examples of small restoration projects may include, but are not limited to:

(1) revegetation of disturbed areas with native plant species;

(2) wetland restoration, the primary purpose of which is to improve conditions for waterfowl or other species that rely on wetland habitat;

(3) stream or river bank revegetation, the primary purpose of which is to improve habitat for amphibians or native fish;

(4) projects to restore or enhance habitat that are carried out principally with hand labor and not mechanized equipment.

(5) stream or river bank stabilization with native vegetation or other bioengineering techniques, the primary purpose of which is to reduce or eliminate erosion and sedimentation; and

(6) culvert replacement conducted in accordance with published guidelines of the Department of Fish and Game or NOAA Fisheries, the primary purpose of which is to improve habitat or reduce sedimentation.

Note: Authority cited: Section 21083, Public Resources Code; Reference: Section 21084, Public Resources Code.

Article 20. Definitions

SECTIONS 15350 TO 15387

15350. GENERAL

The definitions contained in this article apply to terms used throughout the Guidelines unless a term is otherwise defined in a particular section.

Note: Authority cited: Section 21083, Public Resources Code; Reference: Section 21083, Public Resources Code.

15351. APPLICANT

"Applicant" means a person who proposes to carry out a project which needs a lease, permit, license, certificate, or other entitlement for use or financial assistance from one or more public agencies when that person applies for the governmental approval or assistance.

Note: Authority cited: Section 21083, Public Resources Code; Reference: Section 21065, Public Resources Code.

15352. APPROVAL

(a) "Approval" means the decision by a public agency which commits the agency to a definite course of action in regard to a project intended to be carried out by any person. The exact date of approval of any project is a matter determined by each public agency according to its rules, regulations, and ordinances. Legislative action in regard to a project often constitutes approval.

(b) With private projects, approval occurs upon the earliest commitment to issue or the issuance by the public agency of a discretionary contract, grant, subsidy, loan, or other form of financial assistance, lease, permit, license, certificate, or other entitlement for use of the project.

Note: Authority cited: Section 21083, Public Resources Code; Reference: Sections 21061 and 21065, Public Resources Code.

15353. CEQA

"CEQA" means the California Environmental Quality Act, California Public Resources Code Sections 21000 et seq.

Note: Authority cited: Section 21083, Public Resources Code; Reference: Section 21050, Public Resources Code.

15354. CATEGORICAL EXEMPTION

"Categorical exemption" means an exemption from CEQA for a class of projects based on a finding by the Secretary for Resources that the class of projects does not have a significant effect on the environment.

Note: Authority cited: Section 21083, Public Resources Code; Reference: Sections 21080(b)(10) and 21084, Public Resources Code.

15355. CUMULATIVE IMPACTS

"Cumulative impacts" refers to two or more individual effects which, when considered together, are considerable or which compound or increase other environmental impacts.

(a) The individual effects may be changes resulting from a single project or a number of separate projects.

(b) The cumulative impact from several projects is the change in the environment which results from the incremental impact of the project when added to other closely related past, present, and reasonably foreseeable probable future projects. Cumulative impacts can result from individually minor but collectively significant projects taking place over a period of time.

Note: Authority cited: Section 21083, Public Resources Code; Reference: Section 21083(b), Public Resources Code; *Whitman v. Board of Supervisors*, 88 Cal. App. 3d 397, *San Franciscans for Reasonable Growth v. City and County of San Francisco* (1984) 151 Cal. App. 3d 61, Formerly Section 15023.5.

15356. DECISION-MAKING BODY

"Decision-making body" means any person or group of people within a public agency permitted by law to approve or disapprove the project at issue.

Note: Authority cited: Section 21083, Public Resources Code; Reference: Section 21003(b), Public Resources Code; *Kleist v. City of Glendale*, (1976) 56 Cal. App. 3d 770.

15357. DISCRETIONARY PROJECT

"Discretionary project" means a project which requires the exercise of judgment or deliberation when the public agency or body decides to approve or disapprove a particular activity, as distinguished from situations where the public agency or body merely has to determine whether there has been conformity with applicable statutes, ordinances, or regulations. A timber harvesting plan submitted to the State Forester for approval under the requirements of the Z'berg-Nejedly Forest Practice Act of 1973 (Pub. Res. Code Sections 4511 et seq.) constitutes a discretionary project within the meaning of the California Environmental Quality Act. Section 21065(c).

Note: Authority cited: Section 21083, Public Resources Code; Reference: Section 21080(a), Public Resources Code; *Johnson v. State of California*, (1968) 69 Cal. 2d 782; *People v. Department of Housing and Community Development*, (1975) 45 Cal. App. 3d 185; *Day v. City of Glendale*, (1975) 51 Cal. App. 3d 817; *N.R.D.C. v. Arcata National Corp.*, (1976) 59 Cal. App. 3d 959.

15358. EFFECTS

"Effects" and "impacts" as used in these Guidelines are synonymous.

(a) Effects include:

(1) Direct or primary effects which are caused by the project and occur at the same time and place.

(2) Indirect or secondary effects which are caused by the project and are later in time or farther removed in distance, but are still reasonably foreseeable. Indirect or secondary effects may include growth-inducing effects and other effects related to induced changes in the pattern of land use, population density, or growth rate, and related effects on air and water and other natural systems, including ecosystems.

(b) Effects analyzed under CEQA must be related to a physical change.

Note: Authority cited: Section 21083, Public Resources Code; Reference: Sections 21068 and 21100, Public Resources Code.

15359. EMERGENCY

"Emergency" means a sudden, unexpected occurrence, involving a clear and imminent danger, demanding immediate action to prevent or mitigate loss of, or damage to life, health, property, or essential public services. Emergency includes such occurrences as fire, flood, earthquake, or other soil or geologic movements, as well as such occurrences as riot, accident, or sabotage.

Note: Authority cited: Section 21083, Public Resources Code; Reference: Section 21080(b)(2), (3), and (4), Public Resources Code.

15360. ENVIRONMENT

"Environment" means the physical conditions which exist within the area which will be affected by a proposed project including land, air, water, minerals, flora, fauna, ambient noise, and objects of historical or aesthetic significance. The area involved shall be the area in which significant effects would occur either directly or indirectly as a result of the project. The "environment" includes both natural and man-made conditions.

Note: Authority cited: Section 21083, Public Resources Code; Reference: Section 21060.5, Public Resources Code.

15361. ENVIRONMENTAL DOCUMENTS

"Environmental documents" means Initial Studies, Negative Declarations, draft and final EIRs, documents prepared as substitutes for EIRs and Negative Declarations under a program certified pursuant to Public Resources Code Section 21080.5, and documents prepared under NEPA and used by a state or local agency in the place of an Initial Study, Negative Declaration, or an EIR.

Note: Authority cited: Section 21083, Public Resources Code; Reference: Sections 21061, 21080(b), 21080.5, 21108, and 21152, Public Resources Code.

15362. EIR - ENVIRONMENTAL IMPACT REPORT

"EIR" or "Environmental Impact Report" means a detailed statement prepared under CEQA describing and analyzing the significant environmental effects of a project and discussing ways to mitigate or avoid the effects. The contents of an EIR are discussed in Article 9, commencing with Section 15120 of these Guidelines. The term "EIR" may mean either a draft or a final EIR depending on the context.

(a) Draft EIR means an EIR containing the information specified in Sections 15122 through 15131.

(b) Final EIR means an EIR containing the information contained in the draft EIR, comments either verbatim or in summary received in the review process, a list of persons commenting, and the response of the Lead Agency to the comments received. The final EIR is discussed in detail in Section 15132.

Note: Authority cited: Section 21083, Public Resources Code; Reference: Sections 21061, 21100, and 21151, Public Resources Code.

15363. EIS - ENVIRONMENTAL IMPACT STATEMENT

"EIS" or "Environmental Impact Statement" means an environmental impact document prepared pursuant to the National Environmental Policy Act (NEPA). NEPA uses the term EIS in the place of the term EIR which is used in CEQA.

Note: Authority cited: Section 21083, Public Resources Code; Reference: Sections 21083.5, 21083.6, and 21083.7, Public Resources Code; 43 U.S.C.A. 4322(2)(c).

15364. FEASIBLE

"Feasible" means capable of being accomplished in a successful manner within a reasonable period of time, taking into account economic, environmental, legal, social, and technological factors.

Note: Authority cited: Section 21083, Public Resources Code; Reference: Sections 21002, 21002.1, 21004, 21061.1, 21080.5, and 21081, Public Resources Code; Section 4, Chapter 1438 of the Statutes of 1982.

15364.5. GREENHOUSE GAS

"Greenhouse gas" or "greenhouse gases" includes but is not limited to: carbon dioxide, methane, nitrous oxide, hydrofluorocarbons, perfluorocarbons and sulfur hexafluoride.

Note: Authority cited: Sections 21083, 21083.05, Public Resources Code. Reference: Section 38505(g) Health and Safety Code; Section 21083.05, Public Resources Code.

15365. INITIAL STUDY

"Initial Study" means a preliminary analysis prepared by the Lead Agency to determine whether an EIR or a Negative Declaration must be prepared or to identify the significant environmental effects to be analyzed in an EIR. Use of the Initial Study is discussed in Article 5, commencing with Section 15060.

Note: Authority cited: Section 21083, Public Resources Code; Reference: Sections 21080.1, 21080.2, 21080.3, and 21100, Public Resources Code.

15366. JURISDICTION BY LAW

(a) "Jurisdiction by law" means the authority of any public agency:

  (1) To grant a permit or other entitlement for use;

  (2) To provide funding for the project in question; or

  (3) To exercise authority over resources which may be affected by the project.

(b) A city or county will have jurisdiction by law with respect to a project when the city or county having primary jurisdiction over the area involved is:

  (1) The site of the project;

  (2) The area in which the major environmental effects will occur; and/or

  (3) The area in which reside those citizens most directly concerned by any such environmental effects.

(c) Where an agency having jurisdiction by law must exercise discretionary authority over a project in order for the project to proceed, it is also a Responsible Agency, see Section 15381, or the Lead Agency, see Section 15367.

Note: Authority cited: Section 21083, Public Resources Code; Reference: Sections 21080.3, 21080.4, 21104, and 21153, Public Resources Code.

15367. LEAD AGENCY

"Lead Agency" means the public agency which has the principal responsibility for carrying out or approving a project. The Lead Agency will decide whether an EIR or Negative Declaration will be required for the project and will cause the document to be prepared. Criteria for determining which agency will be the Lead Agency for a project are contained in Section 15051.

Note: Authority cited: Section 21083, Public Resources Code; Reference: Section 21165, Public Resources Code.

15368. LOCAL AGENCY

"Local agency" means any public agency other than a state agency, board, or commission. Local agency includes but is not limited to cities, counties, charter cities and counties, districts, school districts, special districts, redevelopment agencies, local agency formation commissions, and any board, commission, or organizational subdivision of a local agency when so designated by order or resolution of the governing legislative body of the local agency.

Note: Authority cited: Section 21083, Public Resources Code; Reference: Sections 21062 and 21151, Public Resources Code.

15369. MINISTERIAL

"Ministerial" describes a governmental decision involving little or no personal judgment by the public official as to the wisdom or manner of carrying out the project. The public official merely applies the law to the facts as presented but uses no special discretion or judgment in reaching a decision. A ministerial decision involves only the use of fixed standards or objective measurements, and the public official cannot use personal, subjective judgment in deciding whether or how the project should be carried out. Common examples of ministerial permits include automobile registrations, dog licenses, and marriage licenses. A building permit is ministerial if the ordinance requiring the permit limits the public official to determining whether the zoning allows the structure to be built in the requested location, the structure would meet the strength requirements in the Uniform Building Code, and the applicant has paid his fee.

Note: Authority cited: Section 21083, Public Resources Code; Reference: Section 21080(b)(1), Public Resources Code; *Johnson v. State of California*, 69 Cal. 2d 782; *Day v. City of Glendale*, 51 Cal. App. 3d 817.

15369.5. MITIGATED NEGATIVE DECLARATION

"Mitigated negative declaration" means a negative declaration prepared for a project when the initial study has identified potentially significant effects on the environment, but (1) revisions in the project plans or proposals made by, or agreed to by, the applicant before the proposed negative declaration and initial study are released for public review would avoid the effects or mitigate the effects to a point where clearly no significant effect on the environment would occur, and (2) there is no substantial evidence in light of the whole record before the public agency that the project, as revised, may have a significant effect on the environment.

Note: Authority cited: Sections 21083 and 21087, Public Resources Code; Reference: Section 21064.5, Public Resources Code.

15370. MITIGATION

"Mitigation" includes:

(a) Avoiding the impact altogether by not taking a certain action or parts of an action.

(b) Minimizing impacts by limiting the degree or magnitude of the action and its implementation.

(c) Rectifying the impact by repairing, rehabilitating, or restoring the impacted environment.

(d) Reducing or eliminating the impact over time by preservation and maintenance operations during the life of the action.

(e) Compensating for the impact by replacing or providing substitute resources or environments.

Note: Authority cited: Section 21083, Public Resources Code; Reference: Sections 21002, 21002.1, 21081, and 21100(c), Public Resources Code.

15371. NEGATIVE DECLARATION

"Negative Declaration" means a written statement by the Lead Agency briefly describing the reasons that a proposed project, not exempt from CEQA, will not have a significant effect on the environment and therefore does not require the preparation of an EIR. The contents of a Negative Declaration are described in Section 15071.

Note: Authority cited: Section 21083, Public Resources Code; Reference: Section 21080(c), Public Resources Code.

15372. NOTICE OF COMPLETION

"Notice of Completion" means a brief notice filed with the Office of Planning and Research by a Lead Agency as soon as it has completed a draft EIR and is prepared to send out copies for review. The contents of this notice are explained in Section 15085.

Note: Authority cited: Section 21083, Public Resources Code; Reference: Section 21161, Public Resources Code.

15373. NOTICE OF DETERMINATION

"Notice of Determination" means a brief notice to be filed by a public agency after it approves or determines to carry out a project which is subject to the requirements of CEQA. The contents of this notice are explained in Sections 15075 and 15094.

Note: Authority cited: Section 21083, Public Resources Code; Reference: Sections 21108(a) and 21152, Public Resources Code.

15374. NOTICE OF EXEMPTION

"Notice of Exemption" means a brief notice which may be filed by a public agency after it has decided to carry out or approve a project and has determined that the project is exempt from CEQA as being ministerial, categorically exempt, an emergency, or subject to another exemption from CEQA. Such a notice may also be filed by an applicant where such a determination has been made by a public agency which must approve the project. The contents of this notice are explained in Section 15062.

Note: Authority cited: Section 21083, Public Resources Code; Reference: Sections 21108(b) and 21152(b), Public Resources Code.

15375. NOTICE OF PREPARATION

"Notice of Preparation" means a brief notice sent by a Lead Agency to notify the Responsible Agencies, Trustee Agencies, the Office of Planning and Research, and involved federal agencies that the Lead Agency plans to prepare an EIR for the project. The purpose of the notice is to solicit guidance from those agencies as to the scope and content of the environmental information to be included in the EIR. Public agencies are free to develop their own formats for this notice. The contents of this notice are described in Section 15082.

Note: Authority cited: Section 21083, Public Resources Code; Reference: Section 21080.4, Public Resources Code.

15376. PERSON

"Person" includes any person, firm, association, organization, partnership, business, trust, corporation, limited liability company, company, district, city, county, city and county, town, the state, and any of the agencies and political subdivisions of such entities, and to the extent permitted by federal law, the United States, or any of its agencies or political subdivisions.

Note: Authority cited: Section 21083, Public Resources Code; Reference: Section 21066, Public Resources Code.

15377. PRIVATE PROJECT

A "private project" means a project which will be carried out by a person other than a governmental agency, but the project will need a discretionary approval from one or more governmental agencies for:

(a) A contract or financial assistance, or

(b) A lease, permit, license, certificate, or other entitlement for use.

Note: Authority cited: Section 21083, Public Resources Code; Reference: Section 21065, Public Resources Code.

15378. PROJECT

(a) "Project" means the whole of an action, which has a potential for resulting in either a direct physical change in the environment, or a reasonably foreseeable indirect physical change in the environment, and that is any of the following:

(1) An activity directly undertaken by any public agency including but not limited to public works construction and related activities clearing or grading of land, improvements to existing public structures, enactment and amendment of zoning ordinances, and the adoption and amendment of local General Plans or elements thereof pursuant to Government Code Sections 65100–65700.

(2) An activity undertaken by a person which is supported in whole or in part through public agency contacts, grants, subsidies, loans, or other forms of assistance from one or more public agencies.

(3) An activity involving the issuance to a person of a lease, permit, license, certificate, or other entitlement for use by one or more public agencies.

(b) Project does not include:

(1) Proposals for legislation to be enacted by the State Legislature;

(2) Continuing administrative or maintenance activities, such as purchases for supplies, personnel-related actions, general policy and procedure making (except as they are applied to specific instances covered above);

(3) The submittal of proposals to a vote of the people of the state or of a particular community that does not involve a public agency sponsored initiative. (*Stein v. City of Santa Monica* (1980) 110 Cal.App.3d 458; *Friends of Sierra Madre v. City of Sierra Madre* (2001) 25 Cal.4th 165);

(4) The creation of government funding mechanisms or other government fiscal activities which do not involve any commitment to any specific project which may result in a potentially significant physical impact on the environment.

(5) Organizational or administrative activities of governments that will not result in direct or indirect physical changes in the environment.

(c) The term "project" refers to the activity which is being approved and which may be subject to several discretionary approvals by governmental agencies. The term "project" does not mean each separate governmental approval.

(d) Where the Lead Agency could describe the project as either the adoption of a particular regulation under subdivision (a)(1) or as a development proposal which will be subject to several governmental approvals under subdivision (a)(2) or (a)(3), the Lead Agency shall describe the project as the development proposal for the purpose of environmental analysis. This approach will implement the Lead Agency principle as described in Article 4.

Note: Authority cited: Section 21083, Public Resources Code; Reference: Section 21065, Public Resources Code; *Kaufman and Broad-South Bay, Inc. v. Morgan Hill Unified School District* (1992) 9 Cal.App.4th 464; *Fullerton Joint Union High School District v. State Board of Education* (1982) 32 Cal.3d 779; *Simi Valley Recreation and Park District v. Local Agency Formation Commission of Ventura County* (1975) 51 Cal.App.3d 648; and *Communities for a Better Environment v. California Resources Agency* (2002) 103 Cal.App.4th 98.

15379. PUBLIC AGENCY

"Public agency" includes any state agency, board, or commission and any local or regional agency, as defined in these Guidelines. It does not include the courts of the state. This term does not include agencies of the federal government.

Note: Authority cited: Section 21083, Public Resources Code; Reference: Section 21063, Public Resources Code.

15380. ENDANGERED, RARE OR THREATENED SPECIES

(a) "Species" as used in this section means a species or subspecies of animal or plant or a variety of plant.

(b) A species of animal or plant is:

(1) "Endangered" when its survival and reproduction in the wild are in immediate jeopardy from one or more causes, including loss of habitat, change in habitat, overexploitation, predation, competition, disease, or other factors; or

(2) "Rare" when either:

(A) Although not presently threatened with extinction, the species is existing in such small numbers throughout all or a significant portion of its range that it may become endangered if its environment worsens; or

(B) The species is likely to become endangered within the foreseeable future throughout all or a significant portion of its range and may be considered "threatened" as that term is used in the Federal Endangered Species Act.

(c) A species of animal or plant shall be presumed to be endangered, rare or threatened, as it is listed in:

(1) Sections 670.2 or 670.5, Title 14, California Code of Regulations; or

(2) Title 50, Code of Federal Regulations Section 17.11 or 17.12 pursuant to the Federal Endangered Species Act as rare, threatened, or endangered.

(d) A species not included in any listing identified in subdivision (c) shall nevertheless be considered to be endangered, rare or threatened, if the species can be shown to meet the criteria in subdivision (b).

(e) This definition shall not include any species of the Class Insecta which is a pest whose protection under the provisions of CEQA would present an overwhelming and overriding risk to man as determined by:

(1) The Director of Food and Agriculture with regard to economic pests; or

(2) The Director of Health Services with regard to health risks.

Note: Authority cited: Section 21083, Public Resources Code; Reference: Section 21001(c), Public Resources Code.

15381. RESPONSIBLE AGENCY

"Responsible Agency" means a public agency which proposes to carry out or approve a project, for which a Lead Agency is preparing or has prepared an EIR or Negative Declaration. For the purposes of CEQA, the term "Responsible Agency" includes all public agencies other than the Lead Agency which have discretionary approval power over the project.

Note: Authority cited: Section 21083, Public Resources Code; Reference: Sections 21002.1, 21069, 21080.1, 21080.3, 21080.4, 21167.2, and 21167.3, Public Resources Code.

15382. SIGNIFICANT EFFECT ON THE ENVIRONMENT

"Significant effect on the environment" means a substantial, or potentially substantial, adverse change in any of the physical conditions within the area affected by the project, including land, air, water, minerals, flora, fauna, ambient noise, and objects of historic or aesthetic significance. An economic or social change by itself shall not be considered a significant effect on the environment. A social or economic change related to a physical change may be considered in determining whether the physical change is significant.

Note: Authority cited: Section 21083, Public Resources Code; Reference: Sections 21068, 21083, 21100, and 21151, Public Resources Code; *Hecton v. People of the State of California*, 58 Cal. App. 3d 653.

15383. STATE AGENCY

"State agency" means a governmental agency in the executive branch of the State Government or an entity which operates under the direction and control of an agency in the executive branch of State Government and is funded primarily by the State Treasury.

Note: Authority cited: Section 21083, Public Resources Code; Reference: Section 21100, Public Resources Code.

15384. SUBSTANTIAL EVIDENCE

(a) "Substantial evidence" as used in these guidelines means enough relevant information and reasonable inferences from this information that a fair argument can be made to support a conclusion, even though other conclusions might also be reached. Whether a fair argument can be made that the project may have a significant effect on the environment is to be determined by examining the whole record before the lead agency. Argument, speculation, unsubstantiated opinion or narrative, evidence which is clearly erroneous or inaccurate, or evidence of social or economic impacts which do not contribute to or are not caused by physical impacts on the environment does not constitute substantial evidence.

(b) Substantial evidence shall include facts, reasonable assumptions predicated upon facts, and expert opinion supported by facts.

Note: Authority cited: Section 21083, Public Resources Code; References: Sections 21080, 21082.2, 21168, and 21168.5, Public Resources Code; *No Oil, Inc. v. City of Los Angeles* (1974) 13 Cal.3d 68; *Running Fence Corp. v. Superior Court* (1975) 51 Cal.App.3d 400; *Friends of B Street v. City of Hayward* (1980) 106 Cal.App.3d 988.

15385. TIERING

"Tiering" refers to the coverage of general matters in broader EIRs (such as on general plans or policy statements) with subsequent narrower EIRs or ultimately site-specific EIRs incorporating by

reference the general discussions and concentrating solely on the issues specific to the EIR subsequently prepared. Tiering is appropriate when the sequence of EIRs is:

(a) From a general plan, policy, or program EIR to a program, plan, or policy EIR of lesser scope or to a site-specific EIR;

(b) From an EIR on a specific action at an early stage to a subsequent EIR or a supplement to an EIR at a later stage. Tiering in such cases is appropriate when it helps the Lead Agency to focus on the issues which are ripe for decision and exclude from consideration issues already decided or not yet ripe.

Note: Authority cited: Sections Section 21083, Public Resources Code; Reference: Sections 21003, 21061, and 21100, Public Resources Code.

15386. TRUSTEE AGENCY

"Trustee Agency" means a state agency having jurisdiction by law over natural resources affected by a project which are held in trust for the people of the State of California. Trustee Agencies include:

(a) The California Department of Fish and Game with regard to the fish and wildlife of the state, to designated rare or endangered native plants, and to game refuges, ecological reserves, and other areas administered by the department;

(b) The State Lands Commission with regard to state owned "sovereign" lands such as the beds of navigable waters and state school lands;

(c) The State Department of Parks and Recreation with regard to units of the State Park System;

(d) The University of California with regard to sites within the Natural Land and Water Reserves System.

Note: Authority cited: Section 21083, Public Resources Code; Reference: Sections 21080.3 and 21080.4, Public Resources Code.

15387. URBANIZED AREA

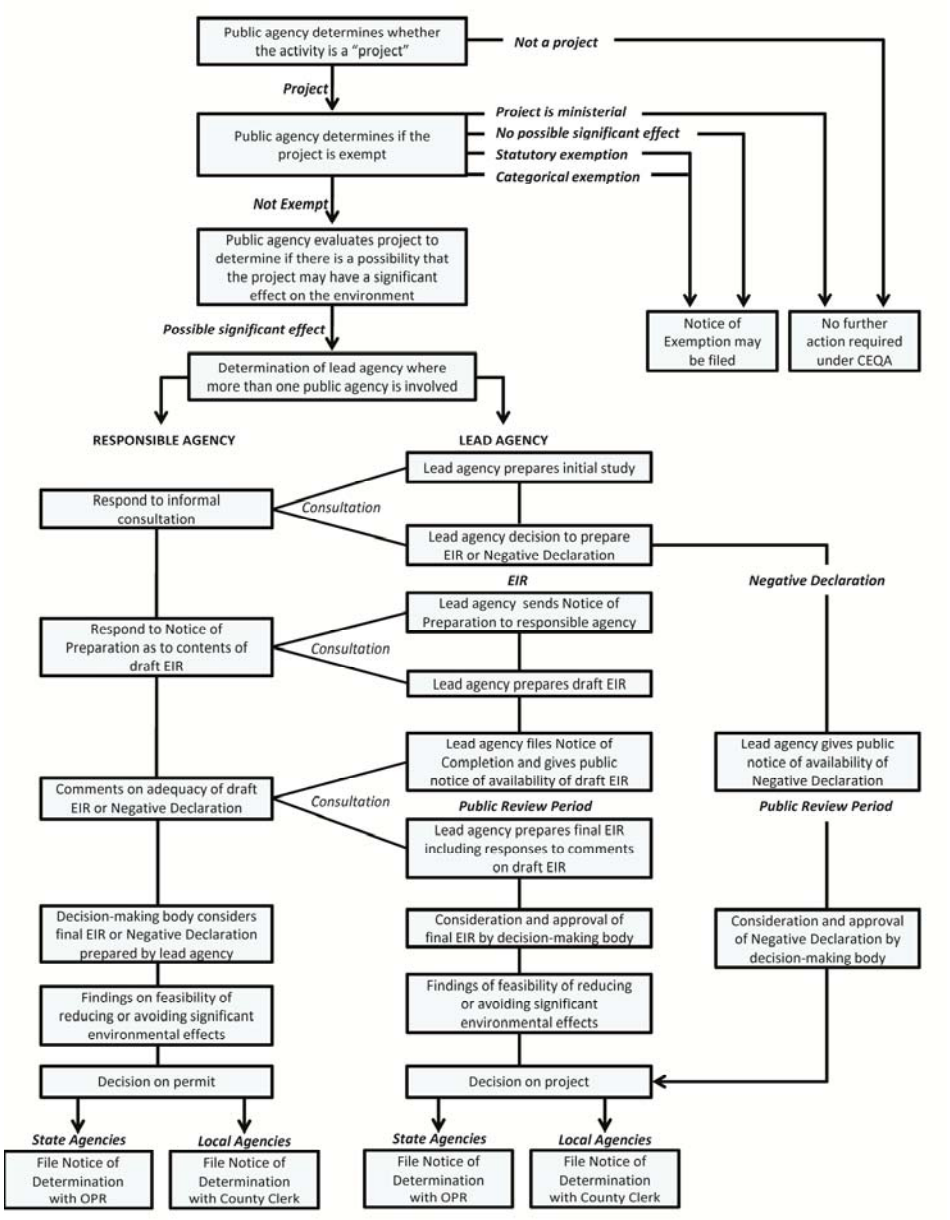
"Urbanized area" means a central city or a group of contiguous cities with a population of 50,000 or more, together with adjacent densely populated areas having a population density of at least 1,000 persons per square mile. A Lead Agency shall determine whether a particular area meets the criteria in this section either by examining the area or by referring to a map prepared by the U.S. Bureau of the Census which designates the area as urbanized. Maps of the designated urbanized areas can be found in the California EIR Monitor of February 7, 1979. The maps are also for sale by the Superintendent of Documents, U.S. Government Printing Office, Washington, D.C. 20402. The maps are sold in sets only as Stock Number 0301-3466. Use of the term "urbanized area" in Section 15182 is limited to areas mapped and designated as urbanized by the U.S. Bureau of the Census.

Note: Authority cited: Sections 21083 and 21087, Public Resources Code; Reference: Sections 21080.7 and 21083, and 21084, Public Resources Code.

CEQA Guidelines Appendices

Appendix A	CEQA Process Flow Chart
Appendix B	Statutory Authority of State Departments
Appendix C	Notice of Completion
Appendix D	Notice of Determination
Appendix E	Notice of Exemption
Appendix F	Energy Conservation
Appendix G	Environmental Checklist Form
Appendix H	Environmental Information Form
Appendix I	Notice of Preparation
Appendix J	Examples of Tiering EIRs
Appendix K	Criteria for Shortened Clearinghouse Review
Appendix L	Notice of Completion of Draft EIR
Appendix M	Performance Standards for lnfill Projects Eligible for Streamlined Review
Appendix N	Proposed Infill Environmental Checklist Form

APPENDIX A:
CEQA PROCESS FLOW CHART



APPENDIX B:
STATUTORY AUTHORITY OF STATE DEPARTMENTS

Bay Conservation and Development Commission	Air Resources Board	Resources Agency		Health Services		Savings and Loan	Real Estate	Caltrans	Dept of Housing and Community Development	Dept of Motor Vehicles	Corporations	California Highway Patrol	Aeronautics		Food and Agriculture	**STATUTORY AUTHORITY OF STATE DEPARTMENTS**
	X			X						X		16	X		1	1. Air quality and air pollution control
				X											X	2. Chemical contamination and food products
26				7												3. Coastal areas, wetlands, estuaries, waterfowl refuges, and beaches
	24			8			X		X							4. Congestion in urban areas, housing, and building displacement
				X											X	5. Disease control
	X			X												6. Electric energy generation and supply
				9			X	X	X							7. Environmental effects with special impact in low-income neighborhoods
							X								X	8. Flood plains and watersheds
				X											X	9. Food additives and food sanitation
		X		X											X	10. Herbicides
								X								11. Historic and archaeological sites
	X			X											2	12. Human ecology
				X											X	13. Microbiological contamination
																14. Mineral land reclamation
																15. Natural gas energy development generation and supply
	16			10									X			16. Navigable airways
25																17. Navigable waterways
				X								X	X			18. Noise control and abatement
25															X	19. Parks, forests, trees and outdoor recreation areas
		X		X											X	20. Pesticides
		X		X												21. Radiation and radiological health
	24			11		X	X	X	X				X			22. Regional comprehensive planning
				X											X	23. Rodent control
				X											3	24. Sanitation and waste systems
				X												25. Shellfish sanitation
															X	26. Soil and plant life, sedimentation, erosion, and hydrologic conditions
				X											X	27. Toxic Materials
				X						X		X			4	28. Transportation and handling of hazardous materials
				X											X	29. Water quality and water pollution control
				12											5	30. Fish and wildlife
25				13												31. Activities with special impact on regional jurisdictions
	24															32. Water project formulation
	24															33. Geothermal energy
																34. Oil and petroleum development, generation and supply
																35. Statewide land use patterns
	24															36. Open space policy
								X								37. Statewide overview — cumulative impact of separate projects
									X							38. Seismic hazards

APPENDIX B

continued

Office of Planning & Research	Native American Heritage Commission	Water Resources	State Water Resources Control Board	State Reclamation Board	State Lands Commission	Solid Waste Mgmt Board	Parks and Recreation	Forestry	Fish and Game	Energy Commission	Conservation	Colorado River Board	CTRPA	Coastal Commission	Boating and Waterways	
			X								X		27			1. Air quality and air pollution control
			X						X							2. Chemical contamination and food products
		X	X		X		X		X		X	14	27	26	X	3. Coastal areas, wetlands, estuaries, waterfowl refuges, and beaches
			21										27	26		4. Congestion in urban areas, housing, and building displacement
			X					22	X			14				5. Disease control
		X					X	23	X	X		14		26	X	6. Electric energy generation and supply
							19									7. Environmental effects with special impact in low-income neighborhoods
		X		20	X		X		X		X	14	27	26		8. Flood plains and watersheds
																9. Food additives and food sanitation
			X				X	22	X			14				10. Herbicides
	X				X		X						27	26		11. Historic and archaeological sites
X							X		X				27	26		12. Human ecology
			X						X			14				13. Microbiological contamination
					X		X		X		X		27	26		14. Mineral land reclamation
					X				15	X	X			26		15. Natural gas energy development generation and supply
									16							16. Navigable airways
				20	X				X			14	27	26	X	17. Navigable waterways
									17							18. Noise control and abatement
	X				X		X		X		X	14	27	26	X	19. Parks, forests, trees and outdoor recreation areas
		X	X				X	22	X							20. Pesticides
									X	X		14				21. Radiation and radiological health
X		X	X		X		X		X	X	X	14	27	26	X	22. Regional comprehensive planning
							X	22	X							23. Rodent control
		X	X			X			18		X	14		26		24. Sanitation and waste systems
			X						X							25. Shellfish sanitation
		X	X		X		X		X		X	14	27	26		26. Soil and plant life, sedimentation, erosion, and hydrologic conditions
			X			X	X		X			14				27. Toxic Materials
			X							X	X					28. Transportation and handling of hazardous materials
		X	X						X		X	14	27	26	X	29. Water quality and water pollution control
			21				X		X			14	27	26		30. Fish and wildlife
		X		20			X					14	27	26		31. Activities with special impact on regional jurisdictions
		X	X	20			X	23	X			14			X	32. Water project formulation
		X	21		X				X	X	X	14				33. Geothermal energy
			21		X				X	X	X			26		34. Oil and petroleum development, generation and supply
X					X				X	X	X		27	26		35. Statewide land use patterns
X	X				X				X		X		27	26		36. Open space policy
X										X						37. Statewide overview — cumulative impact of separate projects
		X								X	X		27	26		38. Seismic hazards

APPENDIX B FOOTNOTES

1. **Food and Agriculture** - Effects on plants and animals.
2. **Food and Agriculture** - Protection of food and fiber.
3. **Food and Agriculture** - Agricultural, dairy and feed lot Systems.
4. **Food and Agriculture** - As pertains to transportation, handling, storage and decontamination of pesticides.
5. **Food and Agriculture** - Pesticide effects, predatory animal control, bird control.
6. **California Highway Patrol** - Enforcement of motor vehicle regulations.
7. **Health Services - Beach sanitation,** water pollution, solid waste and mosquito control.
8. **Health Services** - Pertains to health component.
9. **Health Services** - Most if these are strongly related to health.
10. **Health Services -** Pertains to noise.
11. **Health Services** - Pertains to personal and environmental health components.
12. **Health Services** - As it may pertain to human health hazards.
13. **Health Services** - Pertains to comprehensive health planning.
14. **Colorado River Board** - As pertains to the Colorado, New and Alamo Rivers.
15. **Fish and Game** - As field development and distribution systems may affect fish and wildlife.
16. **Fish and Game** - As may affect migrating and resident wildlife.
17. **Fish and Game -** As excessive noise may affect wildlife.
18. Fish and Game - As water quality may affect fish and wildlife.
19. **Parks and Recreation - In impacted** areas only.
20. **Reclamation Board** - In areas of Board's jurisdiction only — the Sacramento-San Joaquin Valley.
21. **State Water Resources Control Board** - As may pertain to water quality.
22. **Forestry** - With respect to forest land.
23. **Forestry** - (6) and (32) - As related to fire protection or State (fire protection) responsibility land.
24. **Air Resources Board** - (4), (22), (32), (33), and (36) - As may pertain to residential, commercial, industrial or transportation growth.
25. **San Francisco Bay Conservation and Development Commission** - (3), (17), (19), and (30) - With respect to San Francisco Bay, Suisun Bay and adjacent shore areas.
26. **California Coastal Commission -** (3), (4), (6), (8), (11), (12), (14), (15), (17), (19), (22), (23), (26), (29), (30), (31), (34), (35), and (36) - With respect to effects within the California Coastal Zone.
27. **California Tahoe Regional Planning Agency** - With respect to effects in theTahoe Basin.
28. **Native American Heritage Commission** - With respect to places of special religious or social significance to Native Americans including archaeological sites, cemeteries, and places of worship.

NOTE: Authority cited: Section 21083, Public Resources Code; Reference: Sections 21080.3, 21080.4, 21104, and 21153, Public Resources Code.

APPENDIX C:
NOTICE OF COMPLETION & ENVIRONMENTAL DOCUMENT TRANSMITTAL

Appendix C

Notice of Completion & Environmental Document Transmittal

Mail to: State Clearinghouse, P.O. Box 3044, Sacramento, CA 95812-3044 (916) 445-0613
For Hand Delivery/Street Address: 1400 Tenth Street, Sacramento, CA 95814

SCH #

Project Title: _____

Lead Agency: _____ Contact Person: _____

Mailing Address: _____ Phone: _____

City: _____ Zip: _____ County: _____

Project Location: County: _____ City/Nearest Community: _____

Cross Streets: _____ Zip Code: _____

Longitude/Latitude (degrees, minutes and seconds): ____° ____′ ____″ N / ____° ____′ ____″ W Total Acres: _____

Assessor's Parcel No.: _____ Section: _____ Twp.: _____ Range: _____ Base: _____

Within 2 Miles: State Hwy #: _____ Waterways: _____

Airports: _____ Railways: _____ Schools: _____

Document Type:

CEQA: ☐ NOP ☐ Draft EIR NEPA: ☐ NOI Other: ☐ Joint Document
☐ Early Cons ☐ Supplement/Subsequent EIR ☐ EA ☐ Final Document
☐ Neg Dec (Prior SCH No.) _____ ☐ Draft EIS ☐ Other: _____
☐ Mit Neg Dec Other: _____ ☐ FONSI

Local Action Type:

☐ General Plan Update ☐ Specific Plan ☐ Rezone ☐ Annexation
☐ General Plan Amendment ☐ Master Plan ☐ Prezone ☐ Redevelopment
☐ General Plan Element ☐ Planned Unit Development ☐ Use Permit ☐ Coastal Permit
☐ Community Plan ☐ Site Plan ☐ Land Division (Subdivision, etc.) ☐ Other: _____

Development Type:

☐ Residential: Units _____ Acres _____
☐ Office: Sq.ft. _____ Acres _____ Employees _____ ☐ Transportation: Type _____
☐ Commercial: Sq.ft. _____ Acres _____ Employees _____ ☐ Mining: Mineral _____
☐ Industrial: Sq.ft. _____ Acres _____ Employees _____ ☐ Power: Type _____ MW _____
☐ Educational: _____ ☐ Waste Treatment: Type _____ MGD _____
☐ Recreational: _____ ☐ Hazardous Waste: Type _____
☐ Water Facilities: Type _____ MGD _____ ☐ Other: _____

Project Issues Discussed in Document:

☐ Aesthetic/Visual ☐ Fiscal ☐ Recreation/Parks ☐ Vegetation
☐ Agricultural Land ☐ Flood Plain/Flooding ☐ Schools/Universities ☐ Water Quality
☐ Air Quality ☐ Forest Land/Fire Hazard ☐ Septic Systems ☐ Water Supply/Groundwater
☐ Archeological/Historical ☐ Geologic/Seismic ☐ Sewer Capacity ☐ Wetland/Riparian
☐ Biological Resources ☐ Minerals ☐ Soil Erosion/Compaction/Grading ☐ Growth Inducement
☐ Coastal Zone ☐ Noise ☐ Solid Waste ☐ Land Use
☐ Drainage/Absorption ☐ Population/Housing Balance ☐ Toxic/Hazardous ☐ Cumulative Effects
☐ Economic/Jobs ☐ Public Services/Facilities ☐ Traffic/Circulation ☐ Other: _____

Present Land Use/Zoning/General Plan Designation:

Project Description: *(please use a separate page if necessary)*

Note: The State Clearinghouse will assign identification numbers for all new projects. If a SCH number already exists for a project (e.g. Notice of Preparation or previous draft document) please fill in.

Revised 2008

APPENDIX C

continued

Reviewing Agencies Checklist

Lead Agencies may recommend State Clearinghouse distribution by marking agencies below with and "**X**".
If you have already sent your document to the agency please denote that with an "**S**".

_____ Air Resources Board
_____ Boating & Waterways, Department of
_____ California Highway Patrol
_____ Caltrans District # _____
_____ Caltrans Division of Aeronautics
_____ Caltrans Planning
_____ Central Valley Flood Protection Board
_____ Coachella Valley Mtns. Conservancy
_____ Coastal Commission
_____ Colorado River Board
_____ Conservation, Department of
_____ Corrections, Department of
_____ Delta Protection Commission
_____ Education, Department of
_____ Energy Commission
_____ Fish & Game Region # _____
_____ Food & Agriculture, Department of
_____ Forestry and Fire Protection, Department of
_____ General Services, Department of
_____ Health Services, Department of
_____ Housing & Community Development
_____ Integrated Waste Management Board
_____ Native American Heritage Commission
_____ Office of Emergency Services
_____ Office of Historic Preservation
_____ Office of Public School Construction
_____ Parks & Recreation, Department of
_____ Pesticide Regulation, Department of
_____ Public Utilities Commission
_____ Regional WQCB # _____
_____ Resources Agency
_____ S.F. Bay Conservation & Development Comm.
_____ San Gabriel & Lower L.A. Rivers & Mtns. Conservancy
_____ San Joaquin River Conservancy
_____ Santa Monica Mtns. Conservancy
_____ State Lands Commission
_____ SWRCB: Clean Water Grants
_____ SWRCB: Water Quality
_____ SWRCB: Water Rights
_____ Tahoe Regional Planning Agency
_____ Toxic Substances Control, Department of
_____ Water Resources, Department of
_____ Other: _____
_____ Other: _____

Local Public Review Period (to be filled in by lead agency)

Starting Date _____ Ending Date _____

Lead Agency (Complete if applicable):

Consulting Firm: _____
Address: _____
City/State/Zip: _____
Contact: _____
Phone: _____

Applicant: _____
Address: _____
City/State/Zip: _____
Phone: _____

Signature of Lead Agency Representative: _____ **Date:** _____

Authority cited: Section 21083, Public Resources Code. Reference: Section 21161, Public Resources Code.

Revised 2008

APPENDIX D:
NOTICE OF DETERMINATION

Notice of Determination

Appendix D

To:
☐ Office of Planning and Research
For U.S. Mail: P.O. Box 3044 Sacramento, CA 95812-3044
Street Address: 1400 Tenth St. Sacramento, CA 95814

☐ County Clerk
County of: _____
Address: _____

From:
Public Agency: _____
Address: _____
Contact: _____
Phone: _____

Lead Agency (if different from above):
Address: _____
Contact: _____
Phone: _____

SUBJECT: Filing of Notice of Determination in compliance with Section 21108 or 21152 of the Public Resources Code.

State Clearinghouse Number (if submitted to State Clearinghouse): _____

Project Title: _____

Project Location (include county): _____

Project Description:

This is to advise that the _____ has approved the above described project on
☐ Lead Agency or ☐ Responsible Agency
_____ and has made the following determinations regarding the above described project:
(Date)

1. The project [☐ will ☐ will not] have a significant effect on the environment.
2. ☐ An Environmental Impact Report was prepared for this project pursuant to the provisions of CEQA.
   ☐ A Negative Declaration was prepared for this project pursuant to the provisions of CEQA.
3. Mitigation measures [☐ were ☐ were not] made a condition of the approval of the project.
4. A mitigation reporting or monitoring plan [☐ was ☐ was not] adopted for this project.
5. A statement of Overriding Considerations [☐ was ☐ was not] adopted for this project.
6. Findings [☐ were ☐ were not] made pursuant to the provisions of CEQA.

This is to certify that the final EIR with comments and responses and record of project approval, or the Negative Declaration, is available to the General Public at:

Signature (Public Agency) _____ Title _____

Date _____ Date Received for filing at OPR _____

Authority cited: Sections 21083, Public Resources Code.
Reference Section 21000-21174, Public Resources Code.

Revised 2005

APPENDIX E:
NOTICE OF EXEMPTION

Notice of Exemption

Appendix E

To: Office of Planning and Research
P.O. Box 3044, Room 212
Sacramento, CA 95812-3044

County Clerk
County of _____

_____

_____

From: (Public Agency) _____

_____

_____
(Address)

Project Title: _____

Project Location - Specific:

Project Location – City: _____ Project Location – County: _____

Description of Nature, Purpose and Beneficiaries of Project:

Name of Public Agency Approving Project: _____

Name of Person or Agency Carrying Out Project: _____

Exempt Status: **(check one)**

- ☐ Ministerial (Sec. 21080(b)(1); 15268);
- ☐ Declared Emergency (Sec. 21080(b)(3); 15269(a));
- ☐ Emergency Project (Sec. 21080(b)(4); 15269(b)(c));
- ☐ Categorical Exemption. State type and section number: _____
- ☐ Statutory Exemptions. State code number: _____

Reasons why project is exempt:

Lead Agency
Contact Person: _____ Area Code/Telephone/Extension: _____

If filed by applicant:

1. Attach certified document of exemption finding.
2. Has a Notice of Exemption been filed by the public agency approving the project? ☐ Yes ☐ No

Signature: _____ Date: _____ Title: _____

☐ Signed by Lead Agency

☐ Signed by Applicant

Date received for filing at OPR: _____

Revised 2005

APPENDIX F:
ENERGY CONSERVATION

I. Introduction

The goal of conserving energy implies the wise and efficient use of energy. The means of achieving this goal include:

(1) decreasing overall per capita energy consumption,

(2) decreasing reliance on fossil fuels such as coal, natural gas and oil, and

(3) increasing reliance on renewable energy sources.

In order to assure that energy implications are considered in project decisions, the California Environmental Quality Act requires that EIRs include a discussion of the potential energy impacts of proposed projects, with particular emphasis on avoiding or reducing inefficient, wasteful and unnecessary consumption of energy (see Public Resources Code section 21100(b)(3)). Energy conservation implies that a project's cost effectiveness be reviewed not only in dollars, but also in terms of energy requirements. For many projects, cost effectiveness may be determined more by energy efficiency than by initial dollar costs. A lead agency may consider the extent to which an energy source serving the project has already undergone environmental review that adequately analyzed and mitigated the effects of energy production.

II. EIR Contents

Potentially significant energy implications of a project shall be considered in an EIR to the extent relevant and applicable to the project. The following list of energy impact possibilities and potential conservation measures is designed to assist in the preparation of an EIR. In many instances specific items may not apply or additional items may be needed. Where items listed below are applicable or relevant to the project, they should be considered in the EIR.

A. Project Description may include the following items:

1. Energy consuming equipment and processes which will be used during construction, operation and/or removal of the project. If appropriate, this discussion should consider the energy intensiveness of materials and equipment required for the project.
2. Total energy requirements of the project by fuel type and end use.
3. Energy conservation equipment and design features.
4. Identification of energy supplies that would serve the project.
5. Total estimated daily vehicle trips to be generated by the project and the additional energy consumed per trip by mode.

B. Environmental Setting may include existing energy supplies and energy use patterns in the region and locality.

C. Environmental Impacts may include:

1. The project's energy requirements and its energy use efficiencies by amount and fuel type for each stage of the project including construction, operation, maintenance and/or removal. If appropriate, the energy intensiveness of materials maybe discussed.
2. The effects of the project on local and regional energy supplies and on requirements for additional capacity.
3. The effects of the project on peak and base period demands for electricity and other forms of energy.
4. The degree to which the project complies with existing energy standards.
5. The effects of the project on energy resources.

6. The project's projected transportation energy use requirements and its overall use of efficient transportation alternatives.

D. Mitigation Measures may include:

1. Potential measures to reduce wasteful, inefficient and unnecessary consumption of energy during construction, operation, maintenance and/or removal. The discussion should explain why certain measures were incorporated in the project and why other measures were dismissed.
2. The potential of siting, orientation, and design to minimize energy consumption, including transportation energy, increase water conservation and reduce solid waste.
3. The potential for reducing peak energy demand.
4. Alternate fuels (particularly renewable ones) or energy systems.
5. Energy conservation which could result from recycling efforts.

E. Alternatives should be compared in terms of overall energy consumption and in terms of reducing wasteful, inefficient and unnecessary consumption of energy.

F. Unavoidable Adverse Effects may include wasteful, inefficient and unnecessary consumption of energy during the project construction, operation, maintenance and/or removal that cannot be feasibly mitigated.

G. Irreversible Commitment of Resources may include a discussion of how the project preempts future energy development or future energy conservation.

H. Short-Term Gains versus Long-Term Impacts can be compared by calculating the project's energy costs over the project's lifetime.

I. Growth Inducing Effects may include the estimated energy consumption of growth induced by the project.

Note: Authority cited: Sections 21083 and 21087, Public Resources Code. Reference: Sections 21000-21176. Public Resources Code.

Revised 2009

APPENDIX G:
ENVIRONMENTAL CHECKLIST FORM

NOTE: The following is a sample form and may be tailored to satisfy individual agencies' needs and project circumstances. It may be used to meet the requirements for an initial study when the criteria set forth in CEQA Guidelines have been met. Substantial evidence of potential impacts that are not listed on this form must also be considered. The sample questions in this form are intended to encourage thoughtful assessment of impacts, and do not necessarily represent thresholds of significance.

1. Project title: _____
2. Lead agency name and address:

   _____

   _____

   _____
3. Contact person and phone number: _____
4. Project location: _____
5. Project sponsor's name and address:

   _____

   _____

   _____
6. General plan designation: _____ 7. Zoning: _____
8. Description of project: (Describe the whole action involved, including but not limited to later phases of the project, and any secondary, support, or off-site features necessary for its implementation. Attach additional sheets if necessary.)

   _____

   _____

   _____

   _____
9. Surrounding land uses and setting: Briefly describe the project's surroundings:

   _____

   _____

   _____

   _____
10. Other public agencies whose approval is required (e.g., permits, financing approval, or participation agreement.)

    _____

    _____

    _____

    _____

ENVIRONMENTAL FACTORS POTENTIALLY AFFECTED:

The environmental factors checked below would be potentially affected by this project, involving at least one impact that is a "Potentially Significant Impact" as indicated by the checklist on the following pages.

☐ Aesthetics	☐ Agriculture and Forestry Resources	☐ Air Quality
☐ Biological Resources	☐ Cultural Resources	☐ Geology /Soils
☐ Greenhouse Gas Emissions	☐ Hazards & Hazardous Materials	☐ Hydrology / Water Quality
☐ Land Use / Planning	☐ Mineral Resources	☐ Noise
☐ Population / Housing	☐ Public Services	☐ Recreation
☐ Transportation/Traffic	☐ Utilities / Service Systems	☐ Mandatory Findings of Significance

DETERMINATION: (To be completed by the Lead Agency)

On the basis of this initial evaluation:

☐ I find that the proposed project COULD NOT have a significant effect on the environment, and a NEGATIVE DECLARATION will be prepared.

☐ I find that although the proposed project could have a significant effect on the environment, there will not be a significant effect in this case because revisions in the project have been made by or agreed to by the project proponent. A MITIGATED NEGATIVE DECLARATION will be prepared.

☐ I find that the proposed project MAY have a significant effect on the environment, and an ENVIRONMENTAL IMPACT REPORT is required.

☐ I find that the proposed project MAY have a "potentially significant impact" or "potentially significant unless mitigated" impact on the environment, but at least one effect 1) has been adequately analyzed in an earlier document pursuant to applicable legal standards, and 2) has been addressed by mitigation measures based on the earlier analysis as described on attached sheets. An ENVIRONMENTAL IMPACT REPORT is required, but it must analyze only the effects that remain to be addressed.

☐ I find that although the proposed project could have a significant effect on the environment, because all potentially significant effects (a) have been analyzed adequately in an earlier EIR or NEGATIVE DECLARATION pursuant to applicable standards, and (b) have been avoided or mitigated pursuant to that earlier EIR or NEGATIVE DECLARATION, including revisions or mitigation measures that are imposed upon the proposed project, nothing further is required.

_____ _____

Signature Date

_____ _____

Signature Date

EVALUATION OF ENVIRONMENTAL IMPACTS:

1) A brief explanation is required for all answers except "No Impact" answers that are adequately supported by the information sources a lead agency cites in the parentheses following each question. A "No Impact" answer is adequately supported if the referenced information sources show that the impact simply does not apply to projects like the one involved (e.g., the project falls outside a fault rupture zone). A "No Impact" answer should be explained where it is based on project-specific factors as well as general standards (e.g., the project will not expose sensitive receptors to pollutants, based on a project-specific screening analysis).

2) All answers must take account of the whole action involved, including off-site as well as on-site, cumulative as well as project-level, indirect as well as direct, and construction as well as operational impacts.

3) Once the lead agency has determined that a particular physical impact may occur, then the checklist answers must indicate whether the impact is potentially significant, less than significant with mitigation, or less than significant. "Potentially Significant Impact" is appropriate if there is substantial evidence that an effect may be significant. If there are one or more "Potentially Significant Impact" entries when the determination is made, an EIR is required.

4) "Negative Declaration: Less Than Significant With Mitigation Incorporated" applies where the incorporation of mitigation measures has reduced an effect from "Potentially Significant Impact" to a "Less Than Significant Impact." The lead agency must describe the mitigation measures, and briefly explain how they reduce the effect to a less than significant level (mitigation measures from "Earlier Analyses," as described in (5) below, may be cross-referenced).

5) Earlier analyses may be used where, pursuant to the tiering, program EIR, or other CEQA process, an effect has been adequately analyzed in an earlier EIR or negative declaration. Section 15063(c)(3)(D). In this case, a brief discussion should identify the following:

   a) Earlier Analysis Used. Identify and state where they are available for review.

   b) Impacts Adequately Addressed. Identify which effects from the above checklist were within the scope of and adequately analyzed in an earlier document pursuant to applicable legal standards, and state whether such effects were addressed by mitigation measures based on the earlier analysis.

   c) Mitigation Measures. For effects that are "Less than Significant with Mitigation Measures Incorporated," describe the mitigation measures which were incorporated or refined from the earlier document and the extent to which they address site-specific conditions for the project.

6) Lead agencies are encouraged to incorporate into the checklist references to information sources for potential impacts (e.g., general plans, zoning ordinances). Reference to a previously prepared or outside document should, where appropriate, include a reference to the page or pages where the statement is substantiated.

7) Supporting Information Sources: A source list should be attached, and other sources used or individuals contacted should be cited in the discussion.

8) This is only a suggested form, and lead agencies are free to use different formats; however, lead agencies should normally address the questions from this checklist that are relevant to a project's environmental effects in whatever format is selected.

9) The explanation of each issue should identify:

a) the significance criteria or threshold, if any, used to evaluate each question; and

b) the mitigation measure identified, if any, to reduce the impact to less than significance

SAMPLE QUESTION

Issues:

	Potentially Significant Impact	**Less Than Significant with Mitigation Incorporated**	**Less Than Significant Impact**	**No Impact**
I. AESTHETICS. Would the project:				
a) Have a substantial adverse effect on a scenic vista?	☐	☐	☐	☐
b) Substantially damage scenic resources, including, but not limited to, trees, rock outcroppings, and historic buildings within a state scenic highway?	☐	☐	☐	☐
c) Substantially degrade the existing visual character or quality of the site and its surroundings?	☐	☐	☐	☐
d) Create a new source of substantial light or glare which would adversely affect day or nighttime views in the area?	☐	☐	☐	☐
II. AGRICULTURE AND FORESTRY RESOURCES. In determining whether impacts to agricultural resources are significant environmental effects, lead agencies may refer to the California Agricultural Land Evaluation and Site Assessment Model (1997) prepared by the California Dept. of Conservation as an optional model to use in assessing impacts on agriculture and farmland. In determining whether impacts to forest resources, including timberland, are significant environmental effects, lead agencies may refer to information compiled by the California Department of Forestry and Fire Protection regarding the state's inventory of forest land, including the Forest and Range Assessment Project and the Forest Legacy Assessment project; and forest carbon measurement methodology provided in Forest Protocols adopted by the California Air Resources Board. Would the project:				

	Potentially Significant Impact	Less Than Significant with Mitigation Incorporated	Less Than Significant Impact	No Impact
a) Convert Prime Farmland, Unique Farmland, or Farmland of Statewide Importance (Farmland), as shown on the maps prepared pursuant to the Farmland Mapping and Monitoring Program of the California Resources Agency, to non-agricultural use?	☐	☐	☐	☐
b) Conflict with existing zoning for agricultural use, or a Williamson Act contract?	☐	☐	☐	☐
c) Conflict with existing zoning for, or cause rezoning of, forest land (as defined in Public Resources Code section 12220(g)), timberland (as defined by Public Resources Code section 4526), or timberland zoned Timberland Production (as defined by Government Code section 51104(g))?	☐	☐	☐	☐
d) Result in the loss of forest land or conversion of forest land to non-forest use?	☐	☐	☐	☐
e) Involve other changes in the existing environment which, due to their location or nature, could result in conversion of Farmland, to non-agricultural use or conversion of forest land to non-forest use?	☐	☐	☐	☐
III. AIR QUALITY. Where available, the significance criteria established by the applicable air quality management or air pollution control district may be relied upon to make the following determinations. Would the project:				
a) Conflict with or obstruct implementation of the applicable air quality plan?	☐	☐	☐	☐
b) Violate any air quality standard or contribute substantially to an existing or projected air quality violation?	☐	☐	☐	☐
c) Result in a cumulatively considerable net increase of any criteria pollutant for which the project region is non-attainment under an applicable federal or state ambient air quality standard (including releasing emissions which exceed quantitative thresholds for ozone precursors)?	☐	☐	☐	☐

	Potentially Significant Impact	Less Than Significant with Mitigation Incorporated	Less Than Significant Impact	No Impact
d) Expose sensitive receptors to substantial pollutant concentrations?	☐	☐	☐	☐
e) Create objectionable odors affecting a substantial number of people?	☐	☐	☐	☐
IV. BIOLOGICAL RESOURCES: Would the project:				
a) Have a substantial adverse effect, either directly or through habitat modifications, on any species identified as a candidate, sensitive, or special status species in local or regional plans, policies, or regulations, or by the California Department of Fish and Game or U.S. Fish and Wildlife Service?	☐	☐	☐	☐
b) Have a substantial adverse effect on any riparian habitat or other sensitive natural community identified in local or regional plans, policies, regulations or by the California Department of Fish and Game or US Fish and Wildlife Service?	☐	☐	☐	☐
c) Have a substantial adverse effect on federally protected wetlands as defined by Section 404 of the Clean Water Act (including, but not limited to, marsh, vernal pool, coastal, etc.) through direct removal, filling, hydrological interruption, or other means?	☐	☐	☐	☐
d) Interfere substantially with the movement of any native resident or migratory fish or wildlife species or with established native resident or migratory wildlife corridors, or impede the use of native wildlife nursery sites?	☐	☐	☐	☐
e) Conflict with any local policies or ordinances protecting biological resources, such as a tree preservation policy or ordinance?	☐	☐	☐	☐
f) Conflict with the provisions of an adopted Habitat Conservation Plan, Natural Community Conservation Plan, or other approved local, regional, or state habitat conservation plan?	☐	☐	☐	☐

	Potentially Significant Impact	Less Than Significant with Mitigation Incorporated	Less Than Significant Impact	No Impact
V. CULTURAL RESOURCES. Would the project:				
a) Cause a substantial adverse change in the significance of a historical resource as defined in § 15064.5?	☐	☐	☐	☐
b) Cause a substantial adverse change in the significance of an archaeological resource pursuant to § 15064.5?	☐	☐	☐	☐
c) Directly or indirectly destroy a unique paleontological resource or site or unique geologic feature?	☐	☐	☐	☐
d) Disturb any human remains, including those interred outside of formal cemeteries?	☐	☐	☐	☐
VI. GEOLOGY AND SOILS. Would the project:				
a) Expose people or structures to potential substantial adverse effects, including the risk of loss, injury, or death involving:	☐	☐	☐	☐
i) Rupture of a known earthquake fault, as delineated on the most recent Alquist-Priolo Earthquake Fault Zoning Map issued by the State Geologist for the area or based on other substantial evidence of a known fault? Refer to Division of Mines and Geology Special Publication 42.	☐	☐	☐	☐
ii) Strong seismic ground shaking?	☐	☐	☐	☐
iii) Seismic-related ground failure, including liquefaction?	☐	☐	☐	☐
iv) Landslides?	☐	☐	☐	☐
b) Result in substantial soil erosion or the loss of topsoil?	☐	☐	☐	☐
c) Be located on a geologic unit or soil that is unstable, or that would become unstable as a result of the project, and potentially result in on- or off-site landslide, lateral spreading, subsidence, liquefaction or collapse?	☐	☐	☐	☐

	Potentially Significant Impact	**Less Than Significant with Mitigation Incorporated**	**Less Than Significant Impact**	**No Impact**
d) Be located on expansive soil, as defined in Table 18-1-B of the Uniform Building Code (1994), creating substantial risks to life or property?	☐	☐	☐	☐
e) Have soils incapable of adequately supporting the use of septic tanks or alternative waste water disposal systems where sewers are not available for the disposal of waste water?	☐	☐	☐	☐
VII. GREENHOUSE GAS EMISSIONS. Would the project:				
a) Generate greenhouse gas emissions, either directly or indirectly, that may have a significant impact on the environment?	☐	☐	☐	☐
b) Conflict with an applicable plan, policy or regulation adopted for the purpose of reducing the emissions of greenhouse gases?	☐	☐	☐	☐
VIII. HAZARDS AND HAZARDOUS MATERIALS. Would the project:				
a) Create a significant hazard to the public or the environment through the routine transport, use, or disposal of hazardous materials?	☐	☐	☐	☐
b) Create a significant hazard to the public or the environment through reasonably foreseeable upset and accident conditions involving the release of hazardous materials into the environment?	☐	☐	☐	☐
c) Emit hazardous emissions or handle hazardous or acutely hazardous materials, substances, or waste within one-quarter mile of an existing or proposed school?	☐	☐	☐	☐
d) Be located on a site which is included on a list of hazardous materials sites compiled pursuant to Government Code Section 65962.5 and, as a result, would it create a significant hazard to the public or the environment?	☐	☐	☐	☐

	Potentially Significant Impact	Less Than Significant with Mitigation Incorporated	Less Than Significant Impact	No Impact
e) For a project located within an airport land use plan or, where such a plan has not been adopted, within two miles of a public airport or public use airport, would the project result in a safety hazard for people residing or working in the project area?	☐	☐	☐	☐
f) For a project within the vicinity of a private airstrip, would the project result in a safety hazard for people residing or working in the project area?	☐	☐	☐	☐
g) Impair implementation of or physically interfere with an adopted emergency response plan or emergency evacuation plan?	☐	☐	☐	☐
h) Expose people or structures to a significant risk of loss, injury or death involving wildland fires, including where wildlands are adjacent to urbanized areas or where residences are intermixed with wildlands?	☐	☐	☐	☐
IX. HYDROLOGY AND WATER QUALITY. Would the project:				
a) Violate any water quality standards or waste discharge requirements?	☐	☐	☐	☐
b) Substantially deplete groundwater supplies or interfere substantially with groundwater recharge such that there would be a net deficit in aquifer volume or a lowering of the local groundwater table level (e.g., the production rate of pre-existing nearby wells would drop to a level which would not support existing land uses or planned uses for which permits have been granted)?	☐	☐	☐	☐
c) Substantially alter the existing drainage pattern of the site or area, including through the alteration of the course of a stream or river, in a manner which would result in substantial erosion or siltation on- or off-site?	☐	☐	☐	☐

	Potentially Significant Impact	**Less Than Significant with Mitigation Incorporated**	**Less Than Significant Impact**	**No Impact**
d) Substantially alter the existing drainage pattern of the site or area, including through the alteration of the course of a stream or river, or substantially increase the rate or amount of surface runoff in a manner which would result in flooding on- or off-site?	☐	☐	☐	☐
e) Create or contribute runoff water which would exceed the capacity of existing or planned stormwater drainage systems or provide substantial additional sources of polluted runoff?	☐	☐	☐	☐
f) Otherwise substantially degrade water quality?	☐	☐	☐	☐
g) Place housing within a 100-year flood hazard area as mapped on a federal Flood Hazard Boundary or Flood Insurance Rate Map or other flood hazard delineation map?	☐	☐	☐	☐
h) Place within a 100-year flood hazard area structures which would impede or redirect flood flows?	☐	☐	☐	☐
i) Expose people or structures to a significant risk of loss, injury or death involving flooding, including flooding as a result of the failure of a levee or dam?	☐	☐	☐	☐
j) Inundation by seiche, tsunami, or mudflow?	☐	☐	☐	☐
X. LAND USE AND PLANNING. Would the project:				
a) Physically divide an established community?	☐	☐	☐	☐
b) Conflict with any applicable land use plan, policy, or regulation of an agency with jurisdiction over the project (including, but not limited to the general plan, specific plan, local coastal program, or zoning ordinance) adopted for the purpose of avoiding or mitigating an environmental effect?	☐	☐	☐	☐

	Potentially Significant Impact	Less Than Significant with Mitigation Incorporated	Less Than Significant Impact	No Impact
c) Conflict with any applicable habitat conservation plan or natural community conservation plan?	☐	☐	☐	☐
XI. MINERAL RESOURCES. Would the project:				
a) Result in the loss of availability of a known mineral resource that would be of value to the region and the residents of the state?	☐	☐	☐	☐
b) Result in the loss of availability of a locally-important mineral resource recovery site delineated on a local general plan, specific plan or other land use plan?	☐	☐	☐	☐
XII. NOISE -- Would the project result in:				
a) Exposure of persons to or generation of noise levels in excess of standards established in the local general plan or noise ordinance, or applicable standards of other agencies?	☐	☐	☐	☐
b) Exposure of persons to or generation of excessive groundborne vibration or groundborne noise levels?	☐	☐	☐	☐
c) A substantial permanent increase in ambient noise levels in the project vicinity above levels existing without the project?	☐	☐	☐	☐
d) A substantial temporary or periodic increase in ambient noise levels in the project vicinity above levels existing without the project?	☐	☐	☐	☐
e) For a project located within an airport land use plan or, where such a plan has not been adopted, within two miles of a public airport or public use airport, would the project expose people residing or working in the project area to excessive noise levels?	☐	☐	☐	☐
f) For a project within the vicinity of a private airstrip, would the project expose people residing or working in the project area to excessive noise levels?	☐	☐	☐	☐

	Potentially Significant Impact	Less Than Significant with Mitigation Incorporated	Less Than Significant Impact	No Impact
XIII. POPULATION AND HOUSING. Would the project:				
a) Induce substantial population growth in an area, either directly (for example, by proposing new homes and businesses) or indirectly (for example, through extension of roads or other infrastructure)?	☐	☐	☐	☐
b) Displace substantial numbers of existing housing, necessitating the construction of replacement housing elsewhere?	☐	☐	☐	☐
c) Displace substantial numbers of people, necessitating the construction of replacement housing elsewhere?	☐	☐	☐	☐
XIV. PUBLIC SERVICES.				
a) Would the project result in substantial adverse physical impacts associated with the provision of new or physically altered governmental facilities, need for new or physically altered governmental facilities, the construction of which could cause significant environmental impacts, in order to maintain acceptable service ratios, response times or other performance objectives for any of the public services:	☐	☐	☐	☐
Fire protection?	☐	☐	☐	☐
Police protection?	☐	☐	☐	☐
Schools?	☐	☐	☐	☐
Parks?	☐	☐	☐	☐
Other public facilities?	☐	☐	☐	☐
XV. RECREATION.				
a) Would the project increase the use of existing neighborhood and regional parks or other recreational facilities such that substantial physical deterioration of the facility would occur or be accelerated?	☐	☐	☐	☐

	Potentially Significant Impact	**Less Than Significant with Mitigation Incorporated**	**Less Than Significant Impact**	**No Impact**
b) Does the project include recreational facilities or require the construction or expansion of recreational facilities which might have an adverse physical effect on the environment?	☐	☐	☐	☐
XVI. TRANSPORTATION/TRAFFIC. Would the project:				
a) Conflict with an applicable plan, ordinance or policy establishing measures of effectiveness for the performance of the circulation system, taking into account all modes of transportation including mass transit and non-motorized travel and relevant components of the circulation system, including but not limited to intersections, streets, highways and freeways, pedestrian and bicycle paths, and mass transit?	☐	☐	☐	☐
b) Conflict with an applicable congestion management program, including, but not limited to level of service standards and travel demand measures, or other standards established by the county congestion management agency for designated roads or highways?	☐	☐	☐	☐
c) Result in a change in air traffic patterns, including either an increase in traffic levels or a change in location that results in substantial safety risks?	☐	☐	☐	☐
d) Substantially increase hazards due to a design feature (e.g., sharp curves or dangerous intersections) or incompatible uses (e.g., farm equipment)?	☐	☐	☐	☐
e) Result in inadequate emergency access?	☐	☐	☐	☐
f) Conflict with adopted policies, plans, or programs regarding public transit, bicycle, or pedestrian facilities, or otherwise decrease the performance or safety of such facilities?	☐	☐	☐	☐

	Potentially Significant Impact	Less Than Significant with Mitigation Incorporated	Less Than Significant Impact	No Impact
XVII. UTILITIES AND SERVICE SYSTEMS. Would the project:				
a) Exceed wastewater treatment requirements of the applicable Regional Water Quality Control Board?	☐	☐	☐	☐
b) Require or result in the construction of new water or wastewater treatment facilities or expansion of existing facilities, the construction of which could cause significant environmental effects?	☐	☐	☐	☐
c) Require or result in the construction of new storm water drainage facilities or expansion of existing facilities, the construction of which could cause significant environmental effects?	☐	☐	☐	☐
d) Have sufficient water supplies available to serve the project from existing entitlements and resources, or are new or expanded entitlements needed?	☐	☐	☐	☐
e) Result in a determination by the wastewater treatment provider which serves or may serve the project that it has adequate capacity to serve the project's projected demand in addition to the provider's existing commitments?	☐	☐	☐	☐
f) Be served by a landfill with sufficient permitted capacity to accommodate the project's solid waste disposal needs?	☐	☐	☐	☐
g) Comply with federal, state, and local statutes and regulations related to solid waste?	☐	☐	☐	☐
XVIII. MANDATORY FINDINGS OF SIGNIFICANCE.				
a) Does the project have the potential to degrade the quality of the environment, substantially reduce the habitat of a fish or wildlife species, cause a fish or wildlife population to drop below self-sustaining levels, threaten to eliminate a plant or animal community, reduce the number o restrict the range of a rare or endangered plant or animal or eliminate important examples of the major periods of California history or prehistory?	☐	☐	☐	☐

	Potentially Significant Impact	Less Than Significant with Mitigation Incorporated	Less Than Significant Impact	No Impact
b) Does the project have impacts that are individually limited, but cumulatively considerable? ("Cumulatively considerable" means that the incremental effects of a project are considerable when viewed in connection with the effects of past projects, the effects of other current projects, and the effects of probable future projects)?	☐	☐	☐	☐
c) Does the project have environmental effects which will cause substantial adverse effects on human beings, either directly or indirectly?	☐	☐	☐	☐

Note: Authority cited: Sections 21083 and 21083.05, Public Resources Code. Reference: Section 65088.4, Gov. Code; Sections 21080(c), 21080.1, 21080.3, 21083, 21083.05, 21083.3, 21093, 21094, 21095, and 21151, Public Resources Code; *Sundstrom v. County of Mendocino*,(1988) 202 Cal.App.3d 296; *Leonoff v. Monterey Board of Supervisors,* (1990) 222 Cal.App.3d 1337; *Eureka Citizens for Responsible Govt. v. City of Eureka* (2007) 147 Cal.App.4th 357; *Protect the Historic Amador Waterways v. Amador Water Agency* (2004) 116 Cal.App.4th at 1109; *San Franciscans Upholding the Downtown Plan v. City and County of San Francisco* (2002) 102 Cal.App.4th 656.

Revised 2009

APPENDIX H:
ENVIRONMENTAL INFORMATION FORM

(To be Completed by Applicant)

Date Filed _____

General Information

1. Name and address of developer or project sponsor: _____
2. Address of project: _____

   Assessor's Block and Lot Number: _____
3. Name, address, and telephone number of person to be contacted concerning this project:

   _____

   _____
4. Indicate number of the permit application for the project to which this form pertains: _____
5. List and describe any other related permits and other public approvals required for this project, including those required by city, regional, state and federal agencies:

   _____
6. Existing zoning district:: _____
7. Proposed use of site (Project for which this form is filed): _____

   _____

Project Description

8. Site size.
9. Square footage.
10. Number of floors of construction.
11. Amount of off-street parking provided.
12. Attach plans.
13. Proposed scheduling.
14. Associated projects.
15. Anticipated incremental development.
16. If residential, include the number of units, schedule of unit sizes, range of sale prices or rents, and type of household size expected.
17. If commercial, indicate the type, whether neighborhood, city or regionally oriented, square footage of sales area, and loading facilities.
18. If industrial, indicate type, estimated employment per shift, and loading facilities.

19. If institutional, indicate the major function, estimated employment per shift, estimated occupancy, loading facilities, and community benefits to be derived from the project.
20. If the project involves a variance, conditional use or rezoning application, state this and indicate clearly why the application is required.

Are the following items applicable to the project or its effects? Discuss below all items checked yes (attach additional sheets as necessary).

		Yes	No
21.	Change in existing features of any bays, tidelands, beaches, or hills, or substantial alteration of ground contours.	☐	☐
22.	Change in scenic views or vistas from existing residential areas or public lands or roads.	☐	☐
23.	Change in pattern, scale or character of general area of project.	☐	☐
24.	Significant amounts of solid waste or litter.	☐	☐
25.	Change in dust, ash, smoke, fumes or odors in vicinity.	☐	☐
26.	Change in ocean, bay, lake, stream or ground water quality or quantity, or alteration of existing drainage patterns.	☐	☐
27.	Substantial change in existing noise or vibration levels in the vicinity.	☐	☐
28.	Site on filled land or on slope of 10 percent or more.	☐	☐
29.	Use of disposal of potentially hazardous materials, such as toxic substances, flammables or explosives.	☐	☐
30.	Substantial change in demand for municipal services (police, fire, water, sewage, etc.).	☐	☐
31.	Substantially increase fossil fuel consumption (electricity, oil, natural gas, etc.).	☐	☐
32.	Relationship to a larger project or series of projects.	☐	☐

Environmental Setting

33. Describe the project site as it exists before the project, including information on topography, soil stability, plants and animals, and any cultural, historical or scenic aspects. Describe any existing structures on the site, and the use of the structures. Attach photographs of the site. Snapshots or polaroid photos will be accepted.

34. Describe the surrounding properties, including information on plant~ and animals and any cultural, historical or scenic aspects. Indicate the type of land use (residential, commercial, etc.), intensity of land use (one-family, apartment houses, shops, department stores, etc.), and scale of development (height, frontage, set-back, rear yard, etc.). Attach photographs of the vicinity. Snapshots or polaroid photos will be accepted.

Certification

I hereby certify that the statements furnished above and in the attached exhibits present the data and information required for this initial evaluation to the best of my ability, and that the facts, statements, and in formation presented are true and correct to the best of my knowledge and belief.

Date _____ Signature _____

For _____

APPENDIX I:
NOTICE OF PREPARATION

To: _____ From: _____

_____ _____
(Address) (Address)

_____ _____

Subject: **Notice of Preparation of a Draft Environmental Impact Report**

_____ will be the Lead Agency and will prepare an environmental impact report for the project identified below. We need to know the views of your agency as to the scope and content of the environmental information which is germane to your agency's statutory responsibilities in connection with the proposed project. Your agency will need to use the EIR prepared by our agency when considering your permit or other approval for the project.

The project description, location, and the potential environmental effects are contained in the attached materials. A copy of the Initial Study (☐ is ☐ is not) attached.

Due to the time limits mandated by State law, your response must be sent at the earliest possible date but not later than 30 days after receipt of this notice.

Please send your response to _____ at the address shown above. We will need the name for a contact person in your **agency**.

Project Title: _____

Project Applicant, if any: _____

Date _____ Signature _____

Title _____

Telephone _____

Reference: California Code of Regulations, Title 14, (CEQA Guidelines) Sections 15082(a), 15103, 15375.

APPENDIX J:
EXAMPLES OF TIERING EIRS

FIRST TIER EIR (15152)

- project encompasses separate but related projects such as general plan, zoning, development
- later tiers move from general to specific analysis of projects

Later Project EIR

- later project is consistent with general plan or zoning
- initial study must examine significant effects not covered in prior EIR
- later EIR must state lead agency is using tiering concept and must comply with section 15152

STAGED EIR (15167)

- one large project will require a number of discretionary approvals from govt. agencies and one of those approvals will occur more than two years before construction commences

Supplement to the Staged EIR

- supplements to the staged EIR are prepared for later government agency approvals on the same overall project if information available at the time of that later approval would permit consideration of additional environmental impacts, mitigation measures or reasonable alternatives

---

PROGRAM EIR (15168)

- series of actions or activities that can be characterized as one large project and are related either:
- geographically
- as logical parts of a chain of activities
- in connection with rules, regulations, plans or other general criteria governing a continuing program
- as individual activities carried out under common authority (statutory or regulatory) and having similar environmental effects which can be mitigated in similar ways

Subsequent Project EIR

- only if subsequent activity has effects not examined in the previously certified program EIR will additional environmental documentation be required (if subsequent activity has no new effects, that activity is covered by the program EIR)

MASTER EIR (15175)

- alternative to project, staged, or program EIR
- can be used for:
  - general plan (or gen. plan element, amendment, or update)
  - redevelopment plan projects (public or private)
  - project consisting of phases of smaller individual projects
  - other activities described in 15175
- after five years from initial certification, adopting authority must review the Master EIR and prepare subsequent or supplemental EIR if substantial changes have occurred with respect to circumstances under which the original Master EIR was adopted
- no new EIR is required for subsequent projects within the scope of the Master EIR which cause no additional significant effect

Focused EIR (15177)

- a subsequent, Focused EIR is required only where:
  - substantial new/additional information shows adverse environmental effects not examined in Master EIR or more significant than described in EIR, or
  - substantial new/additional information shows mitigation measures previously determined to be infeasible are now feasible and will avoid/reduce the significant effects to a level of insignificance

---

SPECIAL SITUATIONS / EIRs

Multiple-family residential development / residential and commercial or retail mixed-use development (PRC 21158.5 and Guideline §15179.5)

- project is multiple-family residential development up to 100 units or is a residential and commercial or retail mixed-use development of not more than 100,000 square feet
- if project complies with procedures in section 21158.5, only a focused EIR need be prepared, notwithstanding the fact that the project wasn't identified in the Master EIR

Redevelopment Project (15180)

- all public and private activities or undertakings in furtherance of a redevelopment plan (public or private) constitute a single project
- the redevelopment plan EIR is treated as a program EIR

- no subsequent EIR is required for individual components of the redevelopment plan unless substantial changes or substantial new information triggers a subsequent EIR or supplement to an EIR pursuant to (sections 15162 or 15163)

Housing/neighborhood commercial facilities (15181)

- a project involving construction of housing or neighborhood commercial facilities in an urbanized area
- a prior EIR for a specific plan, local coastal program, or port master plan may be used as the EIR for such a project (no new EIR need be prepared) provided section 15181 procedures are complied with

Projects Consistent with Community Plan, General Plan, or Zoning (15183)

- a project which is consistent with a community plan adopted as part of a general plan or zoning ordinance or a general plan of a local agency and where there was an EIR certified for the zoning action or master plan
- the EIR for the residential project need only examine certain significant environmental effects, as outlined in section 15183

Regulations on Pollution Control Equipment (PRC section 21159)

- section 21159 requires environmental analysis of reasonably foreseeable methods of compliance at the time of adoption of rule or regulation requiring the installation of pollution control equipment
- an EIR prepared at the time of adoption of the rule or regulation is deemed to satisfy the requirement of section 21159

Installation of Pollution Control Equipment (PRC section 21159.1)

- a focused EIR is permitted where project 1) consists solely of installation of pollution control equipment; 2) is required by rule or regulation adopted by the State Air Resources Board, an air pollution control district or air quality management district, the State Water Resources Control Board, a California regional water quality control board, the Dept. of Toxic Substances Control, or the California Integrated Waste Management Board; and 3) meets the procedural requirements outlined in section 21159.1

APPENDIX K:
CRITERIA FOR SHORTENED CLEARINGHOUSE REVIEW

Under exceptional circumstances, and when requested in writing by the lead agency, the State Clearinghouse in the Office of Planning and Research (OPR) may shorten the usual review periods for proposed negative declarations, mitigated negative declarations and draft EIRs submitted to the Clearinghouse. A request must be made by the decision-making body of the lead agency, or by a properly authorized representative of the decision-making body.

A shortened review period may be granted when any of the following circumstances exist:

(1) The lead agency is operating under an extension of the one-year period for completion of an EIR and would not otherwise be able to complete the EIR within the extended period.

(2) The public project applicant is under severe time constraints with regard to obtaining financing or exercising options which cannot be met without shortening the review period.

(3) The document is a supplement to a draft EIR or proposed negative declaration or mitigated negative declaration previously submitted to the State Clearinghouse.

(4) The health and safety of the community would be at risk unless the project is approved expeditiously.

(5) The document is a revised draft EIR, or proposed negative declaration or mitigated negative declaration, where changes in the document are primarily the result of comments from agencies and the public.

Shortened review cannot be provided to a draft EIR or proposed negative declaration or mitigated negative declaration which has already begun the usual review process. Prior to requesting shortened review, the lead agency should have already issued a notice of preparation and received comments from applicable State agencies, in the case of an EIR, or consulted with applicable State agencies, in the case of a proposed negative declaration or mitigated negative declaration.

No shortened review period shall be granted unless the lead agency has contacted and obtained prior approval for a shortened review from the applicable state responsible and trustee agencies. No shortened review shall be granted for any project which is of statewide, regional, or areawide significance, as defined in Section 15206 of the guidelines.

APPENDIX L:
NOTICE OF COMPLETION OF DRAFT EIR

Project Title

Project Location – Specific

Project Location – City Project Location – County

Description of Nature, Purpose, and Beneficiaries of Project

Lead Agency Division

Address Where Copy of EIR is Available

Review Period

Contact Person Area Code Phone Extension

Authority cited: Section 21083, Public Resources Code. Reference: Sections 21092, 21152, and 21153, Public Resources Code.
Revised 2005

APPENDIX M: PERFORMANCE STANDARDS FOR INFILL PROJECTS ELIGIBLE FOR STREAMLINED REVIEW

I. Introduction

Section 15183.3 provides a streamlined review process for infill projects that satisfy specified performance standards. This appendix contains those performance standards. The lead agency's determination that the project satisfies the performance standards shall be supported with substantial evidence, which should be documented on the lnfill Checklist in Appendix N. Section II defines terms used in this Appendix. Performance standards that apply to all project types are set forth in Section Ill. Section IV contains performance standards that apply to particular project types (i.e., residential, commercial/retail, office building, transit stations, and schools).

II. Definitions

The following definitions apply to the terms used in this Appendix.

"High-quality transit corridor" means an existing corridor with fixed route bus service with service intervals no longer than 15 minutes during peak commute hours. For the purposes of this Appendix, an "existing stop along a high-quality transit corridor" may include a planned and funded stop that is included in an adopted regional transportation improvement program.
Unless more specifically defined by an air district, city or county, "high-volume roadway" means freeways, highways, urban roads with 100,000 vehicles per day, or rural roads with 50,000 vehicles per day.

"Low vehicle travel area" means a traffic analysis zone that exhibits a below average existing level of travel as determined using a regional travel demand model. For residential projects, travel refers to either home-based or household vehicle miles traveled per capita. For commercial and retail projects, travel refers to non-work attraction trip length; however, where such data are not available, commercial projects reference either home-based or household vehicle miles traveled per capita. For office projects, travel refers to commute attraction vehicle miles traveled per employee; however, where such data are not available, office projects reference either home-based or household vehicle miles traveled per capita.

"Major Transit Stop" means a site containing an existing rail transit station, a ferry terminal served by either a bus or rail transit service, or the intersection of two or more major bus routes with frequencies of service intervals of 15 minutes or less during the morning and afternoon peak commute periods. For the purposes of this Appendix, an "existing major transit stop" may include a planned and funded stop that is included in an adopted regional transportation improvement program.

"Office building" generally refers to centers for governmental or professional services; however, the lead agency shall have discretion in determining whether a project is "commercial" or "office building" for the purposes of this Appendix based on local zoning codes.

"Significant sources of air pollution" include airports, marine ports, rail yards and dist ibution centers that receive more than 100 heavy-duty truck visits per day, as well as stationary sources that are designated major by the Clean Air Act.

A "Traffic Analysis Zone" is an analytical unit used by a travel demand model to estimate vehicle travel within a region.

Ill. Performance Standards Related to Project Design

To be eligible for streamlining pursuant to Section 15183.3, a project must implement all of the following:

Renewable Energy. All non-residential projects shall include on-site renewable power generation, such as solar photovoltaic, solar thermal and wind power generation, or clean backup power supplies, where feasible. Residential projects are also encouraged to include such on-site renewable power generation.

Soil and Water Remediation. If the project site is included on any list compiled pursuant to Section 65962.5 of the Government Code, the project shall document how it has remediated the site, if remediation is completed. Alternatively, the project shall implement the recommendations provided in a preliminary endangerment assessment or comparable document that identifies remediation appropriate for the site.

Residential Units Near High-Volume Roadways and Stationary Sources. If a project includes residential units located within 500 feet, or other distance determined to be appropriate by the local agency or air district based on local conditions, of a high volume roadway or other significant sources of air pollution, the project shall comply with any policies and standards identified in the local general plan, specific plan, zoning code or community risk reduction plan for the protection of public health from such sources of air pollution. If the local government has not adopted such plans or policies, the project shall include measures, such as enhanced air filtration and project design, that the lead agency finds, based on substantial evidence, will promote the protection of public health from sources of air pollution. Those measure may include, among others, the recommendations of the California Air Resources Board, air districts, and the California Air Pollution Control Officers Association.

IV. Additional Performance Standards by Project Type

In addition to the project features described above in Section Ill, specific eligibility requirements are provided below by project type.

Several of the performance standards below refer to "low vehicle travel areas". Such areas can be illustrated on maps based on data developed by the regional Metropolitan Planning Organization (MPO) using its regional travel demand model.

Several of the performance standards below refer to distance to transit. Distance should be calculated so that at least 75 percent of the surface area of the project site is within the specified distance.

A. Residential

To be eligible for streamlining pursuant to Section 15183.3, a project must satisfy one of the following: ·

Projects achieving below average regional per capita vehicle miles traveled (VMT). A residential project is eligible if it is located in a "low vehicle travel area" within the region.

Projects located within % mile of an Existing Major Transit Stop or High Quality Transit Corridor. A residential project is eligible if it is located within Yz mile of an existing major transit stop or an existing stop along a high quality transit corridor.

Low-Income Housing. A residential or mixed-use project consisting of 300 or fewer residential units all of which are affordable to low income households is eligible if the developer of the development project provides sufficient legal commitments to the lead agency to ensure the continued availability and use of the housing units for lower income households, as defined in Section 50079.5 of the Health and Safety Code, for a period of at least 30 years, at monthly housing costs, as determined pursuant to Section 50053 of the Health and Safety Code.

B. Commercial/Retail

To be eligible for streamlining pursuant to Section 15183.3, a project must satisfy one of the following:

Regional Location. A commercial project with no single-building floor-plate greater than 50,000 square feet is eligible if it locates in a "low vehicle travel area."

Proximity to Households. A project with no single-building floor-plate greater than 50,000 square feet located within one-half mile of 1800 households is eligible.

C. Office Building

To be eligible for streamlining pursuant to Section 15183.3, a project must satisfy one of the following:

Regional Location. Office buildings, both commercial and public, are eligible if they. locate in a low vehicle travel area.

Proximity to a Major Transit Stop. Office buildings, both commercial and public, within % mile of an existing major transit stop, or X mile of an existing stop along a high quality transit corridor, are eligible.

D. Transit

Transit stations, as defined in Section 15183.3(e)(1), are eligible.

E. Schools

Elementary schools within one mile of fifty percent of the projected student population are eligible. Middle schools and high schools within two miles of fifty percent of the projected student population are eligible. Alternatively, any school within % mile of an existing major transit stop or an existing stop along a high quality transit corridor is eligible.

Additionally, in order to be eligible, all schools shall provide parking and storage for bicycles and scooters and shall comply with the requirements in Sections 17213, 17213.1 and 17213.2 of the California Education Code.

F. Small Walkable Community Projects

Small walkable community projects, as defined in Section 15183.3, subdivision (e)(6), that implement the project features described in Section Ill above are eligible.

G. Mixed-Use Projects

Where a project includes some combination of residential, commercial and retail, office building, transit station, and/or schools, the performance standards in this Section that apply to the predominant use shall govern the entire project.

Authority: Public Resources Code 21083, 21094.5.5
Reference: Public Resources Code Sections 21094.5 and 21094.5.5

APPENDIX N: INFILL ENVIRONMENTAL CHECKLIST FORM

NOTE: This sample form is intended to assist lead agencies in assessing infill projects according to the procedures provided in Section 21094.5 of the Public Resources Code. Lead agencies may customize this form as appropriate, provided that the content satisfies the requirements in Section 15183.3 of the CEQA Guidelines.

1. Project title: _____
2. Lead agency name and address:
   _____
   _____
3. Contact person and phone number: _____
4. Project location: _____
5. Project sponsor's name and address:
   _____
   _____
6. General plan designation: _____ 7. Zoning: _____
8. Prior Environmental Document(s) Analyzing the Effects of the Infill Project (including State Clearinghouse Number if assigned):_____
   _____
9. Location of Prior Environmental Document(s) Analyzing the Effects of the Infill Project:
   _____
   _____
10. Description of project: (Describe the whole action involved, including but not limited to later phases of the project, and any secondary, support, or off-site features necessary for its implementation. Attach additional sheets if necessary.)
    _____
    _____
    _____
11. Surrounding land uses and setting: Briefly describe the project's surroundings, including any prior uses of the project site, or, if vacant, describe the urban uses that exist on at least 75% of the project's perimeter:
    _____
    _____
    _____
12. Other public agencies whose approval is required (e.g., permits, financing approval, or participation agreement.)
    _____
    _____
    _____

SATISFACTION OF APPENDIX M PERFORMANCE STANDARDS

Provide the information demonstrating that the infill project satisfies the performance standards in Appendix M below. For **mixed-use projects**, the predominant use will determine which performance standards apply to the entire project.

1. Does the non-residential infill project include a renewable energy feature? If so, describe below. If not, explain below why it is not feasible to do so.

_____
_____
_____

2. If the project site is included on any list compiled pursuant to Section 65962.5 of the Government Code, either provide documentation of remediation or describe the recommendations provided in a preliminary endangerment assessment or comparable document that will be implemented as part of the project.

_____
_____

3. If the infill project includes residential units located within 500 feet, or such distance that the local agency or local air district has determined is appropriate based on local conditions, a high volume roadway or other significant source of air pollution, as defined in Appendix M, describe the measures that the project will implement to protect public health. Such measures may include policies and standards identified in the local general plan, specific plans, zoning code or community risk reduction plan, or measures recommended in a health risk assessment, to promote the protection of public health. Identify the policies or standards, or refer to the site specific analysis, below. (Attach additional sheets if necessary.)

_____
_____
_____

4. For **residential** projects, the project satisfies which of the following?

☐ Located within a low vehicle travel area, as defined in Appendix M. (Attach VMT map.)

☐ Located within ½ mile of an existing major transit stop or an existing stop along a high quality transit corridor. (Attach map illustrating proximity to transit.)

☐ Consists of 300 or fewer units that are each affordable to low income households. (Attach evidence of legal commitment to ensure the continued availability and use of the housing units for lower income households, as defined in Section 50079.5 of the Health and Safety Code, for a period of at least 30 years, at monthly housing costs, as determined pursuant to Section 50053 of the Health and Safety Code.)

5. For **commercial** projects with a single building floor-plate below 50,000 square feet, the project satisfies which of the following?

☐ Located within a low vehicle travel area, as defined in Appendix M. (Attach VMT map.)

☐ The project is within one-half mile of 1800 dwelling units. (Attach map illustrating proximity to households.)

6. For **office building** projects, the project satisfies which of the following?

☐ Located within a low vehicle travel area, as defined in Appendix M. (Attach VMT map.)

☐ Located within ½ mile of an existing major transit stop or within ¼ of a stop along a high quality transit corridor. (Attach map illustrating proximity to transit.)

7. For **school** projects, the project does all of the following:

☐ The project complies with the requirements in Sections 17213, 17213.1 and 17213.2 of the California Education Code.

☐ The project is an elementary school and is within one mile of 50% of the student population, or is a middle school or high school and is within two miles of 50% of the student population. Alternatively, the school is within ½ mile of an existing major transit stop or an existing stop along a high quality transit corridor. (Attach map and methodology.)

☐ The project provides parking and storage for bicycles and scooters.

8. For **small walkable community projects**, the project must be a residential project that has a density of at least eight units to the acre or a commercial project with a floor area ratio of at least 0.5, or both.

ENVIRONMENTAL FACTORS POTENTIALLY AFFECTED:

The infill project could potentially result in one or more of the following environmental effects.

☐ Aesthetics	☐ Agriculture and Forestry Resources	☐ Air Quality
☐ Biological Resources	☐ Cultural Resources	☐ Geology /Soils
☐ Greenhouse Gas Emissions	☐ Hazards & Hazardous Materials	☐ Hydrology / Water Quality
☐ Land Use / Planning	☐ Mineral Resources	☐ Noise
☐ Population / Housing	☐ Public Services	☐ Recreation
☐ Transportation/Traffic	☐ Utilities / Service Systems	☐ Mandatory Findings of Significance

DETERMINATION: (To be completed by the Lead Agency)

On the basis of this initial evaluation:

☐ I find that the proposed infill project WOULD NOT have any significant effects on the environment that either have not already been analyzed in a prior EIR or that are more significant than previously analyzed, or that uniformly applicable development policies would not substantially mitigate. Pursuant to Public Resources Code Section 21094.5, CEQA does not apply to such effects. A Notice of Determination (Section 15094) will be filed.

☐ I find that the proposed infill project will have effects that either have not been analyzed in a prior EIR, or are more significant than described in the prior EIR, and that no uniformly applicable development policies would substantially mitigate such effects. With respect to those effects that are subject to CEQA, I find that such effects WOULD NOT be significant and a NEGATIVE DECLARATION, or if the project is a Transit Priority Project a SUSTAINABLE COMMUNITIES ENVIRONMENTAL ASSESSMENT, will be prepared.

☐ I find that the proposed infill project will have effects that either have not been analyzed in a prior EIR, or are more significant than described in the prior EIR, and that no uniformly applicable development policies would substantially mitigate such effects. I find that although those effects could be significant, there will not be a significant effect in this case because revisions in the infill project have been made by or agreed to by the project proponent. A MITIGATED NEGATIVE DECLARATION, or if the project is a Transit Priority Project a SUSTAINABLE COMMUNITIES ENVIRONMENTAL ASSESSMENT, will be prepared.

☐ I find that the proposed infill project would have effects that either have not been analyzed in a prior EIR, or are more significant than described in the prior EIR, and that no uniformly applicable development policies would substantially mitigate such effects. I find that those effects WOULD be significant, and an infill ENVIRONMENTAL IMPACT REPORT is required to analyze those effects that are subject to CEQA.

_____ _____

Signature Date

EVALUATION OF THE ENVIRONMENTAL IMPACTS OF INFILL PROJECTS:

1) A brief explanation is required for all answers except "No Impact" answers that are adequately supported by the information sources a lead agency cites in the parentheses following each question. A "No Impact" answer is adequately supported if the referenced information sources show that the impact simply does not apply to projects like the one involved (e.g., the project falls outside a fault rupture zone). A "No Impact" answer should be explained where it is based on project-specific factors as well as general standards (e.g., the project will not expose sensitive receptors to pollutants, based on a project-specific screening analysis).

2) All answers must take account of the whole action involved, including off-site as well as on-site, cumulative as well as project-level, indirect as well as direct, and construction as well as operational impacts.

3) For the purposes of this checklist, "prior EIR" means the environmental impact report certified for a planning level decision, as supplemented by any subsequent or supplemental environmental impact reports, negative declarations, or addenda to those documents. "Planning level decision" means the enactment or amendment of a general plan, community plan, specific plan, or zoning code. (Section 15183.3(e).)

4) Once the lead agency has determined that a particular physical impact may occur as a result of an infill project, then the checklist answers must indicate whether that impact has already been analyzed in a prior EIR. If the effect of the infill project is not more significant than what has already been analyzed, that effect of the infill project is not subject to CEQA. The brief explanation accompanying this determination should include page and section references to the portions of the prior EIR containing the analysis of that effect. The brief explanation shall also indicate whether the prior EIR included any mitigation measures to substantially lessen that effect and whether those measures have been incorporated into the infill project.

5) If the infill project would cause a significant adverse effect that either is specific to the project or project site and was not analyzed in a prior EIR, or is more significant than what was analyzed in a prior EIR, the lead agency must determine whether uniformly applicable development policies or standards that have been adopted by the lead agency, or city or county, would substantially mitigate that effect. If so, the checklist shall explain how the infill project's implementation of the uniformly applicable development policies will substantially mitigate that effect. That effect of the infill project is not subject to CEQA if the lead agency makes a finding, based upon substantial evidence, that the development policies or standards will substantially mitigate that effect.

6) If all effects of an infill project were either analyzed in a prior EIR or are substantially mitigated by uniformly applicable development policies or standards, CEQA does not apply to the project, and the lead agency shall file a Notice of Determination.

7) Effects of an infill project that either have not been analyzed in a prior EIR, or that uniformly applicable development policies or standards do not substantially mitigate, are subject to CEQA. With respect to those effects of the infill project that are subject to CEQA, the checklist shall indicate whether those effects are significant, less than significant with mitigation, or less than significant. If there are one or more " Significant Impact" entries when the determination is made, an infill EIR is required. The infill EIR should be limited to analysis of those effects determined to be significant. (Sections 15128, 15183.3(d).)

8) "Less Than Significant With Mitigation Incorporated" applies where the incorporation of mitigation measures will reduce an effect of an infill project that is subject to CEQA from " Significant Impact" to a "Less Than Significant Impact." The lead agency must describe the mitigation measures, and briefly explain how those measures reduce the effect to a less than significant level. If the effects of an infill project that are subject to CEQA are less than significant with mitigation incorporated, the lead agency may prepare a Mitigated Negative Declaration. If all of the effects of the infill project that are subject to CEQA are less than significant, the lead agency may prepare a Negative Declaration.

9) This is only a suggested form, and lead agencies are free to use different formats; however, lead agencies should normally address the questions from this checklist that are relevant to an infill project's environmental effects in whatever format is selected.

10) The explanation of each issue should identify:

a) the significance criteria or threshold, if any, used to evaluate each question; and

b) the mitigation measure identified, if any, to reduce the impact to less than significance.

SAMPLE QUESTIONS

Issues:

	Significant Impact	*Less Than Significant or Less than Significant with Mitigation Incorporated*	*No Impact*	**Analyzed in the Prior EIR**	**Substantially Mitigated by Uniformly Applicable Development Policies**
I. AESTHETICS. Would the project:					
a) Have a substantial adverse effect on a scenic vista?	☐	☐	☐	☐	☐
b) Substantially damage scenic resources, including, but not limited to, trees, rock outcroppings, and historic buildings within a state scenic highway?	☐	☐	☐	☐	☐
c) Substantially degrade the existing visual character or quality of the site and its surroundings?	☐	☐	☐	☐	☐
d) Create a new source of substantial light or glare which would adversely affect day or nighttime views in the area?	☐	☐	☐	☐	☐
II. AGRICULTURE AND FORESTRY RESOURCES. In determining whether impacts to agricultural resources are significant					

	Significant Impact	*Less Than Significant or Less than Significant with Mitigation Incorporated*	*No Impact*	**Analyzed in the Prior EIR**	**Substantially Mitigated by Uniformly Applicable Development Policies**
environmental effects, lead agencies may refer to the California Agricultural Land Evaluation and Site Assessment Model (1997) prepared by the California Dept. of Conservation as an optional model to use in assessing impacts on agriculture and farmland. In determining whether impacts to forest resources, including timberland, are significant environmental effects, lead agencies may refer to information compiled by the California Department of Forestry and Fire Protection regarding the state's inventory of forest land, including the Forest and Range Assessment Project and the Forest Legacy Assessment project; and forest carbon measurement methodology provided in Forest Protocols adopted by the California Air Resources Board. Would the project:					

	Significant Impact	*Less Than Significant or Less than Significant with Mitigation Incorporated*	*No Impact*	**Analyzed in the Prior EIR**	**Substantially Mitigated by Uniformly Applicable Development Policies**
a) Convert Prime Farmland, Unique Farmland, or Farmland of Statewide Importance (Farmland), as shown on the maps prepared pursuant to the Farmland Mapping and Monitoring Program of the California Resources Agency, to non-agricultural use?	☐	☐	☐	☐	☐
b) Conflict with existing zoning for agricultural use, or a Williamson Act contract?	☐	☐	☐	☐	☐
c) Conflict with existing zoning for, or cause rezoning of, forest land (as defined in Public Resources Code section 12220(g)), timberland (as defined by Public Resources Code section 4526), or timberland zoned Timberland Production (as defined by Government Code section 51104(g))?	☐	☐	☐	☐	☐
d) Result in the loss of forest land or conversion of forest land to non-forest use?	☐	☐	☐	☐	☐
e) Involve other changes in the existing environment which, due to their location or nature, could result in conversion of Farmland, to non-agricultural use or conversion of forest land to non-forest use?	☐	☐	☐	☐	☐
III. AIR QUALITY. Where available, the significance criteria established by the applicable air quality management or air pollution control district may be relied upon to make the following determinations. Would the project:					
a) Conflict with or obstruct implementation of the applicable air quality plan?	☐	☐	☐	☐	☐
b) Violate any air quality standard or contribute substantially to an existing or projected air quality violation?	☐	☐	☐	☐	☐
c) Result in a cumulatively considerable net increase of any criteria pollutant for which the project region is non-attainment under an applicable federal or state ambient air quality standard (including releasing emissions which exceed quantitative thresholds for ozone precursors)?	☐	☐	☐	☐	☐
d) Expose sensitive receptors to substantial pollutant concentrations?	☐	☐	☐	☐	☐
e) Create objectionable odors affecting a	☐	☐	☐	☐	☐

	Significant Impact	*Less Than Significant or Less than Significant with Mitigation Incorporated*	*No Impact*	**Analyzed in the Prior EIR**	**Substantially Mitigated by Uniformly Applicable Development Policies**
substantial number of people?					
IV. BIOLOGICAL RESOURCES: Would the project:					
a) Have a substantial adverse effect, either directly or through habitat modifications, on any species identified as a candidate, sensitive, or special status species in local or regional plans, policies, or regulations, or by the California Department of Fish and Game or U.S. Fish and Wildlife Service?	☐	☐	☐	☐	☐
b) Have a substantial adverse effect on any riparian habitat or other sensitive natural community identified in local or regional plans, policies, regulations or by the California Department of Fish and Game or US Fish and Wildlife Service?	☐	☐	☐	☐	☐
c) Have a substantial adverse effect on federally protected wetlands as defined by Section 404 of the Clean Water Act (including, but not limited to, marsh, vernal pool, coastal, etc.) through direct removal, filling, hydrological interruption, or other means?	☐	☐	☐	☐	☐
d) Interfere substantially with the movement of any native resident or migratory fish or wildlife species or with established native resident or migratory wildlife corridors, or impede the use of native wildlife nursery sites?	☐	☐	☐	☐	☐
e) Conflict with any local policies or ordinances protecting biological resources, such as a tree preservation policy or ordinance?	☐	☐	☐	☐	☐
f) Conflict with the provisions of an adopted Habitat Conservation Plan, Natural Community Conservation Plan, or other approved local, regional, or state habitat conservation plan?	☐	☐	☐	☐	☐

	Significant Impact	*Less Than Significant or Less than Significant with Mitigation Incorporated*	*No Impact*	**Analyzed in the Prior EIR**	**Substantially Mitigated by Uniformly Applicable Development Policies**
V. CULTURAL RESOURCES. Would the project:					
a) Cause a substantial adverse change in the significance of a historical resource as defined in § 15064.5?	☐	☐	☐	☐	☐
b) Cause a substantial adverse change in the significance of an archaeological resource pursuant to § 15064.5?	☐	☐	☐	☐	☐
c) Directly or indirectly destroy a unique paleontological resource or site or unique geologic feature?	☐	☐	☐	☐	☐
d) Disturb any human remains, including those interred outside of formal cemeteries?	☐	☐	☐	☐	☐
VI. GEOLOGY AND SOILS. Would the project:					
a) Expose people or structures to potential substantial adverse effects, including the risk of loss, injury, or death involving:	☐	☐	☐	☐	☐
i) Rupture of a known earthquake fault, as delineated on the most recent Alquist-Priolo Earthquake Fault Zoning Map issued by the State Geologist for the area or based on other substantial evidence of a known fault? Refer to Division of Mines and Geology Special Publication 42.	☐	☐	☐	☐	☐
ii) Strong seismic ground shaking?	☐	☐	☐	☐	☐
iii) Seismic-related ground failure, including liquefaction?	☐	☐	☐	☐	☐
iv) Landslides?	☐	☐	☐	☐	☐
b) Result in substantial soil erosion or the loss of topsoil?	☐	☐	☐	☐	☐
c) Be located on a geologic unit or soil that is unstable, or that would become unstable as a result of the project, and potentially result in on- or off-site landslide, lateral spreading, subsidence, liquefaction or collapse?	☐	☐	☐	☐	☐

	Significant Impact	*Less Than Significant or Less than Significant with Mitigation Incorporated*	*No Impact*	**Analyzed in the Prior EIR**	**Substantially Mitigated by Uniformly Applicable Development Policies**
d) Be located on expansive soil, as defined in Table 18-1-B of the Uniform Building Code (1994), creating substantial risks to life or property?	☐	☐	☐	☐	☐
e) Have soils incapable of adequately supporting the use of septic tanks or alternative waste water disposal systems where sewers are not available for the disposal of waste water?	☐	☐	☐	☐	☐
VII. GREENHOUSE GAS EMISSIONS. Would the project:					
a) Generate greenhouse gas emissions, either directly or indirectly, that may have a significant impact on the environment?	☐	☐	☐	☐	☐
b) Conflict with an applicable plan, policy or regulation adopted for the purpose of reducing the emissions of greenhouse gases?	☐	☐	☐	☐	☐
VIII. HAZARDS AND HAZARDOUS MATERIALS. Would the project:					
a) Create a significant hazard to the public or the environment through the routine transport, use, or disposal of hazardous materials?	☐	☐	☐	☐	☐
b) Create a significant hazard to the public or the environment through reasonably foreseeable upset and accident conditions involving the release of hazardous materials into the environment?	☐	☐	☐	☐	☐
c) Emit hazardous emissions or handle hazardous or acutely hazardous materials, substances, or waste within one-quarter mile of an existing or proposed school?	☐	☐	☐	☐	☐
d) Be located on a site which is included on a list of hazardous materials sites compiled pursuant to Government Code Section 65962.5 and, as a result, would it create a significant hazard to the public or the environment?	☐	☐	☐	☐	☐

	Significant Impact	*Less Than Significant or Less than Significant with Mitigation Incorporated*	*No Impact*	**Analyzed in the Prior EIR**	**Substantially Mitigated by Uniformly Applicable Development Policies**
e) For a project located within an airport land use plan or, where such a plan has not been adopted, within two miles of a public airport or public use airport, would the project result in a safety hazard for people residing or working in the project area?	☐	☐	☐	☐	☐
f) For a project within the vicinity of a private airstrip, would the project result in a safety hazard for people residing or working in the project area?	☐	☐	☐	☐	☐
g) Impair implementation of or physically interfere with an adopted emergency response plan or emergency evacuation plan?	☐	☐	☐	☐	☐
h) Expose people or structures to a significant risk of loss, injury or death involving wildland fires, including where wildlands are adjacent to urbanized areas or where residences are intermixed with wildlands?	☐	☐	☐	☐	☐
IX. HYDROLOGY AND WATER QUALITY. Would the project:					
a) Violate any water quality standards or waste discharge requirements?	☐	☐	☐	☐	☐
b) Substantially deplete groundwater supplies or interfere substantially with groundwater recharge such that there would be a net deficit in aquifer volume or a lowering of the local groundwater table level (e.g., the production rate of pre-existing nearby wells would drop to a level which would not support existing land uses or planned uses for which permits have been granted)?	☐	☐	☐	☐	☐
c) Substantially alter the existing drainage pattern of the site or area, including through the alteration of the course of a stream or river, in a manner which would result in substantial erosion or siltation on- or off-site?	☐	☐	☐	☐	☐

	Significant Impact	*Less Than Significant or Less than Significant with Mitigation Incorporated*	*No Impact*	**Analyzed in the Prior EIR**	**Substantially Mitigated by Uniformly Applicable Development Policies**
d) Substantially alter the existing drainage pattern of the site or area, including through the alteration of the course of a stream or river, or substantially increase the rate or amount of surface runoff in a manner which would result in flooding on- or off-site?	☐	☐	☐	☐	☐
e) Create or contribute runoff water which would exceed the capacity of existing or planned stormwater drainage systems or provide substantial additional sources of polluted runoff?	☐	☐	☐	☐	☐
f) Otherwise substantially degrade water quality?	☐	☐	☐	☐	☐
g) Place housing within a 100-year flood hazard area as mapped on a federal Flood Hazard Boundary or Flood Insurance Rate Map or other flood hazard delineation map?	☐	☐	☐	☐	☐
h) Place within a 100-year flood hazard area structures which would impede or redirect flood flows?	☐	☐	☐	☐	☐
i) Expose people or structures to a significant risk of loss, injury or death involving flooding, including flooding as a result of the failure of a levee or dam?	☐	☐	☐	☐	☐
j) Inundation by seiche, tsunami, or mudflow?	☐	☐	☐	☐	☐
X. LAND USE AND PLANNING. Would the project:					
a) Physically divide an established community?	☐	☐	☐	☐	☐
b) Conflict with any applicable land use plan, policy, or regulation of an agency with jurisdiction over the project (including, but not limited to the general plan, specific plan, local coastal program, or zoning ordinance) adopted for the purpose of avoiding or mitigating an environmental effect?	☐	☐	☐	☐	☐

	Significant Impact	*Less Than Significant or Less than Significant with Mitigation Incorporated*	*No Impact*	**Analyzed in the Prior EIR**	**Substantially Mitigated by Uniformly Applicable Development Policies**
c) Conflict with any applicable habitat conservation plan or natural community conservation plan?	☐	☐	☐	☐	☐
XI. MINERAL RESOURCES. Would the project:					
a) Result in the loss of availability of a known mineral resource that would be of value to the region and the residents of the state?	☐	☐	☐	☐	☐
b) Result in the loss of availability of a locally-important mineral resource recovery site delineated on a local general plan, specific plan or other land use plan?	☐	☐	☐	☐	☐
XII. NOISE -- Would the project result in:					
a) Exposure of persons to or generation of noise levels in excess of standards established in the local general plan or noise ordinance, or applicable standards of other agencies?	☐	☐	☐	☐	☐
b) Exposure of persons to or generation of excessive groundborne vibration or groundborne noise levels?	☐	☐	☐	☐	☐
c) A substantial permanent increase in ambient noise levels in the project vicinity above levels existing without the project?	☐	☐	☐	☐	☐
d) A substantial temporary or periodic increase in ambient noise levels in the project vicinity above levels existing without the project?	☐	☐	☐	☐	☐
e) For a project located within an airport land use plan or, where such a plan has not been adopted, within two miles of a public airport or public use airport, would the project expose people residing or working in the project area to excessive noise levels?	☐	☐	☐	☐	☐
f) For a project within the vicinity of a private airstrip, would the project expose people residing or working in the project area to excessive noise levels?	☐	☐	☐	☐	☐

	Significant Impact	*Less Than Significant or Less than Significant with Mitigation Incorporated*	*No Impact*	**Analyzed in the Prior EIR**	**Substantially Mitigated by Uniformly Applicable Development Policies**
XIII. POPULATION AND HOUSING. Would the project:					
a) Induce substantial population growth in an area, either directly (for example, by proposing new homes and businesses) or indirectly (for example, through extension of roads or other infrastructure)?	☐	☐	☐	☐	☐
b) Displace substantial numbers of existing housing, necessitating the construction of replacement housing elsewhere?	☐	☐	☐	☐	☐
c) Displace substantial numbers of people, necessitating the construction of replacement housing elsewhere?	☐	☐	☐	☐	☐
XIV. PUBLIC SERVICES.					
a) Would the project result in substantial adverse physical impacts associated with the provision of new or physically altered governmental facilities, need for new or physically altered governmental facilities, the construction of which could cause significant environmental impacts, in order to maintain acceptable service ratios, response times or other performance objectives for any of the public services:	☐	☐	☐	☐	☐
Fire protection?	☐	☐	☐	☐	☐
Police protection?	☐	☐	☐	☐	☐
Schools?	☐	☐	☐	☐	☐
Parks?	☐	☐	☐	☐	☐
Other public facilities?	☐	☐	☐	☐	☐
XV. RECREATION.					
a) Would the project increase the use of existing neighborhood and regional parks or other recreational facilities such that substantial physical deterioration of the facility would occur or be accelerated?	☐	☐	☐	☐	☐

	Significant Impact	*Less Than Significant or Less than Significant with Mitigation Incorporated*	*No Impact*	**Analyzed in the Prior EIR**	**Substantially Mitigated by Uniformly Applicable Development Policies**
b) Does the project include recreational facilities or require the construction or expansion of recreational facilities which might have an adverse physical effect on the environment?	☐	☐	☐	☐	☐
XVI. TRANSPORTATION/TRAFFIC. Would the project:					
a) Conflict with an applicable plan, ordinance or policy establishing measures of effectiveness for the performance of the circulation system, taking into account all modes of transportation including mass transit and non-motorized travel and relevant components of the circulation system, including but not limited to intersections, streets, highways and freeways, pedestrian and bicycle paths, and mass transit?	☐	☐	☐	☐	☐
b) Conflict with an applicable congestion management program, including, but not limited to level of service standards and travel demand measures, or other standards established by the county congestion management agency for designated roads or highways?	☐	☐	☐	☐	☐
c) Result in a change in air traffic patterns, including either an increase in traffic levels or a change in location that results in substantial safety risks?	☐	☐	☐	☐	☐
d) Substantially increase hazards due to a design feature (e.g., sharp curves or dangerous intersections) or incompatible uses (e.g., farm equipment)?	☐	☐	☐	☐	☐
e) Result in inadequate emergency access?	☐	☐	☐	☐	☐
f) Conflict with adopted policies, plans, or programs regarding public transit, bicycle, or pedestrian facilities, or otherwise decrease the performance or safety of such facilities?	☐	☐	☐	☐	☐

	Significant Impact	*Less Than Significant or Less than Significant with Mitigation Incorporated*	*No Impact*	**Analyzed in the Prior EIR**	**Substantially Mitigated by Uniformly Applicable Development Policies**
XVII. UTILITIES AND SERVICE SYSTEMS. Would the project:					
a) Exceed wastewater treatment requirements of the applicable Regional Water Quality Control Board?	☐	☐	☐	☐	☐
b) Require or result in the construction of new water or wastewater treatment facilities or expansion of existing facilities, the construction of which could cause significant environmental effects?	☐	☐	☐	☐	☐
c) Require or result in the construction of new storm water drainage facilities or expansion of existing facilities, the construction of which could cause significant environmental effects?	☐	☐	☐	☐	☐
d) Have sufficient water supplies available to serve the project from existing entitlements and resources, or are new or expanded entitlements needed?	☐	☐	☐	☐	☐
e) Result in a determination by the wastewater treatment provider which serves or may serve the project that it has adequate capacity to serve the project's projected demand in addition to the provider's existing commitments?	☐	☐	☐	☐	☐
f) Be served by a landfill with sufficient permitted capacity to accommodate the project's solid waste disposal needs?	☐	☐	☐	☐	☐
g) Comply with federal, state, and local statutes and regulations related to solid waste?	☐	☐	☐	☐	☐
XVIII. MANDATORY FINDINGS OF SIGNIFICANCE.					
a) Does the project have the potential to degrade the quality of the environment, substantially reduce the habitat of a fish or wildlife species, cause a fish or wildlife population to drop below self-sustaining levels, threaten to eliminate a plant or animal community, reduce the number or restrict the range of a rare or endangered plant or animal or eliminate important examples of the major periods of California history or prehistory?	☐	☐	☐	☐	☐
b) Does the project have impacts that are individually limited, but cumulatively considerable? ("Cumulatively considerable" means that the incremental effects of a project	☐	☐	☐	☐	☐

	Significant Impact	*Less Than Significant or Less than Significant with Mitigation Incorporated*	*No Impact*	**Analyzed in the Prior EIR**	**Substantially Mitigated by Uniformly Applicable Development Policies**
are considerable when viewed in connection with the effects of past projects, the effects of other current projects, and the effects of probable future projects)?					
c) Does the project have environmental effects which will cause substantial adverse effects on human beings, either directly or indirectly?	☐	☐	☐	☐	☐

Authority: Public Resources Code 21083, 21094.5.5
Reference: Public Resources Code Sections 21094.5 and 21094.5.5

INDEX

Note: The electronic version of the CEQA Statute and Guidelines can be searched for keywords at www:califaep.org

A

Acutely Hazardous Material 66, 69, 207
administrative record 157, 175
affordable housing 8, 215, 218, 219
agricultural land 5, 6, 41, 56
Air Pollution Control District 17, 23, 65, 68, 129, 207, 209, 240, 254
Air Quality Management District ... 17, 23, 65, 68, 128, 154, 207, 209, 232, 239, 240, 254
airport.....27, 48, 56, 57, 147, 185, 211, 212
Alquist-Priolo Earthquake Fault Zone 247
Alternatives 2, 3, 4, 5, 13, 14, 16, 17, 30, 31, 34, 40, 42, 51, 59, 62, 70, 71, 78, 80, 81, 82, 83, 110, 119, 122, 124, 131, 143, 144, 151, 152, 155, 158, 162, 168, 169, 170, 171, 174, 175, 176, 181, 184, 185, 188, 189, 191, 192, 195, 196, 198, 206, 210, 222, 228, 232, 233, 234
Amendment.....206
archaeological resources 9, 37, 140, 141, 250
archaeological site.....140, 173
Assembly Committee on Natural Resources..... 18

C

California Attorney General 239
California Coastal Commission 18, 111, 127, 173, 231, 235
California EIR Monitor.....230, 231, 265
California Endangered Species Act 23, 85, 232, 242, 243
California Environmental Quality Act.....1, 4, 118, 125, 227, 256, 257
California Housing Finance Agency..... 18
California Native American tribe.....8, 9, 13, 14, 34, 35
California Register of Historical Resources.....8, 45, 139, 140
California State Library 84
California Wilderness System.....251
categorical exemption 122, 125, 126, 132, 244, 245, 250, 257
categorically exempt 20, 244, 261
certified regulatory program 10, 17, 46, 82, 134, 210
City of Oakland.....245
cogeneration equipment.....254
comment period 112
Congestion Management Program.....10, 238, 239
Consultation..... 13, 14, 33, 34, 35, 45, 50, 62, 68, 131, 135, 140, 152, 153, 161, 208, 226
County Agricultural Commissioner 17, 232
County Clerk.....50, 69, 70, 132, 133, 144, 148, 155, 160
cultural landscape 9
cumulative effect.....52, 178
Cumulative Impact Analysis.....58, 59, 60, 178, 206
cumulative impacts 39, 76, 80, 81, 82, 83, 87, 88, 138, 177, 178, 191, 192, 193, 194, 195, 197, 198, 199, 201, 205, 210, 257

cumulatively considerable 35, 137, 138, 142, 177, 184, 206

D

decision making body 163, 190, 257
Delta Protection Commission 22, 232, 241
Department of Fish and Game 25, 26, 46, 62, 194, 232, 246, 248, 256, 265
Department of Housing and Community Development 18, 241, 257
Department of Toxic Substances Control 65, 67, 83, 207, 209
Department of Transportation 15, 32, 43, 56, 152, 164, 241
Department of Veterans Affairs 249
developed open space 86
disaster 9, 236
Discretionary Project 9, 120, 257
Draft EIR 125, 126, 135, 146, 151, 152, 153, 154, 155, 156, 157, 158, 160, 162, 164, 165, 168, 177, 179, 180, 185, 189, 221, 222, 223, 225, 227, 228, 231, 258, 261, 266, 298

E

economic or social effects 136, 179
emergency 5, 9, 22, 23, 26, 27, 236, 242, 243, 255, 258, 261
endangered species 43, 62, 229
Endangered Species Act 23, 85, 232, 242, 243, 263
Energy 9, 65, 149, 172, 191, 232, 237, 266
entitlement 7, 13, 16, 90, 110, 111, 131, 164, 166, 167, 234, 236, 251, 256, 259, 262
Environmental Benefits 159
environmental damage 1, 119, 120, 124
Environmental Impact Report .. 2, 3, 4, 5, 6, 7, 9, 11, 12, 13, 15, 16, 21, 30, 31, 32, 33, 34, 35, 36, 37, 39, 40, 41, 42, 43, 44, 46, 47, 48, 49, 50, 51, 52, 53, 54, 56, 59, 60, 61, 62, 63, 64, 66, 67, 68, 70, 71, 76, 77, 78, 79, 80, 81, 82, 83, 84, 89, 90, 91, 92, 93, 95, 119, 123, 142, 143, 149, 150, 156, 168, 179, 184, 193, 198, 258
Environmental Impact Statement 41, 42, 60, 142, 177, 228, 239, 259
environmental pollution 1
environmental quality 1, 2, 4, 18, 118, 125, 227, 256, 257
environmental review process 3, 4, 11, 43, 56, 141, 221
environmentally superior alternative 175
exempt 9, 10, 16, 27, 29, 40, 41, 44, 45, 46, 65, 89, 120, 122, 123, 125, 126, 131, 132, 133, 140, 206, 220, 231, 234, 235, 236, 244, 245, 246, 247, 249, 253, 254, 261
exemption 10, 22, 23, 30, 39, 44, 84, 85, 86, 87, 88, 126, 132, 133, 199, 215, 236, 238, 239, 240, 242, 243, 246, 247, 248, 249, 250, 251, 252, 254, 257, 261
Existing Facilities 245, 251, 252, 254

F

fair argument 136, 137, 264
family day care 238, 246
feasible alternatives 2, 3, 16, 42, 78, 124, 174, 176, 195, 228, 234
feasible mitigation measures 2, 3, 16, 39, 78, 82, 158, 162, 192, 195, 200, 209
Final EIR 121, 125, 127, 135, 146, 152, 156, 157, 158, 159, 160, 161, 162, 166, 168, 179, 189, 190, 225, 230, 258

finding..... 4, 8, 26, 30, 35, 39, 44, 46, 52, 68, 69, 78, 80, 81, 98, 109, 110, 126, 132, 134, 135, 143, 147, 158, 169, 180, 185, 189, 198, 200, 208, 222, 233, 240, 243, 244, 257
fiscal emergency 26, 243
flood.....5, 27, 86, 216, 236, 245, 252, 258
Focused Environmental Impact Report (EIR)....60, 67, 78, 80, 81, 82, 194, 196, 197, 198, 210
freeway(s) 30, 31, 50, 62, 67, 68, 144, 154, 179, 207
frivolous claim 110

G

General Plan Amendment(s).....22, 42, 194, 229, 232, 241
geographic scope.....178, 222
Geothermal Exploratory Project 7, 47
Greenhouse Gas Emissions.....44, 138, 170, 174, 182, 200, 205, 206
Greenhouse Gas Reduction Plan.....206
greenhouse gas(es).....36, 138, 259
Growth-inducing impacts.....76, 80, 81, 82, 83, 194, 195, 197, 198, 210, 226

H

Hazardous Conditions.....171
hazardous or toxic wastes 43, 229
hazardous substance.....66, 67, 69, 85, 207, 247, 254
hazardous waste .. 43, 49, 64, 65, 66, 67, 145, 149, 150, 155, 207, 228, 229, 244, 254, 255
historical resource(s)..... 8, 9, 44, 45, 85, 139, 140, 171, 173, 216, 236, 244, 252, 255
Hydroelectric Generating Facilities 253

I

incremental contribution 137, 138
incremental effects..... 53
indirect.....6, 7, 128, 131, 136, 162, 171, 262
infill..... 88
In-fill development 255
initial study 6, 10, 51, 52, 53, 77, 78, 79, 95, 122, 125, 131, 133, 135, 137, 140, 143, 145, 146, 149, 151, 164, 183, 193, 195, 196, 197, 199, 231, 258, 260
International Olympic Committee 9, 237

J

joint EIR/EIS.....193
Judicial Review.....4, 109

K

Keene-Nejedly California Wetlands Preservation Act.....23, 242, 243

L

Land Evaluation and Site Assessment 56
Lead Agency.. 3, 7, 8, 10, 11, 12, 13, 14, 15, 22, 30, 31, 32, 33, 34, 35, 37, 38, 39, 41, 42, 43, 44, 45, 46, 47, 48, 49, 50, 51, 52, 53, 56, 60, 62, 63, 64, 66, 67, 68, 70, 71, 77, 78,

80, 81, 83, 91, 120, 121, 122, 124, 126, 127, 128, 129, 130, 131, 133, 134, 135, 136, 137, 139, 140, 141, 142, 144, 145, 146, 147, 148, 149, 150, 151, 152, 153, 154, 155, 156, 157, 158, 159, 160, 161, 162, 163, 164, 165, 166, 167, 168, 169, 170, 171, 172, 173, 174, 175, 176, 177, 178, 180, 181, 182, 183, 184, 185, 188, 189, 190, 191, 193, 194, 195, 196, 197, 198, 199, 200, 207, 208, 210, 211, 221, 222, 223, 224, 225, 226, 227, 228, 229, 230, 232, 233, 237, 238, 242, 245, 258, 259, 260, 261, 263, 264, 265, 298
leadership project 113, 114, 115
Local Agency Formation Commission 6, 60, 129, 177, 260, 263
lot line adjustments 248

M

Mass Transit Projects 238
Master Environmental Assessment 134, 192, 193
Master Environmental Impact Report (EIR) 46, 76, 77, 78, 79, 80, 81, 134, 184, 193, 194, 195, 196, 197, 198
mediation 98
mediation proceeding 97
military base 42, 43, 77, 170, 194, 227, 228, 229
Ministerial 9, 120, 125, 236, 238, 244, 260, 261
Ministerial Projects 236, 244
Mitigated Negative Declaration ... 11, 13, 31, 32, 33, 34, 35, 47, 63, 78, 79, 81, 83, 84, 95, 136, 137, 143, 144, 145, 146, 147, 148, 149, 163, 164, 165, 185, 195, 196, 198, 210, 222, 223, 260, 298
mitigation 174
Mitigation Measures .. 2, 3, 4, 11, 13, 14, 16, 17, 30, 31, 32, 34, 35, 37, 38, 39, 40, 45, 62, 68, 70, 71, 76, 78, 80, 82, 83, 85, 110, 119, 122, 124, 131, 137, 142, 143, 146, 147, 148, 151, 152, 154, 156, 158, 160, 162, 163, 164, 169, 171, 172, 173, 184, 185, 191, 192, 195, 196, 200, 209, 210, 222, 226, 232, 233
mobilehome park 18, 240
Monitor 206
Monitoring Program 31, 32

N

Napa Valley Wine Train 12
National Environmental Policy Act ... 10, 26, 41, 42, 44, 60, 133, 166, 177, 225, 226, 227, 234, 239, 259
National Register of Historic Places 254
Native American Heritage Commission 8, 14, 140, 141
natural resources 1, 7, 15, 18, 31, 32, 42, 145, 176, 229, 248, 265
Natural Resources Agency 36, 44
Negative Declaration(s) 3, 4, 6, 9, 10, 11, 13, 31, 32, 33, 35, 37, 44, 46, 47, 48, 50, 51, 56, 60, 63, 66, 67, 68, 78, 79, 81, 83, 84, 89, 92, 93, 95, 119, 120, 121, 123, 125, 126, 127, 129, 134, 135, 136, 137, 143, 144, 145, 146, 147, 148, 149, 161, 162, 163, 164, 165, 166, 180, 182, 183, 184, 185, 188, 189, 190, 191, 192, 193, 195, 196, 198, 207, 208, 210, 211, 220, 221, 222, 223, 224, 225, 226, 227, 230, 231, 232, 233, 234, 235, 237, 244, 253, 258, 259, 260, 261, 264, 298
No Project Alternative 42, 175, 176

Notice of Completion....90, 153, 154, 223, 261, 266, 271
Notice of Determination . 112, 148, 152, 160, 161, 162, 167, 185, 196, 199, 261, 266, 273
Notice of Exemption....120, 132, 133, 167, 261, 266, 274
Notice of Intent....144
Notice of Preparation . 43, 48, 60, 67, 83, 95, 126, 150, 151, 152, 161, 165, 170, 171, 175, 211, 227, 229, 261, 266, 294, 298

O

oak woodlands....40, 41
Oak Woodlands Conservation Act.... 40
Office of Planning and Research . 8, 13, 15, 35, 36, 45, 48, 56, 62, 63, 70, 71, 84, 90, 118, 126, 130, 132, 133, 148, 150, 151, 152, 153, 154, 160, 161, 165, 170, 215, 235, 245, 261, 298
overriding consideration.... 52

P

paleontological resources.... 36
performance standard....81, 82, 83, 209, 210
piecemealing.... 89
pipeline....21, 22, 23, 67, 207, 241, 242, 243, 253
Planning and Environmental Review Procedures.... 3
pollution control equipment....81, 82, 209, 210
Porter-Cologne Water Quality Control Act....43, 229
Preliminary Endangerment Assessment.... 85
Program Environmental Impact Report (EIR)...46, 84, 134, 178, 184, 190, 191, 192, 193, 265
Project Alternatives....2, 31, 158, 174, 176
Project Environmental Impact Report (EIR)....46, 188, 193
Project Specific Effect....89, 195, 196
Public Controversy....33, 137
Public Employees Retirement System....249
public higher education....12, 13
public participation....18, 174, 176, 221
public transit....10, 50, 144, 154, 238
Public Utilities Commission....9, 12, 94, 99, 237
publicly owned transit agencies.... 26

Q

Qualified Urban Use.... 87

R

railroad grade separation....19, 240
reasonably foreseeable.... 6, 81, 82, 88, 131, 136, 183, 209, 257, 258, 262
recirculation....11, 146, 147, 156, 157
redevelopment.... 6, 42, 43, 46, 76, 194, 195, 198, 228, 229, 253, 260
Reduction of Emissions....174
Reduction of Greenhouse Gas Emissions....174, 205

Regional Transportation Improvement Program....10, 238
reservation....42, 77, 194, 228, 229
Resources Agency....16, 17, 32, 36, 45, 46, 56, 120, 138, 143, 179, 209, 263
Responsible Agency3, 15, 31, 32, 33, 44, 62, 70, 71, 77, 91, 121, 128, 129, 130, 135, 145, 151, 154, 160, 161, 162, 164, 165, 189, 191, 195, 222, 223, 230, 233, 238, 259, 264
Reuse Plan....42, 43, 64, 150, 227, 228, 229
review period .. 32, 47, 48, 95, 144, 145, 153, 154, 155, 165, 185, 212, 221, 222, 223, 298
Rural Economic Development Infrastructure Panel....240

S

scenic highway....27, 44, 236, 244
scenic resources 44
school....xviii, 20, 32, 66, 67, 68, 77, 125, 207, 208, 240, 250, 252, 260, 265
schoolsite 67, 68
Scoping Meeting....42, 43, 44, 151, 152
Secretary of the Resources Agency 16, 17, 32, 36, 44, 45, 46, 120
Seismic Hazard Zone....86, 247
Senate Committee on Environmental Quality.... 18
Sequester Greenhouse Gases 174
Significant Effect on the Environment... 4, 6, 10, 11, 33, 35, 40, 41, 42, 44, 45, 53, 59, 60, 61, 63, 70, 71, 77, 78, 80, 87, 88, 89, 90, 91, 119, 120, 123, 125, 126, 128, 132, 133, 134, 135, 136, 137, 139, 140, 142, 143, 146, 147, 148, 152, 159, 160, 173, 195, 196, 206, 222, 227, 228, 234, 239, 244, 257, 260, 261, 264
Significant Greenhouse Gas Emissions 205
significant new information....49, 156
Solar Shade Control Act 241
speculative 136, 176, 181
Staged Environmental Impact Report (EIR)....184, 190, 191, 193
State Air Resources Board....62, 69, 83, 154
State CEQA Guidelines 119, 125, 126, 221
State Clearinghouse 33, 35, 47, 48, 126, 145, 148, 152, 153, 155, 160, 165, 190, 222, 223, 224, 298
State Lands Commission....18, 240, 265
State Teachers Retirement System....249
State Transportation Improvement Program....10, 238
State Water Resources Control Board....83, 209, 231, 232, 235
Statement of Overriding Considerations....95, 124, 135, 143, 159, 160, 169
statewide, regional, or areawide significance 32, 43, 50, 144, 154, 223, 224, 298
Statutes of Limitations....167
Statutory Exemptions....234, 240
Streamlining....205
Substantial Evidence.... 6, 10, 11, 17, 31, 33, 39, 78, 98, 99, 119, 120, 133, 134, 135, 136, 137, 138, 139, 141, 142, 143, 146, 157, 158, 159, 168, 174, 188, 190, 200, 205, 206, 208, 222, 239, 260, 264
Supplement Environmental Impact Report (EIR).....79, 91, 162, 185, 189, 197, 198, 199, 210, 229, 265
Surface Mining and Reclamation Act of 1975.... 67
Sustainable Communities Strategy 206

T

Tahoe Regional Planning Compact..... 41
Thermal Power Plant 237
Threshold(s) of Significance.....59, 141, 142
Tier.....205
Tiering..... 7, 51, 53, 54, 123, 134, 178, 183, 184, 205, 264, 265, 266, 295
Timberland Preserve Zones 235
Time Limits 41, 60, 66, 67, 92, 96, 130, 164, 166, 167, 226, 229, 230
Trade Secret.....90, 168
Transportation Planning Agency 32, 50, 164
transportation project(s).....29, 30
transportation projects..... 29
tribal cultural resources.....8, 9, 13, 14, 34, 35, 36, 45
Trustee Agency..... 7, 33, 62, 70, 145, 150, 151, 154, 164, 165, 172, 222, 223, 265

U

Unique Archaeological Resource.....37, 38, 140, 141
United States..... 10, 26, 41, 44, 65, 85, 127, 132, 151, 153, 160, 167, 173, 177, 222, 225, 226, 228, 259, 265
United States Department of Agriculture.....5, 56
urbanized area..... 41, 88, 132, 151, 153, 160, 246, 247, 250, 265

W

waste disposal 1, 67, 69, 145, 155, 207, 209
water supply assessment 186
Williamson Act.....224, 250

CEQA Guidelines
Topics Index

Topic ..... **Section**

Accessory Structures
Categorical Exemption ..... 15303(e)
..... 15311

Addendum to an EIR or Negative Declaration 15164

Adequacy of Document
Decision by Lead Agency 15090
Decision by Responsible Agency 15096
Standards 15151
Use by Responsible Agencies 15231

Adequate Time for Review and Comment 15203

Administrative Appeals
Use of EIRs 15185

Adoption of Coastal Plans and Programs 15265

Advisory Body ..... 15025(c)

Agency Procedures
Additional Notices 15087
Categorical Exemptions 15300.4
Contents 15022
General 15020
Review of Documents 15204

Agricultural Lands
Environmental Checklist ..... Appendix G, Item II

Air Quality Permits 15281

Air Resources Board ..... 15251(d)

Topic ..... **Section**

Alterations in Land Use Limitations
Categorical Exemption 15305

Alternatives
Discussion in EIR 15126.6

Applicability
Generally 15007

Applicant
Data and Information 15084
Defined 15351
Delays 15109
Identifying Responsible Agencies ..... 15084(b)
Meetings 15104
Submission of Draft EIR 15084
Submission of Information 15084

Application of Coatings 15278

Approval
Defined 15352
EIR 15090
Negative Declaration 15074

Archaeological Resources
Environmental Checklist ..... Appendix G, Item V

Archeological Impacts 15064.5

Authority 15000

Authority Provided by CEQA
Public Agencies 15040

Authority to Approve Projects Despite Significant Effects 15043

Topic ..... **Section**

Authority to Comment 15044

Authority to Disapprove Projects 15042

Authority to Mitigate 15041

California Coastal Zone ..... 15206(b)(4)(C)

Categorical Exemption ..... Article 19
- Accessory Structures ..... 15303(e) 15311
- Acquisition of Housing for Housing Assistance Programs 15326
- Acquisition of Lands for Wildlife Conservation Purposes 15313
- Addition of Safety or Health Protection Devices ..... 15301(f)
- Additions to Existing Structures ..... 15301(e)
- Annexations of Existing Facilities 15319
- Bicycle Lanes ..... 15304(h)
- Cogeneration Projects at Existing Facilities 15329
- Condominium Conversions ..... 15301(k)
- Conversion of Small Structures 15303
- Defined 15354
- Demolition of Small Structures ..... 15301(l)
- Educational or Training Programs Involving No Physical Changes 15322
- Enforcement Actions by Regulatory Agencies 15321
- Exceptions 15300.2
- Existing Facilities 15301
- Facilities for Public Gatherings, Normal Operations 15323
- Finding of No Significant Effect 15300
- Fish Stocking ..... 15301(j)
- General 15300
- Grading ..... 15304(a)
- Historical Resource Restoration/Rehabilitation 15331
- Hospitals, Replacement ..... 15302(a)
- Hydroelectric Projects at Existing Facilities 15328
- In-Fill Development Projects 15332
- Information Collection 15306

Topic ..... Section

Inspections 15309
Installation of Small, New Equipment 15303
Leasing New Facilities 15327
Loans 15310
Local Agencies, Changes in Organization 15320
Lots for Exempt Facilities 15319
Maintenance Dredging ..... 15304(g)
Maintenance of Existing Landscaping ..... 15301(h)
Ministerial Projects, Relation to 15300.1
Minor Actions to Prevent, Minimize, Stabilize, Mitigate or Eliminate the Release or Threat of Release of Hazardous Waste or Hazardous Substances 15330
Minor Alterations in Land Use Limitations 15305
Minor Alterations to Land 15304
Minor Land Divisions 15315
Minor Repairs and Alterations of Dams ..... 15301(m)
Minor Temporary Uses of Land ..... 15304(e)
Minor Trenching and Backfilling ..... 15304(f)
New Construction of Small Structures 15303
New Copy on Signs ..... 15301(g)
New Gardening or Landscaping ..... 15304(b)
Notice of Exemption 15062
Open Space Contracts or Easements 15317
Parks, Transfer of Land to Create Parks 15316
Purchases of Mortgages ..... 15310(b)
Reconstruction of Existing Structures 15302
Regulation, Protection of Natural Resources 15307
Regulation, Protection of the Environment 15308
Regulation, Working Conditions 15324
Relation to Ministerial Projects 15300.1
Replacement of Existing Structures 15302
Restoration or Rehabilitation ..... 15301(d)
Reversion to Acreage ..... 15305(c)
Revisions 15300.3
Schools
Minor Additions 15314

Topic ..... Section

Replacement ..... 15302(a)
..... 15311(a)
Signs ..... 15301(g)
Single Family Residences ..... 15303(a)
Small Habitat Restoration Projects 15333
Streets and Highways ..... 15301(c)
Surplus Government Property Sales 15312
Transfers of Ownership of Interest in Land to Preserve Existing Historical Resources 15325
Transfers of Ownership of Interest in Land to Preserve Existing Natural Conditions 15325
Transfers of Ownership of Interest in Land to Preserve Open Space 15325
Use by Public Agencies 15300.4
Utilities ..... 15301(b)
Utility Extensions ..... 15303(d)
Wilderness Area Designation 15318
Working Conditions, Regulation 15324

CEQA
Defined 15353
Process Flow Chart ..... Appendix A
Purposes 15002

Certified Mail
Notice of Preparation ..... 15082(a)(3)

Response to Consultation ..... 15096(b)

Certified State Regulatory Programs
Exemptions ..... Article 17
General 15250
List 15251
Substitute Document 15252
Substitute EIR 15253

Topic ..... **Section**

Checklists
Completed by Applicant ..... Appendix H
Completed by Lead Agency ..... Appendix G
Use in Initial Study ..... 15063(f)

Circulation of Documents 15225

Citation 15148

Coastal Commission
Development Permits ..... 15251(c)
Local Coastal Programs ..... 15251(f)

Coastal Zone
Projects in ..... 15206(b)(4)(C)

Combined EIR-EIS 15170
Consultation 15223
Preparation 15222
Time Limits 15224

Comments
Authority 15044
Failure to Comment 15207
On Initiative of Public Agencies 15209
Part of Final EIR ..... 15088(c)
Public Agencies 15088
..... 15209
Public 15074
..... 15088
..... 15202
Response by Lead Agency 15088
Responsible Agency 15096
Retention 15208

Community Plan Residential Projects 15183

Topic ..... **Section**

Compliance with Performance Standard or Treatment Requirement
Rule or Regulation 15189

Concepts
General 15002
Lead Agency 15050
Tiering 15152

Condominium Conversions
Categorical Exemption ..... 15301(k)

Congestion Management Programs
Exemption 15276

Consideration
Comments 15074
..... 15088
..... 15096(d)
EIR 15090
Environmental Impacts 15126
Preparing EIRs and Negative Declarations ..... Article 10
Mitigated Negative Declaration 15074
Mitigation Measures 15126.4
Negative Declaration 15074
Responsible Agency 15096
Significant Impacts 15126.2

Consultation
Certified Mail ..... 15082(a)(3)
Comments on Draft Documents ..... 15082(b)
..... 15083
Contact Person ..... 15204(d)
Content of Draft EIR ..... 15082(a)(1)
..... 15083

Topic ..... **Section**

Deciding Whether to Prepare an EIR or Negative Declaration 15060
..... 15070
..... 15081
Draft EIR 15086
Federal Agencies ..... 15086(a)(3)
..... 15223
General ..... 15082(a)
Initial Study ..... 15063(g)
List of EIR, Contents, Location ..... 15124(a)
Listings of Agencies ..... 15087(f)
Meetings ..... 15082(c)
Negative Declaration 15072
..... 15073
Notice of Preparation ..... 15082(a)
..... 15082(b)
Preparation of Joint EIR-EIS 15170
..... 15223
Regional and District Offices of State Agencies ..... 15205(f)
Responsible Agency 15096
Scoping 15083
State Responsible Agencies ..... 15082(b)
Use of EIS 15223
Use of State Clearinghouse ..... 15082(e)
..... 15205
Water Agencies 15155

Courts
Defined as Not Public Agencies 15379
Policies Identified by Courts 15003

Criteria for Shortened Clearinghouse Review ..... Appendix K

Cultural Resources
Environmental Checklist ..... Appendix G, Item V
Significant Effect 15064.5

Topic ..... **Section**

Cumulative Impact
Defined 15355
Discussion in EIR 15130
Effect on Categorical Exemptions ..... 15300.2(b)
Mandatory Findings of Significance 15065
Relationship to Larger Undertaking 15165

Deadlines for Compliance with Sections 15188 and 15189 15190

Decision to Prepare a Negative or Mitigated Negative Declaration 15070

Decision to Prepare an EIR 15081
Fair Argument about Significant Effect 15064
Finding of Possible Significant Effect 15064
..... 15091
Public Controversy ..... 15064(f)(4)

Decision-Making Body
Consideration and Approval of Negative Declaration 15074
Consideration of EIR 15090
Defined 15356
Delegation of Authority 15025

Definitions
Affordable Housing 15191
Agricultural Housing 15191
Applicant 15351
Approval 15352
Categorical Exemption 15354
CEQA 15353
Cumulative Impact 15355
Decision-Making Body 15356
Discretionary Project 15357
Draft EIR ..... 15362(a)
Effects 15358

Topic ..... **Section**

EIR ..... 15002(f)
..... 15362
EIS 15363
Emergency 15359
Endangered Species 15380
Environment 15360
Environmental Documents 15361
Evidence, Substantial 15384
Feasible 15364
Final EIR ..... 15362(b)
Impacts 15358
Initial Study 15365
Jurisdiction by Law 15366
Lead Agency 15367
Local Agency 15368
Ministerial Projects 15369
Mitigated Negative Declaration 15369.5
Mitigation 15370
Negative Declaration 15371
Notice of Completion 15372
Notice of Determination 15373
Notice of Exemption 15374
Notice of Preparation 15375
Person 15376
Private Project 15377
Project 15378
Public Agency 15379
Rare Species 15380
Residential Infill Projects 15191
Responsible Agency 15381
Significant Effect on the Environment ..... 15002(g)
..... 15382
State Agency 15383
Substantial Evidence 15384
Threatened Species 15380
Tiering 15385

Topic ..... **Section**

Trustee Agency 15386
Urbanized Area 15387

Degree of Specificity 15146

Delays 15006
..... 15100

Delegation of Responsibilities 15025

Demolition of Small Structures
Categorical Exemption ..... 15301(l)

Determining Significant Effect 15064

Disapprovals 15042

Disaster Relief 15269

Discharge Requirements 15263

Discretionary Project ..... 15002(i)
Defined 15357

Documents
Draft EIR, Defined ..... 15362(a)
EIR ..... 15002(f)
..... 15080 through 15095
..... 15085
Defined 15362
EIS ..... 15220 through 15228
Defined 15363
Final EIR, Defined ..... 15362(b)
Initial Study 15063
Defined 15365
Mitigated Negative Declaration, Defined 15369.5

Topic ..... **Section**

Negative Declaration ..... 15070 through 15075
Defined 15371
Notice of Completion ..... Appendix C
..... 15085
Defined 15372
Notice of Determination ..... Appendix D
Defined 15373
EIR 15094
Mitigated Negative Declaration 15075
Negative Declaration 15075
Notice of Exemption 15062
..... Appendix E
Defined 15374
Notice of Preparation ..... Appendix I
..... 15082
Defined 15375

Draft EIR ..... see EIR Process

Duty to Minimize Environmental Damage and Balance Competing Public Objectives 15021

Duty to Prevent Avoidable Damage 15091

Economic Factors 15131

Educational Programs
Categorical Exemption 15322

Effects Not Found to be Significant 15128

Effects
Defined 15358

EIR
Adequacy 15151

Topic ..... **Section**

All Phases of a Project 15126
Combined with General Plan 15166
Contents
Alternatives 15126.6
Appendices 15147
Cumulative Impacts 15130
Economic and Social Effects 15131
Effects Not Found to be Significant 15128
..... 15143
Energy Conservation ..... Appendix F
..... 15126.2
Environmental Setting 15125
Growth Inducing Impacts ..... 15126(d)
..... 15126.2(d)
Housing Factors ..... 15131(c)
Inconsistencies with Adopted Plans ..... 15125(d)
Incorporation by Reference 15150
Index 15122
Information Submitted by Applicant 15084
Irreversible Commitments ..... 15126(c)
..... 15126.2(c)
..... 15127
Local Project Mandated by State Agency 15184
Location ..... 15124(a)
Maps ..... 15124(a)
Mitigation Measures 15126.4
No Project Alternative ..... 15126.6(e)
Objectives ..... 15124(b)
Page Limits 15141
People Who Prepared 15149
Persons Consulted 15129
Project Description 15124
References 15148
Responses to Comments ..... 15132(d)
Significant Effects 15126.2
Social Effects 15131

Topic ..... **Section**

Speculative Impacts 15145
State Clearinghouse Number ..... 15082(e)
Summary 15123
Table of Contents 15122
Technical Data 15147
Unavoidable Effects ..... 15126(b)
..... 15126.2(b)
Water Quality 15263
Decision to Prepare an EIR 15060
..... 15081
..... Article 10
Defined 15362
Degree of Specificity 15146
Draft EIR, Defined ..... 15362(a)
Engineering Project Report 15148
Evidence ..... 15121(c)
Final EIR 15132
Defined ..... 15362(b)
Format ..... 15120(a)
General ..... 15120 through 15050
General Plan EIR 15166
Informational Document 15121
Interdisciplinary Approach 15142
Language 15140
Lead Agency Evaluation and Analysis 15088
Local Project Mandated by State Agency 15184
Military Base Reuse Plan 15229
Only One EIR with the Same Underlying Activity 15050
Part of Project Report ..... 15004(c)
Preparation ..... Article 10
Professional Services 15149
Program EIR 15168
Project Requiring State Approval or Financial Assistance 15267
Public Review 15201
..... 15203
Required by Statute 15081.5

Topic ..... Section

Staged EIR 15167
Submission of Information by Any Person 15083
..... 15084(c)
Subsequent EIR 15162
Supplement to an EIR 15163
Time of Preparation 15004
Types of EIRs ..... Article 11
Addendum to an EIR 15164
Focused EIR ..... 15063(c)(3)
General Plan EIR 15166
General 15160
Joint EIR-EIS 15170
Master Environmental Assessment 15169
Phased Projects 15165
Program EIR 15168
..... 15161
Staged EIR 15167
Subsequent EIR 15162
Supplement to an EIR 15163
Use of Federal EIS 15221
Use of Single EIR 15153

EIR Monitor 15240
..... Article 16

EIR Process
Approval 15092
Certification of the Final EIR 15090
Completion and Certification of EIR 15108
Consultation, Draft EIR 15086
Direct Contacts 15083
Early Public Consultation 15083
Filing of Final EIR 15095
General 15080
Notice of Completion 15085
Notice of Determination 15094

Topic ..... **Section**

Notice of Preparation 15082
Preparation of Draft EIR ..... Article 9
..... 15084
Preparation of Final EIR 15089
..... 15132
Projects of Statewide, Regional, or Areawide Significance 15206
Projects with Federal Involvement 15083
..... 15110
..... Article 14
Public Notice 15087
Public Review 15087
State Review Period 15205
Use of Final EIR by Responsible Agencies 15096
Use of Libraries ..... 15087(g)

EIS
Consultation 15223
Defined 15363
Public Review 15225
Use as an EIR 15221

Emergency
Defined 15359

Emergency Projects 15269

Emphasis 15143

Endangered Species
Defined 15380

Energy Conservation ..... Appendix F
..... 15126.2

Enforcement Actions
Categorical Exemption 15321

Topic ..... **Section**

Engineering Project Report 15148

Environment
Defined 15360

Environmental Checklist Form ..... Appendix G

Environmental Documents
Defined 15361

Environmental Impacts
Consideration and Discussion of 15126

Environmental Information Form ..... Appendix H

Environmental Review of New Rules and Regulations 15187

Environmental Setting 15125

Evaluation of and Response to Comments 15088

Evidence
Substantial, Defined 15384

Examples of Tiering EIRs ..... Appendix J

Exemptions ..... Article 18
Adoption of Coastal Plans and Programs 15265
Affordable Housing 15194
Agricultural Housing 15193
Categorical Exemptions ..... Article 19
Certified State Regulatory Programs ..... Article 17
Congestion Management Programs 15276
Disapprovals 15270
Disaster Relief 15269
Discharge Requirements 15263

Topic ..... **Section**

Early Activities Related to Thermal Power Plants 15271
Emergency Projects 15269
Emergency Repairs to Public Service Facilities ..... 15269(b)
Feasibility and Planning Studies 15262
Financial Assistance to Low or Moderate Income Housing 15267
Functional Equivalent 15251
General Plan Time Extension 15266
General Rule ..... 15061(b)(3)
General 15260
List of Certified Programs 15251
List of Projects 15061
Local Coastal Programs 15265
Mass Transit 15275
Ministerial Projects 15268
Notice of Exemption 15062
Olympic Games 15272
Ongoing Project 15007
..... 15261
Passenger or Commuter Service on Existing Rail Lines 15275
Preliminary Review 15060
Preventing an Emergency ..... 15269(c)
Rates, Tolls, Fares, and Charges 15273
Residential Infill 15195
Revenue Shortfalls 15285
Review 15060
..... 15061
Statutory ..... Article 18
Thermal Power Plants 15271
Timberland Preserves 15264
Transportation Improvement Programs 15276

Existing Facilities
Categorical Exemption 15301

Expertise of State Agencies ..... Appendix B

Topic ..... **Section**

Facilities for Public Gatherings
Normal Operations, Categorical Exemption 15323

Failure to Comment 15207

Family Day Care Homes 15274

Feasibility and Planning Studies
Defined as Not Projects 15262
Generally 15262

Feasible
Defined 15364

Federal Agency
Will Not Cooperate 15228

Federal Government
Defined as Not a Public Agency Under CEQA 15379
Federal Project ..... Article 14
General 15220
Preparation of a Combined EIR-EIS 15110
..... 15170
..... 15222
State Comments 15227

Fees
Copy of an EIR ..... 15045(b)
For Preparing an EIR or Negative Declaration ..... 15045(a)

Final EIR
Consideration 15090
..... 15096
Contents 15132
Defined ..... 15362(b)

Topic ..... **Section**

Financial Assistance to Low or Moderate Income Housing 15267

Findings
- Agency Lacks Authority ..... 15091(a)(2)
- General 15091
- Project Changed ..... 15091(a)(1)
- Project Changes Infeasible ..... 15091(a)(3)
- Rates, Tolls, Fares, and Charges ..... 15273(a)
- Relationship to Statement of Overriding Considerations ..... 15093(b)
- Responsible Agency 15096
- Substantial Evidence ..... 15091(b)

Fish and Game Commission ..... 15251(b)

Fish Stocking
- Categorical Exemption ..... 15301(j)

Flow Chart ..... Appendix A

Focus of Review 15204

Focused EIR ..... 15063(c)(3)
- Pollution Control Equipment 15188
- Small Projects 15179.5

Food and Agriculture, Department ..... 15251(i)

Forecasting 15144

Forestry
- Board of Forestry ..... 15251(e)
- Department of Forestry ..... 15251(a)
  15357
- Timber Harvesting Plans ..... 15251(a)
  15357

Topic ..... **Section**

Functional Equivalent
Certified Programs 15251
General 15250
Substitute Document 15252
Use of an EIR Substitute by a Responsible Agency 15253

General 15100

General Plan
Analysis in EIR ..... 15146(b)
EIR as Part of General Plan 15166
Inconsistencies of Project with Adopted Plans ..... 15125(d)
Time Extension 15266
Use of General Plan EIR with Subsequent Projects ..... 15168(d)

General Rule Exemption ..... 15061(b)(3)

Grading
Categorical Exemption ..... 15304(a)

Greenhouse Gas Emissions
Cumulative Impacts ..... 15130(b)(1)(B)
Mitigation Measures ..... 15126.4(c)
Tearing and Streamlining 15183.5

Growth Inducing Impacts
Discussion in EIR ..... 15126(d)

Hearings ..... 15087(i)
..... 15202
..... 15232

Historical and Archeological Resources 15064.5
..... 15300.2(f)

Housing Development ..... 15092(c)

Topic ..... **Section**

Housing for Agricultural Employees 15193

Housing Needs Allocation 15283

Impacts
Defined 15358

Incorporation by Reference 15150

Industrial Welfare Commission 15324

Information Collection
Categorical Exemption 15306

Informational Document 15121

Initial Study
Consultation ..... 15063(g)
Contents ..... 15063(d)
Defined 15365
Format ..... 15063(f)
General ..... 15063(a)
Information from Applicant ..... 15063(e)
Prior to Initial Study 15060
Purposes ..... 15063(c)
Submission of Data ..... 15063(e)
Time Limits 15102

Inspections
Categorical Exemption 15309

Interdisciplinary Approach 15142

Irreversible Commitments 15127

Joint Activities 15226

Topic ..... **Section**

Joint EIR-EIS 15170

Jurisdiction by Law
City or County ..... 15366(a)
Defined ..... 15366(b)

Lake Tahoe Basin ..... 15206(b)(4)(A)

Language 15140

Lead Agency
Approval of Final Project 15092
Archeological Sites 15064.5
Authority to Disapprove Projects 15042
Authority to Mitigate 15041
Comments 15044
Defined 15367
Delays 15109
Designation by Agreement ..... 15051(d)
Designation by Office of Planning and Research 15053
Determination of a Lead Agency ..... 15050(c)
Disputes as to Designation ..... 15023(f)
Lead Agency Criteria 15051
Lead Agency Principle ..... 15050(a)
Meetings 15104
Preliminary Review Responsibilities 15060
Shift in Lead Agency Responsibilities 15052
Time Limits 15101
..... 15102

Lead Agency Principle ..... 15050(a)

Limitations on Discussion of Environmental Impact 15127

Limitations on the Use of the Master EIR 15179

Topic ..... **Section**

List of Exemption Projects ..... 15061(c)

Litigation ..... Article 15
Conditional Permits 15233
Request for Hearing 15232
Statutory Reference 15230
Time Limits and Criteria 15230
Use of Documents by Responsible Agencies 15231

Loans for Purchase of Existing Structures
Categorical Exemption 15310

Local Agencies
Changes in Organization, Categorical Exemption 15320

Local Agency
Defined 15368

Local Agency Formation Commission ..... 15127(b)

Local Coastal Programs
CEQA Application 15265
Exemption 15265

Local Projects Mandated by State Agency 15184

Logging ..... 15251(a)
..... 15357

Mandatory Findings of Significance 15065

Mass Transit 15275

Master EIR 15175
Contents 15176

Topic ..... **Section**

Master Environmental Assessment
Contents ..... 15169(b)
General ..... 15169(a)
Preparation ..... 15169(c)
Uses ..... 15169(d)

Master Environmental Impact Report ..... Article 11.5

Meetings 15104
Responsible Agency with Lead Agency ..... 15096(c)

Military Base Reuse Plan EIRs
Baseline Analysis 15229

Ministerial Projects
Defined ..... 15002(i)(1)
..... 15268
..... 15369
Examples ..... 15268(b)
Exemption 15268
Identification in Agency Procedures ..... 15268(c)
Mixed, Ministerial and Discretionary Projects ..... 15268(d)
Relationship to Categorical Exemptions 15300.1

Minor Alterations to Land
Categorical Exemption 15304

Mitigated Negative Declaration 15070
Defined 15369.5
Notice of Determination 15075

Mitigation
Archeological Sites 15064.5
Authority 15041
Defined 15370

Topic ..... **Section**

Mitigation Measures
Adoption ..... 15096(g)
Agencies 15041
Discussion in EIR 15126.4
Findings 15093
Historic Resources ..... 15126.4(b)
Housing Development ..... 15092(c)
Initial Study 15063

Mitigation Monitoring or Reporting 15097

Multiple Projects 15165

Native American Archeological Sites ..... 15064.5(d)

Negative Declaration ..... Article 6
Completion of 15107
Consideration 15074
Contents 15071
Consultation ..... 15063(g)
Defined 15371
Fees 15045
General ..... 15002(f)
..... 15070
Mitigated Negative Declaration 15070
Notice 15072
Notice of Determination 15075
Preparation 15070
..... Article 10
Public Review 15072
..... 15073
Public Review Period 15072
..... 15073
Responsibility for Preparation ..... 15050(a)
State Review Period 15205

Topic ..... Section

When Required 15070
NEPA Document Ready before CEQA Document 15221

NEPA
General 15220
Projects Subject to ..... 15127(c)
..... 15220 through 15228

Notice
Mitigated Negative Declaration 15072
Negative Declaration 15072
Public Notice of Draft EIR 15087
Supplement to an EIR ..... 15163(c)

Notice of Completion
Contents 15085
Defined 15372
Draft EIR ..... Appendix L
Form ..... Appendix C
Use 15085

Notice of Determination
Content 15094
..... 15075
Defined 15373
Filing by a Local Agency ..... 15075(d)
Filing by a State Agency ..... 15075(c)
Filing with Secretary for Resources ..... 15075(c), (d)
Form ..... Appendix D
Responsible Agency ..... 15096(i)
Use of State Clearinghouse ..... 15075(c), (d)
Use with EIR 15094
Use with Negative Declaration ..... 15075(a), (b)

Notice of Exemption
Agricultural Housing, Affordable Housing and Residential Infill Projects 15196

Topic ..... Section

Contents 15062
Defined 15374
Filing by a Local Agency ..... 15062(c)(2)
Filing by a State Agency ..... 15062(c)(1)
Form ..... Appendix E
General 15062
List ..... 15061(c)
Posting Period ..... 15062(c)
Preliminary Review 15062
When Filed by an Applicant ..... 15062(c)(4)

Notice of Preparation
Certified Mail ..... 15082(a)(3)
Comments from Responsible Agency ..... 15082(b) 15103
Contents ..... 15082(a)(1)
Defined 15375
Form ..... Appendix I
General ..... 15082(a)
Procedure for Sending to State Responsible Agencies ..... 15082(d)
Purpose 15375
Sample Format ..... Appendix I
Use of State Clearinghouse ..... 15082(d), (e)

Notification Requirement, Department of Defense 15190.5

Nuclear Power Plants ..... 15206(b)(7)

Office of Planning and Research
Assistance to Other Agencies ..... 15023(d)
Lead Agency Disputes ..... 15023(f)
Monitoring Consultation with State Responsible Agencies ..... 15082(c)
Monitoring State Responsible Agencies ..... 15023(e)
Responsibilities 15023
State Clearinghouse ..... 15023(c) ..... 15082(d), (e)

Topic ..... **Section**

Olympic Games 15272

Ongoing Project 15261

Open Space Contracts or Easements
Categorical Exemption 15317

Organizations and Persons Consulted 15129

Other Statutory Exemptions 15282

Page Limits 15141

Parks, Transfer of Land to Create
Categorical Exemption 15316

Passenger or Commuter Service on Existing Rail Lines
Exemption 15275

Person
Authority to Comment 15044
Defined 15376

Pesticides ..... 15251(i)

Phased Projects 15165

Phase-in of New Requirements 15007

Pipelines 15284

Planning and Review Process
Combined with EIR Process 15095

Planning Commission ..... 15025(c)

Topic ..... **Section**

Power Plants
Exemption for Early Activities 15271
Projects within 10 miles of Nuclear Power Plants ..... 15206(b)(7)

Preapplication Consultation 15060.5

Preliminary Review of Projects 15060
Exemptions 15061
..... 15062

Preparation of Joint Documents 15222

Private Project
Completion and Certification of EIR 15108
Defined 15377
Negative Declaration 15107

Program EIR
Advantages ..... 15168(b)
General ..... 15168(a)
Notice with Later Activities ..... 15168(e)
Use with Later Activities ..... 15168(c)
Use with Subsequent EIRs and Negative Declarations ..... 15168(d)

Project
Activity Being Approved ..... 15378(c)
Authority to Approve Despite Significant Effects 15043
Authority to Disapprove 15042
Certificate ..... 15378(a)(3)
Defined 15378
Entitlement for Use ..... 15378(a)(3)
Exemptions 15061
Financial Assistance ..... 15378(a)(2)
General Plans ..... 15378(a)(1)
Lease ..... 15378(a)(3)

Topic ..... **Section**

License ..... 15378(a)(3)
Multiple Projects 15165
Permit ..... 15378(a)(3)
Phased 15165
Preliminary Review 15060
Public Works ..... 15378(a)(1)
Redevelopment Plan ..... 15180(a)
Scope of Project 15165
Zoning Ordinances ..... 15378(a)(1)

Project Description 15124

Project EIR 15161

Projects Consistent with a Community Plan or Zoning 15183

Projects Located Outside California 15277

Projects near Airports 15154

Projects of Statewide, Regional, or Areawide Significance 15206

Projects with Short Time Periods for Approval 15111

Public Agency
Adoption of Procedures of another Agency 15022
Adoption of Procedures 15022
Adoption of State Guidelines by Reference 15022
Authority 15040
..... 15041
Authority to Approve Despite Significant Effects 15043
Authority to Comment 15044
Authority to Disapprove Projects 15042
Authority to Mitigate 15041
Contents of Procedures 15022
Courts 15379

Topic ..... **Section**

Defined 15379
Exemptions 15061
Implementing Procedures 15022
Objectives, Criteria, and Procedures 15022
Preliminary Review 15060
Responsibilities ..... 15020 through 15022

Public Participation 15201

Public Review ..... 15200 through 15209
Agency Procedures 15201
..... 15203
..... 15204
EIR Process 15087
..... 15105
Focus of Review 15204
Hearings 15202
Length of Review Period 15072
..... 15073
..... 15105
Mitigated Negative Declarations 15073
..... 15105
Negative Declarations 15072
..... 15073
..... 15105
Project Planning 15206
Purpose 15200
Time Limits 15105
..... 15205

Purchases of Mortgages
Categorical Exemption ..... 15310(b)

Purpose of Guidelines 15002

Rare Species

Topic ..... Section

Defined 15380
Rates, Tolls, Fares, and Charges
Exemption ..... 15273(a)
Findings ..... 15273(c)
Increases ..... 15273(b)

Recirculation of a Negative Declaration Prior to Adoption 15073.5

Recirculation of an EIR Prior to Certification 15088.5

Reconstruction of Existing Structures
Categorical Exemption 15302

Redevelopment Plan 15180

Reducing Delay and Paperwork 15006

Regulatory Actions for Protecting Natural Resources
Categorical Exemption 15307

Regulatory Actions for Protecting the Environment
Categorical Exemption 15308

Regulatory Programs
Exemptions ..... Article 17

Removal of Mature & Scenic Trees 15304

Replacement
Existing Structures, Categorical Exemption 15302
Schools and Hospitals, Categorical Exemption ..... 15302(a)

Residential Projects
Consistent with a Community Plan or Zoning 15183
Pursuant to a Specific Plan 15182

Topic ..... **Section**

Response to Consultation
Responsible Agency ..... 15096(b)

Responsible Agencies
Adoption of Alternatives or Mitigation Measures 15041
..... 15096(g)
Authority to Disapprove Projects 15042
Authority to Mitigate 15041
Comments ..... 15096(d)
Conditional Permits 15233
Consideration of Document ..... 15096(f)
Consultation ..... 15096(b)
Decision on Adequacy ..... 15096(e)
Defined 15381
Findings ..... 15096(h)
Meetings 15104
Meetings with Lead Agency ..... 15096(c)
Notice of Determination ..... 15096(i)
Response to Consultation ..... 15096(b)(1)
Time Limits 15101
..... 15103
..... 15205
Use of Document Prepared by Lead Agency ..... 15050(b)
Use of Document Under Litigation 15231

Retention and Availability of Comments 15208

Reuse Plan EIRs
Military Base 15229

Revenue Shortfall 15285

Review by State Agencies 15205

Review for Exemption 15061

Topic ..... **Section**

Review of Application for Completeness 15101

Review of Documents 15105
Agency Procedures 15201
..... 15203
..... 15204
Availability of Documents ..... 15087(e)
Charges for Copies ..... 15045(b)
Comments on Initiative of Public Agencies 15044
..... 15209
Contact Person 15204
Effect on Planning 15203
Failure to Comment 15207
Focus for Review 15204
Hearings 15202
Libraries ..... 15087(g)
Listings of Agencies to be Consulted ..... 15087(f)
Mandatory 15205
..... 15206
Negative Declarations 15072
..... 15073
..... 15105
..... 15205
..... 15206
Projects of Statewide, Regional, or Areawide Significance 15206
Public Participation 15201
..... 15202
Purpose 15200
Retention of Comments 15208
State Clearinghouse 15105
..... 15205
..... 15206
State Review 15105
..... 15205
..... 15206

Topic ..... **Section**

Time Periods 15105
..... 15203
..... 15205(d)

Sacramento-San Joaquin Delta ..... 15206(b)(4)(E)

San Francisco Bay Conservation and Development Commission ..... 15206(b)(4)(G)
..... 15251(h)

Santa Monica Mountains Zone ..... 15206(b)(4)(B)

School Facilities 15186

Schools
Changes in Grade Structure, Categorical Exemption ..... 15322(b)
Education or Training Programs, Categorical Exemption 15322
Minor Additions to, Categorical Exemption 15314

Scoping 15083

Secretary for Resources
Address 15000
Responsibilities 15024

Short Title 15001

Significant Effect
Archeological and Historical Resources 15064.5
Authority to Approve Projects 15043
Consideration and Discussion of 15126.2
Defined 15382
Determining Significant Effect ..... 15002(g)
..... 15064
Examples 15064
..... 15126.2
Findings 15091

Topic ..... Section

Mandatory Findings of Significance 15065
Mitigation Measures 15126.4

Signs
New Copy, Categorical Exemption ..... 15301(g)
On-Premise Signs, Categorical Exemption ..... 15311(a)

Single Family Residences
Categorical Exemption ..... 15303(a)

Social Factors 15131

Special Situations ..... Article 12

Specific Plan
Residential Projects 15182

Speculation 15145

Speculative Impacts 15145

Staged EIR
General 15167
Use with a Supplement ..... 15167(b)
Use with Power Plants ..... 15167(c)

State Agencies
Areas of Expertise ..... Appendix B

State Agency
Defined 15383

State Clearinghouse
Address 15205
Number of Copies Required ..... 15205(e)
Required Review 15105

Topic ..... **Section**

.....15205
.....15206
Responsibilities ..... 15023(c)
Review Periods.....15105
..... 15205(d)
Use of ..... 15082(e)

State Mandated Local Projects 15184

State Policies
Court Declarations.....15003

Statement of Overriding Considerations
General 15093
Relationship to Findings..... 15093(b)

Statute of Limitations.....15112
30 Days ..... 15075(e)
30 Days 15094
Notice of Determination..... 15075(e)
.....15094
Notice of Exemption ..... 15062(d)

Statutory Exemptions (see Exemptions).....Article 18

Subsequent EIR
Conditions Requiring Preparation ..... 15162(a)
Generally.....15162
Preparation by Lead Agency ..... 15162(b)
Preparation by Responsible Agency..... 15162(c)

Subsequent Negative Declaration 15162

Subsequent Projects
Identified in the MEIR 15178

Topic ..... **Section**

Within the Scope of the MEIR 15177

Substantial Evidence
Defined 15384

Substantive Duty
Findings 15091
Responsible Agency 15096
Substitute Document 15252

Substitution of Mitigation Measures in a Proposed Mitigated Negative Declaration 15074.1

Suisin Marsh ..... 15206(b)(4)(F)

Summary 15123

Supplement to an EIR
Circulation ..... 15163(d)
Consideration ..... 15163(e)
Contents ..... 15163(b)
Notice 15163(c)
When Required ..... 15163(a)

Surplus Government Property Sales
Categorical Exemption 15312

Table of Contents or Index 15122

Technical Detail 15147

Terminology
"May" ..... 15005(c)
"Must" ..... 15005(a)
"Shall" ..... 15005(a)
"Should" ..... 15005(b)

Topic ..... **Section**

Thermal Power Plants
Contents of EIR or Negative Declaration ..... 15271(b)
Exemption ..... 15271(a)

Threshold Requirements for Exemptions for Agricultural Housing, Affordable Housing and Residential Infill Projects 15192

Threatened Species
Defined 15380

Thresholds of Significance 15064.7

Tiering 15152
Defined 15385

Timberland Preserves
Exemption 15264

Time Limits ..... Article 8
Determining Type of Document 15102
EIR
1 Year 15108
Extensions 15108
..... 15110
Initial Study 15102
Lead Agency 15101
..... 15102
..... 15104
..... 15110
Litigation 15230
Meeting on Scope of EIR 15104
Negative Declaration 15102
..... 15105
..... 15107
Private Projects 15107
..... 15108

Topic ..... **Section**

Projects Subject to CEQA and NEPA 15110
..... 15224
Public Review 15105
Responsible Agency 15101
..... 15103
..... 15104
Review of Application 15101
Statutes of Limitations 15112
Suspension of Time Periods 15109
Waiver 15110

Timely Compliance 15110

Timing of EIR Preparation
Before Project Plans are Finalized ..... 15004(a)
Early in the Planning Process ..... 15004(b)
Prior to Approval of the Project ..... 15004(a)

Training Program
Categorical Exemption 15322

Transit Agency Responses to Revenue Shortfalls 15285

Transportation Improvement Programs
State and Regional, Exemption 15276

Trustee Agency
Defined 15386

Urbanized Area
Defined 15387

Use of a Single EIR 15153

Use of an EIR from an Earlier Project 15153

Topic ..... **Section**

Use of Registered Professionals in Preparing EIRs 15149

Utility Extensions
Categorical Exemption ..... 15303(d)

Vote of the People
Defined as Not a Project ..... 15378(b)(3)

Water Quality
Discussion in EIR ..... 15206(b)(6)
..... 15263

Water Resources Control Board ..... 15251(g)

Weather Management ..... 15251(j)

Wild and Scenic Rivers ..... 15206(b)(4)(D)

Wilderness Area Designation
Categorical Exemption 15318

Williamson Act ..... 15206(b)(3)

Working Conditions
Regulation of, Categorical Exemption 15324

Zoning
Defined ..... 15378(a)(1)
Residential Projects 15183

Progress on Incorporating Climate Change into Management of California's Water Resources



July 2006
Technical Memorandum Report
California Department of Water Resources

❖ ❖ ❖

Published July 2006

Cover design by Jamie Anderson, Delta Modeling Section.

Copies of this document are available for $20 each for the first 3 copies and $50 for each additional copy. A CD-ROM of the report is included with each copy.

Contact:

Publication Sales
Department of Water Resources
P.O. Box 942836
Sacramento, CA 94236-0001
916-653-1097

This document is available on the web at
http://baydeltaoffice.water.ca.gov/climatechange/reports.cfm

Progress on Incorporating Climate Change into Planning and Management of California's Water Resources

Technical Memorandum Report

July 2006

Department of Water Resources

State of California
Arnold Schwarzenegger, Governor

The Resources Agency
Mike Chrisman, Secretary for Resources

Department of Water Resources
Lester A. Snow, Director

Nancy Saracino
Chief Deputy Director

Brian E. White
Assistant Director Legislative Affairs

David A. Sandino
Acting Chief Counsel

Susan Sims
Assistant Director Public Affairs

Timothy Haines
Deputy Director

Leslie F. Harder, Jr.
Deputy Director

Raphael A. Torres
Deputy Director

Gerald E. Johns
Deputy Director

Bay-Delta Office
Katherine F. Kelly, Chief

Modeling Support Branch
Francis Chung, Chief

Prepared under the direction of:

Francis Chung, Ph.D., P.E. ..... Principal Engineer

Prepared by:

California Department of Water Resources:

Jamie Anderson, Ph.D., P.E. ..... Engineer
Michael Anderson, Ph.D. ..... Acting State Climatologist
Daniel Easton, P.E. ..... Engineer
Michael Floyd, P.E. ..... Senior Engineer
Roy Peterson, Ph.D. ..... Environmental Scientist

Joel Dudas, P.E. ..... Engineer
Messele Ejeta, Ph.D. P.E. ..... Engineer
Brian Heiland, P.E. ..... Engineer
Arthur Hinojosa,Jr., P.E. ..... Supervising Engineer
Jim Goodridge ..... Retired State Climatologist
John King, P.E. ..... Engineer
Bunloeurng Lek, P.E. ..... Engineer
Aaron Miller, P.E. ..... Engineer
Stephen Nemeth, P.E. ..... Engineer
Al Olson, P.E. ..... Engineer
Morteza Orang, Ph.D. ..... Land and Water Use Scientist
Michael Perrone, Ph.D. ..... Environmental Scientist

Prepared by (continued):

California Department of Water Resources (continued):

Tawnly Pranger, P.E. ..... Engineer
David Rizzardo, P.E. ..... Senior Engineer
Maurice Roos, P.E. ..... State Hydrologist
David Todd ..... Land and Water Use Program Manager
Matt Winston ..... Senior Meteorologist
Hongbing Yin, P.E. ..... Senior Engineer

U.S. Bureau of Reclamation:

Levi Brekke, Ph.D., P.E. ..... Engineer
Russell Yaworsky ..... Engineer

University of California, Davis:

Richard Snyder, Ph.D. ..... Biometeorologist

Lawrence Berkeley National Laboratory:

Norman Miller, Ph.D. ..... Staff Scientist

California Energy Commission:

Guido Franco, P.E.. ..... Technical Lead, Climate Change Research

Editorial and design services were provided by:

Mike Durant ..... Research Writer
Gretchen Goettl ..... Research Writer

Table of Contents

Executive Summary I

1 Introduction 1-1
1.1 Background 1-1
1.2 Climate Change and California's Water Resources 1-2
1.3 DWR-Reclamation Climate Change Work Team 1-2
1.4 Report Overview 1-3
1.5 Uses and Limitations 1-4
1.6 Acknowledgements 1-5
1.7 Appendix: Executive Order S-3-05 1-6

2 Potential Impacts of Climate Change on California's Water Resources 2-1
2.1 Introduction 2-1
2.2 Background - California's Water Resources 2-1
2.2.1 Distribution of Precipitation 2-1
2.2.2 California's Water Management Systems 2-3
2.2.3 Climate Change and California's Water Resources 2-5
2.3 The Role of Water Management and Use in Greenhouse Gas Emissions 2-7
2.3.1 Executive Order S-03-05 2-7
2.3.2 Water Supply and Treatment 2-7
2.3.3 Hydroelectric Power 2-7
2.3.4 Future Plans 2-8
2.4 Changes in Air Temperature 2-8
2.4.1 Past Changes 2-8
2.4.2 Causality 2-11
2.4.3 Temperature Projections 2-12
2.5 Changes in Precipitation and Runoff 2-14
2.5.1 Worldwide Precipitation Observations and Projections 2-14
2.5.2 Precipitation Trends in the Western United States and California 2-17
2.5.3 Trends in Snowfall and Related Runoff in California 2-22
2.5.4 Projected Changes in Precipitation for California 2-29
2.5.4.1 Changes in the Amount of Precipitation 2-29
2.5.4.2 Changes in Snowpack 2-30
2.5.4.3 Other Effects 2-31
2.6 Sea Level Rise 2-31
2.6.1 Historical Sea Levels 2-35
2.6.1.1 Sea Level Prior to Recorded History 2-35
2.6.1.2 Sea Level Measurements 2-36
2.6.1.3 Projected Sea Level Rise 2-43
2.6.1.4 Short-Term Changes in Sea Level 2-45

Table of Contents (cont.)

2.6.2 Consequences of Sea Level Rise 2-47
2.6.2.1 Sea Water Intrusion into Estuaries and River Systems....2-47
2.6.2.2 Sea Water Intrusion into Groundwater 2-47
2.6.2.3 Flooding Risk in the Sacramento-San Joaquin River Delta....2-50

2.7 Future Water Demand....2-54
2.7.1 Evapotranspiration 2-58
2.7.2 Agronomic Practices....2-59
2.7.3 Changes in Environmental Water Demand....2-59
2.7.3.1 Delta Salinity Control 2-59
2.7.3.2 Water Temperature Control 2-60
2.7.4 Population 2-61
2.7.5 Technological Innovation 2-62

2.8 Colorado River Basin....2-62
2.8.1 Description of the Colorado River Basin and its Water Resources 2-64
2.8.2 Allocation of Water in the Colorado River Basin....2-68
2.8.3 Climate Change and the Colorado River Basin 2-68
2.8.4 Summary 2-70

2.9 Possible Effects on Fish....2-71
2.9.1 Regional Effects....2-71
2.9.1.1 Region 1- Basins with Snowpack 2-72
2.9.1.2 Region 2 - Basins without Snowpack 2-72
2.9.1.3 Region 3 - Sacramento-San Joaquin River Delta 2-72
2.9.2 Summary 2-73

2.10 Sudden Climate Change....2-73
2.11 Summary 2-75
2.12 References....2-75

3 DWR Climate Change Studies 3-1
3.1 Introduction....3-1
3.2 Background....3-1

3.3 Climate Change Scenarios 3-1
3.3.1 Emissions Scenarios....3-2
3.3.2 Global Climate Models....3-4
3.3.3 Regional Downscaling....3-9

3.4 Water Resources Impacts Approach....3-9
3.5 Acknowledgements....3-11
3.6 References....3-11
3.7 List of Abbreviations 3-12

Table of Contents (cont.)

4 Preliminary Climate Change Impacts Assessment for State Water Project and Central Valley Project Operations 4-1
4.1 Introduction 4-1
4.2 Description of the CVP and SWP 4-2
4.3 Modeling Methodology for Quantifying Climate Change Impacts on CVP and SWP Operations 4-3
4.4 Generating CalSim-II Input from Global Climate Model Output 4-5
4.5 Study Scenarios 4-11
4.5.1 Base Scenario 4-11
4.5.2 Climate Change Scenarios 4-12
4.5.3 Climate Change Impacts Not Considered in the Study Scenarios 4-13
4.6 Results 4-14
4.6.1 Shortages 4-14
4.6.2 Delivery and Storage Analysis 4-16
4.6.3 North-of-Delta Operations Analysis 4-24
4.6.4 Delta Operations Analysis 4-28
4.6.5 Power Supply 4-42
4.6.6 In-Stream Temperature Analysis 4-47
4.7 Conclusion 4-48
4.7.1 Study Limitations 4-49
4.7.2 Results 4-49
4.8 Acknowledgements 4-50
4.9 References 4-51

5 Preliminary Climate Change Impacts Assessment for the Sacramento-San Joaquin Delta 5-1
5.1 Introduction 5-1
5.2 Approach 5-3
5.2.1 Base Case 5-4
5.2.2 Climate Change Scenarios 5-4
5.2.3 Assumptions 5-5
5.2.4 Delta Simulations 5-7
5.3 Climate Change Impacts on Delta Inflows and Exports for Present Sea Level Conditions 5-9
5.4 Climate Change Impacts on Water Quality for Present Sea Level Conditions 5-16
5.4.1 Municipal and Industrial Water Quality for Present Sea Level Conditions 5-17
5.4.1.1 250 mg/l Chloride Standard 5-18
5.4.1.2 150 mg/l Chloride Standard 5-21
5.4.1.3 Chloride Mass Loading Rates 5-23

Table of Contents (cont.)

5.5 Sea Level Rise....5-24
5.5.1 Analysis Approach....5-25
5.5.1.1 Martinez Salinity for Sea Level Rise Scenarios....5-26
5.5.2 Sea Level Rise Effects on Delta Water Quality....5-28
5.5.2.1 250 mg/l Chloride Threshold for Sea Level Rise Scenarios....5-29
5.5.2.2 150 mg/l Chloride Threshold for Sea Level Rise Scenarios....5-30
5.5.2.3 Chloride Mass Loading for Sea Level Rise Scenarios....5-31
5.5.3 Combined Climate Change and Sea Level Rise Effects on Delta Water Quality....5-32
5.5.3.1 250 mg/l Chloride Threshold for Combined Sea Level Rise and Climate Change Scenarios....5-34
5.5.3.2 150 mg/l Chloride Threshold for Combined Sea Level Rise and Climate Change Scenarios....5-36
5.5.3.3 Chloride Mass Loading for Combined Sea Level Rise and Climate Change Scenarios....5-37
5.5.4 Sea Level Rise Effects on Potential to Overtop Delta Levees....5-38
5.6 Summary....5-40
5.6.1 Climate Change for Present Sea Level....5-40
5.6.2 Sea Level Rise....5-40
5.6.3 Combined Climate Change and Sea Level Rise....5-41
5.7 Future Directions....5-41
5.8 Acknowledgements....5-42
5.9 References....5-43
5.10 Abbreviations....5-44
5.11 Appendix A: DSM2 Inputs....5-45
5.12 Appendix B: Additional Chloride Exceedance Plots and Percentile Tables for Present Sea Level Scenarios....5-63
5.13 Appendix C: Additional Chloride Exceedance Plots and Percentile Tables for One-Foot Sea Level Scenarios....5-66
5.14 Appendix D: Additional Chloride Exceedance Plots and Percentile Tables for Combined Climate Change and One-Foot Sea Level Scenarios....5-69

6 Climate Change Impacts on Flood Management....6-1
6.1 Introduction....6-1
6.2 Literature Review of Flood Analysis and Climate Change....6-2
6.3 Historical Precipitation, Temperature, and Runoff Trends....6-4
6.3.1 Precipitation....6-4
6.3.2 Temperature....6-8
6.3.3 Runoff....6-11
6.3.3.1 Annual Runoff....6-12
6.3.3.2 Annual Maximum Flood from Three Day Average Flows....6-18
6.3.4 Historical Trend Summary....6-21

Table of Contents (cont.)

6.4 Climate Change Scenario Simulation Data....6-22
6.4.1 GCM Simulation Results....6-22
6.4.2 Downscaled Results....6-25
6.4.2.1 Precipitation....6-27
6.4.2.2 Temperature....6-27
6.4.2.3 Runoff....6-27
6.4.2.4 Peak Flow Runoff....6-30
6.4.3 Summary of GCM Model Results....6-31
6.5 Potential Impacts....6-31
6.6 Discussion....6-34
6.7 References....6-35

7 Climate Change Impacts on Evapotranspiration....7-1
7.1 Introduction....7-1
7.2 Evaporative Demand for Applied Water in California....7-1
7.2.1 Current settings....7-1
7.2.2 Projected ET changes for the California landscape impacted by climate change....7-7
7.2.3 Landscape influences on ET that complicate climate change effects....7-7
7.2.4 Changes in cropping and irrigation methods that interact with climate change....7-8
7.3 Energy Budget....7-8
7.4 Plant Physiology and Climate Change....7-10
7.4.1 Plant physiological and morphological adaptation....7-10
7.4.2 Transpiration and photosynthesis....7-11
7.4.3 Effect of increased CO2 on plant physiology and morphology....7-13
7.5 A Simulation Model for Estimating ET of Applied Water (SIMETAW)....7-15
7.5.1 SIMEATAW model description....7-15
7.5.2 Input data requirement....7-16
7.5.3 Output files....7-16
7.5.4 Weather simulation....7-17
7.5.4.1 Rainfall....7-17
7.5.4.2 Wind speed....7-17
7.5.4.3 Temperature, solar radiation, and humidity....7-17
7.5.5 Validation of daily simulated weather data of SIMETAW....7-18
7.5.6 Canopy resistance sensitivity test for SIMETAW calculation of ET....7-21

Table of Contents (cont.)

7.6 Using SIMETAW as a DWR Modeling Tool for Climate Change Planning 7-22
7.7 Conclusions 7-23
7.8 Acknowledgments 7-24
7.9 References 7-24

7.10 Appendix 1 Energy Budget Analysis for Climate Change 7-26
7.10.1 Physical bases for temperature, sensible heat and water vapor transfer 7-26
7.10.2 Penman-Monteith equation 7-27
7.10.3 Aerodynamic term response to temperature rise 7-28
7.10.4 Radiation term response to temperature rise 7-29

7.11 Appendix 2 The photosynthesis Response Curve to CO2 7-31
7.12 Appendix 3 The Penman-Monteith equation for reference evapotranspiration (ETo) used in SIMETAW 7-32
7.13 List of Abbreviations 7-33

8 Future Directions 8-1
8.1 Introduction 8-1
8.2 SWP-CVP Operations Impacts 8-1
8.3 Delta Impacts 8-2
8.4 Flood Management 8-2
8.5 Evapotranspiration 8-3
8.6 Modeling Tool Integration 8-4
8.7 Coordination of State Climate Change Research Activities by the California Energy Commission 8-4

8.8 Risk Assessment 8-5
8.8.1 Compilation of Additional Climate Change Scenarios 8-6
8.8.2 Probability Assessments 8-9

8.9 References 8-9
8.10 Abbreviations 8-10

List of Figures

Chapter 1

Figure 1.1: DWR-Reclamation Climate Change Work Team Goals.....1-3

Chapter 2

Figure 2 1 Distribution of Average Annual Precipitation in California, 1961 to 1990 2-2
Figure 2 2 Major Federal, State and Local Water Storage and Conveyance Systems in California 2-4
Figure 2 3 Changes in Air Temperature Over About the Past 400,000 Years.....2-10
Figure 2 4 Trend in Global Average Temperature from 1860 to 2000.....2-10
Figure 2 5 Changes in Atmospheric Carbon Dioxide Concentration Measured at Mauna Loa, Hawaii from 1958 to 2005. 2-12
Figure 2 6 Range of Projections Reported by the Intergovernmental Panel on Climate Change for Increasing Global Average Surface Temperature Through 2100. 2-13
Figure 2 7 Worldwide Precipitation Trend for 1900 to 2000 2-16
Figure 2 8 Long-Term Linear Trend Rates for Annual Precipitation in Western United States 2-17
Figure 2 9 Precipitation Trends for the Western United States and Southwest Canada from 1930 to 1997 (left figure) and 1950 to 1997 (right figure) 2-18
Figure 2 10 Annual Average Precipitation for California from 1890 to 2002 with Linear Trend 2-19
Figure 2 11 Annual Average Precipitation from 1890 to 2002 with Linear Trends by Region 2-20
Figure 2 12 Coefficient of Variation for Annual Average Precipitation in California from 1890 to 2001 with Trend Line.....2-21
Figure 2 13 Annual April through July Unimpaired Runoff for Four Sacramento Valley Rivers Compared to Total Unimpaired Annual Runoff*.....2-23
Figure 2 14 Unimpaired Runoff Volume for Four Sacramento Valley Rivers*.....2-24
Figure 2 15 Annual April through July Unimpaired Runoff for Four San Joaquin Valley Rivers Compared to Total Unimpaired Annual Runoff*.....2-25
Figure 2 16 Total Unimpaired Runoff Volume for Four San Joaquin Valley Rivers*.....2-26
Figure 2 17 Annual April through July Unimpaired Runoff in the Central Valley Compared to Total Unimpaired Annual Runoff 2-27
Figure 2 18 California's Topography and Coastline 2-33
Figure 2 19 Location of the San Francisco Bay, Suisun Marsh and Sacramento-San Joaquin River Delta.....2-34
Figure 2 20 Changes in Global Sea Level over the Past 800,000 Years 2-35
Figure 2 21 Change in Sea Level Over the Past 18,000 Years 2-36

List of Figures (cont.)

Chapter 2 (cont).

Figure 2 22 Relative Change in Sea Level Measured at Six Locations in Northern Europe Beginning at about 1700 AD 2-37
Figure 2 23 Rates of Relative Sea Level Rise Along the Coast of the United States....2-38
Figure 2 24 Location of Coastal Tide Gauges in California....2-39
Figure 2 25 Relative Sea Level Trends for Eight Tide Gauges along California's Coast....2-40
Figure 2 26 Projected Rise in Global Average Sea Level from 1900 to 2100....2-44
Figure 2 27 Graph of Annual Average Relative Sea Level and the 19-Year Running Average Sea Level at the San Francisco Tide Gauge....2-46
Figure 2 28 Graph of Annual Average Relative Sea Level and the 19-Year Running Average Sea Level at the La Jolla Tide Gauge....2-47
Figure 2 29 California's Groundwater Basins....2-49
Figure 2 30 Simplified Cross-Section of a Coastal Aquifer....2-50
Figure 2 31 Sacramento-San Joaquin River Delta....2-51
Figure 2 32 Impact of One Foot of Sea Level Rise on the Relative Effect of Astronomical Tides in the Delta....2-53
Figure 2 33 Historical and Projected Future Population Growth in California....2-61
Figure 2 34 The Colorado River Aqueduct, All American Canal and Their Service Areas..2-63
Figure 2 35 Map of the Colorado River Basin....2-64
Figure 2 36 Distribution of Average Annual Precipitation in the Colorado River Basin....2-66
Figure 2 37 Monthly Storage Volumes in Lake Powell and Lake Mead since their Construction....2-67
Figure 2 38 Size and Locations of Reservoirs in the Colorado River Basin....2-69
Figure 2 39 The Global Thermohaline Circulation System....2-74

Chapter 3

Figure 3.1 Emissions of CO2 from Human Activities for IPCC's SRES Scenarios....3-4
Figure 3.2 Climate Model Forcings used for Climate Change Studies....3-6
Figure 3.3 Approach for Analyzing Potential Water Resources Impacts of Climate Change....3-10

List of Figures (cont.)

Chapter 4

Figure 4.1 Lake Shasta Average Monthly Inflow (1922-1944).....4-8
Figure 4.2 Lake Oroville Average Monthly Inflow (1922-1994).....4-9
Figure 4.3 Folsom Lake Average Monthly Inflow (1922-1994).....4-9
Figure 4.4 Modeling Sequence for Generating CalSim-II Climate Change Scenarios 4-11
Figure 4.5 Exceedance Probability Plot of SWP Table A Deliveries.....4-17
Figure 4.6 Exceedance Probability Plot of SWP Carryover Storage.....4-18
Figure 4.7 Exceedance Probability Plot of SWP Article 21 Deliveries.....4-20
Figure 4.8 Exceedance Probability Plot of CVP South-of-Delta Deliveries 4-21
Figure 4.9 Exceedance Probability Plot of CVP Carryover Storage 4-21
Figure 4.10 Exceedance Probability Plot of CVP North-of-Delta Deliveries 4-23
Figure 4.11 Monthly flood control frequency of Lake Shasta.....4-25
Figure 4.12 Monthly flood control frequency of Lake Oroville.....4-25
Figure 4.13 Monthly flood control frequency of Folsom Lake 4-26
Figure 4.14 MIF requirement control frequency on the Sacramento River during dry periods (1924, 1929-1934, 1976-1977, 1987-1992).....4-27
Figure 4.15 MIF requirement control frequency on the Feather River during dry periods (1924, 1929-1934, 1976-1977, 1987-1992).....4-27
Figure 4.16 MIF requirement control frequency on the American River during dry periods (1924, 1929-1934, 1976-1977, 1987-1992).....4-28
Figure 4.17 Map of the Sacramento – San Joaquin Delta.....4-29
Figure 4.18 Monthly average San Joaquin River Delta inflow at Vernalis (WY1922-1994).....4-31
Figure 4.19 Monthly average Sacramento River--Yolo Bypass Delta inflow (WY1922-1994).....4-31
Figure 4.20 Monthly average Delta outflow (WY1922-1994) 4-33
Figure 4.21 Monthly average total Delta exports (WY1922-1994).....4-34
Figure 4.22 Operational control frequency of Banks permitted capacity.....4-35
Figure 4.23 Operational control frequency of SWP SOD conveyance capacity on Banks exports.....4-36
Figure 4.24 Operational control frequency of the April-May San Joaquin River pulse flow export constraints on Banks pumping 4-36
Figure 4.25 Operational control frequency of Delta water quality standards on Banks pumping 4-37
Figure 4.26 Operational control frequency of Banks pumping by the export-inflow ratio ..4-37
Figure 4.27 Frequency of the decision to favor SWP NOD storage over SWP SOD storage by limiting Oroville releases and Banks pumping 4-39

List of Figures (cont.)

Figure 4.28 Operational control frequency of Tracy pumping capacity and upper Delta-Mendota Canal conveyance capacity 4-39
Figure 4.29 Operational control frequency of CVP SOD conveyance capacity on Tracy exports 4-40
Figure 4.30 Operational control frequency of the April-May San Joaquin River pulse flow export constraints on Tracy pumping 4-40
Figure 4.31 Operational control frequency of water quality standards of Tracy pumping 4-41
Figure 4.32 Operational control frequency of the export-inflow ratio of Tracy pumping 4-41
Figure 4.33 Frequency of the decision to favor CVP NOD storage over CVP SOD storage by limiting Shasta and Folsom releases and Tracy pumping 4-42
Figure 4.34 Monthly Average SWP Power Generation 4-45
Figure 4.35 Monthly Average SWP Power Load 4-46
Figure 4.36 Monthly Average CVP Power Generation 4-46
Figure 4.37 Monthly Average CVP Power Load 4-47

Chapter 5

Figure 5.1: The Sacramento-San Joaquin Delta 5-2
Figure 5.2: Average Annual Delta Inflows, Outflow and Diversions from 1980-1991 5-3
Figure 5.3: Delta Impacts Analysis Approach 5-4
Figure 5.4: Inflows, Exports, Diversions and EC Inputs for DSM2 Simulations 5-8
Figure 5.5: Delta Inflows from the Sacramento River 5-12
Figure 5.6: Delta Inflows from the San Joaquin River 5-13
Figure 5.7: Delta Exports from the State Water Project 5-14
Figure 5.8: Delta Exports from the Central Valley Project 5-15
Figure 5.9: Delta Water Quality Impact Analysis Locations 5-16
Figure 5.10: Probability of Exceedance for Chlorides at Old River at Rock Slough 5-20
Figure 5.11 Historical Annual Mean Sea Level at Golden Gate, 1900-2003 5-24
Figure 5.12 Modeling Domains for RMA and DSM2 5-27
Figure 5.13: Regression Relationship for EC at Martinez for a One-Foot Sea Level Rise. 5-27
Figure 5.14: Probability of Exceedance for Chlorides at Old R. at Rock Sl. for a One-Foot Sea Level Rise and no Changes in System Operations 5-29
Figure 5.15: Probability of Exceedance for Chlorides at Old River at Rock Slough for Climate Change and a One-Foot Sea Level Rise with no Changes in Operations for SLR 5-34
Figure 5.16: Locations of Lowest Levee Elevation on Three Delta Islands 5-39
Figure 5.17: Probability of Exceedance for Chlorides at Old River at Highway 4 5-63
Figure 5.18: Probability of Exceedance for Chlorides at the State Water Project 5-64

List of Figures (cont.)

Figure 5.19: Probability of Exceedance for Chlorides at the Central Valley Project 5-65
Figure 5.20: Probability of Exceedance for Chlorides at Old R. at Hwy 4 for a One-Foot Sea Level Rise and no Changes in System Operations.....5-66
Figure 5.21: Probability of Exceedance for Chlorides at the State Water Project for a One-Foot Sea Level Rise and no Changes in System Operations 5-67
Figure 5.22: Probability of Exceedance for Chlorides at the Central Valley Project for a One-Foot Sea Level Rise and no Changes in System Operations 5-68
Figure 5.23: Probability of Exceedance for Chlorides at Old River at Highway 4 for Climate Change and a One-Foot Sea Level Rise and no Changes in Operations for SLR 5-69
Figure 5.24: Probability of Exceedance for Chlorides at the State Water Project for Climate Change and a One-Foot Sea Level Rise and no Changes in Operations for SLR 5-70
Figure 5.25: Probability of Exceedance for Chlorides at the Central Valley Project for Climate Change and a One-Foot Sea Level Rise and no Changes in Operations for SLR 5-71

Chapter 6

Figure 6 1 Relation of climate change scenario simulations to flood analysis 6-2
Figure 6 2 Average annual precipitation for California 1890-2002 with trend line. 6-5
Figure 6 3 Annual average precipitation with trends by region.....6-6
Figure 6 4 Linear trends of annual precipitation for the past 30 years 6-7
Figure 6 5 Coefficient of variation for statewide average precipitation with trend line.....6-7
Figure 6 6 State average maximum, average, and minimum temperature time series 6-8
Figure 6 7 Variability of annual maximum, average and minimum temperature.....6-9
Figure 6 8 Temperature trend variation with latitude 6-10
Figure 6 9 Temperature trends by county population in California.....6-11
Figure 6 10 Map of Runoff Forecast Points.....6-13
Figure 6 11 Time series of Sacramento River Index water year runoff with fit linear trend.6-14
Figure 6 12 Time series of San Joaquin River Index water year runoff with fit linear trend 6-15
Figure 6 13 Variability of Sacramento and San Joaquin River Index through time.....6-15
Figure 6 14 April-July Runoff as a percent of water year runoff for the Sacramento River System 6-16
Figure 6 15 April-July Runoff as a percent of water year runoff for the San Joaquin River System 6-17
Figure 6 16 Flow centroid day versus time for the Cosumnes River at Michigan Bar.....6-18
Figure 6 17 Map of station location for peak flow analysis 6-19

List of Figures (cont.)

Figure 6 18 GCM precipitation results for Northern California 6-23
Figure 6 19 GCM precipitation results for Southern California 6-23
Figure 6 20 GCM temperature results for Northern California 6-24
Figure 6 21 GCM temperature results for Southern California 6-24
Figure 6 22 Downscaled precipitation time series from VIC model 6-25
Figure 6 23 Downscaled average maximum, and minimum temperature time series 6-26
Figure 6 24 Input hyetograph to HED71 model. 6-32
Figure 6 25 Direct runoff changes due to increasing contributing area of watershed 6-32

Chapter 7

Figure 7 1 Hydrological regions coded by color 7-3
Figure 7 2. Reference evapotranspiration zones 7-4
Figure 7 3 ETo comparison for current and climate change conditions 7-10
Figure 7 4 Relation of transpiration, photosynthesis and nitrogen. 7-12
Figure 7 5. CO2 effects and interactions on C3 plant production. 7-14
Figure 7 6. Comparison of measured and simulated daily solar radiation at Davis 7-18
Figure 7 7. Comparison of measured and simulated air temperature at Davis 7-19
Figure 7 8. Comparison of measured and simulated precipitation at Davis 7-19
Figure 7 9. Comparison of estimated and simulated reference ET at Davis.....7-20
Figure 7 10. Comparison of estimated and simulated reference ET at Oceanside 7-20
Figure 7 11. Comparison of estimated and simulated reference ET at Bishop.....7-21
Figure 7 12. Comparison of simulated daily ETo using the canopy resistance values 70, 85, and 100 s/m and current climate data from Davis 7-22
Figure 7 13. Use of SIMETAW for climate change impacts on water resource planning 7-23
Figure 7 14. A plot of versus canopy resistance for a 3 oC temperature increase as a function of canopy resistance 7-29
Figure 7 15. A plot of versus canopy resistance for a 3 oC temperature increase as a function of canopy resistance. 7-30
Figure 7 16. Photosynthesis Response Curve to CO2 7-32

Chapter 8

Figure 8.1: DWR-Reclamation Climate Change Work Team Goals.....8-6
Figure 8.2: Schematic Representation of 40 Emissions Scenarios 8-7
Figure 8.3: Forcing Factor Represented in Various Global Climate Models 8-8

List of Tables

Chapter 2

Table 2 1 Potential Effects of Climate Change on California's Water Resources and Expected Consequences....2-6
Table 2 2 Abundance of Well-Mixed Greenhouse Gases in 1750 (pre-industrial age) and in 1998 and Radiative Forcing Due to the Change in Abundance....2-11
Table 2 3 Possible Effects of Climate Change on Precipitation in California and Potential Consequences....2-15
Table 2 4 Runoff Statistics and Trends for Selected River Basins in California....2-28
Table 2 5 Areas of the US Coast with Significant Amounts of Uplift or Subsidence....2-39
Table 2 6 Relative Sea Level Trends for Eight Tide Gauges Along the Coast of California with 50 Years or More of Record....2-43
Table 2 7 Summary of the Potential Effects of Climate Change on Future Water Demand....2-53
Table 2 8 Selected Factors Affecting Future Water Demand in California that are Not Directly Related to Climate Change....2-57

Chapter 3

Table 3.1 Model and Emissions Scenario Labels for Four Climate Change Scenarios....3-5
Table 3.2 Air Temperature and Precipitation Trends for Climate Change Scenarios....3-7
Table 3.3 GCM Grid Points in California....3-7
Table 3.4 Air Temperature Projections for Northern California, °C....3-8
Table 3.5 Air Temperature Projections for Southern California, °C....3-8
Table 3.6 Precipitation Projections for Northern California, in/yr....3-8
Table 3.7 Precipitation Projections for Southern California, in/yr....3-8

Chapter 4

Table 4.1 Air Temperature and Precipitation Prediction Trends for Four Scenarios....4-1
Table 4.2 Key CVP Reservoirs....4-2
Table 4.3 Key SWP Reservoirs....4-3
Table 4.4 Streamflow Perturbation Ratios for Scenario GFDL A2....4-6
Table 4.5 Streamflow Perturbation Ratios for Scenario PCM A2....4-6
Table 4.6 Streamflow Perturbation Ratios for Scenario GFDL B1....4-7
Table 4.7 Streamflow Perturbation Ratios for Scenario PCM B1....4-7
Table 4.8 Lake Shasta Annual Average Inflow (TAF)....4-10
Table 4.9 Lake Oroville Annual Average Inflow (TAF)....4-10
Table 4.10 Folsom Lake Annual Average Inflow (TAF)....4-10

List of Tables (cont.)

Table 4.11 Demand Assumptions for the Base Scenario....4-12
Table 4.12 CalSim-II Water Use Prioritization....4-15
Table 4.13 Months of Critical Shortages (Storage at Dead Pool)....4-16
Table 4.14 SWP average and dry year Table A deliveries (TAF)....4-16
Table 4.15 SWP average and dry year Article 21 deliveries (TAF)....4-19
Table 4.16 CVP South-of-Delta contractor deliveries (TAF)....4-20
Table 4.17 CVP North-of-Delta contractor deliveries (TAF)....4-22
Table 4.18 Annual Average Delta Inflow (WY1922-1994)....4-30
Table 4.19 Annual Average Delta Outflow (WY1922 – 1994)....4-32
Table 4.20 Annual Average Delta Exports....4-33
Table 4.21 Generation and Load Facilities Included in Power Supply Analysis....4-43
Table 4.22 Annual Average SWP Power Generation and Load....4-44
Table 4.23 Annual Average CVP Power Generation and Load....4-44
Table 4.24 Average Water Temperatures along the Sacramento River....4-48

Chapter 5
Table 5.1: Air Temperature and Precipitation Projections for 2050....5-5
Table 5.2: Constant EC Concentrations for DSM2 Simulations....5-9
Table 5.3: Average Monthly Change in Sacramento River Inflow to the Delta, cfs....5-10
Table 5.4: Average Monthly Change in San Joaquin River Inflow to the Delta, cfs....5-10
Table 5.5: Average Monthly Change in SWP Exports, cfs....5-10
Table 5.6: Average Monthly Change in CVP Exports, cfs....5-10
Table 5.7: Annual Change in Delta Inflows....5-11
Table 5.8: Annual Change in Delta Exports....5-11
Table 5.9: Delta Water Quality Standards....5-17
Table 5.10: D1641 150 mg/l Chloride Standard....5-17
Table 5.11: Percent of Time Monthly Average Chloride Concentration <225mg/l....5-19
Table 5.12: Chloride Concentration Percentiles for Old River at Rock Slough (mg/l)....5-20
Table 5.13: Municipal and Industrial Intake Chloride Standard Compliance....5-21
Table 5.14: Change in Municipal and Industrial Intake Chloride Standard Compliance....5-21
Table 5.15: Old River at Rock Slough 150mg/l Chloride Standard Compliance....5-22
Table 5.16: Effect of 2 Week Requirement on 150mg/l Chloride Standard Compliance for Two Climate Change Scenarios at Old River at Rock Slough....5-22
Table 5.17: Chloride Mass Loading Percentiles (metric tons/day) for Old River at Rock Slough....5-23
Table 5.18: Chloride Mass Loading Percentiles (metric tons/day) for State Water Project....5-23

List of Tables (cont.)

Table 5.19: Chloride Mass Loading Percentiles (metric tons/day) for Central Valley Project 5-23
Table 5.20: Chloride Concentration Percentiles (mg/l) for Old R. at Rock Sl. for a One-Foot Sea Level Rise and no Changes in System Operations 5-29
Table 5.21: Frequency that Chloride Concentrations were below the 250 mg/l Threshold for a One-Foot Sea Level Rise and no Changes in System Operations..... 5-30
Table 5.22: Change in Frequency that Chloride Concentrations were below the 250mg/l Threshold for a One-Foot Sea Level Rise and no Changes in System Operations Compared to the Base Case 5-30
Table 5.23: Comparison of Chloride Concentrations to the 150 mg/l Threshold at Old River at Rock Sl. for a One-Foot Sea Level Rise and no Changes in System Operations 5-31
Table 5.24: Chloride Mass Loading Percentiles (metric tons/day) for Old River at Rock Slough for a One-Foot Sea Level Rise with no Changes in System Operations ... 5-32
Table 5.25: Chloride Mass Loading Percentiles (metric tons/day) for State Water Project for a One-Foot Sea Level Rise and no Changes in System Operations..... 5-32
Table 5.26: Chloride Mass Loading Percentiles (metric tons/day) for Central Valley Project for a One-Foot Sea Level Rise and no Changes in System Operations 5-32
Table 5.27: Chloride Concentration Percentiles (mg/l) for Old R. at Rock Sl. for Climate Change and a One-Foot Sea Level Rise with no Changes in Operations for SLR 5-34
Table 5.28: Frequency that Chloride Concentrations were below the 250 mg/l Threshold for Climate Change and a 1-ft Sea Level Rise with no Changes to Operations for SLR 5-35
Table 5.29: Change in Frequency that Chloride Concentrations were below the 250mg/l Threshold for Climate Change and a 1ft Sea Level Rise with no Changes to Operations for Sea Level Rise Compared to the Base Case 5-35
Table 5.30: Comparison of Chloride Concentrations to the 150 mg/l Threshold at Old R. at Rock Sl. for Climate Change and a One-Foot Sea Level Rise with no Changes in Operations for SLR 5-36
Table 5.31: Chloride Mass Loading Percentiles (metric tons/day) for Old River at Rock Sl. for Climate Change and a One-Foot Sea Level Rise with no Changes in Operations for SLR 5-37
Table 5.32: Chloride Mass Loading Percentiles (metric tons/day) for the State Water Project for Climate Change and a One-Foot Sea Level Rise with no Changes in Operations for SLR 5-37
Table 5.33: Chloride Mass Loading Percentiles (metric tons/day) for the Central Valley Project for Climate Change and a One-Foot Sea Level Rise with no Changes in Operations for SLR 5-38
Table 5.34: Summary of Levee Overtopping Events for Sea Level Rise Scenarios 5-39
Table 5.35: DSM2 Input from CalSim-II: Sacramento River Flows (cfs) at Sacramento..... 5-46

List of Tables (cont.)

Table 5.36: DSM2 Input from CalSim-II: San Joaquin River Flows (cfs) at Vernalis 5-50
Table 5.37: DSM2 Input from CalSim-II: State Water Project Exports (cfs) 5-54
Table 5.38: DSM2 Input from CalSim-II: Central Valley Project Exports (cfs).....5-58
Table 5.39: DSM2 Input from CalSim-II: Contra Costa Water District Diversions (cfs).....5-62
Table 5.40: Chloride Concentration Percentiles (mg/l) for Old River at Highway 4.....5-63
Table 5.41: Chloride Concentration Percentiles (mg/l) for the State Water Project 5-64
Table 5.42: Chloride Concentration Percentiles (mg/l) for the Central Valley Project.....5-65
Table 5.43: Chloride Concentration Percentiles (mg/l) for Old R. at Hwy 4 for a One-Foot Sea Level Rise and no Changes in System Operations 5-66
Table 5.44: Chloride Concentration Percentiles (mg/l) for the State Water Project for a One-Foot Sea Level Rise and no Changes in System Operations.....5-67
Table 5.45: Chloride Concentration Percentiles (mg/l) for the Central Valley Project for a One-Foot Sea Level Rise and no Changes in System Operations 5-68
Table 5.46: Chloride Concentration Percentiles (mg/l) for Old R. at Highway 4 for Climate Change and a One-Foot Sea Level Rise and no Changes in Operations for SLR 5-69
Table 5.47: Chloride Concentration Percentiles (mg/l) for the State Water Project for Climate Change and a One-Foot Sea Level Rise and no Changes in Operations for SLR 5-70
Table 5.48: Chloride Concentration Percentiles (mg/l) for the Central Valley Project for Climate Change and a One-Foot Sea Level Rise and no Changes in Operations for SLR 5-71

Chapter 6

Table 6 1Climate Change Studies and Runoff in California 6-3
Table 6 2 Average Annual Water Year Runoff for Selected California Watersheds.....6-12
Table 6 3 Comparison of discharge statistics by basin and time period (values in 1000 cfs) 6-20
Table 6 4 Comparison of different return period flows by basin and time period.....6-20
Table 6 5 Percent increase in return period discharges from pre-1955 to post-1955 by basin.....6-20
Table 6 6 Modeled vs Observed Percent Differences in Oct-Mar Runoff Average.....6-28
Table 6 7 Modeled vs Observed Percent Differences in Apr-July Runoff Average 6-28
Table 6 8 Modeled vs Observed Percent Differences in Annual Runoff Average.....6-28
Table 6 9 Modeled vs Observed Percent Differences in Oct-Mar Runoff Standard Deviation.....6-28
Table 6 10 Modeled vs Observed Percent Differences in Apr-Jul Runoff Standard Deviation 6-29

List of Tables (cont.)

Table 6 11 Modeled vs Observed Percent Differences in Annual Runoff Standard Deviation 6-29
Table 6 12 Percent Differences in Future to Present Oct-Mar Runoff Average.....6-30
Table 6 13 Percent Differences in Future to Present Apr-Jul Runoff Average 6-30
Table 6 14 Percent Differences in Future to Present Annual Runoff Average.....6-30
Table 6 15 Snow Covered Area Changes with Temperature for Selected Watersheds.....6-33

Chapter 7

Table 7.1. Monthly and total reference evapotranspiration (ETo) by ETo zone for the California ETo zone map in inches per month. 7-5
Table 7.2 Annual ET of applied water by hydrologic region during the 2000 water year in acre feet per acre from DWR-DPLA 2005.....7-6
Table 7.3 ET of applied water in acre inch per acre for some of the main commodities grown in California. 7-6

Executive Summary

Background

On June 1, 2005, Governor Arnold Schwarzenegger issued Executive Order S-3-05 establishing greenhouse gas emissions targets for California and requiring biennial reports on potential climate change effects on several areas, including water resources. The Governor established a Climate Action Team (CAT) to guide the reporting efforts. The CAT selected four climate change scenarios that reflect two greenhouse gas emissions scenarios represented by two Global Climate Models (GCMs). The CAT requested that those four climate change scenarios be used whenever possible in the climate change reporting efforts.

This report is the Department of Water Resources response to the Executive Order. This report describes progress made incorporating climate change into existing water resources planning and management tools and methodologies.

Climate Change and California's Water Resources

California water planners are concerned about climate change and its potential effects on our water resources. Projected increases in air temperature may lead to changes in the timing, amount and form of precipitation - rain or snow, changes in runoff timing and volume, effects of sea level rise on Delta water quality, and changes in the amount of irrigation water needed due to modified evapotranspiration rates.

More than 20 million Californians rely on two massive water projects: the State Water Project (SWP) and federal Central Valley Project (CVP). These complex water storage and conveyance systems are operated by the California Department of Water Resources (DWR) and the U.S. Bureau of Reclamation (Reclamation) for water supply, flood management, environmental protection and recreation.

DWR and Reclamation have formed a joint Climate Change Work Team to provide qualitative and quantitative information to managers on potential effects and risks of climate change to California's water resources. The mission of the team is to coordinate with other state and federal agencies on the incorporation of climate change science into California's water resources planning and management. The team will provide and regularly update information for decision-makers on potential impacts and risks of climate change, flexibility of existing facilities to cope with climate change, and available mitigation measures. This report is the first product of the Work Team.

Report Overview

This report contains eight chapters that present progress and future directions on incorporating climate change science into management of California's water resources. It focuses on assessment methodologies and preliminary study results. The technical chapters of this report,

Chapters 4-7, were peer-reviewed by experts from water resources-related agencies and research institutions. Policy implications and recommendations are beyond the scope of this report.

Uses and Limitations

The purpose of this report is to demonstrate how various analysis tools currently used by DWR could be used to address issues related to climate change. The methods and results presented in this report could be used to guide future climate change analysis and to identify areas where more information is needed.

All results presented in this report are preliminary, incorporate several assumptions, reflect a limited number of climate change scenarios, and do not address the likelihood of each scenario. Therefore, these results are not sufficient by themselves to make policy decisions.

Chapter 1: Introduction

Chapter 1 describes the purpose of this report, details the DWR-Reclamation Climate Change Work Team's mission and goals, and provides a summary of each chapter of the report. The complete text of Executive Order S-3-05 is in an appendix.

Chapter 2: Potential Impacts of Climate Change on California's Water Resources

Chapter 2 provides a statewide overview of California's water resources. Causes of climate change are summarized with an emphasis on aspects of climate change that pose a potential threat to California's water resources. It identifies measures that could be taken to adapt to or mitigate the effects of climate change. Topics covered in Chapter 2 include:

- Overview of California's water resources
- The role of water management and use in greenhouse gas emissions
- Observed and projected changes in air temperature
- Observed and projected changes in precipitation and runoff
- Observed and projected sea level rise and potential effects on groundwater and the Delta
- Potential effects of climate change on
  - Future water demands
  - Colorado River basin
  - Fish
- Sudden climate change
- Climate change and water supply planning challenges

Chapter 3: DWR Climate Change Studies

Chapter 3 presents the background and approach used for the climate change studies completed for this report. Climate change researchers have used global climate models to simulate projected changes in air temperature and precipitation. The global results were converted to represent regional changes in air temperature and precipitation in a process known as downscaling. DWR staff used the downscaled data to conduct preliminary impacts assessments for water resources. The studies use 2050 climate change projections for precipitation and runoff and 2020 land use estimates. The four climate change scenarios and the impacts assessment methodology are described in this chapter.

Chapter 4: Impacts of Climate Change on the State Water Project and Central Valley Project

Chapter 4 presents potential impacts of the selected climate change scenarios on SWP and CVP operations. Analysis includes changes in reservoir inflows, delivery reliability and annual average carryover storage due to 2050 level climate change induced shifts in precipitation and runoff patterns and 2020-level land use. The chapter discusses interaction of various operating rules and regulations such as water allocations, flood control, in-stream flow requirements, and Delta water quality requirements under climate change scenarios. Current management practices and existing system facilities were used in the analysis for this report. No changes to management practices or system facilities were made to try to mitigate the effects of climate change or sea level rise. Implications for possible changes to operations to mitigate climate change impacts are discussed, however exploring these operations changes is left for future work. The studies presented in this chapter did not incorporate potential effects of sea level rise. Future work will investigate possible changes in system operations and Delta outflow requirements that may be needed to lessen effects of sea level rise on Delta water quality.

Current management practices and existing system facilities were used in the analysis for this report. No changes were made to lessen the effects of climate change or sea level rise.

No changes were made to:

- ❑ System structures, such as added water storage, pumping, or canal capacity
- ❑ Reservoir operating rules, such as changing the space required for flood control
- ❑ Streamflow requirements
- ❑ Water quality standards
- ❑ Delta outflow requirements
- ❑ Operations to account for sea level rise

Some of the main results related to climate change impacts on the SWP and CVP include:

- ❑ In three of the four climate scenarios simulated, there were significant shortages in CVP north-of-Delta reservoirs during droughts. In future studies, operational changes are necessary to avoid these shortages. At this time, it is not clear whether the necessary changes in operations will be insignificant or substantial.

- ❑ Changes in annual average SWP south-of-Delta Table A deliveries ranged from a slight increase of about 1 percent for a wetter scenario to about a 10 percent reduction for one of the drier climate change scenarios.

- Increased winter runoff and lower Table A allocations resulted in slightly higher annual average Article 21 deliveries in the three drier climate change scenarios. The boosts in Article 21 did not offset losses to Table A though. The wetter scenario with higher Table A allocations resulted in fewer Article 21 delivery opportunities and slightly lower annual average Article 21 deliveries.

- Changes in annual average CVP south-of-Delta deliveries ranged from increases of about 2.5 percent for a wetter scenario and decreases of as much as 10 percent for drier climate change scenarios. The CVP results of the drier climate change scenarios are in question due to the north-of-Delta shortages mentioned above. These shortages will have to be addressed in future climate change studies.

- For both the SWP and CVP, carryover storage was negatively impacted in the drier climate change scenarios and somewhat increased in the wetter climate change scenario.

Sea level rise effects on water project operations to repulse a greater salt water intrusion under these conditions were not examined due to lack of existing tools for that type of analysis. Surrogates to provide an indication of the increased operation challenges from sea level rise to repulse sea water are discussed in chapter 5. Future work in this area will include the development of the necessary tools to quantify the impacts of sea level rise on saltwater intrusion and the incremental water supply impacts to repulse greater saltwater intrusion forces into the Delta. As discussed in chapter 5 these water supply impacts are expected to be significant.

Chapter 5: Impacts of Climate Change on the Sacramento-San Joaquin Delta

Chapter 5 focuses on potential impacts of climate change on Delta water quality and water levels. The reservoir operations and Delta exports for the four climate change scenarios determined in the studies for Chapter 4 were used to examine potential effects of climate change on Delta water quality. The Delta impacts reflect adjustments in reservoir operations and Delta exports due to shifting precipitation and runoff patterns. The studies in Chapter 4 include the assumption that meeting Delta water quality standards is a top priority for the SWP and CVP operations. Climate change will make meeting Delta water quality standards a larger challenge in the future. (see Table 4.12 in Chapter 4). In the interest of time, no additional changes were made to system operations in Chapter 5 to try to lessen the effects of climate change on Delta water quality as a result of sea level rise.

Sea level rise is an aspect of climate change of great interest in the Delta. Although current analysis tools are not available to determine changes in system operations required to lessen the effects of increased salt intrusion, there are tools that can estimate how much salt could enter the Delta due to sea level rise. For this report preliminary analyses were conducted to examine potential salt intrusion for a one foot rise in sea level. These results will provide information vital to the development of tools to determine changes in system operations that would be needed to maintain compliance with Delta water quality standards.

For the sea level rise scenarios, simulated water quality constituent concentrations without additional changes in system operations were compared to threshold values as a surrogate for evaluating the effects of sea level rise on water project operations to meet existing standards. Assuming these standards are not changed, this analysis shows that more water will be needed to repulse seawater to meet these standards as sea level rises. Tools are being developed to quantify the incremental impacts of sea level rise on water supplies to counteract increased salt water intrusion. Until these tools become available, the analysis below provides an indication of the water project operational challenges due to sea level rise. Chloride loadings at the urban intakes are also estimated.

Some of the main results related to climate change impacts on the Delta include:

- For the four climate change scenarios, Delta inflows typically increase during the late winter and early spring and decrease during the summer and fall. On average, Delta exports are reduced with the largest reductions occurring during the summer and fall. Inflows and exports are most sensitive to climate change during extremely wet or extremely dry periods.

- Flexibility in the system to modify reservoir operations and Delta exports for the climate change scenarios at present sea level results in minor impacts to compliance with chloride standards at Municipal and Industrial intakes.

- A one foot rise in sea level without any changes to the system operations would result in chloride concentrations below the 250 mg/l threshold 90 percent of the time at Old River at Rock Slough. In real time, operational adjustments will take place so these effects will translate into water supply impacts to the SWP and CVP. As stated above these impacts to water supply cannot be quantified at this time. Maintaining chloride concentrations below the 150 mg/l threshold was also more challenging during critical and dry years. These results indicate the need to develop a tool to quantify the additional water supplies that would need to be dedicated to repulse sea water in order to maintain Delta water quality under sea level rise conditions.

- There was complete compliance with the chloride standards at the SWP and CVP for the climate change at present sea level scenarios. Chloride concentrations remained below threshold values for the sea level rise and combined climate change and sea level rise scenarios.

- Chloride mass loadings at the municipal and industrial intakes are typically reduced for the climate change only scenarios due to lower export rates. Increased intrusion of salt water from the ocean for the sea level rise and combined climate change and sea level rise scenarios lead to increased chloride mass loadings at the municipal and industrial intakes.

- For a one foot rise in sea level, maximum daily water levels exceeded the minimum levee crest elevation on Sherman Island twice during the 16-year analysis period. Water levels did not exceed the minimum crest elevation for present sea level conditions.

Chapter 6: Climate Change Impacts on Flood Management

Chapter 6 discusses implications of climate change for managing floods. It presents historical trends that reflect potential climate change effects. Representation of historical periods by climate projection models are compared to historical data. Data requirements for analysis of climate change effects on flood frequency are also discussed.

Over the past century observed data indicate:

- Increasing maximum, mean, and minimum temperatures
- Increasing precipitation in north; decreasing precipitation in south
- Shift in annual runoff to a greater percentage in October-March vs. April-July
- Annual flood peaks increasing in mean and variance

Estimates of future climate temperatures suggest:

- Higher snow levels
- Larger direct runoff from individual storm events
- Earlier spring melt

Uncertainties in future precipitation prevents further analysis at this time

Chapter 7: Climate Change Impacts on Evapotranspiration

Chapter 7 focuses on potential increases in crop water use under climate change scenarios. California is a semiarid region, and to grow crops, water is needed for irrigation in addition to that supplied by precipitation. On a regional basis, most of the water used in agriculture is consumed by evapotranspiration (ET). There is concern that the ET might increase with climate change, which could increase the demand for developed water. This chapter provides theoretical energy budget analyses of climate change impacts on ET. Physiological processes that influence ET may explain changes in the energy budget for climate change conditions. Application of analysis tools to assess changes in estimated net irrigation requirements for crops is presented.

Some of the main issues related to climate change effects on evapotranspiration include:

- Evapotranspiration is comprised of two parts: (1) evaporation from soil, water and plant surfaces; and (2) transpiration, which occurs when water vaporizes inside the plant leaves and diffuses through the pores (i.e., stomata) to the ambient air. Both of these contributions to ET could be influenced by climate change.

- For a 3°C increase in air temperature, increases in evapotranspiration for a reference grass crop ranged from 3 percent to 6 percent. Although this is a small percentage, the volume of water, when summed over the entire state, is substantial. It is assumed that other crops will show a similar response to climate change.

- Potential higher demands for irrigation water due to increases in evapotranspiration rates could possibly be offset by improved water use efficiencies including adjusting cropping patterns and using more efficient on-farm irrigation methods.

- There is a need for canopy level experiments to validate assumptions relating canopy resistance to elevated atmospheric carbon dioxide concentrations to ensure accurate ET projection in response to climate change.

- The importance of crop life cycles and their physiological responses to expected climate change need more analysis to better project irrigation demand resulting from ET.

- The Simulation of Evapotranspiration and Applied Water (SIMETAW) model shows promise as an analytic tool to investigate potential ET of applied water responses to climate change. SIMETAW could be used in conjunction with other DWR analytic modeling tools to help managers better understand implications of climate change on agricultural water demands in California.

Chapter 8: Future Directions

Chapter 8 presents directions for further work in incorporating climate change into the management of California's water resources. Emphasis is placed on associating probability estimates with potential climate change scenarios in order to provide policymakers with both ranges of impacts and the likelihoods associated with those impacts. A better understanding of the likelihoods associated with potential climate change impacts will aid decision-makers in planning appropriate response strategies.

Future efforts will also involve addressing data and analysis gaps that were identified during these preliminary studies. For these preliminary studies, four scenarios that were readily available were selected by the Climate Action Team mainly for expediency. In collaboration with climate change scientists, criteria will be developed to assist water resource planners in determining which climate change scenarios to examine. For sea level rise studies, a tool will be developed to determine how system operations may need to be modified to maintain Delta water quality under sea level rise conditions. That tool would provide an essential component for a suite of modeling tools for climate change impacts and risk assessment.

With the accomplishments to date and planned future directions, DWR is working with other agencies and researchers to provide leadership in incorporating climate change impacts and risks into the planning and management of California's precious water resources.

Progress on Incorporating Climate Change into Management of California's Water Resources

1st Progress Report
July 2006

Chapter 1: Introduction

Authors:

Jamie Anderson, Ph.D., P.E. and Francis Chung, Ph.D., P.E.
California Department of Water Resources, Bay Delta Office, Modeling Support Branch, Sacramento.

1 Introduction

1.1 Background

Before the United Nations World Environment Day in San Francisco in June 2005, Governor Arnold Schwarzenegger said:

> "As of today California is going to be the leader in the fight against global warming. … I say the debate is over. We know the science. We see the threat. And we know the time for action is now."

Executive Order S-3-05 (see Section 1.7) established the following goals for reducing green house gas emissions:

- By 2010, reduce emissions to the 2000 level
- By 2020, reduce emissions to the 1990 level
- By 2050 reduce emissions to 80 percent below 1990 emissions

The Executive Order requires the secretary of the California Environmental Protection Agency to report to the Governor and legislature biannually on progress toward reaching the goals. Biennial reports are also required on potential climate change impacts and possible mitigation and adaptation plans focusing on these topics:

- Water supply
- Public health
- Agriculture
- California coastline
- Forestry

The first reports were due to the Governor and legislature in January 2006. To meet this deadline, and guide the preparation of the reports, a Climate Action Team (CAT) was formed with members from various State agencies and commissions. In addition to the overview reports being produced under the guidance of the CAT, the California Department of Water Resources (DWR) has established a complimentary report titled "Incorporating Climate Change into Management of California's Water Resources." This report describes progress on incorporating climate change science into water resources planning and management.

1.2 Climate Change and California's Water Resources

California water planners are concerned about climate change and its potential effects on our water resources. More than 20 million Californians rely on two massive water projects: the State Water Project (SWP) and federal Central Valley Project (CVP). These complex water storage and conveyance systems are operated by DWR and the Bureau of Reclamation (Reclamation) for water supply, flood management, environmental protection and recreational uses.

The ability of the SWP and the CVP to meet the water demands of its customers and the environment depends heavily on the accumulation of winter mountain snow melting into spring and summer runoff. A warming planet may reduce this natural water storage mechanism. Projected increases in air temperature may lead to changes in the timing, amount and form of precipitation – rain or snow, changes in runoff timing and volume, sea level rise effects on Delta water quality, and changes in the amount of irrigation water needed due to modified evapotranspiration rates.

1.3 DWR-Reclamation Climate Change Work Team

In the past, climate change was typically considered qualitatively in the planning process. Legislative mandates in California including Executive Order S-3-05 and the latest update to the California Water Plan (Bulletin 160) call for more quantitative assessments of climate change effects. To address these concerns, DWR and Reclamation formed a joint Climate Change Work Team to provide qualitative and quantitative information to managers on potential effects and risks of climate change to California's water resources.

The mission of the Climate Change Work Team is to coordinate with other State and federal agencies on the incorporation of climate change science into California's water resources planning and management. The team will provide and regularly update information for decision-makers on potential impacts and risks of climate change, flexibility of existing facilities to cope with climate change, and available mitigation measures.

In water resources planning, climate change studies often focus on what might happen without providing information about how likely it is to happen. A major long-term objective of the Work Team is to extend impacts analysis to include likelihoods associated with each climate change effect. In order to meet this objective, the Work Team set these goals:

- Build coalitions with experts in climate change and seek their guidance in estimating risk of climate change effects
- Support mandates on climate change
  - Governor's Executive Order S-3-05, June 1, 2005
  - California Water Plan Bulletin 160
- Assess impacts to operations of the SWP and CVP for several climate change scenarios
- Assess risk for the SWP and CVP systems based on impact studies and estimates of impact likelihood
- Evaluate risk-mitigation options

This report presents progress to date by the Work Team on incorporating climate change science into planning and management of California's water resources. This report also provides direction for continued efforts at developing probabilistic risk assessments of climate change impacts for water resources management. Figure 1.1 depicts the progress of the Work Team towards its goals. The target shape of the figure represents the focus of our efforts towards the ultimate goal, or bulls-eye, of probabilistic risk assessments. The components of Figure 1.1 that are shaded blue or white represent progress reflected in this report. The yellow and red components of Figure 1.1 represent future directions.

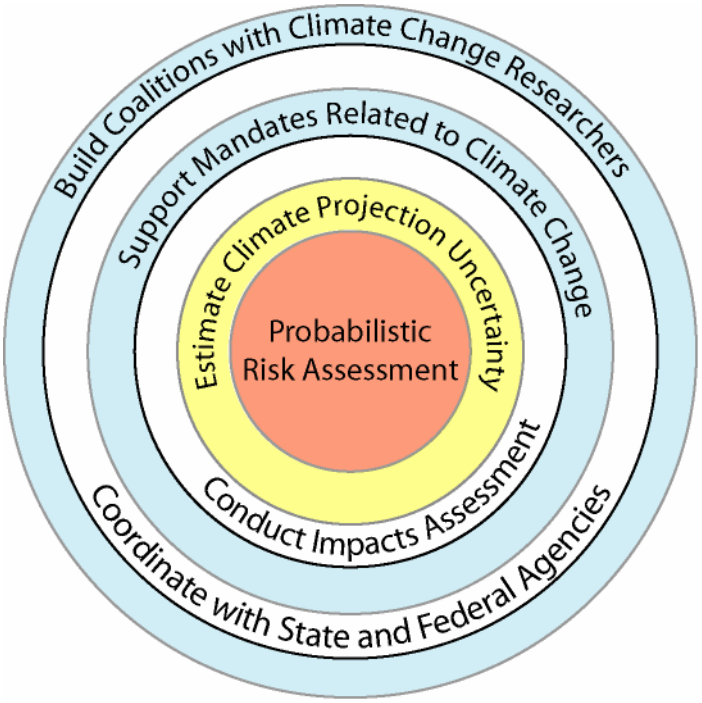


Figure 1.1: DWR-Reclamation Climate Change Work Team Goals

1.4 Report Overview

This report contains eight chapters that present progress and future directions on incorporating climate change science into management of California's water resources. It focuses on assessment methodologies and preliminary study results. The technical chapters of this report, Chapters 4-7, were peer reviewed by experts from water resources related agencies and research institutions. Policy implications and recommendations are beyond the scope of this report.

Chapter 2 provides a statewide overview of California's water resources. Causes of climate change are summarized with an emphasis on aspects of climate change that pose a potential threat to California's water resources. It then identifies measures that could be taken to adapt to or mitigate the effects of climate change.

Chapter 3 presents the background and approach used for the climate change studies completed for this report. It also describes climate change scenarios used in this report.

Chapter 4 presents potential impacts of the selected climate change scenarios on SWP and CVP operations. Analysis includes changes in reservoir inflows, delivery reliability and annual average carryover storage due to climate change induced shifts in precipitation and runoff patterns. It discusses interaction of various operating rules and regulations such as water allocations, flood control, in-stream flow requirements, and Delta water quality requirements under climate change scenarios. It also presents implications for possible changes to operations to mitigate climate change impacts. Exploring these changes is left for future work.

Chapter 5 focuses on potential impacts of climate change on Delta water quality and water levels. It presents effects of modified Delta inflows and exports on compliance with water quality standards. It also discusses implications of sea level rise including a study of levee overtopping potential.

Chapter 6 discusses implications of climate change for managing floods. It presents historical trends that reflect potential climate change effects. Representation of historical periods by climate projection models are compared to historical data. It discusses data requirements for analysis of climate change effects on flood frequency.

Chapter 7 focuses on potential increases in crop water use under climate change scenarios. It discusses potential responses of evapotranspiration to global warming. It characterizes physiological processes that influence ET and might be influenced by climate change. Also, it presents application of analysis tools to assess changes in estimated net irrigation requirements for crops.

Chapter 8 presents directions for further work in incorporating climate change into the management of California's water resources. Emphasis is placed on associating probability estimates with potential climate change scenarios in order to provide policymakers with both ranges of impacts and the likelihoods associated with those impacts.

1.5 Uses and Limitations

The purpose of this report is to demonstrate how various analysis tools currently used by DWR could be used to address issues related to climate change. The methods and results presented in this report could be used to guide future climate change analysis and to identify areas where more information is needed.

Current management practices and existing system facilities were used in the analysis for this report. No changes to management practices or system facilities were made to try to mitigate the effects of climate change or sea level rise. All results presented in this report are preliminary, incorporate several assumptions, reflect a limited number of climate change scenarios, and do not address the likelihood of each scenario. These results are not sufficient by themselves to make policy decisions.

1.6 Acknowledgements

The report authors would like to acknowledge the peer reviewers for their time and valuable technical input on this report:

Chapter 4: Nancy Parker-U.S. Bureau of Reclamation and Richard Palmer-University of Washington

Chapter 5: Paul Hutton-Metropolitan Water District, Leah Orloff-Contra Costa Water District, and K.T. Shum-East Bay Municipal Utility District;

Chapter 6: David Goldman-U.S. Army Corps of Engineer's Cold Regions Lab, and Philip Mote-University of Washington

Chapter 7: Richard Allen-University of Idaho at Kimberley, Hugo Hidalgo-Scripps Institute of Oceanography, and Ted Hsiao-University of California at Davis

This space intentionally left blank.

1.7 Appendix: Executive Order S-3-05

Executive Order

EXECUTIVE DEPARTMENT

STATE OF CALIFORNIA

EXECUTIVE ORDER S-3-05
by the
Governor of the State of California

WHEREAS, California is particularly vulnerable to the impacts of climate change; and

WHEREAS, increased temperatures threaten to greatly reduce the Sierra snowpack, one of the State's primary sources of water; and

WHEREAS, increased temperatures also threaten to further exacerbate California's air quality problems and adversely impact human health by increasing heat stress and related deaths, the incidence of infectious disease, and the risk of asthma, respiratory and other health problems; and

WHEREAS, rising sea levels threaten California's 1,100 miles of valuable coastal real estate and natural habitats; and

WHEREAS, the combined effects of an increase in temperatures and diminished water supply and quality threaten to alter micro-climates within the state, affect the abundance and distribution of pests and pathogens, and result in variations in crop quality and yield; and

WHEREAS, mitigation efforts will be necessary to reduce greenhouse gas emissions and adaptation efforts will be necessary to prepare Californians for the consequences of global warming; and

WHEREAS, California has taken a leadership role in reducing greenhouse gas emissions by: implementing the California Air Resources Board motor vehicle greenhouse gas emission reduction regulations; implementing the Renewable Portfolio Standard that the Governor accelerated; and implementing the most effective building and appliance efficiency standards in the world; and

WHEREAS, California-based companies and companies with significant activities in California have taken leadership roles by reducing greenhouse gas (GHG) emissions, including carbon dioxide, methane, nitrous oxide and hydrofluorocarbons, related to their operations and developing products that will reduce GHG emissions; and

WHEREAS, companies that have reduced GHG emissions by 25 percent to 70 percent have lowered operating costs and increased profits by billions of dollars; and

WHEREAS, technologies that reduce greenhouse gas emissions are increasingly in demand in the worldwide marketplace, and California companies investing in these technologies are well-positioned to profit from this demand, thereby boosting California's economy, creating more jobs and providing increased tax revenue; and

WHEREAS, many of the technologies that reduce greenhouse gas emissions also generate operating cost savings to consumers who spend a portion of the savings across a variety of sectors of the economy; this increased spending creates jobs and an overall benefit to the statewide economy.

NOW, THEREFORE, I, ARNOLD SCHWARZENEGGER, Governor of the State of California, by virtue of the power invested in me by the Constitution and statutes of the State of California, do hereby order effective immediately:

1. That the following greenhouse gas emission reduction targets are hereby established for California: by 2010, reduce GHG emissions to 2000 levels; by 2020, reduce GHG emissions to 1990 levels; by 2050, reduce GHG emissions to 80 percent below 1990 levels; and

2. That the Secretary of the California Environmental Protection Agency ("Secretary") shall coordinate oversight of the efforts made to meet the targets with: the Secretary of the Business, Transportation and Housing Agency, Secretary of the Department of Food and Agriculture, Secretary of the Resources Agency, Chairperson of the Air Resources Board, Chairperson of the Energy Commission, and the President of the Public Utilities Commission; and

3. That the Secretary shall report to the Governor and the State Legislature by January 2006 and biannually thereafter on progress made toward meeting the greenhouse gas emission targets established herein; and

4. That the Secretary shall also report to the Governor and the State Legislature by January 2006 and biannually thereafter on the impacts to California of global warming, including impacts to water supply, public health, agriculture, the coastline, and forestry, and shall prepare and report on mitigation and adaptation plans to combat these impacts; and

5. That as soon as hereafter possible, this Order shall be filed with the Office of the Secretary of State and that widespread publicity and notice be given to this Order.



IN WITNESS WHEREOF I have here unto set my hand and caused the Great Seal of the State of California to be affixed this the first day of June 2005.

/s/ Arnold Schwarzenegger

Governor of California

Progress on Incorporating Climate Change into Management of California's Water Resources

1st Progress Report
July 2006

Chapter 2:
Potential Impacts of Climate Change on California's Water Resources

Authors:

Michael Floyd, P.E.
California Department of Water Resources, Division of Planning and Local Assistance, Sacramento.

Michael Anderson Ph.D. and Maurice Roos P.E.
California Department of Water Resources, Division of Flood Management, Sacramento.

Roy Peterson Ph.D. and Michael Perrone Ph.D.
California Department of Water Resources, Environmental Services Office, Sacramento.

David Todd
California Department of Water Resources, Office of Water Use Efficiency, Sacramento.

Contributors:

Arthur Hinojosa P.E., David Rizzardo P.E., Bunloeurng Lek P.E., Jim Goodridge, Brian Heiland P.E., Tawnly Pranger P.E., Aaron Miller P.E., and Matt Winston, California Department of Water Resources, Division of Flood Management, Sacramento.

Jamie Anderson Ph.D., P.E. and Dan Easton P.E.
California Department of Water Resources, Bay Delta Office, Modeling Support Branch, Sacramento.

Kamyar Guivetchi, P.E.
California Department of Water Resources, Division of Planning and Local Assistance, Sacramento.

2 Potential Impacts of Climate Change on California's Water Resources

2.1 Introduction

The purpose of this chapter is to:

- provide a brief description of California's water resources
- summarize the anthropogenic causes of climate change
- describe the aspects of climate change that pose a potential threat to the State's water management systems

This chapter is general and statewide in scope. It describes impacts that could occur through the end of this century. Subsequent chapters are primarily focused on the effects of climate change on Central Valley water management systems based on selected downscaled climate model projections for mid-century.

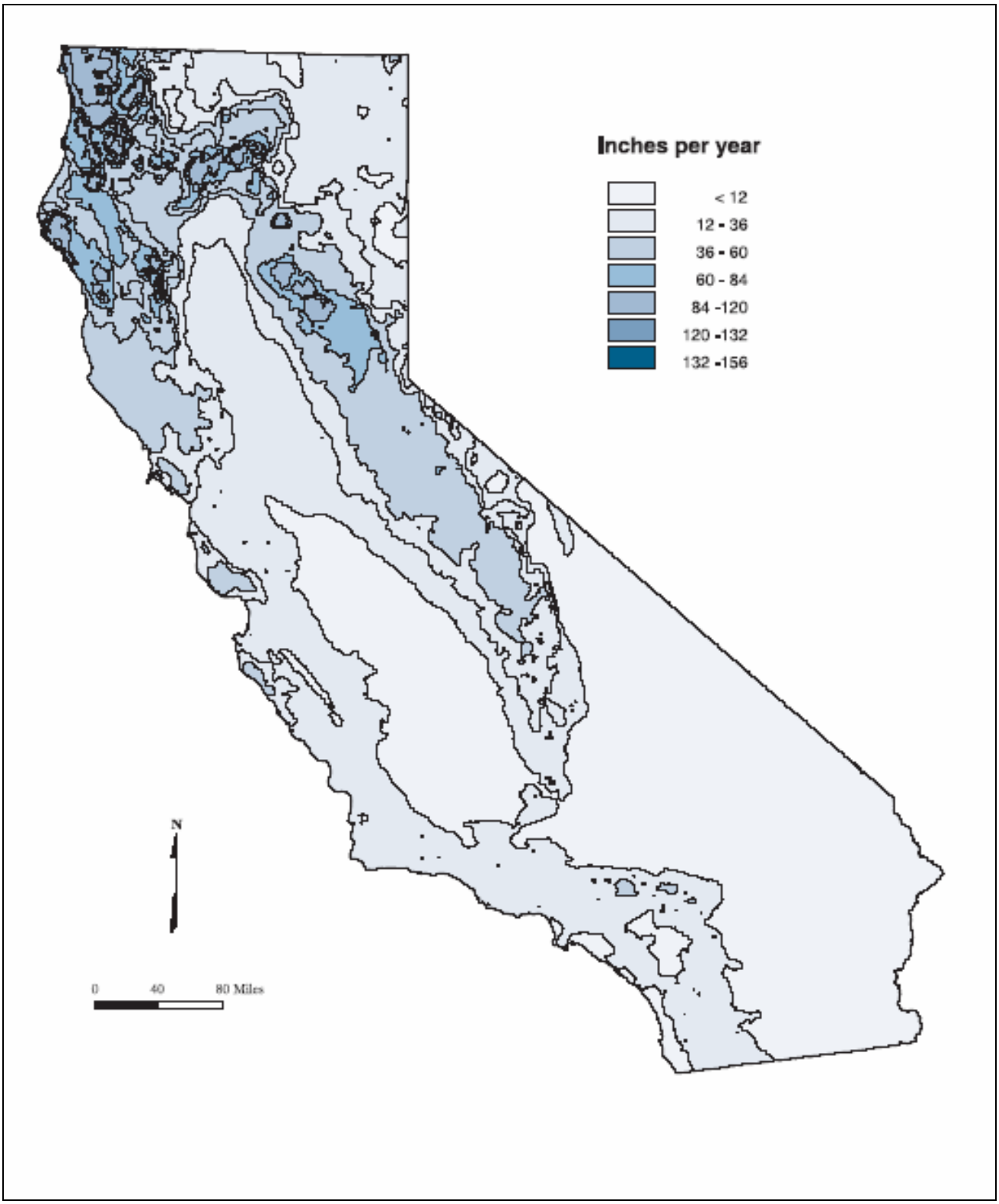
2.2 Background - California's Water Resources

2.2.1 Distribution of Precipitation

California's water resources vary significantly throughout the State as the result of varying climates and the distribution of precipitation. On average, more than 140 inches of precipitation falls annually in the mountains of northwestern California while fewer than four inches falls in parts of the desert in the southeast portion of the State. Figure 2-1 depicts the distribution of average annual precipitation in the State. Statewide average annual precipitation is about 23 inches (DWR, 2003).

Variability in the distribution of precipitation in California is due in part to hemispheric-scale atmospheric circulation patterns. Most winter storms typically move from the Pacific Ocean east across the northern part of the State. A progressively smaller percentage of storms move across the State to the south.

Most of the State's precipitation falls in the northern Coast Range, Klamath and Cascade ranges and the western slope of the Sierra Nevada due to orographic effects. The Mojave Desert, San Joaquin Valley floor and areas east of the Sierra Nevada receive much less precipitation, partly because they are in a rain shadow.



Source: DWR, 2003

Figure 2-1 Distribution of Average Annual Precipitation in California, 1961 to 1990

2.2.2 California's Water Management Systems

The majority of California's population of about 37 million people is concentrated in and near major urban centers. About half of the State's population resides in Southern California where annual precipitation and runoff is much less than in Northern California.

Much of the State's agriculture also is in areas with limited precipitation, including the San Joaquin Valley and the Imperial Valley. Agriculture is critical to the State's economy and usually consumes about 40 percent of the State's total annual developed water supply (DWR, 2005a). California uses this water to produce more than 350 crops, which in 2003 were valued at $29.4 billion. California produces more than half of the vegetables, nuts, and fruits produced in the U.S. (USDA, 2003).

An extensive network of reservoirs and aqueducts has been developed throughout much of California to provide water to major urban and agricultural areas. This network serves to store and transport runoff from where it is plentiful to where it is scarce. It also serves to store winter and early spring runoff so that it will be available when water demand is the highest in the late spring and summer. Figure 2-2 shows the location of major federal, State and local surface reservoirs and aqueducts in California.

The largest system of surface reservoirs and aqueducts in California is in the Central Valley. The historical natural average annual runoff in the Central Valley is about 33.6 million acre-feet, or about 48 percent of California's total natural runoff (DWR, 1951). About two-thirds of the runoff in the Central Valley typically originates in the Sacramento Valley.

Surface reservoirs collecting runoff in the Central Valley have a combined total capacity of about 29 million acre-feet. The two largest water projects in the Central Valley, the State Water Project (SWP) and the federal Central Valley Project (CVP), provide a combined average total of about 10 million acre-feet of water annually for urban and agricultural uses. More than 20 million Californians rely on the SWP and the CVP for at least part of their water supply. These projects irrigate an average of nearly 3.6 million acres of farmland each year (DWR, 2005a).

Other major water storage and conveyance systems in California include the All-American Canal and the Colorado River Aqueduct, both of which divert water from the Colorado River in Southern California. The All-American Canal supplies water to cities and agriculture in the Imperial and Coachella valleys. The Colorado River Aqueduct supplies water to the south coast region. In the recent past, California has diverted as much as 5.3 million acre-feet of water annually from the Colorado River. This is in excess of the State's allotment of 4.4 million acre-feet (DWR, 2005a). Additional discussion of the Colorado River and California's diversions from the river is in Section 2.8.



Figure 2-2 Major Federal, State and Local Water Storage and Conveyance Systems in California

Groundwater also plays a critical role in providing for the State's water needs. In an average year, groundwater meets about 30 percent of California's applied urban and agricultural water demands. This increases to more than 40 percent during drought years. In 1995, an estimated 13 million Californians, nearly 43 percent of the State's population, were served by groundwater (DWR, 2003).

2.2.3 Climate Change and California's Water Resources

Theories concerning climate change and global warming existed as early as the late 1800s. It wasn't until the late 1900s that understanding of the earth's atmosphere had advanced to the point where many climate scientists began to accept that the earth's climate is changing. Today, many climate scientists agree that some warming has occurred over the past century and will continue through this century.

The United Nations Intergovernmental Panel on Climate Change predicts that changes in the earth's climate will continue through the 21st century and that the rate of change may increase significantly in the future because of human activity (IPCC, 2001b). Many researchers studying California's climate believe that changes in the earth's climate have already affected California and will continue to do so in the future.

Climate change may seriously affect the State's water resources. Temperature increases could affect water demand and aquatic ecosystems. Changes in the timing and amount of precipitation and runoff could occur. Sea level rise could adversely affect the Sacramento-San Joaquin River Delta and coastal areas of the State. Some of the projected effects of climate change on California's water resources and the consequences of those effects are summarized in Table 2-1.

Climate change is identified in the 2005 update of the California Water Plan (Bulletin 160-05) as a key consideration in planning for the State's future water management (DWR, 2005a). The 2005 Water Plan update qualitatively describes the effects that climate change may have on the State's water supply. It also describes efforts that should be taken to quantitatively evaluate climate change effects for the next Water Plan update.

Table 2-1 Potential Effects of Climate Change on California's Water Resources and Expected Consequences

Potential Water Resource Impact	Expected Consequence
Reduction of the State's average annual snowpack	• Potential loss of 5 million acre-feet or more of average annual water storage in the State's snowpack • Increased challenges for reservoir management and balancing the competing concerns of flood protection and water supply
Changes in the timing, intensity, location, amount, and variability of precipitation	• Potential increased storm intensity and increased potential for flooding • Possible increased potential for droughts
Long-term changes in watershed vegetation and increased incidence of wildfires	• Changes in the intensity and timing of runoff • Possible increased incidence of flooding and increased sedimentation
Sea level rise	• Inundation of coastal marshes and estuaries • Increased salinity intrusion into the Sacramento-San Joaquin River Delta • Increased potential for Delta levee failure • Increased potential for salinity intrusion into coastal aquifers (groundwater) • Increased potential for flooding near the mouths of rivers due to backwater effects
Increased water temperatures	• Possible critical effects on listed and endangered aquatic species • Increased environmental water demand for temperature control • Possible increased problems with foreign invasive species in aquatic ecosystems • Potential adverse changes in water quality, including the reduction of dissolved oxygen levels
Changes in urban and agricultural water demand	Changes in demand patterns and evapotranspiration rates

2.3 The Role of Water Management and Use in Greenhouse Gas Emissions

2.3.1 Executive Order S-03-05

Executive Order S-3-05, signed by Governor Arnold Schwarzenegger June 1, 2005, establishes aggressive greenhouse gas emission reduction goals for California. These goals are:

- by 2010, reduce emissions to 2000 levels
- by 2020, reduce emissions to 1990 levels
- by 2050, reduce emissions to 80 percent below 1990 levels

Since water management and use are a significant part of California's energy matrix, both in terms of energy generation and consumption, they are an important consideration in meeting the emission reduction goals established by the Governor.

2.3.2 Water Supply and Treatment

In the draft "Statewide Assessment of Energy Used to Manage Water," the California Energy Commission estimated that an average of about 44 million tons of carbon dioxide is emitted into the atmosphere each year to provide water in California. Any reductions in energy consumption related to water will help the State meet its greenhouse gas reduction goals.

California's aqueduct systems are one of the larger users of electricity in the State. Other significant uses of electrical power related to water in California include:

- pumping groundwater from wells
- treating drinking water
- delivering of water to consumers through local distribution systems
- treating wastewater and wastewater reclamation.

Diesel, gasoline, and natural gas-powered pumps are used for some water supply and treatment operations. Diesel-powered pumps are most prevalent in agriculture.

End uses of water also result in the consumption of electrical energy and natural gas, such as heating of water for domestic, commercial, and industrial operations. Various industrial processes that use water also result in energy consumption.

2.3.3 Hydroelectric Power

Hydroelectric power is generated at most publicly-owned water supply reservoirs in California and at many privately-owned reservoirs. Hydroelectric power is also generated by run-of-river hydroelectric plants and by power recovery plants along aqueducts and water distribution systems. Most of California's hydroelectric power is produced in the Sierra Nevada and Cascade

Range. This is due to the relatively large amount of precipitation that falls there and the amount of elevation change available for power generation.

Hydroelectric power production varies from year to year in California with changing hydrologic conditions. Hydroelectric power produced outside of California is also imported into the State to help meet energy needs. Hydroelectric power production is a critical consideration for meeting greenhouse gas emission reduction goals set by Executive Order S-3-05. Other than the construction of hydroelectric power facilities, hydroelectric power production essentially does not result in the emission of greenhouse gasses. As discussed in Section 2.5, climate change could reduce hydroelectric power production by existing facilities, especially at reservoirs in the foothills of the Sierra Nevada. This is due to expected losses in annual snow pack and changes in the timing of annual runoff as the result of climate change.

2.3.4 Future Plans

The 2005 California Water Plan Update (DWR, 2005) estimates that water use efficiency can reduce annual urban water use by 1.1 million to 2.3 million acre-feet by 2030. It is also estimated that water use efficiency can reduce annual agricultural water use by 0.5 million to 2.0 million acre-feet by 2030. Accelerating efforts to attain those water use reductions by 2015 could result in a cumulative reduction of greenhouse gas emissions of approximately 30 million tons by 2030.

The Department of Water Resources is developing water use efficiency measures that can help California meet the greenhouse gas emission reduction goals established by the Governor. These measures are described in a Department staff report titled "Reduction of Greenhouse Gas Emissions through Water Use Efficiency Measures, October, 2005."

In the next sections of this chapter, past and potential future changes in temperature, precipitation, and sea level are described. An overview of the potential impacts of possible future changes is also presented.

2.4 Changes in Air Temperature

2.4.1 Past Changes

The Earth's climate has had numerous periods of cooling and warming in the past. Significant periods of cooling have been marked by massive accumulations of sea and land-based ice extending from the Earth's poles to as far as the mid-latitudes. Periods of cooling have also been marked by lower sea levels due to the accumulation of water as ice, and cooling and contraction of the Earth's oceans. Periods of warming caused recession of the ice toward the poles, warming and thermal expansion of the Earth's oceans, and sea level to rise. More discussion on past changes in sea level is in Section 2.6.

Figure 2-3 depicts significant periods of cooling and warming over about the past 400,000 years based on analysis of ice cores. The causes of the temperature changes are unknown, although

they may be due to changes in solar radiation, the Earth's orbit, the composition of the atmosphere, ocean circulation patterns and other factors. Average temperatures in the Northern Hemisphere appear to have been relatively stable from about 1000 to the mid-1800s based on temperature proxy records from tree rings, corals, ice cores and historical observations (IPCC, 2001a). However, there is a significant amount of uncertainty related to proxy temperature records, especially those extending far back into the past.

The United Nations Intergovernmental Panel on Climate Change stated that the Earth's climate has warmed since the pre-industrial era and that some of this change is attributable to the activities of humans (IPCCb, 2001). Global average near-surface air temperatures and ocean surface temperatures have increased 0.6 ± 0.2°C over the 20th century (IPCCa, 2001). Much of the rise occurred during 1910 to 1945 and 1976 to 2000, as depicted in Figure 2-4.

There is evidence that temperatures in the western United States and California have increased during the past century based on temperature measurements, apparent trends in reduced snowpack and earlier runoff, and other evidence such as changes in the timing of blooming plants (NWS, 2005) (Mote, 2005) (Cayan, 2001). More discussion of observed changes in temperature and related changes in snowpack and runoff in the western United States and California is contained in Section 2.5 and Chapter 6.

This space intentionally left blank.

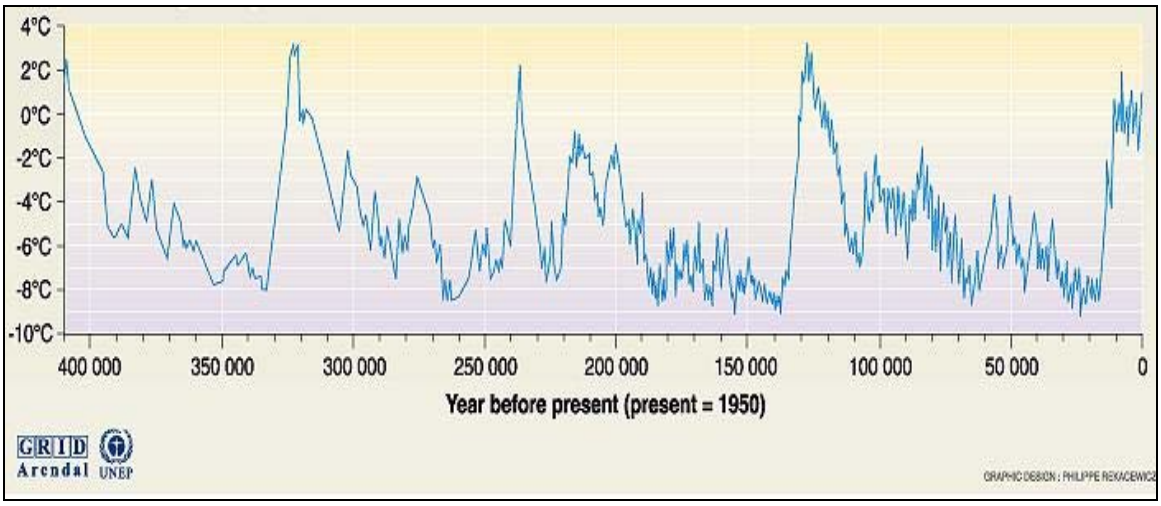


Figure 2-3 Changes in Air Temperature Over About the Past 400,000 Years

Explanation: Graph depicts changes in air temperature as evidenced by isotopic analysis of ice cores obtained at the Russian Vostok station in central east Antarctica. For additional explanation visit: http://cdiac.esd.ornl.gov/trends/temp/vostok/jouz_tem.htm.
Source: United Nation's Environment Programme Global Resource Information Database - Arendal website at http://www.grida.no/climate/vital/02.htm.

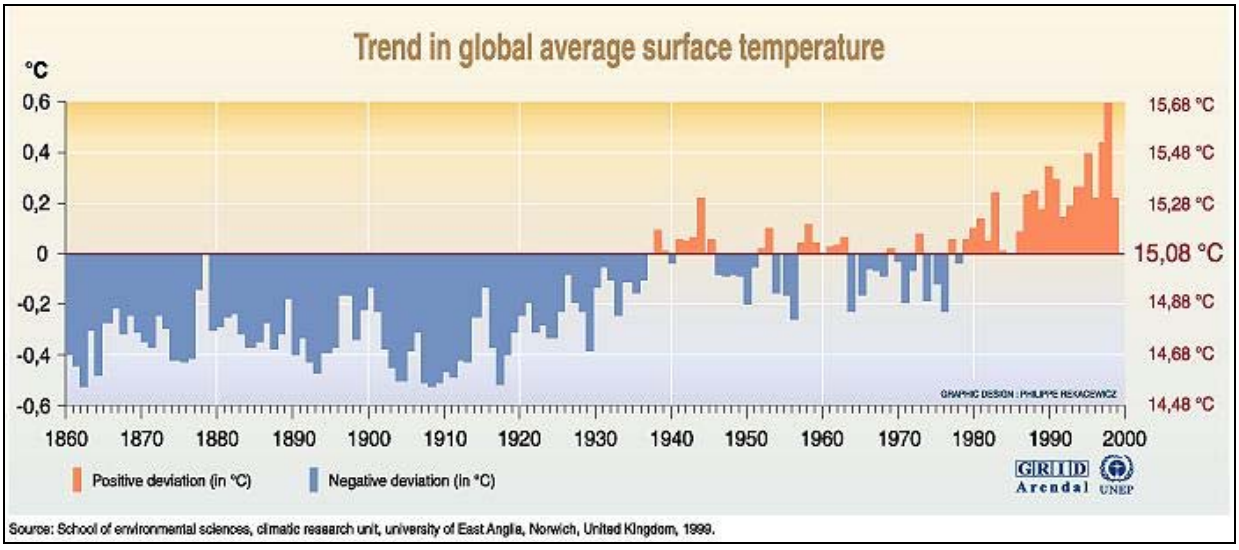


Figure 2-4 Trend in Global Average Temperature from 1860 to 2000

Explanation: The figure depicts global average combined land-surface air and sea surface temperatures from 1861 to 1998 relative to the average temperature between 1961 and 1990. The left vertical scale is in degrees Celsius.
Source: United Nation's Environment Programme Global Resource Information Database - Arendal website at: http://www.grida.no/climate/vital/17.htm.

2.4.2 Causality

Human-induced changes in the Earth's temperature have been tied to increased concentrations of greenhouse gases in the atmosphere caused by the production and burning of fossil fuels and land uses. The primary gases of concern are carbon dioxide, methane, and nitrous oxide. Table 2-2 lists changes in atmospheric concentrations of these gases from 1750 to 1998, as well as their efficacy in causing warming. Figure 2-5 depicts changes in atmospheric carbon dioxide concentration measured at Mauna Loa Hawaii from 1958 to 2005.

Table 2-2 Abundance of Well-Mixed Greenhouse Gases in 1750 (pre-industrial age) and in 1998 and Radiative Forcing Due to the Change in Abundance

Gas	Abundance (Year 1750)	Abundance (Year 1998)	Radiative Forcing (Wm^{-2})
Carbon Dioxide	278	365	1.46
Methane	700	1745	0.48
Nitrous Oxide	270	314	0.15

Source: IPCC, 2001a
Explanation: Volume mixing ratios for carbon dioxide are in parts per million and are in parts per billion for methane and nitrous oxide. Wm^{-2} = watts per square meter.

This space intentionally left blank.

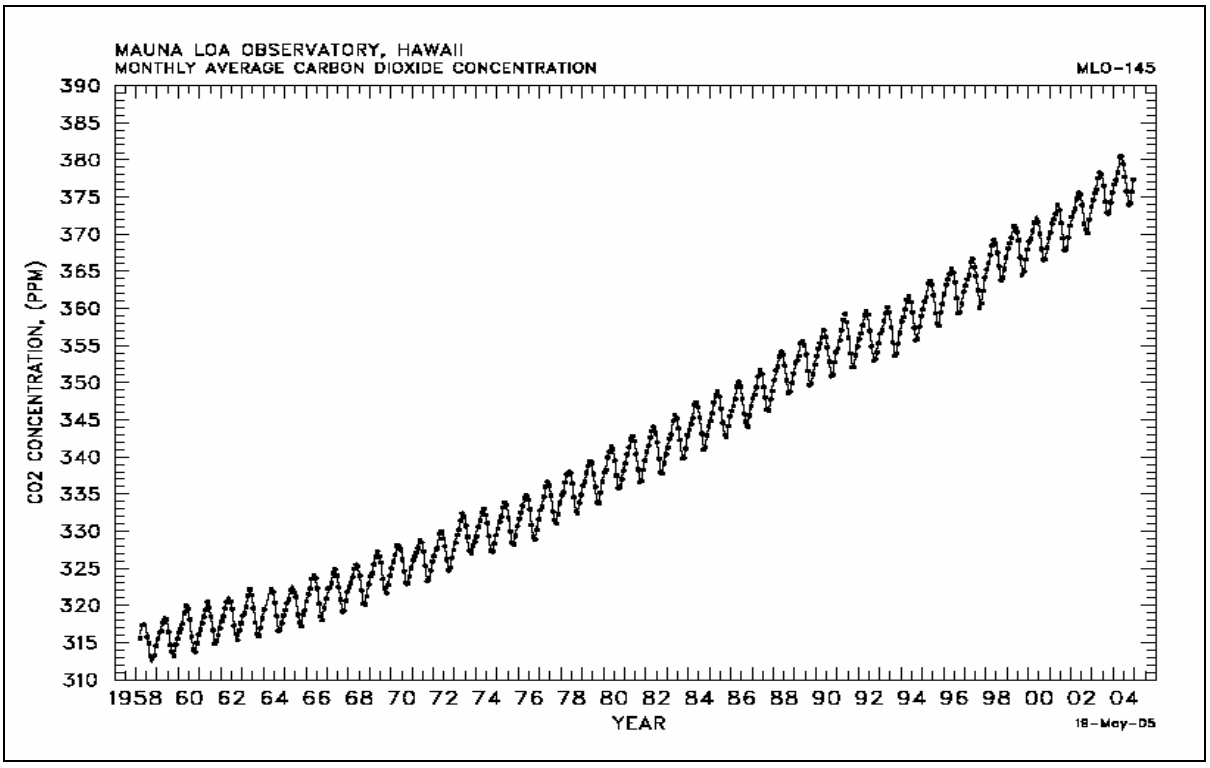


Figure 2-5 Changes in Atmospheric Carbon Dioxide Concentration Measured at Mauna Loa, Hawaii from 1958 to 2005.

Source: United States Department of Energy, Carbon Dioxide Information Analysis Center website at: http://cdiac.esd.ornl.gov/trends/co2/sio-mlo.htm .
Explanation: PPM = parts per million. Annual decreases in atmospheric carbon dioxide concentration at Mauna Loa, Hawaii occur each summer and are due to seasonal increases in plant respiration in the Northern Hemisphere.

2.4.3 Temperature Projections

The United Nations Intergovernmental Panel on Climate Change reports that global average surface temperatures are projected to rise between 1.4 to 5.8°C from 1990 to 2100, based on various climate models and greenhouse gas emission scenarios (IPCC, 2001a). Figure 2-6 is a generalized representation of the range of temperature projections reported by the IPCC in its Third Assessment Report (TAR). Information on the various projections making up the range, as well as their basis can be found in the TAR[1].

[1] Climate Change 2001: The Scientific Basis. Contribution of Working Group I to the Third Assessment Report of the Intergovernmental Panel on Climate Change (IPCC, 2001a). http://www.grida.no/climate/ipcc_tar/wg1/index.htm

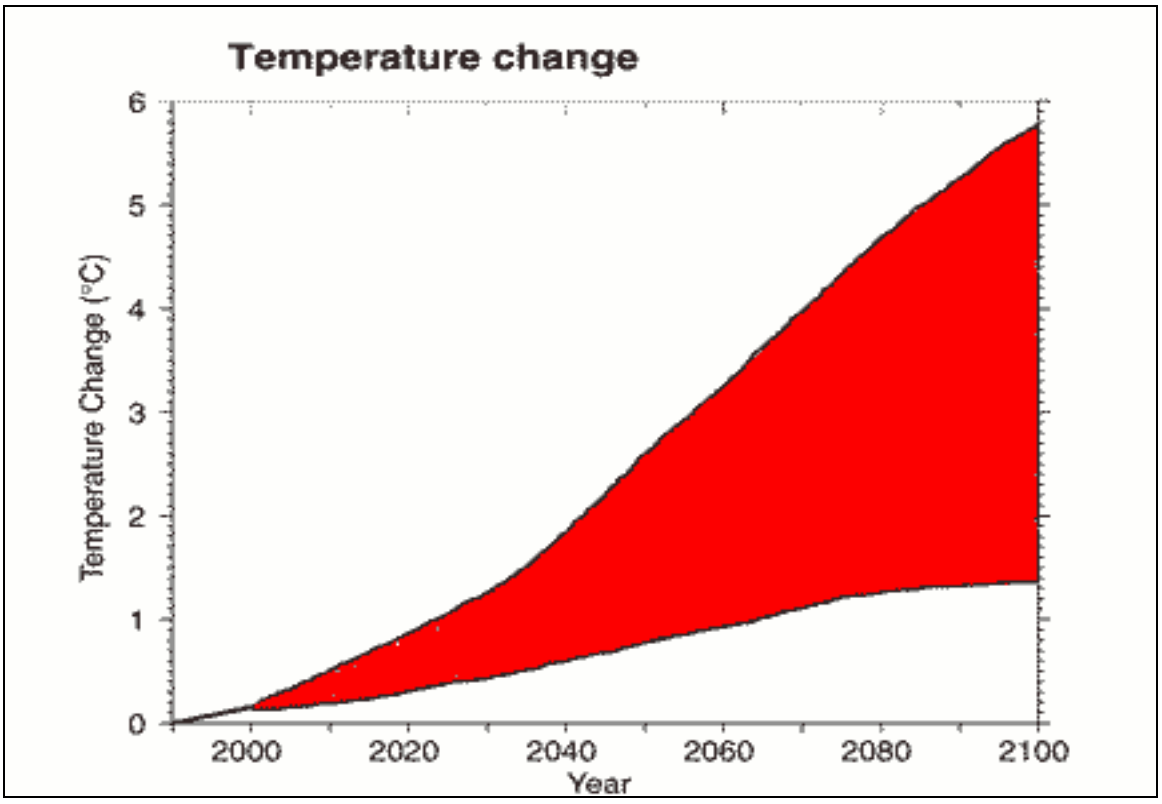


Figure 2-6 Range of Projections Reported by the Intergovernmental Panel on Climate Change for Increasing Global Average Surface Temperature Through 2100.

Source: United States Environmental Protection Agency website at: http://yosemite.epa.gov/oar/globalwarming.nsf/content/ClimateFutureClimateGlobalTemperature.html

Climate change and temperature projections can be developed on a regional basis using techniques to "downscale" from the results of global models. The level of uncertainty related to regional climate change and temperature projections is generally higher than global projections since downscaling adds more uncertainty. One relatively large group of model projections that was recently examined for California provides a range of about 2.5 to 9 degrees Celsius temperature rise for Northern California by 2100. An analysis of the distribution of the projections generally showed a central tendency at about 3 degrees Celsius of rise for 2050, and about 5 degrees Celsius for 2100 (Dettinger, 2005).

2.5 Changes in Precipitation and Runoff

Climate change appears to have already affected precipitation and runoff in California. More changes are expected in the future as additional changes in the Earth's climate occur. Some of the possible effects of climate change on precipitation as well as potential consequences of those effects are listed in Table 2-3.

While all possible changes in precipitation due to climate change are of potential concern for management of the State's water resources, this section deals mainly with potential changes in the amount, form and variability of precipitation. Existing climatologic and hydrologic data are generally suitable for evaluating historical trends for these three factors. Most research and climate change modeling efforts have focused on potential changes in the amount and form of precipitation in California. Historical information and research efforts are not as abundant or as conclusive for other past and possible future changes in precipitation in California.

2.5.1 Worldwide Precipitation Observations and Projections

Worldwide trends in precipitation over land are hard to determine. The difficulties arise from limited measurements worldwide and measurement problems, such as "undercatch" for precipitation gauges (Hulme, 1995). Where available, streamflow measurements and other information can be used as a proxy record for precipitation.

Worldwide precipitation is reported to have increased about 2 percent since 1900. While global average precipitation has been observed to increase, changes in precipitation over the past century vary in different parts of the world. Some areas have experienced increased precipitation while other areas have experienced a decline (NOAA, 2005). Figure 2-7 illustrates worldwide variation in changes in precipitation over the past century.

Precipitation and streamflow records indicate an increase in precipitation over land at a rate of about 0.5 to 1 percent per decade for the middle and high latitudes of the northern hemisphere, except for East Asia. No comparable wide-scale changes in precipitation have been observed for the Southern Hemisphere. Land surface rainfall in the subtropics has decreased an average of about 0.3 percent per decade (IPCC, 2001a).

Total atmospheric water vapor content has been noted to increase at a rate of several percent each decade in the Northern Hemisphere since about 1980 (IPCC, 2001a). Some studies suggest that regional cloudiness has increased over the past century. Satellite data show a general trend for increasing cloud cover over land and the oceans since the early 1980s. This trend appears to have reversed in the early 1990s (NOAA, 2005).

Table 2-3 Possible Effects of Climate Change on Precipitation in California and Potential Consequences

Possible Changes in Precipitation	Potential Consequences
Amount	Increased precipitation could benefit water supplies and improve environmental conditions in some areas, especially where water supply diversions have significantly affected streamflow. Increased precipitation could also increase the incidence of flooding, depending on the timing and intensity of precipitation. Decreased precipitation could have serious consequences for water supplies and the environment.
Form	Climate warming is expected to increase minimum snow elevations in California's mountains and cause more precipitation to fall in the form of rain rather than snow. This will result in reductions of annual snowpack and reduce effective water storage for maintaining spring and summer streamflow/water supply diversions. Reductions in snowpack could also negatively affect hydroelectric power generation and flood control operations.
Intensity, Duration, and Timing of Precipitation Events	Increased intensity or duration of precipitation events could increase the frequency and severity of flooding. Decreases could reduce flooding. Climate change could affect the incidence of precipitation events where rain falls on accumulations of snowpack. If the incidence or severity of such events increase, it could have serious flood control and water supply implications.
Variability	Increased variability in annual precipitation could present significant challenges for water managers in meeting water demands and providing flood control. Increased surface storage capacity, operational changes for reservoirs and additional use of groundwater storage could be required. Decreased variability could benefit water management.
Location	Shifts in the annual average distribution of precipitation in the State, due to possible changes in regional circulation patterns or other possible causes, could benefit some regions and negatively affect others. California's major water storage and conveyance systems are located and designed in accordance with the historic distribution of precipitation. Significant shifts in the distribution of precipitation could pose serious water management challenges, jeopardize the effectiveness of the State's existing water supply infrastructure and alter ecosystems.

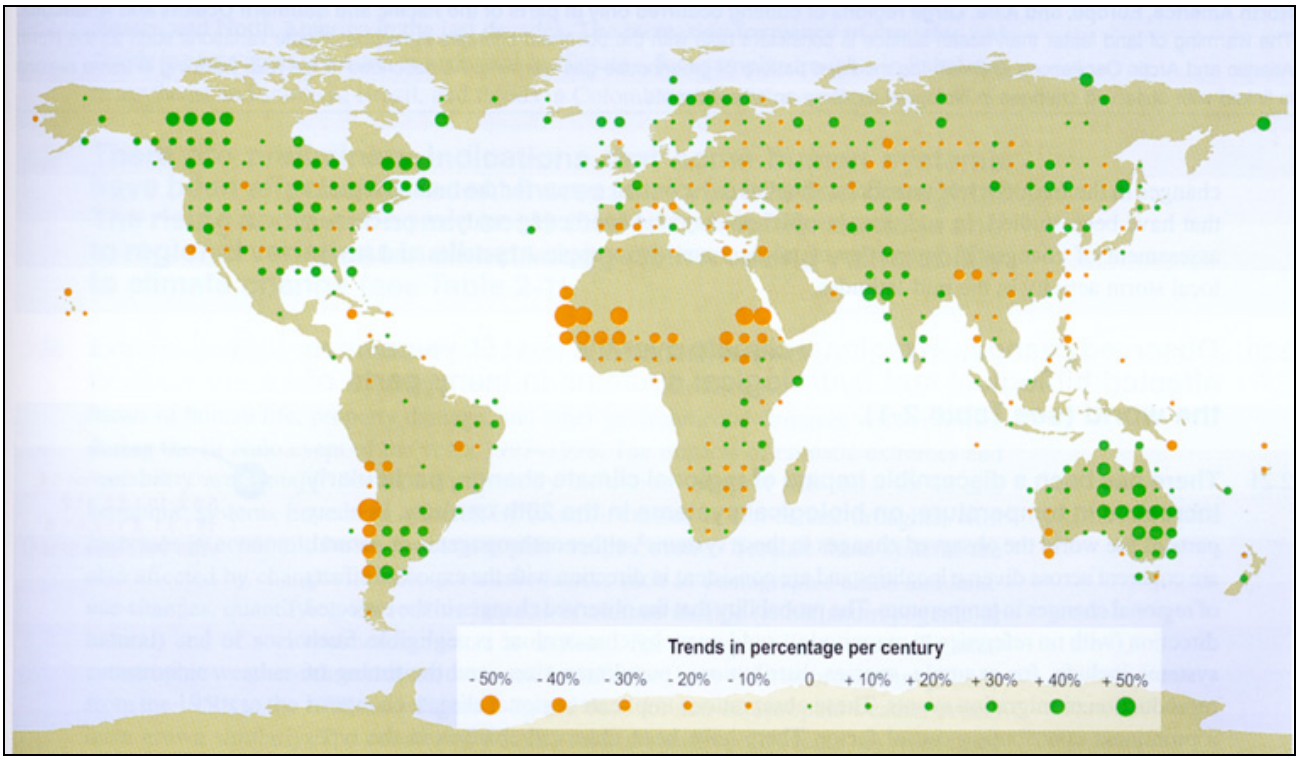


Figure 2-7 Worldwide Precipitation Trend for 1900 to 2000
Source: (IPCC, 2001b) http://www.grida.no/climate/ipcc_tar/vol4/english/fig2-6a.htm

The Intergovernmental Panel on Climate Change predicts that increasing global surface temperatures are very likely to result in changes in precipitation (IPCCb, 2001). Rising temperatures are expected to increase the activity of the world's hydrologic cycle and increase the moisture content of the atmosphere. Water vapor in the atmosphere is a greenhouse gas and will likely provide a positive feedback mechanism for climate warming.

Global average precipitation is expected to increase during the 21st century as the result of climate change based on global climate models for a wide range of greenhouse gas emission scenarios. Regional changes in precipitation will vary (IPCCa 2001). Global climate models are generally not well suited for predicting regional changes in precipitation due to their coarse discretization compared to the scale of regionally-important factors that affect precipitation.

Climate warming may have resulted in an increased occurrence of high-intensity rainfall in various areas with significant regional variation, including the United States (Groisman, 2005; Easterling, 2000). Continued warming through the 21st century may result in further increases in the occurrence of high-intensity rainfall (IPCC, 2001a; Groisman, 2005).

2.5.2 Precipitation Trends in the Western United States and California

An analysis of trends in total annual precipitation in the western United States by the National Weather Service, Climate Prediction Center provides evidence that annual precipitation has increased in much of California, the Colorado River Basin, and the West since the mid-1960s. Figure 2-8 depicts linear trends in annual precipitation in the western United States for areas referred to as "climate divisions."

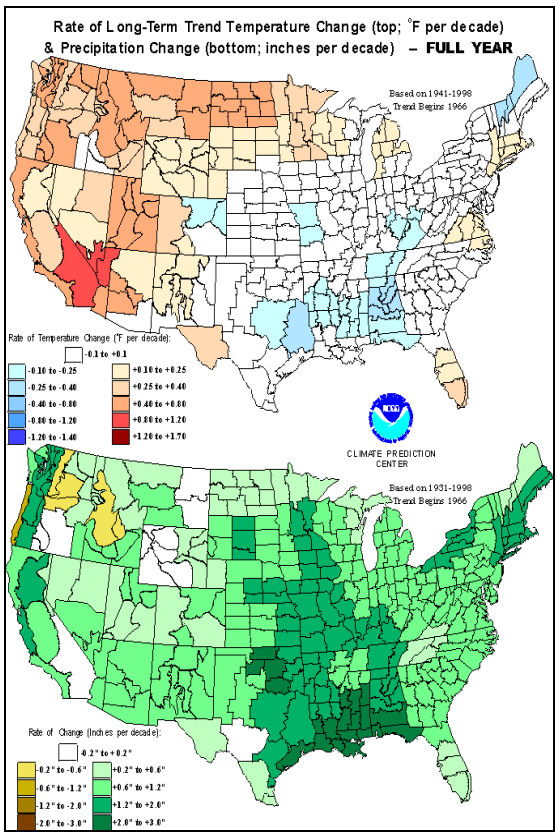


Figure 2-8 Long-Term Linear Trend Rates for Annual Precipitation in Western United States

Explanation: Rate of change is depicted for areas referred to as climate divisions. Trends are based on precipitation data from 1931-1998; however, the linear trends shown are from 1966 to 1998. For additional information concerning this figure and the determination of depicted precipitation trends visit: http://www.cpc.ncep.noaa.gov/trend_text.shtml#limits.

Adapted From: National Weather Service, Climate Prediction Website at http://www.cpc.ncep.noaa.gov/anltrend.gif

Most of the precipitation in the western U.S. falls in November through March, although monsoonal rainfall can be a locally-important factor in the Southwest from July to September. California's precipitation season is generally considered to start about mid-October and end in

April. However, most of the State's precipitation typically falls in the months just before and just after the beginning of each calendar year.

Mote and others (Mote, 2005) evaluated trends in annual November through March precipitation for the western United States and southwest Canada. Figure 2-9 depicts linear trends in November through March precipitation for two periods, 1930 to 1997 and 1950 to 1997. Precipitation trends for most of California and the Southwest are positive (increasing precipitation) during both periods.

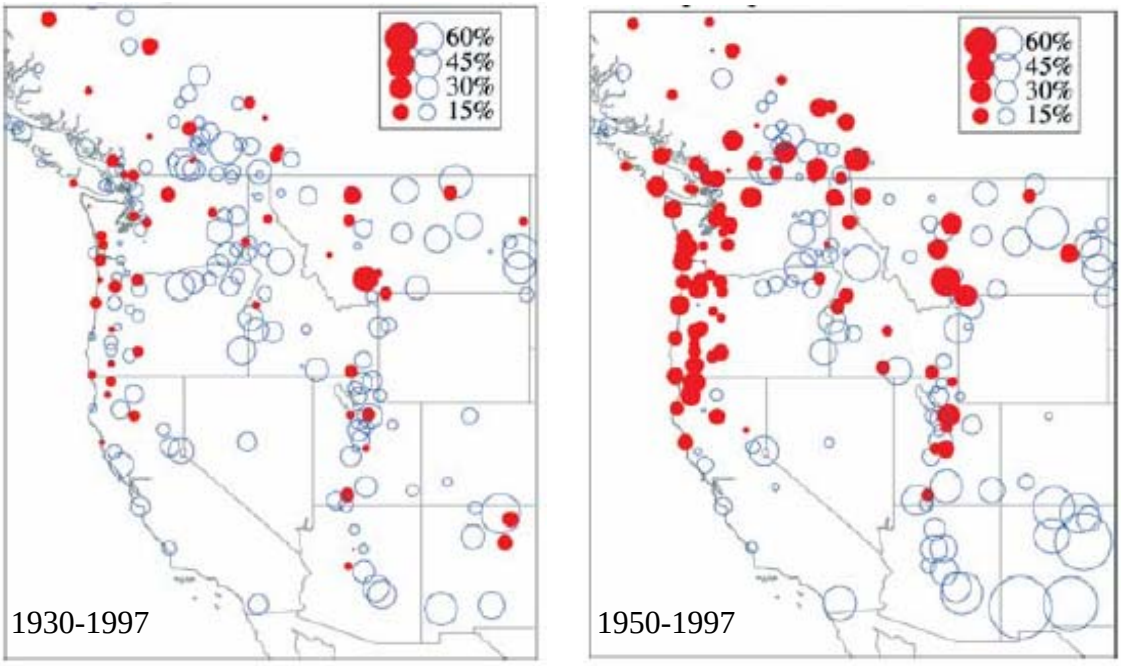


Figure 2-9 Precipitation Trends for the Western United States and Southwest Canada from 1930 to 1997 (left figure) and 1950 to 1997 (right figure)

Explanation: Depicted linear trends are for annual precipitation occurring from November through March. Decreasing precipitation trends are depicted in solid red circles. Increasing precipitation trends are depicted in open blue circles.

Source: Adapted from Mote (2005).

Former State Climatologist James Goodridge compiled an extensive collection of long-term precipitation records from throughout California. These data sets were used to evaluate whether there is a trend in precipitation in the State over the past century. Long-term runoff records in selected watersheds in the State were also examined. Figure 2-10 illustrates the variability in statewide annual average precipitation from 1890-2002. Statewide average precipitation was determined from 102 stations throughout the State. Based on a linear regression of the data, the long-term historical trend for statewide average annual precipitation appears to be relatively flat (no increase or decrease) over the entire record. However, it appears that there may be an upward trend in precipitation toward the latter portion of the record.

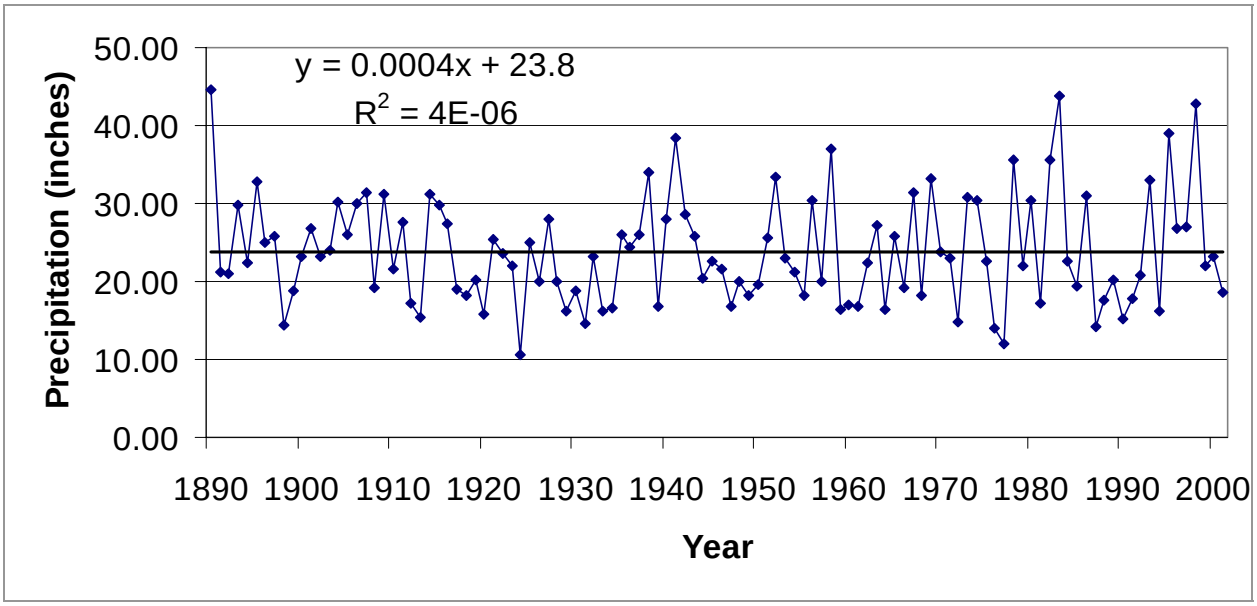


Figure 2-10 Annual Average Precipitation for California from 1890 to 2002 with Linear Trend

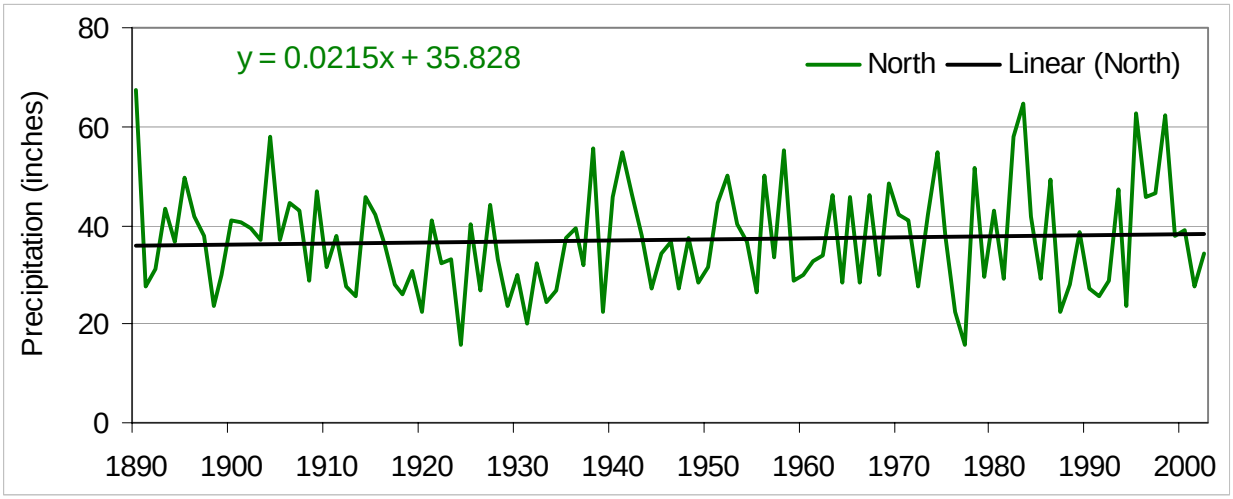
Most of the State's precipitation occurs as the result of storms from the Pacific Ocean. Hemispheric-scale circulation patterns typically cause most of these storms to move eastward across the northern part of the State. The largest amounts of precipitation fall in the mountains due to orographic effects. While a significant number of Pacific storms also cross the central and southern portions of the State, annual precipitation tends to decrease with decreasing latitude.

State precipitation records were sorted into three regions by latitude as follows:

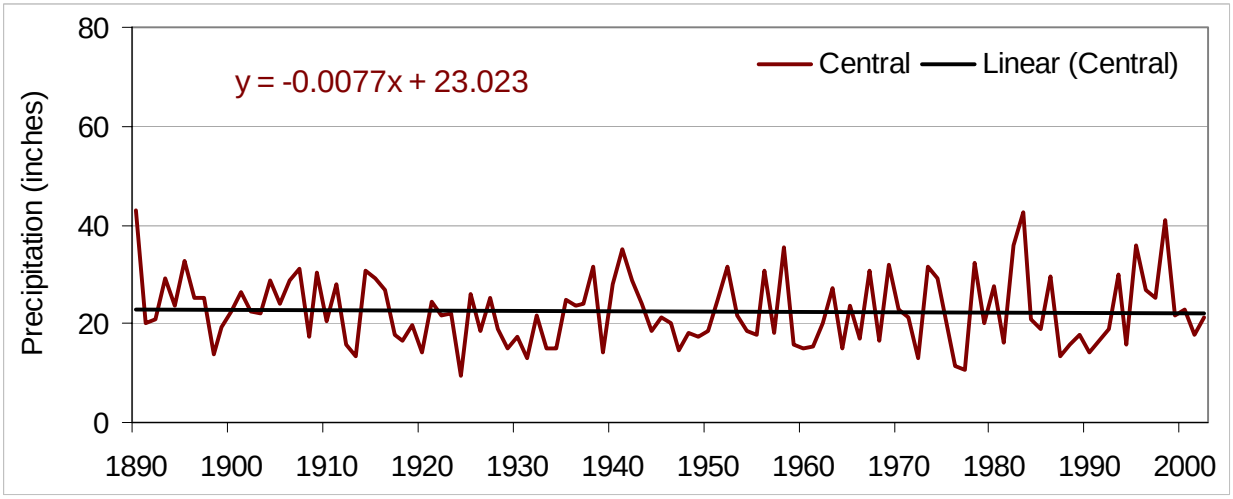
- North; from the California - Oregon border to 39 degrees latitude (latitude where California's eastern border begins to trend northwest at Lake Tahoe);
- Central; 39 to 35 degrees latitude (approximate latitude of Santa Maria); and
- South; 35 degrees latitude to the California – Mexico border.

Annual average precipitation values from 1890 to 2002 are plotted with linear trend lines for these three regions in Figure 2-11. The plots depict decreasing precipitation with decreasing latitude. Precipitation in the northern portion of the State appears to have increased slightly from 1890 to 2002. Increasing runoff trends observed for various Northern California watersheds, as discussed in Section 2.5.3 below, are consistent with the apparent increasing precipitation trend in this part of the State. Precipitation in the central and the southern portions of the State appear to have slightly decreasing trends from 1890 to 2002.

a) Northern Region: California-Oregon border to 39º latitude



b) Central Region: 39º - 35 º latitude



c) Southern Region: 35 º latitude to California-Mexico border

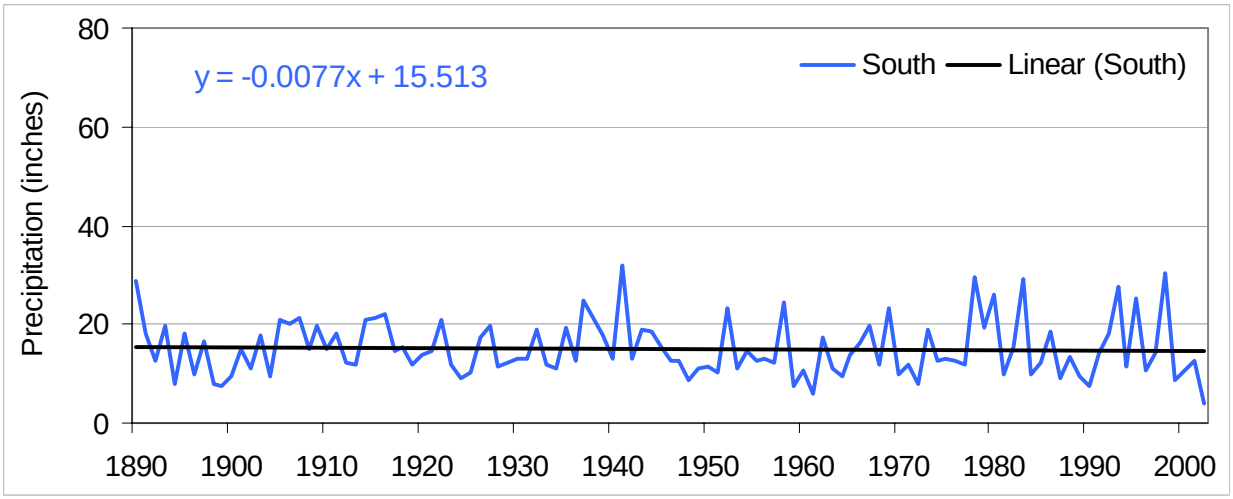


Figure 2-11 Annual Average Precipitation from 1890 to 2002 with Linear Trends by Region

Differences in California precipitation trends between those observed by the National Weather Service, Mote and others, and above analysis are likely due to differences in the:

- the period of analysis
- number and location of precipitation measurement stations used
- geographic regions selected for analysis

While increasing precipitation on a global scale is generally an expected result of climate change, significant regional differences in precipitation trends can be expected. More analysis of precipitation trends in California is probably needed for determining whether changes in California's regional annual precipitation totals have occurred as the result of climate change or other factors.

In addition to possible long-term trends in annual amounts of precipitation, increased variability of annual precipitation is also a possible outcome of climate change. Figure 2-12 depicts the coefficient of variation (standard deviation divided by the mean) based on a 10-year moving average of mean and standard deviation values for statewide annual average precipitation. There appears to be an upward trend in the variability of precipitation over the past century with end-of-period variability values about 75 percent larger than beginning-of-period values. This indicates that there tended to be more extreme wet and dry years at the end of the century than there were at the beginning of the century. This trend may continue with on-going climate change.

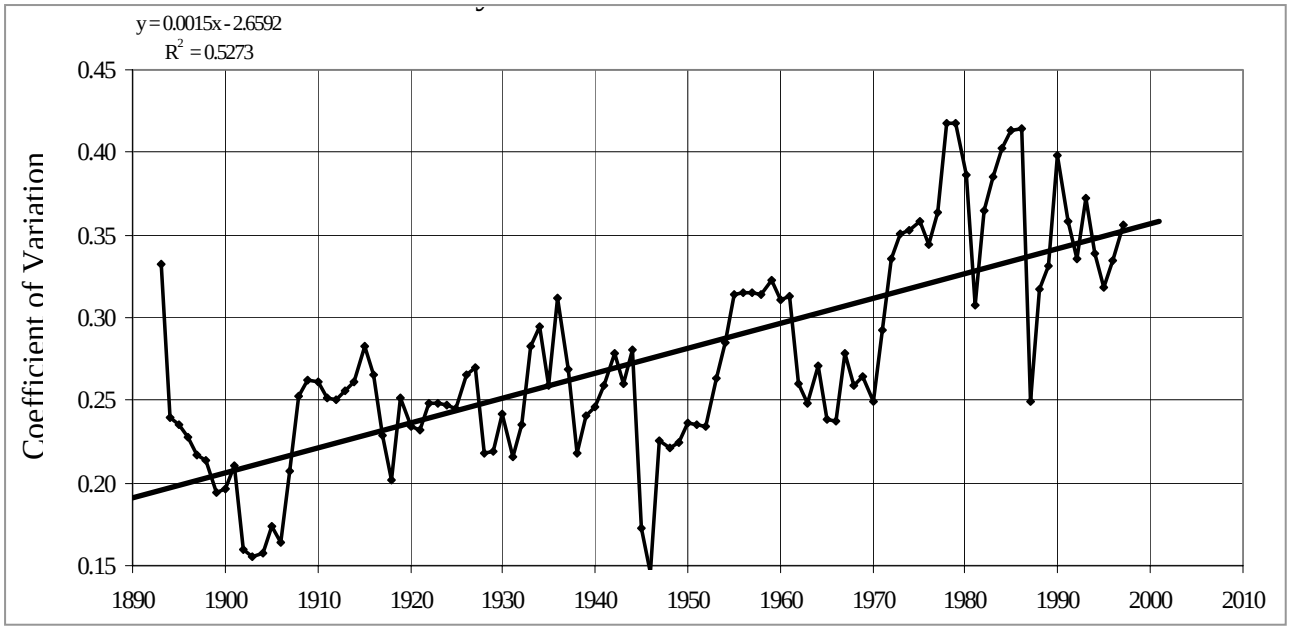


Figure 2-12 Coefficient of Variation for Annual Average Precipitation in California from 1890 to 2001 with Trend Line

2.5.3 Trends in Snowfall and Related Runoff in California

Precipitation in California's higher mountains during the late fall and winter typically falls in the form of snow. Significant accumulations of snow, referred to as snowpack, typically occur each year in the Sierra Nevada along the eastern flank of the Central Valley. A significant annual snowpack also typically occurs in the Cascade Range north and northeast of the Central Valley, and in the Klamath Mountains in the northwest corner of the State. Most of the runoff from the State's snowpack flows into the Central Valley, although snowmelt is also important for flows in rivers and streams on the east slope of the Sierra, such as the Truckee, Carson, and Owens rivers, and for the Klamath River and its tributaries.

California's annual snowpack is, on average, mostly accumulated from November though the end of March. It typically melts from April though July. Snowmelt provides significant quantities of water to streams and reservoirs for several months after the annual storm season has ended. The length and timing of each year's period of snowpack accumulation and melting can vary somewhat due to temperature and precipitation conditions.

California's snowpack is important to the State's annual water supply, because of its volume and when it typically melts. Average runoff from melting snowpack is usually about 20 percent of the State's total annual natural runoff, and probably about 35 percent of the State's total useable annual surface water supply. The State's snowpack is estimated to contribute an average of about 15 million acre-feet of runoff each year, about 14 million acre-feet of which is estimated to occur in the Central Valley. In comparison, total reservoir capacity in the Central Valley is about 24.5 million acre-feet in watersheds with significant annual accumulations of snow (DWR, 2005c).

California's reservoir managers use snowmelt to help fill reservoirs once the threat of large winter and early spring storms and related flooding risks have passed. Water stored in reservoirs is used to help meet downstream water demands when flows from snowmelt begin to recede and are typically not sufficient for satisfying downstream uses.

Some of the annual runoff collected in California's reservoirs is held from one year to the next. Water stored from one year to the next is typically referred to as "carryover storage". California's annual precipitation and snowpack can vary significantly from year to year in California. There may also be decadal-scale variation in precipitation over the Sierra (Freeman, 2002), and possibly other parts of California. Carryover storage can help meet water demand in years where precipitation and runoff is low.

Rising temperatures as the result of climate change threaten California's snowpack. An inchoative analysis of annual runoff trends in the Sacramento Valley was performed by Maurice Roos of DWR in the late 1980s (Roos, 1989). The purpose of the analysis was to determine if changes in the timing of annual runoff in the Sacramento Valley watershed had occurred as the result of possible increasing temperatures and diminished snowpack. It was concluded that, since the beginning of the 20th century, the amount of annual runoff from April though July in the upper Sacramento River watershed had a downward trend compared to each year's total runoff. This was determined to be a possible indication of a long-term reduction in the State's snowpack due to temperature rise.

An updated evaluation of runoff trends was performed for this report. Figure 2-13 presents combined unimpaired April through July runoff for four rivers in the Sacramento Valley (Sacramento, Feather, Yuba, and American rivers) as a percent of total water year runoff from 1906 to 2005. Figure 2-14a presents total April through July unimpaired runoff volume for the same period of record and for the same four rivers. Figure 2-14b presents total unimpaired water year runoff volume for the same period and rivers.

Based on the linear trends depicted in Figure 2-13 and Figure 2-14 for the four Sacramento Valley rivers:

- April through July runoff, as compared to total water year runoff, has declined about 9 percent over the past 100 years
- April through July runoff volume has decreased over the same period and total water year runoff during the same period has remained about the same

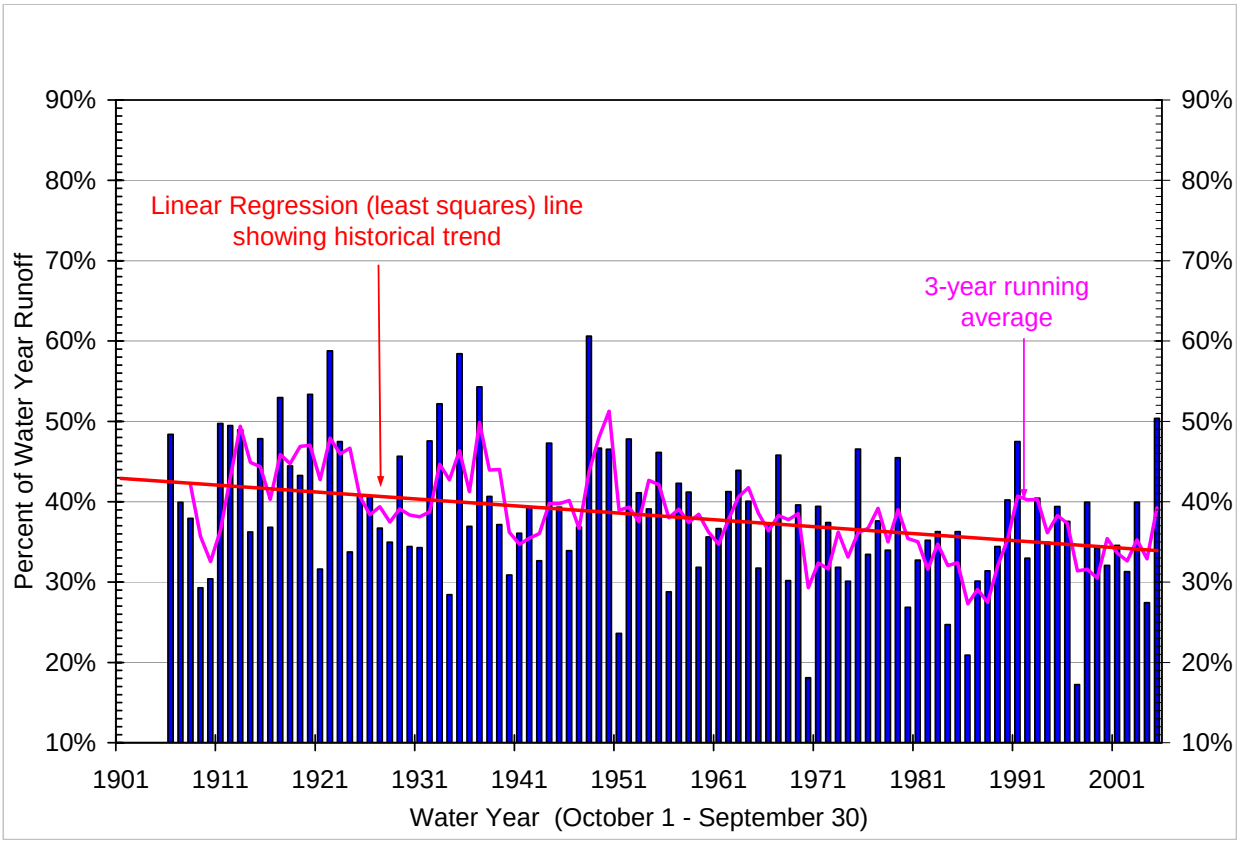
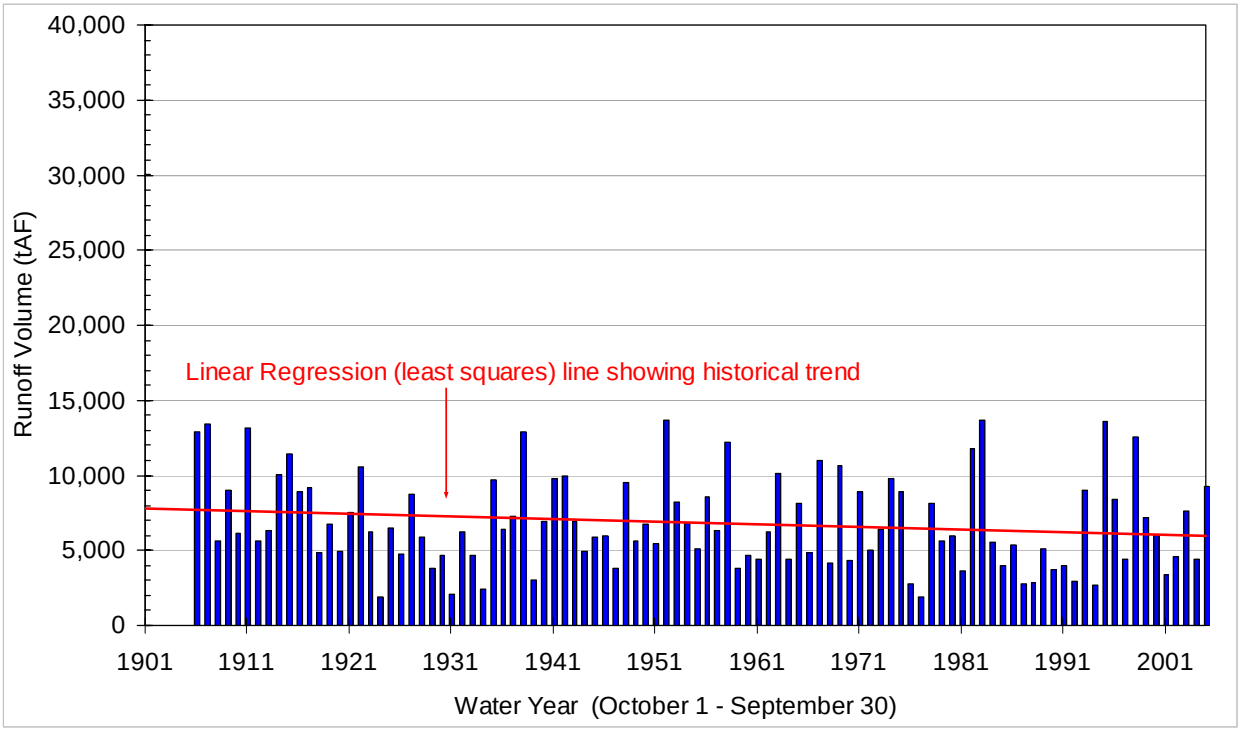


Figure 2-13 Annual April through July Unimpaired Runoff for Four Sacramento Valley Rivers Compared to Total Unimpaired Annual Runoff*

* Based on the flows of four rivers in the Sacramento Valley; Sacramento River at Bend Bridge (near Red Bluff), Feather River into Lake Oroville, Yuba River at Smartville, and American River below Lake Folsom.

a) Annual April through July Runoff Volume



b) Total Water Year Runoff Volume (October-September)

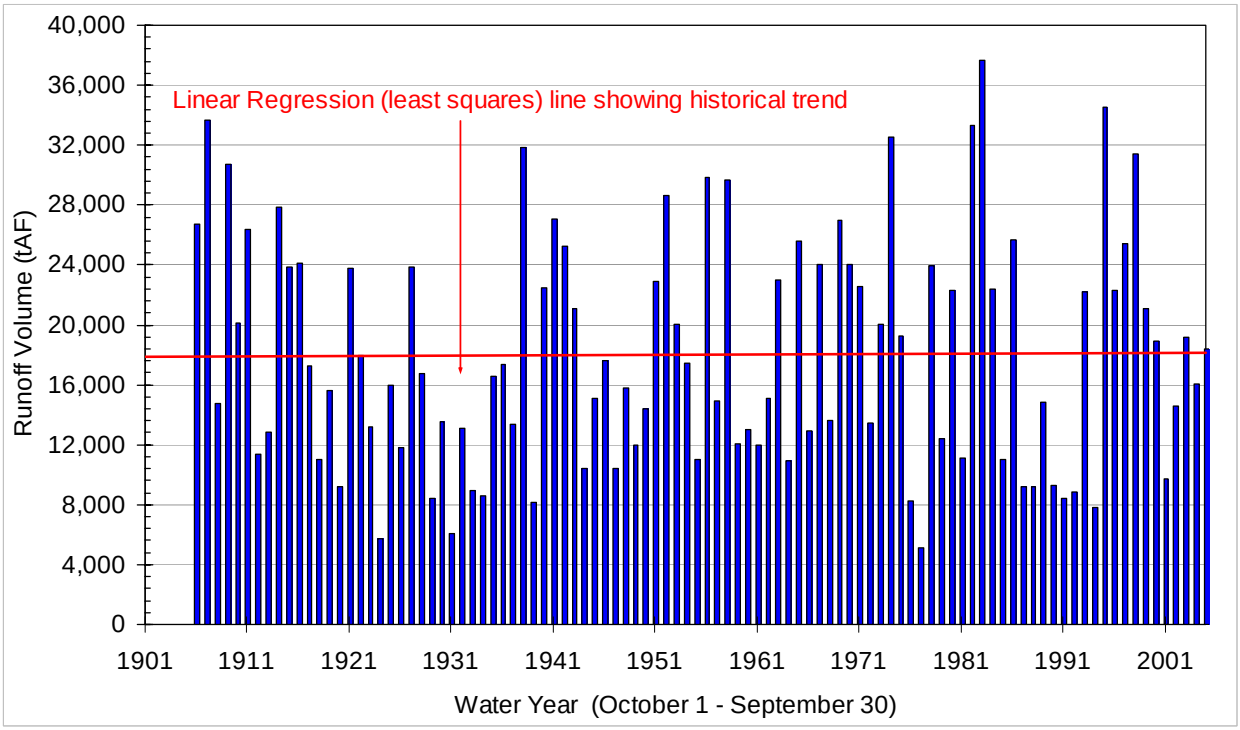


Figure 2-14 Unimpaired Runoff Volume for Four Sacramento Valley Rivers*

* Based on the flows of four rivers in the Sacramento Valley; Sacramento River at Bend Bridge (near Red Bluff), Feather River into Lake Oroville, Yuba River at Smartville, and American River below Folsom Lake. (taf) = thousand acre feet.

Figure 2-15 presents combined unimpaired runoff from April through July for four rivers in the San Joaquin River watershed (Stanislaus, Tuolumne, Merced, and San Joaquin rivers) as a percentage of total water year runoff from 1901 to 2005. Figure 2-16a presents total unimpaired April through July runoff volume for the same four rivers and for the same period of record. Figure 2-16b presents total unimpaired water year runoff volume.

The trends depicted in Figure 2-15 and Figure 2-16 for the four San Joaquin Valley rivers indicate that:

- April through July runoff, as compared to total water year runoff, has declined about 7 percent over about the past 100 years
- while total water year runoff volume decreased somewhat during the past 100 years, April through July runoff volume decreased at even a greater rate.

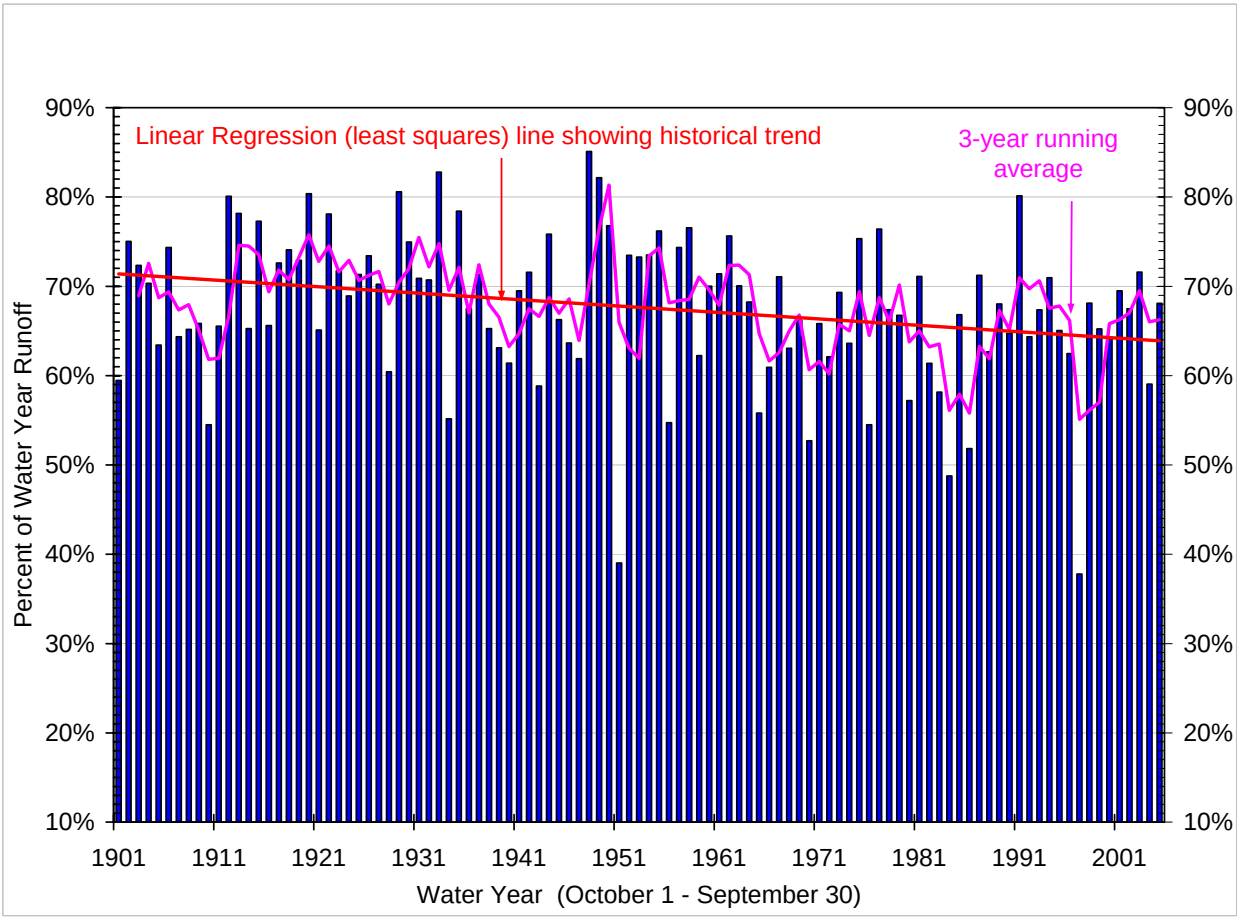
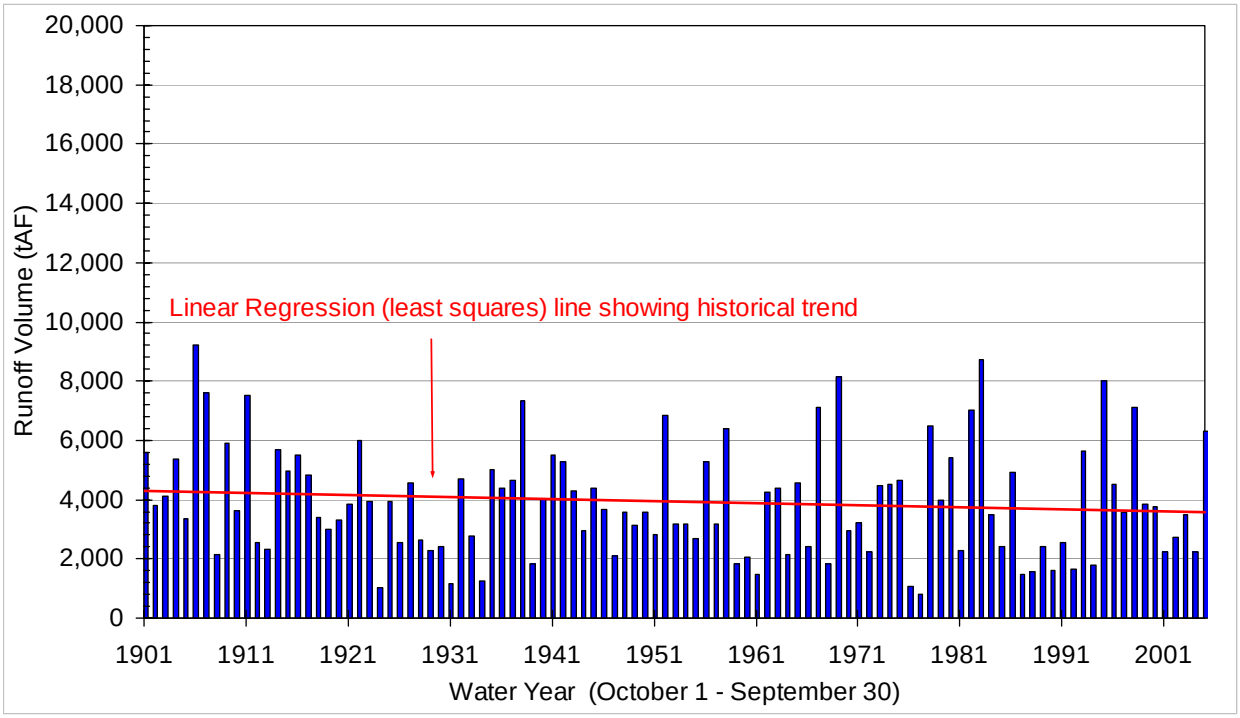


Figure 2-15 Annual April through July Unimpaired Runoff for Four San Joaquin Valley Rivers Compared to Total Unimpaired Annual Runoff*

*Based on the flows of four rivers in the San Joaquin Valley; Stanislaus River into New Melones Reservoir, Tuolumne River into Don Pedro Reservoir, Merced River into Lake McClure, and San Joaquin River into Lake Millerton.

a) Annual April through July Runoff Volume



b) Water Year Runoff Volume

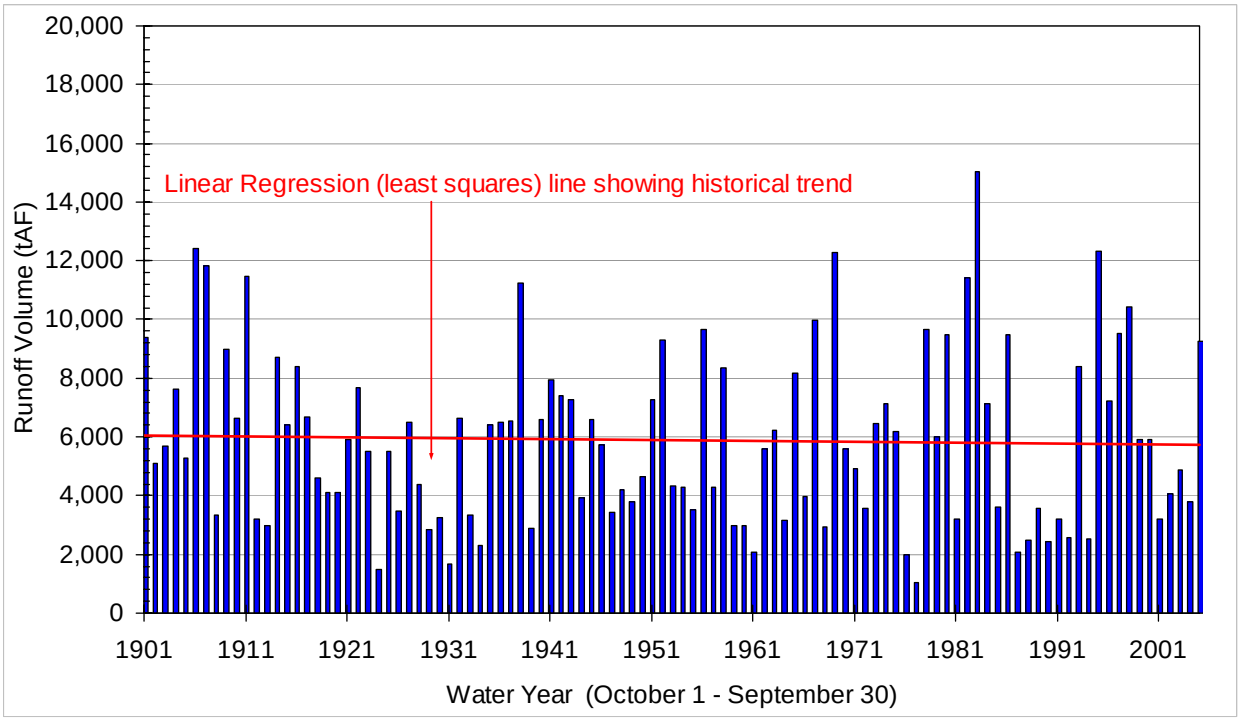


Figure 2-16 Total Unimpaired Runoff Volume for Four San Joaquin Valley Rivers*

*Based on the flows of four rivers in the San Joaquin Valley; Stanislaus River into New Melones Reservoir, Tuolumne River into Don Pedro Reservoir, Merced River into Lake McClure, and San Joaquin River into Lake Millerton. (taf) = thousand acre feet.

Some investigators have evaluated trends in Sierra runoff for different time periods over the past century. Figure 2-17 depicts two trends in April through July runoff as a percentage of total annual runoff for eight western Sierra rivers. No statistically significant downward or upward trend was determined for the period before 1945. However, the trend following 1945 is toward diminished runoff from April through July as compared to total annual runoff (Dettinger, 2005a).

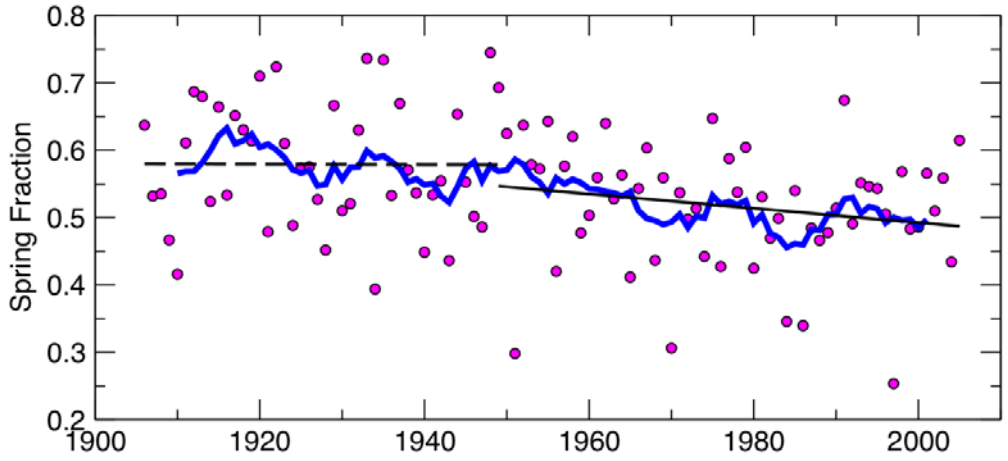


Figure 2-17 Annual April through July Unimpaired Runoff in the Central Valley Compared to Total Unimpaired Annual Runoff

Source: Dettinger, 2005a. (Updated by original author).
Explanation: Individual points depict yearly combined values for the Sacramento River at Bend Bridge (near Red Bluff), Feather River into Lake Oroville, Yuba River at Smartville, American River below Folsom Reservoir, Stanislaus River into New Melones Reservoir, Tuolumne River into Don Pedro Reservoir, Merced River into Lake McClure, and Kings River into Pine Flat Reservoir. The blue curve is the nine-year moving average of annual values. The dashed line is the linear trend prior to 1945. The solid line is the linear trend after 1945.

Updated runoff data for the Sacramento Valley and San Joaquin Valley, as discussed above, continue to support the conclusion from earlier analyses that there appears to be a long-term trend toward reduced April though July runoff compared to total annual runoff from the Sierra. It is reasonable to conclude that this trend is the likely result of climate change and warming and an attendant decline in Sierra snowpack. A portion of the trend may also be attributable to progressively earlier melting of Sierra snowpack due to warming.

The trend toward diminished April through July runoff, as compared to total annual runoff, appears to be stronger for the Sacramento Valley than for the San Joaquin Valley, as evidenced by Figure 2-13 and Figure 2-15. This may be due to elevation differences between the northern and southern Sierra. Rising temperatures could be expected to impact the northern Sierra snowpack to a greater degree than the southern Sierra snowpack because the northern Sierra is generally lower in elevation than the southern Sierra.

Table 2-4 summarizes runoff statistics and linear trends for the Sacramento and San Joaquin Valleys, selected river basins in the two valleys, and selected rivers elsewhere in the State where data could be readily obtained and where unimpaired flows could be determined or inferred. The

long-term trend in April through July runoff volumes for the Sacramento and San Joaquin valleys is downward, as are the trends for individual Sacramento Valley basins listed in the table. April through July runoff volume trends for most of the San Joaquin Valley basins listed in the table are also downward. These trends are consistent with the previously discussed conclusion that the Sierra snowpack is undergoing decline, possibly because of warming. Total water year runoff in the Sacramento Valley has an increasing trend while total water year runoff in the San Joaquin Valley appears to be decreasing on a long-term basis.

Outside of the Central Valley, the most noteworthy temporal change evident in Table 2-4 is an increasing trend in total water year runoff in the major river basins in the north coast portion of the State.

Table 2-4 Runoff Statistics and Trends for Selected River Basins in California

Basin/River System	Period of Record	Period A-J[1] Average (TAF)[3]	Period WY[2] Average (TAF)	Period A-J Linear Trend (TAF/yr)[4]	Period WY Linear Trend (TAF/yr)[4]
Central Valley River Systems					
Sacramento River System[5]	1906-2005	6,847	18,024	-17	3
San Joaquin System[6]	1901-2005	3,922	5,900	-7	-3
Sacramento Valley Basins					
Sacramento at Bend Bridge	1906-2005	2,522	8,476	-3	6
Feather	1906-2005	1,901	4,490	-6	2
Yuba	1901-2005	1,096	2,372	-3	-2
American	1901-2005	1,359	2,739	-5	-3
North San Joaquin Valley Basins					
Cosumnes	1908-2005	127	369	0	0
Mokelumne	1901-2005	487	758	-1	-1
Stanislaus	1901-2005	745	1,175	-2	-1
Tuolumne	1901-2005	1,248	1,911	-1	0
Merced	1901-2005	646	997	-1	0
San Joaquin	1901-2005	1,283	1,816	-2	-1
South San Joaquin Valley Basins					
Kings	1901-2005	1,238	1,683	-2	-1
Kaweah	1901-2005	285	432	0	0
Tule	1930-2005	63	145	0	0
Kern at Isabella	1930-2005	453	697	0	1
Kern at Bakersfield	1901-2005	473	739	0	2

Table 2-4 Runoff Statistics and Trends for Selected River Basins in California (continued)

Basin/River System	Period of Record	Period A-J[1] Average (TAF)[3]	Period WY[2] Average (TAF)	Period A-J Linear Trend (TAF/yr)[4]	Period WY Linear Trend (TAF/yr)[4]
Eastern Sierra Basins					
East Carson and West Walker	1922-2005	326	433	1	2
Truckee	1906-2005	274	452	-1	0
North Coast Basins					
Klamath	1928-2005*	1,665	4,646	1	7
Salmon	1912-2005*	521	1,288	0	2
Eel	1911-2005	914	5,493	0	12
Napa	1930-2005*	8	72	0	0
Russian	1941-2005	101	897	0	1
Central and South Coast Basins					
Arroyo Seco near Soledad	1906-2005	23	122	0	0
Arroyo Seco near Pasadena	1911-2005	2	7	0	0
Nacimiento	1916-2005	23	200	0	0
Santa Ana	1901-2005	21	60	0	0

Footnotes:
[1] A-J = April through July.
[2] WY = Water Year.
[3] TAF = Thousand acre-feet.
[4] Trend rounded to the nearest thousand acre-foot/year.
[5] Composite of runoff data for the Sacramento River at Bend Bridge, Feather River into Lake Oroville, Yuba River at Smartville, and American River below Lake Folsom.
[6] Composite of runoff data for the Stanislaus River into New Melones Reservoir, Tuolumne River into Don Pedro Reservoir, Merced River into Lake McClure, and the Kings River into Pine Flat Reservoir.

2.5.4 Projected Changes in Precipitation for California

2.5.4.1 Changes in the Amount of Precipitation

As discussed above, there are indications that total annual precipitation in some Northern California watersheds has been increasing. While the cause of this apparent change is unknown, it may be due in part to climate change since warming is expected to result in a more active hydrologic cycle.

Climate model projections for changes in total annual precipitation in California through the end of this century are mixed. Models predicting the greatest amount of warming generally predicted

moderate decreases in precipitation. Models projecting smaller increases in temperature tend to predict moderate increases in precipitation. When some of the most extreme projections are underweighted, the central tendency in the projections is toward moderately decreased precipitation (Dettinger, 2005b).

2.5.4.2 Changes in Snowpack

As discussed in Section 2.4, temperatures in California are projected to increase from about 2.5 to about 9 degrees Celsius by the end of this century as the result of climate change. One expected consequence of this is further reduction in the State's annual snowpack and earlier melting of snow.

Historically, average snowline elevations in California have ranged from about 4,500 feet in the north to above 6,000 feet in the southern Sierra. DWR staff estimates that the average snow-covered area totals about 13,200 square miles in the water supply producing basins of the Central Valley and the Trinity River above Lewiston. This is about 8 percent of the State's total land surface. The northern Sierra and Trinity mountains account for about 7,000 square miles of the 13,200 square mile total. The west slope of the southern Sierra accounts for the remainder.

Rising temperatures will cause reductions in the State's snowpack by raising snowline elevations and reducing the area where annual snowpack accumulates. A rudimentary analysis of the impact of rising temperatures on snowpack, shows that a 3 degree Celsius rise will likely cause snowlines to rise about 1,500 feet based on a moist lapse rate of 500 feet per 1 degree Celsius. This would cause a significant reduction in the amount of snow-covered area in the State and an estimated average annual loss of about 5 million acre-feet of effective water storage in snowpack.

Climate model studies support projections for continued reductions in the State's snowpack as the result of warming. Simulations under various amounts of temperature rise indicate that California's snowpack is very vulnerable to warming. One set of simulations by N. Knowles and D. R. Cayan (Knowles, 2002) provide the following projections for loss in April Sierra snowpack snow-water equivalent (in comparison to existing conditions) as a result of rising temperatures:

- 0.6 degree Celsius rise, ~5 percent loss
- 1.6 degrees Celsius rise, ~33 percent loss
- 2.1 degrees Celsius rise, ~50 percent loss

These three levels of average temperature rise were projected by Knowles and Cayan to occur by 2030, 2060 and 2090, respectively.

Losses in snow were projected to occur mainly at low to mid-altitudes. Loss of snowpack was projected to be greater in the northern Sierra and Cascades than in the southern Sierra due to the relative proportions of land at low and mid-elevations. At the highest temperature projection (increase of 2.1 degrees Celsius), the northern Sierra and Cascades were projected to lose 66

percent of their April snowpack, while the southern Sierra was projected to lose 43 percent of its snowpack.

Newer climate model studies, including those for the Intergovernmental Panel on Climate Change's 4th Assessment, due to be published in 2007, will provide a new set of temperature projections in addition to those already available. Most existing temperature projections, as well as those expected from the 4th Assessment, indicate that losses in the State's snowpack are likely to continue increasing through the end of this century.

Warming and loss of the State's snowpack will affect the operation of most major multipurpose reservoirs at low and mid-elevations in the Sierra. Operation of these reservoirs now includes maintaining empty flood-control space during winter months and then gradually allowing them to fill with snowmelt during the spring after the threat of storms and flooding has passed. Higher snow lines and more precipitation falling in the form of rain rather than snow will increase winter inflows to these reservoirs. Higher winter inflows will also likely mean that a greater portion of the total annual runoff volume will occur in the winter. Thus, more annual runoff will likely be passed through reservoirs and will not be available for hydropower production and water supply uses later in the year. Higher winter inflows may also diminish the ability of reservoir managers to store a portion of a year's runoff volume as annual carryover storage.

2.5.4.3 Other Effects

As discussed at the beginning of this section, climate change could affect the intensity, duration, and timing of precipitation events in California. It could also affect the spatial distribution and temporal variability of precipitation. Significant changes in one or more of these factors could have serious consequences for water resources management. While there may be some evidence that year-to-year variation in California's precipitation has increased over the past century, additional work is needed to determine the possible nature and extent of any changes that may already be occurring or could occur as a result of climate change.

2.6 Sea Level Rise

One of the major areas of concern related to global climate change is rising sea level. Worldwide average sea level appears to have risen about 0.3 to 0.6 of a foot over the past century based on tide gauge data (IPCC, 2001a). Rising worldwide average sea level over the past century has primarily been attributed to:

- warming of the world's oceans and the related thermal expansion of ocean waters (steric changes)
- the addition of water to the world's oceans from the melting of land-based ice, such as from Greenland and southeast Alaska (eustatic changes)

Some researchers have attributed most of the worldwide rise to steric changes, although there is some uncertainty about the relative contributions of steric and eustatic changes (Munk, 2002). Worldwide average sea level is projected to rise from between 0.3 of a foot and 2.9 feet by 2100, as discussed below (IPCC, 2001a).

California's coastline is about 1,075 miles in length, not including inland bays, estuaries and offshore islands. The State's coastal features include broad coastal plains and wide beaches in much of Southern California. Extensive stretches of mountainous and rugged coastline occur in the central and northern parts of the State, along with more limited coastal plains than those in Southern California. California's coastal topography is shown in Figure 2-18. The State's coastline also includes major inland bays and estuaries, including the San Francisco Bay and the Sacramento-San Joaquin River Delta (Delta), as shown in Figure 2-19.

Future sea level rise, while projected to be a relatively slow and gradual process, presents a somewhat alarming prospect for California, especially in the case of the more extreme projections. The effects of sea level rise will include:

- increased erosion of beaches, bluffs and other coastal features
- inundation of coastal land and marshes
- local flooding near the mouths of rivers and streams due to backwater effects (especially on coastal plains)
- increased potential for sea water intrusion into coastal aquifers
- increased sea water intrusion into estuaries, including the Sacramento-San Joaquin River Delta
- increased potential for levee failure in the Delta
- potential adverse impacts on flow control and diversion facilities in the Delta
- inundation and critical alteration of aquatic ecosystem habitat development projects in the Delta

.

Of the effects listed above, perhaps the most significant from the standpoint of the State's water resources are increased sea water intrusion and increased potential for levee failure in the Delta. Increased sea water intrusion into the Delta threatens the operations of the State Water Project and the Central Valley Project, as well as other Delta water supply diversions due to water quality degradation. Water quality degradation in the Delta also potentially threatens the Delta's fragile ecosystem, which supports threatened and endangered species. Finally, increased sea water intrusion into the Delta could threaten some groundwater supplies through the interaction of Delta waters with underlying and adjoining portions of the Central Valley groundwater basin.



Figure 2-18 California's Topography and Coastline

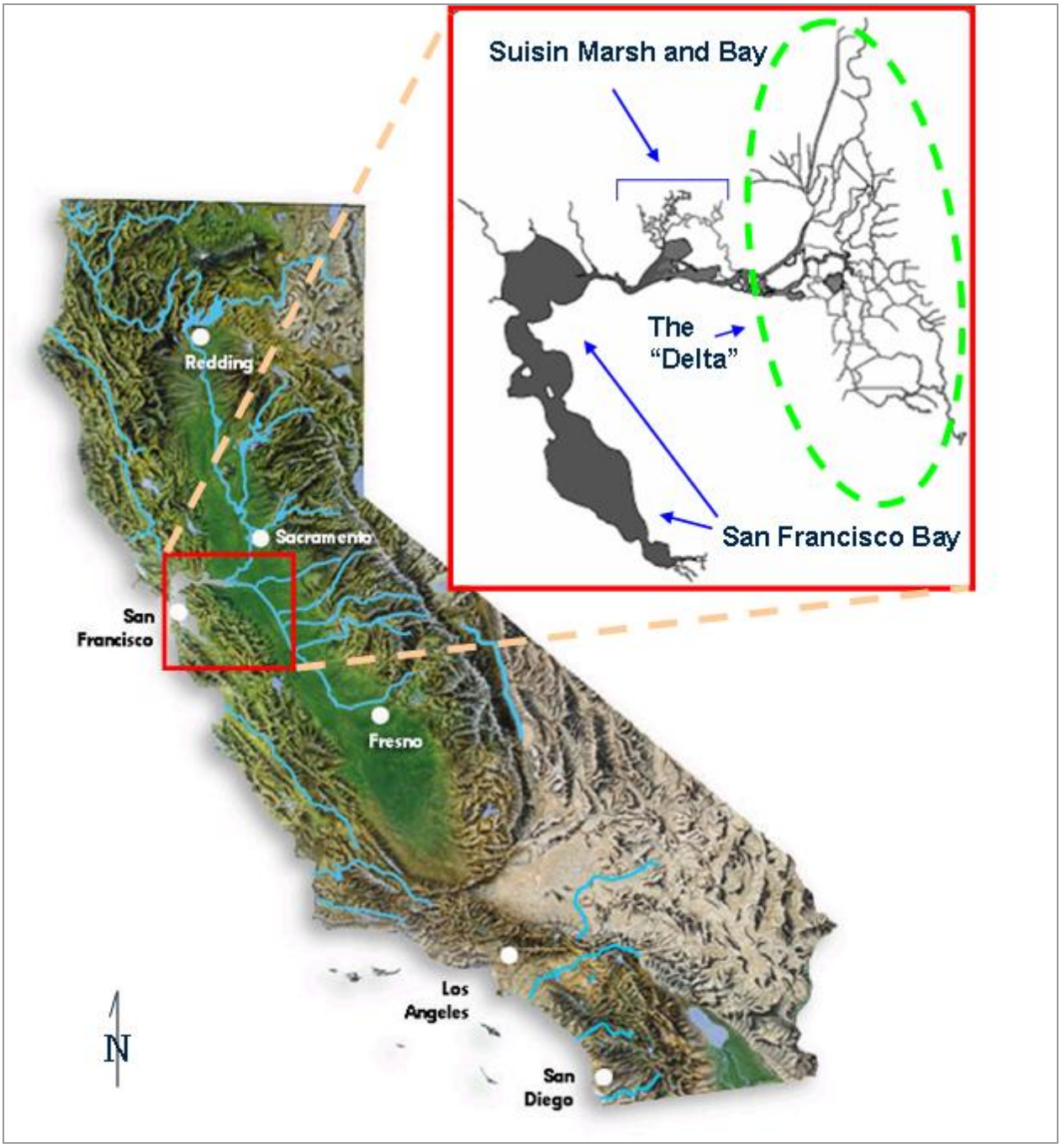


Figure 2-19 Location of the San Francisco Bay, Suisun Marsh and Sacramento-San Joaquin River Delta

2.6.1 Historical Sea Levels

2.6.1.1 Sea Level Prior to Recorded History

The Earth has been subject to many periods of cooling (glacial periods) and warming (interglacial periods). Periods of glaciation are marked by massive accumulations of land- and sea-based ice extending from the Earth's poles sometimes as far as the Earth's mid-latitudes. Interglacial periods are marked by warming and the recession of ice toward the poles. Sea level during glacial periods is lowered as a significant amount of the world's water accumulates as snow and ice through precipitation. Sea level during interglacial periods rises through the melting of massive ice sheets accumulated during glacial periods.

Geologic evidence shows that for the past million years ocean levels have repeatedly risen and fallen on a somewhat cyclical basis. Figure 2-20 depicts several glacial and interglacial periods and fluctuating ocean levels over the past 800,000 years.

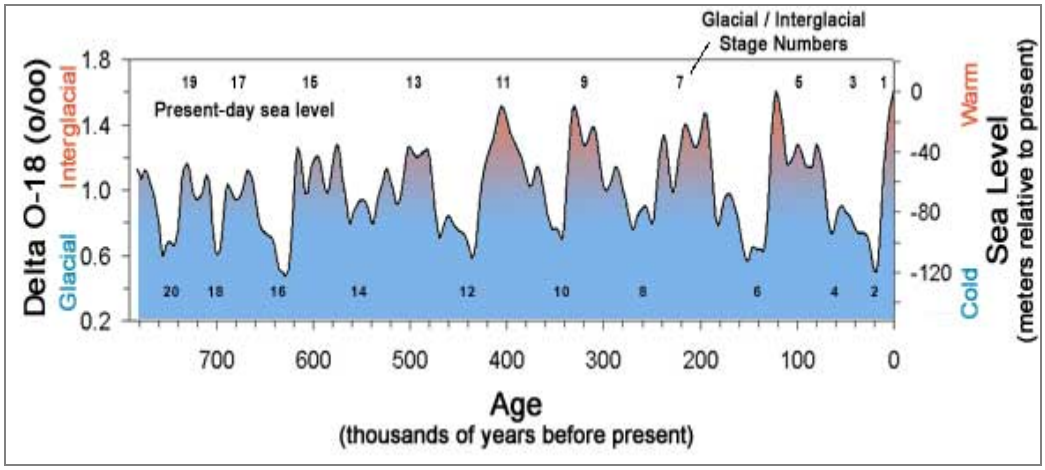


Figure 2-20 Changes in Global Sea Level over the Past 800,000 Years
Adapted from: http://coastalchange.ucsd.edu/st4_climatechange/sealevel.html
Coastal Morphology Group, Integrative Oceanography Division, Scripps Institution of Oceanography

The exact causes for the glacial periods and intervening periods of warming are unknown. Geologic evidence shows that global ocean levels have risen significantly since the most recent period of glaciation. The surface of the world's oceans during the coldest portion of the last glacial period, about 18,000 to 20,000 years ago, is estimated to have been about 400 feet lower than today's level, as shown in Figure 2-21. Most of the rise in sea level since this time was due to the large-scale melting of continental ice sheets, most of which occurred from 6,000 to 15,000 years ago. The average rate of sea level rise from about 6,000 years ago to present may have been about 0.5 mm/yr, or about 0.16 of a foot per century (IPCC, 2001a).

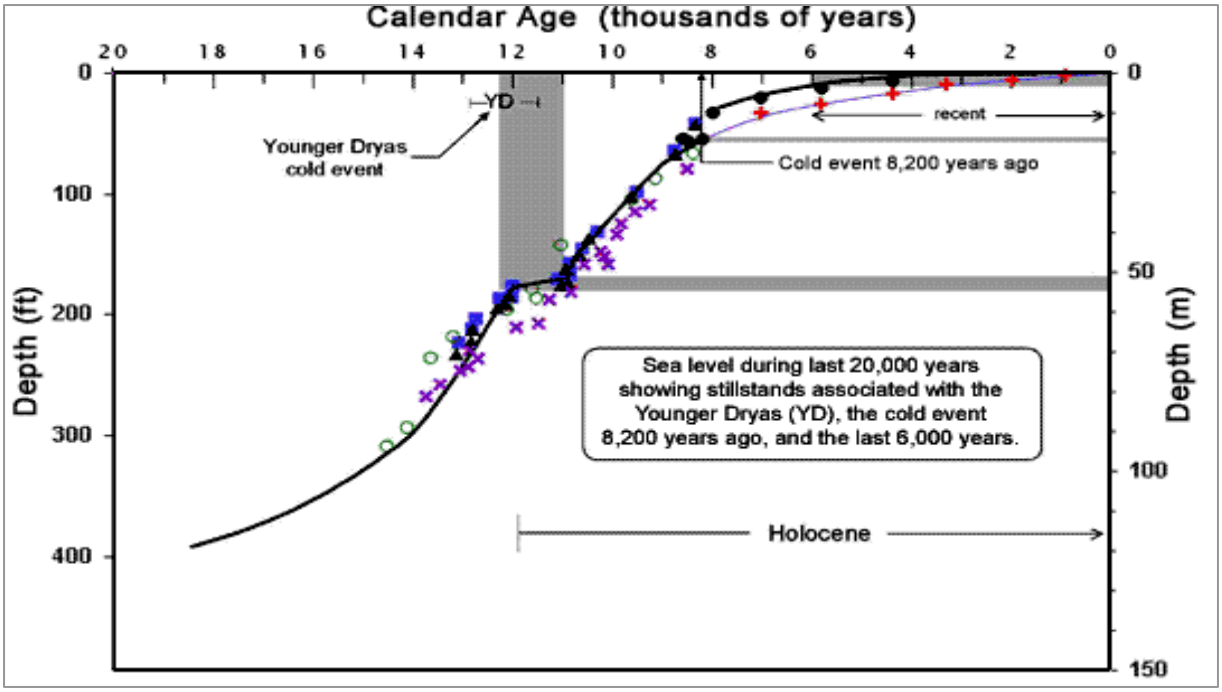


Figure 2-21 Change in Sea Level Over the Past 18,000 Years

Adapted from: Inman, et.al, 2002 http://coastalchange.ucsd.edu/st4_climatechange/sealevel.html
Explanation: The solid black and solid blue lines depict the estimated trend in sea level. The individual points of varying colors depict estimates of sea level at several locations by various researchers. A discussion about the "Younger Dryas" can be found at: http://en.wikipedia.org/wiki/Younger_Dryas#Abrupt_climate_change.

2.6.1.2 Sea Level Measurements

Direct sea level measurements began as early as the beginning of the 18th century in Europe with the use of tide gauges. Measurements for six European tide gauging stations with notably long records are depicted in Figure 2-22. All stations show a rise in relative sea level[2].

Rates of change in relative sea level measured by tide gauges along the coast of the United States over the 20th century are depicted in Figure 2-23. Since global sea level rise during the last century is believed to have been between about 0.3 and 0.6 of a foot, gauges exhibiting rates of sea level rise that significantly exceed this range could be on land masses that are subsiding. Gauges where sea level appears to rising more slowly than the worldwide average, not changing, or declining in comparison to worldwide trends may be on land masses that are rising. Table 2-5 lists areas of the U.S. coast that have been subject to recent subsidence or uplift and the causes for the changes.

Figure 2-24 depicts the locations of tide gauges along the coast of California, including eight gauges that have at least 50 years or more of record. Relative sea level trends for the eight gauges up to 2000 are shown in Figure 2-25. The trends for these gauges are summarized in Table 2-6

[2] See Section 2.6.2.3 for a discussion on "relative" sea level rise.

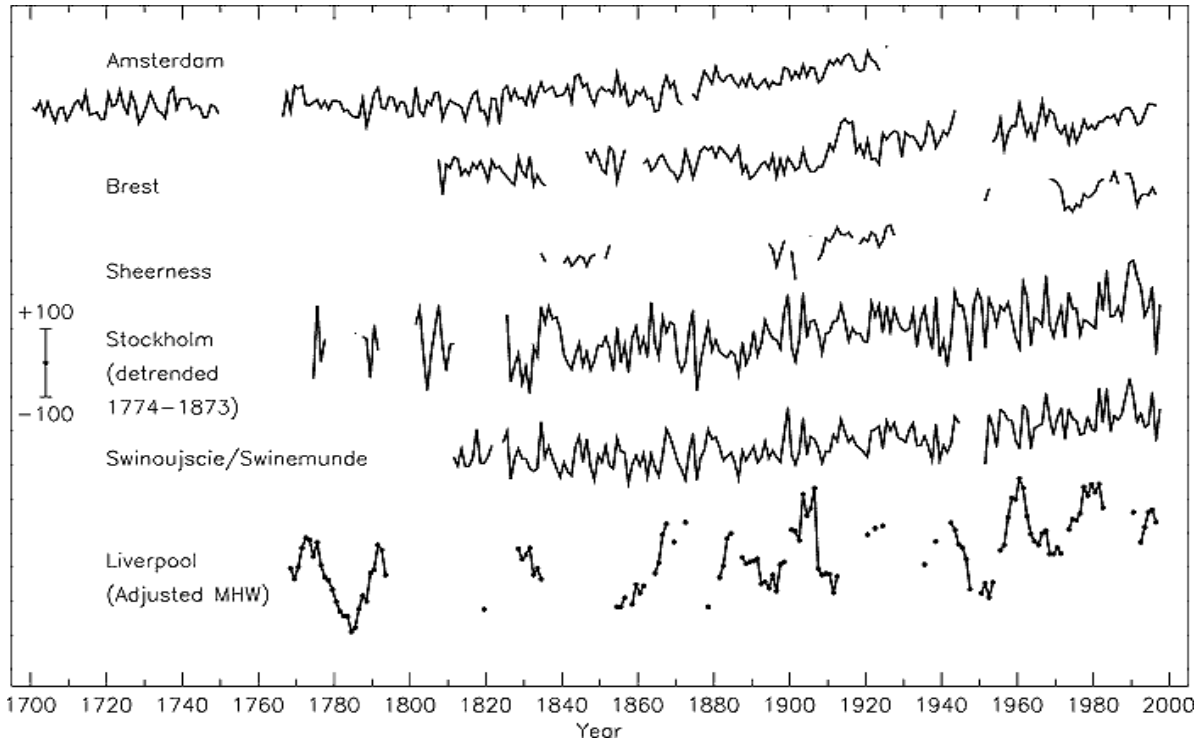


Figure 2-22 Relative Change in Sea Level Measured at Six Locations in Northern Europe Beginning at about 1700 AD

Locations: Amsterdam, Netherlands; Brest, France; Sheerness, UK; Stockholm, Sweden; Swinoujscie, Poland (formerly Swinemunde, Germany); and Liverpool, United Kingdom.
Scale: ± 100 mm.
Note: Data for Stockholm, Sweden is detrended over the period 1774 to 1873 to remove the first order contribution of postglacial rebound; Data for Liverpool, United Kingdom are "Adjusted Mean High Water" rather than Mean Sea Level and include a nodal (18.6 year) term.
Source: IPCCa, 2001
http://www.grida.no/climate/ipcc_tar/wg1/fig11-7.htm

This space intentionally left blank.

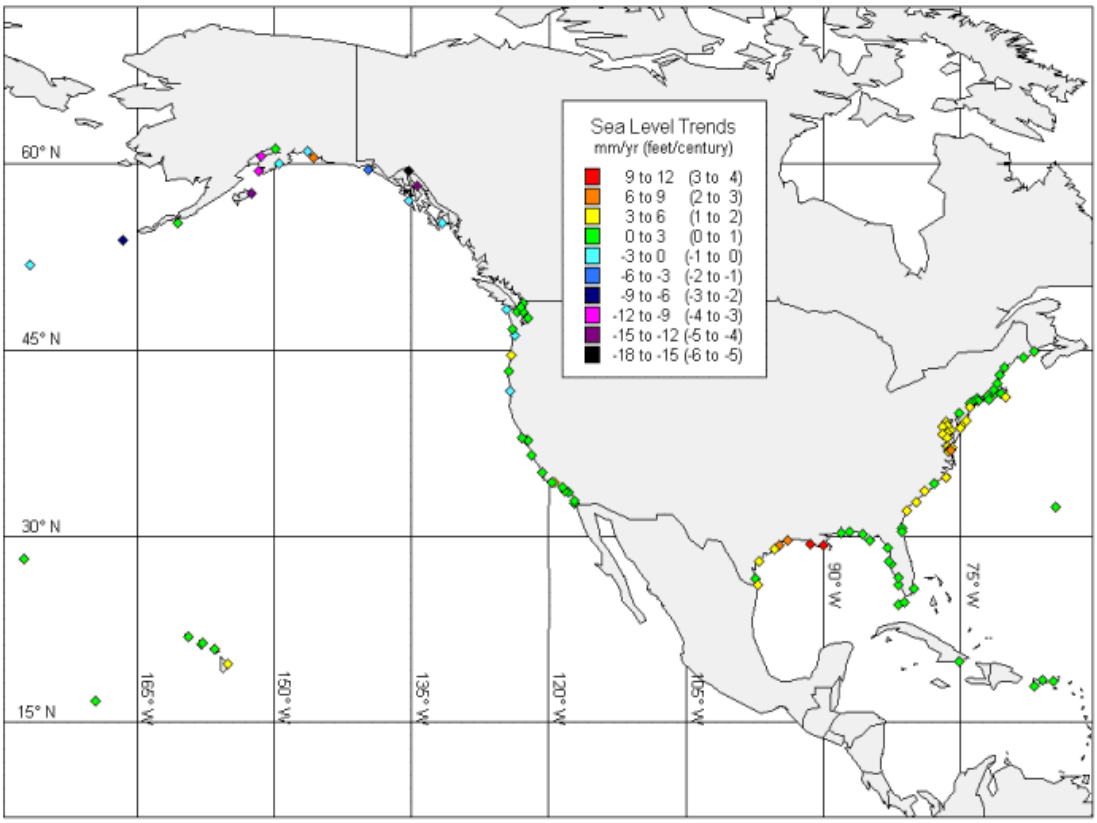


Figure 2-23 Rates of Relative Sea Level Rise Along the Coast of the United States
Source: National Oceanic and Atmospheric Administration, National Ocean Service, Center for Operational Oceanographic Products and Services' website at: http://co-ops.nos.noaa.gov/sltrends/slrmap.shtml .

This space intentionally left blank.

Table 2-5 Areas of the US Coast with Significant Amounts of Uplift or Subsidence

Coastline Area	Elevation Trend	Reason
Mid-Atlantic	Much of the coastline in this area is sinking slowly	Glacial rebound in the Hudson Bay region to the north
Mississippi River Delta region and the Texas coast	Sinking of the coastline--rapid sinking near the Mississippi River Delta	Lithospheric loading and sediment compaction due sediment deposition by the Mississippi River, and subsidence related to oil and gas extraction in some areas
Island of Hawaii	Sinking of the island	Lithospheric loading and local volcanic and seismic activity.
Portions of the coast of Northern California, Oregon, and Washington	Slow uplift	Tectonic effects
Portions of Alaska's coast and the Aleutian Islands	Rapid uplift	Glacial rebound and/or tectonic uplift, depending on the area

Source: Table developed from information obtained at: http://140.90.121.76/sltrends/slrmap.shtml and http://hvo.wr.usgs.gov/volcanowatch/1994/94_10_14.html

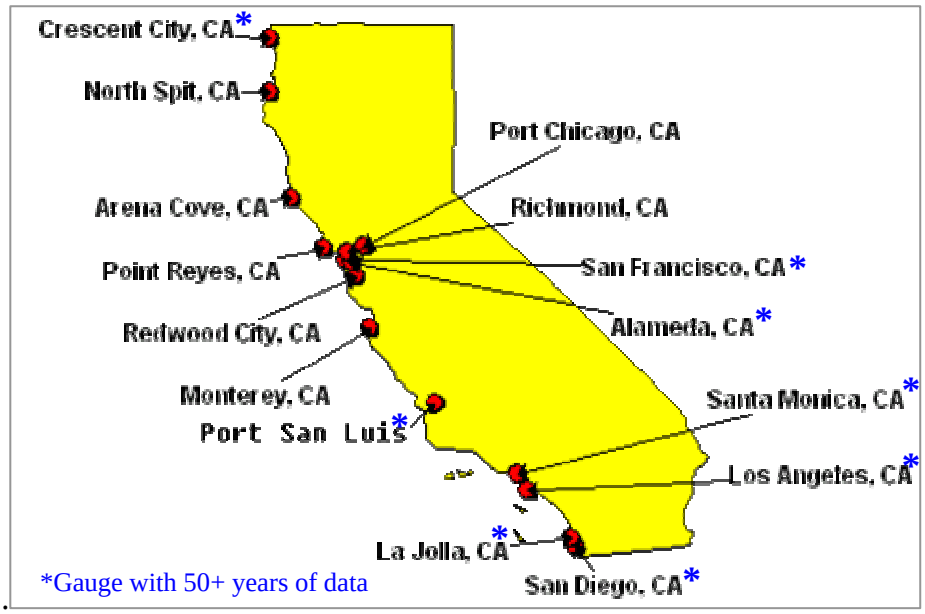
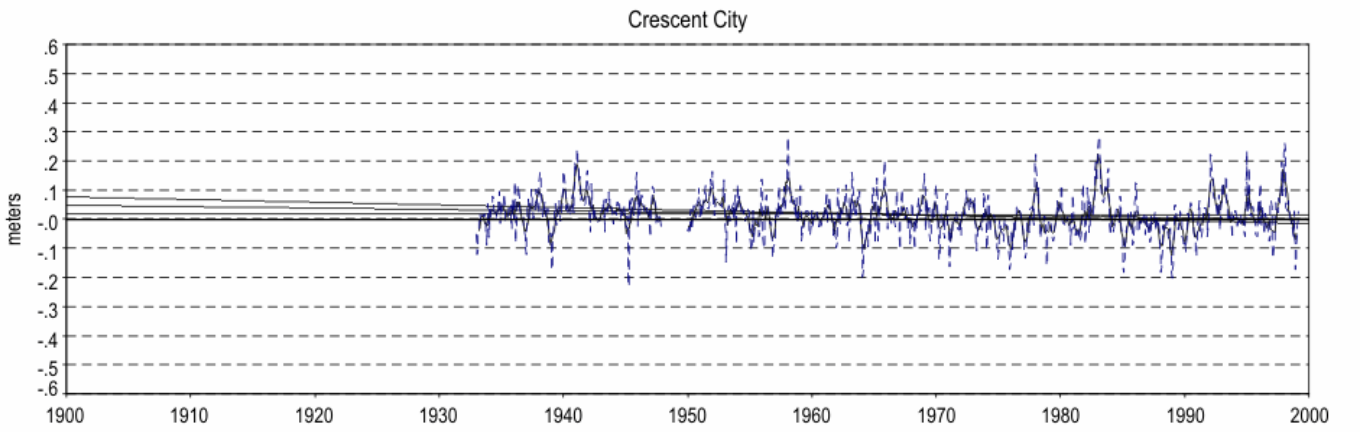
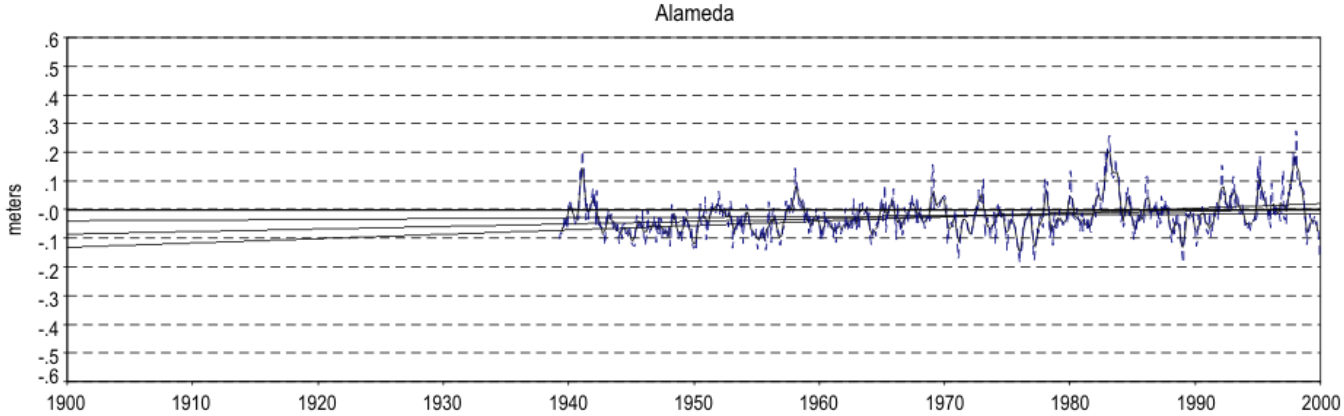


Figure 2-24 Location of Coastal Tide Gauges in California

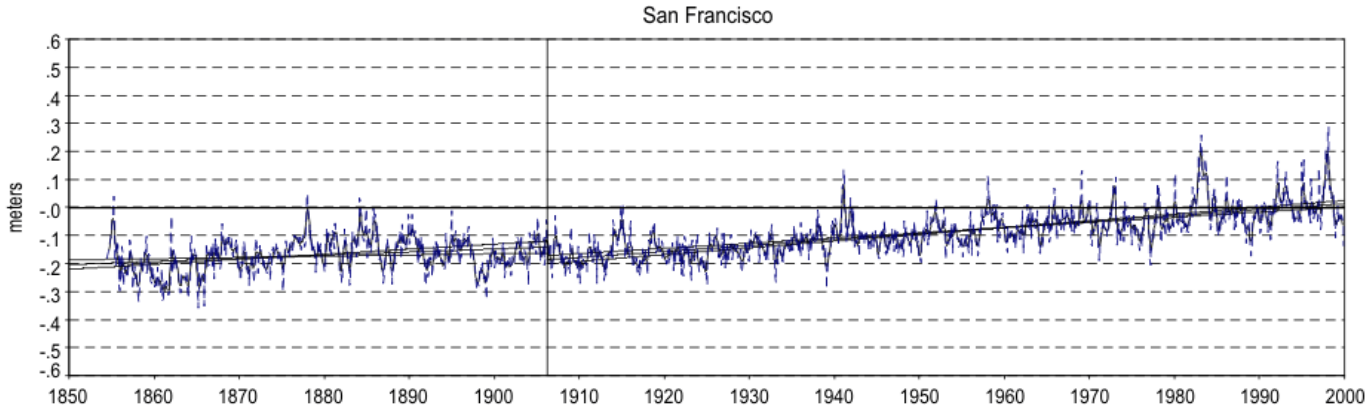
Adapted from: National Oceanic and Atmospheric Administration, National Ocean Service, Center for Operational Oceanographic Products and Services' website at: http://co-ops.nos.noaa.gov/sltrends/slrmap.shtml -- http://140.90.121.76/coastline.shtml?region=ca



Gauge No. 9419750--Crescent City. The mean sea level trend is -0.48 millimeters/year (-0.16 feet/century) with a standard error of 0.23 mm/yr based on monthly mean sea level data from 1933 to 1999.

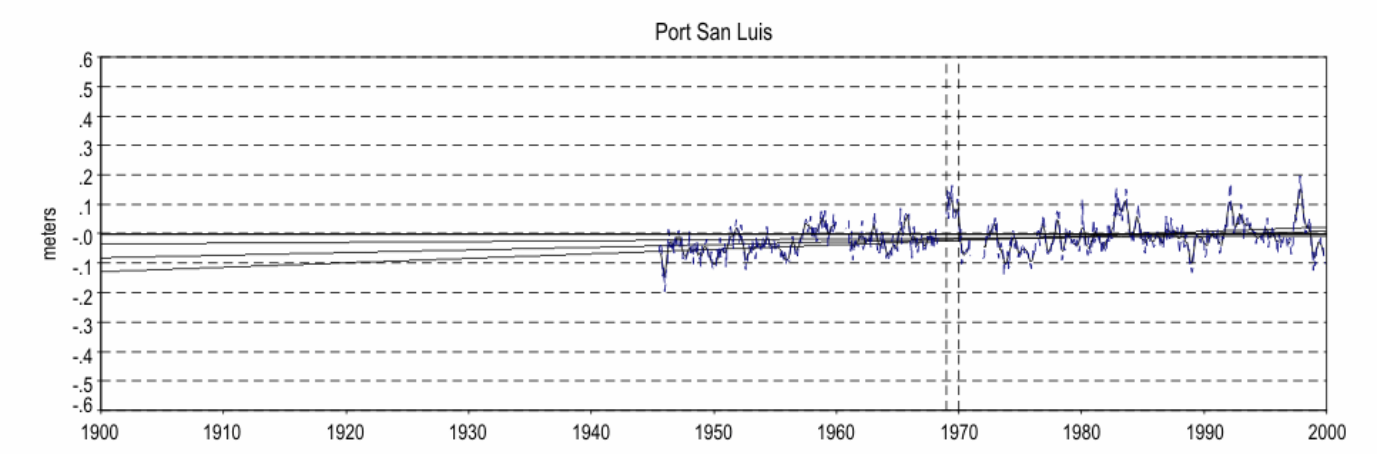


Gauge No. 9414750--Alameda. The mean sea level trend is 0.89 millimeters/year (0.29 feet/century) with a standard error of 0.32 mm/yr based on monthly mean sea level data from 1939 to 1999.

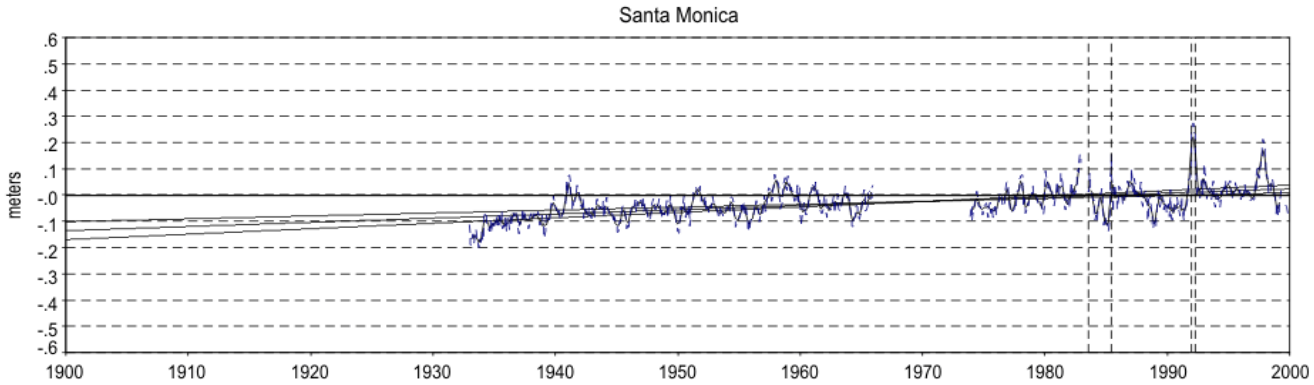


Gauge No. 9414290--San Francisco. The mean sea level trend is 2.13 millimeters/year (0.70 feet/century) with a standard error of 0.14 mm/yr based on monthly mean sea level data from 1906 to 1999.

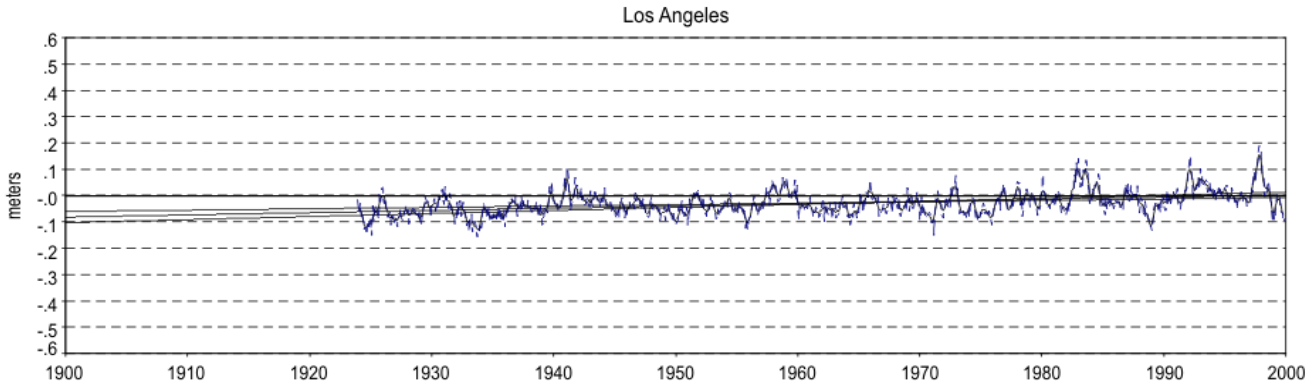
Figure 2-25 Relative Sea Level Trends for Eight Tide Gauges along California's Coast (part 1 of 3)



Gauge No. 9412110--Port San Luis**.** The mean sea level trend is 0.9 millimeters/year (0.30 feet/century) with a standard error of 0.32 mm/yr based on monthly mean sea level data from 1945 to 1999.

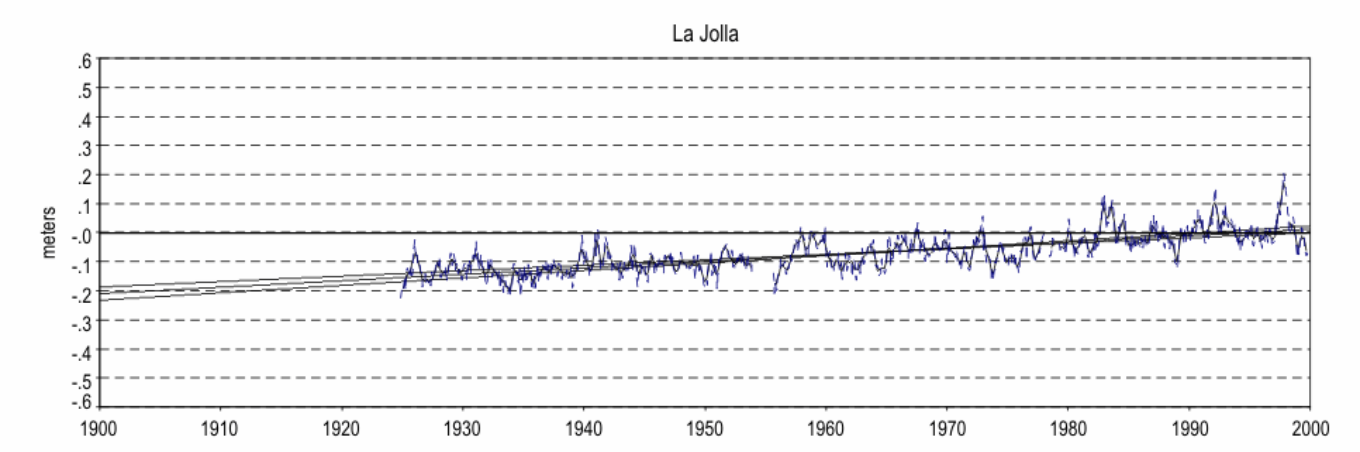


Gauge No. 9410840--Santa Monica. The mean sea level trend is 1.59 millimeters/year (0.52 feet/century) with a standard error of 0.25 mm/yr based on monthly mean sea level data from 1933 to 1999.

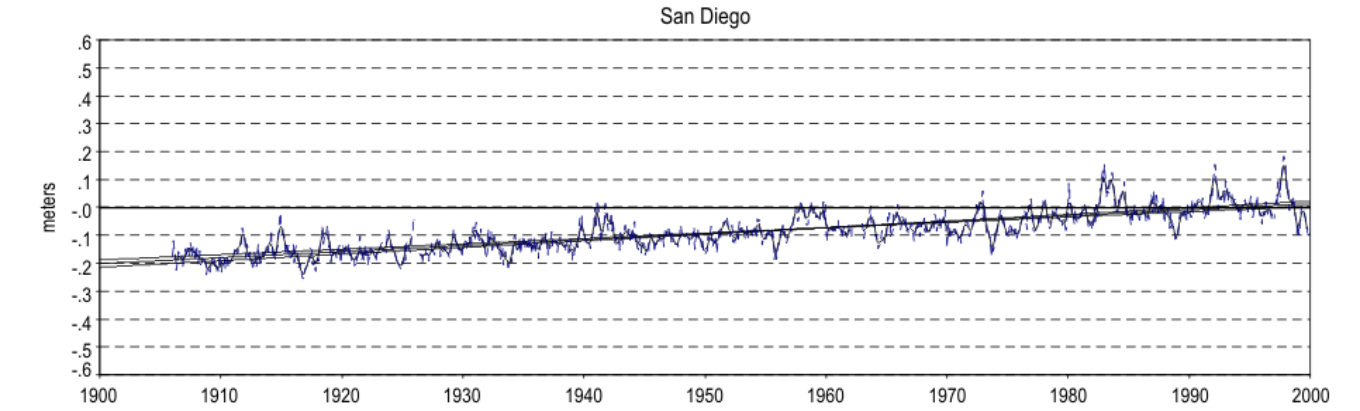


Gauge No. 9410660--Los Angeles. Mean sea level trend is 0.84 millimeters/year (0.28 feet/century) with a standard error of 0.16 mm/yr based on monthly mean sea level data from 1923 to 1999.

Figure 2-25 Relative Sea Level Trends for Eight Tide Gauges along California's Coast (part 2 of 3)



Gauge No. 9410230--La Jolla. The mean sea level trend is 2.22 millimeters/year (0.73 feet/century) with a standard error of 0.17 mm/yr based on monthly mean sea level data from 1924 to 1999.



Gauge No. 9410170--San Diego. The mean sea level trend is 2.15 millimeters/year (0.71 feet/century) with a standard error of 0.12 mm/yr based on monthly mean sea level data from 1906 to 1999.

Figure 2-25 Relative Sea Level Trends for Eight Tide Gauges along California's Coast (part 3 of 3)

Explanation: Solid blue curve is the five-month running average of monthly mean sea level with the average seasonal cycle removed. Linear trend lines illustrate 95 percent confidence interval after accounting for the average seasonal cycle. For most stations, the plotted values are relative to the 1983-2001 mean sea level datum recently established by the National Oceanic and Atmospheric Administration, National Ocean Service, Center for Operational Oceanographic Products (CO-OPS). Solid vertical lines indicate the occurrence of any major earthquakes in the vicinity of the gauge. Dashed vertical lines bracket any periods of questionable data.

Source: Graphs and explanations derived from National Oceanic and Atmospheric Administration, National Ocean Service, Center for Operational Oceanographic Products and Services' website at: http://co-ops.nos.noaa.gov/sltrends/sltrends_states.shtml?region=ca

Table 2-6 Relative Sea Level Trends for Eight Tide Gauges Along the Coast of California with 50 Years or More of Record

CO-OPS Gauge Number--Name	Sea Level Trend (feet/century)
9419750--Crescent City	-0.16
9414750—Alameda	0.29
9414290--San Francisco	0.70
9412110--Port San Luis	0.30
9410840--Santa Monica	0.52
9410660--Los Angeles	0.28
9410230--La Jolla	0.73
9410170--San Diego	0.71

Figure 2-25 and Table 2-6 show relative sea level along the coast of California is rising at all but one of the coastal gauges with 50 years or more of record. The one gauge showing a drop in relative sea level is at Crescent City. The apparent drop in sea level there is likely due to land-mass uplift given the gauge's proximity to the Mendocino Triple Tectonic Plate Junction. Information about this tectonic junction can be found at: http://pubs.usgs.gov/publications/text/Farallon.html.

The rate of relative sea level rise at the seven gauges with 50 years or more of record is fairly consistent with the worldwide sea level rise trend of 0.3 to 0.6 of a foot over the past century. Differences in the rate of rise at the various gauges may be due, at least in part, to changes in land mass elevation.

2.6.1.3 Projected Sea Level Rise

The Intergovernmental Panel on Climate Change projects worldwide average sea level to rise about 0.3 of a foot to 2.9 feet from 1990 to 2100 (IPCC, 2001a). The range in the projections reflects the results of multiple climate models for multiple greenhouse gas emission scenarios. Figure 2-26 depicts the varying sea level rise projections. A study by the U.S. Environmental Protection Agency published in 1995 assigned probability estimates for various magnitudes of sea level rise (Titus, 1995).

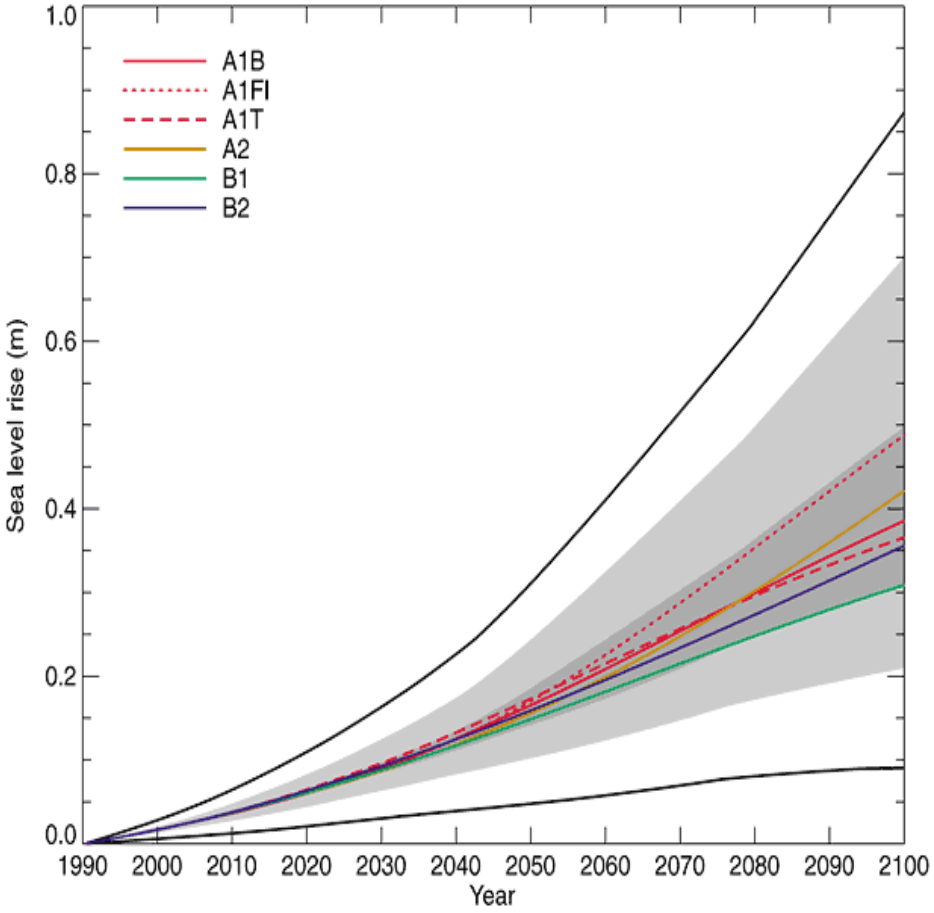


Figure 2-26 Projected Rise in Global Average Sea Level from 1900 to 2100

Source: Adapted from IPCC, 2001a (http://www.grida.no/climate/ipcc_tar/wg1/fig11-12.htm)
Explanation: Global average sea level rise from 1990 to 2100 for the SRES (Special Report on Emission Scenarios; IPCC 2000) scenarios and seven climate models. The region in dark shading shows the range of the average of models for all 35 SRES scenarios. The region in light shading shows the range of all models for all 35 scenarios. The colored lines in the key and in the graph represent the average of modeling results for six GHG emission scenarios. The region delimited by the outermost black lines shows the range of all models and scenarios including uncertainty in land-ice changes, permafrost changes and sediment deposition. This range does not allow for uncertainty relating to ice-dynamic changes in the West Antarctic ice sheet For additional explanation of this figure see IPCC, 2001a (http://www.grida.no/climate/ipcc_tar/wg1/index.htm).

As can be noted from Figure 2-26, many of the model projections for sea level rise show an acceleration in the rate of rise over that observed during the past century. This projected acceleration generally follows the projected acceleration in the rate of global average temperature rise by some climate models for some greenhouse gas emission scenarios (see section 2.4). As mentioned earlier, the rate of relative sea level rise experienced at many locations along California's coast is somewhat consistent with the worldwide average rate of rise observed over the past century. Therefore, it may be reasonable to expect that changes in worldwide average sea level through this century will also be experienced by California's coast.

As mentioned at the beginning of this section, sea level rise poses a significant threat for California. Perhaps the most noteworthy effect of sea level rise on California's water resources will be to the Sacramento-San Joaquin River Delta. Sea level rise over the next century will likely have a significant effect on the Delta's ecosystem, land uses and water supply function, even if the rate of rise over this century is about the same as that observed during the past century. Increased rates of rise, such as those projected for the highest levels of future greenhouse gas emissions and temperature rise could have profound effects on the Delta.

2.6.1.4 Short-Term Changes in Sea Level

Sea level rise at any given location is a function of changes in worldwide average sea level; however, local and regional effects superimposed on global trends can be significant. Rising or falling land elevations can affect what levels an area experiences. Land masses can rise or fall relative to the center of the Earth through tectonic movement. Changes in the elevation of a land mass can also occur due to the activities of humans, such as the extraction of petroleum or groundwater. For example, significant amounts of coastal land subsidence (up to 3 meters) have occurred on the coast of Texas near Houston and Galveston due to petroleum extraction. Groundwater extraction along the Texas coast has also caused subsidence (Gibeaut, 2000). In California, petroleum extraction in Long Beach has resulted in coastal subsidence, but in a limited area. Some coastal area subsidence has also occurred in the Santa Clara Valley south of San Francisco Bay as the result of groundwater extraction (DWR, 1998).

Changes in land elevation as the result of tectonic movement typically occur very slowly (relative to a human timescale), although local land masses have been observed to rise or sink rapidly as the result of seismic activity. As discussed earlier, coastal land masses that are subsiding (sinking) will tend to experience sea levels that appear to be rising faster than the worldwide rate of sea level rise. Coastal areas that are undergoing uplift (rising) will tend to experience sea levels that appear to be going up more slowly than the worldwide average, or will experience sea levels that appear to be declining or not changing compared to worldwide trends.

While rising worldwide average sea level and land mass elevation changes play a long-term role in sea levels experienced at a particular location, other effects can play an important role in the short term. Such effects include:

- gravitational effects of the sun and moon (astronomical tides)
- dynamic interaction of tides with coastlines
- ocean currents
- hydraulic and salinity changes caused by rivers (especially in bays and estuaries)
- barometric pressure
- interannual and decadal changes in ocean temperatures, such as the El Nino Southern Oscillation and the Pacific Decadal Oscillation[3], as well as periodic ocean temperature changes on other timescales
- waves and storm surge

[3] For more information concerning short-term changes in ocean temperature visit: (http://topex-www.jpl.nasa.gov/science/pdo.html)

Of these factors, all but the first two could be affected by climate change. Figure 2-27 and Figure 2-28 illustrate the variability of annual average relative sea level at the San Francisco and La Jolla tide gauges, respectively. These figures also show the 19-year running average of annual average sea level at each gauge for comparison. The 19-year running average was selected since all significant variations in the relative movements of the earth, moon and sun that affect astronomical tides complete their full cycle about every 18.6 years. The San Francisco tide gauge is located a short distance inside of the Golden Gate Bridge on the shore of the San Francisco Presidio. The La Jolla gauge is located at the end of the Scripps Institution of Oceanography pier in La Jolla.

Short-term changes in sea level at a particular location can be quite significant, especially when superimposed on long-term changes. The combined effect could place California's coastal resources and the Delta at an even greater risk than worldwide changes in sea level alone.

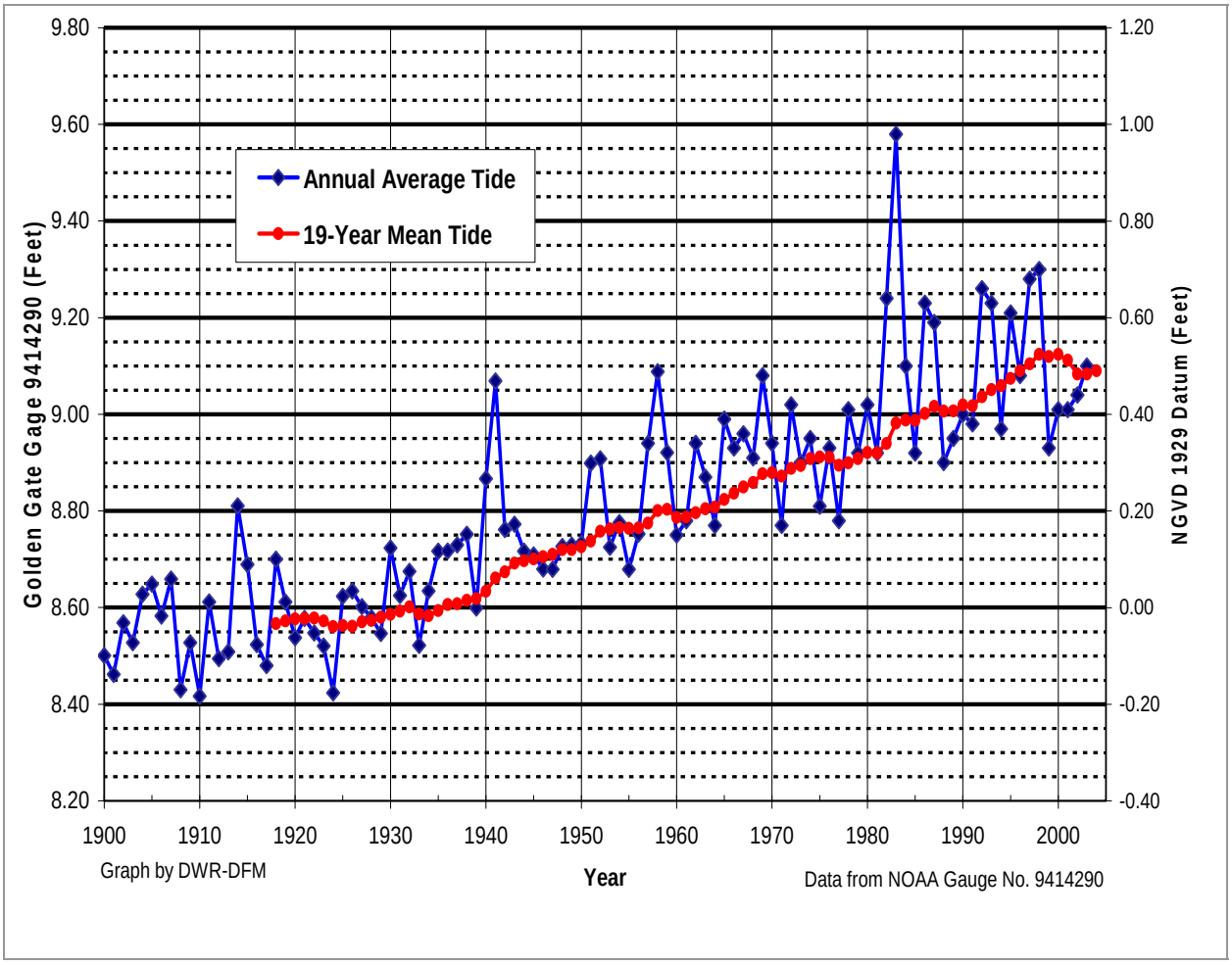


Figure 2-27 Graph of Annual Average Relative Sea Level and the 19-Year Running Average Sea Level at the San Francisco Tide Gauge

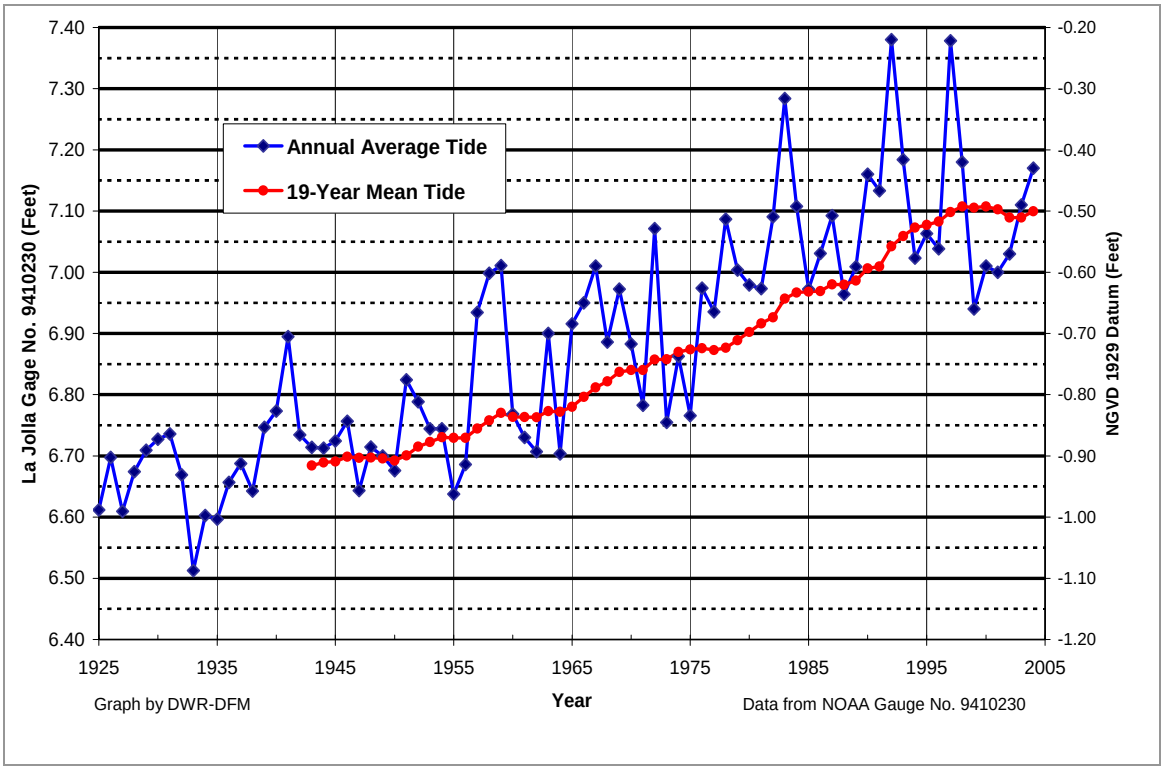


Figure 2-28 Graph of Annual Average Relative Sea Level and the 19-Year Running Average Sea Level at the La Jolla Tide Gauge

2.6.2 Consequences of Sea Level Rise

2.6.2.1 Sea Water Intrusion into Estuaries and River Systems

As mentioned previously, sea level rise during this century will cause increased sea water intrusion into California's coastal marshes and estuaries. Increased intrusion will likely disrupt marsh and estuary ecosystems, especially at the higher projections of sea level rise. Sea water intrusion into the Sacramento - San Joaquin River Delta could cause negative effects on fishes, as discussed in Section 2.9 and increase Delta salinity levels, as discussed in Chapter 5, Section 5.5. Increased salinity levels in the Delta would have a detrimental effect on Delta water supply operations if existing operations in the Delta remain the same and the Delta's configuration is not changed.

2.6.2.2 Sea Water Intrusion into Groundwater

Groundwater plays a significant role in providing California's water supply. In an average year, groundwater meets about 30 percent of California's urban and agricultural water demand. This percentage increases to more than 40 percent during drought years. In 1995, an estimated 13 million Californians, nearly 43 percent of the State's population, were served by groundwater. The demand on groundwater will likely increase as California's population grows (DWR, 2003).

Most of the State's groundwater is produced from alluvial groundwater basins. Alluvial basins are typically valleys that have been partially filled with sediment. Coarser sediment, such as sand, serves to store and transmit significant quantities of water to wells. Layers of finer sediment, such as clay, tend to restrict the movement of groundwater.

DWR has delineated 431 groundwater basins in California beneath about 40 percent of the State's surface area (DWR, 2003). The locations of these basins are illustrated in Figure 2-29.

More than 200 groundwater basins have been identified along the coast of California. Many of these basins play, or could potentially play a significant role in providing a local water supply. Many of California's larger urban areas, including the Los Angeles metropolitan area, overly coastal groundwater basins and derive a significant potion of their supply from groundwater. Regionally and nationally-significant agricultural areas that overlay coastal groundwater basins include the Salinas Valley, Santa Maria Valley and the Ventura-Oxnard Plain.

While most groundwater produced in coastal areas is derived from groundwater basins, groundwater is also produced from mountain and hillside areas underlain by rock, old marine deposits, or volcanic deposits. Such areas typically produce small quantities of groundwater compared to alluvial basins.

Figure 2-30 is a simple illustration of a cross-section of a coastal groundwater basin. The deposits of some coastal groundwater basins in California extend a significant distance beyond the coastline and contain saline ocean water. Under natural conditions, fresh water in coastal aquifers flows toward the ocean keeping saline ocean water from moving inland. However, if inland groundwater levels are lowered through pumping, ocean water may move inland.

Many groundwater basins along California's coast are very susceptible to sea water intrusion, or the intrusion of brackish water from bays and estuaries. Sea water intrusion into California's coastal aquifers was first noted in the 1930s and 1940s. Some of the earliest observations were in Los Angeles and Orange counties. Other areas where a significant amount of seawater intrusion has occurred include Ventura, Santa Cruz and Monterey counties, and some areas around San Francisco Bay and the Sacramento-San Joaquin River Delta. (DWR, 1958; DWR, 1975; DWR, 2003). Sea water intrusion in the Salinas Valley has been observed as far as 5 miles inland (DWR, 1994).

Rising sea level increases the potential for sea water intrusion into coastal groundwater aquifers and other coastal groundwater resources by increasing the pressure of ocean water exerted against water-bearing deposits extending inland from the coast. Rising sea level can also increase the potential for intrusion of sea water into coastal groundwater basins through the inundation of areas that were formerly above sea level.

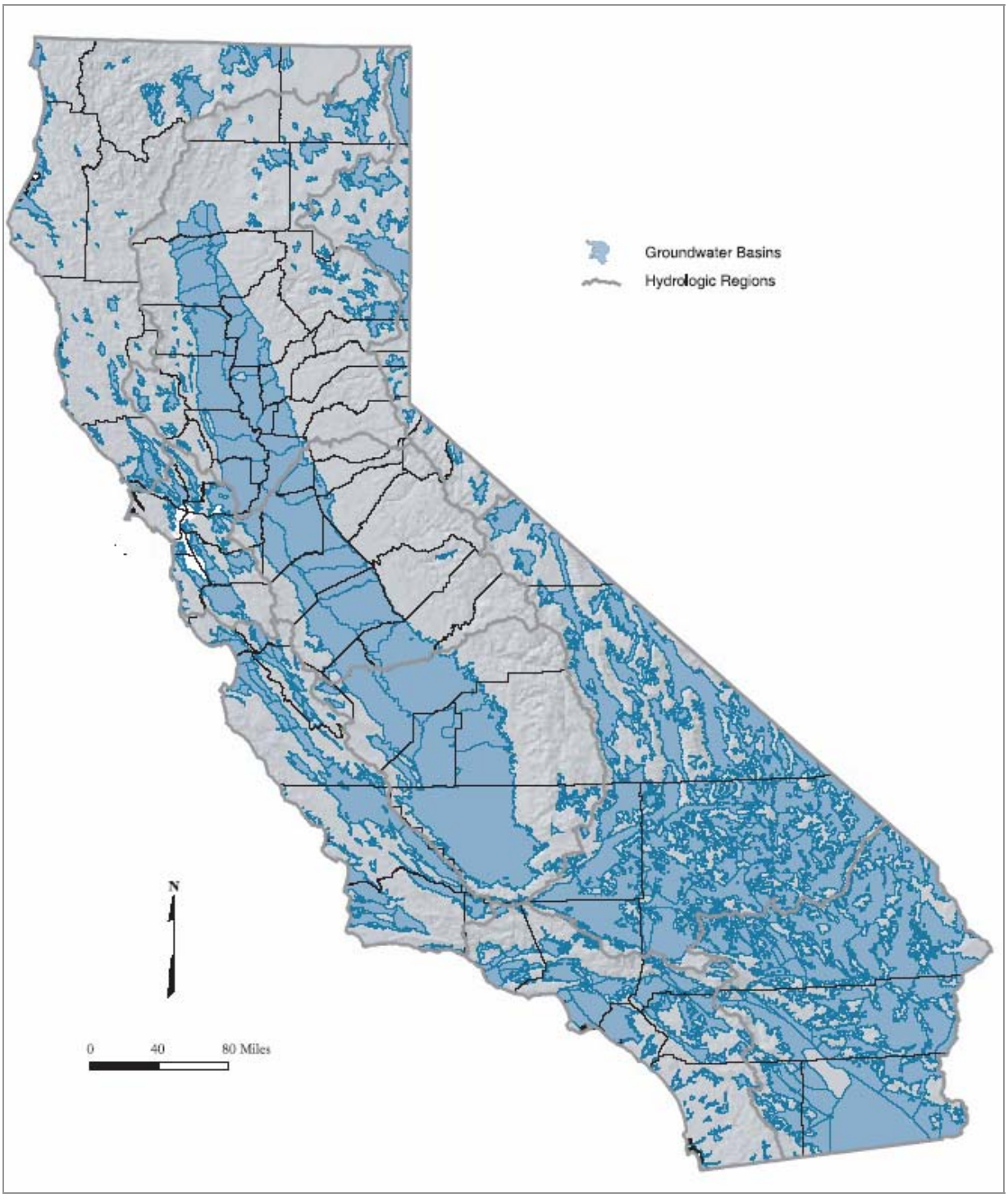


Figure 2-29 California's Groundwater Basins

Source: DWR, 2003

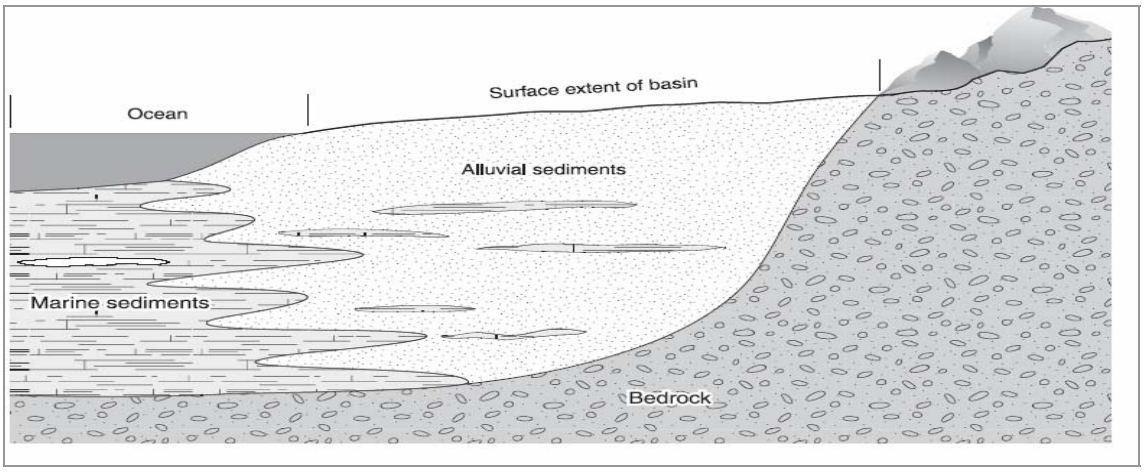


Figure 2-30 Simplified Cross-Section of a Coastal Aquifer
Source: DWR, 2003

The threat posed to coastal groundwater resources by sea level rise can be lessened by various means including controls on well construction and groundwater production, and the operation of hydraulic barrier projects. Hydraulic barrier projects typically involve the injection of treated wastewater or imported water into coastal aquifers to prevent ocean water from moving inland.

The threat to groundwater from the inundation of land by sea level rise can be lessened through shoreline engineering, such as the installation of sea walls. It is anticipated that shoreline engineering projects will be undertaken along many low-lying areas of California's coast to protect areas with high real estate values. Shoreline engineering may be difficult, impractical, or environmentally unacceptable for some of California's bays, estuaries and coastal marshes. Some of these areas might be subject to uncontrolled inundation due to sea level rise.

2.6.2.3 Flooding Risk in the Sacramento-San Joaquin River Delta

The Sacramento-San Joaquin River Delta is highly susceptible to flooding. The Delta includes 70 islands and tracts. Most have land surfaces at or below mean sea level. Land surface on some Delta Islands is as much as 25 feet below mean sea level (DWR, 2005a). The location of the Delta is depicted in Figure 2-19, and a detailed view of the Delta and its islands is shown in Figure 2-31.

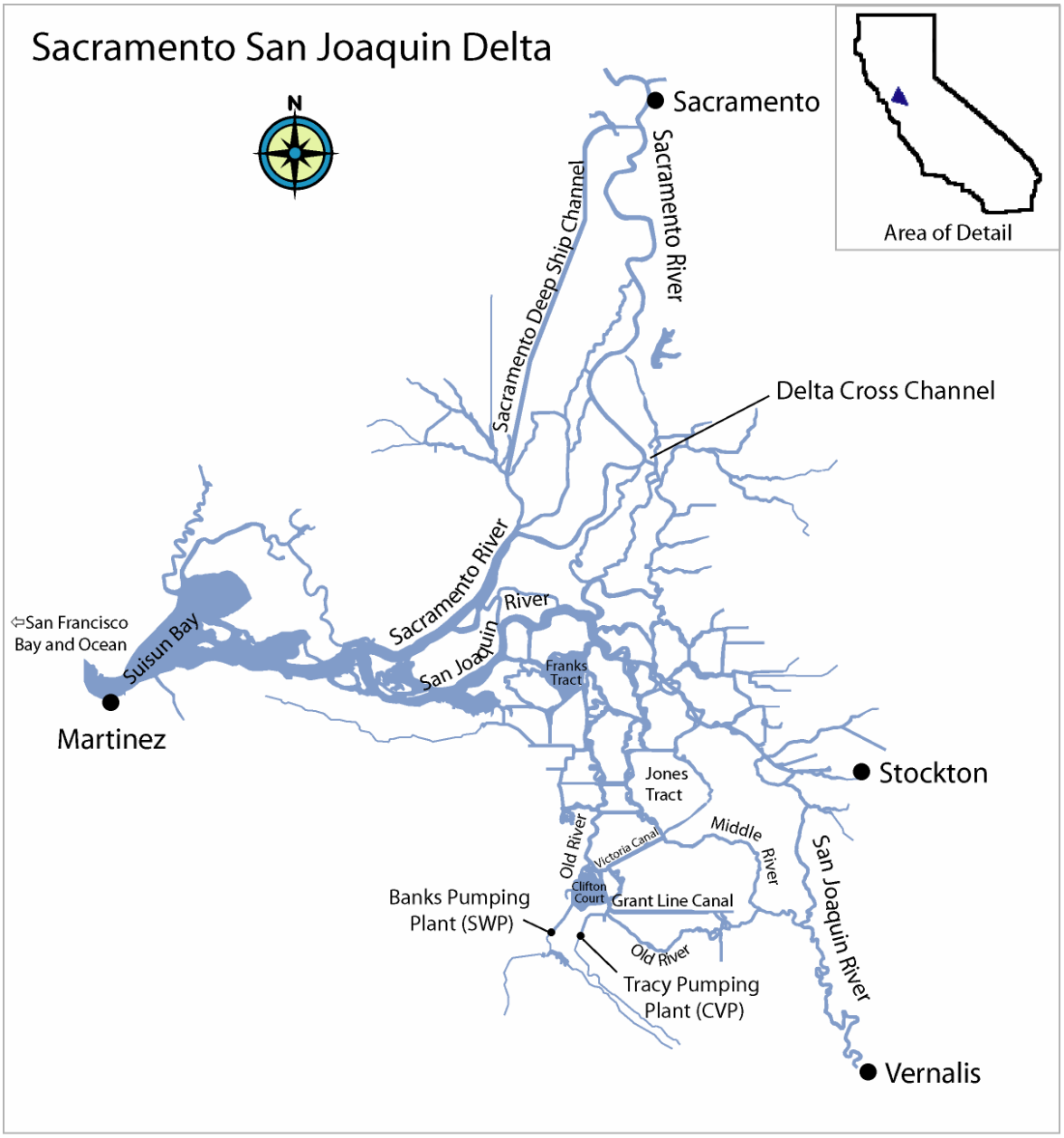


Figure 2-31 Sacramento-San Joaquin River Delta

The islands and tracts of the Delta are protected from the constant threat of inundation by about 1,100 miles of levees. Levee failure can occur due to seepage, piping, slippage, subsidence, sloughing or earthquakes, even during dry weather. Levee failure impacts include potential loss of human life, irreparable harm to the Delta's fragile ecosystem and its listed and endangered species, disruption of utilities and highways and water supply disruption. Water supply disruption can occur when levee failure and island flooding cause salinity levels in the Delta to increase to unacceptable levels due to:

- large amounts of saline ocean water to being drawn into the Delta from the San Francisco Bay, and
- increases in the volume of the Delta's tidal prism and resultant increases in the tidal exchange of saline water in the Delta.

Once a levee fails in the Delta and island flooding occurs, salinity conditions can take weeks or even months to return to normal, depending on the amount and location of levee failures and hydrologic conditions.

2.6.2.3.1 Future Increased Risk of Flooding in the Delta Due to Land Surface Subsidence and Climate Change

Flood risk in the Delta is increasing with time due to land surface subsidence and sea level rise. Land subsidence and sea level rise also increase the consequences of levee failure.

As mentioned earlier, worldwide average sea level rise is projected to be about 0.3 of a foot to 2.9 feet from 1990 to 2100 (IPCC, 2001a). Rising sea levels are likely to have a direct effect on water levels in the Delta because the bottom of essentially all Delta channels and waterways are at or below current mean seal level. Rising sea level will cause backwater effects upstream of the Delta.

Global sea level rise combined with short-term or episodic factors that increase sea level and water levels in the Delta will reduce available levee freeboard unless levees are raised. Short-term and episodic increases in water levels in the Delta include high river flows, ocean/atmosphere phenomena such as El Nino's, storm surge, barometric high tides and high astronomical tides (particularly during perigee, perihelion, and either new or full moon). Figure 2-32 illustrates the relative impact that sea level rise will have on astronomical tides in the Delta. An especially high level of risk would occur if several periodic events were to occur at the same time in the Delta.

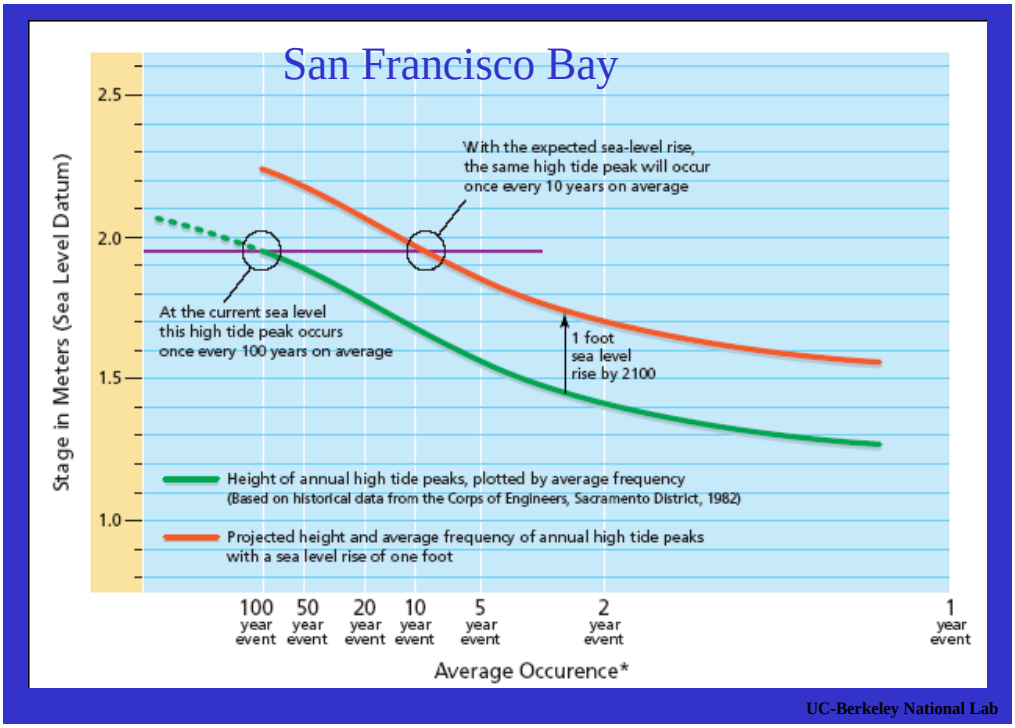


Figure 2-32 Impact of One Foot of Sea Level Rise on the Relative Effect of Astronomical Tides in the Delta

Source: Lawrence Berkeley National Lab (Miller, 1998).

Climate change may affect the magnitude and frequency of flood flows entering the Delta. In their paper on the potential impacts of climate change on California hydrology, Miller and others (2003) present peak river flow data based on climate change simulations. These data show an increased probability of higher annual peak flows for Central Valley rivers. These potential increased flows have yet to be quantified with any confidence. Higher flows will lead to higher water surface elevations in the Delta, especially in its upper reaches.

Ocean temperature anomalies, such as an El Nino, can cause a short-term rise in sea level along California's coast and thus increase water levels in the Delta. For example, the maximum water surface anomaly associated with the 1997-1998 El Nino event increased the level of the ocean along California's coast between about 0.6 to 0.8 of a foot during January 1998 (Bromirski, 2005). This level of rise was due to a combination of steric effects and poleward propagating, coastally-trapped waves. Climate change may increase the frequency or duration of El Nino events (Wara, 2005), although there is a significant amount of uncertainty about possible changes in the nature and occurrence of temperature anomalies in the Pacific as the result of climate change (Kerr, 2005).

Wind driven storm surge can also increase water surface elevations in the Delta. Stronger winds associated with some winter storms would lead to even greater changes in water surface

elevations. Such changes are a function of channel geometry and the distance of open water with respect to wind direction, referred to as "fetch."

Subsidence also must be considered as a risk to Delta levees. The surfaces of many of the Delta's islands and tracts are dominated by soils rich in peat. Peat is a complex organic material that is principally composed of degraded plant matter. Subsidence in the Delta primarily occurs when peat soils are exposed to oxygen and undergo microbial decomposition due to agricultural practices. Subsidence also occurs when peat soils are lost by wind erosion and occasional peat fires. The peat soils of the Sacramento-San Joaquin Delta have subsided at rates of up to about 2 inches per year in the past. Subsidence rates have been the highest in the central Delta islands (Mount, 2004).

Subsidence increases the threat of flooding in the Delta by increasing the differential forces that levees experience. Subsidence also increases the volume of water that can inundate an island or tract when a levee fails. Together, the continued subsidence of Delta islands and rising sea level pose a double-sided threat for Delta levees and flooding. Other factors such as possible increases in peak river flows as the result of climate change further increase the threat to Delta levees.

2.7 Future Water Demand

California's water supply future will be determined by two principal factors, the condition of the State's water resources and water demand. Climate change will likely have a significant effect on California's future water resources, as discussed elsewhere in this report. Climate change will likely also have an effect on future water demand. However, many other factors such as population, land development and economic conditions that are not directly related to climate change will also affect future demand. Table 2-7 provides a summary of some of the potential effects of climate change on future water demand. Table 2-8 lists selected factors that could affect future water demand that will not be directly affected by climate change.

Today there is much uncertainty about future water demand, especially those aspects of future demand that will be directly affected by climate change and warming. While climate change is expected to continue through at least the end of this century, the magnitude and, in some cases, the nature of future changes are uncertain. This uncertainty serves to complicate the analysis of future water demand, especially where the relationship between climate change and its potential effect on water demand is not well understood.

Of the water demand factors that could be directly affected by climate change, potential changes in evapotranspiration, agronomic practices, and environmental water demand might be the most significant for California. Of the changes in demand not directly affected by climate change, changes in demand related to population growth and technological innovation could be the most significant. The following discussion is mostly limited to these aspects of future water demand. Chapter 7 provides additional discussion on evapotranspiration and possible changes in evapotranspiration due to climate change.

Table 2-7 Summary of the Potential Effects of Climate Change on Future Water Demand

Type of Demand	Potential Effect
Crop Irrigation	Increasing temperatures will increase evapotranspiration rates and related water demand where all other factors remain unchanged. Increasing concentrations of atmospheric carbon dioxide may act to reduce increases in plant transpiration (a component of evapotranspiration) in response to increased temperatures. Other factors related to climate change, such as possible changes in humidity, cloudiness and wind could also affect evapotranspiration rates. Evaporation rates from soil and plant surfaces may rise due to temperature increase, depending on changes in other factors that affect evaporation rates. Increased evaporation rates could increase salt accumulation on plant surfaces, especially where overhead irrigation is used. Salt accumulation in surficial soils could also increase. Additional irrigation water demand may result because of possible increased salt control requirements. Some changes in crop type, planting cycles, time of planting, and crop productivity will likely occur as the result of increased temperatures. Statewide and regional irrigation water demand may increase or decrease as the result of these changes. Use of water for frost protection will likely be reduced with increasing temperatures and projected reductions in the annual number of days when frost occurs. Frost protection is typically an important consideration for orchards and vineyards.
Landscape Irrigation	Increased temperatures, as well other atmospheric/climatic factors related to climate change, will affect landscape irrigation in manner similar to that described for crop irrigation, above.
Domestic Water Uses (excluding landscape irrigation)	Domestic water use typically increases with increasing temperature. Increased water demand can occur due to the use of evaporative cooling, increased laundering of clothing, increased bathing, increased drinking water requirements for humans and pets and recreational uses of water.

Table 2-7 Summary of the Potential Effects of Climate Change on Future Water Demand (continued)

Type of Demand	Potential Effect
Commercial and Industrial Water Use (including agro-industrial facilities such as dairies, poultry farms, packing plants, etc.)	Commercial and industrial water use will likely increase as the result of warming due to such factors as increased evaporative cooling demand. Increased consumption of water by concentrated animal feeding facilities, such as dairies and poultry farms, would also likely occur.
Evaporation Losses from Natural Water Bodies and Open Water Storage and Conveyance Facilities	Evaporation losses from water bodies and open conveyances will probably increase as the result of rising temperatures especially in arid portions of the State with low humidity and limited cloud cover.
Environmental Water Requirements	Delta outflow requirements will likely increase to maintain Delta salinity conditions in response to sea level rise; if the Delta's existing configuration, operation of its water supply facilities, and its ecosystem conditions are to remain as they are now. Higher temperatures will likely result in increased environmental water demand for controlling water temperatures for sensitive aquatic species, including anadromous fish. Increased use of reservoir storage and thermal control releases from reservoirs will be required for controlling aquatic habitat temperatures.

Table 2-8 Selected Factors Affecting Future Water Demand in California that are Not Directly Related to Climate Change

Factor	Potential Effect
Population Change	Future increases in population will affect water demand, depending on the location and types of development needed to support an increased population. The conversion of agricultural lands into housing and related community development may not result in a significant increase in water use for a given area, depending on the agricultural use(s) that existed prior to land conversion, and on the type of housing and other facilities constructed. Redevelopment and densification of existing urban land may result in increased water demand in some areas. Development of raw, uncultivated land will directly increase water demand. In general, increases in California's population will tend to increase future water demand.
Changes in Agriculture	Changes in the type and amount of crops grown due to changes in agricultural markets and government crop subsidy programs may help increase or decrease agricultural water demand.
Changes in Landscaping Practices	Changes in consumer preferences and changes in land use ordinances relating to landscaping may affect future landscape water demand.
Changes in Environmental Water Use Requirements	The findings of continuing scientific research related to the condition and preservation of aquatic ecosystems in the State, including the Delta, may affect environmental water demand.
Water Law and Policy	Changes in water law and policy could affect water demand.
Technological Innovation	Lowered consumption rates could result from improvements in water use efficiency for irrigation, domestic, commercial, and industrial uses. Increased reuse of wastewater could help reduce demand on existing and future sources of water. Advances in desalinization technology may reduce demands on the State's freshwater resources, especially in areas along the south coast.

2.7.1 Evapotranspiration

The collective term *evapotranspiration* refers to the vaporization of water from soil and plant surfaces (i.e., evaporation) and vaporization that occurs in plant leaves with water diffusing through pores (stomata) to ambient air (i.e., transpiration). Transpiration is controlled by water availability from the soil, plant morphological and physiological characteristics, and atmospheric conditions which determine how much energy is available to vaporize water inside leaves. Climate and plant type are important determinants of evapotranspiration rates. Even small increases in evapotranspiration rates from crops and landscaping as the possible result of climate change could affect California's overall water demand. This is because of the relatively large amount of the State that is dedicated to irrigated agriculture and the significant amount of landscaping in urban areas.

Increased temperature and atmospheric carbon dioxide concentrations are the two most consistently projected aspects of climate change that will impact evapotranspiration rates for crops and landscaping in California. Hidalgo and others (2005) concluded that a temperature increase of 3 degrees Celsius will result in a 5 percent increase in plant transpiration, unless there is a compensating decrease in solar radiation or other component of the plant energy budget. Increasing carbon dioxide concentrations in the atmosphere may tend to reduce transpiration losses from plants. Other important factors affecting evapotranspiration include wind, dew point (humidity), cloudiness and minimum temperature.

A number of studies related to physiological, biochemical and phenological plant responses to increased atmospheric carbon dioxide concentrations have been published including those studies using data from the 18 free-air carbon dioxide enrichment research sites around the world (Long, 2004). Stomatal responses at elevated atmospheric carbon dioxide concentrations seem to decrease water vapor diffusion; however, more information is needed to better understand the effects of increasing concentrations of atmospheric carbon dioxide on transpiration.

Increased atmospheric carbon dioxide concentrations may also serve to increase vegetal production. Possible increases in production could, in turn, serve to increase total transpiration from individual plants, as well as increase the per-plant water demand for tissue production and direct evaporation from vegetal surfaces. Long and others (2004) found that carbon dioxide concentrations expected by mid-century would increase dry matter production about 20 percent and seed yield by 24 percent for some plant types, including most crops and trees.

Urbanization can affect local evapotranspiration rates through regional greenhouse gas emissions, increasing amounts of plant physiological stressors such as atmospheric ozone, and through higher temperatures associated with urban island heat effects. Slone and others (2005) reported that temperatures over urban centers can be elevated while temperatures over irrigated land tend to be lower than temperatures over undeveloped areas. A significant increase in urbanization in California is expected by the end of this century.

2.7.2 Agronomic Practices

As noted in Table 2-7, climate change and increasing temperatures can affect total crop water demand by inducing changes in crop type, planting cycles and time of planting. Few studies have assessed the possible impacts of climate change on crop patterns in California (Hayhoe, 2004).

Plant physiological responses to increasing temperature will be mixed, therefore there are likely to be varying agronomic responses to climate change. For example, fewer frost days would allow citrus production to extend to higher latitudes and elevations, including in the Central Valley. However, fewer frost days would be detrimental for tree crops having a chill requirement.

There has been a long-term shift toward planting permanent crops in many parts of California, such as trees and vines. Climate change may increase the variability in precipitation and increase the frequency of droughts. Since agricultural water supplies tend to be curtailed before urban supplies during droughts, the possible consequences of increased droughts for agriculture could become more severe because of increased planting of permanent crops. Droughts typically do not cause lasting damage where crops are planted annually.

2.7.3 Changes in Environmental Water Demand

Climate change could have a significant effect on environmental water demand in California. Two aspects of environmental water demand that will likely be impacted the most are salinity control requirements for the Sacramento-San Joaquin River Delta and temperature control demand for various rivers and the Delta.

2.7.3.1 Delta Salinity Control

The Delta is a key component of California's water supply infrastructure. A major portion of the State's agricultural and urban water supply passes through the Delta to State Water Project and Central Valley Project water diversion facilities.

Salinity levels in the Delta depend on outflow from the Delta to the San Francisco Bay and Pacific Ocean. Saline water from the San Francisco Bay is pushed out of the Delta during periods of high Delta outflow. Saline water can enter the Delta and increase salinity a significant distance inland during low outflow.

Delta outflow primarily depends on the amount of freshwater entering the Delta and the diversion of water from the Delta for the Central Valley Project, the State Water Project, and in-Delta uses which collectively reduce outflow. Most of the inflow to the Delta comes from the Sacramento, Cosumnes, Mokelumne, and San Joaquin rivers. Flows from these rivers are typically highest during the winter and spring in response to annual precipitation and snowmelt. The lowest flows typically occur in the late summer and fall.

The greatest challenge for maintaining salinity levels in the Delta typically comes in the late summer and fall when natural Delta inflow is usually the lowest. Reservoir releases during this

time help maintain river flows into the Delta in the absence of enough natural runoff. The rate of pumping from the Delta can be reduced during this period to help maintain Delta outflow and prevent salinity intrusion. Pumping operations have been severely cut back during dry years; especially when reservoir storage levels are very low due to drought.

As discussed in Section 2.5, climate change is expected to cause more precipitation in the form of rain rather than snow, reductions in water storage in annual snowpack, earlier snowmelt and sea level rise. Each of these factors could present significant reservoir management challenges, particularly for reservoirs in the Sierra foothills. These reservoirs will likely experience changes in the rate and timing of inflow. Changes in reservoir operations and reduced annual storage in snowpack could result in less water being available in the summer and fall to meet Delta outflow and salinity control requirements.

2.7.3.2 Water Temperature Control

Increased air temperatures as the result of climate change will likely increase water temperatures in the State's lakes and waterways. Increased water temperatures pose a threat to aquatic species that are sensitive to temperature, including anadromous fish. Increased water temperatures will also cause decreased dissolved oxygen concentrations in water and other water quality changes, and will likely increase production of algae and some aquatic weeds.

Intermittent temperature problems now exist for some aquatic species in some Central Valley rivers and streams, and in portions of the Delta. Intermittent temperature problems also occur in other areas of the State; including in the Klamath, Eel, and Russian river basins. High water-temperature problems typically occur during the summer and early fall.

Water resource managers often release cold water stored in reservoirs to control downstream water temperatures for aquatic life. Most of the water held in the State's reservoirs is accumulated in the winter and spring when temperatures are lower than at other times of the year. Reservoirs that are downstream of significant snowpack receive cold water from snowmelt through the spring and sometimes into the summer.

Climate change and rising temperatures will increase demand for temperature control releases from many reservoirs. However, coldwater storage in reservoirs needed to supply releases may decrease as the result of climate change due to:

- diminished snowpack and less inflow of late-season cold snowmelt, especially for lower elevation reservoirs in the Sierra Nevada
- increased heating of reservoir inflow
- increase heating of reservoir content and releases
- possible loss of reservoir storage for thermal control releases due to changes in reservoir operations in response to changes in runoff timing

Increased temperature control requirements together with a possible decreased capacity to provide temperature control releases from reservoirs as the result of climate change, could pose a double-sided threat for some aquatic species.

2.7.4 Population

California has experienced rapid population growth since the mid 1800s. This growth is due in part to California's strong economy, natural beauty and relatively mild climate.

California's population is approaching 37 million. The California Department of Finance projects the State's population to be about 44 million by 2020 and about 55 million by 2050 (DOF, 2004). California's population could be as high as 90 million by the end of the century (Landis, 2003). Figure 2-33 depicts growth in the State's population from 1850 to 2005, and projected growth to 2050.

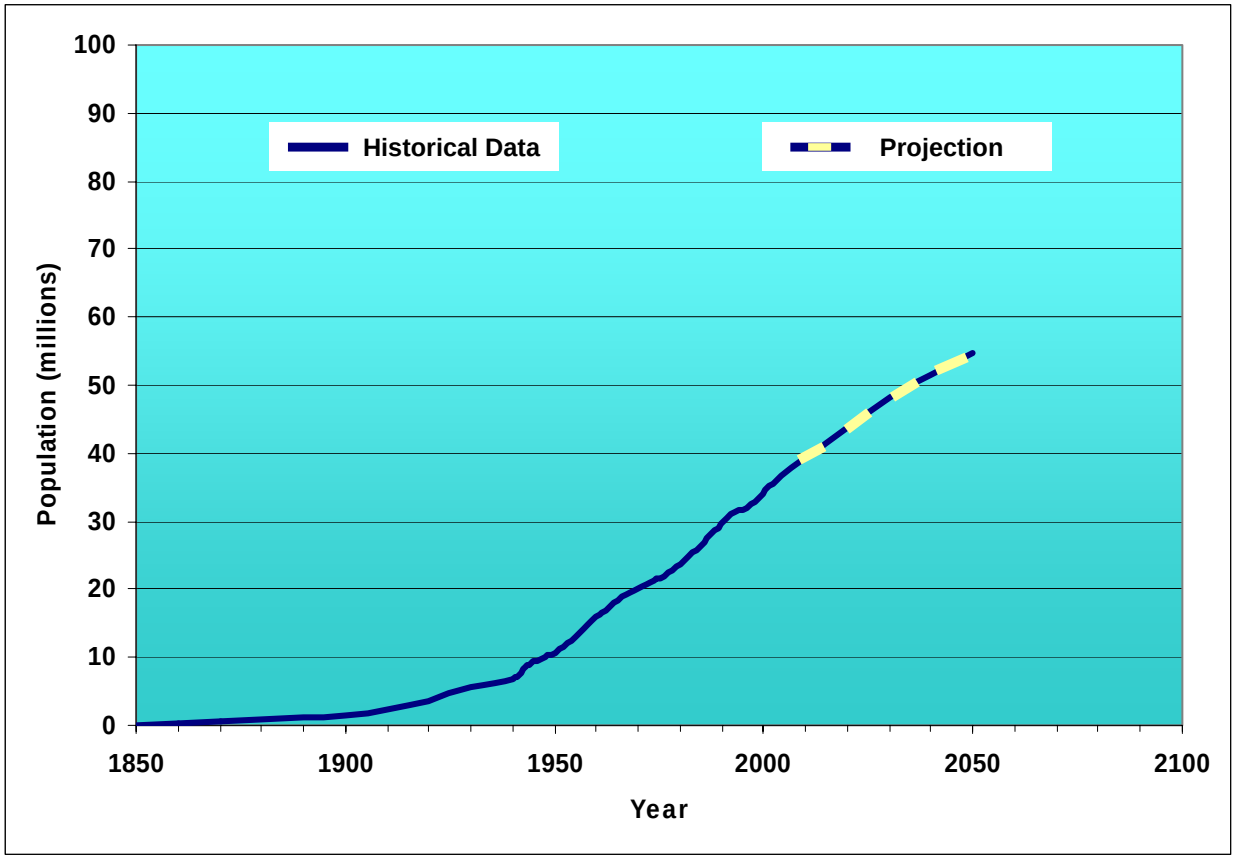


Figure 2-33 Historical and Projected Future Population Growth in California

Data source: DOF (2005)

Future increases in population will affect water demand, depending on the location and types of land development that occur to support an increased population. Much of California's future development is projected to occur on valley floor areas, including in the Central Valley along major transportation systems (Landis, 2003). While climate change is generally not expected to have a major effect on future population growth in California, it could have some effect on the where development occurs.

The conversion of agricultural lands into housing, commercial and industrial uses may not result in an increase in water use for a given area, depending on the agricultural use(s) that existed before conversion and on the specific type of development. Redevelopment and densification of existing urban land may result in increased water demand in some areas. Urbanization of undeveloped land will serve to increase water demand directly. While there is much uncertainty about California's future population growth and development, an increase in the State's population is generally expected to increase the State's total water demand, absent additional measures to conserve water.

2.7.5 Technological Innovation

Technological innovation could play a significant role in determining California's future water demand, as well as future supply. Innovation in water conservation practices could serve to reduce water demand by allowing water to be used more efficiently. Innovation in water resource management could allow California's water resource systems to be managed more efficiently and allow more water supply yield with the same or less environmental impact. Innovation in water resource management and water use would occur with or without climate change. However, given the potential impacts of climate change, there will be an increased impetus for innovation.

A key area for future technological innovation is agricultural water use efficiency. Tanaka and others (2005) have determined that by the year 2100, agricultural water use will fall by 24 percent, while loss of income from agriculture will decrease only 6 percent. This discrepancy between water use and income comes from a predicted shift to higher-value crops and more efficient use of water. A theoretical body of work suggests that horticultural breeding improvements alone can attain a maximum increase in water use efficiency of about 15 percent (Cowan, 1977).

An area of innovation that could affect future water supply conditions, at least in some parts of the State, is sea water desalinization. The unit cost of desalinization has fallen in recent years, however, desalinization remains a relatively expensive and energy-intensive means of obtaining water compared to other water sources. More improvements in desalinization technologies could reduce costs and energy requirements. Desalinization could become a more competitive source of water, especially in coastal areas of Southern California where water is often imported from long distances and at high cost partly because of energy requirements.

2.8 Colorado River Basin

This report is primarily focused on the potential effects of climate change on the Central Valley and associated water resource systems. This is because the Central Valley and its water resource systems supply most of California's water, and because much of the effort to assess the impacts of climate change on the State's water resources has been directed toward the Central Valley. Climate change will affect water resource systems that obtain water from areas outside of the Central Valley. While the timing and scope of this report preclude substantive discussion of most of these systems, it is important to mention the single largest source of water supply for California outside of the Central Valley, the Colorado River.

The Colorado River is an important source of water for Southern California. In the past, California has diverted as much as 5.3 million acre-feet annually from the Colorado River. This is in excess of the State's annual allotment of 4.4 million acre-feet. Even at the allotment of 4.4 million acre-feet per year, the River still supplies about half of Southern California's average annual net water use (DWR, 2005a).

California's diversions from the Colorado River are primarily through the All-American Canal and the Colorado River Aqueduct. The All-American Canal supplies water to cities and agriculture in the Imperial Valley, and to agriculture in the Coachella Valley. The Colorado River Aqueduct supplies water to agriculture and cities of the south coast. Figure 2-34 illustrates the location of the All-American Canal and the Colorado River Aqueduct, as well as the greater service areas for the two systems.

An overview of past, present, and future climate in the Colorado River Basin is presented in a 2005 DWR special report prepared for the Association of California Water Agencies and Colorado Water Users Association conferences (DWR, 2005b). The report discusses hydroclimatic issues for the Colorado River Basin and their implications for water users in the basin. Portions of that report are cited below.



Figure 2-34 The Colorado River Aqueduct, All American Canal and Their Service Areas

Source: California Department of Water Resources, http://www.crss.water.ca.gov/data/ca_service_area.cfm

2.8.1 Description of the Colorado River Basin and its Water Resources

The Colorado River Basin extends into seven western states and Mexico, each of which has strong interests in the river and its water. The states are Arizona, California, Colorado, Nevada, New Mexico, Utah and Wyoming, as shown in Figure 2-35. While the volume of natural runoff in the basin is relatively small in comparison to its area, an average of about 15 million acre-feet of runoff is generated each year in the Colorado River Basin above Lees Ferry. Lees Ferry is labeled as "Compact Point" in Figure 2-35.

The Colorado River and its tributaries are the major source of water for many of the rapidly growing cities of the seven basin states and northern Baja California. The cities include Denver, Salt Lake City, Las Vegas, Phoenix, Tucson, Los Angeles and San Diego and other communities in south coastal California.

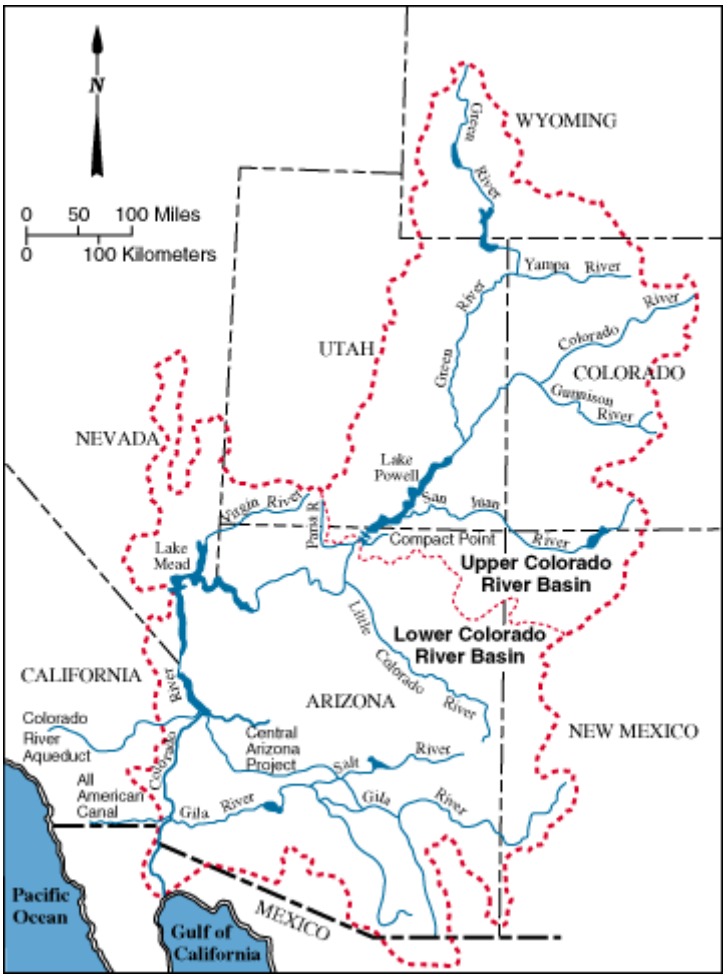


Figure 2-35 Map of the Colorado River Basin

Source: (Dettinger, 1995) http://geochange.er.usgs.gov/sw/changes/natural/codrought/

The Colorado River rises into the snow capped mountains of north central Colorado and flows southwesterly about 1,400 miles to Mexico and the Gulf of California. The River's major tributaries are the Green River, originating in the Wind River Mountains of southwest Wyoming, the Gunnison River from west central Colorado and the San Juan River from southwest Colorado.

The Colorado River basin is estimated to cover an area of about 244,000 square miles, about 8 percent of the land of the conterminous United States. About 2,000 square miles of the basin is in Mexico. The basin is typically considered to consist of two parts, an upper and lower basin, with the dividing point at the Lees Ferry gauging station in north-central Arizona, just downstream of Glen Canyon Dam and Lake Powell.

The upper Colorado River basin is nearly half the total drainage area of the entire basin or 109,300 square miles. Most of the water flowing in the Colorado River originates in the upper basin mountains, but significant tributaries also exist in the lower basin including the Little Colorado River in northeastern Arizona, the Virgin River in southwestern Utah and southeastern Nevada and the Gila River system of south central Arizona and extreme western New Mexico.

The Colorado River basin is one of the driest major watersheds in the United States. Average annual basin precipitation is 13.9 inches, with an annual average of 15.2 inches in the upper basin and 12.9 inches in the lower basin. Much of the Colorado River basin is desert receiving less than 10 inches of precipitation per year. High elevation areas receive significantly more precipitation, over 50 inches at some locations. The wetter areas of the Colorado River Basin consist of the Wind River Mountains in Wyoming, Rocky Mountains in Colorado, San Juan Mountains in southwest Colorado, the Uinta Mountains in northeast Utah and the Mogollon Rim in east central Arizona. The driest areas of the basin are in the basin's southwest corner near Yuma, Arizona. This area receives about 3 inches of annual precipitation. Figure 2-36 illustrates the distribution of average annual precipitation in the basin.

Most of the precipitation in the Colorado River basin is from winter storms originating in the Pacific Ocean. Most of the runoff from these storms comes from the high mountainous areas in the basin's upper reaches. These areas are favored by orographic precipitation and winter snowpacks. While these areas only constitute about 15 percent of the basin's entire area, they generate about 85 percent of its entire natural runoff.

Occasionally, more often in El Nino years, major winter storms from the Pacific Ocean move across Southern California and into the lower portions of the basin. These southern-track storms can provide heavy winter rainfall at low elevations in Arizona, and heavy snow in the San Juan Mountains of southwestern Colorado.

A major factor that sets the climate of the Southwest United States and southern part of the Colorado River Basin apart from the rest of the country is the North American monsoon system. Typically, during the months of July, August, and the first half of September, regional circulation patterns change and cause moisture-laden air to move into the Southwest from the Pacific Ocean, the Gulf of California, and the Gulf of Mexico. As this moist air moves into the

southwest, a combination of orographic uplift and daytime heating from the sun causes thunderstorms to develop.

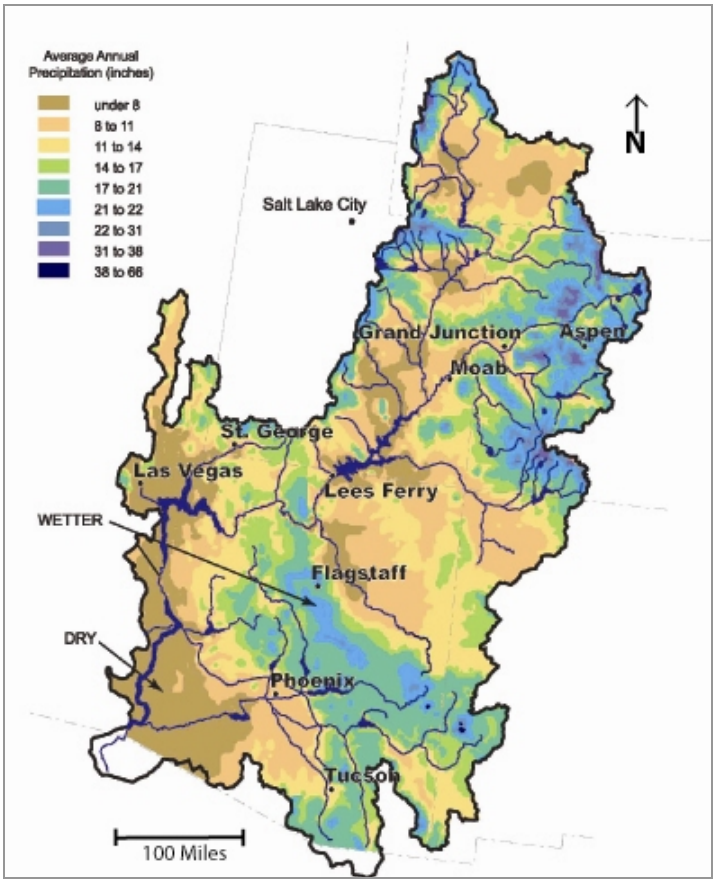


Figure 2-36 Distribution of Average Annual Precipitation in the Colorado River Basin
Adapted from The University of Arizona's Institute for the Study of Planet Earth CLIMAS
http://www.ispe.arizona.edu/climas/learn/swnutshell/sld004.htm

Summer monsoonal rainfall is an important fraction of the total annual precipitation received in southeastern Arizona, much of New Mexico, and southern Colorado. Most of the monsoonal rain is from thunderstorms and is highly localized and sometimes very intense. Although monsoonal rainfall is very important to nourishing watershed vegetation in parts of the southwest, and can cause local flooding, it does not contribute much to flows in the Colorado River or its major tributaries.

Finally, in the summer of some years, the remnants of a Pacific hurricane off the west coast of Mexico will move north over northwestern Mexico and into the Southwest United States. These tropical storms can produce regional rainfall over the desert and flash floods in some of the mountain watersheds.

Since the latter part of 1999, the upper Colorado River basin has experienced an extended severe drought. Water year 2005 saw improved hydrologic conditions in the basin. Figure 2-37 illustrates the volume of water stored in Lake Powell and Lake Mead since the construction of both reservoirs. The decline in reservoir storage after 1999 illustrates the significance of the

recent drought. While hydrologic conditions improved in Water Year 2005 and the severity of drought conditions in the basin has eased somewhat, it is premature to declare that the drought in the upper basin is over (DWR, 2005b).

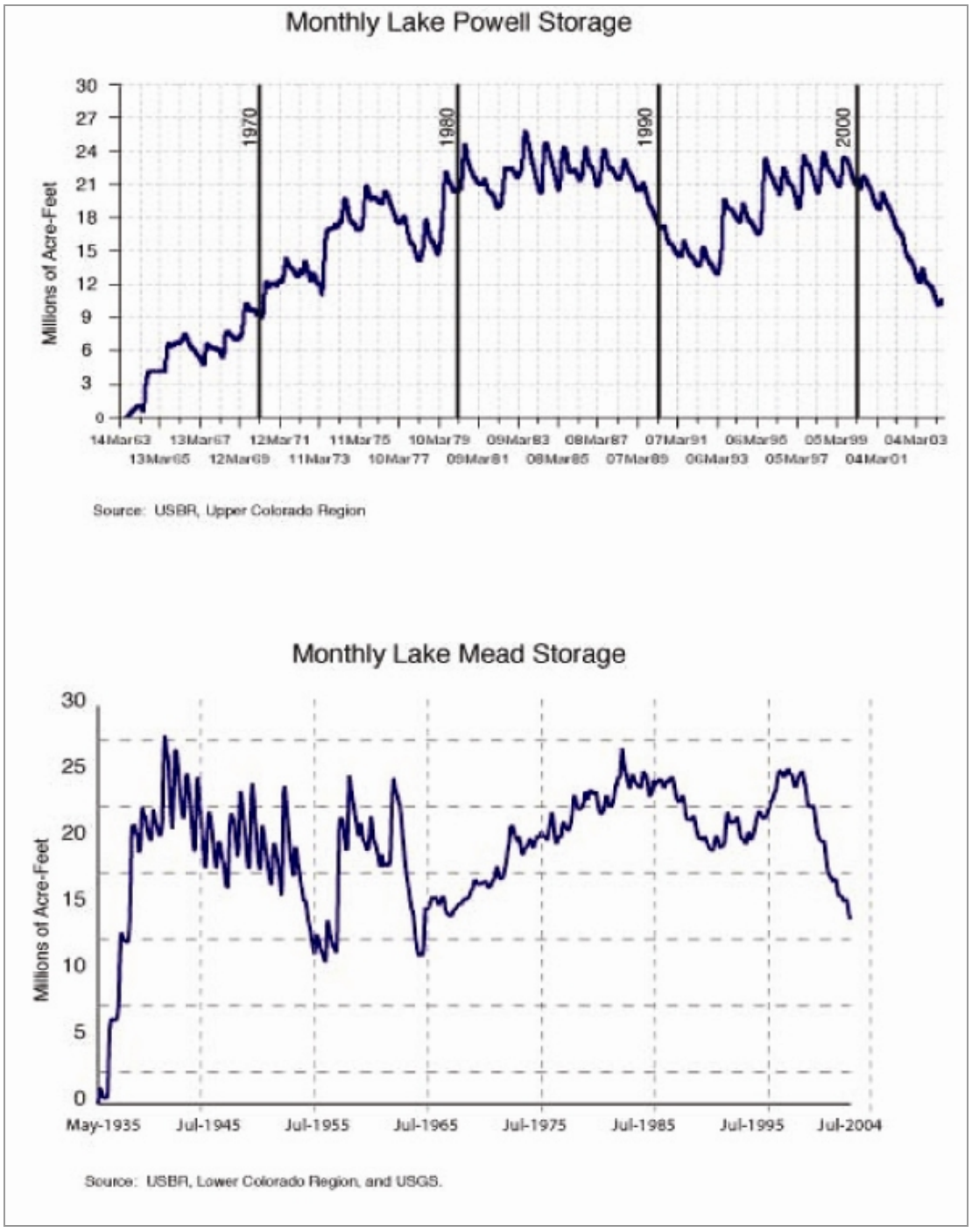


Figure 2-37 Monthly Storage Volumes in Lake Powell and Lake Mead since their Construction

2.8.2 Allocation of Water in the Colorado River Basin

The 1922 Colorado River Compact formally divided the Colorado River basin at Lees Ferry into two parts: an upper basin and lower basin, as described earlier. Each basin was apportioned 7.5 million acre-feet of Colorado River water annually for water supply purposes. A 1944 treaty between the United States and Mexico guarantees Mexico 1.5 million acre-feet annually. The burden of this guarantee is shared equally by the upper and lower basins.

The upper basin states allocated use among themselves in 1948. The allocation of water in the lower basin was decided by the U.S. Supreme Court in 1964. The court decided that the annual apportionment of 7.5 million acre-feet for the lower basin would be allocated as follows: 4.4 million acre-feet to California, 2.8 million acre-feet to Arizona, and 0.3 million acre-feet to Nevada. One of the salient points of the Supreme Court decree was that Arizona's use of Gila River water is not part of its 2.8 million acre-feet allocation. In addition, all lower basin states have the right to use tributary flows before they join the Colorado River without affecting their appropriation of Colorado River water.

2.8.3 Climate Change and the Colorado River Basin

Flows in the upper Colorado River basin are mostly a function of snowmelt. Warmer air temperatures as the projected result of climate change would tend to reduce the basin's middle elevation snowpack. Warmer air temperatures would also tend to cause earlier melting of annual accumulations of snow. Annual snowmelt could begin several weeks sooner than it does now, depending on the amount of warming that occurs.

Warming in the upper Colorado River Basin could cause an increase in winter runoff due to higher minimum snow elevations during winter storms and less precipitation falling and accumulating in the form of snow. Since reservoir storage in the Colorado River Basin is so large in comparison to average annual basin runoff (roughly four times average runoff), a change in the timing of annual runoff in the basin as the result of climate change would not be expected to significantly affect basin yield. Figure 2-38 illustrates locations of the larger reservoirs in the basin.

Recently completed climate model runs for the upcoming Intergovernmental Panel on Climate Change's 4th Assessment indicate a winter temperature increase of 1.1 to 2.0 degrees Celsius in the Colorado River basin by 2050, with continued temperature rise expected through the end of the century. Upper basin runoff from annual snowmelt would likely peak five to 25 days earlier than the average time of peak runoff for the 1951-80 historical period (Garfin, 2005).

Possible changes in amount of precipitation received by the Colorado River basin as the result of climate change could affect basin yield and thus are potentially of more concern for water supplies than predicted changes in the timing of runoff. As discussed previously, about 85 percent of upper basin runoff is contributed by its high elevation watersheds. Therefore, possible changes in high mountain watersheds and the amount runoff from them could be the most important. Although climate models provide precipitation projections, projections for a specific region, such as the Southwest, vary considerably between models and are probably not reliable (Garfin, 2005).



Figure 2-38 Size and Locations of Reservoirs in the Colorado River Basin

From http://www.water.utah.gov/interstate/thecoloradoriverart.pdf

Warmer temperatures from climate change could be expected to cause drying of water-producing areas of the vast Colorado River watershed somewhat sooner each year than what occurs today. One study indicates that a precipitation increase of 10 percent may be required to offset the drying effect of a 2 degree Celsius rise in temperature (Nash and Gleick, 1993).

More extreme precipitation events are generally expected to accompany increasing temperatures associated with climate change. More extreme precipitation events in the Colorado River watershed would in turn be expected to increase sediment production. Basin sediment production would also likely increase given that a higher percentage of the basin's precipitation would likely fall in the form of rain rather than snow due to increased temperatures. If more frequent wild fires were to occur because of earlier drying of watersheds, or simply because of increased summer temperatures, sediment production would be increased further. Increased sediment production would adversely affect water quality and increase the rate of reservoir capacity loss due to sedimentation.

There are likely to be changes in water demand in the Colorado River basin as the result of climate change. Changes in demand at any particular location will probably be small, however, the aggregate change for the basin could be significant since so much land is involved.

One of the key questions concerning possible changes in water demand is what effect climate change will have on evapotranspiration rates for crops and landscaping. Also of concern are possible changes in water use by water loving plants knows as phreatophytes along rivers and streams. Phreatophytes can cause a significant loss in stream flow and shallow groundwater.

As discussed in Section 2.7.1, evapotranspiration rates increase with temperature if other factors that effect evapotranspiration, such as cloudiness, humidity, and atmospheric carbon dioxide content remain the same. However, higher atmospheric carbon dioxide levels expected in the future will act to reduce water consumption by plants, as evidenced by laboratory tests.

Increasing temperatures in the Colorado River Basin will likely increase reservoir evaporation losses. Evaporative losses from open portions of conveyances such as the Central Arizona Project, Colorado River Aqueduct, and the All-American Canal would likely increase as well.

2.8.4 Summary

The Colorado River Basin provides water to Southern California. Expected changes to the Colorado River Basin associated with climate change include:

- Less precipitation falling as snow and an earlier snow melt
- Increased evaporation from reservoirs and conveyance facilities
- Increased sediment production due to more extreme events and more precipitation falling as rain than snow
- Changes in water demand

Changes in the amount of water available to California from the Colorado River Basin may change if long-term decreases in runoff occur.

2.9 Possible Effects on Fish

This section describes aspects of climate change that could affect the abundance of fish in California's inland waters. It focuses on a few key species that have major implications for water management, including rainbow trout, coho and Chinook salmon and Delta smelt. The analysis omits numerous fishes throughout the State for which the influence of climate change and its implications for water management seem less clear.

In California, the timing and amounts of water released from reservoirs and diverted from streams are limited by their effects on various native fishes, especially those that are listed as threatened or endangered under the federal and State endangered species acts. These include winter-run and spring-run Chinook salmon, coho salmon, coastal and Central Valley forms of steelhead rainbow trout, Lahontan cutthroat trout, razorback sucker and Delta smelt. California constitutes the warm, southern end of the geographic range of most of these species.

By 2100, climate change is expected to raise average air temperatures by about 1.4 to 5.8 degrees Celsius in California, raise stream water temperatures by at least as much, greatly reduce California's snowpack, shift the seasonal pattern of surface-water runoff to more in winter and less in spring and summer, and raise sea level by 0.3 of a foot to 2.9 feet (IPCCa, 2001). These physical changes are likely to influence the ecology of aquatic life in California and have several major effects -- all of them negative -- on cold-water fishes.

In many low- and middle-elevation California streams today, summer temperatures often come close to the upper tolerance limits for salmon and trout. Thus, anticipated climate change that raises air temperatures a few degrees Celsius may be enough to raise water temperatures above the tolerance of salmon and trout in many streams, favoring instead non-native fishes such as carp and sunfish.

Unsuitable summer temperatures are a problem because many of the threatened and endangered fishes spend the summer in cold-water streams, either as adults, juveniles, or both. Adults of some populations, such as spring-run Chinook, spend the summer near their upstream spawning grounds waiting for conditions suitable for spawning in fall or winter. Chinook salmon and steelhead, for example, prefer temperatures of less than 18-20 degrees Celsius in mountain streams, although they may tolerate higher temperatures for short periods (Moyle, 2002).

2.9.1 Regional Effects

The specific nature of ecological effects on fishes will differ among regions of the State. The following three regions are important for water supply and will see major effects from climate change:

- Region 1 – Basins with snowpack. River basins that drain the Sierra Nevada and Cascade Range and store water as snowpack;
- Region 2 – Basins without snowpack. River basins without significant snowpack, including all coastal streams south of the Klamath River basin; and
- Region 3 - The Sacramento-San Joaquin River Delta.

Streams on the eastern slope of the Sierra Nevada and in Southern California, as well as the Colorado River, are also important for water supply, but the effects of climate change on fishes there are less clear.

Winter-run and spring-run Chinook salmon, coho salmon, and coastal and Central Valley steelhead trout spawn in Region 1. Coho salmon and steelhead trout occupy coastal streams in the second region. Delta smelt spend their entire lives in the third region, while steelhead trout and Central Valley Chinook salmon migrate through it. All of these fishes are listed under the federal Endangered Species Act.

2.9.1.1 Region 1- Basins with Snowpack

The Sierra-Cascade basins are predicted to get less snow and more rain, more winter and less spring and summer runoff, and warmer runoff. Spring-run Chinook salmon and steelhead trout in some streams migrate upriver into the foothills and mountains early in the year, spend the summer in deep, cold pools, and spawn the following fall (salmon) or winter (steelhead). Adult survival over the summer depends upon the availability of cold water. The combination of streams being both warmer and shallower in the summer due to climate change may diminish most summer habitat for steelhead and potentially all such habitat now used by spring-run salmon.

Many salmon and rainbow trout spawn and rear below dams, or at hatcheries associated with dams. Climate change could reduce the volume of cold water in foothill reservoirs since they would receive less snowmelt and have reduced carryover storage. Thus, releases of cold water to support fish spawning and rearing below such reservoirs may decline and fish production could also decline.

2.9.1.2 Region 2 - Basins without Snowpack

Streams in basins without significant snowpack will likely be warmer in the dry season than now (as well as in the winter), matching the expected rise in air temperature. Warmer inland areas as the result of climate change may increase summer coastal fog which could provide mitigating effects for coastal areas and streams.

Juvenile coho salmon and coastal steelhead trout remain in fresh water through the summer. Climate change could make coastal streams too warm for coho salmon in the summer, especially for the more extreme projections of temperature rise. Steelhead trout could disappear from the more southerly streams in their current range (in Central and Southern California), and would probably be less abundant elsewhere.

2.9.1.3 Region 3 - Sacramento-San Joaquin River Delta

The Sacramento-San Joaquin Delta will become saltier if sea level rise predictions are correct, Delta operations remain the same and the Delta retains its present physical configuration. The predicted decline in natural runoff during the spring, summer and fall could make the Delta even

saltier, and over a larger area. River water at the upstream end of the Delta will still be fresh in summer, but is likely to be warmer than now if measures are not taken.

The Delta smelt occurs in the Sacramento-San Joaquin Estuary and nowhere else. During periods of drought, its center of abundance has been the channel of the Sacramento River in the upstream part of the Delta (Moyle, 2002). Delta smelt rarely occur in waters above 24 degrees Celsius and cannot survive long in water above 25 degrees Celsius (Swanson and others, 2000). Current peak temperatures in the lower Sacramento River at Hood and Rio Vista, for example, are already within a few degrees of these temperature thresholds (CDEC).

In short, a possible result of climate change is that Delta smelt will have little or no suitable habitat in summer. Waters in the lower Delta may be too salty and lacking in food, while fresh water in the upper Delta may be too warm. Thus, the species may become much less numerous or may even go extinct.

2.9.2 Summary

As evident from the above discussion, climate change could have a significant impact on threatened and endangered fish in California. Climate change could also have serious implications for fish that are not now identified as threatened and endangered, but might be affected to a point where they become designated as such.

2.10 Sudden Climate Change

Most global climate models predict that climate change due to human causes will be a continuous and somewhat gradual process through the end of this century. With proper foresight, planning and action, water managers will likely be able to help California adapt to many of the water supply challenges posed by climate change, even at some of the higher projections for change. However, sudden and unexpected changes in climate could leave water managers unprepared and could, in their extreme, have serious implications for California and its water supplies.

Sudden climate change could occur if progressive changes in the earth's climate cause a physical threshold or "trigger point" to be reached where one of the earth's major atmospheric or oceanic systems changes significantly, or ceases to function. One possible example of this that has received a significant amount of attention is a possible change in the global thermohaline circulation system depicted in Figure 2-39.

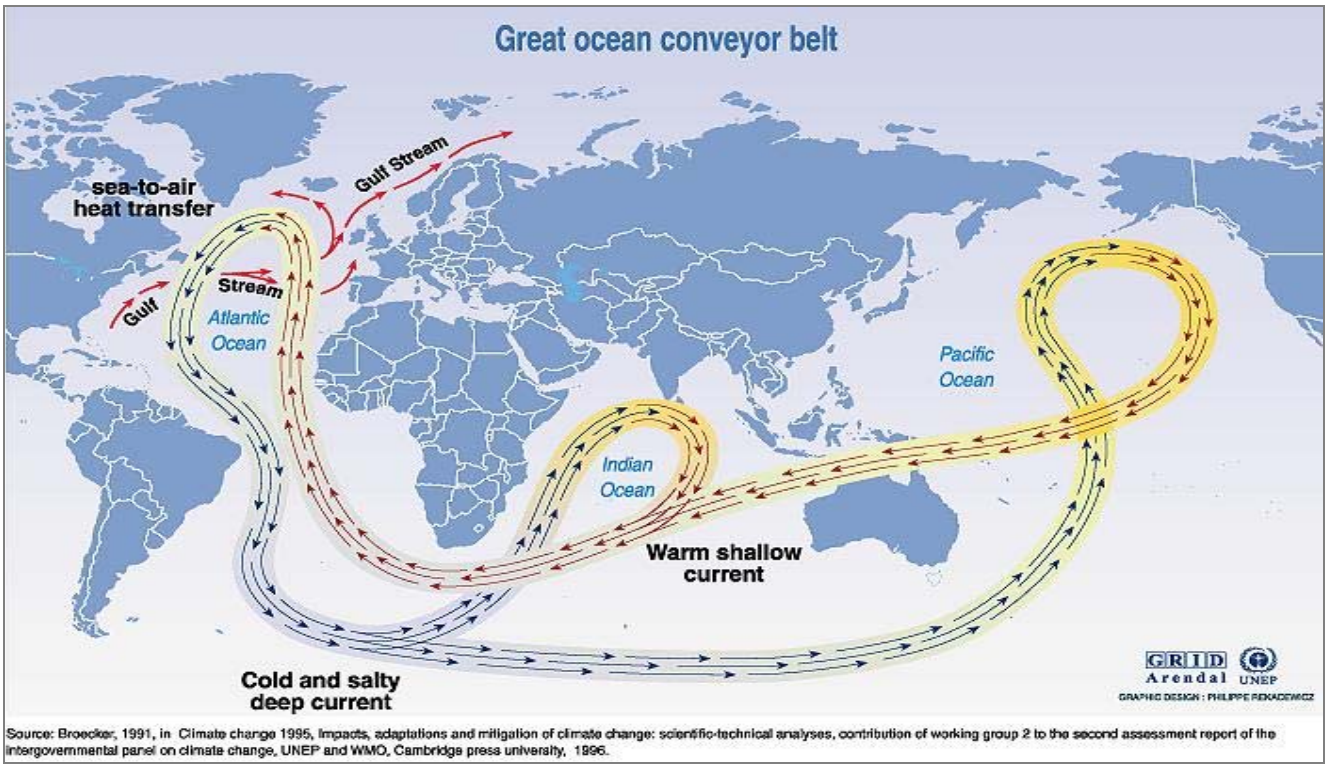


Figure 2-39 The Global Thermohaline Circulation System
Source: GRIDA, 2005.

There is evidence that circulation in the North Atlantic Ocean in relation to the global thermohaline system is slowing (Nature, 2005). While the complete shutdown of the system would likely lead to relatively rapid and significant changes in the earth's climate, such a scenario is considered by most scientists to be unlikely to occur in the next 50 years. The IPCC reports that none of the climate models it used in its evaluations project the complete shutdown of the system before 2100 (IPCC, 2001a).

Relatively sudden and often short-term changes in the climate of California and the western United States have occurred during at least the past 2000 years, as evidenced by precipitation and streamflow measurements over about the past 100 years and paleoclimatological information derived from physical evidence such as annual growth rings in trees. Of particular concern are extreme droughts, some of which appear to have occurred over large areas of the western United States and extended over several decades (MacDonald, 2005, Woodhouse, 2005). The exact cause of these events is unknown. However, there is speculation that some of the more recent droughts may have been due, at least in part, to oscillating conditions in the world's oceans.

Finally, other phenomena that could cause sudden and unexpected changes in the earth's climate include volcanic activity and the impact of meteorites or other extraterrestrial matter with the earth's surface. Large volcanic eruptions during recorded history have been observed to have caused temporary regional and sometimes global-scale cooling from one to several years (Kelly, 1996). While both volcanic eruptions and the impact of large extraterrestrial objects with the

Earth could suddenly affect the State's climate and water resources, the frequency of their occurrence together with their projected effects are extremely difficult to predict.

2.11 Summary

As discussed in previous sections, climate change could cause significant impacts on California's water resources and water demand. Changes in temperature and precipitation patterns in the State have been observed over the past century. Further changes are expected over the next century due to climate change. Changes in sea level are also expected to occur in response to the changing climate. These changes in precipitation and temperature patterns across the State may have profound impacts on ecologic and water resources systems in the State.

There is a significant amount of uncertainty about the magnitude of climate change that will occur over this century. It is unlikely that this level of uncertainty will diminish significantly in the foreseeable future (Dettinger, 2005b). There is also uncertainty about changes in hydrologic conditions, aquatic ecosystems and water demand that could occur as the result of various amounts of climate change. In the following chapters of this report, an initial attempt is made to quantify the impacts of climate change on some aspects of California's water resources.

2.12 References

Sources for illustrations are referenced below each illustration. References cited in the chapter text are listed below.

Bromirski (2005). Dr. Peter Bromirski, Assistant Project Scientist, Scripps Institute of Oceanography, La Jolla, CA, personal communication 10-10-2005.

CDEC [California Data Exchange Center]. California Department of Water Resources.

CRU (2000). Climatic Research Unit, School of Environmental Sciences University of East Anglia, United Kingdom Website. http://www.cru.uea.ac.uk/cru/info/thc/ November 30, 2005.

Cayan (2001). Changes in the Onset of Spring in the Western United States.[Cayan, D.R., Susan A. Kammerdiener, Michael D. Dettinger, Joseph M. Caprio, and David H. Peterson] Bulletin of the American Meteorological Society. Vol. 82, No. 3, March 2001.

Cowan, (1977). *Stomatal diffusion in relation to leaf metabolism and environment*. [Cowan, I.R. and Farquhar, C.D.] Symp. Soc. Exp. Biol. 31, 471-505. 1977.

DOF (2005). *Data File: Historical and Projected Population for California*. California Department of Finance.

DWR (1951). Water Resources of California [California Water Resources Board (now California Department of Water Resources)].

DWR (1958). Sea-Water Intrusion in California, Bulletin 63. [California Department of Water Resources]. November, 1958.

DWR (1975). Sea-Water Intrusion in California, Inventory of Coastal Ground Water Basins, Bulletin 63-5. [California Department of Water Resources]. October, 1975.

DWR (1994). The California Water Plan Update, Bulletin 160-93. [California Department of Water Resources]. October, 1994.

DWR (1998). California Water Plan Update, Bulletin 160-98. [California Department of Water Resources]. 1998.

DWR (2003). *California's Groundwater; Bulletin 118, Update 2003.* [California Department of Water Resources].

DWR (2005a). California Water Plan, Update 2005 (Draft). [California Department of Water Resources]. Final Draft.

DWR (2005b). Special Publication for Association of California Water Agencies and Colorado River Water Users Association Conferences, prepared by the California Department of Water Resources, Sacramento. November, 2005.

DWR (2005c). Water Conditions in California, *California Cooperative Snow Surveys Bulletin 120*. [California Department of Water Resources].

Dettinger (2005a). Changes in Streamflow Timing in the Western United States in Recent Decades. [Michael D. Dettinger] U.S. Geological Survey. Fact Sheet, *http://pubs.usgs.gov/fs/2005/3018/pdf/FS2005_3018.pdf*

Dettinger (2005b). From climate-change spaghetti to climate-change distributions for 21st Century California. [Michael D. Dettinger] San Francisco Estuary and Watershed Science. Vol. 3, Issue 1 (March 2005), Article 4. http://repositories.cdlib.org/jmie/sfews/vol3/iss1/art4

Easterling, (2000). *Observed Variability and Trends in Extreme Climate Events: A Brief Review*. [D.R. Easterling, J.L. Evans, P. Ya. Groisman, T.R. Karl1, K.E. Kunkel, P. Ambenje] Bulletin of the American Meteorological Society, **81**, March 2000, 417-425. http://www.ncdc.noaa.gov/oa/pub/data/special/extr-bams2.pdf

Freeman (2002). Looking for Recent Climatic Trends and Patterns in California's Central Sierra. [Gary J. Freeman]. 2002 PACLIM Conference Proceedings.

Garfin (2005). *Climate and Hydrology in the Colorado River Basin, September 2005 (advance copy)* . [Greg Garfin, University of Arizona].

Gibeaut, J. C. (2000). *Texas Coastal Hazards Atlas Volume 1*. Bureau of Economic Geology, University of Texas, Austin.

Givati (2004). *Quantifying Precipitation Suppression Due to Air Pollution* . [Amir Givati and Daniel Rosenfeld, The Hebrew University of Jerusalem] Journal of Applied Meteorology: Vol. 43, No. 7, pp. 1038–1056.

GRIDA (2005). United Nations Environment Programme, Global Resource Information Database-Arendal (GRIDA) Website at: http://www.grida.no/climate/vital/32.htm. November 30, 2005.

Groisman (2005). *Changes in precipitation distribution spectra and contemporary warming of the extratropics: implications for intense rainfall, droughts, and potential forest fire danger.* [Pavel Ya. Groisman, NOAA/NESDIS/NCDC, Asheville, NC; and R. W. Knight, D. R. Easterling, D. Levinson, R. R. Heim, Jr., T. R. Karl, P. H. Whitfield, G. C. Hegerl, V. N. Razuvaev, B. G. Sherstyukov, J. G. Enloe, and N. S. Stroumentova]. Preceedings of the 16th Conference on Climate Variability and Change, 85th American Meterological Society Meeting, San Diego, CA, January 2005. http://ams.confex.com/ams/Annual2005/techprogram/paper_85857.htm

Hayhoe (2004). *Emissions pathways, climate change, and impacts onCalifornia.* [Hayhoe, K., D. Cayan, C.B. Field, P.C. Frumhoff, E.P. Maurer, N.L. Miller, S.C. Moser, S.H. Schneider, K.N. Cahill, E.E. Cleland, L. Dale, R. Drapek, R.M. Hanemann, L.S. Kalkstein, J. Lenihan, C.K. Lunch, R.P. Neilson, S.C. Sheridan, and J.H. Verville] Proceedings of the National Academy of Sciences of the United States of America 101:12422-12427.

Hidalgo (2005). Sources of variability of evapotranspiration in California. [Hidalgo, H.G., Cayan, D.R., Dettinger, M.D.] J. Hydrometerology. 6, 3-19.

Hulme (1995). *Estimating Global Changes in Precipitation.* Weather, Vol. 50, No. 2, February 1995.

Inman, et. al. (2002). *Facing the Coastal Challenge: Modeling Coastal Erosion in Southern California, October 27, 2002* [Douglas L. Inman, Patricia M. Masters, Scott A. Jenkins, Coastal Morphology Group Integrative Oceanography Division Scripps Institution of Oceanography University of California, San Diego.] (http://repositories.cdlib.org/sio/cmg/12/)

IPCC (2001a). *Climate Change 2001: The Scientific Basis. Contribution of Working Group I to the Third Assessment Report of the Intergovernmental Panel on Climate Change*.[Houghton, J.T.,Y. Ding, D.J. Griggs, M. Noguer, P.J. van der Linden, X. Dai, K.Maskell, and C.A. Johnson (eds.)]. Cambridge University Press, Cambridge, United Kingdom and New York, NY, USA, 881pp. ISBN 0521 80767 0. http://www.grida.no/climate/ipcc_tar/wg1/index.htm

IPCC (2001b). *Climate Change 2001: Synthesis Report. A Contribution of Working Groups I, II, and III to the Third Assessment Report of the Intergovernmental Panel on Climate Change* [Watson, R.T. and the Core Writing Team (eds.)]. Cambridge University Press, Cambridge,United Kingdom, and New York, NY, USA, 398 pp.

IPCC (2000). Intergovernmental Panel on Climate Change, Special Report on Emissions Scenarios, Nebojsa Nakicenovic and Rob Swart (Eds.), Cambridge University Press, UK. pp 570, http://www.grida.no/climate/ipcc/emission/.

Kerr (2005). *El Niño or La Niña? The Past Hints at the Future.* [Richard A Kerr]. Science Vol. 309, 29 July 2005. www.sciencemag.org

Kelly (1996). "The Spatial Response of the Climate System to Explosive Volcanic Eruptions." [Kelly, P. M., Jones, P. D., and Jia Pengqun,] International Journal of Climatology 16 (5), 537-550.

Knowles (2002). *Potential effects of global warming on the Sacramento/San Joaquin watershed and the San Francisco estuary.* [Knowles, N., and D. R. Cayan]. Geophys. Res. Lett., 29(18), 1891, doi:10.1029/2001GL014339.

Lempert (2003). *Shaping the Next One-Hundred Years: New Methods for Quantitative, Long-Term Policy Analysis* [Lempert, R. J., S.W. Popper and S.C. Bankes], RAND Corporation, ISBN 0-08330-3275-5. 2003.

Landis (2003). *How We Will Grow: Baseline Projections of the Growth of California's Urban Footprint through the Year 2100* (August 1, 2003). [John D. Landis and Michael Reilly] Institute of Urban & Regional Development. IURD Working Paper Series. Paper WP-2003-04. http://repositories.cdlib.org/iurd/wps/WP-2003-04 ,

Long (2004). *Rising atmospheric carbon dioxide: plants FACE the future.* [Long, S.P., Ainsworth, E.A., Rogers, A. and Ort, D.R.] (2004) Annu. Rev. Plant Biol. 55, 591-628.

MacDonald (2005). *Southern California and the "Perfect Drought"* [MacDonald G., S. Rian and H. Hildalgo]. Special Publication for Association of California Water Agencies and Colorado River Water Users Association Conferences, November, 2005.

Miller (2003). Miller, N.L., K.E. Bashford, E. Strem, 2003: Potential Impacts of Climate Change on California Hydrology, J. Amer. Water Resoures Assoc., 771-784.

Miller (1998). Climatically Sensitive California: Past, Present, and Future Climate. Presentation at California Workshop on Regional Climate Variability and Change, Santa Barbara, CA 9-11 March 1998

Mote (2005). *Declining mountain snowpack in western North America.* [Mote, P. W., A. F. Hamlet, M. Clark, and D. P. Lettenmaier] Bulletin of the American Meteorological Society 86(1):39-49

Mount (2004). Subsidence, Sea Level Rise, Seismicity in the Sacramento-San Joaquin Delta: Report to the Levee Integrity Subcommittee of the California Bay-Delta Authority Independent Science Board, December 2004. [Jeffery Mount and Robert Twiss, members of the CalFED Independent Science Board]. http://science.calwater.ca.gov/pdf/isb/ISB_subcom_levee_report_120104.pdf#search='mount%20%26%20twiss

Moyle (2002). Inland Fishes of California. University of California Press.

Munk (2002). Twentieth Century Sea Level: An Enigma. [Walter Munk] Proceedings of the National Academy of Sciences, Vol. 99, No. 10, pp. 6550-6555, May 14, 2002.

NOAA (2005). Global Warming, FrequentlyAsked Questions. [National Oceanic and Atmospheric Administration , National Climatic Data Center]. http://lwf.ncdc.noaa.gov/oa/climate/globalwarming.html#Q5 October 23, 2005

NWS (2005). National Weather Service, Climate Prediction Website. December 12, 2005. http://www.cpc.ncep.noaa.gov/charts.shtml

Nash and Gleick (1993). The Colorado River Basin and Climatic Change: The Sensitivity of Streamflow and Water Supply to Variations in Temperature and Precipitation. [Nash, L. and P. Gleick.] U.S. Environmental Protection Agency, EPA230-R-93-009, Washington, D.C. 121 pp.

Nature (2005). *Oceanography: The Atlantic heat conveyor slows.* [Detlef Quadfasel], Nature, Volume 438 Number 7068. December 1, 2005.

PASSC (2005). *Earth Impact Database.* University of New Brunswick, Planetary and Space Science Centre http://www.unb.ca/passc/ImpactDatabase/index.html. December 1, 2005.

Roos (1989). *Possible Climate Change and its Impact on Water Supply in California.* Oceans '89 Conference. [Maurice Roos, California Department of Water Resources]. Institute of Electrical and Electronic Engineering; Seattle, Washington.

Sloan (2005). L. C. Sloan, L. Kueppers, M. Snyder, D. Cayan, M. Tyree, M. Kanamitsu, H. Kanamaru, N. Miller, J. Jin, G. Franco, B. Weare. Have urban and agricultural land use changes affected California's climate? 2nd Annual Climate Research Conference and First Scientific Conference West Coast Governors' Global Warming Initiative. http://www.climatechange.ca.gov/events/2005_conference/presentations/2005-09-14/2005-09-14_SLOAN.PDF

Swanson (2000). Comparative environmental tolerances of threatened delta smelt (Hypomesus transpacificus) and introduced wakasagi (H. nipponensis) in an altered California estuary. [Swanson, C., T. Reid, P.S. Young, and J.J. Cech, Jr.] Oecologia 123: 384-390.

Tanaka (2005). Climate Warming and Water Management Adaptation for California. [Tanaka, S.K., Zhu, T, Lund, J.R., Howitt, R.E., Jenkins, M.W., Pulido, M.A., Tauber, M., Ritzema, R.S., Ferreira, I.C.]. Climatic Change, (in press).

Titus (1995). *The probability of sea level rise.* [James G. Titus, Vijay K. Narayanan]. Washington, D.C.: U.S. Environmental Protection Agency. 186 pp. EPA 230-R95-008. (http://yosemite.epa.gov/OAR/globalwarming.nsf/content/ResourceCenterPublicationsProbability.html)

USDA (2003). *California Agricultural Statistics 2003,* U.S. Department of Agriculture, 2003. .

Wara (2005). *Permanent El Nino–Like Conditions During the Pliocene Warm Period.* [Michael W. Wara, Ana Christina Ravelo, and Margaret L. Delaney]. Science Vol.309, 29 July 2005. www.sciencemag.org

Woodhouse (2005) *Paleoclimate Overview* [Connie Woodhouse]. Special Publication for Association of California Water Agencies and Colorado River Water Users Association Conferences, November, 2005.

Progress on Incorporating Climate Change into Management of California's Water Resources

1st Progress Report
July 2006

Chapter 3:
DWR Climate Change Studies

Author:

Jamie Anderson, Ph.D., P.E.
California Department of Water Resources, Bay Delta Office, Modeling Support Branch, Sacramento.

Contributors:

Michael Anderson, Ph.D.
California Department of Water Resources, Division of Flood Management, Sacramento.

Messele Ejeta, Ph.D., P.E.
California Department of Water Resources, Bay Delta Office, Modeling Support Branch, Sacramento.

3 DWR Climate Change Studies

3.1 Introduction

This chapter provides an overview of climate change studies being conducted by the California Department of Water Resources (DWR). DWR is doing the studies to determine potential effects of climate change on management of California's water resources in support of the governor's Executive Order S-3-05 described below. This chapter explains the background and approach for conducting these climate change studies. It also describes the specific climate change scenarios selected for study. Subsequent chapters of this report will present the results of the studies.

3.2 Background

In June 2005, Gov. Arnold Schwarzenegger issued Executive Order S-3-05 on climate change. It set future greenhouse gas emissions targets for California. It also requires reports every two years on climate change impacts to five areas including water resources. The first of those reports is due to the governor in January 2006. To comply with the Executive Order a Climate Action Team (CAT) was formed with representatives from various state agencies, including the Resources Agency. A subcommittee of the CAT selected four climate change scenarios for analysis for the initial climate change report. The California Energy Commission (CEC) is coordinating the publication of that report.

This report is supplemental and complementary to the CEC report. This report focuses only on water resources. DWR staff has conducted preliminary studies on incorporating climate change into the planning and management of California's water resources. Whenever appropriate, the four climate change scenarios selected by the CAT were used in the DWR studies. DWR has coordinated efforts with other groups conducting modeling studies of climate change impacts on water resources. The groups include the University of California, Berkeley, (CalSim-II); University of California, Davis, (CALVIN); and the Natural Heritage Institute (WEAP).

In addition to these DWR studies for the governor, the California Water Plan Update 2005 includes a qualitative discussion of the possible statewide effects of climate change (DWR, 2005). An expanded, more quantitative discussion of statewide impacts will be included in future Water Plan Updates and will use information from the studies described in this report and other studies done outside DWR.

3.3 Climate Change Scenarios

The four climate change scenarios selected by the CAT were chosen from among several available scenarios compiled for the United Nation's Intergovernmental Panel on Climate Change's (IPCC's) Fourth Assessment Report which is due out in 2007. The four climate change scenarios consist of two greenhouse gas (GHG) emissions scenarios, A2 and B1, each

represented by two different Global Climate Models (GCMs), the Geophysical Fluid Dynamic Lab model (GFDL) and the Parallel Climate Model (PCM). The four climate change scenarios are:

- GFDL A2
- PCM A2
- GFDL B1
- PCM B1

The A2 emissions scenario assumes high growth in population, regional based economic growth, and slow technological changes, which results in significantly higher greenhouse gas emissions. The B1 scenario represents low growth in population, global based economic growth and sustainable development that results in the lowest increase of greenhouse gas emissions of the IPCC scenarios. Both the GFDL and PCM models project future warming. The GFDL model indicates a greater warming trend than the PCM model.

Among the criteria used to select these climate change scenarios were ability of the models to represent El Niño events and availability of the data for analysis to meet the January 2006 governor's deadline for the report (Cayan, 2005). In addition, both models estimated historical climate trends reasonably well. The emissions scenarios and models are described further in later sections of this report.

3.3.1 Emissions Scenarios

The World Meteorological Organization and the United Nations Environment Programme formed the Intergovernmental Panel on Climate Change (IPCC) to periodically evaluate the science, impacts, and socioeconomics of climate change including adaptation and mitigation options. In order to conduct climate change studies, the IPCC has developed scenarios of future greenhouse gas emissions. The first set of IPCC emissions scenarios was released in 1990 and 1992. In 1994, those emissions scenarios were evaluated. And in 1996 a 50-member team representing 18 countries began updating the emissions scenarios. The updated emissions scenarios are documented in the 2000 IPCC Special Report on Emissions Scenarios (SRES).

The SRES emissions scenarios were developed and peer-reviewed using an open process with six major steps (IPCC, 2000):

1. Literature review of existing scenarios
2. Analysis of major scenario characteristics, driving forces, and their relationships
3. Formulation of four narrative scenario storylines to describe alternative futures
4. Quantification of each storyline using a variety of modeling approaches
5. An open review of the resulting emission scenarios and their assumptions
6. Three revisions of the scenarios and the report after the open review: the formal IPCC Expert Review and the final combined IPCC Expert and Government Review

To encompass the vast uncertainty about what may happen by the year 2100, the IPCC developed four storylines. Each story reflects different directions of major greenhouse gas emissions influences, including population, technology and economic factors. Each story evolves dynamically over time. The divergent visions for the future world are intended to represent different combinations of the main greenhouse gas sources, thus spanning the relevant ranges of greenhouse gas emissions. The four stories are referred to as A1, A2, B1 and B2, and the major characteristics of each storyline are summarized below (IPCC, 2000):

A1: The A1 story is about a future with low population growth, rapid economic growth, and rapid introduction of new and more efficient technologies. Other characteristics of the story include convergence among regions, capacity building, and increased cultural and social interactions, with a substantial reduction in regional differences in per capita income.

A2: The A2 story is about a heterogeneous future with high population growth, regional economic growth, and fragmented technological changes. Self reliance and preservation of local identities are major themes in the A2 story.

B1: The B1 story is about a convergent future with low population growth, rapid economic growth, and sustainable technology. Economic growth moves rapidly towards a service- and information-based economy. Use of natural resources is reduced, and clean and resource-efficient technologies are introduced. The B1 storyline emphasizes global solutions to economic, social, and environmental sustainability.

B2: The B2 story envisions a future with moderate population growth, intermediate levels of economic growth, and less rapid and more diverse technological development than the A1 and B1 stories. Local solutions to economic, social, and environmental sustainability are emphasized.

Based on the four stories, the IPCC used six models and various approaches to quantify the characteristics of each story. A total of 40 scenarios were developed, each of which represents an alternative interpretation and quantification of one of the stories. All of the scenarios based on a given story are known as a scenario family. None of the scenarios include future policies that explicitly address climate change such as the United Nations Framework Convention for Climate Change or the Kyoto Protocol greenhouse gas emissions targets. However other policies included in the scenarios may affect greenhouse gas emissions. Disaster scenarios were not considered. The likelihood of each scenario was not evaluated, and thus no SRES scenario was identified as the best-guess or business-as-usual scenario.

The IPCC objectively presents the scenarios by not indicating a preference for any scenario, nor do they assign probabilities of occurrence to any of the scenarios. The IPCC intended for the scenarios to be widely used for climate change assessment: "*We recommend that the new scenarios be used not only in the IPCC's future assessments of climate change, its impacts, and adaptation and mitigation options, but also as the basis for analyses by the wider research and policy community of climate change and other environmental problems*" (IPCC, 2000).

The Climate Action Team has selected scenarios from the A2 and B1 storylines for water resources impact analysis. For these scenarios global population estimates in the year 2100 range from 7 billion people for the B1 scenario to 15 billion people for the A2 scenario (IPCC, 2001). The A2 scenario results in the highest greenhouse gas emissions, and the B1 scenario results in the lowest greenhouse gas emissions of the SRES scenarios (Figure 3.1).

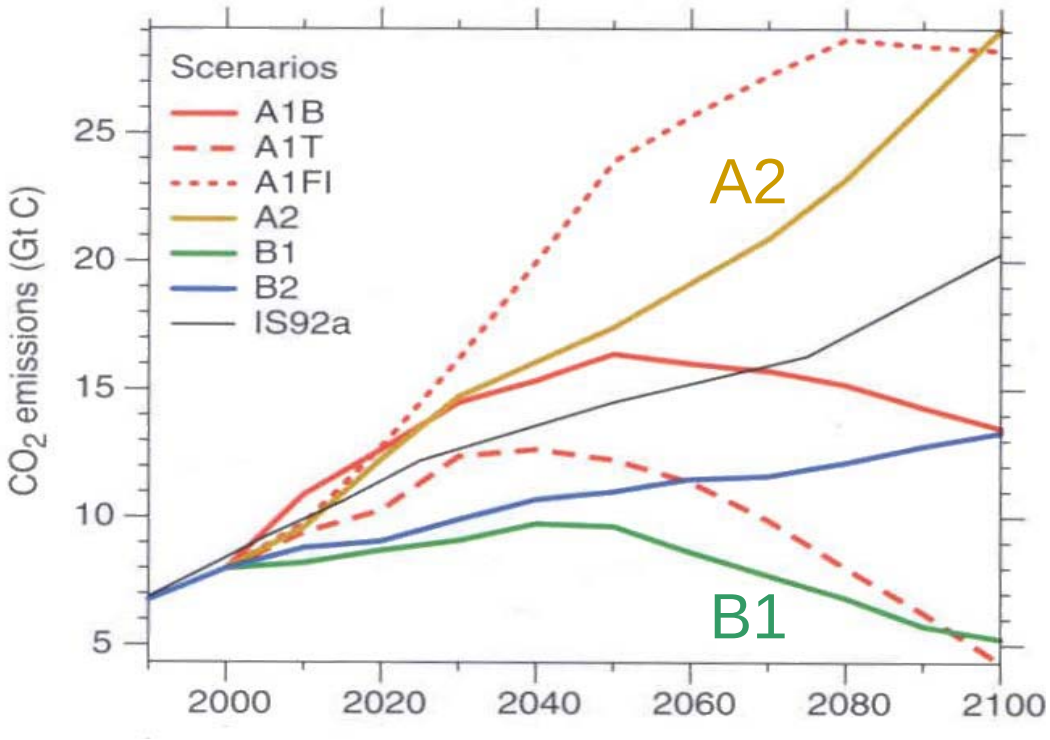


Figure 3.1 Emissions of CO_2 from Human Activities for IPCC's SRES Scenarios
Adapted from Technical Summary Figure 17 (IPCC, 2001)

3.3.2 Global Climate Models

Six Global Climate Models were used to develop IPCC's SRES emissions scenarios. The Climate Action Team (CAT) has selected the A2 and B1 emissions scenarios, each represented by two different global climate models, the Geophysical Fluid Dynamics Lab climate model (GFDL) and Parallel Climate Model (PCM). The Geophysical Fluid Dynamics Lab is part of the National Oceanic and Atmospheric Administration (NOAA). The PCM model was developed by the National Center for Atmospheric Research. The model versions, scenario name and run numbers for the four selected scenarios are given in Table 3.1. For this report, the four scenarios will be referred to by the model and scenario name.

Table 3.1 Model and Emissions Scenario Labels for Four Climate Change Scenarios

Scenario Label for this Report	GCM and SRES Scenario Description
GFDL A2	GFDL version2.1 SRESA2 run1
PCM A2	NCAR PCM version 1 SRESA2 run1
GFDL B1	GFDL version2.1 SRESB1 run1
PCM B1	NCAR PCM version 1 SRESB1 run2

The GFDL and PCM models are both state-of-the-art global climate models that represent linked oceanic, land, and atmospheric processes, including realistic representations of changes in sea surface temperatures due to the El Niño Southern Oscillation (ENSO). The climate processes in a global climate model are driven by factors known as forcings. The forcings used in these two models are summarized in Figure 3.2. Both models include forcings from greenhouse gas emissions, ozone, direct effects of sulfate aerosols, solar irradiance, and volcanic aerosols. In addition, the GFDL model includes forcings from black and organic carbon and land use or land cover. The GFDL model has a resolution of 2.0 degrees latitude by 2.5 degrees longitude, and the PCM model has a resolution of 2.8 degrees latitude by 2.8 degrees longitude. Both models were used to simulate 21st century climate change scenarios for the IPCC fourth assessment report, known as AR4, which is due out in 2007. Those simulations are archived at Lawrence Livermore National Lab's (LLNL's) Program for Climate Model Diagnosis and Intercomparison (PCMDI). The PCMDI website is http://www-pcmdi.llnl.gov/.

Model results and information for the four climate change scenarios selected by the CAT were made available for analysis on the California Climate Change Center's Web site managed by Scripps Institute for Oceanography, http://meteora.ucsd.edu/cap/cccc_model.html. Data are provided for the following variables:

- Surface latent heat flux; W/m^2
- Specific humidity at 925mb and 850mb
- Surface specific humidity; g/kg
- Total precipitation; mm/day
- Sea level pressure; mb
- Downward shortwave at the surface; W/m^2
- Upward shortwave at the surface; W/m^2
- Air temperature at 925mb, 850mb and 500mb; Kelvin
- Surface (2m) air temperature, Kelvin
- Maximum and minimum surface air temperature; Kelvin
- Zonal (east/west) wind at 925mb, 850mb and 500mb; m/s
- Surface (10m) zonal (east/west) wind; m/s
- Meridional (north/south) wind at 925mb, 850mb and 500mb; m/s
- Surface (10m) meridional (north/south) wind; m/s

Model Name/Forcing	G	O	SD	SI	BC	OC	MD	SS	LU	SO	V
GFDL v2.1	■	■	■		■	■			■	■	■
PCM	■	■	■							■	■

Shading indicates that the forcing is included on interannual or longer time scales. Forcings that only varied seasonally are not shaded.

Climate Model Forcing Factors:

G	well mixed greenhouse gases	MD	mineral dust
O	tropospheric and stratospheric ozone	SS	sea salt
SD	sulfate aerosol, direct effects	LU	land use/land cover
SI	sulfate aerosol, indirect effects	SO	solar irradiance
BC	black carbon aerosols	V	volcanic aerosols
OC	organic carbon aerosols		

Figure 3.2 Climate Model Forcings used for Climate Change Studies
Adapted from Table 5.2 (Santer et al., 2006)

A summary of the general air temperature and precipitation trends for the four climate change scenarios at the end of the 21st century is presented in Table 3.2. All four scenarios show an increase in air temperature. The PCM B1 scenario is the only scenario that shows an increase in precipitation.

For the climate change studies presented in this report, a 2050 projection level was used to reflect a water resource planning horizon. For each global climate model, projection data were available at two data points in California (Table 3.3). Average air temperature and precipitation values were computed from the global climate model results for a 30-year historical period from 1961-1990 and for a 30-year future projection period centered around 2050 (2035-2064) (Table 3.4 to Table 3.7). For comparison purposes, average historical air temperature and precipitation data for the 30 year historical period from 1961-1990 are also shown. The historical average values are based on the nearest two data stations for each site. The historical air temperature values were greater than the simulated values since the elevations of the data stations were lower than the elevations of the global climate model output locations (Table 3.3). Thus a temperature correction was applied to the historical average air temperature to adjust the value to a value that corresponds to the elevation of each global climate model output location. The historical average air temperature values for the global climate model output are within acceptable lapse rate (change of temperature with elevation) values for adjusting observed historical values (Table 3.4 and Table 3.5). The precipitation values were not adjusted for elevation since there is no straight forward correlation between precipitation and elevation.

Looking at the 2050 projections increases in air temperature range from 0.8ºC to 2.4ºC (Table 3.4 and Table 3.5). For most scenarios, warming is slightly higher in Northern California than Southern California. Projected changes in precipitation for 2050 are typically less than an inch per year. Values for both the air temperature and the precipitation projections were more

dependent on the global climate model used to represent the emissions scenario than on the emissions scenario. In other words, the projected values from a given global climate model, GFDL or PCM in this case, were closer to each other than the values for a given emissions scenario, A2 or B1 in this case. Additional global climate model results are presented in chapters 2 and 6.

Table 3.2 Air Temperature and Precipitation Trends for Climate Change Scenarios

Scenario	End of 21st Century Projection Trends
GFDL A2	Relatively strong warming Modest drying
PCM A2	Modest warming Modest drying
GFDL B1	Modest warming, Modest drying
PCM B1	Weak temperature warming Weak precipitation increase

Source: Cayan, 2005.

Table 3.3 GCM Grid Points in California

Location	Latitude degrees	Longitude degrees	Elevation m	Avg. Elevation Historical Data m
Northern California				56
GFDL	39.438	121.250	958	
PCM	40.464	120.937	1126	
Southern California				263
GFDL	35.393	118.750	850	
PCM	34.883	118.125	690	

Table 3.4 Air Temperature Projections for Northern California, °C

Northern CA	1961-1990 Average		2035-2064 Average	Difference
Historical Average	13.2		N/A	N/A
Corrected for Elevation	9.5 GFDL	8.9 PCM		
GFDL A2	9.5		11.8	2.3
GFDL B1			11.6	2.1
PCM A2	8.2		9.5	1.3
PCM B1			9.0	0.8

Table 3.5 Air Temperature Projections for Southern California, °C

Southern CA	1961-1990 Average		2035-2064 Average	Difference
Historical	16.2		N/A	N/A
Corrected for Elevation	13.6 GFDL	14.5 PCM		
GFDL A2	12.4		14.7	2.3
GFDL B1			14.5	2.1
PCM A2	14.5		15.7	1.2
PCM B1			15.4	0.9

Table 3.6 Precipitation Projections for Northern California, in/yr

Northern CA	1961-1990 Average	2035-2064 Average	Difference
Historical	27.46	N/A	N/A
GFDL A2	36.56	35.81	-0.75
GFDL B1		36.31	-0.25
PCM A2	25.03	24.41	-0.62
PCM B1		25.86	0.83

Table 3.7 Precipitation Projections for Southern California, in/yr

Southern CA	1961-1990 Average	2035-2064 Average	Difference
Historical	14.24	N/A	N/A
GFDL A2	17.92	17.70	-0.22
GFDL B1		16.15	-1.77
PCM A2	11.36	12.06	0.70
PCM B1		11.28	-0.08

3.3.3 Regional Downscaling

In order to conduct water resources impact analyses for climate change scenarios, the coarse spatial representation of the global climate model data must be refined in a process called downscaling. For the scenarios selected by the CAT, the regional climate data were produced by statistical downscaling of the global climate model output using the Variable Infiltration Capacity (VIC) model. The VIC model provides monthly output at 1/8th degree latitude/longitude resolution for the entire state of California. Daily data were computed by perturbing a historical data set based on the monthly computed climate change data from VIC. For hydrologic analysis, the VIC model output also provides stream flow, snow pack, snowmelt timing and soil moisture content (Maurer and Duffy, 2005; Maurer, 2005). Information on obtaining the downscaled data is available at the California Climate Change Center's Web site http://meteora.ucsd.edu/cap/cccc_model.html. Available climate data for a simulation period from 1950-2100 are:

- Precipitation
- Air temperature
- Wind speed
- Surface air humidity
- Soil moisture in three layers

Stream flow data for the simulation period 1950-2100 are available at the following locations:

- Smith River at Jedediah Smith State Park
- Sacramento River at Shasta Dam
- Feather River at Oroville
- North fork of the American River at North Fork Dam
- American River at Folsom Dam
- Yuba River system outflow at Marysville
- Sacramento River at the Delta
- Stanislaus River at New Melones Dam
- Tuolumne River at Don Pedro
- Merced River at Lake McClure
- King River at Pine Flat Dam

Results of the downscaled climate change data are presented in chapters 2 and 6.

3.4 Water Resources Impacts Approach

As the title of this report suggests, its main goal is to present initial methodologies and results for incorporating climate change into management of California's water resources. This report

presents preliminary studies using existing analysis tools at DWR to quantify potential water resources related effects of climate change. Whenever appropriate, studies focus on the four climate change scenarios selected by the CAT (Figure 3.3). The climate change scenario data were developed by experts in the field of climate change. The goal of DWR staff is to develop methods for incorporating that data into water resources planning and management, not to make predictions about future climate conditions. These initial studies focus on potential effects of climate change to four main California water resources areas:

- State Water Project (SWP) and Central Valley Project (CVP) operations
- Delta water quality including possible increases in sea level
- Flood management and water supply forecasting
- Changes in evapotranspiration rates and thus consumptive use of irrigation water

Each of these topics is covered in detail in separate chapters of this report.

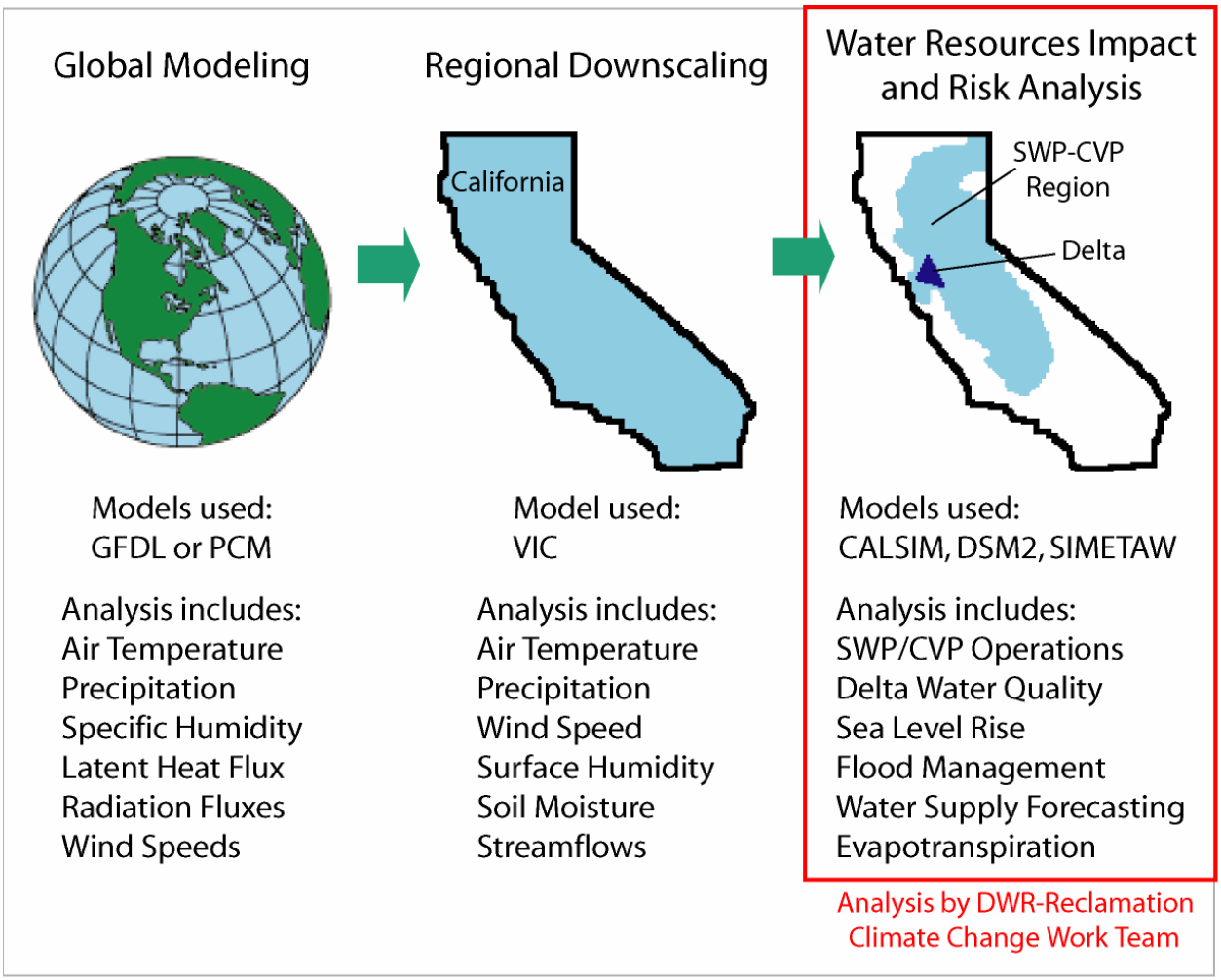


Figure 3.3 Approach for Analyzing Potential Water Resources Impacts of Climate Change

3.5 Acknowledgements

Internal review of this chapter was provided by Rich Juricich.

Analysis of historical and future air temperature and precipitation values from global climate model results were provided by Michael Anderson.

VIC data were processed and provided for download by Mary Tyree and Erik Peterson of Scripps Institution of Oceanography.

VIC data were produced by Ed Maurer at the Santa Clara University.

Information on the Global Climate Model models and emissions scenarios were provided by Dan Cayan from Scripps Institution of Oceanography and Mike Dettinger from the U.S. Geological Survey and Scripps Institution of Oceanography.

3.6 References

Cayan, D., 2005. E-mail dated posted on California Climate Change Center website discussing climate change scenario selection by the CAT. July 25, 2005. http://meteora.ucsd.edu/cap/cccc_model_prelim.html#dan25jul

DWR, 2005. California Water Plan Update 2005, Volume 1-Stategic Plan, Chapter 4: Preparing for an Uncertain Future, California Department of Water Resources, Sacramento, CA, Public Review Draft. http://www.waterplan.water.ca.gov/cwpu2005/index.cfm

IPCC, 2000. Intergovernmental Panel on Climate Change, Special Report on Emissions Scenarios, Nebojsa Nakicenovic and Rob Swart (Eds.), Cambridge University Press, UK. pp 570, http://www.grida.no/climate/ipcc/emission/.

IPCC, 2001. Intergovernmental Panel on Climate Change, Climate Change 2001: The Scientific Basis, Contribution of Working Group I to the Third Assessment Report of the IPCC, J. T. Houghton, Y. Ding, D.J. Griggs, M. Noguer, P. J. van der Linden and D. Xiaosu (Eds.), Cambridge University Press, UK. pp 944. http://www.grida.no/climate/ipcc_tar/wg1/index.htm

Maurer, E.P., 2005, Uncertainty in hydrologic impacts of climate change in the Sierra Nevada Mountains, California under two emissions scenarios, Climatic Change (submitted 29 April 2005)

Maurer, E.P. and P.B. Duffy, 2005, Uncertainty in Projections of Streamflow Changes due to Climate Change in California, Geophys. Res. Let. 32(3), L03704 doi:10.1029/2004GL021462

Santer, B.D., J.E. Penner, and P.W. Thorne, 2006: How well can the observed vertical temperature changes be reconciled with our understanding of the causes of these changes? In: Temperature Trends in the Lower Atmosphere: Steps for Understanding and Reconciling Differences. A Report by the U.S. Climate Change Science Program and the Subcommittee on Global Change Research [Karl, T.R., S.J. Hassol, C.D. Miller, and W.L. Murray (eds.)]. National Oceanic and Atmospheric Administration, National Climatic Data Center, Asheville, NC, USA (in press).

3.7 List of Abbreviations

AR4-IPCC Fourth Assessment Report

CalSim - II-Operations model of the State Water Project and Central Valley Project

CALVIN-Economics driven optimization model of State Water Project and Central Valley Project operations

CAT-Climate Action Team

CEC-California Energy Commission

DWR-California Department of Water Resources

ENSO-El Niño Southern Oscillation

GCM-Global Climate Model

GFDL-Geophysical Fluid Dynamic Lab model

GHG-Greenhouse Gas

IPCC-Intergovernmental Panel on Climate Change

LLNL-Lawrence Livermore National Lab

NCAR-National Center for Atmospheric Research

NOAA-National Oceanic and Atmospheric Administration

PCM-Parallel Climate Model

PCMDI-Program for Climate Model Diagnosis and Intercomparison

SRES-Special Report on Emissions Scenarios [IPCC, 2000]

VIC-Variable Infiltration Capacity Model

WEAP-Water Evaluation and Planning Program

Progress on Incorporating Climate Change into Management of California's Water Resources

1st Progress Report
July 2006

Chapter 4:
Preliminary Climate Change Impacts Assessment for State Water Project and Central Valley Project Operations

Authors:

Daniel Easton, Messele Ejeta, Alan Olson
California Department of Water Resources, Bay-Delta Office, Modeling Support Branch, Sacramento.

Russell Yaworsky
U.S. Bureau of Reclamation, Sacramento.

Peer Reviewers:

Richard Palmer, University of Washington

Nancy Parker, U.S. Bureau of Reclamation, Denver, CO.

4 Preliminary Climate Change Impacts Assessment for State Water Project and Central Valley Project Operations

4.1 Introduction

Planning and design of the Central Valley Project (CVP) and State Water Project (SWP) has, for the most part, assumed an unchanging climate. Of course, it was always accepted that, in California, there would be years of plentiful precipitation followed by years of scarcity; that there would be wet, cool winters followed by hot, dry summers. Weather was expected to change. In fact, it was to overcome these changing weather patterns that the CVP and SWP were primarily built; the people of California needed flood protection during the wet periods and water during the dry. But at a climactic timescale of 30 years or more, it was assumed that the average of the weather patterns would remain about the same; the frequency and severity of future droughts would be much like that of the past; precipitation would continue to fall as winter snow, and the snow would continue to melt in the spring and early summer to fill our reservoirs. That was the assumption, and a changing climate may threaten to destabilize the infrastructure and operations dependent on that assumption.

As titled, this chapter discusses a preliminary assessment of climate change impacts on the SWP and CVP. Impacts were quantified for four scenarios predicted by two global climate models at two carbon dioxide emission rates (see Table 4.1). All four climate scenarios predict a warming trend for California. The effect on annual average precipitation is varied: Three of the scenarios predict a modestly drier climate and one predicts a weak increase in precipitation. The significant change is in the timing of runoff. Most precipitation that feeds the SWP and CVP falls in the Sierra Nevada and the southern end of the Cascades that border the eastern and northern boundaries of the Central Valley. Much of it comes as snow. A warming climate will result in a greater share of rainfall and a more rapid melt of the snowpack. As such, more runoff will occur in the winter and early spring and less during the late spring and early summer.

Table 4.1 Air Temperature and Precipitation Prediction Trends for Four Scenarios

Selected Climate Model	Emission Scenario	Description
PCM	B1	Weak temperature warming Weak precipitation increase in California
PCM	A2	Modest warming Modest drying
GFDL v2.0	B1	Modest warming, Modest drying
GFDL v2.0	A2	Relatively strong warming Modest drying

The focus of this chapter is impacts on water supply. Flood control is only discussed with respect to its operational conflicts with water supply goals. Of course, the SWP and CVP do more than provide water and flood protection to California; among other things, the projects generate and use large quantities of power; they control river temperatures to protect Chinook salmon and steelhead. Climate change effects on these operations will also be discussed.

It is important to note that this is just a starting point for analyzing climate change impacts on SWP and CVP operations. Current management practices and existing system facilities were used in the analysis for this report. No changes were made to lessen the effects of climate change or sea level rise. Only four scenarios are included, and we have not addressed the likelihood of one scenario over another. Furthermore, as will be discussed in the following sections, we have not included all of the ways in which climate change may impact water supply. Therefore, what is written here is not sufficient, by itself, to make final policy decisions. Its sole intent is to introduce readers to the methods of analysis and the potential significance of climate change impacts on CVP and SWP water supply.

4.2 Description of the CVP and SWP

The CVP, operated and maintained by the U.S. Bureau of Reclamation (Reclamation), is the largest surface water storage and delivery system in California, with a geographic scope covering 35 of the state's 58 counties. Authorized project purposes include flood control, navigation, agricultural and domestic water supply, fish and wildlife protection, and power generation. The CVP is composed of some 20 reservoirs with more than 11 million acre-feet (MAF) of storage capacity, 11 power plants, and over 500 miles of major canals and aqueducts. Within the Sacramento Basin, the CVP operates Shasta and Folsom reservoirs, among others. Water is imported from the Trinity River into the Sacramento Basin through Clear Creek Tunnel. Tracy Pumping Plant exports water from the Sacramento-San Joaquin Delta for storage in San Luis Reservoir and delivery to contractors in the San Joaquin Valley. The CVP also operates New Melones Lake on the Stanislaus River and Millerton Lake on the San Joaquin River, and it exports water from the San Joaquin Basin to the Tulare Basin through the Friant-Kern Canal. Overall, the project supplies water to 250 long-term water contractors in the Central Valley, Santa Clara Valley, and the San Francisco Bay Area. Key CVP reservoirs and their storage capacities are listed in Table 4.2.

Table 4.2 Key CVP Reservoirs

Reservoir	Capacity (TAF)
Trinity	2447
Shasta	4552
Folsom	975
San Luis (CVP share)	972
New Melones	2420
Millerton	521

The SWP is operated by DWR. It consists of 32 storage facilities, 660 miles of aqueducts and pipelines, 17 pumping plants, and eight hydroelectric powerplants. Using these facilities, the SWP provides urban and agricultural water supply, flood control, recreation, fish and wildlife enhancement, power generation, and salinity-control in the Sacramento-San Joaquin Delta. The project delivers water to over two-thirds of California's population and approximately 600,000 acres of farmland through 29 urban and agricultural water districts. These agencies have long-term water supply contracts totaling 4.2 million acre-feet per year. The principal storage facility for the SWP is Lake Oroville on the Feather River in the Sacramento Valley. Banks Pumping Plant exports water from the Sacramento-San Joaquin Delta for storage in San Luis Reservoir and delivery to water contractors in the San Francisco Bay Area, San Joaquin Valley, Central Coast, and Southern California. Key SWP reservoirs and their capacities are listed in Table 4.3.

Table 4.3 Key SWP Reservoirs

Reservoir	Capacity (TAF)
Oroville	3558
San Luis (SWP share)	1067

4.3 Modeling Methodology for Quantifying Climate Change Impacts on CVP and SWP Operations

Traditionally, planning simulation models have been used to measure the effects of hydrologic, structural, or regulatory changes on SWP and CVP operations. A base case is simulated to establish expected annual average deliveries and carryover storage if no change is made. Study scenarios are then run by incorporating the expected changes to hydrology, such as those caused by climate change, or planned changes in facilities or project regulations. The impacts of the changes can then be determined by comparing base case operational statistics with those of the study scenarios.

The DWR and Reclamation have jointly developed computer model CalSim-II that simulates much of the water resources infrastructure in the Central Valley of California and Delta region. CalSim-II models all areas that contribute flow to the Delta. The geographical coverage includes: The Sacramento River Valley; the San Joaquin River Valley; the Sacramento-San Joaquin Delta; the Upper Trinity River and the CVP and SWP service areas. CalSim-II simulates operation of the CVP-SWP system for 73 years using a monthly time step. The model assumes that facilities, land use, water supply contracts, and regulatory requirements are constant over this period, representing a fixed level of development. The historical flow record October 1922-Septrember 1994, adjusted for the influence of land-use change and upstream flow regulation, is used to represent the possible range of water supply conditions.

CalSim-II uses optimization techniques to route water through a CVP-SWP system network representation. The network includes over 300 nodes and over 900 arcs, representing 24 surface reservoirs and the interconnected flow system. A linear programming (LP)/mixed integer linear programming (MILP) solver determines an optimal set of decisions for each time period given a

set of weights and system constraints. The physical description of the system is expressed through a user interface with tables outlining the system characteristics. The priority weights and basic constraints are also entered in the system tables. The programming language used, Water Resources Engineering Simulation Language (WRESL), serves as an interface between the user and the LP/MILP solver, time-series database, and relational database. Specialized operating criteria are expressed in WRESL.

The hydrology in CalSim-II was developed jointly by DWR and Reclamation. Water diversion requirements (demands), stream accretions and depletions, rim basin inflows, irrigation efficiency, return flows, non-recoverable losses, and groundwater operation are components that make up the hydrology used in CalSim-II. Demands are preprocessed independent of CalSim-II and vary according to the specified level of development (e.g., 2001, 2020) and according to hydrologic conditions. Agricultural land-use-based demands are calculated from an assumed cropping pattern and a soil moisture budget. Urban demands are typically set to contract amount, but with reductions in wet years based on recent historical data. Both land-use-based demands and contract entitlements serve as upper bound on deliveries. Environmental demands such as minimum reservoir storage requirements, minimum in-stream flows and deliveries to national wildlife refuges, and wildlife management areas are as stipulated in current regulatory requirements and discretionary interagency agreements. Sacramento Valley and tributary rim basin hydrologies are developed using a process designed to adjust the historical sequence of monthly stream flows to represent a sequence of flows at a future level of development. Adjustments to historic water supplies are determined by imposing future level land use on historical meteorological and hydrologic conditions. San Joaquin River basin hydrology is developed using fixed annual demands and regression analysis to develop accretions and depletions. The resulting hydrology represents the water supply available from Central Valley streams to the CVP and SWP at a future level of development. Groundwater has only limited representation in CalSim-II. This resource is modeled as a series of interconnected lumped-parameter basins. Groundwater pumping, recharge from irrigation, stream-aquifer interaction and interbasin flow are calculated dynamically by the model.

CalSim-II uses DWR's Artificial Neural Network (ANN) model to simulate the flow-salinity relationships for the Delta. The ANN model correlates DSM2 model-generated salinity at key locations in the Delta with Delta inflows, Delta exports, and Delta Cross Channel operations. The ANN flow-salinity model estimates electrical conductivity at the following four locations for the purpose of modeling Delta water quality standards: Old River at Rock Slough, San Joaquin River at Jersey Point, Sacramento River at Emmaton, and Sacramento River at Collinsville. In its estimates, the ANN model considers antecedent conditions up to 148 days, and considers a "carriage-water" type of effect associated with Delta exports.

CalSim-II uses logic for determining deliveries to north-of-Delta, and south-of-Delta CVP and SWP contractors. The delivery logic uses runoff forecast information, which incorporates uncertainty and standardized rule curves (i.e. Water Supply Index versus Demand Index Curve). The rule curves relate forecasted water supplies to deliverable "demand," and then use deliverable "demand" to assign subsequent delivery levels to estimate the water available for delivery and carryover storage. Updates of delivery levels occur monthly from January 1 through May 1 for the SWP and March 1 through May 1 for the CVP as runoff forecasts become

more certain. The south-of-Delta SWP delivery is determined based on water supply parameters and operational constraints. The CVP system wide delivery and south-of-Delta delivery are determined similarly upon water supply parameters and operational constraints with specific consideration for export constraints.

4.4 Generating CalSim-II Input from Global Climate Model Output

To simulate the proposed climate change scenarios, CalSim-II climate change input was needed. At a minimum, the input had to represent climate change effects on rainfall and snowmelt runoff. Global climate models (GCMs), listed previously in Table 4.1, provided projected climate data, however, the GCM data were not suitable for direct CalSim-II input for two reasons. First, CalSim-II needed streamflow data whereas the GCMs provided precipitation data. Second, CalSim-II needed data at specific locations, such as inflows to major reservoirs, whereas the GCMs provide data at a coarse resolution of only about six grid points over all of California. In other words, the type and scale of GCM output did not fit as CalSim-II input. An intermediate hydrologic model was needed.

Fortunately, such a hydrologic simulation was available. Ed Maurer, of the University of Santa Clara, had run the GCM results of interest through a macro-scale hydrologic model called the Variable Infiltration Capacity or VIC model. VIC converted the GCM precipitation data into runoff data at a $1/8^{th}$ degree grid. Both rainfall and snowmelt runoff were represented in this model. The runoff data was further processed by SCRIPPS to produce regional scale streamflow data centered on the following locations:

1) Smith River at Jedediah Smith State Park
2) Sacramento River at Shasta Lake
3) Feather River at Lake Oroville
4) Yuba River
5) North Fork of the American River
6) American River at Folsom Lake
7) Stanislaus River at New Melones Reservoir
8) Tuolumne River at New Don Pedro Reservoir
9) Merced River at Lake McClure
10) Kings River at Pine Flat Reservoir

Thus, streamflow data was available, but the regional scale of the data was still too coarse for direct CalSim-II input.

Miller, et al (2001) proposed using perturbation ratios to transfer regional scale climate change behavior to local scale historic data. This technique was used to transfer average climate change effects observed in VIC regional runoff to historic CalSim-II reservoir inflows. First, historic and projected time references were selected – 1976 and 2050 respectively. VIC monthly streamflows were averaged around these years. To adequately represent the effects of climate change, the period of average was thirty years - a recognized climatological time-scale – centered on the reference year; 1976 average monthly streamflows were calculated using the 1961-1990 VIC data, and 2050 average monthly streamflows were calculated using the 2035-2064 VIC data. Finally, perturbation ratios were calculated by dividing the 2050 VIC average

monthly streamflows by their respective 1976 VIC average monthly streamflows. The results are listed in Table 4.4, Table 4.5, Table 4.6, and Table 4.7.

Let's consider the GFDL A2 results listed in Table 4.4. The June perturbation ratio for the Smith River region was 0.62. This shows that, on average, 2050 June streamflows in this region are projected to be 38 percent less (0.62 – 1 = -0.38) than the historic reference 1976 streamflows. For comparison, consider the June perturbation ratio in the Smith River region for scenario PCM B1 – the mildly wetter climate change scenario. Results for this scenario are listed in Table 4.7. A ratio of 0.85 is listed indicating a 15 percent reduction in average streamflow in 2050 as compared to 1976. So while PCM B1 is mildly wetter than current conditions, there is still a projected reduction in runoff in the Smith River region during the late spring.

Table 4.4 Streamflow Perturbation Ratios for Scenario GFDL A2

	OCT	NOV	DEC	JAN	FEB	MAR	APR	MAY	JUN	JUL	AUG	SEP
Smith R at Jed Smith State Park	0.66	0.80	1.19	1.12	1.06	1.01	0.76	0.64	0.62	0.67	0.78	0.85
Stanislaus R at New Melones Dam	0.97	0.78	1.30	1.34	1.20	1.37	1.07	0.72	0.57	0.43	0.64	0.84
Kings R at Pine Flat Dam	0.81	0.83	1.35	1.33	1.36	1.35	1.24	1.00	0.61	0.38	0.52	0.72
Merced R at Lake McClure	0.81	0.56	2.04	1.30	1.10	1.38	1.26	0.83	0.48	0.25	0.39	0.69
Yuba R System Outflow	1.16	0.80	1.37	1.16	1.20	1.24	0.86	0.62	0.49	0.47	0.64	0.77
NF American R at NF Dam	1.34	0.73	1.43	1.07	1.17	1.25	0.83	0.56	0.40	0.26	0.48	0.69
Sacramento R at Shasta Dam	0.90	0.92	1.36	1.12	1.13	1.06	0.84	0.71	0.77	0.78	0.86	0.92
Feather R at Oroville	0.98	0.87	1.31	1.25	1.24	1.22	0.89	0.69	0.58	0.68	0.81	0.84
American R at Folsom Dam	1.22	0.70	1.35	1.13	0.95	1.28	0.77	0.48	0.45	0.44	0.67	0.83
Tuolumne R at New Don Pedro	0.88	0.80	1.36	1.31	1.08	1.31	1.19	0.84	0.49	0.48	0.68	0.81

Table 4.5 Streamflow Perturbation Ratios for Scenario PCM A2

	OCT	NOV	DEC	JAN	FEB	MAR	APR	MAY	JUN	JUL	AUG	SEP
Smith R at Jed Smith State Park	0.65	0.88	0.90	0.91	1.09	1.12	0.87	0.79	0.73	0.76	0.95	1.14
Stanislaus R at New Melones Dam	0.95	1.12	0.72	1.05	1.31	1.11	1.11	0.85	0.81	0.75	0.87	0.92
Kings R at Pine Flat Dam	0.96	1.13	0.83	1.00	1.42	1.19	1.22	1.02	0.81	0.69	0.79	0.89
Merced R at Lake McClure	0.99	1.69	0.84	0.93	1.33	1.18	1.21	0.88	0.70	0.60	0.71	0.89
Yuba R System Outflow	0.69	1.10	0.82	0.95	1.25	1.14	0.95	0.74	0.67	0.67	0.91	0.91
NF American R at NF Dam	0.58	1.19	0.71	1.00	1.26	1.14	0.91	0.69	0.61	0.49	0.90	0.90
Sacramento R at Shasta Dam	0.86	1.02	0.95	0.86	1.06	1.05	0.91	0.78	0.86	0.89	0.94	0.96
Feather R at Oroville	0.81	1.00	0.93	0.90	1.24	1.13	1.00	0.79	0.73	0.85	0.93	0.93
American R at Folsom Dam	0.69	1.13	0.65	1.01	1.35	1.05	0.91	0.65	0.68	0.68	0.92	0.93
Tuolumne R at New Don Pedro	0.98	1.17	0.75	1.02	1.27	1.11	1.15	0.93	0.71	0.81	0.90	0.92

Table 4.6 Streamflow Perturbation Ratios for Scenario GFDL B1

	OCT	NOV	DEC	JAN	FEB	MAR	APR	MAY	JUN	JUL	AUG	SEP
Smith R at Jed Smith State Park	0.56	1.20	1.16	1.18	0.98	1.26	0.85	0.74	0.69	0.74	0.92	0.99
Stanislaus R at New Melones Dam	0.82	1.36	1.13	1.47	0.84	1.03	0.99	0.72	0.55	0.48	0.67	0.85
Kings R at Pine Flat Dam	0.80	0.98	1.03	1.33	0.90	1.05	1.03	0.88	0.57	0.45	0.60	0.75
Merced R at Lake McClure	0.86	1.40	1.50	1.29	0.57	1.20	1.24	0.79	0.47	0.31	0.45	0.71
Yuba R System Outflow	0.77	2.04	1.05	1.33	0.81	1.15	0.87	0.64	0.49	0.50	0.70	0.80
NF American R at NF Dam	0.82	2.89	0.99	1.28	0.60	1.16	0.85	0.59	0.37	0.29	0.54	0.72
Sacramento R at Shasta Dam	0.77	1.26	1.11	1.32	0.96	1.17	0.90	0.78	0.80	0.84	0.91	0.95
Feather R at Oroville	0.72	1.20	1.11	1.38	1.02	1.13	0.89	0.69	0.61	0.72	0.86	0.88
American R at Folsom Dam	0.84	2.54	0.91	1.46	0.56	0.90	0.73	0.56	0.42	0.47	0.72	0.86
Tuolumne R at New Don Pedro	0.83	1.21	1.08	1.41	0.81	1.02	1.13	0.80	0.51	0.55	0.76	0.85

Table 4.7 Streamflow Perturbation Ratios for Scenario PCM B1

	OCT	NOV	DEC	JAN	FEB	MAR	APR	MAY	JUN	JUL	AUG	SEP
Smith R at Jed Smith State Park	0.99	0.90	0.90	1.06	1.00	1.37	1.12	1.02	0.85	0.85	0.95	1.23
Stanislaus R at New Melones Dam	0.96	1.19	0.73	1.26	1.18	1.28	1.20	0.95	0.81	0.83	0.92	0.93
Kings R at Pine Flat Dam	0.94	1.13	0.78	1.16	1.15	1.13	1.12	1.06	0.81	0.85	0.86	0.91
Merced R at Lake McClure	0.95	1.45	0.64	1.20	1.21	1.32	1.19	0.96	0.73	0.80	0.86	0.90
Yuba R System Outflow	0.92	1.09	0.69	1.26	1.10	1.38	1.19	0.94	0.82	0.85	0.97	0.97
NF American R at NF Dam	0.86	1.23	0.60	1.34	1.08	1.47	1.21	0.92	0.73	0.75	0.96	0.94
Sacramento R at Shasta Dam	1.14	0.94	0.90	1.10	0.97	1.30	1.17	1.02	0.97	0.98	0.99	1.00
Feather R at Oroville	0.99	0.94	0.78	1.18	1.11	1.29	1.17	0.97	0.90	0.95	0.99	0.99
American R at Folsom Dam	0.86	1.21	0.60	1.38	1.21	1.40	1.20	0.88	0.74	0.84	0.97	0.97
Tuolumne R at New Don Pedro	0.98	1.18	0.73	1.21	1.16	1.24	1.21	1.03	0.75	0.89	0.93	0.93

The CalSim-II climate change scenario input was produced using the above listed perturbation ratios. Base CalSim-II reservoir inflows were generated from the WY1922-1994 historical record. For each climate change scenario, the historical inflows were perturbed or altered by multiplying the historical inflow timeseries with corresponding perturbation ratios obtained from the VIC streamflow analysis; perturbation ratios were matched with CalSim-II inflow timeseries data based on month and geographic proximity.

The reservoir inflows that constitute the bulk of water supply for the State Water Project (SWP) and the Central Valley Project (CVP) are limited in number. They include the Sacramento River

at Shasta, the Feather River at Oroville, the American River above Folsom, all in the Sacramento Valley, and the Stanislaus, the Tuolumne, the Merced and the San Joaquin Rivers in the San Joaquin Valley. These and others, such as the Trinity River and Yuba River, are the historical inflows that were perturbed for each climate change scenario. Focusing on Sacramento Valley impacts, average monthly Shasta, Oroville and Folsom inflows for the Base and four climate change scenarios are compared in Figure 4.1, Figure 4.2, and Figure 4.3 respectively. The period of average is WY1922-1994. As shown, the climate change perturbations generally resulted in higher flows in the winter and lower in the spring and early summer as expected.

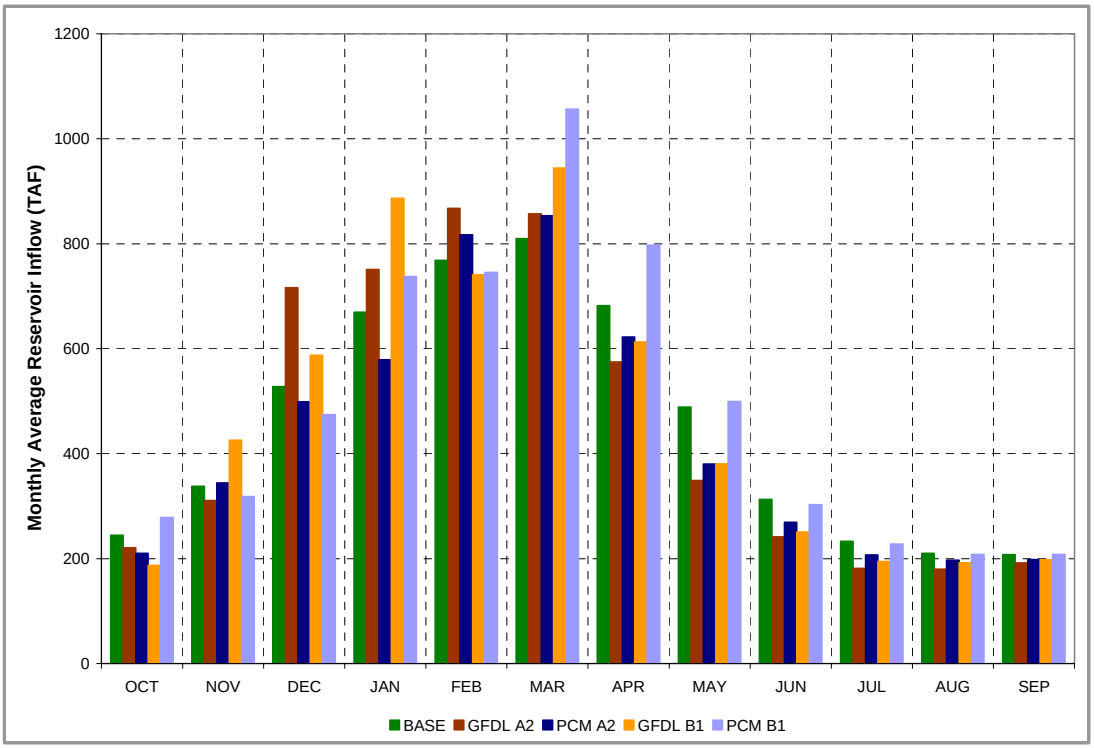


Figure 4.1 Lake Shasta Average Monthly Inflow (1922-1944)

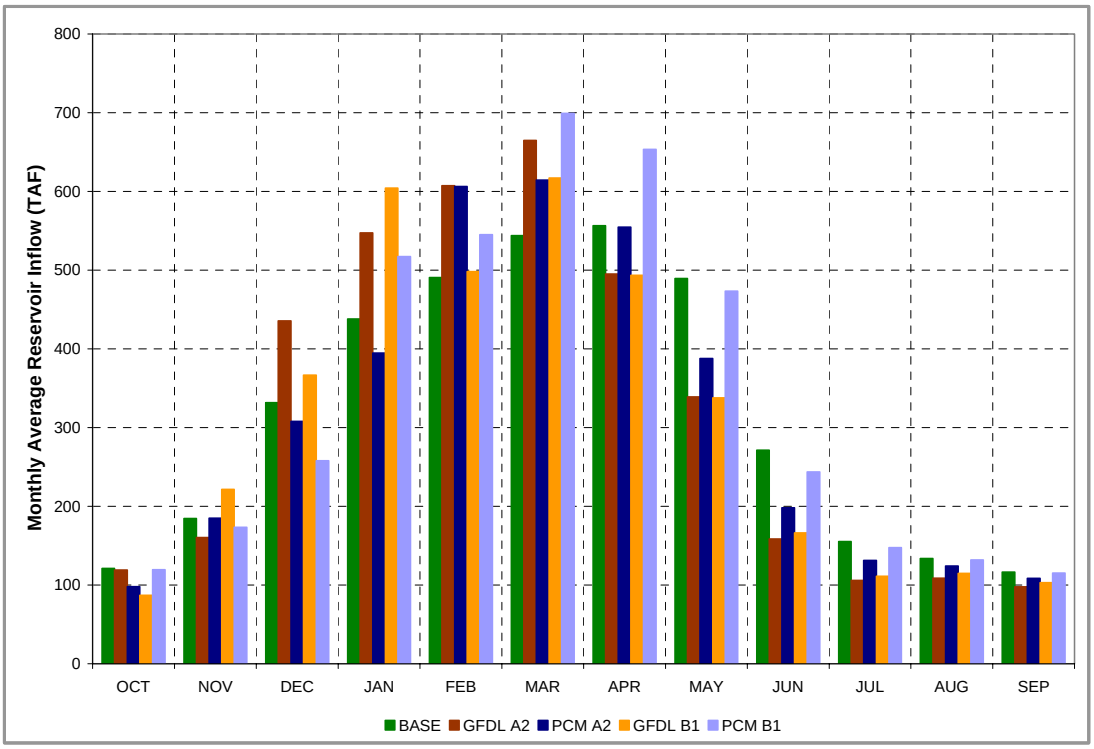


Figure 4.2 Lake Oroville Average Monthly Inflow (1922-1994)

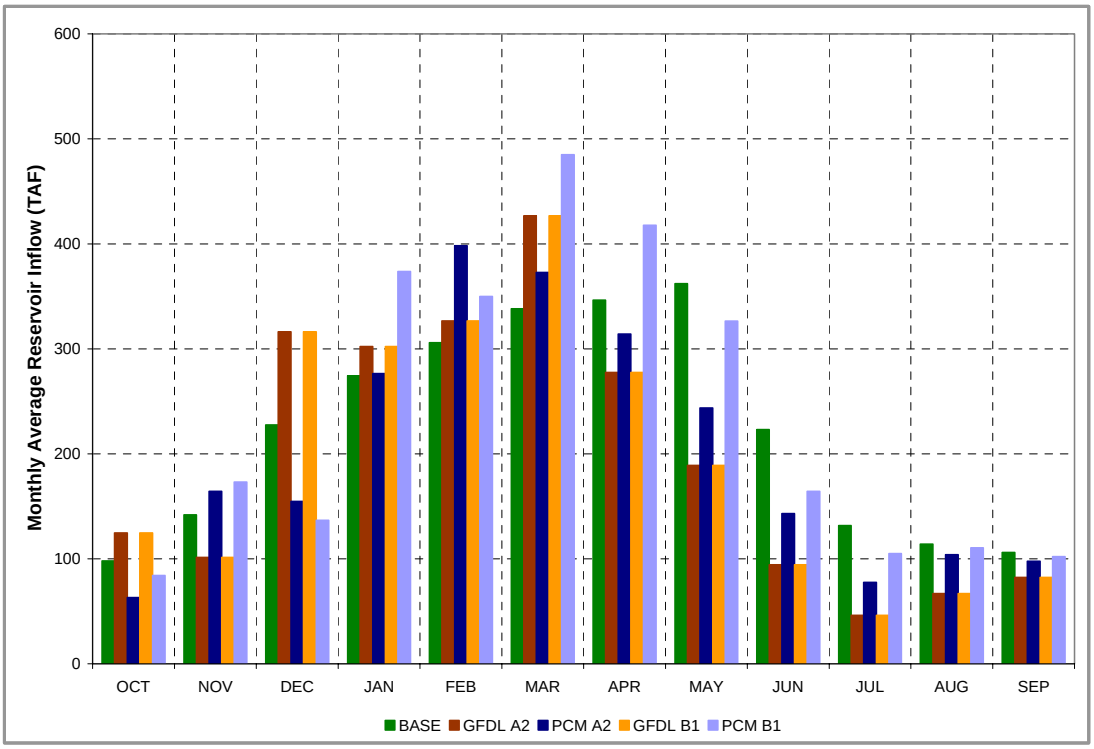


Figure 4.3 Folsom Lake Average Monthly Inflow (1922-1994)

Annual average Shasta, Oroville, and Folsom inflows are listed in Table 4.8, Table 4.9, and Table 4.10. The annual average flows for the climate change scenarios were calculated from the perturbed CalSim-II timeseries input. Inflows were averaged over the 1922 – 1994 historical period, the 1928 – 1934 and 1986 – 1992 droughts, and the 1981 – 1983 wet period.

Table 4.8 Lake Shasta Annual Average Inflow (TAF)

		BASE	GFDL A2	PCM A2	GFDL B1	PCM B1
Long-term (1922 – 1994)	Value	5492	5442	5177	5601	5854
	Change	--	-51	-315	109	362
May 1928 - Oct 1934	Value	3332	3227	3114	3321	3545
	Change	--	-106	-219	-12	213
WY 1987 - WY 1992	Value	3817	3720	3603	3859	4115
	Change	--	-97	-214	42	299
WY 1980 - WY 1983 (Wet Period)	Value	7582	7599	7223	7829	8143
	Change	--	17	-359	247	561

Table 4.9 Lake Oroville Annual Average Inflow (TAF)

		BASE	GFDL A2	PCM A2	GFDL B1	PCM B1
Long-term (1922 – 1994)	Value	3833	3840	3712	3722	4079
	Change	--	6	-122	-111	245
May 1928 - Oct 1934	Value	2174	2109	2061	2038	2282
	Change	--	-66	-113	-136	108
WY 1987 - WY 1992	Value	2002	2032	1968	1964	2163
	Change	--	30	-34	-38	161
WY 1980 - WY 1983 (Wet Period)	Value	6064	6170	5936	5995	6465
	Change	--	106	-128	-69	401

Table 4.10 Folsom Lake Annual Average Inflow (TAF)

		BASE	GFDL A2	PCM A2	GFDL B1	PCM B1
Long-term Annual Average	Value	2670	2355	2410	2368	2829
	Change	--	-315	-260	-302	159
May 1928 - Oct 1934	Value	1519	1281	1321	1277	1552
	Change	--	-238	-198	-242	33
WY 1987 - WY 1992	Value	1355	1225	1237	1239	1479
	Change	--	-130	-117	-116	125
WY 1980 - WY 1983 (Wet Period)	Value	4470	4022	4109	4057	4802
	Change	--	-449	-361	-414	332

So through a sequence of global climate models (GFDL and PCM), a regional hydrologic model (VIC), derivation of climate change runoff perturbation ratios, and, finally, applying those perturbation ratios to CalSim-II historic reservoir inflows, the CalSim-II climate change scenario input was created. The sequence of models is illustrated in Figure 4.4.

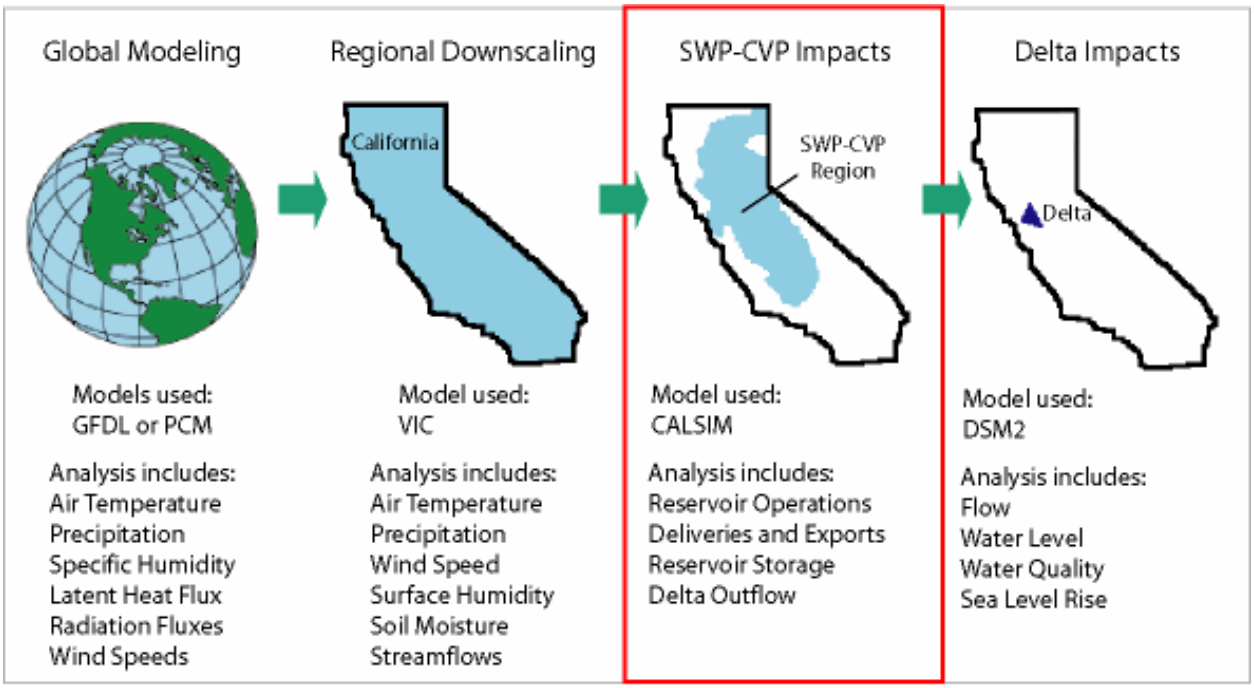


Figure 4.4 Modeling Sequence for Generating CalSim-II Climate Change Scenarios

4.5 Study Scenarios

4.5.1 Base Scenario

The base CalSim-II simulation was adapted from one of the studies presented in 2004 by the Bureau of Reclamation in support of its latest Operations Criteria and Plan (OCAP). Table 4.11 lists project and non-project demand assumptions by region. Regulatory standards and operations criteria are listed in Table 6-2 of Chapter 6 of the report *Long-Term Central Valley Project Operations Criteria and Plan* (USBR 2004). The specific study used from the OCAP analysis was Study D at a 2020 level of development. Some key regulatory and operational assumptions in this study are:

1) Delta exports, outflow and water quality are regulated according to the State Water Resources Control Board D1641 and the Water Quality Control Plan.
2) CVPIA 3406 (b)(2) is NOT included.
3) The Environmental Water Account (EWA) is NOT included.

Table 4.11 Demand Assumptions for the Base Scenario

	Base Condition
Period of Simulation	73 years (1922-1994)
HYDROLOGY **Level of Development (Land Use)**	2020 Level, DWR Bulletin 160-98
Demands **North of Delta (exc American R)**	
CVP	Land Use based, limited by Full Contract
SWP (FRSA)	Land Use based, limited by Full Contract
Non-Project	Land Use based
CVP Refuges	Firm Level 2
American River Basin	
Water rights	2020, Sacramento Water Forum[1]
CVP	2020, Sacramento Water Forum[2]
San Joaquin River Basin	
Friant Unit	Regression of historical
Lower Basin	Fixed annual demands
Stanslaus River Basin	New Melones Interim Operations Plan
South of Delta	
CVP	Full Contract
CCWD	195 TAF/YR[3]
SWP (w/ North Bay Aqueduct)	3.4-4.2 MAF/YR
SWP Article 21 Demand	MWDSC up to 50 TAF/month, Dec-Mar, others up to 84 TAF/month

[1] Sacramento Water Forum 2025 Level Demands defined in the Sacramento Water Forum's EIR
[2] Same as footnote 1
[3] Delta diversions include operations of Los Vaqueros Reservoir operations

4.5.2 Climate Change Scenarios

Four climate change scenarios were simulated for this analysis: GFDL A2, PCM A2, GFDL B1, and PCM B1. GFDL and PCM are the global climate models that generated the climate scenarios. A2 and B1 indicate the different assumed rates of carbon loading in each scenario (see Table 4.1). Global climate model results were downscaled for input as CalSim-II inflow as described in Section 4.4.

The following monthly inflows were perturbed with the factors listed in Table 4.4 - Table 4.7:

1) Trinity River at Trinity Lake
2) Sacramento, McCloud, and Pit Rivers at Shasta Lake
3) Feather River at Lake Oroville
4) Yuba River upstream of the confluence with the Feather River
5) North and South Forks of the American River at Folsom Lake
6) Stanislaus River at New Melones Lake
7) Tuolumne River at New Don Pedro Reservoir
8) Merced River at Lake McClure
9) San Joaquin River at Millerton Lake

Since the monthly perturbation factors repeat themselves on an annual basis, the annual hydrology of both base and climate change scenarios maintain the same pattern of wet years and droughts. Specifically, the droughts of 1929-1934, 1976-1977, and 1987-1992 are preserved and, overall, a wet year in the base is a wet year in the climate change scenarios; there is just modestly less or more precipitation on an annual basis depending on the scenario.

The significant change in inflows between the base and climate change scenarios was in the seasonal distribution of runoff. Generally, as shown in Figure 4.1 - Figure 4.3, more runoff occurred from December through March while less came in the remainder of the year. This seasonal change in runoff was most significant in scenarios GFDL A2 and GFDL B1. It was least significant in PCM B1, and PCM A2 lies somewhere in between. A simple explanation for the change in seasonal runoff patterns is that more precipitation will fall as rain than snow in a warmer climate. More rainfall leads to more runoff in the wet months whereas less snowfall results in a smaller snowpack and less snowmelt in the dry months.

What wasn't changed between the base and climate change scenarios? There were no structural changes – no added storage, pumping, and canal capacity. No changes were made to system regulations. The CVP and SWP continued meeting minimum in-stream flow requirements. The projects continued meeting the Delta outflow and water quality standards established by the State Water Resources Control Board in Decision 1641 and the Water Quality Control Plan. Water use remained at a year 2020 level of development, and operational rules such as flood control and delivery allocations are applied consistently in base and climate change scenarios.

Current management practices and existing system facilities were used in the analysis for this report. No changes were made to lessen the effects of climate change or sea level rise.

No changes were made to:

- ❑ System structures, such as added water storage, pumping, or canal capacity
- ❑ Reservoir operating rules, such as changing the space required for flood control
- ❑ Streamflow requirements
- ❑ Water quality standards
- ❑ Delta outflow requirements
- ❑ Operations to account for sea level rise

4.5.3 Climate Change Impacts Not Considered in the Study Scenarios

There are also some key climate change impacts that were not considered in the study scenarios. With changing rates of evapotranspiration, it is expected that urban (landscaping) and agricultural demand for CVP and SWP water will change accordingly, but no changes in demand were included in the climate change scenarios. Another anticipated result of a warming climate is a rising sea level. While the climate change scenarios are held to the same

Delta salinity standards as in the base scenario, the effect of a rising sea level on the projects' ability to meet those standards was not accounted for; it is assumed in all scenarios that sea level remains unchanged. Future work will include development of a tool for modifying system operations to maintain Delta water quality standards under sea level rise conditions. Note that sea level rise scenarios discussed in Chapter 5 section 5.5 use operations based on present sea level.

Furthermore, the method of downscaling global climate model information for CalSim-II input only captures the general trends of average rainfall and seasonal shifts in runoff. There is no information included about changes in weather variability. In each of the scenarios, the frequency and length of the droughts remained the same. If climate change influences these underlying weather phenomena, then we are missing important information necessary to determine impacts to CVP and SWP operations.

4.6 Results

Results of the CalSim-II base and climate change scenarios are presented and compared in this section. Given that the primary purpose of the CVP and SWP is water supply, the key CVP and SWP operational measures presented are water shortages, contractor deliveries, and carryover storage. Then, to begin the search for operational flexibility in dealing with climate change impacts on water supply, the significance of various operational constraints was analyzed. Of course, the CVP and SWP have other important responsibilities such and fish and wildlife enhancement and power supply. Therefore, at the end of the section, climate change impacts on in-stream temperatures and power supply are also discussed.

Before reviewing the results, though, please note that the purpose of this report is to demonstrate how various analysis tools currently used by DWR could be used to address issues related to climate change. The methods and results presented in this report could be used to guide future climate change analysis and to identify areas where more information is needed. All results presented in this report are preliminary, incorporate several assumptions, reflect a limited number of climate change scenarios, and do not address the likelihood of each scenario. Therefore, these results are not sufficient by themselves to make policy decisions.

4.6.1 Shortages

To discuss CalSim-II shortages, we must first discuss water use priorities. There are many competing demands for the water that flows into the Central Valley. They include farm irrigation, urban and industrial use, ecosystem protection and restoration, and reservoir storage for hydropower production, recreation or for later use in the next inevitable drought. In CalSim-II, distribution of water is prioritized as listed in Table 4.12.

Table 4.12 CalSim-II Water Use Prioritization

First Priority	prior right water users, minimum in-stream flow requirements, WQCP requirements
Second Priority	SWP Table A contractors, CVP contractors
Third Priority	reservoir storage for the next year (carryover)
Fourth Priority	SWP Article 21 deliveries

While CVP and SWP contractor deliveries take precedence over next year's storage, a balance between the two is struck in the allocation decision. During the winter and spring, the SWP and CVP decide how much of contractor demand can be met for the year based on available storage and forecasted runoff. Part of the allocation decision is to ensure that enough water is left in storage at the end of the year in case of impending drought. Once the allocation decision is made though, deliveries to meet that allocation take priority over maintaining the storage carryover target.

Given this simple explanation of prioritization, there are two types of shortages in CalSim-II. One is an acceptable, though not desirable, result of making water allocations based on imperfect forecasts. In wetter years, the SWP and CVP sometimes allocate more south-of-Delta (SOD) deliveries than can be delivered through the pumps due to various export constraints. For the base and four climate change scenarios, this type of shortage is infrequent and, compared to total annual deliveries, insignificant. This type of shortage is also implicitly included in the delivery analysis; if it's not delivered, we don't count it.

The other type of shortage is usually unacceptable. This is when the first priority obligations – prior right contracts, minimum in-stream flow requirements, Delta requirements – are not met. The only way for this shortage to occur in CalSim-II is for one or more North-of-Delta reservoirs to be drawn down to dead storage. At this point, the model has lost control of meeting the watershed's most basic needs not to mention the lawful obligations of the CVP and SWP. Such a simulation is broken. The lower priority metrics are questionable: Could the shortage of high priority water uses be avoided at the expense of lower priority uses through some simple changes in operating rules? And the results of a broken simulation can not be confidently compared to an unbroken simulation.

Table 4.13 shows that Shasta and Folsom reservoirs were at dead storage for a significant number of months in scenarios GFDL A2, PCM A2, and GFDL B1. These months are all concentrated in the critical year of 1924 and the droughts of 1929-1934, 1976-1977, and 1987-1992. During these months, streamflow requirements were not met on the Sacramento and American rivers and the CVP was unable to contribute its Coordinated Operation Agreement defined share of in-basin use. The base scenario had one month of shortage on the American and Sacramento rivers – October 1977. Due to the severity of the 1976-1977 drought, this is frequently unavoidable in CalSim-II simulations.

Table 4.13 Months of Critical Shortages (Storage at Dead Pool)

	Shasta (months)	Oroville (months)	Folsom (months)
BASE	1	0	1
GFDL A2	31	0	28
PCM A2	29	0	22
GFDL B1	21	0	20
PCM B1	0	0	0

The length of shortages in GFDL A2, PCM A2, and GFDL B1 indicate that the delivery results presented for these scenarios in the next section are not always reliable. Too much risk was taken in the delivery allocation decisions of these three scenarios and not enough storage was carried into the drought periods as a result. In future climate change simulations, modifications to the rule that divides available water into delivery and carryover should be investigated as a means to prevent these shortages. Since CVP allocations are dependent on Shasta and Folsom storage, such modifications will likely alter the resulting delivery capability of the CVP as compared to the results presented in the next section.

4.6.2 Delivery and Storage Analysis

As shown previously in Figure 4.1, Figure 4.2, and Figure 4.3, the general effect of climate change on runoff is that more comes in the winter, when we don't need it, and less comes in spring and summer, when we do need it. One would expect that this shift in runoff will make it more difficult for the CVP and SWP to capture water and deliver it to their customers. The resulting annual average deliveries to Table A contractors listed in Table 4.14 fit these expectations for three of the four climate change scenarios. GFDL B1, with 2,861 TAF annual average deliveries, was 10.2 percent less than the Base scenario annual average of 3,186 TAF. PCM A2 and GFDL A2 also reduced Table A deliveries below the Base. On the other hand, in PCM B1, the scenario that was slightly wetter than the Base, the SWP managed to make 1.2 percent more Table A deliveries on an annual average basis – increasing deliveries from 3,186 to 3,224 TAF. The dry year samples of Table A deliveries listed in Table 4.14 show that the SWP did better in the Base scenario than in GFDL A2, PCM A2, and GFDL B1 in most instances. The exception was the single dry year of 1977 – no doubt the result of the higher Table A allocation in the Base scenario for the first year of the 1976-1977 drought. PCM B1 results in higher dry year Table A deliveries than the Base in all instances except for the 1976-1977 drought.

Table 4.14 SWP average and dry year Table A deliveries (TAF)

	Average	*Single dry year 1977*	*2-year drought 1976-1977*	*4-year drought 1931-1934*	*6-year drought 1987-1992*	*6-year drought 1929-1934*
BASE	3186	222	1620	1521	1786	1679
GFDL A2	2879	229	892	1355	1396	1554
PCM A2	2964	279	1049	1343	1651	1458
GFDL B1	2861	285	952	1386	1502	1507
PCM B1	3224	267	1413	1870	1807	1949

While Table 4.14 contrasts annual average deliveries of the Base and climate change scenarios, a more useful comparison is delivery capability. This comparison was made using delivery exceedance probability curves which show the likelihood that some quantity of water or more was delivered in a given scenario. Each curve was assembled from the 73-year annual delivery sample provided by the CalSim-II simulation. For instance, let's say that in one simulation SWP Table A contractors were delivered more than 4 million acre-feet of water in 16 of the 73-year simulation. Therefore, one point on the curve would match the 78 percent (16/73 = 78 percent) probability of exceedance with a delivery of 4 million acre-feet.

Figure 4.5 shows the exceedance probability curves for SWP Table A deliveries. GFDL A2, PCM A2, and GFDL B1, all with slightly drier climates and significant shifts in seasonal runoff, resulted in consistently lower delivery capability. It does not matter whether the deliveries are low or high. PCM B1, with the slightly wetter climate and no significant reduction in runoff in the late spring and summer, resulted in higher delivery capability for SWP Table A contractors at the lower end of the delivery spectrum and roughly equivalent capability at the higher end. This is consistent with the results shown in the dry-period analysis of Table 4.14. The 50 percent exceedance level delivery represents the median delivery of the 73-year simulation. As shown in Figure 4.5, the Base scenario delivery with a 50 percent probability of exceedance was highest at 3551 TAF. PCM B1 was close behind. GFDL A2 has the lowest delivery at 50 percent exceedance; at 3,154 TAF, it is 11.2 percent less than the base scenario.

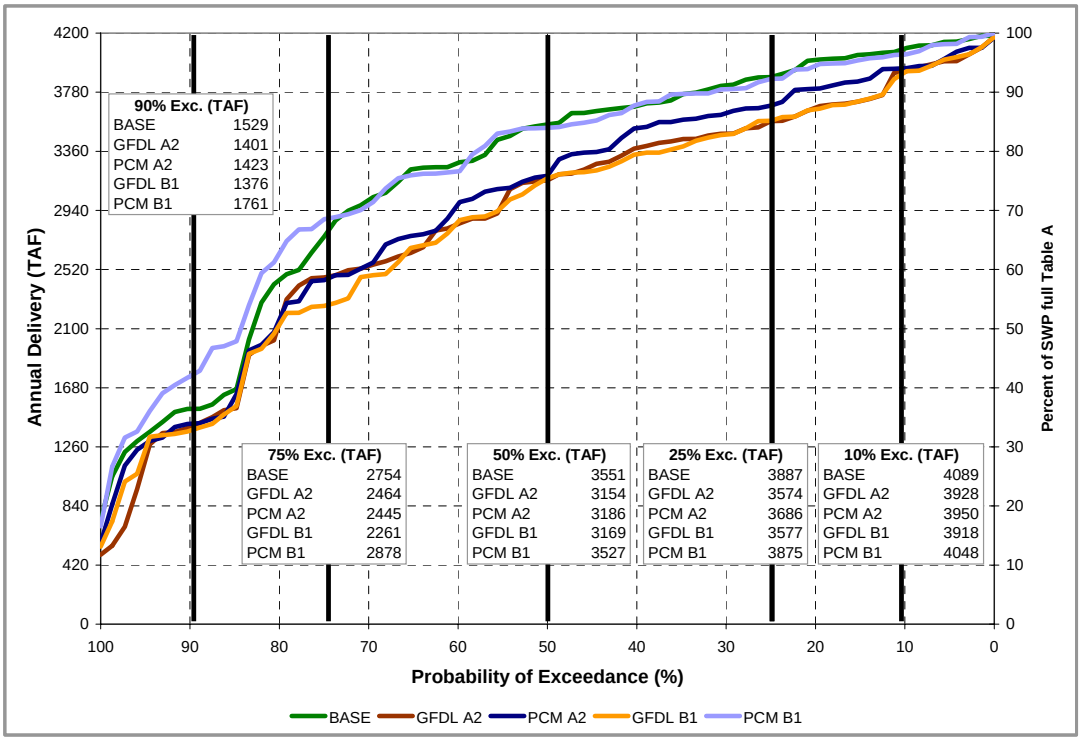


Figure 4.5 Exceedance Probability Plot of SWP Table A Deliveries

Carryover storage was analyzed in a similar fashion. SWP carryover storage is the sum of Oroville storage and SWP San Luis storage on September 30 – the end of the water year. Figure 4.6 shows the probability of exceedance plot for SWP carryover storage. Again, this is constructed from the 73-year simulation sample. As shown, the persistence of SWP carryover storage in scenarios GFDL A2, PCM A2, and GFDL B1 was consistently lower than the Base. The greatest difference was at the 10 percent exceedance level; GFDL B1, at 2,677 TAF carryover, is 28 percent less than the SWP carryover of 3,718 TAF for the Base scenario. However, during the dry years, the SWP was able to change operations and allocations sufficiently to make up for this carryover deficit and avoid unnecessary shortages. Note the convergence of the SWP carryover exceedance curves as you go from 10 percent probability to 90 percent. Base and GFDL A2 carryover were respectively 1,342 TAF and 1,202 TAF at the 90 percent exceedance level. This is a 10 percent reduction in carryover as compared to the 28 percent reduction at the 10 percent exceedance level. Overall, with the drier climate scenarios, less water was delivered to Table A contractors and more risk with SWP carryover storage was taken to do it. The SWP carryover storage in scenario PCM B1 tended to be slightly more dependable than the base for carryover under 2,250 TAF and slightly less dependable than the base for carryover greater than 2,250 TAF. This is also consistent with results shown earlier. The wetter climate of PCM B1 paid off during the drought periods when plenty of storage was available to dampen the added seasonal variability. The SWP was able to capture and deliver this water during the droughts. During the wetter periods though, the storage capacity wasn't available to capture the larger winter runoff. To maintain deliveries, carryover was then reduced.

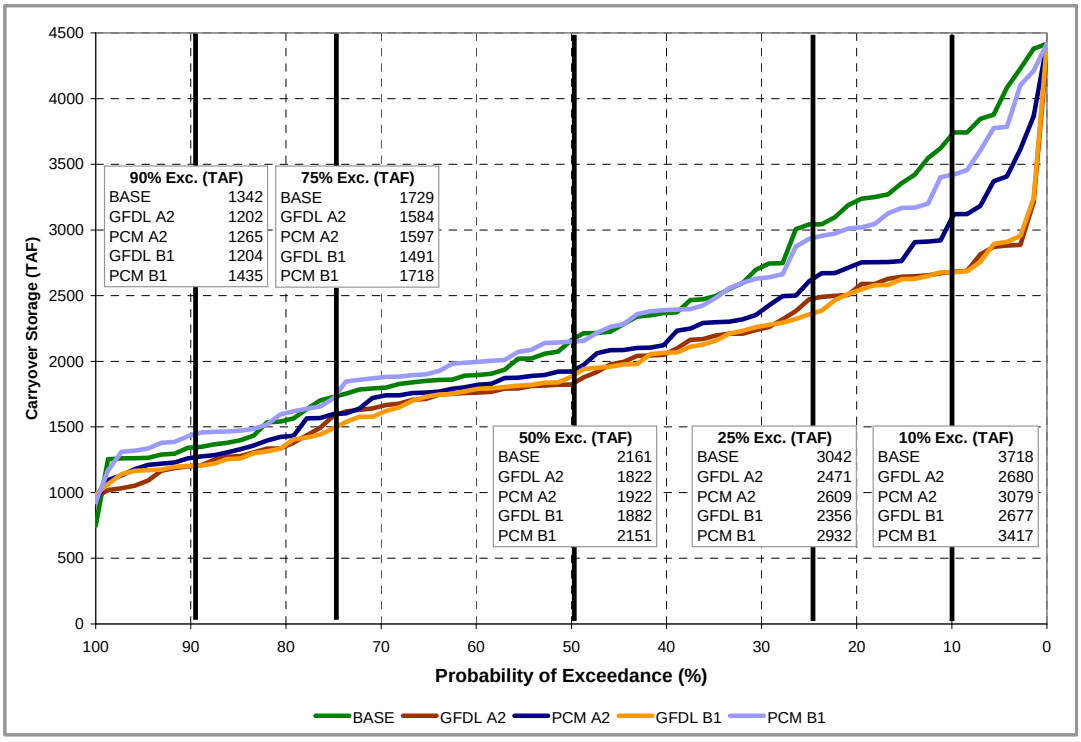


Figure 4.6 Exceedance Probability Plot of SWP Carryover Storage

SWP Article 21 deliveries were not affected by climate change in the same way as Table A deliveries. Having a lower priority than storage, as discussed in Section 4.6.1, Article 21 deliveries were only made when San Luis was full and Delta surplus and Banks pumping capacity were available. Whereas the bulk of Table A deliveries came in the summer and are dependent on the storage of winter precipitation, Article 21 deliveries were primarily made in the winter when surplus conditions existed. The larger winter runoff and lower Table A allocations resulted in higher average Article 21 deliveries for scenarios GFDL A2, PCM A2, and GFDL B1 as shown in Table 4.15. GFDL A2 annual average Article 21 deliveries were increased by 7 TAF from the Base – 99 to 106 TAF. In contrast, GFDL A2 annual average Table A deliveries were decreased 307 TAF from the Base – 3,186 to 2,879 TAF (see Table 4.14). Table 4.15 shows that PCM B1 annual average Article 21 deliveries were reduced in comparison to the Base scenario by 11 TAF. During the 1929-1934 drought, Article 21 contractors lost 69 TAF in scenario PCM B1 as compared to the Base scenario. This happened because higher Table A deliveries were made during this drought in PCM B1 than in the Base. Table 4.14 shows that PCM B1 and Base annual average Table A deliveries during the 1929-1934 drought were 1,949 TAF and 1,679 TAF respectively – a difference of 270 TAF. With higher Table A deliveries, San Luis did not fill as frequently resulting in less Article 21 delivery opportunities.

Table 4.15 SWP average and dry year Article 21 deliveries (TAF)

	Average	*Single dry year 1977*	*2-year drought 1976-1977*	*4-year drought 1931-1934*	*6-year drought 1987-1992*	*6-year drought 1929-1934*
BASE	99	0	0	157	34	111
GFDL A2	106	0	0	188	119	133
PCM A2	103	0	0	194	27	149
GFDL B1	101	0	0	170	52	132
PCM B1	88	0	0	54	39	42

Article 21 delivery capability is illustrated for the Base and climate change scenarios in Figure 4.7. As shown, in all scenarios, no Article 21 deliveries were made in more the 40 percent of the 73 years of simulation. PCM B1 had no Article 21 deliveries in 50 percent of the years. The drier climate change scenarios – GFDL A2, PCM A2, and GFDL B1 – resulted in more frequent Article 21 deliveries. Yet, at the lower probabilities of exceedance, such as 5 percent and 10 percent, the Base and PCM B1 scenarios tended to produce larger Article 21 deliveries.

As expected, the shift in seasonal runoff and slightly drier climate of scenarios GFDL A2, PCM A2 and GFDL B1 reduced annual average deliveries to CVP South-of-Delta contractors. Table 4.16 lists CVP SOD deliveries. The annual average deliveries in the Base and GFDL A2 scenarios were 2,716 and 2,435 TAF respectively – a 10.3 percent reduction. Just as with SWP Table A deliveries, scenario PCM B1 increased annual average CVP SOD deliveries as compared to the Base. The increase was 69 TAF – 2.5 percent of Base CVP SOD deliveries. With the drier climates, less was delivered to CVP SOD contractors during each of the droughts in scenarios GFDL A2, PCM A2, and GFDL B1. Drought CVP SOD deliveries were larger in PCM B1 than in the base in all instances except for 1976-1977.

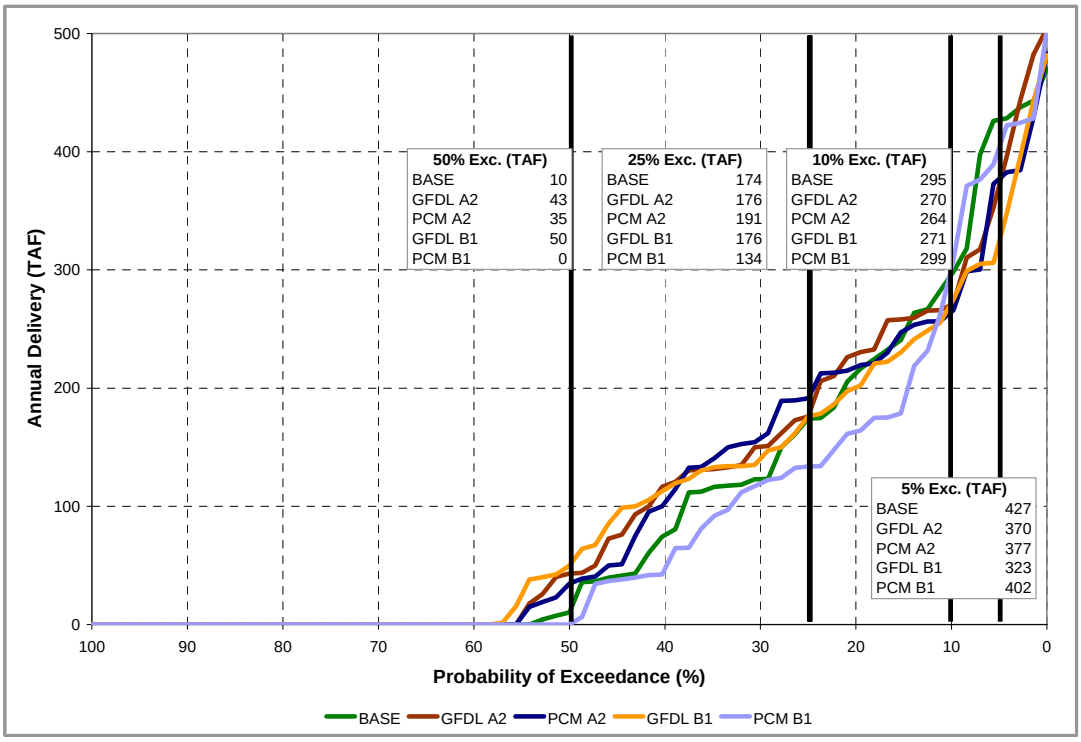


Figure 4.7 Exceedance Probability Plot of SWP Article 21 Deliveries

Table 4.16 CVP South-of-Delta contractor deliveries (TAF)

	Average	*Single dry year 1977*	*2-year drought 1976-1977*	*4-year drought 1931-1934*	*6-year drought 1987-1992*	*6-year drought 1929-1934*
BASE	2716	1358	1704	1362	1806	1538
GFDL A2	2435	1108	1434	1217	1529	1320
PCM A2	2545	1243	1583	1225	1580	1341
GFDL B1	2489	1217	1546	1240	1634	1344
PCM B1	2785	1354	1686	1541	1953	1688

Capability of CVP SOD deliveries decreased for the drier scenarios both at the high and low ends of the probability spectrum. Figure 4.8 shows that the Base median (50 percent exceedance) CVP SOD delivery was 2,963 TAF. The median delivery of scenario GFDL A2 is 2,533 TAF. This equals a 14.5 percent reduction in delivery capability at a 50 percent probability of exceedance. PCM B1 shows more capability than the base in the 60 percent-100 percent exceedance probability range. Annual deliveries of this size (1,500 TAF – 2,750 TAF) typically occurred in the drier years. As such, the higher capability of CVP SOD deliveries in PCM B1 as compared to the base conforms to the higher dry year deliveries shown in Table 4.16.

CVP carryover storage was reduced in the in the drier scenarios and increased in the wetter scenario as compared to the Base. Figure 4.9 plots exceedance probability for CVP carryover storage – defined as the sum of Trinity, Shasta, Folsom, and CVP San Luis storage on September 30, the end of the water year. For GFDL A2, PCM A2, and GFDL B1, higher risks of shortage were taken (lower carryover) and still resulted in lower SOD CVP deliveries. With PCM B1, carryover was more dependable and helped the CVP increase deliveries in the droughts.

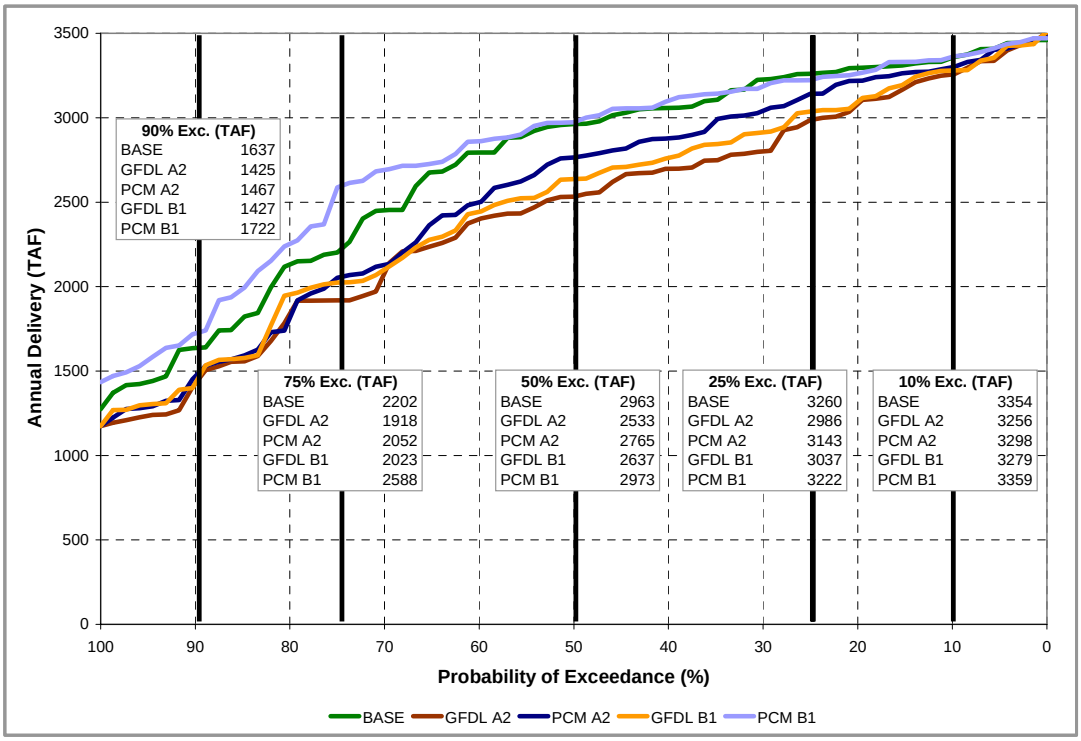


Figure 4.8 Exceedance Probability Plot of CVP South-of-Delta Deliveries

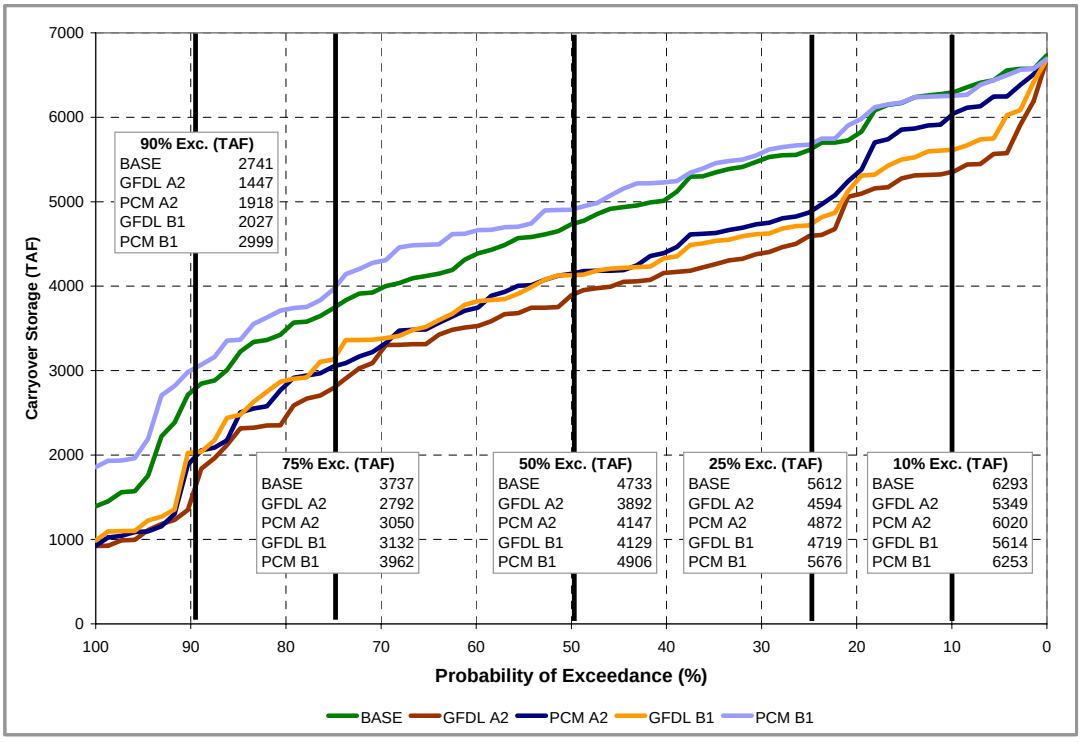


Figure 4.9 Exceedance Probability Plot of CVP Carryover Storage

Table 4.17 shows the annual average CVP north-of-Delta (NOD) deliveries were not as significantly affected by climate change as the CVP SOD deliveries. Base and GFDL A2 annual average CVP NOD deliveries were 2,251 and 2,181 TAF respectively. This equals a 3.1 percent reduction. In contrast, GFDL A2 CVP SOD deliveries were reduced 10.3 percent. There were some significant changes in CVP NOD deliveries during the dry periods. For instance, as shown in Table 4.17, Base and GFDL A2 annual average CVP NOD deliveries during the 1929-1934 drought were 1,940 TAF and 1,742 TAF respectively – a decrease of 10.2 percent. However, this decrease was less of a result of lowered allocations as it was of the critical shortages at Shasta and Folsom. When these reservoirs were drawn down to dead storage during the drought, settlement contractors and refuges were shorted their promised supply. These shortages are reflected in the annual average deliveries presented in Table 4.17.

Table 4.17 CVP North-of-Delta contractor deliveries (TAF)

	Average	*Single dry year 1977*	*2-year drought 1976-1977*	*4-year drought 1931-1934*	*6-year drought 1987-1992*	*6-year drought 1929-1934*
BASE	2251	1847	2076	1815	2061	1940
GFDL A2	2181	1803	2026	1551	1937	1742
PCM A2	2204	1798	2040	1572	1999	1759
GFDL B1	2204	1823	2048	1669	2024	1823
PCM B1	2265	1847	2073	1849	2089	1967

Why were CVP NOD deliveries not as affected by climate change as CVP SOD deliveries? The reason is that different classes of water contracts have different allocation rules. Over 80 percent of CVP NOD deliveries were for settlement contracts or refuges, and delivery allocations for these water users were independent of available storage. NOD settlement contractors and refuges receive 100 percent of contract demand in all years except Shasta critical years; in these years, 75 percent of contract demand is met. (Shasta critical years are defined as years in which Shasta natural inflow totaled less than 3.2 million acre-feet, or as years where the two year total Shasta natural inflow was less than 7.2 million acre-feet and the previous years natural inflow was less than 4 million acre-feet.) SOD exchange contracts and refuges are allocated water in the same way, but these water users represent only around 34 percent of SOD demand. In the Base scenario, nine of the 73 years were Shasta critical. From analysis of Shasta inflow, drier scenarios GFDL A2 and GFDL B1 have exactly the same distribution of Shasta critical years as the Base, drier scenario PCM A2 would add only a single Shasta critical year, and wetter scenario PCM B1 would reduce the number of Shasta critical years by three. For purposes of this study, though, it was assumed that the distribution of Shasta critical years in each climate change scenario remained unchanged from the Base. In the years this assumption was false – one in PCM A2, three in PCM B1 – only small changes in Shasta inflow would be required for the exact definition of Shasta critical to be met. Therefore, the assumption is reasonable. With no change in the number or order of Shasta critical years, water allocations for 80 percent of CVP NOD deliveries and 34 percent of CVP SOD deliveries were the same for the Base and climate scenarios. On the other hand, 66 percent of CVP SOD deliveries and only 20 percent of CVP NOD deliveries were exposed to allocation cuts due to climate change effects on available storage. Thus, total CVP SOD deliveries were more exposed to the negative effects of climate change than CVP NOD deliveries.

Figure 4.10 shows the CVP NOD delivery capability curves for all five scenarios. Capability of these deliveries in the climate change scenarios closely tracked that of the Base in the 0 percent

to 90 percent exceedance probability range. No critical shortages occurred in the years that fall in this range. Given that settlement contract and refuge deliveries were equal in all five scenarios during these years and that these types of deliveries make up more than 80 percent of the total, the fact that the capability curves for CVP NOD deliveries track so closely is expected. In the 0 percent to 90 percent exceedance probability range, GFDL A2, PCM A2, and GFDL B1 have slightly lower deliveries than the Base or PCM B1. This is due to the less than 20 percent of deliveries that are subject to allocation decisions based on available storage. The divergence of the capability curves in the 90 percent to 100 percent exceedance probability range reflects the years of shortage. GFDL A2 shorted settlement contractors and refuges the most. The Base and PCM B1 scenarios continue to track closely in the 90 percent to 100 percent range because neither experienced extreme shortages.

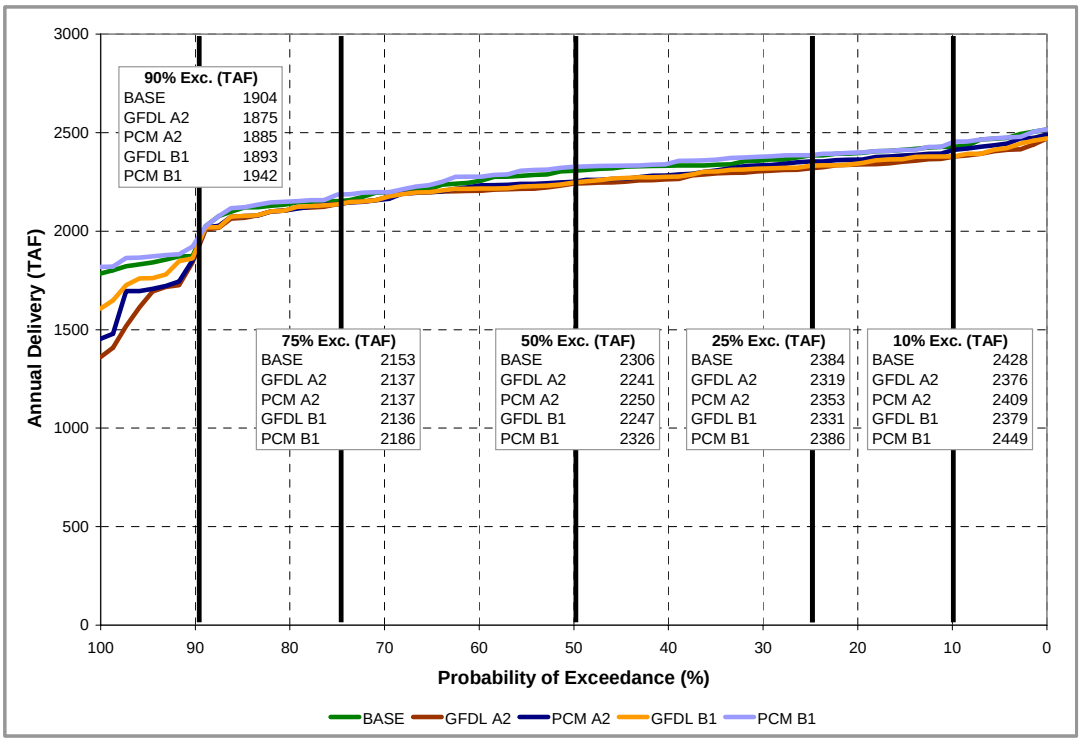


Figure 4.10 Exceedance Probability Plot of CVP North-of-Delta Deliveries

As shown in the above delivery and storage analysis, SWP Table A deliveries and CVP SOD deliveries were negatively affected by the drier climate change scenarios – GFDL A2, PCM A2, and GFDL B1. Carryover was also reduced in these scenarios. With less annual average runoff and a shift in seasonal flows, both projects were less effective capturing, storing, and delivering water. The wetter scenario, PCM B1, had an opposite effect despite the seasonal shift in runoff. During droughts, the additional water was readily captured and delivered with available storage and export capacity. Obviously, the likelihood of a wetter or drier climate will be an important consideration in climate change planning studies. In this case, PCM B1 is the outlier. Does this mean the wetter scenario is less probable than a drier scenario? That is a question that must be addressed.

4.6.3 North-of-Delta Operations Analysis

The purpose of this section is to discuss the interaction between some basic North-of-Delta operational constraints, the climate changed runoff, and impacts to water supply. The constraints of focus are flood control storage and minimum in-stream flow (MIF) requirements. Maintaining flood pool storage in reservoirs during the winter months reduces water supply capacity. Therefore, flood control operations could limit the projects' ability to capture the increased reservoir inflow due to climate change. On the other hand, MIF requirements draw water from NOD storage during extended dry periods. This can lead to a NOD-SOD storage imbalance which adds to the risk of critical NOD shortages like those that occurred in scenarios GFDL A1, PCM A1, and GFDL B1.

Figure 4.11, Figure 4.12, and Figure 4.13 show the monthly frequency that flood pool capacity limited the capture of water for long-term storage in Shasta, Oroville, and Folsom reservoirs respectively. In these frequency plots, flood control included instances that flood pool capacity is zero and the reservoirs were full -- typically in late spring and early summer. It also included late summer and early fall releases to initially free up flood pool capacity. The flood control frequency plots have nothing to do with flooding downstream; they simply show the probability that water was released from a reservoir to preserve flood pool capacity or overtopping of the reservoir in the case that the reservoir was full.

The climate change scenarios, as compared to the Base, increased inflows to Shasta, Oroville and Folsom over the December to March flood season. Shasta and Oroville reserve most of their capacity for water supply, while Folsom's primary function is flood control. It is expected that flood control frequency of Folsom will be greater than that of Shasta or Oroville. As shown in Figure 4.11, Shasta was at flood control capacity less than 40 percent of the time in December and January in all scenarios; therefore, Shasta had a better than 60 percent chance of being able to capture the additional flows in these months. In February, Shasta storage was limited by flood pool less than 45 percent of the time in the five scenarios. While in March, the presence of the flood pool becomes more significant in the GFDL B1 and PCM B1 scenarios with an approximately 50 percent control frequency. Scenarios Base, GFDL A2, and PCM A2 have a Shasta flood control frequency of around 40 percent in March.

Figure 4.12 shows that Oroville is likely to have available capacity to capture increased inflows in December, January, and February in all four climate change scenarios. Only in March does the flood control frequency of Oroville rise above 50 percent for three of the climate change scenarios; at 63 percent flood control frequency, Oroville was least effective capturing the PCM B1 increased inflows in March.

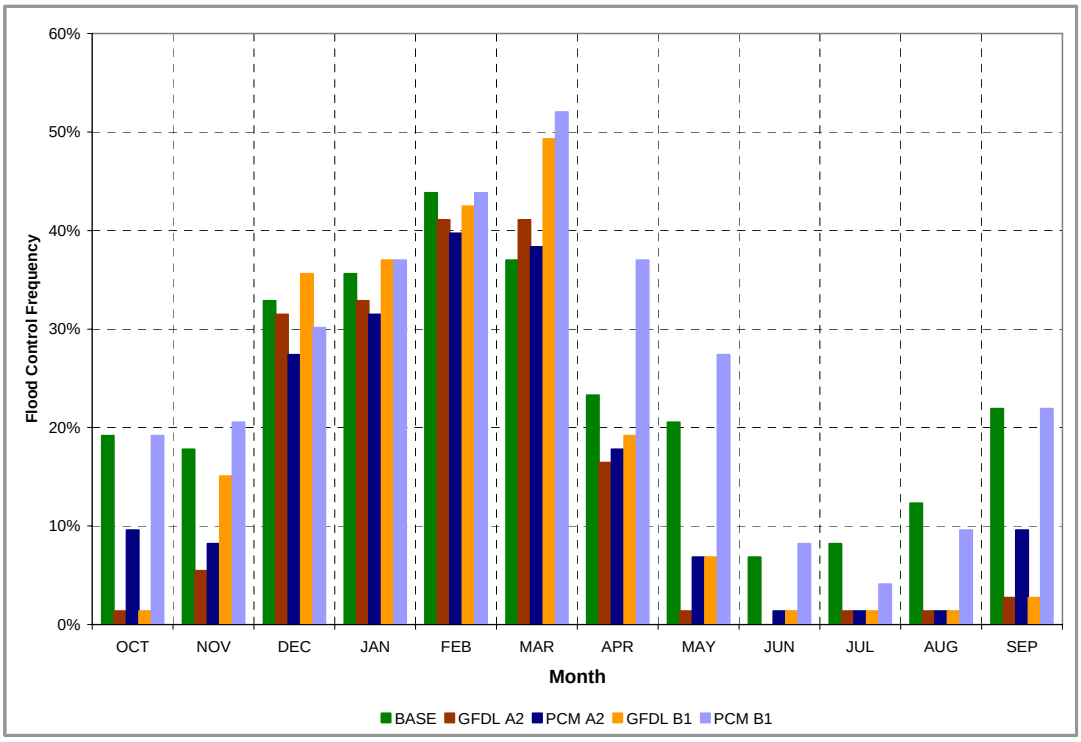


Figure 4.11 Monthly flood control frequency of Lake Shasta

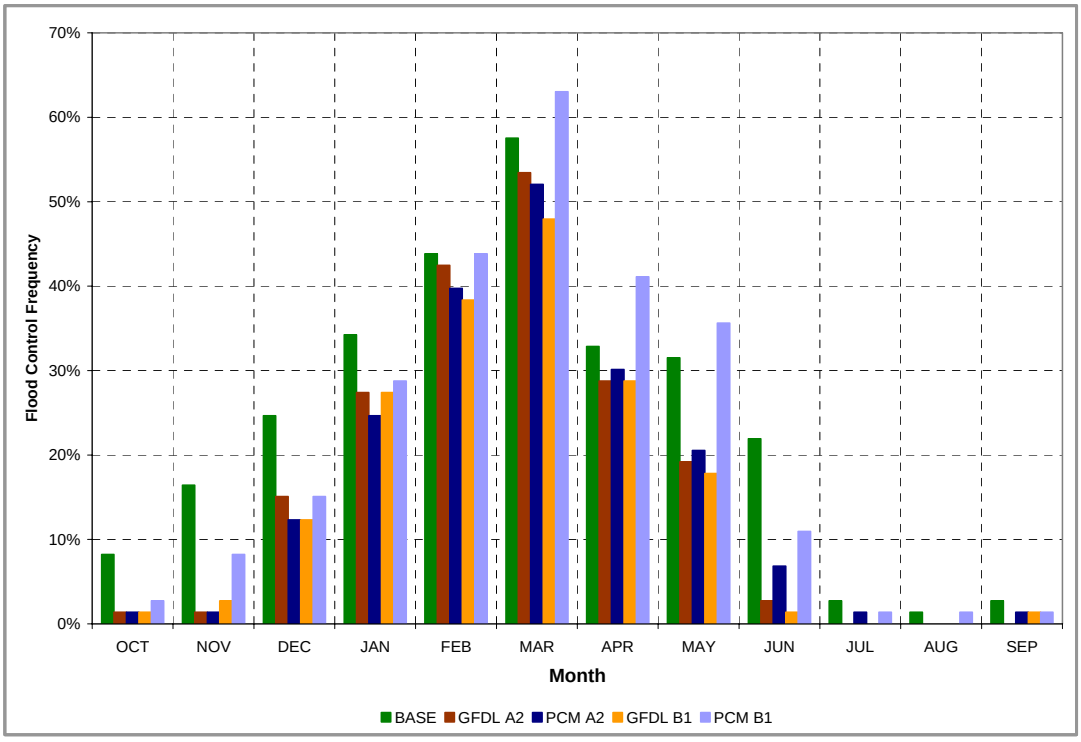


Figure 4.12 Monthly flood control frequency of Lake Oroville

Folsom was the least able of the three reservoirs to capture increased winter inflows. Figure 4.13 shows that in January, February, and March, the Folsom flood control frequency approached or surpassed 70 percent in the four climate change scenarios. PCM B1 reaches nearly 80 percent in February and March. The analysis assumes that flood pool operations will remain consistent with historical rules. However, with increased winter runoff, demands for greater flood protection may further encroach on water supply storage.

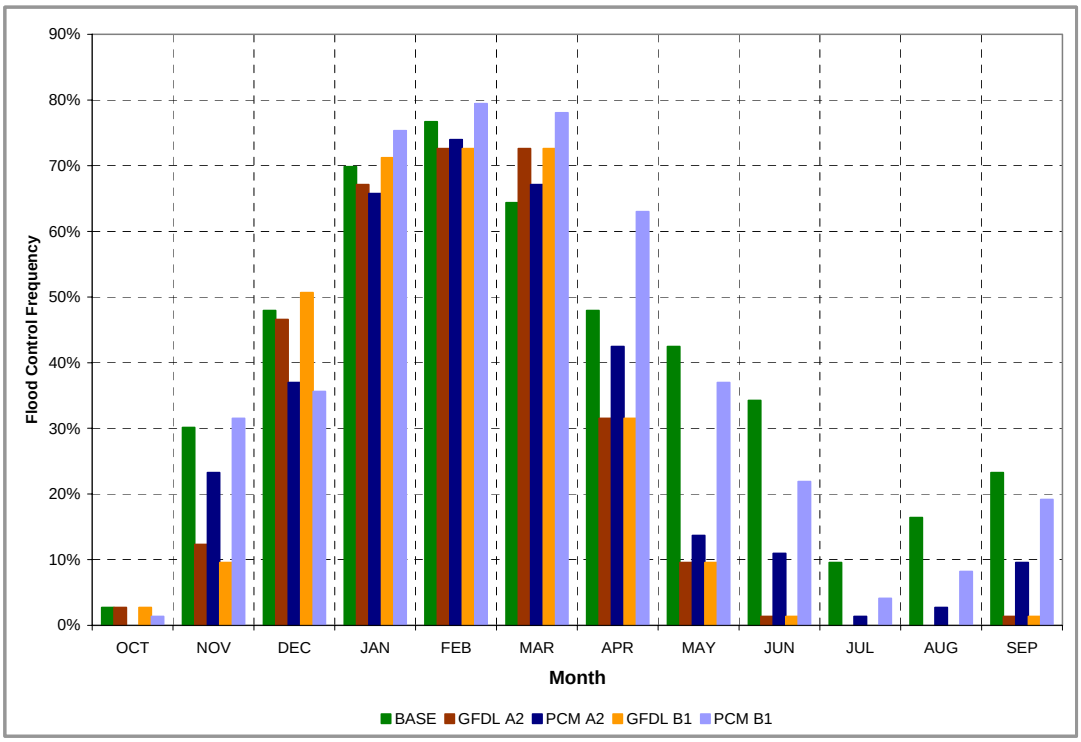


Figure 4.13 Monthly flood control frequency of Folsom Lake

While flood control operations may prevent the capture of increased winter runoff, MIF requirements downstream of the reservoirs will draw down NOD storage when reservoir inflows are low. Figure 4.14, Figure 4.15, and Figure 4.16 show the dry-period frequency that Shasta, Oroville, and Folsom releases are controlled by MIF requirements on the Sacramento, Feather, and American rivers respectively. Each river has 2 to 3 MIF requirements at different locations. When flow is reduced to one of the MIF requirements, reservoir releases on that river have reached a minimum and the MIF requirement is effectively controlling operations.

The reason the control frequency plots for MIF requirements focus on the dry periods – 1924, 1929-1934, 1976-1977, and 1987-1992 – is that those are the periods where there are critical shortages in Shasta and Folsom in the GFDL A2, PCM A2, and GFDL B1 scenarios. Figure 4.14 and Figure 4.16 show that MIF requirements are largely responsible for draining these reservoirs during the dry periods. Of course, there are downstream Delta requirements that are being met by these releases also. One can conclude that changes in SOD delivery allocations during the dry periods will not likely alleviate all of the Shasta and Folsom shortages. The water will have to be released during these years whether it's going South-of-Delta or not. The only way to prevent the shortages with changes in allocation rules is to reduce deliveries in the wet years preceding a drought in hopes of enough carryover storage to get the project through.

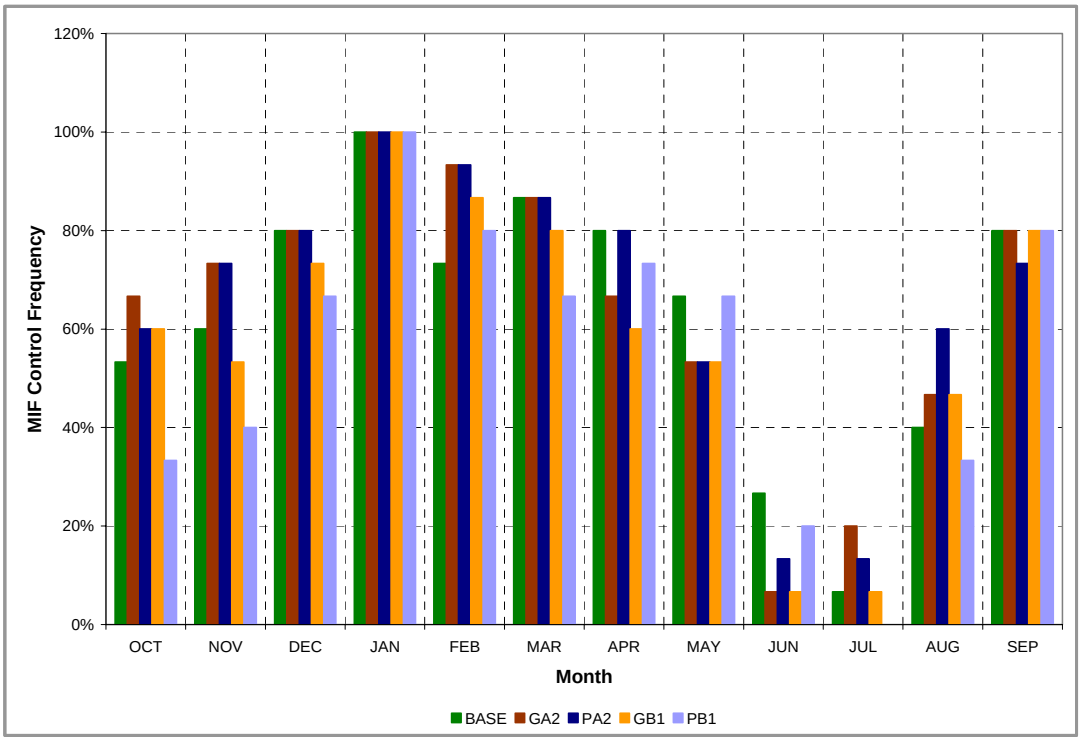


Figure 4.14 MIF requirement control frequency on the Sacramento River during dry periods (1924, 1929-1934, 1976-1977, 1987-1992)

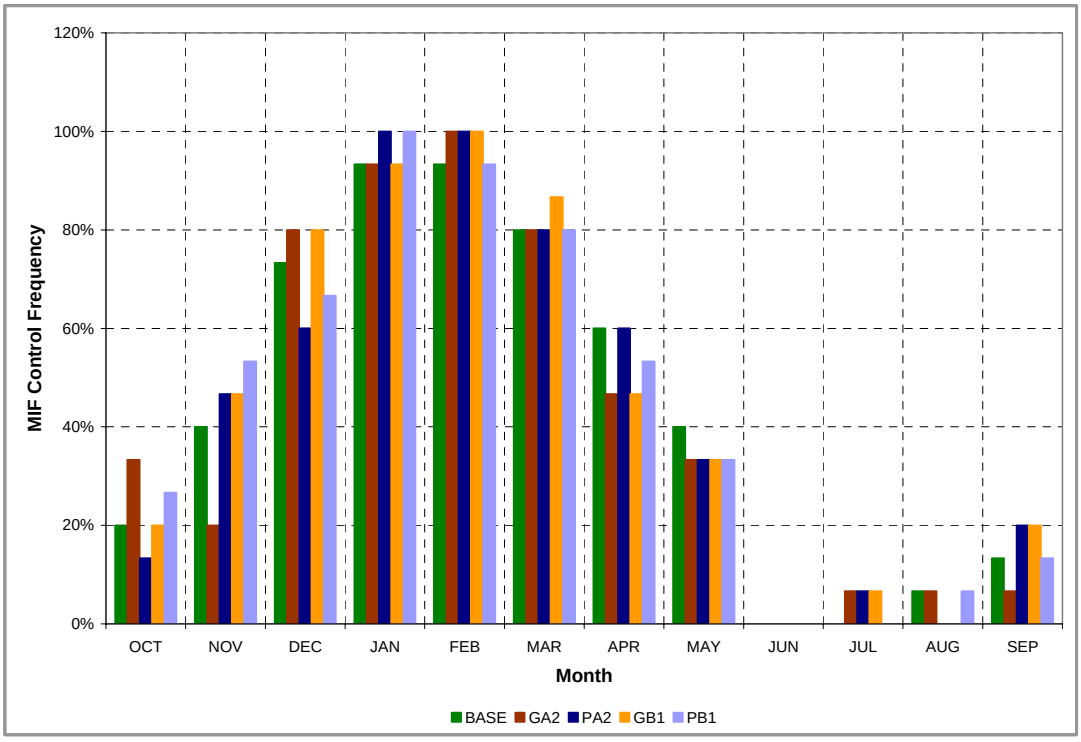


Figure 4.15 MIF requirement control frequency on the Feather River during dry periods (1924, 1929-1934, 1976-1977, 1987-1992)

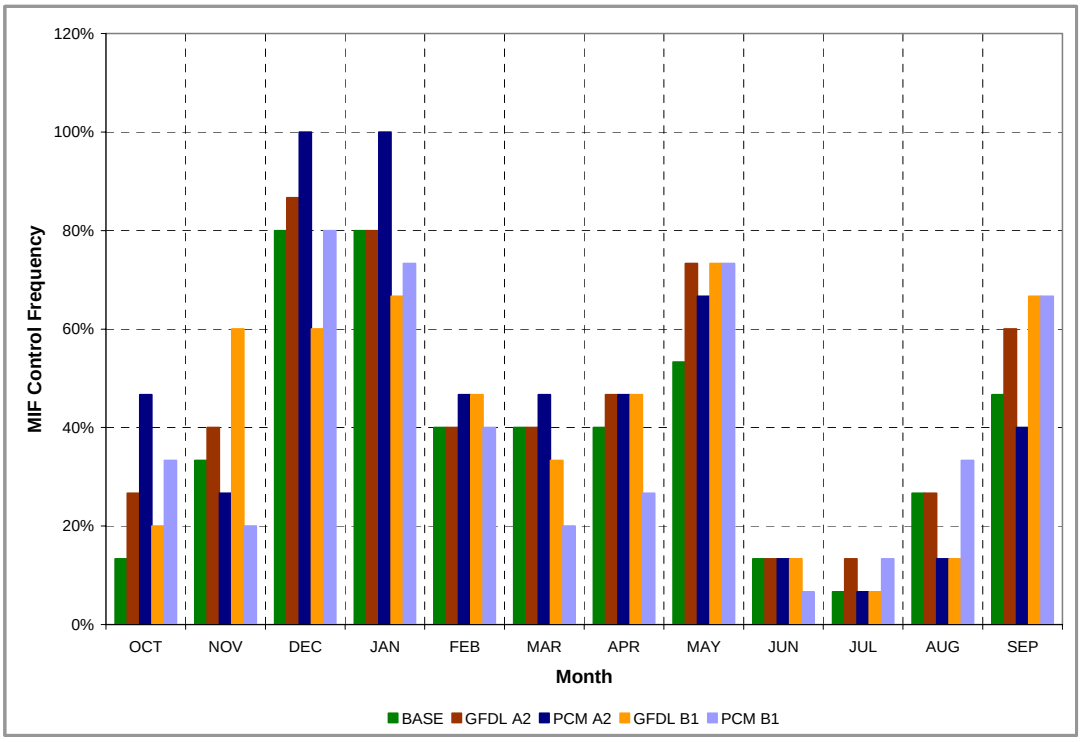


Figure 4.16 MIF requirement control frequency on the American River during dry periods (1924, 1929-1934, 1976-1977, 1987-1992)

4.6.4 Delta Operations Analysis

The CVP and SWP have three mechanisms to operate, or control, the Sacramento-San Joaquin Delta – NOD reservoir releases to the Sacramento River, the Delta Cross Channel, and Tracy and Banks exports. NOD storage releases can be increased to meet Delta outflow requirements, improve water quality, or increase exports. The Delta Cross Channel gates are opened during certain periods of the year to reduce salinity in the Delta interior with water from the Sacramento River and closed for certain periods of the year to prevent migrating fish from getting lost in the interior. Exports can be reduced to protect water quality, fish, or to maintain Delta outflow requirements or increased to capture available surplus water that would otherwise flow out to the San Francisco Bay. Delta locations of the Sacramento River inflow, Cross Channel, and the Banks and Tracy pumping plants are shown in Figure 4.17.

Operation of the Delta Cross Channel gates is largely pre-processed in CalSim-II. The only dynamic decision in the model with respect to the gates is to keep them closed when Delta inflow on the Sacramento River exceeds 25,000 cubic feet per second. While this is a frequent condition, it does not cause many differences in Delta Cross Channel gate operations when comparing the Base and climate change scenarios. There are occasions when the gates are closed in one scenario and open in another, but this is an infrequent occurrence.

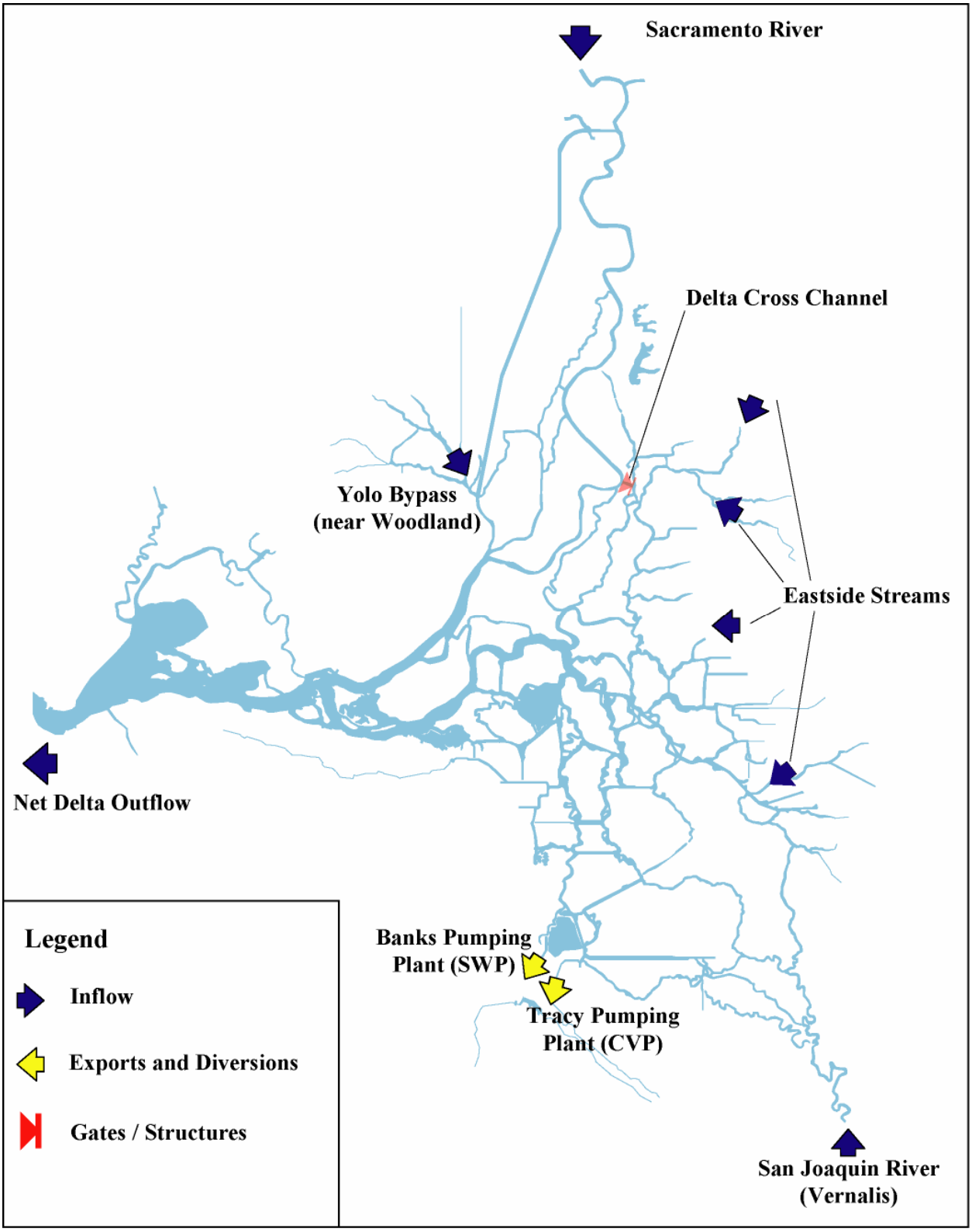


Figure 4.17 Map of the Sacramento – San Joaquin Delta

Annual average changes in Delta inflow are listed in Table 4.18. Total Delta inflow includes the Sacramento River, Yolo Bypass, Eastside streams, San Joaquin River (SJR), and Marsh Creek. Inflow from the Eastside streams and Marsh Creek do not change from the Base to the climate change scenarios. Changes in inflow are centered on the San Joaquin River, Sacramento River, and Yolo Bypass.

Table 4.18 Annual Average Delta Inflow (WY1922-1994)

Study	San Joaquin River			Sacramento River and Yolo Bypass			Total Delta Inflow		
	Annual Average Inflow (TAF)	Change from Base (TAF)	Change from Base (%)	Annual Average Inflow (TAF)	Change from Base (TAF)	Change from Base (%)	Annual Average Inflow (TAF)	Change from Base (TAF)	Change from Base (%)
BASE	2,622	0	0%	17,430	0	0%	20,850	0	0%
GFDL A2	2,508	-114	-4%	16,956	-474	-3%	20,258	-591	-3%
PCM A2	2,542	-81	-3%	16,601	-829	-5%	19,939	-911	-4%
GFDL B1	2,260	-362	-14%	17,018	-412	-2%	20,071	-778	-4%
PCM B1	2,691	69	3%	18,301	870	5%	21,789	939	5%

So far, there has been no discussion of effects in the San Joaquin basin due to the altered reservoir inflows under the climate change scenarios. That will have to wait for another report. However, with respect to Delta operations, it's important to look at the changes in Delta inflow on the San Joaquin River. In the dry months, where SJR Delta inflow is reduced, either exports must be reduced or more NOD storage releases must be made to support Banks and Tracy pumping. Furthermore, Banks permitted pumping capacity is dependent on SJR Delta inflow at Vernalis from December 15 to March 15. During this period, Banks permitted capacity is 6,680 cfs when SJR inflow is at or below 1,000 cfs. One-third of SJR inflow is added to permitted capacity if SJR inflow exceeds 1,000 cfs. Given Banks physical capacity is approximately 8,500 cfs, this permitted capacity condition is significant when SJR monthly inflows are within the range of 60 to 330 TAF per month. Figure 4.18 shows the monthly SJR Delta inflows as averaged over WY1922-1994. From December to March, monthly average inflow falls within this range.

Figure 4.19 shows combined monthly Sacramento River and Yolo Bypass Delta inflows as averaged over WY1922-1994. Average inflows of the climate change scenarios tend to be higher than the base scenario December through March. This is due to increased NOD reservoir inflow in these months when flood control operations were in effect and storage capacity was not available. During the summer and early fall months, Sacramento inflows for scenarios GFDL A2, PCM A2, and GFDL B1 are lower than in the Base. One explanation is that in the Base scenario larger NOD reservoir releases must be made to support the higher exports and SOD deliveries.

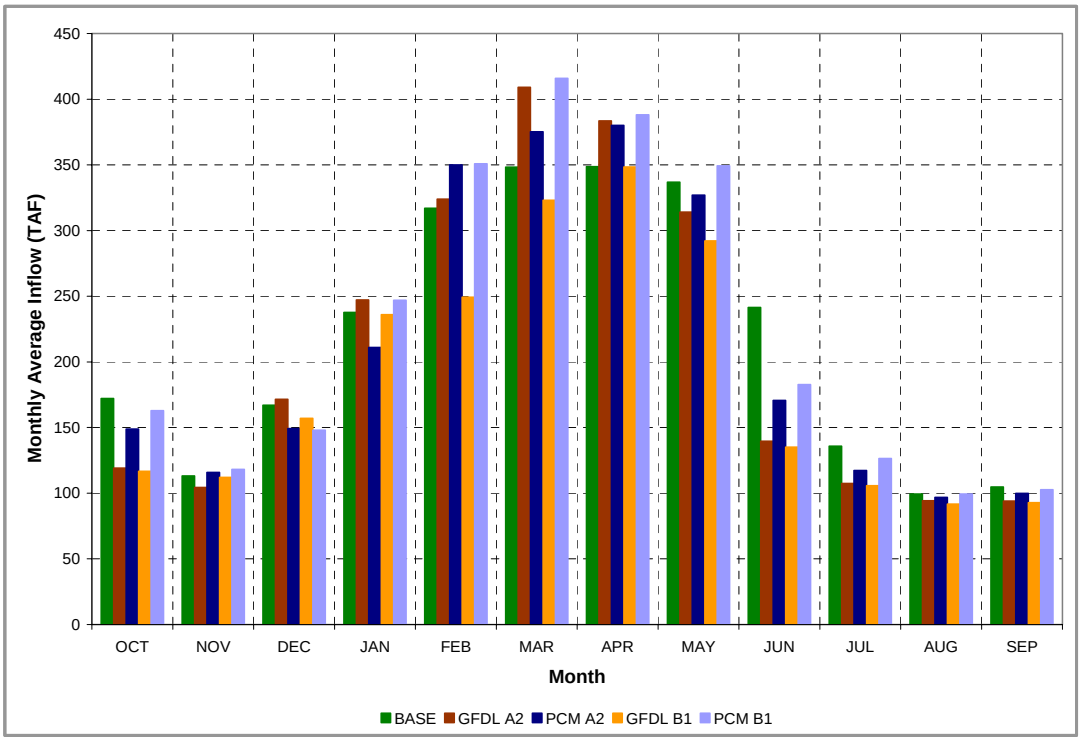


Figure 4.18 Monthly average San Joaquin River Delta inflow at Vernalis (WY1922-1994)

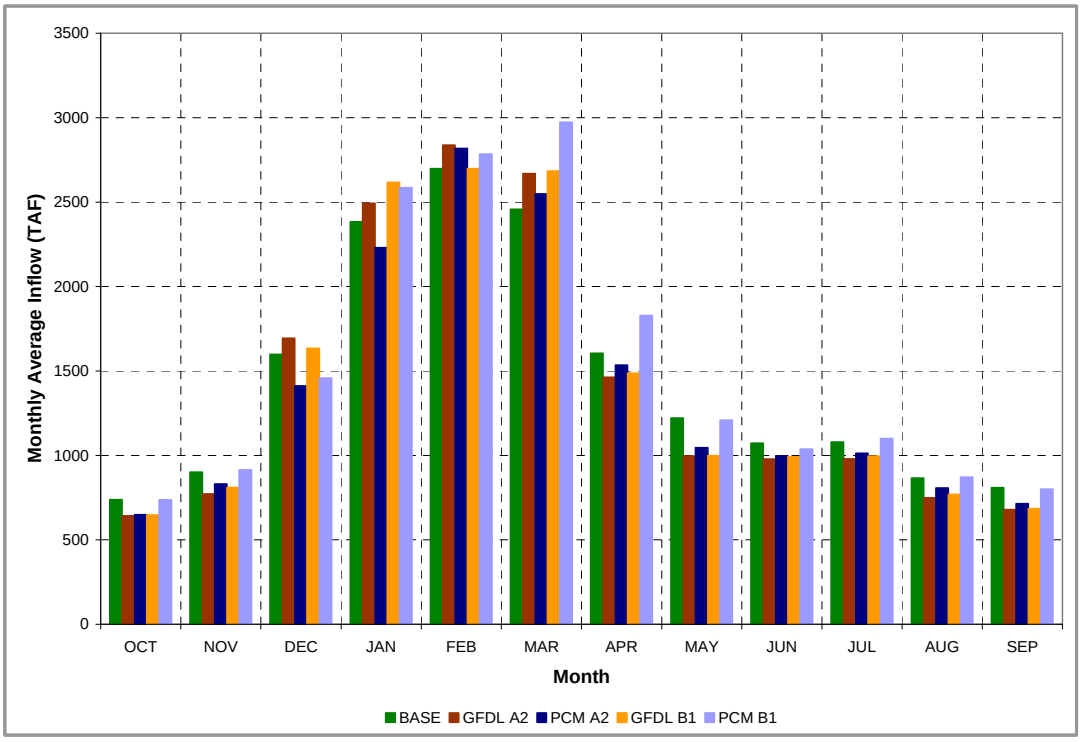


Figure 4.19 Monthly average Sacramento River--Yolo Bypass Delta inflow (WY1922-1994)

Changes in required, surplus, and total Delta outflow, as compared to the Base are listed in Table 4.19. Required Delta outflow is defined in Table 3 of the Water Quality Control Plan (WQCP). It also includes outflow necessary to maintain water quality standards as set in the WQCP. As shown, there are no significant changes in required Delta outflow on an annual average basis. Surplus Delta outflow is where the changes are concentrated. This outflow typically comes in the winter and spring due to rain and snowmelt runoff. In PCM A2, Surplus Delta outflow decreases by 7 percent as compared to the base scenario, while in PCM B1, it increases by 11 percent on average.

Table 4.19 Annual Average Delta Outflow (WY1922 – 1994)

Study	Required Delta Outflow			Surplus Delta Outflow			Total Delta Outflow		
	Annual Average Outflow (TAF)	Change from Base (TAF)	Change from Base (%)	Annual Average Outflow (TAF)	Change from Base (TAF)	Change from Base (%)	Annual Average Outflow (TAF)	Change from Base (TAF)	Change from Base (%)
BASE	5,621	0	0%	8,187	0	0%	13,808	0	0%
GFDL A2	5,627	5	0%	8,170	-18	0%	13,796	-12	0%
PCM A2	5,633	12	0%	7,652	-535	-7%	13,285	-524	-4%
GFDL B1	5,622	1	0%	7,923	-264	-3%	13,546	-263	-2%
PCM B1	5,590	-32	-1%	9,060	872	11%	14,649	841	6%

Figure 4.20 shows monthly Delta outflow as averaged over WY1922-1994. Notice that outflows for the base and climate change scenarios are roughly equivalent on average July-November. As set in Table 3 of the WQCP, required Delta outflow in these months will not change from scenario to scenario. Little surplus would be expected in these months also. The slight increases in base outflows during these months were attributed to maintaining water quality standards with higher exports. This, at times, required higher Delta outflows. In the winter, Delta outflows of the climate change scenarios tended to be higher than those of the base. Given higher Delta inflows during this period and limited pumping capacity, this pattern was expected.

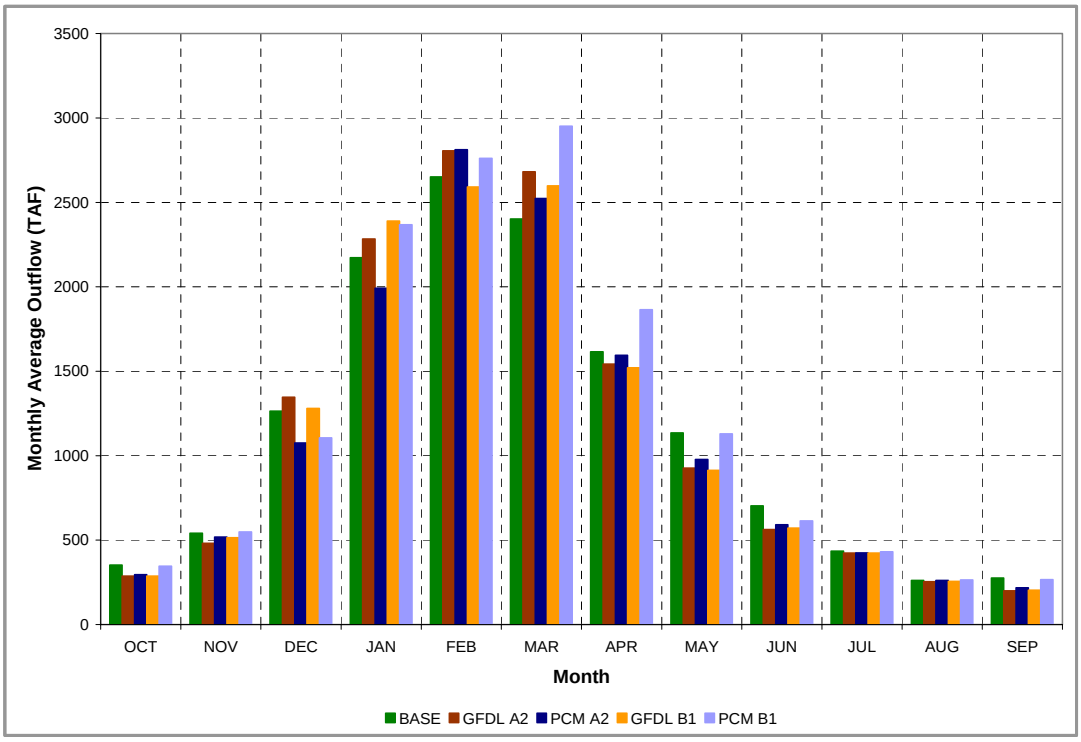


Figure 4.20 Monthly average Delta outflow (WY1922-1994)

Previously, it was shown that the combined SWP and CVP SOD deliveries in the drier climate change scenarios were consistently less than the base scenario. It was expected that SOD exports would decrease also. Table 4.20 lists annual average exports and calculates changes with respect to the base. Total exports in GFDL A2, PCM A2, and GFDL B1 decrease by 10 percent, 6 percent, and 9 percent respectively. Overall, SOD deliveries were increased for the SWP and CVP in scenario PCM B1. A corresponding 2 percent increase in total exports is shown in Table 4.20.

Table 4.20 Annual Average Delta Exports

Study	Tracy Exports			Banks Exports			Total Exports		
	Annual Average Exports (TAF)	Change from Base (TAF)	Change from Base (%)	Annual Average Exports (TAF)	Change from Base (TAF)	Change from Base (%)	Annual Average Exports (TAF)	Change from Base (TAF)	Change from Base (%)
BASE	2554	0	0%	3351	0	0%	5905	0	0%
GFDL A2	2286	-269	-11%	3046	-305	-9%	5332	-573	-10%
PCM A2	2391	-164	-6%	3131	-220	-7%	5522	-383	-6%
GFDL B1	2369	-186	-7%	3027	-324	-10%	5395	-510	-9%
PCM B1	2620	66	3%	3383	33	1%	6004	98	2%

Figure 4.21 shows monthly total Delta exports as averaged over WY1922-1994. During the winter, average exports were not significantly changed from the base to the climate change scenarios. Even with the added Delta inflow of the climate change scenarios during the wet months, exports at Tracy and Banks were unable to capture most of it because of a combination of permitted pumping capacity, physical pumping capacity, SOD conveyance constraints, and the export to inflow ratio of the WQCP. Base and PCM B1 exports were significantly higher in the summer and fall months as compared to the drier climate change scenarios. The higher exports were to support the higher delivery allocations in the Base and PCM B1 scenarios.

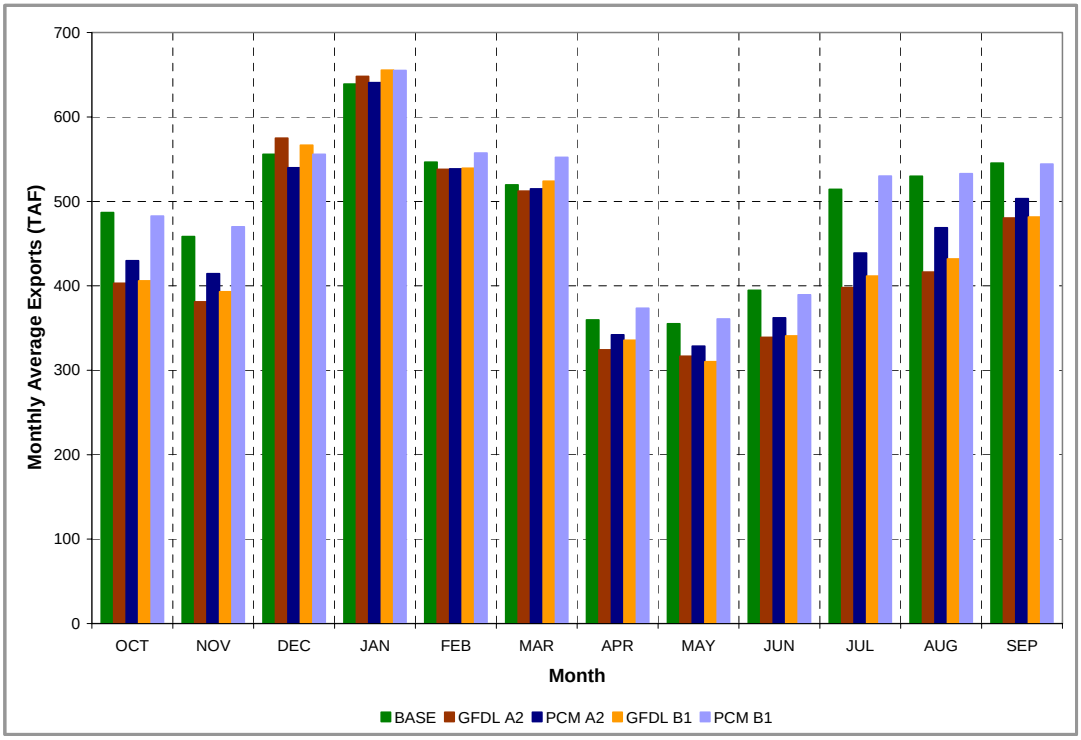


Figure 4.21 Monthly average total Delta exports (WY1922-1994)

There are a number of system constraints, physical and regulatory, that inhibit SWP and CVP Delta exports to SOD contractors. They include:

1) Permitted and physical pumping capacity
2) SOD conveyance capacity including storage capacity, channel and pumping capacity, and contractor demand
3) April-May SJR pulse flow limits on exports (April 15-May15)
4) WQCP water quality standard limits on exports as calculated using ANN
5) WQCP export-inflow ratio

The frequency that these export constraints control exports was quantified for the Base and climate change scenarios. For Banks, the frequency that permitted or physical pumping capacity was reached on a monthly basis is shown in Figure 4.22. This constraint is most significant in

January when surplus Delta outflow was likely. Figure 4.23 shows that SOD conveyance constraints are most likely to constrain exports in March. The April-May pulse flow export limits were applied from April 15 to May 15. Since the simulation time-step is one month, the simulated constraint was actually a day-weighted average of the pulse flow constraint and permitted capacity. As shown in Figure 4.24, the simulated April-May export constraint controlled Banks pumping about 90 percent of the time in these two months in all scenarios. Figure 4.25 shows the frequency that exports are constrained in each simulation by the various WQCP water quality standards; while frequency of water quality constraints varies significantly from month to month and scenario to scenario, November is the month where water quality was most likely to control Banks exports in all five simulations. The frequency that the export-inflow ratio controls Banks is shown in Figure 4.26

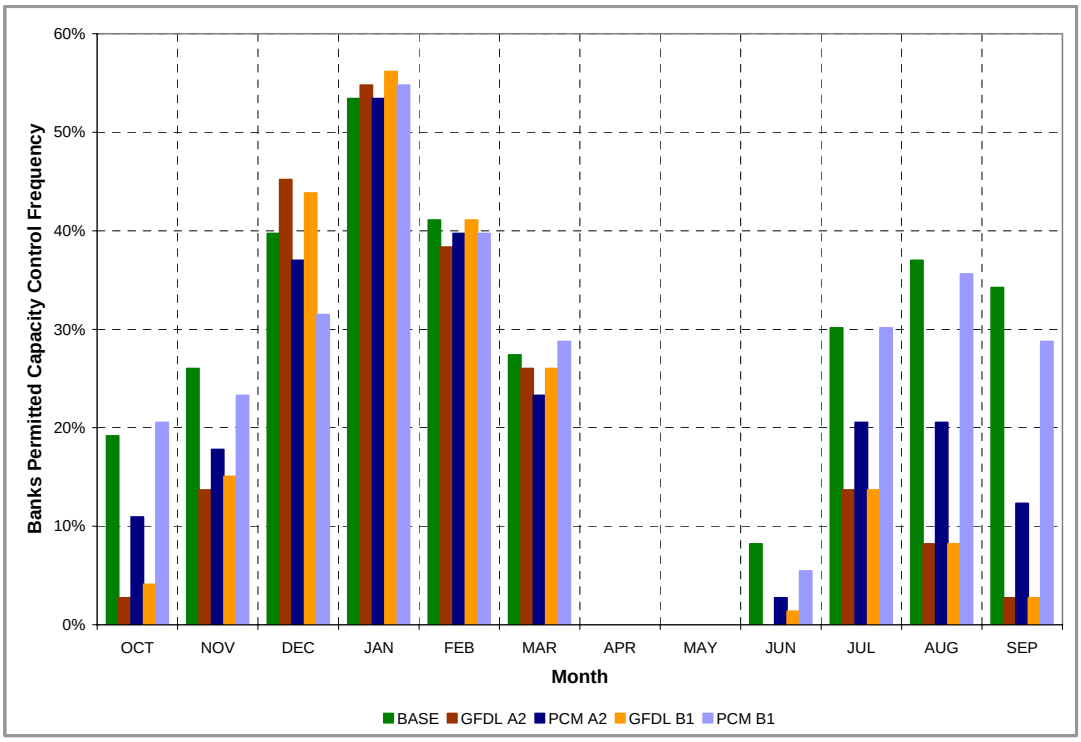


Figure 4.22 Operational control frequency of Banks permitted capacity

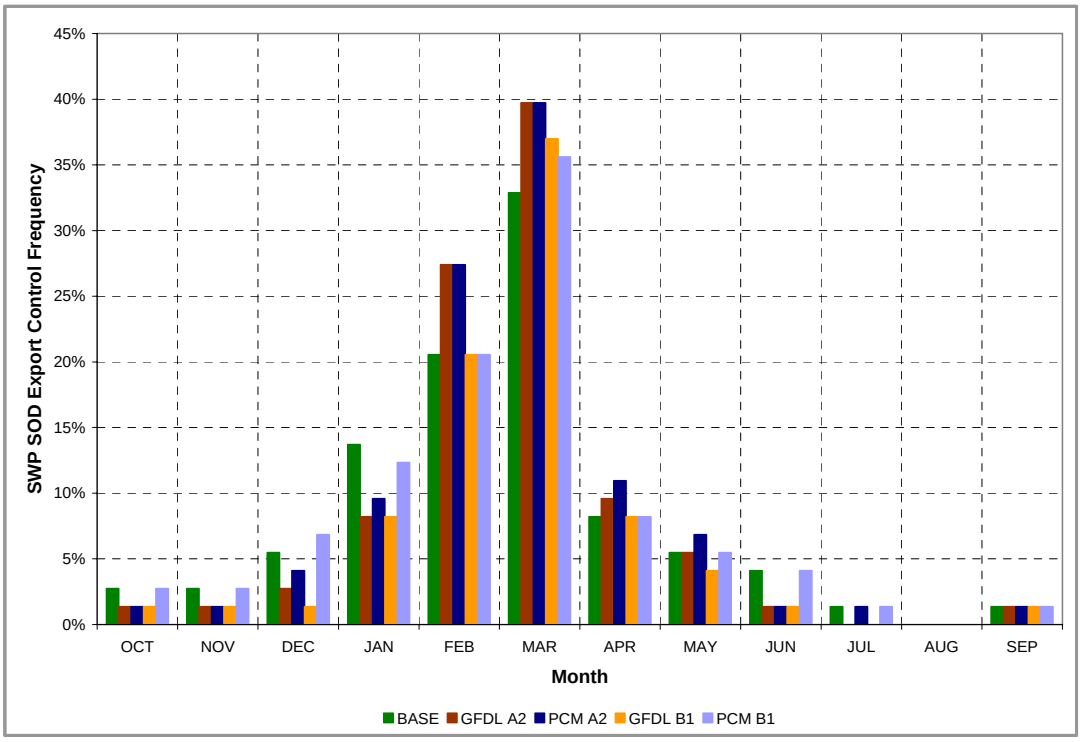


Figure 4.23 Operational control frequency of SWP SOD conveyance capacity on Banks exports

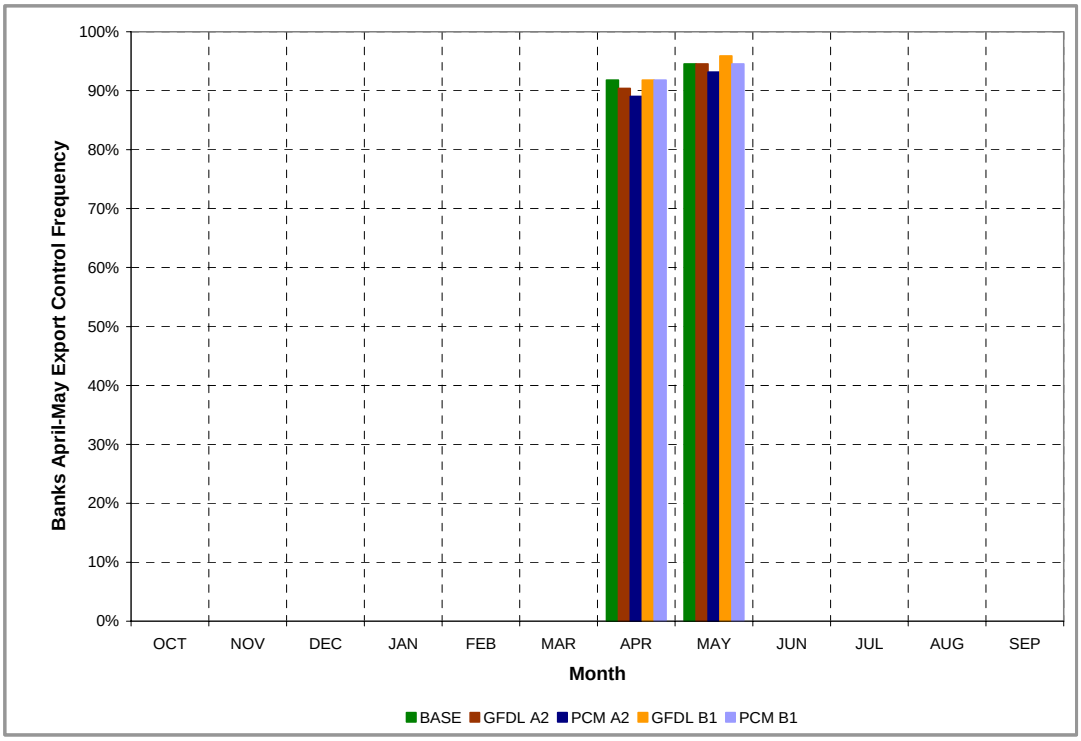


Figure 4.24 Operational control frequency of the April-May San Joaquin River pulse flow export constraints on Banks pumping

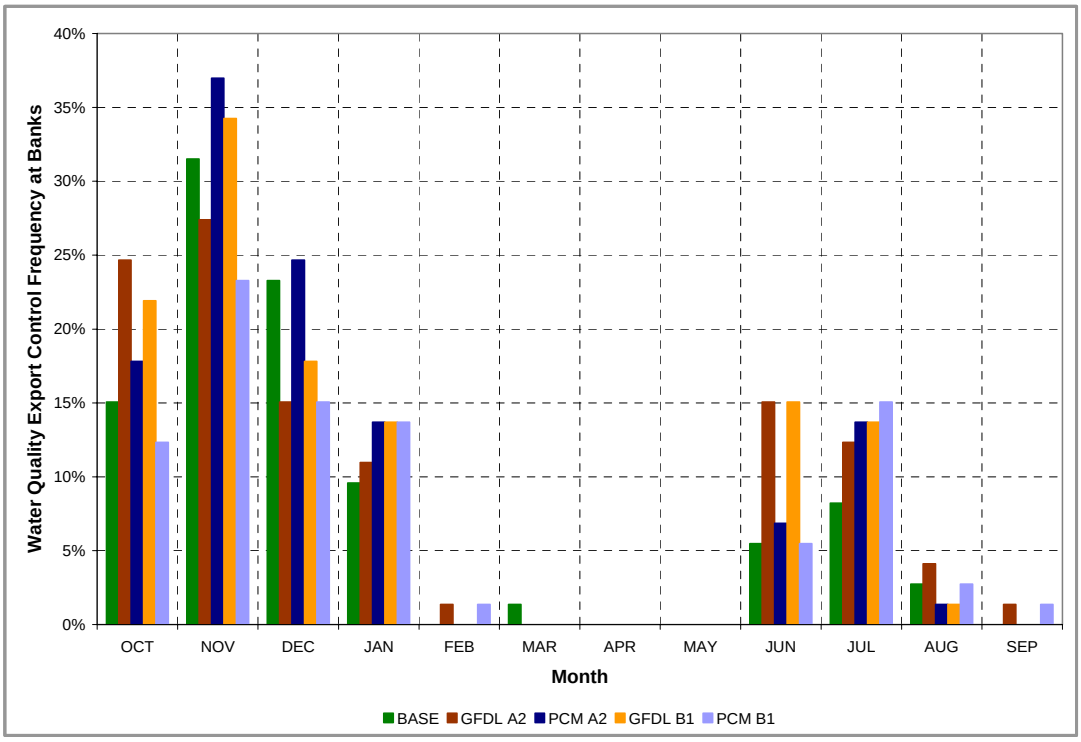


Figure 4.25 Operational control frequency of Delta water quality standards on Banks pumping

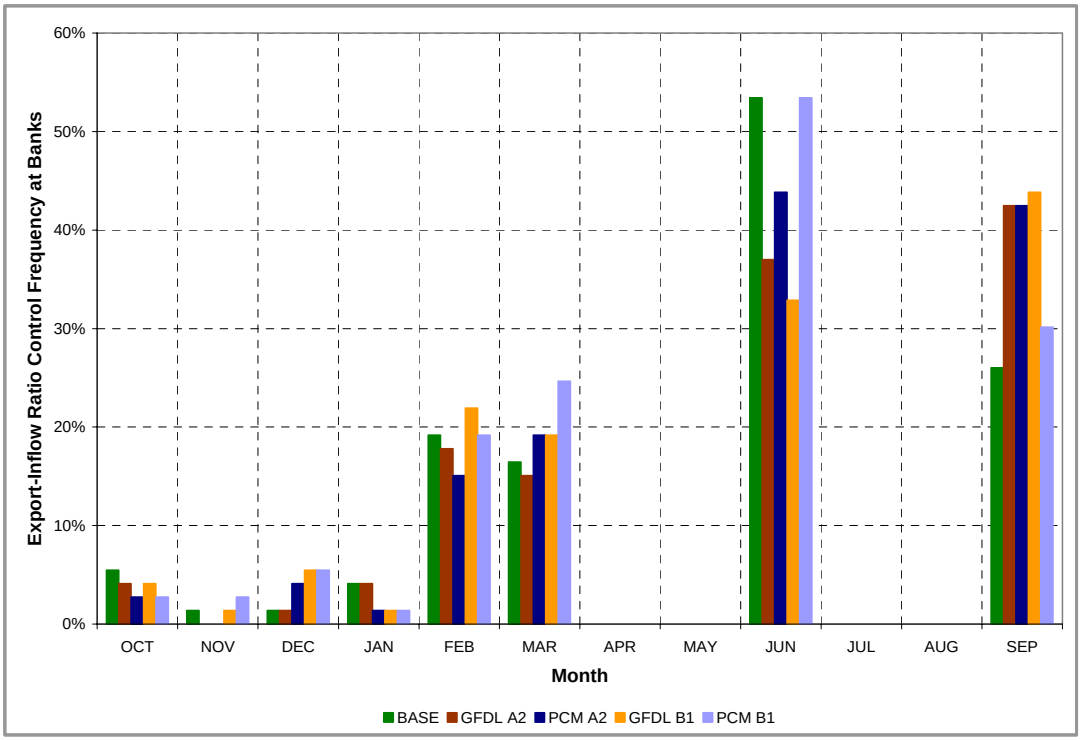


Figure 4.26 Operational control frequency of Banks pumping by the export-inflow ratio

With increased Delta inflow from December to March in the climate change scenarios, it would be useful, from a water supply standpoint, to capture some of the surplus Delta outflow. From the operational control frequency information contained in Figure 4.22 to Figure 4.26, the key constraint in this period was Banks permitted and physical capacity. In March, SWP SOD conveyance often becomes the constraining parameter. This suggests that changes in Banks permitted capacity and SWP SOD conveyance capacity – surface storage, canals, pumps, groundwater banking – should be tested for its potential to compensate for climate change impacts on SOD water supply.

Figure 4.27 shows the frequency that Banks exports are not constrained by physical or permitted capacity, SOD conveyance capacity, April-May export restrictions, water quality, or the export-inflow ratio. In this case, a decision was made to preserve Oroville storage at the expense of San Luis storage. As expected, the least flexibility in Banks pumping is in December-March when it is most needed to capture the additional Delta inflow in the climate change scenarios. Due to decreased exports, there is some unused summer Banks capacity in the drier climate change scenarios as compared to the Base. Would it be helpful to increase San Luis carryover at the expense of Oroville? It is possible that greater available capacity in Oroville would help to capture the increased winter runoff, but no conclusions could be made without further tests. Special Feather River fish criteria from October 15 to November 30 limit Oroville releases for Delta export. So even though there is a high frequency of no export controls in these months, it is likely that Oroville releases could not be made to take advantage. The CVP could take advantage of available Banks capacity for delivery to Cross Valley Canal in the summer and fall. However, given the critical shortages on Shasta and Folsom in the drier climate change scenarios, it is not clear that the CVP would want to release additional water from these reservoirs.

Tracy Pumping Plant has a physical capacity of 4,600 cfs with exports further limited to a range of 4,200 cfs – 4,600 cfs by a constriction on the upper Delta-Mendota canal. Figure 4.28 shows the frequency that the combined physical pumping capacity and upper DMC constraint limit Tracy exports. Sometimes, typically in the winter, there is no place SOD for the CVP to put the water. Figure 4.29 shows the frequency that this occurs. As shown in Figure 4.30, the April-May export constraint regularly limits Tracy exports in these months – just as it did with Banks. However, the April-May constraint does not control Tracy as frequently as Banks because of CVP SOD conveyance limits. Figure 4.31 shows the regularity that the WQCP water quality standards limit Tracy pumping, and Figure 4.32 shows the same information for the export-inflow ratio.

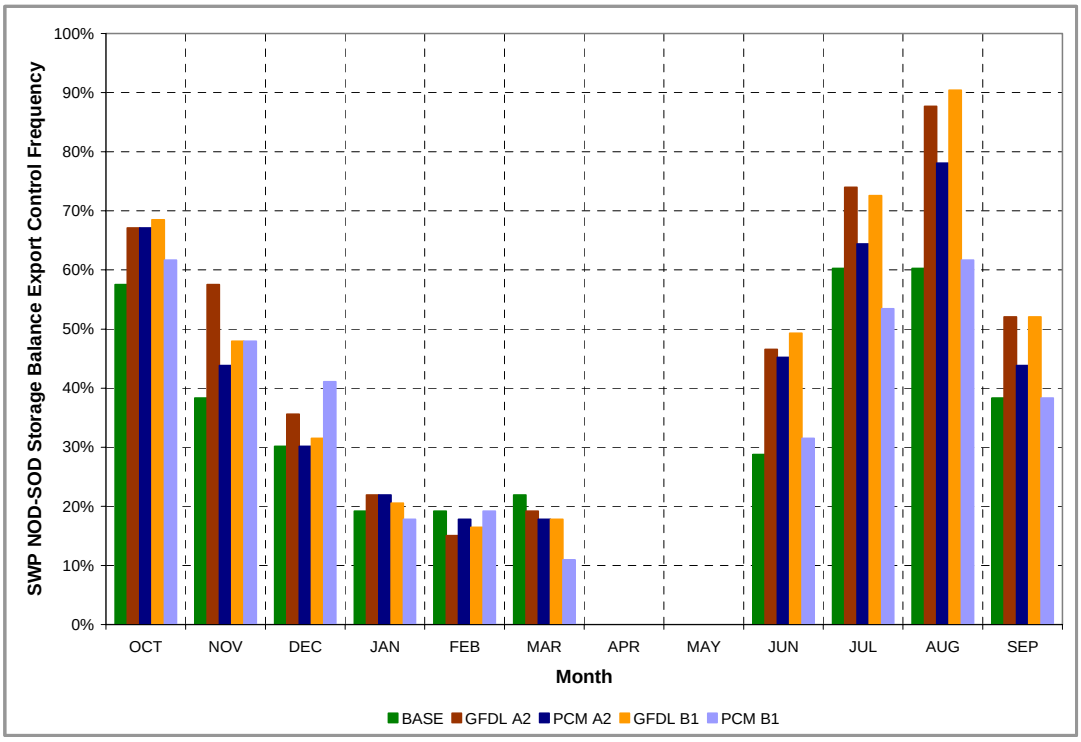


Figure 4.27 Frequency of the decision to favor SWP NOD storage over SWP SOD storage by limiting Oroville releases and Banks pumping

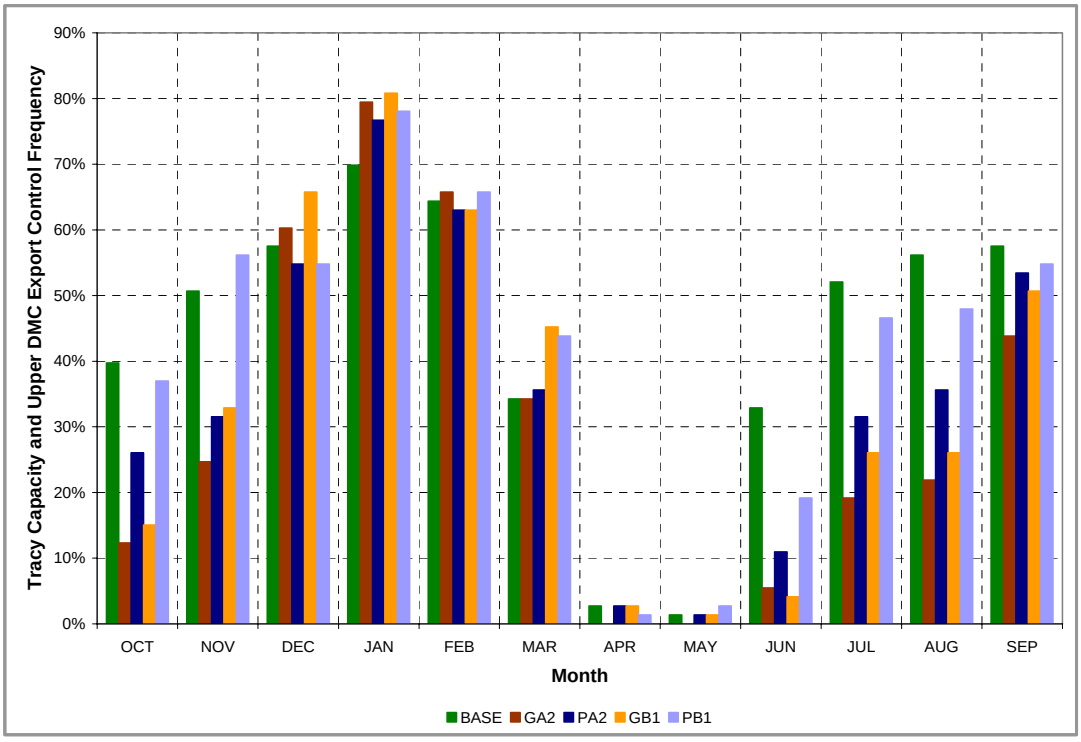


Figure 4.28 Operational control frequency of Tracy pumping capacity and upper Delta-Mendota Canal conveyance capacity

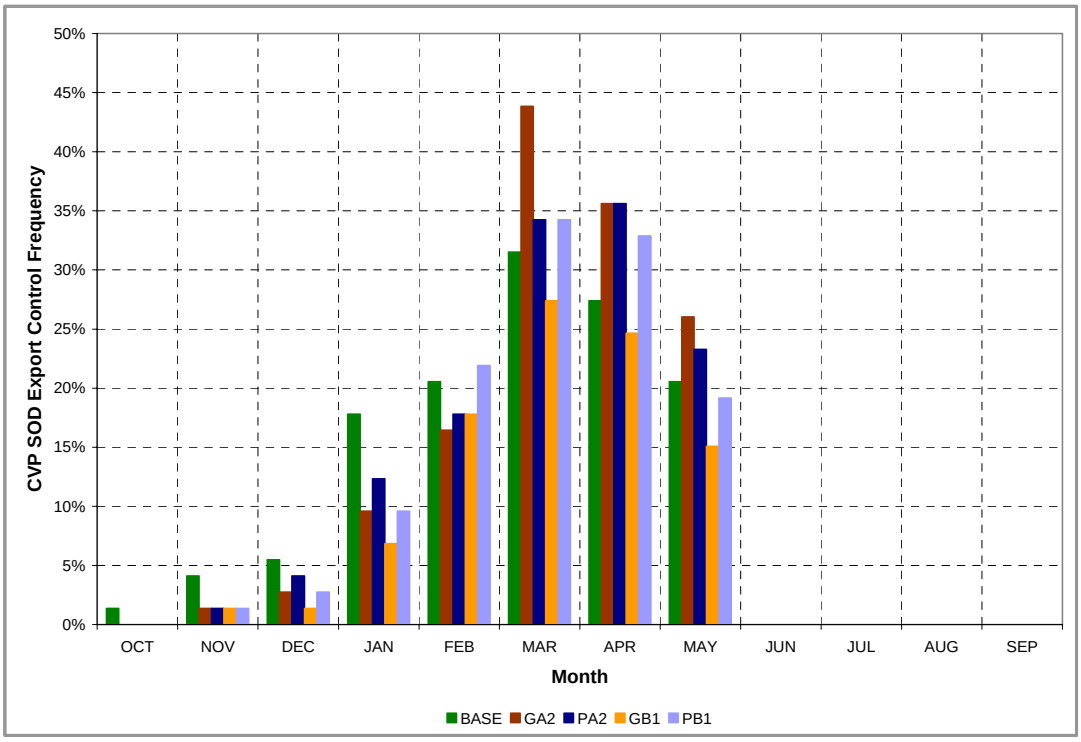


Figure 4.29 Operational control frequency of CVP SOD conveyance capacity on Tracy exports

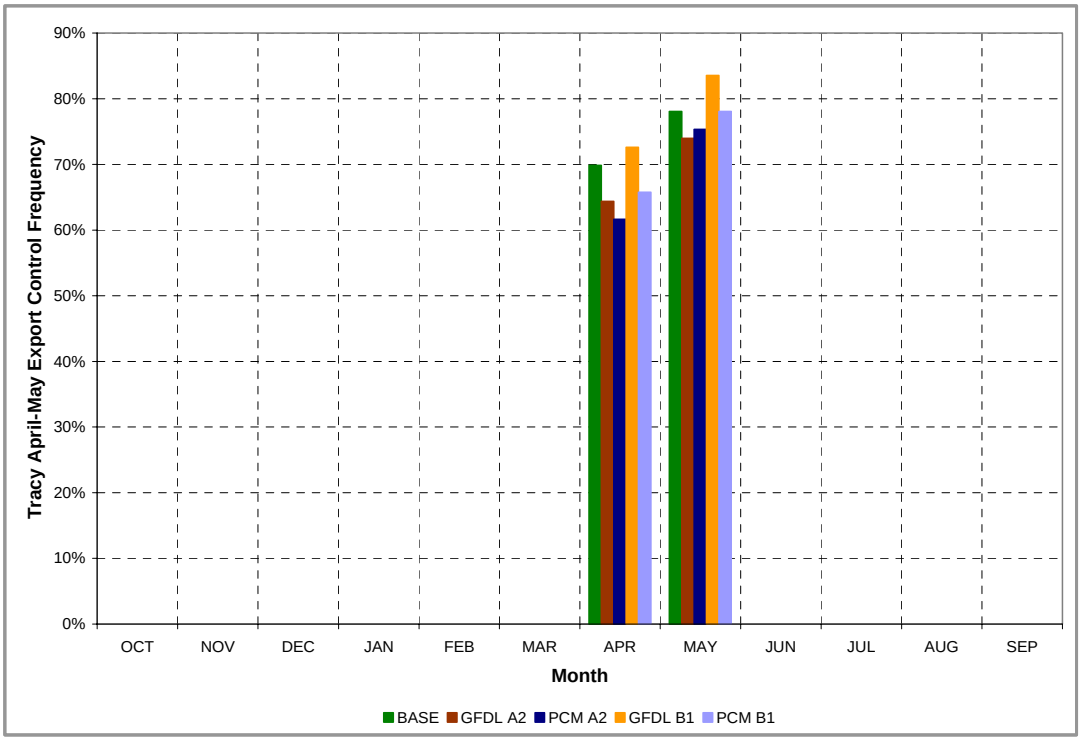


Figure 4.30 Operational control frequency of the April-May San Joaquin River pulse flow export constraints on Tracy pumping

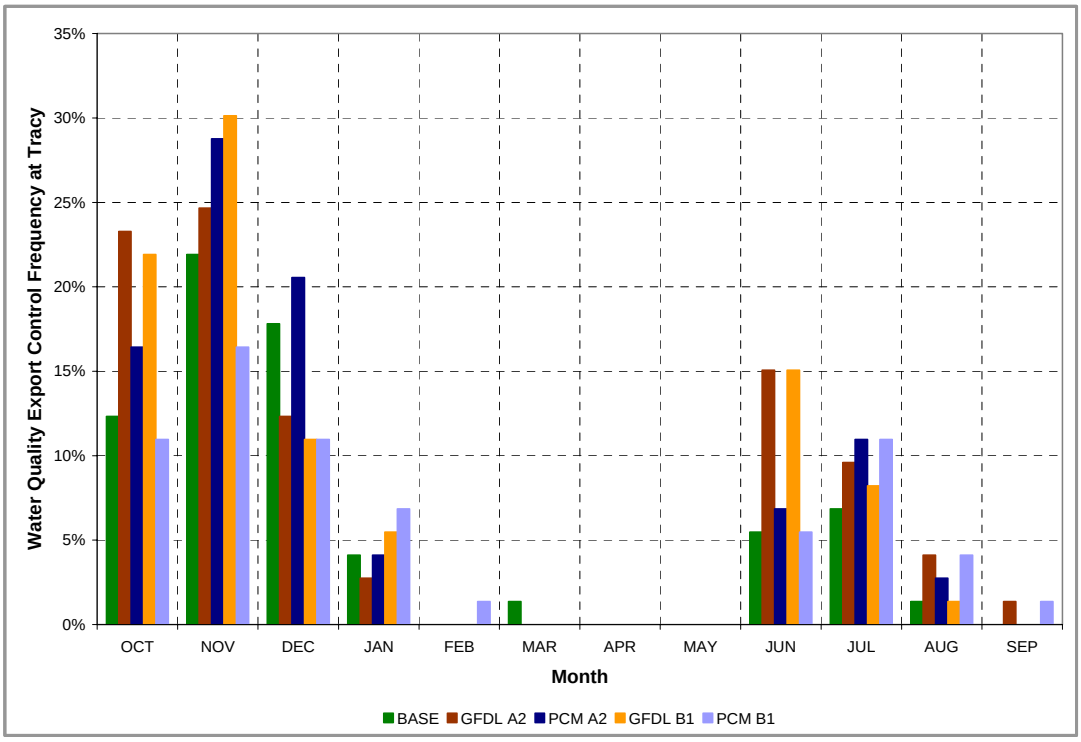


Figure 4.31 Operational control frequency of water quality standards of Tracy pumping

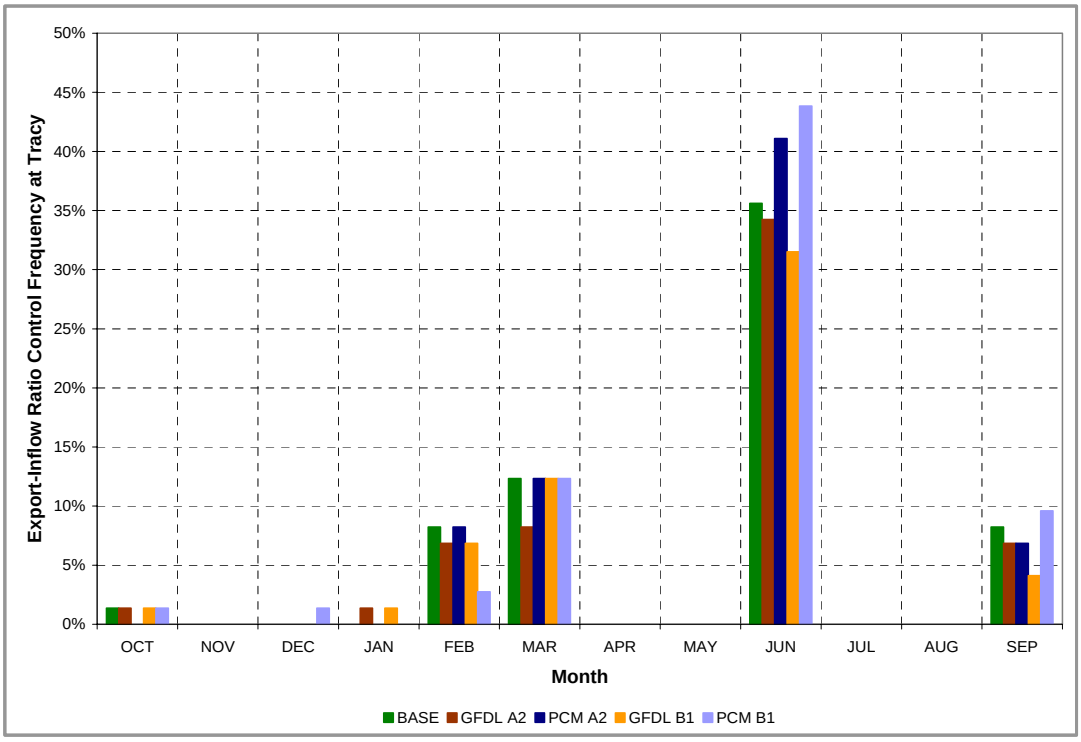


Figure 4.32 Operational control frequency of the export-inflow ratio of Tracy pumping

In the key months of December through March, Tracy exports were most frequently limited by pumping capacity or the upper Delta-Mendota Canal constriction as shown in Figure 4.27. It has been proposed to install an intertie between the Delta-Mendota Canal (DMC) and the California Aqueduct. This would relieve the upper DMC constraint and would be worth more study in the context of climate change.

Figure 4.33 shows the frequency that Tracy Pumping Plant has remaining export capacity -- none of the above mentioned constraints are controlling Tracy exports. Just as with Banks, Tracy is less likely to have available export capacity in the December – March period when it is most needed. In the drier climate change scenarios, there is some flexibility for higher Tracy exports in the summer and fall. However, given the shortages in Shasta and Folsom in these drier scenarios, it is doubtful that higher releases from these reservoirs to support higher exports would be beneficial.

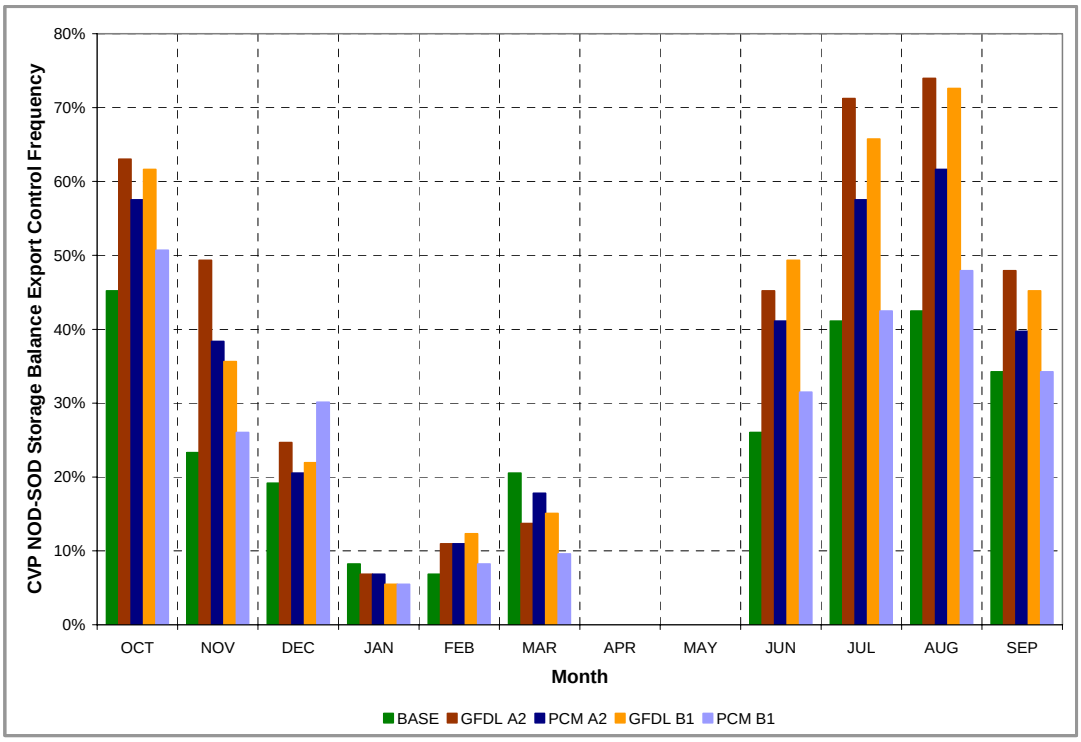


Figure 4.33 Frequency of the decision to favor CVP NOD storage over CVP SOD storage by limiting Shasta and Folsom releases and Tracy pumping

4.6.5 Power Supply

Climate change impacts to CVP and SWP power supply were calculated using Bureau of Reclamation and DWR spreadsheet models. These models estimate monthly power generation using reservoir storage and release data from CalSim-II, and they estimate monthly power loads based on CalSim-II pumping rates. The CVP and SWP facilities included in the power supply analysis are listed in Table 4.21.

Estimates of the average annual SWP power generation and load for each study are compared to the base study in Table 4.22. The summary includes the long-term period of 1922-1993 as well as two six-year droughts. The negative values for net generation indicate that the SWP consumes more power than is generated. For the period 1922-1993, the GFDL A2, PCM A2 and GFDL B1 studies show a decrease in net generation ranging from 7 percent to 11 percent while the PCM B1 study has a smaller decrease of 1 percent. The SWP net power generation effects for the drought of 1929-1934 ranges from a decrease of 11 percent for the PCM A2 study to an increase of 14 percent for the PCM B1 study. For 1987-1992, the GFDL A2, PCM A2 and GFDL B1 studies have a decrease in net generation ranging from 8 percent to 21 percent while the PCM B1 study is only 1 percent less than the base study.

Estimates of the average annual CVP power generation and load for each study are compared to the base study in Table 4.23 for the long-term period of 1922-1994 and the two six-year droughts. For 1922-1994, the GFDL A2, PCM A2 and GFDL B1 studies show a decrease in net generation ranging from 6 percent to 10 percent while the PCM B1 study increases net generation by 6 percent. The CVP net power generation effects for the drought of 1929-1934 ranges from a decrease of 15 percent for the GFDL A2 study to an increase of 7 percent for the PCM B1 study. For 1987-1992, the GFDL A2, PCM A2 and GFDL B1 studies have a decrease in net generation ranging from 3 percent to 12 percent while the PCM B1 study is 8 percent greater than the base study.

Table 4.21 Generation and Load Facilities Included in Power Supply Analysis

SWP Facilities		CVP Facilities	
Generation	Load	Generation	Load
Oroville	Banks	Trinity	Tracy
Thermalito	South Bay	Carr	Banks
Gianelli	Del Valle	Spring Creek	Contra Costa
Alamo	Gianelli	Shasta	O'Neill
Mojave	Dos Amigos	Keswick	San Luis
Devil Canyon	Las Perillas	Folsom	San Felipe
Warne	Badger	Nimbus	Dos Amigos
Castaic	Buena Vista	New Melones	Folsom
	Teerink	San Luis	Corning
	Chrisman	O'Neill	Red Bluff
	Edmonston		San Luis Relift
	Oso		DMC Relift
	Pearblossom		Tehama-Colusa Relift
			Miscellaneous

Table 4.22 Annual Average SWP Power Generation and Load

Calendar year period	Study	Powerplant generation (GWh)	Pumping plant load (GWh)	Net generation (GWh)	Percent change from base
1922-1993	Base	4,840	9,577	-4,737	0%
	GFDL A2	4,552	8,764	-4,212	-11%
	PCM A2	4,576	8,988	-4,412	-7%
	GFDL B1	4,479	8,703	-4,224	-11%
	PCM B1	4,989	9,686	-4,696	-1%
1929-1934	Base	2,666	5,289	-2,623	0%
	GFDL A2	2,577	5,039	-2,462	-6%
	PCM A2	2,453	4,788	-2,335	-11%
	GFDL B1	2,486	4,888	-2,402	-8%
	PCM B1	2,954	5,934	-2,980	14%
1987-1992	Base	2,610	5,386	-2,776	0%
	GFDL A2	2,365	4,561	-2,196	-21%
	PCM A2	2,489	5,057	-2,568	-8%
	GFDL B1	2,368	4,698	-2,330	-16%
	PCM B1	2,721	5,465	-2,745	-1%

Table 4.23 Annual Average CVP Power Generation and Load

Water year period	Study	Powerplant generation (GWh)	Pumping plant load (GWh)	Net generation (GWh)	Percent change from base
1922-1994	Base	4,733	1,313	3,420	0%
	GFDL A2	4,265	1,191	3,074	-10%
	PCM A2	4,310	1,239	3,071	-10%
	GFDL B1	4,440	1,227	3,213	-6%
	PCM B1	4,969	1,355	3,614	6%
1929-1934	Base	2,864	790	2,074	0%
	GFDL A2	2,487	719	1,768	-15%
	PCM A2	2,543	723	1,820	-12%
	GFDL B1	2,641	720	1,922	-7%
	PCM B1	3,077	856	2,221	7%
1987-1992	Base	3,248	840	2,408	0%
	GFDL A2	2,858	736	2,122	-12%
	PCM A2	2,949	743	2,205	-8%
	GFDL B1	3,116	783	2,334	-3%
	PCM B1	3,513	912	2,600	8%

A comparison of monthly average SWP power generation and load and CVP power generation and load are presented in Figure 4.34, Figure 4.35, Figure 4.36 and Figure 4.37, respectively. For the drier scenarios, SWP power generation decreases in all months compared to the Base with the exception of scenario GFDL A2 which has a slight increase in March. The largest decrease occurs in May. For the wetter scenario, PCM B1, SWP power generation increases in February through September and decreases in October through January. The largest increase in SWP power generation occurs in March.

SWP power load decreases in all months for the drier scenarios because of reduced water deliveries. With the wetter scenario, SWP power load increases in all months except January and February.

For the drier scenarios, CVP power generation decreases in all months compared to the Base with the exceptions of scenario GFDL A2 which has a slight increase in March and scenario GFDL B1 which has slight increases in January and March. The largest decreases in CVP power generation occur in September and October when storage impacts are greatest. For the wetter scenario, PCM B1, CVP power generation increases in all months except June and December which have slight decreases. The largest increase in CVP power generation occurs in March.

For the drier scenarios, CVP power load increases slightly in January through March due to higher exports and decreases in other months due to reduced deliveries. With the wetter scenario, there are slight increases in CVP power load in all months except October.

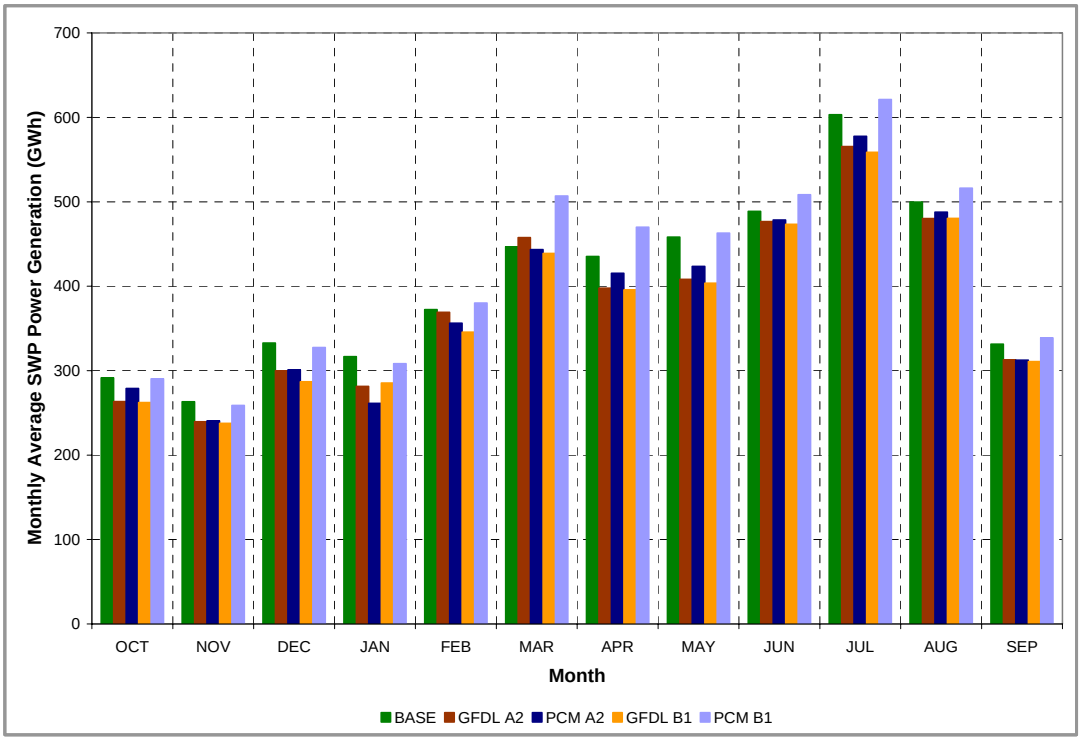


Figure 4.34 Monthly Average SWP Power Generation

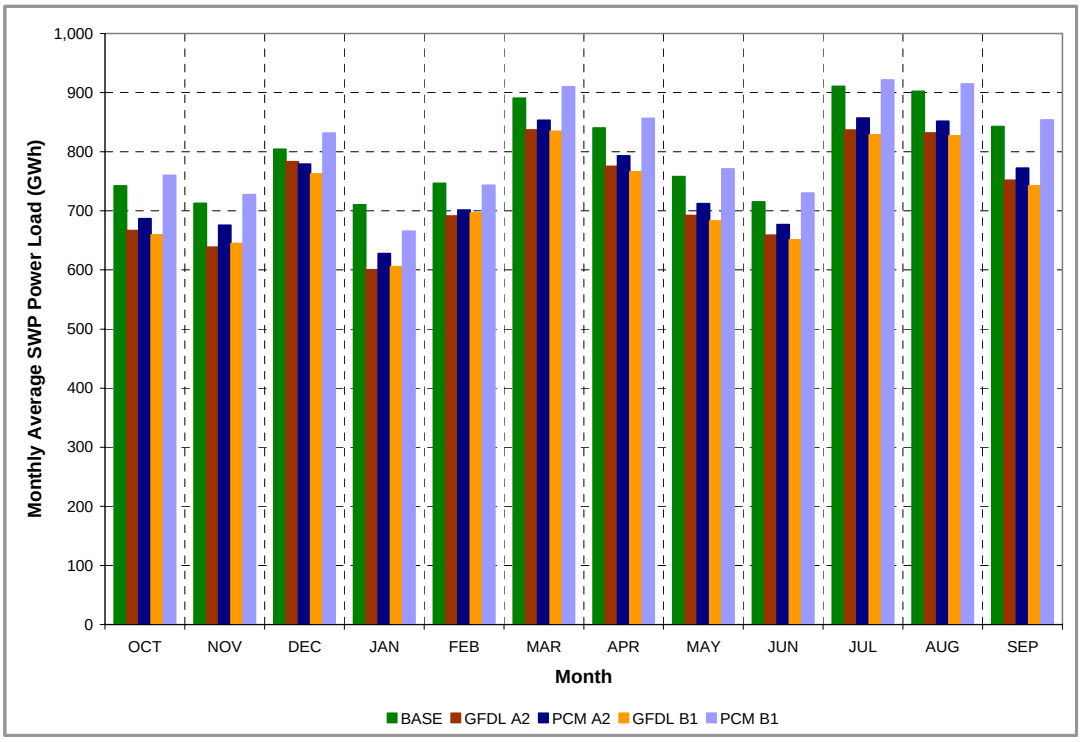


Figure 4.35 Monthly Average SWP Power Load

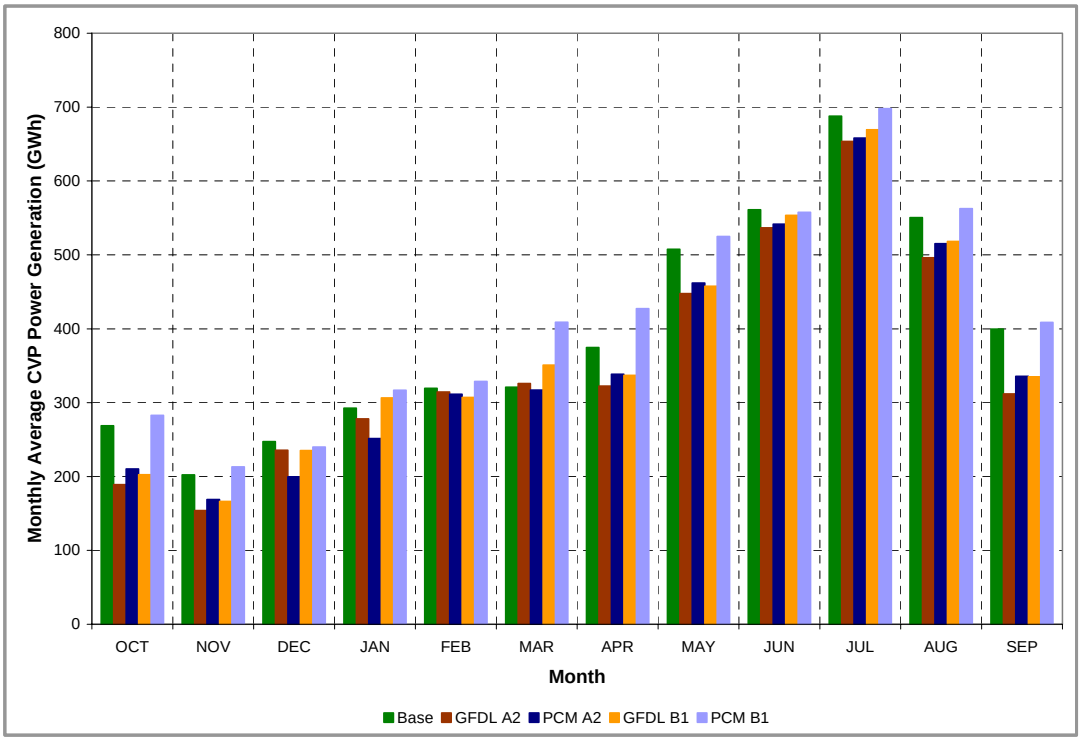


Figure 4.36 Monthly Average CVP Power Generation

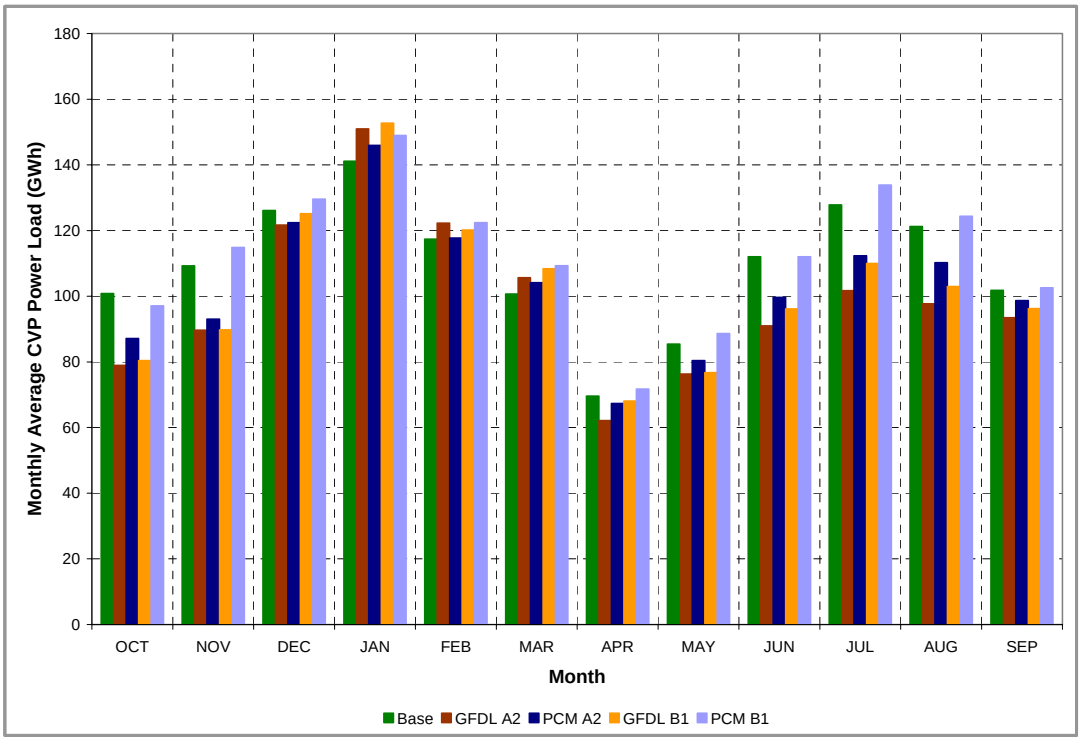


Figure 4.37 Monthly Average CVP Power Load

4.6.6 In-Stream Temperature Analysis

Water temperature has been recognized as key to the habitat needs of steelhead and Chinook salmon in the rivers of the Central Valley. River temperatures that are too high can kill salmon and steelhead by impairing metabolic function, or indirectly by increasing the probability of disease, predation, or other secondary mortality factors. Temperature tolerances also vary by life stage.

The water temperature of the river is a result of several factors: the temperature of water released from the major dams (Shasta, Oroville and Folsom) in the Sacramento Valley (a function of temperature stratification within each reservoir); the depths from which dam releases are made; the seasonal management of the deep cold-water pool reserves; ambient seasonal air temperatures and other climatic conditions; tributary accretions and water temperatures; and residence time in the re-regulating reservoirs downstream of each major dam, and in the river itself. To assist with downstream temperature control, temperature control devices (TCD) were installed at Shasta, Oroville, and Folsom dams. The TCDs can selectively withdraw water from different reservoir levels. The TCDs are generally operated to conserve cold water for the summer and fall months, when river temperatures become critical for fisheries. Therefore, the TCD is operated to make upper-level releases in the winter and spring, mid-level releases in the late spring and summer, and low-level release in the late summer and fall.

To assist in the water temperature impact evaluations of the various climate change scenarios, the Bureau of Reclamation temperature model was used to estimate temperatures in the Trinity,

Sacramento, Feather, American, and Stanislaus river systems. The reservoir component of the temperature model simulates TCD operation. The joint DWR/Bureau of Reclamation simulation model, CALSIM-II, provided monthly CVP/SWP operations input to the temperature model for a 72-year hydrologic period from1922 to 1993.

The climate change scenario impacts on the distribution and volume of reservoir inflow, and its resulting effect on seasonal reservoir storage, influence the cold-water pool volume. Three of the four climate change scenarios indicate an average reduction in reservoir storage, and therefore a corresponding reduction in cold-water pool volume. In addition, all four climate change scenarios show an expected increase in air temperature. This increase is reflected in increased river temperature. A summary of river temperatures at several key locations along the Sacramento River is shown in Table 4.24. Increased air temperature in the winter and early spring is especially important since inflow and air temperature during this period drive accumulation of the cold-water pool.

Table 4.24 Average Water Temperatures along the Sacramento River

	Study 1: Base		Study 2: GFDL A2		Study 3: PCM A2		Study 4: GFDL B1		Study 5: PCM B1	
	Average	1928-1934	Average	1928-1934	Average	1928-1934	Average	1928-1934	Average	1928-1934
American River	59.8	60.5	62.9	63.7	61.4	62.2	62.6	63.4	60.7	61.5
Balls Ferry	52.3	53.9	54.6	56.5	53.8	55.7	54.4	56.1	52.9	54.2
Bend Bridge	53.3	54.7	55.4	57.1	54.6	56.4	55.2	56.7	53.8	55.0
Butte City	57.1	58.3	59.5	61.0	58.5	59.9	59.2	60.6	57.8	58.9
Colusa Basin Drain	59.4	60.4	62.2	63.3	61.0	62.0	61.9	63.0	60.3	61.3
Feather River	59.8	60.6	62.7	63.7	61.3	62.2	62.4	63.3	60.6	61.5
Freeport	59.9	60.7	63.0	63.8	61.5	62.3	62.7	63.6	60.9	61.6
Jellys Ferry	53.1	54.5	55.2	56.9	54.4	56.2	55.0	56.5	53.6	54.7
Keswick	50.6	52.2	53.0	54.8	52.1	54.0	52.8	54.5	51.2	52.5
Keswick Above Spring Creek	50.8	52.3	53.2	55.1	52.3	54.3	53.1	54.8	51.4	52.6
Red Bluff	53.8	55.3	56.0	57.7	55.2	56.9	55.8	57.3	54.4	55.6
Shasta	49.8	51.4	52.1	54.0	51.3	53.2	52.0	53.7	50.5	51.6
Vina	54.8	56.1	57.0	58.6	56.2	57.7	56.8	58.2	55.4	56.5
Wilkins Slough	58.4	59.6	61.1	62.4	60.0	61.2	60.8	62.0	59.2	60.3

4.7 Conclusion

The purpose of this report was to provide a preliminary assessment of climate change impacts on CVP and SWP operations. Results of four climate change scenarios from global climate models GFDL and PCM were downscaled to regional hydrologic data using VIC. The regional streamflows were used to determine average monthly changes in reservoir inflows at a 2050 climate (2035 to 2064) as compared to a historical 1976 climate (1961 to 1990). The resulting perturbation factors were superimposed on historical reservoir inflows to create input for the four climate change simulations of CVP and SWP operations. The perturbed reservoir inflows were input into CalSim-II – the current planning simulation model for the CVP and SWP. Simulation results of the four climate change scenarios were compared to a historic climate simulation scenario in order to determine changes in water deliveries and carryover storage.

4.7.1 Study Limitations

There were some limitations in our analysis. First, the only representation of climate change in the CalSim-II simulations was the perturbed reservoir inflows. No consideration was given in these scenarios to heightened water demand due to changes in evapotranspiration or rainfall; nor was consideration given to increased Delta salinity due to a rising sea level. Both could significantly impact delivery capability.

Also, the method of downscaling global climate model information for CalSim-II input only captures the general trends of average rainfall and seasonal shifts in runoff. There is no information included about changes in weather variability. In each of the scenarios, the frequency and length of the droughts remained the same. If climate change influences these underlying weather phenomena, then we are missing important information necessary to determine impacts to CVP and SWP operations.

Another analytical limitation of our simulated results was the critical shortages of water in Shasta and Folsom during the droughts in scenarios GFDL A2, PCM A2, and GFDL B1. When these reservoirs were at dead storage, the simulated CVP operation was allowed to break rules and contracts that the Base and PCM B1 scenarios otherwise weren't. The result is that CVP deliveries reported for scenarios GFDL A2, PCM A2, and GFDL B1 are likely inaccurate. Alterations to CVP allocation rules governing the balance between deliveries and carryover may be necessary to prevent these shortages.

Given these and other analytical limitations, the results presented in this report are strictly preliminary. They are intended to be used to guide future climate change analysis and to identify areas where more information is needed. The results are not sufficient by themselves to make policy decisions.

4.7.2 Results

While there were limitations to our analysis, the results were nevertheless significant. General shifts in seasonal and annual average runoff, as predicted by the climate change scenarios, resulted in considerable impacts to SWP and CVP delivery capabilities, especially in the drier scenarios. Annual average SWP Table A deliveries were reduced by 10.2 percent in GFDL B1, while GFDL A2, the driest scenario, reduced annual average CVP SOD deliveries by 10.3 percent. SWP Article 21 deliveries tended to be slightly higher in the dry scenarios as compared to the Base because San Luis storage was less aggressively used for Table A and more Delta surplus was available in the winter; as such, San Luis was more likely to fill and the conditions for Article 21 deliveries -- full San Luis, Delta surplus, available Banks capacity -- were more likely to be met. However, the increased Article 21 deliveries did not offset reductions to Table A deliveries. PCM B1, the wetter climate change scenario, generated slightly higher SWP Table A and CVP SOD deliveries and slightly lower Article 21 deliveries; the difference between PCM B1 and the Base was most significant in the dry periods when storage capacity was available to make use of the extra water.

In response to climate change, California will need to search for physical, regulatory, and operational flexibilities in the SWP and CVP systems to maintain project delivery capabilities. With more runoff in the winter, there is likely to be a heightened conflict between the water

supply and flood control uses of North-of-Delta reservoirs. Better storm forecasting technology, allowing for earlier flood releases, or increased storage capacity could reduce the conflict. With higher Delta inflows in the winter months, greater winter SOD exports are desirable. For Banks Pumping Plant, permitted capacity and SOD conveyance including storage, pump, and channel capacity often limited exports from December to March. Therefore, future studies on changes in Banks permitted capacity should consider including climate change scenarios for estimating potential water supply benefits. Tracy exports were often limited by the upper Delta-Mendota Canal constriction. As such, it would be useful to simulate the proposed DMC-California Aqueduct intertie in the context of a climate change scenario.

CalSim-II results were processed to produce net impacts to SWP and CVP power generation. The SWP, using more power than it generates, increased its net load on an annual average basis by 11 percent in both GFDL simulations. The CVP, a net power generator, lost 10 percent of its power production on an annual average basis in both GFDL scenarios. Power generation on average increased for the CVP in scenario PCM B1. Of course, annual average changes in power generation are not as telling as seasonal changes. For the drier climate scenarios, lower storage resulted in reduced SWP and CVP power generation during the key summer months. Summer power generation was slightly higher for PCM B1.

Base and climate change scenario results were input into the Bureau of Reclamation temperature model for in-stream temperature analysis. High temperatures can be hazardous to salmon and steelhead. Therefore, downstream temperature controls are part of CVP and SWP operations of Shasta, Oroville, and Folsom. According to Table 4.24, the climate change scenarios resulted in warming of river temperatures at several key locations on an annual average basis. The timing of impacts will have to be explored in future studies.

As stated in the introduction, this is just the starting point for analyzing climate change impacts on SWP and CVP operations. There is still much work to be done to fully consider climate change effects in project planning studies. Furthermore, future studies should consider measures to relieve the negative effects of climate change. Analysis of the interaction of hydrologic changes and system constraints can suggest where more flexibility would be most useful. Eventually, the accumulated data and analysis can be used by our scientists, engineers, and political leaders to make sound policy decisions concerning the SWP, CVP, and climate change.

4.8 Acknowledgements

VIC data were processed and provided for download by Mary Tyree and Erik Peterson of Scripps Institution of Oceanography.

VIC data were produced by Ed Maurer at the University of Santa Clara.

Information on the Global Climate Models and emissions scenarios were provided by Dan Cayan from Scripps Institution of Oceanography and Mike Dettinger from the U.S. Geological Survey and Scripps Institution of Oceanography.

4.9 References

Miller, Norman L., et al (2001). Climate Change Sensitivity Study of California Hydrology: A Report to the California Energy Commission, *LBNL Technical Report No. 49110.*

United States Bureau of Reclamation (USBR) (2004). Chapter 6: Analytical Approach and Methods. In: *Long-Term Central Valley Project Operations Criteria and Plan.* United States Bureau of Reclamation. Sacramento, CA.

Progress on Incorporating Climate Change into Management of California's Water Resources

1st Progress Report
July 2006

Chapter 5:
Preliminary Climate Change Impacts Assessment for the Sacramento-San Joaquin Delta

Author:
Jamie Anderson Ph.D., P.E.
California Department of Water Resources, Bay Delta Office, Modeling Support Branch, Sacramento.

Contributor:
Joel Dudas P.E.
California Department of Water Resources, Division of Flood Management, Delta-Suisun Marsh Office, Sacramento.

Peer Reviewers:
Paul Hutton, Ph.D., P.E., Metropolitan Water District of Southern California

Leah Orloff, Contra Costa Water District

KT Shum, East Bay Municipal Water District

5 Preliminary Climate Change Impacts Assessment for the Sacramento-San Joaquin Delta

5.1 Introduction

The Sacramento-San Joaquin Delta is a dynamic network of natural and man-made channels. Freshwater from the southward flowing Sacramento River and from the northward flowing San Joaquin River converge with salty tidal flows from San Francisco Bay (Figure 5.1). Historically the Delta was a vast marsh. After the Gold Rush, farmers began building levees in the Delta to reclaim farmland. After years of farming, many of the Delta islands have subsided and are currently below sea level. Today the Delta consists of 57 leveed islands and more than 700 miles of sloughs and channels. This complex ecosystem is home to more than 500 species, including 20 endangered species such as the Delta smelt and salt harvest Suisun Marsh mouse. The Delta is also part of the migration path of young salmon heading out to the ocean and for adult salmon returning to spawn in their natal streams.

The Sacramento-San Joaquin Delta can be considered the hub of California's water supply system. About two-thirds of Californians and millions of acres of farmland rely on water from the Delta. Pumping plants in the south Delta are integral components for water distribution to central and southern California from the State Water Project (SWP) and the federal Central Valley Project (CVP). The Delta also provides local water supply for municipal and industrial and agricultural uses. The Delta supports more than $500 million in annual crop production (DWR, 2006).

The Sacramento River provides most of the freshwater inflow into the Delta (Figure 5.2). From 1980-1991, on average nearly 25 percent of the freshwater inflows to the Delta were used for municipal, industrial and agricultural water supplies, while the remaining 75 percent flowed to San Francisco Bay as Delta outflow. The actual distribution of Delta inflows varies from year to year depending on factors such as the amount and timing of precipitation and operations of upstream reservoirs.

Climate change could affect the Delta water balance shown in Figure 5.2. Warmer air temperatures are expected to shift the timing and form -- rain or snow -- of winter precipitation (see Chapter 2 and Chapter 6). Less snowpack would lead to less spring runoff. These shifting precipitation and runoff patterns would affect reservoir operations and Delta exports (see Chapter 4). Since the major inflows into the Delta are controlled by reservoir releases, Delta inflow patterns would be affected as well. More changes to reservoir releases and Delta exports might be required for compliance with Delta water quality standards. Changes in crop evapotranspiration rates could affect the amount of water needed for agricultural uses (see Chapter 7).

Future projected sea level rise would also affect the Delta. Higher water levels could threaten Delta island levees. Increased saltwater intrusion from the ocean could require increased freshwater releases from upstream reservoirs to maintain compliance with Delta water quality standards.

This chapter presents an initial demonstration of modeling tools use to quantify potential impacts of climate change on Delta water quality and water levels. The results demonstrate advancements on incorporating climate change into existing modeling methodologies, however the results produced are not sufficient by themselves for making management decisions. All results are preliminary and are for illustration purposes only. Sections 5.3 and 5.4 present potential effects of shifting precipitation and runoff patterns on Delta inflows and diversions for present sea level conditions. Section 5.5 addresses potential effects of sea level rise alone and in conjunction with shifting precipitation and runoff patterns.

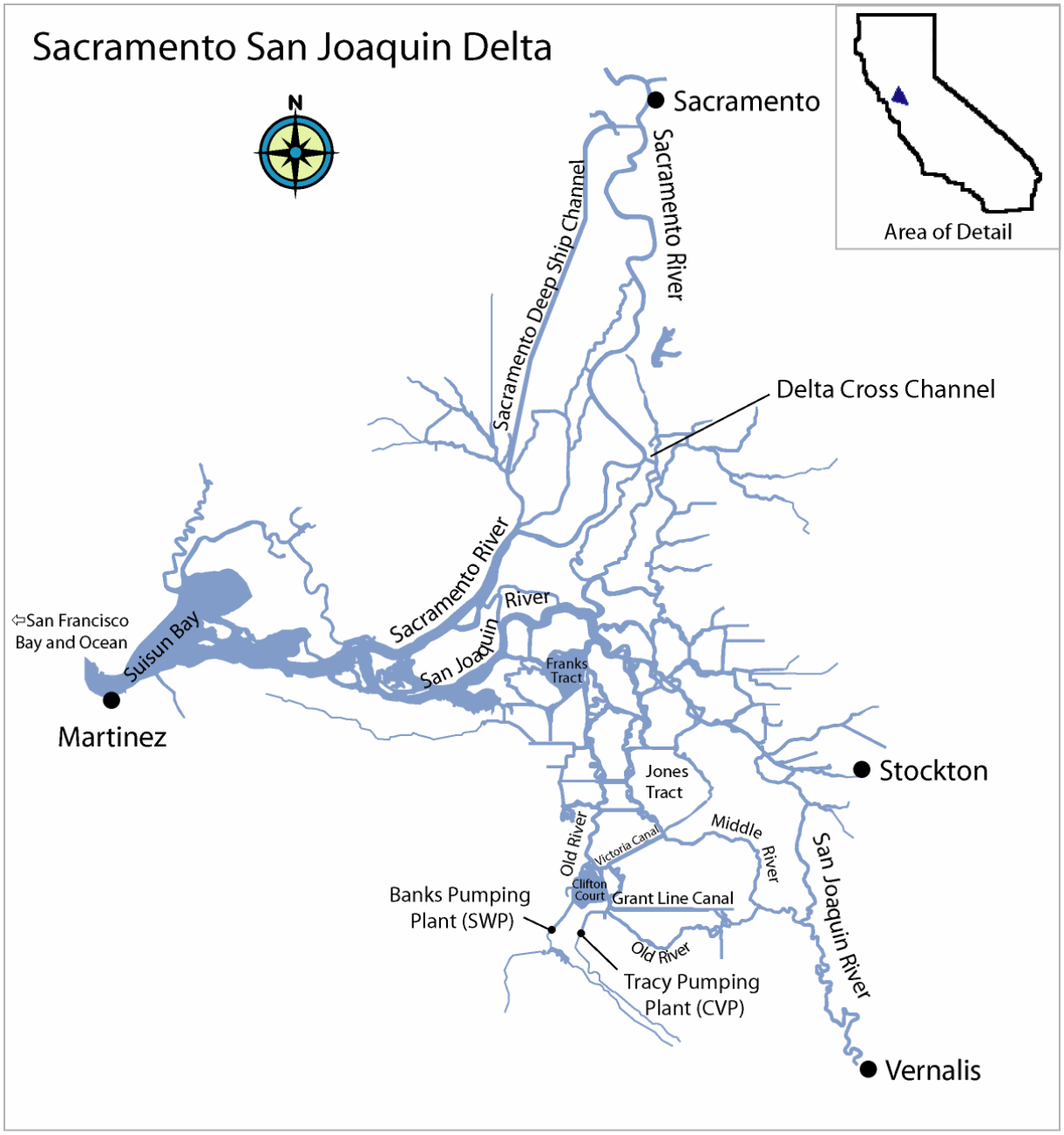


Figure 5.1: The Sacramento-San Joaquin Delta

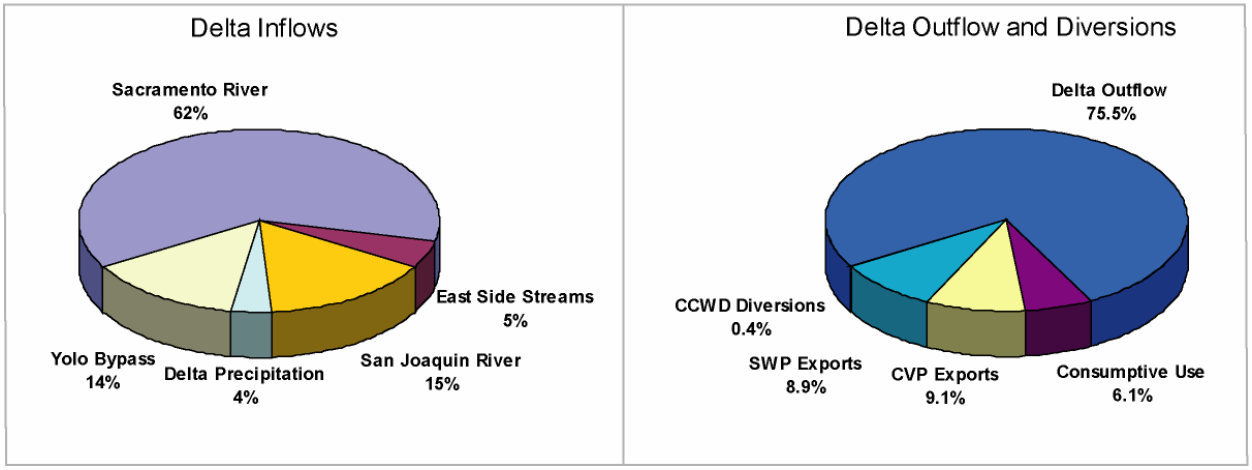


Figure 5.2: Average Annual Delta Inflows, Outflow and Diversions from 1980-1991
Adapted from Delta Atlas (DWR, 1995a)

5.2 Approach

A series of numerical models are being used for preliminary quantification of potential impacts of climate change on Delta flows, water levels and water quality (Figure 5.3). First, climate change scenarios are modeled using a Global Climate Model (GCM) to produce estimates of future air temperature and precipitation changes. These global scale changes are then reduced to a regional scale by a process called downscaling (see Chapter 3). The regional downscaling converts future projections of air temperature and precipitation into estimates of future streamflows. For these studies, the future streamflows are entered into a model, CalSim-II, which then simulates the operations of the SWP and CVP (see Chapter 4 and http://modeling.water.ca.gov/hydro/model/index.html). Using current management practices and existing system facilities, CalSim-II provides estimates of reservoir releases and Delta exports for each climate change scenario. The resulting Delta inflows and exports are then used to drive a model of the flows, water levels and water quality in the Delta, the Delta Simulation Model 2 (DSM2) (http://baydeltaoffice.water.ca.gov/modeling/deltamodeling/models/dsm2/dsm2.cfm). Results of the Delta model are then analyzed for the potential effects on water quality at several key locations. DSM2 is also used to estimate impacts of sea level rise.

All results presented in this report are preliminary. These studies are a starting point for analyzing climate change impacts on Delta hydrodynamics and water quality. Current management practices and existing system facilities were used in the analysis for this report. No changes were made to lessen the effects of climate change or sea level rise. Only four climate change scenarios and one sea level rise scenario were examined, and the likelihood of each scenario was not addressed. Several assumptions were also included in the analyses (see Section 5.2.3). The results presented here are not sufficient by themselves for making final policy decisions. These results are intended to illustrate the application of CalSim-II and DSM2 for climate change impacts assessment. Future efforts will involve improvements of the models and the study assumptions, and will address the likelihood of various climate change scenarios.

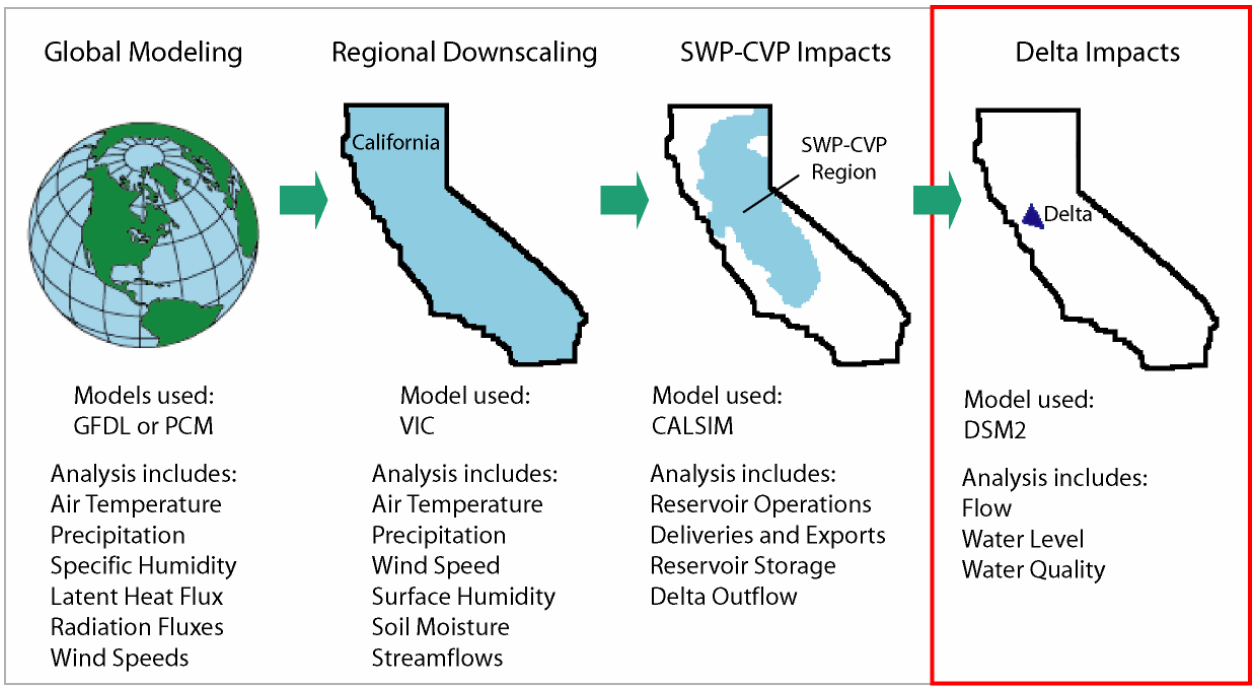


Figure 5.3: Delta Impacts Analysis Approach

5.2.1 Base Case

The base case for these studies is a 2020 level of development scenario using operations based on the "Long-Term Central Valley Project Operations Criteria and Plan" (USBR, 2004). Assumptions for the base case and climate change scenarios are presented later in Section 5.2.3.

5.2.2 Climate Change Scenarios

The studies presented in this report focus on the four climate change scenarios selected by the Climate Action Team appointed in response to the governor's Executive Order S-3-05 on climate change. The four climate change scenarios consist of two greenhouse gas (GHG) emissions scenarios developed by the Intergovernmental Panel on Climate Change (IPCC), known as A2 and B1, each represented by two different GCMs, the Geophysical Fluid Dynamic Lab model (GFDL) and the Parallel Climate Model (PCM) (see Chapter 3).

The A2 emissions scenario assumes high population growth, regional based economic growth, and slow technological changes that result in significantly higher GHG emissions. The B1 scenario represents low population growth, global based economic growth and sustainable development that result in the lowest increase of GHG emissions of the IPCC scenarios. Both the GFDL and PCM models project future warming, with GFDL indicating a greater warming trend than PCM. The PCM B1 scenario is the only scenario that shows a slight increase in precipitation. Precipitation is reduced in the other three scenarios.

Although the GCM models represent climate change through the end of the 21st century, the planning horizon for water resources is typically about 30 years. So the studies presented here focus on the climate change projections at about mid-century (Table 5.1). Thirty years of projected streamflows centered around the year 2050 (2035-2064) were used to develop the climate change influenced runoff patterns simulated in the SWP and CVP operations model, CalSim-II (see Chapter 4). However, land use projections were not available for 2050, so the climate change scenarios use land-use estimates for 2020. Thus when the climate change scenarios are described as being at the 2050 projection level, this refers to the runoff estimates only.

Table 5.1: Air Temperature and Precipitation Projections for 2050

Scenario	Average Change in Air Temperature °C		Average Change in Precipitation, in/yr	
	Northern CA	Southern CA	Northern CA	Southern CA
2050 GFDL A2	2.3	2.3	-0.75	-0.22
2050 PCM A2	2.1	2.1	-0.25	-1.77
2050 GFDL B1	1.3	1.2	-0.62	0.70
2050 PCM B1	0.8	0.9	0.83	-0.08

5.2.3 Assumptions

Major assumptions made in these studies are summarized below:

Runoff Estimations for Climate Change Scenarios (see Chapter 4 section 4.4)

- ❑ Runoff estimates reflect 2050 projections.
- ❑ Climate change scenarios maintain historical hydrologic variability.

CalSim-II Simulations of SWP and CVP Operations (see Chapter 4 section 4.5)

- ❑ Simulations were run for a 73-year analysis period based on wy1922-1994.
- ❑ Operating rules were not modified for climate change scenarios.
- ❑ For climate change scenarios, reservoir inflows reflect 2050 projections.
- ❑ For all scenarios, land use and water demands represent a constant 2020 level of development. The level of development does not change as the simulation progresses through time.

Current management practices and existing system facilities were used in the analysis for this report. No changes were made to lessen the effects of climate change or sea level rise.

No changes were made to:

- ❑ System structures, such as added water storage, pumping, or canal capacity
- ❑ Reservoir operating rules, such as changing the space required for flood control
- ❑ Streamflow requirements
- ❑ Water quality standards
- ❑ Delta outflow requirements
- ❑ Operations to account for sea level rise

- Delta exports, outflow and water quality are regulated according to the State Water Resources Control Board Decision 1641 (D1641) and the Water Quality Control Plan.
- Meeting Delta water quality standards is the top priority when changing SWP and CVP operations. Climate change will make this a larger challenge in the future. (see Table 4.12 in Chapter 4).

CalSim-II Simulations of SWP and CVP Operations (continued)

- Regulations from the Central Valley Project Improvement Act (CVPIA) 3406 (b)(2) are not included.
- The Environmental Water Account (EWA) is not included.
- San Joaquin River hydrology, operations and water quality do not reflect recent improvements subjected to the 2005 California Water and Environmental Modeling Forum (CWEMF)/CALFED peer review.
- New Melones Reservoir operations are governed by the Interim Plan of Operations.
- Operations were not modified to reflect sea level rise conditions

Delta Simulations

- Simulations were run for a 16-year analysis period based on wy1976-1991.
- Delta inflows and exports provided by CalSim-II output were not further modified to try to mitigate for Delta water quality effects of climate change or sea level rise.
- Contra Costa Water District (CCWD) diversions from Old River at Rock Slough and Old River at Highway 4 were combined and diverted from Rock Slough since CalSim-II did not simulate the two diversions separately.
- Operations of south Delta temporary fish and agricultural barriers were not simulated.[1]
- Pulse flows in April and May for the Vernalis Adaptive Management Plan (VAMP) were not simulated.
- Delta Island Consumptive Use for the 2020 level of development was used for all scenarios.
- Delta island return flow water quality varies monthly in a given year, but does not vary from year to year.
- For one-foot sea level rise scenarios, sea level rise was assumed to affect tidal elevation only. Tidal period and amplitude were assumed to be unchanged.
- Martinez EC is either the same or is increased for sea level rise scenarios (see section 5.5.1.1)
- Vernalis EC is the same for present sea level and one-foot sea level rise scenarios.

[1] Barrier operations can significantly influence Delta water quality and circulation patterns. The intent of the preliminary studies was to focus on the effects of climate change without having to separate which impacts were due to climate change and which were due to barrier operations.

5.2.4 Delta Simulations

The base case and four climate change scenarios were evaluated using DSM2 to quantify effects on Delta water quality and water levels. Each scenario was simulated at present sea level and for a one-foot sea level rise. DSM2 is a one dimensional model of flow, water levels and conservative and non-conservative constituent transport. The boundaries of the Delta representation in DSM2 are the I Street Bridge in Sacramento on the Sacramento River, Vernalis on the San Joaquin River, and Martinez downstream of the confluence of the two rivers as they flow into San Francisco Bay (Figure 5.1). Tidal water level fluctuations, river inflows, Delta exports, and irrigation withdrawals and return flows are all represented in DSM2. To represent the effects of the tidal cycle, DSM2 uses a 15-minute computational time step.

For DSM2 planning studies, a 16-year study period based on water years (wy) 1976-1991 (Oct. 1, 1975 to Sept. 30, 1991) is used. The study period reflects the variability in California's hydrology and includes the wettest (wy1983) and driest (wy1977) periods on record.

Reservoir inflows for the study period were modified to reflect climate change by multiplying the base-case runoff by monthly adjustment factors for each climate change scenario (see Chapter 4). Thus these studies reflect potential changes in magnitude and timing of runoff, but they do not represent potential changes in hydrologic variability since the base case represents historical hydrologic variability. System operations were then simulated using CalSim-II. Monthly average results from the CalSim-II simulations provided the following major Delta inflows, exports and diversions (Figure 5.4):

Delta Inflows

- Sacramento River at I Street Bridge in Sacramento
- San Joaquin River at Vernalis
- Eastside Streams (combined Mokelumne and Cosumnes river flows)
- Calaveras River
- Yolo Bypass

Delta Exports and Diversions

- SWP at Banks Pumping Plant
- CVP at Tracy Pumping Plant
- Contra Costa Water District (combined diversions Old River at Rock Slough and at Hwy. 4)
- North Bay Aqueduct
- Vallejo

The Delta inflows, exports and diversions provided from CalSim-II already incorporate mitigation for climate change through system operations using present operating rules. Tidal fluctuations in water level at Martinez are represented in DSM2 on a 15-minute time step by an adjusted astronomical tide that is based on historical data and reflects the spring-neap tidal cycle (Ateljevich, 2001a). Delta Island Consumptive Use (DICU) is represented at more than 250 locations (DWR, 1995b). Delta Cross Channel operations are provided by CalSim-II and did not change for any of the scenarios.

For this study, water quality analysis focused on salinity. DSM2 simulates electrical conductivity (EC) directly. Other salinity constituents such as chlorides can be estimated from the EC concentrations using statistical regression equations. For the DSM2 simulations, EC values must be specified for all Delta inflows. For the Sacramento River, eastside streams, Calaveras River and Yolo Bypass, constant EC values for each location are used in all of the scenarios (Table 5.2). San Joaquin River EC at Vernalis is provided for each scenario from output from the CalSim-II simulations. EC at Martinez is estimated for each scenario using a regression relationship that correlates the astronomical tide and Delta outflow to salinity (Ateljevich, 2001b). Delta Island return flow quality estimates were made based on available field data (DWR, 1995c). The quality of the return flows varies monthly, but does not vary from year to year. The same return flow quality values were used for all scenarios.

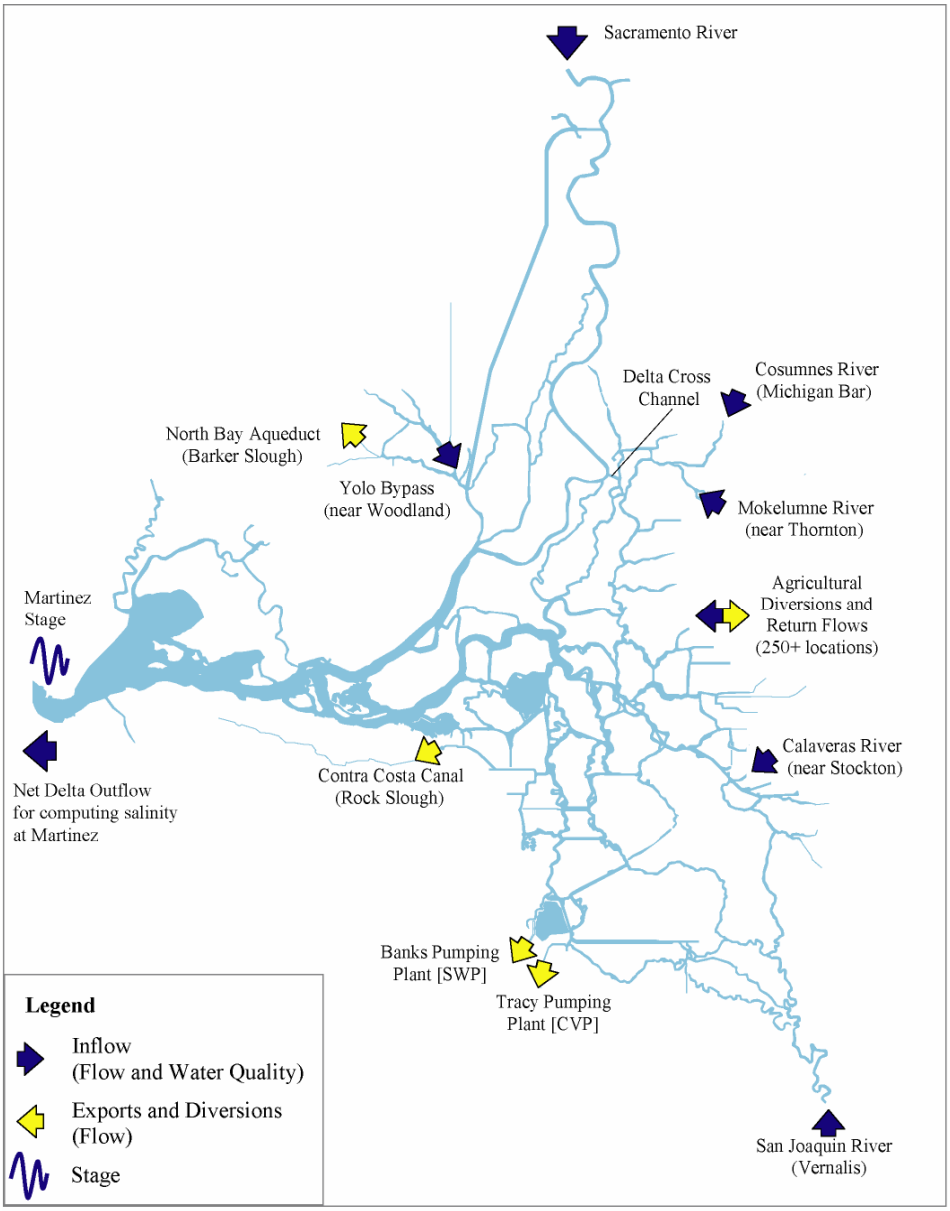


Figure 5.4: Inflows, Exports, Diversions and EC Inputs for DSM2 Simulations

Table 5.2: Constant EC Concentrations for DSM2 Simulations

Location	EC, uS/cm
Sacramento River	175
Eastside Streams	150
Calaveras River	150
Yolo Bypass	175

For sea level rise scenarios (see section 5.5), the tidal elevations at Martinez were raised uniformly by one-foot. This assumes that sea level rise does not affect the period of the tidal cycle. Estimates of additional salt transported from the ocean to Martinez under a one-foot sea level rise were not available. Due to time constraints, a preliminary approach for estimating salinity increases at Martinez for a one-foot sea level rise is applied only to the base case. In order to examine potential combined effects of sea level rise and climate change, scenarios that combined changes in Delta inflows and exports due to climate change with a one-foot sea level rise assumed that the salinity at Martinez for the one-foot sea level rise was the same as the Martinez EC for the present sea level version of that scenario. For example, the specified EC at Martinez was the same for the 2050 GFDL A2 present sea level and one-foot sea level rise scenarios. Since the salinity at Martinez would likely increase with rising sea levels, this assumption provides a lower bound for potential sea level rise effects on water quality for a one-foot rise in sea level. For these studies, system operations were not changed to try to lessen the increased salt intrusion for the sea level rise scenarios.

5.3 Climate Change Impacts on Delta Inflows and Exports for Present Sea Level Conditions

Output from CalSim-II provided Delta inflows and exports for DSM2 simulations of present sea level conditions for the base case and four climate change scenarios (Figure 5.5 to Figure 5.8). Tabular values of selected Delta inflows and exports are provided in the appendix in Section 5.11. Table 5.3 to Table 5.6 show monthly average changes in Delta inflows and exports for the climate change scenarios relative to the base case, and yearly changes are shown in Table 5.7 and Table 5.8. These results are preliminary representations of climate change impacts, and they reflect the assumptions listed in Section 5.2.3. See Chapter 4 for further information on climate change impacts to system operations.

Delta inflows tend to increase during the late winter and early spring and decrease during the summer and fall. The largest reductions in exports tend to occur in summer and fall. Inflows and exports are most sensitive to climate change during extremely wet or extremely dry periods. For example, the largest reduction in the magnitude of Delta inflows occurs during the summer of 1983 when base runoff was very high. For the climate change scenarios, the reduction in inflow for each month is determined by a monthly scaling factor as described in Chapter 4. For example, in the GFDL A2 scenario the June runoff into Shasta and Oroville is reduced by about 30 percent. Since the base runoff for 1983 was very high, the 30 percent reduction in the runoff resulted in the largest Delta inflow reduction. Contra Costa Water District (CCWD) diversions

were the same for all scenarios since they receive a high priority when CalSim-II allocates water. See Chapter 4 for more details on effects of climate change on SWP and CVP operations.

Table 5.3: Average Monthly Change in Sacramento River Inflow to the Delta, cfs

	Oct	Nov	Dec	Jan	Feb	Mar	Apr	May	Jun	Jul	Aug	Sep
GFDL A2	-1,600	-2,156	-1,518	930	265	2,441	-1,040	-2,667	-1,647	-1,571	-1,600	-2,156
PCM A2	-294	-1,056	-1,515	-910	-57	811	-1,010	-2,168	-841	-1,104	-294	-1,056
GFDL B1	-1,175	-1,719	-1,611	1,547	-369	2,456	-728	-2,605	-1,540	-1,205	-1,175	-1,719
PCM B1	254	-163	-178	1,639	386	5,265	1,814	17	-289	272	254	-163

Table 5.4: Average Monthly Change in San Joaquin River Inflow to the Delta, cfs

	Oct	Nov	Dec	Jan	Feb	Mar	Apr	May	Jun	Jul	Aug	Sep
GFDL A2	-1,324	-436	634	479	713	1,921	901	-393	-2,812	-1,173	-115	-426
PCM A2	-410	296	-592	-404	1,447	980	813	-110	-1,847	-705	-67	-196
GFDL B1	-1,362	208	82	364	-1,773	-175	288	-870	-2,866	-1,159	-136	-422
PCM B1	-198	287	-617	361	1,257	1,600	823	255	-1,628	-420	-26	-113

Table 5.5: Average Monthly Change in SWP Exports, cfs

	Oct	Nov	Dec	Jan	Feb	Mar	Apr	May	Jun	Jul	Aug	Sep
GFDL A2	-756	-646	-91	-107	-73	-146	-516	-106	-158	-407	-445	-865
PCM A2	-630	-12	-338	-292	-57	-167	-284	-69	-142	-351	-10	-626
GFDL B1	-756	-489	107	-160	-131	-152	-417	-454	-382	-382	-433	-999
PCM B1	-169	3	-213	-28	-106	198	-117	75	-75	8	91	-75

Table 5.6: Average Monthly Change in CVP Exports, cfs

	Oct	Nov	Dec	Jan	Feb	Mar	Apr	May	Jun	Jul	Aug	Sep
GFDL A2	-474	-36	-266	126	-444	149	-303	-235	-690	-1,143	-867	-305
PCM A2	-306	-94	-255	159	-490	169	-243	-125	-263	-582	-350	-99
GFDL B1	-473	-46	-164	143	-365	219	-215	-178	-447	-754	-554	-81
PCM B1	-16	245	-269	125	-71	130	-48	63	55	122	-4	-37

Table 5.7: Annual Change in Delta Inflows

Water Year	Year Type*	Base Flows TAF		Change in Sacramento River Flows, TAF				Change in San Joaquin River Flows, TAF			
		SAC River	SJR River	GFDL A2	PCM A2	GFDL B1	PCM B1	GFDL A2	PCM A2	GFDL B1	PCM B1
1976	C	9,322	1,345	-1,011	-611	-933	-198	-148	-88	-154	-41
1977	C	6,222	1,086	-511	-157	-145	99	-37	-19	-59	-8
1978	AN	20,144	4,094	826	-148	792	2,021	-260	-148	-787	-94
1979	BN	13,383	2,974	-1,457	-892	-1,562	492	-443	-144	-614	260
1980	AN	20,158	4,794	-622	-175	-430	1,092	101	0	-1,096	367
1981	D	11,976	1,840	-922	-866	-693	251	-343	-38	-360	45
1982	W	31,303	6,056	-585	-373	-573	735	131	61	-796	438
1983	W	35,501	13,934	-5,199	-3,185	-4,618	-130	-1,874	-838	-2,971	-148
1984	W	23,068	5,767	201	56	315	1,196	32	183	-229	340
1985	D	12,050	1,556	-588	-183	-286	78	-204	-56	-216	-10
1986	W	18,784	4,732	-871	-776	-821	208	568	493	-874	589
1987	D	9,765	1,333	-1,008	-828	-988	353	-115	-93	-119	-44
1988	C	8,694	932	-158	-192	-71	314	-25	-19	-26	-3
1989	D	12,086	973	756	-426	838	2,093	-29	-10	-36	4
1990	C	8,128	893	-243	-289	-215	-122	-15	-9	-26	14
1991	C	7,611	965	-535	-145	-136	333	-21	-12	-26	8

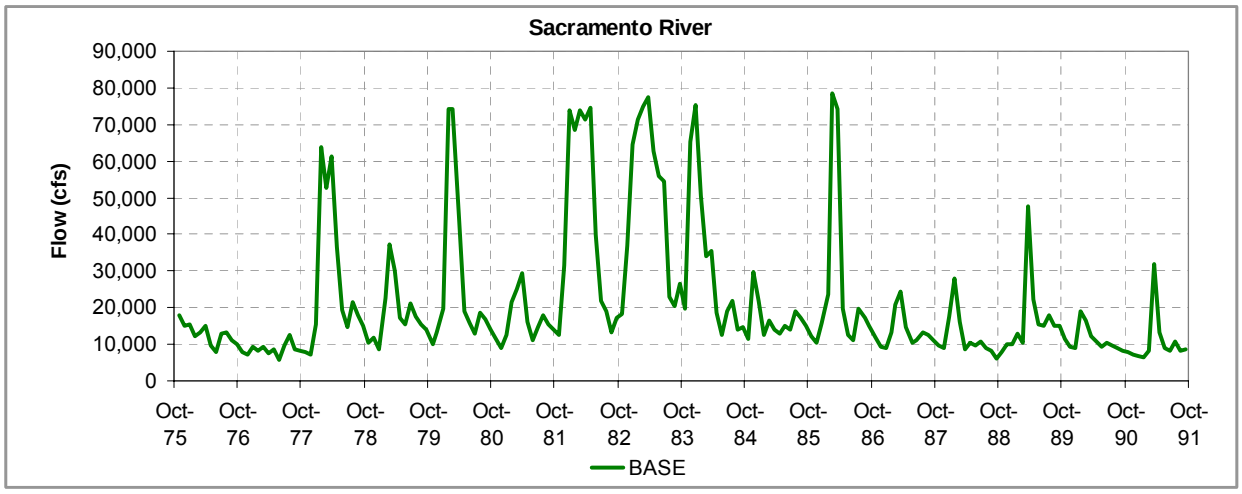
*Sac 40-30-30 water year types: W=Wet, AN=Above Normal, BN=Below Normal, D=Dry, C=Critical

Table 5.8: Annual Change in Delta Exports

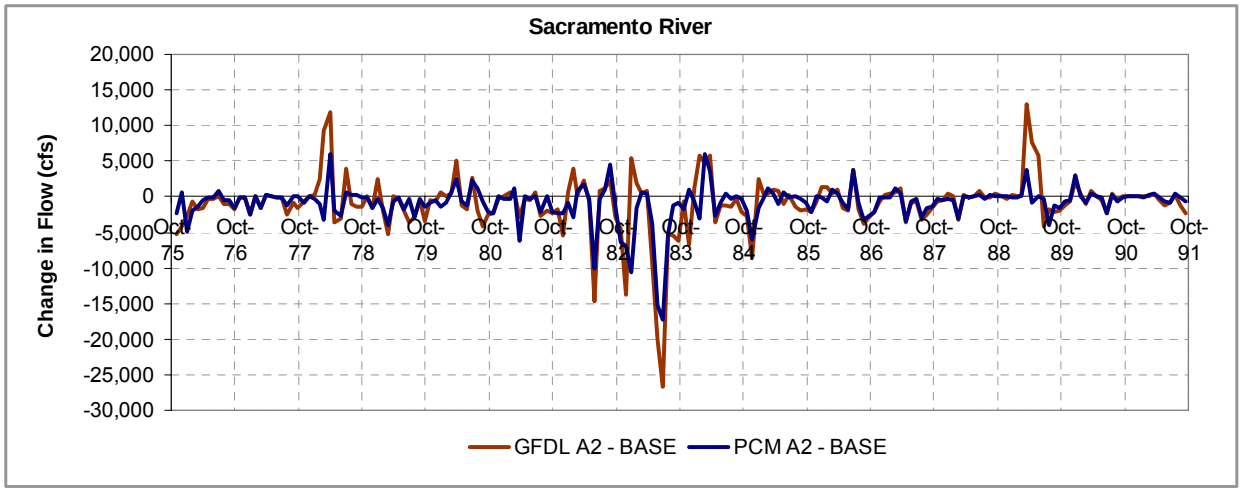
Water Year	Year Type*	Base Exports TAF		Change in SWP Exports TAF				Change in CVP Exports, TAF			
		SWP	CVP	GFDL A2	PCM A2	GFDL B1	PCM B1	GFDL A2	PCM A2	GFDL B1	PCM B1
1976	C	2,967	2,158	-635	-385	-588	-229	-23	45	22	-34
1977	C	995	1,391	-3	-83	-59	75	-462	-97	-153	38
1978	AN	3,608	2,736	-217	-115	-438	-102	-143	-29	-171	19
1979	BN	3,703	2,895	-446	-101	-589	118	-447	-223	-374	62
1980	AN	4,105	2,965	-478	-263	-457	1	-992	-572	-786	-152
1981	D	3,326	2,748	-674	-558	-716	-167	-195	-71	-128	8
1982	W	4,706	3,229	191	244	179	281	-393	-153	-286	-172
1983	W	3,676	2,827	34	0	29	0	176	15	168	14
1984	W	3,417	2,501	-288	-86	-305	-3	-309	-102	-174	-25
1985	D	3,516	2,869	-239	-189	-278	76	-415	-11	-169	-42
1986	W	4,201	2,799	-583	-432	-664	56	-520	-420	-471	-227
1987	D	2,570	1,904	-903	-770	-972	-284	-377	-239	-277	395
1988	C	1,541	1,729	32	-12	20	72	-191	-117	-100	265
1989	D	2,723	2,248	-382	-194	-344	-71	-299	-289	-162	99
1990	C	1,605	1,563	-303	-277	-314	-161	-24	-90	-25	-77
1991	C	1,110	1,495	162	63	-17	161	-574	-143	-149	103

*Sac 40-30-30 water year types: W=Wet, AN=Above Normal, BN=Below Normal, D=Dry, C=Critical

a) Base Case Delta Inflows



b) Change in Inflow for Climate Change A2 Scenarios



c) Change in Inflow for Climate Change B1 Scenarios

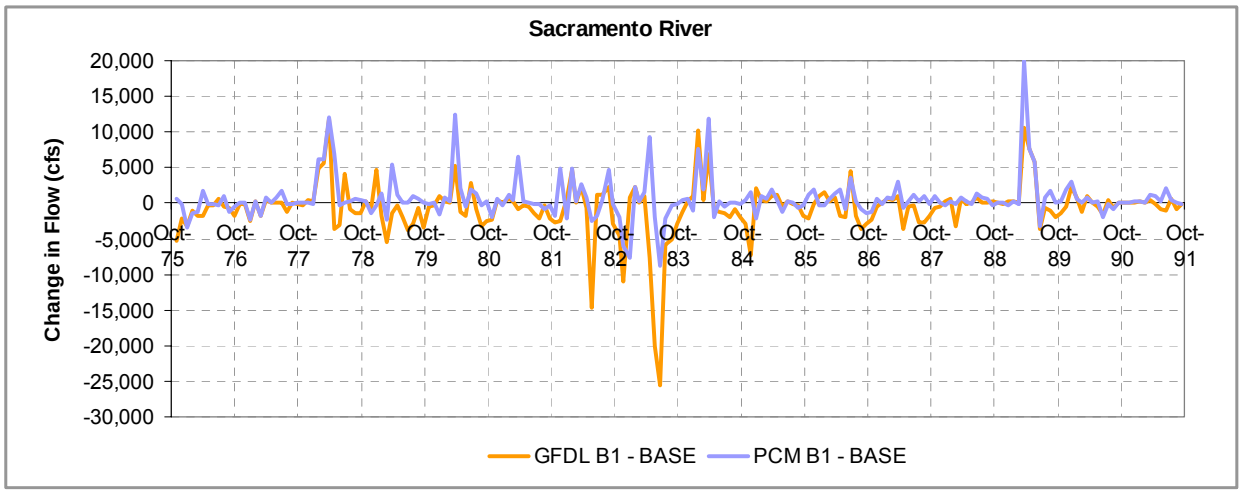
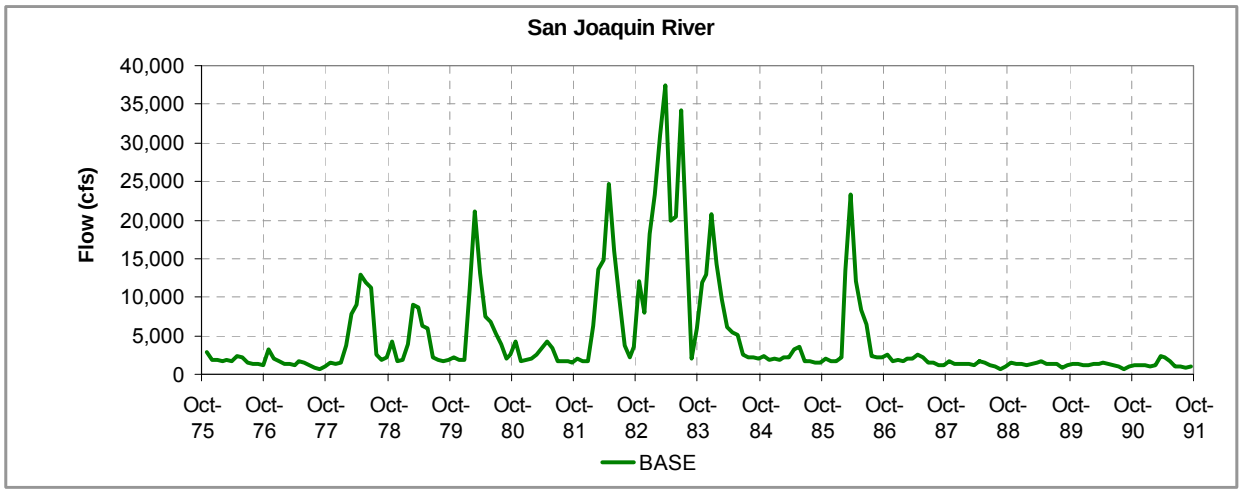
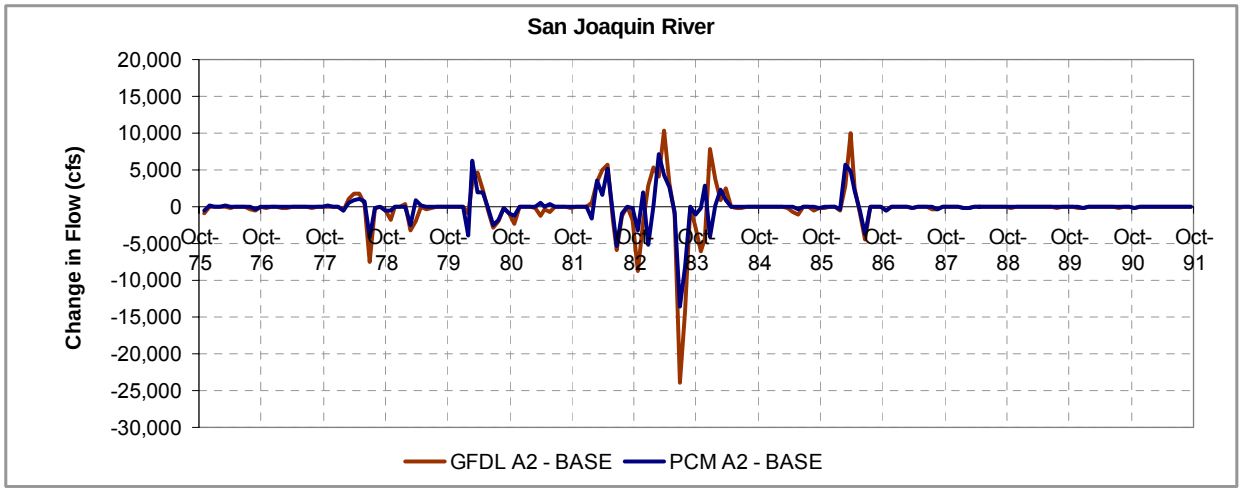


Figure 5.5: Delta Inflows from the Sacramento River

a) Base Case Delta Inflows



b) Change in Inflow for Climate Change A2 Scenarios



c) Change in Inflow for Climate Change B1 Scenarios

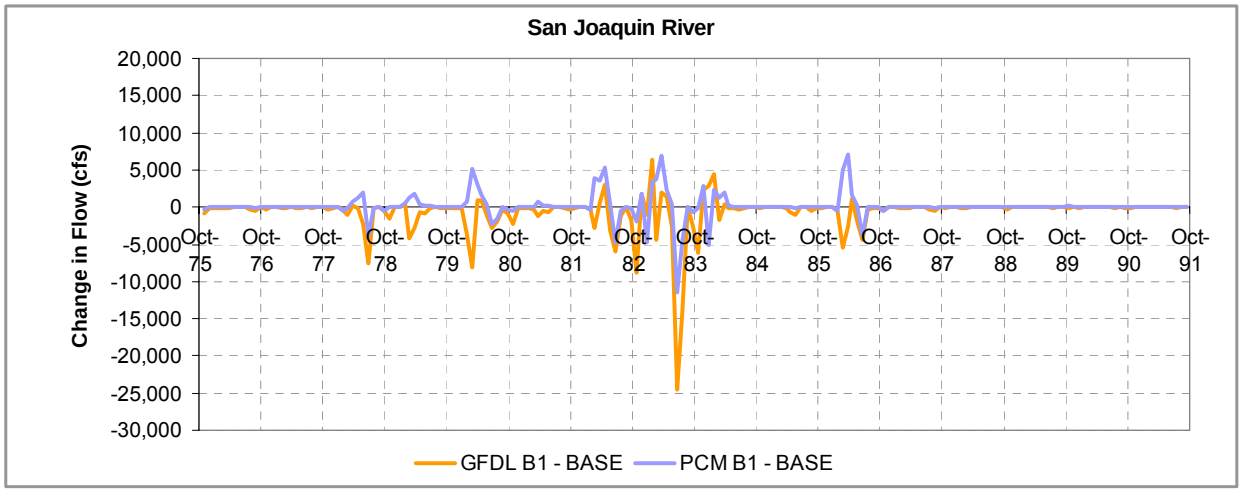
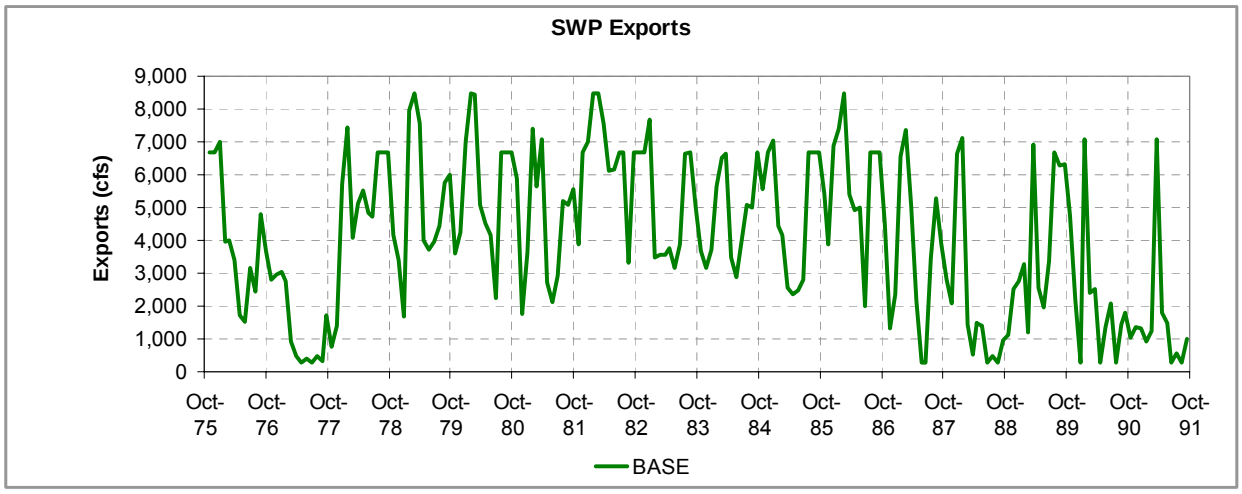
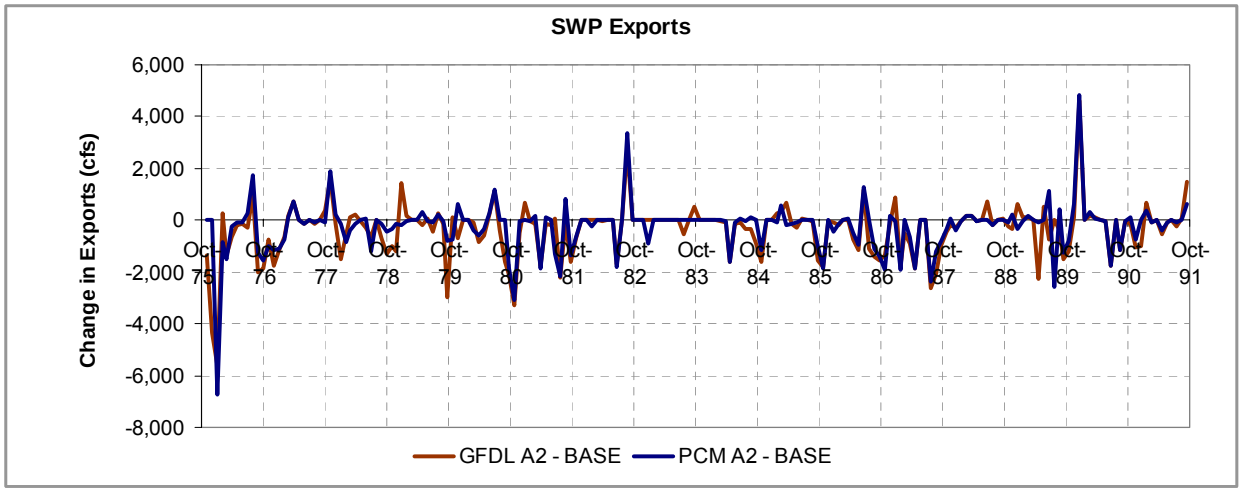


Figure 5.6: Delta Inflows from the San Joaquin River

a) Base Case Delta Exports



b) Change in Exports for Climate Change A2 Scenarios



c) Change in Exports for Climate Change B1 Scenarios

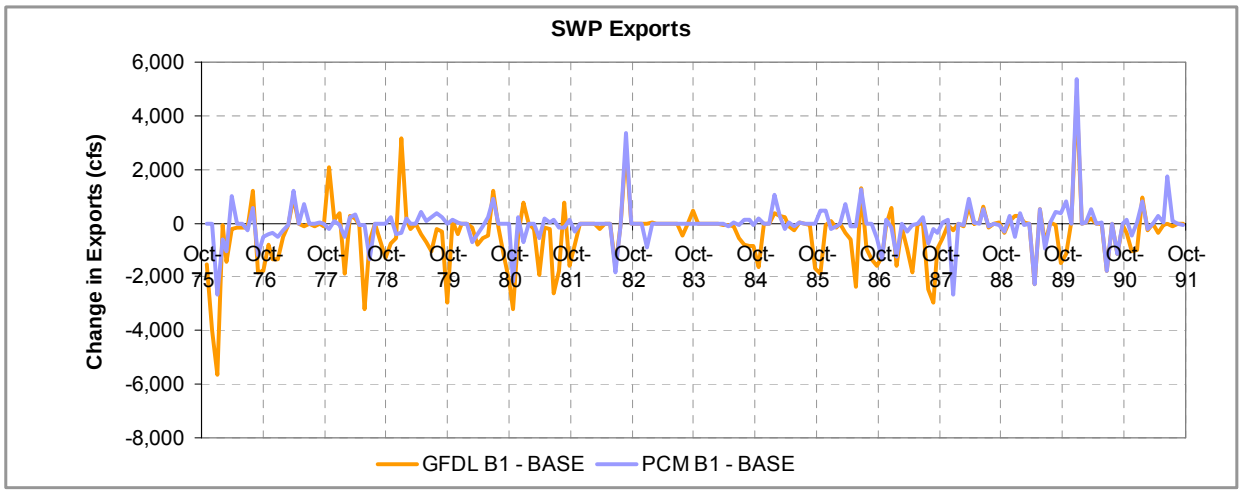
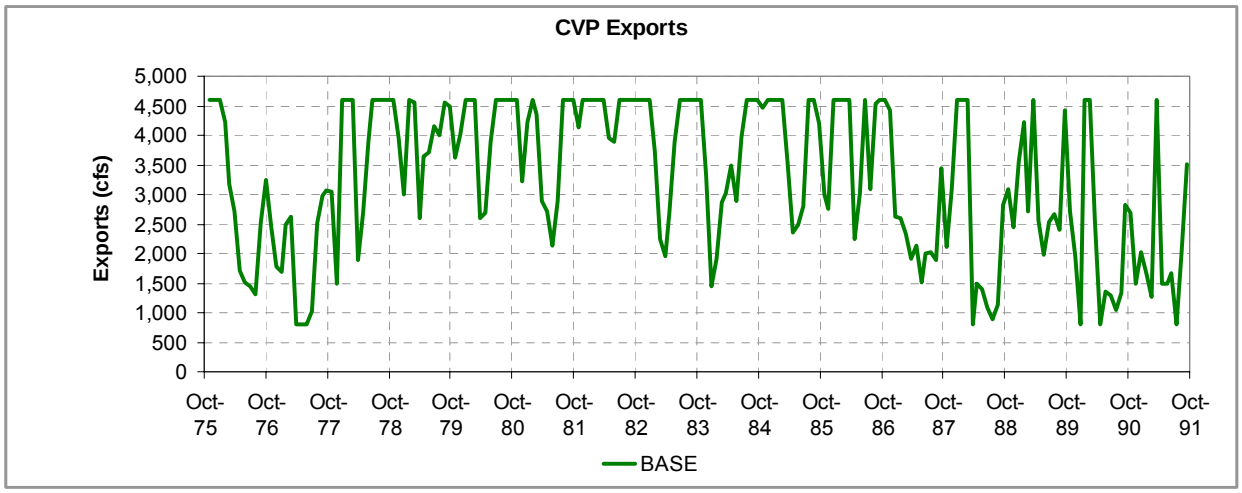
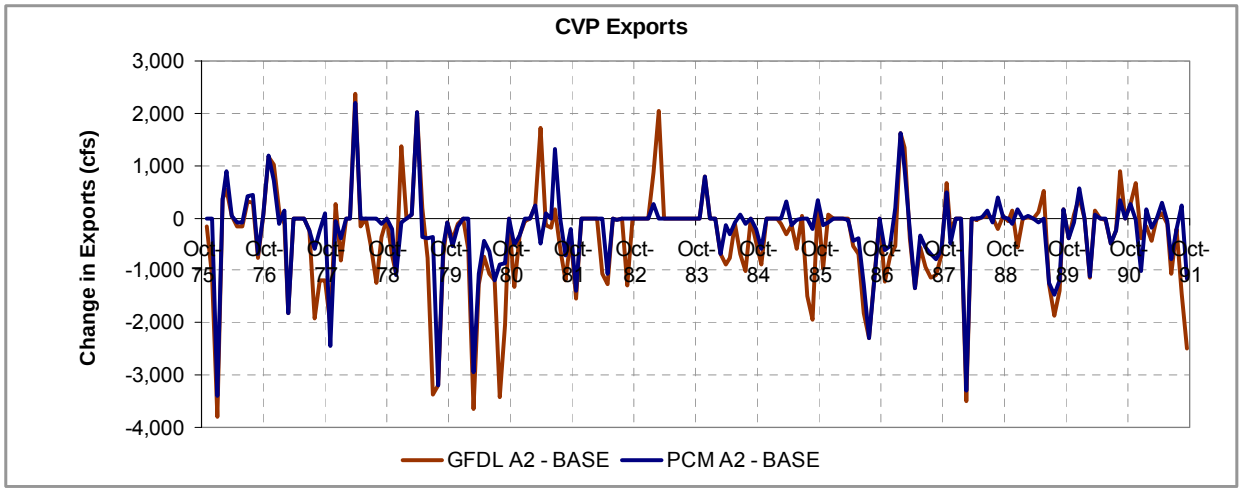


Figure 5.7: Delta Exports from the State Water Project

a) Base Case Delta Exports



b) Change in Exports for Climate Change A2 Scenarios



c) Change in Exports for Climate Change B1 Scenarios

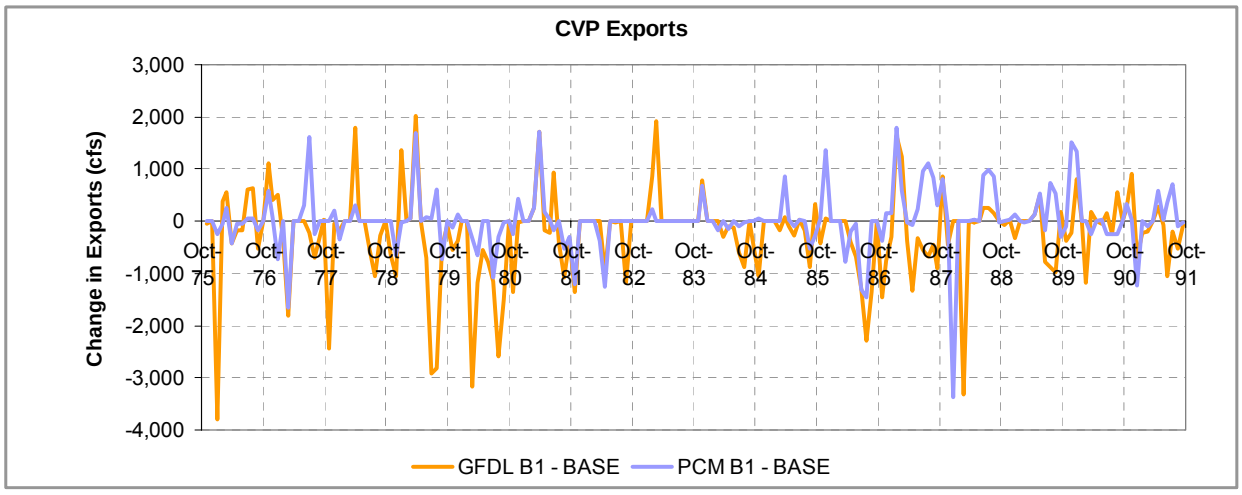


Figure 5.8: Delta Exports from the Central Valley Project

5.4 Climate Change Impacts on Water Quality for Present Sea Level Conditions

Initial analysis of potential impacts of climate change on Delta water quality for present sea level conditions focuses on compliance with selected Delta water quality standards from the Water Quality Control Plan and the State Water Resources Control Board Decision 1641 (D1641) (SWRCB, 1995). Analysis of other water quality parameters of concern, such as disinfection by-product formation potential is beyond the scope of this report. Initial analysis focused on specified limits for chloride concentrations (Table 5.9) at four municipal and industrial intake locations (Figure 5.9). Chloride mass loadings at each intake were also examined. All results are preliminary and incorporate several assumptions (see Section 5.2.3). These preliminary results are intended to illustrate the use of CalSim-II and DSM2 for climate change impacts assessment. The results are not sufficient by themselves for making policy decisions.

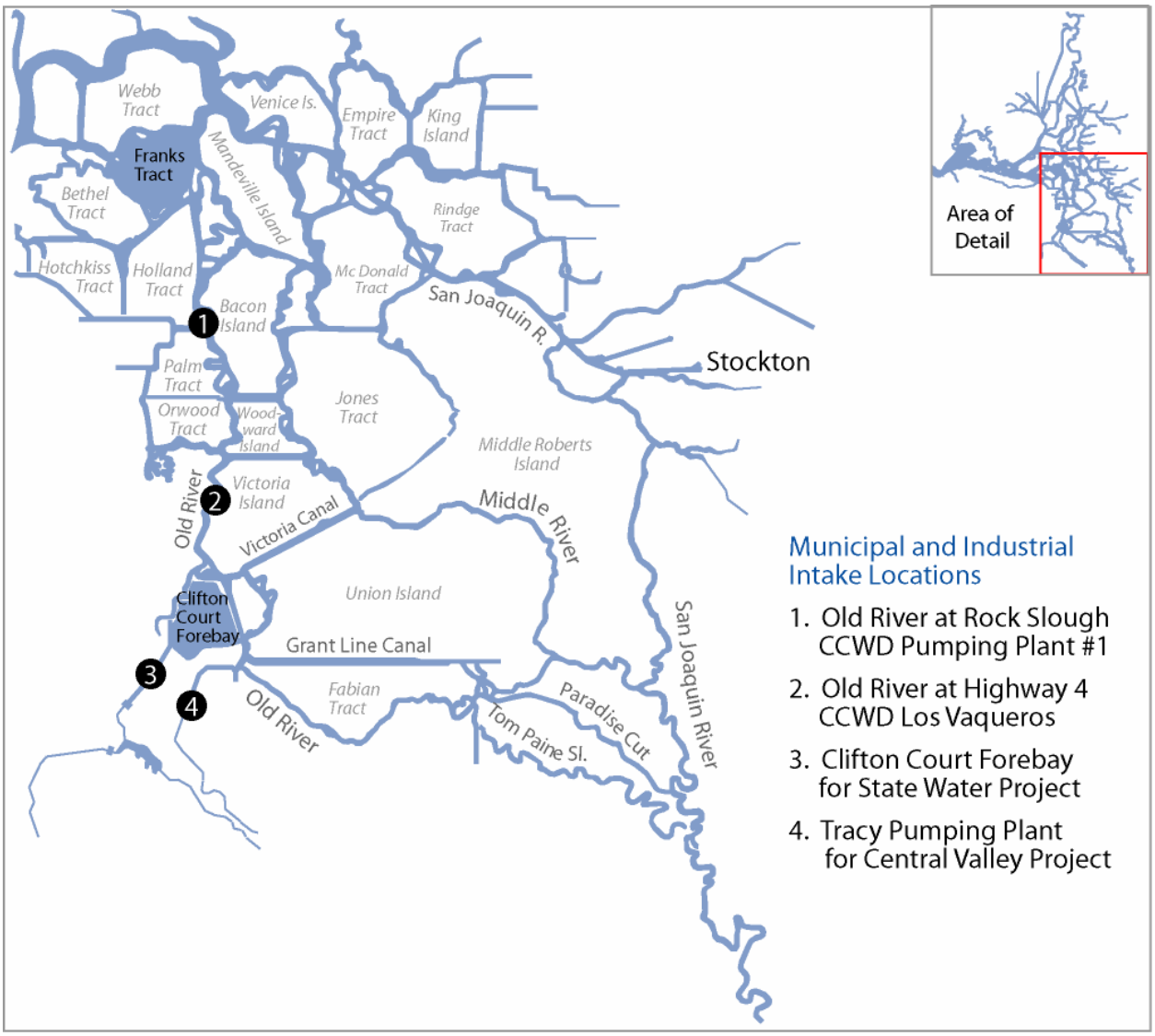


Figure 5.9: Delta Water Quality Impact Analysis Locations

Table 5.9: Delta Water Quality Standards

	Oct	Nov	Dec	Jan	Feb	Mar	Apr	May	Jun	Jul	Aug	Sep
Municipal and Industrial Compliance Locations	Daily average Cl < 250 mg/l											
Contra Costa Pumping Plant #1	Cl<150 mg/l for a required # of days based on year type											

5.4.1 Municipal and Industrial Water Quality for Present Sea Level Conditions

For this study, two municipal and industrial chloride standards from D1641 (SWRCB, 1995) were examined. The first standard specifies that maximum allowable daily average chloride concentrations can not exceed 250mg/l (Table 5.9). The second standard states that daily average chloride concentrations must be less than 150 mg/l for a specified number of days per calendar year based on the water year type (Table 5.10). This second chloride standard also requires that chloride concentration must be less than 150 mg/l for two consecutive weeks before those days can be counted towards meeting the standard.

Table 5.10: D1641 150 mg/l Chloride Standard

Water Year Type	Minimum Number of Days with Chloride Concentration ≤ 150 mg/l
Wet	240 (60% of the time)
Above Normal	190 (52% of the time)
Below Normal	175 (48% of the time)
Dry	165 (45% of the time)
Critical	155 (42% of the time)

*Chloride concentrations must be below 150 mg/l for at least two weeks before those days can be counted towards meeting the standard.

CalSim-II and DSM2 results were analyzed to determine compliance with the chloride standards at four municipal and industrial intakes (Figure 5.9) for the base and climate change scenarios:

- CCWD at Old River diversion at Rock Slough (for Contra Costa Canal)
- CCWD at Old River diversion at Highway 4 (for Los Vaqueros)
- SWP at Clifton Court Forebay
- CVP at Tracy

For these studies in both CalSim-II and DSM2, Contra Costa Water District's diversions were all withdrawn from Old River at Rock Slough[2]. This assumption could have local impacts on hydrodynamics and water quality. Although CCWD diversions were not simulated at Old River at Highway 4, water quality results are presented for that location since it is a potential diversion point.

In CalSim-II, the Artificial Neural Network (ANN) that represents Delta water quality provides chloride concentrations at a few Delta locations. The DSM2 simulations for this study determined EC concentrations throughout the Delta. These EC values can be converted to chloride concentrations using regression relationships based on field data (e.g. Suits, 2001 or Freeport, 2003[3]). For the analysis presented in this chapter, the simulated EC concentrations were converted to chlorides using the following equations from Suits (2001):

Contra Costa Water District Old River Diversion at Rock Slough

$$Cl = \frac{EC - 89.6}{3.73} \qquad \text{Eqn 5.1}$$

Old River at Highway 4, SWP at Clifton Court and CVP at Tracy

$$Cl = \frac{EC - 160.6}{3.66} \qquad \text{Eqn 5.2}$$

where,

Cl = chloride concentration in mg/l

EC = electrical conductivity in uS/cm

5.4.1.1 250 mg/l Chloride Standard

Monthly Average Results

One of the municipal and industrial beneficial use standards in D1641 specifies a maximum daily chloride concentration of 250 mg/l (Table 5.9). CalSim-II simulations attempt to meet this standard at Old River at Rock Slough. Monthly time step CalSim-II simulations represent this standard by setting a monthly average chloride target at Old River at Rock Slough of 225 mg/l. In CalSim-II the monthly average chloride concentrations at Rock Slough are determined by an ANN. CalSim-II tries to operate the system to meet the maximum allowable chloride standard at all time, but that isn't always possible (Table 5.11). For the base case, the 225mg/l chloride

[2] CalSimII calculates CCWD's combined Old River at Rock Slough (Contra Costa Canal) and Old River at Highway 4 (Los Vaqueros) diversions. For DSM2 studies, these combined diversions are taken from Old River at Rock Slough. In order to represent the two diversions separately, it would be necessary to develop a series of rules to emulate the CCWD operation of those diversions.

[3] Examining long term average chloride concentrations at Old River at Rock Slough using two sets of regression relationships, chloride concentrations from the Suits (2001) regression equation were an average of about 15mg/l higher than chloride concentrations determined from the Freeport (2003) regression equations.

target was met about 92 percent of the time for the DSM2 analysis period of wy1976-wy1991. Times when the target maximum chloride concentration was not met occurred in November to January. For the four climate change scenarios, the percent time for meeting the maximum chloride concentration target was met differed from the base case by less than 2 percent.

Table 5.11: Percent of Time Monthly Average Chloride Concentration <225mg/l

	BASE	GFDL A2	PCM A2	GFDL B1	PCM B1
CalSim-II results	92.2	91.1	92.2	90.1	93.8
DSM2 results	92.7	95.3	94.8	95.8	93.8

Monthly system operations from CalSim-II are used to run the more detailed Delta model, DSM2. DSM2 runs on a 15-minute time step and includes physically-based descriptions of flow and water quality constituent transport. DSM2 represents the spring-neap tidal cycle and diversions to and return flows from Delta islands. Thus, chloride concentrations simulated by the physically-based model DSM2 can differ from those estimated by the correlation-based ANN in CalSim-II. For studies in this report, average differences in monthly average chloride concentration at Old River at Rock Slough were about 5mg/l lower for the DSM2 simulations than for the ANN results. For comparison purposes, the percent time that the monthly average chloride concentrations at Rock Slough were less than the 225 mg/l target for both CalSim-II and DSM2 results are shown in Table 5.11. Since the DSM2 simulations tend to have slightly lower chloride concentrations that those estimated by the ANN, the monthly average DSM2 simulation results are less than 225 mg/l a bit more frequently than the CalSim-II results.

Daily Average Results

Daily average EC results from DSM2 for the 16-year simulation period were converted to daily average chloride concentrations using equations 5.1 and 5.2. Exceedance plots for daily average chloride concentrations at Rock Slough are shown in Figure 5.10. Percentiles and average chloride concentrations are shown in Table 5.12. Exceedance plots and percentile tables for other municipal and industrial intake locations are presented in the appendix in section 5.12. The distribution of chloride concentrations is similar for the base case and climate change scenarios at all four municipal and industrial intake locations.

Daily average chloride concentrations based on DSM2 simulation results can be used to examine compliance with the 250 mg/l maximum allowable daily average chloride concentration standard (Table 5.9). Compliance with the maximum daily average chloride concentration standard is given in Table 5.13. Increases in chloride standard compliance for the climate change scenarios relative to the base case are shown in Table 5.14. At Old River at Rock Slough, compliance with the 250 mg/l standard is at least 97 percent for all scenarios. Compliance was reduced in September through February of dry years when freshwater inflows to the Delta are low, which leads to higher salt intrusion from the ocean. Increased winter runoff for the climate change scenarios lead to slight improvements in compliance with the chloride standard at Old River at Rock Slough. There was complete compliance with the 250 mg/l standard for SWP and CVP intakes for all of the scenarios.

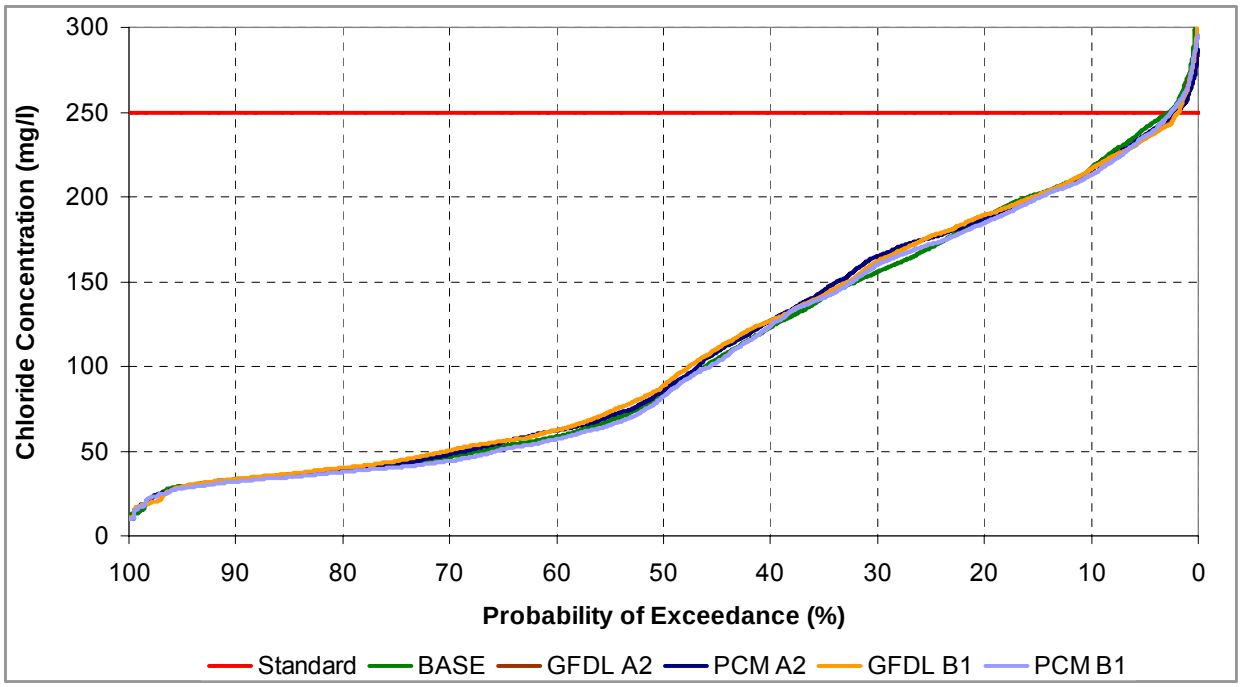


Figure 5.10: Probability of Exceedance for Chlorides at Old River at Rock Slough

Table 5.12: Chloride Concentration Percentiles for Old River at Rock Slough (mg/l)

	5%	10%	25%	50%	75%	90%	95%	Avg
BASE	30	33	42	83	170	217	240	109
GFDL A2	27	33	43	89	175	217	234	110
PCM A2	29	33	43	86	176	216	236	110
GFDL B1	29	34	44	89	177	216	234	111
PCM B1	28	32	40	82	172	213	236	107

Examining the daily average chloride concentrations from DSM2 resulted in higher compliance values for the 250 mg/l maximum chloride concentration standard at Old River at Rock Slough (Table 5.13) than the estimated compliance from examining the monthly average results from CalSim-II relative to the target monthly average chloride concentration of 225mg/l (Table 5.11). For these studies, the 225 mg/l target monthly average chloride concentration in CalSim-II provides a conservative estimate of compliance with of the daily average 250 mg/l maximum chloride concentration standard.

Although the Contra Costa Water District intake at Old River at Highway 4 is not a D1641 compliance location, chloride concentrations were also examined at that location. At Old River at Highway 4, daily average chloride concentrations were less than 250 mg/l 99.9 percent of the time for the base case and 100 percent of the time for the four climate change scenarios. There was complete compliance with the 250 mg/l chloride standard at the SWP and CVP intakes for all scenarios. These results demonstrate that existing flexibility in the system was able to accommodate changing reservoir inflows due to climate change with only minor impacts to compliance with the 250 mg/l chloride standard.

Table 5.13: Municipal and Industrial Intake Chloride Standard Compliance

Scenario/ Location	BASE	GFDL A2	PCM A2	GFDL B1	PCM B1
CCWD-Old River at Rock Sl.	97.2%	98.0%	98.0%	98.2%	97.4%
CCWD-Old River at Hwy 4*	99.9%	100%	100%	100%	100%
SWP-Clifton Court	100%	100%	100%	100%	100%
CVP-Tracy	100%	100%	100%	100%	100%

* Contra Costa Water District's intake at Old River at Highway 4 is not a compliance location for D1641. It is shown for comparison purposes.

Table 5.14: Change in Municipal and Industrial Intake Chloride Standard Compliance

Scenario/ Location	GFDL A2	PCM A2	GFDL B1	PCM B1
CCWD-Old River at Rock Sl.	0.8%	0.8%	0.9%	0.2%
CCWD-Old River at Hwy 4*	0.1%	0.1%	0.1%	0.1%
SWP-Clifton Court	0.0%	0.0%	0.0%	0.0%
CVP-Tracy	0.0%	0.0%	0.0%	0.0%

* Contra Costa Water District's intake at Old River at Highway 4 is not a compliance location for D1641. It is shown for comparison purposes.

5.4.1.2 150 mg/l Chloride Standard

At Old River at Rock Slough, another water quality standard states that the daily average chloride concentration should be below 150 mg/l for a specified number of days per calendar year depending on the water year type (Table 5.9 and Table 5.10). This standard also states that chloride concentrations must be below 150mg/l for at least two weeks before those days can be counted towards meeting the standard. Daily average chloride concentrations were computed from DSM2 EC results using equation 5.1. There was complete compliance with this standard for the base case or the two A2 scenarios (Table 5.15). For the two B1 scenarios, compliance

with the standard was reduced during a dry year. The values in Table 5.15 reflect the requirement that chloride concentrations be less than 150 mg/l for at least two weeks before those days can be counted toward the standard. For these studies, the compliance pattern does not change for any of the scenarios if all days with chloride concentrations less than 150 mg/l are considered. For the two cases that had non-compliance, the number of days with chloride concentrations less than 150 mg/l with and without the 2 consecutive week requirement is shown in Table 5.16. In most cases, existing system flexibility was able to adjust to climate change while maintaining compliance with the 150 mg/l chloride standard.

Table 5.15: Old River at Rock Slough 150mg/l Chloride Standard Compliance
Number of days that chloride concentrations were below 150 mg/l for at least 2 weeks

Year	Yr. Type*	Standard: Min Days Cl≤150 mg/l	Base	GFDL A2	PCM A2	GFDL B1	PCM B1
1976	C	155	177	168	169	167	178
1977	C	155	161	190	169	170	158
1978	AN	190	247	255	250	259	250
1979	BN	175	259	264	239	264	247
1980	AN	190	269	265	262	264	262
1981	D	165	260	275	261	257	261
1982	W	240	365	365	365	365	365
1983	W	240	365	365	365	365	365
1984	W	240	295	306	306	307	296
1985	D	165	216	211	199	215	223
1986	W	240	287	252	259	252	258
1987	D	165	176	196	187	197	217
1988	C	155	230	236	229	234	245
1989	D	165	184	169	170	**153**	**139**
1990	C	155	222	195	195	196	210

*Sac 40-30-30 water year types: W=Wet, AN=Above Normal, BN=Below Normal, D=Dry, C=Critical
Gray shading and bold text indicate non-compliance with the standard.

Table 5.16: Effect of 2 Week Requirement on 150mg/l Chloride Standard Compliance for Two Climate Change Scenarios at Old River at Rock Slough

	Year	Yr. Type*	Standard: Min Days Cl≤150 mg/l	Number of Days Cl≤150 mg/l	
				GFDL B1	PCM B1
# Days with Cl≤150 mg/l for at least 2 weeks	1989	D	165	**153**	**139**
Total # Days with Cl≤150 mg/l	1989	D	165	**156**	**155**

*Sac 40-30-30 water year types: W=Wet, AN=Above Normal, BN=Below Normal, D=Dry, C=Critical
Gray shading and bold text indicate non-compliance with the standard.
Results are only shown for scenarios that did not comply with the standard (see Table 5.15)

5.4.1.3 Chloride Mass Loading Rates

Chloride mass loadings at municipal and industrial intakes were estimated using equation 5.3. The mass loading estimates for CCWD are based on the combined diversion rate for CCWD's Old River diversions at Rock Slough and Highway 4 and the chloride concentrations at Rock Slough (see footnote 2 on page 5-1 for explanation of combined diversions).

$$Cl\ MassLoading\ (metric\ tons/day) = Cl\ (mg/l) * Exports\ (cfs) * \underbrace{2.832x10^{-8}}_{\frac{mg}{l}\ to\ \frac{metric\ tons}{ft3}} * \underbrace{86{,}400}_{\frac{ft^3}{\sec}\ to\ \frac{ft^3}{day}} \qquad \text{Eqn 5.3}$$

Since the export rates at Old River at Rock Slough are the same for all of the scenarios (Table 5.39), the chloride mass loadings are similar for all of the scenarios (Table 5.17). Export rates for the SWP and CVP vary for each scenario (Table 5.37 and Table 5.38). Mass loadings for the SWP and CVP are an order of magnitude higher than those at Rock Slough because the export rates at those locations are also an order of magnitude higher (Table 5.37 and Table 5.38). For the SWP, average chloride mass loadings decrease by 4 percent-9 percent for the climate change scenarios relative to the base case (Table 5.18). For the CVP, the B1 scenarios show little change relative to the base case, while the A2 scenarios have about 5 percent lower chloride mass loadings than the base case (Table 5.19). Reduced chloride mass loadings for the climate change scenarios are due to reduced export rates for those scenarios.

Table 5.17: Chloride Mass Loading Percentiles (metric tons/day) for Old River at Rock Slough

	5%	10%	25%	50%	75%	90%	95%	Avg
BASE	0*	9	19	45	80	115	146	54
GFDL A2	0	7	20	47	77	119	141	54
PCM A2	0	9	20	47	77	113	145	54
GFDL B1	0	8	20	47	78	119	140	55
PCM B1	0	9	19	45	77	115	148	54

*Zero values reflect times when no diversions were made.

Table 5.18: Chloride Mass Loading Percentiles (metric tons/day) for State Water Project

	5%	10%	25%	50%	75%	90%	95%	Avg
BASE	48	80	264	460	1086	1763	2068	711
GFDL A2	48	73	247	480	923	1387	1713	646
PCM A2	48	69	255	451	957	1560	1945	667
GFDL B1	47	71	230	477	951	1495	1883	670
PCM B1	47	75	265	459	1009	1660	1954	685

Table 5.19: Chloride Mass Loading Percentiles (metric tons/day) for Central Valley Project

	5%	10%	25%	50%	75%	90%	95%	Avg
BASE	59	146	317	575	1037	1325	1540	686
GFDL A2	56	145	271	534	1001	1260	1444	648
PCM A2	53	142	314	532	1074	1305	1413	663
GFDL B1	65	164	340	560	1050	1282	1475	686
PCM B1	51	118	337	582	1056	1267	1491	688

5.5 Sea Level Rise

Historical records show that in the 20th century sea levels rose globally with an average increase ranging from 3.9 in to 7.9 in (IPCC, 2001). Over the past 100 years, sea level at Golden Gate has risen more than 8 inches (Figure 5.11) (Roos, 2004). Sea levels are expected to continue to rise under global warming due to thermal expansion of the ocean and melting of glaciers and polar ice caps. Simulations of future climate change for all of the Intergovernmental Panel on Climate Change's (IPCC's) emissions scenarios show increases in global sea levels ranging from 0.3 feet to 2.9 feet (IPCC, 2001).

For California's water supply, the largest effect of sea level rise (SLR) would likely be in the Sacramento-San Joaquin Delta (DWR, 2005). Rising sea levels would increase pressure on the levees that protect the Delta islands, many of which are below sea level. A one-foot increase in sea level is projected to increase the frequency of a 100-year peak tide to a 10-year event (DWR, 2005). Increased intrusion of salt water from the ocean into the Delta could degrade the quality of the freshwater that is pumped out of the Delta for municipal, industrial and agricultural purposes. This could lead to increased releases of water from upstream reservoirs or reduced pumping from the Delta to maintain compliance with Delta water quality standards. Salt water intrusion could also degrade groundwater aquifers. Additional information on sea level rise can be found in Chapter 2 in section 2.6.

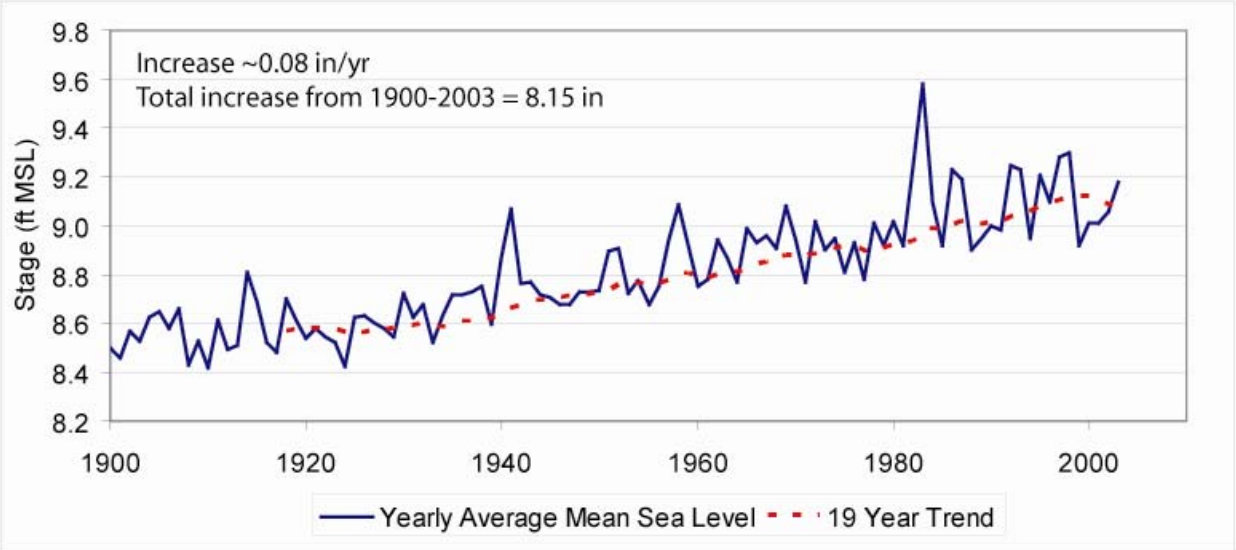


Figure 5.11 Historical Annual Mean Sea Level at Golden Gate, 1900-2003

5.5.1 Analysis Approach

In order to do a complete analysis of potential sea level rise impacts on the Delta, both increased salt intrusion and changes in system operations such as reservoir releases and Delta exports would need to be examined. Currently an analysis tool is not available to determine changes in system operations required to lessen the effects of increased salt intrusion due to sea level rise. However, existing tools can be used to quantify potential salt intrusion into the Delta for sea level rise with present system operations. The results of such studies improve understanding of the salinity transport in the Delta and provide an important starting point for the development of tools and analysis techniques for determining changes in system operations to maintain compliance with Delta water quality standards for sea level rise conditions. In this report water quality concentrations for a one-foot sea level rise without changes in system operations are compared to water quality standards. This information is presented as a surrogate for evaluating the effects of sea level rise on water project operations to meet existing standards.

This report provides preliminary assessments of potential impacts of sea level rise on Delta water quality and on levee overtopping potential assuming present system operations. Additional information on possible effects of sea level rise on the Delta, such as increasing the risk of levee failures, is presented in Chapter 2 in section 2.6. These studies are a first step in developing a more complete sea level rise analysis approach. All results are preliminary and are intended to illustrate the use of DSM2 for sea level rise analysis.

Preliminary modeling studies were conducted to assess potential effects of a one-foot rise in sea level on the Delta. DSM2 simulations were run for

- Present sea level with base case system operations (see section 5.4)
- Present sea level with system operations modified for climate change (see sections 5.4)
- One-foot sea level rise with base case system operations (see sections 5.5.2 and 5.5.4)
- One-foot sea level rise with system operations modified for climate change (see sections 5.5.3 and 5.5.4)

For all of the sea level rise scenarios, the tidal stage (water level) was increased uniformly by one-foot at the DSM2 downstream boundary at Martinez. This assumes that sea level rise does not change the tidal period or amplitude. Representation of Martinez EC for the sea level rise simulations is described in section 5.5.1.1. All other Delta inflows, exports and water quality boundary conditions were identical to the present sea level simulations (see sections 5.3 and 5.11). No operational changes were made to lessen potential effects of sea level rise.

Water quality analysis for the sea level rise scenarios focused on the comparisons of simulated constituent concentrations compared to standard thresholds for the municipal and industrial intakes (Table 5.9). These results are a demonstration of a preliminary application of DSM2 to access water quality changes for a one foot rise in sea level. The results do not reflect operations changes to try to reduce the effects of salt water intrusion from sea level rise, and therefore the results by themselves are not sufficient for making management decisions.

5.5.1.1 Martinez Salinity for Sea Level Rise Scenarios

One area of uncertainty in modeling sea level rise conditions with DSM2 is the representation of salt water intrusion at Martinez, the downstream boundary for DSM2. For this report, two assumptions were used for estimating salinity at Martinez for a one-foot sea level rise (Anderson and Miller, 2005):

- Assume Martinez EC is the same as in the present sea level scenarios
- Increase Martinez EC based on a regression relationship (equation 5.4)

Comparing results for DSM2 studies using each of these assumptions for Martinez EC provides a range of potential effects of a one-foot rise in sea level.

Assume Martinez EC Does Not Change

The first method used to estimate Martinez EC for a one-foot rise in sea level was to assume that the EC is the same as in the present sea level scenario. This provides a lower-bound estimate of salt water intrusion into the Delta for a one-foot increase in sea level.

Assume Martinez EC Increases

The second method used to estimate Martinez EC for a one-foot rise in sea level was to use a preliminary regression relationship based on the Martinez EC for present sea level conditions (Anderson and Miller, 2005):

$$MartinezEC_{1\,ft\,SLR} = 1.0022 * MartinezEC_{Present\,Sea\,Level} + 840.87 \qquad \text{Eqn. 5-4}$$

This regression relationship was based on results from a preliminary one year (calendar year 1992) multi-dimensional modeling study using models from Resource Management Associates (RMA). Since the effects of sea level rise on EC at the DSM2 downstream boundary at Martinez had not been quantified, a multi-dimensional modeling study was done to represent flows and salt water intrusion from Golden Gate into the Delta for a one-foot sea level rise (Figure 5.12). Results from the RMA modeling studies at Martinez for base and one-foot sea level rise conditions were used to develop the regression relationship shown in equation 5-4 (Figure 5.13). This regression relationship can be used to estimate Martinez EC for a one-foot sea level rise for DSM2 simulations.

Equation 5-4 is only applicable for a one-foot rise in sea level. Since this relationship is linear with a coefficient of nearly 1 (1.0022), equation 5-4 indicates that a one-foot rise in sea level at Golden Gate corresponds to an approximate increase in EC at Martinez of 840 uS/cm. Therefore use of this regression equation to estimate the Martinez EC for a one-foot rise in sea level will provide a higher estimate of salt water intrusion than using the assumption that the Martinez EC does not change. An increase in EC of 840 uS/cm is relatively small during time periods when Martinez EC is high (20,000-35,000 uS/cm) and freshwater inflows are low and salt water intrusion is of most concern, typically during the summer and early fall.

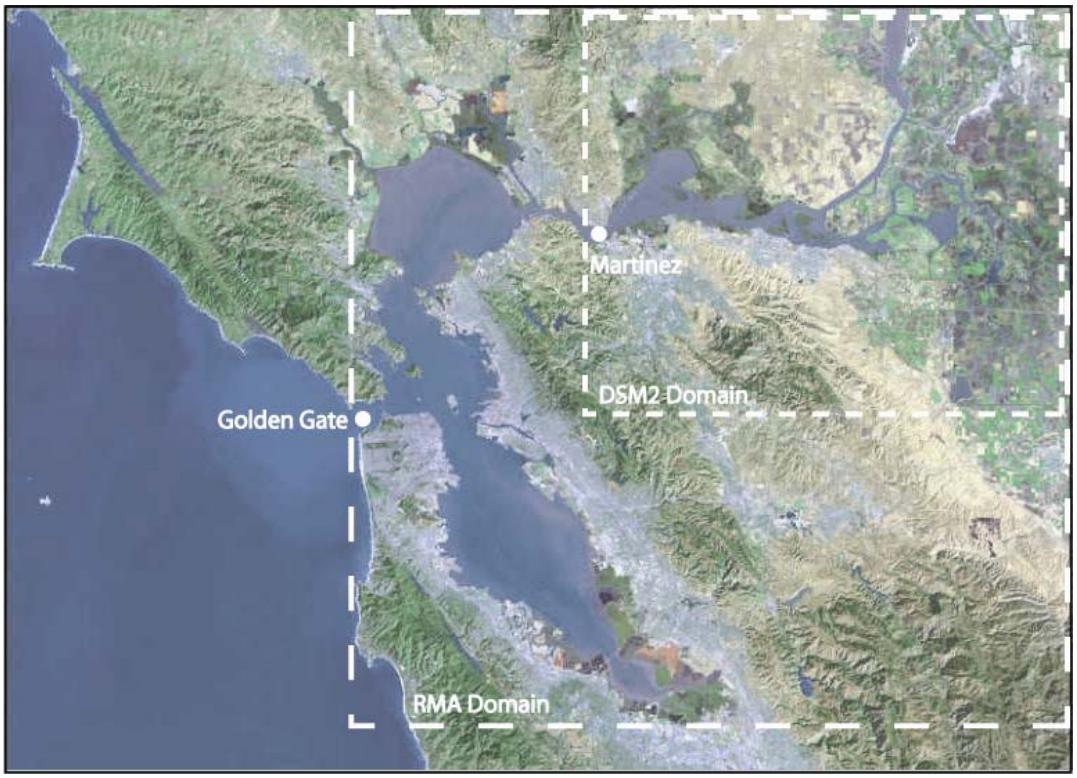


Figure 5.12 Modeling Domains for RMA and DSM2
Satellite image from USGS. (Anderson and Miller, 2005)

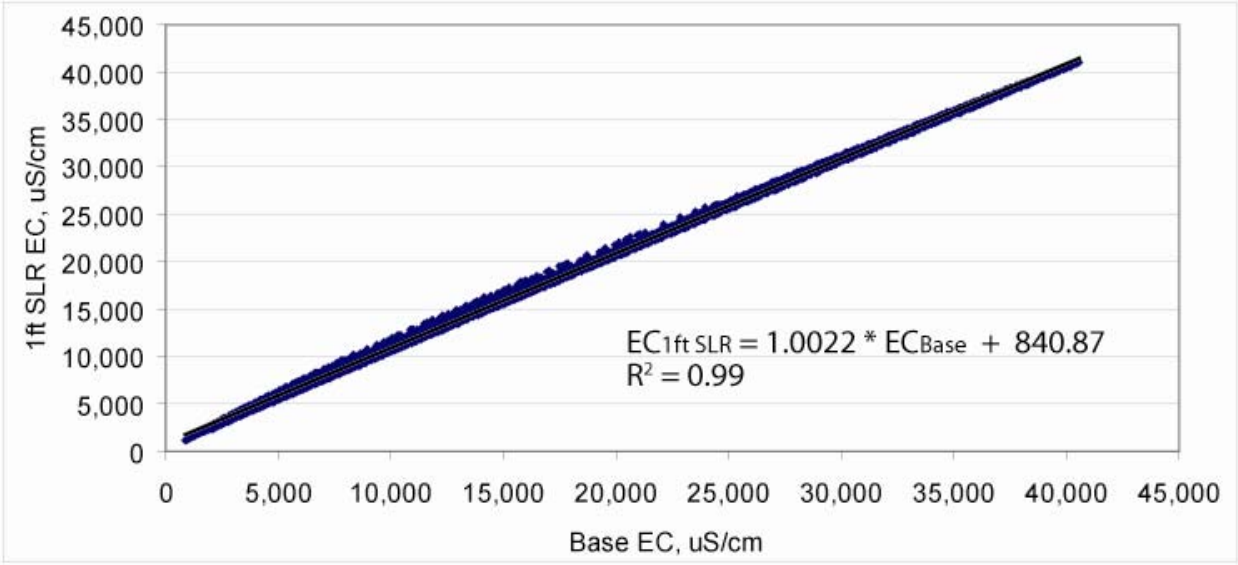


Figure 5.13: Regression Relationship for EC at Martinez for a One-Foot Sea Level Rise.
(Anderson and Miller, 2005)

The RMA modeling study from which the regression relationship in equation 5-4 was developed was a preliminary study that included the following assumptions:

- Historical tidal stage at Golden Gate was increased uniformly by one-foot,
- Ocean salinity is not affected by sea level rise [the same EC boundary condition of a constant ocean salinity was applied for both the base and 1ft SLR scenarios],
- Historical Delta inflows and exports were not modified to mitigate for salt water intrusion due to sea level rise [historical Delta inflows and exports were used for both the base and 1ft SLR scenarios],
- Agricultural return flows do not significantly affect EC at Martinez [Delta island diversions and return flows were not simulated],
- Temporary agricultural and fish barriers in the South Delta were not simulated, and
- Historical Delta inflows and exports for 1992 provide adequate ranges of flows and EC to develop an EC relationship at Martinez for one-foot sea level rise conditions that can be applied for any time period.

5.5.2 Sea Level Rise Effects on Delta Water Quality

Potential effects of a one-foot rise in sea level on Delta water quality were examined for DSM2 results using two different assumptions regarding Martinez EC (see section 5.5.1.1)

- Assume Martinez EC is the same as in the present sea level scenarios
- Assume that Martinez EC increases for a one-foot sea level rise

These results are a preliminary demonstration of the use of DSM2 to estimate a range of impacts given uncertainties in quantifying how much salt would be transported into the Delta under sea level rise with no modifications to system operations to try to reduce the salt water intrusion. Several assumptions that are involved in these studies are described in sections 5.2.3 and 5.5.1.1. Since available methodologies didn't allow consideration of changes to system operations for sea level rise scenarios, simulated constituent concentrations are compared with threshold values for selected water quality standards as a surrogate for evaluating the effects of sea level rise on water project operations to meet existing standards.

Daily average EC results from DSM2 for the 16-year simulation period were converted to daily average chloride concentrations using equations 5.1 and 5.2. Exceedance plots for daily average chloride concentrations at Rock Slough are shown in Figure 5.14. Percentiles and average chloride concentrations are shown in Table 5.20. Exceedance plots and percentile tables for other municipal and industrial intake locations are presented in the appendix in section 5.13. The sea level rise scenarios show an average increase in chloride concentrations of 15-20mg/l compared to the base case. Differences between the two sea level rise scenarios are typically 5-10mg/l. This indicates that raising the water levels at Martinez has more of an impact on chloride concentrations at Old River at Rock Slough than raising the Martinez salt concentrations. For

the SWP and CVP, the average increase in chloride concentrations was about 10 mg/l (see section 5.13). Differences between the two sea level rise scenarios were less than 2mg/l.

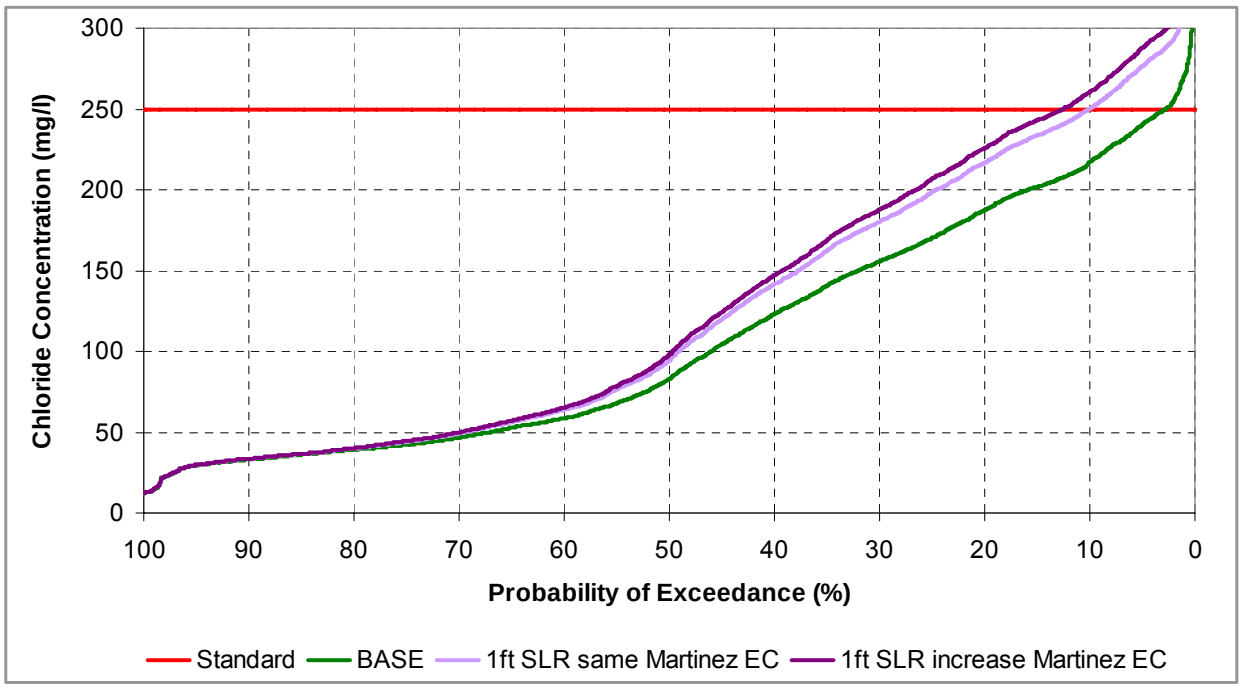


Figure 5.14: Probability of Exceedance for Chlorides at Old R. at Rock Sl. for a One-Foot Sea Level Rise and no Changes in System Operations

Table 5.20: Chloride Concentration Percentiles (mg/l) for Old R. at Rock Sl. for a One-Foot Sea Level Rise and no Changes in System Operations

	5%	10%	25%	50%	75%	90%	95%	Avg
BASE	30	33	42	83	170	217	240	109
1ft SLR same Martinez EC	30	33	44	94	199	250	276	123
1ft SLR increase Martinez EC	30	34	45	98	207	261	288	128

5.5.2.1 250 mg/l Chloride Threshold for Sea Level Rise Scenarios

Daily average chloride concentrations based on DSM2 simulation results for the two sea level rise scenarios without any changes in system operations were compared with the 250 mg/l maximum allowable daily average chloride concentration threshold (Table 5.9). The frequency that chloride concentrations were below the 250 mg/l threshold is presented in Table 5.21. Changes in the frequency that concentrations were below the threshold for sea level rise relative to the base case are shown in Table 5.22. For the base case, chloride concentrations are below the 250 mg/l chloride threshold at Old River at Rock Slough about 97 percent of the time. For the two sea level rise scenarios, chloride concentrations are below the threshold value at Old River at Rock Slough 88 percent to 90 percent of the time. For the scenario that assumes an

increase in EC at Martinez the threshold value is exceeded about 2.5 percent more often than for the scenario that assumes that the EC at Martinez does not change. Chloride concentrations rarely exceeded 250mg/l at Old River at Highway 4 for both the base and the sea level rise scenarios. The 250 mg/l threshold was never exceeded at both the SWP and CVP for the base case and sea level rise scenarios.

Table 5.21: Frequency that Chloride Concentrations were below the 250 mg/l Threshold for a One-Foot Sea Level Rise and no Changes in System Operations

Scenario/ Location	BASE	1ft Sea Level Rise same Martinez EC	1ft Sea Level Rise increase Martinez EC
CCWD-Old River at Rock Sl.	97.2%	89.9%	87.5%
CCWD-Old River at Hwy 4	99.9%	99.7%	99.4%
SWP-Clifton Court	100%	100%	100%
CVP-Tracy	100%	100%	100%

Table 5.22: Change in Frequency that Chloride Concentrations were below the 250mg/l Threshold for a One-Foot Sea Level Rise and no Changes in System Operations Compared to the Base Case

Scenario/ Location	1ft Sea Level Rise same Martinez EC	1ft Sea Level Rise increase Martinez EC
CCWD-Old River at Rock Sl.	-7.3%	-9.8%
CCWD-Old River at Hwy 4	-0.2%	-0.5%
SWP-Clifton Court	0%	0%
CVP-Tracy	0%	0%

5.5.2.2 150 mg/l Chloride Threshold for Sea Level Rise Scenarios

For the two sea level rise scenarios with no changes in system operations, daily average chloride concentrations were computed from DSM2 EC results using equation 5.1, and the results were compared to the 150 mg/l threshold (Table 5.9 and Table 5.10). There was complete compliance with the 150 mg/l standard in the base case (Table 5.23). For the sea level rise scenario that assumed no change in Martinez EC, the 150 mg/l threshold was exceeded in the critically dry years of 1976 and 1977. For the sea level rise scenario that assumed an increase in Martinez EC, the 150 mg/l threshold was exceeded in 1976, 1977, and 1989, a dry year. In most cases, existing operations lead to chloride concentrations below the 150 mg/l threshold, even under sea level rise conditions.

Table 5.23: Comparison of Chloride Concentrations to the 150 mg/l Threshold at Old River at Rock Sl. for a One-Foot Sea Level Rise and no Changes in System Operations Number of days with chloride concentrations below 150 mg/l

Year	Yr. Type*	Min Days Cl≤150 mg/l	Base	1ft SLR same Martinez EC	1ft SLR increase Martinez EC
1976	C	155	177	**126**	**118**
1977	C	155	161	**102**	**94**
1978	AN	190	247	240	237
1979	BN	175	259	226	223
1980	AN	190	269	263	261
1981	D	165	260	232	217
1982	W	240	365	365	365
1983	W	240	365	365	365
1984	W	240	295	289	288
1985	D	165	216	198	197
1986	W	240	287	265	257
1987	D	165	176	168	165
1988	C	155	230	209	206
1989	D	165	184	166	**162**
1990	C	155	222	181	176

*Sac 40-30-30 water year types: W=Wet, AN=Above Normal, BN=Below Normal, D=Dry, C=Critical
Gray shading and bold text indicate values that exceeded the threshold.

5.5.2.3 Chloride Mass Loading for Sea Level Rise Scenarios

Chloride mass loadings at municipal and industrial intakes were estimated based on chloride concentrations and export rates (equation 5.3). The mass loading estimates for CCWD are based on the combined diversion rate for CCWD's Old River diversions at Rock Slough and Highway 4 and the chloride concentrations at Rock Slough (see footnote 2 on page 5-1 for explanation of combined diversions). Since operations were not changed to try to lessen the effects of sea level rise, the export rates for each intake were the same for the base and sea level rise scenarios. Thus differences in mass loading rates are due only to differences in chloride concentrations.

For all intake locations, sea level rise increased the average chloride mass loadings by 13 percent-17 percent for Old River at Rock Slough, by 11 percent-14 percent for the SWP and by 7 percent-9 percent for the CVP. These ranges reflect the two sea level rise assumptions of no change in Martinez EC and increasing Martinez EC. The sea level rise scenarios increased the chloride mass loadings, and the climate change scenarios decreased them (see section 5.4.1.3). The combined affects of sea level rise and climate change are presented in section (5.5.3.3).

Table 5.24: Chloride Mass Loading Percentiles (metric tons/day) for Old River at Rock Slough for a One-Foot Sea Level Rise with no Changes in System Operations

	5%	10%	25%	50%	75%	90%	95%	Avg
Base	0	9	19	45	80	115	146	54
1ft SLR same Martinez EC	0	9	20	50	92	132	165	61
1 ft SLR increase Martinez EC	0	9	20	51	96	138	172	63

Table 5.25: Chloride Mass Loading Percentiles (metric tons/day) for State Water Project for a One-Foot Sea Level Rise and no Changes in System Operations

	5%	10%	25%	50%	75%	90%	95%	Avg
Base	48	80	264	460	1086	1763	2068	711
1ft SLR same Martinez EC	49	84	267	514	1202	1925	2299	786
1 ft SLR increase Martinez EC	50	86	270	527	1238	2014	2394	812

Table 5.26: Chloride Mass Loading Percentiles (metric tons/day) for Central Valley Project for a One-Foot Sea Level Rise and no Changes in System Operations

	5%	10%	25%	50%	75%	90%	95%	Avg
Base	59	146	317	575	1037	1325	1540	686
1ft SLR same Martinez EC	58	147	328	611	1140	1433	1648	734
1 ft SLR increase Martinez EC	58	147	331	618	1163	1461	1696	749

5.5.3 Combined Climate Change and Sea Level Rise Effects on Delta Water Quality

Potential effects of a one-foot rise in sea level coupled with shifting precipitation and runoff patterns from climate change were examined. The results are preliminary and reflect several assumptions (see section 5.2.3) including:

- Martinez EC is the same as in the present sea level scenarios. Due to time constraints for this report, combined sea level rise and climate change scenarios were not run for the increased Martinez EC sea level rise scenario.
- System operations were only modified to reflect the changing precipitation and runoff patterns due to climate change. System operations were not modified to account for sea level rise.

For the combined sea level rise and climate change scenarios, daily average EC results from DSM2 for the 16-year simulation period were converted to daily average chloride concentrations using equations 5.1 and 5.2. Exceedance plots for daily average chloride concentrations at Rock Slough for the combined climate change and one-foot sea level rise scenarios with no changes to system operations for sea level rise are shown in Figure 5.15. Percentiles and average chloride concentrations are shown in Table 5.27. Exceedance plots and percentile tables for other municipal and industrial intake locations are presented in the appendix in section 5.14. For the combined climate change and sea level rise scenarios, average increases in chloride concentrations range from13-17mg/l compared to the base case. For the SWP and CVP, the average increase in chloride concentrations for the combined climate change and sea level rise scenarios was about 10 mg/l (see section 5.14).For all of these intakes, the increases in chloride concentrations are similar to increases due to sea level rise alone.

This space intentionally left blank.

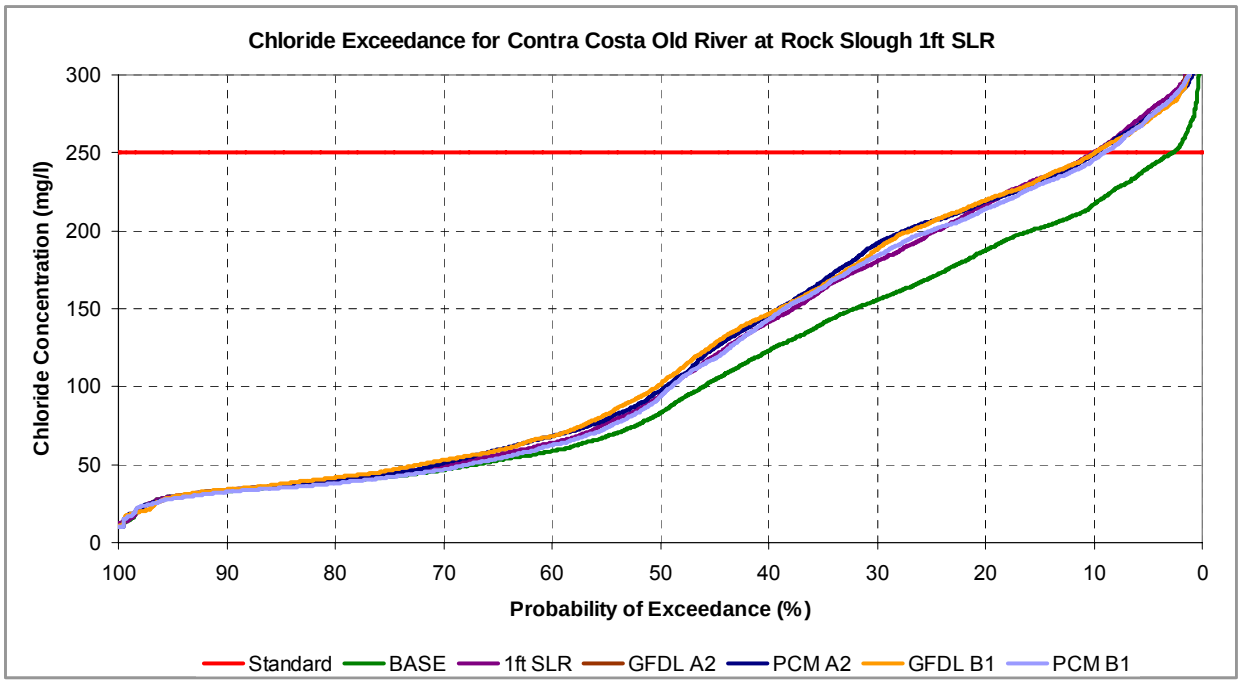


Figure 5.15: Probability of Exceedance for Chlorides at Old River at Rock Slough for Climate Change and a One-Foot Sea Level Rise with no Changes in Operations for SLR

Table 5.27: Chloride Concentration Percentiles (mg/l) for Old R. at Rock Sl. for Climate Change and a One-Foot Sea Level Rise with no Changes in Operations for SLR

	5%	10%	25%	50%	75%	90%	95%	Avg
BASE	30	33	42	83	170	217	240	109
1ft SLR same Mtz EC	30	33	44	94	199	250	276	123
GFDL A2 1ft SLR	27	33	45	102	205	251	272	125
PCM A2 1ft SLR	29	34	44	97	206	249	273	125
GFDL B1 1ft SLR	29	34	46	102	205	250	271	126
PCM B1 1ft SLR	28	33	42	94	200	245	272	122

*All sea level rise scenarios in this table assume that Martinez EC is the same as in the present sea level scenarios.

5.5.3.1 250 mg/l Chloride Threshold for Combined Sea Level Rise and Climate Change Scenarios

For the combined climate change and sea level rise scenarios with no additional changes to system operations for sea level rise, daily average chloride concentrations based on DSM2 simulation results were compared to the 250 mg/l daily average chloride concentration threshold

(Table 5.9). The frequency that chloride concentrations were below the 250 mg/l threshold is given in Table 5.28. Changes in the frequency that chloride concentrations were below the threshold relative to the base case are shown in Table 5.29. For the base case, the 250 mg/l chloride standard is met at Old River at Rock Slough about 97 percent of the time. For the combined climate change and one-foot sea level rise scenarios with no changes in system operations for sea level rise, chloride concentrations at Old River at Rock Slough were less than the threshold value about 90 percent of the time. This result is similar to the sea level rise only scenario (Table 5.21). Chloride concentrations rarely exceeded 250mg/l threshold at Old River at Highway 4 for all scenarios. Chloride concentrations never exceeded the 250 mg/l threshold at both the SWP and CVP for the base and combined climate change and sea level rise scenarios.

Table 5.28: Frequency that Chloride Concentrations were below the 250 mg/l Threshold for Climate Change and a 1-ft Sea Level Rise with no Changes to Operations for SLR

Scenario/ Location	BASE	1ft SLR	GFDL A2 1ft SLR	PCM A2 1ft SLR	GFDL B1 1ft SLR	PCM B1 1ft SLR
Contra Costa-Old R. at Rock Sl.	97.2%	89.9%	89.6%	90.3%	90.1%	90.9%
Contra Costa-Old R at Hwy 4	99.9%	99.7%	100.0%	100.0%	99.8%	99.8%
SWP-Clifton Court	100%	100%	100%	100%	100%	100%
CVP-Tracy	100%	100%	100%	100%	100%	100%

*Note that all sea level rise scenarios shown in this table assume that Martinez EC is the same as in the present sea level scenarios.

Table 5.29: Change in Frequency that Chloride Concentrations were below the 250mg/l Threshold for Climate Change and a 1ft Sea Level Rise with no Changes to Operations for Sea Level Rise Compared to the Base Case

Scenario/ Location	1ft SLR	GFDL A2	PCM A2	GFDL B1	PCM B1
Contra Costa-Old River at Rock Sl.	-7.3%	-7.7%	-6.9%	-7.2%	-6.3%
Contra Costa-Old River at Hwy 4	-0.2%	0.1%	0.1%	-0.1%	-0.1%
SWP-Clifton Court	0%	0%	0%	0%	0%
CVP-Tracy	0%	0%	0%	0%	0%

*Note that all sea level rise scenarios shown in this table assume that Martinez EC is the same as in the present sea level scenarios.

5.5.3.2 150 mg/l Chloride Threshold for Combined Sea Level Rise and Climate Change Scenarios

For the combined climate change and sea level rise scenarios with no additional changes in system operations for sea level rise, daily average chloride concentrations were computed from DSM2 EC results using equation 5.1, and the results were compared to the 150 mg/l chloride threshold (Table 5.9 and Table 5.10). The 150 mg/l threshold was never exceeded in the base case (Table 5.30). For the combined climate change and one-foot sea level rise scenarios with no changes in system operations for sea level rise, the threshold value was exceeded in the critically dry years of 1976 and 1977, and for some of the scenarios in 1989. In most cases, existing operations maintained compliance with the 150 mg/l chloride standard, even under combined climate change and sea level rise conditions.

Table 5.30: Comparison of Chloride Concentrations to the 150 mg/l Threshold at Old R. at Rock Sl. for Climate Change and a One-Foot Sea Level Rise with no Changes in Operations for SLR
Number of Days that Chloride Concentrations were Below 150 mg/l

Year	Yr. Type*	Min Days Cl≤150 mg/l	Base	1ft SLR	GFDL A2 1ft SLR	PCM A2 1ft SLR	GFDL B1 1ft SLR	PCM B1 1ft SLR
1976	C	155	177	**126**	**112**	**113**	**112**	**129**
1977	C	155	161	**102**	**107**	**105**	**113**	**107**
1978	AN	190	247	240	248	245	238	245
1979	BN	175	259	226	231	233	230	240
1980	AN	190	269	263	258	256	255	255
1981	D	165	260	232	240	229	239	241
1982	W	240	365	365	343	365	341	365
1983	W	240	365	365	365	365	365	365
1984	W	240	295	289	299	301	301	291
1985	D	165	216	198	201	198	198	195
1986	W	240	287	265	242	250	242	246
1987	D	165	176	168	180	172	178	181
1988	C	155	230	209	211	207	209	224
1989	D	165	184	166	**152**	165	**142**	**137**
1990	C	155	222	181	182	162	183	162

*Sac 40-30-30 water year types: W=Wet, AN=Above Normal, BN=Below Normal, D=Dry, C=Critical
Gray shading and bold text indicate values that exceed the threshold.
All sea level rise scenarios assume that Martinez EC is the same as in the present sea level scenarios.

5.5.3.3 Chloride Mass Loading for Combined Sea Level Rise and Climate Change Scenarios

Chloride mass loadings at municipal and industrial intakes were estimated based on chloride concentrations and export rates (equation 5.3). The mass loading estimates for CCWD are based on the combined diversion rate for CCWD's Old River diversions at Rock Slough and Highway 4 and the chloride concentrations at Rock Slough (see footnote 2 on page 5-1 for explanation of combined diversions). Diversion rates for CCWD were identical for all scenarios. SWP and CVP operations were changed to reflect shifts in precipitation and runoff due to climate change, but they were not changed to try to lessen the effects of sea level rise.

For all intake locations, sea level rise increased the average chloride mass loadings by about 15 percent for Old River at Rock Slough, by 5 percent for the SWP and by 3 percent-7 percent for the CVP. For Old River at Rock Slough and for the Central Valley Project B1 scenarios, the mass loadings are similar to the sea level rise only scenario. For the SWP and for the CVP A2 scenarios, reduced exports for the climate change scenarios lead to lower mass loadings than in the sea level rise only scenario. This demonstrates that shifts in system operations due to changes in runoff patterns can lessen the effects of sea level rise at the intakes that are further away from the ocean.

Table 5.31: Chloride Mass Loading Percentiles (metric tons/day) for Old River at Rock Sl. for Climate Change and a One-Foot Sea Level Rise with no Changes in Operations for SLR

	5%	10%	25%	50%	75%	90%	95%	Avg
Base	0	9	19	45	80	115	146	54
1ft SLR same Martinez EC	0	9	20	50	92	132	165	61
GFDL A2 1ft SLR same Mtz EC	0	7	21	53	92	137	163	62
PCM A2 1ft SLR same Mtz EC	0	9	22	53	90	129	163	62
GFDL B1 1ft SLR same Mtz EC	0	8	22	54	90	136	157	63
PCM B1 1ft SLR same Mtz EC	0	9	20	48	91	131	167	61

Note: Export rates were identical for all scenarios.

Table 5.32: Chloride Mass Loading Percentiles (metric tons/day) for the State Water Project for Climate Change and a One-Foot Sea Level Rise with no Changes in Operations for SLR

	5%	10%	25%	50%	75%	90%	95%	Avg
Base	48	80	264	460	1086	1763	2068	711
1ft SLR same Martinez EC	49	84	267	514	1202	1925	2299	786
GFDL A2 same Mtz EC	51	74	245	530	1026	1536	1959	718
PCM A2 same Mtz EC	51	70	251	498	1075	1802	2188	740
GFDL B1 same Mtz EC	49	73	254	516	1091	1749	2118	744
PCM B1 same Mtz EC	48	76	262	521	1152	1922	2226	758

Note: Export rates were modified for climate change, but not for sea level rise.

Table 5.33: Chloride Mass Loading Percentiles (metric tons/day) for the Central Valley Project for Climate Change and a One-Foot Sea Level Rise with no Changes in Operations for SLR

	5%	10%	25%	50%	75%	90%	95%	Avg
Base	59	146	317	575	1037	1325	1540	686
1ft SLR same Martinez EC	58	147	328	611	1140	1433	1648	734
GFDL A2 same Mtz EC	55	143	275	563	1099	1360	1576	695
PCM A2 same Mtz EC	53	141	320	569	1168	1408	1549	710
GFDL B1 same Mtz EC	65	175	346	586	1141	1394	1625	735
PCM B1 same Mtz EC	51	121	350	613	1160	1401	1635	736

Note: Export rates were modified for climate change, but not for sea level rise.

5.5.4 Sea Level Rise Effects on Potential to Overtop Delta Levees

This study examined potential effects of a one-foot increase in sea level on the potential to overtop levees on three islands in the western Delta, Sherman Island, Twitchell Island, and Jersey Island. These are the Delta islands closest to the ocean, and so they are most vulnerable to potential overtopping due to sea level rise. The lowest crest elevations on levees on those islands are shown in Figure 5.16. Simulated water levels for present sea level and one-foot sea level rise scenarios were compared to these low-crest elevations to determine potential overtopping (Table 5.34). For the purpose of this analysis, potential overtopping was defined as any time the daily maximum water level in the channel exceeded the minimum crest elevation on the levee. Actual levee overtopping and effects of wind-induced waves were not simulated. Results are preliminary and are presented for illustrative purposes only.

Results for the present sea level scenarios indicated that water levels were never high enough to potentially overtop the study levees, even when Delta inflows were modified by climate change. For all of the one-foot sea level rise scenarios, there were two potential levee overtoppings during the 16-year simulation when simulated water levels exceeded the minimum levee crest elevations. For both the base and climate change sea level rise scenarios, the potential overtoppings occurred at the same time and affected all five study locations. Actual overtopping events and their effects on water levels and water quality were not simulated.

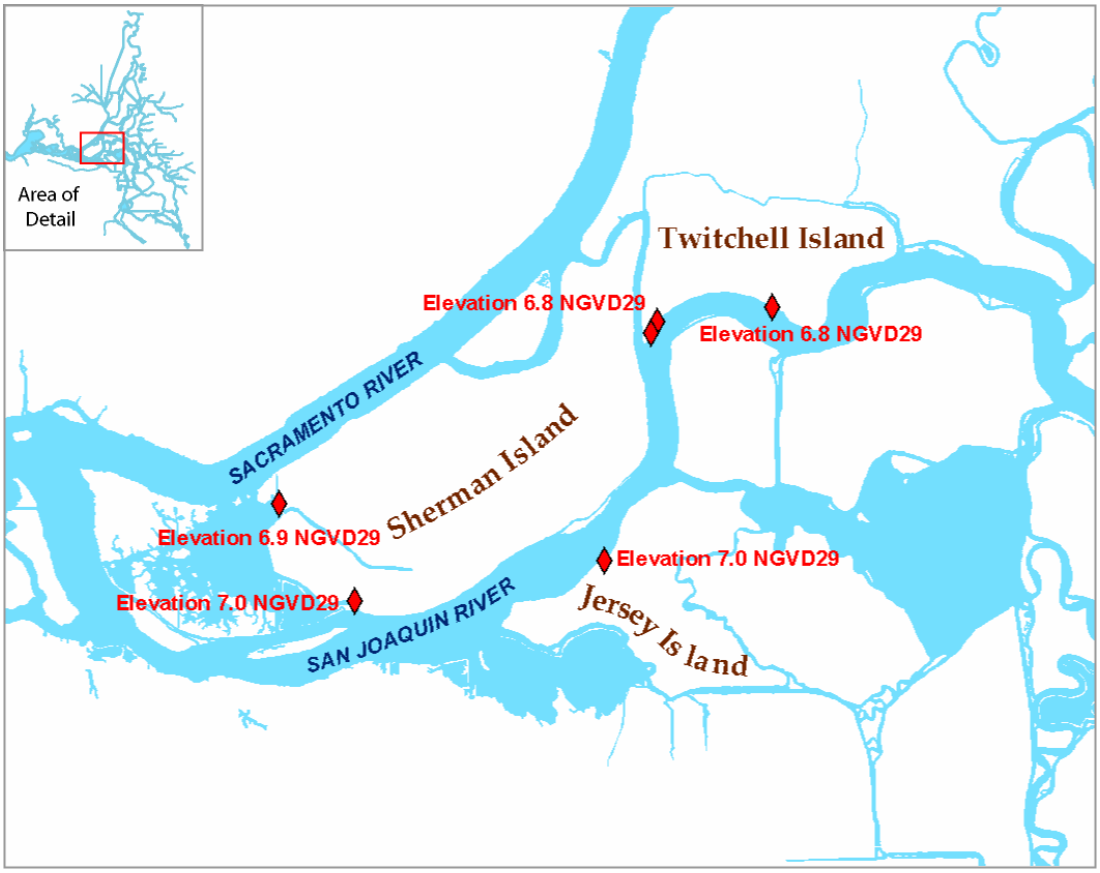


Figure 5.16: Locations of Lowest Levee Elevation on Three Delta Islands

Table 5.34: Summary of Levee Overtopping Events for Sea Level Rise Scenarios

Location	Min Crest Elevation, ft	Number of Potential Overtopping Events in 16 yrs			
		Base	4 Climate Change Scenarios	1 ft SLR	4 Climate Change Scenarios 1ft SLR
NW Sherman Island	6.9	0	0	2	2
SW Sherman Island	7.0	0	0	2	2
SW Twitchell Island	6.8	0	0	2	2
SE Twitchell Island	6.8	0	0	2	2
W Jersey Island	7.0	0	0	2	2

These results indicate that for the scenarios examined, sea level rise is more likely to increase the potential to overtop the study levees than changes in Delta inflows due to climate change. However, this analysis does not provide insight into potential changes in frequency of extreme events due to climate change. Since these climate change studies use perturbation ratios to modify historically-based reservoir inflows (see Chapter 4), the climate change scenarios preserve the historical hydrologic variability and do not reflect any potential changes in the

frequency of extreme events. Thus for the combined sea level rise and climate change scenarios, the potential levee overtoppings occurred at the same time during periods as the sea level rise only scenario. All of the potential overtoppings corresponded to periods with historically high water levels. Levees in other parts of the Delta may be more vulnerable to overtopping due to shifts in reservoir release patterns. Future studies could examine potential effects of sea level rise on levees throughout the Delta.

5.6 Summary

5.6.1 Climate Change for Present Sea Level

The DSM2 model was used for preliminary assessment of potential climate change effects on the Delta for four scenarios. The four scenarios correspond to two greenhouse gas emissions scenarios represented by two global climate models. All four climate change scenarios represent warmer future conditions, and three scenarios reflect drier conditions. The fourth climate change scenario projects slightly wetter conditions.

Projected runoff for the climate change scenarios was used to drive an SWP and CVP operations model that provided Delta inflows and exports (see Chapter 4). These studies include the assumption that meeting Delta water quality standards is a top priority for the SWP and CVP operations. Thus the impacts assessment for the Delta already included some mitigation for climate change through modified system operations for maintaining Delta water quality standards. So Delta water quality effects for the four climate change scenarios were relatively minor. There were no significant changes in compliance with 250 mg/l chloride standard at the municipal and industrial intakes, and there was complete compliance with that standard at the SWP and CVP intakes for all of the scenarios. The only reduction in compliance with the 150mg/l chloride standard occurred for the two B1 climate change scenarios. Chloride mass loadings at the SWP for all climate change scenarios and CVP for the A2 scenarios were reduced for the climate change scenarios due to lower export rates. Overall, existing system flexibility was able to provide Delta water quality compliance for most of the climate change conditions examined.

For the water quality analysis, the choice of global climate model had more influence on the results than the choice of greenhouse gas emissions scenario. One way to address the uncertainties associated with climate models and emissions scenarios is to conduct analysis using multiple climate models representing multiple emissions scenarios.

5.6.2 Sea Level Rise

An analysis tool is not currently available to determine changes in system operations to maintain Delta water quality under sea level rise conditions. As a first step towards developing such a tool, preliminary studies were conducted for a one-foot sea level rise with present system operations. Simulated water quality constituent concentrations for sea level rise conditions with no changes in system operations were compared to threshold values as a surrogate for evaluating the effects of sea level rise on water project operations to meet existing standards.

Preliminary sea level rise studies examined changes in chloride concentrations at municipal and industrial intakes for a one-foot increase in sea level. Due to the uncertainties in how much salt would be transported into the Delta for sea level rise conditions, two scenarios were examined to provide a range of potential impacts. One scenario assumed that the EC at the DSM2 downstream boundary at Martinez did not change relative to present sea level conditions, and the second scenario assumed that Martinez EC increased based on results of a multi-dimensional modeling study.

Without adjusting system operations to try to lessen the effects of sea level rise, chloride concentrations at Old River at Rock Slough were below the 250 mg/l threshold about 90 percent of the time. In real time, operational adjustments will take place so these effects will translate into water supply impacts to the SWP and CVP. As stated above these impacts to water supply cannot be quantified at this time. Increased salt intrusion for the sea level rise scenarios lead to chloride concentrations that exceeded the 150 mg/l standard during some critical and dry years. Chloride mass loadings at all of the urban intakes increased due to higher chloride concentrations. Impacts were similar for the two salt intrusion assumptions.

5.6.3 Combined Climate Change and Sea Level Rise

Preliminary impacts assessments were also conducted for combined climate change and one-foot sea level rise scenarios. System operations were changed to reflect shifts in runoff patterns for climate change, but they were not changed to try to lessen the impacts of sea level rise. Comparisons of chloride concentrations with threshold values at municipal and industrial intakes and potential for overtopping Delta levees were examined. Comparisons of chloride concentrations with threshold values were similar to those for the sea level rise only scenarios. Chloride mass loadings for Old River at Rock Slough were similar for all of the combined climate change and sea level rise scenarios since the export rates were the same. For the SWP and CVP, chloride mass loadings for the combined climate change and sea level rise scenarios were lower than for the sea level rise only scenarios due to reduced export rates.

For the potential levee overtopping analysis, no potential overtoppings occurred for the present sea level conditions. A one-foot rise in sea level resulted in two potential overtoppings during the 16-year analysis. The overtopping potential was not changed when combined sea level rise and climate change conditions were examined. Effects of wind were not considered.

5.7 Future Directions

Future directions for Delta climate change studies may include extending existing analyses, improving analysis tools, investigating mitigation measures, and characterizing uncertainty.

A key area of interest is examining effects of sea level rise alone or combined with climate change on system operations. For the analysis approach presented in this report, an Artificial Neural Network (ANN) could be developed to represent sea level rise effects on Delta water quality. By incorporating a sea level rise ANN into the operations model CalSim-II, changes in system operations to reduce salt water intrusion into the Delta could be determined for sea level rise alone or combined with other climate change factors such as shifting runoff patterns. For

more detailed studies of sea level rise effects on the Delta using DSM2, an improved characterization of potential salt intrusion into the Delta could be developed.

Additional topics related to sea level rise that could be examined included extending the potential levee overtopping analysis to other areas of the Delta. Existing simulation results could be used to estimate sea level rise effects on the stability of Delta levees. Potential effects for a range of increases in sea level could be examined.

Flexibility of the existing system to mitigate for climate change could be explored. Possible mitigation measures could include modifying reservoir releases, Delta exports, Delta Cross Channel operations, and temporary barrier operations. If present system flexibility isn't sufficient for mitigation, additional measures could be investigated such as modifying operating rules or considering new system components such as the proposed South Delta operable gates.

The main focus of future efforts will be to characterize uncertainty related to the climate change projections. For managers to make decisions, information is needed on both the magnitude of potential effects and the likelihood of those effects.

5.8 Acknowledgements

The author would sincerely like to thank the many people who provided data, ideas, technical assistance, and editorial comments for this chapter:

Internal review of this chapter was provided by Parviz Nader-Tehrani, Michael Mierzwa, Tara Smith, Kathy Kelly and Jane Schaefer-Kramer.

Peer review of this chapter was provided by Paul Hutton, Leah Orloff and K.T. Shum.

Assistance with data analysis was provided by Michael Mierzwa, Levi Brekke, Dan Easton and Michael Anderson.

Levee crest elevation data and map were provided by Joel Dudas.

VIC data were processed and provided for download by Mary Tyree and Erik Peterson of Scripps Institution of Oceanography.

VIC data were produced by Ed Maurer at the University of Santa Clara.

Information on the Global Climate Model (GCM) models and emissions scenarios were provided by Dan Cayan from Scripps Institution of Oceanography and Mike Dettinger from the U.S. Geological Survey and Scripps Institution of Oceanography.

5.9 References

Anderson and Miller. (2005). Chapter 5: Estimation of Electrical Conductivity at Martinez for Sea Level Rise Conditions. In: *Methodology for Flow and Salinity Estimates in the Sacramento-San Joaquin Delta and Suisun Marsh. 26th Annual Progress Report to the State Water Resources Control Board*. California Department of Water Resources. Sacramento, CA. October, 2005. http://modeling.water.ca.gov/delta/reports/annrpt/2005/2005Ch5.pdf

Ateljevich E. (2001a). Chapter 10: Planning Tide at the Martinez Boundary. In: *Methodology for Flow and Salinity Estimates in the Sacramento-San Joaquin Delta and Suisun Marsh. 22nd Annual Progress Report to the State Water Resources Control Board*. California Department of Water Resources. Sacramento, CA. http://modeling.water.ca.gov/delta/reports/annrpt/2001/2001Ch10.pdf

Ateljevich E. (2001b). Chapter 11: Improving Estimates of Salinity at the Martinez Boundary. In: *Methodology for Flow and Salinity Estimates in the Sacramento-San Joaquin Delta and Suisun Marsh. 22nd Annual Progress Report to the State Water Resources Control Board*. California Department of Water Resources. Sacramento, CA. http://modeling.water.ca.gov/delta/reports/annrpt/2001/2001Ch11.pdf

DWR (1995a). Sacramento San Joaquin Delta Atlas, California Department of Water Resources, Sacramento, CA, July 1995.

DWR (1995b). Estimation of Delta Island Diversions and Return Flows, California Department of Water Resources, Sacramento, CA, February 1995.

DWR (1995c). Representative Delta Island Return Flow Quality for DSM2, California Department of Water Resources, Sacramento, CA, May 1995.

DWR (2005). California Water Plan Update 2005, Volume 1-Stategic Plan, Chapter 4: Preparing for an Uncertain Future, California Department of Water Resources, Sacramento, CA, Public Review Draft. http://www.waterplan.water.ca.gov/cwpu2005/index.cfm

DWR (2006). http://www.publicaffairs.water.ca.gov/swp/delta.cfm accessed 1-19-06

Freeport (2003). Freeport Regional Water Project Draft EIR-EIS, Volume 3: Modeling Technical Appendix to the Draft Environmental Impact Report/Environmental Impact Statement, U.S. Department of the Interior, U.S. Bureau of Reclamation, the Freeport Regional Water Agency, Sacramento County Water Agency, and East Bay Municipal Water District, July 2003, http://www.freeportproject.org/deir/deir.html. Regression equations are on pg 4-34 of the following document http://www.freeportproject.org/deir/vol3/section04-3.pdf.

IPCC (2001). Intergovernmental Panel on Climate Change, Climate Change 2001: The Scientific Basis, Contribution of Working Group I to the Third Assessment Report of the IPCC, J. T. Houghton, Y. Ding, D.J. Griggs, M. Noguer, P. J. van der Linden and D. Xiaosu (Eds.), Cambridge University Press, UK. pp 944. http://www.grida.no/climate/ipcc_tar/wg1/index.htm

Roos (2004). Maury Roos, California State Hydrologist, California Department of Water Resources, personal communication.

Suits, B. (2001). Relationships between EC, chloride and bromide at Delta export locations. Technical Memo, California Department of Water Resources, Sacramento, CA, May 29, 2001

SWRCB (1995). Water Quality Control Plan for the San Francisco Bay/Sacramento San Joaquin Delta Estuary, 95-1WR, State Water Resources Control Board, California Environmental Protection Agency, Sacramento, CA, May 1995.

USBR (2004). Chapter 6: Analytical Approach and Methods. In: *Long-Term Central Valley Project Operations Criteria and Plan.* United States Bureau of Reclamation. Sacramento, CA. June 2004.

USBR (2005). CALSIM II San Joaquin River Model (Draft), United States Bureau of Reclamation. Sacramento, CA. April, 2005. http://science.calwater.ca.gov/pdf/calsim/CALSIMSJR_DRAFT_072205.pdf

5.10 Abbreviations

ANN-Artificial Neural Network

CalSim-II -SWP and CVP operations model

CCWD-Contra Costa Water District

CVP- Central Valley Project

CVPIA-Central Valley Project Improvement Act

CWEMF-California Water and Environmental Modeling Forum

D1641-State Water Resources Control Board Decision 1641 on Delta water quality standards

DICU-Delta Island Consumptive Use

DSM2-Delta Simulation Model 2

DWR-California Department of Water Resources

EC-Electrical conductivity, a measure of salinity

EWA-Environmental Water Account

GCM-Global Climate Model

GFDL-Geophysical Fluid Dynamic Lab model

GHG-Greenhouse Gas

HWY-Highway

IPCC-Intergovernmental Panel on Climate Change

PCM-Parallel Climate Model

SAC-Sacramento River

SJR-San Joaquin River

SLR-Sea Level Rise

SWP-State Water Project

VIC-Variable Infiltration Capacity Model

WY-Water Year (October 1 to September 30)

5.11 Appendix A: DSM2 Inputs

This appendix provides tables of selected DSM2 input values.

Delta Inflows

- Sacramento River at I Street Bridge in Sacramento (Table 5.35)
- San Joaquin River at Vernalis (Table 5.36)

Delta Exports and Diversions

- State Water Project at Banks Pumping Plant (Table 5.37)
- Central Valley Project at Tracy Pumping Plant (Table 5.38)
- Contra Costa Water District (combined Old River diversions from Rock Slough and Highway 4) (Table 5.39)

Table 5.35: DSM2 Input from CalSim-II: Sacramento River Flows (cfs) at Sacramento

Date	BASE	GFDL A2	PCM A2	GFDL B1	PCM B1
Oct-75	17,863	12,673	15,573	12,573	18,478
Nov-75	15,078	10,890	15,630	12,904	15,027
Dec-75	15,560	12,797	10,636	12,305	12,111
Jan-76	12,235	11,534	10,353	11,179	10,769
Feb-76	13,354	11,566	11,863	11,525	12,199
Mar-76	15,068	13,413	14,648	13,372	16,710
Apr-76	9,702	9,426	9,545	9,416	9,575
May-76	8,046	7,712	7,866	7,698	7,962
Jun-76	12,821	12,959	13,584	13,365	12,460
Jul-76	13,228	12,146	12,819	12,773	14,190
Aug-76	10,993	9,908	10,486	10,253	9,844
Sep-76	10,147	8,321	8,635	8,385	9,643
Oct-76	7,811	7,763	7,771	7,765	7,796
Nov-76	7,248	7,212	7,217	7,214	7,237
Dec-76	9,348	6,752	6,757	6,753	6,959
Jan-77	8,192	8,340	8,205	8,391	8,523
Feb-77	9,469	7,897	7,842	7,662	7,767
Mar-77	7,440	7,684	7,668	7,931	8,175
Apr-77	8,567	8,571	8,571	8,647	8,568
May-77	5,704	5,676	5,676	5,727	6,472
Jun-77	9,537	9,491	9,488	9,584	11,312
Jul-77	12,700	10,150	11,568	11,522	12,680
Aug-77	8,588	7,802	8,600	8,577	8,462
Sep-77	8,245	6,735	8,250	8,155	8,249
Oct-77	7,735	7,075	6,849	7,453	7,737
Nov-77	7,130	7,243	7,144	7,545	7,131
Dec-77	15,471	15,716	15,260	15,648	15,269
Jan-78	63,890	66,446	62,893	68,715	70,086
Feb-78	52,536	61,753	49,313	58,126	58,664
Mar-78	61,373	73,262	67,423	73,271	73,503
Apr-78	36,433	32,776	34,568	32,730	43,377
May-78	19,397	16,344	16,791	16,361	19,043
Jun-78	14,823	18,805	15,368	18,962	14,920
Jul-78	21,490	20,468	21,705	20,659	21,695
Aug-78	17,756	16,396	18,032	16,428	18,322
Sep-78	14,949	13,515	14,838	13,525	15,417
Oct-78	10,305	10,412	10,261	10,496	10,554
Nov-78	11,755	10,079	10,253	10,900	10,332
Dec-78	8,667	11,206	8,289	13,404	8,383
Jan-79	22,527	20,491	20,858	20,771	23,862
Feb-79	37,221	31,858	33,244	31,778	34,859
Mar-79	30,147	30,228	29,440	28,700	35,538
Apr-79	17,240	16,918	17,122	16,936	18,364
May-79	15,250	13,358	13,481	13,342	15,409
Jun-79	21,138	17,435	20,789	17,316	21,275
Jul-79	17,481	14,629	14,538	14,535	18,448
Aug-79	15,445	14,908	15,200	14,721	16,023
Sep-79	14,046	10,527	12,708	10,577	14,030

Table 5.35: DSM2 Input from CalSim-II: Sacramento River Flows (cfs) at Sacramento (cont.)

Date	BASE	GFDL A2	PCM A2	GFDL B1	PCM B1
Oct-79	10,199	9,803	9,370	9,755	10,054
Nov-79	13,383	12,681	12,956	13,059	13,480
Dec-79	19,685	20,398	18,276	20,596	18,114
Jan-80	74,269	74,316	73,465	74,559	75,159
Feb-80	74,367	74,720	75,069	74,488	74,648
Mar-80	44,213	49,229	46,649	49,392	56,602
Apr-80	18,884	17,753	18,154	17,725	20,898
May-80	15,671	13,984	14,392	13,918	15,258
Jun-80	12,820	15,485	15,166	15,686	14,695
Jul-80	18,699	16,812	19,812	17,870	20,024
Aug-80	17,014	12,895	16,269	13,809	16,721
Sep-80	14,012	11,504	11,831	11,526	14,227
Oct-80	11,568	9,276	9,283	9,277	9,655
Nov-80	8,853	8,603	8,892	9,311	9,412
Dec-80	12,513	12,582	12,248	12,624	12,215
Jan-81	21,469	22,017	21,090	22,187	22,650
Feb-81	25,217	25,758	26,399	25,526	25,751
Mar-81	29,580	26,680	23,329	28,722	36,183
Apr-81	16,214	15,974	16,247	15,917	16,484
May-81	10,949	10,411	10,592	10,410	10,949
Jun-81	14,721	15,407	14,771	13,366	14,573
Jul-81	17,771	15,035	15,594	15,589	17,623
Aug-81	15,247	13,362	15,291	15,001	14,382
Sep-81	13,857	11,589	11,746	11,625	13,609
Oct-81	12,566	10,777	10,230	9,964	10,767
Nov-81	31,571	26,160	29,202	29,009	36,384
Dec-81	73,957	74,668	73,141	74,593	71,835
Jan-82	68,660	72,623	65,754	73,359	73,558
Feb-82	73,878	74,226	74,623	74,011	74,190
Mar-82	71,357	73,606	73,039	73,639	74,034
Apr-82	74,475	73,798	74,184	73,832	75,220
May-82	39,827	25,178	29,784	25,134	37,372
Jun-82	21,942	22,822	21,678	23,054	20,123
Jul-82	18,866	20,072	19,778	20,071	19,391
Aug-82	13,160	15,367	17,654	15,486	17,839
Sep-82	17,174	14,366	15,851	14,366	17,032
Oct-82	18,126	13,611	11,672	13,582	16,192
Nov-82	37,037	23,328	30,128	26,130	31,073
Dec-82	64,483	69,855	53,805	65,208	56,758
Jan-83	71,244	73,187	69,680	73,465	73,568
Feb-83	75,088	75,443	75,780	75,178	75,365
Mar-83	77,464	78,354	77,903	78,435	79,055
Apr-83	62,634	53,326	58,813	54,985	71,943
May-83	56,061	36,111	40,874	36,041	54,021
Jun-83	54,463	27,774	37,161	28,819	45,678
Jul-83	23,061	17,810	17,761	17,220	20,917
Aug-83	20,551	15,086	19,287	15,496	20,220
Sep-83	26,629	20,383	25,821	23,725	26,584

Table 5.35: DSM2 Input from CalSim-II: Sacramento River Flows (cfs) at Sacramento (cont.)

Date	BASE	GFDL A2	PCM A2	GFDL B1	PCM B1
Oct-83	19,560	18,926	17,794	18,379	20,092
Nov-83	65,368	58,660	66,296	65,578	66,043
Dec-83	75,185	76,378	74,491	76,092	74,203
Jan-84	50,683	56,494	47,666	60,827	58,266
Feb-84	34,027	38,624	39,952	34,452	36,023
Mar-84	35,425	41,224	38,921	42,305	47,338
Apr-84	18,696	15,098	16,030	17,764	16,792
May-84	12,643	11,476	11,870	11,464	12,820
Jun-84	19,109	17,812	19,570	17,638	18,568
Jul-84	21,758	20,377	21,425	19,743	21,795
Aug-84	14,080	13,763	14,187	13,266	14,183
Sep-84	14,779	12,694	14,475	12,857	14,665
Oct-84	11,554	8,854	9,588	8,693	11,936
Nov-84	29,685	21,119	23,591	22,448	31,207
Dec-84	21,806	24,234	20,176	23,951	19,602
Jan-85	12,452	12,730	12,348	12,856	13,483
Feb-85	16,394	16,905	17,631	16,676	16,981
Mar-85	14,160	15,214	14,520	15,131	16,039
Apr-85	12,790	13,613	11,785	13,992	13,247
May-85	14,989	14,016	15,616	14,531	13,849
Jun-85	14,037	14,331	14,008	14,228	14,252
Jul-85	19,094	17,618	19,092	18,904	19,097
Aug-85	17,293	15,333	16,993	16,981	16,591
Sep-85	14,941	13,139	14,170	13,117	14,585
Oct-85	12,015	9,803	9,836	9,866	13,121
Nov-85	10,466	9,763	10,561	10,429	12,359
Dec-85	15,952	17,338	15,763	16,933	15,634
Jan-86	23,798	25,091	23,209	25,287	23,469
Feb-86	78,551	79,043	79,619	78,795	79,214
Mar-86	74,396	75,360	74,894	75,150	75,843
Apr-86	19,689	18,055	18,799	17,987	21,630
May-86	12,499	10,540	10,741	10,535	11,724
Jun-86	11,145	14,936	14,934	15,649	14,786
Jul-86	19,681	17,973	18,771	17,934	20,008
Aug-86	17,254	13,466	14,070	13,628	16,407
Sep-86	15,048	12,126	12,302	12,172	13,601
Oct-86	11,832	9,715	9,758	9,594	10,523
Nov-86	9,365	8,659	9,277	8,836	9,973
Dec-86	8,963	9,138	8,880	9,095	8,821
Jan-87	13,430	13,782	13,318	14,007	14,193
Feb-87	20,787	21,380	21,964	21,151	21,399
Mar-87	24,272	25,424	24,766	25,359	27,271
Apr-87	14,647	11,084	11,220	11,123	13,941
May-87	10,242	9,405	9,625	9,715	10,549
Jun-87	11,241	10,612	11,017	10,924	12,352
Jul-87	13,153	9,857	10,225	10,409	13,477
Aug-87	12,465	9,952	10,892	9,818	13,397
Sep-87	11,011	9,363	9,597	9,153	10,943

Table 5.35: DSM2 Input from CalSim-II: Sacramento River Flows (cfs) at Sacramento (cont.)

Date	BASE	GFDL A2	PCM A2	GFDL B1	PCM B1
Oct-87	9,814	9,200	9,460	9,197	10,879
Nov-87	8,896	8,497	8,500	8,494	8,944
Dec-87	17,578	17,945	17,358	17,846	17,277
Jan-88	28,123	28,131	27,735	28,818	28,374
Feb-88	16,008	12,799	13,010	12,698	15,957
Mar-88	8,685	8,883	8,847	9,280	9,580
Apr-88	10,475	10,273	10,314	10,294	10,800
May-88	9,754	9,819	9,810	9,811	9,667
Jun-88	10,922	11,737	11,101	11,803	12,339
Jul-88	9,130	8,938	8,823	9,194	9,980
Aug-88	8,130	7,991	8,366	8,236	8,709
Sep-88	6,195	6,589	6,279	6,407	5,882
Oct-88	7,771	7,785	7,777	7,785	7,778
Nov-88	9,993	9,718	10,072	9,933	10,092
Dec-88	9,968	10,284	9,822	10,199	9,732
Jan-89	12,814	12,943	12,666	13,035	13,125
Feb-89	10,328	10,454	10,556	10,346	10,260
Mar-89	47,840	60,757	51,571	58,410	67,796
Apr-89	22,084	29,703	21,145	29,705	29,670
May-89	15,373	21,237	15,441	21,241	21,200
Jun-89	15,170	11,053	14,845	11,523	11,856
Jul-89	18,046	16,272	14,002	17,339	18,780
Aug-89	15,192	13,066	14,029	14,109	16,907
Sep-89	15,211	13,196	13,563	13,237	15,276
Oct-89	11,409	10,180	10,663	9,987	11,725
Nov-89	9,196	8,561	8,707	8,656	11,200
Dec-89	8,934	11,069	11,981	11,185	11,917
Jan-90	18,954	19,488	18,981	19,807	19,642
Feb-90	16,333	15,351	15,533	15,152	16,342
Mar-90	12,359	13,148	12,784	13,440	13,128
Apr-90	10,745	10,735	10,744	10,734	10,737
May-90	9,169	8,763	9,022	8,760	9,371
Jun-90	10,434	8,178	8,183	8,809	8,425
Jul-90	9,577	10,091	9,776	10,097	9,454
Aug-90	8,949	8,485	8,255	8,268	8,017
Sep-90	8,293	8,275	8,246	8,290	8,296
Oct-90	7,745	7,737	7,745	7,736	7,746
Nov-90	7,223	7,216	7,223	7,216	7,223
Dec-90	6,721	6,715	6,721	6,715	7,010
Jan-91	6,576	6,577	6,539	6,808	6,820
Feb-91	8,350	8,366	8,605	8,439	8,472
Mar-91	31,783	32,148	32,136	32,314	33,002
Apr-91	13,266	12,800	13,143	13,105	14,314
May-91	8,786	7,652	8,089	7,999	8,964
Jun-91	8,093	7,229	7,304	7,044	10,171
Jul-91	10,700	11,045	11,079	11,296	11,223
Aug-91	8,100	6,830	7,907	7,336	8,264
Sep-91	8,471	6,190	7,793	8,392	8,355

Table 5.36: DSM2 Input from CalSim-II: San Joaquin River Flows (cfs) at Vernalis

Date	BASE	GFDL A2	PCM A2	GFDL B1	PCM B1
Oct-75	2,946	2,063	2,421	2,019	2,652
Nov-75	1,805	1,753	1,918	1,732	1,856
Dec-75	1,910	1,858	1,885	1,837	1,904
Jan-76	1,721	1,669	1,693	1,648	1,715
Feb-76	1,933	1,879	2,039	1,858	2,021
Mar-76	1,775	1,662	1,690	1,661	1,734
Apr-76	2,450	2,442	2,447	2,445	2,450
May-76	2,262	2,249	2,256	2,254	2,261
Jun-76	1,486	1,449	1,470	1,463	1,483
Jul-76	1,427	1,152	1,407	1,108	1,423
Aug-76	1,347	857	911	858	1,139
Sep-76	1,178	1,160	1,171	1,162	1,179
Oct-76	3,209	3,101	3,131	2,915	3,171
Nov-76	2,100	2,050	2,078	2,050	2,090
Dec-76	1,693	1,642	1,670	1,643	1,682
Jan-77	1,306	1,189	1,220	1,191	1,264
Feb-77	1,383	1,260	1,294	1,265	1,340
Mar-77	1,275	1,268	1,272	1,256	1,275
Apr-77	1,702	1,698	1,700	1,624	1,702
May-77	1,581	1,574	1,577	1,480	1,581
Jun-77	1,236	1,216	1,223	1,209	1,236
Jul-77	798	684	788	685	788
Aug-77	680	646	673	647	680
Sep-77	982	956	975	958	981
Oct-77	1,454	1,442	1,626	1,200	1,454
Nov-77	1,351	1,270	1,350	1,262	1,351
Dec-77	1,524	1,518	1,522	1,535	1,524
Jan-78	3,727	3,247	3,248	3,248	3,251
Feb-78	7,843	8,901	8,385	6,816	7,735
Mar-78	9,089	10,909	10,055	9,268	9,773
Apr-78	12,921	14,729	13,976	12,726	14,273
May-78	11,897	12,235	12,588	9,647	13,952
Jun-78	11,295	3,840	7,262	3,687	7,372
Jul-78	2,470	2,263	2,263	2,263	2,263
Aug-78	1,908	1,908	1,908	1,908	1,908
Sep-78	2,194	1,614	1,614	1,614	1,725
Oct-78	4,206	2,408	3,694	2,621	4,202
Nov-78	1,648	1,606	1,681	1,604	1,650
Dec-78	1,829	1,787	1,823	1,898	1,831
Jan-79	3,851	4,284	3,770	4,278	4,363
Feb-79	9,064	5,809	6,625	4,816	10,257
Mar-79	8,638	6,609	9,480	5,839	10,407
Apr-79	6,349	6,369	6,482	5,729	6,790
May-79	5,904	5,597	5,868	5,008	6,114
Jun-79	2,190	2,093	2,116	2,094	2,334
Jul-79	1,849	1,803	1,818	1,805	1,849
Aug-79	1,764	1,694	1,705	1,695	1,764
Sep-79	1,870	1,820	1,837	1,797	1,883

Table 5.36: DSM2 Input from CalSim-II: San Joaquin River Flows (cfs) at Vernalis (cont.)

Date	BASE	GFDL A2	PCM A2	GFDL B1	PCM B1
Oct-79	2,255	2,200	2,236	2,081	2,281
Nov-79	1,808	1,732	1,788	1,618	1,821
Dec-79	1,945	1,866	1,923	1,752	1,958
Jan-80	11,058	10,135	7,211	7,463	11,747
Feb-80	21,061	24,227	27,335	12,986	26,166
Mar-80	13,100	17,772	15,092	14,019	16,080
Apr-80	7,544	9,844	9,434	8,528	9,136
May-80	6,767	6,218	6,527	5,690	7,183
Jun-80	5,214	2,445	2,766	2,405	2,891
Jul-80	3,864	1,952	2,135	1,920	2,262
Aug-80	2,014	1,788	1,916	1,766	2,006
Sep-80	2,611	1,708	1,770	1,689	2,211
Oct-80	4,278	1,988	2,940	1,979	3,763
Nov-80	1,742	1,688	1,718	1,634	1,740
Dec-80	1,885	1,829	1,859	1,776	1,883
Jan-81	2,106	2,023	2,057	2,019	2,085
Feb-81	2,547	2,280	2,523	2,280	2,604
Mar-81	3,483	2,240	3,957	2,220	4,303
Apr-81	4,327	3,907	4,340	3,906	4,588
May-81	3,461	2,767	3,806	2,710	3,750
Jun-81	1,710	1,671	1,702	1,676	1,683
Jul-81	1,678	1,631	1,668	1,637	1,645
Aug-81	1,625	1,589	1,617	1,486	1,600
Sep-81	1,567	1,311	1,561	1,310	1,549
Oct-81	2,104	2,042	2,100	2,027	2,100
Nov-81	1,708	1,661	1,689	1,657	1,703
Dec-81	1,760	1,711	1,741	1,707	1,754
Jan-82	6,242	6,697	4,673	5,878	5,941
Feb-82	13,580	16,895	17,143	10,856	17,456
Mar-82	14,865	19,929	16,487	15,515	18,363
Apr-82	24,622	30,388	29,743	27,701	29,908
May-82	16,058	14,288	15,150	12,939	16,504
Jun-82	9,692	3,738	4,247	3,738	5,012
Jul-82	3,715	2,511	2,804	2,511	3,191
Aug-82	2,199	2,199	2,199	2,199	2,199
Sep-82	3,563	1,837	3,331	1,837	3,382
Oct-82	12,098	3,340	8,876	3,369	10,131
Nov-82	7,981	5,876	9,890	9,739	9,744
Dec-82	18,184	21,017	13,073	17,211	13,383
Jan-83	23,332	28,727	23,427	29,754	26,805
Feb-83	31,051	35,096	38,220	26,681	34,742
Mar-83	37,383	47,697	41,589	39,407	44,295
Apr-83	19,986	23,136	22,652	21,521	22,363
May-83	20,416	19,270	19,789	17,881	20,879
Jun-83	34,195	10,326	20,598	9,633	22,664
Jul-83	17,655	3,333	9,375	3,997	13,234
Aug-83	2,082	2,082	2,082	2,082	2,082
Sep-83	5,958	3,069	4,827	3,339	5,236

Table 5.36: DSM2 Input from CalSim-II: San Joaquin River Flows (cfs) at Vernalis (cont.)

Date	BASE	GFDL A2	PCM A2	GFDL B1	PCM B1
Oct-83	11,980	5,880	11,773	5,759	11,820
Nov-83	12,960	8,708	15,882	15,330	15,748
Dec-83	20,682	28,501	16,607	23,593	15,626
Jan-84	14,354	18,070	14,455	18,775	16,712
Feb-84	9,683	10,593	12,064	7,987	10,999
Mar-84	6,092	8,591	6,980	6,525	8,034
Apr-84	5,530	5,551	5,552	5,433	5,680
May-84	5,064	4,948	5,015	4,908	5,065
Jun-84	2,627	2,428	2,540	2,356	2,629
Jul-84	2,243	2,184	2,235	2,188	2,243
Aug-84	2,137	2,099	2,135	2,101	2,139
Sep-84	1,969	1,938	1,959	1,932	1,969
Oct-84	2,343	2,301	2,327	2,288	2,343
Nov-84	1,922	1,900	1,914	1,894	1,922
Dec-84	1,971	1,948	1,963	1,942	1,971
Jan-85	1,791	1,764	1,782	1,758	1,791
Feb-85	2,211	2,174	2,201	2,169	2,211
Mar-85	2,191	2,098	2,172	2,081	2,188
Apr-85	3,241	2,573	3,241	2,574	3,241
May-85	3,491	2,376	3,086	2,383	3,419
Jun-85	1,744	1,731	1,745	1,752	1,746
Jul-85	1,651	1,635	1,652	1,660	1,653
Aug-85	1,580	1,133	1,581	1,018	1,582
Sep-85	1,577	1,346	1,339	1,352	1,527
Oct-85	2,119	2,012	2,086	2,001	2,114
Nov-85	1,698	1,740	1,674	1,738	1,695
Dec-85	1,776	1,818	1,753	1,817	1,774
Jan-86	2,182	1,674	1,751	1,662	1,765
Feb-86	13,469	16,280	19,260	7,964	18,396
Mar-86	23,294	33,269	28,189	20,725	30,362
Apr-86	12,075	14,596	14,225	13,234	13,765
May-86	8,356	7,526	7,894	6,515	8,604
Jun-86	6,517	2,130	2,801	2,130	2,752
Jul-86	2,389	2,370	2,378	2,129	2,387
Aug-86	2,169	2,154	2,161	2,070	2,168
Sep-86	2,169	2,153	2,160	2,062	2,167
Oct-86	2,566	2,105	2,112	2,104	2,127
Nov-86	1,748	1,742	1,745	1,696	1,748
Dec-86	1,794	1,787	1,790	1,741	1,794
Jan-87	1,675	1,663	1,669	1,618	1,674
Feb-87	2,041	2,019	2,029	1,974	2,039
Mar-87	1,961	1,855	1,870	1,855	1,934
Apr-87	2,475	2,464	2,467	2,467	2,483
May-87	2,287	2,268	2,274	2,273	2,299
Jun-87	1,531	1,476	1,491	1,491	1,566
Jul-87	1,514	1,205	1,466	1,196	1,555
Aug-87	1,252	825	833	826	1,064
Sep-87	1,197	1,171	1,182	1,173	1,208

Table 5.36: DSM2 Input from CalSim-II: San Joaquin River Flows (cfs) at Vernalis (cont.)

Date	BASE	GFDL A2	PCM A2	GFDL B1	PCM B1
Oct-87	1,676	1,588	1,593	1,590	1,658
Nov-87	1,330	1,279	1,301	1,282	1,327
Dec-87	1,288	1,236	1,258	1,238	1,286
Jan-88	1,280	1,169	1,185	1,173	1,261
Feb-88	1,326	1,206	1,224	1,212	1,313
Mar-88	1,254	1,250	1,250	1,250	1,252
Apr-88	1,719	1,713	1,714	1,713	1,716
May-88	1,586	1,578	1,578	1,577	1,582
Jun-88	1,262	1,239	1,240	1,238	1,251
Jul-88	969	993	1,020	979	1,003
Aug-88	688	670	677	666	685
Sep-88	1,033	1,014	1,022	1,010	1,029
Oct-88	1,554	1,345	1,522	1,309	1,552
Nov-88	1,279	1,201	1,273	1,227	1,278
Dec-88	1,391	1,358	1,384	1,358	1,389
Jan-89	1,183	1,175	1,178	1,176	1,180
Feb-89	1,360	1,349	1,351	1,349	1,355
Mar-89	1,596	1,592	1,595	1,590	1,596
Apr-89	1,727	1,695	1,714	1,696	1,737
May-89	1,439	1,403	1,418	1,407	1,453
Jun-89	1,292	1,255	1,256	1,277	1,322
Jul-89	1,292	1,200	1,286	1,116	1,281
Aug-89	803	789	793	784	811
Sep-89	1,164	1,150	1,154	1,149	1,173
Oct-89	1,370	1,321	1,322	1,308	1,579
Nov-89	1,324	1,225	1,236	1,314	1,328
Dec-89	1,254	1,154	1,161	1,157	1,258
Jan-90	1,194	1,183	1,186	1,188	1,201
Feb-90	1,380	1,363	1,365	1,372	1,392
Mar-90	1,315	1,314	1,314	1,313	1,315
Apr-90	1,570	1,566	1,568	1,564	1,571
May-90	1,307	1,304	1,305	1,301	1,308
Jun-90	1,164	1,162	1,163	1,161	1,164
Jul-90	1,062	935	1,013	907	1,065
Aug-90	728	721	724	716	730
Sep-90	1,085	1,080	1,082	1,007	1,086
Oct-90	1,212	1,051	1,052	1,016	1,257
Nov-90	1,173	1,173	1,173	1,133	1,173
Dec-90	1,130	1,130	1,130	1,130	1,130
Jan-91	1,006	1,004	1,033	1,003	1,033
Feb-91	1,128	1,133	1,149	1,106	1,149
Mar-91	2,387	2,383	2,385	2,383	2,387
Apr-91	2,245	2,230	2,237	2,228	2,246
May-91	1,690	1,672	1,681	1,670	1,692
Jun-91	1,106	1,074	1,092	1,088	1,118
Jul-91	1,073	1,035	1,056	1,006	1,087
Aug-91	777	757	767	755	780
Sep-91	1,026	1,008	1,017	1,008	1,029

Table 5.37: DSM2 Input from CalSim-II: State Water Project Exports (cfs)

Date	BASE	GFDL A2	PCM A2	GFDL B1	PCM B1
Oct-75	6,680	5,334	6,680	5,136	6,680
Nov-75	6,680	2,328	6,680	2,673	6,680
Dec-75	7,013	1,380	300	1,343	4,367
Jan-76	3,972	4,234	3,115	3,903	3,365
Feb-76	3,987	2,609	2,467	2,564	2,921
Mar-76	3,416	2,757	3,199	3,197	4,403
Apr-76	1,721	1,557	1,638	1,551	1,677
May-76	1,517	1,357	1,436	1,352	1,479
Jun-76	3,152	2,884	3,430	2,989	2,909
Jul-76	2,424	3,386	4,162	3,629	2,996
Aug-76	4,808	2,775	3,553	2,984	3,632
Sep-76	3,672	1,828	2,119	1,906	3,174
Oct-76	2,792	2,063	1,780	1,987	2,391
Nov-76	2,945	1,177	1,780	1,582	2,558
Dec-76	3,049	1,888	1,925	1,715	2,558
Jan-77	2,764	2,096	2,013	2,232	2,493
Feb-77	919	1,077	1,034	855	858
Mar-77	497	1,219	1,200	1,455	1,706
Apr-77	300	300	300	300	300
May-77	413	300	300	300	1,105
Jun-77	300	300	300	300	300
Jul-77	461	300	352	329	461
Aug-77	306	300	300	300	342
Sep-77	1,703	2,079	1,609	1,564	1,701
Oct-77	763	2,347	2,634	2,869	542
Nov-77	1,386	1,245	1,623	1,527	1,477
Dec-77	5,717	4,210	5,565	6,102	5,635
Jan-78	7,455	6,934	6,589	5,577	6,930
Feb-78	4,092	4,233	3,679	4,380	4,316
Mar-78	5,115	5,337	4,977	5,280	5,440
Apr-78	5,516	5,490	5,546	5,464	5,452
May-78	4,844	4,532	4,899	1,620	4,758
Jun-78	4,713	4,046	3,490	4,047	3,374
Jul-78	6,680	6,680	6,680	6,680	6,680
Aug-78	6,680	5,991	6,526	6,001	6,680
Sep-78	6,680	5,362	6,227	5,368	6,680
Oct-78	4,174	3,199	3,828	3,427	4,421
Nov-78	3,417	2,198	3,262	2,847	2,991
Dec-78	1,695	3,108	1,504	4,863	1,312
Jan-79	7,964	8,108	7,937	8,106	8,134
Feb-79	8,500	8,500	8,500	8,285	8,500
Mar-79	7,561	7,561	7,561	7,561	7,561
Apr-79	4,020	3,844	4,317	3,626	4,429
May-79	3,718	3,780	3,657	3,018	3,795
Jun-79	3,948	3,494	3,868	2,918	4,188
Jul-79	4,454	4,744	4,676	4,245	4,830
Aug-79	5,754	5,608	5,731	5,436	5,970
Sep-79	6,005	3,021	5,188	3,030	6,006

Table 5.37: DSM2 Input from CalSim-II: State Water Project Exports (cfs) (cont.)

Date	BASE	GFDL A2	PCM A2	GFDL B1	PCM B1
Oct-79	3,597	3,693	2,835	3,676	3,743
Nov-79	4,239	3,534	4,844	3,851	4,279
Dec-79	7,019	7,008	7,015	7,000	7,021
Jan-80	8,500	8,500	8,500	8,500	8,500
Feb-80	8,437	8,347	8,069	8,267	7,726
Mar-80	5,072	4,241	4,471	4,264	4,656
Apr-80	4,535	3,940	4,204	3,967	4,403
May-80	4,163	4,375	4,417	3,682	4,365
Jun-80	2,250	3,405	3,407	3,433	3,181
Jul-80	6,680	6,296	6,680	6,494	6,680
Aug-80	6,680	5,053	6,680	5,478	6,680
Sep-80	6,680	4,577	4,834	4,578	6,680
Oct-80	5,889	2,631	2,791	2,665	3,713
Nov-80	1,759	1,288	1,704	1,299	1,989
Dec-80	3,629	4,282	3,639	4,403	2,941
Jan-81	7,382	7,354	7,366	7,353	7,375
Feb-81	5,654	5,499	5,808	5,418	5,610
Mar-81	7,074	5,293	5,231	5,134	6,529
Apr-81	2,707	2,564	2,801	2,544	2,890
May-81	2,127	1,935	2,126	1,915	2,152
Jun-81	2,909	2,957	1,605	300	3,015
Jul-81	5,219	3,016	3,038	3,425	5,038
Aug-81	5,079	4,970	5,913	5,837	4,900
Sep-81	5,546	3,940	4,198	3,978	5,665
Oct-81	3,896	3,225	3,244	3,092	3,602
Nov-81	6,680	6,680	6,680	6,680	6,680
Dec-81	7,002	6,993	6,998	6,992	7,001
Jan-82	8,500	8,500	8,238	8,500	8,500
Feb-82	8,500	8,500	8,500	8,500	8,500
Mar-82	7,561	7,535	7,561	7,352	7,561
Apr-82	6,125	6,125	6,125	6,125	6,125
May-82	6,177	6,177	6,177	6,177	6,177
Jun-82	6,680	4,984	4,873	5,025	4,869
Jul-82	6,680	6,680	6,680	6,680	6,680
Aug-82	3,304	6,077	6,680	6,115	6,680
Sep-82	6,680	6,680	6,680	6,680	6,680
Oct-82	6,680	6,680	6,680	6,680	6,680
Nov-82	6,680	6,680	6,680	6,680	6,680
Dec-82	7,678	7,678	6,761	7,678	6,755
Jan-83	3,472	3,477	3,476	3,477	3,474
Feb-83	3,548	3,548	3,548	3,548	3,548
Mar-83	3,555	3,555	3,555	3,555	3,555
Apr-83	3,749	3,749	3,749	3,749	3,749
May-83	3,171	3,171	3,171	3,171	3,171
Jun-83	3,877	3,877	3,877	3,877	3,877
Jul-83	6,638	6,119	6,638	6,194	6,638
Aug-83	6,680	6,680	6,680	6,680	6,680
Sep-83	5,039	5,573	5,039	5,496	5,039

Table 5.37: DSM2 Input from CalSim-II: State Water Project Exports (cfs) (cont.)

Date	BASE	GFDL A2	PCM A2	GFDL B1	PCM B1
Oct-83	3,682	3,682	3,682	3,682	3,682
Nov-83	3,144	3,144	3,144	3,144	3,144
Dec-83	3,723	3,723	3,723	3,723	3,723
Jan-84	5,640	5,640	5,640	5,640	5,640
Feb-84	6,531	6,509	6,531	6,506	6,531
Mar-84	6,635	6,564	6,619	6,564	6,635
Apr-84	3,499	1,880	1,914	3,413	3,356
May-84	2,899	2,781	2,825	2,776	2,916
Jun-84	3,974	3,875	4,039	3,425	3,880
Jul-84	5,093	4,771	5,062	4,269	5,198
Aug-84	4,981	4,630	5,090	4,132	5,086
Sep-84	6,680	5,772	6,680	5,850	6,606
Oct-84	5,541	3,916	4,371	3,928	5,726
Nov-84	6,680	6,680	6,680	6,680	6,680
Dec-84	7,040	7,036	7,039	7,035	7,040
Jan-85	4,443	4,703	4,340	4,822	5,478
Feb-85	4,167	4,490	4,719	4,438	4,432
Mar-85	2,560	3,215	2,356	2,791	2,362
Apr-85	2,356	2,230	2,221	2,249	2,393
May-85	2,497	2,183	2,424	2,219	2,387
Jun-85	2,795	2,843	2,790	2,829	2,833
Jul-85	6,680	6,680	6,680	6,680	6,680
Aug-85	6,680	6,647	6,680	6,601	6,680
Sep-85	6,680	5,123	5,685	5,003	6,680
Oct-85	5,411	3,610	3,525	3,524	5,886
Nov-85	3,894	3,880	3,899	3,804	4,363
Dec-85	6,900	6,825	6,480	6,995	6,687
Jan-86	7,407	7,238	7,264	7,234	7,268
Feb-86	8,500	8,500	8,500	8,500	8,500
Mar-86	5,388	5,384	5,460	5,002	6,084
Apr-86	4,901	4,149	4,423	4,276	4,806
May-86	4,988	3,857	4,063	2,623	4,857
Jun-86	2,020	3,206	3,323	3,329	3,288
Jul-86	6,680	5,564	6,680	5,711	6,680
Aug-86	6,680	5,297	5,562	5,319	6,680
Sep-86	6,680	5,134	5,253	5,098	6,102
Oct-86	4,471	3,129	2,563	3,236	3,110
Nov-86	1,302	1,147	1,445	1,251	1,445
Dec-86	2,356	3,245	2,325	2,916	2,166
Jan-87	6,572	4,826	4,640	4,970	5,308
Feb-87	7,360	6,872	7,356	7,210	7,360
Mar-87	5,086	4,197	4,435	4,156	4,764
Apr-87	2,141	300	300	300	2,064
May-87	300	300	300	300	300
Jun-87	300	300	300	300	526
Jul-87	3,445	810	1,071	985	2,692
Aug-87	5,279	3,225	4,076	2,304	5,073
Sep-87	3,863	2,927	3,056	2,910	3,498

Table 5.37: DSM2 Input from CalSim-II: State Water Project Exports (cfs) (cont.)

Date	BASE	GFDL A2	PCM A2	GFDL B1	PCM B1
Oct-87	2,809	2,360	2,481	2,263	2,860
Nov-87	2,071	1,875	2,146	1,985	2,175
Dec-87	6,629	6,341	6,220	6,375	3,961
Jan-88	7,107	7,070	7,075	7,071	7,100
Feb-88	1,428	1,588	1,612	1,322	1,368
Mar-88	511	702	664	1,102	1,424
Apr-88	1,482	1,448	1,464	1,450	1,507
May-88	1,407	1,412	1,411	1,411	1,399
Jun-88	300	1,043	300	892	803
Jul-88	482	300	300	300	382
Aug-88	300	300	300	300	300
Sep-88	942	1,005	950	966	876
Oct-88	1,138	910	1,049	772	820
Nov-88	2,515	2,167	2,742	2,573	2,810
Dec-88	2,780	3,420	2,456	3,057	2,273
Jan-89	3,282	3,395	3,246	3,554	3,660
Feb-89	1,212	1,308	1,377	1,222	1,156
Mar-89	6,937	6,937	6,937	6,936	6,937
Apr-89	2,551	300	2,468	300	300
May-89	1,975	2,489	1,974	2,488	2,504
Jun-89	3,345	2,589	4,465	2,569	2,370
Jul-89	6,670	6,680	4,086	6,680	6,680
Aug-89	6,275	5,862	6,680	6,191	6,680
Sep-89	6,328	4,834	5,076	4,860	6,680
Oct-89	4,778	3,580	3,983	3,617	5,591
Nov-89	2,198	2,299	2,836	2,259	2,158
Dec-89	300	4,944	5,144	5,049	5,641
Jan-90	7,078	7,074	7,075	7,076	7,080
Feb-90	2,385	2,546	2,686	2,391	2,410
Mar-90	2,530	2,667	2,604	2,718	3,041
Apr-90	300	300	300	300	300
May-90	1,358	1,320	1,344	1,318	1,377
Jun-90	2,074	300	300	300	300
Jul-90	300	300	300	300	300
Aug-90	1,430	300	300	300	300
Sep-90	1,794	1,777	1,744	1,719	1,793
Oct-90	1,023	862	1,117	671	1,169
Nov-90	1,361	300	609	300	888
Dec-90	1,306	300	1,324	300	1,351
Jan-91	921	1,591	1,277	1,888	1,710
Feb-91	1,254	1,178	1,173	976	1,048
Mar-91	7,065	7,064	7,065	7,064	7,065
Apr-91	1,801	1,270	1,389	1,419	2,084
May-91	1,478	1,370	1,412	1,400	1,495
Jun-91	300	300	300	300	2,022
Jul-91	555	300	446	423	655
Aug-91	300	382	300	300	300
Sep-91	983	2,475	1,609	967	890

Table 5.38: DSM2 Input from CalSim-II: Central Valley Project Exports (cfs)

Date	BASE	GFDL A2	PCM A2	GFDL B1	PCM B1
Oct-75	4,600	4,449	4,600	4,554	4,600
Nov-75	4,600	3,497	4,600	4,600	4,600
Dec-75	4,600	800	1,200	800	4,342
Jan-76	4,229	4,600	4,600	4,600	4,183
Feb-76	3,174	3,723	4,071	3,740	3,417
Mar-76	2,717	2,757	2,758	2,303	2,291
Apr-76	1,721	1,557	1,638	1,551	1,677
May-76	1,517	1,357	1,436	1,352	1,479
Jun-76	1,436	1,753	1,853	2,031	1,480
Jul-76	1,315	1,602	1,752	1,940	1,357
Aug-76	2,518	1,756	1,830	2,001	2,345
Sep-76	3,242	3,271	3,302	3,257	3,247
Oct-76	2,448	3,625	3,637	3,565	3,024
Nov-76	1,767	2,780	2,481	2,172	1,842
Dec-76	1,689	1,841	1,590	2,197	950
Jan-77	2,489	2,387	2,623	2,134	2,504
Feb-77	2,616	800	800	800	955
Mar-77	800	800	800	800	800
Apr-77	800	800	800	800	800
May-77	800	800	800	800	1,105
Jun-77	1,026	800	800	800	2,643
Jul-77	2,509	600	1,927	1,813	2,272
Aug-77	2,979	1,789	2,732	2,679	2,979
Sep-77	3,078	1,889	3,169	3,101	3,083
Oct-77	3,050	1,013	600	600	3,051
Nov-77	1,489	1,758	1,420	1,444	1,691
Dec-77	4,600	3,795	4,209	4,427	4,257
Jan-78	4,600	4,600	4,600	4,600	4,600
Feb-78	4,600	4,600	4,600	4,600	4,600
Mar-78	1,894	4,262	4,091	3,681	2,206
Apr-78	2,692	2,538	2,692	2,692	2,692
May-78	3,896	3,896	3,896	3,896	3,896
Jun-78	4,600	4,046	4,600	4,047	4,600
Jul-78	4,600	3,354	4,600	3,546	4,600
Aug-78	4,600	4,232	4,488	4,323	4,600
Sep-78	4,600	4,600	4,600	4,600	4,600
Oct-78	4,600	3,885	4,390	3,954	4,600
Nov-78	3,964	2,907	2,872	2,906	3,325
Dec-78	3,010	4,377	2,914	4,377	2,993
Jan-79	4,600	4,600	4,600	4,600	4,600
Feb-79	4,548	4,600	4,600	4,600	4,600
Mar-79	2,589	4,600	4,600	4,600	4,281
Apr-79	3,646	3,844	3,284	3,626	3,647
May-79	3,718	2,948	3,334	3,018	3,795
Jun-79	4,161	800	3,811	1,247	4,211
Jul-79	3,999	800	800	1,191	4,596
Aug-79	4,549	3,838	4,008	4,048	3,822
Sep-79	4,478	4,389	4,401	4,397	4,478

Table 5.38: DSM2 Input from CalSim-II: Central Valley Project Exports (cfs)

Date	BASE	GFDL A2	PCM A2	GFDL B1	PCM B1
Oct-79	3,620	3,220	3,071	3,074	3,495
Nov-79	4,013	3,913	3,844	3,644	4,146
Dec-79	4,600	4,600	4,600	4,600	4,600
Jan-80	4,600	4,015	4,600	4,600	4,600
Feb-80	4,600	943	1,655	1,419	4,273
Mar-80	2,591	1,335	1,537	1,401	1,944
Apr-80	2,699	1,951	2,252	2,155	2,699
May-80	3,884	2,819	3,239	3,102	3,884
Jun-80	4,600	3,405	3,407	3,433	3,512
Jul-80	4,600	1,186	3,720	2,010	4,310
Aug-80	4,600	2,563	3,727	3,105	4,578
Sep-80	4,600	4,600	4,600	4,600	4,600
Oct-80	4,600	3,289	4,083	3,246	4,351
Nov-80	3,231	2,900	2,895	3,212	3,659
Dec-80	4,227	4,159	4,223	4,222	4,227
Jan-81	4,600	4,600	4,600	4,600	4,600
Feb-81	4,349	4,600	4,600	4,600	4,600
Mar-81	2,892	4,600	2,394	4,600	4,600
Apr-81	2,707	2,564	2,801	2,544	2,890
May-81	2,127	1,935	2,126	1,915	2,152
Jun-81	2,897	3,073	4,214	3,833	2,729
Jul-81	4,600	4,023	4,600	4,175	4,600
Aug-81	4,600	3,407	3,893	3,521	4,080
Sep-81	4,600	4,228	4,400	4,247	4,309
Oct-81	4,129	2,581	2,729	2,771	2,912
Nov-81	4,600	4,600	4,600	4,600	4,600
Dec-81	4,600	4,600	4,600	4,600	4,600
Jan-82	4,600	4,600	4,600	4,600	4,600
Feb-82	4,600	4,600	4,600	4,600	4,600
Mar-82	4,600	3,542	4,600	4,600	4,229
Apr-82	3,954	2,690	2,897	2,973	2,690
May-82	3,895	3,895	3,895	3,895	3,895
Jun-82	4,600	4,571	4,571	4,571	4,600
Jul-82	4,600	4,600	4,600	4,600	4,600
Aug-82	4,600	3,302	4,578	3,416	4,600
Sep-82	4,600	4,600	4,600	4,600	4,600
Oct-82	4,600	4,600	4,600	4,600	4,600
Nov-82	4,600	4,600	4,600	4,600	4,600
Dec-82	4,600	4,600	4,600	4,600	4,600
Jan-83	3,741	4,600	3,995	4,600	3,970
Feb-83	2,251	4,298	2,251	4,173	2,251
Mar-83	1,955	1,955	1,955	1,955	1,955
Apr-83	2,687	2,687	2,687	2,687	2,687
May-83	3,892	3,892	3,892	3,892	3,892
Jun-83	4,600	4,600	4,600	4,600	4,600
Jul-83	4,600	4,600	4,600	4,600	4,600
Aug-83	4,600	4,600	4,600	4,600	4,600
Sep-83	4,600	4,600	4,600	4,600	4,600

Table 5.38: DSM2 Input from CalSim-II: Central Valley Project Exports (cfs)

Date	BASE	GFDL A2	PCM A2	GFDL B1	PCM B1
Oct-83	4,600	4,600	4,600	4,600	4,600
Nov-83	3,310	4,093	4,093	4,093	4,006
Dec-83	1,445	1,445	1,445	1,445	1,445
Jan-84	1,919	1,919	1,919	1,919	1,919
Feb-84	2,869	2,173	2,173	2,872	2,692
Mar-84	3,032	2,154	2,898	2,741	3,026
Apr-84	3,499	2,743	3,188	3,413	3,356
May-84	2,899	2,781	2,825	2,776	2,916
Jun-84	3,974	3,274	4,039	3,381	3,880
Jul-84	4,600	3,591	4,483	3,717	4,590
Aug-84	4,600	4,600	4,600	4,600	4,600
Sep-84	4,600	4,128	4,394	4,151	4,600
Oct-84	4,468	3,589	3,888	3,403	4,533
Nov-84	4,600	4,600	4,600	4,600	4,600
Dec-84	4,600	4,600	4,600	4,600	4,600
Jan-85	4,600	4,600	4,600	4,600	4,600
Feb-85	4,600	4,490	4,600	4,438	4,600
Mar-85	3,523	3,204	3,846	3,593	4,378
Apr-85	2,356	2,230	2,221	2,249	2,393
May-85	2,497	1,912	2,469	2,219	2,387
Jun-85	2,795	2,843	2,790	2,829	2,833
Jul-85	4,600	3,103	4,600	4,416	4,600
Aug-85	4,600	2,669	4,386	3,712	4,073
Sep-85	4,191	4,423	4,529	4,532	3,927
Oct-85	3,006	2,036	2,867	2,588	3,049
Nov-85	2,765	2,842	2,671	2,820	4,129
Dec-85	4,600	4,600	4,600	4,600	4,600
Jan-86	4,600	4,600	4,600	4,600	4,600
Feb-86	4,600	4,600	4,600	4,600	4,600
Mar-86	4,600	4,600	4,573	4,600	3,828
Apr-86	2,254	1,725	1,808	1,865	2,049
May-86	3,016	2,318	2,627	2,340	2,962
Jun-86	4,600	2,785	3,323	3,329	3,288
Jul-86	3,097	800	800	800	1,651
Aug-86	4,525	3,383	3,345	3,161	4,522
Sep-86	4,600	4,600	4,600	4,600	4,600
Oct-86	4,600	3,377	3,988	3,145	4,217
Nov-86	4,424	3,683	3,896	3,681	4,569
Dec-86	2,622	2,084	2,822	2,316	2,789
Jan-87	2,590	4,221	4,223	4,221	4,393
Feb-87	2,336	3,676	3,287	3,570	2,926
Mar-87	1,901	1,526	1,677	1,533	1,885
Apr-87	2,141	800	800	800	2,064
May-87	1,507	956	1,182	1,194	1,730
Jun-87	2,001	1,072	1,438	1,458	2,949
Jul-87	2,015	879	1,315	1,339	3,138
Aug-87	1,895	800	1,117	1,436	2,740
Sep-87	3,440	2,715	2,830	2,526	3,751

Table 5.38: DSM2 Input from CalSim-II: Central Valley Project Exports (cfs)

Date	BASE	GFDL A2	PCM A2	GFDL B1	PCM B1
Oct-87	2,102	2,778	2,603	2,960	2,904
Nov-87	3,080	2,841	2,593	2,634	3,024
Dec-87	4,600	4,600	4,600	4,600	1,241
Jan-88	4,600	4,600	4,600	4,600	4,600
Feb-88	4,600	1,106	1,314	1,279	4,600
Mar-88	800	800	800	800	800
Apr-88	1,482	1,448	1,464	1,450	1,507
May-88	1,407	1,412	1,411	1,411	1,399
Jun-88	1,093	1,132	1,245	1,348	1,990
Jul-88	878	883	800	1,125	1,857
Aug-88	1,125	916	1,511	1,280	1,995
Sep-88	2,814	2,849	2,820	2,830	2,785
Oct-88	3,097	3,034	3,089	3,022	3,099
Nov-88	2,434	2,577	2,321	2,463	2,470
Dec-88	3,557	2,995	3,723	3,226	3,696
Jan-89	4,213	4,211	4,211	4,211	4,212
Feb-89	2,720	2,746	2,769	2,721	2,704
Mar-89	4,600	4,600	4,600	4,600	4,600
Apr-89	2,551	2,670	2,468	2,668	2,684
May-89	1,975	2,489	1,974	2,488	2,504
Jun-89	2,544	1,273	1,298	1,778	2,370
Jul-89	2,658	800	1,201	1,781	3,380
Aug-89	2,390	1,009	1,198	1,418	2,914
Sep-89	4,426	4,600	4,600	4,600	4,121
Oct-89	2,719	2,325	2,333	2,337	2,625
Nov-89	1,959	2,019	1,872	1,728	3,475
Dec-89	800	1,189	1,367	1,610	2,128
Jan-90	4,600	4,600	4,600	4,600	4,600
Feb-90	4,600	3,451	3,488	3,413	4,600
Mar-90	2,530	2,667	2,604	2,718	2,287
Apr-90	800	800	800	800	800
May-90	1,358	1,320	1,344	1,318	1,377
Jun-90	1,278	800	800	1,430	1,042
Jul-90	1,039	800	800	800	800
Aug-90	1,339	2,223	1,675	1,887	1,099
Sep-90	2,821	2,821	2,821	2,821	2,826
Oct-90	2,697	2,952	2,955	2,941	3,022
Nov-90	1,485	2,140	1,459	2,397	1,510
Dec-90	2,019	1,631	998	1,327	800
Jan-91	1,668	1,515	1,821	1,449	1,669
Feb-91	1,262	822	1,082	1,056	1,167
Mar-91	4,600	4,600	4,600	4,600	4,600
Apr-91	1,491	1,576	1,793	1,760	2,084
May-91	1,478	1,370	1,412	1,400	1,495
Jun-91	1,656	600	861	600	2,022
Jul-91	800	600	600	600	1,508
Aug-91	2,034	600	2,270	1,498	1,946
Sep-91	3,520	1,017	2,362	3,450	3,498

Table 5.39: DSM2 Input from CalSim-II: Contra Costa Water District Diversions (cfs)

Water Yr	Oct	Nov	Dec	Jan	Feb	Mar	Apr	May	Jun	Jul	Aug	Sep
1976	220	187	148	120	99	197	0	145	249	164	168	279
1977	241	66	49	115	162	197	180	241	249	324	273	279
1978	241	193	177	143	162	99	111	220	281	511	538	464
1979	413	183	172	120	103	200	0	220	474	329	356	264
1980	236	183	146	120	61	99	0	220	418	327	355	264
1981	236	188	146	120	103	99	0	220	430	332	356	264
1982	236	185	145	120	103	34	0	220	479	327	355	264
1983	233	185	145	120	103	99	0	220	410	329	356	279
1984	223	143	181	122	101	99	0	220	435	329	356	281
1985	224	183	145	120	103	99	0	220	434	330	356	264
1986	237	150	145	120	56	150	0	220	420	327	355	264
1987	234	183	145	120	103	99	0	220	437	329	338	264
1988	96	71	99	120	99	99	0	220	281	153	231	103
1989	213	183	145	120	103	99	111	220	481	511	538	264
1990	213	183	145	120	103	197	0	241	249	250	233	166
1991	184	193	177	143	162	197	180	241	249	324	273	279

Note: Values represent combined Old River at Rock Slough and Old River at Highway 4 diversions. CCWD diversions were identical for the base case and all climate change scenarios.

This space intentionally left blank.

5.12 Appendix B: Additional Chloride Exceedance Plots and Percentile Tables for Present Sea Level Scenarios

This appendix provides chloride exceedance plots and percentile tables computed from daily average DSM2 results at selected municipal and industrial intake locations.

- ❑ CCWD at Old River diversion at Highway 4 (Figure 5.17 and Table 5.40)
- ❑ SWP at Clifton Court Forebay (Figure 5.18 and Table 5.41)
- ❑ CVP at Tracy (Figure 5.19 and Table 5.42)

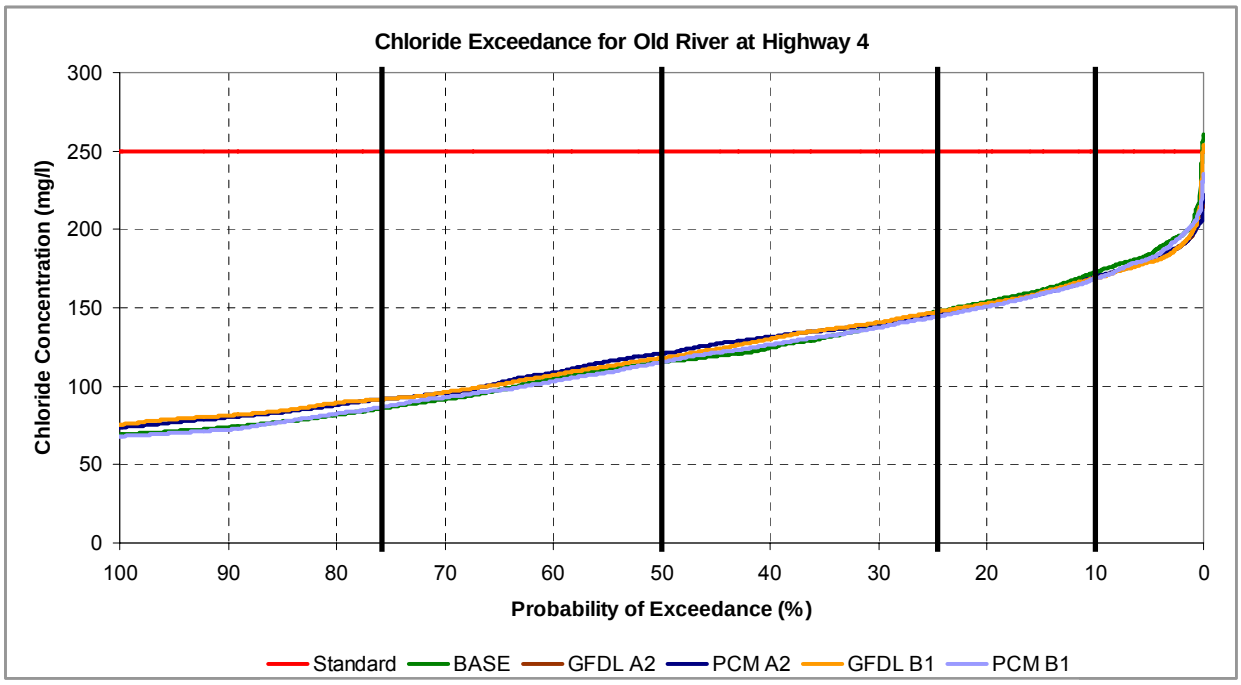


Figure 5.17: Probability of Exceedance for Chlorides at Old River at Highway 4

Table 5.40: Chloride Concentration Percentiles (mg/l) for Old River at Highway 4

	5%	10%	25%	50%	75%	90%	95%	Avg
BASE	11	21	33	69	133	170	183	85
GFDL A2	10	21	33	76	136	166	179	86
PCM A2	10	20	32	74	137	167	180	86
GFDL B1	14	22	35	75	137	167	179	87
PCM B1	10	20	31	68	133	166	181	83

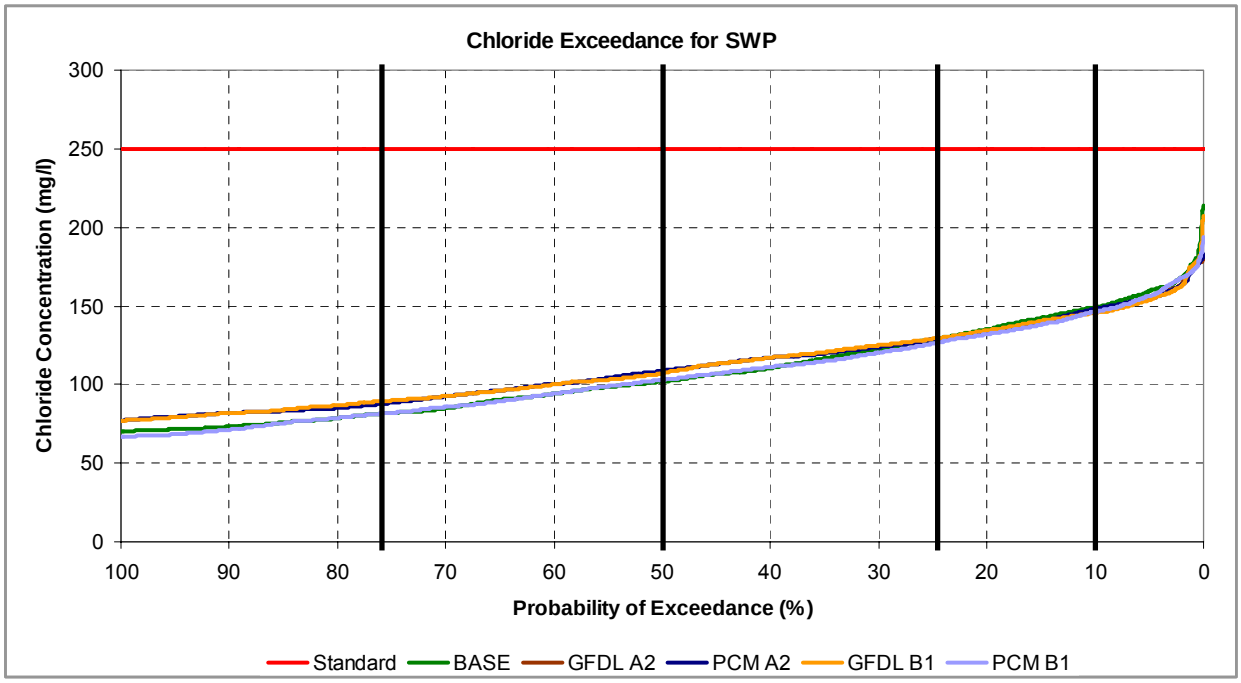


Figure 5.18: Probability of Exceedance for Chlorides at the State Water Project

Table 5.41: Chloride Concentration Percentiles (mg/l) for the State Water Project

	5%	10%	25%	50%	75%	90%	95%	Avg
BASE	10	22	34	70	119	148	158	78
GFDL A2	10	21	37	77	121	146	154	80
PCM A2	10	20	35	77	121	146	154	80
GFDL B1	10	25	39	77	122	145	153	81
PCM B1	10	19	33	67	116	145	156	76

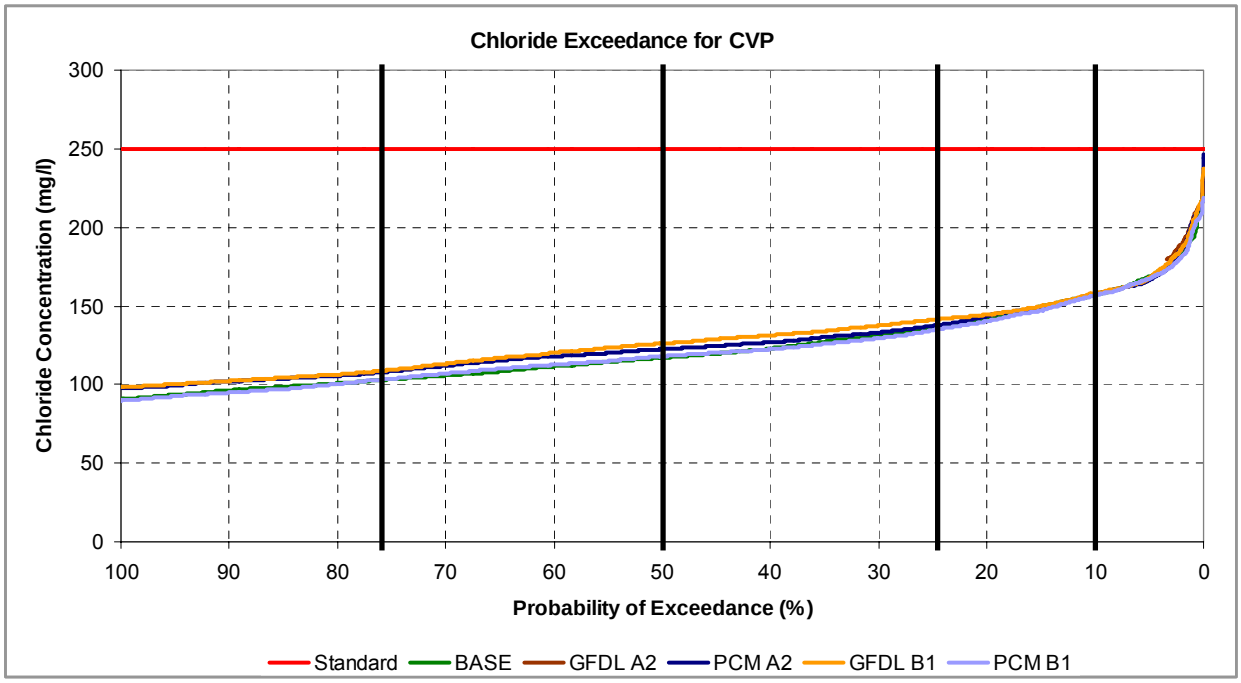


Figure 5.19: Probability of Exceedance for Chlorides at the Central Valley Project

Table 5.42: Chloride Concentration Percentiles (mg/l) for the Central Valley Project

	5%	10%	25%	50%	75%	90%	95%	Avg
BASE	10	16	53	91	129	155	168	91
GFDL A2	10	18	60	100	134	156	169	96
PCM A2	10	15	56	97	131	156	166	94
GFDL B1	11	26	60	99	135	156	167	97
PCM B1	10	15	54	90	127	155	167	90

5.13 Appendix D: Additional Chloride Exceedance Plots and Percentile Tables for One-Foot Sea Level Scenarios

This appendix provides chloride exceedance plots and percentile tables computed from daily average DSM2 results for one-foot sea level rise scenarios at selected municipal and industrial intake locations. No operations changes were made to try to reduce the effects of sea level rise.

- CCWD at Old River diversion at Highway 4 (Figure 5.20 and Table 5.43)
- SWP at Clifton Court Forebay (Figure 5.21 and Table 5.44)
- CVP at Tracy (Figure 5.22 and Table 5.45)

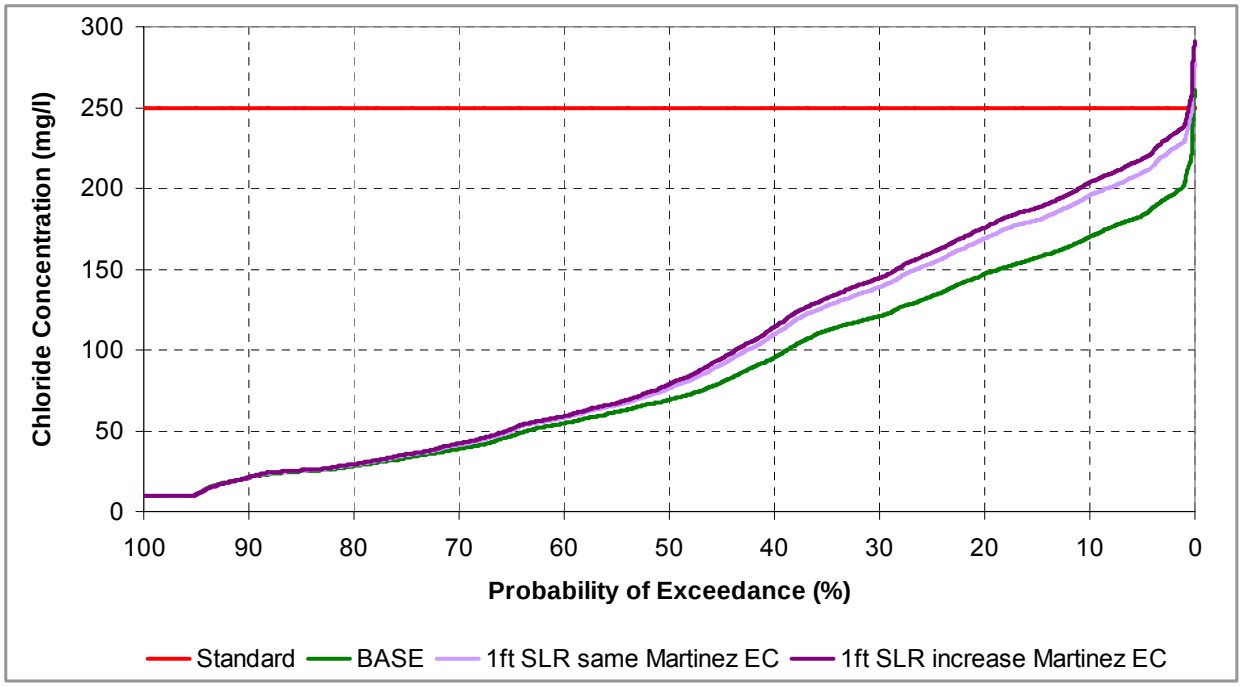


Figure 5.20: Probability of Exceedance for Chlorides at Old R. at Hwy 4 for a One-Foot Sea Level Rise and no Changes in System Operations

Table 5.43: Chloride Concentration Percentiles (mg/l) for Old R. at Hwy 4 for a One-Foot Sea Level Rise and no Changes in System Operations

	5%	10%	25%	50%	75%	90%	95%	Avg
BASE	11	21	33	69	133	170	183	85
1ft SLR same Martinez EC	11	21	35	76	154	196	210	96
1ft SLR increase Martinez EC	11	21	35	79	160	204	218	99

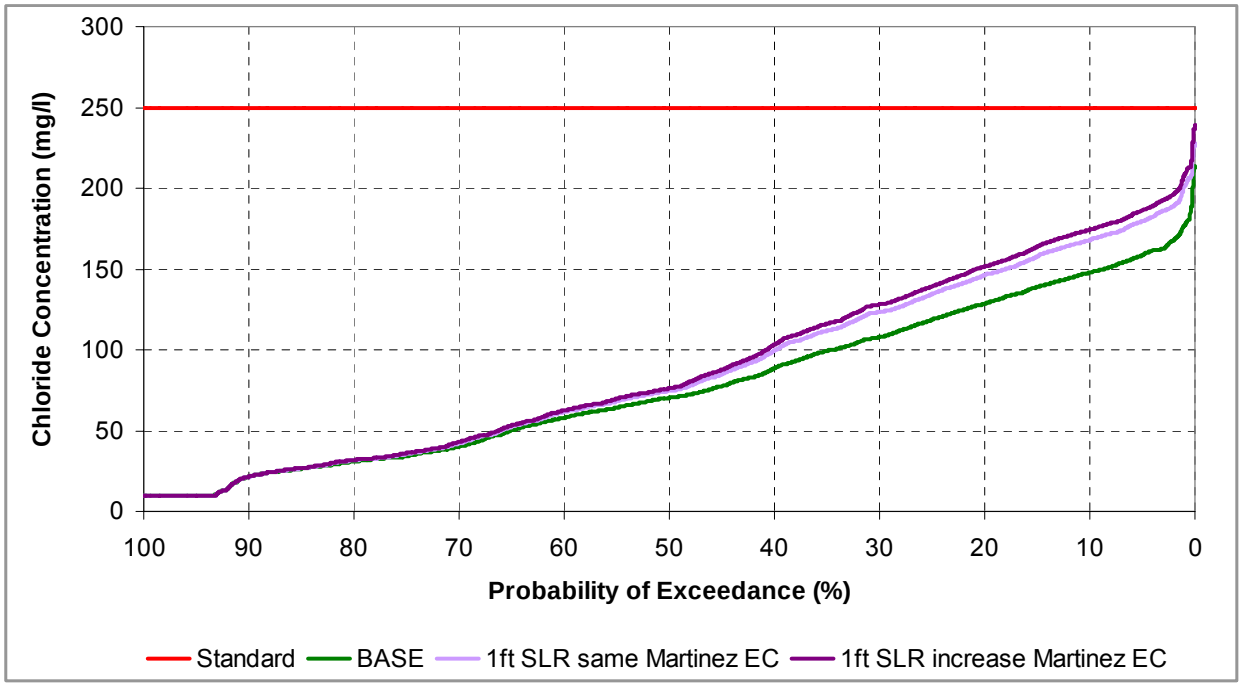


Figure 5.21: Probability of Exceedance for Chlorides at the State Water Project for a One-Foot Sea Level Rise and no Changes in System Operations

Table 5.44: Chloride Concentration Percentiles (mg/l) for the State Water Project for a One-Foot Sea Level Rise and no Changes in System Operations

	5%	10%	25%	50%	75%	90%	95%	Avg
BASE	10	22	34	70	119	148	158	78
1ft SLR same Martinez EC	10	21	36	75	135	168	180	87
1ft SLR increase Martinez EC	10	22	36	76	139	174	186	89

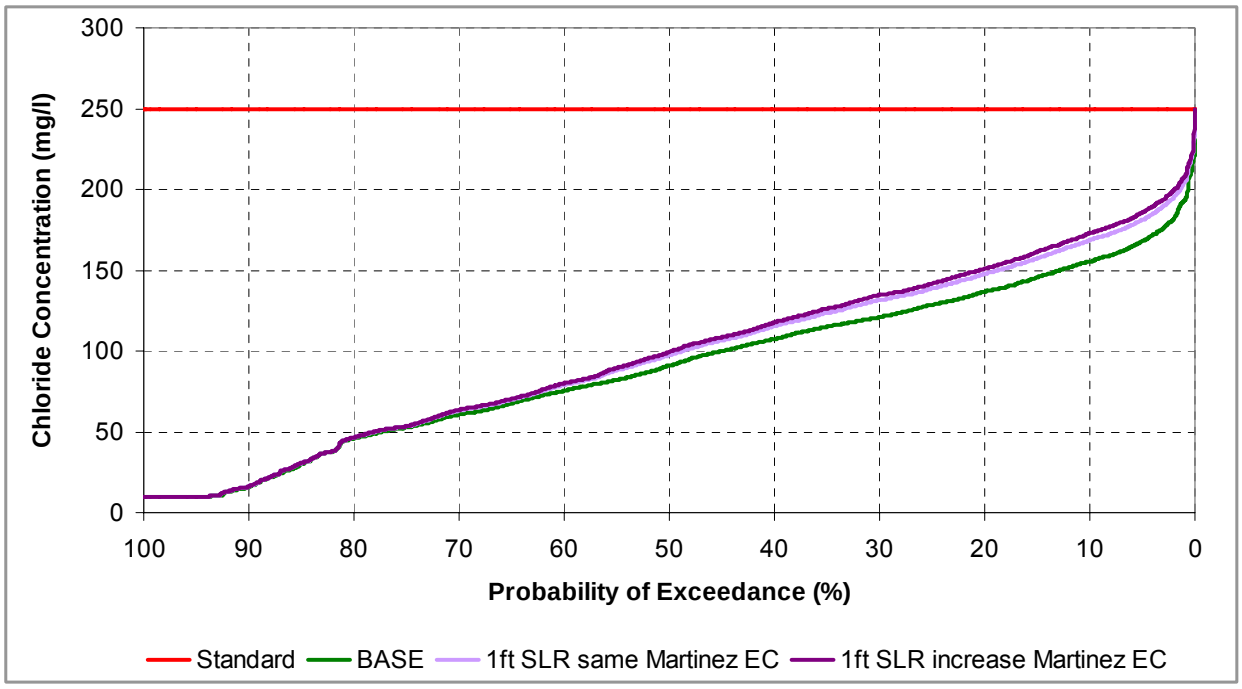


Figure 5.22: Probability of Exceedance for Chlorides at the Central Valley Project for a One-Foot Sea Level Rise and no Changes in System Operations

Table 5.45: Chloride Concentration Percentiles (mg/l) for the Central Valley Project for a One-Foot Sea Level Rise and no Changes in System Operations

	5%	10%	25%	50%	75%	90%	95%	Avg
BASE	10	16	53	91	129	155	168	91
1ft SLR same Martinez EC	10	16	53	97	139	169	181	97
1ft SLR increase Martinez EC	10	16	53	99	142	173	186	98

5.14 Appendix E: Additional Chloride Exceedance Plots and Percentile Tables for Combined Climate Change and One-Foot Sea Level Scenarios

This appendix provides chloride exceedance plots and percentile tables computed from daily average DSM2 results for combined climate change and one-foot sea level rise scenarios at selected municipal and industrial intake locations. No changes in operations were made to account for sea level rise (SLR).

- CCWD at Old River diversion at Highway 4 (Figure 5.23 and Table 5.46)
- SWP at Clifton Court Forebay (Figure 5.24 and Table 5.47)
- CVP at Tracy (Figure 5.25 and Table 5.48)

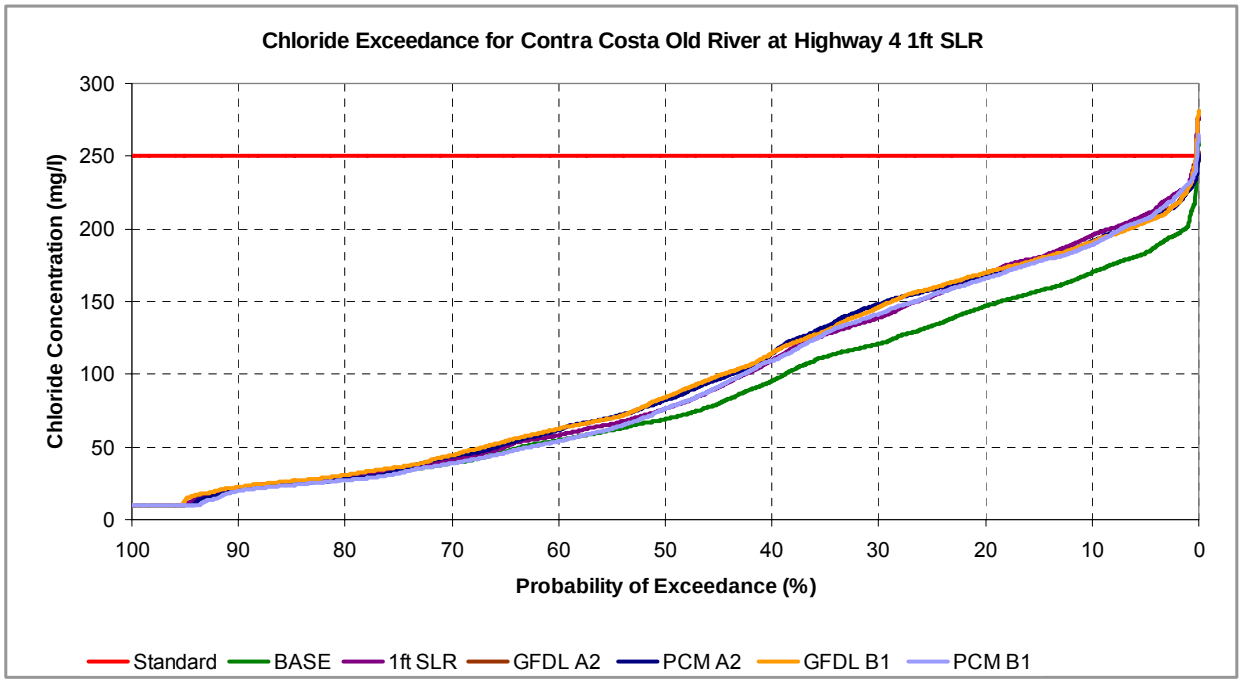


Figure 5.23: Probability of Exceedance for Chlorides at Old River at Highway 4 for Climate Change and a One-Foot Sea Level Rise and no Changes in Operations for SLR

Table 5.46: Chloride Concentration Percentiles (mg/l) for Old R. at Highway 4 for Climate Change and a One-Foot Sea Level Rise and no Changes in Operations for SLR

	5%	10%	25%	50%	75%	90%	95%	Avg
BASE	11	21	33	69	133	170	183	85
1ft SLR same Mtz EC	11	21	35	76	154	196	210	96
GFDL A2 1ft SLR	10	21	35	85	158	191	205	97
PCM A2 1ft SLR	10	21	35	82	158	191	206	97
GFDL B1 1ft SLR	13	22	36	84	159	191	205	98
PCM B1 1ft SLR	10	20	32	76	154	189	207	94

*All sea level rise scenarios in this table assume that Martinez EC is the same as in the present sea level scenarios.

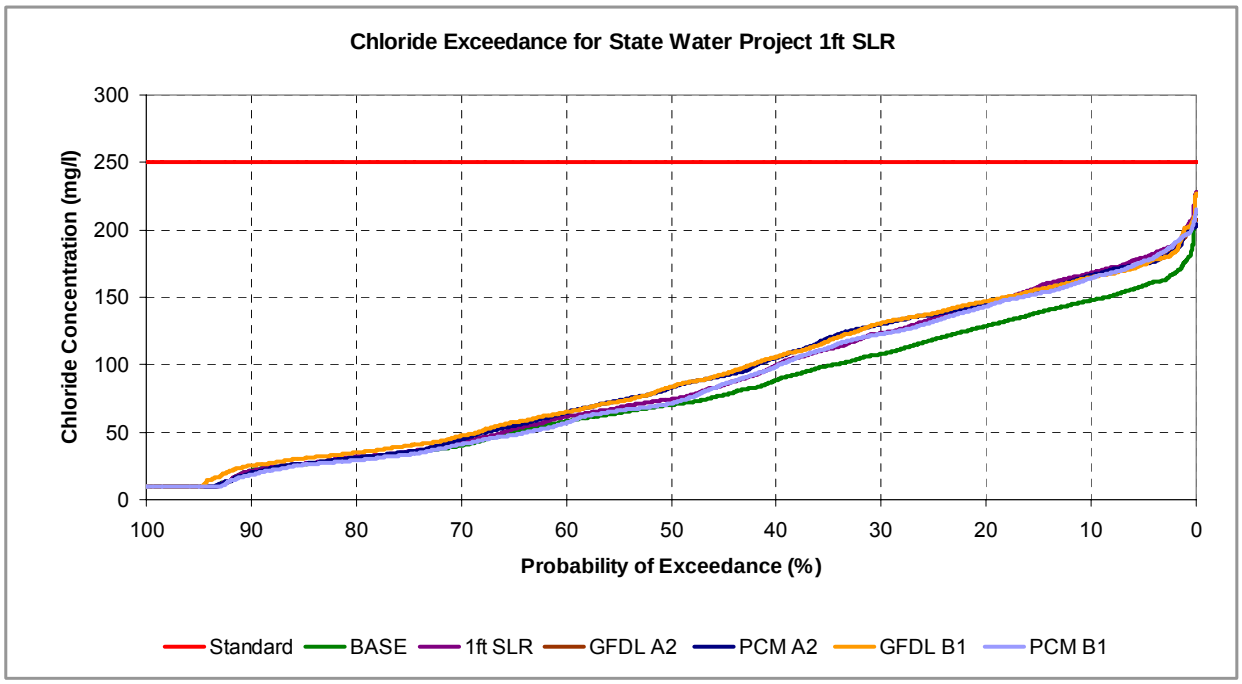


Figure 5.24: Probability of Exceedance for Chlorides at the State Water Project for Climate Change and a One-Foot Sea Level Rise and no Changes in Operations for SLR

Table 5.47: Chloride Concentration Percentiles (mg/l) for the State Water Project for Climate Change and a One-Foot Sea Level Rise and no Changes in Operations for SLR

	5%	10%	25%	50%	75%	90%	95%	Avg
BASE	10	22	34	70	119	148	158	78
1ft SLR same Mtz EC	10	21	36	75	135	168	180	87
GFDL A2 1ft SLR	10	22	38	83	138	166	175	89
PCM A2 1ft SLR	10	20	35	83	137	166	175	89
GFDL B1 1ft SLR	10	25	40	84	138	165	174	90
PCM B1 1ft SLR	10	18	33	71	132	164	177	85

*All sea level rise scenarios in this table assume that Martinez EC is the same as in the present sea level scenarios.

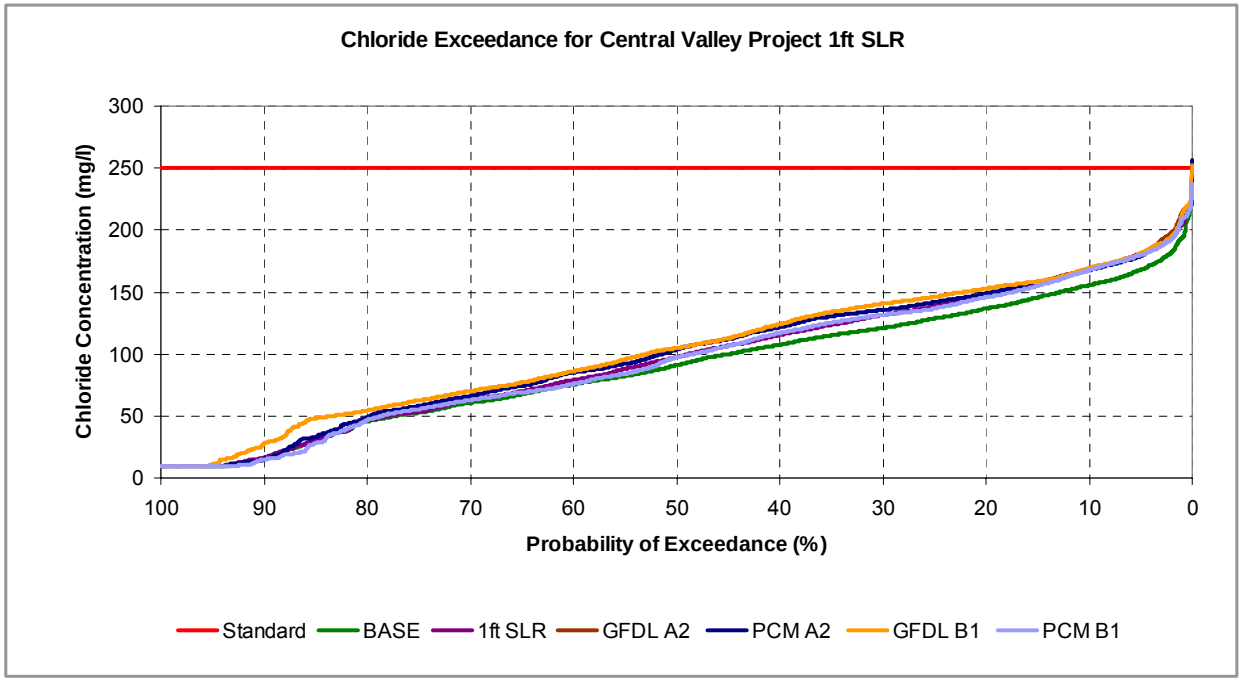


Figure 5.25: Probability of Exceedance for Chlorides at the Central Valley Project for Climate Change and a One-Foot Sea Level Rise and no Changes in Operations for SLR

Table 5.48: Chloride Concentration Percentiles (mg/l) for the Central Valley Project for Climate Change and a One-Foot Sea Level Rise and no Changes in Operations for SLR

	5%	10%	25%	50%	75%	90%	95%	Avg
BASE	10	16	53	91	129	155	168	91
1ft SLR same Mtz EC	10	16	53	97	139	169	181	97
GFDL A2 1ft SLR	10	18	63	105	145	170	182	103
PCM A2 1ft SLR	10	15	58	104	142	168	179	100
GFDL B1 1ft SLR	11	28	63	105	146	169	181	103
PCM B1 1ft SLR	10	15	55	97	137	167	180	96

*All sea level rise scenarios in this table assume that Martinez EC is the same as in the present sea level scenarios.

Progress on Incorporating Climate Change into Management of California's Water Resources

1st Progress Report
July 2006

Chapter 6:
Climate Change Impacts on Flood Management

Author:

Michael Anderson, Ph.D.
California Department of Water Resources, Division of Flood Management, Hydrology Branch, Sacramento.

Contributors:

Norman Miller, Ph.D., Lawrence Berkeley National Lab

Jim Goodridge, Brian Heiland, P.E., John King, P.E., Boone Lek, P.E., Steve Nemeth, P.E., Tawnly Pranger, P.E., Maurice Roos, P.E., Matt Winston
California Department of Water Resources, Division of Flood Management, Hydrology Branch, Sacramento.

Peer Reviewers:

David Goldman, Ph.D., P.E., U.S. Army Corp of Engineers Cold Regions Lab

Philip Mote, Ph.D., University of Washington

6 Climate Change Impacts on Flood Management

6.1 Introduction

Changing climate can have a significant impact on the timing and magnitude of precipitation and runoff in California. Climate is the time-averaged state of temperature, winds, precipitation and runoff. Flooding, however, results from individual weather events which can be considered random phenomena on the time scale of climate (e.g. 30 to 50 years). From year to year, there is a large amount of variability in winter rainfall and associated runoff patterns. This large variability creates uncertainty when evaluating changes in weather events due to climate change.

One way to address this uncertainty is to look at long-term precipitation, temperature, and runoff records in California and identify any trends that may have occurred over the past century. Future change can then be inferred from trends identified in the past record. However, a straight extrapolation of historical trends into the future may not be accurate.

Climate modeling tries to simulate these nonlinear components and their evolution with changing greenhouse gas levels in the atmosphere. Results from these global-scale simulations have been downscaled to provide information on potential changes over California. However, the model results provided relate to climate properties, not weather properties. Because of this, the results cannot be used directly to evaluate changes in specific rainfall and runoff patterns leading to floods or to changes in frequency of floods or droughts.

The climate model simulation data can be used to compare simulated future trends in precipitation, temperature, and runoff to historical trends. The model-derived trends also can be used to guide extrapolation of historical trends. Based on these efforts and using some assumptions, changes in runoff to a given rainfall pattern can be estimated using watershed models.

Such analyses are just the start of work that needs to be completed to evaluate climate change impacts on precipitation and the associated water supply or flood runoff in California. This chapter presents the initial work that has been done and outlines future work and data needed to complete such work. The topics covered in this chapter are illustrated in Figure 6-1. This chapter starts with a literature review of work on climate change and runoff in California. The chapter then examines the historical record for existing trends and investigates the information that can be obtained from the climate change scenarios selected for study by the state's Climate Action Team. After discussing the elements of the climate change scenario data that are not suitable for flood analysis, the chapter concludes with a description of climate change scenario data that would be suitable for analyzing climate change impacts on flood frequency and outlines future work directions. It is important to note that the work presented here is an analysis of past and potential future changes to California hydrology. It is not a recommendation for making changes to existing flood risk, flood frequency, or water supply practices and analyses.

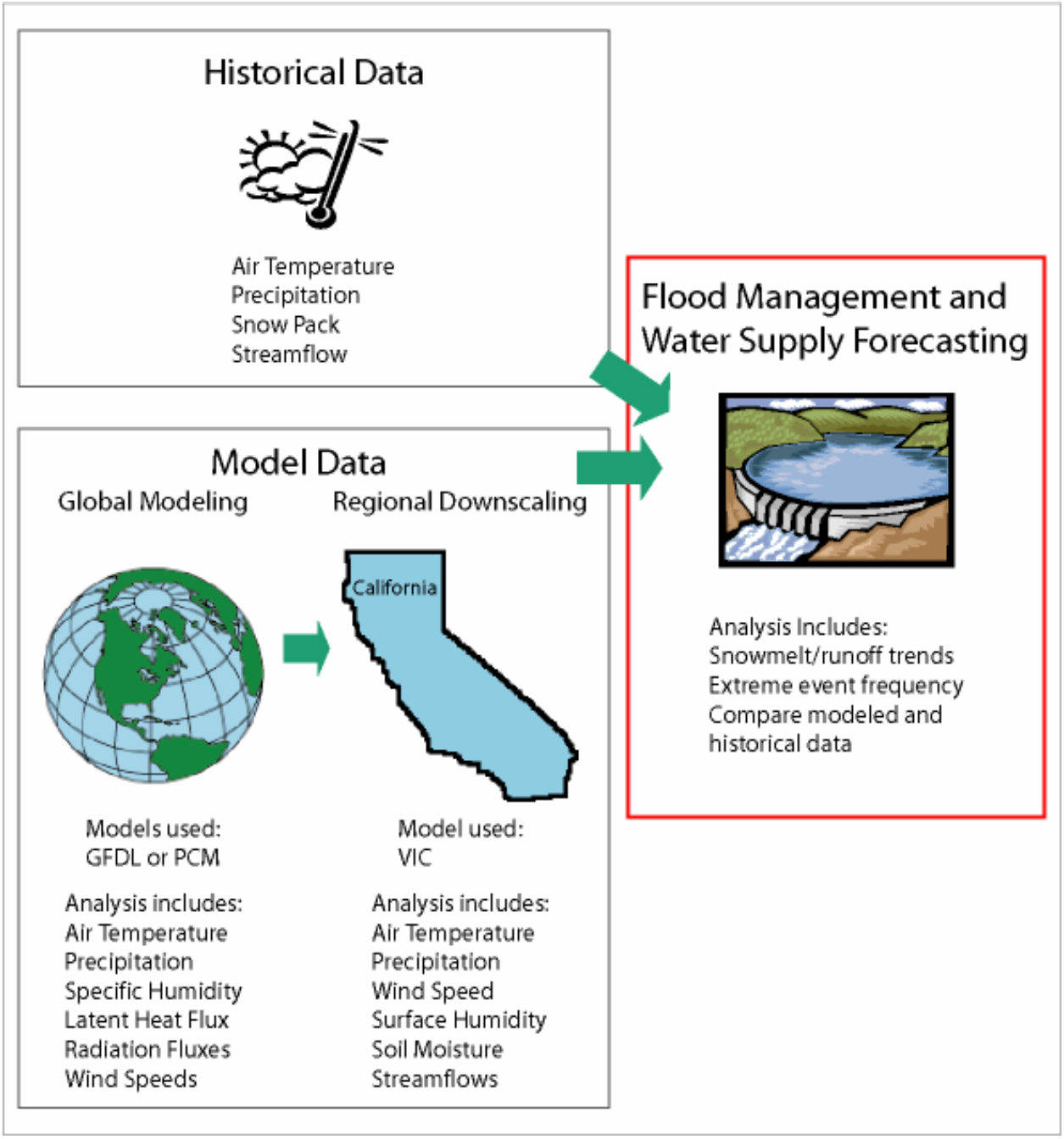


Figure 6-1 Relation of climate change scenario simulations to flood analysis

6.2 Literature Review of Flood Analysis and Climate Change

In 1988, the United Nations Environmental Programme and the World Meteorological Organization established the Intergovernmental Panel on Climate Change (IPCC). It released the First Assessment Report in 1990, the Second Assessment Report in 1995, and the Third Assessment Report in 2001 (IPCC FAR 1990, SAR 1995, TAR 2001). Beginning in 2000, the U.S. Global Climate Change Research Program (USGCRP) has released a series of regional and

sectorial assessment reports. The IPCC TAR and USGCRP Report of the Water Sector (USGCRP Water 2001) provide up-to-date summaries of the potential consequences of global warming.

The IPCC reports that climate model projections with a transient 1 percent annual increase in greenhouse gas emissions show an increase in the global mean near-surface air temperature of 1.4 to 5.8 ^{o}C, with a 95 percent probability interval of 1.7 to 4.9 ^{o}C by 2100 (Wigley and Roper 2001). Both reports indicate that likely changes during the 21st century include: higher maximum and minimum temperatures with a decreasing diurnal range over U.S. land areas, more intense precipitation events, increased summer continental drying, and increased risk of drought. Climate model projections of precipitation amounts remains uncertain, however, the rain to snow ratio, at least in the Sierra Nevada appears to be increasing under the climate change scenarios discussed in the USGCRP Water Sector Report (USGCRP Water 2001).

Further research has been done to investigate the potential impacts of climate change on California hydrology using climate model projections and land surface-hydrology models. Table 6-1 lists the references grouped by the type of study conducted. As can be seen from Table 6-1, there are three main types of studies that have been conducted: regression studies, computer model simulation of watersheds using GCM data directly, and computer model simulation of watersheds using climate change data that has been downscaled. Downscaling means inferring finer detail data from the GCM results. This process is based on statistical properties of a region or through the use of a finer-grid scale dynamic model of the atmosphere and land surface.

Table 6-1Climate Change Studies and Runoff in California

STUDY TYPE	REFERENCES
Regression	Revelle and Waggoner (1983) Stewart et al. (2004)
GCM	Gleick (1987) Lettenmaier and Gan (1990) Dettinger et al. (2004)
GCM with Downscaling	Miller et al. (1999) Knowles and Cayan (2001) Wilby and Dettinger (2000) Miller (2003) Wood et al. (2004) Van Rheenen et al. (2004) Christensen et al. (2004) Kim (2005) Maurer and Duffy (2005)
Other	Jeton et al. (1996) Bardini et al. (2001) Knowles and Cayan (2004)

Also noted in Table 6-1 are studies that do not fit into the above three categories. These studies include watershed studies with set incremental changes to temperature and precipitation (Jeton et al., 1996), an analysis of the changes to the Sacramento and San Joaquin River Delta associated with runoff changes in the upper watersheds (Knowles and Cayan, 2004), and an assessment of climate change data and known impacts to date combined with an assessment of mitigation measures for DWR (Bardini et al., 2001).

The consensus of the above-cited studies is that climate change will impact the timing and magnitude of runoff and flooding patterns in California. Expected impacts include more precipitation falling as rain rather than snow and an earlier melt to the winter snowpack. The uncertainty lies in the magnitude of these changes and any changes associated with the frequency and magnitude of future floods and droughts. The following sections investigate historical changes to precipitation, temperature, and runoff as well as potential changes identified by the latest climate change simulations and their associated consequences.

6.3 Historical Precipitation, Temperature, and Runoff Trends

Former state climatologist James Goodridge compiled an extensive collection of long-term precipitation and temperature data across the state. These data sets have been used to identify precipitation and temperature trends that have occurred in the last 100 years. Long-term runoff records in selected watersheds were also examined for trends. Results are presented below. In order to determine if the identified trends were statistically significant, a t-test with an alpha value of 0.05 was used.

6.3.1 Precipitation

Figure 6-2 shows the statewide average of annual precipitation from 102 stations across California from 1890 to 2002. The average annual precipitation for California of 23.8 inches has not changed significantly over the past century. In an effort to determine if there has been a change in precipitation distribution over the state, the precipitation records were sorted by latitude placed into three categories: south, central, and north. The division between south and central is 35 degrees north latitude and the division between central and north is 39 degrees north latitude.

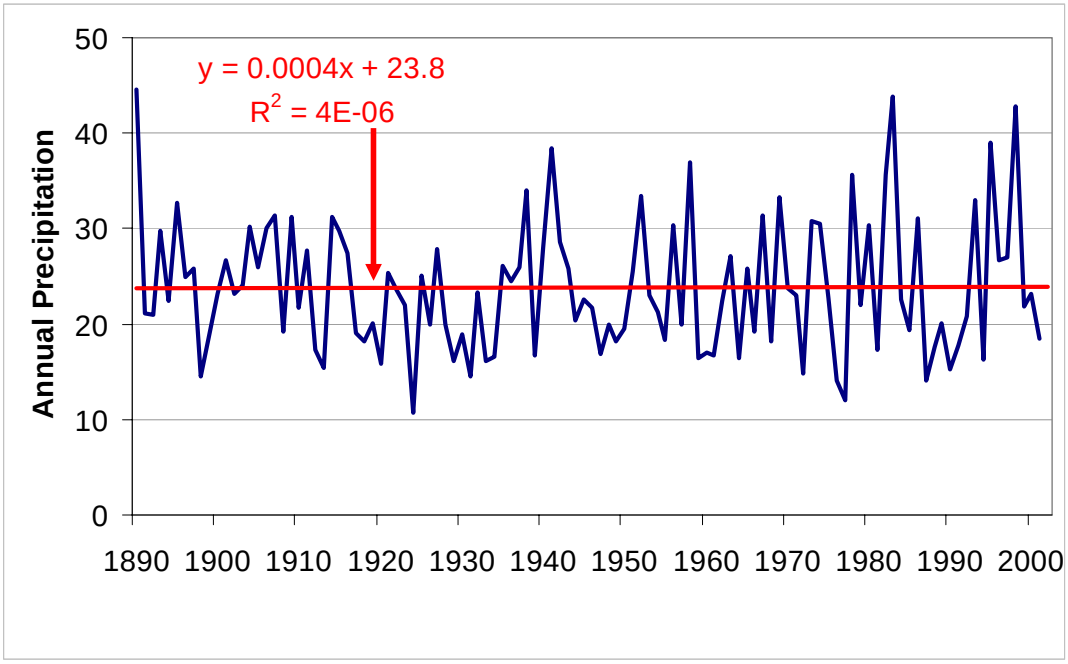


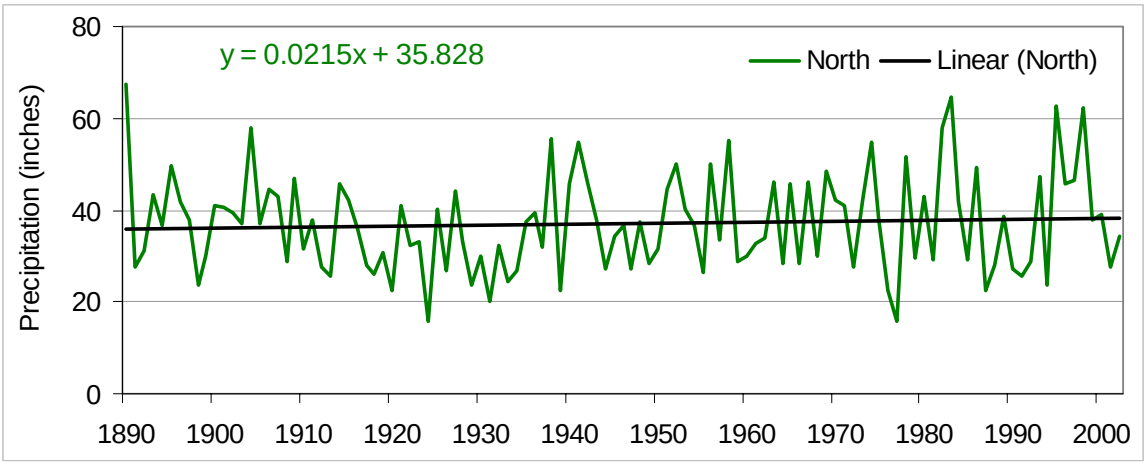
Figure 6-2 Average annual precipitation for California 1890-2002 with trend line.

Average annual precipitation is plotted with trend lines in Figure 6-3 for the south, central, and north regions for 1890-2002. The south and central regions both show a minor decreasing trend in precipitation while the north part of the state shows a minor increase. The trends do not yield a significant change in the average precipitation over the course of the century. But if focus is shifted to the last 30 years, an increasing trend can be found for all three regions as is shown in Figure 6-4. This may be an artifact of the big El Nino seasons of 1983 and 1998. Using the t-test, only the trends for central and northern California were determined to be statistically significant.

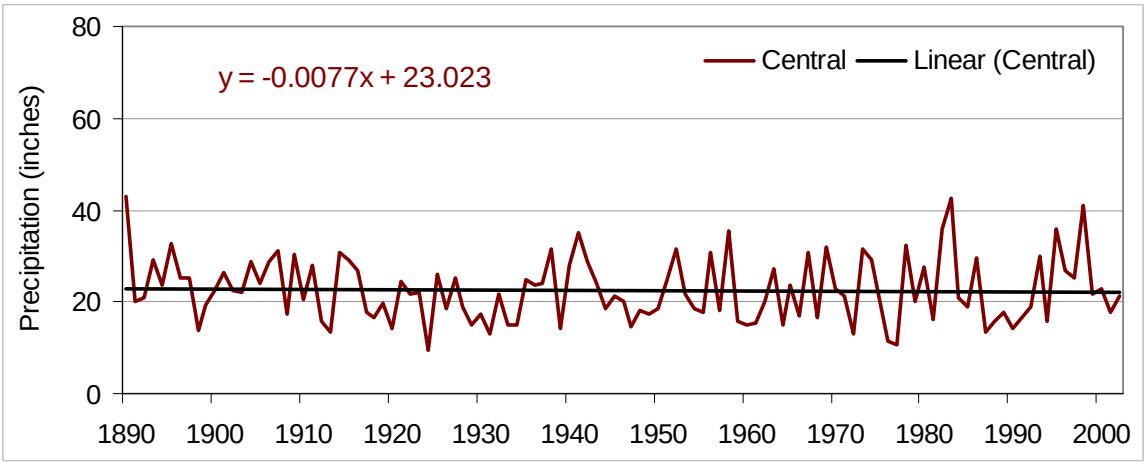
Figure 6-4 depicts annual precipitation for the three regions and a fit linear trend for the past 30 years. This increasing trend over the past 30 years is consistent with the research presented in Chapter 2 which points to increasing precipitation over the state. But it does contradict data presented in Bardini and others (2001). Their data pointed to potential decreasing precipitation. The differences can likely be related to the difference in the period selected to identify the trend. Extremes at the beginning or end of the time series can significantly impact the magnitude of the identified trend.

While the average precipitation has little or no trend over the past century, the variability has a distinct and statistically significant increase, which can be seen in Figure 6-5. Figure 6-5 depicts the coefficient of variation (standard deviation divided by the mean) based on a 10-year moving average of mean and standard deviation values of the annual precipitation time series. There is a distinct upward trend in the variability over the past century with end of period values about 75 percent larger than beginning- of-period values. This increase in variability is much larger than any of the linear trends identified in the average values of the data. There is some evidence from scattered precipitation measurements from 1850 to 1900 that the 19th century was more variable than the 20th.

a) Northern Region: California-Oregon border to 39º latitude



b) Central Region: 35 º - 39º latitude



c) Southern Region: 35 º latitude to California-Mexico border

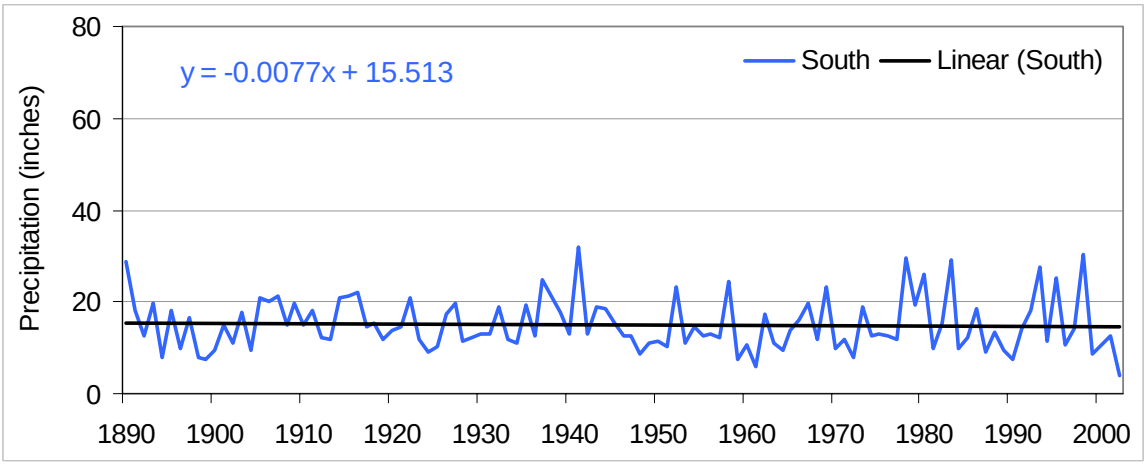


Figure 6-3 Annual average precipitation with trends by region

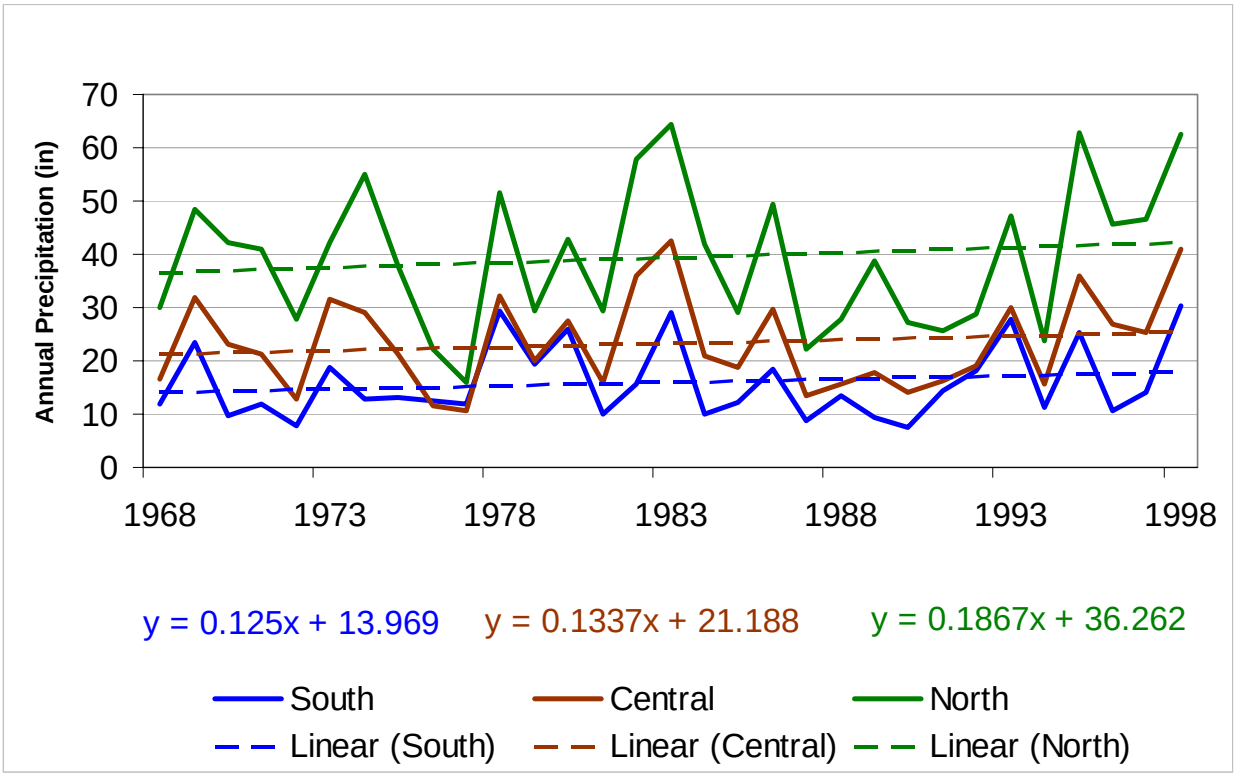


Figure 6-4 Linear trends of annual precipitation for the past 30 years

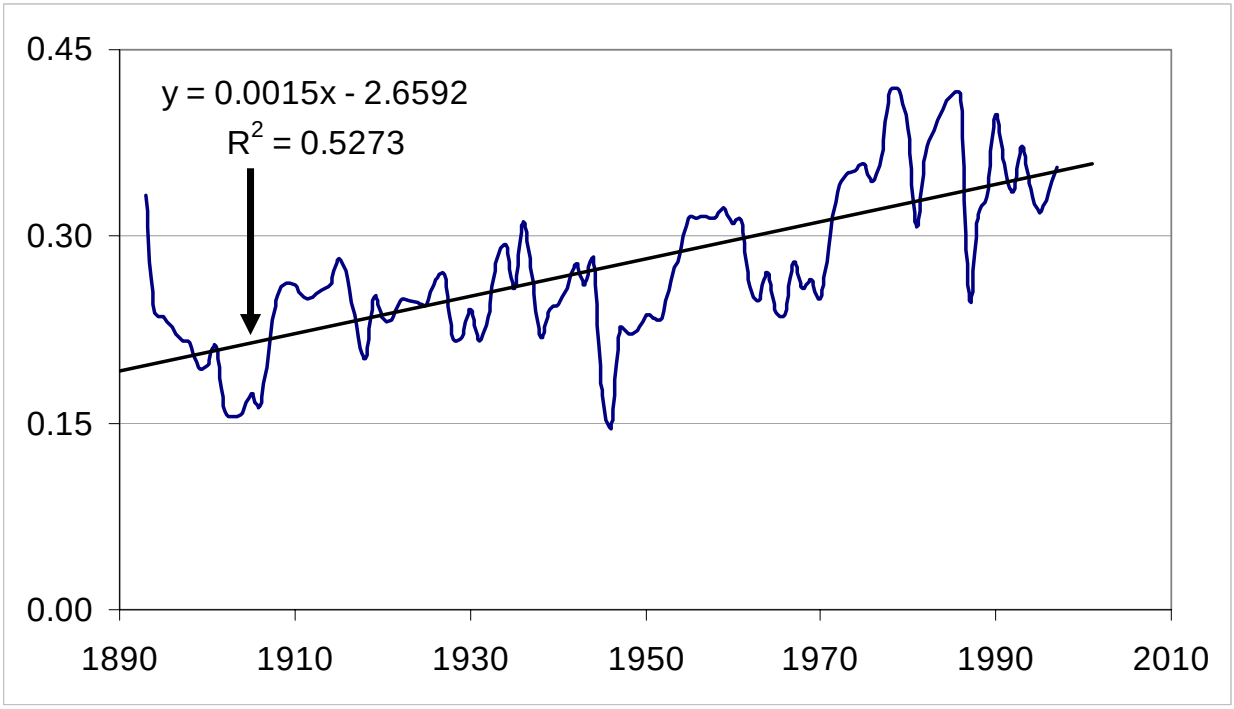


Figure 6-5 Coefficient of variation for statewide average precipitation with trend line

6.3.2 Temperature

In California, increases in atmospheric temperature have already been observed over the past 100 years. Using 226 temperature stations with data record lengths on the order of 100 years, the following trends were identified. The annual maximum, average, and minimum temperatures for California are shown in Figure 6-6. All three time series show a statistically significant increasing trend of about 2 degrees Fahrenheit per century. The minimum temperatures show the largest trend while the maximum temperatures show the smallest.

In terms of variability, Figure 6-7 depicts the trends in the variability of annual maximum, average, and minimum temperatures averaged over the state. For the maximum and average temperatures, there is not a statistically significant trend. For the minimum temperatures, there is a statistically significant decreasing trend in the variability. This, along with the identified trend in state average minimum temperatures indicate that the lower bound of temperature in the state is moving upward and that this upward trend is damping out the variability of the minimum temperature. As a consequence, on average, there may be fewer cold extreme temperature days in the future as a result of global warming. This result is coincident with other studies (see for example Easterling et al, 2000.)

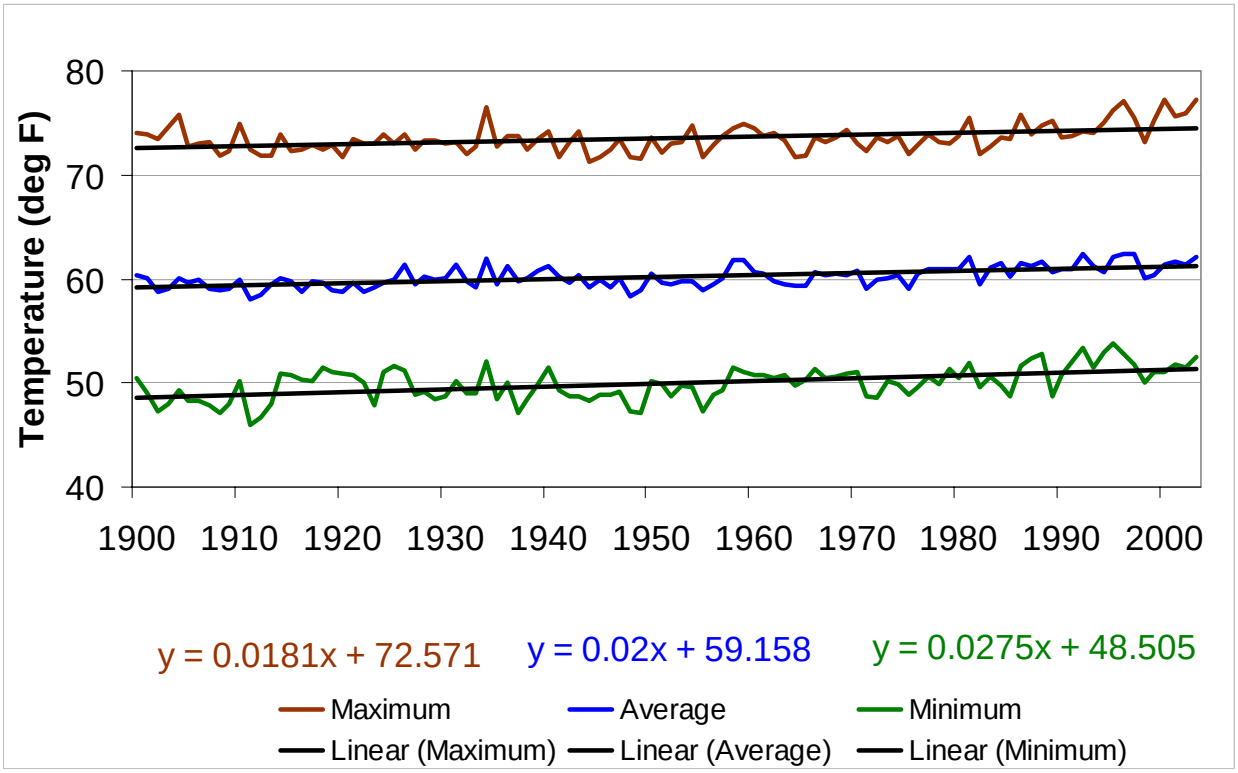
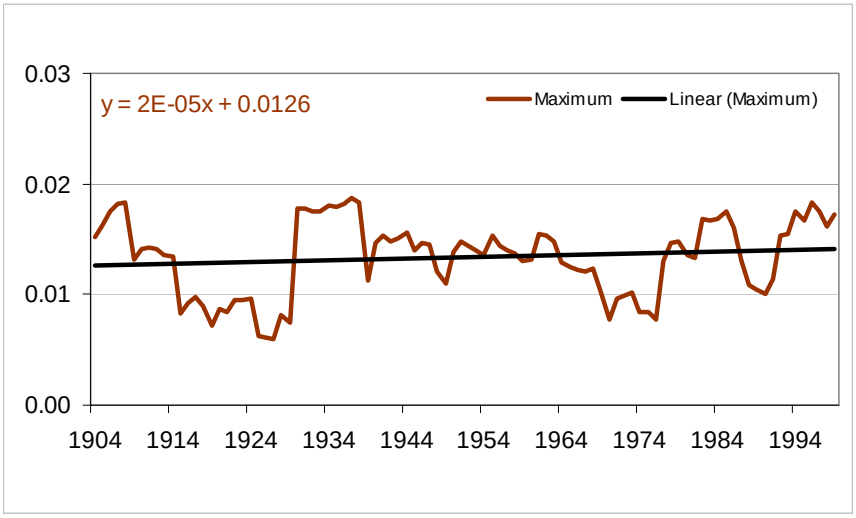
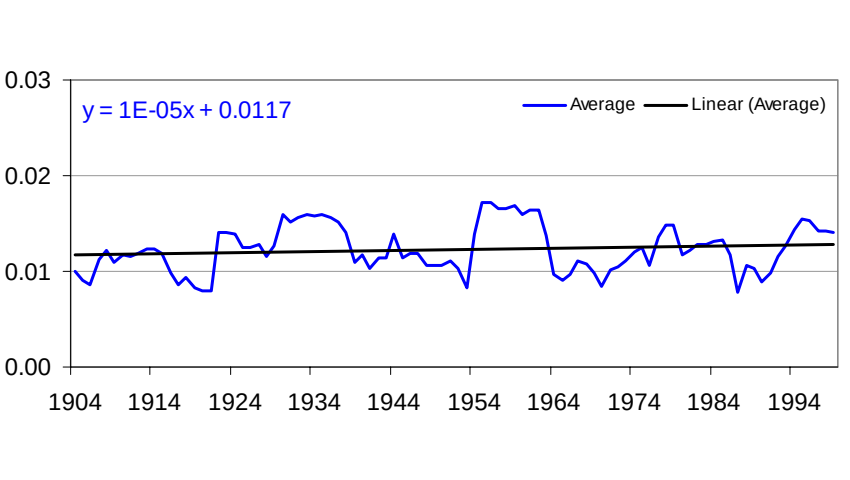


Figure 6-6 State average maximum, average, and minimum temperature time series

a) Coefficient of Variation over time for maximum temperature



b) Coefficient of Variation over time for average temperature



c) Coefficient of Variation over time for minimum temperature

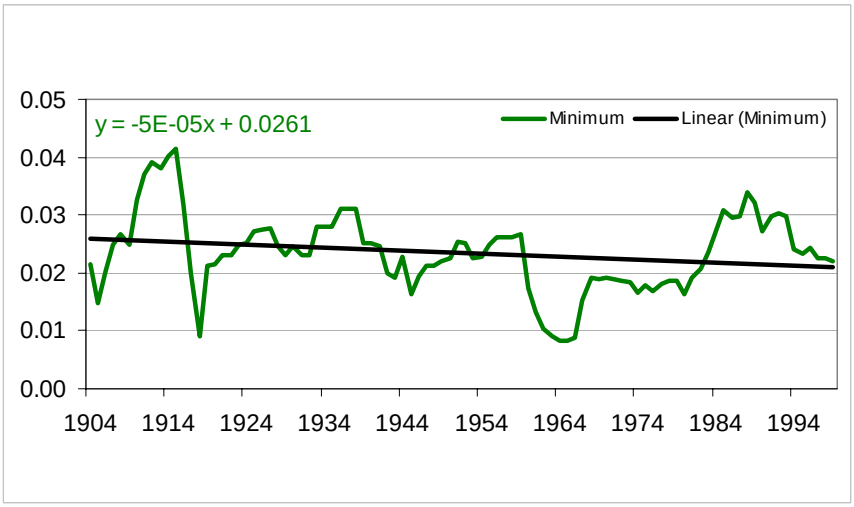


Figure 6-7 Variability of annual maximum, average and minimum temperature

Other state temperature trends can be identified. Figure 6-8 shows the change in trend of average temperature identified over the past 100 years versus latitude in 2.5 degree increments. The magnitude of the temperature trend decreases with latitude from over 3 degrees Fahrenheit per century in the south part of the state to less than a degree Fahrenheit in the northernmost part of the state.

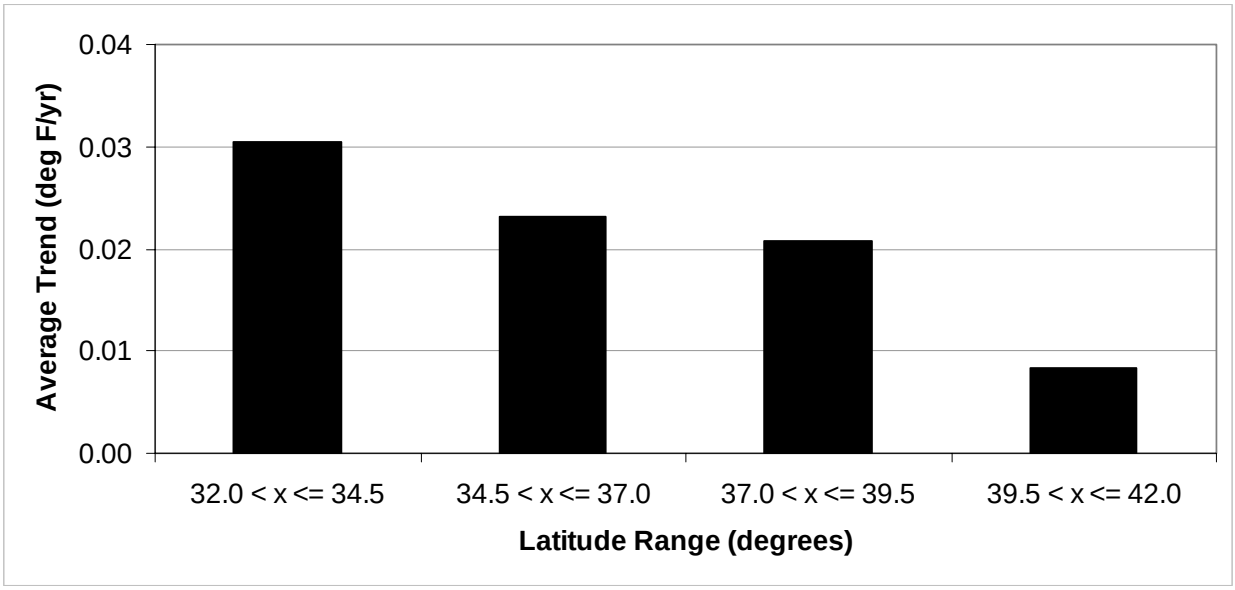


Figure 6-8 Temperature trend variation with latitude

Former state climatologist James Goodridge found a difference in temperature trend with population as seen in Figure 6-9. The lowest trend line is associated with a rural county with a population of less than 100,000 people while the topmost trend line is associated with a highly urbanized county with a population greater than 1 million. As noted in the figure, these trends are based on 65 stations sorted by county population. Note that all three lines show an increasing trend in temperature indicating that temperatures have been increasing even in rural areas. In addition, in urban areas, temperature increases are accentuated indicating that future temperature increases will be even greater in urban areas.

Peterson (2003) of the National Climatic Data Center offers a different point of view. He conducted a study that rigorously removed elevation, equipment, and location variations from temperature records at urban and rural sites. His work indicates that there is no urban heating effect. This is an area of ongoing research and debate among scientists.

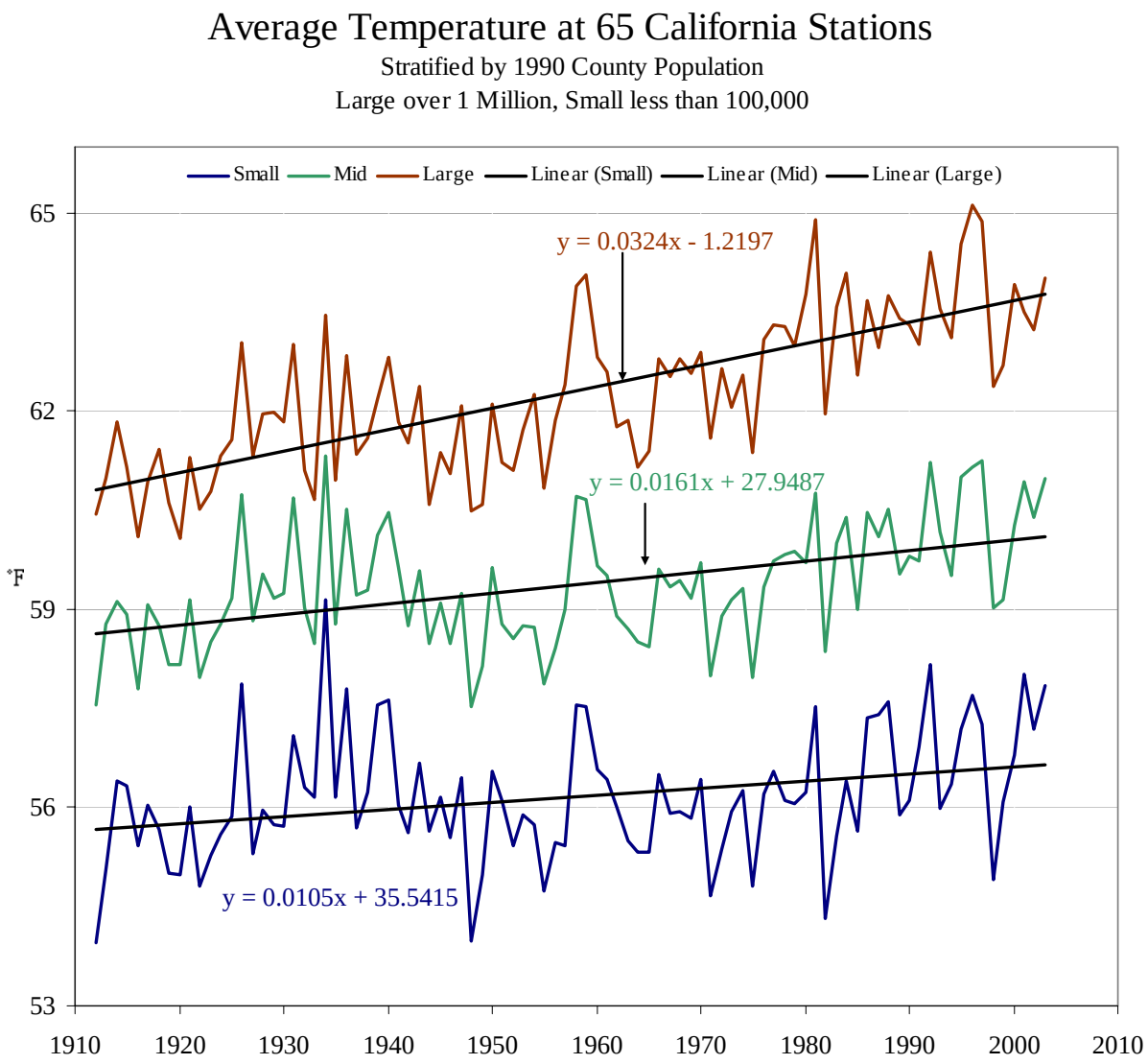


Figure 6-9 Temperature trends by county population in California.

6.3.3 Runoff

Runoff trends can be divided into two categories. The first is trends in annual-water-year-runoff volumes. The second is trends associated with peak runoff for different return periods. Both trends are investigated here.

6.3.3.1 Annual Runoff

Annual water year (October 1 to September 30) unimpaired runoff time series were computed for 24 rivers across the state whose locations are shown in Figure 6-10. The time frame for most basins runs from 1905 to 2005. Total period and split period statistics were generated for each basin. The dividing year for the split period statistics is 1955 which is approximately halfway through the observed record.

Table 6-2 lists the total period, pre-1955 period and post-1955 period average annual runoff in thousand acre-feet for the 25 basins. Table 6-2 also includes the percent change from pre-1955 to post 1955. The sum of all 25 basins shows a 9 percent increase in average annual runoff from 1905-1955 to 1956-2005. In general, the northern rivers show a larger increase in average annual runoff than the southern rivers.

Table 6-2 Average Annual Water Year Runoff for Selected California Watersheds

Station	Total Period (taf)	Pre 1955 (taf)	Post 1955 (taf)	% Change
Klamath Copco to Orleans	4,646	4,144	4,916	19%
Salmon River at Somes Bar	1,288	1,212	1,338	10%
Eel River at Scotia	5,493	4,921	6,007	22%
Russian near Healdsburg	897	817	921	13%
Napa River at St. Helena	72	60	76	27%
Sacramento River at Bend Bridge	8,476	8,052	8,901	11%
Feather River at Oroville	4,490	4,360	4,621	6%
Yuba River at Smartville	2,372	2,375	2,369	0%
American River at Folsom Reservoir	2,739	2,759	2,717	-2%
East Carson and West Walker Rivers	433	396	459	16%
Truckee River at Farad	402	395	408	3%
Cosumnes River at Michigan Bar	369	348	389	12%
Mokelumne River at Pardee Reservoir	758	762	753	-1%
Stanislaus River at New Melones Reservoir	1,175	1,178	1,171	-1%
Tuolumne River at New Don Pedro Reservoir	1,911	1,875	1,951	4%
Merced River at Exchequer Reservoir	997	988	1,008	2%
San Joaquin River at Millerton Reservoir	1,816	1,798	1,835	2%
Kings River at Pine Flat Reservoir	1,683	1,650	1,720	4%
Kaweah River at Terminus Reservoir	432	412	454	10%
Tule River at Lake Success	145	139	148	6%
Kern River at Lake Isabella	697	633	730	15%
Arroyo Seco nr Soledad	122	120	124	3%
Nacimiento River below Nacimiento Dam	200	183	213	16%
Arroyo Seco nr Pasadena	7	6	8	26%
Total	41,620	39,582	43,239	9%



Figure 6-10 Map of Runoff Forecast Points

In addition to the individual basin runoff, runoff of four major rivers is used to compute the Sacramento and San Joaquin River Indices. The index values not only look at current year runoff, but incorporate a term for last year's conditions as well. Figure 6-11 shows the time series plot and linear trend fit for the Sacramento River Index and Figure 6-12 shows the time series plot and linear trend fit for the San Joaquin River Index. From these figures it can be seen that there is a slight decreasing trend in the San Joaquin Index and a slight increasing trend in the Sacramento River Index. These results are consistent with the precipitation trend results over the past century described earlier. However, neither trend was identified as being statistically significant.

In terms of runoff variability, the coefficient of variation is plotted for the Sacramento and San Joaquin River Indices in Figure 6-13. Both time series show an increase with the linear trend fit, but only the Sacramento trend is statistically significant. In fact, the variability increases markedly in both series from the 1970s through the mid-1990s. Since 1995, both series' variability has dropped back to values consistent with the beginning of the period.

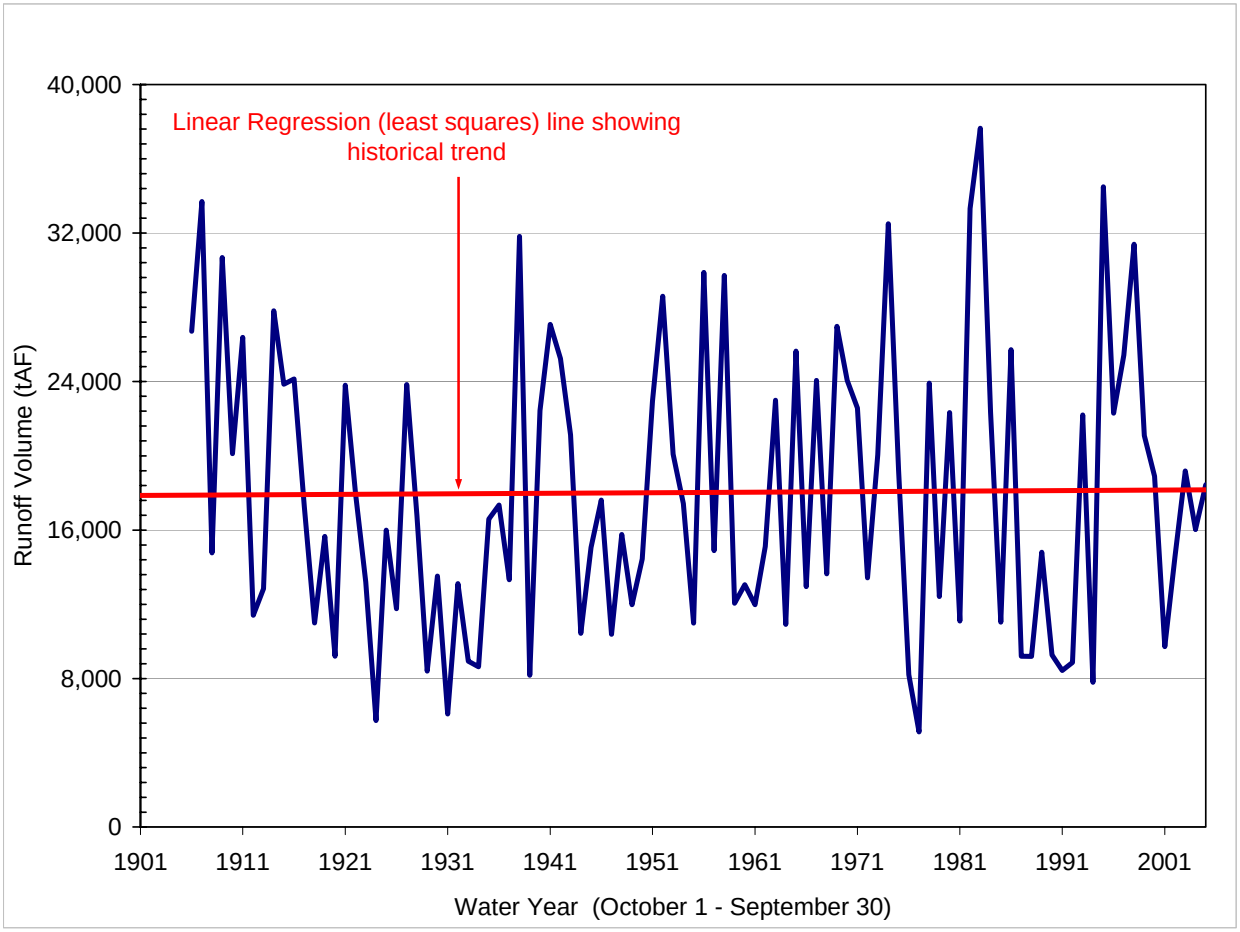


Figure 6-11 Time series of Sacramento River Index water year runoff with fit linear trend

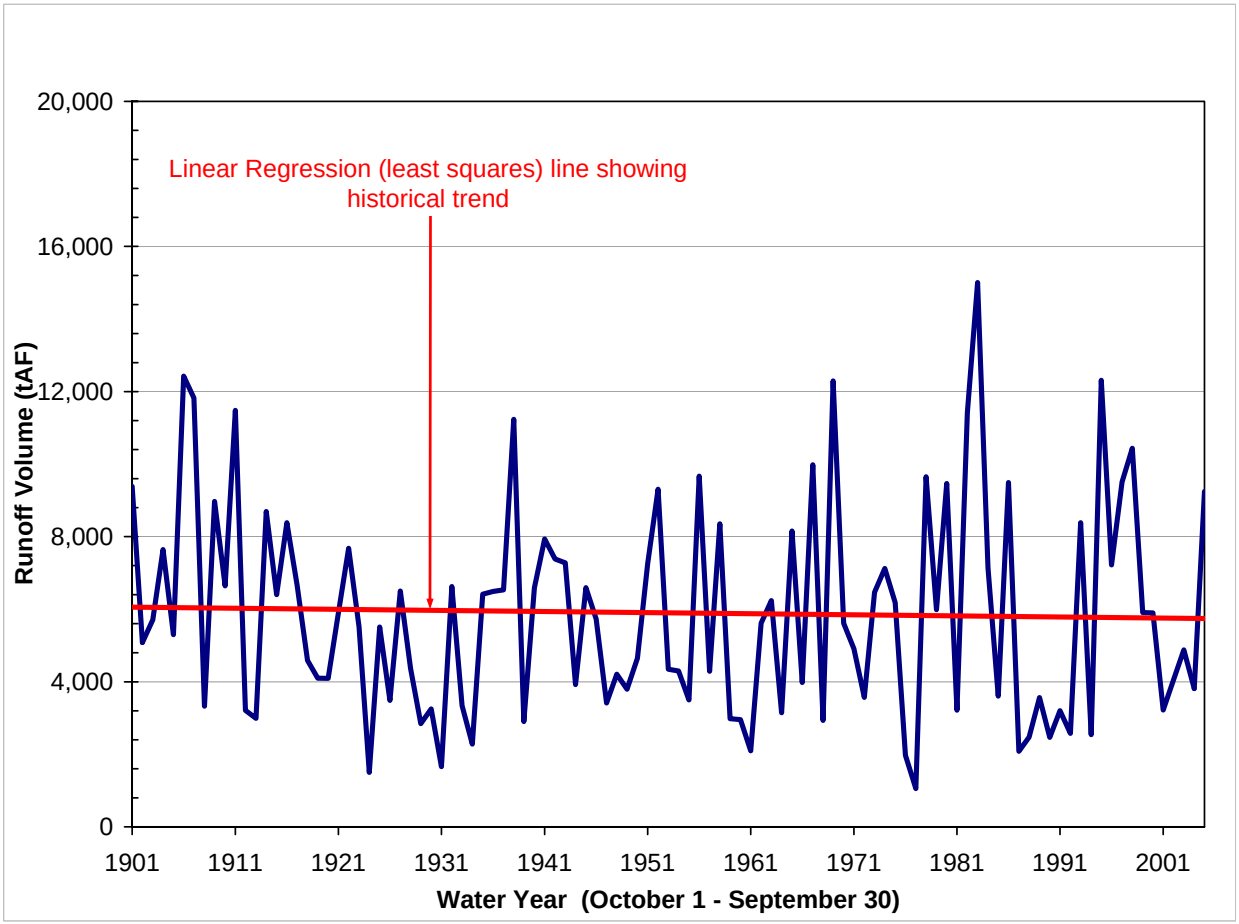


Figure 6-12 Time series of San Joaquin River Index water year runoff with fit linear trend

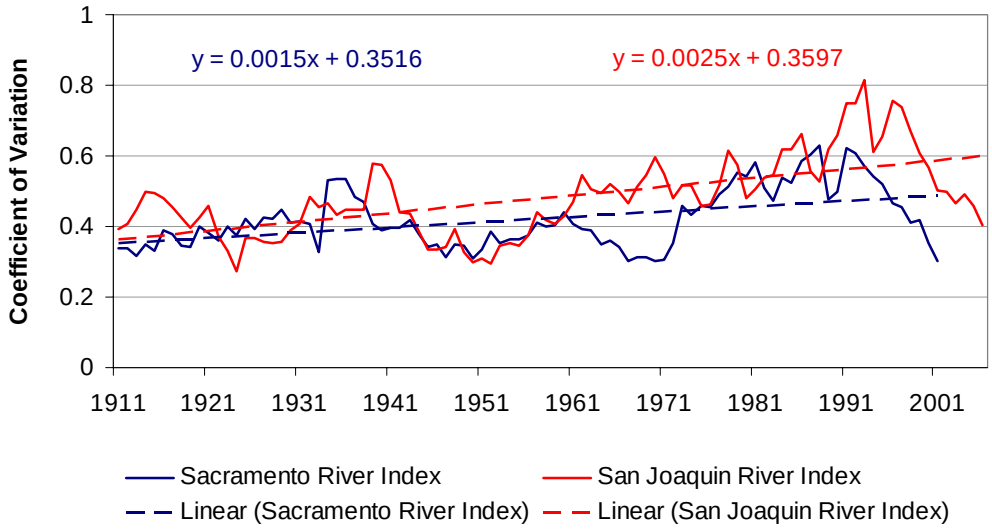


Figure 6-13 Variability of Sacramento and San Joaquin River Index through time

Another element to annual runoff is the timing of that runoff. Winter storms deliver snow to higher elevations that historically has melted in April – July. This spring runoff serves as a significant portion of the water supply for dry summers and falls. The April – July runoff over time is shown in Figure 6-14 for the Sacramento River system and in Figure 6-15 for the San Joaquin River system. Both indices show a decrease in the fraction of annual runoff made up from April – July runoff over the past 100 years. This indicates that a greater percentage of the annual runoff is occurring earlier in the year when flood control needs supersede water storage in reservoirs with flood control and water supply purposes. However, in terms of the t-test for statistical significance, neither trend was identified as statistically significant.

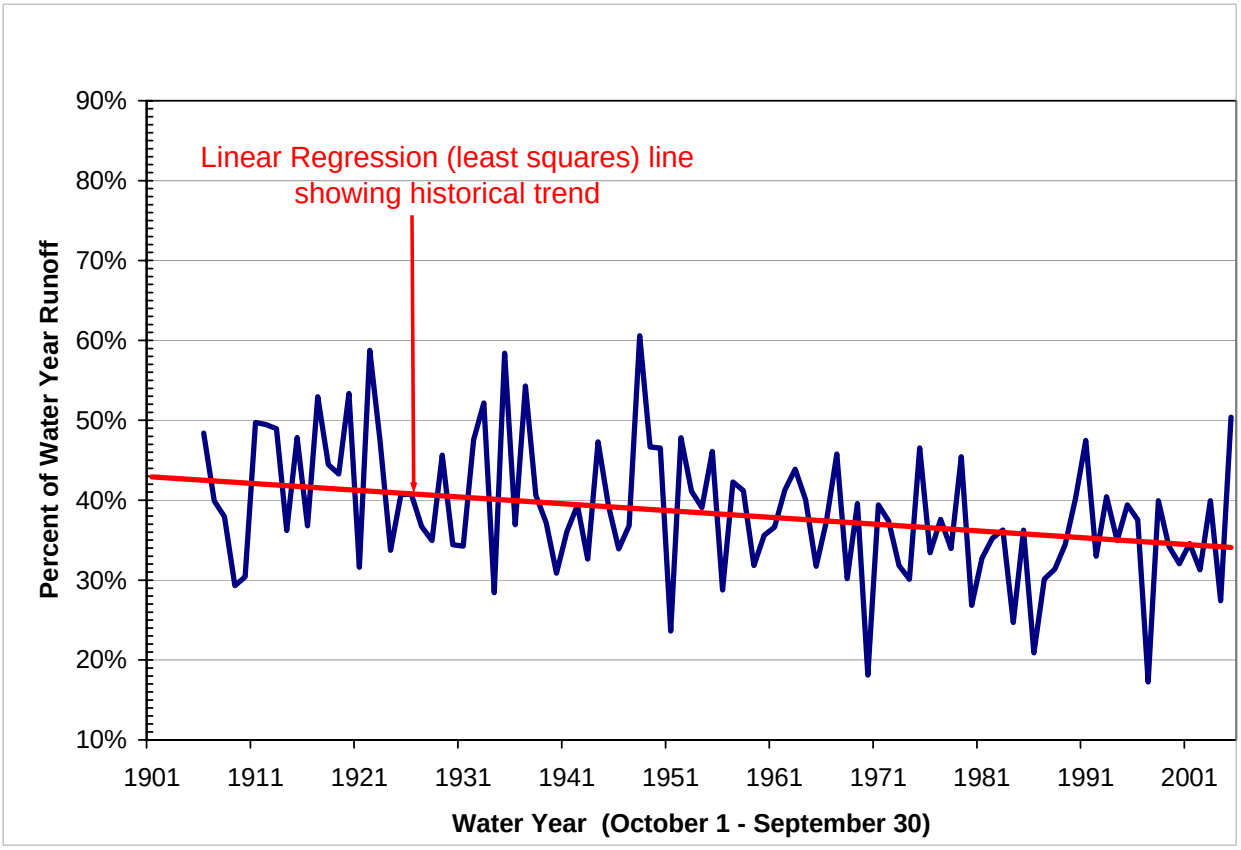


Figure 6-14 April-July Runoff as a percent of water year runoff for the Sacramento River System

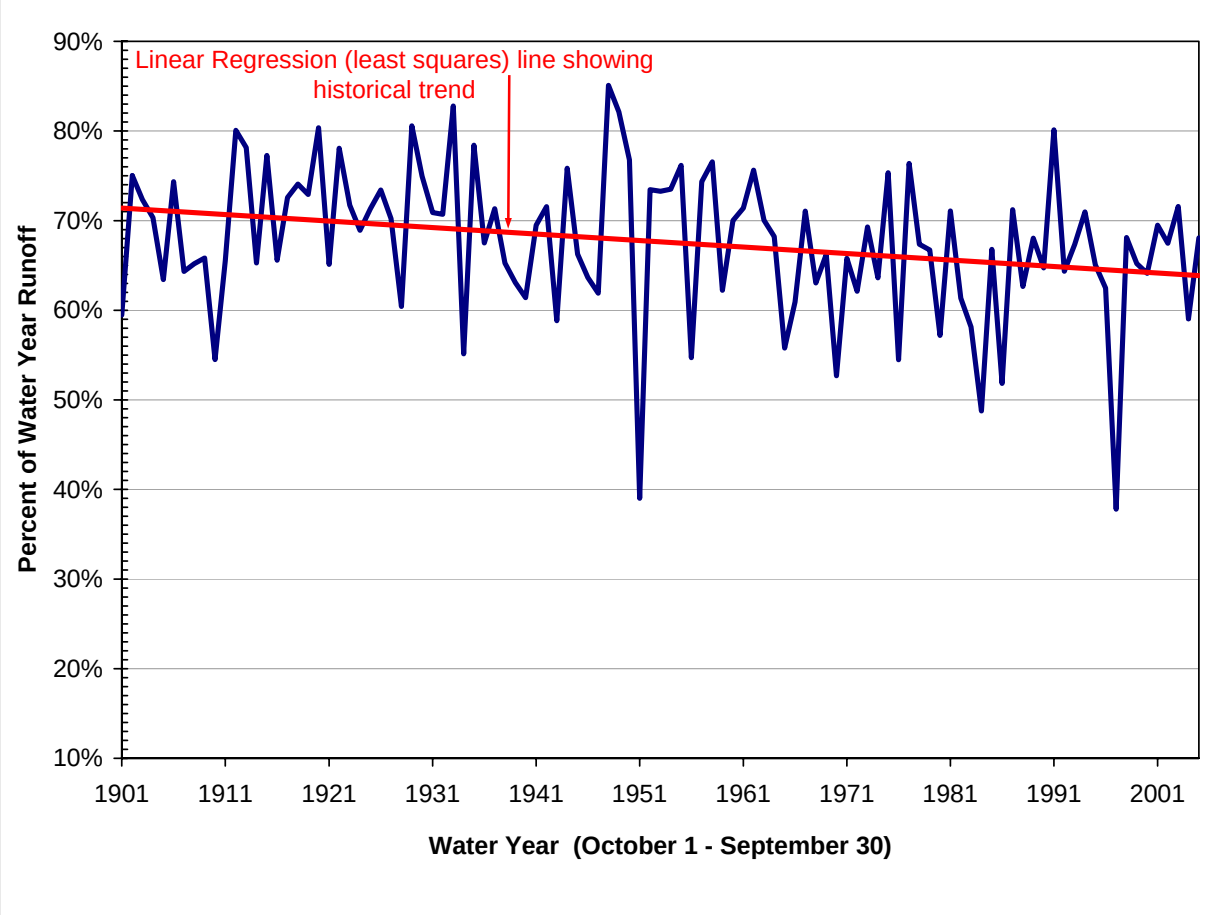


Figure 6-15 April-July Runoff as a percent of water year runoff for the San Joaquin River System

Another indication that spring runoff is occurring earlier in the year can be seen in Figure 6-16. It depicts the flow centroid day at the Michigan Bar stream gage on the Cosumnes River computed from historical flow data. A flow centroid day is the number of days after October 1 for 50 percent of the annual volume to pass. For watersheds with snowmelt, this day is usually in April or May (Julian day 182-243). The Cosumnes River is a lower-elevation watershed with a maximum elevation of slightly less than 8,000 feet. It has a modest snowpack in the upper reaches of the basin. There is also a 40,000 acre-foot reservoir on a tributary to the North Fork (Jenkinson Reservoir) that diverts water from the basin. In the absence of a major runoff event (seen as the sharp downward spikes in the time series such as 1986 and 1997) in the basin, the snowmelt makes up a significant portion of the annual runoff in the watershed and drives the location of the flow centroid day. As can be seen from the above figure, the movement over time of the flow centroid day to earlier in the year indicates that, on average, the snowmelt in the basin is occurring earlier (from mid March in 1908 to the beginning of March in 1998). Based on the linear trend line fit to the data, this change in timing is about 10 days over 90 years. However, based on the t-test, the trend was not identified as statistically significant.

With more of the annual runoff including some snow melt occurring earlier in the year, runoff historically used for water supply starts to overlap the time period when reservoir space is reserved for flood control. This overlap may lead to the need to carefully review early spring reservoir operation.

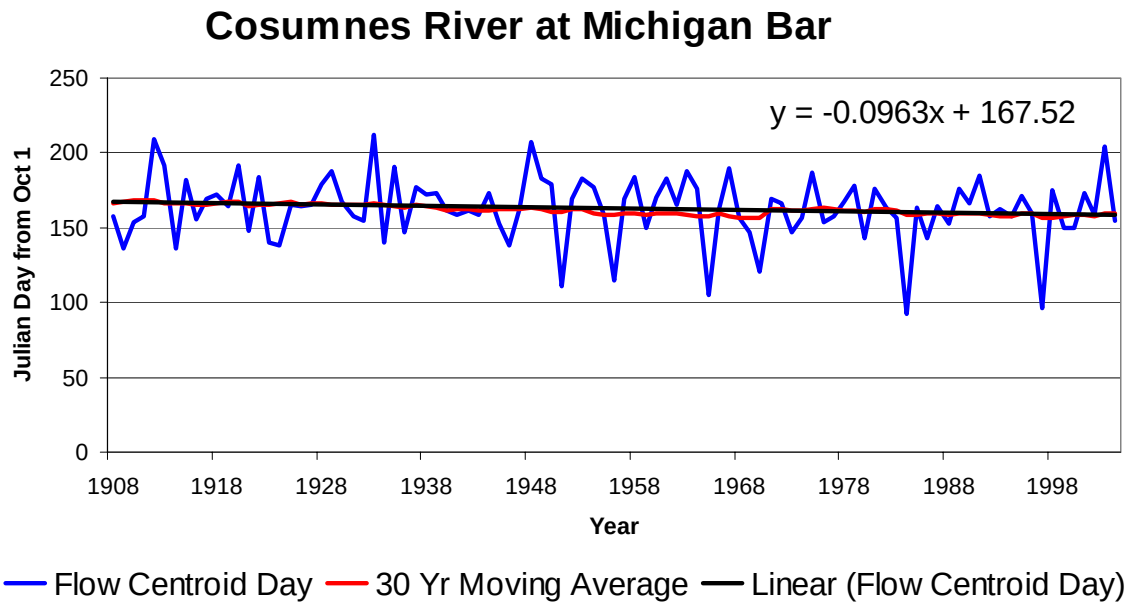


Figure 6-16 Flow centroid day versus time for the Cosumnes River at Michigan Bar

6.3.3.2 Annual Maximum Flood from Three Day Average Flows

For peak runoff analysis, six rivers were chosen with long peak flow records. The peak flows evaluated here are three-day average peak flows. The six rivers chosen include three in the Central Valley: Feather, American, and Tuolumne; and three coastal rivers: the Eel River in the north, the Arroyo Seco in central California, and the Santa Margarita River in the south. Their locations are shown in Figure 6-17.

For the analysis, total period mean, standard deviation, and skew statistics are computed for each river. In addition, the records were divided into two time periods with 1955 as the boundary. The year 1955 was chosen as the boundary because it divides the data sets in half. Mean, standard deviation and skew statistics were computed for the two time periods as well. These values are shown in Table 6-3. As can be seen from Table 6-3, the means and standard deviations all increased from the pre 1955 time period to the post 1955 time period with the exception of the Arroyo Seco mean which remained constant. The skew statistics increased except for the Arroyo Seco which remained constant and the Santa Margarita, which decreased.



Figure 6-17 Map of station location for peak flow analysis

Using these statistics, Bulletin 17-B (Water Resources Council, 1982) procedures were used to compute the 10-year, 50-year, and 100-year return period flows for the six rivers for the total period, pre-1955 period, and post-1955 period. The Bulletin 17-B procedures fit the data to a log-Pearson type III distribution. The flow values for the different return periods are shown in Table 6-4. Percent differences from Pre-1955 conditions to Post-1955 conditions are shown in Table 6-5.

Table 6-3 Comparison of discharge statistics by basin and time period (values in 1000 cfs)

River Basin	American	Feather	Tuolumne	Eel	Arroyo Seco	Santa Margarita
Total Period Mean	32.73	47.61	14.51	110.08	3.12	1.37
Total Period Std Dev	33.68	42.06	15.26	71.13	2.53	2.71
Total Period Skew	2.14	1.89	2.42	2.14	1.02	3.04
Pre55 Mean	28.04	42.38	12.22	92.99	3.09	1.24
Pre55 Standard Deviation	24.23	33.00	10.85	47.97	2.38	2.35
Pre55 Skew	1.76	1.38	1.72	0.47	1.03	3.51
Post55 Mean	37.00	52.23	17.20	123.26	3.09	1.42
Post55 Standard Deviation	41.00	49.68	19.33	84.18	2.71	2.93
Post 55 Skew	1.88	1.81	2.12	2.05	1.02	2.88

Table 6-4Comparison of different return period flows by basin and time period

River Basin (Values in 1000 cfs)	American (1905-2004)	Feather (1904-2004)	Tuolumne (1897-2000)	Eel (1917-2004)	Arroyo Seco (1902-2004)	Santa Margarita (1931-2004)
Total Period Q10	72	101	32	210	7	6
Total Period Q50	150	186	65	334	14	10
Total Period Q100	194	228	83	392	15	12
Pre 1955 Q10	58	88	26	162	6	5
Pre 1955 Q50	103	152	48	236	13	9
Pre 1955 Q100	126	182	58	268	14	11
Post 1955 Q10	88	117	40	257	7	7
Post 1955 Q50	199	221	88	446	14	11
Post 1955 Q100	266	274	117	540	15	13

Table 6-5 Percent increase in return period discharges from pre-1955 to post-1955 by basin

River Basin	American	Feather	Tuolumne	Eel	Arroyo Seco	Santa Margarita
Q10	51%	32%	49%	58%	7%	22%
Q50	92%	46%	85%	88%	10%	23%
Q100	111%	51%	102%	101%	11%	23%

As can be seen from Table 6-5, the 100-year three-day peak flows have more than doubled for the American, Tuolumne, and Eel rivers. The only river with little change in its return period flows is the Arroyo Seco. Examination of the data shows that there was only one major event (defined as a value greater than the mean plus two standard deviations) for the Feather, American, and Tuolumne Rivers in the pre-1955 period. In the post 1955 period, the number of major events jumps to four. For the coastal rivers a similar pattern emerges. From this information it can be seen that the annual peak three-day mean discharges are becoming more variable and larger for many sites in California.

Climate model studies such as Miller and others (2003) and Dettinger and others (2004) indicate that this trend will continue in response to global warming. Stedinger and Crainiceanu (2001) examine frequency analysis issues when the underlying statistical moments are not stationary as has been assumed in this section. They find that the stationary model works just as well at identifying flood risk as more complex models that try to incorporate trends in historical data.

6.3.4 Historical Trend Summary

Over the past 100 years the following trends have been identified and were described in preceding sections:

Precipitation

- No significant trend exists in statewide average precipitation from 1890-2000
- A small increasing trend in statewide precipitation is found from 1970-2000
- A slight increasing trend in precipitation appears in the north part of the state
- A slight decreasing trend in precipitation appears in the south part of the state
- Precipitation variability increased during the 20th century

Temperature

- A slight increasing temperature trend is observed in statewide average of maximum, average and minimum temperatures
- Larger temperature trends are associated with urban areas
- Variability in minimum temperature is slightly decreasing
- Variability in maximum and average temperature is slightly increasing

Runoff – Annual

- Annual runoff shows increasing trend in Sacramento River System
- Annual runoff shows slight decreasing trend in San Joaquin River System
- April-July runoff as percentage of annual runoff is decreasing in both Sacramento and San Joaquin River Systems
- Variability in annual runoff is increasing

Runoff – Peak Flow

- Increase in 10, 50 and 100 year return period peak flows are observed for six basins studied
- Variability in annual peak flows is increasing in six basins studied
- Change between the first and last half of the record are large except for Arroyo Seco

6.4 Climate Change Scenario Simulation Data

6.4.1 GCM Simulation Results

The studies presented in this report focus on the four climate change scenarios selected by the Climate Action Team appointed in response to the governor's Executive Order S-3-05 on climate change. The four climate change scenarios consist to two greenhouse gas (GHG) emissions scenarios developed by the Intergovernmental Panel on Climate Change (IPCC), known as A2 and B1, each represented by two different Global Climate Models (GCMs), the Geophysical Fluid Dynamic Lab model (GFDL) and the Parallel Climate Model (PCM).

The A2 emissions scenario assumes high population growth, regional based economic growth, and slow technological changes which results in significantly higher GHG emissions. The B1 scenario represents low population growth, global based economic growth and sustainable development which results in the lowest increase of GHG emissions of the IPCC scenarios. For more information on the GCMs and scenarios used in this report, refer to Chapter 3. For the following sections examining impacts based on climate change simulation results, the four climate change scenarios are referred to as:

- GFDL A2
- PCM A2
- GFDL B1
- PCM B1

Precipitation and temperature time series for southern and northern California were created using the GCM simulation results. Precipitation results are shown in Figure 6-18 for Northern California and Figure 6-19 for Southern California. Note that scenario simulations for a given GCM do not differ until after year 2000. For both Northern and Southern California, neither model accurately reproduces historical precipitation variability. Because of this, future variability represented by the model can not be considered reliable.

In terms of average precipitation, for Northern California, the GFDL model predicts a 20 percent decrease in precipitation after 2050 for the A2 scenario and a 10 percent decrease for the B1 scenario. The PCM model predicts no change for either scenario. For Southern California, the GFDL model predicts a 10 percent decrease in precipitation after 2050 for both scenarios while the PCM model predicts a 1 percent decrease in precipitation for both scenarios. By 2100 however, the PCM model predicts a 10 percent increase in precipitation for both scenarios.

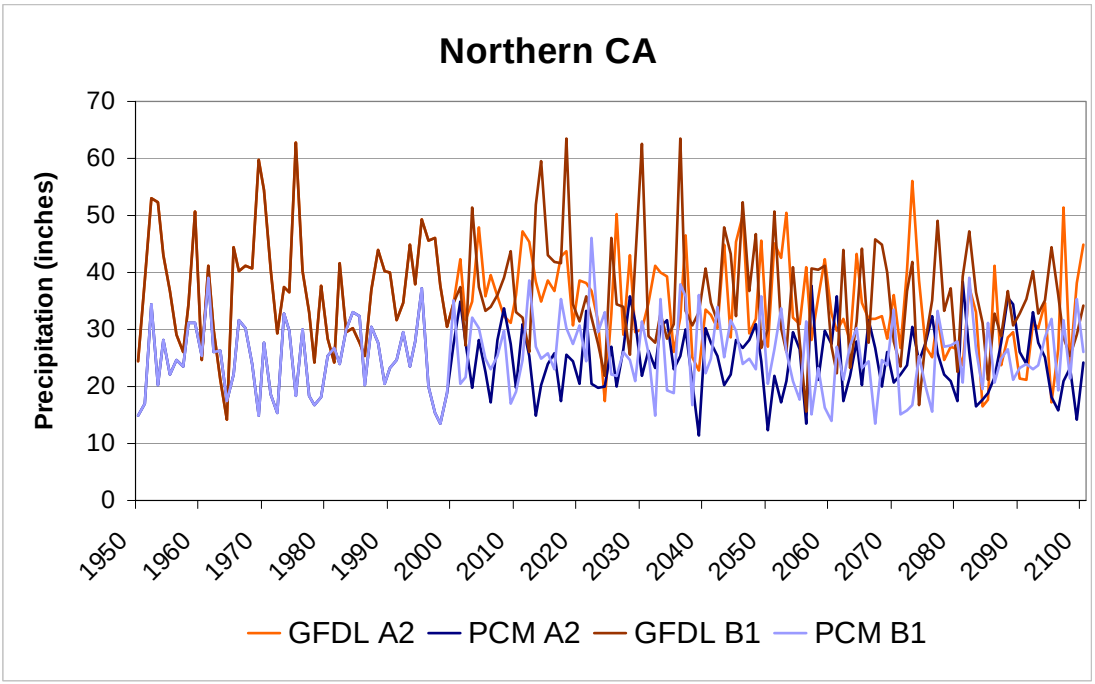


Figure 6-18 GCM precipitation results for Northern California

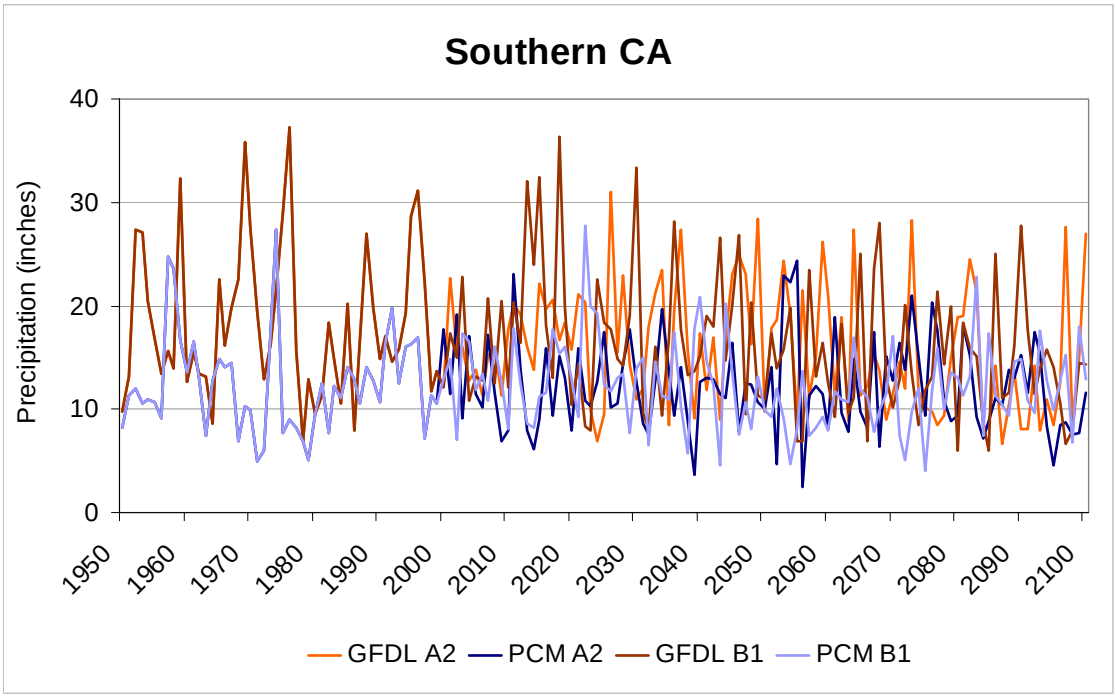


Figure 6-19 GCM precipitation results for Southern California

Temperature results for both models are shown in Figure 6-20 for Northern California and in Figure 6-21 for Southern California. For Northern California, the GFDL model predicts a larger temperature increase than the PCM model. By 2050, the PCM model predicts a one degree Celsius increase in temperature for both scenarios while the GFDL model predicts a 2.25-degree increase for both scenarios. Increases up to 5 degrees C occur by 2100 in the GFDL model.

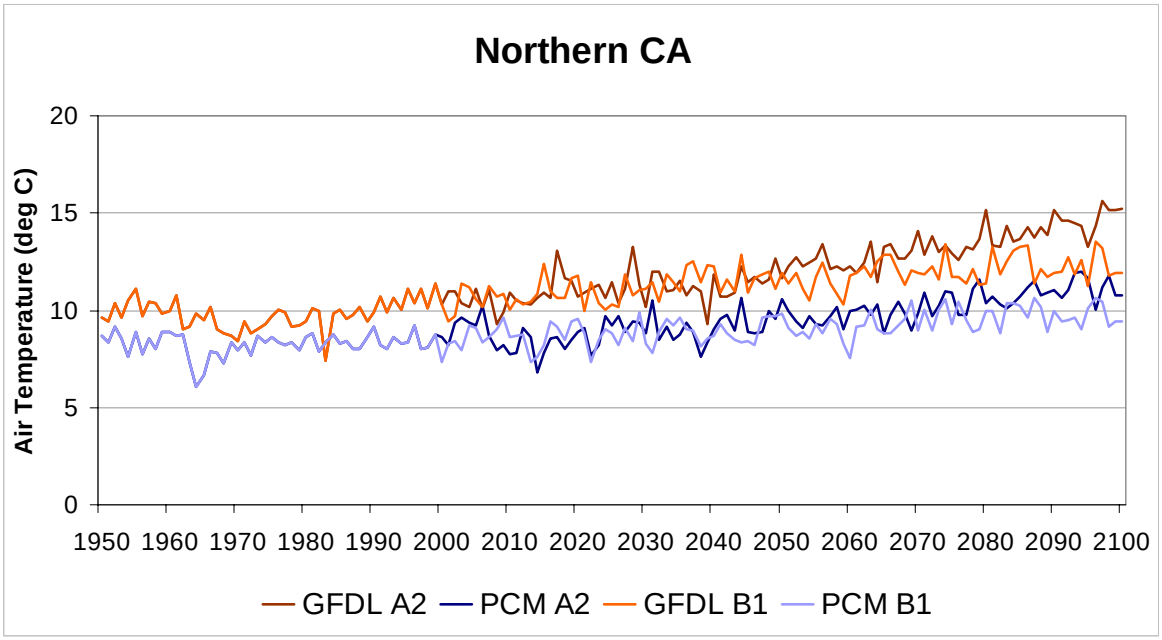


Figure 6-20 GCM temperature results for Northern California

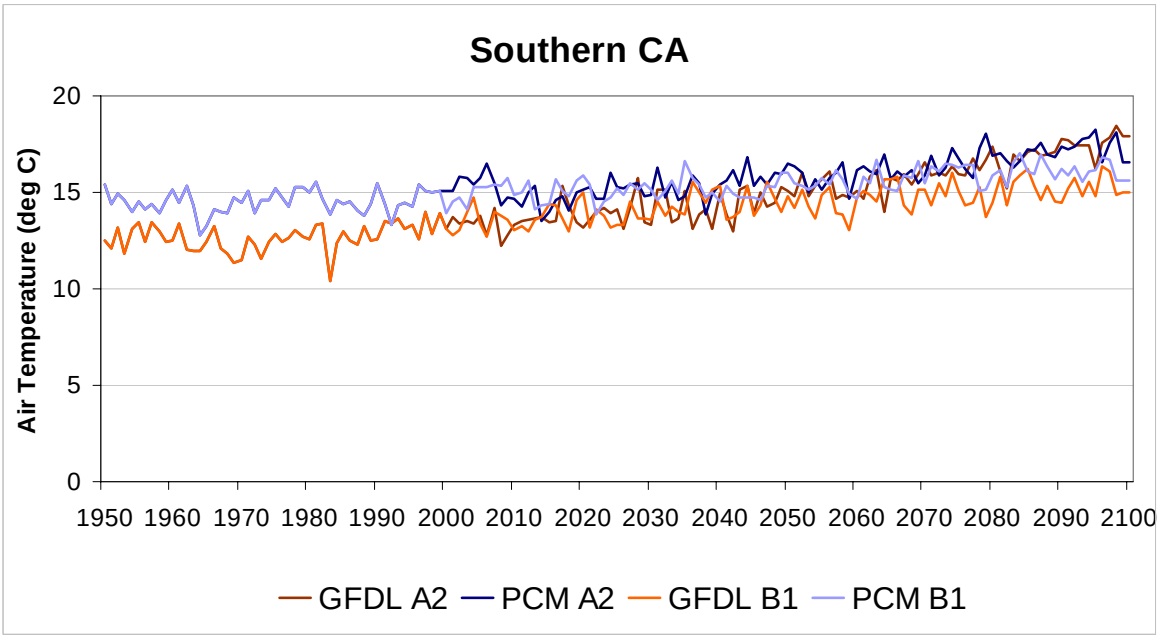


Figure 6-21 GCM temperature results for Southern California

The GCM results presented here are at a scale of about 100-200 km horizontal resolution. California's topography is highly varied which leads to a more complex temperature and precipitation patterns than can be expected from a GCM simulation at this resolution. Because of this, downscaling procedures were carried out on the GCM scale results to create finer resolution (10-20 km) data suitable for analysis over California.

6.4.2 Downscaled Results

Professor Ed Maurer of Santa Clara University statistically downscaled monthly data from each of the GCM simulations to California and then used the data to drive a land surface model known as the VIC (Variable Infiltration Capacity) model. Details of the downscaling and VIC model can be found in Maurer (2005). Data from these simulations were provided to Department of Water Resources staff for analysis. VIC model results for 12 sites across the state were averaged to obtain the precipitation and temperature time-series plots shown in Figure 6-22 and Figure 6-23 respectively. Runoff results from the VIC model were sampled from seven Central Valley watersheds. Annual, October through March, and April through July runoff volumes were analyzed and compared to historical records.

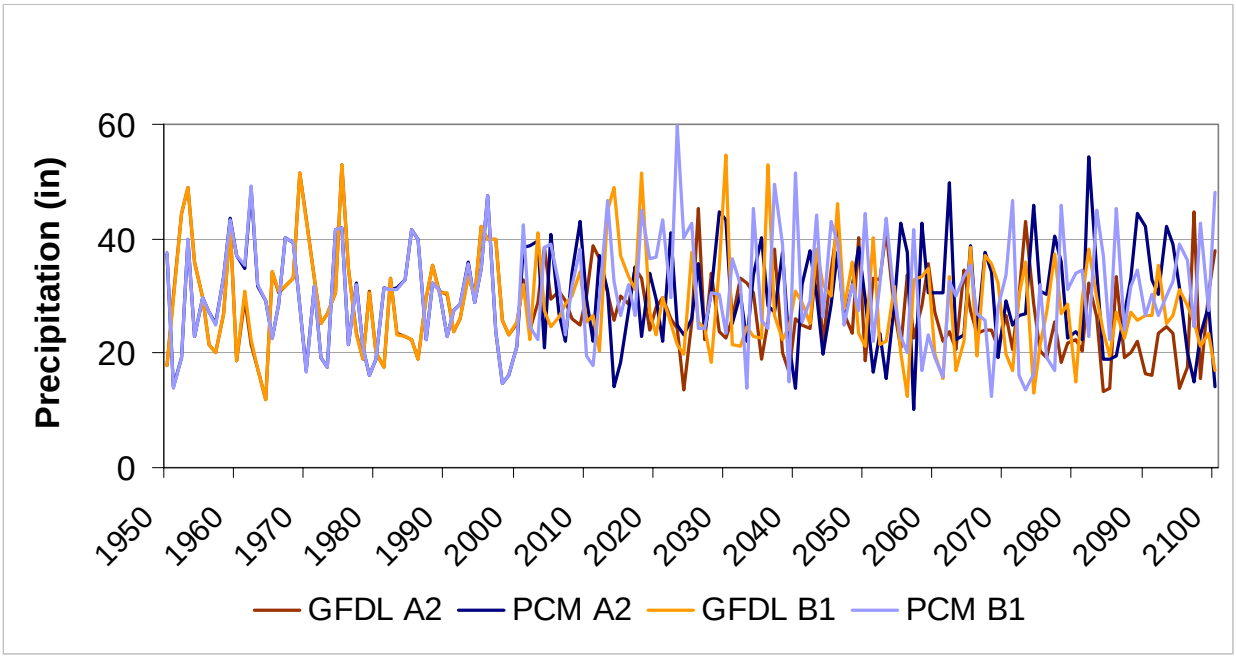
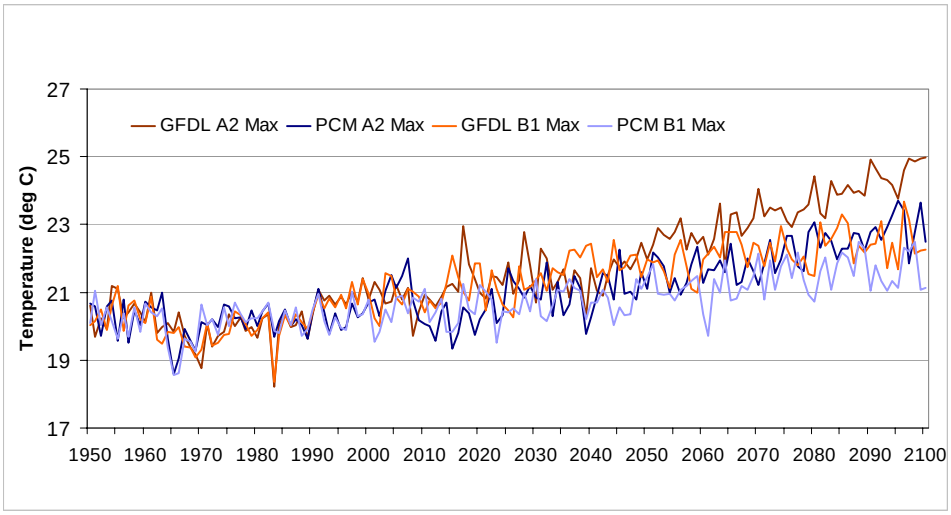
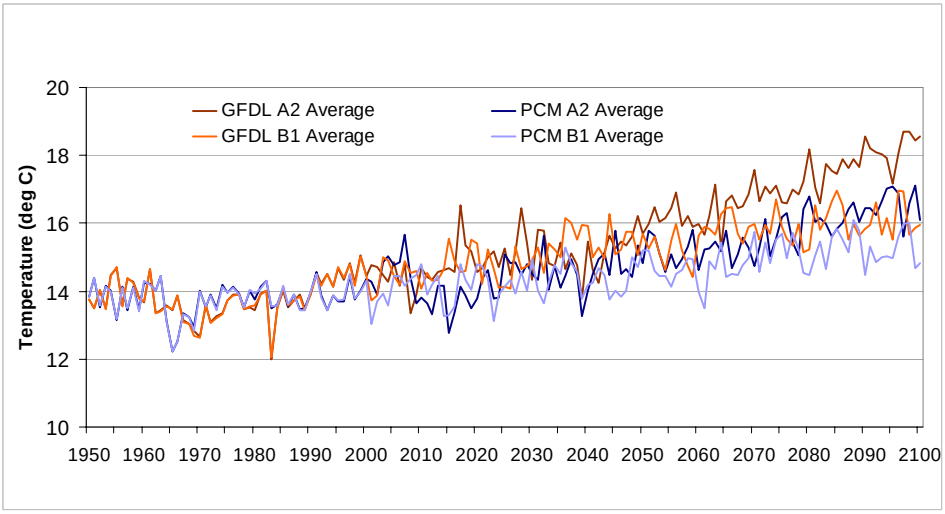


Figure 6-22 Downscaled precipitation time series from VIC model

a) Maximum air temperature from VIC model



b) Average Temperature from VIC model



c) Minimum temperature from VIC model

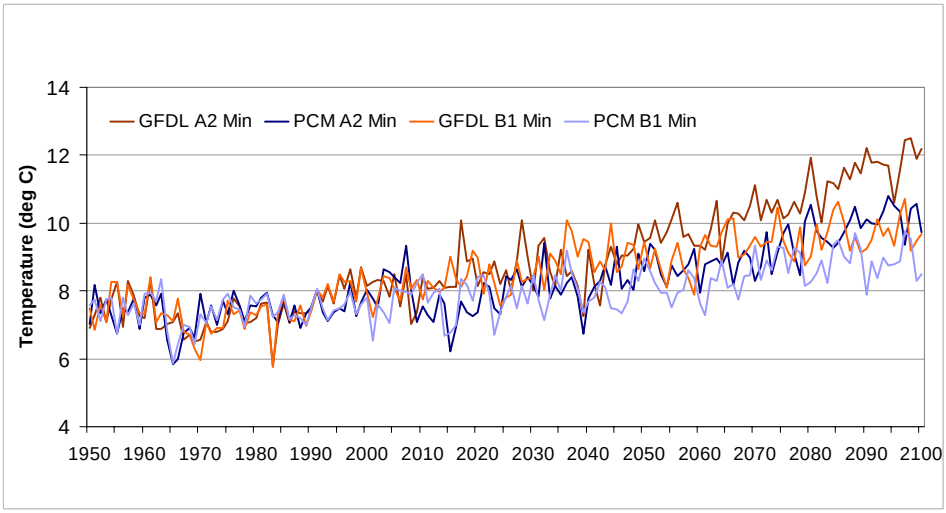


Figure 6-23 Downscaled average maximum, and minimum temperature time series

6.4.2.1 Precipitation

The scenario simulation results shown in Figure 6-22 depict little change in precipitation by 2050. Comparison of 30-year averages for the end of the 20th century and middle 21st century show a 5 percent decrease in precipitation for the GFDL model for both scenarios. The PCM model on the other hand shows no change for the A2 scenario and a 5 percent increase for the B1 scenario.

6.4.2.2 Temperature

For temperature there is a distinct increasing trend in average, maximum, and minimum temperature for both models and both scenarios. By 2050, the PCM model shows an average 1 degree C increase in average, maximum, and minimum temperature, while the GFDL shows an average 2 degree C increase. As in the GCM results, increases up to 5 degrees C exist by 2100 in the GFDL model results.

6.4.2.3 Runoff

In order to verify the ability of the scenario simulation data to represent water supply elements in California, the October-March, April-July, and annual runoff volume averages and standard deviations for the years 1951-2000 were compared for seven basins. The percent differences, computed as (modeled – observed)/observed, from observed average values for October-March are shown in Table 6-6, for April-July in Table 6-7, and annual values in Table 6-8. The percent differences from observed values for the standard deviations are shown in Table 6-9 for October-March, Table 6-10 for April-July, and Table 6-11 for annual values. In general, the simulated runoff values were closer to the observed values during the October-March period. Only the American and Kings basins have errors greater than 10 percent. However, in April-July, which is the important time period for water supply, the simulated data does not match up as well. Two basins, the Feather and Merced watersheds match up within 7 percent or less. The Sacramento and Tuolumne errors are between 10 percent and 20 percent, while the others are all greater than 30 percent.

The standard deviation represents the year-to-year variability in the system. As can be seen from Table 6-9, Table 6-10, and Table 6-11 with a few exceptions, both models had difficulty representing the historical year-to-year variability for the October through March, April through July, and annual periods. Both the GFDL and PCM models show less variability than has been observed. This inability to capture the historical year-to-year variability means that any prolonged dry or wet periods during the future portion of the simulations are suspect and cannot be interpreted as prolonged flood or drought cycles.

Table 6-6 Modeled vs Observed Percent Differences in Oct-Mar Runoff Average

Watershed	Inflow Location	PCM-B1	PCM-A2	GFDL-B1	GFDL-A2
Sacramento	Shasta	2%	1%	3%	2%
Feather	Oroville	7%	6%	8%	8%
American	Folsom	37%	36%	37%	35%
Stanislaus	New Melones	1%	-1%	1%	0%
Merced	Lake McClure	-4%	-3%	-6%	-5%
Tuolumne	Don Pedro	-3%	-4%	-4%	-5%
Kings	Pine Flat	-13%	-14%	-15%	-14%

Table 6-7 Modeled vs Observed Percent Differences in Apr-July Runoff Average

Watershed	Inflow Location	PCM-B1	PCM-A2	GFDL-B1	GFDL-A2
Sacramento	Shasta	18%	16%	20%	19%
Feather	Oroville	6%	7%	2%	4%
American	Folsom	42%	43%	40%	42%
Stanislaus	New Melones	32%	33%	30%	31%
Merced	Lake McClure	5%	3%	6%	6%
Tuolumne	Don Pedro	13%	14%	11%	12%
Kings	Pine Flat	44%	47%	44%	43%

Table 6-8 Modeled vs Observed Percent Differences in Annual Runoff Average

Watershed	Inflow Location	PCM-B1	PCM-A2	GFDL-B1	GFDL-A2
Sacramento	Shasta	25%	25%	9%	9%
Feather	Oroville	7%	6%	-1%	-2%
American	Folsom	-32%	-32%	-35%	-36%
Stanislaus	New Melones	-11%	-11%	-13%	-13%
Merced	Lake McClure	3%	4%	2%	2%
Tuolumne	Don Pedro	2%	3%	1%	1%
Kings	Pine Flat	33%	34%	35%	34%

Table 6-9 Modeled vs Observed Percent Differences in Oct-Mar Runoff Standard Deviation

Watershed	Inflow Location	PCM-B1	PCM-A2	GFDL-B1	GFDL-A2
Sacramento	Shasta	-21%	-21%	-15%	-17%
Feather	Oroville	8%	9%	23%	20%
American	Folsom	12%	12%	22%	21%
Stanislaus	New Melones	11%	9%	21%	24%
Merced	Lake McClure	-18%	-18%	-17%	-13%
Tuolumne	Don Pedro	9%	9%	17%	21%
Kings	Pine Flat	13%	9%	20%	26%

Table 6-10 Modeled vs Observed Percent Differences in Apr-Jul Runoff Standard Deviation

Watershed	Inflow Location	PCM-B1	PCM-A2	GFDL-B1	GFDL-A2
Sacramento	Shasta	8%	14%	27%	21%
Feather	Oroville	33%	33%	16%	25%
American	Folsom	35%	35%	21%	25%
Stanislaus	New Melones	30%	31%	21%	20%
Merced	Lake McClure	10%	7%	3%	0%
Tuolumne	Don Pedro	4%	4%	4%	6%
Kings	Pine Flat	61%	61%	75%	78%

Table 6-11 Modeled vs Observed Percent Differences in Annual Runoff Standard Deviation

Watershed	Inflow Location	PCM-B1	PCM-A2	GFDL-B1	GFDL-A2
Sacramento	Shasta	26%	26%	19%	20%
Feather	Oroville	-15%	-16%	-17%	-16%
American	Folsom	-15%	-16%	-15%	-14%
Stanislaus	New Melones	-20%	-20%	-16%	-16%
Merced	Lake McClure	1%	2%	10%	11%
Tuolumne	Don Pedro	-5%	-6%	1%	1%
Kings	Pine Flat	26%	26%	44%	45%

With the understanding that the simulated runoff does not match historically observed statistics very well, the following tables show the percent change from historical conditions that occurs for the 2035-2064 period relative to the 1961-1990 period. Table 6-12 shows the percent changes in the mean for October through March. The April-July percent changes in the mean are shown in Table 6-13 and the annual changes in the mean are shown in Table 6-14.

While the magnitude of the changes may be suspect due to the large errors in representing the historical conditions, some general trends can be noted. With the exception of the PCM-A2 simulation for inflows to Shasta reservoir, all October through March runoff values are larger in the 30 years centered on 2050 (future) than the 30 years centered on 1975 (present). For the April through July runoff all future values are less than present with the exception of inflows to Shasta and Oroville for the PCM-B1 scenario. On an annual basis, the PCM model predicts changes less than 10 percent for all basins for both scenarios. However, the changes are positive (increase in annual runoff) for the B1 scenario and negative (decrease in annual runoff) for the A2 scenario. The GFDL model predicts less than 20 percent changes all basins for both scenarios. The GFDL predicts decreases in annual runoff with the exception of Shasta and Oroville inflows for the B1 scenario.

Table 6-12 Percent Differences in Future to Present Oct-Mar Runoff Average

Watershed	Inflow Location	PCM-B1	PCM-A2	GFDL-B1	GFDL-A2
Sacramento	Shasta	8%	7%	9%	3%
Feather	Oroville	14%	10%	11%	13%
American	Folsom	13%	17%	0%	4%
Stanislaus	New Melones	16%	12%	9%	14%
Merced	Lake McClure	22%	13%	2%	13%
Tuolomne	Don Pedro	13%	9%	5%	11%
Kings	Pine Flat	15%	17%	4%	11%

Table 6-13 Percent Differences in Future to Present Apr-Jul Runoff Average

Watershed	Inflow Location	PCM-B1	PCM-A2	GFDL-B1	GFDL-A2
Sacramento	Shasta	-9%	0%	-20%	-22%
Feather	Oroville	-14%	-5%	-26%	-30%
American	Folsom	-23%	-13%	-43%	-40%
Stanislaus	New Melones	-13%	-9%	-34%	-33%
Merced	Lk McClure	-10%	-14%	-27%	-29%
Tuolomne	Don Pedro	-6%	-8%	-25%	-26%
Kings	Pine Flat	-6%	-12%	-29%	-28%

Table 6-14 Percent Differences in Future to Present Annual Runoff Average

Watershed	Inflow Location	PCM-B1	PCM-A2	GFDL-B1	GFDL-A2
Sacramento	Shasta	2%	4%	-2%	-6%
Feather	Oroville	3%	4%	-5%	-5%
American	Folsom	-2%	4%	-19%	-15%
Stanislaus	New Melones	1%	1%	-13%	-10%
Merced	Lk McClure	2%	-3%	-16%	-13%
Tuolomne	Don Pedro	1%	-1%	-13%	-11%
Kings	Pine Flat	2%	-2%	-17%	-14%

6.4.2.4 Peak Flow Runoff

Data provided from the GCM simulations is at a monthly time scale. Such data are not suitable to investigate peak flow runoff changes associated with climate change. Peak flows are associated with given weather events that are a fundamentally different scale from climate. In order to generate data appropriate for peak flow runoff analyses, the GCM simulations would have to be able to correctly simulate the magnitude, location, and variability of the atmospheric circulations associated with extreme rainfall and runoff. For future climate scenarios, a large sample of GCM realizations would enable a probabilistic approach to assess changes in extreme precipitation and runoff frequency. At this time, this analysis is left for future work.

6.4.3 Summary of GCM Model Results

There is great uncertainty in the magnitude, timing, and location of precipitation and runoff changes associated with climate change. Historical trends depend on the time frame chosen, although most changes are small. The magnitude of model-derived changes is less than the magnitude of the differences between observed and modeled statistics for the historical period. One way to avoid this problem is to use multiple simulations and compute averages of the multiple simulations. These ensemble averages are then used to analyze expected changes associated with climate change.

It should be noted that maximum, minimum and average temperatures have risen in the past and are expected to continue to rise across the state based on model simulations. There is some range (1 to 5 degrees C) in the amount of warming expected depending on the model and scenario. While changes in flood frequency can not be quantified from the simulation results, some elements of climate change based runoff changes can be quantified. These are explored in the next section.

6.5 Potential Impacts

Changes in runoff associated with climate change can be related to the changes in watershed response due to the modification of the seasonal snowpack. Increasing temperatures will likely push the snow level in watersheds to higher elevations leaving more of the watershed available to contribute to direct winter runoff processes. In addition, higher elevation snow levels decrease the available watershed area for snowpack to develop. Both of these issues are explored in this section. For other studies, see a special issue of Climatic Change (Vol. 62, 2004) which included a number of studies on climate change impacts on California water resources.

A simple hydrologic model of the Feather River watershed, HED71 (Buer, 1988), is used to illustrate the effects of greater contributing area on direct runoff. It is a simple forecasting model and is not a physically based model of the watershed. However, the HED71 model has the ability to specify the elevation where the snowpack starts. Elevations below this are used to generate direct runoff from an input precipitation event. As such the HED71 model can be used to evaluate the relative changes in runoff associated with different contributing areas.

A winter storm pattern of rainfall was chosen which dropped a total of 10 inches of rain in a 72 hour period. This corresponds to a 10-15 year return period event. The timing of the rainfall is shown in Figure 6-24. The HED71 model was run with a base case snow elevation of 4500 feet. Three scenario simulations were run with snow elevations at 5000, 6000, and 7000 feet which are associated with a respective 1, 3, and 5 degree Celsius rise in mean atmospheric temperature. These values are based on the assumption of a 500 foot increase in snow elevation for each 1 degree Celsius increase in mean atmospheric temperature. The percent increases in contributing area over the base case for these three temperature changes are 57 percent, 184 percent, and 250 percent respectively. Note that for the 5 degree increase in temperature, only 2 percent of the watershed is covered with snow and is assumed not to contribute to direct runoff.

Based on these simulations, the peak runoff from this storm increased 23 percent, 83 percent and 131 percent respectively. The runoff hydrographs scaled by the peak flow of the base case are

shown in Figure 6-25. As can be seen from Figure 6-25, there is a significant increase in direct runoff volume associated with higher elevations for snowpack due to the increased contributing area of the watershed. The more than doubling of the peak runoff associated with a 5 degree Celsius increase in mean atmospheric temperature would cause significant changes in the return period of peak runoff associated with a specified rainfall event.

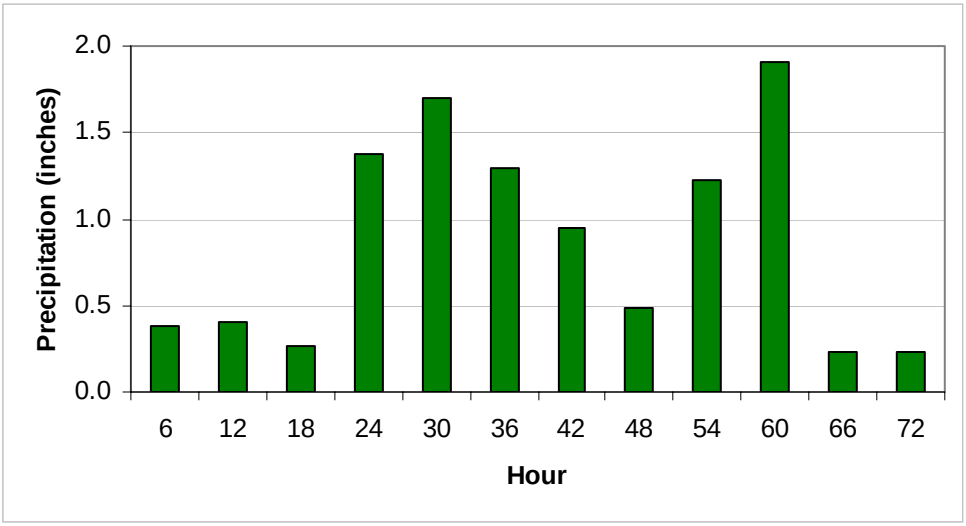


Figure 6-24 Input hyetograph to HED71 model.

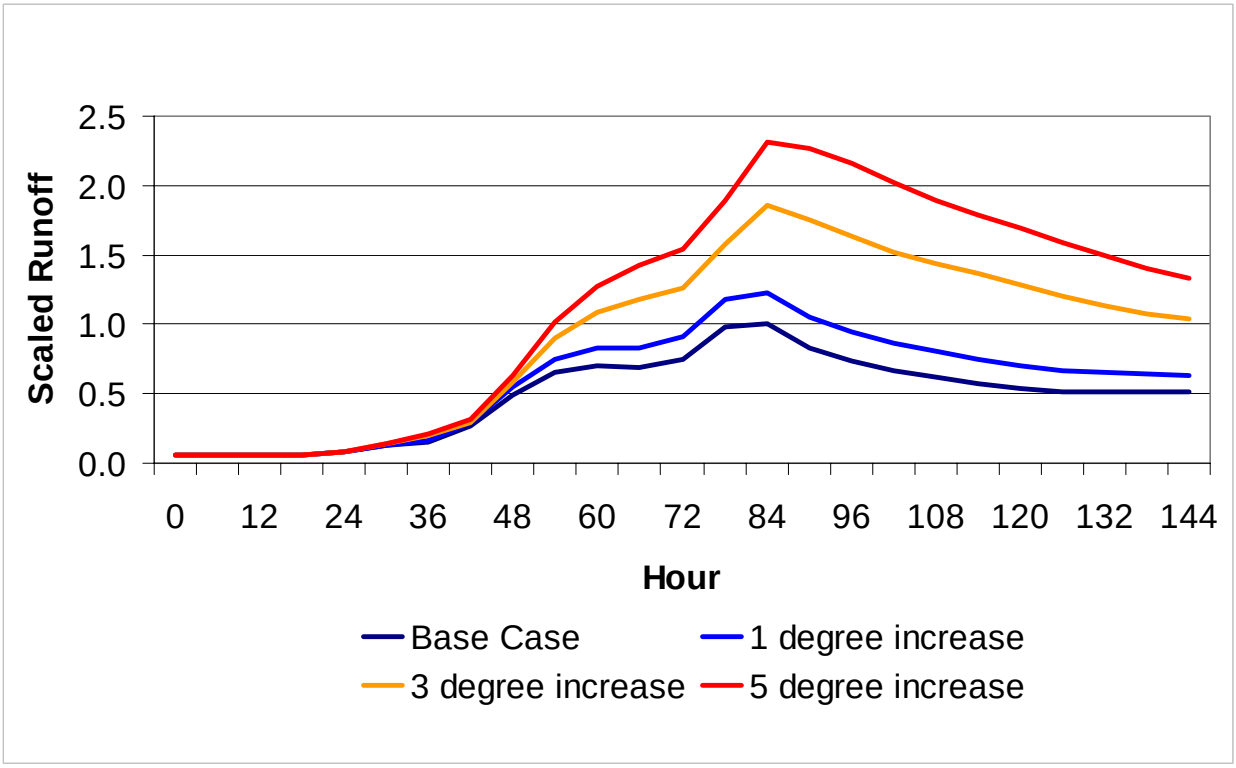


Figure 6-25 Direct runoff changes due to increasing contributing area of watershed

As pointed out earlier, higher snow elevations not only mean more area to contribute to direct runoff for a given winter storm, but there is less area for snowpack to develop at higher elevations. The impact of higher snow elevations due to higher atmospheric temperatures is estimated using area-elevation curves for watersheds. Computations assumed a 500 foot increase in elevation of snowpack for each degree Celsius of atmospheric temperature warming. Table 6-15 lists the percentage of watershed area covered with snow for 25 basins given mean atmospheric temperature increases from 1 to 5 degrees Celsius.

Table 6-15 Snow Covered Area Changes with Temperature for Selected Watersheds

Basin	Mean elevation	Average Apr. 1 snow line	Total area	Snow Covered Area	1° C Rise	2° C Rise	3° C Rise	4° C Rise	5° C Rise
	[ft]	[ft]	[mi2]	[percent of basin]	[% of basin]	[% of basin]	[% of basin]	[% of basin]	[% of basin]
Trinity	4,740	4,000	700	63%	56%	47%	36%	24%	11%
Sac/Delta	4,130	4,000	418	48%	36%	26%	19%	10%	7%
McCloud	4,370	4,000	607	56%	40%	25%	16%	10%	6%
Pit	4,830	4,000	4,768	81%	62%	42%	24%	11%	6%
Shasta	4,550	4,000	6,400	71%	54%	36%	21%	10%	6%
Bend	3,870	4,000	9,030	54%	41%	28%	17%	8%	5%
Feather	4,940	4,500	3,624	72%	56%	36%	20%	9%	2%
Yuba	4,470	4,500	1,191	50%	42%	34%	28%	17%	8%
American	4,300	4,500	1,900	48%	42%	34%	26%	19%	12%
Cosumnes	3,100	4,500	530	25%	15%	9%	6%	3%	1%
Mokelumne	5,030	5,000	575	50%	43%	38%	31%	26%	20%
Stanislaus	5,530	5,000	935	60%	55%	48%	42%	33%	26%
Tuolumne	5,960	5,000	1,530	60%	54%	49%	44%	39%	35%
Merced	5,470	5,500	1,020	47%	43%	42%	38%	32%	26%
San Joaquin	7,130	5,500	1,640	72%	67%	62%	57%	49%	43%
Kings	7,700	5,500	1,540	76%	73%	69%	64%	59%	54%
Kaweah	5,600	6,000	563	44%	39%	34%	27%	23%	18%
Tule	3,950	6,000	390	23%	15%	13%	8%	6%	3%
Kern	7,410	6,000	2,080	73%	65%	56%	49%	41%	33%
Truckee	6,790	5,500	430	100%	84%	58%	35%	17%	8%
Tahoe	7,030	6,000	510	100%	55%	41%	29%	18%	8%
W. Carson	8,050	6,000	70	100%	100%	100%	71%	51%	25%
E. Carson	7,530	6,000	350	86%	77%	66%	54%	47%	22%
W. Walker	8,650	6,500	180	100%	94%	83%	67%	53%	41%
E. Walker	8,250	6,500	360	97%	83%	69%	50%	36%	26%
Average	5,735	5,120	1,654	66%	56%	46%	35%	26%	18%

As can be seen from Table 6-15, the northern watersheds lose the majority of their area for snowpack development once the temperature increases reach or exceed 2 degrees Celsius. Lower elevation basins such as the Cosumnes, may lose their snowpack entirely in drier years. Higher elevation basins tributary to the San Joaquin River are less impacted than the northern basins. However, these basins produce less annual runoff than the basins in the north. Increasing peak flows due to winter storms and smaller snowpacks in terms of the percentage of the watershed

covered can have significant impacts on the operation of flood control and water supply structures in California.

Knowles and Cayan (2004) and Mote and others (2005) discuss how snow responds to climate change based on latitude and elevation. Knowles and Cayan (2004) note that the greatest changes to snowpack due to climate change are in the 4000 to 9000 foot elevation range for the Sacramento River Basin. Mote and others (2005) show that the trends in spring snowpack in the western United States are largely due to long-term warming trends. Year-to-year variability due to changes in the Pacific Ocean like El Nino at most only account for one third of the magnitude of the trend. They also note that future warming will likely change most seasonal snowpack sites to sites that will accumulate and melt several times each year.

6.6 Discussion

Over the past century there have been observed changes to the average, maximum, and minimum temperatures and their variability, changes to the annual precipitation variability, and changes to the three-day peak discharge statistics. Over the past 30 years there has been a small increase in observed statewide average annual precipitation as well.

For this report, four climate-change simulations (two models x two scenarios) were evaluated for information on potential impacts to runoff patterns in California. Increasing temperatures are likely to lead to increased elevations for snowpack formation which leads to a greater contributing area available for winter storm runoff. In a sample calculation, the peak runoff for a given event is shown to double under a 5 degree Celsius warming. The percent decrease in watershed area available for snowpack was also shown for 1 to 5 degree Celsius warming. In addition to these changes, warmer temperatures may lead to early melting of the snowpack. Analysis of observed data indicates that a two-week shift has already occurred for lower elevations. The combination of earlier melt times, greater variability and greater potential for direct storm runoff may challenge the current system of flood protection and water supply in the state. Because of this, future work is needed in the following areas.

In order to better understand the risks associated with global climate change on California's runoff patterns, it is important to be able to quantify the uncertainty in projected changes to flood and drought frequencies and to the quantity and timing of water supply runoff. Future efforts to address these issues include:

- Continue historical data trend and variability evaluation
- Periodically update frequency-based data for design computations
- Evaluate new climate change model-derived data sets
- Develop new water supply forecasting technologies that can adapt to the changing distribution of the state's annual water supply
- Incorporate methodologies to quantify the uncertainty in potential climate change based impacts into the water supply planning process

For flood frequency analysis, future synthetic daily flow datasets may eventually be produced from climate change model output that will be suitable for flood frequency analyses. As these

future datasets become available, they must be evaluated for their ability to represent current magnitude and variability as well as predicted changes due to climate change. At this time there is no dataset that would provide meaningful results.

Another area that may produce useful flood forecasting information examines historical data in order to identify critical atmospheric circulation parameters and their threshold values associated with extreme flooding events. As the circulation patterns in the GCMs improve and are shown to represent current conditions (location, frequency, variability) correctly, circulation patterns under increased greenhouse gas concentrations can be examined for the flood producing patterns or critical threshold characteristics. Improved forecasting technologies will help the implementation of adaptive strategies to mitigate the atmospheric and hydrologic changes that may increase flood risk.

For water supply analyses, it is important to identify potential changes to the land covered by snowpack and to identify changes to the magnitude and timing of snowpack growth and decay. Earlier melt patterns may necessitate new forecast bulletin products such as a March to May runoff forecast being created to complement existing April-July water supply forecasts. The inclusion of March in the forecast process introduces a large element of variability. Uncertainties related to this variability would have to be quantified as part of the water supply forecast product. Improved understanding of the potential future changes to the magnitude and timing of water supply runoff will enable better forecast products which can improve adaptive strategies for water supply operations in the state.

6.7 References

Bardini, G., S. Guillen, B. Pierotti, H. Rooks, S. Sou. 2001. *Climate Change in Califonria: Potential Consequences and strategies to cope and adapt*. California Department of Water Resources Report. 91 pp.

Barnett, T., R. Malone, W. Pennell, D. Stammer, B. Semtner and W. Washington. 2004. "The Effects of Climate Change on Water Resources in the West: Introduction and Overview", *Climatic Change*, 62, 1-11.

Buer, S. 1988. Program Manual: HED71 for Headwater Runoff Forecasting. California Department of Water Resources Division of Flood Management.

Christensen, N.S., A.W. Wood, N. Voisin, D. P. Lettenmaier and R. N. Palmer. 2004. "The effects of climate change on the hydrology and water resources of the Colorado River Basin", *Climatic Change*, 62, 337-363.

Dettinger, M., D. Cayan, M. Meyer, and A. Jeton, 2004. "Simulated hydrologic responses to climate variations and change in the Merced, Carson, and American Rivers, Sierra Nevada, 1900-2099", *Climatic Change*, 62, 283-317.

Easterling, (2000). *Observed Variability and Trends in Extreme Climate Events: A Brief Review*. [D.R. Easterling, J.L. Evans, P. Ya. Groisman, T.R. Karl1, K.E. Kunkel, P. Ambenje] Bulletin of the American Meteorological Society, **81**, March 2000, 417-425. http://www.ncdc.noaa.gov/oa/pub/data/special/extr-bams2.pdf

Gleick, P.H., 1987. "The development and testing of a water balance model for climate impact assessment: Modeling the Sacramento basin", *Water Resources Research*, 23, 1049-1061.

Intergovernmental Panel on Climate Change, 1990. *Climate Change: The IPCC Scientific Assessment*, J.T. Houghton, G.J. Jenkins, and J.J. Ephraums (eds.) Cambridge University Press. Cambridge, UK, 365 pp.

Intergovernmental Panel on Climate Change, 1995. *Climate Change 1995: The Science of Climate Change*, J.T. Houghton, L.G. Meira Filho, B.A. Callander, N. Harris, A. Kattenberg, and K. Maskell (eds.) Cambridge University Press. Cambridge, UK, 572 pp.

Intergovernmental Panel on Climate Change, 2001. *Climate Change 2001: The Scientific Basis*. Cambridge Univ. Press. 881 pp.

Jeton, A.E., M.D. Dettinger, and J.L.. Smith, 1996. "Potential effects of climate change on streamflow: Eastern and western slopes of the Sierra Nevada, California and Nevada". *U.S. Geological Survey, Water Resources Investigations Rep*. 95-4260, 44pp.

Kim, J. 2005. "A projection of the effects of climate change induced by increased CO2 on extreme hydrologic events in the western U.S.", *Climatic Change*, 68, 153-168.

Knowles, N. and D.R. Cayan, 2001. *Global climate change: Potential effects on the Sacramento-San Joaquin watershed and the San Francisco Estuary*.

http://meteora.ucsd.edu/~knowles/papers/Globaland California.pdf

Knowles, N. And D.R. Cayan. 2004. "Elevational dependence of projected hydrologic changes in the san francisco estuary and watershed", *Climatic Change*, 62, 319-336.

Lettenmaier, D.P. and T.Y. Gan, 1990. "Hydrologic sensitivities of the Sacramento-San Joaquin River Basin, California, to global warming". *Water Resources Res*, 26, 69-86.

Maurer, E.P. 2005. "Uncertainty in hydrologic impacts of climate change in the Sierra Nevada Mountains, California under two emissions scenarios", *Climatic Change*, (submitted 29 April 2005).

Maurer, E.P. and P. B. Duffy. 2005. "Uncertainty in projections of streamflow changes due to climate change in California", *Geophysical Research Letters*, 32, L03704.

Miller, N.L., J. Kim, R.K. Hartman, and J. Farrara, 1999. "Downscaled climate and streamflow study of the Southwestern United States", *J. American Water Resources Association*, 35, 1525-1537.

Miller, N.L., K.E. Bashford, and E. Strem, 2003. "Potential impacts of climate change of California hydrology". *J. Amer. Water Resourc. Assoc*, 39, 771-784.

Mote, PW, AF Hamlet, MP Clark, and DP Lettenmaier, 2005. Declining mountain snowpack in western North America, Bulletin of the American Meteorological Society, 86:39-49.

Peterson, T., 2003. "Assessment of Urban Versus Rural In Situ Surface Temperatures in the Contiguous United States: No Difference Found", *Journal of Climate*, 16: 2941–2959.

Revelle, R.R. and P.E. Waggoner,1983. "Effects of a carbon dioxide induced climatic change on water supplies in the Western United States". In *Changing Climate*, National Academy of Sciences Press, Washington, D.C.

Stedinger, J.R, and C. M. Crainiceanu, "Climate Variability and Flood-Risk Management, Risk-Based Decision Making", in *Water Resources IX, Proceedings of the Ninth Conference, United Engineering Foundation , Santa Barbara, CA, Oct. 15-20, 2000*, pp. 77-86, Amer. Society of Civil Engineers, Reston, VA, 2001.

Stewart, I.T., D.R. Cayan and M. D. Dettinger, 2004. "Changes in snowmelt runoff timing in western North America under a `business as usual' climate change scenario", *Climatic Change*, 62, 217-232.

USGRCP Water, 2000. *Water: The potential consequences of climate variabbility and change*. A report of the National Assessment Group for the USGCRP. 151 pp.

VanRheenen, N.T. A.W. Wood, R.N. Palmer and D.P. Lettenmaier. 2004. "Potential implications of pcm climate change scenarios for sacramento–san joaquin river basin hydrology and water resources", *Climatic Change*, 62, 257-281.

Water Resources Council, 1982. Guidelines for determining flood flow frequency, Bulletin 17B, United States Geological Survey Office of Water Data Coordination.

Wigley, T.M.L. and S.C.B. Roper, 2001. "Interpretation of high projections for global-mean warming". *Science*, 293, 451-454.

Wilby, R.L. and M.D. Dettinger, 2000. "Streamflow changes in the Sierra Nevada, California, simulated using statistically downscaled general circulation model output". In *Linking Climate Change to Land Surface Change*, Ed. S. McLaren and D. Kniven, Kluwer Academic Pub., 99-121.

Wood, A.W., L. R. Leung, V. Sridhar and D. P. Lettenmaier. 2004. "Hydrologic implications of dynamical and statistical approaches to downscaling climate model outputs" *Climatic Change*, 62, 189-216.

Acknowledgements: The authors would like to thank the following people for their time and assistance in the preparation of this chapter: Maury Roos, Steve Nemeth, John King, Tawnly Pranger, Brian Heiland, Boone Lek, Matt Winston, Dave Rizzardo, Arthur Hinojosa Jr. and Gary Bardini of the California Department of Water Resources Division of Flood Management for assistance in manuscript preparation and data analysis; James Goodridge, former state climatologist California Department of Water Resources Division of Flood Management for historical data; Jamie Anderson of the California Department of Water Resources Bay Delta Office Modeling Support Branch for graphics and comments; Norman Miller of Lawrence Berkeley National Laboratory for the literature review; Michael Dettinger of the United States Geological Survey/Scripps Institution of Oceanography; Dan Cayan of the Scripps Institution of Oceanography; Mary Tyree of the University of California San Diego; Ed Maurer of Santa Clara University; Marcia Bond and Brian Anderson of the United States Army Corps of Engineers Sacramento District for data and references; and Jery Stedinger of Cornell University for reference and discussion of frequency analysis.

Progress on Incorporating Climate Change into Management of California's Water Resources

1st Progress Report
July 2006

Chapter 7:
Climate Change Impacts on Evapotranspiration

Authors:

Roy M. Peterson, Jr. Ph.D.
California Department of Water Resources, Division Environmental Services, Sacramento.

Richard L. Snyder Ph.D.
Biometeorology Specialist, Department of Land, Air and Water Resources, University of California, Davis.

Morteza N. Orang Ph.D.
California Department of Water Resources, Division Planning and Local Assistance, Sacramento.

Hongbing Yin P.E.
California Department of Water Resources, Bay Delta Office, Sacramento.

Peer Reviewers:

Richard G. Allen, Ph.D., University of Idaho, Kimberly

Hugo G. Hidalgo, Ph.D., Scripps Institute of Oceanography

Theodore C. Hsiao, Ph.D. University of California, Davis

7 Climate Change Impacts on Evapotranspiration

7.1 Introduction

Possible increases in crop water demand and reduced water resource availability due to climate change are a growing concern among scientists and policy makers. We discuss the potential response of evapotranspiration (ET) to global climate change. Evapotranspiration is the vaporization or release of water vapor to the atmosphere from the terrestrial landscape. There are two parts to ET. First is evaporation, which includes vaporization of water from the soil and wet plant surfaces. Second is transpiration, which is vaporization that occurs within the leaves with the water vapor diffusing through pores in the leaves to the atmosphere. Water for transpiration comes from the soil through the plants and to the atmosphere. So the transpiration rate depends on the integration of soil, plant, and atmospheric factors. The evaporation rate depends on soil factors and frequency and amount of precipitation and irrigation, which determine water availability for vaporization.

In this chapter, we provide the current ET demand in California together with possible future ET demand under climate change. Population growth and likely crop pattern shifts are considered as factors that affect climate change ET estimates. An energy budget analysis to examine the net energy flux involved with ET and the physiological processes that influence ET are provided to explain the ET mechanisms affected by climate change. We describe a promising water management simulation model, SIMulation ET of Applied Water (SIMETAW). It is described in relation to climate prediction to estimate future net irrigation needs for crops.

7.2 Evaporative Demand for Applied Water in California

7.2.1 Current settings

California has produced the highest agricultural value in the country for the past 50 years. In 1997, 10.8 million acres of the state were devoted to harvested crops with another 14.4 million acres devoted to pasture and rangeland. Half of the fruits, nuts and vegetables in the country are produced in California. It is the only state producing commercial quantities of almonds, artichokes, clingstone peaches, figs, raisins, walnuts, pistachios, nectarines, olives, dates, and prunes. California also leads the nation in dairy production. In 2003, the latest available information for California agriculture production, California earned $29.4 billion in agriculture income (USDA, 2003).

This land of milk and honey results from a geography of fertile valleys, coastal plains, and gently rolling foothills and sharp tall mountains. The tall mountains in the north and on the eastern side of the state accumulate snow in winter for a water reserve during the next growing season. A semiarid Mediterranean climate provides a long frost-free growing season in most of the state. And there is abundant sunshine, a key to a plentiful agriculture and lush native vegetation.

The native vegetation of the state has a net primary productivity (NPP) that reflects the natural carrying capacity with respect to water and other natural resources. The native NPP is less than that of the state's crop production mainly because of the supplemental irrigation water applied. Figure 7-1 provides a regional map of California with the state's 10 hydrologic regions and Figure 7-2 is a map of 18 reference evapotranspiration (ET_o) zones California. The hydrological zones have traditionally been used for water resources planning and the ETo zone map has further refined ET estimation in California. Reference evapotranspiration is the ET from a vegetated surface with an approximate height of 0.12 m that is similar to clipped, cool-season grass (ASCE-EWRI, 2005). DWR's California Irrigation Management Information System (CIMIS) network (Snyder and Pruitt, 1992) was the main source of data used to develop the ET_o map. The Pruitt and Doorenbos (1977) hourly ET_o equation rather than the hourly ASCE-EWRI Penman-Monteith equation is used in CIMIS. The results, however, are similar for both equations (Ventura et al., 1999). The monthly and annual total ET_o for each of the eighteen zones is listed in Table 7.1 to illustrate the variability through the year and between zones. The ETo rates listed for the zones show the spatial patterns and relative variation of average annual ETo with extremes from 32.9 to 71.6 inches per year.

Rainfall and irrigation water are the principal sources of water for agricultural production. Irrigation water includes groundwater pumped from aquifers and surface water delivered through natural and man-made and watercourses. The surface water generally originates in the mountains as snowmelt and surface runoff from precipitation. It is temporarily stored in reservoirs for later distribution during the peak-demand season. Excluding water used to meet instream flow requirements, Delta water quality, and other environmental uses, 80 percent of the developed water supply supports agriculture while 20 percent serves urban uses.

Most of the agricultural water contributes to crop ET. But water is also used for cultural practices, such as leaching salts and for frost protection. It is also used for groundwater recharge. The term consumptive use is used and it refers to the water vaporized to produce a crop or ET. Evapotranspiration of applied water (ET_{aw}) is equal to ET minus effective precipitation, the amount of rainfall available for use by a crop. Therefore, ET_{aw} is the amount of irrigation water that is consumed by the crop. Additional irrigation water is applied to account for non-uniform distribution of the irrigation water and to control salinity. Most of the applied irrigation water contributes to ET_{aw}, so it is essential information for water resources planning and management. Projections for the actual demand for irrigation water are predicted using estimates of irrigation application efficiency. These estimates depend on the irrigation system and management, water requirements for leaching and other cultural practices, and ET_{aw} or applied irrigation water is transpired by crops and evaporated from soil and plant surfaces.

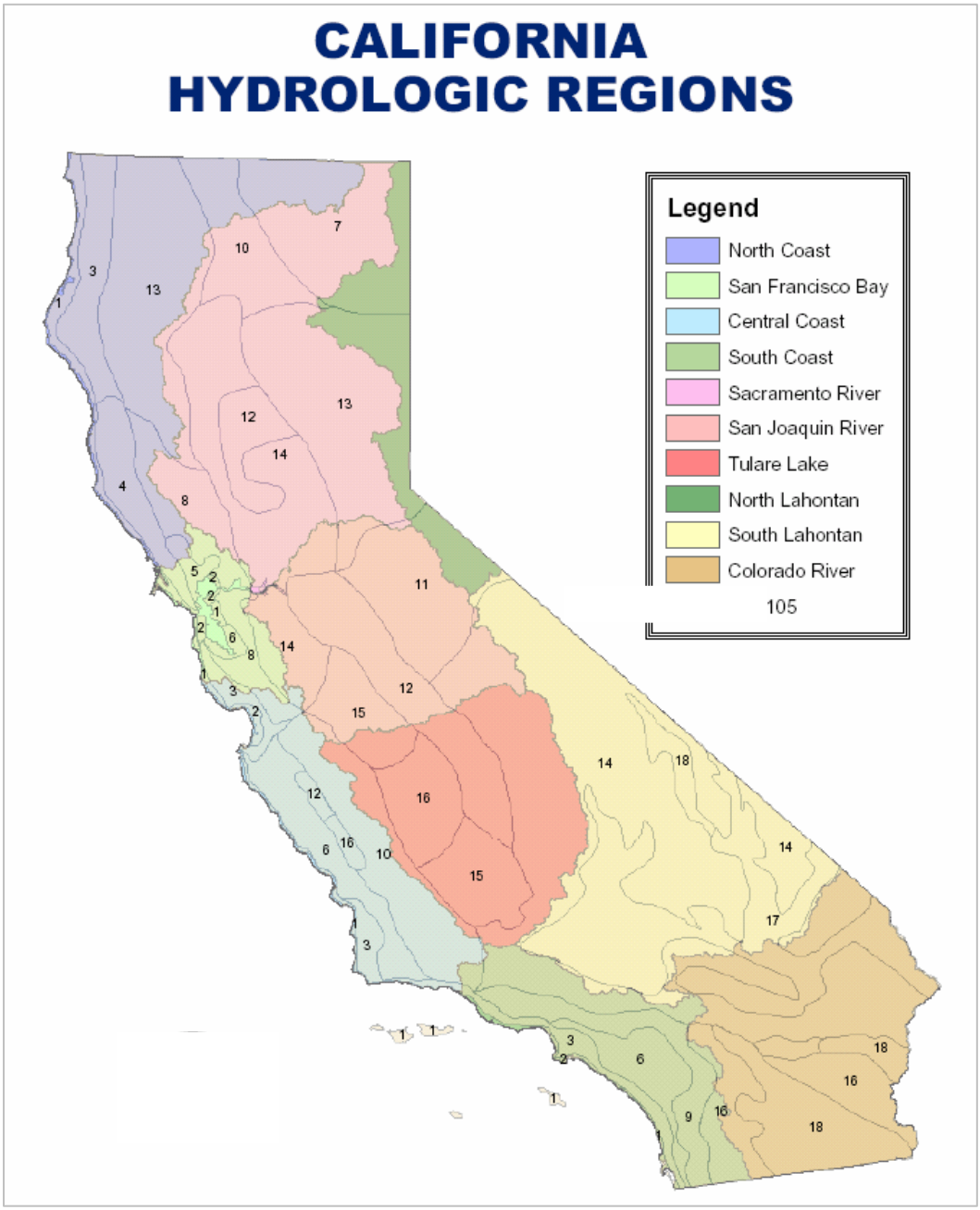


Figure 7-1 Hydrological regions coded by color
(Numbers are the ET zones listed in the legend and coded by color in Figure 7-2)

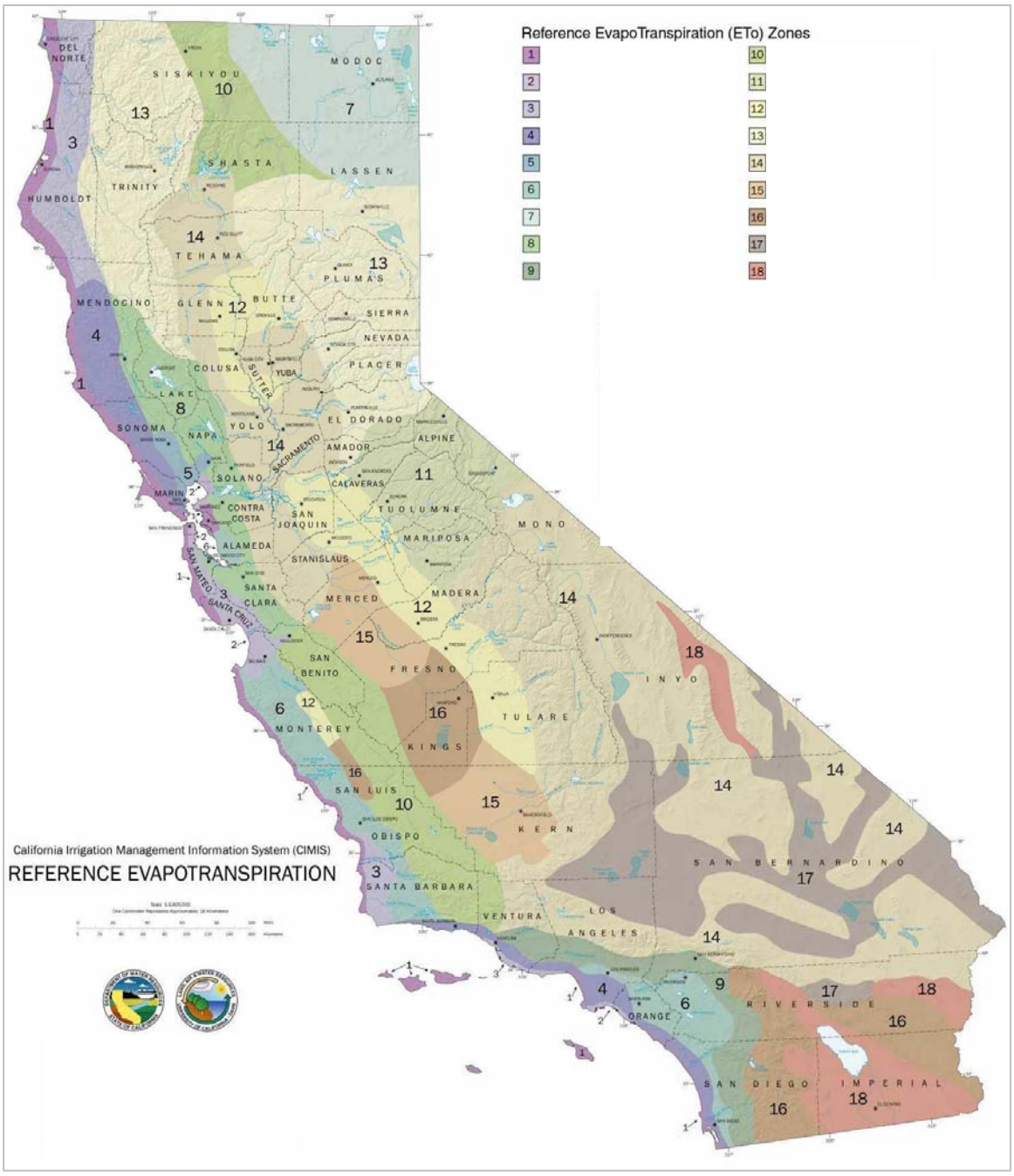


Figure 7-2. Reference evapotranspiration zones

Table 7.1. Monthly and total reference evapotranspiration (ETo) by ETo zone for the California ETo zone map in inches per month.

Zone	Jan	Feb	Mar	Apr	May	Jun	Jul	Aug	Sep	Oct	Nov	Dec	Annual
1	0.9	1.4	2.5	3.3	4.0	4.5	4.7	4.0	3.3	2.5	1.2	0.6	32.9
2	1.2	1.7	3.1	3.9	4.7	5.1	5.0	4.7	3.9	2.8	1.8	1.2	39.0
3	1.9	2.2	3.7	4.8	5.3	5.7	5.6	5.3	4.2	3.4	2.4	1.9	46.3
4	1.9	2.2	3.4	4.5	5.3	5.7	5.9	5.6	4.5	3.4	2.4	1.9	46.6
5	0.9	1.7	2.8	4.2	5.6	6.3	6.5	5.9	4.5	3.1	1.5	0.9	43.9
6	1.9	2.2	3.4	4.8	5.6	6.3	6.5	6.2	4.8	3.7	2.4	1.9	49.7
7	0.6	1.4	2.5	3.9	5.3	6.3	7.4	6.5	4.8	2.8	1.2	0.6	43.3
8	1.2	1.7	3.4	4.8	6.2	6.9	7.4	6.5	5.1	3.4	1.8	0.9	49.4
9	2.2	2.8	4.0	5.1	5.9	6.6	7.4	6.8	5.7	4.0	2.7	1.9	55.1
10	0.9	1.7	3.1	4.5	5.9	7.2	8.1	7.1	5.1	3.1	1.5	0.9	49.1
11	1.6	2.2	3.1	4.5	5.9	7.2	8.1	7.4	5.7	3.7	2.1	1.6	53.1
12	1.2	2.0	3.4	5.1	6.8	7.8	8.1	7.1	5.4	3.7	1.8	0.9	53.4
13	1.2	2.0	3.1	4.8	6.5	7.8	9.0	7.8	5.7	3.7	1.8	0.9	54.3
14	1.6	2.2	3.7	5.1	6.8	7.8	8.7	7.8	5.7	4.0	2.1	1.6	57.0
15	1.2	2.2	3.7	5.7	7.4	8.1	8.7	7.8	5.7	4.0	2.1	1.2	57.9
16	1.6	2.5	4.0	5.7	7.8	8.7	9.3	8.4	6.3	4.3	2.4	1.6	62.5
17	1.9	2.8	4.7	6.0	8.1	9.0	9.9	8.7	6.6	4.3	2.7	1.9	66.5
18	2.5	3.4	5.3	6.9	8.7	9.6	9.6	8.7	6.9	5.0	3.0	2.2	71.6

The average annual ET_{aw} in the state's ten hydrologic regions, during the most recently recorded normal water year 2000 (DWR-DPLA, 2005), ranged from 13.56 acre-inch per acre per year to 44.52 acre-inch per acre per year (Table 7.2). These ET_{aw} values are weighted by the acreages of crops grown in each region. They also reflect the variability in planting and harvest dates, ETo, and effective precipitation for each crop in each hydrologic region. Crop coefficients used to calculate crop ET_{aw} from ET_o came from a variety of sources including DWR Bulletin 113-3, April 1975, Bulletin 113-4, April 1986 and Food and Agriculture Organization of the United Nations Irrigation and Drainage Paper 56 Crop Evapotranspiration, 1998. Soil available water estimates were based on data in soil survey publications from the USDA National Resources Conservation Service. Records of daily precipitation from weather stations located near agricultural areas are used in a model along with ETo data and soil information to estimate the amount of precipitation available for crop consumption. The ET_{aw} values extend from October 1, 1999 through September 30, 2000. ET_{aw} values vary from year-to-year with changes in the proportions of irrigated acreage planted to each crop category, change in cultivars planted, the quantity and distribution (spatial and temporal) of precipitation, water applied for cultural practices, irrigation water management, variation in ETo and other factors.

The statewide average annual ET_{aw} for 20 important agricultural crop categories are listed in Table 7.3. These average ETaw values reflect the distribution of crops across the ETo zones in California. They are based upon the same data from Water Year 2000 used to estimate the average ET_{aw} for each hydrologic region. Safflower used the least water, averaging 9.48 acre-inch per acre while alfalfa used the most, averaging 42.72 acre-inch per acre.

Table 7.2 Estimated Annual ET of applied water by hydrologic region during the 2000 water year in acre feet per acre, from DWR-DPLA 2005

Region	Name	ETaw (acre-inch/acre)
01	North Coast	20.28
02	San Francisco Bay	14.16
03	Central Coast	13.56
04	South Coast	27.60
05	Sacramento River	28.92
06	San Joaquin River	26.04
07	Tulare Lake	26.76
08	North Lahontan	28.92
09	South Lahontan	44.52
10	Colorado River	42.96

Table 7.3 ET of applied water in acre inch per acre for some of the main commodities grown in California.

Commodity	ETaw (acre-in/acre)
Grains	12.72
Rice	37.44
Cotton	28.44
Sugar Beet	30.72
Corn	22.20
Dry Bean	18.36
Safflower	9.48
Other Field Crops	22.44
Alfalfa	42.72
Pasture	34.68
Processing Tomatoes	24.36
Fresh Market Tomatoes	20.40
Cucurbits	18.72
Onions Garlic	29.16
Potatoes	20.04
Other Truck Crops	15.84
Almonds Pistachios	33.12
Other Deciduous Orchards	32.16
Subtropical Crops	30.36
Vineyards	17.3

7.2.2 Projected ET changes for the California landscape impacted by climate change

Hidalgo et al. (2005) investigated the impacts of climate change on irrigation water demand with respect to reference ET (ET_o) in California and found that the highest interseasonal variability of ET_o daily anomalies occurs during the spring, mainly in response to variations in cloudiness. Daily ET_o values were closely associated with net radiation (R_n), relative humidity, and cloud cover, and are less related to average daily temperature. In the next section about energy budget the relationships between climatic factors are discussed along with relative influences they exert. Although Hidalgo et al (2005) concluded that to maintain ET_o in the current condition requires a decrease in R_n of about 6 percent to compensate for a temperature increase of 3ºC, they did not account for increased stomatal resistance that is likely to result from higher CO_2 concentration, which is discussed in detail later in this chapter. Hidalgo et al. were clearly correct in that the effects of climate change on ET_o are difficult to forecast because of the uncertainty of cloud cover and relative humidity. Allen et al. (1991) concluded that a CO_2 induced climate change resulted in an increased ET_o which then translated to an increased ET_{aw}.

7.2.3 Landscape influences on ET that complicate climate change effects

Climate influences biophysical features in the landscape, but the physical landscape also influences climate and affects the interaction between climate and landscape. For example, crop irrigation reduces the air temperature and urban surfaces commonly increase temperature.

Future urban growth affects the statewide ET demand by decreasing irrigated agriculture land. In population studies, Landis and Reilly (2004) reported that the greatest urban expansion is likely to happen on flat land of valley floors. They listed the greatest risk to important farmland as land in the Inland Empire and in the Central Valley.

Increasing urbanization can increase the heat-island effect (a localized elevation in temperature over the ambient air temperature) and could lead to small increases in advection of additional heat to nearby crops. Advection is the horizontal transfer of heat or scalars, such as water vapor or CO_2, that results when wind blows air reflecting characteristics of one surface over another surface with different characteristics. Energy fluxes over irrigated crops are usually vertical, but there can be edge effects when local advection occurs. When there is warm air advection, the horizontal transfer of energy can increase ET on crop edges. This can lead to moderate stress, which reduces plant size, or severe stress that reduces ET and photosynthesis. This is quite noticeable where irrigated fields are surrounded by bare, dry soil. Affected crops are often shorter and appear more stressed on the edges than in the middle of the field. There is also regional warm air advection, which occurs when heat is horizontally transferred over cropped areas. This often happens in the Central Valley where warm air from the drier foothills moves over irrigated land in the middle of the valley. For regional advection, however, the heat transfer is mostly vertical. This means there is more available energy for evaporation than is supplied by net radiation and soil heat flux. The result is a reduced $ET_{c/}ET_{pot}$ ratio because Et_{pot} increases due to advection. Urbanization could lead to some additional warming and it might increased advection. Although small in its reach, increased advection could result from urban expansion into irrigated crops in an increasing dentate edge.

Other effects on ET from growing urbanization next to agricultural land include physiological impacts from air toxicants, most notably ozone, and regional atmospheric dimming from particulates and pollutants above and around urban centers and held in place by inversion due to high atmospheric pressure during the summer growing season.

7.2.4 Changes in cropping and irrigation methods that interact with climate change

Throughout the 150 years of California agriculture, many changes in crop types and shifts in cropping patterns have occurred. In addition to land loss to urbanization, land use conversions for agriculture are driven by irrigation water availability, changes in multiple cropping, and changes in the crops due to economics. Biophysical changes that result from climate change could contribute to these factors. For example, with warming temperatures, citrus production could move farther north in the Central Valley and deciduous orchard crops that have large chill requirements might have reduced production or be forced out of the area. Shifts in cropping patterns are likely to continue with increased water cost and possibly with changes in regional climates. There are, however, no comprehensive studies of projected changes in California agriculture resulting from climate change (Hayhoe et al., 2004). Water resources availability will likely be the main environmental variable determining shifts in crop distribution (Field et al., 1999).

Based on surveys conducted jointly by the University of California and California Department of Water Resources, a definite trend towards growing more perennial crops and using low-volume, pressurized irrigation systems has occurred during the past 30 years (CDWR Bulletin 160-05). While this has improved the economic benefits resulting from irrigation and has likely improved on-farm irrigation efficiency during years with adequate water supplies, growers have reduced ability to adapt during dry periods. For example they don't have annual field or row crops that could be fallowed during droughts. With adequate water supplies, this trend is good, but it is financially dangerous in terms of drought response and mitigation.

The value integration network simulation model (CALVIN) and the statewide water and agricultural production simulation model (SWAP) were developed at the University of California, Davis, and they were coupled to investigate climate change in California by modifying crop yields and amount of irrigated water used (Tanaka et al., 2005). They concluded that by the end of the century there will be a 24 percent decrease in the amount of water devoted to agriculture and only a 6 percent decrease in agricultural income. The differences in water use and income were attributed to growing higher value crops and increased irrigation application efficiency. Higher application efficiencies mean higher ratios of water consumption by evapotranspiration to water applied. This can reduce both diversions for irrigation and reduced return flow. In some instances, this may reduce supplies to downstream projects depending on whether the reduction in diversions or return flow is larger. Generally, if outflows from basins are near minimum values, only reductions in ET upstream will free up water for transfer from irrigated agriculture.

7.3 Energy Budget

An energy budget can account for all input and output energy fluxes to a terrestrial landscape. Among these fluxes is the mass balance of water phase change of liquid water to gaseous water vapor. This accounting is a useful analytic tool to investigate the affect of climate change on

evapotranspiration. The Penman-Monteith equation, which is described in Appendix 1, is a partly empirical algorithm that was derived from energy budget considerations. It was modified by the ASCE-EWRI (2005) to derive a reference evapotranspiration (ETo) rate from meteorological measurements of minimum and maximum temperature, humidity, solar radiation and wind speed. There is, however, a difficulty in estimating crop evapotranspiration (ETc) or ETo for a climate-changed environment because of a lack of knowledge about canopy resistance to water vapor loss in an elevated CO_2 environment. Nonetheless, using FACE measurements of stomatal resistance (Long et al., 2004) for elevated CO_2 and the same approach used by Allen et al. (1989) to estimate canopy from stomatal resistance for use in estimating ETo, an increase in CO_2 concentration to 550 ppm is expected to increase the daily mean canopy resistance from 70 to 87 s m^{-1}.

It is important that the ASCE-EWRI (2005) has fixed the ET_o canopy resistance at 70 s m^{-1} for daily calculations and it is unlikely to be changed in the near future. The equation, however, should be updated if the canopy resistance changes. This is necessary because crop coefficient values were mostly developed by calculating the ratio $K_c = ET_c/ET_o$, where ET_o was the ET of the reference grass surface and ET_c was the crop ET. Consequently, the standardized reference ET equation should provide a good estimate of the ET of a 0.12 m tall, cool-season grass surface or the K_c values will surely be incorrect. It is possible that K_c values could change because of differences in stomatal responses to climate change, but changing the ET_o equation and assuming that the K_c ratio will be conserved is more plausible than maintaining a standardized equation that gives an incorrect estimate of the K_c ratio denominator. To investigate possible ET changes in response to climate change, the daily (24-hour) ASCE-EWRI (2005) ET_o equation is used and the temperatures and canopy resistance are changed to investigate how the ET of a 0.12 m tall, cool-season grass might change. It is assumed that other crops will respond similarly to the grass and the K_c values will not change.

The Consumptive Use Program (CUP) was developed by DWR and the University of California, Davis to estimate crop evapotranspiration for planning purposes. CUP was written, using MS Excel software, as a tool to help California growers and water purveyors obtain accurate estimates of crop water requirement information from monthly mean data. The program takes input weather data and estimates monthly reference evapotranspiration (ETo) using the Penman-Montieth equation. Then the program uses a curve fitting technique to derive one year of daily weather and ETo data from the monthly data. A feature to vary the canopy resistance as well as the temperature allows users to investigate the effects of increasing canopy resistance on ET_o. Current monthly mean climate data from Davis, CA and a canopy resistance of 70 s m^{-1} were input into CUP to calculate ET_o rates using the Penman-Monteith equation. The process was repeated using an elevated 3^oC minimum and maximum temperature, holding all other variables constant. The process was repeated a third time with an increase in the minimum and maximum temperature and the dew point temperature by 3^oC while holding other variables constant. Finally, the combination of the air and dew point temperature increase by 3^oC and a canopy resistance increase to 87 s m^{-1} was computed. Figure 7-3 shows a comparison of the smoothed curves of calculated ET_o for the four scenarios. Increasing only air temperature, resulted in a 18.7 percent increase in ET_o. Increasing the air and dew point temperatures led to a 8.5 percent increase in ET_o. Increasing the temperatures and the canopy resistance to 87 s/m led to a 3.2 percent increase in ET_o over current conditions. While the percentage increase is small when the

canopy resistance is included, the volume of water relative to California is considerable. Other factors like changes in solar radiation due to changes in cloudiness or air pollution and changes in wind speed were not considered.

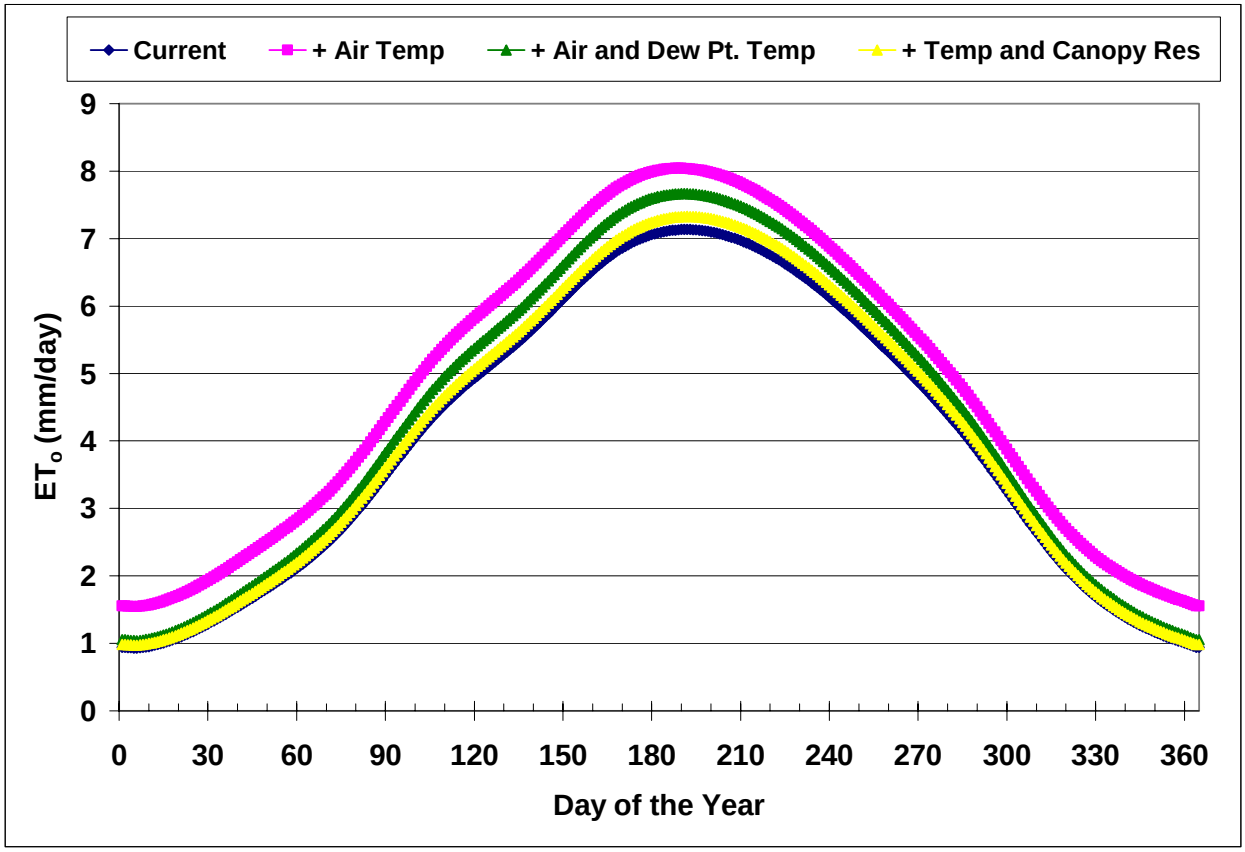


Figure 7-3 ET_o comparison for current and climate change conditions
ETo comparison for current conditions (navy), for minimum and maximum temperature elevated 3°C (pink), for minimum and maximum and dew point temperature elevated by 3°C(green), and for temperature elevated 3°C and canopy resistance increased to 87 s/m (yellow).

7.4 Plant Physiology and Climate Change

7.4.1 Plant physiological and morphological adaptation

Plants adapt to a changed physical environment through physiologically and morphologically modification. For changes in temperature and CO_2, the two main plant adaptations are to control the water continuum between soil and atmosphere and to adjust photosynthetic carbon fixation.

In transpiration, water vaporizes inside leaves and diffuses through stomata (i.e., pores in the leaf surface) to the ambient air. Simultaneously, CO_2 is diffusing from the atmosphere into the leaves through the same stomata. When stomata partially close, CO_2 flow into the leaves and H_2O flow from the leaves are both affected at the same time. However, since mesophyl resistance (i.e., resistance of the cell walls to passage of the CO_2) is typically much higher than stomatal resistance, stomatal closure has less effect on CO_2 uptake than it does on transpiration, which is

restricted by the smaller stomatal aperture. In experiments carried out in enriched CO_2 environments, which are described later, typical agronomic plants exhibited a 20 percent reduction in stomatal conductance and a 20 percent increase in photosynthesis (Long et al., 2004).

In addition to being influenced by the environment, plants also influence their environment. Evaporation from the soil is directly affected by the plant canopy shading. The canopy size and density (i.e., coverage) and the rate of development all influence crop ET. The plant coverage is often quantified with the leaf area index (LAI), which is determined as the ratio of the canopy leaf area per unit ground area under the canopy. Theoretically, there is an optimal LAI that reduces soil evaporation on one hand, which increases water for transpiration and other plant processes, and that minimizes self shading of leaves that decreases growth and reproduction. The rate of canopy growth and closure is often quantified using the relative growth rate (RGR) or the growth per unit of biomass. The RGR optimization depends on below ground and above ground assimilate allocation that influence depth of rooting for water and nutrient attainment as well as canopy development, photosynthesis, and ground shading. To varying degrees, depending on the specific crop or even cultivars, there is a possibility for adaptation during plant growth and development (phenotypic plasticity) or for genetically fixed trait expression regardless of the environment.

What is most important for the ET, is not the total amount of leaf area produced but the rate of canopy development and closure (Hsiao and Xu, 2005), which can take up to two months in herbaceous crops. That is, the LAI is less important than the rate at which the canopy foliage develops and shades the ground. The rate of canopy closure is important for determining the relative contributions of evaporation and transpiration to ET. At planting, soil evaporation comprises 100 percent of the ET_c, but the contribution from the soil decreases until it is small relative to transpiration once a canopy reaches about 75 percent ground cover for field and row crops, and about 70 percent for tree and vine crops. This change occurs because the crop canopy intercepts most of the radiation before it reaches the ground once 75 percent ground cover is attained.

7.4.2 Transpiration and photosynthesis

Several plant physiology processes are often simultaneously influenced by environment factors. Figure 7-4 shows the relation of photosynthesis and transpiration together with the climatological factors influencing the two processes. Nitrogen assimilation, which occurs through the plant roots, can be affected by transpiration rate. It is included because of its importance as a control node in the photosynthetic process. Nitrogen is particularly important as part of the of Rubisco assimilation pathway. Rubisco is said to be the most abundant protein, and is an enzyme with a low efficiency that is pivotal as the initial and limiting step in the fixation of carbon in photosynthesis of most agronomic crops. Appendix 2, detailing the photosynthesis response curve to CO_2, provides a fuller description of Rubisco and photosynthesis).

There are several photosynthetic pathways found in different plant species. In the C_3 pathway, which is the most widespread and is the photosynthetic system of most agriculture plant species, CO_2 is initially fixed by Rubisco during the day (i.e. in the presence of light) and then converted

to a three-carbon intermediate. In the C_4 pathway CO_2 is initially fixed by PEP carboxylase during the day to form four-carbon acids. The C_3 and C_4 plants also differ anatomically, with C_4 plants maintaining a higher c_i (intercellular CO_2 concentration) and a lower stomatal conductance for the same CO_2 assimilation rate.

Both light and dark respiration are included Figure 7-4 because respiration accounts for about 25 percent of plant energy expenditure. Respiration is an intercellular process in which molecules, particularly pyruviate in the citric acid cycle, are oxidized with the release of energy. It involves the complete breakdown of sugar or other organic compounds to CO_2 and H_2O. In addition to respiration relating photosynthesis, transpiration and nitrogen metabolism in an energy currency, optimization respiration is also important in the differential responses of plant biomass production to changes in atmospheric CO_2, which in turn is related to nitrogen form involved in intermediate metabolism. This concept is developed further in the physiological response section.

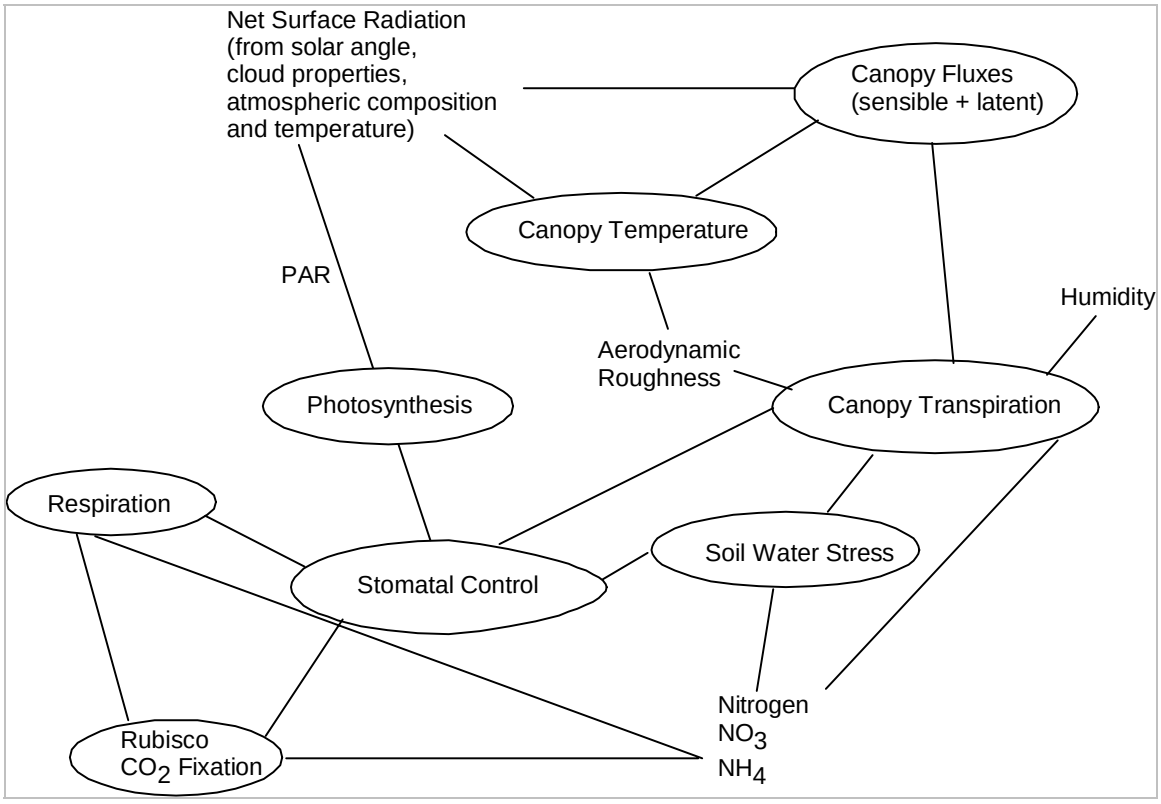


Figure 7-4 Relation of transpiration, photosynthesis and nitrogen.
Photsynthetically available radiation (PAR) indicates the total energy available for photosynthesis

In summary, the relation of the three physiology processes diagramed in Figure 1 are not necessarily direct but rather optimizations which can be either passive or active. Therefore, care is needed in extrapolating relations such as the total leaf area and stomatal density where feedback loops involving Rubisco density and its long term adaptations influence the relation of

stomata function in CO_2 enriched environments. This concept will be discussed in a later section. The water use efficiency (WUE) quantitatively relates assimilation to transpiration. Assimilation is used here as the incorporation of an inorganic resource such as CO_2 or NH_4 into organic compounds; it is often synonymous with net photosynthesis. WUE = A/T, where A is assimilation and T is transpiration. Transpiration efficiency has been used to describe the ratio of carbon gained to water transpired at the whole plant level, that is assimilation per transpiration (Condon and Hall, 1977). In agronomy, WUE is typically regarded as the ratio of carbon fixed per unit water use; so at a crop level it is the amount of dry matter production per unit of total water transpired (T).

7.4.3 Effect of increased CO_2 on plant physiology and morphology

In an atmosphere with increased CO_2, the balance between photosynthesis and transpiration appears to change (Long et al., 2004). Plants adjust their stomatal opening to maintain the CO_2 concentration within the plant leaf intercellular space (c_i) so that it does not limit photosynthesis. Less stomatal opening is required at high atmospheric CO_2 concentration (c_a). Many researchers report that stomatal conductance decreases with rising atmospheric CO_2 concentration to maintain a constant (c_i/c_a) (Long et al, 2004; Hsiao and Jackson, 1999). Because the stomata partially close to maintain the concentration gradient between the air and stomatal cavities under elevated CO_2 concentration and the water vapor gradient is unchanged, the photosynthesis rate is little affected and the transpiration rate declines because of the stomatal closure, resulting in a small increase in WUE though an increase in photosynthetic demand (see Appendix 2 The photosynthesis Response Curve to CO_2).

With increased CO_2 for fixing carbon in photosynthesis, the diffusion of CO_2 into the plant leaf and water vaporization out through the same stomata is influenced by the availability of activation sites for fixing CO_2, which in turn is influenced by the availability of nitrogen to make the sites (i.e. enzymes, which for most crops is Rubisco). New findings suggest respiration could prove important to nitrogen assimilation at elevated CO_2 (Rachmilevitch et al., 2004). The forms of nitrogen used by a plant and elevated CO_2 can influence respiration (Rachmilevitch et al., 2004). The form of nitrogen used in plant intermediate metabolism, whether NO_3 or NH_4, varies between species and even at different growth stages for the same plant. Plants that use NO_3 as their primary nitrogen source are unable to sustain rapid growth under elevated CO_2 because of interferences with respiration.

Figure 7-5 provides response relationships to increased atmospheric CO_2 for processes shown in Figure 7-4. The initial finding for this summarization of responses to CO_2 increase comes from growth chamber studies performed usually on individual leaves or individual plants. More recently, a good body of evidence for plant physiological responses to elevated CO_2 (about 570 µmole mol^{-1}) has been reported from FACE field studies on small plots.

Long et al. (2004) summarized the findings from these FACE sites in a meta analysis, which allows statistical analysis of the studies as a whole to understand elevated CO_2 influences. They found that biomass assimilation increased by about 20 percent while seed production increased about 24 percent. However, nitrogen in the leaves of longer-term plants decreased 17 percent and Rubisco decreased 15 percent. The LAI increased but not significantly.

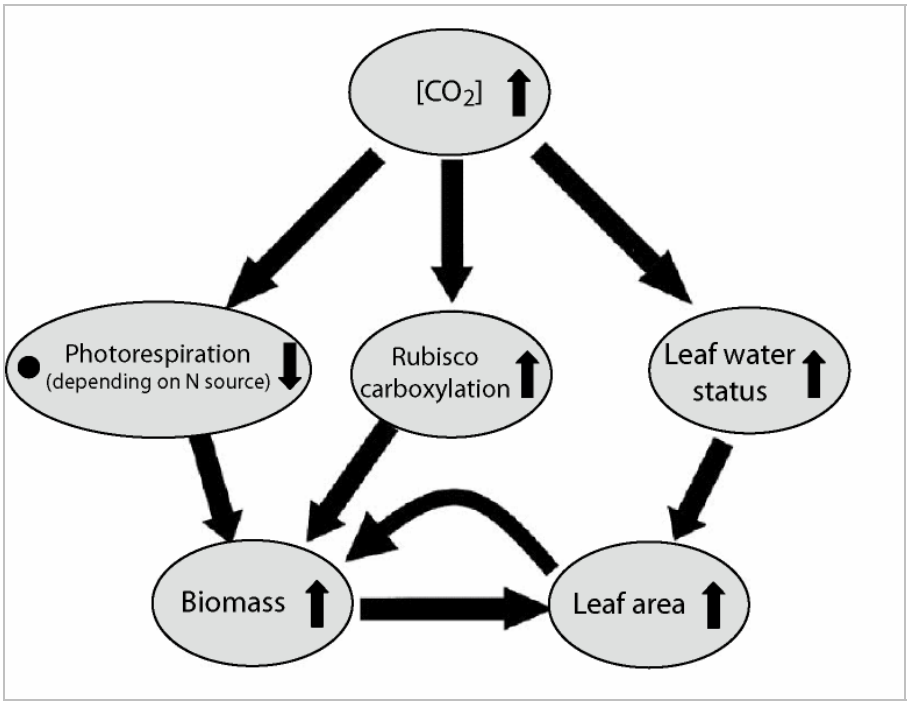


Figure 7-5. CO_2 effects and interactions on C_3 plant production.
CO2 effects and interactions on C3 plant production. The small arrows inside ovals indicate influence of CO2 on process (modified from Long et al, 2004)

Influences of elevated temperature and CO_2 on crop growth and phenology are topics of importance in determining ET for a future California landscape. For both herbaceous plant life and woody perennials, the influence of climate change on leaf senescence needs further study. Physiological changes like the apparent earlier or faster leaf aging in deciduous tress at elevated CO_2 can reduce seasonal ET. Evaporation from the soil is mainly affected by wetness of the soil surface, hydraulic properties of the soil, energy availability, and wind speed beneath the canopy so that advances in regional climate scale models are needed to understand influences of radiation and wind speed trends. Wind speed in particular is difficult to model and projects and accurate modeling of wind speed is unlikely to occur in the near future. Physiological changes like the apparent earlier or faster leaf aging in deciduous tress at elevated CO_2 can reduce seasonal ET and can be estimated.

It is widely held that increased CO_2 concentration could improve WUE, and needs more analysis at least on a whole plant level, if not the plant community level. When using whole plant examination of climate change impact that considers WUE by scaling up from relations such as LAI and stomata conductance there is a need to consider the influence of carbon assimilation from increased carbon fixation efficiency. Groups are using a variety of methods to investigate WUE. The isotope discrimination methodology for WUE is a direct measure that is easily obtained from any tissue in a plant. Seed companies are using this technique to develop plants with increased assimilation relative to transpiration to achieve a better WUE at elevated CO_2 or temperature. There is, however, a likely maximum theoretical upper bound to the gains in plant

WUE that are obtainable (Cowan and Farquhar, 1977). The likely upper bound to WUE brings into focus the need to look at a systems level for both understanding and for possible water use reductions per unit production. A system vision needs to considers the CO_2 and temperature environmental influence on plants, the plants influence on the local ET environment and the on farm water delivery to plants.

7.5 A Simulation Model for Estimating ET of Applied Water (SIMETAW)

7.5.1 SIMEATAW model description

SIMETAW (Simulation of Evapotranspiration of Applied Water) is a computer application program that can simulate several decades of daily weather data from climate records. It is useful for studying the effect of climate change on Crop evapotranspiration (ET_c) and evapotranspiration of applied water (ET_{aw}). SIMETAW was written mainly for use in water demand planning. SIMETAW can use either observed daily climate records or it can simulate daily weather data from monthly means for a specified period of years. The observed or simulated daily data are then used to estimate reference evapotranspiration (ET_o). Crop evapotranspiration is calculated for each day in the period of record using the product of the daily ET_o values and a crop coefficient (K_c) factor. The seasonal change in Kc factors is determined using a slightly modified procedure that was originally presented by Doorenbos and Pruitt (1977). This method enables the representation of day-to-day variations in evaporative demand.

Monthly climate data include solar radiation (R_s), maximum (T_x) and minimum (T_n) air temperature, wind speed at 2 m height (U_2), dew point temperature (T_d), number of rainy days per month (NRD), and monthly total rainfall (Pcp). SIMETAW computes ET_o using the daily (24-hour) Penman-Monteith equation (ASCE-EWRI, 2005). Daily ET_c rates are estimated by multiplying ET_o by a crop coefficient (K_c) factor. In addition, observed or simulated daily rainfall, soil water holding characteristics, effective rooting depths, maximum soil depths, and ET_c are used to determine effective rainfall and to generate hypothetical irrigation schedules to estimate the seasonal and annual ET_{aw}. All of the water balance calculations are done on a daily rather than monthly basis, which improves the estimation of effective rainfall and, hence, ET_{aw}. A two-stage soil evaporation model is used to estimate bare soil evaporation as a function of mean ET_o and wetting frequency in days. The bare soil evaporation rates are used to determine the off-season evapotranspiration and as a base-line for in-season K_c calculations. Since ET_c is unlikely to fall below the evaporation from an unirrigated bare soil, the crop Kc factors are not allowed to fall below the bare soil K_c value on any given date. In addition, SIMETAW accounts for the influence of orchard cover crops on K_c values, and it adjusts for tree and vine crop immaturity.

Combining atmospheric general circulation models (GCMs) with regional landscape models for downscaled model climatic results can provide estimates of future monthly climate variables, which can be used as simulation input for SIMETAW. Daily means of R_s, T_x, T_n, U_2, and T_d by month are used to simulate daily weather data for several decades and the Penman-Monteith equation is then used to estimate daily ET_o for the period of record. Increasing or decreasing one or more of the weather variables in the monthly climate prediction will influence the daily

weather simulation and hence ET_o calculation. For example, changing the rainfall pattern to have more precipitation in the fall and spring with less in the winter can be used to study the impact on the ET_{aw}. The ability to change the canopy resistance in response to higher CO_2 concentration was included in SIMETAW to more accurately estimate the effect of climate change on ET_o by accounting for both canopy resistance and temperature changes.

7.5.2 Input data requirement

Either observed or simulated daily climate data are used in SIMETAW to determine ET_o. When monthly data are input, the daily data are simulated. Data from CIMIS or from a non-CIMIS data source can be input as long as data are in the correct format. For the water balance calculations, soil and crop information are input to calculate ET_c and ET_{aw}.

A main feature of SIMETAW is that it simulates daily weather data from monthly climate data and estimates reference ET_o. Because of this feature, SIMETAW can be used to examine a range of climate scenarios for California's agricultural water demand using GCM scenarios and regional downsizing models. Using four climate change scenarios and a downsizing model to determine a running mean of monthly climate data centered around 2020 and 2050, SIMETAW can simulate daily weather data, and determine ET_o, ET_c, and ET_{aw} for some major crops grown in California. Possible values for canopy resistance can be input into the program to determine the effect of canopy resistance on ET_o.

SIMETAW was developed for water demand planning and it can help to plan for the effects of climate change as well as for current climate conditions. At this time, the limitation is the downscaling of GCMs to a regional scale. When regional long range predictions of R_s, T_x, T_n, T_d, U_2, and precipitation resulting from climate change are available, predicted daily means of the data by month can be input into SIMETAW to provide estimates of agricultural water demand.

7.5.3 Output files

Files created by SIMETAW are listed as following:

- Several years of raw or simulated daily weather data including calculated ET_o from raw or simulated data by weather station
- Several years of daily calculated crop coefficients, crop evapotranspiration and water balance calculations by crop within a study area
- One year mean of simulated or non-simulated daily and monthly ET_c and ET_{aw} data averaged over the data set
- Several years of simulated or non-simulated seasonal and annual total of ET_c and ET_{aw} by crop within a study area
- Simulated or non-simulated seasonal and annual total of ET_c and ET_{aw} averaged over the years of record

7.5.4 Weather simulation

Weather simulation models are often used in conjunction with other models to evaluate possible crop responses to environmental conditions. In SIMETAW, daily climate data are used to estimate ET_o and K_c values are used with the ET_o to estimate ET_c. Rainfall data are then used with estimates of ET_c to determine ET_{aw}. Either daily climate records or simulated daily data can be used for the calculations.

7.5.4.1 Rainfall

Characteristics and patterns of rainfall are highly seasonal and localized, and it is difficult to create a general, seasonal model that is applicable to all locations. Recognizing the fact that rainfall patterns are usually skewed to the right toward extreme heavy amount and that rain status of the previous day tends to affect the present day condition, a gamma distribution and Markov chain modeling approach was applied to described rainfall patterns for periods within which rainfall patterns are relatively uniform. This approach consists of two models: two-state, first order Markov chain and a gamma distribution function. These models require long-term daily rainfall data to estimate model parameters. SIMETAW, however, uses monthly averages of total rainfall amount and number of rain days to obtain all parameters for the Gamma and Markov Chain models.

7.5.4.2 Wind speed

The simulation of wind speed is a simpler procedure, requiring only the gamma distribution function as described for rainfall. Although using a gamma distribution provides good estimates of extreme values of wind speed, there is a tendency to have some unrealistically high wind speed values generated for use in ET_o calculations. Because wind speed depends on atmospheric pressure gradients, no correlation between wind speed and the other weather parameters used to estimate ET_o exists. Therefore, the random matching of high wind speeds with conditions favorable to high evaporation rates leads to unrealistically high ET_o estimates on some days. To eliminate this problem, an upper limit for simulated wind speed was set at twice the mean wind speed. This is believed to be a reasonable upper limit for a weather generator used to estimate ET_o because extreme wind speed values are generally associated with severe storms and ET_o is generally not important during such conditions.

7.5.4.3 Temperature, solar radiation, and humidity

Temperature, solar radiation, and humidity data usually follow a Fourier series distribution. Therefore, the model of these variables may be expressed as:

$$Xki = mki\ (1 + dki\ Cki) \qquad (1)$$

where k = 1, 2 and 3 (k=1 represents maximum temperature; k = 2 represents minimum temperature; and
k =3 represents solar radiation), mki is the estimated daily mean, and Cki is the estimated daily coefficient of variation of the ith day, i = 1, 2, … , 365 and for the kth variable.

SIMETAW simplifies the parameter estimation procedure of Richardson and Wright (1984), requiring only monthly means as inputs. From a study of 34 locations within the United States, the coefficient of variability (CV) values appear to be inversely related to the means. The same approach is used to calculate the daily CV values. In addition, a series of functional relationships were developed between the parameters of the mean curves and the parameters of the coefficient of variation curves, which made it possible to calculate Cki coefficients from mki curves without additional input data requirement.

7.5.5 Validation of daily simulated weather data of SIMETAW

Validity of the SIMETAW model was tested by comparing simulated with observed daily weather data. In this section, nine years of daily measured weather data from the CIMIS station in Davis were compared with 30 years of simulated daily weather data. Figure 7-6, Figure 7-7, and Figure 7-8 show that R_s, T_x, and P values from the simulation were well correlated with values from CIMIS. Similar results were observed for T_n, u_2, and T_d data. Although comparisons are only shown for Davis, similar results were found in other climatic regions of the state.

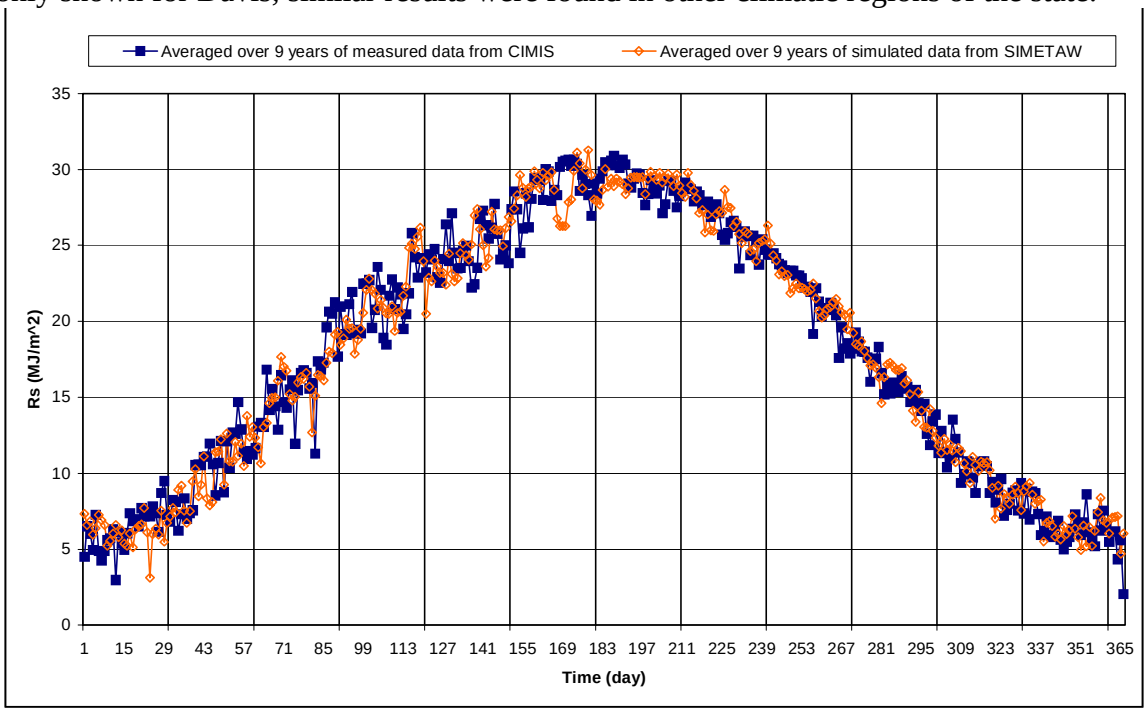


Figure 7-6. Comparison of measured and simulated daily solar radiation at Davis

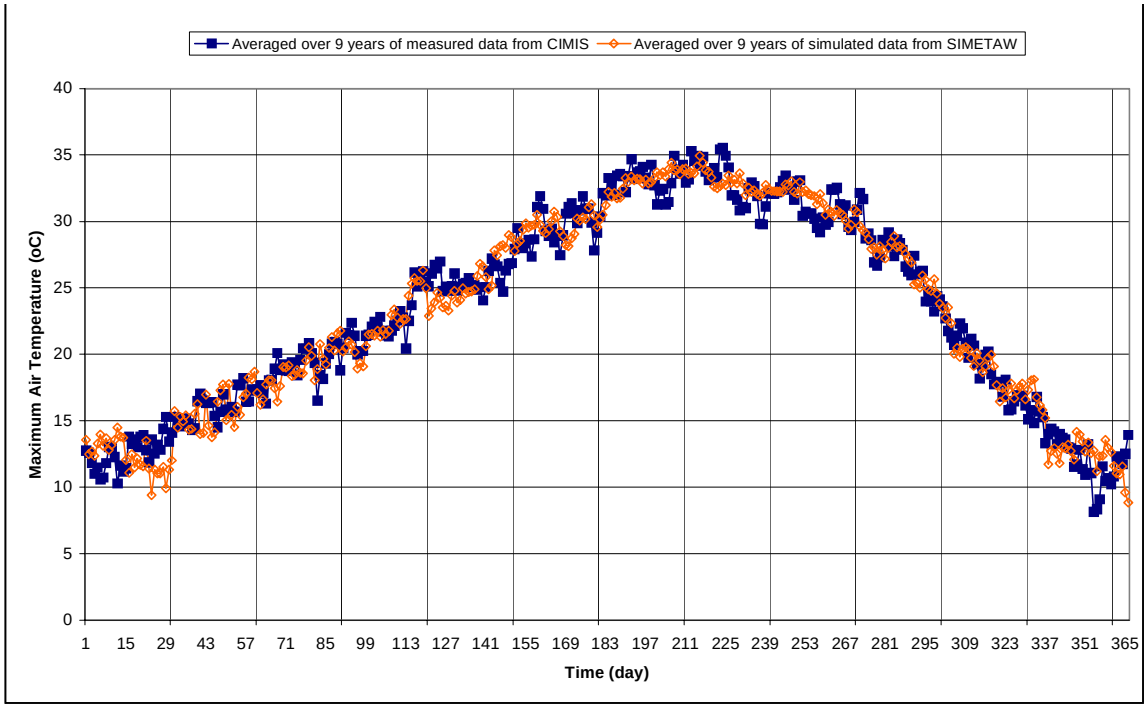


Figure 7-7. Comparison of measured and simulated air temperature at Davis

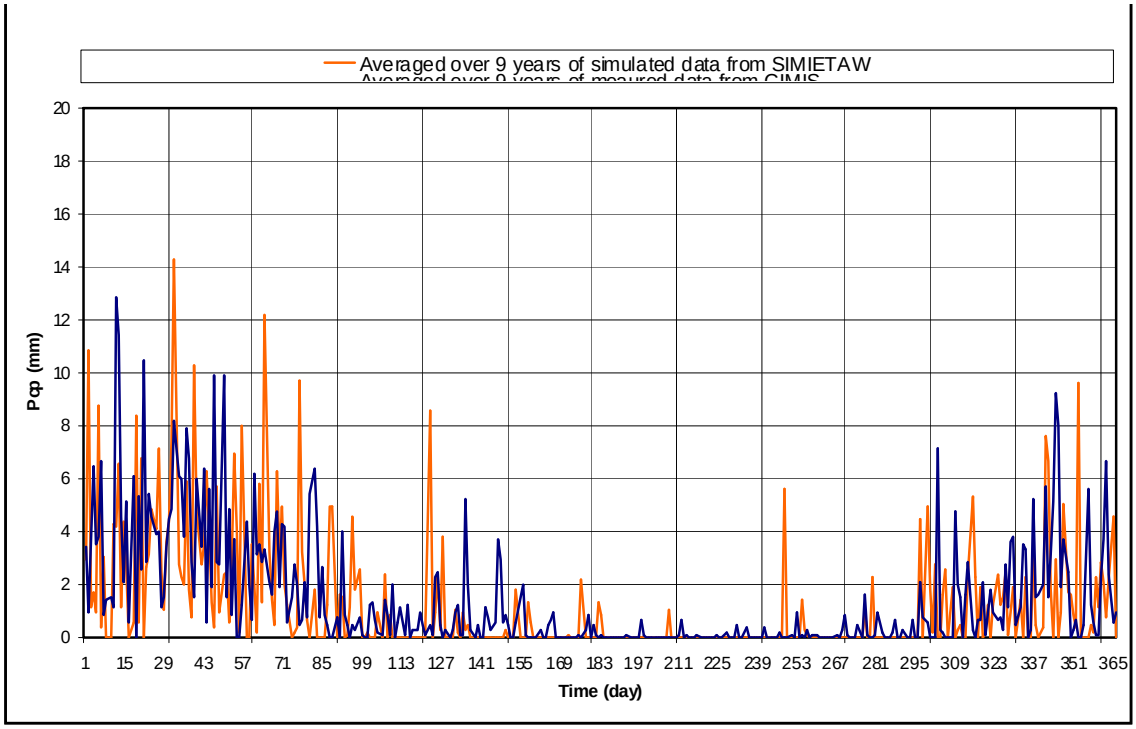


Figure 7-8. Comparison of measured and simulated precipitation at Davis

Using weather data from CIMIS stations near Davis, Oceanside, and Bishop, comparisons were made between ET_o from CIMIS and ET_o simulated from SIMETAW and averaged over the period of record (Figure 7-9, Figure 7-10, and Figure 7-11). CIMIS-based estimates of ET_o closely matched those from the SIMETAW program.

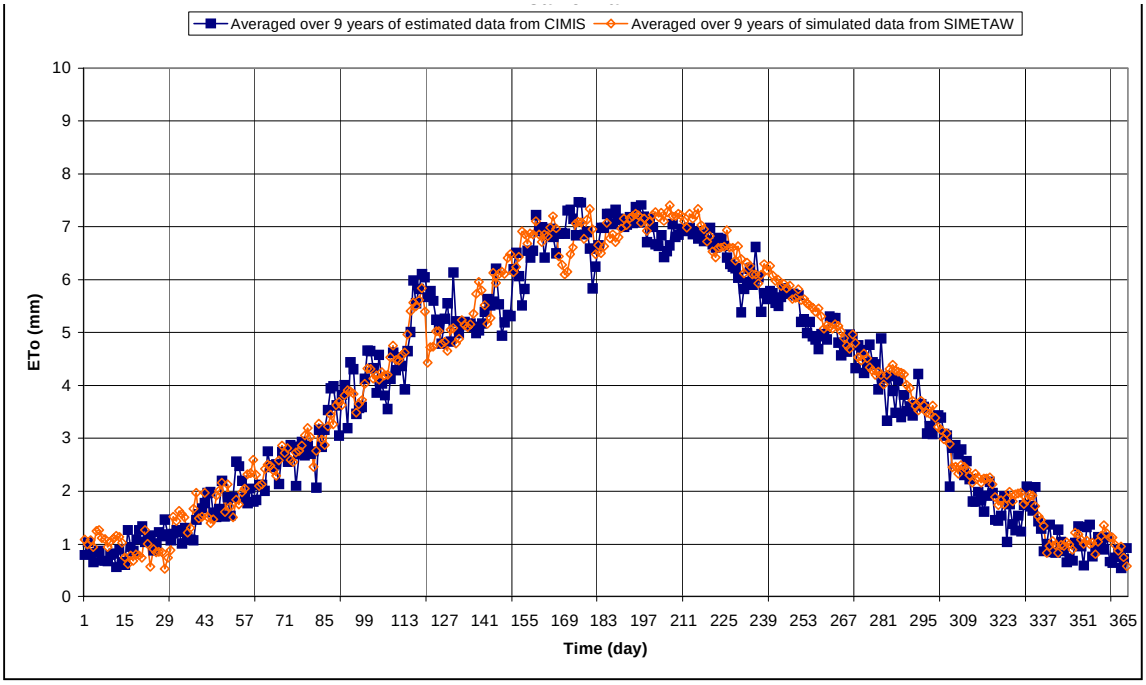


Figure 7-9. Comparison of estimated and simulated reference ET at Davis

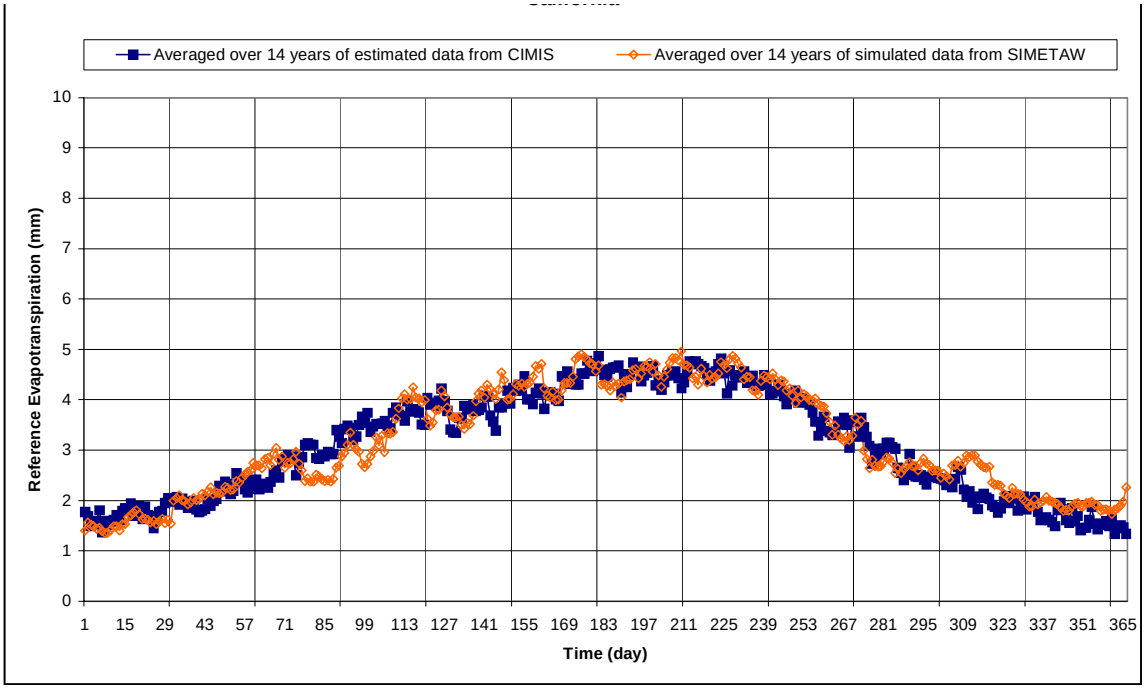


Figure 7-10. Comparison of estimated and simulated reference ET at Oceanside

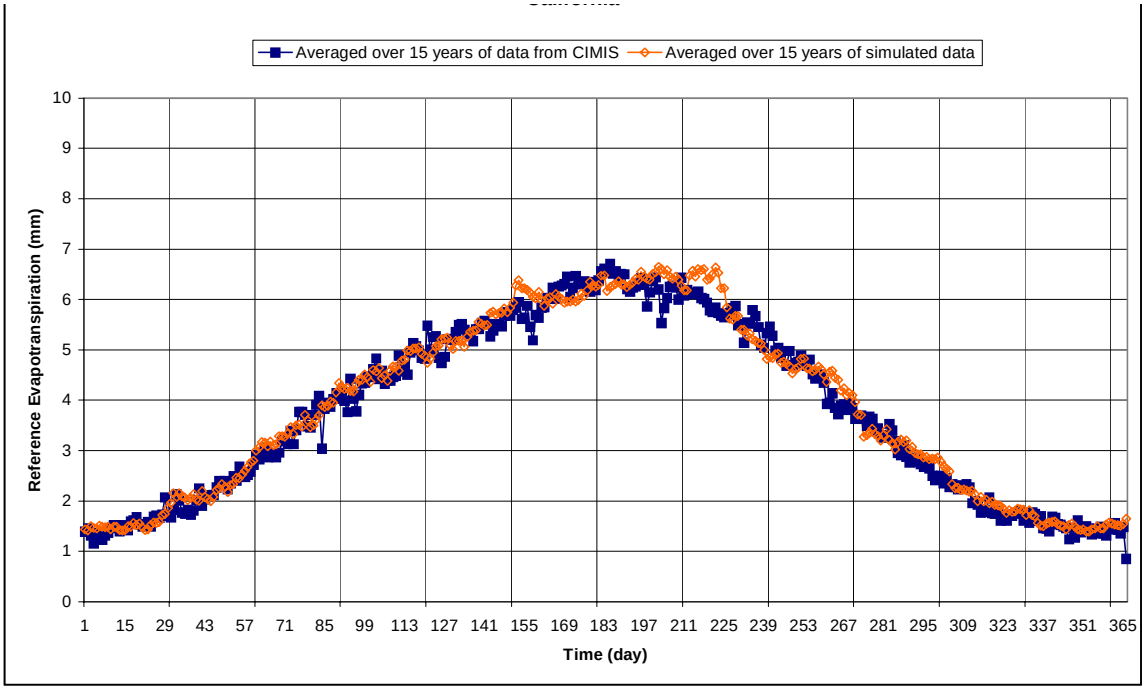


Figure 7-11. Comparison of estimated and simulated reference ET at Bishop

7.5.6 Canopy resistance sensitivity test for SIMETAW calculation of ET

To determine the influence of canopy resistance on ET_o rates, three values of canopy resistance (70, 85, and 100 s m^{-1}) with the current monthly climate data from Davis were used with SIMETAW to simulate 30 years of daily ET_o data. As canopy resistance value increased to 85 and 100 s m^{-1}, the ET_o rate decreased by 4.7 percent and 9.0 percent, respectively (Figure 7-12). The ET_o increase due to a 3°C temperature increase, however, will more than offset the decrease due canopy resistance. The effect of CO_2 concentration on canopy resistance and ET_o rates was roughly estimated and more intensive research on canopy resistance under higher temperature and CO_2 concentrations is needed to confirm the estimates.

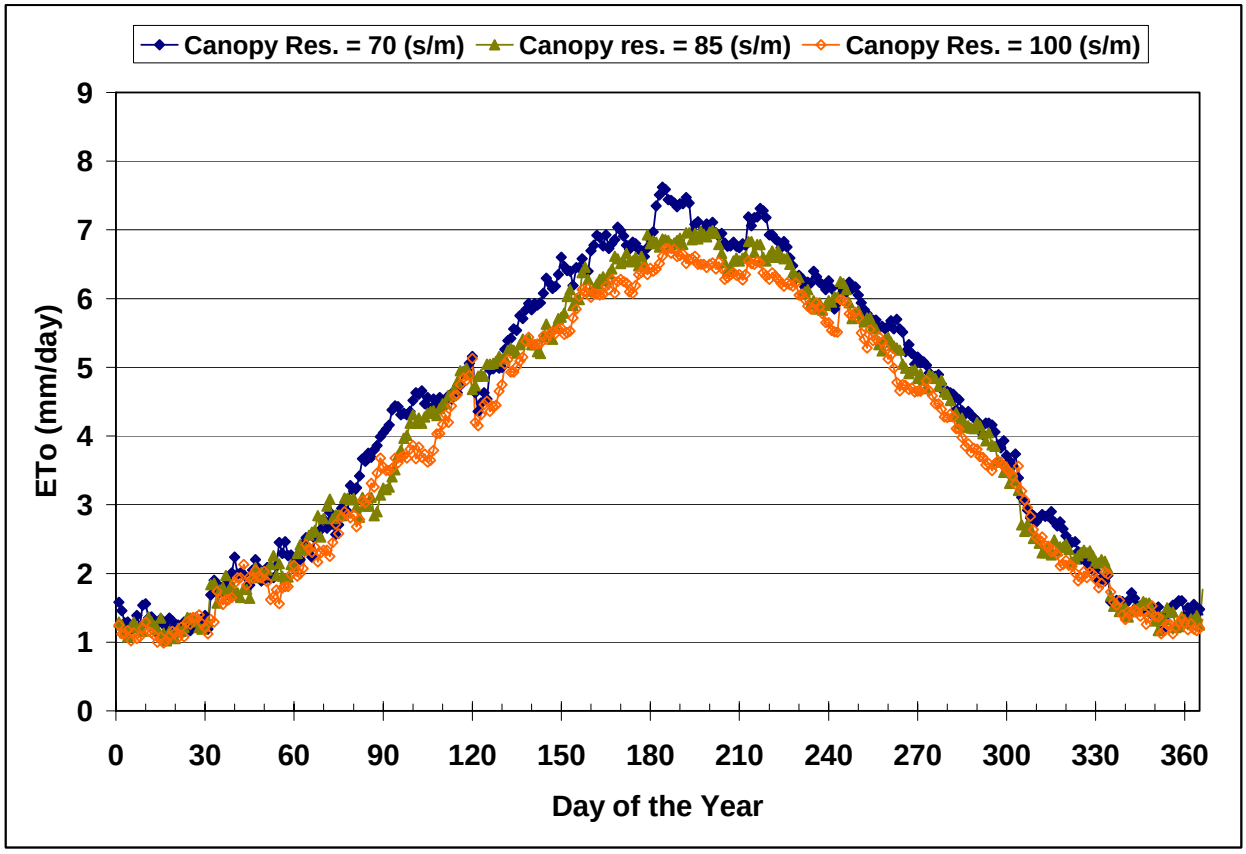


Figure 7-12. Comparison of simulated daily ET_o using the canopy resistance values 70, 85, and 100 s/m and current climate data from Davis

7.6 Using SIMETAW as a DWR Modeling Tool for Climate Change Planning

The preceding sections on using SIMETAW to calculate ET_o, ET_c and ET_{aw} demonstrate the potential to use SIMETAW, with downscaled GCM simulation data as input, for calculation of ET_o, ET_c, and $ET_{aw.}$ SIMETAW has potential as both a stand alone model for evaluating hypothetical climate change impact on ET_c and ET_{aw} or by coupling with downscaled GCM models to provide predictions of future agricultural water needs (Figure 7-13). The ET_c and ET_{aw} output from SIMETAW can serve as input to the DWR Consumptive Use Model to calculate crop water requirement for given planning areas. This possible integration is discussed in Chapter 8 of this report.

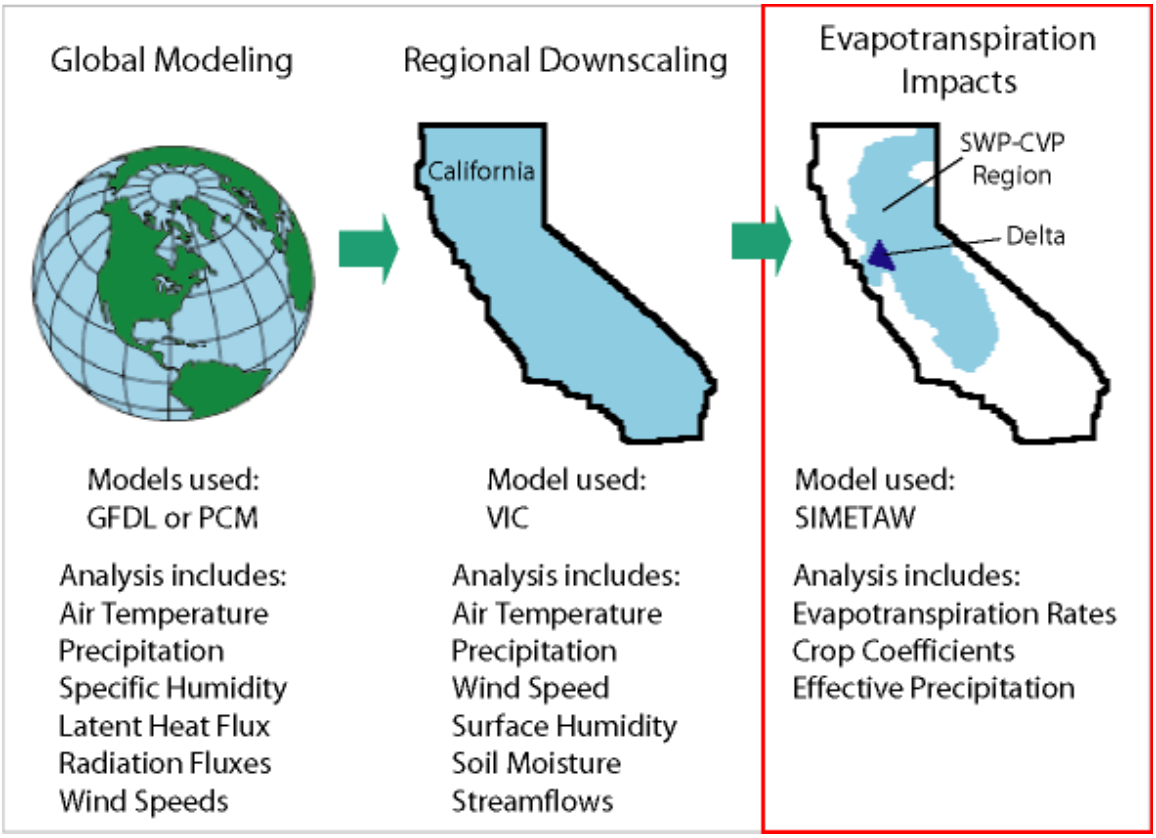


Figure 7-13. Use of SIMETAW for climate change impacts on water resource planning

7.7 Conclusions

It is difficult to accurately estimate the direct effect of global temperature on ET. As long as the minimum temperature and the dew point temperature continue to increase faster than the maximum temperature, the aerodynamic term of the Penman-Monteith ET_o equation is unlikely to increase substantially. This has been the pattern during the past five decades of global temperature rise. Increasing air temperature causes the weighting factor of the radiation-term of the Penman-Monteith equation to increase, but, because of the effect on stomatal closure, increasing CO_2 concentration causes it to decline. Based on limited information, the two effects seem to partially offset one another with the temperature rise resulting in a slightly greater influence on ET than CO_2 in our analysis. Though the net rise in ET we derived is small the influence in water demand for California as a whole is notable. Since natural environments of elevated temperature and CO_2 do not exist on a scale large enough to provide natural boundary layer conditions, it is difficult to study the effects of climate change on ET. More research is needed on the influence of elevated CO_2 and air temperature on canopy resistance.

The SIMETAW model is a promising analytic tool for water management planning that can use input from regional downscaled climate change models. Although it seems that little increase in ET is expected, the net statewide water demand from even a small ET increase is important for

water management. The effect of global change on regional precipitation, wind speed, and cropping pattern shifts are unknown at this time. Climate change could affect California agriculture and water resources, and wise planning is required to avoid serious problems.

7.8 Acknowledgments

We thank Jeff Amthor, Peter Curtis and Arnold Bloom for their thoughtful suggestions. Ed Morris, Jean Woods and Harry Spanglet read and made comments on an earlier version of this chapter for which we are grateful.

7.9 References

Allen, R.G., Jensen, M.E., Wright, J.L., and Burman, R.D. 1989. Operational estimates of reference evapotranspiration. Agron. J. 81: 650-662.

Allen, R.G., F.N. Gichuki and C. Rosenzweig. 1991. CO_2-induced Climatic Changes and Irrig. Water Requirements. J. Wat. Resour. Plan.& Man. ASCE 117(2):157-178.

Allen, R.G., Pereira, L.S., Raes, D., and Smith, M. (1998) "Crop Evapotranspiration: Guidelines for computing crop water requirement." Irrig. And Drain. Paper 56, Food and Agriculture Organization of the United Nations, Rome, 300 pp.

Amthor JS (1999). Increasing atmospheric CO2 concentration, water use, and water stress: scaling up from the plant to the landscape. In: Y Luo, HA Mooney (eds) Carbon Dioxide and Environmental Stress. Academic Press, San Diego, 33-59.

ASCE-EWRI. (2005). The ASCE Standardized Reference Evapotranspiration Equation. Technical Committee report to the Environmental and Water Resources Institute of the American Society of Civil Engineers from the Task Committee on Standardization of Reference Evapotranspiration. 173 p.

California Department of Water Resources, Division of Planning and Local Assistance (2005). Bulletin 160–05: Draft California Water Plan (California Department of Water Resources, Sacramento).

California Department of Water Resources, Division of Planning and Local Assistance (2005).

Condon, A.G. and Hall, A.E. (1997) Adaptation to diverse environments: variation in water-use efficiency within crop species. In L.E. Jackson (ed) Ecology in Agriculture. Academic Press, San Diego, 79-116.

Cowan, I.R. and Farquhar, C.D. (1977). Stomatal diffusion in relation to leaf metabolism and environment. Symp. Soc. Exp. Biol. 31, 471-505.

Field, C. B., Daily, G. C., Davis, F. W., Gaines, S., Matson, P. A., Melack, J. and Miller, N. L. (1999). Confronting Climate Change in California: Ecological Impacts on the Golden State (Union of Concerned Scientists, Cambridge, MA, and Ecological Society of America, Washington, DC).

Gilgen, H., Wild, M. and Ohmura, A. (1998). Means and trends of short wave irradiance at the surface estimated from Global Energy Balance Archive Data. J. of Clim. 11: 2042-2061.

Hayhoe, K., D. Cayan, C.B. Field, P.C. Frumhoff, E.P. Maurer, N.L. Miller, S.C. Moser, S.H. Schneider, K.N. Cahill, E.E. Cleland, L. Dale, R. Drapek, R.M. Hanemann, L.S. Kalkstein, J. Lenihan, C.K. Lunch, R.P. Neilson, S.C. Sheridan, and J.H. Verville. (2004). Emissions pathways, climate change, and impacts on California. Proceedings of the National Academy of Sciences of the United States of America 101:12422-12427.

Hidalgo, H.G., Cayan, D.R., Dettinger, M.D. (2005). Sources of variability of evapotranspiration in California. J. Hydrometerology. 6, 3-19.

Hsiao, T.C. and Jackson, R.B. (1999). Interactive effects of water stress and elevated CO_2 on growth, photosynthesis, and water use efficiency. In: Y Luo, HA Mooney (eds) Carbon Dioxide and Environmental Stress. Academic Press, San Diego, 3-31.

Hsiao, T.C. and Xu, L. (2005). Evapotranspiration and relative contribution by the soil and the plant. In California Department of Water Resources. 2005. Bulletin 160-05 Vol. 4 Reference Guide.

Landis, J.D. and Reilly, M (2004). How We Will Grow: Baseline Projections of the Growth of California's Urban Footprint through the Year 2100 Institute of Urban and Regional Development, University of California, Berkeley.

Long, S.P., Ainsworth, E.A., Rogers, A. and Ort, D.R. (2004). Rising atmospheric carbon dioxide: plants FACE the future. Ann. Rev. Plant Biol. 55, 591-628.

Monteith, J. L.(1965) Evaporation and environment. In: The state and movement of water in living organisms, XIXth symposium, Soc. for Exp. Biol. Swansea, Cambridge University Press, p 205-234.

Penman, H. L. (1948) Natural evaporation from open water, bare soil and grass. Proc. Roy. Soc. London, A193: 120-145.

Pruitt, W. O. and Doorenbos, J. (1977) Empirical calibration, a requisite for evaporation formulae based on daily or longer mean climatic data? ICID conference on Evapotranspiration, Budapest, Hungary, May 26-28, 1977. International Commission on Irrigation and Drainage.

Rachmilevitch, S., Cousins, A.B., Bloom, A.J. (2004). Nitrate assimilation in plant shoots depends on photorespiration. Proceedings of the National Academy of Sciences of the United States of America 101:11506-11510.

Roderick and Farquhar (2002). The cause of decreased pan evaporation over the past 50 years. Science 298: 1410-1411.

Snyder, R. L. and Pruitt, W.O. (1992) Evapotranspiration data management in California. Proceedings/Water Forum '92, August 2-6, 1992, Baltimore, MD.

Stanhill, J. and Cohen, S. (2001). Global dimming: a review of the evidence for a widespread and significant reduction in global radiation with discussion of its probable causes and possible agricultural consequences. Agric. and For. Meteorol. 107: 255-278.

Tanaka, S.K., Zhu, T, Lund, J.R., Howitt, R.E., Jenkins, M.W., Pulido, M.A., Tauber, M., Ritzema, R.S., Ferreira, I.C. (2005). Climate Warming and Water Management Adaptation for California. Climatic Change, (in press).

U.S. Department of Agriculture (2003) California Agricultural Statistics 2003.

Ventura, F., D. Spano, P. Duce and R.L. Snyder. 1999. An evaluation of common evapotranspiration equations. Irrig. Sci. 18:163-170.

7.10 Appendix 1 Energy Budget Analysis for Climate Change

7.10.1 Physical bases for temperature, sensible heat and water vapor transfer

Any moving object has kinetic energy that is proportional to the product of half of the mass and the square of its velocity. Although air molecules have small mass, they move fast (1,600-2,000 km h^{-1}) and there are many (2.65×10^{25}) molecules per cubic meter. Therefore, there are many collisions between air molecules and objects within the air volume. When the air molecules strike an object such as a thermometer some kinetic energy is transferred to the object. In the case of a glass thermometer, the energy resulting from air molecule impacts increases movement of molecules in the glass and transfers by conduction into the instrument where it transfers to the liquid temperature indicator. As energy is absorbed, liquid in the thermometer expands and moves up the thermometer tube. When molecules strike the outside of the thermometer at a faster velocity, and more frequently more heat is transferred and the measured temperature rises. If molecules strike the thermometer at lower velocity and at lower frequency the liquid contracts and the measured temperature drops. The kinetic energy contained in air is commonly called "sensible heat" because it is heat (energy) that one can sense. Generally, small volumes of air have uniform heat content, but big differences can occur between the large air parcels due to energy transfers by radiation, conduction and latent heat exchanges. Wind and turbulence cause

air parcels with different sensible heat content to move and mix with other air parcels and to transfer sensible heat between objects.

Evaporation of liquid water requires energy to break hydrogen bonds between water molecules. It is widely believed that evaporation increases with air temperature. Strictly speaking, it is actually the water temperature at the surface that determines the evaporation rate. Air temperature can affect the evaporation rate if sensible heat is transferred from the air to the water surface. The rate of heat transfer, however, depends on turbulence as well as the temperature difference between the air and water. Sensible heat transfer to a wet surface depends on atmospheric stability, wind speed, and surface roughness. For transpiration from plants, the rate of water vapor transfer is further complicated by plant morphology that affects energy absorption and turbulence and by plant physiology (i.e., stomatal opening and closing) in response to environmental factors including water availability and CO_2 concentration.

Vaporization of water occurs when energy (sensible heat or radiant energy) is used to break hydrogen bonds between the water molecules. Therefore, the rate of energy consumed in the vaporization process provides a measure of the evaporation rate. Evapotranspiration rates are commonly estimated using energy balance by considering the net radiation (R_n), heat conduction into and out of the soil and plants (G), atmospheric sensible heat flux density (H), and atmospheric latent heat flux density (LE). Net radiation is the amount of short- and long-wave radiation absorbed by a surface, and it is the main source of energy for vaporization. Net radiation (R_n) is commonly partitioned into soil heat flux density (*G*), sensible heat flux density, and latent heat flux density (*LE*) and the energy consumed in the evaporation process is therefore expressed as:

$$LE = R_n - G - H \qquad (\text{W m}^{-2}) \qquad (1)$$

where L is the latent heat of vaporization ($L \approx 2454$ J g^{-1} at 20^{o}C) and *E* is the water vapor flux density (g m^{-2} s^{-1}). In equation 1, R_n is positive when the energy flux is towards the surface and LE, G and H are positive for fluxes away from the surface.

Using Equation 1, one could measure R_n, G, and H to estimate LE. Then the rate of evaporation is calculated by dividing LE by L to determine the mass flux density of water vapor. There are methods available to measure the components in Equation 1, but they are not widely used because it is somewhat difficult and expensive to measure the variables, especially H, accurately. Efforts to obtain a simple and inexpensive technique continue, but there is still no perfect method. Other methods to estimate ET using more readily available variables are available.

7.10.2 Penman-Monteith equation

Penman (1948) presented a method to estimate *LE* for short, uniform vegetation using readily available weather variables measured at one level assuming the surface was wet with a canopy resistance $r_c = 0$. Monteith (1966) refined Penman's equation to adjust LE for canopy resistances greater than zero. The so-called Penman-Monteith equation is expressed as:

$$LE = \left(\frac{\Delta}{\Delta + \gamma^*}\right)(R_n - G) + \left(\frac{\rho C_p}{\Delta + \gamma^*}\right)\left(\frac{e_s - e}{r_a}\right) \qquad (\text{W m}^{-2}) \qquad (2)$$

In Equation 2, Δ is the slope of the saturation vapor pressure curve at the air temperature, $\gamma \approx 0.066$ kPa K^{-1} is the psychrometric constant, r_c is the canopy resistance, r_a is the aerodynamic resistance, ρ is the air density (g m^{-3}), C_p is the specific heat at constant pressure (J $g^{-1}K^{-1}$), e_s is the saturation vapor pressure, and *e* is the actual atmospheric vapor pressure. For more information on the variables in Equation 2, see ASCE-EWRI (2005). The parameter $\gamma^* = \gamma\left(1 + \frac{r_c}{r_a}\right)$ in Equation 2 is a modified psychrometric constant, which was introduced by Monteith to account for the effects of canopy resistance on *ET*. The left-hand term of Equation 2 is often called the radiation or available energy term and the right-hand term is called the aerodynamic term because it accounts for the contribution of aerodynamic transfer of sensible heat to *ET*.

Aerodynamic resistance (r_a) is equal to the reciprocal of the aerodynamic conductance (g_a), which is defined as the rate that 1 m of a particular scalar will transfer through 1 m^2 horizontal plane. Therefore, g_a and r_a have the units m s^{-1} and s m^{-1}, respectively. When r_a increases, then g_a decreases, the vertical transfer of sensible and latent heat decreases, and the LE rate falls. Like r_a, the canopy resistance (r_c) equals the reciprocal of the canopy conductance (g_c) and the canopy conductance is the rate at which 1 m^3 of air will pass through 1 m^2 of horizontal plane. When r_c increases, g_c decreases and LE is reduced. The r_c is the resistance to water vapor transfer from the canopy elements and soil to a level near the top of a canopy and r_a is the resistance to vapor transfer from that level to the ambient air above the canopy. The r_a and r_c resistances are in series, so the higher of the two resistances limits the LE rate. As plant stomata close, r_c increases, γ^* increases, and LE decreases (Equation 2). When the surface is wet, then $r_c = 0$, $\gamma^* = \gamma$ and the Penman-Monteith equation reduces to the Penman (1948) form.

7.10.3 Aerodynamic term response to temperature rise

The Penman-Monteith equation is useful to investigate the effect of possible climate change on evapotranspiration. Roderick and Farquar (2002) noted that the global mean maximum and minimum temperatures have increased by approximately 0.1 and 0.2 ^oC per decade during the last 50 years and there has been no observable change in the vapor pressure deficit ($e_s - e$) during the same time period. The minimum temperature is highly correlated with the dew point temperature, which is directly related to the actual vapor pressure of the atmosphere. The fact that the minimum has risen faster than the maximum temperature supports the idea that the dew point temperature and hence the actual vapor pressure (e) have risen and compensated for the temperature induced rise in saturation vapor pressure (e_s).

The temperature weighting function term $\left(\frac{\rho C_p}{\Delta + \gamma^*}\right)$ in Equation 2 decreases with rising temperature and with increasing r_c (Figure 7-14). Since e_s - e has not changed in recent decades and the weighting function decreases with increasing temperature, it is likely that the aerodynamic term of Equation 2 has not changed or slightly decreased with global temperature rise during the past 50 years. Unless the e_s term begins to increase more rapidly than e, the aerodynamic term is unlikely to be greatly affected by global temperature increase.

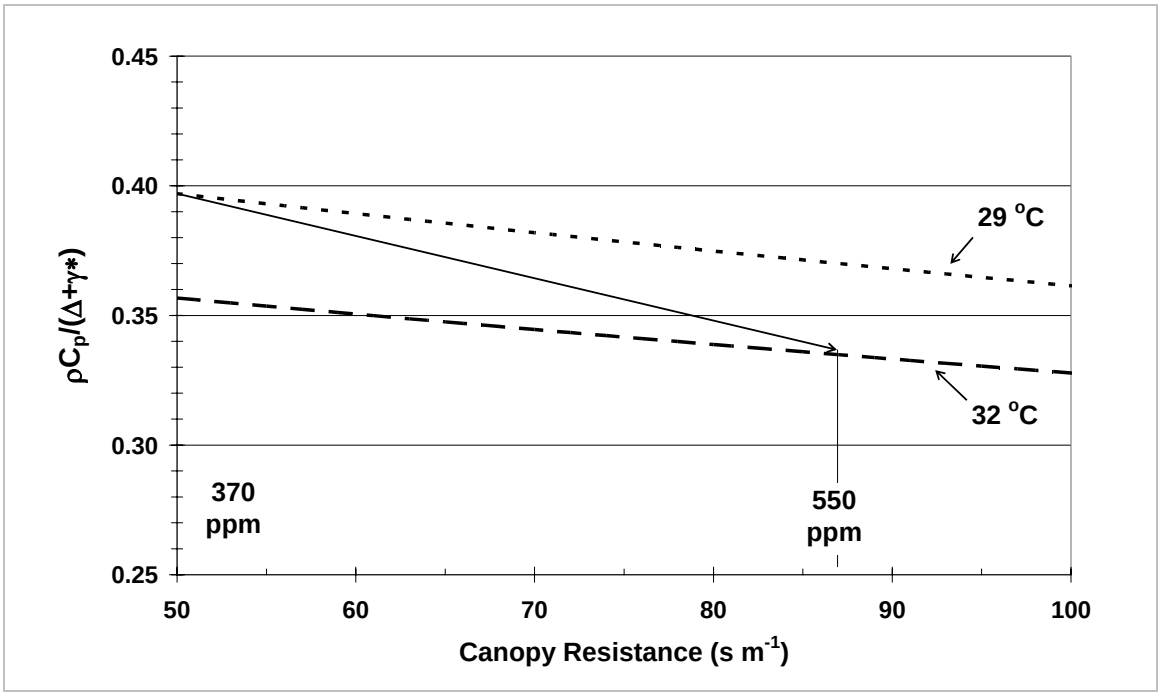


Figure 7-14. A plot of $(\rho C_p)/(\Delta+\gamma^*)$ versus canopy resistance for a 3 °C temperature increase as a function of canopy resistance

7.10.4 Radiation term response to temperature rise

A 3 °C temperature rise will increase the $\left(\frac{\Delta}{\Delta+\gamma^*}\right)$ radiation-term weighting function by about 4.5 percent so the effect is to increase the contribution of the radiation term to LE, causing a higher ET rate. There is, however, some evidence that increased turbidity of the atmosphere has globally decreased the amount of solar (short-wave) radiation reaching the surface (Roderick and Farquar, 2002), and the radiation-term weighting function increase with temperature is partially offset by decreasing solar radiation received at the surface.

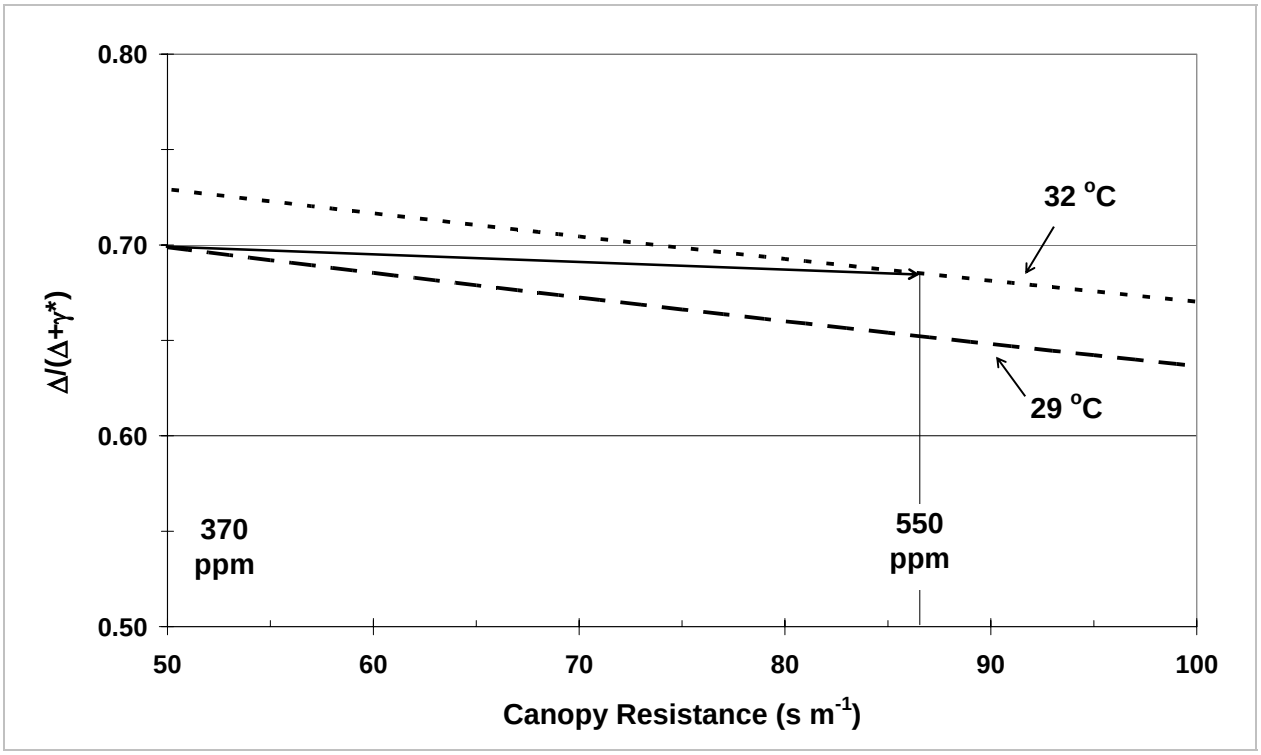


Figure 7-15. A plot of $\Delta/(\Delta+\gamma^*)$ versus canopy resistance for a 3 °C temperature increase as a function of canopy resistance.

Another factor that is often neglected in predictions of temperature effects on ET is the influence of increased CO_2 on stomatal closure and hence canopy resistance. Stomata exhibit partial closure with increasing CO_2 content, but, there is little information on the effect of CO_2 concentration on canopy resistance. The typical enhanced CO_2 concentrations reported in the FACE projects was about 550 ppm, and Long et al. (2004) indicated that the leaf stomatal conductance decreased about 20 percent for C_3 species plants under those conditions. Then using the same procedure to estimate canopy resistance for reference evapotranspiration (Allen et al., 1989) with today's CO_2 concentration, the midday canopy resistance is predicted to increase from about 50 to 87 s m^{-1} as shown in Fig. 7.3. Therefore, if the canopy resistance does increase to 87 s m^{-1}, the increase in the radiation-term weighting factor due to a 3 °C increase in temperature is nearly offset by the higher canopy resistance. For comparison, the midday canopy resistances of tall alfalfa (50 cm) and tall grass (12 cm) are approximately 30 s m^{-1} and 50 s m^{-1}, respectively (ASCE-EWRI, 2005). The r_c is high at night (≥ 200 s m^{-1}) when the stomata are closed. There is a decrease in rc after sunrise to the minimum value and then an increase in the late afternoon as the sun descends toward the horizon. The mean 24-hour r_c is about 70 s m^{-1} for the grass and about 45 s m^{-1} for the alfalfa (ASCE-EWRI, 2005). Again, there is a paucity of research on the effect of CO_2 concentration on canopy resistance, but it clearly will increase and the reduction in the radiation-term weighting function will at least partially offset the increase due to temperature. The magnitude of the change depends on how much the temperature and CO_2 concentration increase. Clearly, more research is needed to determine the influence of temperature and CO_2 concentration on canopy resistance before a truly accurate assessment is possible.

Evaporation from ponds, lakes, rivers, and other bodies of water can also be impacted by climate change. Recently, several groups have reported decreasing evaporation rates from standard pans, and they used this as evidence that the climate is cooling rather than warming. However, the surface resistance of water is zero and the aerodynamic resistance is high, so $\gamma^* = \gamma$ in Equation 2 and the equation simplifies to the Penman (1948) equation. Again, $e_s - e$ has not changed in recent decades, so the change in the aerodynamic term is unlikely to influence evaporation from bodies of water. Increasing temperature does increase the weighting function of the radiation term and there is no stomatal influence, so canopy resistance will not counteract the temperature effect on the radiation term of the ET_o equation. There is some evidence for the reduction in solar radiation due to pollution effects on atmospheric turbidity or perhaps reflectivity of clouds and other factors (Stanhill and Cohen, 2001; Gilgen et al., 1998), and this might be the cause for reduced pan evaporation reported in some regions of the world.

Assuming a little or no increase in the radiation-term weighting function in response to rising temperature, the increasing CO_2 concentration effect on canopy resistance, and a decrease in short-wave radiation at the surface, little or no increase in the radiation term contribution to ET is expected with climate change. Since the aerodynamic term also shows little response to climate change, it is anticipated that the effect of climate change on *ET* will be minimal. Other environmental responses to climate change such as precipitation and wind patterns and changes in cropping and irrigation methods, however, could greatly affect water resource availability and hence irrigation water requirements.

7.11 Appendix 2 The photosynthesis Response Curve to CO_2

The assimilation of CO_2 as a function of intercellular CO_2 is provided in Figure 7-16.
The rate of carbon assimilation is determined by supply and demand for CO_2. The supply of CO_2 is determined by diffusion in the gas and liquid phases. It can be limited by essential constraints in the pathway from the atmosphere to the leaf sites of carbon fixation (carboxylation) most notably at the canopy boundary and at the stomata, which are related to the plants energy budget. The demand for CO_2 is determined by the rate of processing CO_2 in the chloroplast, which is determined most importantly by biochemistry, in particular Rubisco, the first enzyme in the metabolic pathway for assimilation of CO_2. It can also be limited by environmental factors such as irradiance. The electron transport plot relative to CO_2 concentration is included in Figure 7-16 for comparison to the carbon assimilation. The assimilation of CO_2 plot in Figure 7-16 has two principal regions, the first occurs at lower CO_2 concentrations and is referred to as the CO_2 limited region. The second at the higher CO_2 concentrations is the place where available limits to precursors of Rubisco are limiting. Two horizontal lines of Figure 7-16 indicate the intercellular CO_2 concentration at the atmospheric CO_2 concentration given the supply function indicated by the line from the atmospheric concentration to the response curve. The slope of the supply function is the leaf conductance measured. The possible long-term adjustment of plants to elevated CO_2 by sifting the supply curve downward is referred to as downregulation. Long et al (2004) concluded that there is a substantial reduction in Rubisco at elevated CO_2, suggesting acclimation to elevate CO_2, but that there was not downregulation.

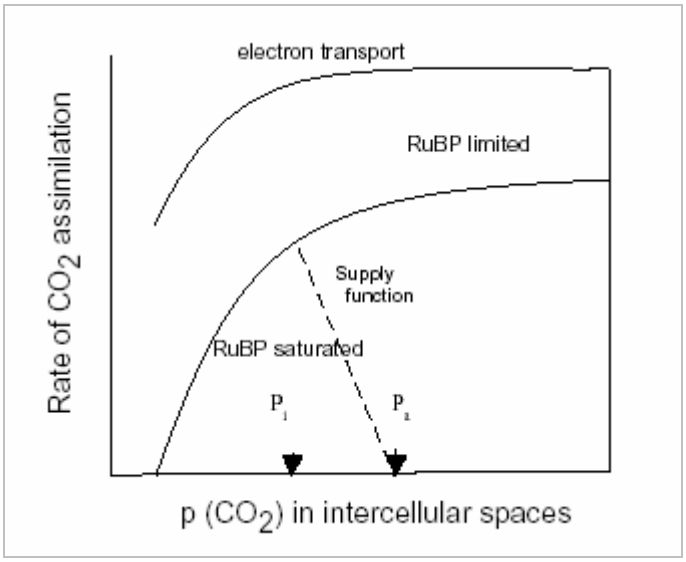


Figure 7-16. Photosynthesis Response Curve to CO_2
(After Lambers et al, 1998)

7.12 Appendix 3 The Penman-Monteith equation for reference evapotranspiration (ET_o) used in SIMETAW

Reference evapotranspiration (ET_o) is estimated from daily weather data using a modified version of the Penman-Monteith equation (Allen et al., 1998; ASCE-EWRI, 2005). The equation is:

$$ET_o = \frac{0.408\ \Delta\ (R_n - G) + \gamma \frac{900}{T + 273}\ u_2\ (e_s - e_a)}{\Delta + \gamma\ (1 + 0.34\ u_2)} \qquad (3)$$

where Δ is the slope of the saturation vapor pressure at mean air temperature curve (kPa $^oC^{-1}$), R_n and G are the net radiation and soil heat flux density in MJ $m^{-2}d^{-1}$, γ is the psychrometric constant (kPa $^oC^{-1}$), T is the daily mean temperature (^oC), u_2 is the mean wind speed in m s^{-1}, e_s is the saturation vapor pressure (kPa) determined as the mean saturation vapor pressure calculated from the daily maximum and minimum air temperature (^oC), and e_a is the actual vapor pressure (kPa) calculated from the mean dew point temperature (^oC) for the day. The coefficient 0.408 converts the R_n – G term from MJ $m^{-2}d^{-1}$ to mm d^{-1}, and the coefficient 900 combines several constants and converts units of the aerodynamic component to mm d^{-1}. The product 0.34 u_2 in the denominator is an estimated ratio of the 0.12-m tall canopy surface resistance (r_c=70 s m^{-1}) to the aerodynamic resistance (r_a=205/u^2 s m^{-1}). It is assumed that the temperature, humidity, and wind speed are measured between 1.5 m (5 ft) and 2.0 m (6.6 ft) above a grass-covered soil surface. For a complete explanation of the equation, see (ASCE-EWRI, 2005).

7.13 List of Abbreviations

ASCE-American Society of Civil Engineers
CALVIN-The California value integration network model
CIMIS-California Irrigation Management Information System
CUP-Consumptive use program
ET-Evapotranspiration
ETo-Reference Evapotranspiration
ETAW-Evapotranspiration of applied water
EWRI- Environmental and Water Resources Institute
FACE-Free-Air Carbon dioxide enrichment
GCM-General Circulation Model
LAI-Leaf Area Index
NPP-Net primary production
PAR-Photosynthetically Available Radiation
RGR-Relative Growth Rate
SIMETAW-SIMulation ET of Applied Water
SWAP-statewide water and agricultural production model (WUE-Water use efficiency
WUE-Water use efficiency

Progress on Incorporating Climate Change into Management of California's Water Resources

1st Progress Report
July 2006

Chapter 8:
Future Directions

Authors:

Jamie Anderson Ph.D. P.E., Francis Chung Ph.D. P.E., Dan Easton P.E., Messele Ejeta, Ph.D. P.E., Hongbing Yin P.E.
California Department of Water Resources, Bay Delta Office, Modeling Support Branch, Sacramento.

Michael Anderson Ph.D.
California Department of Water Resources, Division of Flood Management, Sacramento.

Roy Peterson Ph.D.
California Department of Water Resources, Division of Environmental Services, Sacramento.

Levi Brekke Ph.D. P.E.
U.S. Bureau of Reclamation, Technical Service Center, Denver, CO.

Guido Franco
California Energy Commission, Public Interest Energy Research (PIER) Program, Climate Change Research.

8 Future Directions

8.1 Introduction

This report demonstrates growth in federal and state agency capability to provide planners with relevant information on potential climate change impacts. The joint Department of Water Resources (DWR) and U.S. Bureau of Reclamation (Reclamation) Climate Change Work team has built coalitions with California climate change research groups to improve federal and state agency knowledge on climate modeling and uncertainties in future climate projections. Additional products from work team activities include identification of data and technology gaps and development of innovative analytical approaches using familiar planning tools. The work team will continue to evolve to meet the needs of water resources managers and to use new information and methodologies as they become available. Future activities will focus on probabilistic based potential effects of climate change. A summary of future directions is presented in this chapter.

8.2 SWP-CVP Operations Impacts

The State Water Project (SWP) and Central Valley Project (CVP) operations impacts studies presented in this report only considered climate change affects on runoff patterns. However, a warming climate may lead to changes in the seasonal pattern and magnitude of evaporation/evapotranspiration and, thereby, higher water demands. Rising sea levels would lead to greater fresh water demands in the Delta to maintain water quality. Both increased demands and increased salinity in the Delta could have significant impacts on the ability of the SWP and CVP to meet California's future needs. Impacts from a wider range of climate change effects need to be addressed.

In the climate change scenario studies presented in this report, one significant issue was the critical shortages of water in reservoirs north of the delta that occurred when present operating rules were applied. Future directions would include examining increases in carryover storage in Shasta and Oroville reservoirs to prevent loss of operational control of the Sacramento and Feather rivers during droughts. Corresponding reductions to delivery allocations would be required. If those measures weren't sufficient to provide a reliable water supply, additional measures would be investigated such as rebalancing of the water sharing mechanisms established in the Coordinated Operations Agreement.

System flexibility should be sought to mitigate climate change effects on SWP and CVP deliveries. In the current analysis, flood control spaces were left unchanged. In the future, it is planned to vary the flood control space with different climate change scenarios. Furthermore, refined flood forecasting might allow more runoff to be captured in the early spring than is otherwise possible now. Also, operational rules and regulations will have to be reassessed given a changed hydrology. Current operations studies using the CalSimII model use an Artificial Neural Network (ANN) to represent Delta water quality. Future directions include development

of a new ANN or similar tool that would be incorporated into CalSimII to represent Delta water quality for sea level rise conditions.

Lastly, we need to explore ways of increasing supply to or reducing demand of SWP and CVP contractors. New reservoirs, increased pumping capacity, and groundwater banking are ways that more winter runoff can be captured for later delivery. On the demand side, CalSim-II doesn't deal with specific conservation measures. But the effects of conservation – whether from drip irrigation or low-flow toilets – can be represented in the input water demands and the effects to CVP and SWP operations simulated.

8.3 Delta Impacts

Improving analysis of potential effects of a rising sea level on the Delta will be a focus of future studies. Changes in salt water intrusion from the ocean need to be represented for different sea level increases. Better understanding and mathematical representation of salt water intrusion under conditions of sea-level rise should be incorporated into planning tools such as CalSim-II and DSM2. For this report, results from the sea level rise simulations could be used for levee stability analyses.

Flexibility of the existing water-conveyance system to lessen the effects of climate change will also be explored. In addition to potential changes to system operations mentioned in the previous section, mitigation measures in the Delta could include modifying Delta Cross Channel operations, changing land use patterns and temporary barrier operations. If present system flexibility can't sufficiently decrease the impacts of climate change, other measures will be investigated such as modifying operating rules or considering new system components such as gates proposed to be installed the south Delta.

8.4 Flood Management

In order to better understand the risks associated with global climate change on California's water resources, it is important to be able to quantify climate change effects on the ability to provide adequate flood control and to quantify climate change impacts on seasonal water supply. The Division of Flood Management at DWR will address these issues. It plans to:

1) continue the evaluation of historical data to identify trends and changes in precipitation and runoff patterns
2) periodically update frequency-based data for design computations
3) evaluate new climate change model-derived data for use in flood frequency and water supply forecasting applications
4) develop new forecasting technologies that can adapt to the changing distribution of the state's annual water supply
5) incorporate methodologies to quantify the uncertainty in the expected changes in the annual cycle of water supply into the water supply forecast process

For flood frequency analysis, future efforts at synthetic daily flow data produced from climate change model output may be suitable for traditional flood frequency analyses. As these data become available, they must be evaluated for their ability to represent present-day magnitude and

variability as well as predicted changes caused by climate change. At this time, however, there are no such data that would provide meaningful results.

Another area which may produce useful flood forecasting information examines historical data in order to identify critical atmospheric circulation parameters and their threshold values associated with extreme floods. As the circulation patterns in the GCMs improve and are shown to represent present-day conditions correctly, circulation patterns under increased greenhouse gas concentrations can be examined for the flood producing patterns or critical threshold characteristics. Improved forecasting technologies will help implement adaptive strategies to decrease flood risk changes associated with climate change.

8.5 Evapotranspiration

To further analyze the effects of climate change on evapotranspiration (ET) future efforts will focus on improvements to the SIMETAW (Simulation of Evapotranspiration of Applied Water) model. SIMETAW development and analysis for climate change studies will be a complex process. How will a world with higher atmospheric CO_2 and higher temperatures influence the resistance to water vapor diffusion to the atmosphere (the boundary layer around plants)? No one knows. While we are continuing to search the literature and research programs for boundary-layer data at elevated temperatures and CO_2 concentrations, we need to explore the SIMETAW model's performance by using reasonable analogs for boundary-layer values. Direct measurement of boundary-layer information is limited in the near future, but we are developing an analysis to work around the limitation.

To validate the SIMETAW calculation of ET using downscaled model weather data, a set of comparative simulations is needed using historic California Irrigation Management Information System (CIMIS) data and downscaled regional model output for the same time period. Analysis periods and CIMIS sites will be chosen to obtain a range of extremes of the primary SIMETAW input variables: net radiation, wind speed, relative humidity, temperature and precipitation.

Simulations for several principal herbaceous crops, a row crop, tomatoes, and a field crop, alfalfa, will be tested with SIMETAW first at Central Valley CIMIS stations and then at other CIMIS sites throughout the state. The simulations will be analyzed at 2020 and 2050. The 2020 year is meant to correspond with the current CalSimII capabilities. The 2050 year is the far planning horizon. All four climate change scenarios selected by the Climate Action Team (see Chapter 3) will be analyzed at each location and time. An orchard crop, almonds, will then be added to contrast boundary layer and cropping patterns with the herbaceous crops. Eventually, a wider geographic range and longer list of crops is needed for a comprehensive analysis.

Currently there is no comprehensive study of crop changes or regional cropping pattern shifts in relation to climate change. There are methodologies and experts that we can reach to describe differences in climate change impacts on: (1) crop water use efficiencies (WUE) at a systems level, for the growers' water delivery on site, and as crop differences in WUE, and (2) crop production values both for growers and for water resource planners. This is a high priority need.

As an ad hoc climate change group, it might serve us to establish guidelines for managing regional climate downscaled data. Questions regarding averaging techniques including span of time to use, and quality assurance of the downscaled data are important to address. A workshop including other experts, such as statisticians, would be helpful.

For future SIMETAW studies, an average period is planned to describe the two analysis times. For 2020, we plan to use 2015 through 2025 for averaging; and for 2050, we plan to use 2045 through 2055 for averaging. If possible, we think it is useful to coordinate with the other parts of the work team to have a standard in analysis time sampling.

For an understanding of ET demand there is a need to track irrigation conservation technologies and irrigation system pattern shifts including precision agriculture. This information can help anticipate probable shifts in agricultural applied water.

There is also a need to proportionally sum the evapotranspiration and evaporative demands impacted by different climate change scenarios on an annual perspective over the entire state. The precision of this analysis will improve as we improve our knowledge of evaporative processes and refine the SIMETAW model for climate change study.

8.6 Modeling Tool Integration

Several different mathematical models and analysis techniques can be used to assess impacts of climate change by translating changes in factors such as precipitation, sea level and crop evapotranspiration into water supply changes. Examples of modeling tools used in this report include the SWP-CVP operations model CalSim-II (Chapter 4), the Delta hydrodynamics and water quality model DSM2 (Chapter 5), and the Simulation of Evapotranspiration of Applied Water model SIMETAW (Chapter 7). Additional tools may also be available for climate change studies. Future directions include identifying 1) additional tools that could be used for climate change studies 2) input data requirements for each tool, 3) output produced by each tool and 4) more efficient ways to use these tools separately or in conjunction with other models to address water resources planning and management related climate change issues.

8.7 Coordination of State Climate Change Research Activities by the California Energy Commission

At the national and international levels a considerable amount of funds are being devoted to climate change science. Most of these research initiatives are designed to elucidate fundamental scientific questions such as the role of clouds on climate, or the direct and indirect effect of aerosols. The 2001 National Assessment of the Potential Consequences of Climate Variability and Change was a landmark effort resulting in a series of regional assessments that identified key vulnerabilities to a changing climate. Recently the U.S. Climate Change Science Program has embarked on the production of several synthesis and assessment products designed to support decision making on how to prepare for a changing climate.

Even though all of these national and international efforts are extremely informative, they usually are not adequate to answer policy relevant questions at the state and local levels or for detailed long-term planning in California. For this reason, The California Energy Commission through its Public Interest Energy Research (PIER) Program has created the first state-sponsored climate change research program in the nation designed to complement national and international research efforts producing policy-relevant research products. The Commission has created the California Climate Change Center (Center) with the University of California to implement its research plan on climate change. The Center is producing research products that are directly applicable for the preparation of long-term plans. Examples of such plans are the State Water Plans prepared by the Department of Water Resources and the Integrated Energy Policy Reports prepared by the California Energy Commission.

All the state agencies in California are supporting research on climate change. For example, the Air Resources Board is supporting studies on greenhouse gas tailpipe emissions from automobiles and recently has requested expanding its research program on climate change. The Department of Water Resources has an in-house effort designed to use existing planning modeling tools to better understand the potential effects of climate change on water resources in the state. CALFED is funding projects on the potential effect of climate change in the Delta region. Informally all of these efforts are being coordinated through extensive exchanges of information between technical staff from the different agencies and by the fact that some key researchers are involved in most of these research activities. The annual conferences on climate change organized by the Energy Commission and the California Environmental Protection (CalEPA) Agency are also a forum for exchange of ideas and for coordination.

Governor Schwarzenegger signed an Executive Order on June 1, 2005 requiring, among other things, the preparation of periodic assessment reports on the impacts of climate change on key sectors of the California economy. This effort, headed by CalEPA, is also serving as a catalyst for additional coordination and more intense research efforts.

In short, a great deal of coordinated research activities on climate change is already occurring in California. Formalizing these coordinated activities may be advisable, but extreme care should be taken to avoid hampering these activities with onerous requirements.

8.8 Risk Assessment

A major goal of the work team is to extend the analysis prospective for long-term water resources planning from "assessing impacts" to "assessing risk". Impacts assessment identifies possible outcomes resulting from a given change. Risk assessment takes the impacts assessment and investigates the likelihood or probability of occurrence that a particular outcome may occur. The work team's goal of extending our analyses from impacts assessment to risk assessment is shown in Figure 8.1. The bulls-eye nature of the figure symbolizes the work-team's goal of aiming for risk-based assessments for resource management with respect to climate change.

This report represents an example of an impacts assessment based on four scenarios defining an expected range of potential climate change impacts. Such assessments are good for informing

managers of potential future issues that may require management action. However in order for managers to make decisions related to potential climate change impacts, they need information on the probability that any particular scenario will occur relative to other scenarios under consideration.

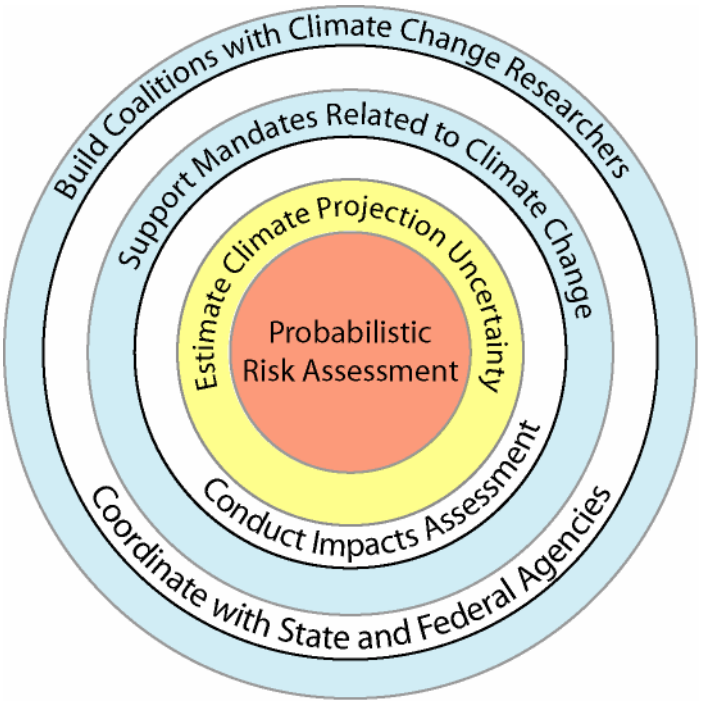


Figure 8.1: DWR-Reclamation Climate Change Work Team Goals
Yellow and red shading indicates future directions.

8.8.1 Compilation of Additional Climate Change Scenarios

An integral component of risk assessment is having as large of a data set as possible to define the range of potential outcomes. The work team plans to collaborate with climate change research groups on the selection of an ensemble of climate change scenarios for analysis, representing a spectrum of climate models and emission scenarios. For this report, analysis focused on four scenarios reflecting two greenhouse gas (GHG) emissions scenarios each represented by two Global Climate Models (GCM's) (see Chapter 3). However, many other emissions scenarios and climate models may be considered for generating future climate scenarios.

Greenhouse Gas Emissions Scenarios

The Intergovernmental Panel on Climate Change's (IPCC's) emissions scenarios cover a wide range of main demographic, economic, and technological driving forces GHG and sulfur emissions and are representative of the literature (IPCC, 2000). Four main storylines representing possible future evolutions of these factors were identified (see Chapter 3).

Scenarios were developed that represent a specific quantitative interpretation of one of the four storylines. All of the scenarios within a given storyline are referred to as a scenario family.

Following an integrated assessment framework, initially six global climate models (GCMs) were used to represent the various climate change scenarios. One advantage of a multi-model approach is that the resultant 40 SRES (Special Report on Emissions Scenarios) encompass the current range of uncertainties of future GHG emissions arising from different characteristics of these models. In addition, the current knowledge of uncertainties that arise from scenario driving forces such as demographic, social and economic, and broad technological developments that drive the models, are described in the storylines. Figure 8.2 shows the SRES emissions scenario tree starting with the four storylines and showing the 40 specific scenarios modeled.

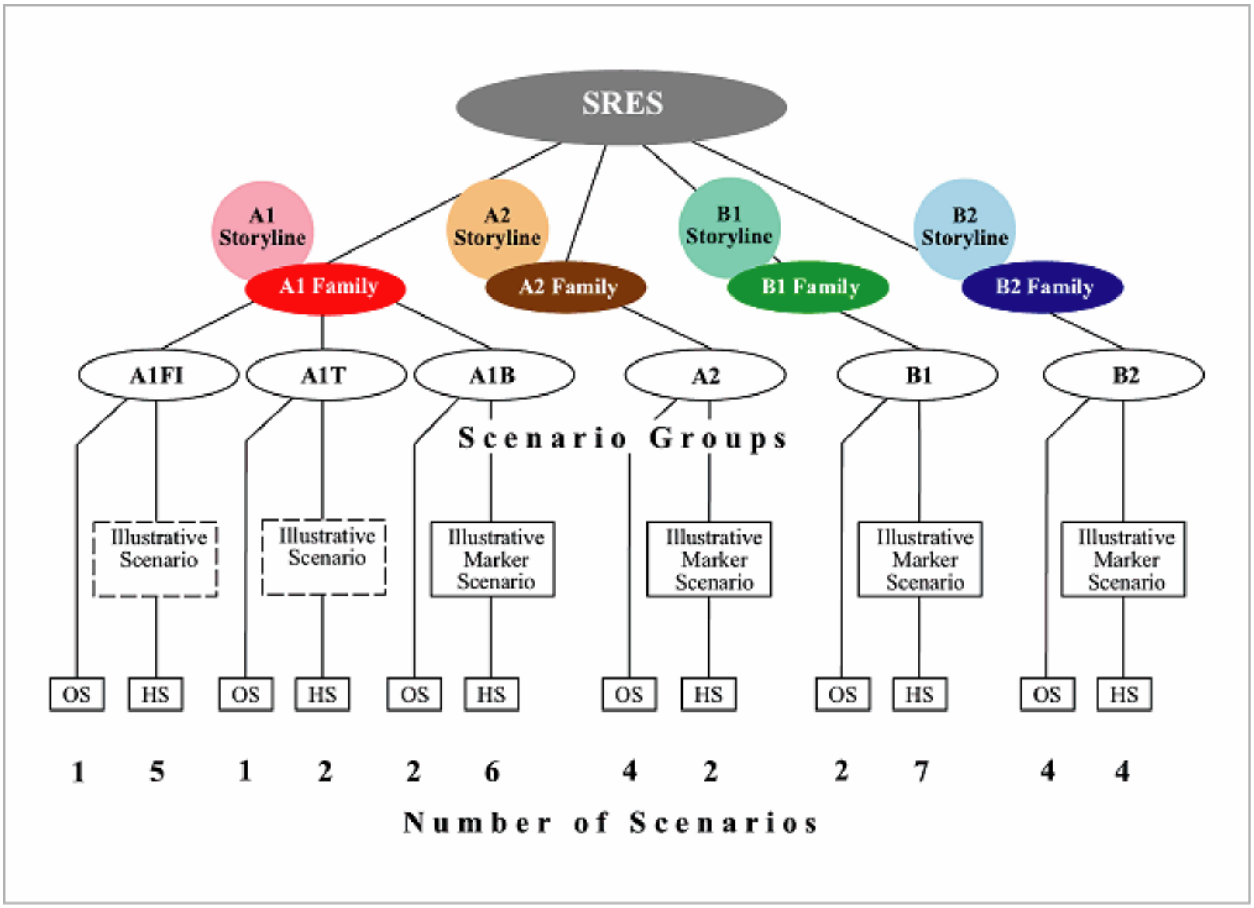


Figure 8.2: Schematic Representation of 40 Emissions Scenarios

Global Climate Models

Nineteen different GGMs have been used to represent the 40 SRES greenhouse gas emissions scenarios (Santer, 2006). The climate processes in a GCM are driven by factors known as forcings, such as greenhouse gas emissions, ozone concentrations, sulfate aerosols, solar irradiance, mineral dust, sea salts, land use/land cover and volcanic aerosols. Different climate

models use different combinations of these forcings to represent the evolution of the climate system (Figure 8.3). The studies presented in this report used climate change projections from two GCMs. Climate change projections produced by additional GCMs are desired to span the range of uncertainty associated with the representation of the climate system.

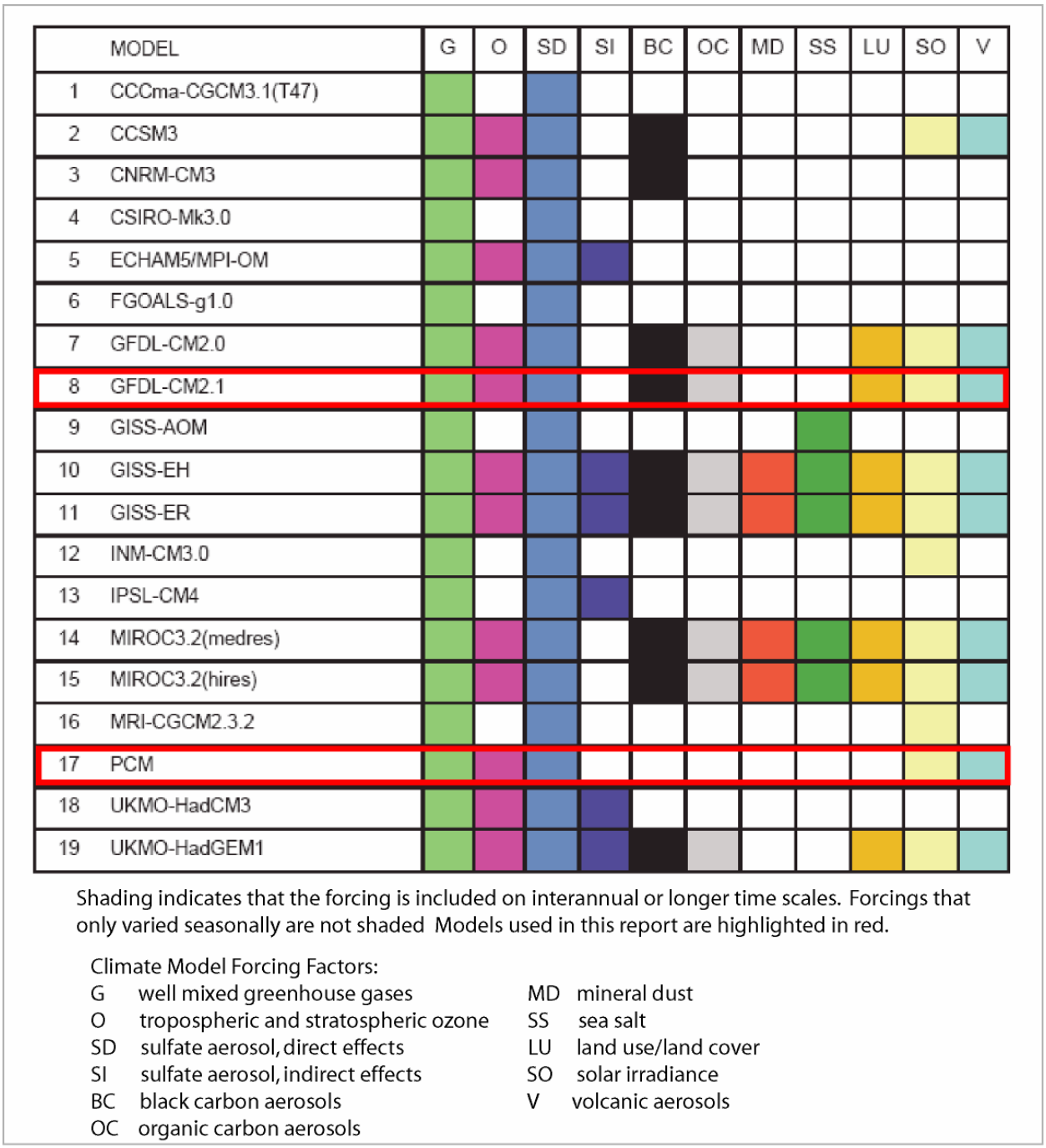


Figure 8.3: Forcing Factor Represented in Various Global Climate Models
Adapted from Table 5.2 (Santer et al., 2006)
Red highlighting indicated models used in this report.

8.8.2 Probability Assessments

As described in the previous section, the work team will compile a larger ensemble of climate change scenarios, hopefully 20 to 30 or more scenarios. The ensemble uncertainty would then be quantified at the regional-scale in terms of probability distributions of annual shifts in precipitation and air temperature. Ensemble members' probabilistic classification (scenario probabilities) would make use of techniques such as those developed by Dettinger (2004). Assumptions would be clearly noted. These scenario probabilities would then be combined with associated impacts assessed using methodologies discussed in this report in order to produce risk information on a variety of system metrics such as annual water deliveries, end-of-September storage, or summer stream temperature. This risk information becomes the baseline for subsequent mitigation studies which look to reduce the risk of negative impacts.

This effort will provide decision makers with both ranges of impacts of climate change and their associated likelihoods. Perceived risk allows planners to make statements about the probability of impacts exceeding certain established thresholds and can be weighed against reliability levels for establishing planning directions. A better understanding of the likelihoods associated with potential climate change impacts will aid decision makers in planning appropriate response strategies. With the accomplishments to date and planned future directions, DWR is collaborating with other agencies and researchers to provide leadership in incorporating climate change impacts and risks into the planning and management of California's precious water resources.

8.9 References

Dettinger, M. (2004). From Climate Change Spaghetti to Climate Change Distributions, Discussion paper prepared for the California Energy Commission, pp25, http://www.energy.ca.gov/reports/2004-04-22_500-04-028.PDF

IPCC. (2000). Intergovernmental Panel on Climate Change, Special Report on Emissions Scenarios, Nebojsa Nakicenovic and Rob Swart (Eds.), Cambridge University Press, UK. pp 570, http://www.grida.no/climate/ipcc/emission/.

Santer, B.D., J.E. Penner, and P.W. Thorne. (2006). How well can the observed vertical temperature changes be reconciled with our understanding of the causes of these changes? In: Temperature Trends in the Lower Atmosphere: Steps for Understanding and Reconciling Differences. A Report by the U.S. Climate Change Science Program and the Subcommittee on Global Change Research [Karl, T.R., S.J. Hassol, C.D. Miller, and W.L. Murray (eds.)]. National Oceanic and Atmospheric Administration, National Climatic Data Center, Asheville, NC, USA (in press).

8.10 Abbreviations

ANN-Artificial Neural Network
CalSimII-Simulation model of the SWP and CVP
CIMIS-California Irrigation Management Information System
CVP-Central Valley Project
GCM-Global Climate Model
GHG-Greenhouse Gas
IPCC-Intergovernmental Panel on Climate Change
SIMETAW-Simulation of Evapotranspiration of Applied Water Model
SRES-IPCC Special Report on Emissions Scenarios
SWP-State Water Project
WUE-Water Use Efficiency



City of Emeryville
Climate Action Plan
November 2008

Environment Equity Economy

Acknowledgements

City of Emeryville Climate Change Task Force Members:

Council Members
- Ruth Atkin
- Nora Davis

Residents
- Deborah Badhia
- Sam Foushee
- Spencer Green
- Pat Hooper
- Jeffrey Koch
- ARobin Orden
- John Scheuerman

Emery Unified School District Board Member
- Cheryl Webb

Emeryville Chamber of Commerce Member
- Denise Pinkston

Emeryville Planning Commission Member
- Gail Donaldson

City Staff - Key Supporting
- Patrick O'Keeffe, City Manager
- Maurice Kaufman, Public Works Director
- Miroo Desai, Senior Planner
- Edmund Suen, Finance Director
- Rebecca Sylvester, Police Service Technician
- Michael Mahoney, Public Works Superintendant
- George Orrego, Assistant Fire Chief

City Staff - Lead and Contact for the Plan:
- Peter Schultze-Allen, Environmental Analyst, Public Works

ICLEI – Cities for Sustainability - Staff
- Timothy Burroughs (former)
- Micah Lang
- Brooke Lee
- Jonathan Strunin
- Ayrin Zahner

StopWaste.org - Staff
- Debra Kaufman
- Teresa Eade
- Wes Sullens

Cover Page photo credits: Emery-Go-Round, Nick Sebastian, Wareham Properties, Siegel and Strain Architects and City Staff

Table of Contents

Executive Summary

Background: The Alameda County Climate Protection Project

1. Introduction

1.1 Introduction to Climate Change Science
1.2 Effects & Impacts of Climate Change
1.3 Action Being Taken on Climate Change

2. Emissions Inventory

2.1 Reasoning, Methodology & Model
2.1.1 Software
2.1.2 Inventory Sources and Data Collection Process
2.2 Alameda County Inventory Results
2.3 Emeryville Inventory Results
2.3.1 Community Emissions Inventory Summary 2004
2.3.2 Community Emissions Inventory Detail 2004
2.3.3 Government Operations Emissions Inventory 2004

3. Forecast for Greenhouse Gas Emissions

4. Greenhouse Gas Emissions Reduction Target

5. Summary of Existing Emissions Reduction Measures

6. Proposed Measures & Policies

6.1 Community-wide Energy and Transportation/Land-use
6.2 Government Energy and Transportation
6.3 Community-wide Solid Waste
6.4 Government Solid Waste

Appendix A – Implementation Table

Appendix B – Baseline Inventory Report (December 2006, Revised August 2008)

Executive Summary

The debate is over. The overwhelming scientific consensus is that human-induced climate change is among the most pressing environmental and social problems facing this generation and those to come.

The time to act is now. Never in the past 1000 years has the planet warmed at a faster rate than during the 20th century, and the most recent decade has been the warmest ever on record. Allowing this trend to continue could result in decreased agricultural output, increased catastrophic weather events such as forest fires, drought and floods and displacement of entire populations due to rising sea levels.

The City of Emeryville must do its part. Although the United States accounts for a mere 4% of the world's population, it produces 20.4% of the world's greenhouse gases, according to Table No. 1 on page 5. The City of Emeryville released an estimated 178,832 tons of carbon dioxide equivalent (CO_2e) in 2004 and, if steps are not taken to achieve reductions, is projected to emit 33% more in 2020. However, in March of 2006 the City of Emeryville pledged to take action against this destructive trend by passing a resolution to join more than 230 U.S. local governments and 770 local governments worldwide in ICLEI's Cities for Climate Protection® (CCP) campaign. In so doing, Emeryville committed to ICLEI's 5-Milestone methodology for combating global warming. In December of 2006, the City approved the baseline inventory report from ICLEI and established a Climate Change Task Force to develop a Climate Action Goal and Plan. Then on May 1st, 2007, the City of Emeryville committed to reducing community-wide greenhouse gas emissions by 25% below 2004 levels by 2020.

Summary of Proposed Actions:

Community-Wide	Affected Sector
Increase Transit Oriented Development	New Development Projects
Adopt a Green Building and Bay-Friendly Ordinance	New Development Projects
Enhance Transportation Demand Management Conditions	New Development Projects
New Pedestrian, Cycling and Transit Programs & Incentives	All Sectors
Increase Transit Service and Ridership	All Sectors
Commercial and Residential Energy Conservation Ordinances	Existing Buildings and Homes
Develop and Incentivize Local Renewable Energy Production	All Sectors
Conserve Potable Water and Develop Rainwater Usage	All Sectors
Reduce 2004 Landfilled Waste Tonnage by 50% by 2020	All Sectors

Government Operations

GB/BFL for buildings and landscapes

Fleet changes – fuel and vehicle types

Reduce 2004 Landfilled Waste Tonnage by 50% by 2020

Environmentally Preferable Purchasing

Alternative Transportation Incentives/Initiatives

Background: The Alameda County Climate Protection Project

In June 2006 eleven local governments in Alameda County, CA committed to becoming members of ICLEI – Local Governments for Sustainability (ICLEI) and participating in the **Alameda County Climate Protection Project (ACCPP)**. The participating jurisdictions include:

Alameda	Berkeley	Newark	San Leandro
Alameda County	Emeryville	Oakland	Union City
Albany	Hayward	Piedmont	

The project was launched by ICLEI in partnership with the Alameda County Waste Management Authority & Recycling Board (StopWaste.Org) and the Alameda County Conference of Mayors. In committing to the project, the jurisdictions embarked on an ongoing, coordinated effort to reduce the emissions that cause global warming, improve air quality, reduce waste, cut energy use and save money. Toward that end, ICLEI and StopWaste.Org assisted each participating jurisdiction to conduct a baseline greenhouse gas emissions inventory, set a community-wide emissions reduction target, and develop a climate action plan that consists of polices and measures that, when implemented, will enable each jurisdiction to meet its target.

A model climate action plan was developed for use by the 11 participating local governments to create tailored climate action plans for their communities. Its purpose is to save participants' time and resources by providing a useful action plan format, background information on the science and impacts of global warming, and detailed suggestions on the types of policies that municipalities can implement to achieve the desired emissions reductions. In developing this resource, ICLEI relied on the expertise of StopWaste.Org staff as well as the experiences of the nationwide network of ICLEI member cities, each of which is working toward similar climate protection goals.

About Alameda County, California

Alameda County is a metropolitan region of the San Francisco Bay Area. The 2005 census estimates the County's population at 1.45 million, the 7th most populous county in the State of California. Like other metropolitan areas, inhabitants of the county and the cities therein contribute to the problem of global warming, while also holding immense potential to contribute to the solution. The energy consumed and the waste produced within the county's boundaries result in thousands of tons of heat-trapping greenhouse gas emissions. But, as is evidenced by the widespread municipal involvement in the Alameda County Climate Protection Project, the local government participants are firmly committed to building on existing efforts to reduce the emissions that cause global warming.

Regional governments and nations across the world can only manage what they measure. The first step in managing greenhouse gas emissions, therefore, is to establish an inventory of those emissions. Below is a chart of global greenhouse gas emissions, which includes the amount of short tons of carbon dioxide equivalent (tons CO_2e) that is generated worldwide, within the United States, the State of California, and in Alameda County. For context, California is the 16th largest emitter in the world - if it were considered a country of its own - second only to Texas in the US. Per capita emissions in California, however, are among the lowest in the US. Further, emissions in Alameda County are significantly less than the California average.

Table (1) World Greenhouse Gas Emissions Scenarios

Locations	GHG – Tons of CO_2e per year	Percent of World GHG Emissions	Percent of U.S.A Emissions	Percent of California Emissions
World (2000)	33,712,900,000	100.0%		
United States (2000)	6,871,700,000	20.4%	100%	
California (2004)	542,184,000	1.6%	7.9%	100.0%
ACCPP Region (2005) [1,2,3]	5,710,393		0.083%	1.105%
ACCPP Governments (2005)	80,532			0.015%

Source: (2000) World and United States emissions from World Resources Institute – Climate Analysis Indicators tool (http://cait.wri.org/). (2004) California emissions from California Energy Commission (http://www.energy.ca.gov/2006publications/CEC-600-2006-013/CEC-600-2006-013-SF.PDF). Figures exclude land use related emissions.

Note: All units in this report are reported in short tons (tons). When source data is found in metric tonnes (MT or tonnes) to convert it into short tons (tons) a conversion factor of 1.102 short ton per metric ton is applied.

Per Capita Fast Facts

2000 Worldwide per capita GHG emissions	**5 tons CO_2e**
2004 US per capita GHG emissions	**23 tons CO_2e**
2004 California per capita GHG emissions	**17 tons CO_2e**

Additional source: 2004, U.S.A. GHG Emissions from EPA (http://www.epa.gov/climatechange/emissions/downloads06/06ES.pdf)

Fast Facts	*Alameda County*	*Emeryville*[5]
Population (2005):	**1.45 Million**	**8,650**
Number of Employees (2005)		**20,000**
Number of Autos (2000):	**4.5 Million**	**4000**
Annual Electricity Usage per Capita (2004):	**6,738 kWh**	
Annual Natural Gas Usage per Capita (2004):	**330 therms**	
Annual Water Usage per Capita (2004):	**46,000 gallons**	
Average Waste per person (2004):	**1.03 tons**	
Average Waste per Business[6] (2004) :	**35.0 tons**	**24.0 tons**
Average Waste Diversion Rate (2004):	**60%**	**64%**
Per capita GHG emissions[4]:	**5.86 tons CO_2e**	

Source: StopWaste.org and City of Emeryville

[1] Data includes the 10 cities in the ACCPP only (Alameda City, Albany, Berkeley, Emeryville, Hayward, Newark, Oakland, Piedmont, San Leandro and Union City).
[2] The Baseline year is 2005 for all cities, except for Albany and Emeryville which inventoried 2004 emissions.
[3] GHG emissions for ACCPP cities are based on ICLEI GHG Emissions Protocol for Local Governments, which includes end use energy, transportation and waste sector within city boundaries. World and U.S.A emissions are based on national GHG inventories which additionally include fugitive emissions, industrial process emissions, and other modes of transportation.
[4] Based on the emissions inventories conducted for the 11 participating local governments.
[5] Per Capita data for the City of Emeryville is not applicable in a predominantly commercial city.
[6] Average Business Waste calculated on estimated 600 businesses with 90% of 2004's 16,000 MSW tons

About the Sponsor: StopWaste.Org

This Alameda County Climate Protection Project was financially sponsored by StopWaste.Org in an effort to support its member agencies in building a region that is continually progressing toward environmentally and economically sound resource management. StopWaste.Org is a public agency formed in 1976 by a Joint Exercise of Powers Agreement among the County of Alameda, each of the fourteen cities within the county, and two sanitary districts. The agency serves as the Alameda County Waste Management Authority and the Alameda County Source Reduction and Recycling Board. In this dual role StopWaste.Org is responsible for the preparation and implementation of the County Integrated Waste Management Plan and Hazardous Waste Management Plan as well as the delivery of voter approved programs in the areas of waste reduction, recycled product procurement, market development and grants to non-profit organizations, to help the County achieve its 75% waste diversion goal.

Key program areas in which StopWaste.Org provides technical and financial assistance to its member agencies include:

→ Business recycling and waste prevention services through the StopWaste Partnership
→ Organics programs, including residential and commercial food waste collection and the promotion of Bay-Friendly Landscaping and gardening
→ Green building and construction and demolition debris recycling
→ Market development
→ Education and outreach, including schools recycling.

As is demonstrated in this document, many of StopWaste.Org's program areas dovetail nicely with municipal efforts to reduce greenhouse gas emissions. While the agency's charge to reduce the waste stream in Alameda County may seem external to traditional emissions reduction strategies, it is working closely with ICLEI in an ongoing way to illustrate the emissions benefits of waste reduction and recycling. Indeed, StopWaste.Org and ICLEI have compiled results in this report that show practices such as residential and commercial recycling and composting, buying recycled products, green building and Bay-Friendly Landscaping play an important role in a local government's emission mitigation strategy. In fact, climate change mitigation can be seen as an umbrella under which the agency's programs play a substantial role.

About ICLEI and the Cities for Climate Protection Campaign

ICLEI's mission is to improve the global environment through local action. The Cities for Climate Protection® (CCP) campaign is ICLEI's flagship campaign designed to educate and empower local governments worldwide to take action on climate change. ICLEI provides resources, tools, and technical assistance to help local governments measure and reduce greenhouse gas emissions in their communities and their internal municipal operations.

ICLEI's CCP campaign was launched in 1993 when municipal leaders, invited by ICLEI, met at the United Nations in New York and adopted a declaration that called for the establishment of a worldwide movement of local governments to reduce greenhouse gas emissions, improve air quality, and enhance urban sustainability. The CCP campaign achieves these results by linking climate change mitigation with actions that improve local air quality, reduce local government operating costs, and improve quality of life by addressing other local concerns. The CCP campaign seeks to achieve significant reductions in U.S. greenhouse gas emissions by assisting local governments in taking action to reduce emissions and realize multiple benefits for their communities.

ICLEI uses the performance-oriented framework and methodology of the CCP campaign's 5-Milestones to assist U.S. local governments in developing and implementing harmonized local approaches for reducing global warming and air pollution emissions, with the additional benefit of improving community livability. The milestone process consists of:

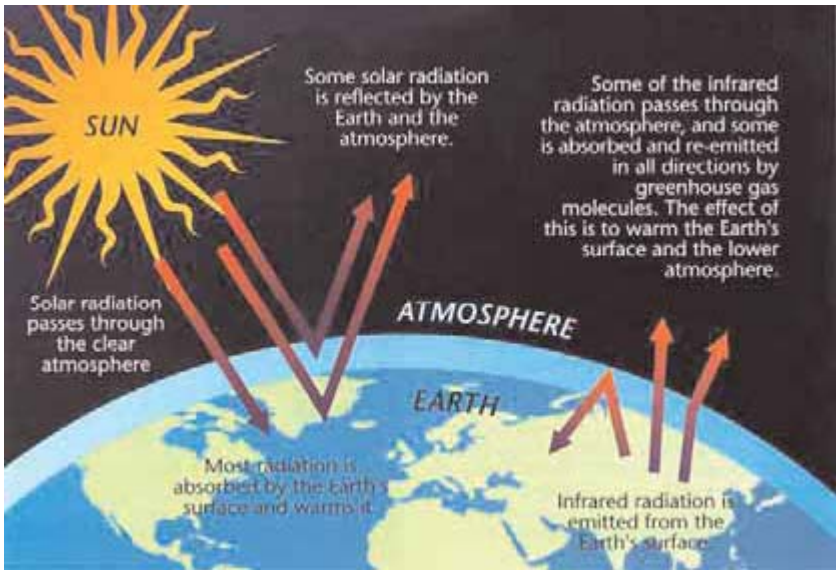
- Milestone 1: Conduct a baseline emissions inventory and forecast
- Milestone 2: Adopt an emissions reduction target
- Milestone 3: Develop a Climate Action Plan for reducing emissions
- Milestone 4: Implement policies and measures
- Milestone 5: Monitor and verify results

1. Introduction

1.1 Introduction to Climate Change Science

The Earth's atmosphere is naturally composed of a number of gases that act like the glass panes of a greenhouse, retaining heat to keep the temperature of the Earth stable and hospitable for life at an average temperature of 60ºF. Carbon dioxide (CO_2) is the most prolific of these gases. Other contributing gases include methane (CH_4), nitrous oxide (NO_2), ozone (0_3) and halocarbons. Without the natural warming effect of these gases the average surface temperature of the Earth would be around 14ºF.

Figure (1) The Greenhouse Gas Phenomenon



Source: US Environmental Protection Agency

However, recently elevated concentrations of these gases in the atmosphere have had a de-stabilizing effect on the global climate, fueling the phenomenon commonly referred to as global warming. The global average surface temperature increased during the 20th century by about 1°F. According to NASA scientists, the 1990s were the warmest decade of the century, and the first decade of the 21st century is well on track to be another record-breaker. The years 2002, 2003, 2004 and 2005, along with 1998, were the warmest five years since the 1890s, with 2005 being the warmest year in over a century.

Scientific Facts and Projections:

- The atmospheric concentration of carbon dioxide (CO_2) during the last two decades has increased at the rate of 0.4% every year.
- Current CO_2 concentrations are higher than they have been in the last 420,000 years, and according to some research, the last 20 million years.
- About three-quarters of the CO_2 emissions produced by human activity during the past 20 years are due to the burning of fossil fuels.

Source: The Intergovernmental Panel on Climate Change

The climate and the atmosphere do not react in a linear fashion to increased greenhouse gases. That is to say that you cannot simply predict the specific degree of warming that each ton of carbon dioxide emitted from a power plant or a vehicle's tailpipe will cause. The Earth's climate has a number of feedback loops and tipping points that scientists fear will accelerate global warming beyond the rate at which it is currently occurring. For example, as CO_2 emissions have increased in recent human history, the oceans have been absorbing a significant portion of these gases, but as the oceans become more permeated with CO_2, scientists anticipate they will reach a saturation point, after which each ton of anthropogenically emitted CO_2 will have a more substantial impact.[5] Another example of this compounding can be found in the polar ice caps. Ice is highly reflective and acts effectively like a giant mirror, reflecting the sun's rays back into space. As the planet warms and some of this ice melts away, a darker land or ocean surface is revealed. This darker surface tends to absorb more heat, accelerating the speed at which the planet warms with each ton of greenhouse gas emitted. As these examples illustrate, the stakes are high, and there is no time to lose in the fight against global warming.

1.2 Effects & Impacts of Climate Change

Global Impacts

In addition to causing an increase in average global surface temperature, rising levels of greenhouse gases have a destabilizing effect on a number of different micro-climates, conditions and systems. According to the Intergovernmental Panel on Climate Change, surface temperatures are on course to increase by between 2.5 and 10.5ºF by the year 2100, with regions in the northern parts of North America and Asia heating by 40% above the mean increase.[6] The increase in the temperature of the oceans is projected to accelerate the water cycle, thereby increasing the severity and rate of both storms and drought, which, along with decreased snow pack, could disrupt ecosystems, agricultural systems and water supplies.

Snow cover has decreased by 10% in the last forty years. Average sea levels have raised between 1/3 and 2/3 of a foot over the course of the 20th century and are projected to rise by at least another 1/3 of a foot and up to almost three feet by the year 2100. These coastal infringements on such a large scale could lead to not only significant environmental and ecosystem disturbances, but also major population displacement and economic upheaval.[7]

Local Impacts

While climate change is a global problem influenced by an array of interrelated factors, climate change is also a local problem with serious impacts foreseen for California, the Bay Area and Emeryville.

***Sea level rise*:** According to the Union of Concerned Scientists, the sea level in the State of California is expected to rise up to 12 inches of the next hundred years. The Pew Center on Climate Change has reported that this would result in the erosion of beaches, bay shores and river deltas, marshes and wetlands and increased salinity of estuaries, marshes, rivers and aquifers.[8]

[5] Intergovernmental Panel on Climate Change (IPCC) Third Assessment Report: "Climate Change 2001: The Scientific Basis."
[6] Intergovernmental Panel on Climate Change (IPCC) Third Assessment Report: "Climate Change 2001: The Scientific Basis."
[7] Intergovernmental Panel on Climate Change (IPCC) Third Assessment Report: "Climate Change 2001: The Scientific Basis."
[8] Neumann, James E. for the Pew Center on Global Climate Change. "Sea Level Rise & Global Climate Change: A Review of Impacts to the US Coasts." February 2000.

This increased salinity has the potential to damage or destroy crops in low-lying farmlands. Infrastructure at or near sea level, such as harbors, bridges, roads and even the San Francisco International and Oakland International Airports are at risk of damage and destruction.

The San Francisco Bay Area Conservation Commission has modeled the impact of a sea level rise of 3 feet (approx 1 meter) on the San Francisco Bay Area. As shown in Figure (2), areas such as the Oakland Airport would be under water as well parts of Alameda, San Leandro, Hayward, Union City, Fremont and Newark, including sections of Interstate 880.

Figure (2) San Francisco Bay Area Land areas Affected by a 1-meter Sea Level Rise



Source: San Francisco Bay Area Conservation Commission

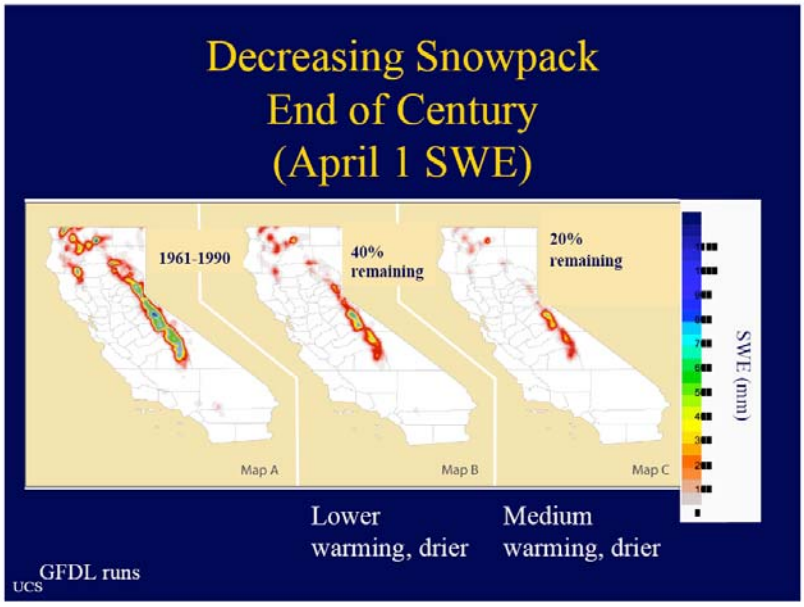
***Natural disasters*:** Climate models predict a 4ºF temperature increase in the next 20 to 40 years, with an increase in the number of long dry spells, as well as a 20-30% increase in precipitation in the spring and fall. More frequent and heavier precipitation cause flooding and mudslides, which would incur considerable costs in damages to property, infrastructure and even human life. Heavy rains during the winter of 2005 offer a glimpse of the potential costly and disruptive effects of such precipitation.

In addition, the increase of wildfires due to continued dry periods and high temperatures is another expected impact of continued climate change. In these conditions, fires burn hotter and spread faster. During 2003, there were 14 reported fires in California which were enhanced due to Santa Ana winds and very low levels of humidity. The estimated damage costs were over $2 Million.

Impacts on water: Water quality and quantity are also at risk as a result of changing temperatures. With warmer average temperatures, more winter precipitation will fall in the form of rain instead of snow, shortening the winter snowfall season and accelerating the rate at which the snowpack melts in the spring. Not only does such snow melt increase the threat for spring flooding, it will decrease the Sierras' capacity as a natural water tower, resulting in decreased water availability for agricultural irrigation, hydro-electric generation and the general needs of a growing population.

The decrease in snow-pack is particularly relevant in the State of California and the Bay Area, as the Sierra snow-pack provides approximately 80% of California's annual water supply, and it is the origin of the Tuolumne River, the primary source of water for the San Francisco regional water system. Figure (3) was provided by the Union of Concern Scientists for the California Climate Action Team Report (2006).

Figure (3) Decreasing Snowpack in California



Source: Union of Concern Scientists

***Impacts on plants and vegetation*:** Native plants and animals are also at risk as temperatures rise. Scientists are reporting more species moving to higher elevations or more northerly latitudes in response. Increased temperatures also provide a foothold for invasive species of weeds, insects and other threats to native species. The increased flow and salinity of water resources could also seriously affect the food web and mating conditions for fish that are of both of economic and recreational interest to residents. In addition, the natural cycle of plant's flowering and pollination, as well as the temperature conditions necessary for a thriving locally adapted agriculture could be affected, with perennial crops such as grapes taking years to recover.

In California, the impacts of climate change on agriculture are estimated to be $30 billion by the Farm Bureau, mostly due to changes in chill hours required per year for cash crops.

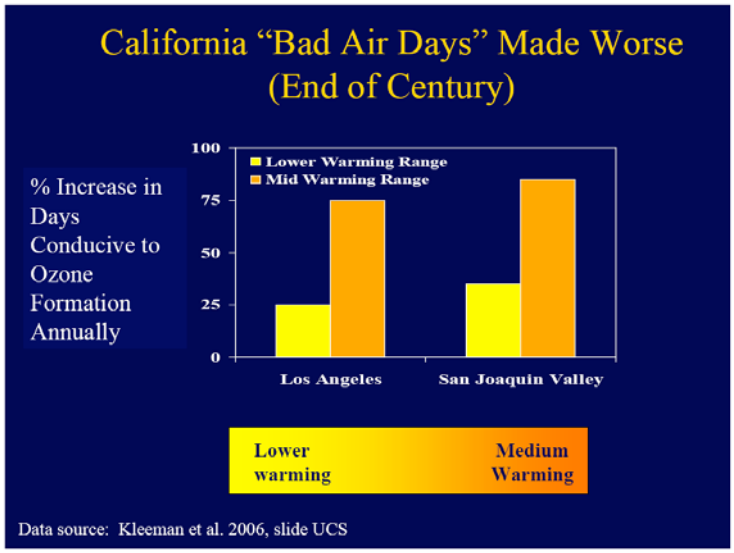
***Public health impact*:** Warming temperatures and increased precipitation can also encourage mosquito-breeding, thus engendering diseases that come with mosquitoes, such as the West Nile

Virus, a disease of growing concern in our region. Heat waves are also expected to have a major impact on public health and be a determinant factor of mortality. According to the IPCC (2004), the summer mortality rates will double by half by 2050 due to hot weather episodes.

Increased temperatures also pose a risk to human health when coupled with high concentrations of ground-level ozone and other air pollutants, which may lead to increased rates of asthma and other pulmonary diseases. Furthermore, anticipated increases in the number and severity of hot days place significant portions of the population, particularly the elderly, young, those already sick, and people who work outdoors, at risk for heat-stroke.

The incidence of bad air days in California's urban areas has increased, mostly in hot summer days. On long, hot, stagnant days, ground level ozone can build up to levels that violate federal and state health-based standards. In the summer of 2006, the Bay Area Air Quality Management District (BAAQMD) registered 11 Spare the Air days and exceeded the California 1-hour standard for ozone (set at 90 ppb) 18 times.

Figure (4) California Bad Air days



Source: Union of Concern Scientists

Given that climate change has local repercussions and effects on weather, water resources, ecosystems, public health, infrastructural stability and economic vitality, local governments have a vested interest in mitigating the amount of greenhouse gases being produced by their communities.

1.3 Action Being Taken on Climate Change

International Action

As evidence of climate change has mounted, groups at the international, federal, state and local level have responded with ways to confront the impending threat. The United Nations Framework Convention on Climate Change (UNFCC) leads international efforts to investigate and combat climate change. Recognizing the problem of potential global climate change, the World Meteorological Organization (WMO) and the United Nations Environment Programme (UNEP) established the Intergovernmental Panel on Climate Change (IPCC) in 1988 to assess on a comprehensive, objective, open and transparent basis the scientific, technical and socio-economic information relevant to understanding the scientific basis of risk associated with human-induced

climate change, its potential impacts and options for adaptation and mitigation, releasing it's most recent assessment in 2007.[9]

In 1997, 10,000 international delegates, observers and journalists gathered in Kyoto, Japan to participate in the drafting and adoption of the Kyoto Protocol, requiring industrialized nations to reduce their collective greenhouse gas emissions 5.2% below 1990 levels. As of January 2007, 162 countries have ratified the Protocol, with the United States and Australia most notably absent from the list. Additionally, since 1995 the annual Conference of the Parties (COP) has met to discuss action and implementation to combat climate change, with the most recent COP, COP-12, being held in Nairobi in 2006.

State and Federal Action

Though adequate attention and action related to combating climate change has been lacking at the federal level, California has taken significant steps at the state level. California has been leading the charge on combating climate change through legislation:

Senate Bill 1078 Sher, 2002 – Established a Renewable Portfolio Standard requiring electricity providers to increase purchases of renewable energy resources by 1% per year until they have attained a portfolio of 20% renewable resources.

Assembly Bill 1493 Pavley, 2002 – Requires the State Air Resources Board to develop and adopt regulations that achieve the maximum feasible reduction of greenhouse gases from vehicles primarily used for non-commercial transportation by January 2005.

Senate Bill 1771 Sher, 2000 – Requires the California Energy Commission (CEC) to prepare an inventory of the state's greenhouse gas emissions, to study data on global climate change, and to provide government agencies and businesses with information on the costs and methods for reducing greenhouse gases. It also established the California Climate Action Registry to serve as a certifying agency for companies and local governments to quantify and register their greenhouse gas emissions for possible future trading systems.

AB 32 Núñez & Pavley, 2006 – Institutes a mandatory limit on greenhouse gas emissions -- reducing emissions in California to 1990 levels by the year 2020, or 25% below forecasted levels. The bill also directs the California Air Resources Board (CARB) to establish a mandatory reporting system to track and monitor emission levels and requires CARB to develop various compliance options and enforcement mechanisms.

On June 1, 2005, Governor Schwarzenegger signed Executive Order #S-3-05 establishing a greenhouse gas reduction target of reducing emissions to 2000 levels by 2010, to 1990 levels by 2020 and 80 percent below 1990 levels by 2050. In April 2006, the California Climate Action Team released its Report to Governor Schwarzenegger and the State Legislature, outlining recommendations and strategies to achieve those reductions.

Local Action

A great deal of work is being done at the local level on climate change as well. ICLEI—Local Governments for Sustainability has been a leader both internationally and domestically for more than ten years, representing over 770 local governments around the world. ICLEI was launched in the United States in 1995 and has grown to more than 230 cities and counties providing national leadership on climate protection and sustainable development. In June 2006, ICLEI launched the California Local Government Climate Task Force as a formal mechanism to provide ongoing input and collaboration into the State of California's climate action process. ICLEI also works in conjunction with the U.S. Conference of Mayors to track progress and implementation of the U.S. Mayors Climate Protection Agreement, launched in 2005, which more than 376 mayors have

[9] Intergovernmental Panel on Climate Change (IPCC) Fourth Assessment Report: "Climate Change 2007"

signed to date pledging to meet or beat the Kyoto Protocol emissions reduction target in their own communities. By the end of 2006, Alameda County mayors from Emeryville, San Leandro, Oakland, Pleasanton, Newark, Hayward, Freemont, Dublin, Berkeley, and Albany signed the U.S. Mayors Climate Protection Agreement.

Climate Protection Efforts by the City of Emeryville

The City of Emeryville has taken several actions on Climate Change in recent years:

On September 7 1999, Council Member Harper asked and received the blessing of the Emeryville City Council to sign onto the "Mayor and Local Official Statement on Global Warming" through the organization "Cities for Climate Protection."

On June 5, 2005, in San Francisco at the United Nations World Environment Day proceedings, the City of Emeryville signed on as a charter member of the United Nations World Environmental Accords - the smallest city in the world to do so. The Accords ask the participating jurisdictions to take one of the 21 action steps each year; the Cities will be evaluated on their voluntary actions in 2012 by the United Nations at a follow-up conference. One of the key action steps of the Accords is to set a goal of reducing green house gas emissions by 25% by 2030 and developing a system to track Greenhouse Gas (GHG) emissions.

Emeryville has already taken many steps toward increasing energy efficiency, reducing air pollution, and reducing solid waste. Examples include:

- Brownfield Redevelopment - Extensive programs since 1996 resulting in urban in-fill projects and reducing the need for urban sprawl. As of 2008 this redevelopment created: 2,290 new residential units for 3,500 residents of which 719 were affordable; and 3.6 million square feet of new commercial space and 800,000 square feet of new retail space creating 8,400 new jobs
- Establishment of the EPA-award-winning Emery-Go-Round: in 2007 shuttled 1.2 million riders between the MacArthur BART station and the City and growing 8% per year.
- Requiring new City Buildings and Landscapes to be LEED Silver Certified and Bay-Friendly Verified
- Reducing building permit fees for single family home solar installations.
- Installing Solar PV panels on the Civic Center roof.
- Requiring vegetated stormwater treatment in all new developments, cleaning the bay, reducing the heat island effect in the City, reducing energy use for cooling and increasing CO2 uptake by plants.
- Increasing Street tree planting standards for new developments ensuring the long-term health of more trees in the City.
- Implementing environmental purchasing decisions such as switching to recycled content copy paper in many City buildings. This practice benefits the community by incentivizing business practices that conserve resources, reduce emissions, and reduce waste.
- Working with the Emeryville Chamber of Commerce to get 21 businesses in Emeryville to "Go Green" and become certified green businesses over since 2003.
- Working with "SmartLights" of the East Bay Energy Watch program to reduce energy use in the lighting of commercial properties in the City.
- Adopting StopWaste.Org's Multi-Family Green Building Guidelines which serve to reduce greenhouse gas emissions by keeping construction and demolition debris out of landfills and increasing energy efficiency in buildings.
- Converting traffic signal lights to more energy efficient LED lamps.
- Requiring new developments to rate their projects using the green building scoring

systems from StopWaste.Org and the United States Green Building Council (USGBC)

- Implementing residential food scrap recycling. Currently approximately 20% percent of households in the single family neighborhoods participate, thereby diverting 9 of tons of food scraps in 2006 from the landfill to a composting facility.
- Requiring landscapes in new developments and city projects to use locally produced compost and mulch partially made of feedstocks from municipal sources.
- Equipping the City Corporation Yard with motion occupancy sensors and energy efficient lighting. These steps save the City money, and reduce the emissions that cause global warming. The Senior Center also received rebate funds for the replacement of the old boiler. Other City facilities are also being considered for lighting retrofits.
- Installing Emeryville's first bike boulevard, adding more bike lanes and building the first phases of the Emeryville Greenway, an urban Rail-to-Trail project, encouraging more people to travel by bike and on foot reducing vehicle emissions.
- Educating the residents of Emeryville at each years Earth Day event in Temescal Creek Park about environmental issues that face the City and the planet.
- Adopting the "Eco Food-ware" ordinance requiring disposable food packaging to be recyclable or compostable for all food prepared in the City and reduce plastic litter washing out to the Bay and ocean.
- Working with the East Bay Green Corridor Partnership to increase the availability of green-collar jobs and green job training
- Starting in 2007, the City has contracted with California Youth Energy Services each summer to give local high school students energy conservation job skills and retrofit existing Emeryville homes with energy conserving devices.
- Joint Bio-Energy Institute - Partnering with UC Berkeley, the Lawrence Berkeley Laboratory and the City of Berkeley, Amyris and others creating 360 green jobs in Emeryville.

2. Emissions Inventory

2.1 Reasoning, Methodology & Model

The City of Emeryville's inventory was conducted by ICLEI in partnership with staff from the municipality. The purpose of the baseline emissions inventory is to determine the levels of greenhouse gas emissions that Emeryville emitted in its base year, 2004.

ICLEI's Cities for Climate Protection inventory methodology allows local governments to systematically estimate and track greenhouse gas emissions from energy and waste related activities at the community-wide scale and those resulting directly form municipal operations. The municipal operations inventory is a subset of the community-scale inventory.

Once completed, these inventories provide the basis for creating an emissions forecast and reduction target, and enable the quantification of emissions reductions associated with implemented and proposed measures.

2.1.1 ICLEI's Emissions Analysis Software

To facilitate local government efforts to identify and reduce greenhouse gas emissions, ICLEI developed the Clean Air and Climate Protection (CACP) software package with Torrie Smith Associates. This software estimates emissions derived from energy consumption and waste generation within a community. The CACP software determines emissions using specific factors (or coefficients) according to the type of fuel used. Emissions are aggregated and reported in terms of carbon dioxide equivalent units, or CO_2e. Converting all emissions to carbon dioxide equivalent units allows for the consideration of different greenhouse gases in comparable terms. For example, methane is twenty-one times more powerful than carbon dioxide in its capacity to trap heat, so the model converts one ton of methane emissions to 21 tons of CO_2e.

The emissions coefficients and methodology employed by the software are consistent with national and international inventory standards established by the Intergovernmental Panel on Climate Change (1996 Revised IPCC Guidelines for the Preparation of National GHG Emissions Inventories), the U.S. Voluntary Greenhouse Gas Reporting Guidelines (EIA form1605), and, for emissions generated from solid waste, the U.S. EPA's Waste Reduction Model (WARM).

The CACP software has been and continues to be used by over 250U.S. local governments to reduce their greenhouse gas emissions. However, it is worth noting that, although the software provides City of Emeryville with a sophisticated and useful tool, calculating emissions from energy use with precision is difficult. The model depends upon numerous assumptions, and it is limited by the quantity and quality of available data. With this in mind, it is useful to think of any specific number generated by the model as an approximation rather than an exact value.

2.1.2 Inventory Sources and Data Collection Process

An inventory of greenhouse gas emissions requires the collection of information from a variety of sectors and sources. For community electricity and natural gas data, ICLEI consulted Pacific Gas & Electric Company (PG&E) and Alameda Power & Telecom[10]. The Metropolitan Transportation Commission (MTC), Bay Area Air Quality Management District (BAAQMD), and Bay Area Rapid Transit (BART) served as sources of transportation data. Solid waste data was gathered from StopWaste.Org, Waste Management, Inc., Alameda County Industries, Republic Services, Inc. and the U.S. Environmental Protection Agency (U.S. EPA). City of Emeryville staff person, Peter Schultze-Allen, was instrumental in providing data on municipal operations.

[10] Exclusively for the City of Alameda

These data were entered into the software to create a community emissions inventory and a municipal emissions inventory. The community inventory represents all the energy used and waste produced within Emeryville and its contribution to greenhouse gas emissions. The municipal inventory is a subset of the community inventory, and includes emissions derived from internal government operations.

There are two main reasons for completing separate emissions inventories for community and municipal operations. First, the government is committed to action on climate change, and has a higher degree of control to achieve reductions in its own municipal emissions than those created by the community at large. Second, by proactively reducing emissions generated by its own activities, the City of Emeryville government takes a visible leadership role in the effort to address climate change. This is important for inspiring local action in Emeryville, as well as for inspiring other communities.

Emeryville's inventory is based on the year 2004. When calculating Emeryville's emissions inventory, all energy consumed in Emeryville was included. This means that, even though the electricity used by Emeryville residents is produced elsewhere, this energy and emissions associated with it appears in Emeryville's inventory. The decision to calculate emissions in this manner reflects the general philosophy that a community should take full ownership of the impacts associated with its energy consumption, regardless of whether the generation occurs within the geographical limits of the community.

2.2 Alameda County Inventory Results

The results for the Alameda County GHG emissions inventory are shown in the following table (2) and figure (5):

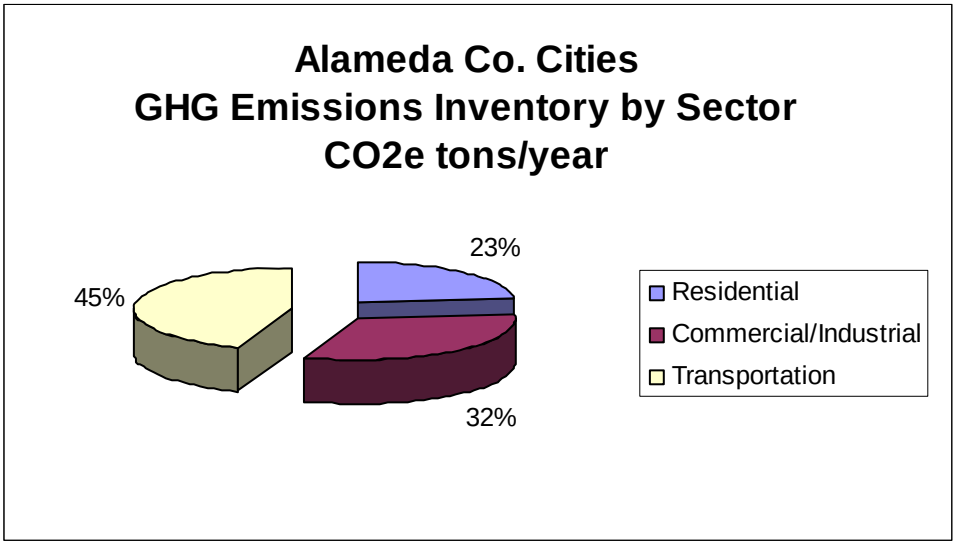
Table (2) GHG Emissions Inventory Results in Alameda County

GHG Emissions Community Inventory Alameda County, CA[1]	**Total CO_2e short tons/year**
	Baseline year[2]
Residential	1,316,481
Commercial/Industrial	1,853,776
Transportation	2,540,136
TOTAL	5,710,393
Households	356,707
Population	974,905
PERCAPITA GHG Emissions (Per capita CO_2e tons/year)	5.86

[1] The above data includes 10 cities (Alameda City, Albany, Berkeley, Emeryville, Hayward, Newark, Oakland, Piedmont, San Leandro and Union City).

[2] The Baseline year is 2005 for all cities, except for Albany and Emeryville which inventoried 2004 emissions. For the presentation of results, data for all cities is included.

Figure (5) GHG Emissions Inventory Results in Alameda County



Source: CACP output

Table (2) and Figure (5) above shows the County's total greenhouse gas emissions from all major sources for the year 2005. The year 2005 was the baseline for all cities except for Albany and Emeryville who used 2004. The County of Alameda is emitting approximately 5,710,393 tons of CO_2e from the residential, commercial/industrial, and transportation sectors. Burning fossil fuels in vehicles and for energy use in buildings and facilities is a major contributor to the County's greenhouse gas emissions. Fuel consumption in the transportation sector is the single largest source of emissions, contributing 45% of total emissions. The residential and commercial/industrial sectors represent emissions that result from electricity and natural gas used in both private and public sector buildings and facilities.

2.3 Emeryville Inventory Results

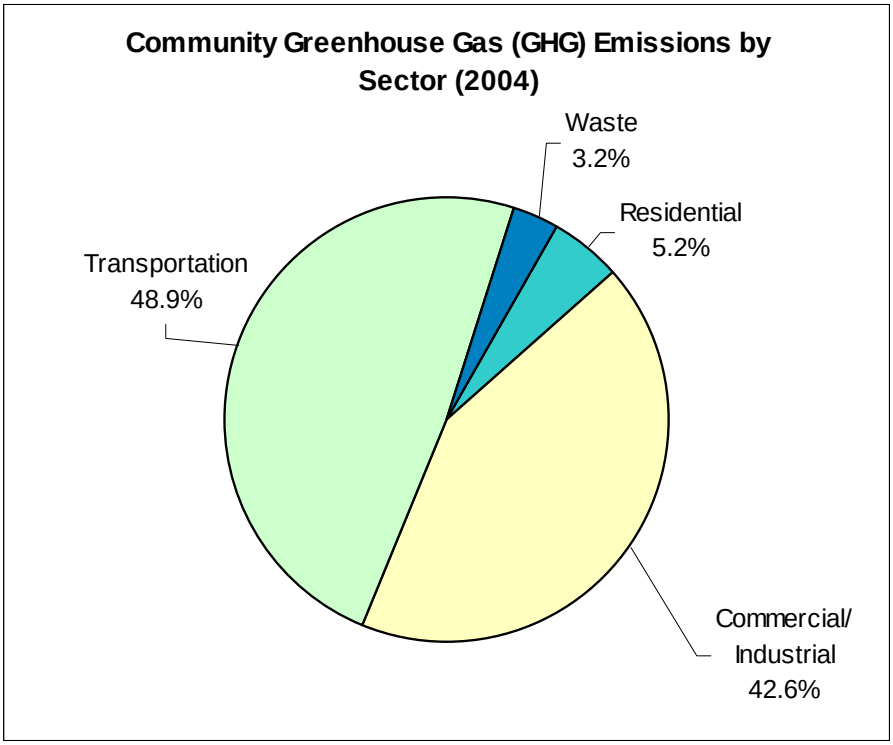
The results below represent the City of Emeryville's completion of the first milestone of ICLEI's CCP campaign. The inventory was first done in 2006 and then updated with Highway emissions in August of 2008. The inventory described below includes those highway emissions.

2.3.1 Community Emissions Inventory Summary – 2004

Table (3) Community Emissions Summary

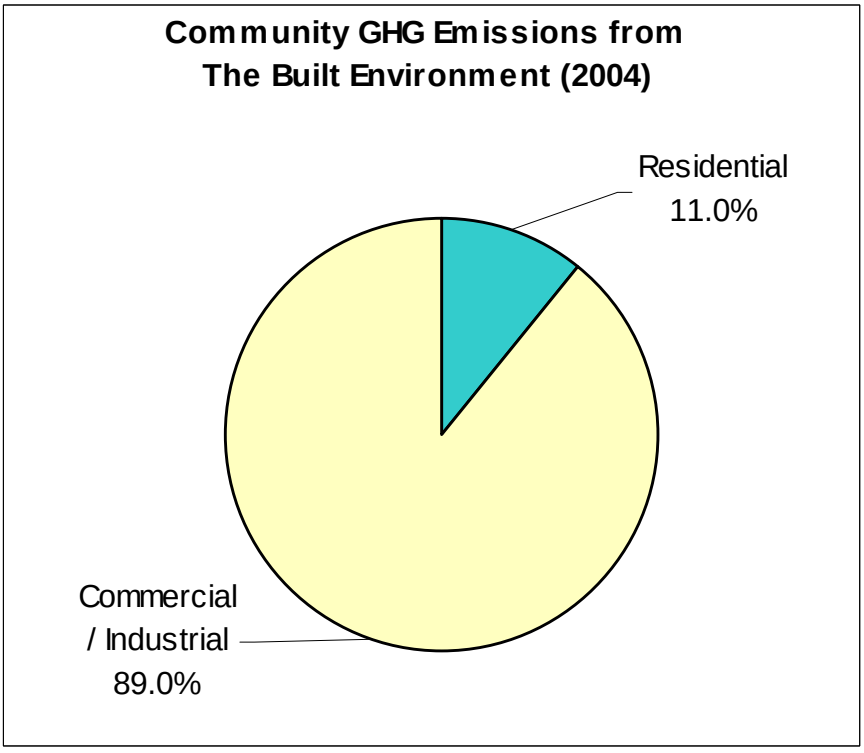
2004 Community Emissions by Sector	Residential	Commercial/ Industrial	Transportation	Waste	TOTAL
CO_2e (metric tons)	9,380	76,204	87,447	5,801	178,832
Percentage of Total CO_2e	5.2%	42.6%	48.9%	3.2%	100.0%
Energy Use (MMBtu)	160,562	1,267,105	262,451	0	1,690,118

Figure (6) Community Emissions by Sector



2.3.2 Community Emissions Inventory Detail – 2004

Figure (7) Community Emissions – Built Environment

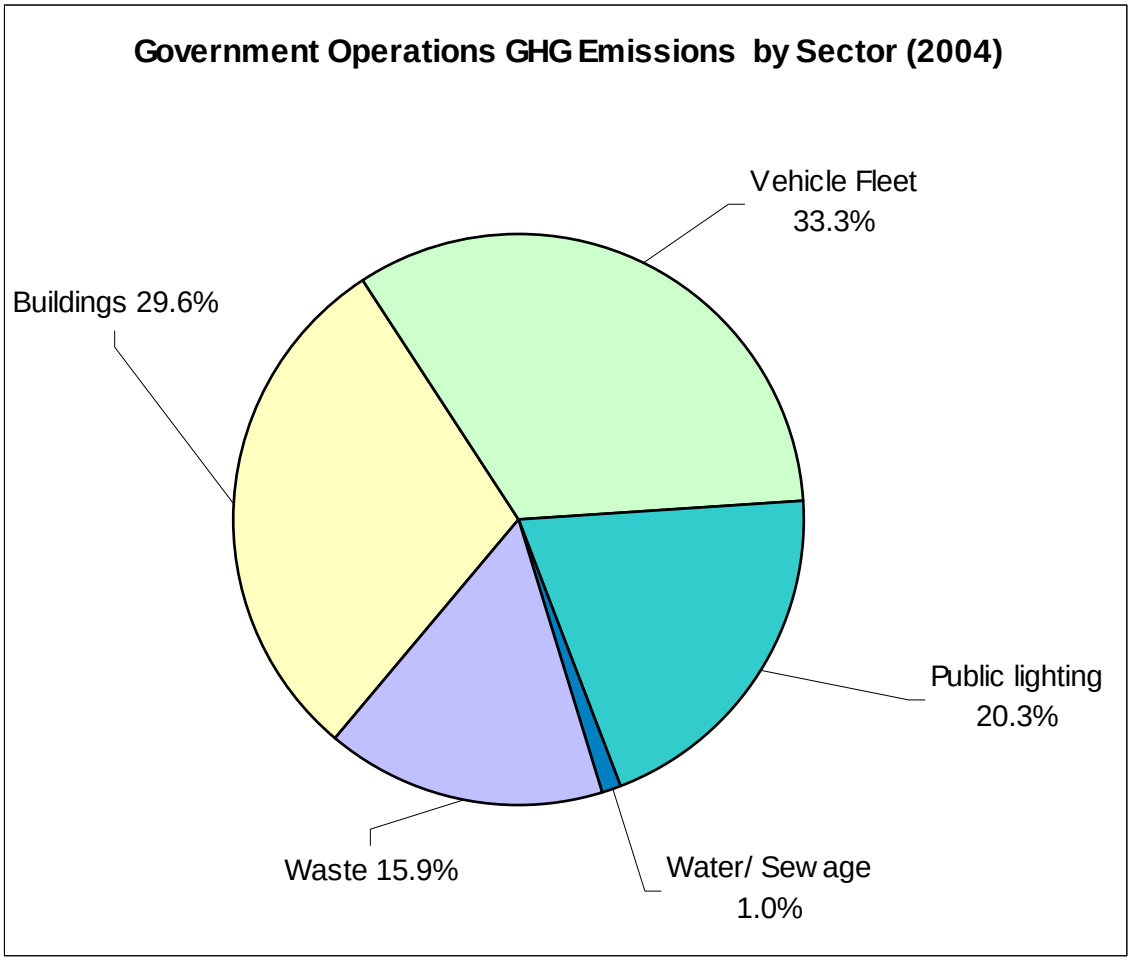


2.3.3 Government Emissions Inventory Summary 2004

Table (4) Government Emissions

Government Emissions 2004	Buildings	Vehicle Fleet	Public Lighting	Water/ Sewage	Waste	TOTAL
CO2e (metric tons)	395	444	271	13	212	1,335
% of Total CO2e	29.6%	33.3%	20.3%	1.0%	15.9%	100.0%
MMBtu	6,633	5,713	4,137	195	-	16,678
Cost ($)	$169,608.00	$118,974.00	$136,974.00	$7,801.00	-	433,357

Figure (8) Government Emissions by Sector



3. Forecast for Greenhouse Gas Emissions – 2020

Table 5 shows the projected new development in the City of Emeryville (taken from the City's draft General Plan - Land Use section.) The row headings are described below:

A. Approved Projects. This includes the various projects that have been approved or are under construction as of November 2007. This development includes 907 housing units and 1.3 million square feet of non-residential space.

B. Gross New Development. This value results from application of average assumed intensities to change areas. Approximately 2,930 housing units and 3.0 million square feet of non-residential space will be added.

C. Existing Development Lost Due to Redevelopment. This value reflects existing underutilized properties that will be replaced by new uses.

D. Net New Development. This reflects the total of the three above categories, and represents the expected development during the life of the General Plan.

E. Existing Development. This reflects existing development, as of November 2007.

F. City at 2030. Totaling net new development and existing development results in the General Plan development potential at 2030. This will result in an increase of approximately 3,800 housing units, a 70 percent increase in the existing population of 9,727 to 16,500, and 2.5 million square feet of total non-residential space, an increase of 21% over 2007 levels.

Table (5) General Plan Development Potential at 2030, by Land Use (draft)

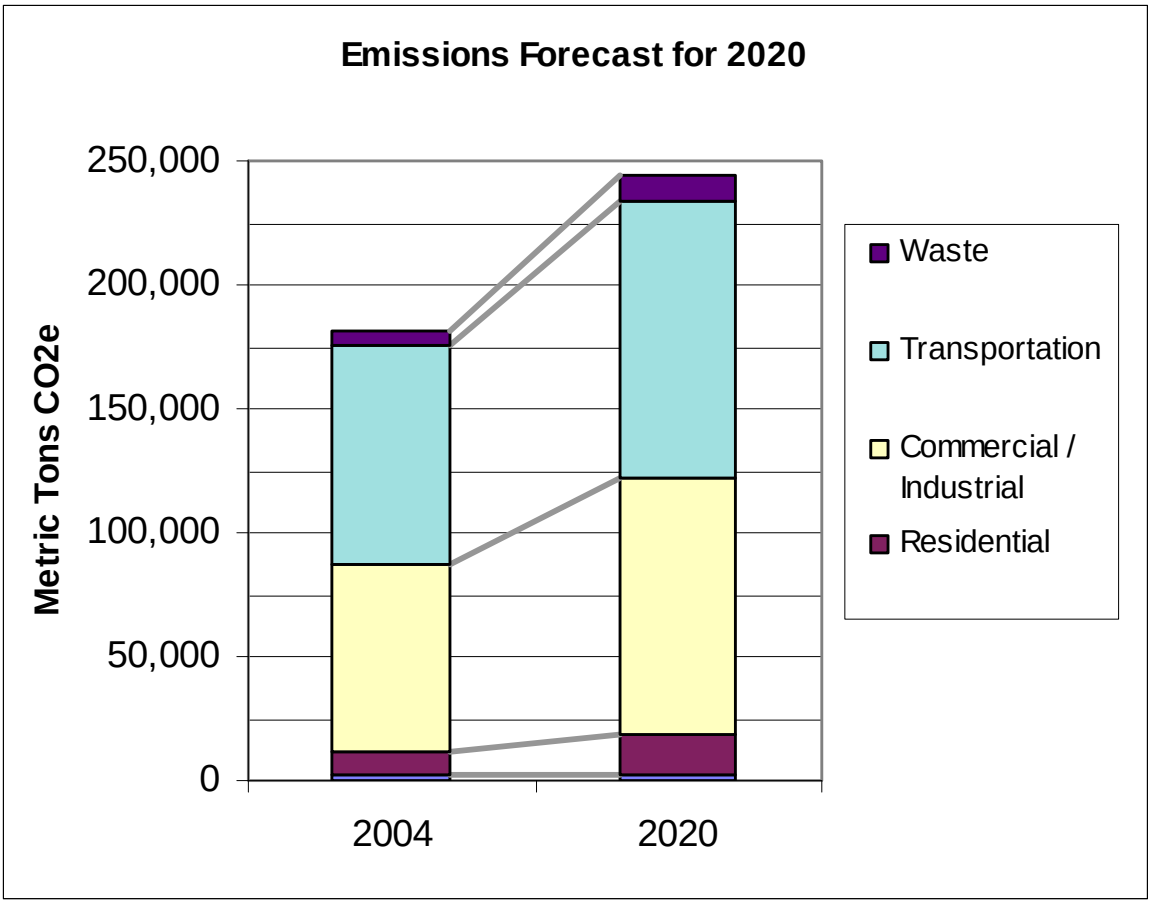
	Residential (units)	Retail (SF)	Hotel (SF)	Office[1] (SF)	Industrial (SF)
A. Approved Development	907	34,461	0	1,313,000	0
B. Gross New Development	2,930	1,075,400	324,600	1,569,700	76,200
C. Existing Lost Due to Redevelopment	70	468,598	14,375	509,740	855,377
D. Net New Development (A+B-C)	3,767	641,263	310,225	2,372,960	-779,177
E. Existing Development	5,988	2,441,660	464,500	4,852,118	4,132,675
F. City at 2030 (D+E)	9,755	3,082,923	774,725	7,225,078	3,353,499

[1]Office includes R&D development.

From 2004 to 2020, under a business-as-usual scenario, the City of Emeryville's emissions will grow by approximately 32.6% from 178,832 to 237,101 metric tons CO2e[11]. To illustrate the potential emissions growth based on projected trends in energy use, driving habits, job growth, and population growth from the baseline year going forward, ICLEI conducted an emissions forecast for the year 2020. Figure 9 and Table 6 show the results of the forecast. A variety of different reports and projections were used to create the emissions forecast.

[11] Transportation growth rates calculated for this forecast assume a base year of 2005, and would be slightly different from 2004.

Figure (9) Community Emissions Forecast



Residential Forecast Methodology

For the residential sector, ICLEI calculated the compounded annual population growth rate[12] between 2005 and 2020, using population projections from Emeryville's draft General Plan. This growth rate (3.444%) was used to estimate average annual compound growth in energy demand. From the Emeryville General Plan, ICLEI estimated that the City's population will be 13,300 in 2020[13].

Commercial / Industrial Forecast Methodology

Analysis contained within "California Energy Demand 2008-2018: Staff Revised Forecast[14]," a report by the California Energy Commission (CEC), shows that commercial floor space and the number of jobs have closely tracked the growth in energy use in the commercial sector. Using job growth projections from the draft Emeryville General Plan, ICLEI calculated that the compounded annual growth in energy use in the commercial sector between 2005 and 2020 will be 1.99%.[15]

[12] Compounded annual growth rate= ((2020 population/2005 population)^(1/15))-1

[13] The General Plan provides population predictions for 2030. To estimate 2020 population, ICLEI used 2000 Census data and assumed an equal growth rate every five years between 2000 and 2030.

[14] http://www.energy.ca.gov/2007publications/CEC-200-2007-015/CEC-200-2007-015-SF2.PDF

[15] The Emeryville General Plan states that 10,000 new jobs will be added by 2030. ICLEI estimated the 2007 number of jobs by assuming a constant growth between 2005 and 2010 from ABAG jobs forecast data and added 10,000 to

Transportation Forecast Methodology

For the transportation sector, projected growth in energy demand was obtained from the CEC 2008 energy demand forecast referenced above. The recently passed federal Corporate Average Fuel Economy standards and the state of California's pending tailpipe emission standards could significantly reduce the demand for transportation fuel in Emeryville. An analysis of potential fuel savings from these measures at a scale that would be useful for the purpose of this report has not been conducted, nor would such an analysis produce a true business-as-usual estimation. Regardless of future changes in the composition of vehicles on the road as a result of state or federal rulemaking, emissions from the transportation sector will continue to be largely determined by growth in vehicle-miles-traveled (VMT). In their report, "Transportation Energy Forecasts for the 2007 Integrated Energy Policy Report," the CEC projects that on-road VMT will increase at an annual rate of 1.51% per year through 2020[16]. This is the number that was used to estimate emission growth in the transportation sector for the Emeryville forecast.

Waste Forecast Methodology

As with the residential sector, the primary determinate for growth in emissions in the waste sector is population. Therefore, the compounded annual population growth rate for 2005 to 2020, which is 3.444%[17] (as calculated from the draft Emeryville General Plan), was used to estimate future emissions in the waste sector.

Table 6 – *Community Emissions Growth Projections by Sector*

Community Emissions Growth Forecast by Sector	2004	2020	Annual Growth Rate	Percent Change from 2004 to 2020
Residential	9,380	15,587	3.444%	66.2%
Commercial / Industrial	76,204	102,407	1.990%	34.4%
Transportation (incl. 2005 State Hwy data)	87,447	109,467	1.509%	25.2%
Waste	5,801	9,640	3.444%	66.2%
TOTAL	**178,832**	**237,101**	**--**	**32.6%**

As Table 6 shows, emissions from the residential and waste sectors will experience a 66.2% increase. Emeryville can dramatically reduce these emissions by ensuring energy and water efficiency standards are met in new residential developments and promoting recycling and composting across the City.

The Municipal operations of the City are not expected to grow in any significant manner, so the business as usual emissions are projected to remain roughly the same. This is reflected in Table 7.

---

estimate 2030 jobs (30,668). This was then prorated in the same manner as population projections to estimate 2020 jobs (27,065).

[16] Report available at: http://www.energy.ca.gov/2007publications/CEC-600-2007-009/CEC-600-2007-009-SF.PDF. Compounded Annual growth rate for 2005-2020 is calculated from Table 4 on page 12. In light of recent fuel cost increases, the calculation assumes high fuel cost scenario.

[17] Ibid

4. Greenhouse Gas Emissions Reduction Target

A reduction target provides a tangible goal for Emeryville's emissions reduction efforts. Our emissions reduction target represents a percentage by which the community aims to decrease emissions, below the 2004 baseline, by 2020.

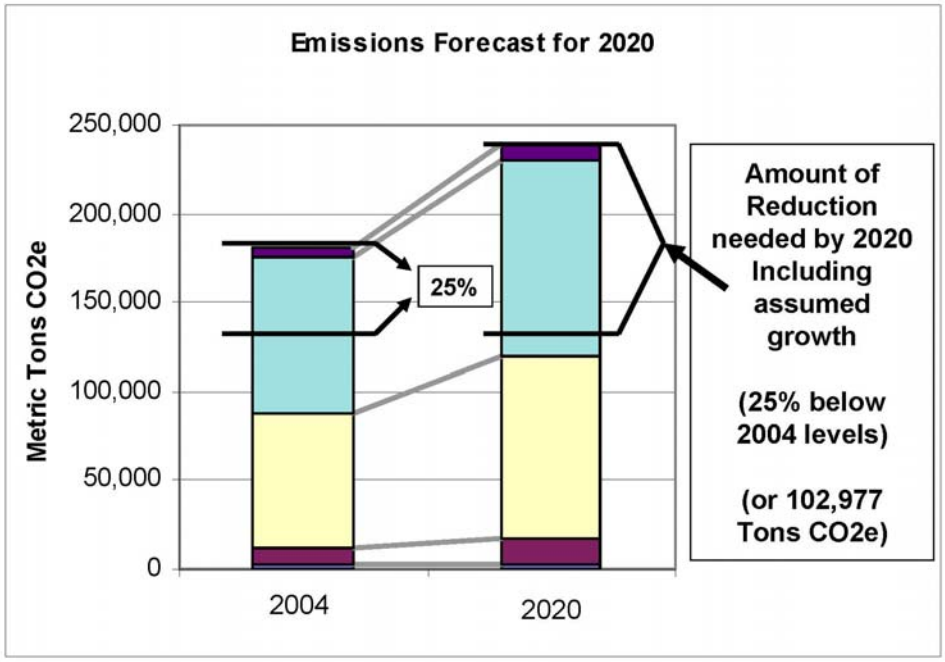
Many factors were considered when selecting Emeryville's reduction target. We strove to choose a target that is both aggressive and achievable given local circumstances. Emeryville's residential and commercial redevelopment is occurring at a rapid level, which provides the City with both challenges and opportunities for climate change actions.

Table (7) Emeryville Emissions Summary

	Community-wide	Government Operations
Base year	2004	2004
Quantity of CO_2e emissions in base year (tons)	178,832	1,335
Target year	2020	2020
Business-as-usual projection of CO_2e emissions in 2020 (tons)	237,101	1,335
Percent CO_2e reduction targeted by target year relative to base year (%)	25%	25%
Quantity of CO_2e reduction targeted relative to base year (tons)	102,977	284

Source: CACP Model Output

Figure (10) Emission Reduction Target Summary



5. Summary of Existing Emissions Reduction Measures

Table (8) Emeryville's Emissions Summary

	Community Analysis	Government Operations Analysis
Base year	2004	2004
Quantity of CO_2e emissions in base year (tons)	178,832	1,335
Target year	2020	2020
Business-as-usual projection of CO_2e emissions in 2020 (tons)	237,101	1,335
Percent CO_2e reduction targeted by target year relative to base year (%)	25%	25%
Quantity of CO_2e reduction targeted relative to base year (tons)	102,977	333
Quantity of CO_2e reduction achieved to date (tons)	0[1]	50[2]
Percent of CO_2e reduction target achieved to date (%)	0%[1]	7%[2]
Quantity of CO_2e reduction pending to reach target (tons)	102,977	284

Source: CACP Model Output

[1] Until the next emissions inventory is performed, it is not possible to accurately estimate the community emission reductions to date.

[2] The Municipal emission reductions to date were estimated from the new programs that have occurred since the end of 2004: solar pv system on City Hall, the police bike patrol program, the lighting retrofit at the Corp Yard, the boiler replacement at the Senior Center, compost and recycling improvements at City facilities and new fleet vehicles with better emissions.

6. Proposed Emissions Reduction Measures & Policies

Based on careful consideration of the emissions reductions needed to achieve our stated targets, the distribution of emissions revealed in our emissions inventory, existing priorities and resources, and the potential costs and benefits of various potential emissions reduction projects, Emeryville has identified a set of emissions reduction measures that should be set into motion as soon as possible. An implementation table prioritizing the measures with costs and scheduling for each measure is attached as Exhibit A. The actions are divided into the following sectors/measure types: transportation, energy efficiency, renewable energy, and solid waste management[18]. Within each of these categories, the measures are further divided into the measures that affect community-wide emissions and measures that affect the emissions that result from municipal operations.

Summary of Proposed Actions:

Community-Wide	Affected Sector
Increase Transit Oriented Development	New Development Projects
Adopt a Green Building and Bay-Friendly Ordinance	New Development Projects
Enhance Transportation Demand Management Conditions	New Development Projects
New Pedestrian, Cycling and Transit Programs & Incentives	All Sectors
Increase Transit Service and Ridership	All Sectors
Commercial and Residential Energy Conservation Ordinances	Existing Buildings and Homes
Develop and Incentivize Local Renewable Energy Production	All Sectors
Conserve Potable Water and Develop Rainwater Usage	All Sectors
Reduce 2004 Landfilled Waste Tonnage by 50% by 2020	All Sectors

Government Operations

GB/BFL for buildings and landscapes

Fleet changes – fuel and vehicle types

Reduce 2004 Landfilled Waste Tonnage by 50% by 2020

Environmentally Preferable Purchasing

Alternative Transportation Incentives/Initiatives

The emissions that result from municipal facilities and operations account for less than 1% percent of Emeryville community-wide emissions. That being said, measures taken to reduce municipal emissions show that the city's elected officials and staff are committed to action on climate change and to inspiring action in both our community and neighboring communities. Emeryville is proud of the emissions reduction efforts implemented to date and is committed to building on those efforts by increasing fleet fuel efficiency, reducing solid waste, and increasing energy efficiency and conservation in municipal buildings.

[18] Waste Management is used in the broader sense to include, waste reduction, recycling, composting and final disposal activities.

6.1 Community-wide Energy and Transportation/Land-Use Measures

Table (9) Proposed Community-wide Energy & Transportation/Land-use Measures
(Source – CAPPA software from ICLEI and WARM model from EPA)

Measure ID#	Measure	CO2e (metric tons)	% towards goal
C58	Transit Oriented Development	17,640	18.00%
C16	Require Green Building for New Construction	10,511	10.73%
C29	Energy Efficiency Education Targeted at Residents	7,514	7.67%
C32	Water Conservation Ordinance	5,341	5.45%
C30	Promote Green Building Through Loans & Incentives	5,256	5.36%
C44	Education on Low-carbon Transportation Options	3,985	4.07%
C23	Require Energy Efficiency Retrofit at Time of Sale	3,757	3.83%
C17	Strict Commercial Energy Code	3,504	3.58%
C22	Energy Efficiency Retrofits of Existing Facilities	3,504	3.58%
C47	Bus Rapid Transit for Emery-Go-Round and AC Transit	3,466	3.54%
C28	Energy Efficiency Education Targeted at Business	3,325	3.39%
C38	Reflective Roofing	2,346	2.39%
C52	Expand Carshare	2,317	2.36%
C18	Strict Residential Energy Code	2,254	2.30%
C19	Offer Loans for Residential Energy Efficiency Improvements	2,254	2.30%
C10	High Efficiency Water Heaters	2,185	2.23%
C21	Energy Efficient Affordable Housing	1,503	1.53%
C36	Low-Maintenance Landscaping	1,480	1.51%
C57	Provide Free High School Bus Passes	1,002	1.07%
C36	Lighting Occupancy Sensors	958	0.98%
C20	Low-income Home Weatherization	881	0.90%
C27	Efficient Lighting Retrofits - T12 lamps to T-8 lamps	821	0.84%
C11	Increase Chiller Efficiency	817	0.83%
C31	Green Business Programs	665	0.68%
C39	Install Solar Photovoltaic (PV) Energy	656	0.67%
C51	Increase BART & AMTRAK Ridership	639	0.65%
C5	Energy Efficient Refrigerators	556	0.57%
C46	Increase Emery-Go-Round Ridership	556	0.57%
C48	Parking Cashout	450	0.46%
C40	Install Solar Hot Water through incentives	390	0.40%
C34	Water Saving Shower Heads	377	0.39%
C1	Energy Efficient Computers	365	0.37%
C2	Energy Efficient Computer Monitors	340	0.35%
C13	HVAC Fan Upgrades	331	0.34%
C14	HVAC Maintenance Tune-ups	317	0.32%
C50	Increase AC Transit Ridership	278	0.28%
C56	Provide Bicycles for Daily Trips	262	0.27%
C8	Energy-Efficient Dish Washers	252	0.26%
C45	Bicycling Paths and Facilities	243	0.25%

C12	Increase Boiler Efficiency	222	0.23%
C6	Energy Efficient Vending Machines	199	0.20%
C37	Green Roofs	196	0.20%
C53	Promote Carpooling and Vanpooling	187	0.19%
C15	Switch Electric Heat to Natural Gas	185	0.19%
C9	Efficient Clothes Washers	172	0.18%
C54	Promote Telecommuting	172	0.18%
C60	Parking and Lane Incentives for Hybrid Vehicles	164	0.17%
C59	Use Hybrid Vehicles - (all sectors)	164	0.17%
C4	Energy Efficient Copiers	150	0.15%
C63	Increase Urban Forest	126	0.13%
C49	Walking Friendly Environments	122	0.12%
C42	Electric Vehicle Charging Stations on Parking Structures	119	0.12%
C61	Use Smaller Fleet Vehicles	92	0.09%
C43	Integrate Bicycles and Transit	81	0.08%
C3	Energy Efficient Printers	74	0.08%
C25	Energy Efficient Exit Signs	54	0.06%
C62	Plant Trees to Shade Buildings	41	0.04%
C33	Water Saving Faucets	38	0.04%
C24	Compact Fluorescent Light Bulb (CFL) Distribution	35	0.04%
C35	High Efficiency Toilets	25	0.03%
C7	Energy Efficient Water Coolers	24	0.02%
C41	Use Wind Energy	20	0.02%
	Sub Total from CAPPA Software	95,961	97.99%
	Waste Measures – See Section 6.3 below (WARM model)	16,766	
	TOTAL TONS REDUCED	112,727	

6.2 Government Energy and Transportation Measures

Table (10): Proposed Government Energy and Transportation Measures
(Source – CAPPA software from ICLEI and WARM model from EPA)

Measure ID #	Measure	CO2e (metric tons)	% of goal
G21	Use Solar Photovoltaic (PV) Energy	65.61	23.12%
G12	Require Green Building for New Construction	26.28	9.26%
G13	Energy Efficiency Retrofits of Existing Facilities	21.90	7.72%
G28	Increase BART & AMTRAK Transit Ridership by employees	16.80	5.92%
G32	Hybrid Vehicles - City Fleet	16.45	5.80%
G22	Use Solar Heat for Public Swimming Pool	15.74	5.55%
G36	Establish/Expand Recycling Programs	13.15	4.63%
G17	Lighting Occupancy Sensors	11.49	4.05%
G35	Fuel Efficient Vehicles for Parking Enforcement	10.55	3.72%
G18	Low-Maintenance Landscaping	9.87	3.48%

G27	Increase Emery-Go-Round Ridership by employees	7.31	2.58%
G25	Police on Bicycles	7.08	2.50%
G16	LED Traffic Signals	4.73	1.67%
G20	Reflective Roofing	4.69	1.65%
G26	Parking Cashout	4.50	1.58%
G8	Increase Chiller Efficiency	4.09	1.44%
G38	Plant Trees to Shade Buildings	4.07	1.44%
G19	Green Roofs	3.92	1.38%
G33	Use Smaller Fleet Vehicles	3.69	1.30%
G7	High Efficiency Water Heaters	3.64	1.28%
G29	Carsharing program for fleet vehicles	3.45	1.22%
G11	HVAC Maintenance Tune-ups	3.17	1.12%
G4	Energy Efficient Copiers	3.00	1.06%
G37	Reuse or Recycling of Construction Materials	2.98	1.05%
G23	Install Solar Hot Water	1.92	0.68%
G1	Energy Efficient Computers	1.83	0.64%
G2	Energy Efficient Computer Monitors	1.70	0.60%
G10	HVAC Fan Upgrades	1.65	0.58%
G3	Energy Efficient Printers	1.48	0.52%
G9	Increase Boiler Efficiency	1.11	0.39%
G14	Energy Efficient Exit Signs	1.09	0.38%
G15	LED Street Lights	1.05	0.37%
G5	Energy Efficient Refrigerators	0.93	0.33%
G30	Promote Telecommuting	0.86	0.30%
G34	Retire Old or Underused Fleet Vehicles	0.75	0.26%
G24	Bicycling Paths and Facilities	0.46	0.16%
G31	Provide Bicycles for Daily Trips	0.45	0.16%
G6	Energy Efficient Water Coolers	0.41	0.14%
	Sub Total from CAPPA Software	285	
	Waste Measures – see Section 6.4 below (WARM model)	50	
	TOTAL TONS REDUCED	335	

6.3 Community-wide Solid Waste Reduction Measures

Table (11): Proposed Community-wide Solid Waste Reduction Measures

Reduce Landfilled Waste in half by 2020 over 2004 levels by:
Increasing participation in commercial recycling/reuse programs for paper, cardboard, metal, glass and plastics – rigid and film.
Participating in StopWaste.Org's audit and technical assistance program
Encouraging businesses to participate in the County Green Business program
Increasing participation in residential recycling programs
Educating residents and businesses about the benefits of Bay-Friendly Landscaping and Gardening
Increasing participation in commercial and residential food waste collection program (for composting).
Revising franchise language as franchises are renegotiated to include language that maximizes diversion (see StopWaste.Org for best practices)
Considering incentives for waste reduction such as new rate structures for refuse and discards collection that credit diversion and allow for reduced rate composting/recycling services for businesses and residents.

6.4 Government Solid Waste Reduction Measures

Table (12): Proposed Government Solid Waste Reduction Measures

Reduce Landfilled Waste in half by 2020 over 2004 levels by:
Implementing a duplex copying/printing policy in municipal office buildings
Reducing Landscape Waste in City landscapes by implementing StopWaste.Org's *Bay-Friendly Landscaping* Program. Include practices such as: Increase on-site composting and mulching of municipal plant debris, using compost as a soil amendment, mulch for weed suppression, including the use of drip irrigation systems, a diverse plant pallet to resist pests, and reducing turf and sheared hedges.
Increasing recycling and composting in municipal facilities
Adopting policies that support reduced waste (and which support other environmental priorities) including the following: Environmental purchasing policy 75% Diversion Goal Construction &Demolition materials recycling ordinance Civic Bay-Friendly/Green Building Ordinance Residential green building resolution Consider mandatory residential & commercial recycling/composting ordinance
Revising franchise language as franchises are renegotiated to include language that maximizes diversion (see StopWaste.Org for best practices)

California Environmental Protection Agency

Air Resources Board

2014 Edition

California Greenhouse Gas Emission Inventory: 2000-2012

May, 2014

This document has been prepared by the staff of the California Air Resources Board. Publication does not signify that the contents reflect the views and policies of the Air Resources Board.

This Page is Intentionally Left Blank

Summary

This report presents an overview of the 2014 Edition of the California greenhouse gas (GHG) emission inventory, which tracks emissions and trends from 2000 through 2012. As California strives to achieve its benchmark goals under AB 32, the California inventory is an increasingly valuable tool to keep track of greenhouse gas emissions from each sector. Maintaining and updating greenhouse gas inventory methodologies and data are imperative for a successful greenhouse gas reduction program.

In 2012, total California greenhouse gas emissions were 459 million metric tons (or tonnes) of carbon dioxide equivalent ($MMTCO_2e$). This represents a 1.7 percent increase in total GHG emissions from 2011 and the first emissions increase since 2007. This increase was driven primarily by strong economic growth in the state, the unexpected closure of the San Onofre Nuclear Generating Station (SONGS), and drought conditions that limited in-state hydropower generation. Since 2000, GHG emissions have decreased by 1.6 percent (from 466 to 459 $MMTCO_2e$) after reaching a peak of 493 $MMTCO_2e$ in 2004.

Emissions in this report are aggregated based on an Economic Sector categorization. In 2012, the transportation sector is the largest source of emissions, accounting for approximately 37 percent of the total emissions. On-road vehicles accounted for more than 90 percent of emissions in the transportation sector. Transportation related GHG emissions have dropped 11 percent since 2006. The industrial sector accounted for approximately 22 percent of the total emissions. Emissions from electricity generation were about 21 percent of total emissions, with higher contribution from in-state than from imported electricity.

Per capita emissions in California have decreased by 12 percent from 2000 to 2012, in spite of the overall 11.4 percent increase in population during the same period. Per capita emissions from in-state electricity generation have declined by 22 percent from 2000 to 2012.

From a broader geographical perspective, California ranks second in the United States in total greenhouse gas emissions; Texas remains as the #1 GHG emitting state. However, from a per capita and per GDP standpoint, California has the 45th and 46th lowest emissions respectively. On an international scale, California has the 20th largest greenhouse gas emissions and the 38th largest per capita emissions for year 2010.

The 2014 edition GHG inventory represents a transition to global warming potentials (GWPs) in the IPCC 4th Assessment Report (AR4). Previous GHG inventories relied on GWPs from IPCC's Second Assessment Report (SAR).

Table of Contents

Contents

Summary i
Table of Contents ii
List of Tables and Figures iii
I. Background 1
II. Overview of Climate Change and Greenhouse Gases 2
A. Greenhouse Gases 2
B. Anthropogenic and Natural Emissions 3
III. California Greenhouse Gas Emission Inventory 4
California Inventory and Other Greenhouse Gas Inventories 4
Inventory Organization 5
IV. Statewide Emission Estimates and Emission Trends 6
Emissions Trends 6
Emissions by Economic Sectors 15
Per Capita Emissions 25
V. Broader Perspective of California Greenhouse Gas Emissions 27
California and Other States 28
California and the Rest of the World 29
VI. Ongoing Work 31
VII. References 32
Appendix A 34

List of Tables and Figures

Tables

Table 1. California Greenhouse Gas Emissions by Gas 9
Table 2. Recent Trends in California Greenhouse Gas Emissions by Inventory Economic Sectors 12
Table 3. Recent Trends in California Greenhouse Gas Emissions by Scoping Plan Categories 13

Figures

Figure 1. Global Warming Potentials of Greenhouse Gases 3
Figure 2. California Greenhouse Gas Emission by Gas 7
Figure 3. Annual Percent Change in California Greenhouse Gas Emissions 10
Figure 4. Cumulative Change in California Greenhouse Gas emissions Relative to 2000 10
Figure 5. Recent Trends in Greenhouse Gas Emissions (U.S. and California) 11
Figure 6. Greenhouse Gas Emission Trends by Economic Sector 14
Figure 7. Contribution of Economic Sectors to Greenhouse Gas Emissions. 15
Figure 8. 2012 Greenhouse Gas Emissions by Economic Sector 16
Figure 9. 2012 Greenhouse Gas Emissions from Agriculture 17
Figure 10. Greenhouse Gas Emission Trends for Agriculture 18
Figure 11. 2012 Greenhouse Gas Emissions from Commercial 19
Figure 12. 2012 Greenhouse Gas Emissions from Electricity Generation 20
Figure 13. Greenhouse Gas Emission Trends from Electricity Generation ... 21
Figure 14. 2012 Greenhouse Gas Emissions from Industry 22
Figure 15. Greenhouse Gas Emission Trends from Industry 22
Figure 16. 2012 Greenhouse Gas Emissions from Transportation 23
Figure 17. Greenhouse Gas Emission Trends from Transportation 24
Figure 18. 2012 Greenhouse Gas Emissions per Capita 26
Figure 19. Total (bars) and Per Capita (markers) California and Other States Greenhouse Gas Emissions (CAIT-U.S. v4.0) 29
Figure 20. Total (bars) and Per Capita (markers) California and Other States Greenhouse Gas Emissions (CAIT-U.S. v4.0) 30

I. Background

A major challenge of today's world is to meet the energy needs of the growing population while protecting the earth and its climate. Governments and organizations at national as well as regional levels have started to take necessary actions to reduce greenhouse gases (AB 32, 2006; United Nations, 2012). The generation of a consistently updated emission inventory with an emission baseline year to monitor the progress of greenhouse gas sources and reductions is vital to these efforts.

The California Legislature and Governor took significant steps to address the concerns raised about climate change with the passage and signing of the Assembly Bill (AB) 32, the Global Warming Solutions Act of 2006 (AB 32, 2006). The California Air Resources Board (ARB) was designated as the lead implementation agency of this landmark legislation. AB 32 set a target to reduce California greenhouse gas emissions to 1990 levels by year 2020. In addition, the Governor signed Executive Order S-3-05 to further require California to reduce greenhouse gas emissions by 80 percent below the 1990 levels by year 2050 (EO, 2005). Parallel to these actions, the California Legislature passed and the Governor signed AB 1803, making the ARB responsible for developing the GHG emission inventory.

Parallel to these actions in 2006, the California Legislature passed and the Governor signed AB 1803 making the ARB responsible to prepare, adopt, and update an inventory of greenhouse gas emissions from all sources located in the state.

The California greenhouse gas emission inventory serves as a foundation for the State's emission reduction goals. ARB regularly updates California's greenhouse gas inventory on its Greenhouse Gas Emission Inventory website (http://www.arb.ca.gov/cc/inventory/inventory.htm). The first set of inventory data covering statewide greenhouse gas emissions and sinks from 1990 through 2004 was published in 2007. In addition, ARB also published a staff report titled "*California 1990 Greenhouse Gas Emissions Level and 2020 Emissions Limit*" that discusses the determination of the 1990 statewide emissions level and provides a summary of the methodologies and main sources of data used to calculate the greenhouse gas emissions (CARB, 2007). These past reports and other inventory related documents are available from ARB's California Greenhouse Gas Emission Inventory website http://www.arb.ca.gov/cc/inventory/inventory.htm.

The 2014 edition of the inventory compiles statewide anthropogenic greenhouse gas emissions from 2000 through 2012. This document presents

a summary of the 2000 to 2012 emissions data, and discusses the statewide greenhouse gas emission trends and relative contributions of emission sources to the total emissions. It is important to note that ARB has updated the estimates of emissions for the full 2000 to 2012 time series, to reflect the latest estimation data and methodologies. This is consistent with the Intergovernmental Panel on Climate Change (IPCC) *Good Practice Guidance and Uncertainty Management in National Greenhouse Gas Inventories* (IPCC, 2000), which states that "It is good practice to recalculate historic emissions when methods are changed or refined, when new source categories are included in the national inventory, or when errors in the estimates are identified and corrected." A comprehensive technical support document detailing the data sources and methods used to develop the 2000 to 2012 inventory is available on the ARB website (CARB, 2014). A technical support document detailing the data sources and methods used to develop the 2000 to 2012 inventory is also available

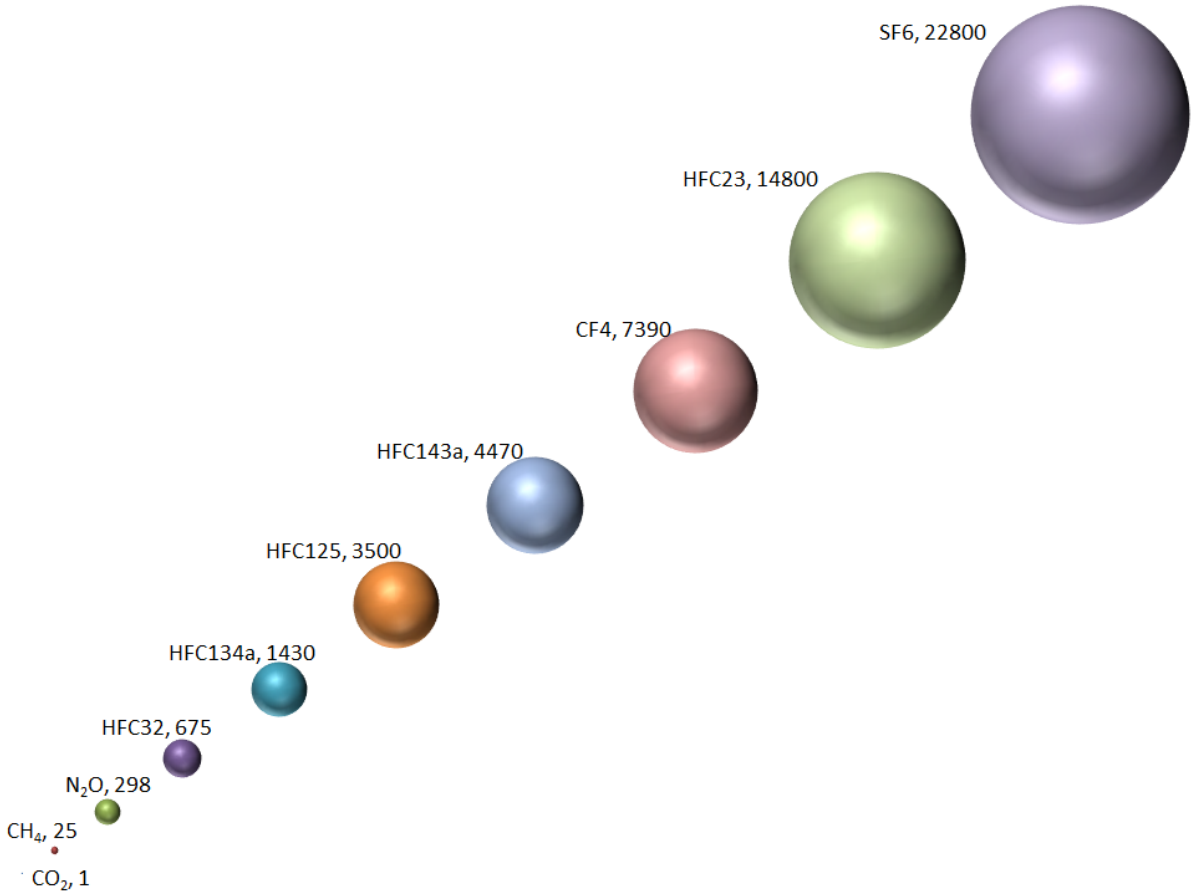
II. Overview of Climate Change and Greenhouse Gases

Emissions of carbon dioxide (CO_2) have increased greatly following the industrial revolution from combustion of fossil fuels, and later from the production of synthetic greenhouse gases such as chlorofluorocarbons (CFCs), hydrofluorocarbons (HFCs), perflurocarbons (PFCs) and sulfur hexafluoride (SF_6). In the past years, numerous scientific studies have shown that the enhanced greenhouse effect causes climatic shifts that will have an adverse effect on human survival (Meehl et al., 2005; Patz et al., 2005; Dettinger and Cayan, 1995). An emission inventory that identifies and quantifies the sources and sinks of these greenhouse gases is essential for addressing climate change.

A. Greenhouse Gases

The Kyoto Protocol identifies the following six gases for emission reduction targets: CO2, methane (CH4), nitrous oxide (N2O), HFCs, PFCs and SF6. Each GHG has a global warming potential (GWP) value, calculated to reflect the relative climate forcing of a kilogram of emissions and how long emissions remain in the atmosphere. The global warming potential allows for a comparison of the warming influence of different greenhouse gases relative to CO2 and provides a single consistent emission unit (IPCC, 2007). For example, it would take 22,800 CO2 molecules to have same effect as one SF6 molecule. This is because SF6 absorbs infrared radiation in a different energy range and has a longer lifetime in the atmosphere than CO2. Thus, small amounts of high GWP gases have a large effect on global warming. GWPs from IPCC's Fourth Assessment Report for greenhouse gases defined in AB 32 are shown in Figure 1.

Figure 1. Global Warming Potentials of Greenhouse Gases



Source: IPCC Fourth Assessment Report

B. Anthropogenic and Natural Emissions

The California GHG inventory is primarily focused on anthropogenic emissions. Anthropogenic emissions directly result from human activities or from human influence on natural and other processes subject to human control (U.S.EPA, 2008). Increases in anthropogenic emissions from pre-industrial times have substantially increased atmospheric greenhouse gas concentrations.

Natural CO_2 emissions are emitted as part of the biogeochemical cycling of carbon and tend to average out over time even though emissions may be significant (IPCC, 2006). For quantification of greenhouse gas fluxes on forest, range, and other natural lands, ARB is updating the methodology under a research contract with UC Berkeley initiated in late 2011. The new quantification procedures under development integrate regularly updated

federal and state ground-based data with geospatial and remotely sensed data and models. Forest and natural lands are not included in the 2014 edition of the inventory while ARB continues to update the methodology.

III. California Greenhouse Gas Emission Inventory

The California greenhouse gas emission inventory serves as the foundation for the State's greenhouse gas emission reduction program. The inventory is a living repository of detailed methodologies for estimating greenhouse gas emissions. The inventory is also a time series of emissions, thus providing a platform to compare the relative contribution of different emission sources and gases to climate change over time.

There are two main types of inventory approaches used to determine the amount of greenhouse gas emissions from a region: the top-down and bottom-up approach (CLIISE, 2007). The California GHG inventory uses both approaches. The top-down approach utilizes nationwide or statewide data, while the bottom-up approach uses facility-specific data to estimate emissions from each source. The total number of emissions from each source are then summed together to generate an inventory for a particular geographic region. For certain industry sectors, ARB draws data from various federal and state government agencies in a top-down approach. For other industry sectors, the data collected through the Regulation for the Mandatory Reporting of Greenhouse Gas Emissions (MRR) program enables ARB to utilize the bottom-up approach. Verified data from the MRR for specific sectors such as in-state power generation, specified electricity imports, refineries and cement manufacturing were used in the 2012 emission inventory.

California Inventory and Other Greenhouse Gas Inventories

The California inventory is developed in a manner consistent with international and national guidelines to the greatest extent possible. Consistency maximizes the comparability of the inventory with similar inventories from other states and nations. This is important as California considers participation in standardized regional, national and international greenhouse gas emission reduction programs.

At an international level, the IPCC has developed standard international guidance for emission inventories (IPCC, 2006). Nations that have adopted the United Nations Framework Convention on Climate Change (UNFCCC) must prepare and report their emissions and sinks of CO_2, CH_4, N_2O, SF_6, PFCs, and HFCs using IPCC methodologies to ensure comparability among national inventories. The IPCC guidelines delineate the sectors and processes for which nations must report their greenhouse gas emissions and

sinks, and how they should report these emissions. They also describe various methodologies to estimate emissions depending on the available data sources (IPCC, 2006). The guidelines allow for use of state-specific data and methodologies rather than the more generic international ones when available. In the California inventory, state-specific emissions data were used whenever possible.

As a nation, the United States follows the IPCC guidelines (with the United States Environmental Protection Agency (U.S.EPA) acting as the lead agency) and submits its national greenhouse gas inventory to UNFCCC Secretariat annually. The U.S.EPA supplements the widely applicable IPCC methodologies with more US-specific methodologies and data (U.S.EPA, 2008).

Inventory Organization

ARB has presented the GHG emissions estimates in California inventory in three formats. First, the GHG emission estimates are presented in the categories outlined in the 2008 Scoping Plan, which focuses on areas for emission reductions. These Scoping Plan sectors include: transportation, electric power, commercial and residential, industrial, recycling and waste, High GWP gases, and agriculture.

Second, the emission estimates are categorized into traditional economic sectors based on economic activity within California, as defined by North American Industry Classification System (NAICS, 2012). These sectors include: agriculture and forestry, commercial, in-state electricity generation, imported electricity, industrial, residential, transportation, and others. The economic sector categorization allows for comparison with other ARB emission inventories, which are similarly categorized. This categorization scheme also provides a familiar reference for readers accustomed to reviewing emission estimates generated by national, state, and local air agencies. The primary difference with Scoping Plan sector categorization is that emissions from High GWP gases are placed under the appropriate sectors of industrial, transportation,

This categorization of the inventory based on economic sectors includes emissions from international and domestic ships operations within California waters under the transportation sector. The aviation category, located within the transportation sector, only includes emissions for intrastate flights. Interstate and international flight emissions are calculated and included as an informational item, but their greenhouse gas emissions are not counted (these are listed as “excluded emissions” in the inventory) in California’s overall inventory. Unless otherwise indicated, emissions estimates in this report are categorized by the economic sectors and emission categories. A small portion of the total emissions could not be

attributed to any of the economic sectors and are therefore aggregated into a "not specified" group[1].

Finally, the emissions data have been categorized by IPCC levels, which is based on groupings of related emission processes and sinks as indicated in the IPCC Guidelines (IPCC, 2006), to ensure comparability with international and national inventories. This version includes five main sectors based on the IPCC categorization: energy; industrial processes and product use; agriculture and other land use; waste; and other.

Changes in the 2000-2012 Inventory

Updates to the methodologies used in the California inventory are an ongoing process. ARB staff regularly evaluates scientific developments in greenhouse gas inventories. In general, the majority of the methodologies and calculations used to generate the emission values have remained constant. However, every year ARB makes improvements to the methods or data used to determine greenhouse gas emissions.

The 2000-2012 GHG inventory represents a transition to global warming potentials (GWPs) in the IPCC's 4th Assessment Report (AR4) compared to previous GHG inventories that relied on GWPs from IPCC's Second Assessment Report (SAR). As a result, the GWP of methane changed from 21 to 25 and also revised the GWPs of other gases to their updated values (IPCC, 2007). For detailed discussions on the updated methodologies and changes to the emission estimates, refer to the Technical Support Document for the 2000 to 2012 inventory (CARB, 2014).

IV. Statewide Emission Estimates and Emission Trends

This section summarizes the latest information on **greenhouse gas emissions and trends in California based on the economic sectors categorization of the inventory**. The estimates reflect revisions to methodologies and data for the 2000 to 2012 time series. Detailed discussions on emission calculations and methodologies are comprehensively discussed in the technical support documents.

Emissions Trends

In 2012, total GHG and per capita emissions increased by 1.7% from 2011 emissions. This increase was driven largely by the increased reliance on natural gas-generation sources of in-state electricity due to the closure of the San Onofre Nuclear Generating Station (SONGS) as well as dry hydrological

[1] Unspecified emissions include emissions from categories that could not be attributed to a particular traditional economic sector.

conditions in 2012 (drought) causing a drop in the in-state hydropower generation. Total statewide greenhouse gas emissions have decreased from 466 million tonnes of carbon dioxide equivalent ($MMTCO_2e$) in 2000 to 459 $MMTCO_2e$ in 2012, a decrease of 1.6 percent.

Figure 2 depicts the general trend in the emissions by greenhouse gas from 2000 to 2012. Figure 2 also shows the percent contribution of each GHG to the 2012 statewide emission total. CO_2 is the largest contributor to statewide greenhouse gas emissions. CO_2 emissions accounted for approximately 88 percent of the emissions in 2000 and 85 percent in 2012. CH_4 and N_2O account for 8.3 and 2.9 percent of the total emissions in 2012, respectively. SF_6 emissions accounted for 0.1 percent of the total emissions. Other halogenated gases constituted approximately 4 percent of the total emissions.

Figure 2. California Greenhouse Gas Emission by Gas

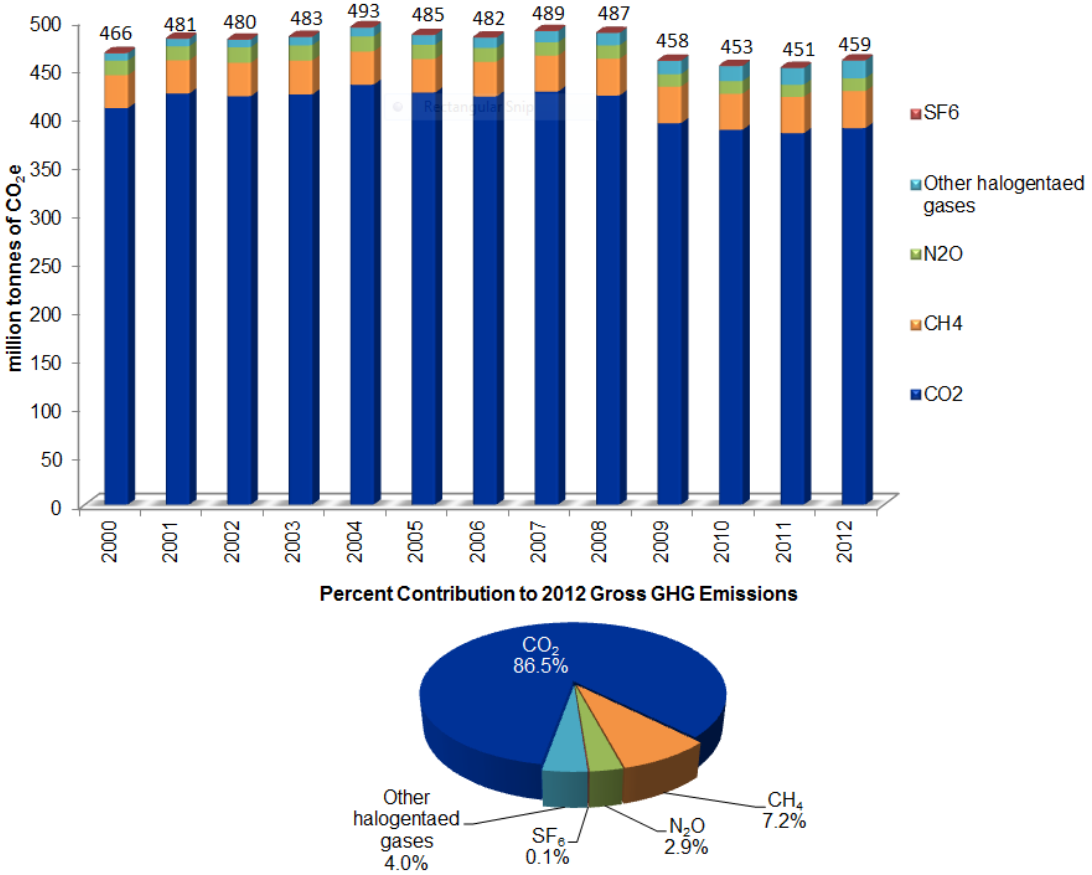


Table 1 shows the total statewide greenhouse gas emissions by gas type. Table 1 shows that the emissions of methane and halogenated gases increased from 2000 to 2012 and CO2, N2O, and SF6 decreased during the same period. Overall, CO2 emissions decreased by 5 percent from 2000 to 2012, and increased by 1.4 percent from 2011 to 2012. N2O and SF6 emissions also decreased by 10.9 and 30.1 percent, respectively, while CH4 and halogenated gas emissions increased by 12.3 and 137 percent respectively, from 2000 to 2012. Though the magnitudes of emissions increase of SF6 and halogenated gases are comparatively smaller from 2000 to 2012, their emissions are significant because of their high GWPs and longer atmospheric lifetimes.

Table 1. California Greenhouse Gas Emissions by Gas

Greenhouse Gas	GHG Gross Emissions ($MMTCO_2e$)*													Percent Change	
	2000	**2001**	**2002**	**2003**	**2004**	**2005**	**2006**	**2007**	**2008**	**2009**	**2010**	**2011**	**2012**	**2000-2012**	**2011-2012**
CO_2	409.3	424.4	421.5	423.4	433.5	425.3	421.4	426.3	422.3	393.8	386.8	383.5	388.7	-5.0%	1.4%
CH_4	34.0	34.3	34.5	35.0	34.3	34.7	35.7	37.3	37.9	37.7	37.3	37.5	38.1	12.3%	1.7%
N_2O	15.0	14.5	16.1	15.8	15.4	14.7	14.4	13.7	14.0	12.9	13.0	12.6	13.4	-10.9%	6.5%
SF_6	0.4	0.4	0.3	0.3	0.3	0.3	0.3	0.3	0.3	0.3	0.3	0.3	0.3	-30.1%	-3.2%
Other Halogentaed Gases	7.6	7.6	7.8	8.5	9.2	10.0	10.8	11.5	12.6	13.7	15.6	17.1	18.1	137.3%	6.3%
Total Gross Emissions	**466.3**	**481.2**	**480.3**	**483.1**	**492.9**	**485.1**	**482.5**	**489.2**	**487.1**	**458.4**	**453.1**	**450.9**	**458.7**	**-1.6%**	**1.7%**

* All greenhouse gases are weighted relative to CO_2 based on the IPCC's 4th Assessment Report.

Figures 3 illustrates the annual percent change in greenhouse gas emissions, where the maximum change occurred from 2008 to 2009 when the emissions decreased by almost 6 percent.

Figure 3. Annual Percent Change in California Greenhouse Gas Emissions

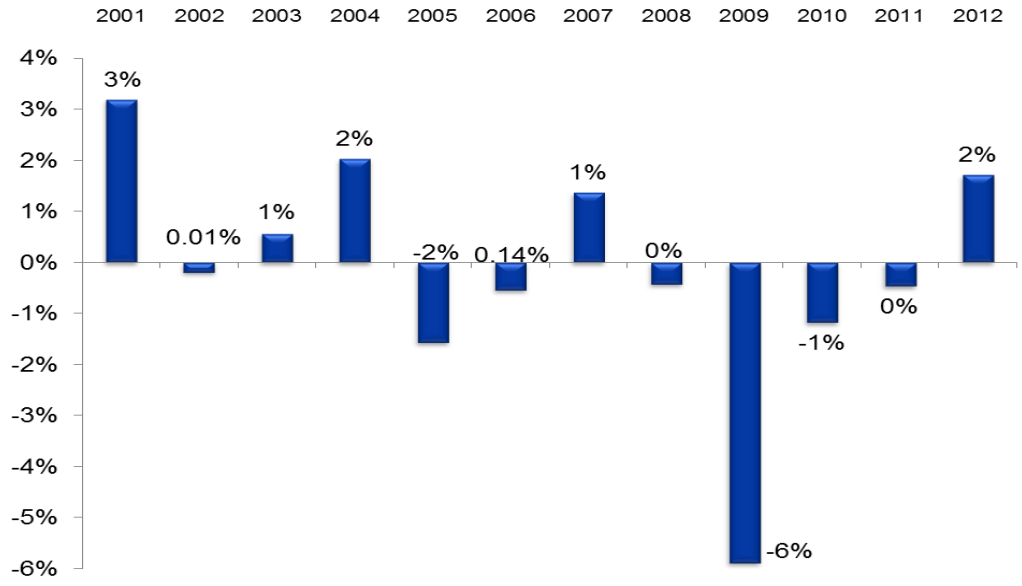


Figure 4 shows the cumulative change in emissions relative to the year 2000. absolute change in emissions from 2000 through 2012 cumulative effect of greenhouse gas emissions change from 2000 to 2012. The decline in the greenhouse gas emissions reversed from in 2012 for the first time since 2008.

Figure 4. Cumulative Change in California Greenhouse Gas emissions Relative to 2000

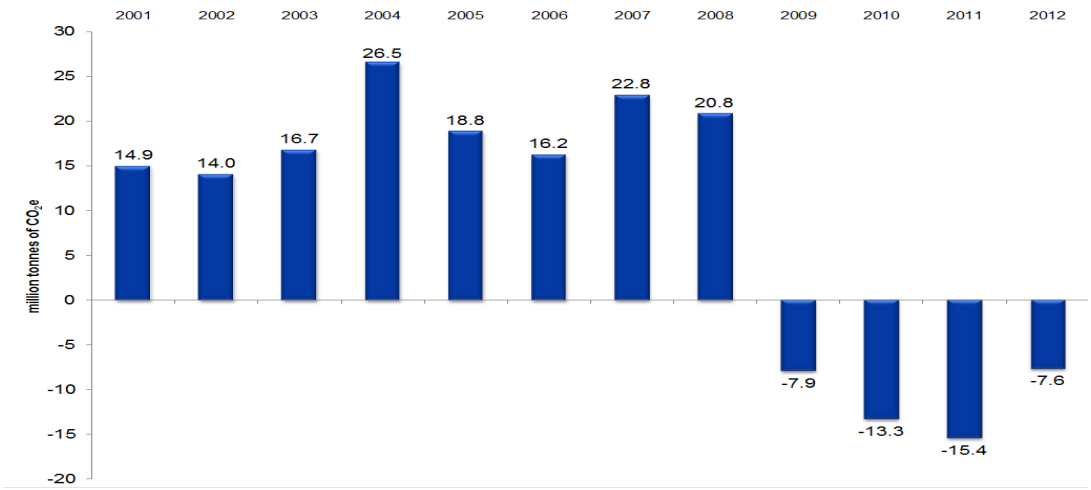


Figure 5 illustrates the trends in greenhouse gas emissions at the national and state level between 2000 and 2012. While the total emissions in 2012 increased by 5.9 percent from 1990 (431 $MMTCO_2e$), the emissions decreased by 5.9 percent from 2008 to 2009, the likely effect of the economic recession that began in late 2007. This decrease in emissions from 2008 to 2009 is also observed in the national emissions, a 7.2 percent decline from 2008 to 2009. From 2010 to 2012, the national emissions and the California emissions exhibit opposite trends. However, it is important to note that California emissions are based on the AR4, while national emissions are based on the SAR.

Figure 5. Recent Trends in Greenhouse Gas Emissions (U.S. and California)



Source: U.S emissions from Inventory of U.S. Greenhouse Gas Emissions and Sinks: 1990-2012 (U.S.EPA, 2014)
Note: CA emissions are based on AR4 while US emissions are based on SAR.

Table 2 summarizes the emissions from these economic sectors in the California inventory in $MMTCO_2e$. The table also presents the percent change in emissions for each of the sectors between 2000 and 2012. The percent changes in the emissions from 2011 to 2012 are also included. Table 3 presents the same 2000 to 2012 emissions by scoping plan categories.

Table 2. Recent Trends in California Greenhouse Gas Emissions by Inventory Economic Sectors

Sector	**GHG Emissions ($MMTCO_2e$)[1]**													**% of Total Emissions in 2012**	**Percent Change**	
	2000	**2001**	**2002**	**2003**	**2004**	**2005**	**2006**	**2007**	**2008**	**2009**	**2010**	**2011**	**2012**		**2000-2012**	**2011-2012**
Transportation	178.5	178.9	186.1	186.0	189.5	192.0	192.1	192.3	181.3	174.9	174.0	171.7	171.0	37.3%	-4%	0%
Industrial	103.3	101.5	101.6	101.2	103.3	101.5	99.7	96.7	97.5	95.2	99.3	99.7	100.7	21.9%	-3%	1%
Electricity Generation (in-state)	59.2	63.2	49.9	48.3	49.4	45.3	50.1	54.3	54.5	53.4	46.9	41.3	51.2	11.2%	*-14%*	*24%*
Electricity Generation (imports)	46.0	59.1	59.1	64.7	66.1	62.9	54.8	59.9	65.9	48.1	43.7	46.9	44.1	9.6%	*-4%*	*-6%*
Agriculture	32.5	32.8	36.0	36.5	36.3	36.5	37.8	37.0	38.0	35.8	35.7	36.3	37.9	8.3%	*16%*	*4%*
Residential	31.8	30.8	30.9	30.4	31.5	30.2	30.6	30.8	31.2	31.0	32.1	33.0	31.6	6.9%	-1%	-4%
Commercial	14.6	14.6	16.6	15.8	16.5	16.6	17.3	17.9	18.5	19.8	21.1	21.8	22.0	4.8%	51%	1%
Unspecified[2]	0.4	0.3	0.2	0.3	0.2	0.2	0.2	0.2	0.2	0.2	0.2	0.2	0.2	0.0%	-43%	0%
Total Gross Emissions[3]	**466.3**	**481.2**	**480.3**	**483.1**	**492.9**	**485.1**	**482.5**	**489.2**	**487.1**	**458.4**	**453.1**	**450.9**	**458.7**	**100.0%**	**-1.6%**	**1.7%**

[1] All greenhouse gases are weighted relative to CO_2 based on the IPCC's 4th Assessment Report.
[2] Unspecified includes emissions from evaporative losses, which could not be attributed to an individual sector.
[3] The sector emissions may not add up exactly to the above listed gross and net total emissions due to rounding.

Table 3. Recent Trends in California Greenhouse Gas Emissions by Scoping Plan Categories

Sector	GHG Emissions ($MMTCO_2e$)[1]													% of Total Emissions in 2012	Percent Change	
	2000	2001	2002	2003	2004	2005	2006	2007	2008	2009	2010	2011	2012		2000-2012	2011-2012
Transportation	176.2	176.6	183.8	183.5	186.9	189.1	189.2	189.3	178.0	171.5	170.5	168.1	167.4	36.5%	-5.0%	-0.4%
Industrial	95.0	93.2	93.1	92.5	94.5	92.3	90.3	87.1	87.5	84.9	88.5	88.3	89.2	19.4%	-6.2%	0.9%
Electric Power (In-state)	59.0	63.0	49.7	48.1	49.2	45.1	49.9	54.1	54.3	53.3	46.7	41.2	51.0	11.1%	-13.5%	23.9%
Electric Power (Imports)	45.9	59.0	59.0	64.6	66.0	62.8	54.7	59.8	65.8	48.0	43.6	46.9	44.1	9.6%	-4.0%	-6.0%
Commercial and Residential	42.3	41.2	43.2	41.5	42.9	41.2	41.9	42.1	42.4	42.7	43.8	44.3	42.3	9.2%	-0.1%	-4.6%
Agriculture	32.5	32.8	36.0	36.5	36.3	36.5	37.8	37.0	38.0	35.8	35.7	36.3	37.9	8.3%	16.4%	4.2%
High GWP	8.0	8.0	8.1	8.8	9.6	10.4	11.1	11.8	12.9	14.0	15.9	17.3	18.4	4.0%	129%	6.1%
Recycling and Waste	7.2	7.4	7.3	7.4	7.4	7.6	7.7	7.8	7.9	8.1	8.2	8.2	8.3	1.9%	15.5%	0.9%
Total Gross Emissions[3]	**466.3**	**481.2**	**480.3**	**483.1**	**492.9**	**485.1**	**482.5**	**489.2**	**487.1**	**458.4**	**453.1**	**450.9**	**458.7**	**100%**	**-1.6%**	**1.7%**

[1] All greenhouse gases are weighted relative to CO_2 based on the IPCC's 4th Assessment Report.
[2] Unspecified includes emissions from evaporative losses, which could not be attributed to an individual sector.
[3] The sector emissions may not add up exactly to the above listed gross and net total emissions due to rounding.

Figures 6 shows the trend in emissions and Figure 7 shows the percent contribution of each inventory economic sector to the total emissions from 2000 through 2012.

Figure 6. Greenhouse Gas Emission Trends by Economic Sector

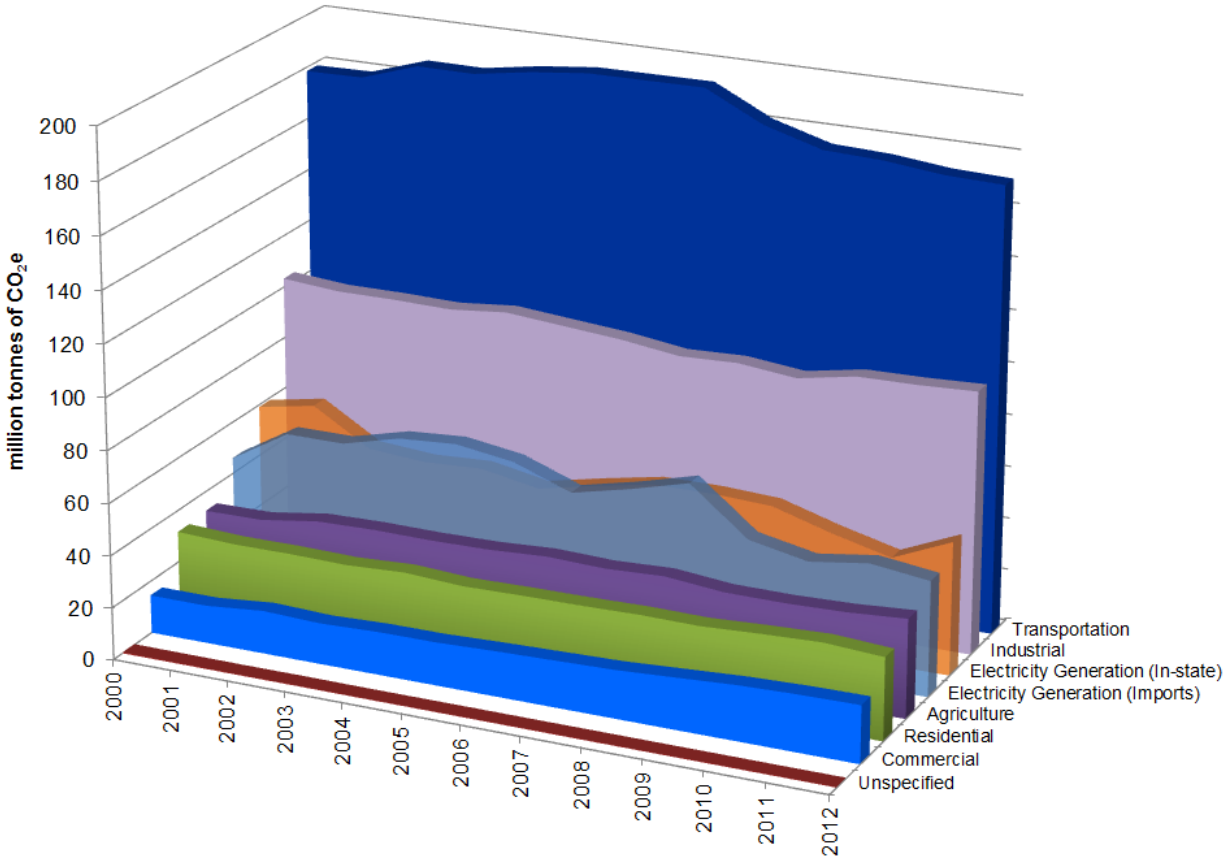
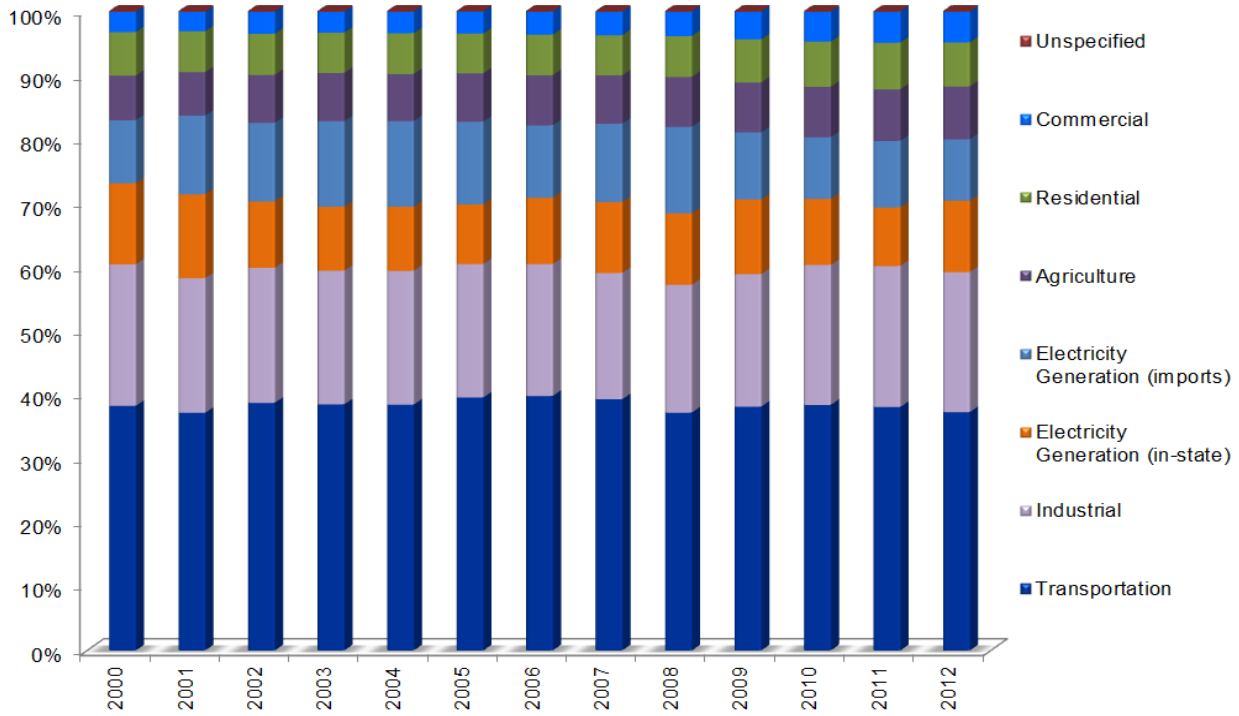


Figure 7. Contribution of Economic Sectors to Greenhouse Gas Emissions



Transportation was the major emitter of greenhouse gases in both 2000 and 2012, producing 171 $MMTCO_2e$ in 2012. The industrial sector was the next largest greenhouse gas contributor, emitting approximately 100 $MMTCO_2e$ in 2012.

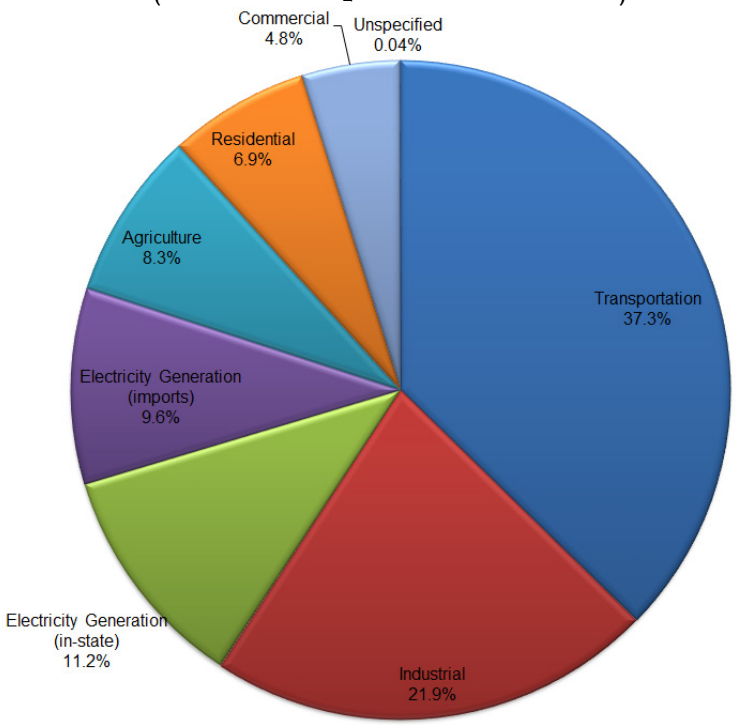
Emissions by Economic Sectors

This section presents the greenhouse gas emissions by the California inventory economic sectors: agriculture, commercial, electricity generation, industry, residential, transportation and unspecified.

Figure 8 displays the sectoral contribution to the total 2012 gross emissions, with transportation at more than 36 percent of statewide emissions thus making it the largest contributor to the total statewide emissions. Emissions from industrial sector, the second largest, accounted for 22 percent of the total emissions. Electricity generation accounted for approximately 21 percent of the total in 2012, with 11 percent in state generation. These three sectors accounted for approximately 80 percent of the statewide greenhouse gas emissions in 2012. Emissions from agriculture (8.3 percent), residential (6.9

percent), and commercial (4.9 percent) sectors accounted for approximately 20 percent of the total.

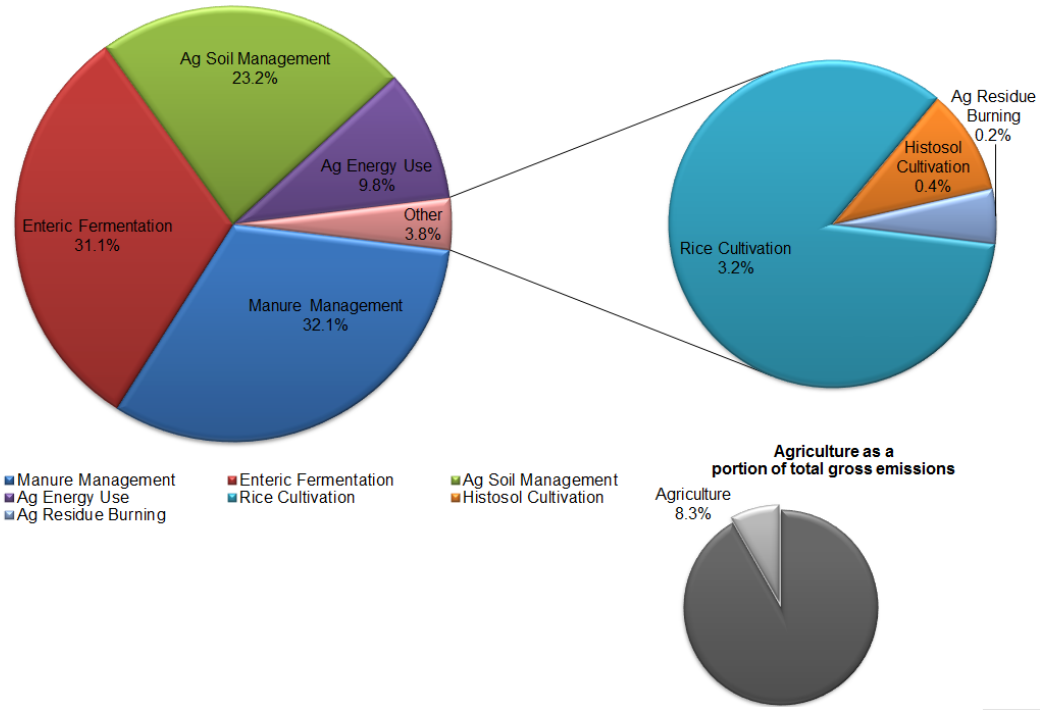
Figure 8. 2012 Greenhouse Gas Emissions by Economic Sector
(459 $MMTCO_2e$ Gross Emissions)



The majority of statewide greenhouse gas emissions were tied to fuel use activities, ranging from transportation to electricity generation to heating buildings. Emissions from fuel combustion comprised 72 percent of overall statewide greenhouse gas emissions in 2012. Primary fuels combusted include natural gas, which was used mainly for in-state electricity generation, residential and industrial uses, and gasoline, which was consumed almost entirely by the transportation sector. Detailed breakdown of the emissions from each of the economic sectors and their relative contribution to the total emissions is discussed in the following sections.

Agriculture: Emissions from agricultural activities were responsible for emissions of 37.9 $MMTCO_2e$, approximately 8.3 percent of total statewide greenhouse gas emissions in 2012. Agricultural emissions represent the sum of emissions from agricultural energy use, agricultural residue burning, agricultural soil management (the practice of utilizing fertilizers, soil amendments, and irrigation to optimize crop yield), enteric fermentation (fermentation that takes place in the digestive system of animals, e.g. cows and sheep), histosol (soils that are composed mainly of organic matter) cultivation, manure management and rice cultivation

Figure 9. 2012 Greenhouse Gas Emissions from Agriculture (38 MMTCO$_2$e Gross Emissions)



The contribution of the categories that contributed towards the 2012 agricultural greenhouse gas emissions is shown in Figure 9. Unlike other economic sectors, N_2O emissions from agricultural soil management and CH_4 emissions from enteric fermentation and manure management contributed towards most of the agricultural sector emissions. The majority of the emission contributions (86 percent) are due to manure management (32 percent), enteric fermentation (31 percent) and agricultural soil management (23 percent). The remaining 14 percent of the agricultural emissions was dominated by emissions from agriculture energy use category (10 percent).

Figure 10. Greenhouse Gas Emission Trends for Agriculture

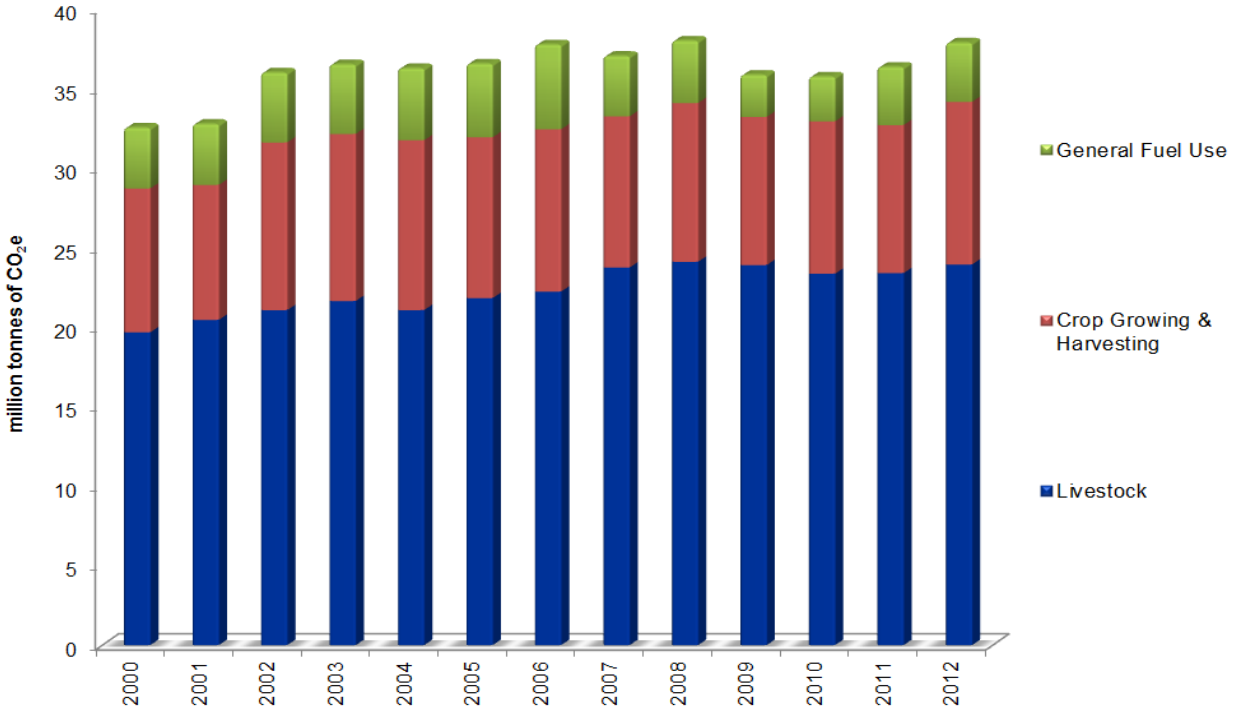
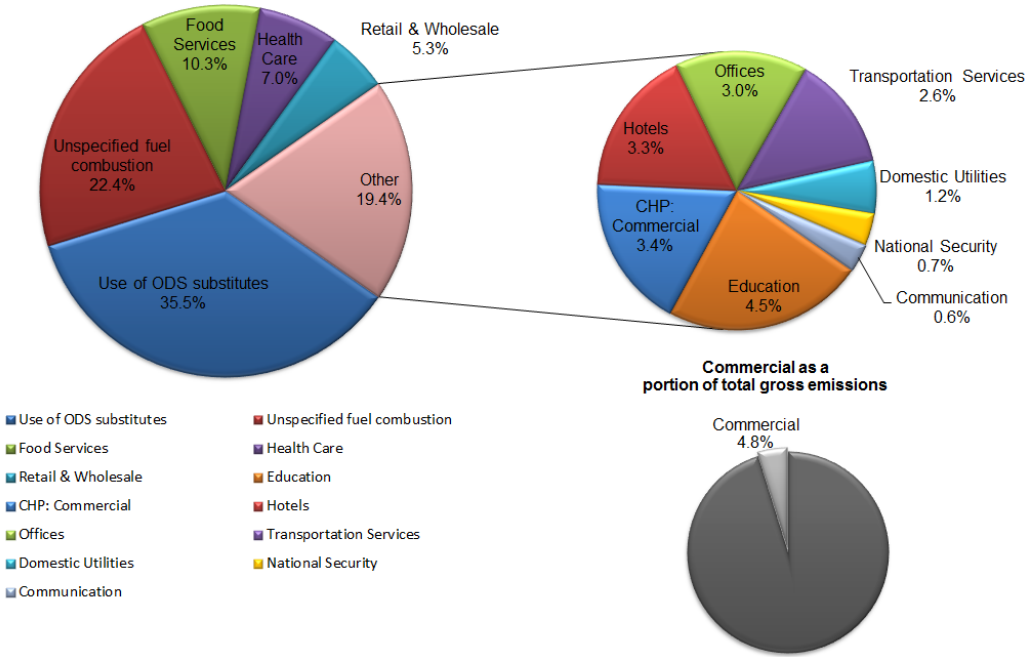


Figure 10 shows the trend in the emissions from each of these categories from 2000 through 2012. The agriculture sector increased its emissions from 32 $MMTCO_2e$ in 2000 to 38 $MMTCO_2e$ in 2012, a 16 percent increase. Agricultural fuel use was the only category that decreased their greenhouse gas emission from 2000 to 2012. Agricultural energy use decreased by 3 percent from 2000 to 2012, while manure management increased 29 percent during the same period.

Commercial: The commercial sector accounted for approximately 4.8 percent of the total statewide emissions in 2012. Greenhouse gas emissions from the commercial sector increased from 14.6 $MMTCO_2e$ in 2000 to 22 $MMTCO_2e$ in 2012. Commercial sector emissions grew approximately 51 percent from 2000 to 2012 and, approximately 1 percent from 2011 to 2012. The commercial sector in this version of the inventory includes the emissions from the substitutes for the ozone depleting substances (ODS).

Figure 11. 2012 Greenhouse Gas Emissions from Commercial
(22 $MMTCO_2e$ Gross Emissions)

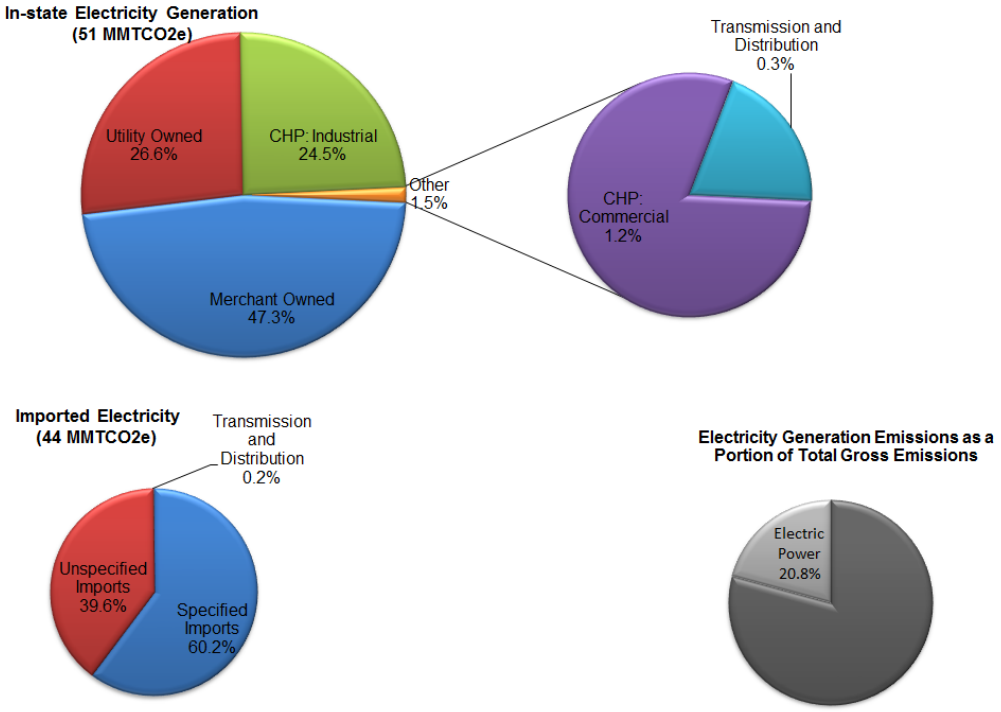


The emission contributions from the commercial sector are from commercial CHP, domestic utilities, education, food services, health care, hotels, national security, offices, retail and wholesale, transportation services, and unspecified sources. The sector includes fuel combustion for all commercial activities such as heating buildings, hot water and steam, and energy for natural gas transmission through pipelines. The primary fuel combusted was natural gas. Approximately 22 percent of the total emissions from this sector are due to natural gas combustion.

The percent contributions of each of these categories to the total 2012 emissions for this sector are shown in Figure 11. The largest contributor to emissions from the commercial sector was the use of ODS substitutes (36 percent). The second largest contributor in the commercial sector was the unspecified combustion of fuels (22 percent). Food services (10 percent) and healthcare (7 percent) were next two major contributors in this sector.

Electricity Generation: Electricity generation, transmission, and distribution accounted for 21 percent of total statewide greenhouse gas emissions in 2012. This sector was the third highest emitting sector in 2012, emitting 95 $MMTCO_2e$ that year. This sector includes power plants and cogenerators that generate electricity for on-site use and for sale to the power grid. This sector specifically includes greenhouse gas emissions from both in-state generated power and imported generation of electricity delivered to and consumed in California. Emissions from transmission line losses of electricity, as well as SF_6 emissions from transmission equipment, are also included. Figures 12 and 13 show the contribution of electricity generation sector to the total emissions and the trends in the emissions.

Figure 12. 2012 Greenhouse Gas Emissions from Electricity Generation
(95 $MMTCO_2e$ Gross Emissions)

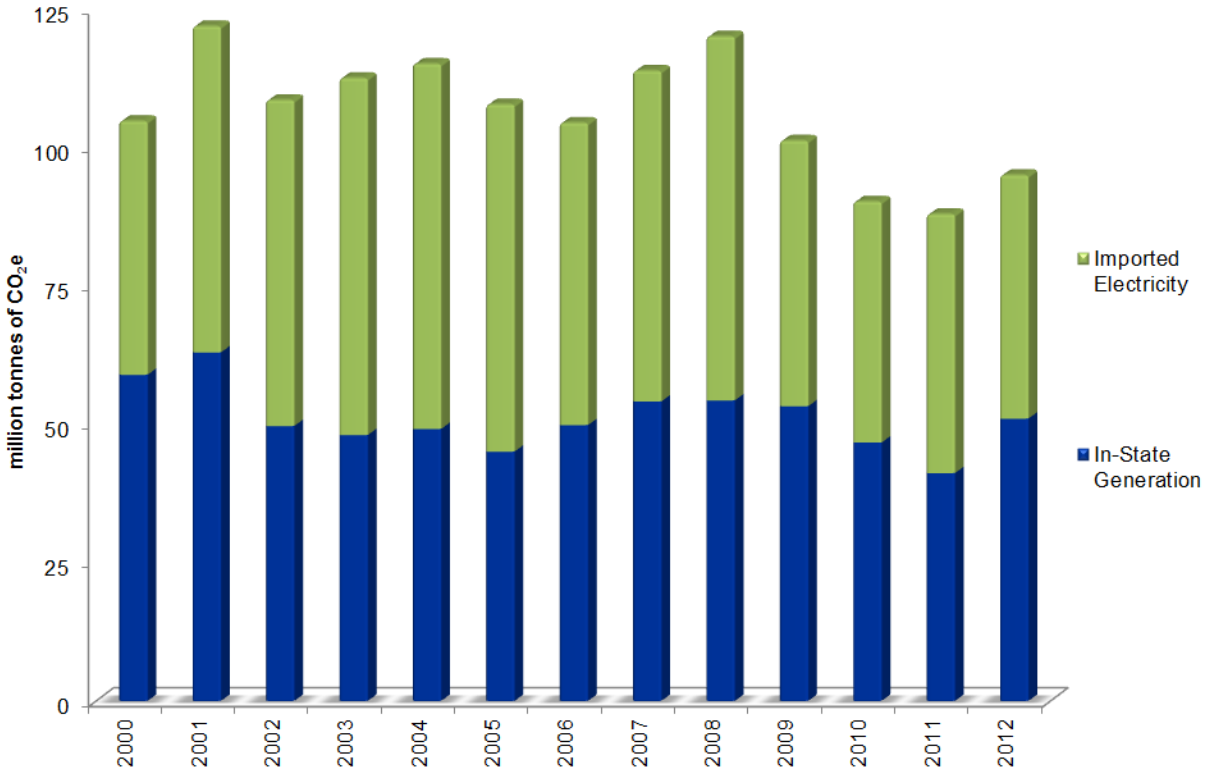


Electricity Generation (imports): The contributions from imported electricity generation are from specified imports (60 percent), unspecified Imports (40 percent) and transmission and distribution (< 1 percent).

Electricity Generation (in-state): Contributions from in-state electricity generation are from categories such as CHP commercial, CHP industrial, merchant owned (privately owned power plant), transmission and distribution, and utility owned (investor-owned power plant). The percent contributions from each of these categories to the total 2011 emissions from this sector are shown in Figure 12.

The merchant owned (47 percent) and CHP industrial (27 percent) contribute most to the in-state electricity generation emissions.

Figure 13. Greenhouse Gas Emission Trends from Electricity Generation



Industrial: Industrial sector includes contributions from CHP industrial, landfills[1], manufacturing, mining, oil and gas extraction, petroleum refining, petroleum marketing, pipelines, wastewater treatment, and other sources. The percent contributions from each of these categories to the 2012 total emissions from this sector are shown in Figure 14. Major contributors from this sector are petroleum refining (30 percent), manufacturing including cement plants (25 percent), oil and gas extraction (17 percent), CHP (11 percent), and landfills (8 percent). Approximately 90 percent of the total emissions from this sector can be attributed to these major categories. For the petroleum refining category, the combustion of fuels is the main source of emissions. Within manufacturing, fuel combustion and clinker production from cement processing are two of the largest sources. Landfills, wastewater treatment, and solid waste treatment, while serving an important societal function, account for only 9 percent of the total emissions from this sector.

[1] Landfill emissions are primarily due to the release of CH_4 (anaerobic decomposition). Carbon dioxide from paper/wood decomposition and from the combustion of landfill gas is included in the flux (See the Technical Support Document for more details).

Figure 14. 2012 Greenhouse Gas Emissions from Industry
(101 MMTCO$_2$e Gross Emissions)

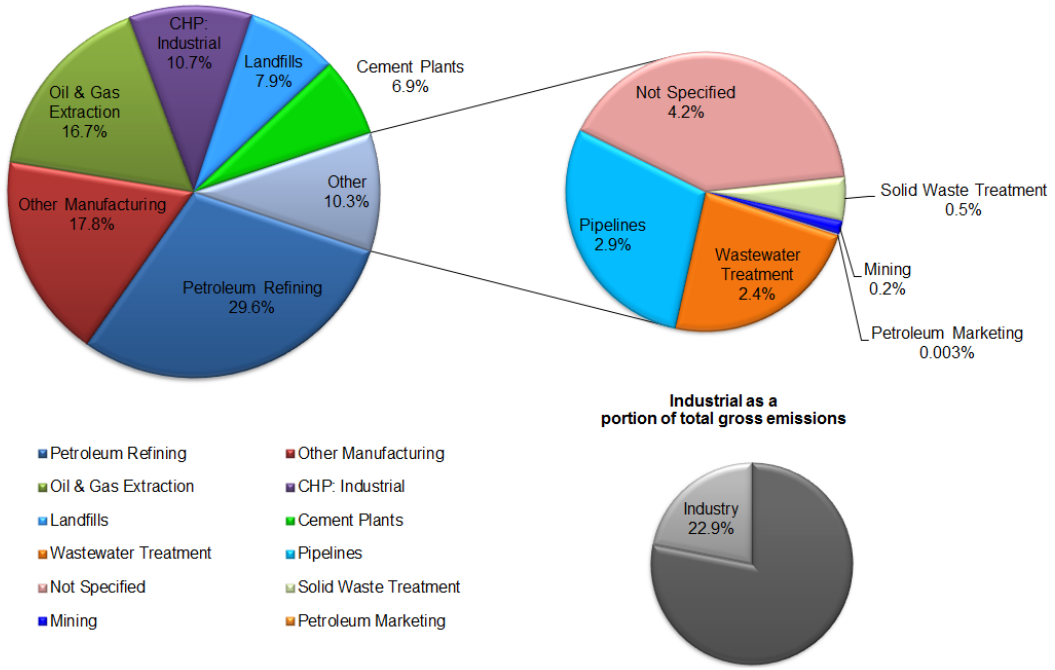
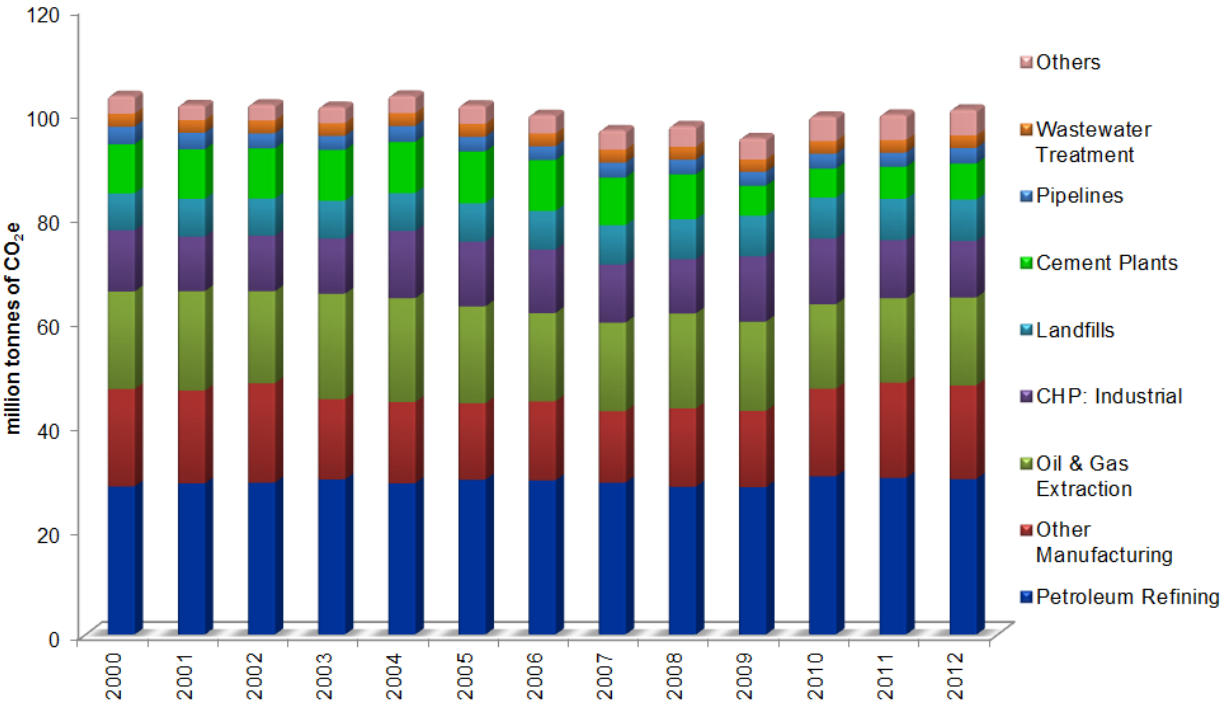


Figure 15. Greenhouse Gas Emission Trends from Industry

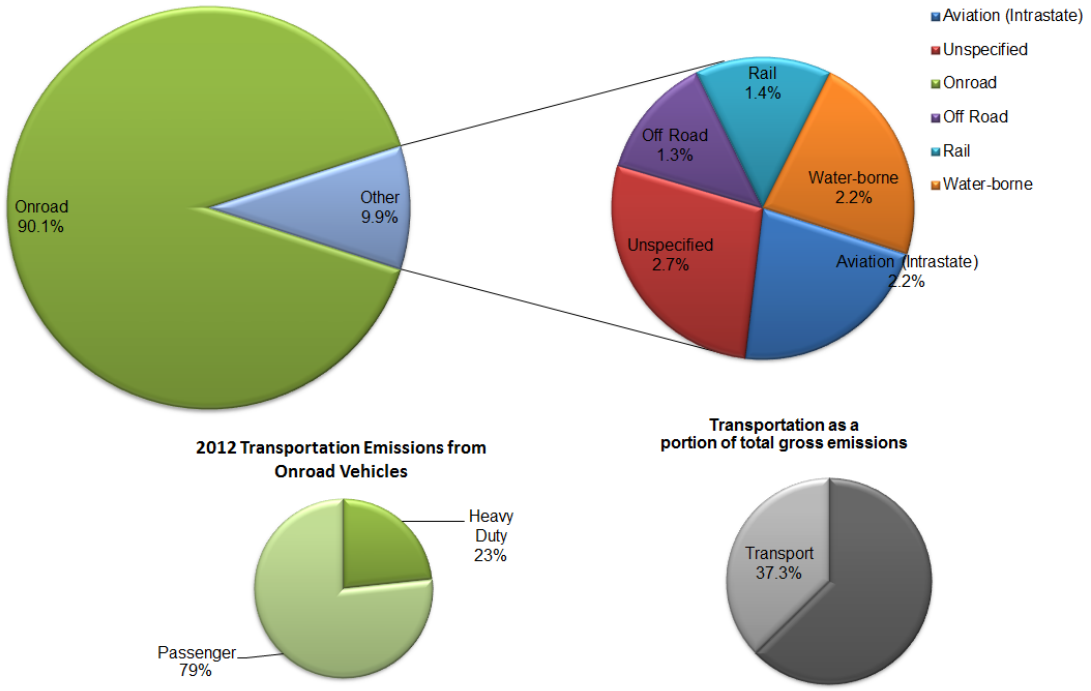


Overall, emissions from industrial sector were 103 $MMTCO_2e$ in 2000 and 101 $MMTCO_2e$ in 2012. The emissions decreased to 95 $MMTCO_2e$ in 2009 mainly due to the decrease in demand for cement.

Residential: The residential sector accounted for 6.9 percent of the total emissions in 2012, and primarily consisted of CO_2 emissions from fossil fuel combustion. Residential emissions are related to the use of fuel for general household needs. Approximately 99 percent of the fuel related emissions are from the burning of natural gas and LPG, with the majority attributed to the burning of natural gas. Emissions from residential fuel use increased from 31.6 $MMTCO_2e$ in 2000 to 32.7 in 2011.

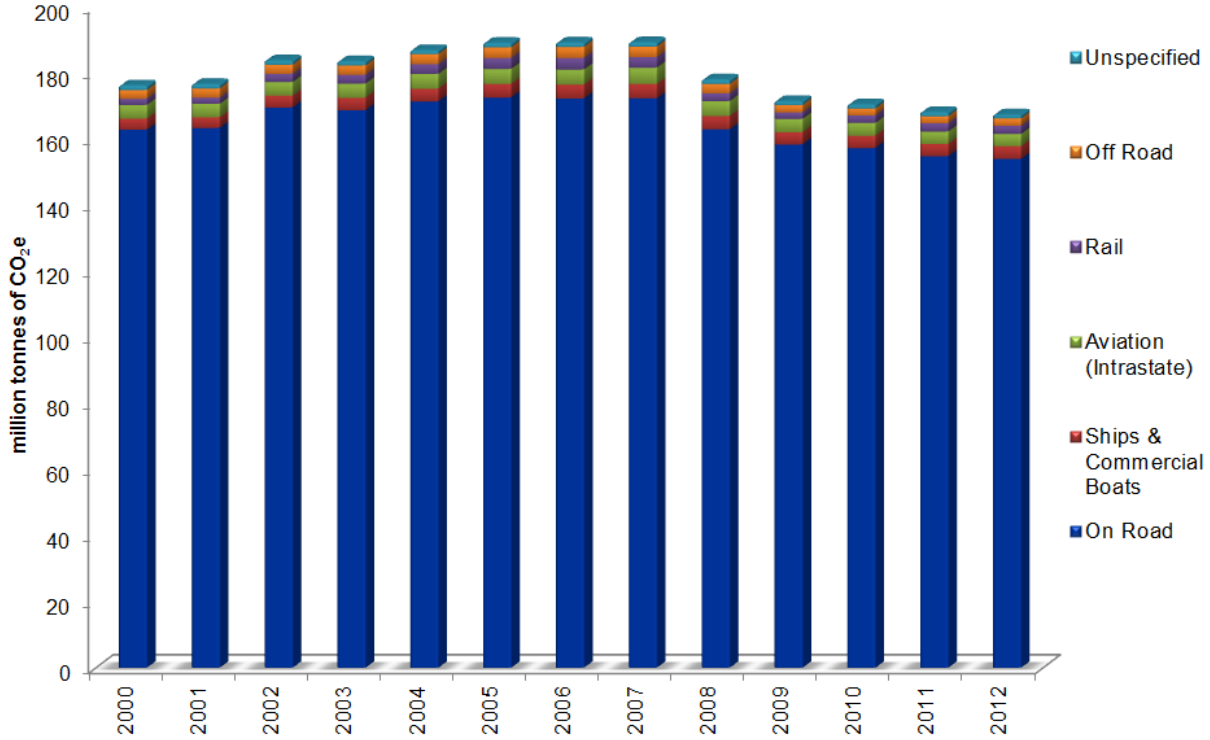
Transportation: Transportation activities accounted for 37.3 percent of the statewide greenhouse gas emissions in 2012. Contributions from the transportation sector include emissions from aviation, on-road, off-road, rail and water-borne and other unspecified sources. Emissions from military transportation activities are not included in the inventory total for the State. The percent contributions from each of these categories to the total emissions from this sector are shown in Figure 16 for 2012.

Figure 16. 2012 Greenhouse Gas Emissions from Transportation
(171 $MMTCO_2e$ Gross Emissions)



An overwhelmingly large majority of emissions from this sector is due to on-road transportation (90 percent). The on-road category also accounts for more than 33 percent of the statewide 2012 greenhouse gas emissions. Of the on-road vehicles, light duty passenger vehicles accounted for approximately 69 percent of the total sector emissions in 2012. Figure 17 shows the trend in emissions for this sector from 2000 through 2012. Transportation emissions showed a marked decline since 2007 (from a high of 192 $MMTCO_2e$ in 2007 to 171 $MMTCO_2e$ in 2012).

Figure 17. Greenhouse Gas Emission Trends from Transportation



Summed together, the above sectors along with the unspecified emissions in the inventory not attributed to any sector, equal the total emissions accounted for in the California inventory. Unspecified emissions include emissions from evaporative losses, which could not be attributed to a specific economic sector. In the previous version of the inventory, emissions from the use of ODS substitutes was categorized in the unspecified emissions. However, in this version, those emissions are attributed to individual sectors. The ODS substitute category includes hydrofluorocarbon (HFC) and perfluorocarbon (PFC) emissions, which are substitutes to chlorofluorocarbons (CFCs), compounds that were phased out under the Montreal Protocol due to their ozone depleting ability.

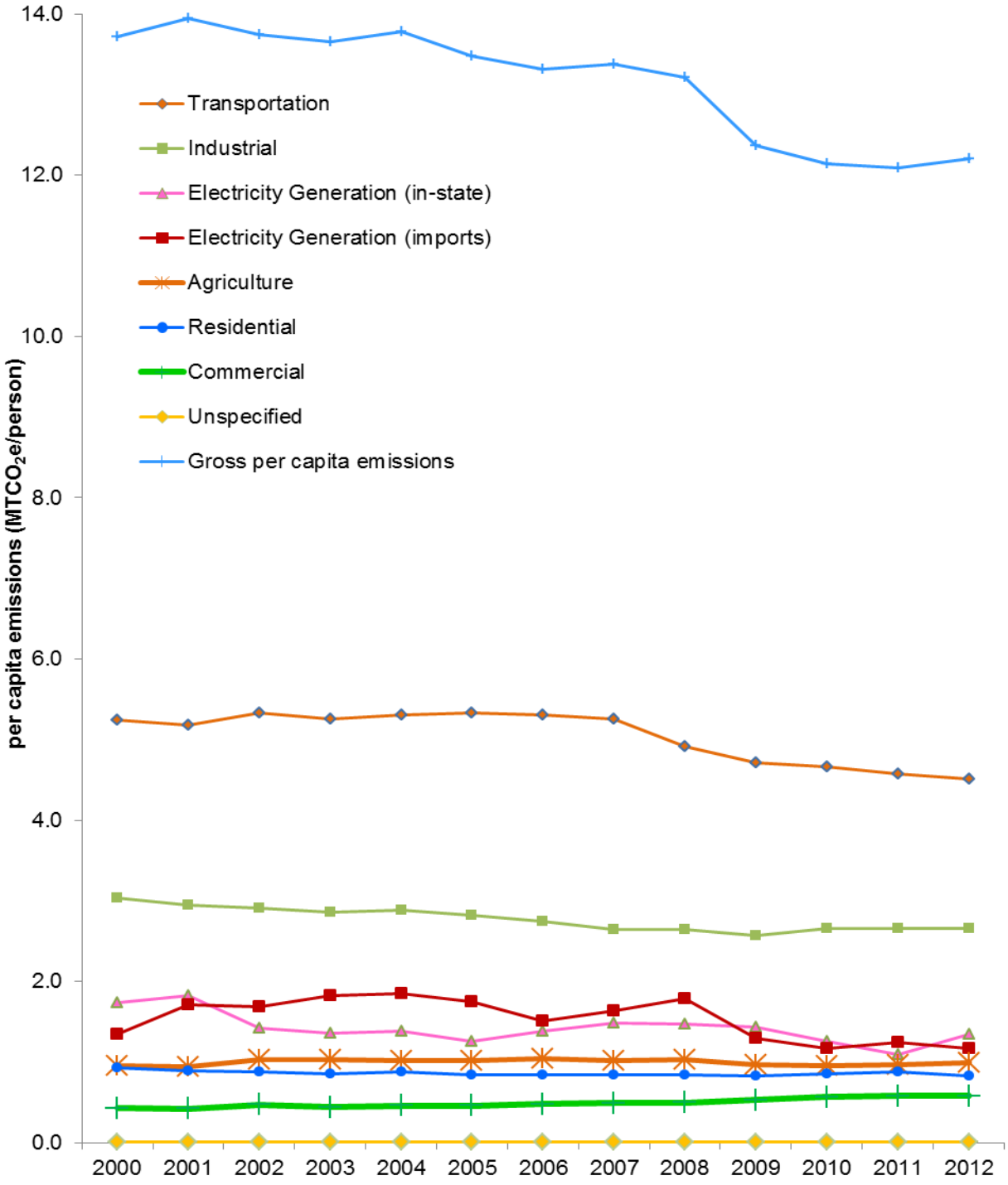
This sector-specific methodology (except for electricity imports and internationally-flagged shipping) generally reflects the reporting methods used by the U.S.EPA and the IPCC.

Per Capita Emissions

For the year 2012, California has a gross per capita emissions of 12.2 $MTCO_2e$ per person (Figure 18). This represents a 12 percent reduction from the 13.7 $MTCO_2e$ per person in 2000 (Figure 18). The population increased by 11.4 percent during the same period.

Per capita emissions from industrial, transportation, and electricity generation (in-state) have decreased from 2000 to 2012, with a 22 percent decrease in the 2012 in-state electricity generation per capita emissions from 2000. The per capita comparison is a useful metric for emissions evaluation because it shows that emissions have not grown consistently with population, indicating that energy conservation may have led to significant emission reductions.

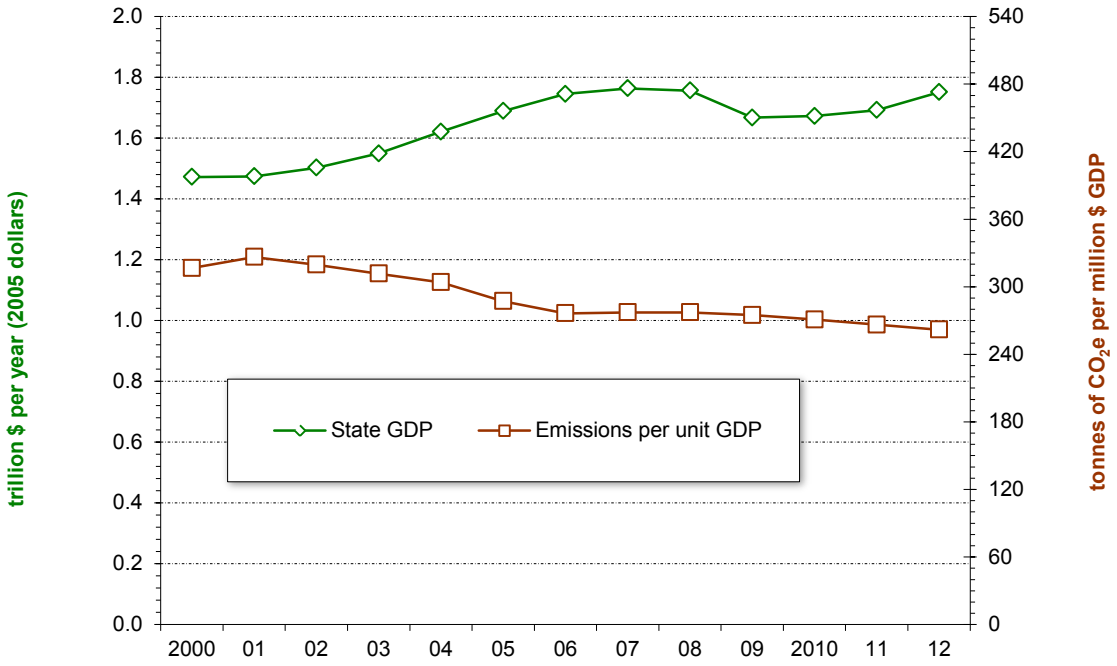
Figure 18. 2012 Greenhouse Gas Emissions per Capita



Carbon Intensity of California Economy - Gross Domestic Product

California's Gross Domestic Product (GDP) increased from $1.47 trillion in 2000 to $1.75 trillion in 2012 (in 2005 dollars)(DoF, 2014). While California's economy has continued to grow, the "carbon intensity" of the economy, the amount of carbon emissions related to the state's overall economy (tonnes CO_2/ GDP$), has continually declined since 2001. The carbon intensity of California's economy has decreased from 316.6 tonnes CO_2e per million dollars in 2000 to 261.9 tonnes per million dollars in 2012. That equates to a 17 percent decrease and California ranks as the 46th lowest state in the nation in terms of carbon intensity.

Carbon Intensity of California's economy



V. Broader Perspective of California Greenhouse Gas Emissions

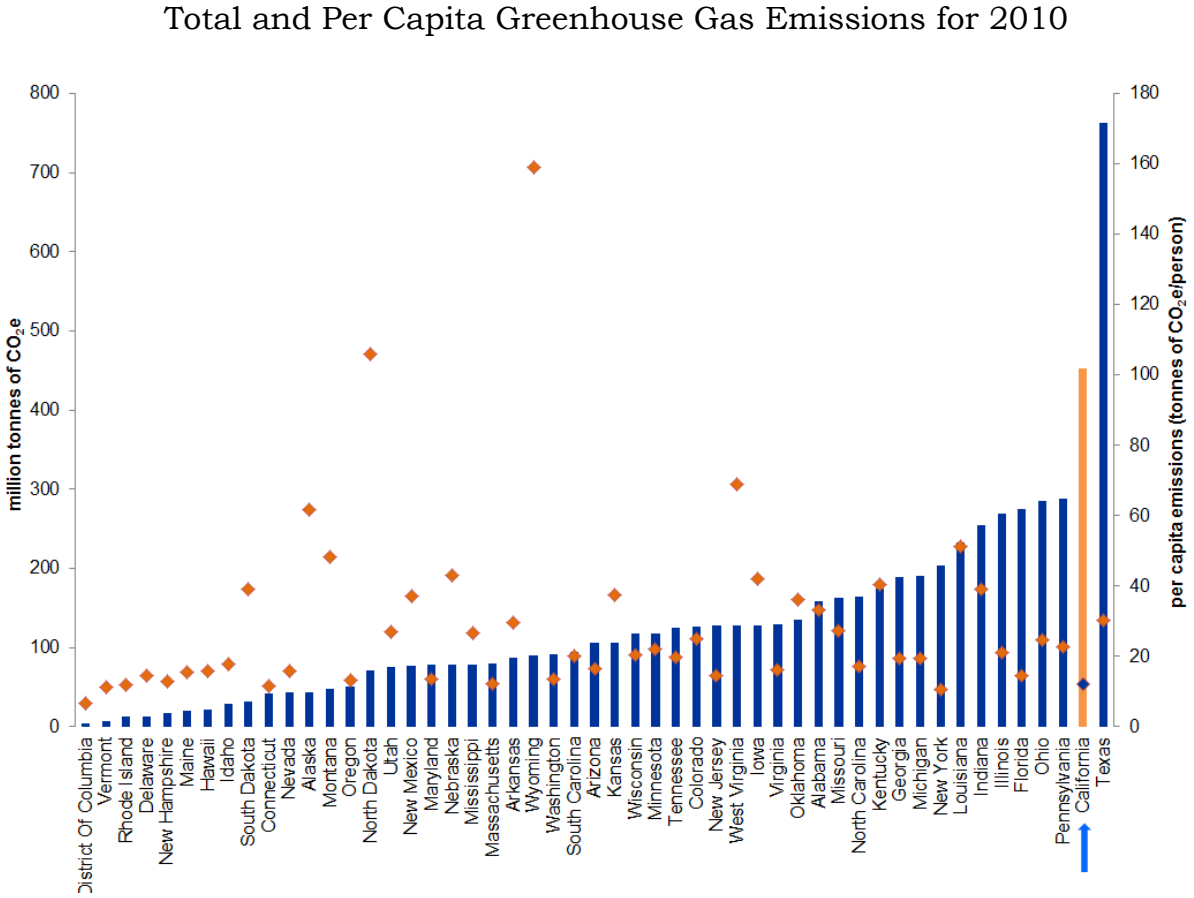
To get a broader perspective of California GHG emissions, it's interesting to compare with other states and nations GHG emissions. Even though the California inventory was designed to facilitate comparability with other nations and states, often the international emissions data is incomplete or of a different time. For this reason, this section uses data from the World Resources Institute (WRI) Climate Analysis Indicators Tool (CAIT) for comparing California's inventory to other states in the United States and other countries around the world (WRI, 2014). CAIT2.0 includes greenhouse gas emissions data for the period 1990-2010. The data include the six major greenhouse gases from most major sources and sinks for over 185 countries as well as state-level data for all 50 U.S. states and the District of Columbia.

California and Other States

The 2010 greenhouse gas emissions data from CAIT 2.0 (WRI, 2014) was the latest available and hence used to compare 2010 emissions from California with emissions from other states in the United States. The data for California emissions for year 2010 was based on the 2000-2012 statewide inventory. The data for all other states was from the WRI CAIT 2.0 tool.

Figure 19 shows the total and per capita greenhouse gas emissions for 2010 for all the states in the country (WRI, 2014). In 2010, California accounted for 6.8 percent of all emissions in the country and ranked second highest among the states with total emissions of 453 $MMTCO_2e$, only behind Texas with 763 $MMTCO_2e$. From a per capita standpoint, California has the 45^{th} lowest emissions with 12.1 $MTCO_2e$/person in 2010.

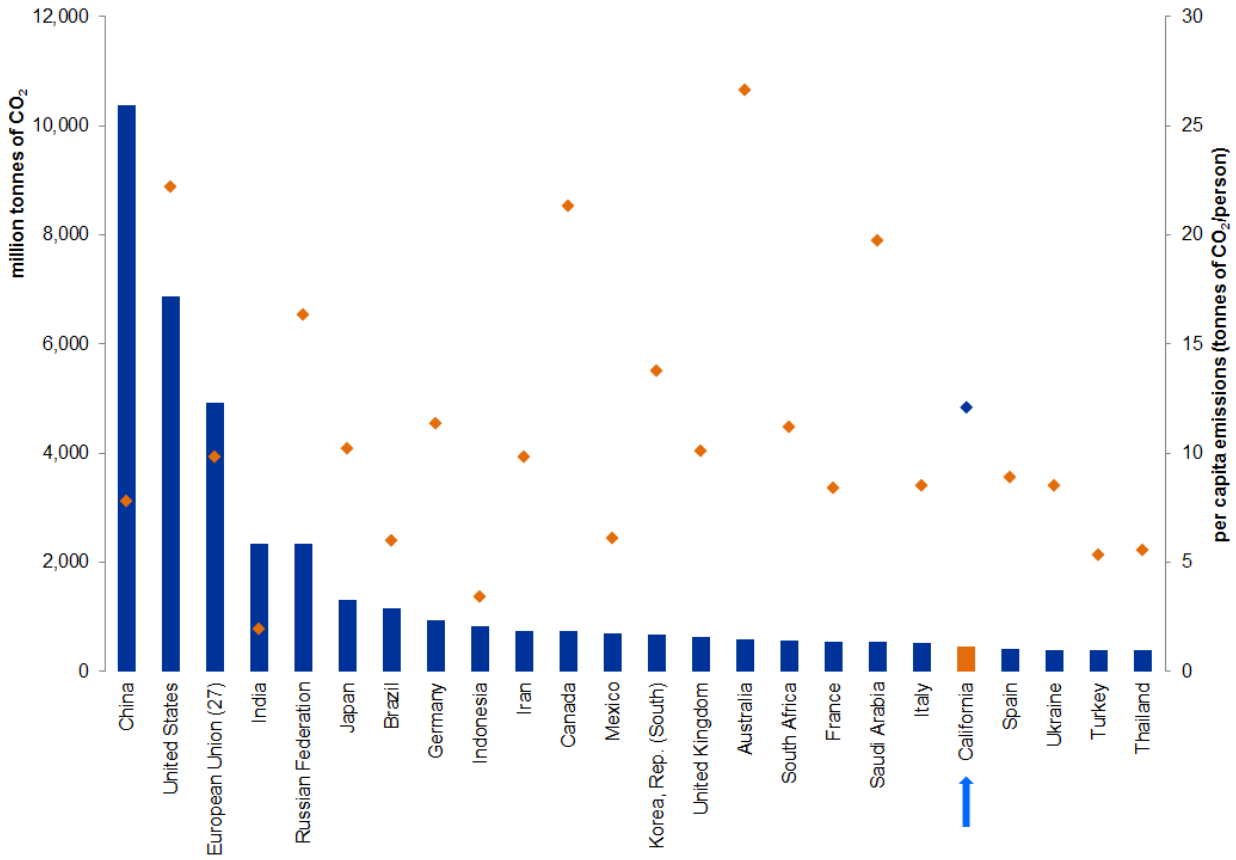
Figure 19. Total (bars) and Per Capita (markers) California and Other States Greenhouse Gas Emissions (CAIT-U.S. v4.0)



California and the Rest of the World

California has substantial greenhouse gas emissions when compared with the nations of the world. CAIT was used to compare 2010 California emissions against 2010 emissions from countries of the world, including the United States (WRI, 2014). A comparison of 2010 total and per capita greenhouse gas emissions as obtained from CAIT for California and the rest of the world is shown in Figure 20.

Figure 20. Total (bars) and Per Capita (markers) California and Other States Greenhouse Gas Emissions (CAIT-U.S. v4.0)
Total and Per Capita CO_2 Emissions for 2010



If California were considered as an independent state, on a global platform in 2010, California would have ranked the 20th highest in CO_2 emissions worldwide. On a per capita emissions basis, California would have ranked 38th in the world with 12.1 $MTCO_2e$/person in 2010, behind United States (including California) at rank 16 with 22.2 $MTCO_2e$/person. Kuwait had the highest per capita emissions at 71.8 $MTCO_2e$/person. The top 10 emitters (individual nations, excluding data for European Union) accounted for a large part of the total global greenhouse gas emissions in 2010 (approximately 70 percent).

VI. Ongoing Work

ARB staff routinely evaluates the methodology used to develop the emissions estimates used in the inventory. In addition, data from a variety of sources are reviewed and compiled for use in updating the inventory each year. ARB regularly releases updated emission inventory data, summary reports, and technical support documents that detail the emission inventory for public use It is anticipated that ARB staff will continue to release updates in the future. All reports are available on ARB's greenhouse gas emission inventory webpage.

VII. References

1. Assembly Bill 32 (AB 32) (2006) Global Warming Solutions Act of 2006 California Statute, Chapter 488, California Health & Safety Code §38500-38599.

2. Assembly Bill 1803 (AB 1803) (2006) Public Resources California Statute, Chapter 77, Amendments to various sections of California Code.

3. CARB (2007) California 1990 Greenhouse Gas Emissions Level and 2020 Emissions Limit, California Air Resources Board, Planning and Technical Support Division.

4. CARB (2014) Technical Support Document for California's 2000-2012 Greenhouse Gas Emission Inventory and 1990 Emissions Level, California Air Resources Board, Air Quality Planning and Science Division.

5. DoF (2014) California Department of Finance – California State Gross Domestic Product (GDP) 1963 – 2012.

6. CLIISE (2007) Greenhouse Gas Inventory of Springfield, Oregon, Climate Leadership Initiative Institute for a Sustainable Environment, University of Oregon.

7. Dettinger M.D. and Cayan D.R. (1995) Large-scale Atmospheric Forcing of Recent Trends toward Early Snowmelt Runoff in California Journal of Climate, 8, 606.

8. DOF (2014) State of California, Department of Finance, E-6. California County Population Estimates and Components of Change by Year, 2010–2012.

9. EO (2005) Executive Order S-3-05, Executive Department, State of California.

10. IPCC (2000) Good Practice Guidance and Uncertainty Management in National Greenhouse Gas Inventories, Penman J., Kruger D., Galbally I., Hiraishi T., Nyenzi B., Emmanuel S., Buendia L., Hoppaus R., Martinsen T., Meijer J., Miwa K., and Tanabe K. (Eds). IPCC/OECD/IEA/IGES, Japan.

11. IPCC (2006) 2006 IPCC Guidelines for National Greenhouse Gas Inventories, National Greenhouse Gas Inventories Programme, Eggleston H.S., Buendia L., Miwa K., Ngara T., and Tanabe K. (eds.), IGES, Japan.

12. IPCC (2007) Climate Change 2007: The Physical Science Basis. Contribution of Working Group I to the Fourth Assessment Report of the Intergovernmental Panel on Climate Change, Solomon S., Qin D., Manning M., Chen Z., Marquis M., Averyt K.B., Tignor M., and Miller H.L. (eds.). Cambridge University Press, Cambridge, United Kingdom and New York, NY, USA. Chapter 2, Table 2.14.

13. Meehl G.A., Washington W.M., Collins W.D., Arblaster J.M., Hu A., Buja L.E., Strand W.G. and Teng H. (2005) How Much More Global Warming and Sea Level Rise? Science, 307, 1769.

14. NAICS (2012) North American Industry Classification System: United States, 2012, Office of Management and Budget.

15. Patz J.A., Campbell-Lendrum D., Holloway T., Foley J.A. (2005) Impact of Regional Climate Change on Human Health Nature, 438, 310.

16. United Nations (2012) Protocol to the United Nations Framework Convention on Climate Change, Adoption of Amendment to the Protocol Articles 1-28, Annexes A-B.

17. U.S.EPA (2014) Inventory of U.S. Greenhouse Gas Emissions and Sinks: 1990-2012, United States Environmental Protection Agency, # EPA 430-R-14-003.

18. WRI (2014) Climate Analysis Indicators Tool (CAIT), Version 2.0, World Resources Institute's Climate Data Explorer. http://cait2.wri.org

Appendix A

2012 Statewide Greenhouse Gas Inventory Emission estimation methodology changes from year 2011:

Inventory-wide change:

- Year 2012 inventory is based on GWP values from IPCC's AR4. Year 2011 GHG inventory was based on the GWP values from the IPCC's second assessment report (SAR).

Sectoral changes are listed below:

Transportation:

- Aviation gasoline data source changed from EIA to BOE.
- On road "gasoline" gallons sold (i.e. gasoline + ethanol) changed slightly due to updates BOE made to the data series back to 2004.
- New methodology uses MRR gasoline and ethanol gallons data to create a percentage mix, instead of using CEC's reported ethanol percentage mix.
- Most water-borne categories changed due to updates in the models on recession and longer term growth forecasts.

Electric Power:

- Combined Heat & Power (CHP) data for 2009-2012 were updated to reflect the same methodology used from 1990-2008, which is the EIA method. (MRR data for these years, produced aberrations in the trend).

Industrial:

- The small amount of Coal and Coke use not reported to MRR was finally determined not to exist (based on EIA data), and was eliminated.
- Off-road Gasoline use now uses MRR totals reconciled to BOE on-road amounts.

Commercial and Residential:

- No methodology changes from year 2011 to 2012.

Agriculture:

- An improved emission factor was derived for rice cultivation for years 2000-2012, in collaboration with USEPA.
- New categories: Dairy calves and beef calves (less than 6 months) have been added for completeness.

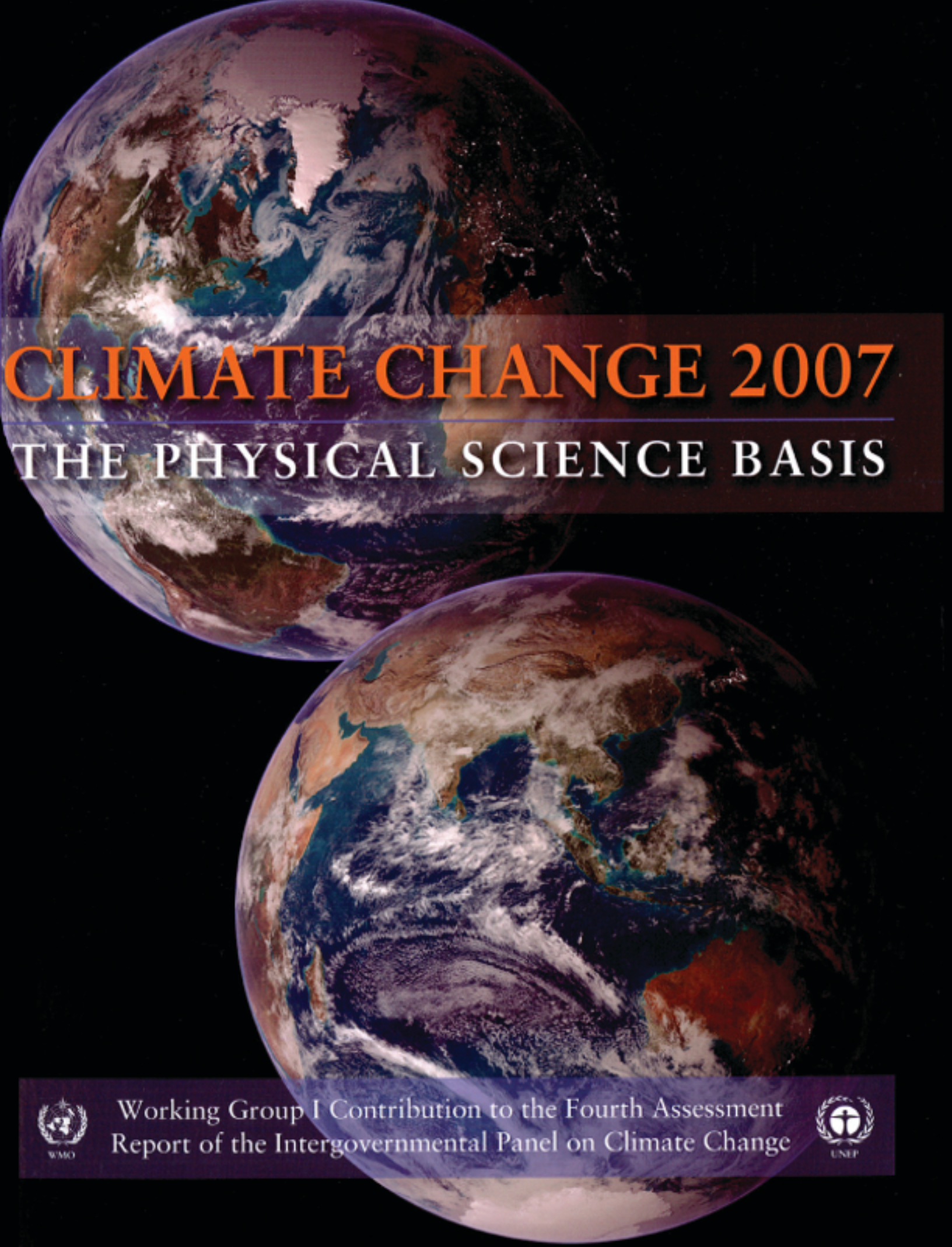
High GWP:

- No methodology changes from year 2011 to 2012.

Recycling and Waste:

- No methodology changes from year 2011 to 2012.

Note: For detailed changes related to each sector, please refer to the Technical Support Document 2000-2012.



CLIMATE CHANGE 2007

THE PHYSICAL SCIENCE BASIS

Working Group I Contribution to the Fourth Assessment Report of the Intergovernmental Panel on Climate Change

WMO

UNEP

Climate Change 2007
The Physical Science Basis

The Intergovernmental Panel on Climate Change (IPCC) was set up jointly by the World Meteorological Organization and the United Nations Environment Programme to provide an authoritative international statement of scientific understanding of climate change. The IPCC's periodic assessments of the causes, impacts and possible response strategies to climate change are the most comprehensive and up-to-date reports available on the subject, and form the standard reference for all concerned with climate change in academia, government and industry worldwide. Through three working groups, many hundreds of international experts assess climate change in this Fourth Assessment Report. The Report consists of three main volumes under the umbrella title Climate Change 2007, all available from Cambridge University Press:

Climate Change 2007 - The Physical Science Basis
Contribution of Working Group I to the Fourth Assessment Report of the IPCC
(ISBN 978 0521 88009-1 Hardback; 978 0521 70596-7 Paperback)

Climate Change 2007 - Impacts, Adaptation and Vulnerability
Contribution of Working Group II to the Fourth Assessment Report of the IPCC
(978 0521 88010-7 Hardback; 978 0521 70597-4 Paperback)

Climate Change 2007 - Mitigation of Climate Change
Contribution of Working Group III to the Fourth Assessment Report of the IPCC
(978 0521 88011-4 Hardback; 978 0521 70598-1 Paperback)

Climate Change 2007 - The Physical Science Basis is the most comprehensive and up-to-date scientific assessment of past, present and future climate change. The report provides:

- the most complete and quantitative assessment of how human activities are affecting the radiative energy balance in the atmosphere
- a more extensive assessment of changes observed throughout the climate system than ever before using the latest measurements covering the atmosphere, land surface, oceans, and snow, ice and frozen ground
- a detailed assessment of past climate change and its causes
- the first probabilistic assessment of climate model simulations and projections using detailed atmosphere-ocean coupled models from 18 modelling centres around the world
- a detailed assessment of climate change observations, modelling, and attribution for every continent

Simply put, this latest assessment of the IPCC will again form the standard scientific reference for all those concerned with climate change and its consequences, including students and researchers in environmental science, meteorology, climatology, biology, ecology and atmospheric chemistry, and policy makers in governments and industry worldwide.

From reviews of the Third Assessment Report – Climate Change 2001:

‘The detail is truly amazing … invaluable works of reference … no reference or science library should be without a set [of the IPCC volumes] … unreservedly recommended to all readers.’
Journal of Meteorology

‘This well-edited set of three volumes will surely be the standard reference for nearly all arguments related with global warming and climate change in the next years. It should not be missing in the libraries of atmospheric and climate research institutes and those administrative and political institutions which have to deal with global change and sustainable development.’
Meteorologische Zeitschrift

‘… likely to remain a vital reference work until further research renders the details outdated by the time of the next survey … another significant step forward in the understanding of the likely impacts of climate change on a global scale.’
International Journal of Climatology

‘The IPCC has conducted what is arguably the largest, most comprehensive and transparent study ever undertaken by mankind … The result is a work of substance and authority, which only the foolish would deride.’
Wind Engineering

‘… the weight of evidence presented, the authority that IPCC commands and the breadth of view can hardly fail to impress and earn respect. Each of the volumes is essentially a remarkable work of reference, containing a plethora of information and copious bibliographies. There can be few natural scientists who will not want to have at least one of these volumes to hand on their bookshelves, at least until further research renders the details outdated by the time of the next survey.’
The Holocene

‘The subject is explored in great depth and should prove valuable to policy makers, researchers, analysts, and students.’
American Meteorological Society

From reviews of the Second Assessment Report – Climate Change 1995:

‘ … essential reading for anyone interested in global environmental change, either past, present or future. … These volumes have a deservedly high reputation’
Geological Magazine

‘… a tremendous achievement of coordinating the contributons of well over a thousand individuals to produce an authoritative, state-of-the-art review which will be of great value to decision-makers and the scientific community at large … an indispensable reference.’
International Journal of Climatology

‘... a wealth of clear, well-organized information that is all in one place ... there is much to applaud.’
Environment International

Climate Change 2007
The Physical Science Basis

Edited by

Susan Solomon
Co-Chair,
IPCC Working Group I

Dahe Qin
Co-Chair,
IPCC Working Group I

Martin Manning
Head, Technical Support Unit
IPCC Working Group I

Melinda Marquis **Kristen Averyt** **Melinda M.B. Tignor** **Henry LeRoy Miller, Jr.**
Technical Support Unit, IPCC Working Group I

Zhenlin Chen
China Meteorological Administration

Contribution of Working Group I
to the Fourth Assessment Report of the
Intergovernmental Panel on Climate Change

Published for the Intergovernmental Panel on Climate Change

CAMBRIDGE
UNIVERSITY PRESS

CAMBRIDGE UNIVERSITY PRESS
Cambridge, New York, Melbourne, Madrid, Cape Town, Singapore, São Paolo, Delhi

Cambridge University Press
32 Avenue of the Americas, New York, NY 10013-2473, USA

www.cambridge.org
Information on this title: www.cambridge.org/9780521880091

© Intergovernmental Panel on Climate Change 2007

This publication is in copyright. Subject to statutory exception and to the provisions of relevant collective licensing agreements, no reproduction of any part may take place without the written permission of
Cambridge University Press.

First published 2007

Printed in Canada by Friesens

A catalog record for this publication is available from the British Library.

ISBN 978-0-521-88009-1 hardback
ISBN 978-0-521-70596-7 paperback

Cambridge University Press has no responsibility for the persistence or accuracy of URLs for external or third-party Internet Web sites referred to in this publication and does not guarantee that any content on such Web sites is, or will remain, accurate or appropriate.

Please use the following reference to the whole report:

IPCC, 2007: *Climate Change 2007: The Physical Science Basis. Contribution of Working Group I to the Fourth Assessment Report of the Intergovernmental Panel on Climate Change* [Solomon, S., D. Qin, M. Manning, Z. Chen, M. Marquis, K.B. Averyt, M. Tignor and H.L. Miller (eds.)]. Cambridge University Press, Cambridge, United Kingdom and New York, NY, USA, 996 pp.

Cover photo:

The Blue Marble western and eastern hemispheres. These images integrate land, ocean, sea ice and clouds into a visual representation of the earth's climate system. They are based on space-borne earth observation data from NASA's MODIS (MODerate resolution Imaging Spectroradiometer) sensor aboard the TERRA and AQUA satellites. These images are part of the Blue Marble dataset which is freely available at http://bluemarble.nasa.gov. They are further documented in Stöckli, R., Vermote, E., Saleous, N., Simmon, R., and Herring, D. (2006). True color earth data set includes seasonal dynamics. EOS, 87(5):49, 55.

Foreword

Representing the first major global assessment of climate change science in six years, "Climate Change 2007 – The Physical Science Basis" has quickly captured the attention of both policymakers and the general public. The report confirms that our scientific understanding of the climate system and its sensitivity to greenhouse gas emissions is now richer and deeper than ever before. It also portrays a dynamic research sector that will provide ever greater insights into climate change over the coming years.

The rigor and credibility of this report owes much to the unique nature of the Intergovernmental Panel on Climate Change (IPCC). Established by the World Meteorological Organization and the United Nations Environment Programme in 1988, the IPCC is both an intergovernmental body and a network of the world's leading climate change scientists and experts.

The chapters forming the bulk of this report describe scientists' assessment of the state-of-knowledge in their respective fields. They were written by 152 coordinating lead authors and lead authors from over 30 countries and reviewed by over 600 experts. A large number of government reviewers also contributed review comments.

The Summary for Policymakers was approved by officials from 113 governments and represents their understanding – and their ownership – of the entire underlying report. It is this combination of expert and government review that constitutes the strength of the IPCC.

The IPCC does not conduct new research. Instead, its mandate is to make policy-relevant – as opposed to policy-prescriptive – assessments of the existing worldwide literature on the scientific, technical and socio-economic aspects of climate change. Its earlier assessment reports helped to inspire governments to adopt and implement the United Nations Framework Convention on Climate Change and the Kyoto Protocol. The current report will also be highly relevant as Governments consider their options for moving forward together to address the challenge of climate change.

Climate Change 2007 – the Physical Science Basis is the first volume of the IPCC's Fourth Assessment Report. The second volume considers climate change impacts, vulnerabilities and adaptation options, while the third volume assesses the opportunities for and the costs of mitigation. A fourth volume provides a synthesis of the IPCC's overall findings.

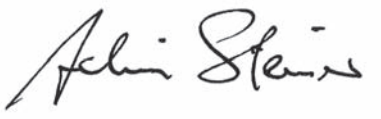
The Physical Science Basis was made possible by the commitment and voluntary labor of the world's leading climate scientists. We would like to express our gratitude to all the Coordinating Lead Authors, Lead Authors, Contributing Authors, Review Editors and Reviewers. We would also like to thank the staff of the Working Group I Technical Support Unit and the IPCC Secretariat for their dedication in coordinating the production of another successful IPCC report.

Many Governments have supported the participation of their resident scientists in the IPCC process and contributed to the IPCC Trust Fund, thus also assuring the participation of experts from developing countries and countries with economies in transition. The governments of Italy, China, New Zealand and Norway hosted drafting sessions, while the Government of France hosted the final plenary that approved and accepted the report. The Government of the United States of America funded the Working Group I Technical Support Unit.

Finally, we would like to thank Dr R.K. Pachauri, Chairman of the IPCC, for his sound direction and tireless and able guidance of the IPCC, and Dr. Susan Solomon and Prof. Dahe Qin, the Co-Chairs of Working Group I, for their skillful leadership of Working Group I through the production of this report.



M. Jarraud
Secretary General
World Meteorological Organization



A. Steiner
Executive Director
United Nations Environment Programme

Preface

This Working Group I contribution to the IPCC's Fourth Assessment Report (AR4) provides a comprehensive assessment of the physical science of climate change and continues to broaden the view of that science, following on from previous Working Group I assessments. The results presented here are based on the extensive scientific literature that has become available since completion of the IPCC's Third Assessment Report, together with expanded data sets, new analyses, and more sophisticated climate modelling capabilities.

This report has been prepared in accordance with rules and procedures established by the IPCC and used for previous assessment reports. The report outline was agreed at the 21st Session of the Panel in November 2003 and the lead authors were accepted at the 31st Session of the IPCC Bureau in April 2004. Drafts prepared by the authors were subject to two rounds of review and revision during which over 30,000 written comments were submitted by over 650 individual experts as well as by governments and international organizations. Review Editors for each chapter have ensured that all substantive government and expert review comments received appropriate consideration. The Summary for Policymakers was approved line-by-line and the underlying chapters were then accepted at the 10th Session of IPCC Working Group I from 29 January to 1 February 2007.

Scope of the Report

The Working Group I report focuses on those aspects of the current understanding of the physical science of climate change that are judged to be most relevant to policymakers. It does not attempt to review the evolution of scientific understanding or to cover all of climate science. Furthermore, this assessment is based on the relevant scientific literature available to the authors in mid-2006 and the reader should recognize that some topics covered here may be subject to further rapid development.

A feature of recent climate change research is the breadth of observations now available for different components of the climate system, including the atmosphere, oceans, and cryosphere. Additional observations and new analyses have broadened our understanding and enabled many uncertainties to be reduced. New information has also led to some new questions in areas such as unanticipated changes in ice sheets, their potential effect on sea level rise, and the implications of complex interactions between climate change and biogeochemistry.

In considering future projections of climate change, this report follows decisions made by the Panel during the AR4 scoping and approval process to use emission scenarios that have been previously assessed by the IPCC for consistency across the three Working Groups. However, the value of information from new climate models related to climate stabilization has also been recognized. In order to address both topics, climate modelling groups have conducted climate simulations that included idealized experiments in which atmospheric composition is held constant. Together with climate model ensemble simulations, including many model runs for the 20th and 21st centuries, this assessment has been able to consider far more simulations than any previous assessment of climate change.

The IPCC assessment of the effects of climate change and of options for responding to or avoiding such effects, are assessed by Working Groups II and III and so are not covered here. In particular, while this Working Group I report presents results for a range of emission scenarios consistent with previous reports, an updated assessment of the plausible range of future emissions can only be conducted by Working Group III.

The Structure of this Report

This Working Group I assessment includes, for the first time, an introductory chapter, Chapter 1, which covers the ways in which climate change science has progressed, including an overview of the methods used in climate change science, the role of climate models and evolution in the treatment of uncertainties.

Chapters 2 and 7 cover the changes in atmospheric constituents (both gases and aerosols) that affect the radiative energy balance in the atmosphere and determine the Earth's climate. Chapter 2 presents a perspective based on observed change in the atmosphere and covers the central concept of radiative forcing. Chapter 7 complements this by considering the interactions between the biogeochemical cycles that affect atmospheric constituents and climate change, including aerosol/cloud interactions.

Chapters 3, 4 and 5 cover the extensive range of observations now available for the atmosphere and surface, for snow, ice and frozen ground, and for the oceans respectively. While observed changes in these components of the climate system are closely inter-related through physical processes, the separate chapters allow a more focused assessment of available data and their uncertainties, including remote sensing data from satellites. Chapter 5 includes observed changes in sea level, recognizing the strong interconnections between these and ocean heat content.

Chapter 6 presents a palaeoclimatic perspective and assesses the evidence for past climate change and the extent to which that is explained by our present scientific understanding. It includes a new assessment of reconstructed temperatures for the past 1300 years.

Chapter 8 covers the ways in which physical processes are simulated in climate models and the evaluation of models against observed climate, including its average state and variability. Chapter 9 covers the closely related issue of the extent to which observed climate change can be attributed to different causes, both natural and anthropogenic.

Chapter 10 covers the use of climate models for projections of global climate including their uncertainties. It shows results for different levels of future greenhouse gases, providing a probabilistic assessment of a range of physical climate system responses and the time scales and inertia associated with such responses. Chapter 11 covers regional climate change projections consistent with the global projections. It includes an assessment of model reliability at regional levels and the factors that can significantly influence regional scale climate change.

The Summary for Policymakers (SPM) and Technical Summary (TS) of this report follow a parallel structure and each includes cross references to the chapter and section where the material being summarized can be found in the underlying report. In this way these summary components of the report provide a road-map to the content of the entire report and the reader is encouraged to use the SPM and TS in that way.

An innovation in this report is the inclusion of 19 Frequently Asked Questions, in which the authors provide scientific answers to a range of general questions in a form that will be useful for a broad range of teaching purposes. Finally the report is accompanied by about 250 pages of supplementary material that was reviewed along with the chapter drafts and is made available on CDRom and in web-based versions of the report to provide an additional level of detail, such as results for individual climate models.

Some key policy-relevant questions and issues addressed in this report and the relevant chapters

Question	Chapters
How has the science of climate change advanced since the IPCC began?	1
What is known about the natural and anthropogenic agents that contribute to climate change, and the underlying processes that are involved?	2, 6, 7
How has climate been observed to change during the period of instrumental measurements?	3, 4, 5
What is known of palaeoclimatic changes, before the instrumental era, over time scales of hundreds to millions of years, and the processes that caused them?	6, 9
How well do we understand human and natural contributions to recent climate change, and how well can we simulate changes in climate using models?	8, 9
How is climate projected to change in the future, globally and regionally?	10, 11
What is known about past and projected changes in sea level, including the role of changes in glaciers and ice sheets?	4, 5, 6, 10
Are extremes such as heavy precipitation, droughts, and heat waves changing and why, and how are they expected to change in the future?	3, 5, 9, 10, 11

Acknowledgments

This assessment has benefited greatly from the very high degree of co-operation that exists within the international climate science community and its coordination by the World Meteorological Organization World Climate Research Program (WCRP) and the International Geosphere Biosphere Program (IGBP). In particular we wish to acknowledge the enormous commitment by the individuals and agencies of 14 climate modelling groups from around the world, as well as the archiving and distribution of an unprecedented amount (over 30 Terabytes) of climate model output by the Program for Climate Model Diagnosis and Intercomparison (PCMDI). This has enabled a more detailed comparison among current climate models and a more comprehensive assessment of the potential nature of long term climate change than ever before.

We must emphasise that this report has been entirely dependent on the expertise, hard work, and commitment to excellence shown throughout by our Coordinating Lead Authors and Lead Authors with important help by many Contributing Authors. In addition we would like to express our sincere appreciation of the work carried out by the expert reviewers and acknowledge the value of the very large number of constructive comments received. Our Review Editors have similarly played a critical role in assisting the authors to deal with these comments.

The Working Group I Bureau, Kansri Boonpragob, Filippo Giorgi, Bubu Jallow, Jean Jouzel, Maria Martelo and David Wratt have played the role of an editorial board in assisting with the selection of authors and with guiding the initial outline of the report. They have provided constructive support to the Working Group Co-Chairs throughout for which we are very grateful.

Our sincere thanks go to the hosts and organizers of the four lead author meetings that were necessary for the preparation of the report and we gratefully acknowledge the support received from governments and agencies in Italy, China, New Zealand and Norway. The final Working Group I approval session was made possible by Mr Marc Gillet through the generosity of the government of France and the session was greatly facilitated by Francis Hayes, the WMO Conference Officer.

It is a pleasure to acknowledge the tireless work of the staff of the Working Group I Technical Support Unit, Melinda Marquis, Kristen Averyt, Melinda Tignor, Roy Miller, Tahl Kestin and Scott Longmore, who were ably assisted by Zhenlin Chen, Barbara Keppler, MaryAnn Pykkonen, Kyle Terran, Lelani Arris, and Marilyn Anderson. Graphics support and layout by Michael Shibao and Paula Megenhardt is gratefully appreciated. We thank Reto Stockli for kindly providing images of the Earth from space for the cover of this report. Assistance in helping the Co-Chairs to organize and edit the Frequently Asked Questions by David Wratt, David Fahey, and Susan Joy Hassol, is also appreciated. We should also like to thank Renate Christ, Secretary of the IPCC, and Secretariat staff Jian Liu, Rudie Bourgeois, Annie Courtin and Joelle Fernandez who provided logistical support for government liaison and travel of experts from developing countries and transitional economy countries.

Rajendra K. Pachauri	Susan Solomon	Dahe Qin	Martin Manning
IPCC Chairman	IPCC WGI Co-Chair	IPCC WGI Co-Chair	IPCC WGI TSU Head

Contents

Foreword v

Preface vii

Summary for Policymakers 1

Technical Summary 19

1 Historical Overview of Climate Change Science 93

2 Changes in Atmospheric Constituents and Radiative Forcing 129

3 Observations: Atmospheric Surface and Climate Change 235

4 Observations: Changes in Snow, Ice and Frozen Ground 337

5 Observations: Ocean Climate Change and Sea Level 385

6 Palaeoclimate 433

7 Coupling Between Changes in the Climate System and Biogeochemistry 499

8 Climate Models and their Evaluation 589

9 Understanding and Attributing Climate Change 663

10 Global Climate Projections 747

11 Regional Climate Projections 847

Annex I: Glossary 941

Annex II: Contributors to the IPCC WGI Fourth Assessment Report 955

Annex III: Reviewers of the IPCC WGI Fourth Assessment Report 969

Annex IV: Acronyms 981

Index 989

A report of Working Group I of the Intergovernmental Panel on Climate Change

Summary for Policymakers

Drafting Authors:

Richard B. Alley, Terje Berntsen, Nathaniel L. Bindoff, Zhenlin Chen, Amnat Chidthaisong, Pierre Friedlingstein, Jonathan M. Gregory, Gabriele C. Hegerl, Martin Heimann, Bruce Hewitson, Brian J. Hoskins, Fortunat Joos, Jean Jouzel, Vladimir Kattsov, Ulrike Lohmann, Martin Manning, Taroh Matsuno, Mario Molina, Neville Nicholls, Jonathan Overpeck, Dahe Qin, Graciela Raga, Venkatachalam Ramaswamy, Jiawen Ren, Matilde Rusticucci, Susan Solomon, Richard Somerville, Thomas F. Stocker, Peter A. Stott, Ronald J. Stouffer, Penny Whetton, Richard A. Wood, David Wratt

Draft Contributing Authors:

J. Arblaster, G. Brasseur, J.H. Christensen, K.L. Denman, D.W. Fahey, P. Forster, E. Jansen, P.D. Jones, R. Knutti, H. Le Treut, P. Lemke, G. Meehl, P. Mote, D.A. Randall, D.A. Stone, K.E. Trenberth, J. Willebrand, F. Zwiers

This Summary for Policymakers should be cited as:

IPCC, 2007: Summary for Policymakers. In: *Climate Change 2007: The Physical Science Basis. Contribution of Working Group I to the Fourth Assessment Report of the Intergovernmental Panel on Climate Change* [Solomon, S., D. Qin, M. Manning, Z. Chen, M. Marquis, K.B. Averyt, M.Tignor and H.L. Miller (eds.)]. Cambridge University Press, Cambridge, United Kingdom and New York, NY, USA.

Introduction

The Working Group I contribution to the IPCC Fourth Assessment Report describes progress in understanding of the human and natural drivers of climate change,[1] observed climate change, climate processes and attribution, and estimates of projected future climate change. It builds upon past IPCC assessments and incorporates new findings from the past six years of research. Scientific progress since the Third Assessment Report (TAR) is based upon large amounts of new and more comprehensive data, more sophisticated analyses of data, improvements in understanding of processes and their simulation in models and more extensive exploration of uncertainty ranges.

The basis for substantive paragraphs in this Summary for Policymakers can be found in the chapter sections specified in curly brackets.

Human and Natural Drivers of Climate Change

Changes in the atmospheric abundance of greenhouse gases and aerosols, in solar radiation and in land surface properties alter the energy balance of the climate system. These changes are expressed in terms of radiative forcing,[2] which is used to compare how a range of human and natural factors drive warming or cooling influences on global climate. Since the TAR, new observations and related modelling of greenhouse gases, solar activity, land surface properties and some aspects of aerosols have led to improvements in the quantitative estimates of radiative forcing.

Global atmospheric concentrations of carbon dioxide, methane and nitrous oxide have increased markedly as a result of human activities since 1750 and now far exceed pre-industrial values determined from ice cores spanning many thousands of years (see Figure SPM.1). The global increases in carbon dioxide concentration are due primarily to fossil fuel use and land use change, while those of methane and nitrous oxide are primarily due to agriculture. {2.3, 6.4, 7.3}

- Carbon dioxide is the most important anthropogenic greenhouse gas (see Figure SPM.2). The global atmospheric concentration of carbon dioxide has increased from a pre-industrial value of about 280 ppm to 379 ppm[3] in 2005. The atmospheric concentration of carbon dioxide in 2005 exceeds by far the natural range over the last 650,000 years (180 to 300 ppm) as determined from ice cores. The annual carbon dioxide concentration growth rate was larger during the last 10 years (1995–2005 average: 1.9 ppm per year), than it has been since the beginning of continuous direct atmospheric measurements (1960–2005 average: 1.4 ppm per year) although there is year-to-year variability in growth rates. {2.3, 7.3}

- The primary source of the increased atmospheric concentration of carbon dioxide since the pre-industrial period results from fossil fuel use, with land-use change providing another significant but smaller contribution. Annual fossil carbon dioxide emissions[4] increased from an average of 6.4 [6.0 to 6.8][5] GtC (23.5 [22.0 to 25.0] $GtCO_2$) per year in the 1990s to 7.2 [6.9 to 7.5] GtC (26.4 [25.3 to 27.5] $GtCO_2$) per year in 2000–2005 (2004 and 2005 data are interim estimates). Carbon dioxide emissions associated with land-use change

[1] *Climate change* in IPCC usage refers to any change in climate over time, whether due to natural variability or as a result of human activity. This usage differs from that in the United Nations Framework Convention on Climate Change, where climate change refers to a change of climate that is attributed directly or indirectly to human activity that alters the composition of the global atmosphere and that is in addition to natural climate variability observed over comparable time periods.

[2] *Radiative forcing* is a measure of the influence that a factor has in altering the balance of incoming and outgoing energy in the Earth-atmosphere system and is an index of the importance of the factor as a potential climate change mechanism. Positive forcing tends to warm the surface while negative forcing tends to cool it. In this report, radiative forcing values are for 2005 relative to pre-industrial conditions defined at 1750 and are expressed in watts per square metre ($W\ m^{-2}$). See Glossary and Section 2.2 for further details.

[3] ppm (parts per million) or ppb (parts per billion, 1 billion = 1,000 million) is the ratio of the number of greenhouse gas molecules to the total number of molecules of dry air. For example, 300 ppm means 300 molecules of a greenhouse gas per million molecules of dry air.

[4] Fossil carbon dioxide emissions include those from the production, distribution and consumption of fossil fuels and as a by-product from cement production. An emission of 1 GtC corresponds to 3.67 $GtCO_2$.

[5] In general, uncertainty ranges for results given in this Summary for Policymakers are 90% uncertainty intervals unless stated otherwise, that is, there is an estimated 5% likelihood that the value could be above the range given in square brackets and 5% likelihood that the value could be below that range. Best estimates are given where available. Assessed uncertainty intervals are not always symmetric about the corresponding best estimate. Note that a number of uncertainty ranges in the Working Group I TAR corresponded to 2 standard deviations (95%), often using expert judgement.

Changes in Greenhouse Gases from Ice Core and Modern Data

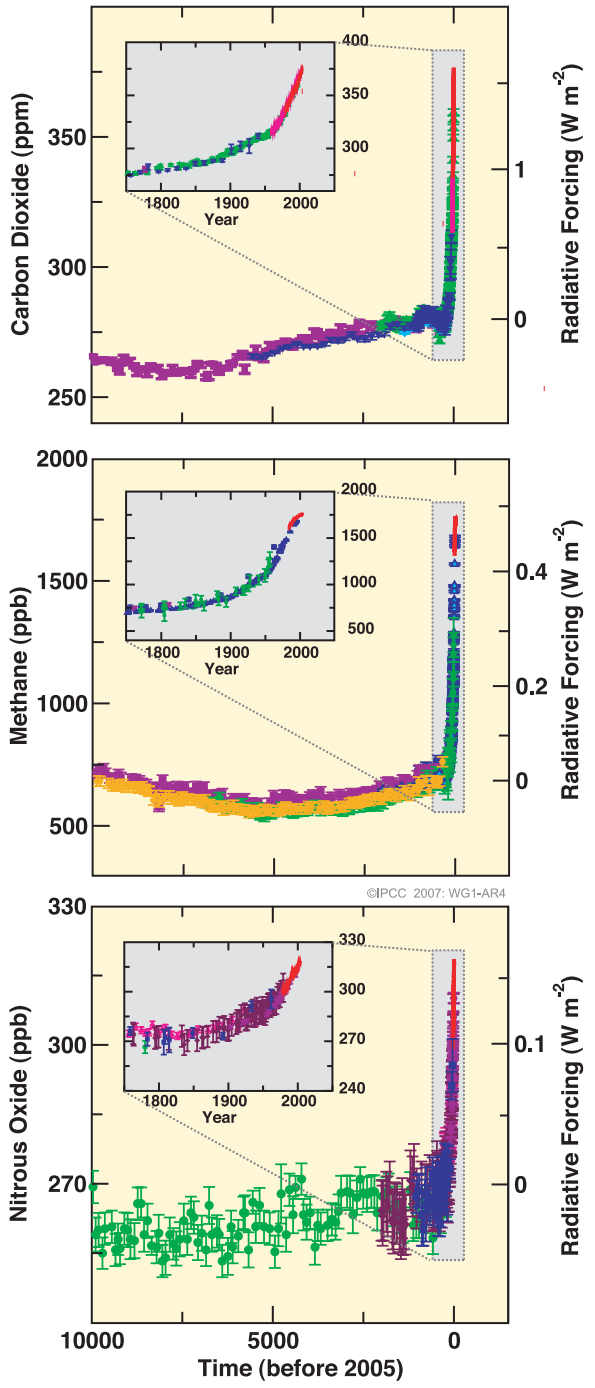


Figure SPM.1. *Atmospheric concentrations of carbon dioxide, methane and nitrous oxide over the last 10,000 years (large panels) and since 1750 (inset panels). Measurements are shown from ice cores (symbols with different colours for different studies) and atmospheric samples (red lines). The corresponding radiative forcings are shown on the right hand axes of the large panels. {Figure 6.4}*

are estimated to be 1.6 [0.5 to 2.7] GtC (5.9 [1.8 to 9.9] $GtCO_2$) per year over the 1990s, although these estimates have a large uncertainty. {7.3}

- The global atmospheric concentration of methane has increased from a pre-industrial value of about 715 ppb to 1732 ppb in the early 1990s, and was 1774 ppb in 2005. The atmospheric concentration of methane in 2005 exceeds by far the natural range of the last 650,000 years (320 to 790 ppb) as determined from ice cores. Growth rates have declined since the early 1990s, consistent with total emissions (sum of anthropogenic and natural sources) being nearly constant during this period. It is *very likely*[6] that the observed increase in methane concentration is due to anthropogenic activities, predominantly agriculture and fossil fuel use, but relative contributions from different source types are not well determined. {2.3, 7.4}

- The global atmospheric nitrous oxide concentration increased from a pre-industrial value of about 270 ppb to 319 ppb in 2005. The growth rate has been approximately constant since 1980. More than a third of all nitrous oxide emissions are anthropogenic and are primarily due to agriculture. {2.3, 7.4}

The understanding of anthropogenic warming and cooling influences on climate has improved since the TAR, leading to *very high confidence*[7] that the global average net effect of human activities since 1750 has been one of warming, with a radiative forcing of +1.6 [+0.6 to +2.4] W m^{-2} (see Figure SPM.2). {2.3., 6.5, 2.9}

- The combined radiative forcing due to increases in carbon dioxide, methane, and nitrous oxide is +2.30 [+2.07 to +2.53] W m^{-2}, and its rate of increase during the industrial era is *very likely* to have been unprecedented in more than 10,000 years (see Figures

[6] In this Summary for Policymakers, the following terms have been used to indicate the assessed likelihood, using expert judgement, of an outcome or a result: *Virtually certain* > 99% probability of occurrence, *Extremely likely* > 95%, *Very likely* > 90%, *Likely* > 66%, *More likely than not* > 50%, *Unlikely* < 33%, *Very unlikely* < 10%, *Extremely unlikely* < 5% (see Box TS.1 for more details).

[7] In this Summary for Policymakers the following levels of confidence have been used to express expert judgements on the correctness of the underlying science: *very high confidence* represents at least a 9 out of 10 chance of being correct; *high confidence* represents about an 8 out of 10 chance of being correct (see Box TS.1)

SPM.1 and SPM.2). The carbon dioxide radiative forcing increased by 20% from 1995 to 2005, the largest change for any decade in at least the last 200 years. {2.3, 6.4}

- Anthropogenic contributions to aerosols (primarily sulphate, organic carbon, black carbon, nitrate and dust) together produce a cooling effect, with a total direct radiative forcing of –0.5 [–0.9 to –0.1] W m^{-2} and an indirect cloud albedo forcing of –0.7 [–1.8 to –0.3] W m^{-2}. These forcings are now better understood than at the time of the TAR due to improved *in situ*, satellite and ground-based measurements and more comprehensive modelling, but remain the dominant uncertainty in radiative forcing. Aerosols also influence cloud lifetime and precipitation. {2.4, 2.9, 7.5}

- Significant anthropogenic contributions to radiative forcing come from several other sources. Tropospheric ozone changes due to emissions of ozone-forming chemicals (nitrogen oxides, carbon monoxide, and hydrocarbons) contribute +0.35 [+0.25 to +0.65] W m^{-2}. The direct radiative forcing due to changes in halocarbons[8] is +0.34 [+0.31 to +0.37] W m^{-2}. Changes in surface albedo, due to land cover changes and deposition of black carbon aerosols on snow, exert

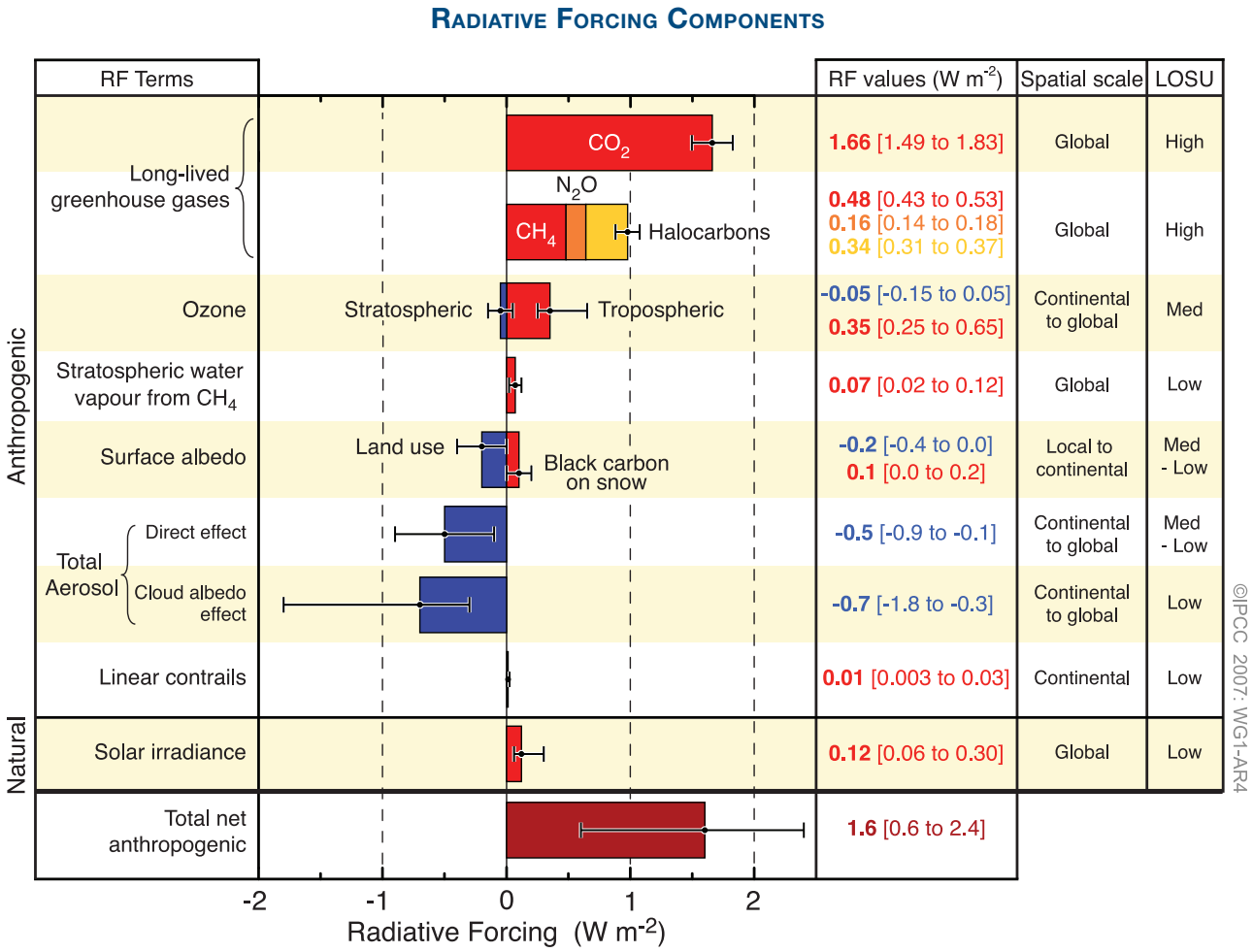


Figure SPM.2. *Global average radiative forcing (RF) estimates and ranges in 2005 for anthropogenic carbon dioxide (CO_2), methane (CH_4), nitrous oxide (N_2O) and other important agents and mechanisms, together with the typical geographical extent (spatial scale) of the forcing and the assessed level of scientific understanding (LOSU). The net anthropogenic radiative forcing and its range are also shown. These require summing asymmetric uncertainty estimates from the component terms, and cannot be obtained by simple addition. Additional forcing factors not included here are considered to have a very low LOSU. Volcanic aerosols contribute an additional natural forcing but are not included in this figure due to their episodic nature. The range for linear contrails does not include other possible effects of aviation on cloudiness. {2.9, Figure 2.20}*

[8] Halocarbon radiative forcing has been recently assessed in detail in *IPCC's Special Report on Safeguarding the Ozone Layer and the Global Climate System* (2005).

respective forcings of –0.2 [–0.4 to 0.0] and +0.1 [0.0 to +0.2] W m^{-2}. Additional terms smaller than ±0.1 W m^{-2} are shown in Figure SPM.2. {2.3, 2.5, 7.2}

- Changes in solar irradiance since 1750 are estimated to cause a radiative forcing of +0.12 [+0.06 to +0.30] W m^{-2}, which is less than half the estimate given in the TAR. {2.7}

Direct Observations of Recent Climate Change

Since the TAR, progress in understanding how climate is changing in space and in time has been gained through improvements and extensions of numerous datasets and data analyses, broader geographical coverage, better understanding of uncertainties, and a wider variety of measurements. Increasingly comprehensive observations are available for glaciers and snow cover since the 1960s, and for sea level and ice sheets since about the past decade. However, data coverage remains limited in some regions.

Warming of the climate system is unequivocal, as is now evident from observations of increases in global average air and ocean temperatures, widespread melting of snow and ice, and rising global average sea level (see Figure SPM.3). {3.2, 4.2, 5.5}

- Eleven of the last twelve years (1995–2006) rank among the 12 warmest years in the instrumental record of global surface temperature[9] (since 1850). The updated 100-year linear trend (1906 to 2005) of 0.74°C [0.56°C to 0.92°C] is therefore larger than the corresponding trend for 1901 to 2000 given in the TAR of 0.6°C [0.4°C to 0.8°C]. The linear warming trend over the last 50 years (0.13°C [0.10°C to 0.16°C] per decade) is nearly twice that for the last 100 years. The total temperature increase from 1850–1899 to 2001–2005 is 0.76°C [0.57°C to 0.95°C]. Urban heat island effects are real but local, and have a negligible influence (less than 0.006°C per decade over land and zero over the oceans) on these values. {3.2}

- New analyses of balloon-borne and satellite measurements of lower- and mid-tropospheric temperature show warming rates that are similar to those of the surface temperature record and are consistent within their respective uncertainties, largely reconciling a discrepancy noted in the TAR. {3.2, 3.4}

- The average atmospheric water vapour content has increased since at least the 1980s over land and ocean as well as in the upper troposphere. The increase is broadly consistent with the extra water vapour that warmer air can hold. {3.4}

- Observations since 1961 show that the average temperature of the global ocean has increased to depths of at least 3000 m and that the ocean has been absorbing more than 80% of the heat added to the climate system. Such warming causes seawater to expand, contributing to sea level rise (see Table SPM.1). {5.2, 5.5}

- Mountain glaciers and snow cover have declined on average in both hemispheres. Widespread decreases in glaciers and ice caps have contributed to sea level rise (ice caps do not include contributions from the Greenland and Antarctic Ice Sheets). (See Table SPM.1.) {4.6, 4.7, 4.8, 5.5}

- New data since the TAR now show that losses from the ice sheets of Greenland and Antarctica have *very likely* contributed to sea level rise over 1993 to 2003 (see Table SPM.1). Flow speed has increased for some Greenland and Antarctic outlet glaciers, which drain ice from the interior of the ice sheets. The corresponding increased ice sheet mass loss has often followed thinning, reduction or loss of ice shelves or loss of floating glacier tongues. Such dynamical ice loss is sufficient to explain most of the Antarctic net mass loss and approximately half of the Greenland net mass loss. The remainder of the ice loss from Greenland has occurred because losses due to melting have exceeded accumulation due to snowfall. {4.6, 4.8, 5.5}

- Global average sea level rose at an average rate of 1.8 [1.3 to 2.3] mm per year over 1961 to 2003. The rate was faster over 1993 to 2003: about 3.1 [2.4 to 3.8] mm per year. Whether the faster rate for 1993 to 2003 reflects decadal variability or an increase in the longer-term trend is unclear. There is *high confidence* that

[9] The average of near-surface air temperature over land and sea surface temperature.

Changes in Temperature, Sea Level and Northern Hemisphere Snow Cover

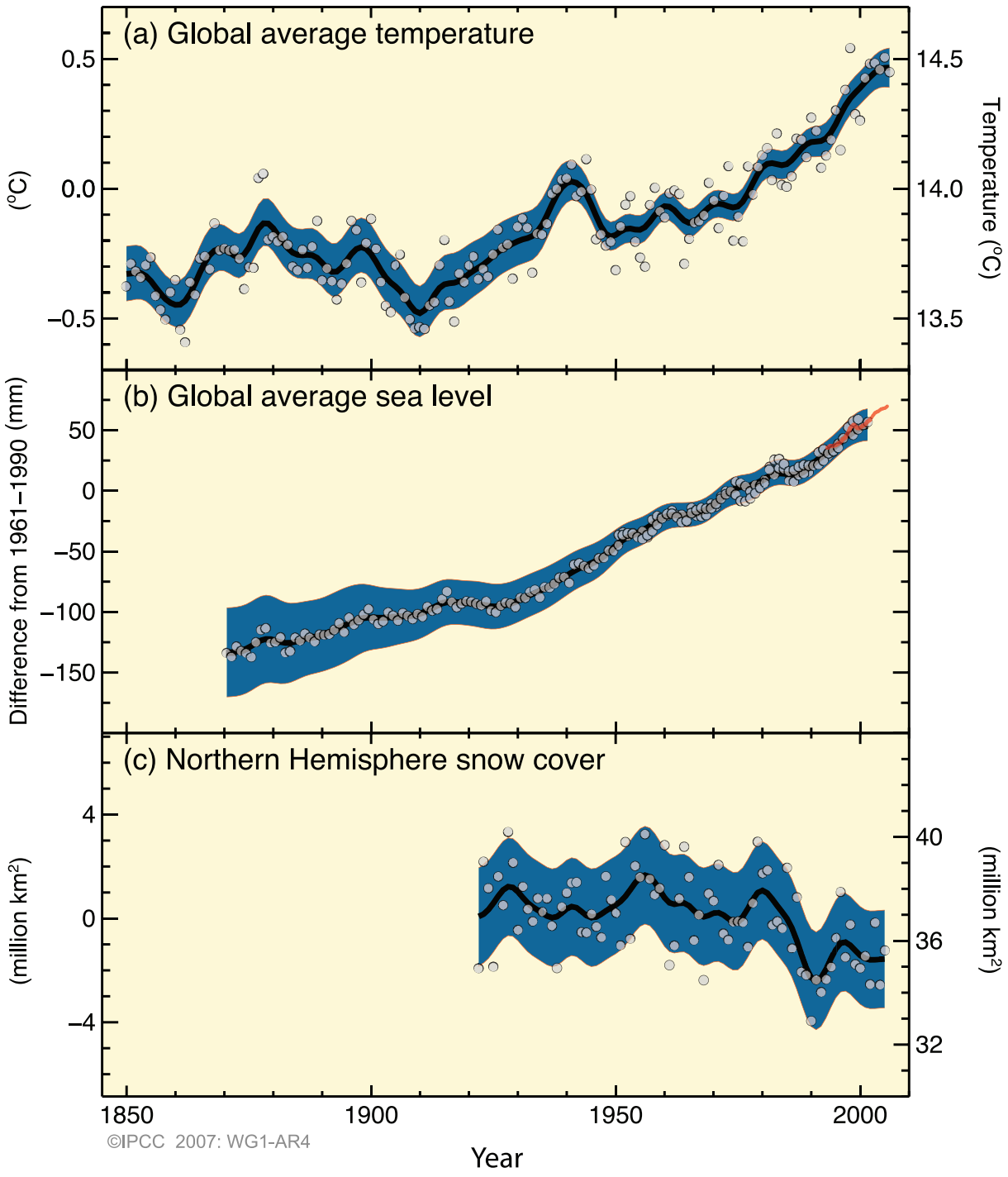


Figure SPM.3. *Observed changes in (a) global average surface temperature, (b) global average sea level from tide gauge (blue) and satellite (red) data and (c) Northern Hemisphere snow cover for March-April. All changes are relative to corresponding averages for the period 1961–1990. Smoothed curves represent decadal average values while circles show yearly values. The shaded areas are the uncertainty intervals estimated from a comprehensive analysis of known uncertainties (a and b) and from the time series (c). {FAQ 3.1, Figure 1, Figure 4.2, Figure 5.13}*

the rate of observed sea level rise increased from the 19th to the 20th century. The total 20th-century rise is estimated to be 0.17 [0.12 to 0.22] m. {5.5}

- For 1993 to 2003, the sum of the climate contributions is consistent within uncertainties with the total sea level rise that is directly observed (see Table SPM.1). These estimates are based on improved satellite and *in situ* data now available. For the period 1961 to 2003, the sum of climate contributions is estimated to be smaller than the observed sea level rise. The TAR reported a similar discrepancy for 1910 to 1990. {5.5}

At continental, regional and ocean basin scales, numerous long-term changes in climate have been observed. These include changes in arctic temperatures and ice, widespread changes in precipitation amounts, ocean salinity, wind patterns and aspects of extreme weather including droughts, heavy precipitation, heat waves and the intensity of tropical cyclones.[10] {3.2, 3.3, 3.4, 3.5, 3.6, 5.2}

- Average arctic temperatures increased at almost twice the global average rate in the past 100 years. Arctic temperatures have high decadal variability, and a warm period was also observed from 1925 to 1945. {3.2}

- Satellite data since 1978 show that annual average arctic sea ice extent has shrunk by 2.7 [2.1 to 3.3]% per decade, with larger decreases in summer of 7.4 [5.0 to 9.8]% per decade. These values are consistent with those reported in the TAR. {4.4}

- Temperatures at the top of the permafrost layer have generally increased since the 1980s in the Arctic (by up to 3°C). The maximum area covered by seasonally frozen ground has decreased by about 7% in the Northern Hemisphere since 1900, with a decrease in spring of up to 15%. {4.7}

- Long-term trends from 1900 to 2005 have been observed in precipitation amount over many large regions.[11] Significantly increased precipitation has been observed in eastern parts of North and South America, northern Europe and northern and central Asia. Drying has been observed in the Sahel, the Mediterranean, southern Africa and parts of southern Asia. Precipitation is highly variable spatially and temporally, and data are limited in some regions. Long-term trends have not been observed for the other large regions assessed.[11] {3.3, 3.9}

- Changes in precipitation and evaporation over the oceans are suggested by freshening of mid- and high-latitude waters together with increased salinity in low-latitude waters. {5.2}

Table SPM.1. *Observed rate of sea level rise and estimated contributions from different sources. {5.5, Table 5.3}*

Source of sea level rise	Rate of sea level rise (mm per year) 1961–2003	1993–2003
Thermal expansion	0.42 ± 0.12	1.6 ± 0.5
Glaciers and ice caps	0.50 ± 0.18	0.77 ± 0.22
Greenland Ice Sheet	0.05 ± 0.12	0.21 ± 0.07
Antarctic Ice Sheet	0.14 ± 0.41	0.21 ± 0.35
Sum of individual climate contributions to sea level rise	1.1 ± 0.5	2.8 ± 0.7
Observed total sea level rise	1.8 ± 0.5[a]	3.1 ± 0.7[a]
Difference (Observed minus sum of estimated climate contributions)	0.7 ± 0.7	0.3 ± 1.0

Table note:
[a] Data prior to 1993 are from tide gauges and after 1993 are from satellite altimetry.

[10] Tropical cyclones include hurricanes and typhoons.

[11] The assessed regions are those considered in the regional projections chapter of the TAR and in Chapter 11 of this report.

- Mid-latitude westerly winds have strengthened in both hemispheres since the 1960s. {3.5}

- More intense and longer droughts have been observed over wider areas since the 1970s, particularly in the tropics and subtropics. Increased drying linked with higher temperatures and decreased precipitation has contributed to changes in drought. Changes in sea surface temperatures, wind patterns and decreased snowpack and snow cover have also been linked to droughts. {3.3}

- The frequency of heavy precipitation events has increased over most land areas, consistent with warming and observed increases of atmospheric water vapour. {3.8, 3.9}

- Widespread changes in extreme temperatures have been observed over the last 50 years. Cold days, cold nights and frost have become less frequent, while hot days, hot nights and heat waves have become more frequent (see Table SPM.2). {3.8}

Table SPM.2. *Recent trends, assessment of human influence on the trend and projections for extreme weather events for which there is an observed late-20th century trend. {Tables 3.7, 3.8, 9.4; Sections 3.8, 5.5, 9.7, 11.2–11.9}*

Phenomenon[a] and direction of trend	Likelihood that trend occurred in late 20th century (typically post 1960)	Likelihood of a human contribution to observed trend[b]	Likelihood of future trends based on projections for 21st century using SRES scenarios
Warmer and fewer cold days and nights over most land areas	*Very likely*[c]	*Likely*[d]	*Virtually certain*[d]
Warmer and more frequent hot days and nights over most land areas	*Very likely*[e]	*Likely (nights)*[d]	*Virtually certain*[d]
Warm spells/heat waves. Frequency increases over most land areas	*Likely*	*More likely than not*[f]	*Very likely*
Heavy precipitation events. Frequency (or proportion of total rainfall from heavy falls) increases over most areas	*Likely*	*More likely than not*[f]	*Very likely*
Area affected by droughts increases	*Likely* in many regions since 1970s	*More likely than not*	*Likely*
Intense tropical cyclone activity increases	*Likely* in some regions since 1970	*More likely than not*[f]	*Likely*
Increased incidence of extreme high sea level (excludes tsunamis)[g]	*Likely*	*More likely than not*[f,h]	*Likely*[i]

Table notes:

[a] See Table 3.7 for further details regarding definitions.

[b] See Table TS.4, Box TS.5 and Table 9.4.

[c] Decreased frequency of cold days and nights (coldest 10%).

[d] Warming of the most extreme days and nights each year.

[e] Increased frequency of hot days and nights (hottest 10%).

[f] Magnitude of anthropogenic contributions not assessed. Attribution for these phenomena based on expert judgement rather than formal attribution studies.

[g] Extreme high sea level depends on average sea level and on regional weather systems. It is defined here as the highest 1% of hourly values of observed sea level at a station for a given reference period.

[h] Changes in observed extreme high sea level closely follow the changes in average sea level. {5.5} It is *very likely* that anthropogenic activity contributed to a rise in average sea level. {9.5}

[i] In all scenarios, the projected global average sea level at 2100 is higher than in the reference period. {10.6} The effect of changes in regional weather systems on sea level extremes has not been assessed.

- There is observational evidence for an increase in intense tropical cyclone activity in the North Atlantic since about 1970, correlated with increases of tropical sea surface temperatures. There are also suggestions of increased intense tropical cyclone activity in some other regions where concerns over data quality are greater. Multi-decadal variability and the quality of the tropical cyclone records prior to routine satellite observations in about 1970 complicate the detection of long-term trends in tropical cyclone activity. There is no clear trend in the annual numbers of tropical cyclones. {3.8}

Some aspects of climate have not been observed to change. {3.2, 3.8, 4.4, 5.3}

- A decrease in diurnal temperature range (DTR) was reported in the TAR, but the data available then extended only from 1950 to 1993. Updated observations reveal that DTR has not changed from 1979 to 2004 as both day- and night-time temperature have risen at about the same rate. The trends are highly variable from one region to another. {3.2}

- Antarctic sea ice extent continues to show interannual variability and localised changes but no statistically significant average trends, consistent with the lack of warming reflected in atmospheric temperatures averaged across the region. {3.2, 4.4}

- There is insufficient evidence to determine whether trends exist in the meridional overturning circulation (MOC) of the global ocean or in small-scale phenomena such as tornadoes, hail, lightning and dust-storms. {3.8, 5.3}

A Palaeoclimatic Perspective

Palaeoclimatic studies use changes in climatically sensitive indicators to infer past changes in global climate on time scales ranging from decades to millions of years. Such proxy data (e.g., tree ring width) may be influenced by both local temperature and other factors such as precipitation, and are often representative of particular seasons rather than full years. Studies since the TAR draw increased confidence from additional data showing coherent behaviour across multiple indicators in different parts of the world. However, uncertainties generally increase with time into the past due to increasingly limited spatial coverage.

Palaeoclimatic information supports the interpretation that the warmth of the last half century is unusual in at least the previous 1,300 years. The last time the polar regions were significantly warmer than present for an extended period (about 125,000 years ago), reductions in polar ice volume led to 4 to 6 m of sea level rise. {6.4, 6.6}

- Average Northern Hemisphere temperatures during the second half of the 20th century were *very likely* higher than during any other 50-year period in the last 500 years and *likely* the highest in at least the past 1,300 years. Some recent studies indicate greater variability in Northern Hemisphere temperatures than suggested in the TAR, particularly finding that cooler periods existed in the 12th to 14th, 17th and 19th centuries. Warmer periods prior to the 20th century are within the uncertainty range given in the TAR. {6.6}

- Global average sea level in the last interglacial period (about 125,000 years ago) was *likely* 4 to 6 m higher than during the 20th century, mainly due to the retreat of polar ice. Ice core data indicate that average polar temperatures at that time were 3°C to 5°C higher than present, because of differences in the Earth's orbit. The Greenland Ice Sheet and other arctic ice fields *likely* contributed no more than 4 m of the observed sea level rise. There may also have been a contribution from Antarctica. {6.4}

Understanding and Attributing Climate Change

This assessment considers longer and improved records, an expanded range of observations and improvements in the simulation of many aspects of climate and its variability based on studies since the TAR. It also considers the results of new attribution studies that have evaluated whether observed changes are quantitatively consistent with the expected response to external forcings and inconsistent with alternative physically plausible explanations.

Most of the observed increase in global average temperatures since the mid-20th century is *very likely* due to the observed increase in anthropogenic greenhouse gas concentrations.[12] This is an advance since the TAR's conclusion that "most of the observed warming over the last 50 years is *likely* to have been due to the increase in greenhouse gas concentrations". Discernible human influences now extend to other aspects of climate, including ocean warming, continental-average temperatures, temperature extremes and wind patterns (see Figure SPM.4 and Table SPM.2). {9.4, 9.5}

- It is *likely* that increases in greenhouse gas concentrations alone would have caused more warming than observed because volcanic and anthropogenic aerosols have offset some warming that would otherwise have taken place. {2.9, 7.5, 9.4}

- The observed widespread warming of the atmosphere and ocean, together with ice mass loss, support the conclusion that it is *extremely unlikely* that global climate change of the past 50 years can be explained without external forcing, and *very likely* that it is not due to known natural causes alone. {4.8, 5.2, 9.4, 9.5, 9.7}

- Warming of the climate system has been detected in changes of surface and atmospheric temperatures in the upper several hundred metres of the ocean, and in contributions to sea level rise. Attribution studies have established anthropogenic contributions to all of these changes. The observed pattern of tropospheric warming and stratospheric cooling is *very likely* due to the combined influences of greenhouse gas increases and stratospheric ozone depletion. {3.2, 3.4, 9.4, 9.5}

- It is *likely* that there has been significant anthropogenic warming over the past 50 years averaged over each continent except Antarctica (see Figure SPM.4). The observed patterns of warming, including greater warming over land than over the ocean, and their changes over time, are only simulated by models that include anthropogenic forcing. The ability of coupled climate models to simulate the observed temperature evolution on each of six continents provides stronger evidence of human influence on climate than was available in the TAR. {3.2, 9.4}

- Difficulties remain in reliably simulating and attributing observed temperature changes at smaller scales. On these scales, natural climate variability is relatively larger, making it harder to distinguish changes expected due to external forcings. Uncertainties in local forcings and feedbacks also make it difficult to estimate the contribution of greenhouse gas increases to observed small-scale temperature changes. {8.3, 9.4}

- Anthropogenic forcing is *likely* to have contributed to changes in wind patterns,[13] affecting extra-tropical storm tracks and temperature patterns in both hemispheres. However, the observed changes in the Northern Hemisphere circulation are larger than simulated in response to 20th-century forcing change. {3.5, 3.6, 9.5, 10.3}

- Temperatures of the most extreme hot nights, cold nights and cold days are *likely* to have increased due to anthropogenic forcing. It is *more likely than not* that anthropogenic forcing has increased the risk of heat waves (see Table SPM.2). {9.4}

[12] Consideration of remaining uncertainty is based on current methodologies.

[13] In particular, the Southern and Northern Annular Modes and related changes in the North Atlantic Oscillation. {3.6, 9.5, Box TS.2}

Global and Continental Temperature Change

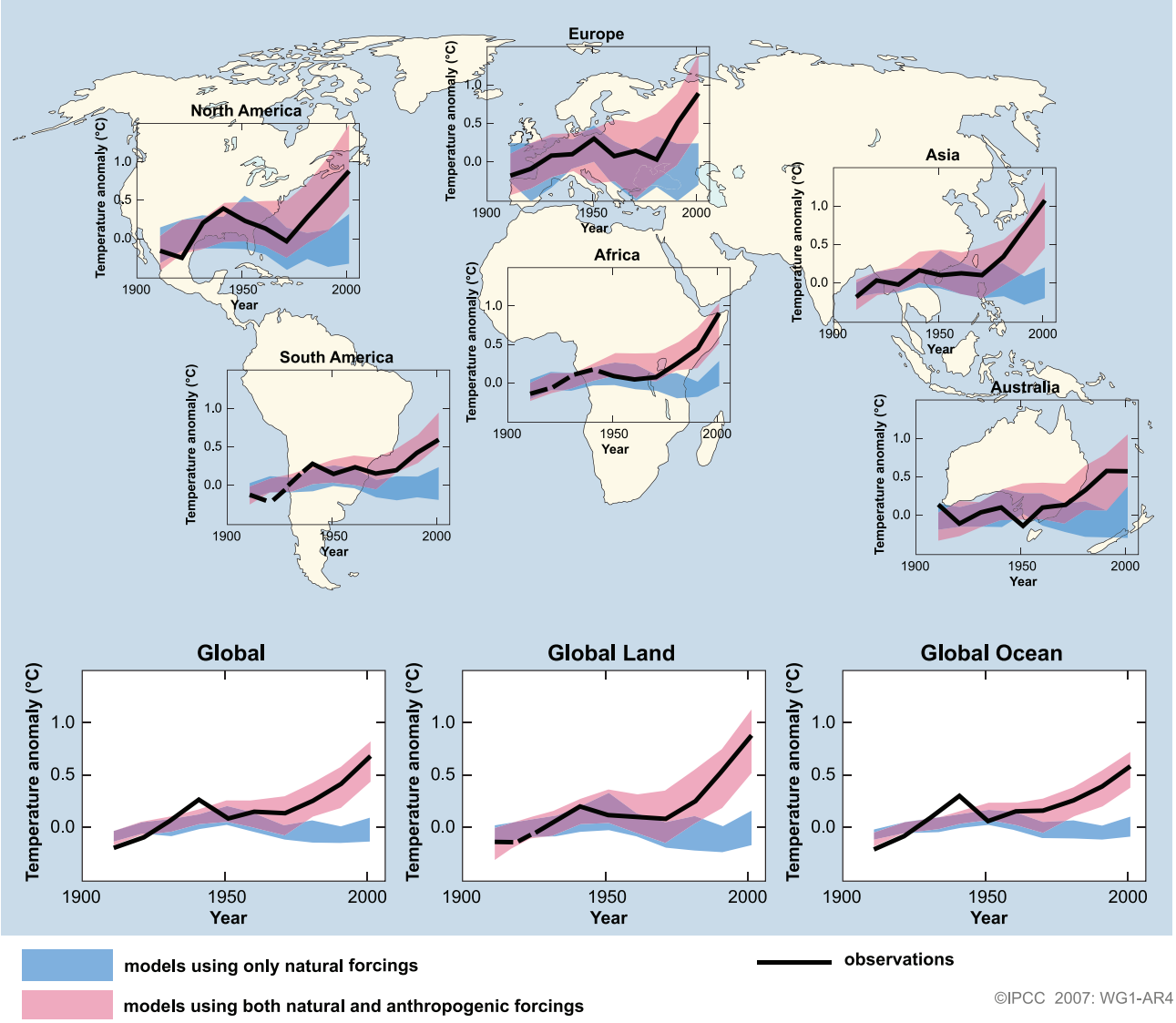


Figure SPM.4. *Comparison of observed continental- and global-scale changes in surface temperature with results simulated by climate models using natural and anthropogenic forcings. Decadal averages of observations are shown for the period 1906 to 2005 (black line) plotted against the centre of the decade and relative to the corresponding average for 1901–1950. Lines are dashed where spatial coverage is less than 50%. Blue shaded bands show the 5–95% range for 19 simulations from five climate models using only the natural forcings due to solar activity and volcanoes. Red shaded bands show the 5–95% range for 58 simulations from 14 climate models using both natural and anthropogenic forcings. {FAQ 9.2, Figure 1}*

Analysis of climate models together with constraints from observations enables an assessed *likely* range to be given for climate sensitivity for the first time and provides increased confidence in the understanding of the climate system response to radiative forcing. {6.6, 8.6, 9.6, Box 10.2}

- The equilibrium climate sensitivity is a measure of the climate system response to sustained radiative forcing. It is not a projection but is defined as the global average surface warming following a doubling of carbon dioxide concentrations. It is *likely* to be in the range 2°C to 4.5°C with a best estimate of about 3°C, and is *very unlikely* to be less than 1.5°C. Values substantially higher than 4.5°C cannot be excluded, but agreement of models with observations is not as good for those values. Water vapour changes represent the largest feedback affecting climate sensitivity and are now better understood than in the TAR. Cloud feedbacks remain the largest source of uncertainty. {8.6, 9.6, Box 10.2}

- It is *very unlikely* that climate changes of at least the seven centuries prior to 1950 were due to variability generated within the climate system alone. A significant fraction of the reconstructed Northern Hemisphere inter-decadal temperature variability over those centuries is *very likely* attributable to volcanic eruptions and changes in solar irradiance, and it is *likely* that anthropogenic forcing contributed to the early 20th-century warming evident in these records. {2.7, 2.8, 6.6, 9.3}

Projections of Future Changes in Climate

A major advance of this assessment of climate change projections compared with the TAR is the large number of simulations available from a broader range of models. Taken together with additional information from observations, these provide a quantitative basis for estimating likelihoods for many aspects of future climate change. Model simulations cover a range of possible futures including idealised emission or concentration assumptions. These include SRES[14] illustrative marker scenarios for the 2000 to 2100 period and model experiments with greenhouse gases and aerosol concentrations held constant after year 2000 or 2100.

For the next two decades, a warming of about 0.2°C per decade is projected for a range of SRES emission scenarios. Even if the concentrations of all greenhouse gases and aerosols had been kept constant at year 2000 levels, a further warming of about 0.1°C per decade would be expected. {10.3, 10.7}

- Since IPCC's first report in 1990, assessed projections have suggested global average temperature increases between about 0.15°C and 0.3°C per decade for 1990 to 2005. This can now be compared with observed values of about 0.2°C per decade, strengthening confidence in near-term projections. {1.2, 3.2}

- Model experiments show that even if all radiative forcing agents were held constant at year 2000 levels, a further warming trend would occur in the next two decades at a rate of about 0.1°C per decade, due mainly to the slow response of the oceans. About twice as much warming (0.2°C per decade) would be expected if emissions are within the range of the SRES scenarios. Best-estimate projections from models indicate that decadal average warming over each inhabited continent by 2030 is insensitive to the choice among SRES scenarios and is *very likely* to be at least twice as large as the corresponding model-estimated natural variability during the 20th century. {9.4, 10.3, 10.5, 11.2–11.7, Figure TS-29}

[14] SRES refers to the *IPCC Special Report on Emission Scenarios* (2000). The SRES scenario families and illustrative cases, which did not include additional climate initiatives, are summarised in a box at the end of this Summary for Policymakers. Approximate carbon dioxide equivalent concentrations corresponding to the computed radiative forcing due to anthropogenic greenhouse gases and aerosols in 2100 (see p. 823 of the TAR) for the SRES B1, A1T, B2, A1B, A2 and A1FI illustrative marker scenarios are about 600, 700, 800, 850, 1250 and 1,550 ppm respectively. Scenarios B1, A1B and A2 have been the focus of model intercomparison studies and many of those results are assessed in this report.

Continued greenhouse gas emissions at or above current rates would cause further warming and induce many changes in the global climate system during the 21st century that would *very likely* be larger than those observed during the 20th century. {10.3}

- Advances in climate change modelling now enable best estimates and *likely* assessed uncertainty ranges to be given for projected warming for different emission scenarios. Results for different emission scenarios are provided explicitly in this report to avoid loss of this policy-relevant information. Projected global average surface warmings for the end of the 21st century (2090–2099) relative to 1980–1999 are shown in Table SPM.3. These illustrate the differences between lower and higher SRES emission scenarios, and the projected warming uncertainty associated with these scenarios. {10.5}

- Best estimates and *likely* ranges for global average surface air warming for six SRES emissions marker scenarios are given in this assessment and are shown in Table SPM.3. For example, the best estimate for the low scenario (B1) is 1.8°C (*likely* range is 1.1°C to 2.9°C), and the best estimate for the high scenario (A1FI) is 4.0°C (*likely* range is 2.4°C to 6.4°C). Although these projections are broadly consistent with the span quoted in the TAR (1.4°C to 5.8°C), they are not directly comparable (see Figure SPM.5). The Fourth Assessment Report is more advanced as it provides best estimates and an assessed likelihood range for each of the marker scenarios. The new assessment of the *likely* ranges now relies on a larger number of climate models of increasing complexity and realism, as well as new information regarding the nature of feedbacks from the carbon cycle and constraints on climate response from observations. {10.5}

- Warming tends to reduce land and ocean uptake of atmospheric carbon dioxide, increasing the fraction of anthropogenic emissions that remains in the atmosphere. For the A2 scenario, for example, the climate-carbon cycle feedback increases the corresponding global average warming at 2100 by more than 1°C. Assessed upper ranges for temperature projections are larger than in the TAR (see Table SPM.3) mainly because the broader range of models now available suggests stronger climate-carbon cycle feedbacks. {7.3, 10.5}

- Model-based projections of global average sea level rise at the end of the 21st century (2090–2099) are shown in Table SPM.3. For each scenario, the midpoint of the range in Table SPM.3 is within 10% of the

Table SPM.3. *Projected global average surface warming and sea level rise at the end of the 21st century. {10.5, 10.6, Table 10.7}*

	Temperature Change (°C at 2090-2099 relative to 1980-1999)[a]		Sea Level Rise (m at 2090-2099 relative to 1980-1999)
Case	Best estimate	*Likely* range	Model-based range excluding future rapid dynamical changes in ice flow
Constant Year 2000 concentrations[b]	0.6	0.3 – 0.9	NA
B1 scenario	1.8	1.1 – 2.9	0.18 – 0.38
A1T scenario	2.4	1.4 – 3.8	0.20 – 0.45
B2 scenario	2.4	1.4 – 3.8	0.20 – 0.43
A1B scenario	2.8	1.7 – 4.4	0.21 – 0.48
A2 scenario	3.4	2.0 – 5.4	0.23 – 0.51
A1FI scenario	4.0	2.4 – 6.4	0.26 – 0.59

Table notes:
[a] These estimates are assessed from a hierarchy of models that encompass a simple climate model, several Earth System Models of Intermediate Complexity and a large number of Atmosphere-Ocean General Circulation Models (AOGCMs).
[b] Year 2000 constant composition is derived from AOGCMs only.

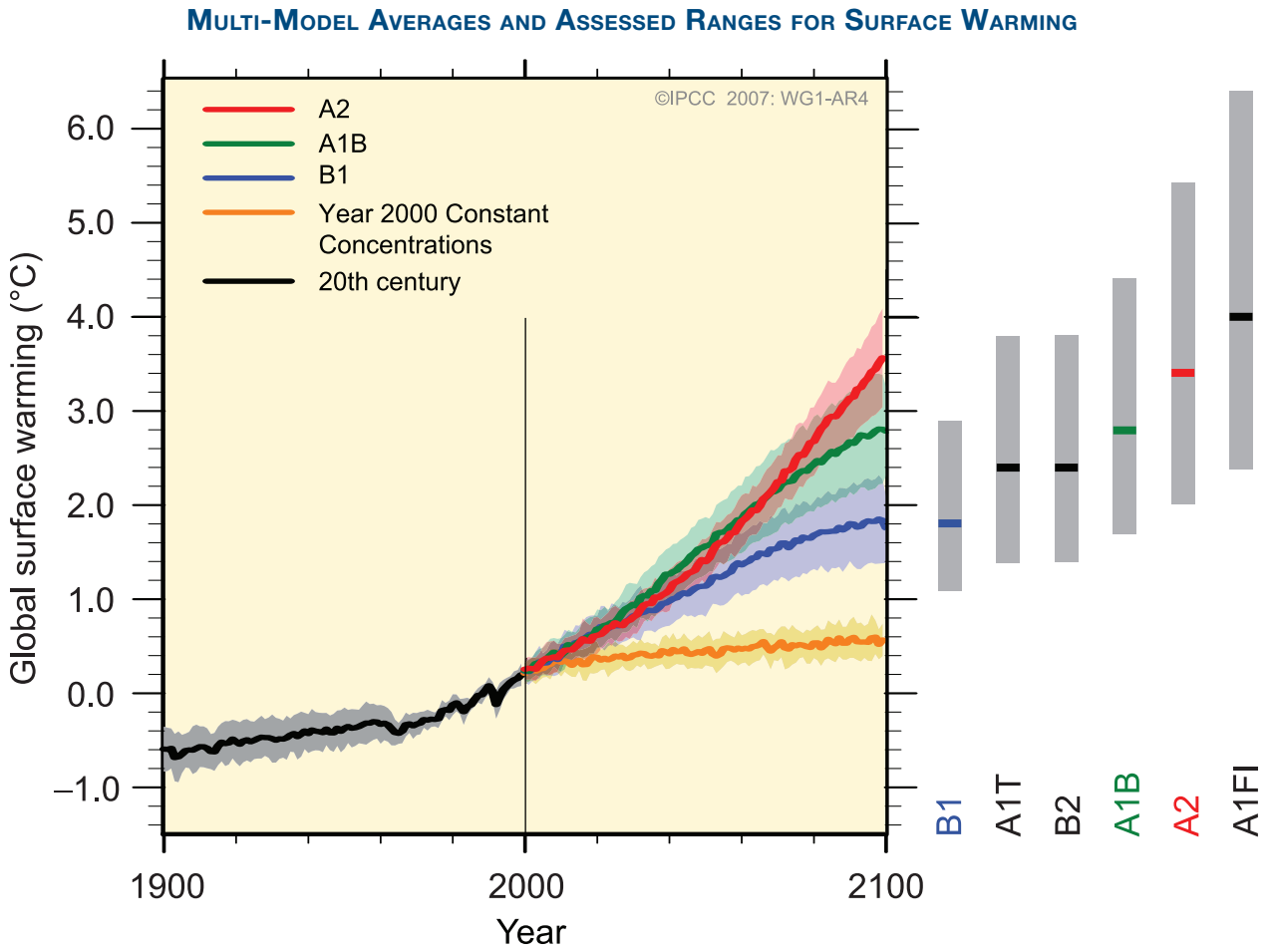


Figure SPM.5. *Solid lines are multi-model global averages of surface warming (relative to 1980–1999) for the scenarios A2, A1B and B1, shown as continuations of the 20th century simulations. Shading denotes the ±1 standard deviation range of individual model annual averages. The orange line is for the experiment where concentrations were held constant at year 2000 values. The grey bars at right indicate the best estimate (solid line within each bar) and the **likely** range assessed for the six SRES marker scenarios. The assessment of the best estimate and **likely** ranges in the grey bars includes the AOGCMs in the left part of the figure, as well as results from a hierarchy of independent models and observational constraints. {Figures 10.4 and 10.29}*

TAR model average for 2090–2099. The ranges are narrower than in the TAR mainly because of improved information about some uncertainties in the projected contributions.[15] {10.6}

- Models used to date do not include uncertainties in climate-carbon cycle feedback nor do they include the full effects of changes in ice sheet flow, because a basis in published literature is lacking. The projections include a contribution due to increased ice flow from Greenland and Antarctica at the rates observed for 1993 to 2003, but these flow rates could increase or decrease in the future. For example, if this contribution were to grow linearly with global average temperature change, the upper ranges of sea level rise for SRES scenarios shown in Table SPM.3 would increase by 0.1 to 0.2 m. Larger values cannot be excluded, but understanding of these effects is too limited to assess their likelihood or provide a best estimate or an upper bound for sea level rise. {10.6}

- Increasing atmospheric carbon dioxide concentrations lead to increasing acidification of the ocean. Projections based on SRES scenarios give reductions in average global surface ocean pH[16] of between 0.14 and 0.35 units over the 21st century, adding to the present decrease of 0.1 units since pre-industrial times. {5.4, Box 7.3, 10.4}

[15] TAR projections were made for 2100, whereas projections in this report are for 2090–2099. The TAR would have had similar ranges to those in Table SPM.3 if it had treated the uncertainties in the same way.

[16] Decreases in pH correspond to increases in acidity of a solution. See Glossary for further details.

There is now higher confidence in projected patterns of warming and other regional-scale features, including changes in wind patterns, precipitation and some aspects of extremes and of ice. {8.2, 8.3, 8.4, 8.5, 9.4, 9.5, 10.3, 11.1}

- Projected warming in the 21st century shows scenario-independent geographical patterns similar to those observed over the past several decades. Warming is expected to be greatest over land and at most high northern latitudes, and least over the Southern Ocean and parts of the North Atlantic Ocean (see Figure SPM.6). {10.3}

- Snow cover is projected to contract. Widespread increases in thaw depth are projected over most permafrost regions. {10.3, 10.6}

- Sea ice is projected to shrink in both the Arctic and Antarctic under all SRES scenarios. In some projections, arctic late-summer sea ice disappears almost entirely by the latter part of the 21st century. {10.3}

- It is *very likely* that hot extremes, heat waves and heavy precipitation events will continue to become more frequent. {10.3}

- Based on a range of models, it is *likely* that future tropical cyclones (typhoons and hurricanes) will become more intense, with larger peak wind speeds and more heavy precipitation associated with ongoing increases of tropical sea surface temperatures. There is less confidence in projections of a global decrease in numbers of tropical cyclones. The apparent increase in the proportion of very intense storms since 1970 in some regions is much larger than simulated by current models for that period. {9.5, 10.3, 3.8}

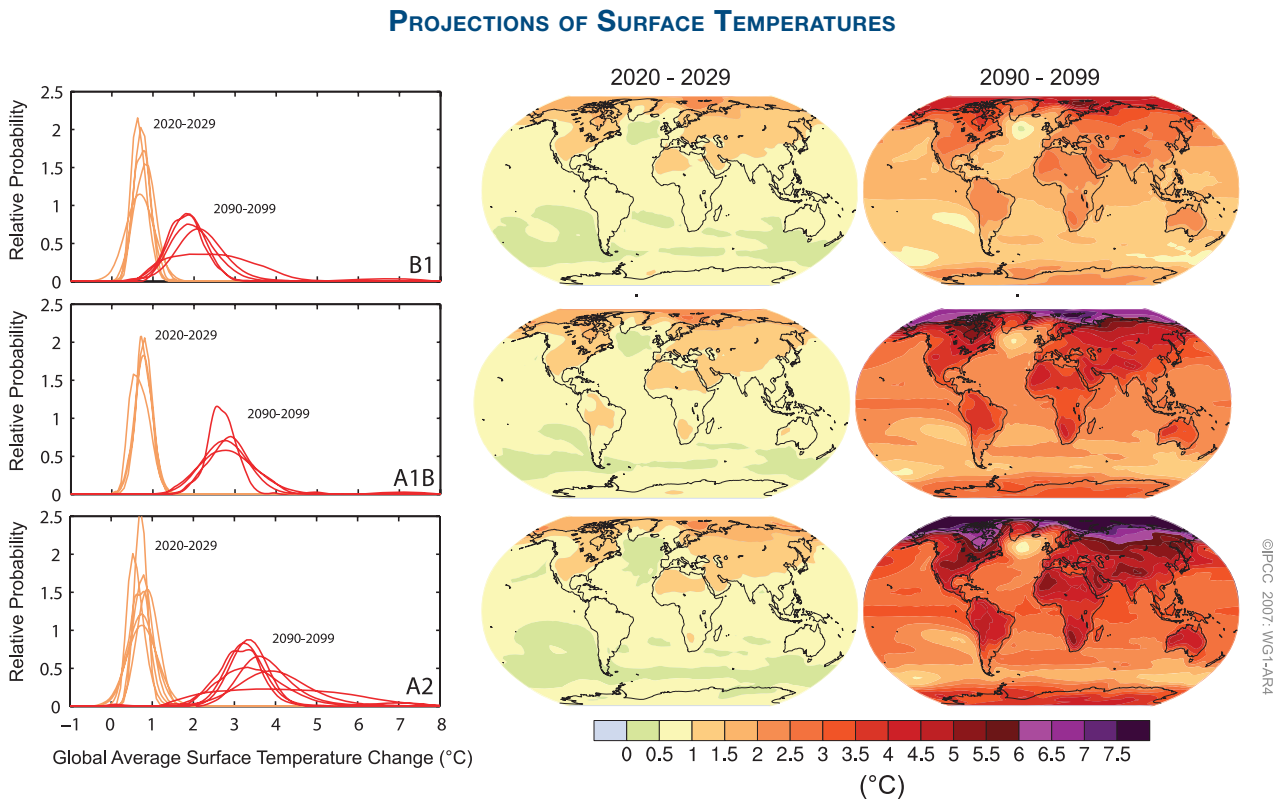


Figure SPM.6. *Projected surface temperature changes for the early and late 21st century relative to the period 1980–1999. The central and right panels show the AOGCM multi-model average projections for the B1 (top), A1B (middle) and A2 (bottom) SRES scenarios averaged over the decades 2020–2029 (centre) and 2090–2099 (right). The left panels show corresponding uncertainties as the relative probabilities of estimated global average warming from several different AOGCM and Earth System Model of Intermediate Complexity studies for the same periods. Some studies present results only for a subset of the SRES scenarios, or for various model versions. Therefore the difference in the number of curves shown in the left-hand panels is due only to differences in the availability of results. {Figures 10.8 and 10.28}*

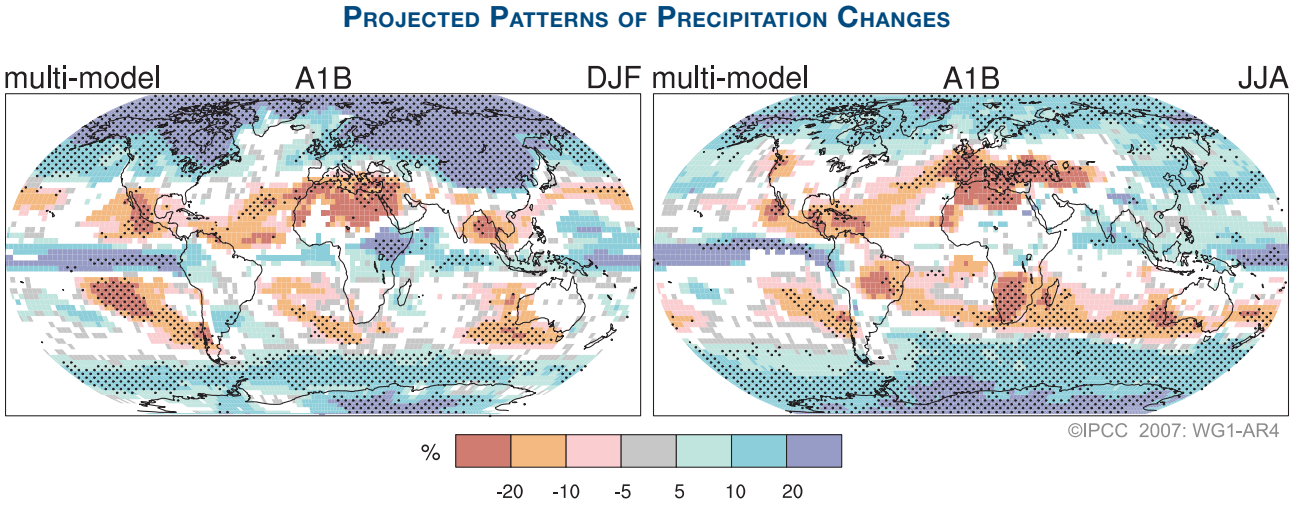


Figure SPM.7. *Relative changes in precipitation (in percent) for the period 2090–2099, relative to 1980–1999. Values are multi-model averages based on the SRES A1B scenario for December to February (left) and June to August (right). White areas are where less than 66% of the models agree in the sign of the change and stippled areas are where more than 90% of the models agree in the sign of the change. {Figure 10.9}*

- Extratropical storm tracks are projected to move poleward, with consequent changes in wind, precipitation and temperature patterns, continuing the broad pattern of observed trends over the last half-century. {3.6, 10.3}

- Since the TAR, there is an improving understanding of projected patterns of precipitation. Increases in the amount of precipitation are *very likely* in high latitudes, while decreases are *likely* in most subtropical land regions (by as much as about 20% in the A1B scenario in 2100, see Figure SPM.7), continuing observed patterns in recent trends. {3.3, 8.3, 9.5, 10.3, 11.2 to 11.9}

- Based on current model simulations, it is *very likely* that the meridional overturning circulation (MOC) of the Atlantic Ocean will slow down during the 21st century. The multi-model average reduction by 2100 is 25% (range from zero to about 50%) for SRES emission scenario A1B. Temperatures in the Atlantic region are projected to increase despite such changes due to the much larger warming associated with projected increases in greenhouse gases. It is *very unlikely* that the MOC will undergo a large abrupt transition during the 21st century. Longer-term changes in the MOC cannot be assessed with confidence. {10.3, 10.7}

Anthropogenic warming and sea level rise would continue for centuries due to the time scales associated with climate processes and feedbacks, even if greenhouse gas concentrations were to be stabilised. {10.4, 10.5, 10.7}

- Climate-carbon cycle coupling is expected to add carbon dioxide to the atmosphere as the climate system warms, but the magnitude of this feedback is uncertain. This increases the uncertainty in the trajectory of carbon dioxide emissions required to achieve a particular stabilisation level of atmospheric carbon dioxide concentration. Based on current understanding of climate-carbon cycle feedback, model studies suggest that to stabilise at 450 ppm carbon dioxide could require that cumulative emissions over the 21st century be reduced from an average of approximately 670 [630 to 710] GtC (2460 [2310 to 2600] $GtCO_2$) to approximately 490 [375 to 600] GtC (1800 [1370 to 2200] $GtCO_2$). Similarly, to stabilise at 1000 ppm, this feedback could require that cumulative emissions be reduced from a model average of approximately 1415 [1340 to 1490] GtC (5190 [4910 to 5460] $GtCO_2$) to approximately 1100 [980 to 1250] GtC (4030 [3590 to 4580] $GtCO_2$). {7.3, 10.4}

- If radiative forcing were to be stabilised in 2100 at B1 or A1B levels[14] a further increase in global average temperature of about 0.5°C would still be expected, mostly by 2200. {10.7}

- If radiative forcing were to be stabilised in 2100 at A1B levels[14], thermal expansion alone would lead to 0.3 to 0.8 m of sea level rise by 2300 (relative to 1980–1999). Thermal expansion would continue for many centuries, due to the time required to transport heat into the deep ocean. {10.7}

- Contraction of the Greenland Ice Sheet is projected to continue to contribute to sea level rise after 2100. Current models suggest that ice mass losses increase with temperature more rapidly than gains due to precipitation and that the surface mass balance becomes negative at a global average warming (relative to pre-industrial values) in excess of 1.9°C to 4.6°C. If a negative surface mass balance were sustained for millennia, that would lead to virtually complete elimination of the Greenland Ice Sheet and a resulting contribution to sea level rise of about 7 m. The corresponding future temperatures in Greenland are comparable to those inferred for the last interglacial period 125,000 years ago, when palaeoclimatic information suggests reductions of polar land ice extent and 4 to 6 m of sea level rise. {6.4, 10.7}

- Dynamical processes related to ice flow not included in current models but suggested by recent observations could increase the vulnerability of the ice sheets to warming, increasing future sea level rise. Understanding of these processes is limited and there is no consensus on their magnitude. {4.6, 10.7}

- Current global model studies project that the Antarctic Ice Sheet will remain too cold for widespread surface melting and is expected to gain in mass due to increased snowfall. However, net loss of ice mass could occur if dynamical ice discharge dominates the ice sheet mass balance. {10.7}

- Both past and future anthropogenic carbon dioxide emissions will continue to contribute to warming and sea level rise for more than a millennium, due to the time scales required for removal of this gas from the atmosphere. {7.3, 10.3}

The Emission Scenarios of the IPCC Special Report on Emission Scenarios (SRES)[17]

A1. The A1 storyline and scenario family describes a future world of very rapid economic growth, global population that peaks in mid-century and declines thereafter, and the rapid introduction of new and more efficient technologies. Major underlying themes are convergence among regions, capacity building and increased cultural and social interactions, with a substantial reduction in regional differences in per capita income. The A1 scenario family develops into three groups that describe alternative directions of technological change in the energy system. The three A1 groups are distinguished by their technological emphasis: fossil-intensive (A1FI), non-fossil energy sources (A1T) or a balance across all sources (A1B) (where balanced is defined as not relying too heavily on one particular energy source, on the assumption that similar improvement rates apply to all energy supply and end use technologies).

A2. The A2 storyline and scenario family describes a very heterogeneous world. The underlying theme is self-reliance and preservation of local identities. Fertility patterns across regions converge very slowly, which results in continuously increasing population. Economic development is primarily regionally oriented and per capita economic growth and technological change more fragmented and slower than other storylines.

B1. The B1 storyline and scenario family describes a convergent world with the same global population, that peaks in mid-century and declines thereafter, as in the A1 storyline, but with rapid change in economic structures toward a service and information economy, with reductions in material intensity and the introduction of clean and resource-efficient technologies. The emphasis is on global solutions to economic, social and environmental sustainability, including improved equity, but without additional climate initiatives.

B2. The B2 storyline and scenario family describes a world in which the emphasis is on local solutions to economic, social and environmental sustainability. It is a world with continuously increasing global population, at a rate lower than A2, intermediate levels of economic development, and less rapid and more diverse technological change than in the B1 and A1 storylines. While the scenario is also oriented towards environmental protection and social equity, it focuses on local and regional levels.

An illustrative scenario was chosen for each of the six scenario groups A1B, A1FI, A1T, A2, B1 and B2. All should be considered equally sound.

The SRES scenarios do not include additional climate initiatives, which means that no scenarios are included that explicitly assume implementation of the United Nations Framework Convention on Climate Change or the emissions targets of the Kyoto Protocol.

[17] Emission scenarios are not assessed in this Working Group I Report of the IPCC. This box summarising the SRES scenarios is taken from the TAR and has been subject to prior line-by-line approval by the Panel.

A report accepted by Working Group I of the Intergovernmental Panel on Climate Change but not approved in detail

"Acceptance" of IPCC Reports at a Session of the Working Group or Panel signifies that the material has not been subject to line-by-line discussion and agreement, but nevertheless presents a comprehensive, objective and balanced view of the subject matter.

Technical Summary

Coordinating Lead Authors:

Susan Solomon (USA), Dahe Qin (China), Martin Manning (USA, New Zealand)

Lead Authors:

Richard B. Alley (USA), Terje Berntsen (Norway), Nathaniel L. Bindoff (Australia), Zhenlin Chen (China), Amnat Chidthaisong (Thailand), Jonathan M. Gregory (UK), Gabriele C. Hegerl (USA, Germany), Martin Heimann (Germany, Switzerland), Bruce Hewitson (South Africa), Brian J. Hoskins (UK), Fortunat Joos (Switzerland), Jean Jouzel (France), Vladimir Kattsov (Russia), Ulrike Lohmann (Switzerland), Taroh Matsuno (Japan), Mario Molina (USA, Mexico), Neville Nicholls (Australia), Jonathan Overpeck (USA), Graciela Raga (Mexico, Argentina), Venkatachalam Ramaswamy (USA), Jiawen Ren (China), Matilde Rusticucci (Argentina), Richard Somerville (USA), Thomas F. Stocker (Switzerland), Ronald J. Stouffer (USA), Penny Whetton (Australia), Richard A. Wood (UK), David Wratt (New Zealand)

Contributing Authors:

J. Arblaster (USA, Australia), G. Brasseur (USA, Germany), J.H. Christensen (Denmark), K.L. Denman (Canada), D.W. Fahey (USA), P. Forster (UK), J. Haywood (UK), E. Jansen (Norway), P.D. Jones (UK), R. Knutti (Switzerland), H. Le Treut (France), P. Lemke (Germany), G. Meehl (USA), D. Randall (USA), D.A. Stone (UK, Canada), K.E. Trenberth (USA), J. Willebrand (Germany), F. Zwiers (Canada)

Review Editors:

Kansri Boonpragob (Thailand), Filippo Giorgi (Italy), Bubu Pateh Jallow (The Gambia)

This Technical Summary should be cited as:

Solomon, S., D. Qin, M. Manning, R.B. Alley, T. Berntsen, N.L. Bindoff, Z. Chen, A. Chidthaisong, J.M. Gregory, G.C. Hegerl, M. Heimann, B. Hewitson, B.J. Hoskins, F. Joos, J. Jouzel, V. Kattsov, U. Lohmann, T. Matsuno, M. Molina, N. Nicholls, J. Overpeck, G. Raga, V. Ramaswamy, J. Ren, M. Rusticucci, R. Somerville, T.F. Stocker, P. Whetton, R.A. Wood and D. Wratt, 2007: Technical Summary. In: *Climate Change 2007: The Physical Science Basis. Contribution of Working Group I to the Fourth Assessment Report of the Intergovernmental Panel on Climate Change* [Solomon, S., D. Qin, M. Manning, Z. Chen, M. Marquis, K.B. Averyt, M. Tignor and H.L. Miller (eds.)]. Cambridge University Press, Cambridge, United Kingdom and New York, NY, USA.

Table of Contents

TS.1 Introduction 21

TS.2 Changes in Human and Natural Drivers of Climate 21

Box TS.1: Treatment of Uncertainties in the Working Group I Assessment 22

TS.2.1 Greenhouse Gases 23

TS.2.2 Aerosols 29

TS.2.3 Aviation Contrails and Cirrus, Land Use and Other Effects 30

TS.2.4 Radiative Forcing Due to Solar Activity and Volcanic Eruptions 30

TS.2.5 Net Global Radiative Forcing, Global Warming Potentials and Patterns of Forcing 31

TS 2.6 Surface Forcing and the Hydrologic Cycle 35

TS.3 Observations of Changes in Climate 35

TS.3.1 Atmospheric Changes: Instrumental Record 35

Box TS.2: Patterns (Modes) of Climate Variability 39

TS.3.2 Changes in the Cryosphere: Instrumental Record 43

Box TS.3: Ice Sheet Dynamics and Stability 44

TS.3.3 Changes in the Ocean: Instrumental Record 47

Box TS.4: Sea Level 51

TS.3.4 Consistency Among Observations 51

Box TS.5: Extreme Weather Events 53

TS.3.5 A Palaeoclimatic Perspective 54

Box TS.6: Orbital Forcing 56

TS.4 Understanding and Attributing Climate Change 58

TS.4.1 Advances in Attribution of Changes in Global-Scale Temperature in the Instrumental Period: Atmosphere, Ocean and Ice 58

Box TS.7: Evaluation of Atmosphere-Ocean General Circulation Models 59

TS.4.2 Attribution of Spatial and Temporal Changes in Temperature 62

TS.4.3 Attribution of Changes in Circulation, Precipitation and Other Climate Variables 64

TS.4.4 Palaeoclimate Studies of Attribution 64

TS.4.5 Climate Response to Radiative Forcing 64

TS.5 Projections of Future Changes in Climate 66

Box TS.8: Hierarchy of Global Climate Models 67

TS.5.1 Understanding Near-Term Climate Change 68

Box TS.9: Committed Climate Change 68

TS.5.2 Large-Scale Projections for the 21st Century 69

TS.5.3 Regional-Scale Projections 74

Box TS.10: Regional Downscaling 74

TS.5.4 Coupling Between Climate Change and Changes in Biogeochemical Cycles 77

TS.5.5 Implications of Climate Processes and their Time Scales for Long-Term Projections 79

TS.6 Robust Findings and Key Uncertainties 81

TS.6.1 Changes in Human and Natural Drivers of Climate 81

TS.6.2 Observations of Changes in Climate 82

TS.6.3 Understanding and Attributing Climate Change 86

TS.6.4 Projections of Future Changes in Climate 87

TS.1 Introduction

In the six years since the IPCC's Third Assessment Report (TAR), significant progress has been made in understanding past and recent climate change and in projecting future changes. These advances have arisen from large amounts of new data, more sophisticated analyses of data, improvements in the understanding and simulation of physical processes in climate models and more extensive exploration of uncertainty ranges in model results. The increased confidence in climate science provided by these developments is evident in this Working Group I contribution to the IPCC's Fourth Assessment Report.

While this report provides new and important policy-relevant information on the scientific understanding of climate change, the complexity of the climate system and the multiple interactions that determine its behaviour impose limitations on our ability to understand fully the future course of Earth's global climate. There is still an incomplete physical understanding of many components of the climate system and their role in climate change. Key uncertainties include aspects of the roles played by clouds, the cryosphere, the oceans, land use and couplings between climate and biogeochemical cycles. The areas of science covered in this report continue to undergo rapid progress and it should be recognised that the present assessment reflects scientific understanding based on the peer-reviewed literature available in mid-2006.

The key findings of the IPCC Working Group I assessment are presented in the Summary for Policymakers. This Technical Summary provides a more detailed overview of the scientific basis for those findings and provides a road map to the chapters of the underlying report. It focuses on key findings, highlighting what is new since the TAR. The structure of the Technical Summary is as follows:

- Section 2: an overview of current scientific understanding of the natural and anthropogenic drivers of changes in climate;
- Section 3: an overview of observed changes in the climate system (including the atmosphere, oceans and cryosphere) and their relationships to physical processes;
- Section 4: an overview of explanations of observed climate changes based on climate models and physical understanding, the extent to which climate change can be attributed to specific causes and a new evaluation of climate sensitivity to greenhouse gas increases;
- Section 5: an overview of projections for both near- and far-term climate changes including the time scales of responses to changes in forcing, and probabilistic information about future climate change; and
- Section 6: a summary of the most robust findings and the key uncertainties in current understanding of physical climate change science.

Each paragraph in the Technical Summary reporting substantive results is followed by a reference in curly brackets to the corresponding chapter section(s) of the underlying report where the detailed assessment of the scientific literature and additional information can be found.

TS.2 Changes in Human and Natural Drivers of Climate

The Earth's global mean climate is determined by incoming energy from the Sun and by the properties of the Earth and its atmosphere, namely the reflection, absorption and emission of energy within the atmosphere and at the surface. Although changes in received solar energy (e.g., caused by variations in the Earth's orbit around the Sun) inevitably affect the Earth's energy budget, the properties of the atmosphere and surface are also important and these may be affected by climate feedbacks. The importance of climate feedbacks is evident in the nature of past climate changes as recorded in ice cores up to 650,000 years old.

Changes have occurred in several aspects of the atmosphere and surface that alter the global energy budget of the Earth and can therefore cause the climate to change. Among these are increases in greenhouse gas concentrations that act primarily to increase the atmospheric absorption of outgoing radiation, and increases in aerosols (microscopic airborne particles or droplets) that act to reflect and absorb incoming solar radiation and change cloud radiative properties. Such changes cause a radiative forcing of the climate system.[1] Forcing agents can differ considerably from one another in terms of the magnitudes of forcing, as well as spatial and temporal features. Positive and negative radiative forcings contribute to increases and decreases, respectively, in

[1] 'Radiative forcing' is a measure of the influence a factor has in altering the balance of incoming and outgoing energy in the Earth-atmosphere system and is an index of the importance of the factor as a potential climate change mechanism. Positive forcing tends to warm the surface while negative forcing tends to cool it. In this report, radiative forcing values are for changes relative to a pre-industrial background at 1750, are expressed in Watts per square metre (W m^{-2}) and, unless otherwise noted, refer to a global and annual average value. See Glossary for further details.

Box TS.1: Treatment of Uncertainties in the Working Group I Assessment

The importance of consistent and transparent treatment of uncertainties is clearly recognised by the IPCC in preparing its assessments of climate change. The increasing attention given to formal treatments of uncertainty in previous assessments is addressed in Section 1.6. To promote consistency in the general treatment of uncertainty across all three Working Groups, authors of the Fourth Assessment Report have been asked to follow a brief set of guidance notes on determining and describing uncertainties in the context of an assessment.[2] This box summarises the way that Working Group I has applied those guidelines and covers some aspects of the treatment of uncertainty specific to material assessed here.

Uncertainties can be classified in several different ways according to their origin. Two primary types are 'value uncertainties' and 'structural uncertainties'. Value uncertainties arise from the incomplete determination of particular values or results, for example, when data are inaccurate or not fully representative of the phenomenon of interest. Structural uncertainties arise from an incomplete understanding of the processes that control particular values or results, for example, when the conceptual framework or model used for analysis does not include all the relevant processes or relationships. Value uncertainties are generally estimated using statistical techniques and expressed probabilistically. Structural uncertainties are generally described by giving the authors' collective judgment of their confidence in the correctness of a result. In both cases, estimating uncertainties is intrinsically about describing the limits to knowledge and for this reason involves expert judgment about the state of that knowledge. A different type of uncertainty arises in systems that are either chaotic or not fully deterministic in nature and this also limits our ability to project all aspects of climate change.

The scientific literature assessed here uses a variety of other generic ways of categorising uncertainties. Uncertainties associated with 'random errors' have the characteristic of decreasing as additional measurements are accumulated, whereas those associated with 'systematic errors' do not. In dealing with climate records, considerable attention has been given to the identification of systematic errors or unintended biases arising from data sampling issues and methods of analysing and combining data. Specialised statistical methods based on quantitative analysis have been developed for the detection and attribution of climate change and for producing probabilistic projections of future climate parameters. These are summarised in the relevant chapters.

The uncertainty guidance provided for the Fourth Assessment Report draws, for the first time, a careful distinction between levels of confidence in scientific understanding and the likelihoods of specific results. This allows authors to express high confidence that an event is extremely unlikely (e.g., rolling a dice twice and getting a six both times), as well as high confidence that an event is about as likely as not (e.g., a tossed coin coming up heads). Confidence and likelihood as used here are distinct concepts but are often linked in practice.

The standard terms used to define levels of confidence in this report are as given in the IPCC Uncertainty Guidance Note, namely:

Confidence Terminology	Degree of confidence in being correct
Very high confidence	At least 9 out of 10 chance
High confidence	About 8 out of 10 chance
Medium confidence	About 5 out of 10 chance
Low confidence	About 2 out of 10 chance
Very low confidence	Less than 1 out of 10 chance

Note that 'low confidence' and 'very low confidence' are only used for areas of major concern and where a risk-based perspective is justified.

Chapter 2 of this report uses a related term 'level of scientific understanding' when describing uncertainties in different contributions to radiative forcing. This terminology is used for consistency with the Third Assessment Report, and the basis on which the authors have determined particular levels of scientific understanding uses a combination of approaches consistent with the uncertainty guidance note as explained in detail in Section 2.9.2 and Table 2.11.

(continued)

[2] The IPCC Uncertainty Guidance Note is included in Supplementary Material for this report.

The standard terms used in this report to define the likelihood of an outcome or result where this can be estimated probabilistically are:

Likelihood Terminology	Likelihood of the occurrence/ outcome
Virtually certain	> 99% probability
Extremely likely	> 95% probability
Very likely	> 90% probability
Likely	> 66% probability
More likely than not	> 50% probability
About as likely as not	33 to 66% probability
Unlikely	< 33% probability
Very unlikely	< 10% probability
Extremely unlikely	< 5% probability
Exceptionally unlikely	< 1% probability

The terms 'extremely likely', 'extremely unlikely' and 'more likely than not' as defined above have been added to those given in the IPCC Uncertainty Guidance Note in order to provide a more specific assessment of aspects including attribution and radiative forcing.

Unless noted otherwise, values given in this report are assessed best estimates and their uncertainty ranges are 90% confidence intervals (i.e., there is an estimated 5% likelihood of the value being below the lower end of the range or above the upper end of the range). Note that in some cases the nature of the constraints on a value, or other information available, may indicate an asymmetric distribution of the uncertainty range around a best estimate. In such cases, the uncertainty range is given in square brackets following the best estimate.

global average surface temperature. This section updates the understanding of estimated anthropogenic and natural radiative forcings.

The overall response of global climate to radiative forcing is complex due to a number of positive and negative feedbacks that can have a strong influence on the climate system (see e.g., Sections 4.5 and 5.4). Although water vapour is a strong greenhouse gas, its concentration in the atmosphere changes in response to changes in surface climate and this must be treated as a feedback effect and not as a radiative forcing. This section also summarises changes in the surface energy budget and its links to the hydrological cycle. Insights into the effects of agents such as aerosols on precipitation are also noted.

TS.2.1 Greenhouse Gases

The dominant factor in the radiative forcing of climate in the industrial era is the increasing concentration of various greenhouse gases in the atmosphere. Several of the major greenhouse gases occur naturally but increases in their atmospheric concentrations over the last 250 years are due largely to human activities. Other greenhouse gases are entirely the result of human activities. The contribution of each greenhouse gas to radiative forcing over a particular period of time is determined by the change in its concentration in the atmosphere over that period and the effectiveness of the gas in perturbing the radiative balance. Current atmospheric concentrations of the different greenhouse gases considered in this report vary by more than eight orders of magnitude (factor of 10^8), and their radiative efficiencies vary by more than four orders of magnitude (factor of 10^4), reflecting the enormous diversity in their properties and origins.

The current concentration of a greenhouse gas in the atmosphere is the net result of the history of its past emissions and removals from the atmosphere. The gases and aerosols considered here are emitted to the atmosphere by human activities or are formed from precursor species emitted to the atmosphere. These emissions are offset by chemical and physical removal processes. With the important exception of carbon dioxide (CO_2), it is generally the case that these processes remove a specific fraction of the amount of a gas in the atmosphere each year and the inverse of this removal rate gives the mean lifetime for that gas. In some cases, the removal rate may vary with gas concentration or other atmospheric properties (e.g., temperature or background chemical conditions).

Long-lived greenhouse gases (LLGHGs), for example, CO_2, methane (CH_4) and nitrous oxide (N_2O), are

chemically stable and persist in the atmosphere over time scales of a decade to centuries or longer, so that their emission has a long-term influence on climate. Because these gases are long lived, they become well mixed throughout the atmosphere much faster than they are removed and their global concentrations can be accurately estimated from data at a few locations. Carbon dioxide does not have a specific lifetime because it is continuously cycled between the atmosphere, oceans and land biosphere and its net removal from the atmosphere involves a range of processes with different time scales.

Short-lived gases (e.g., sulphur dioxide and carbon monoxide) are chemically reactive and generally removed by natural oxidation processes in the atmosphere, by removal at the surface or by washout in precipitation; their concentrations are hence highly variable. Ozone is a significant greenhouse gas that is formed and destroyed by chemical reactions involving other species in the atmosphere. In the troposphere, the human influence on ozone occurs primarily through changes in precursor gases that lead to its formation, whereas in the stratosphere, the human influence has been primarily through changes in ozone removal rates caused by chlorofluorocarbons (CFCs) and other ozone-depleting substances.

TS.2.1.1 Changes in Atmospheric Carbon Dioxide, Methane and Nitrous Oxide

Current concentrations of atmospheric CO_2 and CH_4 far exceed pre-industrial values found in polar ice core records of atmospheric composition dating back 650,000 years. Multiple lines of evidence confirm that the post-industrial rise in these gases does not stem from natural mechanisms (see Figure TS.1 and Figure TS.2). {2.3, 6.3–6.5, FAQ 7.1}

The total radiative forcing of the Earth's climate due to increases in the concentrations of the LLGHGs CO_2, CH_4 and N_2O, and *very likely* the rate of increase in the total forcing due to these gases over the period since 1750, are unprecedented in more than 10,000 years (Figure TS.2). It is *very likely* that the sustained rate of increase in the combined radiative forcing from these greenhouse gases of about +1 W m^{-2} over the past four decades is at least six times faster than at any time during the two millennia before the Industrial Era, the period for which ice core data have the required temporal resolution. The radiative forcing due to these LLGHGs has the highest level of confidence of any forcing agent. {2.3, 6.4}

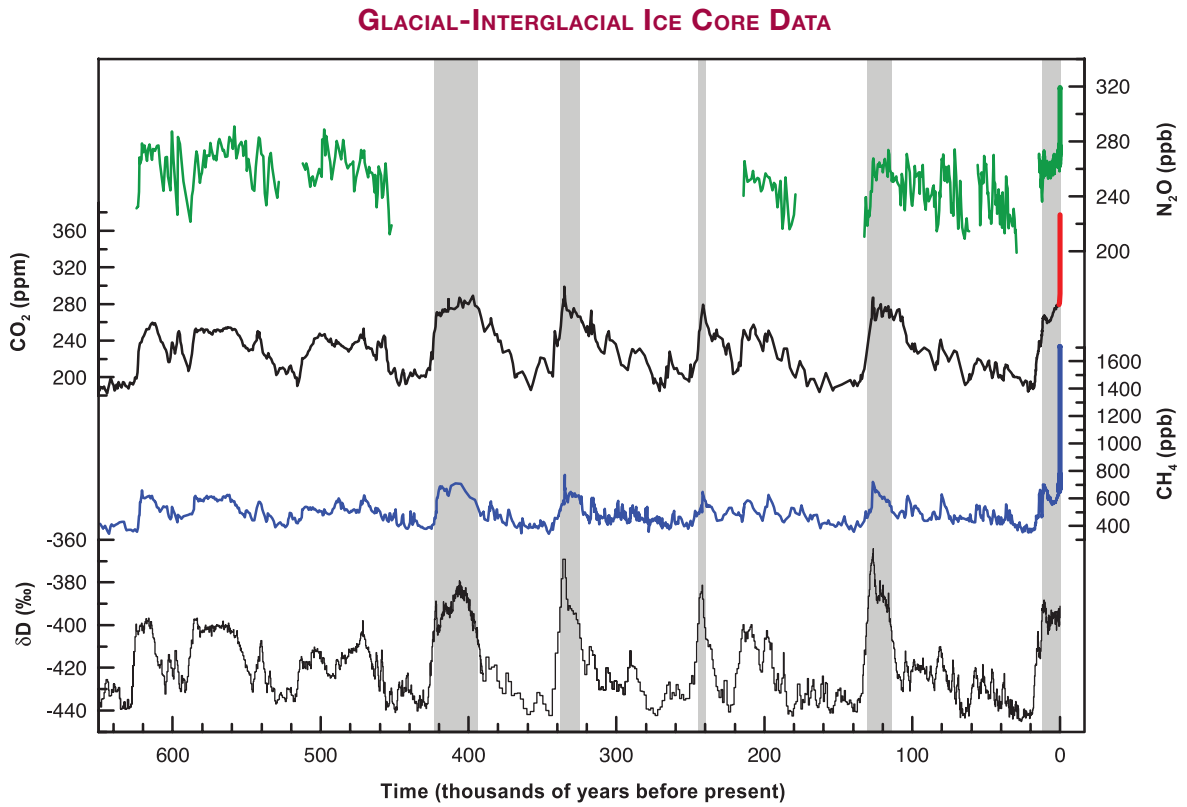


Figure TS.1. *Variations of deuterium (δD) in antarctic ice, which is a proxy for local temperature, and the atmospheric concentrations of the greenhouse gases carbon dioxide (CO_2), methane (CH_4), and nitrous oxide (N_2O) in air trapped within the ice cores and from recent atmospheric measurements. Data cover 650,000 years and the shaded bands indicate current and previous interglacial warm periods. {Adapted from Figure 6.3}*

Changes in Greenhouse Gases from Ice Core and Modern Data

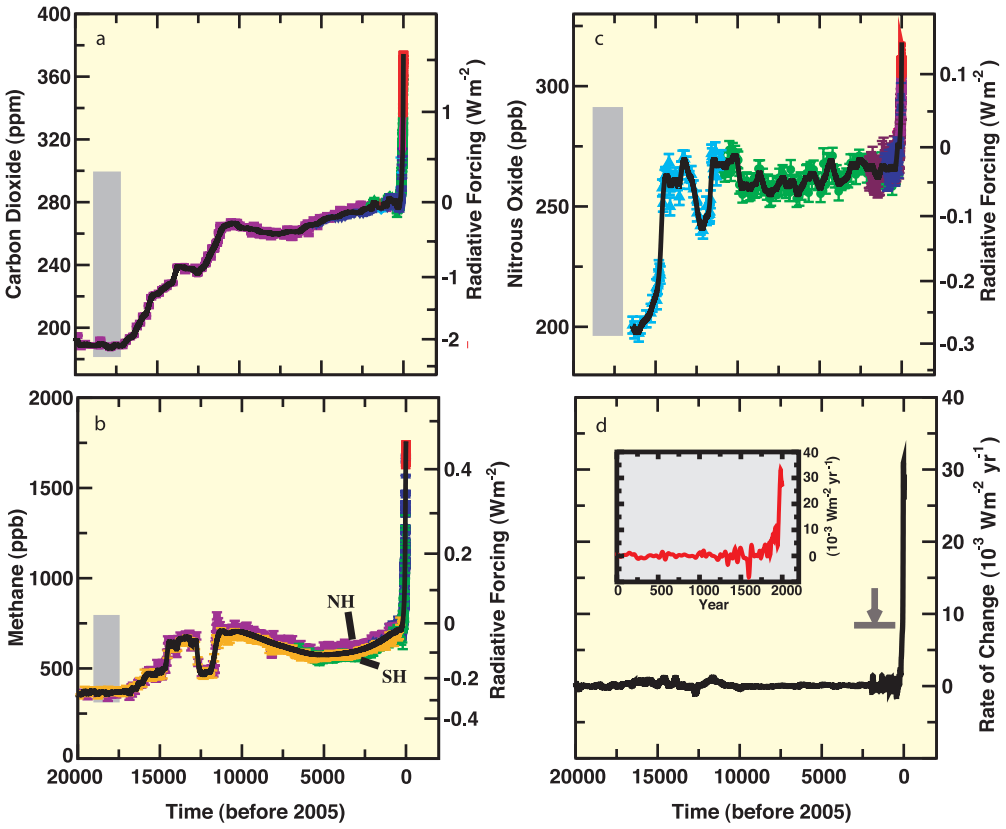


Figure TS.2. *The concentrations and radiative forcing by (a) carbon dioxide (CO_2), (b) methane (CH_4), (c) nitrous oxide (N_2O) and (d) the rate of change in their combined radiative forcing over the last 20,000 years reconstructed from antarctic and Greenland ice and firn data (symbols) and direct atmospheric measurements (panels a,b,c, red lines). The grey bars show the reconstructed ranges of natural variability for the past 650,000 years. The rate of change in radiative forcing (panel d, black line) has been computed from spline fits to the concentration data. The width of the age spread in the ice data varies from about 20 years for sites with a high accumulation of snow such as Law Dome, Antarctica, to about 200 years for low-accumulation sites such as Dome C, Antarctica. The arrow shows the peak in the rate of change in radiative forcing that would result if the anthropogenic signals of CO_2, CH_4, and N_2O had been smoothed corresponding to conditions at the low-accumulation Dome C site. The negative rate of change in forcing around 1600 shown in the higher-resolution inset in panel d results from a CO_2 decrease of about 10 ppm in the Law Dome record. {Figure 6.4}*

The concentration of atmospheric CO_2 has increased from a pre-industrial value of about 280 ppm to 379 ppm in 2005. Atmospheric CO_2 concentration increased by only 20 ppm over the 8000 years prior to industrialisation; multi-decadal to centennial-scale variations were less than 10 ppm and *likely* due mostly to natural processes. However, since 1750, the CO_2 concentration has risen by nearly 100 ppm. The annual CO_2 growth rate was larger during the last 10 years (1995–2005 average: 1.9 ppm yr^{-1}) than it has been since continuous direct atmospheric measurements began (1960–2005 average: 1.4 ppm yr^{-1}). {2.3, 6.4, 6.5}

Increases in atmospheric CO_2 since pre-industrial times are responsible for a radiative forcing of +1.66 ± 0.17 W m^{-2}; a contribution which dominates all other radiative forcing agents considered in this report. For the decade from 1995 to 2005, the growth rate of CO_2 in the atmosphere led to a 20% increase in its radiative forcing. {2.3, 6.4, 6.5}

Emissions of CO_2 from fossil fuel use and from the effects of land use change on plant and soil carbon are the primary sources of increased atmospheric CO_2. Since 1750, it is estimated that about 2/3rds of anthropogenic CO_2 emissions have come from fossil fuel burning and about 1/3rd from land use change. About 45% of this CO_2 has remained in the atmosphere, while about 30% has been taken up by the oceans and the remainder has been taken up by the terrestrial biosphere. About half of a CO_2 pulse to the atmosphere is removed over a time scale of 30 years; a further 30% is removed within a few centuries; and the remaining 20% will typically stay in the atmosphere for many thousands of years. {7.3}

In recent decades, emissions of CO_2 have continued to increase (see Figure TS.3). Global annual fossil

CO_2 emissions[3] increased from an average of 6.4 ± 0.4 GtC yr^{-1} in the 1990s to 7.2 ± 0.3 GtC yr^{-1} in the period 2000 to 2005. Estimated CO_2 emissions associated with land use change, averaged over the 1990s, were[4] 0.5 to 2.7 GtC yr^{-1}, with a central estimate of 1.6 Gt yr^{-1}. Table TS.1 shows the estimated budgets of CO_2 in recent decades. {2.3, 6.4, 7.3, FAQ 7.1}

Since the 1980s, natural processes of CO_2 uptake by the terrestrial biosphere (i.e., the residual land sink in Table TS.1) and by the oceans have removed about 50% of anthropogenic emissions (i.e., fossil CO_2 emissions and land use change flux in Table TS.1). These removal processes are influenced by the atmospheric CO_2 concentration and by changes in climate. Uptake by the oceans and the terrestrial biosphere have been similar in magnitude but the terrestrial biosphere uptake is more variable and was higher in the 1990s than in the 1980s by about 1 GtC yr^{-1}. Observations demonstrate that dissolved CO_2 concentrations in the surface ocean (pCO_2) have been increasing nearly everywhere, roughly following the atmospheric CO_2 increase but with large regional and temporal variability. {5.4, 7.3}

Carbon uptake and storage in the terrestrial biosphere arise from the net difference between uptake due to vegetation growth, changes in reforestation and sequestration, and emissions due to heterotrophic respiration, harvest, deforestation, fire, damage by pollution and other disturbance factors affecting biomass and soils. Increases and decreases in fire frequency in different regions have affected net carbon uptake, and in boreal regions, emissions due to fires appear to have increased over recent decades. Estimates of net CO_2 surface fluxes from inverse studies using networks of atmospheric data demonstrate significant land uptake in the mid-latitudes of the Northern Hemisphere (NH) and near-zero land-atmosphere fluxes in the tropics, implying that tropical deforestation is approximately balanced by regrowth. {7.3}

Short-term (interannual) variations observed in the atmospheric CO_2 growth rate are primarily controlled by changes in the flux of CO_2 between the atmosphere and the terrestrial biosphere, with a smaller but significant fraction due to variability in ocean fluxes (see Figure TS.3). Variability in the terrestrial biosphere flux is driven by climatic fluctuations, which affect the uptake of CO_2 by plant growth and the return of CO_2 to the atmosphere by the decay of organic material through heterotrophic respiration and fires. El Niño-Southern Oscillation (ENSO) events are a major source of interannual variability in atmospheric CO_2 growth rate, due to their effects on fluxes through land and sea surface temperatures, precipitation and the incidence of fires. {7.3}

The direct effects of increasing atmospheric CO_2 on large-scale terrestrial carbon uptake cannot be quantified reliably at present. Plant growth can be stimulated by increased atmospheric CO_2 concentrations and by nutrient deposition (fertilization effects). However, most experiments and studies show that such responses appear to be relatively short lived and strongly coupled

Table TS.1. *Global carbon budget. By convention, positive values are CO_2 fluxes (GtC yr^{-1}) into the atmosphere and negative values represent uptake from the atmosphere (i.e., 'CO$_2$ sinks'). Fossil CO_2 emissions for 2004 and 2005 are based on interim estimates. Due to the limited number of available studies, for the net land-to-atmosphere flux and its components, uncertainty ranges are given as 65% confidence intervals and do not include interannual variability (see Section 7.3). NA indicates that data are not available.*

	1980s	1990s	2000–2005
Atmospheric increase	3.3 ± 0.1	3.2 ± 0.1	4.1 ± 0.1
Fossil carbon dioxide emissions	5.4 ± 0.3	6.4 ± 0.4	7.2 ± 0.3
Net ocean-to-atmosphere flux	–1.8 ± 0.8	–2.2 ± 0.4	–2.2 ± 0.5
Net land-to-atmosphere flux	–0.3 ± 0.9	–1.0 ± 0.6	–0.9 ± 0.6
Partitioned as follows			
Land use change flux	1.4 (0.4 to 2.3)	1.6 (0.5 to 2.7)	NA
Residual land sink	–1.7 (–3.4 to 0.2)	–2.6 (–4.3 to –0.9)	NA

[3] Fossil CO_2 emissions include those from the production, distribution and consumption of fossil fuels and from cement production. Emission of 1 GtC corresponds to 3.67 $GtCO_2$.

[4] As explained in Section 7.3, uncertainty ranges for land use change emissions, and hence for the full carbon cycle budget, can only be given as 65% confidence intervals.

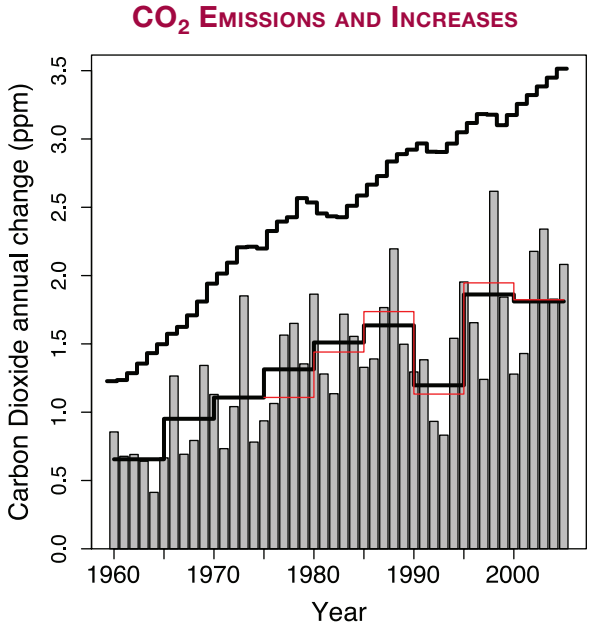


Figure TS.3. *Annual changes in global mean CO_2 concentration (grey bars) and their five-year means from two different measurement networks (red and lower black stepped lines). The five-year means smooth out short-term perturbations associated with strong ENSO events in 1972, 1982, 1987 and 1997. Uncertainties in the five-year means are indicated by the difference between the red and lower black lines and are of order 0.15 ppm. The upper stepped line shows the annual increases that would occur if all fossil fuel emissions stayed in the atmosphere and there were no other emissions. {Figure 7.4}*

to other effects such as availability of water and nutrients. Likewise, experiments and studies of the effects of climate (temperature and moisture) on heterotrophic respiration of litter and soils are equivocal. Note that the effect of climate change on carbon uptake is addressed separately in section TS.5.4. {7.3}

The CH_4 abundance in 2005 of about 1774 ppb is more than double its pre-industrial value. Atmospheric CH_4 concentrations varied slowly between 580 and 730 ppb over the last 10,000 years, but increased by about 1000 ppb in the last two centuries, representing the fastest changes in this gas over at least the last 80,000 years. In the late 1970s and early 1980s, CH_4 growth rates displayed maxima above 1% yr^{-1}, but since the early 1990s have decreased significantly and were close to zero for the six-year period from 1999 to 2005. Increases in CH_4 abundance occur when emissions exceed removals. The recent decline in growth rates implies that emissions now approximately match removals, which are due primarily to oxidation by the hydroxyl radical (OH). Since the TAR, new studies using two independent tracers (methyl chloroform and ^{14}CO) suggest no significant long-term change in the global abundance of OH. Thus, the slowdown in the atmospheric CH_4 growth rate since about 1993 is *likely* due to the atmosphere approaching an equilibrium during a period of near-constant total emissions. {2.3, 7.4, FAQ 7.1}

Increases in atmospheric CH_4 concentrations since pre-industrial times have contributed a radiative forcing of +0.48 ± 0.05 W m^{-2}. Among greenhouse gases, this forcing remains second only to that of CO_2 in magnitude. {2.3}

Current atmospheric CH_4 levels are due to continuing anthropogenic emissions of CH_4, which are greater than natural emissions. Total CH_4 emissions can be well determined from observed concentrations and independent estimates of removal rates. Emissions from individual sources of CH_4 are not as well quantified as the total emissions but are mostly biogenic and include emissions from wetlands, ruminant animals, rice agriculture and biomass burning, with smaller contributions from industrial sources including fossil fuel-related emissions. This knowledge of CH_4 sources, combined with the small natural range of CH_4 concentrations over the past 650,000 years (Figure TS.1) and their dramatic increase since 1750 (Figure TS.2), make it *very likely* that the observed long-term changes in CH_4 are due to anthropogenic activity. {2.3, 6.4, 7.4}

In addition to its slowdown over the last 15 years, the growth rate of atmospheric CH_4 has shown high interannual variability, which is not yet fully explained. The largest contributions to interannual variability during the 1996 to 2001 period appear to be variations in emissions from wetlands and biomass burning. Several studies indicate that wetland CH_4 emissions are highly sensitive to temperature and are also affected by hydrological changes. Available model estimates all indicate increases in wetland emissions due to future climate change but vary widely in the magnitude of such a positive feedback effect. {7.4}

The N_2O concentration in 2005 was 319 ppb, about 18% higher than its pre-industrial value. Nitrous oxide increased approximately linearly by about 0.8 ppb yr^{-1} over the past few decades. Ice core data show that the atmospheric concentration of N_2O varied by less than about 10 ppb for 11,500 years before the onset of the industrial period. {2.3, 6.4, 6.5}

The increase in N_2O since the pre-industrial era now contributes a radiative forcing of +0.16 ± 0.02 W m^{-2} and is due primarily to human activities, particularly agriculture and associated land use change. Current estimates are that about 40% of total N_2O emissions are anthropogenic but individual source estimates remain subject to significant uncertainties. {2.3, 7.4}

TS.2.1.3 Changes in Atmospheric Halocarbons, Stratospheric Ozone, Tropospheric Ozone and Other Gases

CFCs and hydrochlorofluorocarbons (HCFCs) are greenhouse gases that are purely anthropogenic in origin and used in a wide variety of applications. Emissions of these gases have decreased due to their phase-out under the Montreal Protocol, and the atmospheric concentrations of CFC-11 and CFC-113 are now decreasing due to natural removal processes. Observations in polar firn cores since the TAR have now extended the available time series information for some of these greenhouse gases. Ice core and *in situ* data confirm that industrial sources are the cause of observed atmospheric increases in CFCs and HCFCs. {2.3}

The Montreal Protocol gases contributed +0.32 ± 0.03 W m^{-2} to direct radiative forcing in 2005, with CFC-12 continuing to be the third most important long-lived radiative forcing agent. These gases as a group contribute about 12% of the total forcing due to LLGHGs. {2.3}

The concentrations of industrial fluorinated gases covered by the Kyoto Protocol (hydrofluorocarbons (HFCs), perfluorocarbons (PFCs), sulphur hexafluoride (SF_6)) are relatively small but are increasing rapidly. Their total radiative forcing in 2005 was +0.017 W m^{-2}. {2.3}

Tropospheric ozone is a short-lived greenhouse gas produced by chemical reactions of precursor species in the atmosphere and with large spatial and temporal variability. Improved measurements and modelling have advanced the understanding of chemical precursors that lead to the formation of tropospheric ozone, mainly carbon monoxide, nitrogen oxides (including sources and possible long-term trends in lightning) and formaldehyde. Overall, current models are successful in describing the principal features of the present global tropospheric ozone distribution on the basis of underlying processes. New satellite and *in situ* measurements provide important global constraints for these models; however, there is less confidence in their ability to reproduce the changes in ozone associated with large changes in emissions or climate, and in the simulation of observed long-term trends in ozone concentrations over the 20th century. {7.4}

Tropospheric ozone radiative forcing is estimated to be +0.35 [+0.25 to +0.65] W m^{-2} with a *medium* level of scientific understanding. The best estimate of this radiative forcing has not changed since the TAR. Observations show that trends in tropospheric ozone during the last few decades vary in sign and magnitude at many locations, but there are indications of significant upward trends at low latitudes. Model studies of the radiative forcing due to the increase in tropospheric ozone since pre-industrial times have increased in complexity and comprehensiveness compared with models used in the TAR. {2.3, 7.4}

Changes in tropospheric ozone are linked to air quality and climate change. A number of studies have shown that summer daytime ozone concentrations correlate strongly with temperature. This correlation appears to reflect contributions from temperature-dependent biogenic volatile organic carbon emissions, thermal decomposition of peroxyacetylnitrate, which acts as a reservoir for nitrogen oxides (NO_x), and association of high temperatures with regional stagnation. Anomalously hot and stagnant conditions during the summer of 1988 were responsible for the highest surface-level ozone year on record in the north-eastern USA. The summer heat wave in Europe in 2003 was also associated with exceptionally high local ozone at the surface. {Box 7.4}

The radiative forcing due to the destruction of stratospheric ozone is caused by the Montreal Protocol gases and is re-evaluated to be –0.05 ± 0.10 W m^{-2}, weaker than in the TAR, with a medium level of scientific understanding. The trend of greater and greater depletion of global stratospheric ozone observed during the 1980s and 1990s is no longer occurring; however, global stratospheric ozone is still about 4% below pre-1980 values and it is not yet clear whether ozone recovery has begun. In addition to the chemical destruction of ozone, dynamical changes may have contributed to NH mid-latitude ozone reduction. {2.3}

Direct emission of water vapour by human activities makes a negligible contribution to radiative forcing. However, as global mean temperatures increase, tropospheric water vapour concentrations increase and this represents a key feedback but not a forcing of climate change. Direct emission of water to the atmosphere by anthropogenic activities, mainly irrigation, is a possible forcing factor but corresponds to less than 1% of the natural sources of atmospheric water vapour. The direct injection of water vapour into the atmosphere from fossil fuel combustion is significantly lower than that from agricultural activity. {2.5}

Based on chemical transport model studies, the radiative forcing from increases in stratospheric water vapour due to oxidation of CH_4 is estimated to be +0.07 ± 0.05 W m^{-2}. The level of scientific understanding is low because the contribution of CH_4 to the corresponding vertical structure of the water vapour change near the tropopause is uncertain. Other potential human causes of stratospheric water vapour increases that could contribute to radiative forcing are poorly understood. {2.3}

TS.2.2 Aerosols

Direct aerosol radiative forcing is now considerably better quantified than previously and represents a major advance in understanding since the time of the TAR, when several components had a very low level of scientific understanding. A total direct aerosol radiative forcing combined across all aerosol types can now be given for the first time as –0.5 ± 0.4 W m^{-2}, with a medium-low level of scientific understanding. Atmospheric models have improved and many now represent all aerosol components of significance. Aerosols vary considerably in their properties that affect the extent to which they absorb and scatter radiation, and thus different types may have a net cooling or warming effect. Industrial aerosol consisting mainly of a mixture of sulphates, organic and black carbon, nitrates and industrial dust is clearly discernible over many continental regions of the NH. Improved *in situ*, satellite and surface-based measurements (see Figure TS.4) have enabled verification of global aerosol model simulations. These improvements allow quantification of the total direct aerosol radiative forcing for the first time, representing an important advance since the TAR. The direct radiative forcing for individual species remains less certain and is estimated from models to be –0.4 ± 0.2 W m^{-2} for sulphate, –0.05 ± 0.05 W m^{-2} for fossil fuel organic carbon, +0.2 ± 0.15 W m^{-2} for fossil fuel black carbon, +0.03 ± 0.12 W m^{-2} for biomass burning, –0.1 ± 0.1 W m^{-2} for nitrate and –0.1 ± 0.2 W m^{-2} for mineral dust. Two recent emission inventory studies support data from ice cores and suggest that global anthropogenic sulphate emissions decreased over the 1980 to 2000 period and that the geographic distribution of sulphate forcing has also changed. {2.4, 6.6}

Significant changes in the estimates of the direct radiative forcing due to biomass-burning, nitrate and mineral dust aerosols have occurred since the TAR. For biomass-burning aerosol, the estimated direct radiative forcing is now revised from being negative to near zero due to the estimate being strongly influenced by the occurrence of these aerosols over clouds. For the first time, the radiative forcing due to nitrate aerosol is given. For mineral dust, the range in the direct radiative forcing is reduced due to a reduction in the estimate of its anthropogenic fraction. {2.4}

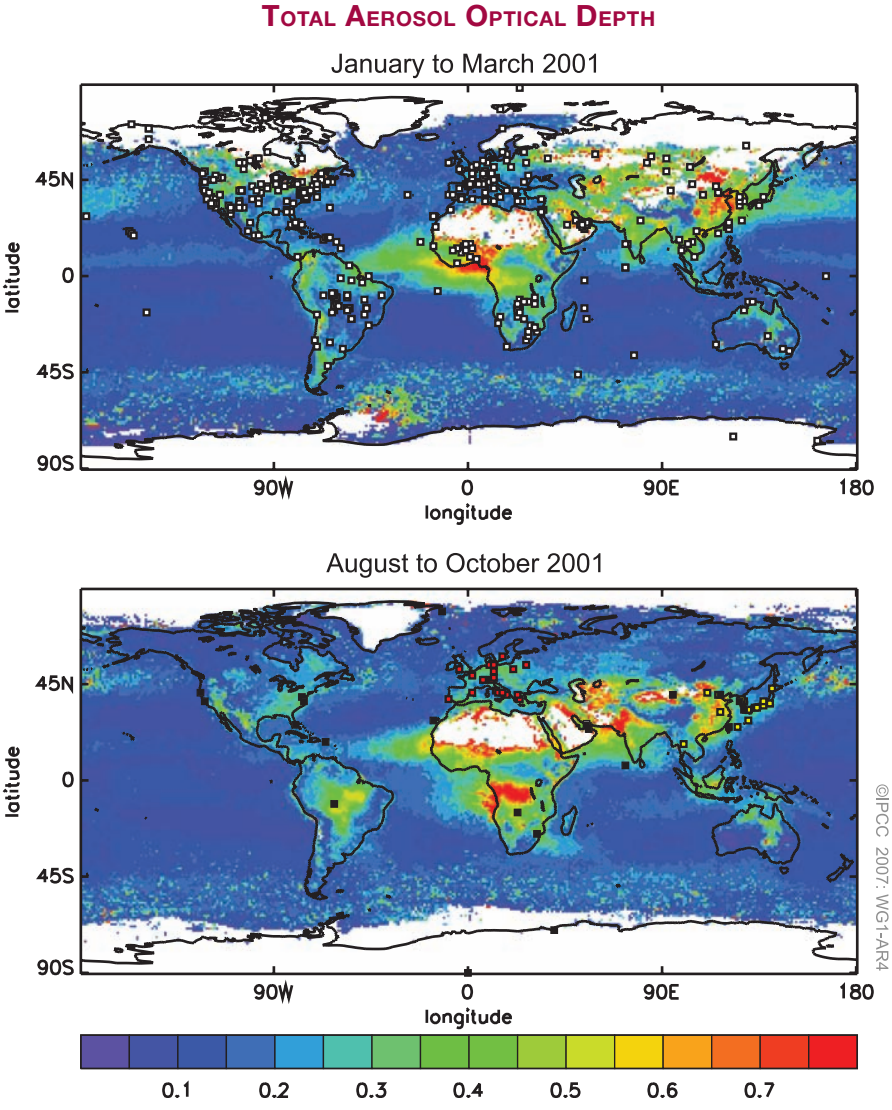


Figure TS.4. *(Top) The total aerosol optical depth (due to natural plus anthropogenic aerosols) at a mid-visible wavelength determined by satellite measurements for January to March 2001 and (bottom) August to October 2001, illustrating seasonal changes in industrial and biomass-burning aerosols. Data are from satellite measurements, complemented by two different kinds of ground-based measurements at locations shown in the two panels (see Section 2.4.2 for details). {Figure 2.11}*

Anthropogenic aerosols effects on water clouds cause an indirect cloud albedo effect (referred to as the first indirect effect in the TAR), which has a best estimate for the first time of –0.7 [–0.3 to –1.8] W m^{-2}. The number of global model estimates of the albedo effect for liquid water clouds has increased substantially since the TAR, and the estimates have been evaluated in a more rigorous way. The estimate for this radiative forcing comes from multiple model studies incorporating more aerosol species and describing aerosol-cloud interaction processes in greater detail. Model studies including more aerosol species or constrained by satellite observations tend to yield a relatively weaker cloud albedo effect. Despite the advances and progress since the TAR and the reduction in the spread of the estimate of the forcing, there remain large uncertainties in both measurements and modelling of processes, leading to a low level of scientific understanding, which is an elevation from the very low rank in the TAR. {2.4, 7.5, 9.2}

Other effects of aerosol include a cloud lifetime effect, a semi-direct effect and aerosol-ice cloud interactions. These are considered to be part of the climate response rather than radiative forcings. {2.4, 7.5}

TS.2.3 Aviation Contrails and Cirrus, Land Use and Other Effects

Persistent linear contrails from global aviation contribute a small radiative forcing of +0.01 [+0.003 to +0.03] W m^{-2}, with a low level of scientific understanding. This best estimate is smaller than the estimate in the TAR. This difference results from new observations of contrail cover and reduced estimates of contrail optical depth. No best estimates are available for the net forcing from spreading contrails. Their effects on cirrus cloudiness and the global effect of aviation aerosol on background cloudiness remain unknown. {2.6}

Human-induced changes in land cover have increased the global surface albedo, leading to a radiative forcing of –0.2 ± 0.2 W m^{-2}, the same as in the TAR, with a medium-low level of scientific understanding. Black carbon aerosols deposited on snow reduce the surface albedo and are estimated to yield an associated radiative forcing of +0.1 ± 0.1 W m^{-2}, with a low level of scientific understanding. Since the TAR, a number of estimates of the forcing from land use changes have been made, using better techniques, exclusion of feedbacks in the evaluation and improved incorporation of large-scale observations. Uncertainties in the estimate include mapping and characterisation of present-day vegetation and historical state, parametrization of surface radiation processes and biases in models' climate variables. The presence of soot particles in snow leads to a decrease in the albedo of snow and a positive forcing, and could affect snowmelt. Uncertainties are large regarding the manner in which soot is incorporated in snow and the resulting optical properties. {2.5}

The impacts of land use change on climate are expected to be locally significant in some regions, but are small at the global scale in comparison with greenhouse gas warming. Changes in the land surface (vegetation, soils, water) resulting from human activities can significantly affect local climate through shifts in radiation, cloudiness, surface roughness and surface temperatures. Changes in vegetation cover can also have a substantial effect on surface energy and water balance at the regional scale. These effects involve non-radiative processes (implying that they cannot be quantified by a radiative forcing) and have a very low level of scientific understanding. {2.5, 7.2, 9.3, Box 11.4}

The release of heat from anthropogenic energy production can be significant over urban areas but is not significant globally. {2.5}

TS.2.4 Radiative Forcing Due to Solar Activity and Volcanic Eruptions

Continuous monitoring of total solar irradiance now covers the last 28 years. The data show a well-established 11-year cycle in irradiance that varies by 0.08% from solar cycle minima to maxima, with no significant long-term trend. New data have more accurately quantified changes in solar spectral fluxes over a broad range of wavelengths in association with changing solar activity. Improved calibrations using high-quality overlapping measurements have also contributed to a better understanding. Current understanding of solar physics and the known sources of irradiance variability suggest comparable irradiance levels during the past two solar cycles, including at solar minima. The primary known cause of contemporary irradiance variability is the presence on the Sun's disk of sunspots (compact, dark features where radiation is locally depleted) and faculae (extended bright features where radiation is locally enhanced). {2.7}

The estimated direct radiative forcing due to changes in the solar output since 1750 is +0.12 [+0.06 to +0.3] W m^{-2}, which is less than half of the estimate given in the TAR, with a low level of scientific understanding. The reduced radiative forcing estimate comes from a re-evaluation of the long-term change in solar irradiance since 1610 (the Maunder Minimum) based upon: a new reconstruction using a model of solar magnetic flux variations that does not invoke geomagnetic,

cosmogenic or stellar proxies; improved understanding of recent solar variations and their relationship to physical processes; and re-evaluation of the variations of Sun-like stars. While this leads to an elevation in the level of scientific understanding from very low in the TAR to low in this assessment, uncertainties remain large because of the lack of direct observations and incomplete understanding of solar variability mechanisms over long time scales. {2.7, 6.6}

Empirical associations have been reported between solar-modulated cosmic ray ionization of the atmosphere and global average low-level cloud cover but evidence for a systematic indirect solar effect remains ambiguous. It has been suggested that galactic cosmic rays with sufficient energy to reach the troposphere could alter the population of cloud condensation nuclei and hence microphysical cloud properties (droplet number and concentration), inducing changes in cloud processes analogous to the indirect cloud albedo effect of tropospheric aerosols and thus causing an indirect solar forcing of climate. Studies have probed various correlations with clouds in particular regions or using limited cloud types or limited time periods; however, the cosmic ray time series does not appear to correspond to global total cloud cover after 1991 or to global low-level cloud cover after 1994. Together with the lack of a proven physical mechanism and the plausibility of other causal factors affecting changes in cloud cover, this makes the association between galactic cosmic ray-induced changes in aerosol and cloud formation controversial. {2.7}

Explosive volcanic eruptions greatly increase the concentration of stratospheric sulphate aerosols. A single eruption can thereby cool global mean climate for a few years. Volcanic aerosols perturb both the stratosphere and surface/troposphere radiative energy budgets and climate in an episodic manner, and many past events are evident in ice core observations of sulphate as well as temperature records. There have been no explosive volcanic events since the 1991 Mt. Pinatubo eruption capable of injecting significant material to the stratosphere. However, the potential exists for volcanic eruptions much larger than the 1991 Mt. Pinatubo eruption, which could produce larger radiative forcing and longer-term cooling of the climate system. {2.7, 6.4, 6.6, 9.2}

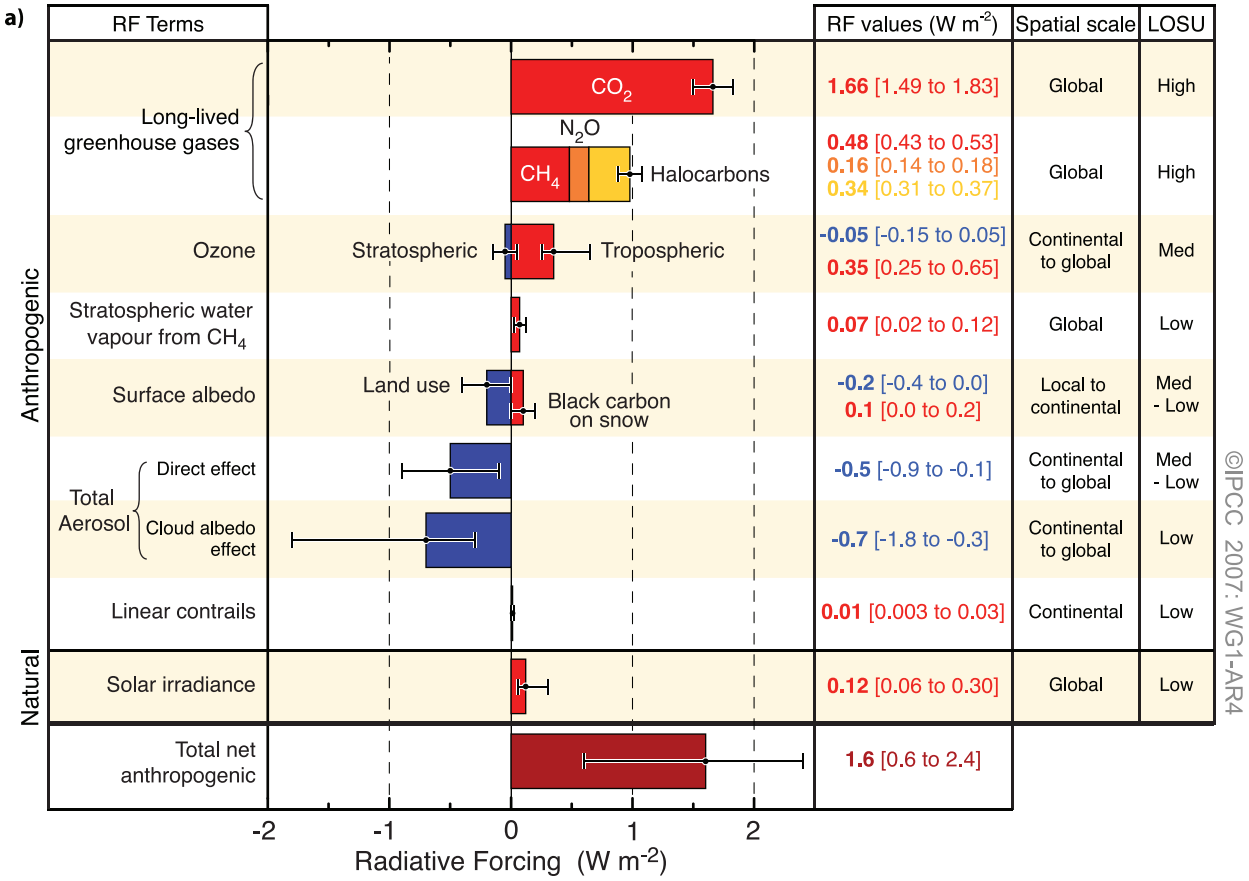
TS.2.5 Net Global Radiative Forcing, Global Warming Potentials and Patterns of Forcing

The understanding of anthropogenic warming and cooling influences on climate has improved since the TAR, leading to *very high confidence* that the effect of human activities since 1750 has been a net positive forcing of +1.6 [+0.6 to +2.4] W m^{-2}. Improved understanding and better quantification of the forcing mechanisms since the TAR make it possible to derive a combined net anthropogenic radiative forcing for the first time. Combining the component values for each forcing agent and their uncertainties yields the probability distribution of the combined anthropogenic radiative forcing estimate shown in Figure TS.5; the most likely value is about an order of magnitude larger than the estimated radiative forcing from changes in solar irradiance. Since the range in the estimate is +0.6 to +2.4 W m^{-2}, there is very high confidence in the net positive radiative forcing of the climate system due to human activity. The LLGHGs together contribute +2.63 ± 0.26 W m^{-2}, which is the dominant radiative forcing term and has the highest level of scientific understanding. In contrast, the total direct aerosol, cloud albedo and surface albedo effects that contribute negative forcings are less well understood and have larger uncertainties. The range in the net estimate is increased by the negative forcing terms, which have larger uncertainties than the positive terms. The nature of the uncertainty in the estimated cloud albedo effect introduces a noticeable asymmetry in the distribution. Uncertainties in the distribution include structural aspects (e.g., representation of extremes in the component values, absence of any weighting of the radiative forcing mechanisms, possibility of unaccounted for but as yet unquantified radiative forcings) and statistical aspects (e.g., assumptions about the types of distributions describing component uncertainties). {2.7, 2.9}

The Global Warming Potential (GWP) is a useful metric for comparing the potential climate impact of the emissions of different LLGHGs (see Table TS.2). Global Warming Potentials compare the integrated radiative forcing over a specified period (e.g., 100 years) from a unit mass pulse emission and are a way of comparing the potential climate change associated with emissions of different greenhouse gases. There are well-documented shortcomings of the GWP concept, particularly in using it to assess the impact of short-lived species. {2.10}

For the magnitude and range of realistic forcings considered, evidence suggests an approximately linear relationship between global mean radiative forcing and global mean surface temperature response. The spatial patterns of radiative forcing vary between different forcing agents. However, the spatial signature of the climate response is not generally expected to match that of the forcing. Spatial patterns of climate response

Global Mean Radiative Forcings



Probability Distribution

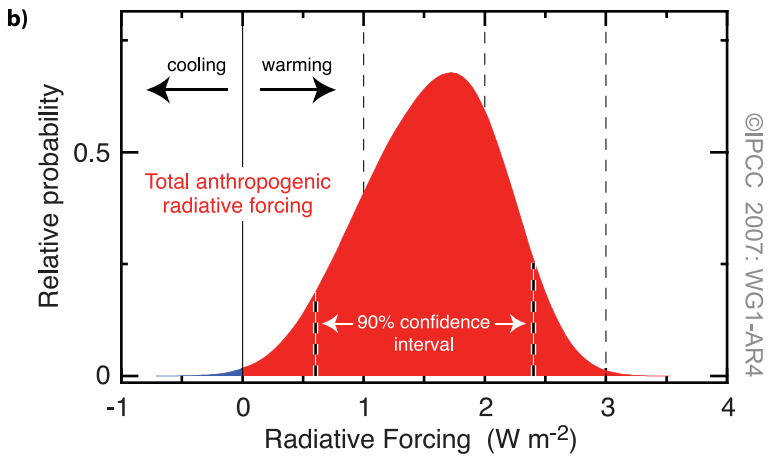


Figure TS.5. *(a) Global mean radiative forcings (RF) and their 90% confidence intervals in 2005 for various agents and mechanisms. Columns on the right-hand side specify best estimates and confidence intervals (RF values); typical geographical extent of the forcing (Spatial scale); and level of scientific understanding (LOSU) indicating the scientific confidence level as explained in Section 2.9. Errors for CH_4, N_2O and halocarbons have been combined. The net anthropogenic radiative forcing and its range are also shown. Best estimates and uncertainty ranges can not be obtained by direct addition of individual terms due to the asymmetric uncertainty ranges for some factors; the values given here were obtained from a Monte Carlo technique as discussed in Section 2.9. Additional forcing factors not included here are considered to have a very low LOSU. Volcanic aerosols contribute an additional form of natural forcing but are not included due to their episodic nature. The range for linear contrails does not include other possible effects of aviation on cloudiness. (b) Probability distribution of the global mean combined radiative forcing from all anthropogenic agents shown in (a). The distribution is calculated by combining the best estimates and uncertainties of each component. The spread in the distribution is increased significantly by the negative forcing terms, which have larger uncertainties than the positive terms. {2.9.1, 2.9.2; Figure 2.20}*

Table TS.2. *Lifetimes, radiative efficiencies and direct (except for CH_4) global warming potentials (GWP) relative to CO_2. {Table 2.14}*

Industrial Designation or Common Name (years)	Chemical Formula	Lifetime (years)	Radiative Efficiency (W m^{-2} ppb^{-1})	Global Warming Potential for Given Time Horizon			
				SAR‡ (100-yr)	20-yr	100-yr	500-yr
Carbon dioxide	CO_2	See below[a]	[b]1.4x10^{-5}	1	1	1	1
Methane[c]	CH_4	12[c]	3.7x10^{-4}	21	72	25	7.6
Nitrous oxide	N_2O	114	3.03x10^{-3}	310	289	298	153
Substances controlled by the Montreal Protocol							
CFC-11	CCl_3F	45	0.25	3,800	6,730	4,750	1,620
CFC-12	CCl_2F_2	100	0.32	8,100	11,000	10,900	5,200
CFC-13	$CClF_3$	640	0.25		10,800	14,400	16,400
CFC-113	CCl_2FCClF_2	85	0.3	4,800	6,540	6,130	2,700
CFC-114	$CClF_2CClF_2$	300	0.31		8,040	10,000	8,730
CFC-115	$CClF_2CF_3$	1,700	0.18		5,310	7,370	9,990
Halon-1301	$CBrF_3$	65	0.32	5,400	8,480	7,140	2,760
Halon-1211	$CBrClF_2$	16	0.3		4,750	1,890	575
Halon-2402	$CBrF_2CBrF_2$	20	0.33		3,680	1,640	503
Carbon tetrachloride	CCl_4	26	0.13	1,400	2,700	1,400	435
Methyl bromide	CH_3Br	0.7	0.01		17	5	1
Methyl chloroform	CH_3CCl_3	5	0.06		506	146	45
HCFC-22	$CHClF_2$	12	0.2	1,500	5,160	1,810	549
HCFC-123	$CHCl_2CF_3$	1.3	0.14	90	273	77	24
HCFC-124	$CHClFCF_3$	5.8	0.22	470	2,070	609	185
HCFC-141b	CH_3CCl_2F	9.3	0.14		2,250	725	220
HCFC-142b	CH_3CClF_2	17.9	0.2	1,800	5,490	2,310	705
HCFC-225ca	$CHCl_2CF_2CF_3$	1.9	0.2		429	122	37
HCFC-225cb	$CHClFCF_2CClF_2$	5.8	0.32		2,030	595	181
Hydrofluorocarbons							
HFC-23	CHF_3	270	0.19	11,700	12,000	14,800	12,200
HFC-32	CH_2F_2	4.9	0.11	650	2,330	675	205
HFC-125	CHF_2CF_3	29	0.23	2,800	6,350	3,500	1,100
HFC-134a	CH_2FCF_3	14	0.16	1,300	3,830	1,430	435
HFC-143a	CH_3CF_3	52	0.13	3,800	5,890	4,470	1,590
HFC-152a	CH_3CHF_2	1.4	0.09	140	437	124	38
HFC-227ea	CF_3CHFCF_3	34.2	0.26	2,900	5,310	3,220	1,040
HFC-236fa	$CF_3CH_2CF_3$	240	0.28	6,300	8,100	9,810	7,660
HFC-245fa	$CHF_2CH_2CF_3$	7.6	0.28		3,380	1030	314
HFC-365mfc	$CH_3CF_2CH_2CF_3$	8.6	0.21		2,520	794	241
HFC-43-10mee	$CF_3CHFCHFCF_2CF_3$	15.9	0.4	1,300	4,140	1,640	500
Perfluorinated compounds							
Sulphur hexafluoride	SF_6	3,200	0.52	23,900	16,300	22,800	32,600
Nitrogen trifluoride	NF_3	740	0.21		12,300	17,200	20,700
PFC-14	CF_4	50,000	0.10	6,500	5,210	7,390	11,200
PFC-116	C_2F_6	10,000	0.26	9,200	8,630	12,200	18,200

Table TS.2 (continued)

Industrial Designation or Common Name (years)	Chemical Formula	Lifetime (years)	Radiative Efficiency (W m^{-2} ppb^{-1})	Global Warming Potential for Given Time Horizon			
				SAR‡ (100-yr)	20-yr	100-yr	500-yr
***Perfluorinated compounds** (continued)*							
PFC-218	C_3F_8	2,600	0.26	7,000	6,310	8,830	12,500
PFC-318	c-C_4F_8	3,200	0.32	8,700	7,310	10,300	14,700
PFC-3-1-10	C_4F_{10}	2,600	0.33	7,000	6,330	8,860	12,500
PFC-4-1-12	C_5F_{12}	4,100	0.41		6,510	9,160	13,300
PFC-5-1-14	C_6F_{14}	3,200	0.49	7,400	6,600	9,300	13,300
PFC-9-1-18	$C_{10}F_{18}$	>1,000[d]	0.56		>5,500	>7,500	>9,500
trifluoromethyl sulphur pentafluoride	SF_5CF_3	800	0.57		13,200	17,700	21,200
Fluorinated ethers							
HFE-125	CHF_2OCF_3	136	0.44		13,800	14,900	8,490
HFE-134	CHF_2OCHF_2	26	0.45		12,200	6,320	1,960
HFE-143a	CH_3OCF_3	4.3	0.27		2,630	756	230
HCFE-235da2	$CHF_2OCHClCF_3$	2.6	0.38		1,230	350	106
HFE-245cb2	$CH_3OCF_2CHF_2$	5.1	0.32		2,440	708	215
HFE-245fa2	$CHF_2OCH_2CF_3$	4.9	0.31		2,280	659	200
HFE-254cb2	$CH_3OCF_2CHF_2$	2.6	0.28		1,260	359	109
HFE-347mcc3	$CH_3OCF_2CF_2CF_3$	5.2	0.34		1,980	575	175
HFE-347pcf2	$CHF_2CF_2OCH_2CF_3$	7.1	0.25		1,900	580	175
HFE-356pcc3	$CH_3OCF_2CF_2CHF_2$	0.33	0.93		386	110	33
HFE-449sl (HFE-7100)	$C_4F_9OCH_3$	3.8	0.31		1,040	297	90
HFE-569sf2 (HFE-7200)	$C_4F_9OC_2H_5$	0.77	0.3		207	59	18
HFE-43-10pccc124 (H-Galden 1040x)	$CHF_2OCF_2OC_2F_4OCHF_2$	6.3	1.37		6,320	1,870	569
HFE-236ca12 (HG-10)	$CHF_2OCF_2OCHF_2$	12.1	0.66		8,000	2,800	860
HFE-338pcc13 (HG-01)	$CHF_2OCF_2CF_2OCHF_2$	6.2	0.87		5,100	1,500	460
Perfluoropolyethers							
PFPMIE	$CF_3OCF(CF_3)CF_2OCF_2OCF_3$	800	0.65		7,620	10,300	12,400
Hydrocarbons and other compounds – Direct Effects							
Dimethylether	CH_3OCH_3	0.015	0.02		1	1	<<1
Methylene chloride	CH_2Cl_2	0.38	0.03		31	8.7	2.7
Methyl chloride	CH_3Cl	1.0	0.01		45	13	4

Notes:

‡ SAR refers to the IPCC Second Assessment Report (1995) used for reporting under the UNFCCC.

[a] The CO_2 response function used in this report is based on the revised version of the Bern Carbon cycle model used in Chapter 10 of this report (Bern2.5CC; Joos et al. 2001) using a background CO_2 concentration value of 378 ppm. The decay of a pulse of CO_2 with time t is given by

$$a_0 + \sum_{i=1}^{3} a_i \cdot e^{-t/\tau_i}$$ where $a_0 = 0.217$, $a_1 = 0.259$, $a_2 = 0.338$, $a_3 = 0.186$, $\tau_1 = 172.9$ years, $\tau_2 = 18.51$ years, and $\tau_3 = 1.186$ years, for $t < 1{,}000$ years.

[b] The radiative efficiency of CO_2 is calculated using the IPCC (1990) simplified expression as revised in the TAR, with an updated background concentration value of 378 ppm and a perturbation of +1 ppm (see Section 2.10.2).

[c] The perturbation lifetime for CH_4 is 12 years as in the TAR (see also Section 7.4). The GWP for CH_4 includes indirect effects from enhancements of ozone and stratospheric water vapour (see Section 2.10) .

[d] The assumed lifetime of 1000 years is a lower limit.

are largely controlled by climate processes and feedbacks. For example, sea ice-albedo feedbacks tend to enhance the high-latitude response. Spatial patterns of response are also affected by differences in thermal inertia between land and sea areas. {2.8, 9.2}

The pattern of response to a radiative forcing can be altered substantially if its structure is favourable for affecting a particular aspect of the atmospheric structure or circulation. Modelling studies and data comparisons suggest that mid- to high-latitude circulation patterns are *likely* to be affected by some forcings such as volcanic eruptions, which have been linked to changes in the Northern Annular Mode (NAM) and North Atlantic Oscillation (NAO) (see Section 3.1 and Box TS.2). Simulations also suggest that absorbing aerosols, particularly black carbon, can reduce the solar radiation reaching the surface and can warm the atmosphere at regional scales, affecting the vertical temperature profile and the large-scale atmospheric circulation. {2.8, 7.5, 9.2}

The spatial patterns of radiative forcings for ozone, aerosol direct effects, aerosol-cloud interactions and land use have considerable uncertainties. This is in contrast to the relatively high confidence in the spatial pattern of radiative forcing for the LLGHGs. The net positive radiative forcing in the Southern Hemisphere (SH) *very likely* exceeds that in the NH because of smaller aerosol concentrations in the SH. {2.9}

TS 2.6 Surface Forcing and the Hydrologic Cycle

Observations and models indicate that changes in the radiative flux at the Earth's surface affect the surface heat and moisture budgets, thereby involving the hydrologic cycle. Recent studies indicate that some forcing agents can influence the hydrologic cycle differently than others through their interactions with clouds. In particular, changes in aerosols may have affected precipitation and other aspects of the hydrologic cycle more strongly than other anthropogenic forcing agents. Energy deposited at the surface directly affects evaporation and sensible heat transfer. The instantaneous radiative flux change at the surface (hereafter called 'surface forcing') is a useful diagnostic tool for understanding changes in the heat and moisture surface budgets and the accompanying climate change. However, unlike radiative forcing, it cannot be used to quantitatively compare the effects of different agents on the equilibrium global mean surface temperature change. Net radiative forcing and surface forcing have different equator-to-pole gradients in the NH, and are different between the NH and SH. {2.9, 7.2, 7.5, 9.5}

TS.3 Observations of Changes in Climate

This assessment evaluates changes in the Earth's climate system, considering not only the atmosphere, but also the ocean and the cryosphere, as well as phenomena such as atmospheric circulation changes, in order to increase understanding of trends, variability and processes of climate change at global and regional scales. Observational records employing direct methods are of variable length as described below, with global temperature estimates now beginning as early as 1850. Observations of extremes of weather and climate are discussed, and observed changes in extremes are described. The consistency of observed changes among different climate variables that allows an increasingly comprehensive picture to be drawn is also described. Finally, palaeoclimatic information that generally employs indirect proxies to infer information about climate change over longer time scales (up to millions of years) is also assessed.

TS.3.1 Atmospheric Changes: Instrumental Record

This assessment includes analysis of global and hemispheric means, changes over land and ocean and distributions of trends in latitude, longitude and altitude. Since the TAR, improvements in observations and their calibration, more detailed analysis of methods and extended time series allow more in-depth analyses of changes including atmospheric temperature, precipitation, humidity, wind and circulation. Extremes of climate are a key expression of climate variability, and this assessment includes new data that permit improved insights into the changes in many types of extreme events including heat waves, droughts, heavy precipitation and tropical cyclones (including hurricanes and typhoons). {3.2–3.4, 3.8}

Furthermore, advances have occurred since the TAR in understanding how a number of seasonal and long-term anomalies can be described by patterns of climate variability. These patterns arise from internal interactions and from the differential effects on the atmosphere of land and ocean, mountains and large changes in heating. Their response is often felt in regions far removed from their physical source through atmospheric teleconnections associated with large-scale waves in the atmosphere. Understanding temperature and precipitation anomalies associated with the dominant patterns of climate variability is essential to understanding many regional climate anomalies and why these may differ from those at the global scale. Changes in storm tracks, the jet streams,

regions of preferred blocking anticyclones and changes in monsoons can also occur in conjunction with these preferred patterns of variability. {3.5–3.7}

TS.3.1.1 Global Average Temperatures

2005 and 1998 were the warmest two years in the instrumental global surface air temperature record since 1850. Surface temperatures in 1998 were enhanced by the major 1997–1998 El Niño but no such strong anomaly was present in 2005. Eleven of the last 12 years (1995 to 2006) – the exception being 1996 – rank among the 12 warmest years on record since 1850. {3.2}

The global average surface temperature has increased, especially since about 1950. The updated 100-year trend (1906–2005) of 0.74°C ± 0.18°C is larger than the 100-year warming trend at the time of the TAR (1901–2000) of 0.6°C ± 0.2°C due to additional warm years. The total temperature increase from 1850-1899 to 2001-2005 is 0.76°C ± 0.19°C. The rate of warming averaged over the last 50 years (0.13°C ± 0.03°C per decade) is nearly twice that for the last 100 years. Three different global estimates all show consistent warming trends. There is also consistency between the data sets in their separate land and ocean domains, and between sea surface temperature (SST) and nighttime marine air temperature (see Figure TS.6). {3.2}

Recent studies confirm that effects of urbanisation and land use change on the global temperature record are negligible (less than 0.006°C per decade over land and zero over the ocean) as far as hemispheric- and continental-scale averages are concerned. All observations are subject to data quality and consistency checks to correct for potential biases. The real but local effects of urban areas are accounted for in the land temperature data sets used. Urbanisation and land use effects are not relevant to the widespread oceanic warming that has been observed. Increasing evidence suggests that urban heat island effects also affect precipitation, cloud and diurnal temperature range (DTR). {3.2}

The global average DTR has stopped decreasing. A decrease in DTR of approximately 0.1°C per decade was reported in the TAR for the period 1950 to 1993. Updated observations reveal that DTR has not changed from 1979 to 2004 as both day- and night time temperature have risen at about the same rate. The trends are highly variable from one region to another. {3.2}

New analyses of radiosonde and satellite measurements of lower- and mid-tropospheric temperature show warming rates that are generally consistent with each other and with those in the surface temperature record within their respective uncertainties for the periods 1958 to 2005 and 1979 to 2005. This largely resolves a discrepancy noted in the TAR (see Figure TS.7). The radiosonde record is markedly less spatially complete than the surface record and increasing evidence suggests that a number of radiosonde data sets are unreliable, especially in the tropics. Disparities remain among different tropospheric temperature trends estimated from satellite Microwave Sounding Unit (MSU) and advanced MSU measurements since 1979, and all likely still contain residual errors. However, trend estimates have been substantially improved and data set differences reduced since the TAR, through adjustments for changing satellites, orbit decay and drift in local crossing time (diurnal cycle effects). It appears that the satellite tropospheric temperature record is broadly consistent with surface temperature trends provided that the stratospheric influence on MSU channel 2 is accounted for. The range across different data sets of global surface warming since 1979 is 0.16°C to 0.18°C per decade, compared to 0.12°C to 0.19°C per decade for MSU-derived estimates of tropospheric temperatures. It is likely that there is increased warming with altitude from the surface through much of the troposphere in the tropics, pronounced cooling in the stratosphere, and a trend towards a higher tropopause. {3.4}

Stratospheric temperature estimates from adjusted radiosondes, satellites and reanalyses are all in qualitative agreement, with a cooling of between 0.3°C and 0.6°C per decade since 1979 (see Figure TS.7). Longer radiosonde records (back to 1958) also indicate stratospheric cooling but are subject to substantial instrumental uncertainties. The rate of cooling increased after 1979 but has slowed in the last decade. It is *likely* that radiosonde records overestimate stratospheric cooling, owing to changes in sondes not yet taken into account. The trends are not monotonic, because of stratospheric warming episodes that follow major volcanic eruptions. {3.4}

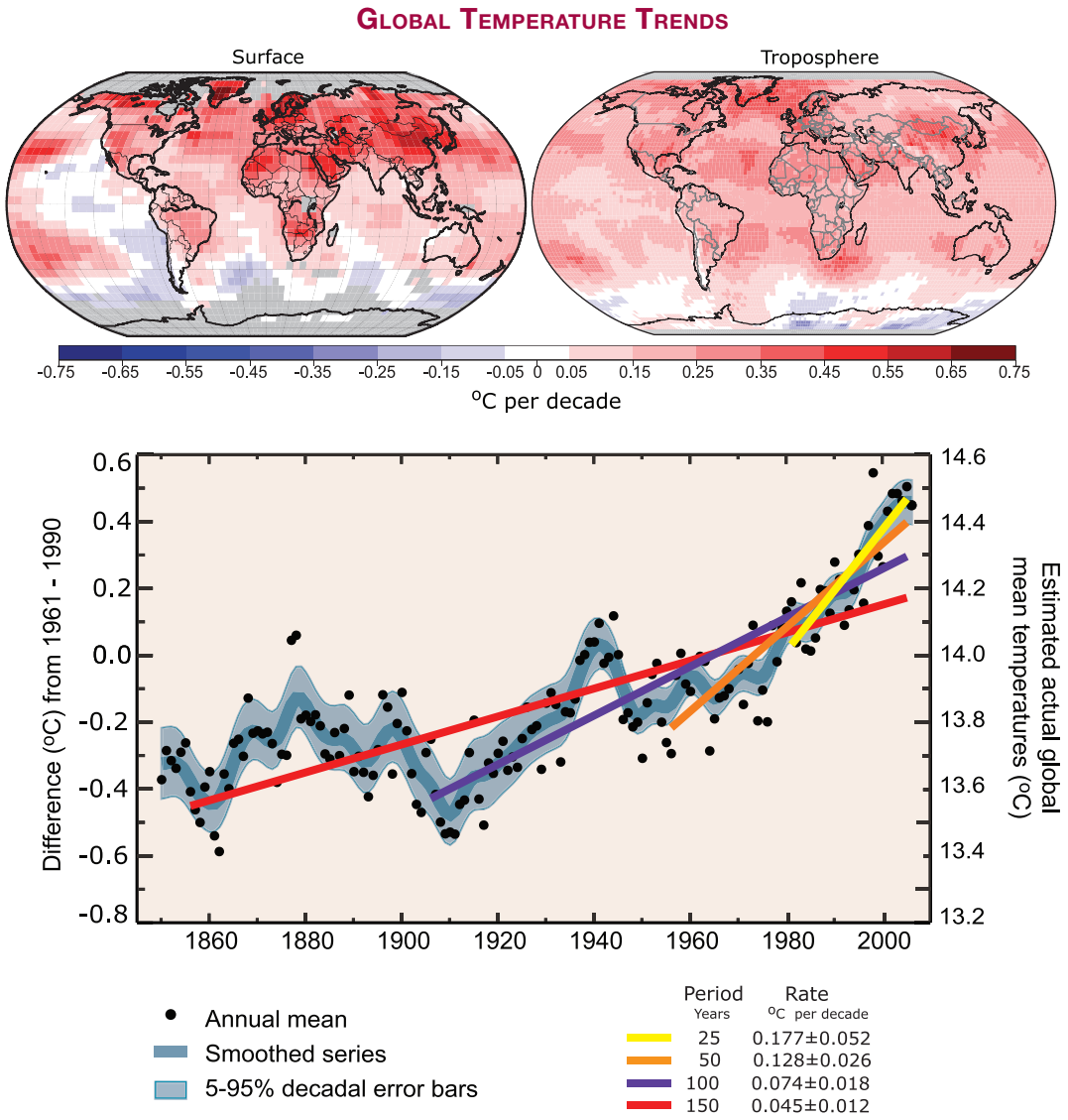


Figure TS.6. *(Top) Patterns of linear global temperature trends over the period 1979 to 2005 estimated at the surface (left), and for the troposphere from satellite records (right). Grey indicates areas with incomplete data. (Bottom) Annual global mean temperatures (black dots) with linear fits to the data. The left hand axis shows temperature anomalies relative to the 1961 to 1990 average and the right hand axis shows estimated actual temperatures, both in °C. Linear trends are shown for the last 25 (yellow), 50 (orange), 100 (purple) and 150 years (red). The smooth blue curve shows decadal variations (see Appendix 3.A), with the decadal 90% error range shown as a pale blue band about that line. The total temperature increase from the period 1850 to 1899 to the period 2001 to 2005 is 0.76°C ± 0.19°C. {FAQ 3.1, Figure 1.}*

TS.3.1.2 Spatial Distribution of Changes in Temperature, Circulation and Related Variables

Surface temperatures over land regions have warmed at a faster rate than over the oceans in both hemispheres. Longer records now available show significantly faster rates of warming over land than ocean in the past two decades (about 0.27°C vs. 0.13°C per decade). {3.2}

The warming in the last 30 years is widespread over the globe, and is greatest at higher northern latitudes. The greatest warming has occurred in the NH winter (DJF) and spring (MAM). Average arctic temperatures have been increasing at almost twice the rate of the rest of the world in the past 100 years. However, arctic temperatures are highly variable. A slightly longer arctic warm period, almost as warm as the present, was observed from 1925 to 1945, but its geographical distribution appears to have been different from the recent warming since its extent was not global. {3.2}

There is evidence for long-term changes in the large-scale atmospheric circulation, such as a poleward shift and strengthening of the westerly winds. Regional climate trends can be very different from the global average, reflecting changes in the circulations and interactions of the atmosphere and ocean and the other components of the climate system. Stronger mid-latitude westerly wind maxima have occurred in both hemispheres in most seasons from at least 1979 to the late 1990s, and poleward displacements of corresponding Atlantic and southern polar front jet streams have been documented. The westerlies in the NH increased from the 1960s to the 1990s but have since returned to values close to the long-term average. The increased strength of the westerlies in the NH changes the flow from oceans to continents, and is a major factor in the observed winter changes in storm tracks and related patterns of precipitation and temperature trends at mid- and high-latitudes. Analyses of wind and significant wave height support reanalysis-based evidence for changes in NH extratropical storms from the start of the reanalysis record in the late 1970s until the late 1990s. These changes are accompanied by a tendency towards stronger winter polar vortices throughout the troposphere and lower stratosphere. {3.2, 3.5}

Many regional climate changes can be described in terms of preferred patterns of climate variability and therefore as changes in the occurrence of indices that characterise the strength and phase of these patterns. The importance, over all time scales, of fluctuations in the westerlies and storm tracks in the North Atlantic has often been noted, and these fluctuations are described by the NAO (see Box TS.2 for an explanation of this and other preferred patterns). The characteristics of fluctuations in the zonally averaged westerlies in the two hemispheres have more recently been described by their respective 'annular modes', the Northern and Southern Annular Modes (NAM and SAM). The observed changes can be expressed as a shift of the circulation towards the structure associated with one sign of these preferred patterns. The increased mid-latitude westerlies in the North Atlantic can be largely viewed as reflecting either NAO or NAM changes; multi-decadal variability is also evident in the Atlantic, both in the atmosphere and the ocean. In the SH, changes in circulation related to an increase in the SAM from the 1960s to the present are associated with strong warming over the Antarctic Peninsula and, to a lesser extent, cooling over parts of continental Antarctica. Changes have also been observed in ocean-atmosphere interactions in the Pacific. The ENSO is the dominant mode of global-scale variability on interannual time scales although there have been times when it is less apparent. The 1976–1977 climate shift, related to the phase change in the Pacific Decadal Oscillation (PDO) towards more El Niño events and changes in the evolution of ENSO, has affected many areas, including most tropical monsoons. For instance, over North America, ENSO and Pacific-

Observed Air Temperatures

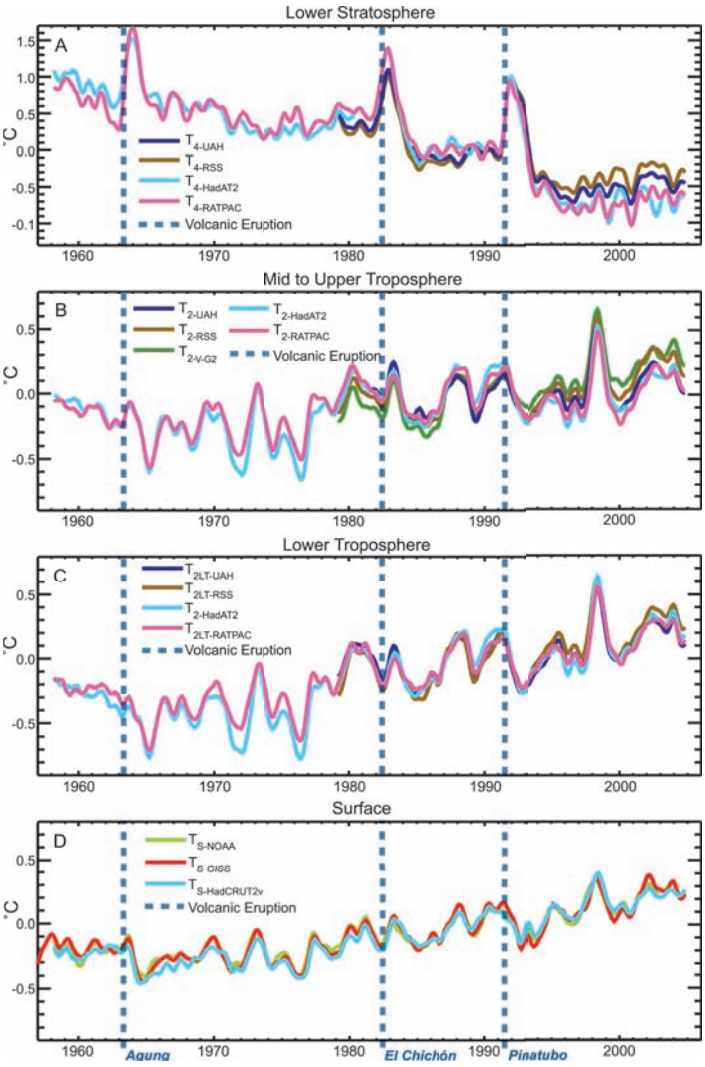


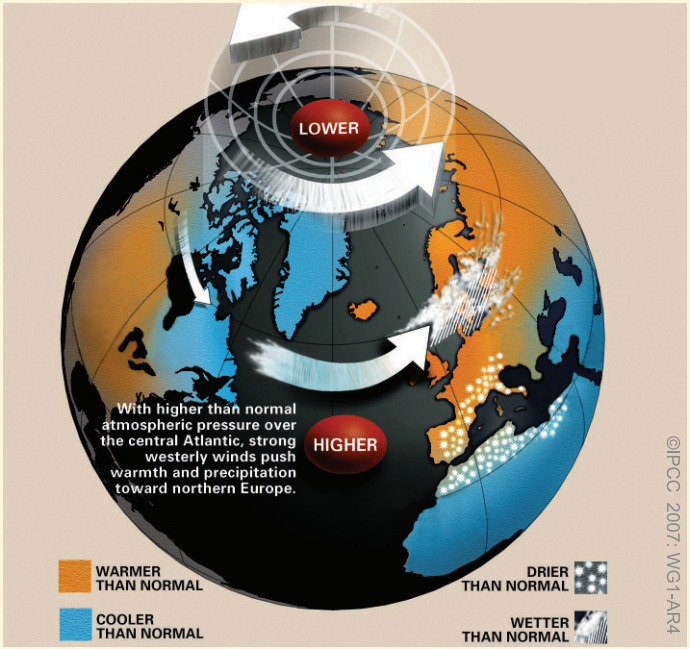
Figure TS.7. *Observed surface (D) and upper air temperatures for the lower troposphere (C), mid- to upper troposphere (B) and lower stratosphere (A), shown as monthly mean anomalies relative to the period 1979 to 1997 smoothed with a seven-month running mean filter. Dashed lines indicate the times of major volcanic eruptions. {Figure 3.17}*

Box TS.2: Patterns (Modes) of Climate Variability

Analysis of atmospheric and climatic variability has shown that a significant component of it can be described in terms of fluctuations in the amplitude and sign of indices of a relatively small number of preferred patterns of variability. Some of the best known of these are:

- El Niño-Southern Oscillation (ENSO), a coupled fluctuation in the atmosphere and the equatorial Pacific Ocean, with preferred time scales of two to about seven years. ENSO is often measured by the difference in surface pressure anomalies between Tahiti and Darwin and the SSTs in the central and eastern equatorial Pacific. ENSO has global teleconnections.
- North Atlantic Oscillation (NAO), a measure of the strength of the Icelandic Low and the Azores High, and of the westerly winds between them, mainly in winter. The NAO has associated fluctuations in the storm track, temperature and precipitation from the North Atlantic into Eurasia (see Box TS.2, Figure 1).
- Northern Annular Mode (NAM), a winter fluctuation in the amplitude of a pattern characterised by low surface pressure in the Arctic and strong mid-latitude westerlies. The NAM has links with the northern polar vortex and hence the stratosphere.
- Southern Annular Mode (SAM), the fluctuation of a pattern with low antarctic surface pressure and strong mid-latitude westerlies, analogous to the NAM, but present year round.
- Pacific-North American (PNA) pattern, an atmospheric large-scale wave pattern featuring a sequence of tropospheric high- and low-pressure anomalies stretching from the subtropical west Pacific to the east coast of North America.
- Pacific Decadal Oscillation (PDO), a measure of the SSTs in the North Pacific that has a very strong correlation with the North Pacific Index (NPI) measure of the depth of the Aleutian Low. However, it has a signature throughout much of the Pacific.

Positive Phase of NAO and NAM



Box TS.2, Figure 1. *A schematic of the changes associated with the positive phase of the NAO and NAM. The changes in pressure and winds are shown, along with precipitation changes. Warm colours indicate areas that are warmer than normal and blue indicates areas that are cooler than normal.*

The extent to which all these preferred patterns of variability can be considered to be true modes of the climate system is a topic of active research. However, there is evidence that their existence can lead to larger-amplitude regional responses to forcing than would otherwise be expected. In particular, a number of the observed 20th-century climate changes can be viewed in terms of changes in these patterns. It is therefore important to test the ability of climate models to simulate them (see Section TS.4, Box TS.7) and to consider the extent to which observed changes related to these patterns are linked to internal variability or to anthropogenic climate change. {3.6, 8.4}

North American (PNA) teleconnection-related changes appear to have led to contrasting changes across the continent, as the western part has warmed more than the eastern part, while the latter has become cloudier and wetter. There is substantial low-frequency atmospheric variability in the Pacific sector over the 20th century, with extended periods of weakened (1900–1924; 1947–1976) as well as strengthened (1925–1946; 1977–2003) circulation. {3.2, 3.5, 3.6}

Changes in extremes of temperature are consistent with warming. Observations show widespread reductions in the number of frost days in mid-latitude regions, increases in the number of warm extremes (warmest 10% of days or nights) and a reduction in the number of daily cold extremes (coldest 10% of days or nights) (see Box TS.5). The most marked changes are for cold nights, which have declined over the 1951 to 2003 period for all regions where data are available (76% of the land). {3.8}

Heat waves have increased in duration beginning in the latter half of the 20th century. The record-breaking heat wave over western and central Europe in the summer of 2003 is an example of an exceptional recent extreme. That summer (JJA) was the warmest since comparable instrumental records began around 1780 (1.4°C above the previous warmest in 1807). Spring drying of the land surface over Europe was an important factor in the occurrence of the extreme 2003 temperatures. Evidence suggests that heat waves have also increased in frequency and duration in other locations. The very strong correlation between observed dryness and high temperatures over land in the tropics during summer highlights the important role moisture plays in moderating climate. {3.8, 3.9}

There is insufficient evidence to determine whether trends exist in such events as tornadoes, hail, lightning and dust storms which occur at small spatial scales. {3.8}

TS.3.1.3 Changes in the Water Cycle: Water Vapour, Clouds, Precipitation and Tropical Storms

Tropospheric water vapour is increasing (Figure TS.8). Surface specific humidity has generally increased since 1976 in close association with higher temperatures over both land and ocean. Total column water vapour has increased over the global oceans by 1.2 ± 0.3% per decade (95% confidence limits) from 1988 to 2004. The observed regional changes are consistent in pattern and amount with the changes in SST and the assumption of a near-constant relative humidity increase in water vapour mixing ratio. The additional atmospheric water vapour implies increased moisture availability for precipitation. {3.4}

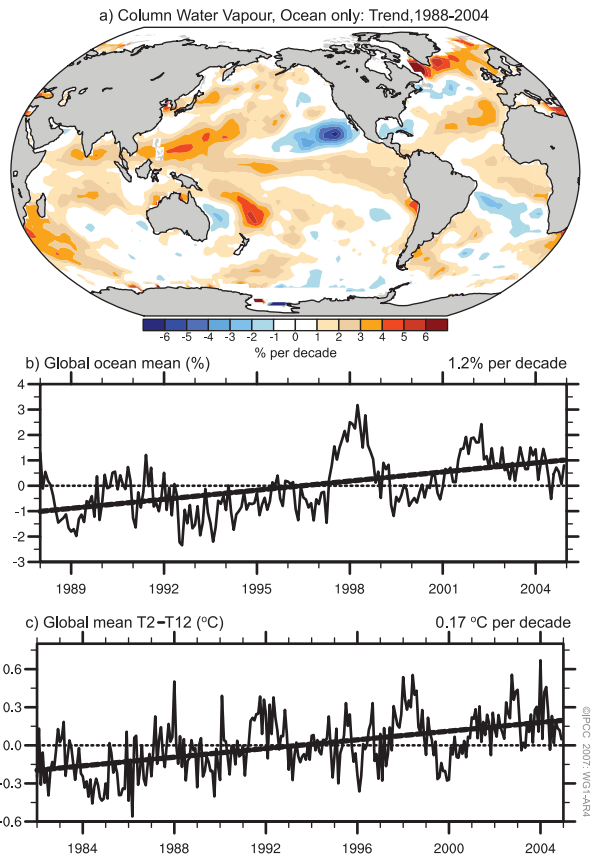


Figure TS.8. *(a) Linear trends in precipitable water (total column water vapour) over the period 1988 to 2004 (% per decade) and (b) the monthly time series of anomalies, relative to the period shown, over the global ocean with linear trend. (c) The global mean (80°N to 80°S) radiative signature of upper-tropospheric moistening is given by monthly time series of combinations of satellite brightness temperature anomalies (°C), relative to the period 1982 to 2004, with the dashed line showing the linear trend of the key brightness temperature in °C per decade. {3.4, Figures 3.20 and 3.21}*

Upper-tropospheric water vapour is also increasing. Due to instrumental limitations, it is difficult to assess long-term changes in water vapour in the upper troposphere, where it is of radiative importance. However, the available data now show evidence for global increases in upper-tropospheric specific humidity over the past two decades (Figure TS.8). These observations are consistent with the observed increase in temperatures and represent an important advance since the TAR. {3.4}

Cloud changes are dominated by ENSO. Widespread (but not ubiquitous) decreases in continental DTR have coincided with increases in cloud amounts. Surface and satellite observations disagree on changes in total and low-level cloud changes over the ocean. However, radiation

changes at the top of the atmosphere from the 1980s to 1990s (possibly related in part to the ENSO phenomenon) appear to be associated with reductions in tropical upper-level cloud cover, and are consistent with changes in the energy budget and in observed ocean heat content. {3.4}

'Global dimming' is not global in extent and it has not continued after 1990. Reported decreases in solar radiation at the Earth's surface from 1970 to 1990 have an urban bias. Further, there have been increases since about 1990. An increasing aerosol load due to human activities decreases regional air quality and the amount of solar radiation reaching the Earth's surface. In some areas, such as Eastern Europe, recent observations of a reversal in the sign of this effect link changes in solar radiation to concurrent air quality improvements. {3.4}

Long-term trends in precipitation amounts from 1900 to 2005 have been observed in many large regions (Figure TS.9). Significantly increased precipitation has been observed in the eastern parts of North and South America, northern Europe and northern and central Asia. Drying has been observed in the Sahel, the Mediterranean, southern Africa and parts of southern Asia. Precipitation is highly variable spatially and temporally, and robust long-term trends have not been established for other large regions.[5] {3.3}

Substantial increases in heavy precipitation events have been observed. It is *likely* that there have been increases in the number of heavy precipitation events (e.g., above the 95th percentile) in many land regions since about 1950, even in those regions where there has been a reduction in total precipitation amount. Increases have also been reported for rarer precipitation events (1 in 50 year return period), but only a few regions have sufficient data to assess such trends reliably (see Figure TS.10). {3.8}

There is observational evidence for an increase of intense tropical cyclone activity in the North Atlantic since about 1970, correlated with increases in tropical SSTs. There are also suggestions of increased intense tropical cyclone activity in some other regions where concerns over data quality are greater. Multi-decadal variability and the quality of the tropical cyclone records prior to routine satellite observations in about 1970 complicate the detection of long-term trends in tropical cyclone activity and there is no clear trend in the annual numbers of tropical cyclones. Estimates of the potential destructiveness of tropical cyclones suggest a substantial upward trend since the mid-1970s, with a trend towards longer lifetimes and greater intensity. Trends are also apparent in SST, a critical variable known to influence

Global Mean Precipitation

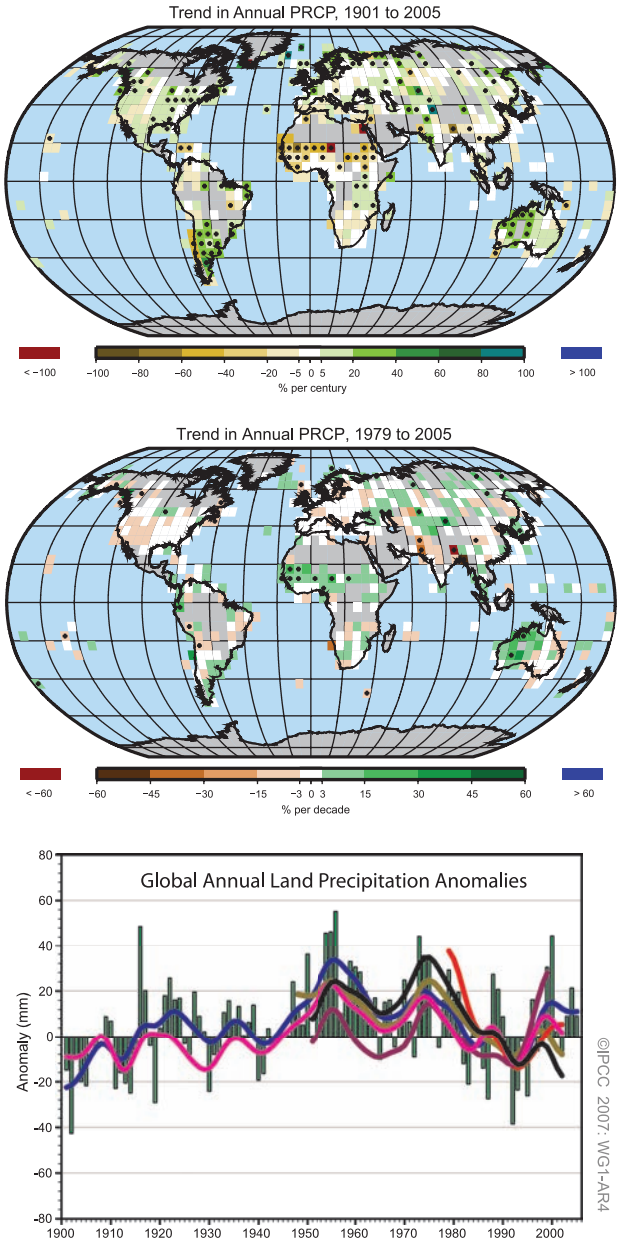


Figure TS.9. *(Top) Distribution of linear trends of annual land precipitation amounts over the period 1901 to 2005 (% per century) and (middle) 1979 to 2005 (% per decade). Areas in grey have insufficient data to produce reliable trends. The percentage is based on the 1961 to 1990 period. (Bottom) Time series of annual global land precipitation anomalies with respect to the 1961 to 1990 base period for 1900 to 2005. The smooth curves show decadal variations (see Appendix 3.A) for different data sets. {3.3, Figures 3.12 and 3.13}*

[5] The assessed regions are those considered in the regional projections chapter of the TAR and in Chapter 11 of this report.

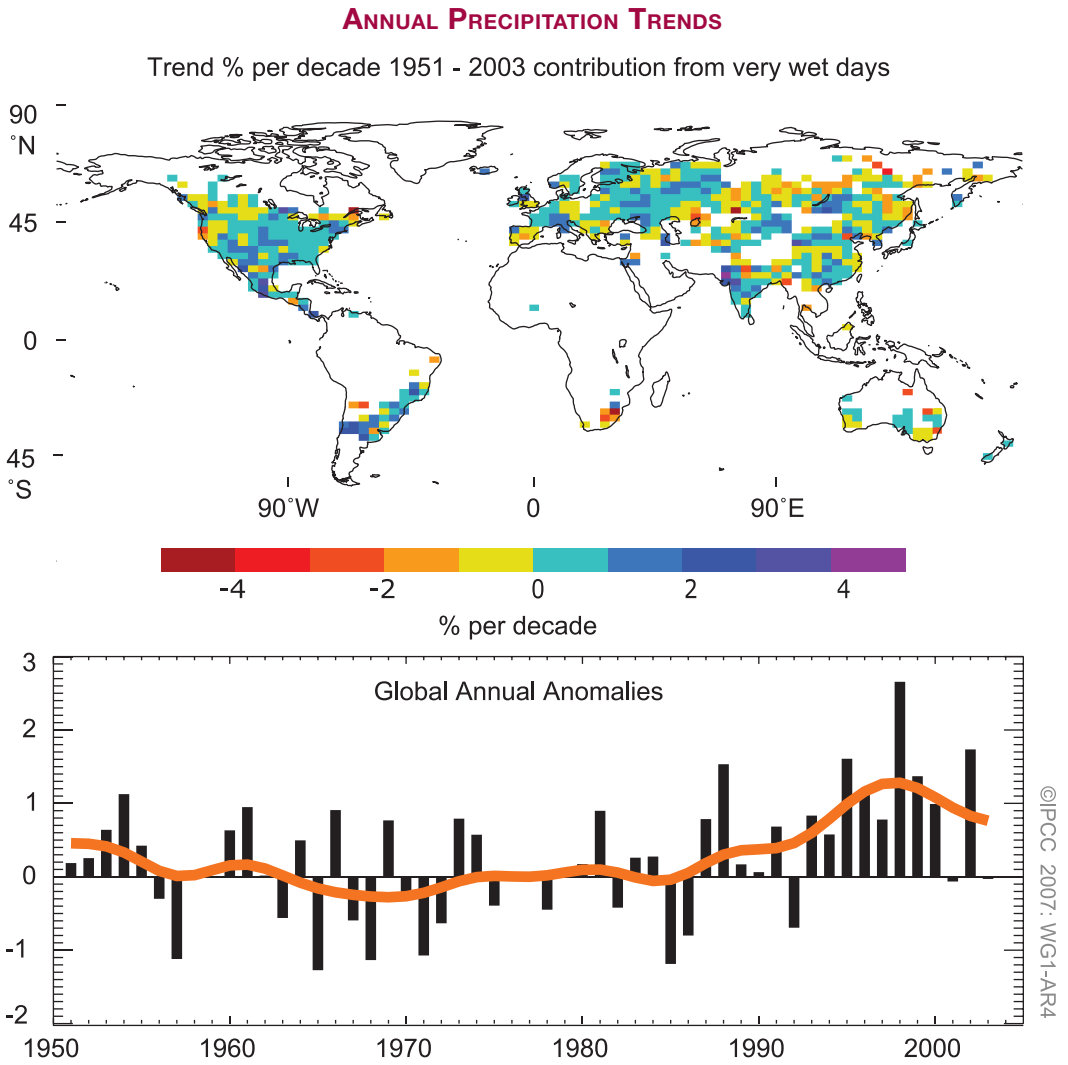


Figure TS.10. *(Top) Observed trends (% per decade) over the period 1951 to 2003 in the contribution to total annual precipitation from very wet days (i.e., corresponding to the 95th percentile and above). White land areas have insufficient data for trend determination. (Bottom) Anomalies (%) of the global (regions with data shown in top panel) annual time series of very wet days (with respect to 1961–1990) defined as the percentage change from the base period average (22.5%). The smooth orange curve shows decadal variations (see Appendix 3.A). {Figure 3.39}*

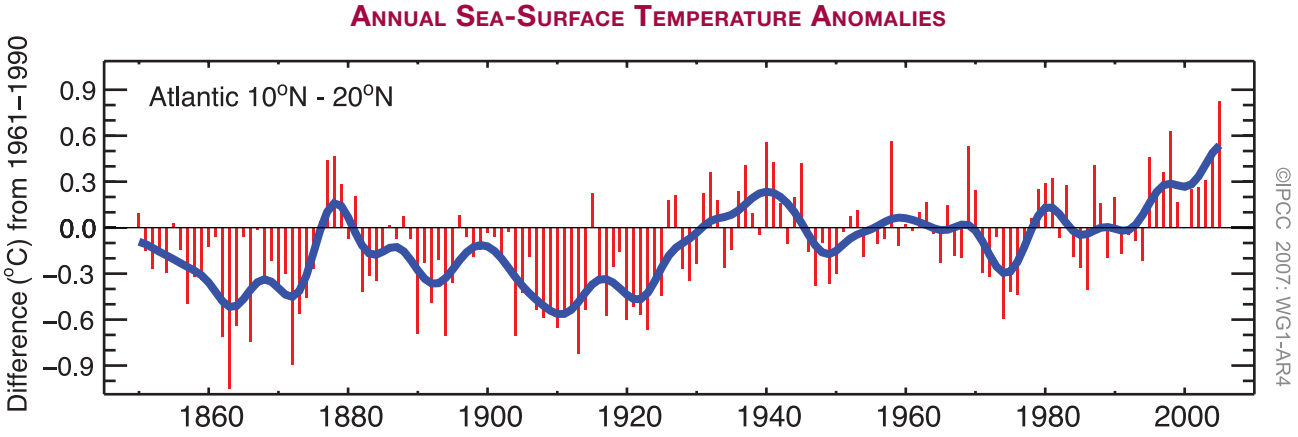


Figure TS.11. *Tropical Atlantic (10°N–20°N) sea surface temperature annual anomalies (°C) in the region of Atlantic hurricane formation, relative to the 1961 to 1990 mean. {Figure 3.33}*

tropical cyclone development (see Figure TS.11). Variations in the total numbers of tropical cyclones result from ENSO and decadal variability, which also lead to a redistribution of tropical storm numbers and tracks. The numbers of hurricanes in the North Atlantic have been above normal (based on 1981–2000) in nine of the years from 1995 to 2005. {3.8}

More intense and longer droughts have been observed over wider areas, particularly in the tropics and subtropics since the 1970s. While there are many different measures of drought, many studies use precipitation changes together with temperature.[6] Increased drying due to higher temperatures and decreased land precipitation have contributed to these changes. {3.3}

TS.3.2 Changes in the Cryosphere: Instrumental Record

Currently, ice permanently covers 10% of the land surface, with only a tiny fraction occurring outside Antarctica and Greenland. Ice also covers approximately 7% of the oceans in the annual mean. In midwinter, snow covers approximately 49% of the land surface in the NH. An important property of snow and ice is its high surface albedo. Because up to 90% of the incident solar radiation is reflected by snow and ice surfaces, while only about 10% is reflected by the open ocean or forested lands, changes in snow and ice cover are important feedback mechanisms in climate change. In addition, snow and ice are effective insulators. Seasonally frozen ground is more extensive than snow cover, and its presence is important for energy and moisture fluxes. Therefore, frozen surfaces play important roles in energy and climate processes. {4.1}

The cryosphere stores about 75% of the world's freshwater. At a regional scale, variations in mountain snowpack, glaciers and small ice caps play a crucial role in freshwater availability. Since the change from ice to liquid water occurs at specific temperatures, ice is a component of the climate system that could be subject to abrupt change following sufficient warming. Observations and analyses of changes in ice have expanded and improved since the TAR, including shrinkage of mountain glacier volume, decreases in snow cover, changes in permafrost and frozen ground, reductions in arctic sea ice extent, coastal thinning of the Greenland Ice Sheet exceeding inland thickening from increased snowfall, and reductions in seasonally frozen ground and river and lake ice cover. These allow an improved understanding of how the cryosphere is changing, including its contributions to recent changes in sea level. The periods from 1961 to the present and from 1993 to the present are a focus of this report, due to the availability of directly measured glacier mass balance data and altimetry observations of the ice sheets, respectively. {4.1}

Snow cover has decreased in most regions, especially in spring. Northern Hemisphere snow cover observed by satellite over the 1966 to 2005 period decreased in every month except November and December, with a stepwise drop of 5% in the annual mean in the late 1980s (see Figure TS.12). In the SH, the few long records or proxies mostly show either decreases or no changes in the past 40 years or more. Northern Hemisphere April snow cover extent is strongly correlated with 40°N to 60°N April temperature, reflecting the feedback between snow and temperature. {4.2}

Decreases in snowpack have been documented in several regions worldwide based upon annual time series of mountain snow water equivalent and snow depth. Mountain snow can be sensitive to small changes in temperature, particularly in temperate climatic zones where the transition from rain to snow is generally closely associated with the altitude of the freezing level. Declines in mountain snowpack in western North America and in the Swiss Alps are largest at lower, warmer elevations. Mountain snow water equivalent has declined since 1950 at 75% of the stations monitored in western North America. Mountain snow depth has also declined in the Alps and in southeastern Australia. Direct observations of snow depth are too limited to determine changes in the Andes, but temperature measurements suggest that the altitude where snow occurs (above the snow line) has probably risen in mountainous regions of South America. {4.2}

Permafrost and seasonally frozen ground in most regions display large changes in recent decades. Changes in permafrost conditions can affect river runoff, water supply, carbon exchange and landscape stability, and can cause damage to infrastructure. Temperature increases at the top of the permafrost layer of up to 3°C since the 1980s have been reported. Permafrost warming has also been observed with variable magnitude in the Canadian Arctic, Siberia, the Tibetan Plateau and Europe. The permafrost base is thawing at a rate ranging from 0.04 m yr^{-1} in Alaska to 0.02 m yr^{-1} on the Tibetan Plateau. {4.7}

The maximum area covered by seasonally frozen ground decreased by about 7% in the NH over the

[6] Precipitation and temperature are combined in the Palmer Drought Severity Index (PDSI), considered in this report as one measure of drought. The PDSI does not include variables such as wind speed, solar radiation, cloudiness and water vapour but is a superior measure to precipitation alone.

Box TS.3: Ice Sheet Dynamics and Stability

Ice sheets are thick, broad masses of ice formed mainly from compaction of snow. They spread under their own weight, transferring mass towards their margins where it is lost primarily by runoff of surface melt water or by calving of icebergs into marginal seas or lakes. Ice sheets flow by deformation within the ice or melt water-lubricated sliding over materials beneath. Rapid basal motion requires that the basal temperature be raised to the melting point by heat from the Earth's interior, delivered by melt water transport, or from the 'friction' of ice motion. Sliding velocities under a given gravitational stress can differ by several orders of magnitude, depending on the presence or absence of deformable sediment, the roughness of the substrate and the supply and distribution of water. Basal conditions are generally poorly characterised, introducing important uncertainties to the understanding of ice sheet stability. {4.6}

Ice flow is often channelled into fast-moving ice streams (that flow between slower-moving ice walls) or outlet glaciers (with rock walls). Enhanced flow in ice streams arises either from higher gravitational stress linked to thicker ice in bedrock troughs, or from increased basal lubrication. {4.6}

Ice discharged across the coast often remains attached to the ice sheet to become a floating ice shelf. An ice shelf moves forward, spreading and thinning under its own weight, and fed by snowfall on its surface and ice input from the ice sheet. Friction at ice shelf sides and over local shoals slows the flow of the ice shelf and thus the discharge from the ice sheet. An ice shelf loses mass by calving icebergs from the front and by basal melting into the ocean cavity beneath. Studies suggest an ocean warming of 1°C could increase ice shelf basal melt by 10 m yr^{-1}, but inadequate knowledge of the largely inaccessible ice shelf cavities restricts the accuracy of such estimates. {4.6}

The palaeo-record of previous ice ages indicates that ice sheets shrink in response to warming and grow in response to cooling, and that shrinkage can be far faster than growth. The volumes of the Greenland and Antarctic Ice Sheets are equivalent to approximately 7 m and 57 m of sea level rise, respectively. Palaeoclimatic data indicate that substantial melting of one or both ice sheets has likely occurred in the past. However, ice core data show that neither ice sheet was completely removed during warm periods of at least the past million years. Ice sheets can respond to environmental forcing over very long time scales, implying that commitments to future changes may result from current warming. For example, a surface warming may take more than 10,000 years to penetrate to the bed and change temperatures there. Ice velocity over most of an ice sheet changes slowly in response to changes in the ice sheet shape or surface temperature, but large velocity changes may occur rapidly in ice streams and outlet glaciers in response to changing basal conditions, penetration of surface melt water to the bed or changes in the ice shelves into which they flow. {4.6, 6.4}

Models currently configured for long integrations remain most reliable in their treatment of surface accumulation and ablation, as for the TAR, but do not include full treatments of ice dynamics; thus, analyses of past changes or future projections using such models may underestimate ice flow contributions to sea level rise, but the magnitude of such an effect is unknown. {8.2}

latter half of the 20th century, with a decrease in spring of up to 15%. Its maximum depth has decreased by about 0.3 m in Eurasia since the mid-20th century. In addition, maximum seasonal thaw depth increased by about 0.2 m in the Russian Arctic from 1956 to 1990. {4.7}

On average, the general trend in NH river and lake ice over the past 150 years indicates that the freeze-up date has become later at an average rate of 5.8 ± 1.9 days per century, while the breakup date has occurred earlier, at a rate of 6.5 ± 1.4 days per century. However, considerable spatial variability has also been observed, with some regions showing trends of opposite sign. {4.3}

Annual average arctic sea ice extent has shrunk by about 2.7 ± 0.6% per decade since 1978 based upon satellite observations (see Figure TS.13). The decline in summer extent is larger than in winter extent, with the summer minimum declining at a rate of about 7.4 ± 2.4% per decade. Other data indicate that the summer decline began around 1970. Similar observations in the Antarctic reveal larger interannual variability but no consistent trends during the period of satellite observations. In contrast to changes in continental ice such as ice sheets and glaciers, changes in sea ice do not directly contribute to sea level change (because this ice is already floating), but can contribute to salinity changes through input of freshwater. {4.4}

During the 20th century, glaciers and ice caps have experienced widespread mass losses and have contributed to sea level rise. Mass loss of glaciers and ice caps (excluding those around the ice sheets of Greenland and Antarctica) is estimated to be 0.50 ± 0.18 mm yr^{-1} in sea level equivalent (SLE) between 1961 and 2003, and 0.77 ± 0.22 mm yr^{-1} SLE between 1991 and 2003. The late 20th-century glacier wastage *likely* has been a response to post-1970 warming. {4.5}

Recent observations show evidence for rapid changes in ice flow in some regions, contributing to sea level rise and suggesting that the dynamics of ice

motion may be a key factor in future responses of ice shelves, coastal glaciers and ice sheets to climate change. Thinning or loss of ice shelves in some near-coastal regions of Greenland, the Antarctic Peninsula and West Antarctica has been associated with accelerated flow of nearby glaciers and ice streams, suggesting that ice shelves (including short ice shelves of kilometres or tens of kilometres in length) could play a larger role in stabilising or restraining ice motion than previously thought. Both oceanic and atmospheric temperatures appear to contribute to the observed changes. Large summer warming in the Antarctic Peninsula region *very likely* played a role in the subsequent rapid breakup of the Larsen B Ice Shelf in 2002 by increasing summer melt water, which drained into crevasses and wedged them open. Models do not accurately capture all of the physical processes that appear to be involved in observed iceberg calving (as in the breakup of Larsen B). {4.6}

Changes in Snow Cover

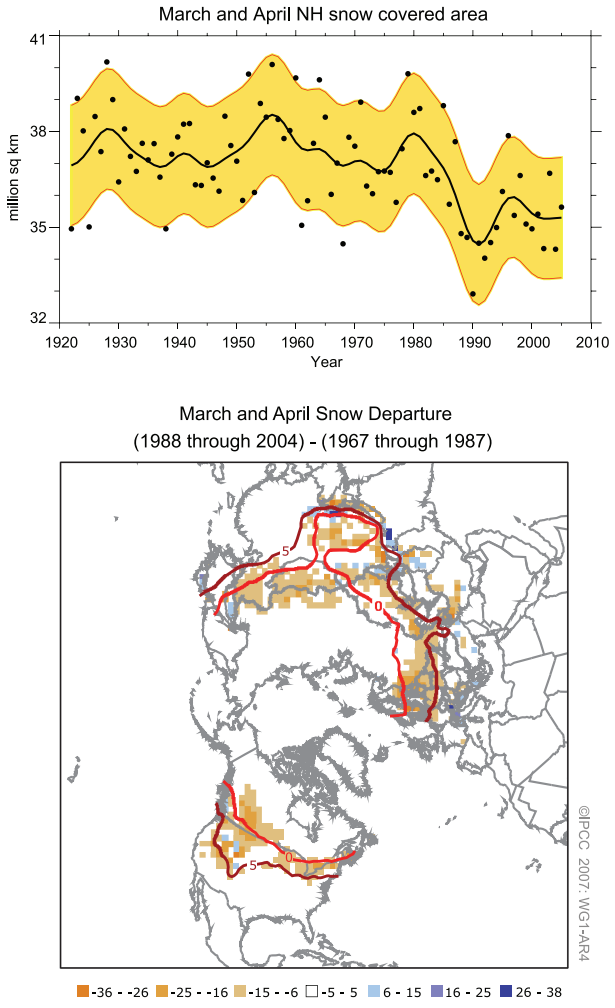


Figure TS.12. *(Top) Northern Hemisphere March-April snow-covered area from a station-derived snow cover index (prior to 1972) and from satellite data (during and after 1972). The smooth curve shows decadal variations (see Appendix 3.A) with the 5 to 95% data range shaded in yellow. (Bottom) Differences in the distribution of March-April snow cover between earlier (1967–1987) and later (1988–2004) portions of the satellite era (expressed in percent coverage). Tan colours show areas where snow cover has declined. Red curves show the 0°C and 5°C isotherms averaged for March-April 1967 to 2004, from the Climatic Research Unit (CRU) gridded land surface temperature version 2 (CRUTEM2v) data. The greatest decline generally tracks the 0°C and 5°C isotherms, reflecting the strong feedback between snow and temperature. {Figures 4.2, 4.3}*

Changes in Sea Ice Extent

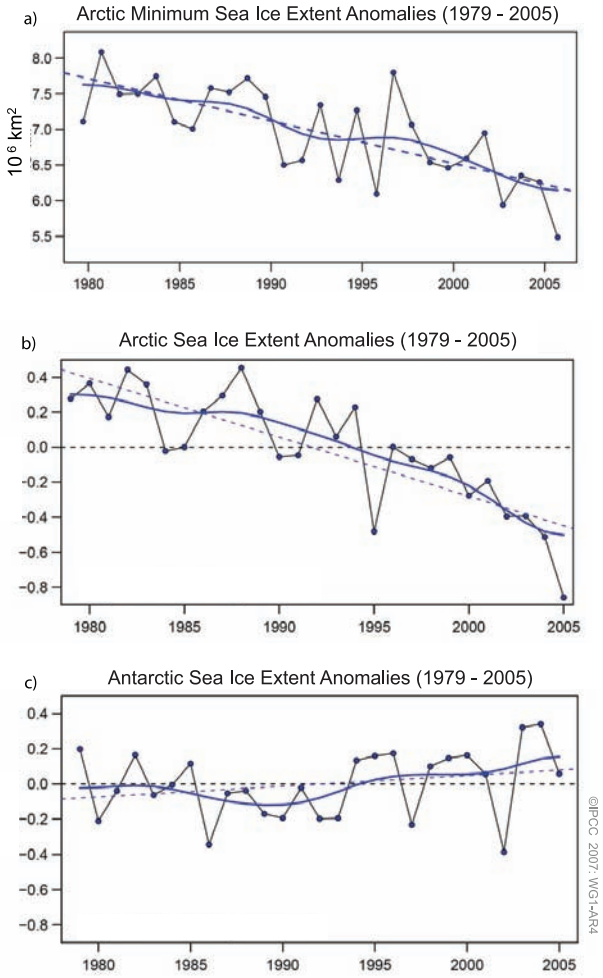


Figure TS.13. *(a) Arctic minimum sea ice extent; (b) arctic sea ice extent anomalies; and (c) antarctic sea ice extent anomalies all for the period 1979 to 2005. Symbols indicate annual values while the smooth blue curves show decadal variations (see Appendix 3.A). The dashed lines indicate the linear trends. (a) Results show a linear trend of –60 ± 20 x 10^3 km^2 yr^{-1}, or approximately -7.4% per decade. (b) The linear trend is –33 ± 7.4 x 10^3 km^2 yr^{-1} (equivalent to approximately –2.7% per decade) and is significant at the 95% confidence level. (c) Antarctic results show a small positive trend of 5.6 ± 9.2 x 10^3 km^2 yr^{-1}, which is not statistically significant. {Figures 4.8 and 4.9}*

The Greenland and Antarctic Ice Sheets taken together have *very likely* contributed to the sea level rise of the past decade. It is *very likely* that the Greenland Ice Sheet shrunk from 1993 to 2003, with thickening in central regions more than offset by increased melting in coastal regions. Whether the ice sheets have been growing or shrinking over time scales of longer than a decade is not well established from observations. Lack of agreement between techniques and the small number of estimates preclude assignment of best estimates or statistically rigorous error bounds for changes in ice sheet mass balances. However, acceleration of outlet glaciers drains ice from the interior and has been observed in both ice sheets (see Figure TS.14). Assessment of the data and techniques suggests a mass balance for the Greenland Ice Sheet of –50 to –100 Gt yr^{-1} (shrinkage contributing to raising global sea level by 0.14 to 0.28 mm yr^{-1}) during 1993 to 2003, with even larger losses in 2005. There are greater uncertainties for earlier time periods and for Antarctica. The estimated range in mass balance for the Greenland Ice Sheet over the period 1961 to 2003 is between growth of 25 Gt yr^{-1} and shrinkage by 60 Gt yr^{-1} (–0.07 to +0.17 mm yr^{-1} SLE). Assessment of all the data yields an estimate for the overall Antarctic Ice Sheet mass balance ranging from growth of 100 Gt yr^{-1} to shrinkage of 200 Gt yr^{-1} (–0.27 to +0.56 mm yr^{-1} SLE) from 1961 to 2003, and from +50 to –200 Gt yr^{-1} (–0.14 to +0.55 mm yr^{-1} SLE) from 1993 to 2003. The recent changes in ice flow are *likely* to be sufficient to explain much or all of the estimated antarctic mass imbalance, with recent changes in ice flow, snowfall and melt water runoff sufficient to explain the mass imbalance of Greenland. {4.6, 4.8}

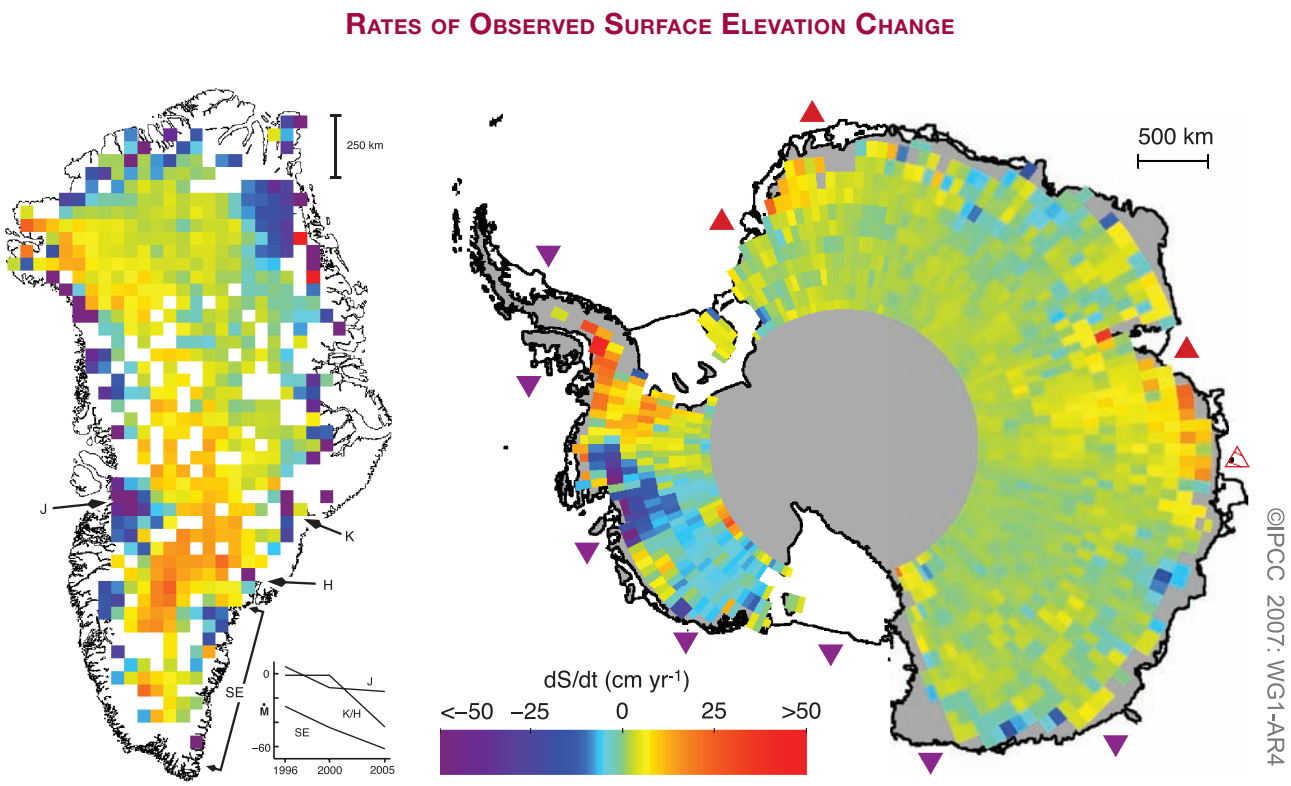


Figure TS.14. *Rates of observed recent surface elevation change for Greenland (left; 1989–2005) and Antarctica (right; 1992–2005). Red hues indicate a rising surface and blue hues a falling surface, which typically indicate an increase or loss in ice mass at a site, although changes over time in bedrock elevation and in near-surface density can be important. For Greenland, the rapidly thinning outlet glaciers Jakobshavn (J), Kangerdlugssuaq (K), Helheim (H) and areas along the southeast coast (SE) are shown, together with their estimated mass balance vs. time (with K and H combined, in Gt yr^{-1}, with negative values indicating loss of mass from the ice sheet to the ocean). For Antarctica, ice shelves estimated to be thickening or thinning by more than 30 cm yr^{-1} are shown by point-down purple triangles (thinning) and point-up red triangles (thickening) plotted just seaward of the relevant ice shelves. {Figures 4.17 and 4.19}*

TS.3.3 Changes in the Ocean: Instrumental Record

The ocean plays an important role in climate and climate change. The ocean is influenced by mass, energy and momentum exchanges with the atmosphere. Its heat capacity is about 1000 times larger than that of the atmosphere and the ocean's net heat uptake is therefore many times greater than that of the atmosphere (see Figure TS.15). Global observations of the heat taken up by the ocean can now be shown to be a definitive test of changes in the global energy budget. Changes in the amount of energy taken up by the upper layers of the ocean also play a crucial role for climate variations on seasonal to interannual time scales, such as El Niño. Changes in the transport of heat and SSTs have important effects upon many regional climates worldwide. Life in the sea is dependent on the biogeochemical status of the ocean and is affected by changes in its physical state and circulation. Changes in ocean biogeochemistry can also feed back into the climate system, for example, through changes in uptake or release of radiatively active gases such as CO_2. {5.1, 7.3}

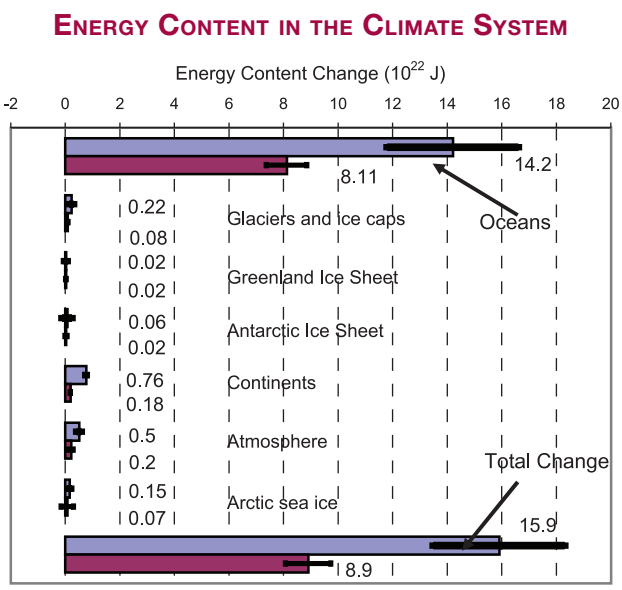


Figure TS.15. *Energy content changes in different components of the Earth system for two periods (1961–2003 and 1993–2003). Blue bars are for 1961 to 2003; burgundy bars are for 1993 to 2003. Positive energy content change means an increase in stored energy (i.e., heat content in oceans, latent heat from reduced ice or sea ice volumes, heat content in the continents excluding latent heat from permafrost changes, and latent and sensible heat and potential and kinetic energy in the atmosphere). All error estimates are 90% confidence intervals. No estimate of confidence is available for the continental heat gain. Some of the results have been scaled from published results for the two respective periods. {Figure 5.4}*

Global mean sea level variations are driven in part by changes in density, through thermal expansion or contraction of the ocean's volume. Local changes in sea level also have a density-related component due to temperature and salinity changes. In addition, exchange of water between oceans and other reservoirs (e.g., ice sheets, mountain glaciers, land water reservoirs and the atmosphere) can change the ocean's mass and hence contribute to changes in sea level. Sea level change is not geographically uniform because processes such as ocean circulation changes are not uniform across the globe (see Box TS.4). {5.5}

Oceanic variables can be useful for climate change detection, in particular temperature and salinity changes below the surface mixed layer where the variability is smaller and signal-to-noise ratio is higher. Observations analysed since the TAR have provided new evidence for changes in global ocean heat content and salinity, sea level, thermal expansion contributions to sea level rise, water mass evolution and biogeochemical cycles. {5.5}

TS.3.3.1 Changes in Ocean Heat Content and Circulation

The world ocean has warmed since 1955, accounting over this period for more than 80% of the changes in the energy content of the Earth's climate system. A total of 7.9 million vertical profiles of ocean temperature allows construction of improved global time series (see Figure TS.16). Analyses of the global oceanic heat budget have been replicated by several independent analysts and are robust to the method used. Data coverage limitations require averaging over decades for the deep ocean and observed decadal variability in the global heat content is not fully understood. However, inadequacies in the distribution of data (particularly coverage in the Southern Ocean and South Pacific) could contribute to the apparent decadal variations in heat content. During the period 1961 to 2003, the 0 to 3000 m ocean layer has taken up about 14.1×10^{22} J, equivalent to an average heating rate of 0.2 W m^{-2} (per unit area of the Earth's surface). During 1993 to 2003, the corresponding rate of warming in the shallower 0 to 700 m ocean layer was higher, about 0.5 ± 0.18 W m^{-2}. Relative to 1961 to 2003, the period 1993 to 2003 had high rates of warming but in 2004 and 2005 there has been some cooling compared to 2003. {5.1–5.3}

Warming is widespread over the upper 700 m of the global ocean. The Atlantic has warmed south of 45°N. The warming is penetrating deeper in the Atlantic Ocean Basin than in the Pacific, Indian and Southern Oceans, due to the

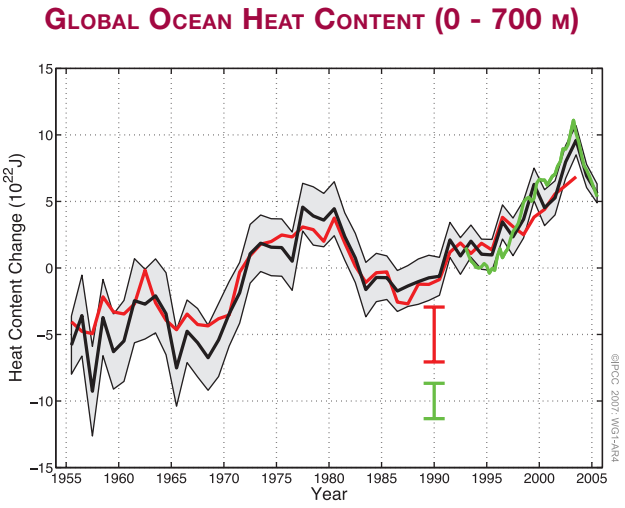


Figure TS.16. *Time series of global ocean heat content (10^{22} J) for the 0 to 700 m layer. The three coloured lines are independent analyses of the oceanographic data. The black and red curves denote the deviation from their 1961 to 1990 average and the shorter green curve denotes the deviation from the average of the black curve for the period 1993 to 2003. The 90% uncertainty range for the black curve is indicated by the grey shading and for the other two curves by the error bars. {Figure 5.1}*

deep overturning circulation cell that occurs in the North Atlantic. The SH deep overturning circulation shows little evidence of change based on available data. However, the upper layers of the Southern Ocean contribute strongly to the overall warming. At least two seas at subtropical latitudes (Mediterranean and Japan/East China Sea) are warming. While the global trend is one of warming, significant decadal variations have been observed in the global time series, and there are large regions where the oceans are cooling. Parts of the North Atlantic, North Pacific and equatorial Pacific have cooled over the last 50 years. The changes in the Pacific Ocean show ENSO-like spatial patterns linked in part to the PDO. {5.2, 5.3}

Parts of the Atlantic meridional overturning circulation exhibit considerable decadal variability, but data do not support a coherent trend in the overturning circulation. {5.3}

TS.3.3.2 Changes in Ocean Biogeochemistry and Salinity

The uptake of anthropogenic carbon since 1750 has led to the ocean becoming more acidic, with an average decrease in surface pH of 0.1 units.[7] Uptake of CO_2 by the ocean changes its chemical equilibrium. Dissolved CO_2 forms a weak acid, so as dissolved CO_2 increases, pH decreases (i.e., the ocean becomes more acidic). The overall pH change is computed from estimates of anthropogenic carbon uptake and simple ocean models. Direct observations of pH at available stations for the last 20 years also show trends of decreasing pH, at a rate of about 0.02 pH units per decade. Decreasing ocean pH decreases the depth below which calcium carbonate dissolves and increases the volume of the ocean that is undersaturated with respect to the minerals aragonite (a meta-stable form of calcium carbonate) and calcite, which are used by marine organisms to build their shells. Decreasing surface ocean pH and rising surface temperatures also act to reduce the ocean buffer capacity for CO_2 and the rate at which the ocean can take up excess atmospheric CO_2. {5.4, 7.3}

The oxygen concentration of the ventilated thermocline (about 100 to 1000 m) decreased in most ocean basins between 1970 and 1995. These changes may reflect a reduced rate of ventilation linked to upper-level warming and/or changes in biological activity. {5.4}

There is now widespread evidence for changes in ocean salinity at gyre and basin scales in the past half century (see Figure TS.17) with the near-surface waters in the more evaporative regions increasing in salinity in almost all ocean basins. These changes in salinity imply changes in the hydrological cycle over the oceans. In the high-latitude regions in both hemispheres, the surface waters show an overall freshening consistent with these regions having greater precipitation, although higher runoff, ice melting, advection and changes in the meridional overturning circulation may also contribute. The subtropical latitudes in both hemispheres are characterised by an increase in salinity in the upper 500 m. The patterns are consistent with a change in the Earth's hydrological cycle, in particular with changes in precipitation and inferred larger water transport in the atmosphere from low latitudes to high latitudes and from the Atlantic to the Pacific. {5.2}

TS.3.3.3 Changes in Sea Level

Over the 1961 to 2003 period, the average rate of global mean sea level rise is estimated from tide gauge data to be 1.8 ± 0.5 mm yr^{-1} (see Figure TS.18). For the purpose of examining the sea level budget, best estimates and 5 to 95% confidence intervals are provided for all land ice contributions. The average

[7] Acidity is a measure of the concentration of H^+ ions and is reported in pH units, where pH = –log(H^+). A pH decrease of 1 unit means a 10-fold increase in the concentration of H^+, or acidity.

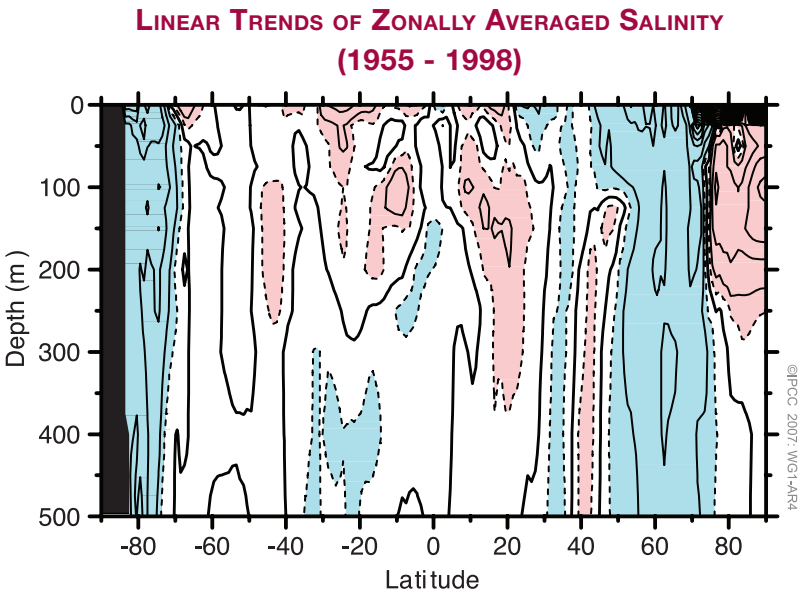


Figure TS.17. *Linear trends (1955–1998) of zonally averaged salinity (Practical Salinity Scale) for the World Ocean. The contour interval is 0.01 per decade and dashed contours are ±0.005 per decade. The dark, solid line is the zero contour. Red shading indicates values equal to or greater than 0.005 per decade and blue shading indicates values equal to or less than –0.005 per decade. {Figure 5.5}*

thermal expansion contribution to sea level rise for this period was 0.42 ± 0.12 mm yr^{-1}, with significant decadal variations, while the contribution from glaciers, ice caps and ice sheets is estimated to have been 0.7 ± 0.5 mm yr^{-1} (see Table TS.3). The sum of these estimated climate-related contributions for about the past four decades thus amounts to 1.1 ± 0.5 mm yr^{-1}, which is less than the best estimate from the tide gauge observations (similar to the discrepancy noted in the TAR). Therefore, the sea level budget for 1961 to 2003 has not been closed satisfactorily. {4.8, 5.5}

The global average rate of sea level rise measured by TOPEX/Poseidon satellite altimetry during 1993 to 2003 is 3.1 ± 0.7 mm yr^{-1}. This observed rate for the recent period is close to the estimated total of 2.8 ± 0.7 mm yr^{-1} for the climate-related contributions due to thermal expansion (1.6 ± 0.5 mm yr^{-1}) and changes in land ice (1.2 ± 0.4 mm yr^{-1}). Hence, the understanding of the budget has improved significantly for this recent period, with the climate contributions constituting the main factors in the sea level budget (which is closed to within known errors). Whether the faster rate for 1993 to 2003 compared to 1961 to 2003 reflects decadal variability or an increase in the longer-term trend is unclear. The tide gauge record indicates that faster rates similar to that observed in 1993 to 2003 have occurred in other decades since 1950. {5.5, 9.5}

There is *high confidence* that the rate of sea level rise accelerated between the mid-19th and the mid-20th centuries based upon tide gauge and geological data. A recent reconstruction of sea level change back to 1870 using the best available tide records provides high confidence that the rate of sea level rise accelerated over the period 1870 to 2000. Geological observations indicate that during the previous 2000 years, sea level change was small, with average rates in the range 0.0 to 0.2 mm yr^{-1}. The use of proxy sea level data from archaeological sources is well established in the Mediterranean and indicates that oscillations in sea level from about AD 1 to AD 1900 did not exceed ±0.25 m. The available evidence indicates that the onset of modern sea level rise started between the mid-19th and mid-20th centuries. {5.5}

Precise satellite measurements since 1993 now provide unambiguous evidence of regional variability of sea level change. In some regions, rates of rise during this period are up to several times the global mean,

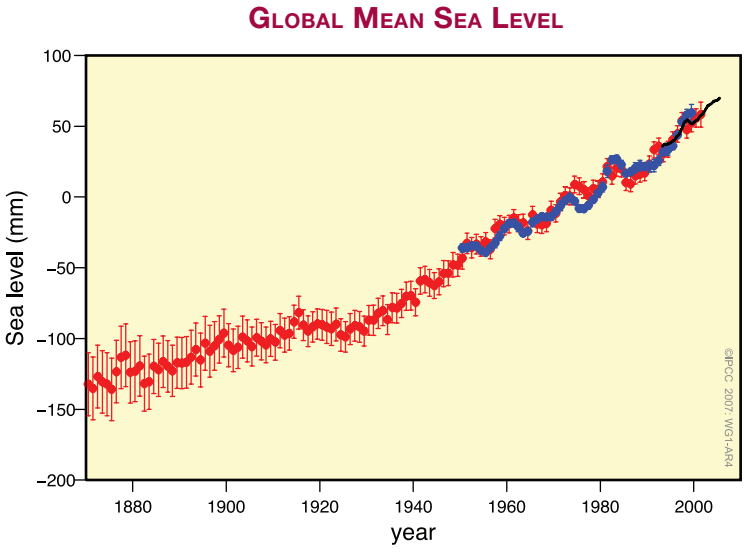


Figure TS.18. *Annual averages of the global mean sea level based on reconstructed sea level fields since 1870 (red), tide gauge measurements since 1950 (blue) and satellite altimetry since 1992 (black). Units are in mm relative to the average for 1961 to 1990. Error bars are 90% confidence intervals. {Figure 5.13}*

Table TS.3. *Contributions to sea level rise based upon observations (left columns) compared to models used in this assessment (right columns; see Section 9.5 and Appendix 10.A for details). Values are presented for 1993 to 2003 and for the last four decades, including observed totals. {Adapted from Tables 5.3 and 9.2}*

	Sea Level Rise (mm yr^{-1})			
	1961–2003		1993–2003	
Sources of Sea Level Rise	Observed	Modelled	Observed	Modelled
Thermal expansion	0.42 ± 0.12	0.5 ± 0.2	1.6 ± 0.5	1.5 ± 0.7
Glaciers and ice caps	0.50 ± 0.18	0.5 ± 0.2	0.77 ± 0.22	0.7 ± 0.3
Greenland Ice Sheet	0.05 ± 0.12[a]		0.21 ± 0.07[a]	
Antarctic Ice Sheet	0.14 ± 0.41[a]		0.21 ± 0.35[a]	
Sum of individual climate contributions to sea level rise	1.1 ± 0.5	1.2 ± 0.5	2.8 ± 0.7	2.6 ± 0.8
Observed total sea level rise	1.8 ± 0.5 (tide gauges)		3.1 ± 0.7 (satellite altimeter)	
Difference (Observed total minus the sum of observed climate contributions)	0.7 ± 0.7		0.3 ± 1.0	

Notes:
[a] prescribed based upon observations (see Section 9.5)

while in other regions sea level is falling. The largest sea level rise since 1992 has taken place in the western Pacific and eastern Indian Oceans (see Figure TS.19). Nearly all of the Atlantic Ocean shows sea level rise during the past decade, while sea level in the eastern Pacific and western Indian Oceans has been falling. These temporal and spatial variations in regional sea level rise are influenced in part by patterns of coupled ocean-atmosphere variability, including ENSO and the NAO. The pattern of observed sea level change since 1992 is similar to the thermal expansion computed from ocean temperature changes, but different from the thermal expansion pattern of the last 50 years, indicating the importance of regional decadal variability. {5.5}

Observations suggest increases in extreme high water at a broad range of sites worldwide since 1975. Longer records are limited in space and under-sampled in time, so a global analysis over the entire 20th century is not feasible. In many locations, the secular changes in extremes were similar to those in mean sea level. At others, changes in atmospheric conditions such as storminess were more important in determining long-term trends. Interannual variability in high water extremes was positively correlated with regional mean sea level, as well as to indices of regional climate such as ENSO in the Pacific and NAO in the Atlantic. {5.5}

Sea Level Change Patterns

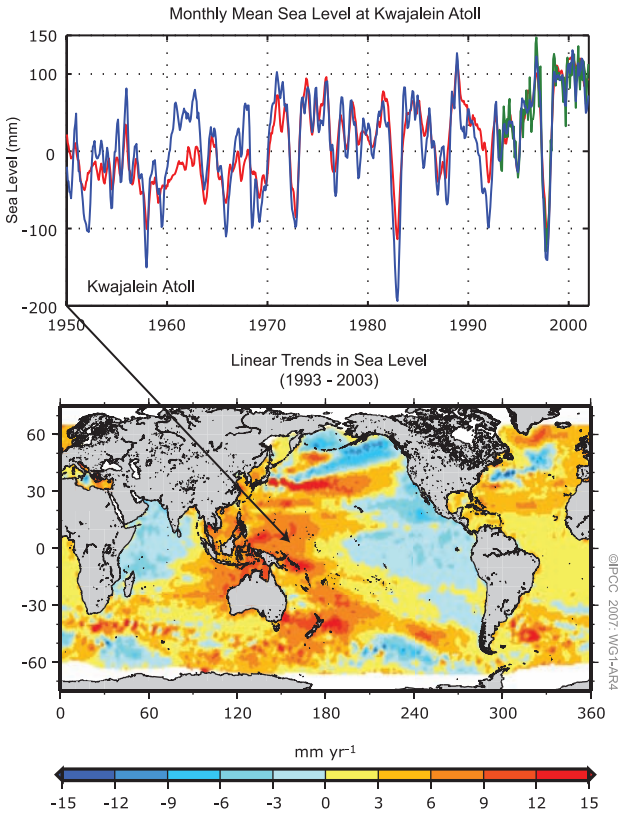


Figure TS.19. *(Top) Monthly mean sea level (mm) curve for 1950 to 2000 at Kwajalein (8°44'N, 167°44'E). The observed sea level (from tide gauge measurements) is in blue, the reconstructed sea level in red and the satellite altimetry record in green. Annual and semiannual signals have been removed from each time series and the tide gauge data have been smoothed. (Bottom) Geographic distribution of short-term linear trends in mean sea level for 1993 to 2003 (mm yr^{-1}) based on TOPEX/Poseidon satellite altimetry. {Figures 5.15 and 5.18}*

Box TS.4: Sea Level

The level of the sea at the shoreline is determined by many factors that operate over a great range of temporal scales: hours to days (tides and weather), years to millennia (climate), and longer. The land itself can rise and fall and such regional land movements need to be accounted for when using tide gauge measurements for evaluating the effect of oceanic climate change on coastal sea level. Coastal tide gauges indicate that global average sea level rose during the 20th century. Since the early 1990s, sea level has also been observed continuously by satellites with near-global coverage. Satellite and tide gauge data agree at a wide range of spatial scales and show that global average sea level has continued to rise during this period. Sea level changes show geographical variation because of several factors, including the distributions of changes in ocean temperature, salinity, winds and ocean circulation. Regional sea level is affected by climate variability on shorter time scales, for instance associated with El Niño and the NAO, leading to regional interannual variations which can be much greater or weaker than the global trend.

Based on ocean temperature observations, the thermal expansion of seawater as it warms has contributed substantially to sea level rise in recent decades. Climate models are consistent with the ocean observations and indicate that thermal expansion is expected to continue to contribute to sea level rise over the next 100 years. Since deep ocean temperatures change only slowly, thermal expansion would continue for many centuries even if atmospheric concentrations of greenhouse gases were stabilised.

Global average sea level also rises or falls when water is transferred from land to ocean or vice versa. Some human activities can contribute to sea level change, especially by the extraction of groundwater and construction of reservoirs. However, the major land store of freshwater is the water frozen in glaciers, ice caps and ice sheets. Sea level was more than 100 m lower during the glacial periods because of the ice sheets covering large parts of the NH continents. The present-day retreat of glaciers and ice caps is making a substantial contribution to sea level rise. This is expected to continue during the next 100 years. Their contribution should decrease in subsequent centuries as this store of freshwater diminishes.

The Greenland and Antarctic Ice Sheets contain much more ice and could make large contributions over many centuries. In recent years the Greenland Ice Sheet has experienced greater melting, which is projected to increase further. In a warmer climate, models suggest that the ice sheets could accumulate more snowfall, tending to lower sea level. However, in recent years any such tendency has probably been outweighed by accelerated ice flow and greater discharge observed in some marginal areas of the ice sheets. The processes of accelerated ice flow are not yet completely understood but could result in overall net sea level rise from ice sheets in the future.

The greatest climate- and weather-related impacts of sea level are due to extremes on time scales of days and hours, associated with tropical cyclones and mid-latitude storms. Low atmospheric pressure and high winds produce large local sea level excursions called 'storm surges', which are especially serious when they coincide with high tide. Changes in the frequency of occurrence of these extreme sea levels are affected both by changes in mean sea level and in the meteorological phenomena causing the extremes. {5.5}

TS.3.4 Consistency Among Observations

In this section, variability and trends within and across different climate variables including the atmosphere, cryosphere and oceans are examined for consistency based upon conceptual understanding of physical relationships between the variables. For example, increases in temperature will enhance the moisture-holding capacity of the atmosphere. Changes in temperature and/or precipitation should be consistent with those evident in glaciers. Consistency between independent observations using different techniques and variables provides a key test of understanding, and hence enhances confidence. {3.9}

Changes in the atmosphere, cryosphere and ocean show unequivocally that the world is warming. {3.2, 3.9, 4.2, 4.4–4.8, 5.2, 5.5}

Both land surface air temperatures and SSTs show warming. In both hemispheres, land regions have warmed at a faster rate than the oceans in the past few decades, consistent with the much greater thermal inertia of the oceans. {3.2}

The warming of the climate is consistent with observed increases in the number of daily warm extremes, reductions in the number of daily cold extremes and reductions in the number of frost days at mid-latitudes. {3.2, 3.8}

Surface air temperature trends since 1979 are now consistent with those at higher altitudes. It is *likely* that there is slightly greater warming in the troposphere than at the surface, and a higher tropopause, consistent with expectations from basic physical processes and observed increases in greenhouse gases together with depletion of stratospheric ozone. {3.4, 9.4}

Changes in temperature are broadly consistent with the observed nearly worldwide shrinkage of the cryosphere. There have been widespread reductions in mountain glacier mass and extent. Changes in climate consistent with warming are also indicated by decreases in snow cover, snow depth, arctic sea ice extent, permafrost thickness and temperature, the extent of seasonally frozen ground and the length of the freeze season of river and lake ice. {3.2, 3.9, 4.2–4.5, 4.7}

Observations of sea level rise since 1993 are consistent with observed changes in ocean heat content and the cryosphere. Sea level rose by 3.1 ± 0.7 mm yr^{-1} from 1993 to 2003, the period of availability of global altimetry measurements. During this time, a near balance was observed between observed total sea level rise and contributions from glacier, ice cap and ice sheet retreat together with increases in ocean heat content and associated ocean expansion. This balance gives increased

Table TS.4. *Recent trends, assessment of human influence on trends, and projections of extreme weather and climate events for which there is evidence of an observed late 20th-century trend. An asterisk in the column headed 'D' indicates that formal detection and attribution studies were used, along with expert judgement, to assess the likelihood of a discernible human influence. Where this is not available, assessments of likelihood of human influence are based on attribution results for changes in the mean of a variable or changes in physically related variables and/or on the qualitative similarity of observed and simulated changes, combined with expert judgement. {3.8, 5.5, 9.7, 11.2–11.9; Tables 3.7, 3.8, 9.4}*

Phenomenon[a] and direction of trend	Likelihood that trend occurred in late 20th century (typically post-1960)	Likelihood of a human contribution to observed trend	D	Likelihood of future trend based on projections for 21st century using SRES[b] scenarios
Warmer and fewer cold days and nights over most land areas	*Very likely*[c]	*Likely*[e]	*	*Virtually certain*[e]
Warmer and more frequent hot days and nights over most land areas	*Very likely*[d]	*Likely* (nights)[e]	*	*Virtually certain*[e]
Warm spells / heat waves: Frequency increases over most land areas	*Likely*	*More likely than not*		*Very likely*
Heavy precipitation events. Frequency (or proportion of total rainfall from heavy falls) increases over most areas	*Likely*	*More likely than not*		*Very likely*
Area affected by droughts increases	*Likely* in many regions since 1970s	*More likely than not*	*	*Likely*
Intense tropical cyclone activity increases	*Likely* in some regions since 1970	*More likely than not*		*Likely*
Increased incidence of extreme high sea level (excludes tsunamis)[f]	*Likely*	*More likely than not*[g]		*Likely*[h]

Notes:
[a] See Table 3.7 for further details regarding definitions.
[b] SRES refers to the IPCC Special Report on Emission Scenarios. The SRES scenario families and illustrative cases are summarised in a box at the end of the Summary for Policymakers.
[c] Decreased frequency of cold days and nights (coldest 10%)
[d] Increased frequency of hot days and nights (hottest 10%)
[e] Warming of the most extreme days/nights each year
[f] Extreme high sea level depends on average sea level and on regional weather systems. It is defined here as the highest 1% of hourly values of observed sea level at a station for a given reference period.
[g] Changes in observed extreme high sea level closely follow the changes in average sea level {5.5.2.6}. It is *very likely* that anthropogenic activity contributed to a rise in average sea level. {9.5.2}
[h] In all scenarios, the projected global average sea level at 2100 is higher than in the reference period {10.6}. The effect of changes in regional weather systems on sea level extremes has not been assessed.

confidence that the observed sea level rise is a strong indicator of warming. However, the sea level budget is not balanced for the longer period 1961 to 2003. {5.5, 3.9}

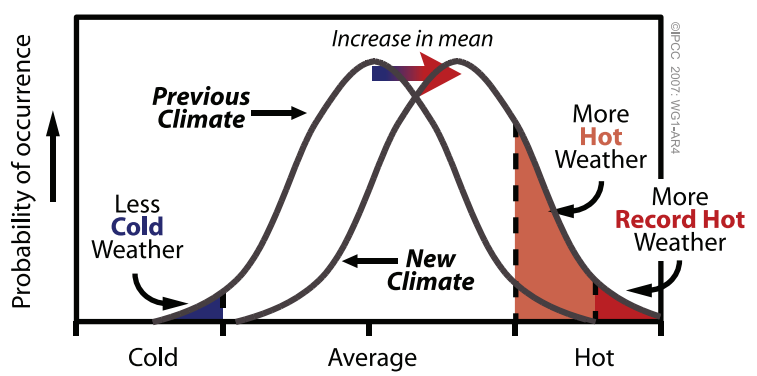
Observations are consistent with physical understanding regarding the expected linkage between water vapour and temperature, and with intensification of precipitation events in a warmer world. Column and upper-tropospheric water vapour have increased, providing important support for the hypothesis of simple physical models that specific humidity increases in a warming world and represents an important positive feedback to climate change. Consistent with rising amounts of water vapour in the atmosphere, there are widespread increases in the numbers of heavy precipitation events and increased likelihood of flooding events in many land regions, even those where there has been a reduction in total precipitation. Observations of changes in ocean salinity independently support the view

Box TS.5: Extreme Weather Events

People affected by an extreme weather event (e.g., the extremely hot summer in Europe in 2003, or the heavy rainfall in Mumbai, India in July 2005) often ask whether human influences on the climate are responsible for the event. A wide range of extreme weather events is expected in most regions even with an unchanging climate, so it is difficult to attribute any individual event to a change in the climate. In most regions, instrumental records of variability typically extend only over about 150 years, so there is limited information to characterise how extreme rare climatic events could be. Further, several factors usually need to combine to produce an extreme event, so linking a particular extreme event to a single, specific cause is problematic. In some cases, it may be possible to estimate the anthropogenic contribution to such changes in the probability of occurrence of extremes.

However, simple statistical reasoning indicates that substantial changes in the frequency of extreme events (and in the maximum feasible extreme, e.g., the maximum possible 24-hour rainfall at a specific location) can result from a relatively small shift of the distribution of a weather or climate variable.

Extremes are the infrequent events at the high and low end of the range of values of a particular variable. The probability of occurrence of values in this range is called a probability distribution function (PDF) that for some variables is shaped similarly to a 'Normal' or 'Gaussian' curve (the familiar 'bell' curve). Box TS.5, Figure 1 shows a schematic of a such a PDF and illustrates the effect a small shift (corresponding to a small change in the average or centre of the distribution) can have on the frequency of extremes at either end of the distribution. An increase in the frequency of one extreme (e.g., the number of hot days) will often be accompanied by a decline in the opposite extreme (in this case the number of cold days such as frosts). Changes in the variability or shape of the distribution can complicate this simple picture.



Box TS.5, Figure 1. *Schematic showing the effect on extreme temperatures when the mean temperature increases, for a normal temperature distribution.*

The IPCC Second Assessment Report noted that data and analyses of extremes related to climate change were sparse. By the time of the TAR, improved monitoring and data for changes in extremes was available, and climate models were being analysed to provide projections of extremes. Since the TAR, the observational basis of analyses of extremes has increased substantially, so that some extremes have now been examined over most land areas (e.g., daily temperature and rainfall extremes). More models have been used in the simulation and projection of extremes, and multiple integrations of models with different starting conditions (ensembles) now provide more robust information about PDFs and extremes. Since the TAR, some climate change detection and attribution studies focussed on changes in the global statistics of extremes have become available (Table TS.4). For some extremes (e.g., tropical cyclone intensity), there are still data concerns and/or inadequate models. Some assessments still rely on simple reasoning about how extremes might be expected to change with global warming (e.g., warming could be expected to lead to more heat waves). Others rely on qualitative similarity between observed and simulated changes. The assessed likelihood of anthropogenic contributions to trends is lower for variables where the assessment is based on indirect evidence.

that the Earth's hydrologic cycle has changed, in a manner consistent with observations showing greater precipitation and river runoff outside the tropics and subtropics, and increased transfer of freshwater from the ocean to the atmosphere at lower latitudes. {3.3, 3.4, 3.9, 5.2}

Although precipitation has increased in many areas of the globe, the area under drought has also increased. Drought duration and intensity has also increased. While regional droughts have occurred in the past, the widespread spatial extent of current droughts is broadly consistent with expected changes in the hydrologic cycle under warming. Water vapour increases with increasing global temperature, due to increased evaporation where surface moisture is available, and this tends to increase precipitation. However, increased continental temperatures are expected to lead to greater evaporation and drying, which is particularly important in dry regions where surface moisture is limited. Changes in snowpack, snow cover and in atmospheric circulation patterns and storm tracks can also reduce available seasonal moisture, and contribute to droughts. Changes in SSTs and associated changes in the atmospheric circulation and precipitation have contributed to changes in drought, particularly at low latitudes. The result is that drought has become more common, especially in the tropics and subtropics, since the 1970s. In Australia and Europe, direct links to global warming have been inferred through the extremes in high temperatures and heat waves accompanying recent droughts. {3.3, 3.8, 9.5}

TS.3.5 A Palaeoclimatic Perspective

Palaeoclimatic studies make use of measurements of past change derived from borehole temperatures, ocean sediment pore-water change and glacier extent changes, as well as proxy measurements involving the changes in chemical, physical and biological parameters that reflect past changes in the environment where the proxy grew or existed. Palaeoclimatic studies rely on multiple proxies so that results can be cross-verified and uncertainties better understood. It is now well accepted and verified that many biological organisms (e.g., trees, corals, plankton, animals) alter their growth and/or population dynamics in response to changing climate, and that these climate-induced changes are well recorded in past growth in living and dead (fossil) specimens or assemblages of organisms. Networks of tree ring width and tree ring density chronologies are used to infer past temperature changes based on calibration with temporally overlapping instrumental data. While these methods are heavily used, there are concerns regarding the distributions of available measurements, how well these sample the globe, and such issues as the degree to which the methods have spatial and seasonal biases or apparent divergence in the relationship with recent climate change. {6.2}

It is *very likely* that average NH temperatures during the second half of the 20th century were warmer than any other 50-year period in the last 500 years and *likely* the warmest in at least the past 1300 years. The data supporting these conclusions are most extensive over summer extratropical land areas (particularly for the longer time period; see Figure TS.20). These conclusions are based upon proxy data such as the width and density of a tree ring, the isotopic composition of various elements in ice or the chemical composition of a growth band in corals, requiring analysis to derive temperature information and associated uncertainties. Among the key uncertainties are that temperature and precipitation are difficult to separate in some cases, or are representative of particular seasons rather than full years. There are now improved and expanded data since the TAR, including, for example, measurements at a larger number of sites, improved analysis of borehole temperature data and more extensive analyses of glaciers, corals and sediments. However, palaeoclimatic data are more limited than the instrumental record since 1850 in both space and time, so that statistical methods are employed to construct global averages, and these are subject to uncertainties as well. Current data are too limited to allow a similar evaluation of the SH temperatures prior to the period of instrumental data. {6.6, 6.7}

Some post-TAR studies indicate greater multi-centennial NH variability than was shown in the TAR, due to the particular proxies used and the specific statistical methods of processing and/or scaling them to represent past temperatures. The additional variability implies cooler conditions, predominantly during the 12th to 14th, the 17th and the 19th centuries; these are *likely* linked to natural forcings due to volcanic eruptions and/or solar activity. For example, reconstructions suggest decreased solar activity and increased volcanic activity in the 17th century as compared to current conditions. One reconstruction suggests slightly warmer conditions in the 11th century than those indicated in the TAR, but within the uncertainties quoted in the TAR. {6.6}

The ice core CO_2 record over the past millennium provides an additional constraint on natural climate variability. The amplitudes of the pre-industrial, decadal-scale NH temperature changes from the proxy-based reconstructions (<1°C) are broadly consistent with the ice core CO_2 record and understanding of the strength

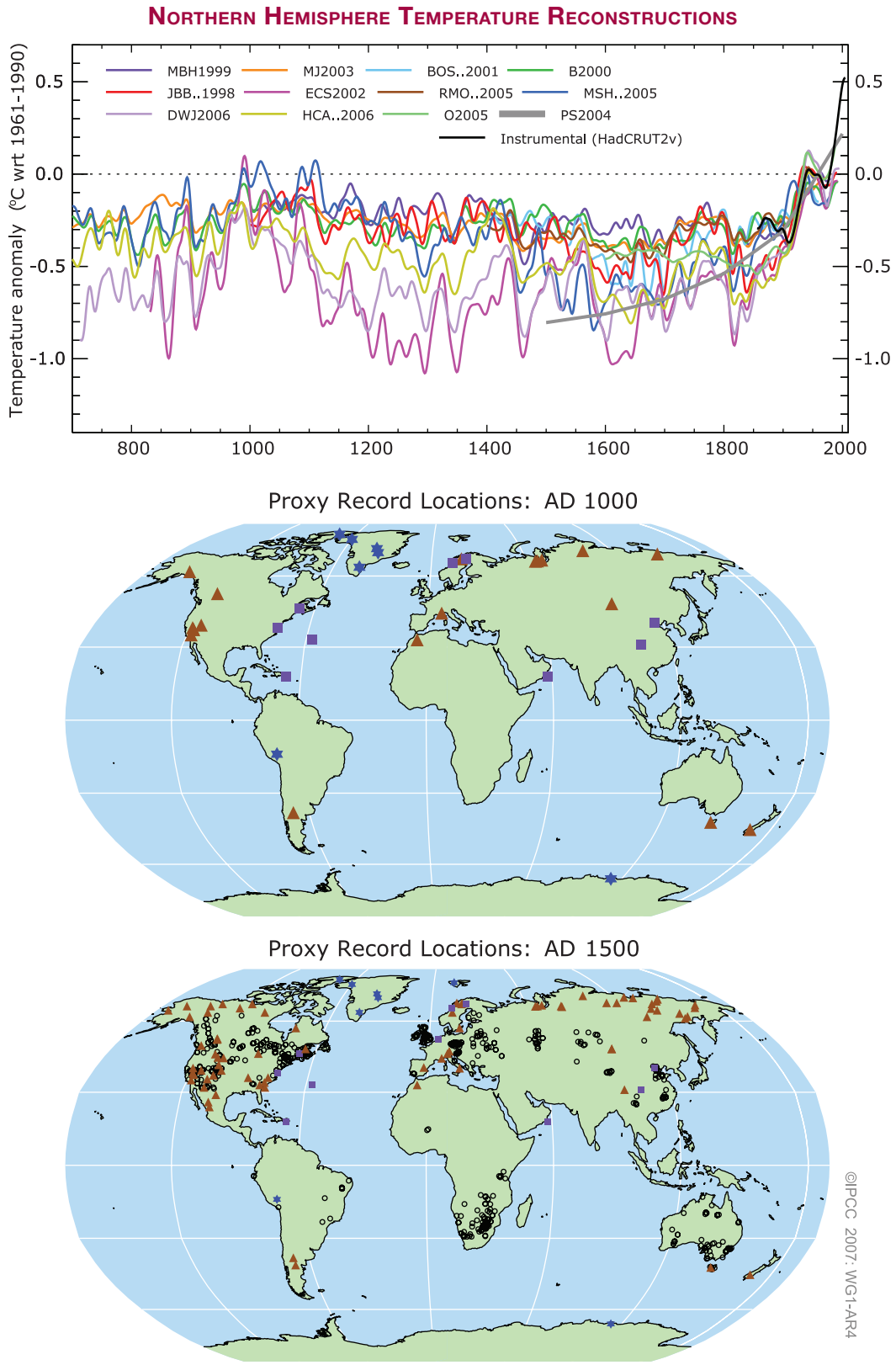


Figure TS.20. *(Top) Records of Northern Hemisphere temperature variation during the last 1300 years with 12 reconstructions using multiple climate proxy records shown in colour and instrumental records shown in black. (Middle and Bottom) Locations of temperature-sensitive proxy records with data back to AD 1000 and AD 1500 (tree rings: brown triangles; boreholes: black circles; ice core/ice boreholes: blue stars; other records including low-resolution records: purple squares). Data sources are given in Table 6.1, Figure 6.10 and are discussed in Chapter 6. {Figures 6.10 and 6.11}*

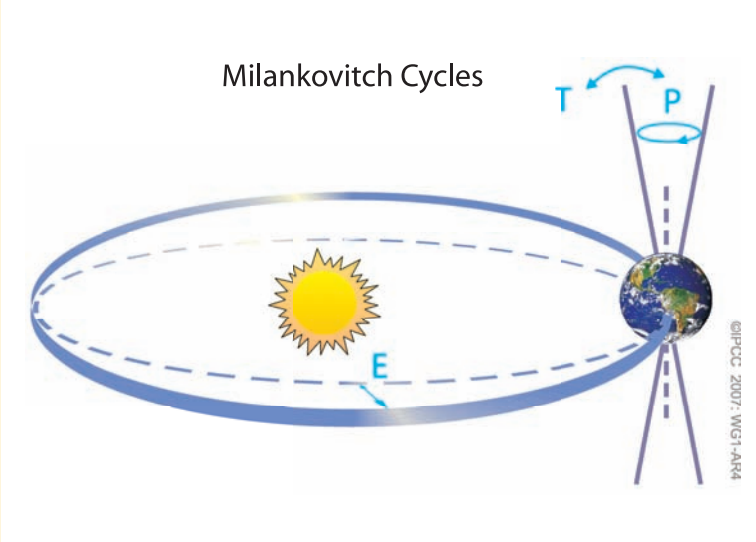
Box TS.6: Orbital Forcing

It is well known from astronomical calculations that periodic changes in characteristics of the Earth's orbit around the Sun control the seasonal and latitudinal distribution of incoming solar radiation at the top of the atmosphere (hereafter called 'insolation'). Past and future changes in insolation can be calculated over several millions of years with a high degree of confidence. {6.4}

Precession refers to changes in the time of the year when the Earth is closest to the Sun, with quasi-periodicities of about 19,000 and 23,000 years. As a result, changes in the position and duration of the seasons on the orbit strongly modulate the latitudinal and seasonal distribution of insolation. Seasonal changes in insolation are much larger than annual mean changes and can reach 60 W m^{-2} (Box TS.6, Figure 1).

The obliquity (tilt) of the Earth's axis varies between about 22° and 24.5° with two neighbouring quasi-periodicities of around 41,000 years. Changes in obliquity modulate seasonal contrasts as well as annual mean insolation changes with opposite effects at low vs. high latitudes (and therefore no effect on global average insolation) {6.4}.

The eccentricity of the Earth's orbit around the Sun has longer quasi-periodicities at 400,000 years and around 100,000 years. Changes in eccentricity alone have limited impacts on insolation, due to the resulting very small changes in the distance between the Sun and the Earth. However, changes in eccentricity interact with seasonal effects induced by obliquity and precession of the equinoxes. During periods of low eccentricity, such as about 400,000 years ago and during the next 100,000 years, seasonal insolation changes induced by precession are not as large as during periods of larger eccentricity (Box TS.6, Figure 1). {6.4}



Box TS.6, Figure 1. *Schematic of the Earth's orbital changes (Milankovitch cycles) that drive the ice age cycles. 'T' denotes changes in the tilt (or obliquity) of the Earth's axis, 'E' denotes changes in the eccentricity of the orbit and 'P' denotes precession, that is, changes in the direction of the axis tilt at a given point of the orbit. {FAQ 6.1, Figure 1}*

The Milankovitch, or 'orbital' theory of the ice ages is now well developed. Ice ages are generally triggered by minima in high-latitude NH summer insolation, enabling winter snowfall to persist through the year and therefore accumulate to build NH glacial ice sheets. Similarly, times with especially intense high-latitude NH summer insolation, determined by orbital changes, are thought to trigger rapid deglaciations, associated climate change and sea level rise. These orbital forcings determine the pacing of climatic changes, while the large responses appear to be determined by strong feedback processes that amplify the orbital forcing. Over multi-millennial time scales, orbital forcing also exerts a major influence on key climate systems such as the Earth's major monsoons, global ocean circulation and the greenhouse gas content of the atmosphere. {6.4}

Available evidence indicates that the current warming will not be mitigated by a natural cooling trend towards glacial conditions. Understanding of the Earth's response to orbital forcing indicates that the Earth would not naturally enter another ice age for at least 30,000 years. {6.4, FAQ 6.1}

of the carbon cycle-climate feedback. Atmospheric CO_2 and temperature in Antarctica co-varied over the past 650,000 years. Available data suggest that CO_2 acts as an amplifying feedback. {6.4, 6.6}

Changes in glaciers are evident in Holocene data, but these changes were caused by different processes than the late 20th-century retreat. Glaciers of several mountain regions in the NH retreated in response to orbitally forced regional warmth between 11,000 and 5000 years ago, and were smaller than at the end of the 20th century (or even absent) at times prior to 5000 years ago. The current near-global retreat of mountain glaciers cannot be due to the same causes, because decreased summer insolation during the past few thousand years in the NH should be favourable to the growth of glaciers. {6.5}

Palaeoclimatic data provide evidence for changes in many regional climates. The strength and frequency of ENSO events have varied in past climates. There is evidence that the strength of the Asian monsoon, and hence precipitation amount, can change abruptly. The palaeoclimatic records of northern and eastern Africa and of North America indicate that droughts lasting decades to centuries are a recurrent feature of climate in these regions, so that recent droughts in North America and northern Africa are not unprecedented. Individual decadal-resolution palaeoclimatic data sets support the existence of regional quasi-periodic climate variability, but it is *unlikely* that these regional signals were coherent at the global scale. {6.5, 6.6}

Strong evidence from ocean sediment data and from modelling links abrupt climate changes during the last glacial period and glacial-interglacial transition to changes in the Atlantic Ocean circulation. Current understanding suggests that the ocean circulation can become unstable and change rapidly when critical thresholds are crossed. These events have affected temperature by up to 16°C in Greenland and have influenced tropical rainfall patterns. They were probably associated with a redistribution of heat between the NH and SH rather than with large changes in global mean temperature. Such events have not been observed during the past 8000 years. {6.4}

The Arctic and the Last Interglacial

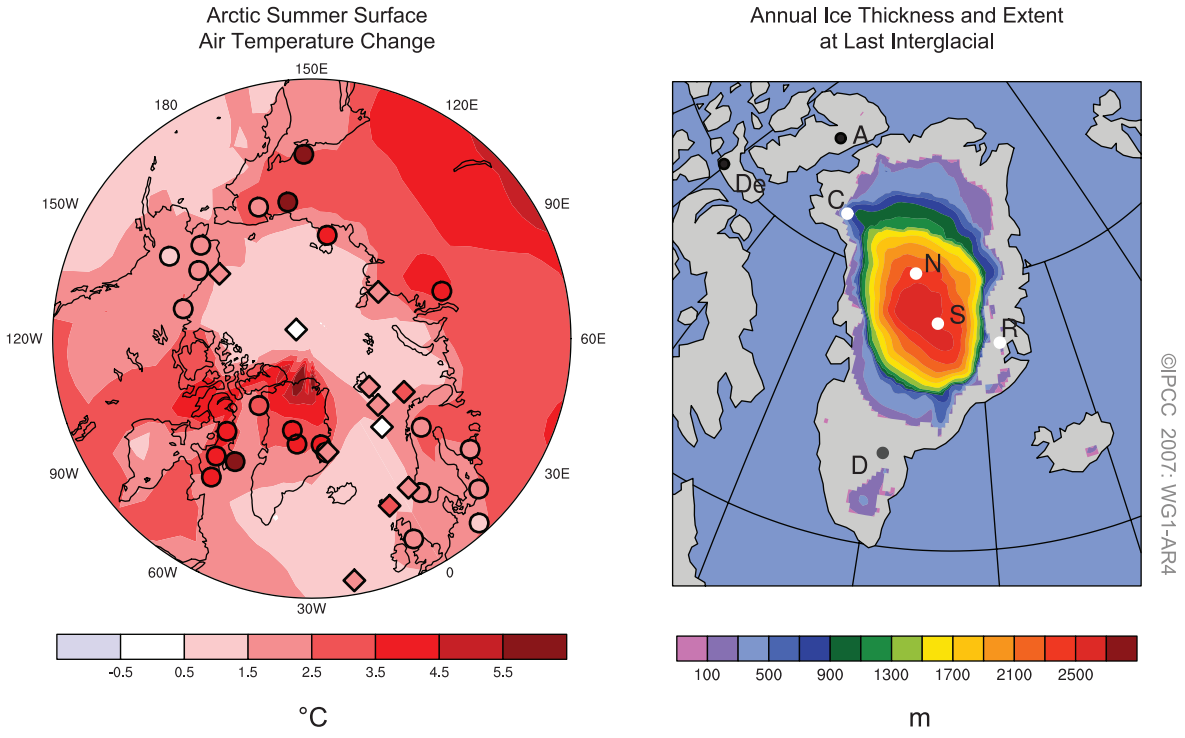


Figure TS.21. *Summer surface air temperature change relative to the present over the Arctic (left) and ice thickness and extent for Greenland and western arctic glaciers (right) for the last interglacial, approximately 125,000 years ago, from a multi-model and multi-proxy synthesis. (Left) A multi-model simulation of summer warming during the last interglacial is overlain by proxy estimates of maximum summer warming from terrestrial (circles) and marine (diamonds) sites. (Right) Extents and thicknesses of the Greenland Ice Sheet and western Canadian and Iceland glaciers at their minimum extent during the last interglacial, shown as a multi-model average from three ice models. Ice core observations indicate ice during the last interglacial at sites (white dots), Renland (R), North Greenland Ice Core Project (N), Summit (S, GRIP and GISP2) and possibly Camp Century (C), but no ice at sites (black dots): Devon (De) and Agassiz (A).Evidence for LIG ice at Dye-3 (D, grey dot) is equivocal. {Figure 6.6}*

Confidence in the understanding of past climate change and changes in orbital forcing is strengthened by the improved ability of current models to simulate past climate conditions. The Last Glacial Maximum (LGM; the last 'ice age' about 21,000 years ago) and the mid-Holocene (6000 years ago) were different from the current climate not because of random variability, but because of altered seasonal and global forcing linked to known differences in the Earth's orbit (see Box TS.6). Biogeochemical and biogeophysical feedbacks amplified the response to orbital forcings. Comparisons between simulated and reconstructed conditions in the LGM demonstrate that models capture the broad features of inferred changes in the temperature and precipitation patterns. For the mid-Holocene, coupled climate models are able to simulate mid-latitude warming and enhanced monsoons, with little change in global mean temperature (<0.4°C), consistent with our understanding of orbital forcing. {6.2, 6.4, 6.5, 9.3}

Global average sea level was likely between 4 and 6 m higher during the last interglacial period, about 125,000 years ago, than during the 20th century, mainly due to the retreat of polar ice (Figure TS.21). Ice core data suggest that the Greenland Summit region was ice-covered during this period, but reductions in the ice sheet extent are indicated in parts of southern Greenland. Ice core data also indicate that average polar temperatures at that time were 3°C to 5°C warmer than the 20th century because of differences in the Earth's orbit. The Greenland Ice Sheet and other arctic ice fields likely contributed no more than 4 m of the observed sea level rise, implying that there may also have been a contribution from Antarctica. {6.4}

TS.4 Understanding and Attributing Climate Change

Attribution evaluates whether observed changes are consistent with quantitative responses to different forcings obtained in well-tested models, and are not consistent with alternative physically plausible explanations. The first IPCC Assessment Report (FAR) contained little observational evidence of a detectable anthropogenic influence on climate. Six years later, the IPCC Second Assessment Report (SAR) concluded that the balance of evidence suggested a discernible human influence on the climate of the 20th century. The TAR concluded that 'most of the observed warming over the last 50 years is likely to have been due to the increase in greenhouse gas concentrations'. Confidence in the assessment of the human contributions to recent climate change has increased considerably since the TAR, in part because of stronger signals obtained from longer records, and an expanded and improved range of observations allowing attribution of warming to be more fully addressed jointly with other changes in the climate system. Some apparent inconsistencies in the observational record (e.g., in the vertical profile of temperature changes) have been largely resolved. There have been improvements in the simulation of many aspects of present mean climate and its variability on seasonal to inter-decadal time scales, although uncertainties remain (see Box TS.7). Models now employ more detailed representations of processes related to aerosol and other forcings. Simulations of 20th-century climate change have used many more models and much more complete anthropogenic and natural forcings than were available for the TAR. Available multi-model ensembles increase confidence in attribution results by providing an improved representation of model uncertainty. An anthropogenic signal has now more clearly emerged in formal attribution studies of aspects of the climate system beyond global-scale atmospheric temperature, including changes in global ocean heat content, continental-scale temperature trends, temperature extremes, circulation and arctic sea ice extent. {9.1}

TS.4.1 Advances in Attribution of Changes in Global-Scale Temperature in the Instrumental Period: Atmosphere, Ocean and Ice

Anthropogenic warming of the climate system is widespread and can be detected in temperature observations taken at the surface, in the free atmosphere and in the oceans. {3.2, 3.4, 9.4}

Evidence of the effect of external influences, both anthropogenic and natural, on the climate system has continued to accumulate since the TAR. Model and data improvements, ensemble simulations and improved representations of aerosol and greenhouse gas forcing along with other influences lead to greater confidence that most current models reproduce large-scale forced variability of the atmosphere on decadal and inter-decadal time scales quite well. These advances confirm that past climate variations at large spatial scales have been strongly influenced by external forcings. However, uncertainties still exist in the magnitude and temporal evolution of estimated contributions from individual forcings other than well-mixed greenhouse gases, due, for

Box TS.7: Evaluation of Atmosphere-Ocean General Circulation Models

Atmosphere-ocean general circulation models (AOGCMs) are the primary tool used for understanding and attribution of past climate variations, and for future projections. Since there are no historical perturbations to radiative forcing that are fully analogous to the human-induced perturbations expected over the 21st century, confidence in the models must be built from a number of indirect methods, described below. In each of these areas there have been substantial advances since the TAR, increasing overall confidence in models. {8.1}

Enhanced scrutiny and analysis of model behaviour has been facilitated by internationally coordinated efforts to collect and disseminate output from model experiments performed under common conditions. This has encouraged a more comprehensive and open evaluation of models, encompassing a diversity of perspectives. {8.1}

Projections for different scales and different periods using global climate models. Climate models project the climate for several decades or longer into the future. Since the details of individual weather systems are not being tracked and forecast, the initial atmospheric conditions are much less important than for weather forecast models. For climate projections, the forcings are of much greater importance. These forcings include the amount of solar energy reaching the Earth, the amount of particulate matter from volcanic eruptions in the atmosphere, and the concentrations of anthropogenic gases and particles in the atmosphere. As the area of interest moves from global to regional to local, or the time scale of interest shortens, the amplitude of variability linked to weather increases relative to the signal of long-term climate change. This makes detection of the climate change signal more difficult at smaller scales. Conditions in the oceans are important as well, especially for interannual and decadal time scales. {FAQ 1.2, 9.4, 11.1}

Model formulation. The formulation of AOGCMs has developed through improved spatial resolution and improvements to numerical schemes and parametrizations (e.g., sea ice, atmospheric boundary layer, ocean mixing). More processes have been included in many models, including a number of key processes important for forcing (e.g., aerosols are now modelled interactively in many models). Most models now maintain a stable climate without use of flux adjustments, although some long-term trends remain in AOGCM control integrations, for example, due to slow processes in the ocean. {8.2, 8.3}

Simulation of present climate. As a result of improvements in model formulation, there have been improvements in the simulation of many aspects of present mean climate. Simulations of precipitation, sea level pressure and surface temperature have each improved overall, but deficiencies remain, notably in tropical precipitation. While significant deficiencies remain in the simulation of clouds (and corresponding feedbacks affecting climate sensitivity), some models have demonstrated improvements in the simulation of certain cloud regimes (notably marine stratocumulus). Simulation of extreme events (especially extreme temperature) has improved, but models generally simulate too little precipitation in the most extreme events. Simulation of extratropical cyclones has improved. Some models used for projections of tropical cyclone changes can simulate successfully the observed frequency and distribution of tropical cyclones. Improved simulations have been achieved for ocean water mass structure, the meridional overturning circulation and ocean heat transport. However most models show some biases in their simulation of the Southern Ocean, leading to some uncertainty in modelled ocean heat uptake when climate changes. {8.3, 8.5, 8.6}

Simulation of modes of climate variability. Models simulate dominant modes of extratropical climate variability that resemble the observed ones (NAM/SAM, PNA, PDO) but they still have problems in representing aspects of them. Some models can now simulate important aspects of ENSO, while simulation of the Madden-Julian Oscillation remains generally unsatisfactory. {8.4}

Simulation of past climate variations. Advances have been made in the simulation of past climate variations. Independently of any attribution of those changes, the ability of climate models to provide a physically self-consistent explanation of observed climate variations on various time scales builds confidence that the models are capturing many key processes for the evolution of 21st-century climate. Recent advances include success in modelling observed changes in a wider range of climate variables over the 20th century (e.g., continental-scale surface temperatures and extremes, sea ice extent, ocean heat content trends and land precipitation). There has also been progress in the ability to model many of the general features of past, very different climate states such as the mid-Holocene and the LGM using identical or related models to those used for studying current climate. Information on factors treated as boundary conditions in palaeoclimate calculations include the different states of ice sheets in those periods. The broad predictions of earlier climate models, of increasing global temperatures in response to increasing greenhouse gases, have been borne out by subsequent observations. This strengthens confidence in near-term climate projections and understanding of related climate change commitments. {6.4, 6.5, 8.1, 9.3–9.5}

(continued)

Weather and seasonal prediction using climate models. A few climate models have been tested for (and shown) capability in initial value prediction, on time scales from weather forecasting (a few days) to seasonal climate variations, when initialised with appropriate observations. While the predictive capability of models in this mode of operation does not necessarily imply that they will show the correct response to changes in climate forcing agents such as greenhouse gases, it does increase confidence that they are adequately representing some key processes and teleconnections in the climate system. {8.4}

Measures of model projection accuracy. The possibility of developing model capability measures ('metrics'), based on the above evaluation methods, that can be used to narrow uncertainty by providing quantitative constraints on model climate projections, has been explored for the first time using model ensembles. While these methods show promise, a proven set of measures has yet to be established. {8.1, 9.6, 10.5}

example, to uncertainties in model responses to forcing. Some potentially important forcings such as black carbon aerosols have not yet been considered in most formal detection and attribution studies. Uncertainties remain in estimates of natural internal climate variability. For example, there are discrepancies between estimates of ocean heat content variability from models and observations, although poor sampling of parts of the world ocean may explain this discrepancy. In addition, internal variability is difficult to estimate from available observational records since these are influenced by external forcing, and because records are not long enough in the case of instrumental data, or precise enough in the case of proxy reconstructions, to provide complete descriptions of variability on decadal and longer time scales (see Figure TS.22 and Box TS.7). {8.2–8.4, 8.6, 9.2–9.4}

It is *extremely unlikely* (<5%) that the global pattern of warming observed during the past half century can be explained without external forcing. These changes took place over a time period when non-anthropogenic forcing factors (i.e., the sum of solar and volcanic forcing) would be *likely* to have produced cooling, not warming (see Figure TS.23). Attribution studies show that it is *very likely* that these natural forcing factors alone cannot account for the observed warming (see Figure TS.23). There is also increased confidence that natural internal variability cannot account for the observed changes, due in part to improved studies demonstrating that the warming occurred in both oceans and atmosphere, together with observed ice mass losses. {2.9, 3.2, 5.2, 9.4, 9.5, 9.7}

It is *very likely* that anthropogenic greenhouse gas increases caused most of the observed increase in global average temperatures since the mid-20th century. Without the cooling effect of atmospheric aerosols, it is *likely* that greenhouse gases alone would have caused a greater global mean temperature rise than that observed during the last 50 years. A key factor in identifying the aerosol fingerprint, and therefore the amount of cooling counteracting greenhouse warming, is the temperature change through time (see Figure TS.23), as well as the hemispheric warming contrast. The conclusion that greenhouse gas forcing has been dominant takes into account observational and forcing uncertainties, and is robust to the use of different climate models, different methods for estimating the responses to external forcing and different analysis techniques. It also allows for possible amplification of the response to solar forcing. {2.9, 6.6, 9.1, 9.2, 9.4}

Widespread warming has been detected in ocean temperatures. Formal attribution studies now suggest that it is *likely* that anthropogenic forcing has contributed to the observed warming of the upper several hundred metres of the global ocean during the latter half of the 20th century. {5.2, 9.5}

Anthropogenic forcing has *likely* contributed to recent decreases in arctic sea ice extent. Changes in arctic sea ice are expected given the observed enhanced arctic warming. Attribution studies and improvements in the modelled representation of sea ice and ocean heat transport strengthen the confidence in this conclusion. {3.3, 4.4, 8.2, 8.3, 9.5}

It is *very likely* that the response to anthropogenic forcing contributed to sea level rise during the latter half of the 20th century, but decadal variability in sea level rise remains poorly understood. Modelled estimates of the contribution to sea level rise from thermal expansion are in good agreement with estimates based on observations during 1961 to 2003, although the budget for sea level rise over that interval is not closed. The observed increase in the rate of loss of mass from glaciers and ice caps is proportional to the global average temperature rise, as expected qualitatively from physical considerations (see Table TS.3). The greater rate of sea level rise in 1993 to 2003 than in 1961 to 2003 may be linked to increasing anthropogenic forcing, which has

Global and Continental Temperature Change

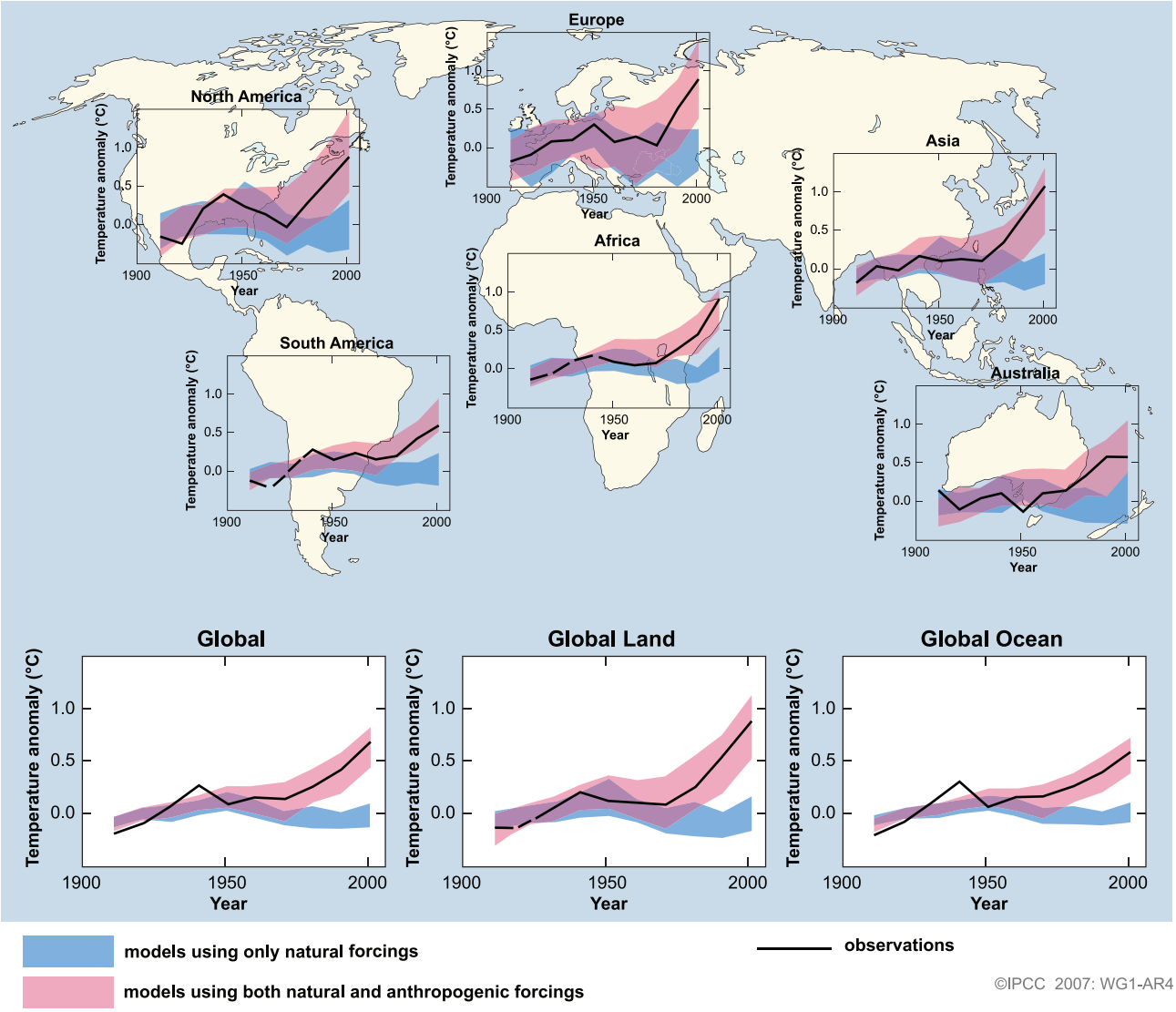


Figure TS.22. *Comparison of observed continental- and global-scale changes in surface temperature with results simulated by climate models using natural and anthropogenic forcings. Decadal averages of observations are shown for the period 1906 to 2005 (black line) plotted against the centre of the decade and relative to the corresponding average for 1901 to 1950. Lines are dashed where spatial coverage is less than 50%. Blue shaded bands show the 5% to 95% range for 19 simulations from 5 climate models using only the natural forcings due to solar activity and volcanoes. Red shaded bands show the 5% to 95% range for 58 simulations from 14 climate models using both natural and anthropogenic forcings. Data sources and models used are described in Section 9.4, FAQ 9.2, Table 8.1 and the supplementary information for Chapter 9. {FAQ 9.2, Figure 1}*

likely contributed to the observed warming of the upper ocean and widespread glacier retreat. On the other hand, the tide gauge record of global mean sea level suggests that similarly large rates may have occurred in previous 10-year periods since 1950, implying that natural internal variability could also be a factor in the high rates for 1993 to 2003 period. Observed decadal variability in the tide gauge record is larger than can be explained by variability in observationally based estimates of thermal expansion and land ice changes. Further, the observed decadal variability in thermal expansion is larger than simulated by models for the 20th century. Thus, the physical causes of the variability seen in the tide gauge record are uncertain. These unresolved issues relating to sea level change and its decadal variability during 1961 to 2003 make it unclear how much of the higher rate of sea level rise in 1993 to 2003 is due to natural internal variability and how much to anthropogenic climate change. {5.5, 9.5}

TS.4.2 Attribution of Spatial and Temporal Changes in Temperature

The observed pattern of tropospheric warming and stratospheric cooling is *very likely* due to the influence of anthropogenic forcing, particularly that due to greenhouse gas increases and stratospheric ozone depletion. New analyses since the TAR show that this pattern corresponds to an increase in the height of the tropopause that is *likely* due largely to greenhouse gas and stratospheric ozone changes. Significant uncertainty remains in the estimation of tropospheric temperature trends, particularly from the radiosonde record. {3.2, 3.4, 9.4}

It is *likely* that there has been a substantial anthropogenic contribution to surface temperature increases averaged over every continent except Antarctica since the middle of the 20th century. Antarctica has insufficient observational coverage to make an assessment. Anthropogenic warming has also been identified in some sub-continental land areas. The ability of coupled climate models to simulate the temperature evolution on each of six continents provides stronger evidence of human influence on the global climate than was available in the TAR. No coupled global climate model that has used natural forcing only has reproduced the observed global mean warming trend, or the continental mean warming trends in individual

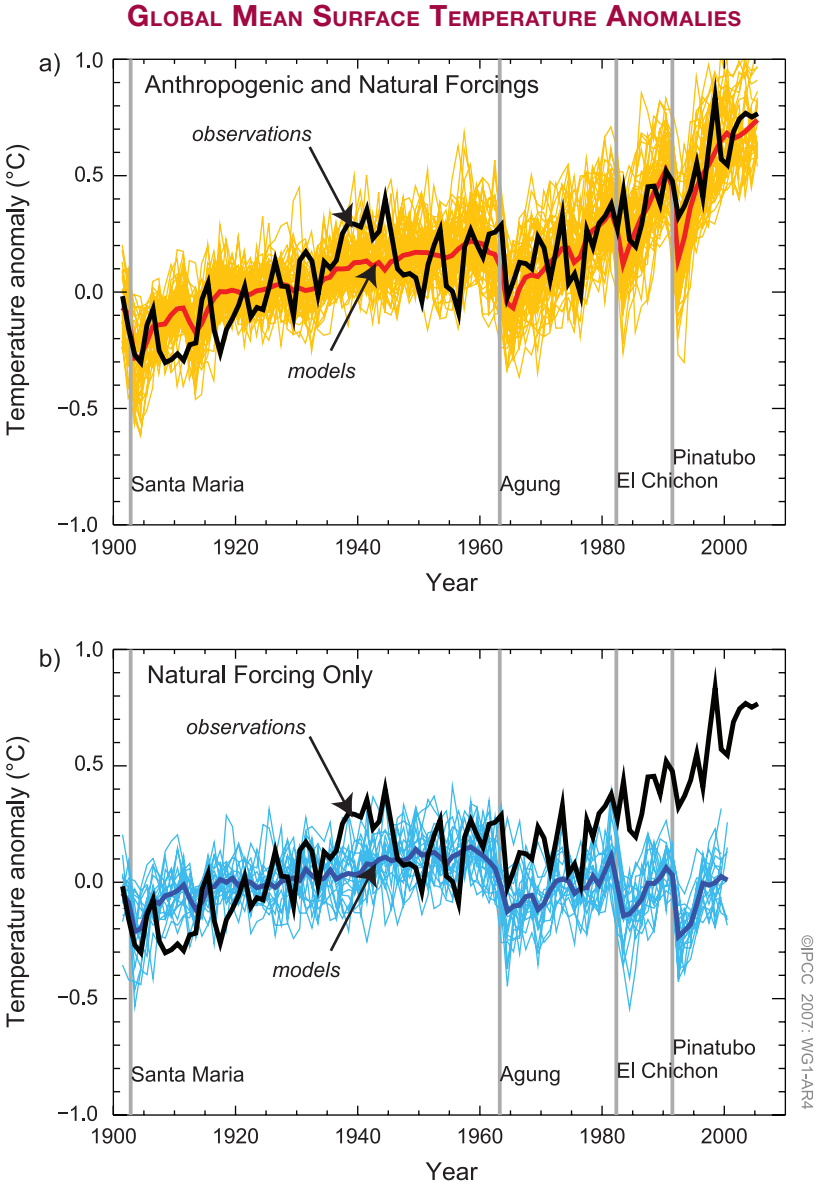


Figure TS.23. *(a) Global mean surface temperature anomalies relative to the period 1901 to 1950, as observed (black line) and as obtained from simulations with both anthropogenic and natural forcings. The thick red curve shows the multi-model ensemble mean and the thin yellow curves show the individual simulations. Vertical grey lines indicate the timing of major volcanic events. (b) As in (a), except that the simulated global mean temperature anomalies are for natural forcings only. The thick blue curve shows the multi-model ensemble mean and the thin lighter blue curves show individual simulations. Each simulation was sampled so that coverage corresponds to that of the observations. {Figure 9.5}*

continents (except Antarctica) over the second half of the 20th century. {9.4}

Difficulties remain in attributing temperature changes at smaller than continental scales and over time scales of less than 50 years. Attribution results at these scales have, with limited exceptions, not been established. Averaging over smaller regions reduces the natural variability less than does averaging over large regions, making it more difficult to distinguish between changes expected from external forcing and variability. In addition, temperature changes associated with some modes of variability are poorly simulated by models in some regions and seasons. Furthermore, the small-scale details of external forcing and the response simulated by models are less credible than large-scale features. {8.3, 9.4}

Surface temperature extremes have *likely* been affected by anthropogenic forcing. Many indicators of extremes, including the annual numbers and most extreme values of warm and cold days and nights, as well as numbers of frost days, show changes that are consistent with warming. Anthropogenic influence has been detected in some of these indices, and there is evidence that anthropogenic forcing may have substantially increased the risk of extremely warm summer conditions regionally, such as the 2003 European heat wave. {9.4}

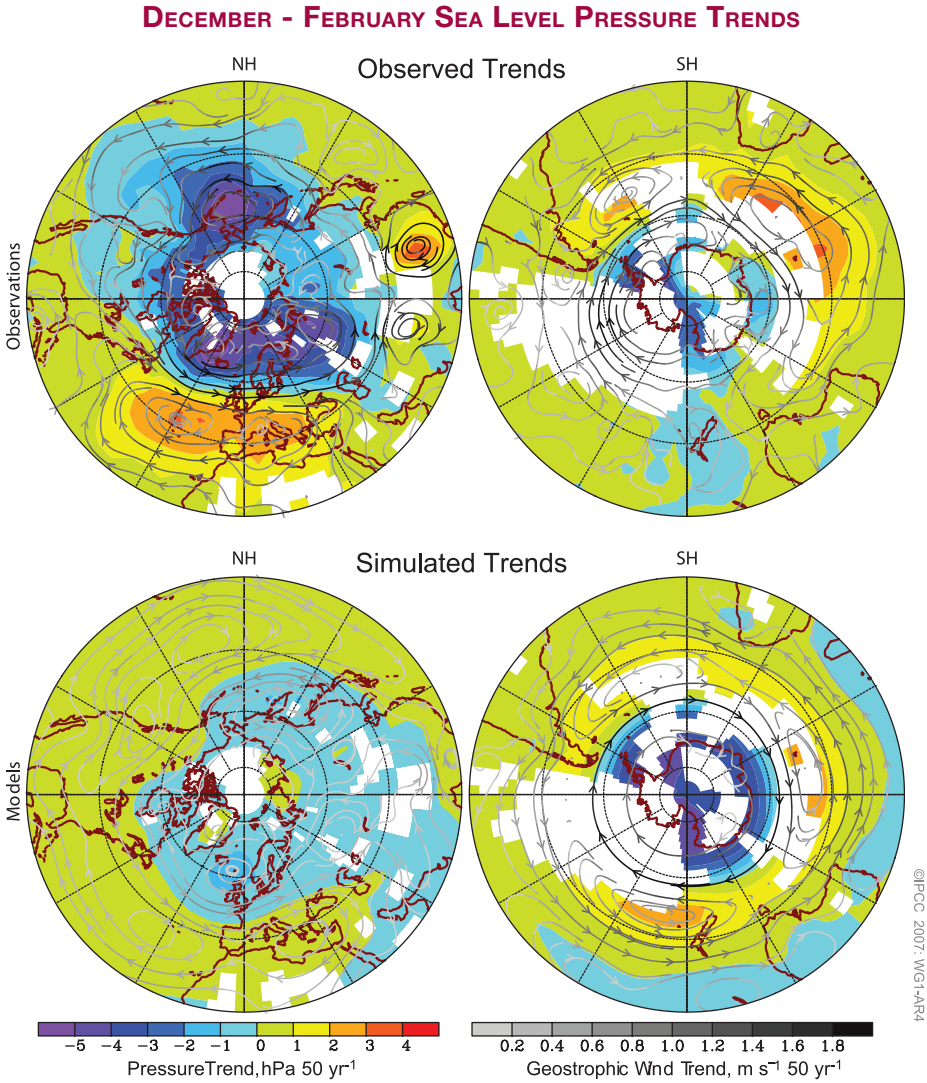


Figure TS.24. *December through February sea level pressure trends based on decadal means for the period 1955 to 2005. (Top) Trends estimated from an observational data set and displayed in regions where there is observational coverage. (Bottom) Mean trends simulated in response to natural and anthropogenic forcing changes in eight coupled models. The model-simulated trends are displayed only where observationally based trends are displayed. Streamlines, which are not masked, indicate the direction of the trends in the geostrophic wind derived from the trends in sea level pressure, and the shading of the streamlines indicates the magnitude of the change, with darker streamlines corresponding to larger changes in geostrophic wind. Data sources and models are described in Chapter 9 and its supplementary material, and Table 8.1 provides model details. {Figure 9.16}*

TS.4.3 Attribution of Changes in Circulation, Precipitation and Other Climate Variables

Trends in the Northern and Southern Annular Modes over recent decades, which correspond to sea level pressure reductions over the poles and related changes in atmospheric circulation, are *likely* related in part to human activity (see Figure TS.24). Models reproduce the sign of the NAM trend, but the simulated response is smaller than observed. Models including both greenhouse gas and stratospheric ozone changes simulate a realistic trend in the SAM, leading to a detectable human influence on global sea level pressure that is also consistent with the observed cooling trend in surface climate over parts of Antarctica. These changes in hemispheric circulation and their attribution to human activity imply that anthropogenic effects have *likely* contributed to changes in mid- and high-latitude patterns of circulation and temperature, as well as changes in winds and storm tracks. However, quantitative effects are uncertain because simulated responses to 20th century forcing change for the NH agree only qualitatively and not quantitatively with observations of these variables. {3.6, 9.5, 10.3}

There is some evidence of the impact of external influences on the hydrological cycle. The observed large-scale pattern of changes in land precipitation over the 20th century is qualitatively consistent with simulations, suggestive of a human influence. An observed global trend towards increases in drought in the second half of the 20th century has been reproduced with a model by taking anthropogenic and natural forcing into account. A number of studies have now demonstrated that changes in land use, due for example to overgrazing and conversion of woodland to agriculture, are *unlikely* to have been the primary cause of Sahelian and Australian droughts. Comparisons between observations and models suggest that changes in monsoons, storm intensities and Sahelian rainfall are related at least in part to changes in observed SSTs. Changes in global SSTs are expected to be affected by anthropogenic forcing, but an association of regional SST changes with forcing has not been established. Changes in rainfall depend not just upon SSTs but also upon changes in the spatial and temporal SST patterns and regional changes in atmospheric circulation, making attribution to human influences difficult. {3.3, 9.5, 10.3, 11.2}

TS.4.4 Palaeoclimate Studies of Attribution

It is *very likely* that climate changes of at least the seven centuries prior to 1950 were not due to unforced variability alone. Detection and attribution studies indicate that a substantial fraction of pre-industrial NH inter-decadal temperature variability contained in reconstructions for those centuries is *very likely* attributable to natural external forcing. Such forcing includes episodic cooling due to known volcanic eruptions, a number of which were larger than those of the 20th century (based on evidence such as ice cores), and long-term variations in solar irradiance, such as reduced radiation during the Maunder Minimum. Further, it is *likely* that anthropogenic forcing contributed to the early 20th-century warming evident in these records. Uncertainties are unlikely to lead to a spurious agreement between temperature reconstructions and forcing reconstructions as they are derived from independent proxies. Insufficient data are available to make a similar SH evaluation. {6.6, 9.3}

TS.4.5 Climate Response to Radiative Forcing

Specification of a *likely* range and a most *likely* value for equilibrium climate sensitivity[8] in this report represents significant progress in quantifying the climate system response to radiative forcing since the TAR and an advance in challenges to understanding that have persisted for over 30 years. A range for equilibrium climate sensitivity – the equilibrium global average warming expected if CO_2 concentrations were to be sustained at double their pre-industrial values (about 550 ppm) – was given in the TAR as between 1.5°C and 4.5°C. It has not been possible previously to provide a best estimate or to estimate the probability that climate sensitivity might fall outside that quoted range. Several approaches are used in this assessment to constrain climate sensitivity, including the use of AOGCMs, examination of the transient evolution of temperature (surface, upper air and ocean) over the last 150 years and examination of the rapid response of the global climate system to changes in the forcing caused by volcanic eruptions (see Figure TS.25). These are complemented by estimates based upon palaeoclimate studies such as reconstructions of the NH temperature record of the past millennium and the LGM. Large ensembles of climate model simulations have shown that the ability of models to simulate present climate has value in constraining climate sensitivity. {8.1, 8.6, 9.6, Box 10.2}

[8] See the Glossary for a detailed definition of climate sensitivity.

Analysis of models together with constraints from observations suggest that the equilibrium climate sensitivity is *likely* to be in the range 2°C to 4.5°C, with a best estimate value of about 3°C. It is *very unlikely* to be less than 1.5°C. Values substantially higher than 4.5°C cannot be excluded, but agreement with observations is not as good for those values. Probability density functions derived from different information and approaches generally tend to have a long tail towards high values exceeding 4.5°C. Analysis of climate and forcing evolution over previous centuries and model ensemble studies do not rule out climate sensitivity being as high as 6°C or more. One factor in this is the possibility of small net radiative forcing over the 20th century if aerosol indirect cooling effects were at the upper end of their uncertainty range, thus cancelling most of the positive forcing due to greenhouse gases. However, there is no well-established way of estimating a single probability distribution function from individual results taking account of the different assumptions in each study. The lack of strong constraints limiting high climate sensitivities prevents the specification of a 95th percentile bound or a very likely range for climate sensitivity. {Box 10.2}

There is now increased confidence in the understanding of key climate processes that are important to climate sensitivity due to improved analyses and comparisons of models to one another and to observations. Water vapour changes dominate the feedbacks affecting climate sensitivity and are now better understood. New observational and modelling evidence strongly favours a combined water vapour-lapse rate[9] feedback of around the strength found in General Circulation Models (GCMs), that is, approximately 1 W m^{-2} per degree global temperature increase, corresponding to about a 50% amplification of global mean warming. Such GCMs have demonstrated an ability to simulate seasonal to inter-decadal humidity variations in the upper troposphere over land and ocean, and have successfully simulated the observed surface temperature and humidity changes associated with volcanic eruptions. Cloud feedbacks (particularly from low clouds) remain the largest source of uncertainty. Cryospheric feedbacks such as changes in snow cover have been shown to contribute less to the spread in model estimates of climate sensitivity than cloud or water vapour feedbacks, but they

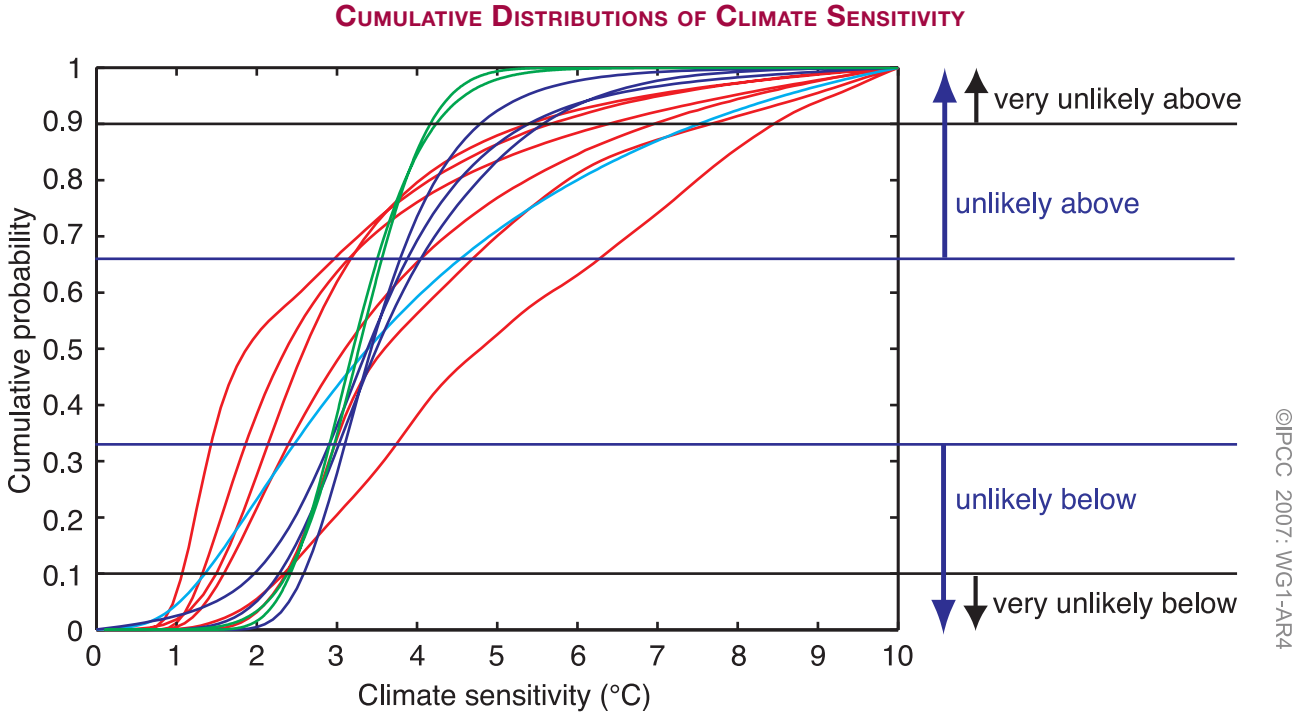


Figure TS.25. *Cumulative distributions of climate sensitivity derived from observed 20th-century warming (red), model climatology (blue), proxy evidence (cyan) and from climate sensitivities of AOGCMs (green). Horizontal lines and arrows mark the boundaries of the likelihood estimates defined in the IPCC Fourth Assessment Uncertainty Guidance Note (see Box TS.1). {Box 10.2, Figures 1 and 2}*

[9] The rate at which air temperature decreases with altitude.

can be important for regional climate responses at mid- and high latitudes. A new model intercomparison suggests that differences in radiative transfer formulations also contribute to the range. {3.4, 8.6, 9.3, 9.4, 9.6, 10.2, Box 10.2}

Improved quantification of climate sensitivity allows estimation of best estimate equilibrium temperatures and ranges that could be expected if concentrations of CO_2 were to be stabilised at various levels based on global energy balance considerations (see Table TS.5). As in the estimate of climate sensitivity, a very likely upper bound cannot be established. Limitations to the concept of radiative forcing and climate sensitivity should be noted. Only a few AOGCMs have been run to equilibrium under elevated CO_2 concentrations, and some results show that climate feedbacks may change over long time scales, resulting in substantial deviations from estimates of warming based on equilibrium climate sensitivity inferred from mixed layer ocean models and past climate change. {10.7}

Agreement among models for projected transient climate change has also improved since the TAR. The range of transient climate responses (defined as the global average surface air temperature averaged over a 20-year period centred at the time of CO_2 doubling in a 1% yr^{-1} increase experiment) among models is smaller than the range in the equilibrium climate sensitivity. This parameter is now better constrained by multi-model ensembles and comparisons with observations; it is *very likely* to be greater than 1°C and *very unlikely* to be greater than 3°C. The transient climate response is related to sensitivity in a nonlinear way such that high sensitivities are not immediately manifested in the short-term response. Transient climate response is strongly affected by the rate of ocean heat uptake. Although the ocean models have improved, systematic model biases and limited ocean temperature data to evaluate transient ocean heat uptake affect the accuracy of current estimates. {8.3, 8.6, 9.4, 9.6, 10.5}

Table TS.5. *Best estimate, likely ranges and very likely lower bounds of global mean equilibrium surface temperature increase (°C) over pre-industrial temperatures for different levels of CO_2-equivalent radiative forcing, as derived from the climate sensitivity.*

Equilibrium CO_2–eq (ppm)	Temperature Increase (°C)		
	Best Estimate	*Very Likely* Above	*Likely* in the Range
350	1.0	0.5	0.6–1.4
450	2.1	1.0	1.4–3.1
550	2.9	1.5	1.9–4.4
650	3.6	1.8	2.4–5.5
750	4.3	2.1	2.8–6.4
1000	5.5	2.8	3.7–8.3
1200	6.3	3.1	4.2–9.4

TS.5 Projections of Future Changes in Climate

Since the TAR, there have been many important advances in the science of climate change projections. An unprecedented effort has been initiated to make new model results available for prompt scrutiny by researchers outside of the modelling centres. A set of coordinated, standard experiments was performed by 14 AOGCM modelling groups from 10 countries using 23 models. The resulting multi-model database of outputs, analysed by hundreds of researchers worldwide, forms the basis for much of this assessment of model results. Many advances have come from the use of multi-member ensembles from single models (e.g., to test the sensitivity of response to initial conditions) and from multi-model ensembles. These two different types of ensembles allow more robust studies of the range of model results and more quantitative model evaluation against observations, and provide new information on simulated statistical variability. {8.1, 8.3, 9.4, 9.5, 10.1}

A number of methods for providing probabilistic climate change projections, both for global means and geographical depictions, have emerged since the TAR and are a focus of this report. These include methods based on results of AOGCM ensembles without formal application of observational constraints as well as methods based on detection algorithms and on large model ensembles that provide projections consistent with observations of climate change and their uncertainties. Some methods now explicitly account for key uncertainty sources such as climate feedbacks, ocean heat uptake, radiative forcing and the carbon cycle. Short-term projections are similarly constrained by observations of recent trends. Some studies have probed additional probabilistic issues, such as the likelihood of future changes in extremes such as heat waves that could occur due to human influences. Advances have also occurred since the TAR through broader ranges

of studies of committed climate change and of carbon-climate feedbacks. {8.6, 9.6, 10.1, 10.3, 10.5}

These advances in the science of climate change modelling provide a probabilistic basis for distinguishing projections of climate change for different SRES marker scenarios. This is in contrast to the TAR where ranges for different marker scenarios could not be given in probabilistic terms. As a result, this assessment identifies and quantifies the difference in character between uncertainties that arise in climate modelling and those that arise from a lack of prior knowledge of decisions that will affect greenhouse gas emissions. A loss of policy-relevant information would result from combining probabilistic projections. For these reasons, projections for different emission scenarios are not combined in this report.

Model simulations used here consider the response of the physical climate system to a range of possible future conditions through use of idealised emissions or concentration assumptions. These include experiments with greenhouse gases and aerosols held constant at year 2000 levels, CO_2 doubling and quadrupling experiments, SRES marker scenarios for the 2000 to 2100 period, and experiments with greenhouse gases and aerosols held constant after 2100, providing new information on the physical aspects of long-term climate change and stabilisation. The SRES scenarios did not include climate initiatives. This Working Group I assessment does not evaluate the plausibility or likelihood of any specific emission scenario. {10.1, 10.3}

A new multi-model data set using Earth System Models of Intermediate Complexity (EMICs) complements AOGCM experiments to extend the time horizon for several more centuries in the future. This provides a more comprehensive range of model responses in this assessment as well as new information on climate change over long time scales when greenhouse gas and aerosol concentrations are held constant. Some AOGCMs and EMICs contain prognostic carbon cycle components, which permit estimation of the likely effects and associated uncertainties of carbon cycle feedbacks. {10.1}

Box TS.8: Hierarchy of Global Climate Models

Estimates of change in global mean temperature and sea level rise due to thermal expansion can be made using Simple Climate Models (SCMs) that represent the ocean-atmosphere system as a set of global or hemispheric boxes, and predict global surface temperature using an energy balance equation, a prescribed value of climate sensitivity and a basic representation of ocean heat uptake. Such models can also be coupled to simplified models of biogeochemical cycles and allow rapid estimation of the climate response to a wide range of emission scenarios. {8.8, 10.5}

Earth System Models of Intermediate Complexity (EMICs) include some dynamics of the atmospheric and oceanic circulations, or parametrizations thereof, and often include representations of biogeochemical cycles, but they commonly have reduced spatial resolution. These models can be used to investigate continental-scale climate change and long-term, large-scale effects of coupling between Earth system components using large ensembles of model runs or runs over many centuries. For both SCMs and EMICs it is computationally feasible to sample parameter spaces thoroughly, taking account of parameter uncertainties derived from tuning to more comprehensive climate models, matching observations and use of expert judgment. Thus, both types of model are well suited to the generation of probabilistic projections of future climate and allow a comparison of the 'response uncertainty' arising from uncertainty in climate model parameters with the 'scenario range' arising from the range of emission scenarios being considered. Earth System Models of Intermediate Complexity have been evaluated in greater depth than previously and intercomparison exercises have demonstrated that they are useful for studying questions involving long time scales or requiring large ensembles of simulations. {8.8, 10.5, 10.7}

The most comprehensive climate models are the AOGCMs. They include dynamical components describing atmospheric, oceanic and land surface processes, as well as sea ice and other components. Much progress has been made since the TAR (see Box TS.7), and there are over 20 models from different centres available for climate simulations. Although the large-scale dynamics of these models are comprehensive, parametrizations are still used to represent unresolved physical processes such as the formation of clouds and precipitation, ocean mixing due to wave processes and the formation of water masses, etc. Uncertainty in parametrizations is the primary reason why climate projections differ between different AOGCMs. While the resolution of AOGCMs is rapidly improving, it is often insufficient to capture the fine-scale structure of climatic variables in many regions. In such cases, the output from AOGCMs can be used to drive limited-area (or regional climate) models that combine the comprehensiveness of process representations comparable to AOGCMs with much higher spatial resolution. {8.2}

TS.5.1 Understanding Near-Term Climate Change

Knowledge of the climate system together with model simulations confirm that past changes in greenhouse gas concentrations will lead to a committed warming (see Box TS.9 for a definition) and future climate change. New model results for experiments in which concentrations of all forcing agents were held constant provide better estimates of the committed changes in atmospheric variables that would follow because of the long response time of the climate system, particularly the oceans. {10.3, 10.7}

Previous IPCC projections of future climate changes can now be compared to recent observations, increasing confidence in short-term projections and the underlying physical understanding of committed climate change over a few decades. Projections for 1990 to 2005 carried out for the FAR and the SAR suggested global mean temperature increases of about 0.3°C and 0.15°C per decade, respectively.[10] The difference between the two was due primarily to the inclusion of aerosol cooling effects in the SAR, whereas there was no quantitative basis for doing so in the FAR. Projections given in the TAR were similar to those of the SAR. These results are comparable to observed values of about 0.2°C per decade, as shown in Figure TS.26, providing broad confidence in such short-term projections. Some of this warming is the committed effect of changes in the concentrations of greenhouse gases prior to the times of those earlier assessments. {1.2, 3.2}

Committed climate change (see Box TS.9) due to atmospheric composition in the year 2000 corresponds to a warming trend of about 0.1°C per decade over the next two decades, in the absence of large changes in volcanic or solar forcing. About twice as much warming (0.2°C per decade) would be expected if emissions were to fall within the range of the SRES marker scenarios. This result is insensitive to the choice among the SRES marker scenarios, none of which considered climate initiatives. By 2050, the range of expected warming shows limited sensitivity to the choice among SRES scenarios (1.3°C to 1.7°C relative to 1980–1999) with about a quarter being due to the committed climate change if all radiative forcing agents were stabilised today. {10.3, 10.5, 10.7}

Sea level is expected to continue to rise over the next several decades. During 2000 to 2020 under the SRES A1B scenario in the ensemble of AOGCMs, the rate of thermal expansion is projected to be 1.3 ± 0.7 mm yr^{-1}, and is not significantly different under the A2 or B1 scenarios. These projected rates are within the uncertainty of the observed contribution of thermal expansion for 1993 to 2003 of 1.6 ± 0.6 mm yr^{-1}. The ratio of committed thermal expansion, caused by constant atmospheric composition at year 2000 values, to total thermal expansion (that is the ratio of expansion occurring after year 2000 to that occurring before and after) is larger than the corresponding ratio for global average surface temperature. {10.6, 10.7}

Box TS.9: Committed Climate Change

If the concentrations of greenhouse gases and aerosols were held fixed after a period of change, the climate system would continue to respond due to the thermal inertia of the oceans and ice sheets and their long time scales for adjustment. 'Committed warming' is defined here as the further change in global mean temperature after atmospheric composition, and hence radiative forcing, is held constant. Committed change also involves other aspects of the climate system, in particular sea level. Note that holding concentrations of radiatively active species constant would imply that ongoing emissions match natural removal rates, which for most species would be equivalent to a large reduction in emissions, although the corresponding model experiments are not intended to be considered as emission scenarios. {FAQ 10.3}

The troposphere adjusts to changes in its boundary conditions over time scales shorter than a month or so. The upper ocean responds over time scales of several years to decades, and the deep ocean and ice sheet response time scales are from centuries to millennia. When the radiative forcing changes, internal properties of the atmosphere tend to adjust quickly. However, because the atmosphere is strongly coupled to the oceanic mixed layer, which in turn is coupled to the deeper oceanic layer, it takes a very long time for the atmospheric variables to come to an equilibrium. During the long periods where the surface climate is changing very slowly, one can consider that the atmosphere is in a quasi-equilibrium state, and most energy is being absorbed by the ocean, so that ocean heat uptake is a key measure of climate change. {10.7}

[10] See IPCC First Assessment Report, Policymakers Summary, and Second Assessment Report, Technical Summary, Figure 18.

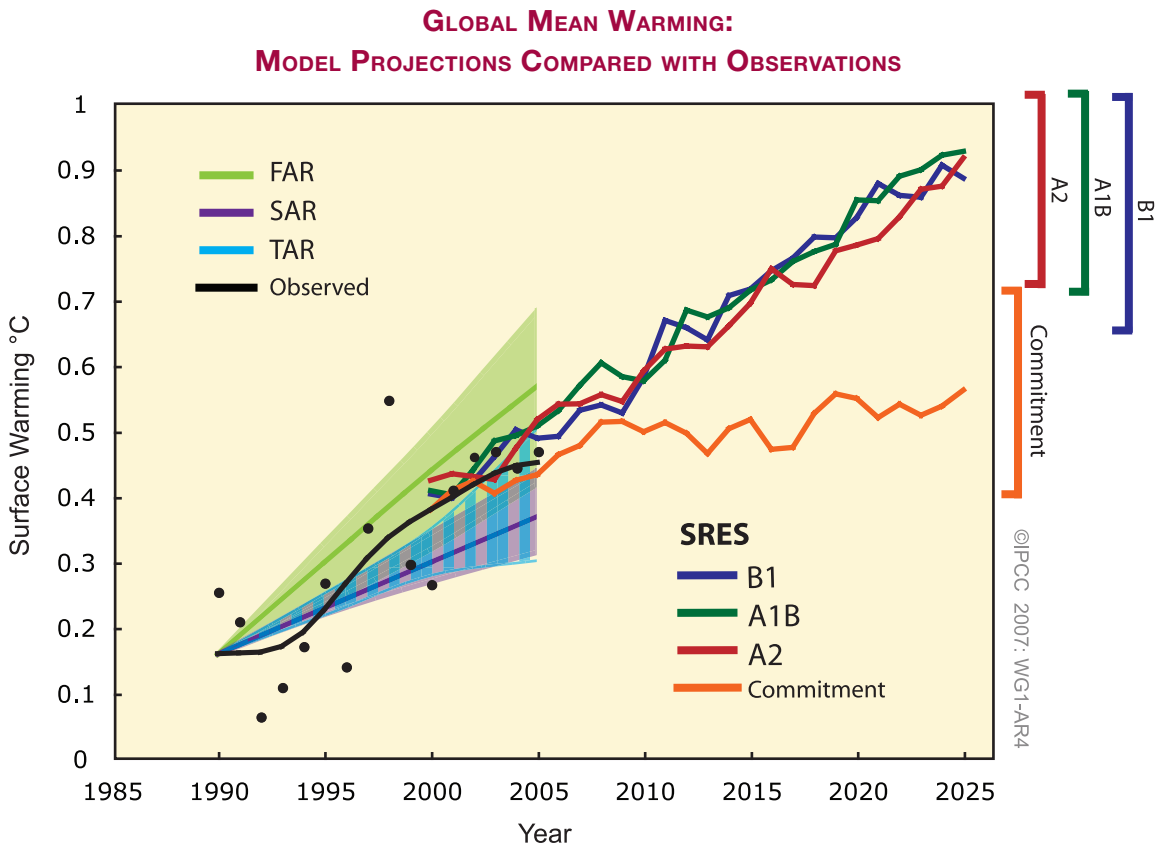


Figure TS.26. *Model projections of global mean warming compared to observed warming. Observed temperature anomalies, as in Figure TS.6, are shown as annual (black dots) and decadal average values (black line). Projected trends and their ranges from the IPCC First (FAR) and Second (SAR) Assessment Reports are shown as green and magenta solid lines and shaded areas, and the projected range from the TAR is shown by vertical blue bars. These projections were adjusted to start at the observed decadal average value in 1990. Multi-model mean projections from this report for the SRES B1, A1B and A2 scenarios, as in Figure TS.32, are shown for the period 2000 to 2025 as blue, green and red curves with uncertainty ranges indicated against the right-hand axis. The orange curve shows model projections of warming if greenhouse gas and aerosol concentrations were held constant from the year 2000 – that is, the committed warming. {Figures 1.1 and 10.4}*

TS.5.2 Large-Scale Projections for the 21st Century

This section covers advances in understanding global-scale climate projections and the processes that will influence their large-scale patterns in the 21st century. More specific discussion of regional-scale changes follows in TS.5.3.

Projected global average surface warming for the end of the 21st century (2090–2099) is scenario-dependent and the actual warming will be significantly affected by the actual emissions that occur. Warmings compared to 1980 to 1999 for six SRES scenarios[11] and for constant year 2000 concentrations, given as best estimates and corresponding *likely* ranges, are shown in Table TS.6. These results are based on AOGCMs, observational constraints and other methods to quantify the range of model response (see Figure TS.27). The combination of multiple lines of evidence allows likelihoods to be assigned to the resulting ranges, representing an important advance since the TAR. {10.5}

Assessed uncertainty ranges are larger than those given in the TAR because they consider a more complete range of models and climate-carbon cycle feedbacks. Warming tends to reduce land and ocean uptake of atmospheric CO_2, increasing the fraction of anthropogenic emissions that remains in the atmosphere. For the A2 scenario for example, the CO_2 feedback increases the corresponding global average warming in 2100 by more than 1°C. {7.3, 10.5}

[11] Approximate CO_2 equivalent concentrations corresponding to the computed radiative forcing due to anthropogenic greenhouse gases and aerosols in 2100 (see p. 823 of the TAR) for the SRES B1, A1T, B2, A1B, A2 and A1FI illustrative marker scenarios are about 600, 700, 800, 850, 1,250 and 1,550 ppm respectively. Constant emission at year 2000 levels would lead to a concentration for CO_2 alone of about 520 ppm by 2100.

Table TS.6. *Projected global average surface warming and sea level rise at the end of the 21st century. {10.5, 10.6, Table 10.7}*

Case	Temperature Change (°C at 2090-2099 relative to 1980-1999) [a]		Sea Level Rise (m at 2090-2099 relative to 1980-1999)
	Best estimate	*Likely* range	Model-based range excluding future rapid dynamical changes in ice flow
Constant Year 2000 concentrations [b]	0.6	0.3 – 0.9	NA
B1 scenario	1.8	1.1 – 2.9	0.18 – 0.38
A1T scenario	2.4	1.4 – 3.8	0.20 – 0.45
B2 scenario	2.4	1.4 – 3.8	0.20 – 0.43
A1B scenario	2.8	1.7 – 4.4	0.21 – 0.48
A2 scenario	3.4	2.0 – 5.4	0.23 – 0.51
A1FI scenario	4.0	2.4 – 6.4	0.26 – 0.59

Notes:
[a] These estimates are assessed from a hierarchy of models that encompass a simple climate model, several Earth Models of Intermediate Complexity (EMICs), and a large number of Atmosphere-Ocean Global Circulation Models (AOGCMs).
[b] Year 2000 constant composition is derived from AOGCMs only.

Projected global-average sea level rise at the end of the 21st century (2090 to 2099), relative to 1980 to 1999 for the six SRES marker scenarios, given as 5% to 95% ranges based on the spread of model results, are shown in Table TS.6. Thermal expansion contributes 70 to 75% to the best estimate for each scenario. An improvement since the TAR is the use of AOGCMs to evaluate ocean heat uptake and thermal expansion. This has also reduced the projections as compared to the simple model used in the TAR. In all the SRES marker scenarios except B1, the average rate of sea level rise during the 21st century *very likely* exceeds the 1961–2003 average rate (1.8 ± 0.5 mm yr^{-1}). For an average model, the scenario spread in sea level rise is only 0.02 m by the middle of the century, but by the end of the century it is 0.15 m. These ranges do not include uncertainties in carbon-cycle feedbacks or ice flow processes because a basis in published literature is lacking. {10.6, 10.7}

For each scenario, the midpoint of the range given here is within 10% of the TAR model average for 2090–2099, noting that the TAR projections were given for 2100, whereas projections in this report are for 2090–2099. The uncertainty in these projections is less than in the TAR for several reasons: uncertainty in land ice models is assumed independent of uncertainty in temperature and expansion projections; improved observations of recent mass loss from glaciers provide a better observational constraint; and the present report gives uncertainties as 5% to 95% ranges, equivalent to ±1.65 standard deviations, whereas the TAR gave uncertainty ranges of ±2 standard deviations. The TAR would have had similar ranges for sea level projections to those in this report if it had treated the uncertainties in the same way. {10.6, 10.7}

Changes in the cryosphere will continue to affect sea level rise during the 21st century. Glaciers, ice caps and the Greenland Ice Sheet are projected to lose mass in the 21st century because increased melting will exceed increased snowfall. Current models suggest that the Antarctic Ice Sheet will remain too cold for widespread melting and may gain mass in future through increased snowfall, acting to reduce sea level rise. However, changes in ice dynamics could increase the contributions of both Greenland and Antarctica to 21st-century sea level rise. Recent observations of some Greenland outlet glaciers give strong evidence for enhanced flow when ice shelves are removed. The observations in west-central Greenland of seasonal variation in ice flow rate and of a correlation with summer temperature variation suggest that surface melt water may join a sub-glacially routed drainage system lubricating the ice flow. By both of these mechanisms, greater surface melting during the 21st century could cause acceleration of ice flow and discharge and increase the sea level contribution. In some parts of West Antarctica, large accelerations of ice flow have recently occurred, which may have been caused by thinning of ice shelves due to ocean warming. Although this has not been formally attributed to anthropogenic climate change due to greenhouse gases, it suggests that future warming could cause faster mass loss and greater

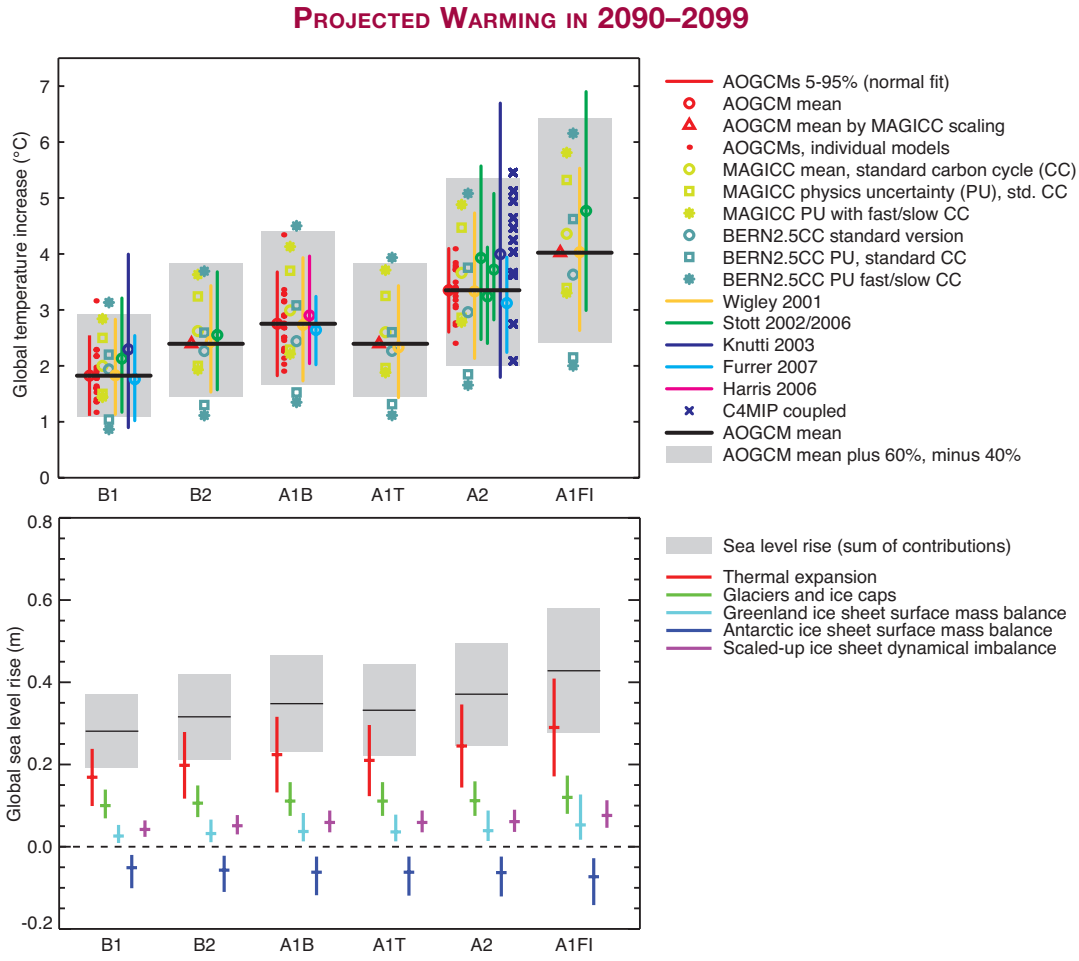


Figure TS.27. *(Top) Projected global mean temperature change in 2090 to 2099 relative to 1980 to 1999 for the six SRES marker scenarios based on results from different and independent models. The multi-model AOGCM mean and the range of the mean minus 40% to the mean plus 60% are shown as black horizontal solid lines and grey bars, respectively. Carbon cycle uncertainties are estimated for scenario A2 based on Coupled Carbon Cycle Climate Model Intercomparison Project (C⁴MIP) models (dark blue crosses), and for all marker scenarios using an EMIC (pale blue symbols). Other symbols represent individual studies (see Figure 10.29 for details of specific models). (Bottom) Projected global average sea level rise and its components in 2090 to 2099 (relative to 1980–1999) for the six SRES marker scenarios. The uncertainties denote 5 to 95% ranges, based on the spread of model results, and not including carbon cycle uncertainties. The contributions are derived by scaling AOGCM results and estimating land ice changes from temperature changes (see Appendix 10.A for details). Individual contributions are added to give the total sea level rise, which does not include the contribution shown for ice sheet dynamical imbalance, for which the current level of understanding prevents a best estimate from being given. {Figures 10.29 and 10.33}*

sea level rise. Quantitative projections of this effect cannot be made with confidence. If recently observed increases in ice discharge rates from the Greenland and Antarctic Ice Sheets were to increase linearly with global average temperature change, that would add 0.1 to 0.2 m to the upper bound of sea level rise. Understanding of these effects is too limited to assess their likelihood or to give a best estimate. {4.6, 10.6}

Many of the global and regional patterns of temperature and precipitation seen in the TAR projections remain in the new generation of models and across ensemble results (see Figure TS.28). Confidence in the robustness of these patterns is increased by the fact that they have remained largely unchanged while overall model simulations have improved (Box TS.7). This adds to confidence that these patterns reflect basic physical constraints on the climate system as it warms. {8.3–8.5, 10.3, 11.2–11.9}

The projected 21st-century temperature change is positive everywhere. It is greatest over land and at most high latitudes in the NH during winter, and increases going from the coasts into the continental interiors. In otherwise geographically similar areas, warming is typically larger in arid than in moist regions. {10.3, 11.2–11.9}

In contrast, warming is least over the southern oceans and parts of the North Atlantic Ocean. Temperatures are projected to increase, including over the North Atlantic and Europe, despite a projected slowdown of the meridional overturning circulation (MOC) in most models, due to the much larger influence of the increase in greenhouse gases. The projected pattern of zonal mean temperature change in the atmosphere displays a maximum warming in the upper tropical troposphere and cooling in the stratosphere. Further zonal mean warming in the ocean is expected to occur first near the surface and in the northern mid-latitudes, with the warming gradually reaching the ocean interior, most evident at high latitudes where vertical mixing is greatest. The projected pattern of change is very similar among the late-century cases irrespective of the scenario. Zonally averaged fields normalised by the mean warming are very similar for the scenarios examined (see Figure TS.28). {10.3}

It is *very likely* that the Atlantic MOC will slow down over the course of the 21st century. The multi-model average reduction by 2100 is 25% (range from zero to about 50%) for SRES emission scenario A1B. Temperatures in the Atlantic region are projected to increase despite such changes due to the much larger warming associated with projected increases of greenhouse gases. The projected reduction of the Atlantic MOC is due to the combined effects of an increase in high latitude temperatures and precipitation, which reduce the density of the surface waters in the North Atlantic. This could lead to a significant reduction in Labrador Sea Water formation. Very few AOGCM studies have included the impact of additional freshwater from melting of the Greenland Ice Sheet, but those that have do not suggest that this will lead to a complete MOC shutdown. Taken together, it is *very likely* that the MOC will reduce, but very *unlikely* that the MOC will undergo a large abrupt transition during the course of the 21st century. Longer-term changes in the MOC cannot be assessed with confidence. {8.7, 10.3}

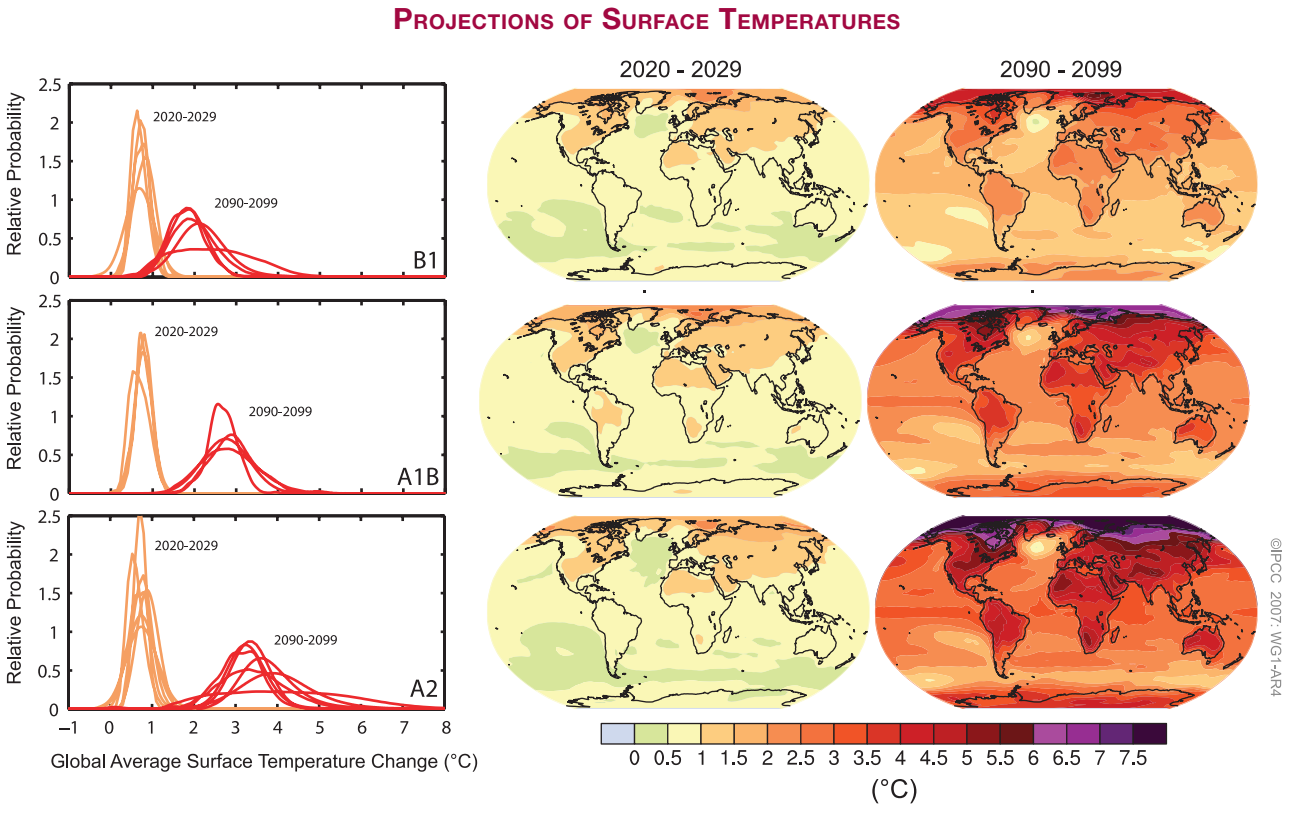


Figure TS.28. *Projected surface temperature changes for the early and late 21st century relative to the period 1980 to 1999. The central and right panels show the AOGCM multi-model average projections (°C) for the B1 (top), A1B (middle) and A2 (bottom) SRES scenarios averaged over the decades 2020 to 2029 (centre) and 2090 to 2099 (right). The left panel shows corresponding uncertainties as the relative probabilities of estimated global average warming from several different AOGCM and EMIC studies for the same periods. Some studies present results only for a subset of the SRES scenarios, or for various model versions. Therefore the difference in the number of curves, shown in the left-hand panels, is due only to differences in the availability of results. {Adapted from Figures 10.8 and 10.28}*

Models indicate that sea level rise during the 21st century will not be geographically uniform. Under scenario A1B for 2070 to 2099, AOGCMs give a median spatial standard deviation of 0.08 m, which is about 25% of the central estimate of the global average sea level rise. The geographic patterns of future sea level change arise mainly from changes in the distribution of heat and salinity in the ocean and consequent changes in ocean circulation. Projected patterns display more similarity across models than those analysed in the TAR. Common features are a smaller than average sea level rise in the Southern Ocean, larger than average sea level rise in the Arctic and a narrow band of pronounced sea level rise stretching across the southern Atlantic and Indian Oceans. {10.6}

Projections of changes in extremes such as the frequency of heat waves are better quantified than in the TAR, due to improved models and a better assessment of model spread based on multi-model ensembles. The TAR concluded that there was a risk of increased temperature extremes, with more extreme heat episodes in a future climate. This result has been confirmed and expanded in more recent studies. Future increases in temperature extremes are projected to follow increases in mean temperature over most of the world except where surface properties (e.g., snow cover or soil moisture) change. A multi-model analysis, based on simulations of 14 models for three scenarios, investigated changes in extreme seasonal (DJF and JJA) temperatures where 'extreme' is defined as lying above the 95th percentile of the simulated temperature distribution for the 20th century. By the end of the 21st century, the projected probability of extreme warm seasons rises above 90% in many tropical areas, and reaches around 40% elsewhere. Several recent studies have addressed possible future changes in heat waves, and found that, in a future climate, heat waves are expected to be more intense, longer lasting and more frequent. Based on an eight-member multi-model ensemble, heat waves are simulated to have been increasing for the latter part of the 20th century, and are projected to increase globally and over most regions. {8.5, 10.3}

For a future warmer climate, models project a 50 to 100% decline in the frequency of cold air outbreaks relative to the present in NH winters in most areas. Results from a nine-member multi-model ensemble show simulated decreases in frost days for the 20th century continuing into the 21st century globally and in most regions. Growing season length is related to frost days and is projected to increase in future climates. {10.3, FAQ 10.1}

Snow cover is projected to decrease. Widespread increases in thaw depth are projected to occur over most permafrost regions. {10.3}

Under several different scenarios (SRES A1B, A2 and B1), large parts of the Arctic Ocean are expected to no longer have year-round ice cover by the end of the 21st century. Arctic sea ice responds sensitively to warming. While projected changes in winter sea ice extent are moderate, late-summer sea ice is projected to disappear almost completely towards the end of the 21st century under the A2 scenario in some models. The reduction is accelerated by a number of positive feedbacks in the climate system. The ice-albedo feedback allows open water to receive more heat from the Sun during summer, the insulating effect of sea ice is reduced and the increase in ocean heat transport to the Arctic further reduces ice cover. Model simulations indicate that the late-summer sea ice cover decreases substantially and generally evolves over the same time scale as global warming. Antarctic sea ice extent is also projected to decrease in the 21st century. {8.6, 10.3, Box 10.1}

Sea level pressure is projected to increase over the subtropics and mid-latitudes, and decrease over high latitudes associated with an expansion of the Hadley Circulation and annular mode changes (NAM/NAO and SAM, see Box TS.2). A positive trend in the NAM/NAO as well as the SAM index is projected by many models. The magnitude of the projected increase is generally greater for the SAM, and there is considerable spread among the models. As a result of these changes, storm tracks are projected to move poleward, with consequent changes in wind, precipitation and temperature patterns outside the tropics, continuing the broad pattern of observed trends over the last half century. Some studies suggest fewer storms in mid-latitude regions. There are also indications of changes in extreme wave height associated with changing storm tracks and circulation. {3.6, 10.3}

In most models, the central and eastern equatorial Pacific SSTs warm more than those in the western equatorial Pacific, with a corresponding mean eastward shift in precipitation. ENSO interannual variability is projected to continue in all models, although changes differ from model to model. Large inter-model differences in projected changes in El Niño amplitude, and the inherent centennial time-scale variability of El Niño in the models, preclude a definitive projection of trends in ENSO variability. {10.3}

Recent studies with improved global models, ranging in resolution from about 100 to 20 km, suggest future changes in the number and intensity of future tropical cyclones (typhoons and hurricanes).

A synthesis of the model results to date indicates, for a warmer future climate, increased peak wind intensities and increased mean and peak precipitation intensities in future tropical cyclones, with the possibility of a decrease in the number of relatively weak hurricanes, and increased numbers of intense hurricanes. However, the total number of tropical cyclones globally is projected to decrease. The apparent observed increase in the proportion of very intense hurricanes since 1970 in some regions is in the same direction but much larger than predicted by theoretical models. {10.3, 8.5, 3.8}

Since the TAR, there is an improving understanding of projected patterns of precipitation. Increases in the amount of precipitation are *very likely* at high latitudes while decreases are *likely* in most subtropical land regions (by as much as about 20% in the A1B scenario in 2100). Poleward of 50°, mean precipitation is projected to increase due to the increase in water vapour in the atmosphere and the resulting increase in vapour transport from lower latitudes. Moving equatorward, there is a transition to mostly decreasing precipitation in the subtropics (20°–40° latitude). Due to increased water vapour transport out of the subtropics and a poleward expansion of the subtropical high-pressure systems, the drying tendency is especially pronounced at the higher-latitude margins of the subtropics (see Figure TS.30). {8.3, 10.3, 11.2–11.9}

Models suggest that changes in mean precipitation amount, even where robust, will rise above natural variability more slowly than the temperature signal. {10.3, 11.1}

Available research indicates a tendency for an increase in heavy daily rainfall events in many regions, including some in which the mean rainfall is projected to decrease. In the latter cases, the rainfall decrease is often attributable to a reduction in the number of rain days rather than the intensity of rain when it occurs. {11.2–11.9}

TS.5.3 Regional-Scale Projections

For each of the continental regions, the projected warming over 2000 to 2050 resulting from the SRES emissions scenarios is greater than the global average and greater than the observed warming over the past century. The warming projected for the next few decades of the 21st century, when averaged over the continents individually, would substantially exceed estimated 20th-century natural forced and unforced variability in all cases except Antarctica (Figure TS.29). Model best-estimate projections indicate that decadal average warming over each continent except Antarctica by 2030 is *very likely* to be at least twice as large as the corresponding model-estimated natural variability during the 20th century. The simulated warming over this period is not very sensitive to the choice of scenarios across the SRES set as is illustrated in Figure TS.32. Over longer time scales, the choice of scenario is more important, as shown in Figure TS.28. The projected warming in the SRES scenarios over 2000 to 2050 also exceeds estimates of natural variability when averaged over most sub-continental regions. {11.1}

Box TS.10. Regional Downscaling

Simulation of regional climates has improved in AOGCMs and, as a consequence, in nested regional climate models and in empirical downscaling techniques. Both dynamic and empirical downscaling methodologies show improving skill in simulating local features in present-day climates when the observed state of the atmosphere at scales resolved by current AOGCMs is used as input. The availability of downscaling and other regionally focused studies remains uneven geographically, causing unevenness in the assessments that can be provided, particularly for extreme weather events. Downscaling studies demonstrate that local precipitation changes can vary significantly from those expected from the large-scale hydrological response pattern, particularly in areas of complex topography. {11.10}

There remain a number of important sources of uncertainty limiting the ability to project regional climate change. While hydrological responses are relatively robust in certain core subpolar and subtropical regions, there is uncertainty in the precise location of these boundaries between increasing and decreasing precipitation. There are some important climate processes that have a significant effect on regional climate, but for which the climate change response is still poorly known. These include ENSO, the NAO, blocking, the thermohaline circulation and changes in tropical cyclone distribution. For those regions that have strong topographical controls on their climatic patterns, there is often insufficient climate change information at the fine spatial resolution of the topography. In some regions there has been only very limited research on extreme weather events. Further, the projected climate change signal becomes comparable to larger internal variability at smaller spatial and temporal scales, making it more difficult to utilise recent trends to evaluate model performance. {Box 11.1, 11.2–11.9}

Continental Surface Temperature Anomalies: Observations and Projections

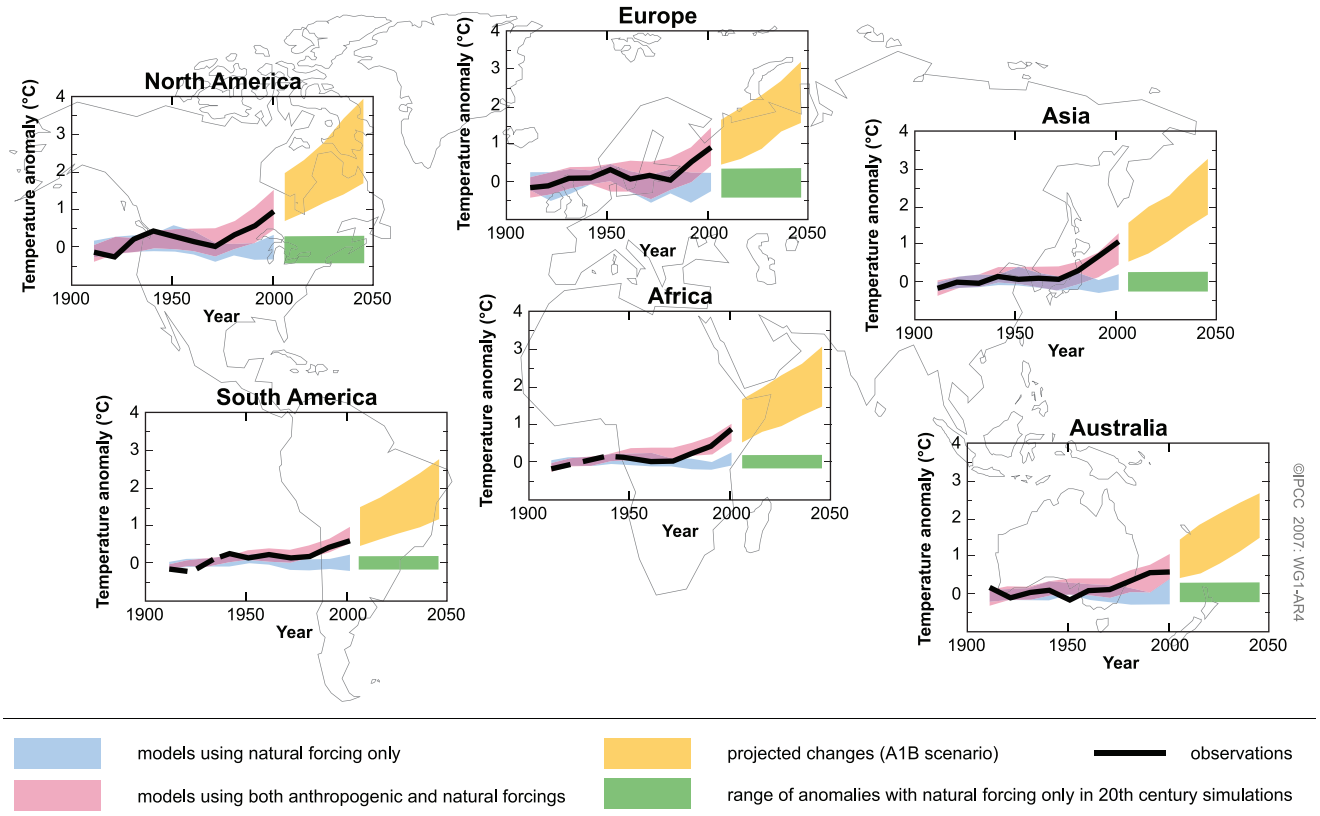


Figure TS.29. *Decadal mean continental surface temperature anomalies (°C) in observations and simulations for the period 1906 to 2005 and in projections for 2001 to 2050. Anomalies are calculated from the 1901 to 1950 average. The black lines represent the observations and the red and blue bands show simulated average temperature anomalies as in Figure TS.22 for the 20th century (i.e., red includes anthropogenic and natural forcings and blue includes only natural forcings). The yellow shading represents the 5th to 95th percentile range of projected changes according to the SRES A1B emissions scenario. The green bar denotes the 5th to 95th percentile range of decadal mean anomalies from the 20th-century simulations with only natural forcings (i.e., a measure of the natural decadal variability). For the observed part of these graphs, the decadal averages are centred on calendar decade boundaries (i.e., the last point is at 2000 for 1996 to 2005), whereas for the future period they are centred on calendar decade mid-points (i.e., the first point is at 2005 for 2001 to 2010). To construct the ranges, all simulations from the set of models involved were considered independent realisations of the possible evolution of the climate given the forcings applied. This involved 58 simulations from 14 models for the red curve, 19 simulations from 5 models (a subset of the 14) for the blue curve and green bar and 47 simulations from 18 models for the yellow curve. {FAQ 9.2.1, Figure 1 and Box 11.1, Figure 1}*

In the NH a robust pattern of increased subpolar and decreased subtropical precipitation dominates the projected precipitation pattern for the 21st century over North America and Europe, while subtropical drying is less evident over Asia (see Figure TS.30). Nearly all models project increased precipitation over most of northern North America and decreased precipitation over Central America, with much of the continental USA and northern Mexico in a more uncertain transition zone that moves north and south following the seasons. Decreased precipitation is confidently projected for southern Europe and Mediterranean Africa, with a transition to increased precipitation in northern Europe. In both continents, summer drying is extensive due both to the poleward movement of this transition zone in summer and to increased evaporation. Subpolar increases in precipitation are projected over much of northern Asia but with the subtropical drying spreading from the Mediterranean displaced by distinctive monsoonal signatures as one moves from central Asia eastward. {11.2–11.5}

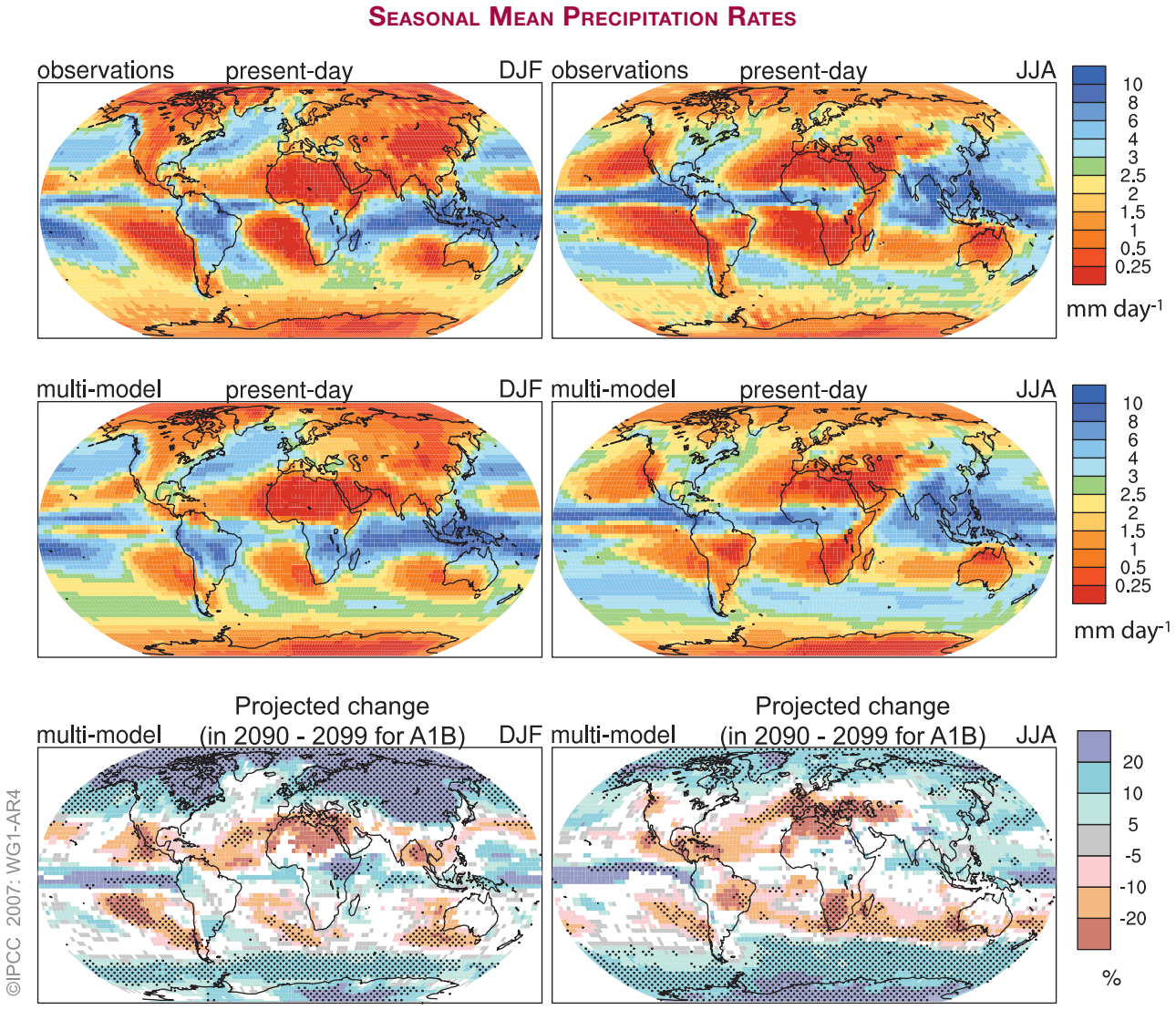


Figure TS.30. *Spatial patterns of observed (top row) and multi-model mean (middle row) seasonal mean precipitation rate (mm day^{-1}) for the period 1979 to 1993 and the multi-model mean for changes by the period 2090 to 2099 relative to 1980 to 1999 (% change) based on the SRES A1B scenario (bottom row). December to February means are in the left column, June to August means in the right column. In the bottom panel, changes are plotted only where more than 66% of the models agree on the sign of the change. The stippling indicates areas where more than 90% of the models agree on the sign of the change. {Based on same datasets as shown in Figures 8.5 and 10.9}*

In the SH, there are few land areas in the zone of projected subpolar moistening during the 21st century, with the subtropical drying more prominent (see Figure TS.30). The South Island of New Zealand and Tierra del Fuego fall within the subpolar precipitation increase zone, with southernmost Africa, the southern Andes in South America and southern Australia experiencing the drying tendency typical of the subtropics. {11.2, 11.6, 11.7}

Projections of precipitation over tropical land regions are more uncertain than those at higher latitudes, but, despite significant inadequacies in modelling tropical convection and atmosphere-ocean interactions, and the added uncertainty associated with tropical cyclones, some robust features emerge in models. Rainfall in the summer monsoon season of South and Southeast Asia increases in most models, as does rainfall in East Africa. The sign of the precipitation response is considered less certain over both the Amazon and the African Sahel. These are regions in which there is added uncertainty due to potential vegetation-climate links, and there is less robustness across models even when vegetation feedbacks are not included. {8.3, 11.2, 11.4, 11.6}

TS.5.4 Coupling Between Climate Change and Changes in Biogeochemical Cycles

All models that treat the coupling of the carbon cycle to climate change indicate a positive feedback effect with warming acting to suppress land and ocean uptake of CO_2, leading to larger atmospheric CO_2 increases and greater climate change for a given emissions scenario, but the strength of this feedback effect varies markedly among models. Since the TAR, several new projections based on fully coupled carbon cycle-climate models have been performed and compared. For the SRES A2 scenario, and based on a range of model results, the projected increase in atmospheric CO_2 concentration over the 21st century is *likely* between 10 and 25% higher than projections without this feedback, adding more than 1°C to projected mean warming by 2100 for higher emission SRES scenarios. Correspondingly, the reduced CO_2 uptake caused by this effect reduces the CO_2 emissions that are consistent with a target stabilisation level. However, there are still significant uncertainties due, for example, to limitations in the understanding of the dynamics of land ecosystems and soils. {7.3, 10.4}

Increasing atmospheric CO_2 concentrations lead directly to increasing acidification of the surface ocean. Projections based on SRES scenarios give reductions in pH of between 0.14 and 0.35 units in the 21st century (depending on scenario), extending the present decrease of 0.1 units from pre-industrial times. Ocean acidification would lead to dissolution of shallow-water carbonate sediments. Southern Ocean surface waters are projected to exhibit undersaturation with regard to calcium carbonate ($CaCO_3$) for CO_2 concentrations higher than 600 ppm, a level exceeded during the second half of the 21st century in most of the SRES scenarios. Low-latitude regions and the deep ocean will be affected as well. These changes could affect marine organisms that form their exoskeletons out of $CaCO_3$, but the net effect on the biological cycling of carbon in the oceans is not well understood. {Box 7.3, 10.4}

Committed climate change due to past emissions varies considerably for different forcing agents because of differing lifetimes in the Earth's atmosphere (see Box TS.9*).* The committed climate change due to past emissions takes account of both (i) the time lags in the responses of the climate system to changes in radiative forcing; and (ii) the time scales over which different forcing agents persist in the atmosphere after their emission because of their differing lifetimes. Typically the committed climate change due to past emissions includes an initial period of further increase in temperature, for the reasons discussed above, followed by a long-term decrease as radiative forcing decreases. Some greenhouse gases have relatively short atmospheric lifetimes (decades or less), such as CH_4 and carbon monoxide, while others such as N_2O have lifetimes of the order of a century, and some have lifetimes of millennia, such as SF_6 and PFCs. Atmospheric concentrations of CO_2 do not decay with a single well-defined lifetime if emissions are stopped. Removal of CO_2 emitted to the atmosphere occurs over multiple time scales, but some CO_2 will stay in the atmosphere for many thousands of years, so that emissions lead to a very long commitment to climate change. The slow long-term buffering of the ocean, including $CaCO_3$-sediment feedback, requires 30,000 to 35,000 years for atmospheric CO_2 concentrations to reach equilibrium. Using coupled carbon cycle components, EMICs show that the committed climate change due to past CO_2 emissions persists for more than 1000 years, so that even over these very long time scales, temperature and sea level do not return to pre-industrial values. An indication of the long time scales of committed climate change is obtained by prescribing anthropogenic CO_2 emissions following a path towards stabilisation at 750 ppm, but arbitrarily setting emissions to zero at year 2100. In this test case, it takes about 100 to 400 years in the different models for the atmospheric CO_2 concentration to drop from the maximum (ranges between 650 to 700 ppm) to below the level of two times the pre-industrial CO_2 concentration (about 560 ppm), owing to a continuous but slow transfer of carbon from the atmosphere and terrestrial reservoirs to the ocean (see Figure TS.31). {7.3, 10.7}

Future concentrations of many non-CO_2 greenhouse gases and their precursors are expected to be coupled to future climate change. Insufficient understanding of the causes of recent variations in the CH_4 growth rate suggests large uncertainties in future projections for this gas in particular. Emissions of CH_4 from wetlands are *likely* to increase in a warmer and wetter climate and to decrease in a warmer and drier climate. Observations also suggest increases in CH_4 released from northern peatlands that are experiencing permafrost melt, although the large-scale magnitude of this effect is not well quantified. Changes in temperature, humidity and clouds could also affect biogenic emissions of ozone precursors, such as volatile organic compounds. Climate change is also expected to affect tropospheric ozone through changes in chemistry and transport. Climate change could induce changes in OH through changes in humidity, and could alter stratospheric ozone concentrations and hence solar ultraviolet radiation in the troposphere. {7.4, 4.7}

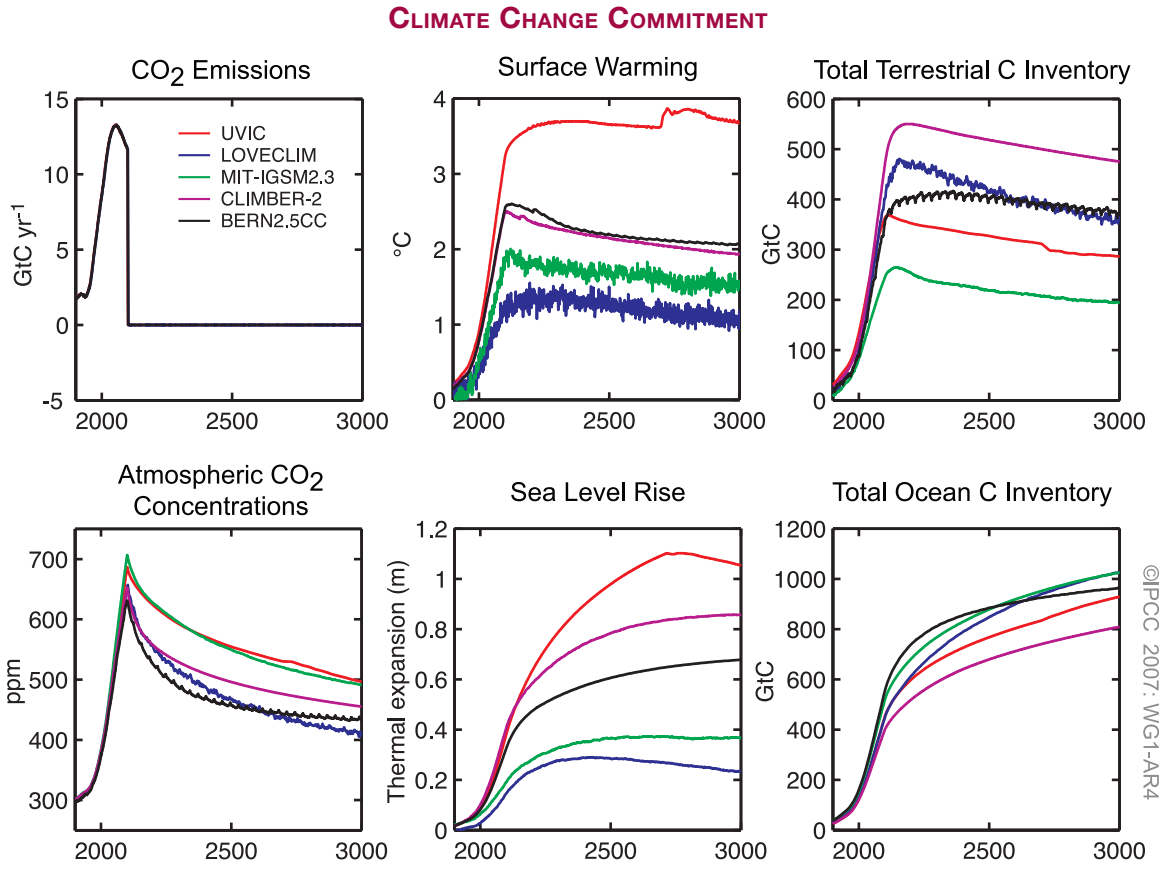


Figure TS.31. *Calculation of climate change commitment due to past emissions for five different EMICs and an idealised scenario where emissions follow a pathway leading to stabilisation of atmospheric CO_2 at 750 ppm, but before reaching this target, emissions are reduced to zero instantly at year 2100. (Left) CO_2 emissions and atmospheric CO_2 concentrations; (centre) surface warming and sea level rise due to thermal expansion; (right) change in total terrestrial and oceanic carbon inventory since the pre-industrial era. {Figure 10.35}*

Future emissions of many aerosols and their precursors are expected to be affected by climate change. Estimates of future changes in dust emissions under several climate and land use scenarios suggest that the effects of climate change are more important in controlling future dust emissions than changes in land use. Results from one study suggest that meteorology and climate have a greater influence on future Asian dust emissions and associated Asian dust storm occurrences than desertification. The biogenic emission of volatile organic compounds, a significant source of secondary organic aerosols, is known to be highly sensitive to (and increase with) temperature. However, aerosol yields decrease with temperature and the effects of changing precipitation and physiological adaptation are uncertain. Thus, change in biogenic secondary organic aerosol production in a warmer climate could be considerably lower than the response of biogenic volatile organic carbon emissions. Climate change may affect fluxes from the ocean of dimethyl sulphide (which is a precursor for some sulphate aerosols) and sea salt aerosols, however, the effects on temperature and precipitation remain very uncertain. {7.5}

While the warming effect of CO_2 represents a commitment over many centuries, aerosols are removed from the atmosphere over time scales of only a few days, so that the negative radiative forcing due to aerosols could change rapidly in response to any changes in emissions of aerosols or aerosol precursors. Because sulphate aerosols are *very likely* exerting a substantial negative radiative forcing at present, future net forcing is very sensitive to changes in sulphate emissions. One study suggests that the hypothetical removal from the atmosphere of the entire current burden of anthropogenic sulphate aerosol particles would produce a rapid increase in global mean temperature of about 0.8°C within a decade or two. Changes in aerosols are also likely to influence precipitation. Thus, the effect of environmental strategies aimed at mitigating climate change requires consideration of changes in both greenhouse gas and aerosol emissions.

Changes in aerosol emissions may result from measures implemented to improve air quality which may therefore have consequences for climate change. {Box 7.4, 7.6, 10.7}

Climate change would modify a number of chemical and physical processes that control air quality and the net effects are *likely* to vary from one region to another. Climate change can affect air quality by modifying the rates at which pollutants are dispersed, the rate at which aerosols and soluble species are removed from the atmosphere, the general chemical environment for pollutant generation and the strength of emissions from the biosphere, fires and dust. Climate change is also expected to decrease the global ozone background. Overall, the net effect of climate change on air quality is highly uncertain. {Box 7.4}

TS.5.5 Implications of Climate Processes and their Time Scales for Long-Term Projections

The commitments to climate change after stabilisation of radiative forcing are expected to be about 0.5 to 0.6°C, mostly within the following century. The multi-model average when stabilising concentrations of greenhouse gases and aerosols at year 2000 values after a 20th-century climate simulation, and running an additional 100 years, is about 0.6°C of warming (relative to 1980–1999) at year 2100 (see Figure TS.32). If the B1 or A1B scenarios were to characterise 21st-century emissions followed by stabilisation at those levels, the additional warming after stabilisation is similar, about 0.5°C, mostly in the subsequent hundred years. {10.3, 10.7}

The magnitude of the positive feedback between climate change and the carbon cycle is uncertain. This leads to uncertainty in the trajectory of CO_2 emissions required to achieve a particular stabilization level of atmospheric CO_2 concentration. Based upon current understanding of climate-carbon cycle feedback, model studies suggest that, in order to stabilise CO_2 at 450 ppm, cumulative emissions in the 21st century could be reduced from a model average of approximately 670 [630 to 710] GtC to approximately 490 [375 to 600] GtC. Similarly, to stabilise CO_2 at 1000 ppm, the cumulative emissions could be reduced by this feedback from a model average of

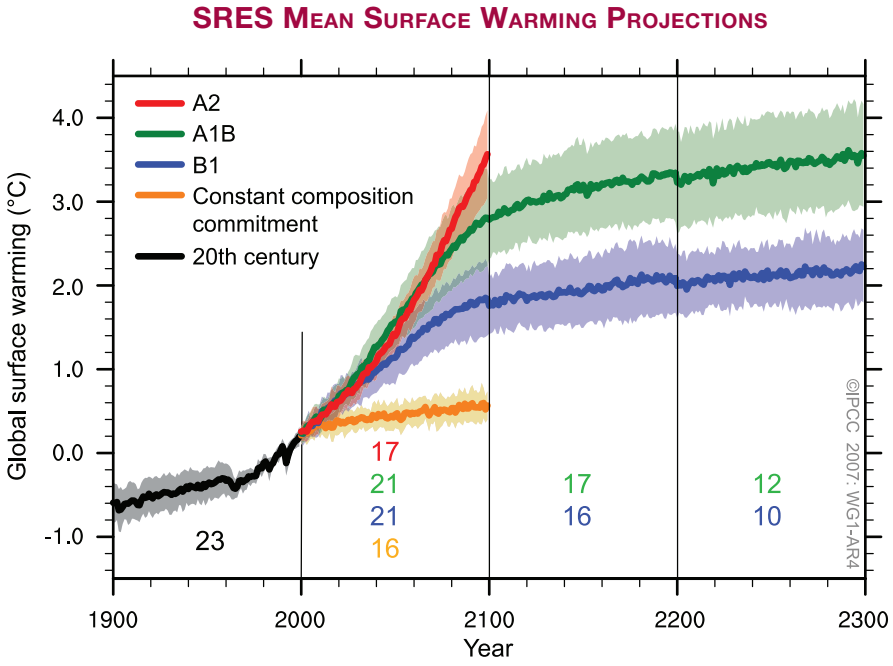


Figure TS.32. *Multi-model means of surface warming (compared to the 1980–1999 base period) for the SRES scenarios A2 (red), A1B (green) and B1 (blue), shown as continuations of the 20th-century simulation. The latter two scenarios are continued beyond the year 2100 with forcing kept constant (committed climate change as it is defined in Box TS.9). An additional experiment, in which the forcing is kept at the year 2000 level is also shown (orange). Linear trends from the corresponding control runs have been removed from these time series. Lines show the multi-model means, shading denotes the ±1 standard deviation range. Discontinuities between different periods have no physical meaning and are caused by the fact that the number of models that have run a given scenario is different for each period and scenario (numbers indicated in figure). For the same reason, uncertainty across scenarios should not be interpreted from this figure (see Section 10.5 for uncertainty estimates). {Figure 10.4}*

approximately 1415 [1340 to 1490] GtC to approximately 1100 [980 to 1250] GtC. {7.3, 10.4}

If radiative forcing were to be stabilised in 2100 at A1B concentrations, thermal expansion alone would lead to 0.3 to 0.8 m of sea level rise by 2300 (relative to 1980–1999) and would continue at decreasing rates for many centuries, due to slow processes that mix heat into the deep ocean. {10.7}

Contraction of the Greenland Ice Sheet is projected to continue to contribute to sea level rise after 2100. For stabilisation at A1B concentrations in 2100, a rate of 0.03 to 0.21 m per century due to thermal expansion is projected. If a global average warming of 1.9°C to 4.6°C relative to pre-industrial temperatures were maintained for millennia, the Greenland Ice Sheet would largely be eliminated except for remnant glaciers in the mountains. This would raise sea level by about 7 m and could be irreversible. These temperatures are comparable to those inferred for the last interglacial period 125,000 years ago, when palaeoclimatic information suggests reductions of polar ice extent and 4 to 6 m of sea level rise. {6.4, 10.7}

Dynamical processes not included in current models but suggested by recent observations could increase the vulnerability of the ice sheets to warming, increasing future sea level rise. Understanding of these processes is limited and there is no consensus on their likely magnitude. {4.6, 10.7}

Current global model studies project that the Antarctic Ice Sheet will remain too cold for widespread surface melting and will gain in mass due to increased snowfall. However, net loss of ice mass could occur if dynamical ice discharge dominates the ice sheet mass balance. {10.7}

While no models run for this assessment suggest an abrupt MOC shutdown during the 21st century, some models of reduced complexity suggest MOC shutdown as a possible long-term response to sufficiently strong warming. However, the likelihood of this occurring cannot be evaluated with confidence. The few available simulations with models of different complexity rather suggest a centennial-scale slowdown. Recovery of the MOC is *likely* if the radiative forcing is stabilised but would take several centuries. Systematic model comparison studies have helped establish some key processes that are responsible for variations between models in the response of the ocean to climate change (especially ocean heat uptake). {8.7, FAQ 10.2, 10.3}

TS.6 Robust Findings and Key Uncertainties

TS.6.1 Changes in Human and Natural Drivers of Climate

Robust Findings:

Current atmospheric concentrations of CO_2 and CH_4, and their associated positive radiative forcing, far exceed those determined from ice core measurements spanning the last 650,000 years. {6.4}

Fossil fuel use, agriculture and land use have been the dominant cause of increases in greenhouse gases over the last 250 years. {2.3, 7.3, 7.4}

Annual emissions of CO_2 from fossil fuel burning, cement production and gas flaring increased from a mean of 6.4 ± 0.4 GtC yr^{-1} in the 1990s to 7.2 ± 0.3 GtC yr^{-1} for 2000 to 2005. {7.3}

The sustained rate of increase in radiative forcing from CO_2, CH_4 and N_2O over the past 40 years is larger than at any time during at least the past 2000 years. {6.4}

Natural processes of CO_2 uptake by the oceans and terrestrial biosphere remove about 50 to 60% of anthropogenic emissions (i.e., fossil CO_2 emissions and land use change flux). Uptake by the oceans and the terrestrial biosphere are similar in magnitude over recent decades but that by the terrestrial biosphere is more variable. {7.3}

It is *virtually certain* that anthropogenic aerosols produce a net negative radiative forcing (cooling influence) with a greater magnitude in the NH than in the SH. {2.9, 9.2}

From new estimates of the combined anthropogenic forcing due to greenhouse gases, aerosols and land surface changes, it is *extremely likely* that human activities have exerted a substantial net warming influence on climate since 1750. {2.9}

Solar irradiance contributions to global average radiative forcing are considerably smaller than the contribution of increases in greenhouse gases over the industrial period. {2.5, 2.7}

***Key Uncertainties*:**

The full range of processes leading to modification of cloud properties by aerosols is not well understood and the magnitudes of associated indirect radiative effects are poorly determined. {2.4, 7.5}

The causes of, and radiative forcing due to stratospheric water vapour changes are not well quantified. {2.3}

The geographical distribution and time evolution of the radiative forcing due to changes in aerosols during the 20th century are not well characterised. {2.4}

The causes of recent changes in the growth rate of atmospheric CH_4 are not well understood. {7.4}

The roles of different factors increasing tropospheric ozone concentrations since pre-industrial times are not well characterised. {2.3}

Land surface properties and land-atmosphere interactions that lead to radiative forcing are not well quantified. {2.5}

Knowledge of the contribution of past solar changes to radiative forcing on the time scale of centuries is not based upon direct measurements and is hence strongly dependent upon physical understanding. {2.7}

TS.6.2 Observations of Changes in Climate

TS.6.2.1 Atmosphere and Surface

Robust Findings:

Global mean surface temperatures continue to rise. Eleven of the last 12 years rank among the 12 warmest years on record since 1850. {3.2}

Rates of surface warming increased in the mid-1970s and the global land surface has been warming at about double the rate of ocean surface warming since then. {3.2}

Changes in surface temperature extremes are consistent with warming of the climate. {3.8}

Estimates of mid- and lower-tropospheric temperature trends have substantially improved. Lower-tropospheric temperatures have slightly greater warming rates than the surface from 1958 to 2005. {3.4}

Long-term trends from 1900 to 2005 have been observed in precipitation amount in many large regions. {3.3}

Increases have occurred in the number of heavy precipitation events. {3.8}

Droughts have become more common, especially in the tropics and subtropics, since the 1970s. {3.3}

Tropospheric water vapour has increased, at least since the 1980s. {3.4}

Key Uncertainties:

Radiosonde records are much less complete spatially than surface records and evidence suggests a number of radiosonde records are unreliable, especially in the tropics. It is likely that all records of tropospheric temperature trends still contain residual errors. {3.4}

While changes in large-scale atmospheric circulation are apparent, the quality of analyses is best only after 1979, making analysis of, and discrimination between, change and variability difficult. {3.5, 3.6}

Surface and satellite observations disagree on total and low-level cloud changes over the ocean. {3.4}

Multi-decadal changes in DTR are not well understood, in part because of limited observations of changes in cloudiness and aerosols. {3.2}

Difficulties in the measurement of precipitation remain an area of concern in quantifying trends in global and regional precipitation. {3.3}

Records of soil moisture and streamflow are often very short, and are available for only a few regions, which impedes complete analyses of changes in droughts. {3.3}

The availability of observational data restricts the types of extremes that can be analysed. The rarer the event, the more difficult it is to identify long-term changes because there are fewer cases available. {3.8}

Information on hurricane frequency and intensity is limited prior to the satellite era. There are questions about the interpretation of the satellite record. {3.8}

There is insufficient evidence to determine whether trends exist in tornadoes, hail, lightning and dust storms at small spatial scales. {3.8}

TS.6.2.2 Snow, Ice and Frozen Ground

Robust Findings:

The amount of ice on the Earth is decreasing. There has been widespread retreat of mountain glaciers since the end of the 19th century. The rate of mass loss from glaciers and the Greenland Ice Sheet is increasing. {4.5, 4.6}

The extent of NH snow cover has declined. Seasonal river and lake ice duration has decreased over the past 150 years. {4.2, 4.3}

Since 1978, annual mean arctic sea ice extent has been declining and summer minimum arctic ice extent has decreased. {4.4}

Ice thinning occurred in the Antarctic Peninsula and Amundsen shelf ice during the 1990s. Tributary glaciers have accelerated and complete breakup of the Larsen B Ice Shelf occurred in 2002. {4.6}

Temperature at the top of the permafrost layer has increased by up to 3°C since the 1980s in the Arctic. The maximum extent of seasonally frozen ground has decreased by about 7% in the NH since 1900, and its maximum depth has decreased by about 0.3 m in Eurasia since the mid-20th century. {4.7}

Key Uncertainties:

There is no global compilation of *in situ* snow data prior to 1960. Well-calibrated snow water equivalent data are not available for the satellite era. {4.2}

There are insufficient data to draw any conclusions about trends in the thickness of antarctic sea ice. {4.4}

Uncertainties in estimates of glacier mass loss arise from limited global inventory data, incomplete area-volume relationships and imbalance in geographic coverage. {4.5}

Mass balance estimates for ice shelves and ice sheets, especially for Antarctica, are limited by calibration and validation of changes detected by satellite altimetry and gravity measurements. {4.6}

Limited knowledge of basal processes and of ice shelf dynamics leads to large uncertainties in the understanding of ice flow processes and ice sheet stability. {4.6}

TS.6.2.3 Oceans and Sea Level

Robust Findings:

The global temperature (or heat content) of the oceans has increased since 1955. {5.2}

Large-scale regionally coherent trends in salinity have been observed over recent decades with freshening in subpolar regions and increased salinity in the shallower parts of the tropics and subtropics. These trends are consistent with changes in precipitation and inferred larger water transport in the atmosphere from low latitudes to high latitudes and from the Atlantic to the Pacific. {5.2}

Global average sea level rose during the 20th century. There is high confidence that the rate of sea level rise increased between the mid-19th and mid-20th centuries. During 1993 to 2003, sea level rose more rapidly than during 1961 to 2003. {5.5}

Thermal expansion of the ocean and loss of mass from glaciers and ice caps made substantial contributions to the observed sea level rise. {5.5}

The observed rate of sea level rise from 1993 to 2003 is consistent with the sum of observed contributions from thermal expansion and loss of land ice. {5.5}

The rate of sea level change over recent decades has not been geographically uniform. {5.5}

As a result of uptake of anthropogenic CO_2 since 1750, the acidity of the surface ocean has increased. {5.4, 7.3}

Key Uncertainties:

Limitations in ocean sampling imply that decadal variability in global heat content, salinity and sea level changes can only be evaluated with moderate confidence. {5.2, 5.5}

There is low confidence in observations of trends in the MOC. {Box 5.1}

Global average sea level rise from 1961 to 2003 appears to be larger than can be explained by thermal expansion and land ice melting. {5.5}

TS.6.2.4 Palaeoclimate

***Robust Findings**:*

During the last interglacial, about 125,000 years ago, global sea level was *likely* 4 to 6 m higher than present, due primarily to retreat of polar ice. {6.4}

A number of past abrupt climate changes were *very likely* linked to changes in Atlantic Ocean circulation and affected the climate broadly across the NH. {6.4}

It is *very unlikely* that the Earth would naturally enter another ice age for at least 30,000 years. {6.4}

Biogeochemical and biogeophysical feedbacks have amplified climatic changes in the past. {6.4}

It is *very likely* that average NH temperatures during the second half of the 20th century were warmer than in any other 50-year period in the last 500 years and *likely* that this was also the warmest 50-year period in the past 1300 years. {6.6}

Palaeoclimate records indicate with high confidence that droughts lasting decades or longer were a recurrent feature of climate in several regions over the last 2000 years. {6.6}

Key Uncertainties:

Mechanisms of onset and evolution of past abrupt climate change and associated climate thresholds are not well understood. This limits confidence in the ability of climate models to simulate realistic abrupt change. {6.4}

The degree to which ice sheets retreated in the past, the rates of such change and the processes involved are not well known. {6.4}

Knowledge of climate variability over more than the last few hundred years in the SH and tropics is limited by the lack of palaeoclimatic records. {6.6}

Differing amplitudes and variability observed in available millennial-length NH temperature reconstructions, as well as the relation of these differences to choice of proxy data and statistical calibration methods, still need to be reconciled. {6.6}

The lack of extensive networks of proxy data for temperature in the last 20 years limits understanding of how such proxies respond to rapid global warming and of the influence of other environmental changes. {6.6}

TS.6.3 Understanding and Attributing Climate Change

Robust Findings:

Greenhouse gas forcing has *very likely* caused most of the observed global warming over the last 50 years. Greenhouse gas forcing alone during the past half century would *likely* have resulted in greater than the observed warming if there had not been an offsetting cooling effect from aerosol and other forcings. {9.4}

It is *extremely unlikely* (<5%) that the global pattern of warming during the past half century can be explained without external forcing, and *very unlikely* that it is due to known natural external causes alone. The warming occurred in both the ocean and the atmosphere and took place at a time when natural external forcing factors would *likely* have produced cooling. {9.4, 9.7}

It is *likely* that anthropogenic forcing has contributed to the general warming observed in the upper several hundred metres of the ocean during the latter half of the 20th century. Anthropogenic forcing, resulting in thermal expansion from ocean warming and glacier mass loss, has *very likely* contributed to sea level rise during the latter half of the 20th century. {9.5}

A substantial fraction of the reconstructed NH inter-decadal temperature variability of the past seven centuries is *very likely* attributable to natural external forcing (volcanic eruptions and solar variability). {9.3}

Key Uncertainties:

Confidence in attributing some climate change phenomena to anthropogenic influences is currently limited by uncertainties in radiative forcing, as well as uncertainties in feedbacks and in observations. {9.4, 9.5}

Attribution at scales smaller than continental and over time scales of less than 50 years is limited by larger climate variability on smaller scales, by uncertainties in the small-scale details of external forcing and the response simulated by models, as well as uncertainties in simulation of internal variability on small scales, including in relation to modes of variability. {9.4}

There is less confidence in understanding of forced changes in precipitation and surface pressure than there is of temperature. {9.5}

The range of attribution statements is limited by the absence of formal detection and attribution studies, or their very limited number, for some phenomena (e.g., some types of extreme events). {9.5}

Incomplete global data sets for extremes analysis and model uncertainties still restrict the regions and types of detection studies of extremes that can be performed. {9.4, 9.5}

Despite improved understanding, uncertainties in model-simulated internal climate variability limit some aspects of attribution studies. For example, there are apparent discrepancies between estimates of ocean heat content variability from models and observations. {5.2, 9.5}

Lack of studies quantifying the contributions of anthropogenic forcing to ocean heat content increase or glacier melting together with the open part of the sea level budget for 1961 to 2003 are among the uncertainties in quantifying the anthropogenic contribution to sea level rise. {9.5}

TS.6.4 Projections of Future Changes in Climate

TS.6.4.1 Model Evaluation

Robust Findings:

Climate models are based on well-established physical principles and have been demonstrated to reproduce observed features of recent climate and past climate changes. There is considerable confidence that AOGCMs provide credible quantitative estimates of future climate change, particularly at continental scales and above. Confidence in these estimates is higher for some climate variables (e.g., temperature) than for others (e.g., precipitation). {FAQ 8.1}

Confidence in models has increased due to:

- improvements in the simulation of many aspects of present climate, including important modes of climate variability and extreme hot and cold spells;
- improved model resolution, computational methods and parametrizations and inclusion of additional processes;
- more comprehensive diagnostic tests, including tests of model ability to forecast on time scales from days to a year when initialised with observed conditions; and
- enhanced scrutiny of models and expanded diagnostic analysis of model behaviour facilitated by internationally coordinated efforts to collect and disseminate output from model experiments performed under common conditions. {8.4}

Key Uncertainties:

A proven set of model metrics comparing simulations with observations, that might be used to narrow the range of plausible climate projections, has yet to be developed. {8.2}

Most models continue to have difficulty controlling climate drift, particularly in the deep ocean. This drift must be accounted for when assessing change in many oceanic variables. {8.2}

Models differ considerably in their estimates of the strength of different feedbacks in the climate system. {8.6}

Problems remain in the simulation of some modes of variability, notably the Madden-Julian Oscillation, recurrent atmospheric blocking and extreme precipitation. {8.4}

Systematic biases have been found in most models' simulations of the Southern Ocean that are linked to uncertainty in transient climate response. {8.3}

Climate models remain limited by the spatial resolution that can be achieved with present computer resources, by the need for more extensive ensemble runs and by the need to include some additional processes. {8.1–8.5}

TS.6.4.2 Equilibrium and Transient Climate Sensitivity

Robust Findings:

Equilibrium climate sensitivity is *likely* to be in the range 2°C to 4.5°C with a most likely value of about 3°C, based upon multiple observational and modelling constraints. It is *very unlikely* to be less than 1.5°C. {8.6, 9.6, Box 10.2}

The transient climate response is better constrained than the equilibrium climate sensitivity. It is *very likely* larger than 1°C and *very unlikely* greater than 3°C. {10.5}

There is a good understanding of the origin of differences in equilibrium climate sensitivity found in different models. Cloud feedbacks are the primary source of inter-model differences in equilibrium climate sensitivity, with low cloud being the largest contributor. {8.6}

New observational and modelling evidence strongly supports a combined water vapour-lapse rate feedback of a strength comparable to that found in AOGCMs. {8.6}

Key Uncertainties:

Large uncertainties remain about how clouds might respond to global climate change. {8.6}

TS.6.4.3 Global Projections

Robust Findings:

Even if concentrations of radiative forcing agents were to be stabilised, further committed warming and related climate changes would be expected to occur, largely because of time lags associated with processes in the oceans. {10.7}

Near-term warming projections are little affected by different scenario assumptions or different model sensitivities, and are consistent with that observed for the past few decades. The multi-model mean warming, averaged over 2011 to 2030 relative to 1980 to 1999 for all AOGCMs considered here, lies in a narrow range of 0.64°C to 0.69°C for the three different SRES emission scenarios B1, A1B and A2. {10.3}

Geographic patterns of projected warming show the greatest temperature increases at high northern latitudes and over land, with less warming over the southern oceans and North Atlantic. {10.3}

Changes in precipitation show robust large-scale patterns: precipitation generally increases in the tropical precipitation maxima, decreases in the subtropics and increases at high latitudes as a consequence of a general intensification of the global hydrological cycle. {10.3}

As the climate warms, snow cover and sea ice extent decrease; glaciers and ice caps lose mass and contribute to sea level rise. Sea ice extent decreases in the 21st century in both the Arctic and Antarctic. Snow cover reduction is accelerated in the Arctic by positive feedbacks and widespread increases in thaw depth occur over much of the permafrost regions. {10.3}

Based on current simulations, it is *very likely* that the Atlantic Ocean MOC will slow down by 2100. However, it is *very unlikely* that the MOC will undergo a large abrupt transition during the course of the 21st century. {10.3}

Heat waves become more frequent and longer lasting in a future warmer climate. Decreases in frost days are projected to occur almost everywhere in the mid- and high latitudes, with an increase in growing season length. There is a tendency for summer drying of the mid-continental areas during summer, indicating a greater risk of droughts in those regions. {10.3, FAQ 10.1}

Future warming would tend to reduce the capacity of the Earth system (land and ocean) to absorb anthropogenic CO_2. As a result, an increasingly large fraction of anthropogenic CO_2 would stay in the atmosphere under a warmer climate. This feedback requires reductions in the cumulative emissions consistent with stabilisation at a given atmospheric CO_2 level compared to the hypothetical case of no such feedback. The higher the stabilisation scenario, the larger the amount of climate change and the larger the required reductions. {7.3, 10.4}

Key Uncertainties:

The likelihood of a large abrupt change in the MOC beyond the end of the 21st century cannot yet be assessed reliably. For low and medium emission scenarios with atmospheric greenhouse gas concentrations stabilised beyond 2100, the MOC recovers from initial weakening within one to several centuries. A permanent reduction in the MOC cannot be excluded if the forcing is strong and long enough. {10.7}

The model projections for extremes of precipitation show larger ranges in amplitude and geographical locations than for temperature. {10.3, 11.1}

The response of some major modes of climate variability such as ENSO still differs from model to model, which may be associated with differences in the spatial and temporal representation of present-day conditions. {10.3}

The robustness of many model responses of tropical cyclones to climate change is still limited by the resolution of typical climate models. {10.3}

Changes in key processes that drive some global and regional climate changes are poorly known (e.g., ENSO, NAO, blocking, MOC, land surface feedbacks, tropical cyclone distribution). {11.2–11.9}

The magnitude of future carbon cycle feedbacks is still poorly determined. {7.3, 10.4}

TS.6.4.4 Sea Level

Robust Findings:

Sea level will continue to rise in the 21st century because of thermal expansion and loss of land ice. Sea level rise was not geographically uniform in the past and will not be in the future. {10.6}

Projected warming due to emission of greenhouse gases during the 21st century will continue to contribute to sea level rise for many centuries. {10.7}

Sea level rise due to thermal expansion and loss of mass from ice sheets would continue for centuries or millennia even if radiative forcing were to be stabilised. {10.7}

Key Uncertainties:

Models do not yet exist that address key processes that could contribute to large rapid dynamical changes in the Antarctic and Greenland Ice Sheets that could increase the discharge of ice into the ocean. {10.6}

The sensitivity of ice sheet surface mass balance (melting and precipitation) to global climate change is not well constrained by observations and has a large spread in models. There is consequently a large uncertainty in the magnitude of global warming that, if sustained, would lead to the elimination of the Greenland Ice Sheet. {10.7}

TS.6.4.5 Regional Projections

Robust Findings:

Temperatures averaged over all habitable continents and over many sub-continental land regions will *very likely* rise at greater than the global average rate in the next 50 years and by an amount substantially in excess of natural variability. {10.3, 11.2–11.9}

Precipitation is *likely* to increase in most subpolar and polar regions. The increase is considered especially robust, and *very likely* to occur, in annual precipitation in most of northern Europe, Canada, the northeast USA and the Arctic, and in winter precipitation in northern Asia and the Tibetan Plateau. {11.2–11.9}

Precipitation is *likely* to decrease in many subtropical regions, especially at the poleward margins of the subtropics. The decrease is considered especially robust, and *very likely* to occur, in annual precipitation in European and African regions bordering the Mediterranean and in winter rainfall in south-western Australia. {11.2–11.9}

Extremes of daily precipitation are *likely* to increase in many regions. The increase is considered as *very likely* in northern Europe, south Asia, East Asia, Australia and New Zealand – this list in part reflecting uneven geographic coverage in existing published research. {11.2–11.9}

Key Uncertainties:

In some regions there has been only very limited study of key aspects of regional climate change, particularly with regard to extreme events. {11.2–11.9}

Atmosphere-Ocean General Circulation Models show no consistency in simulated regional precipitation change in some key regions (e.g., northern South America, northern Australia and the Sahel). {10.3, 11.2–11.9}

In many regions where fine spatial scales in climate are generated by topography, there is insufficient information on how climate change will be expressed at these scales. {11.2–11.9}

1

Historical Overview of Climate Change Science

Coordinating Lead Authors:
Hervé Le Treut (France), Richard Somerville (USA)

Lead Authors:
Ulrich Cubasch (Germany), Yihui Ding (China), Cecilie Mauritzen (Norway), Abdalah Mokssit (Morocco), Thomas Peterson (USA), Michael Prather (USA)

Contributing Authors:
M. Allen (UK), I. Auer (Austria), J. Biercamp (Germany), C. Covey (USA), J.R. Fleming (USA), R. García-Herrera (Spain), P. Gleckler (USA), J. Haigh (UK), G.C. Hegerl (USA, Germany), K. Isaksen (Norway), J. Jones (Germany, UK), J. Luterbacher (Switzerland), M. MacCracken (USA), J.E. Penner (USA), C. Pfister (Switzerland), E. Roeckner (Germany), B. Santer (USA), F. Schott (Germany), F. Sirocko (Germany), A. Staniforth (UK), T.F. Stocker (Switzerland), R.J. Stouffer (USA), K.E. Taylor (USA), K.E. Trenberth (USA), A. Weisheimer (ECMWF, Germany), M. Widmann (Germany, UK)

Review Editors:
Alphonsus Baede (Netherlands), David Griggs (UK)

This chapter should be cited as:
Le Treut, H., R. Somerville, U. Cubasch, Y. Ding, C. Mauritzen, A. Mokssit, T. Peterson and M. Prather, 2007: Historical Overview of Climate Change. In: *Climate Change 2007: The Physical Science Basis. Contribution of Working Group I to the Fourth Assessment Report of the Intergovernmental Panel on Climate Change* [Solomon, S., D. Qin, M. Manning, Z. Chen, M. Marquis, K.B. Averyt, M. Tignor and H.L. Miller (eds.)]. Cambridge University Press, Cambridge, United Kingdom and New York, NY, USA.

Table of Contents

Executive Summary 95

1.1 Overview of the Chapter 95

1.2 The Nature of Earth Science 95

1.3 Examples of Progress in Detecting and Attributing Recent Climate Change 100

1.3.1 The Human Fingerprint on Greenhouse Gases 100

1.3.2 Global Surface Temperature 100

1.3.3 Detection and Attribution 102

1.4 Examples of Progress in Understanding Climate Processes 103

1.4.1 The Earth's Greenhouse Effect 103

1.4.2 Past Climate Observations, Astronomical Theory and Abrupt Climate Changes 106

1.4.3 Solar Variability and the Total Solar Irradiance 107

1.4.4 Biogeochemistry and Radiative Forcing 108

1.4.5 Cryospheric Topics 110

1.4.6 Ocean and Coupled Ocean-Atmosphere Dynamics 111

1.5 Examples of Progress in Modelling the Climate 112

1.5.1 Model Evolution and Model Hierarchies 112

1.5.2 Model Clouds and Climate Sensitivity 114

1.5.3 Coupled Models: Evolution, Use, Assessment 117

1.6 The IPCC Assessments of Climate Change and Uncertainties 118

Box 1.1: Treatment of Uncertainties in the Working Group I Assessment 120

1.7 Summary 121

Frequently Asked Questions

FAQ 1.1: *What Factors Determine Earth's Climate?* 96

FAQ 1.2: *What is the Relationship between Climate Change and Weather?* 104

FAQ 1.3: *What is the Greenhouse Effect?* 115

References 122

Executive Summary

Awareness and a partial understanding of most of the interactive processes in the Earth system that govern climate and climate change predate the IPCC, often by many decades. A deeper understanding and quantification of these processes and their incorporation in climate models have progressed rapidly since the IPCC First Assessment Report in 1990.

As climate science and the Earth's climate have continued to evolve over recent decades, increasing evidence of anthropogenic influences on climate change has been found. Correspondingly, the IPCC has made increasingly more definitive statements about human impacts on climate.

Debate has stimulated a wide variety of climate change research. The results of this research have refined but not significantly redirected the main scientific conclusions from the sequence of IPCC assessments.

1.1 Overview of the Chapter

To better understand the science assessed in this Fourth Assessment Report (AR4), it is helpful to review the long historical perspective that has led to the current state of climate change knowledge. This chapter starts by describing the fundamental nature of earth science. It then describes the history of climate change science using a wide-ranging subset of examples, and ends with a history of the IPCC.

The concept of this chapter is new. There is no counterpart in previous IPCC assessment reports for an introductory chapter providing historical context for the remainder of the report. Here, a restricted set of topics has been selected to illustrate key accomplishments and challenges in climate change science. The topics have been chosen for their significance to the IPCC task of assessing information relevant for understanding the risks of human-induced climate change, and also to illustrate the complex and uneven pace of scientific progress.

In this chapter, the time frame under consideration stops with the publication of the Third Assessment Report (TAR; IPCC, 2001a). Developments subsequent to the TAR are described in the other chapters of this report, and we refer to these chapters throughout this first chapter.

1.2 The Nature of Earth Science

Science may be stimulated by argument and debate, but it generally advances through formulating hypotheses clearly and testing them objectively. This testing is the key to science. In fact, one philosopher of science insisted that to be genuinely scientific, a statement must be susceptible to testing that could potentially show it to be false (Popper, 1934). In practice, contemporary scientists usually submit their research findings to the scrutiny of their peers, which includes disclosing the methods that they use, so their results can be checked through replication by other scientists. The insights and research results of individual scientists, even scientists of unquestioned genius, are thus confirmed or rejected in the peer-reviewed literature by the combined efforts of many other scientists. It is not the belief or opinion of the scientists that is important, but rather the results of this testing. Indeed, when Albert Einstein was informed of the publication of a book entitled *100 Authors Against Einstein*, he is said to have remarked, 'If I were wrong, then one would have been enough!' (Hawking, 1988); however, that one opposing scientist would have needed proof in the form of testable results.

Thus science is inherently self-correcting; incorrect or incomplete scientific concepts ultimately do not survive repeated testing against observations of nature. Scientific theories are ways of explaining phenomena and providing insights that can be evaluated by comparison with physical reality. Each successful prediction adds to the weight of evidence supporting the theory, and any unsuccessful prediction demonstrates that the underlying theory is imperfect and requires improvement or abandonment. Sometimes, only certain kinds of questions tend to be asked about a scientific phenomenon until contradictions build to a point where a sudden change of paradigm takes place (Kuhn, 1996). At that point, an entire field can be rapidly reconstructed under the new paradigm.

Despite occasional major paradigm shifts, the majority of scientific insights, even unexpected insights, tend to emerge incrementally as a result of repeated attempts to test hypotheses as thoroughly as possible. Therefore, because almost every new advance is based on the research and understanding that has gone before, science is cumulative, with useful features retained and non-useful features abandoned. Active research scientists, throughout their careers, typically spend large fractions of their working time studying in depth what other scientists have done. Superficial or amateurish acquaintance with the current state of a scientific research topic is an obstacle to a scientist's progress. Working scientists know that a day in the library can save a year in the laboratory. Even Sir Isaac Newton (1675) wrote that if he had 'seen further it is by standing on the shoulders of giants'. Intellectual honesty and professional ethics call for scientists to acknowledge the work of predecessors and colleagues.

The attributes of science briefly described here can be used in assessing competing assertions about climate change. Can the statement under consideration, in principle, be proven false? Has it been rigorously tested? Did it appear in the peer-reviewed literature? Did it build on the existing research record where appropriate? If the answer to any of these questions is no, then less credence should be given to the assertion until it is tested and independently verified. The IPCC assesses the scientific literature to create a report based on the best available science (Section 1.6). It must be acknowledged, however, that the IPCC also contributes to science by identifying the key uncertainties and by stimulating and coordinating targeted research to answer important climate change questions.

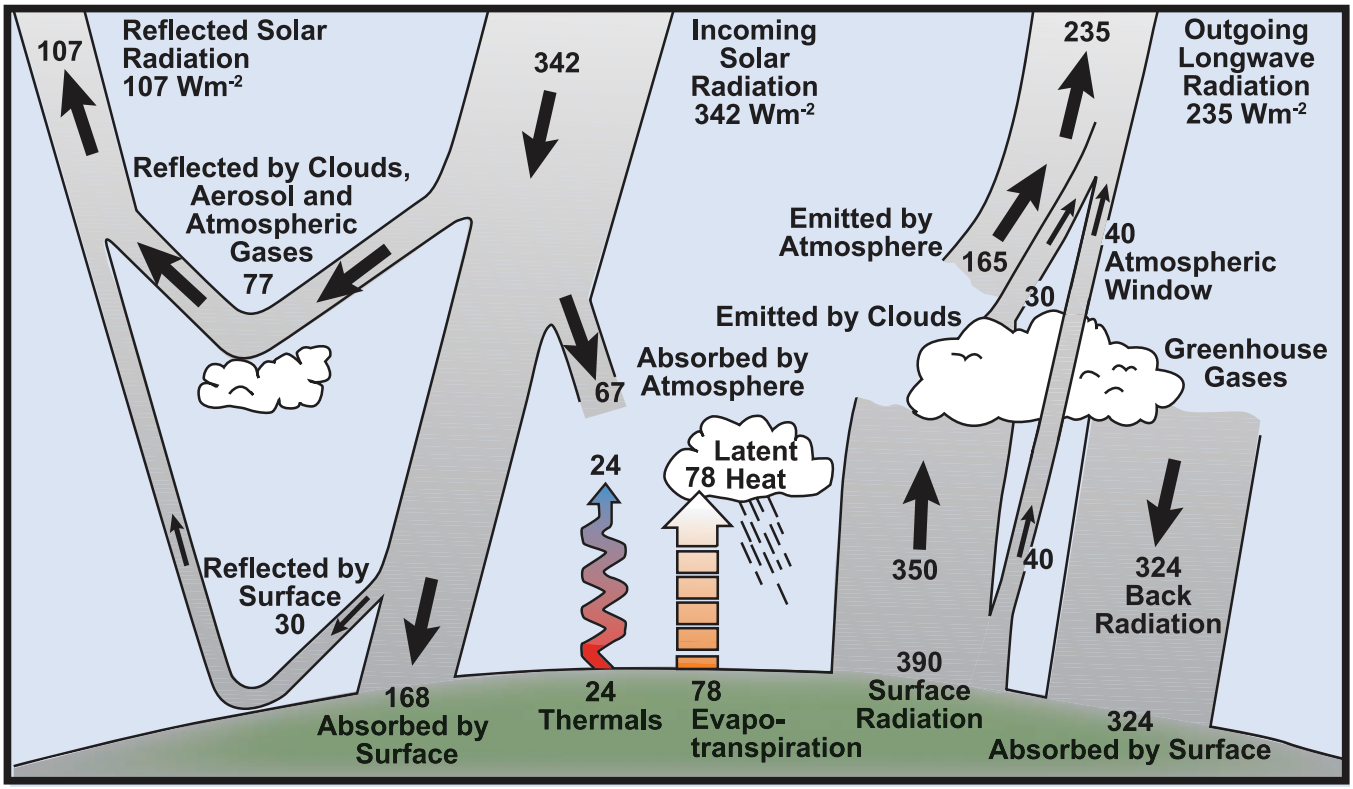
Frequently Asked Question 1.1

What Factors Determine Earth's Climate?

The climate system is a complex, interactive system consisting of the atmosphere, land surface, snow and ice, oceans and other bodies of water, and living things. The atmospheric component of the climate system most obviously characterises climate; climate is often defined as 'average weather'. Climate is usually described in terms of the mean and variability of temperature, precipitation and wind over a period of time, ranging from months to millions of years (the classical period is 30 years). The climate system evolves in time under the influence of its own internal dynamics and due to changes in external factors that affect climate (called 'forcings'). External forcings include natural phenomena such as volcanic eruptions and solar variations, as well as human-induced changes in atmospheric composition. Solar radiation powers the climate system. There are three fundamental ways to change the radiation balance of the Earth: 1) by changing the incoming solar radiation (e.g., by changes in Earth's orbit or in the Sun itself); 2) by changing the fraction of solar radiation that is reflected (called 'albedo'; e.g., by changes in cloud cover, atmospheric particles or vegetation); and 3) by altering the longwave radiation from Earth back towards space (e.g., by changing greenhouse gas concentrations). Climate, in turn, responds directly to such changes, as well as indirectly, through a variety of feedback mechanisms.

The amount of energy reaching the top of Earth's atmosphere each second on a surface area of one square metre facing the Sun during daytime is about 1,370 Watts, and the amount of energy per square metre per second averaged over the entire planet is one-quarter of this (see Figure 1). About 30% of the sunlight that reaches the top of the atmosphere is reflected back to space. Roughly two-thirds of this reflectivity is due to clouds and small particles in the atmosphere known as 'aerosols'. Light-coloured areas of Earth's surface – mainly snow, ice and deserts – reflect the remaining one-third of the sunlight. The most dramatic change in aerosol-produced reflectivity comes when major volcanic eruptions eject material very high into the atmosphere. Rain typically

(continued)



FAQ 1.1, Figure 1. *Estimate of the Earth's annual and global mean energy balance. Over the long term, the amount of incoming solar radiation absorbed by the Earth and atmosphere is balanced by the Earth and atmosphere releasing the same amount of outgoing longwave radiation. About half of the incoming solar radiation is absorbed by the Earth's surface. This energy is transferred to the atmosphere by warming the air in contact with the surface (thermals), by evapotranspiration and by longwave radiation that is absorbed by clouds and greenhouse gases. The atmosphere in turn radiates longwave energy back to Earth as well as out to space. Source: Kiehl and Trenberth (1997).*

clears aerosols out of the atmosphere in a week or two, but when material from a violent volcanic eruption is projected far above the highest cloud, these aerosols typically influence the climate for about a year or two before falling into the troposphere and being carried to the surface by precipitation. Major volcanic eruptions can thus cause a drop in mean global surface temperature of about half a degree celsius that can last for months or even years. Some man-made aerosols also significantly reflect sunlight.

The energy that is not reflected back to space is absorbed by the Earth's surface and atmosphere. This amount is approximately 240 Watts per square metre (W m^{-2}). To balance the incoming energy, the Earth itself must radiate, on average, the same amount of energy back to space. The Earth does this by emitting outgoing longwave radiation. Everything on Earth emits longwave radiation continuously. That is the heat energy one feels radiating out from a fire; the warmer an object, the more heat energy it radiates. To emit 240 W m^{-2}, a surface would have to have a temperature of around –19°C. This is much colder than the conditions that actually exist at the Earth's surface (the global mean surface temperature is about 14°C). Instead, the necessary –19°C is found at an altitude about 5 km above the surface.

The reason the Earth's surface is this warm is the presence of greenhouse gases, which act as a partial blanket for the longwave radiation coming from the surface. This blanketing is known as the natural greenhouse effect. The most important greenhouse gases are water vapour and carbon dioxide. The two most abundant constituents of the atmosphere – nitrogen and oxygen – have no such effect. Clouds, on the other hand, do exert a blanketing effect similar to that of the greenhouse gases; however, this effect is offset by their reflectivity, such that on average, clouds tend to have a cooling effect on climate (although locally one can feel the warming effect: cloudy nights tend to remain warmer than clear nights because the clouds radiate longwave energy back down to the surface). Human activities intensify the blanketing effect through the release of greenhouse gases. For instance, the amount of carbon dioxide in the atmosphere has increased by about 35% in the industrial era, and this increase is known to be due to human activities, primarily the combustion of fossil fuels and removal of forests. Thus, humankind has dramatically altered the chemical composition of the global atmosphere with substantial implications for climate.

Because the Earth is a sphere, more solar energy arrives for a given surface area in the tropics than at higher latitudes, where sunlight strikes the atmosphere at a lower angle. Energy is transported from the equatorial areas to higher latitudes via atmospheric and oceanic circulations, including storm systems. Energy is also required to evaporate water from the sea or land surface, and this energy, called latent heat, is released when water vapour condenses in clouds (see Figure 1). Atmospheric circulation is primarily driven by the release of this latent heat. Atmospheric circulation in turn drives much of the ocean circulation through the action of winds on the surface waters of the ocean, and through changes in the ocean's surface temperature and salinity through precipitation and evaporation.

Due to the rotation of the Earth, the atmospheric circulation patterns tend to be more east-west than north-south. Embedded in the mid-latitude westerly winds are large-scale weather systems that act to transport heat toward the poles. These weather systems are the familiar migrating low- and high-pressure systems and their associated cold and warm fronts. Because of land-ocean temperature contrasts and obstacles such as mountain ranges and ice sheets, the circulation system's planetary-scale atmospheric waves tend to be geographically anchored by continents and mountains although their amplitude can change with time. Because of the wave patterns, a particularly cold winter over North America may be associated with a particularly warm winter elsewhere in the hemisphere. Changes in various aspects of the climate system, such as the size of ice sheets, the type and distribution of vegetation or the temperature of the atmosphere or ocean will influence the large-scale circulation features of the atmosphere and oceans.

There are many feedback mechanisms in the climate system that can either amplify ('positive feedback') or diminish ('negative feedback') the effects of a change in climate forcing. For example, as rising concentrations of greenhouse gases warm Earth's climate, snow and ice begin to melt. This melting reveals darker land and water surfaces that were beneath the snow and ice, and these darker surfaces absorb more of the Sun's heat, causing more warming, which causes more melting, and so on, in a self-reinforcing cycle. This feedback loop, known as the 'ice-albedo feedback', amplifies the initial warming caused by rising levels of greenhouse gases. Detecting, understanding and accurately quantifying climate feedbacks have been the focus of a great deal of research by scientists unravelling the complexities of Earth's climate.

A characteristic of Earth sciences is that Earth scientists are unable to perform controlled experiments on the planet as a whole and then observe the results. In this sense, Earth science is similar to the disciplines of astronomy and cosmology that cannot conduct experiments on galaxies or the cosmos. This is an important consideration, because it is precisely such whole-Earth, system-scale experiments, incorporating the full complexity of interacting processes and feedbacks, that might ideally be required to fully verify or falsify climate change hypotheses (Schellnhuber et al., 2004). Nevertheless, countless empirical tests of numerous different hypotheses have built up a massive body of Earth science knowledge. This repeated testing has refined the understanding of numerous aspects of the climate system, from deep oceanic circulation to stratospheric chemistry. Sometimes a combination of observations and models can be used to test planetary-scale hypotheses. For example, the global cooling and drying of the atmosphere observed after the eruption of Mt. Pinatubo (Section 8.6) provided key tests of particular aspects of global climate models (Hansen et al., 1992).

Another example is provided by past IPCC projections of future climate change compared to current observations. Figure 1.1 reveals that the model projections of global average temperature from the First Assessment Report (FAR; IPCC, 1990) were higher than those from the Second Assessment Report (SAR; IPCC, 1996). Subsequent observations (Section 3.2) showed that the evolution of the actual climate system fell midway between the FAR and the SAR 'best estimate' projections and were within or near the upper range of projections from the TAR (IPCC, 2001a).

Not all theories or early results are verified by later analysis. In the mid-1970s, several articles about possible global cooling appeared in the popular press, primarily motivated by analyses indicating that Northern Hemisphere (NH) temperatures had decreased during the previous three decades (e.g., Gwynne, 1975). In the peer-reviewed literature, a paper by Bryson and Dittberner (1976) reported that increases in carbon dioxide (CO_2) should be associated with a decrease in global temperatures. When challenged by Woronko (1977), Bryson and Dittberner (1977) explained that the cooling projected by their model was due to aerosols (small particles in the atmosphere) produced by the same combustion that caused the increase in CO_2. However, because aerosols remain in the atmosphere only a short time compared to CO_2, the results were not applicable for long-term climate change projections. This example of a prediction of global cooling is a classic illustration of the self-correcting nature of Earth science. The scientists involved were reputable researchers who followed the accepted paradigm of publishing in scientific journals, submitting their methods and results to the scrutiny of their peers (although the peer-review did not catch this problem), and responding to legitimate criticism.

A recurring theme throughout this chapter is that climate science in recent decades has been characterised by the increasing rate of advancement of research in the field and by the notable evolution of scientific methodology and tools, including the models and observations that support and enable the research. During the last four decades, the rate at which scientists have added to the body of knowledge of atmospheric and oceanic processes has accelerated dramatically. As scientists incrementally increase the totality of knowledge, they publish their results in peer-reviewed journals. Between 1965 and 1995, the number of articles published per year in atmospheric science journals tripled (Geerts, 1999). Focusing more narrowly, Stanhill (2001) found that the climate change science literature grew approximately exponentially with a doubling time of 11 years for the period 1951 to 1997. Furthermore, 95% of all the climate change science literature since 1834 was published after 1951. Because science is cumulative, this represents considerable growth in the knowledge of climate processes and in the complexity of climate research. An important example of this is the additional physics incorporated in climate models over the last several decades, as illustrated in Figure 1.2. As a result of the cumulative nature of science, climate science today is an interdisciplinary synthesis of countless tested and proven physical processes and principles painstakingly compiled and verified over several centuries of detailed laboratory measurements, observational experiments and theoretical analyses; and is now far more wide-ranging and physically comprehensive than was the case only a few decades ago.

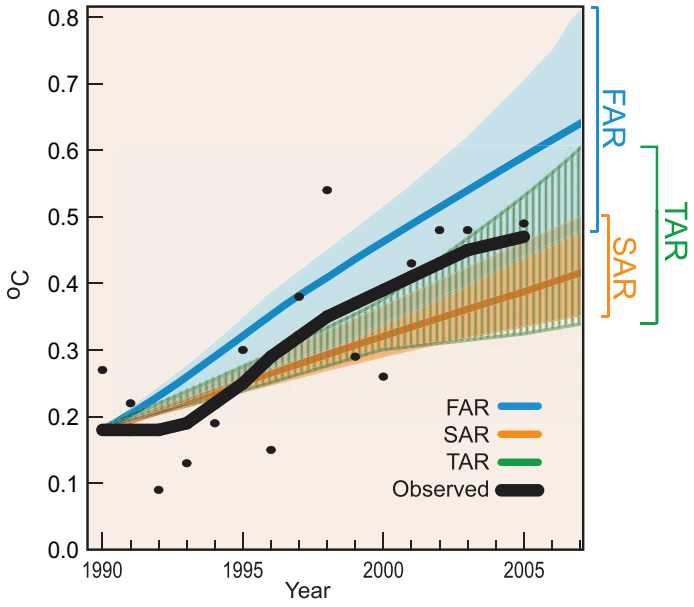


Figure 1.1. *Yearly global average surface temperature (Brohan et al., 2006), relative to the mean 1961 to 1990 values, and as projected in the FAR (IPCC, 1990), SAR (IPCC, 1996) and TAR (IPCC, 2001a). The 'best estimate' model projections from the FAR and SAR are in solid lines with their range of estimated projections shown by the shaded areas. The TAR did not have 'best estimate' model projections but rather a range of projections. Annual mean observations (Section 3.2) are depicted by black circles and the thick black line shows decadal variations obtained by smoothing the time series using a 13-point filter.*

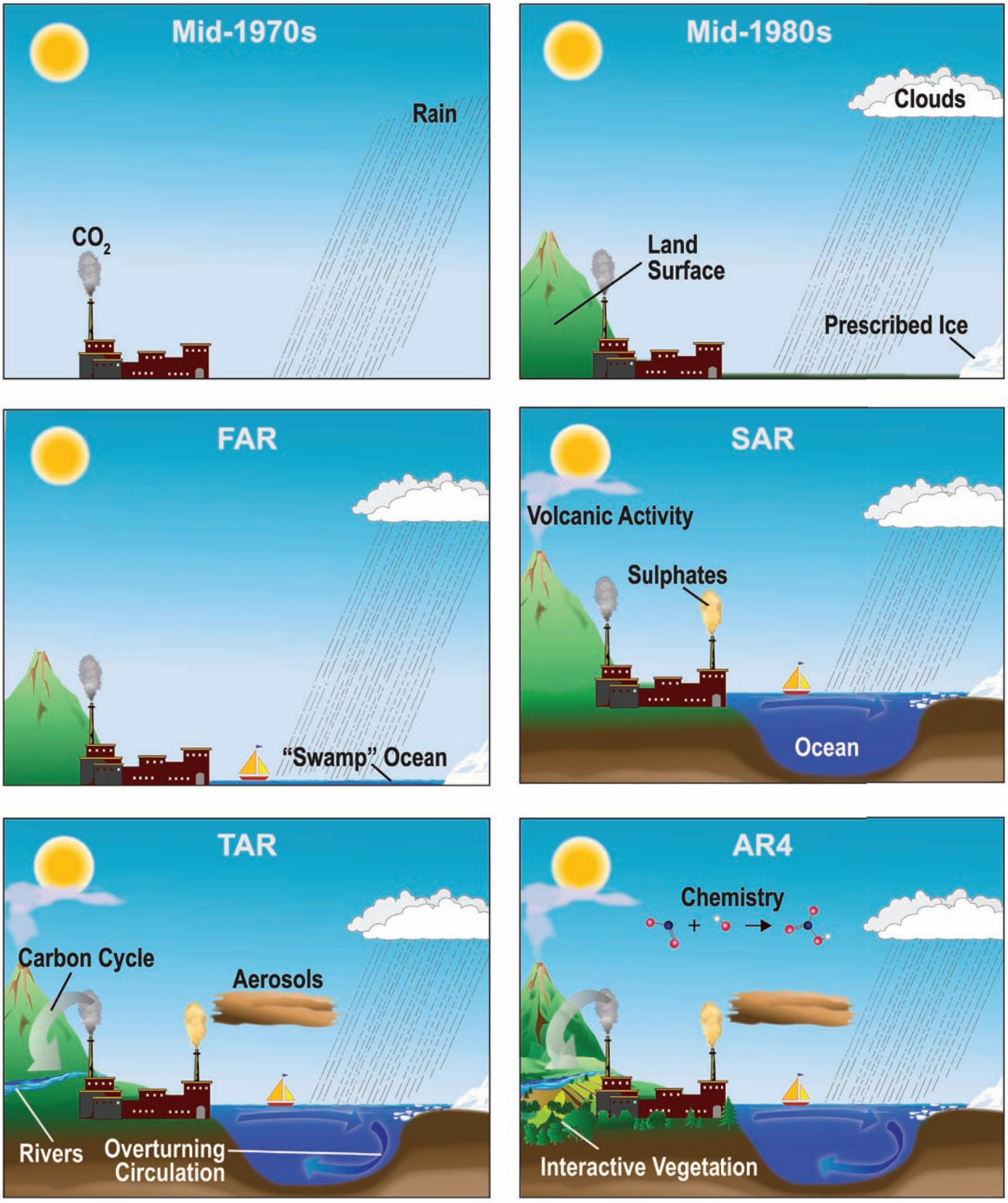


Figure 1.2. *The complexity of climate models has increased over the last few decades. The additional physics incorporated in the models are shown pictorially by the different features of the modelled world.*

1.3 Examples of Progress in Detecting and Attributing Recent Climate Change

1.3.1 The Human Fingerprint on Greenhouse Gases

The high-accuracy measurements of atmospheric CO_2 concentration, initiated by Charles David Keeling in 1958, constitute the master time series documenting the changing composition of the atmosphere (Keeling, 1961, 1998). These data have iconic status in climate change science as evidence of the effect of human activities on the chemical composition of the global atmosphere (see FAQ 7.1). Keeling's measurements on Mauna Loa in Hawaii provide a true measure of the global carbon cycle, an effectively continuous record of the burning of fossil fuel. They also maintain an accuracy and precision that allow scientists to separate fossil fuel emissions from those due to the natural annual cycle of the biosphere, demonstrating a long-term change in the seasonal exchange of CO_2 between the atmosphere, biosphere and ocean. Later observations of parallel trends in the atmospheric abundances of the $^{13}CO_2$ isotope (Francey and Farquhar, 1982) and molecular oxygen (O_2) (Keeling and Shertz, 1992; Bender et al., 1996) uniquely identified this rise in CO_2 with fossil fuel burning (Sections 2.3, 7.1 and 7.3).

To place the increase in CO_2 abundance since the late 1950s in perspective, and to compare the magnitude of the anthropogenic increase with natural cycles in the past, a longer-term record of CO_2 and other natural greenhouse gases is needed. These data came from analysis of the composition of air enclosed in bubbles in ice cores from Greenland and Antarctica. The initial measurements demonstrated that CO_2 abundances were significantly lower during the last ice age than over the last 10 kyr of the Holocene (Delmas et al., 1980; Berner et al., 1980; Neftel et al., 1982). From 10 kyr before present up to the year 1750, CO_2 abundances stayed within the range 280 ± 20 ppm (Indermühle et al., 1999). During the industrial era, CO_2 abundance rose roughly exponentially to 367 ppm in 1999 (Neftel et al., 1985; Etheridge et al., 1996; IPCC, 2001a) and to 379 ppm in 2005 (Section 2.3.1; see also Section 6.4).

Direct atmospheric measurements since 1970 (Steele et al., 1996) have also detected the increasing atmospheric abundances of two other major greenhouse gases, methane (CH_4) and nitrous oxide (N_2O). Methane abundances were initially increasing at a rate of about 1% yr^{-1} (Graedel and McRae, 1980; Fraser et al., 1981; Blake et al., 1982) but then slowed to an average increase of 0.4% yr^{-1} over the 1990s (Dlugokencky et al., 1998) with the possible stabilisation of CH_4 abundance (Section 2.3.2). The increase in N_2O abundance is smaller, about 0.25% yr^{-1}, and more difficult to detect (Weiss, 1981; Khalil and Rasmussen, 1988). To go back in time, measurements were made from firn air trapped in snowpack dating back over 200 years, and these data show an accelerating rise in both CH_4 and N_2O into the 20th century (Machida et al., 1995; Battle et al., 1996). When ice core measurements extended the CH_4 abundance back 1 kyr, they showed a stable, relatively constant abundance of 700 ppb until the 19th century when a steady increase brought CH_4 abundances to 1,745 ppb in 1998 (IPCC, 2001a) and 1,774 ppb in 2005 (Section 2.3.2). This peak abundance is much higher than the range of 400 to 700 ppb seen over the last half-million years of glacial-interglacial cycles, and the increase can be readily explained by anthropogenic emissions. For N_2O the results are similar: the relative increase over the industrial era is smaller (15%), yet the 1998 abundance of 314 ppb (IPCC, 2001a), rising to 319 ppb in 2005 (Section 2.3.3), is also well above the 180-to-260 ppb range of glacial-interglacial cycles (Flückiger et al., 1999; see Sections 2.3, 6.2, 6.3, 6.4, 7.1 and 7.4)

Several synthetic halocarbons (chlorofluorocarbons (CFCs), hydrofluorocarbons, perfluorocarbons, halons and sulphur hexafluoride) are greenhouse gases with large global warming potentials (GWPs; Section 2.10). The chemical industry has been producing these gases and they have been leaking into the atmosphere since about 1930. Lovelock (1971) first measured CFC-11 ($CFCl_3$) in the atmosphere, noting that it could serve as an artificial tracer, with its north-south gradient reflecting the latitudinal distribution of anthropogenic emissions. Atmospheric abundances of all the synthetic halocarbons were increasing until the 1990s, when the abundance of halocarbons phased out under the Montreal Protocol began to fall (Montzka et al., 1999; Prinn et al., 2000). In the case of synthetic halocarbons (except perfluoromethane), ice core research has shown that these compounds did not exist in ancient air (Langenfelds et al., 1996) and thus confirms their industrial human origin (see Sections 2.3 and 7.1).

At the time of the TAR scientists could say that the abundances of all the well-mixed greenhouse gases during the 1990s were greater than at any time during the last half-million years (Petit et al, 1999), and this record now extends back nearly one million years (Section 6.3). Given this daunting picture of increasing greenhouse gas abundances in the atmosphere, it is noteworthy that, for simpler challenges but still on a hemispheric or even global scale, humans have shown the ability to undo what they have done. Sulphate pollution in Greenland was reversed in the 1980s with the control of acid rain in North America and Europe (IPCC, 2001b), and CFC abundances are declining globally because of their phase-out undertaken to protect the ozone layer.

1.3.2 Global Surface Temperature

Shortly after the invention of the thermometer in the early 1600s, efforts began to quantify and record the weather. The first meteorological network was formed in northern Italy in 1653 (Kington, 1988) and reports of temperature observations were published in the earliest scientific journals (e.g., Wallis and Beale, 1669). By the latter part of the 19th century, systematic observations of the weather were being made in almost all inhabited areas of the world. Formal international coordination of meteorological observations from ships commenced in 1853 (Quetelet, 1854).

Inspired by the paper *Suggestions on a Uniform System of Meteorological Observations* (Buys-Ballot, 1872), the International Meteorological Organization (IMO) was formed in 1873. Its successor, the World Meteorological Organization (WMO), still works to promote and exchange standardised meteorological observations. Yet even with uniform observations, there are still four major obstacles to turning instrumental observations into accurate global time series: (1) access to the data in usable form; (2) quality control to remove or edit erroneous data points; (3) homogeneity assessments and adjustments where necessary to ensure the fidelity of the data; and (4) area-averaging in the presence of substantial gaps.

Köppen (1873, 1880, 1881) was the first scientist to overcome most of these obstacles in his quest to study the effect of changes in sunspots (Section 2.7). Much of his data came from Dove (1852), but wherever possible he used data directly from the original source, because Dove often lacked information about the observing methods. Köppen considered examination of the annual mean temperature to be an adequate technique for quality control of far distant stations. Using data from more than 100 stations, Köppen averaged annual observations into several major latitude belts and then area-averaged these into a near-global time series shown in Figure 1.3.

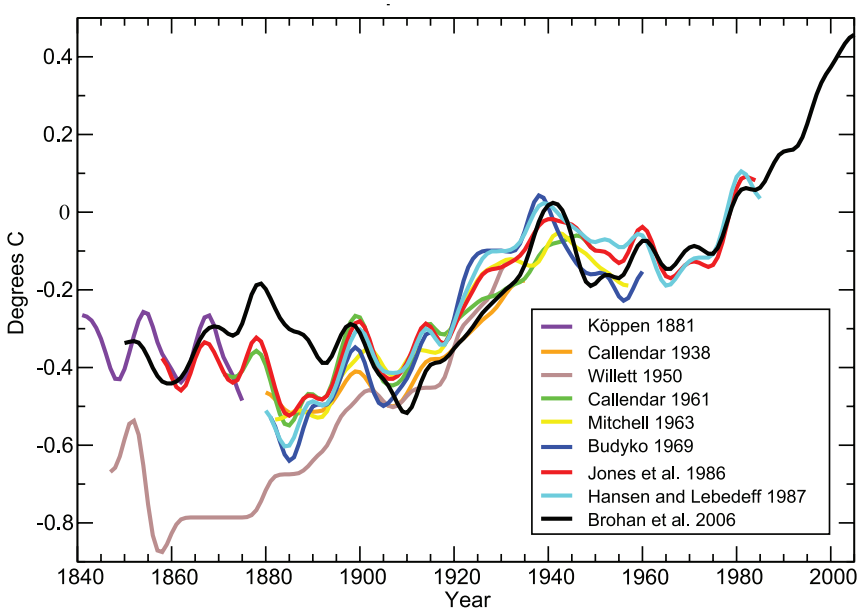


Figure 1.3. *Published records of surface temperature change over large regions. Köppen (1881) tropics and temperate latitudes using land air temperature. Callendar (1938) global using land stations. Willett (1950) global using land stations. Callendar (1961) 60°N to 60°S using land stations. Mitchell (1963) global using land stations. Budyko (1969) Northern Hemisphere using land stations and ship reports. Jones et al. (1986a,b) global using land stations. Hansen and Lebedeff (1987) global using land stations. Brohan et al. (2006) global using land air temperature and sea surface temperature data is the longest of the currently updated global temperature time series (Section 3.2). All time series were smoothed using a 13-point filter. The Brohan et al. (2006) time series are anomalies from the 1961 to 1990 mean (°C). Each of the other time series was originally presented as anomalies from the mean temperature of a specific and differing base period. To make them comparable, the other time series have been adjusted to have the mean of their last 30 years identical to that same period in the Brohan et al. (2006) anomaly time series.*

Callendar (1938) produced the next global temperature time series expressly to investigate the influence of CO_2 on temperature (Section 2.3). Callendar examined about 200 station records. Only a small portion of them were deemed defective, based on quality concerns determined by comparing differences with neighbouring stations or on homogeneity concerns based on station changes documented in the recorded metadata. After further removing two arctic stations because he had no compensating stations from the antarctic region, he created a global average using data from 147 stations.

Most of Callendar's data came from World Weather Records (WWR; Clayton, 1927). Initiated by a resolution at the 1923 IMO Conference, WWR was a monumental international undertaking producing a 1,196-page volume of monthly temperature, precipitation and pressure data from hundreds of stations around the world, some with data starting in the early 1800s. In the early 1960s, J. Wolbach had these data digitised (National Climatic Data Center, 2002). The WWR project continues today under the auspices of the WMO with the digital publication of decadal updates to the climate records for thousands of stations worldwide (National Climatic Data Center, 2005).

Willett (1950) also used WWR as the main source of data for 129 stations that he used to create a global temperature time series going back to 1845. While the resolution that initiated WWR called for the publication of long and homogeneous records, Willett took this mandate one step further by carefully selecting a subset of stations with as continuous and homogeneous a record as possible from the most recent update of WWR, which included data through 1940. To avoid over-weighting certain areas such as Europe, only one record, the best available, was included from each 10° latitude and longitude square. Station monthly data were averaged into five-year periods and then converted to anomalies with respect to the five-year period 1935 to 1939. Each station's anomaly was given equal weight to create the global time series.

Callendar in turn created a new near-global temperature time series in 1961 and cited Willett (1950) as a guide for some of his improvements. Callendar (1961) evaluated 600 stations with about three-quarters of them passing his quality checks. Unbeknownst to Callendar, a former student of Willett, Mitchell (1963), in work first presented in 1961, had created his own updated global temperature time series using slightly fewer than 200 stations and averaging the data into latitude bands. Landsberg and Mitchell (1961) compared Callendar's results with Mitchell's and stated that there was generally good agreement except in the data-sparse regions of the Southern Hemisphere.

Meanwhile, research in Russia was proceeding on a very different method to produce large-scale time series. Budyko (1969) used smoothed, hand-drawn maps of monthly temperature anomalies as a starting point. While restricted to analysis of the NH, this map-based approach not only allowed the inclusion of an increasing number of stations over time (e.g., 246 in 1881, 753 in 1913, 976 in 1940 and about 2,000 in 1960) but also the utilisation of data over the oceans (Robock, 1982).

Increasing the number of stations utilised has been a continuing theme over the last several decades with considerable effort being spent digitising historical station data as well as addressing the continuing problem of acquiring up-to-date data, as there can be a long lag between making an observation and the data getting into global data sets. During the 1970s and 1980s, several teams produced global temperature time series. Advances especially worth noting during this period include the extended spatial interpolation and station averaging technique of Hansen and Lebedeff (1987) and the Jones et al. (1986a,b) painstaking assessment of homogeneity and adjustments to account for discontinuities in the record of each of the thousands of stations in a global data set. Since then, global and national data sets have been rigorously adjusted for homogeneity using a variety of statistical and metadata-based approaches (Peterson et al., 1998).

One recurring homogeneity concern is potential urban heat island contamination in global temperature time series. This concern has been addressed in two ways. The first is by adjusting the temperature of urban stations to account for assessed urban heat island effects (e.g., Karl et al., 1988; Hansen et al., 2001). The second is by performing analyses that, like Callendar (1938), indicate that the bias induced by urban heat islands in the global temperature time series is either minor or non-existent (Jones et al., 1990; Peterson et al., 1999).

As the importance of ocean data became increasingly recognised, a major effort was initiated to seek out, digitise and quality-control historical archives of ocean data. This work has since grown into the International Comprehensive Ocean-Atmosphere Data Set (ICOADS; Worley et al., 2005), which has coordinated the acquisition, digitisation and synthesis of data ranging from transmissions by Japanese merchant ships to the logbooks of South African whaling boats. The amount of sea surface temperature (SST) and related data acquired continues to grow.

As fundamental as the basic data work of ICOADS was, there have been two other major advances in SST data. The first was adjusting the early observations to make them comparable to current observations (Section 3.2). Prior to 1940, the majority of SST observations were made from ships by hauling a bucket on deck filled with surface water and placing a thermometer in it. This ancient method eventually gave way to thermometers placed in engine cooling water inlets, which are typically located several metres below the ocean surface. Folland and Parker (1995) developed an adjustment model that accounted for heat loss from the buckets and that varied with bucket size and type, exposure to solar radiation, ambient wind speed and ship speed. They verified their results using time series of night marine air temperature. This adjusted the early bucket observations upwards by a few tenths of a degree celsius.

Most of the ship observations are taken in narrow shipping lanes, so the second advance has been increasing global coverage in a variety of ways. Direct improvement of coverage has been achieved by the internationally coordinated placement of drifting and moored buoys. The buoys began to be numerous enough to make significant contributions to SST analyses in the mid-1980s (McPhaden et al., 1998) and have subsequently increased to more than 1,000 buoys transmitting data at any one time. Since 1982, satellite data, anchored to *in situ* observations, have contributed to near-global coverage (Reynolds and Smith, 1994). In addition, several different approaches have been used to interpolate and combine land and ocean observations into the current global temperature time series (Section 3.2). To place the current instrumental observations into a longer historical context requires the use of proxy data (Section 6.2).

Figure 1.3 depicts several historical 'global' temperature time series, together with the longest of the current global temperature time series, that of Brohan et al. (2006; Section 3.2). While the data and the analysis techniques have changed over time, all the time series show a high degree of consistency since 1900. The differences caused by using alternate data sources and interpolation techniques increase when the data are sparser. This phenomenon is especially illustrated by the pre-1880 values of Willett's (1950) time series. Willett noted that his data coverage remained fairly constant after 1885 but dropped off dramatically before that time to only 11 stations before 1850. The high degree of agreement between the time series resulting from these many different analyses increases the confidence that the changes they are indicating are real.

Despite the fact that many recent observations are automatic, the vast majority of data that go into global surface temperature calculations – over 400 million individual readings of thermometers at land stations and over 140 million individual *in situ* SST observations – have depended on the dedication of tens of thousands of individuals for well over a century. Climate science owes a great debt to the work of these individual weather observers as well as to international organisations such as the IMO, WMO and the Global Climate Observing System, which encourage the taking and sharing of high-quality meteorological observations. While modern researchers and their institutions put a great deal of time and effort into acquiring and adjusting the data to account for all known problems and biases, century-scale global temperature time series would not have been possible without the conscientious work of individuals and organisations worldwide dedicated to quantifying and documenting their local environment (Section 3.2).

1.3.3 Detection and Attribution

Using knowledge of past climates to qualify the nature of ongoing changes has become a concern of growing importance during the last decades, as reflected in the successive IPCC reports. While linked together at a technical level, detection and attribution have separate objectives. Detection of climate

change is the process of demonstrating that climate has changed in some defined statistical sense, without providing a reason for that change. Attribution of causes of climate change is the process of establishing the most likely causes for the detected change with some defined level of confidence. Using traditional approaches, unequivocal attribution would require controlled experimentation with our climate system. However, with no spare Earth with which to experiment, attribution of anthropogenic climate change must be pursued by: (a) detecting that the climate has changed (as defined above); (b) demonstrating that the detected change is consistent with computer model simulations of the climate change 'signal' that is calculated to occur in response to anthropogenic forcing; and (c) demonstrating that the detected change is not consistent with alternative, physically plausible explanations of recent climate change that exclude important anthropogenic forcings.

Both detection and attribution rely on observational data and model output. In spite of the efforts described in Section 1.3.2, estimates of century-scale natural climate fluctuations remain difficult to obtain directly from observations due to the relatively short length of most observational records and a lack of understanding of the full range and effects of the various and ongoing external influences. Model simulations with no changes in external forcing (e.g., no increases in atmospheric CO_2 concentration) provide valuable information on the natural internal variability of the climate system on time scales of years to centuries. Attribution, on the other hand, requires output from model runs that incorporate historical estimates of changes in key anthropogenic and natural forcings, such as well-mixed greenhouse gases, volcanic aerosols and solar irradiance. These simulations can be performed with changes in a single forcing only (which helps to isolate the climate effect of that forcing), or with simultaneous changes in a whole suite of forcings.

In the early years of detection and attribution research, the focus was on a single time series – the estimated global-mean changes in the Earth's surface temperature. While it was not possible to detect anthropogenic warming in 1980, Madden and Ramanathan (1980) and Hansen et al. (1981) predicted it would be evident at least within the next two decades. A decade later, Wigley and Raper (1990) used a simple energy-balance climate model to show that the observed change in global-mean surface temperature from 1867 to 1982 could not be explained by natural internal variability. This finding was later confirmed using variability estimates from more complex coupled ocean-atmosphere general circulation models (e.g., Stouffer et al., 1994).

As the science of climate change progressed, detection and attribution research ventured into more sophisticated statistical analyses that examined complex patterns of climate change. Climate change patterns or 'fingerprints' were no longer limited to a single variable (temperature) or to the Earth's surface. More recent detection and attribution work has made use of precipitation and global pressure patterns, and analysis of vertical profiles of temperature change in the ocean and atmosphere. Studies with multiple variables make it easier to address attribution issues. While two different climate forcings may yield similar changes in global mean temperature, it is highly unlikely that they will produce exactly the same 'fingerprint' (i.e., climate changes that are identical as a function of latitude, longitude, height, season and history over the 20th century).

Such model-predicted fingerprints of anthropogenic climate change are clearly statistically identifiable in observed data. The common conclusion of a wide range of fingerprint studies conducted over the past 15 years is that observed climate changes cannot be explained by natural factors alone (Santer et al., 1995, 1996a,b,c; Hegerl et al., 1996, 1997, 2000; Hasselmann, 1997; Barnett et al., 1999; Tett et al., 1999; Stott et al., 2000). A substantial anthropogenic influence is required in order to best explain the observed changes. The evidence from this body of work strengthens the scientific case for a discernible human influence on global climate.

1.4 Examples of Progress in Understanding Climate Processes

1.4.1 The Earth's Greenhouse Effect

The realisation that Earth's climate might be sensitive to the atmospheric concentrations of gases that create a greenhouse effect is more than a century old. Fleming (1998) and Weart (2003) provided an overview of the emerging science. In terms of the energy balance of the climate system, Edme Mariotte noted in 1681 that although the Sun's light and heat easily pass through glass and other transparent materials, heat from other sources (*chaleur de feu*) does not. The ability to generate an artificial warming of the Earth's surface was demonstrated in simple greenhouse experiments such as Horace Benedict de Saussure's experiments in the 1760s using a 'heliothermometer' (panes of glass covering a thermometer in a darkened box) to provide an early analogy to the greenhouse effect. It was a conceptual leap to recognise that the air itself could also trap thermal radiation. In 1824, Joseph Fourier, citing Saussure, argued 'the temperature [of the Earth] can be augmented by the interposition of the atmosphere, because heat in the state of light finds less resistance in penetrating the air, than in repassing into the air when converted into non-luminous heat'. In 1836, Pouillit followed up on Fourier's ideas and argued 'the atmospheric stratum…exercises a greater absorption upon the terrestrial than on the solar rays'. There was still no understanding of exactly what substance in the atmosphere was responsible for this absorption.

In 1859, John Tyndall (1861) identified through laboratory experiments the absorption of thermal radiation by complex molecules (as opposed to the primary bimolecular atmospheric constituents O_2 and molecular nitrogen). He noted that changes in the amount of any of the radiatively active constituents of the atmosphere such as water (H_2O) or CO_2 could have produced 'all the mutations of climate which the researches of geologists

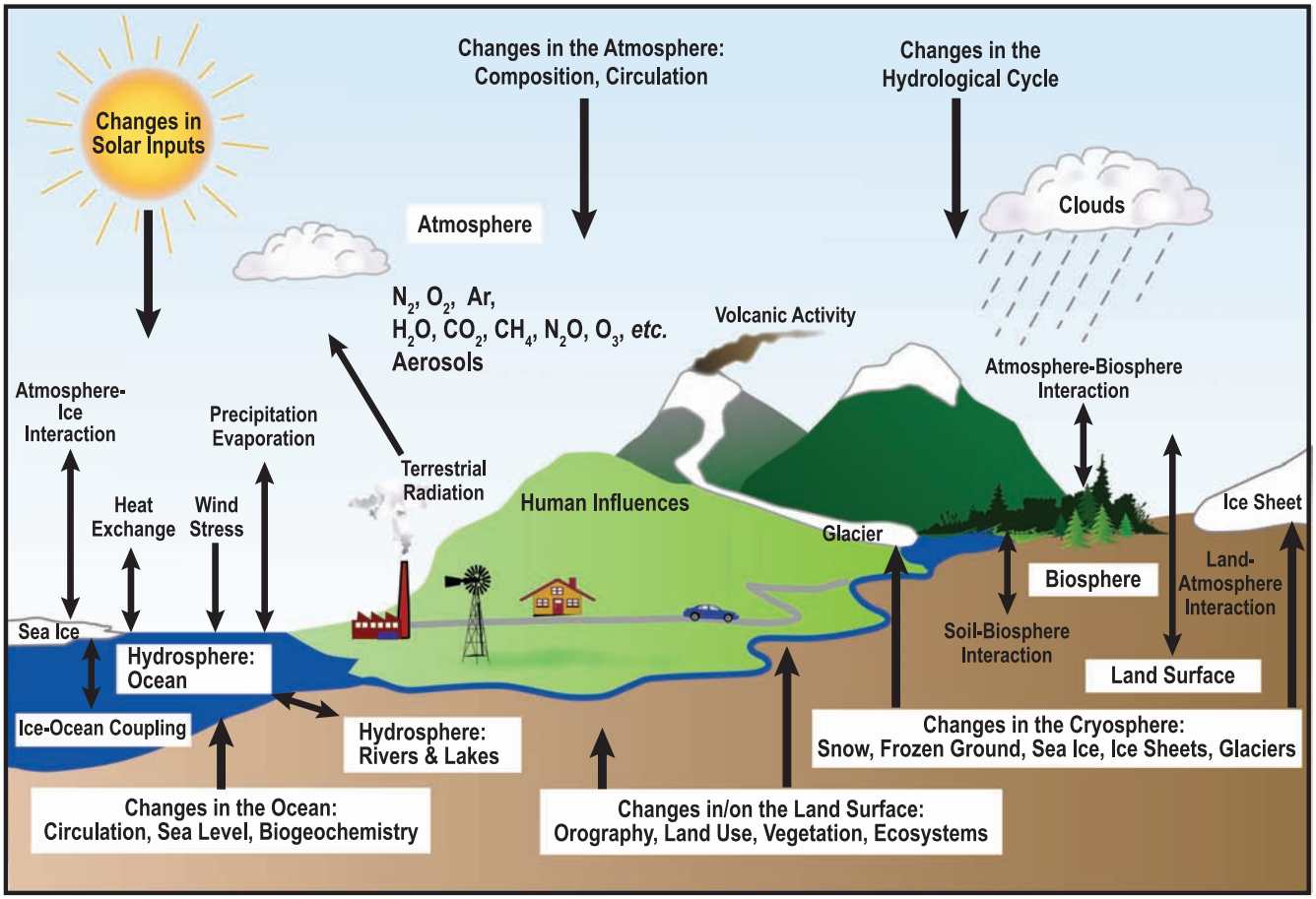
Frequently Asked Question 1.2

What is the Relationship between Climate Change and Weather?

Climate is generally defined as average weather, and as such, climate change and weather are intertwined. Observations can show that there have been changes in weather, and it is the statistics of changes in weather over time that identify climate change. While weather and climate are closely related, there are important differences. A common confusion between weather and climate arises when scientists are asked how they can predict climate 50 years from now when they cannot predict the weather a few weeks from now. The chaotic nature of weather makes it unpredictable beyond a few days. Projecting changes in climate (i.e., long-term average weather) due to changes in atmospheric composition or other factors is a very different and much more manageable issue. As an analogy, while it is impossible to predict the age at which any particular man will die, we can say with high confidence that the average age of death for men in industrialised countries is about 75. Another common confusion of these issues is thinking that a cold winter or a cooling spot on the globe is evidence against global warming. There are always extremes of hot and cold, although their frequency and intensity change as climate changes. But when weather is averaged over space and time, the fact that the globe is warming emerges clearly from the data.

Meteorologists put a great deal of effort into observing, understanding and predicting the day-to-day evolution of weather systems. Using physics-based concepts that govern how the atmosphere moves, warms, cools, rains, snows, and evaporates water, meteorologists are typically able to predict the weather successfully several days into the future. A major limiting factor to the predictability of weather beyond several days is a fundamental dynamical property of the atmosphere. In the 1960s, meteorologist Edward Lorenz discovered that very slight differences in initial conditions can produce very different forecast results.

(continued)



FAQ 1.2, Figure 1. *Schematic view of the components of the climate system, their processes and interactions.*

This is the so-called butterfly effect: a butterfly flapping its wings (or some other small phenomenon) in one place can, in principle, alter the subsequent weather pattern in a distant place. At the core of this effect is chaos theory, which deals with how small changes in certain variables can cause apparent randomness in complex systems.

Nevertheless, chaos theory does not imply a total lack of order. For example, slightly different conditions early in its history might alter the day a storm system would arrive or the exact path it would take, but the average temperature and precipitation (that is, climate) would still be about the same for that region and that period of time. Because a significant problem facing weather forecasting is knowing all the conditions at the start of the forecast period, it can be useful to think of climate as dealing with the background conditions for weather. More precisely, climate can be viewed as concerning the status of the entire Earth system, including the atmosphere, land, oceans, snow, ice and living things (see Figure 1) that serve as the global background conditions that determine weather patterns. An example of this would be an El Niño affecting the weather in coastal Peru. The El Niño sets limits on the probable evolution of weather patterns that random effects can produce. A La Niña would set different limits.

Another example is found in the familiar contrast between summer and winter. The march of the seasons is due to changes in the geographical patterns of energy absorbed and radiated away by the Earth system. Likewise, projections of future climate are shaped by fundamental changes in heat energy in the Earth system, in particular the increasing intensity of the greenhouse effect that traps heat near Earth's surface, determined by the amount of carbon dioxide and other greenhouse gases in the atmosphere. Projecting changes in climate due to changes in greenhouse gases 50 years from now is a very different and much more easily solved problem than forecasting weather patterns just weeks from now. To put it another way, long-term variations brought about by changes in the composition of the atmosphere are much more predictable than individual weather events. As an example, while we cannot predict the outcome of a single coin toss or roll of the dice, we can predict the statistical behaviour of a large number of such trials.

While many factors continue to influence climate, scientists have determined that human activities have become a dominant force, and are responsible for most of the warming observed over the past 50 years. Human-caused climate change has resulted primarily from changes in the amounts of greenhouse gases in the atmosphere, but also from changes in small particles (aerosols), as well as from changes in land use, for example. As climate changes, the probabilities of certain types of weather events are affected. For example, as Earth's average temperature has increased, some weather phenomena have become more frequent and intense (e.g., heat waves and heavy downpours), while others have become less frequent and intense (e.g., extreme cold events).

reveal'. In 1895, Svante Arrhenius (1896) followed with a climate prediction based on greenhouse gases, suggesting that a 40% increase or decrease in the atmospheric abundance of the trace gas CO_2 might trigger the glacial advances and retreats. One hundred years later, it would be found that CO_2 did indeed vary by this amount between glacial and interglacial periods. However, it now appears that the initial climatic change preceded the change in CO_2 but was enhanced by it (Section 6.4).

G. S. Callendar (1938) solved a set of equations linking greenhouse gases and climate change. He found that a doubling of atmospheric CO_2 concentration resulted in an increase in the mean global temperature of 2°C, with considerably more warming at the poles, and linked increasing fossil fuel combustion with a rise in CO_2 and its greenhouse effects: 'As man is now changing the composition of the atmosphere at a rate which must be very exceptional on the geological time scale, it is natural to seek for the probable effects of such a change. From the best laboratory observations it appears that the principal result of increasing atmospheric carbon dioxide… would be a gradual increase in the mean temperature of the colder regions of the Earth.' In 1947, Ahlmann reported a 1.3°C warming in the North Atlantic sector of the Arctic since the 19th century and mistakenly believed this climate variation could be explained entirely by greenhouse gas warming. Similar model predictions were echoed by Plass in 1956 (see Fleming, 1998): 'If at the end of this century, measurements show that the carbon dioxide content of the atmosphere has risen appreciably and at the same time the temperature has continued to rise throughout the world, it will be firmly established that carbon dioxide is an important factor in causing climatic change' (see Chapter 9).

In trying to understand the carbon cycle, and specifically how fossil fuel emissions would change atmospheric CO_2, the interdisciplinary field of carbon cycle science began. One of the first problems addressed was the atmosphere-ocean exchange of CO_2. Revelle and Suess (1957) explained why part of the emitted CO_2 was observed to accumulate in the atmosphere rather than being completely absorbed by the oceans. While CO_2 can be mixed rapidly into the upper layers of the ocean, the time to mix with the deep ocean is many centuries. By the time of the TAR, the interaction of climate change with the oceanic circulation and biogeochemistry was projected to reduce the fraction of anthropogenic CO_2 emissions taken up by the oceans in the future, leaving a greater fraction in the atmosphere (Sections 7.1, 7.3 and 10.4).

In the 1950s, the greenhouse gases of concern remained CO_2 and H_2O, the same two identified by Tyndall a century earlier. It was not until the 1970s that other greenhouse gases – CH_4, N_2O and CFCs – were widely recognised as

important anthropogenic greenhouse gases (Ramanathan, 1975; Wang et al., 1976; Section 2.3). By the 1970s, the importance of aerosol-cloud effects in reflecting sunlight was known (Twomey, 1977), and atmospheric aerosols (suspended small particles) were being proposed as climate-forcing constituents. Charlson and others (summarised in Charlson et al., 1990) built a consensus that sulphate aerosols were, by themselves, cooling the Earth's surface by directly reflecting sunlight. Moreover, the increases in sulphate aerosols were anthropogenic and linked with the main source of CO_2, burning of fossil fuels (Section 2.4). Thus, the current picture of the atmospheric constituents driving climate change contains a much more diverse mix of greenhouse agents.

1.4.2 Past Climate Observations, Astronomical Theory and Abrupt Climate Changes

Throughout the 19th and 20th centuries, a wide range of geomorphology and palaeontology studies has provided new insight into the Earth's past climates, covering periods of hundreds of millions of years. The Palaeozoic Era, beginning 600 Ma, displayed evidence of both warmer and colder climatic conditions than the present; the Tertiary Period (65 to 2.6 Ma) was generally warmer; and the Quaternary Period (2.6 Ma to the present – the ice ages) showed oscillations between glacial and interglacial conditions. Louis Agassiz (1837) developed the hypothesis that Europe had experienced past glacial ages, and there has since been a growing awareness that long-term climate observations can advance the understanding of the physical mechanisms affecting climate change. The scientific study of one such mechanism – modifications in the geographical and temporal patterns of solar energy reaching the Earth's surface due to changes in the Earth's orbital parameters – has a long history. The pioneering contributions of Milankovitch (1941) to this astronomical theory of climate change are widely known, and the historical review of Imbrie and Imbrie (1979) calls attention to much earlier contributions, such as those of James Croll, originating in 1864.

The pace of palaeoclimatic research has accelerated over recent decades. Quantitative and well-dated records of climate fluctuations over the last 100 kyr have brought a more comprehensive view of how climate changes occur, as well as the means to test elements of the astronomical theory. By the 1950s, studies of deep-sea cores suggested that the ocean temperatures may have been different during glacial times (Emiliani, 1955). Ewing and Donn (1956) proposed that changes in ocean circulation actually could initiate an ice age. In the 1960s, the works of Emiliani (1969) and Shackleton (1967) showed the potential of isotopic measurements in deep-sea sediments to help explain Quaternary changes. In the 1970s, it became possible to analyse a deep-sea core time series of more than 700 kyr, thereby using the last reversal of the Earth's magnetic field to establish a dated chronology. This deep-sea observational record clearly showed the same periodicities found in the astronomical forcing, immediately providing strong support to Milankovitch's theory (Hays et al., 1976).

Ice cores provide key information about past climates, including surface temperatures and atmospheric chemical composition. The bubbles sealed in the ice are the only available samples of these past atmospheres. The first deep ice cores from Vostok in Antarctica (Barnola et al., 1987; Jouzel et al., 1987, 1993) provided additional evidence of the role of astronomical forcing. They also revealed a highly correlated evolution of temperature changes and atmospheric composition, which was subsequently confirmed over the past 400 kyr (Petit et al., 1999) and now extends to almost 1 Myr. This discovery drove research to understand the causal links between greenhouse gases and climate change. The same data that confirmed the astronomical theory also revealed its limits: a linear response of the climate system to astronomical forcing could not explain entirely the observed fluctuations of rapid ice-age terminations preceded by longer cycles of glaciations.

The importance of other sources of climate variability was heightened by the discovery of abrupt climate changes. In this context, 'abrupt' designates regional events of large amplitude, typically a few degrees celsius, which occurred within several decades – much shorter than the thousand-year time scales that characterise changes in astronomical forcing. Abrupt temperature changes were first revealed by the analysis of deep ice cores from Greenland (Dansgaard et al., 1984). Oeschger et al. (1984) recognised that the abrupt changes during the termination of the last ice age correlated with cooling in Gerzensee (Switzerland) and suggested that regime shifts in the Atlantic Ocean circulation were causing these widespread changes. The synthesis of palaeoclimatic observations by Broecker and Denton (1989) invigorated the community over the next decade. By the end of the 1990s, it became clear that the abrupt climate changes during the last ice age, particularly in the North Atlantic regions as found in the Greenland ice cores, were numerous (Dansgaard et al., 1993), indeed abrupt (Alley et al., 1993) and of large amplitude (Severinghaus and Brook, 1999). They are now referred to as Dansgaard-Oeschger events. A similar variability is seen in the North Atlantic Ocean, with north-south oscillations of the polar front (Bond et al., 1992) and associated changes in ocean temperature and salinity (Cortijo et al., 1999). With no obvious external forcing, these changes are thought to be manifestations of the internal variability of the climate system.

The importance of internal variability and processes was reinforced in the early 1990s with analysis of records with high temporal resolution. New ice cores (Greenland Ice Core Project, Johnsen et al., 1992; Greenland Ice Sheet Project 2, Grootes et al., 1993), new ocean cores from regions with high sedimentation rates, as well as lacustrine sediments and cave stalagmites produced additional evidence for unforced climate changes, and revealed a large number of abrupt changes in many regions throughout the last glacial cycle. Long sediment cores from the deep ocean were used to reconstruct the thermohaline circulation connecting deep and surface waters (Bond et al., 1992; Broecker, 1997) and to demonstrate the participation of the ocean in these abrupt climate changes during glacial periods.

By the end of the 1990s, palaeoclimate proxies for a range of climate observations had expanded greatly. The analysis of deep corals provided indicators for nutrient content and mass exchange from the surface to deep water (Adkins et al., 1998), showing abrupt variations characterised by synchronous changes in surface and deep-water properties (Shackleton et al., 2000). Precise measurements of the CH_4 abundances (a global quantity) in polar ice cores showed that they changed in concert with the Dansgaard-Oeschger events and thus allowed for synchronisation of the dating across ice cores (Blunier et al., 1998). The characteristics of the antarctic temperature variations and their relation to the Dansgaard-Oeschger events in Greenland were consistent with the simple concept of a bipolar seesaw caused by changes in the thermohaline circulation of the Atlantic Ocean (Stocker, 1998). This work underlined the role of the ocean in transmitting the signals of abrupt climate change.

Abrupt changes are often regional, for example, severe droughts lasting for many years have changed civilizations, and have occurred during the last 10 kyr of stable warm climate (deMenocal, 2001). This result has altered the notion of a stable climate during warm epochs, as previously suggested by the polar ice cores. The emerging picture of an unstable ocean-atmosphere system has opened the debate of whether human interference through greenhouse gases and aerosols could trigger such events (Broecker, 1997).

Palaeoclimate reconstructions cited in the FAR were based on various data, including pollen records, insect and animal remains, oxygen isotopes and other geological data from lake varves, loess, ocean sediments, ice cores and glacier termini. These records provided estimates of climate variability on time scales up to millions of years. A climate proxy is a local quantitative record (e.g., thickness and chemical properties of tree rings, pollen of different species) that is interpreted as a climate variable (e.g., temperature or rainfall) using a transfer function that is based on physical principles and recently observed correlations between the two records. The combination of instrumental and proxy data began in the 1960s with the investigation of the influence of climate on the proxy data, including tree rings (Fritts, 1962), corals (Weber and Woodhead, 1972; Dunbar and Wellington, 1981) and ice cores (Dansgaard et al., 1984; Jouzel et al., 1987). Phenological and historical data (e.g., blossoming dates, harvest dates, grain prices, ships' logs, newspapers, weather diaries, ancient manuscripts) are also a valuable source of climatic reconstruction for the period before instrumental records became available. Such documentary data also need calibration against instrumental data to extend and reconstruct the instrumental record (Lamb, 1969; Zhu, 1973; van den Dool, 1978; Brazdil, 1992; Pfister, 1992). With the development of multi-proxy reconstructions, the climate data were extended not only from local to global, but also from instrumental data to patterns of climate variability (Wanner et al., 1995; Mann et al., 1998; Luterbacher et al., 1999). Most of these reconstructions were at single sites and only loose efforts had been made to consolidate records. Mann et al. (1998) made a notable advance in the use of proxy data by ensuring that the dating of different records lined up. Thus, the true spatial patterns of temperature variability and change could be derived, and estimates of NH average surface temperatures were obtained.

The Working Group I (WGI) WGI FAR noted that past climates could provide analogues. Fifteen years of research since that assessment has identified a range of variations and instabilities in the climate system that occurred during the last 2 Myr of glacial-interglacial cycles and in the super-warm period of 50 Ma. These past climates do not appear to be analogues of the immediate future, yet they do reveal a wide range of climate processes that need to be understood when projecting 21st-century climate change (see Chapter 6).

1.4.3 Solar Variability and the Total Solar Irradiance

Measurement of the absolute value of total solar irradiance (TSI) is difficult from the Earth's surface because of the need to correct for the influence of the atmosphere. Langley (1884) attempted to minimise the atmospheric effects by taking measurements from high on Mt. Whitney in California, and to estimate the correction for atmospheric effects by taking measurements at several times of day, for example, with the solar radiation having passed through different atmospheric pathlengths. Between 1902 and 1957, Charles Abbot and a number of other scientists around the globe made thousands of measurements of TSI from mountain sites. Values ranged from 1,322 to 1,465 W m^{-2}, which encompasses the current estimate of 1,365 W m^{-2}. Foukal et al. (1977) deduced from Abbot's daily observations that higher values of TSI were associated with more solar faculae (e.g., Abbot, 1910).

In 1978, the Nimbus-7 satellite was launched with a cavity radiometer and provided evidence of variations in TSI (Hickey et al., 1980). Additional observations were made with an active cavity radiometer on the Solar Maximum Mission, launched in 1980 (Willson et al., 1980). Both of these missions showed that the passage of sunspots and faculae across the Sun's disk influenced TSI. At the maximum of the 11-year solar activity cycle, the TSI is larger by about 0.1% than at the minimum. The observation that TSI is highest when sunspots are at their maximum is the opposite of Langley's (1876) hypothesis.

As early as 1910, Abbot believed that he had detected a downward trend in TSI that coincided with a general cooling of climate. The solar cycle variation in irradiance corresponds to an 11-year cycle in radiative forcing which varies by about 0.2 W m^{-2}. There is increasingly reliable evidence of its influence on atmospheric temperatures and circulations, particularly in the higher atmosphere (Reid, 1991; Brasseur, 1993; Balachandran and Rind, 1995; Haigh, 1996; Labitzke and van Loon, 1997; van Loon and Labitzke, 2000). Calculations with three-dimensional models (Wetherald and Manabe, 1975; Cubasch et al., 1997; Lean and Rind, 1998; Tett et al., 1999; Cubasch and Voss, 2000) suggest that the changes in solar radiation could cause surface temperature changes of the order of a few tenths of a degree celsius.

For the time before satellite measurements became available, the solar radiation variations can be inferred from cosmogenic isotopes (^{10}Be, ^{14}C) and from the sunspot number. Naked-eye observations of sunspots date back to ancient times, but it was only after the invention of the telescope in 1607 that it became possible to routinely monitor the number, size and position of these 'stains' on the surface of the Sun. Throughout the 17th and 18th centuries, numerous observers noted the variable concentrations and ephemeral nature of sunspots, but very few sightings were reported between 1672 and 1699 (for an overview see Hoyt et al., 1994). This period of low solar activity, now known as the Maunder Minimum, occurred during the climate period now commonly referred to as the Little Ice Age (Eddy, 1976). There is no exact agreement as to which dates mark the beginning and end of the Little Ice Age, but from about 1350 to about 1850 is one reasonable estimate.

During the latter part of the 18th century, Wilhelm Herschel (1801) noted the presence not only of sunspots but of bright patches, now referred to as faculae, and of granulations on the solar surface. He believed that when these indicators of activity were more numerous, solar emissions of light and heat were greater and could affect the weather on Earth. Heinrich Schwabe (1844) published his discovery of a '10-year cycle' in sunspot numbers. Samuel Langley (1876) compared the brightness of sunspots with that of the surrounding photosphere. He concluded that they would block the emission of radiation and estimated that at sunspot cycle maximum the Sun would be about 0.1% less bright than at the minimum of the cycle, and that the Earth would be 0.1°C to 0.3°C cooler.

These satellite data have been used in combination with the historically recorded sunspot number, records of cosmogenic isotopes, and the characteristics of other Sun-like stars to estimate the solar radiation over the last 1,000 years (Eddy, 1976; Hoyt and Schatten, 1993, 1997; Lean et al., 1995; Lean, 1997). These data sets indicated quasi-periodic changes in solar radiation of 0.24 to 0.30% on the centennial time scale. These values have recently been re-assessed (see, e.g., Chapter 2).

The TAR states that the changes in solar irradiance are not the major cause of the temperature changes in the second half of the 20th century unless those changes can induce unknown large feedbacks in the climate system. The effects of galactic cosmic rays on the atmosphere (via cloud nucleation) and those due to shifts in the solar spectrum towards the ultraviolet (UV) range, at times of high solar activity, are largely unknown. The latter may produce changes in tropospheric circulation via changes in static stability resulting from the interaction of the increased UV radiation with stratospheric ozone. More research to investigate the effects of solar behaviour on climate is needed before the magnitude of solar effects on climate can be stated with certainty.

1.4.4 Biogeochemistry and Radiative Forcing

The modern scientific understanding of the complex and interconnected roles of greenhouse gases and aerosols in climate change has undergone rapid evolution over the last two decades. While the concepts were recognised and outlined in the 1970s (see Sections 1.3.1 and 1.4.1), the publication of generally accepted quantitative results coincides with, and was driven in part by, the questions asked by the IPCC beginning in 1988. Thus, it is instructive to view the evolution of this topic as it has been treated in the successive IPCC reports.

The WGI FAR codified the key physical and biogeochemical processes in the Earth system that relate a changing climate to atmospheric composition, chemistry, the carbon cycle and natural ecosystems. The science of the time, as summarised in the FAR, made a clear case for anthropogenic interference with the climate system. In terms of greenhouse agents, the main conclusions from the WGI FAR Policymakers Summary are still valid today: (1) 'emissions resulting from human activities are substantially increasing the atmospheric concentrations of the greenhouse gases: CO_2, CH_4, CFCs, N_2O'; (2) 'some gases are potentially more effective (at greenhouse warming)'; (3) feedbacks between the carbon cycle, ecosystems and atmospheric greenhouse gases in a warmer world will affect CO_2 abundances; and (4) GWPs provide a metric for comparing the climatic impact of different greenhouse gases, one that integrates both the radiative influence and biogeochemical cycles. The climatic importance of tropospheric ozone, sulphate aerosols and atmospheric chemical feedbacks were proposed by scientists at the time and noted in the assessment. For example, early global chemical modelling results argued that global tropospheric ozone, a greenhouse gas, was controlled by emissions of the highly reactive gases nitrogen oxides (NO_x), carbon monoxide (CO) and non-methane hydrocarbons (NMHC, also known as volatile organic compounds, VOC). In terms of sulphate aerosols, both the direct radiative effects and the indirect effects on clouds were acknowledged, but the importance of carbonaceous aerosols from fossil fuel and biomass combustion was not recognised (Chapters 2, 7 and 10).

The concept of radiative forcing (RF) as the radiative imbalance (W m^{-2}) in the climate system at the top of the atmosphere caused by the addition of a greenhouse gas (or other change) was established at the time and summarised in Chapter 2 of the WGI FAR. Agents of RF included the direct greenhouse gases, solar radiation, aerosols and the Earth's surface albedo. What was new and only briefly mentioned was that 'many gases produce indirect effects on the global radiative forcing'. The innovative global modelling work of Derwent (1990) showed that emissions of the reactive but non-greenhouse gases – NO_x, CO and NMHCs – altered atmospheric chemistry and thus changed the abundance of other greenhouse gases. Indirect GWPs for NO_x, CO and VOCs were proposed. The projected chemical feedbacks were limited to short-lived increases in tropospheric ozone. By 1990, it was clear that the RF from tropospheric ozone had increased over the 20th century and stratospheric ozone had decreased since 1980 (e.g., Lacis et al., 1990), but the associated RFs were not evaluated in the assessments. Neither was the effect of anthropogenic sulphate aerosols, except to note in the FAR that 'it is conceivable that this radiative forcing has been of a comparable magnitude, but of opposite sign, to the greenhouse forcing earlier in the

century'. Reflecting in general the community's concerns about this relatively new measure of climate forcing, RF bar charts appear only in the underlying FAR chapters, but not in the FAR Summary. Only the long-lived greenhouse gases are shown, although sulphate aerosols direct effect in the future is noted with a question mark (i.e., dependent on future emissions) (Chapters 2, 7 and 10).

The cases for more complex chemical and aerosol effects were becoming clear, but the scientific community was unable at the time to reach general agreement on the existence, scale and magnitude of these indirect effects. Nevertheless, these early discoveries drove the research agendas in the early 1990s. The widespread development and application of global chemistry-transport models had just begun with international workshops (Pyle et al., 1996; Jacob et al., 1997; Rasch, 2000). In the Supplementary Report (IPCC, 1992) to the FAR, the indirect chemical effects of CO, NO_x and VOC were reaffirmed, and the feedback effect of CH_4 on the tropospheric hydroxyl radical (OH) was noted, but the indirect RF values from the FAR were retracted and denoted in a table with '+', '0' or '–'. Aerosol-climate interactions still focused on sulphates, and the assessment of their direct RF for the NH (i.e., a cooling) was now somewhat quantitative as compared to the FAR. Stratospheric ozone depletion was noted as causing a significant and negative RF, but not quantified. Ecosystems research at this time was identifying the responses to climate change and CO_2 increases, as well as altered CH_4 and N_2O fluxes from natural systems; however, in terms of a community assessment it remained qualitative.

By 1994, with work on SAR progressing, the Special Report on Radiative Forcing (IPCC, 1995) reported significant breakthroughs in a set of chapters limited to assessment of the carbon cycle, atmospheric chemistry, aerosols and RF. The carbon budget for the 1980s was analysed not only from bottom-up emissions estimates, but also from a top-down approach including carbon isotopes. A first carbon cycle assessment was performed through an international model and analysis workshop examining terrestrial and oceanic uptake to better quantify the relationship between CO_2 emissions and the resulting increase in atmospheric abundance. Similarly, expanded analyses of the global budgets of trace gases and aerosols from both natural and anthropogenic sources highlighted the rapid expansion of biogeochemical research. The first RF bar chart appears, comparing all the major components of RF change from the pre-industrial period to the present. Anthropogenic soot aerosol, with a positive RF, was not in the 1995 Special Report but was added to the SAR. In terms of atmospheric chemistry, the first open-invitation modelling study for the IPCC recruited 21 atmospheric chemistry models to participate in a controlled study of photochemistry and chemical feedbacks. These studies (e.g., Olson et al., 1997) demonstrated a robust consensus about some indirect effects, such as the CH_4 impact on atmospheric chemistry, but great uncertainty about others, such as the prediction of tropospheric ozone changes. The model studies plus the theory of chemical feedbacks in the CH_4-CO-OH system (Prather, 1994) firmly established that the atmospheric lifetime of a perturbation (and hence climate impact and GWP) of CH_4 emissions was about 50% greater than reported in the FAR. There was still no consensus on quantifying the past or future changes in tropospheric ozone or OH (the primary sink for CH_4) (Chapters 2, 7 and 10).

In the early 1990s, research on aerosols as climate forcing agents expanded. Based on new research, the range of climate-relevant aerosols was extended for the first time beyond sulphates to include nitrates, organics, soot, mineral dust and sea salt. Quantitative estimates of sulphate aerosol indirect effects on cloud properties and hence RF were sufficiently well established to be included in assessments, and carbonaceous aerosols from biomass burning were recognised as being comparable in importance to sulphate (Penner et al., 1992). Ranges are given in the special report (IPCC, 1995) for direct sulphate RF (–0.25 to –0.9 W m^{-2}) and biomass-burning aerosols (–0.05 to –0.6 W m^{-2}). The aerosol indirect RF was estimated to be about equal to the direct RF, but with larger uncertainty. The injection of stratospheric aerosols from the eruption of Mt. Pinatubo was noted as the first modern test of a known radiative forcing, and indeed one climate model accurately predicted the temperature response (Hansen et al., 1992). In the one-year interval between the special report and the SAR, the scientific understanding of aerosols grew. The direct anthropogenic aerosol forcing (from sulphate, fossil-fuel soot and biomass-burning aerosols) was reduced to –0.5 W m^{-2}. The RF bar chart was now broken into aerosol components (sulphate, fossil-fuel soot and biomass burning aerosols) with a separate range for indirect effects (Chapters 2 and 7; Sections 8.2 and 9.2).

Throughout the 1990s, there were concerted research programs in the USA and EU to evaluate the global environmental impacts of aviation. Several national assessments culminated in the IPCC Special Report on Aviation and the Global Atmosphere (IPCC, 1999), which assessed the impacts on climate and global air quality. An open invitation for atmospheric model participation resulted in community participation and a consensus on many of the environmental impacts of aviation (e.g., the increase in tropospheric ozone and decrease in CH_4 due to NO_x emissions were quantified). The direct RF of sulphate and of soot aerosols was likewise quantified along with that of contrails, but the impact on cirrus clouds that are sometimes generated downwind of contrails was not. The assessment re-affirmed that RF was a first-order metric for the global mean surface temperature response, but noted that it was inadequate for regional climate change, especially in view of the largely regional forcing from aerosols and tropospheric ozone (Sections 2.6, 2.8 and 10.2).

By the end of the 1990s, research on atmospheric composition and climate forcing had made many important advances. The TAR was able to provide a more quantitative evaluation in some areas. For example, a large, open-invitation modelling workshop was held for both aerosols (11 global models) and tropospheric ozone-OH chemistry (14 global models). This workshop brought together as collaborating authors most of the international scientific community involved in developing and testing global models of atmospheric composition. In terms of atmospheric chemistry, a strong consensus was reached for the first time

that science could predict the changes in tropospheric ozone in response to scenarios for CH_4 and the indirect greenhouse gases (CO, NO_x, VOC) and that a quantitative GWP for CO could be reported. Further, combining these models with observational analysis, an estimate of the change in tropospheric ozone since the pre-industrial era – with uncertainties – was reported. The aerosol workshop made similar advances in evaluating the impact of different aerosol types. There were many different representations of uncertainty (e.g., a range in models versus an expert judgment) in the TAR, and the consensus RF bar chart did not generate a total RF or uncertainties for use in the subsequent IPCC Synthesis Report (IPCC, 2001b) (Chapters 2 and 7; Section 9.2).

1.4.5 Cryospheric Topics

The cryosphere, which includes the ice sheets of Greenland and Antarctica, continental (including tropical) glaciers, snow, sea ice, river and lake ice, permafrost and seasonally frozen ground, is an important component of the climate system. The cryosphere derives its importance to the climate system from a variety of effects, including its high reflectivity (albedo) for solar radiation, its low thermal conductivity, its large thermal inertia, its potential for affecting ocean circulation (through exchange of freshwater and heat) and atmospheric circulation (through topographic changes), its large potential for affecting sea level (through growth and melt of land ice), and its potential for affecting greenhouse gases (through changes in permafrost) (Chapter 4).

Studies of the cryospheric albedo feedback have a long history. The albedo is the fraction of solar energy reflected back to space. Over snow and ice, the albedo (about 0.7 to 0.9) is large compared to that over the oceans (<0.1). In a warming climate, it is anticipated that the cryosphere would shrink, the Earth's overall albedo would decrease and more solar energy would be absorbed to warm the Earth still further. This powerful feedback loop was recognised in the 19th century by Croll (1890) and was first introduced in climate models by Budyko (1969) and Sellers (1969). But although the principle of the albedo feedback is simple, a quantitative understanding of the effect is still far from complete. For instance, it is not clear whether this mechanism is the main reason for the high-latitude amplification of the warming signal.

The potential cryospheric impact on ocean circulation and sea level are of particular importance. There may be 'large-scale discontinuities' (IPCC, 2001a) resulting from both the shutdown of the large-scale meridional circulation of the world oceans (see Section 1.4.6) and the disintegration of large continental ice sheets. Mercer (1968, 1978) proposed that atmospheric warming could cause the ice shelves of western Antarctica to disintegrate and that as a consequence the entire West Antarctic Ice Sheet (10% of the antarctic ice volume) would lose its land connection and come afloat, causing a sea level rise of about five metres.

The importance of permafrost-climate feedbacks came to be realised widely only in the 1990s, starting with the works of Kvenvolden (1988, 1993), MacDonald (1990) and Harriss et al. (1993). As permafrost thaws due to a warmer climate, CO_2 and CH_4 trapped in permafrost are released to the atmosphere. Since CO_2 and CH_4 are greenhouse gases, atmospheric temperature is likely to increase in turn, resulting in a feedback loop with more permafrost thawing. The permafrost and seasonally thawed soil layers at high latitudes contain a significant amount (about one-quarter) of the global total amount of soil carbon. Because global warming signals are amplified in high-latitude regions, the potential for permafrost thawing and consequent greenhouse gas releases is thus large.

In situ monitoring of the cryosphere has a long tradition. For instance, it is important for fisheries and agriculture. Seagoing communities have documented sea ice extent for centuries. Records of thaw and freeze dates for lake and river ice start with Lake Suwa in Japan in 1444, and extensive records of snowfall in China were made during the Qing Dynasty (1644–1912). Records of glacial length go back to the mid-1500s. Internationally coordinated, long-term glacier observations started in 1894 with the establishment of the International Glacier Commission in Zurich, Switzerland. The longest time series of a glacial mass balance was started in 1946 at the Storglaciären in northern Sweden, followed by Storbreen in Norway (begun in 1949). Today a global network of mass balance monitoring for some 60 glaciers is coordinated through the World Glacier Monitoring Service. Systematic measurements of permafrost (thermal state and active layer) began in earnest around 1950 and were coordinated under the Global Terrestrial Network for Permafrost.

The main climate variables of the cryosphere (extent, albedo, topography and mass) are in principle observable from space, given proper calibration and validation through *in situ* observing efforts. Indeed, satellite data are required in order to have full global coverage. The polar-orbiting Nimbus 5 satellite, launched in 1972, yielded the earliest all-weather, all-season imagery of global sea ice, using microwave instruments (Parkinson et al., 1987), and enabled a major advance in the scientific understanding of the dynamics of the cryosphere. Launched in 1978, the Television Infrared Observation Satellite (TIROS-N) yielded the first monitoring from space of snow on land surfaces (Dozier et al., 1981). The number of cryospheric elements now routinely monitored from space is growing, and current satellites are now addressing one of the more challenging elements, variability of ice volume.

Climate modelling results have pointed to high-latitude regions as areas of particular importance and ecological vulnerability to global climate change. It might seem logical to expect that the cryosphere overall would shrink in a warming climate or expand in a cooling climate. However, potential changes in precipitation, for instance due to an altered hydrological cycle, may counter this effect both regionally and globally. By the time of the TAR, several climate models incorporated physically based treatments of ice dynamics, although the land ice processes were only rudimentary. Improving representation of the cryosphere in climate models is still an area of intense research and continuing progress (Chapter 8).

1.4.6 Ocean and Coupled Ocean-Atmosphere Dynamics

Developments in the understanding of the oceanic and atmospheric circulations, as well as their interactions, constitute a striking example of the continuous interplay among theory, observations and, more recently, model simulations. The atmosphere and ocean surface circulations were observed and analysed globally as early as the 16th and 17th centuries, in close association with the development of worldwide trade based on sailing. These efforts led to a number of important conceptual and theoretical works. For example, Edmund Halley first published a description of the tropical atmospheric cells in 1686, and George Hadley proposed a theory linking the existence of the trade winds with those cells in 1735. These early studies helped to forge concepts that are still useful in analysing and understanding both the atmospheric general circulation itself and model simulations (Lorenz, 1967; Holton, 1992).

A comprehensive description of these circulations was delayed by the lack of necessary observations in the higher atmosphere or deeper ocean. The balloon record of Gay-Lussac, who reached an altitude of 7,016 m in 1804, remained unbroken for more than 50 years. The stratosphere was independently discovered near the turn of the 20th century by Aßmann (1902) and Teisserenc de Bort (1902), and the first manned balloon flight into the stratosphere was made in 1901 (Berson and Süring, 1901). Even though it was recognised over 200 years ago (Rumford, 1800; see also Warren, 1981) that the oceans' cold subsurface waters must originate at high latitudes, it was not appreciated until the 20th century that the strength of the deep circulation might vary over time, or that the ocean's Meridional Overturning Circulation (MOC; often loosely referred to as the 'thermohaline circulation', see the Glossary for more information) may be very important for Earth's climate.

By the 1950s, studies of deep-sea cores suggested that the deep ocean temperatures had varied in the distant past. Technology also evolved to enable measurements that could confirm that the deep ocean is not only not static, but in fact quite dynamic (Swallow and Stommel's 1960 subsurface float experiment Aries, referred to by Crease, 1962). By the late 1970s, current meters could monitor deep currents for substantial amounts of time, and the first ocean observing satellite (SeaSat) revealed that significant information about subsurface ocean variability is imprinted on the sea surface. At the same time, the first estimates of the strength of the meridional transport of heat and mass were made (Oort and Vonder Haar, 1976; Wunsch, 1978), using a combination of models and data. Since then the technological developments have accelerated, but monitoring the MOC directly remains a substantial challenge (see Chapter 5), and routine observations of the subsurface ocean remain scarce compared to that of the atmosphere.

In parallel with the technological developments yielding new insights through observations, theoretical and numerical explorations of multiple (stable or unstable) equilibria began. Chamberlain (1906) suggested that deep ocean currents could reverse in direction, and might affect climate. The idea did not gain momentum until fifty years later, when Stommel (1961) presented a mechanism, based on the opposing effects that temperature and salinity have on density, by which ocean circulation can fluctuate between states. Numerical climate models incorporating models of the ocean circulation were developed during this period, including the pioneering work of Bryan (1969) and Manabe and Bryan (1969). The idea that the ocean circulation could change radically, and might perhaps even feel the attraction of different equilibrium states, gained further support through the simulations of coupled climate models (Bryan and Spelman, 1985; Bryan, 1986; Manabe and Stouffer, 1988). Model simulations using a hierarchy of models showed that the ocean circulation system appeared to be particularly vulnerable to changes in the freshwater balance, either by direct addition of freshwater or by changes in the hydrological cycle. A strong case emerged for the hypothesis that rapid changes in the Atlantic meridional circulation were responsible for the abrupt Dansgaard-Oeschger climate change events.

Although scientists now better appreciate the strength and variability of the global-scale ocean circulation, its roles in climate are still hotly debated. Is it a passive recipient of atmospheric forcing and so merely a diagnostic consequence of climate change, or is it an active contributor? Observational evidence for the latter proposition was presented by Sutton and Allen (1997), who noticed SST anomalies propagating along the Gulf Stream/North Atlantic Current system for years, and therefore implicated internal oceanic time scales. Is a radical change in the MOC likely in the near future? Brewer et al. (1983) and Lazier (1995) showed that the water masses of the North Atlantic were indeed changing (some becoming significantly fresher) in the modern observational record, a phenomenon that at least raises the possibility that ocean conditions may be approaching the point where the circulation might shift into Stommel's other stable regime. Recent developments in the ocean's various roles in climate can be found in Chapters 5, 6, 9 and 10.

Studying the interactions between atmosphere and ocean circulations was also facilitated through continuous interactions between observations, theories and simulations, as is dramatically illustrated by the century-long history of the advances in understanding the El Niño-Southern Oscillation (ENSO) phenomenon. This coupled air-sea phenomenon originates in the Pacific but affects climate globally, and has raised concern since at least the 19th century. Sir Gilbert Walker (1928) describes how H. H. Hildebrandsson (1897) noted large-scale relationships between interannual trends in pressure data from a worldwide network of 68 weather stations, and how Lockyer and Lockyer (1902) confirmed Hildebrandsson's discovery of an apparent 'seesaw' in pressure between South America and the Indonesian region. Walker named this seesaw pattern the 'Southern Oscillation' and related it to occurrences of drought and heavy rains in India, Australia, Indonesia and Africa. He also proposed that there must be a certain level of predictive skill in that system.

El Niño is the name given to the rather unusual oceanic conditions involving anomalously warm waters occurring in

the eastern tropical Pacific off the coast of Peru every few years. The 1957–1958 International Geophysical Year coincided with a large El Niño, allowing a remarkable set of observations of the phenomenon. A decade later, a mechanism was presented that connected Walker's observations to El Niño (Bjerknes, 1969). This mechanism involved the interaction, through the SST field, between the east-west atmospheric circulation of which Walker's Southern Oscillation was an indicator (Bjerknes appropriately referred to this as the 'Walker Circulation') and variability in the pool of equatorial warm water of the Pacific Ocean. Observations made in the 1970s (e.g., Wyrtki, 1975) showed that prior to ENSO warm phases, the sea level in the western Pacific often rises significantly. By the mid-1980s, after an unusually disruptive El Niño struck in 1982 and 1983, an observing system (the Tropical Ocean Global Atmosphere (TOGA) array; see McPhaden et al., 1998) had been put in place to monitor ENSO. The resulting data confirmed the idea that the phenomenon was inherently one involving coupled atmosphere-ocean interactions and yielded much-needed detailed observational insights. By 1986, the first experimental ENSO forecasts were made (Cane et al., 1986; Zebiak and Cane, 1987).

The mechanisms and predictive skill of ENSO are still under discussion. In particular, it is not clear how ENSO changes with, and perhaps interacts with, a changing climate. The TAR states '...increasing evidence suggests the ENSO plays a fundamental role in global climate and its interannual variability, and increased credibility in both regional and global climate projections will be gained once realistic ENSOs and their changes are simulated'.

Just as the phenomenon of El Niño has been familiar to the people of tropical South America for centuries, a spatial pattern affecting climate variability in the North Atlantic has similarly been known by the people of Northern Europe for a long time. The Danish missionary Hans Egede made the following well-known diary entry in the mid-18th century: 'In Greenland, all winters are severe, yet they are not alike. The Danes have noticed that when the winter in Denmark was severe, as we perceive it, the winter in Greenland in its manner was mild, and conversely' (van Loon and Rogers, 1978).

Teisserenc de Bort, Hann, Exner, Defant and Walker all contributed to the discovery of the underlying dynamic structure. Walker, in his studies in the Indian Ocean, actually studied global maps of sea level pressure correlations, and named not only the Southern Oscillation, but also a Northern Oscillation, which he subsequently divided into a North Pacific and a North Atlantic Oscillation (Walker, 1924). However, it was Exner (1913, 1924) who made the first correlation maps showing the spatial structure in the NH, where the North Atlantic Oscillation (NAO) pattern stands out clearly as a north-south oscillation in atmospheric mass with centres of action near Iceland and Portugal.

The NAO significantly affects weather and climate, ecosystems and human activities of the North Atlantic sector. But what is the underlying mechanism? The recognition that the NAO is associated with variability and latitudinal shifts in the westerly flow of the jet stream originates with the works of Willett, Namias, Lorenz, Rossby and others in the 1930s, 1940s and 1950s (reviewed by Stephenson et al., 2003). Because atmospheric planetary waves are hemispheric in nature, changes in one region are often connected with changes in other regions, a phenomenon dubbed 'teleconnection' (Wallace and Gutzler, 1981).

The NAO may be partly described as a high-frequency stochastic process internal to the atmosphere. This understanding is evidenced by numerous atmosphere-only model simulations. It is also considered an expression of one of Earth's 'annular modes' (See Chapter 3). It is, however, the low-frequency variability of this phenomenon (Hurrell, 1995) that fuels continued investigations by climate scientists. The long time scales are the indication of potential predictive skill in the NAO. The mechanisms responsible for the correspondingly long 'memory' are still debated, although they are likely to have a local or remote oceanic origin. Bjerknes (1964) recognised the connection between the NAO index (which he referred to as the 'zonal index') and sea surface conditions. He speculated that ocean heat advection could play a role on longer time scales. The circulation of the Atlantic Ocean is radically different from that of the Indian and Pacific Oceans, in that the MOC is strongest in the Atlantic with warm water flowing northwards, even south of the equator, and cold water returning at depth. It would therefore not be surprising if the oceanic contributions to the NAO and to the Southern Oscillation were different.

Earth's climate is characterised by many modes of variability, involving both the atmosphere and ocean, and also the cryosphere and biosphere. Understanding the physical processes involved in producing low-frequency variability is crucial for improving scientists' ability to accurately predict climate change and for allowing the separation of anthropogenic and natural variability, thereby improving the ability to detect and attribute anthropogenic climate change. One central question for climate scientists, addressed in particular in Chapter 9, is to determine how human activities influence the dynamic nature of Earth's climate, and to identify what would have happened without any human influence at all.

1.5 Examples of Progress in Modelling the Climate

1.5.1 Model Evolution and Model Hierarchies

Climate scenarios rely upon the use of numerical models. The continuous evolution of these models over recent decades has been enabled by a considerable increase in computational capacity, with supercomputer speeds increasing by roughly a factor of a million in the three decades from the 1970s to the present. This computational progress has permitted a corresponding increase in model complexity (by including more and more components and processes, as depicted in Figure 1.2), in the length of the simulations, and in spatial resolution,

as shown in Figure 1.4. The models used to evaluate future climate changes have therefore evolved over time. Most of the pioneering work on CO_2-induced climate change was based on atmospheric general circulation models coupled to simple 'slab' ocean models (i.e., models omitting ocean dynamics), from the early work of Manabe and Wetherald (1975) to the review of Schlesinger and Mitchell (1987). At the same time the physical content of the models has become more comprehensive (see in Section 1.5.2 the example of clouds). Similarly, most of the results presented in the FAR were from atmospheric models, rather than from models of the coupled climate system, and were used to analyse changes in the equilibrium climate resulting from a doubling of the atmospheric CO_2 concentration. Current climate projections can investigate time-dependent scenarios of climate evolution and can make use of much more complex coupled ocean-atmosphere models, sometimes even including interactive chemical or biochemical components.

A parallel evolution toward increased complexity and resolution has occurred in the domain of numerical weather prediction, and has resulted in a large and verifiable improvement in operational weather forecast quality. This example alone shows that present models are more realistic than were those of a decade ago. There is also, however, a continuing awareness that models do not provide a perfect simulation of reality, because resolving all important spatial or time scales remains far beyond current capabilities, and also because the behaviour of such a complex nonlinear system may in general be chaotic.

It has been known since the work of Lorenz (1963) that even simple models may display intricate behaviour because of their nonlinearities. The inherent nonlinear behaviour of the climate system appears in climate simulations at all time scales (Ghil, 1989). In fact, the study of nonlinear dynamical systems has become important for a wide range of scientific disciplines, and the corresponding mathematical developments are essential to interdisciplinary studies. Simple models of ocean-atmosphere interactions, climate-biosphere interactions or climate-economy interactions may exhibit a similar behaviour, characterised by partial unpredictability, bifurcations and transition to chaos.

In addition, many of the key processes that control climate sensitivity or abrupt climate changes (e.g., clouds, vegetation, oceanic convection) depend on very small spatial scales. They cannot be represented in full detail in the context of global models, and scientific understanding of them is still notably incomplete. Consequently, there is a continuing need to assist in the use and interpretation of complex models through models that are either conceptually simpler, or limited to a number of processes or to a specific region, therefore enabling a deeper understanding of the processes at work or a more relevant comparison with observations. With the development of computer capacities, simpler models have not disappeared; on the contrary, a stronger emphasis has been given to the concept of a 'hierarchy of models' as the only way to provide a linkage between theoretical understanding and the complexity of realistic models (Held, 2005).

The list of these 'simpler' models is very long. Simplicity may lie in the reduced number of equations (e.g., a single

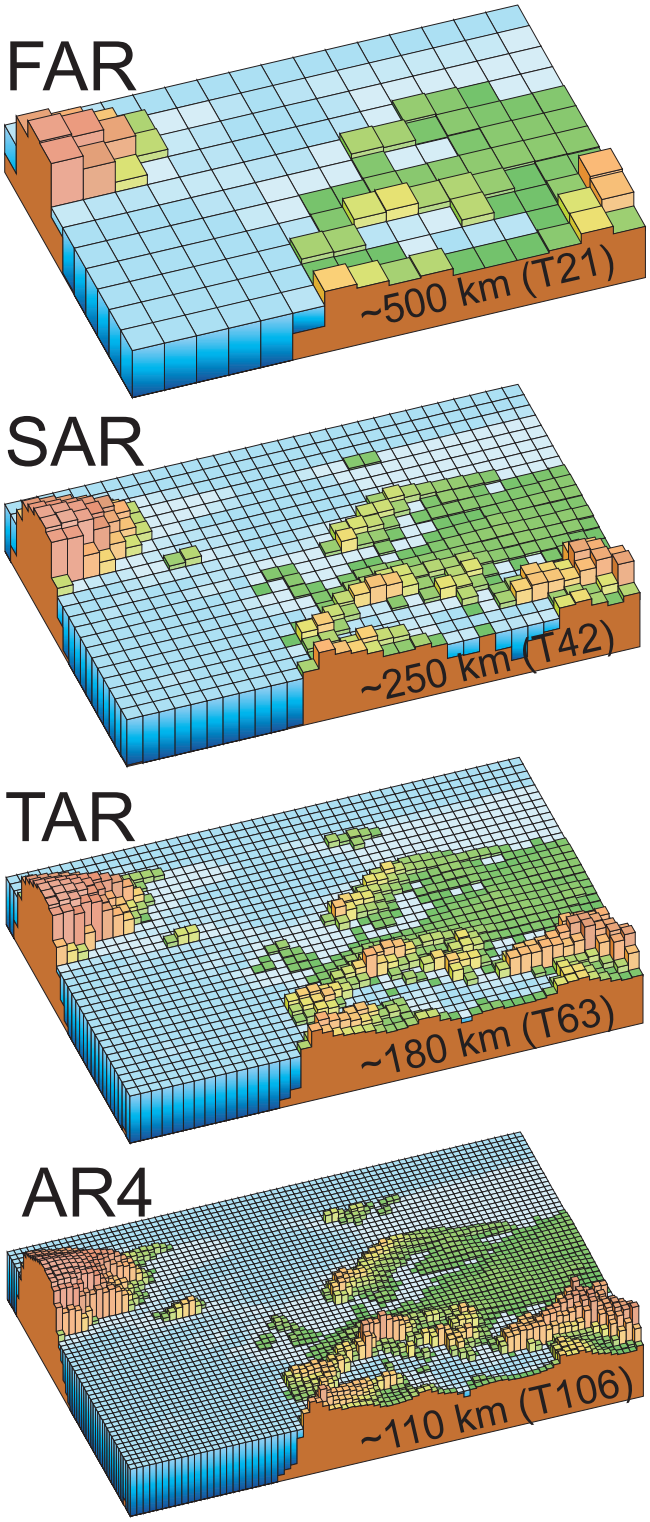


Figure 1.4. *Geographic resolution characteristic of the generations of climate models used in the IPCC Assessment Reports: FAR (IPCC, 1990), SAR (IPCC, 1996), TAR (IPCC, 2001a), and AR4 (2007). The figures above show how successive generations of these global models increasingly resolved northern Europe. These illustrations are representative of the most detailed horizontal resolution used for short-term climate simulations. The century-long simulations cited in IPCC Assessment Reports after the FAR were typically run with the previous generation's resolution. Vertical resolution in both atmosphere and ocean models is not shown, but it has increased comparably with the horizontal resolution, beginning typically with a single-layer slab ocean and ten atmospheric layers in the FAR and progressing to about thirty levels in both atmosphere and ocean.*

equation for the global surface temperature); in the reduced dimensionality of the problem (one-dimension vertical, one-dimension latitudinal, two-dimension); or in the restriction to a few processes (e.g., a mid-latitude quasi-geostrophic atmosphere with or without the inclusion of moist processes). The notion of model hierarchy is also linked to the idea of scale: global circulation models are complemented by regional models that exhibit a higher resolution over a given area, or process oriented models, such as cloud resolving models or large eddy simulations. Earth Models of Intermediate Complexity are used to investigate long time scales, such as those corresponding to glacial to interglacial oscillations (Berger et al., 1998). This distinction between models according to scale is evolving quickly, driven by the increase in computer capacities. For example, global models explicitly resolving the dynamics of convective clouds may soon become computationally feasible.

Many important scientific debates in recent years have had their origin in the use of conceptually simple models. The study of idealised atmospheric representations of the tropical climate, for example by Pierrehumbert (1995) who introduced a separate representation of the areas with ascending and subsiding circulation in the tropics, has significantly improved the understanding of the feedbacks that control climate. Simple linearized models of the atmospheric circulation have been used to investigate potential new feedback effects. Ocean box models have played an important role in improving the understanding of the possible slowing down of the Atlantic thermohaline circulation (Birchfield et al., 1990), as emphasized in the TAR. Simple models have also played a central role in the interpretation of IPCC scenarios: the investigation of climate scenarios presented in the SAR or the TAR has been extended to larger ensembles of cases using idealised models.

1.5.2 Model Clouds and Climate Sensitivity

The modelling of cloud processes and feedbacks provides a striking example of the irregular pace of progress in climate science. Representation of clouds may constitute the area in which atmospheric models have been modified most continuously to take into account increasingly complex physical processes. At the time of the TAR clouds remained a major source of uncertainty in the simulation of climate changes (as they still are at present: e.g., Sections 2.4, 2.6, 3.4.3, 7.5, 8.2, 8.4.11, 8.6.2.2, 8.6.3.2, 9.2.1.2, 9.4.1.8, 10.2.1.2, 10.3.2.2, 10.5.4.3, 11.8.1.3, 11.8.2.2).

In the early 1980s, most models were still using prescribed cloud amounts, as functions of location and altitude, and prescribed cloud radiative properties, to compute atmospheric radiation. The cloud amounts were very often derived from the zonally averaged climatology of London (1957). Succeeding generations of models have used relative humidity or other simple predictors to diagnose cloudiness (Slingo, 1987), thus providing a foundation of increased realism for the models, but at the same time possibly causing inconsistencies in the representation of the multiple roles of clouds as bodies interacting with radiation, generating precipitation and influencing small-scale convective or turbulent circulations. Following the pioneering studies of Sundqvist (1978), an explicit representation of clouds was progressively introduced into climate models, beginning in the late 1980s. Models first used simplified representations of cloud microphysics, following, for example, Kessler (1969), but more recent generations of models generally incorporate a much more comprehensive and detailed representation of clouds, based on consistent physical principles. Comparisons of model results with observational data presented in the TAR have shown that, based on zonal averages, the representation of clouds in most climate models was also more realistic in 2000 than had been the case only a few years before.

In spite of this undeniable progress, the amplitude and even the sign of cloud feedbacks was noted in the TAR as highly uncertain, and this uncertainty was cited as one of the key factors explaining the spread in model simulations of future climate for a given emission scenario. This cannot be regarded as a surprise: that the sensitivity of the Earth's climate to changing atmospheric greenhouse gas concentrations must depend strongly on cloud feedbacks can be illustrated on the simplest theoretical grounds, using data that have been available for a long time. Satellite measurements have indeed provided meaningful estimates of Earth's radiation budget since the early 1970s (Vonder Haar and Suomi, 1971). Clouds, which cover about 60% of the Earth's surface, are responsible for up to two-thirds of the planetary albedo, which is about 30%. An albedo decrease of only 1%, bringing the Earth's albedo from 30% to 29%, would cause an increase in the black-body radiative equilibrium temperature of about 1°C, a highly significant value, roughly equivalent to the direct radiative effect of a doubling of the atmospheric CO_2 concentration. Simultaneously, clouds make an important contribution to the planetary greenhouse effect. In addition, changes in cloud cover constitute only one of the many parameters that affect cloud radiative interactions: cloud optical thickness, cloud height and cloud microphysical properties can also be modified by atmospheric temperature changes, which adds to the complexity of feedbacks, as evidenced, for example, through satellite observations analysed by Tselioudis and Rossow (1994).

The importance of simulated cloud feedbacks was revealed by the analysis of model results (Manabe and Wetherald, 1975; Hansen et al, 1984), and the first extensive model intercomparisons (Cess et al., 1989) also showed a substantial model dependency. The strong effect of cloud processes on climate model sensitivities to greenhouse gases was emphasized further through a now-classic set of General Circulation Model (GCM) experiments, carried out by Senior and Mitchell (1993). They produced global average surface temperature changes (due to doubled atmospheric CO_2 concentration) ranging from 1.9°C to 5.4°C, simply by altering the way that cloud radiative properties were treated in the model. It is somewhat unsettling that the results of a complex climate model can be so drastically altered by substituting one reasonable cloud parametrization for another, thereby approximately replicating the overall inter-model range of sensitivities. Other GCM groups have also

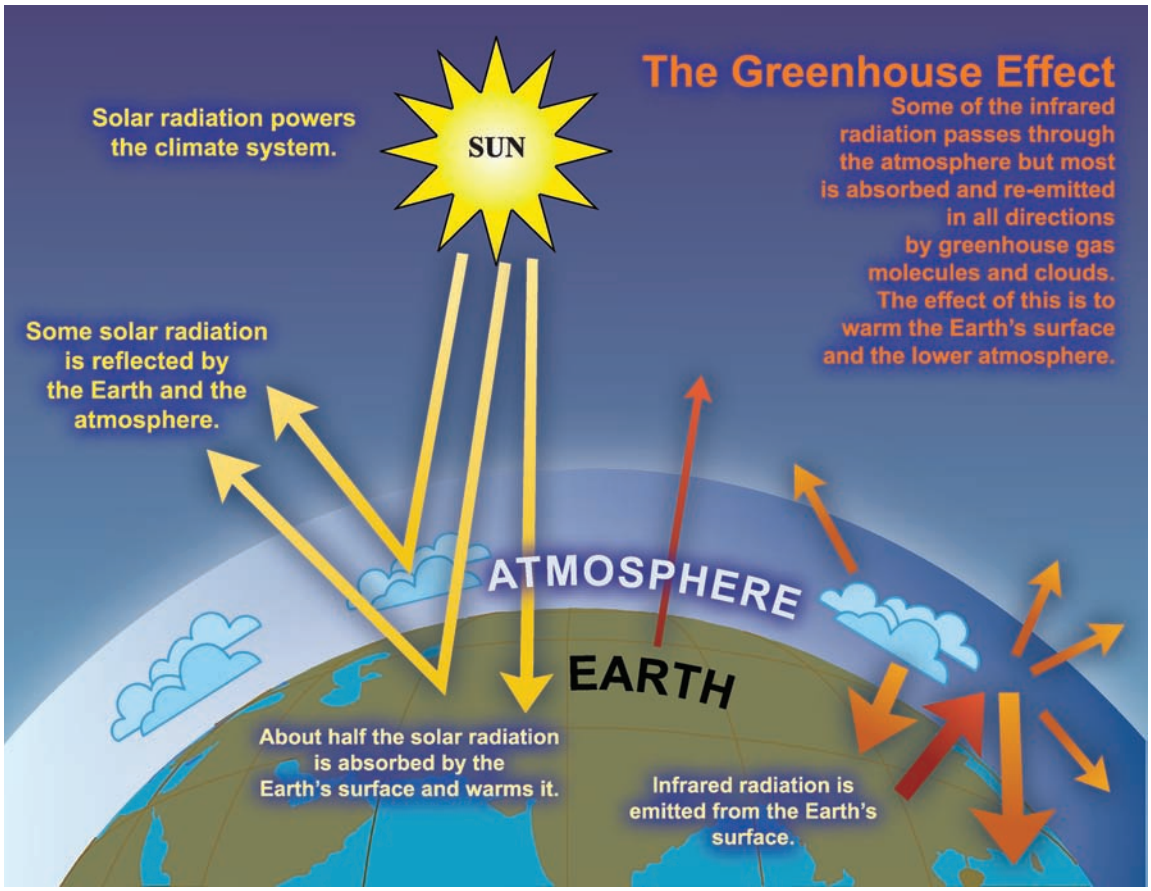
Frequently Asked Question 1.3

What is the Greenhouse Effect?

The Sun powers Earth's climate, radiating energy at very short wavelengths, predominately in the visible or near-visible (e.g., ultraviolet) part of the spectrum. Roughly one-third of the solar energy that reaches the top of Earth's atmosphere is reflected directly back to space. The remaining two-thirds is absorbed by the surface and, to a lesser extent, by the atmosphere. To balance the absorbed incoming energy, the Earth must, on average, radiate the same amount of energy back to space. Because the Earth is much colder than the Sun, it radiates at much longer wavelengths, primarily in the infrared part of the spectrum (see Figure 1). Much of this thermal radiation emitted by the land and ocean is absorbed by the atmosphere, including clouds, and reradiated back to Earth. This is called the greenhouse effect. The glass walls in a greenhouse reduce airflow and increase the temperature of the air inside. Analogously, but through a different physical process, the Earth's greenhouse effect warms the surface of the planet. Without the natural greenhouse effect, the average temperature at Earth's surface would be below the freezing point of water. Thus, Earth's natural greenhouse effect makes life as we know it possible. However, human activities, primarily the burning of fossil fuels and clearing of forests, have greatly intensified the natural greenhouse effect, causing global warming.

The two most abundant gases in the atmosphere, nitrogen (comprising 78% of the dry atmosphere) and oxygen (comprising 21%), exert almost no greenhouse effect. Instead, the greenhouse effect comes from molecules that are more complex and much less common. Water vapour is the most important greenhouse gas, and carbon dioxide (CO_2) is the second-most important one. Methane, nitrous oxide, ozone and several other gases present in the atmosphere in small amounts also contribute to the greenhouse effect. In the humid equatorial regions, where there is so much water vapour in the air that the greenhouse effect is very large, adding a small additional amount of CO_2 or water vapour has only a small direct impact on downward infrared radiation. However, in the cold, dry polar regions, the effect of a small increase in CO_2 or

(continued)



FAQ 1.3, Figure 1. *An idealised model of the natural greenhouse effect. See text for explanation.*

water vapour is much greater. The same is true for the cold, dry upper atmosphere where a small increase in water vapour has a greater influence on the greenhouse effect than the same change in water vapour would have near the surface.

Several components of the climate system, notably the oceans and living things, affect atmospheric concentrations of greenhouse gases. A prime example of this is plants taking CO_2 out of the atmosphere and converting it (and water) into carbohydrates via photosynthesis. In the industrial era, human activities have added greenhouse gases to the atmosphere, primarily through the burning of fossil fuels and clearing of forests.

Adding more of a greenhouse gas, such as CO_2, to the atmosphere intensifies the greenhouse effect, thus warming Earth's climate. The amount of warming depends on various feedback mechanisms. For example, as the atmosphere warms due to rising levels of greenhouse gases, its concentration of water vapour increases, further intensifying the greenhouse effect. This in turn causes more warming, which causes an additional increase in water vapour, in a self-reinforcing cycle. This water vapour feedback may be strong enough to approximately double the increase in the greenhouse effect due to the added CO_2 alone.

Additional important feedback mechanisms involve clouds. Clouds are effective at absorbing infrared radiation and therefore exert a large greenhouse effect, thus warming the Earth. Clouds are also effective at reflecting away incoming solar radiation, thus cooling the Earth. A change in almost any aspect of clouds, such as their type, location, water content, cloud altitude, particle size and shape, or lifetimes, affects the degree to which clouds warm or cool the Earth. Some changes amplify warming while others diminish it. Much research is in progress to better understand how clouds change in response to climate warming, and how these changes affect climate through various feedback mechanisms.

consistently obtained widely varying results by trying other techniques of incorporating cloud microphysical processes and their radiative interactions (e.g., Roeckner et al., 1987; Le Treut and Li, 1991), which differed from the approach of Senior and Mitchell (1993) through the treatment of partial cloudiness or mixed-phase properties. The model intercomparisons presented in the TAR showed no clear resolution of this unsatisfactory situation.

The scientific community realised long ago that using adequate data to constrain models was the only way to solve this problem. Using climate changes in the distant past to constrain the amplitude of cloud feedback has definite limitations (Ramstein et al., 1998). The study of cloud changes at decadal, interannual or seasonal time scales therefore remains a necessary path to constrain models. A long history of cloud observations now runs parallel to that of model development. Operational ground-based measurements, carried out for the purpose of weather prediction, constitute a valuable source of information that has been gathered and analysed by Warren et al. (1986, 1988). The International Satellite Cloud Climatology Project (ISCCP; Rossow and Schiffer, 1991) has developed an analysis of cloud cover and cloud properties using the measurements of operational meteorological satellites over a period of more than two decades. These data have been complemented by other satellite remote sensing data sets, such as those associated with the Nimbus-7 Temperature Humidity Infrared Radiometer (THIR) instrument (Stowe et al., 1988), with high-resolution spectrometers such as the High Resolution Infrared Radiation Sounder (HIRS) (Susskind et al., 1987), and with microwave absorption, as used by the Special Sensor Microwave/Imager (SSM/I). Chapter 8 provides an update of this ongoing observational effort.

A parallel effort has been carried out to develop a wider range of ground-based measurements, not only to provide an adequate reference for satellite observations, but also to make possible a detailed and empirically based analysis of the entire range of space and time scales involved in cloud processes. The longest-lasting and most comprehensive effort has been the Atmospheric Radiation Measurement (ARM) Program in the USA, which has established elaborately instrumented observational sites to monitor the full complexity of cloud systems on a long-term basis (Ackerman and Stokes, 2003). Shorter field campaigns dedicated to the observation of specific phenomena have also been established, such as the TOGA Coupled Ocean-Atmosphere Response Experiment (COARE) for convective systems (Webster and Lukas, 1992), or the Atlantic Stratocumulus Transition Experiment (ASTEX) for stratocumulus (Albrecht et al., 1995).

Observational data have clearly helped the development of models. The ISCCP data have greatly aided the development of cloud representations in climate models since the mid-1980s (e.g., Le Treut and Li, 1988; Del Genio et al., 1996). However, existing data have not yet brought about any reduction in the existing range of simulated cloud feedbacks. More recently, new theoretical tools have been developed to aid in validating parametrizations in a mode that emphasizes the role of cloud processes participating in climatic feedbacks. One such approach has been to focus on comprehensively observed episodes of cloudiness for which the large-scale forcing is observationally known, using single-column models (Randall et al., 1996; Somerville, 2000) and higher-resolution cloud-resolving models to evaluate GCM parametrizations. Another approach is to make use of the more global and continuous satellite data, on a statistical basis, through an investigation of the correlation between climate forcing and cloud parameters (Bony et al., 1997), in such a way as to provide a test of feedbacks between different climate variables. Chapter 8 assesses recent progress in this area.

1.5.3 Coupled Models: Evolution, Use, Assessment

The first National Academy of Sciences of the USA report on global warming (Charney et al., 1979), on the basis of two models simulating the impact of doubled atmospheric CO_2 concentrations, spoke of a range of global mean equilibrium surface temperature increase of between 1.5°C and 4.5°C, a range that has remained part of conventional wisdom at least as recently as the TAR. These climate projections, as well as those treated later in the comparison of three models by Schlesinger and Mitchell (1987) and most of those presented in the FAR, were the results of atmospheric models coupled with simple 'slab' ocean models (i.e., models omitting all changes in ocean dynamics).

The first attempts at coupling atmospheric and oceanic models were carried out during the late 1960s and early 1970s (Manabe and Bryan, 1969; Bryan et al., 1975; Manabe et al., 1975). Replacing 'slab' ocean models by fully coupled ocean-atmosphere models may arguably have constituted one of the most significant leaps forward in climate modelling during the last 20 years (Trenberth, 1993), although both the atmospheric and oceanic components themselves have undergone highly significant improvements. This advance has led to significant modifications in the patterns of simulated climate change, particularly in oceanic regions. It has also opened up the possibility of exploring transient climate scenarios, and it constitutes a step toward the development of comprehensive 'Earth-system models' that include explicit representations of chemical and biogeochemical cycles.

Throughout their short history, coupled models have faced difficulties that have considerably impeded their development, including: (i) the initial state of the ocean is not precisely known; (ii) a surface flux imbalance (in either energy, momentum or fresh water) much smaller than the observational accuracy is enough to cause a drifting of coupled GCM simulations into unrealistic states; and (iii) there is no direct stabilising feedback that can compensate for any errors in the simulated salinity. The strong emphasis placed on the realism of the simulated base state provided a rationale for introducing 'flux adjustments' or 'flux corrections' (Manabe and Stouffer, 1988; Sausen et al., 1988) in early simulations. These were essentially empirical corrections that could not be justified on physical principles, and that consisted of arbitrary additions of surface fluxes of heat and salinity in order to prevent the drift of the simulated climate away from a realistic state. The National Center for Atmospheric Research model may have been the first to realise non-flux-corrected coupled simulations systematically, and it was able to achieve simulations of climate change into the 21st century, in spite of a persistent drift that still affected many of its early simulations. Both the FAR and the SAR pointed out the apparent need for flux adjustments as a problematic feature of climate modelling (Cubasch et al., 1990; Gates et al., 1996).

By the time of the TAR, however, the situation had evolved, and about half the coupled GCMs assessed in the TAR did not employ flux adjustments. That report noted that 'some non-flux-adjusted models are now able to maintain stable climatologies of comparable quality to flux-adjusted models' (McAvaney et al., 2001). Since that time, evolution away from flux correction (or flux adjustment) has continued at some modelling centres, although a number of state-of-the-art models continue to rely on it. The design of the coupled model simulations is also strongly linked with the methods chosen for model initialisation. In flux-adjusted models, the initial ocean state is necessarily the result of preliminary and typically thousand-year-long simulations to bring the ocean model into equilibrium. Non-flux-adjusted models often employ a simpler procedure based on ocean observations, such as those compiled by Levitus et al. (1994), although some spin-up phase is even then necessary. One argument brought forward is that non-adjusted models made use of *ad hoc* tuning of radiative parameters (i.e., an implicit flux adjustment).

This considerable advance in model design has not diminished the existence of a range of model results. This is not a surprise, however, because it is known that climate predictions are intrinsically affected by uncertainty (Lorenz, 1963). Two distinct kinds of prediction problems were defined by Lorenz (1975). The first kind was defined as the prediction of the actual properties of the climate system in response to a given initial state. Predictions of the first kind are initial-value problems and, because of the nonlinearity and instability of the governing equations, such systems are not predictable indefinitely into the future. Predictions of the second kind deal with the determination of the response of the climate system to changes in the external forcings. These predictions are not concerned directly with the chronological evolution of the climate state, but rather with the long-term average of the statistical properties of climate. Originally, it was thought that predictions of the second kind do not at all depend on initial conditions. Instead, they are intended to determine how the statistical properties of the climate system (e.g., the average annual global mean temperature, or the expected number of winter storms or hurricanes, or the average monsoon rainfall) change as some external forcing parameter, for example CO_2 content, is altered. Estimates of future climate scenarios as a function of the concentration of atmospheric greenhouse gases are typical examples of predictions of the second kind. However, ensemble simulations show that the projections tend to form clusters around a number of attractors as a function of their initial state (see Chapter 10).

Uncertainties in climate predictions (of the second kind) arise mainly from model uncertainties and errors. To assess and disentangle these effects, the scientific community has organised a series of systematic comparisons of the different existing models, and it has worked to achieve an increase in the number and range of simulations being carried out in order to more fully explore the factors affecting the accuracy of the simulations.

An early example of systematic comparison of models is provided by Cess et al. (1989), who compared results of documented differences among model simulations in their

representation of cloud feedback to show how the consequent effects on atmospheric radiation resulted in different model response to doubling of the CO_2 concentration. A number of ambitious and comprehensive 'model intercomparison projects' (MIPs) were set up in the 1990s under the auspices of the World Climate Research Programme to undertake controlled conditions for model evaluation. One of the first was the Atmospheric Model Intercomparison Project (AMIP), which studied atmospheric GCMs. The development of coupled models induced the development of the Coupled Model Intercomparison Project (CMIP), which studied coupled ocean-atmosphere GCMs and their response to idealised forcings, such as a 1% yearly increase in the atmospheric CO_2 concentration. It proved important in carrying out the various MIPs to standardise the model forcing parameters and the model output so that file formats, variable names, units, etc., are easily recognised by data users. The fact that the model results were stored separately and independently of the modelling centres, and that the analysis of the model output was performed mainly by research groups independent of the modellers, has added confidence in the results. Summary diagnostic products such as the Taylor (2001) diagram were developed for MIPs.

The establishment of the AMIP and CMIP projects opened a new era for climate modelling, setting standards of quality control, providing organisational continuity and ensuring that results are generally reproducible. Results from AMIP have provided a number of insights into climate model behaviour (Gates et al., 1999) and quantified improved agreement between simulated and observed atmospheric properties as new versions of models are developed. In general, results of the MIPs suggest that the most problematic areas of coupled model simulations involve cloud-radiation processes, the cryosphere, the deep ocean and ocean-atmosphere interactions.

Comparing different models is not sufficient, however. Using multiple simulations from a single model (the so-called Monte Carlo, or ensemble, approach) has proved a necessary and complementary approach to assess the stochastic nature of the climate system. The first ensemble climate change simulations with global GCMs used a set of different initial and boundary conditions (Cubasch et al., 1994; Barnett, 1995). Computational constraints limited early ensembles to a relatively small number of samples (fewer than 10). These ensemble simulations clearly indicated that even with a single model a large spread in the climate projections can be obtained.

Intercomparison of existing models and ensemble model studies (i.e., those involving many integrations of the same model) are still undergoing rapid development. Running ensembles was essentially impossible until recent advances in computer power occurred, as these systematic comprehensive climate model studies are exceptionally demanding on computer resources. Their progress has marked the evolution from the FAR to the TAR, and is likely to continue in the years to come.

1.6 The IPCC Assessments of Climate Change and Uncertainties

The WMO and the United Nations Environment Programme (UNEP) established the IPCC in 1988 with the assigned role of assessing the scientific, technical and socioeconomic information relevant for understanding the risk of human-induced climate change. The original 1988 mandate for the IPCC was extensive: '(a) Identification of uncertainties and gaps in our present knowledge with regard to climate changes and its potential impacts, and preparation of a plan of action over the short-term in filling these gaps; (b) Identification of information needed to evaluate policy implications of climate change and response strategies; (c) Review of current and planned national/international policies related to the greenhouse gas issue; (d) Scientific and environmental assessments of all aspects of the greenhouse gas issue and the transfer of these assessments and other relevant information to governments and intergovernmental organisations to be taken into account in their policies on social and economic development and environmental programs.' The IPCC is open to all members of UNEP and WMO. It does not directly support new research or monitor climate-related data. However, the IPCC process of synthesis and assessment has often inspired scientific research leading to new findings.

The IPCC has three Working Groups and a Task Force. Working Group I (WGI) assesses the scientific aspects of the climate system and climate change, while Working Groups II (WGII) and III (WGIII) assess the vulnerability and adaptation of socioeconomic and natural systems to climate change, and the mitigation options for limiting greenhouse gas emissions, respectively. The Task Force is responsible for the IPCC National Greenhouse Gas Inventories Programme. This brief history focuses on WGI and how it has described uncertainty in the quantities presented (See Box 1.1).

A main activity of the IPCC is to provide on a regular basis an assessment of the state of knowledge on climate change, and this volume is the fourth such Assessment Report of WGI. The IPCC also prepares Special Reports and Technical Papers on topics for which independent scientific information and advice is deemed necessary, and it supports the United Nations Framework Convention on Climate Change (UNFCCC) through its work on methodologies for National Greenhouse Gas Inventories. The FAR played an important role in the discussions of the Intergovernmental Negotiating Committee for the UNFCCC. The UNFCCC was adopted in 1992 and entered into force in 1994. It provides the overall policy framework and legal basis for addressing the climate change issue.

The WGI FAR was completed under the leadership of Bert Bolin (IPCC Chair) and John Houghton (WGI Chair) in a plenary at Windsor, UK in May 1990. In a mere 365 pages with eight colour plates, it made a persuasive, but not quantitative, case for anthropogenic interference with the climate system. Most conclusions from the FAR were non-quantitative and

remain valid today (see also Section 1.4.4). For example, in terms of the greenhouse gases, 'emissions resulting from human activities are substantially increasing the atmospheric concentrations of the greenhouse gases: CO_2, CH_4, CFCs, N_2O' (see Chapters 2 and 3; Section 7.1). On the other hand, the FAR did not foresee the phase-out of CFCs, missed the importance of biomass-burning aerosols and dust to climate and stated that unequivocal detection of the enhanced greenhouse effect was more than a decade away. The latter two areas highlight the advance of climate science and in particular the merging of models and observations in the new field of detection and attribution (see Section 9.1).

The Policymakers Summary of the WGI FAR gave a broad overview of climate change science and its Executive Summary separated key findings into areas of varying levels of confidence ranging from 'certainty' to providing an expert 'judgment'. Much of the summary is not quantitative (e.g., the radiative forcing bar charts do not appear in the summary). Similarly, scientific uncertainty is hardly mentioned; when ranges are given, as in the projected temperature increases of 0.2°C to 0.5°C per decade, no probability or likelihood is assigned to explain the range (see Chapter 10). In discussion of the climate sensitivity to doubled atmospheric CO_2 concentration, the combined subjective and objective criteria are explained: the range of model results was 1.9°C to 5.2°C; most were close to 4.0°C; but the newer model results were lower; and hence the best estimate was 2.5°C with a range of 1.5°C to 4.5°C. The likelihood of the value being within this range was not defined. However, the importance of identifying those areas where climate scientists had high confidence was recognised in the Policymakers Summary.

The Supplementary Report (IPCC, 1992) re-evaluated the RF values of the FAR and included the new IPCC scenarios for future emissions, designated IS92a–f. It also included updated chapters on climate observations and modelling (see Chapters 3, 4, 5, 6 and 8). The treatment of scientific uncertainty remained as in the FAR. For example, the calculated increase in global mean surface temperature since the 19th century was given as 0.45°C ± 0.15°C, with no quantitative likelihood for this range (see Section 3.2).

The SAR, under Bert Bolin (IPCC Chair) and John Houghton and Gylvan Meira Filho (WGI Co-chairs), was planned with and coupled to a preliminary Special Report (IPCC, 1995) that contained intensive chapters on the carbon cycle, atmospheric chemistry, aerosols and radiative forcing. The WGI SAR culminated in the government plenary in Madrid in November 1995. The most cited finding from that plenary, on attribution of climate change, has been consistently reaffirmed by subsequent research: 'The balance of evidence suggests a discernible human influence on global climate' (see Chapter 9). The SAR provided key input to the negotiations that led to the adoption in 1997 of the Kyoto Protocol to the UNFCCC.

Uncertainty in the WGI SAR was defined in a number of ways. The carbon cycle budgets used symmetric plus/minus ranges explicitly defined as 90% confidence intervals, whereas the RF bar chart reported a 'mid-range' bar along with a plus/minus range that was estimated largely on the spread of published values. The likelihood, or confidence interval, of the spread of published results was not given. These uncertainties were additionally modified by a declaration that the confidence of the RF being within the specified range was indicated by a stated confidence level that ranged from 'high' (greenhouse gases) to 'very low' (aerosols). Due to the difficulty in approving such a long draft in plenary, the Summary for Policy Makers (SPM) became a short document with no figures and few numbers. The use of scientific uncertainty in the SPM was thus limited and similar to the FAR: a range in the mean surface temperature increase since 1900 was given as 0.3°C to 0.6°C with no explanation as to likelihood of this range. While the underlying report showed projected future warming for a range of different climate models, the Technical Summary focused on a central estimate.

The IPCC Special Report on Aviation and the Global Atmosphere (IPCC, 1999) was a major interim assessment involving both WGI and WGIII and the Scientific Assessment Panel to the Montreal Protocol on Substances that Deplete the Ozone Layer. It assessed the impacts of civil aviation in terms of climate change and global air quality as well as looking at the effect of technology options for the future fleet. It was the first complete assessment of an industrial sub-sector. The summary related aviation's role relative to all human influence on the climate system: 'The best estimate of the radiative forcing in 1992 by aircraft is 0.05 W m^{-2} or about 3.5% of the total radiative forcing by all anthropogenic activities.' The authors took a uniform approach to assigning and propagating uncertainty in these RF values based on mixed objective and subjective criteria. In addition to a best value, a two-thirds likelihood (67% confidence) interval is given. This interval is similar to a one-sigma (i.e., one standard deviation) normal error distribution, but it was explicitly noted that the probability distribution outside this interval was not evaluated and might not have a normal distribution. A bar chart with 'whiskers' (two-thirds likelihood range) showing the components and total (without cirrus effects) RF for aviation in 1992 appeared in the SPM (see Sections 2.6 and 10.2).

The TAR, under Robert Watson (IPCC Chair) and John Houghton and Ding YiHui (WGI Co-chairs), was approved at the government plenary in Shanghai in January 2001. The predominant summary statements from the TAR WGI strengthened the SAR's attribution statement: 'An increasing body of observations gives a collective picture of a warming world and other changes in the climate system', and 'There is new and stronger evidence that most of the warming observed over the last 50 years is attributable to human activities.' The TAR Synthesis Report (IPCC, 2001b) combined the assessment reports from the three Working Groups. By combining data on global (WGI) and regional (WGII) climate change, the Synthesis Report was able to strengthen the conclusion regarding human influence: 'The Earth's climate system has demonstrably changed on both global and regional scales since the pre-industrial era, with some of these changes attributable to human activities' (see Chapter 9).

Box 1.1: Treatment of Uncertainties in the Working Group I Assessment

The importance of consistent and transparent treatment of uncertainties is clearly recognised by the IPCC in preparing its assessments of climate change. The increasing attention given to formal treatments of uncertainty in previous assessments is addressed in Section 1.6. To promote consistency in the general treatment of uncertainty across all three Working Groups, authors of the Fourth Assessment Report have been asked to follow a brief set of guidance notes on determining and describing uncertainties in the context of an assessment .[1] This box summarises the way that Working Group I has applied those guidelines and covers some aspects of the treatment of uncertainty specific to material assessed here.

Uncertainties can be classified in several different ways according to their origin. Two primary types are 'value uncertainties' and 'structural uncertainties'. Value uncertainties arise from the incomplete determination of particular values or results, for example, when data are inaccurate or not fully representative of the phenomenon of interest. Structural uncertainties arise from an incomplete understanding of the processes that control particular values or results, for example, when the conceptual framework or model used for analysis does not include all the relevant processes or relationships. Value uncertainties are generally estimated using statistical techniques and expressed probabilistically. Structural uncertainties are generally described by giving the authors' collective judgment of their confidence in the correctness of a result. In both cases, estimating uncertainties is intrinsically about describing the limits to knowledge and for this reason involves expert judgment about the state of that knowledge. A different type of uncertainty arises in systems that are either chaotic or not fully deterministic in nature and this also limits our ability to project all aspects of climate change.

The scientific literature assessed here uses a variety of other generic ways of categorising uncertainties. Uncertainties associated with 'random errors' have the characteristic of decreasing as additional measurements are accumulated, whereas those associated with 'systematic errors' do not. In dealing with climate records, considerable attention has been given to the identification of systematic errors or unintended biases arising from data sampling issues and methods of analysing and combining data. Specialised statistical methods based on quantitative analysis have been developed for the detection and attribution of climate change and for producing probabilistic projections of future climate parameters. These are summarised in the relevant chapters.

The uncertainty guidance provided for the Fourth Assessment Report draws, for the first time, a careful distinction between levels of confidence in scientific understanding and the likelihoods of specific results. This allows authors to express high confidence that an event is extremely unlikely (e.g., rolling a dice twice and getting a six both times), as well as high confidence that an event is about as likely as not (e.g., a tossed coin coming up heads). Confidence and likelihood as used here are distinct concepts but are often linked in practice.

The standard terms used to define levels of confidence in this report are as given in the IPCC Uncertainty Guidance Note, namely:

Confidence Terminology	Degree of confidence in being correct
Very high confidence	At least 9 out of 10 chance
High confidence	About 8 out of 10 chance
Medium confidence	About 5 out of 10 chance
Low confidence	About 2 out of 10 chance
Very low confidence	Less than 1 out of 10 chance

Note that 'low confidence' and 'very low confidence' are only used for areas of major concern and where a risk-based perspective is justified.

Chapter 2 of this report uses a related term 'level of scientific understanding' when describing uncertainties in different contributions to radiative forcing. This terminology is used for consistency with the Third Assessment Report, and the basis on which the authors have determined particular levels of scientific understanding uses a combination of approaches consistent with the uncertainty guidance note as explained in detail in Section 2.9.2 and Table 2.11.

[1] See Supplementary Material for this report

The standard terms used in this report to define the likelihood of an outcome or result where this can be estimated probabilistically are:

Likelihood Terminology	Likelihood of the occurrence/ outcome
Virtually certain	> 99% probability
Extremely likely	> 95% probability
Very likely	> 90% probability
Likely	> 66% probability
More likely than not	> 50% probability
About as likely as not	33 to 66% probability
Unlikely	< 33% probability
Very unlikely	< 10% probability
Extremely unlikely	< 5% probability
Exceptionally unlikely	< 1% probability

The terms 'extremely likely', 'extremely unlikely' and 'more likely than not' as defined above have been added to those given in the IPCC Uncertainty Guidance Note in order to provide a more specific assessment of aspects including attribution and radiative forcing.

Unless noted otherwise, values given in this report are assessed best estimates and their uncertainty ranges are 90% confidence intervals (i.e., there is an estimated 5% likelihood of the value being below the lower end of the range or above the upper end of the range). Note that in some cases the nature of the constraints on a value, or other information available, may indicate an asymmetric distribution of the uncertainty range around a best estimate.

In an effort to promote consistency, a guidance paper on uncertainty (Moss and Schneider, 2000) was distributed to all Working Group authors during the drafting of the TAR. The WGI TAR made some effort at consistency, noting in the SPM that when ranges were given they generally denoted 95% confidence intervals, although the carbon budget uncertainties were specified as ±1 standard deviation (68% likelihood). The range of 1.5°C to 4.5°C for climate sensitivity to atmospheric CO_2 doubling was reiterated but with no confidence assigned; however, it was clear that the level of scientific understanding had increased since that same range was first given in the Charney et al. (1979) report. The RF bar chart noted that the RF components could not be summed (except for the long-lived greenhouse gases) and that the 'whiskers' on the RF bars each meant something different (e.g., some were the range of models, some were uncertainties). Another failure in dealing with uncertainty was the projection of 21st-century warming: it was reported as a range covering (i) six Special Report on Emission Scenarios (SRES) emissions scenarios and (ii) nine atmosphere-ocean climate models using two grey envelopes without estimates of likelihood levels. The full range (i.e., scenario plus climate model range) of 1.4°C to 5.8°C is a much-cited finding of the WGI TAR but the lack of discussion of associated likelihood in the report makes the interpretation and useful application of this result difficult.

1.7 Summary

As this chapter shows, the history of the centuries-long effort to document and understand climate change is often complex, marked by successes and failures, and has followed a very uneven pace. Testing scientific findings and openly discussing the test results have been the key to the remarkable progress that is now accelerating in all domains, in spite of inherent limitations to predictive capacity. Climate change science is now contributing to the foundation of a new interdisciplinary approach to understanding our environment. Consequently, much published research and many notable scientific advances have occurred since the TAR, including advances in the understanding and treatment of uncertainty. Key aspects of recent climate change research are assessed in Chapters 2 through 11 of this report.

References

Abbot, C.G., 1910: The solar constant of radiation. *Smithsonian Institution Annual Report*, p. 319.

Ackerman, T., and G. Stokes, 2003: The Atmospheric Radiation Measurement Program. *Phys. Today*, **56**, 38–44.

Adkins, J.F., et al., 1998: Deep-sea coral evidence for rapid change in ventilation of the deep North Atlantic 15,400 years ago. *Science*, **280**, 725–728.

Agassiz, L., 1837: Discours d'ouverture sur l'ancienne extension des glaciers. *Société Helvétique des Sciences Naturelles*, Neufchâtel.

Albrecht, B.A., et al., 1995: The Atlantic Stratocumulus Transition Experiment – ASTEX. *Bull. Am. Meteorol. Soc*., **76**, 889–904.

Alley, R.B., et al., 1993: Abrupt increase in Greenland snow accumulation at the end of the Younger Dryas event. *Nature*, **362**, 527–529.

Arrhenius, S., 1896: On the influence of carbonic acid in the air upon the temperature on the ground, *Philos. Mag.*, **41**, 237–276.

Aßmann, R., 1902: Über die Existenz eines wärmeren Luftstromes in der Höhe von 10 bis 15 km. *Sitzungsbericht der Königlich-Preußischen Akademie der Wissenschaften zu Berlin, Sitzung der physikalisch-mathematischen Klasse vom 1. Mai 1902*, **XXIV**, 1–10.

Balachandran, N.K., and D. Rind, 1995: Modeling the effects of UV-variability and the QBO on the troposphere-stratosphere system. Part I: The middle atmosphere. *J. Clim.*, **8**, 2058–2079.

Barnett, T.P., 1995: Monte Carlo climate forecasting. *J. Clim.*, **8**, 1005–1022.

Barnett, T.P., et al., 1999: Detection and attribution of recent climate change: A status report. *Bull. Am. Meteorol. Soc.*, **80**, 2631–2660.

Barnola, J.-M., D. Raynaud, Y.S. Korotkevich, and C. Lorius, 1987: Vostok ice core provides 160,000-year record of atmospheric CO_2. *Nature*, **329**, 408–414.

Battle, M., et al., 1996: Atmospheric gas concentrations over the past century measured in air from firn at South Pole. *Nature*, **383**, 231–235.

Bender, M., et al., 1996: Variability in the O-2/N-2 ratio of southern hemisphere air, 1991-1994: Implications for the carbon cycle. *Global Biogeochem. Cycles*, **1**, 9–21.

Berger, A., M.F. Loutre, and H. Gallée, 1998: Sensitivity of the LLN climate model to the astronomical and CO_2 forcings over the last 200 kyr. *Clim. Dyn.*, **14**, 615–629.

Berner, W., H. Oeschger, and B. Stauffer, 1980: Information on the CO_2 cycle from ice core studies. *Radiocarbon*, **22**, 227–235.

Berson, A., and R. Süring, 1901: Ein ballonaufstieg bis 10 500m. *Illustrierte Aeronautische Mitteilungen*, Heft 4, 117–119.

Birchfield, G.E., H. Wang, and M. Wyant, 1990: A bimodal climate response controlled by water vapor transport in a coupled ocean-atmosphere box model. *Paleoceanography*, **5**, 383–395.

Bjerknes, J., 1964: Atlantic air-sea interaction. *Adv. Geophys*., **10**, 1–82.

Bjerknes, J., 1969: Atmospheric teleconnections from the equatorial Pacific. *Mon. Weather Rev.*, **97**, 163–172.

Blake, D.R., et al., 1982: Global increase in atmospheric methane concentrations between 1978 and 1980. *Geophys. Res. Lett.*, **9**, 477–480.

Blunier, T., et al., 1998: Asynchrony of Antarctic and Greenland climate change during the last glacial period. *Nature*, **394**, 739–743.

Bond, G., et al., 1992: Evidence for massive discharges of icebergs into the glacial Northern Atlantic. *Nature*, **360**, 245–249.

Bony, S., K.-M. Lau, and Y.C. Sud, 1997: Sea surface temperature and large-scale circulation influences on tropical greenhouse effect and cloud radiative forcing. *J. Clim.*, **10**, 2055–2077.

Brasseur, G., 1993: The response of the middle atmosphere to long term and short term solar variability: A two dimensional model. *J. Geophys. Res.*, **28**, 23079–23090.

Brazdil, R., 1992: Reconstructions of past climate from historical sources in the Czech lands. In: *Climatic Variations and Forcing Mechanisms of the Last 2000 Years* [Jones, P.D., R.S. Bradley, and J. Jouzel (eds.)]. Springer Verlag, Berlin and Heidelberg, 649 pp.

Brewer, P.G., et al., 1983: A climatic freshening of the deep North Atlantic (north of 50° N) over the past 20 years. *Science*, **222**, 1237–1239.

Broecker, W.S., 1997: Thermohaline circulation, the Achilles heel of our climate system: will man-made CO_2 upset the current balance? *Science*, **278**, 1582–1588.

Broecker, W.S., and G.H. Denton, 1989: The role of ocean-atmosphere reorganizations in glacial cycles. *Geochim. Cosmochim. Acta*, **53**, 2465–2501.

Brohan P., et al., 2006: Uncertainty estimates in regional and global observed temperature changes: A new data set from 1850. *J. Geophys. Res.*, **111**, D12106, doi:10.1029/2005JD006548.

Bryan, F., 1986: High-latitude salinity effects and interhemispheric thermohaline circulations. *Nature*, **323**, 301–304.

Bryan, K., 1969: A numerical method for the study of the circulation of the world ocean. *J. Comput. Phys.*, **4**, 347–376.

Bryan, K., and M.J. Spelman, 1985: The ocean's response to a CO_2-induced warming. *J. Geophys. Res.*, **90**, 679–688.

Bryan, K., S. Manabe, and R.C. Pacanowski, 1975: A global ocean-atmosphere climate model. Part II. The oceanic circulation. *J. Phys. Oceanogr*., **5**, 30–46.

Bryson, R.A., and G.J. Dittberner, 1976: A non-equilibrium model of hemispheric mean surface temperature. *J. Atmos. Sci.*, **33**, 2094–2106.

Bryson, R.A., and G.J. Dittberner, 1977: Reply. *J. Atmos. Sci*., **34**, 1821–1824.

Budyko, M.I., 1969: The effect of solar radiation variations on the climate of the Earth. *Tellus*, **21**, 611–619.

Buys Ballot, C.H.D., 1872: *Suggestions on a Uniform System of Meteorological Observations*. Publication No. 37, Royal Netherlands Meteorological Institute, Utrecht, 56 pp.

Callendar, G.S., 1938: The artificial production of carbon dioxide and its influence on temperature. *Q. J. R. Meteorol. Soc.*, **64**, 223–237.

Callendar, G.S., 1961: Temperature fluctuations and trends over the Earth. *Q. J. R. Meteorol. Soc.*, **87**, 1–12.

Cane, M.A., S.C. Dolan, and S.E. Zebiak, 1986: Experimental forecasts of the El Niño. *Nature*, **321**, 827–832.

Cess, R.D., et al., 1989: Interpretation of cloud-climate feedback as produced by 14 atmospheric general circulation models. *Science*, **245**, 513–516.

Chamberlain, T.C., 1906: On a possible reversal of deep-sea circulation and its influence on geologic climates. *J. Geol.*, **14**, 371–372.

Charlson, R.J., J. Langner, and H. Rodhe, 1990: Sulfur, aerosol, and climate. *Nature*, **22**, 348.

Charney, J.G., et al., 1979: *Carbon Dioxide and Climate: A Scientific Assessment*. National Academy of Sciences, Washington, DC, 22 pp.

Clayton, H.H., 1927: *World Weather Records*. Smithsonian Miscellaneous Collection, Volume 79, Washington, DC, 1196 pp.

Cortijo, E., et al., 1999: Changes in meridional temperature and salinity gradients in the North Atlantic Ocean (30 degrees-72 degrees N) during the last interglacial period. *Paleoceanography*, **14**, 23–33.

Crease, J., 1962: Velocity measurements in the deep water of the western North Atlantic. *J. Geophys. Res.*, **67**, 3173–3176.

Croll, J., 1890: *Climate and Time in Their Geological Relations: A Theory of Secular Changes of the Earth's Climate*, 2nd ed. Appleton, New York, 577 pp.

Cubasch, U., and R. Voss, 2000: The influence of total solar irradiance on climate. *Space Sci. Rev.*, **94**, 185–198.

Cubasch, U., et al., 1990: Processes and modelling. In: *Climate Change: The IPCC Scientific Assessment* [Houghton, J.T., G.J. Jenkins, and J.J. Ephraums (eds.)]. Cambridge University Press, Cambridge, United Kingdom and New York, NY, USA, pp. 69–91.

Cubasch, U., et al., 1994: Monte Carlo climate change forecasts with a global coupled ocean-atmosphere model. *Clim. Dyn.*, **10**, 1–19.

Cubasch, U., et al., 1997: Simulation with an O-AGCM of the influence of variations of the solar constant on the global climate. *Clim. Dyn.*, **13**, 757–767.

Dansgaard, W., et al., 1984: North Atlantic climatic oscillations revealed by deep Greenland ice cores. In: *Climate Processes and Climate Sensitivity* [Hansen, J.E., and T. Takahashi (eds.)]. American Geophysical Union, Washington, DC, pp. 288–298.

Dansgaard, W., et al., 1993: Evidence for general instability of past climate from a 250-kyr ice-core record. *Nature*, **364**, 218–220.

Del Genio, A.D., M.-S. Yao, W. Kovari, and K.K.-W. Lo, 1996: A prognostic cloud water parameterization for global climate models. *J. Clim.*, **9**, 270–304, doi:10.1175/1520-0442.

Delmas, R.J., J.M. Ascencio, and M. Legrand, 1980: Polar ice evidence that atmospheric CO_2 20,000 yr BP was 50% of present. *Nature*, **284**, 155–157.

deMenocal, P.B., 2001: Cultural responses during the late Holocene. *Science*, **292**, 667–673.

Derwent, R., 1990: *Trace Gases and Their Relative Contribution to the Greenhouse Effect*. Report AERE- R13716, Atomic Energy Research Establishment, Harwell, Oxon, UK. 95 pp.

Dlugokencky, E.J., K.A. Masarie, P.M. Lang, and P.P. Tans, 1998: Continuing decline in the growth rate of the atmospheric methane burden. *Nature*, **393**, 447–450.

Dove, H.W., 1852: Über die geographische Verbreitung gleichartiger Witterungserscheinungen (Über die nichtperiodischen Änderungen der Temperaturverteilung auf der Oberfläche der Erde). *Abh. Akad. Wiss. Berlin*, V Teil, **42**, 3–4.

Dozier, J., S.R. Schneider, and D.F. McGinnis Jr., 1981: Effect of grain size and snowpack water equivalence on visible and near-infrared satellite observations of snow. *Water Resour. Res.*, **17**, 1213–1221.

Dunbar, R.B., and G.M. Wellington, 1981: Stable isotopes in a branching coral monitor seasonal temperature variation. *Nature*, **298**, 453–455.

Eddy, J.A., 1976: The Maunder Minimum. *Science*, **192**, 1189–1202

Emiliani, C., 1955: Pleistocene temperatures. *J. Geol.*, **63**, 538–578.

Emiliani, C., 1969: Interglacials, high sea levels and the control of Greenland ice by the precession of the equinoxes. *Science*, **166**, 1503–1504.

Etheridge, D.M., et al., 1996: Natural and anthropogenic changes in atmospheric CO_2 over the last 1000 years from air in Antarctic ice and firn. *J. Geophys. Res*., **101**, 4115–4128.

Ewing, M., and W.L. Donn, 1956: A theory of ice ages. *Science*, **123**, 1061–1065.

Exner, F.M., 1913: Übermonatliche Witterungsanomalien auf der nördlichen Erdhälfte im Winter. *Sitzungsberichte d. Kaiserl, Akad. der Wissenschaften*, **122**, 1165–1241.

Exner, F.M., 1924: Monatliche Luftdruck- und Temperaturanomalien auf der Erde. *Sitzungsberichte d. Kaiserl, Akad. der Wissenschaften*, **133**, 307–408.

Fleming, J.R., 1998: *Historical Perspectives on Climate Change*. Oxford University Press, New York, 208pp.

Flückiger, J., et al., 1999: Variations in atmospheric N_2O concentration during abrupt climatic changes. *Science*, **285**, 227–230.

Folland, C.K., and D.E. Parker, 1995: Correction of instrumental biases in historical sea surface temperature data. *Q. J. R. Meteorol. Soc.*, **121**, 319–367.

Foukal, P.V., P.E. Mack, and J.E. Vernazza, 1977: The effect of sunspots and faculae on the solar constant. *Astrophys. J.*, **215**, 952-959.

Francey, R.J., and G.D. Farquhar, 1982: An explanation of C-13/C-12 variations in tree rings. *Nature*, **297**, 28–31.

Fraser, P.J., M.A.K. Khalil, R.A. Rasmussen, and A.J. Crawford, 1981: Trends of atmospheric methane in the southern hemisphere. *Geophys. Res. Lett*., **8**, 1063–1066.

Fritts, H.C., 1962: An approach to dendroclimatology: screening by means of multiple regression techniques. *J. Geophys. Res*., **67**, 1413–1420.

Gates, W.L., et al., 1996: Climate models – evaluation. In: *Climate 1995: The Science of Climate Change* [Houghton, J.T., et al. (eds.)]. Cambridge University Press, Cambridge, United Kingdom and New York, NY, USA, pp. 229–284.

Gates, W.L., et al., 1999: An overview of the results of the Atmospheric Model Intercomparison Project (AMIP I). *Bull. Am. Meteorol. Soc.*, **80**, 29–55.

Geerts, B., 1999: Trends in atmospheric science journals. *Bull. Am. Meteorol. Soc.*, **80**, 639–652.

Grootes, P.M., et al., 1993: Comparison of oxygen isotope records from the GISP2 and GRIP Greenland ice cores. *Nature*, **366**, 552–554.

Ghil, M., 1989: Deceptively-simple models of climatic change. In: *Climate and Geo-Sciences* [Berger, A., J.-C. Duplessy, and S.H. Schneider (eds.)]. D. Reidel, Dordrecht, Netherlands and Hingham, MA, pp. 211–240.

Graedel, T.E., and J.E. McRae, 1980: On the possible increase of atmospheric methane and carbon monoxide concentrations during the last decade. *Geophys. Res. Lett*., **7**, 977–979.

Gwynne, P., 1975: The cooling world. *Newsweek*, April 28, 64.

Haigh, J., 1996: The impact of solar variability on climate. *Science*, **272**, 981–985.

Hansen, J., and S. Lebedeff, 1987: Global trends of measured surface air temperature. *J. Geophys. Res.*, **92**, 13345–13372.

Hansen, J., A. Lacis, R. Ruedy, and M. Sato, 1992: Potential climate impact of Mount-Pinatubo eruption. *Geophys. Res. Lett*., **19**, 215–218.

Hansen, J., et al., 1981: Climate impact of increasing atmospheric carbon dioxide. *Science*, **213**, 957–966.

Hansen, J., et al., 1984: Climate sensitivity: Analysis of feedback mechanisms. In: *Climate Processes and Climate Sensitivity* [Hansen, J.E., and T. Takahashi (eds.)]. Geophysical Monograph 29, American Geophysical Union, Washington, DC, pp. 130–163.

Hansen, J., et al., 2001: A closer look at United States and global surface temperature change. *J. Geophys. Res.*, **106**, 23947–23963.

Harriss, R., K. Bartlett, S. Frolking, and P. Crill, 1993: Methane emissions from northern high-latitude wetlands. In: *Biogeochemistry of Global Change* [Oremland, R.S. (ed.)]. Chapman & Hall, New York, pp. 449–486.

Hasselmann, K., 1997: Multi-pattern fingerprint method for detection and attribution of climate change. *Clim. Dyn.*, **13**, 601–612.

Hawking, S., 1988: *A Brief History of Time.* Bantam Press, New York, 224 pp.

Hays, J.D., J. Imbrie, and N.J. Shackleton, 1976: Variations in the Earth's orbit: Pace-maker of the ice ages. *Science*, **194**, 1121–1132.

Hegerl, G.C., et al., 1996: Detecting greenhouse-gas-induced climate change with an optimal fingerprint method. *J. Clim.*, **9**, 2281–2306.

Hegerl, G.C., et al., 1997: Multi-fingerprint detection and attribution of greenhouse-gas and aerosol-forced climate change. *Clim. Dyn.*, **13**, 613–634.

Hegerl, G.C., et al., 2000: Optimal detection and attribution of climate change: Sensitivity of results to climate model differences. *Clim. Dyn.*, **16**, 737–754.

Held, I.M., 2005: The gap between simulation and understanding in climate modelling. *Bull. Am. Meteorol. Soc*., **86**, 1609–1614.

Herschel, W., 1801: Observations tending to investigate the nature of the sun, in order to find the causes or symptoms of its variable emission of light and heat. *Philos. Trans. R. Soc. London*, **91**, 265-318.

Hickey, J.R., et al., 1980: Initial solar irradiance determinations from Nimbus 7 cavity radiometer measurements. *Science*, **208**, 281–283.

Hildebrandsson, H.H., 1897: Quelques recherches sur les centres d'action de l'atmosphère. *Svenska Vet. Akad. Handlingar*, 36 pp.

Holton, J.R., 1992: *An Introduction to Dynamic Meteorology*, 3rd ed. Volume 48 of International Geophysics Series. Academic Press, San Diego, 511 pp.

Hoyt, D.V., and K.H. Schatten, 1993: A discussion of plausible solar irradiance variations 1700-1992. *J. Geophys. Res.*, **98**, 18895–18906

Hoyt, D.V., and K.H. Schatten, 1997: *The Role of the Sun in Climate Change*. Oxford University Press, Oxford, 279 pp.

Hoyt, D.V., K.H. Schatten, and E. Nesmes-Ribes, 1994: The hundredth year of Rudolf Wolf's death: Do we have the correct reconstruction of solar activity? *Geophys. Res. Lett.*, **21**, 2067–2070.

Hurrell, J.W., 1995: Decadal trends in the North Atlantic Oscillation: Regional temperatures and precipitation. *Science*, **269**, 676–679.

Imbrie, J., and K.P. Imbrie, 1979: *Ice Ages: Solving the Mystery*. Harvard University Press, Cambridge, 224pp.

Indermühle, A., et al., 1999: Holocene carbon-cycle dynamics based on CO_2 trapped in ice at Taylor Dome, Antarctica. *Nature*, **398**, 121–126.

IPCC, 1990: *Climate Change: The IPCC Scientific Assessment* [Houghton, J.T., G.J. Jenkins, and J.J. Ephraums (eds.)]. Cambridge University Press, Cambridge, United Kingdom and New York, NY, USA, 365 pp.

IPCC, 1992: *Climate Change 1992: The Supplementary Report to the IPCC Scientific Assessment* [Houghton, J.T., B.A. Callander, and S.K. Varney (eds.)]. Cambridge University Press, Cambridge, United Kingdom and New York, NY, USA, 200 pp.

IPCC, 1995: *Climate Change 1994: Radiative Forcing of Climate Change and an Evaluation of the IPCC IS92 Emission Scenarios* [Houghton, J.T., et al. (eds.)]. Cambridge University Press, Cambridge, United Kingdom and New York, NY, USA, 339 pp.

IPCC, 1996: *Climate Change 1995: The Science of Climate Change* [Houghton, J.T., et al. (eds.)]. Cambridge University Press, Cambridge, United Kingdom and New York, NY, USA, 572 pp.

IPCC, 1999: *Special Report on Aviation and the Global Atmosphere* [Penner, J.E., et al. (eds.)]. Cambridge University Press, Cambridge, United Kingdom and New York, NY, USA, 373 pp.

IPCC, 2001a: *Climate Change 2001: The Scientific Basis. Contribution of Working Group I to the Third Assessment Report of the Intergovernmental Panel on Climate Change* [Houghton, J.T., et al. (eds.)]. Cambridge University Press, Cambridge, United Kingdom and New York, NY, USA, 881 pp.

IPCC, 2001b: *Climate Change 2001: Synthesis Report. A contribution of Working Groups I, II, and III to the Third Assessment Report of the Intergovernmental Panel on Climate Change* [Watson, R.T., et al. (eds.)]. Cambridge University Press, Cambridge, United Kingdom and New York, NY, USA, 398 pp.

Jacob, D.J., et al., 1997: Evaluation and intercomparison of global atmospheric transport models using ^{222}Rn and other short-lived tracers. *J. Geophys. Res*., **102**, 5953–5970.

Johnsen, S.J., et al., 1992: Irregular glacial interstadials recorded in a new Greenland ice core. *Nature*, **359**, 311–313.

Jones, P.D., S.C.B. Raper, and T.M.L. Wigley, 1986a: Southern Hemisphere surface air temperature variations: 1851-1984. *J. Appl. Meteorol.*, **25**, 1213–1230.

Jones, P.D., et al., 1986b: Northern Hemisphere surface air temperature variations: 1851-1984. *J. Clim. Appl. Meteorol.*, **25**, 161–179.

Jones, P.D., et al., 1990: Assessment of urbanization effects in time series of surface air temperature over land. *Nature*, **347**, 169–172.

Jouzel, J., et al., 1987: Vostok ice core: a continuous isotope temperature record over the last climatic cycle (160,000 years). *Nature*, **329**, 402–408.

Jouzel, J., et al., 1993: Extending the Vostok ice-core record of palaeoclimate to the penultimate glacial period. *Nature*, **364**, 407–412.

Karl, T.R., H.F. Diaz, and G. Kukla, 1988: Urbanization: Its detection and effect in the United States climate record. *J. Clim.*, **1**, 1099–1123.

Keeling, C.D., 1961: The concentration and isotopic abundances of carbon dioxide in rural and marine air. *Geochim. Cosmochim. Acta*, **24**, 277–298.

Keeling, C.D., 1998: Rewards and penalties of monitoring the Earth. *Annu. Rev. Energy Environ.*, **23**, 25–82.

Keeling, R.F., and S.R. Shertz, 1992: Seasonal and interannual variations in atmospheric oxygen and implications for the global carbon-cycle. *Nature*, **358**, 723–727.

Kessler, E., 1969: *On the Distribution and Continuity of Water Substance in Atmospheric Circulation*. Meteorological Monograph Series, Vol. 10, No. 32, American Meteorological Society, Boston, MA, 84 pp.

Khalil, M.A.K., and R.A. Rasmussen, 1988: Nitrous oxide: Trends and global mass balance over the last 3000 years. *Ann. Glaciol.*, **10**, 73–79.

Kiehl, J., and K. Trenberth, 1997: Earth's annual global mean energy budget. *Bull. Am. Meteorol. Soc.*, **78**, 197–206.

Kington, J., 1988: *The Weather of the 1780s over Europe*. Cambridge University Press, Cambridge, UK, 164 pp.

Köppen, W., 1873: Über mehrjährige Perioden der Witterung, insbesondere über die 11-jährige Periode der Temperatur. *Zeitschrift der Österreichischen Gesellschaft für Meteorologie*, **Bd VIII**, 241–248 and 257–267.

Köppen, W., 1880: Kleinere Mittheilungen (Conferenz des permanenten internationalen Meteorologen-Comitè's). *Zeitschrift der Österreichischen Gesellschaft für Meteorologie*, **Bd XV**, 278–283.

Köppen, W., 1881: Über mehrjährige Perioden der Witterung – III. Mehrjährige Änderungen der Temperatur 1841 bis 1875 in den Tropen der nördlichen und südlichen gemässigten Zone, an den Jahresmitteln. untersucht. *Zeitschrift der Österreichischen Gesellschaft für Meteorologie*, **Bd XVI**, 141–150.

Kuhn, T.S., 1996: *The Structure of Scientific Revolutions,* 3rd edition. University of Chicago Press, Chicago, 226 pp.

Kvenvolden, K.A., 1988: Methane hydrate – a major reservoir of carbon in the shallow geosphere? *Chem. Geol.*, **71**, 41–51.

Kvenvolden, K.A., 1993: Gas hydrates – geological perspective and global change. *Rev. Geophys.*, **31**, 173–187.

Labitzke, K., and H. van Loon, 1997: The signal of the 11-year sunspot cycle in the upper troposphere-lower stratosphere. *Space Sci. Rev.*, **80**, 393–410.

Lacis, A.A., D.J. Wuebbles, and J.A. Logan, 1990: Radiative forcing of climate by changes in the vertical distribution of ozone. *J. Geophys. Res.*, **95**, 9971–9981.

Lamb, H.H., 1969: The new look of climatology. *Nature*, **223**, 1209–1215.

Landsberg, H.E., and J.M. Mitchell Jr., 1961: Temperature fluctuations and trends over the Earth. *Q. J. R. Meteorol. Soc.*, **87**, 435–436.

Langenfelds, R.L., et al., 1996: The Cape Grim Air Archive: The first seventeen years. In: *Baseline Atmospheric Program Australia, 1994-95* [Francey, R.J., A.L. Dick, and N. Derek (eds.)]. Bureau of Meteorology and CSIRO Division of Atmospheric Research, Melbourne, Australia**,** pp. 53–70.

Langley, S.P., 1876: Measurement of the direct effect of sun-spots on terrestrial climates. *Mon. Not. R. Astron. Soc.*, **37**, 5–11.

Langley, S.P., 1884: *Researches on the Solar Heat and its Absorption by the Earth's Atmosphere. A Report of the Mount Whitney Expedition*. Signal Service Professional Paper 15, Washington, DC.

Lazier, J.R.N., 1995: The salinity decrease in the Labrador Sea over the past thirty years. In: *Natural Climate Variability on Decade-to-Century Time Scales* [Martinson, D.G., et al. (eds.)]. National Academy Press, Washington, DC, pp. 295–302.

Le Treut, H., and Z.-X. Li, 1988: Using meteosat data to validate a prognostic cloud generation scheme. *Atmos. Res.*, **21**, 273–292.

Le Treut, H., and Z.-X. Li, 1991: Sensitivity of an atmospheric general circulation model to prescribed SST changes: feedback effects associated with the simulation of cloud optical properties. *Clim. Dyn.*, **5**, 175–187.

Lean, J., 1997: The sun's variable radiation and its relevance to Earth. *Annu. Rev. Astron. Astrophys*., **35**, 33–67.

Lean, J., and D. Rind, 1998: Climate forcing by changing solar radiation. *J. Clim.*, **11**, 3069–3093.

Lean, J., J. Beer, and R. Bradley, 1995: Reconstruction of solar irradiance since 1610: Implications for climate change. *Geophys. Res. Lett.*, **22**, 3195–3198.

Levitus, S., J. Antonov, and T. Boyer, 1994: Interannual variability of temperature at a depth of 125 m in the North Atlantic Ocean. *Science*, **266**, 96–99.

Lockyer, N., and W.J.S. Lockyer, 1902: On some phenomena which suggest a short period of solar and meteorological changes. *Proc. R. Soc. London*, **70**, 500–504.

London, J., 1957: *A Study of Atmospheric Heat Balance*. Final Report, Contract AF 19(122)-165, AFCRC-TR57-287, College of Engineering, New York University, New York, NY. 99 pp.

Lorenz, E.N., 1963: Deterministic nonperiodic flow. *J. Atmos. Sci.*, **20**, 130–141.

Lorenz, E.N., 1967: *On the Nature and Theory of the General Circulation of the Atmosphere*. Publication No. 218, World Meteorological Association, Geneva, 161 pp.

Lorenz, E.N., 1975: The physical bases of climate and climate modelling. In: *Climate Predictability*. GARP Publication Series 16, World Meteorological Association, Geneva, pp. 132–136.

Lovelock, J.E., 1971: Atmospheric fluorine compounds as indicators of air movements. *Nature*, **230**, 379–381.

Luterbacher, J., et al., 1999: Reconstruction of monthly NAO and EU indices back to AD 1675. *Geophys. Res. Lett*., **26**, 2745–2748.

MacDonald, G.J., 1990: Role of methane clathrates in past and future climates. *Clim. Change*, **16**, 247–281.

Machida, T., et al., 1995: Increase in the atmospheric nitrous oxide concentration during the last 250 years. *Geophys. Res. Lett.*, **22**, 2921–2924.

Madden, R.A., and V. Ramanathan, 1980: Detecting climate change due to increasing carbon dioxide. *Science*, **209**, 763–768.

Manabe, S., and K. Bryan, 1969: Climate calculations with a combined ocean-atmosphere model. *J. Atmos. Sci.*, **26**, 786–789.

Manabe, S., and R.T. Wetherald, 1975: The effects of doubling the CO_2 concentration on the climate of a general circulation model. *J. Atmos. Sci.*, **32**, 3–15.

Manabe, S., and R.J. Stouffer, 1988: Two stable equilibria of a coupled ocean-atmosphere model. *J. Clim.*, **1**, 841–866.

Manabe, S., K. Bryan, and M.J. Spelman, 1975: A global ocean-atmosphere climate model. Part I. The atmospheric circulation. *J. Phys. Oceanogr*., **5**, 3–29.

Mann, M.E., R.S. Bradley, and M.K. Hughes, 1998: Global-scale temperature patterns and climate forcing over the past six centuries. *Nature*, **392**, 779–787.

McAvaney, B.J., et al., 2001: Model evaluation. In: *Climate Change 2001: The Scientific Basis* [Houghton, J.T., et al. (eds.)]. Cambridge University Press, Cambridge, United Kingdom and New York, NY, USA, pp. 471–521.

McPhaden, M.J., et al., 1998: The Tropical Ocean – Global Atmosphere (TOGA) observing system: a decade of progress. *J. Geophys. Res*., **103**(C7), 14169–14240.

Mercer, J.H., 1968: Antarctic ice and Sangamon sea level. *Int. Assoc. Sci. Hydrol. Symp*., **79**, 217–225.

Mercer, J.H., 1978: West Antarctic ice sheet and CO_2 greenhouse effect: a threat of disaster. *Nature*, **271**, 321–325.

Milankovitch, M., 1941: *Kanon der Erdbestrahlungen und seine Anwendung auf das Eiszeitenproblem*. Belgrade. English translation by Pantic, N., 1998: *Canon of Insolation and the Ice Age Problem*. Alven Global, 636 pp.

Mitchell, J.M. Jr., 1963: On the world-wide pattern of secular temperature change. In: *Changes of Climate. Proceedings of the Rome Symposium Organized by UNESCO and the World Meteorological Organization, 1961*. Arid Zone Research Series No. 20, UNESCO, Paris, pp. 161–181.

Montzka, S. A., et al., 1999: Present and future trends in the atmospheric burden of ozone-depleting halogens. *Nature*, **398**, 690–694.

Moss, R., and S. Schneider, 2000: Uncertainties. In: *Guidance Papers on the Cross Cutting Issues of the Third Assessment Report of the IPCC* [Pachauri, R., T. Taniguchi, and K. Tanaka (eds.)]. Intergovernmental Panel on Climate Change, Geneva, pp. 33-51.

National Climatic Data Center, 2002: *Data Documentation for Data Set 9645 World Weather Records – NCAR Surface (World Monthly Surface Station Climatology)*. U.S. Department of Commerce, NOAA, National Climatic Data Center, Asheville, NC, 17 pp.

National Climatic Data Center, 2005: *World Meteorological Organization, World Weather Records, 1991-2000, Volumes I-VI*. U.S. Department of Commerce, NOAA, National Climatic Data Center, Asheville, NC, CD-ROM format.

Neftel, A., E. Moor, H. Oeschger, and B. Stauffer, 1985: Evidence from polar ice cores for the increase in atmospheric CO_2 in the past 2 centuries. *Nature*, **315**, 45–47.

Neftel, A., et al., 1982: Ice core sample measurements give atmospheric CO_2 content during the Past 40,000 Yr. *Nature*, **295**, 220–223.

Newton, I., 1675: Letter to Robert Hooke, February 5, 1675. In: Andrews, R., 1993: *The Columbia Dictionary of Quotations*. Columbia University Press, New York, 1090 pp.

Oeschger, H., et al., 1984: Late glacial climate history from ice cores. In: *Climate Processes and Climate Sensitivity* [Hansen, J.E., and T. Takahashi (eds.)]. American Geophysical Union, Washington, DC, pp. 299–306.

Olson, J., et al., 1997: Results from the Intergovernmental Panel on Climatic Change Photochemical Model Intercomparison (PhotoComp). *J. Geophys. Res*., **102**(D5), 5979–5991.

Oort, A.H., and T.H. Vonder Haar, 1976: On the observed annual cycle in the ocean-atmosphere heat balance over the Northern Hemisphere. *J. Phys. Oceanogr*., **6**, 781–800.

Parkinson, C.L., et al., 1987: *Arctic Sea Ice, 1973-1976: Satellite Passive-Microwave Observations*. NASA SP-489, National Aeronautics and Space Administration, Washington, DC, 296 pp.

Penner, J., R. Dickinson, and C. O'Neill, 1992: Effects of aerosol from biomass burning on the global radiation budget. *Science*, **256**, 1432–1434.

Peterson, T.C., et al., 1998: Homogeneity adjustments of in situ atmospheric climate data: A review. *Int. J. Climatol.*, **18**, 1493–1517.

Peterson, T.C., et al., 1999: Global rural temperature trends. *Geophys. Res. Lett.*, **26**, 329–332.

Petit, J.R., et al., 1999: Climate and atmospheric history of the past 420,000 years from the Vostok ice core, Antarctica. *Nature*, **399**, 429–436.

Pfister, C., 1992: Monthly temperature and precipitation in central Europe 1525-1979: quantifying documentary evidence on weather and its effects. In: *Climatic Variations and Forcing Mechanisms of the Last 2000 Years*. [Jones, P.D., R.S. Bradley, and J. Jouzel (eds.)]. Springer Verlag, Berlin and Heidelberg, 649 pp.

Pierrehumbert, R.T., 1995: Thermostats, radiator fins, and the local runaway greenhouse. *J. Atmos. Sci.*, **52**, 1784–1806.

Popper, K.R., 1934: *The Logic of Scientific Discovery*. English edition: Routledge, London (1992), 544 pp.

Prather, M., 1994: Lifetimes and eigenstates in atmospheric chemistry. *Geophys. Res. Lett*., **21**, 801–804.

Prinn, R.G., et al., 2000: A history of chemically and radiatively important gases in air deduced from ALE/GAGE/AGAGE. *J. Geophys. Res*., **105**, 17751–17792.

Pyle, J., et al., 1996: *Global Tracer Transport Models: Report of a Scientific Symposium, Bermuda, 10-13 Dec. 1990*. WCRP CAS/JSC Report No. 24 (World Meteorological Organization, TD-No.770, Geneva, Switzerland), 186 pp.

Quetelet, A., 1854: Rapport de la Conférence, tenue à Bruxelles, sur l'invitation du gouvernement des Etats-Unis d'Amérique, à l'effet de s'entendre sur un système uniform d'observations météorologiques à la mer. *Annuaire de l'Observatoire Royal de Belgique*, **21**, 155–167.

Ramanathan, V., 1975: Greenhouse effect due to chlorofluorocarbons: Climatic implications. *Science*, **190**, 50–52.

Ramstein, G., et al., 1998: Cloud processes associated with past and future climate changes, *Clim. Dyn.*, **14**, 233–247.

Randall, D.A., K.-M. Xu, R.C.J. Somerville, and S. Iacobellis, 1996: Single-column models and cloud ensemble models as links between observations and climate models. *J. Clim.*, **9**, 1683–1697.

Rasch, P.J., 2000: A comparison of scavenging and deposition processes in global models: results from the WCRP Cambridge Workshop of 1995. *Tellus*, **52B**, 1025–1056.

Reid, G.C., 1991: Solar irradiance variations and the global sea surface temperature record. *J. Geophys. Res.*, **96**, 2835–2844.

Revelle, R., and H.E. Suess, 1957: Carbon dioxide exchange between atmosphere and ocean and the question of an increase of atmospheric CO_2 during the past decades. *Tellus*, **9**, 18–27.

Reynolds, R.W., and T.M. Smith, 1994: Improved global sea surface temperature analyses using optimum interpolation. *J. Clim.*, **7**, 929–948.

Robock, A., 1982: The Russian surface temperature data set. *J. Appl. Meteorol.*, **21**, 1781–1785.

Roeckner, E., U. Schlese, J. Biercamp, and P. Loewe, 1987: Cloud optical depth feedbacks and climate modelling. *Nature*, **329**, 138–140.

Rossow, W.B., and R.A. Schiffer, 1991: ISCCP cloud data products. *Bull. Am. Meteorol. Soc.*, **72**, 2–20.

Rumford, B., Count, 1800: Essay VII. The propagation of heat in fluids. In: *Essays, Political, Economical, and Philosophical, A New Edition*. T. Cadell, Jr., and W. Davies. London, pp. 197–386. Also in: *Collected Works of Count Rumford, 1, The Nature of Heat* [Brown, S.C. (ed.)]. Harvard University Press, Cambridge, MA (1968), pp. 117–285.

Santer, B.D., J.S. Boyle, and D.E. Parker, 1996a: Human effect on global climate? Reply. *Nature*, **384**, 524.

Santer, B.D., T.M.L. Wigley, T.P. Barnett, and E. Anyamba, 1996b: Detection of climate change, and attribution of causes. In: *Climate Change 1995: The Science of Climate Change* [Houghton, J.T., et al. (eds.)]. Cambridge University Press, Cambridge, United Kingdom and New York, NY, USA, pp. 407–443.

Santer, B.D., et al., 1995: Towards the detection and attribution of an anthropogenic effect on climate. *Clim. Dyn.*, **12**, 77–100.

Santer, B.D., et al., 1996c: A search for human influences on the thermal structure of the atmosphere. *Nature*, **382**, 39–46.

Sausen, R., K. Barthel, and K. Hasselman, 1988: Coupled ocean-atmosphere models with flux correction. *Clim. Dyn.*, **2**, 145–163.

Schellnhuber, H.J., et al. (eds.), 2004: *Earth System Analysis for Sustainability*. MIT Press, Cambridge, MA, 352 pp.

Schlesinger, M.E., and J.F.B. Mitchell, 1987: Climate model simulations of the equilibrium climatic response to increased carbon-dioxide. *Rev. Geophys.*, **25**, 760–798.

Schwabe, S.H., 1844: Sonnen-Beobachtungen im Jahre 1843. *Astronomische Nachrichten*, **21**, 233.

Sellers, W.D., 1969: A climate model based on the energy balance of the Earth-atmosphere system. *J. Appl. Meteorol.*, **8**, 392–400.

Senior, C.A., and J.F.B. Mitchell, 1993: Carbon dioxide and climate: the impact of cloud parameterization. *J. Clim.*, **6**, 393–418.

Severinghaus, J.P., and E.J. Brook, 1999: Abrupt climate change at the end of the last glacial period inferred from trapped air in polar ice. *Science*, **286**, 930–934.

Shackleton, N., 1967: Oxygen isotope analyses and Pleistocene temperatures reassessed. *Nature*, **215**, 15–17.

Shackleton, N.J., M.A. Hall, and E. Vincent, 2000: Phase relationships between millennial-scale events 64,000–24,000 years ago. *Paleoceanography*, **15**, 565–569.

Slingo, J., 1987: The development and verification of a cloud prediction scheme for the ECMWF model. *Q. J. R. Meteorol. Soc.*, **113**, 899–927.

Somerville, R.C.J., 2000: Using single-column models to improve cloud-radiation parameterizations. In: *General Circulation Model Development: Past, Present and Futur*e [Randall, D.A. (ed.)]. Academic Press, San Diego and London, pp. 641–657.

Stanhill, G., 2001: The growth of climate change science: A scientometric study. *Clim. Change*, **48**, 515–524.

Steele, L.P., et al., 1996: Atmospheric methane, carbon dioxide, carbon monoxide, hydrogen, and nitrous oxide from Cape Grim air samples analysed by gas chromatography. In: *Baseline Atmospheric Program Australia, 1994-95* [Francey, R.J., A.L. Dick, and N. Derek (eds.)]. Bureau of Meteorology and CSIRO Division of Atmospheric Research, Melbourne, Australia, pp. 107–110.

Stephenson, D.B., H. Wanner, S. Brönnimann, and J. Luterbacher, 2003: The history of scientific research on the North Atlantic Oscillation. In: *The North Atlantic Oscillation: Climatic Significance and Environmental Impact* [Hurrell, J.W., et al. (eds.)]. Geophysical Monograph 134, American Geophysical Union, Washington, DC, doi:10.1029/134GM02.

Stocker, T.F., 1998: The seesaw effect. *Science*, **282**, 61–62.

Stommel, H., 1961: Thermohaline convection with two stable regimes of flow. *Tellus*, **13**, 224–230.

Stott, P.A., et al., 2000: External control of 20th century temperature by natural and anthropogenic forcings. *Science*, **290**, 2133–2137.

Stouffer, R.J., S. Manabe, and K.Y. Vinnikov, 1994: Model assessment of the role of natural variability in recent global warming. *Nature*, **367**, 634–636.

Stowe, L., et al., 1988: Nimbus-7 global cloud climatology. Part I: Algorithms and validation. *J. Clim.*, **1**, 445–470.

Sundqvist, H., 1978: A parametrization scheme for non-convective condensation including prediction of cloud water content. *Q. J. R. Meteorol. Soc.*, **104**, 677–690.

Susskind, J., D. Reuter, and M.T. Chahine, 1987: Clouds fields retrieved from HIRS/MSU data. *J. Geophys. Res.*, **92**, 4035–4050.

Sutton, R., and M. Allen, 1997: Decadal predictability of North Atlantic sea surface temperature and climate. *Nature*, **388**, 563–567.

Taylor, K.E., 2001: Summarizing multiple aspects of model performance in a single diagram. *J. Geophys. Res.*, **106**, 7183–7192.

Teisserenc de Bort, L.P., 1902: Variations de la température de l'air libre dans la zona comprise entre 8km et 13km d'altitude. *Comptes Rendus de l'Acad. Sci. Paris*, **134**, 987–989.

Tett, S.F.B., et al., 1999: Causes of twentieth century temperature change. *Nature*, **399**, 569–572.

Trenberth, K. (ed.), 1993: *Climate System Modeling*. Cambridge University Press, Cambridge, UK, 818 pp.

Tselioudis, G., and W.B. Rossow, 1994: Global, multiyear variations of optical thickness with temperature in low and cirrus clouds. *Geophys. Res. Lett.*, **21**, 2211–2214, doi:10.1029/94GL02004.

Twomey, S., 1977: Influence of pollution on shortwave albedo of clouds. *J. Atmos. Sci.*, **34**, 1149–1152.

Tyndall, J., 1861: On the absorption and radiation of heat by gases and vapours, and on the physical connection, *Philos. Mag.*, **22**, 277–302.

Van den Dool, H.M., H.J. Krijnen, and C.J.E. Schuurmans, 1978: Average winter temperatures at de Bilt (the Netherlands): 1634-1977. *Clim. Change*, **1**, 319–330.

Van Loon, H., and J. C. Rogers, 1978: The seesaw in winter temperatures between Greenland and northern Europe. Part 1: General descriptions. *Mon. Weather Rev.*, **106**, 296–310.

Van Loon, H., and K. Labitzke, 2000: The influence of the 11-year solar cycle on the stratosphere below 30 km: A review. *Space Sci. Rev.*, **94**, 259–278.

Vonder Haar, T.H., and V.E. Suomi, 1971: Measurements of the Earth's radiation budget from satellites during a five-year period. Part 1: Extended time and space means. *J. Atmos. Sci.*, **28**, 305–314.

Walker, G.T., 1924: Correlation in seasonal variation of weather. *IX Mem. Ind. Met. Dept.*, **25**, 275–332.

Walker, G.T., 1928: World weather: III. *Mem. Roy. Meteorol. Soc.*, **2**, 97–106.

Wallace, J.M., and D.S. Gutzler, 1981: Teleconnections in the geopotential height field during the Northern Hemisphere winter. *Mon. Weather Rev.*, **109**, 784–812.

Wallis, I., and I. Beale, 1669: Some observations concerning the baroscope and thermoscope, made and communicated by Doctor I. Wallis at Oxford, and Dr. I Beale at Yeovil in Somerset, deliver'd here according to the several dates, when they were imparted. Dr. Beale in those letters of his dated Decemb.18. Decemb. 29. 1669. and Januar. 3. 1670. *Philosophical Transactions (1665-1678)*, **4**, 1113–1120.

Wang, W. C., et al., 1976: Greenhouse effects due to man-made perturbations of trace gases. *Science*, **194**, 685–690.

Wanner, H., et al., 1995. Wintertime European circulation patterns during the late maunder minimum cooling period (1675-1704). *Theor. Appl. Climatol.*, **51**, 167–175.

Warren, B.A., 1981: Deep circulation of the World Ocean. In: *Evolution of Physical Oceanography* [Warren, B.A., and C. Wunsch (eds.)]. MIT Press, Cambridge, MA, pp. 6–41.

Warren, S.G., et al., 1986: *Global Distribution of Total Cloud Cover and Cloud Type Amounts Over Land*. DOE/ER/60085-H1, NCAR/TN-273 + STR, National Center for Atmospheric Research, Boulder, CO.

Warren, S.G., et al., 1988: *Global Distribution of Total Cloud Cover and Cloud Type Amounts Over the Ocean*. DOE/ER-0406, NCAR/FN-317 + STR, National Center for Atmospheric Research, Boulder, CO.

Weart, S., 2003: *The Discovery of Global Warming*. Harvard University Press, Cambridge, MA, 240 pp.

Weber, J.N., and P.M.J. Woodhead, 1972: Temperature dependence of oxygen-18 concentration in reef coral carbonates. *J. Geophys. Res*., **77**, 463–473.

Webster, P.J., and R. Lukas, 1992: TOGA-COARE: The coupled ocean-atmosphere response experiment. *Bull. Am. Meteorol. Soc*., **73**, 1377–1416.

Weiss, R.F., 1981: The temporal and spatial distribution of tropospheric nitrous oxide. *J. Geophys. Res*., **86**, 7185–7195.

Wetherald, R.T., and S. Manabe, 1975: The effects of changing solar constant on the climate of a general circulation model. *J. Atmos. Sci*., **32**, 2044–2059.

Wigley, T.M.L., and S.C.B. Raper, 1990: Natural variability of the climate system and detection of the greenhouse effect. *Nature*, **344**, 324–327.

Willett, H.C., 1950: Temperature trends of the past century. In: *Centenary Proceedings of the Royal Meteorological Society*. Royal Meteorological Society, London. pp. 195–206.

Willson, R.C., C.H. Duncan, and J. Geist, 1980: Direct measurements of solar luminosity variation. *Science*, **207**, 177–179.

Worley, S.J., et al., 2005: ICOADS release 2.1 data and products. *Int. J. Climatol.*, **25**, 823–842.

Woronko, S.F., 1977: Comments on "a non-equilibrium model of hemispheric mean surface temperature". *J. Atmos. Sci.*, **34**, 1820–1821.

Wunsch, C., 1978: The North Atlantic general circulation west of 50°W determined by inverse methods. *Rev. Geophys. Space Phys.*, **16**, 583–620.

Wyrtki, K., 1975: El Niño – the dynamic response of the equatorial Pacific Ocean to atmospheric forcing. *J. Phys. Oceanogr*., **5**, 572–584.

Zebiak, S.E., and M.A. Cane, 1987: A model El Nino-Southern Oscillation. *Mon. Weather Rev*., **115**, 2262–2278.

Zhu, K., 1973: A preliminary study on the climate changes since the last 5000 years in China. *Science in China*, **2**, 168–189.

2

Changes in Atmospheric Constituents and in Radiative Forcing

Coordinating Lead Authors:

Piers Forster (UK), Venkatachalam Ramaswamy (USA)

Lead Authors:

Paulo Artaxo (Brazil), Terje Berntsen (Norway), Richard Betts (UK), David W. Fahey (USA), James Haywood (UK), Judith Lean (USA), David C. Lowe (New Zealand), Gunnar Myhre (Norway), John Nganga (Kenya), Ronald Prinn (USA, New Zealand), Graciela Raga (Mexico, Argentina), Michael Schulz (France, Germany), Robert Van Dorland (Netherlands)

Contributing Authors:

G. Bodeker (New Zealand), O. Boucher (UK, France), W.D. Collins (USA), T.J. Conway (USA), E. Dlugokencky (USA), J.W. Elkins (USA), D. Etheridge (Australia), P. Foukal (USA), P. Fraser (Australia), M. Geller (USA), F. Joos (Switzerland), C.D. Keeling (USA), R. Keeling (USA), S. Kinne (Germany), K. Lassey (New Zealand), U. Lohmann (Switzerland), A.C. Manning (UK, New Zealand), S. Montzka (USA), D. Oram (UK), K. O'Shaughnessy (New Zealand), S. Piper (USA), G.-K. Plattner (Switzerland), M. Ponater (Germany), N. Ramankutty (USA, India), G. Reid (USA), D. Rind (USA), K. Rosenlof (USA), R. Sausen (Germany), D. Schwarzkopf (USA), S.K. Solanki (Germany, Switzerland), G. Stenchikov (USA), N. Stuber (UK, Germany), T. Takemura (Japan), C. Textor (France, Germany), R. Wang (USA), R. Weiss (USA), T. Whorf (USA)

Review Editors:

Teruyuki Nakajima (Japan), Veerabhadran Ramanathan (USA)

This chapter should be cited as:

Forster, P., V. Ramaswamy, P. Artaxo, T. Berntsen, R. Betts, D.W. Fahey, J. Haywood, J. Lean, D.C. Lowe, G. Myhre, J. Nganga, R. Prinn, G. Raga, M. Schulz and R. Van Dorland, 2007: Changes in Atmospheric Constituents and in Radiative Forcing. *In: Climate Change 2007: The Physical Science Basis. Contribution of Working Group I to the Fourth Assessment Report of the Intergovernmental Panel on Climate Change* [Solomon, S., D. Qin, M. Manning, Z. Chen, M. Marquis, K.B. Averyt, M.Tignor and H.L. Miller (eds.)]. Cambridge University Press, Cambridge, United Kingdom and New York, NY, USA.

Table of Contents

Executive Summary 131

2.1 Introduction and Scope 133

2.2 Concept of Radiative Forcing 133

2.3 Chemically and Radiatively Important Gases 137

2.3.1 Atmospheric Carbon Dioxide 137
2.3.2 Atmospheric Methane 140
2.3.3 Other Kyoto Protocol Gases 143
2.3.4 Montreal Protocol Gases 145
2.3.5 Trends in the Hydroxyl Free Radical 147
2.3.6 Ozone 149
2.3.7 Stratospheric Water Vapour 152
2.3.8 Observations of Long-Lived Greenhouse Gas Radiative Effects 153

2.4 Aerosols 153

2.4.1 Introduction and Summary of the Third Assessment Report 153
2.4.2 Developments Related to Aerosol Observations 154
2.4.3 Advances in Modelling the Aerosol Direct Effect 159
2.4.4 Estimates of Aerosol Direct Radiative Forcing 160
2.4.5 Aerosol Influence on Clouds (Cloud Albedo Effect) 171

2.5 Anthropogenic Changes in Surface Albedo and the Surface Energy Budget 180

2.5.1 Introduction 180
2.5.2 Changes in Land Cover Since 1750 182
2.5.3 Radiative Forcing by Anthropogenic Surface Albedo Change: Land Use 182
2.5.4 Radiative Forcing by Anthropogenic Surface Albedo Change: Black Carbon in Snow and Ice 184
2.5.5 Other Effects of Anthropogenic Changes in Land Cover 185
2.5.6 Tropospheric Water Vapour from Anthropogenic Sources 185
2.5.7 Anthropogenic Heat Release 185
2.5.8 Effects of Carbon Dioxide Changes on Climate via Plant Physiology: 'Physiological Forcing' 185

2.6 Contrails and Aircraft-Induced Cloudiness 186

2.6.1 Introduction 186
2.6.2 Radiative Forcing Estimates for Persistent Line-Shaped Contrails 186
2.6.3 Radiative Forcing Estimates for Aviation-Induced Cloudiness 187
2.6.4 Aviation Aerosols 188

2.7 Natural Forcings 188

2.7.1 Solar Variability 188
2.7.2 Explosive Volcanic Activity 193

2.8 Utility of Radiative Forcing 195

2.8.1 Vertical Forcing Patterns and Surface Energy Balance Changes 196
2.8.2 Spatial Patterns of Radiative Forcing 196
2.8.3 Alternative Methods of Calculating Radiative Forcing 196
2.8.4 Linearity of the Forcing-Response Relationship 197
2.8.5 Efficacy and Effective Radiative Forcing 197
2.8.6 Efficacy and the Forcing-Response Relationship 199

2.9 Synthesis 199

2.9.1 Uncertainties in Radiative Forcing 199
2.9.2 Global Mean Radiative Forcing 200
2.9.3 Global Mean Radiative Forcing by Emission Precursor 205
2.9.4 Future Climate Impact of Current Emissions 206
2.9.5 Time Evolution of Radiative Forcing and Surface Forcing 208
2.9.6 Spatial Patterns of Radiative Forcing and Surface Forcing 209

2.10 Global Warming Potentials and Other Metrics for Comparing Different Emissions 210

2.10.1 Definition of an Emission Metric and the Global Warming Potential 210
2.10.2 Direct Global Warming Potentials 211
2.10.3 Indirect GWPs 214
2.10.4 New Alternative Metrics for Assessing Emissions 215

Frequently Asked Question

FAQ 2.1: *How Do Human Activities Contribute to Climate Change and How Do They Compare With Natural Influences?* 135

References 217

Executive Summary

Radiative forcing (RF)[1] is a concept used for quantitative comparisons of the strength of different human and natural agents in causing climate change. Climate model studies since the Working Group I Third Assessment Report (TAR; IPCC, 2001) give *medium* confidence that the equilibrium global mean temperature response to a given RF is approximately the same (to within 25%) for most drivers of climate change.

For the first time, the combined RF for all anthropogenic agents is derived. Estimates are also made for the first time of the separate RF components associated with the emissions of each agent.

The combined anthropogenic RF is estimated to be +1.6 [–1.0, +0.8][2] W m^{-2}, indicating that, since 1750, it is *extremely likely*[3] that humans have exerted a substantial warming influence on climate. This RF estimate is *likely* to be at least five times greater than that due to solar irradiance changes. For the period 1950 to 2005, it is *exceptionally unlikely* that the combined natural RF (solar irradiance plus volcanic aerosol) has had a warming influence comparable to that of the combined anthropogenic RF.

Increasing concentrations of the long-lived greenhouse gases (carbon dioxide (CO_2), methane (CH_4), nitrous oxide (N_2O), halocarbons and sulphur hexafluoride (SF_6); hereinafter LLGHGs) have led to a combined RF of +2.63 [±0.26] W m^{-2}. Their RF has a *high* level of scientific understanding.[4] The 9% increase in this RF since the TAR is the result of concentration changes since 1998.

— The global mean concentration of CO_2 in 2005 was 379 ppm, leading to an RF of +1.66 [±0.17] W m^{-2}. Past emissions of fossil fuels and cement production have *likely* contributed about three-quarters of the current RF, with the remainder caused by land use changes. For the 1995 to 2005 decade, the growth rate of CO_2 in the atmosphere was 1.9 ppm yr^{-1} and the CO_2 RF increased by 20%: this is the largest change observed or inferred for any decade in at least the last 200 years. From 1999 to 2005, global emissions from fossil fuel and cement production increased at a rate of roughly 3% yr^{-1}.

— The global mean concentration of CH_4 in 2005 was 1,774 ppb, contributing an RF of +0.48 [±0.05] W m^{-2}. Over the past two decades, CH_4 growth rates in the atmosphere have generally decreased. The cause of this is not well understood. However, this decrease and the negligible long-term change in its main sink (the hydroxyl radical OH) imply that total CH_4 emissions are not increasing.

— The Montreal Protocol gases (chlorofluorocarbons (CFCs), hydrochlorofluorocarbons (HCFCs), and chlorocarbons) as a group contributed +0.32 [±0.03] W m^{-2} to the RF in 2005. Their RF peaked in 2003 and is now beginning to decline.

— Nitrous oxide continues to rise approximately linearly (0.26% yr^{-1}) and reached a concentration of 319 ppb in 2005, contributing an RF of +0.16 [±0.02] W m^{-2}. Recent studies reinforce the large role of emissions from tropical regions in influencing the observed spatial concentration gradients.

— Concentrations of many of the fluorine-containing Kyoto Protocol gases (hydrofluorocarbons (HFCs), perfluorocarbons, SF_6) have increased by large factors (between 4.3 and 1.3) between 1998 and 2005. Their total RF in 2005 was +0.017 [±0.002] W m^{-2} and is rapidly increasing by roughly 10% yr^{-1}.

— The reactive gas, OH, is a key chemical species that influences the lifetimes and thus RF values of CH_4, HFCs, HCFCs and ozone; it also plays an important role in the formation of sulphate, nitrate and some organic aerosol species. Estimates of the global average OH concentration have shown no detectable net change between 1979 and 2004.

Based on newer and better chemical transport models than were available for the TAR, the RF from increases in tropospheric ozone is estimated to be +0.35 [–0.1, +0.3] W m^{-2}, with a *medium* level of scientific understanding. There are indications of significant upward trends at low latitudes.

The trend of greater and greater depletion of global stratospheric ozone observed during the 1980s and 1990s is no longer occurring; however, it is not yet clear whether these recent changes are indicative of ozone recovery. The RF is largely due to the destruction of stratospheric ozone by the Montreal Protocol gases and it is re-evaluated to be –0.05 [±0.10] W m^{-2}, with a *medium* level of scientific understanding.

Based on chemical transport model studies, the RF from the increase in stratospheric water vapour due to oxidation of CH_4 is estimated to be +0.07 [± 0.05] W m^{-2}, with a *low* level of scientific understanding. Other potential human causes of water vapour increase that could contribute an RF are poorly understood.

The total direct aerosol RF as derived from models and observations is estimated to be –0.5 [±0.4] W m^{-2}, with a

[1] The RF represents the stratospherically adjusted radiative flux change evaluated at the tropopause, as defined in the TAR. Positive RFs lead to a global mean surface warming and negative RFs to a global mean surface cooling. Radiative forcing, however, is not designed as an indicator of the detailed aspects of climate response. Unless otherwise mentioned, RF here refers to global mean RF. Radiative forcings are calculated in various ways depending on the agent: from changes in emissions and/or changes in concentrations, and from observations and other knowledge of climate change drivers. In this report, the RF value for each agent is reported as the difference in RF, unless otherwise mentioned, between the present day (approximately 2005) and the beginning of the industrial era (approximately 1750), and is given in units of W m^{-2}.

[2] 90% confidence ranges are given in square brackets. Where the 90% confidence range is asymmetric about a best estimate, it is given in the form A [–X, +Y] where the lower limit of the range is (A – X) and the upper limit is (A + Y).

[3] The use of '*extremely likely*' is an example of the calibrated language used in this document, it represents a 95% confidence level or higher; '*likely*' (66%) is another example (See Box TS.1).

[4] Estimates of RF are accompanied by both an uncertainty range (value uncertainty) and a level of scientific understanding (structural uncertainty). The value uncertainties represent the 5 to 95% (90%) confidence range, and are based on available published studies; the level of scientific understanding is a subjective measure of structural uncertainty and represents how well understood the underlying processes are. Climate change agents with a *high* level of scientific understanding are expected to have an RF that falls within their respective uncertainty ranges (See Section 2.9.1 and Box TS.1 for more information).

medium-low level of scientific understanding. The RF due to the cloud albedo effect (also referred to as first indirect or Twomey effect), in the context of liquid water clouds, is estimated to be –0.7 [–1.1, +0.4] W m^{-2}, with a *low* level of scientific understanding.

— Atmospheric models have improved and many now represent all aerosol components of significance. Improved *in situ*, satellite and surface-based measurements have enabled verification of global aerosol models. The best estimate and uncertainty range of the total direct aerosol RF are based on a combination of modelling studies and observations.

— The direct RF of the individual aerosol species is less certain than the total direct aerosol RF. The estimates are: sulphate, –0.4 [±0.2] W m^{-2}; fossil fuel organic carbon, –0.05 [±0.05] W m^{-2}; fossil fuel black carbon, +0.2 [±0.15] W m^{-2}; biomass burning, +0.03 [±0.12] W m^{-2}; nitrate, –0.1 [±0.1] W m^{-2}; and mineral dust, –0.1 [±0.2] W m^{-2}. For biomass burning, the estimate is strongly influenced by aerosol overlying clouds. For the first time best estimates are given for nitrate and mineral dust aerosols.

— Incorporation of more aerosol species and improved treatment of aerosol-cloud interactions allow a best estimate of the cloud albedo effect. However, the uncertainty remains large. Model studies including more aerosol species or constrained by satellite observations tend to yield a relatively weaker RF. Other aspects of aerosol-cloud interactions (e.g., cloud lifetime, semi-direct effect) are not considered to be an RF (see Chapter 7).

Land cover changes, largely due to net deforestation, have increased the surface albedo giving an RF of –0.2 [±0.2] W m^{-2}, with a *medium-low* level of scientific understanding. Black carbon aerosol deposited on snow has reduced the surface albedo, producing an associated RF of +0.1 [±0.1] W m^{-2}, with a *low* level of scientific understanding. Other surface property changes can affect climate through processes that cannot be quantified by RF; these have a *very low* level of scientific understanding.

Persistent linear contrails from aviation contribute an RF of +0.01 [–0.007, +0.02] W m^{-2}, with a *low* level of scientific understanding; the best estimate is smaller than in the TAR. No best estimates are available for the net forcing from spreading contrails and their effects on cirrus cloudiness.

The direct RF due to increases in solar irradiance since 1750 is estimated to be +0.12 [–0.06, +0.18] W m^{-2}, with a *low* level of scientific understanding. This RF is less than half of the TAR estimate.

— The smaller RF is due to a re-evaluation of the long-term change in solar irradiance, namely a smaller increase from the Maunder Minimum to the present. However, uncertainties in the RF remain large. The total solar irradiance, monitored from space for the last three decades, reveals a well-established cycle of 0.08% (cycle minimum to maximum) with no significant trend at cycle minima.

— Changes (order of a few percent) in globally averaged column ozone forced by the solar ultraviolet irradiance 11-year cycle are now better understood, but ozone profile changes are less certain. Empirical associations between solar-modulated cosmic ray ionization of the atmosphere and globally averaged low-level cloud cover remain ambiguous.

The global stratospheric aerosol concentrations in 2005 were at their lowest values since satellite measurements began in about 1980. This can be attributed to the absence of significant explosive volcanic eruptions since Mt. Pinatubo in 1991. Aerosols from such episodic volcanic events exert a transitory negative RF; however, there is limited knowledge of the RF associated with eruptions prior to Mt. Pinatubo.

The spatial patterns of RFs for non-LLGHGs (ozone, aerosol direct and cloud albedo effects, and land use changes) have considerable uncertainties, in contrast to the relatively high confidence in that of the LLGHGs. The Southern Hemisphere net positive RF *very likely* exceeds that in Northern Hemisphere because of smaller aerosol contributions in the Southern Hemisphere. The RF spatial pattern is not indicative of the pattern of climate response.

The total global mean surface forcing[5] is *very likely* negative. By reducing the shortwave radiative flux at the surface, increases in stratospheric and tropospheric aerosols are principally responsible for the negative surface forcing. This is in contrast to LLGHG increases, which are the principal contributors to the total positive anthropogenic RF.

[5] Surface forcing is the instantaneous radiative flux change at the surface; it is a useful diagnostic tool for understanding changes in the heat and moisture surface budgets. However, unlike RF, it cannot be used for quantitative comparisons of the effects of different agents on the equilibrium global mean surface temperature change.

2.1 Introduction and Scope

This chapter updates information taken from Chapters 3 to 6 of the IPCC Working Group I Third Assessment Report (TAR; IPCC, 2001). It concerns itself with trends in forcing agents and their precursors since 1750, and estimates their contribution to the radiative forcing (RF) of the climate system. Discussion of the understanding of atmospheric composition changes is limited to explaining the trends in forcing agents and their precursors. Areas where significant developments have occurred since the TAR are highlighted. The chapter draws on various assessments since the TAR, in particular the 2002 World Meteorological Organization (WMO)-United Nations Environment Programme (UNEP) Scientific Assessment of Ozone Depletion (WMO, 2003) and the IPCC-Technology and Economic Assessment Panel (TEAP) special report on Safeguarding the Ozone Layer and the Global Climate System (IPCC/TEAP, 2005).

The chapter assesses anthropogenic greenhouse gas changes, aerosol changes and their impact on clouds, aviation-induced contrails and cirrus changes, surface albedo changes and natural solar and volcanic mechanisms. The chapter reassesses the 'radiative forcing' concept (Sections 2.2 and 2.8), presents spatial and temporal patterns of RF, and examines the radiative energy budget changes at the surface.

For the long-lived greenhouse gases (carbon dioxide (CO_2), methane (CH_4), nitrous oxide (N_2O), chlorofluorocarbons (CFCs), hydrochlorofluorocarbons (HCFCs), hydrofluorocarbons (HFCs), perfluorocarbons (PFCs) and sulphur hexafluoride (SF_6), hereinafter collectively referred to as the LLGHGs; Section 2.3), the chapter makes use of new global measurement capabilities and combines long-term measurements from various networks to update trends through 2005. Compared to other RF agents, these trends are considerably better quantified; because of this, the chapter does not devote as much space to them as previous assessments (although the processes involved and the related budgets are further discussed in Sections 7.3 and 7.4). Nevertheless, LLGHGs remain the largest and most important driver of climate change, and evaluation of their trends is one of the fundamental tasks of both this chapter and this assessment.

The chapter considers only 'forward calculation' methods of estimating RF. These rely on observations and/or modelling of the relevant forcing agent. Since the TAR, several studies have attempted to constrain aspects of RF using 'inverse calculation' methods. In particular, attempts have been made to constrain the aerosol RF using knowledge of the temporal and/or spatial evolution of several aspects of climate. These include temperatures over the last 100 years, other RFs, climate response and ocean heat uptake. These methods depend on an understanding of – and sufficiently small uncertainties in – other aspects of climate change and are consequently discussed in the detection and attribution chapter (see Section 9.2).

Other discussions of atmospheric composition changes and their associated feedbacks are presented in Chapter 7. Radiative forcing and atmospheric composition changes before 1750 are discussed in Chapter 6. Future RF scenarios that were presented in Ramaswamy et al. (2001) are not updated in this report; however, they are briefly discussed in Chapter 10.

2.2 Concept of Radiative Forcing

The definition of RF from the TAR and earlier IPCC assessment reports is retained. Ramaswamy et al. (2001) define it as 'the change in net (down minus up) irradiance (solar plus longwave; in W m^{-2}) at the tropopause after allowing for stratospheric temperatures to readjust to radiative equilibrium, but with surface and tropospheric temperatures and state held fixed at the unperturbed values'. Radiative forcing is used to assess and compare the anthropogenic and natural drivers of climate change. The concept arose from early studies of the climate response to changes in solar insolation and CO_2, using simple radiative-convective models. However, it has proven to be particularly applicable for the assessment of the climate impact of LLGHGs (Ramaswamy et al., 2001). Radiative forcing can be related through a linear relationship to the global mean equilibrium temperature change at the surface (ΔT_s): $\Delta T_s = \lambda RF$, where λ is the climate sensitivity parameter (e.g., Ramaswamy et al., 2001). This equation, developed from these early climate studies, represents a linear view of global mean climate change between two equilibrium climate states. Radiative forcing is a simple measure for both quantifying and ranking the many different influences on climate change; it provides a limited measure of climate change as it does not attempt to represent the overall climate response. However, as climate sensitivity and other aspects of the climate response to external forcings remain inadequately quantified, it has the advantage of being more readily calculable and comparable than estimates of the climate response. Figure 2.1 shows how the RF concept fits within a general understanding of climate change comprised of 'forcing' and 'response'. This chapter also uses the term 'surface forcing' to refer to the instantaneous perturbation of the surface radiative balance by a forcing agent. Surface forcing has quite different properties than RF and should not be used to compare forcing agents (see Section 2.8.1). Nevertheless, it is a useful diagnostic, particularly for aerosols (see Sections 2.4 and 2.9).

Since the TAR a number of studies have investigated the relationship between RF and climate response, assessing the limitations of the RF concept; related to this there has been considerable debate whether some climate change drivers are better considered as a 'forcing' or a 'response' (Hansen et al., 2005; Jacob et al., 2005; Section 2.8). Emissions of forcing agents, such as LLGHGs, aerosols and aerosol precursors, ozone precursors and ozone-depleting substances, are the more fundamental drivers of climate change and these emissions can be used in state-of-the-art climate models to interactively evolve forcing agent fields along with their associated climate change. In such models, some 'response' is necessary to evaluate the

RF. This 'response' is most significant for aerosol-related cloud changes, where the tropospheric state needs to change significantly in order to create a radiative perturbation of the climate system (Jacob et al., 2005).

Over the palaeoclimate time scales that are discussed in Chapter 6, long-term changes in forcing agents arise due to so-called 'boundary condition' changes to the Earth's climate system (such as changes in orbital parameters, ice sheets and continents). For the purposes of this chapter, these 'boundary conditions' are assumed to be invariant and forcing agent changes are considered to be external to the climate system. The natural RFs considered are solar changes and volcanoes; the other RF agents are all attributed to humans. For the LLGHGs it is appropriate to assume that forcing agent concentrations have not been significantly altered by biogeochemical responses (see Sections 7.3 and 7.4), and RF is typically calculated in off-line radiative transfer schemes, using observed changes in concentration (i.e., humans are considered solely responsible for their increase). For the other climate change drivers, RF is often estimated using general circulation model (GCM) data employing a variety of methodologies (Ramaswamy et al., 2001; Stuber et al., 2001b; Tett et al., 2002; Shine et al., 2003; Hansen et al., 2005; Section 2.8.3). Often, alternative RF calculation methodologies that do not directly follow the TAR definition of a stratospheric-adjusted RF are used; the most important ones are illustrated in Figure 2.2. For most aerosol constituents (see Section 2.4), stratospheric adjustment has little effect on the RF, and the instantaneous RF at either the top of the atmosphere or the tropopause can be substituted. For the climate change drivers discussed in Sections 7.5 and 2.5, that are not initially radiative in nature, an RF-like quantity can be evaluated by allowing the tropospheric state to change: this is the zero-surface-temperature-change RF in Figure 2.2 (see Shine et al., 2003; Hansen et al., 2005; Section 2.8.3). Other water vapour and cloud changes are considered climate feedbacks and are evaluated in Section 8.6.

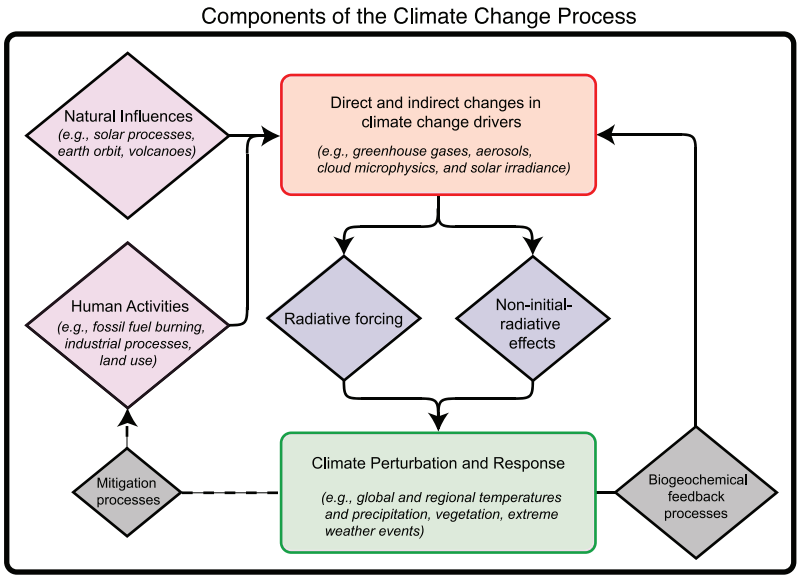


Figure 2.1. *Diagram illustrating how RF is linked to other aspects of climate change assessed by the IPCC. Human activities and natural processes cause direct and indirect changes in climate change drivers. In general, these changes result in specific RF changes, either positive or negative, and cause some non-initial radiative effects, such as changes in evaporation. Radiative forcing and non-initial radiative effects lead to climate perturbations and responses as discussed in Chapters 6, 7 and 8. Attribution of climate change to natural and anthropogenic factors is discussed in Chapter 9. The coupling among biogeochemical processes leads to feedbacks from climate change to its drivers (Chapter 7). An example of this is the change in wetland emissions of CH_4 that may occur in a warmer climate. The potential approaches to mitigating climate change by altering human activities (dashed lines) are topics addressed by IPCC's Working Group III.*

Climate change agents that require changes in the tropospheric state (temperature and/or water vapour amounts) prior to causing a radiative perturbation are aerosol-cloud lifetime effects, aerosol semi-direct effects and some surface

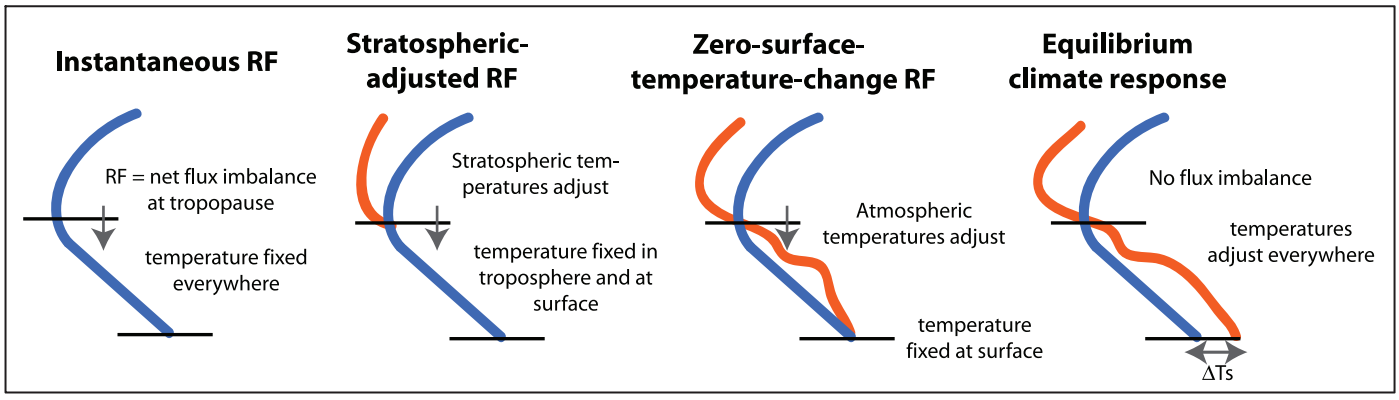


Figure 2.2. *Schematic comparing RF calculation methodologies. Radiative forcing, defined as the net flux imbalance at the tropopause, is shown by an arrow. The horizontal lines represent the surface (lower line) and tropopause (upper line). The unperturbed temperature profile is shown as the blue line and the perturbed temperature profile as the orange line. From left to right: Instantaneous RF: atmospheric temperatures are fixed everywhere; stratospheric-adjusted RF: allows stratospheric temperatures to adjust; zero-surface-temperature-change RF: allows atmospheric temperatures to adjust everywhere with surface temperatures fixed; and equilibrium climate response: allows the atmospheric and surface temperatures to adjust to reach equilibrium (no tropopause flux imbalance), giving a surface temperature change (ΔT_s).*

Frequently Asked Question 2.1

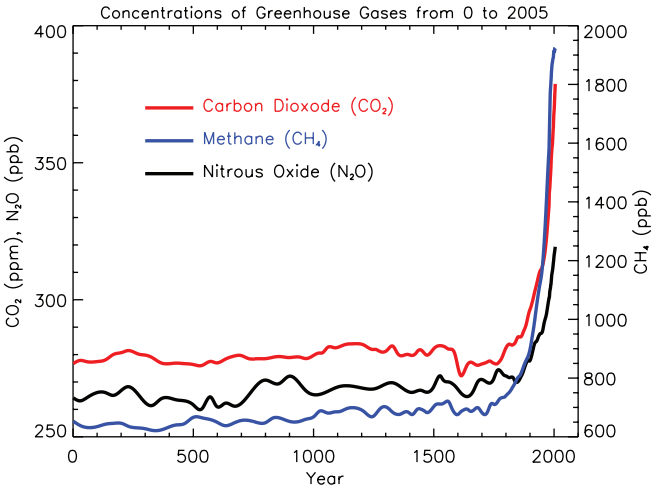
How do Human Activities Contribute to Climate Change and How do They Compare with Natural Influences?

Human activities contribute to climate change by causing changes in Earth's atmosphere in the amounts of greenhouse gases, aerosols (small particles), and cloudiness. The largest known contribution comes from the burning of fossil fuels, which releases carbon dioxide gas to the atmosphere. Greenhouse gases and aerosols affect climate by altering incoming solar radiation and outgoing infrared (thermal) radiation that are part of Earth's energy balance. Changing the atmospheric abundance or properties of these gases and particles can lead to a warming or cooling of the climate system. Since the start of the industrial era (about 1750), the overall effect of human activities on climate has been a warming influence. The human impact on climate during this era greatly exceeds that due to known changes in natural processes, such as solar changes and volcanic eruptions.

Greenhouse Gases

Human activities result in emissions of four principal greenhouse gases: carbon dioxide (CO_2), methane (CH_4), nitrous oxide (N_2O) and the halocarbons (a group of gases containing fluorine, chlorine and bromine). These gases accumulate in the atmosphere, causing concentrations to increase with time. Significant increases in all of these gases have occurred in the industrial era (see Figure 1). All of these increases are attributable to human activities.

- Carbon dioxide has increased from fossil fuel use in transportation, building heating and cooling and the manufacture of cement and other goods. Deforestation releases CO_2 and reduces its uptake by plants. Carbon dioxide is also released in natural processes such as the decay of plant matter.
- Methane has increased as a result of human activities related to agriculture, natural gas distribution and landfills. Methane is also released from natural processes that occur, for example, in wetlands. Methane concentrations are not currently increasing in the atmosphere because growth rates decreased over the last two decades.
- Nitrous oxide is also emitted by human activities such as fertilizer use and fossil fuel burning. Natural processes in soils and the oceans also release N_2O.
- Halocarbon gas concentrations have increased primarily due to human activities. Natural processes are also a small source. Principal halocarbons include the chlorofluorocarbons (e.g., CFC-11 and CFC-12), which were used extensively as refrigeration agents and in other industrial processes before their presence in the atmosphere was found to cause stratospheric ozone depletion. The abundance of chlorofluorocarbon gases is decreasing as a result of international regulations designed to protect the ozone layer.



FAQ 2.1, Figure 1. *Atmospheric concentrations of important long-lived greenhouse gases over the last 2,000 years. Increases since about 1750 are attributed to human activities in the industrial era. Concentration units are parts per million (ppm) or parts per billion (ppb), indicating the number of molecules of the greenhouse gas per million or billion air molecules, respectively, in an atmospheric sample. (Data combined and simplified from Chapters 6 and 2 of this report.)*

- Ozone is a greenhouse gas that is continually produced and destroyed in the atmosphere by chemical reactions. In the troposphere, human activities have increased ozone through the release of gases such as carbon monoxide, hydrocarbons and nitrogen oxide, which chemically react to produce ozone. As mentioned above, halocarbons released by human activities destroy ozone in the stratosphere and have caused the ozone hole over Antarctica.
- Water vapour is the most abundant and important greenhouse gas in the atmosphere. However, human activities have only a small direct influence on the amount of atmospheric water vapour. Indirectly, humans have the potential to affect water vapour substantially by changing climate. For example, a warmer atmosphere contains more water vapour. Human activities also influence water vapour through CH_4 emissions, because CH_4 undergoes chemical destruction in the stratosphere, producing a small amount of water vapour.
- Aerosols are small particles present in the atmosphere with widely varying size, concentration and chemical composition. Some aerosols are emitted directly into the atmosphere while others are formed from emitted compounds. Aerosols contain both naturally occurring compounds and those emitted as a result of human activities. Fossil fuel and biomass burning have increased aerosols containing sulphur compounds, organic compounds and black carbon (soot). Human activities such as

(continued)

surface mining and industrial processes have increased dust in the atmosphere. Natural aerosols include mineral dust released from the surface, sea salt aerosols, biogenic emissions from the land and oceans and sulphate and dust aerosols produced by volcanic eruptions.

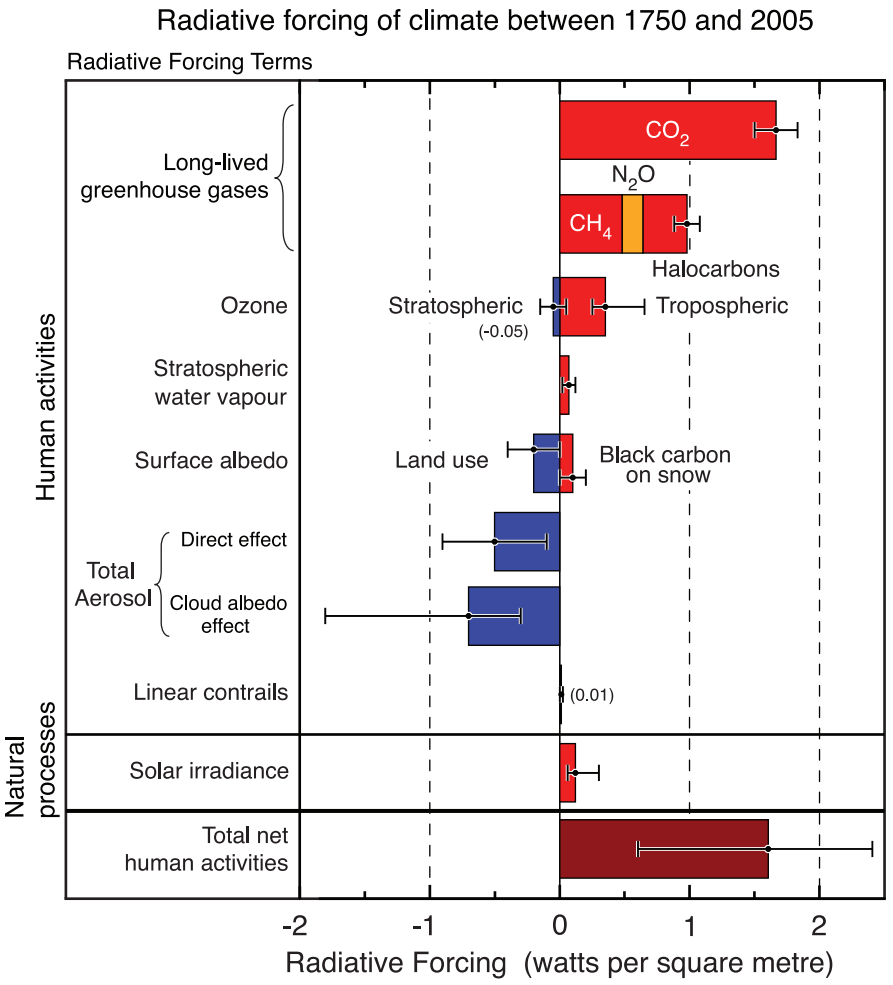
Radiative Forcing of Factors Affected by Human Activities

The contributions to radiative forcing from some of the factors influenced by human activities are shown in Figure 2. The values reflect the total forcing relative to the start of the industrial era (about 1750). The forcings for all greenhouse gas increases, which are the best understood of those due to human activities, are positive because each gas absorbs outgoing infrared radiation in the atmosphere. Among the greenhouse gases, CO_2 increases have caused the largest forcing over this period. Tropospheric ozone increases have also contributed to warming, while stratospheric ozone decreases have contributed to cooling.

Aerosol particles influence radiative forcing directly through reflection and absorption of solar and infrared radiation in the atmosphere. Some aerosols cause a positive forcing while others cause a negative forcing. The direct radiative forcing summed over all aerosol types is negative. Aerosols also cause a negative radiative forcing indirectly through the changes they cause in cloud properties.

Human activities since the industrial era have altered the nature of land cover over the globe, principally through changes in

(continued)



FAQ 2.1, Figure 2. *Summary of the principal components of the radiative forcing of climate change. All these radiative forcings result from one or more factors that affect climate and are associated with human activities or natural processes as discussed in the text. The values represent the forcings in 2005 relative to the start of the industrial era (about 1750). Human activities cause significant changes in long-lived gases, ozone, water vapour, surface albedo, aerosols and contrails. The only increase in natural forcing of any significance between 1750 and 2005 occurred in solar irradiance. Positive forcings lead to warming of climate and negative forcings lead to a cooling. The thin black line attached to each coloured bar represents the range of uncertainty for the respective value. (Figure adapted from Figure 2.20 of this report.)*

FAQ 2.1, Box 1: What is Radiative Forcing?

What is radiative forcing? The influence of a factor that can cause climate change, such as a greenhouse gas, is often evaluated in terms of its radiative forcing. Radiative forcing is a measure of how the energy balance of the Earth-atmosphere system is influenced when factors that affect climate are altered. The word radiative arises because these factors change the balance between incoming solar radiation and outgoing infrared radiation within the Earth's atmosphere. This radiative balance controls the Earth's surface temperature. The term forcing is used to indicate that Earth's radiative balance is being pushed away from its normal state.

Radiative forcing is usually quantified as the 'rate of energy change per unit area of the globe as measured at the top of the atmosphere', and is expressed in units of 'Watts per square metre' (see Figure 2). When radiative forcing from a factor or group of factors is evaluated as positive, the energy of the Earth-atmosphere system will ultimately increase, leading to a warming of the system. In contrast, for a negative radiative forcing, the energy will ultimately decrease, leading to a cooling of the system. Important challenges for climate scientists are to identify all the factors that affect climate and the mechanisms by which they exert a forcing, to quantify the radiative forcing of each factor and to evaluate the total radiative forcing from the group of factors.

croplands, pastures and forests. They have also modified the reflective properties of ice and snow. Overall, it is likely that more solar radiation is now being reflected from Earth's surface as a result of human activities. This change results in a negative forcing.

Aircraft produce persistent linear trails of condensation ('contrails') in regions that have suitably low temperatures and high humidity. Contrails are a form of cirrus cloud that reflect solar radiation and absorb infrared radiation. Linear contrails from global aircraft operations have increased Earth's cloudiness and are estimated to cause a small positive radiative forcing.

Radiative Forcing from Natural Changes

Natural forcings arise due to solar changes and explosive volcanic eruptions. Solar output has increased gradually in the industrial era, causing a small positive radiative forcing (see Figure 2). This is in addition to the cyclic changes in solar radiation that follow an 11-year cycle. Solar energy directly heats the climate system and can also affect the atmospheric abundance of some greenhouse gases, such as stratospheric ozone. Explosive volcanic eruptions can create a short-lived (2 to 3 years) negative forcing through the temporary increases that occur in sulphate aerosol in the stratosphere. The stratosphere is currently free of volcanic aerosol, since the last major eruption was in 1991 (Mt. Pinatubo).

The differences in radiative forcing estimates between the present day and the start of the industrial era for solar irradiance changes and volcanoes are both very small compared to the differences in radiative forcing estimated to have resulted from human activities. As a result, in today's atmosphere, the radiative forcing from human activities is much more important for current and future climate change than the estimated radiative forcing from changes in natural processes.

change effects. They need to be accounted for when evaluating the overall effect of humans on climate and their radiative effects as discussed in Sections 7.2 and 7.5. However, in both this chapter and the Fourth Assessment Report they are not considered to be RFs, although the RF definition could be altered to accommodate them. Reasons for this are twofold and concern the need to be simple and pragmatic. Firstly, many GCMs have some representation of these effects inherent in their climate response and evaluation of variation in climate sensitivity between mechanisms already accounts for them (see 'efficacy', Section 2.8.5). Secondly, the evaluation of these tropospheric state changes rely on some of the most uncertain aspects of a climate model's response (e.g., the hydrologic cycle); their radiative effects are very climate-model dependent and such a dependence is what the RF concept was designed to avoid. In practice these effects can also be excluded on practical grounds – they are simply too uncertain to be adequately quantified (see Sections 7.5, 2.4.5 and 2.5.6).

The RF relationship to transient climate change is not straightforward. To evaluate the overall climate response associated with a forcing agent, its temporal evolution and its spatial and vertical structure need to be taken into account. Further, RF alone cannot be used to assess the potential climate change associated with emissions, as it does not take into account the different atmospheric lifetimes of the forcing agents. Global Warming Potentials (GWPs) are one way to assess these emissions. They compare the integrated RF over a specified period (e.g., 100 years) from a unit mass pulse emission relative to CO_2 (see Section 2.10).

2.3 Chemically and Radiatively Important Gases

2.3.1 Atmospheric Carbon Dioxide

This section discusses the instrumental measurements of CO_2, documenting recent changes in atmospheric mixing ratios needed for the RF calculations presented later in the section. In addition, it provides data for the pre-industrial levels of CO_2 required as the accepted reference level for the RF calculations. For dates before about 1950 indirect measurements are relied upon. For these periods, levels of atmospheric CO_2 are usually determined from analyses of air bubbles trapped in polar ice cores. These time periods are primarily considered in Chapter 6.

A wide range of direct and indirect measurements confirm that the atmospheric mixing ratio of CO_2 has increased globally by about 100 ppm (36%) over the last 250 years, from a range of 275 to 285 ppm in the pre-industrial era (AD 1000–1750) to 379 ppm in 2005 (see FAQ 2.1, Figure 1). During this period, the absolute growth rate of CO_2 in the atmosphere increased substantially: the first 50 ppm increase above the pre-industrial value was reached in the 1970s after more than 200 years, whereas the second 50 ppm was achieved in about 30 years. In the 10 years from 1995 to 2005 atmospheric CO_2 increased by about 19 ppm; the highest average growth rate recorded for any decade since direct atmospheric CO_2 measurements began in the 1950s. The average rate of increase in CO_2 determined by these direct instrumental measurements over the period 1960 to 2005 is 1.4 ppm yr^{-1}.

High-precision measurements of atmospheric CO_2 are essential to the understanding of the carbon cycle budgets discussed in Section 7.3. The first *in situ* continuous measurements of atmospheric CO_2 made by a high-precision non-dispersive infrared gas analyser were implemented by C.D. Keeling from the Scripps Institution of Oceanography (SIO) (see Section 1.3). These began in 1958 at Mauna Loa, Hawaii, located at 19°N (Keeling et al., 1995). The data documented for the first time that not only was CO_2 increasing in the atmosphere, but also that it was modulated by cycles caused by seasonal changes in photosynthesis in the terrestrial biosphere. These measurements were followed by continuous *in situ* analysis programmes at other sites in both hemispheres (Conway et al., 1994; Nakazawa et al., 1997; Langenfelds et al., 2002). In Figure 2.3, atmospheric CO_2 mixing ratio data at Mauna Loa in the Northern Hemisphere (NH) are shown with contemporaneous measurements at Baring Head, New Zealand in the Southern Hemisphere (SH; Manning et al., 1997; Keeling and Whorf, 2005). These two stations provide the longest continuous records of atmospheric CO_2 in the NH and SH, respectively. Remote sites such as Mauna Loa, Baring Head, Cape Grim (Tasmania) and the South Pole were chosen because air sampled at such locations shows little short-term variation caused by local sources and sinks of CO_2 and provided the first data from which the global increase of atmospheric CO_2 was documented. Because CO_2 is a LLGHG and well mixed in the atmosphere, measurements made at such sites provide an integrated picture of large parts of the Earth including continents and city point sources. Note that this also applies to the other LLGHGs reported in Section 2.3.

In the 1980s and 1990s, it was recognised that greater coverage of CO_2 measurements over continental areas was required to provide the basis for estimating sources and sinks of atmospheric CO_2 over land as well as ocean regions. Because continuous CO_2 analysers are relatively expensive to maintain and require meticulous on-site calibration, these records are now widely supplemented by air sample flask programmes, where air is collected in glass and metal containers at a large number of continental and marine sites. After collection, the filled flasks are sent to central well-calibrated laboratories for analysis. The most extensive network of international air sampling sites is operated by the National Oceanic and Atmospheric Administration's Global Monitoring Division (NOAA/GMD; formerly NOAA/Climate Monitoring and Diagnostics Laboratory (CMDL)) in the USA. This organisation collates measurements of atmospheric CO_2 from six continuous analyser locations as well as weekly flask air samples from a global network of almost 50 surface sites. Many international laboratories make atmospheric CO_2 observations and worldwide databases of their measurements are maintained by the Carbon Dioxide Information Analysis Center (CDIAC) and by the World Data Centre for Greenhouse Gases (WDCGG) in the WMO Global Atmosphere Watch (GAW) programme.[6]

The increases in global atmospheric CO_2 since the industrial revolution are mainly due to CO_2 emissions from the combustion of fossil fuels, gas flaring and cement production. Other sources include emissions due to land use changes such as deforestation (Houghton, 2003) and biomass burning (Andreae and Merlet, 2001; van der Werf, 2004). After entering the atmosphere, CO_2 exchanges rapidly with the short-lived components of the terrestrial biosphere and surface ocean, and is then redistributed on time scales of hundreds of years among all active carbon reservoirs including the long-lived terrestrial biosphere and

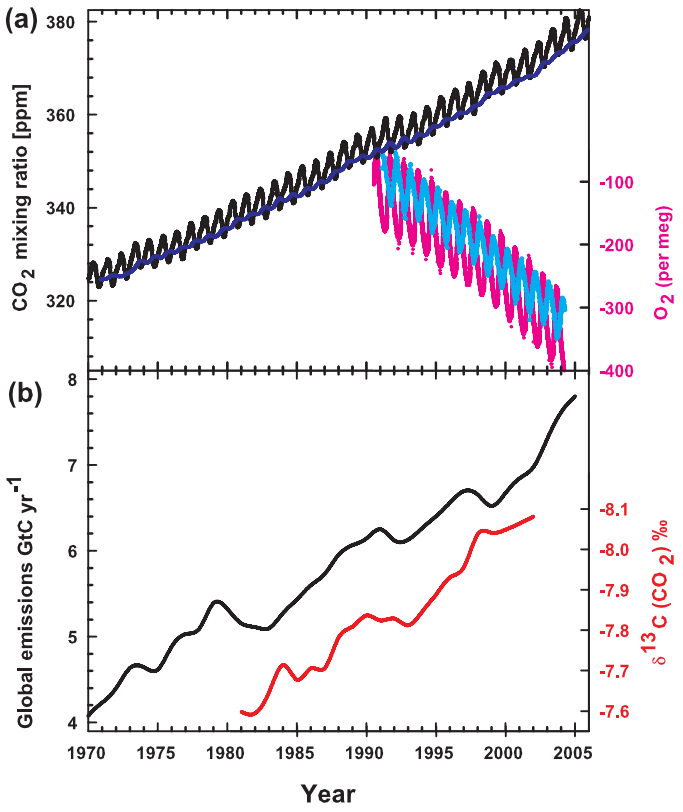


Figure 2.3. *Recent CO_2 concentrations and emissions. (a) CO_2 concentrations (monthly averages) measured by continuous analysers over the period 1970 to 2005 from Mauna Loa, Hawaii (19°N, black; Keeling and Whorf, 2005) and Baring Head, New Zealand (41°S, blue; following techniques by Manning et al., 1997). Due to the larger amount of terrestrial biosphere in the NH, seasonal cycles in CO_2 are larger there than in the SH. In the lower right of the panel, atmospheric oxygen (O_2) measurements from flask samples are shown from Alert, Canada (82°N, pink) and Cape Grim, Australia (41°S, cyan) (Manning and Keeling, 2006). The O_2 concentration is measured as 'per meg' deviations in the O_2/N_2 ratio from an arbitrary reference, analogous to the 'per mil' unit typically used in stable isotope work, but where the ratio is multiplied by 10^6 instead of 10^3 because much smaller changes are measured. (b) Annual global CO_2 emissions from fossil fuel burning and cement manufacture in GtC yr^{-1} (black) through 2005, using data from the CDIAC website (Marland et al, 2006) to 2003. Emissions data for 2004 and 2005 are extrapolated from CDIAC using data from the BP Statistical Review of World Energy (BP, 2006). Land use emissions are not shown; these are estimated to be between 0.5 and 2.7 GtC yr^{-1} for the 1990s (Table 7.2). Annual averages of the $^{13}C/^{12}C$ ratio measured in atmospheric CO_2 at Mauna Loa from 1981 to 2002 (red) are also shown (Keeling et al, 2005). The isotope data are expressed as $\delta^{13}C(CO_2)$ ‰ (per mil) deviation from a calibration standard. Note that this scale is inverted to improve clarity.*

[6] CDIAC, http://cdiac.esd.ornl.gov/; WDCGG, http://gaw.kishou.go.jp/wdcgg.html.

deep ocean. The processes governing the movement of carbon between the active carbon reservoirs, climate carbon cycle feedbacks and their importance in determining the levels of CO_2 remaining in the atmosphere, are presented in Section 7.3, where carbon cycle budgets are discussed.

The increase in CO_2 mixing ratios continues to yield the largest sustained RF of any forcing agent. The RF of CO_2 is a function of the change in CO_2 in the atmosphere over the time period under consideration. Hence, a key question is 'How is the CO_2 released from fossil fuel combustion, cement production and land cover change distributed amongst the atmosphere, oceans and terrestrial biosphere?'. This partitioning has been investigated using a variety of techniques. Among the most powerful of these are measurements of the carbon isotopes in CO_2 as well as high-precision measurements of atmospheric oxygen (O_2) content. The carbon contained in CO_2 has two naturally occurring stable isotopes denoted ^{12}C and ^{13}C. The first of these, ^{12}C, is the most abundant isotope at about 99%, followed by ^{13}C at about 1%. Emissions of CO_2 from coal, gas and oil combustion and land clearing have $^{13}C/^{12}C$ isotopic ratios that are less than those in atmospheric CO_2, and each carries a signature related to its source. Thus, as shown in Prentice et al. (2001), when CO_2 from fossil fuel combustion enters the atmosphere, the $^{13}C/^{12}C$ isotopic ratio in atmospheric CO_2 decreases at a predictable rate consistent with emissions of CO_2 from fossil origin. Note that changes in the $^{13}C/^{12}C$ ratio of atmospheric CO_2 are also caused by other sources and sinks, but the changing isotopic signal due to CO_2 from fossil fuel combustion can be resolved from the other components (Francey et al., 1995). These changes can easily be measured using modern isotope ratio mass spectrometry, which has the capability of measuring $^{13}C/^{12}C$ in atmospheric CO_2 to better than 1 part in 10^5 (Ferretti et al., 2000). Data presented in Figure 2.3 for the $^{13}C/^{12}C$ ratio of atmospheric CO_2 at Mauna Loa show a decreasing ratio, consistent with trends in both fossil fuel CO_2 emissions and atmospheric CO_2 mixing ratios (Andres et al., 2000; Keeling et al., 2005).

Atmospheric O_2 measurements provide a powerful and independent method of determining the partitioning of CO_2 between the oceans and land (Keeling et al., 1996). Atmospheric O_2 and CO_2 changes are inversely coupled during plant respiration and photosynthesis. In addition, during the process of combustion O_2 is removed from the atmosphere, producing a signal that decreases as atmospheric CO_2 increases on a molar basis (Figure 2.3). Measuring changes in atmospheric O_2 is technically challenging because of the difficulty of resolving changes at the part-per-million level in a background mixing ratio of roughly 209,000 ppm. These difficulties were first overcome by Keeling and Shertz (1992), who used an interferometric technique to show that it is possible to track both seasonal cycles and the decline of O_2 in the atmosphere at the part-per-million level (Figure 2.3). Recent work by Manning and Keeling (2006) indicates that atmospheric O_2 is decreasing at a faster rate than CO_2 is increasing, which demonstrates the importance of the oceanic carbon sink. Measurements of both the $^{13}C/^{12}C$ ratio in atmospheric CO_2 and atmospheric O_2 levels are valuable tools used to determine the distribution of fossil-fuel derived CO_2 among the active carbon reservoirs, as discussed in Section 7.3. In Figure 2.3, recent measurements in both hemispheres are shown to emphasize the strong linkages between atmospheric CO_2 increases, O_2 decreases, fossil fuel consumption and the $^{13}C/^{12}C$ ratio of atmospheric CO_2.

From 1990 to 1999, a period reported in Prentice et al. (2001), the emission rate due to fossil fuel burning and cement production increased irregularly from 6.1 to 6.5 GtC yr^{-1} or about 0.7% yr^{-1}. From 1999 to 2005 however, the emission rate rose systematically from 6.5 to 7.8 GtC yr^{-1} (BP, 2006; Marland et al., 2006) or about 3.0% yr^{-1}, representing a period of higher emissions and growth in emissions than those considered in the TAR (see Figure 2.3). Carbon dioxide emissions due to global annual fossil fuel combustion and cement manufacture combined have increased by 70% over the last 30 years (Marland et al., 2006). The relationship between increases in atmospheric CO_2 mixing ratios and emissions has been tracked using a scaling factor known as the apparent 'airborne fraction', defined as the ratio of the annual increase in atmospheric CO_2 to the CO_2 emissions from annual fossil fuel and cement manufacture combined (Keeling et al., 1995). On decadal scales, this fraction has averaged about 60% since the 1950s. Assuming emissions of 7 GtC yr^{-1} and an airborne fraction remaining at about 60%, Hansen and Sato (2004) predicted that the underlying long-term global atmospheric CO_2 growth rate will be about 1.9 ppm yr^{-1}, a value consistent with observations over the 1995 to 2005 decade.

Carbon dioxide emissions due to land use changes during the 1990s are estimated as 0.5 to 2.7 GtC yr^{-1} (Section 7.3, Table 7.2), contributing 6% to 39% of the CO_2 growth rate (Brovkin et al., 2004). Prentice et al. (2001) cited an inventory-based estimate that land use change resulted in net emissions of 121 GtC between 1850 and 1990, after Houghton (1999, 2000). The estimate for this period was revised upwards to 134 GtC by Houghton (2003), mostly due to an increase in estimated emissions prior to 1960. Houghton (2003) also extended the inventory emissions estimate to 2000, giving cumulative emissions of 156 GtC since 1850. In carbon cycle simulations by Brovkin et al. (2004) and Matthews et al. (2004), land use change emissions contributed 12 to 35 ppm of the total CO_2 rise from 1850 to 2000 (Section 2.5.3, Table 2.8). Historical changes in land cover are discussed in Section 2.5.2, and the CO_2 budget over the 1980s and 1990s is discussed further in Section 7.3.

In 2005, the global mean average CO_2 mixing ratio for the SIO network of 9 sites was 378.75 ± 0.13 ppm and for the NOAA/GMD network of 40 sites was 378.76 ± 0.05 ppm, yielding a global average of almost 379 ppm. For both networks, only sites in the remote marine boundary layer are used and high-altitude locations are not included. For example, the Mauna Loa site is excluded due to an 'altitude effect' of about 0.5 ppm. In addition, the 2005 values are still pending final reference gas calibrations used to measure the samples.

New measurements of CO_2 from Antarctic ice and firn (MacFarling Meure et al., 2006) update and extend those from Etheridge et al. (1996) to AD 0. The CO_2 mixing ratio in 1750 was 277 ± 1.2 ppm.[7] This record shows variations between 272 and 284 ppm before 1800 and also that CO_2 mixing ratios dropped by 5 to 10 ppm between 1600 and 1800 (see Section 6.3). The RF calculations usually take 1750 as the pre-industrial index (e.g., the TAR and this report). Therefore, using 1750 may slightly overestimate the RF, as the changes in the mixing ratios of CO_2, CH_4 and N_2O after the end of this naturally cooler period may not be solely attributable to anthropogenic emissions. Using 1860 as an alternative start date for the RF calculations would reduce the LLGHG RF by roughly 10%. For the RF calculation, the data from Law Dome ice cap in the Antarctic are used because they show the highest age resolution (approximately 10 years) of any ice core record in existence. In addition, the high-precision data from the cores are connected to direct observational records of atmospheric CO_2 from Cape Grim, Tasmania.

The simple formulae for RF of the LLGHG quoted in Ramaswamy et al. (2001) are still valid. These formulae are based on global RF calculations where clouds, stratospheric adjustment and solar absorption are included, and give an RF of +3.7 W m^{-2} for a doubling in the CO_2 mixing ratio. (The formula used for the CO_2 RF calculation in this chapter is the IPCC (1990) expression as revised in the TAR. Note that for CO_2, RF increases logarithmically with mixing ratio.) Collins et al. (2006) performed a comparison of five detailed line-by-line models and 20 GCM radiation schemes. The spread of line-by-line model results were consistent with the ±10% uncertainty estimate for the LLGHG RFs adopted in Ramaswamy et al. (2001) and a similar ±10% for the 90% confidence interval is adopted here. However, it is also important to note that these relatively small uncertainties are not always achievable when incorporating the LLGHG forcings into GCMs. For example, both Collins et al. (2006) and Forster and Taylor (2006) found that GCM radiation schemes could have inaccuracies of around 20% in their total LLGHG RF (see also Sections 2.3.2 and 10.2).

Using the global average value of 379 ppm for atmospheric CO_2 in 2005 gives an RF of 1.66 ± 0.17 W m^{-2}; a contribution that dominates that of all other forcing agents considered in this chapter. This is an increase of 13 to 14% over the value reported for 1998 in Ramaswamy et al. (2001). This change is solely due to increases in atmospheric CO_2 and is also much larger than the RF changes due to other agents. In the decade 1995 to 2005, the RF due to CO_2 increased by about 0.28 W m^{-2} (20%), an increase greater than that calculated for any decade since at least 1800 (see Section 6.6 and FAQ 2.1, Figure 1).

Table 2.1 summarises the present-day mixing ratios and RF for the LLGHGs, and indicates changes since 1998. The RF from CO_2 and that from the other LLGHGs have a high level of scientific understanding (Section 2.9, Table 2.11). Note that the uncertainty in RF is almost entirely due to radiative transfer assumptions and not mixing ratio estimates, therefore trends in RF can be more accurately determined than the absolute RF. From Section 2.5.3, Table 2.8, the contribution from land use change to the present CO_2 RF is likely to be about 0.4 W m^{-2} (since 1850). This implies that fossil fuel and cement production have likely contributed about three-quarters of the current RF.

2.3.2 Atmospheric Methane

This section describes the current global measurement programmes for atmospheric CH_4, which provide the data required for the understanding of its budget and for the calculation of its RF. In addition, this section provides data for the pre-industrial levels of CH_4 required as the accepted reference level for these calculations. Detailed analyses of CH_4 budgets and its biogeochemistry are presented in Section 7.4.

Methane has the second-largest RF of the LLGHGs after CO_2 (Ramaswamy et al., 2001). Over the last 650 kyr, ice core records indicate that the abundance of CH_4 in the Earth's atmosphere has varied from lows of about 400 ppb during glacial periods to highs of about 700 ppb during interglacials (Spahni et al., 2005) with a single measurement from the Vostok core reaching about 770 ppb (see Figure 6.3).

In 2005, the global average abundance of CH_4 measured at the network of 40 surface air flask sampling sites operated by NOAA/GMD in both hemispheres was 1,774.62 ± 1.22 ppb.[8] This is the most geographically extensive network of sites operated by any laboratory and it is important to note that the calibration scale it uses has changed since the TAR (Dlugokencky et al., 2005). The new scale (known as NOAA04) increases all previously reported CH_4 mixing ratios from NOAA/GMD by about 1%, bringing them into much closer agreement with the Advanced Global Atmospheric Gases Experiment (AGAGE) network. This scale will be used by laboratories participating in the WMO's GAW programme as a 'common reference'. Atmospheric CH_4 is also monitored at five sites in the NH and SH by the AGAGE network. This group uses automated systems to make 36 CH_4 measurements per day at each site, and the mean for 2005 was 1,774.03 ± 1.68 ppb with calibration and methods described by Cunnold et al. (2002). For the NOAA/GMD network, the 90% confidence interval is calculated with a Monte Carlo technique, which only accounts for the uncertainty due to the distribution of sampling sites. For both networks, only sites in the remote marine boundary layer are used and continental sites are not included. Global databases of atmospheric CH_4 measurements for these and other CH_4 measurement programmes (e.g., Japanese, European and Australian) are maintained by the CDIAC and by the WDCGG in the GAW programme.

Present atmospheric levels of CH_4 are unprecedented in at least the last 650 kyr (Spahni et al., 2005). Direct atmospheric

[7] For consistency with the TAR, the pre-industrial value of 278 ppm is retained in the CO_2 RF calculation.

[8] The 90% confidence range quoted is from the normal standard deviation error for trace gas measurements assuming a normal distribution (i.e., multiplying by a factor of 1.645).

Table 2.1. *Present-day concentrations and RF for the measured LLGHGs. The changes since 1998 (the time of the TAR estimates) are also shown.*

	Concentrations[b] and their changes[c]		Radiative Forcing[d]	
Species[a]	2005	Change since 1998	2005 ($W m^{-2}$)	Change since 1998 (%)
CO_2	**379 ± 0.65 ppm**	**+13 ppm**	**1.66**	**+13**
CH_4	**1,774 ± 1.8 ppb**	**+11 ppb**	**0.48**	**-**
N_2O	**319 ± 0.12 ppb**	**+5 ppb**	**0.16**	**+11**
	ppt	ppt		
CFC-11	251 ± 0.36	–13	0.063	–5
CFC-12	538 ± 0.18	+4	0.17	+1
CFC-113	79 ± 0.064	–4	0.024	–5
HCFC-22	169 ± 1.0	+38	0.033	+29
HCFC-141b	18 ± 0.068	+9	0.0025	+93
HCFC-142b	15 ± 0.13	+6	0.0031	+57
CH_3CCl_3	19 ± 0.47	–47	0.0011	–72
CCl_4	93 ± 0.17	–7	0.012	–7
HFC-125	3.7 ± 0.10[e]	+2.6[f]	0.0009	+234
HFC-134a	35 ± 0.73	+27	0.0055	+349
HFC-152a	3.9 ± 0.11[e]	+2.4[f]	0.0004	+151
HFC-23	18 ± 0.12[g,h]	+4	0.0033	+29
SF_6	5.6 ± 0.038[i]	+1.5	0.0029	+36
CF_4 (PFC-14)	74 ± 1.6[j]	-	0.0034	-
C_2F_6 (PFC-116)	2.9 ± 0.025[g,h]	+0.5	0.0008	+22
CFCs Total[k]			**0.268**	**–1**
HCFCs Total			**0.039**	**+33**
Montreal Gases			**0.320**	**–1**
Other Kyoto Gases (HFCs + PFCs + SF_6)			**0.017**	**+69**
Halocarbons			**0.337**	**+1**
Total LLGHGs			**2.63**	**+9**

Notes:

[a] See Table 2.14 for common names of gases and the radiative efficiencies used to calculate RF.

[b] Mixing ratio errors are 90% confidence ranges of combined 2005 data, including intra-annual standard deviation, measurement and global averaging uncertainty. Standard deviations were multiplied by 1.645 to obtain estimates of the 90% confidence range; this assumes normal distributions. Data for CO_2 are combined measurements from the NOAA Earth System Research Laboratory (ESRL) and SIO networks (see Section 2.3.1); CH_4 measurements are combined data from the ESRL and Advanced Global Atmospheric Gases Experiment (AGAGE) networks (see Section 2.3.2); halocarbon measurements are the average of ESRL and AGAGE networks. University of East Anglia (UEA) and Pennsylvania State University (PSU) measurements were also used (see Section 2.3.3).

[c] Pre-industrial values are zero except for CO_2 (278 ppm), CH_4 (715 ppb; 700 ppb was used in the TAR), N_2O (270 ppb) and CF_4 (40 ppt).

[d] 90% confidence ranges for RF are not shown but are approximately 10%. This confidence range is almost entirely due to radiative transfer assumptions, therefore trends remain valid when quoted to higher accuracies. Higher precision data are used for totals and affect rounding of the values. Percent changes are calculated relative to 1998.

[e] Data available from AGAGE network only.

[f] Data for 1998 not available; values from 1999 are used.

[g] Data from UEA only.

[h] Data from 2003 are used due to lack of available data for 2004 and 2005.

[i] Data from ESRL only.

[j] 1997 data from PSU (Khalil et al., 2003, not updated) are used.

[k] CFC total includes a small 0.009 $W m^{-2}$ RF from CFC-13, CFC-114, CFC-115 and the halons, as measurements of these were not updated.

measurements of the gas made at a wide variety of sites in both hemispheres over the last 25 years show that, although the abundance of CH_4 has increased by about 30% during that time, its growth rate has decreased substantially from highs of greater than 1% yr^{-1} in the late 1 70s and early 1980s (Blake and Rowland, 1988) to lows of close to zero towards the end of the 1990s (Dlugokencky et al., 1998; Simpson et al., 2002). The slowdown in the growth rate began in the 1980s, decreasing from 14 ppb yr^{-1} (about 1% yr^{-1}) in 1984 to close to zero during 1999 to 2005, for the network of surface sites maintained by NOAA/GMD (Dlugokencky et al., 2003). Measurements by Lowe et al. (2004) for sites in the SH and Cunnold et al. (2002) for the network of GAGE/AGAGE sites show similar features. A key feature of the global growth rate of CH_4 is its current interannual variability, with growth rates ranging from a high of 14 ppb yr^{-1} in 1998 to less than zero in 2001, 2004 and 2005. (Figure 2.4)

The reasons for the decrease in the atmospheric CH_4 growth rate and the implications for future changes in its atmospheric burden are not understood (Prather et al., 2001) but are clearly related to changes in the imbalance between CH_4 sources and sinks. Most CH_4 is removed from the atmosphere by reaction with the hydroxyl free radical (OH), which is produced photochemically in the atmosphere. The role of OH in controlling atmospheric CH_4 levels is discussed in Section 2.3.5. Other minor sinks include reaction with free chlorine (Platt et al., 2004; Allan et al., 2005), destruction in the stratosphere and soil sinks (Born et al., 1990).

The total global CH_4 source is relatively well known but the strength of each source component and their trends are not. As detailed in Section 7.4, the sources are mostly biogenic and include wetlands, rice agriculture, biomass burning and ruminant animals. Methane is also emitted by various industrial sources including fossil fuel mining and distribution. Prather et al. (2001) documented a large range in 'bottom-up' estimates for the global source of CH_4. New source estimates published since then are documented in Table 7.6. However, as reported by Bergamaschi et al. (2005), national inventories based on 'bottom-up' studies can grossly underestimate emissions and 'top-down' measurement-based assessments of reported emissions will be required for verification. Keppler et al. (2006) reported the discovery of emissions of CH_4 from living vegetation and estimated that this contributed 10 to 30% of the global CH_4 source. This work extrapolates limited measurements to a global source and has not yet been confirmed by other laboratories, but lends some support to space-borne observations of CH_4 plumes above tropical rainforests reported by Frankenberg et al. (2005). That such a potentially large source of CH_4 could have been missed highlights the large uncertainties involved in current 'bottom-up' estimates of components of the global source (see Section 7.4).

Several wide-ranging hypotheses have been put forward to explain the reduction in the CH_4 growth rate and its variability. For example, Hansen et al. (2000) considered that economic incentives have led to a reduction in anthropogenic CH_4 emissions. The negligible long-term change in its main sink (OH; see Section 2.3.5 and Figure 2.8) implies that CH_4 emissions are not increasing. Similarly, Dlugokencky et al. (1998) and Francey et al. (1999) suggested that the slowdown in the growth rate reflects a stabilisation of CH_4 emissions, given that the observations are consistent with stable emissions and lifetime since 1982.

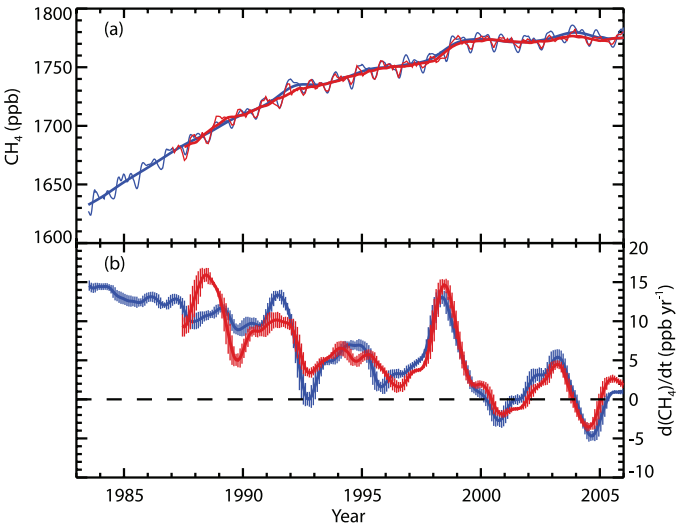


Figure 2.4. *Recent CH_4 concentrations and trends. (a) Time series of global CH_4 abundance mole fraction (in ppb) derived from surface sites operated by NOAA/GMD (blue lines) and AGAGE (red lines). The thinner lines show the CH_4 global averages and the thicker lines are the de-seasonalized global average trends from both networks. (b) Annual growth rate (ppb yr^{-1}) in global atmospheric CH_4 abundance from 1984 through the end of 2005 (NOAA/GMD, blue), and from 1988 to the end of 2005 (AGAGE, red). To derive the growth rates and their uncertainties for each month, a linear least squares method that takes account of the autocorrelation of residuals is used. This follows the methods of Wang et al. (2002) and is applied to the de-seasonalized global mean mole fractions from (a) for values six months before and after the current month. The vertical lines indicate ±2 standard deviation uncertainties (95% confidence interval), and 1 standard deviation uncertainties are between 0.1 and 1.4 ppb yr^{-1} for both AGAGE and NOAA/GMD. Note that the differences between AGAGE and NOAA/GMD calibration scales are determined through occasional intercomparisons.*

Relatively large anomalies occurred in the growth rate during 1991 and 1998, with peak values reaching 15 and 14 ppb yr^{-1}, respectively (about 1% yr^{-1}). The anomaly in 1991 was followed by a dramatic drop in the growth rate in 1992 and has been linked with the Mt. Pinatubo volcanic eruption in June 1991, which injected large amounts of ash and (sulphur dioxide) SO_2 into the lower stratosphere of the tropics with subsequent impacts on tropical photochemistry and the removal of CH_4 by atmospheric OH (Bekki et al., 1994; Dlugokencky et al., 1996). Lelieveld et al. (1998) and Walter et al. (2001a,b) proposed that lower temperatures and lower precipitation in the aftermath of the Mt. Pinatubo eruption could have suppressed CH_4 emissions from wetlands. At this time, and in parallel with the growth rate anomaly in the CH_4 mixing ratio, an anomaly was observed in the $^{13}C/^{12}C$ ratio of CH_4 at surface sites in the SH. This was attributed to a decrease in emissions from an isotopically heavy source such as biomass burning (Lowe et al., 1997; Mak et al., 2000), although these data were not confirmed by lower frequency measurements from the same period made by Francey et al. (1999).

For the relatively large increase in the CH_4 growth rate reported for 1998, Dlugokencky et al. (2001) suggested that wetland and boreal biomass burning sources might have contributed to the anomaly, noting that 1998 was the warmest year globally since surface instrumental temperature records began. Using an inverse method, Chen and Prinn (2006) attributed the same event primarily to increased wetland and rice region emissions and secondarily to biomass burning. The same conclusion was reached by Morimoto et al. (2006), who used carbon isotopic measurements of CH_4 to constrain the relative contributions of biomass burning (one-third) and wetlands (two-thirds) to the increase.

Based on ice core measurements of CH_4 (Etheridge et al., 1998), the pre-industrial global value for CH_4 from 1700 to 1800 was 715 ± 4 ppb (it was also 715 ± 4 ppb in 1750), thus providing the reference level for the RF calculation. This takes into account the inter-polar difference in CH_4 as measured from Greenland and Antarctic ice cores.

The RF due to changes in CH_4 mixing ratio is calculated with the simplified yet still valid expression for CH_4 given in Ramaswamy et al. (2001). The change in the CH_4 mixing ratio from 715 ppb in 1750 to 1,774 ppb (the average mixing ratio from the AGAGE and GMD networks) in 2005 gives an RF of +0.48 ± 0.05 W m^{-2}, ranking CH_4 as the second highest RF of the LLGHGs after CO_2 (Table 2.1). The uncertainty range in mixing ratios for the present day represents intra-annual variability, which is not included in the pre-industrial uncertainty estimate derived solely from ice core sampling precision. The estimate for the RF due to CH_4 is the same as in Ramaswamy et al. (2001) despite the small increase in its mixing ratio. The spectral absorption by CH_4 is overlapped to some extent by N_2O lines (taken into account in the simplified expression). Taking the overlapping lines into account using current N_2O mixing ratios instead of pre-industrial mixing ratios (as in Ramaswamy et al., 2001) reduces the current RF due to CH_4 by 1%.

Collins et al. (2006) confirmed that line-by-line models agree extremely well for the calculation of clear-sky instantaneous RF from CH_4 and N_2O when the same atmospheric background profile is used. However, GCM radiation schemes were found to be in poor agreement with the line-by-line models, and errors of over 50% were possible for CH_4, N_2O and the CFCs. In addition, a small effect from the absorption of solar radiation was found with the line-by-line models, which the GCMs did not include (Section 10.2).

2.3.3 Other Kyoto Protocol Gases

At the time of the TAR, N_2O had the fourth largest RF among the LLGHGs behind CO_2, CH_4 and CFC-12. The TAR quoted an atmospheric N_2O abundance of 314 ppb in 1998, an increase of 44 ppb from its pre-industrial level of around 270 ± 7 ppb, which gave an RF of +0.15 ± 0.02 W m^{-2}. This RF is affected by atmospheric CH_4 levels due to overlapping absorptions. As N_2O is also the major source of ozone-depleting nitric oxide (NO) and nitrogen dioxide (NO_2) in the stratosphere, it is routinely reviewed in the ozone assessments; the most recent assessment (Montzka et al., 2003) recommended an atmospheric lifetime of 114 years for N_2O. The TAR pointed out large uncertainties in the major soil, agricultural, combustion and oceanic sources of N_2O. Given these emission uncertainties, its observed rate of increase of 0.2 to 0.3% yr^{-1} was not inconsistent with its better-quantified major sinks (principally stratospheric destruction). The primary driver for the industrial era increase of N_2O was concluded to be enhanced microbial production in expanding and fertilized agricultural lands.

Ice core data for N_2O have been reported extending back 2,000 years and more before present (MacFarling Meure et al., 2006; Section 6.6). These data, as for CO_2 and CH_4, show relatively little changes in mixing ratios over the first 1,800 years of this record, and then exhibit a relatively rapid rise (see FAQ 2.1, Figure 1). Since 1998, atmospheric N_2O levels have steadily risen to 319 ± 0.12 ppb in 2005, and levels have been increasing approximately linearly (at around 0.26% yr^{-1}) for the past few decades (Figure 2.5). A change in the N_2O mixing ratio

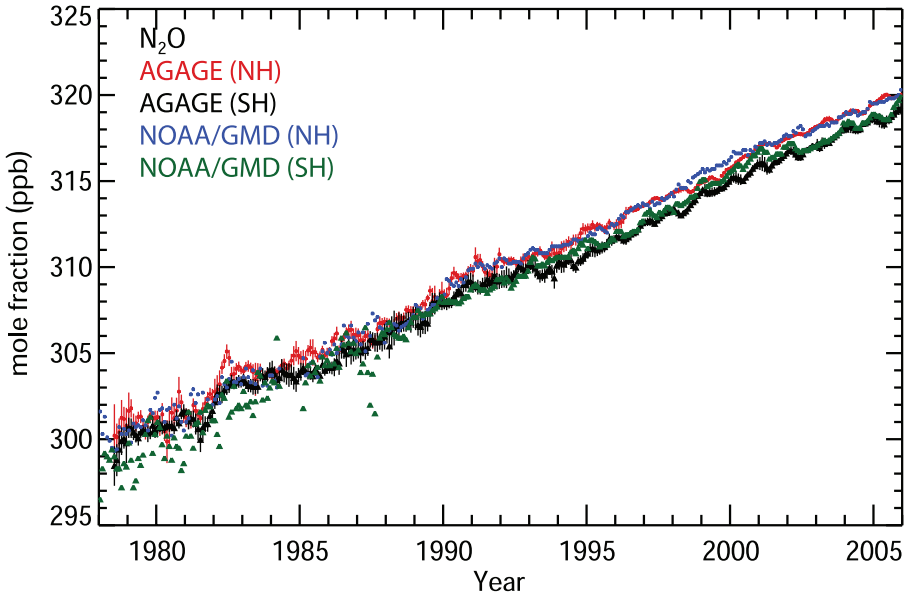


Figure 2.5. *Hemispheric monthly mean N_2O mole fractions (ppb) (crosses for the NH and triangles for the SH). Observations (*in situ*) of N_2O from the Atmospheric Lifetime Experiment (ALE) and GAGE (through the mid-1990s) and AGAGE (since the mid-1990s) networks (Prinn et al., 2000, 2005b) are shown with monthly standard deviations. Data from NOAA/GMD are shown without these standard deviations (Thompson et al., 2004). The general decrease in the variability of the measurements over time is due mainly to improved instrumental precision. The real signal emerges only in the last decade.*

from 270 ppb in 1750 to 319 ppb in 2005 results in an RF of $+0.16 \pm 0.02$ W m^{-2}, calculated using the simplified expression given in Ramaswamy et al. (2001). The RF has increased by 11% since the time of the TAR (Table 2.1). As CFC-12 levels slowly decline (see Section 2.3.4), N_2O should, with its current trend, take over third place in the LLGHG RF ranking.

Since the TAR, understanding of regional N_2O fluxes has improved. The results of various studies that quantified the global N_2O emissions from coastal upwelling areas, continental shelves, estuaries and rivers suggest that these coastal areas contribute 0.3 to 6.6 TgN yr^{-1} of N_2O or 7 to 61% of the total oceanic emissions (Bange et al., 1996; Nevison et al., 2004b; Kroeze et al., 2005; see also Section 7.4). Using inverse methods and AGAGE Ireland measurements, Manning et al. (2003) estimated EU N_2O emissions of 0.9 ± 0.1 TgN yr^{-1} that agree well with the United Nations Framework Convention on Climate Change (UNFCCC) N_2O inventory (0.8 ± 0.1 TgN yr^{-1}). Melillo et al. (2001) provided evidence from Brazilian land use sequences that the conversion of tropical forest to pasture leads to an initial increase but a later decline in emissions of N_2O relative to the original forest. They also deduced that Brazilian forest soils alone contribute about 10% of total global N_2O production. Estimates of N_2O sources and sinks using observations and inverse methods had earlier implied that a large fraction of global N_2O emissions in 1978 to 1988 were tropical: specifically 20 to 29% from 0° to 30°S and 32 to 39% from 0° to 30°N compared to 11 to 15% from 30°S to 90°S and 22 to 34% from 30°N to 90°N (Prinn et al., 1990). These estimates were uncertain due to their significant sensitivity to assumed troposphere-stratosphere exchange rates that strongly influence inter-hemispheric gradients. Hirsch et al. (2006) used inverse modelling to estimate significantly lower emissions from 30°S to 90°S (0 to 4%) and higher emissions from 0° to 30°N (50 to 64%) than Prinn et al. (1990) during 1998 to 2001, with 26 to 36% from the oceans. The stratosphere is also proposed to play an important role in the seasonal cycles of N_2O (Nevison et al., 2004a). For example, its well-defined seasonal cycle in the SH has been interpreted as resulting from the net effect of seasonal oceanic outgassing of microbially produced N_2O, stratospheric intrusion of low-N_2O air and other processes (Nevison et al., 2005). Nevison et al. also estimated a Southern Ocean (30°S–90°S) N_2O source of 0.9 TgN yr^{-1}, or about 5% of the global total. The complex seasonal cycle in the NH is more difficult to reconcile with seasonal variations in the northern latitude soil sources and stratospheric intrusions (Prinn et al., 2000; T. Liao et al., 2004). The destruction of N_2O in the stratosphere causes enrichment of its heavier isotopomers and isotopologues, providing a potential method to differentiate stratospheric and surface flux influences on tropospheric N_2O (Morgan et al., 2004).

Human-made PFCs, HFCs and SF_6 are very effective absorbers of infrared radiation, so that even small amounts of these gases contribute significantly to the RF of the climate system. The observations and global cycles of the major HFCs, PFCs and SF_6 were reviewed in Velders et al. (2005), and this section only provides a brief review and an update for these species. Table 2.1 shows the present mixing ratio and recent trends in the halocarbons and their RFs. Absorption spectra of most halocarbons reviewed here and in the following section are characterised by strongly overlapping spectral lines that are not resolved at tropospheric pressures and temperatures, and there is some uncertainty in cross section measurements. Apart from the uncertainties stemming from the cross sections themselves, differences in the radiative flux calculations can arise from the spectral resolution used, tropopause heights, vertical, spatial and seasonal distributions of the gases, cloud cover and how stratospheric temperature adjustments are performed. IPCC/TEAP (2005) concluded that the discrepancy in the RF calculation for different halocarbons, associated with uncertainties in the radiative transfer calculation and the cross sections, can reach 40%. Studies reviewed in IPCC/TEAP (2005) for the more abundant HFCs show that an agreement better than 12% can be reached for these when the calculation conditions are better constrained (see Section 2.10.2).

The HFCs of industrial importance have lifetimes in the range 1.4 to 270 years. The HFCs with the largest observed mole fractions in 1998 (as reported in the TAR) were, in descending order, HFC-23, HFC-134a and HFC-152a. In 2005, the observed mixing ratios of the major HFCs in the atmosphere were 35 ppt for HFC-134a, 17.5 ppt for HFC-23 (2003 value), 3.7 ppt for HFC-125 and 3.9 ppt for HFC-152a (Table 2.1). Within the uncertainties in calibration and emissions estimates, the observed mixing ratios of the HFCs in the atmosphere can be explained by the anthropogenic emissions. Measurements are available from GMD (Thompson et al., 2004) and AGAGE (Prinn et al., 2000; O'Doherty et al., 2004; Prinn et al., 2005b) networks as well as from University of East Anglia (UEA) studies in Tasmania (updated from Oram et al., 1998; Oram, 1999). These data, summarised in Figure 2.6, show a continuation of positive HFC trends and increasing latitudinal gradients (larger trends in the NH) due to their predominantly NH sources. The air conditioning refrigerant HFC-134a is increasing at a rapid rate in response to growing emissions arising from its role as a replacement for some CFC refrigerants. With a lifetime of about 14 years, its current trends are determined primarily by its emissions and secondarily by its atmospheric destruction. Emissions of HFC-134a estimated from atmospheric measurements are in approximate agreement with industry estimates (Huang and Prinn, 2002; O'Doherty et al., 2004). IPCC/TEAP (2005) reported that global HFC-134a emissions started rapidly increasing in the early 1990s, and that in Europe, sharp increases in emissions are noted for HFC-134a from 1995 to 1998 and for HFC-152a from 1996 to 2000, with some levelling off through 2003. The concentration of the foam blower HFC-152a, with a lifetime of only about 1.5 years, is rising approximately exponentially, with the effects of increasing emissions only partly offset by its rapid atmospheric destruction. Hydrofluorocarbon-23 has a very long atmospheric lifetime (approximately 270 years) and is mainly produced as a by-product of HCFC-22 production. Its concentrations are rising approximately linearly, driven by these emissions, with its destruction being only a minor factor in its budget. There are

also smaller but rising concentrations of HFC-125 and HFC-143a, which are both refrigerants.

The PFCs, mainly CF_4 (PFC-14) and C_2F_6 (PFC-116), and SF_6 have very large radiative efficiencies and lifetimes in the range 1,000 to 50,000 years (see Section 2.10, Table 2.14), and make an essentially permanent contribution to RF. The SF_6 and C_2F_6 concentrations and RFs have increased by over 20% since the TAR (Table 2.1 and Figure 2.6), but CF_4 concentrations have not been updated since 1997. Both anthropogenic and natural sources of CF_4 are important to explain its observed atmospheric abundance. These PFCs are produced as by-products of traditional aluminium production, among other activities. The CF_4 concentrations have been increasing linearly since about 1960 and CF_4 has a natural source that accounts for about one-half of its current atmospheric content (Harnisch et al., 1996). Sulphur hexafluoride (SF_6) is produced for use as an electrical insulating fluid in power distribution equipment and also deliberately released as an essentially inert tracer to study atmospheric and oceanic transport processes. Its concentration was 4.2 ppt in 1998 (TAR) and has continued to increase linearly over the past decade, implying that emissions are approximately constant. Its very long lifetime ensures that its emissions accumulate essentially unabated in the atmosphere.

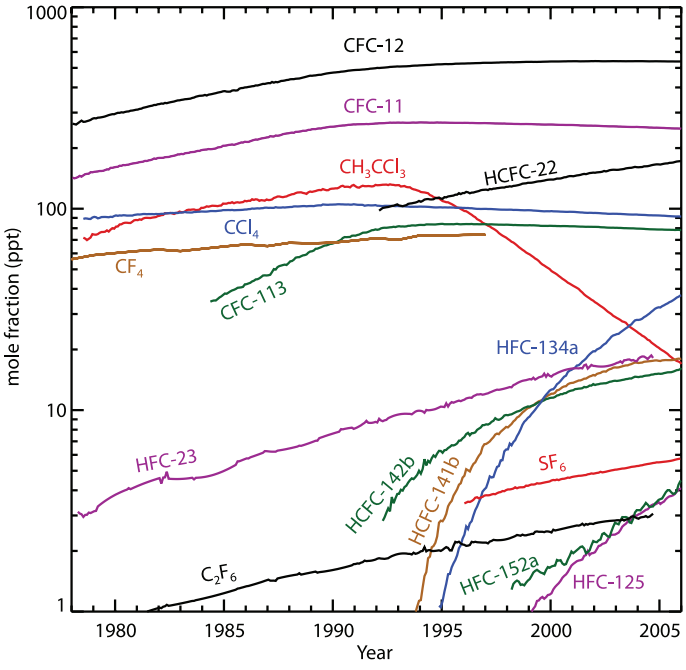


Figure 2.6. *Temporal evolution of the global average dry-air mole fractions (ppt) of the major halogen-containing LLGHGs. These are derived mainly using monthly mean measurements from the AGAGE and NOAA/GMD networks. For clarity, the two network values are averaged with equal weight when both are available. While differences exist, these network measurements agree reasonably well with each other (except for CCl_4 (differences of 2 – 4% between networks) and HCFC-142b (differences of 3 – 6% between networks)), and with other measurements where available (see text for references for each gas).*

2.3.4 Montreal Protocol Gases

The Montreal Protocol on Substances that Deplete the Ozone Layer regulates many radiatively powerful greenhouse gases for the primary purpose of lowering stratospheric chlorine and bromine concentrations. These gases include the CFCs, HCFCs, chlorocarbons, bromocarbons and halons. Observations and global cycles of these gases were reviewed in detail in Chapter 1 of the 2002 Scientific Assessment of Ozone Depletion (WMO, 2003) and in IPCC/TEAP (2005). The discussion here focuses on developments since these reviews and on those gases that contribute most to RF rather than to halogen loading. Using observed 2005 concentrations, the Montreal Protocol gases have contributed 12% (0.320 W m^{-2}) to the direct RF of all LLGHGs and 95% to the halocarbon RF (Table 2.1). This contribution is dominated by the CFCs. The effect of the Montreal Protocol on these gases has been substantial. IPCC/TEAP (2005) concluded that the combined CO_2-equivalent emissions of CFCs, HCFCs and HFCs decreased from a peak of about 7.5 $GtCO_2$-eq yr^{-1} in the late 1980s to about 2.5 $GtCO_2$-eq yr^{-1} by the year 2000, corresponding to about 10% of that year's CO_2 emissions due to global fossil fuel burning.

Measurements of the CFCs and HCFCs, summarised in Figure 2.6, are available from the AGAGE network (Prinn et al., 2000, 2005b) and the GMD network (Montzka et al., 1999 updated; Thompson et al., 2004). Certain flask measurements are also available from the University of California at Irvine (UCI; Blake et al., 2001 updated) and UEA (Oram et al., 1998; Oram, 1999 updated). Two of the major CFCs (CFC-11 and CFC-113) have both been decreasing in the atmosphere since the mid-1990s. While their emissions have decreased very substantially in response to the Montreal Protocol, their long lifetimes of around 45 and 85 years, respectively, mean that their sinks can reduce their levels by only about 2% and 1% yr^{-1}, respectively. Nevertheless, the effect of the Montreal Protocol has been to substantially reduce the growth of the halocarbon RF, which increased rapidly from 1950 until about 1990. The other major CFC (CFC-12), which is the third most important LLGHG, is finally reaching a plateau in its atmospheric levels (emissions equal loss) and may have peaked in 2003. Its 100-year lifetime means that it can decrease by only about 1% yr^{-1} even when emissions are zero. The levelling off for CFC-12 and approximately linear downward trends for CFC-11 and CFC-113 continue. Latitudinal gradients of all three are very small and decreasing as expected. The combined CFC and HCFC RF has been slowly declining since 2003. Note that the 1998 concentrations of CFC-11 and CFC-12 were overestimated in Table 6.1 of the TAR. This means that the total halocarbon RF quoted for 2005 in Table 2.1 (0.337 W m^{-2}) is slightly smaller than the 0.34 W m^{-2} quoted in the TAR, even though the measurements indicate a small 1% rise in the total halocarbon RF since the time of the TAR (Table 2.1).

The major solvent, methyl chloroform (CH_3CCl_3), is of special importance regarding RFs, not because of its small RF (see Table 2.1 and Figure 2.6), but because this gas is widely

used to estimate concentrations of OH, which is the major sink species for CH_4, HFCs, and HCFCs and a major production mechanism for sulphate, nitrate and some organic aerosols as discussed in Section 2.3.5. The global atmospheric methyl chloroform concentration rose steadily from 1978 to reach a maximum in 1992 (Prinn et al., 2001; Montzka et al., 2003). Since then, concentrations have decreased rapidly, driven by a relatively short lifetime of 4.9 years and phase-out under the Montreal Protocol, to levels in 2003 less than 20% of the levels when AGAGE measurements peaked in 1992 (Prinn et al., 2005a). Emissions of methyl chloroform determined from industry data (McCulloch and Midgley, 2001) may be too small in recent years. The 2000 to 2003 emissions from Europe estimated using surface observations (Reimann et al., 2005) show that 1.2 to 2.3 Gg yr^{-1} need to be added over this 4-year period to the above industry estimates for Europe. Estimates of European emissions in 2000 exceeding 20 Gg (Krol et al., 2003) are not supported by analyses of the above extensive surface data (Reimann et al., 2005). From multi-year measurements, Li et al. (2005) estimated 2001 to 2002 emissions from the USA of 2.2 Gg yr^{-1} (or about half of those estimated from more temporally but less geographically limited measurements by Millet and Goldstein, 2004), and suggested that 1996 to 1998 US emissions may be underestimated by an average of about 9.0 Gg yr^{-1} over this 3-year period. East Asian emissions deduced from aircraft data in 2001 are about 1.7 Gg above industry data (Palmer et al., 2003; see also Yokouchi et al., 2005) while recent Australian and Russian emissions are negligible (Prinn et al., 2001; Hurst et al., 2004).

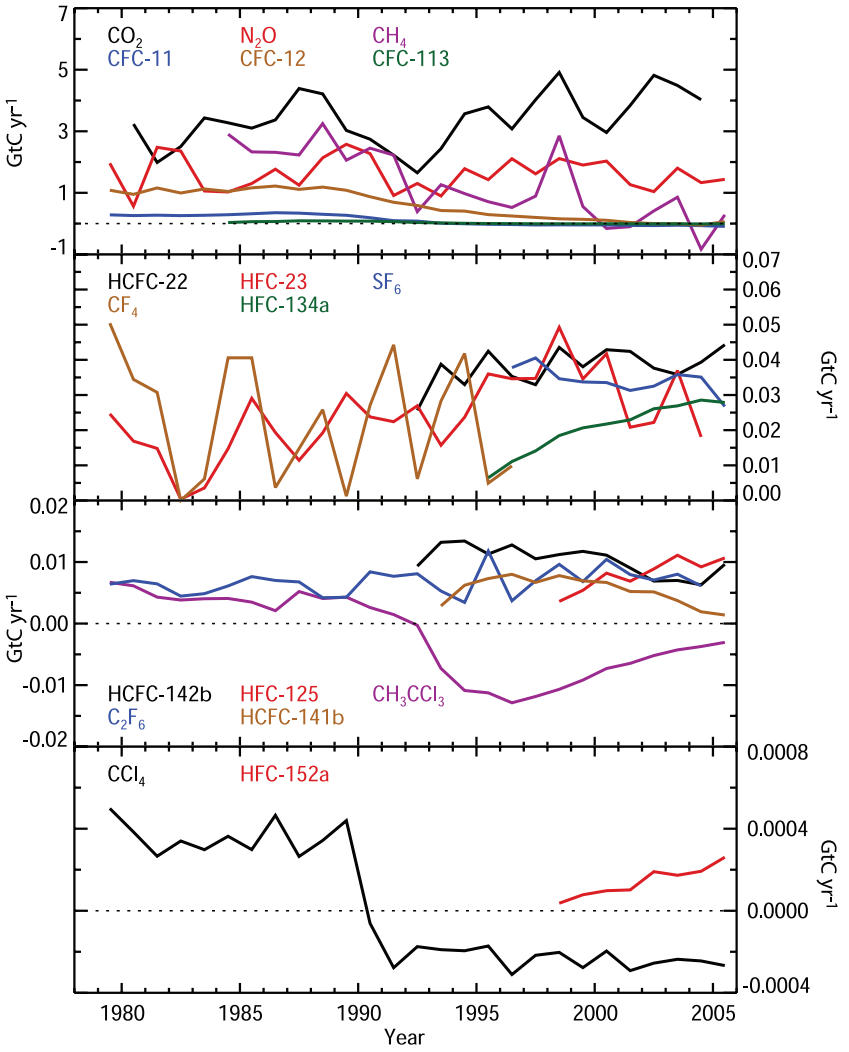


Figure 2.7. *Annual rates of change in the global atmospheric masses of each of the major LLGHGs expressed in common units of GtC yr^{-1}. These rates are computed from their actual annual mass changes in Gt yr^{-1} (as derived from their observed global and annual average mole fractions presented in Figures 2.3 to 2.6 and discussed in Sections 2.3.1 to 2.3.4) by multiplying them by their GWPs for 100-year time horizons and then dividing by the ratio of the CO_2 to carbon (C) masses (44/12). These rates are positive or negative whenever the mole fractions are increasing or decreasing, respectively. Use of these common units provides an approximate way to intercompare the fluxes of LLGHGs, using the same approach employed to intercompare the values of LLGHG emissions under the Kyoto Protocol (see, e.g., Prinn, 2004). Note that the negative indirect RF of CFCs and HCFCs due to stratospheric ozone depletion is not included. The oscillations in the CF_4 curve may result partly from truncation in reported mole fractions.*

Carbon tetrachloride (CCl_4) is the second most rapidly decreasing atmospheric chlorocarbon after methyl chloroform. Levels peaked in early 1990 and decreased approximately linearly since then (Figure 2.7). Its major use was as a feedstock for CFC manufacturing. Unlike methyl chloroform, a significant inter-hemispheric CCl_4 gradient still exists in 2005 in spite of its moderately long lifetime of 20 to 30 years, resulting from a persistence of significant NH emissions.

HCFCs of industrial importance have lifetimes in the range of 1.3 to 20 years. Global and regional emissions of the CFCs and HCFCs have been derived from observed concentrations and can be used to check emission inventory estimates. Montzka et al. (2003) and IPCC/TEAP (2005) concluded that global emissions of HCFC-22 rose steadily over the period 1975 to 2000, while those of HCFC-141b and HCFC-142b started increasing quickly in the early 1990s and then began to decrease after 2000.

To provide a direct comparison of the effects on global warming due to the annual changes in each of the non-CO_2 greenhouse gases (discussed in Sections 2.3.2, 2.3.3 and 2.3.4) relative to CO_2, Figure 2.7 shows these annual changes in atmospheric mass multiplied by the GWP (100-year horizon) for each gas (e.g., Prinn, 2004). By expressing them in this way, the observed changes in all non-CO_2 gases in GtC equivalents and the significant roles of CH_4, N_2O and many halocarbons are very evident. This highlights the importance of considering the full suite of greenhouse gases for RF calculations.

2.3.5 Trends in the Hydroxyl Free Radical

The hydroxyl free radical (OH) is the major oxidizing chemical in the atmosphere, destroying about 3.7 Gt of trace gases, including CH_4 and all HFCs and HCFCs, each year (Ehhalt, 1999). It therefore has a very significant role in limiting the LLGHG RF. IPCC/TEAP (2005) concluded that the OH concentration might change in the 21st century by –18 to +5% depending on the emission scenario. The large-scale concentrations and long-term trends in OH can be inferred indirectly using global measurements of trace gases for which emissions are well known and the primary sink is OH. The best trace gas used to date for this purpose is methyl chloroform; long-term measurements of this gas are reviewed in Section 2.3.4. Other gases that are useful OH indicators include ^{14}CO, which is produced primarily by cosmic rays (Lowe and Allan, 2002). While the accuracy of the ^{14}CO cosmic ray and other ^{14}CO source estimates and the frequency and spatial coverage of its measurements do not match those for methyl chloroform, the ^{14}CO lifetime (2 months) is much shorter than that of methyl chloroform (4.9 years). As a result, ^{14}CO provides estimates of average concentrations of OH that are more regional, and is capable of resolving shorter time scales than those estimated from methyl chloroform. The ^{14}CO source variability is better defined than its absolute magnitude so it is better for inferring relative rather than absolute trends. Another useful gas is the industrial chemical HCFC-22. It yields OH concentrations similar to those derived from methyl chloroform, but with less accuracy due to greater uncertainties in emissions and less extensive measurements (Miller et al., 1998). The industrial gases HFC-134a, HCFC-141b and HCFC-142b are potentially useful OH estimators, but the accuracy of their emission estimates needs improvement (Huang and Prinn, 2002; O'Doherty et al., 2004).

Indirect measurements of OH using methyl chloroform have established that the globally weighted average OH concentration in the troposphere is roughly 10^6 radicals per cubic centimetre (Prinn et al., 2001; Krol and Lelieveld, 2003). A similar average concentration is derived using ^{14}CO (Quay et al., 2000), although the spatial weighting here is different. Note that methods to infer global or hemispheric average OH concentrations may be insensitive to compensating regional OH changes such as OH increases over continents and decreases over oceans (Lelieveld et al., 2002). In addition, the quoted absolute OH concentrations (but not their relative trends) depend on the choice of weighting (e.g., Lawrence et al., 2001). While the global average OH concentration appears fairly well defined by these indirect methods, the temporal trends in OH are more difficult to discern since they require long-term measurements, optimal inverse methods and very accurate calibrations, model transports and methyl chloroform emissions data. From AGAGE methyl chloroform measurements, Prinn et al. (2001) inferred that global OH levels grew between 1979 and 1989, but then declined between 1989 and 2000, and also exhibited significant interannual variations. They concluded that these decadal global variations were driven principally by NH OH, with SH OH decreasing from 1979 to 1989 and staying essentially constant after that. Using the same AGAGE data and identical methyl chloroform emissions, a three-dimensional model analysis (Krol and Lelieveld, 2003) supported qualitatively (but not quantitatively) the earlier result (Prinn et al., 2001) that OH concentrations increased in the 1980s and declined in the 1990s. Prinn et al. (2001) also estimated the emissions required to provide a zero trend in OH. These required methyl chloroform emissions differed substantially from industry estimates by McCulloch and Midgley (2001) particularly for 1996 to 2000. However, Krol and Lelieveld (2003) argued that the combination of possible underestimated recent emissions, especially the >20 Gg European emissions deduced by Krol et al. (2003), and the recent decreasing effectiveness of the stratosphere as a sink for tropospheric methyl chloroform, may be sufficient to yield a zero deduced OH trend. As discussed in Section 2.3.4, estimates of European emissions by Reimann et al. (2005) are an order of magnitude less than those of Krol et al. (2003). In addition, Prinn et al. (2005a) extended the OH estimates through 2004 and showed that the Prinn et al. (2001) decadal and interannual OH estimates remain valid even after accounting for the additional recent methyl chloroform emissions discussed in Section 2.3.4. They also reconfirmed the OH maximum around 1989 and a larger OH minimum around 1998, with OH concentrations then recovering so that in 2003 they were comparable to those in 1979. They noted that the 1997 to 1999 OH minimum coincides with, and is likely caused by, major global wildfires and an intense El Niño at that time. The 1997 Indonesian fires alone have been estimated to have lowered global late-1997 OH levels by 6% due to carbon monoxide (CO) enhancements (Duncan et al., 2003).

Methyl chloroform is also destroyed in the stratosphere. Because its stratospheric loss frequency is less than that in the troposphere, the stratosphere becomes a less effective sink for tropospheric methyl chloroform over time (Krol and Lelieveld, 2003), and even becomes a small source to the troposphere beginning in 1999 in the reference case in the Prinn et al. (2001, 2005a) model. Loss to the ocean has usually been considered irreversible, and its rates and uncertainties have been obtained from observations (Yvon-Lewis and Butler, 2002). However, Wennberg et al. (2004) recently proposed that the polar oceans may have effectively stored methyl chloroform during the pre-1992 years when its atmospheric levels were rising, but began re-emitting it in subsequent years, thus reducing the overall oceanic sink. Prinn et al. (2005a) tried both approaches and found that their inferred interannual and decadal OH variations were present using either formulation, but inferred OH was lower in the pre-1992 years and higher after that using the Wennberg et al. (2004) formulation.

More recently, Bousquet et al. (2005) used an inverse method with a three-dimensional model and methyl chloroform measurements and concluded that substantial year-to-year variations occurred in global average OH concentrations between 1980 and 2000. This conclusion was previously reached by Prinn et al. (2001), but subsequently challenged by Krol and Lelieveld (2003) who argued that these variations

were caused by model shortcomings and that models need, in particular, to include observationally-based, interannually varying meteorology to provide accurate annual OH estimates. Neither the two-dimensional Prinn et al. (2001) nor the three-dimensional Krol et al. (2003) inversion models used interannually varying circulation. However, the Bousquet et al. (2005) analysis, which uses observationally based meteorology and estimates OH on monthly time scales, yields interannual OH variations that agree very well with the Prinn et al. (2001) and equivalent Krol and Lelieveld (2003) estimates (see Figure 2.8). However, when Bousquet et al. (2005) estimated both OH concentrations and methyl chloroform emissions (constrained by their uncertainties as reported by McCulloch and Midgley, 2001), the OH variations were reduced by 65% (dashed line in Figure 2.8). The error bars on the Prinn et al. (2001, 2005a) OH estimates, which account for these emission uncertainties using Monte Carlo ensembles of inversions, also easily allow such a reduction in OH variability (thin vertical bars in Figure 2.8). This implies that these interannual OH variations are real, but only their phasing and not their amplitude, is well defined. Bousquet et al. (2005) also deduced that OH in the SH shows a zero to small negative trend, in qualitative agreement with Prinn et al. (2001). Short-term variations in OH were also recently deduced by Manning et al. (2005) using 13 years of ^{14}CO measurements in New Zealand and Antarctica. They found no significant long-term trend between 1989 and 2003 in SH OH but provided evidence for recurring multi-month OH variations of around 10%. They also deduced even larger (20%) OH decreases in 1991 and 1997, perhaps triggered by the 1991 Mt. Pinatubo eruption and the 1997 Indonesian fires. The similarity

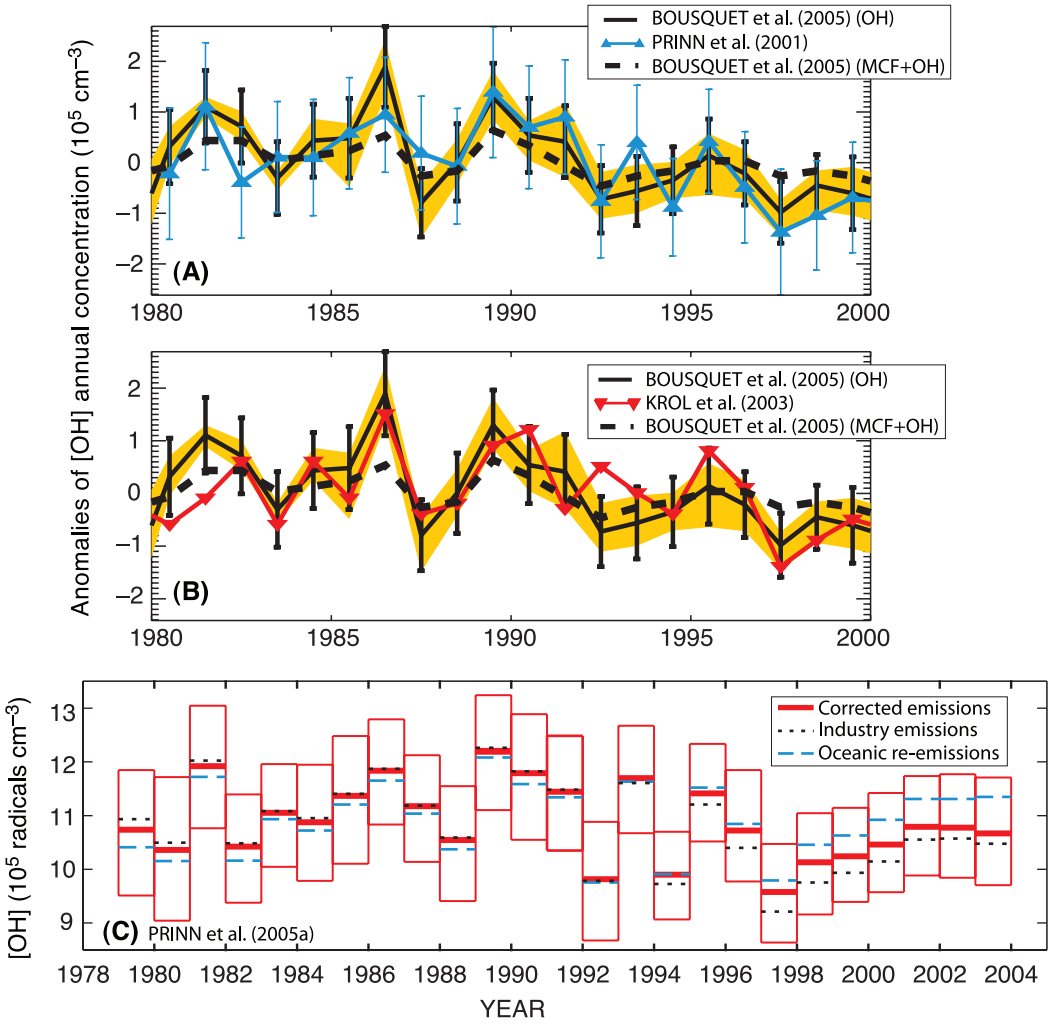


Figure 2.8. *Estimates used to evaluate trends in weighted global average OH concentrations. (A) and (B): comparison of 1980 to 1999 OH anomalies (relative to their long-term means) inferred by Bousquet et al. (2005), Prinn et al. (2001) and Krol et al. (2003) from AGAGE methyl chloroform observations, and by Bousquet et al. (2005) when methyl chloroform emissions as well as OH are inferred; error bars for Bousquet et al. (2005) refer to 1 standard deviation inversion errors while yellow areas refer to the envelope of their 18 OH inversions. (C) OH concentrations for 1979 to 2003 inferred by Prinn et al. (2005a) (utilising industry emissions corrected using recent methyl chloroform observations), showing the recovery of 2003 OH levels to 1979 levels; also shown are results assuming uncorrected emissions and estimates of recent oceanic re-emissions. Error bars in Prinn et al. (2001, 2005a) are 1 standard deviation and include inversion, model, emission and calibration errors from large Monte Carlo ensembles (see Section 2.3.5 for details and references).*

of many of these results to those from methyl chloroform discussed above is very important, given the independence of the two approaches.

RF calculations of the LLGHGs are calculated from observed trends in the LLGHG concentrations and therefore OH concentrations do not directly affect them. Nevertheless OH trends are needed to quantify LLGHG budgets (Section 7.4) and for understanding future trends in the LLGHGs and tropospheric ozone.

2.3.6 Ozone

In the TAR, separate estimates for RF due to changes in tropospheric and stratospheric ozone were given. Stratospheric ozone RF was derived from observations of ozone change from roughly 1979 to 1998. Tropospheric ozone RF was based on chemical model results employing changes in precursor hydrocarbons, CO and nitrogen oxides (NO_x). Over the satellite era (since approximately 1980), stratospheric ozone trends have been primarily caused by the Montreal Protocol gases, and in Ramaswamy et al. (2001) the stratospheric ozone RF was implicitly attributed to these gases. Studies since then have investigated a number of possible causes of ozone change in the stratosphere and troposphere and the attribution of ozone trends to a given precursor is less clear. Nevertheless, stratospheric ozone and tropospheric ozone RFs are still treated separately in this report. However, the RFs are more associated with the vertical location of the ozone change than they are with the agent(s) responsible for the change.

2.3.6.1 Stratospheric Ozone

The TAR reported that ozone depletion in the stratosphere had caused a negative RF of –0.15 W m^{-2} as a best estimate over the period since 1750. A number of recent reports have assessed changes in stratospheric ozone and the research into its causes, including Chapters 3 and 4 of the 2002 Scientific Assessment of Ozone Depletion (WMO, 2003) and Chapter 1 of IPCC/TEAP (2005). This section summarises the material from these reports and updates the key results using more recent research.

Global ozone amounts decreased between the late 1970s and early 1990s, with the lowest values occurring during 1992 to 1993 (roughly 6% below the 1964 to 1980 average), and slightly increasing values thereafter. Global ozone for the period 2000 to 2003 was approximately 4% below the 1964 to 1980 average values. Whether or not recently observed changes in ozone trends (Newchurch et al., 2003; Weatherhead and Andersen, 2006) are already indicative of recovery of the global ozone layer is not yet clear and requires more detailed attribution of the drivers of the changes (Steinbrecht et al., 2004a (see also comment and reply: Cunnold et al., 2004 and Steinbrecht et al., 2004b); Hadjinicolaou et al., 2005; Krizan and Lastovicka, 2005; Weatherhead and Andersen, 2006). The largest ozone changes since 1980 have occurred during the late winter and spring over Antarctica where average total column ozone in September and October is about 40 to 50% below pre-1980 values (WMO, 2003). Ozone decreases over the Arctic have been less severe than have those over the Antarctic, due to higher temperature in the lower stratosphere and thus fewer polar stratospheric clouds to cause the chemical destruction. Arctic stratospheric ozone levels are more variable due to interannual variability in chemical loss and transport.

The temporally and seasonally non-uniform nature of stratospheric ozone trends has important implications for the resulting RF. Global ozone decreases result primarily from changes in the lower stratospheric extratropics. Total column ozone changes over the mid-latitudes of the SH are significantly larger than over the mid-latitudes of the NH. Averaged over the period 2000 to 2003, SH values are 6% below pre-1980 values, while NH values are 3% lower. There is also significant seasonality in the NH ozone changes, with 4% decreases in winter to spring and 2% decreases in summer, while long-term SH changes are roughly 6% year round (WMO, 2003). Southern Hemisphere mid-latitude ozone shows significant decreases during the mid-1980s and essentially no response to the effects of the Mt. Pinatubo volcanic eruption in June 1991; both of these features remain unexplained. Pyle et al. (2005) and Chipperfield et al. (2003) assessed several studies that show that a substantial fraction (roughly 30%) of NH mid-latitude ozone trends are not directly attributable to anthropogenic chemistry, but are related to dynamical effects, such as tropopause height changes. These dynamical effects are likely to have contributed a larger fraction of the ozone RF in the NH mid-latitudes. The only study to assess this found that 50% of the RF related to stratospheric ozone changes between 20°N to 60°N over the period 1970 to 1997 is attributable to dynamics (Forster and Tourpali, 2001). These dynamical changes may well have an anthropogenic origin and could even be partly caused by stratospheric ozone changes themselves through lower stratospheric temperature changes (Chipperfield et al., 2003; Santer et al., 2004), but are not directly related to chemical ozone loss.

At the time of writing, no study has utilised ozone trend observations after 1998 to update the RF values presented in Ramaswamy et al. (2001). However, Hansen et al. (2005) repeated the RF calculation based on the same trend data set employed by studies assessed in Ramaswamy et al. (2001) and found an RF of roughly –0.06 W m^{-2}. A considerably stronger RF of –0.2 ± 0.1 W m^{-2} previously estimated by the same group affected the Ramaswamy et al. (2001) assessment. The two other studies assessed in Ramaswamy et al. (2001), using similar trend data sets, found RFs of –0.01 W m^{-2} and –0.10 W m^{-2}. Using the three estimates gives a revision of the observationally based RF for 1979 to 1998 to about –0.05 ± 0.05 W m^{-2}.

Gauss et al. (2006) compared results from six chemical transport models that included changes in ozone precursors to simulate both the increase in the ozone in the troposphere and the ozone reduction in the stratosphere over the industrial era. The 1850 to 2000 annually averaged global mean stratospheric ozone column reduction for these models ranged between 14 and 29 Dobson units (DU). The overall pattern of the ozone changes from the models were similar but the magnitude of the ozone

changes differed. The models showed a reduction in the ozone at high latitudes, ranging from around 20 to 40% in the SH and smaller changes in the NH. All models have a maximum ozone reduction around 15 km at high latitudes in the SH. Differences between the models were also found in the tropics, with some models simulating about a 10% increase in the lower stratosphere and other models simulating decreases. These differences were especially related to the altitude where the ozone trend switched from an increase in the troposphere to a decrease in the stratosphere, which ranged from close to the tropopause to around 27 km. Several studies have shown that ozone changes in the tropical lower stratosphere are very important for the magnitude and sign of the ozone RF (Ramaswamy et al., 2001). The resulting stratospheric ozone RF ranged between –0.12 and +0.07 W m^{-2}. Note that the models with either a small negative or a positive RF also had a small increase in tropical lower stratospheric ozone, resulting from increases in tropospheric ozone precursors; most of this increase would have occurred before the time of stratospheric ozone destruction by the Montreal Protocol gases. These RF calculations also did not include any negative RF that may have resulted from stratospheric water vapour increases. It has been suggested (Shindell and Faluvegi, 2002) that stratospheric ozone during 1957 to 1975 was lower by about 7 DU relative to the first half of the 20th century as a result of possible stratospheric water vapour increases; however, these long-term increases in stratospheric water vapour are uncertain (see Sections 2.3.7 and 3.4).

The stratospheric ozone RF is assessed to be –0.05 ± 0.10 W m^{-2} between pre-industrial times and 2005. The best estimate is from the observationally based 1979 to 1998 RF of –0.05 ± 0.05 W m^{-2}, with the uncertainty range increased to take into account ozone change prior to 1979, using the model results of Gauss et al. (2006) as a guide. Note that this estimate takes into account causes of stratospheric ozone change in addition to those due to the Montreal Protocol gases. The level of scientific understanding is medium, unchanged from the TAR (see Section 2.9, Table 2.11).

2.3.6.2 Tropospheric Ozone

The TAR identified large regional differences in observed trends in tropospheric ozone from ozonesondes and surface observations. The TAR estimate of RF from tropospheric ozone was +0.35 ± 0.15 W m^{-2}. Due to limited spatial and temporal coverage of observations of tropospheric ozone, the RF estimate is based on model simulations. In the TAR, the models considered only changes in the tropospheric photochemical system, driven by estimated emission changes (NO_x, CO, non-methane volatile organic compounds (NMVOCs), and CH_4) since pre-industrial times. Since the TAR, there have been major improvements in models. The new generation models include several Chemical Transport Models (CTMs) that couple stratospheric and tropospheric chemistry, as well as GCMs with on-line chemistry (both tropospheric and stratospheric). While the TAR simulations did not consider changes in ozone within the troposphere caused by reduced influx of ozone from the stratosphere (due to ozone depletion in the stratosphere), the new models include this process (Gauss et al., 2006). This advancement in modelling capabilities and the need to be consistent with how the RF due to changes in stratospheric ozone is derived (based on observed ozone changes) have led to a change in the definition of RF due to tropospheric ozone compared with that in the TAR. Changes in tropospheric ozone due to changes in transport of ozone across the tropopause, which are in turn caused by changes in stratospheric ozone, are now included.

Trends in anthropogenic emissions of ozone precursors for the period 1990 to 2000 have been compiled by the Emission Database for Global Atmospheric Research (EDGAR) consortium (Olivier and Berdowski, 2001 updated). For specific regions, there is significant variability over the period due to variations in the emissions from open biomass burning sources. For all components (NO_x, CO and volatile organic compounds (VOCs)) industrialised regions like the USA and Organisation for Economic Co-operation and Development (OECD) Europe show reductions in emissions, while regions dominated by developing countries show significant growth in emissions. Recently, the tropospheric burdens of CO and NO_2 were estimated from satellite observations (Edwards et al., 2004; Richter et al., 2005), providing much needed data for model evaluation and very valuable constraints for emission estimates.

Assessment of long-term trends in tropospheric ozone is difficult due to the scarcity of representative observing sites with long records. The long-term tropospheric ozone trends vary both in terms of sign and magnitude and in the possible causes for the change (Oltmans et al., 2006). Trends in tropospheric ozone at northern middle and high latitudes have been estimated based on ozonesonde data by WMO (2003), Naja et al. (2003), Naja and Akimoto (2004), Tarasick et al. (2005) and Oltmans et al. (2006). Over Europe, ozone in the free troposphere increased from the early 20th century until the late 1980s; since then the trend has levelled off or been slightly negative. Naja and Akimoto (2004) analysed 33 years of ozonesonde data from Japanese stations, and showed an increase in ozone in the lower troposphere (750–550 hPa) between the periods 1970 to 1985 and 1986 to 2002 of 12 to 15% at Sapporo and Tsukuba (43°N and 36°N) and 35% at Kagoshima (32°N). Trajectory analysis indicates that the more southerly station, Kagoshima, is significantly more influenced by air originating over China, while Sapporo and Tsukuba are more influenced by air from Eurasia. At Naha (26°N) a positive trend (5% per decade) is found between 700 and 300 hPa (1990–2004), while between the surface and 700 hPa a slightly negative trend is observed (Oltmans et al., 2006). Ozonesondes from Canadian stations show negative trends in tropospheric ozone between 1980 and 1990, and a rebound with positive trends during 1991 to 2001 (Tarasick et al., 2005). Analysis of stratosphere-troposphere exchange processes indicates that the rebound during the 1990s may be partly a result of small changes in atmospheric circulation.

Trends are also derived from surface observations. Jaffe et al. (2003) derived a positive trend of 1.4% yr^{-1} between 1988

and 2003 using measurements from Lassen Volcanic Park in California (1,750 m above sea level), consistent with the trend derived by comparing two aircraft campaigns (Parrish et al., 2004). However, a number of other sites show insignificant changes over the USA over the last 15 years (Oltmans et al., 2006). Over Europe and North America, observations from Whiteface Mountain, Wallops Island, Hohenpeisenberg, Zugspitze and Mace Head (flow from the European sector) show small trends or reductions during summer, while there is an increase during winter (Oltmans et al., 2006). These observations are consistent with reduced NO_x emissions (Jonson et al., 2005). North Atlantic stations (Mace Head, Izana and Bermuda) indicate increased ozone (Oltmans et al., 2006). Over the North Atlantic (40°N–60°N) measurements from ships (Lelieveld et al., 2004) show insignificant trends in ozone, however, at Mace Head a positive trend of 0.49 ± 0.19 ppb yr^{-1} for the period 1987 to 2003 is found, with the largest contribution from air coming from the Atlantic sector (Simmonds et al., 2004).

In the tropics, very few long-term ozonesonde measurements are available. At Irene in South Africa (26°S), Diab et al. (2004) found an increase between the 1990 to 1994 and 1998 to 2002 periods of about 10 ppb close to the surface (except in summer) and in the upper troposphere during winter. Thompson et al. (2001) found no significant trend during 1979 to 1992, based on Total Ozone Mapping Spectrometer (TOMS) satellite data. More recent observations (1994 to 2003, *in situ* data from the Measurement of Ozone by Airbus In-service Aircraft (MOZAIC) program) show significant trends in free-tropospheric ozone (7.7 to 11.3 km altitude) in the tropics: 1.12 ± 0.05 ppb yr^{-1} and 1.03 ± 0.08 ppb yr^{-1} in the NH tropics and SH tropics, respectively (Bortz and Prather, 2006). Ozonesonde measurements over the southwest Pacific indicate an increased frequency of near-zero ozone in the upper troposphere, suggesting a link to an increased frequency of deep convection there since the 1980s (Solomon et al., 2005).

At southern mid-latitudes, surface observations from Cape Point, Cape Grim, the Atlantic Ocean (from ship) and from sondes at Lauder (850–700 hPa) show positive trends in ozone concentrations, in particular during the biomass burning season in the SH (Oltmans et al., 2006). However, the trend is not accompanied by a similar trend in CO, as expected if biomass burning had increased. The increase is largest at Cape Point, reaching 20% per decade (in September). At Lauder, the increase is confined to the lower troposphere.

Changes in tropospheric ozone and the corresponding RF have been estimated in a number of recent model studies (Hauglustaine and Brasseur, 2001; Mickley et al., 2001; Shindell et al., 2003a; Mickley et al., 2004; Wong et al., 2004; Liao and Seinfeld, 2005; Shindell et al., 2005). In addition, a multi-model experiment including 10 global models was organised through the Atmospheric Composition Change: an European Network (ACCENT; Gauss et al., 2006). Four of the ten ACCENT models have detailed stratospheric chemistry. The adjusted RF for all models was calculated by the same radiative transfer model. The normalised adjusted RF for the ACCENT models was $+0.032 \pm 0.006$ W m^{-2} DU^{-1}, which is significantly lower than the TAR estimate of $+0.042$ W m^{-2} DU^{-1}.

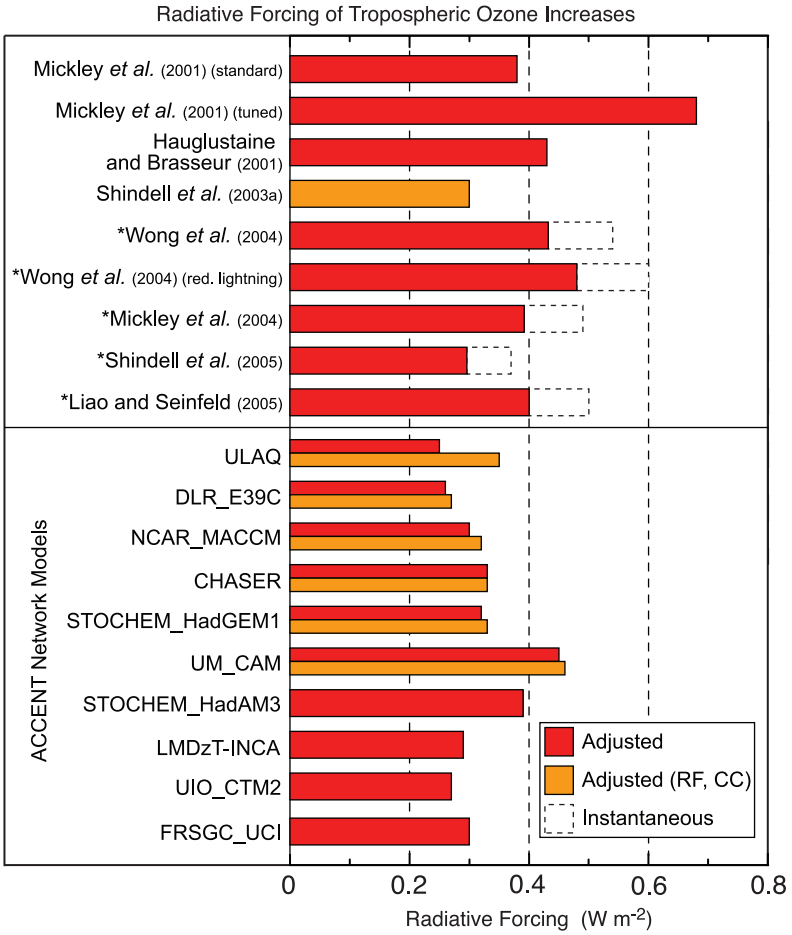


Figure 2.9. *Calculated RF due to tropospheric ozone change since pre-industrial time based on CTM and GCM model simulations published since the TAR. Estimates with GCMs including the effect of climate change since 1750 are given by orange bars (Adjusted RF, CC). Studies denoted with an (*) give only the instantaneous RF in the original publications. Stratospheric-adjusted RFs for these are estimated by reducing the instantaneous RF (indicated by the dashed bars) by 20%. The instantaneous RF from Mickley et al. (2001) is reported as an adjusted RF in Gauss et al. (2006). ACCENT models include ULAQ: University of L'Aquila; DLR_E39C: Deutsches Zentrum für Luft- und Raumfahrt European Centre Hamburg Model; NCAR_MACCM: National Center for Atmospheric Research Middle Atmosphere Community Climate Model; CHASER: Chemical Atmospheric GCM for Study of Atmospheric Environment and Radiative Forcing; STOCHEM_HadGEM1: United Kingdom Meteorological Office global atmospheric chemistry model /Hadley Centre Global Environmental Model 1; UM_CAM: United Kingdom Meteorological Office Unified Model GCM with Cambridge University chemistry; STOCHEM_HadAM3: United Kingdom Meteorological Office global atmospheric chemistry model/ Hadley Centre Atmospheric Model; LMDzT-INCA: Laboratoire de Météorologie Dynamique GCM-INteraction with Chemistry and Aerosols; UIO_CTM2: University of Oslo CTM; FRSGC_UCI: Frontier Research System for Global Change/University of California at Irvine CTM.*

The simulated RFs for tropospheric ozone increases since 1750 are shown in Figure 2.9. Most of the calculations used the same set of assumptions about pre-industrial emissions (zero anthropogenic emissions and biomass burning sources reduced by 90%). Emissions of NO_x from soils and biogenic hydrocarbons were generally assumed to be natural and were thus not changed (see, e.g., Section 7.4). In one study (Hauglustaine and Brasseur, 2001), pre-industrial NO_x emissions from soils were reduced based on changes in the use of fertilizers. Six of the ACCENT models also made coupled climate-chemistry simulations including climate change since pre-industrial times. The difference between the RFs in the coupled climate-chemistry and the chemistry-only simulations, which indicate the possible climate feedback to tropospheric ozone, was positive in all models but generally small (Figure 2.9).

A general feature of the models is their inability to reproduce the low ozone concentrations indicated by the very uncertain semi-quantitative observations (e.g., Pavelin et al., 1999) during the late 19th century. Mickley et al. (2001) tuned their model by reducing pre-industrial lightning and soil sources of NO_x and increasing natural NMVOC emissions to obtain close agreement with the observations. The ozone RF then increased by 50 to 80% compared to their standard calculations. However, there are still several aspects of the early observations that the tuned model did not capture.

The best estimate for the RF of tropospheric ozone increases is +0.35 W m^{-2}, taken as the median of the RF values in Figure 2.9 (adjusted and non-climate change values only, i.e., the red bars). The best estimate is unchanged from the TAR. The uncertainties in the estimated RF by tropospheric ozone originate from two factors: the models used (CTM/GCM model formulation, radiative transfer models), and the potential overestimation of pre-industrial ozone levels in the models. The 5 to 95% confidence interval, assumed to be represented by the range of the results in Figure 2.9, is +0.25 to +0.65 W m^{-2}. A medium level of scientific understanding is adopted, also unchanged from the TAR (see Section 2.9, Table 2.11).

2.3.7 Stratospheric Water Vapour

The TAR noted that several studies had indicated long-term increases in stratospheric water vapour and acknowledged that these trends would contribute a significant radiative impact. However, it only considered the stratospheric water vapour increase expected from CH_4 increases as an RF, and this was estimated to contribute 2 to 5% of the total CH_4 RF (about +0.02 W m^{-2}).

Section 3.4 discusses the evidence for stratospheric water vapour trends and presents the current understanding of their possible causes. There are now 14 years of global stratospheric water vapour measurements from Halogen Occultation Experiment (HALOE) and continued balloon-based measurements (since 1980) at Boulder, Colorado. There is some evidence of a sustained long-term increase in stratospheric water vapour of around 0.05 ppm yr^{-1} from 1980 until roughly 2000, since then water vapour concentrations in the lower stratosphere have been decreasing (see Section 3.4 for details and references). As well as CH_4 increases, several other indirect forcing mechanisms have been proposed, including: a) volcanic eruptions (Considi ne et al., 2001; Joshi and Shine, 2003); b) biomass burning aerosol (Sherwood, 2002); c) tropospheric (SO_2; Notholt et al., 2005) and d) changes in CH_4 oxidation rates from changes in stratospheric chlorine, ozone and OH (Rockmann et al., 2004). These are mechanisms that can be linked to an external forcing agent. Other proposed mechanisms are more associated with climate feedbacks and are related to changes in tropopause temperatures or circulation (Stuber et al., 2001a; Fueglistaler et al., 2004). From these studies, there is little quantification of the stratospheric water vapour change attributable to different causes. It is also likely that different mechanisms are affecting water vapour trends at different altitudes.

Since the TAR, several further calculations of the radiative balance change due to changes in stratospheric water vapour have been performed (Forster and Shine, 1999; Oinas et al., 2001; Shindell, 2001; Smith et al., 2001; Forster and Shine, 2002). Smith et al. (2001) estimated a +0.12 to +0.2 W m^{-2} per decade range for the RF from the change in stratospheric water vapour, using HALOE satellite data. Shindell (2001) estimated an RF of about +0.2 W m^{-2} in a period of two decades, using a GCM to estimate the increase in water vapour in the stratosphere from oxidation of CH_4 and including climate feedback changes associated with an increase in greenhouse gases. Forster and Shine (2002) used a constant 0.05 ppm yr^{-1} trend in water vapour at pressures of 100 to 10 hPa and estimated the RF to be +0.29 W m^{-2} for 1980 to 2000. GCM radiation codes can have a factor of two uncertainty in their modelling of this RF (Oinas et al., 2001). For the purposes of this chapter, the above RF estimates are not readily attributable to forcing agent(s) and uncertainty as to the causes of the observed change precludes all but the component due to CH_4 increases being considered a forcing. Two related CTM studies have calculated the RF associated with increases in CH_4 since pre-industrial times (Hansen and Sato, 2001; Hansen et al., 2005), but no dynamical feedbacks were included in those estimates. Hansen et al. (2005) estimated an RF of +0.07 ± 0.01 W m^{-2} for the stratospheric water vapour changes over 1750 to 2000, which is at least a factor of three larger than the TAR value. The RF from direct injection of water vapour by aircraft is believed to be an order of magnitude smaller than this, at about +0.002 W m^{-2} (IPCC, 1999). There has been little trend in CH_4 concentration since 2000 (see Section 2.3.2); therefore the best estimate of the stratospheric water vapour RF from CH_4 oxidation (+0.07 W m^{-2}) is based on the Hansen et al. (2005) calculation. The 90% confidence range is estimated as ±0.05 W m^{-2}, from the range of the RF studies that included other effects. There is a low level of scientific understanding in this estimate, as there is only a partial understanding of the vertical profile of CH_4-induced stratospheric water vapour change (Section 2.9, Table 2.11). Other human causes of stratospheric water vapour change are unquantified and have a very low level of scientific understanding.

2.3.8 Observations of Long-Lived Greenhouse Gas Radiative Effects

Observations of the clear-sky radiation emerging at the top of the atmosphere and at the surface have been conducted. Such observations, by their nature, do not measure RF as defined here. Instead, they yield a perspective on the influence of various species on the transfer of radiation in the atmosphere. Most importantly, the conditions involved with these observations involve varying thermal and moisture profiles in the atmosphere such that they do not conform to the conditions underlying the RF definition (see Section 2.2). There is a more comprehensive discussion of observations of the Earth's radiative balance in Section 3.4.

Harries et al. (2001) analysed spectra of the outgoing longwave radiation as measured by two satellites in 1970 and 1997 over the tropical Pacific Ocean. The reduced brightness temperature observed in the spectral regions of many of the greenhouse gases is experimental evidence for an increase in the Earth's greenhouse effect. In particular, the spectral signatures were large for CO_2 and CH_4. The halocarbons, with their large change between 1970 and 1997, also had an impact on the brightness temperature. Philipona et al. (2004) found an increase in the measured longwave downward radiation at the surface over the period from 1995 to 2002 at eight stations over the central Alps. A significant increase in the clear-sky longwave downward flux was found to be due to an enhanced greenhouse effect after combining the measurements with model calculations to estimate the contribution from increases in temperature and humidity. While both types of observations attest to the radiative influences of the gases, they should not be interpreted as having a direct linkage to the value of RFs in Section 2.3.

2.4 Aerosols

2.4.1 Introduction and Summary of the Third Assessment Report

The TAR categorised aerosol RFs into direct and indirect effects. The direct effect is the mechanism by which aerosols scatter and absorb shortwave and longwave radiation, thereby altering the radiative balance of the Earth-atmosphere system. Sulphate, fossil fuel organic carbon, fossil fuel black carbon, biomass burning and mineral dust aerosols were all identified as having a significant anthropogenic component and exerting a significant direct RF. Key parameters for determining the direct RF are the aerosol optical properties (the single scattering albedo, ω_o, specific extinction coefficient, k_e and the scattering phase function), which vary as a function of wavelength and relative humidity, and the atmospheric loading and geographic distribution of the aerosols in the horizontal and vertical, which vary as a function of time (e.g., Haywood and Boucher, 2000; Penner et al., 2001; Ramaswamy et al., 2001). Scattering aerosols exert a net negative direct RF, while partially absorbing aerosols may exert a negative top-of-the-atmosphere (TOA) direct RF over dark surfaces such as oceans or dark forest surfaces, and a positive TOA RF over bright surfaces such as desert, snow and ice, or if the aerosol is above cloud (e.g., Chylek and Wong, 1995; Haywood and Shine, 1995). Both positive and negative TOA direct RF mechanisms reduce the shortwave irradiance at the surface. The longwave direct RF is only substantial if the aerosol particles are large and occur in considerable concentrations at higher altitudes (e.g., Tegen et al., 1996). The direct RF due to tropospheric aerosols is most frequently derived at TOA rather than at the tropopause because shortwave radiative transfer calculations have shown a negligible difference between the two (e.g., Haywood and Shine, 1997; Section 2.2). The surface forcing will be approximately the same as the direct RF at the TOA for scattering aerosols, but for partially absorbing aerosols the surface forcing may be many times stronger than the TOA direct RF (e.g., Ramanathan et al., 2001b and references therein).

The indirect effect is the mechanism by which aerosols modify the microphysical and hence the radiative properties, amount and lifetime of clouds (Figure 2.10). Key parameters for determining the indirect effect are the effectiveness of an aerosol particle to act as a cloud condensation nucleus, which is a function of the size, chemical composition, mixing state and ambient environment (e.g., Penner et al., 2001). The microphysically induced effect on the cloud droplet number concentration and hence the cloud droplet size, with the liquid water content held fixed has been called the 'first indirect effect' (e.g., Ramaswamy et al., 2001), the 'cloud albedo effect' (e.g., Lohmann and Feichter, 2005), or the 'Twomey effect' (e.g., Twomey, 1977). The microphysically induced effect on the liquid water content, cloud height, and lifetime of clouds has been called the 'second indirect effect' (e.g., Ramaswamy et al., 2001), the 'cloud lifetime effect' (e.g., Lohmann and Feichter, 2005) or the 'Albrecht effect' (e.g., Albrecht, 1989). The TAR split the indirect effect into the first indirect effect, and the second indirect effect. Throughout this report, these effects are denoted as 'cloud albedo effect' and 'cloud lifetime effect', respectively, as these terms are more descriptive of the microphysical processes that occur. The cloud albedo effect was considered in the TAR to be an RF because global model calculations could be performed to describe the influence of increased aerosol concentration on the cloud optical properties while holding the liquid water content of the cloud fixed (i.e., in an entirely diagnostic manner where feedback mechanisms do not occur). The TAR considered the cloud albedo effect to be a key uncertainty in the RF of climate but did not assign a best estimate of the RF, and showed a range of RF between 0 and –2 W m^{-2} in the context of liquid water clouds. The other indirect effects were not considered to be RFs because, in suppressing drizzle, increasing the cloud height or the cloud lifetime in atmospheric models (Figure 2.10), the hydrological cycle is invariably altered (i.e., feedbacks occur; see Section

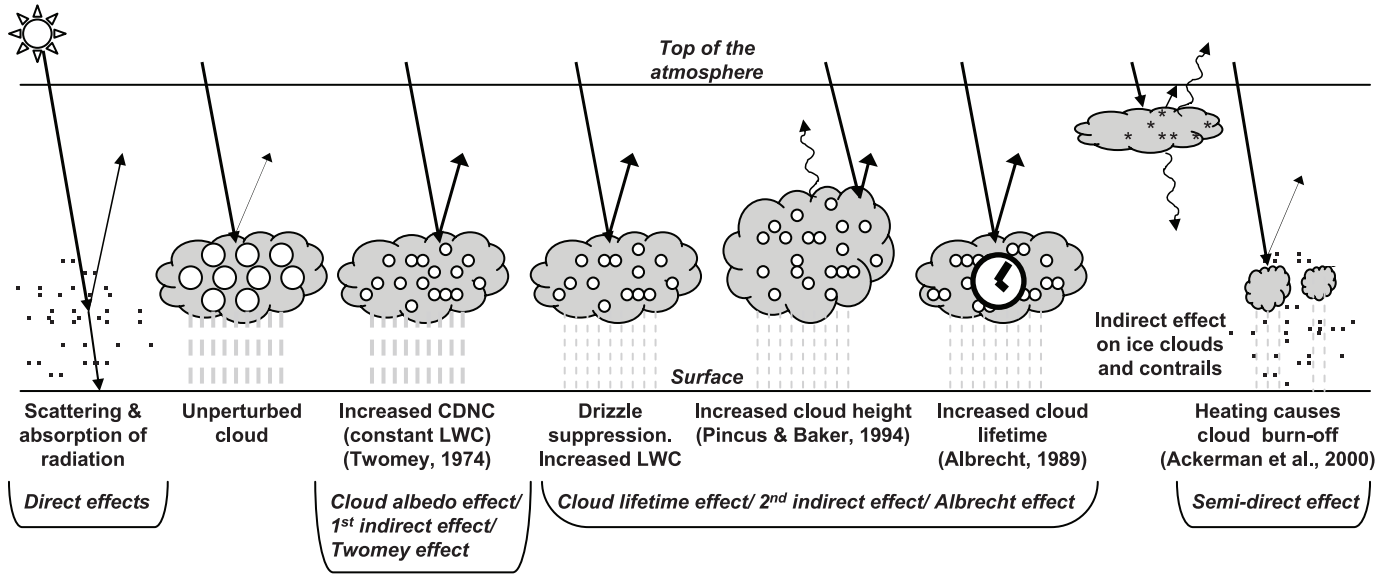


Figure 2.10. *Schematic diagram showing the various radiative mechanisms associated with cloud effects that have been identified as significant in relation to aerosols (modified from Haywood and Boucher, 2000). The small black dots represent aerosol particles; the larger open circles cloud droplets. Straight lines represent the incident and reflected solar radiation, and wavy lines represent terrestrial radiation. The filled white circles indicate cloud droplet number concentration (CDNC). The unperturbed cloud contains larger cloud drops as only natural aerosols are available as cloud condensation nuclei, while the perturbed cloud contains a greater number of smaller cloud drops as both natural and anthropogenic aerosols are available as cloud condensation nuclei (CCN). The vertical grey dashes represent rainfall, and LWC refers to the liquid water content.*

7.5). The TAR also discussed the impact of anthropogenic aerosols on the formation and modification of the physical and radiative properties of ice clouds (Penner et al., 2001), although quantification of an RF from this mechanism was not considered appropriate given the host of uncertainties and unknowns surrounding ice cloud nucleation and physics.

The TAR did not include any assessment of the semi-direct effect (e.g., Hansen et al., 1997; Ackerman et al., 2000a; Jacobson, 2002; Menon et al., 2003; Cook and Highwood, 2004; Johnson et al., 2004), which is the mechanism by which absorption of shortwave radiation by tropospheric aerosols leads to heating of the troposphere that in turn changes the relative humidity and the stability of the troposphere and thereby influences cloud formation and lifetime. In this report, the semi-direct effect is not strictly considered an RF because of modifications to the hydrological cycle, as discussed in Section 7.5 (see also Sections 2.2, 2.8 and 2.4.5).

Since the TAR, there have been substantial developments in observations and modelling of tropospheric aerosols; these are discussed in turn in the following sections.

2.4.2 Developments Related to Aerosol Observations

Surface-based measurements of aerosol properties such as size distribution, chemical composition, scattering and absorption continue to be performed at a number of sites, either at long-term monitoring sites, or specifically as part of intensive field campaigns. These *in situ* measurements provide essential validation for global models, for example, by constraining aerosol concentrations at the surface and by providing high-quality information about chemical composition and local trends. In addition, they provide key information about variability on various time scales. Comparisons of *in situ* measurements against those from global atmospheric models are complicated by differences in meteorological conditions and because *in situ* measurements are representative of conditions mostly at or near the surface while the direct and indirect RFs depend on the aerosol vertical profile. For example, the spatial resolution of global model grid boxes is typically a few degrees of latitude and longitude and the time steps for the atmospheric dynamics and radiation calculations may be minutes to hours depending on the process to be studied; this poses limitations when comparing with observations conducted over smaller spatial extent and shorter time duration.

Combinations of satellite and surface-based observations provide near-global retrievals of aerosol properties. These are discussed in this subsection; the emissions estimates, trends and *in situ* measurements of the physical and optical properties are discussed with respect to their influence on RF in Section 2.4.4. Further detailed discussions of the recent satellite observations of aerosol properties and a satellite-measurement based assessment of the aerosol direct RF are given by Yu et al. (2006).

2.4.2.1 Satellite Retrievals

Satellite retrievals of aerosol optical depth in cloud-free regions have improved via new generation sensors (Kaufman et al., 2002) and an expanded global validation program (Holben et al., 2001). Advanced aerosol retrieval products such as aerosol fine-mode fraction and effective particle radius have been

developed and offer potential for improving estimates of the aerosol direct radiative effect. Additionally, efforts have been made to determine the anthropogenic component of aerosol and associated direct RF, as discussed by Kaufman et al. (2002) and implemented by Bellouin et al. (2005) and Chung et al. (2005). However, validation programs for these advanced products have yet to be developed and initial assessments indicate some systematic errors (Levy et al., 2003; Anderson et al., 2005a; Chu et al., 2005), suggesting that the routine differentiation between natural and anthropogenic aerosols from satellite retrievals remains very challenging.

2.4.2.1.1 Satellite retrievals of aerosol optical depth

Figure 2.11 shows an example of aerosol optical depth τ_{aer} (mid-visible wavelength) retrieved over both land and ocean, together with geographical positions of aerosol instrumentation. Table 2.2 provides a summary of aerosol data currently available from satellite instrumentation, together with acronyms for the instruments. τ_{aer} from the Moderate Resolution Imaging Spectrometer (MODIS) instrument for the January to March 2001 average (Figure 2.11, top panel) clearly differs from that for the August to October 2001 average (Figure 2.11, bottom panel) (Kaufman et al., 1997; Tanré et al., 1997). Seasonal variability in τ_{aer} can be seen; biomass burning aerosol is most strongly evident over the Gulf of Guinea in Figure 2.11 (top panel) but shifts to southern Africa in Figure 2.11 (bottom panel). Likewise, the biomass burning in South America is most evident in Figure 2.11 (bottom panel). In Figure 2.11 (top panel), transport of mineral dust from Africa to South America is discernible while in Figure 2.11 (bottom panel) mineral dust is transported over the West Indies and Central America. Industrial aerosol, which consists of a mixture of sulphates, organic and black carbon,

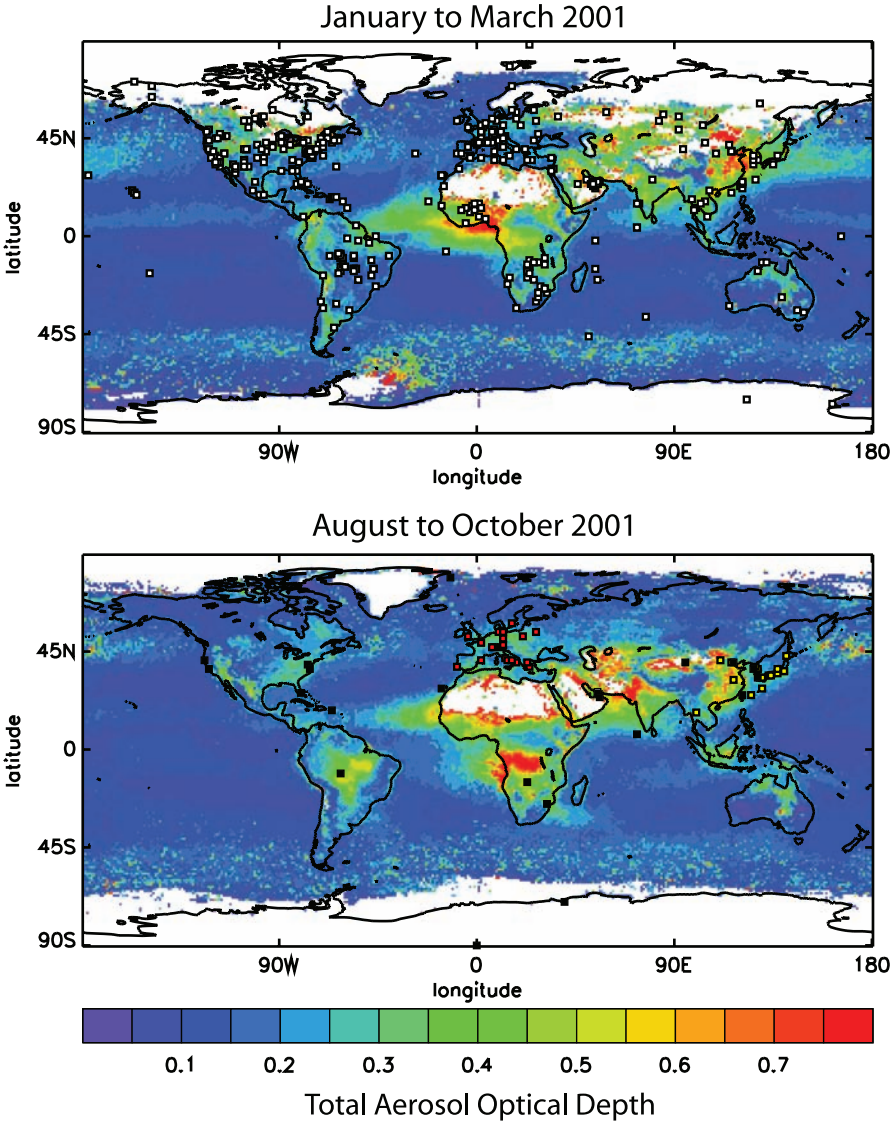


Figure 2.11. *Aerosol optical depth, τ_{aer}, at 0.55 µm (colour bar) as determined by the MODIS instrument for the January to March 2001 mean (top panel) and for the August to October 2001 mean (bottom panel). The top panel also shows the location of AERONET sites (white squares) that have been operated (not necessary continuously) since 1996. The bottom panel also shows the location of different aerosol lidar networks (red: EARLINET, orange: ADNET, black: MPLNET).*

Table 2.2. *Periods of operation, spectral bands and products available from various different satellite sensors that have been used to retrieve aerosol properties.*

Satellite Instrument	Period of Operation	Spectral Bands	Products[a]	Comment and Reference
AVHRR (Advanced Very High Resolution Radiometer) α	1979 to present	5 bands (0.63, 0.87, 3.7, 10.5 and 11.5 μm)	τ_{aer}, α	1-channel retrieval gives $\tau_{\lambda=0.63}$ over ocean (Husar et al., 1997; Ignatov and Stowe, 2002) 2-channel using 0.63 μm and 0.86 μm gives $\tau_{\lambda=0.55}$ and α over ocean assuming mono-modal aerosol size distribution (Mishchenko et al., 1999) 2-channel using 0.63 μm and 0.86 μm gives $\tau_{\lambda=0.55}$ and α over dark forests and lake surfaces (Soufflet et al., 1997) 2-channel using 0.64 μm and 0.83 μm gives $\tau_{\lambda=0.55}$ and α over ocean assuming a bimodal aerosol size distribution (Higurashi and Nakajima, 1999; Higurashi et al., 2000)
TOMS[b] (Total Ozone Mapping Spectrometer)	1979 to present	0. 33 μm, 0.36 μm	Aerosol Index, τ_{aer}	Aerosol index to τ_{aer} conversion sensitive to the altitude of the 8 mono-modal aerosol models used in the retrieval (Torres et al., 2002).
POLDER (Polarization and Directionality of the Earth's Reflectances)	Nov 1996 to June 1997; Apr 2003 to Oct 2003; Jan 2005 to present	8 bands (0.44 to 0.91 μm)	τ_{aer}, α, DRE	Multiple view angles and polarization capabilities. 0.67 μm and 0.86 μm radiances used with 12 mono-modal aerosol models over ocean (Goloub et al., 1999; Deuzé et al., 2000). Polarization allows fine particle retrieval over land (Herman et al., 1997; Goloub and Arino, 2000). DRE determined over ocean (Boucher and Tanré, 2000; Bellouin et al., 2003).
OCTS (Ocean Colour and Temperature Scanner)	Nov 1996 to Jun 1997; Apr 2003 to Oct 2003	9 bands (0.41 to 0.86 μm) and 3.9 μm	τ_{aer}, α	0.67 μm and 0.86 μm retrieval gives $\tau_{\lambda=0.50}$ and α over ocean. Bi-modal aerosol size distribution assumed (Nakajima and Higurashi, 1998; Higurashi et al., 2000).
MODIS (Moderate Resolution Imaging Spectrometer)	2000 to present	12 bands (0.41 to 2.1 μm)	τ_{aer}, α, DRE	Retrievals developed over ocean surfaces using bi-modal size distributions (Tanré et al., 1997; Remer et al., 2002). Retrievals developed over land except bright surfaces (Kaufman et al., 1997; Chu et al., 2002). Optical depth speciation and DRE determined over ocean and land (e.g., Bellouin et al., 2005; Kaufman et al., 2005a).
MISR (Multi-angle Imaging Spectro-Radiometer)	2000 to present	4 bands (0.47 to 0.86 μm)	τ_{aer}, α	9 different viewing angles. Five climatological mixing groups composed of four component particles are used in the retrieval algorithm (Kahn et al., 2001; Kahn et al., 2005). Retrievals over bright surfaces are possible (Martonchik et al., 2004).
CERES (Clouds and the Earth's Radiant Energy System)	1998 to present		DRE	DRE determined by a regression of, for example, Visible Infrared Scanner (VIRS; AVHRR-like) τ_{aer} against upwelling irradiance (Loeb and Kato; 2002).
GLAS (Geoscience Laser Altimeter System)	2003 to present	Active lidar (0.53, 1.06 μm)	Aerosol vertical profile	Lidar footprint roughly 70 m at 170 m intervals. 8-day repeat orbiting cycle (Spinhirne et al., 2005).
ATSR-2/AATSR (Along Track Scanning Radiometer/Advanced ATSR)	1996 to present	4 bands (0.56 to 1.65 μm)	τ_{aer}, α	Nadir and 52° forward viewing geometry. 40 aerosol climatological mixtures containing up to six aerosol species are used in the retrievals (Veefkind et al., 1998; Holzer-Popp et al., 2002).
SeaWiFS (Sea-Viewing Wide Field-of-View Sensor)	1997 to present	0.765 and 0.865 μm (ocean) 0.41 to 0.67 μm (land)	τ_{aer}, α	2-channel using 0.765 μm and 0.856 μm gives $\tau_{\lambda=0.856}$ and α over ocean. Bi-modal aerosol size distribution assumed (M. Wang et al., 2005). Retrievals over land and ocean using six visible channels from 0.41 to 0.67μm (von Hoyningen-Huene, 2003; Lee et al., 2004) also developed.

Notes: [a] DRE is the direct radiative effect and includes both natural and anthropogenic sources (see Table 2.3). The Angstrom exponent, α, is the wavelength dependence of τ_{aer} and is defined by $\alpha = -\ln(\tau_{aer\lambda 1}/\tau_{aer\lambda 2}) / \ln(\lambda_1 / \lambda_2)$ where λ_1 = wavelength 1 and λ_2 = wavelength 2.

[b] TOMS followed up by the Ozone Monitoring Instrument (OMI) on the Earth Observing System (EOS) Aura satellite, launched July 2004.

nitrates and industrial dust, is evident over many continental regions of the NH. Sea salt aerosol is visible in oceanic regions where the wind speed is high (e.g., south of 45°S). The MODIS aerosol algorithm is currently unable to make routine retrievals over highly reflective surfaces such as deserts, snow cover, ice and areas affected by ocean glint, or over high-latitude regions when the solar insolation is insufficient.

Early retrievals for estimating τ_{aer} include the Advanced Very High Resolution Radiometer (AVHRR) single channel retrieval (e.g., Husar et al., 1997; Ignatov and Stowe, 2002), and the ultraviolet-based retrieval from the TOMS (e.g., Torres et al., 2002). A dual channel AVHRR retrieval has also been developed (e.g., Mishchenko et al., 1999; Geogdzhayev et al., 2002). Retrievals by the AVHRR are generally only performed over ocean surfaces where the surface reflectance characteristics are relatively well known, although retrievals are also possible over dark land surfaces such as boreal forests and lakes (Soufflet et al., 1997). The TOMS retrieval is essentially independent of surface reflectance thereby allowing retrievals over both land and ocean (Torres et al., 2002), but is sensitive to the altitude of the aerosol, and has a relatively low spatial resolution. While these retrievals only use a limited number of spectral bands and lack sophistication compared to those from dedicated satellite instruments, they have the advantage of offering continuous long-term data sets (e.g., Geogdzhayev et al., 2002).

Early retrievals have been superseded by those from dedicated aerosol instruments (e.g., Kaufman et al., 2002). Polarization and Directionality of the Earth's Reflectance (POLDER) uses a combination of spectral channels (0.44–0.91 μm) with several viewing angles, and measures polarization of radiation. Aerosol optical depth and Ångstrom exponent (α) over ocean (Deuzé et al., 2000), τ_{aer} over land (Deuzé et al., 2001) and the direct radiative effect of aerosols (Boucher and Tanré, 2000; Bellouin et al., 2003) have all been developed. Algorithms for aerosol retrievals using MODIS have been developed and validated over both ocean (Tanré et al., 1997) and land surfaces (Kaufman et al., 1997). The uncertainty in these retrievals of τ_{aer} is necessarily higher over land (Chu et al., 2002) than over oceans (Remer et al., 2002) owing to uncertainties in land surface reflectance characteristics, but can be minimised by careful selection of the viewing geometry (Chylek et al., 2003). In addition, new algorithms have been developed for discriminating between sea salt, dust or biomass burning and industrial pollution over oceans (Bellouin et al., 2003, 2005; Kaufman et al., 2005a) that allow for a more comprehensive comparison against aerosol models. Multi-angle Imaging Spectro-Radiometer (MISR) retrievals have been developed using multiple viewing capability to determine aerosol parameters over ocean (Kahn et al., 2001) and land surfaces, including highly reflective surfaces such as deserts (Martonchik et al., 2004). Five typical aerosol climatologies, each containing four aerosol components, are used in the retrievals, and the optimum radiance signature is determined for nine viewing geometries and two different radiances. The results have been validated against those from the Aerosol RObotic NETwork (AERONET; see Section 2.4.3). Along Track Scanning Radiometer (ATSR) and ATSR-2 retrievals (Veefkind et al., 1998; Holzer-Popp et al., 2002) use a relatively wide spectral range (0.56–1.65 μm), and two viewing directions and aerosol climatologies from the Optical Parameters of Aerosols and Clouds (OPAC) database (Hess et al., 1998) to make τ_{aer} retrievals over both ocean and land (Robles-Gonzalez et al., 2000). The Ocean Colour and Temperature Scanner (OCTS) retrieval has a basis similar to the dual wavelength retrieval from AVHRR and uses wavelengths over the range 0.41 to 0.86 μm to derive τ_{aer} and α over oceans (e.g., Higurashi et al., 2000) using a bi-modal aerosol size distribution. The Sea-Viewing Wide Field-of-View Sensor (SeaWiFs) uses 0.765 μm and 0.856 μm radiances to provide $\tau_{\lambda=0.856}$ and α over ocean using a bi-modal aerosol size distribution (M. Wang et al., 2005). Further SeaWiFs aerosol products have been developed over both land and ocean using six and eight visible channels, respectively (e.g., von Hoyningen-Heune et al., 2003; Lee et al., 2004).

Despite the increased sophistication and realism of the aerosol retrieval algorithms, discrepancies exist between retrievals of τ_{aer} even over ocean regions (e.g., Penner et al., 2002; Myhre et al., 2004a, 2005b; Jeong et al., 2005; Kinne et al., 2006). These discrepancies are due to different assumptions in the cloud clearing algorithms, aerosol models, different wavelengths and viewing geometries used in the retrievals, different parametrizations of ocean surface reflectance, etc. Comparisons of these satellite aerosol retrievals with the surface AERONET observations provide an opportunity to objectively evaluate as well as improve the accuracy of these satellite retrievals. Myhre et al. (2005b) showed that dedicated instruments using multi-channel and multi-view algorithms perform better when compared against AERONET than the simple algorithms that they have replaced, and Zhao et al. (2005) showed that retrievals based on dynamic aerosol models perform better than those based on globally fixed aerosol models. While some systematic biases in specific satellite products exist (e.g., Jeong et al., 2005; Remer et al., 2005), these can be corrected for (e.g., Bellouin et al., 2005; Kaufman et al., 2005b), which then enables an assessment of the direct radiative effect and the direct RF from an observational perspective, as detailed below.

2.4.2.1.2 Satellite retrievals of direct radiative effect

The solar direct radiative effect (DRE) is the sum of the direct effects due to anthropogenic and natural aerosol species while the direct RF only considers the anthropogenic components. Satellite estimates of the global clear-sky DRE over oceans have advanced since the TAR, owing to the development of dedicated aerosol instruments and algorithms, as summarised by Yu et al. (2006) (see Table 2.3). Table 2.3 suggests a reasonable agreement of the global mean, diurnally averaged clear-sky DRE from various studies, with a mean of –5.4 W m^{-2} and a standard deviation of 0.9 W m^{-2}. The clear-sky DRE is converted to an all-sky DRE by Loeb and Manalo-Smith (2005) who estimated an all-sky DRE over oceans of –1.6 to –2.0 W m^{-2} but assumed no aerosol contribution to the DRE from

cloudy regions; such an assumption is not valid for optically thin clouds or if partially absorbing aerosols exist above the clouds (see Section 2.4.4.4).

Furthermore, use of a combination of sensors on the same satellite offers the possibility of concurrently deriving τ_{aer} and the DRE (e.g., Zhang and Christopher, 2003; Zhang et al., 2005), which enables estimation of the DRE efficiency, that is, the DRE divided by τ_{aer} (W m^{-2} τ_{aer}^{-1}). Because the DRE efficiency removes the dependence on the geographic distribution of τ_{aer} it is a useful parameter for comparison of models against observations (e.g., Anderson et al., 2005b); however, the DRE efficiency thus derived is not a linear function of τ_{aer} at high τ_{aer} such as those associated with intense mineral dust, biomass burning or pollution events.

2.4.2.1.3. Satellite retrievals of direct radiative forcing

Kaufman et al. (2005a) estimated the anthropogenic-only component of the aerosol fine-mode fraction from the MODIS product to deduce a clear sky RF over ocean of –1.4 W m^{-2}. Christopher et al. (2006) used a combination of the MODIS fine-mode fraction and Clouds and the Earth's Radiant Energy System (CERES) broadband TOA fluxes and estimated an identical value of –1.4 ± 0.9 W m^{-2}. Bellouin et al. (2005) used a combination of MODIS τ_{aer} and fine-mode fraction together with data from AeroCom (see Section 2.4.3) to determine an all-sky RF of aerosols over both land and ocean of –0.8 ± 0.2 W m^{-2}, but this does not include the contribution to the RF and associated uncertainty from cloudy skies. Chung et al. (2005) performed a similar satellite/AERONET/model analysis, but included the contribution from cloudy areas to deduce an RF of –0.35 W m^{-2} or –0.50 W m^{-2} depending upon whether the anthropogenic fraction is determined from a model or from the MODIS fine-mode fraction and suggest an overall uncertainty range of –0.1 to –0.6 W m^{-2}. Yu et al. (2006) used several measurements to estimate a direct RF of –0.5 ± 0.33 W m^{-2}. These estimates of the RF are compared to those obtained from modelling studies in Section 2.4.4.7.

2.4.2.2 Surface-Based Retrievals

A significant advancement since the TAR is the continued deployment and development of surface based remote sensing sun-photometer sites such as AERONET (Holben et al., 1998), and the establishment of networks of aerosol lidar systems such

Table 2.3. *The direct aerosol radiative effect (DRE) estimated from satellite remote sensing studies (adapted and updated from Yu et al., 2006).*

Reference	Instrument[a]	Data Analysed	Brief Description	Clear Sky DRE (W m^{-2}) ocean
Bellouin et al. (2005)	MODIS; TOMS; SSM/I	2002	MODIS fine and total τ_{aer} with TOMS Aerosol Index and SSM/I to discriminate dust from sea salt.	–6.8
Loeb and Manalo-Smith (2005)	CERES; MODIS	Mar 2000 to Dec 2003	CERES radiances/irradiances and angular distribution models and aerosol properties from either MODIS or from NOAA-NESDIS[b] algorithm used to estimate the direct radiative effect.	–3.8 (NESDIS) to –5.5 (MODIS)
Remer and Kaufman (2006)	MODIS	Aug 2001 to Dec 2003	Best-prescribed aerosol model fitted to MODIS data. τ_{aer} from fine-mode fraction.	–5.7 ± 0.4
Zhang et al. (2005); Christopher and Zhang (2004)	CERES; MODIS	Nov 2000 to Aug 2001	MODIS aerosol properties, CERES radiances/irradiances and angular distribution models used to estimate the direct radiative effect.	–5.3 ± 1.7
Bellouin et al. (2003)	POLDER	Nov 1996 to Jun 1997	Best-prescribed aerosol model fitted to POLDER data	–5.2
Loeb and Kato (2002)	CERES; VIRS	Jan 1998 to Aug 1998; Mar 2000.	τ_{aer} from VIRS regressed against the TOA CERES irradiance (35°N to 35°S)	–4.6 ± 1.0
Chou et al. (2002)	SeaWiFs	1998	Radiative transfer calculations with SeaWiFS τ_{aer} and prescribed optical properties	–5.4
Boucher and Tanré (2000)	POLDER	Nov 1996 to Jun 1997	Best-prescribed aerosol model fitted to POLDER data	–5 to –6
Haywood et al. (1999)	ERBE	Jul 1987 to Dec 1988	DRE diagnosed from GCM-ERBE TOA irradiances	–6.7
Mean (standard deviation)				**–5.4 (0.9)**

Notes:

[a] SSM/I: Special Sensor Microwave/Imager; VIRS: Visible Infrared Scanner; ERBE: Earth Radiation Budget Experiment.

[b] NESDIS: National Environmental Satellite, Data and Information Service.

as the European Aerosol Research Lidar Network (EARLINET, Matthias et al., 2004), the Asian Dust Network (ADNET, Murayama et al., 2001), and the Micro-Pulse Lidar Network (MPLNET, Welton et al., 2001).

The distribution of AERONET sites is also shown in Figure 2.11 (top panel). Currently there are approximately 150 sites operating at any one time, many of which are permanent to enable determination of climatological and interannual column-averaged monthly and seasonal means. In addition to measurements of τaer as a function of wavelength, new algorithms have been developed that measure sky radiance as a function of scattering angle (Nakajima et al., 1996; Dubovik and King, 2000). From these measurements, the column-averaged size distribution and, if the τaer is high enough ($\tau_{aer} > 0.5$), the aerosol single scattering albedo, ω_o, and refractive indices may be determined at particular wavelengths (Dubovik et al., 2000), allowing partitioning between scattering and absorption. While these inversion products have not been comprehensively validated, a number of studies show encouraging agreement for both the derived size distribution and ω_o when compared against *in situ* measurements by instrumented aircraft for different aerosol species (e.g., Dubovik et al., 2002; Haywood et al., 2003a; Reid et al., 2003; Osborne et al., 2004). A climatology of the aerosol DRE based on the AERONET aerosols has also been derived (Zhou et al., 2005).

The MPLNET Lidar network currently consists of 11 lidars worldwide; 9 are co-located with AERONET sites and provide complementary vertical distributions of aerosol backscatter and extinction. Additional temporary MPLNET sites have supported major aerosol field campaigns (e.g., Campbell et al., 2003). The European-wide lidar network EARLINET currently has 15 aerosol lidars making routine retrievals of vertical profiles of aerosol extinction (Mathias et al., 2004), and ADNET is a network of 12 lidars making routine measurements in Asia that have been used to assess the vertical profiles of Asian dust and pollution events (e.g., Husar et al., 2001; Murayama et al., 2001).

2.4.3 Advances in Modelling the Aerosol Direct Effect

Since the TAR, more complete aerosol modules in a larger number of global atmospheric models now provide estimates of the direct RF. Several models have resolutions better than 2° by 2° in the horizontal and more than 20 to 30 vertical levels; this represents a considerable enhancement over the models used in the TAR. Such models now include the most important anthropogenic and natural species. Tables 2.4, 2.5 and 2.6 summarise studies published since the TAR. Some of the more complex models now account explicitly for the dynamics of the aerosol size distribution throughout the aerosol atmospheric lifetime and also parametrize the internal/external mixing of the various aerosol components in a more physically realistic way than in the TAR (e.g., Adams and Seinfeld, 2002; Easter et al., 2004; Stier et al., 2005). Because the most important aerosol species are now included, a comparison of key model output parameters, such as the total τ_{aer}, against satellite retrievals and surface-based sun photometer and lidar observations is possible (see Sections 2.4.2 and 2.4.4). Progress with respect to modelling the indirect effects due to aerosol-cloud interactions is detailed in Section 2.4.5 and Section 7.5. Several studies have explored the sensitivity of aerosol direct RF to current parametrization uncertainties. These are assessed in the following sections.

Major progress since the TAR has been made in the documentation of the diversity of current aerosol model simulations. Sixteen groups have participated in the Global Aerosol Model Intercomparison (AeroCom) initiative (Kinne et al., 2006). Extensive model outputs are available via a dedicated website (Schulz et al., 2004). Three model experiments (named A, B, and PRE) were analysed. Experiment A models simulate the years 1996, 1997, 2000 and 2001, or a five-year mean encompassing these years. The model emissions and parametrizations are those determined by each research group, but the models are driven by observed meteorological fields to allow detailed comparisons with observations, including those from MODIS, MISR and the AERONET sun photometer network. Experiment B models use prescribed AeroCom aerosol emissions for the year 2000, and experiment PRE models use prescribed aerosol emissions for the year 1750 (Dentener et al., 2006; Schulz et al., 2006). The model diagnostics included information on emission and deposition fluxes, vertical distribution and sizes, thus enabling a better understanding of the differences in lifetimes of the various aerosol components in the models.

This paragraph discusses AeroCom results from Textor et al. (2006). The model comparison study found a wide range in several of the diagnostic parameters; these, in turn, indicate which aerosol parametrizations are poorly constrained and/or understood. For example, coarse aerosol fractions are responsible for a large range in the natural aerosol emission fluxes (dust: ±49% and sea salt: ±200%, where uncertainty is 1 standard deviation of inter-model range), and consequently in the dry deposition fluxes. The complex dependence of the source strength on wind speed adds to the problem of computing natural aerosol emissions. Dust emissions for the same time period can vary by a factor of two or more depending on details of the dust parametrization (Luo et al., 2003; Timmreck and Schulz, 2004; Balkanski et al., 2004; Zender, 2004), and even depend on the reanalysis meteorological data set used (Luo et al., 2003). With respect to anthropogenic and natural emissions of other aerosol components, modelling groups tended to make use of similar best guess information, for example, recently revised emissions information available via the Global Emissions Inventory Activity (GEIA). The vertical aerosol distribution was shown to vary considerably, which is a consequence of important differences in removal and vertical mixing parametrizations. The inter-model range for the fraction of sulphate mass below 2.5 km to that of total sulphate is 45 ± 23%. Since humidification takes place mainly in the boundary layer, this source of inter-model variability increases the range of modelled direct RF. Additionally, differences in the parametrization of the wet deposition/vertical mixing process

become more pronounced above 5 km altitude. Some models have a tendency to accumulate insoluble aerosol mass (dust and carbonaceous aerosols) at higher altitudes, while others have much more efficient wet removal schemes. Tropospheric residence times, defined here as the ratio of burden over sinks established for an equilibrated one-year simulation, vary by 20 to 30% for the fine-mode aerosol species. These variations are of interest, since they express the linearity of modelled emissions to aerosol burden and eventually to RF.

Considerable progress has been made in the systematic evaluation of global model results (see references in Tables 2.4 to 2.6). The simulated global τ_{aer} at a wavelength of 0.55 μm in models ranges from 0.11 to 0.14. The values compare favourably to those obtained by remote sensing from the ground (AERONET, about 0.135) and space (satellite composite, about 0.15) (Kinne et al., 2003, 2006), but significant differences exist in regional and temporal distributions. Modelled absorption optical thickness has been suggested to be underestimated by a factor of two to four when compared to observations (Sato et al., 2003) and DRE efficiencies have been shown to be lower in models both for the global average and regionally (Yu et al., 2006) (see Section 2.4.4.7). A merging of modelled and observed fields of aerosol parameters through assimilation methods of different degrees of complexity has also been performed since the TAR (e.g., Yu et al., 2003; Chung et al., 2005). Model results are constrained to obtain present-day aerosol fields consistent with observations. Collins et al. (2001) showed that assimilation of satellite-derived fields of τ_{aer} can reduce the model bias down to 10% with respect to daily mean τ_{aer} measured with a sun photometer at the Indian Ocean Experiment (INDOEX) station Kaashidhoo. Liu et al. (2005) demonstrated similar efficient reduction of errors in τ_{aer}. The magnitude of the global dust cycle has been suggested to range between 1,500 and 2,600 Tg yr^{-1} by minimising the bias between model and multiple dust observations (Cakmur et al., 2006). Bates et al. (2006) focused on three regions downwind of major urban/population centres and performed radiative transfer calculations constrained by intensive and extensive observational parameters to derive 24-hour average clear-sky DRE of –3.3 ± 0.47, –14 ± 2.6 and –6.4 ± 2.1 W m^{-2} for the north Indian Ocean, the northwest Pacific and the northwest Atlantic, respectively. By constraining aerosol models with these observations, the uncertainty associated with the DRE was reduced by approximately a factor of two.

2.4.4 Estimates of Aerosol Direct Radiative Forcing

Unless otherwise stated, this section discusses the TOA direct RF of different aerosol types as a global annual mean quantity inclusive of the effects of clouds. Where possible, statistics from model results are used to assess the uncertainty in the RF. Recently published results and those grouped within AeroCom are assessed. Because the AeroCom results assessed here are based on prescribed emissions, the uncertainty in these results is lowered by having estimates of the uncertainties in the emissions. The quoted uncertainties therefore include the structural uncertainty (i.e., differences associated with the model formulation and structure) associated with the RF, but do not include the full range of parametric uncertainty (i.e., differences associated with the choice of key model parameters), as the model results are essentially best estimates constrained by observations of emissions, wet and dry deposition, size distributions, optical parameters, hygroscopicity, etc. (Pan et al., 1997). The uncertainties are reported as the 5 to 95% confidence interval to allow the uncertainty in the RF of each species of aerosol to be quantitatively intercompared.

2.4.4.1 Sulphate Aerosol

Atmospheric sulphate aerosol may be considered as consisting of sulphuric acid particles that are partly or totally neutralized by ammonia and that are present as liquid droplets or partly crystallized. Sulphate is formed by aqueous phase reactions within cloud droplets, oxidation of SO_2 via gaseous phase reactions with OH, and by condensational growth onto pre-existing particles (e.g., Penner et al., 2001). Emission estimates are summarised by Haywood and Boucher (2000). The main source of sulphate aerosol is via SO_2 emissions from fossil fuel burning (about 72%), with a small contribution from biomass burning (about 2%), while natural sources are from dimethyl sulphide emissions by marine phytoplankton (about 19%) and by SO_2 emissions from volcanoes (about 7%). Estimates of global SO_2 emissions range from 66.8 to 92.4 TgS yr^{-1} for anthropogenic emissions in the 1990s and from 91.7 to 125.5 TgS yr^{-1} for total emissions. Emissions of SO_2 from 25 countries in Europe were reduced from approximately 18 TgS yr^{-1} in 1980 to 4 TgS yr^{-1} in 2002 (Vestreng et al., 2004). In the USA, the emissions were reduced from about 12 to 8 TgS yr^{-1} in the period 1980 to 2000 (EPA, 2003). However, over the same period SO_2 emissions have been increasing significantly from Asia, which is estimated to currently emit 17 TgS yr^{-1} (Streets et al., 2003), and from developing countries in other regions (e.g., Lefohn et al., 1999; Van Aardenne et al., 2001; Boucher and Pham, 2002). The most recent study (Stern, 2005) suggests a decrease in global anthropogenic emissions from approximately 73 to 54 TgS yr^{-1} over the period 1980 to 2000, with NH emission falling from 64 to 43 TgS yr^{-1} and SH emissions increasing from 9 to 11 TgS yr^{-1}. Smith et al. (2004) suggested a more modest decrease in global emissions, by some 10 TgS yr^{-1} over the same period. The regional shift in the emissions of SO_2 from the USA, Europe, Russia, Northern Atlantic Ocean and parts of Africa to Southeast Asia and the Indian and Pacific Ocean areas will lead to subsequent shifts in the pattern of the RF (e.g., Boucher and Pham, 2002; Smith et al., 2004; Pham et al., 2005). The recently used emission scenarios take into account effective injection heights and their regional and seasonal variability (e.g., Dentener et al., 2006).

The optical parameters of sulphate aerosol have been well documented (see Penner et al., 2001 and references therein). Sulphate is essentially an entirely scattering aerosol across the solar spectrum (ω_o = 1) but with a small degree of absorption in the near-infrared spectrum. Theoretical and experimental

data are available on the relative humidity dependence of the specific extinction coefficient, f_{RH} (e.g., Tang et al., 1995). Measurement campaigns concentrating on industrial pollution, such as the Tropospheric Aerosol Radiative Forcing Experiment (TARFOX; Russell et al., 1999), the Aerosol Characterization Experiment (ACE-2; Raes et al., 2000), INDOEX (Ramanathan et al., 2001b), the Mediterranean Intensive Oxidants Study (MINOS, 2001 campaign), ACE-Asia (2001), Atmospheric Particulate Environment Change Studies (APEX, from 2000 to 2003), the New England Air Quality Study (NEAQS, in 2003) and the Chesapeake Lighthouse and Aircraft Measurements for Satellites (CLAMS; Smith et al., 2005), continue to show that sulphate contributes a significant fraction of the sub-micron aerosol mass, anthropogenic τ_{aer} and RF (e.g., Hegg et al., 1997; Russell and Heintzenberg, 2000; Ramanathan et al., 2001b; Magi et al., 2005; Quinn and Bates, 2005). However, sulphate is invariably internally and externally mixed to varying degrees with other compounds such as biomass burning aerosol (e.g., Formenti et al., 2003), fossil fuel black carbon (e.g., Russell and Heintzenberg, 2000), organic carbon (Novakov et al., 1997; Brock et al., 2004), mineral dust (e.g., Huebert et al., 2003) and nitrate aerosol (e.g., Schaap et al., 2004). This results in a composite aerosol state in terms of effective refractive indices, size distributions, physical state, morphology, hygroscopicity and optical properties.

The TAR reported an RF due to sulphate aerosol of –0.40 W m^{-2} with an uncertainty of a factor of two, based on global modelling studies that were available at that time. Results from model studies since the TAR are summarised in Table 2.4. For models A to L, the RF ranges from approximately –0.21 W m^{-2} (Takemura et al., 2005) to –0.96 W m^{-2} (Adams et al., 2001) with a mean of –0.46 W m^{-2} and a standard deviation of 0.20 W m^{-2}. The range in the RF per unit τ_{aer} is substantial due to differing representations of aerosol mixing state, optical properties, cloud, surface reflectance, hygroscopic growth, sub-grid scale effects, radiative transfer codes, etc. (Ramaswamy et al., 2001). Myhre et al. (2004b) performed several sensitivity studies and found that the uncertainty was particularly linked to the hygroscopic growth and that differences in the model relative humidity fields could cause differences of up to 60% in the RF. The RFs from the models M to U participating in the AeroCom project are slightly weaker than those obtained from the other studies, with a mean of approximately –0.35 W m^{-2} and a standard deviation of 0.15 W m^{-2}; the standard deviation is reduced for the AeroCom models owing to constraints on aerosol emissions, based on updated emission inventories (see Table 2.4). Including the uncertainty in the emissions reported in Haywood and Boucher (2000) increases the standard deviation to 0.2 W m^{-2}. As sulphate aerosol is almost entirely scattering, the surface forcing will be similar or marginally stronger than the RF diagnosed at the TOA. The uncertainty in the RF estimate relative to the mean value remains relatively large compared to the situation for LLGHGs.

The mean and median of the sulphate direct RF from grouping all these studies together are identical at –0.41 W m^{-2}. Disregarding the strongest and weakest direct RF estimates to approximate the 90% confidence interval leads to an estimate of –0.4 ± 0.2 W m^{-2}.

2.4.4.2 Organic Carbon Aerosol from Fossil Fuels

Organic aerosols are a complex mixture of chemical compounds containing carbon-carbon bonds produced from fossil fuel and biofuel burning and natural biogenic emissions. Organic aerosols are emitted as primary aerosol particles or formed as secondary aerosol particles from condensation of organic gases considered semi-volatile or having low volatility. Hundreds of different atmospheric organic compounds have been detected in the atmosphere (e.g., Hamilton et al., 2004; Murphy, 2005), which makes definitive modelling of the direct and indirect effects extremely challenging (McFiggans et al., 2006). Emissions of primary organic carbon from fossil fuel burning have been estimated to be 10 to 30 TgC yr^{-1} (Liousse et al., 1996; Cooke et al., 1999; Scholes and Andreae, 2000). More recently, Bond et al. (2004) provided a detailed analysis of primary organic carbon emissions from fossil fuels, biofuels and open burning, and suggested that contained burning (approximately the sum of fossil fuel and biofuel) emissions are in the range of 5 to 17 TgC yr^{-1}, with fossil fuel contributing only 2.4 TgC yr^{-1}. Ito and Penner (2005) estimated global fossil fuel particulate organic matter (POM, which is the sum of the organic carbon and the other associated chemical elements) emissions of around 2.2 Tg(POM) yr^{-1}, and global biofuel emissions of around 7.5 Tg(POM) yr^{-1}. Ito and Penner (2005) estimated that emissions of fossil and biofuel organic carbon increased by a factor of three over the period 1870 to 2000. Subsequent to emission, the hygroscopic, chemical and optical properties of organic carbon particles continue to change because of chemical processing by gas-phase oxidants such as ozone, OH, and the nitrate radical (NO_3) (e.g., Kanakidou et al., 2005). Atmospheric concentrations of organic aerosol are frequently similar to those of industrial sulphate aerosol. Novakov et al. (1997) and Hegg et al. (1997) measured organic carbon in pollution off the East Coast of the USA during the TARFOX campaign, and found organic carbon primarily from fossil fuel burning contributed up to 40% of the total submicron aerosol mass and was frequently the most significant contributor to τ_{aer}. During INDOEX, which studied the industrial plume over the Indian Ocean, Ramanathan et al. (2001b) found that organic carbon was the second largest contributor to τ_{aer} after sulphate aerosol.

Observational evidence suggests that some organic aerosol compounds from fossil fuels are relatively weakly absorbing but do absorb solar radiation at some ultraviolet and visible wavelengths (e.g., Bond et al., 1999; Jacobson, 1999; Bond, 2001) although organic aerosol from high-temperature combustion such as fossil fuel burning (Dubovik et al., 1998; Kirchstetter et al., 2004) appears less absorbing than from low-temperature combustion such as open biomass burning. Observations suggest that a considerable fraction of organic carbon is soluble to some degree, while at low relative humidity more water is often associated with the organic fraction than

Table 2.4. *The direct radiative forcing for sulphate aerosol derived from models published since the TAR and from the AeroCom simulations where different models used identical emissions. Load and aerosol optical depth (τ_{aer}) refer to the anthropogenic sulphate; $\tau_{aer\ ant}$ is the fraction of anthropogenic sulphate to total sulphate τ_{aer} for present day, NRFM is the normalised RF by mass, and NRF is the normalised RF per unit τ_{aer}.*

No	Model[a]	LOAD (mg(SO_4) m^{-2})	τ_{aer} (0.55 µm)	$\tau_{aer\ ant}$ (%)	RF (W m^{-2})	NRFM (W g^{-1})	NRF (W m^{-2} τ_{aer}^{-1})	Reference
Published since IPCC, 2001								
A	CCM3	2.23			–0.56	–251		(Kiehl et al., 2000)
B	GEOSCHEM	1.53	0.018		–0.33	–216	–18	(Martin et al., 2004)
C	GISS	3.30	0.022		–0.65	–206	–32	(Koch, 2001)
D	GISS	3.27			–0.96	–293		(Adams et al., 2001)
E	GISS	2.12			–0.57	–269		(Liao and Seinfeld, 2005)
F	SPRINTARS	1.55	0.015	72	–0.21	–135	–8	(Takemura et al., 2005)
G	LMD	2.76			–0.42	–152		(Boucher and Pham., 2002)
H	LOA	3.03	0.030		–0.41	–135	–14	(Reddy et al., 2005b)
I	GATORG	3.06			–0.32	–105		(Jacobson, 2001a)
J	PNNL	5.50	0.042		–0.44	–80	–10	(Ghan et al., 2001)
K	UIO_CTM	1.79	0.019		–0.37	–207	–19	(Myhre et al., 2004b)
L	UIO_GCM	2.28			–0.29	–127		(Kirkevag and Iversen, 2002)
AeroCom: identical emissions used for year 1750 and 2000								
M	UMI	2.64	0.020	58	–0.58	–220	–28	(Liu and Penner, 2002)
N	UIO_CTM	1.70	0.019	57	–0.35	–208	–19	(Myhre et al., 2003)
O	LOA	3.64	0.035	64	–0.49	–136	–14	(Reddy and Boucher, 2004)
P	LSCE	3.01	0.023	59	–0.42	–138	–18	(Schulz et al., 2006)
Q	ECHAM5-HAM	2.47	0.016	60	–0.46	–186	–29	(Stier et al., 2005)
R	GISS	1.34	0.006	41	–0.19	–139	–31	(Koch, 2001)
S	UIO_GCM	1.72	0.012	59	–0.25	–145	–21	(Iversen and Seland, 2002; Kirkevag and Iversen, 2002)
T	SPRINTARS	1.19	0.013	59	–0.16	–137	–13	(Takemura et al., 2005)
U	ULAQ	1.62	0.020	42	–0.22	–136	–11	(Pitari et al., 2002)
	Average A to L	2.80	0.024		–0.46	–176	–17	
	Average M to U	2.15	0.018	55	–0.35	–161	–20	
	Minimum A to U	1.19	0.006	41	–0.96	–293	–32	
	Maximum A to U	5.50	0.042	72	–0.16	–72	–8	
	Std. dev. A to L	1.18	0.010		0.20	75	9	
	Std. dev. M to U	0.83	0.008	8	0.15	34	7	

Notes:

[a] CCM3: Community Climate Model; GEOSCHEM: Goddard Earth Observing System-Chemistry; GISS: Goddard Institute for Space Studies; SPRINTARS: Spectral Radiation-Transport Model for Aerosol Species; LMD: Laboratoire de Météorologie Dynamique; LOA: Laboratoire d'Optique Atmospherique; GATORG: Gas, Aerosol, Transport, Radiation, and General circulation model; PNNL: Pacific Northwest National Laboratory; UIO_CTM: University of Oslo CTM; UIO_GCM: University of Oslo GCM; UMI: University of Michigan; LSCE: Laboratoire des Sciences du Climat et de l'Environnement; ECHAM5-HAM: European Centre Hamburg with Hamburg Aerosol Module; ULAQ: University of L'Aquila.

with inorganic material. At higher relative humidities, the hygroscopicity of organic carbon is considerably less than that of sulphate aerosol (Kotchenruther and Hobbs, 1998; Kotchenruther et al., 1999).

Based on observations and fundamental chemical kinetic principles, attempts have been made to formulate organic carbon composition by functional group analysis in some main classes of organic chemical species (e.g., Decesari et al., 2000, 2001; Maria et al., 2002; Ming and Russell, 2002), capturing some general characteristics in terms of refractive indices, hygroscopicity and cloud activation properties. This facilitates improved parametrizations in global models (e.g., Fuzzi et al., 2001; Kanakidou et al., 2005; Ming et al., 2005a).

Organic carbon aerosol from fossil fuel sources is invariably internally and externally mixed to some degree with other combustion products such as sulphate and black carbon (e.g., Novakov et al., 1997; Ramanathan et al., 2001b). Theoretically, coatings of essentially non-absorbing components such

as organic carbon or sulphate on strongly absorbing core components such as black carbon can increase the absorption of the composite aerosol (e.g., Fuller et al., 1999; Jacobson, 2001a; Stier et al., 2006a), with results backed up by laboratory studies (e.g., Schnaiter et al., 2003). However, coatings of organic carbon aerosol on hygroscopic aerosol such as sulphate may lead to suppression of the rate of water uptake during cloud activation (Xiong et al., 1998; Chuang, 2003).

Current global models generally treat organic carbon using one or two tracers (e.g., water-insoluble tracer, water-soluble tracer) and highly parametrized schemes have been developed to represent the direct RF. Secondary organic carbon is highly simplified in the global models and in many cases treated as an additional source similar to primary organic carbon. Considerable uncertainties still exist in representing the refractive indices and the water of hydration associated with the particles because the aerosol properties will invariably differ depending on the combustion process, chemical processing in the atmosphere, mixing with the ambient aerosol, etc. (e.g., McFiggans et al., 2006).

The TAR reported an RF of organic carbon aerosols from fossil fuel burning of –0.10 W m^{-2} with a factor of three uncertainty. Many of the modelling studies performed since the TAR have investigated the RF of organic carbon aerosols from both fossil fuel and biomass burning aerosols, and the combined RF of both components. These studies are summarised in Table 2.5. The RF from total organic carbon (POM) from both biomass burning and fossil fuel emissions from recently published models A to K and AeroCom models (L to T) is –0.24 W m^{-2} with a standard deviation of 0.08 W m^{-2} and –0.16 W m^{-2} with a standard deviation of 0.10 W m^{-2}, respectively. Where the RF due to organic carbon from fossil fuels is not explicitly accounted for in the studies, an approximate scaling based on the source apportionment of 0.25:0.75 is applied for fossil fuel organic carbon:biomass burning organic carbon (Bond et al., 2004). The mean RF of the fossil fuel component of organic carbon from those studies other than in AeroCom is –0.06 W m^{-2}, while those from AeroCom produce an RF of –0.03 W m^{-2} with a range of –0.01 W m^{-2} to –0.06 W m^{-2} and a standard deviation of around 0.02 W m^{-2}. Note that these RF estimates, to a large degree, only take into account primary emitted organic carbon. These studies all use optical properties for organic carbon that are either entirely scattering or only weakly absorbing and hence the surface forcing is only slightly stronger than that at the TOA.

The mean and median for the direct RF of fossil fuel organic carbon from grouping all these studies together are identical at –0.05 W m^{-2} with a standard deviation of 0.03 W m^{-2}. The standard deviation is multiplied by 1.645 to approximate the 90% confidence interval.[9] This leads to a direct RF estimate of –0.05 ± 0.05 W m^{-2}.

2.4.4.3 Black Carbon Aerosol from Fossil Fuels

Black carbon (BC) is a primary aerosol emitted directly at the source from incomplete combustion processes such as fossil fuel and biomass burning and therefore much atmospheric BC is of anthropogenic origin. Global, present-day fossil fuel emission estimates range from 5.8 to 8.0 TgC yr^{-1} (Haywood and Boucher, 2000 and references therein). Bond et al. (2004) estimated the total current global emission of BC to be approximately 8 TgC yr^{-1}, with contributions of 4.6 TgC yr^{-1} from fossil fuel and biofuel combustion and 3.3 TgC yr^{-1} from open biomass burning, and estimated an uncertainty of about a factor of two. Ito and Penner (2005) suggested fossil fuel BC emissions for 2000 of around 2.8 TgC yr^{-1}. The trends in emission of fossil fuel BC have been investigated in industrial areas by Novakov et al. (2003) and Ito and Penner (2005). Novakov et al. (2003) reported that significant decreases were recorded in the UK, Germany, the former Soviet Union and the USA over the period 1950 to 2000, while significant increases were reported in India and China. Globally, Novakov et al. (2003) suggested that emissions of fossil fuel BC increased by a factor of three between 1950 and 1990 (2.2 to 6.7 TgC yr^{-1}) owing to the rapid expansion of the USA, European and Asian economies (e.g., Streets et al., 2001, 2003), and have since fallen to around 5.6 TgC yr^{-1} owing to further emission controls. Ito and Penner (2005) determined a similar trend in emissions over the period 1950 to 2000 of approximately a factor of three, but the absolute emissions are smaller than in Novakov et al. (2003) by approximately a factor of 1.7.

Black carbon aerosol strongly absorbs solar radiation. Electron microscope images of BC particles show that they are emitted as complex chain structures (e.g., Posfai et al., 2003), which tend to collapse as the particles age, thereby modifying the optical properties (e.g., Abel et al., 2003). The Indian Ocean Experiment (Ramanathan et al., 2001b and references therein) focussed on emissions of aerosol from the Indian sub-continent, and showed the importance of absorption by aerosol in the atmospheric column. These observations showed that the local surface forcing (–23 W m^{-2}) was significantly stronger than the local RF at the TOA (–7 W m^{-2}). Additionally, the presence of BC in the atmosphere above highly reflective surfaces such as snow and ice, or clouds, may cause a significant positive RF (Ramaswamy et al., 2001). The vertical profile is therefore important, as BC aerosols or mixtures of aerosols containing a relatively large fraction of BC will exert a positive RF when located above clouds. Both microphysical (e.g., hydrophilic-to-hydrophobic nature of emissions into the atmosphere, aging of the aerosols, wet deposition) and meteorological aspects govern the horizontal and vertical distribution patterns of BC aerosols, and the residence time of these aerosols is thus sensitive to these factors (Cooke et al., 2002; Stier et al., 2006b).

The TAR assessed the RF due to fossil fuel BC as being +0.2 W m^{-2} with an uncertainty of a factor of two. Those models since the TAR that explicitly model and separate out the RF

[9] 1.645 is the factor relating the standard deviation to the 90% confidence interval for a normal distribution.

Table 2.5. *Estimates of anthropogenic carbonaceous aerosol forcing derived from models published since the TAR and from the AeroCom simulations where different models used identical emissions. POM: particulate organic matter; BC: black carbon; BCPOM: BC and POM; FFBC: fossil fuel black carbon; FFPOM: fossil fuel particulate organic matter; BB: biomass burning sources included.*

No	Model[a]	LOAD POM (mgPOM m^{-2})	τ_{aer} POM	τ_{aer} POM_{ant} (%)	LOAD BC (mg m^{-2})	RF BCPOM (W m^{-2})	RF POM (W m^{-2})	RF BC (W m^{-2})	RF FFPOM (W m^{-2})	RF FFBC (W m^{-2})	RF BB (W m^{-2})	Reference
Published since IPCC, 2001												
A	SPRINT					0.12	–0.24	0.36	–0.05	0.15	–0.01	(Takemura et al., 2001)
B	LOA	2.33	0.016		0.37	0.30	–0.25	0.55	–0.02	0.19	0.14	(Reddy et al., 2005b)
C	GISS	1.86	0.017		0.29	0.35	–0.26	0.61	–0.13	0.49	0.065	(Hansen et al., 2005)
D	GISS	1.86	0.015		0.29	0.05	–0.30	0.35	–0.08[b]	0.18[b]	–0.05[b]	(Koch, 2001)
E	GISS	2.39			0.39	0.32	–0.18	0.50	–0.05[b]	0.25[b]	0.12[b]	(Chung and Seinfeld., 2002)
F	GISS	2.49			0.43	0.30	–0.23	0.53	–0.06[b]	0.27[b]	0.09[b]	(Liao and Seinfeld, 2005)
G	SPRINTARS	2.67	0.029	82	0.53	0.15	–0.27	0.42	–0.07[b]	0.21[b]	0.01[b]	(Takemura et al., 2005)
H	GATORG	2.55			0.39	0.47	–0.06	0.55	–0.01[b]	0.27[b]	0.22[b]	(Jacobson, 2001b)
I	MOZGN	3.03	0.018				–0.34					(Ming et al., 2005a)
J	CCM				0.33			0.34				(Wang, 2004)
K	UIO-GCM				0.30			0.19				(Kirkevag and Iversen, 2002)
AeroCom: identical emissions used for year 1750 and 2000 (Schulz et al., 2006)												
L	UMI	1.16	0.0060	53	0.19	0.02	–0.23	0.25	–0.06[b]	0.12[b]	–0.01	(Liu and Penner, 2002)
M	UIO_CTM	1.12	0.0058	55	0.19	0.02	–0.16[b]	0.22[b]	–0.04	0.11	–0.05	(Myhre et al., 2003)
N	LOA	1.41	0.0085	52	0.25	0.14	–0.16[c]	0.32[c]	–0.04[b]	0.16[b]	0.02[b]	(Reddy and Boucher, 2004)
O	LSCE	1.50	0.0079	46	0.25	0.13	–0.17	0.30	–0.04[b]	0.15[b]	0.02[b]	(Schulz et al., 2006)
P	ECHAM5-HAM	1.00	0.0077		0.16	0.09	–0.10[c]	0.20[c]	–0.03[b]	0.10[b]	0.01	(Stier et al., 2005)
Q	GISS	1.22	0.0060	51	0.24	0.08	–0.14	0.22	–0.03[b]	0.11[b]	0.01[b]	(Koch, 2001)
R	UIO_GCM	0.88	0.0046	59	0.19	0.24	–0.06	0.36	–0.02[b]	0.18[b]	0.08[b]	(Iversen and Seland, 2002)
S	SPRINTARS	1.84	0.0200	49	0.37	0.22	–0.10	0.32	–0.01	0.13	0.06	(Takemura et al., 2005)
T	ULAQ	1.71	0.0075	58	0.38	–0.01	–0.09	0.08	–0.02[b]	0.04[b]	–0.03[b]	(Pitari et al., 2002)
Average A–K		2.38	0.019		0.38	0.26	–0.24	0.44	–0.06	0.25	0.07	
Average L–T		1.32	0.008	53	0.25	0.10	–0.13	0.25	–0.03	0.12	0.01	
Stddev A–K		0.42	0.006		0.08	0.14	0.08	0.13	0.04	0.11	0.09	
Stddev L–T		0.32	0.005	4	0.08	0.09	0.05	0.08	0.01	0.04	0.04	

Notes:
[a] MOZGN: MOZART (Model for OZone and Related chemical Tracers-GFDL(Geophysical Fluid Dynamics Laboratory)-NCAR (National Center for Atmospheric Research); for other models see Note (a) in Table 2.4.
[b] Models A to C are used to provide a split in sources derived from total POM and total BC: FFPOM = POM × 0.25; FFBC = BC × 0.5; BB = (BCPOM) – (FFPOM + FFBC); BC = 2 × FFBC; POM = 4 × FFPOM.
[c] Models L, O and Q to T are used to provide a split in components: POM = BCPOM × (–1.16); BC = BCPOM × 2.25.

due to BC from fossil fuels include those from Takemura et al. (2000), Reddy et al. (2005a) and Hansen et al. (2005) as summarised in Table 2.5. The results from a number of studies that continue to group the RF from fossil fuel with that from biomass burning are also shown. Recently published results (A to K) and AeroCom studies (L to T) suggest a combined RF from both sources of +0.44 ± 0.13 W m^{-2} and +0.29 ± 0.15 W m^{-2} respectively. The stronger RF estimates from the models A to K appear to be primarily due to stronger sources and column loadings as the direct RF/column loading is similar at approximately 1.2 to 1.3 W mg^{-1} (Table 2.5). Carbonaceous aerosol emission inventories suggest that approximately 34 to 38% of emissions come from biomass burning sources and the remainder from fossil fuel burning sources. Models that separate fossil fuel from biomass burning suggest an equal split in RF. This is applied to those estimates where the BC emissions are not explicitly separated into emission sources to provide an estimate of the RF due to fossil fuel BC. For the AeroCom results, the fossil fuel BC RF ranges from +0.08 to +0.18 W m^{-2} with a mean of +0.13 W m^{-2} and a standard deviation of 0.03 W m^{-2}. For model results A to K, the RFs range from +0.15 W m^{-2} to approximately +0.27 W m^{-2}, with a mean of +0.25 W m^{-2} and a standard deviation of 0.11 W m^{-2}.

The mean and median of the direct RF for fossil fuel BC from grouping all these studies together are +0.19 and +0.16 W m^{-2}, respectively, with a standard deviation of nearly 0.10 W m^{-2}. The standard deviation is multiplied by 1.645 to approximate the 90% confidence interval and the best estimate is rounded upwards slightly for simplicity, leading to a direct RF estimate of +0.20 ± 0.15 W m^{-2}. This estimate does not include the semi-direct effect or the BC impact on snow and ice surface albedo (see Sections 2.5.4 and 2.8.5.6)

2.4.4.4 Biomass Burning Aerosol

The TAR reported a contribution to the RF of roughly –0.4 W m^{-2} from the scattering components (mainly organic carbon and inorganic compounds) and +0.2 W m^{-2} from the absorbing components (BC) leading to an estimate of the RF of biomass burning aerosols of –0.20 W m^{-2} with a factor of three uncertainty. Note that the estimates of the BC RF from Hansen and Sato (2001), Hansen et al. (2002), Hansen and Nazarenko (2004) and Jacobson (2001a) include the RF component of BC from biomass burning aerosol. Radiative forcing due to biomass burning (primarily organic carbon, BC and inorganic compounds such as nitrate and sulphate) is grouped into a single RF, because biomass burning emissions are essentially uncontrolled. Emission inventories show more significant differences for biomass burning aerosols than for aerosols of fossil fuel origin (Kasischke and Penner, 2004). Furthermore, the pre-industrial levels of biomass burning aerosols are also difficult to quantify (Ito and Penner, 2005; Mouillot et al., 2006).

The Southern African Regional Science Initiative (SAFARI 2000: see Swap et al., 2002, 2003) took place in 2000 and 2001. The main objectives of the aerosol research were to investigate pyrogenic and biogenic emissions of aerosol in southern Africa (Eatough et al., 2003; Formenti et al., 2003; Hély et al., 2003), validate the remote sensing retrievals (Haywood et al., 2003b; Ichoku et al., 2003) and to study the influence of aerosols on the radiation budget via the direct and indirect effects (e.g., Bergstrom et al., 2003; Keil and Haywood, 2003; Myhre et al., 2003; Ross et al., 2003). The physical and optical properties of fresh and aged biomass burning aerosol were characterised by making intensive observations of aerosol size distributions, optical properties, and DRE through *in situ* aircraft measurements (e.g., Abel et al., 2003; Formenti et al., 2003; Haywood et al., 2003b; Magi and Hobbs, 2003; Kirchstetter et al., 2004) and radiometric measurements (e.g., Bergstrom et al., 2003; Eck et al., 2003). The ω_o at 0.55 µm derived from near-source AERONET sites ranged from 0.85 to 0.89 (Eck et al., 2003), while ω_o at 0.55 µm for aged aerosol was less absorbing at approximately 0.91 (Haywood et al., 2003b). Abel et al. (2003) showed evidence that ω_o at 0.55 µm increased from approximately 0.85 to 0.90 over a time period of approximately two hours subsequent to emission, and attributed the result to the condensation of essentially non-absorbing organic gases onto existing aerosol particles. Fresh biomass burning aerosols produced by boreal forest fires appear to have weaker absorption than those from tropical fires, with ω_o at 0.55 µm greater than 0.9 (Wong and Li 2002). Boreal fires may not exert a significant direct RF because a large proportion of the fires are of natural origin and no significant change over the industrial era is expected. However, Westerling et al. (2006) showed that earlier spring and higher temperatures in USA have increased wildfire activity and duration. The partially absorbing nature of biomass burning aerosol means it exerts an RF that is larger at the surface and in the atmospheric column than at the TOA (see Figure 2.12).

Modelling efforts have used data from measurement campaigns to improve the representation of the physical and optical properties as well as the vertical profile of biomass burning aerosol (Myhre et al., 2003; Penner et al., 2003; Section 2.4.5). These modifications have had important consequences for estimates of the RF due to biomass burning aerosols because the RF is significantly more positive when biomass burning aerosol overlies cloud than previously estimated (Keil and Haywood, 2003; Myhre et al., 2003; Abel et al., 2005). While the RF due to biomass burning aerosol in clear skies is certainly negative, the overall RF of biomass burning aerosol may be positive. In addition to modelling studies, observations of this effect have been made with satellite instruments. Hsu et al. (2003) used SeaWiFs, TOMS and CERES data to show that biomass burning aerosol emitted from Southeast Asia is frequently lifted above the clouds, leading to a reduction in reflected solar radiation over cloudy areas by up to 100 W m^{-2}, and pointed out that this effect could be due to a combination of direct and indirect effects. Similarly, Haywood et al. (2003a) showed that remotely sensed cloud liquid water and effective radius underlying biomass burning aerosol off the coast of Africa are subject to potentially large systematic biases. This may have important consequences for studies that use

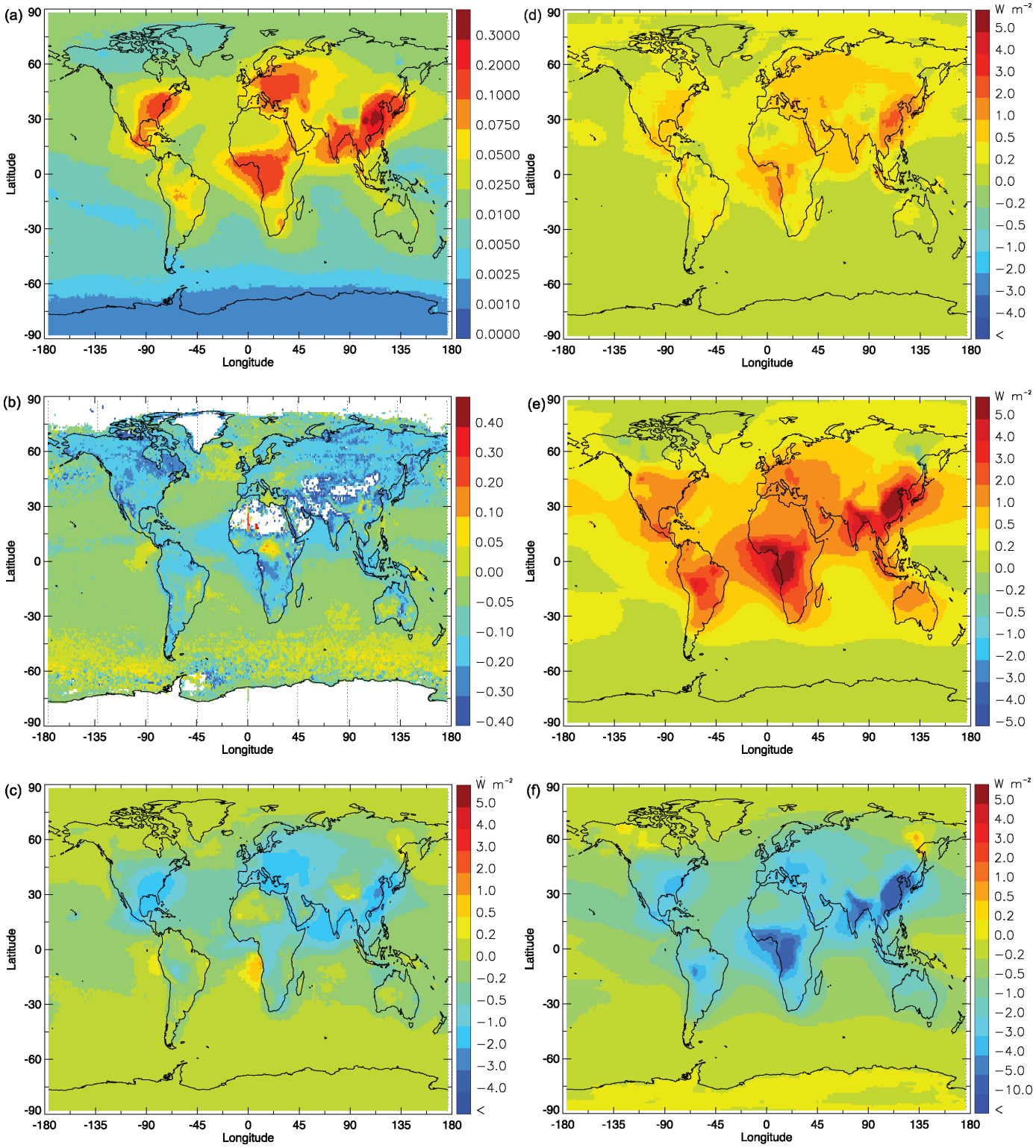


Figure 2.12. *Characteristic aerosol properties related to their radiative effects, derived as the mean of the results from the nine AeroCom models listed in Table 2.5. All panels except (b) relate to the combined anthropogenic aerosol effect. Panel (b) considers the total (natural plus anthropogenic) aerosol optical depth from the models. (a) Aerosol optical depth. (b) Difference in total aerosol optical depth between model and MODIS data. (c) Shortwave RF. (d) Standard deviation of RF from the model results. (e) Shortwave forcing of the atmosphere. (f) Shortwave surface forcing.*

correlations of τ_{aer} and cloud effective radius in estimating the indirect radiative effect of aerosols.

Since the biomass burning aerosols can exert a significant positive RF when above clouds, the aerosol vertical profile is critical in assessing the magnitude and even the sign of the direct RF in cloudy areas. Textor et al. (2006) showed that there are significant differences in aerosol vertical profiles between global aerosol models. These differences are evident in the results from the recently published studies and AeroCom models in Table 2.5. The most negative RF of –0.05 W m^{-2} is from the model of Koch (2001) and from the Myhre et al. (2003) AeroCom submission, while several models have RFs that are slightly positive. Hence, even the sign of the RF due to biomass burning aerosols is in question.

The mean and median of the direct RF for biomass burning aerosol from grouping all these studies together are similar at +0.04 and +0.02 W m^{-2}, respectively, with a standard deviation of 0.07 W m^{-2}. The standard deviation is multiplied by 1.645 to approximate the 90% confidence interval, leading to a direct RF estimate of +0.03 ± 0.12 W m^{-2}. This estimate of the direct RF is more positive than that of the TAR owing to improvements in the models in representing the absorption properties of the aerosol and the effects of biomass burning aerosol overlying clouds.

2.4.4.5 Nitrate Aerosol

Atmospheric ammonium nitrate aerosol forms if sulphate aerosol is fully neutralised and there is excess ammonia. The direct RF due to nitrate aerosol is therefore sensitive to atmospheric concentrations of ammonia as well as NO_x emissions. In addition, the weakening of the RF of sulphate aerosol in many regions due to reduced emissions (Section 2.4.4.1) will be partially balanced by increases in the RF of nitrate aerosol (e.g., Liao and Seinfeld, 2005). The TAR did not quantify the RF due to nitrate aerosol owing to the large discrepancies in the studies available at that time. Van Dorland (1997) and Jacobson (2001a) suggested relatively minor global mean RFs of –0.03 and –0.05 W m^{-2}, respectively, while Adams et al. (2001) suggested a global mean RF as strong as –0.22 W m^{-2}. Subsequent studies include those of Schaap et al. (2004), who estimated that the RF of nitrate over Europe is about 25% of that due to sulphate aerosol, and of Martin et al. (2004), who reported –0.04 to –0.08 W m^{-2} for global mean RF due to nitrate. Further, Liao and Seinfeld (2005) estimated a global mean RF due to nitrate of –0.16 W m^{-2}. In this study, heterogeneous chemistry reactions on particles were included; this strengthens the RF due to nitrate and accounts for 25% of its RF. Feng and Penner (2007) estimated a large, global, fine-mode nitrate burden of 0.58 mg NO_3 m^{-2}, which would imply an equivalent of 20% of the mean anthropogenic sulphate burden. Surface observations of fine-mode nitrate particles show that high concentrations are mainly found in highly industrialised regions, while low concentrations are found in rural areas (Malm et al., 2004; Putaud et al., 2004). Atmospheric nitrate is essentially non-absorbing in the visible spectrum, and laboratory studies have been performed to determine the hygroscopicity of the aerosols (e.g., Tang 1997; Martin et al., 2004 and references therein). In the AeroCom exercise, nitrate aerosols were not included so fewer estimates of this compound exist compared to the other aerosol species considered.

The mean direct RF for nitrate is estimated to be –0.10 W m^{-2} at the TOA, and the conservative scattering nature means a similar flux change at the surface. However, the uncertainty in this estimate is necessarily large owing to the relatively small number of studies that have been performed and the considerable uncertainty in estimates, for example, of the nitrate τ_{aer}. Thus, a direct RF of –0.10 ± 0.10 W m^{-2} is tentatively adopted, but it is acknowledged that the number of studies performed is insufficient for accurate characterisation of the magnitude and uncertainty of the RF.

2.4.4.6 Mineral Dust Aerosol

Mineral dust from anthropogenic sources originates mainly from agricultural practices (harvesting, ploughing, overgrazing), changes in surface water (e.g., Caspian and Aral Sea, Owens Lake) and industrial practices (e.g., cement production, transport) (Prospero et al., 2002). The TAR reported that the RF due to anthropogenic mineral dust lies in the range of +0.4 to –0.6 W m^{-2}, and did not assign a best estimate because of the difficulties in determining the anthropogenic contribution to the total dust loading and the uncertainties in the optical properties of dust and in evaluating the competing shortwave and longwave radiative effects. For the sign and magnitude of the mineral dust RF, the most important factor for the shortwave RF is the single scattering albedo whereas the longwave RF is dependent on the vertical profile of the dust.

Tegen and Fung (1995) estimated the anthropogenic contribution to mineral dust to be 30 to 50% of the total dust burden in the atmosphere. Tegen et al. (2004) provided an updated, alternative estimate by comparing observations of visibility, as a proxy for dust events, from over 2,000 surface stations with model results, and suggested that only 5 to 7% of mineral dust comes from anthropogenic agricultural sources. Yoshioka et al. (2005) suggested that a model simulation best reproduces the North African TOMS aerosol index observations when the cultivation source in the Sahel region contributes 0 to 15% to the total dust emissions in North Africa. A 35-year dust record established from Barbados surface dust and satellite observations from TOMS and the European geostationary meteorological satellite (Meteosat) show the importance of climate control and Sahel drought for interannual and decadal dust variability, with no overall trend yet documented (Chiapello et al., 2005). As further detailed in Section 7.3, climate change and CO_2 variations on various time scales can change vegetation cover in semi-arid regions. Such processes dominate over land use changes as defined above, which would give rise to anthropogenic dust emissions (Mahowald and Luo, 2003; Moulin and Chiapello, 2004; Tegen et al., 2004). A best

guess of 0 to 20% anthropogenic dust burden from these works is used here, but it is acknowledged that a very large uncertainty remains because the methods used cannot exclude either a reduction of 24% in present-day dust nor a large anthropogenic contribution of up to 50% (Mahowald and Luo, 2003; Mahowald et al., 2004; Tegen et al., 2005). The RF efficiency of anthropogenic dust has not been well differentiated from that of natural dust and it is assumed that they are equal. The RF due to dust emission changes induced by circulation changes between 1750 and the present are difficult to quantify and not included here (see also Section 7.5).

In situ measurements of the optical properties of local Saharan dust (e.g., Haywood et al., 2003c; Tanré et al., 2003), transported Saharan mineral dust (e.g., Kaufman et al., 2001; Moulin et al., 2001; Coen et al., 2004) and Asian mineral dust (Huebert et al., 2003; Clarke et al., 2004; Shi et al., 2005; Mikami et al., 2006) reveal that dust is considerably less absorbing in the solar spectrum than suggested by previous dust models such as that of WMO (1986). These new, spectral, simultaneous remote and *in situ* observations suggest that the single scattering albedo (ω_o) of pure dust at a wavelength of 0.67 µm is predominantly in the range 0.90 to 0.99, with a central global estimate of 0.96. This is in accordance with the bottom-up modelling of ω_o based on the haematite content in desert dust sources (Claquin et al., 1999; Shi et al., 2005). Analyses of ω_o from long-term AERONET sites influenced by Saharan dust suggest an average ω_o of 0.95 at 0.67 µm (Dubovik et al., 2002), while unpolluted Asian dust during the Aeolian Dust Experiment on Climate (ADEC) had an average ω_o of 0.93 at 0.67 µm (Mikami et al., 2006 and references therein). These high ω_o values suggest that a positive RF by dust in the solar region of the spectrum is unlikely. However, absorption by particles from source regions with variable mineralogical distributions is generally not represented by global models.

Measurements of the DRE of mineral dust over ocean regions, where natural and anthropogenic contributions are indistinguishably mixed, suggest that the local DRE may be extremely strong: Haywood et al. (2003b) made aircraft-based measurements of the local instantaneous shortwave DRE of as strong as –130 W m^{-2} off the coast of West Africa. Hsu et al. (2000) used Earth Radiation Budget Experiment (ERBE) and TOMS data to determine a peak monthly mean shortwave DRE of around –45 W m^{-2} for July 1985. Interferometer measurements from aircraft and the surface have now measured the spectral signature of mineral dust for a number of cases (e.g., Highwood et al., 2003) indicating an absorption peak in the centre of the 8 to 13 µm atmospheric window. Hsu et al. (2000) determined a longwave DRE over land areas of North Africa of up to +25 W m^{-2} for July 1985; similar results were presented by Haywood et al. (2005) who determined a peak longwave DRE of up to +50 W m^{-2} at the top of the atmosphere for July 2003.

Recent model simulations report the total anthropogenic and natural dust DRE, its components and the net effect as follows (shortwave / longwave = net TOA, in W m^{-2}): H. Liao et al. (2004): –0.21 / +0.31 = +0.1; Reddy et al. (2005a): –0.28 / +0.14 = –0.14; Jacobson (2001a): –0.20 / +0.07 = –0.13; reference case and [range] of sensitivity experiments in Myhre and Stordal (2001a, except case 6 and 7): –0.53 [–1.4 to +0.2] / +0.13 [+0.0 to +0.8] = –0.4 [–1.4 to +1.0]; and from AeroCom database models, GISS: –0.75 / (+0.19) = (–0.56); UIO-CTM*: –0.56 / (+0.19) = (–0.37); LSCE*: –0.6 / +0.3 = –0.3; UMI*: –0.54 / (+0.19) = (–0.35). (See Table 2.4, Note (a) for model descriptions.) The (*) star marked models use a single scattering albedo (approximately 0.96 at 0.67 µm) that is more representative of recent measurements and show more negative shortwave effects. A mean longwave DRE of 0.19 W m^{-2} is assumed for GISS, UMI and UIO-CTM. The scatter of dust DRE estimates reflects the fact that dust burden and τ_{aer} vary by ±40 and ±44%, respectively, computed as standard deviation from 16 AeroCom A model simulations (Textor et al., 2006; Kinne et al., 2006). Dust emissions from different studies range between 1,000 and 2,150 Tg yr^{-1} (Zender, 2004). Finally, a major effect of dust may be in reducing the burden of anthropogenic species at sub-micron sizes and reducing their residence time (Bauer and Koch, 2005; see Section 2.4.5.7).

The range of the reported dust net DRE (–0.56 to +0.1 W m^{-2}), the revised anthropogenic contribution to dust DRE of 0 to 20% and the revised absorption properties of dust support a small negative value for the anthropogenic direct RF for dust of –0.1 W m^{-2}. The 90% confidence level is estimated to be ±0.2 W m^{-2}, reflecting the uncertainty in total dust emissions and burdens and the range of possible anthropogenic dust fractions. At the limits of this uncertainty range, anthropogenic dust RF is as negative as –0.3 W m^{-2} and as positive as +0.1 W m^{-2}. This range includes all dust DREs reported above, assuming a maximum 20% anthropogenic dust fraction, except the most positive DRE from Myhre and Stordal (2001a).

2.4.4.7 Direct RF for Combined Total Aerosol

The TAR reported RF values associated with several aerosol components but did not provide an estimate of the overall aerosol RF. Improved and intensified *in situ* observations and remote sensing of aerosols suggest that the range of combined aerosol RF is now better constrained. For model results, extensive validation now exists for combined aerosol properties, representing the whole vertical column of the atmosphere, such as τ_{aer}. Using a combined estimate implicitly provides an alternative procedure to estimating the RF uncertainty. This approach may be more robust than propagating uncertainties from all individual aerosol components. Furthermore, a combined RF estimate accounts for nonlinear processes due to aerosol dynamics and interactions between radiation field and aerosols. The role of nonlinear processes of aerosol dynamics in RF has been recently studied in global aerosol models that account for the internally mixed nature of aerosol particles (Jacobson, 2001a; Kirkevåg and Iversen, 2002; Liao and Seinfeld, 2005; Takemura et al., 2005; Stier et al., 2006b). Mixing of aerosol particle populations influences the radiative properties of the combined aerosol, because mixing changes size, chemical composition, state and shape, and this feed backs to the aerosol removal and formation processes itself. Chung

and Seinfeld (2002), in reviewing studies where BC is mixed either externally or internally with various other components, showed that BC exerts a stronger positive direct RF when mixed internally. Although the source-related processes for anthropogenic aerosols favour their submicron nature, natural aerosols enter the picture by providing a condensation surface for aerosol precursor gases. Heterogeneous reactions on sea salt and dust can reduce the sub-micron sulphate load by 28% (H. Liao et al., 2004) thereby reducing the direct and indirect RFs. Bauer and Koch (2005) estimated the sulphate RF to weaken from –0.25 to –0.18 W m^{-2} when dust is allowed to interact with the sulphur cycle. It would be useful to identify the RF contribution attributable to different source categories (Section 2.9.3 investigates this). However, few models have separated out the RF from specific emission source categories. Estimating the combined aerosol RF is a first step to quantify the anthropogenic perturbation to the aerosol and climate system caused by individual source categories.

A central model-derived estimate for the aerosol direct RF is based here on a compilation of recent simulation results using multi-component global aerosol models (see Table 2.6). This is a robust method for several reasons. The complexity of multi-component aerosol simulations captures nonlinear effects. Combining model results removes part of the errors in individual model formulations. As shown by Textor et al. (2006), the model-specific treatment of transport and removal processes is partly responsible for the correlated dispersion of the different aerosol components. A less dispersive model with smaller burdens necessarily has fewer scattering and absorbing aerosols interacting with the radiation field. An error in accounting for cloud cover would affect the all-sky RF from all aerosol components. Such errors result in correlated RF efficiencies for major aerosol components within a given model. Directly combining aerosol RF results gives a more realistic aerosol RF uncertainty estimate. The AeroCom compilation suggests significant differences in the modelled local and regional composition of the aerosol (see also Figure 2.12), but an overall reproduction of the total τ_{aer} variability can be performed (Kinne et al., 2006). The scatter in model performance suggests that currently no preference or weighting of individual model results can be used (Kinne et al., 2006). The aerosol RF taken together from several models is more robust than an analysis per component or by just one model. The mean estimate from Table 2.6 of the total aerosol direct RF is –0.2 W m^{-2}, with a standard deviation of ±0.2 W m^{-2}. This is a low-end estimate for both the aerosol RF and uncertainty because nitrate (estimated as –0.1 W m^{-2}, see Section 2.4.4.5) and anthropogenic mineral dust (estimated as –0.1 W m^{-2}, see Section 2.4.4.6) are missing in most of the model simulations. Adding their contribution yields an overall model-derived aerosol direct RF of –0.4 W m^{-2} (90% confidence interval: 0 to –0.8 W m^{-2}).

Three satellite-based measurement estimates of the aerosol direct RF have become available, which all suggest a more negative aerosol RF than the model studies (see Section 2.4.2.1.3). Bellouin et al. (2005) computed a TOA aerosol RF of –0.8 ± 0.1 W m^{-2}. Chung et al. (2005), based upon similarly extensive calculations, estimated the value to be –0.35 ± 0.25 W m^{-2}, and Yu et al. (2006) estimated it to be –0.5 ± 0.33 W m^{-2}. A central measurement-based estimate would suggest an aerosol direct RF of –0.55 W m^{-2}. Figure 2.13 shows the observationally based aerosol direct RF estimates together with the model estimates published since the TAR.

The discrepancy between measurements and models is also apparent in oceanic clear-sky conditions where the measurement-based estimate of the combined aerosol DRE including natural aerosols is considered unbiased. In these areas, models underestimate the negative aerosol DRE by 20 to 40% (Yu et al., 2006). The anthropogenic fraction of τ_{aer} is similar between model and measurement based studies. Kaufman et al. (2005a) used satellite-observed fine-mode τ_{aer} to estimate the anthropogenic τ_{aer}. Correcting for fine-mode τ_{aer}

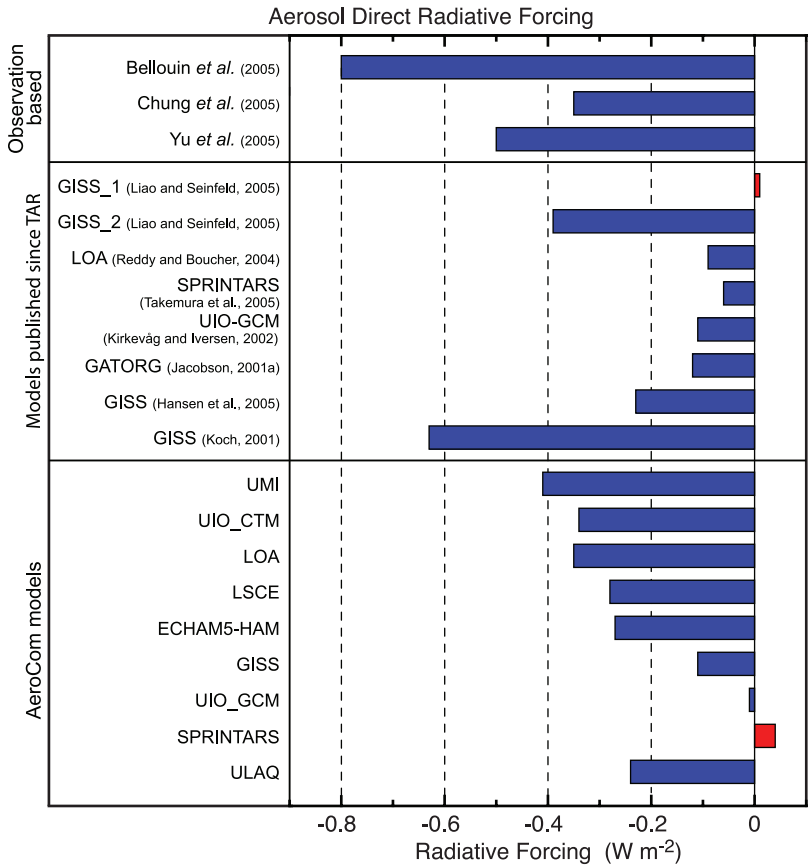


Figure 2.13. *Estimates of the direct aerosol RF from observationally based studies, independent modelling studies, and AeroCom results with identical aerosol and aerosol precursor emissions. GISS_1 refers to a study employing an internal mixture of aerosol, and GISS_2 to a study employing an external mixture. See Table 2.4, Note (a) for descriptions of models.*

Table 2.6. *Quantities related to estimates of the aerosol direct RF. Recent estimates of anthropogenic aerosol load (LOAD), anthropogenic aerosol optical depth (τ_{aer}), its fraction of the present-day total aerosol optical depth ($\tau_{aer\ ant}$), cloud cover in aerosol model, total aerosol direct radiative forcing (RF) for clear sky and all sky conditions, surface forcing and atmospheric all-sky forcing.*

No	Model[a]	LOAD (mg m^{-2})	τ_{aer} (0.55 µm)	$\tau_{aer\ ant}$ (0.55 µm) (%)	Cloud Cover (%)	RF top clear sky (W m^{-2})	RF top all sky (W m^{-2})	Surface Forcing all sky (W m^{-2})	Atmospheric Forcing all sky (W m^{-2})	Reference
Published since IPCC, 2001										
							–0.39[b]	–1.98[b]	1.59[b]	
A	GISS	5.0			79%		+0.01[c]	–2.42[c]	2.43[c]	(Liao and Seinfeld, 2005)
B	LOA	6.0	0.049	34%	70%	–0.53	–0.09			(Reddy and Boucher, 2004)
C	SPRINTARS	4.8	0.044	50%	63%	–0.77	–0.06	–1.92	1.86	(Takemura et al., 2005)
D	UIO-GCM	2.7			57%		–0.11			(Kirkevag and Iversen, 2002)
E	GATORG	6.4[d]			62%	–0.89	–0.12	–2.5	2.38	(Jacobson, 2001a)
F	GISS	6.7	0.049				–0.23			(Hansen et al., 2005)
G	GISS	5.6	0.040				–0.63			(Koch, 2001)
AeroCom: identical emissions used for year 1750 and 2000 (Schulz et al., 2006)										
H	UMI	4.0	0.028	25%	63%	–0.80	–0.41	–1.24	0.84	(Liu and Penner, 2002)
I	UIO_CTM	3.0	0.026	19%	70%	–0.85	–0.34	–0.95	0.61	(Myhre et al., 2003)
J	LOA	5.3	0.046	28%	70%	–0.80	–0.35	–1.49	1.14	(Reddy and Boucher, 2004)
K	LSCE	4.8	0.033	40%	62%	–0.94	–0.28	–0.93	0.66	(Schulz et al., 2006)
L	ECHAM5	4.3	0.032	30%	62%	–0.64	–0.27	–0.98	0.71	(Stier et al., 2005)
M	GISS	2.8	0.014	11%	57%	–0.29	–0.11	–0.81	0.79	(Koch, 2001)
N	UIO_GCM	2.8	0.017	11%	57%		–0.01	–0.84	0.84	(Kirkevag and Iversen, 2002)
O	SPRINTARS	3.2	0.036	44%	62%	–0.35	+0.04	–0.91	0.96	(Takemura et al., 2005)
P	ULAQ	3.7	0.030	23%		–0.79	–0.24			(Pitari et al., 2002)
Average A–G		5.1	0.046	42%	67%	–0.73	–0.23	–2.21	2.07	
Average H–P		3.8	0.029	26%	63%	–0.68	–0.22	–1.02	0.82	
Stddev A–G		1.4	0.004			0.18	0.21			
Stddev H–P		0.9	0.010	11%	5%	0.24	0.16	0.23	0.17	
Average A–P		4.3	0.035	29%	64%	–0.70	–0.22	–1.21	1.24	
Stddev A–P		1.3	0.012	13%	7%	0.26	0.18	0.44	0.65	
Minimum A–P		2.7	0.014	11%	57%	–0.94	–0.63	–1.98	0.61	
Maximum A–P		6.7	0.049	50%	79%	–0.29	0.04	–0.81	2.43	

Notes:
[a] See Note (a) in Table 2.4 for model information.
[b] External mixture.
[c] Internal mixture.
[d] The load excludes that of mineral dust, some of which was considered anthropogenic in Jacobson (2001a).

contributions from dust and sea salt, they found 21% of the total τ_{aer} to be anthropogenic, while Table 2.6 suggests that 29% of τ_{aer} is anthropogenic. Finally, cloud contamination of satellite products, aerosol absorption above clouds, not accounted for in some of the measurement-based estimates, and the complex assumptions about aerosol properties in both methods can contribute to the present discrepancy and increase uncertainty in aerosol RF.

A large source of uncertainty in the aerosol RF estimates is associated with aerosol absorption. Sato et al. (2003) determined the absorption τ_{aer} from AERONET measurements and suggested that aerosol absorption simulated by global aerosol models is underestimated by a factor of two to four. Schuster et al. (2005) estimated the BC loading over continental-scale regions. The results suggest that the model concentrations and absorption τ_{aer} of BC from models are lower than those derived from AERONET. Some of this difference in concentrations could be explained by the assumption that all aerosol absorption is due to BC (Schuster et al., 2005), while a significant fraction may be due to absorption by organic aerosol and mineral dust (see Sections 2.4.4.2, and 2.4.4.6). Furthermore, Reddy et al. (2005a) show that comparison of the aerosol absorption τ_{aer} from models against those from AERONET must be performed very carefully, reducing the discrepancy between their model and AERONET derived aerosol absorption τ_{aer} from a factor of 4 to a factor of 1.2 by careful co-sampling of AERONET and model data. As mentioned above, uncertainty in the vertical position of absorbing aerosol relative to clouds can lead to large uncertainty in the TOA aerosol RF.

The partly absorbing nature of the aerosol is responsible for a heating of the lower-tropospheric column and also results in the surface forcing being considerably more negative than TOA RF, results that have been confirmed through several experimental and observational studies as discussed in earlier sections. Table 2.6 summarises the surface forcing obtained in the different models. Figure 2.12 depicts the regional distribution of several important parameters for assessing the regional impact of aerosol RF. The results are based on a mean model constructed from AeroCom simulation results B and PRE. Anthropogenic τ_{aer} (Figure 2.12a) is shown to have local maxima in industrialised regions and in areas dominated by biomass burning. The difference between simulated and observed τ_{aer} shows that regionally τ_{aer} can be up to 0.1 (Figure 2.12b). Figure 2.12c suggests that there are regions off Southern Africa where the biomass burning aerosol above clouds leads to a local positive RF. Figure 2.12d shows the local variability as the standard deviation from nine models of the overall RF. The largest uncertainties of ±3 W m^{-2} are found in East Asia and in the African biomass burning regions. Figure 2.12e reveals that an average of 0.9 W m^{-2} heating can be expected in the atmospheric column as a consequence of absorption by anthropogenic aerosols. Regionally, this can reach annually averaged values exceeding 5 W m^{-2}. These regional effects and the negative surface forcing in the shortwave (Figure 2.12f) is expected to exert an important effect on climate through alteration of the hydrological cycle.

An uncertainty estimate for the model-derived aerosol direct RF can be based upon two alternative error analyses:

1) An error propagation analysis using the errors given in the sections on sulphate, fossil fuel BC and organic carbon, biomass burning aerosol, nitrate and anthropogenic mineral dust. Assuming linear additivity of the errors, this results in an overall 90% confidence level uncertainty of 0.4 W m^{-2}.

2) The standard deviation of the aerosol direct RF results in Table 2.6, multiplied by 1.645, suggests a 90% confidence level uncertainty of 0.3 W m^{-2}, or 0.4 W m^{-2} when mineral dust and nitrate aerosol are accounted for.

Therefore, the results summarised in Table 2.6 and Figure 2.13, together with the estimates of nitrate and mineral dust RF combined with the measurement-based estimates, provide an estimate for the combined aerosol direct RF of –0.50 ± 0.40 W m^{-2}. The progress in both global modelling and measurements of the direct RF of aerosol leads to a medium-low level of scientific understanding (see Section 2.9, Table 2.11).

2.4.5 Aerosol Influence on Clouds (Cloud Albedo Effect)

As pointed out in Section 2.4.1, aerosol particles affect the formation and properties of clouds. Only a subset of the aerosol population acts as cloud condensation nuclei (CCN) and/or ice nuclei (IN). Increases in ambient concentrations of CCN and IN due to anthropogenic activities can modify the microphysical properties of clouds, thereby affecting the climate system (Penner et al., 2001; Ramanathan et al., 2001a, Jacob et al., 2005). Several mechanisms are involved, as presented schematically in Figure 2.10. As noted in Ramaswamy et al. (2001), enhanced aerosol concentrations can lead to an increase in the albedo of clouds under the assumption of fixed liquid water content (Junge, 1975; Twomey, 1977); this mechanism is referred to in this report as the 'cloud albedo effect'. The aerosol enhancements have also been hypothesised to lead to an increase in the lifetime of clouds (Albrecht, 1989); this mechanism is referred to in this report as the 'cloud lifetime effect' and discussed in Section 7.5.

The interactions between aerosol particles (natural and anthropogenic in origin) and clouds are complex and can be nonlinear (Ramaswamy et al., 2001). The size and chemical composition of the initial nuclei (e.g., anthropogenic sulphates, nitrates, dust, organic carbon and BC) are important in the activation and early growth of the cloud droplets, particularly the water-soluble fraction and presence of compounds that affect surface tension (McFiggans et al., 2006 and references therein). Cloud optical properties are a function of wavelength. They depend on the characteristics of the droplet size distributions and ice crystal concentrations, and on the morphology of the various cloud types.

The interactions of increased concentrations of anthropogenic particles with shallow (stratocumulus and shallow cumulus) and deep convective clouds (with mixed phase) are discussed in this subsection. This section presents new observations and model estimates of the albedo effect. The associated RF in the context of liquid water clouds is assessed. In-depth discussion of the induced changes that are not considered as RFs (e.g., semi-direct and cloud cover and lifetime effects, thermodynamic response and changes in precipitation development) are presented in Section 7.5. The impacts of contrails and aviation-induced cirrus are discussed in Section 2.6 and the indirect impacts of aerosol on snow albedo are discussed in Section 2.5.4.

2.4.5.1 Link Between Aerosol Particles and Cloud Microphysics

The local impact of anthropogenic aerosols has been known for a long time. For example, smoke from sugarcane and forest fires was shown to reduce cloud droplet sizes in early case studies utilising *in situ* aircraft observations (Warner and Twomey, 1967; Eagan et al., 1974). On a regional scale, studies have shown that heavy smoke from forest fires in the Amazon Basin have led to increased cloud droplet number concentrations and to reduced cloud droplet sizes (Reid et al., 1999; Andreae et al., 2004; Mircea et al., 2005). The evidence concerning aerosol modification of clouds provided by the ship track observations reported in the TAR has been further confirmed, to a large extent qualitatively, by results from a number of studies using *in situ* aircraft and satellite data, covering continental cases and regional studies. Twohy et al. (2005) explored the relationship between aerosols and clouds in nine stratocumulus cases, indicating an inverse relationship between particle number and droplet size, but no correlation was found between albedo and particle concentration in the entire data set. Feingold et al. (2003), Kim et al. (2003) and Penner et al. (2004) presented evidence of an increase in the reflectance in continental stratocumulus cases, utilising remote sensing techniques at specific field sites. The estimates in Feingold et al. (2003) confirm that the relationship between aerosol and cloud droplet number concentrations is nonlinear, that is $N_d \approx (N_a)^b$, where N_d is the cloud drop number density and N_a is the aerosol number concentration. The parameter b in this relationship can vary widely, with values ranging from 0.06 to 0.48 (low values of b correspond to low hygroscopicity). This range highlights the sensitivity to aerosol characteristics (primarily size distribution), updraft velocity and the usage of aerosol extinction as a proxy for CCN (Feingold, 2003). Disparity in the estimates of b (or equivalent) based on satellite studies (Nakajima et al., 2001; Breon et al., 2002) suggests that a quantitative estimate of the albedo effect from remote sensors is problematic (Rosenfeld and Feingold 2003), particularly since measurements are not considered for similar liquid water paths.

Many recent studies highlight the importance of aerosol particle composition in the activation process and droplet spectral evolution (indicated in the early laboratory work of Gunn and Philips, 1957), but the picture that emerges is not complete. Airborne aerosol mass spectrometers provide firm evidence that ambient aerosols consist mostly of internal mixtures, for example, biomass burning components, organics and soot are mixed with other aerosol components (McFiggans et al., 2006). Mircea et al. (2005) showed the importance of the organic aerosol fraction in the activation of biomass burning aerosol particles. The presence of internal mixtures (e.g., sea salt and organic compounds) can affect the uptake of water and the resulting optical properties compared to a pure sea salt particle (Randles et al., 2004). Furthermore, the varying contents of water-soluble and insoluble substances in internally mixed particles, the vast diversity of organics, and the resultant effects on cloud droplet sizes, makes the situation even more complex. Earlier observations of fog water (Facchini et al., 1999, 2000) suggested that the presence of organic aerosols would reduce surface tension and lead to a significant increase in the cloud droplet number concentration (Nenes et al., 2002; Rissler et al., 2004; Lohmann and Leck, 2005; Ming et al., 2005a; McFiggans et al., 2006). On the other hand, Feingold and Chuang (2002) and Shantz et al. (2003) indicated that organic coating on CCN delayed activation, leading to a reduction in drop number and a broadening of the cloud droplet spectrum, which had not been previously considered. Ervens et al. (2005) addressed numerous composition effects in unison to show that the effect of composition on droplet number concentration is much less than suggested by studies that address individual composition effects, such as surface tension. The different relationships observed between cloud optical depth and liquid water path in clean and polluted stratocumulus clouds (Penner et al., 2004) have been explained by differences in sub-cloud aerosol particle distributions, while some contribution can be attributed to CCN composition (e.g., internally mixed insoluble dust; Asano et al., 2002). Nevertheless, the review by McFiggans et al. (2006) points to the remaining difficulties in quantitatively explaining the relationship between aerosol size and composition and the resulting droplet size distribution. Dusek et al. (2006) concluded that the ability of a particle to act as a CCN is largely controlled by size rather than composition.

The complexity of the aerosol-cloud interactions and local atmospheric conditions where the clouds are developing are factors in the large variation evidenced for this phenomenon. Advances have been made in the understanding of the regional and/or global impact based on observational studies, particularly for low-level stratiform clouds that constitute a simpler cloud system to study than many of the other cloud types. Column aerosol number concentration and column cloud droplet concentration over the oceans from the AVHRR (Nakajima et al., 2001) indicated a positive correlation, and an increase in shortwave reflectance of low-level, warm clouds with increasing cloud optical thickness, while liquid water path (LWP) remained unmodified. While these results are only applicable over the oceans and are based on data for only four months, the positive correlation between an increase in cloud reflectance and an enhanced ambient aerosol concentration has been confirmed by

other studies (Brenguier et al., 2000a,b; Rosenfeld et al., 2002). However, other studies highlight the sensitivity to LWP, linking high pollution entrained into clouds to a decrease in LWP and a reduction in the observed cloud reflectance (Jiang et al., 2002; Brenguier et al., 2003; Twohy et al., 2005). Still others (Han et al., 2002, using AVHRR observations) have reported an absence of LWP changes in response to increases in the column-averaged droplet number concentration, this occurred for one-third of the cloud cases studied for which optical depths ranged between 1 and 15. Results of large-eddy simulations of stratocumulus (Jiang et al., 2002; Ackerman et al., 2004; Lu and Seinfeld, 2005) and cumulus clouds (Jiang and Feingold, 2006; Xue and Feingold, 2006) seem to confirm the lack of increase in LWP due to increases in aerosols; they point to a dependence on precipitation rate and relative humidity above the clouds (Ackerman et al., 2004). The studies above highlight the difficulty of devising observational studies that can isolate the albedo effect from other effects (e.g., meteorological variability, cloud dynamics) that influence LWP and therefore cloud RF.

Results from the POLDER satellite instrument, which retrieves both submicron aerosol loading and cloud droplet size, suggest much larger cloud effective radii in remote oceanic regions than in the highly polluted continental source areas and downwind adjacent oceanic areas, namely from a maximum of 14 µm down to 6 µm (Bréon et al., 2002). This confirms earlier studies of hemispheric differences using AVHRR. Further, the POLDER- and AVHRR-derived correlations between aerosol and cloud parameters are consistent with an aerosol indirect effect (Sekiguchi et al., 2003). These results suggest that the impact of aerosols on cloud microphysics is global. Note that the satellite measurements of aerosol loading and cloud droplet size are not coincident, and an aerosol index is not determined in the presence of clouds. Further, there is a lack of simultaneous measurements of LWP, which makes assessment of the cloud albedo RF difficult.

The albedo effect is also estimated from studies that combined satellite retrievals with a CTM, for example, in the case of two pollution episodes over the mid-latitude Atlantic Ocean. Results indicated a brightening of clouds over a time scale of a few days in instances when LWP did not undergo any significant changes (Hashvardhan et al., 2002; Schwartz et al., 2002; Krüger and Graβl, 2002). There have been fewer studies on aerosol-cloud relationships under more complex meteorological conditions (e.g., simultaneous presence of different cloud types).

The presence of insoluble particles within ice crystals constituting clouds formed at cold temperatures has a significant influence on the radiation transfer. The inclusions of scattering and absorbing particles within large ice crystals (Macke et al., 1996) suggest a significant effect. Hence, when soot particles are embedded, there is an increase in the asymmetry parameter and thus forward scattering. In contrast, inclusions of ammonium sulphate or air bubbles lead to a decrease in the asymmetry parameter of ice clouds. Given the recent observations of partially insoluble nuclei in ice crystals (Cziczo et al., 2004) and the presence of small crystal populations, there is a need to further develop the solution for radiative transfer through such systems.

2.4.5.2 Estimates of the Radiative Forcing from Models

General Circulation Models constitute an important and useful tool to estimate the global mean RF associated with the cloud albedo effect of anthropogenic aerosols. The model estimates of the changes in cloud reflectance are based on forward calculations, considering emissions of anthropogenic primary particles and secondary particle production from anthropogenic gases. Since the TAR, the cloud albedo effect has been estimated in a more systematic and rigorous way (allowing, for example, for the relaxation of the fixed LWC criterion), and more modelling results are now available. Most climate models use parametrizations to relate the cloud droplet number concentration to aerosol concentration; these vary in complexity from simple empirical fits to more physically based relationships. Some models are run under an increasing greenhouse gas concentration scenario and include estimates of present-day aerosol loadings (including primary and secondary aerosol production from anthropogenic sources). These global modelling studies (Table 2.7) have a limitation arising from the underlying uncertainties in aerosol emissions (e.g., emission rates of primary particles and of secondary particle precursors). Another limitation is the inability to perform a meaningful comparison between the various model results owing to differing formulations of relationships between aerosol particle concentrations and cloud droplet or ice crystal populations; this, in turn, yields differences in the impact of microphysical changes on the optical properties of clouds. Further, even when the relationships used in different models are similar, there are noticeable differences in the spatial distributions of the simulated low-level clouds. Individual models' physics have undergone considerable evolution, and it is difficult to clearly identify all the changes in the models as they have evolved. While GCMs have other well-known limitations, such as coarse spatial resolution, inaccurate representation of convection and hence updraft velocities leading to aerosol activation and cloud formation processes, and microphysical parametrizations, they nevertheless remain an essential tool for quantifying the global cloud albedo effect. In Table 2.7, differences in the treatment of the aerosol mixtures (internal or external, with the latter being the more frequently employed method) are noted. Case studies of droplet activation indicate a clear sensitivity to the aerosol composition (McFiggans et al., 2006); additionally, radiative transfer is sensitive to the aerosol composition and the insoluble fraction present in the cloud droplets.

All models estimate a negative global mean RF associated with the cloud albedo effect, with the range of model results varying widely, from –0.22 to –1.85 W m^{-2}. There are considerable differences in the treatment of aerosol, cloud processes and aerosol-cloud interaction processes in these models. Several models include an interactive sulphur cycle and anthropogenic aerosol particles composed of sulphate, as

Table 2.7. *Published model studies of the RF due to cloud albedo effect, in the context of liquid water clouds, with a listing of the relevant modelling details.*

Model	Model type[a]	Aerosol species[b]	Aerosol mixtures[c]	Cloud types included	Microphysics	Radiative Forcing (W m^{-2})[d]
Lohmann et al. (2000)	AGCM + sulphur cycle (ECHAM4)	S, OC, BC, SS, D	I	warm and mixed phase	Droplet number concentration and LWC, Beheng (1994); Sundqvist et al. (1989). Also, mass and number from field observations	–1.1 (total) **–0.45 (albedo)**
			E			–1.5 (total)
Jones et al. (2001)	AGCM + sulphur cycle, fixed SST (Hadley)	S, SS, D (a crude attempt for D over land, no radiation)	E	stratiform and shallow cumulus	Droplet number concentration and LWC, Wilson and Ballard (1999); Smith (1990); Tripoli and Cotton (1980); Bower et al. (1994). Warm and mixed phase, radiative treatment of anvil cirrus, non-spherical ice particles	–1.89 (total) **–1.34 (albedo)**
Williams et al. (2001b)	GCM with slab ocean + sulphur cycle (Hadley)	S, SS	E	stratiform and shallow cumulus	Jones et al. (2001)	–1.69 (total) **–1.37 (albedo)**
	AGCM, fixed SST					–1.62 (total) **–1.43(albedo)**
Rotstayn and Penner (2001)	AGCM (CSIRO), fixed SST and sulphur loading	S	n.a.	warm and mixed phase	Rotstayn (1997); Rotstayn et al. (2000)	**–1.39 (albedo)**
Rotstayn and Liu (2003)	Interactive sulphur cycle				Inclusion of dispersion	12 to 35% decrease **–1.12 (albedo, mid value decreased)**
Ghan et al. (2001)	AGCM (PNNL) + chemistry (MIRAGE), fixed SST	S, OC, BC, SS, N, D	E (for different modes); I (within modes)	warm and mixed phase	Droplet number concentration and LWC, crystal concentration and ice water content. Different processes affecting the various modes	–1.7 (total) **–0.85 (albedo)**
Chuang et al. (2002)	CCM1 (NCAR) + chemistry (GRANTOUR), fixed SST	S, OC, BC, SS, D	E (for emitted particles); I: when growing by condensation	warm and mixed phase	Modified from Chuang and Penner (1995), no collision/coalescence	**–1.85 (albedo)**
Menon et al. (2002a)	GCM (GISS) + sulphur cycle, fixed SST	S,OC, SS	E	warm	Droplet number concentration and LWC, Del Genio et al. (1996), Sundqvist et al. (1989). Warm and mixed phase, improved vertical distribution of clouds (but only nine layers).Global aerosol burdens poorly constrained	–2.41 (total) **–1.55 (albedo)**
Kristjansson (2002)	CCM3 (NCAR) fixed SST	S, OC, BC, SS, D	E (for nucleation mode and fossil fuel BC); I (for accumulation mode)	warm and mixed phase	Rasch and Kristjánsson (1998). Stratiform and detraining convective clouds	–1.82 (total) **–1.35 (albedo)**
Suzuki et al. (2004)	AGCM (Japan), fixed SST	S, OC, BC, SS	E	stratiform	Berry(1967), Sundqvist(1978)	**0.54 (albedo)**
Quaas et al. (2004)	AGCM (LMDZ) + interactive sulphur cycle, fixed SST	S	n.a.	warm and mixed phase	Aerosol mass and cloud droplet number concentration, Boucher and Lohmann (1995); Boucher et al. (1995)	**–1.3 (albedo)**

Table 2.7 (continued)

Model	Model type[a]	Aerosol species[b]	Aerosol mixtures[c]	Cloud types included	Microphysics	Radiative Forcing (W m^{-2})[d]
Hansen et al. (2005)	GCM (GISS) + 3 different ocean parametrizations	S, OC, BC, SS, N, D (D not included in clouds)	E	warm and shallow (below 720hPa)	Schmidt et al. (2005), 20 vertical layers. Droplet number concentration (Menon and Del Genio, 2007)	**–0.77 (albedo)**
Kristjansson et al. (2005)	CCM3 (NCAR) + sulphur and carbon cycles slab ocean	S, OC, BC, SS, D	E (for nucleation mode and fossil fuel BC); I (for accumulation mode)	warm and mixed phase	Kristjansson (2002). Stratiform and detraining convective clouds	–1.15 (total, at the surface)
Quaas and Boucher (2005)	AGCM (LMDZ) + interactive sulphur cycle, fixed SST	S, OC, BC, SS, D	E	warm and mixed phase	Aerosol mass and cloud droplet number concentration, Boucher and Lohmann (1995); Boucher et al. (1995) control run	**–0.9 (albedo)**
					fit to POLDER data fit to MODIS data	**–0.5 (albedo)[e]** **–0.3 (albedo)[e]**
Quaas et al. (2005)	AGCM (LMDZ and ECHAM4)	S, OC, BC, SS, D	E	warm and mixed phase	Aerosol mass and cloud droplet number concentration, Boucher and Lohmann, (1995), control runs (ctl)	–0.84 (total LMDZ-ctl) –1.54 (total (ECHAM4-ctl)
					Aerosol mass and cloud droplet number concentration fitted to MODIS data	–0.53 (total LMDZ)[e] –0.29 (total (ECHAM4)[e]
Dufresne et al. (2005)	AGCM (LMDZ) + interactive sulphur cycle, fixed SST	S	n.a.	warm	Aerosol mass and cloud droplet number concentration, Boucher and Lohmann, (1995), fitted to POLDER data	**–0.22 (albedo)[e]**
Takemura et al. (2005)	AGCM (SPRINTARS) + slab ocean	S, OC, BC, SS, D	E (50% BC from fossil fuel); I (for OC and BC)	warm	Activation based on Kohler theory and updraft velocity	–0.94 (total) **–0.52 (albedo)**
Chen and Penner (2005)	AGCM (UM) + fixed SST	S, SS, D, OC, BC	I	warm and mixed phase	Aerosol mass and cloud droplet number concentration (lognormal) Control (Abdul-Razzak and Ghan, 2002) Relationship between droplet concentration and dispersion coefficient: High Relationship between droplet concentration and dispersion coefficient: Medium Updraft velocity Relationship between droplet concentration and dispersion coefficient: Low Chuang et al. (1997) Nenes and Seinfeld (2003)	 **–1.30 (albedo, UM_ctrl)[f]** **–0.75 (albedo, UM_1)[f]** **–0.86 (albedo, UM_2)[f]** **–1.07 (albedo, UM_3)[f]** **–1.10 (albedo, UM_4)[f]** **–1.29 (albedo, UM_5)[f]** **–1.79 (albedo, UM_6)[f]**

Table 2.7 (continued)

Model	Model type[a]	Aerosol species[b]	Aerosol mixtures[c]	Cloud types included	Microphysics	Radiative Forcing (W m^{-2})[d]
Ming et al. (2005b)	AGCM (GFDL), fixed SST and sulphur loading	S	n.a.	warm	Rotstayn et al. (2000), Khainroutdinov and Kogan (2000). Aerosols off-line	–2.3 (total) **–1.4 (albedo)**
Penner et al. (2006) results from experiment 1	LMDZ, Oslo and CCSR	S, SS, D, OC, BC	E	warm and mixed phase	Aerosol mass and cloud droplet number concentration; Boucher and Lohmann, (1995); Chen and Penner (2005); Sundqvist (1978)	**–0.65 (albedo Oslo)** **–0.68 (albedo LMDZ)** **–0.74 (albedo CCSR)**

Notes:

[a] AGCM: Atmospheric GCM; SST: sea surface temperature; CSIRO: Commonwealth Scientific and Industrial Research Organisation; MIRAGE: Model for Integrated Research on Atmospheric Global Exchanges; GRANTOUR: Global Aerosol Transport and Removal model; GFDL: Geophysical Fluid Dynamics Laboratory; CCSR: Centre for Climate System Research; see Table 2.4, Note (a) for listing of other models and modelling centres listed in this column.

[b] S: sulphate; SS: sea salt; D: mineral dust; BC: black carbon; OC: organic carbon; N: nitrate.

[c] E: external mixtures; I: internal mixtures.

[d] Only the bold numbers were used to construct Figure 2.16.

[e] These simulations have been constrained by satellite observations, using the same empirical fit to relate aerosol mass and cloud droplet number concentration.

[f] The notation UM corresponds to University of Michigan, as listed in Figure 2.14.

well as naturally produced sea salt, dust and continuously outgassing volcanic sulphate aerosols. Lohmann et al. (2000) and Chuang et al. (2002) included internally mixed sulphate, black and organic carbon, sea salt and dust aerosols, resulting in the most negative estimate of the cloud albedo indirect effect. Takemura et al. (2005) used a global aerosol transport-radiation model coupled to a GCM to estimate the direct and indirect effects of aerosols and their associated RF. The model includes a microphysical parametrization to diagnose the cloud droplet number concentration using Köhler theory, which depends on the aerosol particle number concentration, updraft velocity, size distributions and chemical properties of each aerosol species. The results indicate a global decrease in cloud droplet effective radius caused by anthropogenic aerosols, with the global mean RF calculated to be –0.52 W m^{-2}; the land and oceanic contributions are –1.14 and –0.28 W m^{-2}, respectively. Other modelling results also indicate that the mean RF due to the cloud albedo effect is on average somewhat larger over land than over oceans; over oceans there is a more consistent response from the different models, resulting in a smaller inter-model variability (Lohmann and Feichter, 2005).

Chen and Penner (2005), by systematically varying parameters, obtained a less negative RF when the in-cloud updraft velocity was made to depend on the turbulent kinetic energy. Incorporating other cloud nucleation schemes, for example, changing from Abdul-Razzak and Ghan (2002) to the Chuang et al. (1997) parametrization resulted in no RF change, while changing to the Nenes and Seinfeld (2003) parametrization made the RF more negative. Rotstayn and Liu (2003) found a 12 to 35% decrease in the RF when the size dispersion effect was included in the case of sulphate particles. Chen and Penner (2005) further explored the range of parameters used in Rotstayn and Liu (2003) and found the RF to be generally less negative than in the standard integration.

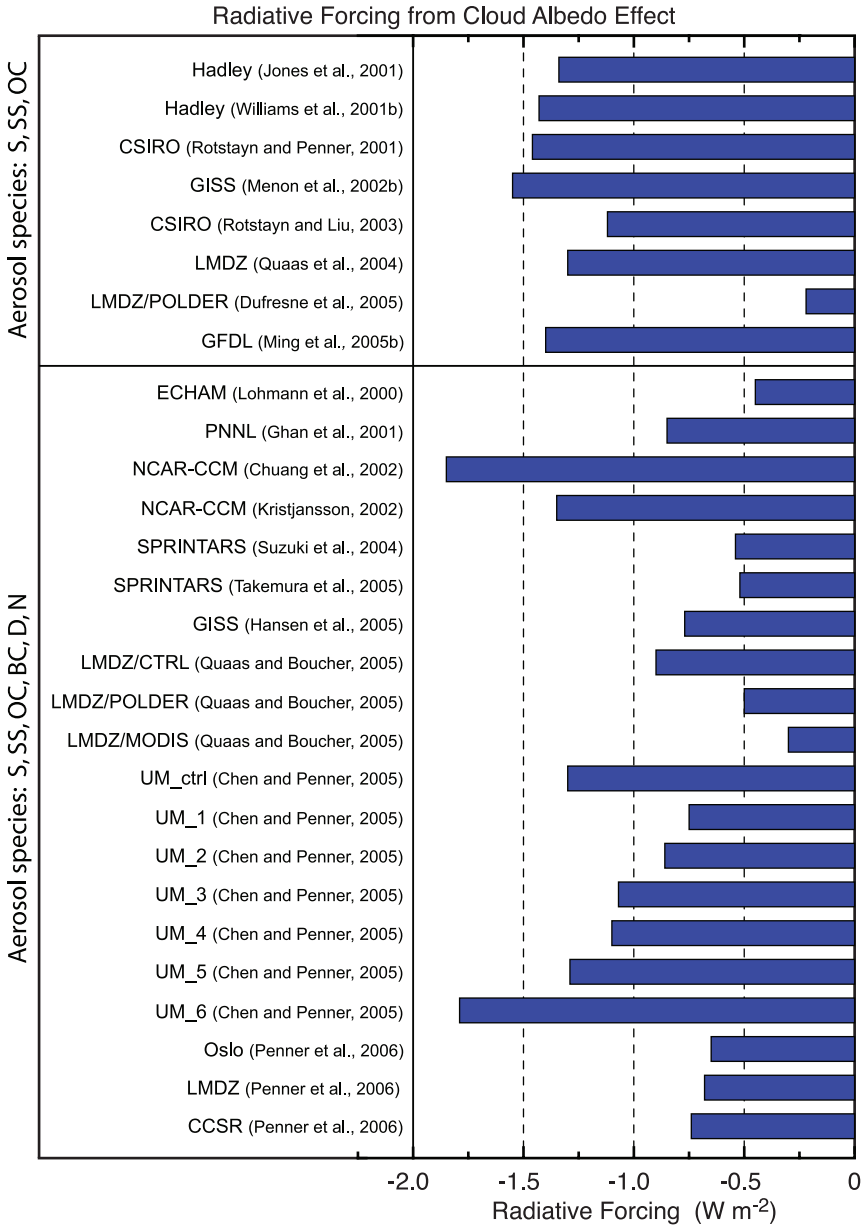


Figure 2.14. *Radiative forcing due to the cloud albedo effect, in the context of liquid water clouds, from the global climate models that appear in Table 2.7. The labels next to the bars correspond to the published study; the notes of Table 2.7 explain the species abbreviations listed on the left hand side. Top panel: results for models that consider a limited number of species, primarily anthropogenic sulphate (S). Bottom panel: results from studies that include a variety of aerosol compositions and mixtures; the estimates here cover a larger range than those in the top panel. Chen and Penner (2005) presented a sensitivity study obtained by changing parametrizations in their model, so the results can be considered independent and are thus listed separately. Penner et al. (2006) is an intercomparison study, so the results of the individual models are listed separately.*

A model intercomparison study (Penner et al., 2006) examined the differences in cloud albedo effect between models through a series of controlled experiments that allowed examination of the uncertainties. This study presented results from three models, which were run with prescribed aerosol mass-number concentration (from Boucher and Lohmann, 1995), aerosol field (from Chen and Penner, 2005) and precipitation efficiency (from Sundqvist, 1978). The cloud albedo RFs in the three models do not vary widely: –0.65, –0.68 and –0.74 W m^{-2}, respectively. Nevertheless, changes in the autoconversion scheme led to a differing response of the LWP between the models, and this is identified as an uncertainty.

A closer inspection of the treatment of aerosol species in the models leads to a broad separation of the results into two groups: models with only a few aerosol species and those that include a more complex mixture of aerosols of different composition. Thus, in Figure 2.14, RF results are grouped according to the

type of aerosol species included in the simulations. In the top panel of Figure 2.14, which shows estimates from models that mainly include anthropogenic sulphate, there is an indication that the results are converging, even though the range of models comes from studies published between 2001 and 2006. These studies show much less scatter than in the TAR, with a mean and standard deviation of –1.37 ± 0.14 W m^{-2}. In contrast, in the bottom panel of Figure 2.14, which shows the studies that include more species, a much larger variability is found. These latter models (see Table 2.7) include 'state of the art' parametrizations of droplet activation for a variety of aerosols, and include both internal and external mixtures.

Some studies have commented on inconsistencies between some of the earlier estimates of the cloud albedo RF from forward and inverse calculations (Anderson et al., 2003). Notwithstanding the fact that these two streams of calculations rely on very different formulations, the results here appear to be within range of the estimates from inverse calculations.

2.4.5.3 Estimates of the Radiative Forcing from Observations and Constrained Models

It is difficult to obtain a best estimate of the cloud albedo RF from pre-industrial times to the present day based solely on observations. The satellite record is not long enough, and other long-term records do not provide the pre-industrial aerosol and cloud microphysical properties needed for such an assessment. Some studies have attempted to estimate the RF by incorporating empirical relationships derived from satellite observations. This approach is valid as long as the observations are robust, but problems still remain, particularly with the use of the aerosol optical depth as proxy for CCN (Feingold et al., 2003), droplet size and cloud optical depth from broken clouds (Marshak et al., 2006), and relative humidity effects (Kapustin et al., 2006) to discriminate between hydrated aerosols and cloud. Radiative forcing estimates constrained by satellite observations need to be considered with these caveats in mind.

By assuming a bimodal lognormal size distribution, Nakajima et al. (2001) determined the Ångstrom exponent from AVHRR data over the oceans (for a period of four months), together with cloud properties, optical thickness and effective radii. The nonlinear relationship between aerosol number concentration and cloud droplet concentration ($N_d \approx (N_a)^b$) obtained is consistent with Twomey's hypothesis; however, the parameter b is smaller than previous estimates (0.5 compared with 0.7 to 0.8; Kaufman et al., 1991), but larger than the 0.26 value obtained by Martin et al. (1994). Using this relationship, Nakajima et al. (2001) provided an estimate of the cloud albedo RF in the range between –0.7 and –1.7 W m^{-2}, with a global average of –1.3 W m^{-2}. Lohmann and Lesins (2002) used POLDER data to estimate aerosol index and cloud droplet radius; they then scaled the results of the simulations with the European Centre Hamburg (ECHAM4) model. The results show that changes in N_a lead to larger changes in N_d in the model than in observations, particularly over land, leading to an overestimate of the cloud albedo effect. The scaled values using the constraint from POLDER yield a global cloud albedo RF of –0.85 W m^{-2}, an almost 40% reduction from their previous estimate. Sekiguchi et al. (2003) presented results from the analysis of AVHRR data over the oceans, and of POLDER data over land and ocean. Assuming that the aerosol column number concentration increased by 30% from the pre-industrial era, they estimated the effect due to the aerosol influence on clouds as the difference between the forcing under present and pre-industrial conditions. They estimated a global effect due to the total aerosol influence on clouds (sum of cloud albedo and lifetime effects) to be between –0.6 and –1.2 W m^{-2}, somewhat lower than the Nakajima et al. (2001) ocean estimate. When the assumption is made that the liquid water content is constant, the cloud albedo RF estimated from AVHRR data is –0.64 ± 0.16 W m^{-2} and the estimate using POLDER data is –0.37 ± 0.09 W m^{-2}. The results from these two studies are very sensitive to the magnitude of the increase in the aerosol concentration from pre-industrial to current conditions, and the spatial distributions.

Quaas and Boucher (2005) used the POLDER and MODIS data to evaluate the relationship between cloud properties and aerosol concentrations on a global scale in order to incorporate it in a GCM. They derived relationships corresponding to marine stratiform clouds and convective clouds over land that show a decreasing effective radius as the aerosol optical depth increases. These retrievals involve a variety of assumptions that introduce uncertainties in the relationships, in particular the fact that the retrievals for aerosol and cloud properties are not coincident and the assumption that the aerosol optical depth can be linked to the sub-cloud aerosol concentration. When these empirical parametrizations are included in a climate model, the simulated RF due to the cloud albedo effect is reduced by 50% from their baseline simulation. Quaas et al. (2005) also utilised satellite data to establish a relationship between cloud droplet number concentration and fine-mode aerosol optical depth, minimising the dependence on cloud liquid water content but including an adiabatic assumption that may not be realistic in many cases. This relationship is implemented in the ECHAM4 and Laboratoire de Météorologie Dynamique Zoom (LMDZ) climate models and the results indicate that the original parametrizations used in both models overestimated the magnitude of the cloud albedo effect. Even though both models show a consistent weakening of the RF, it should be noted that the original estimates of their respective RFs are very different (by almost a factor of two); the amount of the reduction was 37% in LMDZ and 81% in ECHAM4. Note that the two models have highly different spatial distributions of low clouds, simulated aerosol concentrations and anthropogenic fractions.

When only sulphate aerosols were considered, Dufresne et al. (2005) obtained a weaker cloud albedo RF. Their model used a relationship between aerosol mass concentration and cloud droplet number concentration, modified from that originally proposed by Boucher and Lohmann (1995) and adjusted to POLDER data. Their simulations give a factor of two weaker RF compared to the previous parametrization, but it is noted that the results are highly sensitive to the distribution of clouds over land.

2.4.5.4 Uncertainties in Satellite Estimates

The improvements in the retrievals and satellite instrumentation have provided valuable data to begin observation-motivated assessments of the effect of aerosols on cloud properties, even though satellite measurements cannot unambiguously distinguish natural from anthropogenic aerosols. Nevertheless, an obvious advantage of the satellite data is their global coverage, and such extensive coverage can be analysed to determine the relationships between aerosol and cloud properties at a number of locations around the globe. Using these data some studies (Sekiguchi et al., 2003; Quaas et al., 2004) indicate that the magnitude of the RF is resolution dependent, since the representation of convection and clouds in the GCMs and the simulation of updraft velocity that affects activation themselves are resolution dependent. The rather low spatial and temporal resolution of some of the satellite data sets can introduce biases by failing to distinguish aerosol species with different properties. This, together with the absence of coincident LWP measurements in several instances, handicaps the inferences from such studies, and hinders an accurate analysis and estimate of the RF. Furthermore, the ability to separate meteorological from chemical influences in satellite observations depends on the understanding of how clouds respond to meteorological conditions.

Retrievals involve a variety of assumptions that introduce uncertainties in the relationships. As mentioned above, the retrievals for aerosol and cloud properties are not coincident and the assumption is made that the aerosol optical depth can be linked to the aerosol concentration below the cloud. The POLDER instrument may underestimate the mean cloud-top droplet radius due to uncertainties in the sampling of clouds (Rosenfeld and Feingold, 2003). The retrieval of the aerosol index over land may be less reliable and lead to an underestimate of the cloud albedo effect over land. There is an indication of a systematic bias between MODIS-derived cloud droplet radius and that derived from POLDER (Breon and Doutriaux-Boucher, 2005), as well as differences in the aerosol optical depth retrieved from those instruments (Myhre et al., 2004a) that need to be resolved.

2.4.5.5 Uncertainties Due to Model Biases

One of the large sources of uncertainties is the poor knowledge of the amount and distribution of anthropogenic aerosols used in the model simulations, particularly for pre-industrial conditions. Some studies show a large sensitivity in the RF to the ratio of pre-industrial to present-day aerosol number concentrations.

All climate models discussed above include sulphate particles; some models produce them from gaseous precursors over oceans, where ambient concentrations are low, while some models only condense mass onto pre-existing particles over the continents. Some other climate models also include sea salt and dust particles produced naturally, typically relating particle production to wind speed. Some models include anthropogenic nitrate, BC and organic compounds, which in turn affect activation. Models also have weaknesses in representing convection processes and aerosol distributions, and simulating updraft velocities and convection-cloud interactions. Even without considering the existing biases in the model-generated clouds, differences in the aerosol chemical composition and the subsequent treatment of activation lead to uncertainties that are difficult to quantify and assess. The presence of organic carbon, owing to its distinct hygroscopic and absorption properties, can be particularly important for the cloud albedo effect in the tropics (Ming et al., 2007).

Modelling the cloud albedo effect from first principles has proven difficult because the representation of aerosol-cloud and convection-cloud interactions in climate models are still crude (Lohmann and Feichter, 2005). Clouds often do not cover a complete grid box and are inhomogeneous in terms of droplet concentration, effective radii and LWP, which introduces added complications in the microphysical and radiative transfer calculations. Model intercomparisons (e.g., Lohmann et al., 2001; Menon et al., 2003) suggest that the predicted cloud distributions vary significantly between models, particularly their horizontal and vertical extents; also, the vertical resolution and parametrization of convective and stratiform clouds are quite different between models (Chen and Penner, 2005). Even high-resolution models have difficulty in accurately estimating the amount of cloud liquid and ice water content in a grid box.

It has proven difficult to compare directly the results from the different models, as uncertainties are not well identified and quantified. All models could be suffering from similar biases, and modelling studies do not often quote the statistical significance of the RF estimates that are presented. Ming et al. (2005b) demonstrated that it is only in the mid-latitude NH that their model yields a RF result at the 95% confidence level when compared to the unforced model variability. There are also large differences in the way that the different models treat the appearance and evolution of aerosol particles and the subsequent cloud droplet formation. Differences in the horizontal and vertical resolution introduce uncertainties in their ability to accurately represent the shallow warm cloud layers over the oceans that are most susceptible to the changes due to anthropogenic aerosol particles. A more fundamental problem is that GCMs do not resolve the small scales (order of hundreds of metres) at which aerosol-cloud interactions occur. Chemical composition and size distribution spectrum are also likely insufficiently understood at a microphysical level, although some modelling studies suggest that the albedo effect is more sensitive to the size than to aerosol composition (Feingold, 2003; Ervens et al., 2005; Dusek et al., 2006). Observations indicate that aerosol particles in nature tend to be composed of several compounds and can be internally or externally mixed. The actual conditions are difficult to simulate and possibly lead to differences among climate models. The calculation of the cloud albedo effect is sensitive to the details of particle chemical composition (activation) and state of the mixture (external or internal). The relationship between ambient aerosol particle concentrations and resulting cloud

droplet size distribution is important during the activation process; this is a critical parametrization element in the climate models. It is treated in different ways in different models, ranging from simple empirical functions (Menon et al., 2002a) to more complex physical parametrizations that also tend to be more computationally costly (Abdul-Razzak and Ghan, 2002; Nenes and Seinfeld, 2003; Ming et al., 2006). Finally, comparisons with observations have not yet risen to the same degree of verification as, for example, those for the direct RF estimates; this is not merely due to model limitations, since the observational basis also has not yet reached a sound footing.

Further uncertainties may be due to changes in the droplet spectral shape, typically considered invariant in climate models under clean and polluted conditions, but which can be substantially different in typical atmospheric conditions (e.g., Feingold et al., 1997; Ackerman et al., 2000b; Erlick et al., 2001; Liu and Daum, 2002). Liu and Daum (2002) estimated that a 15% increase in the width of the size distribution can lead to a reduction of between 10 and 80% in the estimated RF of the cloud albedo indirect effect. Peng and Lohmann (2003), Rotstayn and Liu (2003) and Chen and Penner (2005) studied the sensitivity of their estimates to this dispersion effect. These studies confirm that their estimates of the cloud albedo RF, without taking the droplet spectra change into account, are overestimated by about 15 to 35%.

The effects of aerosol particles on heterogeneous ice formation are currently insufficiently understood and present another level of challenge for both observations and modelling. Ice crystal concentrations cannot be easily measured with present *in situ* instrumentation because of the difficulty of detecting small particles (Hirst et al., 2001) and frequent shattering of ice particles on impact with the probes (Korolev and Isaac, 2005). Current GCMs do not have sufficiently rigorous microphysics or sub-grid scale processes to accurately predict cirrus clouds or super-cooled clouds explicitly. Ice particles in clouds are often represented by simple shapes (e.g., spheres), even though it is well known that few ice crystals are like that in reality. The radiative properties of ice particles in GCMs often do not effectively simulate the irregular shapes that are normally found, nor do they simulate the inclusions of crustal material or soot in the crystals.

2.4.5.6 Assessment of the Cloud Albedo Radiative Forcing

As in the TAR, only the aerosol interaction in the context of liquid water clouds is assessed, with knowledge of the interaction with ice clouds deemed insufficient. Since the TAR, the cloud albedo effect has been estimated in a more systematic way, and more modelling results are now available. Models now are more advanced in capturing the complexity of the aerosol-cloud interactions through forward computations. Even though major uncertainties remain, clear progress has been made, leading to a convergence of the estimates from the different modelling efforts. Based on the results from all the modelling studies shown in Figure 2.14, compared to the TAR it is now possible to present a best estimate for the cloud albedo RF of –0.7 W m^{-2} as the median, with a 5 to 95% range of –0.3 to –1.8 W m^{-2}. The increase in the knowledge of the aerosol-cloud interactions and the reduction in the spread of the cloud albedo RF since the TAR result in an elevation of the level of scientific understanding to low (Section 2.9, Table 2.11).

2.5 Anthropogenic Changes in Surface Albedo and the Surface Energy Budget

2.5.1 Introduction

Anthropogenic changes to the physical properties of the land surface can perturb the climate, both by exerting an RF and by modifying other processes such as the fluxes of latent and sensible heat and the transfer of momentum from the atmosphere. In addition to contributing to changes in greenhouse gas concentrations and aerosol loading, anthropogenic changes in the large-scale character of the vegetation covering the landscape ('land cover') can affect physical properties such as surface albedo. The albedo of agricultural land can be very different from that of a natural landscape, especially if the latter is forest. The albedo of forested land is generally lower than that of open land because the greater leaf area of a forest canopy and multiple reflections within the canopy result in a higher fraction of incident radiation being absorbed. Changes in surface albedo induce an RF by perturbing the shortwave radiation budget (Ramaswamy et al., 2001). The effect is particularly accentuated when snow is present, because open land can become entirely snow-covered and hence highly reflective, while trees can remain exposed above the snow (Betts, 2000). Even a snow-covered canopy exhibits a relatively low albedo as a result of multiple reflections within the canopy (Harding and Pomeroy, 1996). Surface albedo change may therefore provide the dominant influence of mid- and high-latitude land cover change on climate (Betts, 2001; Bounoua et al., 2002). The TAR cited two estimates of RF due to the change in albedo resulting from anthropogenic land cover change relative to potential natural vegetation (PNV), –0.4 W m^{-2} and –0.2 W m^{-2}, and assumed that the RF relative to 1750 was half of that relative to PNV, so gave a central estimate of the RF due to surface albedo change of –0.2 W m^{-2} ± 0.2 W m^{-2}.

Surface albedo can also be modified by the settling of anthropogenic aerosols on the ground, especially in the case of BC on snow (Hansen and Nazarenko, 2004). This mechanism may be considered an RF mechanism because diagnostic calculations may be performed under the strict definition of RF (see Sections 2.2 and 2.8). This mechanism was not discussed in the TAR.

Land cover change can also affect other physical properties such as surface emissivity, the fluxes of moisture through evaporation and transpiration, the ratio of latent to sensible heat fluxes (the Bowen ratio) and the aerodynamic roughness, which exerts frictional drag on the atmosphere and also affects

turbulent transfer of heat and moisture. All these processes can affect the air temperature near the ground, and also modify humidity, precipitation and wind speed. Direct human perturbations to the water cycle, such as irrigation, can affect surface moisture fluxes and hence the surface energy balance. Changes in vegetation cover can affect the production of dust, which then exerts an RF. Changes in certain gases, particularly CO_2 and ozone, can also exert an additional influence on climate by affecting the Bowen ratio, through plant responses that affect transpiration. These processes are discussed in detail in Section 7.2. While such processes will act as anthropogenic perturbations to the climate system (Pielke et al., 2002) and will fall at least partly within the 'forcing' component of the forcing-feedback-response conceptual model, it is difficult to unequivocally quantify the pure forcing component as distinct from feedbacks and responses. The term 'non-radiative forcing' has been proposed (Jacob et al., 2005) and this report adopts the similar term 'non-initial radiative effect', but no quantitative metric separating forcing from feedback and response has yet been implemented for climatic perturbation processes that do not act directly on the radiation budget (see Section 2.2).

Energy consumption by human activities, such as heating buildings, powering electrical appliances and fuel combustion by vehicles, can directly release heat into the environment. This was not discussed in the TAR. Anthropogenic heat release is not an RF, in that it does not directly perturb the radiation budget; the mechanisms are not well identified and so it is here referred to as a non-initial radiative effect. It can, however, be quantified as a direct input of energy to the system in terms of W m^{-2}.

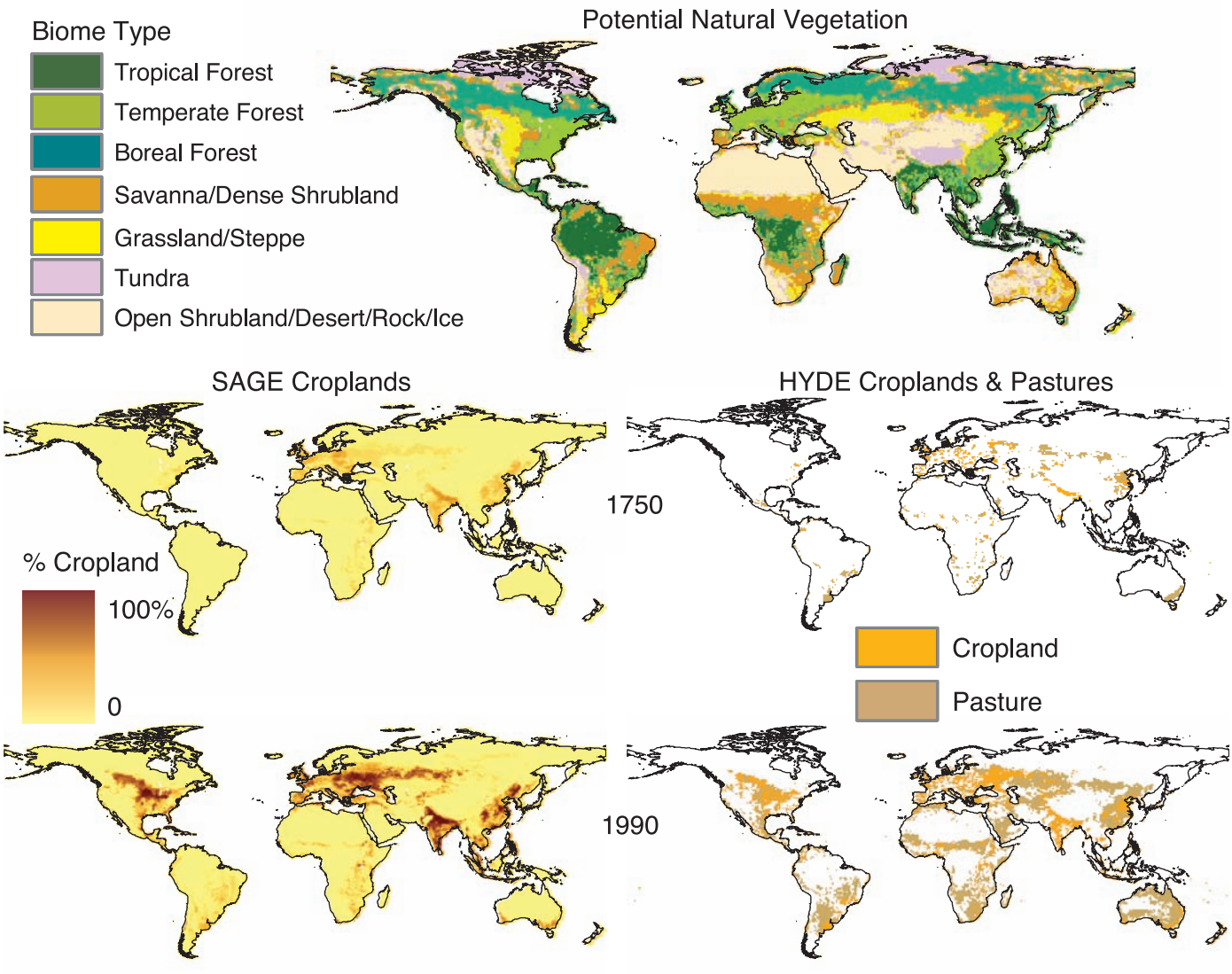


Figure 2.15. *Anthropogenic modifications of land cover up to 1990. Top panel: Reconstructions of potential natural vegetation (Haxeltine and Prentice, 1996). Lower panels: reconstructions of croplands and pasture for 1750 and 1990. Bottom left: fractional cover of croplands from Centre for Sustainability and the Global Environment (SAGE; Ramankutty and Foley, 1999) at 0.5° resolution. Bottom right: reconstructions from the HistorY Database of the Environment (HYDE; Klein Goldewijk, 2001), with one land cover classification per 0.5° grid box.*

2.5.2 Changes in Land Cover Since 1750

In 1750, 7.9 to 9.2 million km^2 (6 to 7% of the global land surface) were under cultivation or pasture (Figure 2.15), mainly in Europe, the Indo-Gangetic Plain and China (Ramankutty and Foley, 1999; Klein Goldewijk, 2001). Over the next hundred years, croplands and pasture expanded and intensified in these areas, and new agricultural areas emerged in North America. The period 1850 to 1950 saw a more rapid rate of increase in cropland and pasture areas. In the last 50 years, several regions of the world have seen cropland areas stabilise, and even decrease. In the USA, as cultivation shifted from the east to the Midwest, croplands were abandoned along the eastern seaboard around the turn of the century and the eastern forests have regenerated over the last century. Similarly, cropland areas have decreased in China and Europe. Overall, global cropland and pasture expansion was slower after 1950 than before. However, deforestation is occurring more rapidly in the tropics. Latin America, Africa and South and Southeast Asia experienced slow cropland expansion until the 20th century, but have had exponential increases in the last 50 years. By 1990, croplands and pasture covered 45.7 to 51.3 million km^2 (35% to 39% of global land), and forest cover had decreased by roughly 11 million km^2 (Ramankutty and Foley, 1999; Klein Goldewijk, 2001; Table 2.8).

Overall, until the mid-20th century most deforestation occurred in the temperate regions (Figure 2.15). In more recent decades, however, land abandonment in Western Europe and North America has been leading to reforestation while deforestation is now progressing rapidly in the tropics. In the 1990s compared to the 1980s, net removal of tropical forest cover had slowed in the Americas but increased in Africa and Asia.

2.5.3 Radiative Forcing by Anthropogenic Surface Albedo Change: Land Use

Since the TAR, a number of estimates of the RF from land use changes over the industrial era have been made (Table 2.8). Unlike the main TAR estimate, most of the more recent studies are 'pure' RF calculations with the only change being land cover; feedbacks such as changes in snow cover are excluded. Brovkin et al. (2006) estimated the global mean RF relative to 1700 to be –0.15 W m^{-2}, considering only cropland changes (Ramankutty and Foley, 1999) and not pastures. Hansen et al. (2005) also considered only cropland changes (Ramankutty and Foley, 1999) and simulated the RF relative to 1750 to be –0.15 W m^{-2}. Using historical reconstructions of both croplands (Ramankutty and Foley, 1999) and pasturelands (Klein Goldewijk, 2001), Betts et al. (2007) simulated an RF of –0.18 W m^{-2} since 1750. This study also estimated the RF relative to PNV to be –0.24 W m^{-2}. Other studies since the TAR have also estimated the RF at the present day relative to PNV (Table 2.8). Govindasamy et al. (2001a) estimated this RF as –0.08 W m^{-2}. Myhre et al. (2005a) used land cover and albedo data from MODIS (Friedl et al., 2002; Schaaf et al., 2002) and estimated this RF as –0.09 W m^{-2}. The results of Betts et al. (2007) and Brovkin et al. (2006) suggest that the RF relative to 1750 is approximately 75% of that relative to PNV. Therefore, by employing this factor published RFs relative to PNV can be used to estimate the RF relative to 1750 (Table 2.8).

In all the published studies, the RF showed a very high degree of spatial variability, with some areas showing no RF in 1990 relative to 1750 while values more negative than –5 W m^{-2} were typically found in the major agricultural areas of North America and Eurasia. The local RF depends on local albedo changes, which depend on the nature of the PNV replaced by agriculture (see top panel of Figure 2.15). In historical simulations, the spatial patterns of RF relative to the PNV remain generally similar over time, with the regional RFs in 1750 intensifying and expanding in the area covered. The major new areas of land cover change since 1750 are North America and central and eastern Russia.

Changes in the underlying surface albedo could affect the RF due to aerosols if such changes took place in the same regions. Similarly, surface albedo RF may depend on aerosol concentrations. Estimates of the temporal evolution of aerosol RF and surface albedo RF may need to consider changes in each other (Betts et al., 2007).

2.5.3.1 Uncertainties

Uncertainties in estimates of RF due to anthropogenic surface albedo change arise from several factors.

2.5.3.1.1 Uncertainties in the mapping and characterisation of present-day vegetation

The RF estimates reported in the TAR used atlas-based data sets for present-day vegetation (Matthews, 1983; Wilson and Henderson-Sellers, 1985). More recent data sets of land cover have been obtained from satellite remote sensing. Data from the AVHRR in 1992 to 1993 were used to generate two global land cover data sets at 1 km resolution using different methodologies (Hansen and Reed, 2000; Loveland et al., 2000) The International Geosphere-Biosphere Programme Data and Information System (IGBP-DIS) data set is used as the basis for global cropland maps (Ramankutty and Foley, 1999) and historical reconstructions of croplands, pasture and other vegetation types (Ramankutty and Foley, 1999; Klein Goldewijk, 2001) (Table 2.8). The MODIS (Friedl et al., 2002) and Global Land Cover 2000 (Bartholome and Belward, 2005) provide other products. The two interpretations of the AVHRR data agree on the classification of vegetation as either tall (forest and woody savannah) or short (all other land cover) over 84% of the land surface (Hansen and Reed, 2000). However, some of the key disagreements are in regions subject to anthropogenic land cover change so may be important for the estimation of anthropogenic RF. Using the Hadley Centre Atmospheric Model (HadAM3) GCM, Betts et al. (2007) found that the estimate of RF relative to PNV varied from –0.2 W m^{-2} with the Wilson and Henderson-Sellers (1985) atlas-based land use data set to –0.24 W m^{-2} with a version of the Wilson and Henderson-

Table 2.8. *Estimates of forest area, contribution to CO_2 increase from anthropogenic land cover change, and RF due to the land use change-induced CO_2 increase and surface albedo change, relative to pre-industrial vegetation and PNV. The CO_2 RFs are for 2000 relative to 1850, calculated from the land use change contribution to the total increase in CO_2 from 1850 to 2000 simulated with both land use and fossil fuel emissions by the carbon cycle models. Carbon emissions from land cover change for the 1980s and 1990s are discussed in Section 7.3 and Table 7.2.*

Main Source of Land Cover Data	Forest Area PNV 10^6 km^2	Forest Area circa 1700 10^6 km^2	Forest Area circa 1990 10^6 km^2	Contribution to CO_2 Increase 1850–2000[a] (ppm)	CO_2 RF (W m^{-2})	Albedo RF vs. PNV (W m^{-2})	Albedo RF vs. 1750 (W m^{-2})
Ramankutty and Foley (1999)	55.27	52.77[b]	43.97[c]	16[d]	0.27	–0.24[e] –0.29 to +0.02[f] –0.2[g]	–0.18[e] –0.22 to +0.02[h] –0.14[g,i] –0.15 to –0.28[i,j] –0.15[k] –0.075 to –0.325[i,l]
Klein Goldewijk (2001)	58.6	54.4	41.5	12[d]	0.20	–0.66 to +0.1[f]	–0.50 to +0.08[h] –0.275[i,l]
Houghton (1983[m], 2003)		62.15	50.53[n]	35[d] 26[o]	0.57 0.44		
MODIS (Schaaf et al., 2002)						–0.09[p]	–0.07[h]
Wilson and Henderson-Sellers (1985)						–0.2[q] –0.29[f]	–0.15[h] –0.22[h]
SARB[r]						–0.11 to –0.55[f]	–0.08 to –0.41[h]
Matthews (1983)						–0.12[f] –0.4[s] –0.08[t]	–0.09[h] –0.3[h] –0.06[h]

Notes:

[a] The available literature simulates CO_2 rises with and without land use relative to 1850.

[b] 1750 forest area reported as 51.85 x 10^6 km^2.

[c] 1992 forest area.

[d] Land use contribution CO_2 rise from Brovkin et al. (2004).

[e] Albedo RF from Betts et al. (2007). Land cover data combined from Ramankutty and Foley (1999), Klein Goldelwijk (2001) and Wilson and Henderson-Sellers (1985).

[f] Albedo RF from Myhre and Myhre (2003). Range of estimate for each land cover data set arises from use of different albedo values.

[g] Albedo RF from model of Goosse et al. (2005) in Brovkin et al. (2006).

[h] RF relative to 1750 estimated here as 0.75 of RF relative to PNV following Betts et al. (2007) and Brovkin et al. (2006).

[i] Estimate relative to 1700.

[j] Albedo RF from Matthews et al. (2003).

[k] Albedo RF from Hansen et al. (2005).

[l] Albedo RF from Matthews et al. (2004).

[m] Forest areas aggregated by Richards (1990).

[n] 1980 forest area.

[o] Land use contribution to CO_2 rise from Matthews et al. (2004). Estimate only available relative to 1850 not 1750.

[p] Albedo RF from Myhre et al. (2005a).

[q] Albedo RF from Betts (2001).

[r] Surface and Atmosphere Radiation Budget; http://www-surf.larc.nasa.gov/surf/.

[s] Albedo RF from Hansen et al. (1997).

[t] Albedo RF from Govindasamy et al. (2001a).

Sellers (1985) data set adjusted to agree with the cropland data of Ramankutty and Foley (1999). Myhre and Myhre (2003) found the RF relative to PNV to vary from –0.66 W m^{-2} to 0.29 W m^{-2} according to whether the present-day land cover was from Wilson and Henderson-Sellers (1985), Ramankutty and Foley (1999) or other sources.

2.5.3.1.2 Uncertainties in the mapping and characterisation of the reference historical state

Reconstructions of historical land use states require information or assumptions regarding the nature and extent of land under human use and the nature of the PNV. Ramankutty and Foley (1999) reconstructed the fraction of land under crops at 0.5° resolution from 1700 to 1990 (Figure 2.15, Table 2.8) by combining the IGBP Global Land Cover Dataset with historical inventory data, assuming that all areas of past vegetation occur within areas of current vegetation. Klein Goldewijk (2001) reconstructed all land cover types from 1700 to 1990 (Figure 2.15, Table 2.8), combining cropland and pasture inventory data with historical population density maps and PNV. Klein Goldewijk used a Boolean approach, which meant that crops, for example, covered either 100% or 0% of a 0.5° grid box. The total global cropland of Klein Goldewijk is generally 25% less than that reconstructed by Ramankutty and Foley (1999) throughout 1700 to 1990. At local scales, the disagreement is greater due to the high spatial heterogeneity in both data sets. Large-scale PNV (Figure 2.15) is reconstructed either with models or by assuming that small-scale examples of currently undisturbed vegetation are representative of the PNV at the large scale. Matthews et al. (2004) simulated RF relative to 1700 as –0.20 W m^{-2} and –0.28 W m^{-2} with the above land use reconstructions.

2.5.3.1.3 Uncertainties in the parametrizations of the surface radiation processes

The albedo for a given land surface or vegetation type may either be prescribed or simulated on the basis of more fundamental characteristics such as vegetation leaf area. But either way, model parameters are set on the basis of observational data that may come from a number of conflicting sources. Both the AVHRR and MODIS (Schaaf et al., 2002; Gao et al., 2005) instruments have been used to quantify surface albedo for the IGBP vegetation classes in different regions and different seasons, and in some cases the albedo for a given vegetation type derived from one source can be twice that derived from the other (e.g., Strugnell et al., 2001; Myhre et al., 2005a). Myhre and Myhre (2003) examined the implications of varying the albedo of different vegetation types either together or separately, and found the RF relative to PNV to vary from –0.65 W m^{-2} to +0.47 W m^{-2}; however, the positive RFs occurred in only a few cases and resulted from large reductions in surface albedo in semi-arid regions on conversion to pasture, so were considered unrealistic by the study's authors. The single most important factor for the uncertainty in the study by Myhre and Myhre (2003) was found to be the surface albedo for cropland. In simulations where only the cropland surface albedo was varied between 0.15, 0.18 and 0.20, the resulting RFs relative to PNV were –0.06, –0.20 and –0.29 W m^{-2}, respectively. Similar results were found by Matthews et al. (2003) considering only cropland changes and not pasture; with cropland surface albedos of 0.17 and 0.20, RFs relative to 1700 were –0.15 and –0.28 W m^{-2}, respectively.

2.5.3.1.3 Uncertainties in other parts of the model

When climate models are used to estimate the RF, uncertainties in other parts of the model also affect the estimates. In particular, the simulation of snow cover affects the extent to which land cover changes affect surface albedo. Betts (2000) estimated that the systematic biases in snow cover in HadAM3 introduced errors of up to approximately 10% in the simulation of local RF due to conversion between forest and open land. Such uncertainties could be reduced by the use of an observational snow climatology in a model that just treats the radiative transfer (Myhre and Myhre, 2003). The simulation of cloud cover affects the extent to which the simulated surface albedo changes affect planetary albedo – too much cloud cover could diminish the contribution of surface albedo changes to the planetary albedo change.

On the basis of the studies assessed here, including a number of new estimates since the TAR, the assessment is that the best estimate of RF relative to 1750 due to land-use related surface albedo change should remain at –0.2 ± 0.2 W m^{-2}. In the light of the additional modelling studies, the exclusion of feedbacks, the improved incorporation of large-scale observations and the explicit consideration of land use reconstructions for 1750, the level of scientific understanding is raised to medium-low, compared to low in the TAR (Section 2.9, Table 2.11).

2.5.4 Radiative Forcing by Anthropogenic Surface Albedo Change: Black Carbon in Snow and Ice

The presence of soot particles in snow could cause a decrease in the albedo of snow and affect snowmelt. Initial estimates by Hansen et al. (2000) suggested that BC could thereby exert a positive RF of +0.2 W m^{-2}. This estimate was refined by Hansen and Nazarenko (2004), who used measured BC concentrations within snow and ice at a wide range of geographic locations to deduce the perturbation to the surface and planetary albedo, deriving an RF of +0.15 W m^{-2}. The uncertainty in this estimate is substantial due to uncertainties in whether BC and snow particles are internally or externally mixed, in BC and snow particle shapes and sizes, in voids within BC particles, and in the BC imaginary refractive index. Jacobson (2004) developed a global model that allows the BC aerosol to enter snow via precipitation and dry deposition, thereby modifying the snow albedo and emissivity. They found modelled concentrations of BC within snow that were in reasonable agreement with those from many observations. The model study found that BC on snow and sea ice caused a decrease in the surface albedo of 0.4% globally and 1% in the NH, although RFs were not reported. Hansen et al. (2005) allowed the albedo change to be

proportional to local BC deposition according to Koch (2001) and presented a further revised estimate of 0.08 W m^{-2}. They also suggested that this RF mechanism produces a greater temperature response by a factor of 1.7 than an equivalent CO_2 RF, that is, the 'efficacy' may be higher for this RF mechanism (see Section 2.8.5.7). This report adopts a best estimate for the BC on snow RF of +0.10 ± 0.10 W m^{-2}, with a low level of scientific understanding (Section 2.9, Table 2.11).

2.5.5 Other Effects of Anthropogenic Changes in Land Cover

Anthropogenic land use and land cover change can also modify climate through other mechanisms, some directly perturbing the Earth radiation budget and some perturbing other processes. Impacts of land cover change on emissions of CO_2, CH_4, biomass burning aerosols and dust aerosols are discussed in Sections 2.3 and 2.4. Land cover change itself can also modify the surface energy and moisture budgets through changes in evaporation and the fluxes of latent and sensible heat, directly affecting precipitation and atmospheric circulation as well as temperature. Model results suggest that the combined effects of past tropical deforestation may have exerted regional warmings of approximately 0.2°C relative to PNV, and may have perturbed the global atmospheric circulation affecting regional climates remote from the land cover change (Chase et al., 2000; Zhao et al., 2001; Pielke et al., 2002; Chapters 7, 9 and 11).

Since the dominant aspect of land cover change since 1750 has been deforestation in temperate regions, the overall effect of anthropogenic land cover change on global temperature will depend largely on the relative importance of increased surface albedo in winter and spring (exerting a cooling) and reduced evaporation in summer and in the tropics (exerting a warming) (Bounoua et al., 2002). Estimates of global temperature responses from past deforestation vary from 0.01°C (Zhao et al., 2001) to –0.25°C (Govindasamy et al., 2001a; Brovkin et al., 2006). If cooling by increased surface albedo dominates, then the historical effect of land cover change may still be adequately represented by RF. With tropical deforestation becoming more significant in recent decades, warming due to reduced evaporation may become more significant globally than increased surface albedo. Radiative forcing would then be less useful as a metric of climate change induced by land cover change recently and in the future.

2.5.6 Tropospheric Water Vapour from Anthropogenic Sources

Anthropogenic use of water is less than 1% of natural sources of water vapour and about 70% of the use of water for human activity is from irrigation (Döll, 2002). Several regional studies have indicated an impact of irrigation on temperature, humidity and precipitation (Barnston and Schickedanz, 1984; Lohar and Pal, 1995; de Ridder and Gallée, 1998; Moore and Rojstaczer, 2001; Zhang et al., 2002). Boucher et al. (2004) used a GCM to show that irrigation has a global impact on temperature and humidity. Over Asia where most of the irrigation takes place, the simulations showed a change in the water vapour content in the lower troposphere of up to 1%, resulting in an RF of +0.03 W m^{-2}. However, the effect of irrigation on surface temperature was dominated by evaporative cooling rather than by the excess greenhouse effect and thus a decrease in surface temperature was found. Irrigation affects the temperature, humidity, clouds and precipitation as well as the natural evaporation through changes in the surface temperature, raising questions about the strict use of RF in this case. Uncertainties in the water vapour flow to the atmosphere from irrigation are significant and Gordon et al. (2005) gave a substantially higher estimate compared to that of Boucher et al. (2004). Most of this uncertainty is likely to be linked to differences between the total withdrawal for irrigation and the amount actually used (Boucher et al., 2004). Furthermore, Gordon et al. (2005) also estimated a reduced water vapour flow to the atmosphere from deforestation, most importantly in tropical areas. This reduced water vapour flow is a factor of three larger than the water vapour increase due to irrigation in Boucher et al. (2004), but so far there are no estimates of the effect of this on the water vapour content of the atmosphere and its RF. Water vapour changes from deforestation will, like irrigation, affect the surface evaporation and temperature and the water cycle in the atmosphere. Radiative forcing from anthropogenic sources of tropospheric water vapour is not evaluated here, since these sources affect surface temperature more significantly through these non-radiative processes, and a strict use of the RF is problematic. The emission of water vapour from fossil fuel combustion is significantly lower than the emission from changes in land use (Boucher et al., 2004).

2.5.7 Anthropogenic Heat Release

Urban heat islands result partly from the physical properties of the urban landscape and partly from the release of heat into the environment by the use of energy for human activities such as heating buildings and powering appliances and vehicles ('human energy production'). The global total heat flux from this is estimated as 0.03 W m^{-2} (Nakicenovic, 1998). If this energy release were concentrated in cities, which are estimated to cover 0.046% of the Earth's surface (Loveland et al., 2000) the mean local heat flux in a city would be 65 W m^{-2}. Daytime values in central Tokyo typically exceed 400 W m^{-2} with a maximum of 1,590 W m^{-2} in winter (Ichinose et al., 1999). Although human energy production is a small influence at the global scale, it may be very important for climate changes in cities (Betts and Best, 2004; Crutzen, 2004).

2.5.8 Effects of Carbon Dioxide Changes on Climate via Plant Physiology: 'Physiological Forcing'

As well as exerting an RF on the climate system, increasing concentrations of atmospheric CO_2 can perturb the climate system through direct effects on plant physiology. Plant stomatal apertures open less under higher CO_2 concentrations (Field et

al., 1995), which directly reduces the flux of moisture from the surface to the atmosphere through transpiration (Sellers et al., 1996). A decrease in moisture flux modifies the surface energy balance, increasing the ratio of sensible heat flux to latent heat flux and therefore warming the air near the surface (Sellers et al., 1996; Betts et al., 1997; Cox et al., 1999). Betts et al. (2004) proposed the term 'physiological forcing' for this mechanism. Although no studies have yet explicitly quantified the present-day temperature response to physiological forcing, the presence of this forcing has been detected in global hydrological budgets (Gedney et al., 2006; Section 9.5). This process can be considered a non-initial radiative effect, as distinct from a feedback, since the mechanism involves a direct response to increasing atmospheric CO_2 and not a response to climate change. It is not possible to quantify this with RF. Reduced global transpiration would also be expected to reduce atmospheric water vapour causing a negative forcing, but no estimates of this have been made.

Increased CO_2 concentrations can also 'fertilize' plants by stimulating photosynthesis, which models suggest has contributed to increased vegetation cover and leaf area over the 20th century (Cramer et al., 2001). Increases in the Normalized Difference Vegetation Index, a remote sensing product indicative of leaf area, biomass and potential photosynthesis, have been observed (Zhou et al., 2001), although other causes including climate change itself are also likely to have contributed. Increased vegetation cover and leaf area would decrease surface albedo, which would act to oppose the increase in albedo due to deforestation. The RF due to this process has not been evaluated and there is a very low scientific understanding of these effects.

2.6 Contrails and Aircraft-Induced Cloudiness

2.6.1 Introduction

The IPCC separately evaluated the RF from subsonic and supersonic aircraft operations in the Special Report on Aviation and the Global Atmosphere (IPCC, 1999), hereinafter designated as IPCC-1999. Like many other sectors, subsonic aircraft operations around the globe contribute directly and indirectly to the RF of climate change. This section only assesses the aspects that are unique to the aviation sector, namely the formation of persistent condensation trails (contrails), their impact on cirrus cloudiness, and the effects of aviation aerosols. Persistent contrail formation and induced cloudiness are indirect effects from aircraft operations because they depend on variable humidity and temperature conditions along aircraft flight tracks. Thus, future changes in atmospheric humidity and temperature distributions in the upper troposphere will have consequences for aviation-induced cloudiness. Also noted here is the potential role of aviation aerosols in altering the properties of clouds that form later in air containing aircraft emissions.

2.6.2 Radiative Forcing Estimates for Persistent Line-Shaped Contrails

Aircraft produce persistent contrails in the upper troposphere in ice-supersaturated air masses (IPCC, 1999). Contrails are thin cirrus clouds, which reflect solar radiation and trap outgoing longwave radiation. The latter effect is expected to dominate for thin cirrus (Hartmann et al., 1992; Meerkötter et al., 1999), thereby resulting in a net positive RF value for contrails. Persistent contrail cover has been calculated globally from meteorological data (e.g., Sausen et al., 1998) or by using a modified cirrus cloud parametrization in a GCM (Ponater et al., 2002). Contrail cover calculations are uncertain because the extent of supersaturated regions in the atmosphere is poorly known. The associated contrail RF follows from determining an optical depth for the computed contrail cover. The global RF values for contrail and induced cloudiness are assumed to vary linearly with distances flown by the global fleet if flight ambient conditions remain unchanged. The current best estimate for the RF of persistent linear contrails for aircraft operations in 2000 is +0.010 W m^{-2} (Table 2.9; Sausen et al., 2005). The value is based on independent estimates derived from Myhre and Stordal (2001b) and Marquart et al. (2003) that were updated for increased aircraft traffic in Sausen et al. (2005) to give RF estimates of +0.015 W m^{-2} and +0.006 W m^{-2}, respectively. The uncertainty range is conservatively estimated to be a factor of three. The +0.010 W m^{-2} value is also considered to be the best estimate for 2005 because of the slow overall growth in aviation fuel use in the 2000 to 2005 period. The decrease in the best estimate from the TAR by a factor of two results from reassessments of persistent contrail cover and lower optical depth estimates (Marquart and Mayer, 2002; Meyer et al., 2002; Ponater et al., 2002; Marquart et al., 2003). The new estimates

Table 2.9. *Radiative forcing terms for contrail and cirrus effects caused by global subsonic aircraft operations.*

	Radiative forcing (W m^{-2})[a]		
	1992 IPCC[b]	2000 IPCC[c]	2000[d]
CO_2[d]	0.018	0.025	0.025
Persistent linear contrails	0.020	0.034	0.010 (0.006 to 0.015)
Aviation-induced cloudiness without persistent contrails	0 to 0.040	n.a.	
Aviation-induced cloudiness with persistent contrails			0.030 (0.010 to 0.080)

Notes:

[a] Values for contrails are best estimates. Values in parentheses give the uncertainty range.

[b] Values from IPCC-1999 (IPCC, 1999).

[c] Values interpolated from 1992 and 2015 estimates in IPCC-1999 (Sausen et al., 2005).

[d] Sausen et al. (2005). Values are considered valid (within 10%) for 2005 because of slow growth in aviation fuel use between 2000 and 2005.

include diurnal changes in the solar RF, which decreases the net RF for a given contrail cover by about 20% (Myhre and Stordal, 2001b). The level of scientific understanding of contrail RF is considered low, since important uncertainties remain in the determination of global values (Section 2.9, Table 2.11). For example, unexplained regional differences are found in contrail optical depths between Europe and the USA that have not been fully accounted for in model calculations (Meyer et al., 2002; Ponater et al., 2002; Palikonda et al., 2005).

2.6.3 Radiative Forcing Estimates for Aviation-Induced Cloudiness

Individual persistent contrails are routinely observed to shear and spread, covering large additional areas with cirrus cloud (Minnis et al., 1998). Aviation aerosol could also lead to changes in cirrus cloud (see Section 2.6.4). Aviation-induced cloudiness (AIC) is defined to be the sum of all changes in cloudiness associated with aviation operations. Thus, an AIC estimate includes persistent contrail cover. Because spreading contrails lose their characteristic linear shape, a component of AIC is indistinguishable from background cirrus. This basic ambiguity, which prevented the formulation of a best estimate of AIC amounts and the associated RF in IPCC-1999, still exists for this assessment. Estimates of the ratio of induced cloudiness cover to that of persistent linear contrails range from 1.8 to 10 (Minnis et al., 2004; Mannstein and Schumann, 2005[10]), indicating the uncertainty in estimating AIC amounts. Initial attempts to quantify AIC used trend differences in cirrus cloudiness between regions of high and low aviation fuel consumption (Boucher, 1999). Since IPCC-1999, two studies have also found significant positive trends in cirrus cloudiness in some regions of high air traffic and found lower to negative trends outside air traffic regions (Zerefos et al., 2003; Stordal et al., 2005). Using the International Satellite Cloud Climatology Project (ISCCP) database, these studies derived cirrus cover trends for Europe of 1 to 2% per decade over the last one to two decades. A study with the Television Infrared Observation Satellite (TIROS) Operational Vertical Sounder (TOVS) provides further support for these trends (Stubenrauch and Schumann, 2005). However, cirrus trends that occurred due to natural variability, climate change or other anthropogenic effects could not be accounted for in these studies. Cirrus trends over the USA (but not over Europe) were found to be consistent with changes in contrail cover and frequency (Minnis et al., 2004). Thus, significant uncertainty remains in attributing observed cirrus trends to aviation.

Regional cirrus trends were used as a basis to compute a global mean RF value for AIC in 2000 of +0.030 W m^{-2} with a range of +0.01 to +0.08 W m^{-2} (Stordal et al., 2005). This value is not considered a best estimate because of the uncertainty in the optical properties of AIC and in the assumptions used to derive AIC cover. However, this value is in good agreement with the upper limit estimate for AIC RF in 1992 of +0.026 W m^{-2} derived from surface and satellite cloudiness observations (Minnis et al., 2004). A value of +0.03 W m^{-2} is close to the upper-limit estimate of +0.04 W m^{-2} derived for non-contrail cloudiness in IPCC-1999. Without an AIC best estimate, the best estimate of the total RF value for aviation-induced cloudiness (Section 2.9.2, Table 2.12 and Figure 2.20) includes only that due to persistent linear contrails. Radiative forcing estimates for AIC made using cirrus trend data necessarily cannot distinguish between the components of aviation cloudiness, namely persistent linear contrails, spreading contrails and other aviation aerosol effects. Some aviation effects might be more appropriately considered feedback processes rather than an RF (see Sections 2.2 and 2.4.5). However, the low understanding of the processes involved and the lack of quantitative approaches preclude reliably making the forcing/feedback distinction for all aviation effects in this assessment.

Two issues related to the climate response of aviation cloudiness are worth noting here. First, Minnis et al. (2004, 2005) used their RF estimate for total AIC over the USA in an empirical model, and concluded that the surface temperature response for the period 1973 to 1994 could be as large as the observed surface warming over the USA (around 0.3°C per decade). In response to the Minnis et al. conclusion, contrail RF was examined in two global climate modelling studies (Hansen et al., 2005; Ponater et al., 2005). Both studies concluded that the surface temperature response calculated by Minnis et al. (2004) is too large by one to two orders of magnitude. For the Minnis et al. result to be correct, the climate efficacy or climate sensitivity of contrail RF would need to be much greater than that of other larger RF terms, (e.g., CO_2). Instead, contrail RF is found to have a smaller efficacy than an equivalent CO_2 RF (Hansen et al., 2005; Ponater et al., 2005) (see Section 2.8.5.7), which is consistent with the general ineffectiveness of high clouds in influencing diurnal surface temperatures (Hansen et al., 1995, 2005). Several substantive explanations for the incorrectness of the enhanced response found in the Minnis et al. study have been presented (Hansen et al., 2005; Ponater et al., 2005; Shine, 2005).

The second issue is that the absence of AIC has been proposed as the cause of the increased diurnal temperature range (DTR) found in surface observations made during the short period when all USA air traffic was grounded starting on 11 September 2001 (Travis et al., 2002, 2004). The Travis et al. studies show that during this period: (i) DTR was enhanced across the conterminous USA, with increases in the maximum temperatures that were not matched by increases of similar magnitude in the minimum temperatures, and (ii) the largest DTR changes corresponded to regions with the greatest contrail cover. The Travis et al. conclusions are weak because they are based on a correlation rather than a quantitative model and rely (necessarily) on very limited data (Schumann, 2005). Unusually clear weather across the USA during the shutdown period also has been proposed to account for the observed DTR changes (Kalkstein and Balling, 2004). Thus, more evidence and a

[10] A corrigendum to this paper has been submitted for publication by these authors but has not been assessed here.

quantitative physical model are needed before the validity of the proposed relationship between regional contrail cover and DTR can be considered further.

2.6.4 Aviation Aerosols

Global aviation operations emit aerosols and aerosol precursors into the upper troposphere and lower stratosphere (IPCC, 1999; Hendricks et al., 2004). As a result, aerosol number and/or mass are enhanced above background values in these regions. Aviation-induced cloudiness includes the possible influence of aviation aerosol on cirrus cloudiness amounts. The most important aerosols are those composed of sulphate and BC (soot). Sulphate aerosols arise from the emissions of fuel sulphur and BC aerosol results from incomplete combustion of aviation fuel. Aviation operations cause enhancements of sulphate and BC in the background atmosphere (IPCC, 1999; Hendricks et al., 2004). An important concern is that aviation aerosol can act as nuclei in ice cloud formation, thereby altering the microphysical properties of clouds (Jensen and Toon, 1997; Kärcher, 1999; Lohmann et al., 2004) and perhaps cloud cover. A modelling study by Hendricks et al. (2005) showed the potential for significant cirrus modifications by aviation caused by increased numbers of BC particles. The modifications would occur in flight corridors as well as in regions far away from flight corridors because of aerosol transport. In the study, aviation aerosols either increase or decrease ice nuclei in background cirrus clouds, depending on assumptions about the cloud formation process. Results from a cloud chamber experiment showed that a sulphate coating on soot particles reduced their effectiveness as ice nuclei (Möhler et al., 2005). Changes in ice nuclei number or nucleation properties of aerosols can alter the radiative properties of cirrus clouds and, hence, their radiative impact on the climate system, similar to the aerosol-cloud interactions discussed in Sections 2.4.1, 2.4.5 and 7.5. No estimates are yet available for the global or regional RF changes caused by the effect of aviation aerosol on background cloudiness, although some of the RF from AIC, determined by correlation studies (see Section 2.6.3), may be associated with these aerosol effects.

2.7 Natural Forcings

2.7.1 Solar Variability

The estimates of long-term solar irradiance changes used in the TAR (e.g., Hoyt and Schatten, 1993; Lean et al., 1995) have been revised downwards, based on new studies indicating that bright solar faculae likely contributed a smaller irradiance increase since the Maunder Minimum than was originally suggested by the range of brightness in Sun-like stars (Hall and Lockwood, 2004; M. Wang et al., 2005). However, empirical results since the TAR have strengthened the evidence for solar forcing of climate change by identifying detectable tropospheric changes associated with solar variability, including during the solar cycle (Section 9.2; van Loon and Shea, 2000; Douglass and Clader, 2002; Gleisner and Thejll, 2003; Haigh, 2003; Stott et al., 2003; White et al., 2003; Coughlin and Tung, 2004; Labitzke, 2004; Crooks and Gray, 2005). The most likely mechanism is considered to be some combination of direct forcing by changes in total solar irradiance, and indirect effects of ultraviolet (UV) radiation on the stratosphere. Least certain, and under ongoing debate as discussed in the TAR, are indirect effects induced by galactic cosmic rays (e.g., Marsh and Svensmark, 2000a,b; Kristjánsson et al., 2002; Sun and Bradley, 2002).

2.7.1.1 Direct Observations of Solar Irradiance

2.7.1.1.1 Satellite measurements of total solar irradiance

Four independent space-based instruments directly measure total solar irradiance at present, contributing to a database extant since November 1978 (Fröhlich and Lean, 2004). The Variability of Irradiance and Gravity Oscillations (VIRGO) experiment on the Solar Heliospheric Observatory (SOHO) has been operating since 1996, the ACRIM III on the Active Cavity Radiometer Irradiance Monitor Satellite (ACRIMSAT) since 1999 and the Earth Radiation Budget Satellite (ERBS) (intermittently) since 1984. Most recent are the measurements made by the Total Solar Irradiance Monitor (TIM) on the Solar Radiation and Climate Experiment (SORCE) since 2003 (Rottman, 2005).

2.7.1.1.2 Observed decadal trends and variability

Different composite records of total solar irradiance have been constructed from different combinations of the direct radiometric measurements. The Physikalisch-Meteorologisches Observatorium Davos (PMOD) composite (Fröhlich and Lean, 2004), shown in Figure 2.16, combines the observations by the ACRIM I on the Solar Maximum Mission (SMM), the Hickey-Friedan radiometer on Nimbus 7, ACRIM II on the Upper Atmosphere Research Satellite (UARS) and VIRGO on SOHO by analysing the sensitivity drifts in each radiometer prior to determining radiometric offsets. In contrast, the ACRIM composite (Willson and Mordvinov, 2003), also shown in Figure 2.16, utilises ACRIMSAT rather than VIRGO observations in recent times and cross calibrates the reported data assuming that radiometric sensitivity drifts have already been fully accounted for. A third composite, the Space Absolute Radiometric Reference (SARR) composite, uses individual absolute irradiance measurements from the shuttle to cross calibrate satellite records (Dewitte et al., 2005). The gross temporal features of the composite irradiance records are very similar, each showing day-to-week variations associated with the Sun's rotation on its axis, and decadal fluctuations arising from the 11-year solar activity cycle. But the linear slopes differ among the three different composite records, as do levels at solar activity minima (1986 and 1996). These differences are the result of different cross calibrations and drift adjustments applied to individual radiometric sensitivities when constructing the composites (Fröhlich and Lean, 2004).

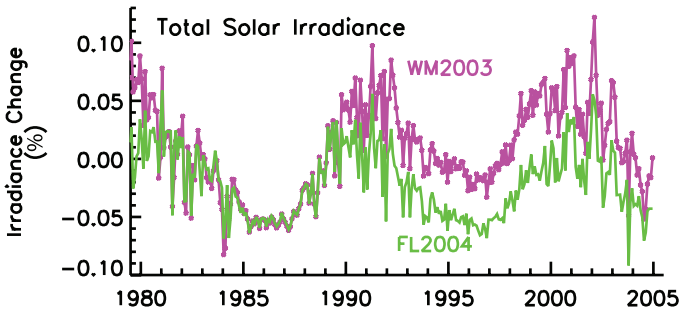


Figure 2.16. *Percentage change in monthly values of the total solar irradiance composites of Willson and Mordvinov (2003; WM2003, violet symbols and line) and Fröhlich and Lean (2004; FL2004, green solid line).*

Solar irradiance levels are comparable in the two most recent cycle minima when absolute uncertainties and sensitivity drifts in the measurements are assessed (Fröhlich and Lean, 2004 and references therein). The increase in excess of 0.04% over the 27-year period of the ACRIM irradiance composite (Willson and Mordvinov, 2003), although incompletely understood, is thought to be more of instrumental rather than solar origin (Fröhlich and Lean, 2004). The irradiance increase in the ACRIM composite is indicative of an episodic increase between 1989 and 1992 that is present in the Nimbus 7 data (Lee et al., 1995; Chapman et al., 1996). Independent, overlapping ERBS observations do not show this increase; nor do they suggest a significant secular trend (Lee et al., 1995). Such a trend is not present in the PMOD composite, in which total irradiance between successive solar minima is nearly constant, to better than 0.01% (Fröhlich and Lean, 2004). Although a long-term trend of order 0.01% is present in the SARR composite between successive solar activity minima (in 1986 and 1996), it is not statistically significant because the estimated uncertainty is ±0.026% (Dewitte et al., 2005).

Current understanding of solar activity and the known sources of irradiance variability suggests comparable irradiance levels during the past two solar minima. The primary known cause of contemporary irradiance variability is the presence on the Sun's disk of sunspots (compact, dark features where radiation is locally depleted) and faculae (extended bright features where radiation is locally enhanced). Models that combine records of the global sunspot darkening calculated directly from white light images and the magnesium (Mg) irradiance index as a proxy for the facular signal do not exhibit a significant secular trend during activity minima (Fröhlich and Lean, 2004; Preminger and Walton, 2005). Nor do the modern instrumental measurements of galactic cosmic rays, 10.7 cm flux and the *aa* geomagnetic index since the 1950s (Benestad, 2005) indicate this feature. While changes in surface emissivity by magnetic sunspot and facular regions are, from a theoretical view, the most effective in altering irradiance (Spruit, 2000), other mechanisms have also been proposed that may cause additional, possibly secular, irradiance changes. Of these, changes in solar diameter have been considered a likely candidate (e.g., Sofia and Li, 2001). But recent analysis of solar imagery, primarily from the Michelson Doppler Imager (MDI) instrument on SOHO, indicates that solar diameter changes are no more than a few kilometres per year during the solar cycle (Dziembowski et al., 2001), for which associated irradiance changes are 0.001%, two orders of magnitude less than the measured solar irradiance cycle.

2.7.1.1.3 Measurements of solar spectral irradiance

The solar UV spectrum from 120 to 400 nm continues to be monitored from space, with SORCE observations extending those made since 1991 by two instruments on the UARS (Woods et al., 1996). SORCE also monitors, for the first time from space, solar spectral irradiance in the visible and near-infrared spectrum, providing unprecedented spectral coverage that affords a detailed characterisation of solar spectral irradiance variability. Initial results (Harder et al., 2005; Lean et al., 2005) indicate that, as expected, variations occur at all wavelengths, primarily in response to changes in sunspots and faculae. Ultraviolet spectral irradiance variability in the extended database is consistent with that seen in the UARS observations since 1991, as described in the TAR.

Radiation in the visible and infrared spectrum has a notably different temporal character than the spectrum below 300 nm. Maximum energy changes occur at wavelengths from 400 to 500 nm. Fractional changes are greatest at UV wavelengths but the actual energy change is considerably smaller than in the visible spectrum. Over the time scale of the 11-year solar cycle, bolometric facular brightness exceeds sunspot blocking by about a factor of two, and there is an increase in spectral irradiance at most, if not all, wavelengths from the minimum to the maximum of the solar cycle. Estimated solar cycle changes are 0.08% in the total solar irradiance. Broken down by wavelength range these irradiance changes are 1.3% at 200 to 300 nm, 0.2% at 315 to 400 nm, 0.08% at 400 to 700 nm, 0.04% at 700 to 1,000 nm and 0.025% at 1,000 to 1,600 nm.

However, during episodes of strong solar activity, sunspot blocking can dominate facular brightening, causing decreased irradiance at most wavelengths. Spectral irradiance changes on these shorter time scales now being measured by SORCE provide tests of the wavelength-dependent sunspot and facular parametrizations in solar irradiance variability models. The modelled spectral irradiance changes are in good overall agreement with initial SORCE observations but as yet the SORCE observations are too short to provide definitive information about the amplitude of solar spectral irradiance changes during the solar cycle.

2.7.1.2 Estimating Past Solar Radiative Forcing

2.7.1.2.1 Reconstructions of past variations in solar irradiance

Long-term solar irradiance changes over the past 400 years may be less by a factor of two to four than in the reconstructions employed by the TAR for climate change simulations. Irradiance reconstructions such as those of Hoyt and Schatten (1993), Lean et al. (1995), Lean (2000), Lockwood and Stamper (1999) and Solanki and Fligge (1999), used in the TAR, assumed the

existence of a long-term variability component in addition to the known 11-year cycle, in which the 17th-century Maunder Minimum total irradiance was reduced in the range of 0.15% to 0.3% below contemporary solar minima. The temporal structure of this long-term component, typically associated with facular evolution, was assumed to track either the smoothed amplitude of the solar activity cycle or the cycle length. The motivation for adopting a long-term irradiance component was three-fold. Firstly, the range of variability in Sun-like stars (Baliunas and Jastrow, 1990), secondly, the long-term trend in geomagnetic activity, and thirdly, solar modulation of cosmogenic isotopes, all suggested that the Sun is capable of a broader range of activity than witnessed during recent solar cycles (i.e., the observational record in Figure 2.16). Various estimates of the increase in total solar irradiance from the 17th-century Maunder Minimum to the current activity minima from these irradiance reconstructions are compared with recent results in Table 2.10.

Each of the above three assumptions for the existence of a significant long-term irradiance component is now questionable. A reassessment of the stellar data was unable to recover the original bimodal separation of lower calcium (Ca) emission in non-cycling stars (assumed to be in Maunder-Minimum type states) compared with higher emission in cycling stars (Hall and Lockwood, 2004), which underpins the Lean et al. (1995) and Lean (2000) irradiance reconstructions. Rather, the current Sun is thought to have 'typical' (rather than high) activity relative to other stars. Plausible lowest brightness levels inferred from stellar observations are higher than the peak of the lower mode of the initial distribution of Baliunas and Jastrow (1990). Other studies raise the possibility of long-term instrumental drifts in historical indices of geomagnetic activity (Svalgaard et al., 2004), which would reduce somewhat the long-term trend in the Lockwood and Stamper (1999) irradiance reconstruction. Furthermore, the relationship between solar irradiance and geomagnetic and cosmogenic indices is complex, and not necessarily linear. Simulations of the transport of magnetic flux on the Sun and propagation of open flux into the heliosphere indicate that 'open' magnetic flux (which modulates geomagnetic activity and cosmogenic isotopes) can accumulate on inter-cycle time scales even when closed flux (such as in sunspots and faculae) does not (Lean et al., 2002; Y. Wang et al., 2005).

A new reconstruction of solar irradiance based on a model of solar magnetic flux variations (Y. Wang et al., 2005), which does not invoke geomagnetic, cosmogenic or stellar proxies, suggests that the amplitude of the background component is significantly less than previously assumed, specifically 0.27 times that of Lean (2000). This estimate results from simulations of the eruption, transport and accumulation of magnetic flux during the past 300 years using a flux transport model with variable meridional flow. Variations in both the total flux and in just the flux that extends into the heliosphere (the open flux) are estimated, arising from the deposition of bipolar magnetic regions (active regions) and smaller-scale bright features (ephemeral regions) on the Sun's surface in strengths and numbers proportional to the sunspot number. The open flux compares reasonably well with the cosmogenic isotopes for which variations arise, in part, from heliospheric modulation. This gives confidence that the approach is plausible. A small accumulation of total flux (and possibly ephemeral regions) produces a net increase in facular brightness, which, in combination with sunspot blocking, permits the reconstruction of total solar irradiance shown in Figure 2.17. There is a 0.04% increase from the Maunder Minimum to present-day cycle minima.

Prior to direct telescopic measurements of sunspots, which commenced around 1610, knowledge of solar activity is inferred indirectly from the ^{14}C and ^{10}Be cosmogenic isotope records in tree rings and ice cores, respectively, which exhibit solar-related cycles near 90, 200 and 2,300 years. Some studies of cosmogenic isotopes (Jirikowic and Damon, 1994) and spectral analysis of the sunspot record (Rigozo et al., 2001) suggest that solar activity during the 12th-century Medieval Solar Maximum was comparable to the present Modern Solar Maximum. Recent work attempts to account for the chain of physical processes in which solar magnetic fields modulate the heliosphere, in turn altering the penetration of the galactic cosmic rays, the flux of which produces the cosmogenic isotopes that are subsequently deposited in the terrestrial system following additional transport and chemical processes. An initial effort reported exceptionally high levels of solar activity in the past 70 years, relative to the preceding 8,000 years (Solanki et al., 2004). In contrast, when differences among isotopes records are taken into account and the ^{14}C record corrected for fossil fuel burning, current levels of solar activity are found to be historically high, but not exceptionally so (Muscheler et al., 2007).

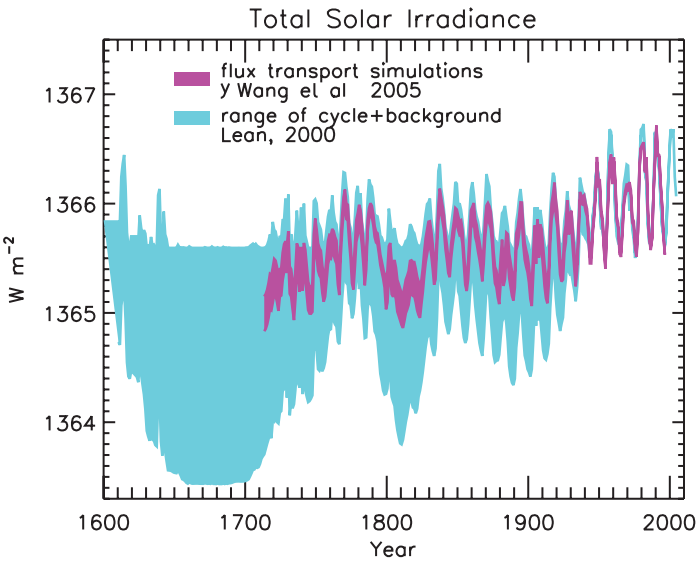


Figure 2.17. *Reconstructions of the total solar irradiance time series starting as early as 1600. The upper envelope of the shaded regions shows irradiance variations arising from the 11-year activity cycle. The lower envelope is the total irradiance reconstructed by Lean (2000), in which the long-term trend was inferred from brightness changes in Sun-like stars. In comparison, the recent reconstruction of Y. Wang et al. (2005) is based on solar considerations alone, using a flux transport model to simulate the long-term evolution of the closed flux that generates bright faculae.*

Table 2.10. *Comparison of the estimates of the increase in RF from the 17th-century Maunder Minimum (MM) to contemporary solar minima, documenting new understanding since the TAR.*

Reference	Assumptions and Technique	RF Increase from the Maunder Minimum to Contemporary Minima (W m^{-2})[a]	Comment on Current Understanding
Schatten and Orosz (1990)	Extrapolation of the 11-year irradiance cycle to the MM, using the sunspot record.	~ 0	Irradiance levels at cycle minima remain approximately constant.
Lean et al. (1992)	No spots, plage or network in Ca images assumed during MM.	0.26	Maximum irradiance increase from a non-magnetic sun, due to changes in known bright features on contemporary solar disk.
Lean et al. (1992)	No spots, plage or network and reduced basal emission in cell centres in Ca images to match reduced brightness in non-cycling stars, assumed to be MM analogues.	0.45	New assessment of stellar data (Hall and Lockwood, 2004) does not support original stellar brightness distribution, or the use of the brightness reduction in the Baliunas and Jastrow (1990) 'non-cycling' stars as MM analogues.
Hoyt and Schatten (1993)[b]	Convective restructuring implied by changes in sunspot umbra/penumbra ratios from MM to present: amplitude of increase from MM to present based on brightness of non-cycling stars, from Lean et al. (1992).	0.65	As above
Lean et al. (1995)	Reduced brightness of non-cycling stars, relative to those with active cycles, assumed typical of MM.	0.45	As above
Solanki and Fligge (1999)[b]	Combinations of above.	0.68	As above
Lean (2000)	Reduced brightness of non-cycling stars (revised solar-stellar calibration) assumed typical of MM.	0.38	As above
Foster (2004) Model	Non-magnetic sun estimates by removing bright features from MDI images assumed for MM.	0.28	Similar approach to removal of spots, plage and network by Lean et al. (1992).
Y. Wang et al. (2005)[b]	Flux transport simulations of total magnetic flux evolution from MM to present.	0.1	Solar model suggests that modest accumulation of magnetic flux from one solar cycle to the next produces a modest increase in irradiance levels at solar cycle minima.
Dziembowski et al. (2001)	Helioseismic observations of solar interior oscillations suggest that the historical Sun could not have been any dimmer than current activity minima.	~ 0	

Notes:

[a] The RF is the irradiance change divided by 4 (geometry) and multiplied by 0.7 (albedo). The solar activity cycle, which was negligible during the Maunder Minimum and is of order 1 W m^{-2} (minimum to maximum) during recent cycles, is superimposed on the irradiance changes at cycle minima. When smoothed over 20 years, this cycle increases the net RF in the table by an additional 0.09 W m^{-2}.

[b] These reconstructions extend only to 1713, the end of the Maunder Minimum.

2.7.1.2.2 Implications for solar radiative forcing

In terms of plausible physical understanding, the most likely secular increase in total irradiance from the Maunder Minimum to current cycle minima is 0.04% (an irradiance increase of roughly 0.5 W m^{-2} in 1,365 W m^{-2}), corresponding to an RF[11] of +0.1 W m^{-2}. The larger RF estimates in Table 2.10, in the range of +0.38 to +0.68 W m^{-2}, correspond to assumed changes in solar irradiance at cycle minima derived from brightness fluctuations in Sun-like stars that are no longer valid. Since the 11-year cycle amplitude has increased from the Maunder Minimum to the present, the total irradiance increase to the present-day cycle mean is 0.08%. From 1750 to the present there was a net 0.05% increase in total solar irradiance, according to the 11-year smoothed total solar irradiance time series of Y. Wang et al. (2005), shown in Figure 2.17. This corresponds to an RF of +0.12 W m^{-2}, which is more than a factor of two less than the solar RF estimate in the TAR, also from 1750 to the present. Using the Lean (2000) reconstruction (the lower envelope in Figure 2.17) as an upper limit, there is a 0.12% irradiance increase since 1750, for which the RF is +0.3 W m^{-2}. The lower limit of the irradiance increase from 1750 to the present is 0.026% due to the increase in the 11-year cycle only. The corresponding lower limit of the RF is +0.06 W m^{-2}. As with solar cycle changes, long-term irradiance variations are expected to have significant spectral dependence. For example, the Y. Wang et al. (2005) flux transport estimates imply decreases during the Maunder Minimum relative to contemporary activity cycle minima of 0.43% at 200 to 300 nm, 0.1% at 315 to 400 nm, 0.05% at 400 to 700 nm, 0.03% at 700 to 1,000 nm and 0.02% at 1,000 to 1,600 nm (Lean et al., 2005), compared with 1.4%, 0.32%, 0.17%, 0.1% and 0.06%, respectively, in the earlier model of Lean (2000).

2.7.1.3 Indirect Effects of Solar Variability

Approximately 1% of the Sun's radiant energy is in the UV portion of the spectrum at wavelengths below about 300 nm, which the Earth's atmosphere absorbs. Although of considerably smaller absolute energy than the total irradiance, solar UV radiation is fractionally more variable by at least an order of magnitude. It contributes significantly to changes in total solar irradiance (15% of the total irradiance cycle; Lean et al., 1997) and creates and modifies the ozone layer, but is not considered as a direct RF because it does not reach the troposphere. Since the TAR, new studies have confirmed and advanced the plausibility of indirect effects involving the modification of the stratosphere by solar UV irradiance variations (and possibly by solar-induced variations in the overlying mesosphere and lower thermosphere), with subsequent dynamical and radiative coupling to the troposphere (Section 9.2). Whether solar wind fluctuations (Boberg and Lundstedt, 2002) or solar-induced heliospheric modulation of galactic cosmic rays (Marsh and Svensmark, 2000b) also contribute indirect forcings remains ambiguous.

As in the troposphere, anthropogenic effects, internal cycles (e.g., the Quasi-Biennial Oscillation) and natural influences all affect the stratosphere. It is now well established from both empirical and model studies that solar cycle changes in UV radiation alter middle atmospheric ozone concentrations (Fioletov et al., 2002; Geller and Smyshlyaev, 2002; Hood, 2003), temperatures and winds (Ramaswamy et al., 2001; Labitzke et al., 2002; Haigh, 2003; Labitzke, 2004; Crooks and Gray, 2005), including the Quasi-Biennial Oscillation (McCormack, 2003; Salby and Callaghan, 2004). In their recent survey of solar influences on climate, Gray et al. (2005) noted that updated observational analyses have confirmed earlier 11-year cycle signals in zonally averaged stratospheric temperature, ozone and circulation with increased statistical confidence. There is a solar-cycle induced increase in global total ozone of 2 to 3% at solar cycle maximum, accompanied by temperature responses that increase with altitude, exceeding 1°C around 50 km. However, the amplitudes and geographical and altitudinal patterns of these variations are only approximately known, and are not linked in an easily discernible manner to the forcing. For example, solar forcing appears to induce a significant lower stratospheric response (Hood, 2003), which may have a dynamical origin caused by changes in temperature affecting planetary wave propagation, but it is not currently reproduced by models.

When solar activity is high, the more complex magnetic configuration of the heliosphere reduces the flux of galactic cosmic rays in the Earth's atmosphere. Various scenarios have been proposed whereby solar-induced galactic cosmic ray fluctuations might influence climate (as surveyed by Gray et al., 2005). Carslaw et al. (2002) suggested that since the plasma produced by cosmic ray ionization in the troposphere is part of an electric circuit that extends from the Earth's surface to the ionosphere, cosmic rays may affect thunderstorm electrification. By altering the population of CCN and hence microphysical cloud properties (droplet number and concentration), cosmic rays may also induce processes analogous to the indirect effect of tropospheric aerosols. The presence of ions, such as produced by cosmic rays, is recognised as influencing several microphysical mechanisms (Harrison and Carslaw, 2003). Aerosols may nucleate preferentially on atmospheric cluster ions. In the case of low gas-phase sulphuric acid concentrations, ion-induced nucleation may dominate over binary sulphuric acid-water nucleation. In addition, increased ion nucleation and increased scavenging rates of aerosols in turbulent regions around clouds seem likely. Because of the difficulty in tracking the influence of one particular modification brought about by

[11] To estimate RF, the change in total solar irradiance is multiplied by 0.25 to account for Earth-Sun geometry and then multiplied by 0.7 to account for the planetary albedo (e.g., Ramaswamy et al., 2001). Ideally this resulting RF should also be reduced by 15% to account for solar variations in the UV below 300 nm (see Section 2.7.1.3) and further reduced by about 4% to account for stratospheric absorption of solar radiation above 300 nm and the resulting stratospheric adjustment (Hansen et al., 1997). However, these corrections are not made to the RF estimates in this report because they: 1) represent small adjustments to the RF; 2) may in part be compensated by indirect effects of solar-ozone interaction in the stratosphere (see Section 2.7.1.3); and 3) are not routinely reported in the literature.

ions through the long chain of complex interacting processes, quantitative estimates of galactic cosmic-ray induced changes in aerosol and cloud formation have not been reached.

Many empirical associations have been reported between globally averaged low-level cloud cover and cosmic ray fluxes (e.g., Marsh and Svensmark, 2000a,b). Hypothesised to result from changing ionization of the atmosphere from solar-modulated cosmic ray fluxes, an empirical association of cloud cover variations during 1984 to 1990 and the solar cycle remains controversial because of uncertainties about the reality of the decadal signal itself, the phasing or anti-phasing with solar activity, and its separate dependence for low, middle and high clouds. In particular, the cosmic ray time series does not correspond to global total cloud cover after 1991 or to global low-level cloud cover after 1994 (Kristjánsson and Kristiansen, 2000; Sun and Bradley, 2002) without unproven de-trending (Usoskin et al., 2004). Furthermore, the correlation is significant with low-level cloud cover based only on infrared (not visible) detection. Nor do multi-decadal (1952 to 1997) time series of cloud cover from ship synoptic reports exhibit a relationship to cosmic ray flux. However, there appears to be a small but statistically significant positive correlation between cloud over the UK and galactic cosmic ray flux during 1951 to 2000 (Harrison and Stephenson, 2006). Contrarily, cloud cover anomalies from 1900 to 1987 over the USA do have a signal at 11 years that is anti-phased with the galactic cosmic ray flux (Udelhofen and Cess, 2001). Because the mechanisms are uncertain, the apparent relationship between solar variability and cloud cover has been interpreted to result not only from changing cosmic ray fluxes modulated by solar activity in the heliosphere (Usoskin et al., 2004) and solar-induced changes in ozone (Udelhofen and Cess, 2001), but also from sea surface temperatures altered directly by changing total solar irradiance (Kristjánsson et al., 2002) and by internal variability due to the El Niño-Southern Oscillation (Kernthaler et al., 1999). In reality, different direct and indirect physical processes (such as those described in Section 9.2) may operate simultaneously.

The direct RF due to increase in solar irradiance is reduced from the TAR. The best estimate is +0.12 W m^{-2} (90% confidence interval: +0.06 to +0.30 W m^{-2}). While there have been advances in the direct solar irradiance variation, there remain large uncertainties. The level of scientific understanding is elevated to low relative to TAR for solar forcing due to direct irradiance change, while declared as very low for cosmic ray influences (Section 2.9, Table 2.11).

2.7.2 Explosive Volcanic Activity

2.7.2.1 Radiative Effects of Volcanic Aerosols

Volcanic sulphate aerosols are formed as a result of oxidation of the sulphur gases emitted by explosive volcanic eruptions into the stratosphere. The process of gas-to-particle conversion has an e-folding time of roughly 35 days (Bluth et al., 1992; Read et al., 1993). The e-folding time (by mass) for sedimentation of sulphate aerosols is typically about 12 to 14 months (Lambert et al., 1993; Baran and Foot, 1994; Barnes and Hoffman, 1997; Bluth et al., 1997). Also emitted directly during an eruption are volcanic ash particulates (siliceous material). These are particles usually larger than 2 μm that sediment out of the stratosphere fairly rapidly due to gravity (within three months or so), but could also play a role in the radiative perturbations in the immediate aftermath of an eruption. Stratospheric aerosol data incorporated for climate change simulations tends to be mostly that of the sulphates (Sato et al., 1993; Stenchikov et al., 1998; Ramachandran et al., 2000; Hansen et al., 2002; Tett et al., 2002; Ammann et al., 2003). As noted in the Second Assessment Report (SAR) and the TAR, explosive volcanic events are episodic, but the stratospheric aerosols resulting from them yield substantial transitory perturbations to the radiative energy balance of the planet, with both shortwave and longwave effects sensitive to the microphysical characteristics of the aerosols (e.g., size distribution).

Long-term ground-based and balloon-borne instrumental observations have resulted in an understanding of the optical effects and microphysical evolution of volcanic aerosols (Deshler et al., 2003; Hofmann et al., 2003). Important ground-based observations of aerosol characteristics from pre-satellite era spectral extinction measurements have been analysed by Stothers (2001a,b), but they do not provide global coverage. Global observations of stratospheric aerosol over the last 25 years have been possible owing to a number of satellite platforms, for example, TOMS and TOVS have been used to estimate SO_2 loadings from volcanic eruptions (Krueger et al., 2000; Prata et al., 2003). The Stratospheric Aerosol and Gas Experiment (SAGE) and Stratospheric Aerosol Measurement (SAM) projects (e.g., McCormick, 1987) have provided vertically resolved stratospheric aerosol spectral extinction data for over 20 years, the longest such record. This data set has significant gaps in coverage at the time of the El Chichón eruption in 1982 (the second most important in the 20th century after Mt. Pinatubo in 1991) and when the aerosol cloud is dense; these gaps have been partially filled by lidar measurements and field campaigns (e.g., Antuña et al., 2003; Thomason and Peter, 2006).

Volcanic aerosols transported in the atmosphere to polar regions are preserved in the ice sheets, thus recording the history of the Earth's volcanism for thousands of years (Bigler et al., 2002; Palmer et al., 2002; Mosley-Thompson et al., 2003). However, the atmospheric loadings obtained from ice records suffer from uncertainties due to imprecise knowledge of the latitudinal distribution of the aerosols, depositional noise that can affect the signal for an individual eruption in a single ice core, and poor constraints on aerosol microphysical properties.

The best-documented explosive volcanic event to date, by way of reliable and accurate observations, is the 1991 eruption of Mt. Pinatubo. The growth and decay of aerosols resulting from this eruption have provided a basis for modelling the RF due to explosive volcanoes. There have been no explosive and climatically significant volcanic events since Mt. Pinatubo. As pointed out in Ramaswamy et al. (2001), stratospheric

aerosol concentrations are now at the lowest concentrations since the satellite era and global coverage began in about 1980. Altitude-dependent stratospheric optical observations at a few wavelengths, together with columnar optical and physical measurements, have been used to construct the time-dependent global field of stratospheric aerosol size distribution formed in the aftermath of volcanic events. The wavelength-dependent stratospheric aerosol single-scattering characteristics calculated for the solar and longwave spectrum are deployed in climate models to account for the resulting radiative (shortwave plus longwave) perturbations.

Using available satellite- and ground-based observations, Hansen et al. (2002) constructed a volcanic aerosols data set for the 1850 to 1999 period (Sato et al., 1993). This has yielded zonal mean vertically resolved aerosol optical depths for visible wavelengths and column average effective radii. Stenchikov et al. (2006) introduced a slight variation to this data set, employing UARS observations to modify the effective radii relative to Hansen et al. (2002), thus accounting for variations with altitude. Ammann et al. (2003) developed a data set of total aerosol optical depth for the period since 1890 that does not include the Krakatau eruption. The data set is based on empirical estimates of atmospheric loadings, which are then globally distributed using a simplified parametrization of atmospheric transport, and employs a fixed aerosol effective radius (0.42 µm) for calculating optical properties. The above data sets have essentially provided the bases for the volcanic aerosols implemented in virtually all of the models that have performed the 20th-century climate integrations (Stenchikov et al., 2006). Relative to Sato et al. (1993), the Ammann et al. (2003) estimate yields a larger value of the optical depth, by 20 to 30% in the second part of the 20th century, and by 50% for eruptions at the end of 19th and beginning of 20th century, for example, the 1902 Santa Maria eruption (Figure 2.18).

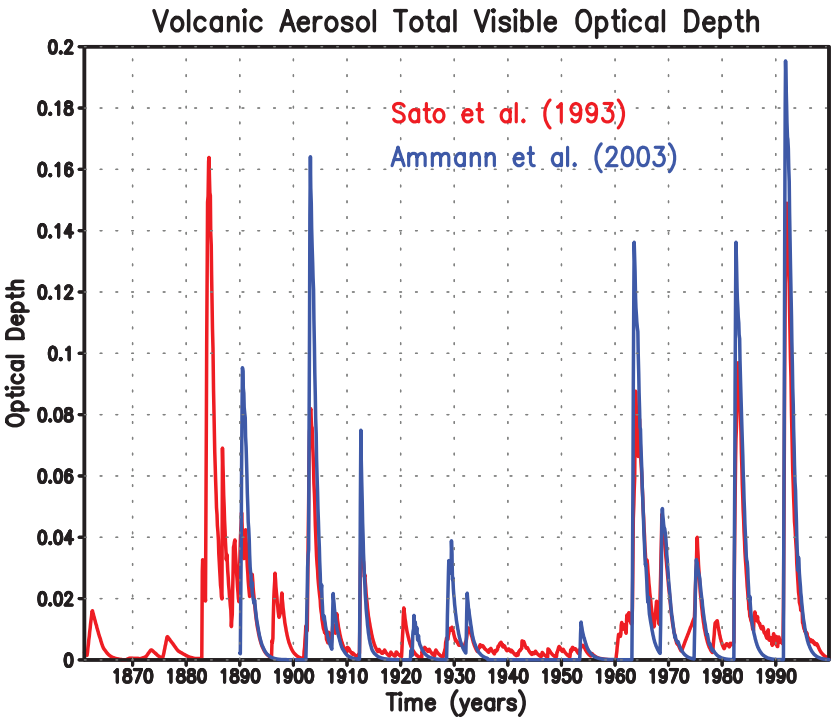


Figure 2.18. *Visible (wavelength 0.55 µm) optical depth estimates of stratospheric sulphate aerosols formed in the aftermath of explosive volcanic eruptions that occurred between 1860 and 2000. Results are shown from two different data sets that have been used in recent climate model integrations. Note that the Ammann et al. (2003) data begins in 1890.*

The global mean RF calculated using the Sato et al. (1993) data yields a peak in radiative perturbation of about –3 W m^{-2} for the strong (rated in terms of emitted SO_2) 1860 and 1991 eruptions of Krakatau and Mt. Pinatubo, respectively. The value is reduced to about –2 W m^{-2} for the relatively less intense El Chichón and Agung eruptions (Hansen et al., 2002). As expected from the arguments above, Ammann's RF is roughly 20 to 30% larger than Sato's RF.

Not all features of the aerosols are well quantified, and extending and improving the data sets remains an important area of research. This includes improved estimates of the aerosol size parameters (Bingen et al., 2004), a new approach for calculating aerosol optical characteristics using SAGE and UARS data (Bauman et al., 2003), and intercomparison of data from different satellites and combining them to fill gaps (Randall et al., 2001). While the aerosol characteristics are better constrained for the Mt. Pinatubo eruption, and to some extent for the El Chichón and Agung eruptions, the reliability degrades for aerosols from explosive volcanic events further back in time as there are few, if any, observational constraints on their optical depth and size evolution.

The radiative effects due to volcanic aerosols from major eruptions are manifest in the global mean anomaly of reflected solar radiation; this variable affords a good estimate of radiative effects that can actually be tested against observations. However, unlike RF, this variable contains effects due to feedbacks (e.g., changes in cloud distributions) so that it is actually more a signature of the climate response. In the case of the Mt. Pinatubo eruption, with a peak global visible optical depth of about 0.15, simulations yield a large negative perturbation as noted above of about –3 W m^{-2} (Ramachandran et al., 2000; Hansen et al., 2002) (see also Section 9.2). This modelled estimate of reflected solar radiation compares reasonably with ERBS observations (Minnis et al., 1993). However, the ERBS observations were for a relatively short duration, and the model-observation comparisons are likely affected by differing cloud effects in simulations and measurements. It is interesting to note (Stenchikov et al., 2006) that, in the Mt. Pinatubo case, the Goddard Institute for Space Studies (GISS) models that use the Sato et al. (1993) data yield an even greater solar reflection than the National Center for Atmospheric Research (NCAR) model that uses the larger (Ammann et al., 2003) optical depth estimate.

2.7.2.2 *Thermal, Dynamical and Chemistry Perturbations Forced by Volcanic Aerosols*

Four distinct mechanisms have been invoked with regards to the climate response to volcanic aerosol RF. First, these forcings can directly affect the Earth's radiative balance and thus alter surface temperature. Second, they introduce horizontal and vertical heating gradients; these can alter the stratospheric circulation, in turn affecting the troposphere. Third, the forcings can interact with internal climate system variability (e.g., El Niño-Southern Oscillation, North Atlantic Oscillation, Quasi-Biennial Oscillation) and dynamical noise, thereby triggering, amplifying or shifting these modes (see Section 9.2; Yang and Schlesinger, 2001; Stenchikov et al., 2004). Fourth, volcanic aerosols provide surfaces for heterogeneous chemistry affecting global stratospheric ozone distributions (Chipperfield et al., 2003) and perturbing other trace gases for a considerable period following an eruption. Each of the above mechanisms has its own spatial and temporal response pattern. In addition, the mechanisms could depend on the background state of the climate system, and thus on other forcings (e.g., due to well-mixed gases, Meehl et al., 2004), or interact with each other.

The complexity of radiative-dynamical response forced by volcanic impacts suggests that it is important to calculate aerosol radiative effects interactively within the model rather than prescribe them (Andronova et al., 1999; Broccoli et al., 2003). Despite differences in volcanic aerosol parameters employed, models computing the aerosol radiative effects interactively yield tropical and global mean lower-stratospheric warmings that are fairly consistent with each other and with observations (Ramachandran et al., 2000; Hansen et al., 2002; Yang and Schlesinger, 2002; Stenchikov et al., 2004; Ramaswamy et al., 2006b); however, there is a considerable range in the responses in the polar stratosphere and troposphere. The global mean warming of the lower stratosphere is due mainly to aerosol effects in the longwave spectrum, in contrast to the flux changes at the TOA that are essentially due to aerosol effects in the solar spectrum. The net radiative effects of volcanic aerosols on the thermal and hydrologic balance (e.g., surface temperature and moisture) have been highlighted by recent studies (Free and Angell, 2002; Jones et al., 2003; see Chapter 6; and see Chapter 9 for significance of the simulated responses and model-observation comparisons for 20th-century eruptions). A mechanism closely linked to the optical depth perturbation and ensuing warming of the tropical lower stratosphere is the potential change in the cross-tropopause water vapour flux (Joshi and Shine, 2003; see Section 2.3.7).

Anomalies in the volcanic-aerosol induced global radiative heating distribution can force significant changes in atmospheric circulation, for example, perturbing the equator-to-pole heating gradient (Stenchikov et al., 2002; Ramaswamy et al., 2006a; see Section 9.2) and forcing a positive phase of the Arctic Oscillation that in turn causes a counterintuitive boreal winter warming at middle and high latitudes over Eurasia and North America (Perlwitz and Graf, 2001; Stenchikov et al., 2002, 2004, 2006; Shindell et al., 2003b, 2004; Perlwitz and Harnik, 2003; Rind et al., 2005; Miller et al., 2006).

Stratospheric aerosols affect the chemistry and transport processes in the stratosphere, resulting in the depletion of ozone (Brasseur and Granier, 1992; Tie et al., 1994; Solomon et al., 1996; Chipperfield et al., 2003). Stenchikov et al. (2002) demonstrated a link between ozone depletion and Arctic Oscillation response; this is essentially a secondary radiative mechanism induced by volcanic aerosols through stratospheric chemistry. Stratospheric cooling in the polar region associated with a stronger polar vortex initiated by volcanic effects can increase the probability of formation of polar stratospheric clouds and therefore enhance the rate of heterogeneous chemical destruction of stratospheric ozone, especially in the NH (Tabazadeh et al., 2002). The above studies indicate effects on the stratospheric ozone layer in the wake of a volcanic eruption and under conditions of enhanced anthropogenic halogen loading. Interactive microphysics-chemistry-climate models (Rozanov et al., 2002, 2004; Shindell et al., 2003b; Timmreck et al., 2003; Dameris et al., 2005) indicate that aerosol-induced stratospheric heating affects the dispersion of the volcanic aerosol cloud, thus affecting the spatial RF. However the models' simplified treatment of aerosol microphysics introduces biases; further, they usually overestimate the mixing at the tropopause level and intensity of meridional transport in the stratosphere (Douglass et al., 2003; Schoeberl et al., 2003). For present climate studies, it is practical to utilise simpler approaches that are reliably constrained by aerosol observations.

Because of its episodic and transitory nature, it is difficult to give a best estimate for the volcanic RF, unlike the other agents. Neither a best estimate nor a level of scientific understanding was given in the TAR. For the well-documented case of the explosive 1991 Mt. Pinatubo eruption, there is a good scientific understanding. However, the limited knowledge of the RF associated with prior episodic, explosive events indicates a low level of scientific understanding (Section 2.9, Table 2.11).

2.8 Utility of Radiative Forcing

The TAR and other assessments have concluded that RF is a useful tool for estimating, to a first order, the relative global climate impacts of differing climate change mechanisms (Ramaswamy et al., 2001; Jacob et al., 2005). In particular, RF can be used to estimate the relative equilibrium globally averaged surface temperature change due to different forcing agents. However, RF is not a measure of other aspects of climate change or the role of emissions (see Sections 2.2 and 2.10). Previous GCM studies have indicated that the climate sensitivity parameter was more or less constant (varying by less than 25%) between mechanisms (Ramaswamy et al., 2001; Chipperfield et al., 2003). However, this level of agreement was found not to hold for certain mechanisms such as ozone changes at some altitudes and changes in absorbing aerosol.

Because the climate responses, and in particular the equilibrium climate sensitivities, exhibited by GCMs vary by much more than 25% (see Section 9.6), Ramaswamy et al. (2001) and Jacob et al. (2005) concluded that RF is the most simple and straightforward measure for the quantitative assessment of climate change mechanisms, especially for the LLGHGs. This section discusses the several studies since the TAR that have examined the relationship between RF and climate response. Note that this assessment is entirely based on climate model simulations.

2.8.1 Vertical Forcing Patterns and Surface Energy Balance Changes

The vertical structure of a forcing agent is important both for efficacy (see Section 2.8.5) and for other aspects of climate response, particularly for evaluating regional and vertical patterns of temperature change and also changes in the hydrological cycle. For example, for absorbing aerosol, the surface forcings are arguably a more useful measure of the climate response (particularly for the hydrological cycle) than the RF (Ramanathan et al., 2001a; Menon et al., 2002b). It should be noted that a perturbation to the surface energy budget involves sensible and latent heat fluxes besides solar and longwave irradiance; therefore, it can quantitatively be very different from the RF, which is calculated at the tropopause, and thus is not representative of the energy balance perturbation to the surface-troposphere (climate) system. While the surface forcing adds to the overall description of the total perturbation brought about by an agent, the RF and surface forcing should not be directly compared nor should the surface forcing be considered in isolation for evaluating the climate response (see, e.g., the caveats expressed in Manabe and Wetherald, 1967; Ramanathan, 1981). Therefore, surface forcings are presented as an important and useful diagnostic tool that aids understanding of the climate response (see Sections 2.9.4 and 2.9.5).

2.8.2 Spatial Patterns of Radiative Forcing

Each RF agent has a unique spatial pattern (see, e.g., Figure 6.7 in Ramaswamy et al., 2001). When combining RF agents it is not just the global mean RF that needs to be considered. For example, even with a net global mean RF of zero, significant regional RFs can be present and these can affect the global mean temperature response (see Section 2.8.5). Spatial patterns of RF also affect the pattern of climate response. However, note that, to first order, very different RF patterns can have similar patterns of surface temperature response and the location of maximum RF is rarely coincident with the location of maximum response (Boer and Yu, 2003b). Identification of different patterns of response is particularly important for attributing past climate change to particular mechanisms, and is also important for the prediction of regional patterns of future climate change. This chapter employs RF as the method for ranking the effect of a forcing agent on the equilibrium global temperature change, and only this aspect of the forcing-response relationship is discussed. However, patterns of RF are presented as a diagnostic in Section 2.9.5.

2.8.3 Alternative Methods of Calculating Radiative Forcing

RFs are increasingly being diagnosed from GCM integrations where the calculations are complex (Stuber et al., 2001b; Tett et al., 2002; Gregory et al., 2004). This chapter also discusses several mechanisms that include some response in the troposphere, such as cloud changes. These mechanisms are not initially radiative in nature, but will eventually lead to a radiative perturbation of the surface-troposphere system that could conceivably be measured at the TOA. Jacob et al. (2005) refer to these mechanisms as non-radiative forcings (see also Section 2.2). Alternatives to the standard stratospherically adjusted RF definition have been proposed that may help account for these processes. Since the TAR, several studies have employed GCMs to diagnose the zero-surface-temperature-change RF (see Figure 2.2 and Section 2.2). These studies have used a number of different methodologies. Shine et al. (2003) fixed both land and sea surface temperatures globally and calculated a radiative energy imbalance: this technique is only feasible in GCMs with relatively simple land surface parametrizations. Hansen et al. (2005) fixed sea surface temperatures and calculated an RF by adding an extra term to the radiative imbalance that took into account how much the land surface temperatures had responded. Sokolov (2006) diagnosed the zero-surface-temperature-change RF by computing surface-only and atmospheric-only components of climate feedback separately in a slab model and then modifying the stratospherically adjusted RF by the atmospheric-only feedback component. Gregory et al. (2004; see also Hansen et al., 2005; Forster and Taylor, 2006) used a regression method with a globally averaged temperature change ordinate to diagnose the zero-surface-temperature-change RF: this method had the largest uncertainties. Shine et al. (2003), Hansen et al. (2005) and Sokolov (2006) all found that that the fixed-surface-temperature RF was a better predictor of the equilibrium global mean surface temperature response than the stratospherically adjusted RF. Further, it was a particularly useful diagnostic for changes in absorbing aerosol where the stratospherically adjusted RF could fail as a predictor of the surface temperature response (see Section 2.8.5.5). Differences between the zero-surface-temperature-change RF and the stratospherically adjusted RF can be caused by semi-direct and cloud-aerosol interaction effects beyond the cloud albedo RF. For most mechanisms, aside from the case of certain aerosol changes, the difference is likely to be small (Shine et al., 2003; Hansen et al., 2005; Sokolov, 2006). These calculations also remove problems associated with defining the tropopause in the stratospherically adjusted RF definition (Shine et al., 2003; Hansen et al., 2005). However, stratospherically adjusted RF has the advantage that it does not depend on relatively uncertain components of a GCM's response, such as cloud

changes. For the LLGHGs, the stratospherically adjusted RF also has the advantage that it is readily calculated in detailed off-line radiation codes. For these reasons, the stratospherically adjusted RF is retained as the measure of comparison used in this chapter (see Section 2.2). However, to first order, all methods are comparable and all prove useful for understanding climate response.

2.8.4 Linearity of the Forcing-Response Relationship

Reporting findings from several studies, the TAR concluded that responses to individual RFs could be linearly added to gauge the global mean response, but not necessarily the regional response (Ramaswamy et al., 2001). Since then, studies with several equilibrium and/or transient integrations of several different GCMs have found no evidence of any nonlinearity for changes in greenhouse gases and sulphate aerosol (Boer and Yu, 2003b; Gillett et al., 2004; Matthews et al., 2004; Meehl et al., 2004). Two of these studies also examined realistic changes in many other forcing agents without finding evidence of a nonlinear response (Meehl et al., 2004; Matthews et al., 2004). In all four studies, even the regional changes typically added linearly. However, Meehl et al. (2004) observed that neither precipitation changes nor all regional temperature changes were linearly additive. This linear relationship also breaks down for global mean temperatures when aerosol-cloud interactions beyond the cloud albedo RF are included in GCMs (Feichter et al., 2004; see also Rotstayn and Penner, 2001; Lohmann and Feichter, 2005). Studies that include these effects modify clouds in their models, producing an additional radiative imbalance. Rotstayn and Penner (2001) found that if these aerosol-cloud effects are accounted for as additional forcing terms, the inference of linearity can be restored (see Sections 2.8.3 and 2.8.5). Studies also find nonlinearities for large negative RFs, where static stability changes in the upper troposphere affect the climate feedback (e.g., Hansen et al., 2005). For the magnitude and range of realistic RFs discussed in this chapter, and excluding cloud-aerosol interaction effects, there is high confidence in a linear relationship between global mean RF and global mean surface temperature response.

2.8.5 Efficacy and Effective Radiative Forcing

Efficacy (E) is defined as the ratio of the climate sensitivity parameter for a given forcing agent (λ_i) to the climate sensitivity parameter for CO_2 changes, that is, $E_i = \lambda_i / \lambda_{CO_2}$ (Joshi et al., 2003; Hansen and Nazarenko, 2004). Efficacy can then be used to define an effective RF ($= E_i\ RF_i$) (Joshi et al., 2003; Hansen et al., 2005). For the effective RF, the climate sensitivity parameter is independent of the mechanism, so comparing this forcing is equivalent to comparing the equilibrium global mean surface temperature change. That is, $\Delta T_s = \lambda_{CO_2} \times E_i \times RF_i$ Preliminary studies have found that efficacy values for a number of forcing agents show less model dependency than the climate sensitivity values (Joshi et al., 2003). Effective RFs have been used get one step closer to an estimator of the likely surface temperature response than can be achieved by using RF alone (Sausen and Schumann, 2000; Hansen et al., 2005; Lohmann and Feichter, 2005). Adopting the zero-surface-temperature-change RF, which has efficacies closer to unity, may be another way of achieving similar goals (see Section 2.8.3). This section assesses the efficacy associated with stratospherically adjusted RF, as this is the definition of RF adopted in this chapter (see Section 2.2). Therefore, cloud-aerosol interaction effects beyond the cloud albedo RF are included in the efficacy term. The findings presented in this section are from an assessment of all the studies referenced in the caption of Figure 2.19, which presents a synthesis of efficacy results. As space is limited not all these studies are explicitly discussed in the main text.

2.8.5.1 Generic Understanding

Since the TAR, several GCM studies have calculated efficacies and a general understanding is beginning to emerge as to how and why efficacies vary between mechanisms. The initial climate state, and the sign and magnitude of the RF have less importance but can still affect efficacy (Boer and Yu, 2003a; Joshi et al., 2003; Hansen et al., 2005). These studies have also

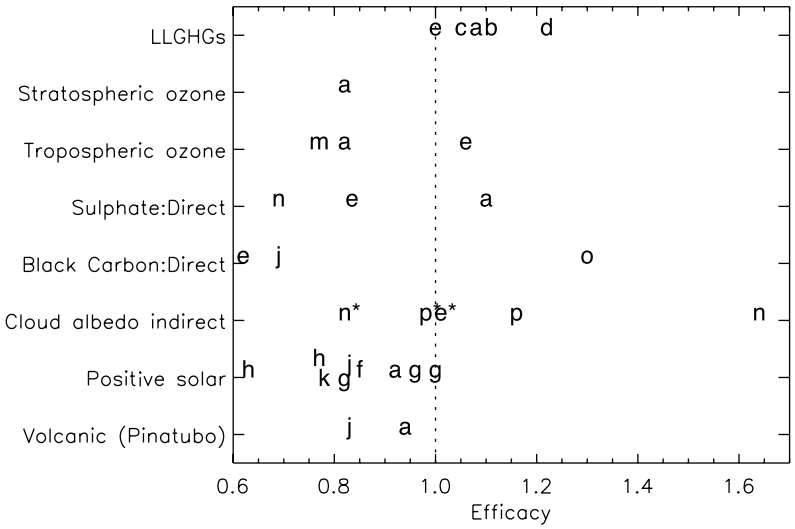


Figure 2.19. *Efficacies as calculated by several GCM models for realistic changes in RF agents. Letters are centred on efficacy value and refer to the literature study that the value is taken from (see text of Section 2.8.5 for details and further discussion). In each RF category, only one result is taken per model or model formulation. Cloud-albedo efficacies are evaluated in two ways: the standard letters include cloud lifetime effects in the efficacy term and the letters with asterisks exclude these effects. Studies assessed in the figure are: a) Hansen et al. (2005); b) Wang et al. (1991); c) Wang et al. (1992); d) Govindasamy et al. (2001b); e) Lohmann and Feichter (2005); f) Forster et al. (2000); g) Joshi et al. (2003; see also Stuber et al., 2001a); h) Gregory et al. (2004); j) Sokolov (2006); k) Cook and Highwood (2004); m) Mickley et al. (2004); n) Rotstayn and Penner (2001); o) Roberts and Jones (2004) and p) Williams et al. (2001a).*

developed useful conceptual models to help explain variations in efficacy with forcing mechanism. The efficacy primarily depends on the spatial structure of the forcings and the way they project onto the various different feedback mechanisms (Boer and Yu, 2003b). Therefore, different patterns of RF and any nonlinearities in the forcing response relationship affects the efficacy (Boer and Yu, 2003b; Joshi et al., 2003; Hansen et al., 2005; Stuber et al., 2005; Sokolov, 2006). Many of the studies presented in Figure 2.19 find that both the geographical and vertical distribution of the forcing can have the most significant effect on efficacy (in particular see Boer and Yu, 2003b; Joshi et al., 2003; Stuber et al., 2005; Sokolov, 2006). Nearly all studies that examine it find that high-latitude forcings have higher efficacies than tropical forcings. Efficacy has also been shown to vary with the vertical distribution of an applied forcing (Hansen et al., 1997; Christiansen, 1999; Joshi et al., 2003; Cook and Highwood, 2004; Roberts and Jones, 2004; Forster and Joshi, 2005; Stuber et al., 2005; Sokolov, 2006). Forcings that predominately affect the upper troposphere are often found to have smaller efficacies compared to those that affect the surface. However, this is not ubiquitous as climate feedbacks (such as cloud and water vapour) will depend on the static stability of the troposphere and hence the sign of the temperature change in the upper troposphere (Govindasamy et al., 2001b; Joshi et al., 2003; Sokolov, 2006).

2.8.5.2 Long-Lived Greenhouse Gases

The few models that have examined efficacy for combined LLGHG changes generally find efficacies slightly higher than 1.0 (Figure 2.19). Further, the most recent result from the NCAR Community Climate Model (CCM3) GCM (Govindasamy et al., 2001b) indicates an efficacy of over 1.2 with no clear reason of why this changed from earlier versions of the same model. Individual LLGHG efficacies have only been analysed in two or three models. Two GCMs suggest higher efficacies from individual components (over 30% for CFCs in Hansen et al., 2005). In contrast another GCM gives efficacies for CFCs (Forster and Joshi, 2005) and CH_4 (Berntsen et al., 2005) that are slightly less than one. Overall there is medium confidence that the observed changes in the combined LLGHG changes have an efficacy close to 1.0 (within 10%), but there are not enough studies to constrain the efficacies for individual species.

2.8.5.3 Solar

Solar changes, compared to CO_2, have less high-latitude RF and more of the RF realised at the surface. Established but incomplete knowledge suggests that there is partial compensation between these effects, at least in some models, which leads to solar efficacies close to 1.0. All models with a positive solar RF find efficacies of 1.0 or smaller. One study finds a smaller efficacy than other models (0.63: Gregory et al., 2004). However, their unique methodology for calculating climate sensitivity has large uncertainties (see Section 2.8.4). These studies have only examined solar RF from total solar irradiance change; any indirect solar effects (see Section 2.7.1.3) are not included in this efficacy estimate. Overall, there is medium confidence that the direct solar efficacy is within the 0.7 to 1.0 range.

2.8.5.4 Ozone

Stratospheric ozone efficacies have normally been calculated from idealised ozone increases. Experiments with three models (Stuber et al., 2001a; Joshi et al., 2003; Stuber et al., 2005) found higher efficacies for such changes; these were due to larger than otherwise tropical tropopause temperature changes which led to a positive stratospheric water vapour feedback. However, this mechanism may not operate in the two versions of the GISS model, which found smaller efficacies. Only one study has used realistic stratospheric ozone changes (see Figure 2.19); thus, knowledge is still incomplete. Conclusions are only drawn from the idealised studies where there is (1) medium confidence that the efficacy is within a 0.5 to 2.0 range and (2) established but incomplete physical understanding of how and why the efficacy could be larger than 1.0. There is medium confidence that for realistic tropospheric ozone perturbations the efficacy is within the 0.6 to 1.1 range.

2.8.5.5 Scattering Aerosol

For idealised global perturbations, the efficacy for the direct effect of scattering aerosol is very similar to that for changes in the solar constant (Cook and Highwood, 2004). As for ozone, realistic perturbations of scattering aerosol exhibit larger changes at higher latitudes and thus have a higher efficacy than solar changes (Hansen et al., 2005). Although the number of modelling results is limited, it is expected that efficacies would be similar to other solar effects; thus there is medium confidence that efficacies for scattering aerosol would be in the 0.7 to 1.1 range. Efficacies are likely to be similar for scattering aerosol in the troposphere and stratosphere.

With the formulation of RF employed in this chapter, the efficacy of the cloud albedo RF accounts for cloud lifetime effects (Section 2.8.3). Only two studies contained enough information to calculate efficacy in this way and both found efficacies higher than 1.0. However, the uncertainties in quantifying the cloud lifetime effect make this efficacy very uncertain. If cloud lifetime effects were excluded from the efficacy term, the cloud albedo efficacy would very likely be similar to that of the direct effect (see Figure 2.19).

2.8.5.6 Absorbing Aerosol

For absorbing aerosols, the simple ideas of a linear forcing-response relationship and efficacy can break down (Hansen et al., 1997; Cook and Highwood, 2004; Feichter et al., 2004; Roberts and Jones, 2004; Hansen et al., 2005; Penner et al., 2007). Aerosols within a particular range of single scattering albedos have negative RFs but induce a global mean warming, that is, the efficacy can be negative. The surface albedo and

height of the aerosol layer relative to the cloud also affects this relationship (Section 7.5; Penner et al., 2003; Cook and Highwood, 2004; Feichter et al., 2004; Johnson et al., 2004; Roberts and Jones, 2004; Hansen et al., 2005). Studies that increase BC in the planetary boundary layer find efficacies much larger than 1.0 (Cook and Highwood, 2004; Roberts and Jones, 2004; Hansen et al., 2005). These studies also find that efficacies are considerably smaller than 1.0 when BC aerosol is changed above the boundary layer. These changes in efficacy are at least partly attributable to a semi-direct effect whereby absorbing aerosol modifies the background temperature profile and tropospheric cloud (see Section 7.5). Another possible feedback mechanism is the modification of snow albedo by BC aerosol (Hansen and Nazarenko, 2004; Hansen et al., 2005); however, this report does not classify this as part of the response, but rather as a separate RF (see Section 2.5.4 and 2.8.5.7). Most GCMs likely have some representation of the semi-direct effect (Cook and Highwood, 2004) but its magnitude is very uncertain (see Section 7.5) and dependent on aspects of cloud parametrizations within GCMs (Johnson, 2005). Two studies using realistic vertical and horizontal distributions of BC find that overall the efficacy is around 0.7 (Hansen et al., 2005; Lohmann and Feichter, 2005). However, Hansen et al. (2005) acknowledge that they may have underestimated BC within the boundary layer and another study with realistic vertical distribution of BC changes finds an efficacy of 1.3 (Sokolov, 2006). Further, Penner et al. (2007) also modelled BC changes and found efficacies very much larger and very much smaller than 1.0 for biomass and fossil fuel carbon, respectively (Hansen et al. (2005) found similar efficacies for biomass and fossil fuel carbon). In summary there is no consensus as to BC efficacy and this may represent problems with the stratospherically adjusted definition of RF (see Section 2.8.3).

2.8.5.7 Other Forcing Agents

Efficacies for some other effects have been evaluated by one or two modelling groups. Hansen et al. (2005) found that land use albedo RF had an efficacy of roughly 1.0, while the BC-snow albedo RF had an efficacy of 1.7. Ponater et al. (2005) found an efficacy of 0.6 for contrail RF and this agrees with a suggestion from Hansen et al. (2005) that high-cloud changes should have smaller efficacies. The results of Hansen et al. (2005) and Forster and Shine (1999) suggest that stratospheric water vapour efficacies are roughly one.

2.8.6 Efficacy and the Forcing-Response Relationship

Efficacy is a new concept introduced since the TAR and its physical understanding is becoming established (see Section 2.8.5). When employing the stratospherically adjusted RF, there is medium confidence that efficacies are within the 0.75 to 1.25 range for most realistic RF mechanisms aside from aerosol and stratospheric ozone changes. There is medium confidence that realistic aerosol and ozone changes have efficacies within the 0.5 to 2.0 range. Further, zero-surface-temperature-change RFs are very likely to have efficacies significantly closer to 1.0 for all mechanisms. It should be noted that efficacies have only been evaluated in GCMs and actual climate efficacies could be different from those quoted in Section 2.8.5.

2.9 Synthesis

This section begins by synthesizing the discussion of the RF concept. It presents summaries of the global mean RFs assessed in earlier sections and discusses time evolution and spatial patterns of RF. It also presents a brief synthesis of surface forcing diagnostics. It breaks down the analysis of RF in several ways to aid and advance the understanding of the drivers of climate change.

RFs are calculated in various ways depending on the agent: from changes in emissions and/or changes in concentrations; and from observations and other knowledge of climate change drivers. Current RF depends on present-day concentrations of a forcing agent, which in turn depend on the past history of emissions. Some climate response to these RFs is expected to have already occurred. Additionally, as RF is a comparative measure of equilibrium climate change and the Earth's climate is not in an equilibrium state, additional climate change in the future is also expected from present-day RFs (see Sections 2.2 and 10.7). As previously stated in Section 2.2, RF alone is not a suitable metric for weighting emissions; for this purpose, the lifetime of the forcing agent also needs to be considered (see Sections 2.9.4 and 2.10).

RFs are considered external to the climate system (see Section 2.2). Aside from the natural RFs (solar, volcanoes), the other RFs are considered to be anthropogenic (i.e., directly attributable to human activities). For the LLGHGs it is assumed that all changes in their concentrations since pre-industrial times are human-induced (either directly through emissions or from land use changes); these concentration changes are used to calculate the RF. Likewise, stratospheric ozone changes are also taken from satellite observations and changes are primarily attributed to Montreal-Protocol controlled gases, although there may also be a climate feedback contribution to these trends (see Section 2.3.4). For the other RFs, anthropogenic emissions and/or human-induced land use changes are used in conjunction with CTMs and/or GCMs to estimate the anthropogenic RF.

2.9.1 Uncertainties in Radiative Forcing

The TAR assessed uncertainties in global mean RF by attaching an error bar to each RF term that was 'guided by the range of published values and physical understanding'. It also quoted a level of scientific understanding (LOSU) for each RF, which was a subjective judgment of the estimate's reliability.

The concept of LOSU has been slightly modified based on the IPCC Fourth Assessment Report (AR4) uncertainty guidelines. Error bars now represent the 5 to 95% (90%)

confidence range (see Box TS.1). Only 'well-established' RFs are quantified. 'Well established' implies that there is qualitatively both sufficient evidence and sufficient consensus from published results to estimate a central RF estimate and a range. 'Evidence' is assessed by an A to C grade, with an A grade implying strong evidence and C insufficient evidence. Strong evidence implies that observations have verified aspects of the RF mechanism and that there is a sound physical model to explain the RF. 'Consensus' is assessed by assigning a number between 1 and 3, where 1 implies a good deal of consensus and 3 insufficient consensus. This ranks the number of studies, how well studies agree on quantifying the RF and especially how well observation-based studies agree with models. The product of 'Evidence' and 'Consensus' factors give the LOSU rank. These ranks are high, medium, medium-low, low or very low. Ranks of very low are not evaluated. The quoted 90% confidence range of RF quantifies the value uncertainty, as derived from the expert assessment of published values and their ranges. For most RFs, many studies have now been published, which generally makes the sampling of parameter space more complete and the value uncertainty more realistic, compared to the TAR. This is particularly true for both the direct and cloud albedo aerosol RF (see Section 2.4). Table 2.11 summarises the key certainties and uncertainties and indicates the basis for the 90% confidence range estimate. Note that the aerosol terms will have added uncertainties due to the uncertain semi-direct and cloud lifetime effects. These uncertainties in the response to the RF (efficacy) are discussed in Section 2.8.5.

Table 2.11 indicates that there is now stronger evidence for most of the RFs discussed in this chapter. Some effects are not quantified, either because they do not have enough evidence or because their quantification lacks consensus. These include certain mechanisms associated with land use, stratospheric water vapour and cosmic rays. Cloud lifetime and the semi-direct effects are also excluded from this analysis as they are deemed to be part of the climate response (see Section 7.5). The RFs from the LLGHGs have both a high degree of consensus and a very large amount of evidence and, thereby, place understanding of these effects at a considerably higher level than any other effect.

2.9.2 Global Mean Radiative Forcing

The RFs discussed in this chapter, their uncertainty ranges and their efficacies are summarised in Figure 2.20 and Table 2.12. Radiative forcings from forcing agents have been combined into their main groupings. This is particularly useful for aerosol as its total direct RF is considerably better constrained than the RF from individual aerosol types (see Section 2.4.4). Table 2.1 gives a further component breakdown of RF for the LLGHGs. Radiative forcings are the stratospherically adjusted RF and they have not been multiplied by efficacies (see Sections 2.2 and 2.8).

In the TAR, no estimate of the total combined RF from all anthropogenic forcing agents was given because: a) some of the forcing agents did not have central or best estimates; b) a degree of subjectivity was included in the error estimates; and c) uncertainties associated with the linear additivity assumption and efficacy had not been evaluated. Some of these limitations still apply. However, methods for objectively adding the RF of individual species have been developed (e.g., Schwartz and Andreae, 1996; Boucher and Haywood, 2001). In addition, as efficacies are now better understood and quantified (see Section 2.8.5), and as the linear additivity assumption has been more thoroughly tested (see Section 2.8.4), it becomes scientifically justifiable for RFs from different mechanisms to be combined, with certain exceptions as noted below. Adding together the anthropogenic RF values shown in panel (A) of Figure 2.20 and combining their individual uncertainties gives the probability density functions (PDFs) of RF that are shown in panel (B). Three PDFs are shown: the combined RF from greenhouse gas changes (LLGHGs and ozone); the combined direct aerosol and cloud albedo RFs and the combination of all anthropogenic RFs. The solar RF is not included in any of these distributions. The PDFs are generated by combining the 90% confidence estimates for the RFs, assuming independence and employing a one-million point Monte Carlo simulation to derive the PDFs (see Boucher and Haywood, 2001; and Figure 2.20 caption for details).

The PDFs show that LLGHGs and ozone contribute a positive RF of +2.9 ± 0.3 W m^{-2}. The combined aerosol direct and cloud albedo effect exert an RF that is virtually certain to be negative, with a median RF of –1.3 W m^{-2} and a –2.2 to –0.5 W m^{-2} 90% confidence range. The asymmetry in the combined aerosol PDF is caused by the estimates in Tables 2.6 and 2.7 being non-Gaussian. The combined net RF estimate for all anthropogenic drivers has a value of +1.6 W m^{-2} with a 0.6 to 2.4 W m^{-2} 90% confidence range. Note that the RFs from surface albedo change, stratospheric water vapour change and persistent contrails are only included in the combined anthropogenic PDF and not the other two.

Statistically, the PDF shown in Figure 2.20 indicates just a 0.2% probability that the total RF from anthropogenic agents is negative, which would suggest that it is virtually certain that the combined RF from anthropogenic agents is positive. Additionally, the PDF presented here suggests that it is extremely likely that the total anthropogenic RF is larger than +0.6 W m^{-2}. This combined anthropogenic PDF is better constrained than that shown in Boucher and Haywood (2001) because each of the individual RFs have been quantified to 90% confidence levels, enabling a more definite assessment, and because the uncertainty in some of the RF estimates is considerably reduced. For example, modelling of the total direct RF due to aerosols is better constrained by satellite and surface-based observations (Section 2.4.2), and the current estimate of the cloud albedo indirect effect has a best estimate and uncertainty associated with it, rather than just a range. The LLGHG RF has also increased by 0.20 W m^{-2} since 1998, making a positive RF more likely than in Boucher and Haywood (2001).

Nevertheless, there are some structural uncertainties associated with the assumptions used in the construction of

Table 2.11. *Uncertainty assessment of forcing agents discussed in this chapter. Evidence for the forcing is given a grade (A to C), with A implying strong evidence and C insufficient evidence. The degree of consensus among forcing estimates is given a 1, 2 or 3 grade, where grade 1 implies a good deal of consensus and grade 3 implies an insufficient consensus. From these two factors, a level of scientific understanding is determined (LOSU). Uncertainties are in approximate order of importance with first-order uncertainties listed first.*

	Evidence	Consensus	LOSU	Certainties	Uncertainties	Basis of RF range
LLGHGs	A	1	High	Past and present concentrations; spectroscopy	Pre-industrial concentrations of some species; vertical profile in stratosphere; spectroscopic strength of minor gases	Uncertainty assessment of measured trends from different observed data sets and differences between radiative transfer models
Stratospheric ozone	A	2	Medium	Measured trends and its vertical profile since 1980; cooling of stratosphere; spectroscopy	Changes prior to 1970; trends near tropopause; effect of recent trends	Range of model results weighted to calculations employing trustworthy observed ozone trend data
Tropospheric ozone	A	2	Medium	Present-day concentration at surface and some knowledge of vertical and spatial structure of concentrations and emissions; spectroscopy	Pre-industrial values and role of changes in lightning; vertical structure of trends near tropopause; aspects of emissions and chemistry	Range of published model results, upper bound increased to account for anthropogenic trend in lightning
Stratospheric water vapour from CH_4	A	3	Low	Global trends since 1990; CH_4 contribution to trend; spectroscopy	Global trends prior to 1990; radiative transfer in climate models; CTM models of CH_4 oxidation	Range based on uncertainties in CH_4 contribution to trend and published RF estimates
Direct aerosol	A	2 to 3	Medium to Low	Ground-based and satellite observations; some source regions and modelling	Emission sources and their history vertical structure of aerosol, optical properties, mixing and separation from natural background aerosol	Range of published model results with allowances made for comparisons with satellite data
Cloud albedo effect (all aerosols)	B	3	Low	Observed in case studies – e.g., ship tracks; GCMs model an effect	Lack of direct observational evidence of a global forcing	Range of published model results and published results where models have been constrained by satellite data
Surface albedo (land use)	A	2 to 3	Medium to Low	Some quantification of deforestation and desertification	Separation of anthropogenic changes from natural	Based on range of published estimates and published uncertainty analyses
Surface albedo (BC aerosol on snow)	B	3	Low	Estimates of BC aerosol on snow; some model studies suggest link	Separation of anthropogenic changes from natural; mixing of snow and BC aerosol; quantification of RF	Estimates based on a few published model studies
Persistent linear Contrails	A	3	Low	Cirrus radiative and microphysical properties; aviation emissions; contrail coverage in certain regions	Global contrail coverage and optical properties	Best estimate based on recent work and range from published model results

Table 2.11 (continued)

	Evidence	Consensus	LOSU	Certainties	Uncertainties	Basis of RF range
Solar irradiance	B	3	Low	Measurements over last 25 years; proxy indicators of solar activity	Relationship between proxy data and total solar irradiance; indirect ozone effects	Range from available reconstructions of solar irradiance and their qualitative assessment
Volcanic aerosol	A	3	Low	Observed aerosol changes from Mt. Pinatubo and El Chichón; proxy data for past eruptions; radiative effect of volcanic aerosol	Stratospheric aerosol concentrations from pre-1980 eruptions; atmospheric feedbacks	Past reconstructions/estimates of explosive volcanoes and observations of Mt. Pinatubo aerosol
Stratospheric water vapour from causes other than CH_4 oxidation	C	3	Very Low	Empirical and simple model studies suggest link; spectroscopy	Other causes of water vapour trends poorly understood	Not given
Tropospheric water vapour from irrigation	C	3	Very Low	Process understood; spectroscopy; some regional information	Global injection poorly quantified	Not given
Aviation-induced cirrus	C	3	Very Low	Cirrus radiative and microphysical properties; aviation emissions; contrail coverage in certain regions	Transformation of contrails to cirrus; aviation's effect on cirrus clouds	Not given
Cosmic rays	C	3	Very Low	Some empirical evidence and some observations as well as microphysical models suggest link to clouds	General lack/doubt regarding physical mechanism; dependence on correlation studies	Not given
Other surface effects	C	3	Very Low	Some model studies suggest link and some evidence of relevant processes	Quantification of RF and interpretation of results in forcing feedback context difficult	Not given

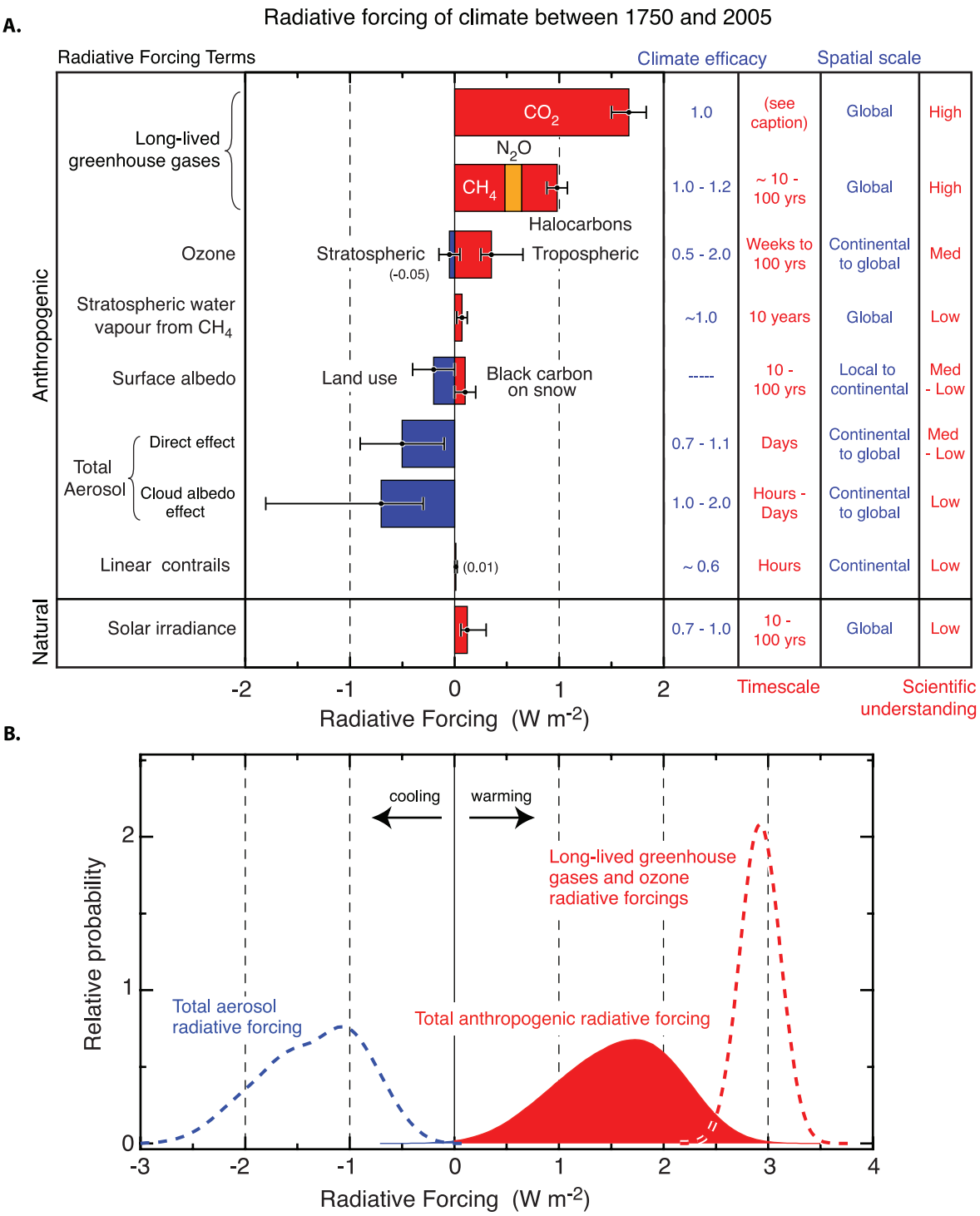


Figure 2.20. *(A) Global mean RFs from the agents and mechanisms discussed in this chapter, grouped by agent type. Anthropogenic RFs and the natural direct solar RF are shown. The plotted RF values correspond to the bold values in Table 2.12. Columns indicate other characteristics of the RF; efficacies are not used to modify the RFs shown. Time scales represent the length of time that a given RF term would persist in the atmosphere after the associated emissions and changes ceased. No CO_2 time scale is given, as its removal from the atmosphere involves a range of processes that can span long time scales, and thus cannot be expressed accurately with a narrow range of lifetime values. The scientific understanding shown for each term is described in Table 2.11. (B) Probability distribution functions (PDFs) from combining anthropogenic RFs in (A). Three cases are shown: the total of all anthropogenic RF terms (block filled red curve; see also Table 2.12); LLGHGs and ozone RFs only (dashed red curve); and aerosol direct and cloud albedo RFs only (dashed blue curve). Surface albedo, contrails and stratospheric water vapour RFs are included in the total curve but not in the others. For all of the contributing forcing agents, the uncertainty is assumed to be represented by a normal distribution (and 90% confidence intervals) with the following exceptions: contrails, for which a lognormal distribution is assumed to account for the fact that the uncertainty is quoted as a factor of three; and tropospheric ozone, the direct aerosol RF (sulphate, fossil fuel organic and black carbon, biomass burning aerosols) and the cloud albedo RF, for which discrete values based on Figure 2.9, Table 2.6 and Table 2.7 are randomly sampled. Additional normal distributions are included in the direct aerosol effect for nitrate and mineral dust, as these are not explicitly accounted for in Table 2.6. A one-million point Monte Carlo simulation was performed to derive the PDFs (Boucher and Haywood, 2001). Natural RFs (solar and volcanic) are not included in these three PDFs. Climate efficacies are not accounted for in forming the PDFs.*

Table 2.12. *Global mean radiative forcings since 1750 and comparison with earlier assessments. Bold rows appear on Figure 2.20. The first row shows the combined anthropogenic RF from the probability density function in panel B of Figure 2.20. The sum of the individual RFs and their estimated errors are not quite the same as the numbers presented in this row due to the statistical construction of the probability density function.*

	Global mean radiative forcing (W m^{-2})[a]			
	SAR (1750–1993)	TAR (1750–1998)	AR4 (1750–2005)	Summary comments on changes since the TAR
Combined Anthropogenic RF	**Not evaluated**	**Not evaluated**	**1.6 [–1.0, +0.8]**	**Newly evaluated. Probability density function estimate**
Long-lived Greenhouse gases (Comprising CO_2, CH_4, N_2O, and halocarbons)	**+2.45 [15%] (CO_2 1.56; CH_4 0.47; N_2O 0.14; Halocarbons 0.28)**	**+2.43 [10%] (CO_2 1.46; CH_4 0.48; N_2O 0.15; Halocarbons 0.34[b])**	**+2.63 [±0.26] (CO_2 1.66 [±0.17]; CH_4 0.48 [±0.05]; N_2O 0.16 [±0.02]; Halocarbons 0.34 [±0.03])**	**Total increase in RF, due to upward trends, particularly in CO_2. Halocarbon RF trend is positive[b]**
Stratospheric ozone	**–0.1 [2x]**	**–0.15 [67%]**	**–0.05 [±0.10]**	**Re-evaluated to be weaker**
Tropospheric ozone	**+0.40 [50%]**	**+0.35 [43%]**	**+0.35 [–0.1, +0.3]**	**Best estimate unchanged. However, a larger RF could be possible**
Stratospheric water vapour from CH_4	**Not evaluated**	**+0.01 to +0.03**	**+0.07 [±0.05]**	**Re-evaluated to be higher**
Total direct aerosol	**Not evaluated**	**Not evaluated**	**–0.50 [±0.40]**	**Newly evaluated**
Direct sulphate aerosol	–0.40 [2x]	–0.40 [2x]	–0.40 [±0.20]	Better constrained
Direct fossil fuel aerosol (organic carbon)	Not evaluated	–0.10 [3x]	–0.05 [±0.05]	Re-evaluated to be weaker
Direct fossil fuel aerosol (BC)	+0.10 [3x]	+0.20 [2x]	+0.20 [±0.15]	Similar best estimate to the TAR. Response affected by semi-direct effects
Direct biomass burning aerosol	–0.20 [3x]	–0.20 [3x]	+0.03 [±0.12]	Re-evaluated and sign changed. Response affected by semi-direct effects
Direct nitrate aerosol	Not evaluated	Not evaluated	–0.10 [±0.10]	Newly evaluated
Direct mineral dust aerosol	Not evaluated	–0.60 to +0.40	–0.10 [±0.20]	Re-evaluated to have a smaller anthropogenic fraction
Cloud albedo effect	**0 to –1.5 (sulphate only)**	**0.0 to –2.0 (all aerosols)**	**–0.70 [–1.1, +0.4] (all aerosols)**	**Best estimate now given**
Surface albedo (land use)	**Not evaluated**	**–0.20 [100%]**	**–0.20 [±0.20]**	**Additional studies**
Surface albedo (BC aerosol on snow)	**Not evaluated**	**Not evaluated**	**+0.10 [±0.10]**	**Newly evaluated**
Persistent linear contrails	**Not evaluated**	**0.02 [3.5x]**	**0.01 [–0.007, +0.02]**	**Re-evaluated to be smaller**
Solar irradiance	**+0.30 [67%]**	**+0.30 [67%]**	**+0.12 [–0.06, +0.18]**	**Re-evaluated to be less than half**

Notes: [a] For the AR4 column, 90% value uncertainties appear in brackets: when adding these numbers to the best estimate the 5 to 95% confidence range is obtained. When two numbers are quoted for the value uncertainty, the distribution is non-normal. Uncertainties in the SAR and the TAR had a similar basis, but their evaluation was more subjective. [15%] indicates 15% relative uncertainty, [2x], etc. refer to a factor of two, etc. uncertainty and a lognormal distribution of RF estimates.

[b] The TAR RF for halocarbons and hence the total LLGHG RF was incorrectly evaluated some 0.01 W m^{-2} too high. The actual trends in these RFs are therefore more positive than suggested by numbers in this table (Table 2.1 shows updated trends).

the PDF and the assumptions describing the component uncertainties. Normal distributions are assumed for most RF mechanisms (with the exceptions noted in the caption); this may not accurately capture extremes. Additionally, as in Boucher and Haywood (2001), all of the individual RF mechanisms are given equal weighting, even though the level of scientific understanding differs between forcing mechanisms. Note also that variation in efficacy and hence the semi-direct and cloud lifetime effects are not accounted for, as these are not considered to be RFs in this report (see Section 2.2). Adding these effects, together with other potential mechanisms that have so far not been defined as RFs and quantified, would introduce further uncertainties but give a fuller picture of the role of anthropogenic drivers. Introducing efficacy would give a broader PDF and a large cloud lifetime effect would reduce the median estimate. Despite these caveats, from the current knowledge of individual forcing mechanisms presented here it remains extremely likely that the combined anthropogenic RF is both positive and substantial (best estimate: +1.6 W m^{-2}).

2.9.3 Global Mean Radiative Forcing by Emission Precursor

The RF due to changes in the concentration of a single forcing agent can have contributions from emissions of several compounds (Shindell et al., 2005). The RF of CH_4, for example, is affected by CH_4 emissions, as well as NO_x emissions. The CH_4 RF quoted in Table 2.12 and shown in Figure 2.20 is a value that combines the effects of both emissions. As an anthropogenic or natural emission can affect several forcing agents, it is useful to assess the current RF caused by each primary emission. For example, emission of NO_x affects CH_4, tropospheric ozone and tropospheric aerosols. Based on a development carried forward from the TAR, this section assesses the RF terms associated with each principal emission including indirect RFs related to perturbations of other forcing agents, with the results shown in Figure 2.21. The following indirect forcing mechanisms are considered:

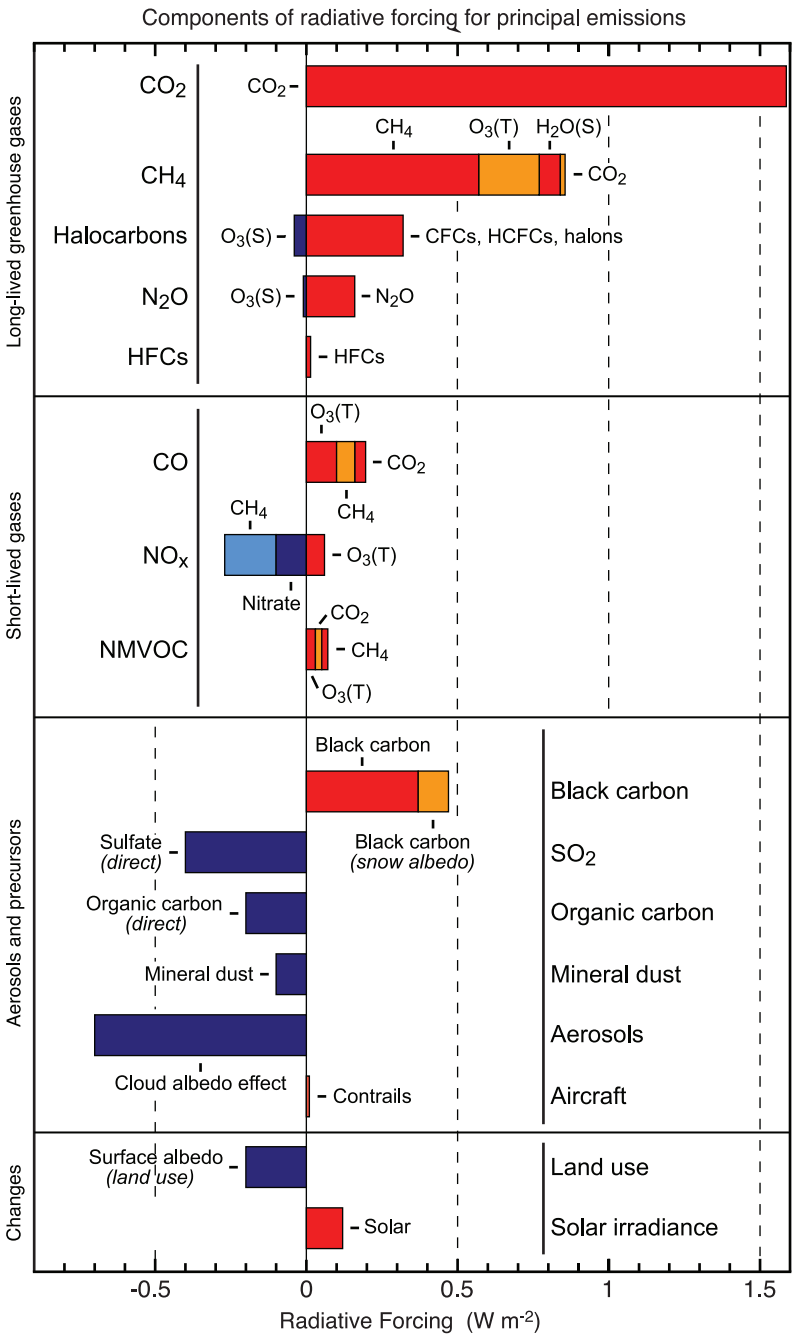


Figure 2.21. *Components of RF for emissions of principal gases, aerosols and aerosol precursors and other changes. Values represent RF in 2005 due to emissions and changes since 1750. (S) and (T) next to gas species represent stratospheric and tropospheric changes, respectively. The uncertainties are given in the footnotes to Table 2.13. Quantitative values are displayed in Table 2.13.*

- fossil carbon from non-CO_2 gaseous compounds, which eventually increase CO_2 in the atmosphere (from CO, CH_4, and NMVOC emissions);
- changes in stratospheric ozone (from N_2O and halocarbon (CFCs, HCFC, halons, etc.) emissions);
- changes in tropospheric ozone (from CH_4, NO_x, CO, and NMVOC emissions);
- changes in OH affecting the lifetime of CH_4 (from CH_4, CO, NO_x, and NMVOC emissions); and
- changing nitrate and sulphate aerosols through changes in NO_x and SO_2 emissions, respectively.

For some of the principal RFs (e.g., BC, land use and mineral dust) there is not enough quantitative information available to assess their indirect effects, thus their RFs are the same as those

presented in Table 2.12. Table 2.5 gives the total (fossil and biomass burning) direct RFs for BC and organic carbon aerosols that are used to obtain the average shown in Figure 2.21. Table 2.13 summarises the direct and indirect RFs presented in Figure 2.21, including the methods used for estimating the RFs and the associated uncertainty. Note that for indirect effects through changes in chemically active gases (e.g., OH or ozone), the emission-based RF is not uniquely defined since the effect of one precursor will be affected by the levels of the other precursors. The RFs of indirect effects on CH_4 and ozone by NO_x, CO and VOC emissions are estimated by removing the anthropogenic emissions of one precursor at a time. A sensitivity analysis by Shindell et al. (2005) indicates that the nonlinear effect induced by treating the precursors separately is of the order of 10% or less. Very uncertain indirect effects are not included in Table 2.13 and Figure 2.21. These include ozone changes due to solar effects, changes in secondary organic aerosols through changes in the ozone/OH ratio and apportioning of the cloud albedo changes to each aerosol type (Hansen et al., 2005).

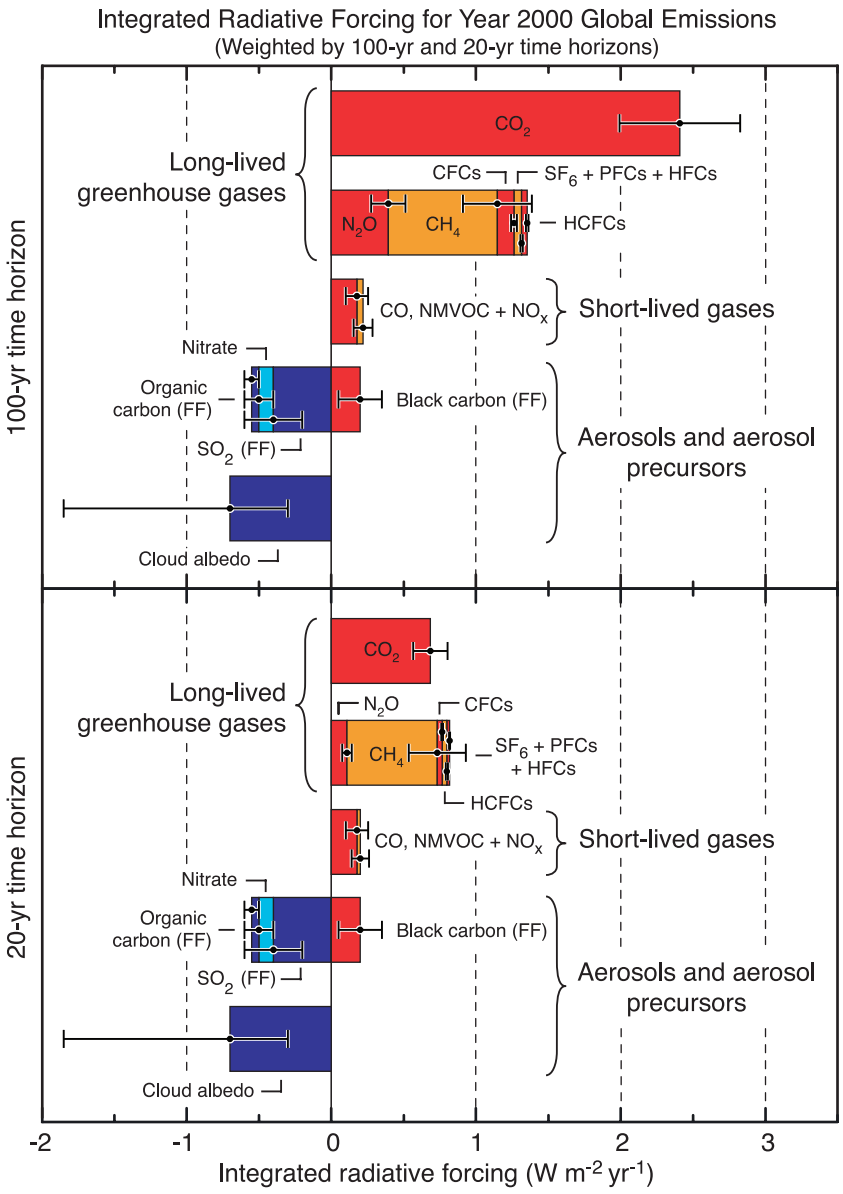


Figure 2.22. *Integrated RF of year 2000 emissions over two time horizons (20 and 100 years). The figure gives an indication of the future climate impact of current emissions. The values for aerosols and aerosol precursors are essentially equal for the two time horizons. It should be noted that the RFs of short-lived gases and aerosol depend critically on both when and where they are emitted; the values given in the figure apply only to total global annual emissions. For organic carbon and BC, both fossil fuel (FF) and biomass burning emissions are included. The uncertainty estimates are based on the uncertainties in emission sources, lifetime and radiative efficiency estimates.*

2.9.4 Future Climate Impact of Current Emissions

The changes in concentrations since pre-industrial time of the long-lived components causing the RF shown in Figure 2.20 are strongly influenced by the past history of emissions. A different perspective is obtained by integrating RF over a future time horizon for a one-year 'pulse' of global emissions (e.g., Jacobson (2002) used this approach to compare fossil fuel organic and BC aerosols to CO_2). Comparing the contribution from each forcing agent as shown in Figure 2.22 gives an indication of the future climate impact for current (year 2000) emissions of the different forcing agents. For the aerosols, the integrated RF is obtained based on the lifetimes, burdens and RFs from the AeroCom experiments, as summarised in Tables 2.4 and 2.5. For ozone precursors (CO, NO_x and NMVOCs), data are taken from Derwent et al. (2001), Collins et al. (2002), Stevenson et al. (2004) and Berntsen et al. (2005), while for the long-lived species the radiative efficiencies and lifetimes are used, as well as a response function for CO_2 (see Section 2.10.2, Table 2.14). Uncertainties in the estimates of the integrated RF originate from uncertainties in lifetimes, optical properties and current global emissions.

Figure 2.22 shows the integrated RF for both a 20- and 100-year time horizon. Choosing the longer time horizon of 100 years, as was done in the GWPs for the long-lived species included in the Kyoto Protocol, reduces the apparent importance of the shorter-lived species. It should be noted that the compounds with long lifetimes and short emission histories will tend to contribute more to the total with this 'forward looking' perspective than in the standard 'IPCC RF bar chart diagram' (Figure 2.20).

Table. 2.13. *Emission-based RFs for emitted components with radiative effects other than through changes in their atmospheric abundance. Minor effects where the estimated RF is less than 0.01 W m^{-2} are not included. Effects on sulphate aerosols are not included since SO_2 emission is the only significant factor affecting sulphate aerosols. Method of calculation and uncertainty ranges are given in the footnotes. Values represent RF in 2005 due to emissions and changes since 1750. See Figure 2.21 for graphical presentation of these values.*

	CO_2	CH_4	CFC/ HCFC	N_2O	HFC/ PFC/SF_6	BC-direct	BC snow albedo	Organic carbon	O_3(T)[a]	O_3(S)[b]	H_2O(S)[c]	Nitrate aerosols	Indirect cloud albedo effect
Component emitted	**Atmospheric or surface change directly causing radiative forcing**												
CO_2	1.56[d]												
CH_4	0.016[d]	0.57[e]							0.2[e]		0.07[f]		
CFC/HCFC/halons			0.32[g]							–0.04[h]			
N_2O				0.15[g]						–0.01[h]			
HFC/PFC/SF_6					0.017[g]								
CO/VOC	0.06[d]	0.08[e]							0.13[e]				
NOx		–0.17[e]							0.06[e]			–0.10[i]	X[j]
BC						0.34[k]	0.1[l]						X[j]
OC								–0.19[k]					X[j]
SO_2													X[j]

Notes:

[a] tropospheric ozone.

[b] stratospheric ozone.

[c] stratospheric water vapour.

[d] Derived from the total RF of the observed CO_2 change (Table 2.12), with the contributions from CH_4, CO and VOC emissions from fossil sources subtracted. Historical emissions of CH_4, CO and VOCs from Emission Database for Global Atmospheric Research (EDGAR)-HistorY Database of the Environment (HYDE) (Van Aardenne et al., 2001), CO_2 contribution from these sources calculated with CO_2 model described by Joos et al. (1996).

[e] Derived from the total RF of the observed CH_4 change (Table 2.12). Subtracted from this were the contributions through lifetime changes caused by emissions of NO_x, CO and VOC that change OH concentrations. The effects of NO_x, CO and VOCs are from Shindell et al. (2005). There are significant uncertainties related to these relations. Following Shindell et al. (2005) the uncertainty estimate is taken to be ±20% for CH_4 emissions, and ±50% for CO, VOC and NO_x emissions.

[f] All the radiative forcing from changes in stratospheric water vapour is attributed to CH_4 emissions (Section 2.3.7 and Table 2.12).

[g] RF calculated based on observed concentration change, see Table 2.12 and Section 2.3

[h] 80% of RF from observed ozone depletion in the stratosphere (Table 2.12) is attributed to CFCs/HFCs, remaining 20% to N_2O (Based on Nevison et al., 1999 and WMO, 2003).

[i] RF from Table 2.12, uncertainty ±0.10 W m^{-2}.

[j] Uncertainty too large to apportion the indirect cloud albedo effect to each aerosol type (Hansen et al., 2005).

[k] Mean of all studies in Table 2.5, includes fossil fuel, biofuel and biomass burning. Uncertainty (90% confidence ranges) ±0.25 W m^{-2} (BC) and ±0.20 W m^{-2} (organic carbon) based on range of reported values in Table 2.5.

[l] RF from Table 2.12, uncertainty ±0.10 W m^{-2}.

2.9.5 Time Evolution of Radiative Forcing and Surface Forcing

There is a good understanding of the time evolution of the LLGHG concentrations from *in situ* measurements over the last few decades and extending further back using firn and ice core data (see Section 2.3, FAQ 2.1, Figure 1 and Chapter 6). Increases in RF are clearly dominated by CO_2. Halocarbon RF has grown rapidly since 1950, but the RF growth has been cut dramatically by the Montreal Protocol (see Section 2.3.4). The RF of CFCs is declining; in addition, the combined RF of all ozone-depleting substances (ODS) appears to have peaked at 0.32 W m^{-2} during 2003. However, substitutes for ODS are growing at a slightly faster rate, so halocarbon RF growth is still positive (Table 2.1). Although the trend in halocarbon RF since the time of the TAR has been positive (see Table 2.1), the halocarbon RF in this report, as shown in Table 2.12, is the same as in the TAR; this is due to a re-evaluation of the TAR results.

Radiative forcing time series for the natural (solar, volcanic aerosol) forcings are reasonably well known for the past 25 years; estimates further back are prone to uncertainties (Section 2.7). Determining the time series for aerosol and ozone RF is far more difficult because of uncertainties in the knowledge of past emissions and chemical-microphysical modelling. Several time series for these and other RFs have been constructed (e.g., Myhre et al., 2001; Ramaswamy et al., 2001; Hansen et al., 2002). General Circulation Models develop their own time evolution of many forcings based on the temporal history of the relevant concentrations. As an example, the temporal evolution of the global and annual mean, instantaneous, all-sky RF and surface forcing due to the principal agents simulated by the Model for Interdisciplinary Research on Climate (MIROC) + Spectral Radiation-Transport Model for Aerosol Species (SPRINTARS) GCM (Nozawa et al., 2005; Takemura et al., 2005) is illustrated in Figure 2.23. Although there are differences between models with regards to the temporal reconstructions and thus present-day forcing estimates, they typically have a qualitatively similar temporal evolution since they often base the temporal histories on similar emissions data.

General Circulation Models compute the climate response based on the knowledge of the forcing agents and their temporal evolution. While most current GCMs incorporate the trace gas RFs, aerosol direct effects, solar and volcanoes, a few have in addition incorporated land use change and cloud albedo effect. While LLGHGs have increased rapidly over the past 20 years and contribute the most to the present RF (refer also to Figure 2.20 and FAQ 2.1, Figure 1), Figure 2.23 also indicates that the combined positive RF of the greenhouse gases exceeds the contributions due to all other anthropogenic agents throughout the latter half of the 20th century.

The solar RF has a small positive value. The positive solar irradiance RF is likely to be at least five times smaller than the combined RF due to all anthropogenic agents, and about an order of magnitude less than the total greenhouse gas contribution (Figures 2.20 and 2.23 and Table 2.12; see also the Foukal et al., 2006 review). The combined natural RF consists of the solar RF plus the large but transitory negative RF from episodic, explosive volcanic eruptions of which there have been several over the past half century (see Figure 2.18). Over particularly the 1950 to 2005 period, the combined natural forcing has been either negative or slightly positive (less than approximately 0.2 W m^{-2}), reaffirming and extending the conclusions in the

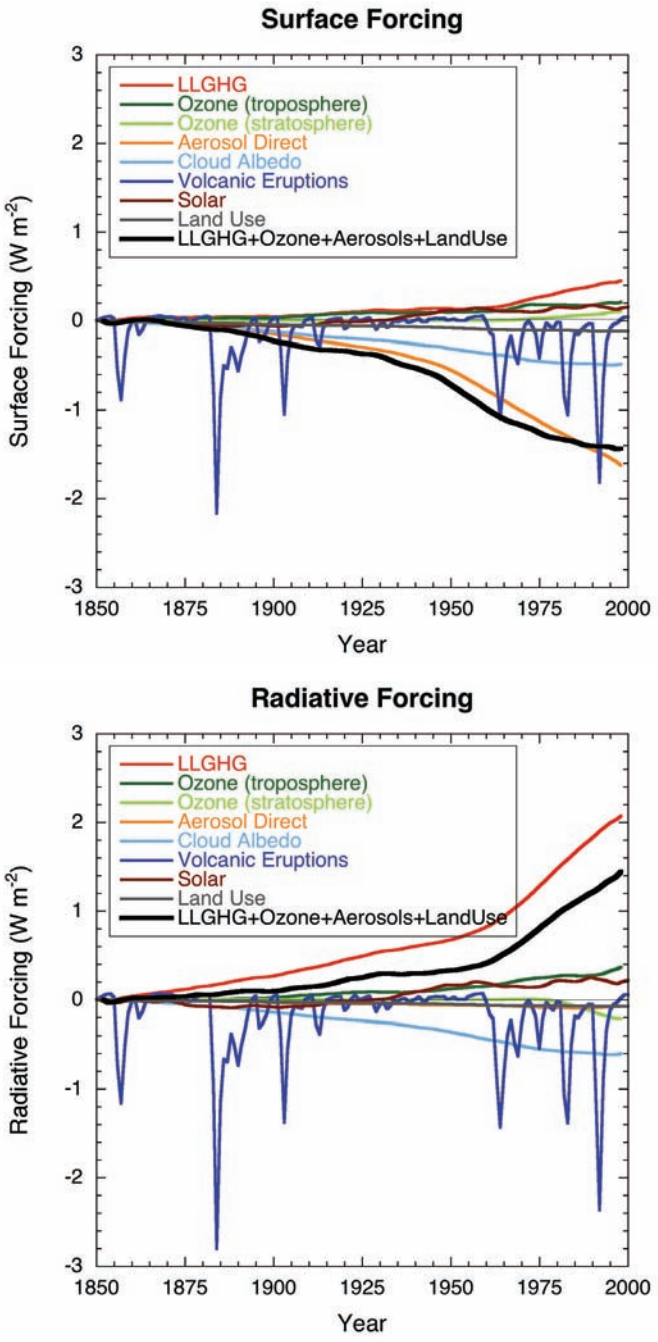


Figure 2.23. *Globally and annually averaged temporal evolution of the instantaneous all-sky RF (top panel) and surface forcing (bottom panel) due to various agents, as simulated in the MIROC+SPRINTARS model (Nozawa et al., 2005; Takemura et al., 2005). This is an illustrative example of the forcings as implemented and computed in one of the climate models participating in the AR4. Note that there could be differences in the RFs among models. Most models simulate roughly similar evolution of the LLGHGs' RF.*

TAR. Therefore, it is exceptionally unlikely that natural RFs could have contributed a positive RF of comparable magnitude to the combined anthropogenic RF term over the period 1950 to 2005 (Figure 2.23). Attribution studies with GCMs employ the available knowledge of the evolution of the forcing over the 20th century, and particularly the features distinguishing the anthropogenic from the natural agents (see also Section 9.2).

The surface forcing (Figure 2.23, top panel), in contrast to RF, is dominated by the strongly negative shortwave effect of the aerosols (tropospheric and the episodic volcanic ones), with the LLGHGs exerting a small positive effect. Quantitative values of the RFs and surface forcings by the agents differ across models in view of the differences in model physics and in the formulation of the forcings due to the short-lived species (see Section 10.2, Collins et al. (2006) and Forster and Taylor (2006) for further discussion on uncertainties in GCMs' calculation of RF and surface forcing). As for RF, it is difficult to specify uncertainties in the temporal evolution, as emissions and concentrations for all but the LLGHGs are not well constrained.

2.9.6 Spatial Patterns of Radiative Forcing and Surface Forcing

Figure 6.7 of Ramaswamy et al. (2001) presented examples of the spatial patterns for most of the RF agents discussed in this chapter; these examples still hold. Many of the features seen in Figure 6.7 of Ramaswamy et al. (2001) are generic. However, additional uncertainties exist for the spatial patterns compared to those for the global-mean RF. Spatial patterns of the aerosol RF exhibit some of the largest differences between models, depending on the specification of the aerosols and their properties, and whether or not indirect cloud albedo effects are included. The aerosol direct and cloud albedo effect RF also depend critically on the location of clouds, which differs between the GCMs. Figure 2.24 presents illustrative examples of the spatial pattern of the instantaneous RF between 1860 and present day, due to natural plus anthropogenic agents, from two GCMs. Volcanic aerosols play a negligible role in this calculation owing to the end years considered and their virtual absence during these years. The MIROC+SPRINTARS model includes

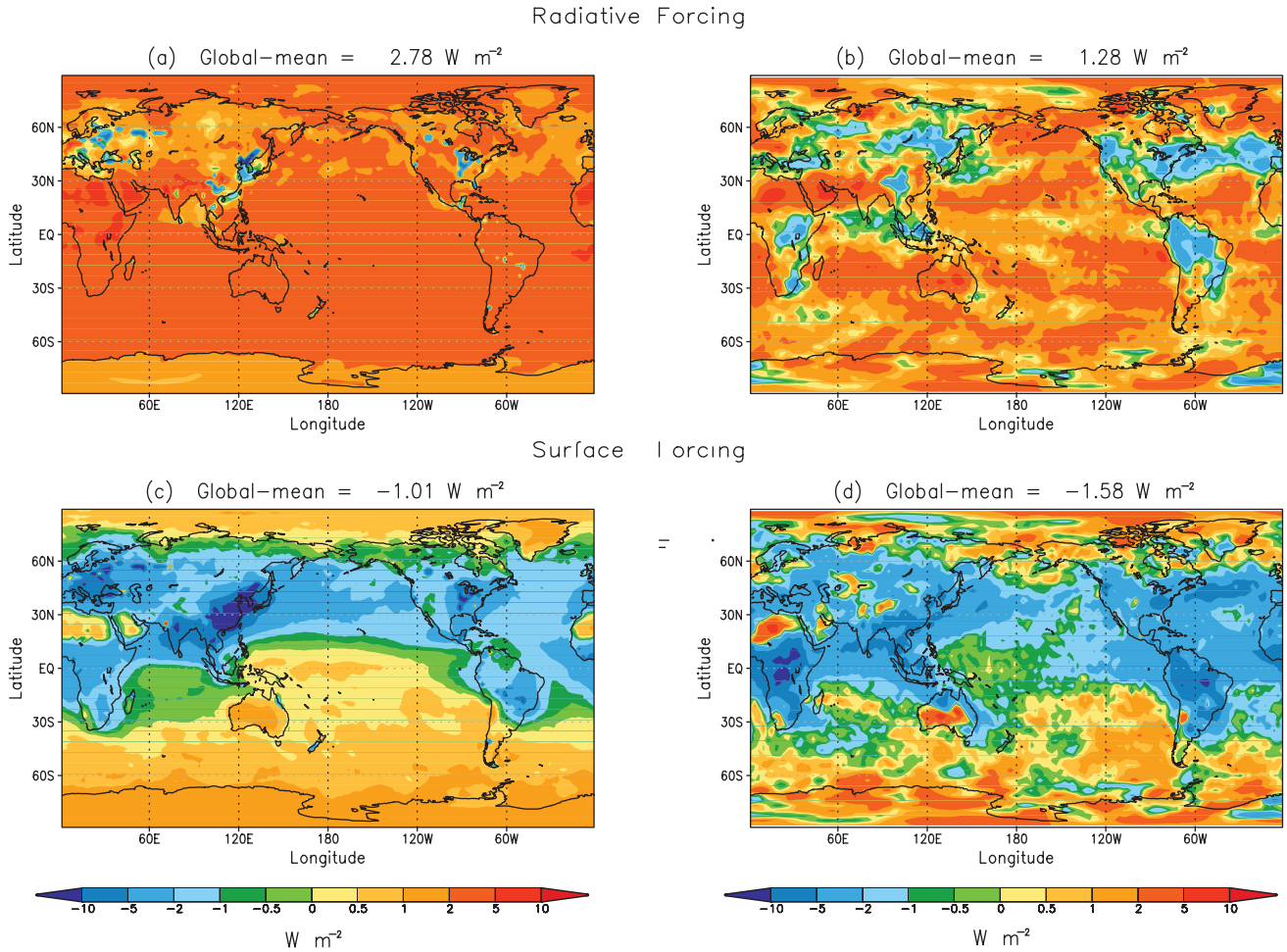


Figure 2.24. *Instantaneous change in the spatial distribution of the net (solar plus longwave) radiative flux (W m^{-2}) due to natural plus anthropogenic forcings between the years 1860 and 2000. Results here are intended to be illustrative examples of these quantities in two different climate models. (a) and (c) correspond to tropopause and surface results using the GFDL CM 2.1 model (adapted from Knutson et al., 2006). (b) and (d) correspond to tropopause and surface results using the MIROC+SPRINTARS model (adapted from Nozawa et al., 2005 and Takemura et al., 2005). Note that the MIROC+SPRINTARS model takes into account the aerosol cloud albedo effect while the CM 2.1 model does not.*

an aerosol cloud albedo effect while the Geophysical Fluid Dynamics Laboratory Coupled Climate Model (GFDL CM2.1) (Delworth et al., 2005; Knutson et al., 2006) does not. Radiative forcing over most of the globe is positive and is dominated by the LLGHGs. This is more so for the SH than for the NH, owing to the pronounced aerosol presence in the mid-latitude NH (see also Figure 2.12), with the regions of substantial aerosol RF clearly manifest over the source-rich continental areas. There are quantitative differences between the two GCMs in the global mean RF, which are indicative of the uncertainties in the RF from the non-LLGHG agents, particularly aerosols (see Section 2.4 and Figure 2.12d). The direct effect of aerosols is seen in the total RF of the GFDL model over NH land regions, whereas the cloud albedo effect dominates the MIROC+SPRINTARS model in the stratocumulus low-latitude ocean regions. Note that the spatial pattern of the forcing is not indicative of the climate response pattern.

Wherever aerosol presence is considerable (namely the NH), the surface forcing is negative, relative to pre-industrial times (Figure 2.24). Because of the aerosol influence on the reduction of the shortwave radiation reaching the surface (see also Figure 2.12f), there is a net (sum of shortwave and longwave) negative surface forcing over a large part of the globe (see also Figure 2.23). In the absence of aerosols, LLGHGs increase the atmospheric longwave emission, with an accompanying increase in the longwave radiative flux reaching the surface. At high latitudes and in parts of the SH, there are fewer anthropogenic aerosols and thus the surface forcing has a positive value, owing to the LLGHGs.

These spatial patterns of RF and surface forcing imply different changes in the NH equator-to-pole gradients for the surface and tropopause. These, in turn, imply different changes in the amount of energy absorbed by the troposphere at low and high latitudes. The aerosol influences are also manifest in the difference between the NH and SH in both RF and surface forcing.

2.10 Global Warming Potentials and Other Metrics for Comparing Different Emissions

2.10.1 Definition of an Emission Metric and the Global Warming Potential

Multi-component abatement strategies to limit anthropogenic climate change need a framework and numerical values for the trade-off between emissions of different forcing agents. Global Warming Potentials or other emission metrics provide a tool that can be used to implement comprehensive and cost-effective policies (Article 3 of the UNFCCC) in a decentralised manner so that multi-gas emitters (nations, industries) can compose mitigation measures, according to a specified emission constraint, by allowing for substitution between different climate agents. The metric formulation will differ depending on whether a long-term climate change constraint has been set (e.g., Manne and Richels, 2001) or no specific long-term constraint has been agreed upon (as in the Kyoto Protocol). Either metric formulation requires knowledge of the contribution to climate change from emissions of various components over time. The metrics assessed in this report are purely physically based. However, it should be noted that many economists have argued that emission metrics need also to account for the economic dimensions of the problem they are intended to address (e.g., Bradford, 2001; Manne and Richels, 2001; Godal, 2003; O'Neill, 2003). Substitution of gases within an international climate policy with a long-term target that includes economic factors is discussed in Chapter 3 of IPCC WGIII AR4. Metrics based on this approach will not be discussed in this report.

A very general formulation of an emission metric is given by (e.g., Kandlikar, 1996):

$$AM_i = \int_0^{\infty} [(I(\Delta C_{(r+i)}(t)) - I(\Delta C_r(t))) \times g(t)]dt$$

where $I(\Delta C_i(t))$ is a function describing the impact (damage and benefit) of change in climate (ΔC) at time t. The expression $g(t)$ is a weighting function over time (e.g., $g(t) = e^{-kt}$ is a simple discounting giving short-term impacts more weight) (Heal, 1997; Nordhaus, 1997). The subscript r refers to a baseline emission path. For two emission perturbations i and j the absolute metric values AM_i and AM_j can be calculated to provide a quantitative comparison of the two emission scenarios. In the special case where the emission scenarios consist of only one component (as for the assumed pulse emissions in the definition of GWP), the ratio between AM_i and AM_j can be interpreted as a relative emission index for component i versus a reference component j (such as CO_2 in the case of GWP).

There are several problematic issues related to defining a metric based on the general formulation given above (Fuglestvedt et al., 2003). A major problem is to define appropriate impact functions, although there have been some initial attempts to do this for a range of possible climate impacts (Hammitt et al., 1996; Tol, 2002; den Elzen et al., 2005). Given that impact functions can be defined, AM calculations would require regionally resolved climate change data (temperature, precipitation, winds, etc.) that would have to be based on GCM results with their inherent uncertainties (Shine et al., 2005a). Other problematic issues include the definition of the temporal weighting function $g(t)$ and the baseline emission scenarios.

Due to these difficulties, the simpler and purely physical GWP index, based on the time-integrated global mean RF of a pulse emission of 1 kg of some compound (i) relative to that of 1 kg of the reference gas CO_2, was developed (IPCC, 1990) and adopted for use in the Kyoto Protocol. The GWP of component i is defined by

$$GWP_i \equiv \frac{\int_0^{TH} RF_i(t)\,dt}{\int_0^{TH} RF_r(t)\,dt} = \frac{\int_0^{TH} a_i \cdot [C_i(t)]\,dt}{\int_0^{TH} a_r \cdot [C_r(t)]\,dt}$$

where TH is the time horizon, RF_i is the global mean RF of component i, a_i is the RF per unit mass increase in atmospheric abundance of component i (radiative efficiency), $[C_i(t)]$ is the time-dependent abundance of i, and the corresponding quantities for the reference gas (r) in the denominator. The numerator and denominator are called the absolute global warming potential (AGWP) of i and r respectively. All GWPs given in this report use CO_2 as the reference gas. The simplifications made to derive the standard GWP index include (1) setting $g(t) = 1$ (i.e., no discounting) up until the time horizon (TH) and then $g(t) = 0$ thereafter, (2) choosing a 1-kg pulse emission, (3) defining the impact function, $I(\Delta C)$, to be the global mean RF, (4) assuming that the climate response is equal for all RF mechanisms and (5) evaluating the impact relative to a baseline equal to current concentrations (i.e., setting $I(\Delta C_r(t)) = 0$). The criticisms of the GWP metric have focused on all of these simplifications (e.g., O'Neill, 2000; Smith and Wigley, 2000; Bradford, 2001; Godal, 2003). However, as long as there is no consensus on which impact function ($I(\Delta C)$) and temporal weighting functions to use (both involve value judgements), it is difficult to assess the implications of the simplifications objectively (O'Neill, 2000; Fuglestvedt et al., 2003).

The adequacy of the GWP concept has been widely debated since its introduction (O'Neill, 2000; Fuglestvedt et al., 2003). By its definition, two sets of emissions that are equal in terms of their total GWP-weighted emissions will not be equivalent in terms of the temporal evolution of climate response (Fuglestvedt et al., 2000; Smith and Wigley, 2000). Using a 100-year time horizon as in the Kyoto Protocol, the effect of current emissions reductions (e.g., during the first commitment period under the Kyoto Protocol) that contain a significant fraction of short-lived species (e.g., CH_4) will give less temperature reductions towards the end of the time horizon, compared to reductions in CO_2 emissions only. Global Warming Potentials can really only be expected to produce identical changes in one measure of climate change – integrated temperature change following emissions impulses – and only under a particular set of assumptions (O'Neill, 2000). The Global Temperature Potential (GTP) metric (see Section 2.10.4.2) provides an alternative approach by comparing global mean temperature change at the end of a given time horizon. Compared to the GWP, the GTP gives equivalent climate response at a chosen time, while putting much less emphasis on near-term climate fluctuations caused by emissions of short-lived species (e.g., CH_4). However, as long as it has not been determined, neither scientifically, economically nor politically, what the proper time horizon for evaluating 'dangerous anthropogenic interference in the climate system' should be, the lack of temporal equivalence does not invalidate the GWP concept or provide guidance as to how to replace it. Although it has several known shortcomings, a multi-gas strategy using GWPs is very likely to have advantages over a CO_2-only strategy (O'Neill, 2003). Thus, GWPs remain the recommended metric to compare future climate impacts of emissions of long-lived climate gases.

Globally averaged GWPs have been calculated for short-lived species, for example, ozone precursors and absorbing aerosols (Fuglestvedt et al., 1999; Derwent et al., 2001; Collins et al., 2002; Stevenson et al., 2004; Berntsen et al., 2005; Bond and Sun, 2005). There might be substantial co-benefits realised in mitigation actions involving short-lived species affecting climate and air pollutants (Hansen and Sato, 2004); however, the effectiveness of the inclusion of short-lived forcing agents in international agreements is not clear (Rypdal et al., 2005). To assess the possible climate impacts of short-lived species and compare those with the impacts of the LLGHGs, a metric is needed. However, there are serious limitations to the use of global mean GWPs for this purpose. While the GWPs of the LLGHGs do not depend on location and time of emissions, the GWPs for short-lived species will be regionally and temporally dependent. The different response of precipitation to an aerosol RF compared to a LLGHG RF also suggests that the GWP concept may be too simplistic when applied to aerosols.

2.10.2 Direct Global Warming Potentials

All GWPs depend on the AGWP for CO_2 (the denominator in the definition of the GWP). The AGWP of CO_2 again depends on the radiative efficiency for a small perturbation of CO_2 from the current level of about 380 ppm. The radiative efficiency per kilogram of CO_2 has been calculated using the same expression as for the CO_2 RF in Section 2.3.1, with an updated background CO_2 mixing ratio of 378 ppm. For a small perturbation from 378 ppm, the RF is 0.01413 W m^{-2} ppm^{-1} (8.7% lower than the TAR value). The CO_2 response function (see Table 2.14) is based on an updated version of the Bern carbon cycle model (Bern2.5CC; Joos et al. 2001), using a background CO_2 concentration of 378 ppm. The increased background concentration of CO_2 means that the airborne fraction of emitted CO_2 (Section 7.3) is enhanced, contributing to an increase in the AGWP for CO_2. The AGWP values for CO_2 for 20, 100, and 500 year time horizons are 2.47×10^{-14}, 8.69×10^{-14}, and 28.6×10^{-14} W m^{-2} yr (kg CO_2)$^{-1}$, respectively. The uncertainty in the AGWP for CO_2 is estimated to be ±15%, with equal contributions from the CO_2 response function and the RF calculation.

Updated radiative efficiencies for well-mixed greenhouse gases are given in Table 2.14. Since the TAR, radiative efficiencies have been reviewed by Montzka et al. (2003) and Velders et al. (2005). Gohar et al. (2004) and Forster et al. (2005) investigated HFC compounds, with up to 40% differences from earlier published results. Based on a variety of radiative transfer codes, they found that uncertainties could be reduced to around 12% with well-constrained experiments. The HFCs studied were HFC-23, HFC-32, HFC-134a and HFC-227ea. Hurley et al. (2005) studied the infrared spectrum and RF of perfluoromethane ($C\Omega F_4$) and derived a 30% higher GWP value than given in the TAR. The RF calculations for the GWPs for CH_4, N_2O and halogen-containing well-mixed greenhouse gases employ the simplified formulas given in Ramaswamy et al. (2001; see Table 6.2 of the TAR). Table 2.14 gives GWP values for time horizons of 20, 100 and 500 years. The species in Table 2.14 are those for which either significant concentrations or large trends in concentrations have been

Table 2.14. *Lifetimes, radiative efficiencies and direct (except for CH_4) GWPs relative to CO_2. For ozone-depleting substances and their replacements, data are taken from IPCC/TEAP (2005) unless otherwise indicated.*

Industrial Designation or Common Name (years)	Chemical Formula	Lifetime (years)	Radiative Efficiency (W m^{-2} ppb^{-1})	Global Warming Potential for Given Time Horizon			
				SAR‡ (100-yr)	20-yr	100-yr	500-yr
Carbon dioxide	CO_2	See below[a]	[b]1.4x10^{-5}	1	1	1	1
Methane[c]	CH_4	12[c]	3.7x10^{-4}	21	72	25	7.6
Nitrous oxide	N_2O	114	3.03x10^{-3}	310	289	298	153
Substances controlled by the Montreal Protocol							
CFC-11	CCl_3F	45	0.25	3,800	6,730	4,750	1,620
CFC-12	CCl_2F_2	100	0.32	8,100	11,000	10,900	5,200
CFC-13	$CClF_3$	640	0.25		10,800	14,400	16,400
CFC-113	CCl_2FCClF_2	85	0.3	4,800	6,540	6,130	2,700
CFC-114	$CClF_2CClF_2$	300	0.31		8,040	10,000	8,730
CFC-115	$CClF_2CF_3$	1,700	0.18		5,310	7,370	9,990
Halon-1301	$CBrF_3$	65	0.32	5,400	8,480	7,140	2,760
Halon-1211	$CBrClF_2$	16	0.3		4,750	1,890	575
Halon-2402	$CBrF_2CBrF_2$	20	0.33		3,680	1,640	503
Carbon tetrachloride	CCl_4	26	0.13	1,400	2,700	1,400	435
Methyl bromide	CH_3Br	0.7	0.01		17	5	1
Methyl chloroform	CH_3CCl_3	5	0.06		506	146	45
HCFC-22	$CHClF_2$	12	0.2	1,500	5,160	1,810	549
HCFC-123	$CHCl_2CF_3$	1.3	0.14	90	273	77	24
HCFC-124	$CHClFCF_3$	5.8	0.22	470	2,070	609	185
HCFC-141b	CH_3CCl_2F	9.3	0.14		2,250	725	220
HCFC-142b	CH_3CClF_2	17.9	0.2	1,800	5,490	2,310	705
HCFC-225ca	$CHCl_2CF_2CF_3$	1.9	0.2		429	122	37
HCFC-225cb	$CHClFCF_2CClF_2$	5.8	0.32		2,030	595	181
Hydrofluorocarbons							
HFC-23	CHF_3	270	0.19	11,700	12,000	14,800	12,200
HFC-32	CH_2F_2	4.9	0.11	650	2,330	675	205
HFC-125	CHF_2CF_3	29	0.23	2,800	6,350	3,500	1,100
HFC-134a	CH_2FCF_3	14	0.16	1,300	3,830	1,430	435
HFC-143a	CH_3CF_3	52	0.13	3,800	5,890	4,470	1,590
HFC-152a	CH_3CHF_2	1.4	0.09	140	437	124	38
HFC-227ea	CF_3CHFCF_3	34.2	0.26	2,900	5,310	3,220	1,040
HFC-236fa	$CF_3CH_2CF_3$	240	0.28	6,300	8,100	9,810	7,660
HFC-245fa	$CHF_2CH_2CF_3$	7.6	0.28		3,380	1030	314
HFC-365mfc	$CH_3CF_2CH_2CF_3$	8.6	0.21		2,520	794	241
HFC-43-10mee	$CF_3CHFCHFCF_2CF_3$	15.9	0.4	1,300	4,140	1,640	500
Perfluorinated compounds							
Sulphur hexafluoride	SF_6	3,200	0.52	23,900	16,300	22,800	32,600
Nitrogen trifluoride	NF_3	740	0.21		12,300	17,200	20,700
PFC-14	CF_4	50,000	0.10	6,500	5,210	7,390	11,200
PFC-116	C_2F_6	10,000	0.26	9,200	8,630	12,200	18,200

Table 2.14 (continued)

Industrial Designation or Common Name	Chemical Formula	Lifetime (years)	Radiative Efficiency (W m^{-2} ppb^{-1})	Global Warming Potential for Given Time Horizon			
				SAR‡ (100-yr)	20-yr	100-yr	500-yr
***Perfluorinated compounds** (continued)*							
PFC-218	C_3F_8	2,600	0.26	7,000	6,310	8,830	12,500
PFC-318	c-C_4F_8	3,200	0.32	8,700	7,310	10,300	14,700
PFC-3-1-10	C_4F_{10}	2,600	0.33	7,000	6,330	8,860	12,500
PFC-4-1-12	C_5F_{12}	4,100	0.41		6,510	9,160	13,300
PFC-5-1-14	C_6F_{14}	3,200	0.49	7,400	6,600	9,300	13,300
PFC-9-1-18	$C_{10}F_{18}$	>1,000[d]	0.56		>5,500	>7,500	>9,500
trifluoromethyl sulphur pentafluoride	SF_5CF_3	800	0.57		13,200	17,700	21,200
Fluorinated ethers							
HFE-125	CHF_2OCF_3	136	0.44		13,800	14,900	8,490
HFE-134	CHF_2OCHF_2	26	0.45		12,200	6,320	1,960
HFE-143a	CH_3OCF_3	4.3	0.27		2,630	756	230
HCFE-235da2	$CHF_2OCHClCF_3$	2.6	0.38		1,230	350	106
HFE-245cb2	$CH_3OCF_2CHF_2$	5.1	0.32		2,440	708	215
HFE-245fa2	$CHF_2OCH_2CF_3$	4.9	0.31		2,280	659	200
HFE-254cb2	$CH_3OCF_2CHF_2$	2.6	0.28		1,260	359	109
HFE-347mcc3	$CH_3OCF_2CF_2CF_3$	5.2	0.34		1,980	575	175
HFE-347pcf2	$CHF_2CF_2OCH_2CF_3$	7.1	0.25		1,900	580	175
HFE-356pcc3	$CH_3OCF_2CF_2CHF_2$	0.33	0.93		386	110	33
HFE-449sl (HFE-7100)	$C_4F_9OCH_3$	3.8	0.31		1,040	297	90
HFE-569sf2 (HFE-7200)	$C_4F_9OC_2H_5$	0.77	0.3		207	59	18
HFE-43-10pccc124 (H-Galden 1040x)	$CHF_2OCF_2OC_2F_4OCHF_2$	6.3	1.37		6,320	1,870	569
HFE-236ca12 (HG-10)	$CHF_2OCF_2OCHF_2$	12.1	0.66		8,000	2,800	860
HFE-338pcc13 (HG-01)	$CHF_2OCF_2CF_2OCHF_2$	6.2	0.87		5,100	1,500	460
Perfluoropolyethers							
PFPMIE	$CF_3OCF(CF_3)CF_2OCF_2OCF_3$	800	0.65		7,620	10,300	12,400
Hydrocarbons and other compounds – Direct Effects							
Dimethylether	CH_3OCH_3	0.015	0.02		1	1	<<1
Methylene chloride	CH_2Cl_2	0.38	0.03		31	8.7	2.7
Methyl chloride	CH_3Cl	1.0	0.01		45	13	4

Notes:

[a] The CO_2 response function used in this report is based on the revised version of the Bern Carbon cycle model used in Chapter 10 of this report (Bern2.5CC; Joos et al. 2001) using a background CO_2 concentration value of 378 ppm. The decay of a pulse of CO_2 with time t is given by

$$a_0 + \sum_{i=1}^{3} a_i \cdot e^{-t/\tau_i}$$

Where $a_0 = 0.217$, $a_1 = 0.259$, $a_2 = 0.338$, $a_3 = 0.186$, $\tau_1 = 172.9$ years, $\tau_2 = 18.51$ years, and $\tau_3 = 1.186$ years.

[b] The radiative efficiency of CO_2 is calculated using the IPCC (1990) simplified expression as revised in the TAR, with an updated background concentration value of 378 ppm and a perturbation of +1 ppm (see Section 2.10.2).

[c] The perturbation lifetime for methane is 12 years as in the TAR (see also Section 7.4). The GWP for methane includes indirect effects from enhancements of ozone and stratospheric water vapour (see Section 2.10.3.1).

[d] Shine et al. (2005c), updated by the revised AGWP for CO_2. The assumed lifetime of 1,000 years is a lower limit.

[e] Hurley et al. (2005)

[f] Robson et al. (2006)

[g] Young et al. (2006)

observed or a clear potential for future emissions has been identified. The uncertainties of these direct GWPs are taken to be ±35% for the 5 to 95% (90%) confidence range.

2.10.3 Indirect GWPs

Indirect radiative effects include the direct effects of degradation products or the radiative effects of changes in concentrations of greenhouse gases caused by the presence of the emitted gas or its degradation products. Direct effects of degradation products for the greenhouse gases are not considered to be significant (WMO, 2003). The indirect effects discussed here are linked to ozone formation or destruction, enhancement of stratospheric water vapour, changes in concentrations of the OH radical with the main effect of changing the lifetime of CH_4, and secondary aerosol formation. Uncertainties for the indirect GWPs are generally much higher than for the direct GWPs. The indirect GWP will in many cases depend on the location and time of the emissions. For some species (e.g., NO_x) the indirect effects can be of opposite sign, further increasing the uncertainty of the net GWP. This can be because background levels of reactive species (e.g., NO_x) can affect the chemical response nonlinearly, and/or because the lifetime or the radiative effects of short-lived secondary species formed can be regionally dependent. Thus, the usefulness of the global mean GWPs to inform policy decisions can be limited. However, they are readily calculable and give an indication of the total potential of mitigating climate change by including a certain forcing agent in climate policy. Following the approach taken by the SAR and the TAR, the CO_2 produced from oxidation of CH_4, CO and NMVOCs of fossil origin is not included in the GWP estimates since this carbon has been included in the national CO_2 inventories. This issue may need to be reconsidered as inventory guidelines are revised.

2.10.3.1 Methane

Four indirect radiative effects of CH_4 emissions have been identified (see Prather et al., 2001; Ramaswamy et al., 2001). Methane enhances its own lifetime through changes in the OH concentration: it leads to changes in tropospheric ozone, enhances stratospheric water vapour levels, and produces CO_2. The GWP given in Table 2.14 includes the first three of these effects. The lifetime effect is included by adopting a perturbation lifetime of 12 years (see Section 7.4). The effect of ozone production is still uncertain, and as in the TAR, it is included by enhancing the net of the direct and the lifetime effect by 25%. The estimate of RF caused by an increase in stratospheric water vapour has been increased significantly since the TAR (see Section 2.3.7). This has also been taken into account in the GWP estimate for CH_4 by increasing the enhancement factor from 5% (TAR) to 15%. As a result, the 100-year GWP for CH_4 has increased from 23 in the TAR to 25.

2.10.3.2 Carbon Monoxide

The indirect effects of CO occur through reduced OH levels (leading to enhanced concentrations of CH_4) and enhancement of ozone. The TAR gave a range of 1.0 to 3.0 for the 100-year GWP. Since the TAR, Collins et al. (2002) and Berntsen et al. (2005) have calculated GWPs for CO emissions that range between 1.6 and 2.0, depending on the location of the emissions. Berntsen et al. (2005) found that emissions of CO from Asia had a 25% higher GWP compared to European emissions. Averaging over the TAR values and the new estimates give a mean of 1.9 for the 100-year GWP for CO.

2.10.3.3 Non-methane Volatile Organic Compounds

Collins et al. (2002) calculated indirect GWPs for 10 NMVOCs with a global three-dimensional Lagrangian chemistry-transport model. Impacts on tropospheric ozone, CH_4 (through changes in OH) and CO_2 have been considered, using either an 'anthropogenic' emission distribution or a 'natural' emission distribution depending on the main sources for each gas. The indirect GWP values are given in Table 2.15. Weighting these GWPs by the emissions of the respective compounds gives a weighted average 100-year GWP of 3.4. Due to their short lifetimes and the nonlinear chemistry involved in ozone and OH chemistry, there are significant uncertainties in the calculated GWP values. Collins et al. (2002) estimated an uncertainty range of –50% to +100%.

2.10.3.4 Nitrogen Oxides

The short lifetime and complex nonlinear chemistry, which cause two opposing indirect effects through ozone enhancements and CH_4 reductions, make calculations of GWP for NO_x emissions very uncertain (Shine et al., 2005a). In addition, the effect of nitrate aerosol formation (see Section 2.4.4.5), which has not yet been included in model studies calculating GWPs for NO_x, can be significant. Due to the nonlinear chemistry, the net RF of NO_x emissions will depend strongly on the location of emission and, with a strict definition of a pulse emission for the GWP, also on timing (daily, seasonal) of the emissions (Fuglestvedt et al., 1999; Derwent et al., 2001; Wild et al., 2001; Stevenson et al., 2004; Berntsen et al., 2005, 2006). Due to the lack of agreement even on the sign of the global mean GWP for NO_x among the different studies and the omission of the nitrate aerosol effect, a central estimate for the 100-year GWP for NO_x is not presented.

2.10.3.5 Halocarbons

Chlorine- and bromine-containing halocarbons lead to ozone depletion when the halocarbon molecules are broken down in the stratosphere and chlorine or bromine atoms are released. Indirect GWPs for ozone-depleting halocarbons are estimated in Velders et al. (2005; their Table 2.7). These are based on

observed ozone depletion between 1980 and 1990 for 2005 emissions using the Daniel et al. (1995) formulation. Velders et al. (2005) did not quote net GWPs, pointing out that the physical characteristics of the CFC warming effect and ozone cooling effect were very different from each other.

2.10.3.6 Hydrogen

The main loss of hydrogen (H_2) is believed to be through surface deposition, but about 25% is lost through oxidation by OH. In the stratosphere, this enhances the water vapour concentrations and thus also affects the ozone concentrations. In the troposphere, the chemical effects are similar to those of CO, leading to ozone production and CH_4 enhancements (Prather, 2003). Derwent et al. (2001) calculated an indirect 100-year GWP for the tropospheric effects of H_2 of 5.8, which includes the effects of CH_4 lifetime and tropospheric ozone.

2.10.4 New Alternative Metrics for Assessing Emissions

While the GWP is a simple and straightforward index to apply for policy makers to rank emissions of different greenhouse gases, it is not obvious on what basis 'equivalence' between emissions of different species is obtained (Smith and Wigley, 2000; Fuglestvedt et al., 2003). The GWP metric is also problematic for short-lived gases or aerosols (e.g., NO_x or BC aerosols), as discussed above. One alternative, the RF index (RFI) introduced by IPCC (1999), should not be used as an emission metric since it does not account for the different residence times of different forcing agents.

2.10.4.1 Revised GWP Formulations

2.10.4.1.2 Including the climate efficacy in the GWP

As discussed in Section 2.8.5, the climate efficacy can vary between different forcing agents (within 25% for most realistic RFs). Fuglestvedt et al. (2003) proposed a revised GWP concept that includes the efficacy of a forcing agent. Berntsen et al. (2005) calculated GWP values in this way for NO_x and CO emissions in Europe and in South East Asia. The efficacies are less uncertain than climate sensitivities. However, Berntsen et al. (2005) showed that for ozone produced by NO_x emissions the climate efficacies will also depend on the location of the emissions.

2.10.4.2 The Global Temperature Potential

Shine et al. (2005b) proposed the GTP as a new relative emission metric. The GTP is defined as the ratio between the

Table 2.15. *Indirect GWPs (100-year) for 10 NMVOCs from Collins et al. (2002) and for NO_x emissions (on N-basis) from Derwent et al. (2001), Wild et al. (2001), Berntsen et al. (2005) and Stevenson et al. (2004). The second and third columns respectively represent the methane and ozone contribution to the net GWP and the fourth column represents the net GWP.*

Organic Compound/Study	GWP^{CH_4}	GWP^{O_3}	GWP
Ethane (C_2H_6)	2.9	2.6	5.5
Propane (C_3H_8)	2.7	0.6	3.3
Butane (C_4H_{10})	2.3	1.7	4.0
Ethylene (C_2H_4)	1.5	2.2	3.7
Propylene (C_3H_6)	–2.0	3.8	1.8
Toluene (C_7H_8)	0.2	2.5	2.7
Isoprene (C_5H_8)	1.1	1.6	2.7
Methanol (CH_3OH)	1.6	1.2	2.8
Acetaldehyde (CH_3CHO)	–0.4	1.7	1.3
Acetone (CH_3COCH_3)	0.3	0.2	0.5
Derwent et al. NH surface NO_x[a,b]	–24	11	–12
Derwent et al. SH surface NO_x[a,b]	–64	33	–31
Wild et al., industrial NO_x	–44	32	–12
Berntsen et al., surface NO_x Asia	–31 to –42[c]	55 to 70[c]	25 to 29[c]
Berntsen et al., surface NO_x Europe	–8.6 to –11[c]	8.1 to 12.7	–2.7 to +4.1[c]
Derwent et al., Aircraft NO_x[a,b]	–145	246	100
Wild et al., Aircraft NO_x	–210	340	130
Stevenson et al. Aircraft NO_x	–159	155	–3

Notes:

[a] Corrected values as described in Stevenson et al. (2004).

[b] For January pulse emissions.

[c] Range from two three-dimensional chemistry transport models and two radiative transfer models.

global mean surface temperature change at a given future time horizon (TH) following an emission (pulse or sustained) of a compound x relative to a reference gas r (e.g., CO_2):

$$GTP_x^{TH} = \frac{\Delta T_x^H}{\Delta T_r^H}$$

where ΔT_x^H denotes the global mean surface temperature change after H years following an emission of compound x. The GTPs do not require simulations with AOGCMs, but are given as transparent and simple formulas that employ a small number of input parameters required for calculation. Note that while the GWP is an integral quantity over the time horizon (i.e., the contribution of the RF at the beginning and end of the time horizon is exactly equal), the GTP uses the temperature change at time H (i.e., RF closer to time H contributes relatively more). The GTP metric requires knowledge of the same parameters as the GWP metric (radiative efficiency and lifetimes), but in addition, the response times for the climate system must be known, in particular if the lifetime of component x is very different from the lifetime of the reference gas. Differences in climate efficacies can easily be incorporated into the GTP metric. Due to the inclusion of the response times for the climate system, the GTP values for pulse emissions of gases with shorter lifetimes than the reference gas will be lower than the corresponding GWP values. As noted by Shine et al. (2005b), there is a near equivalence between the GTP for sustained emission changes and the pulse GWP. The GTP metric has the potential advantage over GWP that it is more directly related to surface temperature change.

References

Abdul-Razzak, H., and S.J. Ghan, 2002: A parametrization of aerosol activation: 3. Sectional representation. *J. Geophys. Res.*, **107**(D3), 4026, doi:10.1029/2001JD000483.

Abel, S.J., E.J. Highwood, J.M. Haywood, and M.A. Stringer, 2005: The direct radiative effect of biomass burning aerosol over southern Africa. *Atmos. Chem. Phys. Discuss.*, **5**, 1165–1211.

Abel, S.J., et al., 2003: Evolution of biomass burning aerosol properties from an agricultural fire in southern Africa. *Geophys. Res. Lett.*, **30**(15), 1783, doi:10.1029/2003GL017342.

Ackerman, A.S, M.P. Kirkpatrick, D.E. Stevens, and O.B. Toon, 2004: The impact of humidity above stratiform clouds on indirect aerosol climate forcing. *Nature*, **432**, 1014–1017.

Ackerman, A.S., et al., 2000a: Reduction of tropical cloudiness by soot. *Science*, **288**, 1042–1047.

Ackerman, A.S., et al., 2000b: Effects of aerosols on cloud albedo: evaluation of Twomey's parametrization of cloud susceptibility using measurements of ship tracks. *J. Atmos. Sci.*, **57**, 2684–2695.

Adams, P.J. and J.H. Seinfeld, 2002: Predicting global aerosol size distributions in general circulation models. *J. Geophys. Res.*, **107**(D19), 4370, doi:10.1029/2001JD001010.

Adams, P.J., et al., 2001: General circulation model assessment of direct radiative forcing by the sulfate-nitrate-ammonium-water inorganic aerosol system. *J. Geophys. Res.*, **106**(D1), 1097–1112.

Albrecht, B., 1989: Aerosols, cloud microphysics and fractional cloudiness. *Science*, **245**, 1227–1230.

Allan, W., et al., 2005: Interannual variation of ^{13}C in tropospheric methane: Implications for a possible atomic chlorine sink in the marine boundary layer. *J. Geophys. Res.*, **110**, D11306, doi:10.1029/2004JD005650.

Ammann, C.M., G.A. Meehl, W.M. Washington, and C.S. Zender, 2003: A monthly and latitudinally varying volcanic forcing dataset in simulations of 20th century climate. *Geophys. Res. Lett.*, **30**(12), 1657, doi:10.1029/2003GL016875.

Anderson, T.L., et al., 2003: Climate forcing by aerosols: a hazy picture. *Science*, **300**, 1103–1104.

Anderson, T.L., et al., 2005a. Testing the MODIS satellite retrieval of aerosol fine-mode fraction. *J. Geophys. Res.*, **110,** D18204, doi:10.1029/2005JD005978.

Anderson, T.L., et al., 2005b: An "A-Train" strategy for quantifying direct climate forcing by anthropogenic aerosols. *Bull. Am. Meteorol. Soc.*, **86**, 1795–1809.

Andreae, M.O., and P. Merlet, 2001: Emission of trace gases and aerosols from biomass burning. *Global Biogeochem. Cycles*, **15**(4), 955–966, doi:10.1029/2000GB001382.

Andreae, M.O., et al., 2004: Atmospheric science: smoking rain clouds over the Amazon. *Science*, **303**(5662), 1337–1341.

Andres, R.J., G. Marland, T. Boden, and S. Bischof, 2000: Carbon dioxide emissions from fossil fuel consumption and cement manufacture, 1751-1991, and an estimate of their isotopic composition and latitudinal distribution. In: *The Carbon Cycle* [Wigley, T.M.L., and D.S. Schimel (eds.)]. Cambridge University Press, Cambridge, UK, pp. 53–62.

Andronova, N.G., et al., 1999: Radiative forcing by volcanic aerosols from 1850 to 1994. *J. Geophys. Res.*, **104**(D14), 16807–16826.

Antuña, J.C., et al., 2003: Spatial and temporal variability of the stratospheric aerosol cloud produced by the 1991 Mount Pinatubo eruption. *J. Geophys. Res.*, **108**, 4624, doi:10.1029/2003JD003722.

Asano, S., et al., 2002: Two case studies of winter continental-type water and mixed-phased stratocumuli over the sea. II: Absorption of solar radiation. *J. Geophys. Res.*, **107**(D21), 4570, doi:10.1029/2001JD001108.

Baliunas, S., and R. Jastrow, 1990: Evidence for long-term brightness changes of solar-type stars. *Nature*, **348**, 520–522.

Balkanski, Y., et al., 2004: Global emissions of mineral aerosol: formulation and validation using satellite imagery. In: *Emission of Atmospheric Trace Compounds* [Granier, C., P. Artaxo, and C.E. Reeves (eds.)]. Kluwer, Amsterdam, pp. 239–267.

Bange, H.W., S. Rapsomanikis, and M.O. Andreae, 1996: Nitrous oxide in coastal waters. *Global Biogeochem. Cycles*, **10**(1), 197–207.

Baran, A.J., and J.S. Foot, 1994: A new application of the operational sounder HIRS in determining a climatology of sulfuric acid aerosol from the Pinatubo eruption. *J. Geophys. Res.*, **99**(D12), 25673–25679.

Barnes, J.E., and D.J. Hoffman, 1997: Lidar measurements of stratospheric aerosol over Mauna Loa Observatory. *Geophys. Res. Lett.*, **24**(15), 1923–1926.

Barnston, A.G., and P.T. Schickedanz, 1984: The effect of irrigation on warm season precipitation in the southern Great Plains. *J. Appl. Meteorol.*, **23**, 865–888.

Bartholome, E., and A.S. Belward, 2005: GLC2000: a new approach to global land cover mapping from Earth observation data. *Int. J. Remote Sens.*, **26**, 1959–1977.

Bates, T.S., et al., 2006: Aerosol direct radiative effects over the northwest Atlantic, northwest Pacific, and North Indian Oceans: estimates based on in situ chemical and optical measurements and chemical transport modelling. *Atmos. Chem. Phys. Discuss.*, **6**, 175–362.

Bauer, S.E., and D. Koch, 2005: Impact of heterogeneous sulfate formation at mineral dust surfaces on aerosol loads and radiative forcing in the Goddard Institute for Space Studies general circulation model. *J. Geophys. Res.*, **110**, D17202, doi:10.1029/2005JD005870.

Bauman, J.J., P.B. Russell, M.A. Geller, and P. Hamill, 2003: A stratospheric aerosol climatology from SAGE II and CLAES measurements: 2. Results and comparisons, 1984-1999. *J. Geophys. Res.*, **108**(D13), 4383, doi:10.1029/2002JD002993.

Beheng, K.D., 1994: A parametrization of warm cloud microphysical conversion process. *Atmos. Res.*, **33**, 193–206.

Bekki, S., K. Law, and J. Pyle, 1994: Effect of ozone depletion on atmospheric CH_4 and CO concentrations. *Nature*, **371**, 595–597.

Bellouin, N., O. Boucher, D. Tanré, and O. Dubovik, 2003: Aerosol absorption over the clear-sky oceans deduced from POLDER-1 and AERONET observations. *Geophys. Res. Lett.*, **30**(14), 1748, doi:10.1029/2003GL017121.

Bellouin, N., O. Boucher, J. Haywood, and M.S. Reddy, 2005: Global estimates of aerosol direct radiative forcing from satellite measurements. *Nature*, **438**, 1138–1141.

Benestad, R.E., 2005: A review of the solar cycle length estimates. *Geophys. Res. Lett.*, **32**, L15714, doi:10.1029/2005GL023621.

Bergamaschi, P., et al., 2005: Inverse modelling of national and European CH_4 emissions using the atmospheric zoom model TM5. *Atmos. Chem. Phys.*, **5**, 2431–2460.

Bergstrom, R.W., P. Pilewskie, B. Schmid, and P.B. Russell, 2003: Estimates of the spectral aerosol single scattering albedo and aerosol radiative effects during SAFARI 2000. *J. Geophys. Res.*, **108**(D13), 8474, doi:10.1029/2002JD002435.

Berntsen, T.K., et al., 2005: Climate response to regional emissions of ozone precursors; sensitivities and warming potentials. *Tellus*, **4B**, 283–304.

Berntsen, T.K., et al., 2006: Abatement of greenhouse gases: does location matter? *Clim. Change*, **74**, 377–411.

Berry, E.X., 1967: Cloud droplet growth by collection. *J. Atmos. Sci.*, **24**, 688–701.

Betts, R.A., 2000: Offset of the potential carbon sink from boreal forestation by decreases in surface albedo. *Nature*, **408**(6809), 187–189.

Betts, R.A., 2001: Biogeophysical impacts of land use on present-day climate: near-surface temperature change and radiative forcing. *Atmos. Sci. Lett.*, **2**(1–4), doi:1006/asle.2001.0023.

Betts, R.A., and M.J. Best, 2004: *Relative impact of radiative forcing, landscape effects and local heat sources on simulated climate change in urban areas.* BETWIXT Technical Briefing Note No. 6, Met Office, Exeter, UK, 15 pp.

Betts, R.A., P.M. Cox, S.E. Lee, and F.I. Woodward, 1997: Contrasting physiological and structural vegetation feedbacks in climate change simulations. *Nature*, **387**, 796–799.

Betts, R.A., P.D. Falloon, K.K. Goldewijk, and N. Ramankutty, 2007: Biogeophysical effects of land use on climate: model simulations of radiative forcing and large-scale temperature change. *Agric. For. Meteorol*., 142, 216-233.

Betts, R.A., et al., 2004: The role of ecosystem-atmosphere interactions in simulated Amazonian precipitation decrease and forest dieback under global climate warming. *Theor. Appl. Climatol*., **78**, 157–175.

Bigler, M., et al., 2002: Sulphate record from a northeast Greenland ice core over the last 1200 years based on continuous flow analysis. *Ann. Glaciol*., 35, 250–256.

Bingen, C., D. Fussen, and F. Vanhellemont, 2004: A global climatology of stratospheric aerosol size distribution parameters derived from SAGE II data over the period 1984-2000: 2. Reference data. *J. Geophys. Res.*, **109**, D06202, doi:10.1029/2003JD003511.

Blake, D., and F. Rowland, 1988: Continuing worldwide increase in tropospheric methane, 1978 to 1987. *Science*, **239**, 1129–1131.

Blake, N.J., et al., 2001: Large-scale latitudinal and vertical distributions of NMHCs and selected halocarbons in the troposphere over the Pacific Ocean during the March-April 1999 Pacific Exploratory Mission (PEM-Tropics B). *J. Geophys. Res*., **106**, 32627–32644.

Bluth, G.J.S., W.I. Rose, I.E. Sprod, and A.J. Krueger, 1997: Stratospheric loading of sulfur from explosive volcanic eruptions. *J. Geol*., **105**, 671–683.

Bluth, G.J.S., et al., 1992: Global tracking of the SO_2 clouds from the June 1991 Mount Pinatubo eruptions. *Geophys. Res. Lett*., **19**(2), 151–154, doi:10.1029/91GL02792.

Boberg, F., and H. Lundstedt, 2002: Solar wind variations related to fluctuations of the North Atlantic Oscillation. *Geophys. Res. Lett*., **29**(15), doi:10.1029/2002GL014903.

Boer, G.J., and B. Yu, 2003a: Climate sensitivity and climate state. *Clim. Dyn.*, **21**, 167–176.

Boer, G.J., and B. Yu, 2003b: Climate sensitivity and response. *Clim. Dyn*., **20**, 415–429.

Bond, T.C., 2001: Spectral dependence of visible light absorption by carbonaceous particles emitted from coal combustion. *Geophys. Res. Lett.*, **28**(21), 4075–4078.

Bond, T.C., and H. Sun, 2005: Can reducing black carbon emissions counteract global warming? *Environ. Sci. Technol*., **39**, 5921–5926.

Bond, T.C., et al., 1999: Light absorption by primary particle emissions from a lignite burning plant. *Environ. Sci.Technol.*, **33**, 3887–3891.

Bond, T.C., et al., 2004: A technology-based global inventory of black and organic carbon emissions from combustion. *J. Geophys. Res*., **109**, D14203, doi:10.1029/2003JD003697.

Born, M., H. Dorr, and I. Levin, 1990: Methane consumption in aerated soils of the temperate zone. *Tellus* , **42B**, 2–8.

Bortz, S.E., and M.J. Prather, 2006: Ozone, water vapor, and temperature in the upper tropical troposphere: Variations over a decade of MOZAIC Measurements. *J. Geophys. Res*., **111**, D05305, doi:10.1029/2005JD006512.

Boucher, O., 1999: Air traffic may increase cirrus cloudiness. *Nature*, **397**, 30–31.

Boucher, O., and U. Lohmann, 1995: The sulfate-CCN-cloud albedo effect: a sensitivity study using two general circulation models. *Tellus*, **47B**, 281–300.

Boucher, O., and D. Tanré, 2000: Estimation of the aerosol perturbation to the Earth's radiative budget over oceans using POLDER satellite aerosol retrievals. *Geophys. Res. Lett.*, **27**(8), 1103–1106.

Boucher, O., and J. Haywood, 2001: On summing the components of radiative forcing of climate change. *Clim. Dyn*., **18**, 297–302.

Boucher, O., and M. Pham, 2002: History of sulfate aerosol radiative forcings. *Geophys. Res. Lett*., **29**(9), 22–25.

Boucher, O., H. Le Treut, and M.B. Baker, 1995: Precipitation and radiation modeling in a general circulation model: introduction of cloud microphysical processes. *J. Geophys. Res.*, **100**(D8), 16395–16414.

Boucher, O., G. Myhre, and A. Myhre, 2004: Direct human influence of irrigation on atmospheric water vapour and climate. *Clim. Dyn*., **22**, 597–604.

Bounoua, L., et al., 2002: Effects of land cover conversion on surface climate. *Clim. Change*, **52**, 29–64.

Bousquet, P., et al., 2005: Two decades of OH variability as inferred by an inversion of atmospheric transport and chemistry of methyl chloroform. *Atmos. Chem. Phys.*, **5**, 1679–1731.

Bower, K.N., et al., 1994: A parametrization of warm clouds for use in atmospheric general circulation models. *J. Atmos. Sci*., **51**, 2722–2732.

BP, 2006: *Quantifying Energy: BP Statistical Review of World Energy June 2006*. BP p.l.c., London, 45 pp., http://www.bp.com/productlanding.do?categoryId=6842&contentId=7021390.

Bradford, D.F., 2001: Global change: time, money and tradeoffs. *Nature*, **410**, 649–650, doi:10.1038/35070707.

Brasseur, G., and C. Granier, 1992: Mount Pinatubo aerosols, chlorofluorocarbons and ozone depletion. *Science*, **257**, 1239–1242.

Brenguier, J.L., H. Pawlowska, and L. Schuller, 2003: Cloud microphysical and radiative properties for parametrization and satellite monitoring of the indirect effect of aerosol on climate. *J. Geophys. Res.*, **108**(D15), 8632, doi:10.1029/2002JD002682.

Brenguier, J.L., et al., 2000a: Radiative properties of boundary layer clouds: droplet effective radius versus number concentration. *J. Atmos. Sci*., **57**, 803–821.

Brenguier, J.L., et al., 2000b: An overview of the ACE-2 CLOUDYCOLUMN closure experiment. *Tellus*, **52B**, 815–827.

Bréon, F-M., and M. Doutriaux-Boucher, 2005: A comparison of cloud droplet radii measured from space. *IEEE Trans. Geosci. Remote. Sens.*, **43**, 1796–1805, doi:10.1109/TGRS.2005.852838.

Bréon, F.-M., D. Tanré, and S. Generoso, 2002: Aerosol effect on cloud droplet size monitored from satellite. *Science*, **295**, 834–838.

Broccoli, A.J., et al., 2003: Twentieth-century temperature and precipitation trends in ensemble climate simulations including natural and anthropogenic forcing. *J. Geophys. Res.*, **108**(D24), 4798, doi:10.1029/2003JD003812.

Brock, C.A., et al., 2004: Particle characteristics following cloud-modified transport from Asia to North America. *J. Geophys. Res*., **109**, 1–17.

Brovkin, V.M., et al., 2004. Role of land cover changes for atmospheric CO_2 increase and climate change during the last 150 years. *Global Change Biol.*, **10**, 1253–1266.

Brovkin, V.M., et al., 2006: Biogeophysical effects of historical land cover changes simulated by six earth system models of intermediate complexity. *Clim. Dyn*., **26**(6), 587–600.

Cakmur, R.V., et al., 2006: Constraining the magnitude of the global dust cycle by minimizing the difference between a model and observations. *J. Geophys. Res.*, **111**, doi:10.1029/2005JD005791.

Campbell, J.R., et al., 2003: Micropulse Lidar observations of tropospheric aerosols over northeastern South Africa during the ARREX and SAFARI-2000 dry season experiments. *J. Geophys. Res*., **108**(D13), 8497, doi:10.1029/2002JD002563.

Carslaw, K.S., R.G. Harrison, and J. Kirkby, 2002: Atmospheric science: Cosmic rays, clouds, and climate. *Science*, **298**, 1732–1737.

Chapman, G.A., A.M. Cookson, and J.J. Dobias, 1996: Variations in total solar irradiance during solar cycle 22. *J. Geophys. Res*., **101**, 13541–13548.

Chase, T.N., et al., 2000: Simulated impacts of historical land cover changes on global climate in northern winter. *Clim. Dyn*., **16**, 93–105.

Chen, Y., and J.E. Penner, 2005: Uncertainty analysis of the first indirect aerosol effect. *Atmos. Chem. Phys*., **5**, 2935–2948.

Chen, Y.-H., and R.G. Prinn, 2005: Atmospheric modelling of high- and low-frequency methane observations: Importance of interannually varying transport. *J. Geophys. Res*., **110**, D10303, doi:10.1029/2004JD005542.

Chen, Y.-H., and R.G. Prinn, 2006: Estimation of atmospheric methane emissions between 1996-2001 using a 3D global chemical transport model. *J. Geophys. Res.*, **111**, D10307, doi:10.1029/2005JD006058.

Chiapello, I., C. Moulin, and J.M. Prospero, 2005: Understanding the long-term variability of African dust transport across the Atlantic as recorded in both Barbados surface concentrations and large-scale Total Ozone Mapping Spectrometer (TOMS) optical thickness. *J. Geophys. Res.*, **110**, D18S10, doi:10.1029/2004JD005132.

Chipperfield, M.P., W.J. Randel, G.E. Bodeker, and P. Johnston, 2003: Global ozone: past and future. In: *Scientific Assessment of Ozone Depletion: 2002* [Ennis, C.A. (ed.)]. World Meteorological Organization, Geneva, pp. 4.1–4.90.

Chou, M.-D., P.-K. Chan, and M. Wang, 2002: Aerosol radiative forcing derived from SeaWiFS-retrieved aerosol optical properties. *J. Atmos. Sci.*, **59**, 748–757.

Christiansen, B., 1999: Radiative forcing and climate sensitivity: the ozone experience. *Q. J. R. Meteorol. Soc.*, **125**, 3011–3035.

Christopher, S.A., and J. Zhang, 2004: Cloud-free shortwave aerosol radiative effect over oceans: strategies for identifying anthropogenic forcing from Terra satellite measurements. *Geophys. Res. Lett.*, **31**, L18101, doi:10.1029/2004GL020510.

Christopher, S.A., J. Zhang, Y.J. Kaufman, and L. Remer, 2006: Satellite-based assessment of the top of the atmosphere anthropogenic aerosol radiative forcing over cloud-free oceans. *Geophys Res. Lett*., **111**, L15816, doi:10.1029/2005GL025535.

Chu, D.A., et al., 2002: Validation of MODIS aerosol optical depth retrieval over land. *Geophys. Res. Lett*., **29**(12), doi:10.1029/2001GL013205.

Chu, D.A., et al., 2005: Evaluation of aerosol properties over ocean from Moderate Resolution Imaging Spectroradiometer (MODIS) during ACE-Asia. *J. Geophys. Res*., **110**, D07308, doi:10.1029/2004JD005208.

Chuang, C.C., and J.E. Penner, 1995: Effects of anthropogenic sulfate on cloud drop nucleation and optical properties. *Tellus*, **47B**, 566–577.

Chuang, C.C., et al., 1997: An assessment of the radiative effects of anthropogenic sulfate. *J. Geophys. Res*., **102**(D3), 3761–3778.

Chuang, C.C., et al., 2002: Cloud susceptibility and the first aerosol indirect forcing: Sensitivity to black carbon and aerosol concentrations. *J. Geophys. Res*., **107**(D21), 4564, doi:10.1029/2000JD000215.

Chuang, P.Y., 2003: Measurement of the timescale of hygroscopic growth for atmospheric aerosols. *J. Geophys. Res.*, **108**(D9), 5–13.

Chung, C.E., V. Ramanathan, D. Kim, and I.A. Podgorny, 2005: Global anthropogenic aerosol direct forcing derived from satellite and ground-based observations. *J. Geophys. Res*., **110**, D24207, doi:10.1029/2005JD006356.

Chung, S.H., and J.H. Seinfeld, 2002: Global distribution and climate forcing of carbonaceous aerosols. *J. Geophys. Res.*, **107**, doi:10.1029/2001JD001397.

Chylek, P., and J. Wong, 1995: Effect of absorbing aerosols on global radiation budget. *Geophys. Res. Lett*., **22**(8), 929–931.

Chylek, P., B. Henderson, and M. Mishchenko, 2003: Aerosol radiative forcing and the accuracy of satellite aerosol optical depth retrieval. *J. Geophys. Res*., **108**(D24), 4764, doi:10.1029/2003JD004044.

Clarke, A.D., et al., 2004: Size distributions and mixtures of dust and black carbon aerosol in Asian outflow: Physiochemistry and optical properties. *J. Geophys. Res.*, **109**, D15S09, doi:10.1029/2003JD004378.

Claquin, T., M. Schulz, and Y. Balkanski, 1999: Modeling the mineralogy of atmospheric dust. *J. Geophys. Res.*, **104**(D18), 22243–22256.

Coen, M.C., et al., 2004: Saharan dust events at the Jungfraujoch: detection by wavelength dependence of the single scattering albedo and first climatology analysis. *Atmos. Chem. Phys*., **4**, 2465–2480.

Collins, W.D., et al., 2001: Simulating aerosols using a chemical transport model with assimilation of satellite aerosol retrievals: Methodology for INDOEX. *J. Geophys. Res*., **106**(D7), 7313–7336.

Collins, W.D., et al., 2006: Radiative forcing by well-mixed greenhouse gases: Estimates from climate models in the IPCC AR4. *J. Geophys. Res.*, **111**, D14317, doi:10.1029/2005JD006713.

Collins, W.J., R.G. Derwent, C.E. Johnson, and D.S. Stevenson, 2002: The oxidation of organic compounds in the troposphere and their global warming potentials. *Clim. Change*, **52**, 453–479.

Considine, D.B., J.E. Rosenfield, and E.L. Fleming, 2001: An interactive model study of the influence of the Mount Pinatubo aerosol on stratospheric methane and water trends. *J. Geophys. Res*., **106**(D21), 27711–27727.

Conway, T.J., et al., 1994: Evidence for interannual variability of the carbon cycle from the NOAA/CMDL sampling network. *J. Geophys. Res*., **99**(D11), 22831–22855.

Cook, J., and E.J. Highwood, 2004: Climate response to tropospheric absorbing aerosols in an intermediate general-circulation model. *Q. J. R. Meteorol. Soc*., **130**, 175–191.

Cooke, W.F., V. Ramaswamy, and P. Kasibhatla, 2002: A general circulation model study of the global carbonaceous aerosol distribution. *J. Geophys. Res*., **107**(D16), doi:10.1029/2001JD001274.

Cooke, W.F., C. Liousse, H. Cachier, and J. Feichter, 1999: Construction of a 1° x 1° fossil fuel emission data set for carbonaceous aerosol and implementation and radiative impact in the ECHAM4 model. *J. Geophys. Res.*, **104**(D18), 22137–22162.

Coughlin, K., and K.K. Tung, 2004: Eleven-year solar cycle signal throughout the lower atmosphere. *J. Geophys. Res.*, **109**, D21105, doi:10.1029/2004JD004873.

Cox, P.M., et al., 1999: The impact of new land surface physics on the GCM simulation of climate and climate sensitivity. *Clim. Dyn*. **15**, 183–203.

Cramer, W., et al., 2001: Global response of terrestrial ecosystem structure and function to CO_2 and climate change: Results from six dynamic global vegetation models. *Global Change Biol.*, **7**, 357–373.

Crooks, S.A., and L.J. Gray, 2005: Characterization of the 11-year solar signal using a multiple regression analysis of the ERA-40 dataset. *J. Clim.*, **18**, 996–1015.

Crutzen, P.J., 2004: New directions: the growing urban heat and pollution "island" effect - impact on chemistry and climate. *Atmos. Environ.*, **38**, 3539–3540.

Cunnold, D.M., et al., 2002: In situ measurements of atmospheric methane at GAGE/AGAGE sites during 1985-2000 and resulting source inferences. *J. Geophys. Res*., **107**(D14), doi:10.1029/2001JD001226.

Cunnold, D.M., et al., 2004: Comment on "Enhanced upper stratospheric ozone: Sign of recovery or solar cycle effect?" by W. Steinbrecht et al. *J. Geophys. Res*., **109**, D14305, doi:10.1029/2004JD004826.

Cziczo, D.J., D.M. Murphy, P.K. Hudson, and D.S. Thompson, 2004: Single particle measurements of the chemical composition of cirrus ice residue from CRYSTAL-FACE. *J. Geophys. Res*., **109**, D04201, doi:10.1029/2003JD004032.

Dameris, M., et al., 2005: Long-term changes and variability in a transient simulation with a chemistry-climate model employing realistic forcing. *Atmos. Chem. Phys. Discuss.*, **5**, 2121–2145.

Daniel, J.S., S. Solomon, and D.L. Albritton, 1995: On the evaluation of halocarbon radiative forcing and global warming potentials. *J. Geophys. Res*., **100**(D1), 1271–1286, doi:10.1029/94JD02516.

de Ridder, K., and H. Gallée, 1998: Land surface-induced regional climate change in southern Israel. *J. Appl. Meteorol*., **37**, 1470–1485.

Decesari, S., M.C. Facchini, S. Fuzzi, and E. Tagliavini, 2000: Characterization of water-soluble organic compounds in atmospheric aerosol: a new approach. *J. Geophys. Res*., **105**(D1), 1481–1489.

Decesari, S., et al., 2001: Chemical features and seasonal variation of fine aerosol water-soluble organic compounds in the Po Valley, Italy. *Atmos. Environ.*, **35**, 3691–3699.

Del Genio, A.D., M.S. Yao, and K.-W. Lo, 1996: A prognostic cloud water parametrization for global climate models. *J. Clim.*, **9**, 270–304.

Delworth, T.L., V. Ramaswamy, and G.L. Stenchikov, 2005: The impact of aerosols on simulated ocean temperature and heat content in the 20th century. *Geophys. Res. Lett*., **32**, L24709, doi:10.1029/2005GL024457.

den Elzen, M., et al., 2005. Analysing countries' contribution to climate change: Scientific and policy-related choices. *Environ. Sci. Technol.*, **8**(6), 614–636.

Dentener, F., et al., 2006: Emissions of primary aerosol and precursor gases in the years 2000 and 1750 - prescribed data-sets for AeroCom. *Atmos. Chem. Phys. Discuss.*, **6**, 2703–2763.

Derwent, R.G., W.J. Collins, C.E. Johnson, and D.S. Stevenson, 2001: Transient behaviour of tropospheric ozone precursors in a global 3-D CTM and their indirect greenhouse effects. *Clim. Change*, **49**, 463–487.

Deshler, T., et al., 2003: Thirty years of in situ stratospheric aerosol size distribution measurements from Laramie, Wyoming (41N), using balloon-borne instruments. *J. Geophys. Res*., **108**(D5), 4167, doi:10.1029/2002JD002514.

Deuzé, J.L., et al., 2000: Estimate of the aerosol properties over the ocean with POLDER. *J. Geophys. Res*., **105**, 15329–15346.

Deuzé, J.L., et al., 2001: Remote sensing of aerosols over land surfaces from POLDER-ADEOS-1 polarized measurements. *J. Geophys. Res*., **106**, 4913–4926.

Dewitte, S., D. Crommelynck, S. Mekaoui, and A. Joukoff, 2005: Measurement and uncertainty of the long-term total solar irradiance trend. *Sol. Phys*., **224**, 209–216.

Diab, R.D., et al., 2004: Tropospheric ozone climatology over Irene, South Africa, from 1990 to 1994 and 1998 to 2002. *J. Geophys. Res*., **109**, D20301, doi:10.1029/2004JD004793.

Dlugokencky, E.J., K.A. Masarie, P.M. Lang, and P.P. Tans, 1998: Continuing decline in the growth rate of atmospheric methane. *Nature*, **393**, 447–450.

Dlugokencky, E.J., et al., 1996: Changes in CH_4 and CO growth rates after the eruption of Mt. Pinatubo and their link with changes in tropical tropospheric UV flux. *Geophys. Res. Lett*., **23**(20), 2761–2764.

Dlugokencky, E.J., et al., 2001: Measurements of an anomalous global methane increase during 1998. *Geophys. Res. Lett*., **28**(3), 499–502.

Dlugokencky, E.J., et al., 2003: Atmospheric methane levels off: Temporary pause or a new steady-state? *Geophys. Res. Lett*., **30**(19), doi:10.1029/2003GL018126.

Dlugokencky, E.J., et al., 2005: Conversion of NOAA CMDL atmospheric dry air CH_4 mole fractions to a gravimetrically prepared standard scale. *J. Geophys. Res*., **110**, D18306, doi:10.1029/2005JD006035.

Döll, P., 2002: Impact of climate change and variability on irrigation requirements: a global perspective. *Clim. Change*, **54**, 269–293.

Douglass, A., M. Schoeberl, R. Rood, and S. Pawson, 2003: Evaluation of transport in the lower tropical stratosphere in a global chemistry and transport model. *J. Geophys. Res*., **108**(D9), 4259, doi:10.1029/2002JD002696.

Douglass, D.H., and B.D. Clader, 2002: Climate sensitivity of the Earth to solar irradiance. *Geophys. Res. Lett.*, **29**(16), 33–36.

Dubovik, O., and M.D. King, 2000: A flexible inversion algorithm for retrieval of aerosol optical properties from Sun and sky radiance measurements. *J. Geophys. Res*., **105**, 20673–20696.

Dubovik, O., et al., 1998: Single-scattering albedo of smoke retrieved from the sky radiance and solar transmittance measured from ground. *J. Geophys. Res*., **103**(D24), 31903–31923.

Dubovik, O., et al., 2000: Accuracy assessments of aerosol optical properties retrieved from Aerosol Robotic Network (AERONET) Sun and sky radiance measurements. *J. Geophys. Res*., **105**, 9791–9806.

Dubovik, O., et al., 2002: Variability of absorption and optical properties of key aerosol types observed in worldwide locations. *J. Atmos. Sci*., **59**, 590–608.

Dufresne, L.-L., et al., 2005: Contrasts in the effects on climate of anthropogenic sulfate aerosols between the 20th and the 21st century. *Geophys. Res. Lett*., **32**, L21703, doi:10.1029/2005GL023619.

Duncan, B.N., et al., 2003: Indonesian wildfires of 1997: Impact on tropospheric chemistry. *J. Geophys. Res*., **108**(D15), 4458, doi:10.1029/2002JD003195.

Dusek, U., et al., 2006: Size matters more than chemistry for cloud-nucleating ability of aerosol particles. *Science*, **312**, 1375–1378.

Dziembowski, W.A., P.R. Goode, and J. Schou, 2001: Does the sun shrink with increasing magnetic activity? *Astrophys. J*., **553**, 897–904.

Eagan, R., P.V. Hobbs, and L. Radke, 1974: Measurements of CCN and cloud droplet size distributions in the vicinity of forest fires. *J. Appl. Meteorol*., **13**, 537–553.

Easter, R., et al., 2004: MIRAGE: Model description and evaluation of aerosols and trace gases. *J. Geophys. Res*. **109**, D20210, doi:10.1029/2004JD004571.

Eatough, D.J., et al., 2003: Semivolatile particulate organic material in southern Africa during SAFARI 2000. *J. Geophys. Res*., **108**(D13), 8479, doi:10.1029/2002JD002296.

Eck, T.F., et al., 2003: Variability of biomass burning aerosol optical characteristics in southern Africa during the SAFARI 2000 dry season campaign and a comparison of single scattering albedo estimates from radiometric measurements. *J. Geophys. Res.*, **108**(D13), 8477, doi:10.1029/2002JD002321.

Edwards, D.P., et al., 2004: Observations of carbon monoxide and aerosols from the Terra satellite: Northern Hemisphere variability. *J. Geophys. Res*., **109**, D24202, doi:10.1029/2004JD004727.

Ehhalt, D.H., 1999: Gas phase chemistry of the troposphere. In: *Global Aspects of Atmospheric Chemistry, Vol. 6* [Baumgaertel, H., W. Gruenbein, and F. Hensel (eds.)]. Springer Verlag, Darmstadt, pp. 21–110.

EPA, 2003: *National Air Quality and Emissions Trends Report, 2003 Special Studies Edition*. Publication No. EPA 454/R-03-005, U. S. Environmental Protection Agency, Washington, DC, 190pp, http://www.epa.gov/air/airtrends/aqtrnd03/

Erlick, C., L.M. Russell, and V. Ramaswamy, 2001: A microphysics-based investigation of the radiative effects of aerosol-cloud interactions for two MAST Experiment case studies. *J. Geophys. Res*., **106**(D1), 1249–1269.

Ervens, B., G. Feingold, and S.M. Kreidenweis, 2005: The influence of water-soluble organic carbon on cloud drop number concentration. *J. Geophys. Res*., **110**, D18211, doi:10.1029/2004JD005634.

Etheridge, D.M., L.P. Steele, R.J. Francey, and R.L. Langenfelds, 1998: Atmospheric methane between 1000 A.D. and present: Evidence of anthropogenic emissions and climatic variability. *J. Geophys. Res*., **103**(D13), 15979–15993.

Etheridge, D.M., et al., 1996: Natural and anthropogenic changes in atmospheric CO_2 over the last 1000 years from air in Antarctic ice and firn. *J. Geophys. Res*., **101**(D2), 4115–4128.

Facchini, M.C., M. Mircea, S. Fuzzi, and R.J. Charlson, 1999: Cloud albedo enhancement by surface-active organic solutes in growing droplets. *Nature*, **401**, 257–259.

Facchini, M.C., et al., 2000: Surface tension of atmospheric wet aerosol and cloud/fog droplets in relation to their organic carbon content and chemical composition. *Atmos. Environ.*, **34**, 4853–4857.

Feichter, J., E. Roeckner, U. Lohmann, and B. Liepert, 2004: Nonlinear aspects of the climate response to greenhouse gas and aerosol forcing. *J. Clim.*, **17**, 2384–2398.

Feingold, G., 2003: Modelling of the first indirect effect: Analysis of measurement requirements. *Geophys. Res. Lett.*, **30**(19), 1997, doi:10.1029/2003GL017967.

Feingold, G., and P.Y. Chuang, 2002: Analysis of influence of film-forming compounds on droplet growth: Implications for cloud microphysical processes and climate. *J. Atmos. Sci*., **59**, 2006–2018.

Feingold, G., R. Boers, B. Stevens, and W.R. Cotton, 1997: A modelling study of the effect of drizzle on cloud optical depth and susceptibility. *J. Geophys. Res*., **102**(D12), 13527–13534.

Feingold, G., W.L. Eberhard, D.E. Veron, and M. Previdi, 2003: First measurements of the Twomey indirect effect using ground-based remote sensors. *Geophys. Res. Lett*., **30**(6), 1287, doi:10.1029/2002GL016633.

Feng, Y., and J. Penner. 2007: Global modeling of nitrate and ammonium: Interaction of aerosols and tropospheric chemistry. *J. Geophys. Res*., **112**(D01304), doi:10.1029/2005JD006404.

Ferretti, D.F., D.C. Lowe, R.J. Martin, and G.W. Brailsford, 2000: A new GC-IRMS technique for high precision, N_2O-free analysis of $\delta^{13}C$ and $\delta^{18}O$ in atmospheric CO_2 from small air samples. *J. Geophys. Res.*, **105**(D5), 6709–6718.

Field, C.B., R.B. Jackson, and H.A. Mooney, 1995: Stomatal responses to increased CO_2: implications from the plant to the global scale. *Plant Cell Environ.*, **18**, 1214–1225.

Fioletov, V.E., et al., 2002: Global and zonal total ozone variations estimated from ground-based and satellite measurements: 1964-2000. *J. Geophys. Res.*, **107**(D22), 4647, doi:10.1029/2001JD001350.

Formenti, P., et al., 2003: Inorganic and carbonaceous aerosols during the Southern African Regional Science Initiative (SAFARI 2000) experiment: Chemical characteristics, physical properties, and emission data or smoke from African biomass burning. *J. Geophys. Res*., **108**(D13), 8488, doi:10.1029/2002JD002408.

Forster, P.M.F., and K.P. Shine, 1999: Stratospheric water vapour changes as a possible contributor to observed stratospheric cooling. *Geophys. Res. Lett*., **26**(21), 3309–3312.

Forster, P.M.F., and K. Tourpali, 2001: Effect of tropopause height changes on the calculation of ozone trends and their radiative forcing. *J. Geophys. Res*., **106**(D11), 12241–12251.

Forster, P.M.F., and K.P. Shine, 2002: Assessing the climate impact of trends in stratospheric water vapor. *Geophys. Res. Lett.*, **29**(6), doi:10.1029/2001GL013909.

Forster, P.M.F., and M.J. Joshi, 2005: The role of halocarbons in the climate change of the troposphere and stratosphere. *Clim. Change*, **70**, 249–266.

Forster, P.M.F., and K.E. Taylor, 2006: Climate forcings and climate sensitivities diagnosed from coupled climate model integrations. *J. Clim.*, **19**, 6181–6194.

Forster, P.M.F., M. Blackburn, R. Glover, and K.P. Shine, 2000: An examination of climate sensitivity for idealised climate change experiments in an intermediate general circulation model. *Clim. Dyn*., **16**, 833–849.

Forster, P.M.F., et al., 2005: Resolving uncertainties in the radiative forcing of HFC-134s. *J. Quant. Spectrosc. Radiative Transfer*, **93**, 447–460.

Foster, S.S., 2004: *Reconstruction of Solar Irradiance Variations for use in Studies of Global Climate Change: Application of Recent SOHO Observations with Historic Data from the Greenwich Observatory.* PhD Thesis, University of Southampton, Faculty of Science, Southampton, 231 p.

Foukal, P., C. Frohlich, H. Spruit, and T.M.L. Wigley, 2006: Variations in solar luminosity and their effect on the Earth's climate. *Nature*, **443**, 161–166.

Francey, R.J., et al., 1995: Changes in oceanic and terrestrial carbon uptake since 1982. *Nature*, **373**, 326–330.

Francey, R.J., et al., 1999: A history of $\delta^{13}C$ in atmospheric CH_4 from the Cape Grim Air Archive and Antarctic firn air. *J. Geophys. Res*., **104**(D19), 23633–23643.

Frankenberg, C., et al., 2005: Assessing methane emissions from global space-borne observations. *Science*, **308**, 1010–1014.

Free, M., and J. Angell, 2002: Effect of volcanoes on the vertical temperature profile in radiosonde data. *J. Geophys. Res.*, **107**(D10), doi:10.1029/2001JD001128.

Friedl, M.A., et al., 2002: Global land cover mapping from MODIS: algorithms and early results. *Remote Sens. Environ.*, **83**, 287–302.

Fröhlich, C., and J. Lean, 2004: Solar radiative output and its variability: Evidence and mechanisms. *Astron. Astrophys. Rev.*, **12**, 273–320.

Fueglistaler, S., H. Wernli, and T. Peter, 2004: Tropical troposphere-to-stratosphere transport inferred from trajectory calculations. *J. Geophys. Res*., **109**, D03108, doi:10.1029/2003JD004069.

Fuglestvedt, J.S., T.K. Berntsen, O. Godal, and T. Skodvin, 2000: Climate implications of GWP-based reductions in greenhouse gas emissions. *Geophys. Res. Lett*., **27**(3), 409–412, doi:10.1029/1999GL010939**.**

Fuglestvedt, J.S., et al., 1999: Climatic forcing of nitrogen oxides through changes in tropospheric ozone and methane; global 3D model studies. *Atmos. Environ.*, **33**, 961–977.

Fuglestvedt, J.S., et al., 2003: Metrics of climate change: assessing radiative forcing and emission indices. *Clim. Change*, **58**, 267–331.

Fuller, K.A., W.C. Malm, and S.M. Kreidenweis, 1999: Effects of mixing on extinction by carbonaceous particles. *J. Geophys. Res*., **104**(D13), 15941–15954.

Fuzzi, S., et al., 2001; A simplified model of the water soluble organic component of atmospheric aerosols. *Geophys. Res. Lett*., **28**(21), 4079–4082.

Gao, F., et al., 2005: MODIS bidirectional reflectance distribution function and albedo Climate Modeling Grid products and the variability of albedo for major global vegetation types. *J. Geophys. Res.*, **110**, D01104, doi:10.1029/2004JD005190.

Gauss, M., et al., 2006: Radiative forcing since preindustrial times due to ozone changes in the troposphere and the lower stratosphere. *Atmos. Chem. Phys*., **6**, 575–599.

Gedney, N., et al., 2006: Detection of a direct carbon dioxide effect in continental river runoff records. *Nature*, **439**, 835–838, doi:10.1038/nature04504.

Geller, M.A., and S.P. Smyshlyaev, 2002: A model study of total ozone evolution 1979-2000: The role of individual natural and anthropogenic effects. *Geophys. Res. Lett*., **29**(22), 5–8.

Geogdzhayev, I.V., et al., 2002: Global two-channel AVHRR retrievals of aerosol properties over the ocean for the period of NOAA-9 observations and preliminary retrievals using NOAA-7 and NOAA-11 data. *J. Atmos. Sci*., **59**, 262–278.

Ghan, S., et al., 2001: Evaluation of aerosol direct radiative forcing in MIRAGE. *J. Geophys. Res*., **106**(D6), 5295–5316.

Gillett, N.P., M.F. Wehner, S.F.B. Tett, and A.J. Weaver, 2004: Testing the linearity of the response to combined greenhouse gas and sulfate aerosol forcing. *Geophys. Res. Lett*., **31**, L14201, doi:10.1029/2004GL020111.

Gleisner, H., and P. Thejll, 2003: Patterns of tropospheric response to solar variability. *Geophys. Res. Lett*., **30**(13), 1711, doi:10.1029/2003GL017129.

Godal, O., 2003: The IPCC assessment of multidisciplinary issues: The choice of greenhouse gas indices. *Clim. Change*, **58**, 243–249.

Gohar, L.K., G. Myhre, and K.P. Shine, 2004: Updated radiative forcing estimates of four halocarbons. *J. Geophys. Res*., **109**, D01107, doi:10.1029/2003JD004320.

Goloub, P., and O. Arino, 2000: Verification of the consistency of POLDER aerosol index over land with ATSR-2/ERS-2 fire product. *Geophys. Res. Lett*., **27**(6), 899–902.

Goloub, P., et al., 1999: Validation of the first algorithm applied for deriving the aerosol properties over the ocean using the POLDER/ADEOS measurements. *IEEE Trans. Remote Sens.*, **37**, 1586–1596.

Goosse, H., H. Renssen, A. Timmermann, and R.S. Bradley, 2005: Internal and forced climate variability during the last millennium: a model-data comparison using ensemble simulations. *Quat. Sci. Rev*., **24,** 1345–1360.

Gordon, L.J., et al., 2005: Human modification of global water vapor flows from the land surface. *Proc. Natl. Acad. Sci. U.S.A.*, **102**, 7612–7617.

Govindasamy, B., P.B. Duffy, and K. Caldeira, 2001a: Land use changes and Northern Hemisphere cooling. *Geophys. Res. Lett*., **28**(2), 291–294.

Govindasamy, B., et al., 2001b: Limitations of the equivalent CO_2 approximation in climate change simulations. *J. Geophys. Res.*, **106**(D19), 22593–22603.

Gray, L.J., J.D. Haigh, and R.G. Harrison, 2005: *Review of the Influences of Solar Changes on the Earth's Climate.* Hadley Centre Technical Note No. 62, Met Office, Exeter, 82 pp.

Gregory, J.M., et al., 2004: A new method for diagnosing radiative forcing and climate sensitivity. *Geophys. Res. Lett.*, **31**, L03205, doi:10.1029/2003GL018747.

Gunn, R., and B.B. Phillips, 1957: An experimental investigation of the effect of air pollution on the initiation of rain. *J. Meteorol*., **14**(3), 272–280.

Hadjinicolaou, P., J.A. Pyle, and N.R.P. Harris, 2005: The recent turnaround in stratospheric ozone over northern middle latitudes: a dynamical modeling perspective. *Geophys. Res. Lett.*, **32**, L12821**,** doi:10.1029/2005GL022476.

Haigh, J.D., 2003: The effects of solar variability on the Earth's climate. *Phil. Trans. R. Soc. London Ser. A*, **361**, 95–111.

Hall, J.C., and G.W. Lockwood, 2004: The chromospheric activity and variability of cycling and flat activity solar-analog stars. *Astrophys. J.*, **614**, 942–946.

Hamilton, J.F., et al., 2004: Partially oxidised organic components in urban aerosol using GCXGC-TOF/MS. *Atmos. Chem. Phys.*, **4**, 1279–1290.

Hammitt, J.K., A.K. Jain, J.L. Adams, and D.J. Wuebbles, 1996: A welfare-based index for assessing environmental effects of greenhouse-gas emissions. *Nature*, **381**, 301–303.

Han, Q., W.B. Rossow, J. Zeng, and R. Welch, 2002: Three different behaviors of liquid water path of water clouds in aerosol-cloud interactions. *J. Atmos. Sci.*, **59**, 726–735.

Hansen, J., and M. Sato, 2001: Trends of measured climate forcing agents. *Proc. Natl. Acad. Sci. U.S.A.*, **98**, 14778–14783.

Hansen, J., and L. Nazarenko, 2004: Soot climate forcing via snow and ice albedos. *Proc. Natl. Acad. Sci. U.S.A.*, **101**, 423–428.

Hansen, J., and M. Sato, 2004: Greenhouse gas growth rates. *Proc. Natl. Acad. Sci. U.S.A.*, **101**, 16109–16114.

Hansen, J., M. Sato, and R. Reudy, 1995: Long-term changes of the diurnal temperature cycle: Implications about mechanisms of global climate change. *Atmos. Res.*, **37**, 175–209.

Hansen, J., M. Sato, and R. Ruedy, 1997: Radiative forcing and climate response. *J. Geophys. Res.*, **102**(D6), 6831–6864.

Hansen, J., et al., 2000: Global warming in the twenty-first century: An alternative scenario. *Proc. Natl. Acad. Sci. U.S.A.*, **97**, 9875–9880.

Hansen, J., et al., 2002: Climate forcings in Goddard Institute for Space Studies SI2000 simulations. *J. Geophys. Res.*, **107**(D18), 4347, doi:10.1029/2001JD001143.

Hansen, J., et al., 2005: Efficacy of climate forcings. *J. Geophys. Res.*, **110**, D18104, doi:10.1029/2005JD005776.

Hansen, M.C., and B. Reed, 2000: A comparison of the IGBP DISCover and University of Maryland 1km global land cover products. *Int. J. Remote Sens.*, **21**, 1365–1373.

Harder, J., et al., 2005: The spectral irradiance monitor I. Scientific requirements, instrument design and operation modes. *Sol. Phys.*, **230**, 141–167.

Harding, R.J., and J.W. Pomeroy, 1996: The energy balance of the winter boreal landscape. *J. Clim.*, **9**, 2778–2787.

Harnisch, J., R.R. Borchers, P.P. Fabian, and M.M. Maiss, 1996: Tropospheric trends for CF_4 and C_2F_6 since 1982 derived from SF_6 dated stratospheric air. *Geophys. Res. Lett.*, **23**(10), 1099–1102.

Harries, J.E., H.E. Brindley, P.J. Sagoo, and R.J. Bantges, 2001: Increases in greenhouse forcing inferred from the outgoing longwave radiation spectra of the Earth in 1970 and 1997. *Nature*, **410**, 355–357.

Harrison, R.G., and K.S. Carslaw, 2003: Ion-aerosol-cloud processes in the lower atmosphere. *Rev. Geophys.*, **41**, 1021.

Harrison, R.G., and D.B. Stephenson, 2006: Empirical evidence for a nonlinear effect of galactic cosmic rays on clouds. *Proc. Roy. Soc. London Ser. A*, **462**, 1221–1233.

Hartmann, D.L., M.E. Ockert-Bell, and M.L. Michelsen, 1992: The effect of cloud type on Earth's energy balance: global analysis. *J. Clim.*, **5,** 1281–1304.

Hashvardhan, S.E. Schwartz, C.E. Benkovitz, and G. Guo, 2002: Aerosol influence on cloud microphysics examined by satellite measurements and chemical transport modelling. *J. Atmos. Sci.*, **59**, 714–725.

Hauglustaine, D.A., and G.P. Brasseur, 2001: Evolution of tropospheric ozone under anthropogenic activities and associated radiative forcing of climate. *J. Geophys. Res.*, **106**(D23), 32337–32360, doi:10.1029/2001JD900175.

Haxeltine, A., and I.C. Prentice, 1996: BIOME3: An equilibrium terrestrial biosphere model based on ecophysiological constraints, resource availability, and competition among plant functional types. *Global Biogeochem. Cycles*, **10**(4), 693–709.

Haywood, J.M., and K.P. Shine, 1995: The effect of anthropogenic sulfate and soot aerosol on the clear sky planetary radiation budget. *Geophys. Res. Lett.*, **22**(5), 603–606.

Haywood, J.M., and K.P. Shine. 1997: Multi-spectral calculations of the direct radiative forcing of tropospheric sulphate and soot aerosols using a column model. *Q. J. R. Meteorol. Soc*. **123**, 1907–1930.

Haywood, J.M., and O. Boucher, 2000: Estimates of the direct and indirect radiative forcing due to tropospheric aerosols: A review. *Rev. Geophys.*, **38**, 513–543.

Haywood, J.M., V. Ramaswamy, and B.J. Soden, 1999: Tropospheric aerosol climate forcing in clear-sky satellite observations over the oceans. *Science*, **283**, 1299–1305.

Haywood, J.M., et al., 2003a: Comparison of aerosol size distributions, radiative properties, and optical depths determined by aircraft observations and Sun photometers during SAFARI 2000. *J. Geophys. Res.*, **108**(D13), 8471, doi:10.1029/2002JD002250.

Haywood, J.M., et al., 2003b: The mean physical and optical properties of regional haze dominated by biomass burning aerosol measured from the C-130 aircraft during SAFARI 2000. *J. Geophys. Res*., **108**(D13), 8473, doi:10.1029/2002JD002226.

Haywood, J.M, et al., 2003c: Radiative properties and direct radiative effect of Saharan dust measured by the C-130 aircraft during SHADE: 1. Solar spectrum. *J. Geophys. Res.*, **108**(D18), 8577, doi:10.1029/2002JD002687.

Haywood, J.M., et al., 2005: Can desert dust explain the outgoing longwave radiation anomaly over the Sahara during July 2003? *J. Geophys. Res*., **110**, D05105, doi:10.1029/2004JD005232.

Heal, G., 1997: Discounting and climate change: an editorial comment. *Clim. Change*, **37**, 335–343.

Hegg, D.A., et al., 1997: Chemical apportionment of aerosol column optical depth off the mid-Atlantic coast of the United States. *J. Geophys. Res*., **102**(D21), 25293–25303.

Hély, C., et al., 2003: Release of gaseous and particulate carbonaceous compound from biomass burning during the SAFARI 2000 dry season field campaign. *J. Geophys. Res*., **108**(D13), 8470, doi:10.1029/2002JD002482.

Hendricks, J., B. Kärcher, U. Lohmann, and M. Ponater, 2005: Do aircraft black carbon emissions affect cirrus clouds on the global scale? *Geophys. Res. Lett*., **32**, L12814, doi:10.1029/2005GL022740.

Hendricks, J., et al., 2004: Simulating the global atmospheric black carbon cycle: a revisit to the contribution of aircraft. *Atmos. Chem. Phys.*, **4**, 2521–2541.

Herman, M., et al., 1997: Remote sensing of aerosols over land surfaces including polarization measurements and application to POLDER measurements. *J. Geophys. Res*., **102**(D14), 17039–17050, doi:10.1029/96JD02109.

Hess, M., P. Koepke, and I. Schult, 1998: Optical properties of aerosols and clouds: the software package OPAC. *Bull. Am. Meteorol. Soc*., **79**, 831–844.

Highwood, E.J., et al., 2003: Radiative properties and direct effect of Saharan dust measured by the C-130 aircraft during Saharan Dust Experiment (SHADE): 2. Terrestrial spectrum. *J. Geophys. Res*., **108**(D18), 8577, doi:10.1029/2002JD002552.

Higurashi, A., and T. Nakajima. 1999. Development of a two-channel aerosol retrieval algorithm on a global scale using NOAA AVHRR. *J. Atmos. Sci*., **56,** 924–941.

Higurashi, A., et al., 2000: A study of global aerosol optical climatology with two-channel AVHRR remote sensing. *J. Clim.*, **13**, 2011–2027.

Hirsch, A.I., et al., 2006: Inverse modeling estimates of the global nitrous oxide surface flux from 1998–2001. *Global Biogeochem. Cycles*, **20**, GB1008, doi:10.1029/2004GB002443.

Hirst, E., et al., 2001: Discrimination of micrometre-sized ice and super-cooled droplets in mixed-phase cloud. *Atmos. Environ*., **35**, 33–47.

Hofmann, D., 2003: et al., Surface-based observations of volcanic emissions to stratosphere. In: *Volcanism and the Earth's Atmosphere* [Robock, A., and C. Oppenheimer (eds.)]. Geophysical Monograph 139, American Geophysical Union, Washington, DC, pp. 57–73.

Holben, B.N., et al., 1998: AERONET: A federated instrument network and data archive for aerosol characterization. *Remote Sens. Environ.*, **66**, 1–16.

Holben, B.N., et al., 2001: An emerging ground-based aerosol climatology: aerosol optical depth from AERONET. *J. Geophys. Res*., **106**(D11), 12067–12097.

Holzer-Popp, T., M. Schroedter, and G. Gesell, 2002: Retrieving aerosol optical depth and type in the boundary layer over land and ocean from simultaneous GOME spectrometer and ATSR-2 radiometer measurements - 2. Case study application and validation. *J. Geophys. Res*., **107**(D21), 4578, doi:10.1029/2002JD002777.

Hood, L.L., 2003: Thermal response of the tropical tropopause region to solar ultraviolet variations. *Geophys. Res. Lett.*, **30**, 2215, doi:10.1029/2003GL018364.

Houghton, R.A., 1999: The annual net flux of carbon to the atmosphere from changes in land use 1850-1990. *Tellus*, **51B**, 298–313.

Houghton, R.A., 2000: A new estimate of global sources and sinks of carbon from land use change. *Eos*, **81**(19), S281.

Houghton, R.A., 2003: Revised estimates of the annual net flux of carbon to the atmosphere from changes in land use and land management. *Tellus*, **55B**, 378–390.

Houghton, R.A., et al., 1983: Changes in the carbon content of terrestrial biota and soils between 1860 and 1980: a net release of CO_2 to the atmosphere. *Ecol. Monogr.*, **53**, 235–262, doi:10.2307/1942531.

Hoyt, D.V., and K.H. Schatten, 1993: A discussion of plausible solar irradiance variations, 1700-1992. *J. Geophys. Res*., **98**(A11), 18895–18906.

Hsu, N.C., J.R. Herman, and C. Weaver, 2000: Determination of radiative forcing of Saharan dust using combined TOMS and ERBE data. *J. Geophys. Res*., **105**(D16), 20649–20661.

Hsu, N.C., J.R. Herman, and S.C. Tsay, 2003: Radiative impacts from biomass burning in the presence of clouds during boreal spring in southeast Asia. *Geophys. Res. Lett*., **30**(5), 28, doi:10.1029/2002GL016485.

Huang, J., and R.G. Prinn, 2002: Critical evaluation of emissions of potential new gases for OH estimation. *J. Geophys. Res*., **107**(D24), 4784, doi:10.1029/2002JD002394.

Huebert, B.J., et al., 2003: An overview of ACE-Asia: Strategies for quantifying the relationships between Asian aerosols and their climatic impacts. *J. Geophys. Res*., **108**(D23), 8633, doi:10.1029/2003JD003550.

Hurley, M.D., et al., 2005: IR spectrum and radiative forcing of CF_4 revisited. *J. Geophys. Res*., **110**, D02102, doi:10.1029/2004JD005201.

Hurst, D.F., et al., 2004: Emissions of ozone-depleting substances in Russia during 2001. *J. Geophys. Res*., **109**, D14303, doi:10.1029/2004JD004633.

Husar, R.B., J.M. Prospero, and L.L. Stowe, 1997: Characterization of tropospheric aerosols over the oceans with the NOAA advanced very high resolution radiometer optical thickness operational product. *J. Geophys. Res*., **102**(D14), 16889–16910.

Husar, R.B., et al., 2001: Asian dust events of April 1998. *J. Geophys. Res.*, **106**(D16), 18317–18330.

Ichinose, T., K. Shimodozono, and K. Hanaki, 1999: Impact of anthropogenic heat on urban climate in Tokyo. *Atmos. Environ.*, **33**, 3897–3909.

Ichoku, C., et al., 2003: MODIS observation of aerosols and estimation of aerosol radiative forcing over southern Africa during SAFARI 2000. *J. Geophys. Res*., **108**(D13), 8499, doi:10.1029/2002JD002366.

Ignatov, A., and L. Stowe, 2002: Aerosol retrievals from individual AVHRR channels. Part I: Retrieval algorithm and transition from Dave to 6S Radiative Transfer Model. *J. Atmos. Sci*., **59**, 313–334.

IPCC, 1990: *Climate Change: The Intergovernmental Panel on Climate Change Scientific Assessment* [Houghton, J.T., G.J. Jenkins, and J.J. Ephraums (eds.)]. Cambridge University Press, Cambridge, United Kingdom and New York, NY, USA, 364 pp.

IPCC, 1999: *Aviation and the Global Atmosphere: A Special Report of IPCC Working Groups I and III* [Penner, J.E., et al. (eds.)]. Cambridge University Press, Cambridge, United Kingdom and New York, NY, USA, 373 pp.

IPCC, 2001: *Climate Change 2001: The Scientific Basis. Contribution of Working Group I to the Third Assessment Report of the Intergovernmental Panel on Climate Change* [Houghton, J.T., et al. (eds.)]. Cambridge University Press, Cambridge, United Kingdom and New York, NY, USA, 881 pp.

IPCC/TEAP, 2005: *Special Report on Safeguarding the Ozone Layer and the Global Climate System: Issues Related to Hydrofluorocarbons and Perfluorocarbons* [Metz, B., et al. (eds.)]. Cambridge University Press, Cambridge, United Kingdom and New York, NY, USA, 488 pp.

Ito, A., and J.E. Penner, 2005: Historical emissions of carbonaceous aerosols from biomass and fossil fuel burning for the period 1870–2000. *Global Biogeochem. Cycles*, **19**, GB2028, doi:10.1029/2004GB002374.

Iversen, T., and O. Seland, 2002: A scheme for process-tagged SO_4 and BC aerosols in NCAR CCM3: Validation and sensitivity to cloud processes. *J. Geophys. Res*., **107**(D24), 4751, doi:10.1029/2001JD000885.

Jacob, D.J., et al., 2005: *Radiative Forcing of Climate Change*. The National Academies Press, Washington, DC, 207 pp.

Jacobson, M.Z., 1999: Isolating nitrated and aromatic aerosols and nitrated aromatic gases as sources of ultraviolet light absorption. *J. Geophys. Res*., **104**(D3), 3527–3542.

Jacobson, M.Z., 2001a: Global direct radiative forcing due to multicomponent anthropogenic and natural aerosols. *J. Geophys. Res*., **106**(D2), 1551–1568.

Jacobson, M.Z., 2001b: Strong radiative heating due to the mixing state of black carbon in atmospheric aerosols. *Nature*, **409**, 695–697.

Jacobson, M.Z., 2002: Control of fossil-fuel particulate black carbon and organic matter, possibly the most effective method of slowing global warming. *J. Geophys. Res*., **107**(D19), 4410, doi:10.1029/2001JD001376.

Jacobson, M.Z., 2004: Climate response of fossil fuel and biofuel soot, accounting for soot's feedback to snow and sea ice albedo and emissivity. *J. Geophys. Res*., **109**, D21201, doi:10.1029/2004JD004945.

Jaffe, D., et al., 2003: Increasing background ozone during spring on the west coast of North America. *Geophys. Res. Lett.*, **30**, 1613, doi:10.1029/2003GL017024.

Jensen, E.J., and O.B. Toon, 1997: The potential impact of soot particles from aircraft exhaust on cirrus clouds. *Geophys. Res. Lett*., **24**(3), 249–252.

Jeong, M.J., Z.Q. Li, D.A. Chu, and S.C. Tsay, 2005: Quality and compatibility analyses of global aerosol products derived from the advanced very high resolution radiometer and Moderate Resolution Imaging Spectroradiometer. *J. Geophys. Res*., **110**, D10S09, doi:10.1029/2004JD004648.

Jiang, H., and G. Feingold, 2006: Effect of aerosol on warm convective clouds: Aerosol-clouds-surface flux feedbacks in a new coupled large eddy model. *J. Geophys. Res*., **111**, D01202, doi:10.1029/2005JD006138.

Jiang, H., G. Feingold, and W.R. Cotton, 2002: Simulations of aerosol-cloud-dynamical feedbacks resulting from of entrainment of aerosols into the marine boundary layer during the Atlantic Stratocumulus Transition Experiment. *J. Geophys. Res*., **107**(D24), 4813, doi:10.1029/2001JD001502.

Jirikowic, J.L., and P.E. Damon, 1994: The Medieval solar activity maximum. *Clim. Change*, **26**, 309–316.

Johnson, B.T., 2005: The semidirect aerosol effect: comparison of a single-column model with large eddy simulation for marine stratocumulus. *J. Clim.*, **18**, 119–130.

Johnson, B.T., K.P. Shine, and P.M. Forster, 2004: The semi-direct aerosol effect: Impact of absorbing aerosols on marine stratocumulus. *Q. J. R. Meteorol. Soc*., **130**, 1407–1422.

Jones, A., D.L. Roberts, and M.J. Woodage, 2001: Indirect sulphate aerosol forcing in a climate model with an interactive sulphur cycle. *J. Geophys. Res*., **106**(D17), 20293–20301.

Jones, P.D., A. Moberg, T.J. Osborn, and K.R. Briffa, 2003: Surface climate responses to explosive volcanic eruptions seen in long European temperature records and mid-to-high latitude tree-ring density around the Northern Hemisphere. In: *Volcanism and the Earth's Atmosphere* [Robock, A., and C. Oppenheimer (eds.)]. Geophysical Monograph 139, American Geophysical Union, Washington, DC, pp. 239–254.

Jonson, J.E., D. Simpson, H. Fagerli, and S. Solberg, 2005: Can we explain the trends in European ozone levels? *Atmos. Chem. Phys. Discuss.*, **5**, 5957–5985.

Joos, F., et al., 1996. An efficient and accurate representation of complex oceanic and biospheric models of anthropogenic carbon uptake. *Tellus*, **48B**, 397–417.

Joos, F., et al., 2001. Global warming feedbacks on terrestrial carbon uptake under the Intergovernmental Panel on Climate Change (IPCC) emission scenarios. *Global Biogeochem. Cycles*, **15**, 891-908, 2001

Joshi, M.M., and K.P. Shine, 2003: A GCM study of volcanic eruptions as a cause of increased stratospheric water vapor. *J. Clim.*, **16**, 3525–3534.

Joshi, M., et al., 2003: A comparison of climate response to different radiative forcings in three general circulation models: Towards an improved metric of climate change. *Clim. Dyn*., **20**, 843–854.

Junge, C.E., 1975: The possible influence of aerosols on the general circulation and climate and possible approaches for modelling. In: *The Physical Basis of Climate and Climate Modelling: Report of the International Study Conference in Stockholm, 29 July-10 August 1974: organised by WMO and ICSU and supported by UNEP Global Atmospheric Research Programme (GARP), WMO-ICSU Joint Organising Committee*. World Meteorological Organization, Geneva, pp. 244–251.

Kahn, R., P. Banerjee, and D. McDonald, 2001: Sensitivity of multiangle imaging to natural mixtures of aerosols over ocean. *J. Geophys. Res*., **106**(D16), 18219–18238.

Kahn, R.A., et al., 2005: Multiangle Imaging Spectroradiometer (MISR) global aerosol optical depth validation based on 2 years of coincident Aerosol Robotic Network (AERONET) observation. *J. Geophys. Res*., **110**, D10S04, doi:10.1029/2004JD004706.

Kalkstein, A.J., and R.C. Balling Jr., 2004: Impact of unusually clear weather on United States daily temperature range following 9/11/2001. *Clim. Res.*, **26**, 1–4.

Kanakidou, M., et al., 2005: Organic aerosol and global climate modelling: a review. *Atmos. Chem. Phys*., **5**, 1053–1123.

Kandlikar, M., 1996: Indices for comparing greenhouse gas emissions: integrating science and economics. *Energy Econ*., **18**, 265–282.

Kapustin, V.N., et al., 2006: On the determination of a cloud condensation nuclei from satellite: challenges and possibilities. *J. Geophys. Res*., **111**, D04202, doi:10.1029/2004JD005527.

Kärcher, B., 1999: Aviation-produced aerosols and contrails. *Surv. Geophys.*, **20**, 113–167.

Kasischke, E.S., and J.E. Penner, 2004: Improving global estimates of atmospheric emissions from biomass burning. *J. Geophys. Res*., **109**, D14S01, doi:10.1029/2004JD004972.

Kaufman, Y.J., C.J. Tucker, and R.L Mahoney, 1991: Fossil fuel and biomass burning effect on climate: Heating or cooling? *J. Clim.*, **4**, 578–588.

Kaufman, Y.J., D. Tanré, and O. Boucher, 2002: A satellite view of aerosols in the climate system. *Nature*, **419**, 215–223.

Kaufman, Y.J., et al., 1997: Operational remote sensing of tropospheric aerosols over the land from EOS-MODIS. *J. Geophys. Res*., **102**(D14), 17051–17068.

Kaufman, Y.J., et al., 2001: Absorption of sunlight by dust as inferred from satellite and ground-based remote sensing. *Geophys. Res. Lett*., **28**(8), 1479–1482.

Kaufman Y.J., et al., 2005a: Aerosol anthropogenic component estimated from satellite data. *Geophys. Res. Lett*., **32**, L17804, doi:10.1029/2005GL023125.

Kaufman, Y.J., et al., 2005b: A critical examination of the residual cloud contamination and diurnal sampling effects on MODIS estimates of aerosol over ocean. *IEEE Trans. Geosci. Remote*, **43**(12), 2886–2897.

Keeling, C.D., and T.P. Whorf, 2005: Atmospheric CO_2 records from sites in the SIO air sampling network. In: *Trends: A Compendium of Data on Global Change*. Carbon Dioxide Information Analysis Center, Oak Ridge National Laboratory, U.S. Department of Energy, Oak Ridge, TN, http://cdiac.esd.ornl.gov/trends/co2/sio-keel-flask/sio-keel-flask.html.

Keeling, C.D., A.F. Bollenbacher, and T.P. Whorf, 2005: Monthly atmospheric $^{13}C/^{12}C$ isotopic ratios for 10 SIO stations. In: *Trends: A Compendium of Data on Global Change*. Carbon Dioxide Information Analysis Center, Oak Ridge National Laboratory, U.S. Department of Energy, Oak Ridge, TN, http://cdiac.ornl.gov/trends/co2/iso-sio/iso-sio.html.

Keeling, C.D., T.P. Whorf, M. Wahlen, and J. van der Plicht, 1995: Interannual extremes in the rate of rise of atmospheric carbon dioxide since 1980. *Nature*, **375**, 666–670.

Keeling, R.F., and S.R. Shertz, 1992: Seasonal and interannual variations in atmospheric oxygen and implications for the global carbon cycle. *Nature*, **358**, 723–727.

Keeling, R.F., S.C. Piper, and M. Heimann, 1996: Global and hemispheric CO_2 sinks deduced from changes in atmospheric O_2 concentration. *Nature*, **381**, 218–221.

Keil, A., and J.M. Haywood, 2003: Solar radiative forcing by biomass burning aerosol particles during SAFARI 2000: A case study based on measured aerosol and cloud properties. *J. Geophys. Res*., **108** (D13), 8467, doi:10.1029/2002JD002315.

Keppler, F., J.T.G. Hamilton, M. Brass, and T. Röckmann, 2006: Methane emissions from terrestrial plants under aerobic conditions. *Nature*, **439**, 187–191, doi:10.1038/nature04420.

Kernthaler, S.C., R. Toumi, and J.D. Haigh, 1999: Some doubts concerning a link between cosmic ray fluxes and global cloudiness. *Geophys. Res. Lett*., **26**(7), 863–866, doi:10.1029/1999GL900121.

Khainroutdinov, M., and Y. Kogan, 2000: A new cloud physics parametrization in a large-eddy simulation model of marine stratocumulus. *Mon. Weather Rev*., **128**, 229–243.

Khalil, M.A.K., et al., 2003: Atmospheric perfluorocarbons. *Environ. Sci. Technol.*, **37**, 4358–4361.

Kiehl, J.T., et al., 2000: Radiative forcing due to sulfate aerosols from simulations with the National Center for Atmospheric Research Community Climate Model, Version 3. *J. Geophys. Res*., **105**(D1), 1441–1457.

Kim, B.-G., S.E. Schwartz, and M.A. Miller, 2003: Effective radius of cloud droplets by ground-based remote sensing: Relationship to aerosol. *J. Geophys. Res*., **108**(D23), doi:10.1029/2003JD003721.

Kinne, S., et al., 2003: Monthly averages of aerosol properties: a global comparison among models, satellite data, and AERONET ground data. *J. Geophys. Res*., **108** (D20), 4634, doi:10.1029/2001JD001253.

Kinne, S., et al., 2006: An AeroCom initial assessment: optical properties in aerosol component modules of global models. *Atmos. Chem. Phys*. **6**, 1815–1834.

Kirchstetter, T.W., T. Novakov, and P.V. Hobbs, 2004: Evidence that the spectral dependence of light absorption by aerosols is affected by organic carbon. *J. Geophys. Res*., **109**, D21208, doi:10.1029/2004JD004999.

Kirkevåg, A., and T. Iversen, 2002: Global direct radiative forcing by process-parametrized aerosol optical properties. *J. Geophys. Res*., **107**(D20), 4433, doi:10.1029/2001JD000886.

Klein Goldewijk, K., 2001: Estimating global land use change over the past 300 years: The HYDE database. *Global Biogeochem. Cycles*, **15**, 417–433.

Knutson, T.R., et al., 2006: Assessment of twentieth-century regional surface temperature trends using the GFDL CM2 coupled models. *J. Clim.*, **10**(9), 1624–1651.

Koch, D., 2001: Transport and direct radiative forcing of carbonaceous and sulfate aerosols in the GISS GCM. *J. Geophys. Res*., **106**(D17), 20311–20332.

Korolev, A.V., and G.A. Isaac, 2005: Shattering during sampling OAPs and HVPS. Part I: snow particles. *J. Atmos. Ocean. Technol*., **22**, 528–542.

Kotchenruther, R.A., and P.V. Hobbs, 1998: Humidification factors of aerosols from biomass burning in Brazil. *J. Geophys. Res*., **103**(D24), 32081–32089.

Kotchenruther, R.A., P.V. Hobbs, and D.A. Hegg, 1999: Humidification factors for atmospheric aerosols off the mid-Atlantic coast of the United States. *J. Geophys. Res*., **104**(D2), 2239–2251.

Kristjánsson, J.E., and J. Kristiansen, 2000: Is there a cosmic ray signal in recent variations in global cloudiness and cloud radiative forcing? *J. Geophys. Res*., **105**(D9), 11851–11863.

Kristjánsson, J.E., A. Staple, J. Kristiansen, and E. Kaas, 2002: A new look at possible connections between solar activity, clouds and climate. *Geophys. Res. Lett*., **29**, doi:10.1029/2002GL015646.

Kristjánsson, J.E., et al., 2005: Response of the climate system to aerosol direct and indirect forcing: the role of cloud feedbacks. *J. Geophys. Res*., **110**, D24206, doi:10.1029/2005JD006299.

Krizan P., and J. Lastovicka, 2005: Trends in positive and negative ozone laminae in the Northern Hemisphere. *J. Geophys. Res*., **110**, D10107, doi:10.1029/2004JD005477.

Kroeze, C., E. Dumont, and S.P. Seitzinger, 2005: New estimates of global emissions of N_2O from rivers, estuaries and continental shelves. *Environ. Sci.*, 2(2–3), 159–165.

Krol, M., and J. Lelieveld, 2003: Can the variability in tropospheric OH be deduced from measurements of 1,1,1-trichloroethane (methyl chloroform)? *J. Geophys. Res*., **108**(D3), 4125**,** doi:10.1029/2002JD002423.

Krol, M., et al., 2003: Continuing emissions of methyl chloroform from Europe. *Nature*, **421**, 131–135.

Krueger, A.J., et al., 2000: Ultraviolet remote sensing of volcanic emissions. In: *Remote Sensing of Active Volcanism* [Mouginis-Mark, P.J., J.A. Crisp, and J.H. Fink (eds.)]. Geophysical Monograph 116, American Geophysical Union, Washington, DC, pp. 25–43.

Krüger, O., and H. Graßl, 2002: The indirect aerosol effect over Europe. *Geophys. Res. Lett*., **29**, doi:10.1029/2001GL14081.

Labitzke, K., 2004: On the signal of the 11-year sunspot cycle in the stratosphere and its modulation by the quasi-biennial oscillation. *J. Atmos. Solar Terr. Phys.*, **66**, 1151–1157.

Labitzke, K., et al., 2002: The global signal of the 11-year solar cycle in the stratosphere: observations and models. *J. Atmos. Solar Terr. Phys.*, **64**, 203–210.

Lambert, A., et al., 1993: Measurements of the evolution of the Mt. Pinatubo aerosol cloud by ISAMS. *Geophys. Res. Lett*., **20**(12), 1287–1290.

Langenfelds, R.L., et al., 2002: Interannual growth rate variations of atmospheric CO_2 and its delta C-13, H-2, CH_4, and CO between 1992 and 1999 linked to biomass burning. *Global Biogeochem. Cycles*, **16**, doi:10.1029/2001GB001466.

Lawrence, M.G., P. Jöckel, and R. von Kuhlmann, 2001: What does the global mean OH concentration tell us? *Atmos. Chem. Phys*., **1**, 43–74.

Lean, J., 2000: Evolution of the sun's spectral irradiance since the Maunder Minimum. *Geophys. Res. Lett*., **27**, 2425–2428.

Lean, J., A. Skumanich, and O.White, 1992: Estimating the sun's radiative output during the Maunder Minimum. *Geophys. Res. Lett.*, **19**(15), 1595–1598.

Lean, J., J. Beer, and R. Bradley, 1995: Reconstruction of solar irradiance since 1610: implications for climate change. *Geophys. Res. Lett*., **22**, 3195–3198.

Lean, J.L., Y.M. Wang, and N.R. Sheeley, 2002: The effect of increasing solar activity on the Sun's total and open magnetic flux during multiple cycles: Implications for solar forcing of climate. *Geophys. Res. Lett*., **29**(24), 2224, doi:10.1029/2002GL015880.

Lean, J., G. Rottman, J. Harder, and G. Kopp, 2005: SORCE contribution to new understanding of global change and solar variability. *Solar Phys*., **230**, 27–53.

Lean, J.L., et al., 1997: Detection and parametrization of variations in solar mid and near ultraviolet radiation (200 to 400 nm). *J. Geophys. Res*., **102**(D25), 29939–29956.

Lee, K.H., Y.J. Kim, and W. von Hoyningen-Huene, 2004: Estimation of regional aerosol optical thickness from satellite observations during the 2001 ACE-Asia IOP. *J. Geophys. Res*. **109,** D19S16, doi:10.1029/2003JD004126.

Lee, R.B. III, M.A. Gibson, R.S. Wilson, and S. Thomas, 1995: Long-term total solar irradiance variability during sunspot cycle 22. *J. Geophys. Res*., **100**(A2), 1667–1675.

Lefohn, A.S., J.D. Husar, and R.B. Husar, 1999: Estimating historical anthropogenic global sulfur emission patterns for the period 1850-1990. *Atmos. Environ.*, **33**, 3435–3444.

Lelieveld, J., P.J. Crutzen, and F.J. Dentener, 1998: Changing concentration, lifetime and climate forcing of atmospheric methane. *Tellus*, **50B**, 128–150.

Lelieveld, J., W. Peters, F.J. Dentener, and M.C. Krol, 2002: Stability of tropospheric hydroxyl chemistry. *J. Geophys. Res*., **107**(D23), 4715, doi:10.1029/2002JD002272.

Lelieveld, J., et al., 2004: Increasing ozone over the Atlantic Ocean. *Science*, **304**, 1483–1487.

Levy, R.C., et al., 2003: Evaluation of the Moderate-Resolution Imaging Spectroradiometer (MODIS) retrievals of dust aerosol over the ocean during PRIDE. *J. Geophys. Res*., **108**(D19), 8594, doi:10.1029/2002JD002460.

Li, J., et al., 2005: Halocarbon emissions estimated from AGAGE measured pollution events at Trinidad Head, California. *J. Geophys. Res*., **110**, D14308, doi:10.1029/2004JD005739.

Liao, H., and J.H. Seinfeld, 2005: Global impacts of gas-phase chemistry-aerosol interactions on direct radiative forcing by anthropogenic aerosols and ozone. *J. Geophys. Res*., **110**, D18208, doi:10.1029/2005JD005907.

Liao, H., J.H. Seinfeld, P.J. Adams, and L.J. Mickley, 2004: Global radiative forcing of coupled tropospheric ozone and aerosols in a unified general circulation model. *J. Geophys. Res*., **109**, D16207, doi:10.1029/2003JD004456.

Liao, T., C.D. Camp, and Y.L. Yung, 2004: The seasonal cycle of N_2O. *Geophys. Res. Lett*., **31**, L17108, doi:10.1029/2004GL020345.

Liousse, C., et al., 1996: A global three-dimensional model study of carbonaceous aerosols. *J. Geophys. Res*., **101**(D14), 19411–19432.

Liu, H.Q., R.T. Pinker, and B.N. Holben, 2005: A global view of aerosols from merged transport models, satellite, and ground observations. *J. Geophys. Res*., **110**(D10), doi:10.1029/2004JD004695.

Liu, X.H., and J.E. Penner, 2002: Effect of Mount Pinatubo H_2SO_4/H_2O aerosol on ice nucleation in the upper troposphere using a global chemistry and transport model. *J. Geophys. Res*., **107**(D12), doi:10.1029/2001JD000455.

Liu, Y., and P.H. Daum, 2002: Indirect warming effect from dispersion forcing. *Nature*, **419**, 580–581.

Lockwood, M., and R. Stamper, 1999: Long-term drift of the coronal source magnetic flux and the total solar irradiance. *Geophys. Res. Lett.*, **26**(16), 2461–2464.

Loeb, N.G., and S. Kato, 2002: Top-of-atmosphere direct radiative effect of aerosols over the tropical oceans from the Clouds and the Earth's Radiant Energy System (CERES) satellite instrument. *J. Clim.*, **15**, 1474–1484.

Loeb, N.G., and N. Manalo-Smith, 2005: Top-of-atmosphere direct radiative effect of aerosols over global oceans from merged CERES and MODIS observations. *J. Clim.*, **18**, 3506–3526.

Lohar, D., and B. Pal, 1995: The effect of irrigation on premonsoon season precipitation over south west Bengal, India. *J. Clim.*, **8**, 2567–2570.

Lohmann, U., and G. Lesins, 2002: Stronger constraints on the anthropogenic indirect aerosol effect. *Science*, **298**, 1012–1016.

Lohmann, U., and J. Feichter, 2005: Global indirect aerosol effects: A review. *Atmos. Chem. Phys.*, **5**, 715–737.

Lohmann, U. and C. Leck, 2005: Importance of submicron surface active organic aerosols for pristine Arctic clouds. *Tellus*, **57B**, 261–268.

Lohmann, U., B. Kärcher, and J. Hendrichs, 2004: Sensitivity studies of cirrus clouds formed by heterogeneous freezing in ECHAM GCM. *J. Geophys. Res*., **109**, D16204, doi:10.1029/2003JD004443.

Lohmann, U., J. Feichter, J.E. Penner, and W.R. Leaitch, 2000: Indirect effect of sulfate and carbonaceous aerosols: a mechanistic treatment. *J. Geophys. Res*., **105**(D10), 12193–12206.

Lohmann, U., et al., 2001: Vertical distributions of sulfur species simulated by large scale atmospheric models in COSAM: comparison with observations. *Tellus*, **53B**, 646–672.

Loveland, T.R., et al., 2000: Development of a global land cover characteristics database and IGBP DISCover from 1 km AVHR R data. *Int. J. Remote Sens.*, **21**, 1303–1330.

Lowe, D.C., and W. Allan, 2002: A simple procedure for evaluating global cosmogenic ^{14}C production in the atmosphere using neutron monitor data. *Radiocarbon*, **44**, 149–157.

Lowe, D.C., M.R. Manning, G.W. Brailsford, and A.M. Bromley, 1997: The 1991-1992 atmospheric methane anomaly: Southern hemisphere ^{13}C decrease and growth rate fluctuations. *Geophys. Res. Lett*., **24**(8), 857–860.

Lowe, D.C., et al., 2004: Seasonal cycles of mixing ratio and ^{13}C in atmospheric methane at Suva, Fiji. *J. Geophys. Res.*, **109**, D23308 doi:10.1029/2004JD005166.

Lu, M.-L., and J. Seinfeld, 2005: Study of the aerosol indirect effect by large-eddy simulation of marine stratocumulus. *J. Atmos. Sci*., **62**, 3909–3932.

Luo, C., N.M. Mahowald, and J. del Corral, 2003: Sensitivity study of meteorological parameters on mineral aerosol mobilization, transport, and distribution, *J. Geophys. Res*., **108** (D15), 4447, doi:10.1029/2003JD003483.

MacFarling Meure, C., et al., 2006: The Law Dome CO_2, CH_4 and N_2O ice core records extended to 2000 years BP. *Geophys. Res. Lett.*, **33**, L14810, doi:10.1029/2006GL026152.

Macke, A., M. Mishchenko, and B. Cairns, 1996: The influence of inclusions on light scattering by large ice particles. *J. Geophys. Res*., **101**(D18), 23311–23316.

Magi, B.I., and P.V. Hobbs, 2003: Effects of humidity on aerosols in southern Africa during the biomass burning season. *J. Geophys. Res*., **108**(D13), 8495, doi:10.1029/2002JD002144.

Magi, B.I., et al., 2005: Properties and chemical apportionment of aerosol optical depth at locations off the U.S. East Coast in July and August 2001. *J. Atmos. Sci*., **62**(4), 919–933, doi:10.1175/JAS3263.1.

Mahowald, N.M., and C. Luo, 2003: A less dusty future? *Geophys. Res. Lett*., **30**(17), doi:10.1029/2003GL017880.

Mahowald, N.M., G.C. Rivera, and C. Luo, 2004: Comment on Tegen et al. 2004, on the "Relative importance of climate and land use in determining present and future global soil dust emissions". *Geophys. Res. Lett*., **31**, L24105, doi:10.1029/2004GL021272.

Mak, J.E., M.R. Manning, and D.C. Lowe, 2000: Aircraft observations of $\delta^{13}C$ of atmospheric methane over the Pacific in August 1991 and 1993: evidence of an enrichment in $^{13}CH_4$ in the Southern Hemisphere. *J. Geophys. Res*., **105**(D1), 1329–1335.

Malm, W.C., et al., 2004: Spatial and monthly trends in speciated fine particle concentration in the United States. *J. Geophys. Res*., **109**, D03306, doi:10.1029/2003JD003739.

Manabe, S., and R.T. Wetherald, 1967: Thermal equilibrium of the atmosphere with a given distribution of relative humidity. *J. Atmos. Sci*., **24**, 241–259.

Manne, A.S., and R.G. Richels, 2001: An alternative approach to establishing trade-offs among greenhouse gases. *Nature*, **410**, 675–676.

Manning, A.C., and R.F. Keeling, 2006: Global oceanic and land biotic carbon sinks from the Scripps atmospheric oxygen flask sampling network. *Tellus*, **58B**, 95–116.

Manning, A.J., et al., 2003: Estimating European emissions of ozone-depleting and greenhouse gases using observations and a modelling back-attribution technique. *J. Geophys. Res*., **108** (D14), 4405, doi:10.1029/2002JD002312.

Manning, M.R., A. Gomez, and G.W. Brailsford, 1997: Annex B11: The New Zealand CO_2 measurement programme. In: *Report of the Ninth WMO Meeting of Experts on Carbon Dioxide Concentration and Related Tracer Measurement Techniques*. WMO Global Atmosphere Watch No. 132; WMO TD No. 952, Commonwealth Scientific and Industrial Research Organisation, Melbourne, pp. 120–123.

Manning, M.R., et al., 2005: Short term variations in the oxidizing power of the atmosphere. *Nature*, **436**, 1001–1004.

Mannstein, H., and U. Schumann, 2005: Aircraft induced contrail cirrus over Europe. *Meteorol. Z.*, **14**, 549–544.

Maria, S., F. Russell, L.M. Turpin, and R.J. Porcja, 2002: FTIR measurements of functional groups and organic mass in aerosol samples over the Caribbean. *Atmos. Environ*., **36**, 5185–5196.

Marland, G., T.A. Boden, and R.J. Andres, 2006: Global, regional, and national CO_2 emissions. In: *Trends: A Compendium of Data on Global Change*. Carbon Dioxide Information Analysis Center, Oak Ridge National Laboratory, U.S. Department of Energy, Oak Ridge, TN, http://cdiac.esd.ornl.gov/trends/emis/tre_glob.htm.

Marquart, S., and B. Mayer, 2002: Towards a reliable GCM estimation of contrail radiative forcing. *Geophys. Res. Lett*., **29**(8), doi:10.1029/2001GL014075.

Marquart, S., M. Ponater, F. Mager, and R. Sausen, 2003: Future development of contrail cover, optical depth, and radiative forcing: Impacts of increasing air traffic and climate change. *J. Clim.*, **16**, 2890–2904.

Marsh, N.D., and H. Svensmark, 2000a: Low cloud properties influenced by cosmic rays. *Phys. Rev. Lett*., **85**, 5004–5007.

Marsh, N.D., and H. Svensmark, 2000b: Cosmic rays, clouds, and climate. *Space Sci. Rev*., **94**, 215–230.

Marshak, A., et al., 2006: Impact of three-dimensional radiative effects on satellite retrievals of cloud droplet sizes. *J. Geophys. Res*., **111**, D09207, doi:10.1029/2005JD006686.

Martin, G.M., D.W. Johnson, and A. Spice, 1994: The measurement and parametrization of effective radius of droplets in warm stratiform clouds. *J. Atmos. Sci*., **51**, 1823–1842.

Martin, S.T., et al., 2004: Effects of the physical state of tropospheric ammonium-sulfate-nitrate particles on global aerosol direct radiative forcing. *Atmos. Chem. Phys.*, **4**, 183–214.

Martonchik, J.V., et al., 2004: Comparison of MISR and AERONET aerosol optical depths over desert sites. *Geophys. Res. Lett*., **31**, L16102, doi:10.1029/2004GL019807.

Matthews, E., 1983: Global vegetation and land-use: new high-resolution data-bases for climate studies. *J. Clim. Appl. Meteorol.*, **22**, 474–487.

Matthews, H.D., A.J. Weaver, M. Eby, and K.J. Meissner, 2003: Radiative forcing of climate by historical land cover change. *Geophys. Res. Lett*., **30**(2), 271–274.

Matthews, H.D., et al., 2004: Natural and anthropogenic climate change: Incorporating historical land cover change, vegetation dynamics and the global carbon cycle. *Clim. Dyn*., **22**, 461–479.

Matthias, I., et al., 2004: Multiyear aerosol observations with dual wavelength Raman lidar in the framework of EARLINET. *J. Geophys. Res*., **109**, D13203, doi:10.1029/2004JD004600.

McCormack, J.P., 2003: The influence of the 11-year solar cycle on the quasi-biennial oscillation. *Geophys. Res. Lett*., **30** (22), 2162, doi:10.1029/2003GL018314.

McCormick, M.P., 1987: SAGE II: An overview. *Adv. Space Res*., **7**, 219–226.

McCulloch, A., and P.M. Midgley, 2001: The history of methyl chloroform emissions: 1951-2000. *Atmos. Environ.*, **35**, 5311–5319.

McFiggans, G., et al., 2006: The effect of aerosol composition and properties on warm cloud droplet activation. *Atmos. Chem. Phys*., **6**, 2593–2649.

Meehl, G.A., et al., 2004: Combinations of natural and anthropogenic forcings in twentieth-century climate. *J. Clim.*, **17**, 3721–3727.

Meerkötter, R., et al., 1999: Radiative forcing by contrails. *Ann. Geophys.*, **17**, 1080–1094.

Melillo, J.M., et al., 2001: Nitrous oxide emissions from forests and pastures of various ages in the Brazilian Amazon. *J. Geophys. Res*., **106**(D24), 34179–34188.

Menon, S., and A. Del Genio, 2007: Evaluating the impacts of carbonaceous aerosols on clouds and climate. In: *Human-Induced Climate Change: An Interdisciplinary Assessment* [Schlesinger, M., et al. (eds.)]. Cambridge University Press, Cambridge, UK, in press.

Menon, S., A.D. Del Genio, D. Koch, and G. Tselioudis, 2002a: GCM simulations of the aerosol indirect effect: sensitivity to cloud parametrization and aerosol burden. *J. Atmos. Sci.*, **59**, 692–713.

Menon, S., J. Hansen, L. Nazarenko, and Y. Luo, 2002b: Climate effects of black carbon aerosols in China and India. *Science*, **297**, 2250–2253.

Menon, S., et al., 2003: Evaluating aerosol/cloud/radiation process parametrizations with single-column models and Second Aerosol Characterization Experiment (ACE-2) cloudy column observations. *J. Geophys. Res*., **108**(D24), 4762, doi:10.1029/2003JD003902.

Meyer, R., et al., 2002: Regional radiative forcing by line-shaped contrails derived from satellite data. *J. Geophys. Res*., **107**(D10), 4104, doi:10.1029/2001JD000426.

Mickley, L.J., D.J. Jacob, and D. Rind, 2001: Uncertainty in preindustrial abundance of tropospheric ozone: implications for radiative forcing calculations. *J. Geophys. Res*., **106**(D4), 3389–3399 doi:10.1029/2000JD900594.

Mickley, L.J., D.J. Jacob, B.D. Field, and D. Rind, 2004: Climate response to the increase in tropospheric ozone since preindustrial times: a comparison between ozone and equivalent CO_2 forcings. *J. Geophys. Res*., **109**, D05106, doi:10.1029/2003JD003653.

Mikami, M., et al., 2006: Aeolian dust experiment on climate impact: an overview of Japan-China Joint Project ADEC. *Global Planet. Change*, **52**, 142–172, doi:10.1016/j.gloplacha.2006.03.001.

Miller, B.R., et al., 1998: Atmospheric trend and lifetime of chlorodifluoromethane (HCFC-22) and the global tropospheric OH concentration. *J. Geophys. Res*., **103**(D11), 13237–13248, doi:10.1029/98JD00771.

Miller, R.L., G.A. Schmidt, and D.T. Shindell, 2006: Forced annular variations in the 20th century IPCC AR4 models. *J. Geophys. Res.*, **111**, D18101, doi:10.1029/2005JD006323.

Millet, D.B., and A.H. Goldstein, 2004: Evidence of continuing methylchloroform emissions from the United States. *Geophys. Res. Lett*., **31**, L17101, doi:10.1029/2004GL020166.

Ming, Y., and L.M. Russell, 2002: Thermodynamic equilibrium of organic-electrolyte mixtures in aerosol particles. *Am. Inst. Chem. Eng. J.*, **48**, 1331–1348.

Ming, Y., V. Ramaswamy, P.A. Ginoux, and L.H. Horowitz, 2005a: Direct radiative forcing of anthropogenic organic aerosol. *J. Geophys. Res.*, **110**, D20208, doi:10.1029/2004JD005573.

Ming, Y., V. Ramaswamy, L.J. Donner, and V.T.J. Phillips, 2006: A new parametrization of cloud droplet activation applicable to general circulation models. *J. Atmos. Sci*., **63**(4), 1348–1356.

Ming, Y., et al., 2005b: Geophysical Fluid Dynamics Laboratory general circulation model investigation of the indirect radiative effects of anthropogenic sulfate aerosol. *J. Geophys. Res.*, **110**, D22206, doi:10.1029/2005JD006161.

Ming, Y., et al., 2007: Modelling the interactions between aerosols and liquid water clouds with a self-consistent cloud scheme in a general circulation model. *J. Atmos. Sci*., **64**(4), 1189–1209.

Minnis, P., 2005: Reply. *J. Clim.*, **18**, 2783–2784.

Minnis, P., J.K. Ayers, R. Palikonda, and D. Phan, 2004: Contrails, cirrus trends, and climate. *J. Clim.*, **17**, 1671–1685.

Minnis, P., et al., 1993: Radiative climate forcing by the Mt. Pinatubo eruption. *Science*, **259**, 1411–1415.

Minnis, P., et al., 1998: Transformation of contrails into cirrus during SUCCESS. *Geophys. Res. Lett*., **25**, 1157–1160.

Mircea, M., et al., 2005: Importance of the organic aerosol fraction for modeling aerosol hygroscopic growth and activation: a case study in the Amazon Basin. *Atmos. Chem. Phys*., **5**, 3111–3126.

Mishchenko, M.I., et al., 1999: Aerosol retrievals over the ocean by use of channels 1 and 2 AVHRR data: sensitivity analysis and preliminary results. *Appl. Opt.*, **38**, 7325–7341.

Möhler, O., et al., 2005: Effect of sulfuric acid coating on heterogeneous ice nucleation by soot aerosol particles. *J. Geophys. Res*., **110**, D11210, doi:10.1029/2004JD005169.

Montzka, S.A., et al., 1999: Present and future trends in the atmospheric burden of ozone-depleting halogens. *Nature*, **398**, 690–694.

Montzka, S.A., et al., 2003: Controlled substances and other source gases. In: *Scientific Assessment of Ozone Depletion: 2002*. World Meteorological Organization, Geneva, pp. 1.1–1.83.

Moore, N., and S. Rojstaczer, 2001: Irrigation-induced rainfall and the Great Plains. *J. Appl. Meteorol*., **40**, 1297–1309.

Morgan, C.G., et al., 2004: Isotopic fractionation of nitrous oxide in the stratosphere: Comparison between model and observations. *J. Geophys. Res*., **109**, D04305, doi:10.1029/2003JD003402.

Morimoto, S., S. Aoki, T. Nakazawa, and T. Yamanouchi , 2006: Temporal variations of the carbon isotopic ratio of atmospheric methane observed at Ny Ålesund, Svalbard from 1996 to 2004. *Geophys. Res. Lett.*, **33**, L01807, doi:10.1029/2005GL024648.

Mosley-Thompson, E., T.A. Mashiotta, and L.G. Thompson, 2003: High resolution ice core records of Late Holocene volcanism: Current and future contributions from the Greenland PARCA cores. In: *Volcanism and the Earth's Atmosphere* [Robock, A., and C. Oppenheimer (eds.)]. Geophysical Monograph 139, American Geophysical Union, Washington, DC, pp. 153–164.

Mouillot, F., et al., 2006: Global carbon emissions from biomass burning in the 20th century. *Geophys. Res. Lett*., **33**, L01801, doi:10.1029/2005GL024707.

Moulin, C., and I. Chiapello, 2004: Evidence of the control of summer atmospheric transport of African dust over the Atlantic by Sahel sources from TOMS satellites (1979-2000). *Geophys. Res. Lett*., **31**, L02107, doi:10.1029/2003GL018931.

Moulin, C., H.R. Gordon, V.F. Banzon, and R.H. Evans, 2001: Assessment of Saharan dust absorption in the visible from SeaWiFS imagery. *J. Geophys. Res.*, **106**(D16), 18239–18249.

Murayama, T., et al., 2001: Ground-based network observation of Asian dust events of April 1998 in East Asia. *J. Geophys. Res*., **106**, 18345–18360.

Murphy, D.M., 2005: Something in the air. *Science*, **307**, 1888–1890.

Muscheler, R., et al., 2007: Solar activity during the last 1000 yr inferred from radionuclide records. *Quat. Sci. Rev.*, **26**, 82-97, doi:10.1016/j.quascirev.2006.07.012.

Myhre, G., and F. Stordal, 2001a: Global sensitivity experiments of the radiative forcing due to mineral aerosols. *J. Geophys. Res*., **106**, 18193–18204.

Myhre, G., and F. Stordal, 2001b: On the tradeoff of the solar and thermal infrared radiative impact of contrails. *Geophys. Res. Lett*., **28**, 3119–3122.

Myhre, G., and A. Myhre, 2003: Uncertainties in radiative forcing due to surface albedo changes caused by land-use changes. *J. Clim.*, **16**, 1511–1524.

Myhre, G., A. Myhre, and F. Stordal, 2001: Historical evolution of radiative forcing of climate. *Atmos. Environ.*, **35**, 2361–2373.

Myhre, G., M.M. Kvalevåg, and C.B. Schaaf, 2005a: Radiative forcing due to anthropogenic vegetation change based on MODIS surface albedo data. *Geophys. Res. Lett*., **32**, L21410, doi:10.1029/2005GL024004.

Myhre, G., et al., 2003: Modelling the solar radiative impact of aerosols from biomass burning during the Southern African Regional Science Initiative (SAFARI 2000) experiment. *J. Geophys. Res*., **108**, 8501, doi:10.1029/2002JD002313.

Myhre, G., et al., 2004a: Intercomparison of satellite retrieved aerosol optical depth over ocean. *J. Atmos. Sci*., **61**, 499–513.

Myhre, G., et al., 2004b: Uncertainties in the radiative forcing due to sulfate aerosols. *J. Atmos. Sci*., **61**, 485–498.

Myhre, G., et al., 2005b: Intercomparison of satellite retrieved aerosol optical depth over ocean during the period September 1997 to December 2000. *Atmos. Chem. Phys.*, **5**, 1697–1719.

Naja, M., and H. Akimoto, 2004: Contribution of regional pollution and long-range transport to the Asia-Pacific region: Analysis of long-term ozonesonde data over Japan. *J. Geophys. Res*., **109**, 1306, doi:10.1029/2004JD004687.

Naja, M., H. Akimoto, and J. Staehelin, 2003: Ozone in background and photochemically aged air over central Europe: analysis of long-term ozonesonde data from Hohenpeissenberg and Payerne. *J. Geophys. Res*., **108**, 4063, doi:10.1029/2002JD002477.

Nakajima, T., and A. Higurashi, 1998: A use of two-channel radiances for an aerosol characterization from space. *Geophys. Res. Lett*., **25**, 3815–3818.

Nakajima, T., A. Higurashi, K. Kawamoto, and J. Penner, 2001: A possible correlation between satellite-derived cloud and aerosol microphysical parameters, *Geophys. Res. Lett*., **28**, 1171–1174.

Nakajima, T., et al., 1996: Aerosol optical properties in the Iranian region obtained by ground-based solar radiation measurements in the summer of 1991. *J. Appl. Meteorol*., **35**, 1265–1278.

Nakazawa, T., S. Moromoto, S. Aoki, and M. Tanaka, 1997: Temporal and spatial variations of the carbon isotopic ratio of atmospheric carbon dioxide in the Western Pacific region. *J. Geophys. Res*., **102**, 1271–1285.

Nakicenovic, N., A. Grübler, and A. McDonald (eds), 1998: *Global Energy Perspectives*. Cambridge University Press, New York, NY, 299 pp.

Nenes, A., and J.H. Seinfeld, 2003: Parametrization of cloud droplet formation in global climate models. *J. Geophys. Res*., **108**, doi:10.1029/2002JD002911.

Nenes, A., et al., 2002: Can chemical effects on cloud droplet number rival the first indirect effect? *Geophys. Res. Lett*., **29**, 1848, doi:10.1029/2002GL015295.

Nevison, C.D., S. Solomon, and R.S. Gao, 1999: Buffering interactions in the modeled response of stratospheric O_3 to increased NO_x and HO_x. *J. Geophys. Res*., **104**(D3), 3741–3754, 10.1029/1998JD100018.

Nevison, C.D., D.E. Kinnison, and R.F. Weiss, 2004a: Stratospheric influences on the tropospheric seasonal cycles of nitrous oxide and chlorofluorocarbons. *Geophys. Res. Lett*., **31**, L20103, doi:10.1029/2004GL020398.

Nevison, C., T. Lueker, and R.F. Weiss, 2004b: Quantifying the nitrous oxide source from coastal upwelling. *Global Biogeochem. Cycles*, **18**, GB1018, doi:10.1029/2003GB002110.

Nevison, C.D., et al., 2005: Southern Ocean ventilation inferred from seasonal cycles of atmospheric N_2O and O_2/N_2 at Cape Grim, Tasmania. *Tellus*, **57B**, 218–229.

Newchurch, M.J., et al., 2003: Evidence for slowdown in stratospheric ozone loss: first stage of ozone recovery. *J. Geophys. Res*., **108**(D16), 4507, doi:10.1029/2003JD003471.

Nordhaus, W.D., 1997: Discounting in economics and climate change: an editorial comment. *Clim. Change*, **37**, 315–328.

Notholt, J., et al., 2005: Influence of tropospheric SO_2 emissions on particle formation and the stratospheric humidity. *Geophys. Res. Lett*., **32**, L07810, doi:10.1029/2004GL022159.

Novakov, T., D.A. Hegg, and P.V. Hobbs, 1997: Airborne measurements of carbonaceous aerosols on the East coast of the United States. *J. Geophys. Res*., **102**(D25), 30023–20030.

Novakov, T., et al., 2003: Large historical changes of fossil-fuel black carbon aerosols. *Geophys. Res. Lett*., **30**(6), 1324, doi:10.1029/2002GL016345.

Nozawa, T., T. Nagashima, H. Shiogama, and S.A. Crooks, 2005: Detecting natural influence on surface air temperature change in the early twentieth century. *Geophys. Res. Lett*., **32**, L20719, doi:10.1029/2005GL023540.

O'Doherty, S., et al., 2004: Rapid growth of hydrofluorocarbon 134a and hydrochlorofluorocarbons 141b, 142b, and 22 from Advanced Global Atmospheric Gases Experiment (AGAGE) observations at Cape Grim, Tasmania, and Mace Head, Ireland. *J. Geophys. Res*., **109**, D06310, doi:10.1029/2003JD004277.

Oinas, V., et al., 2001: Radiative cooling by stratospheric water vapor: big differences in GCM results. *Geophys. Res. Lett*., **28**, 2791–2794.

Olivier, J.G.J., and J.J.M. Berdowski, 2001: Global emissions sources and sinks. In: *The Climate System* [Berdowski, J., R. Guicherit, and B.J. Heij (eds.)]. A.A. Balkema/Swets & Zeitlinger, Lisse, The Netherlands, pp. 33–78, updated at http://www.mnp.nl/edgar/.

Oltmans, S.J., et al., 2006: Long-term changes in tropospheric ozone. *Atmos. Environ.*, **40**, 3156–3173.

O'Neill, B.C., 2000: The jury is still out on global warming potentials. *Clim. Change*, **44**, 427–443.

O'Neill, B., 2003: Economics, natural science, and the costs of global warming potentials. *Clim. Change*, **58**, 251–260.

Oram, D.E., 1999: *Trends of Long-Lived Anthropogenic Halocarbons in the Southern Hemisphere and Model Calculations of Global Emissions*. PhD Thesis, University of East Anglia, Norwich, UK, 249 pp.

Oram, D.E., et al., 1998: Growth of fluoroform (CHF_3, HFC-23) in the background atmosphere. *Geophys. Res. Lett*., **25**, 35–38, doi:10.1029/97GL03483.

Osborne, S.R., J.M. Haywood, P.N. Francis, and O. Dubovik, 2004: Shortwave radiative effects of biomass burning aerosol during SAFARI2000. *Q. J. R. Meteorol. Soc*., **130**, 1423–1448.

Palikonda, R., P. Minnis, D.P. Duda, and H. Mannstein, 2005: Contrail coverage derived from 2001 AVHRR data over the continental United States of America and surrounding area. *Meteorol. Z.*, **14**, 525–536.

Palmer, A.S., et al., 2002: Antarctic volcanic flux ratios from Law Dome ice cores. *Ann. Glaciol.*, **35**, 329–332.

Palmer, P.I., et al., 2003: Eastern Asian emissions of anthropogenic halocarbons deduced from aircraft concentration data. *J. Geophys. Res*., **108**(D24), 4753, doi:10.1029/2003JD003591.

Pan, W., M.A. Tatang, G.J. McRae, and R.G. Prinn, 1997: Uncertainty analysis of direct radiative forcing by anthropogenic sulfate aerosols. *J. Geophys. Res*., **102**(D18), 21915–21924.

Parrish, D.D., et al., 2004: Changes in the photochemical environment of the temperate North Pacific troposphere in response to increased Asian emissions. *J. Geophys. Res*., **109**, D23S18, doi:10.1029/2004JD004978.

Pavelin, E.G., C.E. Johnson, S. Rughooputh, and R. Toumi, 1999: Evaluation of pre-industrial surface ozone measurements made using Schönbein's method. *Atmos. Environ.*, **33**, 919–929.

Peng, Y., and U. Lohmann, 2003: Sensitivity study of the spectral dispersion of the cloud droplet size distribution on the indirect aerosol effect. *Geophys. Res. Lett*., **30**(10), 1507, doi:10.1029/2003GL017192.

Penner, J.E., S.Y. Zhang, and C.C. Chuang, 2003: Soot and smoke aerosol may not warm climate. *J. Geophys. Res*., **108**(D21), 4657, doi:10.1029/2003JD003409.

Penner, J.E., X. Dong, and Y. Chen, 2004: Observational evidence of a change in radiative forcing due to the indirect aerosol effect. *Nature*, **427**, 231–234.

Penner, J.E., et al., 2001: Aerosols, their direct and indirect effects. In: *Climate Change 2001: The Scientific Basis. Contribution of Working Group I to the Third Assessment Report of the Intergovernmental Panel on Climate Change* [Houghton, J.T., et al. (eds.)]. Cambridge University Press, Cambridge, United Kingdom and New York, NY, USA, pp. 289–348.

Penner, J. E., et al., 2002: A comparison of model- and satellite-derived aerosol optical depth and reflectivity. *J. Atmos. Sci*., **59**, 441–460.

Penner, J.E., et al., 2006: Model intercomparison of indirect aerosol effects. *Atmos. Chem. Phys. Discuss.*, **6**, 1579–1617.

Penner, J.E., et al., 2007: Effect of black carbon on mid-troposphere and surface temperature trends. In: *Human-Induced Climate Change: An Interdisciplinary Assessment* [Schlesinger, M., et al., (eds.)]. Cambridge University Press, Cambridge, UK, in press.

Perlwitz, J., and H.-F. Graf, 2001: Troposphere-stratosphere dynamic coupling under strong and weak polar vortex conditions. *Geophys. Res. Lett.*, **28**, 271–274.

Perlwitz, J., and N. Harnik, 2003: Observational evidence of a stratospheric influence on the troposphere by planetary wave reflection. *J. Clim.*, **16**, 3011–3026.

Pham, M., O. Boucher, and D. Hauglustaine, 2005: Changes in atmospheric sulfur burdens and concentrations and resulting radiative forcings under IPCC SRES emission scenarios for 1990-2100. *J. Geophys. Res.*, **110**, D06112, doi:10.1029/2004JD005125.

Philipona, R., et al., 2004: Radiative forcing - measured at Earth's surface - corroborate the increasing greenhouse effect. *Geophys. Res. Lett.*, **31**, L03202, doi:10.1029/2003GL018765.

Pielke, R.A. Sr., et al., 2002: The influence of land-use change and landscape dynamics on the climate system - relevance to climate change policy beyond the radiative effect of greenhouse gases. *Philos. Trans. R. Soc. London Ser. A*, **360**, 1705–1719.

Pitari, G., E. Mancini, V. Rizi, and D.T. Shindell, 2002: Impact of future climate and emissions changes on stratospheric aerosols and ozone. *J. Atmos. Sci.*, **59**, 414–440.

Platt, U., W. Allan, and D.C. Lowe, 2004: Hemispheric average Cl atom concentration from $^{13}C/^{12}C$ ratios in atmospheric methane. *Atmos. Chem. Phys.*, **4**, 2393–2399.

Ponater, M., S. Marquart, and R. Sausen, 2002: Contrails in a comprehensive global climate model: Parametrization and radiative forcing results. *J. Geophys. Res.*, **107**(D13), doi:10.1029/2001JD000429.

Ponater, M., S. Marquart, R. Sausen, and U. Schumann, 2005: On contrail climate sensitivity. *Geophys. Res. Lett.*, **32**, L10706, doi:10.1029/2005GL022580.

Posfai, M., et al., 2003: Individual aerosol particles from biomass burning in southern Africa: 1. Compositions and size distributions of carbonaceous particles. *J. Geophys. Res.*, **108**(D13), 8483, doi:10.1029/2002JD002291.

Prata, A., W. Rose, S. Self, and D. O'Brien, 2003: Global, long-term sulphur dioxide measurements from TOVS data: a new tool for studying explosive volcanism and climate. In: *Volcanism and the Earth's Atmosphere* [Robock, A., and C. Oppenheimer (eds).]. Geophysical Monograph 139, American Geophysical Union, Washington, DC, pp. 75–92.

Prather, M.J., 2003: Atmospheric science: an environmental experiment with H_2? *Science*, **302**, 581–583.

Prather, M.J., et al., 2001: Atmospheric chemistry and greenhouse gases. In: *Climate Change 2001: The Scientific Basis. Contribution of Working Group I to the Third Assessment Report of the Intergovernmental Panel on Climate Change* [Houghton, J.T., et al. (eds.)]. Cambridge University Press, Cambridge, United Kingdom and New York, NY, USA, pp. 239–287.

Preminger, D.G., and S.R. Walton, 2005: A new model of total solar irradiance based on sunspot areas. *Geophys. Res. Lett.*, **32**, L14109, doi:10.1029/2005GL022839.

Prentice, I.C., et al., 2001: The carbon cycle and atmospheric carbon dioxide. In: *Climate Change 2001: The Scientific Basis. Contribution of Working Group I to the Third Assessment Report of the Intergovernmental Panel on Climate Change* [Houghton, J.T., et al. (eds.)]. Cambridge University Press, Cambridge, United Kingdom and New York, NY, USA, pp. 184–238.

Prinn, R.G., 2004: Non-CO_2 greenhouse gases. In: *The Global Carbon Cycle* [Field, C., and M. Raupach (eds.)]. Island Press, Washington, DC, pp. 205–216.

Prinn, R.G., et al., 1990: Atmospheric emissions and trends of nitrous oxide deduced from ten years of ALE-GAGE data. *J. Geophys. Res.*, **95**, 18369–18385.

Prinn, R.G., et al., 2000: A history of chemically and radiatively important gases in air deduced from ALE/GAGE/AGAGE. *J. Geophys. Res.*, **105**(D14), 17751–17792.

Prinn, R.G., et al., 2001: Evidence for substantial variations of atmospheric hydroxyl radicals in the past two decades. *Science*, **292**, 1882–1888.

Prinn, R.G., et al., 2005a: Evidence for variability of atmospheric hydroxyl radicals over the past quarter century. *Geophys. Res. Lett.*, **32**, L07809, doi:10.1029/2004GL022228.

Prinn, R.G., et al., 2005b: *The ALE/GAGE/AGAGE Network: DB1001*. Carbon Dioxide Information and Analysis World Data Center, http://cdiac.esd.ornl.gov/ndps/alegage.html.

Prospero, J.M., et al., 2002: Environmental characterization of global sources of atmospheric soil dust identified with the Nimbus 7 Total Ozone Mapping Spectrometer (TOMS) absorbing aerosol product. *Rev. Geophys.*, **40**(1), doi:10.1029/2000RG000095.

Putaud, J.P., et al., 2004: European aerosol phenomenology-2: chemical characteristics of particulate matter at kerbside, urban, rural and background sites in Europe. *Atmos. Environ.*, **38**, 2579–2595.

Pyle, J., et al., 2005: Ozone and climate: a review of interconnections. In: *Special Report on Safeguarding the Ozone Layer and Global Climate System: Issues Related to Hydrofluorocarbons and Perfluorocarbons* [Metz., B., et al. (eds.)]. Cambridge University Press, Cambridge, United Kingdom and New York, NY, USA, pp. 83–132.

Quaas, J., and O. Boucher, 2005: Constraining the first aerosol indirect radiative forcing in the LMDZ GCM using POLDER and MODIS satellite data. *Geophys. Res. Lett.*, **32**, L17814, doi:10.1029/2005GL023850.

Quaas, J., O. Boucher, and F.-M. Breon, 2004: Aerosol indirect effects in POLDER satellite data and the Laboratoire de Météorologie Dynamique-Zoom (LMDZ) general circulation model. *J. Geophys. Res.*, **109**, D08205, doi:10.1029/2003JD004317.

Quaas, J., O. Boucher, and U. Lohmann, 2005: Constraining the total aerosol indirect effect in the LMDZ and ECHAM4 GCMs using MODIS satellite data. *Atmos. Chem. Phys.*, **5**, 9669–9690.

Quay, P., et al., 2000: Atmospheric (CO)-C-14: A tracer of OH concentration and mixing rates. *J. Geophys. Res.*, **105**(D12), 15147–15166.

Quinn, P.K., and T.S. Bates, 2005: Regional aerosol properties: comparisons from ACE 1, ACE 2, Aerosols99, INDOEX, ACE Asia, TARFOX, and NEAQS. *J. Geophys. Res.*, **110**, D14202, doi:10.1029/2004JD004755.

Raes, F., T. Bates, F. McGovern, and M. Van Liedekerke, 2000: The 2nd Aerosol Characterization Experiment (ACE-2): general overview and main results. *Tellus*, **52B**, 111–125.

Ramachandran, S., V. Ramaswamy, G.L. Stenchikov, and A. Robock, 2000: Radiative impact of the Mt. Pinatubo volcanic eruption: Lower stratospheric response. *J. Geophys. Res.*, **105**(D19), 24409–24429.

Ramanathan, V., 1981: The role of ocean-atmosphere interactions in the CO_2 climate problem. *J. Atmos. Sci.*, **38**, 918–930.

Ramanathan, V., P.J. Crutzen, J.T. Kiehl, and D. Rosenfeld, 2001a: Atmosphere: aerosols, climate, and the hydrological cycle. *Science*, **294**, 2119–2124.

Ramanathan, V., et al., 2001b: Indian Ocean experiment: An integrated analysis of the climate forcing and effects of the great Indo-Asian haze. *J. Geophys. Res.*, **106**(D22), 28371–28398.

Ramankutty, N., and J.A. Foley, 1999: Estimating historical changes in global land cover: croplands from 1700 to 1992. *Global Biogeochem. Cycles*, **14**, 997–1027.

Ramaswamy, V., S. Ramachandran, G. Stenchikov, and A. Robock, 2006a: A model study of the effect of Pinatubo volcanic aerosols on the stratospheric temperatures. In: *Frontiers of Climate Modeling* [Kiehl, J.T., and V. Ramanathan (eds.)]. Cambridge University Press, Cambridge, UK, pp. 152–178.

Ramaswamy, V., et al., 2001: Radiative forcing of climate change. In: *Climate Change 2001: The Scientific Basis. Contribution of Working Group I to the Third Assessment Report of the Intergovernmental Panel on Climate Change* [Houghton, J.T., et al. (eds.)]. Cambridge University Press, Cambridge, United Kingdom and New York, NY, USA, pp. 349–416.

Ramaswamy, V., et al., 2006b: Anthropogenic and natural influences in the evolution of lower stratospheric cooling. *Science*, **311**, 1138–1141.

Randall, C.E., R.M. Bevilacqua, J.D. Lumpe, and K.W. Hoppel, 2001: Validation of POAM III aerosols: Comparison to SAGE II and HALOE. *J. Geophys. Res.*, **106**, 27525–27536.

Randles, C.A., L.M. Russell, and V. Ramaswamy, 2004: Hygroscopic and optical properties of organic sea salt aerosol and consequences for climate forcing. *Geophys. Res. Lett.*, **31**, L16108, doi:10.1029/2004GL020628.

Rasch, P.J., and J.E. Kristjánsson, 1998. A comparison of the CCM3 model climate using diagnosed and predicted condensate parametrizations. *J. Clim.*, **11**, 1587–1614.

Read, W.G., L. Froidevaux, and J.W. Waters, 1993: Microwave limb sounder measurements of stratospheric SO_2 from the Mt. Pinatubo volcano. *Geophys. Res. Lett.*, **20**(12), 1299–1302.

Reddy, M.S., and O. Boucher, 2004: A study of the global cycle of carbonaceous aerosols in the LMDZT general circulation model. *J. Geophys. Res.*, **109**, D14202, doi:10.1029/2003JD004048.

Reddy, M.S., O. Boucher, Y. Balanski, and M. Schulz, 2005a: Aerosol optical depths and direct radiative perturbations by species and source type. *Geophys. Res. Lett.*, **32**, L12803, doi:10.1029/2004GL021743.

Reddy, M.S., et al., 2005b: Estimates of global multicomponent aerosol optical depth and direct radiative perturbation in the Laboratoire de Météorologie Dynamique general circulation model. *J. Geophys. Res.*, **110**, D10S16, doi:10.1029/2004JD004757.

Reid, J.S., et al., 1999: Use of the Angstrom exponent to estimate the variability of optical and physical properties of aging smoke particles in Brazil. *J. Geophys. Res.*, **104**(D22), 27473–27490.

Reid, J.S., et al., 2003: Analysis of measurements of Saharan dust by airborne and ground-based remote sensing methods during the Puerto Rico Dust Experiment (PRIDE). *J. Geophys. Res.*, **108**(D19), 8586, doi:10.1029/2002JD002493.

Reimann, S., et al., 2005: Low methyl chloroform emissions inferred from long-term atmospheric measurements. *Nature*, **433**, 506–508, doi:10.1038/nature03220.

Remer, L.A., and Y.J. Kaufman, 2006: Aerosol direct radiative effect at the top of the atmosphere over cloud free oceans derived from four years of MODIS data. *Atmos. Chem. Phys.*, **6**, 237–253.

Remer, L.A., et al., 2002: Validation of MODIS aerosol retrieval over ocean. *Geophys. Res. Lett.*, **29**(12), doi:10.1029/2001GL013204.

Remer, L.A., et al., 2005: The MODIS aerosol algorithm, products, and validation. *J. Atmos. Sci.*, **62**, 947–973.

Richards, J.F, 1990: Land transformation. In: *The Earth as Transformed by Human Action* [Turner, B.L. II, et al. (eds.)]. Cambridge University Press, New York, NY, pp. 163–178.

Richter, A., et al., 2005: Increase in tropospheric nitrogen dioxide over China observed from space. *Nature*, **437**, 129–132.

Rigozo, N.R., E. Echer, L.E.A. Vieira, and D.J.R. Nordemann, 2001: Reconstruction of Wolf sunspot numbers on the basis of spectral characteristics and estimates of associated radio flux and solar wind parameters for the last millennium. *Sol. Phys.*, **203**, 179–191.

Rind, D., J. Perlwitz, and P. Lonergan, 2005: AO/NAO response to climate change: 1. Respective influences of stratospheric and tropospheric climate changes. *J. Geophys. Res.*, **110**, D12107, doi:10.1029/2004JD005103.

Rissler, J., et al., 2004: Physical properties of the sub-micrometer aerosol over the Amazon rain forest during the wet-to-dry season transition – Comparison of modeled and measured CCN concentrations. *Atmos. Chem. Phys.*, **4**, 2119–2143.

Roberts, D.L., and A. Jones, 2004: Climate sensitivity to black carbon aerosol from fossil fuel combustion. *J. Geophys. Res.*, **109**, D16202, doi:10.1029/2004JD004676.

Robles-Gonzalez, C., J.P. Veefkind, and G. de Leeuw, 2000: Mean aerosol optical depth over Europe in August 1997 derived from ATSR-2 data. *Geophys. Res. Lett.* **27**(7), 955–959.

Robson, J.I., et al., 2006: Revised IR spectrum, radiative efficiency and global warming potential of nitrogen trifluoride. *Geophys. Res. Lett.*, **33**, L10817, doi:10.1029/2006GL026210.

Rockmann, T., J. Grooss, and R. Muller, 2004: The impact of anthropogenic chlorine emissions, stratospheric ozone change and chemical feedbacks on stratospheric water. *Atmos. Chem. Phys.*, **4**, 693–699.

Rosenfeld, D., and G. Feingold, 2003: Explanation of discrepancies among satellite observations of the aerosol indirect effects. *Geophys. Res. Lett.*, **30**(14), 1776, doi:10.1029/2003GL017684.

Rosenfeld, D., R. Lahav, A. Khain, and M. Pinsky, 2002: The role of sea spray in cleansing air pollution over the ocean via cloud processes. *Science*, **297**, 1667–1670.

Ross, K.E., et al., 2003: Spatial and seasonal variations in CCN distribution and the aerosol-CCN relationship over southern Africa. *J. Geophys. Res.*, **108**(D13), 8481, doi:10.1029/2002JD002384.

Rotstayn, L.D., 1997: A physically based scheme for the treatment of stratiform clouds and precipitation in large-scale models. I: Description and evaluation of the microphysical processes. *Q. J. R. Meteorol. Soc.*, **123,** 1227–1282.

Rotstayn, L.D., and J.E. Penner, 2001: Indirect aerosol forcing, quasi forcing, and climate response. *J. Clim.*, **14**, 2960–2975.

Rotstayn, L.D., and Y. Liu, 2003: Sensitivity of the first indirect aerosol effect to an increase of the cloud droplet spectral dispersion with droplet number concentration. *J. Clim.*, **16**, 3476–3481.

Rotstayn, L.D., B.F. Ryan, and J. Katzfey, 2000: A scheme for calculation of the liquid fraction in mixed-phase clouds in large scale models. *Mon. Weather Rev.*, **128**, 1070–1088.

Rottman, G., 2005: The SORCE Mission. *Solar Phys.*, **230**, 7–25.

Rozanov, E.V., et al., 2002: Climate/chemistry effect of the Pinatubo volcanic eruption simulated by the UIUC stratosphere/troposphere GCM with interactive photochemistry. *J. Geophys. Res.*, **107**, 4594, doi:10.1029/2001JD000974.

Rozanov, E.V., et al., 2004: Atmospheric response to the observed increase of solar UV radiation from solar minimum to solar maximum simulated by the University of Illinois at Urbana-Champaign climate-chemistry model. *J. Geophys. Res.*, **109**, D01110, doi:10.1029/2003JD003796.

Russell, P.B., and J. Heintzenberg, 2000: An overview of the ACE-2 clear sky column closure experiment (CLEARCOLUMN). *Tellus*, **52B**, 463–483, doi:10.1034/j.1600-0889.2000.00013.x.

Russell, P.B., P.V. Hobbs, and L.L. Stowe, 1999: Aerosol properties and radiative effects in the United States East Coast haze plume: An overview of the Tropospheric Aerosol Radiative Forcing Observational Experiment (TARFOX). *J. Geophys. Res.*, **104**(D2), 2213–2222.

Rypdal, K., et al., 2005: Tropospheric ozone and aerosols in climate agreements: scientific and political challenges. *Environ. Sci. Policy*, **8**, 29–43.

Salby, M., and P. Callaghan, 2004: Evidence of the solar cycle in the general circulation of the stratosphere. *J. Clim.*, **17**, 34–46.

Santer, B.D., et al., 2004: Identification of anthropogenic climate change using a second-generation reanalysis. *J. Geophys. Res.*, **109**, D21104, doi:10.1029/2004JD005075.

Sato, M., J.E. Hansen, M.P. McCormick, and J.B. Pollack, 1993: Stratospheric aerosol optical depths, 1850-1990. *J. Geophys. Res.*, **98**(D12), 22987–22994.

Sato, M., et al., 2003: Global atmospheric black carbon inferred from AERONET. *Proc. Natl. Acad. Sci. U.S.A.*, **100**, 6319–6324.

Sausen, R., and U. Schumann, 2000: Estimates of the climate response to aircraft CO_2 and NO(x) emissions scenarios. *Clim. Change*, **44**, 27–58.

Sausen, R., K. Gierens, M. Ponater, and U. Schumann, 1998: A diagnostic study of the global distribution of contrails part I: Present day climate. *Theor. Appl. Climatol.*, **61**, 127–141.

Sausen, R., et al., 2005: Aviation radiative forcing in 2000: An update on IPCC (1999). *Meteorol. Z.*, **14**, 1–7.

Schaaf, C.B., et al., 2002: First operational BRDF, albedo nadir reflectance products from MODIS. *Remote Sens. Environ.*, **83**, 135–148.

Schaap, M., et al., 2004: Secondary inorganic aerosol simulations for Europe with special attention to nitrate. *Atmos. Chem. Phys.*, **4,** 857–874.

Schatten, K.H., and J.A. Orosz, 1990: Solar constant secular changes. *Sol. Phys.*, **125**, 179–184.

Schmidt, G.A., et al., 2005: Present day atmospheric simulations using GISS ModelE: Comparison to in situ, satellite and reanalysis data. *J. Clim.*, **19**, 153–192.

Schnaiter, M., et al., 2003: UV-VIS-NIR spectral optical properties of soot and soot-containing aerosols. *J. Aerosol Sci.*, **34**(10), 1421–1444.

Schoeberl, M., A. Douglass, Z. Zhu, and S. Pawson, 2003: A comparison of the lower stratospheric age spectra derived from a general circulation model and two data assimilation systems. *J. Geophys. Res*., **108**, L4113, doi:10.1029/2002JD002652.

Scholes, M., and M.O. Andreae, 2000: Biogenic and pyrogenic emissions from Africa and their impact on the global atmosphere. *Ambio*, **29**, 23–29.

Schulz, M., S. Kinne, C. Textor, and S. Guibert, 2004: *AeroCom Aerosol Model Intercomparison*. http://nansen.ipsl.jussieu.fr/AEROCOM/.

Schulz, M., et al., 2006: Radiative forcing by aerosols as derived from the AeroCom present-day and pre-industrial simulations. *Atmos. Chem. Phys. Discuss.*, **6**, 5095–5136.

Schumann, U., 2005: Formation, properties, and climatic effects of contrails. *Comptes Rendus Physique*, **6**, 549–565.

Schuster, G.L., O. Dubovik, B.N. Holben, and E.E. Clothiaux, 2005: Inferring black carbon content and specific absorption from Aerosol Robotic Network (AERONET) aerosol retrievals. *J. Geophys. Res*., **110**, D10S17, doi:10.1029/2004JD004548.

Schwartz, S.E., and M.O. Andreae, 1996: Uncertainty in climate change caused by aerosols. *Science*, **272**, 1121–1122.

Schwartz, S.E., D.W. Harshvardhan, and C.M. Benkovitz, 2002: Influence of anthropogenic aerosol on cloud optical depth and albedo shown by satellite measurements and chemical transport modeling. *Proc. Natl. Acad. Sci. U.S.A.*, **99**, 1784–1789.

Sekiguchi, M., et al., 2003: A study of the direct and indirect effects of aerosols using global satellite datasets of aerosol and cloud parameters. *J. Geophys. Res*., **108**(D22), 4699, doi:10.1029/2002JD003359.

Sellers, P.J., et al., 1996: Comparison of radiative and physiological effects of doubled atmospheric CO_2 on climate. *Science*, **271**, 1402–1406.

Shantz, N.C., W.R. Leaitch, and P. Caffrey, 2003: Effect of organics of low solubility on the growth rate of cloud droplets. *J. Geophys. Res.*, **108**(D5), doi:10.1029/2002JD002540.

Sherwood, S., 2002: A microphysical connection among biomass burning, cumulus clouds, and stratospheric moisture. *Science*, **295**, 1272–1275.

Shi, G.Y., et al., 2005: Sensitivity experiments on the effects of optical properties of dust aerosols on their radiative forcing under clear sky condition. *J. Meteorol. Soc. Japan*, **83A**, 333–346.

Shindell, D.T., 2001: Climate and ozone response to increased stratospheric water vapor. *Geophys. Res. Lett*., **28**, 1551–1554.

Shindell, D.T., and G. Faluvegi, 2002: An exploration of ozone changes and their radiative forcing prior to the chlorofluorocarbon era. *Atmos. Chem. Phys.*, **2**, 363–374.

Shindell, D.T., G. Faluvegi, and N. Bell, 2003a: Preindustrial-to-present day radiative forcing by tropospheric ozone from improved simulations with the GISS chemistry-climate GCM. *Atmos. Chem. Phys.*, **3**, 1675–1702.

Shindell, D.T., G.A. Schmidt, R.L. Miller, and M. Mann, 2003b: Volcanic and solar forcing of climate change during the preindustrial era. *J. Clim.*, **16**, 4094–4107.

Shindell, D.T., G.A. Schmidt, M. Mann, and G. Faluvegi, 2004: Dynamic winter climate response to large tropical volcanic eruptions since 1600. *J. Geophys. Res*., **109**, D05104, doi:10.1029/2003JD004151.

Shindell, D.T., G. Faluvegi, N. Bell, and G. Schmidt, 2005: An emissions-based view of climate forcing by methane and tropospheric ozone. *Geophys. Res. Lett*., **32**, L04803, doi:10.1029/2004GL021900.

Shine, K.P., 2005: Comment on 'Contrails, cirrus, trends, and climate'. *J. Clim.*, **18**, 2781–2782.

Shine, K.P., J. Cook, E.J. Highwood, and M.M. Joshi, 2003: An alternative to radiative forcing for estimating the relative importance of climate change mechanisms. *Geophys. Res. Lett*., **30** (20), 2047, doi:10.1029/2003GL018141.

Shine, K.P., T.K. Berntsen, J.S. Fuglestvedt, and R. Sausen, 2005a: Scientific issues in the design of metrics for inclusion of oxides of nitrogen in global climate agreements. *Proc. Natl. Acad. Sci. U.S.A.*, **102**, 15768–15773.

Shine, K.P., J.S. Fuglestvedt, K. Hailemariam, and N. Stuber, 2005b: Alternatives to the global warming potential for comparing climate impacts of emissions of greenhouse gases. *Clim. Change*, **68**, 281–302.

Shine, K.P, et al., 2005c: Perfluorodecalin: global warming potential and first detection in the atmosphere. *Atmos. Environ.*, **39**, 1759–1763.

Simmonds, P.G., R. Derwent, A. Manning, and G. Spain, 2004: Significant growth in surface ozone at Mace Head, Ireland ,1987-2003. *Atmos. Environ.*, **38**, 4769–4778.

Simpson, I.J., D.R. Blake, F.S. Rowland, and T.Y. Chen, 2002: Implications of the recent fluctuations in the growth rate of tropospheric methane. *Geophys. Res. Lett*., **29**(10), doi:10.1029/2001GL014521.

Smith, C.A., J.D. Haigh, and R. Toumi, 2001: Radiative forcing due to trends in stratospheric water vapour. *Geophys. Res. Lett*., **28**(1), 179–182.

Smith, R.N.B., 1990: A scheme for predicting layer clouds and their water content in a general circulation model. *Q. J. R. Meteorol. Soc*., **116**, 435–460.

Smith, S.J., and T.M.L. Wigley, 2000: Global warming potentials: 2. Accuracy. *Clim. Change*, **44**, 459–469.

Smith, S.J., E. Conception, R. Andres, and J. Lurz, 2004: *Historical Sulphur Dioxide Emissions 1850-2000: Methods and Results*. Research Report No. PNNL-14537, Joint Global Change Research Institute, College Park, MD, 16 pp.

Smith, W.L. Jr., et al., 2005: EOS terra aerosol and radiative flux validation: an overview of the Chesapeake Lighthouse and Aircraft Measurements for Satellites (CLAMS) experiment. *J. Atmos. Sci*., **62**(4), 903–918, doi:10.1175/JAS3398.1.

Sofia, S., and L.H. Li, 2001: Solar variability and climate. *J. Geophys. Res*., **106**(A7), 12969–12974.

Sokolov, A., 2006: Does model sensitivity to changes in CO_2 provide a measure of sensitivity to the forcing of different nature. *J. Clim.*, **19**, 3294–3306.

Solanki, S.K., and M. Fligge, 1999: A reconstruction of total solar irradiance since 1700. *Geophys. Res. Lett*., **26**(16), 2465–2468.

Solanki, S.K., et al., 2004: Unusual activity of the Sun during recent decades compared to the previous 11,000 years. *Nature*, **431**, 1084–1087.

Solomon, S., et al., 1996: The role of aerosol variations in anthropogenic ozone depletion at northern midlatitudes. *J. Geophys. Res.*, **101**(D3), 6713–6727.

Solomon, S., et al., 2005: On the distribution and variability of ozone in the tropical upper troposphere: Implications for tropical deep convection and chemical-dynamical coupling. *Geophys. Res. Lett*., **32**, L23813, doi:10.1029/2005GL024323.

Soufflet, V., D. Tanre, A. Royer, and N.T. O'Neill, 1997: Remote sensing of aerosols over boreal forest and lake water from AVHRR data. *Remote Sens. Environ.*, **60**, 22–34.

Spahni, R., et al., 2005: Atmospheric methane and nitrous oxide of the late Pleistocene from Antarctic ice cores. *Science*, **310**, 1317–1321.

Spinhirne, J.D., et al., 2005: Cloud and aerosol measurements from GLAS: overview and initial results. *Geophys. Res. Lett*., **32**, L22S03, doi:10.1029/2005GL023507.

Spruit, H., 2000: Theory of solar irradiance variations. *Space Sci. Rev.*, **94**, 113–126.

Steinbrecht, W., H. Claude, and P. Winkler, 2004a: Enhanced upper stratospheric ozone: sign of recovery or solar cycle effect? *J. Geophys. Res*., **109**, D020308, doi:10.1029/2003JD004284.

Steinbrecht, W., H. Claude, and P. Winkler, 2004b: Reply to comment by D. M. Cunnold et al. on "Enhanced upper stratospheric ozone: Sign of recovery or solar cycle effect?". *J. Geophys. Res*., **109**, D14306, doi:10.1029/2004JD004948.

Stenchikov, G.L., et al., 1998: Radioactive forcing from the 1991 Mount Pinatubo volcanic eruption. *J. Geophys. Res*., **103**(D12), 13837–13857.

Stenchikov, G.L., et al., 2002: Arctic Oscillation response to the 1991 Mount Pinatubo eruption: effects of volcanic aerosols and ozone depletion. *J. Geophys. Res*., **107**(D24), 4803, doi:10.1029/2002JD002090.

Stenchikov, G., et al., 2004: Arctic Oscillation response to the 1991 Pinatubo eruption in the SKYHI GCM with a realistic quasi-biennial oscillation. *J. Geophys. Res*., **109**, D03112, doi:10.1029/2003JD003699.

Stenchikov, G., et al., 2006: Arctic Oscillation response to volcanic eruptions in the IPCC AR4 climate models. *J. Geophys. Res*., **111**, D07107, doi:10.1029/2005JD006286.

Stern, D.I., 2005: Global sulfur emissions from 1850 to 2000. *Chemosphere*, **58**, 163–175.

Stevenson, D.S., et al., 2004: Radiative forcing from aircraft NO_x emissions: mechanisms and seasonal dependence. *J. Geophys. Res*., **109**, D17307, doi:10.1029/2004JD004759.

Stier, P., et al., 2005: The aerosol-climate model ECHAM5-HAM. *Atmos. Chem. Phys*., **5**, 1125–1156.

Stier, P., et al., 2006a: Impact of nonabsorbing anthropogenic aerosols on clear-sky atmospheric absorption. *J. Geophys. Res.*, **111**, D18201, doi:10.1029/2006JD007147.

Stier, P., et al., 2006b: Emission-induced nonlinearities in the global aerosol system: results from the ECHAM5-HAM aerosol-climate model. *J. Clim.*, **19**, 3845–3862.

Stordal, F., et al., 2005: Is there a trend in cirrus cloud cover due to aircraft traffic? *Atmos. Chem. Phys.*, **5**, 2155–2162.

Stothers, R., 2001a: Major optical depth perturbations to the stratosphere from volcanic eruptions: Stellar extinction period, 1961-1978. *J. Geophys. Res*., **106**(D3), 2993–3003.

Stothers, R., 2001b: A chronology of annual mean radii of stratospheric aerosol from volcanic eruptions during the twentieth century as derived from ground-based spectral extinction measurements. *J. Geophys. Res*., **106**(D23), 32043–32049.

Stott P.A., G.S. Jones, and J.F.B. Mitchell, 2003: Do models underestimate the solar contribution to recent climate change? *J. Clim.*, **16**, 4079–4093.

Streets, D.G., et al., 2001: Black carbon emissions in China. *Atmos. Environ*., **35**, 4281–4296.

Streets, D.G., et al., 2003: An inventory of gaseous and primary aerosol emissions in Asia in the year 2000. *J. Geophys. Res*., **108**(D21), 8809, doi:10.1029/2002JD003093.

Strugnell, N.C., W. Lucht, and C. Schaaf, 2001: A global albedo data set derived from AVHRR data for use in climate simulations. *Geophys. Res. Lett*., **28**(1), 191–194.

Stubenrauch, C.J., and U. Schumann, 2005: Impact of air traffic on cirrus coverage. *Geophys. Res. Lett*., **32**, L14813, doi:10.1029/2005GL022707.

Stuber, N., M. Ponater, and R. Sausen, 2001a: Is the climate sensitivity to ozone perturbations enhanced by stratospheric water vapor feedback? *Geophys. Res. Lett*., **28**(15), 2887–2890.

Stuber, N., R. Sausen, and M. Ponater, 2001b: Stratosphere adjusted radiative forcing calculations in a comprehensive climate model. *Theor. Appl. Climatol*., **68**, 125–135.

Stuber, N., M. Ponater, and R. Sausen, 2005: Why radiative forcing might fail as a predictor of climate change. *Clim. Dyn*., **24**, 497–510.

Sun, B., and R.S. Bradley, 2002: Solar influences on cosmic rays and cloud formation: a re-assessment. *J. Geophys. Res*., **107**(D14), doi:10.1029/2001JD000560.

Sundqvist, H., 1978: A parametrization scheme for non-convective condensation including prediction of cloud water content. *Q. J. R. Meteorol. Soc*., **104**, 677–690.

Sundqvist, H., E. Berge, and J.E. Kristjánsson, 1989: Condensation and cloud parametrization studies with a mesoscale numerical weather prediction model. *Mon. Weather Rev*., **117**, 1641–1657.

Suzuki, K., et al., 2004: A study of the aerosol effect on a cloud field with simultaneous use of GCM modeling and satellite observation. *J. Atmos. Sci*., **61**, 179–194.

Svalgaard, L., E.W. Cliver, and P. Le Sager, 2004: IHV: A new long-term geomagnetic index. *Adv. Space Res.*, **34**, 436–439.

Swap, R.J., et al., 2002: The Southern African Regional Science Initiative (SAFARI 2000): overview of the dry season field campaign. *S. Afr. J. Sci.*, **98**, 125–130.

Swap, R.J., et al., 2003: Africa burning: a thematic analysis of the Southern African Regional Science Initiative (SAFARI 2000). *J. Geophys. Res*., **108**(D13), 8465, doi:10.1029/2003JD003747.

Tabazadeh, A., et al., 2002: Arctic "ozone hole" in cold volcanic stratosphere. *Proc. Natl. Acad. Sci. U.S.A.*, **99**, 2609–2612.

Takemura, T., T. Nakajima, T. Nozawa, and K. Aoki, 2001: Simulation of future aerosol distribution, radiative forcing, and long-range transport in East Asia. *J. Meteorol. Soc. Japan*, **2**, 79, 1139–1155.

Takemura, T., et al., 2000: Global three-dimensional simulation of aerosol optical thickness distribution of various origins. *J. Geophys. Res.*, **105**(D14), 17853–17874.

Takemura, T., et al., 2005: Simulation of climate response to aerosol direct and indirect effects with aerosol transport-radiation model. *J. Geophys. Res*., **110**, D02202, doi:10.1029/2004JD005029.

Tang, I.N., 1997: Thermodynamic and optical properties of mixed-salt aerosols of atmospheric importance. *J. Geophys. Res*., **102**(D2), 1883–1893.

Tang, I.N., K.H. Fung, D.G. Imre, and H.R. Munkelwitz, 1995: Phase transformation and metastability of hygroscopic microparticles. *Aerosol Sci. Tech.*, **23**, 443.

Tanré, D., Y.J. Kaufman, M. Herman, and S. Mattoo, 1997: Remote sensing of aerosol properties over oceans using the MODIS/EOS spectral radiances. *J. Geophys. Res*., **102**(D14), 16971–16988.

Tanré, D., et al., 2003: Measurement and modeling of the Saharan dust radiative impact: overview of the SaHAran Dust Experiment (SHADE). *J. Geophys. Res*., **108**(D18), doi:10.1029/2002JD003273.

Tarasick, D.W., et al., 2005: Changes in the vertical distribution of ozone over Canada from ozonesondes: 1980-2001. *J. Geophys. Res*., **110**, D02304, doi:10.1029/2004JD004643.

Tegen, I., and I. Fung, 1995: Contribution to the atmospheric mineral aerosol load from land surface modification. *J. Geophys. Res*., **100**, 18707–18726.

Tegen, I., A.A. Lacis, and I. Fung, 1996: The influence on climate forcing of mineral aerosols from disturbed soils. *Nature*, **380**, 419–421.

Tegen, I., M. Werner, S.P. Harrison, and K.E. Kohfeld, 2004: Relative importance of climate and land use in determining present and future global soil dust emission. *Geophys. Res. Lett.*, **31**, L05105, doi:10.1029/2003GL019216.

Tegen, I., M. Werner, S.P. Harrison, and K.E. Kohfeld, 2005: Reply to comment by N. M. Mahowald et al. on "Relative importance of climate and land use in determining present and future global soil dust emission". *Geophys. Res. Lett.*, **32**, doi:10.1029/2004GL021560.

Tett, S.F.B., et al., 2002: Estimation of natural and anthropogenic contributions to twentieth century temperature change. *J. Geophys. Res.*, **107**(D16), 4306, doi:10.1029/2000JD000028.

Textor, C., et al., 2006: AeroCom: The status quo of global aerosol modelling. *Atmos. Chem. Phys*., **6**, 1777–1813.

Tie, X.X., G.P. Brasseur, B. Breiglib, and C. Granier, 1994: Two dimensional simulation of Pinatubo aerosol and its effect on stratospheric chemistry. *J. Geophys. Res*., **99**(D10), 20545–20562.

Thomason, L., and T. Peter, 2006: *Assessment of Stratospheric Aerosol Properties (ASAP): Report on the Assessment Kick-Off Workshop, Paris, France, 4-6 November 2001*. SPARC Report No. 4, WCRP-124, WMO/TD No. 1295, http://www.aero.jussieu.fr/~sparc/News18/18_Thomason.html.

Thompson, A.M., et al., 2001: Tropical tropospheric ozone and biomass burning. *Science*, **291**, 2128–2132.

Thompson, T.M., et al., 2004: Halocarbons and other atmospheric trace species. In: *Climate Monitoring and Diagnostics Laboratory, Summary Report No. 27* [Schnell, R.C., A.-M. Buggle, and R.M. Rosson (eds.)]. NOAA CMDL, Boulder, CO, pp. 115–135.

Timmreck, C., and M. Schulz, 2004: Significant dust simulation differences in nudged and climatological operation mode of the AGCM ECHAM. *J. Geophys. Res*., **109**, D13202, doi:10.1029/2003JD004381.

Timmreck, C., H.-F. Graf, and B. Steil, 2003: Aerosol chemistry interactions after the Mt. Pinatubo Eruption. In: *Volcanism and the Earth's Atmosphere* [Robock, A., and C. Oppenheimer (eds.)]. Geophysical Monograph 139, American Geophysical Union, Washington, DC, pp. 227–236.

Tol, R.S.J., 2002: Estimates of the damage costs of climate change, Part II. Dynamic estimates. *Environ. Resour. Econ.*, **21**, 135–160.

Torres, O., et al., 2002: A long-term record of aerosol optical depth from TOMS: Observations and comparison to AERONET measurements. *J. Atmos. Sci.*, **59**, 398–413.

Travis, D.J., A.M. Carleton, and R.G. Lauritsen, 2002: Contrails reduce daily temperature range. *Nature*, **418**, 601–602.

Travis, D.J., A.M. Carleton, and R.G. Lauritsen, 2004: Regional variations in U.S. diurnal temperature range for the 11-14 September 2001 aircraft groundings: evidence of jet contrail influence on climate. *J. Clim.*, **17**, 1123–1134.

Tripoli, G.J., and W.R. Cotton, 1980: A numerical investigation of several factors contributing to the observed variable intensity of deep convection over South Florida. *J. Appl. Meteorol*., **19**, 1037–1063.

Twohy, C.H., et al., 2005: Evaluation of the aerosol indirect effect in marine stratocumulus clouds: droplet number, size, liquid water path, and radiative impact. *J. Geophys.Res*., **110**, D08203, doi:10.1029/2004JD005116.

Twomey, S.A., 1977: The influence of pollution on the shortwave albedo of clouds. *J. Atmos. Sci*., **34**, 1149–1152.

Udelhofen, P.M., and R.D. Cess, 2001: Cloud cover variations over the United States: An influence of cosmic rays or solar variability? *Geophys. Res. Lett*., **28**(13), 2617–2620.

Usoskin, I.G., et al., 2004: Latitudinal dependence of low cloud amount on cosmic ray induced ionization. *Geophys. Res. Lett*., **31**, L16109, doi:10.1029/2004GL019507.

Van Aardenne, J.A., et al., 2001: A 1 x 1 degree resolution dataset of historical anthropogenic trace gas emissions for the period 1890-1990. *Global Biogeochem. Cycles*, **15**, 909–928.

van der Werf, et al., 2004: Continental-scale partitioning of fire emissions during the 1997 to 2001 El Nino/La Nina period. *Science*, **303**, 73–76.

Van Dorland, R., F.J. Dentener, and J. Lelieveld, 1997: Radiative forcing due to tropospheric ozone and sulfate aerosols. *J. Geophys. Res*., **102**(D23), 28079–28100.

van Loon, H., and D.J. Shea, 2000: The global 11-year solar signal in July-August. *Geophys. Res. Lett*., **27**(18), 2965–2968.

Veefkind, J.P., G. de Leeuw, and P.A. Durkee, 1998: Retrieval of aerosol optical depth over land using two-angle view satellite radiometry. *Geophys. Res. Lett*. **25**(16), 3135–3138.

Velders, et al., 2005: Chemical and radiative effects of halocarbons and their replacement compounds. In: *Special Report on Safeguarding the Ozone Layer and the Global Climate System: Issues Related to Hydrofluorocarbons and Perfluorocarbons* [Metz, B., et al. (eds.)]. Cambridge University Press, Cambridge, United Kingdom and New York, NY, USA, pp. 133–180.

Vestreng, V., M. Adams, and J. Goodwin, 2004: *Inventory Review 2004: Emission Data Reported to CLRTAP and the NEC Directive*. EMEP/EEA Joint Review Report, Norwegian Meteorological Institute, Norway, 120 pp.

von Hoyningen-Huene, W., M. Freitag, and J.B. Burrows, 2003: Retrieval of aerosol optical thickness over land surfaces from top-of-atmosphere radiance. *J. Geophys. Res*., **108**(D9), 4260, doi:10.1029/2001JD002018.

Walter, B.P., M. Heimann, and E. Matthews, 2001a: Modeling modern methane emissions from natural wetlands 2. Interannual variations 1982-1993. *J. Geophys. Res*., **106**(D24), 34207–34220.

Walter, B.P., M. Heimann, and E. Matthews, 2001b: Modeling modern methane emissions from natural wetlands 1. Model description and results. *J. Geophys. Res*., **106**(D24), 34189–34206.

Wang, C., 2004: A modeling study on the climate impacts of black carbon aerosols. *J. Geophys. Res*., **109**, D03106, doi:10.1029/2003JD004084.

Wang, H.J., et al., 2002: Assessment of SAGE version 6.1 ozone data quality. *J. Geophys. Res*., **107**(D23), 4691, doi:10.1029/2002JD002418.

Wang, M.H., K.D. Knobelspiesse, and C.R. McClain, 2005: Study of the Sea-Viewing Wide Field-of-View Sensor (SeaWiFS) aerosol optical property data over ocean in combination with the ocean color products. *J. Geophys. Res*., **110**, D10S06, doi:10.1029/2004JD004950.

Wang, W.-C., M.P. Dudek, and X.-Z. Liang, 1992: Inadequacy of effective CO_2 as a proxy in assessing the regional climate change due to other radiatively active gases. *Geophys. Res. Lett*., **19**, 1375–1378.

Wang, W.-C., M.P. Dudek, X.-Z. Liang, and J.T. Kiehl, 1991: Inadequacy of effective CO_2 as a proxy in simulating the greenhouse effect of other radiatively active gases. *Nature*, **350**, 573–577.

Wang, Y.M., J.L. Lean, and N.R. Sheeley, 2005: Modeling the sun's magnetic field and irradiance since 1713. *Astrophys. J.*, **625**, 522–538.

Warner, J., and S.A. Twomey, 1967: The production and cloud nuclei by cane fires and the effect on cloud droplet concentration. *J. Atmos. Sci*., **24**, 704–706.

Warwick, N.J., et al., 2002: The impact of meteorology on the interannual growth rate of atmospheric methane. *Geophys. Res. Lett*., **29**(26), doi:10.1029/2002/GL015282.

Weatherhead, E.C., and S. B. Andersen, 2006: The search for signs of recovery of the ozone layer. *Nature*, **441**, 39–45.

Welton, E.J., J.R. Campbell, J.D. Spinhirne, and V.S. Scott, 2001: Global monitoring of clouds and aerosols using a network of micro-pulse lidar systems. In: *Lidar Remote Sensing for Industry and Environmental Monitoring* [Singh, U.N., T. Itabe, and N. Sugimoto (eds.)]. SPIE, Bellingham, WA, pp. 151–158.

Wennberg, P.O., S. Peacock, J.T. Randerson, and R. Bleck, 2004: Recent changes in the air-sea gas exchange of methyl chloroform. *Geophys. Res. Lett*., **31**, L16112, doi:10.1029/2004GL020476.

Westerling, A.L., H.G. Hidalgo, D.R. Cayan, and T.W. Swetnam, 2006: Warming and earlier spring increase western U.S. forest wildfire activity. *Science*, **313**, 940–943.

White, W.B., M.D. Dettinger, and D.R. Cayan, 2003: Sources of global warming of the upper ocean on decadal period scales. *J. Geophys. Res*., **108**(C8), doi:10.1029/2002JC001396.

Wild, O., M.J. Prather, and H. Akimoto, 2001: Indirect long-term global radiative cooling from NO_x emissions. *Geophys. Res. Lett*., **28**(9), 1719–1722.

Williams, K.D., C.A. Senior, and J.F.B. Mitchell, 2001a: Transient climate change in the Hadley Centre models: the role of physical processes. *J. Clim.*, **14**, 2659–2674.

Williams, K.D., et al., 2001b: The response of the climate system to the indirect effects of anthropogenic sulfate aerosols. *Clim. Dyn*., **17**, 846–856.

Willson, R.C., and A.V. Mordvinov, 2003: Secular total solar irradiance trend during solar cycles 21-23. *Geophys. Res. Lett*., **30**(5), 3–6.

Wilson, D.R., and S.P. Ballard, 1999: A microphysically based precipitation scheme for the UK Meteorological Office Unified Model. *Q. J. R. Meteorol. Soc*., **125**, 1607–1636.

Wilson, M.F., and A. Henderson-Sellers, 1985: A global archive of land cover and soils data for use in general-circulation climate models. *J. Climatol.*, **5**, 119–143.

WMO, 1986: *Atmospheric Ozone 1985*. Global Ozone Research and Monitoring Project Report No.16, World Meteorological Organisation, Geneva, Volume 3.

WMO, 2003: *Scientific Assessment of Ozone Depletion: 2002*. Global Ozone Research and Monitoring Project Report No. 47, World Meteorological Organization, Geneva, 498 pp.

Wong, J., and Z. Li, 2002: Retrieval of optical depth for heavy smoke aerosol plumes: uncertainties and sensitivities to the optical properties. *J. Atmos. Sci*., **59**, 250–261.

Wong, S., et al., 2004: A global climate-chemistry model study of present-day tropospheric chemistry and radiative forcing from changes in tropospheric O_3 since the preindustrial period. *J. Geophys. Res*., **109**, D11309, doi:10.1029/2003JD003998.

Woods, T.N., et al., 1996: Validation of the UARS solar ultraviolet irradiances: comparison with the ATLAS 1 and 2 measurements. *J. Geophys. Res*., **101**(D6), 9541–9569.

Xiong, J.Q., et al., 1998: Influence of organic films on the hygroscopicity of ultrafine sulfuric acid aerosol. *Environ. Sci. Technol*., **32**, 3536–3541.

Xue, H., and G. Feingold, 2006: large eddy simulations of trade-wind cumuli: investigation of aerosol indirect effects. *J. Atmos. Sci*., **63**, 1605–1622.

Yang, F., and M. Schlesinger, 2001: Identification and separation of Mount Pinatubo and El Nino-Southern Oscillation land surface temperature anomalies. *J. Geophys. Res*., **106**(D14), 14757–14770.

Yang, F., and M. Schlesinger, 2002: On the surface and atmospheric temperature changes following the 1991 Pinatubo volcanic eruption: a GCM study. *J. Geophys. Res*., **107**(D8), doi:10.1029/2001JD000373.

Yokouchi, et al., 2005: Estimates of ratios of anthropogenic halocarbon emissions from Japan based on aircraft monitoring over Sagami Bay, Japan. *J. Geophys. Res*., **110**, D06301, doi:10.1029/2004JD005320.

Yoshioka, M., N. Mahowald, J.L. Dufresne, and C. Luo, 2005: Simulation of absorbing aerosol indices for African dust. *J. Geophys. Res*., **110**, D18S17, doi:10.1029/2004JD005276.

Yu, H., et al., 2003: Annual cycle of global distributions of aerosol optical depth from integration of MODIS retrievals and GOCART model simulations. *J. Geophys. Res*., **108**(D3), 4128, doi:10.1029/2002JD002717.

Yu, H., et al., 2006: A review of measurement-based assessments of the aerosol direct radiative effect and forcing. *Atmos. Chem. Phys.*, **6**, 613–666.

Yvon-Lewis, S.A., and J.H. Butler, 2002: Effect of oceanic uptake on atmospheric lifetimes of selected trace gases. *J. Geophys. Res*., **107**(D20), 4414, doi:10.1029/2001JD001267.

Zender, C.S., 2004: Quantifying mineral dust mass budgets: terminology, constraints, and current estimates. *Eos*, **85**, 509–512.

Zerefos, C.S., et al., 2003: Evidence of impact of aviation on cirrus cloud formation. *Atmos. Chem. Phys.*, **3**, 1633–1644.

Zhang, J., and S. Christopher, 2003: Longwave radiative forcing of Saharan dust aerosols estimated from MODIS, MISR and CERES observations on Terra. *Geophys. Res. Lett*., **30**(23), doi:10.1029/2003GL018479.

Zhang, J., S.A. Christopher, L.A. Remer, and Y.J. Kaufman, 2005: Shortwave aerosol radiative forcing over cloud-free oceans from Terra: 2. Seasonal and global distributions. *J. Geophys. Res*., **110**, D10S24, doi:10.1029/2004JD005009.

Zhang, J.P., Z. Yang, D.J. Wang, and X.B. Zhang, 2002: Climate change and causes in the Yuanmou dry-hot valley of Yunnan China. *J. Arid Environ.*, **51**, 153–162.

Zhao, M., A. Pitman, and T.N. Chase, 2001: The impacts of land cover change on the atmospheric circulation. *Clim. Dyn*., **17**, 467–477.

Zhao, T.X.P., I. Laszlo, P. Minnis, and L. Remer, 2005: Comparison and analysis of two aerosol retrievals over the ocean in the terra/clouds and the earth's radiant energy system: moderate resolution imaging spectroradiometer single scanner footprint data: 1. Global evaluation. *J. Geophys. Res*., **110**, D21208, doi:10.1029/2005JD005851.

Zhou, L.M., et al., 2001: Variations in northern vegetation activity inferred from satellite data of vegetation index during 1981 to 1999. *J. Geophys. Res*., **106**(D17), 20069–20083.

Zhou, M., et al., 2005: A normalized description of the direct effect of key aerosol types on solar radiation as estimated from aerosol robotic network aerosols and moderate resolution imaging spectroradiometer albedos. *J. Geophys. Res*., **110**, D19202, doi:10.1029/2005JD005909.

3

Observations: Surface and Atmospheric Climate Change

Coordinating Lead Authors:
Kevin E. Trenberth (USA), Philip D. Jones (UK)

Lead Authors:
Peter Ambenje (Kenya), Roxana Bojariu (Romania), David Easterling (USA), Albert Klein Tank (Netherlands), David Parker (UK), Fatemeh Rahimzadeh (Iran), James A. Renwick (New Zealand), Matilde Rusticucci (Argentina), Brian Soden (USA), Panmao Zhai (China)

Contributing Authors:
R. Adler (USA), L. Alexander (UK, Australia, Ireland), H. Alexandersson (Sweden), R. Allan (UK), M.P. Baldwin (USA), M. Beniston (Switzerland), D. Bromwich (USA), I. Camilloni (Argentina), C. Cassou (France), D.R. Cayan (USA), E.K.M. Chang (USA), J. Christy (USA), A. Dai (USA), C. Deser (USA), N. Dotzek (Germany), J. Fasullo (USA), R. Fogt (USA), C. Folland (UK), P. Forster (UK), M. Free (USA), C. Frei (Switzerland), B. Gleason (USA), J. Grieser (Germany), P. Groisman (USA, Russian Federation), S. Gulev (Russian Federation), J. Hurrell (USA), M. Ishii (Japan), S. Josey (UK), P. Kållberg (ECMWF), J. Kennedy (UK), G. Kiladis (USA), R. Kripalani (India), K. Kunkel (USA), C.-Y. Lam (China), J. Lanzante (USA), J. Lawrimore (USA), D. Levinson (USA), B. Liepert (USA), G. Marshall (UK), C. Mears (USA), P. Mote (USA), H. Nakamura (Japan), N. Nicholls (Australia), J. Norris (USA), T. Oki (Japan), F.R. Robertson (USA), K. Rosenlof (USA), F.H. Semazzi (USA), D. Shea (USA), J.M. Shepherd (USA), T.G. Shepherd (Canada), S. Sherwood (USA), P. Siegmund (Netherlands), I. Simmonds (Australia), A. Simmons (ECMWF, UK), C. Thorncroft (USA, UK), P. Thorne (UK), S. Uppala (ECMWF), R. Vose (USA), B. Wang (USA), S. Warren (USA), R. Washington (UK, South Africa), M. Wheeler (Australia), B. Wielicki (USA), T. Wong (USA), D. Wuertz (USA)

Review Editors:
Brian J. Hoskins (UK), Thomas R. Karl (USA), Bubu Jallow (The Gambia)

This chapter should be cited as:
Trenberth, K.E., P.D. Jones, P. Ambenje, R. Bojariu, D. Easterling, A. Klein Tank, D. Parker, F. Rahimzadeh, J.A. Renwick, M. Rusticucci, B. Soden and P. Zhai, 2007: Observations: Surface and Atmospheric Climate Change. In: *Climate Change 2007: The Physical Science Basis*. Contribution of Working Group I to the Fourth Assessment Report of the Intergovernmental Panel on Climate Change [Solomon, S., D. Qin, M. Manning, Z. Chen, M. Marquis, K.B. Averyt, M. Tignor and H.L. Miller (eds.)]. Cambridge University Press, Cambridge, United Kingdom and New York, NY, USA.

Table of Contents

Executive Summary 237

3.1 Introduction 240

3.2 Changes in Surface Climate: Temperature 241

3.2.1 Background 241

3.2.2 Temperature in the Instrumental Record for Land and Oceans 241

3.3 Changes in Surface Climate: Precipitation, Drought and Surface Hydrology 254

3.3.1 Background 254

3.3.2 Changes in Large-scale Precipitation 254

3.3.3 Evapotranspiration 260

3.3.4 Changes in Soil Moisture, Drought, Runoff and River Discharge 260

Box 3.1: Drought Terminology and Determination 261

3.3.5 Consistency and Relationships between Temperature and Precipitation 264

3.3.6 Summary 265

3.4 Changes in the Free Atmosphere 265

3.4.1 Temperature of the Upper Air: Troposphere and Stratosphere 265

3.4.2 Water Vapour 271

3.4.3 Clouds 275

3.4.4 Radiation 277

Box 3.2: The Dimming of the Planet and Apparent Conflicts in Trends of Evaporation and Pan Evaporation 279

3.5 Changes in Atmospheric Circulation 280

3.5.1 Surface or Sea Level Pressure 280

3.5.2 Geopotential Height, Winds and the Jet Stream 280

3.5.3 Storm Tracks 281

3.5.4 Blocking 282

3.5.5 The Stratosphere 283

3.5.6 Winds, Waves and Surface Fluxes 283

Box 3.3: Stratospheric-Tropospheric Relations and Downward Propagation 284

3.5.7 Summary 285

3.6 Patterns of Atmospheric Circulation Variability 286

3.6.1 Teleconnections 286

Box 3.4: Defining the Circulation Indices 287

3.6.2 El Niño-Southern Oscillation and Tropical/Extratropical Interactions 287

3.6.3 Pacific Decadal Variability 289

3.6.4 The North Atlantic Oscillation and Northern Annular Mode 290

3.6.5 The Southern Hemisphere and Southern Annular Mode 292

3.6.6 Atlantic Multi-decadal Oscillation 293

3.6.7 Other Indices 294

3.6.8 Summary 295

3.7 Changes in the Tropics and Subtropics, and in the Monsoons 295

3.7.1 Asia 297

3.7.2 Australia 297

3.7.3 The Americas 298

3.7.4 Africa 298

3.7.5 Summary 299

3.8 Changes in Extreme Events 299

3.8.1 Background 299

3.8.2 Evidence for Changes in Variability or Extremes 300

3.8.3 Evidence for Changes in Tropical Storms 304

Box 3.5: Tropical Cyclones and Changes in Climate 305

Box 3.6: Recent Extreme Events 310

3.8.4 Evidence for Changes in Extratropical Storms and Extreme Events 312

3.8.5 Summary 316

3.9 Synthesis: Consistency Across Observations 317

Frequently Asked Questions

FAQ 3.1: *How are Temperatures on the Earth Changing?* 252

FAQ 3.2: *How is Precipitation Changing?* 262

FAQ 3.3: *Has there Been a Change in Extreme Events like Heat Waves, Droughts, Floods and Hurricanes?* 308

References 319

Appendix 3.A: Low-Pass Filters and Linear Trends 336

Supplementary Material

The following Supplementary Material is available on CD-ROM and in on-line versions of this report.

Appendix 3.B: *Techniques, Error Estimation and Measurement Systems*

Executive Summary

Global mean surface temperatures have risen by 0.74°C ± 0.18°C when estimated by a linear trend over the last 100 years (1906–2005). The rate of warming over the last 50 years is almost double that over the last 100 years (0.13°C ± 0.03°C vs. 0.07°C ± 0.02°C per decade). Global mean temperatures averaged over land and ocean surfaces, from three different estimates, each of which has been independently adjusted for various homogeneity issues, are consistent within uncertainty estimates over the period 1901 to 2005 and show similar rates of increase in recent decades. The trend is not linear, and the warming from the first 50 years of instrumental record (1850–1899) to the last 5 years (2001–2005) is 0.76°C ± 0.19°C.

2005 was one of the two warmest years on record. The warmest years in the instrumental record of global surface temperatures are 1998 and 2005, with 1998 ranking first in one estimate, but with 2005 slightly higher in the other two estimates. 2002 to 2004 are the 3rd, 4th and 5th warmest years in the series since 1850. Eleven of the last 12 years (1995 to 2006) – the exception being 1996 – rank among the 12 warmest years on record since 1850. Surface temperatures in 1998 were enhanced by the major 1997–1998 El Niño but no such strong anomaly was present in 2005. Temperatures in 2006 were similar to the average of the past 5 years.

Land regions have warmed at a faster rate than the oceans. Warming has occurred in both land and ocean domains, and in both sea surface temperature (SST) and nighttime marine air temperature over the oceans. However, for the globe as a whole, surface air temperatures over land have risen at about double the ocean rate after 1979 (more than 0.27°C per decade vs. 0.13°C per decade), with the greatest warming during winter (December to February) and spring (March to May) in the Northern Hemisphere.

Changes in extremes of temperature are also consistent with warming of the climate. A widespread reduction in the number of frost days in mid-latitude regions, an increase in the number of warm extremes and a reduction in the number of daily cold extremes are observed in 70 to 75% of the land regions where data are available. The most marked changes are for cold (lowest 10%, based on 1961–1990) nights, which have become rarer over the 1951 to 2003 period. Warm (highest 10%) nights have become more frequent. Diurnal temperature range (DTR) decreased by 0.07°C per decade averaged over 1950 to 2004, but had little change from 1979 to 2004, as both maximum and minimum temperatures rose at similar rates. The record-breaking heat wave over western and central Europe in the summer of 2003 is an example of an exceptional recent extreme. That summer (June to August) was the hottest since comparable instrumental records began around 1780 (1.4°C above the previous warmest in 1807) and is very likely to have been the hottest since at least 1500.

Recent warming is strongly evident at all latitudes in SSTs over each of the oceans. There are inter-hemispheric differences in warming in the Atlantic, the Pacific is punctuated by El Niño events and Pacific decadal variability that is more symmetric about the equator, while the Indian Ocean exhibits steadier warming. These characteristics lead to important differences in regional rates of surface ocean warming that affect the atmospheric circulation.

Urban heat island effects are real but local, and have not biased the large-scale trends. A number of recent studies indicate that effects of urbanisation and land use change on the land-based temperature record are negligible (0.006ºC per decade) as far as hemispheric- and continental-scale averages are concerned because the very real but local effects are avoided or accounted for in the data sets used. In any case, they are not present in the SST component of the record. Increasing evidence suggests that urban heat island effects extend to changes in precipitation, clouds and DTR, with these detectable as a 'weekend effect' owing to lower pollution and other effects during weekends.

Average arctic temperatures increased at almost twice the global average rate in the past 100 years. Arctic temperatures have high decadal variability. A slightly longer warm period, almost as warm as the present, was also observed from the late 1920s to the early 1950s, but appears to have had a different spatial distribution than the recent warming.

Lower-tropospheric temperatures have slightly greater warming rates than those at the surface over the period 1958 to 2005. The radiosonde record is markedly less spatially complete than the surface record and increasing evidence suggests that it is very likely that a number of records have a cooling bias, especially in the tropics. While there remain disparities among different tropospheric temperature trends estimated from satellite Microwave Sounding Unit (MSU and advanced MSU) measurements since 1979, and all likely still contain residual errors, estimates have been substantially improved (and data set differences reduced) through adjustments for issues of changing satellites, orbit decay and drift in local crossing time (i.e., diurnal cycle effects). It appears that the satellite tropospheric temperature record is broadly consistent with surface temperature trends provided that the stratospheric influence on MSU channel 2 is accounted for. The range (due to different data sets) of global surface warming since 1979 is 0.16°C to 0.18°C per decade compared to 0.12°C to 0.19°C per decade for MSU estimates of tropospheric temperatures. It is likely, however, that there is slightly greater warming in the troposphere than at the surface, and a higher tropopause, with the latter due also to pronounced cooling in the stratosphere.

Lower stratospheric temperatures feature cooling since 1979. Estimates from adjusted radiosondes, satellites (MSU channel 4) and reanalyses are in qualitative agreement, suggesting a lower-stratospheric cooling of between 0.3°C and 0.6°C per decade since 1979. Longer radiosonde records (back

to 1958) also indicate cooling but the rate of cooling has been significantly greater since 1979 than between 1958 and 1978. It is likely that radiosonde records overestimate stratospheric cooling, owing to changes in sondes not yet accounted for. Because of the stratospheric warming episodes following major volcanic eruptions, the trends are far from being linear.

Precipitation has generally increased over land north of 30°N over the period 1900 to 2005 but downward trends dominate the tropics since the 1970s. From 10°N to 30°N, precipitation increased markedly from 1900 to the 1950s, but declined after about 1970. Downward trends are present in the deep tropics from 10°N to 10°S, especially after 1976/1977. Tropical values dominate the global mean. It has become significantly wetter in eastern parts of North and South America, northern Europe, and northern and central Asia, but drier in the Sahel, the Mediterranean, southern Africa and parts of southern Asia. Patterns of precipitation change are more spatially and seasonally variable than temperature change, but where significant precipitation changes do occur they are consistent with measured changes in streamflow.

Substantial increases are found in heavy precipitation events. It is likely that there have been increases in the number of heavy precipitation events (e.g., 95th percentile) within many land regions, even in those where there has been a reduction in total precipitation amount, consistent with a warming climate and observed significant increasing amounts of water vapour in the atmosphere. Increases have also been reported for rarer precipitation events (1 in 50 year return period), but only a few regions have sufficient data to assess such trends reliably.

Droughts have become more common, especially in the tropics and subtropics, since the 1970s. Observed marked increases in drought in the past three decades arise from more intense and longer droughts over wider areas, as a critical threshold for delineating drought is exceeded over increasingly widespread areas. Decreased land precipitation and increased temperatures that enhance evapotranspiration and drying are important factors that have contributed to more regions experiencing droughts, as measured by the Palmer Drought Severity Index. The regions where droughts have occurred seem to be determined largely by changes in SSTs, especially in the tropics, through associated changes in the atmospheric circulation and precipitation. In the western USA, diminishing snow pack and subsequent reductions in soil moisture also appear to be factors. In Australia and Europe, direct links to global warming have been inferred through the extreme nature of high temperatures and heat waves accompanying recent droughts.

Tropospheric water vapour is increasing. Surface specific humidity has generally increased after 1976 in close association with higher temperatures over both land and ocean. Total column water vapour has increased over the global oceans by 1.2 ± 0.3% per decade from 1988 to 2004, consistent in pattern and amount with changes in SST and a fairly constant relative humidity. Strong correlations with SST suggest that total column water vapour has increased by 4% since 1970. Similar upward trends in upper-tropospheric specific humidity, which considerably enhance the greenhouse effect, have also been detected from 1982 to 2004.

'Global dimming' is neither global in extent nor has it continued after 1990. Reported decreases in solar radiation at the Earth's surface from 1970 to 1990 have an urban bias and have reversed in sign. Although records are sparse, pan evaporation is estimated to have decreased in many places due to decreases in surface radiation associated with increases in clouds, changes in cloud properties and/or increases in air pollution (aerosols), especially from 1970 to 1990. However, in many of the same places, actual evapotranspiration inferred from surface water balance exhibits an increase in association with enhanced soil wetness from increased precipitation, as the actual evapotranspiration becomes closer to the potential evaporation measured by the pans. Hence, in determining evapotranspiration there is a trade-off between less solar radiation and increased surface wetness, with the latter generally dominant.

Cloud changes are dominated by the El Niño-Southern Oscillation and appear to be opposite over land and ocean. Widespread (but not ubiquitous) decreases in continental DTR since the 1950s coincide with increases in cloud amounts. Surface and satellite observations disagree about total and low-level cloud changes over the ocean. However, radiation changes at the top of the atmosphere from the 1980s to 1990s, possibly related in part to the El Niño-Southern Oscillation (ENSO) phenomenon, appear to be associated with reductions in tropical upper-level cloud cover, and are linked to changes in the energy budget at the surface and changes in observed ocean heat content.

Changes in the large-scale atmospheric circulation are apparent. Atmospheric circulation variability and change is largely described by relatively few major patterns. The dominant mode of global-scale variability on interannual time scales is ENSO, although there have been times when it is less apparent. The 1976–1977 climate shift, related to the phase change in the Pacific Decadal Oscillation and more frequent El Niños, has affected many areas and most tropical monsoons. For instance, over North America, ENSO and Pacific-North American teleconnection-related changes appear to have led to contrasting changes across the continent, as the west has warmed more than the east, while the latter has become cloudier and wetter. There are substantial multi-decadal variations in the Pacific sector over the 20th century with extended periods of weakened (1900–1924; 1947–1976) as well as strengthened circulation (1925–1946; 1976–2005). Multi-decadal variability is also evident in the Atlantic as the Atlantic Multi-decadal Oscillation in both the atmosphere and the ocean.

Mid-latitude westerly winds have generally increased in both hemispheres. These changes in atmospheric circulation are predominantly observed as 'annular modes', related to the zonally averaged mid-latitude westerlies, which strengthened in most seasons from the 1960s to at least the mid-1990s, with poleward displacements of corresponding Atlantic and southern polar front jet streams and enhanced storm tracks. These were accompanied by a tendency towards stronger winter polar vortices throughout the troposphere and lower stratosphere. On monthly time scales, the southern and northern annular modes (SAM and NAM, respectively) and the North Atlantic Oscillation (NAO) are the dominant patterns of variability in the extratropics and the NAM and NAO are closely related. The westerlies in the Northern Hemisphere, which increased from the 1960s to the 1990s but which have since returned to about normal as part of NAO and NAM changes, alter the flow from oceans to continents and are a major cause of the observed changes in winter storm tracks and related patterns of precipitation and temperature anomalies, especially over Europe. In the Southern Hemisphere, SAM increases from the 1960s to the present are associated with strong warming over the Antarctic Peninsula and, to a lesser extent, cooling over parts of continental Antarctica. Analyses of wind and significant wave height support reanalysis-based evidence for an increase in extratropical storm activity in the Northern Hemisphere in recent decades until the late 1990s.

Intense tropical cyclone activity has increased since about 1970. Variations in tropical cyclones, hurricanes and typhoons are dominated by ENSO and decadal variability, which result in a redistribution of tropical storm numbers and their tracks, so that increases in one basin are often compensated by decreases over other oceans. Trends are apparent in SSTs and other critical variables that influence tropical thunderstorm and tropical storm development. Globally, estimates of the potential destructiveness of hurricanes show a significant upward trend since the mid-1970s, with a trend towards longer lifetimes and greater storm intensity, and such trends are strongly correlated with tropical SST. These relationships have been reinforced by findings of a large increase in numbers and proportion of hurricanes reaching categories 4 and 5 globally since 1970 even as total number of cyclones and cyclone days decreased slightly in most basins. The largest increase was in the North Pacific, Indian and southwest Pacific Oceans. However, numbers of hurricanes in the North Atlantic have also been above normal (based on 1981–2000 averages) in 9 of the last 11 years, culminating in the record-breaking 2005 season. Moreover, the first recorded tropical cyclone in the South Atlantic occurred in March 2004 off the coast of Brazil.

The temperature increases are consistent with observed changes in the cryosphere and oceans. Consistent with observed changes in surface temperature, there has been an almost worldwide reduction in glacier and small ice cap (not including Antarctica and Greenland) mass and extent in the 20th century; snow cover has decreased in many regions of the Northern Hemisphere; sea ice extents have decreased in the Arctic, particularly in spring and summer (Chapter 4); the oceans are warming; and sea level is rising (Chapter 5).

3.1 Introduction

This chapter assesses the observed changes in surface and atmospheric climate, placing new observations and new analyses made during the past six years (since the Third Assessment Report – TAR) in the context of the previous instrumental record. In previous IPCC reports, palaeo-observations from proxy data for the pre-instrumental past and observations from the ocean and ice domains were included within the same chapter. This helped the overall assessment of the consistency among the various variables and their synthesis into a coherent picture of change. However, the amount of information became unwieldy and is now spread over Chapters 3 to 6. Nevertheless, a short synthesis and scrutiny of the consistency of all the observations is included here (see Section 3.9).

In the TAR, surface temperature trends were examined from 1860 to 2000 globally, for 1901 to 2000 as maps and for three sub-periods (1910–1945, 1946–1975 and 1976–2000). The first and third sub-periods had rising temperatures, while the second sub-period had relatively stable global mean temperatures. The 1976 divide is the date of a widely acknowledged 'climate shift' (e.g., Trenberth, 1990) and seems to mark a time (see Chapter 9) when global mean temperatures began a discernible upward trend that has been at least partly attributed to increases in greenhouse gas concentrations in the atmosphere (see the TAR; IPCC, 2001). The picture prior to 1976 has essentially not changed and is therefore not repeated in detail here. However, it is more convenient to document the sub-period after 1979, rather than 1976, owing to the availability of increased and improved satellite data since then (in particular Television InfraRed Observation Satellite (TIROS) Operational Vertical Sounder (TOVS) data) in association with the Global Weather Experiment (GWE) of 1979. The post-1979 period allows, for the first time, a global perspective on many fields of variables, such as precipitation, that was not previously available. For instance, the reanalyses of the global atmosphere from the National Centers for Environmental Prediction/National Center for Atmospheric Research (NCEP/NCAR, referred to as NRA; Kalnay et al., 1996; Kistler et al., 2001) and the European Centre for Medium Range Weather Forecasts (ECMWF, referred to as ERA-40; Uppala et al., 2005) are markedly more reliable after 1979, and spurious discontinuities are present in the analysed record at the end of 1978 (Santer et al., 1999; Bengtsson et al., 2004; Bromwich and Fogt, 2004; Simmons et al., 2004; Trenberth et al., 2005a). Therefore, the availability of high-quality data has led to a focus on the post-1978 period, although physically this new regime seems to have begun in 1976/1977.

Documentation of the climate has traditionally analysed global and hemispheric means, and land and ocean means, and has presented some maps of trends. However, climate varies over all spatial and temporal scales: from the diurnal cycle to El Niño to multi-decadal and millennial variations. Atmospheric waves naturally create regions of temperature and moisture of opposite-signed departures from the zonal mean, as moist warm conditions are favoured in poleward flow while cool dry conditions occur in equatorward flow. Although there is an infinite variety of weather systems, one area of recent substantial progress is recognition that a few preferred patterns (or modes) of variability determine the main seasonal and longer-term climate anomalies (Section 3.6). These patterns arise from the differential effects on the atmosphere of land and ocean, mountains, and anomalous heating, such as occurs during El Niño events. The response is generally felt in regions far removed from the anomalous forcing through atmospheric teleconnections, associated with large-scale waves in the atmosphere. This chapter therefore documents some aspects of temperature and precipitation anomalies associated with these preferred patterns, as they are vitally important for understanding regional climate anomalies (such as observed cooling in parts of the northern North Atlantic from 1901 to 2005; see Section 3.2.2.7, Figure 3.9) and why they differ from global means. Changes in storm tracks, the jet streams, regions of preferred blocking anticyclones and changes in monsoons all occur in conjunction with these preferred patterns and other climate anomalies. Therefore the chapter not only documents changes in variables, but also changes in phenomena (such as El Niño) or patterns, in order to increase understanding of the character of change.

Extremes of climate, such as droughts and wet spells, are very important because of their large impacts on society and the environment, but they are an expression of the variability. Therefore, the nature of variability at different spatial and temporal scales is vital to our understanding of extremes. The global means of temperature and precipitation are most readily linked to global mean radiative forcing and are important because they clearly indicate if unusual change is occurring. However, the local or regional response can be complex and perhaps even counter-intuitive, such as changes in planetary waves in the atmosphere induced by global warming that result in regional cooling. As an indication of the complexity associated with temporal and spatial scales, Table 3.1 provides measures of the magnitude of natural variability of surface temperature in which climate signals are embedded. The measures used are indicators of the range: the mean range of the diurnal and annual cycles, and the estimated 5th to 95th percentiles range of anomalies. These are based on the standard deviation and assumed normal distribution, which is a reasonable approximation in many places for temperature, with the exception of continental interiors in the cold season, which have strongly negatively skewed temperature distributions owing to cold extremes. For the global mean, the variance is somewhat affected by the observed trend, which inflates this estimate of the range slightly. The comparison highlights the large diurnal cycle and daily variability. Daily variability is, however, greatly reduced by either spatial or temporal averaging that effectively averages over synoptic weather systems. Nevertheless, even continental-scale averages contain much greater variability than the global mean in association with planetary-scale waves and events such as El Niño.

Table 3.1. *Typical ranges of surface temperature at different spatial and temporal scales for a sample mid-latitude mid-continental station (Boulder, Colorado; based on 80 years of data) and for monthly mean anomalies (diurnal and annual cycles removed) for the USA as a whole and the globe for the 20th century. For the diurnal and annual cycles, the monthly mean range is given, while other values are the difference between the 5th and 95th percentiles.*

Temporal and Spatial Scale	Temperature Range (°C)
Boulder diurnal cycle	13.1 (December) to 15.1 (September)
Boulder annual cycle	23
Boulder daily anomalies	15
Boulder monthly anomalies	7.0
USA monthly anomalies	3.9
Global mean monthly anomalies	0.79

Throughout the chapter, the authors try to consistently indicate the degree of confidence and uncertainty in trends and other results, as given by Box TS.1 in the Technical Summary. Quantitative estimates of uncertainty include: for the mean, the 5th and 95th percentiles; and for trends, statistical significance at the 0.05 (5%) significance level. This allows assessment of what is unusual. The chapter mainly uses the word 'trend' to designate a generally monotonic change in the level of a variable. Where numerical values are given, they are equivalent linear trends, though more complex changes in the variable will often be clear from the description. The chapter also assesses, if possible, the physical consistency among different variables, which helps to provide additional confidence in trends.

3.2 Changes in Surface Climate: Temperature

3.2.1 Background

Improvements have been made to both land surface air temperature and sea surface temperature (SST) databases during the six years since the TAR was published. Jones and Moberg (2003) revised and updated the Climatic Research Unit (CRU) monthly land-surface air temperature record, improving coverage particularly in the Southern Hemisphere (SH) in the late 19th century. Further revisions by Brohan et al. (2006) include a comprehensive reassessment of errors together with an extension back to 1850. Under the auspices of the World Meteorological Organization (WMO) and the Global Climate Observing System (GCOS), daily temperature (together with precipitation and pressure) data for an increasing number of land stations have also become available, allowing more detailed assessment of extremes (see Section 3.8), as well as potential urban influences on both large-scale temperature averages and microclimate. A new gridded data set of monthly maximum and minimum temperatures has updated earlier work (Vose et al., 2005a). For the oceans, the International Comprehensive Ocean-Atmosphere Data Set (ICOADS) has been extended by blending the former COADS with the UK's Marine Data Bank and newly digitised data, including the US Maury Collection and Japan's Kobe Collection. As a result, coverage has been improved substantially before 1920, especially over the Pacific, with further modest improvements up to 1950 (Worley et al., 2005; Rayner et al., 2006). Improvements have also been made in the bias reduction of satellite-based infrared (Reynolds et al., 2002) and microwave (Reynolds et al., 2004; Chelton and Wentz, 2005) retrievals of SST for the 1980s onwards. These data represent ocean skin temperature (Section 3.2.2.3), not air temperature or SST, and so must be adjusted to match the latter. Satellite infrared and microwave imagery can now also be used to monitor land surface temperature (Peterson et al., 2000; Jin and Dickinson, 2002; Kwok and Comiso, 2002b). Microwave imagery must allow for variations in surface emissivity and cannot act as a surrogate for air temperature over either snow-covered (Peterson et al., 2000) or sea-ice areas. As satellite-based records are still short in duration, all regional and hemispheric temperature series shown in this section are based on conventional surface-based data sets, except where stated.

Despite these improvements, substantial gaps in data coverage remain, especially in the tropics and the SH, particularly Antarctica. These gaps are largest in the 19th century and during the two world wars. Accordingly, advanced interpolation and averaging techniques have been applied when creating global data sets and hemispheric and global averages (Smith and Reynolds, 2005), and advanced techniques have also been used in the estimation of errors (Brohan et al., 2006), both locally and on a global basis (see Appendix 3.B.1). These errors, as well as the influence of decadal and multi-decadal variability in the climate, have been taken into account when estimating linear trends and their uncertainties (see Appendix 3.A). Estimates of surface temperature from ERA-40 reanalyses have been shown to be of climate quality (i.e., without major time-varying biases) at large scales from 1979 (Simmons et al., 2004). Improvements in ERA-40 over NRA arose from both improved data sources and better assimilation techniques (Uppala et al., 2005). The performance of ERA-40 was degraded prior to the availability of satellite data in the mid-1970s (see Appendix 3.B.5).

3.2.2 Temperature in the Instrumental Record for Land and Oceans

3.2.2.1 Land-Surface Air Temperature

Figure 3.1 shows annual global land-surface air temperatures, relative to the period 1961 to 1990, from the improved analysis (CRU/Hadley Centre gridded land-surface air temperature version 3; CRUTEM3) of Brohan et al. (2006). The long-term variations are in general agreement with those from the operational version of the Global Historical Climatology Network

(GHCN) data set (National Climatic Data Center (NCDC); Smith and Reynolds, 2005; Smith et al. 2005), and with the National Aeronautics and Space Administration's (NASA) Goddard Institute for Space Studies (GISS; Hansen et al., 2001) and Lugina et al. (2005) analyses (Figure 3.1). Most of the differences arise from the diversity of spatial averaging techniques. The global average for CRUTEM3 is a land-area weighted sum (0.68 × NH + 0.32 × SH). For NCDC it is an area-weighted average of the grid-box anomalies where available worldwide. For GISS it is the average of the anomalies for the zones 90°N to 23.6°N, 23.6°N to 23.6°S and 23.6°S to 90°S with weightings 0.3, 0.4 and 0.3, respectively, proportional to their total areas. For Lugina et al. (2005) it is (NH + 0.866 × SH) / 1.866 because they excluded latitudes south of 60°S. As a result, the recent global trends are largest in CRUTEM3 and NCDC, which give more weight to the NH where recent trends have been greatest (Table 3.2).

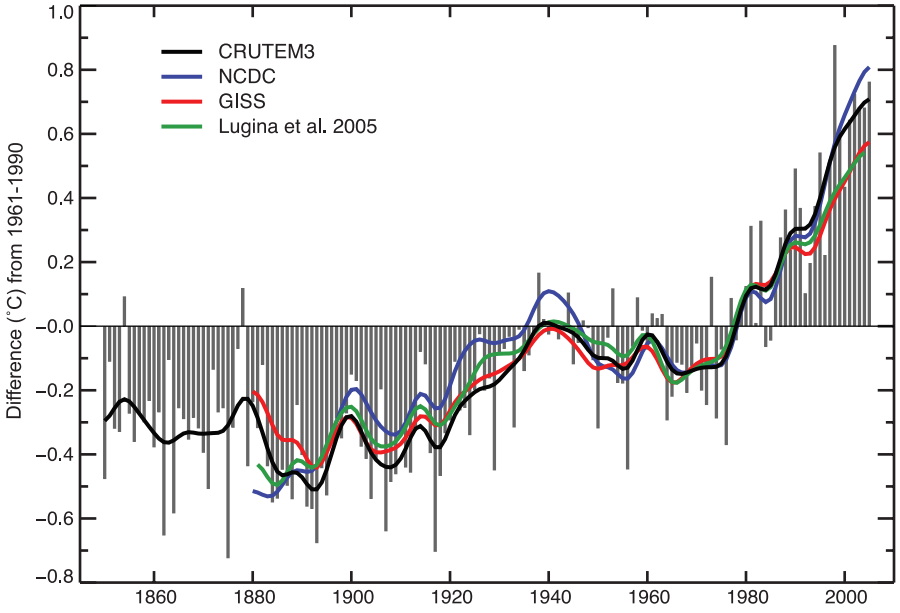


Figure 3.1. *Annual anomalies of global land-surface air temperature (°C), 1850 to 2005, relative to the 1961 to 1990 mean for CRUTEM3 updated from Brohan et al. (2006). The smooth curves show decadal variations (see Appendix 3.A). The black curve from CRUTEM3 is compared with those from NCDC (Smith and Reynolds, 2005; blue), GISS (Hansen et al., 2001; red) and Lugina et al. (2005; green).*

Further, small differences arise from the treatment of gaps in the data. The GISS gridding method favours isolated island and coastal sites, thereby reducing recent trends, and Lugina et al. (2005) also obtain reduced recent trends owing to their optimal interpolation method that tends to adjust anomalies towards zero where there are few observations nearby (see, e.g., Hurrell and Trenberth, 1999). The NCDC analysis, which begins in 1880, is higher than CRUTEM3 by between 0.1°C and 0.2°C in the first half of the 20th century and since the late 1990s. This is probably because its anomalies have been interpolated to be spatially complete: an earlier but very similar version (CRUTEM2v; Jones and Moberg, 2003) agreed very closely with NCDC when the global averages were calculated in the same way (Vose et al., 2005b). Differences may also arise because the numbers of stations used by CRUTEM3, NCDC and GISS differ (4,349, 7,230 and >7,200 respectively), although many of the basic station data are in common. Differences in station numbers relate principally to CRUTEM3 requiring series to have sufficient data between 1961 and 1990 to allow the calculation of anomalies (Brohan et al., 2006). Further differences may have arisen from differing homogeneity adjustments (see also Appendix 3.B.2).

Trends and low-frequency variability of large-scale surface air temperature from the ERA-40 reanalysis and from CRUTEM2v (Jones and Moberg, 2003) are in general agreement from the late 1970s onwards (Simmons et al., 2004). When ERA-40 is sub-sampled to match the Jones and Moberg coverage, correlations between monthly hemispheric- and continental-scale averages exceed 0.96, although trends in ERA-40 are then 0.03°C and 0.07°C per decade (NH and SH, respectively) lower than Jones and Moberg (2003). The ERA-40 reanalysis is more homogeneous than previous reanalyses (see Section 3.2.1 and Appendix 3.B.5.4) but is not completely independent of the Jones and Moberg data (Simmons et al., 2004). The warming trends continue to be greatest over the continents of the NH (see maps in Section 3.2.2.7, Figures 3.9 and 3.10), in line with the TAR. Issues of homogeneity of terrestrial air temperatures are discussed in Appendix 3.B.2.

Table 3.2 provides trend estimates from a number of hemispheric and global temperature databases. Warming since 1979 in CRUTEM3 has been 0.27°C per decade for the globe, but 0.33°C and 0.13°C per decade for the NH and SH, respectively. Brohan et al. (2006) and Rayner et al. (2006) (see Section 3.2.2.3) provide uncertainties for annual estimates, incorporating the effects of measurement and sampling error, and uncertainties regarding biases due to urbanisation and earlier methods of measuring SST. These factors are taken into account, although ignoring their serial correlation. In Table 3.2, the effects of persistence on error bars are accommodated using a red noise approximation, which effectively captures the main influences. For more extensive discussion see Appendix 3.A

From 1950 to 2004, the annual trends in minimum and maximum land-surface air temperature averaged over regions with data were 0.20°C per decade and 0.14°C per decade, respectively, with a trend in diurnal temperature range (DTR) of –0.07°C per decade (Vose et al., 2005a; Figure 3.2). This is consistent with the TAR where data extended from 1950 to 1993; spatial coverage is now 71% of the terrestrial surface instead of 54% in the TAR, although tropical areas are still under-represented. Prior to 1950, insufficient data are available to develop global-scale maps of maximum and minimum temperature trends. For 1979 to 2004, the corresponding linear trends for the land areas where data are available were 0.29°C

Table 3.2. *Linear trends in hemispheric and global land-surface air temperatures, SST (shown in table as HadSST2) and Nighttime Marine Air Temperature (NMAT; shown in table as HadMAT1). Annual averages, with estimates of uncertainties for CRU and HadSST2, were used to estimate trends. Trends with 5 to 95% confidence intervals and levels of significance (**bold: <1%**; italic, 1–5%) were estimated by Restricted Maximum Likelihood (REML; see Appendix 3.A), which allows for serial correlation (first order autoregression AR1) in the residuals of the data about the linear trend. The Durbin Watson D-statistic (not shown) for the residuals, after allowing for first-order serial correlation, never indicates significant positive serial correlation.*

	Temperature Trend (°C per decade)		
Dataset	**1850–2005**	**1901–2005**	**1979–2005**
Land: Northern Hemisphere			
CRU (Brohan et al., 2006)	**0.063 ± 0.015**	**0.089 ± 0.025**	**0.328 ± 0.087**
NCDC (Smith and Reynolds, 2005)		**0.072 ± 0.026**	**0.344 ± 0.096**
GISS (Hansen et al., 2001)		**0.083 ± 0.025**	**0.294 ± 0.074**
Lugina et al. (2006)		**0.079 ± 0.029**	**0.301 ± 0.075**
Land: Southern Hemisphere			
CRU (Brohan et al., 2006)	*0.036 ± 0.024*	**0.077 ± 0.029**	*0.134 ± 0.070*
NCDC (Smith and Reynolds, 2005)		**0.057 ± 0.017**	**0.220 ± 0.093**
GISS (Hansen et al., 2001)		**0.056 ± 0.012**	*0.085 ± 0.055*
Lugina et al. (2005)		**0.058 ± 0.011**	**0.091 ± 0.048**
Land: Globe			
CRU (Brohan et al., 2006)	**0.054 ± 0.016**	**0.084 ± 0.021**	**0.268 ± 0.069**
NCDC (Smith and Reynolds, 2005)		**0.068 ± 0.024**	**0.315 ± 0.088**
GISS (Hansen et al., 2001)		**0.069 ± 0.017**	**0.188 ± 0.069**
Lugina et al. (2005)		**0.069 ± 0.020**	**0.203 ± 0.058**
Ocean: Northern Hemisphere			
UKMO HadSST2 (Rayner et al., 2006)	**0.042 ± 0.016**	**0.071 ± 0.029**	*0.190 ± 0.134*
UKMO HadMAT1 (Rayner et al., 2003) from 1861	**0.038 ± 0.011**	**0.065 ± 0.020**	**0.186 ± 0.060**
Ocean: Southern Hemisphere			
UKMO HadSST2 (Rayner et al., 2006)	**0.036 ± 0.013**	**0.068 ± 0.015**	**0.089 ± 0.041**
UKMO HadMAT1 (Rayner et al., 2003) from 1861	**0.040 ± 0.012**	**0.069 ± 0.011**	**0.092 ± 0.050**
Ocean: Globe			
UKMO HadSST2 (Rayner et al., 2006)	**0.038 ± 0.011**	**0.067 ± 0.015**	**0.133 ± 0.047**
UKMO HadMAT1 (Rayner et al., 2003) from 1861	**0.039 ± 0.010**	**0.067 ± 0.013**	**0.135 ± 0.044**

per decade for both maximum and minimum temperature with no trend for DTR. Diurnal temperature range is particularly sensitive to observing techniques, and monitoring it requires adherence to GCOS monitoring principles (GCOS, 2004). A map of the trend of annual DTR over the period 1979 to 2004 (Section 3.2.2.7, Figure 3.11) is discussed later in the chapter.

3.2.2.2 Urban Heat Islands and Land Use Effects

The modified land surface in cities affects the storage and radiative and turbulent transfers of heat and its partition into sensible and latent components (see Section 7.2 and Box 7.2). The relative warmth of a city compared with surrounding rural areas, known as the urban heat island (UHI) effect, arises from these changes and may also be affected by changes in water runoff, pollution and aerosols. Urban heat island effects are often very localised and depend on local climate factors such as windiness and cloudiness (which in turn depend on season), and on proximity to the sea. Section 3.3.2.4 discusses impacts of urbanisation on precipitation.

Many local studies have demonstrated that the microclimate within cities is on average warmer, with a smaller DTR, than if

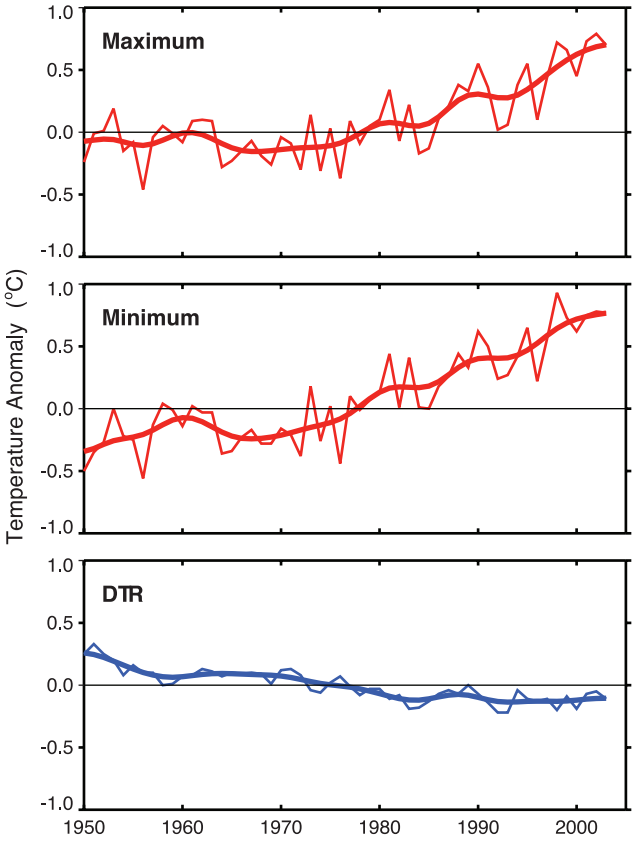


Figure 3.2. *Annual anomalies of maximum and minimum temperatures and DTR (°C) relative to the 1961 to 1990 mean, averaged for the 71% of global land areas where data are available for 1950 to 2004. The smooth curves show decadal variations (see Appendix 3.A). Adapted from Vose et al. (2005a).*

the city were not there. However, the key issue from a climate change standpoint is whether urban-affected temperature records have significantly biased large-scale temporal trends. Studies that have looked at hemispheric and global scales conclude that any urban-related trend is an order of magnitude smaller than decadal and longer time-scale trends evident in the series (e.g., Jones et al., 1990; Peterson et al., 1999). This result could partly be attributed to the omission from the gridded data set of a small number of sites (<1%) with clear urban-related warming trends. In a worldwide set of about 270 stations, Parker (2004, 2006) noted that warming trends in night minimum temperatures over the period 1950 to 2000 were not enhanced on calm nights, which would be the time most likely to be affected by urban warming. Thus, the global land warming trend discussed is very unlikely to be influenced significantly by increasing urbanisation (Parker, 2006). Over the conterminous USA, after adjustment for time-of-observation bias and other changes, rural station trends were almost indistinguishable from series including urban sites (Peterson, 2003; Figure 3.3, and similar considerations apply to China from 1951 to 2001 (Li et al., 2004). One possible reason for the patchiness of UHIs is the location of observing stations in parks where urban influences are reduced (Peterson, 2003). In summary, although some individual sites may be affected, including some small rural locations, the UHI effect is not pervasive, as all global-scale studies indicate it is a very small component of large-scale averages. Accordingly, this assessment adds the same level of urban warming uncertainty as in the TAR: 0.006°C per decade since 1900 for land, and 0.002°C per decade since 1900 for blended land with ocean, as ocean UHI is zero. These uncertainties are added to the cool side of the estimated temperatures and trends, as explained by Brohan et al. (2006), so that the error bars in Section 3.2.2.4, Figures 3.6 and 3.7 and FAQ 3.1, Figure 1 are slightly asymmetric. The statistical significances of the trends in Table 3.2 and Section 3.2.2.4, Table 3.3 take account of this asymmetry.

McKitrick and Michaels (2004) and De Laat and Maurellis (2006) attempted to demonstrate that geographical patterns of warming trends over land are strongly correlated with geographical patterns of industrial and socioeconomic development, implying that urbanisation and related land surface changes have caused much of the observed warming. However, the locations of greatest socioeconomic development are also those that have been most warmed by atmospheric circulation changes (Sections 3.2.2.7 and 3.6.4), which exhibit large-scale coherence. Hence, the correlation of warming with industrial and socioeconomic development ceases to be statistically significant. In addition, observed warming has been, and transient greenhouse-induced warming is expected to be, greater over land than over the oceans (Chapter 10), owing to the smaller thermal capacity of the land.

Comparing surface temperature estimates from the NRA with raw station time series, Kalnay and Cai (2003) concluded that more than half of the observed decrease in DTR in the eastern USA since 1950 was due to changes in land use, including urbanisation. This conclusion was based on the fact that the reanalysis did not explicitly include these factors, which would affect the observations. However, the reanalysis also did not explicitly include many other natural and anthropogenic

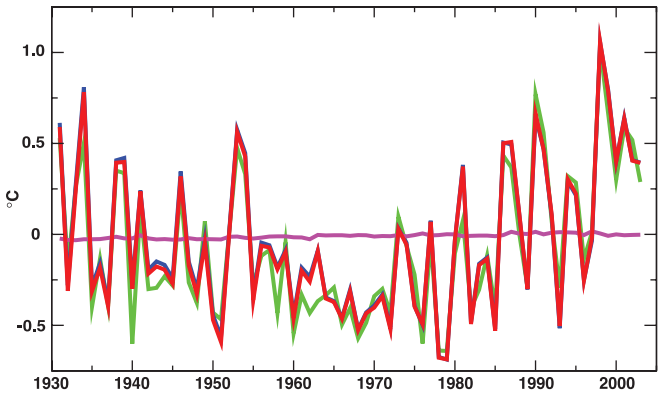


Figure 3.3. *Anomaly (°C) time series relative to the 1961 to 1990 mean of the full US Historical Climatology Network (USHCN) data (red), the USHCN data without the 16% of the stations with populations of over 30,000 within 6 km in the year 2000 (blue), and the 16% of the stations with populations over 30,000 (green). The full USHCN set minus the set without the urban stations is shown in magenta. Both the full data set and the data set without the high-population stations had stations in all of the 2.5° latitude by 3.5° longitude grid boxes during the entire period plotted, but the subset of high-population stations only had data in 56% of these grid boxes. Adapted from Peterson and Owen (2005).*

effects, such as increasing greenhouse gases and observed changes in clouds or soil moisture (Trenberth, 2004). Vose et al. (2004) showed that the adjusted station data for the region (for homogeneity issues, see Appendix 3.B.2) do not support Kalnay and Cai's conclusions. Nor are Kalnay and Cai's results reproduced in the ERA-40 reanalysis (Simmons et al., 2004). Instead, most of the changes appear related to abrupt changes in the type of data assimilated into the reanalysis, rather than to gradual changes arising from land use and urbanisation changes. Current reanalyses may be reliable for estimating trends since 1979 (Simmons et al., 2004) but are in general unsuited for estimating longer-term global trends, as discussed in Appendix 3.B.5.

Nevertheless, changes in land use can be important for DTR at the local-to-regional scale. For instance, land degradation in northern Mexico resulted in an increase in DTR relative to locations across the border in the USA (Balling et al., 1998), and agriculture affects temperatures in the USA (Bonan, 2001; Christy et al., 2006). Desiccation of the Aral Sea since 1960 raised DTR locally (Small et al., 2001). By processing maximum and minimum temperature data as a function of day of the week, Forster and Solomon (2003) found a distinctive 'weekend effect' in DTR at stations examined in the USA, Japan, Mexico and China. The weekly cycle in DTR has a distinctive large-scale pattern with geographically varying sign, and strongly suggests an anthropogenic effect on climate, likely through changes in pollution and aerosols (Jin et al., 2005). Section 7.2 provides fuller discussion of the effects of land use changes.

3.2.2.3 Sea Surface Temperature and Marine Air Temperature

Most analyses of SST estimate the subsurface bulk temperature (i.e., the temperature in the uppermost few metres of the ocean), not the ocean skin temperature measured by satellites. For maximum resolution and data coverage, polar-orbiting infrared satellite data since 1981 can be used so long as the satellite ocean skin temperatures are adjusted to estimate bulk SST values through a calibration procedure (see e.g., Reynolds et al., 2002; Rayner et al., 2003, 2006; Appendix 3.B.3). But satellite SST data alone have not been used as a major resource for estimating climate change because of their strong time-varying biases which are hard to completely remove, for example, as shown in Reynolds et al. (2002) for the Pathfinder polar orbiting satellite SST data set (Kilpatrick et al., 2001). Figures 3.9 and 3.10 (Section 3.2.2.7) do, however, make use of spatial relationships based on adjusted satellite SST estimates after November 1981 to provide nearer-to-global coverage for the 1979 to 2005 period, and O'Carroll et al. (2006) have developed an analysis based on Along-Track Scanning Radiometers (ATSRs) with potential for the future. However, satellite data are unable to fill in estimates of surface temperature over or near sea ice areas.

Recent bulk SSTs estimated using ship and buoy data also have time-varying biases (e.g., Christy et al., 2001; Kent and Kaplan, 2006) that are larger than originally estimated by Folland et al. (1993), but not large enough to prejudice conclusions about recent warming (see Appendix 3.B.3). As reported in the TAR, a combined physical-empirical method (Folland and Parker, 1995) is mainly used to estimate adjustments to ship SST data obtained up to 1941 to compensate for heat losses from uninsulated (mainly canvas) or partly insulated (mainly wooden) buckets. Details are given in Appendix 3.B.3.

The SST analyses of Rayner et al. (2003) and Smith and Reynolds (2004) are interpolated to fill missing data areas. The main problem for estimating climate variations in the presence of large data gaps is underestimation of change, as most interpolation procedures tend to bias the analysis towards the modern climatologies used in these data sets (Hurrell and Trenberth, 1999). To address non-stationary aspects, Rayner et al. (2003) extracted the leading global covariance pattern, which represents long-term changes, before interpolating using reduced-space optimal interpolation (see Appendix 3.B.1); and Smith and Reynolds removed a smoothed, moving 15-year-average field before interpolating by a related technique.

Figure 3.4a shows annual and decadally smoothed anomalies of global SST from the new, uninterpolated Hadley Centre SST data set version 2 (HadSST2) analysis (Rayner et al., 2006). Figure 3.4a also shows NMAT (referred to as HadMAT: Hadley Centre Marine Air Temperature data set), which is used to avoid daytime heating of ship decks (Bottomley et al., 1990). The global averages are ocean-area weighted sums (0.44 × NH + 0.56 × SH). The HadMAT analysis includes limited optimal interpolation (Rayner et al., 2003) and was chosen because of the demonstration by Folland et al. (2003) of its skill in the sparsely observed South Pacific from the late 19th century onwards, but major gaps (e.g., the Southern Ocean) are not interpolated. Although HadMAT data have been corrected for warm biases during World War II they may still be too warm in the NH and too cool in the SH at that time (Figure 3.4c,d). However, global HadSST2 and HadMAT generally agree well, especially after the 1880s. The SST analysis in the TAR is included in Figure 3.4a. The changes in SST since the TAR are generally fairly small, though the new SST analysis is warmer around 1880 and cooler in the 1950s. The peak warmth in the early 1940s is likely to have arisen partly from closely spaced multiple El Niño events (Brönnimann et al., 2004; see also Section 3.6.2) and also due to the warm phase of the Atlantic Multi-decadal Oscillation (AMO; see Section 3.6.6). The HadMAT data generally confirm the hemispheric SST trends in the 20th century (Figure 3.4c,d and Table 3.2). Overall, the SST data should be regarded as more reliable because averaging of fewer samples is needed for SST than for HadMAT to remove synoptic weather noise. However, the changes in SST relative to NMAT since 1991 in the tropical Pacific may be partly real (Christy et al., 2001). As the atmospheric circulation changes, the relationship between SST and surface air temperature anomalies can change along with surface fluxes. Interannual variations in the heat fluxes to the atmosphere can exceed 100 W m^{-2} locally in individual months, but the main prolonged variations occur with the El Niño-Southern Oscillation (ENSO), where changes in the central tropical Pacific exceed ±50 W m^{-2} for many months during major ENSO events (Trenberth et al., 2002a).

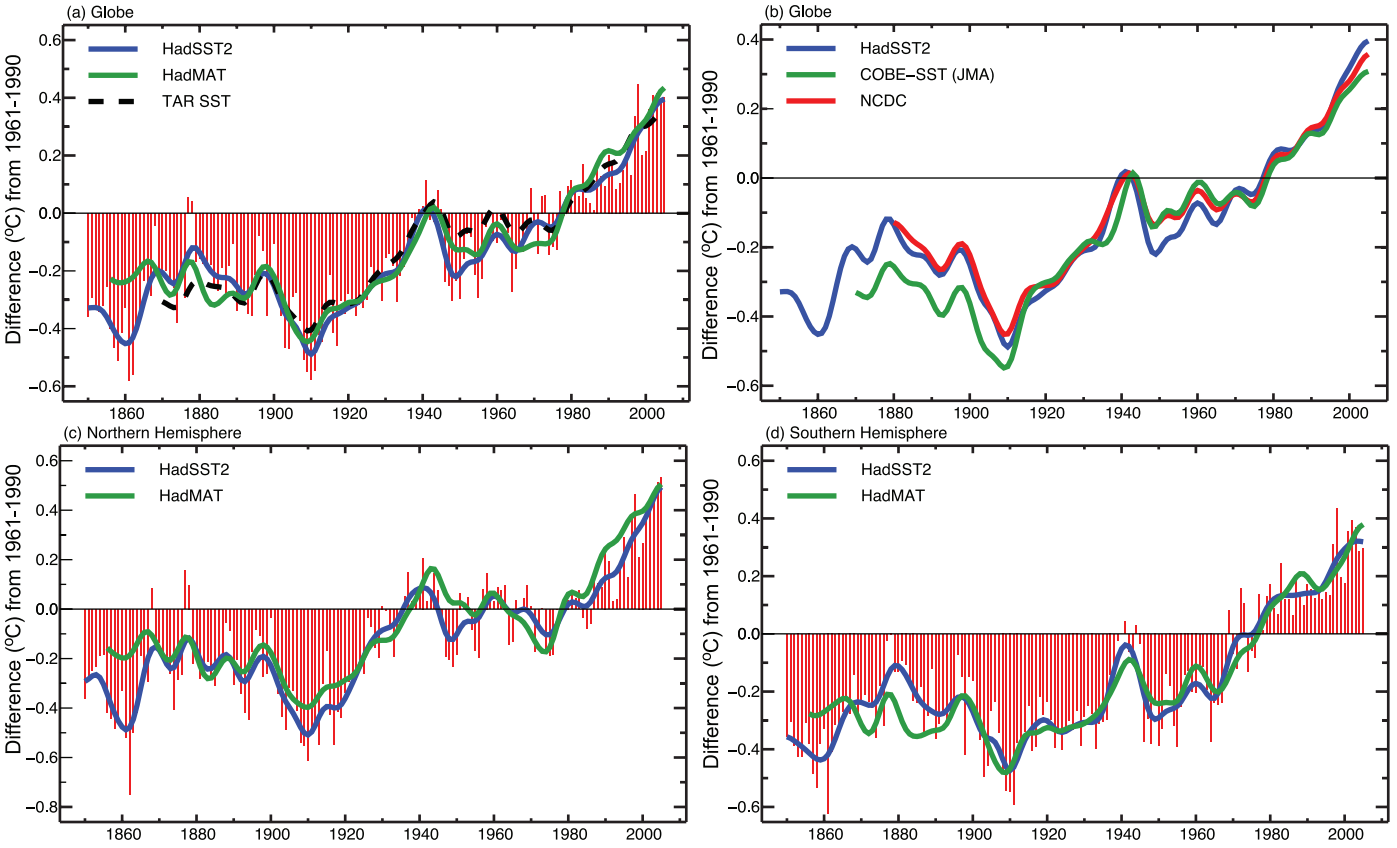


Figure 3.4. *(a) Annual anomalies of global SST (HadSST2; red bars and blue solid curve), 1850 to 2005, and global NMAT (HadMAT, green curve), 1856 to 2005, relative to the 1961 to 1990 mean (°C) from the UK Meteorological Office (UKMO; Rayner et al., 2006). The smooth curves show decadal variations (see Appendix 3.A). The dashed black curve shows equivalent smoothed SST anomalies from the TAR. (b) Smoothed annual global SST anomalies, relative to 1961 to 1990 (°C), from HadSST2 (blue line, as in (a)), from NCDC (Smith et al., 2005; red line) and from COBE-SST (Ishii et al., 2005; green line). The latter two series begin later in the 19th century than HadSST2. (c,d) As in (a) but for the NH and SH showing only the UKMO series.*

Figure 3.4b shows three time series of changes in global SST. Neither the HadSST2 series (as in Figure 3.4a) nor the NCDC series include polar-orbiting satellite data because of possible time-varying biases that remain difficult to correct fully (Rayner et al., 2003). The Japanese series (Ishii et al., 2005; referred to as Centennial *in-situ* Observation-Based Estimates of SSTs (COBE-SST) from the Japan Meteorological Agency (JMA)) is also *in situ* except for the specification of sea ice. The warmest year globally in each SST record was 1998 (0.44°C, 0.38°C and 0.37°C above the 1961 to 1990 average for HadSST2, NCDC and COBE-SST, respectively). The five warmest years in all analyses have occurred after 1995.

Understanding of the variability and trends in different oceans is still developing, but it is already apparent that they are quite different. The Pacific is dominated by ENSO and modulated by the Pacific Decadal Oscillation (PDO), which may provide ways of moving heat from the tropical ocean to higher latitudes and out of the ocean into the atmosphere (Trenberth et al., 2002a), thereby greatly altering how trends are manifested. In the Atlantic, observations reveal the role of the AMO (Folland et al., 1999; Delworth and Mann, 2000; Enfield et al., 2001; Goldenberg et al., 2001; Section 3.6.6 and Figure 3.33). The AMO is likely to be associated with the Thermohaline Circulation (THC), which transports heat northwards, thereby moderating the tropics and warming the high latitudes. In the Indian Ocean, interannual variability is small compared with the trend. Figure 3.5 presents latitude-time sections from 1900 for SSTs (from HadSST2) for the zonal mean across each ocean, filtered to remove fluctuations of less than about six years, including the ENSO signal. In the Pacific, the long-term warming is clearly evident, but punctuated by cooler episodes centred in the tropics, and no doubt linked to the PDO. The prolonged 1939–1942 El Niño shows up as a warm interval. In the Atlantic, the warming from the 1920s to about 1940 in the NH was focussed on higher latitudes, with the SH remaining cool. This inter-hemispheric contrast is believed to be one signature of the THC (Zhang and Delworth, 2005). The subsequent relative cooling in the NH extratropics and the more recent intense warming in NH mid-latitudes was predominantly a multi-decadal variation of SST; only in the last decade is an overall warming signal clearly emerging. Therefore, the recent strong warming appears to be related in part to the AMO in addition to a global warming signal (Section 3.6.6). The cooling in the northwestern North Atlantic just south of Greenland, reported in the SAR, has now been replaced by strong warming (see also Section 3.2.2.7, Figures 3.9 and 3.10; also Figures

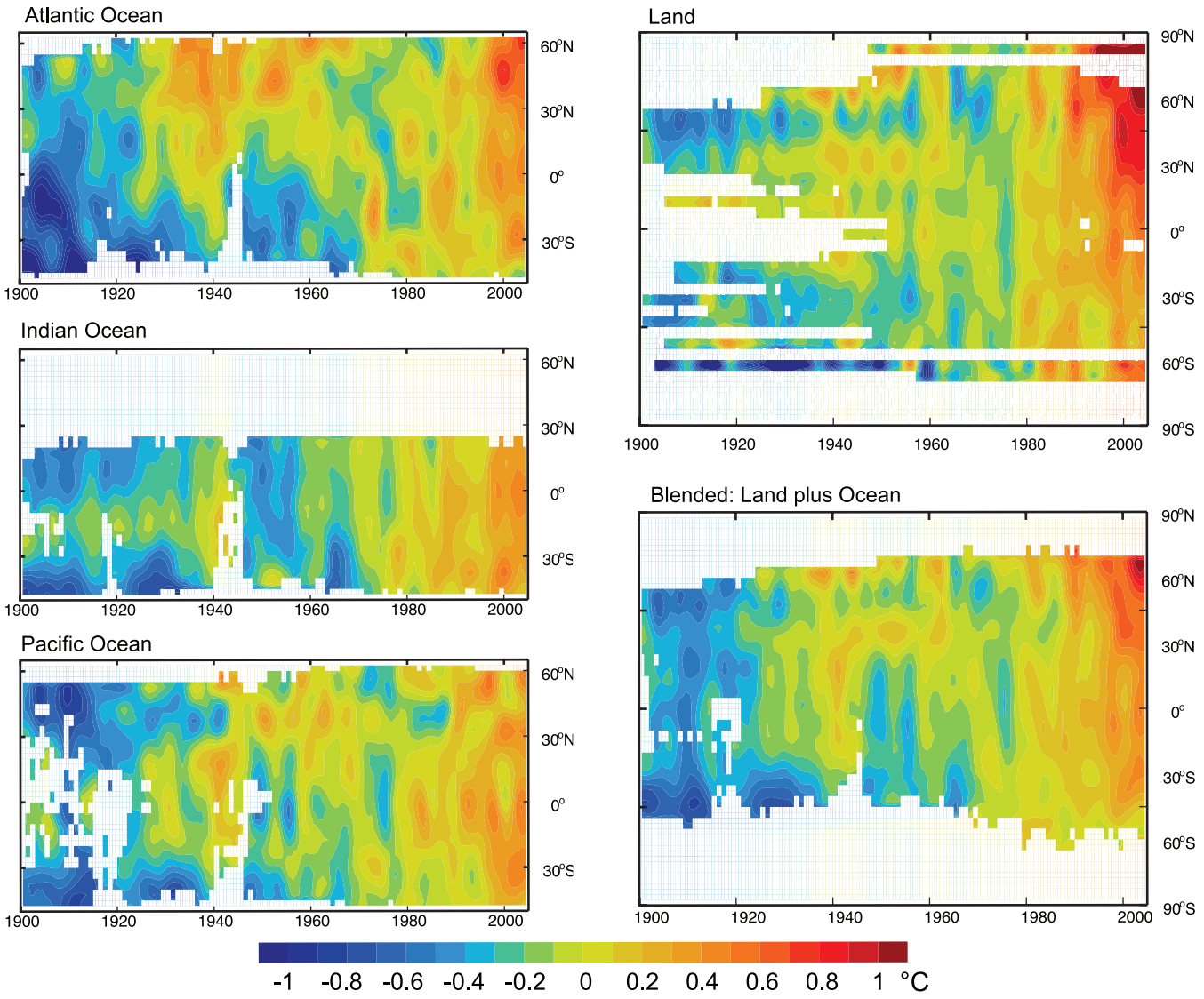


Figure 3.5. *Latitude-time sections of zonal mean temperature anomalies (°C) from 1900 to 2005, relative to the 1961 to 1990 mean. Left panels: SST annual anomalies across each ocean from HadSST2 (Rayner et al., 2006). Right panels: Surface temperature annual anomalies for land (top, CRUTEM3) and land plus ocean (bottom, HadCRUT3). Values are smoothed with the 5-point filter to remove fluctuations of less than about six years (see Appendix 3.A); and white areas indicate missing data.*

5.1 and 5.2 for ocean heat content). The Indian Ocean also reveals a poorly observed warm interval in the early 1940s, and further shows the fairly steady warming in recent years. The multi-decadal variability in the Atlantic has a much longer time scale than that in the Pacific, but it is noteworthy that all oceans exhibit a warm period around the early 1940s.

3.2.2.4 *Land and Sea Combined Temperature: Global, Northern Hemisphere, Southern Hemisphere and Zonal Means*

Gridded data sets combining land-surface air temperature and SST anomalies have been developed and maintained by three groups: CRU with the UKMO Hadley Centre in the UK (HadCRUT3; Brohan et al., 2006) and NCDC (Smith and Reynolds, 2005) and GISS (Hansen et al., 2001) in the USA. Although the component data sets differ slightly (see Sections 3.2.2.1 and 3.2.2.3) and the combination methods also differ, trends are similar. Table 3.3 provides comparative estimates of linear trends. Overall warming since 1901 has been a little less in the NCDC and GISS analysis than in the HadCRUT3 analysis. All series indicate that the warmest five years have occurred after 1997, although there is slight disagreement about the ordering. The HadCRUT3 data set shows 1998 as warmest, while 2005 is warmest in NCDC and GISS data. Thus the year 2005, with no El Niño, was about as warm globally as 1998 with its major El Niño effects. The GISS analysis of 2005 interpolated the exceptionally warm conditions in the extreme north of Eurasia and North America over the Arctic Ocean (see Figure 3.5). If the GISS data for 2005 are averaged only south of 75°N, then 2005 is cooler than 1998. In addition, there were relatively cool anomalies in 2005 in HadCRUT3 in parts of Antarctica and the Southern Ocean, where sea ice coverage (see Chapter 4) has not declined.

Table 3.3. *Linear trends (°C per decade) in hemispheric and global combined land-surface air temperatures and SST. Annual averages, along with estimates of uncertainties for CRU/UKMO (HadCRUT3), were used to estimate trends. For CRU/UKMO, global annual averages are the simple average of the two hemispheres. For NCDC and GISS the hemispheres are weighted as in Section 3.2.2.1. Trends are estimated and presented as in Table 3.2. R^2 is the squared trend correlation (%). The Durbin Watson D-statistic (not shown) for the residuals, after allowing for first-order serial correlation, never indicated significant positive serial correlation, and plots of the residuals showed virtually no long-range persistence.*

	Temperature Trend (°C per decade)		
Dataset	**1850–2005**	**1901–2005**	**1979–2005**
Northern Hemisphere			
CRU/UKMO (Brohan et al., 2006)	**0.047 ± 0.013 R^2=54**	**0.075 ± 0.023 R^2=63**	**0.234 ± 0.070 R^2=69**
NCDC (Smith and Reynolds, 2005)		**0.063 ± 0.022 R^2=55**	**0.245 ± 0.062 R^2=72**
Southern Hemisphere			
CRU/UKMO (Brohan et al., 2006)	**0.038 ± 0.014 R^2=51**	**0.068 ± 0.017 R^2=74**	**0.092 ± 0.038 R^2=48**
NCDC (Smith and Reynolds, 2005)		**0.066 ± 0.009 R^2=82**	**0.096 ± 0.038 R^2=58**
Globe			
CRU/UKMO (Brohan et al., 2006)	**0.042 ± 0.012 R^2=57**	**0.071 ± 0.017 R^2=74**	**0.163 ± 0.046 R^2=67**
NCDC (Smith and Reynolds, 2005)		**0.064 ± 0.016 R^2=71**	**0.174 ± 0.051 R^2=72**
GISS (Hansen et al., 2001)		**0.060 ± 0.014 R^2=70**	**0.170 ± 0.047 R^2=67**

Hemispheric and global series based on Brohan et al. (2006) are shown in Figure 3.6 and tropical and polar series in Figure 3.7. Owing to the sparsity of SST data, the polar series are for land only. The recent warming is strongest in the NH extratropics, while El Niño events are clearly evident in the tropics, particularly the 1997–1998 event that makes 1998 the warmest year in HadCRUT3. The warming over land in the Arctic north of 65°N (Figure 3.7) is more than double the warming in the global mean from the 19th century to the 21st century and also from about the late 1960s to the present. In the arctic series, 2005 is the warmest year. A slightly longer warm period, almost as warm as the present, was observed from the late 1920s to the early 1950s. Although data coverage was limited in the first half of the 20th century, the spatial pattern of the earlier warm period appears to have been different from that of the current warmth. In particular, the current warmth is partly linked to the Northern Annular Mode (NAM; see Section 3.6.4) and affects a broader region (Polyakov et al., 2003). Temperatures over mainland Antarctica (south of 65°S) have not warmed in recent decades (Turner et al., 2005), but it is virtually certain that there has been strong warming over the last 50 years in the Antarctic Peninsula region (Turner et al., 2005; see the discussion of changes in the Southern Annular Mode (SAM) and Figure 3.32 in Section 3.6.5).

3.2.2.5 *Consistency between Land and Ocean Surface Temperature Changes*

The course of temperature change over the 20th century, revealed by the independent analysis of land air temperatures, SST and NMAT, is generally consistent (Figure 3.8). Warming occurred in two distinct phases (1915–1945 and since 1975), and it has been substantially stronger over land than over the oceans in the later phase, as shown also by the trends in Table 3.2. The land component has also been more variable from year to year (compare Figures 3.1 and 3.4a,c,d). Much of the recent difference between global SST (and NMAT) and global land air temperature trends has arisen from accentuated warming over the continents in the mid-latitude NH (Section 3.2.2.7, Figures 3.9 and 3.10). This is likely to be related to greater evaporation and heat storage in the ocean, and in particular to atmospheric circulation changes in the winter half-year due to the North Atlantic Oscillation (NAO)/NAM (see discussion in Section 3.6.4). Accordingly the differences between NH and SH temperatures follow a course similar to the plot of land air temperature minus SST shown in Figure 3.8.

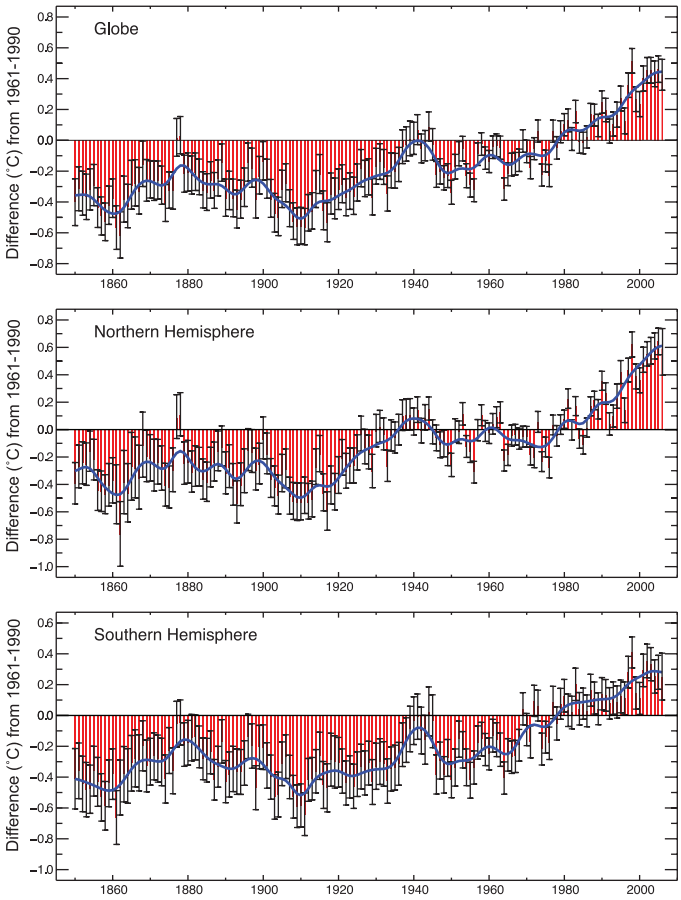


Figure 3.6. *Global and hemispheric annual combined land-surface air temperature and SST anomalies (°C) (red) for 1850 to 2006 relative to the 1961 to 1990 mean, along with 5 to 95% error bar ranges, from HadCRUT3 (adapted from Brohan et al., 2006). The smooth blue curves show decadal variations (see Appendix 3.A).*

3.2.2.6 Temporal Variability of Global Temperatures and Recent Warming

The standard deviation of the HadCRUT3 annual average temperatures for the globe for 1850 to 2005 shown in Figure 3.6 is 0.24°C. The greatest difference between two consecutive years in the global average since 1901 is 0.29°C between 1976 and 1977, demonstrating the importance of the 0.75°C and 0.74°C temperature increases (the HadCRUT3 linear trend estimates for 1901 to 2005 and 1906 to 2005, respectively) in a centennial time-scale context. However, both trends are small compared with interannual variations at one location, and much smaller than day-to-day variations (Table 3.1).

The principal conclusion from the three global analyses is that the global average surface temperature trend has very likely been slightly more than 0.65°C ± 0.2°C over the period from 1901 to 2005 (Table 3.3), a warming greater than any since at least the 11th century (see Chapter 6). A HadCRUT3 linear trend over the 1906 to 2005 period yields a warming of 0.74°C ± 0.18°C, but this rate almost doubles for the last 50 years (0.64°C ± 0.13°C for 1956 to 2005; see FAQ 3.1). Clearly, the changes are not linear and can also be characterised as level prior to about 1915, a warming to about 1945, levelling out or even a slight decrease until the 1970s, and a fairly linear upward trend since then (Figure 3.6 and FAQ 3.1). Considered this way, the overall warming from the average of the first 50-year period (1850–1899) through 2001 to 2005 is 0.76°C ± 0.19°C. Clearly, the world's surface temperature has continued to increase since the TAR and the trend when computed in the same way as in the TAR remains 0.6°C over the 20th century. In view of Section 3.2.2.2 and the dominance of the globe by ocean, the influence of urbanisation on these estimates is estimated to be very small. The last 12 complete years (1995–2006) now contain 11 of the 12 warmest years since 1850, the earliest year for which comparable records are available. Only 1996 is not in this list – replaced by 1990. 2002 to 2005 are the 3rd, 4th, 5th and 2nd warmest years in the series, with 1998 the warmest in HadCRUT3 but with 2005 and 1998 switching order in GISS and NCDC. The HadCRUT3 surface warming

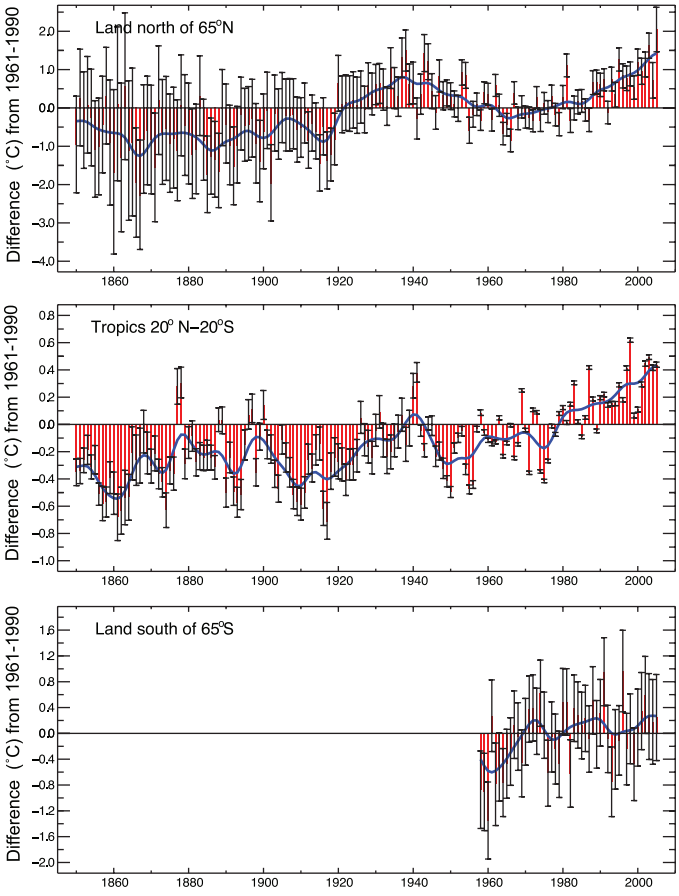


Figure 3.7. *Annual temperature anomalies (°C) up to 2005, relative to the 1961 to 1990 mean (red) with 5 to 95% error bars. The tropical series (middle) is combined land-surface air temperature and SST from HADCRUT3 (adapted from Brohan et al., 2006). The polar series (top and bottom) are land-only from CRUTEM3, because SST data are sparse and unreliable in sea ice zones. The smooth blue curves show decadal variations (see Appendix 3.A).*

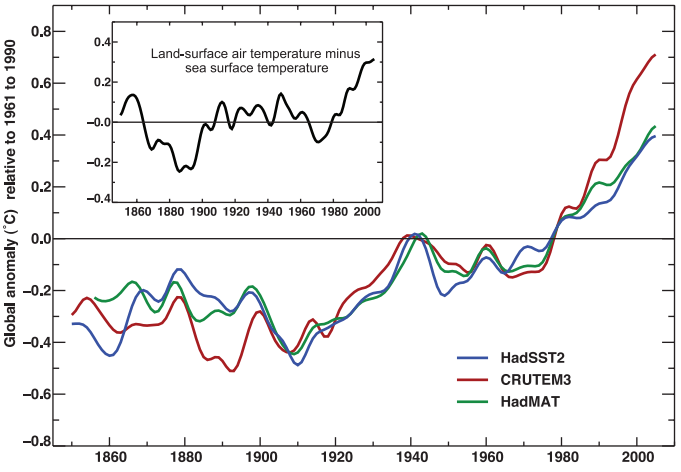


Figure 3.8. *Annual anomalies (°C) of global average SST (blue curve, begins 1850), NMAT (green curve, begins 1856) and land-surface air temperature (red curve, begins 1850) to 2005, relative to their 1961 to 1990 means (Brohan et al., 2006; Rayner et al., 2006). The smooth curves show decadal variations (see Appendix 3.A). Inset shows the smoothed differences between the land-surface air temperature and SST anomalies (i.e., red minus blue).*

trend over 1979 to 2005 was more than 0.16°C per decade, that is, a total warming of 0.44°C ± 0.12°C (the error bars overlap those of NCDC and GISS). During 2001 to 2005, the global average temperature anomaly has been 0.44°C above the 1961–1990 average. The value for 2006 is close to the 2001 to 2005 average.

3.2.2.7 Spatial Trend Patterns

Figure 3.9 illustrates the spatial patterns of annual surface temperature changes for 1901 to 2005 and 1979 to 2005, and Figure 3.10 shows seasonal trends for 1979 to 2005. All maps clearly indicate that differences in trends between locations can be large, particularly for shorter time periods. For the century-long period, warming is statistically significant over most of the world's surface with the exception of an area south of Greenland and three smaller regions over the southeastern USA and parts of Bolivia and the Congo basin. The lack of significant warming at about 20% of the locations (Karoly and Wu, 2005), and the enhanced warming in other places, is likely to be a result of changes in atmospheric circulation (see Section 3.6). Warming is strongest over the continental interiors of Asia and northwestern North America and over some mid-latitude ocean regions of the SH as well as southeastern Brazil. In the recent period, some regions have warmed substantially while a few have cooled slightly on an annual basis (Figure 3.9). Southwest China has cooled since the mid-20th century (Ren et al., 2005), but most of the cooling locations since 1979 have been oceanic and in the SH, possibly through changes in atmospheric and oceanic circulation related to the PDO and SAM (see discussion in Section 3.6.5). Warming dominates most of the seasonal maps for the period 1979 onwards, but weak cooling has affected a few regions, especially the mid-latitudes of the SH oceans, but also over eastern Canada in spring, possibly in relation to the strengthening NAO (see Section 3.6.4, Figure 3.30). Warming in this period was strongest over western North America, northern Europe and China in winter, Europe and northern and eastern Asia in spring, Europe and North Africa in summer and northern North America, Greenland and eastern Asia in autumn (Figure 3.10).

No single location follows the global average, and the only way to monitor the globe with any confidence is to include observations from as many diverse places as possible. The importance of regions without adequate records is determined from complete model reanalysis fields (Simmons et al., 2004). The importance of the missing areas for hemispheric and global averages is incorporated into the errors bars in Figure 3.6 (see Brohan et al., 2006). Error bars are generally larger in the more data-sparse SH than in the NH; they are larger before the 1950s and largest of all in the 19th century.

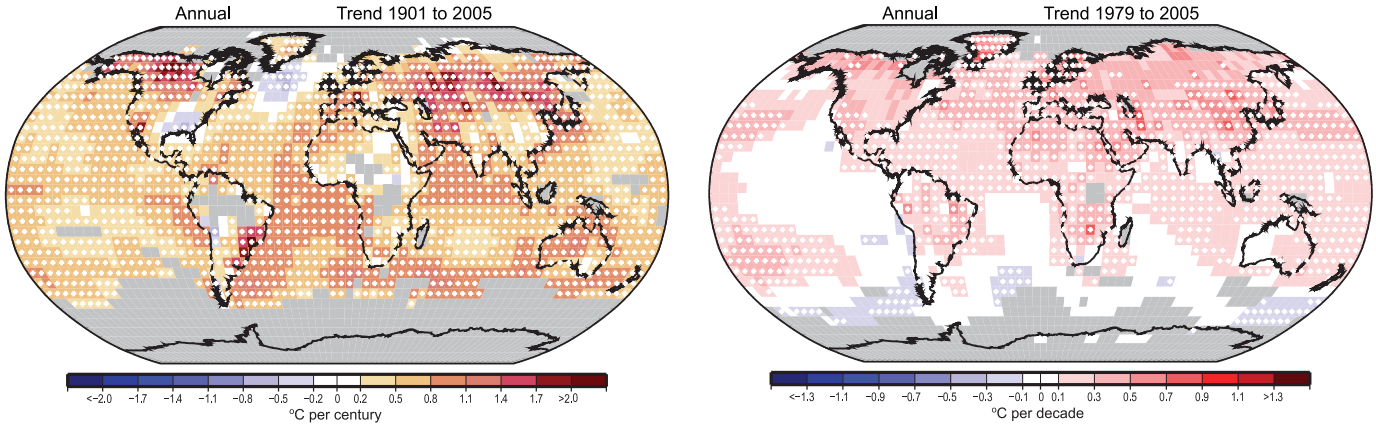


Figure 3.9. *Linear trend of annual temperatures for 1901 to 2005 (left; °C per century) and 1979 to 2005 (right; °C per decade). Areas in grey have insufficient data to produce reliable trends. The minimum number of years needed to calculate a trend value is 66 years for 1901 to 2005 and 18 years for 1979 to 2005. An annual value is available if there are 10 valid monthly temperature anomaly values. The data set used was produced by NCDC from Smith and Reynolds (2005). Trends significant at the 5% level are indicated by white + marks.*

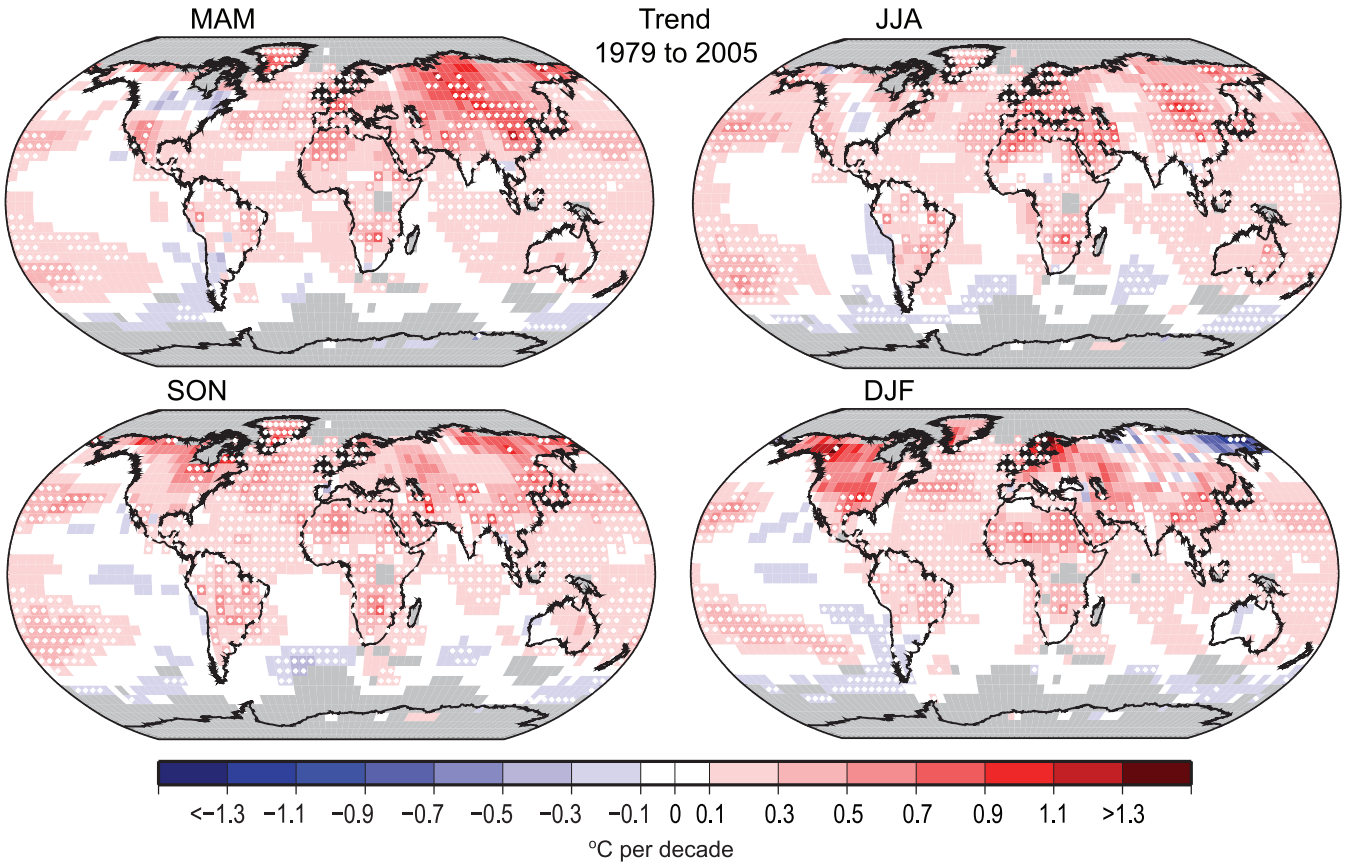


Figure 3.10. *Linear trend of seasonal MAM, JJA, SON and DJF temperature for 1979 to 2005 (°C per decade). Areas in grey have insufficient data to produce reliable trends. The minimum number of years required to calculate a trend value is 18. A seasonal value is available if there are two valid monthly temperature anomaly values. The dataset used was produced by NCDC from Smith and Reynolds (2005). Trends significant at the 5% level are indicated by white + marks.*

Figure 3.11 shows annual trends in DTR from 1979 to 2004. The decline in DTR since 1950 reported in the TAR has now ceased, as confirmed by Figure 3.2. Since 1979, daily minimum temperature increased in most areas except western Australia and southern Argentina, and parts of the western Pacific Ocean; and daily maximum temperature also increased in most regions except northern Peru, northern Argentina, northwestern Australia, and parts of the North Pacific Ocean (Vose et al., 2005a). The changes reported here appear inconsistent with Dai et al. (2006) who reported decreasing DTR in the USA, but this arises partly because Dai et al. (2006) included the high DTR years 1976 to 1978. Furthermore, Figure 3.11 is supported by many other recent regional-scale analyses.

Changes in cloud cover and precipitation explained up to 80% of the variance in historical DTR series for the USA, Australia, mid-latitude Canada and the former Soviet Union during the 20th century (Dai et al., 1999). Cloud cover accounted for nearly half of the change in the DTR in Fennoscandia during the 20th century (Tuomenvirta et al., 2000). Variations in atmospheric circulation also affect DTR. Changes in the frequency of certain synoptic weather types resulted in a decline in DTR during the cold half-year in the Arctic (Przybylak, 2000). A positive phase of the NAM (see Section 3.6.4) is associated with increased DTR in the northeastern USA and Canada (Wettstein and Mearns, 2002). Variations in sea level pressure patterns and associated changes in cloud cover partially accounted for increasing trends in cold-season DTR in the northwestern USA and decreasing trends in the south-central USA (Durre and Wallace, 2001). The relationship between DTR and anthropogenic forcings is complex, as these forcings can affect atmospheric circulation, as well as clouds through both greenhouses gases and aerosols.

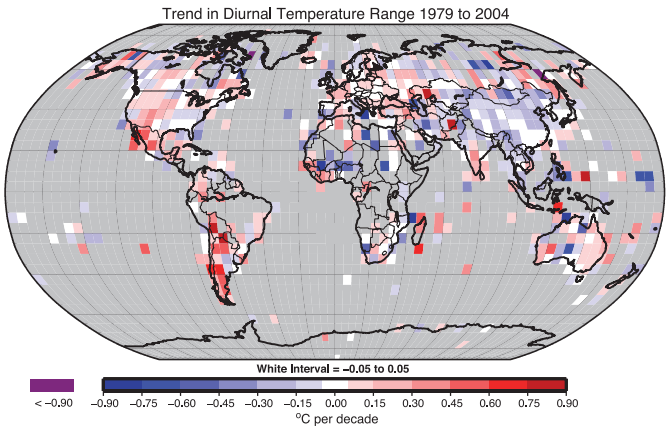


Figure 3.11. *Linear trend in annual mean DTR for 1979 to 2004 (°C per decade). Grey regions indicate incomplete or missing data (after Vose et al., 2005a).*

Frequently Asked Question 3.1

How are Temperatures on Earth Changing?

Instrumental observations over the past 157 years show that temperatures at the surface have risen globally, with important regional variations. For the global average, warming in the last century has occurred in two phases, from the 1910s to the 1940s (0.35°C), and more strongly from the 1970s to the present (0.55°C). An increasing rate of warming has taken place over the last 25 years, and 11 of the 12 warmest years on record have occurred in the past 12 years. Above the surface, global observations since the late 1950s show that the troposphere (up to about 10 km) has warmed at a slightly greater rate than the surface, while the stratosphere (about 10–30 km) has cooled markedly since 1979. This is in accord with physical expectations and most model results. Confirmation of global warming comes from warming of the oceans, rising sea levels, glaciers melting, sea ice retreating in the Arctic and diminished snow cover in the Northern Hemisphere.

There is no single thermometer measuring the global temperature. Instead, individual thermometer measurements taken every day at several thousand stations over the land areas of the world are combined with thousands more measurements of sea surface temperature taken from ships moving over the oceans to produce an estimate of global average temperature every month. To obtain consistent changes over time, the main analysis is actually of anomalies (departures from the climatological mean at each site) as these are more robust to changes in data availability. It is now possible to use these measurements from 1850 to the present, although coverage is much less than global in the second half of the 19th century, is much better after 1957 when measurements began in Antarctica, and best after about 1980, when satellite measurements began.

Expressed as a global average, surface temperatures have increased by about 0.74°C over the past hundred years (between 1906 and 2005; see Figure 1). However, the warming has been neither steady nor the same in different seasons or in different locations. There was not much overall change from 1850 to about 1915, aside from ups and downs associated with natural variability but which may have also partly arisen from poor sampling. An increase (0.35°C) occurred in the global average temperature from the 1910s to the 1940s, followed by a slight cooling (0.1°C), and then a rapid warming (0.55°C) up to the end of 2006 (Figure 1). The warmest years of the series are 1998 and 2005 (which are statistically indistinguishable), and 11 of the 12 warmest years have occurred in the last 12 years (1995 to 2006). Warming, particularly since the 1970s, has generally been greater over land than over the oceans. Seasonally, warming has been slightly greater in the winter hemisphere. Additional warming occurs in cities and urban areas (often referred to as the urban heat island effect), but is confined in spatial extent, and its effects are allowed for both by excluding as many of the affected sites as possible from the global temperature data and by increasing the error range (the blue band in the figure).

A few areas have cooled since 1901, most notably the northern North Atlantic near southern Greenland. Warming during this time has been strongest over the continental interiors of Asia and northern North America. However, as these are areas with large year-to-year variability, the most evident warming signal has occurred in parts of the middle and lower latitudes, particularly the tropical oceans. In the lower left panel of Figure 1, which shows temperature trends since 1979, the pattern in the Pacific Ocean features warming and cooling regions related to El Niño.

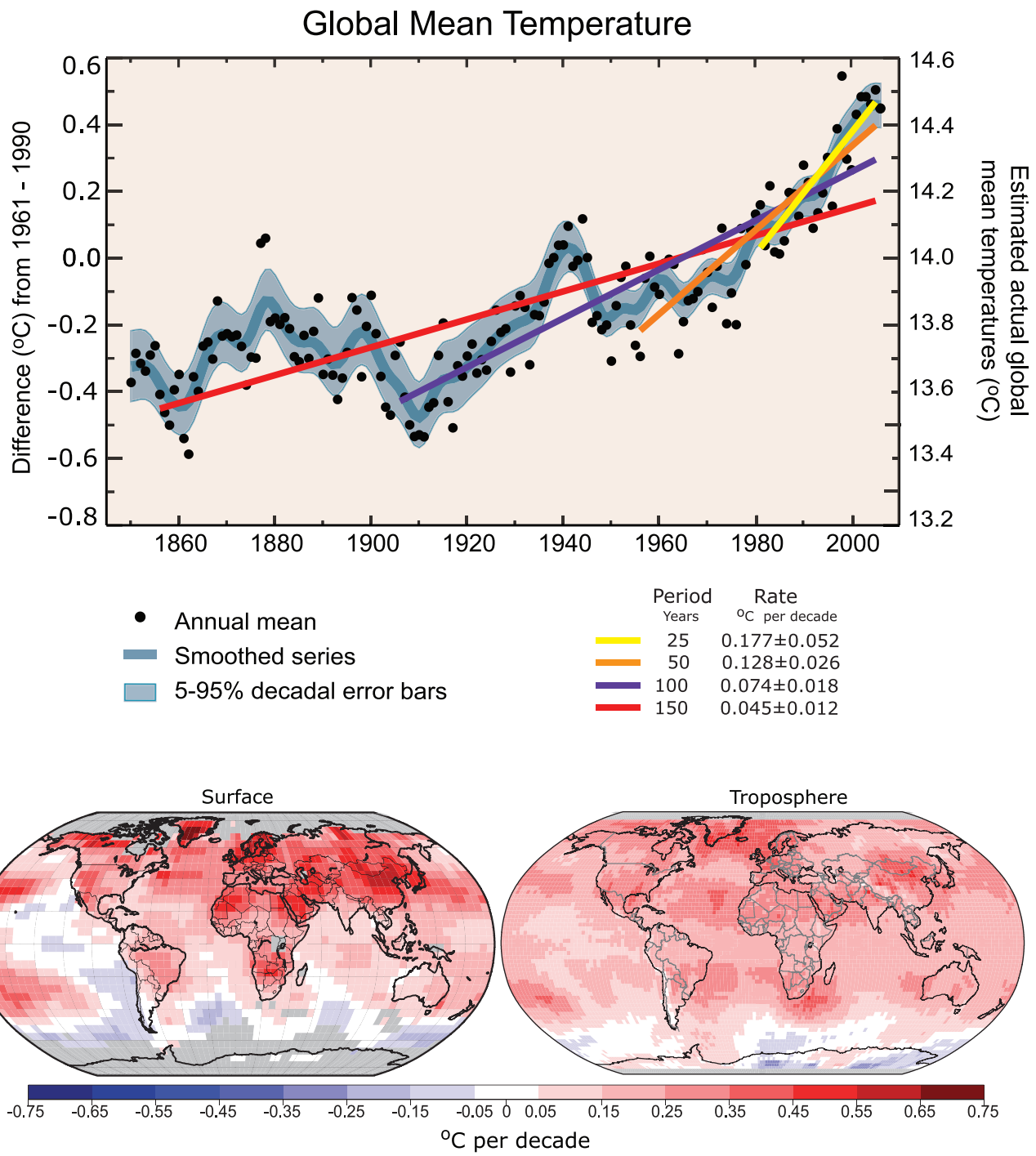
Analysis of long-term changes in daily temperature extremes has recently become possible for many regions of the world (parts of North America and southern South America, Europe, northern and eastern Asia, southern Africa and Australasia). Especially since the 1950s, these records show a decrease in the number of very cold days and nights and an increase in the number of extremely hot days and warm nights (see FAQ 3.3). The length of the frost-free season has increased in most mid- and high-latitude regions of both hemispheres. In the Northern Hemisphere, this is mostly manifest as an earlier start to spring.

In addition to the surface data described above, measurements of temperature above the surface have been made with weather balloons, with reasonable coverage over land since 1958, and from satellite data since 1979. All data are adjusted for changes in instruments and observing practices where necessary. Microwave satellite data have been used to create a 'satellite temperature record' for thick layers of the atmosphere including the troposphere (from the surface up to about 10 km) and the lower stratosphere (about 10 to 30 km). Despite several new analyses with improved cross-calibration of the 13 instruments on different satellites used since 1979 and compensation for changes in observing time and satellite altitude, some uncertainties remain in trends.

For global observations since the late 1950s, the most recent versions of all available data sets show that the troposphere has warmed at a slightly greater rate than the surface, while the stratosphere has cooled markedly since 1979. This is in accord with physical expectations and most model results, which demonstrate the role of increasing greenhouse gases in tropospheric warming and stratospheric cooling; ozone depletion also contributes substantially to stratospheric cooling.

Consistent with observed increases in surface temperature, there have been decreases in the length of river and lake ice seasons. Further, there has been an almost worldwide reduction in glacial mass and extent in the 20th century; melting of the Greenland Ice Sheet has recently become apparent; snow cover has decreased in many Northern Hemisphere regions; sea ice thickness and extent have decreased in the Arctic in all seasons, most dramatically in spring and summer; the oceans are warming; and sea level is rising due to thermal expansion of the oceans and melting of land ice.

(continued)



FAQ 3.1, Figure 1. *(Top) Annual global mean observed temperatures[1] (black dots) along with simple fits to the data. The left hand axis shows anomalies relative to the 1961 to 1990 average and the right hand axis shows the estimated actual temperature (°C). Linear trend fits to the last 25 (yellow), 50 (orange), 100 (purple) and 150 years (red) are shown, and correspond to 1981 to 2005, 1956 to 2005, 1906 to 2005, and 1856 to 2005, respectively. Note that for shorter recent periods, the slope is greater, indicating accelerated warming. The blue curve is a smoothed depiction to capture the decadal variations. To give an idea of whether the fluctuations are meaningful, decadal 5% to 95% (light grey) error ranges about that line are given (accordingly, annual values do exceed those limits). Results from climate models driven by estimated radiative forcings for the 20th century (Chapter 9) suggest that there was little change prior to about 1915, and that a substantial fraction of the early 20th-century change was contributed by naturally occurring influences including solar radiation changes, volcanism and natural variability. From about 1940 to 1970 the increasing industrialisation following World War II increased pollution in the Northern Hemisphere, contributing to cooling, and increases in carbon dioxide and other greenhouse gases dominate the observed warming after the mid-1970s. (Bottom) Patterns of linear global temperature trends from 1979 to 2005 estimated at the surface (left), and for the troposphere (right) from the surface to about 10 km altitude, from satellite records. Grey areas indicate incomplete data. Note the more spatially uniform warming in the satellite tropospheric record while the surface temperature changes more clearly relate to land and ocean.*

[1] *From the HadCRUT3 data set.*

3.3 Changes in Surface Climate: Precipitation, Drought and Surface Hydrology

3.3.1 Background

Temperature changes are one of the more obvious and easily measured changes in climate, but atmospheric moisture, precipitation and atmospheric circulation also change, as the whole system is affected. Radiative forcing alters heating, and at the Earth's surface this directly affects evaporation as well as sensible heating (see Box 7.1). Further, increases in temperature lead to increases in the moisture-holding capacity of the atmosphere at a rate of about 7% per °C (Section 3.4.2). Together these effects alter the hydrological cycle, especially characteristics of precipitation (amount, frequency, intensity, duration, type) and extremes (Trenberth et al., 2003). In weather systems, convergence of increased water vapour leads to more intense precipitation, but reductions in duration and/or frequency, given that total amounts do not change much. The extremes are addressed in Section 3.8.2.2. Expectations for changes in overall precipitation amounts are complicated by aerosols. Because aerosols block the Sun, surface heating is reduced. Absorption of radiation by some, notably carbonaceous, aerosols directly heats the aerosol layer that may otherwise have been heated by latent heat release following surface evaporation, thereby reducing the strength of the hydrological cycle. As aerosol influences tend to be regional, the net expected effect on precipitation over land is especially unclear. This section discusses most aspects of the surface hydrological cycle, except that surface water vapour is included with other changes in atmospheric water vapour in Section 3.4.2.

Difficulties in the measurement of precipitation remain an area of concern in quantifying the extent to which global- and regional-scale precipitation has changed (see Appendix 3.B.4). *In situ* measurements are especially affected by wind effects on the gauge catch, particularly for snow but also for light rain. For remotely sensed measurements (radar and space-based), the greatest problems are that only measurements of instantaneous rate can be made, together with uncertainties in algorithms for converting radiometric measurements (radar, microwave, infrared) into precipitation rates at the surface. Because of measurement problems, and because most historical *in situ*-based precipitation measurements are taken on land leaving the majority of the global surface area under-sampled, it is useful to examine the consistency of changes in a variety of complementary moisture variables. These include both remotely-sensed and gauge-measured precipitation, drought, evaporation, atmospheric moisture, soil moisture and stream flow, although uncertainties exist with all of these variables as well (Huntington, 2006).

3.3.2 Changes in Large-scale Precipitation

3.3.2.1 Global Land Areas

Trends in global annual land precipitation were analysed using data from the GHCN, using anomalies with respect to the 1981 to 2000 base period (Vose et al., 1992; Peterson and Vose, 1997). The observed GHCN linear trend (Figure 3.12) over the 106-year period from 1900 to 2005 is statistically insignificant, as is the CRU linear trend up to 2002 (Table 3.4b). However, the global mean land changes (Figure 3.12) are not at all linear, with an overall increase until the 1950s, a decline until the early 1990s and then a recovery. Although the global land mean is an indicator of a crucial part of the global hydrological cycle, it is difficult to interpret as it is often made up of large regional anomalies of opposite sign.

There are several other global land precipitation data sets covering more recent periods: Table 3.4a gives their characteristics, and the linear trends and their significance are given in Table 3.4b. There are a number of differences in processing, data sources and time periods that lead to the differences in the trend estimates. All but one data set (GHCN) are spatially infilled by either interpolation or the use of satellite estimates of precipitation. The Precipitation Reconstruction over Land (PREC/L) data (Chen et al., 2002) include GHCN data, synoptic data from the National Oceanic and Atmospheric Administration (NOAA) Climate Prediction Center's Climate Anomaly Monitoring System (CAMS), and the Global Precipitation Climatology Project (GPCP) data (Adler et al., 2003), and are a blend of satellite and gauge data. The Global Precipitation Climatology Centre (GPCC; updated from Rudolf et al., 1994) provides monthly data from surface gauges on several grids constructed using GPCC sources (including data

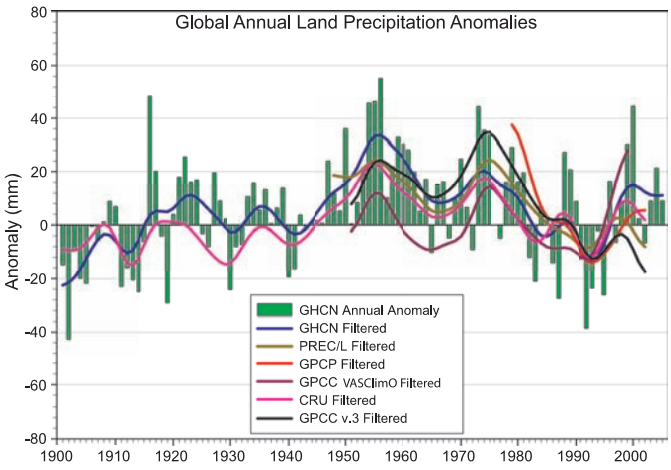


Figure 3.12. *Time series for 1900 to 2005 of annual global land precipitation anomalies (mm) from GHCN with respect to the 1981 to 2000 base period. The smooth curves show decadal variations (see Appendix 3.A) for the GHCN (Peterson and Vose, 1997), PREC/L (Chen et al., 2002), GPCP (Adler et al., 2003), GPCC (Rudolf et al., 1994) and CRU (Mitchell and Jones, 2005) data sets.*

Table 3.4. *(a) Characteristics and references of the six global land-area precipitation data sets used to calculate trends. (b) Global land precipitation trends (mm per decade). Trends with 5 and 95% confidence intervals and levels of significance (italic, 1–5%) were estimated by REML (see Appendix 3.A), which allows for serial correlation in the residuals of the data about the linear trend. All trends are based on annual averages without estimates of intrinsic uncertainties.*

(a)

Series	Period of Record	Gauge only	Satellite and gauge	Spatial infilling	Reference
GHCN	1900–2005	X		No	Vose et al., 1992
PREC/L	1948–2002	X		Yes	Chen et al., 2002
GPCP	1979–2002		X	Yes	Adler et al., 2003
GPCC VASClimO	1951–2000	X		Yes	Beck et al., 2005
GPCC v.3	1951–2002	X		Yes	Rudolf et al., 1994
CRU	1901–2002	X		Yes	Mitchell and Jones, 2005

(b)

Series	Precipitation Trend (mm per decade)		
	1901–2005	1951–2005	1979–2005
PREC/L		*–5.10 ± 3.25*[a]	–6.38 ± 8.78[a]
CRU	1.10 ± 1.50[a]	–3.87 ± 3.89[a]	–0.90 ± 16.24[a]
GHCN	1.08 ± 1.87	–4.56 ± 4.34	4.16 ± 12.44
GPCC VASClimO		1.82 ± 5.32[b]	12.82 ± 21.45[b]
GPCC v.3		*–6.63 ± 5.18*[a]	–14.64 ± 11.67[a]
GPCP			–15.60 ± 19.84[a]

Notes:
[a] Series ends at 2002
[b] Series ends at 2000

from CRU, GHCN, a Food and Agriculture Organization (FAO) database and many nationally provided data sets). The data set designated GPCC VASClimO (Beck et al., 2005) uses only those quasi-continuous stations whose long-term homogeneity can be assured, while GPCC v.3 has used all available stations to provide more complete spatial coverage. Gridding schemes also vary and include optimal interpolation and grid-box averaging of areally weighted station anomalies. The CRU data set is from Mitchell and Jones (2005).

For 1951 to 2005, trends range from –7 to +2 mm per decade and 5 to 95% error bars range from 3.2 to 5.3 mm per decade. Only the updated PREC/L series (Chen et al., 2002) trend and the GPCC v.3 trend appear to be statistically significant, but the uncertainties, as seen in the different estimates, undermine that result. For 1979 to 2005, GPCP data are added and trends range from –16 to +13 mm per decade but none is significant. Nevertheless, the discrepancies in trends are substantial, and highlight the difficulty of monitoring a variable such as precipitation that has large variability in both space and time. On the other hand, Figure 3.12 also suggests that interannual fluctuations have some overall reproducibility for land as a whole. The lag-1 autocorrelation of the residuals from the fitted trend (i.e., the de-trended persistence) is in the range 0.3 to 0.5 for the PREC/L, CRU and GHCN series but 0.5 to 0.7 for the two GPCC and the GPCP series. This suggests that either the limited sampling by *in situ* gauge data adds noise, or systematic biases lasting a few years (the lifetime of a satellite) are afflicting the GPCP data, or a combination of the two.

3.3.2.2 Spatial Patterns of Precipitation Trends

The spatial patterns of trends in annual precipitation (% per century or per decade) during the periods 1901 to 2005 and 1979 to 2005 are shown in Figure 3.13. The observed trends over land areas were calculated using GHCN station data interpolated to a 5° × 5° latitude/longitude grid. For most of North America, and especially over high-latitude regions in Canada, annual precipitation has increased during the 105-year period. The primary exception is over the southwest USA, northwest Mexico and the Baja Peninsula, where the trend in

annual precipitation has been negative (1 to 2% per decade) as drought has prevailed in recent years. Across South America, increasingly wet conditions were observed over the Amazon Basin and southeastern South America, including Patagonia, while negative trends in annual precipitation were observed over Chile and parts of the western coast of the continent. The largest negative trends in annual precipitation were observed over western Africa and the Sahel. After having concluded that the effect of changing rainfall-gauge networks on Sahel rainfall time series is small, Dai et al. (2004b) noted that Sahel rainfall in the 1990s has recovered considerably from the severe dry years in the early 1980s (see Section 3.7.4 and Figure 3.37). A drying trend is also evident over southern Africa since 1901. Over much of northwestern India the 1901 to 2005 period shows increases of more than 20% per century, but the same area shows a strong decrease in annual precipitation for the 1979 to 2005 period. Northwestern Australia shows areas with moderate to strong increases in annual precipitation over both periods. Over most of Eurasia, increases in precipitation outnumber decreases for both periods.

To assess the expected large regional variations in precipitation trends, Figure 3.14 presents time series of annual precipitation. The regions are 19 of those defined in Table 11.1 (see Section 11.1) and illustrated in Figure 11.26. The GHCN precipitation data set from NCDC was used, and the CRU decadal values allow the reproducibility to be assessed. Based on this, plots for four additional regions (Greenland, Sahara, Antarctica and the Tibetan Plateau) were not included, as precipitation data for these were not considered sufficiently reliable, nor was the first part of the Alaskan series (prior to 1935). Some discrepancies between the decadal variations are still evident at times, mostly owing to different subsets of stations and some stations coming in or dropping out, but overall the confidence in what is presented is quite high. Figure 3.15 presents a latitude-time series of zonal averages over land.

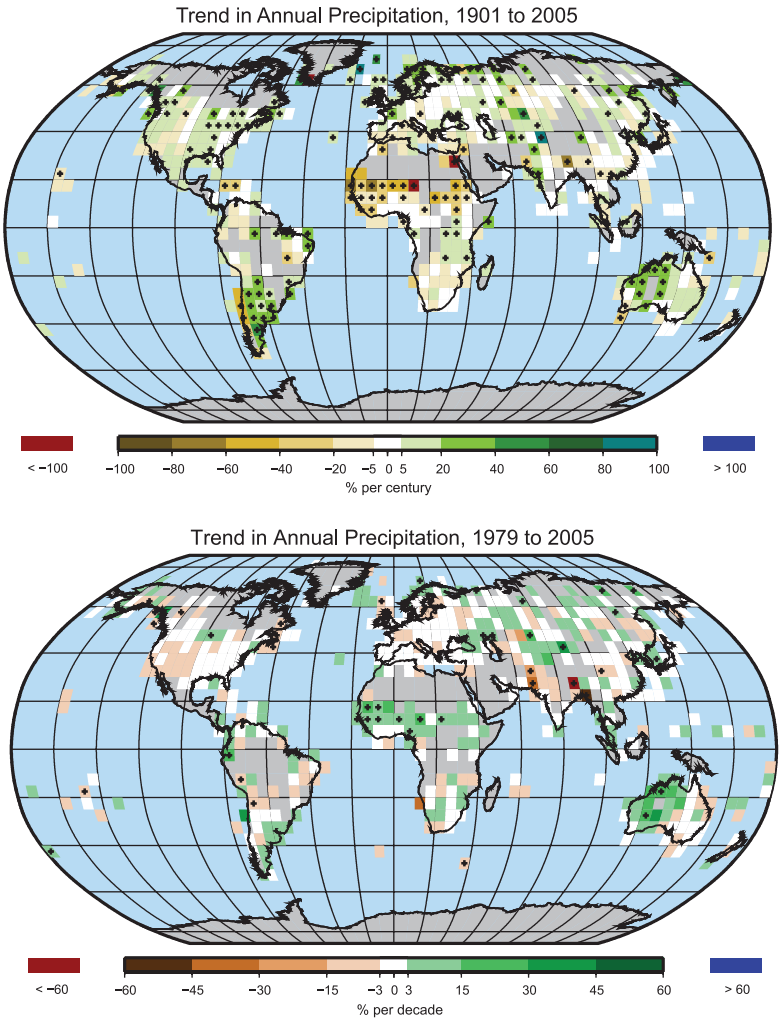


Figure 3.13. *Trend of annual land precipitation amounts for 1901 to 2005 (top, % per century) and 1979 to 2005 (bottom, % per decade), using the GHCN precipitation data set from NCDC. The percentage is based on the means for the 1961 to 1990 period. Areas in grey have insufficient data to produce reliable trends. The minimum number of years required to calculate a trend value is 66 for 1901 to 2005 and 18 for 1979 to 2005. An annual value is complete for a given year if all 12 monthly percentage anomaly values are present. Note the different colour bars and units in each plot. Trends significant at the 5% level are indicated by black + marks.*

In the tropics, precipitation is highly seasonal, consisting of a dry season and a wet season in association with the summer monsoon. These aspects are discussed in more detail in Section 3.7. Downward trends are strongest in the Sahel (see Section 3.7.4) but occur in both western and eastern Africa in the past 50 years, and are reflected in the zonal means. The downward trends in this zone are also found in southern Asia. The linear trends of rainfall decreases for 1900 to 2005 were 7.5% in both the western Africa and southern Asia regions (significant at <1%). The area of the latter region is much greater than India, whose rainfall features strong variability but little in the way of a century-scale trend. Southern Africa also features a strong overall downward trend, although with strong multi-decadal variability present. Often the change in rainfall in these regions occurs fairly abruptly, and in several cases occurs around the same time in association with the 1976–1977 climate shift (Wang and Ding, 2006). The timing is not the same everywhere, however, and the downward shift occurred earlier in the Sahel (see also Section 3.7.4, Figure 3.37). The main location with different trends at low latitudes is over Australia, but it is clear that large interannual variability, mostly ENSO-related, is dominant (note also the expanded vertical scales for Australia). The apparent upward trend occurs due to two rather wet spells in northern Australia in the early 1970s and 1990s, when it was dry in Southeast Asia (see also Section 3.7.2). Also of note in Australia is the marked downward trend in the far southwest characterised by a downward shift around 1975 (Figure 3.13).

At higher latitudes, especially from 30°N to 85°N, quite distinct upward trends are evident in many regions and these are reflected in the zonal means (Figure 3.15). Central North America, eastern North America, northern Europe, northern

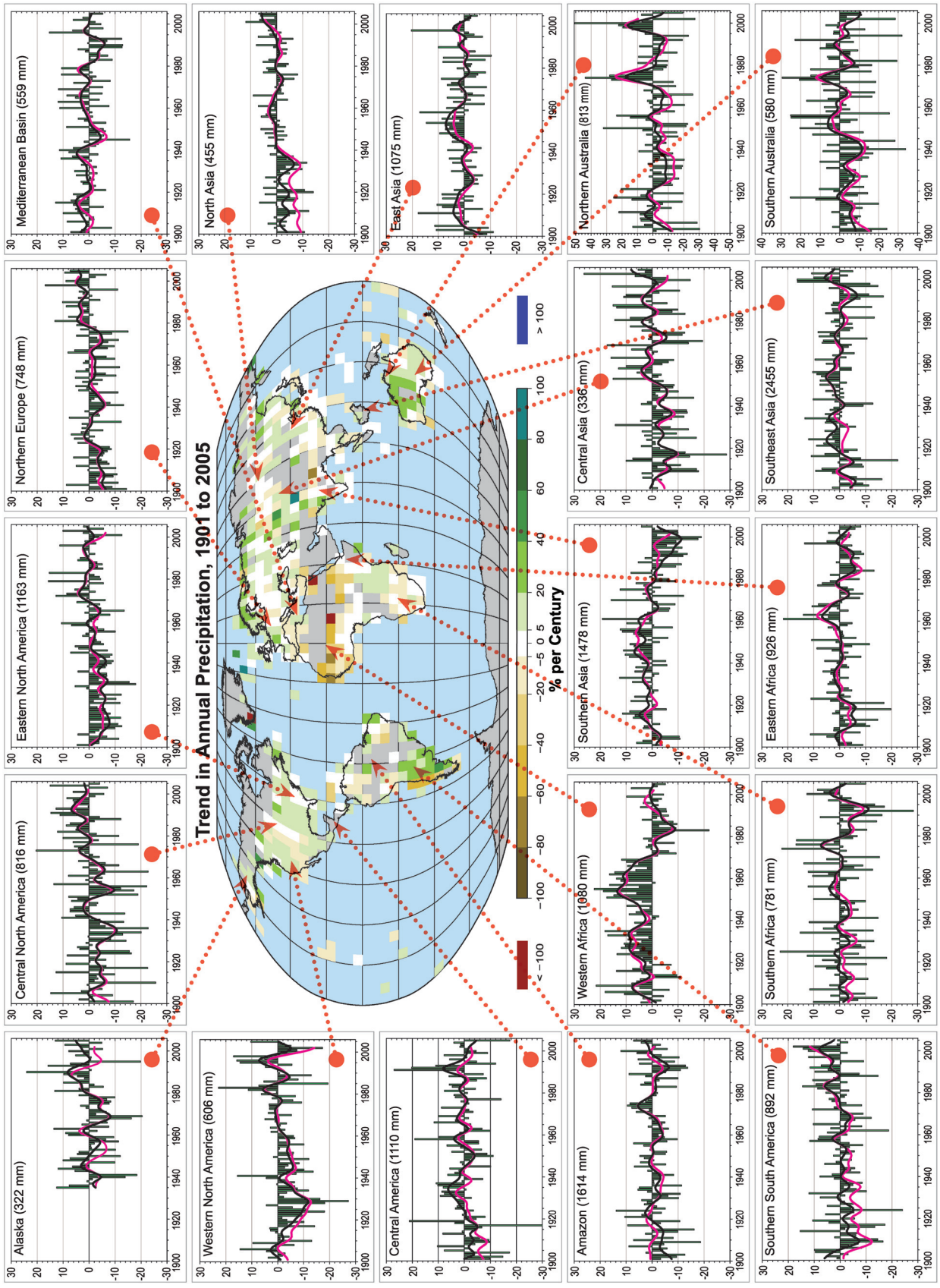


Figure 3.14. *Precipitation for 1900 to 2005. The central map shows the annual mean trends (% per century). Areas in grey have insufficient data to produce reliable trends. The surrounding time series of annual precipitation displayed (% of mean, with the mean given at top for 1961 to 1990) are for the named regions as indicated by the red arrows. The GHCN precipitation from NCDC was used for the annual green bars and black for decadal variations (see Appendix 3.A), and for comparison the CRU decadal variations are in magenta. The range is +30 to −30% except for the two Australian panels. The regions are a subset of those defined in Table 11.1 (Section 11.1) and include: Central North America, Western North America, Alaska, Central America, Eastern North America, Mediterranean, Northern Europe, North Asia, East Asia, Central Asia, Southeast Asia, Southern Asia, Northern Australia, Southern Australia, Eastern Africa, Western Africa, Southern Africa, Southern South America, and the Amazon.*

Asia and central Asia (east of the Caspian Sea) all experienced upward linear trends of between 6 and 8% from 1900 to 2005 (all significant at <5%). These regions all experience snowfall (see also Section 3.3.2.3) and part of the upward trend may arise from changes in efficiency of catching snow, especially in northern Asia. However, there is ample evidence that these trends are real (see Section 3.3.4), and they extend from North America to Europe across the North Atlantic as evidenced by ocean freshening, documented in Sections 5.2.3 and 5.3.2. Western North America shows longer time-scale variability, principally due to the severe drought in the 1930s and lesser events more recently. Note the tendency for inverse variations between northern Europe and the Mediterranean, associated with changes in the NAO (see Section 3.6.4). Southern Europe and parts of central Europe, as well as North Africa, are characterised by a drier winter (DJF) during the positive phase of the NAO, while the reverse is true in the British Isles, Fennoscandia and northwestern Russia.

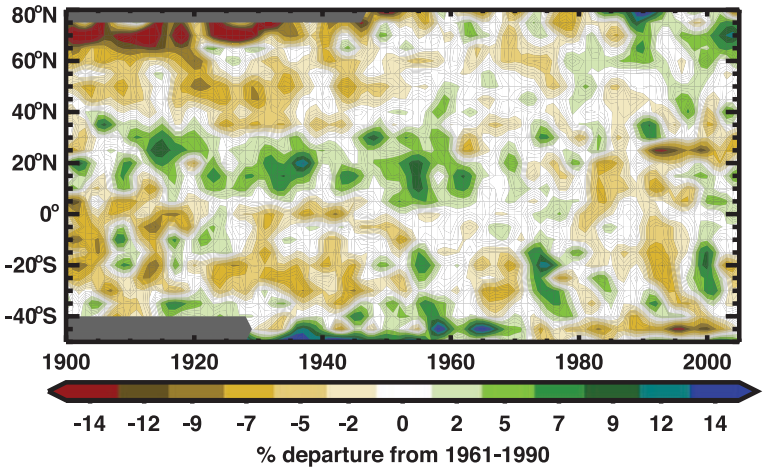


Figure 3.15. *Latitude-time section of zonal average annual anomalies for precipitation (%) over land from 1900 to 2005, relative to their 1961 to 1990 means. Values are smoothed with the 5-point filter to remove fluctuations of less than about six years (see Appendix 3.A). The colour scale is nonlinear and grey areas indicate missing data.*

In the SH, Amazonia and southern South America feature opposite changes, as the South American monsoon features shifted southwards (see Section 3.7.3). This movement was in association with changes in ENSO and the 1976–1977 climate shift. The result is a pronounced upward trend in Argentina and the La Plata River Basin, but not in Chile (where the main declines in precipitation are evident in the austral summer (DJF) and autumn (MAM; Figure 3.13). Decadal-scale variations over Amazonia are also out of phase with the Central American region to the north, which in turn has out-of-phase variations with western North America, again suggestive of latitudinal changes in monsoon features. East and Southeast Asia show hardly any long-term changes, with both having plentiful rains in the 1950s. At interannual time scales there are a number of surprisingly strong correlations: Amazonia is correlated with northern Australia (0.44, significant at <1%) and also Southeast Asia (0.55, <1%), while southern South America is inversely correlated with western Africa (–0.51, <1%). The correlations are surprising because they are based on high-frequency relationships and barely change when the smoothed series are used.

3.3.2.3 Changes in Snowfall

Winter precipitation has increased at high latitudes, although uncertainties exist because of changes in undercatch, especially as snow changes to rain. Snow cover changes are discussed in Section 4.2. Annual precipitation for the circumpolar region north of 50°N has increased during the past 50 years (not shown) by approximately 4% but this increase has not been homogeneous in time and space (Groisman et al., 2003, 2005). Statistically significant increases were documented over Fennoscandia, coastal regions of northern North America (Groisman et al., 2005), most of Canada (particularly northern regions) up until at least 1995 when the analysis ended (Stone et al., 2000), the permafrost-free zone of Russia (Groisman and Rankova, 2001) and the entire Great Russian Plain (Groisman et al., 2005, 2007). However, there were no discernible changes in summer and annual precipitation totals over northern Eurasia east of the Ural Mountains (Gruza et al., 1999; Sun and Groisman, 2000; Groisman et al., 2005, 2007). Rainfall (liquid precipitation) has increased during the past 50 years over western portions of North America and Eurasia north of 50°N by about 6%. Rising temperatures have generally resulted in rain rather than snow in locations and seasons where climatological average (1961–1990) temperatures were close to 0°C. The liquid precipitation season has become longer by up to three weeks in some regions of the boreal high latitudes over the last 50 years (Cayan et al., 2001; Groisman et al., 2001; Easterling, 2002; Groisman et al., 2005, 2007) owing, in particular, to an earlier onset of spring. Therefore, in some regions (southern Canada and western Russia), snow has provided a declining fraction of total annual precipitation (Groisman et al., 2003, 2005, 2007). In other regions, particularly north of 55°N, the fraction of annual precipitation falling as snow in winter has changed little.

Berger et al. (2002) found a trend towards fewer snowfall events during winter across the lower Missouri River Basin from 1948 to 2002, but little or no trend in snowfall occurrences within the plains region to the south. In New England, there has been a decrease in the proportion of precipitation occurring as snow at many locations, caused predominantly by a decrease in snowfall, with a lesser contribution from increased rainfall (Huntington et al., 2004). By contrast, Burnett et al. (2003) found large increases in lake-effect snowfall since 1951 for locations near the North American Great Lakes, consistent with the observed decrease in ice cover for most of the Great Lakes since the early 1980s (Assell et al., 2003). In addition to snow data, Burnett et al. (2003) used lake sediment reconstructions for locations south of Lake Ontario to indicate that these increases have been ongoing since the beginning of the 20th century. Ellis and Johnson (2004) found that the increases in snowfall across

the regions to the lee of Lakes Erie and Ontario are due to increases in the frequency of snowfall at the expense of rainfall events, an increase in the intensity of snowfall events, and to a lesser extent an increase in the water equivalent of the snow. In Canada, the frequency of heavy snowfall events has decreased since the 1970s in the south and increased in the north (Zhang et al., 2001a).

3.3.2.4 Urban Areas

As noted in Section 3.2.2.2 (see also Box 7.2), the microclimates in cities are clearly different than in neighbouring rural areas. The presence of a city affects runoff, moisture availability and precipitation. Crutzen (2004) pointed out that while human energy production is relatively small globally compared with the Sun, it is locally important in cities, where it can reach 20 to 70 W m^{-2}. Urban effects can lead to increased precipitation (5 to 25% over background values) during the summer months within and 50 to 75 km downwind of the city (Changnon et al., 1981). More frequent or intense storms have been linked to city growth in Phoenix, Arizona (Balling and Brazel, 1987) and Mexico City (Jauregui and Romales, 1996). More recent observational studies (Bornstein and Lin, 2000; Changnon and Westcott, 2002; Shepherd et al., 2002; Diem and Brown, 2003; Dixon and Mote, 2003; Fujibe, 2003; Shepherd and Burian, 2003; Inoue and Kimura, 2004; Shepherd et al., 2004; Burian and Shepherd, 2005) have continued to link urban-induced dynamic processes to precipitation anomalies. Nor is land use change confined to urban areas (see Section 7.2). Other changes in land use also affect precipitation. A notable example arises from deforestation in the Amazon, where Chagnon and Bras (2005) found large changes in local rainfall with increases in deforested areas, associated with local atmospheric circulations that are changed by gradients in vegetation, and also found changes in seasonality.

Suggested mechanisms for urban-induced rainfall include: (1) enhanced convergence due to increased surface roughness in the urban environment (e.g., Changnon et al., 1981; Bornstein and Lin, 2000; Thielen et al., 2000); (2) destabilisation due to UHI thermal perturbation of the boundary layer and resulting downstream translation of the UHI circulation or UHI-generated convective clouds (e.g., Shepherd et al., 2002; Shepherd and Burian, 2003); (3) enhanced aerosols in the urban environment for cloud condensation nuclei sources (e.g., Diem and Brown, 2003; Molders and Olson, 2004); or (4) bifurcating or diverting of precipitating systems by the urban canopy or related processes (e.g., Bornstein and Lin, 2000). The 'weekend effect' noted in Section 3.2.2.2 likely arises from some of these mechanisms. The diurnal cycle in precipitation, which varies over the USA from late afternoon maxima in the Southeast to nocturnal maxima in the Great Plains (Dai and Trenberth, 2004), may be modified in some regions by urban environments. Dixon and Mote (2003) found that a growing UHI effect in Atlanta, Georgia (USA) enhanced and possibly initiated thunderstorms, especially in July (summer) just after midnight. Low-level moisture was found to be a key factor.

3.3.2.5 Ocean Precipitation

Remotely sensed precipitation measurements over the ocean are based on several different sensors in the microwave and infrared that are combined in different ways. Many experimental products exist. Operational merged products seem to perform best in replicating island-observed monthly amounts (Adler et al., 2001). This does not mean they are best for trends or low-frequency variability, because of the changing mixes of input data. The main global data sets available for precipitation, and which therefore include ocean coverage, have been the GPCP (Huffman et al., 1997; Adler et al., 2003) and the NOAA Climate Prediction Center (CPC) Merged Analysis of Precipitation (CMAP; Xie and Arkin, 1997). Comparisons of these data sets and others (Adler et al., 2001; Yin et al., 2004) reveal large discrepancies over the ocean; however, there is better agreement among the passive microwave products even using different algorithms. Over the tropical oceans, mean amounts in CMAP and GPCP differ by 10 to 15%. Calibration using observed rainfall from small atolls in CMAP was extended throughout the tropics in ways that are now recognised as incorrect. However, evaluation of GPCP reveals that it is biased low by 16% at such atolls (Adler et al., 2003), also raising questions about the ocean GPCP values. Differences arise due to sampling and algorithms. Polar-orbiting satellites each obtain only two instantaneous rates per day over any given location, and thus suffer from temporal sampling deficiencies that are offset by using geostationary satellites. However, only less-accurate infrared sensors are available with the latter. Model-based (including reanalysis) products perform poorly in the evaluation of Adler et al. (2001) and are not currently suitable for climate monitoring. Robertson et al. (2001b) examined monthly anomalies from several satellite-derived precipitation data sets (using different algorithms) over the tropical oceans. The expectation in the TAR was that measurements from the Tropical Rainfall Measuring Mission (TRMM) Precipitation Radar (PR) and passive TRMM microwave imager (TMI) would clarify the reasons for the discrepancies, but this has not yet been the case. Robertson et al. (2003) documented poorly correlated behaviour (correlation 0.12) between the monthly, tropical ocean-averaged precipitation anomalies from the PR and TMI sensors. Although the TRMM PR responds directly to precipitation size hydrometeors, it operates with a single attenuating frequency (13.8 GHz) that necessitates significant microphysical assumptions regarding drop size distributions for relating reflectivity, signal attenuation and rainfall, and uncertainties in microphysical assumptions for the primary TRMM algorithm (2A25) remain problematic.

The large regional signals from monsoons and ENSO that emphasise large-scale shifts in precipitation are reasonably well captured in GPCP and CMAP (see Section 3.6.2), but cancel out when area-averaged over the tropics, and the trends and variability of the tropical average are quite different in the two products. Global precipitation from GPCP (updated from Adler et al., 2003, but not shown) has monthly variability with a standard deviation of about 2% of the mean. The variability in the ocean

and land areas when examined separately is larger, about 3%, and with variations related to ENSO events (Curtis and Adler, 2003). During El Niño events, area-averaged precipitation increases over the oceans but decreases over land.

Although the trend over 25 years in global total precipitation in the GPCP data set (Adler et al., 2003) is very small, there is a small increase (about 4% over the 25 years) over the oceans in the latitude range 25°S to 25°N, with a partially compensating decrease over land (2%) in the same latitude belt. Northern mid-latitudes show a decrease over land and ocean. Over a slightly longer time frame, precipitation increased over the North Atlantic between 1960 to 1974 and 1975 to 1989 (Josey and Marsh, 2005) and is reflected in changes in salinity in the oceans (Section 5.2.3). The inhomogeneous nature of the data sets and the large ENSO variability limit what can be said about the validity of changes, both globally and regionally.

3.3.3 Evapotranspiration

There are very limited direct measurements of actual evapotranspiration over global land areas. Over oceans, estimates of evaporation depend on bulk flux estimates that contain large errors. Evaporation fields from the ERA-40 and NRA are not considered reliable because they are not well constrained by precipitation and radiation (Betts et al., 2003; Ruiz-Barradas and Nigam, 2005). The physical processes related to changes in evapotranspiration are discussed in Section 7.2 and Section 3.4, Box 3.2.

Decreasing trends during recent decades are found in sparse records of pan evaporation (measured evaporation from an open water surface in a pan) over the USA (Peterson et al., 1995; Golubev et al., 2001; Hobbins et al., 2004), India (Chattopadhyay and Hulme, 1997), Australia (Roderick and Farquhar, 2004), New Zealand (Roderick and Farquhar, 2005), China (Liu et al., 2004a; Qian et al., 2006b) and Thailand (Tebakari et al., 2005). Pan measurements do not represent actual evaporation (Brutsaert and Parlange, 1998), and any trend is more likely caused by decreasing surface solar radiation over the USA and parts of Europe and Russia (Abakumova et al., 1996; Liepert, 2002) and decreased sunshine duration over China (Kaiser and Qian, 2002) that may be related to increases in air pollution and atmospheric aerosols (Liepert et al., 2004; Qian et al., 2006a) and increases in cloud cover (Dai et al., 1999). Whether actual evapotranspiration decreases or not also depends on how surface wetness changes (see Section 3.4, Box 3.2). Changes in evapotranspiration are often calculated using empirical models as a function of precipitation, wind and surface net radiation (Milly and Dunne, 2001), or land surface models (LSMs; e.g., van den Dool et al., 2003; Qian et al., 2006a).

The TAR reported that actual evapotranspiration increased during the second half of the 20th century over most dry regions of the USA and Russia (Golubev et al., 2001), resulting from greater availability of surface moisture due to increased precipitation and larger atmospheric moisture demand due to higher temperature. One outcome is a larger surface latent heat flux (increased evapotranspiration) but decreased sensible heat flux (Trenberth and Shea, 2005). Using observed precipitation, temperature, cloudiness-based surface solar radiation and a comprehensive land surface model, Qian et al. (2006a) found that global land evapotranspiration closely follows variations in land precipitation. Global precipitation values (Figure 3.12) peaked in the early 1970s and then decreased somewhat, but reflect mainly tropical values, and precipitation has increased more generally over land at higher latitudes (Figures 3.13 and 3.14). Changes in evapotranspiration depend not only on moisture supply but also on energy availability and surface wind (see Section 3.4, Box 3.2).

3.3.4 Changes in Soil Moisture, Drought, Runoff and River Discharge

Historical records of soil moisture content measured *in situ* are available for only a few regions and often are very short (Robock et al., 2000). A rare 45-year record of soil moisture over agricultural areas of the Ukraine shows a large upward trend, which was stronger during the first half of the period (Robock et al., 2005). Among over 600 stations from a large variety of climates, including the former Soviet Union, China, Mongolia, India and the USA, Robock et al. (2000) showed an increasing long-term trend in surface (top 1 m) soil moisture content during summer for the stations with the longest records.

One method to examine long-term changes in soil moisture uses calculations based on formulae or LSMs. Since the *in situ* observational record and global estimates of remotely sensed soil moisture data are limited, global soil moisture variations during the 20th century have been estimated by LSM simulations. However, the results depend critically on the 'forcings' used, namely the radiation (clouds), precipitation, winds and other weather variables, which are not sufficiently reliable to determine trends. Consequently the estimates based on simulations disagree. Instead, the primary approach has been to calculate Palmer Drought Severity Index (PDSI; see Box 3.1) values from observed precipitation and temperature (e.g., Dai et al., 2004a). In some locations, much longer proxy extensions have been derived from earlier tree ring data (see Section 6.6.1; e.g., Cook et al., 1999). The longer instrumental-based PDSI estimations are used to look at trends and some recent extreme PDSI events in different regions are placed in a longer-term context (see specific cases in Section 3.8, Box 3.6). As with LSM-based studies, the version of the PDSI used is crucial, and it can partly determine some aspects of the results found (Box 3.1).

Using the PDSI, Dai et al. (2004a) found a large drying trend over NH land since the middle 1950s, with widespread drying over much of Eurasia, northern Africa, Canada and Alaska. In the SH, land surfaces were wet in the 1970s and relatively dry in the 1960s and 1990s, and there was a drying trend from 1974 to 1998 although trends over the entire 1948 to 2002 period were small. Overall patterns of trends in the PDSI are given in FAQ 3.2, Figure 1. Although the long-term (1901–2004) land-based precipitation trend shows a small increase (Figure 3.12), decreases in land precipitation in recent decades are the main

Box 3.1: Drought Terminology and Determination

In general terms, drought is a 'prolonged absence or marked deficiency of precipitation', a 'deficiency of precipitation that results in water shortage for some activity or for some group' or a 'period of abnormally dry weather sufficiently prolonged for the lack of precipitation to cause a serious hydrological imbalance' (Heim, 2002). Drought has been defined in a number of ways. 'Agricultural drought' relates to moisture deficits in the topmost one metre or so of soil (the root zone) that impact crops, 'meteorological drought' is mainly a prolonged deficit of precipitation, and 'hydrologic drought' is related to below-normal streamflow, lake and groundwater levels.

Drought and its severity can be numerically defined using indices that integrate temperature, precipitation and other variables that affect evapotranspiration and soil moisture. Several indices in different countries assess precipitation deficits in various ways, such as the Standardized Precipitation Index. Other indices make use of additional weather variables. An example is the Keetch-Byrum Drought Index (Keetch and Byrum, 1988), which assesses the severity of drought in soils based on rainfall and temperature estimates to assess soil moisture deficiencies. However, the most commonly used index is the PDSI (Palmer, 1965; Heim, 2002) that uses precipitation, temperature and local available water content data to assess soil moisture. Although the PDSI is not an optimal index, since it does not include variables such as wind speed, solar radiation, cloudiness and water vapour, it is widely used and can be calculated across many climates as it requires only precipitation and temperature data for the calculation of potential evapotranspiration (PET) using Thornthwaite's (1948) method. Because these data are readily available for most parts of the globe, the PDSI provides a measure of drought for comparison across many regions.

However, PET is considered to be more reliably calculated using Penman (1948) type approaches that incorporate the effects of wind, water vapour and solar and longwave radiation. In addition, there has been criticism of most Thornthwaite-based estimates of the PDSI because the empirical constants have not been re-computed for each climate (Alley, 1984). Hence, a self-calibrating version of the PDSI has recently been developed to ensure consistency with the climate at any location (Wells et al., 2004). Also, studies that compute changes or trends in the PDSI effectively remove influences of biases in the absolute values. As the effects of temperature anomalies on the PDSI are small compared to precipitation anomalies (Guttman, 1991), the PDSI is largely controlled by precipitation changes.

cause for the drying trends, although large surface warming during the last two to three decades has likely contributed to the drying. Dai et al. (2004a) showed that globally, very dry areas (defined as land areas with a PDSI of less than –3.0) more than doubled (from ~12 to 30%) since the 1970s, with a large jump in the early 1980s due to an ENSO-related precipitation decrease over land and subsequent increases primarily due to surface warming. However, results are dependent on the version of the PDSI model used, since the empirical constants used in a global PDSI model may not be adequately adjusted for the local climate (see Box 3.1).

In Canada, the summer PDSI averaged for the entire country indicates dry conditions during the 1940s and 1950s, generally wet conditions from the 1960s to 1995, but much drier conditions after 1995 (Shabbar and Skinner, 2004) with a relationship between recent increasing summer droughts and the warming trend in SST. Groisman et al. (2007) found increased dryness based on the Keetch-Byrum forest-fire drought index in northern Eurasia, a finding supported by Dai et al. (2004a) using the PDSI. Long European records (van der Schrier et al., 2006) reveal no trend in areas affected by extreme PDSI values (thresholds of either ±2 or ±4) over the 20th century. Nevertheless, recently Europe has suffered prolonged drought, including the 2003 episode associated with the severe summer heat wave (see Section 3.8.4, Box 3.6).

Although there was no significant trend from 1880 to 1998 during summer (JJA) in eastern China, precipitation for 1990 to 1998 was the highest on record for any period of comparable length (Gong and Wang, 2000). Zou et al. (2005) found that for China as a whole there were no long-term trends in the percentage areas of droughts (defined as PDSI < –1.0) during 1951 to 2003. However, increases in drought areas were found in much of northern China (but not in northwest China; Zou et al., 2005), aggravated by warming and decreasing precipitation (Ma and Fu, 2003; Wang and Zhai, 2003), consistent with Dai et al. (2004a).

A severe drought affecting central and southwest Asia in recent years (see Section 3.8.4, Box 3.6) appears to be the worst since at least 1980 (Barlow et al., 2002). In the Sahel region of Africa, rainfall has recovered somewhat in recent years, after large decreasing rainfall trends from the late 1960s to the late 1980s (Dai et al., 2004b; see also Section 3.3.2.2 and Section 3.7.4, Figure 3.37). Large multi-year oscillations appear to be more frequent and extreme after the late 1960s than previously in the century. A severe drought affected Australia in 2002 and 2003; precipitation deficits were not as severe as during a few episodes earlier in the 20th century, but higher temperatures exacerbated the impacts (see Section 3.8.4, Box 3.6). There have been marked multi-year rainfall deficits and drought since the mid- to late-1990s in several parts of Australia, particularly the far southwest, parts of the southeast and along sections of the east coast.

A multi-decadal period of relative wetness characterised the latter portion of the 20th century in the continental USA, in terms of precipitation (Mauget, 2003a), streamflow (Groisman et al., 2004) and annual moisture surplus (precipitation minus potential evapotranspiration; McCabe and Wolock, 2002). Despite this overall national trend towards wetter conditions,

Frequently Asked Question 3.2
How is Precipitation Changing?

Observations show that changes are occurring in the amount, intensity, frequency and type of precipitation. These aspects of precipitation generally exhibit large natural variability, and El Niño and changes in atmospheric circulation patterns such as the North Atlantic Oscillation have a substantial influence. Pronounced long-term trends from 1900 to 2005 have been observed in precipitation amount in some places: significantly wetter in eastern North and South America, northern Europe and northern and central Asia, but drier in the Sahel, southern Africa, the Mediterranean and southern Asia. More precipitation now falls as rain rather than snow in northern regions. Widespread increases in heavy precipitation events have been observed, even in places where total amounts have decreased. These changes are associated with increased water vapour in the atmosphere arising from the warming of the world's oceans, especially at lower latitudes. There are also increases in some regions in the occurrences of both droughts and floods.

Precipitation is the general term for rainfall, snowfall and other forms of frozen or liquid water falling from clouds. Precipitation is intermittent, and the character of the precipitation when it occurs depends greatly on temperature and the weather situation. The latter determines the supply of moisture through winds and surface evaporation, and how it is gathered together in storms as clouds. Precipitation forms as water vapour condenses, usually in rising air that expands and hence cools. The upward motion comes from air rising over mountains, warm air riding over cooler air (warm front), colder air pushing under warmer air (cold front), convection from local heating of the surface, and other weather and cloud systems. Hence, changes in any of these aspects alter precipitation. As precipitation maps tend to be spotty, overall trends in precipitation are indicated by the Palmer Drought Severity Index (see Figure 1), which is a measure of soil moisture using precipitation and crude estimates of changes in evaporation.

A consequence of increased heating from the human-induced enhanced greenhouse effect is increased evaporation, provided that adequate surface moisture is available (as it always is over the oceans and other wet surfaces). Hence, surface moisture effectively acts as an 'air conditioner', as heat used for evaporation acts to moisten the air rather than warm it. An observed consequence of this is that summers often tend to be either warm and dry or cool and wet. In the areas of eastern North and South America where it has become wetter (Figure 1), temperatures have therefore increased less than elsewhere (see FAQ 3.3, Figure 1 for changes in warm days). Over northern continents in winter, however, more precipitation is associated with higher temperatures, as the water holding capacity of the atmosphere increases in the warmer conditions. However, in these regions, where precipitation has generally increased somewhat, increases in temperatures (FAQ 3.1) have increased drying, making the precipitation changes less evident in Figure 1.

As climate changes, several direct influences alter precipitation amount, intensity, frequency and type. Warming accelerates land surface drying and increases the potential incidence and severity of droughts, which has been observed in many places worldwide (Figure 1). However, a well-established physical law (the Clausius-Clapeyron relation) determines that the water-holding capacity of the atmosphere increases by about 7% for every 1°C rise in temperature. Observations of trends in relative humidity are uncertain but suggest that it has remained about the same overall, from the surface throughout the troposphere, and hence increased temperatures will have resulted in increased water vapour. Over the 20th century, based on changes in sea surface temperatures, it is estimated that atmospheric water vapour increased by about 5% in the atmosphere over the oceans. Because precipitation comes mainly from weather systems that feed on the water vapour stored in the atmosphere, this has generally increased precipitation intensity and the risk of heavy rain and snow events. Basic theory, climate model simulations and empirical evidence all confirm that warmer climates, owing to increased water vapour, lead to more intense precipitation events even when the total annual precipitation is reduced slightly, and with prospects for even stronger events when the overall precipitation amounts increase. The warmer climate therefore increases risks of both drought – where it is not raining – and floods – where it is – but at different times and/or places. For instance, the summer of 2002 in Europe brought widespread floods but was followed a year later in 2003 by record-breaking heat waves and drought. The distribution and timing of floods and droughts is most profoundly affected by the cycle of El Niño events, particularly in the tropics and over much of the mid-latitudes of Pacific-rim countries.

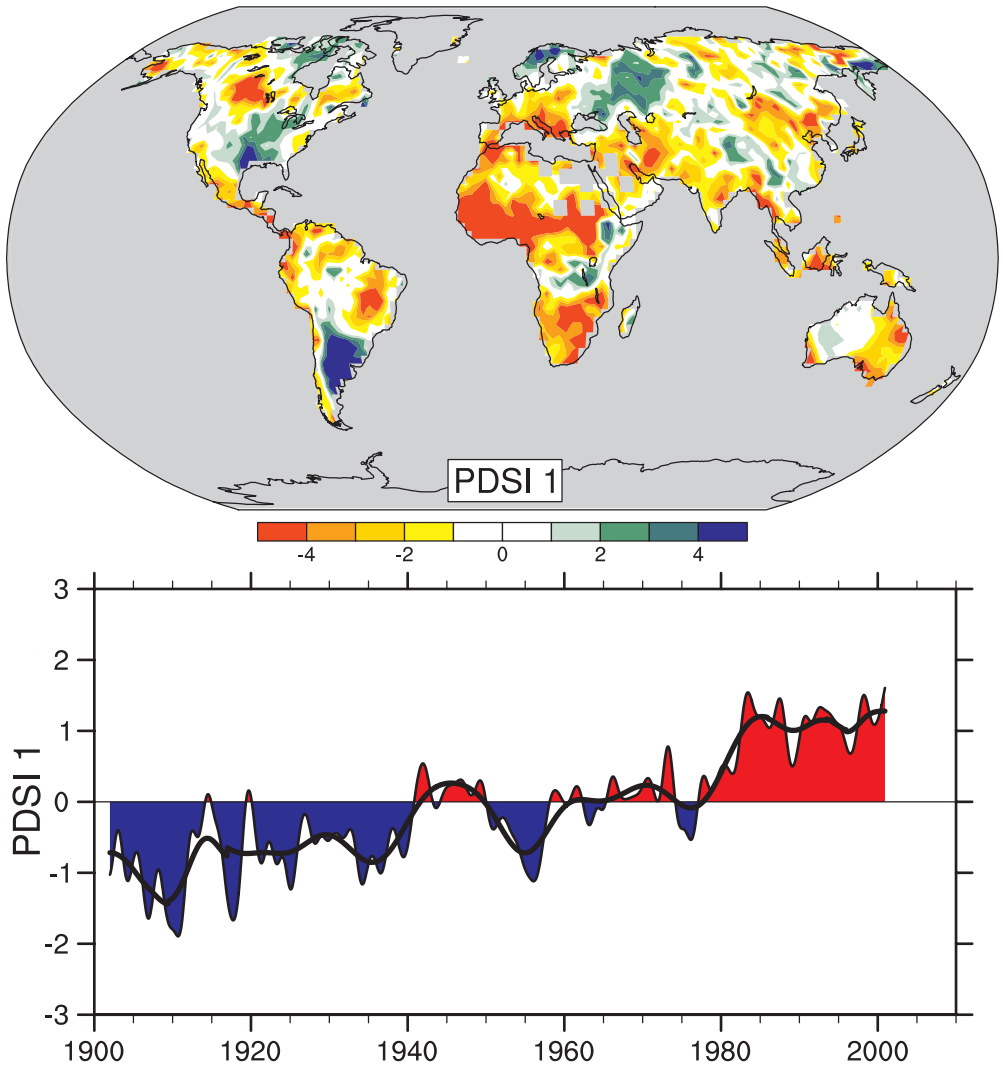
In areas where aerosol pollution masks the ground from direct sunlight, decreases in evaporation reduce the overall moisture supply to the atmosphere. Hence, even as the potential for heavier precipitation results from increased water vapour amounts, the duration and frequency of events may be curtailed, as it takes longer to recharge the atmosphere with water vapour.

Local and regional changes in the character of precipitation also depend a great deal on atmospheric circulation patterns determined by El Niño, the North Atlantic Oscillation (NAO; a measure of westerly wind strength over the North Atlantic in winter) and other patterns of variability. Some of these observed circulation changes are associated with climate change. An associated shift in the storm track makes some regions wetter and some – often nearby – drier, making for complex patterns of change. For instance, in the European sector a more positive NAO in the 1990s led to wetter conditions in northern Europe and drier conditions over the Mediterranean and northern African regions (Figure 1). The prolonged drought in the Sahel (see Figure 1), which was pronounced from the late 1960s to the late 1980s,

(continued)

continues although it is not quite as intense as it was; it has been linked, through changes in atmospheric circulation, to changes in tropical sea surface temperature patterns in the Pacific, Indian and Atlantic Basins. Drought has become widespread throughout much of Africa and more common in the tropics and subtropics.

As temperatures rise, the likelihood of precipitation falling as rain rather than snow increases, especially in autumn and spring at the beginning and end of the snow season, and in areas where temperatures are near freezing. Such changes are observed in many places, especially over land in middle and high latitudes of the Northern Hemisphere, leading to increased rains but reduced snowpacks, and consequently diminished water resources in summer, when they are most needed. Nevertheless, the often spotty and intermittent nature of precipitation means observed patterns of change are complex. The long-term record emphasizes that patterns of precipitation vary somewhat from year to year, and even prolonged multi-year droughts are usually punctuated by a year of heavy rains; for instance as El Niño influences are felt. An example may be the wet winter of 2004-2005 in the southwestern USA following a six-year drought and below-normal snowpack.



FAQ 3.2, Figure 1. *The most important spatial pattern (top) of the monthly Palmer Drought Severity Index (PDSI) for 1900 to 2002. The PDSI is a prominent index of drought and measures the cumulative deficit (relative to local mean conditions) in surface land moisture by incorporating previous precipitation and estimates of moisture drawn into the atmosphere (based on atmospheric temperatures) into a hydrological accounting system. The lower panel shows how the sign and strength of this pattern has changed since 1900. Red and orange areas are drier (wetter) than average and blue and green areas are wetter (drier) than average when the values shown in the lower plot are positive (negative). The smooth black curve shows decadal variations. The time series approximately corresponds to a trend, and this pattern and its variations account for 67% of the linear trend of PDSI from 1900 to 2002 over the global land area. It therefore features widespread increasing African drought, especially in the Sahel, for instance. Note also the wetter areas, especially in eastern North and South America and northern Eurasia. Adapted from Dai et al. (2004b).*

a severe drought affected the western USA from 1999 to November 2004 (see Section 3.8.4, Box 3.6).

Available streamflow gauge records cover only about two-thirds of the global actively drained land areas and they often have gaps and vary in record length (Dai and Trenberth, 2002). Estimates of total continental river discharge are therefore often based on incomplete gauge records (e.g., Probst and Tardy, 1987, 1989; Guetter and Georgakakos, 1993), reconstructed streamflow time series (Labat et al., 2004) or methods to account for the runoff contribution from the unmonitored areas (Dai and Trenberth, 2002). These estimates show large decadal to multi-decadal variations in continental and global freshwater discharge (excluding groundwater; Guetter and Georgakakos, 1993; Labat et al., 2004).

Streamflow records for the world's major rivers show large decadal to multi-decadal variations, with small secular trends for most rivers (Cluis and Laberge, 2001; Lammers et al., 2001; Mauget, 2003b; Pekárová et al., 2003; Dai et al., 2004a). Increased streamflow during the latter half of the 20th century has been reported over regions with increased precipitation, such as many parts of the USA (Lins and Slack, 1999; Groisman et al., 2004) and southeastern South America (Genta et al., 1998). Decreased streamflow was reported over many Canadian river basins during the last 30 to 50 years (Zhang et al., 2001b), where precipitation has also decreased during the period. Déry and Wood (2005) also found decreases in river discharge into the Arctic and North Atlantic Oceans from high-latitude Canadian rivers, with potential implications for salinity levels in these oceans and possibly the North Atlantic THC. These changes are consistent with observed precipitation decreases in high-latitude Canada from 1963 to 2000. Further, Milly et al. (2002) showed significant trends towards more extreme flood events from streamflow measurements in 29 very large basins, but Kundzewicz et al. (2005) found both increases (in 27 cases) and decreases (in 31 cases) as well as no significant (at the 10% level) long-term changes in annual extreme flows for 137 of the 195 rivers examined worldwide. Recent extreme flood events in central Europe (on the Elbe and some adjacent catchments) are discussed in Section 3.8.4, Box 3.6.

Large changes and trends in seasonal streamflow rates for many of the world's major rivers (Lammers et al., 2001; Cowell and Stoudt, 2002; Ye et al., 2003; Yang et al., 2004) should be interpreted with caution, since many of these streams have been affected by the construction of large dams and reservoirs that increase low flow and reduce peak flow. Nevertheless, there is evidence that the rapid warming since the 1970s has induced earlier snowmelt and associated peak streamflow in the western USA (Cayan et al., 2001) and New England, USA (Hodgkins et al., 2003) and earlier breakup of river ice in Russian Arctic rivers (Smith, 2000) and many Canadian rivers (Zhang et al., 2001b).

River discharges in the La Plata River Basin in southeastern South America exhibit large interannual variability. Consistent evidence linking the Paraná and Uruguay streamflows and ENSO has been found (Bischoff et al., 2000; Camilloni and Barros, 2000, 2003; Robertson et al., 2001a; Berri et al., 2002; Krepper et al., 2003), indicating that monthly and extreme flows during El Niño are generally larger than those observed during La Niña events. For the Paraguay River, most of the major discharges at the Pantanal wetland outlet occurred in the neutral phases of ENSO, but in the lower reaches of the river the major discharge events occurred during El Niño events (Barros et al., 2004). South Atlantic SST anomalies also modulate regional river discharges through effects on rainfall in southeastern South America (Camilloni and Barros, 2000). The Paraná River shows a positive trend in its annual mean discharge since the 1970s in accordance with the regional rainfall trends (García and Vargas, 1998; Barros et al., 2000a; Liebmann et al., 2004), as do the Paraguay and Uruguay Rivers since 1970 (Figure 3.14).

For 1935 to 1999 in the Lena River Basin in Siberia, Yang et al. (2002) found significant increases in temperature and streamflow and decreases in ice thickness during the cold season. Strong spring warming resulted in earlier snowmelt with a reduced maximum streamflow pulse in June. During the warm season, smaller streamflow increases are related to an observed increase in precipitation. Streamflow in the Yellow River Basin in China decreased significantly during the latter half of the 20th century, even after accounting for increased human water consumption (Yu et al., 2004a). Temperatures have increased over the basin, but precipitation has shown no change, suggesting an increase in evaporation.

In Africa from 1950 to 1995, Jury (2003) found that the Niger and Senegal Rivers show the effects of the Sahel drying trend with a decreasing trend in flow. The Zambezi also exhibits reduced flows, but rainfall over its catchment area appears to be stationary. Other major African rivers, including the Blue and White Nile, Congo and inflow into Lake Malawi show high variability, consistent with interannual variability of SSTs in the Atlantic, Indian and Pacific Oceans. A composite index of streamflow for these rivers shows that the five highest flow years occurred prior to 1979, and the five lowest flow years occurred after 1971.

3.3.5 Consistency and Relationships between Temperature and Precipitation

Observed changes in regional temperature and precipitation can often be physically related to one another. This section assesses the consistencies of these relationships in the observed trends. Significant large-scale correlations between observed monthly mean temperature and precipitation (Madden and Williams, 1978) for North America and Europe have stood up to the test of time and been expanded globally (Trenberth and Shea, 2005). In the warm season over continents, higher temperatures accompany lower precipitation amounts and vice versa. Hence, over land, strong negative correlations dominate, as dry conditions favour more sunshine and less evaporative cooling, while wet summers are cool. However, at latitudes poleward of 40° in winter, positive correlations dominate as the water-holding capacity of the atmosphere limits precipitation amounts in cold conditions and warm air advection in cyclonic storms

is accompanied by precipitation. Where ocean conditions drive the atmosphere, higher surface air temperatures are associated with precipitation, as during El Niño events. For South America, Rusticucci and Penalba (2000) showed that warm summers are associated with low precipitation, especially in northeast and central-western Argentina, southern Chile, and Paraguay. Cold season (JJA) correlations are weak but positive to the west of 65°W, as stratiform cloud cover produces a higher minimum temperature. For stations in coastal Chile, the correlation is always positive and significant, as it is adjacent to the ocean, especially in the months of rainfall (May to September), showing that high SSTs favour convection.

This relationship of higher warm-season temperatures with lower precipitation appears to apply also to trends (Trenberth and Shea, 2005). An example is Australia, which exhibits evidence of increased drought severity, consistent with the observed warming during the latter half of the 20th century (Nicholls, 2004). Mean maximum and minimum temperatures during the 2002 Australian drought were much higher than during the previous droughts in 1982 and 1994, suggesting enhanced potential evaporation as well (see Section 3.8.4, Box 3.6). Record-high maximum temperatures also accompanied the dry conditions in 2005.

3.3.6 Summary

Substantial uncertainty remains in trends of hydrological variables because of large regional differences, gaps in spatial coverage and temporal limitations in the data (Huntington, 2006). At present, documenting interannual variations and trends in precipitation over the oceans remains a challenge. Global precipitation averages over land are not very meaningful and mask large regional variations. Precipitation generally increased over the 20th century from 30°N to 85°N over land, and over Argentina, but notable decreases have occurred in the past 30 to 40 years from 10°S to 30°N. Salinity decreases in the North Atlantic and south of 25°S suggest similar precipitation changes over the ocean (Sections 5.3.2 and 5.5.3). Runoff and river discharge generally increased at higher latitudes, along with soil moisture, consistent with precipitation changes. River discharges in many tropical areas of Africa and South America are strongly affected by ENSO, with greater discharges from the Paraná River after the 1976–1977 climate shift but lower discharges from some major African rivers since then.

However, the PDSI suggests there has likely been a large drying trend since the mid-1950s over many land areas, with widespread drying over much of Africa, southern Eurasia, Canada and Alaska. In the SH, there was a drying trend from 1974 to 1998, although trends over the entire 1948 to 2002 period are small. Seasonal decreases in land precipitation since the 1950s are the main cause for some of the drying trends, although large surface warming during the last two to three decades has also likely contributed to the drying. Based on the PDSI data, very dry areas (defined as land areas with a PDSI of less than –3.0) have more than doubled in extent since the 1970s, with a large jump in the early 1980s due to an ENSO-induced precipitation decrease over land and subsequent increases primarily due to surface warming.

Hence, the observed marked increases in drought in the past three decades arise from more intense and longer droughts over wider areas, as a critical threshold for delineating drought is exceeded over increasingly widespread areas. Overall, consistent with the findings of Huntington (2006), the evidence for increases in both severe droughts and heavy rains (Section 3.8.2) in many regions of the world makes it likely that hydrologic conditions have become more intense.

3.4 Changes in the Free Atmosphere

3.4.1 Temperature of the Upper Air: Troposphere and Stratosphere

Within the community that constructs and actively analyses satellite- and radiosonde-based temperature records there is agreement that the uncertainties about long-term change are substantial. Changes in instrumentation and protocols pervade both sonde and satellite records, obfuscating the modest long-term trends. Historically there is no reference network to anchor the record and establish the uncertainties arising from these changes – many of which are both barely documented and poorly understood. Therefore, investigators have to make seemingly reasonable choices of how to handle these sometimes known but often unknown influences. It is difficult to make quantitatively defensible judgments as to which, if any, of the multiple, independently derived estimates is closer to the true climate evolution. This reflects almost entirely upon the inadequacies of the historical observing network and points to the need for future network design that provides the reference sonde-based ground truth. Karl et al. (2006) provide a comprehensive review of this issue.

3.4.1.1 Radiosondes

Since the TAR, considerable effort has been devoted to assessing and improving the quality of the radiosonde temperature record (see Appendix 3.B.5.1). A particular aim has been to reduce artificial changes arising from instrumental and procedural developments during the seven decades (1940s–2000s) of the radiosonde record (Free and Seidel, 2005; Thorne et al., 2005a; Karl et al., 2006). Comparisons of several adjustment methods showed that they gave disparate results when applied to a common set of radiosonde station data (Free et al., 2002). One approach, based on the physics of heat transfer within the radiosonde, performed poorly when evaluated against satellite temperature records (Durre et al., 2002). Another method, comparison with satellite data (HadRT (Hadley Centre Radiosonde Temperature Data Set); Parker et al., 1997), is limited to the satellite era and to events with available metadata, and causes a reduction in spatial consistency of the data. A comprehensive intercomparison (Seidel et al., 2004)

showed that five radiosonde data sets yielded consistent signals for higher-frequency events such as ENSO, the Quasi-Biennial Oscillation (QBO) and volcanic eruptions, but inconsistent signals for long-term trends.

Several approaches have been used to create new adjusted data sets since the TAR. The Lanzante-Klein-Seidel (LKS; Lanzante et al., 2003a,b) data set, using 87 carefully selected stations, has subjectively derived bias adjustments throughout the length of its record but terminates in 1997. It has been updated using the Integrated Global Radiosonde Archive (IGRA; Durre et al., 2006) by applying a different bias adjustment technique (Free et al., 2004b) after 1997, creating a new archive (Radiosonde Atmospheric Temperature Products for Assessing Climate; RATPAC). Another new radiosonde record, HadAT2 (Hadley Centre Atmospheric Temperature Data Set Version 2, successor to HadRT), uses a neighbour comparison approach to build spatial as well as temporal consistency. A third approach (Haimberger, 2005) uses the bias adjustments estimated during data assimilation into model-based reanalyses to identify and reduce inhomogeneities in radiosonde data. Despite the risk of contamination by other biased data or by model bias, the resulting adjustments agree with those estimated by other methods. Rather than adjusting the data, Angell (2003) tried to reduce data quality problems by removing several tropical stations from his radiosonde network.

Despite these efforts to produce homogeneous data sets, recent analyses of radiosonde data indicate that significant problems remain. Sherwood et al. (2005) found substantial changes in the diurnal cycle in unadjusted radiosonde data. These changes are probably a consequence of improved sensors and radiation error adjustments. Relative to nighttime values, they found a daytime warming of sonde temperatures prior to 1971 that is likely to be spurious and then a spurious daytime cooling from 1979 to 1997. They estimated that there was probably a spurious overall downward trend in sonde temperature records during the satellite era (since 1978) throughout the atmosphere of order 0.1°C per decade globally. The assessed spurious cooling is greatest in the tropics (0.16°C per decade for the 850 to 300 hPa layer) and least in the NH extratropics (0.04°C per decade). Randel and Wu (2006) used collocated MSU data to show that cooling biases remain in some of the LKS and RATPAC radiosonde data for the tropical stratosphere and upper troposphere due to changes in instruments and radiation correction adjustments. They also identified problems in night data as well as day, indicating that negative biases are not limited to daytime observations. However, a few stations may have positive biases (Christy and Spencer, 2005).

The radiosonde data set is limited to land areas, and coverage is poor over the tropics and SH. Accordingly, when global estimates based solely on radiosondes are presented, there are

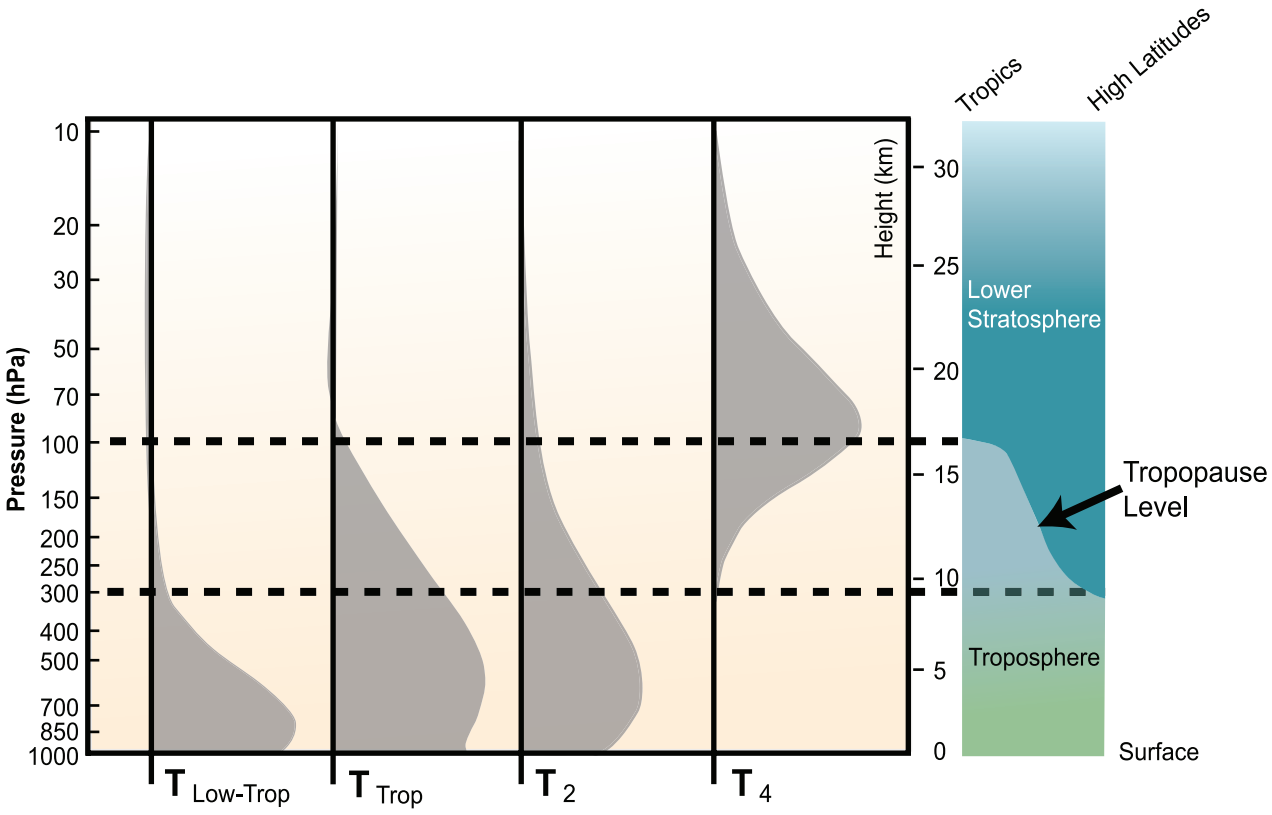


Figure 3.16. *Vertical weighting functions (grey) depicting the layers sampled by satellite MSU measurements and their derivatives, and used also for radiosonde and reanalysis records. The right panel schematically depicts the variation in the tropopause (that separates the stratosphere and troposphere) from the tropics (left) to the high latitudes (right). The fourth panel depicts T4 in the lower stratosphere, the third panel shows T2, the second panel shows the troposphere as a combination of T2 and T4 (Fu et al., 2004a) and the first panel shows $T2_{LT}$ from the UAH for the low troposphere. Adapted from Karl et al. (2006).*

considerable uncertainties (Hurrell et al., 2000; Agudelo and Curry, 2004) and denser networks – which perforce still omit oceanic areas – may not yield more reliable 'global' trends (Free and Seidel, 2005). Radiosonde records have an advantage of starting in the 1940s regionally, and near-globally from about 1958. They monitor the troposphere and lower stratosphere; the layers analysed are described below and in Figure 3.16. Radiosonde-based global mean temperature estimates are given in Figure 3.17, presented later.

3.4.1.2 The Satellite Microwave Sounding Unit Record

3.4.1.2.1 Summary of satellite capabilities and challenges

Satellite-borne microwave sounders estimate the temperature of thick layers of the atmosphere by measuring microwave emissions (radiances) that are proportional to the thermal state of emission of oxygen molecules from a complex of emission lines near 60 GHz. By making measurements at different frequencies near 60 GHz, different atmospheric layers can be sampled. A series of nine instruments called Microwave Sounding Units (MSUs) began making this kind of measurement in late 1978. Beginning in mid-1998, a subsequent series of instruments, the Advanced MSUs (AMSUs), began operation. Unlike infrared sounders, microwave sounders are not affected by most clouds, although some effects are experienced from precipitation and clouds with high liquid water content. Figure 3.16 illustrates the lower troposphere (referred to as $T2_{LT}$), troposphere, and MSU channel 2 (referred to as T2) and channel 4 (lower stratosphere, referred to as T4) layers.

The main advantage of satellite measurements compared to radiosondes is the excellent coverage of the measurements, with complete global coverage every few days. However, like radiosondes, temporal continuity is a major challenge for climate assessment, as data from all the satellites in the series must be merged together. The merging procedure must accurately account for a number of error sources. The most important are: (1) offsets in calibration between satellites; (2) orbital decay and drift and associated long-term changes in the time of day that the measurements are made at a particular location, which combine with the diurnal cycle in atmospheric temperature to produce diurnal drifts in the estimated temperatures; (3) drifts in satellite calibration that are correlated with the temperature of the on-board calibration target. Since the calibration target temperatures vary with the satellite diurnal drift, the satellite calibration and diurnal drift corrections are intricately coupled together (Fu and Johanson 2005). Independent teams of investigators have used different methods to determine and correct for these 'structural' and other sources of error (Thorne et al., 2005b). Appendix 3.B.5.3 discusses adjustments to the data in more detail.

3.4.1.2.2 Progress since the TAR

Since the TAR, several important developments and advances have occurred in the analysis of satellite measurements of atmospheric temperatures. Existing data sets have been scrutinised and problems identified, leading to new versions as described below. A number of new data records have been constructed from the MSU measurements, as well as from global reanalyses (see Section 3.4.1.3). Further, new insights have come from statistical combinations of the MSU records from different channels that have minimised the influence of the stratosphere on the tropospheric records (Fu et al., 2004a,b; Fu and Johanson, 2004, 2005). These new data sets and analyses are very important because the differences highlight assumptions and it becomes possible to estimate the uncertainty in satellite-derived temperature trends that arises from different methods and approaches to the construction of temporally consistent records.

Analyses of MSU channels 2 and 4 have been conducted by the University of Alabama in Huntsville (UAH; Christy et al., 2000, 2003) and by Remote Sensing Systems (RSS; Mears et al., 2003; Mears and Wentz, 2005). Another analysis of channel 2 is that of Vinnikov and Grody (2003; version 1 – VG1), now superseded by Grody et al. (2004) and Vinnikov et al. (2006; version 2 – VG2). MSU channel 2 (T2) measures a thick layer of the atmosphere, with approximately 75 to 80% of the signal coming from the troposphere, 15% from the lower stratosphere, and the remaining 5 to 10% from the surface. MSU channel 4 (T4) is primarily sensitive to temperature in the lower stratosphere (Figure 3.16).

Global time series from each of the MSU records are shown in Figure 3.17 and calculated global trends are depicted in Figure 3.18. These show a global cooling of the stratosphere (T4) of –0.32°C to –0.47 °C per decade and a global warming of the troposphere (T2) of 0.04°C to 0.20°C per decade for the period 1979 to 2004. The large spread in T2 trends stems from differences in the inter-satellite calibration and merging technique, and differences in the corrections for orbital drift, diurnal cycle change and the hot-point calibration temperature (Christy et al., 2003; Mears et al., 2003; Christy and Norris, 2004; Grody et al., 2004; Fu and Johanson, 2005; Mears and Wentz, 2005; Vinnikov et al., 2006; see also Appendix 3.B.5.3)

The RSS results for T2 indicate nearly 0.1°C per decade more warming in the troposphere than UAH (see Figure 3.18) and most of the difference arises from the use of different amounts of data to determine the parameters of the calibration target effect (Appendix 3.B.5.3). The UAH analysis yields parameters for the NOAA-9 satellite (1985–1987) outside of the physical bounds expected by Mears et al. (2003). Hence, the large difference in the calibration parameters for the single instrument mounted on the NOAA-9 satellite accounted for a substantial part of the difference between the UAH and RSS T2 trends. The rest arises from differences in merging parameters for other satellites; differences in the correction for the drift in measurement time, especially for the NOAA-11 satellite (Mears et al., 2003; Christy and Norris, 2004); and differences in the ways the hot-point temperature is corrected for (Grody et al., 2004; Fu and Johanson, 2005). In the tropics, these accounted for differences in T2 trends of about 0.07°C per decade after 1987 and discontinuities were also present in 1992 and 1995 at times of satellite transitions (Fu and Johanson, 2005). The T2 data record of Grody et al. (2004) and Vinnikov et al. (2006) (VG2) shows slightly more warming in the troposphere than

the RSS data record (Figure 3.18). See also Appendix 3.B.5.3 for discussion of the VG2 analysis.

Although the T4 from RSS has about 0.1°C per decade less cooling than the UAH product (Figure 3.18), both data sets support the conclusions that the stratosphere has undergone strong cooling since 1979. Because about 15% of the signal for T2 comes from the lower stratosphere, the observed cooling causes the reported T2 trends to underestimate tropospheric warming. By creating a weighted combination of T2 and T4, this effect has been greatly reduced (Fu et al., 2004a; see Figure 3.16). This technique for estimating the global mean temperature implies small negative weights at some stratospheric levels, but because of vertical coherence these merely compensate for other positive weights nearby and it is the integral that matters (Fu and Johanson, 2004). From 1979 to 2001 the stratospheric contribution to the trend in T2 is about –0.08°C per decade. Questions about this technique (Tett and Thorne, 2004) have led to clearer interpretation of its application to the tropics (Fu et al., 2004b). The technique has also been successfully applied to model results (Gillett et al., 2004; Kiehl et al., 2005), although model biases in depicting stratospheric cooling can affect results. In a further development, weighted combinations of T2, MSU channel 3 (T3) and T4 since 1987 have formed tropical series for the upper, lower and whole troposphere (Fu and Johanson, 2005).

By differencing T2 measurements made at different slant angles, the UAH group produced an updated data record weighted for the lower and mid troposphere, $T2_{LT}$ (Christy et al., 2003). This retrieval also has the effect of removing the stratospheric influence on long-term trends, but its uncertainties are augmented by the need to compensate for orbital decay and by computing a small residual from two large values (Wentz and Schabel, 1998). $T2_{LT}$ retrievals include a large signal from the surface and so are adversely affected by changes in surface emissivity, including changes in sea ice cover (Swanson, 2003). Fu and Johanson (2005) found that the $T2_{LT}$ trends were physically inconsistent compared with those of the surface, T2 and T4, even if taken from the UAH record. They also showed that the large trend bias is mainly attributed to the periods when a satellite had substantial drifts in local equator crossing time that caused large changes in calibration target temperatures and large diurnal drifts. Mears and Wentz (2005) further found that the adjustments for diurnal cycle required from satellite drift had the wrong sign in the UAH record in the tropics. Corrections have been made (version 5.2; Christy and Spencer, 2005) and are reflected in Figure 3.18, but the trend in the tropics is still smaller for most periods than both those in the troposphere (using T2 and T4) and those at the surface. Mears and Wentz (2005) computed their own alternative $T2_{LT}$ record and found a $T2_{LT}$ trend nearly 0.1°C per decade larger than the revised UAH trend. After 1987, when MSU channel 3 became available, Fu and Johanson (2005), using RSS data, found a systematic trend of increasing temperature with altitude throughout the tropics.

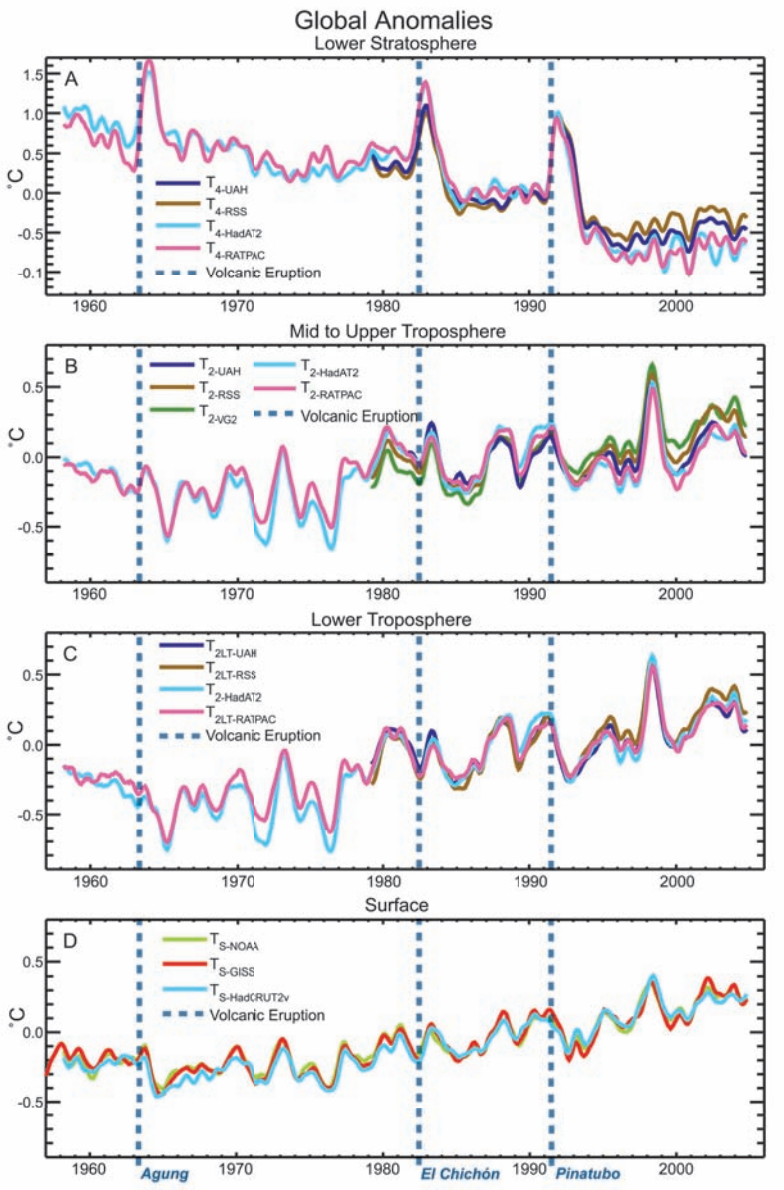


Figure 3.17. *Observed surface and upper-air temperature anomalies (°C). (A) Lower stratospheric T4, (B) Tropospheric T2, (C) Lower tropospheric $T2_{LT}$ from UAH, RSS and VG2 MSU satellite analyses and UKMO HadAT2 and NOAA RATPAC radiosonde observations; and (D) Surface records from NOAA, NASA/GISS and UKMO/CRU (HadCRUT2v). All time series are monthly mean anomalies relative to the period 1979 to 1997 smoothed with a seven-month running mean filter. Major volcanic eruptions are indicated by vertical blue dashed lines. Adapted from Karl et al. (2006).*

Comparisons of tropospheric radiosonde station data with collocated satellite data (Christy and Norris, 2004) show considerable scatter, and root mean square differences between UAH satellite data and radiosondes are substantial (Hurrell et al., 2000). Although Christy and Norris (2004) found good agreement between median radiosonde temperature trends and UAH trends, comparisons are more likely to be biased by spurious cooling than by spurious warming in unhomogenised

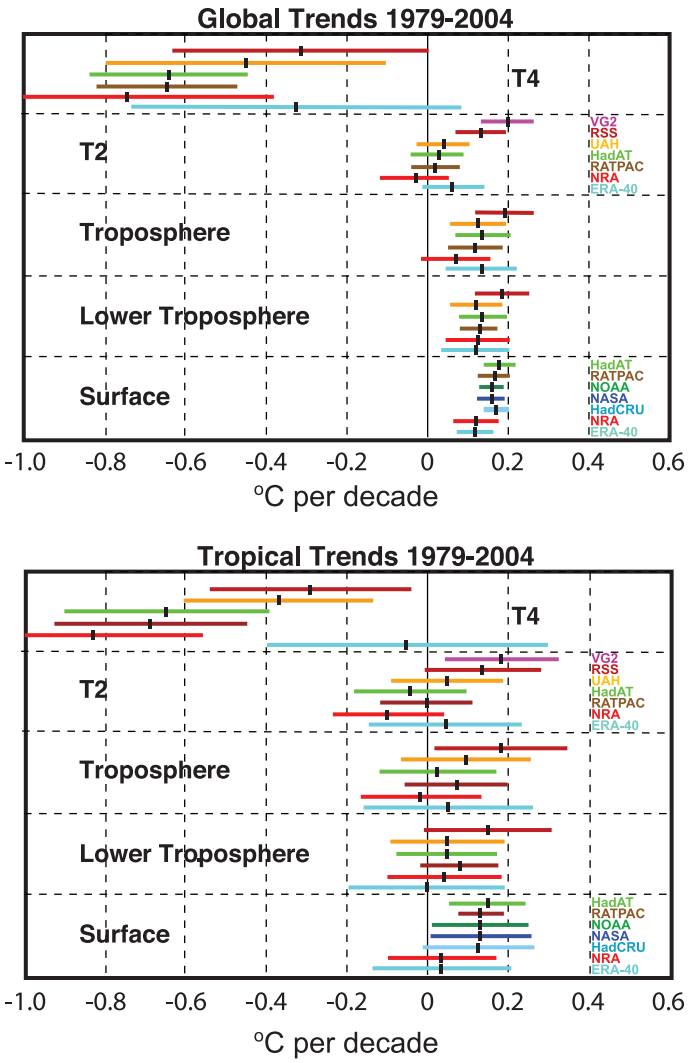


Figure 3.18. *Linear temperature trends (°C per decade) for 1979 to 2004 for the globe (top) and tropics (20°N to 20°S; bottom) for the MSU channels T4 (top panel) and T2 (second panel) or equivalent for radiosondes and reanalyses; for the troposphere (third panel) based on T2 with T4 used to statistically remove stratospheric influences (Fu et al., 2004a); for the lower troposphere (fourth panel) based on the UAH retrieval profile; and for the surface (bottom panel). Surface records are from NOAA/NCDC (green), NASA/GISS (blue) and HadCRUT2v (light blue). Satellite records are from UAH (orange), RSS (dark red) and VG2 (magenta); radiosonde-based records are from NOAA RATPAC (brown) and HadAT2 (light green); and atmospheric reanalyses are from NRA (red) and ERA-40 (cyan). The error bars are 5 to 95% confidence limits associated with sampling a finite record with an allowance for autocorrelation. Where the confidence limits exceed –1, the values are truncated. ERA-40 trends are only for 1979 to August 2002. Data from Karl et al. (2006; D. Seidel courtesy of J. Lanzante; and J. Christy).*

(Sherwood et al., 2005) and even homogenised (Randel and Wu, 2006) radiosonde data (see Section 3.4.1.1 and Appendix 3.B.5.1). In the stratosphere, radiosonde trends are more negative than both MSU retrievals, especially when compared with RSS, and this is very likely due to changes in sondes and their processing for radiation corrections (Randel and Wu, 2006).

Geographical patterns of the linear trend in tropospheric temperature from 1979 to 2004 (Figure 3.19) are qualitatively similar in the RSS and UAH MSU data sets. Both show coherent warming over most of the NH, but UAH shows cooling over parts of the tropical Pacific and tropospheric temperature trends differ south of 45°S where UAH indicate more cooling than RSS.

3.4.1.3 Reanalyses

A comprehensive global reanalysis completed since the TAR, ERA-40 (Uppala et al., 2005), extends from September 1957 to August 2002. Reanalysis is designed to prevent changes in the analysis system from contaminating the climate record, as occurs with global analyses from operational numerical weather prediction, and it compensates for some but not all of the effects of changes in the observing system (see Appendix 3.B.5.4). Unlike the earlier NRA that assimilated satellite retrievals, ERA-40 assimilated bias-adjusted radiances including MSU data (Harris and Kelly, 2001; Uppala et al., 2005), and the assimilation procedure itself accounts for orbital drift and change in satellite height – factors that have to be addressed in direct processing of MSU radiances for climate studies (e.g., Christy et al., 2003; Mears et al., 2003; Mears and Wentz, 2005). Onboard calibration biases are treated indirectly via the influence of other data sets. Nonetheless, the veracity of low-frequency variability in atmospheric temperatures is compromised in ERA-40 by residual problems in bias corrections.

Trends and low-frequency variability in large-scale surface air temperature from ERA-40 and from the monthly climate station data analysed by Jones and Moberg (2003) are in generally good agreement from the late 1970s onwards (see also Section 3.2.2.1). Temperatures from ERA-40 vary quite coherently throughout the planetary boundary layer over this period, and earlier for regions with consistently good coverage from both surface and upper-air observations (Simmons et al., 2004).

Processed MSU records of layer temperature have been compared with equivalents derived from the ERA-40 analyses (Santer et al., 2004). The use of deep layers conceals disparate trends at adjacent tropospheric levels in ERA-40.

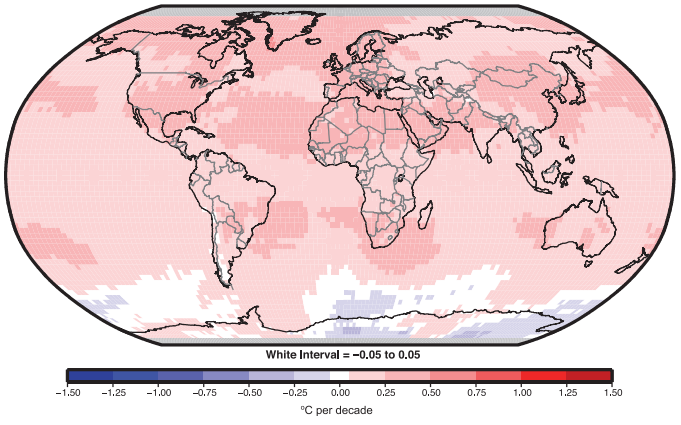


Figure 3.19. *Linear tropospheric temperature trends (°C per decade) for 1979 to 2005 from RSS (based on T2 and T4 adjusted as in Fu et al., 2004a). Courtesy Q. Fu.*

Relatively cold tropospheric values before the satellite era arose from a combination of scarcity of radiosonde data over the extratropical SH and a cold bias of the assimilating model, giving a tropospheric warming trend that is clearly too large when taken over the full period of the reanalysis (Bengtsson et al., 2004; Simmons et al., 2004; Karl et al., 2006). ERA-40 also exhibits a middle-tropospheric cooling over most of the tropics and subtropics since the 1970s that is certainly too strong owing to a warm bias in the analyses for the early satellite years.

Tropospheric patterns of trends from ERA-40 are similar to Figure 3.19, with coherent warming over the NH, although with discrepancies south of 45°S. These differences are not fully understood, although the treatment of surface emissivity anomalies over snow- and ice-covered surfaces may contribute (Swanson, 2003). At high southern latitudes, ERA-40 shows strong positive temperature trends in JJA in the period 1979 to 2001, in good accord with antarctic radiosonde data (Turner et al., 2006). The large-scale patterns of stratospheric cooling are similar in ERA-40 and the MSU data sets (Santer et al., 2004). However, the ERA-40 analyses in the lower stratosphere are biased cold relative to radiosonde data in the early satellite years, reducing downward trends. Section 3.5 relates the trends to atmospheric circulation changes.

3.4.1.4 The Tropopause

The tropopause marks the division between the troposphere and stratosphere and generally a minimum in the vertical profile of temperature. The height of the tropopause is affected by the heat balance of both the troposphere and the stratosphere. For example, when the stratosphere warms owing to absorption of radiation by volcanic aerosol, the tropopause is lowered. Conversely, a warming of the troposphere raises the tropopause, as does a cooling of the stratosphere. The latter is expected as a result of increasing greenhouse gas concentrations and stratospheric ozone depletion. Accordingly, changes in the height of the tropopause provide a sensitive indicator of human effects on climate. Inaccuracies and spurious trends in NRA preclude their use in determining tropopause trends (Randel et al., 2000) although they were found useful for interannual variability. Over 1979 to 2001, tropopause height increased by nearly 200 m (as a global average) in ERA-40, partly due to tropospheric warming plus stratospheric cooling (Santer et al., 2004). Atmospheric temperature changes in the UAH and RSS satellite MSU data sets (see Section 3.4.1.2) were found to be more highly correlated with changes in ERA-40 than with those in NRA, illustrating the improved quality of ERA-40 and satellite data. The Santer et al. (2004) results provide support for warming of the troposphere and cooling of the lower stratosphere over the last four decades of the 20th century, and indicate that both of these changes in atmospheric temperature have contributed to an overall increase in tropopause height. The radiosonde-based analyses of Randel et al. (2000), Seidel et al. (2001) and Highwood et al. (2000) also show increases in tropical tropopause height.

3.4.1.5 Synthesis and Comparison with the Surface Temperatures

Figure 3.17 presents the radiosonde and satellite global time series and Figure 3.18 gives a summary of the linear trends for 1979 to 2004 for global and tropical (20°N to 20°S) averages. Values at the surface are from NOAA (NCDC), NASA (GISS), UKMO/CRU (HadCRUT2v) and the NRA and ERA-40 reanalyses. Trends aloft are for the lower troposphere corresponding to $T2_{LT}$, T2, T4 and also the linear combination of T2 and T4 to better depict the entire troposphere as given by Fu et al. (2004a). In addition to the reanalyses, the results from the satellite-based methods from UAH, RSS and VG2 are given along with radiosonde estimates from HadAT2 and RATPAC. The ERA-40 trends only extend through August 2002, and VG2 is available only for T2. The error bars plotted here are 5 to 95% confidence limits associated with sampling a finite record where an allowance has been made for temporal autocorrelation in computing degrees of freedom (Appendix 3.A). However, the error bars do not include spatial sampling uncertainty, which increases the noise variance. Noise typically cuts down on temporal autocorrelation and reduces the temporal sampling error bars, which is why the RATPAC error bars are often smaller than the rest. Other sources of 'structural' and 'internal' errors of order 0.08°C for 5 to 95% levels (Mears and Wentz, 2005; see Appendix 3.B.5) are also not explicitly accounted for here. Structural uncertainties and parametric errors (Thorne et al., 2005b) reflect divergence between different data sets after the common climate variability has been accounted for and are better illustrated by use of difference time series, as seen for instance in T2 for RSS vs. UAH in Fu and Johanson (2005; see also Karl et al., 2006).

From Figure 3.17 the first dominant impression is that overall, the records agree remarkably well, especially in the timing and amplitude of interannual variations. This is especially true at the surface, and even the tropospheric records from the two radiosonde data sets agree reasonably well, although HadAT2 has lower values in the 1970s. In the lower stratosphere, all records replicate the dominant variations and the pulses of warming following the volcanic eruptions indicated in the figure. The sonde records differ prior to 1963 in the lower stratosphere when fewer observations were available, and differences also emerge among all data sets after about 1992, with the sonde values lower than the satellite temperatures. The focus on linear trends tends to emphasize these relatively small differences.

A linear trend over the long term is often not a very good approximation of what has occurred (Seidel and Lanzante, 2004; Thorne et al., 2005a,b); alternative interpretations are to factor in the abrupt 1976–1977 climate regime shift (Trenberth, 1990) and episodic stratospheric warming and tropospheric cooling for the two years following major volcanic eruptions. Hence, the confidence limits for linear trends (Figure 3.18) are very large in the lower stratosphere owing to the presence of the large warming perturbations from volcanic eruptions. In the troposphere, the confidence limits are much wider in the tropics

than globally, reflecting the strong interannual variability associated with ENSO.

Radiosonde, satellite observations and reanalyses agree that there has been global stratospheric cooling since 1979 (Figures 3.17 and 3.18), although radiosondes almost certainly still overestimate the cooling owing to residual effects of changes in instruments and processing (such as for radiation corrections; Lanzante et al., 2003b; Sherwood et al., 2005; Randel and Wu, 2006) and possibly increased sampling of cold conditions owing to stronger balloons (Parker and Cox, 1995). As the stratosphere is cooling and T2 has a 15% signal from there, it is virtually certain that the troposphere must be warming at a significantly greater rate than indicated by T2 alone. Thus, the tropospheric record adjusted for the stratospheric contribution to T2 has warmed more than T2 in every case. The differences range from 0.06°C per decade for ERA-40 to 0.09°C per decade for both radiosonde and NRA data sets. For UAH and RSS the difference is 0.07°C per decade.

The weakest tropospheric trends occur for NRA. However, unlike ERA-40, the NRA did not allow for changes in greenhouse gas increases over the record (Trenberth, 2004), resulting in errors in radiative forcing and in satellite retrievals in the infrared and making trends unreliable (Randel et al., 2000); indeed, upward trends at high surface mountain stations are stronger than NRA free-atmosphere temperatures at nearby locations (Pepin and Seidel, 2005). The records suggest that since 1979, the global and tropical tropospheric trends are similar to those at the surface although RSS, and by inference VG2, indicate greater tropospheric than surface warming. The reverse is indicated by the UAH and the radiosonde record although these data are subject to significant imperfections discussed above. Amplification occurs in the tropics for the RSS fields, especially after 1987 when there are increasing trends with altitude throughout the troposphere based on T2, T3 and T4 (Fu and Johanson, 2005). In the tropics, the theoretically expected amplification of temperature perturbations with height is borne out by interannual fluctuations (ENSO) in radiosonde, RSS, UAH and model data (Santer et al., 2005), but it is not borne out in the trends of the radiosonde records and UAH data.

The global mean trends since 1979 disguise many regional differences. In particular, in winter much larger temperature trends are present at the surface over northern continents than at higher levels (Karl et al., 2006) (see Figures 3.9 and 3.10; FAQ 3.1, Figure 1). These are associated with weakening of shallow winter temperature inversions and the strong stable surface layers that have little signature in the main troposphere. Such changes are related to changes in surface winds and atmospheric circulation (see Section 3.6.4).

In summary, for the period since 1958, overall global and tropical tropospheric warming estimated from radiosondes has slightly exceeded surface warming (Figure 3.17 and Karl et al., 2006). The climate shift of 1976 appeared to yield greater tropospheric than surface warming (Figure 3.17); such climate variations make differences between the surface and tropospheric temperature trends since 1979 unsurprising. After 1979, there has also been global and tropical tropospheric warming; however, it is uncertain whether tropospheric warming has exceeded that at the surface because the spread of trends among tropospheric data sets encompasses the surface warming trend. The range (due to different data sets, but not including the reanalyses) of global surface warming since 1979 from Figure 3.18 is 0.16°C to 0.18°C per decade compared to 0.12°C to 0.19°C per decade for MSU estimates of tropospheric temperatures. A further complexity is that surface trends have been greater over land than over ocean. Substantial cooling has occurred in the lower stratosphere. Compensation for the effects of stratospheric cooling trends on the T2 record (a cooling of about 0.08°C per decade) has been an important development. However, a linear trend is a poor fit to the data in the stratosphere and the tropics at all levels. The overall global variability is well replicated by all records, although small relative trends exacerbate the differences between records. Inadequacies in the observations and analytical methods result in structural uncertainties that still contribute to the differences between surface and tropospheric temperature trends, and revisions continue to be made. Changes in the height of the tropopause since 1979 are consistent with overall tropospheric warming as well as stratospheric cooling.

3.4.2 Water Vapour

Water vapour is a key climate variable. In the lower troposphere, condensation of water vapour into precipitation provides latent heating which dominates the structure of tropospheric diabatic heating (Trenberth and Stepaniak, 2003a,b). Water vapour is also the most important gaseous source of infrared opacity in the atmosphere, accounting for about 60% of the natural greenhouse effect for clear skies (Kiehl and Trenberth, 1997), and provides the largest positive feedback in model projections of climate change (Held and Soden, 2000).

Water vapour at the land surface has been measured since the late 19th century, but only observations made since the 1950s have been compiled into a database suitable for climate studies. The concentration of surface water vapour is typically reported as the vapour pressure, dew point temperature or relative humidity. Using physical relationships, it is possible to convert from one to the other, but the conversions are exact only for instantaneous values. As the relationships are nonlinearly related to air temperature, errors accumulate as data are averaged to daily and monthly periods. Slightly more comprehensive data exist for oceanic areas, where the dew point temperature is included as part of the ICOADS database, but few analyses have taken place for periods before the 1950s.

The network of radiosonde measurements provides the longest record of water vapour measurements in the atmosphere, dating back to the mid-1940s. However, early radiosonde sensors suffered from significant measurement biases, particularly for the upper troposphere, and changes in instrumentation with time often lead to artificial discontinuities in the data record (e.g., see Elliott et al., 2002). Consequently, most of the analysis of radiosonde humidity has focused on trends for altitudes below 500 hPa

and is restricted to those stations and periods for which stable instrumentation and reliable moisture soundings are available.

Additional information on water vapour can be obtained from satellite observations and reanalysis products. Satellite observations provide near-global coverage and thus represent an important source of information over the oceans, where radiosonde observations are scarce, and in the upper troposphere, where radiosonde sensors are often unreliable.

3.4.2.1 Surface and Lower-Tropospheric Water Vapour

Boundary layer moisture strongly determines the longwave (LW) radiative flux from the atmosphere to the surface. It also accounts for a significant proportion of the direct absorption of solar radiation by the atmosphere. The TAR reported widespread increases in surface water vapour in the NH. The overall sign of these trends has been confirmed from analysis of specific humidity over the USA (Robinson, 2000) and over China from 1951 to 1994 (Wang and Gaffen, 2001), particularly for observations made at night. Differences in the spatial, seasonal and diurnal patterns of these changes were found with strong sensitivity of the results to the network choice. Philipona et al. (2004) inferred rapid increases in surface water vapour over central Europe from cloud-cleared LW radiative flux measured over the period 1995 to 2003. Subsequent analyses (Philipona et al., 2005) confirmed that changes in integrated water vapour for this region are strongly coupled to the surface temperature, with regions of warming experiencing increasing moisture and regions of cooling experiencing decreasing moisture. For central Europe, Auer et al. (2007) demonstrated increasing moisture trends. Their vapour pressure series from the Greater Alpine Region closely follow the decadal- to centennial-scale warming at both urban lowland and rural summit sites. In Canada, van Wijngaarden and Vincent (2005) found a decrease in relative humidity of several percent in the spring for 75 stations, after correcting for instrumentation changes, but little change in relative humidity elsewhere or for other seasons. Ishii et al. (2005) reported that globally averaged dew points over the ocean have risen by about 0.25°C between 1950 and 2000. Increasing extremes in summer dew points, and increased humidity during summer heat waves, were found at three stations in northeastern Illinois (Sparks et al., 2002; Changnon et al., 2003) and attributed in part to changes in agricultural practices in the region.

Dai (2006) analysed near-global (60°S–75°N) synoptic data for 1976 to 2005 from ships and buoys and more than 15,000 land stations for specific humidity, temperature and relative humidity. Nighttime relative humidity was found to be greater than daytime by 2 to 15% over most land areas, as temperatures undergo a diurnal cycle, while moisture does not change much. The global trends of near-surface relative humidity are very small. Trends in specific humidity tend to follow surface temperature trends with a global average increase of 0.06 g kg^{-1} per decade (1976–2004). The rise in specific humidity corresponds to about 4.9% per 1°C warming over the globe. Over the ocean, the observed surface specific humidity increases at 5.7% per 1°C warming, which is consistent with a constant relative humidity. Over land, the rate of increase is slightly smaller (4.3% per 1°C), suggesting a modest reduction in relative humidity as temperatures increase, as expected in water-limited regions.

For the lower troposphere, water vapour information has been available from the TOVS since 1979 and from the Scanning Multichannel Microwave Radiometer (SMMR) from 1979 to 1984. However, the main improvement occurred with the introduction of the Special Sensor Microwave/Imager (SSM/I) in mid-1987 (Wentz and Schabel, 2000). Retrievals of column-integrated water vapour from SSM/I are generally regarded as providing the most reliable measurements of lower-tropospheric water vapour over the oceans, although issues pertaining to the merging of records from successive satellites do arise (Trenberth et al., 2005a; Sohn and Smith, 2003).

Significant interannual variability of column-integrated water vapour has been observed using TOVS, SMMR and SSM/I data. In particular, column water vapour over the tropical oceans increased by 1 to 2 mm during the 1982–1983, 1986–1987 and 1997–1998 El Niño events (Soden and Schroeder, 2000; Allan et al., 2003; Trenberth et al., 2005a) and decreased by a smaller magnitude in response to global cooling following the eruption of Mt. Pinatubo in 1991 (Soden et al., 2002; Trenberth and Smith, 2005; see also Section 8.6.3.1). The linear trend based on monthly SSM/I data over the oceans was 1.2% per decade (0.40 ± 0.09 mm per decade) for 1988 to 2004 (Figure 3.20).

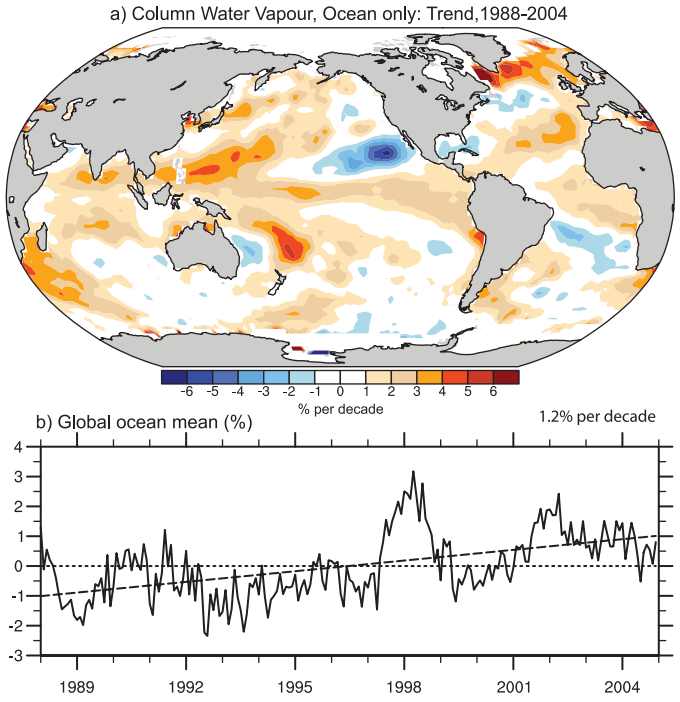


Figure 3.20. *Linear trends in precipitable water (total column water vapour) in % per decade (top) and monthly time series of anomalies relative to the 1988 to 2004 period in % over the global ocean plus linear trend (bottom), from RSS SSM/I (updated from Trenberth et al., 2005a).*

Since the trends are similar in magnitude to the interannual variability, it is likely that the latter affects the magnitude of the linear trends. The trends are overwhelmingly positive in spatial structure, but also suggestive of an ENSO influence. As noted by Trenberth et al. (2005a), most of the patterns associated with the interannual variability and linear trends can be reproduced from the observed SST changes over this period by assuming a constant relative humidity increase in water vapour mixing ratio. Given observed SST increases, this implies an overall increase in water vapour of order 5% over the 20th century and about 4% since 1970.

An independent check on globally vertically integrated water vapour amounts is whether the change in water vapour mass is reflected in the surface pressure field, as this is the only significant influence on the global atmospheric mass to within measurement accuracies. As Trenberth and Smith (2005) showed, such checks indicate considerable problems prior to 1979 in reanalyses, but results are in better agreement thereafter for ERA-40. Evaluations of column integrated water vapour from the NASA Water Vapor Project (NVAP; Randel et al., 1996), and reanalysis data sets from NRA, NCEP-2 and ERA-15/ERA-40 (see Appendix 3.B.5.4) reveal several deficiencies and spurious trends, which limit their utility for climate monitoring (Zveryaev and Chu, 2003; Trenberth et al., 2005a; Uppala et al., 2005). The spatial distributions, trends and interannual variability of water vapour over the tropical oceans are not always well reproduced by reanalyses, even after the 1970s (Allan et al., 2002, 2004; Trenberth et al., 2005a).

To summarise, global, local and regional studies all indicate increases in moisture in the atmosphere near the surface, but highlight differences between regions and between day and night. Satellite observations of oceanic lower-tropospheric water vapour reveal substantial variability during the last two decades. This variability is closely tied to changes in surface temperatures, with the water vapour mass changing at roughly the same rate at which the saturated vapour pressure does. A significant upward trend is observed over the global oceans and some NH land areas, although the calculated trend is likely influenced by large interannual variability in the record.

3.4.2.2 Upper-Tropospheric Water Vapour

Water vapour in the middle and upper troposphere accounts for a large part of the atmospheric greenhouse effect and is believed to be an important amplifier of climate change (Held and Soden, 2000). Changes in upper-tropospheric water vapour in response to a warming climate have been the subject of significant debate.

Due to instrumental limitations, long-term changes in water vapour in the upper troposphere are difficult to assess. Wang et al. (2001) found an increasing trend of 1 to 5% per decade in relative humidity during 1976 to 1995, with the largest increases in the upper troposphere, using 17 radiosonde stations in the tropical west Pacific. Conversely, a combination of Microwave Limb Sounder (MLS) and Halogen Occultation Experiment (HALOE) measurements at 215 hPa suggested increases in water vapour with increasing temperature (Minschwaner and Dessler, 2004) on interannual time scales, but at a rate smaller than expected from constant relative humidity.

Maistrova et al. (2003) reported an increase in specific humidity at 850 hPa and a decrease from 700 to 300 hPa for 1959 to 2000 in the Arctic, based on data from ships and temporary stations as well as permanent stations. In general, the radiosonde trends are highly suspect owing to the poor quality of, and changes over time in, the humidity sensors (e.g., Wang et al., 2002a). Comparisons of water vapour sensors during recent intensive field campaigns have produced a renewed appreciation of random and systematic errors in radiosonde measurements of upper-tropospheric water vapour and of the difficulty in developing accurate corrections for these measurements (Guichard et al., 2000; Revercombe et al., 2003; Turner et al., 2003; Wang et al., 2003; Miloshevich et al., 2004; Soden et al., 2004).

Information on the decadal variability of upper-tropospheric relative humidity is now provided by 6.7 μm thermal radiance measurements from Meteosat (Picon et al., 2003) and the High-resolution Infrared Radiation Sounder (HIRS) series of instruments flying on NOAA operational polar-orbiting satellites (Bates and Jackson, 2001; Soden et al., 2005). These products rely on the merging of many different satellites to ensure uniform calibration. The HIRS channel 12 (T12) data have been most extensively analysed for variability and show linear trends in relative humidity of order ±1% per decade at various latitudes (Bates and Jackson, 2001), but these trends are difficult to separate from larger interannual fluctuations due to ENSO (McCarthy and Toumi, 2004) and are negligible when averaging over the tropical oceans (Allan et al., 2003).

In the absence of large changes in relative humidity, the observed warming of the troposphere (see Section 3.4.1) implies that the specific humidity in the upper troposphere should have increased. As the upper troposphere moistens, the emission level for T12 increases due to the increasing opacity of water vapour along the satellite line of sight. In contrast, the emission level for the MSU T2 remains constant because it depends primarily on the concentration of oxygen, which does not vary by any appreciable amount. Therefore, if the atmosphere moistens, the brightness temperature difference (T2 − T12) will increase over time due to the divergence of their emission levels (Soden et al., 2005). This radiative signature of upper-tropospheric moistening is evident in the positive trends of T2 − T12 for the period 1982 to 2004 (Figure 3.21). If the specific humidity in the upper troposphere had not increased over this period, the emission level for T12 would have remained unchanged and T2 − T12 would show little trend over this period (dashed line in Figure 3.21).

Clear-sky outgoing longwave radiation (OLR) is also highly sensitive to upper-tropospheric water vapour and a number of scanning instruments have made well-calibrated but non-overlapping measurements since 1985 (see Section 3.4.3). Over this period, the small changes in clear-sky OLR can be explained by the observed temperature changes while maintaining a constant relative humidity (Wong et al., 2000; Allan and Slingo,

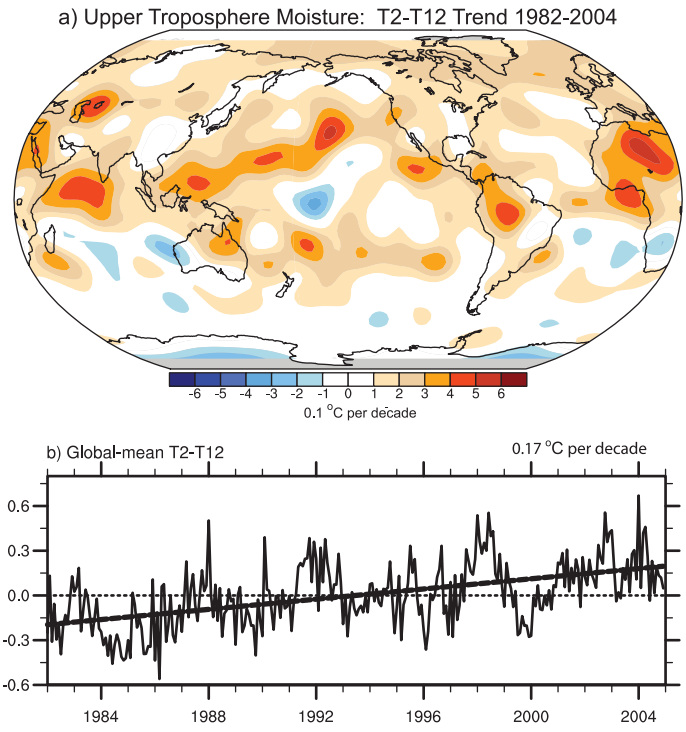


Figure 3.21. *The radiative signature of upper-tropospheric moistening is given by upward linear trends in T2–T12 for 1982 to 2004 (0.1 ºC per decade; top) and monthly time series of the global-mean (80°N to 80°S) anomalies relative to 1982 to 2004 (ºC) and linear trend (dashed; bottom). Data are from the RSS T2 and HIRS T12 (Soden et al., 2005). The map is smoothed to spectral truncation T31 resolution.*

2002) and changes in well-mixed greenhouse gases (Allan et al., 2003). This again implies a positive relationship between specific humidity and temperature in the upper troposphere.

To summarise, the available data do not indicate a detectable trend in upper-tropospheric relative humidity. However, there is now evidence for global increases in upper-tropospheric specific humidity over the past two decades, which is consistent with the observed increases in tropospheric temperatures and the absence of any change in relative humidity.

3.4.2.4 Stratospheric Water Vapour

The TAR noted an apparent increase of roughly 1% yr^{-1} in stratospheric water vapour content (~0.05 ppm yr^{-1}) during the last half of the 20th century (Kley et al., 2000; Rosenlof et al., 2001). This was based on data taken at mid-latitudes, and from multiple instruments. However, the longest series of data come from just two locations in North America with no temporal overlap. The combination of measurement uncertainties and relatively large variability on time scales from months to years warrants some caution when interpreting the longer-term trends (Kley et al., 2000; Fueglistaler and Haynes, 2005). The moistening is more convincingly documented during the 1980s and most of the 1990s than earlier, due to a longer continuous record (the NOAA Climate Monitoring and Diagnostics Laboratory (CMDL) frost-point balloon record from Boulder, Colorado; Oltmans et al., 2000) and the availability of satellite observations during much of this period. However, discrepancies between satellite- and balloon-measured variations are apparent at decadal time scales, largely over the latter half of the 1990s (Randel et al., 2004a).

An increase in stratospheric water vapour has important radiative and chemical consequences (see also Section 2.3.8). These may include a contribution to the recent observed cooling of the lower stratosphere and/or warming of the surface (Forster and Shine, 1999, 2002; Smith et al., 2001), although the exact magnitude is difficult to quantify (Oinas et al., 2001; Forster and Shine, 2002). Some efforts to reconcile observed rates of cooling in the stratosphere with those expected based on observed changes in ozone and carbon dioxide (CO_2) since 1979 (Langematz et al., 2003; Shine et al., 2003) have found discrepancies in the lower stratosphere consistent with an additional cooling effect of a stratospheric water vapour increase. However, Shine et al. (2003) noted that because the water vapour observations over the period of consideration are not global in extent, significant uncertainties remain as to whether radiative effects of a water vapour change are a significant contributor to the stratospheric temperature changes. Moreover, other studies which account for uncertainties in the ozone profiles and temperature trends, and natural variability, can reconcile the observed stratospheric temperature changes without the need for sizable water vapour changes (Ramaswamy and Schwarzkopf, 2002; Schwarzkopf and Ramaswamy, 2002).

Although methane oxidation is a major source of water in the stratosphere, and has been increasing over the industrial period, the noted stratospheric trend in water vapour is too large to attribute to methane oxidation alone (Kley et al., 2000; Oltmans et al., 2000). Therefore, other contributors to an increase in stratospheric water vapour are under active investigation. It is likely that different mechanisms are affecting water vapour trends at different altitudes. Aviation emits a small but potentially significant amount of water vapour directly into the stratosphere (IPCC, 1999). Several indirect mechanisms have also been considered including: a) volcanic eruptions (Considine et al., 2001; Joshi and Shine, 2003); b) biomass-burning aerosol (Sherwood, 2002; Andreae et al., 2004); c) tropospheric sulphur dioxide (Notholt et al., 2005); and d) changes to methane oxidation rates from changes in stratospheric chlorine, ozone and the hydroxyl radical (Röckmann et al., 2004). Other proposed mechanisms relate to changes in tropopause temperatures or circulation (Stuber et al., 2001; Zhou et al., 2001; Rosenlof, 2002; Nedoluha et al., 2003; Dessler and Sherwood, 2004; Fueglistaler et al., 2004; Roscoe, 2004).

It has been assumed that temperatures near the tropical tropopause control stratospheric water vapour according to equilibrium thermodynamics, importing more water vapour into the stratosphere when temperatures are warmer. However, tropical tropopause temperatures have cooled slightly over the period of the stratospheric water vapour increase (see Section 3.4.1; Seidel et al., 2001; Zhou et al, 2001). This makes the

mid-latitude lower-stratospheric increases harder to explain (Fueglistaler and Haynes, 2005). Satellite observations (Read et al., 2004) show water vapour injected above the tropical tropopause by deep convective clouds, bypassing the traditional control point. Changes in the amount of condensate sublimating in this layer may have contributed to the upward trend, but to what degree is uncertain (Sherwood, 2002). Another suggested source for temperature-independent variability is changes in the efficiency with which air is circulated through the coldest regions before entering the stratosphere (Hatsushika and Yamazaki, 2003; Bonnazola and Haynes, 2004; Dessler and Sherwood, 2004; Fueglistaler et al., 2004). However, it is not yet clear that a circulation-based mechanism can explain the observed trend (Fueglistaler and Haynes, 2005).

The TAR noted a stalling of the upward trend in water vapour during the last few years of observations available at that time. This change in behaviour has persisted, with a near-zero trend in stratospheric water vapour between 1996 and 2000 (Nedoluha et al., 2003; Randel et al., 2004a). The upward trend of methane is also smaller and is currently close to zero (see Section 2.3.2). Further, at the end of 2000 there was a dramatic drop in water vapour in the tropical lower stratosphere as observed by both satellite and CMDL balloon data (Randel et al., 2004a). Temperatures observed near the tropical tropopause also dropped, but the processes producing the tropical tropopause cooling itself are currently not fully understood. The propagation of this recent decrease through the stratosphere should ensure flat or decreasing stratospheric moisture for at least the next few years.

To summarise, water vapour in the stratosphere has shown significant long-term variability and an apparent upward trend over the last half of the 20th century but with no further increases since 1996. It does not appear that this behaviour is a straightforward consequence of known climate changes. Although ideas have been put forward, there is no consensus as to what caused either the upward trend or its recent disappearance.

3.4.3 Clouds

Clouds play an important role in regulating the flow of radiation at the top of the atmosphere and at the surface. They are also integral to the atmospheric hydrological cycle via their integral influence on the balance between radiative and latent heating. The response of cloud cover to increasing greenhouse gases currently represents the largest uncertainty in model predictions of climate sensitivity (see Chapter 8). Surface observations made at weather stations and onboard ships, dating back over a century, provide the longest available records of cloud cover changes. Surface observers report the all-sky conditions, which include the sides as well as bottoms of clouds, but are unable to report upper-level clouds that may be obscured from the observer's view. Although limited by potential inhomogeneities in observation times and methodology, the surface-observed cloud changes are often associated with physically consistent changes in correlative data, strengthening their credibility. Since the mid-1990s, especially in the USA and Canada, human observations at the surface have been widely replaced with automated ceilometer measurements, which measure only directly overhead low clouds rather than all-sky conditions. In contrast, satellites generally only observe the uppermost level of clouds and have difficulty detecting optically thin clouds. While satellite measurements do provide much better spatial and temporal sampling than can be obtained from the surface, their record is much shorter in length. These disparities in how cloud cover is observed contribute to the lack of consistency between surface- and satellite-measured changes in cloudiness. Condensation trails ('contrails') from aircraft exhaust may expand to form cirrus clouds and these and cosmic ray relations to clouds are addressed in Chapter 2.

3.4.3.1 Surface Cloud Observations

As noted in the TAR and extended with more recent studies, surface observations suggest increased total cloud cover since the middle of the last century over many continental regions including the USA (Sun, 2003; Groisman et al., 2004; Dai et al., 2006), the former USSR (Sun and Groisman, 2000; Sun et al., 2001), Western Europe, mid-latitude Canada, and Australia (Henderson-Sellers, 1992). This increasing cloudiness since 1950 is consistent with an increase in precipitation and a reduction in DTR (Dai et al., 2006). However, decreasing cloudiness over this period has been reported over China (Kaiser, 1998), Italy (Maugeri et al., 2001) and over central Europe (Auer et al.,2007). If the analyses are restricted to after about 1971, changes in continental cloud cover become less coherent. For example, using a worldwide analysis of cloud data (Hahn and Warren, 2003; Minnis et al., 2004) regional reductions were found since the early 1970s over western Asia and Europe but increases over the USA.

Changes in total cloud cover along with an estimate of precipitation over global and hemispheric land (excluding North America) from 1976 to 2003 are shown in Figure 3.22. During this period, secular trends over land are small. The small variability evident in land cloudiness appears to be correlated with precipitation changes, particularly in the SH (Figure 3.22). Note that surface observations from North America are excluded from this figure due to the declining number of human cloud observations since the early 1990s over the USA and Canada, as human observers have been replaced with Automated Surface Observation Systems (ASOS) from which cloud amounts are less reliable and incompatible with previous records (Dai et al., 2006). However, independent human observations from military stations suggest an increasing trend (~1.4% of sky per decade) in total cloud cover over the USA.

The TAR also noted multi-decadal trends in cloud cover over the ocean. An updated analysis of this information (Norris, 2005a) documented substantial decadal variability and decreasing trends in upper-level cloud cover over mid- and low-latitude oceans since 1952. However, there are no direct observations of upper-level clouds from the surface and instead Norris (2005a) infers them from reported total and low cloud cover assuming

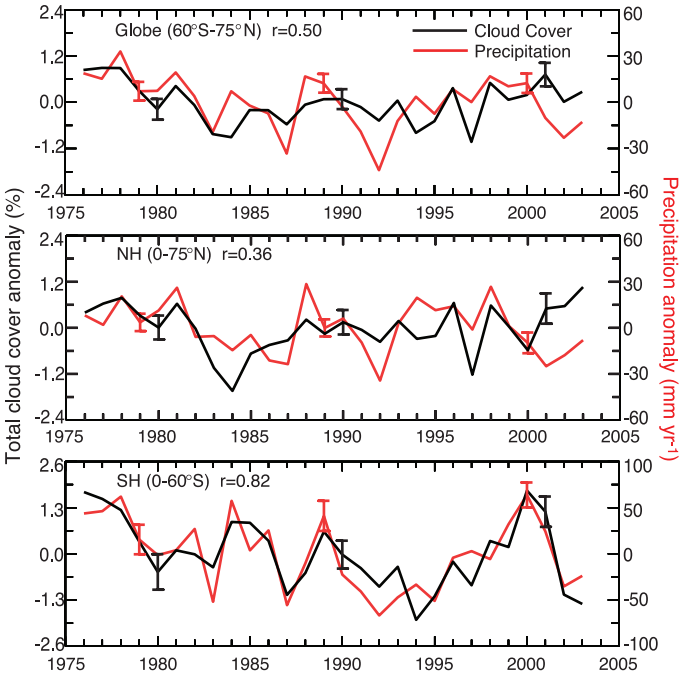


Figure 3.22. *Annual total land (excluding the USA and Canada) cloud cover (black) and precipitation (red) anomalies from 1976 to 2003 over global (60°S–75°N), NH and SH regions, with the correlation coefficient (r) shown at the top. The cloud cover is derived by gridding and area-averaging synoptic observations and the precipitation is updated from Chen et al. (2002). Typical 5 to 95% error bars for each decade are estimates using inter-grid-box variations (from Dai et al., 2006).*

a random overlap. These results partially reverse the finding of increasing trends in mid-level cloud amount in the northern mid-latitude oceans that was reported in the TAR, although the new study does not distinguish between high and middle clouds. Norris (2005b) found that upper-level cloud cover had increased over the equatorial South Pacific between 1952 and 1997 and decreased over the adjacent subtropical regions, the tropical Western Pacific, and the equatorial Indian Ocean. This pattern is consistent with decadal changes in precipitation and atmospheric circulation over these regions noted in the TAR, which further supports their validity. Deser et al. (2004) found similar spatial patterns in inter-decadal variations in total cloud cover, SST and precipitation over the tropical Pacific and Indian Oceans during 1900 to 1995. In contrast, low-cloud cover increased over almost all of the tropical Indian and Pacific Oceans, but this increase bears little resemblance to changes in atmospheric circulation over this period, suggesting that it may be spurious (Norris, 2005b). When averaged globally, oceanic cloud cover appears to have increased over the last 30 years or more (e.g., Ishii et al., 2005).

During El Niño events, cloud cover generally decreases over land throughout much of the tropics and subtropics, but increases over the ocean in association with precipitation changes (Curtis and Adler, 2003). Multi-decadal variations are affected by the 1976–1977 climate shift (Deser et al., 2004), and these dominate the low-latitude trends from 1971 to 1996 found in Hahn and Warren (2003).

3.4.3.2 Satellite Cloud Observations

Since the TAR, there has been considerable effort in the development and analysis of satellite data sets for documenting changes in global cloud cover over the past few decades. The most comprehensive cloud climatology is that of the International Satellite Cloud Climatology Project (ISCCP), begun in July 1983. The ISCCP shows an increase in globally averaged total cloud cover of about 2% from 1983 to 1987, followed by a decline of about 4% from 1987 to 2001 (Rossow and Dueñas, 2004). Cess and Udelhofen (2003) documented decreasing ISCCP total cloud cover in all latitude zones between 40°S and 40°N. Norris (2005a) found that both ISCCP and ship synoptic reports show consistent reductions in middle- or high-level cloud cover from the 1980s to the 1990s over low- and mid-latitude oceans. Minnis et al. (2004) also found consistent trends in high-level cloud cover between ISCCP and surface observations over most areas, except for the North Pacific where they differed by almost 2% per decade. In addition, an analysis of Stratospheric Aerosol and Gas Experiment II (SAGE II) data revealed a decline in cloud frequency above 12 km between 1985 and 1998 (Wang et al., 2002b) that is consistent with the decrease in upper-level cloud cover noted in ISCCP and ocean surface observations. The decline in upper-level cloud cover since 1987 may also be consistent with a decrease in reflected shortwave (SW) radiation during this period as measured by the Earth Radiation Budget Satellite (ERBS; see Section 3.4.4). Radiative transfer calculations, which use the ISCCP cloud properties as input, are able to independently reproduce the decadal changes in outgoing LW and reflected SW radiation reported by ERBS (Zhang et al., 2004c).

Analyses of the spatial trends in ISCCP cloud cover reveal changing biases arising from changes in satellite view angle and coverage that affect the global mean anomaly time series (Norris, 2000; Dai et al., 2006). The ISCCP spurious variability may occur primarily in low-level clouds with the least optical thickness (the ISCCP 'cumulus' category; Norris, 2005a), due to discontinuities in satellite view angles associated with changes in satellites. Such biases likely contribute to ISCCP's negative cloud cover trend, although their magnitude and impact on radiative flux calculations using ISCCP cloud data are not yet known. Additional artefacts, including radiometric noise, navigation and rectification errors are present in the ISCCP data (Norris, 2000), but the effects of known and unknown artefacts on ISCCP cloud and flux data have not yet been quantified.

Other satellite data sets show conflicting decadal changes in total cloud cover. For example, analysis of cloud cover changes from the HIRS shows a slight increase in cloud cover between 1985 and 2001 (Wylie et al., 2005). However, spurious changes have also been identified in the HIRS data set, which may affect its estimates of decadal variability. One important source of uncertainty results from the drift in Equatorial Crossing Time (ECT) of polar-orbiting satellite measurements (e.g., HIRS and the Advanced Very High Resolution Radiometer; AVHRR), which aliases the large diurnal cycle of clouds into spurious lower-frequency variations. After correcting for ECT drift and

other small calibration errors in AVHRR measurements of cloudiness, Jacobowitz et al. (2003) found essentially no trend in cloud cover for the tropics from 1981 to 2000.

While the variability in surface-observed upper-level cloud cover has been shown to be consistent with that observed by ISCCP (Norris, 2005a), the variability in total cloud cover is not, implying differences between ISCCP and surface-observed low cloud cover. Norris (2005a) shows that even after taking into account the difference between surface and satellite views of low-level clouds, the decadal changes between the ISCCP and surface data sets still disagree. The extent to which this results from differences in spatial and temporal sampling or differences in viewing perspective is unclear.

In summary, while there is some consistency between ISCCP, ERBS, SAGE II and surface observations of a reduction in high cloud cover during the 1990s relative to the 1980s, there are substantial uncertainties in decadal trends in all data sets and at present there is no clear consensus on changes in total cloudiness over decadal time scales.

3.4.4 Radiation

Measuring the radiation balance accurately is fundamental in quantifying the radiative forcing of the system as well as diagnosing the radiative properties of the atmosphere and surface, which are crucial for understanding radiative feedback processes. At the top of the atmosphere, satellites provide excellent spatial coverage but poorer temporal sampling. The reverse is true at the surface with only a limited number of high-quality point measurements but with excellent temporal coverage.

3.4.4.1 Top-of-Atmosphere Radiation

One important development since the TAR is the apparent unexpectedly large changes in tropical mean radiation flux reported by ERBS (Wielicki et al., 2002a,b). It appears to be related in part to changes in the nature of tropical clouds (Wielicki et al., 2002a), based on the smaller changes in the clear-sky component of the radiative fluxes (Wong et al., 2000; Allan and Slingo, 2002), and appears to be statistically distinct from the spatial signals associated with ENSO (Allan and Slingo, 2002; Chen et al., 2002). A recent reanalysis of the ERBS active-cavity broadband data corrects for a 20 km change in satellite altitude between 1985 and 1999 and changes in the SW filter dome (Wong et al., 2006). Based upon the revised (Edition 3_Rev1) ERBS record (Figure 3.23), outgoing LW radiation over the tropics appears to have increased by about 0.7 W m^{-2} while the reflected SW radiation decreased by roughly 2.1 W m^{-2} from the 1980s to 1990s (Table 3.5).

These conclusions depend upon the calibration stability of the ERBS non-scanner record, which is affected by diurnal sampling issues, satellite altitude drifts and changes in calibration following a three-month period when the sensor was powered off (Trenberth, 2002). Moreover, rather than a trend, the reflected SW radiation change may stem mainly from a jump in late 1992 in the ERBS record that is also observed in the ISCCP (version FD) record (Zhang et al., 2004c) but not in the AVHRR Pathfinder record (Jacobowitz et al., 2003). However, careful inspection of the sensor calibration revealed no known issues that can explain the decadal shift in the fluxes despite corrections to the ERBS time series relating to diurnal aliasing and satellite altitude changes (Wielicki et al., 2002b; Wong et al., 2006).

As noted in Section 3.4.3, the low-latitude changes in the radiation budget appear consistent with reduced cloud fraction from ISCCP. Detailed radiative transfer computations, using ISCCP cloud products along with additional global data sets, show broad agreement with the ERBS record of tropical radiative fluxes (Hatzianastassiou et al., 2004; Zhang et al., 2004c; Wong et al., 2006). However, the decrease in reflected SW radiation from the 1980s to the 1990s may be inconsistent with the increase in total and low cloud cover over oceans reported by surface observations (Norris, 2005a), which show increased low cloud occurrence. The degree of inconsistency, however, is difficult to ascertain without information on possible changes in low-level cloud albedo.

While the ERBS satellite provides the only continuous long-term top-of-atmosphere (TOA) flux record from broadband active-cavity instruments, narrow spectral band radiometers have made estimates of both reflected SW and outgoing LW radiation trends using regressions to broadband data, or using radiative transfer theory to estimate unmeasured portions of the spectrum of radiation. Table 3.5 shows the 1980s to 1990s TOA tropical mean flux changes for the ERBS Edition 3 data (Wong et al., 2006), the HIRS Pathfinder data (Mehta and Susskind, 1999), the AVHRR Pathfinder data (Jacobowitz et al., 2003) and the ISCCP FD data (Zhang et al., 2004c).

The most accurate of the data sets in Table 3.5 is believed to be the ERBS Edition 3 Rev 1 active-cavity wide field of view data (Wielicki et al., 2005). The ERBS stability is estimated as better than 0.5 W m^{-2} over the 1985 to 1999 period and the spatial and temporal sampling noise is less than 0.5 W m^{-2} on annual time scales (Wong et al., 2006). The outgoing LW radiation changes from ERBS are similar to the decadal changes in the HIRS Pathfinder and ISCCP FD records, but disagree with the AVHRR Pathfinder data (Wong et al., 2006). The AVHRR Pathfinder data also do not support the TOA SW radiation trends. However, calibration issues, conversion from narrow to broadband, and satellite orbit changes are thought to render the AVHRR record less reliable for decadal changes compared to ERBS (Wong et al., 2006). Estimates of the stability of the ISCCP time series for long-term TOA flux records are 3 to 5 W m^{-2} for SW radiative flux and 1 to 2 W m^{-2} for LW radiative flux (Brest et al., 1997), although the time series agreement of the ISCCP and ERBS records are much closer than these estimated calibration drift uncertainties (Zhang et al., 2004c).

The changes in SW radiation measured by ERBS Edition 3 Rev 1 are larger than the clear-sky flux changes due to humidity variations (Wong et al., 2000) or anthropogenic

radiative forcing (see Chapter 2). If correct, the large decrease in reflected SW radiation with little change in outgoing LW radiation implies a reduction in tropical low cloud cover over this period. However, specific information on cloud radiative forcing is not available from ERBS after 1989 and, as noted in Section 3.4.3, surface data sets suggest an increase in low cloud cover over this period.

Since most of the net tropical heating of 1.4 W m^{-2} is a decrease in reflected SW radiative flux, the change implies a similar increase in solar insolation at the surface that, if unbalanced by other changes in surface fluxes, would increase the amount of ocean heat storage. Wong et al. (2006) showed that the changes in global net radiation are consistent with a new ocean heat-storage data set from Willis et al. (2004; see Chapter 5 and Figure 5.1). Differences between the two data sets are roughly 0.4 W m^{-2}, in agreement with the estimated annual sampling noise in the ocean heat-storage data.

Using astronomical observations of visible wavelength solar photons reflected from parts of the Earth to the moon and then back to the Earth at a surface-based observatory, Pallé et al. (2004) estimated a dramatic increase of Earth-reflected SW radiative flux of 5.5 W m^{-2} over three years. This is unlikely to be real, as over the same time period (2000–2003), the Clouds and the Earth's Radiant Energy System (CERES) broadband data indicate a decrease in SW radiative flux of almost 1 W m^{-2}, which is much smaller and the opposite sign (Wielicki et al., 2005). In addition, changes in ocean heat storage are more consistent with the CERES data than with the Earthshine indirect observation.

The only long-term time series (1979–2001) of energy divergence in the atmosphere (Trenberth and Stepaniak, 2003b) are based on NRA, which, although not reliable for depicting trends, are reliable on interannual times scales for which they show substantial variability associated with ENSO. Analyses by Trenberth and Stepaniak (2003b) reveal more divergence of energy out of the deep tropics in the 1990s compared with the 1980s due to differences in ENSO, which may account for at least some of the changes discussed above.

In summary, although there is independent evidence for decadal changes in TOA radiative fluxes over the last two decades, the evidence is equivocal. Changes in the planetary and tropical TOA radiative fluxes are consistent with independent global ocean heat-storage data, and are expected to be dominated by changes in cloud radiative forcing. To the extent that they are real, they may simply reflect natural low-frequency variability of the climate system.

3.4.4.2 Surface Radiation

The energy balance at the surface requires net radiative heating to be balanced by turbulent energy fluxes and thus determines the evolution of surface temperature and the cycling of water, which are key parameters of climate change (see Box 7.1). In recent years, several studies have focused on observational evidence of changing surface radiative heating.

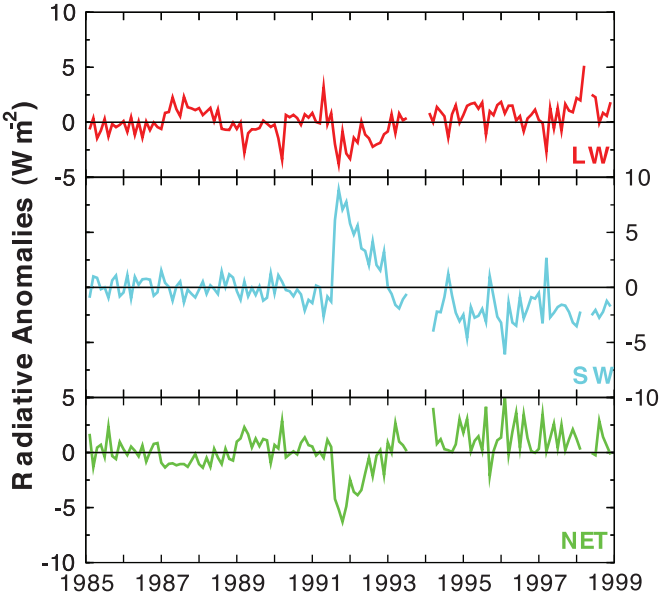


Figure 3.23. *Tropical mean (20°S to 20°N) TOA flux anomalies from 1985 to 1999 (W m^{-2}) for LW, SW, and NET radiative fluxes [NET = –(LW + SW)]. Coloured lines are observations from ERBS Edition 3_Rev1 data from Wong et al. (2006) updated from Wielicki et al. (2002a), including spacecraft altitude and SW dome transmission corrections.*

Reliable SW radiative measurement networks have existed since the 1957–1958 International Geophysical Year.

A reduction in downward solar radiation ('dimming') of about 1.3% per decade or about 7 W m^{-2} was observed from 1961 to 1990 at land stations around the world (Gilgen et al., 1998; Liepert, 2002). Additional studies also found declines in surface solar radiation in the Arctic and Antarctic (Stanhill and Cohen, 2001) as well as at sites in the former Soviet Union (Russak, 1990; Abakumova et al., 1996), around the Mediterranean Sea (Aksoy, 1997; Omran, 2000), China (Ren et al., 2005), the USA (Liepert, 2002) and southern Africa (Power and Mills, 2005). Stanhill and Cohen (2001) claim an overall globally averaged reduction of 2.7% per decade but used only 30 records. However, the stations where these analyses took place are quite limited in domain and dominated by large urban areas, and the dimming is much less at rural sites (Alpert et al., 2005) or even missing altogether over remote areas, except for

Table 3.5. *Top-of-atmosphere (TOA) radiative flux changes from the 1980s to 1990s (W m^{-2}). Values are given as tropical means (20°S to 20°N) for the 1994 to 1997 period minus the 1985 to 1989 period. Dashes are shown where no data are available. From Wong et al. (2006).*

Data Source	Radiative Flux Change (W m^{-2})		
	TOA LW	TOA SW	TOA Net
ERBS Edition 3 Rev 1	0.7	–2.1	1.4
HIRS Pathfinder	0.2	–	–
AVHRR Pathfinder	–1.4	0.7	0.7
ISCCP FD	0.5	–2.4	1.8

Box 3.2: The Dimming of the Planet and Apparent Conflicts in Trends of Evaporation and Pan Evaporation

Several reports have defined the term 'global dimming' (e.g., Cohen et al., 2004). This refers to a widespread reduction of solar radiation received at the surface of the Earth, at least up until about 1990 (Wild et al., 2005). However, recent studies (Alpert et al., 2005; Schwartz, 2005) found that dimming is not global but is rather confined only to large urban areas. At the same time there is considerable confusion in the literature over conflicting trends in pan evaporation and actual evaporation (Ohmura and Wild, 2002; Roderick and Farquhar, 2002, 2004, 2005; Hobbins et al., 2004; Wild et al., 2004, 2005) although the framework for explaining observed changes exists (Brutsaert and Parlange, 1998).

Surface evaporation, or more generally evapotranspiration, depends upon two key components. The first is available energy at the surface, especially solar radiation. The second is the availability of surface moisture, which is not an issue over oceans, but which is related to soil moisture amounts over land. Evaporation pans provide estimates of the potential evaporation that would occur if the surface were wet. Actual evaporation is generally not measured, except at isolated flux towers, but may be computed using bulk flux formulae or estimated as a residual from the surface moisture balance.

The evidence is strong that a key part of the solution to the paradox of conflicting trends in evaporation and pan evaporation lies in changes in the atmospheric circulation and the hydrological cycle. There has been an increase in clouds and precipitation, which reduce solar radiation available for actual and potential evapotranspiration but also increase soil moisture and make the actual evapotranspiration closer to the potential evapotranspiration. An increase in both clouds and precipitation has occurred over many parts of the land surface (Dai et al., 1999, 2004a, 2006), although not in the tropics and subtropics (which dominate the global land mean; Section 3.3.2.2). This reduces solar radiation available for evapotranspiration, as observed since the late 1950s or early 1960s over the USA (Liepert, 2002), parts of Europe and Siberia (Peterson et al., 1995; Abakumova et al., 1996), India (Chattopadhyay and Hulme, 1997), China (Liu et al., 2004a) and over land more generally (Wild et al., 2004). However, increased precipitation also increases soil moisture and thereby increases actual evapotranspiration (Milly and Dunne, 2001). Moreover, increased clouds impose a greenhouse effect and reduce outgoing LW radiation (Philipona and Dürr, 2004), so that changes in net radiation can be quite small or even of reversed sign. Recent re-assessments suggest increasing trends of evapotranspiration over southern Russia during the last 40 years (Golubev et al., 2001) and over the USA during the past 40 or 50 years (Golubev et al., 2001; Walter et al., 2004) in spite of decreases in pan evaporation. Hence, in most, but not all, places the net result has been an increase in actual evaporation but a decrease in pan evaporation. Both are related to observed changes in atmospheric circulation and associated weather.

It is an open question as to how much the changes in cloudiness are associated with other effects, notably impacts of changes in aerosols. Dimming seems to be predominant in large urban areas where pollution plays a role (Alpert et al., 2005). Increases in aerosols are apt to redistribute cloud liquid water over more and smaller droplets, brightening clouds, decreasing the potential for precipitation and perhaps changing the lifetime of clouds (e.g., Rosenfeld, 2000; Ramanathan et al., 2001; Kaufman et al., 2002; see Sections 2.4 and 7.5). Increases in aerosols also reduce direct radiation at the surface under clear skies (e.g., Liepert, 2002), and this appears to be a key part of the explanation in China (Ren et al., 2005).

Another apparent paradox raised by Wild et al. (2004) is that if surface radiation decreases then it should be compensated by a decrease in evaporation from a surface energy balance standpoint, especially given an observed increase in surface air temperature. Of course, back radiation from greenhouse gases and clouds operate in the opposite direction (Philipona and Dürr, 2004). Also, a primary change (not considered by Wild et al., 2004) is in the partitioning of sensible vs. latent heat at the surface and thus in the Bowen ratio. Increased soil moisture means that more heating goes into evapotranspiration at the expense of sensible heating, reducing temperature increases locally (Trenberth and Shea, 2005). Temperatures are affected above the surface where latent heating from precipitation is realised, but then the full dynamics of the atmospheric motions (horizontal advection, adiabatic cooling in rising air and warming in compensating subsiding air) come into play. The net result is a non-local energy balance.

identifiable effects of volcanic eruptions, such as Mt. Pinatubo in 1991 (Schwartz, 2005). At the majority of 421 analysed sites, the decline in surface solar radiation ended around 1990 and a recovery of about 6 W m^{-2} occurred afterwards (Wild et al., 2004; 2005). The increase in surface solar radiation ('brightening') agrees with satellite and surface observations of reduced cloud cover (Wang et al., 2002b; Wielicki et al., 2002a; Rossow and Dueñas, 2004; Norris, 2005b; Pinker et al., 2005), although there is evidence that some of these changes are spurious (see Section 3.4.3). In addition, the satellite-observed increase in surface radiation noted by Pinker et al. (2005) occured primarily over ocean, whereas the increase observed by Wild et al. (2005) was restricted to land stations.

From 1981 to 2003 over central Europe, Philipona and Dürr (2004) showed that decreases in surface solar radiation from increases in clouds were cancelled by opposite changes in LW radiation and that increases in net radiative flux were dominated by the clear-sky LW radiation component relating to an enhanced

water vapour greenhouse effect. Alpert et al. (2005) provided evidence that a significant component of the reductions may relate to increased urbanisation and anthropogenic aerosol concentrations over the period (see also Section 7.5). This has been detected in solar radiation reductions for polluted regions (e.g., China; Luo et al., 2001), but cloudiness changes must also play a major role, as shown for European sites and the USA (Liepert, 2002; Dai et al., 2006). In the USA increasing cloud optical thickness and a shift from cloud-free to more cloudy skies are the dominating factors compared to the aerosol direct effects. Possible causes of the 1990s reversal are reduced cloudiness and increased cloud-free atmospheric transparency due to the reduction of anthropogenic aerosol concentrations and recovery from the effects of the 1991 eruption of Mt. Pinatubo. See Box 3.2 for more discussion and a likely explanation of these aspects.

3.5 Changes in Atmospheric Circulation

Changes in the circulation of the atmosphere and ocean are an integral part of climate variability and change. Accordingly, regional variations in climate can be complex and sometimes counter-intuitive. For example, a rise in global mean temperatures does not mean warming everywhere, but can result in cooling in some places, due to circulation changes.

This section assesses research since the TAR on atmospheric circulation changes, through analysis of global-scale data sets of mean sea level pressure (MSLP), geopotential heights, jet streams and storm tracks. Related quantities at the surface over the ocean, including winds, waves and surface fluxes, are also considered. Many of the results discussed are based on reanalysis data sets. Reanalyses provide a global synthesis of all available observations, but are subject to spurious changes over time as observations change, especially in the late 1970s with the improved satellite and aircraft data and observations from drifting buoys over the SH. See Appendix 3.B.5 for a discussion of the quality of reanalyses from a climate perspective.

3.5.1 Surface or Sea Level Pressure

Maps of MSLP synthesize the atmospheric circulation status. Hurrell and van Loon (1994) noted MSLP changes in the SH beginning in the 1970s while major changes were also occurring over the North Pacific in association with the 1976–1977 climate shift (Trenberth, 1990; Trenberth and Hurrell, 1994). More recently, analyses of sea level pressure from 1948 to 2005 for DJF found decreases over the Arctic, Antarctic and North Pacific, an increase over the subtropical North Atlantic, southern Europe and North Africa (Gillett et al., 2003, 2005), and a weakening of the Siberian High (Gong et al., 2001). The strength of mid-latitude MSLP gradients and associated westerly circulation appears to have increased in both hemispheres, especially during DJF, since at least the late 1970s.

The increase in MSLP gradients in the NH appears to significantly exceed simulated internal and anthropogenically forced variability (Gillett et al., 2003, 2005). However, the significance of changes over the SH is less clear, especially over the oceans prior to satellite observations in the late 1970s, as spurious trends are evident in both major reanalyses (NRA and ERA-40; Marshall, 2003; Bromwich and Fogt, 2004; Trenberth and Smith, 2005; Wang et al., 2006a; see also Appendix 3.B.5). Consistent changes, validated with long-term station-based data, do however seem to be present since the mid-1970s and are often interpreted in terms of time-averaged signatures of weather regimes (Cassou et al., 2004) or annular modes in both hemispheres (Thompson et al., 2000; Marshall, 2003; Bromwich and Fogt, 2004; see Section 3.6).

3.5.2 Geopotential Height, Winds and the Jet Stream

Mean changes in geopotential heights resemble in many ways their MSLP counterparts (Hurrell et al., 2004). Linear trends in 700 hPa height during the solstitial seasons, from ERA-40, are shown in Figure 3.24. The 700 hPa level was used as it is the first atmospheric level to lie largely above the East Antarctic Ice Sheet. The NRA and ERA-40 trends agree closely between 1979 and 2001. Over the NH between 1960 and 2000, winter (DJF) and annual means of geopotential height at 850, 500 and 200 hPa decreased over high latitudes and increased over the mid-latitudes, as for MSLP, albeit shifted westward (Lucarini and Russell, 2002). Using NRA, Frauenfeld and Davis (2003) identified a statistically significant expansion of the NH circumpolar vortex at 700, 500 and 300 hPa from 1949 to 1970. But the vortex has contracted significantly at all levels since then (until 2000) and Angell (2006) found a downward trend in the size of the polar vortex from 1963 to 2001, consistent with warming of the vortex core and analysed increases in 850 to 300 hPa thickness temperatures.

In the NH for 1979 to 2001 during DJF, increases in geopotential height occurred between 30°N and 50°N at many longitudes, notably over the central North Pacific (Figure 3.24). North of 60°N, height changes are consistent with recent occurrences of more neutral phases of the mean polar vortex. Increases in the 700 hPa height outweigh decreases in the northern summer (JJA) during 1979 to 2001. At SH high latitudes, the largest changes are seen in the solstitial seasons (Figure 3.24), with changes of opposite sign in many areas between DJF and JJA. Changes during DJF reflect the increasing strength of the positive phase of the SAM (see Marshall, 2003; Section 3.6.5), with large height decreases over Antarctica and corresponding height increases in the mid-latitudes, through the depth of the troposphere and into the stratosphere. The corresponding enhancement of the near-surface circumpolar westerlies at about 60°S, and associated changes in meridional winds in some sectors, is consistent with a warming trend observed at weather stations over the Antarctic Peninsula and Patagonia (Thompson and Solomon, 2002; see also Sections 3.2.2.4 and 3.6.5). In winter (JJA), there have been height

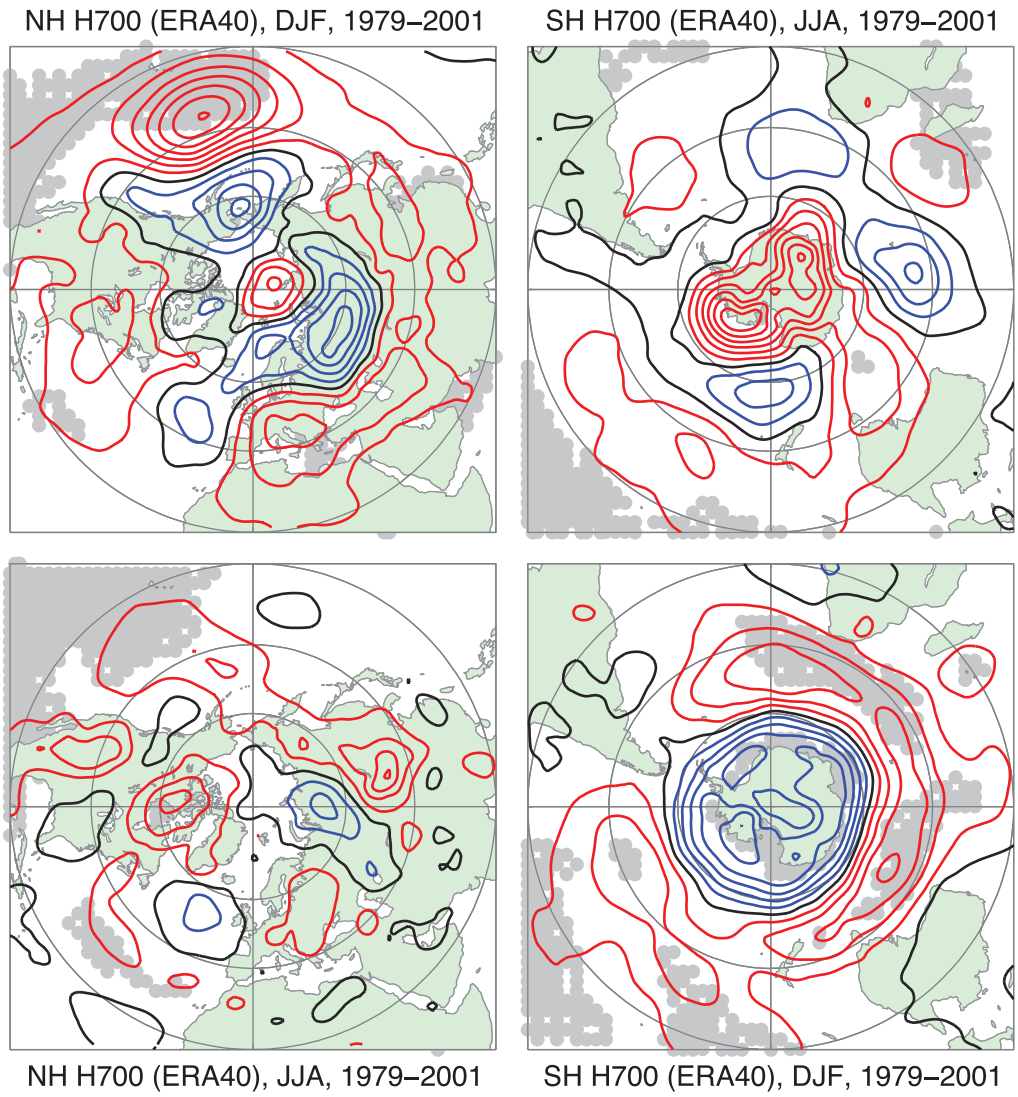


Figure 3.24. *Linear trends in ERA-40 700 hPa geopotential height from 1979 to 2001 for DJF (top left and bottom right) and JJA (bottom left and top right), for the NH (left) and SH (right). Trends are contoured in 5 gpm per decade and are calculated from seasonal means of daily 1200 UTC fields. Red contours are positive, blue negative and black zero; the grey background indicates 1% statistical significance using a standard least squares F-test and assuming independence between years.*

increases over Antarctica since 1979, with a zonal wave 3 to wave 4 pattern of rises and falls in southern mid-latitudes. Trends up to 2001 are relatively strong and statistically significant, with annular modes in both hemispheres strongly positive during the 1990s, although less so in recent years. Hence, geopotential height trends in DJF in the SH through 2004 have weakened in magnitude and significance, but with little change in spatial trend patterns.

Hemispheric teleconnections are strongly influenced by jet streams, which alter waves and storm tracks (Branstator, 2002). Using NRA from 1979 to 1995, Nakamura et al. (2002) found a weakening of the North Pacific winter jet since 1987, allowing efficient vertical coupling of upper-level disturbances with the surface temperature gradients (Nakamura and Sampe, 2002; Nakamura et al., 2004). A trend from the 1970s to the 1990s towards a deeper polar vortex and Iceland Low associated with a positive phase of the NAM in winter (Hurrell, 1995; Thompson et al., 2000; Ostermeier and Wallace, 2003) was accompanied by intensification and poleward displacement of the Atlantic polar frontal jet and associated enhancement of the Atlantic storm track activity (Chang and Fu, 2002; Harnik and Chang, 2003). Analogous trends have also been found in the SH (Gallego et al., 2005).

3.5.3 Storm Tracks

A number of recent studies suggest that cyclone activity over both hemispheres has changed over the second half of the 20th century. General features include a poleward shift in storm track location, increased storm intensity, but a decrease in total storm numbers (e.g., Simmonds and Keay, 2000; Gulev et al., 2001; McCabe et al., 2001). In the NH, McCabe et al. (2001) found that there has been a significant decrease in mid-latitude cyclone activity and an increase in high-latitude

cyclone frequency, suggesting a poleward shift of the storm track, with storm intensity increasing over the North Pacific and North Atlantic. In particular, Wang et al. (2006a) found that the North Atlantic storm track has shifted about 180 km northward in winter (JFM) during the past half century. The above findings are corroborated by Paciorek et al. (2002), Simmonds and Keay (2002) and Zhang et al. (2004b).

Several results suggest that cyclone activity in the NH mid-latitudes has increased during the past 40 years. Increases in storm track activity have been found in eddy statistics, based on NRA data. North Pacific storm track activity, identified as poleward eddy heat transport at 850 hPa, was significantly stronger during the late 1980s and early 1990s than during the early 1980s (Nakamura et al., 2002). A striking signal of decadal variability in Pacific storm track activity was its midwinter enhancement since 1987, despite a concurrent weakening of the Pacific jet, concomitant with the sudden weakening of the Siberian High (Nakamura et al., 2002; Chang, 2003). Significant increasing trends over both the Pacific and Atlantic are found in eddy meridional velocity variance at 300 hPa and other statistics (Chang and Fu, 2002; Paciorek et al., 2002). Since 1980, there was an increase in the amount of eddy kinetic energy in the NH due to an increase in the efficiency in the conversion from potential to kinetic energy (Hu et al., 2004). Graham and Diaz (2001) also found an increase in MSLP variance over the Pacific.

There are, however, significant uncertainties with such analyses, with some studies (Bromirski et al., 2003; Chang and Fu, 2003) suggesting that storm track activity during the last part of the 20th century may not be more intense than the activity prior to the 1950s. Eddy meridional velocity variance at 300 hPa in the NRA appears to be biased low prior to the mid-1970s, especially over east Asia and the western USA (Harnik and Chang, 2003). Hence, the increases in eddy variance in the NRA reanalysis data are nearly twice as large as that computed from rawinsonde observations. Better agreement is found for the Atlantic storm track exit region over Europe. Major differences between radiosonde and NRA temperature variance at 500 hPa over Asia (Iskenderian and Rosen, 2000; Paciorek et al., 2002) also cast doubts on the magnitude of the increase in storm track activity, especially over the Pacific.

Station pressure data over the Atlantic-European sector (where records are long and consistent) show a decline of storminess from high levels during the late 19th century to a minimum around 1960 and then a quite rapid increase to a maximum around 1990, followed again by a slight decline (Alexandersson et al., 2000; Bärring and von Storch, 2004; see also Section 3.8.4.1). However, changes in storm tracks are expected to be complex and depend on patterns of variability, and in practice, the noise present in the observations makes the detection of long-term changes in extratropical storm activity difficult. A more relevant approach seems to be the analysis of regional storminess in relation to spatial shifts and strength changes in teleconnection patterns (see Section 3.6).

Significant decreases in cyclone numbers, and increases in mean cyclone radius and depth over the southern extratropics over the last two or three decades (Simmonds and Keay, 2000; Keable et al., 2002; Simmonds, 2003; Simmonds et al., 2003) have been associated with the observed trend in the SAM. Such changes, derived from NRA data, have been related to reductions in mid-latitude winter rainfall (e.g., the drying trend observed in south-western Australia (Karoly, 2003) and to a circumpolar signal of increased precipitation off the coast of Antarctica (Cai et al., 2003). However, there are significant differences between ERA-40 and NRA in the SH: higher strong-cyclone activity and less weak-cyclone activity over all oceanic areas south of 40°S in all seasons, and stronger cyclone activity over the subtropics in the warm season in ERA-40, especially in the early decades (Wang et al., 2006a).

3.5.4 Blocking

Blocking events, associated with persistent high-latitude ridging and a displacement of mid-latitude westerly winds lasting typically a week or two, are an important component of total circulation variability on intra-seasonal time scales. In the NH, the preferred locations for the blocking are over the Atlantic and the Pacific (Tibaldi et al., 1994), with a spring maximum and summer minimum in the Atlantic-European region (Andrea et al., 1998; Trigo et al., 2004). Observations show that in the Euro-Atlantic sector, long-lasting (>10 day) blockings are clearly associated with the negative NAO phase (Quadrelli et al., 2001; Barriopedro et al., 2006), whereas the blockings of 5 to 10 day duration exhibit no such relationship, pointing to the dynamical links between the life cycles of NAO and blocking events (Scherrer et al, 2006; Schwierz et al., 2006). Wiedenmann et al. (2002) did not find any long-term statistically significant trends in NH blocking intensity. However, in the Pacific sector, Barriopedro et al. (2006) found a significant increase from 1948 to 2002 in western Pacific blocking days and events (57 and 62%, respectively). They also found less intense North Atlantic region blocking, with statistically significant decreases in events and days. Wiedenmann et al. (2002) found that blocking events, especially in the North Pacific region, were significantly weaker during El Niño years.

In the SH, blocking occurrence is maximised over the southern Pacific (Renwick and Revell, 1999; Renwick, 2005), with secondary blocking regions over the southern Atlantic and over the southern Indian Ocean and the Great Australian Bight. The frequency of blocking occurrence over the southeast Pacific is strongly ENSO-modulated (Rutllant and Fuenzalida, 1991; Renwick, 1998), while in other regions, much of the interannual variability in occurrence appears to be internally generated (Renwick, 2005). A decreasing trend in blocking frequency and intensity for the SH as a whole from NRA (Wiedenmann et al., 2002) is consistent with observed increases in zonal winds across the southern oceans. However, an overall increasing trend in the frequency of long-lived positive height anomalies is evident in the reanalyses over the SH in the 1970s (Renwick, 2005), apparently related to the introduction of satellite observations. Given data limitations, it may be too early to reliably define trends in SH blocking occurrence.

3.5.5 The Stratosphere

The dynamically stable stratospheric circulation is dominated in mid-latitudes by westerlies in the winter hemisphere and easterlies in the summer hemisphere, and the associated meridional overturning 'Brewer-Dobson' circulation. In the tropics, zonal winds reverse direction approximately every two years, in the downward-propagating QBO (Andrews et al., 1987). Ozone is formed predominantly in the tropics and transported to higher latitudes by the Brewer-Dobson circulation. Climatological stratospheric zonal-mean zonal winds (i.e., the westerly wind averaged over latitude circles) from different data sets show overall good agreement in the extratropics, whereas relatively large differences occur in the tropics (Randel et al., 2004b).

The breaking of vertically propagating waves, originating from the troposphere, decelerates the stratospheric westerlies (see Box 3.3). This sometimes triggers 'sudden warmings' when the westerly polar vortex breaks down with an accompanying warming of the polar stratosphere, which can quickly reverse the latitudinal temperature gradient (Kodera et al., 2000). While no major warming occurred in the NH in nine consecutive winters during 1990 to 1998, seven major warmings occurred during 1999 to 2004 (Manney et al., 2005). As noted by Naujokat et al. (2002), many of the recent stratospheric warmings after 2000 have been atypically early and the cold vortex recovered in March. In September 2002, a major warming was observed for the first time in the SH (e.g., Krüger et al., 2005; Simmons et al., 2005). This major warming followed a relatively weak winter polar vortex (Newman and Nash, 2005).

The analysis of past stratospheric changes relies on a combination of radiosonde information (available since the 1950s), satellite information (available from the 1970s) and global reanalyses. During the mid-1990s, the NH exhibited a number of years when the Arctic winter vortex was colder, stronger (Kodera and Koide, 1997; Pawson and Naujokat, 1999) and more persistent (Waugh et al., 1999; Zhou et al., 2000). Some analyses show a downward trend in the NH wave forcing in the period 1979 to 2000, particularly in January and February (Newman and Nash, 2000; Randel et al., 2002). Trend calculations are, however, very sensitive to the month and period of calculation, so the detection of long-term change from a relatively short stratospheric data series is still problematic (Labitzke and Kunze, 2005).

In the SH, using radiosonde data, Thompson and Solomon (2002) reported a significant decrease of the lower-stratospheric geopotential height averaged over the SH polar cap in October to March and May between 1969 and 1998. The ERA-40 and NRA stratospheric height reanalyses indicate a trend towards a strengthening antarctic vortex since 1980 during summer (DJF; Renwick, 2004; Section 3.5.2), largely related to ozone depletion (Ramaswamy et al., 2001; Gillett and Thompson, 2003). The ozone hole has led to a cooling of the stratospheric polar vortex in late spring (October–November; Randel and Wu, 1999), and to a two- to three-week delay in vortex breakdown (Waugh et al., 1999).

3.5.6 Winds, Waves and Surface Fluxes

Changes in atmospheric circulation imply associated changes in winds, wind waves and surface fluxes. Surface wind and meteorological observations from Voluntary Observing Ships (VOS) became systematic around 150 years ago and are assembled in ICOADS (Worley et al., 2005). Apparent significant trends in scalar wind should be considered with caution as VOS wind observations are influenced by time-dependent biases (Gulev et al., 2007), resulting from the rising proportion of anemometer measurements, increasing anemometer heights, changes in definitions of Beaufort wind estimates (Cardone et al., 1990), growing ship size, inappropriate evaluation of the true wind speed from the relative wind (Gulev and Hasse, 1999) and time-dependent sampling biases (Sterl, 2001; Gulev et al., 2007). Consideration of time series of local surface pressure gradients (Ward and Hoskins, 1996) does not support the existence of any significant globally averaged trends in marine wind speeds, but reveals regional patterns of upward trends in the tropical North Atlantic and extratropical North Pacific and downward trends in the equatorial Atlantic, tropical South Atlantic and subtropical North Pacific (see also Sections 3.5.1 and 3.5.3).

Visual VOS observations of wind waves for more than a century, often measured as significant wave height (SWH, the highest one-third of wave (sea and swell) heights), have been less affected than marine winds by changes in observational practice, although they may suffer from time-dependent sampling uncertainty, which was somewhat higher at the beginning of the record. Local wind speed directly affects only the wind-sea component of SWH, while the swell component is largely influenced by the frequency and intensity of remote storms. Linear trends in the annual mean SWH from ship data (Gulev and Grigorieva, 2004) for 1900 to 2002 were significantly positive almost everywhere in the North Pacific, with a maximum upward trend of 8 to 10 cm per decade (up to 0.5% yr^{-1}). These are supported by buoy records for 1978 to 1999 (Allan and Komar, 2000; Gower, 2002) for annual and winter (October to March) mean SWH and confirmed by the long-term estimates of storminess derived from the tide gauge residuals (Bromirski et al., 2003) and hindcast data (Graham and Diaz, 2001), although Tuller (2004) found primarily negative trends in wind off the west coast of Canada. In the Atlantic, centennial time series (Gulev and Grigorieva, 2004) show weak but statistically significant negative trends along the North Atlantic storm track, with a decrease of 5.2 cm per decade (0.25% yr^{-1}) in the western Atlantic storm formation region. Regional model hindcasts (e.g., Vikebo et al., 2003; Weisse et al., 2005) show growing SWH in the northern North Atlantic over the last 118 years.

Linear trends in SWH for the period 1950 to 2002 (Figure 3.25) are statistically significant and positive over most of the mid-latitudinal North Atlantic and North Pacific, as well as in the western subtropical South Atlantic, the eastern equatorial Indian Ocean and the East China and South China Seas. The largest upward trends (14 cm per decade) occur in the northwest

Box 3.3: Stratospheric-Tropospheric Relations and Downward Propagation

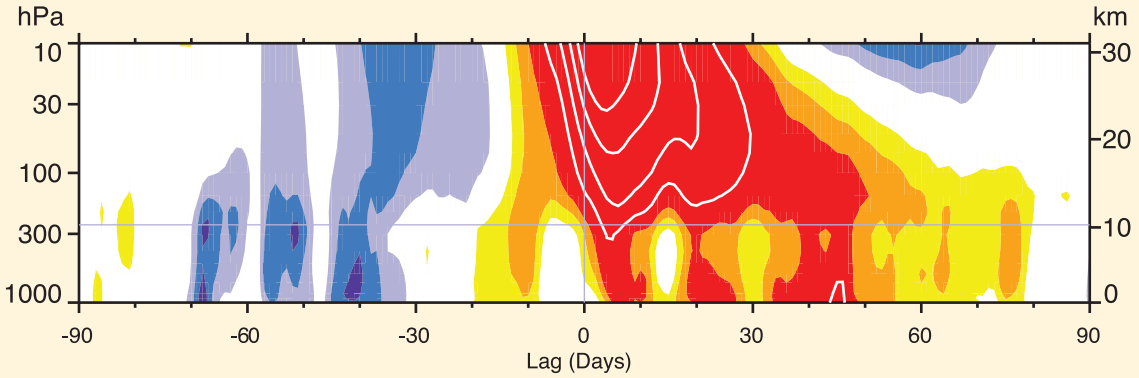
The troposphere influences the stratosphere mainly through planetary-scale waves that propagate upward during the extended winter season when stratospheric winds are westerly. The stratosphere responds to this forcing from below to produce long-lived changes to the strength of the polar vortices. In turn, these fluctuations in the strength of the stratospheric polar vortices are observed to couple downward to surface climate (Baldwin and Dunkerton, 1999, 2001; Kodera et al., 2000; Limpasuvan et al., 2004; Thompson et al., 2005). This relationship occurs in the zonal wind and can be seen clearly in annular modes, which explain a large fraction of the intra-seasonal and interannual variability in the troposphere (Thompson and Wallace, 2000) and most of the variability in the stratosphere (Baldwin and Dunkerton, 1999). Annular modes appear to arise naturally as a result of internal interactions within the troposphere and stratosphere (Limpasuvan and Hartmann, 2000; Lorenz and Hartmann, 2001, 2003).

The relationship between NAM anomalies in the stratosphere and troposphere can be seen in Box 3.3, Figure 1, in which the NAM index at 10 hPa is used to define events when the stratospheric polar vortex was extremely weak (stratospheric warmings). On average, weak vortex conditions in the stratosphere tend to descend to the troposphere and are followed by negative NAM anomalies at the surface for more than two months. Anomalously strong vortex conditions propagate downwards in a similar way.

Long-lived annular mode anomalies in the lowermost stratosphere appear to lengthen the time scale of the surface NAM. The tropospheric annular mode time scale is longest during winter in the NH, but longest during late spring (November–December) in the SH (Baldwin et al., 2003). In both hemispheres, the time scale of the tropospheric annular modes is longest when the variance of the annular modes is greatest in the lower stratosphere.

Downward coupling to the surface depends on having large circulation anomalies in the lowermost stratosphere. In such cases, the stratosphere can be used as a statistical predictor of the monthly mean surface NAM on time scales of up to two months (Baldwin et al., 2003; Scaife et al., 2005). Similarly, SH trends in temperature and geopotential height, associated with the ozone hole, appear to couple downward to affect high-latitude surface climate (Thompson and Solomon, 2002; Gillett and Thompson, 2003). As the stratospheric circulation changes with ozone depletion or increasing greenhouse gases, those changes will likely be reflected in changes to surface climate. Thompson and Solomon (2005) showed that the spring strengthening and cooling of the SH polar stratospheric vortex preceded similarly signed trends in the SH tropospheric circulation by one month in the interval 1973 to 2003. They argued that similar downward coupling is not evident in the NH geopotential trends computed using monthly radiosonde data. An explanation for this difference may be that the stratospheric signal is stronger in the SH, mainly due to ozone depletion, giving a more robust downward coupling.

The dynamical mechanisms by which the stratosphere influences the troposphere are not well understood, but the relatively large surface signal implies that the stratospheric signal is amplified. The processes likely involve planetary waves (Song and Robinson, 2004) and synoptic-scale waves (Wittman et al., 2004), which interact with stratospheric zonal wind anomalies near the tropopause. The altered waves would be expected to affect tropospheric circulation and induce surface pressure changes corresponding to the annular modes (Wittman et al., 2004).



Box 3.3, Figure 1. *Composites of time-height development of the NAM index for 18 weak vortex events. The events are selected by the dates on which the 10 hPa annular mode index crossed –3.0. Day 0 is the start of the weak vortex event. The indices are non-dimensional; the contour interval for the colour shading is 0.25, and 0.5 for the white lines. Values between –0.25 and 0.25 are not shaded. Yellow and red shading indicates negative NAM indices and blue shading indicates positive indices. The thin horizontal lines indicate the approximate boundary between the troposphere and the stratosphere. Modified from Baldwin and Dunkerton (2001).*

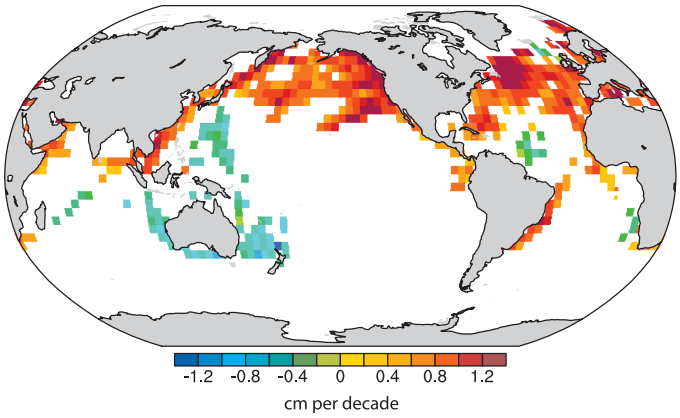


Figure 3.25. *Estimates of linear trends in significant wave height (cm per decade) for regions along the major ship routes of the global ocean for 1950 to 2002. Trends are shown only for locations where they are significant at the 5% level. Adapted from Gulev and Grigorieva (2004).*

Atlantic and the northeast Pacific. Statistically significant negative trends are observed in the western Pacific tropics, the Tasman Sea and the south Indian Ocean (–11 cm per decade). Hindcasts of waves with global and basin-scale models by Wang and Swail (2001, 2002) and Sterl and Caires (2005), based on NRA and ERA-40 winds, respectively, show an increasing mean SWH as well as intensification of SWH extremes during the last 40 years, with the 99% extreme of the winter SWH increasing in the northeast Atlantic by a maximum of 0.4 m per decade. Wave height hindcasts driven with NRA surface winds suggest that worsening wave conditions in the northeastern North Atlantic during the latter half of the 20th century were connected to a northward displacement in the storm track, with decreasing wave heights in the southern North Atlantic (Lozano and Swail, 2002). Increases of SWH in the North Atlantic mid-latitudes are further supported by a 14-year (1988–2002) time series of the merged TOPography EXperiment (TOPEX)/Poseidon and European Remote Sensing (ERS-1/2) satellite altimeter data (Woolf et al., 2002).

Since the TAR, research into surface fluxes has continued to be directed at improving the accuracy of the mean air-sea exchange fields (particularly of heat) with less work on long-term trends. Significant uncertainties remain in global fields of the net heat exchange, stemming from problems in obtaining accurate estimates of the different heat flux components. Estimates of surface flux variability from reanalyses are strongly influenced by inhomogeneous data assimilation input, especially in the Southern Ocean, and Sterl (2004) reported that variability of the surface latent heat flux in the Southern Ocean became much more reliable after 1979, when observations increased. Recent evaluations of heat flux estimates from reanalyses and *in situ* observations indicate some improvements but there are still global biases of several tens of watts per square metre in unconstrained products based on VOS observations (Grist and Josey, 2003). Estimates of the implied ocean heat transport from the NRA, indirect residual techniques and some coupled models are in reasonable agreement with hydrographic observations (Trenberth and Caron, 2001; Grist and Josey, 2003). However, the hydrographic observations also contain significant uncertainties (see Chapter 5) due to both interannual variability and assumptions made in the computation of the heat transport, and these must be recognised when using them to evaluate the various flux products. For the North Atlantic, there are indications of positive trends in the net heat flux from the ocean of 10 W m^{-2} per decade in the western subpolar gyre and coherent negative changes in the eastern subtropical gyre, closely correlated with the NAO variability in the interval 1948 to 2002 (Marshall et al., 2001; Visbeck et al., 2003; Gulev et al., 2007).

3.5.7 Summary

Changes from the late 1970s to recent years generally reveal decreases in tropospheric geopotential heights over high latitudes of both hemispheres and increases over the mid-latitudes in DJF. The changes amplify with altitude up to the lower stratosphere, but remain similar in shape to lower atmospheric levels and are associated with the intensification and poleward displacement of corresponding Atlantic and southern polar front jet streams and enhanced storm track activity. Based on a variety of measurements at the surface and in the upper troposphere, it is likely that there has been an increase and a poleward shift in NH winter storm-track activity over the second half of the 20th century, but there are still significant uncertainties in the magnitude of the increase due to time-dependent biases in the reanalyses. Analysed decreases in cyclone numbers over the southern extratropics and increases in mean cyclone radius and depth over much of the SH over the last two decades are subject to even larger uncertainties.

The decrease in long-lasting blocking frequency over the North Atlantic-European sector over recent decades is dynamically consistent with NAO variability (see Section 3.6), but given data limitations, it may be too early to define the nature of any trends in SH blocking occurrence, despite observed trends in the SAM. After the late 1990s in the NH, occurrences of major sudden warmings seem to have increased in the polar stratosphere, associated with the occurrence of more neutral states of the tropospheric and stratospheric vortex. In the SH, there has been a strengthening tropospheric antarctic vortex during summer in association with the ozone hole, which has led to a cooling of the stratospheric polar vortex in late spring and to a two- to three-week delay in vortex breakdown. In September 2002, a major warming was observed for the first and only time in the SH. Analysis of observed wind and SWH support the reanalysis-based evidence for an increase in storm activity in the extratropical NH in recent decades (see also Section 3.6) until the late 1990s. For heat flux, there seem to have been NAO-related variations over the Labrador Sea, which is a key region for deep water formation.

3.6 Patterns of Atmospheric Circulation Variability

3.6.1 Teleconnections

The global atmospheric circulation has a number of preferred patterns of variability, all of which have expressions in surface climate. Box 3.4 discusses the main patterns and associated indices. Regional climates in different locations may vary out of phase, owing to the action of such 'teleconnections', which modulate the location and strength of the storm tracks (Section 3.5.3) and poleward fluxes of heat, moisture and momentum. A comprehensive review by Hurrell et al. (2003) has been updated by new analyses, notably from Quadrelli and Wallace (2004) and Trenberth et al. (2005b). Understanding the nature of teleconnections and changes in their behaviour is central to understanding regional climate variability and change. Such seasonal and longer time-scale anomalies have direct impacts on humans, as they are often associated with droughts, floods, heat waves and cold waves and other changes that can severely disrupt agriculture, water supply and fisheries, and can modulate air quality, fire risk, energy demand and supply and human health.

The analysis of teleconnections has typically employed a linear perspective, which assumes a basic spatial pattern with varying amplitude and mirror image positive and negative polarities (Hurrell et al., 2003; Quadrelli and Wallace, 2004). In contrast, nonlinear interpretations would identify preferred climate anomalies as recurrent states of a specific polarity (e.g., Corti et al., 1999; Cassou and Terray, 2001; Monahan et al., 2001). Climate change may result through changes from one quasi-stationary state to another, as a preference for one polarity of a pattern (Palmer, 1999), or through a change in the nature or number of states (Straus and Molteni, 2004).

In the NH, one-point correlation maps illustrate the Pacific-North American (PNA) pattern and the NAO (Figure 3.26), but in the SH, wave structures do not emerge as readily owing to the dominance of the SAM. Although teleconnections are best defined over a grid, simple indices based on a few key station locations remain attractive as the series can often be carried back in time long before complete gridded fields were available (see Section 3.6.4, Figure 3.31); the disadvantage is increased noise from the reduced spatial sampling. For instance, Hurrell et al. (2003) found that the residence time of the NAO in its positive phase in the early 20th century was not as great as indicated by the positive NAO index for that period.

Many teleconnections have been identified, but combinations of only a small number of patterns can account for much of the interannual variability in the circulation and surface climate. Quadrelli and Wallace (2004) found that many patterns of NH interannual variability can be reconstructed as linear combinations of the first two Empirical Orthogonal Functions (EOFs) of sea level pressure (approximately the NAM and the PNA). Trenberth et al. (2005b) analysed global atmospheric mass and found four key rotated EOF patterns: the two annular modes (SAM and NAM), a global ENSO-related pattern and a fourth closely related to the North Pacific Index and the PDO, which in turn is closely related to ENSO and the PNA pattern.

Teleconnection patterns tend to be most prominent in the winter (especially in the NH), when the mean circulation is

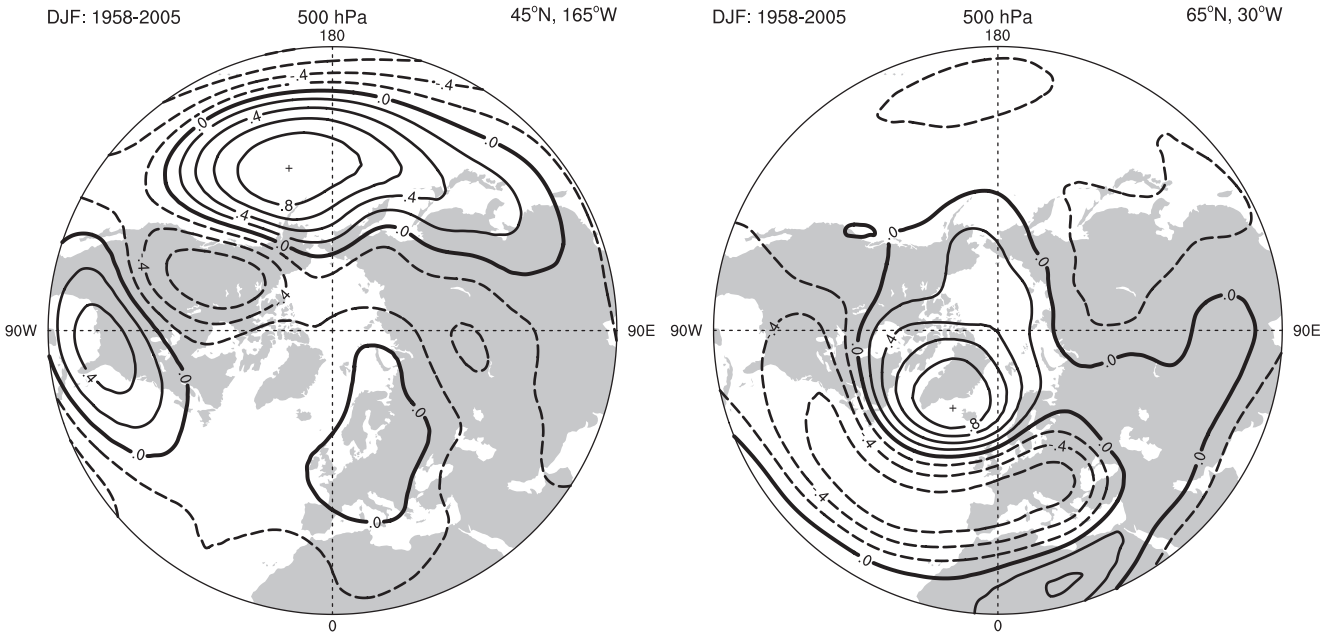


Figure 3.26. *The PNA (left) and NAO (right) teleconnection patterns, shown as one-point correlation maps of 500 hPa geopotential heights for boreal winter (DJF) over 1958 to 2005. In the left panel, the reference point is 45°N, 165°W, corresponding to the primary centre of action of the PNA pattern, given by the + sign. In the right panel, the NAO pattern is illustrated based on a reference point of 65°N, 30°W. Negative correlation coefficients are dashed, and the contour increment is 0.2. Adapted from Hurrell et al. (2003).*

Box 3.4: Defining the Circulation Indices

A teleconnection is made up of a fixed spatial pattern with an associated index time series showing the evolution of its amplitude and phase. Teleconnections are best defined by values over a grid but it is often convenient to devise simplified indices based on key station values. A classic example is the Southern Oscillation (SO), encompassing the entire tropical Pacific, yet encapsulated by a simple SO Index (SOI), based on differences between Tahiti (eastern Pacific) and Darwin (western Pacific) MSLP anomalies.

A number of teleconnections have historically been defined from either station data (SOI, NAO) or from gridded fields (NAM, SAM, PDO/NPI and PNA):

- **Southern Oscillation Index (SOI).** The MSLP anomaly difference of Tahiti minus Darwin, normalised by the long-term mean and standard deviation of the MSLP difference (Troup, 1965; Können et al., 1998). Available from the 1860s. Darwin can be used alone, as its data are more consistent than Tahiti prior to 1935.
- **North Atlantic Oscillation (NAO) Index.** The difference of normalised MSLP anomalies between Lisbon, Portugal and Stykkisholmur, Iceland has become the most widely used NAO index and extends back in time to 1864 (Hurrell, 1995), and to 1821 if Reykjavik is used instead of Stykkisholmur and Gibraltar instead of Lisbon (Jones et al., 1997).
- **Northern Annular Mode (NAM) Index.** The amplitude of the pattern defined by the leading empirical orthogonal function of winter monthly mean NH MSLP anomalies poleward of 20°N (Thompson and Wallace, 1998, 2000). The NAM has also been known as the Arctic Oscillation (AO), and is closely related to the NAO.
- **Southern Annular Mode (SAM) Index.** The difference in average MSLP between SH middle and high latitudes (usually 45°S and 65°S), from gridded or station data (Gong and Wang, 1999; Marshall, 2003), or the amplitude of the leading empirical orthogonal function of monthly mean SH 850 hPa height poleward of 20°S (Thompson and Wallace, 2000). Formerly known as the Antarctic Oscillation (AAO) or High Latitude Mode (HLM).
- **Pacific-North American pattern (PNA) Index.** The mean of normalised 500 hPa height anomalies at 20°N, 160°W and 55°N, 115°W minus those at 45°N, 165°W and 30°N, 85°W (Wallace and Gutzler, 1981).
- **Pacific Decadal Oscillation (PDO) Index and North Pacific Index (NPI).** The NPI is the average MSLP anomaly in the Aleutian Low over the Gulf of Alaska (30°N–65°N, 160°E–140°W; Trenberth and Hurrell, 1994) and is an index of the PDO, which is also defined as the pattern and time series of the first empirical orthogonal function of SST over the North Pacific north of 20°N (Mantua et al., 1997; Deser et al., 2004). The PDO broadened to cover the whole Pacific Basin is known as the Inter-decadal Pacific Oscillation (IPO: Power et al., 1999b). The PDO and IPO exhibit virtually identical temporal evolution (Folland et al., 2002).

strongest. The strength of teleconnections and the way they influence surface climate also vary over long time scales. Both the NAO and ENSO exhibited marked changes in their surface climate expressions on multi-decadal time scales during the 20th century (e.g., Power et al., 1999b; Jones et al., 2003). Multi-decadal changes in influence are often real and not due just to poorer data quality in earlier decades.

3.6.2 El Niño-Southern Oscillation and Tropical/Extratropical Interactions

3.6.2.1 El Niño-Southern Oscillation

El Niño-Southern Oscillation events are a coupled ocean-atmosphere phenomenon. El Niño involves warming of tropical Pacific surface waters from near the International Date Line to the west coast of South America, weakening the usually strong SST gradient across the equatorial Pacific, with associated changes in ocean circulation. Its closely linked atmospheric counterpart, the Southern Oscillation (SO), involves changes in trade winds, tropical circulation and precipitation. Historically, El Niño events occur about every 3 to 7 years and alternate with the opposite phases of below-average temperatures in the eastern tropical Pacific (La Niña). Changes in the trade winds, atmospheric circulation, precipitation and associated atmospheric heating set up extratropical responses. Wavelike extratropical teleconnections are accompanied by changes in the jet streams and storm tracks in mid-latitudes (Chang and Fu, 2002).

The El Niño-Southern Oscillation has global impacts, manifested most strongly in the northern winter months (November–March). Anomalies in MSLP are much greater in the extratropics while the tropics feature large precipitation variations. Associated patterns of surface temperature and precipitation anomalies around the globe are given in Figure 3.27 (Trenberth and Caron, 2000), and the evolution of these patterns and links to global mean temperature perturbations are given by Trenberth et al. (2002b).

The nature of ENSO has varied considerably over time. Strong ENSO events occurred from the late 19th century through the first 25 years of the 20th century and again after about 1950, but there were few events of note from 1925 to 1950 with the exception of the major 1939–1941 event (Figure 3.27). The 1976–1977 climate shift (Trenberth, 1990; see Figure 3.27 and Section 3.6.3, Figure 3.28) was associated with marked changes in El Niño evolution (Trenberth and Stepaniak, 2001), a shift to generally above-normal SSTs in the eastern and central equatorial Pacific and a tendency towards more prolonged and

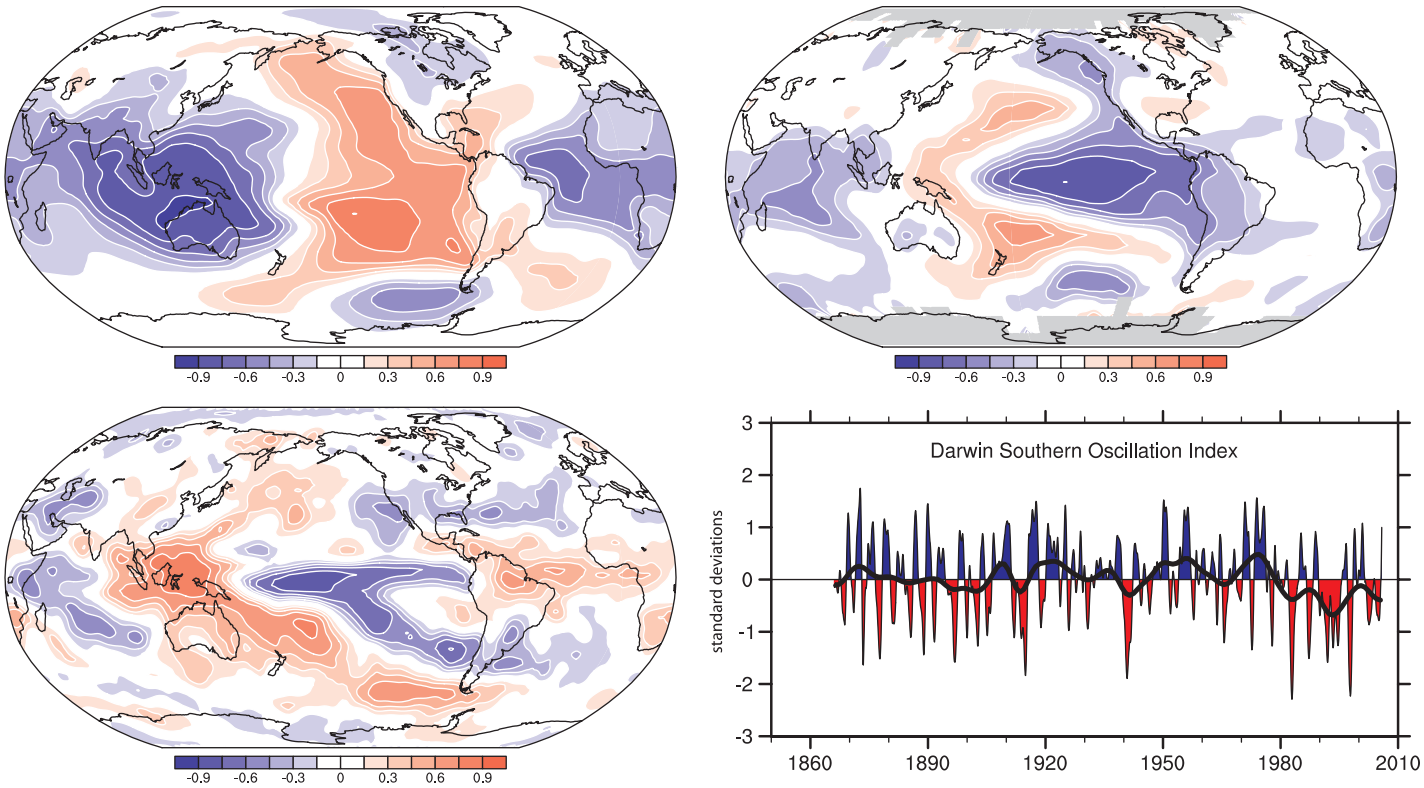


Figure 3.27. *Correlations with the SOI, based on normalised Tahiti minus Darwin sea level pressures, for annual (May to April) means for sea level pressure (top left) and surface temperature (top right) for 1958 to 2004, and GPCP precipitation for 1979 to 2003 (bottom left), updated from Trenberth and Caron (2000). The Darwin-based SOI, in normalized units of standard deviation, from 1866 to 2005 (Können et al., 1998; lower right) features monthly values with an 11-point low-pass filter, which effectively removes fluctuations with periods of less than eight months (Trenberth, 1984). The smooth black curve shows decadal variations (see Appendix 3.A). Red values indicate positive sea level pressure anomalies at Darwin and thus El Niño conditions.*

stronger El Niños. Since the TAR, there has been considerable work on decadal and longer-term variability of ENSO and Pacific climate. Such decadal atmospheric and oceanic variations (Section 3.6.3) are more pronounced in the North Pacific and across North America than in the tropics but are also present in the South Pacific, with evidence suggesting they are at least in part forced from the tropics (Deser et al., 2004).

El Niño-Southern Oscillation events involve large exchanges of heat between the ocean and atmosphere and affect global mean temperatures. The 1997–1998 event was the largest on record in terms of SST anomalies and the global mean temperature in 1998 was the highest on record (at least until 2005). Trenberth et al. (2002b) estimated that global mean surface air temperatures were 0.17°C higher for the year centred on March 1998 owing to the El Niño. Extremes of the hydrological cycle such as floods and droughts are common with ENSO and are apt to be enhanced with global warming (Trenberth et al., 2003). For example, the modest 2002–2003 El Niño was associated with a drought in Australia, made much worse by record-breaking heat (Nicholls, 2004; and see Section 3.8.4, Box 3.6). Thus, whether observed changes in ENSO behaviour are physically linked to global climate change is a research question of great importance.

3.6.2.2 Tropical-Extratropical Teleconnections: PNA and PSA

Circulation variability over the extratropical Pacific features wave-like patterns emanating from the subtropical western Pacific, characteristic of Rossby wave propagation associated with anomalous tropical heating (Horel and Wallace, 1981; Hoskins and Karoly, 1981). These are known as the PNA and Pacific-South American (PSA) patterns and can arise naturally through atmospheric dynamics as well as in response to heating. Over the NH in winter, the PNA pattern lies across North America from the subtropical Pacific, with four centres of action (Figure 3.26). While the PNA pattern can be illustrated by taking a single point correlation, this is not so easy for the PSA pattern (not shown), as its spatial centres of action are not fixed. However, the PSA pattern can be present at all times of year, lying from Australasia over the southern Pacific and Atlantic (Mo and Higgins, 1998; Kidson, 1999; Mo, 2000).

The PNA, or a variant of it (Straus and Shukla, 2002), is associated with modulation of the Aleutian Low, the Asian jet, and the Pacific storm track, affecting precipitation in western North America and the frequency of Alaskan blocking events and associated cold air outbreaks over the western USA in winter (Compo and Sardeshmukh, 2004). The PSA is associated with

modulation of the westerlies over the South Pacific, effects of which include significant rainfall variations over New Zealand, changes in the nature and frequency of blocking events across the high-latitude South Pacific, and interannual variations in antarctic sea ice across the Pacific and Atlantic sectors (Renwick and Revell, 1999; Kwok and Comiso, 2002a; Renwick, 2002). While both PNA and PSA activity have varied with decadal modulation of ENSO, no systematic changes in their behaviour have been reported.

3.6.3 Pacific Decadal Variability

Decadal to inter-decadal variability of the atmospheric circulation is most prominent in the North Pacific, where fluctuations in the strength of the winter Aleutian Low pressure system co-vary with North Pacific SST in the PDO. These are linked to decadal variations in atmospheric circulation, SST and ocean circulation throughout the whole Pacific Basin in the Inter-decadal Pacific Oscillation (IPO; Trenberth and Hurrell, 1994; Gershunov and Barnett, 1998; Folland et al., 2002; McPhaden and Zhang, 2002; Deser et al., 2004). Key measures of Pacific decadal variability are the North Pacific Index (NPI; Trenberth and Hurrell, 1994), PDO index (Mantua et al., 1997) and the IPO index (Power et al., 1999b; Folland et al., 2002; see Figures 3.28 and 3.29). Modulation of ENSO by the PDO significantly modifies regional teleconnections around the Pacific Basin (Power et al., 1999b; Salinger et al., 2001), and affects the evolution of the global mean climate.

The PDO/IPO has been described as a long-lived El Niño-like pattern of Indo-Pacific climate variability (Knutson and Manabe, 1998; Evans et al., 2001; Deser et al., 2004; Linsley et al., 2004) or as a low-frequency residual of ENSO variability on multi-decadal time scales (Newman et al., 2003). Indeed, the symmetry of the SST anomaly pattern between the NH and SH may be a reflection of common tropical forcing. However, Folland et al. (2002) showed that the IPO significantly affects the movement of the South Pacific Convergence Zone in a way independent of ENSO (see also Deser et al., 2004). Other results indicate that the extratropical phenomena are generic components of the PDO (Deser et al., 1996, 1999, 2003; Gu and Philander, 1997). The extratropics may also contribute to the tropical SST changes via an 'atmospheric bridge', confounding the simple interpretation of a tropical origin (Barnett et al., 1999; Vimont et al., 2001).

The inter-decadal time scale of tropical Indo-Pacific SST variability is likely due to oceanic processes. Extratropical ocean influences are also likely to play a role as changes in the ocean gyre evolve and heat anomalies are subducted and re-emerge (Deser et al., 1996, 1999, 2003; Gu and Philander, 1997). It is also possible that there is no well-defined coupled ocean-atmosphere 'mode' of variability in the Pacific on decadal to inter-decadal time scales, since instrumental records are too short to provide a robust assessment and palaeoclimate records conflict regarding time scales (Biondi et al., 2001; Gedalof et al., 2002). Schneider and Cornuelle (2005) suggested that the PDO is not itself a mode of variability but is a blend of three

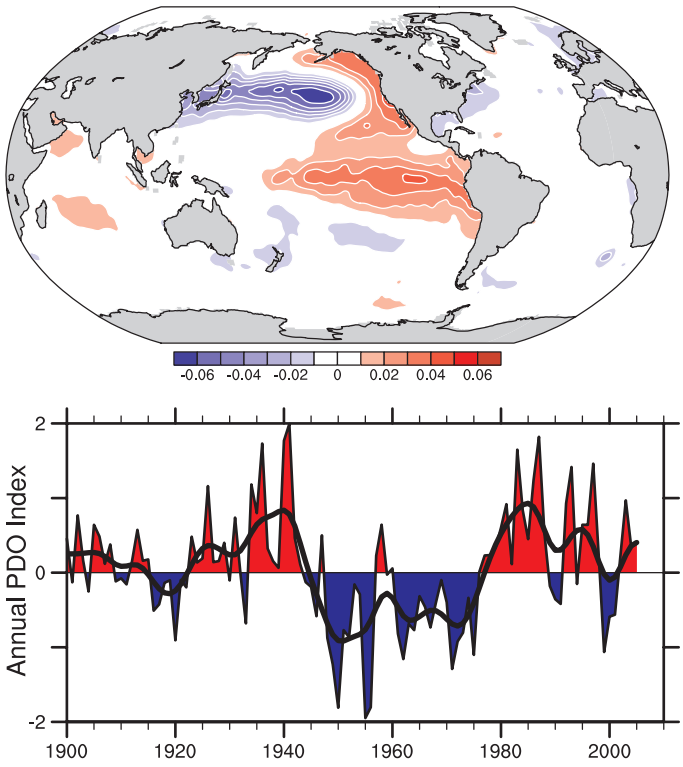


Figure 3.28. *Pacific Decadal Oscillation: (top) SST based on the leading EOF SST pattern for the Pacific basin north of 20°N for 1901 to 2004 (updated; see Mantua et al., 1997; Power et al., 1999b) and projected for the global ocean (units are nondimensional); and (bottom) annual time series (updated from Mantua et al., 1997). The smooth black curve shows decadal variations (see Appendix 3.A).*

phenomena. They showed that the observed PDO pattern and evolution can be recovered from a reconstruction of North Pacific SST anomalies based on a first order autoregressive model and forcing by variability of the Aleutian low, ENSO and oceanic zonal advection in the Kuroshio-Oyashio Extension. The latter results from oceanic Rossby waves that are forced by North Pacific Ekman pumping. The SST response patterns to these processes are not completely independent, but they determine the spatial characteristics of the PDO. Under this hypothesis, the key physical variables for measuring Pacific climate variability are ENSO and NPI (Aleutian Low) indices, rather than the PDO index.

Figure 3.29 (top) shows a time series of the NPI for 1900 to 2005 (Deser et al., 2004). There is substantial low-frequency variability, with extended periods of predominantly high values indicative of a weakened circulation (1900–1924 and 1947–1976) and predominantly low values indicative of a strengthened circulation (1925–1946 and 1977–2005). The well-known decrease in pressure from 1976 to 1977 is analogous to transitions that occurred from 1946 to 1947 and from 1924 to 1925, and these earlier changes were also associated with SST fluctuations in the tropical Indian (Figure 3.29, lower) and Pacific Oceans although not in the upwelling zone of the equatorial eastern Pacific (Minobe, 1997; Deser et al., 2004). In addition, the NPI exhibits variability on shorter time scales, interpreted in part as a bi-decadal rhythm (Minobe, 1999).

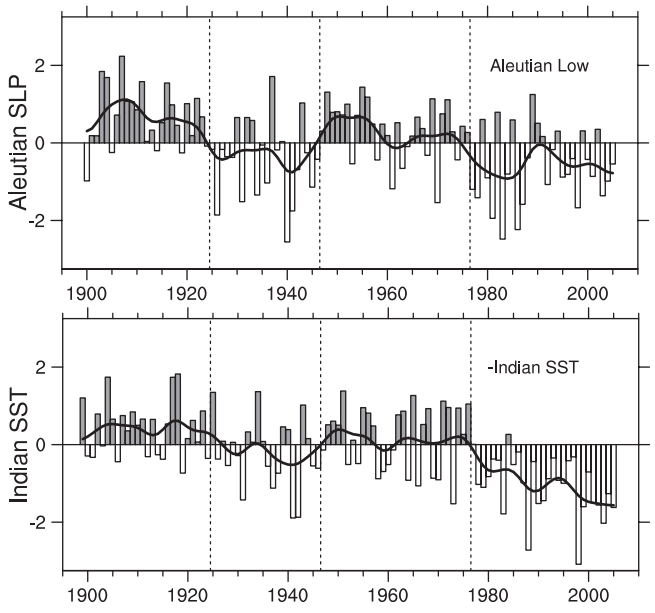


Figure 3.29. *(Top) Time series of the NPI (sea level pressure during December through March averaged over the North Pacific, 30°N to 65°N, 160°E to 140°W) from 1900 to 2005 expressed as normalised departures from the long-term mean (each tick mark on the ordinate represents two standard deviations, or 5.5 hPa). This record reflects the strength of the winter Aleutian Low pressure system, with positive (negative) values indicative of a weak (strong) Aleutian Low. The bars give the winter series and the smooth black curves show decadal variations (see Appendix 3.A). Values were updated and extended to earlier decades from Trenberth and Hurrell (1994). (Bottom) As above but for SSTs averaged over the tropical Indian Ocean (10°S–20°N, 50°E –125°E; each tick mark represents two standard deviations, or 0.36°C). This record has been inverted to facilitate comparison with the top panel. The dashed vertical lines mark years of transition in the Aleutian Low record (1925, 1947, 1977). Updated from Deser et al. (2004).*

There is observational and modelling evidence (Pierce, 2001; Schneider and Cornuelle, 2005) suggesting the PDO/IPO does not excite the climate shifts in the Pacific area, but they share the same forcing. The 1976–1977 climate shift in the Pacific, associated with a phase change in the PDO from negative to positive, was associated with significant changes in ENSO evolution (Trenberth and Stepaniak, 2001) and with changes in ENSO teleconnections and links to precipitation and surface temperatures over North and South America, Asia and Australia (Trenberth, 1990; Trenberth and Hurrell, 1994; Power et al., 1999a; Salinger et al., 2001; Mantua and Hare, 2002; Minobe and Nakanowatari, 2002; Trenberth et al., 2002b; Deser et al., 2004; Marengo, 2004). Schneider and Cornuelle (2005) added extra credence to the hypothesis that the 1976–1977 climate shift is of tropical origin.

3.6.4 The North Atlantic Oscillation and Northern Annular Mode

The only teleconnection pattern prominent throughout the year in the NH is the NAO (Barnston and Livezey, 1987). It is primarily a north-south dipole in sea level pressure characterised by simultaneous out-of-phase pressure and height anomalies between temperate and high latitudes over the Atlantic sector, and therefore corresponds to changes in the westerlies across the North Atlantic into Europe (Figure 3.30). The NAO has the strongest signature in the winter months (December to March) when its positive (negative) phase exhibits an enhanced (diminished) Iceland Low and Azores High (Hurrell et al., 2003). The NAO is the dominant pattern of near-surface atmospheric circulation variability over the North Atlantic, accounting for one third of the total variance in monthly MSLP in winter. It is closely related to the NAM, which has similar structure over the Atlantic but is more zonally symmetric. The leading winter pattern of variability in the lower stratosphere is also annular, but the MSLP anomaly pattern that is associated with it is confined almost entirely to the Arctic and Atlantic sectors and coincides with the spatial structure of the NAO (Deser, 2000; see also Section 3.5.5 and Box 3.3).

There is considerable debate over whether the NAO or the NAM is more physically relevant to the winter circulation (Deser, 2000; Ambaum et al., 2001, 2002), but the time series are highly correlated in winter (Figure 3.31). As Quadrelli and Wallace (2004) showed, they are near neighbours in terms of their spatial patterns and their temporal evolution. The annular modes are intimately linked to the configuration of the extratropical storm tracks and jet streams. Changes in the phase of the annular modes appear to occur as a result of interactions between the eddies and the mean flow, and external forcing is not required to sustain them (De Weaver and Nigam, 2000). In the NH, stationary waves provide most of the eddy momentum fluxes, although transient eddies are also important. To the extent that the intrinsic excitation of the NAO/NAM pattern is limited to a period less than a few days (Feldstein, 2002), it should not exhibit year-to-year autocorrelation in conditions of constant forcing. Proxy and instrumental data, however, show evidence for intervals with prolonged positive and negative NAO index values in the last few centuries (Cook et al., 2002; Jones et al., 2003). In winter, a reversal occurred from the minimum index values in the late 1960s to strongly positive NAO index values in the mid-1990s. Since then, NAO values have declined to near the long-term mean (Figure 3.31). In summer, Hurrell et al. (2001, 2002) identified significant interannual to multi-decadal fluctuations in the NAO pattern, and the trend towards persistent anticyclonic flow over northern Europe has contributed to anomalously warm and dry conditions in recent decades (Rodwell, 2003).

Feldstein (2002) suggested that the trend and increase in the variance of the NAO/NAM index from 1968 through 1997 was greater than would be expected from internal variability alone, while NAO behaviour during the first 60 years of the 20th century was consistent with atmospheric internal variability. However, the results are not so clear if based on just the period 1975 to 2004 (Overland and Wang, 2005). Although monthly-scale NAO variability is strong (Czaja et al., 2003; Thompson et al., 2003), there may be predictability from stratospheric influences (Thompson et al., 2002; Scaife et al., 2005; see Box 3.3). There is mounting evidence that the recent observed inter-decadal NAO variability comes from tropical and extratropical ocean influences (Hurrell et al., 2003, 2004), land surface

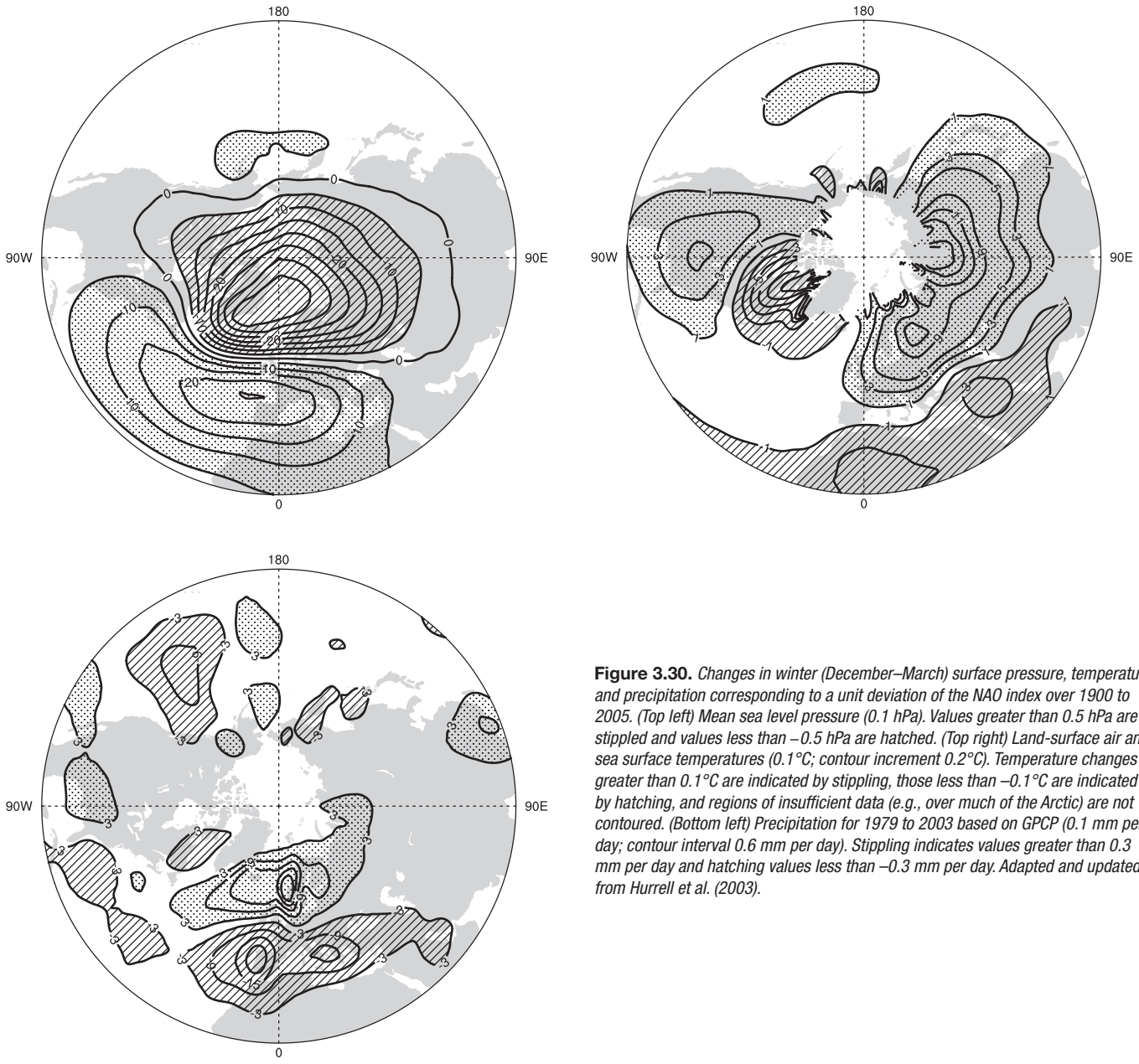


Figure 3.30. *Changes in winter (December–March) surface pressure, temperature, and precipitation corresponding to a unit deviation of the NAO index over 1900 to 2005. (Top left) Mean sea level pressure (0.1 hPa). Values greater than 0.5 hPa are stippled and values less than –0.5 hPa are hatched. (Top right) Land-surface air and sea surface temperatures (0.1°C; contour increment 0.2°C). Temperature changes greater than 0.1°C are indicated by stippling, those less than –0.1°C are indicated by hatching, and regions of insufficient data (e.g., over much of the Arctic) are not contoured. (Bottom left) Precipitation for 1979 to 2003 based on GPCP (0.1 mm per day; contour interval 0.6 mm per day). Stippling indicates values greater than 0.3 mm per day and hatching values less than –0.3 mm per day. Adapted and updated from Hurrell et al. (2003).*

forcing (Gong et al., 2003; Bojariu and Gimeno, 2003) and from other external factors (Gillett et al., 2003).

The NAO exerts a dominant influence on winter surface temperatures across much of the NH (Figure 3.30), and on storminess and precipitation over Europe and North Africa. When the NAO index is positive, enhanced westerly flow across the North Atlantic in winter moves warm moist maritime air over much of Europe and far downstream, with dry conditions over southern Europe and northern Africa and wet conditions in northern Europe, while stronger northerly winds over Greenland and northeastern Canada carry cold air southward and decrease land temperatures and SST over the northwest Atlantic. Temperature variations over North Africa and the Middle East (cooling) and the southeastern USA (warming), associated with the stronger clockwise flow around the subtropical Atlantic high-pressure centre, are also notable. Following on from Hurrell (1996), Thompson et al. (2000) showed that for JFM from 1968 to 1997, the NAM accounted for 1.6°C of the 3.0°C warming in Eurasian surface temperatures, 4.9 hPa of the 5.7 hPa decrease in sea level pressure from 60°N to 90°N; 37% out of the 45% increase in Norwegian-area precipitation (55°N–65°N, 5°E–10°E), and 33% out of the 49% decrease in Spanish-region rainfall (35°N–45°N, 10°W–0°W). There were also significant effects on ocean heat content, sea ice, ocean currents and ocean heat transport.

Positive NAO index winters are associated with a northeastward shift in the Atlantic storm activity, with enhanced activity from Newfoundland into northern Europe and a modest decrease to the south (Hurrell and van Loon, 1997; Alexandersson et al., 1998). Positive NAO index winters are also typified by more intense and frequent storms in the vicinity of Iceland and the Norwegian Sea (Serreze et al., 1997;

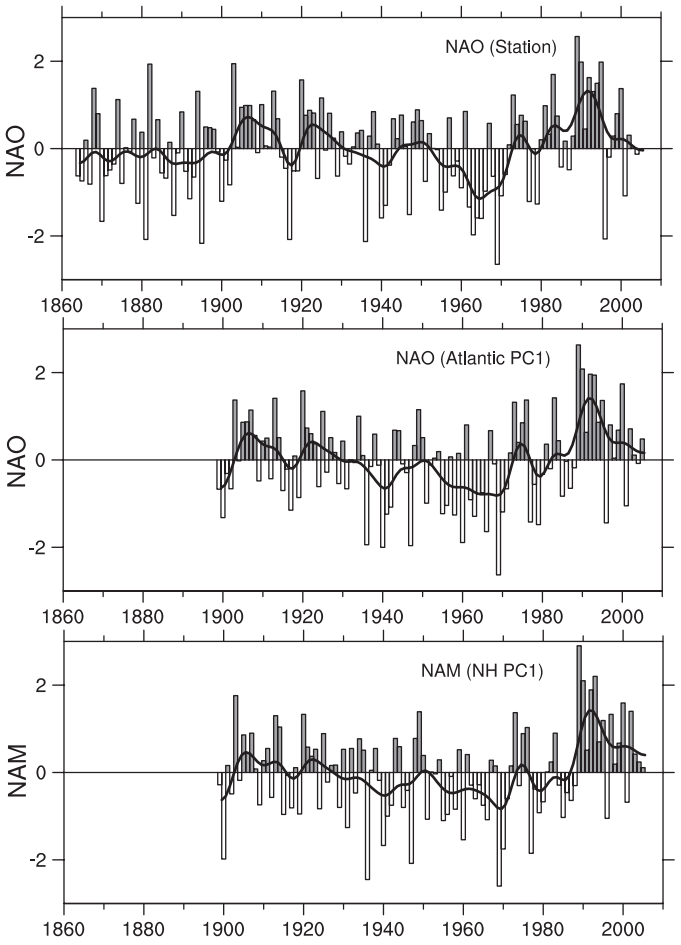


Figure 3.31. *Normalised indices (units of standard deviation) of the mean winter (December–March) NAO developed from sea level pressure data. In the top panel, the index is based on the difference of normalised sea level pressure between Lisbon, Portugal and Stykkisholmur/Reykjavik, Iceland from 1864 to 2005. The average winter sea level pressure data at each station were normalised by dividing each seasonal pressure anomaly by the long-term (1864 to 1983) standard deviation. In the middle panel, the index is the principal component time series of the leading EOF of Atlantic-sector sea level pressure. In the lower panel, the index is the principal component time series of the leading EOF of NH sea level pressure. The smooth black curves show decadal variations (see Appendix 3.A). The individual bar corresponds to the January of the winter season (e.g., 1990 is the winter of 1989/1990). Updated from Hurrell et al. (2003); see http://www.cgd.ucar.edu/cas/jhurrell/indices.html for updated time series.*

Deser et al., 2000). The correlation between the NAO index and cyclone activity is highly negative in eastern Canada and positive in western Canada (Wang et al., 2006b). The upward trend towards more positive NAO index winters from the mid-1960s to the mid-1990s has been associated with increased wave heights over the northeast Atlantic and decreased wave heights south of 40°N (Carter, 1999; Wang and Swail, 2001; see also Section 3.5.6).

The NAO/NAM modulates the transport and convergence of atmospheric moisture and the distribution of evaporation and precipitation (Dickson et al., 2000). Evaporation exceeds precipitation over much of Greenland and the Canadian Arctic and more precipitation than normal falls from Iceland through Scandinavia during winters with a high NAO index, while the reverse occurs over much of central and southern Europe, the Mediterranean and parts of the Middle East (Dickson et al., 2000). Severe drought has persisted throughout parts of Spain and Portugal as well (Hurrell et al., 2003). As far eastward as Turkey, river runoff is significantly correlated with NAO variability (Cullen and deMenocal, 2000). There are many NAO-related effects on ocean circulation, such as the freshwater balance of the Atlantic Ocean (see Chapter 5), on the cryosphere (see Chapter 4), and on many aspects of the north Atlantic/European biosphere (see the Working Group II contribution to the IPCC Fourth Assessment Report).

3.6.5 The Southern Hemisphere and Southern Annular Mode

The principal mode of variability of the atmospheric circulation in the SH extratropics is now known as the SAM (see Figure 3.32). It is essentially a zonally symmetric structure, but with a zonal wave three pattern superimposed. It is associated with synchronous pressure or height anomalies of opposite sign in mid- and high-latitudes, and therefore reflects changes in the main belt of subpolar westerly winds. Enhanced Southern Ocean westerlies occur in the positive phase of the SAM. The SAM contributes a significant proportion of SH mid-latitude circulation variability on many time scales (Hartmann and Lo, 1998; Kidson, 1999; Thompson and Wallace, 2000; Baldwin, 2001). Trenberth et al. (2005b) showed that the SAM is the leading mode in an EOF analysis of monthly mean global atmospheric mass, accounting for around 10% of total global variance. As with the NAM, the structure and variability of the SAM results mainly from the internal dynamics of the atmosphere and the SAM is an expression of storm track and jet stream variability (e.g., Hartmann and Lo, 1998; Limpasuvan and Hartmann, 2000; Box 3.3). Poleward eddy momentum fluxes interact with the zonal mean flow to sustain latitudinal displacements of the mid-latitude westerlies (Limpasuvan and Hartmann, 2000; Rashid and Simmonds, 2004, 2005).

Gridded reanalysis data sets have been utilised to derive time series of the SAM, particularly the NRA (e.g., Gong and Wang, 1999; Thompson et al., 2000) and more recently ERA-40 (Renwick, 2004; Trenberth et al., 2005b). However, a declining positive bias in pressure at high southern latitudes in both reanalyses before 1979 (Hines et al., 2000; Trenberth and Smith, 2005) means that derived trends in the SAM are too large. Marshall (2003) produced a SAM index based on appropriately located station observations. His index reveals a general increase in the SAM index beginning in the 1960s (Figure 3.32) consistent with a strengthening of the circumpolar vortex and intensification of the circumpolar westerlies, as observed in northern Antarctic Peninsula radiosonde data (Marshall, 2002).

The observed SAM trend has been related to stratospheric ozone depletion (Sexton, 2001; Thompson and Solomon, 2002; Gillett and Thompson, 2003) and to greenhouse gas increases (Hartmann et al., 2000; Marshall et al., 2004; see also Section 9.5.3.3). Jones and Widmann (2004) reconstructed century-

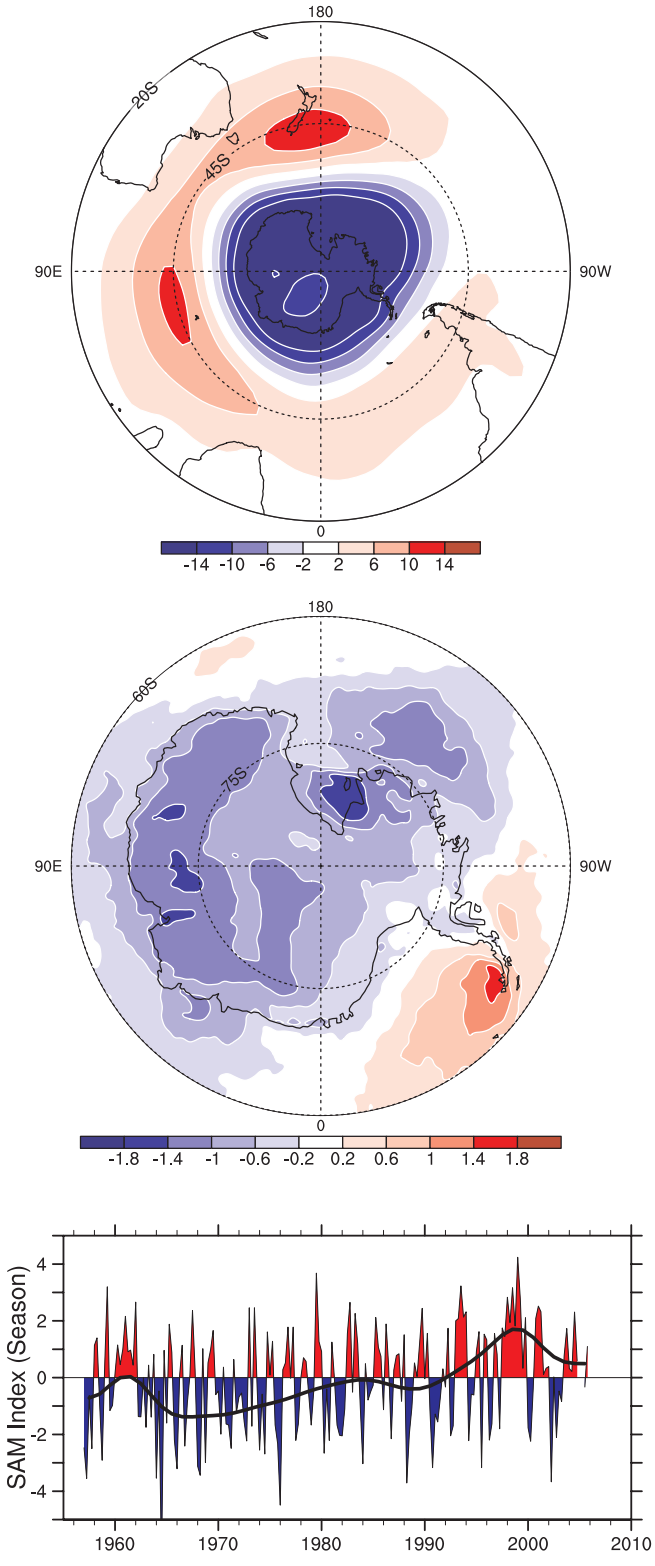


Figure 3.32. *(Bottom) Seasonal values of the SAM index calculated from station data (updated from Marshall, 2003). The smooth black curve shows decadal variations (see Appendix 3.A). (Top) The SAM geopotential height pattern as a regression based on the SAM time series for seasonal anomalies at 850 hPa (see also Thompson and Wallace, 2000). (Middle) The regression of changes in surface temperature (°C) over the 23-year period (1982 to 2004) corresponding to a unit change in the SAM index, plotted south of 60°S. Values exceeding about 0.4°C in magnitude are significant at the 1% significance level (adapted from Kwok and Comiso, 2002b).*

scale records based on proxies of the SAM that indicate that the magnitude of the recent trend may not be unprecedented, even during the 20th century. There is also recent evidence that ENSO variability can influence the SAM in the southern summer (e.g., L'Heureux and Thompson, 2006).

The trend in the SAM, which is statistically significant annually and in summer and autumn (Marshall et al., 2004), has contributed to antarctic temperature trends (Kwok and Comiso, 2002b; Thompson and Solomon, 2002; van den Broeke and van Lipzig, 2003; Schneider et al., 2004); specifically a strong summer warming in the Peninsula region and little change or cooling over much of the rest of the continent (Turner et al., 2005; see Figure 3.32). Through the wave component, the positive SAM is associated with low pressure west of the Peninsula (e.g., Lefebvre et al., 2004) leading to increased poleward flow, warming and reduced sea ice in the region (Liu et al., 2004b). Orr et al. (2004) proposed that this scenario yields a higher frequency of warmer maritime air masses passing over the Peninsula, leading to the marked northeast Peninsula warming observed in summer and autumn (December–May). The positive trend in the SAM has led to more cyclones in the circumpolar trough (Sinclair et al., 1997) and hence a greater contribution to antarctic precipitation from these near-coastal systems that is reflected in $\delta^{18}O$ levels in the snow (Noone and Simmonds, 2002). The SAM also affects spatial patterns of precipitation variability in Antarctica (Genthon et al., 2003) and southern South America (Silvestri and Vera, 2003).

The imprint of SAM variability on the Southern Ocean system is observed as a coherent sea level response around Antarctica (Aoki, 2002; Hughes et al., 2003) and by its regulation of Antarctic Circumpolar Current flow through the Drake Passage (Meredith et al., 2004). Changes in oceanic circulation directly alter the THC (Oke and England, 2004) and may explain recent patterns of observed temperature change at SH high latitudes described by Gille (2002).

3.6.6 Atlantic Multi-decadal Oscillation

Over the instrumental period (since the 1850s), North Atlantic SSTs show a 65 to 75 year variation (0.4°C range), with a warm phase during 1930 to 1960 and cool phases during 1905 to 1925 and 1970 to 1990 (Schlesinger and Ramankutty, 1994), and this feature has been termed the AMO (Kerr, 2000), as shown in Figure 3.33. Evidence (e.g., Enfield et al., 2001; Knight et al., 2005) of a warm phase in the AMO from 1870 to 1900 is revealed as an artefact of the de-trending used (Trenberth and Shea, 2006). The cycle appears to have returned to a warm phase beginning in the mid-1990s, and tropical Atlantic SSTs were at record high levels in 2005. Instrumental observations capture only two full cycles of the AMO, so the robustness of the signal has been addressed using proxies. Similar oscillations in a 60- to 110-year band are seen in North Atlantic palaeoclimatic reconstructions through the last four centuries (Delworth and Mann, 2000; Gray et al., 2004). Both observations and model simulations implicate changes in the strength of the THC as the primary source of the multi-decadal variability, and suggest a

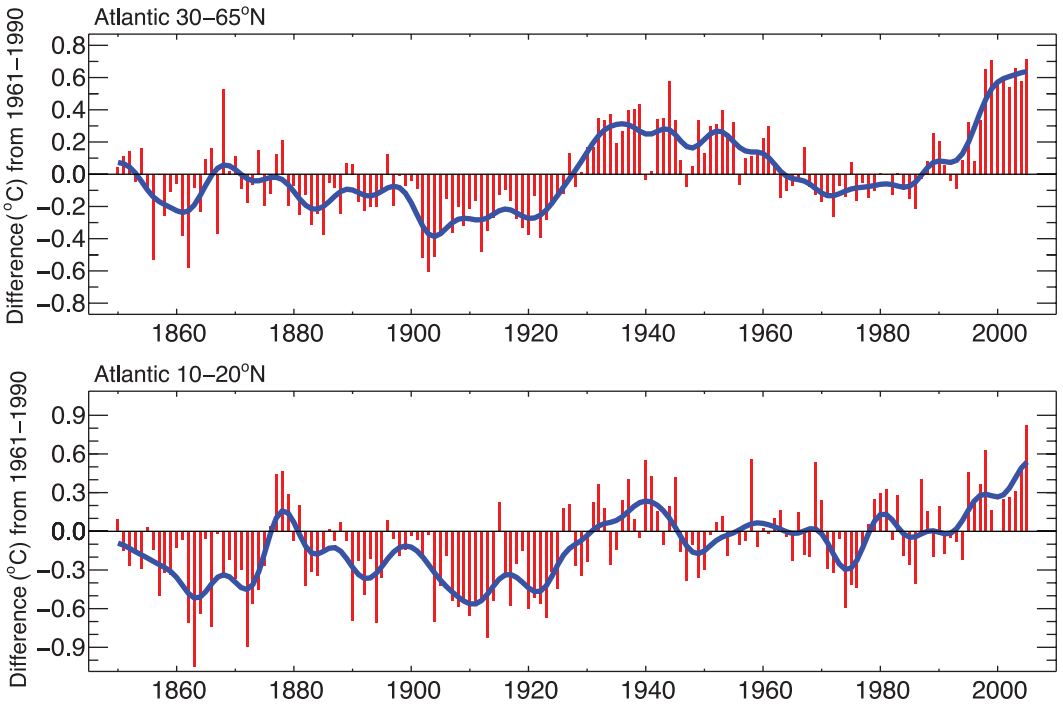


Figure 3.33. *Atlantic Multi-decadal Oscillation index from 1850 to 2005 represented by annual anomalies of SST in the extratropical North Atlantic (30–65°N; top), and in a more muted fashion in the tropical Atlantic (10°N –20°N) SST anomalies (bottom). Both series come from HadSST2 (Rayner et al., 2006) and are relative to the 1961 to 1990 mean (°C). The smooth blue curves show decadal variations (see Appendix 3.A).*

possible oscillatory component to its behaviour (Delworth and Mann, 2000; Latif, 2001; Sutton and Hodson, 2003; Knight et al., 2005). Trenberth and Shea (2006) proposed a revised AMO index, subtracting the global mean SST from the North Atlantic SST. The revised index is about 0.35°C lower than the original after 2000, highlighting the fact that most of the recent warming is global in scale.

The AMO has been linked to multi-year precipitation anomalies over North America, and appears to modulate ENSO teleconnections (Enfield et al., 2001; McCabe et al., 2004; Shabbar and Skinner, 2004). Multi-decadal variability in the North Atlantic also plays a role in Atlantic hurricane formation (Goldenberg et al., 2001; see also Section 3.8.3.2). The revised AMO index (Trenberth and Shea, 2006) indicates that North Atlantic SSTs have recently been about 0.3°C warmer than during 1970 to 1990, emphasizing the role of the AMO in suppressing tropical storm activity during that period. The AMO is likely to be a driver of multi-decadal variations in Sahel droughts, precipitation in the Caribbean, summer climate of both North America and Europe, sea ice concentration in the Greenland Sea and sea level pressure over the southern USA, the North Atlantic and southern Europe (e.g., Venegas and Mysak, 2000; Goldenberg et al., 2001; Sutton and Hodson, 2005; Trenberth and Shea, 2006). Walter and Graf (2002) identified a non-stationary relationship between the NAO and the AMO. During the negative phase of the AMO, the North Atlantic SST is strongly correlated with the NAO index. In contrast, the NAO index is only weakly correlated with the North Atlantic SST during the AMO positive phase. Chelliah and Bell (2004) defined a tropical multi-decadal pattern related to the AMO, the PDO and winter NAO with coherent variations in tropical convection and surface temperatures in the West African monsoon region, the central tropical Pacific, the Amazon Basin and the tropical Indian Ocean.

3.6.7 Other Indices

As noted earlier, many patterns of variability (sometimes referred to as 'modes') in the climate system have been identified over the years, but few stand out as robust and dynamically significant features in relation to understanding regional climate change. This section discusses two climate signals that have recently drawn the attention of scientific community: the Antarctic Circumpolar Wave and the Indian Ocean Dipole.

3.6.7.1 Antarctic Circumpolar Wave

The Antarctic Circumpolar Wave (ACW) is described as a pattern of variability with an approximately four-year period in the southern high-latitude ocean-atmosphere system, characterised by the eastward propagation of anomalies in antarctic sea ice extent, and coupled to anomalies in SST, sea surface height, MSLP and wind (Jacobs and Mitchell, 1996; White and Peterson, 1996; White and Annis, 2004). Since its initial formulation (White and Peterson, 1996), questions have arisen concerning many aspects of the ACW: the robustness of the ACW on inter-decadal time scales (Carril and Navarra, 2001;

Connolley, 2003; Simmonds, 2003), its generating mechanisms (Cai and Baines, 2001; Venegas, 2003; White et al., 2004; White and Simmonds, 2006) and even its very existence (Park et al., 2004).

3.6.7.2 Indian Ocean Dipole

Large interannual variability of SST in the Indian Ocean has been associated with the Indian Ocean Dipole (IOD), also referred to as the Indian Ocean Zonal Mode (IOZM; Saji et al., 1999; Webster et al., 1999). This pattern manifests through a zonal gradient of tropical SST, which in one extreme phase in boreal autumn shows cooling off Sumatra and warming off Somalia in the west, combined with anomalous easterlies along the equator. The magnitude of the secondary rainfall maximum from October to December in East Africa is strongly correlated with positive IOD events (Xie et al., 2002). Several recent IOD events have occurred simultaneously with ENSO events and there is a significant debate on whether the IOD is an Indian Ocean pattern or whether it is triggered by ENSO in the Pacific Ocean (Allan et al., 2001). The strongest IOD episode ever observed occurred in 1997 to 1998 and was associated with catastrophic flooding in East Africa. Trenberth et al. (2002b) showed that Indian Ocean SSTs tend to rise about five months after the peak of ENSO in the Pacific. Monsoon variability and the SAM (Lau and Nath, 2004) are also likely to play a role in triggering or intensifying IOD events. One argument for an independent IOD was the large episode in 1961 when no ENSO event occurred (Saji et al., 1999). Saji and Yamagata (2003), analysing observations from 1958 to 1997, concluded that 11 out of the 19 episodes identified as moderate to strong IOD events occurred independently of ENSO. However, this was disputed by Allan et al. (2001), who found that accounting for varying lag correlations removes the apparent independence from ENSO. Decadal variability in correlations between SST-based indices of the IOD and ENSO has been documented (Clark et al., 2003). At inter-decadal time scales, the SST patterns associated with the inter-decadal variability of ENSO indices are very similar to the SST patterns associated with the Indian monsoon rainfall (Krishnamurthy and Goswami, 2000) and with the North Pacific inter-decadal variability (Deser et al., 2004), raising the issue of coupled mechanisms modulating both ENSO-monsoon system and IOD variability (e.g., Terray et al., 2005).

3.6.8 Summary

Decadal variations in teleconnections considerably complicate the interpretation of climate change. Since the TAR, it has become clear that a small number of teleconnection patterns account for much of the seasonal to interannual variability in the extratropics. On monthly time scales, the SAM, NAM and NAO are dominant in the extratropics. The NAM and NAO are closely related, and are mostly independent from the SAM, except perhaps on decadal time scales. Many other patterns can be explained through combinations of the NAM and PNA in the NH, and the SAM and PSA in the SH, plus ENSO-related global patterns. Both the NAM/NAO and the SAM have exhibited trends towards their positive phase (strengthened mid-latitude westerlies) over the last three to four decades, although both have returned to near their long-term mean state in the last five years. In the NH, this trend has been associated with the observed winter change in storm tracks, precipitation and temperature patterns. In the SH, SAM changes are related to contrasting trends of strong warming in the Antarctic Peninsula and a cooling over most of interior Antarctica. The increasing positive phase of the SAM has been linked to stratospheric ozone depletion and to greenhouse gas increases. Multi-decadal variability is also evident in the Atlantic, and appears to be related to the THC. Other teleconnection patterns discussed (PNA, PSA) exhibit decadal variations, but have not been shown to have systematic long-term changes.

ENSO has exhibited considerable inter-decadal variability in the past century, in association with the PDO (or IPO). Systematic changes in ENSO behaviour have also been observed, in particular the different evolution of ENSO events and enhanced El Niño activity since the 1976–1977 climate shift. Over North America, ENSO- and PNA-related changes appear to have led to contrasting changes across the continent, as the west has warmed more than the east, while the latter has become cloudier and wetter. Over the Indian Ocean, ENSO, monsoon and SAM variability are related to a zonal gradient of tropical SST associated with anomalous easterlies along the equator, and opposite precipitation and thermal anomalies in East Africa and over the Maritime Continent. The tropical Pacific variability is influenced by interactions with the tropical Atlantic and Indian Oceans, and by the extratropical North and South Pacific. Responses of the extratropical ocean become more important as the time scale is extended, and processes such as subduction, gyre changes and the THC come into play.

3.7 Changes in the Tropics and Subtropics, and in the Monsoons

The global monsoon system embraces an overturning circulation that is intimately associated with the seasonal variation of monsoon precipitation over all major continents and adjacent oceans (Trenberth et al., 2000). It involves the Hadley Circulation, the zonal mean meridional overturning mass flow between the tropics and subtropics entailing the Inter-Tropical Convergence Zone (ITCZ), and the Walker Circulation, which is the zonal east-west overturning. The South Pacific Convergence Zone (SPCZ) is a semi-permanent cloud band extending from around the Coral Sea southeastward towards the extratropical South Pacific, while the South Atlantic Convergence Zone (SACZ) is a more transient feature over and southeast of Brazil that transports moisture originating over the Amazon into the South Atlantic (Liebmann et al., 1999).

Tropical SSTs determine where the upward branch of the Hadley Circulation is located over the oceans, and the dominant variations in the energy transports by the Hadley cell, reflecting its strength, relate to ENSO (Trenberth et al., 2002a; Trenberth and Stepaniak, 2003a). During El Niño, elevated SST causes an increase in convection and relocation of the ITCZ and SPCZ to near the equator over the central and eastern tropical Pacific, with a tendency for drought conditions over Indonesia. There follows a weakening of the Walker Circulation and a strengthening of the Hadley Circulation (Oort and Yienger, 1996; Trenberth and Stepaniak, 2003a), leading to drier conditions over many subtropical regions during El Niño, especially over the Pacific sector. As discussed in Section 3.4.4.1, increased divergence of energy out of the tropics in the 1990s relative to the 1980s (Trenberth and Stepaniak, 2003a) is associated with more frequent El Niño events and especially the major 1997–1998 El Niño event, so these conditions play a role in inter-decadal variability (Gong and Ho, 2002; Mu et al., 2002; Deser et al., 2004). Examination of the Hadley Circulation in several data sets (Mitas and Clement, 2005) suggests some strengthening, although discrepancies among reanalysis data sets and known deficiencies raise questions about the robustness of this strengthening, especially prior to the satellite era (1979).

Monsoons are generally referred to as tropical and subtropical seasonal reversals in both the surface winds and associated precipitation. The strongest monsoons occur over the tropics of southern and eastern Asia and northern Australia, and parts of western and central Africa. Rainfall is the most important monsoon variable because the associated latent heat release drives atmospheric circulations, and because of its critical role in the global hydrological cycle and its vital socioeconomic impacts. Thus, other regions that have an annual reversal in precipitation with an intense rainy summer and a dry winter have been recently recognised as monsoon regions, even though these regions have no explicit seasonal reversal of the surface winds (Wang, 1994; Webster et al., 1998). The latter regions include Mexico and the southwest USA, and parts of South America and South Africa. Owing to the lack of sufficiently reliable and long-term oceanic observations, analyses of observed long-term changes have mainly relied on land-based rain gauge data.

Because the variability of regional monsoons is often the result of interacting circulations from other regions, simple indices of monsoonal strength in adjacent regions may give contradictory indications of strength (Webster and Yang, 1992; Wang and Fan, 1999). Decreasing trends in precipitation over the Indonesian Maritime Continent, equatorial parts of western and central Africa, Central America, Southeast Asia and eastern Australia have been found for 1948 to 2003 (Chen et al., 2004; see Figure 3.13), while increasing trends were evident over the USA and northwestern Australia (see also Section 3.3.2.2 and Figure 3.14), consistent with Dai et al. (1997). Using NRA, Chase et al. (2003) found diminished monsoonal circulations since 1950 and no trends since 1979, but results based on NRA suffer severely from artefacts arising from changes in the observing system (Kinter et al., 2004).

Two precipitation data sets (Chen et al., 2002; GHCN, see Section 3.3) yield very similar patterns of change in the seasonal precipitation contrasts between 1976 to 2003 and 1948 to 1975 (Figure 3.34), despite some differences in details and discrepancies in northwest India. Significant decreases in the annual range (wet minus dry season) were observed over the NH tropical monsoon regions (e.g., Southeast Asia and Central America). Over the East Asian monsoon region, the change over these periods involves increased rainfall in the Yangtze River valley and Korea but decreased rainfall over the lower reaches of the Yellow River and northeast China. In the Indonesian-Australian monsoon region, the change between the two periods is characterised by an increase in northwest Australia and Java but a decrease in northeast Australia and a northeastward movement in the SPCZ (Figure 3.34). However, the average monsoonal rainfall in East Asia, Indonesia-Australia and South America in summer mostly shows no long-term trend

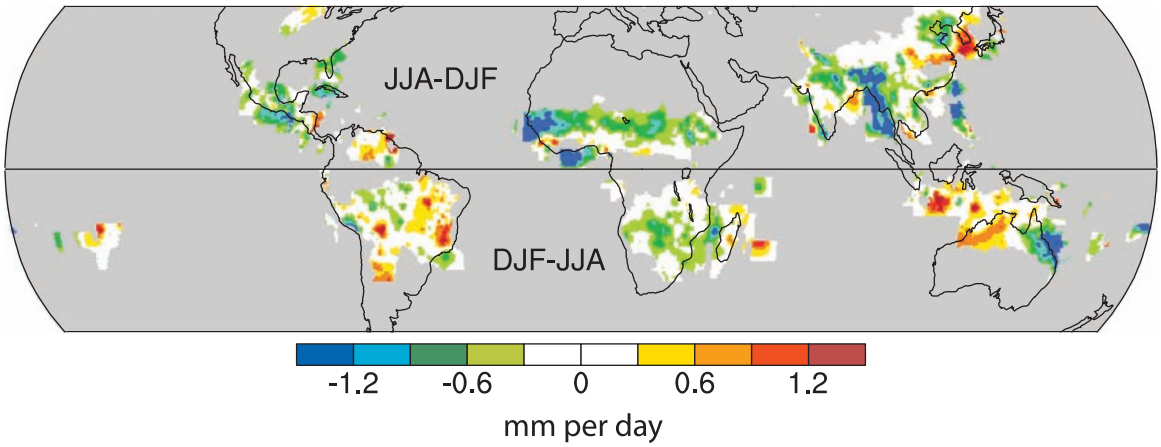


Figure 3.34. *Change in the mean annual range of precipitation: 1976 to 2003 minus 1948 to 1975 periods (mm per day). Blue/green (red/yellow) colour denotes a decreasing (increasing) annual range of the monsoon rainfall. Grey areas indicate missing values (oceans) or areas with insignificant annual changes. Data were from PREC/L (Chen et al., 2002; see Wang and Ding, 2006).*

but significant interannual and inter-decadal variations. In the South African monsoon region there is a slight decrease in the annual range of rainfall (Figure 3.34), and a decreasing trend in area-averaged precipitation (Figure 3.14).

Monsoon variability depends on many factors, from regional air-sea interaction and land processes (e.g., snow cover fluctuations) to teleconnection influences (e.g., ENSO, NAO/NAM, PDO, IOD). New evidence, relevant to climate change, indicates that increased aerosol loading in the atmosphere may have strong impacts on monsoon evolution (Menon et al., 2002) through changes in local heating of the atmosphere and land surface (see also Box 3.2 and Chapter 2).

3.7.1 Asia

The Asian monsoon can be divided into the East Asian and the South Asian or Indian monsoon systems (Ding et al., 2004). Based on a summer monsoon index derived from MSLP gradients between land and ocean in the East Asian region, Guo et al. (2003) found a systematic reduction in the East Asian summer monsoon during 1951 to 2000, with a stronger monsoon dominant in the first half of the period and a weaker monsoon prevailing in the second half (Figure 3.35). This long-term change in the East Asian monsoon index is consistent with a tendency for a southward shift of the summer rain belt over eastern China (Zhai et al., 2004). However, Figure 3.35, based on the newly developed Hadley Centre MSLP data set version 2 (HadSLP2; Allan and Ansell, 2006), suggests that although there exists a weakening trend starting in the 1920s, it is not reflected in the longer record extending back to the 1850s, which shows marked decadal-scale variability before the 1940s.

There is other evidence that changes in the Asian monsoon occurred about the time of the 1976–1977 climate shift (Wang, 2001) along with changes in ENSO (Huang et al., 2003; Qian et al., 2003), and declines in land precipitation are evident in southern Asia and, to some extent, in Southeast Asia (see Figure 3.14). Gong and Ho (2002) suggested that the change in summer rainfall over the Yangtze River valley was due to a southward rainfall shift and Ho et al. (2003) noted a sudden change in Korea. These occurred about the same time as a change in the 500 hPa geopotential height and typhoon tracks in summer over the northern Pacific (Gong et al., 2002; see Section 3.6.3) related to the enlargement, intensification and southwestward extension of the northwest Pacific subtropical high. When the equatorial central and eastern Pacific is in a decadal warm period, summer monsoon rainfall is stronger in the Yangtze River valley but weaker in North China. A strong tropospheric cooling trend is found in East Asia during July and August. Accompanying this summer cooling, the upper-level westerly jet stream over East Asia shifts southward and the East Asian summer monsoon weakens, which results in the tendency towards increased droughts in northern China and floods in the Yangtze River valley (Yu et al., 2004b).

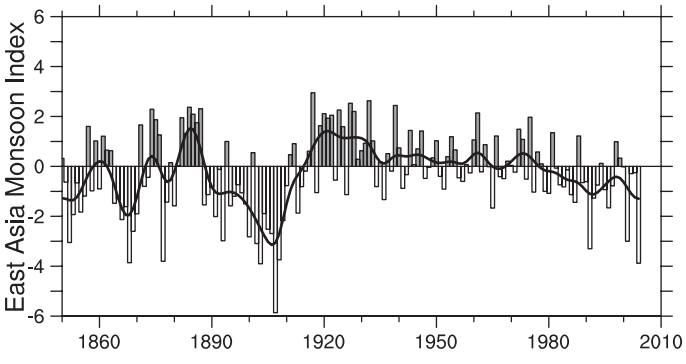


Figure 3.35. *Annual values of the East Asia summer monsoon index derived from MSLP gradients between land and ocean in the East Asia region. The definition of the index is based on Guo et al. (2003) but was recalculated based on the HadSLP2 (Allan and Ansell, 2006) data set. The smooth black curve shows decadal variations (see Appendix 3.A).*

Rainfall during the Indian monsoon season, which runs from June to September and accounts for about 70% of annual rainfall, exhibits decadal variability. Observational studies have shown that the impact of El Niño is more severe during the below-normal epochs, while the impact of La Niña is more severe during the above-normal epochs (Kripalani and Kulkarni, 1997a; Kripalani et al., 2001, 2003). Such modulation of ENSO impacts by the decadal monsoon variability was also observed in the rainfall regimes over Southeast Asia (Kripalani and Kulkarni, 1997b). Links between monsoon-related events (rainfall over South Asia, rainfall over East Asia, NH circulation, tropical Pacific circulation) weakened between 1890 and 1930 but strengthened during 1930 to 1970 (Kripalani and Kulkarni, 2001). The strong inverse relationship between El Niño events and Indian monsoon rainfalls that prevailed for more than a century prior to about 1976 has weakened substantially since then (Kumar et al., 1999; Krishnamurthy and Goswami, 2000; Sarkar et al., 2004), involving large-scale changes in atmospheric circulation. Shifts in the Walker Circulation and enhanced land-sea contrasts appear to be countering effects of increased El Niño activity. Ashok et al. (2001) also found that the IOD (see Section 3.6.7.2) plays an important role as a modulator of Indian rainfall. The El Niño-Southern Oscillation is also related to atmospheric fluctuations both in the Indian sector and in northeastern China (Kinter et al., 2002).

3.7.2 Australia

The Australian monsoon covers the northern third of continental Australia and surrounding seas and, considering its closely coincident location and annual evolution, is often studied in conjunction with the monsoon over the islands of Indonesia and Papua New Guinea. The Australian monsoon exhibits large interannual and intra-seasonal variability, largely associated with the effects of ENSO, the Madden-Julian Oscillation (MJO) and tropical cyclone activity (McBride, 1998; Webster et al., 1998; Wheeler and McBride, 2005). Using rain-gauge data, Hennessy et al. (1999) found an increase in calendar-year total rainfall in the Northern Territory of 18% from 1910 to 1995, attributed mostly to enhanced monsoon rainfall in the 1970s and coincident with an almost 20% increase in the number of rain

days. With data updated to 2002, Smith (2004) demonstrated that increased monsoon rainfall has become statistically significant over northern, western and central Australia. Northern Australian wet season rainfall (Jones et al., 2004), updated through 2004–2005 (Figure 3.36), shows the positive trend and the contribution of the anomalously wet period of the mid-1970s as well as the more recent anomalously wet period around 2000 (see also Smith, 2004). Wardle and Smith (2004) argued that the upward rainfall trend is consistent with the upward trend in land surface temperatures that has been observed in the south of the continent, independent of changes over the oceans. Strong decadal variations in Australian precipitation have also been noted (Figure 3.36). Using northeastern Australian rainfall, Latif et al. (1997) showed that rainfall was much increased during decades when the tropical Pacific was anomalously cold (the 1950s and 1970s). This strong relationship does not extend to the Australian monsoon as a whole, however, as the rainfall time series (Figure 3.36) has only a weak negative correlation (approximately –0.2) with the IPO. The fact that the long-term trends in rainfall and Pacific SSTs are both positive, the opposite of their interannual relationship (Power et al., 1998), explains only a portion of why the correlation is reduced at decadal time scales.

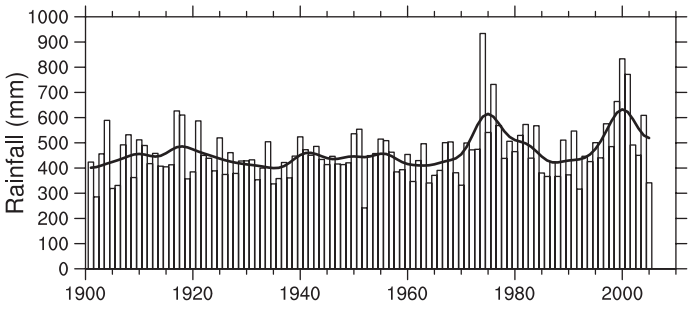


Figure 3.36. *Time series of northern Australian (north of 26°S) wet season (October–April) rainfall (mm) from 1900/1901 to 2004/2005. The individual bar corresponds to the January of the summer season (e.g., 1990 is the summer of 1989/1990). The smooth black curve shows decadal variations (see Appendix 3.A). Data from the Australian Bureau of Meteorology.*

3.7.3 The Americas

The North American Monsoon System (NAMS) is characterised by ocean-land contrasts including summer heating of higher-elevation mountain and plateau regions of Mexico and the southwestern USA, a large-scale upper-level anticyclonic circulation, a lower-level thermal low and a strong subsidence region to the west in the cool stratus regime of the eastern North Pacific (Vera et al., 2006). The NAMS contains a strong seasonal structure (Higgins and Shi, 2000), with rapid onset of monsoon rains in southwestern Mexico in June, a later northward progression into the southwest USA during its mature phase in July and August and a gradual decay in September and October.

Timing of the start of the northern portion of the NAMS has varied considerably, with some years starting as early as mid-June and others starting as late as early August (Higgins and Shi, 2000). Since part of NAMS variability is governed by larger-scale climate conditions, it is susceptible to interannual and multi-decadal variations. Higgins and Shi (2000) further suggested that the northern portion of the NAMS may be affected by the PDO, wherein anomalous winter precipitation over western North America is correlated with North American monsoon conditions in the subsequent summer.

The South American Monsoon System (SAMS) is evident over South America in the austral summer (Barros et al., 2002; Nogués-Paegle et al., 2002; Vera et al., 2006). It is a key factor for the warm season precipitation regime. In northern Brazil, different precipitation trends (see Figure 3.14 for the Amazon and southern South America regions) have been observed over northern and southern Amazonia, showing a dipole structure (Marengo, 2004) that suggests a southward shift of the SAMS. This is consistent with Rusticucci and Penalba (2000), who found a significant positive trend in the amplitude of the annual precipitation cycle, indicating a long-term climate change of the monsoon regime over the semi-arid region of the La Plata Basin. In addition, the mean wind speed of the low-level jet, a component of the SAMS that transports moisture from the Amazon to the south and southwest, showed a positive trend (Marengo et al., 2004). Positive SST anomalies in the western subtropical South Atlantic are associated with positive rainfall anomalies over the SACZ region (Doyle and Barros, 2002; Robertson et al., 2003). Barros et al. (2000b) found that, during summer, the SACZ was displaced northward (southward) and was more intense (weaker) with cold (warm) SST anomalies to its south. The convergence zone is modulated in part by surface features, including the gradient of SST over the equatorial Atlantic (Chang et al., 1999; Nogués-Paegle et al., 2002), and it modulates the interannual variability of seasonal rainfall over eastern Amazonia and northeastern Brazil (Nobre and Shukla, 1996; Folland et al., 2001).

3.7.4 Africa

Since the TAR, a variety of studies have firmly established that ENSO and SSTs in the Indian Ocean are the dominant sources of climate variability over eastern Africa (Goddard and Graham, 1999; Yu and Rienecker, 1999; Indeje et al., 2000; Clark et al., 2003). Further, Schreck and Semazzi (2004) isolated a secondary but significant pattern of regional climate variability based on seasonal (OND) rainfall data. In distinct contrast to the ENSO-related spatial pattern, the trend pattern in their analysis is characterised by positive rainfall anomalies over the northeastern sector of eastern Africa (Ethiopia, Somalia, Kenya and northern Uganda) and opposite conditions over the southwestern sector (Tanzania, southern parts of the Democratic Republic of the Congo and southwestern Uganda). This signal significantly strengthened in recent decades. Warming is associated with an earlier onset of the rainy season over the northeastern Africa region and a late start over the southern sector.

West Africa experiences marked multi-decadal variability in rainfall (e.g., Le Barbe et al., 2002; Dai et al., 2004b). Wet conditions in the 1950s and 1960s gave way to much drier conditions in the 1970s, 1980s and 1990s. The rainfall deficit in this region during 1970 to 1990 was relatively uniform across the region, implying that the deficit was not due to a spatial shift in the peak rainfall (Le Barbe et al., 2002) and was mainly linked to a reduction in the number of significant rainfall events occurring during the peak monsoon period (JAS) in the Sahel and during the first rainy season south of about 9°N. The decreasing rainfall and devastating droughts in the Sahel region during the last three decades of the 20th century (Figure 3.37) are among the largest climate changes anywhere. Dai et al. (2004b) provided an updated analysis of the normalised Sahel rainfall index based on the years 1920 to 2003 (Figure 3.37). Following the major 1982–1983 El Niño event, rainfall reached a minimum of 170 mm below the long-term mean of about 506 mm. Since 1982, there is some evidence for a recovery (see also lower panel of Figure 3.13) but despite this, the mean of the last decade is still well below the pre-1970 level. These authors also noted that large multi-year oscillations appear to be more frequent and extreme after the late 1980s than previously.

ENSO affects the West African monsoon, and the correlation between Sahel rainfall and ENSO during JJA varied between 1945 and 1993 (Janicot et al., 2001). The correlation was always negative but was not significant during the 1960s to the mid-1970s when the role of the tropical Atlantic was relatively more important. Years when ENSO has a larger impact tend to be associated with same-signed rainfall anomalies over the West African region whereas years when the tropical Atlantic is more important tend to have a so-called anomalous 'dipole' pattern, with the Sahel and Guinea Coast having opposite-signed rainfall anomalies (Ward, 1998). Giannini et al. (2003) suggested that both interannual and decadal variability of Sahel rainfall results from the response of the African summer monsoon to oceanic forcing, amplified by land-atmosphere interaction.

While other parts of Africa have experienced statistically significant weakening of the monsoon circulation, analyses of long-term southern African rainfall totals in the wet season (JFM) have reported no trends (Fauchereau et al., 2003). Decreases in rainfall are evident in analyses of shorter periods, such as the decade from 1986 to 1995 that was the driest of the 20th century. New et al. (2006) reported a decrease in average rainfall intensity and an increase in dry spell length (number of consecutive dry days) for 1961 to 2000.

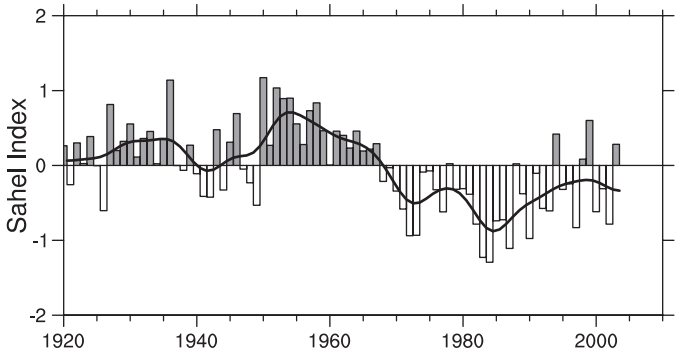


Figure 3.37. *Time series of Sahel (10ºN –20ºN, 18ºW–20ºE) regional rainfall (April–October) from 1920 to 2003 derived from gridding normalised station anomalies and then averaging using area weighting (adapted from Dai et al., 2004a). The smooth black curve shows decadal variations (see Appendix 3.A).*

3.7.5 Summary

Variability at multiple time scales strongly affects monsoon systems. Large interannual variability associated with ENSO dominates the Hadley and Walker Circulations, the ITCZ and monsoons. There is also good evidence for decadal changes associated with monsoonal rainfall changes in many monsoon systems, especially across the 1976–1977 climate shift, but data uncertainties compromise evidence for trends. Some monsoons, especially the East Asian monsoon system, have experienced a dipole change in precipitation with increases in one region and decreases in the other during the last 50 years.

3.8 Changes in Extreme Events

3.8.1 Background

There is increasing concern that extreme events may be changing in frequency and intensity as a result of human influences on climate. Climate change may be perceived most through the impacts of extremes, although these are to a large degree dependent on the system under consideration, including its vulnerability, resiliency and capacity for adaptation and mitigation; see the Working Group II contribution to the IPCC Fourth Assessment Report. Improvements in technology mean that people hear about extremes in most parts of the world within a few hours of their occurrence. Pictures shot by camcorders on the news may foster a belief that weather-related extremes are increasing in frequency, whether they are or not. An extreme weather event becomes a disaster when society and/or ecosystems are unable to cope with it effectively. Growing human vulnerability (due to growing numbers of people living in exposed and marginal areas or due to the development of more high-value property in high-risk zones) is increasing the risk, while human endeavours (such as by local governments) try to mitigate possible effects.

The assessment of extremes in this section is based on long-term observational series of weather elements. As in the TAR, extremes refer to rare events based on a statistical model of particular weather elements, and changes in extremes may relate to changes in the mean and variance in complicated ways. Changes in extremes are assessed at a range of temporal and spatial scales, for example, from extremely warm years globally to peak rainfall intensities locally, and examples are given in Box 3.6. To span this entire range, data are required at a daily (or shorter) time scale. However, the availability of

observational data restricts the types of extremes that can be analysed. The rarer the event, the more difficult it is to identify long-term changes, simply because there are fewer cases to evaluate (Frei and Schär, 2001; Klein Tank and Können, 2003). Identification of changes in extremes is also dependent on the analysis technique employed (Zhang et al., 2004a; Trömel and Schönwiese, 2005). To avoid excessive statistical limitations, trend analyses of extremes have traditionally focused on standard and robust statistics that describe moderately extreme events. In percentile terms, these are events occurring between 1 and 10% of the time at a particular location in a particular reference period (generally 1961 to 1990). Unless stated otherwise, this section focuses on changes in these extremes.

Global studies of daily temperature and precipitation extremes over land (e.g., Frich et al., 2002; see also the TAR) suffer from both a scarcity of data and regions with missing data. The main reason is that in various parts of the globe there is a lack of homogeneous observational records with daily | resolution covering multiple decades that are part of integrated digitised data sets (GCOS, 2003). In addition, existing records are often inhomogeneous; for instance as a result of changes in observing practices or UHI effects (DeGaetano and Allen, 2002; Vincent et al., 2002; Wijngaard et al., 2003). This affects, in particular, the understanding of extremes, because changes in extremes are often more sensitive to inhomogeneous climate monitoring practices than changes in the mean (see Appendix 3.B.2 and 3.B.4). Consistent observing is also a problem when assessing long-term changes in the frequency and severity of tropical and extratropical storms. Similar difficulties are encountered when trying to find worldwide observational evidence for changes in severe local weather events like tornadoes, hail, thunderstorms and dust storms. Analyses of trends in extremes are also sensitive to the analysis period, for example, the inclusion of the exceptionally hot European summer of 2003 may have a marked influence on results if the period is short.

Since the TAR, the situation with observational data sets has improved, although efforts to update and exchange data must be continued (e.g., GCOS, 2004). Results are now available from newly established regional- and continental-scale daily data sets; from denser networks, from temporally more extended high-quality time series and from many existing national data archives, which have been expanded to cover longer time periods. Moreover, the systematic use and exchange of time series of standard indices of extremes, with common definitions, provides an unprecedented global picture of changes in daily temperature and precipitation extremes (Alexander et al., 2006, updating the results of Frich et al., 2002 presented in the TAR).

As an alternative, but not independent data source, reanalyses can also be analysed for changes in extremes (see Appendix 3.B.5.4). Although spatially and temporally complete, under-representation of certain types of extremes (Kharin and Zwiers, 2000) and spurious trends in the reanalyses (especially in the tropics and in the SH) remain problematic, in particular before the start of the modern satellite era in 1979 (Marshall, 2002, 2003; Sturaro, 2003; Sterl, 2004; Trenberth et al., 2005a). For instance, Bengtsson et al. (2004) found that analysed global kinetic energy rose by almost 5% in 1979 as a direct consequence of the inclusion of improved satellite information over the oceans, which is expected to significantly affect analysed storm activity over the southern oceans, where ship data are sparse.

In this section, observational evidence for changes in extremes is assessed for temperature, precipitation, tropical and extratropical cyclones and severe local weather events. Most studies of extremes consider the period since about 1950 with even greater emphasis on the last few decades (since 1979), although longer data sets exist for a few regions, enabling more recent events to be placed in a longer context. The section discusses mostly the changes observed in the daily weather elements, where most progress has been made since the TAR. Droughts (although they are considered extremes) are covered in Section 3.3.4 as they are more related to longer periods of anomalous climate.

3.8.2 Evidence for Changes in Variability or Extremes

3.8.2.1 Temperature

For temperature extremes in the 20th century, the TAR highlighted the lengthening of the growing or frost-free season in most mid- and high-latitude regions, a reduction in the frequency of extreme low monthly and seasonal average temperatures and smaller increases in the frequency of extreme high average temperatures. In addition, there was evidence to suggest a decrease in the intra-annual temperature variability with consistent reductions in frost days and increases in warm nighttime temperatures across much of the globe.

Evidence for changes in observed interannual variability (such as standard deviations of seasonal averages) is still sparse. Scherrer et al. (2005) investigated standardised distribution changes for seasonal mean temperature in central Europe and found that temperature variability showed a weak increase (decrease) in summer (winter) for 1961 to 2004, but these changes are not statistically significant at the 10% level. On the daily time scale, regional studies have been completed for southern South America (Vincent et al., 2005), Central America and northern South America (Aguilar et al., 2005), the Caribbean (Peterson et al., 2002), North America (Kunkel et al., 2004; Vincent and Mekis, 2006), the Arctic (Groisman et al., 2003), central and northern Africa (Easterling et al., 2003), southern and western Africa (New et al., 2006), the Middle East (Zhang et al., 2005), Western Europe and east Asia (Kiktev et al., 2003), Australasia and southeast Asia (Griffiths et al., 2005), China (Zhai and Pan, 2003) and central and southern Asia (Klein Tank et al., 2006). They all show patterns of changes in extremes consistent with a general warming, although the observed changes of the tails of the temperature distributions are often more complicated than a simple shift of the entire distribution would suggest (see Figure 3.38). In addition, uneven trends are observed for nighttime and daytime

temperature extremes. In southern South America, significant increasing trends were found in the occurrence of warm nights and decreasing trends in the occurrence of cold nights, but no consistent changes in the indices based on daily maximum temperature. In Central America and northern South America, high extremes of both minimum and maximum temperature have increased. Warming of both the nighttime and daytime extremes was also found for the other regions where data have been analysed. For Australasia and Southeast Asia, the dominant distribution change at rural stations for both maximum and minimum temperature involved a change in the mean, affecting either one or both distribution tails, with no significant change in standard deviation (Griffiths et al., 2005). For urbanised stations, however, the dominant change also involved a change in the standard deviation. This result was particularly evident for minimum temperature.

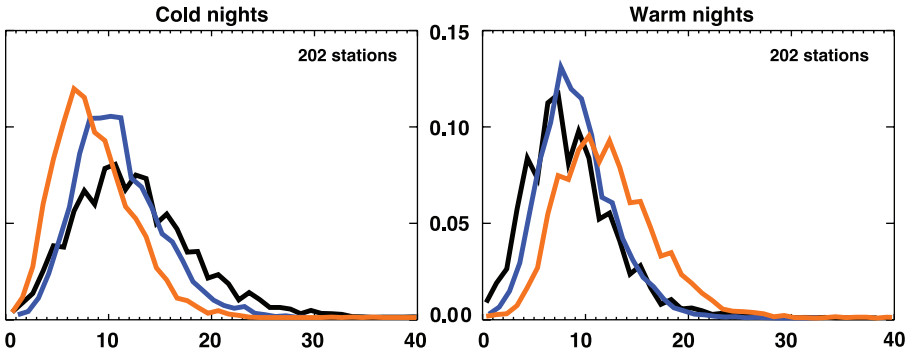


Figure 3.38. *Annual probability distribution functions for temperature indices for 202 global stations with at least 80% complete data between 1901 and 2003 for three time periods: 1901 to 1950 (black), 1951 to 1978 (blue) and 1979 to 2003 (red). The x-axis represents the percentage of time during the year when the indicators were below the 10th percentile for cold nights (left) or above the 90th percentile for warm nights (right). From Alexander et al. (2006).*

Few other studies have considered mutual changes in both the high and low tail of the same daily (minimum, maximum or mean) temperature distribution. Klein Tank and Können (2003) analysed such changes over Europe using standard indices, and found that the annual number of warm extremes (above the 90th percentile for 1961 to 1990) of the daily minimum and maximum temperature distributions increased twice as fast during the last 25 years than expected from the corresponding decrease in the number of cold extremes (lowest 10%). Moberg and Jones (2005) found that both the high and the low tail (defined by the 90th and 10th percentile) of the daily minimum and maximum temperature distribution over Europe in winter increased over the 20th century as a whole, with the low tail of minimum temperature warming significantly in summer. For an even longer period, Yan et al. (2002) found decreasing warm extremes in Europe and China up to the late 19th century, decreasing cold extremes since then, and increasing warm extremes only since 1961, especially in summer (JJA). Brunet et al. (2006) analysed 22 Spanish records for the period 1894 to 2003 and found greater reductions in the number of cold days than increases in hot days. However, since 1973 warm days have been rising dramatically, particularly near the Mediterranean coast. Beniston and Stephenson (2004) showed that changes in extremes of daily temperature in Switzerland were due to changes in both the mean and the variance of the daily temperatures. Vincent and Mekis (2006) found progressively fewer extreme cold nights and cool days but more extreme warm nights and hot days for Canada from 1900 to 2003 and Robeson (2004) found intense warming of the lowest daily minimum temperatures over western and central North America. In Argentina, the strong positive changes in minimum temperature seen during 1959 to 1998 were associated with significant increases in the frequency of warm nights; there were also decreases in cold days (Rusticucci and Barrucand, 2004).

Alexander et al. (2006) and Caesar et al. (2006) have brought all these and other regional results together, gridding the common indices or data for the period since 1946. Over 74% of the global land area sampled showed a significant decrease in the annual occurrence of cold nights; a significant increase in the annual occurrence of warm nights took place over 73% of the area (Table 3.6, Figure 3.38 and FAQ 3.3). This implies a positive shift in the distribution of daily minimum temperature T_{min} throughout the globe. Changes in the occurrence of cold and warm days show warming as well, but generally less marked. This is consistent with T_{min} increasing more than maximum temperature T_{max}, leading to a reduction in DTR since 1951 (see Sections 3.2.2.1 and 3.2.2.7). The change in the four extremes indices (Table 3.6) also show that the distribution of T_{min} and T_{max} have not only shifted, but also changed in shape. The indices for the number of cold and warm events have changed almost equally, which for a near-Gaussian distributed quantity indicates that the cold tails of the distributions have warmed considerably more than the warm tails over the last 50 years. Considering the last 25 years only, such a change in shape is not seen (Table 3.6).

3.8.2.2 Precipitation

The conceptual basis for changes in precipitation has been given by Allen and Ingram (2002) and Trenberth et al. (2003; see Section 3.3 and FAQ 3.2). Issues relate to changes in type, amount, frequency, intensity and duration of precipitation. Observed increases in atmospheric water vapour (see Section 3.4.2) imply increases in intensity, but this will lead to reduced frequency or duration if the total evaporation rate from the Earth's surface (land and ocean) is unchanged. The TAR states that it is likely that there has been a statistically significant 2 to 4% increase in the frequency of heavy and extreme precipitation events when averaged across the middle and high latitudes. Since then a more refined understanding of the observed changes in precipitation extremes has been achieved.

Table 3.6. *Global trends in extremes of temperature and precipitation as measured by the 10th and 90th percentiles (for 1961–1990). Trends with 5 and 95% confidence intervals and levels of significance (**bold**: <1%) were estimated by REML (see Appendix 3.A), which allows for serial correlation in the residuals of the data about the linear trend. All trends are based on annual averages. Values are % per decade. Based on Alexander et al. (2006).*

Series	Trend (% per decade) 1951–2003	1979–2003
TN10: % incidence of T_{min} below coldest decile.	**–1.17 ± 0.20**	**–1.24 ± 0.44**
TN90: % incidence of T_{min} above warmest decile.	**1.43 ± 0.42**	**2.60 ± 0.81**
TX10: % incidence of T_{max} below coldest decile.	**–0.63 ± 0.16**	**–0.91 ± 0.48**
TX90: % incidence of T_{max} above warmest decile.	**0.71 ± 0.35**	**1.74 ± 0.72**
PREC: % contribution of very wet days (above the 95th percentile) to the annual precipitation total.	**0.21 ± 0.10**	0.41 ± 0.38

Many analyses indicate that the evolution of rainfall statistics through the second half of the 20th century is dominated by variations on the interannual to inter-decadal time scale and that trend estimates are spatially incoherent (Manton et al., 2001; Peterson et al., 2002; Griffiths et al., 2003; Herath and Ratnayake, 2004). In Europe, there is a clear majority of stations with increasing trends in the number of moderately and very wet days (defined as wet days (≥1 mm of rain) that exceed the 75th and 95th percentiles, respectively) during the second half of the 20th century (Klein Tank and Können, 2003; Haylock and Goodess, 2004). Similarly, for the contiguous USA, Kunkel et al. (2003) and Groisman et al. (2004) confirmed earlier results and found statistically significant increases in heavy (upper 5%) and very heavy (upper 1%) precipitation of 14 and 20%, respectively. Much of this increase occurred during the last three decades of the 20th century and is most apparent over the eastern parts of the country. In addition, there is new evidence from Europe and the USA that the relative increase in precipitation extremes is larger than the increase in mean precipitation, and this is manifested as an increasing contribution of heavy events to total precipitation (Klein Tank and Können, 2003; Groisman et al., 2004).

Despite a decrease in mean annual rainfall, an increase in the fraction from heavy events was inferred for large parts of the Mediterranean (Alpert et al., 2002; Brunetti et al., 2004; Maheras et al., 2004). Further, Kostopoulou and Jones (2005) noted contrasting trends of heavy rainfall events between an increase in the central Mediterranean (Italy) and a decrease over the Balkans. In South Africa, Siberia, central Mexico, Japan and the northeastern part of the USA, an increase in heavy precipitation was also observed, while total precipitation and/or the frequency of days with an appreciable amount of precipitation (wet days) was either unchanged or decreasing (Easterling et al., 2000; Fauchereau et al., 2003; Sun and Groisman, 2004; Groisman et al., 2005).

A number of recent regional studies have been completed for southern South America (Haylock et al., 2006), Central America and northern South America (Aguilar et al., 2005), southern and western Africa (New et al., 2006), the Middle East (Zhang et al., 2005) and central and southern Asia (Klein Tank et al., 2006). For southern South America, the pattern of trends for extremes between 1960 and 2000 was generally the same as that for total annual rainfall (Haylock et al., 2006). A majority of stations showed a change to wetter conditions, related to the generally lower value of the SOI since 1976/1977, with the exception of southern Peru and southern Chile, where a decrease was observed in many precipitation indices. In the latter region, the change in ENSO has led to a weakening of the continental trough resulting in a southward shift in storm tracks and an important effect on the observed rainfall trends. No significant increases in total precipitation amounts were found over Central America and northern South America (see also Figure 3.14), but rainfall intensities have increased related to changes in SST of tropical Atlantic waters. Over southern and western Africa, and the Middle East, there are no spatially coherent patterns of statistically significant trends in precipitation indices. Averaged over central and southern Asia, a slight indication of disproportionate changes in the precipitation extremes compared with the total amounts is seen. In the Indian sub-continent Sen Roy and Balling (2004) found that about two- thirds of all considered time series exhibit increasing trends in indices of precipitation extremes and that there are coherent regions with increases and decreases.

Alexander et al. (2006) also gridded the extreme indices for precipitation (as for temperature in Section 3.8.2.1). Changes in precipitation extremes are much less coherent than for temperature, but globally averaged over the land area with sufficient data, the percentage contribution to total annual precipitation from very wet days (upper 5%) is greater in recent decades than earlier decades (Figure 3.39, top panel, and Table 3.6, last line). Observed changes in intense precipitation (with geographically varying thresholds between the 90th and 99.9th percentile of daily precipitation events) for more than one half of the global land area indicate an increasing probability of intense precipitation events beyond that expected from changes in the mean for many extratropical regions (Groisman et al., 2005; Figure 3.39, bottom panel). This finding supports the disproportionate changes in the precipitation extremes described in the majority of regional studies above, in particular for the mid-latitudes since about 1950. It is still difficult to draw a consistent picture of changes in the tropics and the subtropics,

where many areas are not analysed and data are not readily available.

As well as confirming previous findings, the new analyses provide seasonal detail and insight into longer-term variations for the mid-latitudes. While the increase in the USA is found primarily in the warm season (Groisman et al., 2004), central and northern Europe exhibited changes primarily in winter (DJF) and changes were insignificant in summer (JJA), but the studies did not include the extreme European summers of 2002 (very wet) and 2003 (very dry) (Osborn and Hulme, 2002; Haylock and Goodess, 2004; Schmidli and Frei, 2005). Although data are not as good, the frequencies of precipitation extremes in the USA were at comparable levels from 1895 into the early 1900s and during the 1980s to 1990s (Kunkel et al., 2003). For Canada (excluding the high-latitude Arctic), Zhang et al. (2001a) and Vincent and Mekis (2006) found that the frequency of precipitation days significantly increased during the 20th century, but averaged for the country as a whole, there is no identifiable trend in precipitation extremes. Nevertheless, Groisman et al. (2005) found significant increases in the frequency of heavy and very heavy (between the 95th and 99.7th percentile of daily precipitation events) precipitation in British Columbia south of 55°N for 1910 to 2001, and in other areas (Figure 3.39, bottom panel).

Since the TAR, several regional analyses have been undertaken for statistics with return periods much longer than in the previous studies. For the UK, Fowler and Kilsby (2003a,b), using extreme value statistics, estimated that the recurrence of 10-day precipitation totals with a 50-year return period (based on data for 1961 to 1990) had increased by a factor of two to five by the 1990s in northern England and Scotland. Their results for long return periods are qualitatively similar to changes obtained for traditional (moderate) statistics (Osborn et al., 2000; Osborn and Hulme, 2002), but there are differences in the relative magnitude of the change between seasons (Fowler and Kilsby, 2003b). For the contiguous USA, Kunkel et al. (2003) and Groisman et al. (2004) analysed return periods of 1 to 20 years, and interannual to inter-decadal variations during the 20th century exhibit a high correlation between all return periods. Similar results were obtained for several extratropical regions (Groisman et al., 2005), including the central USA, the northwestern coast of North America, southern Brazil, Fennoscandia, the East European Plain, South Africa, southeastern Australia and Siberia. In summary, from the available analyses there is evidence that the changes at the extreme tail of the distribution (several-decade return periods) are consistent with changes inferred for more robust statistics based on percentiles between the 75th and 95th levels, but practically no regions have sufficient data to assess such trends reliably.

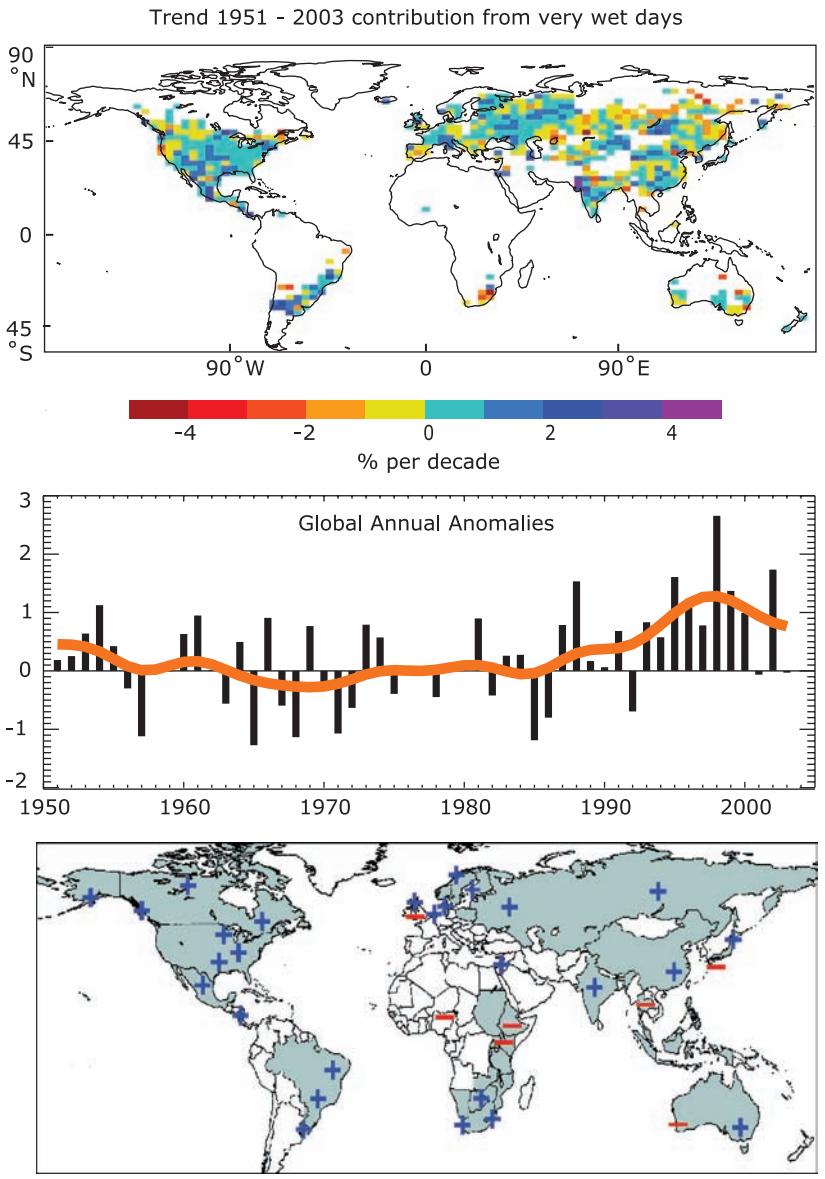


Figure 3.39. *(Top) Observed trends (% per decade) for 1951 to 2003 in the contribution to total annual precipitation from very wet days (95th percentile). Trends were only calculated for grid boxes where both the total and the 95th percentile had at least 40 years of data during this period and had data until at least 1999. (Middle) Anomalies (%) of the global annual time series (with respect to 1961 to 1990) defined as the percentage change of contributions of very wet days from the base period average (22.5%). The smooth orange curve shows decadal variations (see Appendix 3.A). From Alexander et al. (2006). (Bottom) Regions where disproportionate changes in heavy and very heavy precipitation during the past decades were documented as either an increase (+) or decrease (–) compared to the change in the annual and/or seasonal precipitation (updated from Groisman et al., 2005). Thresholds used to define "heavy" and "very heavy" precipitation vary by season and region. However, changes in heavy precipitation frequencies are always greater than changes in precipitation totals and, in some regions, an increase in heavy and/or very heavy precipitation occurred while no change or even a decrease in precipitation totals was observed.*

3.8.3 Evidence for Changes in Tropical Storms

The TAR noted that evidence for changes in tropical cyclones (both in number and in intensity) across the various ocean basins is often hampered by classification changes. In addition, considerable inter-decadal variability reduces significance of any long-term trends. Careful interpretation of observational records is therefore required. Traditional measures of tropical cyclones, hurricanes and typhoons have varied in different regions of the globe, and typically have required thresholds of estimated wind speed to be crossed for the system to be called a tropical storm, named storm, cyclone, hurricane or typhoon, or major hurricane or super typhoon. Many other measures or terms exist, such as 'named storm days', 'hurricane days', 'intense hurricanes', 'net tropical cyclone activity', and so on.

The ACE index (see Box 3.5), is essentially a wind energy index, defined as the sum of the squares of the estimated six-hour maximum sustained wind speed (knots) for all named systems while they are at least tropical storm strength. Since this index represents a continuous spectrum of both system duration and intensity, it does not suffer as much from the discontinuities inherent in more widely used measures of activity such as the number of tropical storms, hurricanes or major hurricanes. However, the ACE values reported here are not adjusted for known inhomogeneities in the record (discussed below). The ACE index is also used to define above-, near-, and below-normal hurricane seasons (based on the 1981 to 2000 period). The index has the same meaning in every region. Figure 3.40 shows the ACE index for six regions (adapted from Levinson, 2005, and updated through early 2006). Prior to about 1970, there was no satellite imagery to help estimate the intensity and size of tropical storms, so the estimates of ACE are less reliable, and values are not given prior to about the mid- or late 1970s in the Indian Ocean, South Pacific or Australian regions. Values are given for the Atlantic and two North Pacific regions after 1948, although reliability improves over time, and trends contain unquantified uncertainties.

The Potential Intensity (PI) of tropical cyclones (Emanuel, 2003) can be computed from observational data based primarily on vertical profiles of temperature and humidity (see Box 3.5) and on SSTs. In analysing CAPE (see Box 3.5) from selected radiosonde stations throughout the tropics for the period 1958 to 1997, Gettelman et al. (2002) found mostly positive trends. DeMott and Randall (2004) found more mixed results, although their data may have been contaminated by spurious adjustments (Durre et al., 2002). Further, Free et al. (2004a) found that trends in PI were small and statistically insignificant at a scattering of stations in the tropics. As all of these studies were probably contaminated by problems with tropical radiosondes (Sherwood et al., 2005; Randel and Wu, 2006; see Section 3.4.1 and Appendix 3.B.5), definitive results are not available.

The PDI index of the total power dissipation for the North Atlantic and western North Pacific (Emanuel, 2005a; see also Box 3.5) showed substantial upward trends beginning in the mid-1970s. Because the index depends on wind speed cubed, it is very sensitive to data quality, and the initial Emanuel (2005a) report has been revised to show the PDI increasing by about 75% (vs. about 100%) since the 1970s (Emanuel, 2005b). The

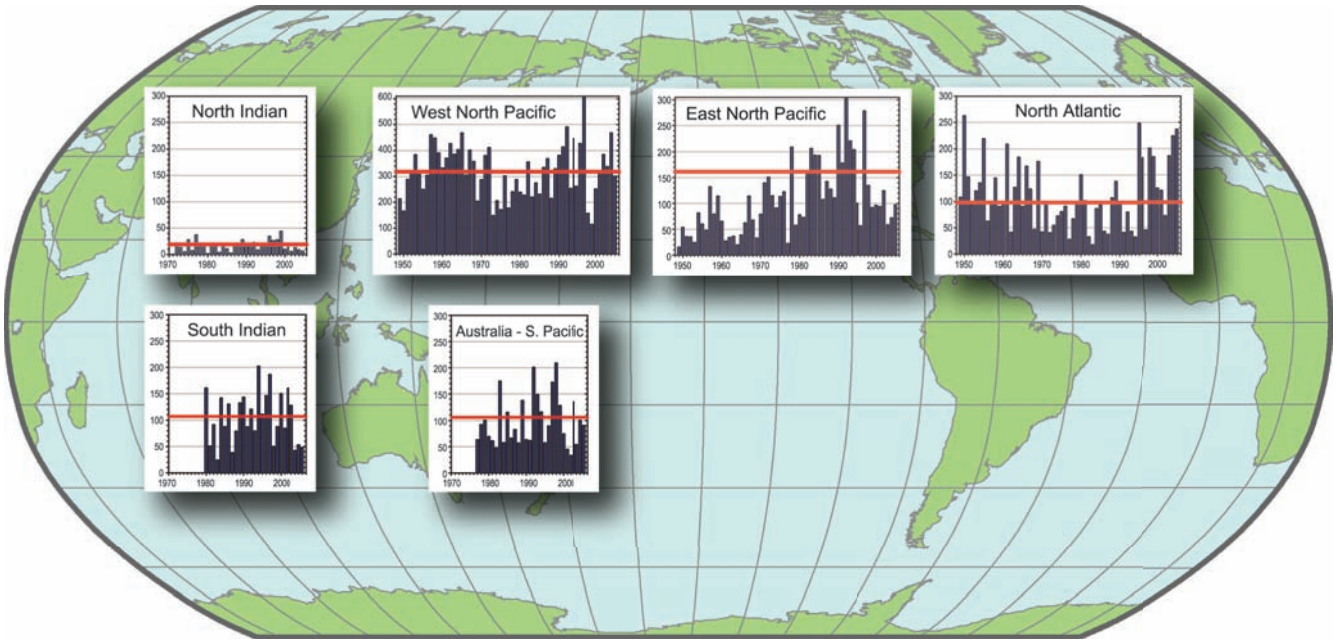


Figure 3.40. *Seasonal values of the ACE index for the North Indian, South Indian, West North Pacific, East North Pacific, North Atlantic and combined Australian-South Pacific regions. The vertical scale in the West North Pacific is twice as large as that of other basins. The SH values are those for the season from July the year before to June of the year plotted. The timeline runs from 1948 or 1970 through 2005 in the NH and through June 2006 in the SH. The ACE index accounts for the combined strength and duration of tropical storms and hurricanes during a given season by computing the sum of squares of the six-hour maximum sustained surface winds in knots while the storm is above tropical storm intensity. Adapted and updated from Levinson (2005).*

Box 3.5: Tropical Cyclones and Changes in Climate

In the summer tropics, outgoing longwave radiative cooling from the surface to space is not effective in the high water vapour, optically thick environment of the tropical oceans. Links to higher latitudes are weakest in the summer tropics, and transports of energy by the atmosphere, such as occur in winter, are also not an effective cooling mechanism, while monsoonal circulations between land and ocean redistribute energy in areas where they are active. However, tropical storms cool the ocean surface through mixing with cooler deeper ocean layers and through evaporation. When the latent heat is realised in precipitation in the storms, the energy is transported high into the troposphere where it can radiate to space, with the system acting somewhat like a Carnot cycle (Emanuel, 2003). Hence, tropical cyclones appear to play a key role in alleviating the heat from the summer Sun over the oceans.

As the climate changes and SSTs continue to increase (see Section 3.2.2.3), the environment in which tropical storms form is changed. Higher SSTs are generally accompanied by increased water vapour in the lower troposphere (see Section 3.4.2.1 and Figure 3.20), thus the moist static energy that fuels convection and thunderstorms is also increased. Hurricanes and typhoons currently form from pre-existing disturbances only where SSTs exceed about 26°C and, as SSTs have increased, it thereby potentially expands the areas over which such storms can form. However, many other environmental factors also influence the generation and tracks of disturbances, and wind shear in the atmosphere greatly influences whether or not these disturbances can develop into tropical storms. The El Niño-Southern Oscillation and variations in monsoons as well as other factors also affect where storms form and track (e.g., Gray, 1984). Whether the large-scale thermodynamic environment and atmospheric static stability (often measured by Convective Available Potential Energy, CAPE) becomes more favourable for tropical storms depends on how changes in atmospheric circulation, especially subsidence, affect the static stability of the atmosphere, and how the wind shear changes. The potential intensity, defined as the maximum wind speed achievable in a given thermodynamic environment (e.g., Emanuel, 2003), similarly depends critically on SSTs and atmospheric structure. The tropospheric lapse rate is maintained mostly by convective transports of heat upwards, in thunderstorms and thunderstorm complexes, including mesoscale disturbances, various waves and tropical storms, while radiative processes serve to cool the troposphere. Increases in greenhouse gases decrease radiative cooling aloft, thus potentially stabilising the atmosphere. In models, the parametrization of sub-grid scale convection plays a critical role in determining whether this stabilisation is realised and whether CAPE is released or not. All of these factors, in addition to SSTs, determine whether convective complexes become organised as rotating storms and form a vortex.

While attention has often been focussed simply on the frequency or number of storms, the intensity, size and duration likely matter more. NOAA's Accumulated Cyclone Energy (ACE) index (Levinson and Waple, 2004) approximates the collective intensity and duration of tropical storms and hurricanes during a given season and is proportional to maximum surface sustained winds squared. The power dissipation of a storm is proportional to the wind speed cubed (Emanuel, 2005a), as the main dissipation is from surface friction and wind stress effects, and is measured by a Power Dissipation Index (PDI). Consequently, the effects of these storms are highly nonlinear and one big storm may have much greater impacts on the environment and climate system than several smaller storms.

From an observational perspective then, key issues are the tropical storm formation regions, the frequency, intensity, duration and tracks of tropical storms, and associated precipitation. For landfalling storms, the damage from winds and flooding, as well as storm surges, are especially of concern, but often depend more on human factors, including whether people place themselves in harm's way, their vulnerability and their resilience through such things as building codes.

increase comes about because of longer storm lifetimes and greater storm intensity, and the index is strongly correlated with tropical SST. These relationships have been reinforced by Webster et al. (2005, 2006) who found a large increase in numbers and proportion of hurricanes reaching categories 4 and 5 globally since 1970 even as the total number of cyclones and cyclone days decreased slightly in most basins. The largest increase was in the North Pacific, Indian and Southwest Pacific Oceans.

These studies have been challenged by several scientists (e.g., Landsea, 2005; Chan, 2006) who have questioned the quality of the data and the start date of the 1970s. In addition, different centres may assign different intensities to the same storm. The historical record typically records the central pressure and the maximum winds, but these turn out not to be physically consistent in older records, mainly prior to about the early 1970s. However, attempts at mutual adjustments result in increases in some years and decreases in others, with little effect on overall trends. In particular, in the satellite era after about 1970, the trends found by Emanuel (2005a) and Webster et al. (2005) appear to be robust in strong association with higher SSTs (Emanuel, 2005b). There is no doubt that active periods have occurred in the more distant past, notably in the North Atlantic (see below), but the PDI was evidently not as high in the earlier years (Emanuel, 2005a).

There is a clear El Niño connection in most regions, and strong negative correlations between regions in the Pacific and Atlantic, so that the total tropical storm activity is more nearly constant than ACE values in any one basin. During an El Niño event, the incidence of hurricanes typically decreases in the Atlantic (Gray, 1984; Bove et al., 1998) and far western Pacific and Australian regions, while it increases in the central North and South Pacific and especially in the western North Pacific typhoon region (Gray, 1984; Lander, 1994; Kuleshov and de

Hoedt, 2003; Chan and Liu, 2004), emphasizing the change in locations for tropical storms to preferentially form and track with ENSO. Formation and tracks of tropical storms favour either the Australian or South Pacific region depending on the phase of ENSO (Basher and Zheng, 1995; Kuleshov and de Hoedt, 2003), and these two regions have been combined.

The ACE values have been summed over all regions to produce a global value, as given in Klotzbach (2006), beginning in 1986. The highest ACE year through 2005 is 1997, when a major El Niño event began and surface temperatures were subsequently the highest on record (see Section 3.2), and this is followed by 1992, a moderate El Niño year. Such years contain low values in the Atlantic, but much higher values in the Pacific, and they highlight the critical role of SSTs in the distribution and formation of hurricanes. Next in ranking are 1994 and 2004, while 2005 is close to the 1981 to 2000 mean. The PDI also peaks in the late 1990s about the time of the 1997–1998 El Niño for the combined Atlantic and West Pacific regions, although 2004 is almost as high. Webster et al. (2005) found that numbers of intense (category 4 and 5) hurricanes after 1990 are much greater than from 1970 to 1989. Klotzbach (2006) considers ACE values only from 1986 and his record is not long enough to provide reliable trends, given the substantial variability.

3.8.3.1 Western North Pacific

In the western North Pacific, long-term trends are masked by strong inter-decadal variability for 1960 to 2004 (Chan and Liu, 2004; Chan, 2006), but results also depend on the statistics used and there are uncertainties in the data prior to the mid-1980s (Klotzbach, 2006). Further increases in activity have occurred in the last few years after Chan and Liu (2004) was completed (Figure 3.40). Tropical cyclones making landfall in China are a small fraction of the total storms, and no obvious long-term trend can be discerned (He et al., 2003; Liu and Chan, 2003; Chan and Liu, 2004). However, Emanuel (2005a) and Webster et al. (2005, 2006) indicated that the typhoons have become more intense in this region, with almost a doubling of PDI values since the 1950s and an increase of about 30% in the number of category 4 and 5 storms from 1990 to 2004 compared with 1975 to 1989. The post-1985 record analysed by Klotzbach (2006) is too short to provide reliable trends.

The main modulating influence on tropical cyclone activity in the western North Pacific appears to be the changes in atmospheric circulation associated with ENSO, rather than local SSTs (Liu and Chan, 2003; Chan and Liu, 2004). In El Niño years, tropical cyclones tend to be more intense and longer-lived than in La Niña years (Camargo and Sobel, 2004) and occur in different locations. In the summer (JJA) and autumn (SON) of strong El Niño years, tropical cyclone numbers increase markedly in the southeastern quadrant of the western North Pacific (0°N–17°N, 140°E–180°E) and decrease in the northwestern quadrant (17°N–30°N, 120°E–140°E; Wang and Chan, 2002). In SON of El Niño years from 1961 to 2000, significantly fewer tropical cyclones made landfall in the western North Pacific compared with neutral years, although in Japan and the Korean Peninsula no statistically significant change was detected. In contrast, in SON of La Niña years, significantly more landfalls were reported in China (Wu et al., 2004). Overall in 2004, the number of tropical depressions, tropical storms and typhoons was slightly above the 1971 to 2000 median but the number of typhoons (21) was well above the median (17.5) and second highest to 1997, when 23 developed. Moreover, a record number of 10 tropical cyclones or typhoons made landfall in Japan; the previous record was 6 (Levinson, 2005). The ACE index was very close to normal for the 2005 season (Figure 3.40).

3.8.3.2 North Atlantic

The North Atlantic hurricane record begins in 1851 and is the longest among cyclone series. Values are considered fairly reliable after about 1950 when measurements from reconnaissance aircraft began. Methods of estimating wind speed from aircraft have evolved over time and, unfortunately, changes were not always well documented. The record is most reliable after the early 1970s (Landsea, 2005). The North Atlantic record shows a fairly active period from the 1930s to the 1960s followed by a less active period in the 1970s and 1980s, similar to the fluctuations of the AMO (Figure 3.33).

Beginning with 1995, all but two Atlantic hurricane seasons have been above normal (relative to the 1981 to 2000 base period). The exceptions are the two El Niño years of 1997 and 2002. As noted in Section 3.8.3, El Niño acts to reduce activity and La Niña acts to increase activity in the North Atlantic. The increased activity after 1995 contrasts sharply with the generally below-normal seasons observed during the previous 25-year period (1970–1994). These multi-decadal fluctuations in hurricane activity result nearly entirely from differences in the number of hurricanes and major hurricanes forming from tropical storms first named in the tropical Atlantic and Caribbean Sea. The change from the negative phase of the AMO in the 1970s and 1980s (see Section 3.6.6) to the post-1995 period has been a contributing factor to the increased hurricane activity (Goldenberg et al., 2001) and is well depicted in Atlantic SSTs (Figure 3.33), including those in the tropics. Nevertheless, it appears likely that most of the warming since the 1970s can be associated with global SST increases rather than the AMO (Trenberth and Shea, 2006; see Section 3.6.6).

During 1995 to 2004, hurricane seasons averaged 13.6 tropical storms, 7.8 hurricanes and 3.8 major hurricanes, and have an average ACE index of 159% of the median. The record-breaking 2005 season is documented in more detail in Section 3.8.4, Box 3.6. In contrast, during the preceding 1970 to 1994 period, hurricane seasons averaged 8.6 tropical storms, 5 hurricanes and 1.5 major hurricanes, and had an average ACE index of only 70% of the median. NOAA classifies 12 (almost one-half) of these 25 seasons as being below normal, and only three as being above normal (1980, 1988, 1989), with the remainder as normal. The positive phase of the AMO was also present during the above-

normal hurricane decades of the 1950s and 1960s, as indicated by comparing Atlantic SSTs (Figure 3.33) and seasonal ACE values (Figure 3.40). In 2004, there were 15 named storms, of which 9 were hurricanes, and an unprecedented 4 hit Florida, causing extensive damage (Levinson, 2005). In 2005, record-high SSTs (Figure 3.33) and favourable atmospheric conditions enabled the most active season on record (by many measures), but this was not fully reflected in the ACE index (see also Section 3.8.4, Box 3.6). In 2005, the North Atlantic ACE was the third highest since 1948, while the PDI was the highest on record, exceeding the previous high reached in 2004.

Key factors in the recent increase in Atlantic activity (Chelliah and Bell, 2004) include: (1) warmer SSTs across the tropical Atlantic; (2) an amplified subtropical ridge at upper levels across the central and eastern North Atlantic; (3) reduced vertical wind shear in the deep tropics over the central North Atlantic, which results from an expanded area of easterly winds in the upper atmosphere and weaker easterly trade winds in the lower atmosphere; and (4) a configuration of the African easterly jet that favours hurricane development from tropical disturbances moving westward from the African coast. The vertical shear in the main development region where most Atlantic hurricanes form (Aiyyer and Thorncroft, 2006) fluctuates interannually with ENSO, and with a multi-decadal variation that is correlated with Sahel precipitation. The latter switched sign around 1970 and remained in that phase until the early 1990s, consistent with the AMO variability. It has been argued that the QBO is also a factor in interannual variability (Gray, 1984). The most recent decade has the highest SSTs on record in the tropical North Atlantic (Figure 3.33), apparently as part of global warming and a favourable phase of the AMO. In the Atlantic generally, the changing environmental conditions (Box 3.5) have been more favourable in the past decade for tropical storms to develop.

3.8.3.3 Eastern North Pacific

Tropical cyclone activity (both frequency and intensity) in this region is related especially to SSTs, the phase of ENSO and the phase of the QBO in the tropical lower stratosphere. Above-normal tropical cyclone activity during El Niño years and the lowest activity typically associated with La Niña years is the opposite of the North Atlantic Basin (Landsea et al., 1998). Tropical cyclones tend to attain a higher intensity when the QBO is in its westerly phase at 30 hPa in the tropical lower stratosphere. A well-defined peak in the seasonal ACE occurred in early 1990s, with the largest annual value in 1992 (Figure 3.40), but values are unreliable prior to 1970 in the pre-satellite era. In general, seasonal hurricane activity, including the ACE index, has been below average since 1995, with the exception of the El Niño year of 1997, and is inversely related to the observed increase in activity in the North Atlantic basin over the same time period. This pattern is associated with the AMO (Levinson, 2005) and ENSO. Nevertheless, there has been an increase in category 4 and 5 storms (Webster et al., 2005).

3.8.3.4 Indian Ocean

The North Indian Ocean tropical cyclone season extends from May to December, with peaks in activity during May to June and November when the monsoon trough lies over tropical waters in the basin. Tropical cyclones are usually short-lived and weak, quickly moving into the sub-continent. Tropical storm activity in the northern Indian Ocean has been near normal in recent years (Figure 3.40).

The tropical cyclone season in the South Indian Ocean is normally active from December through April and thus the data are summarised by season in Figure 3.40, rather than by calendar year. The basin extends from the African coastline, where tropical cyclones affect Madagascar, Mozambique and the Mascarene Islands, including Mauritius, to 110°E (tropical cyclones east of 110°E are included in the Australian summary), and from the equator southward, although most cyclones develop south of 10°S. The intensity of tropical cyclones in the South Indian Ocean is reduced during El Niño events (Figure 3.40; Levinson, 2005). Lack of historical record keeping severely hinders trend analysis.

3.8.3.5 Australia and the South Pacific

The tropical cyclone season in the South Pacific-Australia region typically extends over the period November through April, with peak activity from December through March. Tropical cyclone activity in the Australian region (105°E–160°E) apparently declined somewhat over the past decade (Figure 3.40), although this may be partly due to improved analysis and discrimination of weak cyclones that previously were estimated at minimum tropical storm strength (Plummer et al., 1999). Increased cyclone activity in the Australian region has been associated with La Niña years, while below-normal activity has occurred during El Niño years (Plummer et al., 1999; Kuleshov and de Hoedt, 2003). In contrast, in the South Pacific east of 160°E, the opposite signal has been observed, and the most active years have been associated with El Niño events, especially during the strong 1982–1983 and 1997–1998 events (Levinson, 2005), and maximum ACE values occurred from January through March 1998 (Figure 3.40). Webster et al. (2005) found more than a doubling in the numbers of category 4 and 5 hurricanes in the southwest Pacific region between 1975 to 1989 and 1990 to 2004. In the 2005–2006 season, La Niña influences shifted tropical storm activity away from the South Pacific to the Australian region and in March and April 2006, four category 5 typhoons (Floyd, Glenda, Larry and Monica) occurred.

3.8.3.6 South Atlantic

In late March 2004 in the South Atlantic, off the coast of Brazil, the first and only documented hurricane in that region occurred (Pezza and Simmonds, 2005). It came ashore in the Brazilian state of Santa Catarina on 28 March 2004 with winds,

Frequently Asked Question 3.3

Has there been a Change in Extreme Events like Heat Waves, Droughts, Floods and Hurricanes?

Since 1950, the number of heat waves has increased and widespread increases have occurred in the numbers of warm nights. The extent of regions affected by droughts has also increased as precipitation over land has marginally decreased while evaporation has increased due to warmer conditions. Generally, numbers of heavy daily precipitation events that lead to flooding have increased, but not everywhere. Tropical storm and hurricane frequencies vary considerably from year to year, but evidence suggests substantial increases in intensity and duration since the 1970s. In the extratropics, variations in tracks and intensity of storms reflect variations in major features of the atmospheric circulation, such as the North Atlantic Oscillation.

In several regions of the world, indications of changes in various types of extreme climate events have been found. The extremes are commonly considered to be the values exceeded 1, 5 and 10% of the time (at one extreme) or 90, 95 and 99% of the time (at the other extreme). The warm nights or hot days (discussed below) are those exceeding the 90th percentile of temperature, while cold nights or days are those falling below the 10th percentile. Heavy precipitation is defined as daily amounts greater than the 95th (or for 'very heavy', the 99th) percentile.

In the last 50 years for the land areas sampled, there has been a significant decrease in the annual occurrence of cold nights and a significant increase in the annual occurrence of warm nights (Figure 1). Decreases in the occurrence of cold days and increases in hot days, while widespread, are generally less marked. The distributions of minimum and maximum temperatures have not only shifted to higher values, consistent with overall warming, but the cold extremes have warmed more than the warm extremes over the last 50 years (Figure 1). More warm extremes imply an increased frequency of heat waves. Further supporting indications include the observed trend towards fewer frost days associated with the average warming in most mid-latitude regions.

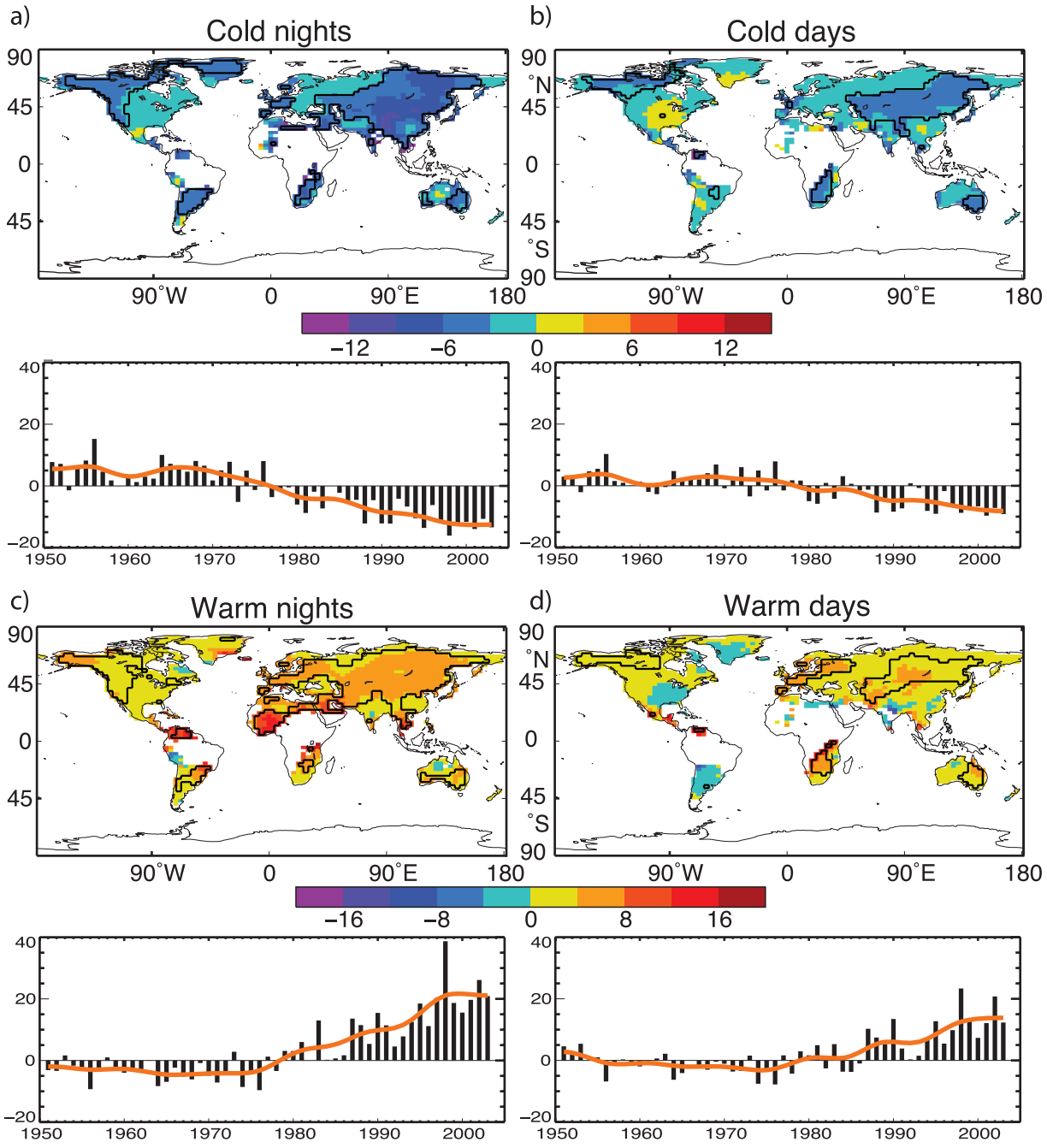
A prominent indication of a change in extremes is the observed evidence of increases in heavy precipitation events over the mid-latitudes in the last 50 years, even in places where mean precipitation amounts are not increasing (see also FAQ 3.2). For very heavy precipitation events, increasing trends are reported as well, but results are available for few areas.

Drought is easier to measure because of its long duration. While there are numerous indices and metrics of drought, many studies use monthly precipitation totals and temperature averages combined into a measure called the Palmer Drought Severity Index (PDSI). The PDSI calculated from the middle of the 20th century shows a large drying trend over many Northern Hemisphere land areas since the mid-1950s, with widespread drying over much of southern Eurasia, northern Africa, Canada and Alaska (FAQ 3.2, Figure 1), and an opposite trend in eastern North and South America. In the Southern Hemisphere, land surfaces were wet in the 1970s and relatively dry in the 1960s and 1990s, and there was a drying trend from 1974 to 1998. Longer-duration records for Europe for the whole of the 20th century indicate few significant trends. Decreases in precipitation over land since the 1950s are the likely main cause for the drying trends, although large surface warming during the last two to three decades has also likely contributed to the drying. One study shows that very dry land areas across the globe (defined as areas with a PDSI of less than –3.0) have more than doubled in extent since the 1970s, associated with an initial precipitation decrease over land related to the El Niño-Southern Oscillation and with subsequent increases primarily due to surface warming.

Changes in tropical storm and hurricane frequency and intensity are masked by large natural variability. The El Niño-Southern Oscillation greatly affects the location and activity of tropical storms around the world. Globally, estimates of the potential destructiveness of hurricanes show a substantial upward trend since the mid-1970s, with a trend towards longer storm duration and greater storm intensity, and the activity is strongly correlated with tropical sea surface temperature. These relationships have been reinforced by findings of a large increase in numbers and proportion of strong hurricanes globally since 1970 even as total numbers of cyclones and cyclone days decreased slightly in most basins. Specifically, the number of category 4 and 5 hurricanes increased by about 75% since 1970. The largest increases were in the North Pacific, Indian and Southwest Pacific Oceans. However, numbers of hurricanes in the North Atlantic have also been above normal in 9 of the last 11 years, culminating in the record-breaking 2005 season.

Based on a variety of measures at the surface and in the upper troposphere, it is likely that there has been a poleward shift as well as an increase in Northern Hemisphere winter storm track activity over the second half of the 20th century. These changes are part of variations that have occurred related to the North Atlantic Oscillation. Observations from 1979 to the mid-1990s reveal a tendency towards a stronger December to February circumpolar westerly atmospheric circulation throughout the troposphere and lower stratosphere, together with poleward displacements of jet streams and increased storm track activity. Observational evidence for changes in small-scale severe weather phenomena (such as tornadoes, hail and thunderstorms) is mostly local and too scattered to draw general conclusions; increases in many areas arise because of increased public awareness and improved efforts to collect reports of these phenomena.

(continued)



FAQ 3.3, Figure 1. *Observed trends (days per decade) for 1951 to 2003 in the frequency of extreme temperatures, defined based on 1961 to 1990 values, as maps for the 10th percentile: (a) cold nights and (b) cold days; and 90th percentile: (c) warm nights and (d) warm days. Trends were calculated only for grid boxes that had at least 40 years of data during this period and had data until at least 1999. Black lines enclose regions where trends are significant at the 5% level. Below each map are the global annual time series of anomalies (with respect to 1961 to 1990). The orange line shows decadal variations. Trends are significant at the 5% level for all the global indices shown. Adapted from Alexander et al. (2006).*

Box 3.6: Recent Extreme Events

Single extreme events cannot be simply and directly attributed to anthropogenic climate change, as there is always a finite chance the event in question might have occurred naturally. However, when a pattern of extreme weather persists for some time, it may be classed as an extreme climate event, perhaps associated with anomalies in SSTs (such as El Niño). This box provides examples of some recent (post-TAR) notable extreme climate events. A lack of long and homogeneous observational data often makes it difficult to place some of these events in a longer-term context. The odds may have shifted to make some of them more likely than in an unchanging climate, but attribution of the change in odds typically requires extensive model experiments, a topic taken up in Chapter 9. It may be possible, however, to say that the occurrence of recent events is consistent with physically based expectations arising from climate change. Some examples of these recent events are described below (in response to the questions posed to IPCC by the governments) and placed in a long-term perspective.

Drought in Central and Southwest Asia, 1998–2003

Between 1999 and 2003 a severe drought hit much of southwest Asia, including Afghanistan, Kyrgyzstan, Iran, Iraq, Pakistan, Tajikistan, Turkmenistan, Uzbekistan and parts of Kazakhstan (Waple and Lawrimore, 2003; Levinson and Waple, 2004). Most of the area is a semiarid steppe, receiving precipitation only during winter and early spring through orographic capture of eastward-propagating mid-latitude cyclones from the Atlantic Ocean and the Mediterranean Sea (Martyn, 1992). Precipitation between 1998 and 2001 was on average less than 55% of the long-term average, making the drought conditions in 2000 the worst in 50 years (Waple et al., 2002). By June 2000, some parts of Iran had reported no measurable rainfall for 30 consecutive months. In December 2001 and January 2002, snowfall at higher altitudes brought relief for some areas, although the combination of above-average temperatures and early snowmelt, substantial rainfall and hardened ground desiccated by prolonged drought resulted in flash flooding during spring in parts of central and southern Iran, northern Afghanistan and Tajikistan. Other regions in the area continued to experience drought through 2004 (Levinson, 2005). In these years, an anomalous ridge in the upper-level circulation was a persistent feature during the cold season in central and southern Asia. The pattern served to both inhibit the development of baroclinic storm systems and deflect eastward-propagating storms to the north of the drought-affected area. Hoerling and Kumar (2003) linked the drought in certain areas of the mid-latitudes to common global oceanic influences. Both the prolonged duration of the 1998–2002 cold phase ENSO (La Niña) event and the unusually warm ocean waters in the western Pacific and eastern Indian Oceans appear to contribute to the severity of the drought (Nazemosadat and Cordery, 2000; Barlow et al., 2002; Nazemosadat and Ghasemi, 2004).

Drought in Australia, 2002–2003

A severe drought affected Australia during 2002, associated with a moderate El Niño event (Watkins, 2002). However, droughts in 1994 and 1982 were about as dry as the 2002 drought. Earlier droughts in the first half of the 20th century may well have been even drier. The 2002 drought came after several years of good rainfall (averaged across the country), rather than during an extended period of low rainfall such as occurred in the 1940s. If only rainfall is considered, the 2002 drought alone does not provide evidence of Australian droughts becoming more extreme. However, daytime temperatures during the 2002 drought were much higher than during previous droughts. The mean annual maximum temperature for 2002 was 0.5°C warmer than in 1994 and 1.0°C warmer than in 1982. So in this sense, the 2002 drought and associated heat waves were more extreme than the earlier droughts, because the impact of the low rainfall was exacerbated by high potential evaporation (Karoly et al., 2003; Nicholls, 2004). The very high maximum temperatures during 2002 could not simply be attributed to the low rainfall, although there is a strong negative correlation between rainfall and maximum temperature. Severe long-term drought, stemming from at least three years of rainfall deficits, continued during 2005, especially in the eastern third of Australia, although above-normal rainfall in winter and spring 2005 brought some relief. These conditions also have been accompanied by record high maximum temperatures over Australia during 2005 (a comparable national series is only available since 1951).

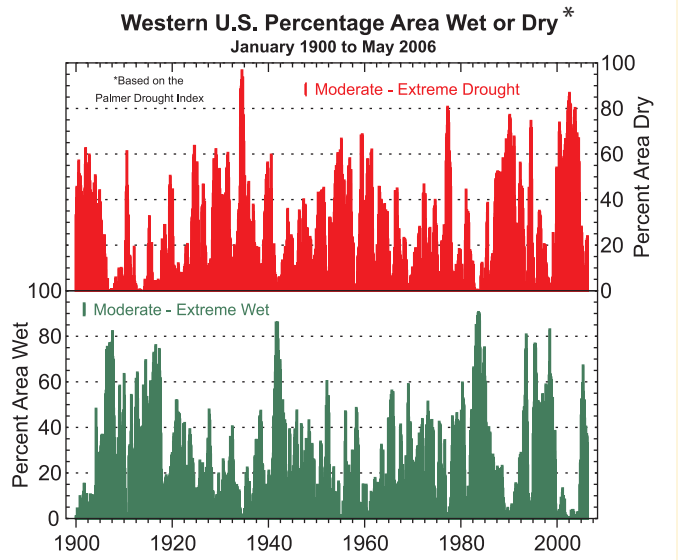
Drought in Western North America, 1999–2004

The western USA, southern Canada and northwest Mexico experienced a recent pervasive drought (Lawrimore et al., 2002), with dry conditions commencing as early as 1999 and persisting through the end of 2004 (Box 3.6, Figure 1). Drought conditions were recorded by several hydrologic measures, including precipitation, streamflow, lake and reservoir levels and soil moisture (Piechota et al., 2004). The period 2000 through 2004 was the first instance of five consecutive years of below-average flow in the Colorado River since the beginning of modern records in 1922 (Pagano et al., 2004). Cook et al. (2004) provided a longer-term context for this drought. In the western conterminous USA, the area under moderate to extreme drought, as given by the PDSI, rose above 20% in November 1999 and stayed above this level persistently until October 2004. At its peak (August 2002), this drought affected 87% of the West (Rocky Mountains westward), making it the second most extensive and one of the longest droughts in the last 105 years. The impacts of this drought have been exacerbated by depleted or earlier than average melting of the mountain snowpack, due to warm springs,

(continued)

as observed changes in timing from 1948 to 2000 trended earlier by one to two weeks in many parts of the West (Cayan et al., 2001; Regonda et al., 2005; Stewart et al., 2005). Within this episode, the spring of 2004 was unusually warm and dry, resulting in record early snowmelt in several western watersheds (Pagano et al., 2004).

Hoerling and Kumar (2003) attributed the drought to changes in atmospheric circulation associated with warming of the western tropical Pacific and Indian oceans, while McCabe et al. (2004) have produced evidence suggesting that the confluence of both Pacific decadal and Atlantic multi-decadal fluctuations is involved. In the northern winter of 2004 to 2005, the weak El Niño was part of a radical change in atmospheric circulation and storm track across the USA, ameliorating the drought in the Southwest, although lakes remain low.



Box 3.6, Figure 1. *Percentage of the USA west of the Rocky Mountains (the 11 states west of and including Montana to New Mexico) that was dry (top) or wet (bottom), based on the Palmer Drought Severity Index for classes of moderate to extreme drought or wet. From NOAA, NCDC.*

Floods in Europe, Summer 2002

A catastrophic flood occurred along several central European rivers in August 2002. The floods resulting from extraordinarily high precipitation were enhanced by the fact that the soils were completely saturated and the river water levels were already high because of previous rain (Rudolf and Rapp, 2003; Ulbrich et al., 2003a,b). Hence, it was part of a pattern of weather over an extended period. In the flood, the water levels of the Elbe at Dresden reached a maximum mark of 9.4 m, which is the highest level since records began in 1275 (Ulbrich et al., 2003a). Some small villages in the Ore Mountains (on tributaries of the Elbe) were hit by extraordinary flash floods. The river Vltava inundated the city of Prague before contributing to the Elbe flood. A return period of 500 years was estimated for the flood levels at Prague (Grollmann and Simon, 2002). The central European floods were caused by two heavy precipitation episodes. The first, on 6–7 August, was situated mainly over Lower Austria, the southwestern part of the Czech Republic and southeastern Germany. The second took place on 11–13 August 2002 and most severely affected the Ore Mountains and western parts of the Czech Republic. A persistent low-pressure system moved slowly from the Mediterranean Sea to central Europe on a path over or near the eastern Alps and led to large-scale, strong and quasi-stationary frontal lifting of air with very high liquid water content. Additional to this advective rain were convective precipitation processes (showers and thunderstorms) and a significant orographic lifting (mainly over the Ore Mountains). A maximum 24-hour precipitation total of 353 mm was observed at the German station Zinnwald-Georgenfeld, a new record for Germany. The synoptic situation leading to floods is well known to meteorologists of the region. Similar situations led to the summer floods of the River Oder in 1997 and the River Vistula in 2001 (Ulbrich et al., 2003b). Average summer precipitation trends in the region are negative but barely significant (Schönwiese and Rapp, 1997) and there is no significant trend in flood occurrences of the Elbe within the last 500 years (Mudelsee et al., 2003). However, the observed increase in precipitation variability at a majority of German precipitation stations during the last century (Trömel and Schönwiese, 2005) is indicative of an enhancement of the probability of both floods and droughts.

Heat Wave in Europe, Summer 2003

The heat wave that affected many parts of Europe during the course of summer 2003 produced record-breaking temperatures particularly during June and August (Beniston, 2004; Schär et al., 2004; see Box 3.6, Figure 2). Absolute maximum temperatures exceeded the record highest temperatures observed in the 1940s and early 1950s in many locations in France, Germany, Switzerland, Spain, Italy and the UK, according to the information supplied by national weather agencies (WMO, 2004). Gridded instrumental temperatures (from CRUTEM2v for the region 35°N–50°N, 0–20°E) show that the summer was the hottest since comparable records began in 1780: 3.8°C above the 1961 to 1990 average and 1.4°C hotter than any other summer in this period (the second hottest was 1807). Based on early documentary records, Luterbacher et al. (2004) estimated that 2003 is very likely to have been the hottest summer since at least 1500. The 2003 heat wave was associated with a very robust and persistent blocking high-pressure system that may be a manifestation of an exceptional northward extension of the Hadley Cell (Black et al., 2004; Fink et al., 2004). Already a record month in terms of maximum temperatures, June exhibited high geopotential values that penetrated northwards towards the British Isles, with the

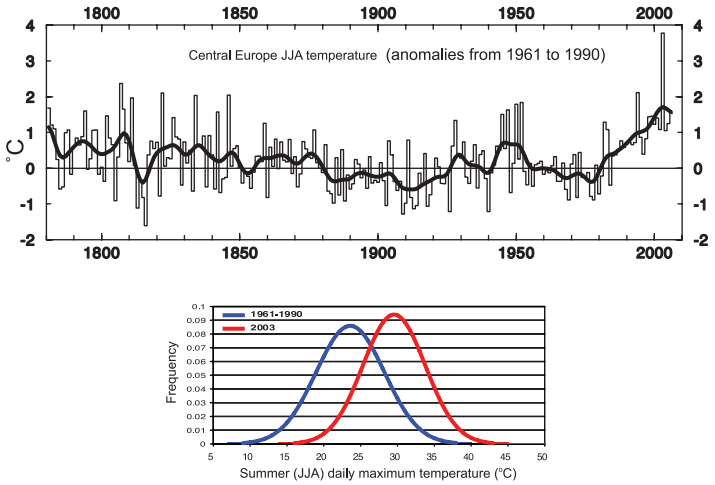
(continued)

greatest northward extension and longest persistence of record-high temperatures observed in August. An exacerbating factor for the temperature extremes was the lack of precipitation in many parts of western and central Europe, leading to much-reduced soil moisture and surface evaporation and evapotranspiration, and thus to a strong positive feedback effect (Beniston and Diaz, 2004).

The 2005 Tropical Storm Season in the North Atlantic

The 2005 North Atlantic hurricane season (1 June to 30 November) was the most active on record by several measures, surpassing the very active season of 2004 (e.g., Levinson, 2005) and causing an unprecedented level of damage. Even before the peak in the seasonal activity, the seven tropical storms in June and July were the most ever, and hurricane Dennis was the strongest on record in July and the earliest ever fourth-named storm. The record 2005 North Atlantic hurricane season featured the largest number of named storms (28; sustained winds greater than 17 m s^{-1}) and is the only time names have ventured into the Greek alphabet. It had the largest number of hurricanes (15; sustained winds greater than 33 m s^{-1}) recorded, and is the only time there have been four category 5 storms (maximum sustained winds greater than 67 m s^{-1}). These included the most intense Atlantic storm on record (Wilma, with recorded surface pressure in the eye of 882 hPa), the most intense storm in the Gulf of Mexico (Rita, 897 hPa), and Katrina. Tropical storm Vince was the first ever to make landfall in Portugal and Spain. In spite of these metrics, the ACE index, although very high and surpassing the 2004 value (Figure 3.40), was not the highest on record, as several storms were quite short lived. Six of the eight most damaging storms on record for the USA occurred from August 2004 to September 2005 (Charlie, Ivan, Francis, Katrina, Rita, Wilma) while another storm in 2005 (Stan) caused severe flooding and mudslides as well as about 2,000 fatalities in central America (Guatemala, El Salvador and southern Mexico).

SSTs in the tropical North Atlantic region critical for hurricanes (10°N to 20°N) were at record-high levels (0.9°C above the 1901 to 1970 normal) in the extended summer (June to October) of 2005 (Figure 3.33), and these high values were a major reason for the very active hurricane season along with favourable atmospheric conditions (see Box 3.5). A substantial component of this warming was the global mean SST increase (Trenberth and Shea, 2006; see Sections 3.2 and 3.6.6).



Box 3.6, Figure 2. *Long time series of JJA temperature anomalies in Central Europe relative to the 1961 to 1990 mean (top). The smooth curve shows decadal variations (see Appendix 3.A). In the summer of 2003, the value of 3.8°C far exceeded the next largest anomaly of 2.4°C in 1807, and the highly smoothed Gaussian distribution (bottom) of maximum temperatures (red) compared with normal (blue) at Basel, Switzerland (Beniston and Diaz, 2004) shows how the whole distribution shifted.*

estimated by the U.S. National Hurricane Center, of near 40 m s^{-1}, causing much damage to property and some loss of life (see Levinson, 2005). The Brazilian meteorologists dubbed it 'Catarina'. This event appears to be unprecedented although records are poor before the satellite era. Pezza and Simmonds (2005) suggest that a key factor in the hurricane development was the more favourable atmospheric circulation regime associated with the positive trend in the SAM (see Section 3.6).

3.8.4 Evidence for Changes in Extratropical Storms and Extreme Events

3.8.4.1 Extratropical Cyclones

Intense extratropical cyclones are often associated with extreme weather, particularly with severe windstorms. Significant increases in the number or strength of intense extratropical cyclone systems have been documented in a number of studies (e.g., Lambert, 1996; Gustafsson, 1997; McCabe et al., 2001; Wang et al., 2006a) with associated changes in the preferred tracks of storms as described in Section 3.5.3. As with tropical cyclones, detection of long-term changes

in cyclone measures is hampered by incomplete and changing observing systems. Some earlier results have been questioned because of changes in the observation system (e.g., Graham and Diaz, 2001).

Results from NRA and ERA-40 show that an increase in the number of deep cyclones is apparent over the North Pacific and North Atlantic (Graham and Diaz, 2001; Gulev et al., 2001), with statistically significant winter increases over both ocean basins (Simmonds and Keay, 2002; Wang et al., 2006a). Geng and Sugi (2001) found that cyclone density, deepening rate, central pressure gradient and translation speed have all been increasing in the winter North Atlantic. Caires and Sterl (2005) compared global estimates of 100-year return values of wind speed and SWH in ERA-40, with linear bias corrections based on buoy data, for three different 10-year periods. They showed that the differences in the storm tracks can be attributed to decadal variability in the NH, linked to changes in global circulation patterns, most notably to the NAO (see also Section 3.5.6).

Using NCEP-2 reanalysis data, Lim and Simmonds (2002) showed that for 1979 to 1999, increasing trends in the annual number of explosively developing (deepening by 1 hPa per hour or more) extratropical cyclones are significant in the SH and over the globe (0.56 and 0.78 more systems per year, respectively), while the positive trend did not achieve significance in the NH. Simmonds and Keay (2002) obtained similar results for the change in the number of cyclones in the decile for deepest cyclones averaged over the North Pacific and over the North Atlantic in winter over the period 1958 to 1997.

As noted in Sections 3.5.3 and 3.5.7, the time-dependent biases in the reanalysis cause uncertainties in the trends reported above. Besides reanalyses, station data may also be used to indicate evidence for changes in extratropical cyclone activity. Instead of direct station wind measurements, which may suffer from a lack of consistency of instrumentation, methodology and exposure, values based on pressure gradients have been derived that are more reliable for discerning long-term changes. Alexandersson et al. (2000) used station pressure observations for 21 stations over northwestern Europe back to 1881, from which geostrophic winds were calculated using 'pressure-triangle' methods. They found a decline of storminess expressed by the 95th and 99th percentiles from high levels during the late 19th century to a minimum around 1960 and then a quite rapid increase to a maximum around 1990, followed again by a decline (Figure 3.41). Positive NAO winters are typically associated with more intense and frequent storms (see Section 3.6.4). Similar results were obtained by Schmith et al. (1998) using simpler indices based on pressure tendency. Bärring and von Storch (2004), using both pressure tendencies and the number of very low pressure values, confirmed these results on the basis of two especially long station series in southern Sweden dating back to about 1800. Studies of rapid pressure changes at stations indicate an increase in the frequency, duration and intensity of winter cyclone activity over the lower Canadian Arctic and in the number and intensity of severe storms over the southern

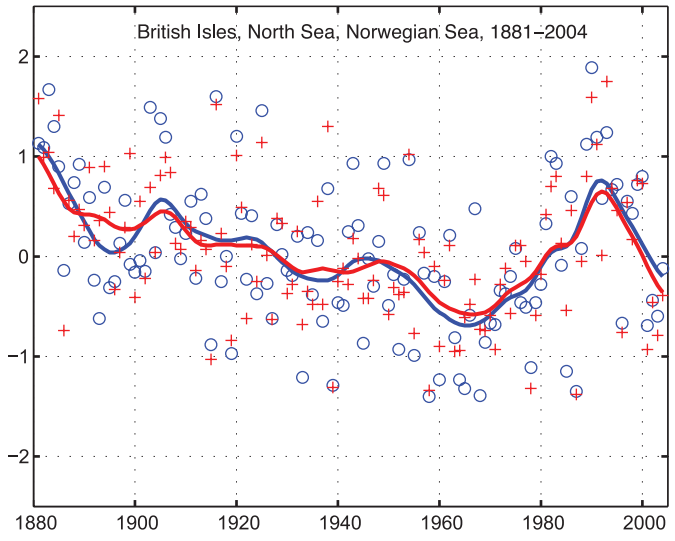


Figure 3.41. *Storm index for the British Isles, North Sea and Norwegian Sea, 1881 to 2004. Blue circles are 95th percentiles and red crosses 99th percentiles of standardised geostrophic winds averaged over 10 sets of triangles of stations. The smoothed curves are a decadal filter (updated from Alexandersson et al., 2000).*

UK since the 1950s, but a decrease over southern Canada and Iceland (Wang et al., 2006b; Alexander et al., 2005). Besides a northward shift of the storm track (see 3.5.3), the station pressure data for parts of the North Atlantic region show a modest increase in severe storms in recent decades. However, decadal-scale fluctuations of similar magnitude have occurred earlier in the 19th and 20th centuries.

Direct surface wind measurements have, however, been used in a few studies. An analysis of extreme pressure differences and surface winds (Salinger et al., 2005) showed a significant increasing trend over the last 40 years in westerly wind extremes over the southern part of New Zealand and the oceans to the south. The trends are consistent with the increased frequency of El Niño events in recent decades, associated with Pacific decadal variability (see Section 3.6.3). While the zonal pressure gradient and extreme westerly wind frequency have both increased over southern New Zealand, the frequency of extreme easterly winds has also increased there, suggesting more variability in the circulation generally. However, trends in pressure differences (based on the ERA-40, NRA and station data) are not always consistent with changes in surface windiness (e.g., Smits et al., 2005). Based on observed winds at 10 m height over the Netherlands, Smits et al. (2005) found a decline in strong (greater than about 8 on the Beaufort scale) wind events over the last 40 years. Differences cannot entirely be explained by changes in surface aerodynamic roughness, and they concluded that inhomogeneities in the reanalyses are the cause. However, local differences can be important and intensity and severity of storms may not always be synonymous with local extreme surface winds and gusts.

Table 3.7. *Definition of phenomena used to assess extremes in Table 3.8*

PHENOMENON	Definition
Low-temperature days/ nights and frost days	Percentage of days with temperature (maximum for days, minimum for nights) not exceeding some threshold, either fixed (frost days) or varying regionally (cold days/cold nights), based on the 10th percentile of the daily distribution in the reference period (1961–1990).
High-temperature days/nights	See low-temperature days/nights, but now exceeding the 90th percentile.
Cold spells/snaps	Episode of several consecutive low-temperature days/nights.
Warm spells (heat waves)	Episode of several consecutive high-temperature days/nights.
Cool seasons/warm seasons	Seasonal averages (rather than daily temperatures) exceeding some threshold.
Heavy precipitation events (events that occur every year)	Percentage of days (or daily precipitation amount) with precipitation exceeding some threshold, either fixed or varying regionally, based on the 95th or 99th percentile of the daily distribution in the reference period (1961–1990).
Rare precipitation events (with return periods >~10 yr)	As for heavy precipitation events, but for extremes further into the tail of the distribution.
Drought (season/year)	Precipitation deficit; or based on the PDSI (see Box 3.1).
Tropical cyclones (frequency, intensity, track, peak wind, peak precipitation)	Tropical storm with thresholds crossed in terms of estimated wind speed and organisation. Hurricanes in categories 1 to 5, according to the Saffir-Simpson scale, are defined as storms with wind speeds of 33 to 42 m s^{-1}, 43 to 49 m s^{-1}, 50 to 58 m s^{-1}, 59 to 69 m s^{-1}, and >70 m s^{-1}, respectively. NOAA's ACE index is a measure of the total seasonal activity that accounts for the collective intensity and duration of tropical storms and hurricanes during a given tropical cyclone season.
Extreme extratropical storms (frequency, intensity, track, surface wind, wave height)	Intense low-pressure systems that occur throughout the mid-latitudes of both hemispheres fueled by temperature gradients and acting to reduce them.
Small-scale severe weather phenomena	Extreme events, such as tornadoes, hail, thunderstorms, dust storms and other severe local weather.

Table 3.8. *Change in extremes for phenomena over the specified region and period, with the level of confidence and section where the phenomenon is discussed in detail.*

PHENOMENON	Change	Region	Period	Confidence	Section
Low-temperature days/nights and frost days	Decrease, more so for nights than days	Over 70% of global land area	1951–2003 (last 150 years for Europe and China)	*Very likely*	3.8.2.1
High-temperature days/nights	Increase, more so for nights than days	Over 70% of global land area	1951–2003	*Very likely*	3.8.2.1
Cold spells/snaps (episodes of several days)	Insufficient studies, but daily temperature changes imply a decrease				
Warm spells (heat waves) (episodes of several days)	Increase: implicit evidence from changes of daily temperatures	Global	1951–2003	*Likely*	FAQ 3.3
Cool seasons/ warm seasons (seasonal averages)	Some new evidence for changes in inter-seasonal variability	Central Europe	1961–2004	*Likely*	3.8.2.1
Heavy precipitation events (that occur every year)	Increase, generally beyond that expected from changes in the mean (disproportionate)	Many mid-latitude regions (even where reduction in total precipitation)	1951–2003	*Likely*	3.8.2.2
Rare precipitation events (with return periods > ~10 yr)	Increase	Only a few regions have sufficient data for reliable trends (e.g., UK and USA)	Various since 1893	*Likely* (consistent with changes inferred for more robust statistics)	3.8.2.2
Drought (season/year)	Increase in total area affected	Many land regions of the world	Since 1970s	*Likely*	3.3.4 and FAQ 3.3
Tropical cyclones	Trends towards longer lifetimes and greater storm intensity, but no trend in frequency	Tropics	Since 1970s	*Likely;* more confidence in frequency and intensity	3.8.3 and FAQ 3.3
Extreme extratropical storms	Net increase in frequency/intensity and poleward shift in track	NH land	Since about 1950	*Likely*	3.8.4, 3.5, and FAQ 3.3
Small-scale severe weather phenomena	Insufficient studies for assessment				

3.8.4.2 Tornadoes, Hail, Thunderstorms, Dust Storms and Other Severe Local Weather

Evidence for changes in the number or intensity of tornadoes relies entirely on local reports. In the USA, databases for tornado reporting are well established, although changes in procedures for evaluating the intensity of tornadoes introduced significant discontinuities in the record. In particular, the apparent decrease in strong tornadoes in the USA from the early period of the official record (1950s–1970s) to the more recent period is, in large part, a result of the way damage from the earlier events was evaluated. Trapp et al. (2005) also questioned the completeness of the tornado record and argued that about 12% of squall-line tornadoes remain unreported. In many European countries, the number of tornado reports has increased considerably over the last decade (Snow, 2003), leading to a much higher estimate of tornado activity (Dotzek, 2003). Bissolli et al. (2007) showed that the increase in Germany between 1950 and 2003 mainly concerns weak tornadoes (F0 and F1 on the Fujita scale), thus paralleling the evolution of tornado reports in the USA after 1950 (see, e.g., Dotzek et al., 2005) and making it likely that the increase in reports in Europe is at least dominated (if not solely caused) by enhanced detection and reporting efficiency. Doswell et al. (2005) highlighted the difficulties encountered when trying to find observational evidence for changes in extreme events at local scales connected to severe thunderstorms. In light of the very strong spatial variability of small-scale severe weather phenomena, the density of surface meteorological observing stations is too coarse to measure all such events. Moreover, homogeneity of existing station series is questionable. While remote sensing techniques allow detection of thunderstorms even in remote areas, they do not always uniquely identify severe weather events from these storms. Another approach links severe thunderstorm occurrence to larger-scale environmental conditions in places where the observations of events are fairly good and then consider the changes in the distribution of those environments (Brooks et al., 2003; Bissolli et al., 2007).

Although a decreasing trend in dust storms was observed from the mid-1950s to the mid-1990s in northern China, the number of dust storm days increased from 1997 to 2002 (Li and Zhai, 2003; Zhou and Zhang, 2003). The decreasing trend appears linked to the reduced cyclone frequency and increasing winter (DJF) temperatures (Qian et al., 2002). The recent increase is associated with vegetation degradation and drought, plus increased surface wind speed (Wang and Zhai, 2004; Zou and Zhai, 2004).

3.8.5 Summary

Even though the archived data sets are not yet sufficient for determining long-term trends in extremes, there are new findings on observed changes for different types of extremes. The definitions of the phenomena are summarised in Table 3.7. A summary of the changes in extremes by phenomena, region and time is given in Table 3.8 along with an assessment of the confidence in these changes.

New analyses since the TAR confirm the picture of a gradual reduction of the number of frost days over most of the mid-latitudes in recent decades. In agreement with this warming trend, the number of warm nights increased between 1951 and 2003, cold nights decreased, and trends in the number of cold and warm days are also consistent with warming, but are less marked than at night.

For precipitation, analysis of updated trends and results for regions that were missing at the time of the TAR show increases in heavy events for the majority of observation stations, with some increase in flooding. This result applies both for areas where total precipitation has increased and for areas where total precipitation has even decreased. Increasing trends are also reported for more rare precipitation events, although results for such extremes are available only for a few areas. Mainly because of lack of data, it remains difficult to draw a consistent picture of changes in extreme precipitation for the tropics and subtropics.

Tropical cyclones, hurricanes and typhoons exhibit large variability from year to year and limitations in the quality of data compromise evaluations of trends. Nonetheless, clear evidence exists for increases in category 4 and 5 storms globally since 1970 along with increases in the PDI due to increases in intensity and duration of storms. The 2005 season in the North Atlantic broke many records. The global view of tropical storm activity highlights the important role of ENSO in all basins, and the most active year was 1997, when a very strong El Niño began, suggesting that observed record high SSTs played a key role.

For extratropical cyclones, positive trends in storm frequency and intensity dominate for recent decades in most regional studies performed. Longer records for the northeastern Atlantic suggest that the recent extreme period may be similar in level to that of the late 19th century.

As noted in Section 3.3.4, the PDSI shows a large drying trend over NH land areas since the mid-1950s and a drying trend in the SH from 1974 to 1998. Decreases in land precipitation, especially since the early 1980s are the main cause for the drying trends, although large surface warming during the last two to three decades has also likely contributed to the drying.

3.9 Synthesis: Consistency Across Observations

This section briefly compares variability and trends within and across different climate variables to see if a physically consistent picture enhances confidence in the realism of apparent recent observed changes. Therefore, this section looks ahead to the subsequent observational chapters on the cryosphere (Chapter 4) and oceans (Chapter 5), which focus on changes in those domains. The emphasis here is on inter-relationships. For example, increases in temperature should enhance the moisture-holding capacity of the atmosphere as a whole and changes in temperature and/or precipitation should be consistent with those evident in circulation indices. Variables treated in this chapter are summarised in the executive summary, with some discussion below. The example of increases in temperature that should also reduce snow seasons and sea ice and cause widespread glacier retreat involves cross-chapter variables. The main sections where more detailed information can be found are given in parentheses following each bullet.

- The observed temperature increases are consistent with the observed nearly worldwide reduction in glacier and small ice cap (not including Antarctica and Greenland) mass and extent in the 20th century. Glaciers and ice caps respond not only to temperatures but also to changes in precipitation, and both winter accumulation and summer melting have increased over the last half century in association with temperature increases. In some regions, moderately increased accumulation observed in recent decades is consistent with changes in atmospheric circulation and associated increases in winter precipitation (e.g., southwestern Norway, parts of coastal Alaska, Patagonia, Karakoram, and Fjordland of the South Island of New Zealand), even though enhanced ablation has led to marked declines in mass balances in Alaska and Patagonia. Tropical glacier changes are synchronous with higher-latitude ones and all have shown declines in recent decades; local temperature records all show a slight warming, but not of the magnitude required to explain the rapid reduction in mass of such glaciers (e.g., on Kilimanjaro). Other factors in recent ablation include changes in cloudiness, water vapour, albedo due to snowfall frequency and the associated radiation balance (Sections 3.2.2, 3.3.3, 3.4.3 and 4.5).

- Snow cover has decreased in many NH regions, particularly in spring, consistent with greater increases in spring as opposed to autumn temperatures in mid-latitude regions, and more precipitation falling as rain instead of snow. These changes are consistent with changes in permafrost: temperatures of the permafrost in the Arctic and subarctic have increased by up to 3°C since the 1980s with permafrost warming also observed on the Tibetan Plateau and in the European mountain permafrost regions. Active layer thickness has increased and seasonally frozen ground depth has decreased over the Eurasian continent (Sections 3.2.2, 3.3.2, 4.2 and 4.8).

- Sea ice extents have decreased in the Arctic, particularly in spring and summer, and patterns of the changes are consistent with regions showing a temperature increase, although changes in winds are also a major factor. Sea ice extents were at record low values in 2005, which was also the warmest year since records began in 1850 for the Arctic north of 65°N. There have also been decreases in sea ice thickness. In contrast to the Arctic, antarctic sea ice does not exhibit any significant trend since the end of the 1970s, which is consistent with the lack of trend in surface temperature south of 65°S over that period. However, along the Antarctic Peninsula, where significant warming has occurred, progressive breakup of ice shelves has occurred beginning in the late 1980s, culminating in the breakup of the Larsen-B ice shelf in 2002. Decreases are found in the length of the freeze season of river and lake ice (Sections 3.2.2, 3.6.5, 4.3 and 4.4).

- Radiation changes at the top of the atmosphere from the 1980s to 1990s, possibly ENSO-related in part, appear to be associated with reductions in tropical cloud cover, and are linked to changes in the energy budget at the surface and in observed ocean heat content in a consistent way (Sections 3.4.3, 3.4.4, 3.6.2 and 5.2.2).

- Reported decreases in solar radiation from 1970 to 1990 at the surface have an urban bias. Although records are sparse, pan evaporation is estimated to have decreased in many places due to decreases in surface radiation associated with increases in clouds, changes in cloud properties and/or increases in air pollution (aerosol), especially from 1970 to 1990. There is evidence to suggest that the solar radiation decrease has reversed in recent years (Sections 2.4.5, 2.4.6, 3.3.3, 3.4.4, 7.2 and 7.5).

- Droughts have increased in spatial extent in various parts of the world. The regions where they have occurred seem to be determined largely by changes in SSTs, especially in the tropics, through changes in the atmospheric circulation and precipitation. Inferred enhanced evapotranspiration and drying associated with warming are additional factors in drought increases, but decreased precipitation is the dominant factor. In the western USA, diminishing snowpack and subsequent summer soil moisture reductions have also been a factor. In Australia and Europe, direct links to warming have been inferred through the extreme nature of high temperatures and heat waves accompanying drought (Sections 3.3.4 and 4.2, FAQ 3.2 and Box 3.6).

- Changes in the freshwater balance of the Atlantic Ocean over the past four decades have been pronounced, as freshening has occurred in the North Atlantic and south of 25°S, while salinity has increased in the tropics and subtropics, especially in the upper 500 m. The implication is that there have been increases in moisture transport by the atmosphere from the subtropics to higher latitudes, in association with changes in atmospheric circulation, including the NAO, thereby producing the observed increases in precipitation over the northern oceans and adjacent land areas (Sections 3.3.2, 3.6.4, 5.3.2 and 5.5.3).

- Sea level likely rose 1.7 ± 0.5 mm yr^{-1} during the 20th century, but the rate increased to 3.1 ± 0.7 mm yr^{-1} from 1993 through 2003, when confidence increases from global altimetry measurements. Increases in ocean heat content and associated ocean expansion are estimated to have contributed 0.4 ± 0.1 mm yr^{-1} from 1961 to 2003, increasing to an estimated value of 1.6 ± 0.5 mm yr^{-1} for 1993 to 2003. In the same interval, glacier and land ice melt has increased ocean mass by approximately 1.2 ± 0.4 mm yr^{-1}. Changes in land water storage are uncertain but may have reduced water in the ocean. The near balance for 1993 to 2003 gives increased confidence that the observed sea level rise is a strong indicator of warming, and an integrator of the cumulative energy imbalance at the top of atmosphere (Sections 4.5, 4.6, 4.8, 5.2 and 5.5).

In summary, global mean temperatures have increased since the 19th century, especially since the mid-1970s. Temperatures have increased nearly everywhere over land, and SSTs and marine air temperatures have also increased, reinforcing the evidence from land. However, temperatures have increased neither monotonically nor in a spatially uniform manner, especially over shorter time intervals. The atmospheric circulation has also changed: in particular, increasing zonal flow is observed in most seasons in both hemispheres, and the mid- to high-latitude annular modes strengthened until the mid-1990s in the NH and up until the present in the SH. In the NH, this brought milder maritime air into Europe and much of high-latitude Asia from the North Atlantic in winter, enhancing warming there. In the SH, where the ozone hole has played a role, it has resulted in cooling over 1971 to 2000 for parts of the interior of Antarctica but large warming in the Antarctic Peninsula region and Patagonia. Temperatures generally have risen more than average where flow has become more poleward, and less than average or even cooled where flow has become more equatorward, reflecting the PDO and other patterns of variability.

Over land, a strong negative correlation is observed between precipitation and surface temperature in summer and at low latitudes throughout the year, and areas that have become wetter, such as the eastern USA and Argentina, have not warmed as much as other land areas (see especially FAQs 3.2 and 3.3). Increased precipitation is associated with increases in cloud and surface wetness, and thus increased evapotranspiration. The inferred increased evapotranspiration and reduced temperature increase is physically consistent with enhanced latent vs. sensible heat fluxes from the surface in wetter conditions.

Consistent with the expectations noted above for a warmer climate, surface specific humidity has generally increased after 1976 in close association with higher temperatures over both land and ocean. Total column water vapour has increased over the global oceans by 1.2 ± 0.3% per decade from 1988 to 2004, consistent in patterns and amount with changes in SST and a fairly constant relative humidity. Upper-tropospheric water vapour has also increased in ways such that relative humidity remains about constant, providing a major positive feedback to radiative forcing. In turn, widespread observed increases in the fraction of heavy precipitation events are consistent with the increased water vapour amounts.

The three main ocean basins are unique and contain very different wind systems, SST patterns and currents, leading to vastly different variability associated, for instance, with ENSO in the Pacific, and the THC in the Atlantic. Consequently, the oceans have not warmed uniformly, especially at depth. SSTs in the tropics have warmed at different rates and help drive, through coupling with tropical convection and winds, teleconnections around the world. This has changed the atmospheric circulation through ENSO, the PDO, the AMO, monsoons and the Hadley and Walker Circulations. Changes in precipitation and storm tracks are not as well documented but clearly respond to these changes on interannual and decadal time scales. When precipitation increases over the ocean, as it has in recent years in the tropics, it decreases over land, although it has increased over land at higher latitudes. Droughts have increased over many tropical and mid-latitude land areas, in part because of decreased precipitation over land since the 1970s but also from increased evapotranspiration arising from increased atmospheric demand associated with warming.

Changes in the cryosphere (Chapter 4), ocean and land strongly support the view that the world is warming, through observed decreases in snow cover and sea ice, thinner sea ice, shorter freezing seasons of lake and river ice, glacier melt, decreases in permafrost extent, increases in soil temperatures and borehole temperature profiles (see Section 6.6), and sea level rise (Section 5.5).

Acknowledgments

The authors gratefully acknowledge the valuable assistance of Sara Veasey (NCDC, Asheville) and Lisa Butler (NCAR, Boulder) in the development of diagrams and text formatting.

References

Abakumova, G.M., et al., 1996: Evaluation of long-term changes in radiation, cloudiness, and surface temperature on the territory of the former Soviet Union. *J. Clim.*, **9**, 1319–1327.

Adler, R.F., et al., 2001: Intercomparison of global precipitation products: The Third Precipitation Intercomparison Project (PIP-3). *Bull. Am. Meteorol. Soc.*, **82**, 1377–1396.

Adler, R.F., et al., 2003: The version 2 Global Precipitation Climatology Project (GPCP) monthly precipitation analysis (1979–present). *J. Hydrometeorol*., **4**, 1147–1167.

Agudelo, P.A., and J.A. Curry, 2004: Analysis of spatial distribution in tropospheric temperature trends. *Geophys. Res. Lett.*, **31**, L22207, doi:10.1029/2004GL02818.

Aguilar, E., et al., 2005: Changes in precipitation and temperature extremes in Central America and northern South America, 1961–2003. *J. Geophys. Res*., **110**, D23107, doi:10.1029/2005JD006119.

Aiyyer, A.R., and C. Thorncroft, 2006: Climatology of vertical wind shear over the tropical Atlantic. *J. Clim.*, **19**, 2969–2983.

Aksoy, B., 1997: Variations and trends in global solar radiation for Turkey. *Theor. Appl. Climatol*., **58**, 71–77.

Alexander, L.V., S.F.B. Tett, and T. Jónsson, 2005: Recent observed changes in severe storms over the United Kingdom and Iceland. *Geophys. Res. Lett*., **32**, L13704, doi:10.1029/2005GL022371.

Alexander, L.V., et al., 2006: Global observed changes in daily climate extremes of temperature and precipitation. *J. Geophys. Res*., **111**, D05109, doi:10.1029/2005JD006290.

Alexandersson, H., et al., 1998: Long-term variations of the storm climate over NW Europe. *Global Atmos. Ocean System*, **6**, 97–120.

Alexandersson, H., et al., 2000: Trends of storms in NW Europe derived from an updated pressure data set. *Clim. Res.*, **14**, 71–73.

Allan, J., and P. Komar, 2000: Are ocean wave heights increasing in the eastern North Pacific? *Eos*, **81**, 561–567.

Allan, R.J., and T. Ansell, 2006: A new globally complete monthly historical gridded mean sea level pressure data set (HadSLP2); 1850–2003. *J. Clim.*, **19**, 5816–5842.

Allan, R.P., and A. Slingo, 2002: Can current climate model forcings explain the spatial and temporal signatures of decadal OLR variations? *Geophys. Res. Lett*., **29**, 1141, doi:10.1029/2001GL014620.

Allan, R.P., A. Slingo, and V. Ramaswamy, 2002: Analysis of moisture variability in the European Centre for Medium-Range Weather Forecasts 15-year reanalysis over tropical oceans. *J. Geophys. Res.*, **107**, doi:10.1029/2001JD001132.

Allan, R.P., M.A. Ringer, and A. Slingo, 2003: Evaluation of moisture in the Hadley Centre Climate Model using simulations of HIRS water vapour channel radiances. *Q. J. R. Meteorol. Soc*., **128**, 1–18.

Allan, R.P., et al., 2001: Is there an equatorial Indian Ocean dipole, and is it independent of the El Niño Southern Oscillation? *CLIVAR Exchanges*, **21**, 1–3.

Allan, R.P., et al., 2004: Simulation of the Earth's radiation budget by the European Centre for Medium-Range Weather Forecasts 40-year reanalysis (ERA40). *J. Geophys. Res*., **109**, D18107, doi:10.1029/2004JD004816.

Allen, M.R., and W.J. Ingram, 2002: Constraints on future changes in climate and the hydrological cycle. *Nature*, **419**, 2224–2232.

Alley, W.M., 1984: The Palmer Drought Severity Index: limitation and assumptions. *J. Clim. Appl. Meteorol*., **23**, 1100–1109.

Alpert, P., et al., 2002: The paradoxical increase of Mediterranean extreme daily rainfall in spite of decrease in total values. *Geophys. Res. Lett*., **29**(11), doi:10.1029/2001GL013554.

Alpert, P., et al., 2005: Global dimming or local dimming?: Effect of urbanization on sunlight availability. *Geophys. Res. Lett*., **32**, L17802, doi:10.1029/2005GL023320.

Ambaum, M.H.P., B.J. Hoskins, and D.B. Stephenson, 2001: Arctic Oscillation or North Atlantic Oscillation? *J. Clim.*, **14**, 3495–3507.

Ambaum, M.H.P., B.J. Hoskins, and D.B. Stephenson, 2002: Corrigendum: Arctic Oscillation or North Atlantic Oscillation? *J. Clim.*, **15**, 553.

Andrea, F., et al., 1998: Northern Hemisphere atmospheric blocking as simulated by 15 atmospheric general circulation models in the period 1979–1988. *Clim. Dyn.*, **14**, 385–407.

Andreae, M.O., et al., 2004: Smoking rain clouds over the Amazon. *Science*, **303**, 1337–1342.

Andrews, D.G., J.R. Holton, and C.B. Leovy, 1987: *Middle Atmosphere Dynamics*. Academic Press, San Diego, CA, 489 pp.

Angell, J.K., 2003: Effect of exclusion of anomalous tropical stations on temperature trends from a 63-station radiosonde network, and comparison with other analyses. *J. Clim.*, **16**, 2288–2295.

Angell, J.K., 2006: Changes in the 300 mb north circumpolar vortex, 1963–2001. *J. Clim.*, **19**, 2984–2994.

Aoki, S., 2002: Coherent sea level response to the Antarctic Oscillation. *Geophys. Res. Lett.*, **29**, 1950, doi:10.1029/2002GL15733.

Ashok, K., Z. Guan, and T. Yamagata, 2001: Impact of the Indian Ocean Dipole on the decadal relationship between the Indian monsoon rainfall and ENSO. *Geophys. Res. Lett*., **28**, 4499–4502.

Assell, R., K. Cronk, and D. Norton, 2003: Recent trends in Laurentian Great Lakes ice cover. *Clim. Change*, **57**, 185–204.

Auer, I., et al., 2007: HISTALP -- Historical Instrumental Climatological Surface Time Series of the Greater Alpine Region. *Int. J. Climatol.*, **27**, 17-46.

Baldwin, M.P., 2001: Annular modes in global daily surface pressure. *Geophys. Res. Lett.*, **28**, 4115–4118.

Baldwin, M.P., and T. Dunkerton, 1999: Downward propagation of the Arctic Oscillation from the stratosphere to the troposphere. *J. Geophys. Res*., **104**, 30937–30946.

Baldwin, M.P., and T.J. Dunkerton, 2001: Stratospheric harbingers of anomalous weather regimes. *Science*, **244**, 581–584.

Baldwin, M.P., et al., 2003: Stratospheric memory and extended-range weather forecasts. *Science*, **301**, 636–640.

Balling, R.C. Jr., and S. Brazel, 1987: Recent changes in Phoenix summertime diurnal precipitation patterns. *Theor. Appl. Climatol*., **38**, 50–54.

Balling, R.C. Jr., et al., 1998: Impacts of land degradation on historical temperature records from the Sonoran Desert. *Clim. Change*, **40**, 669–681.

Barlow, M., H. Cullen, and B. Lyon, 2002: Drought in central and southwest Asia: La Niña, the warm pool, and Indian Ocean precipitation. *J. Clim.*, **15**, 697–700.

Barnett, T.P., et al., 1999: Interdecadal interactions between the tropics and midlatitudes in the Pacific basin. *Geophys. Res. Lett*., **26**, 615–618.

Barnston, A.G., and R.E. Livezey, 1987: Classification, seasonality and persistence of low frequency atmospheric circulation patterns. *Mon. Weather Rev.*, **115**, 1083–1126.

Bärring, L., and H. von Storch, 2004: Scandinavian storminess since about 1800. *Geophys. Res. Lett.*, **31**, L20202, doi:10.1029/2004GL020441.

Barriopedro, D., et al., 2006: A climatology of Northern Hemisphere blocking. *J. Clim.*, **19**, 1042–1063.

Barros, V.R., M.E. Castañeda, and M.E. Doyle, 2000a: Recent precipitation trends in southern South America east of the Andes: An indication of climatic variability. In: *Southern Hemisphere Paleo- and Neoclimates. Key Sites, Methods, Data and Models* [Smolka, P.P., and W. Volkheimer (eds.)]. Springer Verlag, Berlin, pp. 187–206.

Barros, V.R., et al., 2000b: Influence of the South Atlantic Convergence Zone and South Atlantic sea surface temperature on interannual summer rainfall variability in southeastern South America. *Theor. Appl. Climatol*., **67**, 123–133.

Barros, V.R., et al., 2002: Climate variability over South America and the South America monsoon: A review. *Meteorologica*, **27**, 33–57.

Barros, V.R., et al., 2004: The major discharge events in the Paraguay River: magnitudes, source regions and climate forcings. *J. Hydrometeorol.*, **6**, 1161–1170.

Basher, R.E., and X. Zheng, 1995: Tropical cyclones in the southwest Pacific: Spatial patterns and relationships to Southern Oscillation and sea surface temperature. *J. Clim.*, **8**, 1249–1260.

Bates, J.J., and D.L. Jackson, 2001: Trends in upper-tropospheric humidity. *Geophys. Res. Lett*., **28**, 1695–1698.

Beck, C., J. Grieser, and B. Rudolf, 2005: A new monthly precipitation climatology for the global land areas for the period 1951 to 2000. *Climate Status Report, 2004*. German Meteorological Service, pp. 181–190, http://www.dwd.de/de/FundE/Klima/KLIS/prod/KSB/ksb04/28_precipitation.pdf

Bengtsson, L., S. Hagemann, and K.L. Hodges, 2004: Can climate trends be calculated from reanalysis data? *J. Geophys. Res*., **109**, D11111, doi:10.1029/2004JD004536.

Beniston, M., 2004: The 2003 heat wave in Europe. A shape of things to come? *Geophys. Res. Lett.*, **31**, L02022, doi:10.1029/2003GL018857.

Beniston, M., and H.F. Diaz, 2004: The 2003 heat wave as an example of summers in a greenhouse climate? Observations and climate model simulations for Basel, Switzerland. *Global Planet. Change*, **44**, 73–81.

Beniston, M., and D.B. Stephenson, 2004: Extreme climatic events and their evolution under changing climatic conditions. *Global Planet. Change*, **44**, 1–9.

Berger, C.L., et al., 2002: A climatology of northwest Missouri snowfall events: Long-term trends and interannual variability. *Phys. Geogr*., **23**, 427–448.

Berri, G.S., M.A. Ghietto, and N.O. García, 2002: The influence of ENSO in the flows of the Upper Paraná River of South America over the past 100 years. *J. Hydrometeorol.*, **3**, 57–65.

Betts, A.K., J.H. Ball, and P. Viterbo, 2003: Evaluation of the ERA-40 surface water budget and surface temperature for the Mackenzie River Basin. *J. Hydrometeorol.*, **4**, 1194–1211.

Biondi, F., A. Gershunov, and D.R. Cayan, 2001: North Pacific decadal climate variability since AD 1661. *J. Clim.*, **14**, 5–10.

Bischoff, S.A., et al., 2000: Climate variability and Uruguay River flows. *Water International*, **25**, 446–456.

Bissolli, P., J. Grieser, N. Dotzek, and M. Welsch, 2007: Tornadoes in Germany 1950-2003 and their relation to particular weather conditions. *Global Planet. Change*, **46**, doi:10.1016/j.gloplacha.2006.11.007

Black, E.M., et al., 2004: Factors contributing to the summer 2003 European heatwave. *Weather*, **59**, 217–223.

Bojariu, R., and L. Gimeno, 2003: The influence of snow cover fluctuations on multiannual NAO persistence. *Geophys. Res. Lett.*, **30**, 1156, doi:10.1029/2002GL015651.

Bonan, G.B., 2001: Observational evidence for reduction of daily maximum temperature by croplands in the midwest United States. *J. Clim.*, **14**, 2430–2442.

Bonnazola, M., and P.H. Haynes, 2004: A trajectory-based study of the tropical tropopause region. *J. Geophys. Res*., **109**, D020112, doi:10.1029/2003JD004356.

Bornstein, R., and Q. Lin, 2000: Urban heat islands and summertime convective thunderstorms in Atlanta: three cases studies. *Atmos. Environ*., **34**, 507–516.

Bottomley, M., et al., 1990: *Global Ocean Surface Temperature Atlas "GOSTA"*. HMSO, London, 20 pp.+iv, 313 plates.

Bove, M.C., et al., 1998: Effect of El Niño on U.S. landfalling hurricanes, revisited. *Bull. Am. Meteorol. Soc.*, **79**, 2477–2482.

Branstator, G., 2002: Circum-global teleconnections, the jetstream waveguide, and the North Atlantic Oscillation. *J. Clim.*, **15**, 1893–1910.

Brest, C.L., W.B. Rossow, and M. Roiter, 1997: Update of radiance calibrations for ISCCP. *J. Atmos. Ocean Technol.*, **14**, 1091–1109.

Brohan, P., et al., 2006: Uncertainty estimates in regional and global observed temperature changes: A new dataset from 1850. *J. Geophys. Res.*, **111**, D12106, doi:10.1029/2005JD006548.

Bromirski, P.D., R.E. Flick, and D.R. Cayan, 2003: Storminess variability along the California coast: 1858–2000. *J. Clim.*, **16**, 982–993.

Bromwich, D.H., and R.L. Fogt, 2004: Strong trends in the skill of the ERA-40 and NCEP–NCAR reanalyses in the high and middle latitudes of the Southern Hemisphere, 1958–2001. *J. Clim.*, **17**, 4603–4619.

Brönnimann, S., et al., 2004: Extreme climate of the global troposphere and stratosphere in 1940–42 related to El Niño. *Nature*, **431**, doi:10.1038/nature02982.

Brooks, H.E., J.W. Lee, and J.P. Craven, 2003: The spatial distribution of severe thunderstorm and tornado environments from global reanalysis data. *Atmos. Res.*, **67–68**, 73–94.

Brunet, M., et al., 2006: The development of a new dataset of Spanish daily adjusted temperature series (SDATS) (1850-2003). *Int. J. Climatol.*, **26**, 1777–1802.

Brunetti, M., et al., 2004: Changes in daily precipitation frequency and distribution in Italy over the last 120 years. *J. Geophys. Res*., **109**, D05102, doi:10.1029/2003JD004296.

Brutsaert, W., and M.B. Parlange, 1998: Hydrologic cycle explains the evaporation paradox. *Nature*, **396**, 30.

Burian, S.J., and J.M. Shepherd, 2005: Effects of urbanization on the diurnal rainfall pattern in Houston. *Hydrological Processes*: *Special Issue on Rainfall and Hydrological Processes*, **19**, 1089–1103.

Burnett, A.W., et al., 2003: Increasing Great Lake-effect snowfall during the Twentieth Century: A regional response to global warming? *J. Clim.*, **16**, 3535–3541.

Caesar, J., L. Alexander, and R. Vose, 2006: Large-scale changes in observed daily maximum and minimum temperatures: Creation and analysis of a new gridded data set. *J. Geophys. Res.*, **111**, D05101, doi:10.1029/2005JD006280.

Cai, W., and P.G. Baines, 2001: Forcing of the Antarctic Circumpolar Wave by El Niño-Southern Oscillation teleconnections. *J. Geophys. Res.*, **106**, 9019–9038.

Cai, W., P.H. Whetton, and D.J. Karoly, 2003: The response of the Antarctic Oscillation to increasing and stabilized atmospheric CO_2. *J. Clim.*, **16**, 1525–1538.

Caires, S., and A. Sterl, 2005: 100-year return value estimates for wind speed and significant wave height from the ERA-40 data. *J. Clim.*, **18**, 1032–1048.

Camargo, S.J., and A.H. Sobel, 2004: *Western North Pacific Tropical Cyclone Intensity and ENSO*. Technical Report No. 04-03, International Research Institute for Climate Prediction, Palisades, NY, 25 pp.

Camilloni, I.A., and V.R. Barros, 2000: The Paraná River response to El Niño 1982–83 and 1997–98 events. *J. Hydrometeorol.*, **1**, 412–430.

Camilloni, I.A., and V.R. Barros, 2003: Extreme discharge events in the Paraná River and their climate forcing. *J. Hydrol.*, **278**, 94–106.

Cardone, V.J., J.G. Greenwood, and M.A. Cane, 1990: On trends in historical marine wind data. *J. Clim.*, **3**, 113–127.

Carril, A.F., and A. Navarra, 2001: Low-frequency variability of the Antarctic Circumpolar Wave. *Geophys. Res. Lett*., **28**, 4623–4626.

Carter, D.J.T., 1999: Variability and trends in the wave climate of the North Atlantic: a review. In: *Proceedings of the 9th International Offshore and Polar Engineering Conference*, *Brest, France,* vol. III. International Society of Offshore and Polar Engineers, Golden, CO, pp. 12–18.

Cassou, C., and L. Terray, 2001: Dual influence of Atlantic and Pacific SST anomalies on the North Atlantic/Europe winter climate. *Geophys. Res. Lett.*, **28**, 3195–3198.

Cassou, C., et al., 2004: North Atlantic winter climate regimes: spatial asymmetry, stationarity with time and oceanic forcing. *J. Clim.*, **17**, 1055–1068.

Cayan, D.R., et al., 2001: Changes in the onset of spring in the western United States. *Bull. Am. Meteorol. Soc.*, **82**, 399–415.

Cess, R.D., and P.M. Udelhofen, 2003: Climate change during 1985–1999: Cloud interactions determined from satellite measurements. *Geophys. Res. Lett*., **30**, 1019, doi:10.1029/2002GL016128.

Chagnon, F.J.F., and R. L. Bras, 2005: Contemporary climate change in the Amazon. *Geophys. Res. Lett*., **32**, L13703, doi:10.1029/2005GL022722.

Chan, J.C.L., 2006: Comment on "Changes in tropical cyclone number, duration, and intensity in a warming environment". *Science*, **311**, 1713.

Chan, J.C.L., and K.S. Liu, 2004: Global warming and Western North Pacific typhoon activity from an observational perspective. *J. Clim.*, **17**, 4590–4602.

Chang, C.P., Y. Zhang, and T. Li, 1999: Interannual and interdecadal variations of the East Asian summer monsoon and tropical Pacific SSTs. Pt I: Roles of the subtropical ridge. *J. Clim.*, **13**, 4310–4325.

Chang, E.K.M., 2003: Midwinter suppression of the Pacific storm track activity as seen in aircraft observations. *J. Atmos. Sci*., **60**, 1345–1358.

Chang, E.K.M., and Y. Fu, 2002: Interdecadal variations in Northern Hemisphere winter storm track intensity. *J. Clim.*, **15**, 642–658.

Chang, E.K.M., and Y. Fu, 2003: Using mean flow change as a proxy to infer interdecadal storm track variability. *J. Clim.*, **16**, 2178–2196.

Changnon, D., M. Sandstrom, and C. Schaffer, 2003: Relating changes in agricultural practices to increasing dew points in extreme Chicago heat waves. *Clim. Res*., **24**, 243–254.

Changnon, S.A., and N.E. Westcott, 2002: Heavy rainstorms in Chicago: Increasing frequency, altered impacts, and future implications. *J. Am. Water Res. Assoc*., **38**, 1467–1475.

Changnon, S.A., et al., 1981: *METROMEX: A Review and Summary*. Meteorological Monograph 18, American Meteorological Society, Boston, MA, 81 pp.

Chase, T.N., J.A. Knaff, R.A. Pielke Sr., and E. Kalnay, 2003: Changes in global monsoon circulation since 1950. *Natural Hazards*, **29**, 229–254.

Chattopadhyay, N., and M. Hulme, 1997: Evaporation and potential evapotranspiration in India under conditions of recent and future climate change. *Agric. For. Meteorol*., **87**, 55–73.

Chelliah, M., and G.D. Bell, 2004: Tropical multidecadal and interannual climate variability in the NCEP–NCAR Reanalysis. *J. Clim.*, **17**, 1777–1803.

Chelton, D.B., and F.J. Wentz, 2005: Global microwave satellite observations of sea surface temperature for numerical weather prediction and climate research. *Bull. Am. Meteorol. Soc.*, **86**, 1097–1115.

Chen, M., P. Xie, and J.E. Janowiak, 2002: Global land precipitation: a 50-yr monthly analysis based on gauge observations. *J. Hydrometeorol.*, **3**, 249–266.

Chen, T.-C., et al., 2004: Variation of the East Asian summer monsoon rainfall. *J. Clim.*, **17**, 744–762.

Christy, J.R., and W.B. Norris, 2004: What may we conclude about tropospheric temperature trends? *Geophys. Res. Lett*., **31**, L0621, doi:10.1029/2003GL019361.

Christy, J. R., and R.W. Spencer, 2005: Correcting temperature data sets. *Science*, **310**, 972.

Christy, J.R., R.W. Spencer, and W.D. Braswell, 2000: MSU tropospheric temperatures: Dataset construction and radiosonde comparisons. *J. Atmos. Ocean. Technol*., **17**, 1153–1170.

Christy, J.R., et al., 2001: Differential trends in tropical sea surface and atmospheric temperature since 1979. *Geophys. Res. Lett.*, **28**, 183–186.

Christy, J.R., et al., 2003: Error estimates of version 5.0 of MSU/AMSU bulk atmospheric temperatures. *J. Atmos. Ocean. Technol.*, **20**, 613–629.

Christy, J.R., et al., 2006: Methodology and results of calculating Central California surface temperature trends: Evidence of human-induced climate change? *J. Clim.*, **19**, 548–563.

Clark, C.O., P.J. Webster, and J.E. Cole, 2003: Interdecadal variability of the relationship between the Indian Ocean zonal mode and east African coastal rainfall anomalies. *J. Clim.*, **16**, 548–554.

Cluis, D., and C. Laberge, 2001: Climate change and trend detection in selected rivers within the Asia-Pacific region. *Water International*, **26**, 411–424.

Cohen, S., B. Liepert, and G. Stanhill, 2004: Global dimming comes of age. *Eos*, **85**, 362.

Cohn, T., and H.J. Lins, 2005: Nature's style: Naturally trendy. *Geophys. Res. Lett.*, **32**, L23402, doi:10.1029/2005GL024476.

Compo, G.P., and P.D. Sardeshmukh, 2004: Storm track predictability on seasonal and decadal scales. *J. Clim.*, **17**, 3701–3720.

Connolley, W.M., 2003: Long-term variation of the Antarctic Circumpolar Wave. *J. Geophys. Res*., **108**, 8076, doi:10.1029/2000JC000380.

Considine, D.B., et al., 2001: An interactive model study of the influence of the Mount Pinatubo aerosol on stratospheric methane and water trends. *J. Geophys. Res*., **106**, 27711–27728.

Cook, E.R., R.D. D'Arrigo, and M.E. Mann, 2002: A well-verified, multiproxy reconstruction of the winter North Atlantic Oscillation index since A.D. 1400. *J. Clim.*, **15**, 1754–1764.

Cook, E.R., et al., 1999: Drought reconstructions for the continental United States. *J. Clim.*, **12**, 1145–1162.

Cook, E.R., et al., 2004: Long-term aridity changes in the western United States. *Science*, **306**, 1015–1018.

Corti, S., F. Molteni, and T.N. Palmer, 1999: Signature of recent climate change in frequencies of natural atmospheric circulation regimes. *Nature*, **398**, 799–802.

Cowell, C.M., and R.T. Stoudt, 2002: Dam-induced modifications to upper Allegheny River streamflow patterns and their biodiversity implications. *J. Am. Water Res. Assoc.*, **38**, 187–196.

Crutzen, P.J., 2004: New Directions: The growing urban heat and pollution "island" effect—impact on chemistry and climate. *Atmos. Environ.*, **38**, 3539–3540.

Cullen, H., and P.B. deMenocal, 2000: North Atlantic influence on Tigris-Euphrates streamflow. *Int. J. Climatol*., **20**, 853–863.

Curtis, S., and R.F. Adler, 2003: The evolution of El Niño-precipitation relationships from satellites and gauges. *J. Geophys. Res.*, **108**, 4153, doi:10.1029/2002JD002690.

Czaja, A., A.W. Robertson, and T. Huck: 2003: The role of Atlantic ocean-atmosphere coupling in affecting North Atlantic Oscillation variability. In: *The North Atlantic Oscillation: Climatic Significance and Environmental Impact* [Hurrell, J.W., et al. (eds.)]. Geophysical Monograph 134, American Geophysical Union, Washington, DC, pp. 147–172.

Dai, A., 2006: Recent climatology, variability and trends in global surface humidity. *J. Clim.*, **19**, 3589–3606.

Dai, A., and K.E. Trenberth, 2002: Estimates of freshwater discharge from continents: Latitudinal and seasonal variations. *J. Hydrometeorol*., **3**, 660–687.

Dai, A., and K.E. Trenberth, 2004: The diurnal cycle and its depiction in the Community Climate System Model. *J. Clim.*, **17**, 930–995.

Dai, A., I.Y. Fung, and A.D. Del Genio, 1997: Surface observed global land precipitation during 1900–1988. *J. Clim.*, **10**, 2943–2962.

Dai, A., K.E. Trenberth, and T.R. Karl, 1999: Effects of clouds, soil moisture, precipitation and water vapor on diurnal temperature range. *J. Clim.*, **12**, 2451–2473.

Dai A., K.E. Trenberth, and T. Qian, 2004a: A global data set of Palmer Drought Severity Index for 1870–2002: Relationship with soil moisture and effects of surface warming. *J. Hydrometeorol.*, **5**, 1117–1130.

Dai, A., et al., 2004b: The recent Sahel drought is real. *Int. J. Climatol*., **24**, 1323–1331.

Dai, A., et al., 2006: Recent trends in cloudiness over the United States: A tale of monitoring inadequacies. *Bull. Am. Meteorol. Soc*, **87**, 597–606.

De Laat, A.T.J., and A.N. Maurellis, 2006: Evidence for influence of anthropogenic surface processes on lower tropospheric and surface temperature trends. *Int. J. Climatol*., **26**, 897–913.

DeGaetano, A.T., and R.J. Allen, 2002: Trends in twentieth-century extremes across the United States. *J. Clim.*, **15**, 3188–3205.

Delworth, T.L., and M.E. Mann, 2000: Observed and simulated multidecadal variability in the Northern Hemisphere. *Clim. Dyn.*, **16**, 661–676.

DeMott, C.A., and D.A. Randall, 2004: Observed variations of tropical convective available potential energy. *J. Geophys. Res*., **109**, D02102, doi:10.1029/2003JD003784.

Déry, S.J., and E.F. Wood, 2005: Decreasing river discharge in northern Canada. *Geophys. Res. Lett*., **32**, L10401, doi:10.1029/2005GL022845.

Deser, C., 2000: On the teleconnectivity of the Arctic Oscillation. *Geophys. Res. Lett.*, **27**, 779–782.

Deser, C., M.A. Alexander, and M.S. Timlin, 1996: Upper-ocean thermal variations in the North Pacific during 1970–1991. *J. Clim.*, **9**, 1840–1855.

Deser, C., M.A. Alexander, and M.S. Timlin, 1999: Evidence for a wind-driven intensification of the Kuroshio Current Extension from the 1970s to the 1980s. *J. Clim.*, **12**, 1697–1706.

Deser, C., J.E. Walsh, and M.S. Timlin, 2000: Arctic sea ice variability in the context of recent atmospheric circulation trends. *J. Clim.*, **13**, 617–633.

Deser, C., M.A. Alexander, and M. S. Timlin, 2003: Understanding the persistence of sea surface temperature anomalies in midlatitudes. *J. Clim.*, **16**, 57–72.

Deser, C., A.S. Phillips, and J.W. Hurrell, 2004: Pacific interdecadal climate variability: Linkages between the tropics and the north Pacific during boreal winter since 1900. *J. Clim.*, **17**, 3109–3124.

Dessler, A.E., and S.C. Sherwood, 2004: Effect of convection on the summertime extratropical lower stratosphere, *J. Geophys. Res*., **109**, D23301, doi:10.1029/2004JD005209.

DeWeaver, E., and S. Nigam, 2000: Zonal-eddy dynamics of the North Atlantic Oscillation. *J. Clim.*, 13, 3893–3914.

Dickson, R.R., et al., 2000: The Arctic Ocean response to the North Atlantic Oscillation. *J. Clim.*, **13**, 2671–2696.

Diem, J.E., and D.P. Brown, 2003: Anthropogenic impacts on summer precipitation in central Arizona, U.S.A. *Professional Geogr.*, **55**, 343–355.

Diggle, P.J., K.Y. Liang, and S.L. Zeger, 1999: *Analysis of Longitudinal Data*. Clarendon Press, Oxford, UK, 253 pp.

Ding, Y.H, C.Y. Li, and Y.J. Liu, 2004: Overview of the South China Seas monsoon experiment. *Adv. Atmos. Sci.*, **21**, 343–360.

Dixon, P.G., and T.L. Mote, 2003: Patterns and causes of Atlanta's urban heat island-initiated precipitation. *J. Appl. Meteorol.*, **42**, 1273–1284.

Doswell, C.A., H.E. Brooks, and M.P. Kay, 2005: Climatological estimates of daily local nontornadic severe thunderstorm probability for the United States. *Weather Forecasting*, **20**, 577–595.

Dotzek, N., 2003: An updated estimate of tornado occurrence in Europe. *Atmos. Res*., **67–68**, 153–161.

Dotzek, N., et al., 2005: Observational evidence for exponential tornado intensity distributions over specific kinetic energy. *Geophys. Res. Lett*., **32**, L24813, doi:10.1029/2005GL024583.

Doyle, M.E., and V.R. Barros, 2002: Midsummer low-level circulation and precipitation in subtropical South America and related sea surface temperature anomalies in the South Atlantic. *J. Clim.*, **15**, 3394–3410.

Duchon, C.E., 1979: Lanczos filtering in one and two dimensions. *J Appl. Meteorol.*, **18**, 1016–1022.

Durre, I., and J.M. Wallace, 2001: Factors influencing the cold-season diurnal temperature range in the United States. *J. Clim.*, **14**, 3263–3278.

Durre, I., T. Peterson, and R. Vose, 2002: Evaluation of the effect of the Luers-Eskridge radiation adjustments on radiosonde temperature homogeneity. *J. Clim.*, **15**, 1335–1347.

Durre, I., R.S. Vose, and D.B. Wuertz, 2006: Overview of the integrated global radiosonde archive. *J. Clim.*, **19**, 53–68.

Easterling, D.R., 2002: Recent changes in frost days and the frost-free season in the United States. *Bull. Am. Meteorol. Soc*., **83**, 1327–1332.

Easterling, D.R., et al., 2000: Observed variability and trends in extreme climate events: A brief review. *Bull. Am. Meteorol. Soc*., **81**, 417–425.

Easterling, D.R., et al., 2003: CCl/CLIVAR workshop to develop priority climate indices. *Bull. Am. Meteorol. Soc.*, **84**, 1403–1407.

Elliott, W.P., R.J. Ross, and W.H. Blackmore, 2002: Recent changes in NWS upper-air observations with emphasis on changes from VIZ to Vaisala radiosondes. *Bull. Am. Meteorol. Soc*., **83**, 1003–1017.

Ellis, A.W., and J.J. Johnson, 2004: Hydroclimatic analysis of snowfall trends associated with the North American Great Lakes. *J. Hydrometeorol.*, **5**, 471–486.

Emanuel, K., 2003: Tropical cyclones. *Annu. Rev. Earth. Planet. Sci*., **31**, 75–104.

Emanuel, K., 2005a: Increasing destructiveness of tropical cyclones over the past 30 years. *Nature*, **436**, 686–688.

Emanuel, K., 2005b: Emanuel replies. *Nature*, **438**, E13, doi:10.1038/nature04427.

Enfield, D.B., A.M. Mestas-Nuñez, and P.J Trimble, 2001: The Atlantic Multidecadal Oscillation and its relation to rainfall and river flows in the continental US. *Geophys. Res. Lett.*, **28**, 2077–2080.

Evans, M.N., et al., 2001: Support for tropically-driven Pacific decadal variability based on paleoproxy evidence. *Geophys. Res. Lett*., **28**, 3689–3692.

Fauchereau, N., et al., 2003: Rainfall variability and changes in Southern Africa during the 20th century in the global warming context. *Natural Hazards*, **29**, 139–154.

Feldstein, S.B., 2002: The recent trend and variance increase of the Annular Mode. *J. Clim.*, **15**, 88–94.

Fink, A.H., et al., 2004: The 2003 European summer heatwaves and drought – synoptic diagnosis and impacts. *Weather*, **59**, 209–216.

Folland, C.K., and D.E. Parker, 1995: Correction of instrumental biases in historical sea surface temperature data. *Q. J. R. Meteorol. Soc.*, **121**, 319–367.

Folland, C.K., et al., 1993: A study of six operational sea surface temperature analyses. *J. Clim.*, **6**, 96–113.

Folland, C.K., et al., 1999: Large scale modes of ocean surface temperature since the late nineteenth century. In: *Beyond El Niño: Decadal and Interdecadal Climate Variability* [Navarra, A. (ed.)]. Springer-Verlag, Berlin, pp. 73–102.

Folland, C.K., et al., 2001: Predictability of North East Brazil rainfall and real-time forecast skill, 1987-1998. *J. Clim.*, **14**, 1937–1958.

Folland, C.K., et al., 2002: Relative influences of the interdecadal Pacific oscillation and ENSO on the South Pacific convergence zone. *Geophys. Res. Lett.*, **29**(13), doi:10.1029/2001GL014201.

Folland, C.K., et al., 2003: Trends and variations in South Pacific island and ocean surface temperature. *J. Clim.*, **16**, 2859–2874.

Forster, P.M.D., and K.P. Shine, 1999: Stratospheric water vapour changes as a possible contributor to observed stratospheric cooling. *Geophys. Res. Lett.*, **26**, 3309–3312.

Forster, P.M.D., and K.P. Shine, 2002: Assessing the climate impact of trends in stratospheric water vapor. *Geophys. Res. Lett*, **29**, 1086, doi:10.1029/2001GL013909.

Forster, P.M.D., and S. Solomon, 2003: Observations of a "weekend effect" in diurnal temperature range. *Proc. Natl. Acad. Sci. U.S.A.*, **100**, 11225–11230.

Fowler, H.J., and C.G. Kilsby, 2003a: Implications of changes in seasonal and annual extreme rainfall. *Geophys. Res. Lett*., **30**, 1720, doi:10.1029/2003GL017327.

Fowler, H.J., and C.G. Kilsby, 2003b: A regional frequency analysis of United Kingdom extreme rainfall from 1961 to 2000. *Int. J. Climatol*., **23**, 1313–1334.

Frauenfeld, O.W., and R.E. Davis, 2003: Northern Hemisphere circumpolar vortex trends and climate change implications. *J. Geophys. Res*., **108**, 4423, doi:10.1029/2002JD002958.

Free, M., and D. Seidel, 2005: Causes of differing temperature trends in radiosonde upper-air datasets. *J. Geophys. Res.*, **110**, D07101, doi:10.1029/2004JD005481.

Free, M., M. Bister, and K. Emanuel, 2004a: Potential intensity of tropical cyclones: comparison of results from radiosonde and reanalysis data. *J. Clim.*, **17**, 1722–1727.

Free, M., et al., 2002: Creating climate reference datasets: CARDS workshop on adjusting radiosonde temperature data for climate monitoring. *Bull. Am. Meteorol. Soc*., **83**, 891–899.

Free, M., et al., 2004b: Using first differences to reduce inhomogeneity in radiosonde temperature datasets. *J. Clim.*, **17**, 4171–4179.

Frei, C., and C. Schär, 2001: Detection of probability of trends in rare events: Theory and application to heavy precipitation in the Alpine region. *J. Clim.*, **14**, 1568–1584.

Frich, P., et al., 2002: Observed coherent changes in climatic extremes during the second half of the twentieth century. *Clim. Res.*, **19**, 193–212.

Fu, Q., and C.M. Johanson, 2004: Stratospheric influence on MSU-derived tropospheric temperature trends: A direct error analysis. *J. Clim.*, **17**, 4636–4640.

Fu, Q., and C.M. Johanson, 2005: Satellite-derived vertical dependence of tropical tropospheric temperature trends. *Geophys. Res. Lett.*, **32**, L10703, doi:10.1029/2004GL022266.

Fu, Q., et al., 2004a: Contribution of stratospheric cooling to satellite-inferred tropospheric temperature trends. *Nature*, **429**, 55–58.

Fu, Q., et al., 2004b: Stratospheric cooling and the troposphere (reply). *Nature*, **432**, doi:10.1038/nature03210.

Fueglistaler, S., and P.H. Haynes, 2005: Control of interannual and longer-term variability of stratospheric water vapour. *J. Geophys. Res.*, **110**, D24108, doi:10.1029/2005JD006019.

Fueglistaler, S., H. Wernli, and T. Peter, 2004: Tropical troposphere-to-stratosphere transport inferred from trajectory calculations. *J. Geophys. Res.*, **109**, D03108, doi:10.1029/2003JD004069.

Fujibe, F., 2003: Long-term surface wind changes in the Tokyo metropolitan area in the afternoon of sunny days in the warm season. *J. Meteorol. Soc. Japan*, **81**, 141–149.

Gallego, D., et al., 2005: A new look at the Southern Hemisphere jet stream. *Clim. Dyn.*, **24**, 607–621.

García, N.O., and W.M. Vargas, 1998: The temporal climatic variability in the 'Río de la Plata' basin displayed by the river discharges. *Clim. Change*, **38**, 359–379.

GCOS, 2003: *The Second Report on the Adequacy of the Global Observing Systems for Climate in Support of the UNFCCC*. GCOS-82, WMO/TD No. 1143, Global Climate Observing System, 74 pp.

GCOS, 2004: *GCOS Implementation Plan for the Global Observing System for Climate in support of UNFCCC*. GCOS-92, WMO/TD 1219, Global Climate Observing System, 136 pp.

Gedalof, Z., N.J. Mantua, and D.L. Peterson, 2002: A multi-century perspective of variability in the Pacific Decadal Oscillation: new insights from tree rings and coral. *Geophys. Res. Lett.*, **29**, 2204, doi:10.1029/2002GL015824.

Geng, Q., and M. Sugi, 2001: Variability of the North Atlantic cyclone activity in winter analyzed from NCEP-NCAR reanalysis data. *J. Clim.*, **14**, 3863–3873.

Genta, J.L., G. Perez-Iribarren, and C.R. Mechoso, 1998: A recent increasing trend in the streamflow of rivers in southeastern South America. *J. Clim.*, **11**, 2858–2862.

Genthon, C., G. Krinner, and M. Sacchettini, 2003: Interannual Antarctic tropospheric circulation and precipitation variability. *Clim. Dyn.*, **21**, 289–307.

Gershunov, A., and T.P. Barnett, 1998: Interdecadal modulation of ENSO teleconnections. *Bull. Am. Meteorol. Soc.*, **79**, 2715–2725.

Gettelman, A., et al., 2002: Multi-decadal trends in tropical convective available potential energy. *J. Geophys. Res.*, **107**, 4606, doi:10.1029/2001JD001082.

Giannini, A., R. Saravannan, and P. Chang, 2003: Ocean forcing of Sahel rainfall on interannual to interdecadal time scales. *Science*, **302**, 1027–1030.

Gilgen, H., M. Wild, and A. Ohmura, 1998: Means and trends of shortwave irradiance at the surface estimated from global energy balance archive data. *J. Clim.*, **11**, 2042–2061.

Gille, S.T., 2002: Warming of the Southern Ocean since the 1950s. *Science*, **295**, 1275–1277.

Gillett, N.P., and D. Thompson, 2003: Simulation of recent Southern Hemisphere climate change. *Science*, **302**, 273–275.

Gillett, N.P., B.D. Santer, and A.J. Weaver, 2004: Stratospheric cooling and the troposphere. *Nature*, **432**, doi:10.1038/nature03209.

Gillett, N.P., R.J. Allan, and T.J. Ansell, 2005: Detection of external influence on sea level pressure with a multi-model ensemble. *Geophys. Res. Lett.*, **32**, L19714, doi:10.1029/2005GL023640.

Gillett, N.P., et al., 2003: Detection of human influence on sea-level pressure. *Nature*, **422**, 292–294.

Goddard, L., and N.E. Graham, 1999: Importance of the Indian Ocean for simulating rainfall anomalies over eastern and southern Africa. *J. Geophys. Res.*, **104**, 19099–19116.

Goldenberg, S.B et al., 2001: The recent increase in Atlantic hurricane activity: causes and implications. *Science*, **293**, 474–479.

Golubev, V.S., et al., 2001: Evaporation changes over the contiguous United States and the former USSR: A reassessment. *Geophys. Res. Lett.*, **28**, 2665–2668.

Gong, D.Y., and S.W. Wang, 1999: Definition of Antarctic oscillation index. *Geophys. Res. Lett.*, **26**, 459–462.

Gong D.Y., and S.W. Wang, 2000: Severe summer rainfall in China associated with enhanced global warming. *Clim. Res.*, **16**, 51–59.

Gong, D.Y., and C.-H. Ho, 2002: Shift in the summer rainfall over the Yangtze River valley in the late 1970s. *Geophys. Res. Lett*., **29**(3), doi:10.1029/2001GL014523.

Gong, D.Y., S.W. Wang, and J.H. Zhu, 2001: East Asian winter monsoon and Arctic Oscillation. *Geophys. Res. Lett*., **28**, 2073–2076.

Gong, G., D. Entekhabi, and J. Cohen, 2002: A large-ensemble model study of the wintertime AO-NAO and the role of interannual snow perturbations. *J. Clim.*, **15**, 3488–3499.

Gong, G., D. Entekhabi, and J. Cohen, 2003: Modeled Northern Hemisphere winter climate response to realistic Siberian snow anomalies. *J. Clim.*, **16**, 3917–3931.

Gower, J.F.R., 2002: Temperature, wind and wave climatologies, and trends from marine meteorological buoys in the northeast Pacific. *J. Clim.*, **15**, 3709–3718.

Graham, N.E., and H.F. Diaz, 2001: Evidence for intensification of North Pacific winter cyclones since 1948. *Bull. Am. Meteorol. Soc*., **82**, 1869–1893.

Gray, S.T., et al., 2004: A tree-ring based reconstruction of the Atlantic Multidecadal Oscillation since 1567 A.D. *Geophys. Res. Lett*., **31**, L12205, doi:10.1029/2004GL019932.

Gray, W.M., 1984: Atlantic seasonal hurricane frequency: Part I: El Niño and 30-mb quasi-biennial oscillation influences. *Mon. Weather Rev.*, **112**, 1649–1668.

Grieser, J., S. Trömel, and C.-D. Schönwiese, 2002: Statistical time series decomposition into significant components and application to European temperature. *Theor. Appl. Climatol*., **71**, 171–183.

Griffiths, G.M., M.J. Salinger, and I. Leleu, 2003: Trends in extreme daily rainfall in the South Pacific and relations to the South Pacific Convergence Zone. *Int. J. Climatol*., **23**, 847–869.

Griffiths, G.M., et al., 2005: Change in mean temperature as a predictor of extreme temperature change in the Asia-Pacific region. *Int. J. Climatol.*, **25**, 1301–1330.

Grist, J.P., and S.A. Josey, 2003: Inverse analysis of the SOC air-sea flux climatology using ocean heat transport constraints. *J. Clim.*, **16**, 3274–3295.

Grody, N.C., et al., 2004: Calibration of multi-satellite observations for climatic studies: Microwave sounding unit (MSU). *J. Geophys. Res*., **109**, D24104, doi:10.1029/2004JD005079.

Groisman, P.Ya., and E.Ya. Rankova, 2001: Precipitation trends over the Russian permafrost-free zone: removing the artifacts of pre-processing. *Int. J. Climatol.*, **21**, 657–678.

Groisman, P.Ya., R.W. Knight, and T.R. Karl, 2001: Heavy precipitation and high streamflow in the contiguous United States: Trends in the 20th century. *Bull. Am. Meteorol. Soc*., **82**, 219–246.

Groisman, P.Ya., et al., 2003. Contemporary climate changes in high latitudes of the Northern Hemisphere: Daily time resolution. In: *Proceedings of the International Symposium on Climate Change, Beijing, China, 31 March–3 April, 2003*. WMO/TD No. 1172, China Meteorological Press, Beijing, China, pp. 51–55.

Groisman, P.Ya., et al., 2004: Contemporary changes of the hydrological cycle over the contiguous United States: Trends derived from *in situ* observations. *J. Hydrometeorol.*, **5**, 64–85.

Groisman, P.Ya., et al., 2005: Trends in intense precipitation in the climate record. *J. Clim.*, **18**, 1326–1350.

Groisman, P.Ya., et al., 2007: Potential forest fire danger over northern Eurasia: Changes during the 20th century. *Global Planet. Change*, **46**, doi:10.1016/j.gloplacha.2006.07.029.

Grollmann, T., and S. Simon, 2002: Flutkatastrophen – Boten des klimawandels. *Z. Versicher.*, **53**, 682–689.

Gruza, G.V., et al., 1999: Indicators of climatic change for the Russian Federation. *Clim. Change*, **42**, 219–242.

Gu, D.F., and S.G.H. Philander, 1997: Interdecadal climate fluctuations that depend on exchanges between the tropics and extratropics. *Science*, **275**, 805–807.

Guetter, A.K., and K.P. Georgakakos, 1993: River outflow of the conterminous United States, 1939–1988. *Bull. Am. Meteorol. Soc.*, **74**, 1873–1891.

Guichard, F., D. Parsons, and E. Miller, 2000: Thermodynamic and radiative impact of the correction of sounding humidity bias in the tropics. *J. Clim.*, **13**, 3611–3624.

Gulev, S.K., and L. Hasse, 1999: Changes of wind waves in the North Atlantic over the last 30 years. *Int. J. Climatol.*, **19**, 1091–1117.

Gulev, S.K., and V. Grigorieva, 2004: Last century changes in ocean wind wave height from global visual wave data. *Geophys. Res. Lett.*, **31**, L24302, doi:10.1029/2004GL021040.

Gulev, S. K., O. Zolina, and S. Grigoriev, 2001: Extratropical cyclone variability in the Northern Hemisphere winter from the NCEP/NCAR reanalysis data. *Clim. Dyn.*, **17**, 795–809.

Gulev, S.K., T. Jung, and E. Ruprecht, 2007: Estimation of the impact of sampling errors in the VOS observations on air-sea fluxes. Part II. Impact on trends and interannual variability. *J. Clim.*, **20**, 302–315.

Guo, Q.Y., et al., 2003: Interdecadal variability of East-Asian summer monsoon and its impact on the climate of China. *Acta Geogr. Sin.*, **4**, 569–576.

Gustafsson, M.E.R., 1997: Raised levels of marine aerosol deposition owing to increased storm frequency: A cause of forest decline in southern Sweden? *Agric. For. Meteorol.*, **84**, 169–177.

Guttman, N., 1991: A sensitivity analysis of the Palmer Hydrologic Drought Index. *Water Resour. Bull.*, **27**, 797–807.

Hahn, C.J., and S.G. Warren, 2003: *Cloud Climatology for Land Stations Worldwide, 1971–1996*. Report NDP-026D, Carbon Dioxide Information Analysis Center, Oak Ridge, TN, USA, 35 pp., http://cdiac.ornl.gov/epubs/ndp/ndp026d/ndp026d.html.

Haimberger, L., 2005: *Homogenization of Radiosonde Temperature Time Series Using ERA-40 Analysis Feedback Information*. ERA-40 Project Report Series 23, European Centre for Medium Range Weather Forecasts, Reading, UK, 68 pp.

Hansen, J., et al., 2001: A closer look at United States and global surface temperature change. *J. Geophys. Res.*, **106**, 23947–23963.

Harnik, N., and E.K.M. Chang, 2003: Storm track variations as seen in radiosonde observations and reanalysis data. *J. Clim.*, **16**, 480–495.

Harris, B.A., and G.A Kelly, 2001: A satellite radiance bias correction scheme for data assimilation. *Q. J. R. Meteorol. Soc.*, **127**, 1453–1468.

Hartmann, D.L., and F. Lo, 1998: Wave-driven flow vacillation in the Southern Hemisphere. *J. Atmos. Sci.*, **55**, 1303–1315.

Hartmann, D.L., et al., 2000: Can ozone depletion and global warming interact to produce rapid climate change? *Proc. Natl. Acad. Sci. U.S.A.*, **97**, 1412–1417.

Hatsushika, H., and K. Yamazaki, 2003: The stratospheric drain over Indonesia and dehydration within the tropical tropopause layer diagnosed by air parcel trajectories. *J. Geophys. Res.*, **108**, 4610, doi:10.1029/2002JD002986.

Hatzianastassiou, N., et al., 2004: Long-term global distribution of Earth's shortwave radiation budget at the top of atmosphere. *Atmos. Chem. Phys.*, **4**, 1217–1235.

Haylock, M.R., and C.M. Goodess, 2004: Interannual variability of extreme European winter rainfall and links with mean large-scale circulation. *Int. J. Climatol.*, **24**, 759–776.

Haylock M.R., et al., 2006. Trends in total and extreme South American rainfall in1960-2000 and links with sea surface temperature. *J. Clim.*, **19**, 1490–1512.

He, H., et al., 2003: Some climatic features of the tropical cyclones landed onto Guangdong Province during the recent 50 years. *Sci. Meteorol. Sin.*, **23**, 401–409 (in Chinese with English abstract).

Heim, R.R., 2002: A review of twentieth-century drought indices used in the United States. *Bull. Am. Meteorol. Soc.*, **83**, 1149–1165.

Held, I.M., and B.J. Soden, 2000: Water vapor feedback and global warming. *Annu. Rev. Energy Environ.*, **25**, 441–475.

Henderson-Sellers, A., 1992: Continental cloudiness changes this century. *GeoJournal*, **27**, 255–262.

Hennessy, K.J., R. Suppiah, and C.M. Page, 1999: Australian rainfall changes, 1910–1995. *Aust. Meteorol. Mag.*, **48**, 1–13.

Herath, S., and U. Ratnayake, 2004: Monitoring rainfall trends to predict adverse impacts – a case study from Sri Lanka (1964–1993). *Global Environ. Change*, **14**, 71–79.

Higgins, R.W., and W. Shi, 2000: Dominant factors responsible for interannual variability of the summer monsoon in the southwestern United States. *J. Clim.*, **13**, 759–776.

Highwood, E.J., B.J. Hoskins, and P. Berrisford, 2000: Properties of the Arctic tropopause. *Q. J. R. Meteorol. Soc.*, **126**, 1515–1532.

Hines, K.M., D.H. Bromwich, and G.J. Marshall, 2000: Artificial surface pressure trends in the NCEP-NCAR reanalysis over the Southern Ocean and Antarctica. *J. Clim.*, **13**, 3940–3952.

Ho, C.-H., et al., 2003: A sudden change summer rainfall characteristics in Korea during the late 1970s. *Int. J. Climatol.*, **23**, 117–128.

Hobbins, M.T., J.A. Ramirez, and T.C. Brown, 2004: Trends in pan evaporation and actual evapotranspiration across the conterminous U.S.: Paradoxical or complementary? *Geophys. Res. Lett.*, **31**, L13503, doi:10/10029/2004GL019846.

Hodgkins, G.A., R.W. Dudley, and T.G. Huntington, 2003: Changes in the timing of high river flows in New England over the 20th century. *J. Hydrol.*, **278**, 244–252.

Hoerling, M., and A. Kumar, 2003: The perfect ocean for drought. *Science*, **299**, 691–694.

Horel, J.D., and J.M. Wallace, 1981: Planetary-scale atmospheric phenomena associated with the Southern Oscillation. *Mon. Weather Rev.*, **109**, 813–829.

Hoskins, B.J., and D.J. Karoly, 1981: Steady linear response of a spherical atmosphere to thermal and orographic forcing. *J. Atmos. Sci.*, **38**, 1179–1196.

Hu, Q., Y. Tawaye, and S. Feng, 2004: Variations of the Northern Hemisphere atmospheric energetics: 1948–2000. *J. Clim.*, **17**, 1975–1986.

Huang, R.H., L. Zhou, and W. Chen, 2003: The progresses of recent studies on the variabilities of the East Asian monsoon and their causes. *Adv. Atmos. Sci.*, **1**, 55–69.

Huffman, G., et al., 1997: The Global Precipitation Climatology Project (GPCP): combined precipitation dataset. *Bull Am. Meteorol. Soc.*, **78**, 5–20.

Hughes, C.W., et al., 2003: Coherence of Antarctic sea levels, Southern Hemisphere Annular Mode, and flow through the Drake Passage. *Geophys. Res. Lett.*, **30**, 1464, doi:10.1029/2003GL017240.

Huntington, T.G., 2006: Evidence for intensification of the global water cycle: Review and synthesis. *J. Hydrol.*, **319**, 83–95.

Huntington, T.G., et al., 2004: Changes in the proportion of precipitation occurring as snow in New England (1949–2000). *J. Clim.*, **17**, 2626–2636.

Hurrell, J.W., 1995: Decadal trends in the North Atlantic Oscillation and relationships to regional temperature and precipitation. *Science*, **269**, 676–679.

Hurrell, J.W., 1996: Influence of variations in extratropical wintertime teleconnections on Northern Hemisphere temperature. *Geophys. Res. Lett.*, **23**, 665–668.

Hurrell, J.W., and H. van Loon, 1994: A modulation of the atmospheric annual cycle in the Southern Hemisphere. *Tellus*, **46A**, 325–338.

Hurrell, J.W., and H. van Loon, 1997: Decadal variations associated with the North Atlantic Oscillation. *Clim. Change*, **36**, 301–326.

Hurrell, J.W., and K.E. Trenberth, 1999: Global sea surface temperature analyses: multiple problems and their implications for climate analysis, modeling and reanalysis. *Bull. Am. Meteorol. Soc.*, **80**, 2661–2678.

Hurrell, J.W., M.P. Hoerling, and C.K. Folland, 2001: Climatic variability over the North Atlantic. In: *Meteorology at the Millennium* [Pearce, R. (ed.)]. Academic Press, London, pp. 143–151.

Hurrell, J.W., et al., 2000: Comparison of tropospheric temperatures from radiosondes and satellites: 1979–98. *Bull. Am. Meteorol. Soc*., **81**, 2165–2177.

Hurrell, J.W., et al., 2002: The relationship between tropical Atlantic rainfall and the summer circulation over the North Atlantic. In: *Proc. U. S. CLIVAR Atlantic Conf.*, June 12-14, 2001, Boulder, CO, [Legler, D. (ed.)]. U.S. CLIVAR Office, 193pp. 108–110.

Hurrell, J.W., et al., 2003: An overview of the North Atlantic Oscillation. In: *The North Atlantic Oscillation: Climatic Significance and Environmental Impact* [Hurrell, J.W., et al. (eds.)]. Geophysical Monograph 134, American Geophysical Union, Washington, DC, pp. 1–35.

Hurrell, J.W., et al., 2004: Twentieth century North Atlantic climate change. Pt I: Assessing determinism. *Clim. Dyn.*, **23**, 371–389.

Indeje, M., H.F.M. Semazzi, and L.J.Ogallo, 2000. ENSO signals in East African rainfall seasons. *Int. J. Climatol.*, **20**, 19–46.

Inoue, T., and F. Kimura, 2004: Urban effects on low-level clouds around the Tokyo metropolitan area on clear summer days. *Geophys. Res. Lett.*, **31**, L05103, doi:10.1029/2003GL018908.

IPCC, 1999: *Aviation and the Global Atmosphere* [Penner, J. E., et al. (eds.)]. Cambridge University Press, Cambridge, United Kingdom and New York, NY, USA, 384pp.

IPCC, 2001: *Climate Change 2001: The Scientific Basis. Contribution of Working Group I to the Third Assessment Report of the Intergovernmental Panel on Climate Change* [Houghton, J.T., et al. (eds.)]. Cambridge University Press, Cambridge, United Kingdom and New York, NY, USA, 881 pp.

Ishii, M., et al., 2005: Objective analysis of SST and marine meteorological variables for the 20th Century using ICOADS and the Kobe Collection. *Int. J. Climatol.*, **25**, 865–879.

Iskenderian, H., and R. Rosen, 2000: Low-frequency signals in mid-tropospheric submonthly temperature variance. *J. Clim.*, **13**, 2323–2333.

Jacobowitz, H., et al., 2003: The Advanced Very High Resolution Radiometer Pathfinder Atmosphere (PATMOS) climate dataset: A resource for climate research. *Bull. Am. Meteorol. Soc*., **84**, 785–793.

Jacobs, G.A., and J.L. Mitchell, 1996: Ocean circulation variations associated with the Antarctic Circumpolar Wave. *Geophys. Res. Lett.*, **23**, 2947–2950.

Janicot, S., S. Trzaska, and I. Poccard, 2001: Summer Sahel-ENSO teleconnection and decadal time scale SST variations. *Clim. Dyn.*, **18**, 303–320.

Jauregui, E., and E. Romales, 1996: Urban effects on convective precipitation in Mexico City. *Atmos. Environ*., **30**, 3383–3389.

Jin, M., and R.E. Dickinson, 2002: New observational evidence for global warming from satellite. *Geophys. Res. Lett.*, **29**(10), doi:10.1029/2001GL013833.

Jin, M., J.M. Shepherd, and M.D. King, 2005: Urban aerosols and their interaction with clouds and rainfall: A case study for New York and Houston. *J. Geophys. Res*., **110**, D10S20, doi:10.1029/2004JD005081.

Jones, D., et al., 2004. A new tool for tracking Australia's climate variability and change. *Bull. Aust. Meteorol. Oceanogr. Soc.*, **17**, 65–69.

Jones, J.M., and M. Widmann, 2004: Variability of the Antarctic Oscillation during the 20th century. *Nature*, **432**, 290–291.

Jones, P.D., and A. Moberg, 2003: Hemispheric and large-scale surface air temperature variations: An extensive revision and update to 2001. *J. Clim.*, **16**, 206–223.

Jones, P.D., T. Jónsson, and D. Wheeler, 1997: Extension to the North Atlantic Oscillation using early instrumental pressure observations from Gibraltar and south-west Iceland. *Int. J. Climatol.*, **17**, 1433–1450.

Jones, P.D., T.J. Osborn, and K.R. Briffa, 2003: Pressure-based measures of the North Atlantic Oscillation (NAO): A comparison and an assessment of changes in the strength of the NAO and in its influence on surface climate parameters. In: *The North Atlantic Oscillation: Climatic Significance and Environmental Impact* [Hurrell, J.W., et al. (eds.)]. Geophysical Monograph 134, American Geophysical Union, Washington, DC, pp. 51–62.

Jones, P.D., et al., 1990: Assessment of urbanization effects in time series of surface air temperature over land. *Nature*, **347**, 169–172.

Josey, S.A., and R. Marsh, 2005: Surface freshwater flux variability and recent freshening of the North Atlantic in the eastern subpolar gyre. *J. Geophys. Res.*, **110**, C05008, doi:10.1029/2004JC002521.

Joshi, M.M., and K.P. Shine, 2003: A GCM study of volcanic eruptions as a cause of increased stratospheric water vapour. *J. Clim.*, **16**, 3525–3534.

Jury, M.R., 2003: The coherent variability of African river flows: composite climate structure and the Atlantic Circulation. *Water SA*, **29**, 1–10.

Kaiser, D.P., 1998: Analysis of total cloud amount over China, 1951–1994. *Geophys. Res. Lett*, **25**, 3599–3602.

Kaiser, D.P., and Y. Qian, 2002: Decreasing trends in sunshine duration over China for 1954–1998: Indication of increased haze pollution? *Geophys. Res. Lett*., **29**, 2042, doi:10.1029/2002GL016057.

Kalnay, E., and M. Cai, 2003: Impact of urbanization and land-use change on climate. *Nature*, **423**, 528–531.

Kalnay, E., et al., 1996: The NCEP/NCAR Reanalysis Project. *Bull. Am. Meteorol. Soc*., **77**, 437–471.

Karl, T.R., S.J. Hassol, C.D. Miller, and W.L. Murray (eds.), 2006: *Temperature Trends in the Lower Atmosphere: Steps for Understanding and Reconciling Differences*. A report by the Climate Change Science Program and Subcommittee on Global Change Research, Washington, DC, 180pp., http://www.climatescience.gov/Library/sap/sap1-1/finalreport/default.htm.

Karoly, D.J., 2003: Ozone and climate change. *Science*, **302**, 236–237.

Karoly, D.J., and Q. Wu, 2005: Detection of regional surface temperature trends. *J. Clim.*, **18**, 4337–4343.

Karoly, D.J., et al., 2003: Global warming contributes to Australia's worst drought. *Australasian Science*, April, 14–17.

Kaufman, Y.J., D. Tanré, and O. Boucher, 2002: A satellite view of aerosols in the climate system. *Nature*, **419**, 215–223.

Keable, M., I. Simmonds, and K. Keay, 2002: Distribution and temporal variability of 500 hPa cyclone characteristics in the Southern Hemisphere. *Int. J. Climatol.*, **22**, 131–150.

Keetch, J.J., and G.M. Byrum, 1988: *A Drought Index for Forest Fire Control*. Research Paper SE-38, US Department of Agriculture, Asheville, NC, 32 pp., http://www.fl-dof.com/fire_weather/information/se038_keetchbyram_di.pdf.

Kent, E.C., and A. Kaplan, 2006: Toward estimating climatic trends in SST data, part 3: Systematic biases. *J. Atmos. Ocean. Technol.*, **23**, 487–500.

Kerr, R., 2000: A North Atlantic climate pacemaker for the centuries. *Science*, **288**, 1984–1985.

Kharin, V.V., and F.W. Zwiers, 2000: Changes in extremes in an ensemble of transient climate simulations with a coupled atmosphere-ocean GCM. *J. Clim.*, **13**, 3760–3780.

Kidson, J.W., 1999: Principal modes of Southern Hemisphere low frequency variability obtained from NCEP-NCAR reanalyses. *J. Clim.*, **12**, 2808–2830.

Kiehl, J.T., and K.E. Trenberth, 1997: Earth's annual global mean energy budget. *Bull. Am. Meteorol. Soc.*, **78**, 197–208.

Kiehl, J.T., J.M. Caron, and J.J. Hack, 2005: On using global climate model simulations to assess the accuracy of MSU retrieval methods for tropospheric warming trends. *J. Clim.*, **18**, 2533–2539.

Kiktev, D., et al., 2003: Comparison of modeled and observed trends in indices of daily climate extremes. *J. Clim.*, **16**, 3560–3571.

Kilpatrick, K.A., G.P. Podesta, and R. Evans, 2001: Overview of the NOAA/NASA advanced very high resolution radiometer Pathfinder algorithm for sea surface temperature and associated matchup database. *J. Geophys. Res.*, **106**, 9179–9198.

Kinter III, J.L., K. Miyakoda, and S. Yang, 2002: Recent change in the connection from the Asia monsoon to ENSO. *J. Clim.*, **15**, 1203–1215.

Kinter III, J.L., et al., 2004: An evaluation of the apparent interdecadal shift in the tropical divergent circulation in the NCEP–NCAR reanalysis. *J. Clim.*, **17**, 349–361.

Kistler, R., et al., 2001: The NCEP-NCAR 50-year reanalysis: Month means CD-ROM and documentation. *Bull. Am. Meteorol. Soc.*, **82**, 247–268.

Klein Tank, A.M.G., and G.P. Können, 2003: Trends in indices of daily temperature and precipitation extremes in Europe, 1946–1999. *J. Clim.*, **16**, 3665–3680.

Klein Tank, A.M.G., et al., 2006: Changes in daily temperature and precipitation extremes in central and south Asia. *J. Geophys. Res.*, **111**, D16105, doi:10.1029/2005JD006316.

Kley, D., J.M. Russell, and C. Phillips, 2000: *SPARC Assessment of Upper Tropospheric and Stratospheric Water Vapour*. WCRP Report No. 113, WMO/TD Report No. 1043, World Climate Research Programme, Geneva, 325 pp.

Klotzbach, P.J., 2006: Trends in global tropical cyclone activity over the past twenty years (1986–2005). *Geophys. Res. Lett.*, **33**, L10805, doi:10.1029/2006GL025881.

Knight, J., et al., 2005: A signature of persistent natural thermohaline circulation cycles in observed climate. *Geophys. Res. Lett.*, **32**, L20708, doi: 1029/2005GL024233.

Knutson, T.R., and S. Manabe, 1998: Model assessment of decadal variability and trends in the Tropical Pacific Ocean. *J. Clim.*, **11**, 2273–2296

Kodera, K., and H. Koide, 1997: Spatial and seasonal characteristics of recent decadal trends in the northern hemispheric troposphere and stratosphere. *J. Geophys. Res.*, **102**, 19433–19447.

Kodera, K., Y. Kuroda, and S. Pawson, 2000: Stratospheric sudden warmings and slowly propagating zonal-mean zonal wind anomalies. *J. Geophys. Res.*, **105**, 12351–12359.

Können, G.P., et al., 1998: Pre-1866 extensions of the Southern Oscillation index using early Indonesian and Tahitian meteorological readings. *J. Clim.*, **11**, 2325–2339.

Kostopoulou, E., and P.D. Jones, 2005: Assessment of climate extremes in the eastern Mediterranean. *Meteorol. Atmos. Phys.*, **89**, 69–85.

Krepper, C.M., N.O. García, and P.D. Jones, 2003: Interannual variability in the Uruguay River basin. *Int. J. Climatol.*, **23**, 103–115.

Kripalani, R.H., and A. Kulkarni, 1997a: Climatic impact of El Niño / La Niña on the Indian monsoon: A new perspective. *Weather*, **52**, 39–46.

Kripalani, R.H., and A. Kulkarni, 1997b: Rainfall variability over Southeast Asia: Connections with Indian monsoon and ENSO extremes: New perspectives. *Int. J. Climatol.*, **17**, 1155–1168.

Kripalani, R.H., and A. Kulkarni, 2001: Monsoon rainfall variations and teleconnections over South and East Asia. *Int. J. Climatol.*, **21**, 603–616.

Kripalani, R.H., A. Kulkarni, and S.S. Sabade, 2001: El Niño Southern Oscillation, Eurasian snow cover and the Indian monsoon rainfall. *Proc. Indian Nat. Sci. Acad.*, **67A**, 361–368.

Kripalani, R.H., et al., 2003: Indian monsoon variability in a global warming scenario. *Natural Hazards*, **29**, 189–206.

Krishnamurthy, V., and B.N. Goswami, 2000: Indian monsoon-ENSO relationship on interdecadal timescale. *J. Clim.*, **13**, 579–595.

Krüger, K., B. Naujokat, and K. Labitzke, 2005: The unusual midwinter warming in the southern hemisphere stratosphere in 2002: A comparison to northern hemisphere phenomena. *J. Atmos. Sci.*, **62**, 602–613.

Kuleshov, Y., and G. de Hoedt, 2003: Tropical cyclone activity in the Southern Hemisphere. *Bull. Aust. Meteorol. Oceanogr. Soc.*, **16**, 135–137.

Kumar, K.K., B. Rajagopalan, and A.M. Cane, 1999: On the weakening relationship between the Indian monsoon and ENSO. *Science*, **284**, 2156–2159.

Kundzewicz, Z.W., et al., 2005: Trend detection in river flow: 1. Annual maximum flow. *Hydrolog. Sci.*, **50**, 797–810.

Kunkel, K.E., et al., 2003: Temporal variations of extreme precipitation events in the United States: 1895–2000. *Geophys. Res. Lett.*, **30**, 1900, doi:10.1029/2003GL018052.

Kunkel, K.E., et al., 2004: Temporal variations in frost-free season in the United States: 1895–2000. *Geophys. Res. Lett.*, **31**, L03201, doi:10.1029/2003GL018624.

Kwok, R., and J.C. Comiso, 2002a: Southern ocean climate and sea ice anomalies associated with the Southern Oscillation. *J. Clim.*, **15**, 487–501.

Kwok, R., and J.C. Comiso, 2002b: Spatial patterns of variability in Antarctic surface temperature: Connections to the Southern Hemisphere Annular Mode and the Southern Oscillation. *Geophys. Res. Lett.*, **29**, 1705, doi:10.1029/2002GL015415.

Labat, D., et al., 2004: Evidence for global runoff increase related to climate warming. *Adv. Water Resour.*, **27**, 631–642.

Labitzke, K., and M. Kunze, 2005: Stratospheric temperature over the Arctic: Comparison of three data sets. *Meteorol. Z.*, **14**, 65–74.

Lambert, S.J., 1996: Intense extratropical Northern Hemisphere winter cyclone events: 1899–1991. *J. Geophys. Res.*, **101**, 21319–21325.

Lammers, R.B., et al., 2001: Assessment of contemporary Arctic river runoff based on observational discharge records. *J. Geophys. Res.*, **106**, 3321–3334.

Lander, M., 1994: An exploratory analysis of the relationship between tropical storm formation in the Western North Pacific and ENSO. *Mon. Weather Rev.*, **122**, 636–651.

Landsea, C.W., 2005: Hurricanes and global warming: Arising from Emanuel 2005a. *Nature*, **438**, E11–E13, doi:10.1038/nature04477.

Landsea, C.W., et al., 1998: The extremely active 1995 Atlantic hurricane season: Environmental conditions and verification of seasonal forecasts. *Mon. Weather Rev.*, **126**, 1174–1193.

Langematz, U., et al., 2003: Thermal and dynamical changes of the stratosphere since 1979 and their link to ozone and CO_2 changes. *J. Geophys. Res.*, **108**, 4027, doi:10.1029/2002JD002069.

Lanzante, J.R., S.A. Klein, and D.J. Seidel, 2003a: Temporal homogenization of monthly radiosonde temperature data. Pt I: Methodology. *J. Clim.*, **16**, 224–240.

Lanzante, J.R., S.A. Klein, and D.J. Seidel, 2003b: Temporal homogenization of monthly radiosonde temperature data. Pt II: Trends, sensitivities, and MSU comparison. *J. Clim.*, **16**, 241–262.

Latif, M., 2001: Tropical Pacific/Atlantic ocean interactions at multi-decadal time scales. *Geophys. Res. Lett.*, **28**, 539–542.

Latif, M., R. Kleeman, and C. Eckert, 1997: Greenhouse warming, decadal variability, or El Nino? An attempt to understand the anomalous 1990s. *J. Clim.*, **10**, 2221–2239.

Lau, N-C., and M.J. Nath, 2004: Coupled GCM simulation of atmosphere-ocean variability associated with zonally asymmetric SST changes in the tropical Indian Ocean. *J. Clim.*, **17**, 245–265.

Lawrimore, J., et al., 2002: Beginning a new era of drought monitoring across North America. *Bull. Am. Meteorol. Soc.*, **83**, 1191–1192.

Le Barbe, L., T. Lebel, and D. Tapsoba, 2002: Rainfall variability in West Africa during the years 1950–1990. *J. Clim.*, **15**, 187–202.

Lefebvre, W., et al., 2004: Influence of the Southern Annular Mode on the sea ice-ocean system. *J. Geophys. Res.*, **109**, C09005, doi:10.1029/2004JC002403.

Levinson, D.H. (ed.), 2005: State of the climate in 2004. *Bull. Am. Meteorol. Soc.*, **86**(6), S1–S84.

Levinson, D.H., and A.M. Waple (eds.), 2004: State of the climate in 2003. *Bull. Am. Meteorol. Soc.*, **85**(6), S1–S72.

L'Heureux, M.L., and D.W.J. Thompson, 2006: Observed relationships between the El Niño–Southern Oscillation and the extratropical zonal-mean circulation. *J. Clim.*, **19**, 276–287.

Li, Q., et al., 2004: Urban heat island effect on annual mean temperature during the last 50 years in China. *Theor. Appl.Climatol.*, **79**, 165–174.

Li, W., and P.M. Zhai, 2003: Variability in occurrence of China's spring dust storm and its relationship with atmospheric general circulation. *Acta Meteorol. Sin.*, **17**(4), 396–405.

Liebmann, B., et al., 1999: Submonthly convective variability over South America and the South Atlantic convergence zone. *J. Clim.*, **12**, 1877–1891.

Liebmann, B., et al., 2004: An observed trend in Central South American precipitation. *J. Clim.*, **22**, 4357–4367.

Liepert, B.G., 2002: Observed reductions of surface solar radiation at sites in the United States and worldwide from 1961 to 1990. *Geophys. Res. Lett.*, **29**, 1421, 10.1029/2002GL014910.

Liepert, B.G., et al., 2004: Can aerosols spin down the water cycle in a warmer and moister world? *Geophys. Res. Lett.*, **31**, doi:10.1029/2003GL019060.

Lim, E.-P., and I. Simmonds, 2002: Explosive cyclone development in the Southern Hemisphere and a comparison with Northern Hemisphere events. *Mon. Weather Rev.*, **130**, 2188–2209.

Limpasuvan, V., and D.L. Hartmann, 2000: Wave-maintained annular modes of climate variability. *J. Clim.*, **13**, 4414–4429.

Limpasuvan, V., D. Thompson and D. Hartmann, 2004: The life cycle of northern hemispheric sudden stratospheric warmings. *J. Clim.*, **17**, 2584–2596.

Lins, H.F., and J.R. Slack, 1999: Streamflow trends in the United States. *Geophys. Res. Lett.*, **26**, 227–230.

Linsley, B.K., et al., 2004: Geochemical evidence from corals for changes in the amplitude and spatial pattern of South Pacific interdecadal climate variability over the last 300 years. *Clim. Dyn.*, **22**, doi:10.1007/s00382-003-0364-y.

Liu, B.H., et al., 2004a: A spatial analysis of pan evaporation trends in China, 1955–2000. *J. Geophys. Res.*, **109**, D15102, doi:10.1029/2004JD004511.

Liu, J., J.A. Curry, and D.G. Martinson, 2004b: Interpretation of recent Antarctic sea ice variability. *Geophys. Res. Lett.*, **31**, L02205, doi:10.1029/2003GL018732.

Liu, K.S., and J.C.L. Chan, 2003: Climatological characteristics and seasonal forecasting of tropical cyclones making landfall along the south China coast. *Mon. Weather Rev.*, **131**, 1650–1662.

Lorenz, D.J., and D.L. Hartmann, 2001: Eddy–zonal flow feedback in the Southern Hemisphere. *J. Atmos. Sci.*, **58**, 3312–3327.

Lorenz, D.J., and D.L. Hartmann, 2003: Eddy-zonal flow feedback in the Northern Hemisphere winter. *J. Clim.*, **16**, 1212–1227.

Lozano, I., and V. Swail, 2002: The link between wave height variability in the North Atlantic and the storm track activity in the last four decades. *Atmos.-Ocean*, **40**, 377–388.

Lucarini, V., and G.L. Russell, 2002: Comparison of mean climate trends in the Northern Hemisphere between National Centers for Environmental Prediction and two atmosphere-ocean model forced runs. *J. Geophys. Res.*, **107**, 4269, doi:10.1029/2001JD001247.

Lugina, K.M., et al., 2005: Monthly surface air temperature time series area-averaged over the 30-degree latitudinal belts of the globe, 1881-2004. In: *Trends: A Compendium of Data on Global Change.* Carbon Dioxide Information Analysis Center, Oak Ridge National Laboratory, US Department of Energy, Oak Ridge, TN, http://cdiac.esd.ornl.gov/trends/temp/lugina/lugina.html.

Luo, Y., et al., 2001: Characteristics of spatial distribution of yearly variation of aerosol optical depth over China in the last 30 years. *J. Geophys. Res.*, **106**(D13), 14501–14513.

Luterbacher, J., et al., 2004: European seasonal and annual temperature variability, trends, and extremes since 1500. *Science*, **303**, 1499–1503.

Ma, Z.G., and C.B. Fu, 2003: Interannual characteristics of the surface hydrological variables over the arid and semi-arid areas of northern China. *Global Planet. Change*, **37**, 189-200.

Madden, R.A., and J. Williams, 1978: The correlation between temperature and precipitation in the United States and Europe. *Mon. Weather Rev.*, **106**, 142–147.

Maheras, P., et al., 2004: On the relationships between circulation types and changes in rainfall variability in Greece. *Int. J. Climatol.*, **24**, 1695–1712.

Maistrova, V.V., et al., 2003: Long-term trends in temperature and specific humidity of free atmosphere in the Northern Polar region. *Dokl. Earth Sci.*, **391**, 755–759.

Mann, M.E., 2004: On smoothing potentially non-stationary climate time series. *Geophys. Res. Lett.*, **31**, L07214, doi:10.1029/2004GL019569.

Manney, G., et al., 2005: The remarkable 2003–2004 winter and other recent warm winters in the Arctic stratosphere since the late 1990s. *J. Geophys. Res.*, **110**, D04107, doi:10.1029/2004JD005367.

Manton, M.J., et al., 2001: Trends in extreme daily rainfall and temperature in Southeast Asia and the South Pacific: 1961–1998. *Int. J. Climatol.*, **21**, 269–284.

Mantua, N.J., and S.J. Hare, 2002: The Pacific Decadal Oscillation. *J. Oceanogr.*, **58**, 35–44.

Mantua, N.J., et al., 1997: A Pacific interdecadal climate oscillation with impacts on salmon production. *Bull. Am. Meteorol. Soc.*, **78**, 1069–1079.

Marengo, J., 2004: Interdecadal variability and trends of rainfall across the Amazon Basin. *Theor. Appl. Climatol.*, **78**, 79–96.

Marengo, J.A., et al., 2004: Climatology of the low-level jet east of the Andes as derived from the NCEP–NCAR Reanalyses: Characteristics and temporal variability. *J. Clim.*, **17**, 2261–2280.

Marshall, G.J., 2002: Analysis of recent circulation and thermal advection change on the northern Antarctic Peninsula. *Int. J. Climatol.*, **22**, 1557–1567.

Marshall, G.J., 2003: Trends in the Southern Annular Mode from observations and reanalyses. *J. Clim.*, **16**, 4134–4143.

Marshall, G.J., et al., 2004: Causes of exceptional atmospheric circulation changes in the Southern Hemisphere. *Geophys. Res. Lett.*, **31**, L14205, doi:10.1029/2004GL019952.

Marshall, J., H. Johnson, and J. Goodman, 2001: A study of the interaction of the North Atlantic Oscillation with the ocean circulation. *J. Clim.*, **14**, 1399–1421.

Martyn, D., 1992: *Climates of the World.* Elsevier, Amsterdam, 436 pp.

Maugeri, M., et al., 2001: Trends in Italian cloud amount 1951-1996. *Geophys. Res. Lett.*, **28**, 4551–4554.

Mauget, S.A., 2003a: Intra- to multidecadal climate variability over the continental United States: 1932–99. *J. Clim.*, **16**, 2215–2231.

Mauget, S.A., 2003b: Multidecadal regime shifts in US streamflow, precipitation, and temperature at the end of the twentieth century. *J. Clim.*, **16**, 3905–3916.

McBride, J.L., 1998: Indonesia, Papua New Guinea, and tropical Australia: The southern hemisphere monsoon. In: *Meteorology of the Southern Hemisphere* [Karoly, D., and D. Vincent (eds.)]. American Meteorological Society, Boston, MA, pp. 89–99.

McCabe, G.J., and D.M. Wolock, 2002: Trends and temperature sensitivity of moisture conditions in the conterminous United States. *Clim. Res.*, **20**, 19–29.

McCabe, G.J., M.P. Clark, and M.C. Serreze, 2001: Trends in Northern Hemisphere surface cyclone frequency and intensity. *J. Clim.*, **14**, 2763–2768.

McCabe, G.J., M. Palecki, and J.L. Betancourt, 2004: Pacific and Atlantic Ocean influences on multi-decadal drought frequency in the United States. *Proc. Natl. Acad. Sci. U.S.A.*, **101**, 4136–4141.

McCarthy, M.P., and R. Toumi, 2004: Observed interannual variability of tropical troposphere relative humidity. *J. Clim.*, **17**, 3181–3191.

McKitrick, R., and P.J. Michaels, 2004: A test of corrections for extraneous signals in gridded surface temperature data. *Clim. Res.*, **26**, 159–173.

McPhaden, M.J., and D. Zhang, 2002: Slowdown of the meridional overturning circulation of the upper Pacific ocean. *Nature*, **415**, 603–608.

Mears, C.A., and F.J. Wentz, 2005: The effect of diurnal correction on satellite-derived lower tropospheric temperature. *Science*, **309**, 1548–1551.

Mears, C.A., M.C. Schabel, and F.J. Wentz, 2003: A reanalysis of the MSU channel 2 tropospheric temperature record. *J. Clim.*, **16**, 3650–3664.

Mehta, A., and J. Susskind, 1999: Outgoing longwave radiation from the TOVS Pathfinder Path A data set. *J. Geophys. Res*., **104**, 12193–12212.

Menon, S., et al., 2002: Climate effects of black carbon aerosols in China and India. *Science*, **297**, 2250–2253.

Meredith, M.P., et al., 2004: Changes in the ocean transport through Drake Passage during the 1980s and 1990s, forced by changes in the Southern Annular Mode. *Geophys. Res. Lett*., **31**, L21305, doi:10.1029/2004GL021169.

Milly, P.C.D., and K.A. Dunne, 2001: Trends in evaporation and surface cooling in the Mississippi River basin. *Geophys. Res. Lett.*, **28**, 1219–1222.

Milly, P.C.D., et al., 2002: Increasing risk of great floods in a changing climate. *Nature*, **415**, 514–517.

Miloshevich, L.M., et al., 2004: Development and validation of a time-lag correction for Vaisala radiosonde humidity measurements. *J. Atmos. Ocean. Technol.*, **21**, 1305–1327.

Minnis, P., et al., 2004: Contrails, cirrus trends, and climate. *J. Clim.*, **17**, 1671–1685.

Minschwaner, K., and A.E. Dessler, 2004: Water vapor feedback in the tropical upper troposphere: Model results and observations. *J. Clim.*, **17**, 1272–1282.

Minobe, S., 1997: A 50–70 year climatic oscillation over the North Pacific and North America. *Geophys. Res. Lett.*, **24**, 683–686.

Minobe, S., 1999: Resonance in bidecadal and pentadecadal oscillations over the North Pacific: Role in climate regime shifts. *Geophys. Res. Lett*., **26**, 855–858.

Minobe, S., and T. Nakanowatari, 2002: Global structure of bidecadal precipitation variability in boreal winter. *Geophys. Res. Lett*., **29**, 1396, doi:10.1029/2001GL014447.

Mitas, C.M., and A. Clement, 2005: Has the Hadley cell been strengthening in recent decades? *Geophys. Res. Lett*., **32**, L03809, doi:10.1029/2004GL021765.

Mitchell, T.D., and P.D. Jones, 2005: An improved method of constructing a database of monthly climate observations and associated high-resolution grids. *Int. J. Climatol*., **25**, 693–712

Mo, K.C., 2000: Relationships between low-frequency variability in the Southern Hemisphere and sea surface temperature anomalies. *J. Clim.*, **13**, 3599–3610.

Mo, K.C., and R.W. Higgins, 1998: The Pacific-South American modes and tropical convection during the Southern Hemisphere winter. *Mon. Weather Rev.*, **126**, 1581–1596.

Moberg, A., and P.D. Jones, 2005: Trends in indices for extremes of daily temperature and precipitation in central and western Europe 1901–1999. *Int. J. Climatol.*, **25**, 1173–1188.

Molders, N., and M.A. Olson, 2004: Impact of urban effects on precipitation in high latitudes. *J. Hydrometeorol*., **5**, 409–429.

Monahan, A.H., L. Pandolfo, and J.C. Fyfe, 2001: The preferred structure of variability of the Northern Hemisphere atmospheric circulation. *Geophys. Res. Lett.*, **28**, 1019–1022.

Mu, Q.Z., et al., 2002: Simulation study on variation of Western Pacific subtropical high during the last hundred years. *Chin. Sci. Bull.*, **7**, 550–553.

Mudelsee, M., et al., 2003: No upward trends in the occurrence of extreme floods in central Europe. *Nature*, **425**, 166–169.

Nakamura, H., and T. Sampe, 2002: Trapping of synoptic-scale disturbances into the North-Pacific subtropical jet core in midwinter. *Geophys. Res. Lett*., **29**(16), doi:10.1029/2002GL015535.

Nakamura, H., T. Izumi, and T. Sampe, 2002: Interannual and decadal modulations recently observed in the Pacific storm track activity and East Asia winter monsoon. *J. Clim.*, **15**, 1855–1874.

Nakamura, H., et al., 2004: Observed associations among storm tracks, jet streams and midlatitude oceanic fronts. In: *Earth's Climate: The Ocean-Atmosphere Interaction* [Wang, C., S.-P. Xie, and J. A. Carton (eds.)]. Geophysical Monograph 147, American Geophysical Union, Washington, DC, pp. 329–346.

Naujokat, B., et al., 2002: The early major warming in December 2001 – Exceptional? *Geophys. Res. Lett*., **29**, 2023, doi:10.1029/2002GL015316.

Nazemosadat, M.J., and I. Cordery, 2000: On the relationships between ENSO and autumn rainfall in Iran. *Int. J. Climatol*., **20**, 47–61.

Nazemosadat, M.J., and A.R. Ghasemi, 2004: Quantifying the ENSO-related shifts in the intensity and probability of drought and wet periods in Iran. *J. Clim.*, **17**, 4005–4018.

Nedoluha, G.E., et al., 2003: An evaluation of trends in middle atmospheric water vapor as measured by HALOE, WVMS, and POAM. *J. Geophys. Res*., **108**, 4391, doi:10.1029/2002JD003332.

New, M., et al., 2006: Evidence of trends in daily climate extremes over southern and West Africa. *J. Geophys. Res.*, **111**, D14102, doi:10.1029/2005JD006289.

Newman, M., G. Compo, and M.A. Alexander, 2003: ENSO-forced variability of the Pacific Decadal Oscillation. *J. Clim.*, **23**, 3853–3857.

Newman, P.A., and E.R. Nash, 2000: Quantifying the wave drinking of the stratosphere. *J. Geophys. Res*., **105**, 12485–12497.

Newman, P.A., and E.R. Nash, 2005: The unusual Southern Hemisphere stratosphere winter of 2002. *J. Atmos. Sci.*, **62**, doi:10.1175/JAS-3323.1.

Nicholls, N., 2004: The changing nature of Australian droughts. *Clim. Change*, **63**, 323–336.

Nobre, P., and J. Shukla, 1996: Variations of sea surface temperature, wind stress, and rainfall over the tropical Atlantic and South America. *J. Clim.*, **9**, 2464–2479.

Nogués-Paegle, J., et al., 2002: Progress in Pan American CLIVAR research: Understanding the South American monsoon. *Meteorologica*, **27**, 3–32.

Noone, D., and I. Simmonds, 2002: Annular variations in moisture transport mechanisms and the abundance of $\delta^{18}O$ in Antarctic snow. *J. Geophys. Res.*, **107**, 4742, doi:10.1029/2002JD002262.

Norris, J.R., 2000: What can cloud observations tell us about climate variability? *Space Sci. Rev*., **94**, 375–380.

Norris, J.R., 2005a: Multidecadal changes in near-global cloud cover and estimated cloud cover radiative forcing. *J. Geophys. Res.*, **110**, D08206, doi:10.1029/2004JD005600.

Norris, J.R., 2005b: Trends in upper-level cloud cover and atmospheric circulation over the Indo-Pacific region between 1952 and 1997. *J. Geophys. Res*., **110**, D21110, doi:10.1029/2005JD006183.

Notholt, J., et al., 2005: Influence of tropospheric SO_2 emissions on particle formation and the stratospheric humidity. *Geophys. Res. Lett*., **32**, L07810, doi:10.1029/2004GL022159.

O'Carroll, A.G., R.W. Saunders, and J.G. Watts, 2006: The measurement of the sea surface temperature climatology by satellites from 1991 to 2005. *J. Atmos. Ocean. Technol.*, **23**,1573-1582.

Ohmura, A., and M. Wild, 2002: Is the hydrological cycle accelerating? *Science*, **298**, 1345–1346.

Oinas, V., et al., 2001: Radiative cooling by stratospheric water vapor: big differences in GCM results. *Geophys. Res. Lett*., **28**, 2791–2794.

Oke, P.R., and M.H. England, 2004: Oceanic response to changes in the latitude of the Southern Hemisphere subpolar westerly winds. *J. Clim*., **17**, 1040–1054.

Oltmans, S.J., et al., 2000: The increase in stratospheric water vapor from balloon borne, frostpoint hygrometer measurements at Washington, DC, and Boulder, Colorado. *Geophys. Res. Lett*, **27**, 3453–3456.

Omran, M.A., 2000: Analysis of solar radiation over Egypt. *Theor. Appl. Climatol*., **67**, 225–240.

Oort, A.H., and J.J.Yienger, 1996: Observed interannual variability in the Hadley circulation and its connection to ENSO. *J. Clim.*, **9**, 2751–2767.

Orr, A., et al., 2004: A 'low-level' explanation for the recent large warming trend over the western Antarctic Peninsula involving blocked winds and changes in zonal circulation. *Geophys. Res. Lett.*, **31**, L06204, doi:10.1029/2003GL019160.

Osborn, T.J., and M. Hulme, 2002: Evidence for trends in heavy rainfall events over the U.K. *Philos. Trans. R. Soc. London Ser. A*, **360**, 1313–1325.

Osborn, T.J., et al., 2000: Observed trends in the daily intensity of United Kingdom precipitation. *Int. J. Climatol.*, **20**, 347–364.

Ostermeier, G.M., and J.M. Wallace, 2003: Trends in the North Atlantic Oscillation – Northern Hemisphere annular mode during the twentieth century. *J. Clim.*, **16**, 336–341.

Overland, J. E., and M. Wang, 2005: The Arctic climate paradox: The recent decrease of the Arctic Oscillation. *Geophys. Res. Lett.*, **32**, L23808, doi:10.1029/2005GL024254.

Paciorek, C.J., et al., 2002: Multiple indices of Northern Hemisphere cyclone activity, winters 1949–99. *J. Clim.*, **15**, 1573–1590.

Pagano, T., et al., 2004: Water year 2004: Western water managers feel the heat. *Eos*, **85**, 392–393.

Pallé, E., et al., 2004: Changes in Earth's reflectance over the past two decades. *Science*, **304**, 1299–1301.

Palmer, T.N., 1999: A nonlinear dynamical perspective on climate prediction. *J. Clim.*, **12**, 575–591.

Palmer, W.C., 1965: *Meteorological Drought*. Research Paper 45, US Department of Commerce, Weather Bureau, Washington, DC, 58 pp. [Available from NOAA Library and Information Services Division, Washington, DC 20852.]

Park, Y., F. Roquet, and F. Vivier, 2004: Quasi-stationary ENSO wave signals versus the Antarctic Circumpolar Wave scenario. *Geophys. Res. Lett.*, **31**, L09315, doi:10.1029/2004GL019806.

Parker, D.E., 2004: Large-scale warming is not urban. *Nature*, **432**, 290–290.

Parker, D.E., 2006: A demonstration that large-scale warming is not urban. *J. Clim.*, **19**, 2882–2895.

Parker, D.E., and D.I. Cox, 1995: Towards a consistent global climatological rawinsonde data-base. *Int. J. Climatol.*, **15**, 473–496.

Parker, D.E., et al., 1997: A new global gridded radiosonde temperature data base and recent temperature trends. *Geophys. Res. Lett.*, **24**, 1499–1502.

Pawson, S., and B. Naujokat, 1999: The cold winters of the middle 1990s in the northern lower stratosphere. *J. Geophys. Res.*, **104**, 14209–14222.

Pekárová, P., P. Miklánek, and J. Pekár, 2003: Spatial and temporal runoff oscillation analysis of the main rivers of the world during the 19th–20th centuries. *J. Hydrol.*, **274**, 62–79.

Penman, H.L., 1948: Natural evaporation from open water, bare soil and grass. *Proc. R. Soc. London Ser. A*, **193**, 120–145.

Pepin, N.C., and D.J. Seidel, 2005: A global comparison of surface and free-air temperatures at high elevations. *J. Geophys. Res.*, **110**, D03104, doi:10.1029/2004JD005047.

Peterson, T.C., 2003: Assessment of urban versus rural *in situ* surface temperatures in the contiguous United States: no difference found. *J. Clim.*, **16**, 2941–2959.

Peterson, T.C., and R.S. Vose, 1997: An overview of the Global Historical Climatology Network temperature database. *Bull. Am. Meteorol. Soc.*, **78**, 2837–2848.

Peterson, T.C., and T.W. Owen, 2005: Urban heat island assessment: Metadata are important. *J. Clim.*, **18**, 2637–2646.

Peterson, T.C., V.S. Golubev, and P.Ya. Groisman, 1995: Evaporation losing its strength. *Nature*, **377**, 687–688.

Peterson, T.C., et al., 1999: Global rural temperature trends. *Geophys. Res. Lett.*, **26**, 329–332.

Peterson, T.C., et al., 2000: A blended satellite – *in situ* near-global surface temperature dataset. *Bull. Am. Meteorol. Soc.*, **81**, 2157–2164.

Peterson, T.C., et al., 2002: Recent changes in climate extremes in the Caribbean region. *J. Geophys. Res.*, **107**, 4601, doi:10.1029/2002JD002251.

Pezza, A.B., and I. Simmonds, 2005: The first South Atlantic hurricane: unprecedented blocking, low shear and climate change. *Geophys. Res. Lett.*, **32**, L15712, doi:10.1029/2005GL023390.

Philipona, R., and B. Dürr, 2004: Greenhouse forcing outweighs decreasing solar radiation driving rapid temperature rise over land. *Geophys. Res. Lett.*, **31**, L22208, doi:10.1029/2004GL020937.

Philipona, R., et al., 2004: Radiative forcing - measured at Earth's surface - corroborate the increasing greenhouse effect. *Geophys. Res. Lett.*, **31**, L15712, doi:10.1029/2003GL018765.

Philipona, R., et al., 2005: Anthropogenic greenhouse forcing and strong water vapor feedback increase temperature in Europe. *Geophys. Res. Lett.*, **32**, L19809, doi:1029/ 2005GL023624.

Picon, L., et al., 2003: A new METEOSAT "water vapor" archive for climate studies. *J. Geophys. Res.*, **108**, 4301, doi:10.1029/2002JD002640.

Piechota, T., et al., 2004: The western drought: How bad is it? *Eos*, **85**(32), 301.

Pierce, D.W., 2001: Distinguishing coupled ocean–atmosphere interactions from background noise in the North Pacific. *Prog. Oceanogr.*, **49**, 331–352.

Pinker, R.T., B. Zhang, and E.G. Dutton, 2005: Do satellites detect trends in surface solar radiation? *Science*, **308**, 850–854.

Plummer, N., et al., 1999: Changes in climate extremes over the Australian region and New Zealand during the Twentieth Century. *Clim. Change*, **42**, 183–202.

Polyakov, I.V., et al., 2003: Variability and trends of air temperature in the Maritime Arctic, 1875–2000. *J. Clim.*, **16**, 2067–2077.

Power, H.C., and D.M. Mills, 2005: Solar radiation climate change over South Africa and an assessment of the radiative impact of volcanic eruptions. *Int. J. Climatol.*, **25**, 295–318.

Power, S., et al., 1998: Australian temperature, Australian rainfall and the Southern Oscillation, 1910–1992: coherent variability and recent changes. *Aust. Meteorol. Mag.*, **47**, 85–101.

Power, S., et al., 1999a: Decadal climate variability in Australia during the twentieth century. *Int. J. Climatol.*, **19**, 169–184.

Power, S., et al., 1999b: Inter-decadal modulation of the impact of ENSO on Australia. *Clim. Dyn.*, **15**, 319–324.

Probst, J.L., and Y. Tardy, 1987: Long-range streamflow and world continental runoff fluctuations since the beginning of this century. *J. Hydrol.*, **94**, 289–311.

Probst, J.L., and Y. Tardy, 1989: Global runoff fluctuations during the last 80 years in relation to world temperature-change. *Am. J. Sci.*, **289**, 267–285.

Przybylak, R., 2000: Diurnal temperature range in the Arctic and its relation to hemispheric and Arctic circulation patterns. *Int. J. Climatol.*, **20**, 231–253.

Qian, T., et al., 2006a: Simulation of global land surface conditions from 1948–2004. Pt I: Forcing data and evaluations. *J. Hydrometeorol.*, **7**, 953–975.

Qian, W.H., L.S. Quan, and S.Y. Shi, 2002: Variations of the dust storm in China and its climatic control. *J. Clim.*, **15**, 1216–1229.

Qian, W.H., et al., 2003: Centennial-scale dry-wet variations in East Asia. *Clim. Dyn.*, **21**, 77–89.

Qian, Y., et al., 2006b: More frequent cloud-free sky and less surface solar radiation in China from 1955 to 2000. *Geophys. Res. Lett.*, **33**, L01812, doi:10.1029/2005GL024586.

Quadrelli, R., and J.M. Wallace, 2004: A simplified linear framework for interpreting patterns of Northern Hemisphere wintertime climate variability. *J. Clim.*, **17**, 3728–3744.

Quadrelli, R., V. Pavan, and F. Molteni, 2001: Wintertime variability of Mediterranean precipitation and its links with large-scale circulation anomalies. *Clim. Dyn.*, **17**, 457–466.

Ramanathan, V., et al., 2001: Aerosols, climate and the hydrological cycle. *Science*, **294**, 2119–2124.

Ramaswamy, V., and M. Schwarzkopf, 2002: Effects of ozone and well-mixed gases on annual-mean stratospheric temperature trends. *Geophys. Res. Lett.*, **29**, 2064, doi:10.1029/2002GL05141.

Ramaswamy, V., et al., 2001: Stratospheric temperature changes: observations and model simulations. *Rev. Geophys.*, **39**, 71–122.

Randel, D.L., et al., 1996: A new global water vapor dataset. *Bull. Am. Meteorol. Soc.*, **77**, 1233–1246.

Randel, W.J., and F. Wu, 1999: Cooling of the Arctic and Antarctic polar stratospheres due to ozone depletion. *J. Clim.*, **12**, 1467–1479.

Randel, W.J., and F. Wu, 2006: Biases in stratospheric temperature trends derived from historical radiosonde data. *J. Clim.*, **19**, 2094–2104.

Randel, W.J., F. Wu, and D.J. Gaffen, 2000: Interannual variability of the tropical tropopause derived from radiosonde data and NCEP reanalyses. *J. Geophys. Res.*, **105**, 15509–15524.

Randel, W.J, F. Wu, and R. Stolarski, 2002: Changes in column ozone correlated with the stratospheric EP flux. *J. Meteorol. Soc. Japan*, **80**, 849–862.

Randel, W.J., et al., 2004a: Interannual changes of stratospheric water vapor and correlations with tropical tropopause temperatures. *J. Atmos. Sci.*, **61**, 2133–2148.

Randel, W.J., et al., 2004b: The SPARC intercomparison of middle-atmosphere climatologies. *J. Clim.*, **17**, 986–1003.

Rashid, H.A., and I. Simmonds, 2004: Eddy-zonal flow interactions associated with the Southern Hemisphere annular mode: Results from NCEP-DOE reanalysis and a quasi-linear model. *J. Atmos. Sci.*, **61**, 873–888.

Rashid, H.A., and I. Simmonds, 2005: Southern Hemisphere annular mode variability and the role of optimal nonmodal growth. *J. Atmos. Sci.*, **62**, 1947–1961

Rayner, N.A., et al., 2003: Global analyses of sea surface temperature, sea ice, and night marine air temperature since the late nineteenth century. *J. Geophys. Res.*, **108**, 4407, doi:10.1029/2002JD002670.

Rayner, N.A., et al., 2006: Improved analyses of changes and uncertainties in sea surface temperature measured *in situ* since the mid-nineteenth century: the HadSST2 dataset. *J. Clim.*, **19**, 446–469.

Read, W.G., et al., 2004: Dehydration in the tropical tropopause layer: Implications from the UARS Microwave Limb Sounder. *J. Geophys. Res.*, **109**, D06110, doi:10.1029/2003JD004056.

Regonda, S.K., et al., 2005: Seasonal cycle shifts in hydroclimatology over the Western U.S. *J. Clim..*, **18**, 372–384.

Ren, G.Y., et al., 2005: Climate changes of mainland China over the past half century, *Acta Meteorol. Sin.*, **63** (6): 942–955 (in Chinese).

Renwick, J.A., 1998: ENSO-related variability in the frequency of South Pacific blocking. *Mon. Weather Rev.*, **126**, 3117–3123.

Renwick, J.A., 2002: Southern Hemisphere circulation and relations with sea ice and sea surface temperature. *J. Clim.*, **15**, 3058–3068.

Renwick, J.A., 2004: Trends in the Southern Hemisphere polar vortex in NCEP and ECMWF reanalyses. *Geophys. Res. Lett.*, **31**, L07209, doi:10.1029/2003GL019302.

Renwick, J.A., 2005: Persistent positive anomalies in the Southern Hemisphere circulation. *Mon. Weather Rev.*, **133**, 977–988.

Renwick, J.A., and M.J. Revell, 1999: Blocking over the South Pacific and Rossby wave propagation. *Mon. Weather Rev.*, **127**, 2233–2247.

Revercombe, H.E., et al., 2003: The ARM program's water vapor intensive observation periods: Overview, initial accomplishments, and future challenges. *Bull. Am. Meteorol. Soc*., **84**, 217–236.

Reynolds, R.W., C.L. Gentemann, and F. Wentz, 2004: Impact of TRMM SSTs on a climate-scale SST analysis. *J. Clim.*, **17**, 2938–2952.

Reynolds, R.W., et al., 2002: An improved in situ and satellite SST analysis for climate. *J. Clim.*, **15**, 1609–1625.

Robertson, A.W., C.R. Mechoso, and N.O. García, 2001a: Interannual prediction of the Paraná River. *Geophys. Res. Lett*., **28**, 4235–4238.

Robertson, F.R., R.W. Spencer, and D.E. Fitzjarrald, 2001b: A new satellite deep convective ice index for tropical climate monitoring: possible implications for existing oceanic precipitation data sets, *Geophys. Res. Lett*., **28**, 251–254.

Robertson F.R., D.E. Fitzjarrald, and C.D. Kummerow, 2003: Effects of uncertainty in TRMM precipitation radar path integrated attenuation on interannual variations of tropical oceanic rainfall. *Geophys. Res. Lett*., **30**, 1180, doi:10.1029/2002GL016416.

Robeson, S., 2004: Trends in time-varying percentiles of daily minimum and maximum temperature over North America. *Geophys. Res. Lett*, **31**, L04203, doi:10.1029/2003GL019019.

Robinson, P.J., 2000: Temporal trends in United States dew point temperatures. *Int. J. Climatol.*, **20**, 985–1002.

Robock, A., et al., 2000: The global soil moisture data bank. *Bull. Am. Meteorol. Soc.*, **81**, 1281–1299.

Robock, A., et al., 2005: Forty five years of observed soil moisture in Ukraine: No summer desiccation (yet). *Geophys. Res. Lett.*, **32**, L03401, doi:10.0129/2004GL021914.

Röckmann, T., et al., 2004: The impact of anthropogenic chlorine emissions, stratospheric ozone change and chemical feedbacks on stratospheric water. *Atmos. Chem. Phys*., **4**, 693–699.

Roderick, M.L., and G.D. Farquhar, 2002: The cause of decreased pan evaporation over the past 50 years. *Science*, **298**, 1410–1411.

Roderick, M.L., and G.D. Farquhar, 2004: Changes in Australian pan evaporation from 1970–2002. *Int. J. Climatol.*, **24**, 1077–1090.

Roderick, M.L., and G.D. Farquhar, 2005: Changes in New Zealand pan evaporation since the 1970s. *Int. J. Climatol.*, **25**, 2031–2039.

Rodwell, M.J., 2003: On the predictability of North Atlantic climate. In: *The North Atlantic Oscillation: Climatic significance and environmental impact* [Hurrell, J.W., et al. (eds.)]. Geophysical Monograph 134, American Geophysical Union, Washington, DC, pp. 173–192.

Roscoe, H.K., 2004: A review of stratospheric H_2O and NO_2. *Adv. Space Res.*, **34**, 1747–1754.

Rosenfeld, D., 2000: Suppression of rain and snow by urban and industrial air pollution. *Science*, **287**, 1793–1796.

Rosenlof, K.H., 2002: Transport changes inferred from HALOE water and methane measurements. *J. Meteorol. Soc. Japan*, **80**, 831–848.

Rosenlof, K.H., et al., 2001: Stratospheric water vapor increases over the past half-century. *Geophys. Res. Lett*, **28**, 1195–1198.

Rossow, W.B., and E.N. Dueñas, 2004: The International Satellite Cloud Climatology Project (ISCCP) web site. *Bull. Am. Meteorol. Soc*., **85**, 167–172.

Rudolf, B., and J. Rapp, 2003: The century flood of the River Elbe in August 2002: Synoptic weather development and climatological aspects. In: *Quart. Rep. German NWP-System Deutscher Wetterdienst*, No. 2, Pt 1, pp. 8–23.

Rudolf, B., et al., 1994: Terrestrial precipitation analysis: Operational method and required density of point measurements. In: *Global Precipitations and Climate Change* [M. Bubois, and F. Désalmand (eds.)]. NATO ASI Series I, **26**, Springer Verlag, Berlin, 173–186.

Ruiz-Barradas, A., and S. Nigam, 2005: Warm-season rainfall variability over the US Great Plains in observations, NCEP and ERA-40 reanalyses, and NCAR and NASA atmospheric model simulations: Intercomparisons for NAME. *J. Clim.*, **18**, 1808–1830.

Russak, V., 1990: Trends of solar radiation, cloudiness and atmospheric transparency during recent decades in Estonia. *Tellus*, **42B**, 206–210.

Rusticucci, M., and O. Penalba, 2000: Precipitation seasonal cycle over southern South America. *Clim. Res*., **16**, 1–15.

Rusticucci, M., and M. Barrucand, 2004: Observed trends and changes in temperature extremes over Argentina. *J. Clim.*, **17**, 4099–4107.

Rutllant, J., and H. Fuenzalida, 1991: Synoptic aspects of the central Chile rainfall variability associated with the Southern Oscillation. *Int. J. Climatol.*, **11**, 63–76.

Saji, N.H., and T. Yamagata, 2003: Structure of SST and surface wind variability during Indian Ocean dipole mode events: COADS observations. *J. Clim.*, **16**, 2735–2751.

Saji, N.H., et al., 1999: A dipole mode in the tropical Indian Ocean. *Nature*, **401**, 360–363.

Salinger, M.J., J.A. Renwick, and A.B. Mullan, 2001: Interdecadal Pacific Oscillation and South Pacific climate. *Int. J. Climatol.*, **21**, 1705–1721.

Salinger, M.J., G.M. Griffiths, and A. Gosai, 2005: Extreme pressure differences at 0900 NZST and winds across New Zealand. *Int. J. Climatol.*, **25**, 1203–1222.

Santer, B.D., et al., 1999: Uncertainties in observationally based estimates of temperature change in the free atmosphere. *J. Geophys. Res*., **104**, 6305–6333.

Santer, B.D., et al., 2004: Identification of anthropogenic climate change using a second-generation reanalysis. *J. Geophys. Res.*, **109**, D21104, doi:1029/2004/JD005075.

Santer, B.D., et al., 2005: Amplification of surface temperature trends and variability in the tropical atmosphere. *Science*, **309**, 1551–1556.

Sarkar, S., R.P. Singh, and M. Kafatos, 2004: Further evidences for the weakening relationship of Indian rainfall and ENSO over India. *Geophys. Res. Lett*., **31**, L13209, doi:10.1029/2004GL020259.

Scaife A.A., et al., 2005: A stratospheric influence on the winter NAO and North Atlantic surface climate, *Geophys. Res. Lett.*, **32**, L18715, doi:10.1029/2005GL023226.

Schär, C., et al., 2004: The role of increasing temperature variability in European summer heat waves. *Nature*, **427**, 332–336.

Scherrer, S.C., et al., 2005: European temperature distribution changes in observations and climate change scenarios. *Geophys. Res. Lett.*, **32**, L19705, doi:10.1029/2005GL024108.

Scherrer, S.C., et al., 2006: Two dimensional indices of atmospheric blocking and their statistical relationship with winter climate patterns in the Euro-Atlantic region. *Int. J. Climatol.*, **20**, 233–249.

Schlesinger, M.E., and N. Ramankutty, 1994: An oscillation in the global climate system of period 65–70 years. *Nature*, **367**, 723–726.

Schmidli, J., and C. Frei, 2005: Trends of heavy precipitation and wet and dry spells in Switzerland during the 20th century. *Int. J. Climatol*., **25**, 753–771.

Schmith, T., E. Kaas, and T.-S. Li, 1998: Northeast Atlantic winter storminess 1875–1995 re-analysed. *Clim. Dyn.*, **14**, 529–536.

Schneider, D.P., E.J. Steig, and J.C. Comiso, 2004: Recent climate variability in Antarctica from satellite-derived temperature data. *J. Clim.*, **17**, 1569–1583.

Schneider, N., and B.D. Cornuelle, 2005: The forcing of the Pacific Decadal Oscillation. *J. Clim.*, **18**, 4355–4373.

Schönwiese, C.-D., and J. Rapp, 1997: *Climate Trend Atlas of Europe Based on Observations 1891–1990*. Kluwer Academic Press, Dordrecht, 228 pp.

Schreck, C.J. III, and F.H.M. Semazzi, 2004: Variability of the recent climate of Eastern Africa. *Int. J. Climatol.*, **24**, 681–701.

Schwartz, R.D., 2005: Global dimming: clear sky atmospheric transmission from astronomical extinction measurements. *J. Geophys. Res.*, **110**, D14210, doi:10.1029/2005JD005882.

Schwarzkopf, M., and V. Ramaswamy, 2002: Effects of changes in well-mixed gases and ozone on stratospheric seasonal temperatures. *Geophys. Res. Lett*., **29**, 2184, doi:10.1029/2002GL015759.

Schwierz, C., et al., 2006: Challenges posed by and approaches to the study of seasonal-to-decadal climate variability. *Clim. Change*, **79**, 31–63.

Seidel, D.J., and J. Lanzante, 2004: An assessment of three alternatives to linear trends for characterizing global atmospheric temperature changes. *J. Geophys. Res.*, **109**, D14108, doi:10.1029/2003JD004414.

Seidel, D.J., et al., 2001: Climatological characteristics of the tropical tropopause as revealed by radiosondes. *J. Geophys. Res.*, **106**, 7857–7878.

Seidel, D.J., et al., 2004: Uncertainty in signals of large-scale climate variations in radiosonde and satellite upper-air temperature datasets. *J. Clim.*, **17**, 2225–2240.

Sen Roy, S., and R.C. Balling, 2004: Trends in extreme daily rainfall indices in India. *Intl. J. Climatol*., **24**, 457–466.

Serreze, M.C., et al., 1997: Icelandic low cyclone activity: climatological features, linkages with the NAO, and relationships with recent changes in the Northern Hemisphere circulation. *J. Clim.*, **10**, 453–464.

Sexton, D.M.H., 2001: The effect of stratospheric ozone depletion on the phase of the Antarctic Oscillation. *Geophys. Res. Lett.*, **28**, 3697–3700.

Shabbar, A., and W. Skinner, 2004: Summer drought patterns in Canada and the relationship to global sea surface temperatures. *J. Clim.*, **17**, 2866–2880.

Shepherd, J.M., and S.J. Burian, 2003: Detection of urban-induced rainfall anomalies in a major coastal city. *Earth Interactions*, **7**, 1–17.

Shepherd, J.M., H. Pierce, and A.J. Negri, 2002: Rainfall modification by major urban areas: Observations from spaceborne rain radar on the TRMM satellite. *J. Appl. Meteorol*., **41**, 689–701.

Shepherd, J.M., L. Taylor, and C. Garza, 2004: A dynamic multi-criteria technique for siting NASA-Clark Atlanta rain gauge network. *J. Atmos. Ocean. Technol.*, **21**, 1346–1363.

Sherwood, S.C., 2002: A microphysical connection among biomass burning, cumulus clouds, and stratospheric moisture. *Science*, **295**, 1271–1275.

Sherwood, S.C., J. Lanzante, and C. Meyer, 2005: Radiosonde daytime biases and late 20th century warming. *Science*, **309**, 1556–1559.

Shine, K.P., et al., 2003: A comparison of model-simulated trends in stratospheric temperatures. *Q. J. R. Meteorol. Soc.*, **129**, 1565–1588.

Silvestri, G.E., and C.S. Vera, 2003: Antarctic Oscillation signal on precipitation anomalies over southeastern South America. *Geophys. Res. Lett.*, **30**, 2115, doi:10.1029/2003GL018277.

Simmonds, I., 2003: Modes of atmospheric variability over the Southern Ocean. *J. Geophys. Res.*, **108**, 8078, doi:10.1029/2000JC000542.

Simmonds, I., and K. Keay, 2000: Variability of Southern Hemisphere extratropical cyclone behavior 1958–97. *J. Clim.*, **13**, 550–561.

Simmonds, I., and K. Keay, 2002: Surface fluxes of momentum and mechanical energy over the North Pacific and North Atlantic Oceans. *Meteorol. Atmos. Phys.*, **80**, 1–18.

Simmonds, I., K. Keay, and E.-P. Lim, 2003: Synoptic activity in the seas around Antarctica. *Mon. Weather Rev.*, **131**, 272–288.

Simmons, A.J., et al., 2004: Comparison of trends and low-frequency variability in CRU, ERA-40 and NCEP/NCAR analyses of surface air temperature. *J. Geophys. Res*., **109**, D24115, doi:10.1029/2004JD005306.

Simmons, A.J., et al., 2005: ECMWF analyses and forecasts of stratospheric winter polar vortex breakup: September 2002 in the Southern Hemisphere and related events. *J. Atmos. Sci*., **62**, 668–689.

Sinclair, M.R., J.A. Renwick, and J.W. Kidson, 1997: Low-frequency variability of Southern Hemisphere sea level pressure and weather system activity. *Mon. Weather Rev.*, **125**, 2531–2543.

Small, E.E., L.C. Sloan, and R. Nychka, 2001: Changes in surface air temperature caused by desiccation of the Aral Sea. *J. Clim.*, **14**, 284–299.

Smith, C.A., J.D. Haigh, and R. Toumi, 2001: Radiative forcing due to trends in stratospheric water vapour. *Geophys. Res. Lett.*, **28**, 179–182.

Smith, I., 2004: An assessment of recent trends in Australian rainfall. *Aust. Meteorol. Mag.*, **53**, 163–173.

Smith, L.C., 2000: Trends in Russian Arctic river-ice formation and breakup, 1917 to 1994. *Phys. Geogr.*, **21**, 46–56.

Smith, T.M., and R.W. Reynolds, 2004: Improved extended reconstruction of SST (1854–1997). *J. Clim.*, **17**, 2466–2477.

Smith, T.M., and R.W. Reynolds, 2005: A global merged land and sea surface temperature reconstruction based on historical observations (1880–1997). *J. Clim.*, **18**, 2021–2036.

Smith, T.M., et al., 2005: New surface temperature analyses for climate monitoring. *Geophys. Res. Lett.*, **32**, L14712, doi:10.1029/2005GL023402.

Smits, A., A.M.G. Klein Tank, and G.P. Können, 2005: Trends in storminess over the Netherlands, 1962–2002. *Int. J. Climatol*., **25**, 1331–1344.

Snow, J.T. (ed.), 2003: Special Issue: European Conference on Severe Storms. *Atmos. Res.*, **67–68**, 703pp.

Soden, B.J., and S.R. Schroeder, 2000: Decadal variations in tropical water vapor: A comparison of observations and a model simulation. *J. Clim.*, **13**, 3337–3340.

Soden, B.J., et al., 2002: Global cooling after the eruption of Mount Pinatubo: A test of climate feedback by water vapor. *Science*, **296**, 727–730.

Soden, B.J., et al., 2004: An analysis of satellite, radiosonde, and lidar observations of upper tropospheric water vapor from the Atmospheric Radiation Measurement Program. *J. Geophys. Res*., **109**, D04105, doi:10.1029/2003JD003828.

Soden, B.J., et al., 2005: The radiative signature of upper tropospheric moistening. *Science*, **310**, 841–844.
Sohn, B.-J., and E.A. Smith, 2003: Explaining sources of discrepancy in SSM/I water vapor algorithms. *J. Clim.*, **16**, 3229–3255.
Song, Y., and W.A. Robinson, 2004: Dynamical mechanisms for stratospheric influences on the troposphere. *J. Atmos. Sci.*, **61**, 1711–1725.
Sparks, J., D. Changnon, and J. Starke, 2002: Changes in the frequency of extreme warm-season surface dewpoints in northeastern Illinois: Implications for cooling-system design and operation. *J. Appl. Meteorol.*, **41**, 890–898.
Stanhill, G., and S. Cohen, 2001: Global dimming, a review of the evidence for a widespread and significant reduction in global radiation with a discussion of its probable causes and possible agricultural consequences. *Agric. For. Meteorol*., **107**, 255–278.
Sterl, A., 2001: On the impact of gap-filling algorithms on variability patterns of reconstructed oceanic surface fields. *J. Geophys. Res*., **28**, 2473–2476.
Sterl, A., 2004: On the (in)homogeneity of reanalysis products. *J. Clim.*, **17**, 3866–3873.
Sterl, A., and S. Caires, 2005: Climatology, variability and extrema of ocean waves: the Web-based KNMI/ERA-40 wave atlas. *Int. J. Climatol*., **25**, 963–977.
Stewart, I.T., D.R. Cayan, and M.D. Dettinger, 2005: Changes towards earlier streamflow timing across western North America. *J. Clim.*, **18**, 1136–1155.
Stone, D.A., A.J. Weaver, and F.W. Zwiers, 2000: Trends in Canadian precipitation intensity. *Atmos.-Ocean*, **38**, 321–347.
Straus, D.M., and J. Shukla, 2002: Does ENSO force the PNA? *J. Clim.*, **15**, 2340–2358.
Straus, D.M., and F. Molteni, 2004: Circulation regimes and SST forcing: Results from large GCM ensembles. *J. Clim.*, **17**, 1641–1656.
Stuber, N., et al., 2001: Is the climate sensitivity to ozone perturbations enhanced by stratospheric water vapor feedback? *Geophys. Res. Lett*., **28**, 2887–2890.
Sturaro, G., 2003: A closer look at the climatological discontinuities present in the NCEP/NCAR reanalysis temperature due to the introduction of satellite data. *Clim. Dyn.*, **21**, 309–316.
Sun, B.M., 2003: Cloudiness over the contiguous United States: Contemporary changes observed using ground-based and ISCCP D2 data. *Geophys. Res. Lett.*, **30**, doi:10.1029/2002GL015887.
Sun, B.M., and P.Ya. Groisman, 2000: Cloudiness variations over the former Soviet Union. *Int. J. Climatol.*, **20**, 1097–1111.
Sun, B.M., and P.Ya. Groisman, 2004: Variations in low cloud cover over the United States during the second half of the twentieth century. *J. Clim.*, **17**, 1883–1888.
Sun, B.M., P.Ya. Groisman, and I.I. Mokhov, 2001: Recent changes in cloud-type frequency and inferred increases in convection over the United States and the former USSR. *J. Clim.*, **14**, 1864–1880.
Sutton, R.T., and D.L.R. Hodson, 2003: Influence of the ocean on North Atlantic climate variability 1871–1999. *J. Clim.*, **16**, 3296–3313.
Sutton, R.T., and D.L.R. Hodson, 2005: Atlantic Ocean forcing of North American and European summer climate. *Science*, **290**, 2133–2137.
Swanson, R.E., 2003: Evidence of possible sea-ice influence on Microwave Sounding Unit tropospheric temperature trends in polar regions. *Geophys. Res. Lett.*, **30**, 2040, doi:10.1029/2003GL017938.
Tebakari, T., J. Yoshitani, and C. Suvanpimol, 2005: Time-space trend analysis in pan evaporation over kingdom of Thailand. *J. Hydrol. Eng*., **10**, 205–215.
Terray, P., S. Dominiak, and P. Delecluse, 2005: Role of the southern Indian Ocean in the transition of the monsoon-ENSO system during recent decades. *Clim. Dyn*., **24**, 169–195.
Tett, S.F.B., and P.W. Thorne, 2004: Tropospheric temperature series from satellites. *Nature*, **429**, doi:10.1038/nature03208.
Thielen, J., et al., 2000: The possible influence of urban surfaces on rainfall development: a sensitivity study in 2D in the meso-gamma scale. *Atmos. Res*., **54**, 15–39.
Thompson, D.W.J., and J.M. Wallace, 1998: The Arctic Oscillation signature in the wintertime geopotential height and temperature fields. *Geophys. Res. Lett.*, **25**, 1297–1300.
Thompson, D.W.J., and J.M. Wallace, 2000: Annular modes in the extratropical circulation, Pt I: Month-to-month variability. *J. Clim.*, **13**, 1000–1016.
Thompson, D.W.J., and S. Solomon, 2002: Interpretation of recent Southern Hemisphere climate change. *Science*, **296**, 895–899.
Thompson, D.W.J., and S. Solomon, 2005: Recent stratospheric climate trends: Global structure and tropospheric linkages. *J. Clim.*, **18**, 4785–4795.
Thompson, D.W.J., J.M. Wallace, and G.C. Hegerl, 2000: Annular modes in the extratropical circulation. Part II: Trends. *J. Clim.*, **13**, 1018–1036.
Thompson, D.W.J., M.P. Baldwin, and J.M. Wallace, 2002: Stratospheric connection to Northern Hemisphere wintertime weather: Implications for prediction. *J. Clim.*, **15**, 1421–1428.
Thompson, D.W.J., S. Lee, and M.P. Baldwin, 2003: Atmospheric processes governing the Northern Hemisphere Annular Mode/North Atlantic Oscillation. In: *The North Atlantic Oscillation: Climatic Significance and Environmental Impact* [Hurrell, J.W., et al. (eds.)]. Geophysical Monograph 134, American Geophysical Union, Washington, DC, pp. 81–112.
Thompson, D.W.J., M.P. Baldwin, and S. Solomon, 2005: Stratosphere/troposphere coupling in the Southern Hemisphere. *J. Atmos. Sci*., **62**, 708–715.
Thorne, P.W., et al., 2005a: Revisiting radiosonde upper air temperatures from 1958 to 2002. *J. Geophys. Res*., **110**, D18105, doi:10.1029/2004JD005753.
Thorne, P.W., et al., 2005b: Uncertainties in climate trends: Lessons from upper-air temperature records. *Bull. Am. Meteorol. Soc*., **86**, 1437–1442.
Thornthwaite, C.W., 1948: An approach toward a rational classification of climate. *Geogr. Rev.*, **38**, 55–94.
Tibaldi, S., et al., 1994: Northern and Southern Hemisphere seasonal variability of blocking frequency and predictability. *Mon. Weather Rev*., **122**, 1971–2003.
Trapp, R.J., et al., 2005: Tornadoes from squall lines and bow echoes. Pt I: Climatological distribution. *Weather Forecasting*, **20**, 23–34.
Trenberth, K.E., 1984: Signal versus noise in the Southern Oscillation. *Mon. Weather Rev.*, **112**, 326–332.
Trenberth, K.E., 1990: Recent observed interdecadal climate changes in the Northern Hemisphere. *Bull. Am. Meteorol. Soc.*, **71**, 988–993.
Trenberth, K.E., 2002: Changes in tropical clouds and radiation. *Science*, **296**, 2095a (online), http://www/sciencemag.org/cgi/content/full/296/5576/2095a.
Trenberth, K.E., 2004: Rural land-use change and climate. *Nature*, **427**, 213.
Trenberth, K.E., and J.W. Hurrell, 1994: Decadal atmosphere–ocean variations in the Pacific. *Clim. Dyn.*, **9**, 303–319.
Trenberth, K.E., and J.M. Caron, 2000: The Southern Oscillation revisited: Sea level pressures, surface temperatures and precipitation. *J. Clim.*, **13**, 4358–4365.
Trenberth, K.E., and J.M. Caron, 2001: Estimates of meridional atmosphere and ocean heat transports. *J. Clim.*, **14**, 3433–3443.
Trenberth, K.E., and D. P. Stepaniak, 2001: Indices of El Niño evolution. *J. Clim.*, **14**, 1697–1701.
Trenberth, K.E., and D.P. Stepaniak, 2003a: Co-variability of components of poleward atmospheric energy transports on seasonal and interannual timescales. *J. Clim.*, **16**, 3690–3704.
Trenberth, K.E., and D.P. Stepaniak, 2003b: Seamless poleward atmospheric energy transports and implications for the Hadley circulation. *J. Clim.*, **16**, 3705–3721.
Trenberth, K.E., and D.J. Shea, 2005: Relationships between precipitation and surface temperature. *Geophys. Res. Lett.*, **32**, L14703, doi:10.1029/2005GL022760.

Trenberth, K.E., and L. Smith, 2005: The mass of the atmosphere: A constraint on global analyses. *J. Clim.*, **18**, 864–875.

Trenberth, K.E., and D.J. Shea, 2006: Atlantic hurricanes and natural variability in 2005, *Geophys. Res. Lett.*, **33**, L12704, doi:10.1029/2006GL026894.

Trenberth, K.E., D.P. Stepaniak, and J.M. Caron, 2000: The global monsoon as seen through the divergent atmospheric circulation. *J. Clim.*, **13**, 3969–3993.

Trenberth, K.E., D.P. Stepaniak, and J.M. Caron, 2002a: Interannual variations in the atmospheric heat budget. *J. Geophys. Res*., **107**, 4066, doi:10.1029/2000JD000297.

Trenberth, K.E., J. Fasullo, and L. Smith, 2005a: Trends and variability in column integrated atmospheric water vapor. *Clim. Dyn.*, **24**, 741–758.

Trenberth, K.E., D.P. Stepaniak, and L. Smith, 2005b: Interannual variability of the patterns of atmospheric mass distribution. *J. Clim.*, **18**, 2812–2825.

Trenberth, K.E., et al., 2002b: The evolution of ENSO and global atmospheric temperatures. *J. Geophys. Res*., **107**, 4065, doi:10.1029/2000JD000298.

Trenberth, K.E., et al., 2003: The changing character of precipitation. *Bull. Am. Meteorol. Soc.*, **84**, 1205–1217.

Trigo, R.M., et al., 2004: Climate impact of the European winter blocking episodes from the NCEP/NCAR Reanalyses. *Clim. Dyn.*, **23**, 17–28.

Trömel, S., and C.-D. Schönwiese, 2005: A generalized method of time series decomposition into significant components including probability assessments of extreme events and application to observed German precipitation data. *Meteorol. Z.*, **14**, 417–427.

Troup, A.J., 1965: The Southern Oscillation. *Q. J. R. Meteorol. Soc.*, **91**, 490–506.

Tuller, S.E., 2004: Measured wind speed trends on the west coast of Canada. *Int. J. Climatol*., **24**, 1359–1374.

Tuomenvirta, R.H., et al., 2000: Trends in Nordic and Arctic temperature extremes. *J. Clim.*, **13**, 977–990.

Turner, D.D., et al., 2003: Dry bias and variability in Vaisala RS80-H radiosondes: The ARM experience. *J. Atmos. Ocean. Technol.*, **20**, 117–132.

Turner, J., et al., 2005: Antarctic climate change during the last 50 years. *Int. J. Climatol.*, **25**, 279–294.

Turner, J., et al., 2006: Significant warming of the Antarctic winter troposphere. *Science*, **311**, 1914–1917.

Ulbrich, U., et al., 2003a: The central European floods of August 2002: Pt. 1 – Rainfall periods and flood development. *Weather*, **58**, 371–377.

Ulbrich, U., et al., 2003b: The central European floods of August 2002: Pt. 2 – Synoptic causes and considerations with respect to climatic change. *Weather*, **58**, 434–442.

Uppala, S.M., et al., 2005: The ERA-40 reanalysis. *Q. J. R. Meteorol. Soc.*, **131**, 2961–3012.

van den Broeke, M.R., and N.P.M. van Lipzig, 2003: Response of wintertime Antarctic temperatures to the Antarctic Oscillation: Results of a regional climate model. In: *Antarctic Peninsula Climate Variability: Historical and Paleoenvironmental Perspectives* [Domack, E., et al. (eds.)]. Antarctic Research Series 79, American Geophysical Union, Washington, DC, pp. 43–58.

van den Dool, H., J. Huang, and Y. Fan, 2003: Performance and analysis of the constructed analogue method applied to U.S. soil moisture over 1981–2001. *J. Geophys. Res*., **108**, 8617, doi:10.1029/2002JD003114.

van der Schrier, G., et al., 2006: Summer moisture variability across Europe. *J. Clim.*, **19**, 2818–2834.

van Wijngaarden, W.A., and L.A. Vincent, 2005: Examination of discontinuities in hourly surface relative humidity in Canada during 1953-2003. *J. Geophys. Res.*, **110**, D22102, doi:10.1029/2005JD005925.

Venegas, S.A., 2003: The Antarctic Circumpolar Wave: A combination of two signals? *J. Clim.*, **16**, 2509–2525.

Venegas, S.A., and L.A. Mysak, 2000: Is there a dominant timescale of natural climate variability in the Arctic? *J. Clim.*, **13**, 3412–3434.

Vera, C., et al., 2006: A unified view of the American monsoon systems. *J. Clim.*, **19**, 4977–5000.

Vikebo, F., et al., 2003: Wave height variations in the North Sea and on the Norwegian continental shelf, 1881-1999. *Continental Shelf Res.*, **23**, 251–263.

Vimont, D.J., D.S. Battisti, and A.C. Hirst, 2001: Footprinting: A seasonal connection between the Tropics and midlatitudes. *Geophys. Res. Lett*., **28**, 3923–2936.

Vincent, L.A., and É. Mekis, 2006: Changes in daily and extreme temperature and precipitation indices for Canada over the 20th century. *Atmos.-Ocean*, **44**, 177–193.

Vincent, L.A., et al., 2002: Homogenization of daily temperatures over Canada.. *J. Clim.*, **15**, 1322–1334.

Vincent, L.A., et al., 2005: Observed trends in indices of daily temperature extremes in South America 1960–2000. *J. Clim.*, **18**, 5011–5023.

Vinnikov, K.Y., and N.C. Grody, 2003: Global warming trend of mean tropospheric temperature observed by satellites. *Science*, **302**, 269–272.

Vinnikov, K.Y., et al., 2006: Temperature trends at the surface and in the troposphere. *J. Geophys. Res.*, **111**, D03106, doi:10.1029/2005JD006392.

Visbeck, M., et al., 2003: The ocean's response to North Atlantic Oscillation variability. In: *The North Atlantic Oscillation: Climatic Significance and Environmental Impact* [Hurrell, J.W., et al. (eds.)]. Geophysical Monograph 134, American Geophysical Union, Washington, DC, pp. 113–145.

Vose, R.S., D.R. Easterling, and B. Gleason, 2005a: Maximum and minimum temperature trends for the globe: An update through 2004. *Geophys. Res. Lett.*, **32**, L23822, doi:10.1029/2004GL024379.

Vose, R.S., et al., 1992: *The Global Historical Climatology Network: Long-Term Monthly Temperature, Precipitation, Sea Level Pressure, and Station Pressure Data*. ORNL/CDIAC-53, NDP-041, Carbon Dioxide Information Analysis Center, Oak Ridge National Laboratory, Oak Ridge, TN, 325 pp.

Vose, R.S., et al., 2004: Impact of land-use change on climate. *Nature*, **427**, 213–214.

Vose, R.S., et al., 2005b: An intercomparison of surface air temperature analyses at the global, hemispheric and grid-box scale. *Geophys. Res. Lett*., **32**, L18718, doi:10.1029/2005GL023502.

Wallace, J.M., and D.S. Gutzler, 1981: Teleconnections in the geopotential height field during the Northern Hemisphere winter. *Mon. Weather Rev.*, **109**, 784–812.

Walter, K., and H.-F. Graf, 2002: On the changing nature of the regional connection between the North Atlantic Oscillation and sea surface temperature. *J. Geophys. Res*., **107**, 4338, doi:10.1029/2001JD000850.

Walter, M.T., et al., 2004: Increasing evapotranspiration from the conterminous United States. *J. Hydrometeorol.*, **5**, 405–408.

Wang, B., 1994: Climatic regimes of tropical convection and rainfall. *J. Clim.*, **7**, 1109–1118.

Wang, B., and Z. Fan, 1999: Choice of South Asian summer monsoon indices. *Bull. Am. Meteorol. Sci.*, **80**, 629–638.

Wang, B., and J.C.L. Chan, 2002: How strong ENSO events affect tropical storm activity over the western North Pacific. *J. Clim.*, **15**, 1643–1658.

Wang, B., and Q. Ding, 2006: Changes in global monsoon precipitation over the past 56 years. *Geophys. Res. Lett.*, **33**, L06711, doi:10.1029/2005GL025347.

Wang, H.J., 2001: The weakening of the Asian monsoon circulation after the end of 1970's. *Adv. Atmos. Sci.*, **18**, 376–386.

Wang, J., et al., 2003: Performance of operational radiosonde humidity sensors in direct comparison with a chilled mirror dew-point hygrometer and its climate implication. *Geophys. Res. Lett*., **30**, 1860, 10.129/2003GL016985.

Wang, J.H., H.L. Cole, and D.J. Carlson, 2001: Water vapor variability in the tropical western Pacific from 20-year radiosonde data. *Adv. Atmos. Sci.*, **18**, 752–766.

Wang, J.H., et al., 2002a: Corrections of humidity measurement errors from the Vaisala RS80 radiosonde – Application to TOGA COARE data. *J. Atmos. Ocean. Technol.*, **19**, 981–1002.

Wang, J.X.L., and D.J. Gaffen, 2001: Trends in extremes of surface humidity, temperatures and summertime heat stress in China. *Adv. Atmos. Sci.*, **18**, 742–751.

Wang, P.H., et al., 2002b: Satellite observations of long-term changes in tropical cloud and outgoing longwave radiation from 1985 to 1998. *Geophys. Res. Lett.*, **29**, 1397, doi:10.1029/2001GL014264.

Wang, X.L., and V.R. Swail, 2001: Changes of extreme wave heights in Northern Hemisphere oceans and related atmospheric circulation regimes. *J. Clim.*, **14**, 2204–2201.

Wang, X.L., and V.R. Swail, 2002: Trends of Atlantic wave extremes as simulated in a 40-yr wave hindcast using kinematically reanalyzed wind fields**.** *J. Clim.*, **15**, 1020–1035.

Wang, X.L., and P.M. Zhai, 2004: Variation of spring dust storms in China and its association with surface winds and sea level pressures. *Acta Meteorol. Sin.*, **62**, 96–103 (in Chinese).

Wang, X.L., V.R. Swail, and F.W. Zwiers, 2006a: Climatology and changes of extratropical storm tracks and cyclone activity: Comparison of ERA-40 with NCEP/NCAR Reanalysis for 1958–2001. *J. Clim.*, **19**, 3145–3166.

Wang, X.L., H. Wan, and V.R. Swail, 2006b: Observed changes in cyclone activity in Canada and their relationships to major circulation regimes. *J. Clim.*, **19**, 896–915.

Wang, Z.W., and P.M. Zhai, 2003: Climate change in drought over northern China during 1950–2000. *Acta Geogr. Sin.*, **58**(supplement), 61–68 (in Chinese).

Waple, A.M., and J.H. Lawrimore, 2003: State of the climate in 2002. *Bull. Am. Meteorol. Soc*., **84**(6), S1–S68.

Waple, A.M., et al., 2002: Climate assessment for 2001. *Bull. Am. Meteorol. Soc*., **83**(6), S1–S62.

Ward, M.N., 1998: Diagnosis and short-lead time prediction of summer rainfall in tropical North Africa at interannual and multidecadal timescales. *J. Clim.*, **11**, 3167–3191.

Ward, M.N., and B.J. Hoskins, 1996: Near surface wind over the global ocean 1949–1988. *J. Clim.*, **9**, 1877–1895.

Wardle, R., and I. Smith, 2004: Modeled response of the Australian monsoon to changes in land surface temperatures. *Geophys. Res. Lett.*, **31**, L16205, doi:10.1029/2004GL020157.

Watkins, A., 2002: 2002 Australian climate summary: Dry and warm conditions dominate. *Bull. Aust. Meteorol. Oceanogr. Soc.*, **15**, 109–114.

Waugh, D., et al., 1999: Persistence of the lower stratospheric polar vortices. *J. Geophys. Res*., **104**, 27191–27201.

Webster, P.J., and S. Yang, 1992: Monsoon and ENSO: selective interactive systems. *Q. J. R. Meteorol. Soc.*, **118**, 877–926.

Webster, P.J., et al., 1998: Monsoons: processes, predictability, and the prospects for prediction. *J. Geophys. Res.*, **103**, 14451–14510.

Webster, P.J., et al., 1999: Coupled ocean-atmosphere dynamics in the Indian Ocean during 1997-98. *Nature*, **401**, 356–360.

Webster, P.J., et al., 2005: Changes in tropical cyclone number, duration and intensity in a warming environment. *Science*, **309**, 1844–1846.

Webster, P. J., et al., 2006: Response to comment on "Changes in tropical cyclone number, duration, and intensity in a warming environment". *Science*, **311**, 1713c.

Weisse, R., H. von Storch, and F. Feser, 2005: Northeast Atlantic and North Sea storminess as simulated by a regional climate model during 1958-2001 and comparison with observations. *J. Clim.*, **18**, 465–479.

Wells, N., S. Goddard, and M.J. Hayes, 2004: A self-calibrating Palmer Drought Severity Index. *J. Clim.*, **17**, 2335–2351.

Wentz, F.J., and M. Schabel, 1998: Effects of satellite orbital decay on MSU lower tropospheric temperature trends. *Nature*, **394**, 661–664.

Wentz, F.J., and M. Schabel, 2000: Precise climate monitoring using complementary satellite data sets. *Nature*, **403**, 414–416.

Wettstein, J.J., and L.O. Mearns, 2002: The influence of the North Atlantic-Arctic Oscillation on mean, variance, and extremes of temperature in the northeastern United States and Canada. *J. Clim.*, **15**, 3586–3600.

Wheeler, M.C., and J.L. McBride, 2005: Australian-Indonesian monsoon. In: *Intraseasonal Variability of the Atmosphere-Ocean Climate System* [Lau, W.K.M., and D.E. Waliser, (eds.)]. Praxis Publishing, Chichester, UK, pp. 125–173.

White, W.B., and R.G. Peterson, 1996: An Antarctic Circumpolar Wave in surface pressure, wind, temperature and sea-ice extent. *Nature*, **380**, 699–702.

White, W.B., and J. Annis, 2004: Influence of the Antarctic Circumpolar Wave on El Niño and its multidecadal changes from 1950 to 2001. *J. Geophys. Res.*, **109**, C06019, doi:10.1029/2002JC001666.

White, W.B., and I. Simmonds, 2006: SST-induced cyclogenesis in the Antarctic Circumpolar Wave. *J. Geophys. Res.*, **111**, C08011, doi:10.1029/2004JC002395.

White, W.B., P. Gloersen, and I. Simmonds, 2004: Tropospheric response in the Antarctic Circumpolar Wave along the sea ice edge around Antarctica. *J. Clim.*, **17**, 2765–2779.

Wiedenmann, J.M., et al., 2002: The climatology of blocking anticyclones for the Northern and Southern Hemispheres: Block intensity as a diagnostic. *J. Clim.*, **15**, 3459–3473.

Wielicki, B.A., et al., 2002a: Evidence for large decadal variability in the tropical mean radiative energy budget. *Science*, **295**, 841–844.

Wielicki, B.A., et al., 2002b: Response. *Science*, **296**, http://www/sciencemag.org/cgi/content/full/296/5576/2095a.

Wielicki, B.A., et al., 2005: Change in Earth's albedo measured by satellite. *Science*, **308**, 825.

Wijngaard, J.B., A.M.G. Klein Tank, and G.P. Können, 2003: Homogeneity of 20th century European daily temperature and precipitation series. *Int. J. Climatol.*, **23**, 679–692.

Wild, M.A., et al., 2004: On the consistency of trends in radiation and temperature records and implications for the global hydrological cycle. *Geophys. Res. Lett*., **31**, L11201, doi:10.1029/2003GL019188.

Wild, M.A., et al., 2005: From dimming to brightening: Decadal changes in solar radiation at Earth's surface. *Science*, **308**, 847–850.

Willis, J.K., D. Roemmich, and B. Cornuelle, 2004: Interannual variability in upper-ocean heat content, temperature and thermosteric expansion on global scales. *J. Geophys. Res.*, **109**, C12036, doi:10.1029/2003JC002260.

Wittman, M.A.H., et al., 2004: Stratospheric influence on baroclinic lifecycles and its connection to the Arctic Oscillation. *Geophys. Res. Lett*., **31**, L16113, doi:10.1029/2004GL020503.

WMO, 2004: *World Meteorological Organization Statement on the Status of Global Climate in 2003*. World Meteorological Organization, Geneva, 12 pp.

Wong, T.D.F., M.H. Young, and S. Weckmann, 2000: Validation of the CERES/TRMM ERBE-like monthly mean clear-sky longwave dataset and the effects of the 1998 ENSO event. *J. Clim.*, **13**, 4256–4267.

Wong, T., et al., 2006: Re-examination of the observed decadal variability of Earth Radiation Budget using altitude-corrected ERBE/ERBS nonscanner WFOV data. *J. Clim.*, **19**, 4028–4040.

Woolf, D.K., P.G. Challenor, and P.D. Cotton, 2002: The variability and predictability of North Atlantic wave climate. *J. Geophys. Res*., **107**, 3145, doi:10.1029/2001JC001124.

Worley, S.J., et al., 2005: ICOADS release 2.1 data and products. *Int. J. Climatol*., **25**, 823–842.

Wu, M.C., W.L. Chang, and W.M. Leung, 2004: Impacts of El Niño-Southern Oscillation events on tropical cyclone landfalling activity in the western North Pacific. *J. Clim.*, **17**, 1419–1428.

Wylie, D.P., et al., 2005: Trends in global cloud cover in two decades of HIRS observations. *J. Clim.*, **18**, 3021–3031.

Xie, P., and Arkin, P.A. 1997: Global precipitation: A 17-year monthly analysis based on gauge observations, satellite estimates and numerical model outputs. *Bull. Am. Meteorol. Soc.*, **78**, 2539–2558.

Xie, S.P., et al., 2002: Structure and mechanisms of South Indian Ocean climate variability. *J. Clim.*, **15**, 864–878.

Yan, Z., et al., 2002: Trends of extreme temperatures in Europe and China based on daily observations. *Clim. Change*, **53**, 355–392.

Yang, D., B. Ye, and D.L. Kane, 2004: Streamflow changes over Siberian Yenisei River Basin. *J. Hydrol.*, **296**, 59–80.

Yang, D., et al., 2002: Siberian Lena River hydrologic regime and recent change. *J. Geophys. Res.*, **107**, 4694, doi:10.1029/2002JD002542.

Ye, B.S., D.Q. Yang, and D.L. Kane, 2003: Changes in Lena River streamflow hydrology: Human impacts versus natural variations. *Water Resour. Res.*, **39**, 1200, doi:10.1029/2003WR001991.

Yin, X., A. Gruber, and P. Arkin, 2004: Comparison of the GPCP and CMAP merged gauge-satellite monthly precipitation products for the period 1979–2001. *J. Hydrometeorol.*, **5**, 1207–1222.

Yu, L.S., and M.M. Rienecker, 1999: Mechanisms for the Indian Ocean warming during the 1997–1998 El Niño. *Geophys. Res. Lett*., **26**, 735–738.

Yu, R., B. Wang, and T. Zhou, 2004a: Climate effects of the deep continental stratus clouds generated by the Tibetan Plateau. *J. Clim.*, **17**, 2702–2713.

Yu, R., B. Wang, and T. Zhou, 2004b: Tropospheric cooling and summer monsoon weakening trend over East Asia. *Geophys.Res. Lett.*, **31**, L22212, doi:10.1029/2004GL021270.

Zhai, P.M., and X.H. Pan, 2003: Trends in temperature extremes during 1951–1999 in China. *Geophys. Res. Lett.*, **30**, 1913, doi:10.1029/203GL018004.

Zhai, P.M., et al., 2004: Trends in total precipitation and frequency of daily precipitation extremes over China. *J. Clim.*, **18**, 1096–1108.

Zhang, R., and T.L. Delworth, 2005: Simulated tropical response to a substantial weakening of the Atlantic thermohaline circulation. *J. Clim.*, **18**, 1853–1860.

Zhang, X., W.D. Hogg, and E. Mekis, 2001a: Spatial and temporal characteristics of heavy precipitation events over Canada. *J. Clim.*, **14**, 1923–1936.

Zhang, X., F.W. Zwiers, and G. Li, 2004a: Monte Carlo experiments on the detection of trends in extreme values. *J. Clim.*, **17**, 1945–1952.

Zhang, X., et al., 2001b: Trends in Canadian streamflow. *Water Resour. Res.*, **37**, 987–998.

Zhang, X., et al., 2004b: Climatology and interannual variability of Arctic cyclone activity: 1948–2002. *J. Clim.*, **17**, 2300–2317.

Zhang, X., et al., 2005: Trends in Middle East climate extremes indices from 1950 to 2003. *J. Geophys. Res*., **110**, D22104, doi:10.1029/2005JD006181.

Zhang, Y., et al., 2004c: Calculation of radiative fluxes from the surface to top of atmosphere based on ISCCP and other global data sets: refinements of the radiative transfer model and the input data. *J. Geophys. Res*., **109**, D19105, doi:10.1029/2003JD004457.

Zheng, X., and R.E. Basher, 1999: Structural time series models and trend detection in global and regional temperature series. *J. Clim.*, **12**, 2347–2358.

Zhou, S., et al., 2000: An inter-hemisphere comparison of the persistent stratospheric polar vortex. *Geophys. Res. Lett*., **27**, 1123–1126.

Zhou, X.L., M.A. Geller, and M.H. Zhang, 2001: Cooling trend of the tropical cold point tropopause temperatures and its implications. *J. Geophys. Res*., **106**, 1511–1522.

Zhou, Z.J., and G.C. Zhang, 2003: Typical severe dust storms in northern China (1954–2002). *Chinese Sci. Bull.*, ***48***, 1224–1228 (in Chinese).

Zou, X.K., and P.M. Zhai, 2004: Relationship between vegetation coverage and spring dust storms over northern China. *J. Geophys. Res.*, **109**, D03104, doi:10.1029/2003JD003913.

Zou, X.K., P.M. Zhai, and Q. Zhang, 2005: Variations in droughts over China: 1951–2003. *Geophys. Res. Lett.*, **32**, L04707, doi:10.1029/2004GL021853.

Zveryaev, I.I., and P.S. Chu, 2003: Recent climate changes in precipitable water in the global tropics as revealed in National Centers for Environmental Prediction/National Center for Atmospheric Research reanalysis. *J. Geophys. Res.*, **108**, 4311, doi:10.129/2002JD002476.

Appendix 3.A: Low-Pass Filters and Linear Trends

The time series used in this report have undergone diverse quality controls that have, for example, led to removal of outliers, thereby building in some smoothing. In order to highlight decadal and longer time-scale variations and trends, it is often desirable to apply some kind of low-pass filter to the monthly, seasonal or annual data. In the literature cited for the many indices used in this chapter, a wide variety of schemes was employed. In this chapter, the same filter was used wherever it was reasonable to do so. The desirable characteristics of such filters are 1) they should be easily understood and transparent; 2) they should avoid introducing spurious effects such as ripples and ringing (Duchon, 1979); 3) they should remove the high frequencies; and 4) they should involve as few weighting coefficients as possible, in order to minimise end effects. The classic low-pass filters widely used have been the binomial set of coefficients that remove $2\Delta t$ fluctuations, where Δt is the sampling interval. However, combinations of binomial filters are usually more efficient, and those have been chosen for use here, for their simplicity and ease of use. Mann (2004) discusses smoothing time series and especially how to treat the ends. This chapter uses the 'minimum slope' constraint at the beginning and end of all time series, which effectively reflects the time series about the boundary. If there is a trend, it will be conservative in the sense that this method will underestimate the anomalies at the end.

The first filter (e.g., Figure 3.5) is used in situations where only the smoothed series is shown, and it is designed to remove interannual fluctuations and those on El Niño time scales. It has 5 weights 1/12 [1-3-4-3-1] and its response function (ratio of amplitude after to before) is 0.0 at 2 and $3\Delta t$, 0.5 at $6\Delta t$, 0.69 at $8\Delta t$, 0.79 at $10\Delta t$, 0.91 at $16\Delta t$, and 1 for zero frequency, so for yearly data ($\Delta t = 1$) the half-amplitude point is for a 6-year period, and the half-power point is near 8.4 years.

The second filter used in conjunction with annual values ($\Delta t = 1$) or for comparisons of multiple curves (e.g., Figure 3.8) is designed to remove fluctuations on less than decadal time scales. It has 13 weights 1/576 [1-6-19-42-71-96-106-96-71-42-19-6-1]. Its response function is 0.0 at 2, 3 and $4\Delta t$, 0.06 at $6\Delta t$, 0.24 at $8\Delta t$, 0.41 at $10\Delta t$, 0.54 at $12\Delta t$, 0.71 at $16\Delta t$, 0.81 at $20\Delta t$, and 1 for zero frequency, so for yearly data the half-amplitude point is about a 12-year period, and the half-power point is 16 years. This filter has a very similar response function to the 21-term binomial filter used in the TAR.

Another low-pass filter, widely used and easily understood, is to fit a linear trend to the time series although there is generally no physical reason why trends should be linear, especially over long periods. The overall change in the time series is often inferred from the linear trend over the given time period, but can be quite misleading. Such measures are typically not stable and are sensitive to beginning and end points, so that adding or subtracting a few points can result in marked differences in the estimated trend. Furthermore, as the climate system exhibits highly nonlinear behaviour, alternative perspectives of overall change are provided by comparing low-pass-filtered values (see above) near the beginning and end of the major series.

The linear trends are estimated by Restricted Maximum Likelihood regression (REML, Diggle et al., 1999), and the estimates of statistical significance assume that the terms have serially uncorrelated errors and that the residuals have an AR1 structure. Brohan et al. (2006) and Rayner et al. (2006) provide annual uncertainties, incorporating effects of measurement and sampling error and uncertainties regarding biases due to urbanisation and earlier methods of measuring SST. These are taken into account, although ignoring their serial correlation. The error bars on the trends, shown as 5 to 95% ranges, are wider and more realistic than those provided by the standard ordinary least squares technique. If, for example, a century-long series has multi-decadal variability as well as a trend, the deviations from the fitted linear trend will be autocorrelated. This will cause the REML technique to widen the error bars, reflecting the greater difficulty in distinguishing a trend when it is superimposed on other long-term variations and the sensitivity of estimated trends to the period of analysis in such circumstances. Clearly, however, even the REML technique cannot widen its error estimates to take account of variations outside the sample period of record. Robust methods for the estimation of linear and nonlinear trends in the presence of episodic components became available recently (Grieser et al., 2002).

As some components of the climate system respond slowly to change, the climate system naturally contains persistence. Hence, the statistical significances of REML AR1-based linear trends could be overestimated (Zheng and Basher, 1999; Cohn and Lins, 2005). Nevertheless, the results depend on the statistical model used, and more complex models are not as transparent and often lack physical realism. Indeed, long-term persistence models (Cohn and Lins, 2005) have not been shown to provide a better fit to the data than simpler models.

Appendix 3.B: Techniques, Error Estimation and Measurement Systems: See Supplementary Material

This material is included in the supplementary material. Please note that the many references that are cited only in Appendix 3.B have not been included in the list above, but are just as valuable in formulating the report.

4

Observations: Changes in Snow, Ice and Frozen Ground

Coordinating Lead Authors:
Peter Lemke (Germany), Jiawen Ren (China)

Lead Authors:
Richard B. Alley (USA), Ian Allison (Australia), Jorge Carrasco (Chile), Gregory Flato (Canada), Yoshiyuki Fujii (Japan), Georg Kaser (Austria, Italy), Philip Mote (USA), Robert H. Thomas (USA, Chile), Tingjun Zhang (USA, China)

Contributing Authors:
J. Box (USA), D. Bromwich (USA), R. Brown (Canada), J.G. Cogley (Canada), J. Comiso (USA), M. Dyurgerov (Sweden, USA), B. Fitzharris (New Zealand), O. Frauenfeld (USA, Austria), H. Fricker (USA), G. H. Gudmundsson (UK, Iceland), C. Haas (Germany), J.O. Hagen (Norway), C. Harris (UK), L. Hinzman (USA), R. Hock (Sweden), M. Hoelzle (Switzerland), P. Huybrechts (Belgium), K. Isaksen (Norway), P. Jansson (Sweden), A. Jenkins (UK), Ian Joughin (USA), C. Kottmeier (Germany), R. Kwok (USA), S. Laxon (UK), S. Liu (China), D. MacAyeal (USA), H. Melling (Canada), A. Ohmura (Switzerland), A. Payne (UK), T. Prowse (Canada), B.H. Raup (USA), C. Raymond (USA), E. Rignot (USA), I. Rigor (USA), D. Robinson (USA), D. Rothrock (USA), S.C. Scherrer (Switzerland), S. Smith (Canada), O. Solomina (Russian Federation), D. Vaughan (UK), J. Walsh (USA), A. Worby (Australia), T. Yamada (Japan), L. Zhao (China)

Review Editors:
Roger Barry (USA), Toshio Koike (Japan)

This chapter should be cited as:
Lemke, P., J. Ren, R.B. Alley, I. Allison, J. Carrasco, G. Flato, Y. Fujii, G. Kaser, P. Mote, R.H. Thomas and T. Zhang, 2007: Observations: Changes in Snow, Ice and Frozen Ground. In: *Climate Change 2007: The Physical Science Basis. Contribution of Working Group I to the Fourth Assessment Report of the Intergovernmental Panel on Climate Change* [Solomon, S., D. Qin, M. Manning, Z. Chen, M. Marquis, K.B. Averyt, M. Tignor and H.L. Miller (eds.)]. Cambridge University Press, Cambridge, United Kingdom and New York, NY, USA.

Table of Contents

Executive Summary 339

4.1 Introduction 341

4.2 Changes in Snow Cover 343

4.2.1 Background 343

4.2.2 Observations of Snow Cover, Snow Duration and Snow Quantity? 343

4.3 Changes in River and Lake Ice 346

4.3.1 Background 346

4.3.2 Changes in Freeze-up and Breakup Dates 346

4.4 Changes in Sea Ice 350

4.4.1 Background 350

4.4.2 Sea Ice Extent and Concentration 350

4.4.3 Sea Ice Thickness 352

4.4.4 Pack Ice Motion 355

4.5 Changes in Glaciers and Ice Caps 356

4.5.1 Background 356

4.5.2 Large and Global-Scale Analyses 356

4.5.3 Special Regional Features 359

4.6 Changes and Stability of Ice Sheets and Ice Shelves 361

4.6.1 Background 361

4.6.2 Mass Balance of the Ice Sheets and Ice Shelves 361

4.6.3 Causes of Changes 366

Box 4.1: Ice Sheet Dynamics and Stability 367

4.7 Changes in Frozen Ground 369

4.7.1 Background 369

4.7.2 Changes in Permafrost 369

4.7.3 Changes in Seasonally Frozen Ground 372

4.8 Synthesis 374

Frequently Asked Question

FAQ 4.1: *Is the Amount of Snow and Ice on the Earth Decreasing?* 376

References 378

Executive Summary

In the climate system, the cryosphere (which consists of snow, river and lake ice, sea ice, glaciers and ice caps, ice shelves and ice sheets, and frozen ground) is intricately linked to the surface energy budget, the water cycle, sea level change and the surface gas exchange. The cryosphere integrates climate variations over a wide range of time scales, making it a natural sensor of climate variability and providing a visible expression of climate change. In the past, the cryosphere has undergone large variations on many time scales associated with ice ages and with shorter-term variations like the Younger Dryas or the Little Ice Age (see Chapter 6). Recent decreases in ice mass are correlated with rising surface air temperatures. This is especially true for the region north of 65°N, where temperatures have increased by about twice the global average from 1965 to 2005.

- Snow cover has decreased in most regions, especially in spring and summer. Northern Hemisphere (NH) snow cover observed by satellite over the 1966 to 2005 period decreased in every month except November and December, with a stepwise drop of 5% in the annual mean in the late 1980s. In the Southern Hemisphere, the few long records or proxies mostly show either decreases or no changes in the past 40 years or more. Where snow cover or snowpack decreased, temperature often dominated; where snow increased, precipitation almost always dominated. For example, NH April snow cover extent is strongly correlated with 40°N to 60°N April temperature, reflecting the feedback between snow and temperature, and declines in the mountains of western North America and in the Swiss Alps have been largest at lower elevations.

- Freeze-up and breakup dates for river and lake ice exhibit considerable spatial variability (with some regions showing trends of opposite sign). Averaged over available data for the NH spanning the past 150 years, freeze-up date has occurred later at a rate of 5.8 ± 1.6 days per century, while the breakup date has occurred earlier at a rate of 6.5 ± 1.2 days per century. (The uncertainty range given throughout this chapter denotes the 5 to 95% confidence interval.)

- Satellite data indicate a continuation of the 2.7 ± 0.6% per decade decline in annual mean arctic sea ice extent since 1978. The decline for summer extent is larger than for winter, with the summer minimum declining at a rate of 7.4 ± 2.4% per decade since 1979. Other data indicate that the summer decline began around 1970. Similar observations in the Antarctic reveal larger interannual variability but no consistent trends.

- Submarine-derived data for the central Arctic indicate that the average sea ice thickness in the central Arctic has *very likely* decreased by up to 1 m from 1987 to 1997. Model-based reconstructions support this, suggesting an arctic-wide reduction of 0.6 to 0.9 m over the same period. Large-scale trends prior to 1987 are ambiguous.

- Mass loss of glaciers and ice caps is estimated to be 0.50 ± 0.18 mm yr^{-1} in sea level equivalent (SLE) between 1961 and 2004, and 0.77 ± 0.22 mm yr^{-1} SLE between 1991 and 2004. The late 20th-century glacier wastage likely has been a response to post-1970 warming. Strongest mass losses per unit area have been observed in Patagonia, Alaska and northwest USA and southwest Canada. Because of the corresponding large areas, the biggest contributions to sea level rise came from Alaska, the Arctic and the Asian high mountains.

- Taken together, the ice sheets in Greenland and Antarctica have *very likely* been contributing to sea level rise over 1993 to 2003. Thickening in central regions of Greenland has been more than offset by increased melting near the coast. Flow speed has increased for some Greenland and Antarctic outlet glaciers, which drain ice from the interior. The corresponding increased ice sheet mass loss has often followed thinning, reduction or loss of ice shelves or loss of floating glacier tongues. Assessment of the data and techniques suggests a mass balance of the Greenland Ice Sheet of between +25 and –60 Gt yr^{-1} (–0.07 to 0.17 mm yr^{-1} SLE) from 1961 to 2003, and –50 to –100 Gt yr^{-1} (0.14 to 0.28 mm yr^{-1} SLE) from 1993 to 2003, with even larger losses in 2005. Estimates for the overall mass balance of the Antarctic Ice Sheet range from +100 to –200 Gt yr^{-1} (–0.28 to 0.55 mm yr^{-1} SLE) for 1961 to 2003, and from +50 to –200 Gt yr^{-1} (–0.14 to 0.55 mm yr^{-1} SLE) for 1993 to 2003. The recent changes in ice flow are *likely* to be sufficient to explain much or all of the estimated antarctic mass imbalance, with changes in ice flow, snowfall and melt water runoff sufficient to explain the mass imbalance of Greenland.

- Temperature at the top of the permafrost layer has increased by up to 3°C since the 1980s in the Arctic. The permafrost base has been thawing at a rate ranging up to 0.04 m yr^{-1} in Alaska since 1992 and 0.02 m yr^{-1} on the Tibetan Plateau since the 1960s. Permafrost degradation is leading to changes in land surface characteristics and drainage systems.

- The maximum extent of seasonally frozen ground has decreased by about 7% in the NH from 1901 to 2002, with a decrease in spring of up to 15%. Its maximum depth has decreased about 0.3 m in Eurasia since the mid-20th century. In addition, maximum seasonal thaw depth over permafrost has increased about 0.2 m in the Russian Arctic from 1956 to 1990. Onset dates of thaw in spring and freeze in autumn advanced five to seven days in Eurasia from 1988 to 2002, leading to an earlier growing season but no change in duration.

- Results summarised here indicate that the total cryospheric contribution to sea level change ranged from 0.2 to 1.2 mm yr^{-1} between 1961 and 2003, and from 0.8 to 1.6 mm yr^{-1} between 1993 and 2003. The rate increased over the 1993 to 2003 period primarily due to increasing losses from mountain glaciers and ice caps, from increasing surface melt on the Greenland Ice Sheet and from faster flow of parts of the Greenland and Antarctic Ice Sheets. Estimates of changes in the ice sheets are highly uncertain, and no best estimates are given for their mass losses or gains. However, strictly for the purpose of considering the possible contributions to the sea level budget, a total cryospheric contribution of 1.2 ± 0.4 mm yr^{-1} SLE is estimated for 1993 to 2003 assuming a midpoint mean plus or minus uncertainties and Gaussian error summation.

4.1 Introduction

The main components of the cryosphere are snow, river and lake ice, sea ice, glaciers and ice caps, ice shelves, ice sheets, and frozen ground (Figure 4.1). In terms of the ice mass and its heat capacity, the cryosphere is the second largest component of the climate system (after the ocean). Its relevance for climate variability and change is based on physical properties, such as its high surface reflectivity (albedo) and the latent heat associated with phase changes, which have a strong impact on the surface energy balance. The presence (absence) of snow or ice in polar regions is associated with an increased (decreased) meridional temperature difference, which affects winds and ocean currents. Because of the positive temperature-ice albedo feedback, some cryospheric components act to amplify both changes and variability. However, some, like glaciers and permafrost, act to average out short-term variability and so are sensitive indicators of climate change. Elements of the cryosphere are found at all latitudes, enabling a near-global assessment of cryosphere-related climate changes.

The cryosphere on land stores about 75% of the world's freshwater. The volumes of the Greenland and Antarctic Ice Sheets are equivalent to approximately 7 m and 57 m of sea level rise, respectively. Changes in the ice mass on land have contributed to recent changes in sea level. On a regional scale, many glaciers and ice caps play a crucial role in freshwater availability.

Presently, ice permanently covers 10% of the land surface, of which only a tiny fraction lies in ice caps and glaciers outside Antarctica and Greenland (Table 4.1). Ice also covers approximately 7% of the oceans in the annual mean. In midwinter, snow covers approximately 49% of the land surface in the Northern Hemisphere (NH). Frozen ground has the largest area of any component of the cryosphere. Changes in the components of the cryosphere occur at different time scales, depending on their dynamic and thermodynamic characteristics (Figure 4.1). All parts of the cryosphere contribute to short-term climate changes, with permafrost, ice shelves and ice sheets also contributing to longer-term changes including the ice age cycles.

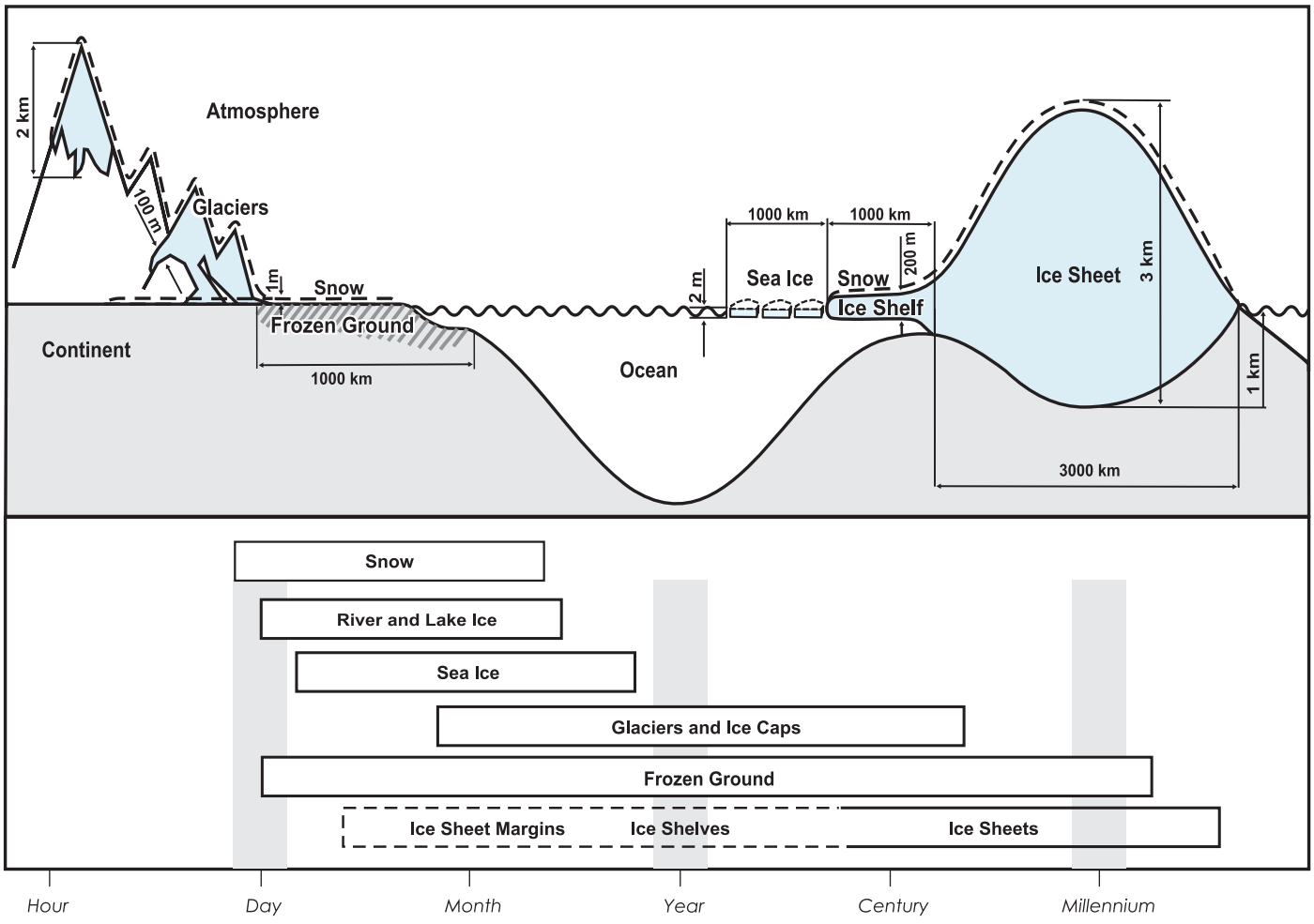


Figure 4.1. *Components of the cryosphere and their time scales.*

Seasonally, the area covered by snow in the NH ranges from a mean maximum in January of 45.2×10^6 km^2 to a mean minimum in August of 1.9×10^6 km^2 (1966–2004). Snow covers more than 33% of lands north of the equator from November to April, reaching 49% coverage in January. The role of snow in the climate system includes strong positive feedbacks related to albedo and other, weaker feedbacks related to moisture storage, latent heat and insulation of the underlying surface (M.P. Clark et al., 1999), which vary with latitude and season.

High-latitude rivers and lakes develop an ice cover in winter. Although the area and volume are small compared to other components of the cryosphere, this ice plays an important role in freshwater ecosystems, winter transportation, bridge and pipeline crossings, etc. Changes in the thickness and duration of these ice covers can therefore have consequences for both the natural environment and human activities. The breakup of river ice is often accompanied by 'ice jams' (blockages formed by accumulation of broken ice); these jams impede the flow of water and may lead to severe flooding.

At maximum extent arctic sea ice covers more than 15×10^6 km^2, reducing to only 7×10^6 km^2 in summer. Antarctic sea ice is considerably more seasonal, ranging from a winter maximum of over 19×10^6 km^2 to a minimum extent of about 3×10^6 km^2. Sea ice less than one year old is termed 'first-year ice' and that which survives more than one year is called 'multi-year ice'. Most sea ice is part of the mobile 'pack ice', which circulates in the polar oceans, driven by winds and surface currents. This pack ice is extremely inhomogeneous, with differences in ice thicknesses and age, snow cover, open water distribution, etc. occurring at spatial scales from metres to hundreds of kilometres.

Glaciers and ice caps adapt to a change in climate conditions much more rapidly than does a large ice sheet, because they have a higher ratio between annual mass turnover and their total mass. Changes in glaciers and ice caps reflect climate variations, in many cases providing information in remote areas where no direct climate records are available, such as at high latitudes or on the high mountains that penetrate high into the middle troposphere. Glaciers and ice caps contribute to sea level changes and affect the freshwater availability in many mountains and surrounding regions. Formation of large and hazardous lakes is occurring as glacier termini retreat from prominent Little Ice Age moraines, especially in the steep Himalaya and Andes.

The ice sheets of Greenland and Antarctica are the main reservoirs capable of affecting sea level. Ice formed from snowfall spreads under gravity towards the coast, where it melts or calves into the ocean to form icebergs. Until recently (including IPCC, 2001) it was assumed that the spreading velocity would not change rapidly, so that impacts of climate change could be estimated primarily from expected changes in snowfall and surface melting. Observations of rapid ice flow changes since IPCC (2001) have complicated this picture, with strong indications that floating ice shelves 'regulate' the motion of tributary glaciers, which can accelerate manyfold following ice shelf breakup.

Frozen ground includes seasonally frozen ground and permafrost. The permafrost region occupies approximately

Table 4.1: *Area, volume and sea level equivalent (SLE) of cryospheric components. Indicated are the annual minimum and maximum for snow, sea ice and seasonally frozen ground, and the annual mean for the other components. The sea ice area is represented by the extent (area enclosed by the sea ice edge). The values for glaciers and ice caps denote the smallest and largest estimates excluding glaciers and ice caps surrounding Greenland and Antarctica.*

Cryospheric Component	Area (10^6 km^2)	Ice Volume (10^6 km^3)	Potential Sea Level Rise (SLE) (m)[g]
Snow on land (NH)	1.9–45.2	0.0005–0.005	0.001–0.01
Sea ice	19–27	0.019–0.025	~0
Glaciers and ice caps			
Smallest estimate[a]	0.51	0.05	0.15
Largest estimate[b]	0.54	0.13	0.37
Ice shelves[c]	1.5	0.7	~0
Ice sheets	14.0	27.6	63.9
Greenland[d]	1.7	2.9	7.3
Antarctica[c]	12.3	24.7	56.6
Seasonally frozen ground (NH)[e]	5.9–48.1	0.006–0.065	~0
Permafrost (NH)[f]	22.8	0.011–0.037	0.03–0.10

Notes:
[a] Ohmura (2004); glaciers and ice caps surrounding Greenland and Antarctica are excluded.
[b] Dyurgerov and Meier (2005); glaciers and ice caps surrounding Greenland and Antarctica are excluded.
[c] Lythe et al. (2001).
[d] Bamber et al. (2001).
[e] Zhang et al. (2003).
[f] Zhang et al. (1999) , excluding permafrost under ocean, ice sheets and glaciers.
[g] Assuming an oceanic area of 3.62×10^8 km^2, an ice density of 917 kg m^{-3}, a seawater density of 1,028 kg m^{-3}, and seawater replacing grounded ice below sea level.

23×10^6 km^2 or 24% of the land area in the NH. On average, the long-term maximum areal extent of the seasonally frozen ground, including the active layer over permafrost, is about 48×10^6 km^2 or 51% of the land area in the NH. In terms of areal extent, frozen ground is the single largest cryospheric component. Permafrost also acts to record air temperature and snow cover variations, and under changing climate can be involved in feedbacks related to moisture and greenhouse gas exchange with the atmosphere.

4.2 Changes in Snow Cover

4.2.1 Background

The high albedo of snow (0.8 to 0.9 for fresh snow) has an important influence on the surface energy budget and on Earth's radiative balance (e.g., Groisman et al., 1994). Snow albedo, and hence the strength of the feedback, depends on a number of factors such as the depth and age of a snow cover, vegetation height, the amount of incoming solar radiation and cloud cover. The albedo of snow may be decreasing because of anthropogenic soot (Hansen and Nazarenko, 2004; see Section 2.5.4 for details).

In addition to the direct snow-albedo feedback, snow may influence climate through indirect feedbacks (i.e., those in which there are more than two causal steps), such as to summer soil moisture. Indirect feedbacks to atmospheric circulation may involve two types of circulation, monsoonal (e.g., Lo and Clark, 2001) and annular (e.g., Saito and Cohen, 2003; see Section 3.6.4), although there are large uncertainties in the physical mechanisms involved (Bamzai, 2003; Robock et al., 2003).

In this section, observations of snow cover extent are updated from IPCC (2001). In addition, several new topics are covered: changes in snow depth and snow water equivalent; relationships of snow to temperature and precipitation; and observations and estimates of changes in snow in the Southern Hemisphere (SH). Changes in the fraction of precipitation falling as snow or other frozen forms are covered in Section 3.3.2.3. This section covers only snow on land; snow on various forms of ice is covered in subsequent sections.

4.2.2 Observations of Snow Cover, Snow Duration and Snow Quantity

4.2.2.1 Sources of Snow Data

Daily observations of the depth of snow and of new snowfall have been made by various methods in many countries, dating to the late 1800s in a few countries (e.g., Switzerland, USA, the former Soviet Union and Finland). Measurements of snow depth and snow water equivalent (SWE) became widespread by 1950 in the mountains of western North America and Europe, and a few sites in the mountains of Australia have been monitored since 1960. *In situ* snow data are affected by changes in station location, observing practices and land cover, and are not uniformly distributed.

The premier data set used to evaluate large-scale snow covered area (SCA), which dates to 1966 and is the longest satellite-derived environmental data set of any kind, is the weekly visible wavelength satellite maps of NH snow cover produced by the US National Oceanic and Atmospheric Administration's (NOAA) National Environmental Satellite Data and Information Service (NESDIS; Robinson et al., 1993). Trained meteorologists produce the weekly NESDIS snow product from visual analyses of visible satellite imagery. These maps are well validated against surface observations, although changes in mapping procedures in 1999 affected the continuity of data series at a small number of mountain and coastal grid points. For the SH, mapping of SCA began only in 2000 with the advent of Moderate Resolution Imaging Spectroradiometer (MODIS) satellite data.

Space-borne passive microwave sensors offer the potential for global monitoring since 1978 of not just snow cover, but also snow depth and SWE, unimpeded by cloud cover and winter darkness. In order to generate homogeneous depth or SWE data series, differences between Scanning Multichannel Microwave Radiometer (SMMR; 1978 to 1987) and Special Sensor Microwave/Imager (SSM/I; 1987 to present) in 1987 must be resolved (Derksen et al., 2003). Estimates of SCA from microwave satellite data compare moderately well with visible data except in autumn (when microwave estimates are too low) and over the Tibetan plateau (microwave too high; Armstrong and Brodzik, 2001). Work is ongoing to develop reliable depth and SWE retrievals from passive microwave for areas with heavy forest or deep snowpacks, and the relatively coarse spatial resolution (~10–25 km) still limits applications over mountainous regions.

4.2.2.2 Variability and Trends in Northern Hemisphere Snow Cover

In this subsection, following the hemispheric view provided by the large-scale analyses by Brown (2000) and Robinson et al. (1993), regional and national-scale studies are discussed. The mean annual NH SCA (1966–2004) is 23.9×10^6 km^2, not including the Greenland Ice Sheet. Interannual variability of SCA is largest not in winter, when mean SCA is greatest, but in autumn (in absolute terms) or summer (in relative terms). Monthly standard deviations range from 1.0×10^6 km^2 in August and September to 2.7×10^6 km^2 in October, and are generally just below 2×10^6 km^2 in non-summer months.

Since the early 1920s, and especially since the late 1970s, SCA has declined in spring (Figure 4.2) and summer, but not substantially in winter (Table 4.2) despite winter warming (see Section 3.2.2). Recent declines in SCA in the months of

February through August have resulted in (1) a shift in the month of maximum SCA from February to January; (2) a statistically significant decline in annual mean SCA; and (3) a shift towards earlier spring melt by almost two weeks in the 1972 to 2000 period (Dye, 2002). Early in the satellite era, between 1967 and 1987, mean annual SCA was 24.4 × 10^6 km^2. An abrupt transition occurred between 1986 and 1988, and since 1988 the mean annual extent has been 23.1 × 10^6 km^2, a statistically significant (T test, p <0.01) reduction of approximately 5% (Robinson and Frei, 2000). Over the longer 1922 to 2005 period (updated from Brown, 2000), the linear trend in March and April NH SCA (Figure 4.2) is a statistically significant reduction of 2.7 ± 1.5 × 10^6 km^2 or 7.5 ± 3.5%.

Temperature variations and trends play a significant role in variability and trends of NH SCA, by determining whether precipitation falls as rain or snow, and by determining snowmelt. In almost every month, SCA is correlated with temperature in the latitude band of greatest variability in SCA, owing to the snow-albedo feedback. For example, temperature in the 40°N to 60°N band and NH SCA are highly correlated in spring (r = –0.68; updated from Brown, 2000) and the largest reductions in March-April average snow cover occurred roughly between the 0°C and 5°C isotherms (Figure 4.3). The snow-albedo feedback also helps determine the longer-term trends (for temperature see Section 3.2.2; see also M.P. Clark et al., 1999; Groisman et al., 1994).

The following paragraphs discuss regional details, including information not available or missing from the satellite data and from Brown's (2000) hemispheric reconstruction.

4.2.2.2.1 North America

From 1915 to 2004, North American SCA increased in November, December and January owing to increases in precipitation (Section 3.3.2; Groisman et al., 2004). Decreases in snow cover are mainly confined to the latter half of the 20th century, and are most apparent in the spring period over western North America (Groisman et al., 2004). Shifts towards earlier melt by about eight days since the mid-1960s were also observed in northern Alaska (Stone et al., 2002).

Another dimension of change in snow is provided by the annual measurements of mountain SWE near April 1 in western North America, which indicate declines since 1950 at about 75% of locations monitored (Mote et al., 2005). The date of maximum mountain SWE appears to have shifted earlier by about two weeks since 1950, as inferred from streamflow measurements (Stewart et al., 2005). That these reductions are predominantly due to warming is shown by regression analysis of streamflow (Stewart et al., 2005) and SWE (Mote, 2006) on temperature and precipitation, and by the dependence of trends in SWE (Mote et al., 2005) on elevation or equivalently mean winter temperature (Figure 4.4a), with the largest percentage changes near the 0°C level.

4.2.2.2.2 Europe and Eurasia

Snow cover trends in mountain regions of Europe are characterised by large regional and altitudinal variations. Recent declines in snow cover have been documented in the mountains of Switzerland (e.g., Scherrer et al., 2004) and Slovakia (Vojtek et al., 2003), but no change was observed in Bulgaria over the 1931 to 2000 period (Petkova et al., 2004). Declines, where observed, were largest at lower elevations, and Scherrer et al.

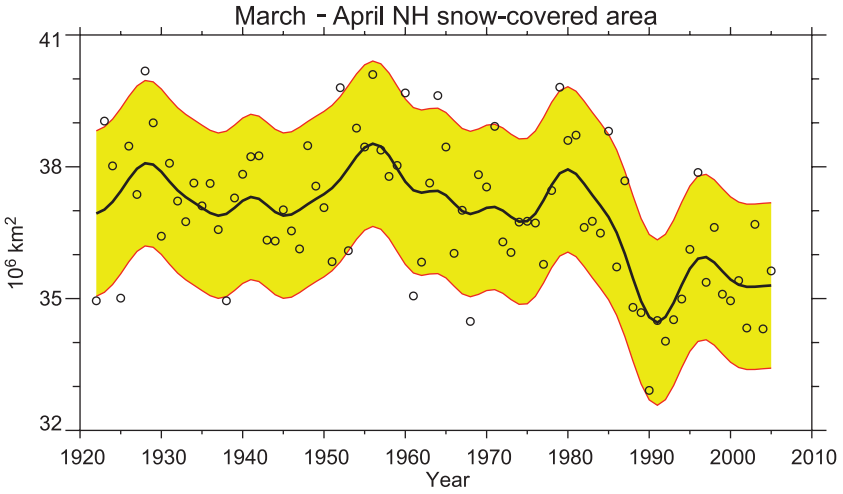


Figure 4.2. *Update of NH March-April average snow-covered area (SCA) from Brown (2000). Values of SCA before 1972 are based on the station-derived snow cover index of Brown (2000); values beginning in 1972 are from the NOAA satellite data set. The smooth curve shows decadal variations (see Appendix 3.A), and the shaded area shows the 5 to 95% range of the data estimated after first subtracting the smooth curve.*

Table 4.2. *Trend (10^6 km^2 per decade) in monthly NH SCA from satellite data (Rutgers-corrected, D. Robinson) over the 1966 to 2005 period and for three months covering the 1922 to 2005 period based on the NH SCA reconstruction of Brown (2000).*

Years	Jan	Feb	Mar	Apr	May	Jun	Jul	Aug	Sep	Oct	Nov	Dec	Ann
1966–2005	–0.11	–0.49	–0.80[a]	–0.74[a]	–0.57	–1.10[a]	–1.17[a]	–0.82[a]	–0.20	–0.36	0.12	0.19	–0.33[a]
1922–2005	n/a	n/a	–0.25[a]	–0.35[a]	n/a	n/a	n/a	n/a	n/a	0.24[a]	n/a	n/a	n/a

Notes:
[a] Statistically significant at the 0.05 level of confidence.
n/a: not available.

(2004) statistically attributed the declines in the Swiss Alps to warming, as is clear when trends are plotted against winter temperature (Figure 4.4b).

Lowland areas of central Europe are characterised by recent reductions in annual snow cover duration by about 1 day yr^{-1} (e.g., Falarz, 2002). Trends towards greater maximum snow depth but shorter snow season have been noted in Finland (Hyvärinen, 2003), the former Soviet Union from 1936 to 1995 (Ye and Ellison, 2003), and in the Tibetan Plateau (Zhang et al., 2004) since the late 1970s. Qin et al. (2006) reported no trends in snow depth or snow cover in western China since 1957.

4.2.2.3 Southern Hemisphere

Outside of Antarctica (see Section 4.6), very little land area in the SH experiences snow cover. Long-term records of snow cover, snowfall, snow depth or SWE are scarce. In some cases, proxies for snow line can be used, but the quality of data is much lower than for most NH areas.

4.2.2.3.1 South America

Estimates from microwave satellite observations for mid-latitude alpine regions of South America for the period of

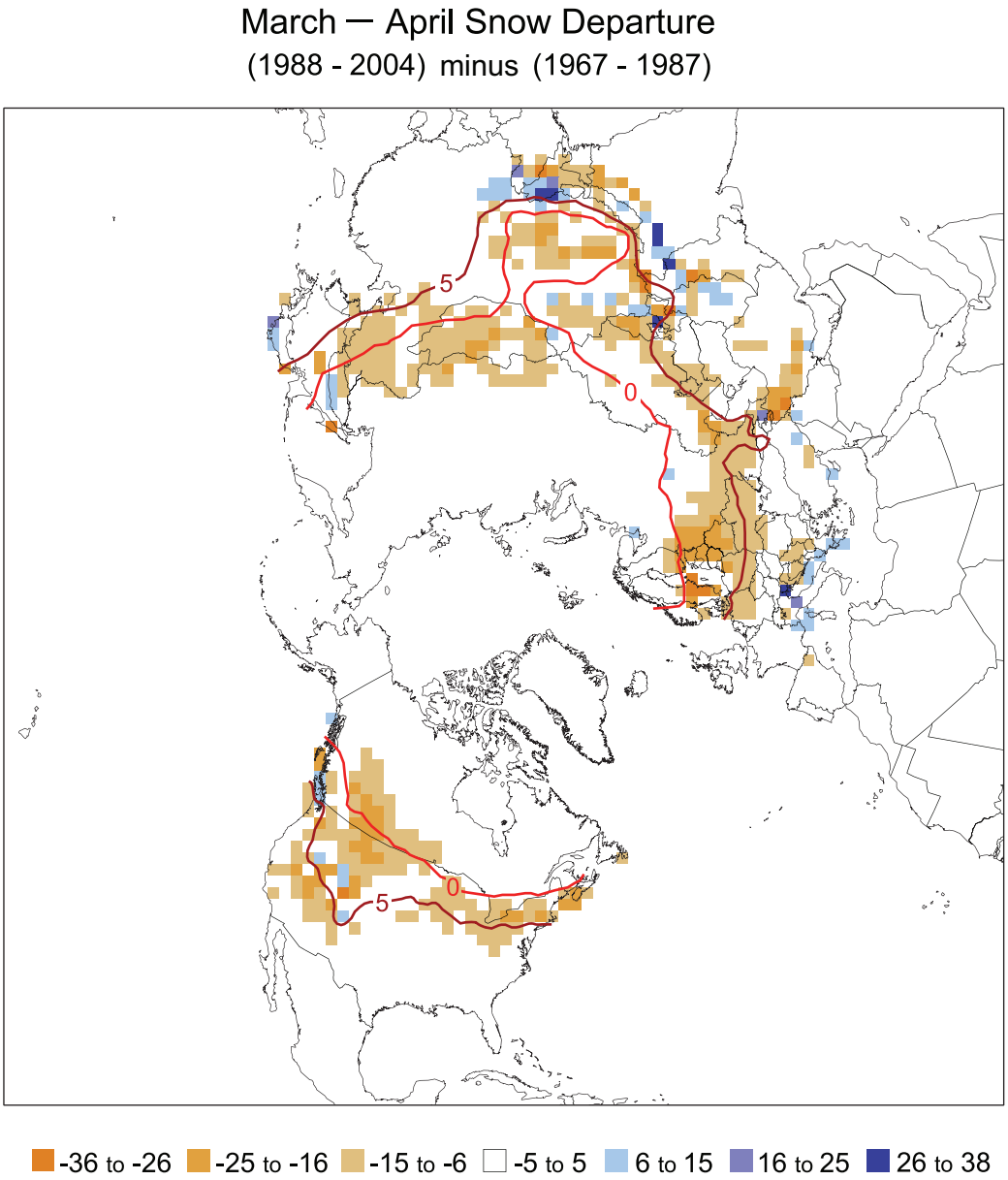


Figure 4.3. *Differences in the distribution of Northern Hemisphere March-April average snow cover between earlier (1967–1987) and later (1988–2004) portions of the satellite era (expressed in % coverage). Negative values indicate greater extent in the earlier portion of the record. Extents are derived from NOAA/NESDIS snow maps. Red curves show the 0°C and 5°C isotherms averaged for March and April 1967 to 2004, from the Climatic Research Unit (CRU) gridded land surface temperature version 2 (CRUTEM2v) data.*

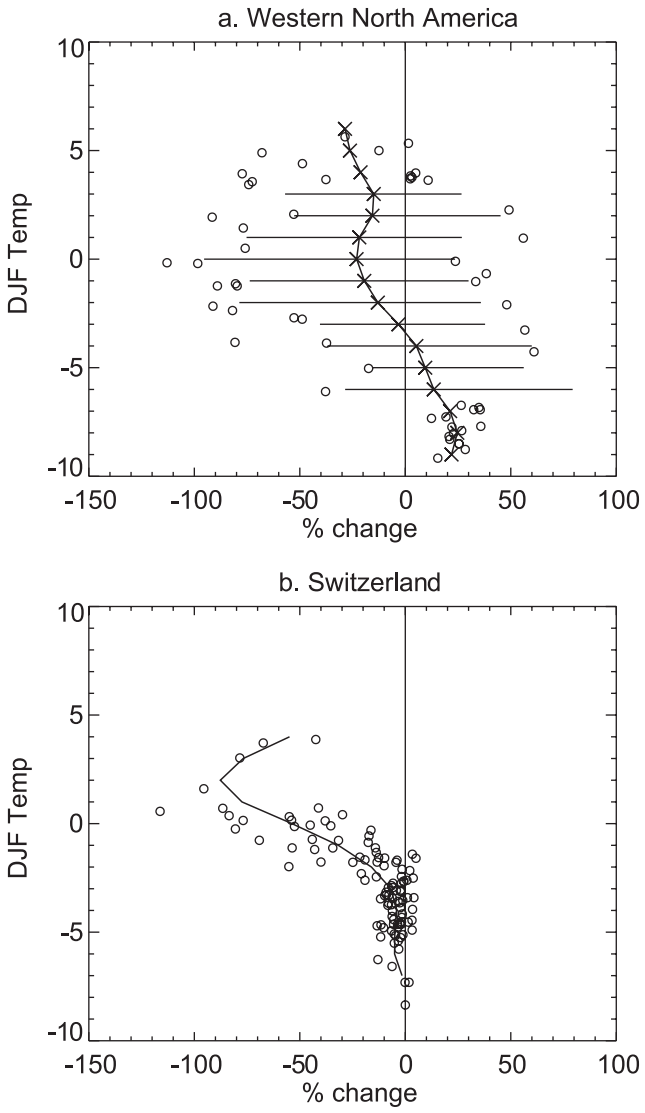


Figure 4.4. *Dependence of trends in snow on mean winter temperature (°C) at each location. (a) Relative trends in 1 April SWE, 1950 to 2000, in the mountains of western North America (British Columbia, Washington, Oregon and California), binned by mean December to February (DJF) temperature. For each 1°C temperature bin, '×' symbols indicate the mean trend, bars indicate the span of the 5 to 95% confidence interval for bins with at least 10 points, and circles indicate outliers. Total number of data points is 323 (adapted from Mote et al., 2005). (b) Relative trend in days of winter (DJF) snow cover at 109 sites in Switzerland, 1958 to 1999, binned by mean DJF temperature (adapted from Scherrer et al., 2004).*

record 1979 to 2002 show substantial interannual variability with little or no long-term trend. A long-term increasing trend in the number of snow days was found in the eastern side of the central Andes region (33°S) from 1885 to 1996, derived from newspaper reports of Mendoza City (Prieto et al., 2001).

Other approaches suggest some response of snow line to warming in South America. The 0°C isotherm altitude (ZIA), an indication of snow line, has been derived from the daily temperature profile obtained from radiosonde data located at Quintero (32°47'S, 71°33'W, 8 m above sea level; Carrasco et al., 2005), which represents the snow line behaviour in the western Andes from about 30°S to 36°S. Over the 1975 to 2001 period of record, the linear change in winter ZIA was 121.9 ± 7.7 m, and the positive trend was dominated by atmospheric conditions on dry days (enhancing melt) with no trend on wet days (accumulation zone unchanged).

4.2.2.3.2 Australia and New Zealand

For the mountainous south-eastern area of Australia, studies of late winter (August–September) snow depth have shown some significant declines (as much as 40%) since 1962. Trends in maximum snow depth were more modest. The stronger declines in late winter are attributed to spring season warming, while maximum snow depth is largely determined by winter precipitation, which has declined only slightly (Hennessy et al., 2003; Nicholls, 2005).

In New Zealand, annual observations of end-of-summer snow line on 47 glaciers have been made by airplane since 1977, and reveal large interannual variability primarily associated with atmospheric circulation anomalies (Clare et al., 2002); it is noteworthy, however, that the four years with highest snow line occurred in the 1990s. The only study of seasonal snow cover in the Southern Alps found no trend over the 1930 to 1985 period (Fitzharris and Garr, 1995) and has not been updated.

4.3 Changes in River and Lake Ice

4.3.1 Background

Because of its importance to many human activities, freeze-up and breakup dates of river and lake ice have been recorded for a long time at many locations. These records provide useful climate information, although they must be interpreted with care. In the case of rivers, both freeze-up and breakup at a given location can be strongly affected by conditions far upstream (for example, heavy rains or snowmelt in a distant portion of the watershed). In the case of lakes, the historical observations have typically been made at coastal locations (often protected bays and harbours) and so may not be representative of the lake as a whole, or comparable to more recent satellite-based observations. Nevertheless, these observations represent some of the longest records of cryospheric change available.

Observations of ice thickness are considerably sparser and are generally made using direct drilling methods. Long-term records are available at a few locations; however it should be noted that, just as for sea ice, changes in lake and river ice thickness are a consequence not just of temperature and radiative forcing, but also of changes in snowfall (via the insulating effect of snow).

4.3.2 Changes in Freeze-up and Breakup Dates

Freeze-up is defined conceptually as the time at which a continuous and immobile ice cover forms; however, operational definitions range from local observations of the presence

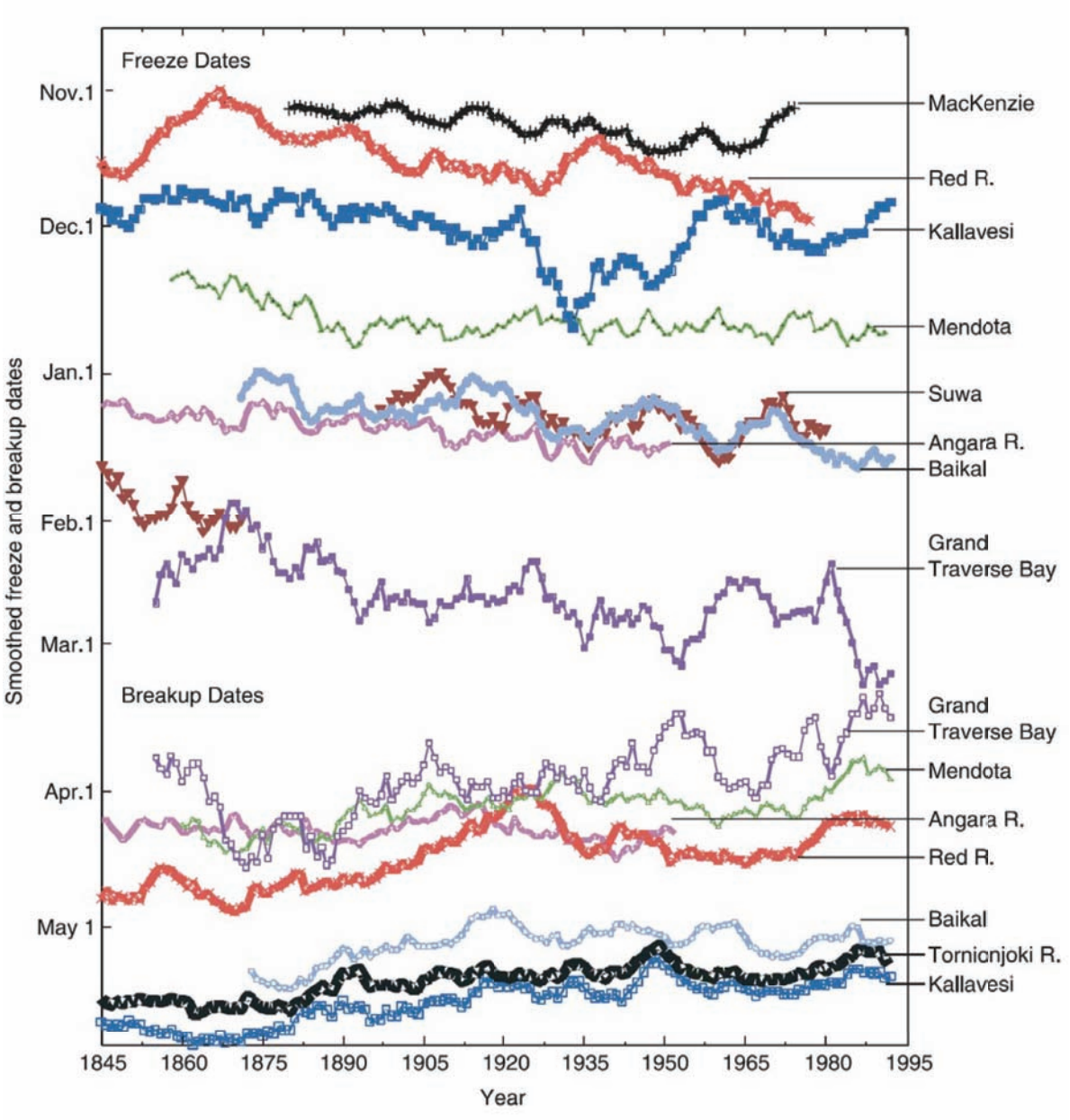


Figure 4.5. *Time series of freeze-up and breakup dates from several northern lakes and rivers (reprinted with permission from Magnuson et al., 2000, copyright AAAS). Dates have been smoothed with a 10-year moving average. See the cited publication for locations and other details.*

or absence of ice to inferences drawn from river discharge measurements. Breakup is typically the time when the ice cover begins to move downstream in a river or when open water becomes extensive at the measurement location for lakes. Here again, there is some ambiguity in the specific date, and in the extent to which local observations reflect conditions elsewhere on a large lake or in a large river basin.

Selected time series from a recent compilation of river and lake freeze-up and breakup records by Magnuson et al. (2000) are shown in Figure 4.5. They limited consideration to records spanning at least 150 years. Eleven out of 15 records showed significant trends towards later freeze-up and 17 out of 25 records showed significant trends towards earlier breakup. When averaged together, the freeze-up date has become later at a rate of 5.8 ± 1.6 days per century, while the breakup date has occurred earlier at a rate of 6.5 ± 1.2 days per century.

A larger sample of Canadian rivers spanning the last 30 to 50 years was analysed by Zhang et al. (2001). These freeze-up and breakup estimates (based on inferences from streamflow data) exhibit considerable variability, with a trend towards earlier freeze-up and breakup over much of the country. The earlier freeze-up dominates, however, leading to a significant decrease in open water duration at many locations as shown in Figure 4.6. A recent analysis of Russian river data by Smith (2000) revealed a trend towards earlier freeze-up of western Russian rivers and later freeze-up in rivers of eastern Siberia over the last 50 to 70 years. Breakup dates did not exhibit statistically significant trends.

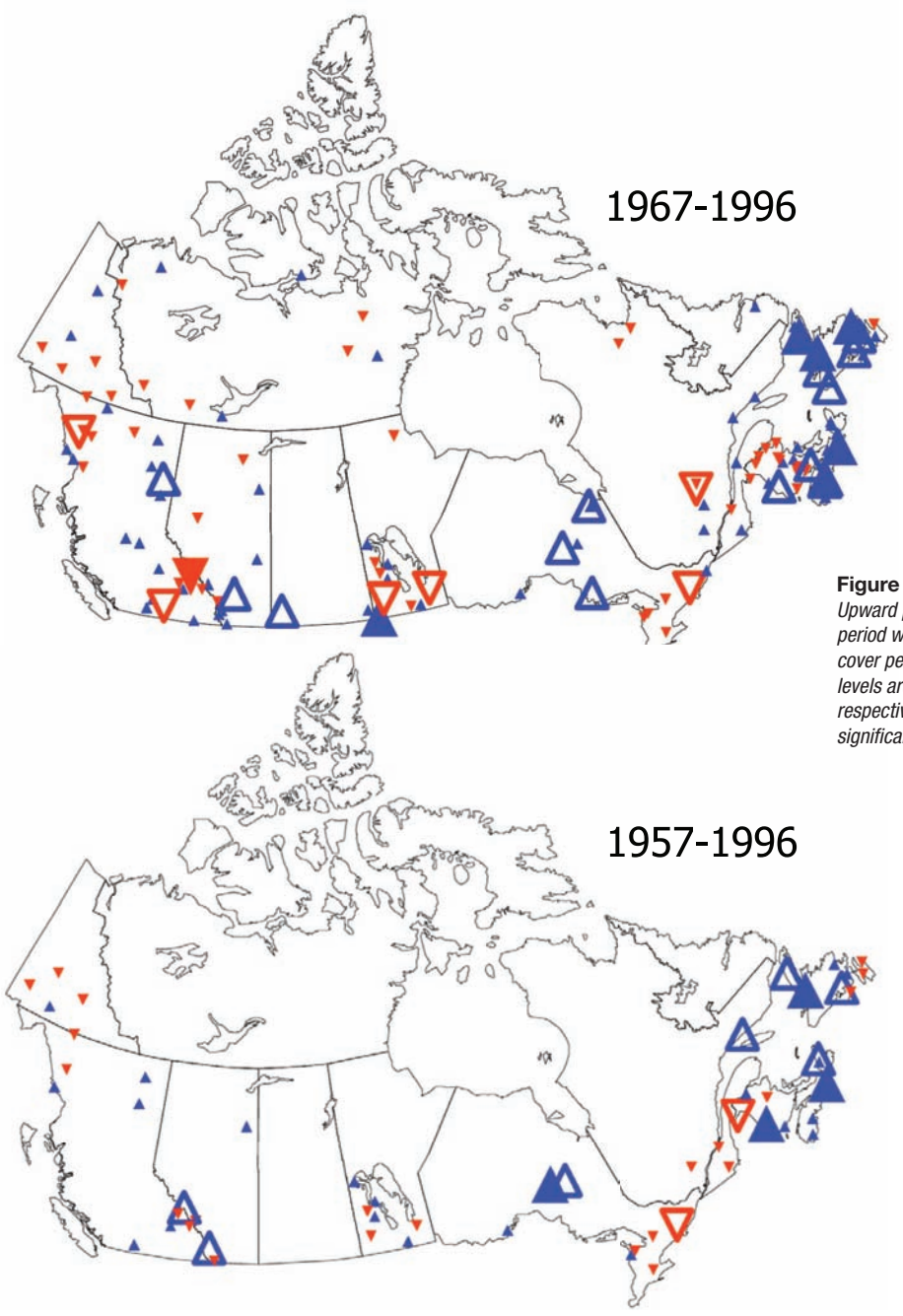


Figure 4.6. *Trends in river ice cover duration in Canada. Upward pointing triangles indicate lengthening of the ice cover period while downward triangles indicate shortening of the ice cover period. Trends significant at the 99 and 90% confidence levels are marked by larger filled and hollow triangles, respectively. Smaller triangles indicate trends that are not significant at the 90% level (Zhang et al., 2001).*

A comparable analysis of freeze-up and breakup dates for Canadian lakes has recently been completed by Duguay et al. (2006). These results (shown in Figure 4.7) indicate a fairly general trend towards earlier breakup (particularly in western Canada), while freeze-up exhibited a mix of early and later dates.

There are insufficient published data on river and lake ice thickness to allow assessment of trends. Modelling studies (e.g., Duguay et al., 2003) indicate that, as with the landfast sea ice case, much of the variability in maximum ice thickness and breakup date is driven by variations in snowfall.

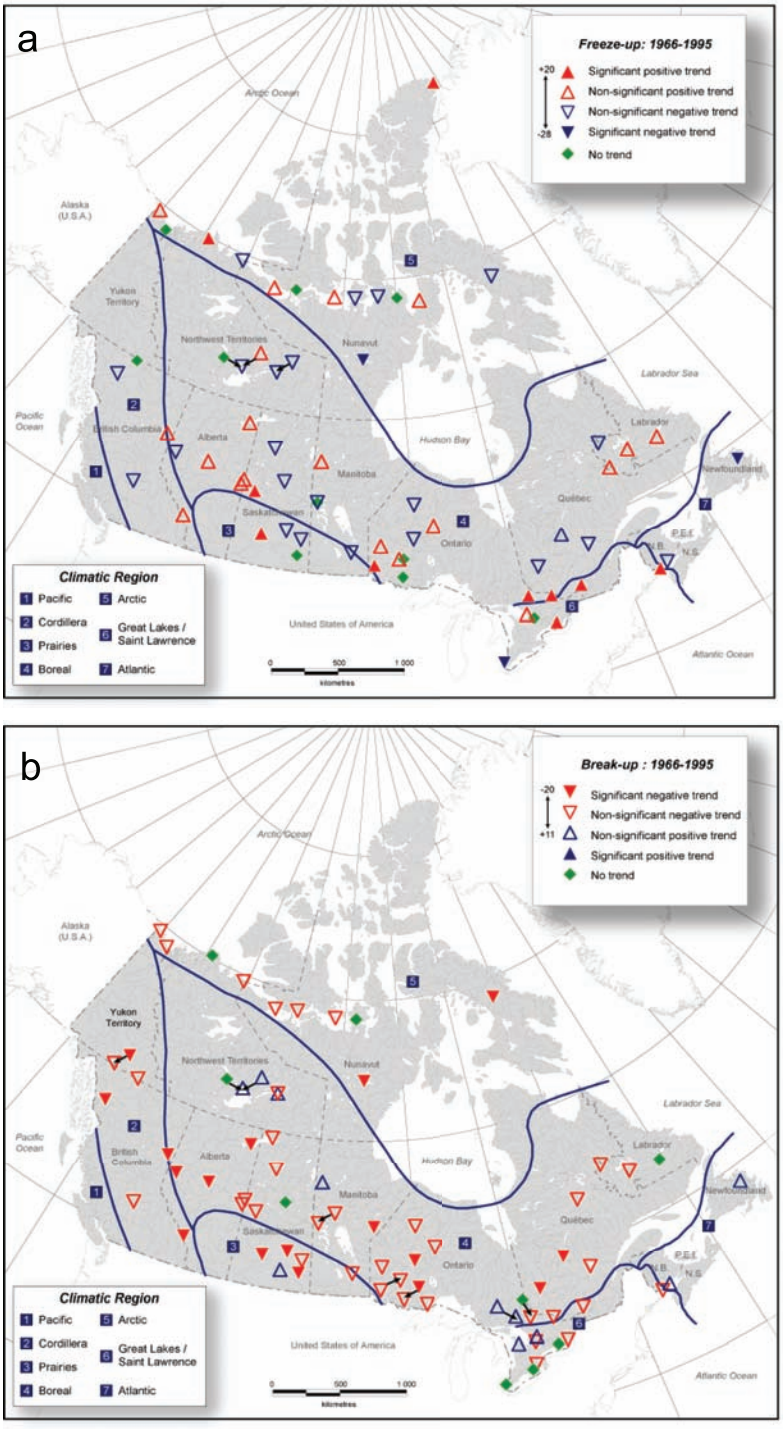


Figure 4.7. *Trends in (a) freeze-up and (b) breakup dates observed at lakes in Canada over the period 1965 to 1995. Downward pointing arrows indicate a trend towards earlier dates; upward pointing arrows, a trend towards later dates. Open symbols indicate that the trend is not significant while solid symbols indicate that the trend is significant at the 90% confidence level (modified from Duguay et al., 2006).*

4.4 Changes in Sea Ice

4.4.1 Background

Sea ice is formed by freezing of seawater in the polar oceans. It is an important, interactive component of the global climate system because: a) it is central to the powerful 'ice-albedo' feedback mechanism that enhances climate response at high latitudes (see Chapter 2); b) it modifies the exchange of heat, gases and momentum between the atmosphere and polar oceans; and c) it redistributes freshwater via the transport and subsequent melt of relatively fresh sea ice, and hence alters ocean buoyancy forcing.

The thickness of sea ice is a consequence of past growth, melt and deformation, and so is an important indicator of climatic conditions. Ice thickness is also closely connected to ice strength, and so changes in thickness are important to navigability by ships, to the stability of the ice as a platform for use by humans and marine mammals, to light transmission through the ice cover, etc. Sea ice increases in thickness as bottom freezing balances heat conduction through the ice to the surface (heat conduction is strongly influenced by the insulating thickness of the ice itself and the snow on it). Most of the inhomogeneity in the pack results from deformation of the ice due to differential movement of individual pieces of ice (called 'floes'). Open water areas created within the ice pack under divergence or shear (called 'leads') are a major contributor to ocean-atmosphere heat exchange (turbulent heat loss from the ocean in winter and shortwave heating in the summer). In some locations, due either to persistent ice divergence or to persistent upwelling of oceanic heat, open water areas within an otherwise ice-covered region can be sustained over much of the winter. These are called 'polynyas' and are important feeding areas for marine mammals and birds.

Under convergence, thin ice sheets may 'raft' on top of each other, doubling the ice thickness, and under strong convergence (for example, when wind drives sea ice against a coast), the ice buckles and crushes to form sinuous 'ridges' of thick ice. In the Arctic, ridges can be tens of metres thick, account for nearly half of the total ice volume and constitute a major impediment to transportation on, through, or under the ice. Although ridging is generally less severe in the Antarctic, ice deformation is still an important process in thickening the ice cover.

Near the shore, in bays and fjords, and among islands like those of the Canadian Arctic Archipelago, sea ice can be attached to land and therefore be immobile. This is termed 'landfast' ice. In the Arctic such ice (and in particular its freeze-up and breakup) is of special importance to local residents as it is used as a platform for hunting and fishing, and is an impediment to shipping.

Some climatically important characteristics of sea ice include: its concentration (that fraction of the ocean covered by ice); its extent (the area enclosed by the ice edge – operationally defined as the 15% concentration contour); the total area of ice within its extent (i.e., extent weighted by concentration); the area of multi-year ice within the total extent; its thickness (and the thickness of the snow cover on it); its velocity; and its growth and melt rates (and hence salt or freshwater flux into the ocean). Ice extent, or ice edge position, is the only sea ice variable for which observations are available for more than a few decades. Expansion or retreat of the ice edge may be amplified by the ice-albedo feedback.

4.4.2 Sea Ice Extent and Concentration

4.4.2.1 Data Sources and Time Periods Covered

The most complete record of sea ice extent is provided by passive microwave data from satellites that are available since the early 1970s. Prior to that, aircraft, ship and coastal observations are available at certain times and in certain locations. Portions of the North Atlantic are unique in having ship observations extending well back into the 19th century. Far fewer historic data exist from the SH, with one notable exception being the record of annual landfast ice duration from the sub-antarctic South Orkney islands starting in 1903 (Murphy et al., 1995).

Estimation of sea ice properties from passive microwave emission requires an algorithm to convert observed radiance into ice concentration (and type). Several such algorithms are available (e.g., Steffen et al., 1992) and their accuracy has been evaluated using high-resolution satellite and aircraft imagery (e.g., Cavalieri, 1992; Kwok, 2002) and operational ice charts (e.g., Agnew and Howell, 2003). The accuracy of satellite-derived ice concentration is usually 5% or better, although errors of 10 to 20% can occur during the melt season. The accuracy of the ice edge (relevant to estimating ice extent) is largely determined by the spatial resolution of the satellite radiometer, and is of the order of 25 km (recently launched instruments provide improved resolution of about 12.5 km). Summer concentration errors do lead to a bias in estimated ice-covered area in both the NH and SH warm seasons (Agnew and Howell, 2003; Worby and Comiso, 2004). This is an important consideration when comparing the satellite period with older proxy records of ice extent.

Distinguishing between first-year and multi-year ice from passive microwave data is more difficult, although algorithms are improving (e.g., Johannessen et al., 1999). However, the summer minimum ice extent, which is by definition the multi-year ice extent at that time of year, is not as prone to algorithm errors (e.g., Comiso, 2002).

4.4.2.2 Hemispheric, Regional and Seasonal Time Series from Passive Microwave

Most analyses of variability and trend in ice extent using the satellite record have focussed on the period after 1978 when the satellite sensors have been relatively constant. Different estimates, obtained using different retrieval algorithms, produce

very similar results for hemispheric extent, and all show an asymmetry between changes in the Arctic and Antarctic. As an example, an updated version of the analysis done by Comiso (2003), spanning the period from November 1978 through December 2005, is shown in Figure 4.8. The annual mean ice extent anomalies are shown. There is a significant decreasing trend in arctic sea ice extent of $-33 \pm 7.4 \times 10^3$ km^2 yr^{-1} (equivalent to -2.7 ± 0.6% per decade), whereas the antarctic results show a small positive trend of $5.6 \pm 9.2 \times 10^3$ km^2 yr^{-1} (0.47 ± 0.8% per decade), which is not statistically significant. The uncertainties represent the 90% confidence interval around the trend estimate and the percentages are based on the 1978 to 2005 mean. In both hemispheres, the trends are larger in summer and smaller in winter. In addition, there is considerable variation in the magnitude, and even the sign, of the trend from region to region within each hemisphere.

The most remarkable change observed in the arctic ice cover has been the decrease in ice that survives the summer, shown in Figure 4.9. The trend in the minimum arctic sea ice extent, between 1979 and 2005, was $-60 \pm 20 \times 10^3$ km^2 yr^{-1} (-7.4 ± 2.4% per decade). These trends are superimposed on substantial interannual to decadal variability, which is associated with variability in atmospheric circulation (Belchansky et al., 2005).

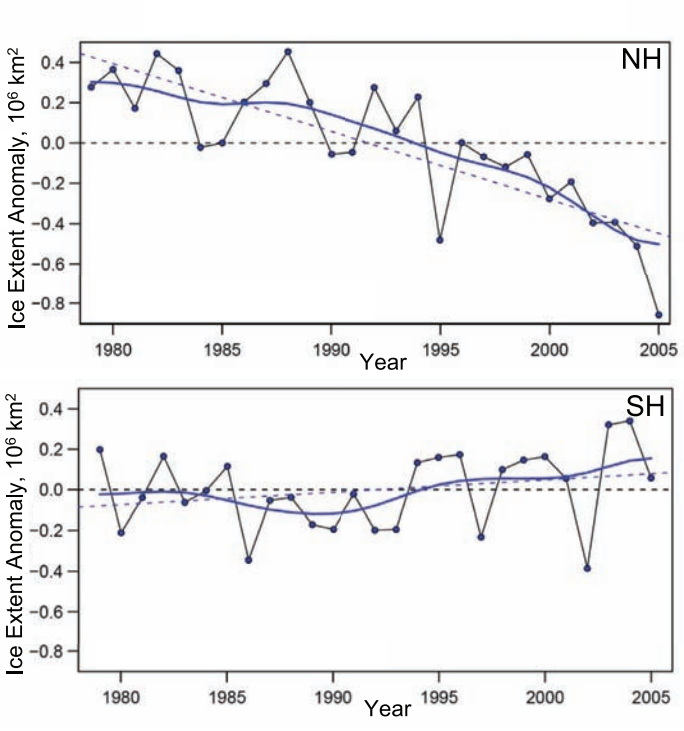


Figure 4.8. *Sea ice extent anomalies (computed relative to the mean of the entire period) for (a) the NH and (b) the SH, based on passive microwave satellite data. Symbols indicate annual mean values while the smooth blue curves show decadal variations (see Appendix 3.A). Linear trend lines are indicated for each hemisphere. For the Arctic, the trend is $-33 \pm 7.4 \times 10^3$ km^2 yr^{-1} (equivalent to approximately –2.7% per decade), whereas the Antarctic results show a small positive trend of $5.6 \pm 9.2 \times 10^3$ km^2 yr^{-1}. The negative trend in the NH is significant at the 90% confidence level whereas the small positive trend in the SH is not significant (updated from Comiso, 2003).*

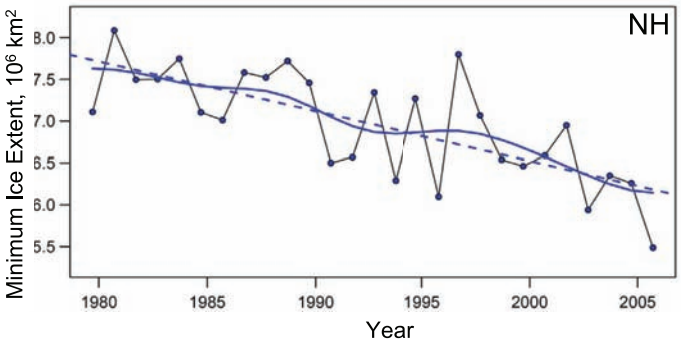


Figure 4.9. *Summer minimum arctic sea ice extent from 1979 to 2005. Symbols indicate annual mean values while the smooth blue curve shows decadal variations (see Appendix 3.A). The dashed line indicates the linear trend, which is $-60 \pm 20 \times 10^3$ km^2 yr^{-1}, or approximately –7.4% per decade (updated from Comiso, 2002).*

4.4.2.3 Longer Records of Hemispheric Extent

The lack of comprehensive sea ice data prior to the satellite era hampers estimates of hemispheric-scale trends over longer time scales. Rayner et al. (2003) compiled a data set of sea ice extent for the 20th century from available sources and accounted for the inhomogeneity between them (Figure 4.10). There is a clear indication of sustained decline in arctic ice extent since about the early 1970s, particularly in summer. On a regional basis, portions of the North Atlantic have sufficient historical data, based largely on ship reports and coastal observations, to permit trend assessments over periods exceeding 100 years. Vinje (2001) compiled information from ship reports in the Nordic Seas to estimate April sea ice extent in this region for the period since about 1860. This time series is also shown in Figure 4.10 and indicates a generally continuous decline from the start of the record to the end. Ice extent data from Russian sources have recently been published (Polyakov et al., 2003), and cover essentially the entire 20th century for the Russian coastal seas (Kara, Laptev, East Siberian and Chukchi). These data, which exhibit large inter-decadal variability, show a declining trend since the 1960s until a reversal in the late 1990s. The Russian data indicate anomalously little ice during the 1940s and 1950s, whereas the Nordic Sea data indicate anomalously large extent at this time, showing the importance of regional variability.

Omstedt and Chen (2001) obtained a proxy record of the annual maximum extent of sea ice in the region of the Baltic Sea over the period 1720 to 1997. This record showed a substantial decline in sea ice that occurred around 1877, and greater variability in sea ice extent in the colder 1720 to 1877 period than in the warmer 1878 to 1997 period. Hill et al. (2002) have examined sea ice information for the Canadian maritime region and deduced that sea ice incursions occurred during the 19th century in the Grand Banks and surrounding areas that are now ice-free. Although there are problems with homogeneity of all these data (with quality declining further back in history), and with the disparity in spatial scales represented by each, they are all consistent in terms of the declining ice extent during the latter decades of the 20th century, with the decline beginning

prior to the satellite era. Those data that extend far enough back in time imply, with high confidence, that sea ice was more extensive in the North Atlantic during the 19th century.

Continuous long-term data records for the Antarctic are lacking, as systematic information on the entire Southern Ocean ice cover became available only with the advent of routine microwave satellite reconnaissance in the early 1970s. Parkinson (1990) examined ice edge observations from four exploration voyages in the late 18th and early 19th centuries. Her analysis suggested that the summer antarctic sea ice was more extensive in the eastern Weddell Sea in 1772 and in the Amundsen Sea in 1839 than the present day range from satellite observations. However, many of the early observations are within the present range for the same time of year. An analysis of whaling records by de la Mare (1997) suggested a step decline in antarctic sea ice coverage of 25% (a 2.8° poleward shift in average ice edge latitude) between the mid-1950s and the early 1970s. A reanalysis by Ackley et al. (2003), which accounted for offsets between satellite-derived ice edge and whaling ship locations, challenged evidence of significant change in ice edge location. Curran et al. (2003) made use of a correlation between methanesulphonic acid concentration (a by-product of marine phytoplankton) in a near-coastal antarctic ice core and the regional sea ice extent in the sector from 80°E to 140°E to infer a quasi-decadal pattern of interannual variability in the ice extent in this region, along with a roughly 20% decline (approximately two degrees of latitude) since the 1950s.

In summary, the antarctic data provide evidence of a decline in sea ice extent in some regions, but there are insufficient data to draw firm conclusions about hemispheric changes prior to the satellite era.

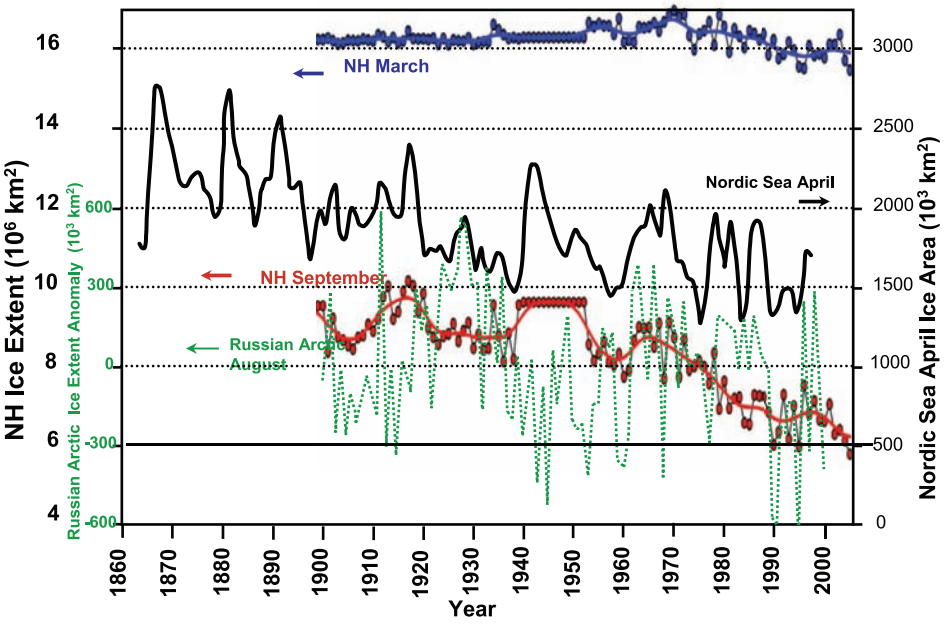


Figure 4.10. *Time series of NH sea ice extent for March and September from the Hadley Centre Sea Ice and Sea Surface Temperature (HadISST) data set (the blue and red curves, updated from Rayner et al., 2003), the April Nordic Sea ice extent (the black curve, redrafted from Vinje, 2001) and the August ice extent anomaly (computed relative to the mean of the entire period) in the Russian Arctic seas – Kara, Laptev, East Siberian and Chukchi (dotted green curve, redrafted from Polyakov et al., 2003). For the NH time series, the symbols indicate yearly values while the curves show the decadal variation (see Appendix 3.A).*

4.4.3 Sea Ice Thickness

4.4.3.1 Sea Ice Thickness Data Sources and Time Periods Covered

Until recently there have been no satellite remote sensing techniques capable of mapping sea ice thickness, and this parameter has primarily been determined by drilling or by under-ice sonar measurement of draft (the submerged portion of sea ice).

Subsea sonar from submarines or moored instruments can be used to measure ice draft over a footprint of 1 to 10 m diameter. Draft is converted to thickness, assuming an average density for the measured floe, including its snow cover. The principal challenges to accurate observation with sonar are uncertainties in sound speed and atmospheric pressure, and the identification of spurious targets. Upward-looking sonar has been on submarines operating beneath arctic pack ice since 1958. US and UK naval data are now being released for science, and some dedicated arctic submarine missions were made for science during 1993 to 1999. Ice draft measurement by moored ice-profiling sonar, best suited to studies of ice transport or change at fixed sites, began in the Arctic in the late 1980s. Instruments have operated since 1990 in the Beaufort and Greenland Seas and for shorter intervals in other areas, but few records span more than 10 years. In the SH there are no data from submarines and only short time series from moored sonar.

Other techniques, such as electromagnetic induction sounders deployed on the ice surface, ships or aircraft, or airborne laser altimetry to measure freeboard (the portion of sea ice above the waterline), have limited applicability to wide-scale climate analysis of sea ice thickness. Indirect estimates, based on measurement of surface gravity waves, are available in some regions for the 1970s and 1980s (Nagurnyi et al., 1999 as reported in Johannessen et al., 2004), but the accuracy of these estimates is difficult to quantify.

Quantitative data on the thickness of antarctic pack ice only started to become available in the 1980s from sparsely scattered drilling programs covering only small areas and primarily for use in validating other techniques. Visual observations of ice

characteristics from ships (Worby and Ackley, 2000) are not adequate for climate monitoring, but are providing one of the first broad pictures of antarctic sea ice thickness.

4.4.3.2 Evidence of Changes in Arctic Pack Ice Thickness from Submarine Sonar

Estimates of thickness change over limited regions are possible when submarine transects are repeated (e.g., Wadhams, 1992). The North Pole is a common waypoint in many submarine cruises and this allowed McLaren et al. (1994) to analyse data from 12 submarine cruises near the pole between 1958 and 1992. They found considerable interannual variability, but no significant trend. Shy and Walsh (1996) examined the same data in relation to ice drift and found that much of the thickness variability was due to the source location and path followed by the ice prior to arrival at the pole.

Rothrock et al. (1999) provided the first 'basin-scale' analysis and found that ice draft in the mid-1990s was less than that measured between 1958 and 1977 at every available location (including the North Pole). The change was least (–0.9 m) in the southern Canada Basin and greatest (–1.7 m) in the Eurasian Basin (with an estimated overall error of less than 0.3 m). The decline averaged about 42% of the average 1958 to 1977 thickness. Their study included very few data within the seasonal sea ice zone and none within 300 km of Canada or Greenland.

Subsequent studies indicate that the reduction in ice thickness was not gradual, but occurred abruptly before 1991. Winsor (2001) found no evidence of thinning along 150°W from six spring cruises during 1991 to 1996, but Tucker et al. (2001), using spring observations from 1976 to 1994 along the same meridian, noted a decrease in ice draft sometime between the mid-1980s and early 1990s, with little subsequent change. The observed change in mean draft resulted from a decrease in the fraction of thick ice (draft of more than 3.5 m) and an increase in the fraction of thin ice, which was probably due to reduced storage of multi-year ice in a smaller Beaufort Gyre and the export of 'surplus' via Fram Strait. Yu et al. (2004) presented evidence of a similar change in ice thickness over a wider area. However, ice thickness varies considerably from year to year at a given location and so the rather sparse temporal sampling provided by submarine data makes inferences regarding long-term change difficult.

4.4.3.3 Other Evidence of Sea Ice Thickness Change in the Arctic and Antarctic

Haas (2004, and references therein) used ground-based electromagnetic induction measurements to show a decrease of approximately 0.5 m between 1991 and 2001 in the modal thickness (i.e., the most commonly observed thickness) of ice floes in the Arctic Trans-Polar Drift. Their survey of 120 km of ice on 146 floes during four cruises is biased by an absence of ice-free and thin-ice fractions and underestimation of ridged ice, but the data are descriptive of floes that are safe to traverse in summer, and the observed changes are most likely due to thermodynamic forcing.

An emerging new technique, using satellite radar or laser altimetry to estimate ice freeboard from the measured ranges to the ice and sea surface in open leads (and assuming an average floe density and snow depth), offers promise for future monitoring of large-scale sea ice thickness. Laxon et al. (2003) estimated average arctic sea ice thickness over the cold months (October–March) for 1993 to 2001 from satellite-borne radar altimeter measurements. Their data reveal a realistic geographic variation in thickness (increasing from about 2 m near Siberia to 4.5 m off the coasts of Canada and Greenland) and a significant (9%) interannual variability in winter ice thickness, but no indication of a trend over this time.

There are no available data on change in the thickness of antarctic sea ice, much of which is considerably thinner and less ridged than ice in the Arctic Basin.

4.4.3.4 Model-Based Estimates of Change

Physically based sea ice models, forced with winds and temperatures from atmospheric reanalyses and sometimes constrained by observed ice concentration fields, can provide continuous time series of sea ice extent and thickness that can be compared to the sparse observations, and used to interpret the observational record. Models such as those described by Rothrock et al. (2003) and references therein are able to reproduce the observed interannual variations in ice thickness, at least when averaged over fairly large regions. In particular, model studies can elucidate some of the forcing agents responsible for observed changes in ice thickness.

A comparison of various model simulations of historical arctic ice thickness or volume is shown in Figure 4.11. All the models indicate a marked reduction in ice thickness of 0.6 to 0.9 m starting in the late 1980s, but disagree somewhat with respect to trends and/or variations earlier in the century. Most models indicate a maximum in ice thickness in the mid-1960s, with local maxima around 1980 and 1990 as well. There is an emerging suggestion from both models and observations that much of the decrease in thickness occurred between the late 1980s and late 1990s.

It is not possible to attribute the abrupt decrease in thickness inferred from submarine observations entirely to the (rather slow) observed warming in the Arctic, and some of the dramatic decrease may be a consequence of spatial redistribution of ice volume over time (e.g., Holloway and Sou, 2002). Low-frequency, large-scale modes of atmospheric variability (such as interannual changes in circulation connected to the Northern Annular Mode) affect both wind-driving of sea ice and heat transport in the atmosphere, and therefore contribute to interannual variations in ice formation, growth and melt (e.g., Rigor et al., 2002; Dumas et al., 2003).

For the Antarctic, Fichefet et al. (2003) conducted one of the few long-term simulations of ice thickness using observationally based atmospheric forcing covering the period 1958 to 1999. They noted pronounced decadal variability, with area-average

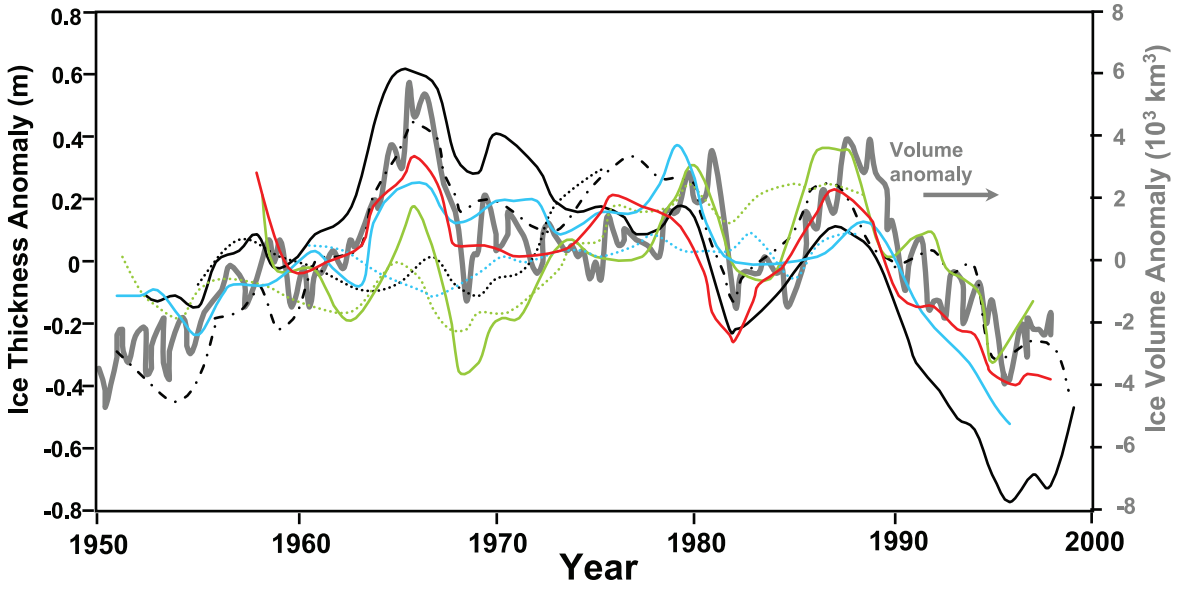


Figure 4.11. *Comparison of model-based time series of the annual mean average sea ice thickness anomaly (computed relative to the mean of the entire period) in the Arctic Basin, obtained from a variety of models (redrafted from Rothrock et al., 2003; see this paper for identification of the individual models and their attributes), along with the sea ice volume anomalies in the Arctic Basin (grey curve and right-hand scale; computed by Koeberle and Gerdes, 2003).*

ice thickness varying by ±0.1 m (over a mean thickness of roughly 0.9 m), but no long-term trend.

4.4.3.5 Landfast Ice Changes

Interannual variations in landfast ice thickness for selected stations in northern Canada were analysed by Brown and Coté (1992). At each of the four sites studied, where ice typically thickens to about 2 m at the end of winter, they detected both positive and negative trends in ice thickness, but no spatially coherent pattern. Interannual variation in ice thickness at the end of the season was determined principally by variation in the amount and timing of snow accumulation, not variation in air temperature. An analysis of several half-century records in Siberian seas has provided evidence that trends in landfast ice thickness over the past century in this area have been small, diverse and generally not statistically significant. Some of the variability is correlated with multi-decadal atmospheric variability (Polyakov et al., 2003).

For the Antarctic, a combined record of the seasonal duration of fast ice in the South Orkney Islands (60.6°S, 45.6°W) has been compiled for observations from two correlated sites for the period 1903 to 1992 (Murphy et al., 1995). The ice duration in these coastal locations is linked to the cycle of pack ice extent in the Weddell Sea, and the duration shows a likely decrease of 7.3 days per decade. This decrease is not linear over the 90-year period and occurs within a strong 7- to 9-year cyclical component of variability over the latter 30 to 40 years of the record. Fast ice thickness measurements have been intermittently made at the coastal sites of Mawson (67.6°S, 62.9°E) and Davis (68.6°S, 78.0°E) for about the last 50 years. Although there is no long-term trend in maximum ice thickness, at both sites there is a trend for the date of maximum thickness to become later at a rate of about four days per decade (Heil and Allison, 2002).

4.4.3.6 Snow on Sea Ice

Warren et al. (1999) analysed 37 years (1954–1991) of snow depth and density measurements made at Soviet drifting stations on multi-year arctic sea ice. They found a weak negative trend for all months, with the largest trend a decrease of 8 cm (23%) over 37 years in May, the month of maximum snow depth.

There are few data on snow cover and distribution in the Antarctic, and none adequate for detecting any trend in snow cover. Massom et al. (2001) collated available ship observations (between 1981 and 1987) to show that average antarctic snow thickness is typically 0.15 to 0.20 m, and varies widely both seasonally and regionally. An important process in the antarctic sea ice zone is the formation of snow-ice, which occurs when a snow loading depresses thin sea ice below sea level, causing seawater flooding of the near-surface snow and subsequent rapid freezing.

4.4.3.7 Assessment of Changes in Sea Ice Thickness

Sea ice thickness is one of the most difficult geophysical parameters to measure at large scales and, because of the large variability inherent in the sea-ice-climate system, evaluation of ice thickness trends from the available observational data is difficult. Nevertheless, on the basis of submarine sonar data and interpolation of the average sea ice thickness in the Arctic Basin from a variety of physically based sea ice models, it is very likely that the average sea ice thickness in the central Arctic

has decreased by up to 1 m since the late 1980s, and that most of this decrease occurred between the late 1980s and the late 1990s. The steady decrease in the area of the summer minimum arctic sea ice cover since the 1980s, resulting in less-thick multi-year ice at the start of the next growth season, is consistent with this. This recent decrease, however, occurs within the context of longer-term decadal variability, with strong maxima in arctic ice thickness in the mid-1960s and around 1980 and 1990, due to both dynamic and thermodynamic forcing of the ice by circulation changes associated with low-frequency modes of atmospheric variability.

There are insufficient data to draw any conclusions about trends in the thickness of antarctic sea ice.

4.4.4 Pack Ice Motion

Pack ice motion influences ice mass locally, through deformation and creation of open water areas; regionally, through advection of ice from one area to another; and globally through export of ice from polar seas to lower latitudes where it melts. The drift of sea ice is primarily forced by the winds and ocean currents. On time scales of days to weeks, winds are responsible for most of the variance in sea ice motion. On longer time scales, the patterns of ice motion follow surface currents and the evolving patterns of wind forcing. Here we consider whether there are trends in the pattern of ice motion.

4.4.4.1 Data Sources and Time Periods Covered

Sea ice motion data are primarily derived from the drift of ships, manned stations and buoys set on or in the pack ice. Although some individual drift trajectories date back to the late 19th century in the Arctic and the early 20th century in the Antarctic, a coordinated observing program did not begin until the International Arctic Buoy Programme (IABP) in the late 1970s. The IABP currently maintains an array of about 25 buoys at any given time and produces gridded fields of ice motion from these using objective analysis (Rigor et al., 2002 and references therein).

Sea ice motion may also be derived from satellite data by estimating the displacement of sea ice features found in two consecutive images from a variety of satellite instruments (e.g., Agnew et al., 1997; Kwok, 2000). The passive microwave sensors provide the longest period of coverage (1979 to present) but their spatial resolution limits the precision of motion estimates. The optimal interpolation of satellite and buoy data (e.g., Kwok et al., 1998) seems to be the most consistent data set to assess interannual variability of sea ice motion.

In the Antarctic, buoy deployments have only been reasonably frequent since the late 1980s. Since 1995, buoy operations have been organised within the World Climate Research Programme (WCRP) International Programme for Antarctic Buoys (IPAB), although spatial and temporal coverage remain poor. A digital atlas of antarctic sea ice has been compiled from two decades of combined passive microwave and IPAB buoy data (Schmitt et al., 2004).

4.4.4.2 Changes in Patterns of Sea Ice Motion and Modes of Climate Variability that Affect Sea Ice Motion

Gudkovich (1961) hypothesised the existence of two regimes of arctic ice motion driven by large-scale variations in atmospheric circulation. Using a coupled atmosphere-ocean-ice model, Proshutinsky and Johnson (1997) showed that the regimes proposed by Gudkovich (1961) alternated on five- to seven-year intervals. Similarly, Rigor et al. (2002) showed that the changes in the patterns of sea ice motion from the 1980s to the 1990s are related to the Northern Annular Mode (NAM). There is, however, no indication of a long-term trend in ice motion.

In the Antarctic, ice motion undergoes an annual cycle caused by stronger winds in winter. Interannual oscillations are found in all regions, most regularly in the Ross, Amundsen and Bellingshausen Seas with periods of about three to six years (Venegas et al., 2001). These wind-driven ice drift oscillations account for the ice extent oscillations seen in the Antarctic Circumpolar Wave (see Section 3.6.6.2). As for the Arctic, no trend in ice motion is apparent based on the limited data available.

4.4.4.3 Ice Export and Advection

The sea ice outflow through Fram Strait is a major component of the ice mass balance of the Arctic Ocean. Approximately 14% of the sea ice mass is exported each year through Fram Strait. Vinje (2001) constructed a time series of ice export during 1950 to 2000 using available moored ice-profiling sonar observations and a parametrization based on geostrophic wind. He found substantial inter-decadal variability in export but no trend.

Kwok and Rothrock (1999) assembled an 18-year time series of ice area and volume flux through Fram Strait based on satellite-derived ice motion and concentration estimates. They found a mean annual area flux of 919×10^3 km^2 yr^{-1} (nearly 10% of the Arctic Ocean area), with large interannual variability that is positively correlated in part with the NAM or North Atlantic Oscillation (NAO) index. Using the thickness data of Vinje et al. (1998), they estimated a mean annual volume flux of 2,366 km^3. Subsequent modelling by Hilmer and Jung (2000) indicated that the correlation between NAO (or nearly equivalently, the NAM) and Fram Strait ice outflow is somewhat transient, with significant correlation during the period 1978 to 1997, but no correlation during 1958 to 1977 (Figure 4.12). This was a consequence of rather subtle shifts in the spatial pattern of surface pressure (and hence wind) anomalies associated with the NAO. A recent update of this time series (Kwok et al., 2004) to 24 years (ending in 2002) shows only minor variations in the mean volume and area flux and the correlation with NAO persists.

Overall, while there is considerable low-frequency variability in the pattern of sea ice motion, there is no evidence of a trend in either hemisphere.

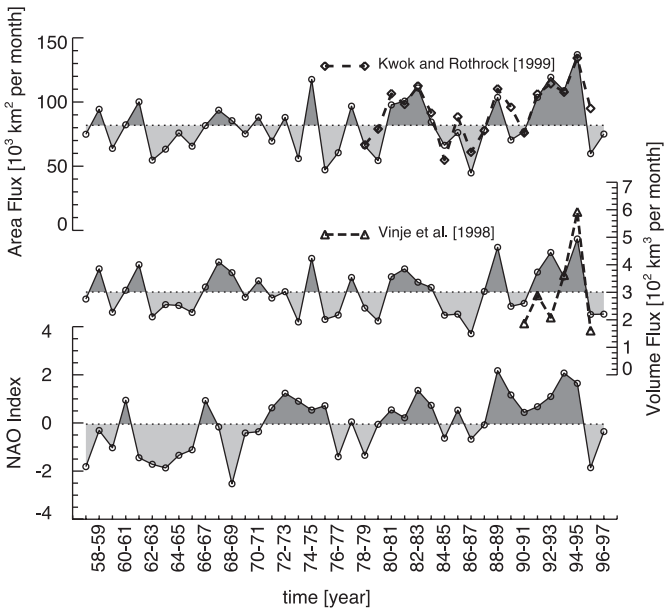


Figure 4.12. *Time series of modelled Fram Strait sea ice area and volume flux, along with the NAO index. Also shown are observational estimates of area flux (Kwok and Rothrock, 1999) and volume flux (Vinje et al., 1998). Reproduced from Hilmer and Jung (2000).*

4.5 Changes in Glaciers and Ice Caps

4.5.1 Background

Those glaciers and ice caps not immediately adjacent to the large ice sheets of Greenland and Antarctica cover an area between 512 × 10^3 and 546 × 10^3 km^2 according to inventories from different authors (Table 4.3); volume estimates differ considerably from 51 × 10^3 to 133 × 10^3 km^3, representing sea level equivalent (SLE) of between 0.15 and 0.37 m. Including the glaciers and ice caps surrounding the Greenland Ice Sheet and West Antarctica, but excluding those on the Antarctic Peninsula and those surrounding East Antarctica, yields 0.72 ± 0.2 m SLE. These new estimates are about 40% higher than those given in IPCC (2001), but area inventories are still incomplete and volume measurements more so, despite increasing efforts.

Glaciers and ice caps provide among the most visible indications of the effects of climate change. The mass balance at the surface of a glacier (the gain or loss of snow and ice over a hydrological cycle) is determined by the climate. At high and mid-latitudes, the hydrological cycle is determined by the annual cycle of air temperature, with accumulation dominating in winter and ablation in summer. In wide parts of the Himalaya most accumulation and ablation occur during summer (Fujita and Ageta, 2000), in the tropics ablation occurs year round and the seasonality in precipitation controls accumulation (Kaser and Osmaston, 2002). A climate change will affect the magnitude of the accumulation and ablation terms and the length of the mass balance seasons. The glacier will then change its extent towards a size that makes the total mass balance (the mass gain or loss over the entire glacier) zero. However, climate variability and the time lag of the glacier response mean that static equilibrium is never attained. Changes in glacier extent lag behind climate changes by only a few years on the short, steep and shallow glaciers of the tropical mountains with year-round ablation (Kaser et al., 2003), but by up to several centuries on the largest glaciers and ice caps with small slopes and cold ice (Paterson, 2004). Glaciers also lose mass by iceberg calving: this does not have an immediate and straightforward link to climate, but general relations to climate can often be discerned. Mass loss by basal melting is considered negligible at a global or large regional scale.

4.5.2 Large and Global-Scale Analyses

Records of glacier length changes (WGMS(ICSI-IAHS), various years-a) go far back in time – written reports as far back as 1600 in a few cases – and are directly related to low-frequency climate change. From 169 glacier length records, Oerlemans (2005) compiled mean length variations of glacier tongues for large-scale regions between 1700 and 2000 (Figure 4.13).

Table 4.3. *Extents of glaciers and ice caps as given by different authors.*

Reference	Area (10^3 km^2)	Volume (10^3 km^3)	SLE[f] (m)
Raper and Braithwaite, 2005[a,c]	522 ± 42	87 ± 10	0.24 ± 0.03
Ohmura, 2004[a,d]	512	51	0.15
Dyurgerov and Meier, 2005[a,e]	546 ± 30	133 ± 20	0.37 ± 0.06
Dyurgerov and Meier, 2005[b,e]	785 ± 100	260 ± 65	0.72 ± 0.2
IPCC, 2001[b]	680	180 ± 40	0.50 ± 0.1

Notes:
[a] glaciers and ice caps surrounding Greenland and Antarctic Ice Sheets are excluded.
[b] glaciers and ice caps surrounding Greenland and West Antarctic Ice Sheets are included.
[c] volume derived from hypsometry and volume/area scaling within 1° × 1° grid cells.
[d] volume derived from a statistical relationship between glacier volume and area, calibrated with 61 glacier volumes derived from radio-echo-sounding measurements.
[e] volume derived from a statistical relationship between glacier volume and area, calibrated with 144 glacier volumes derived from radio-echo-sounding measurements.
[f] calculated for the ocean surface area of 362 × 10^6 km^2.

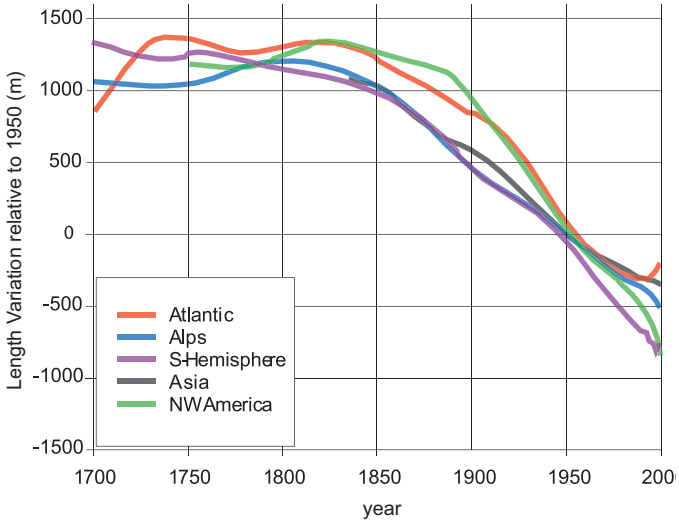


Figure 4.13. *Large-scale regional mean length variations of glacier tongues (Oerlemans, 2005). The raw data are all constrained to pass through zero in 1950. The curves shown are smoothed with the Stineman (1980) method and approximate this. Glaciers are grouped into the following regional classes: SH (tropics, New Zealand, Patagonia), northwest North America (mainly Canadian Rockies), Atlantic (South Greenland, Iceland, Jan Mayen, Svalbard, Scandinavia), European Alps and Asia (Caucasus and central Asia).*

Although much local, regional and high-frequency variability is superimposed, the smoothed series give an apparently homogeneous signal. General retreat of glacier tongues started after 1800, with considerable mean retreat rates in all regions after 1850 lasting throughout the 20th century. A slow down of retreat between about 1970 and 1990 is more evident in the raw data (Oerlemans, 2005). Retreat was again generally rapid in the 1990s; the Atlantic and the SH curves reflect precipitation-driven growth and advances of glaciers in western Scandinavia and New Zealand during the late 1990s (Chinn et al., 2005).

Records of directly measured glacier mass balances are few and stretch back only to the mid-20th century. Because of the very intensive fieldwork required, these records are biased towards logistically and morphologically 'easy' glaciers. Uncertainty in directly measured annual mass balance is typically ±200 kg m^{-2} yr^{-1} due to measurement and analysis errors (Cogley, 2005). Mass balance data are archived and distributed by the World Glacier Monitoring Service (WGMS(ICSI-IAHS), various years-b). From these and from several other new and historical sources, quality checked time series of the annual mean specific mass balance (the total mass balance of a glacier or ice cap divided by its total surface area) for about 300 individual glaciers have been constructed, analysed and presented in three databases (Ohmura, 2004; Cogley, 2005; Dyurgerov and Meier, 2005). Dyurgerov and Meier (2005) also incorporated recent findings from repeat altimetry of glaciers and ice caps in Alaska (Arendt et al., 2002) and Patagonia (Rignot et al., 2003). Only a few individual series stretch over the entire period. From these statistically small samples, global estimates have been obtained as five-year (pentadal) means by arithmetic averaging (C05a in Figure 4.14), area-weighted averaging (DM05 and O04) and spatial interpolation (C05i). Although mass balances reported from individual glaciers include the effect of changing glacier area, deficiencies in the inventories do not allow for general consideration of area changes. The effect of this inaccuracy is considered minor. Table 4.4 summarises the data plotted in Figure 4.14.

The time series of globally averaged mean specific mass balance from different authors have very similar shapes despite some offsets in magnitude. Around 1970, mass balances were close to zero or slightly positive in most regions (Figure 4.15) and close to zero in the global mean (Figure 4.14), indicating near-equilibration with climate after the strong earlier mass loss. This gives confidence that the glacier wastage in the late 20th century is essentially a response to post-1970 global warming (Greene, 2005). Strong mass losses are indicated for the 1940s but uncertainty is great since the arithmetic mean values (C05a in Figure 4.14) are from only a few glaciers. The most recent period consists of four years only (2000/2001–2003/2004) and does not cover all regions completely. The shortage of data from Alaska and Patagonia likely causes a positive bias on the area-weighted and interpolated analyses (DM05, O04, C05i) due to the large ice areas in these regions. There is probably also a negative bias in the arithmetic mean (C05a), due to the strongly negative northern mid-latitudes mass balances in 2002/2003, particularly in the European Alps (Zemp et al., 2005). Mass loss rates for 1990/1991 to 2003/2004 are roughly double those for 1960/1961 to 1989/1990 (Table 4.4).

Over the last half century, both global mean winter accumulation and summer melting have increased steadily (Ohmura, 2004; Dyurgerov and Meier, 2005; Greene, 2005). At least in the NH, winter accumulation and summer melting correlate positively with hemispheric air temperature, whereas the mean specific mass balance correlates negatively with hemispheric air temperature (Greene, 2005). Dyurgerov and Dwyer (2000) analysed time series of 21 NH glaciers and found a rather uniformly increased mass turnover rate, qualitatively consistent with moderately increased precipitation and substantially increased low-altitude melting. This general trend is also indicated for Alaska (Arendt et al., 2002), the Canadian Arctic Archipelago (Abdalati et al., 2004) and Patagonia (Rignot et al., 2003).

Regional analyses by Dyurgerov and Meier (2005) show strongest negative mean specific mass balances in Patagonia, the northwest USA and southwest Canada, and Alaska, with losses especially rapid in Patagonia and Alaska after the mid-1990s (Figure 4.15a). A cumulative mean specific mass balance of -10×10^3 kg m^{-2} corresponds to a loss of 10 m of water, or about 11 m of ice, averaged over the glacier area; cumulative losses in Patagonia since 1960 are approximately 40 m of ice thickness averaged over the glaciers. Only Europe showed a mean value close to zero, with strong mass losses in the Alps compensated by mass gains in maritime Scandinavia until the end of the 20th century. High spatial variability in climate and, thus, in glacier variations, also exists in other large regions such as in the high mountains of Asia (Liu et al., 2004; Dyurgerov

Table 4.4. *Global average mass balance of glaciers and ice caps for different periods, showing mean specific mass balance (kg m^{-2} yr^{-1}); total mass balance (Gt yr^{-1}); and SLE (mm yr^{-1}) derived from total mass balance and an ocean surface area of 362 × 10^6 km^2. Values for glaciers and ice caps excluding those around the ice sheets (total area 546 × 10^3 km^2) are derived from MB values in Figure 4.14. Values for glaciers and ice caps including those surrounding Greenland and West Antarctica (total area 785.0 × 10^3 km^2) are modified from Dyurgerov and Meier (2005) by applying pentadal DM05 to MB ratios. Uncertainties are for the 90% confidence level. Sources: Ohmura (2004), Cogley (2005) and Dyurgerov and Meier (2005), all updated to 2003/2004.*

Period	Mean Specific Mass Balance[a] (kg m^{-2} yr^{-1})	Total Mass Balance[a] (Gt yr^{-1})	Sea Level Equivalent[a] (mm yr^{-1})	Mean Specific Mass Balance[b] (kg m^{-2} yr^{-1})	Total Mass Balance[b] (Gt yr^{-1})	Sea Level Equivalent[b] (mm yr^{-1})
1960/1961–2003/2004	–283 ± 102	–155 ± 55	0.43 ± 0.15	–231 ± 82	–182 ± 64	0.50 ± 0.18
1960/1961–1989/1990	–219 ± 92	–120 ± 50	0.33 ± 0.14	–173 ± 73	–136 ± 57	0.37 ± 0.16
1990/1991–2003/2004	–420 ± 121	–230 ± 66	0.63 ± 0.18	–356 ± 101	–280 ± 79	0.77 ± 0.22

Notes:
[a] Excluding glaciers and ice caps around ice sheets
[b] Including glaciers and ice caps around ice sheets

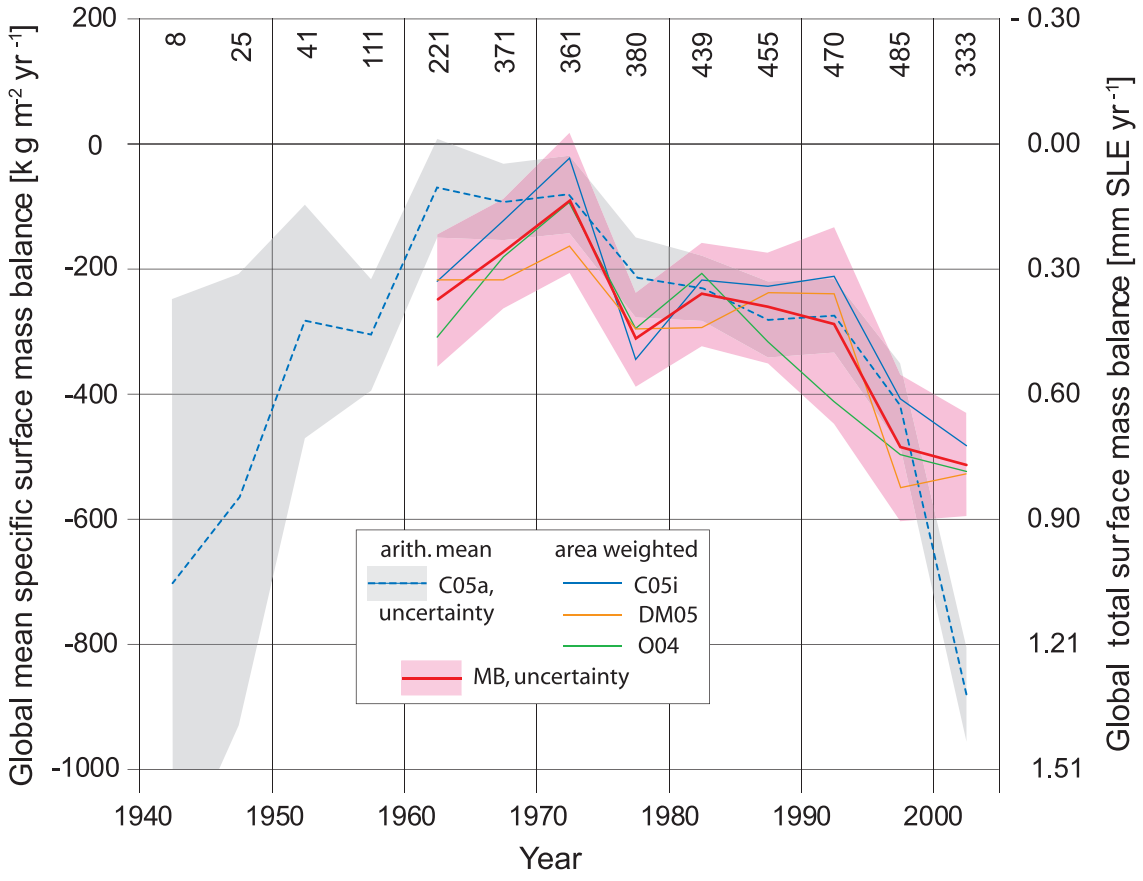


Figure 4.14. *Pentadal (five-year) average mass balance of the world's glaciers and ice caps excluding those around the ice sheets of Greenland and Antarctica. Mean specific mass balance (left axis) is converted to total mass balance and to SLE (right axis) using the total ice surface area of 546 × 10^3 km^2 (Table 4.3) and the ocean surface area of 362 × 10^6 km^2. C05a is an arithmetic mean over all annual measurements within each pentade (Cogley, 2005); the grey envelope is the 90% confidence level of the C05a data and represents the spatial variability of the measured mass balances. The number of measurements in each time period is given at the top of the graph. C05i is obtained by spatial interpolation (Cogley, 2005), while DM05 (Dyurgerov and Meier, 2005) and O04 (Ohmura, 2004) are area-weighted global numbers. MB is the arithmetic mean of C05i, DM05 and O04, and its uncertainty (red shading) combines the spatial variability and the structural uncertainty calculated for the 90% confidence level. This does not include uncertainties that derive from uncertainties in the glacier area inventories. The authors performed area weighting and spatial interpolation only after 1960, when up to 100 measured mass balances were available. The most recent period consists of four years only (2000/2001 to 2003/2004).*

and Meier, 2005). Values for Patagonia and Alaska are mainly derived from altimetry evaluations made by Arendt et al. (2002) and Rignot et al. (2003), and authors of both papers note that the observed mass losses cannot be explained by surface mass loss only, but also include increased ice discharge due to enhanced ice velocity. The latter, in turn, has possibly been triggered by previous negative mass balances of glaciers calving icebergs, as well as by increased melt water production that enhances basal sliding. Some glaciers exhibit quasi-periodic internal instabilities (surging), which can affect data from those glaciers (Arendt et al., 2002; Rignot et al., 2003), but these effects are expected to average very close to zero over large regions and many years or decades. Because of a lack of suitable information, the temporal variation of the mass loss of the Patagonian ice fields has been interpolated to match the time series of Alaskan mass balances assuming similar climate regimes (Dyurgerov and Meier, 2005).

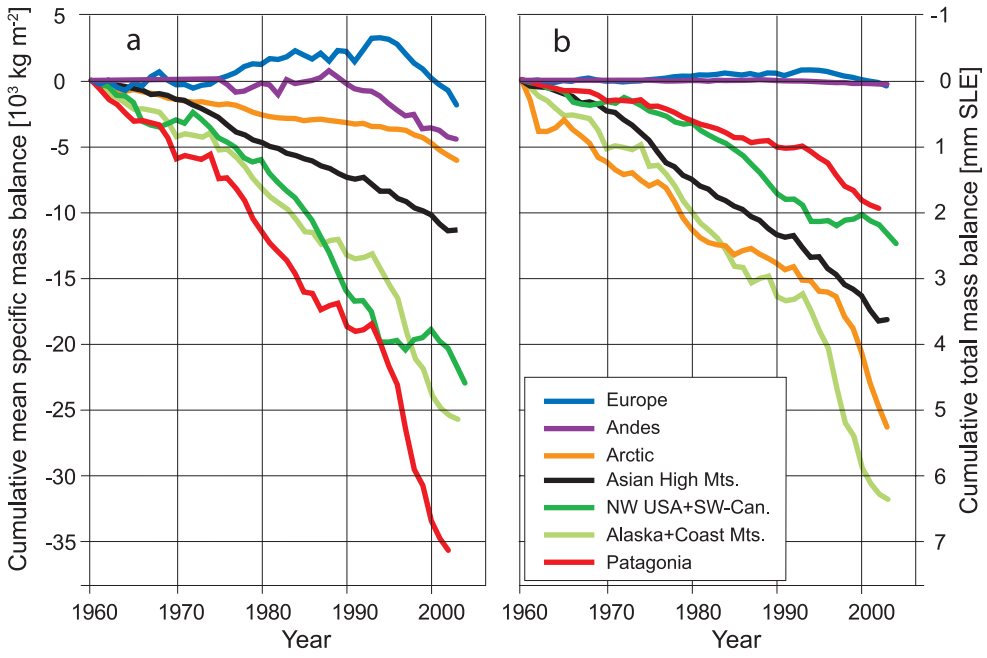


Figure 4.15. *Cumulative mean specific mass balances (a) and cumulative total mass balances (b) of glaciers and ice caps, calculated for large regions (Dyurgerov and Meier, 2005). Mean specific mass balance shows the strength of climate change in the respective region. Total mass balance is the contribution from each region to sea level rise.*

The surface mass balance of snow and ice is determined by a complex interaction of energy fluxes towards and away from the surface and the occurrence of solid precipitation. Nevertheless, glacier fluctuations show a strong statistical correlation with air temperature at least at a large spatial scale throughout the 20th century (Greene, 2005), and a strong physical basis exists to explain why warming would cause mass loss (Ohmura, 2001). Changes in snow accumulation also matter, and may dominate in response to strong circulation changes or when temperature is not changing greatly. For example, analyses of glacier mass balances, volume changes, length variations and homogenised temperature records for the western portion of the European Alps (Vincent et al., 2005) clearly indicate the role of precipitation changes in glacier variations in the 18th and 19th centuries. Similarly, Nesje and Dahl (2003) explained glacier advances in southern Norway in the early 18th century as being due to increased winter precipitation rather than colder temperatures.

Total mass balances are the integration of mean specific mass balances (which have a climate signal) over the existing glacier area. Consequently, the biggest mass losses and, thus, contributions to sea level rise are from Alaska with 0.11 mm yr^{-1} SLE from 1960/1961 to 1989/1990 and 0.24 mm yr^{-1} SLE from 1990/1991 to 2002/2003, the Arctic (0.09 and 0.19), and the high mountains of Asia (0.08 and 0.10) (Figure 4.15b).

4.5.3 Special Regional Features

Although reports on individual glaciers or limited glacier areas support the global picture of ongoing strong ice shrinkage in almost all regions, some exceptional results indicate the complexity of both regional- to local-scale climate and respective glacier regimes.

For glaciers in the dry and cold Taylor Valley, Antarctica, Fountain et al. (2004) hypothesised that an increase in average air temperature of 2°C alone can explain the observed glacier advance through ice softening.

Altimetric measurements in Svalbard suggested a small ice cap growth (Bamber et al., 2004), however, an alternative evaluation of mass balance processes indicates a slight sea level contribution of 0.01 mm yr^{-1} for the last three decades of the 20th century (Hagen et al., 2003). Svalbard glaciers were recently close to balance, which is exceptional for the Arctic.

In Scandinavia, Norwegian coastal glaciers, which advanced in the 1990s due to increased accumulation in response to a positive phase of the NAO (Nesje et al., 2000), started to shrink around 2000 as a result of a combination of reduced winter accumulation and greater summer melting (Kjøllmoen, 2005). Norwegian glacier tongues farther inland have retreated continuously at a moderate rate. Warming is also indicated by a change in temperature distribution in northern Sweden's Storglaciären where, between 1989 and 2001, 8.3 m of the cold surface layer (or 22% of the long-term average thickness of this cold layer) warmed to the melting point. This is attributed

primarily to increased winter temperatures yielding a longer melt season; summer ablation was normal (Pettersson et al., 2003). As with coastal Scandinavia, glaciers in the New Zealand Alps advanced during the 1990s, but have started to shrink since 2000. Increased precipitation may have caused the glacier growth (Chinn et al., 2005).

In the European Alps, exceptional mass loss during 2003 removed an average of 2,500 kg m^{-2} yr^{-1} over nine measured Alpine glaciers, almost 60% higher than the previous record of 1,600 kg m^{-2} yr^{-1} loss in 1996 and four times more than the mean loss from 1980 to 2001 (600 kg m^{-2} yr^{-1}; Zemp et al., 2005). This was caused by extraordinarily high air temperatures over a long period, extremely low precipitation, and albedo feedback from Sahara dust depositions and a previous series of negative mass balance years (see Box 3.6.).

Whereas glaciers in the Asian high mountains have generally shrunk at varying rates (Su and Shi, 2002; Ren et al., 2004; Solomina et al., 2004; Dyurgerov and Meier, 2005), several high glaciers in the central Karakoram are reported to have advanced and/or thickened at their tongues (Hewitt, 2005), probably due to enhanced precipitation.

Tropical glaciers have shrunk from a maximum in the mid-19th century, following the global trend (Figure 4.16). Strong shrinkage rates in the 1940s were followed by relatively stable extents that lasted into the 1970s. Since then, shrinkage has become stronger again; as in other mountain ranges, the smallest glaciers are more strongly affected. Since the publication of IPCC (2001), evidence has increased that changes in the mass balance of tropical glaciers are mainly driven by coupled changes in energy and mass fluxes related to interannual variations of regional-scale hygric seasonality (Wagnon et al., 2001; Francou et al., 2003, 2004). Variations in atmospheric moisture content affect incoming solar radiation, precipitation and albedo, atmospheric longwave emission, and sublimation (Wagnon et al., 2001; Kaser and Osmaston, 2002; Mölg et al., 2003a; Favier et al., 2004; Mölg and Hardy, 2004; Sicart et al., 2005). At a large scale, the mass balance of tropical glaciers strongly correlates with tropical sea surface temperature anomalies and related atmospheric circulation modes (Francou et al., 2003, 2004; Favier et al., 2004). Glaciers on Kilimanjaro behaved exceptionally throughout the 20th century (Figure 4.16). The geometry of the volcano and the dry climate above the freezing level maintain vertical ice walls around the tabular ice on the summit plateau and these retreat at about 0.9 m yr^{-1} (Thompson et al., 2002) forced by solar radiation (Mölg et al., 2003b). Their retreat is responsible for the steady shrinkage of the ice area on the summit plateau (Figure 4.16, insert) (Cullen et al., 2006). In contrast, the slope glaciers, which extend from the plateau rim onto the steep slopes of the volcano, decreased strongly at the beginning of the 20th century, but more slowly recently. This shrinkage is interpreted as an ongoing response to a dramatic change from a wetter to a drier regime, supposedly around 1880, and a subsequent negative trend in mid-troposphere atmospheric moisture content over East Africa (Cullen et al., 2006).

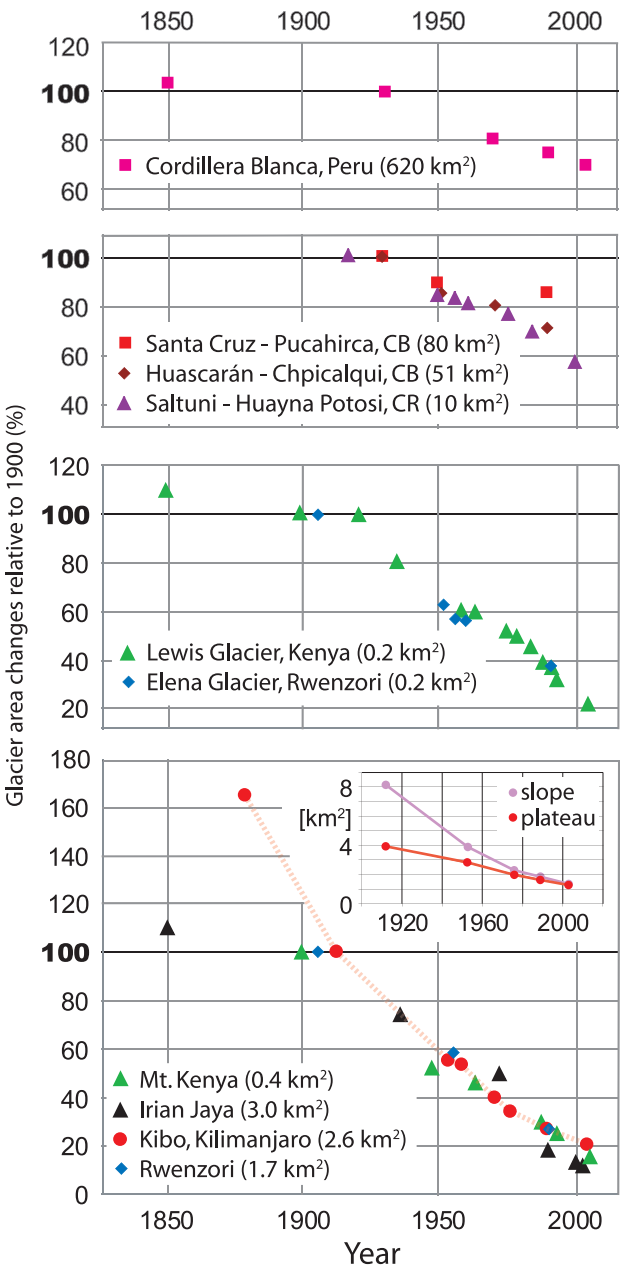


Figure 4.16. *Changes in the surface area of tropical glaciers relative to their extent around 1900, grouped according to different glacier sizes. The sizes are given for 1990 or the closest available date to 1990. The broken red line highlights the retreat of Kilimanjaro glaciers. The insert shows the area change (km²) of the Kilimanjaro plateau (red) and slope (purple) glaciers as separated by the 5,700 m contour line (Kaser and Osmaston, 2002 (updated courtesy of S. Lieb); Mölg et al., 2003b; Georges, 2004; Hastenrath, 2005; Cullen et al., 2006; Klein and Kincaid, 2006).*

4.6 Changes and Stability of Ice Sheets and Ice Shelves

New and improved observational techniques, and extended time series, reveal changes in many parts of the large ice sheets. Greenland has experienced mass loss recently in response to increases in near-coastal melting and in ice flow velocity more than offsetting increases in snowfall. Antarctica appears to be losing mass at least partly in response to recent ice flow acceleration in some near-coastal regions, although with greater uncertainty in overall balance than for Greenland. Shortcomings in forcing, physics and resolution in comprehensive ice flow models have prevented them from fully capturing the ice flow changes.

4.6.1 Background

The ice sheets of Greenland and Antarctica hold enough ice to raise sea level about 64 m if fully melted (Bamber et al., 2001; Lythe et al., 2001). Even a modest change in ice sheet balance could strongly affect future sea level and freshwater flux to the oceans, with possible climatic implications. These ice sheets consist of vast central reservoirs of slow-moving ice drained by rapidly moving, ice-walled ice streams or rock-walled outlet glaciers typically flowing into floating ice shelves or narrower ice tongues, or directly into the ocean. Ice shelves often form in embayments, or run aground on local bedrock highs to produce ice rumples or ice rises, and friction with embayment sides or local grounding points helps restrain the motion of the ice shelves and their tributaries. About half of the ice lost from Greenland is by surface melting and runoff into the sea, but surface melting is much less important to the mass balance of Antarctica. Dynamics of the slow-moving ice and of ice shelves are reasonably well understood and can be modelled adequately, but this is not so for fast-moving ice streams and outlet glaciers. Until recently (including IPCC, 2001), it was assumed that velocities of these outlet glaciers and ice streams cannot change rapidly, and impacts of climate change were estimated primarily as changes in snowfall and surface melting. Recent observations show that outlet glacier and ice stream speeds can change rapidly, for reasons that are still under investigation. Consequently, this assessment will not adequately quantify such effects.

4.6.2 Mass Balance of the Ice Sheets and Ice Shelves

The current state of balance of the Greenland and Antarctic Ice Sheets is discussed here, focussing on the substantial progress made since IPCC (2001). Possible future changes are considered in Chapter 10, and in Chapter 19 of the Working Group II contribution to the IPCC Fourth Assessment Report.

4.6.2.1 Techniques

Several techniques are used to measure the mass balance of large ice masses. The mass budget approach compares input from snow accumulation with output from ice flow and melt water runoff. Repeated altimetry measures surface elevation changes. Temporal variations in gravity over the ice sheets reveal mass changes. Changes in day length and in the direction of the Earth's rotation axis also reveal mass redistribution.

4.6.2.1.1 Mass budget

Snow accumulation is often estimated from annual layering in ice cores, with interpolation between core sites using satellite microwave measurements or radar sounding (Jacka et al., 2004). Increasingly, atmospheric modelling techniques are also applied (e.g., Monaghan et al., 2006). Ice discharge is calculated from radar or seismic measurements of ice thickness, and from *in situ* or remote measurements of ice velocity, usually where the ice begins to float and velocity is nearly depth-independent. A major advance since IPCC (2001) has been widespread application of Interferometric Synthetic Aperture Radar (InSAR) techniques from satellites to measure ice velocity over very large areas of the ice sheets (e.g., Rignot et al., 2005). Calculation of mass discharge also requires estimates for runoff of surface melt water, which is large for low-elevation regions of Greenland and parts of the Antarctic Peninsula but small or zero elsewhere on the ice sheets. Surface melt amounts usually are estimated from modelling driven by atmospheric reanalyses, global models or climatology, and often calibrated against surface observations where available (e.g., Hanna et al., 2005; Box et al., 2006). The typically small mass loss by melting beneath grounded ice is usually estimated from models. Mass loss from melting beneath ice shelves can be large, and is difficult to measure; it is generally calculated as the remainder after accounting for other mass inputs and outputs.

Ice sheet mass inputs and outputs are difficult to estimate with high accuracy. For example, van de Berg et al. (2006) summarised six estimates of net accumulation on the grounded section of Antarctica published between 1999 and 2006, which ranged from 1,811 to 2,076 Gt yr^{-1} or ±7% about the midpoint. Transfer of 360 Gt of grounded (non-floating) ice to the ocean would raise sea level about 1 mm. Uncertainty in the Greenland accumulation rate is probably about 5% (Hanna et al., 2005; Box et al., 2006). Although broad InSAR coverage and progressively improving estimates of grounding-line ice thickness have substantially improved ice discharge estimates, incomplete data coverage implies uncertainties in discharge estimates of a few percent. Uncorrelated errors of 5% on input and output would imply mass budget uncertainties of about 40 Gt yr^{-1} for Greenland and 140 Gt yr^{-1} for Antarctica. Large interannual variability and trends also complicate interpretation. Box et al. (2006) estimated average accumulation on the Greenland Ice Sheet of 543 Gt yr^{-1} from 1988 to 2004, but with an annual minimum of 482 Gt yr^{-1}, a maximum of 613 Gt yr^{-1} and a

best-fit linear trend yielding an increase of 68 Gt yr^{-1} during the period. Glacier velocities can change substantially, sometimes in months or years, adding to the overall uncertainty of mass budget calculations.

4.6.2.1.2 Repeated altimetry

Surface elevation changes reveal ice sheet mass changes after correction for changes in depth-density profiles and in bedrock elevation, or for hydrostatic equilibrium if the ice is floating. Satellite radar altimetry (SRALT) has been widely used to estimate elevation changes (Shepherd et al., 2002; Davis et al., 2005; Johannessen et al., 2005; Zwally et al., 2006), together with laser altimetry from airplanes (Krabill et al., 2004) and from the Ice, Cloud and land Elevation Satellite (ICESat; Thomas et al., 2006). Modelled corrections for isostatic changes in bedrock elevation are small (a few millimetres per year), but with uncertainties nearly as large as the corrections in some cases (Zwally et al., 2006). Corrections for near-surface firn density changes are larger (>10 mm yr^{-1}; Cuffey, 2001) and also uncertain.

Radar altimetry has provided long-term and widespread coverage for more than a decade, but with important challenges (described by Legresy et al., 2006). The available SRALT data are from altimeters with a beam width of 20 km or more, designed and demonstrated to make accurate measurements over the almost flat, horizontal ocean. Data interpretation is more complex over sloping, undulating ice sheet surfaces with spatially and temporally varying dielectric properties and thus penetration into near-surface firn. Empirical corrections are applied for some of these effects, and for inter-satellite biases. The correction for the offset between the European Remote Sensing Satellite (ERS-1 and ERS-2) altimeters is reported by Zwally et al. (2006) to affect mass change estimates for the interval 1992 to 2002 by about 50 Gt yr^{-1} for Greenland, and to differ from the corresponding correction of Johannessen et al. (2005) by about 20 Gt yr^{-1}, although some of this difference may reflect differences in spatial coverage of the studies combined with spatial dependence of the correction. Changes in surface dielectric properties affect the returned waveform and thus the measured range, so a correction is made for elevation changes correlated to returned-power changes. This effect is small averaged over an ice sheet but often of the same magnitude as the remaining signal at a point, and could remove part or all of the signal if climate change affected both elevation and surface character, hence returned power.

The SRALT tracking algorithms use leading edges of reflected radar waveforms, thus primarily sampling higher-elevation parts of the large footprint. This probably introduces only small errors over most of an ice sheet, where surfaces are nearly flat. However, glaciers and ice streams often flow in surface depressions that can be narrower than the radar footprint, so that SRALT-derived elevation changes are weighted towards slower-moving ice at the glacier sides (Thomas et al., 2006). This is of most concern in Greenland, where other studies show thinning along outlet glaciers just a few kilometres wide (Abdalati et al., 2001). Elevation-change estimates from SRALT have not been validated against independent data except at higher elevations, where surfaces are nearly flat and horizontal and dielectric properties nearly unchanging (Thomas et al., 2001). Although SRALT coverage is lacking within 900 km of the poles, and some data are lost in steep regions, coverage has now been achieved for about 90% of the Greenland Ice Sheet and 80% of the Antarctic Ice Sheet (Zwally et al., 2006) (Figure 4.19).

Laser altimeters reduce some of the difficulties with SRALT by having negligible penetration of near-surface layers and a smaller footprint (about 1 m for airborne laser, and 60 m for ICESat). However, clouds limit data acquisition, and accuracy is affected by atmospheric conditions and particularly by laser pointing errors. Airborne surveys over Greenland in 1993/1994 and 1998/1999 yielded estimates of elevation change accurate to ±14 mm yr^{-1} along survey tracks (Krabill et al., 2002). However, the large gaps between flight lines must be filled, often by simple interpolation in regions of weak variability or by interpolation using physical models in more complex regions (Krabill et al., 2004; Figure 4.17).

4.6.2.1.3 Geodetic measurements, including measurement of temporal variations in Earth gravity

Since 2002, the Gravity Recovery and Climate Experiment (GRACE) satellite mission has been providing routine measurement of the Earth's gravity field and its temporal variability. After removing the effects of tides, atmospheric loading, etc., high-latitude data contain information on temporal changes in the mass distribution of the ice sheets and underlying rock (Velicogna and Wahr, 2005). Estimates of ice sheet mass balance are sensitive to modelled estimates of bedrock vertical motion, primarily arising from response to changes in mass loading from the end of the last ice age. Velicogna and Wahr (2005) estimated a correction for Greenland Ice Sheet mass balance of 5 ± 17 Gt yr^{-1} for the bedrock motion, with an equivalent value of 177 ± 73 Gt yr^{-1} for Antarctica (Velicogna and Wahr, 2006). (Note that stated uncertainties for ice sheet mass balances referenced to published papers are given here as published. Some papers include error terms that were estimated without formal statistical derivations, and other papers note omission of estimates for certain possible systematic errors, so that these as-published errors generally cannot be interpreted as representing any specific confidence interval such as 5 to 95%.)

Other geodetic data provide constraints on mass changes at high latitudes. These data include the history of changing length of day from eclipse records, the related ongoing changes in the spherical-harmonic coefficients of the geopotential, and true polar wander (changes in the planet's rotation vector; Peltier, 1998; Munk, 2002; Mitrovica et al., 2006). At present, unique solutions are not possible from these techniques, but hypothesised histories of ice sheet changes can be tested against the data for consistency, and progress is rapidly being made.

4.6.2.2 Measured Balance of the Ice Sheets and Ice Shelves

Mass balance of the large ice sheets was summarised by Rignot and Thomas (2002) and Alley et al. (2005a).

4.6.2.2.1 Greenland

Many recent studies have addressed Greenland mass balance. They yield a broad picture (Figure 4.17) of inland thickening (Thomas et al., 2001; Johannessen et al., 2005; Thomas et al., 2006; Zwally et al., 2006), faster near-coastal thinning primarily in the south along fast-moving outlet glaciers (Abdalati et al., 2001; Rignot and Kanagaratnam, 2006), and a recent acceleration in overall shrinkage.

Analysis of GRACE data showed total losses of 75 ± 26 Gt yr^{-1} between April 2002 and July 2004 (Velicogna and Wahr, 2005). Ramillien et al. (2006), also working from GRACE data, found a mass loss of 129 ± 15 Gt yr^{-1} for July 2002 to March 2005. Because of the low spatial resolution of GRACE, these include losses from isolated mountain glaciers and ice caps near the coast, whereas the results discussed next do not.

Mass loss from the ice sheet surface (net snow accumulation minus melt water runoff) has increased recently. Box et al. (2006) used calibrated atmospheric modelling and a single approximation for ice flow discharge to estimate average ice sheet mass loss of more than 100 Gt yr^{-1} during 1988 to 2004; they also found acceleration of surface mass loss during this interval of 43 Gt yr^{-1}. A similar analysis by Hanna et al. (2005) for 1961 to 2003 found somewhat higher net accumulation but similar trends, with ice sheet growth of 22 ± 51 Gt yr^{-1} from 1961 to 1990, shifting to shrinkage of 14 ± 55 Gt yr^{-1} from 1993 to 1998 and shrinkage of 36 ± 59 Gt yr^{-1} from 1998 to 2003. Again, ice flow acceleration was not included in these estimates.

In a study especially using SRALT but incorporating laser elevation measurements from aircraft and a correction for the effect of changing temperature on near-surface density, Zwally et al. (2006) estimated slight growth of the ice sheet by 11 ± 3 Gt yr^{-1} from 1992 to 2002. However, they noted that mass loss of 18 ± 2 Gt yr^{-1} would be indicated if the thickness changes at higher elevations are largely low-density firn rather than high-density ice, as might apply if the effects of increasing accumulation rate were also taken into account (Hanna et al., 2005; Box et al., 2006). The more spatially limited results of Johannessen et al. (2005) from the same radar data indicated slightly less shrinkage or slightly more growth than found by Zwally et al. (2006) in regions of overlap. Krabill et al. (2000) also found thickening of central regions (~10 mm yr^{-1}) from laser measurements covering 1993/1994 to 1998/1999.

Krabill et al. (2004) used repeat laser altimetry and modelled surface mass balance to estimate mass loss of about 45 Gt yr^{-1} from 1993/1994 to 1998/1999, with acceleration to a loss of 73 ± 11 Gt yr^{-1} during the overlapping interval 1997 to 2003. These values may underestimate total losses, because they do not take account of rapid thinning in sparsely surveyed regions such as the southeast, where mass budget studies show large losses (Rignot and Kanagaratnam, 2006). Thomas et al. (2006) extended these results to 2004 using ICESat data to include approximate corrections for density changes in the near surface. Results showed ice sheet mass loss of 27 ± 23 Gt yr^{-1} for 1993/1994 to 1998/1999, loss of 55 ± 25 Gt yr^{-1} for 1997 to 2003, with an updated loss of 81 ± 24 Gt yr^{-1} from 1998/1999 to 2004.

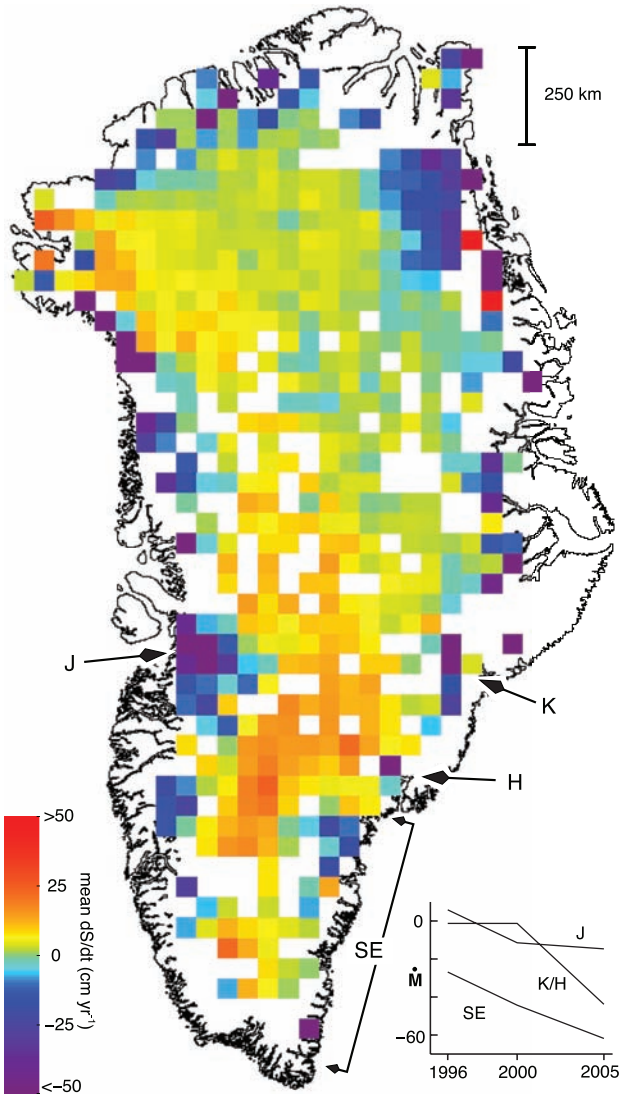


Figure 4.17. *Rates of surface elevation change (dS/dt) derived from laser altimeter measurements at more than 16,000 locations on the Greenland Ice Sheet where ICESat data from 2005 overlay aircraft surveys in 1998/1999 (using methods described by Thomas et al., 2006). Locations of rapidly thinning outlet glaciers at Jakobshavn (J), Kangerdlugssuaq (K), Helheim (H) and along the southeast coast (SE) are shown, together with an inset showing their estimated total mass balance (***Ṁ***, Gt* yr^{-1}*) between 1996 and 2005 (Rignot and Kanagaratnam, 2006).*

Rignot and Kanagaratnam (2006) combined several data sets, with special focus on the acceleration in velocity of outlet glaciers measured by Synthetic Aperture Radar (SAR) interferometry. Starting from an estimated excess ice flow discharge of 51 ± 28 Gt yr^{-1} in 1996, these authors estimated that the ice flow loss increased to 83 ± 27 Gt yr^{-1} in 2000 and 150 ± 36 Gt yr^{-1} in 2005. Adding surface mass balance deviations

from the long-term average as calculated by Hanna et al. (2005) yielded mass losses of 82 ± 28 Gt yr^{-1} in 1996, 124 ± 28 Gt yr^{-1} in 2000 and 202 ± 37 Gt yr^{-1} in 2005. The more pronounced ice flow accelerations were restricted to regions south of 66°N before 2000 but extended to 70°N by 2005. These estimates of rapid mass loss would be reduced somewhat if ice surface velocities are higher than depth-averaged velocities, which may apply in some places.

Greenland Ice Sheet mass balance estimates are summarised in Figure 4.18 (top). Most results indicate accelerating mass loss from Greenland during the 1990s up to 2005. The different estimates are not fully independent (there is, for example, some commonality in the isostatic corrections used for GRACE and altimetry estimates, and other overlaps can be found), but sufficient independence remains to increase confidence in the result. Different techniques have not fully converged quantitatively, with mismatches larger than formal error estimates suggesting structural uncertainties in the analyses, some of which were discussed above. The SRALT results showing overall near-balance or slight thickening, in contrast to other estimates, may result from the SRALT limitations over narrow glaciers discussed earlier.

Assessment of the data and techniques suggests a mass balance for the Greenland Ice Sheet ranging between growth of 25 Gt yr^{-1} and shrinkage of 60 Gt yr^{-1} for 1961 to 2003, shrinkage of 50 to 100 Gt yr^{-1} for 1993 to 2003 and shrinkage at even higher rates between 2003 and 2005. Lack of agreement between techniques and the small number of estimates preclude assignment of statistically rigorous error bounds. Interannual variability is very large, driven mainly by variability in summer melting, but also by sudden glacier accelerations (Rignot and Kanagaratnam, 2006). Consequently, the short time interval covered by instrumental data is of concern in separating fluctuations from trends.

4.6.2.2.2 Antarctica

Recent estimates of Antarctic Ice Sheet mass balance are summarised in Figure 4.18 (bottom). Rignot and Thomas (2002) combined several data sets including improved estimates of glacier velocities from InSAR to obtain antarctic mass budget estimates. For East Antarctica, growth of 20 ± 21 Gt yr^{-1} was indicated, with estimated losses of 44 ± 13 Gt yr^{-1} from West Antarctica. The balance of the Antarctic Peninsula was not assessed. Combining the East and West Antarctic numbers yielded a loss of 24 ± 25 Gt yr^{-1} for the region monitored. The time interval covered by these estimates is not tightly constrained, because ice input was estimated from data sets of varying length; output data were determined primarily in the few years before 2002.

Zwally et al. (2006) obtained SRALT coverage for about 80% of the ice sheet, including some portions of the Antarctic Peninsula, and interpolated to the rest of the ice sheet. The resulting balance included West Antarctic loss of 47 ± 4 Gt yr^{-1}, East Antarctic gain of 17 ± 11 Gt yr^{-1} and overall loss of 30 ± 12 Gt yr^{-1}. If all the ice thickness changes were low-density firn rather than ice, the loss would be smaller (14 ± 5 Gt yr^{-1}).

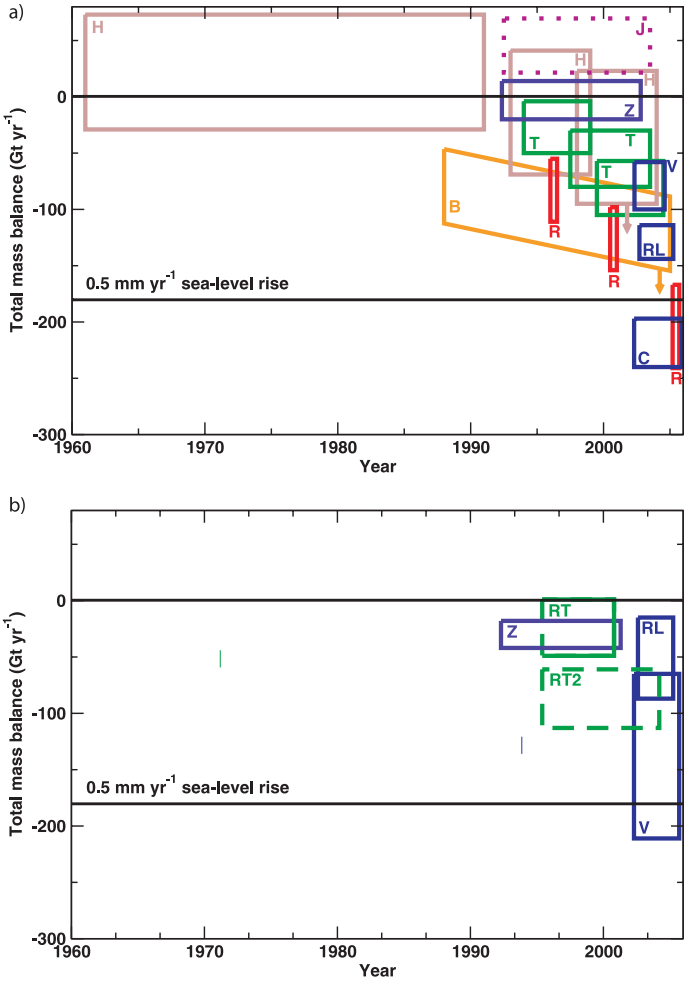


Figure 4.18. *(Top) Mass balance estimates for Greenland. The coloured rectangles, following Thomas et al. (2006), indicate the time span over which the measurements apply and the estimated range, given as (mean + uncertainty) and (mean – uncertainty) as reported in the original papers. Code: B (orange; Box et al, 2006), surface mass balance, using stated trend in accumulation, ice flow discharge (assumed constant), and standard error on regression of accumulation trend, with added arrow indicating additional loss from ice flow acceleration; H (brown; Hanna et al., 2005), surface mass balance, with arrow as for B; T (dark green; Thomas et al., 2006), laser altimetry, showing new results and revision of Krabill et al. (2004) to include firn densification changes; Z (violet; Zwally et al., 2006), primarily radar altimetry, with uncertainty reflecting the difference between a thickness change due to ice everywhere and that due to low-density firn in the accumulation zone; R (red; Rignot and Kanagaratnam, 2006), ice discharge combined with surface mass balance; V (blue; Velicogna and Wahr, 2005) GRACE gravity; RL (blue; Ramillen et al., 2006) GRACE gravity; J (magenta dashed; Johannessen et al., 2005), radar altimetry without firn densification correction and applying only to central regions that are thickening but omitting thinning of coastal regions. (Bottom) Mass balance estimates for grounded ice of Antarctica. Coloured rectangles show age span and error range as in the top panel. Code: Z (violet; Zwally et al., 2006), radar altimetry, with uncertainty reflecting the difference between a thickness change due to ice everywhere and that due to low-density firn everywhere; RT (dark green; Rignot and Thomas, 2002), ice discharge and surface mass balance, with dashed end line because some of the accumulation rate data extend beyond the time limits shown; RT2 (dark green; Rignot and Thomas, 2002), updated to include additional mass losses indicated by Thomas et al. (2004) and Rignot et al. (2005), dashed because the original authors did not produce this as an estimate for the whole ice sheet nor are accumulation rates updated; V (blue; Velicogna and Wahr, 2006), GRACE gravity; RL (blue; Ramillen et al., 2006), GRACE gravity.*

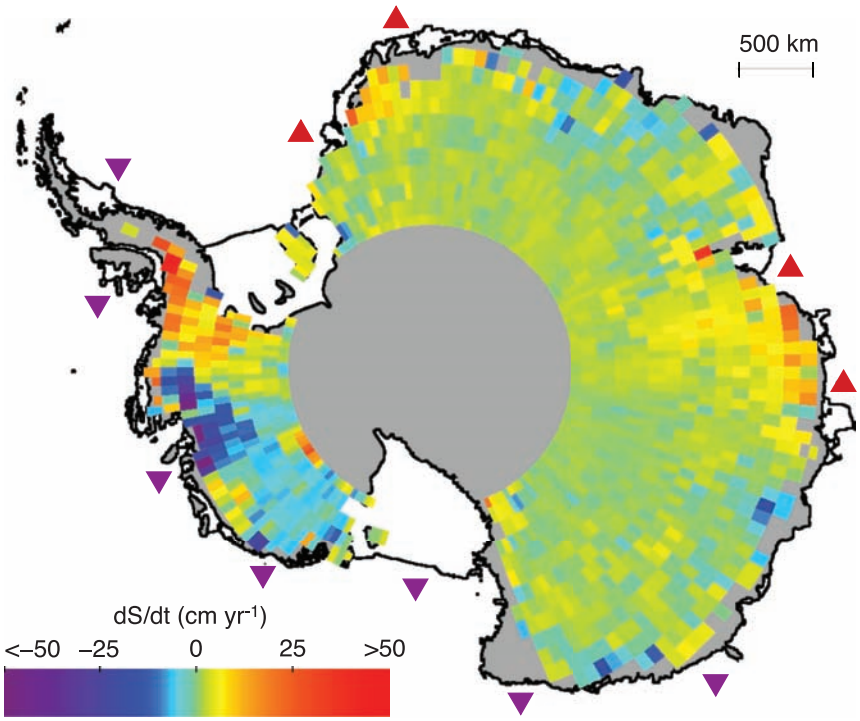


Figure 4.19. *Rates of surface elevation change (dS/dt) derived from ERS radar-altimeter measurements between 1992 and 2003 over the Antarctic Ice Sheet (Davis et al., 2005). Locations of ice shelves estimated to be thickening or thinning by more than 30 cm yr^{-1} (Zwally et al., 2006) are shown by red triangles (thickening) and purple triangles (thinning).*

Davis et al. (2005) compiled SRALT data for about 70% of the ice sheet, and did not interpolate to the rest. The same pattern of East Antarctic thickening and West Antarctic thinning was observed (Figure 4.19). Davis et al. (2005) suggested that the East Antarctic change was primarily from increased snowfall. Assigning all thickness change to low-density firn produces growth of the monitored portions of the ice sheet of 45 ± 8 Gt yr^{-1}; if all thickness changes were ice, this growth would be 105 ± 20 Gt yr^{-1}. Following the suggestion that the East Antarctic changes are from increased snow accumulation and the West Antarctic changes are more likely to be ice-dynamical would yield growth of monitored regions of 33 ± 9 Gt yr^{-1}. Note, however, that Monaghan et al. (2006) did not find the strong increase in snow accumulation suggested by Davis et al. (2005) in arguing for use of low-density firn in East Antarctic changes.

Rignot et al. (2005) documented discharges 84 ± 30% larger than accumulation rates for the glaciers that feed the Wordie Ice Shelf on the west coast of the northern Antarctic Peninsula (which shrank greatly between 1966 and 1989), a region largely absent from the SRALT studies. Consideration of strong imbalances in glaciers feeding the former Larsen B Ice Shelf across the Peninsula, and extrapolation of the results to undocumented basins, suggested mass loss from the ice in the northern part of the Antarctic Peninsula of 42 ± 7 Gt yr^{-1}. Observation of widespread glacier front retreat in the region (Cook et al., 2005) motivates the extrapolation, although mass loss would be overestimated if snow accumulation has been systematically underestimated (van de Berg et al., 2006).

Taking the Rignot and Thomas (2002), Zwally et al. (2006) and Rignot et al. (2005) results as providing the most complete antarctic coverage suggests ice sheet thinning of about 60 Gt yr^{-1}, with uncertainty of similar magnitude to the signal. Consideration of acceleration of some near-coastal glaciers, discussed below, and the difficulty of SRALT sampling of such regions, might allow slightly faster mass loss. The time interval considered is not uniform; the Rignot et al. (2005) results include changes after the collapse of the Larsen B Ice Shelf in 2002, more recent than data in the other studies, and suggest the possibility of accelerating mass loss. Use of the more spatially restricted Davis et al. (2005) SRALT data rather than the Zwally et al. (2006) results illustrates the persistent uncertainties; depending on the assumed density structure of the changes, Davis et al. (2005) combined with the Rignot et al. (2005) estimate for the Antarctic Peninsula would suggest near-balance or antarctic growth.

Interpretations of GRACE satellite gravity data indicate mass loss from the Antarctic Ice Sheet, including the Antarctic Peninsula and small glaciers and ice caps nearby, of 139 ± 73 Gt yr^{-1} between April 2002 and July 2005 (Velicogna and Wahr, 2006). Near-balance was indicated for East Antarctica, at 0 ± 51 Gt yr^{-1}, with mass loss in West Antarctica of 136 ± 21 Gt yr^{-1}. Independent analyses by Ramillien et al. (2006) found, for July 2002 to March 2005, East Antarctic growth of 67 ± 28 Gt yr^{-1}, West Antarctic shrinkage of 107 ± 23 Gt yr^{-1} and a net antarctic loss of 40 ± 36 Gt yr^{-1}.

Assessment of the data and techniques suggests overall Antarctic Ice Sheet mass balance ranging from growth of 50 Gt yr^{-1} to shrinkage of 200 Gt yr^{-1} from 1993 to 2003. As in the case of Greenland, the small number of measurements, lack of agreement between techniques, and existence of systematic errors that cannot be estimated accurately preclude formal error analyses and confidence limits. There is no implication that the midpoint of the range given provides the best estimate. Lack of older data complicates a similar estimate for the period 1961 to 2003. Acceleration of mass loss is likely to have occurred, but not so dramatically as in Greenland. Considering the lack of estimated strong trends in accumulation rate, assessment of the possible acceleration and the slow time scales affecting central regions of the ice sheets, it is reasonable to estimate that the behaviour from 1961 to 2003 falls between ice sheet growth of 100 Gt yr^{-1} and shrinkage of 200 Gt yr^{-1}.

Simply summing the 1993 to 2003 contributions from Greenland and Antarctica produces a range from balance

(0 Gt yr^{-1}) to shrinkage of 300 Gt yr^{-1}, or a contribution to sea level rise of 0 to 0.8 mm yr^{-1}. Because it is very unlikely that each of the ice sheets would exhibit the upper limit of its estimated mass balance range, it is very likely that, taken together, the ice sheets in Greenland and Antarctica have been contributing to sea level rise over the period 1993 to 2003. For 1961 to 2003, the same calculation spans growth of 125 Gt yr^{-1} to shrinkage of 260 Gt yr^{-1}, with 1993 to 2003 likely having the fastest mass loss of any decade in the 1961 to 2003 interval. Geodetic data on Earth rotation and polar wander provide additional insight (Peltier, 1998). Although Munk (2002) suggested that the geodetic data did not allow much contribution to sea level rise from ice sheets, subsequent reassessment of the errors involved in some of the data sets and analyses allows an anomalous late 20th century sea level rise of up to about 1 mm yr^{-1} (360 Gt yr^{-1}) from land ice (Mitrovica et al., 2006). Estimated mountain glacier contributions do not supply this, so a contribution from the polar ice sheets is consistent with the geodetic constraints, although little change in polar ice is also consistent.

4.6.2.2.3 Ice shelves

Changes in the mass of ice shelves, which are already floating, do not directly affect sea level, but ice shelf changes can affect flow of adjacent ice that is not floating, and thus affect sea level indirectly. Most ice shelves are in Antarctica, where they cover an area of about 1.5×10^6 km^2, or 11% of the entire ice sheet, and where nearly all ice streams and outlet glaciers flow into ice shelves. By contrast, Greenland ice shelves occupy only a few thousand square kilometres, and many are little more than floating glacier tongues. Mass loss by surface melt water runoff is not important for most ice shelf regions, which lose mass primarily by iceberg calving and basal melting, although basal freeze-on occurs in some regions.

Developments since IPCC (2001) include improved velocity and thickness data to estimate fluxes, and interpretation of repeated SRALT surveys over ice shelves to infer thickening or thinning rates. Melting of up to tens of metres per year has been estimated beneath deeper ice near grounding lines (Rignot and Jacobs, 2002; Joughin and Padman, 2003). Significant changes are observed on most ice shelves, with both positive and negative trends, and with faster changes on smaller shelves. Overall, Zwally et al. (2006) estimated mass loss from ice shelves fed by glaciers flowing from West Antarctica of 95 ± 11 Gt yr^{-1}, and mass gain to ice shelves fed by glaciers flowing from East Antarctica of 142 ± 10 Gt yr^{-1}. Rapid thinning of more than 1 m yr^{-1}, and locally more than 5 m yr^{-1}, was observed between 1992 and 2001 for many small ice shelves in the Amundsen Sea and along the Antarctic Peninsula. Thinning of about 1 m yr^{-1} (Shepherd et al., 2003; Zwally et al., 2006) preceded the fragmentation of almost all (3,300 km^2) of the Larsen B Ice Shelf along the Antarctic Peninsula in fewer than five weeks in early 2002 (Scambos et al., 2003).

4.6.3 Causes of Changes

4.6.3.1 Changes in Snowfall and Surface Melting

For Greenland, modelling driven by reanalyses and calibrated against surface observations indicates recent increases in temperature, precipitation minus evaporation, surface melt water runoff and net mass loss from the surface of the ice sheet, as well as areal expansion of melting and reduction in albedo (Hanna et al., 2005, 2006; Box et al., 2006). High interannual variability means that many of the trends are not highly significant, but the trends are supported by the consistency between the various component data sets and results from different groups. Estimated net snowfall minus melt water runoff includes an increase in the Greenland contribution to sea level rise of 58 Gt yr^{-1} between the 1961 to 1990 and 1998 to 2003 intervals (Hanna et al., 2005), or of 43 Gt yr^{-1} from 1998 to 2004 (Box et al., 2006).

For Antarctica, the recent summaries by van de Berg et al. (2006), van den Broeke et al. (2006) and Monaghan et al. (2006) have updated trends in accumulation rate. Contrary to some earlier work, these new studies found no continent-wide significant trends in accumulation over the interval 1980 to 2004 (van de Berg et al., 2006; van den Broeke et al., 2006) or 1985 to 2001 (Monaghan et al., 2006) from atmospheric reanalysis products (National Centers for Environmental Prediction (NCEP), the European Centre for Medium Range Weather Forecasts (ECMWF), Japanese), or from two mesoscale models driven by ECMWF and one by NCEP reanalyses. Strong interannual variability was found, approaching 5% for the continent, and important regional and seasonal trends that fit into larger climatic patterns, including an upward trend in accumulation in the Antarctic Peninsula. Studies of surface temperature (e.g., van den Broeke, 2000; Vaughan et al., 2001; Thompson and Solomon, 2002; Doran et al., 2002; Schneider et al., 2004; Turner et al., 2005) similarly showed regional patterns including strong warming in the Antarctic Peninsula region, and cooling at some other stations. Long-term data are very sparse, precluding confident identification of continent-wide trends.

4.6.3.2 Ongoing Dynamic Ice Sheet Response to Past Forcing

Because some portions of ice sheets respond only slowly to climate changes (decades to thousands of years or longer), past forcing may be influencing ongoing changes (Box 4.1). Some geologic data support recent and perhaps ongoing antarctic mass loss (e.g., Stone et al., 2003). A comprehensive attempt to discern such long-term trends contributing to recently measured imbalances was made by Huybrechts (2002) and Huybrechts et al. (2004). They found little long-term trend in volume of the Greenland Ice Sheet, but a trend in antarctic shrinkage of about 90 Gt yr^{-1}, primarily because of retreat of the West Antarctic grounding line in response to the end of the last ice age. Models project that this trend will largely disappear over

Box 4.1: Ice Sheet Dynamics and Stability

The ice sheets of Antarctica and Greenland could raise sea level greatly. Central parts of these ice sheets have been observed to change only slowly, but near the coast rapid changes over quite large areas have been observed. In these areas, uncertainties about glacier basal conditions, ice deformation and interactions with the surrounding ocean seriously limit the ability to make accurate projections.

Ice sheets are thick, broad masses of ice formed mainly from compaction of snow (Paterson, 2004). They spread under their own weight, transferring mass towards their margins where it is lost primarily by runoff of surface melt water or by calving of icebergs into marginal seas or lakes. Water vapour fluxes (sublimation and condensation), and basal melting or freezing (especially beneath ice shelves) may also be important processes of mass gain and loss.

Ice sheets flow by internal deformation, basal sliding or a combination of both. Deformation in ice occurs through solid-state processes analogous to those involved in polycrystalline metals that are relatively close to their melting points. Deformation rates depend on the gravitational stress (which increases with ice thickness and with the slope of the upper surface), temperature, impurities, and size and orientation of the crystals (which in turn depend in part on the prior deformational history of the ice). While these characteristics are not completely known, model tuning allows slow ice flow by deformation to be simulated with reasonable accuracy.

For basal sliding to be an important component of the total motion, melt water or deformable wet sediment slurries at the base are required for lubrication. While the central regions of ice sheets (typically above 2,000 m elevation) seldom experience surface melting, the basal temperature may be raised to the melting point by heat conducted from the earth's interior, delivered by melt water transport, or from the 'friction' of ice motion. Sliding velocities under a given gravitational stress can differ by orders of magnitude, depending on the presence or absence of unconsolidated sediment, the roughness of the substrate and the supply and distribution of water. Basal conditions are well characterised in few regions, introducing important uncertainties to the modelling of basal motion.

Ice flow is often channelled into fast-moving ice streams (which flow between slower-moving ice walls) or outlet glaciers (with rock walls). Enhanced flow in ice streams arises either from higher gravitational stress linked to thicker ice in bedrock troughs, or from increased basal lubrication.

Ice flowing into a marginal sea or lake may break off immediately to form icebergs, or may remain attached to the ice sheet to become a floating ice shelf. An ice shelf moves forward, spreading and thinning under its own weight, and fed by snowfall on its surface and ice input from the ice sheet. Friction at ice shelf sides and over local shoals slows the flow of the ice shelf and thus the discharge from the ice sheet. An ice shelf loses mass by calving icebergs from the front and by basal melting into the ocean cavity beneath. Estimates based on available data suggest a 1°C ocean warming could increase ice shelf basal melt by 10 m yr^{-1}, but inadequate knowledge of the bathymetry and circulation in the largely inaccessible ice shelf cavities restricts the accuracy of such estimates.

Ice deformation is nonlinear, increasing approximately proportional to the cube of the applied stress. Moreover, an increase in any of the six independent applied stresses (three stretching stresses and three shear stresses) increases the deformation rate for all other stresses. For computational efficiency, most long simulations with comprehensive ice flow models use a simplified stress distribution, but recent changes in ice sheet margins and ice streams cannot be simulated accurately with these models, demonstrating a need for resolving the full stress configuration. Development of such models is still in its infancy, with few results yet available.

Ice sheets respond to environmental forcing over numerous time scales. A surface warming may take more than 10,000 years to penetrate to the bed and change temperatures there, while a crevasse filled with melt water might penetrate to the bed and affect the temperature locally within minutes. Ice velocity over most of an ice sheet changes slowly in response to changes in the ice sheet shape or surface temperature, but large velocity changes may occur rapidly on ice streams and outlet glaciers in response to changing basal conditions or changes in the ice shelves into which they flow.

The palaeo-record of previous ice ages indicates that ice sheets shrink in response to warming and grow in response to cooling. The data also indicate that shrinkage can be far faster than growth. Understanding of the processes suggests that this arises both because surface melting rates can be much larger than the highest snowfall rates, and because ice discharge may be accelerated by strong positive feedbacks (Paterson, 1994; P.U. Clark et al., 1999). Thawing of the bed, loss of restraint from ice shelves or changes in melt water supply and transmission can increase flow speed greatly. The faster flow may then generate additional lubrication from frictional heating and from erosion to produce wet sediment slurries. Surface lowering as the faster flow thins the ice will enhance surface melting, and will reduce basal friction where the thinner ice becomes afloat. Despite competition from stabilising feedbacks, warming-induced changes have led to rapid shrinkage and loss of ice sheets in the past, with possible implications for the future.

the next millennium. In tests of the sensitivity of this result to various model parameters, Huybrechts (2002) found a modern thinning trend in most simulations but an opposite trend in one; in addition, simulated trends for today depend on the poorly known timing of retreat in West Antarctica. Moreover, the ice flow model responds too slowly to some forcings owing to the coarse model grid and lack of some stresses and processes (see Section 4.6.3.3), perhaps causing the modelled long-term trend to end more slowly than it should.

The recent ice flow accelerations discussed in Section 4.6.3.3 are likely to be sufficient to explain much or all of the estimated antarctic mass imbalance, and ice flow and surface mass balance changes are sufficient to explain the mass imbalance in Greenland. This points to little or no contribution from long-term trends to modern ice sheet balance, although with considerable uncertainties.

4.6.3.3 Dynamic Response to Recent Forcing

Numerous papers since IPCC (2001) have documented rapid changes in marginal regions of the ice sheets. Attention has especially focused on increased flow velocity of glaciers along the Antarctic Peninsula (Scambos et al., 2004; Rignot et al., 2004, 2005), the glaciers draining into Pine Island Bay and nearby parts of the Amundsen Sea from West Antarctica (Shepherd et al., 2004; Thomas et al., 2004) and Greenland's Jakobshavn Glacier (Thomas et al., 2003; Joughin et al., 2004) and other glaciers south of about 70°N (Howat et al., 2005; Rignot and Kanagaratnam, 2006). Accelerations may have occurred in some coastal parts of East Antarctica (Zwally et al., 2006), and ice flow deceleration has been observed on Whillans and Bindschadler Ice Streams on the Siple Coast of West Antarctica (Joughin and Tulaczyk, 2002). Rignot and Kanagaratnam (2006) estimated that ice discharge increase in Greenland caused mass loss in 2005 to be about 100 Gt yr^{-1} larger than in 1996; consideration of the changes in the Amundsen Sea and Antarctic Peninsula regions of West Antarctica (and the minor opposing trend on Whillans and Bindschadler Ice Streams) suggests an antarctic signal of similar magnitude, although with greater uncertainty and occurring perhaps over a longer interval (Joughin and Tulaczyk, 2002; Thomas et al., 2004; Rignot et al., 2005; van den Broeke et al., 2006).

Most of the other coastal changes appear to have involved inland acceleration following reduction or loss of ice shelves. Very soon after breakup of the Larsen B Ice Shelf along the Antarctic Peninsula, the speeds of tributary glaciers increased up to eight-fold, but with little change in velocity of adjacent ice still buttressed by the remaining ice shelf (Rignot et al., 2004; Scambos et al., 2004). Thinning and breakup of the floating ice tongue of Jakobshavn Glacier were accompanied by approximate doubling of the ice flow velocity (Thomas et al., 2003; Joughin et al., 2004; Thomas, 2004). Ice shelf thinning has occurred with the acceleration of tributary glaciers entering the Amundsen Sea (Shepherd et al., 2002, 2004; Joughin et al., 2003).

Because of drag between ice shelves and embayment sides or localised re-grounding points on seabed topographic highs, shortening or thinning of ice shelves is expected to accelerate ice flow (Thomas, 1979), with even small ice shelves potentially important (Dupont and Alley, 2006). Targeted models addressing acceleration of particular glaciers in response to ice shelf reduction are capable of simulating the observed time scales (notable changes in years or less) and patterns of change (largest thinning and acceleration near the coast, decreasing inland and following ice streams; Payne et al., 2004; Dupont and Alley, 2005). Comprehensive model runs for ice sheet behaviour over the last century, using known forcings and flow processes but omitting full stress coupling with ice shelves and poorly known details of oceanographic changes beneath the ice shelves, match overall ice sheet trends rather well (Huybrechts et al., 2004) but fail to show these rapid marginal thinning events. This suggests that the changes are in response to processes (either forcings from ocean temperature or ocean circulation changes, or ice flow processes) not included in the comprehensive modelling, or that the coarse spatial resolution of the comprehensive models slows their simulated response rates enough to be important.

The acceleration of Helheim Glacier in Greenland may be akin to changes linked to ice shelves. Enhanced calving may have removed not-quite-floating ice at Helheim, reducing restraint on the remaining ice and allowing faster flow (Howat et al., 2005).

Other ice flow changes have occurred that are not linked to ice shelf reduction. The changes in Siple Coast, Antarctica, likely reflect inherent flow variability rather than recent forcing (Parizek et al., 2003). Zwally et al. (2002) showed for one site near the equilibrium line on the west coast of Greenland that the velocity of comparatively slow-moving ice increased just after the seasonal onset of drainage of surface melt water into the ice sheet, and that greater melt water input produced greater ice flow acceleration. The total acceleration was not large (of the order of 10%), but the effect is not included in most ice flow models. Inclusion in one model (Parizek and Alley, 2004) somewhat increased the sensitivity of the ice sheet to various specified warmings, mostly beyond the year 2100. Much uncertainty remains, especially related to whether fast-moving glaciers and ice streams are similarly affected, and whether access of melt water to the bed through more than 1 km of cold ice would migrate inland if warming caused surface melting to migrate inland (Alley et al., 2005b). This could thaw ice that is frozen to the bed, allowing faster flow through enhanced basal sliding or sub-glacial sediment deformation. Data are not available to assess whether effects of increased surface melting in Greenland have been transmitted to the bed and contributed to ice flow acceleration.

4.6.3.4 Melting and Calving of Ice Shelves

Many of the largest and fastest ice sheet changes thus appear to be at least in part responses to ice shelf shrinkage or loss. Although ice shelf shrinkage does not directly contribute to sea level change because shelf ice is already floating, the very tight coupling to inland ice means that ice shelf balance does matter to sea level. The available data suggest that the ice shelf changes have resulted from environmental warming, with both oceanic and atmospheric temperatures important, although changes in oceanic circulation cannot be ruled out as important contributors.

The southward-progressing loss of ice shelves along the Antarctic Peninsula is consistent with a thermal limit to ice shelf viability (Morris and Vaughan, 2003). Cook et al. (2005) found that no ice shelves exist on the warmer side of the –5°C mean annual isotherm, whereas no ice shelves on the colder side of the –9°C isotherm have broken up. Before the 2002 breakup of the Larsen B Ice Shelf, local air temperatures had increased by more than 1.5°C over the previous 50 years (Vaughan et al., 2003), increasing summer melting and formation of large melt ponds on the ice shelf. These likely contributed to breakup by draining into and wedging open surface crevasses that linked to bottom crevasses filled with seawater (Scambos et al., 2000). Large ice flow models do not accurately capture the physical processes involved in such dramatic iceberg calving, or in more common calving behaviour.

Despite an increased ice supply from tributary glaciers, thinning of up to several metres per year has been measured for ice shelves on the Amundsen Sea coastline in the absence of large surface mass balance changes. This suggests that increased basal ice melting is responsible for the thinning (Shepherd et al., 2003, 2004). Similarly, the 15-km floating ice tongue of Jakobshavn Glacier survived air temperatures during the 1950s similar to or even warmer than those associated with thinning and collapse near the end of the 20th century, implicating oceanic heat transport in the more recent changes, although air temperature increases may have contributed (Thomas et al., 2003).

The basal mass balance of an ice shelf depends on temperature and ocean circulation beneath it. Isolation from direct wind forcing means that the main drivers of circulation below an ice shelf are tidal and density (thermohaline) forces. Lack of knowledge of sub-ice bathymetry has hampered the use of three-dimensional models to simulate circulation beneath the thinning ice shelves. Both the west side of the Antarctic Peninsula and the Amundsen Sea coast are exposed to warm Circumpolar Deep Water (CDW; Hellmer et al., 1998), capable of causing rapid ice shelf basal melting. Increased melting in the Amundsen Sea is consistent with observed recent warming by 0.2°C of ocean waters seaward of the continental shelf break (Jacobs et al., 2002; Robertson et al., 2002). Simple regression analysis of available data including those from the Amundsen Sea indicated that 1°C warming of waters below an ice shelf increases basal melt rate by about 10 m yr^{-1} (Shepherd et al., 2004).

4.7 Changes in Frozen Ground

4.7.1 Background

Frozen ground, in a broad sense, includes near-surface soil affected by short-term freeze-thaw cycles, seasonally frozen ground and permafrost. In terms of areal extent, frozen ground is the single largest component of the cryosphere. The presence of frozen ground depends on the ground temperature, which is controlled by the surface energy balance. While the climate is an important factor determining the distribution of frozen ground, local factors are also important, such as vegetation conditions, snow cover, physical and thermal properties of soils and soil moisture conditions. The permafrost temperature regime is a sensitive indicator of decadal to centennial climatic variability (Lachenbruch and Marshall, 1986; Osterkamp, 2005). Thawing of ice-rich permafrost can lead to subsidence of the ground surface as masses of ground ice melt and to the formation of uneven topography know as thermokarst, generating dramatic changes in ecosystems, landscape and infrastructure performance (Nelson et al., 2001; Walsh et al., 2005). Surface soil freezing and thawing processes play a significant role in the land surface energy and moisture balance, hence in climate and hydrologic systems. The primary controls on local hydrological processes in northern regions are the presence or absence of permafrost and the thickness of the active layer (Hinzman et al., 2003). Changes in soil seasonal freeze-thaw processes have a strong influence on spatial patterns, seasonal to interannual variability, and long-term trends in terrestrial carbon budgets and surface-atmosphere trace gas exchange, both directly through biophysical controls on photosynthesis and respiration and indirectly through controls on soil nutrient availability.

4.7.2 Changes in Permafrost

4.7.2.1 Data Sources

Although there are some earlier measurements, systematic permafrost temperature monitoring in Russia started in the 1950s at hydrometeorological stations to depths of up to 3.2 m (Zhang et al., 2001) and in boreholes greater than 100 m deep (Pavlov, 1996). Permafrost temperatures in northern Alaska have been measured from deep boreholes (generally >200 m) since the 1940s (Lachenbruch and Marshall, 1986) and from shallow boreholes (generally <80 m) since the mid-1980s (Osterkamp, 2005). Some permafrost temperature measurements on the Tibetan Plateau were conducted in the early 1960s, while continuous permafrost monitoring only started in the late 1980s (Zhao et al., 2003). Monitoring of permafrost temperatures mainly started in the early 1980s in northern Canada (S.L. Smith et al., 2005) and in the 1990s in Europe (Harris et al., 2003).

4.7.2.2 Changes in Permafrost Temperature

Permafrost in the NH has typically warmed in recent decades (Table 4.5), although at a few sites there was little warming or even a cooling trend. For example, measurements (Osterkamp, 2003) and modelling results (see Hinzman et al., 2005; Walsh et al., 2005) indicate that permafrost temperature has increased by up to 2°C to 3°C in northern Alaska since the 1980s. Changes in air temperature alone over the same period cannot account for the permafrost temperature increase, and so changes in the insulation provided by snow may be responsible for some of the change (Zhang, 2005). Data from the northern Mackenzie Valley in the continuous permafrost zone show that permafrost temperature between depths of 20 to 30 m has increased about 1°C in the 1990s (S.L. Smith et al., 2005), with smaller changes in the central Mackenzie Valley. There is no significant trend in temperatures at the top of permafrost in the southern Mackenzie Valley, where permafrost is thin (less than 10 to 15 m thick) and warmer than –0.3°C (S.L. Smith et al., 2005, Couture et al., 2003). The absence of a trend is likely due to the absorption of latent heat required to melt ice. Similar results are reported for warm permafrost in the southern Yukon Territory (Haeberli and Burn, 2002). Cooling of permafrost was observed from the late 1980s to the early 1990s at a depth of 5 m at Iqaluit in the eastern Canadian Arctic. This cooling, however, was followed by warming of 0.4°C yr^{-1} between 1993 and 2000 (S.L. Smith

Table 4.5. *Recent trends in permafrost temperature (updated from Romanovsky et al., 2002 and Walsh et al., 2005).*

Region	Depth (m)	Period of Record	Permafrost Temperature Change (°C)	Reference
United States				
Northern Alaska	~1	1910s–1980s	2–4	Lachenbruch and Marshall, 1986
Northern Alaska	20	1983–2003	2–3	Osterkamp, 2005
Interior of Alaska	20	1983–2003	0.5–1.5	Osterkamp, 2005
Canada				
Alert, Nunavut	15	1995–2000	0.8	S.L. Smith et al., 2003
Northern Mackenzie Valley	20–30	1990–2002	0.3–0.8	S.L. Smith et al., 2005
Central Mackenzie Valley	10–20	Mid-1980s–2003	0.5	S.L. Smith et al., 2005
Southern Mackenzie Valley & Southern Yukon Territory	~20	Mid-1980s–2003	0	Haeberli and Burn, 2002
Northern Quebec	10	Late 1980s–mid-1990s	<–1	Allard et al., 1995
Northern Quebec	10	1996–2001	1.0	DesJarlais, 2004
Lake Hazen	2.5	1994–2000	1.0	Broll et al., 2003
Iqaluit, Eastern Canadian Arctic	5	1993–2000	2.0	S.L. Smith et al., 2005
Russia				
East Siberia	1.6–3.2	1960–2002	~1.3	Walsh et al., 2005
Northern West Siberia	10	1980–1990	0.3–0.7	Pavlov, 1996
European north of Russia, continuous permafrost zone	6	1973–1992	1.6–2.8	Pavlov, 1996
Northern European Russia	6	1970–1995	1.2–2.8	Oberman and Mazhitova, 2001
Europe				
Juvvasshoe, Southern Norway	~3	Past 30–40 years	0.5–1.0	Isaksen et al., 2001
Janssonhaugen, Svalbard	~2	Past 60–80 years	1–2	Isaksen et al., 2001
Murtel-Corvatsch	11.5	1987–2001	1.0	Vonder Muhll et al., 2004
China				
Tibetan Plateau	~10	1970s–1990s	0.2–0.5	Zhao et al., 2004
Qinghai-Xizang Highway	3–5	1995–2002	Up to 0.5	Wu and Liu, 2003; Zhao et al., 2004
Tianshan Mountains	16–20	1973–2002	0.2–0.4	Qiu et al., 2000; Zhao et al., 2004
Da Hinggan Mountains, Northeastern China	~2	1978–1991	0.7–1.5	Zhou et al., 1996

et al., 2005). This trend is similar to that observed in Northern Quebec, where permafrost cooling was observed between the mid-1980s and mid-1990s at a depth of 10 m (Allard et al., 1995) followed by warming beginning in 1996 (Brown et al., 2000). Warming of permafrost at depths of 15 to 30 m since the mid-1990s has also been observed in the Canadian High Arctic (Smith et al., 2003).

There is also evidence of permafrost warming in the Russian Arctic. Permafrost temperature increased approximately 1°C at depths between 1.6 and 3.2 m from the 1960s to the 1990s in East Siberia, about 0.3°C to 0.7°C at a depth of 10 m in northern West Siberia (Pavlov, 1996) and about 1.2°C to 2.8°C at a depth of 6 m from 1973 through 1992 in northern European Russia (Oberman and Mazhitova, 2001). Fedorov and Konstantinov (2003) reported that permafrost temperatures from three central Siberian stations did not show an apparent trend between 1991 and 2000. Mean annual temperature in Central Mongolia at depths from 10 to 90 m increased 0.05°C to 0.15°C per decade over 30 years (Sharkhuu, 2003).

At the Murtèl-Corvatsch borehole in the Swiss Alps, permafrost temperatures in 2001 and 2003, at a depth of 11.5 m in ice-rich frozen debris, were only slightly below –1°C, and were the highest since readings began in 1987 (Vonder Mühll et al., 2004). Analysis of the long-term thermal record from this site has shown that in addition to summer air temperatures, the depth and duration of snow cover, particularly in early winter, have a major influence on permafrost temperatures (Harris et al., 2003). Results from six years of ground temperature monitoring at Janssonhaugen, Svalbard, indicate that the permafrost has warmed at a rate of about 0.5°C per decade at a depth of 20 m (Isaksen et al., 2001). Results from Juvvasshøe, in southern Norway, indicate that ground temperature has increased by about 0.3°C at a depth of 15 m from 1999 to 2006. At both these sites, wind action prevents snow accumulation in winter and so a close relationship is observed between air, ground surface and ground subsurface temperatures, which makes the geothermal records from Janssonhaugen and Juvvasshøe more direct indicators of climate change.

Permafrost temperature increased about 0.2°C to 0.5°C from the 1970s to 1990s over the hinterland of the Tibetan Plateau (Zhao et al., 2003), up to 0.5°C along the Qinghai-Xizang Highway over a period from 1995 to 2002 (Wu and Liu, 2003; Zhao et al., 2004) and about 0.2°C to 0.4°C from 1973 to 2002 at depths of 16 to 20 m in Tianshan Mountain regions (Qiu et al., 2000; Zhao et al., 2004). Over the Da Hinggan Mountains in north-eastern China, permafrost surface temperature increased about 0.7°C to 1.5°C over a period from 1978 through 1991 from the valley bottom to the north-facing slopes (Zhou et al., 1996). Permafrost temperature at the depth of the zero annual temperature variation increased about 2.1°C on the valley bottom, 0.7°C on the north-facing slopes and 0.8°C on south-facing slopes. In areas of the south-facing slopes where no permafrost exists, soil temperature at depths of 2 to 3 m increased about 2.4°C (Zhou et al., 1996).

4.7.2.3 Permafrost Degradation

Permafrost degradation refers to a naturally or artificially caused decrease in the thickness and/or areal extent of permafrost. Evidence of change in the southern boundary of the discontinuous permafrost zone in the past decades has been reported. In North America, the southern boundary has migrated northward in response to warming since the Little Ice Age, and continues to do so today (Halsey et al., 1995). In recent years, widespread permafrost warming and thawing have occurred on the Tibetan Plateau, China. Based on data from ground penetration radar and *in situ* measurements, the lower limit of permafrost has moved upward about 25 m from 1975 through 2002 on the north-facing slopes of the Kunlun Mountains (Nan et al., 2003). From Amdo to Liangdehe along the Qinghai-Xizang Highway on the Tibetan Plateau, areal extent of permafrost islands decreased approximately 36% over the past three decades (Wang, 2002). Areal extent of taliks (areas of unfrozen ground within permafrost) expanded about 1.2 km on both sides of the Tongtian River (Wang, 2002). Overall, the northern limit of permafrost retreated about 0.5 to 1.0 km southwards and the southern limit moved northwards about 1.0 to 2.0 km along the Qinghai-Xizang (Tibet) Highway (Wang and Zhao, 1997; Wu and Liu, 2003).

When the warming at the top of permafrost eventually penetrates to the base of permafrost and the new surface temperature remains stable, thawing at the base of the ice-bearing permafrost occurs (i.e., basal thawing), especially for thin discontinuous permafrost. At Gulkana, Alaska, permafrost thickness is about 50 to 60 m and the basal thawing of permafrost has averaged 0.04 m yr^{-1} since 1992 (Osterkamp, 2003). Over the Tibetan Plateau, basal thawing of 0.01 to 0.02 m yr^{-1} was observed since the 1960s in permafrost of less than 100 m thickness (Zhao et al., 2003). It is expected that the basal thawing rate will accelerate over the Tibetan Plateau as the permafrost surface continues to warm.

If ice-rich permafrost thaws, the ground surface subsides. This downward displacement of the ground surface is called thaw settlement. Typically, thaw settlement does not occur uniformly and so yields a chaotic surface with small hills and wet depressions known as thermokarst terrain; this is particularly common in areas underlain by ice wedges. On slopes, thawing of ice-rich, near-surface permafrost layers can create mechanical discontinuities in the substrate, leading to active-layer detachment slides (Lewkowicz, 1992), which have the capacity to damage structures similar to other types of rapid mass movements. Thermokarst processes pose a serious threat to arctic biota through either oversaturation or drying (Hinzman et al., 2005; Walsh et al., 2005). Extensive thermokarst development has been discovered near Council, Alaska (Yoshikawa and Hinzman, 2003) and in central Yakutia (Gavrilov and Efremov, 2003). Significant expansion and deepening of thermokarst lakes were observed near Yakutsk (Fedorov and Konstantinov, 2003) between 1992 and 2001. The largest subsidence rates of 17 to 24 cm yr^{-1} were observed

in depressions holding young thermokarst lakes. Satellite data reveal that in the continuous permafrost zone of Siberia, total lake area increased by about 12% and lake number rose by 4% during the past three decades (L.C. Smith et al., 2005). Over the discontinuous permafrost zone, total area and lake number decreased by up to 9% and 13%, respectively, probably due to lake water drainage through taliks.

The most sensitive regions of permafrost degradation are coasts with ice-bearing permafrost that are exposed to the Arctic Ocean. Mean annual erosion rates vary from 2.5 to 3.0 m yr^{-1} for the ice-rich coasts to 1.0 m yr^{-1} for the ice-poor permafrost coasts along the Russian Arctic Coast (Rachold et al., 2003). Over the Alaskan Beaufort Sea Coast, mean annual erosion rates range from 0.7 to 3.2 m yr^{-1} with maximum rates up to 16.7 m yr^{-1} (Jorgenson and Brown, 2005).

4.7.2.4 Subsea Permafrost

Subsea (or offshore) permafrost refers to permafrost occurring beneath the seabed. It exists in continental shelves of the polar regions. Subsea permafrost formed either in response to the negative mean annual sea-bottom temperature or as the result of sea level rise so that terrestrial permafrost was covered by seawater. Although the potential release of methane trapped within subsea permafrost may provide a positive feedback to climate warming, available observations do not permit an assessment of changes that might have occurred.

4.7.3 Changes in Seasonally Frozen Ground

Seasonally frozen ground refers to a soil layer that freezes and thaws annually regardless of whether there is underlying permafrost. It includes both seasonal soil freeze-thaw in non-permafrost regions and the active layer over permafrost. Significant changes in seasonally frozen ground have been observed worldwide.

4.7.3.1 Changes in the Active Layer

The active layer is that portion of the soil above permafrost that thaws and freezes seasonally. It plays an important role in cold regions because most ecological, hydrological, biogeochemical and pedogenic (soil-forming) activity takes place within it (Kane et al., 1991; Hinzman et al., 2003). Changes in active layer thickness are influenced by many factors, including surface temperature, physical and thermal properties of the surface cover and substrate, vegetation, soil moisture and duration and thickness of snow cover (Brown et al., 2000; Frauenfeld et al., 2004; Zhang et al., 2005). The interannual and spatial variations in thaw depth at point locations can be large, an artefact of year-to-year and microtopographic variations in both surface

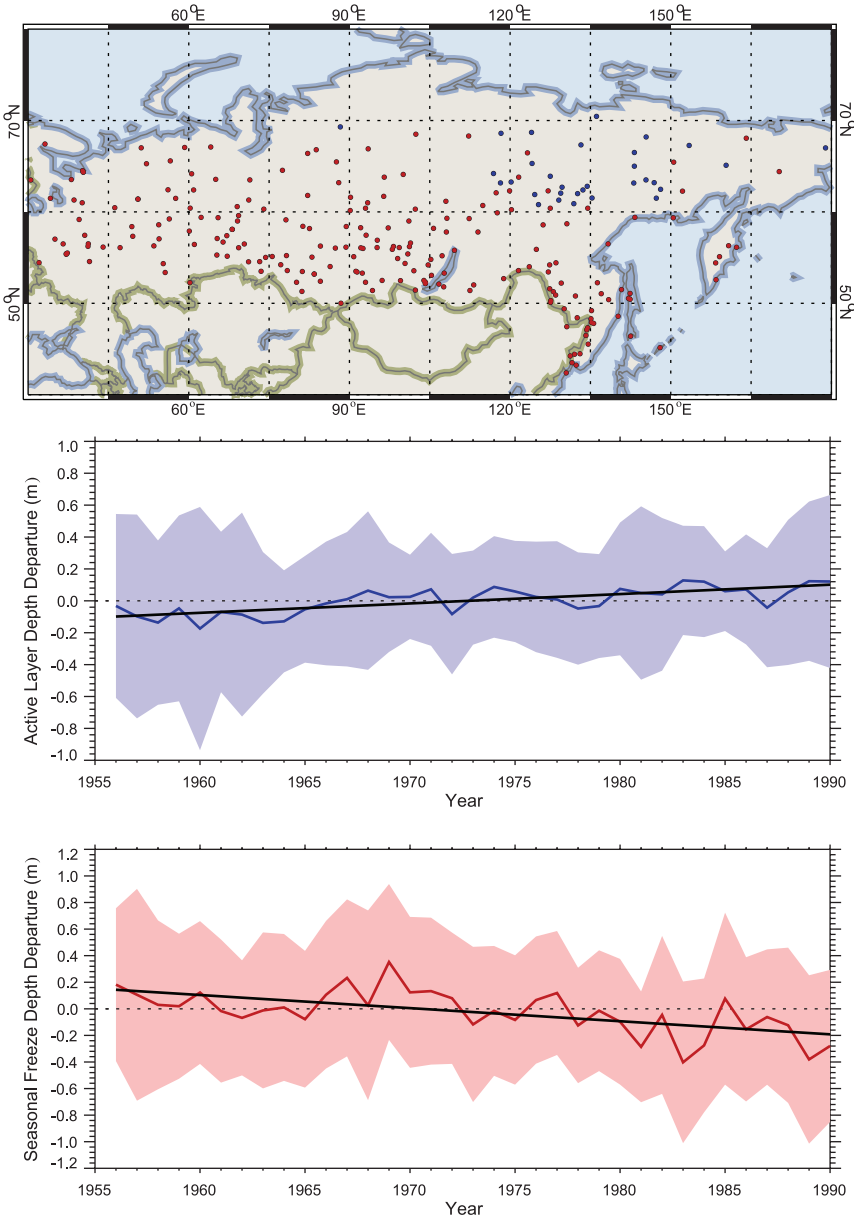


Figure 4.20. *Variations in the thickness of the active layer over permafrost (middle) and maximum soil freeze depth in non-permafrost areas (bottom) in Russia from 1956 through 1990. Active layer thickness has increased by about 20 cm while seasonal freeze depth has decreased by about 34 cm over the period of record (black lines in middle and lower panels). The anomaly in active layer thickness (blue line) is an average of anomalies from 31 stations (blue dots in the top panel) after removing the mean over the period of record for each station. The anomaly in maximum soil freeze depth (red line) is an average of anomalies from 211 stations (red dots in the top panel) after removing the mean over the period of record for each station. The shaded area represents the 5 to 95% confidence interval from the mean for each year, and the dashed line is the zero reference (from Frauenfeld et al., 2004).*

temperature and soil moisture, and so presents monitoring challenges. When the other conditions remain constant, changes in active layer thickness could be expected to increase in response to climate warming, especially in summer.

Long-term monitoring of the active layer has been conducted over the past several decades in Russia. By the early 1990s, there were about 25 stations, each containing 8 to 10 plots and 20 to 30 boreholes to a depth of 10 to 15 m (Pavlov, 1996). Measurements of soil temperature in the active layer and permafrost at depths up to 3.20 m have been carried out in Russia from 31 hydrometeorological stations, most of them started in the 1950s but a few as early as in the 1930s (Figure 4.20). Active layer thickness can be estimated using these daily soil temperature measurements. Over the period 1956 to 1990, the active layer exhibited a statistically significant deepening of about 21 cm. Increases in summer air temperature and winter snow depth are responsible for the increase in active layer thickness.

Monitoring of the active layer was developed at a global scale in the 1990s and currently incorporates more than 125 sites in the Arctic, the Antarctic and several mid-latitude mountain ranges (Brown et al., 2000; Nelson, 2004a,b; Figure 4.21). These sites were designed to observe the response of the active layer and near-surface permafrost to climate change. The results from northern high-latitude sites demonstrate substantial interannual and inter-decadal fluctuations in active layer thickness in response to air temperature variations. During the mid- to late 1990s in Alaska and north-western Canada, maximum and minimum thaw depths were observed in 1998 and in 2000, corresponding to the warmest and coolest summers, respectively. There is evidence of an increase in active layer thickness and thermokarst development, indicating degradation of warmer permafrost (Brown et al., 2000). Evidence from European monitoring sites indicates that active layer thickness has been the greatest in the summers of 2002 and 2003, approximately 20% greater than in previous years (Harris et al., 2003). Active layer thickness has increased by up to 1.0 m along the Qinghai-Xizang Highway over the Tibetan Plateau since the early 1980s (Zhao et al., 2004).

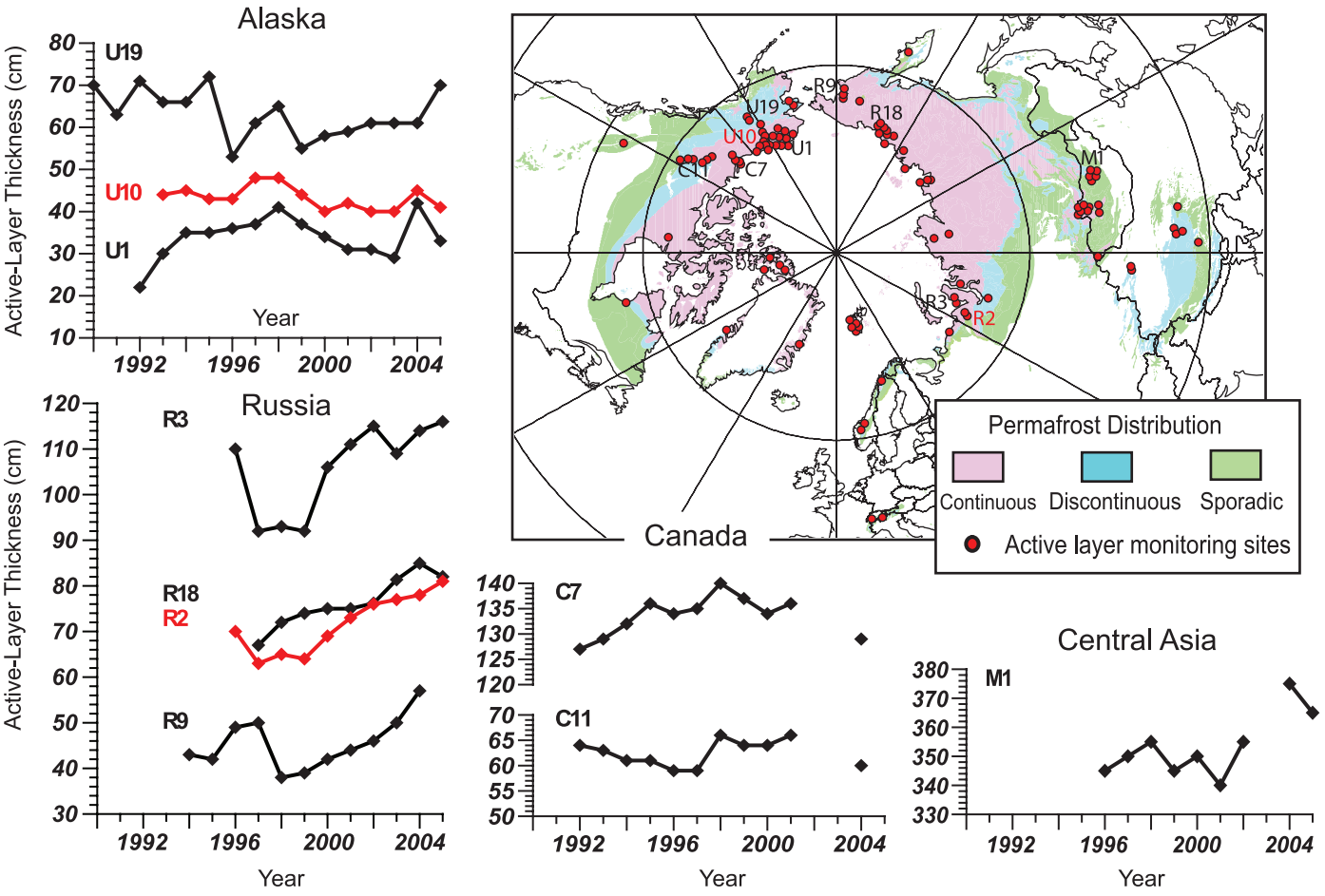


Figure 4.21. *Locations of sites and changes in active layer thickness from selected sites (after Nelson, 2004a,b).*

4.7.3.2 Seasonally Frozen Ground in Non-Permafrost Areas

The thickness of seasonally frozen ground has decreased by more than 0.34 m from 1956 through 1990 in Russia (Figure 4.20), primarily controlled by the increase in winter air temperature and snow depth (Frauenfeld et al., 2004). Over the Tibetan Plateau, the thickness of seasonally frozen ground has decreased by 0.05 to 0.22 m from 1967 through 1997 (Zhao et al., 2004). The driving force for the decrease in thickness of the seasonally frozen ground is the significant warming in cold seasons, while changes in snow depth play a minor role. The duration of seasonally frozen ground decreased by more than 20 days from 1967 through 1997 over the Tibetan Plateau, mainly due to the earlier onset of thaw in spring (Zhao et al., 2004).

The estimated maximum extent of seasonally frozen ground has decreased by about 7% in the NH from 1901 to 2002, with a decrease in spring of up to 15% (Figure 4.22; Zhang et al., 2003). There was little change in the areal extent of seasonally frozen ground during the early and midwinters.

4.7.3.3 Near-Surface Soil Freeze-Thaw Cycle

Satellite remote sensing data have been used to detect the near-surface soil freeze-thaw cycle at regional and hemispheric scales. Evidence from the satellite record indicates that the onset dates of thaw in spring and freeze in autumn advanced five to seven days in Eurasia over the period 1988 to 2002, leading to an earlier start to the growing season but no change in its length (Smith et al., 2004). In North America, a trend towards later freeze dates in autumn by about five days led, in part, to a lengthening of the growing season by eight days. Overall, the timing of seasonal thawing and subsequent initiation of the growing season in early spring has advanced by approximately eight days from 1988 to 2001 for the pan-arctic basin and Alaska (McDonald et al., 2004).

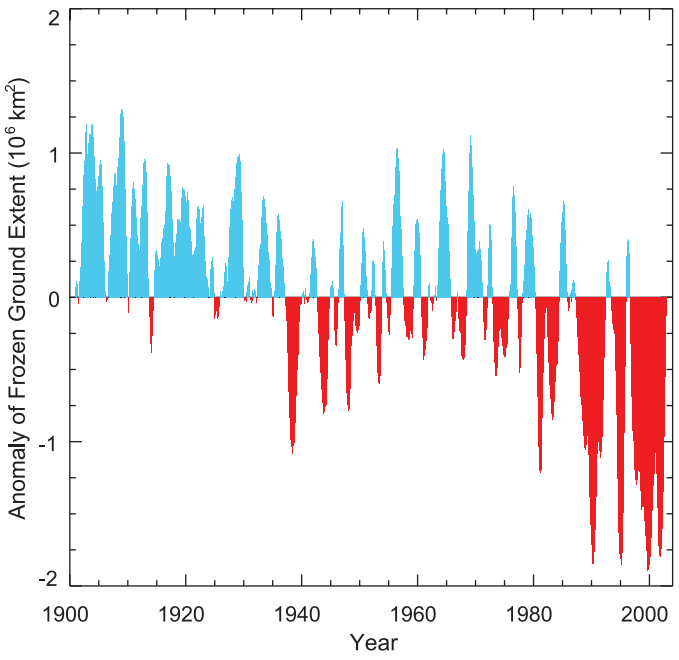


Figure 4.22. *Historical variations in the monthly areal extent (10^6 km^2) of seasonally frozen ground (including the active layer over permafrost) for the period from 1901 through 2002 in the NH. The positive anomaly (blue) represents above-average monthly extent, while the negative anomaly (red) represents below-average extent. The time series is smoothed with a low-pass filter (after Zhang et al., 2003).*

4.8 Synthesis

Observations show a consistent picture of surface warming and reduction in all components of the cryosphere (FAQ 4.1, Figure 1),[1] except antarctic sea ice, which exhibits a small positive but insignificant trend since 1978 (Figure 4.23).

Since IPCC (2001) the cryosphere has undergone significant changes, such as the substantial retreat of arctic sea ice, especially in summer; the continued shrinking of mountain glaciers; the decrease in the extent of snow cover and seasonally frozen ground, particularly in spring; the earlier breakup of river and lake ice; and widespread thinning of antarctic ice shelves along the Amundsen Sea coast, indicating increased basal melting due to increased ocean heat fluxes in the cavities below the ice shelves. An additional new feature is the increasingly visible fast dynamic response of ice shelves, for example, the dramatic breakup of the Larsen B Ice Shelf in 2002, and the acceleration of tributary glaciers and ice streams, with possible consequences for the adjacent part of the ice sheets.

One difficulty with using cryospheric quantities as indicators of climate change is the sparse historical database. Although 'extent' of ice (sea ice and glacier margins for example) has been observed for a long time at a few locations, the 'amount' of ice (thickness or depth) is difficult to measure. Therefore, reconstructions of past mass balance are often not possible.

Table 4.6. *Estimates of cryospheric contributions to sea level change.*

Cryospheric component	Sea Level Equivalent (mm yr^{-1}) 1961–2003	1993–2003
Glaciers and Ice Caps	+0.32 to +0.68	+0.55 to +0.99
Greenland	–0.07 to +0.17	+0.14 to +0.28
Antarctica	–0.28 to +0.55	–0.14 to +0.55
Total (adding ranges)	–0.03 to +1.40	+0.55 to +1.82
Total (Gaussian error summation)	+0.22 to +1.15	+0.77 to +1.60

[1] Surface air temperature data are updated from Jones and Moberg, 2003; sea ice data are updated from Comiso, 2003; frozen ground data are from Zhang et al., 2003; snow cover data are updated from Brown et al., 2000; glacier mass balance data are from Ohmura, 2004; Cogley, 2005; and Dyurgerov and Meier, 2005.

The most important cryospheric contributions to sea level variations (see Chapter 5) arise from changes in the ice on land (e.g., glaciers, ice caps and ice sheets). In IPCC (2001), the contribution of glaciers and ice caps to sea level rise during the 20th century was estimated as 0.2 to 0.4 mm yr^{-1} (of 1 to 2 mm yr^{-1} total sea level rise). New results presented here indicate that all glaciers contributed about 0.50 ± 0.18 mm yr^{-1} during 1961 to 2003, increasing to 0.77 ± 0.22 mm yr^{-1} from 1993 to 2003 (interpolation from five-year analyses in Table 4.4). Estimates for both ice sheets combined give a contribution ranging from –0.35 to +0.72 mm yr^{-1} for 1961 to 2003, increasing to 0 to 0.8 mm yr^{-1} for 1993 to 2003. A conservative error estimate in terms of summing ranges is given in Table 4.6. Assuming a midpoint mean, interpreting the range as uncertainty and using Gaussian error summation of estimates for glaciers and both ice sheets suggests that the total ice contribution to sea level rise was approximately 0.7 ± 0.5 mm yr^{-1} during 1961 to 2003 and 1.2 ± 0.4 mm yr^{-1} during 1993 to 2003.

The large uncertainties reflect the difficulties in estimating the global ice mass and its variability, because global monitoring of ice thickness is impossible (even the total area of glaciers is not exactly known) and extrapolation from local measurements is therefore necessary. A regional extension of the monitored ice masses and an improvement of measurement and extrapolation techniques are urgently required.

In spite of the large uncertainties, the data that are available portray a rather consistent picture of a cryosphere in decline over the 20th century, increasingly so during 1993 to 2003.

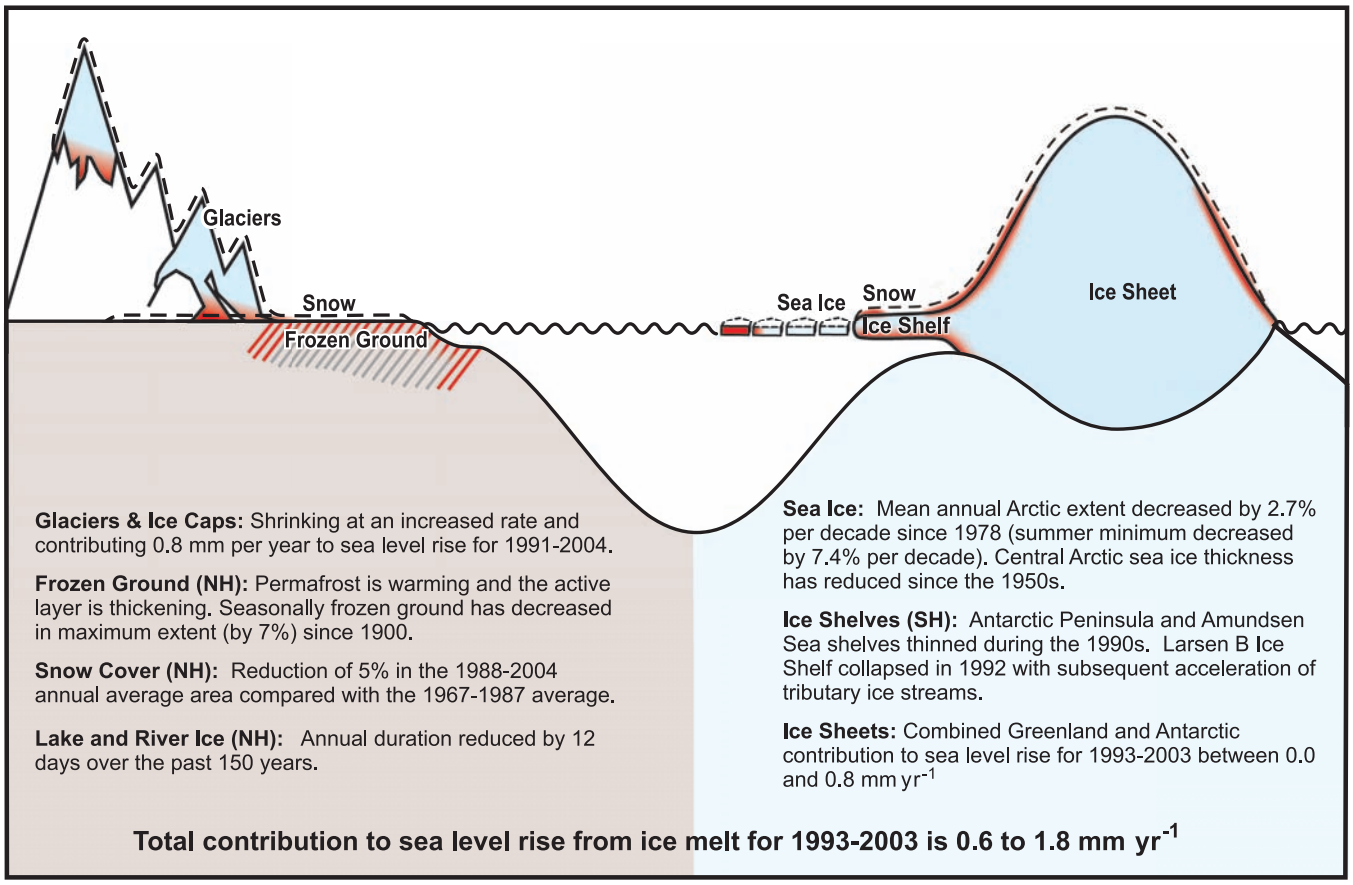


Figure 4.23. *Summary of observed variations in the cryosphere.*

Frequently Asked Question 4.1

Is the Amount of Snow and Ice on the Earth Decreasing?

Yes. Observations show a global-scale decline of snow and ice over many years, especially since 1980 and increasing during the past decade, despite growth in some places and little change in others (Figure 1). Most mountain glaciers are getting smaller. Snow cover is retreating earlier in the spring. Sea ice in the Arctic is shrinking in all seasons, most dramatically in summer. Reductions are reported in permafrost, seasonally frozen ground and river and lake ice. Important coastal regions of the ice sheets on Greenland and West Antarctica, and the glaciers of the Antarctic Peninsula, are thinning and contributing to sea level rise. The total contribution of glacier, ice cap and ice sheet melt to sea level rise is estimated as 1.2 ± 0.4 mm yr^{-1} for the period 1993 to 2003.

Continuous satellite measurements capture most of the Earth's seasonal snow cover on land, and reveal that Northern Hemisphere spring snow cover has declined by about 2% per decade since 1966, although there is little change in autumn or early winter. In many places, the spring decrease has occurred despite increases in precipitation.

Satellite data do not yet allow similarly reliable measurement of ice conditions on lakes and rivers, or in seasonally or permanently frozen ground. However, numerous local and regional reports have been published, and generally seem to indicate warming of permafrost, an increase in thickness of the summer thawed layer over permafrost, a decrease in winter freeze depth in seasonally frozen areas, a decrease in areal extent of permafrost and a decrease in duration of seasonal river and lake ice.

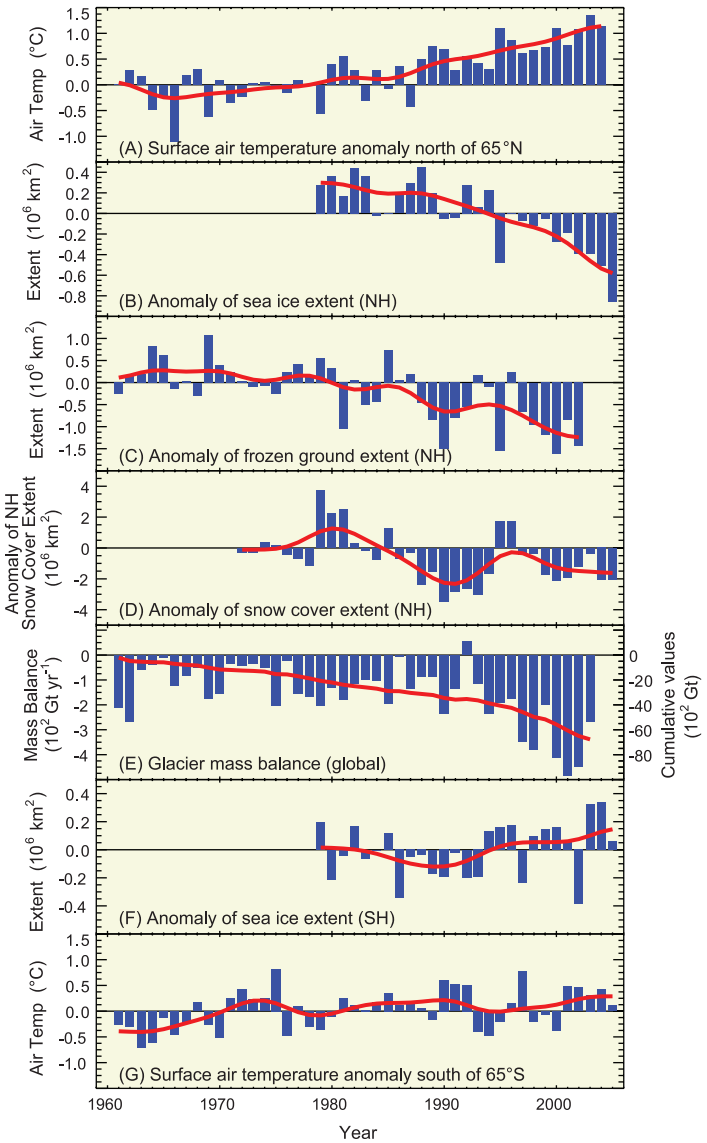
Since 1978, satellite data have provided continuous coverage of sea ice extent in both polar regions. For the Arctic, average annual sea ice extent has decreased by 2.7 ± 0.6% per decade, while summer sea ice extent has decreased by 7.4 ± 2.4% per decade. The antarctic sea ice extent exhibits no significant trend. Thickness data, especially from submarines, are available but restricted to the central Arctic, where they indicate thinning of approximately 40% between the period 1958 to 1977 and the 1990s. This is likely an overestimate of the thinning over the entire arctic region however.

Most mountain glaciers and ice caps have been shrinking, with the retreat probably having started about 1850. Although many Northern Hemisphere glaciers had a few years of near-balance around 1970, this was followed by increased shrinkage. Melting of glaciers and ice caps contributed 0.77 ± 0.22 mm yr^{-1} to sea level rise between 1991 and 2004

Taken together, the ice sheets of Greenland and Antarctica are very likely shrinking, with Greenland contributing about 0.2 ± 0.1 mm yr^{-1} and Antarctica contributing 0.2 ± 0.35 mm yr^{-1} to sea level rise over the period 1993 to 2003. There is evidence of accelerated loss through 2005. Thickening of high-altitude, cold regions of Greenland and East Antarctica, perhaps from increased snowfall, has been more than offset by thinning in coastal regions of Greenland and West Antarctica in response to increased ice outflow and increased Greenland surface melting.

Ice interacts with the surrounding climate in complex ways, so the causes of specific changes are not always clear. Nonetheless, it is an unavoidable fact that ice melts when the local temperature is

(continued)



FAQ 4.1, Figure 1. *Anomaly time series (departure from the long-term mean) of polar surface air temperature (A, G), arctic and antarctic sea ice extent (B, F), Northern Hemisphere (NH) frozen ground extent (C), NH snow cover extent (D) and global glacier mass balance (E). The solid red line in E denotes the cumulative global glacier mass balance; in the other panels it shows decadal variations (see Appendix 3.A).*

above the freezing point. Reductions in snow cover and in mountain glaciers have occurred despite increased snowfall in many cases, implicating increased air temperatures. Similarly, although snow cover changes affect frozen ground and lake and river ice, this does not seem sufficient to explain the observed changes, suggesting that increased local air temperatures have been important. Observed arctic sea ice reductions can be simulated fairly well in models driven by historical circulation and temperature changes. The observed increases in snowfall on ice sheets in some cold central regions, surface melting in coastal regions and sub-ice-shelf melting along many coasts are all consistent with warming. The geographically widespread nature of these snow and ice changes suggests that widespread warming is the cause of the Earth's overall loss of ice.

References

Abdalati, W., et al., 2001: Outlet glacier and margin elevation changes: Near-coastal thinning of the Greenland ice sheet. *J. Geophys. Res.*, **106**(D24), 33729–33741.

Abdalati, W., et al., 2004: Elevation changes of ice caps in the Canadian Arctic Archipelago. *J. Geophys. Res.*, **109**, F04007, doi:10.1029/2003JF000045.

Ackley, S., P. Wadhams, J.C. Comiso, and A.P. Worby, 2003: Decadal decrease of Antarctic sea ice extent inferred from whaling records revisited on the basis of historical and modern sea ice records. *Polar Res.*, **22**(1), 19–25.

Agnew, T. and S. Howell, 2003: The use of operational ice charts for evaluating passive microwave ice concentration data. *Atmos.-Ocean*, **41**(4), 317–331.

Agnew, T., H. Le, and T. Hirose, 1997: Estimation of large-scale sea-ice motion from SSM/I 85.5 GHz imagery. *Ann. Glaciol.*, **25**, 305–311.

Allard, M., B. Wang, and J.A. Pilon, 1995: Recent cooling along the southern shore of Hudson Strait Quebec, Canada, documented from permafrost temperature measurements. *Arctic and Alpine Res.*, **27**, 157–166.

Alley, R.B., P.U. Clark, P. Huybrechts, and I. Joughin, 2005a: Ice-sheet and sea-level changes. *Science*, **310**, 456–460.

Alley, R.B., T.K. Dupont, B.R. Parizek, and S. Anandakrishnan, 2005b: Access of surface meltwater to beds of sub-freezing glaciers: preliminary insights. *Ann. Glaciol.*, **40**, 8–14.

Arendt, A.A., et al., 2002: Rapid wastage of Alaska glaciers and their contribution to rising sea level. *Science*, **297**, 382–386.

Armstrong, R.L. and M.J. Brodzik, 2001: Recent Northern Hemisphere snow extent: A comparison of data derived from visible and microwave satellite sensors. *Geophys. Res. Lett.*, **28**, 3673–3676.

Bamber, J.L., R.L. Layberry, and S.P. Gogineni, 2001: A new ice thickness and bed data set for the Greenland ice sheet, 1. Measurement, data reduction, and errors. *J. Geophys. Res.*, **106**, 33733–33780.

Bamber, J.L., W. Krabill, V. Raper, and J. Dowdeswell, 2004: Anomalous recent growth of part of a large Arctic ice cap: Austfonna, Svalbard. *Geophys. Res. Lett.*, **31**(12), L12402, doi: 10.1029/2004GL019667.

Bamzai, A.S., 2003: Relationship between snow cover variability and Arctic Oscillation Index on a hierarchy of time scales. *Int. J. Climatol.*, **23**, 131–142.

Belchansky, G. I., D.C. Douglas, V.A. Eremeev, and N.G. Platonov, 2005: Variations in the Arctic's multiyear sea ice cover: A neural network analysis of SMMR-SSM/I data, 1979-2004. *Geophys. Res. Lett.*, **32**, L09605, doi:10.1029/2005GL022395.

Box, J.E., et al., 2006: Greenland ice-sheet surface mass balance variability (1988-2004) from calibrated Polar MM5 output. *J. Clim.*, **19**(12), 2783–2800.

Broll, G., C. Tarnocai, and J. Gould, 2003: Long-term high Arctic ecosystem monitoring in Quttinirpaaq National Park, Ellesmere Island, Canada. In: *Proceedings of the 8th International Conference on Permafrost, 21-25 July 2003, Zurich, Switzerland* [Phillips, M., S.M. Springman, and L.U. Arenson (eds.)]. A.A. Balkema, Lisse, the Netherlands, pp. 89–94.

Brown, J., K.M. Hinkel, and F.E. Nelson, 2000: The Circumpolar Active Layer Monitoring (CALM) program: research design and initial results. *Polar Geogr.*, **24**(3), 166–258.

Brown, R.D., 2000: Northern hemisphere snow cover variability and change, 1915-97. *J. Clim.*, **13**, 2339–2355.

Brown, R.D., and P. Coté, 1992: Interannual variability of landfast ice thickness in the Canadian high Arctic, 1950-1989. *Arctic*, **45**, 273–284.

Carrasco, J.F., G. Casassa, and J. Quintana, 2005: Changes of the 0°C isotherm and the equilibrium line altitude in central Chile during the last quarter of the XXth century. *Hydrolog. Sci. J.*, **50**, 933–948.

Cavalieri, D.J., 1992: The validation of geophysical products using multisensor data. In: *Microwave Remote Sensing of Sea Ice* [Carsey, F.D. (ed.)]. Geophysical Monograph 68, American Geophysical Union, Washington, DC, pp 233–242.

Chinn, T.J.H., S. Winkler, M.J. Salinger, and N. Haakensen, 2005: Recent glacier advances in Norway and New Zealand: a comparison of their glaciological and meteorological causes. *Geografiska Annaler*, **87A**(1), 141–157.

Clare, G.R., B.B. Fizharris, T.J.H. Chinn, and M.J. Salinger, 2002: Interannual variation in end-of-summer snowlines of the Southern Alps of New Zealand, and relationships with Southern Hemisphere atmospheric circulation and sea surface temperature patterns. *Int. J. Climatol.*, **22**, 107–120.

Clark, M.P., M.C. Serreze, and D.A. Robinson, 1999: Atmospheric controls on Eurasian snow extent. *Int. J. Climatol.*, **19**, 27–40.

Clark, P.U., R.B. Alley, and D. Pollard, 1999: Northern hemisphere ice-sheet influences on global climate change. *Science*, **286**, 1103–1111.

Cogley, J.G., 2005: Mass and energy balances of glaciers and ice sheets. In: *Encyclopedia of Hydrological Sciences* [Anderson, M. (ed.)]. John Wiley & Sons, Ltd, Chichester, pp 2555–2573.

Comiso, J.C., 2002: A rapidly declining perennial sea ice cover in the Arctic. *Geophys. Res. Lett.*, **29**, 1956–1959.

Comiso, J.C., 2003: Large scale characteristics and variability of the global sea ice cover. In: *Sea Ice - An Introduction to its Physics, Biology, Chemistry, and Geology* [Thomas, D. and G.S. Dieckmann (eds.)]. Blackwell Science, Oxford, UK, pp. 112–142.

Cook, A., A. Fox, D. Vaughan, and J. Ferigno, 2005: Retreating glacier fronts on the Antarctic Peninsula over the past half century. *Science*, **308**, 541–544.

Couture, R., et al., 2003: On the hazards to infrastructure in the Canadian North associated with thawing of permafrost. In: *Proceedings of Geohazards 2003, 3rd Canadian Conference on Geotechnique and Natural Hazards*. Canadian Geotechnical Society, Alliston, Ontario, pp. 97–104.

Cuffey, K.M., 2001: Interannual variability of elevation on the Greenland ice sheet: effects of firn densification, and establishment of a benchmark. *Journal of Glaciol.*, **47**(158), 369–377.

Cullen, N.J., et al., 2006: Kilimanjaro glaciers: Recent areal extent from satellite data and new interpretation of observed 20th century retreat rates. *Geophys. Res. Lett.*, **33**, L16502, doi:10.1029/2006GL027084.

Curran, M.A.J., et al., 2003: Ice core evidence for Antarctic sea ice decline since the 1950s. *Science*, **302**(14), 1203–1206.

Davis, C.H., et al., 2005: Snowfall-driven growth in East Antarctic ice sheet mitigates recent sea-level rise. *Science*, **308**, 1898–1901, doi:10.1126/science.1110662.

de la Mare, W.K., 1997: Abrupt mid-20th century decline in Antarctic sea ice extent from whaling records. *Nature*, **389**, 57–61.

Derksen, C., A. Walker, E. LeDrew, and B. Goodison, 2003: Combining SMMR and SSM/I data for time series analysis of central North American snow water equivalent. *J. Hydrometeorol.*, **4**(2), 304–316.

DesJarlais, C., 2004: *S'adapter aux Changements Climatiques*. Ouranos, Montreal, 91pp.

Doran, P.T., et al., 2002: Antarctic climate cooling and terrestrial ecosystem response. *Nature*, **415**, 517–520.

Duguay, C.R., et al., 2003: Ice-cover variability on shallow lakes at high latitudes: model simulations and observations. *Hydrolog. Process.*, **17**, 3465–3483.

Duguay, C.R., et al., 2006: Recent trends in Canadian lake ice cover. *Hydrological Processes*, **20**, 781–801.

Dumas, J.A., G.M. Flato, and A.J. Weaver, 2003: The impact of varying atmospheric forcing on the thickness of arctic multi-year sea ice. *Geophys. Res. Lett.*, **30**(18), 1918–1921.

Dupont, T.K., and R.B. Alley, 2005: Assessment of the importance of ice-shelf buttressing to ice-sheet flow. *Geophys. Res. Lett.*, **32**, L04503, doi:10.1029/2004GL022024.

Dupont, T.K., and R.B. Alley, 2006: The importance of small ice shelves in sea-level rise. *Geophys. Res. Lett.*, **33**, L09503, doi:10.1029/2005GL025665.

Dye, D.G., 2002: Variability and trends in the annual snow-cover cycle in Northern Hemisphere land areas, 1972–2000. *Hydrolog. Process.*, **16**, 3065–3077.

Dyurgerov, M., and J. Dwyer, 2000. The steepening of glacier mass balance gradients with Northern Hemisphere warming. *Zeitschrift für Gletscherkunde und Glazialgeologie*, **36**, 107–118.

Dyurgerov, M., and M.F. Meier, 2005: *Glaciers and the Changing Earth System: A 2004 Snapshot*. Occasional Paper 58, Institute of Arctic and Alpine Research, University of Colorado, Boulder, CO, 118 pp.

Falarz, M., 2002: Long-term variability in reconstructed and observed snow cover over the last 100 winter seasons in Cracow and Zakopane (southern Poland). *Clim. Res.*, **19**(3), 247–256.

Favier, V., P. Wagnon, and P. Ribstein, 2004: Glaciers of the outer and inner tropics: A different behaviour but a common response to climatic forcing. *Geophys. Res. Lett.*, **31**, L16403, doi:10.1029/2004GL020654.

Fedorov, A., and P. Konstantinov, 2003: Observations of surface dynamics with thermokarst initiation, Yukechi site, central Yakutia. In: *Proceedings of the 8th International Conference on Permafrost, 21-25 July 2003, Zurich, Switzerland* [Phillips, M., S.M. Springman, and L.U. Arenson (eds.)]. A.A. Balkema, Lisse, the Netherlands, pp. 239–243.

Fichefet, T., B. Tartinville, and H. Goosse, 2003: Antarctic sea ice variability during 1958-1999: A simulation with a global ice-ocean model. *J. Geophys. Res*., **108**(C3), 3102–3113.

Fitzharris, B.B., and C.E. Garr, 1995: Simulation of past variability in seasonal snow in the Southern Alps, New Zealand. *Ann. Glaciol*., **21**, 377–382.

Fountain, A.G., T.A. Neumann, P.L. Glenn, and T. Chinn, 2004: Can warming induce advances of polar glaciers, Taylor Valley, Antarctica. *J. Glaciol.*, **50**(171), 556–564.

Francou, B., et al., 2003: Tropical climate change recorded by a glacier in the central Andes during the last decades of the twentieth century: Chacaltaya, Bolivia, 16°S. *J. Geophys. Res.*, **108**(D5), 4154, doi:10.1029/2002JD002959.

Francou, B., M. Vuille, V. Favier, and B. Cáceres, 2004: New evidence for an ENSO impact on low-latitude glaciers: Antizana 15, Andes of Ecuador, 0°28'S. *J. Geophys. Res.*, **109**, D18106, doi:10.1029/2003JD004484.

Frauenfeld, O.W., T. Zhang, R.G. Barry, and D. Gilichinsky, 2004: Interdecadal changes in seasonal freeze and thaw depths in Russia. *J. Geophys. Res.*, **109**, D5101, doi:10.1029/2003JD004245.

Fujita, K., and Y. Ageta, 2000: Effect of summer accumulation on glacier mass balance on the Tibetan Plateau revealed by mass-balance model. *J. Glaciol.*, **46**(153), 244–252.

Gavrilov, P.P. and P.V. Efremov, 2003: Effects of cryogenic processes on Yakutia landscapes under climate warming. In: *Proceedings of the 8th International Conference on Permafrost, 21-25 July 2003, Zurich, Switzerland* [Phillips, M., S.M. Springman, and L.U. Arenson (eds.)]. A.A. Balkema, Lisse, the Netherlands, pp. 277–282.

Georges, C., 2004: The 20th century glacier fluctuations in the Cordillera Blanca (Perú). *Arctic, Antarctic, and Alpine Res.*, **36**(1), 100–107.

Greene, A.M., 2005: A time constant for hemispheric glacier mass balance. *J. Glaciol.*, **51**(174), 353–362.

Groisman, P.Ya, T.R. Karl, and R.W. Knight, 1994: Observed impact of snow cover on the heat balance and the rise of continental spring temperatures. *Science*, **263**, 198–200.

Groisman, P.Ya., et al., 2004: Contemporary changes of the hydrological cycle over the contiguous United States: Trends derived from in situ observations. *J. Hydrometeorol.*, **5**, 64–85.

Gudkovich, Z.M., 1961: Relation of the ice drift in the Arctic Basin to ice conditions in the Soviet Arctic seas. *Tr. Okeanogr. Kom. Akad. Nauk SSSR*, **11**, 14–21 (in Russian).

Haas, C., 2004: Late-summer sea ice thickness variability in the Arctic Transpolar Drift 1991–2001 derived from ground-based electromagnetic sounding. *Geophys. Res. Lett.*, **31**, L09402, doi:10.1029/2003GL019394.

Haeberli, W., and C.R. Burn, 2002: Natural hazards in forests: glacier and permafrost effects as related to climate change. In: *Environmental Change and Geomorphic Hazards in Forests* [Sidle, R.C. (ed.)]. IUFRO Research Series 9, CABI Publishing, Wallingford and New York, pp. 167–202.

Hagen, J.O., K. Melvold, F. Pinglot, and J.A. Dowdeswell, 2003: On the net mass balance of the glaciers and ice caps in Svalbard, Norwegian Arctic. *Arctic, Antarctic, and Alpine Res.*, **35**(2), 264–270.

Halsey, L.A., D.H. Vitt, and S.C. Zoltai, 1995: Disequilibrium response of permafrost in boreal continental western Canada to climate change. *Clim. Change*, **30**, 57–73.

Hanna, E., et al., 2005: Runoff and mass balance of the Greenland ice sheet: 1958-2003. *J. Geophys. Res.*, **110**, D13108, doi:10.1029/2004JD005641.

Hanna, E., et al., 2006: Observed and modeled Greenland Ice Sheet snow accumulation, 1958–2003, and links with regional climate forcing. *J. Clim.*, **19**(3), 344–358.

Hansen, J., and L. Nazarenko, 2004: Soot climate forcing via snow and ice albedos. *Proc. Natl. Acad. Sci. U.S.A.*, **101**(2), 423–428.

Harris, C., et al., 2003: Warming permafrost in European mountains. *Global Planet. Change*, **39**, 215–225.

Hastenrath, S., 2005: The glaciers of Mount Kenya 1899-2004. *Erdkunde*, **59**, 120–125.

Heil, P., and I. Allison, 2002: Long-term fast-ice variability off Davis and Mawson stations, Antarctica. In: *Ice in the Environment: Proceedings of the 16th IAHR International Symposium on Ice (Volume 1), Dunedin, New Zealand, 2-6 December 2002* [Squire, V., and P. Langhorne (eds)]. University of Otago, Dunedin, NZ, pp. 360–367.

Hellmer, H., S. Jacobs, and A. Jenkins, 1998: Oceanic erosion of a floating Antarctic glacier in the Amundsen Sea. In: *Ocean, Ice, and Atmosphere: Interactions at the Antarctic Continental Margin* [Jacobs, S. and R. Weiss (eds.)]. Antarctic Research Series 75, American Geophysical Union, Washington, DC, pp. 83–99.

Hennessy, K.J., et al., 2003: *The Impact of Climate Change on Snow Conditions in Mainland Australia*. CSIRO Atmospheric Research, Aspendale, Australia, 47 pp, http://www.cmar.csiro.au/e-print/open/hennessy_2003a.pdf.

Hewitt, K., 2005: The Karakoram anomaly? Glacier expansion and the "elevation effect", Karakoram Himalaya. *Mountain Research and Development*, **25**(4), 332–340.

Hill, B.T., A. Ruffman, and K. Drinkwater. 2002: Historical record of the incidence of sea ice on the Scotian Shelf and the Gulf of St. Lawrence. In: *Ice in the Environment: Proceedings of the 16th IAHR International Symposium on Ice (Volume 1). Dunedin, New Zealand, 2-6 December 2002* [Squire, V., and P. Langhorne (eds)]. University of Otago, Dunedin, NZ.

Hilmer, M., and T. Jung, 2000: Evidence for a recent change in the link between the North Atlantic Oscillation and Arctic sea ice export. *Geophys. Res. Lett.*, **27**, 989–992.

Hinzman, L.D., et al., 2003: Hydrological variations among watersheds with varying degrees of permafrost. *Proceedings of the 8th International Conference on Permafrost, 21-25 July 2003, Zurich, Switzerland* [Phillips, M., S.M. Springman, and L.U. Arenson (eds.)]. A.A. Balkema, Lisse, the Netherlands, pp. 407–411.

Hinzman, L.D., et al., 2005: Evidence and implications of recent climate change in northern Alaska and other arctic regions. *Clim. Change*, **72**(3), 251–298.

Holloway, G., and T. Sou, 2002: Has Arctic sea ice rapidly thinned? *J. Clim.*, **15**, 1691–1701.

Howat, I.M., I. Joughin, S. Tulaczyk, and S. Gogineni, 2005: Rapid retreat and acceleration of Helheim Glacier, east Greenland. *Geophys. Res. Lett.*, **32**, L22502, doi: 10.1029/2005GL024737.

Huybrechts, P., 2002: Sea-level changes at the LGM from ice-dynamic reconstructions of the Greenland and Antarctic ice sheets during the glacial cycles. *Quat. Sci. Rev.*, **21**(1–3), 203–231.

Huybrechts, P., J. Gregory, I. Janssens, and M. Wild, 2004: Modelling Antarctic and Greenland volume changes during the 20th and 21st centuries forced by GCM time slice integrations. *Global Planet. Change*, **42**(1–4), 83–105.

Hyvärinen, V., 2003: Trends and characteristics of hydrological time series in Finland. *Nord. Hydrol.*, **34**(1–2), 71–90.

IPCC, 2001: *Climate Change 2001: The Scientific Basis. Contribution of Working Group I to the Third Assessment Report of the Intergovernmental Panel on Climate Change* [Houghton, J.T., et al. (eds)]. Cambridge University Press, Cambridge, United Kingdom and New York, NY, USA, 881 pp.

Isaksen, K., P. Holmlund, J.L. Sollid, and C. Harris, 2001: Three deep alpine-permafrost boreholes in Svalbard and Scandinavia. *Permafrost and Periglacial Processes*, **12**, 13–25.

Jacka, T.H., et al., 2004: Recommendations for the collection and synthesis of Antarctic Ice Sheet mass balance data. *Global Planet. Change*, **42**(1–4), 1–15.

Jacobs, S.S., C.F. Giulivi, and P.A. Mele, 2002: Freshening of the Ross Sea during the late 20th century. *Science*, **297**(5580), 386–389.

Johannessen, O.M, E.V. Shalina, and M.W. Miles, 1999: Satellite evidence for an Arctic sea ice cover in transformation. *Science*, 286, 1937–1939.

Johannessen, O.M., K. Khvorostovsky, M.W. Miles, and L.P. Bobylev, 2005: Recent ice-sheet growth in the interior of Greenland. *Science*, **310**, 1013–1016.

Johannessen, O.M., et al., 2004: Arctic climate change – observed and modelled temperature and sea ice. *Tellus*, **56A**, 328–341.

Jones, P.D., and A. Moberg, 2003: Hemispheric and large-scale surface air temperature variations: an extensive revision and an update to 2001. *J Climate*, **16**, 206–223.

Jorgenson, M.T., and J. Brown, 2005: Classification of the Alaskan Beaufort Sea Coast and estimation of carbon and sediment inputs from coastal erosion. *Geo-Marine Lett.*, **25**, 69–80.

Joughin, I., and S. Tulaczyk, 2002: Positive mass balance of the Ross Ice Streams, West Antarctica. *Science*, **295**(5554), 476–480.

Joughin, I., and L. Padman, 2003: Melting and freezing beneath Filchner-Ronne Ice Shelf, Antarctica. *Geophys. Res. Lett.*, **30**(9), 1477, doi:10.1029/2003GL016941.

Joughin, I., W. Abdalati, and M. Fahnestock, 2004: Large fluctuations in speed on Greenland's Jakobshavn Isbræ glacier. *Nature*, **432**, 608–610.

Joughin, I., et al., 2003: Timing of recent accelerations of Pine Island Glacier, Antarctica. *Geophys. Res. Lett.*, **30**(13), 1706, doi:10.1029/2003GL017609.

Kane, D.L., L.D. Hinzman, and J.P. Zarling, 1991: Thermal response of the active layer to climate warming in a permafrost environment. *Cold Regions Sci. Technol.*, **19**, 111–122.

Kaser, G., and H. Osmaston, 2002: *Tropical Glaciers*. UNESCO International Hydrological Series. Cambridge University Press, Cambridge, UK, 207pp.

Kaser, G., et al., 2003: The impact of glaciers on the runoff and the reconstruction of mass balance history from hydrological data in the tropical Cordillera Blanca, Peru. *J. Hydrol.*, **282**, 130–144.

Kjøllmoen, B.E., 2005: *Glaciological Investigations in Norway in 2004*. Norwegian Water Resources and Energy Directorate, Oslo, http://www.nve.no/FileArchive/176/Glac_invest2004.pdf.

Klein, A.G., and J.L. Kincaid, 2006: Retreat of glaciers on Puncak Jaya, Irian Jaya, determined from 2000 and 2002 IKONOS satellite images. *J. Glaciol.*, **52**(176), 65–79.

Koeberle, C., and R. Gerdes, 2003: Mechanisms determining the variability of Arctic sea ice conditions and export. *J. Clim.*, **16**, 2843–2858.

Krabill, W.B., et al., 2000: Greenland Ice Sheet: High elevation balance and peripheral thinning. *Science*, **289**, 428–430.

Krabill, W.B., et al., 2002: Aircraft laser altimetry measurement of elevation changes of the Greenland ice sheet: Technique and accuracy assessment. *J. Geodyn.*, **34**, 357–376.

Krabill, W.B., et al., 2004: Greenland Ice Sheet: Increased coastal thinning. *Geophys. Res. Lett.*, **31**, L24402, doi:10.1029/2004GL021533.

Kwok, R., 2000: Recent changes of the Arctic Ocean sea ice motion associated with the North Atlantic Oscillation. *Geophys. Res. Lett*, **27**(6), 775–778.

Kwok, R., 2002: Sea ice concentration from passive microwave radiometry and openings from SAR ice motion. *Geophys. Res. Lett*, **29**(10), doi:10.1029/2002GL014787.

Kwok, R., and D.A. Rothrock, 1999: Variability of Fram Strait ice flux and North Atlantic Oscillation. *J. Geophys. Res*., **104**, 5177–5189.

Kwok, R., G.F. Cunningham, and S.S. Pang, 2004: Fram Strait sea ice outflow. *J. Geophys. Res*., **109**, C01009, doi:10.1029/2003JC001785.

Kwok, R., et al., 1998: Assessment of sea ice motion from sequential passive microwave observations with ERS and buoy ice motions. *J. Geophys. Res*., **103**(C4), 8191–8213.

Lachenbruch, A.H., and B.V. Marshall, 1986: Changing climate: geothermal evidence from permafrost in the Alaskan Arctic. *Science*, **234**, 689–696.

Laxon, S., N. Peacock, and D. Smith, 2003: High interannual variability of sea ice thickness in the Arctic region. *Nature*, **425**, 947–950.

Legresy, B., F. Remy, and F. Blarel, 2006: Along track repeat altimetry for ice sheets and continental surface studies. In: *Proceedings of the Symposium on 15 years of Progress in Radar Altimetry, Venice, Italy, 13-18 March 2006* [Danesy, D. (ed.)]. ESA-SP614, Paper 181, European Space Agency Publications Division, Noordwijk, The Netherlands, 4 pp., http://earth.esa.int/workshops/venice06/participants/181/paper_181_legrsy.pdf.

Lewkowicz, A.G., 1992: Factors influencing the distribution and initiation of active-layer detachment slides on Ellesmere Island, arctic Canada. In: *Periglacial Geomorphology* [Dixon, J.C. and A.D. Abrahams (eds.)]. Wiley, New York, pp. 223–250.

Liu, S., et al., 2004: Recent progress in glaciological studies in China. *J. Geogr. Sci.*, **14**(4), 401–410.

Lo, F., and M.P. Clark, 2001: Relationships between spring snow mass and summer precipitation in the southwestern US associated with the North American monsoon system. *J. Clim.*, **15**, 1378–1385.

Lythe, M.B., D.G. Vaughan, and the BEDMAP Group, 2001: BEDMAP: A new ice thickness and subglacial topographic model of Antarctica. *J. Geophys. Res.*, **106**(B6), 11335–11351.

Magnuson, J.J., et al., 2000: Historical trends in lake and river ice cover in the Northern Hemisphere. *Science*, **289**, 1743–1746.

Massom, R.A., et al., 2001: Snow on Antarctic sea ice: a review of physical characteristics. *Rev. Geophys.*, **39**(3), 413–445

McDonald, K.C., et al., 2004: Variability in springtime thaw in the terrestrial high latitudes: monitoring a major control on the biospheric assimilation of atmospheric CO_2 with spaceborne microwave remote sensing. *Earth Interactions*, **8**, Paper No. 20.

McLaren, A.S., R.H. Bourke, J.E. Walsh, and R.L. Weaver, 1994: Variability in sea-ice thickness over the North Pole from 1958 to 1992. In: *The Polar Oceans and Their Role in Shaping the Global Environment* [Johannessen, O.M., R.D. Muench, and J.E. Overland (eds.)]. American Geophysical Union, Washington, DC, pp. 363–371.

Mitrovica, J.X., et al., 2006: Reanalysis of ancient eclipse, astronomic and geodetic data: A possible route to resolving the enigma of global sea level rise. *Earth Planet. Sci. Lett.*, **243**, 390–399.

Mölg, T., and D.R. Hardy, 2004: Ablation and associated energy balance of a horizontal glacier surface on Kilimanjaro. *J. Geophys. Res.*, **109**, 1–13, D16104, doi:10.1029/2003JD004338.

Mölg, T., C. Georges, and G. Kaser, 2003a: The contribution of increased incoming shortwave radiation to the retreat of the Rwenzori Glaciers, East Africa, during the 20th century. *Int. J. Climatol.*, **23**, 291–303, doi:10.1002/joc.877.

Mölg, T., D.R. Hardy, and G. Kaser, 2003b: Solar-radiation-maintained glacier recession on Kilimanjaro drawn from combined ice-radiation geometry modeling. *J. Geophys. Res.*, **108**(D23), 4731, doi:10.1029/2003JD003546.

Monaghan, A.J., et al., 2006: Insignificant change in Antarctic snowfall since the International Geophysical Year. *Science*, **313**(5788), 827–831.

Morris, E.M., and D. G. Vaughan, 2003: Glaciological climate relationships spatial and temporal variation of surface temperature on the Antarctic Peninsula and the limit of viability of ice shelves. In: *Antarctic Peninsula Climate Variability: Historical and Paleoenvironmental Perspectives* [Domack, E., et al. (eds.)]. Antarctic Research Series 79, American Geophysical Union, Washington, DC, pp. 61–68.

Mote, P.W., 2006: Climate-driven variability and trends in mountain snowpack in western North America. *J. Clim.*, **19**(23), 6209–6220.

Mote, P.W., A.F. Hamlet, M.P. Clark, and D.P. Lettenmaier, 2005: Declining mountain snowpack in western North America. *Bull. Am. Meteorol. Soc.*, **86**, 39–49, doi:10.1175/BAMS-86-1-39.

Munk, W., 2002: Twentieth century sea level: An enigma. *Proc. Natl. Acad. Sci. U.S.A.*, **99**, 6550–6555.

Murphy, E.J., A. Clarke, C. Symon, and J. Priddle, 1995: Temporal variation in Antarctic sea-ice: analysis of a long term fast-ice record from the South Orkney Islands. *Deep-Sea. Res.*, **42**, l045–1062.

Nagurnyi, A.P., V.G. Korostolev, and V.V. Ivanov, 1999: Multiyear variability of sea ice thickness in the Arctic basin measured by elastic-gravity waves on the ice surface. *Meteorol. Hydrol.*, **3**, 72–78 (in Russian).

Nan, Z., Z. Gao, S. Li, and T. Wu, 2003: Permafrost changes in the northern limit of permafrost on the Qinghai-Tibet Plateau in the last 30 years. *Acta Geogr. Sin.*, **58**(6), 817–823 (in Chinese).

Nelson, F.E., O.A. Anisimov, and N.I. Shiklomanov, 2001: Subsidence risk from thawing permafrost. *Nature*, **410**, 889–890.

Nelson, F.E. (ed.), 2004a: Circumpolar Active Layer Monitoring (CALM) Workshop. *Permafrost and Periglacial Processes*, **15**(2), 99–188.

Nelson, F.E. (ed.), 2004b: Eurasian contributions to the Circumpolar Active Layer Monitoring (CALM) Workshop. *Polar Geogr.*, **28**(4), 253–340.

Nesje, A., and S.O. Dahl, 2003: The 'Little Ice Age' - only temperature? *The Holocene*, **13**(1), 139–145.

Nesje, A., Ø. Lie, and S.O. Dahl, 2000: Is the North Atlantic Oscillation reflected in Scandinavian glacier mass balance records? *J. Quat. Sci.*, **15**(6), 587–601.

Nicholls, N., 2005: Climate variability, climate change and the Australian snow season. *Aust. Meteorol. Mag.*, **54**, 177–185.

Oberman, N.G., and G.G. Mazhitova, 2001: Permafrost dynamics in the northeast of European Russia at the end of the 20th century. *Norwegian J. Geogr.*, **55**, 241–244.

Oerlemans, J., 2005: Extracting a climate signal from 169 glacier records. *Science*, **308**, 675-677.

Ohmura, A., 2001: Physical basis for the temperature/melt-index method. *J. Appl. Meteorol.*, **40**, 753–761.

Ohmura, A., 2004: Cryosphere during the twentieth century. In: *The State of the Planet: Frontiers and Challenges in Geophysics* [Sparks, R.S.J. and C.J. Hawkesworth (eds.)]. Geophysical Monograph 150, International Union of Geodesy and Geophysics, Boulder, CO and American Geophysical Union, Washington, DC, pp. 239–257.

Omstedt, A., and D. Chen, 2001: Influence of atmospheric circulation on the maximum ice extent in the Baltic Sea. *J. Geophys. Res.*, **106**, 4493–4500.

Osterkamp, T.E., 2003: A thermal history of permafrost in Alaska. In: *Proceedings of the 8th International Conference on Permafrost, 21-25 July 2003, Zurich, Switzerland* [Phillips, M., S.M. Springman, and L.U. Arenson (eds.)]. A.A. Balkema, Lisse, the Netherlands, pp. 863–867.

Osterkamp, T.E., 2005: The recent warming of permafrost in Alaska. *Global Planet. Change*, **49**, 187–202, doi: 10.1016/j.gloplacha.2005.09.001.

Parizek, B.R., and R.B. Alley, 2004: Implications of increased Greenland surface melt under global-warming scenarios: ice-sheet simulations. *Quat. Sci. Rev.*, **23**(9–10), 1013–1027.

Parizek, B.R., R.B. Alley, and C.L. Hulbe, 2003: Subglacial thermal balance permits ongoing grounding-line retreat along the Siple Coast of West Antarctica. *Ann. Glaciol.*, **36**, 251–256.

Parkinson, C.L., 1990: Search for the Little Ice Age in Southern Ocean sea-ice records. *Ann. Glaciol.*, **14**, 221–225.

Paterson, W.S.B., 2004: *The Physics of Glaciers*, Ed. 3.A, Elsevier, Oxford, UK, 496pp.

Pavlov, A.V., 1996: Permafrost-climate monitoring of Russia: analysis of field data and forecast. *Polar Geogr.*, **20**(1), 44–64.

Payne, A.J., et al., 2004: Recent dramatic thinning of largest West Antarctic ice stream triggered by oceans. *Geophys. Res. Lett.*, **31**, L23401, doi:10.1029/2004GL021284.

Peltier, W.R., 1998: Postglacial variations in the level of the sea: implications for climate dynamics and solid-earth geophysics. *Rev. Geophys.*, **36**, 603–689.

Petkova, N., E. Koleva, and V. Alexandrov, 2004: Snow cover variability and change in mountainous regions of Bulgaria, 1931-2000. *Meteorol. Z.*, **13**(1), 19–23.

Pettersson, R., P. Jansson, and P. Holmlund, 2003: Cold surface layer thinning on Storglaciären, Sweden, observed by repeated ground penetrating radar surveys. *J. Geophys. Res.*, **108**(F1), 6004, doi:10.1029/2003JF000024.

Polyakov, I.V., et al., 2003: Long-term ice variability in Arctic marginal seas. *J. Clim.*, **16**, 2078–2085.

Prieto, R, et al., 2001: Interannual oscillations and trend of snow occurrence in the Andes region since 1885. *Aust. Meteorol. Mag.*, **50**(2), 164.

Proshutinsky, A.Y., and M.A. Johnson, 1997: Two circulation regimes of the wind-driven Arctic Ocean. *J. Geophys. Res.*, **102**(C6), 12493–12514.

Qin, D., S. Liu, and P. Li, 2006: Snow cover distribution, variability, and response to climate change in Western China. *J. Clim.*, **19**, 1820–1833.

Qiu, G., Y. Zhou, D. Guo, and Y. Wang, 2000: The map of geocryological regionalization and classification in China. In: *Geocryology in China* [Zhou, Y., D. Guo, G. Qiu, G. Cheng, and S. Li (eds.)]. Science Press, Beijing (in Chinese). The digital version of the map is available at the National Snow and Ice Data Center, University of Colorado at Boulder, Boulder, CO, http://nsidc.org/data/ggd603.html.

Rachold, V., et al., 2003: Modern terrigenous organic carbon input to the Arctic Ocean. In: *Organic Carbon Cycle in the Arctic Ocean: Present and Past* [Stein, R., and R.W. Macdonald (eds.)]. Springer Verlag, Berlin, pp. 33–55.

Ramillien, G., et al., 2006: Interannual variations of the mass balance of the Antarctica and Greenland ice sheets from GRACE. *Global Planet. Change*, **53**, 198–208.

Randerson, J.T., C.B. Field, I.Y. Fung, and C.B. Tans, 1999: Increases in early season ecosystem uptake explain recent changes in the seasonal cycle of the atmospheric CO_2 at high northern latitudes. *Geophys. Res. Lett.*, **26**, 2765–2768.

Raper, S.C.B., and R.J. Braithwaite, 2005: The potential for sea level rise: New estimates from glacier and ice cap area and volume distribution. *Geophys. Res. Lett.*, **32**, L05502, doi:10.1029/2004GL021981.

Rayner, N.A., et al., 2003: Global analyses of sea surface temperature, sea ice and night marine air temperature since the late nineteenth century. *J. Geophys. Res.*, **108**(D14), 4407, doi: 10.1029/2002JD002670.

Ren, J., et al., 2004: Glacier variations and climate warming and drying in the central Himalayas. *Chin. Sci. Bull.*, **49**(1), 65–69.

Rignot, E., and S. Jacobs, 2002: Rapid bottom melting widespread near Antarctic Ice Sheet grounding lines. *Science*, **296**, 2020–2023.

Rignot, E., and R.H. Thomas, 2002: Mass balance of polar ice sheets. *Science*, **297**(5586), 1502–1506.

Rignot, E., and P. Kanagaratnam, 2006: Changes in the velocity structure of the Greenland Ice Sheet. *Science*, **311**, 986–990.

Rignot, E., A. Rivera, and G. Casassa, 2003: Contribution of the Patagonia Icefields of South America to sea level rise. *Science*, **302**, 434–437.

Rignot, E., et al., 2004: Accelerated ice discharge from the Antarctic Peninsula following the collapse of Larsen B ice shelf. *Geophys. Res. Lett.*, **31**(18), L18401, doi:10.1029/2004GL020697.

Rignot, E., et al., 2005: Recent ice loss from the Fleming and other glaciers, Wordie Bay, West Antarctic Peninsula. *Geophys. Res. Lett.*, **32**(7), 1–4.

Rigor, I.G., J.M. Wallace, and R.L. Colony, 2002: Response of sea ice to the arctic oscillation. *J. Clim.*, **15**, 2648– 2663.

Robertson, R., M. Visbek, A. Gordon, and E. Fahrbach, 2002: Long term temperature trends in the deep waters of the Weddell. *Deep-Sea Res.*, **49**, 4791–4802.

Robinson, D.A., and A. Frei, 2000: Seasonal variability of northern hemisphere snow extent using visible satellite data. *Professional Geogr.*, **51**, 307–314.

Robinson, D.A., K.F. Dewey, and R.R. Heim Jr., 1993: Global snow cover monitoring: an update. *Bull. Am. Meteorol. Soc.*, **74**, 1689–1696.

Robock, A., M. Mu, K. Vinnikov, and D. Robinson, 2003: Land surface conditions over Eurasia and Indian summer monsoon rainfall. *J. Geophys. Res.*, **108**(D4), 4131, doi: 10.1029/2002JD002286.

Romanovsky, V.E., et al., 2002: Permafrost temperature records: Indicator of climate change. *Eos*, **83**(50), 589, 593–594.

Rothrock, D.A., Y. Yu, and G.A. Maykut, 1999: Thinning of the Arctic sea-ice cover. *Geophys. Res. Lett.*, **26**(23), 3469.

Rothrock, D.A., J. Zhang, and Y. Yu., 2003: The arctic ice thickness anomaly of the 1990s: A consistent view from observations and models. *J. Geophys. Res*., **108**(C3), 3083, doi:10.1029/2001JC001208.

Saito, K., and J. Cohen, 2003: The potential role of snow cover in forcing interannual variability of the major Northern Hemisphere mode. *Geophys. Res. Lett.*, **30**, 1302, doi:10.1029/2002GL016341.

Scambos, T., C. Hulbe, and M. Fahnestock, 2003: Climate-induced ice shelf disintegration in the Antarctic Peninsula. In: *Antarctic Peninsula Climate Variability: Historical and Paleoenvironmental Perspectives* [Domack, E., et al. (eds.)]. Antarctic Research Series 79, American Geophysical Union, Washington, DC, pp. 79–92.

Scambos, T., C. Hulbe, M. Fahnestock, and J. Bohlander, 2000: The link between climate warming and break-up of ice shelves in the Antarctic Peninsula. *J. Glaciol.*, **46**, 516–530.

Scambos, T., J. Bohlander, C. Shuman, and P. Skvarca, 2004: Glacier acceleration and thinning after ice shelf collapse in the Larsen B embayment, Antarctica. *Geophys. Res. Lett.*, **31**, L18401, doi:10.1029/2004GL020670.

Scherrer, S.C., C. Appenzeller, and M. Laternser, 2004: Trends in Swiss alpine snow days – the role of local and large scale climate variability. *Geophys. Res. Lett.*, **31**, L13215, doi:10.1029/2004GL020255.

Schmitt, C., Ch. Kottmeier, S. Wassermann, and M. Drinkwater, 2004: *Atlas of Antarctic Sea Ice Drift*. University of Karlsruhe, Karlsruhe, http://imkhp7.physik.uni-karlsruhe.de/~eisatlas/eisatlas_start.html.

Schneider, D.P., E.J. Steig, and J.C. Comiso, 2004: Recent climate variability in Antarctica from satellite-derived temperature data. *J. Clim.*, **17**, 1569–1583.

Sharkhuu, N., 2003: Recent changes in the permafrost of Mongolia. In: *Proceedings of the 8th International Conference on Permafrost, 21-25 July 2003, Zurich, Switzerland* [Phillips, M., S.M. Springman, and L.U. Arenson (eds.)]. A.A. Balkema, Lisse, the Netherlands, pp. 1029–1034.

Shepherd, A., D.J. Wingham, and J.A.D. Mansley, 2002: Inland thinning of the Amundsen Sea sector, West Antarctica. *Geophys. Res. Lett.*, **29**(10), 1364.

Shepherd, A., D. Wingham, and E. Rignot, 2004: Warm ocean is eroding West Antarctic Ice Sheet. *Geophys. Res. Lett.*, **31**(23), 1–4.

Shepherd, A., D. Wingham, T. Payne, and P. Skvarca, 2003: Larsen Ice Shelf has progressively thinned. *Science*, **302**, 856–859.

Shy, T.L., and J.E. Walsh, 1996: North Pole ice thickness and association with ice motion history. *Geophys. Res. Lett.*, **23**(21), 2975–2978.

Sicart, J.E., P. Wagnon, and P. Ribstein, 2005: Atmospheric controls of the heat balance of Zongo Glacier (16°S, Bolivia). *J. Geophys. Res.*, **110**, D12106, doi:10.1029/2004JD005732.

Smith, L.C., 2000: Trends in Russian Arctic river-ice formation and breakup, 1917-1994. *Phys. Geogr.*, **21**, 46–56.

Smith, L.C., Y. Sheng, G.M. MacDonald, and L.D. Hinzman, 2005: Disappearing Arctic lakes. *Science*, **308**, 1429.

Smith, N.V., S.S. Saatchi, and T. Randerson, 2004: Trends in high latitude soil freeze and thaw cycles from 1988 to 2002. *J. Geophys. Res.*, **109**, D12101, doi:10.1029/2003JD004472.

Smith, S.L., M.M. Burgess, and A.E. Taylor, 2003: High Arctic permafrost observatory at Alert, Nunavut – analysis of a 23 year data set. In: *Proceedings of the 8th International Conference on Permafrost, 21-25 July 2003, Zurich, Switzerland* [Phillips, M., S.M. Springman, and L.U. Arenson (eds.)]. A.A. Balkema, Lisse, the Netherlands, pp. 1073–1078.

Smith, S.L., M.M. Burgess, D. Riseborough, and F.M. Nixon, 2005: Recent trends from Canadian permafrost thermal monitoring network sites. *Permafrost and Periglacial Processes*, **16**, 19–30.

Solomina, O., R. Barry, and M. Bodnya, 2004: The retreat of Tien Shan glaciers (Kyrgyzstan) since the Little Ice Age estimated from aerial photographs, lichonometric and historical data. *Geografiska Annaler*, **86A**(2), 205–215.

Steffen, K., et al., 1992: The estimation of geophysical parameters using passive microwave algorithms. In: *Microwave Remote Sensing of Sea Ice* [Carsey, F.D. (ed.)]. Geophysical Monograph 68, American Geophysical Union, Washington, DC, pp 201–231.

Stewart, I.T., D.R. Cayan, and M.D. Dettinger, 2005: Changes towards earlier streamflow timing across western North America. *J. Clim.*, **18**, 1136–1155.

Stineman, R.W., 1980: A consistently well-behaved method of interpolation. *Creative Computing*, July 1980, 54–57.

Stone, J.O., et al., 2003: Holocene deglaciation of Marie Byrd Land, West Antarctica. *Science*, **299**, 99–102.

Stone, R.S., E.G. Dutton, J.M. Harris, and D. Longnecker, 2002: Earlier spring snowmelt in northern Alaska as an indicator of climate change. *J. Geophys. Res.*, **107**(D10), doi:10.1029/2000JD000286.

Su, Z., and Shi, Y., 2002: Response of monsoonal temperate glaciers to global warming since the Littel Ice Age. *Quat. Int.*, **97–98**, 123–131.

Thomas, R.H., 1979: The dynamics of marine ice sheets. *J. Glaciol.*, **24**, 167–177.

Thomas, R., 2004: Force-perturbation analysis of recent thinning and acceleration of Jakobshavn Isbrae, Greenland. *J. Glaciol.*, **50**, 57–66.

Thomas, R., et al., 2001: Mass balance of higher-elevation parts of the Greenland ice sheet. *J. Geophys. Res.*, **106D**, 33707–33716.

Thomas, R., et al., 2003: Investigation of surface melting and dynamic thinning on Jakobshavn Isbrae, Greenland. *J. Glaciol.*, **49**, 231–239.

Thomas, R., et al., 2004: Accelerated sea-level rise from West Antarctica. *Science*, **306**(5694), 255–258.

Thomas, R., et al., 2006: Progressive increase in ice loss from Greenland. *Geophys. Res. Lett.*, **33**, L10503, doi: 10.1029/2006GL026075.

Thompson, D.W.J., and S. Solomon, 2002: Interpretation of recent Southern Hemisphere climate change. *Science*, **296**, 895–899.

Thompson, L.G., et al., 2002: Kilimanjaro ice core records: Evidence of Holocene climate change in tropical Africa. *Science*, **298**, 589–593.

Tucker, W.B. III, et al., 2001: Evidence for the rapid thinning of sea ice in the western Arctic Ocean at the end of the 1980s. *Geophys. Res. Lett.*, **28**(14), 2851–2854.

Turner, J., et al., 2005: Antarctic climate change during the last 50 years. *Int. J. Climatol.*, **25**(3), 279–294.

van de Berg, W.J., M.R. van den Broeke, C.H. Reijmer, and E. van Meijgaard, 2006: Reassessment of the Antarctic surface mass balance using calibrated output of a regional atmospheric climate model. *J. Geophys. Res.*, **111**, D11104, doi:10.1029/2005JD006495.

van den Broeke, M.R., 2000: On the interpretation of Antarctic temperature trends. *J. Clim.*, **13**(21), 3885–3889.

van den Broeke, M.R., W.J. van de Berg, and E. van Meijgaard, 2006: Snowfall in coastal West Antarctica much greater than previously assumed. *Geophys. Res. Lett.*, **33**, L02505, doi:10.1029/2005GL025239.

Vaughan, D.G., et al., 2001: Climate change – Devil in the detail. *Science*, **293**(5536), 1777–1779.

Vaughan, D.G., et al., 2003: Recent rapid regional climate warming on the Antarctic Peninsula. *Clim. Change*, **60**, 243–274.

Velicogna, I., and J. Wahr, 2005: Greenland mass balance from GRACE. *Geophys. Res. Lett.*, **32**, L18505, doi:10.1029/2005GL023955.

Velicogna, I., and J. Wahr, 2006: Measurements of time variable gravity show mass loss in Antarctica. *Science*, **311**(5768), 1754–1756, doi:10.1126/science.1123785.

Venegas, S.A., M.R. Drinkwater, and G. Shaffer, 2001: Coupled oscillations in Antarctic sea ice and atmosphere in the South Pacific sector. *Geophys. Res. Lett.*, **28**,(17), 3301–3304.

Vincent, C., E. Le Meur, D. Six, and M. Funk, 2005: Solving the paradox of the end of the Little Ice Age in the Alps. *Geophys. Res. Lett.*, **32**, L09706, doi:10.1029/2005GL022552.

Vinje, T., 2001: Anomalies and trends of sea ice extent and atmospheric circulation in the Nordic Seas during the period 1864-1998. *J. Clim.*, **14**, 255–267.

Vinje, T., N. Nordlund, and A. Kvambekk, 1998: Monitoring ice thickness in Fram Strait. *J. Geophys. Res.*, **103**(C5), 10437–10450.

Vojtek, M., P. Fasko, and P. St'astny, 2003: Some selected snow climate trends in Slovakia with respect to altitude. *Acta Meteorologica Universitatis Comenianae*, **32**, 17–27.

Vonder Mühll, D., J. Nötzli, K. Makowski, and R. Delaloye, 2004: *Permafrost in Switzerland 2000/2001 and 2001/2002*. Glaciological Report (Permafrost) No. 2/3, Glaciological Commission of the Swiss Academy of Sciences, Zurich, 86 pp.

Wadhams, P., 1992: Sea ice thickness distribution in the Greenland Sea and Eurasian Basin, May 1987. *J. Geophys. Res.*, **97**, 5331–5348.

Wagnon, P., P. Ribstein, B. Francou, and J.E. Sicart, 2001. Anomalous heat and mass budget of Glaciar Zongo, Bolivia during the 1997/98 El Niño year. *J. Glaciol.*, **47**(156), 21–28.

Walsh, J., et al., 2005: Cryosphere and hydrology. In: *Arctic Climate Impact Assessment*. Cambridge University Press, Cambridge and New York, pp. 183–242.

Wang, S., 2002: Permafrost degradation, desertification and CH_4 release. In: *Dynamic Characteristic of Cryosphere in the Central Section of Qinghai-Tibet Plateau* [Yao, T., et al. (eds.)]. Geology Press, Beijing, 234–255 (in Chinese).

Wang, S., and Zhao, X., 1997: Environmental change in patchy permafrost zone in the south section of Qinghai-Tibet Highway. *J. Glaciol. Geocryol.*, **19**, 231–239 (in Chinese).

Warren, S.G., et al., 1999: Snow depth on arctic sea ice. *J. Clim.*, **12**, 1814–1829.

WGMS(ICSI-IAHS), various years-a: *Fluctuations of Glaciers*. World Glacier Monitoring Service, Zurich.

WGMS(ICSI-IAHS), various years-b: *Mass Balance Bulletin*. World Glacier Monitoring Service, Zurich, http://www.wgms.ch/mbb.html.

Winsor, P., 2001: Arctic sea ice thickness remained constant during the 1990s. *Geophys. Res. Lett.*, **28**(6), 1039–1041.

Worby, A.P., and S.F. Ackley, 2000: Antarctic research yields circumpolar sea ice thickness data. *Eos*, **81**(17), 181, 184–185.

Worby, A.P., and J.C. Comiso, 2004: Studies of the Antarctic sea ice edge and ice extent from satellite and ship observations. *Remote Sensing of Environment*, **92**, 98–111.

Wu, Q., and Y. Liu, 2003: Ground temperature monitoring and its recent change in Qinghai–Tibet Plateau. *Cold Regions Sci. Technol.*, **18**, 85–92.

Ye, H.C., and M. Ellison, 2003: Changes in transitional snowfall season length in northern Eurasia. *Geophys. Res. Lett.*, **30**(5), 1252.

Yoshikawa, K., and L.D. Hinzman, 2003: Shrinking thermokarst ponds and groundwater dynamics in discontinuous permafrost. *Permafrost and Periglacial Processes*, **14**(2), 151–160.

Yu, Y., G.A. Maykut, and D.A. Rothrock, 2004: Changes in the thickness distribution of Arctic sea ice between 1958-1970 and 1993-1997. *J. Geophys. Res.*, **109**, C08004, doi:10.1029/2003JC001982.

Zemp, M., R. Frauenfelder, W. Haeberli, and M. Hoelzle, 2005: Worldwide glacier mass balance measurements: general trends and first results of the extraordinary year 2003 in Central Europe. In: *XIII Glaciological Symposium, Shrinkage of the Glaciosphere: Facts and Analyses, St. Petersburg, Russia* [Science, R.A.O. (ed.)]. Data of Glaciological Studies [Materialy glyatsiologicheskikh issledovaniy], Moscow, Russia, pp. 3–12.

Zhang, T., 2005: Influence of the seasonal snow cover on the ground thermal regime: An overview. *Rev. Geophys.*, **43**, RG4002, doi:10.1029/2004RG000157.

Zhang, T., et al., 1999: Statistics and characteristics of permafrost and ground-ice distribution in the Northern Hemisphere. *Polar Geogr.*, 23(2), 132–154.

Zhang, T., et al., 2003: Distribution of seasonally and perennially frozen ground in the Northern Hemisphere. In: *Proceedings of the 8th International Conference on Permafrost, 21-25 July 2003, Zurich, Switzerland* [Phillips, M., S.M. Springman, and L.U. Arenson (eds.)]. A.A. Balkema, Lisse, the Netherlands, pp. 1289–1294.

Zhang, T., et al., 2005: Spatial and temporal variability in active layer thickness over the Russian Arctic drainage basin. *J. Geophys. Res.*, **110**, D16101, doi:10.1029/2004JD005642.

Zhang, X., L.A. Vincent, W.D. Hogg, and A. Niitsoo, 2000: Temperature and precipitation trends in Canada during the 20th century. *Atmos-Ocean*, **38**(3), 395–429.

Zhang, X., K.D. Harvey, W.D. Hogg, and T.R. Yuzyk, 2001: Trends in Canadian streamflow. *Water Resour. Res.*, **37**(4), 987–998.

Zhang, Y.S., T. Li, and B. Wang, 2004: Decadal change of the spring snow depth over the Tibetan Plateau: The associated circulation and influence on the East Asian summer monsoon. *J. Clim.*, **17**(14), 2780–2793.

Zhao, L., G. Cheng, and Li, S., 2003: Changes of plateau frozen-ground and environmental engineering effects. In: *The Formation Environment and Development of Qinghai-Tibet Plateau* [Zheng, D., et al. (eds)]. Heibei Science and Technology Press, Shijiazhang, pp. 143–150 (in Chinese).

Zhao, L., et al., 2004: Changes of climate and seasonally frozen ground over the past 30 years in Qinghai-Xizang (Tibetan) Plateau, China. *Global Planet. Change*, **43**, 19–31.

Zhou, Y., X. Gao, and Y. Wang,1996: The ground temperature changes of seasonally freeze-thaw layers and climate warming in Northeast China in the past 40 years. In: *Proceeding of the 5th Chinese Conference on Glaciology and Geocryology (Volume 1)*. Gansu Culture Press, Lanzhou, pp. 3–9 (in Chinese).

Zwally, H.J., et al., 2002: Surface melt-induced acceleration of Greenland ice-sheet flow. *Science*, **297**(5579), 218–222.

Zwally, H.J., et al., 2006: Mass changes of the Greenland and Antarctic ice sheets and shelves and contributions to sea level rise: 1992-2002. *J. Glaciol.*, **51**, 509–527.

5

Observations: Oceanic Climate Change and Sea Level

Coordinating Lead Authors:

Nathaniel L. Bindoff (Australia), Jürgen Willebrand (Germany)

Lead Authors:

Vincenzo Artale (Italy), Anny Cazenave (France), Jonathan M. Gregory (UK), Sergey Gulev (Russian Federation), Kimio Hanawa (Japan), Corrine Le Quéré (UK, France, Canada), Sydney Levitus (USA), Yukihiro Nojiri (Japan), C.K. Shum (USA), Lynne D. Talley (USA), Alakkat S. Unnikrishnan (India)

Contributing Authors:

J. Antonov (USA, Russian Federation), N.R. Bates (Bermuda), T. Boyer (USA), D. Chambers (USA), B. Chao (USA), J. Church (Australia), R. Curry (USA), S. Emerson (USA), R. Feely (USA), H. Garcia (USA), M. González-Davíla (Spain), N. Gruber (USA, Switzerland), S. Josey (UK), T. Joyce (USA), K. Kim (Republic of Korea), B. King (UK), A. Koertzinger (Germany), K. Lambeck (Australia), K. Laval (France), N. Lefevre (France), E. Leuliette (USA), R. Marsh (UK), C. Mauritzen (Norway), M. McPhaden (USA), C. Millot (France), C. Milly (USA), R. Molinari (USA), R.S. Nerem (USA), T. Ono (Japan), M. Pahlow (Canada), T.-H. Peng (USA), A. Proshutinsky (USA), B. Qiu (USA), D. Quadfasel (Germany), S. Rahmstorf (Germany), S. Rintoul (Australia), M. Rixen (NATO, Belgium), P. Rizzoli (USA, Italy), C. Sabine (USA), D. Sahagian (USA), F. Schott (Germany), Y. Song (USA), D. Stammer (Germany), T. Suga (Japan), C. Sweeney (USA), M. Tamisiea (USA), M. Tsimplis (UK, Greece), R. Wanninkhof (USA), J. Willis (USA), A.P.S. Wong (USA, Australia), P. Woodworth (UK), I. Yashayaev (Canada), I. Yasuda (Japan)

Review Editors:

Laurent Labeyrie (France), David Wratt (New Zealand)

This chapter should be cited as:

Bindoff, N.L., J. Willebrand, V. Artale, A, Cazenave, J. Gregory, S. Gulev, K. Hanawa, C. Le Quéré, S. Levitus, Y. Nojiri, C.K. Shum, L.D. Talley and A. Unnikrishnan, 2007: Observations: Oceanic Climate Change and Sea Level. In: *Climate Change 2007: The Physical Science Basis*. *Contribution of Working Group I to the Fourth Assessment Report of the Intergovernmental Panel on Climate Change* [Solomon, S., D. Qin, M. Manning, Z. Chen, M. Marquis, K.B. Averyt, M. Tignor and H.L. Miller (eds.)]. Cambridge University Press, Cambridge, United Kingdom and New York, NY, USA.

Table of Contents

Executive Summary 387

5.1 Introduction 389

5.2 Changes in Global-Scale Temperature and Salinity 389

5.2.1 Background 389

5.2.2 Ocean Heat Content 390

5.2.3 Ocean Salinity 393

5.2.4 Air-Sea Fluxes and Meridional Transports 393

5.3 Regional Changes in Ocean Circulation and Water Masses 394

5.3.1 Introduction 394

5.3.2 Atlantic and Arctic Oceans 395

Box 5.1: Has the Meridional Overturning Circulation in the Atlantic Changed? 397

5.3.3 Pacific Ocean 399

5.3.4 Indian Ocean 400

5.3.5 Southern Ocean 401

5.3.6 Relation of Regional to Global Changes 402

5.4 Ocean Biogeochemical Changes 403

5.4.1 Introduction 403

5.4.2 Carbon 403

5.4.3 Oxygen 406

5.4.4 Nutrients 406

5.4.5 Biological Changes Relevant to Ocean Biogeochemistry 408

5.4.6 Consistency with Physical Changes 408

5.5 Changes in Sea Level 408

5.5.1 Introductory Remarks 408

5.5.2 Observations of Sea Level Changes 410

5.5.3 Ocean Density Changes 414

5.5.4 Interpretation of Regional Variations in the Rate of Sea Level Change 416

5.5.5 Ocean Mass Change 417

5.5.6 Total Budget of the Global Mean Sea Level Change 419

5.6 Synthesis 420

Frequently Asked Question

FAQ 5.1: *Is Sea Level Rising?* 409

References 422

Appendix 5.A: Techniques, Error Estimation and Measurement Systems 429

Executive Summary

- The oceans are warming. Over the period 1961 to 2003, global ocean temperature has risen by 0.10°C from the surface to a depth of 700 m. Consistent with the Third Assessment Report (TAR), global ocean heat content (0–3,000 m) has increased during the same period, equivalent to absorbing energy at a rate of 0.21 ± 0.04 W m^{-2} globally averaged over the Earth's surface. Two-thirds of this energy is absorbed between the surface and a depth of 700 m. Global ocean heat content observations show considerable interannual and inter-decadal variability superimposed on the longer-term trend. Relative to 1961 to 2003, the period 1993 to 2003 has high rates of warming but since 2003 there has been some cooling.

- Large-scale, coherent trends of salinity are observed for 1955 to 1998, and are characterised by a global freshening in subpolar latitudes and a salinification of shallower parts of the tropical and subtropical oceans. Freshening is pronounced in the Pacific while increasing salinities prevail over most of Atlantic and Indian Oceans. These trends are consistent with changes in precipitation and inferred larger water transport in the atmosphere from low latitudes to high latitudes and from the Atlantic to the Pacific. Observations do not allow for a reliable estimate of the global average change in salinity in the oceans.

- Key oceanic water masses are changing; however, there is no clear evidence for ocean circulation changes. Southern Ocean mode waters and Upper Circumpolar Deep Waters have warmed from the 1960s to about 2000. A similar but weaker pattern of warming in the Gulf Stream and Kuroshio mode waters in the North Atlantic and North Pacific has been observed. Long-term cooling is observed in the North Atlantic subpolar gyre and in the central North Pacific. Since 1995, the upper North Atlantic subpolar gyre has been warming and becoming more saline. It is *very likely* that up to the end of the 20th century, the Atlantic meridional overturning circulation has been changing significantly at interannual to decadal time scales. Over the last 50 years, no coherent evidence for a trend in the strength of the meridional overturning circulation has been found.

- Ocean biogeochemistry is changing. The total inorganic carbon content of the oceans has increased by 118 ± 19 GtC between the end of the pre-industrial period (about 1750) and 1994 and continues to increase. It is *more likely than not* that the fraction of emitted carbon dioxide that was taken up by the oceans has decreased, from 42 ± 7% during 1750 to 1994 to 37 ± 7% during 1980 to 2005. This would be consistent with the expected rate at which the oceans can absorb carbon, but the uncertainty in this estimate does not allow firm conclusions. The increase in total inorganic carbon caused a decrease in the depth at which calcium carbonate dissolves, and also caused a decrease in surface ocean pH by an average of 0.1 units since 1750. Direct observations of pH at available time series stations for the last 20 years also show trends of decreasing pH at a rate of 0.02 pH units per decade. There is evidence for decreased oxygen concentrations, likely driven by reduced rates of water renewal, in the thermocline (~100–1,000 m) in most ocean basins from the early 1970s to the late 1990s.

- Global mean sea level has been rising. From 1961 to 2003, the average rate of sea level rise was 1.8 ± 0.5 mm yr^{-1}. For the 20th century, the average rate was 1.7 ± 0.5 mm yr^{-1}, consistent with the TAR estimate of 1 to 2 mm yr^{-1}. There is *high confidence* that the rate of sea level rise has increased between the mid-19th and the mid-20th centuries. Sea level change is highly non-uniform spatially, and in some regions, rates are up to several times the global mean rise, while in other regions sea level is falling. There is evidence for an increase in the occurrence of extreme high water worldwide related to storm surges, and variations in extremes during this period are related to the rise in mean sea level and variations in regional climate.

- The rise in global mean sea level is accompanied by considerable decadal variability. For the period 1993 to 2003, the rate of sea level rise is estimated from observations with satellite altimetry as 3.1 ± 0.7 mm yr^{-1}, significantly higher than the average rate. The tide gauge record indicates that similar large rates have occurred in previous 10-year periods since 1950. It is unknown whether the higher rate in 1993 to 2003 is due to decadal variability or an increase in the longer-term trend.

- There are uncertainties in the estimates of the contributions to sea level change but understanding has significantly improved for recent periods. For the period 1961 to 2003, the average contribution of thermal expansion to sea level rise was 0.4 ± 0.1 mm yr^{-1}. As reported in the TAR, it is *likely* that the sum of all known contributions for this period is smaller than the observed sea level rise, and therefore it is not possible to satisfactorily account for the processes causing sea level rise. However, for the period 1993 to 2003, for which the observing system is much better, the contributions from thermal expansion (1.6 ± 0.5 mm yr^{-1}) and loss of mass from glaciers, ice caps and the Greenland and Antarctic Ice Sheets together give 2.8 ± 0.7 mm yr^{-1}. For the latter period, the climate contributions constitute the main factors in the sea level budget, which is closed to within known errors.

- The patterns of observed changes in global ocean heat content and salinity, sea level, thermal expansion, water mass evolution and biogeochemical parameters described in this chapter are broadly consistent with the observed ocean surface changes and the known characteristics of the large-scale ocean circulation.

5.1 Introduction

The ocean has an important role in climate variability and change. The ocean's heat capacity is about 1,000 times larger than that of the atmosphere, and the oceans net heat uptake since 1960 is around 20 times greater than that of the atmosphere (Levitus et al., 2005a). This large amount of heat, which has been mainly stored in the upper layers of the ocean, plays a crucial role in climate change, in particular variations on seasonal to decadal time scales. The transport of heat and freshwater by ocean currents can have an important effect on regional climates, and the large-scale Meridional Overturning Circulation (MOC; also referred to as thermohaline circulation) influences the climate on a global scale (e.g., Vellinga and Wood, 2002). Life in the sea is dependent on the biogeochemical status of the ocean and is influenced by changes in the physical state and circulation. Changes in ocean biogeochemistry can directly feed back to the climate system, for example, through changes in the uptake or release of radiatively active gases such as carbon dioxide. Changes in sea level are also important for human society, and are linked to changes in ocean circulation. Finally, oceanic parameters can be useful for detecting climate change, in particular temperature and salinity changes in the deeper layers and in different regions where the short-term variability is smaller and the signal-to-noise ratio is higher.

The large-scale, three-dimensional ocean circulation and the formation of water masses that ventilate the main thermocline together create pathways for the transport of heat, freshwater and dissolved gases such as carbon dioxide from the surface ocean into the density-stratified deeper ocean, thereby isolating them from further interaction with the atmosphere. These pathways are also important for the transport of anomalies in these parameters caused by changes in the surface conditions. Furthermore, changes in the storage of heat and in the distribution of ocean salinity cause the ocean to expand or contract and hence change the sea level both regionally and globally.

The ocean varies over a broad range of time scales, from seasonal (e.g., in the surface mixed layer) to decadal (e.g., circulation in the main subtropical gyres) to centennial and longer (associated with the MOC). The main modes of climate variability, which are described in Chapter 3, are the El Niño-Southern Oscillation (ENSO), the Pacific Decadal Oscillation (PDO), the Northern Annular Mode (NAM), which is related to the North Atlantic Oscillation (NAO), and the Southern Annular Mode (SAM). Forcing of the oceans is often related to these modes, which cause changes in ocean circulation through changed patterns of winds and changes in surface ocean density.

The Third Assessment Report (TAR) discussed some aspects of the ocean's role. Folland et al. (2001) concluded that the global ocean has significantly warmed since the late 1950's. This assessment provides updated estimates of temperature changes for the oceans. Furthermore, it discusses new evidence for changes in the ocean freshwater budget and the ocean circulation. The TAR estimate of the total inorganic carbon increase in the ocean (Prentice et al., 2001) was based entirely on indirect evidence. This assessment provides updated indirect estimates and reports on new and direct evidence for changes in total carbon increase and for changes in ocean biogeochemistry (including pH and oxygen). Church et al. (2001) determined a range of 1 to 2 mm yr^{-1} for the observed global average sea level rise in the 20th century. This assessment provides new estimates for sea level change and the climate-related contributions to sea level change from thermal expansion and melting of ice sheets, glaciers and ice caps. The focus of this chapter is on observed changes in the global ocean basins, however some regional changes in the ocean state are also considered.

Many ocean observations are poorly sampled in space and time, and regional distributions often are quite heterogeneous. Furthermore, the observational records only cover a relatively short period of time (e.g., the 1950s to the present). Many of the observed changes have significant decadal variability associated with them, and in some cases decadal variability and/or poor sampling may prevent detection of long-term trends. When time series of oceanic parameters are considered, linear trends are often computed in order to quantify the observed long-term changes; however, this does not imply that the original signal is best represented by a linear increase in time. For plotting time series, this chapter generally uses the difference (anomaly) from the average value for the years 1961 to 1990. Wherever possible, error bars are provided to quantify the uncertainty of the observations. As in other parts of this report, 90% confidence intervals are used throughout. If not otherwise stated, values with error bars given as $x \pm e$ should hence be interpreted as a 90% chance that the true value is in the range $x - e$ to $x + e$.

5.2 Changes in Global-Scale Temperature and Salinity

5.2.1 Background

Among the major challenges in understanding the climate system are quantifying the Earth's heat balance and the freshwater balance (hydrological cycle), which both have a substantial contribution from the World Ocean. This chapter presents observational evidence that directly or indirectly helps to quantify changes in these balances.

The TAR included estimates of ocean heat content changes for the upper 3,000 m of the World Ocean. Ocean heat content change is closely proportional to the average temperature change in a volume of seawater, and is defined here as the deviation from a reference period. This section reports on updates of this estimate and presents estimates for the upper 700 m based on additional modern and historical data (Willis et al., 2004; Levitus et al., 2005b; Ishii et al., 2006). The section also presents new estimates of the temporal variability of salinity. The data used for temperature and heat content estimates are based on the World Ocean Database 2001 (e.g., Boyer et al.,

2002; Conkright et al., 2002), which has been updated with more recent data. Temperature data include measurements from reversing thermometers, expendable bathythermographs, mechanical bathythermographs, conductivity-temperature-depth instruments, Argo profiling floats, moored buoys and drifting buoys. The salinity data are described by Locarnini et al. (2002) and Stephens et al. (2002).

5.2.2 Ocean Heat Content

5.2.2.1 Long-Term Temperature Changes

Figure 5.1 shows two time series of ocean heat content for the 0 to 700 m layer of the World Ocean, updated from Ishi et al. (2006) and Levitus et al. (2005a) for 1955 to 2005, and a time series for 0 to 750 m for 1993 to 2005 updated from Willis et al. (2004). Approximately 7.9 million temperature profiles were used in constructing the two longer time series. The three heat content analyses cover different periods but where they overlap in time there is good agreement. The time series shows an overall trend of increasing heat content in the World Ocean with interannual and inter-decadal variations superimposed on this trend. The root mean square difference between the three data sets is 1.5×10^{22} J. These year-to-year differences, which are due to differences in quality control and data used, are small and now approaching the accuracies required to close the Earth's radiation budget (e.g., Carton et al., 2005). On longer time scales, the two longest time series (using independent criteria for selection, quality control, interpolation and analysis of similar data sets) show good agreement about long-term trends and also on decadal time scales.

For the period 1993 to 2003, the Levitus et al. (2005a) analysis has a linear global ocean trend of 0.42 ± 0.18 W m^{-2}, Willis et al. (2004) has a trend of 0.66 ± 0.18 W m^{-2} and Ishii et al. (2006) a trend of 0.33 ± 0.18 W m^{-2}. Overall, we assess the trend for this period as 0.5 ± 0.18 W m^{-2}. For the 0 to 700 m layer and the period 1955 to 2003 the heat content change is $10.9 \pm 3.1 \times 10^{22}$ J or 0.14 ± 0.04 W m^{-2} (data from Levitus et al., 2005a). All of these estimates are per unit area of Earth surface. Despite the fact that there are differences between these three ocean heat content estimates due to the data used, quality control applied, instrumental biases, temporal and spatial averaging and analysis methods (Appendix 5.A.1), they are consistent with each other giving a high degree of confidence for their use in climate change studies. The global increase in ocean heat content during the period 1993 to 2003 in two ocean models constrained by assimilating altimetric sea level and other observations (Carton et al., 2005; Köhl et al., 2006) is considerably larger than these observational estimates. We assess the heat content change from both of the long time series (0 to 700 m layer and the 1961 to 2003 period) to be $8.11 \pm 0.74 \times 10^{22}$ J, corresponding to an average warming of 0.1°C or 0.14 ± 0.04 W m^{-2}, and conclude that the available heat content estimates from 1961 to 2003 show a significant increasing trend in ocean heat content.

The data used in estimating the Levitus et al. (2005a) ocean temperature fields (for the above heat content estimates) do not include sea surface temperature (SST) observations,

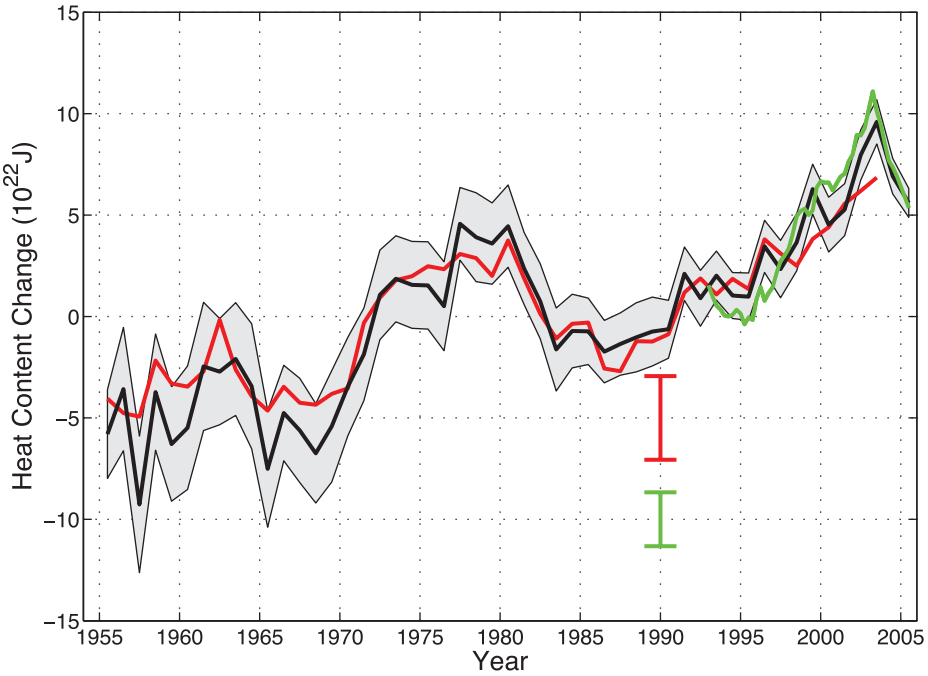


Figure 5.1. *Time series of global annual ocean heat content (10^{22} J) for the 0 to 700 m layer. The black curve is updated from Levitus et al. (2005a), with the shading representing the 90% confidence interval. The red and green curves are updates of the analyses by Ishii et al. (2006) and Willis et al. (2004, over 0 to 750 m) respectively, with the error bars denoting the 90% confidence interval. The black and red curves denote the deviation from the 1961 to 1990 average and the shorter green curve denotes the deviation from the average of the black curve for the period 1993 to 2003.*

which are discussed in Chapter 3. However, comparison of the global, annual mean time series of near-surface temperature (approximately 0 to 5 m depth) from this analysis and the corresponding SST series based on a subset of the International Comprehensive Ocean-Atmosphere Data Set (ICOADS) database (approximately 134 million SST observations; Smith and Reynolds, 2003 and additional data) shows a high correlation (r = 0.96) for the period 1955 to 2005. The consistency between these two data sets gives confidence in the ocean temperature data set used for estimating depth-integrated heat content, and supports the trends in SST reported in Chapter 3.

There is a contribution to the global heat content integral from depths greater than 700 m as documented by Levitus et al. (2000; 2005a). However, due to the lack of data with increasing depth the data must be composited using five-year running pentads in order to have enough data for a meaningful analysis in the deep ocean. Even then, there are not enough deep ocean data to extend the time series for the upper 3,000 m past the 1994–1998 pentad. There is a close correlation between the 0 to 700 and 0 to 3,000 m time series of Levitus et al. (2005a). A comparison of the linear trends from these two series indicates that about 69% of the increase in ocean heat content during 1955 to 1998 (the period when estimates from both time series are available) occurred in the upper 700 m of the World Ocean. Based on the linear trend, for the 0 to 3,000 m layer for the period 1961 to 2003 there has been an increase of ocean heat content of approximately $14.2 \pm 2.4 \times 10^{22}$ J, corresponding to a global ocean volume mean temperature increase of 0.037°C during this period. This increase in ocean heat content corresponds to an average heating rate of 0.21 ± 0.04 W m^{-2} for the Earth's surface.

The geographical distribution of the linear trend of 0 to 700 m heat content for 1955 to 2003 for the World Ocean is shown in Figure 5.2. These trends are non-uniform in space, with some regions showing cooling and others warming. Most of the Atlantic Ocean exhibits warming with a major exception being the subarctic gyre. The Atlantic Ocean accounts for approximately half of the global linear trend of ocean heat content (Levitus et al., 2005a). Much of the Indian Ocean has warmed since 1955 with a major exception being the 5°S to 20°S latitude belt. The Southern Ocean (south of 35°S) in the Atlantic, Indian and Pacific sectors has generally warmed. The Pacific Ocean is characterised by warming with major exceptions along 40°N and the western tropical Pacific.

Figure 5.3 shows the linear trends (1955 to 2003) of zonally averaged temperature anomalies (0 to 1,500 m) for the World Ocean and individual basins based on yearly anomaly fields (Levitus et al., 2005a). The strongest trends in these anomalies are concentrated in the upper ocean. Warming occurs at most latitudes in all three of the ocean basins. The regions that exhibit cooling are mainly in the shallow equatorial areas and in some high-latitude regions. In the Indian Ocean, cooling occurs at subsurface depths centred on 12°S at 150 m depth and in the Pacific centred on the equator and 150 m depth. Cooling also occured in the 32°N to 48°N region of the Pacific Ocean and the 49°N to 60°N region of the Atlantic Ocean. Regional temperature changes are discussed further in Section 5.3.

5.2.2.2 Variability of Heat Content

A major feature of Figure 5.1 is the relatively large increase in global ocean heat content during 1969 to 1980 and a sharp

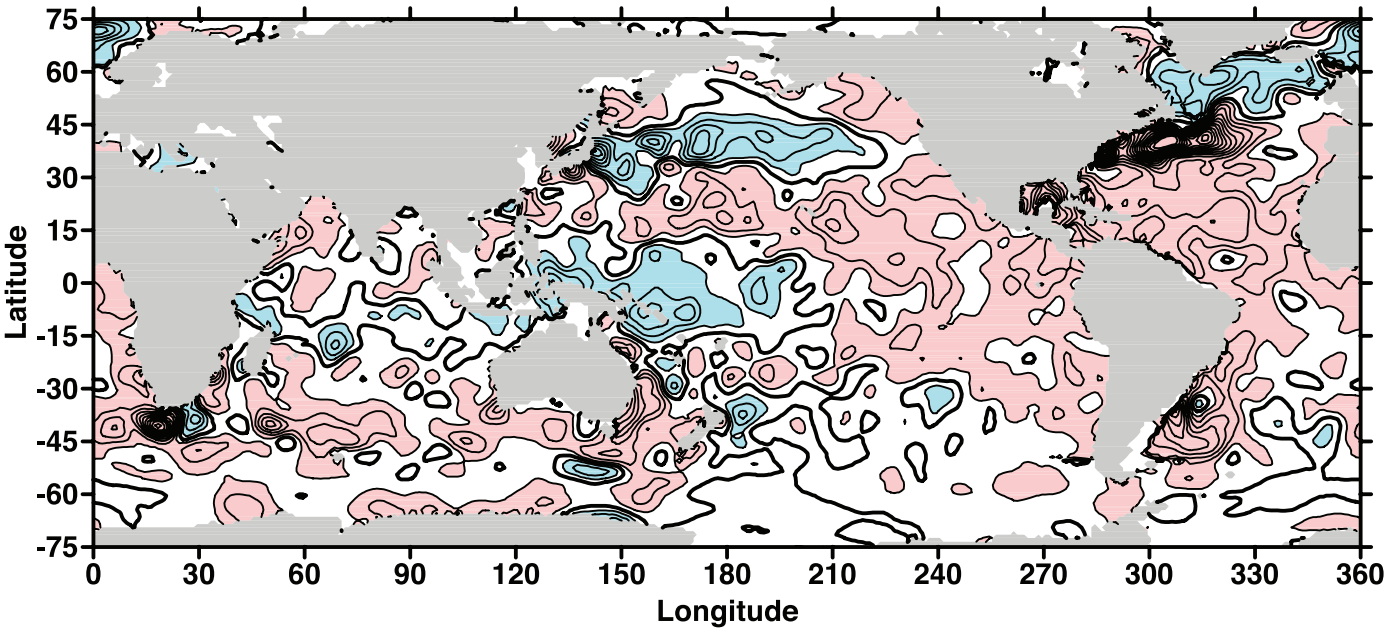


Figure 5.2. *Linear trends (1955–2003) of change in ocean heat content per unit surface area (W m^{-2}) for the 0 to 700 m layer, based on the work of Levitus et al. (2005a). The linear trend is computed at each grid point using a least squares fit to the time series at each grid point. The contour interval is 0.25 W m^{-2}. Red shading indicates values equal to or greater than 0.25 W m^{-2} and blue shading indicates values equal to or less than –0.25 W m^{-2}.*

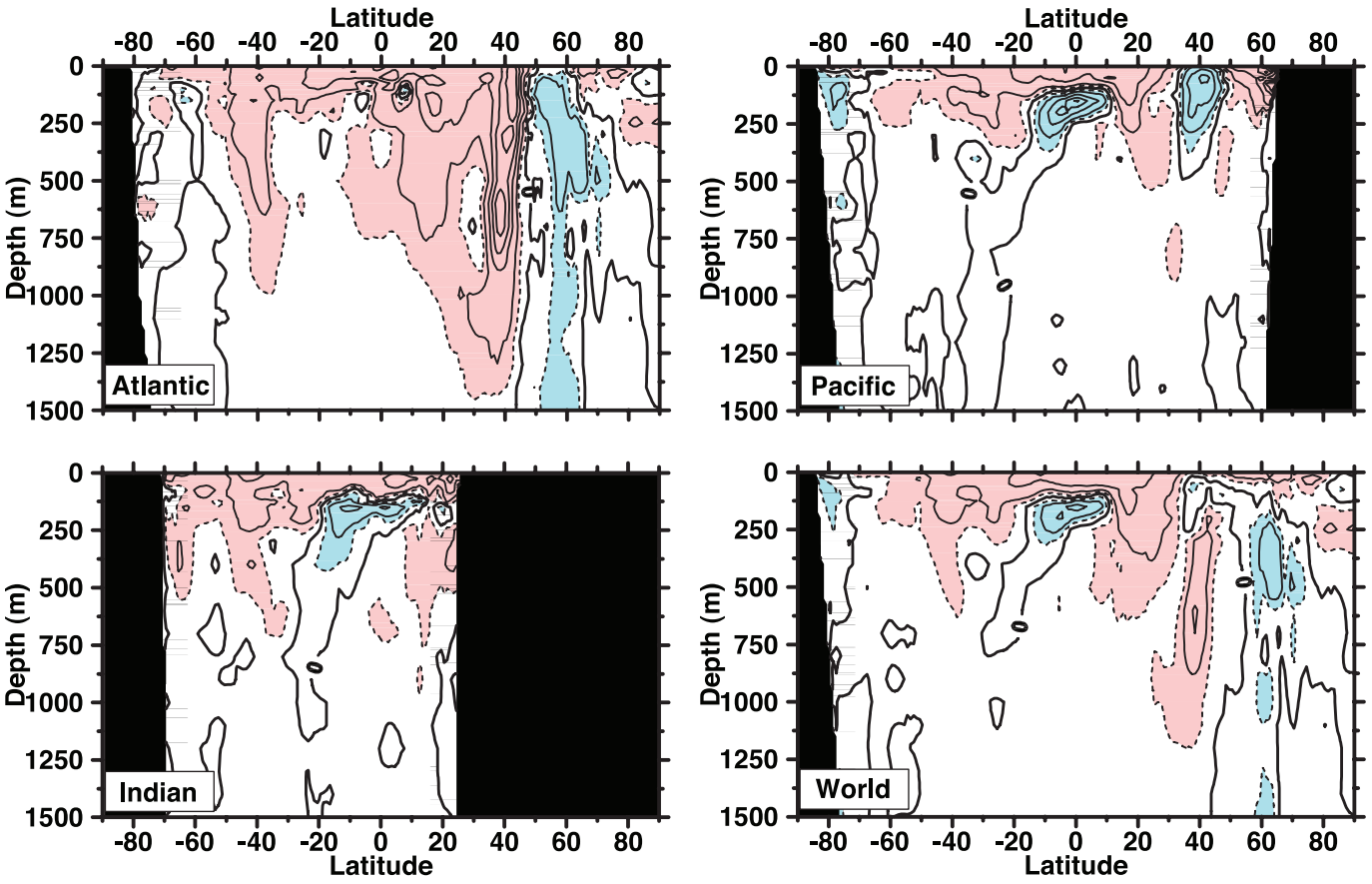


Figure 5.3. *Linear trend (1955–2003) of zonally averaged temperature in the upper 1,500 m of the water column of the Atlantic, Pacific, Indian and World Oceans. The contour interval is 0.05°C per decade, and the dark solid line is the zero contour. Red shading indicates values equal to or greater than 0.025°C per decade and blue shading indicates values equal to or less than –0.025°C per decade. Based on the work of Levitus et al. (2005a).*

decrease during 1980 to 1983. The 0 to 700 m layer cooled at a rate of 1.2 W m^{-2} during this period. Most of this cooling occurred in the Pacific Ocean and may have been associated with the reversal in polarity of the PDO (Stephens et al., 2001; Levitus et al., 2005c, see also Section 3.6.3). Examination of the geographical distribution of the differences in 0 to 700 m heat content between the 1977–1981 and 1965–1969 pentads and the 1986–1990 and 1977–1981 pentads shows that the pattern of heat content change has spatial scales of entire ocean basins and is also found in similar analyses by Ishii et al. (2006). The Pacific Ocean dominates the decadal variations of global heat content during these two periods. The origin of this variability is not well understood.

Based on model experiments, it has been suggested that errors resulting from the highly inhomogeneous distribution of ocean observations in space and time (see Appendix 5.A.1) could lead to spurious variability in the analysis (e.g., Gregory et al., 2004, AchutaRao et al., 2006). As discussed in the appendix, even in periods with overall good coverage in the observing system, large regions in Southern Hemisphere (SH) are not well sampled, and their contribution to global heat content variability is less certain. However, the large-scale nature of heat content variability, the similarity of the Levitus et al. (2005a) and the Ishii et al. (2006) analyses and new results showing a decrease in the global heat content in a period with much better data coverage (Lyman et al., 2006), gives confidence that there is substantial inter-decadal variability in global ocean heat content.

5.2.2.3 Implications for Earth's Heat Balance

To place the changes of ocean heat content in perspective, Figure 5.4 provides updated estimates of the change in heat content of various components of the Earth's climate system for the period 1961 to 2003 (Levitus et al., 2005a). This includes changes in heat content of the lithosphere (Beltrami et al., 2002), the atmosphere (e.g., Trenberth et al., 2001) and the total heat of fusion due to melting of i) glaciers, ice caps and the Antarctic and Greenland Ice Sheets (see Chapter 4) and ii) arctic sea ice (Hilmer and Lemke, 2000). The increase in ocean heat content is much larger than any other store of energy in the Earth's heat balance over the two periods 1961 to 2003 and 1993 to 2003, and accounts for more than 90% of the possible increase in heat content of the Earth system during these periods. Ocean heat content variability is thus a critical variable for detecting the effects of the observed increase in greenhouse gases in the Earth's atmosphere and for resolving the Earth's overall energy balance. It is noteworthy that whereas ice melt from glaciers, ice caps and ice sheets is very important in the sea level budget

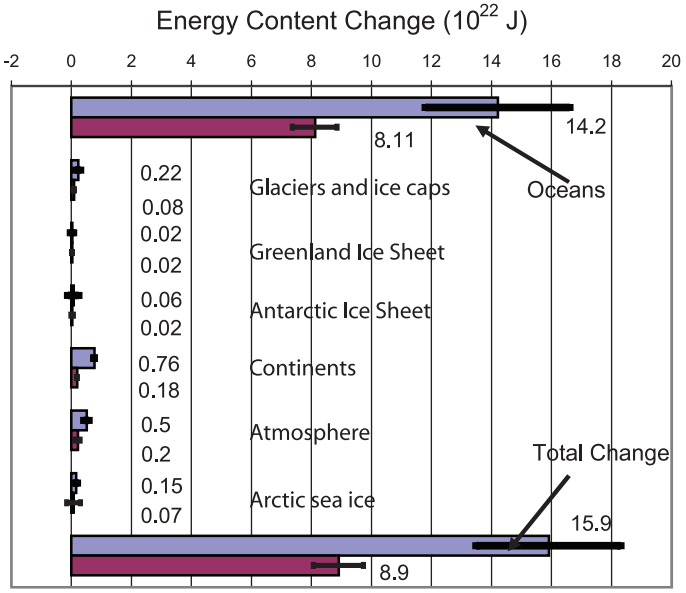


Figure 5.4. *Energy content changes in different components of the Earth system for two periods (1961–2003 and 1993–2003). Blue bars are for 1961 to 2003, burgundy bars for 1993 to 2003. The ocean heat content change is from this section and Levitus et al. (2005c); glaciers, ice caps and Greenland and Antarctic Ice Sheets from Chapter 4; continental heat content from Beltrami et al. (2002); atmospheric energy content based on Trenberth et al. (2001); and arctic sea ice release from Hilmer and Lemke (2000). Positive energy content change means an increase in stored energy (i.e., heat content in oceans, latent heat from reduced ice or sea ice volumes, heat content in the continents excluding latent heat from permafrost changes, and latent and sensible heat and potential and kinetic energy in the atmosphere). All error estimates are 90% confidence intervals. No estimate of confidence is available for the continental heat gain. Some of the results have been scaled from published results for the two respective periods. Ocean heat content change for the period 1961 to 2003 is for the 0 to 3,000 m layer. The period 1993 to 2003 is for the 0 to 700 m (or 750 m) layer and is computed as an average of the trends from Ishii et al. (2006), Levitus et al. (2005a) and Willis et al. (2004).*

(contributing about 40%), the energy associated with ice melt contributes only about 1% to the Earth's energy budget.

5.2.3 Ocean Salinity

Ocean salinity changes are an indirect but potentially sensitive indicator for detecting changes in precipitation, evaporation, river runoff and ice melt. The patterns of salinity change can be used to infer changes in the Earth's hydrological cycle over the oceans (Wong et al., 1999; Curry et al., 2003) and are an important complement to atmospheric measurements. Figure 5.5 shows the linear trends (based on pentadal anomaly fields) of zonally averaged salinity in the upper 500 m of the World Ocean and individual ocean basins (Boyer et al., 2005) from 1955 to 1998. A total of 2.3 million salinity profiles were used in this analysis, about one-third of the amount of data used in the ocean heat content estimates in Section 5.2.2.

Estimates of changes in the freshwater content of the global ocean have suggested that the global ocean is freshening (e.g., Antonov et al., 2002), however, sampling limitations due to data sparsity in some regions, particularly the SH, means that such estimates have an uncertainty that is not possible to quantify.

Between 15°S and 42°N in the Atlantic Ocean there is a salinity increase in the upper 500 m layer. This region includes the North Atlantic subtropical gyre. In the 42°N to 72°N region, including the Labrador, Irminger and Icelandic Seas, there is a freshening trend (discussed further in Section 5.3). The increase in salinity north of 72°N (Arctic Ocean) is highly uncertain because of the paucity of data in this region.

South of 50°S in the polar region of the Southern Ocean, there is a relatively weak freshening signal. Freshening occurs throughout most of the Pacific with the exception of the South Pacific subtropical gyre between 8°S and 32°S and above 300 m where there is an increase in salinity. The near-surface Indian Ocean is characterised mainly by increasing salinity. However, in the latitude band 5°S to 42°S (South Indian gyre) in the depth range of 200 to 1,000 m, there is a freshening of the water column.

The results shown here document that ocean salinity and hence freshwater are changing on gyre and basin scales, with the near-surface waters in the more evaporative regions increasing in salinity in almost all ocean basins. In the high-latitude regions in both hemispheres the surface waters are freshening consistent with these regions having greater precipitation, although higher runoff, ice melting, advection and changes in the MOC (Häkkinen, 2002) may also contribute. In addition to these meridional changes, the Atlantic is becoming saltier over much of the water column (Figure 5.5 and Boyer et al., 2005). Although the South Pacific subtropical region is becoming saltier, on average the whole water column in the Pacific Basin is becoming fresher (Boyer et al., 2005). The increasing difference in volume-averaged salinity between the Atlantic and Pacific Oceans suggests changes in freshwater transport between these two ocean basins.

We are confident that vertically coherent gyre and basin scale changes have occurred in the salinity (freshwater content) of parts of the World Ocean during the past several decades. While the available data and their analyses are insufficient to identify in detail the origin of these changes, the patterns are consistent with a change in the Earth's hydrological cycle, in particular with changes in precipitation and inferred larger water transport in the atmosphere from low latitudes to high latitudes and from the Atlantic to the Pacific (see Section 3.3.2).

5.2.4 Air-Sea Fluxes and Meridional Transports

The global average changes in ocean heat content discussed above are driven by changes in the air-sea net energy flux (see Section 5.2.2.1). At regional scales, few estimates of heat flux changes have been possible. During the last 50 years, net heat fluxes from the ocean to the atmosphere demonstrate locally decreasing values (up to 1 W m^{-2} yr^{-1}) over the southern flank of the Gulf Stream and positive trends (up to 0.5 W m^{-2} yr^{-1}) in the Atlantic central subpolar regions (Gulev et al., 2006). At the global scale, the accuracy of the flux observations is insufficient to permit a direct assessment of changes in heat flux. Air-sea fluxes are discussed in Section 3.5.6.

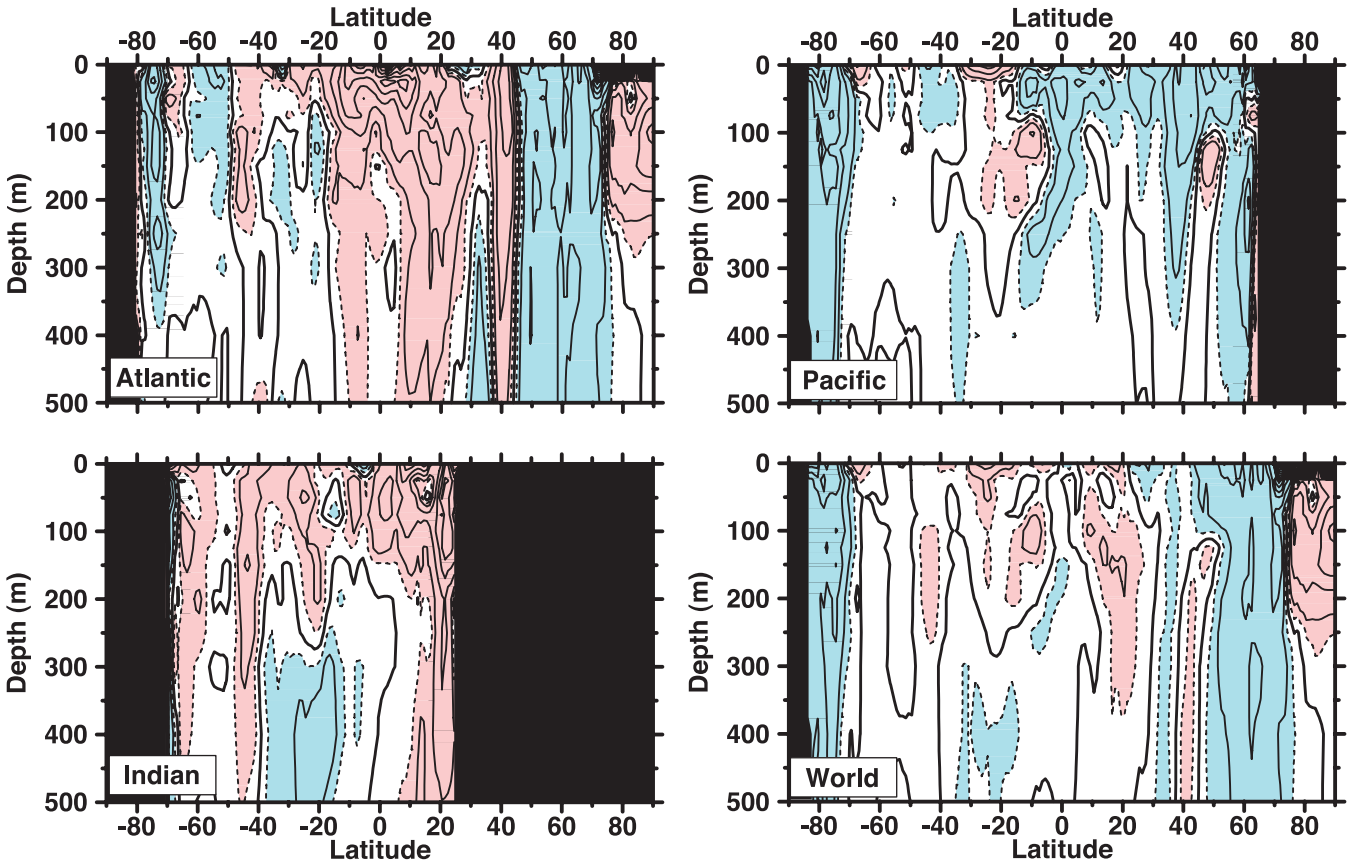


Figure 5.5: *Linear trends (1955–1998) of zonally averaged salinity (psu) in the upper 500 m of the Atlantic, Pacific, Indian and World Oceans. The contour interval is 0.01 psu per decade and dashed contours are ±0.005 psu per decade. The dark solid line is the zero contour. Red shading indicates values equal to or greater than 0.005 psu per decade and blue shading indicates values equal to or less than –0.005 psu per decade. Based on the work of Boyer et al. (2005).*

Estimates of the climatological mean oceanic meridional heat transport derived from atmospheric observations (e.g., Trenberth and Caron, 2001) and from oceanographic cross sections (e.g., Ganachaud and Wunsch, 2003) are in fair agreement, despite considerable uncertainties (see Appendix 5.A.2). The ocean heat transport estimate derived from integration of climatological air-sea heat flux fields (e.g., Grist and Josey, 2003) is in good agreement with an independent oceanographic cross section at 32°S. Estimates of changes in the Atlantic meridional heat transport are discussed in Section 5.3.2.

5.3 Regional Changes in Ocean Circulation and Water Masses

5.3.1 Introduction

Robust long-term trends in global- and basin-scale ocean heat content and basin-scale salinity were shown in Section 5.2. The observed heat and salinity trends are linked to changes in ocean circulation and other manifestations of global change such as oxygen and carbon system parameters (see Section 5.4). Global ocean changes result from regional changes in these properties, assessed in this section. Evidence for change in temperature, salinity and circulation is described globally and then for each of the major oceans. Two marginal seas with multi-decadal time series are also examined as examples of regional variations.

The upper ocean in all regions is close to the atmospheric forcing and has the largest variability; it is also the best sampled. For these reasons, Section 5.2 mainly assessed upper-ocean observations for long-term trends in heat content and salinity. However, there are important changes in heat and salinity at intermediate and abyssal depths, restricted to regions that are relatively close to the main sources of deep and intermediate waters. These sources are most vigorous in the northern North Atlantic and the Southern Ocean around Antarctica. This is illustrated well in salinity differences shown for the Atlantic (1985–1999 minus 1955–1969) and Pacific (1980s minus 1960s) in Figure 5.6. Striking changes in salinity are found from the surface to the bottom in the northern North Atlantic near water mass formation sites that fill the water column (Section 5.3.2); bottom changes elsewhere are small, being most prevalent at the under-sampled southern ends of both sections. At mid-depth (500 to 2,000 m), the Atlantic and southern end of the Pacific section show widespread change, but the North Pacific signal is weaker and shallower because it has only weak intermediate water formation (and no deep water formation). Changes in intermediate and deep waters can ultimately affect

the ocean's vertical stratification and overturning circulation; the topic of the overturning circulation in the North Atlantic is considered in Section 5.3.2.

The observed changes in salinity are of global scale, with similar patterns in different ocean basins (Figure 5.6). The subtropical waters have increased in salinity and the subpolar surface and intermediate waters have freshened in both the Atlantic and Pacific Oceans during the period from the 1960s to the 1990s and in both hemispheres in each ocean. The waters that underlie the near-surface subtropical waters have freshened due to equatorward circulation of the freshened subpolar surface waters; in particular, the fresh intermediate water layer (at ~1,000 m) in the SH has freshened in both the Atlantic and Pacific Oceans. In the Northern Hemisphere (NH), the Pacific intermediate waters have freshened, and the underlying deep waters did not change, consistent with no local bottom water source in the North Pacific. In the central North Atlantic, the intermediate layer (approximately 900–1,200 m) became saltier due to increased salinity in the outflow from the Mediterranean that feeds this layer.

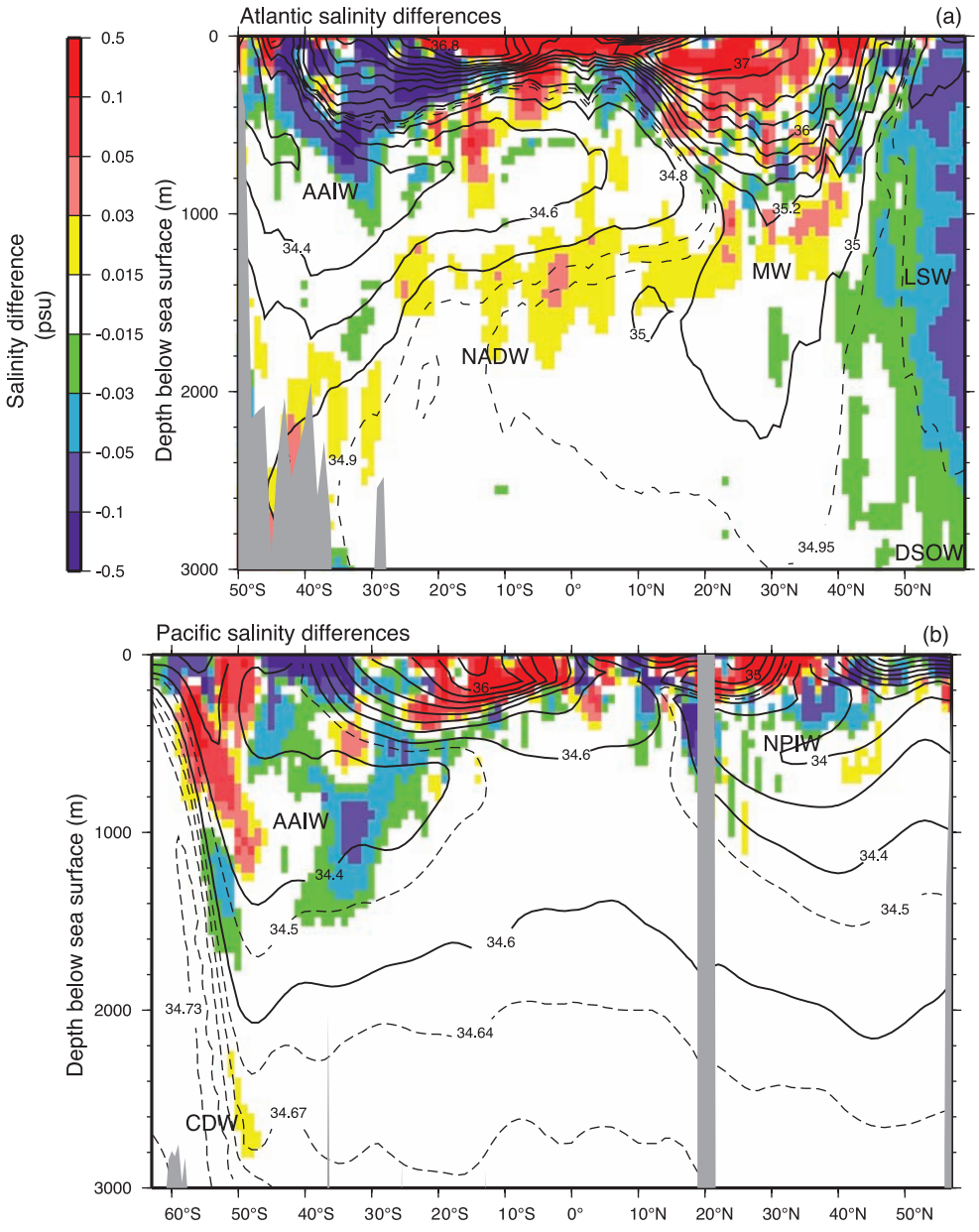


Figure 5.6. *Meridional sections of differences in salinity (psu) of the a) Atlantic Ocean for the period 1985 to 1999 minus 1955 to 1969 and b) Pacific Ocean for the World Ocean Circulation Experiment (WOCE) 150°W section (1991–1992) and historical data from 1968 plus or minus 7.5 years. Contours are the mean salinity fields along each section and show the key features. The salinity differences are differences along isopycnals that have been mapped to pressure surfaces. The Atlantic section is along the western side of the Atlantic Ocean and the Pacific section is along 150°W. The two figures are redrafted from Curry et al. (2003) and Wong et al (2001). Water masses shown include Antarctic Intermediate Water (AAIW), Circumpolar Deep Water (CDW), North Atlantic Deep Water (NADW), Mediterranean Water (MW), Labrador Sea Water (LSW), Denmark Strait Overflow Water (DSOW) and North Pacific Intermediate Water NPIW). The areas shaded in grey represent the seafloor and oceanic crust.*

5.3.2 Atlantic and Arctic Oceans

The North Atlantic Ocean has a special role in long-term climate assessment because it is central to one of the two global-scale MOCs (see Box 5.1), the other location being the Southern Ocean. The long-term trends in depth-integrated Atlantic heat content for the period 1955 to 2003 (Figure 5.2) are broadly consistent with the warming tendencies identified from the global analyses of SST (see Section 3.2.2.3). The subtropical gyre warmed and the subpolar gyre cooled over that period, consistent with a predominantly positive phase of the NAO during the last several decades. The warming extended down to below 1,000 m, deeper than anywhere else in the World Ocean (Figure 5.3 Atlantic), and was particularly pronounced under the Gulf Stream and North Atlantic Current near 40°N. Long-term trends in salinity towards freshening in the subpolar regions and increased salinity in the subtropics through the mid-1990s (Figure 5.5 Atlantic and Figure 5.6a) are consistent with the global tendencies for freshening of relatively fresher regions and increased salinity in saltier regions (Section 5.2.3).

5.3.2.1 North Atlantic Subpolar Gyre, Labrador Sea and Nordic Seas

In the North Atlantic subpolar gyre, Labrador Sea and Nordic Seas, large salinity changes have been observed that have been associated with changed inputs of fresh water (ice melt, ocean circulation and river runoff) and with the NAO. Advection of these surface and deep salinity anomalies has been traced around the whole subpolar gyre including the Labrador and Nordic Seas. These anomalies are often called 'Great Salinity Anomalies' (GSAs; e.g., Dickson et al., 1988; Belkin, 2004). During a positive phase of the NAO, the subpolar gyre strengthens and expands towards the east, resulting in lower surface salinity in the central subpolar region (Levitus, 1989; Reverdin et al., 1997; Bersch, 2002). Three GSAs have been thoroughly documented: one from 1968 to 1978, one in the 1980s and one in the 1990s. Observational and modelling studies show that the relative influence of local events and advection differ between different GSA events and regions (Houghton and Visbeck, 2002; Josey and Marsh, 2005).

These surface salinity anomalies have affected the Labrador Sea and the production of Labrador Sea Water (LSW), a major component of the North Atlantic Deep Water (NADW) and contributor to the lower limb of the MOC. The LSW appears to alternate between dense, cold types and less dense, warm types (Yashayaev et al., 2003; Kieke et al., 2006) possibly with more production of dense LSW during years of positive-phase NAO (Dickson et al., 1996). Since 1965 to 1970, the LSW has had a significant freshening trend with a superimposed variability consisting of three saltier periods, coinciding with warmer water, and two freshening and cooling periods in the 1970s and 1990s (Figure 5.7). During the period 1988 to 1994, an exceptionally large volume of cold, fresh and dense LSW was produced (Sy et al., 1997; Lazier et al., 2002), unprecedented in the sparse time series that extends back to the 1930s (Talley and McCartney, 1982). The Labrador Sea has now returned to a warmer, more saline state; most of the excess volume of the dense LSW has disappeared, the mid-layers became warmer and saltier, and the production of LSW shifted to the warmer type (e.g., Lazier et al., 2002; Yashayaev et al., 2003; Stramma et al., 2004). This warming and increased salinity and reduction in LSW was associated with the weakening of the North Atlantic subpolar gyre, seen also in satellite altimetry data (Häkkinen and Rhines, 2004).

The eastern half of the subpolar North Atlantic also freshened through the 1980s and into the 1990s, but the upper ocean has been increasing in salinity or remaining steady since then, depending on location. About two-thirds of the freshening in this region has been attributed to an increase in precipitation associated with a climate pattern known as the East Atlantic Pattern (Josey and Marsh, 2005), with the NAO playing a secondary role. From 1965 to 1995, the subpolar freshening amounted to an equivalent freshwater layer of approximately 3 m spread evenly over its total area (Belkin, 2004; Curry and Mauritzen, 2005).

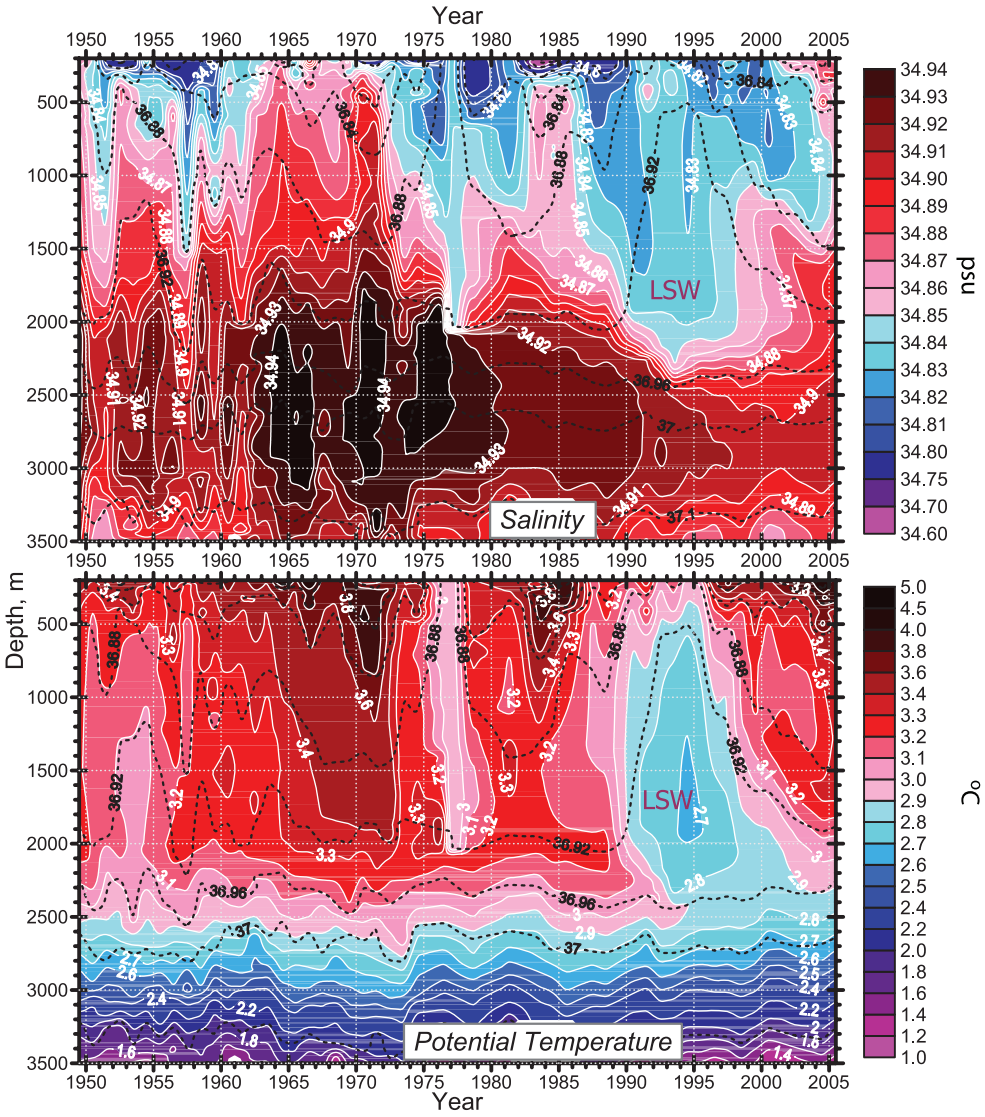


Figure 5.7. *The longest available time series of salinity (psu; upper panel) and potential temperature (°C, lower panel) in the central Labrador Sea from 1949 to 2005 (updated from Yashayaev et al., 2003). The dashed lines are contours of potential density (kg m^{-3}, difference from 1,000 kg m^{-3}) and are the same on both panels.*

Box 5.1: Has the Meridional Overturning Circulation in the Atlantic Changed?

The global Meridional Overturning Circulation consists primarily of dense waters that sink to the abyssal ocean at high latitudes in the North Atlantic Ocean and near Antarctica. These dense waters then spread across the equator with comparable flows of approximately 17 and 14 Sv (10^6 m^3 s^{-1}), respectively (Orsi et al., 2002; Talley et al., 2003a). The North Atlantic overturning circulation (henceforth 'MOC') is characterised by an inflow of warm, saline upper-ocean waters from the south that gradually increase in density from cooling as they move northward through the subtropical and subpolar gyres. They also freshen, which reduces the density increase. The inflows reach the Nordic Seas (Greenland, Iceland and Norwegian Seas) and the Labrador Sea, where they are subject to deep convection, sill overflows and vigorous mixing. Through these processes NADW is formed, constituting the southward-flowing lower limb of the MOC.

Climate models show that the Earth's climate system responds to changes in the MOC (e.g., Vellinga and Wood, 2002), and also suggest that the MOC might gradually decrease in transport in the 21st century as a consequence of anthropogenic warming and additional freshening in the North Atlantic (Bi et al., 2001; Gregory et al., 2005; see also Chapter 10). However, observations of changes in the MOC strength and variability are fragmentary; the best evidence for observational change comes from the North Atlantic.

There is evidence for a link between the MOC and abrupt changes in surface climate during the past 120 kyr, although the exact mechanism is not clear (Clark et al., 2002). At the end of the last glacial period, as the climate warmed and ice sheets melted, there were a number of abrupt oscillations, for example, the Younger Dryas and the 8.2 ka cold event (see Section 6.4), which may have been caused by changes in ocean circulation. The variability of the MOC during the Holocene after the 8.2 ka cooling event is clearly much smaller than during glacial times (Keigwin et al., 1994; see Section 6.4).

Observed changes in MOC transport, water properties and water mass formation are inconclusive about changes in the MOC strength (see Section 5.3.2.2). This is partially due to decadal variability and partially due to inadequate long-term observations. From repeated hydrographic sections in the subtropics, Bryden et al. (2005) concluded that the MOC transport at 25°N had decreased by 30% between 1957 and 2004, but the presence of significant unsampled variability in time and the lack of supporting direct current measurements reduces confidence in this estimate. Direct measurements of the two major sill overflows have shown considerable variability in the dominant Denmark Strait Overflow without enough years of coverage to discern long-term trends (Macrander et al., 2005). The observed freshening of the overflows and the associated reduction in density from 1965 to 2000 (see Section 5.3.2) has so far not led to a significant weakening of the MOC (Dickson et al., 2003; Curry and Mauritzen, 2005). Moreover, large decadal variability observed since 1960 in salinity and temperature of the surface waters, including the recent increase in salinity of the surface waters feeding the MOC, obscures the long-term trend (Hátún et al., 2005; ICES 2005) and hence conclusions about potential MOC changes.

Changes in the MOC can also be caused by changes in Labrador Sea convection, with strong convection corresponding to higher MOC. Convection was strong from the 1970s to 1995, but thereafter the Labrador Sea warmed and re-stratified (Lazier et al., 2002; Yashayaev et al., 2003) and convection has been weaker. Based on observed SST patterns, it was concluded that the MOC transport has increased by about 10% from 1970 to the 1990s (Knight et al., 2005; Latif et al., 2006). From direct current meter observations at the exit of the subpolar North Atlantic, Schott et al. (2004) concluded that the Deep Water outflow, while varying at shorter time scales, had no significant trend during the 1993 to 2001 period.

In summary, it is very likely that up to the end of the 20th century the MOC was changing significantly at interannual to decadal time scales. Given the above evidence from components of the MOC as well as uncertainties in the observational records, over the modern instrumental record no coherent evidence for a trend in the mean strength of the MOC has been found.

Subsurface salinity in the Nordic Seas has also decreased markedly since the 1970s (Dickson et al., 2003), directly affecting the salinity of the Nordic Sea overflow waters that contribute to NADW. This decrease in subsurface salinity was associated with lower salinity of the Atlantic waters entering the Nordic seas and related to the high NAO index and intensification of the subpolar gyre. Since 1994, the salinity of the inflow from the North Atlantic has been increasing, reaching the highest values since 1948, largely due to a weakening of the subpolar gyre circulation that allowed more warm water into the Nordic Seas, associated with a decreasing NAO index (Hátún et al., 2005).

The densest waters contributing to NADW and to the deep limb of the MOC arise as overflows from the upper 1,500 m of the Nordic Seas through the Denmark Strait and Faroe Channel. The marked freshening of the overflow water masses exiting the Arctic was associated with growing sea ice export from the Arctic and precipitation in the Nordic Seas (Dickson et al., 2002, 2003). The transports of the overflow waters, of which the largest component is through Denmark Strait, have varied by about 30% (Macrander et al., 2005), but there has been no clear trend in this location. Overall, the overflows that contribute to NADW from the Nordic Seas have remained constant to within the known variability.

The overall pattern of change in the North Atlantic subpolar gyre is one of a trend towards fresher values over most of the water column from the mid-1960s until the mid-1990s. Since then, there has been a return to warmer and more saline waters

(Figure 5.7), which coincides with the change in NAO and East Atlantic Pattern. However, this return to saltier waters has not been sustained for a long enough period to change the sign of the long-term trends (Figure 5.5 Atlantic).

5.3.2.2 Arctic Ocean

Climate change in the Arctic Ocean and Nordic Seas is closely linked to the North Atlantic subpolar gyre (Østerhus et al., 2005). Within the Arctic Ocean and Nordic Seas, surface temperature has increased since the mid-1980s and continues to increase (Comiso, 2003). In the Atlantic waters entering the Nordic Seas, a temperature increase in the late 1980s and early 1990s (Quadfasel et al., 1991; Carmack et al., 1995) has been associated with the transition in the 1980s towards more positive NAO states. Warm Atlantic waters have also been observed to enter the Arctic as pulses via Fram Strait and then along the slope to the Laptev Sea (Polyakov et al., 2005); the increased heat content and increased transport in the pulses both contribute to net warming of the arctic waters (Schauer et al., 2004). Multi-decadal variability in the temperature of the Atlantic Water core affecting the top 400 m in the Arctic Ocean has been documented (Polyakov et al., 2004). Within the Arctic, salinity increased in the upper layers of the Amundsen and Makarov Basins, while salinity of the upper layers in the Canada Basin decreased (Morison et al., 1998). Compared to the 1980s, the area of upper waters of Pacific origin has decreased (McLaughlin et al., 1996; Steele and Boyd, 1998).

During the 1990s, changed winds caused eastward redirection of river runoff from the Laptev Sea (Lena River, etc.), reducing the low-salinity surface layer in the central Arctic Ocean (Steele and Boyd, 1998), thus allowing greater convection and heat transport into the surface arctic layer from the more saline subsurface Atlantic layer. Thereafter, however, the stratification in the central Arctic (Amundsen Basin) increased and a low-salinity mixed layer was again observed at the North Pole in 2001, possibly due to a circulation change that restored the river water input (Björk et al., 2002). Circulation variability that shifts the balance of fresh and saline surface waters in the Arctic, with associated changes in sea ice, might be associated with the NAM (Proshutinsky and Johnson, 1997; Rigor et al., 2002), however, the long-term decline in arctic sea ice cover appears to be independent of the NAM (Comiso, 2002). While there is significant decadal variability in the Arctic Ocean, no systematic long-term trend in subsurface arctic waters has been identified.

5.3.2.3 Subtropical and Equatorial Atlantic

In the North Atlantic subtropical gyre, circulation, SST, the thickness of near-surface Subtropical Mode Water (STMW, Hanawa and Talley, 2001) and thermocline ventilation are all highly correlated with the NAO, with some time lags. A more positive NAO state, with westerlies shifted northwards, results in a decreased Florida Current transport (Baringer and Larsen, 2001), a likely delayed northward shift of the Gulf Stream position (Joyce et al., 2000; Seager et al., 2001; Molinari, 2004), and decreased subtropical eddy variability (Penduff et al., 2004). In the STMW, low thickness and production and higher temperature result from a high NAO index (e.g., Talley, 1996; e.g., Hazeleger and Drijfhout, 1998; Marsh, 2000). The volume of STMW is likely to lag changes in the NAO by two to three years, and low (high) volumes are associated with high (low) surface layer temperatures because of changes in both convective forcing and location of STMW formation. While quasi-cyclic variability in STMW renewal is apparent over the 1960 to 1980 period, the total volume of STMW has remained low through 2000 since a peak in 1983 to 1984, associated with a relatively persistent positive NAO phase during the late 1980s and early 1990s (Lazier et al., 2002; Kwon and Riser, 2004).

In the subtropics at depths of 1,000 to 2,000 m, the temperature has increased since the late 1950s at Bermuda, at 24°N, and at 52°W and 66°W in the Gulf Stream (Bryden et al., 1996; Joyce and Robbins, 1996; Joyce et al., 1999). These warming trends reflect reduced production of LSW (Lazier, 1995) and increased salinity and temperature of the waters from the Mediterranean (Roether et al., 1996; Potter and Lozier, 2004). After the mid-1990s at greater depths (1,500–2,500 m), temperature and salinity decreased, reversing the previous warming trend, most likely due to delayed appearance of the new colder and fresher Labrador Sea Water produced in the mid-1990s.

Intermediate water (800–1,200 m) in the mid-latitude eastern North Atlantic is strongly influenced by the saline Mediterranean Water (MW; Section 5.3.2.3). This saline layer joins the southward-flowing NADW and becomes part of it in the tropical Atlantic. This layer has warmed and become more saline since at least 1957 (Bryden et al., 1996), continuing during the last decade (1994–2003) at a rate of more than 0.2°C per decade with a rate of 0.4°C per decade at some levels (Vargas-Yáñez et al., 2004). In the Bay of Biscay (44°N; González-Pola et al., 2005) and at Gibraltar (Millot et al., 2006), similar warming was observed through the thermocline and into the core of the MW. From 1955 to 1993, the trend was about 0.1°C per decade in a zone west of Gibraltar (Potter and Lozier, 2004), and of almost the same magnitude even west of the mid-Atlantic Ridge (Curry et al., 2003).

Surface waters in the Southern Ocean, including the high-latitude South Atlantic, set the initial conditions for bottom water in the (SH). This extremely dense Antarctic Bottom Water (AABW), which is formed around the coast of Antarctica (see Section 5.3.5.2), spreads equatorward and enters the Brazil Basin through the narrow Vema Channel of the Rio Grande Rise at 31°S. Ongoing observations of the lowest bottom temperatures there have revealed a slow but consistent increase of the order 0.002°C yr^{-1} in the abyssal layer over the last 30 years (Hogg and Zenk, 1997).

In the tropical Atlantic, the surface water changes are partly associated with the variability of the marine Inter-tropical Convergence Zone, which has strong seasonal variability (Mitchell and Wallace, 1992; Biasutti et al., 2003; Stramma et al., 2003). Tropical Atlantic variability on interannual to decadal time scales can be influenced by a South Atlantic dipole in SST

(Venegas et al., 1998), associated with latent heat fluxes related to changes in the subtropical high (Sterl and Hazeleger, 2003). The South Equatorial Current provides a region for subduction of the water masses (Hazeleger et al., 2003) and may also maintain a propagation pathway for water mass anomalies towards the north (Lazar et al., 2002).

The North Atlantic Oscillation is an important driver of the oceanic water mass variations in the upper North Atlantic subtropical gyre. Its effects are also observed at depths greater than 1,500 m within the subtropical gyre consistent with the large-scale circulation and changes in source waters in the North Atlantic Ocean. While there are coherent changes in the long-term trends in temperature and salinity (Section 5.2), decadal variations are an important climate signal for this region.

5.3.2.4 Mediterranean Sea

Marked changes in thermohaline properties have been observed throughout the Mediterranean (Manca et al., 2002). In the western basin, the Western Mediterranean Deep Water (WMDW), formed in the Gulf of Lions, warmed during the last 50 years, interrupted by a short period of cooling in the early 1980s, the latter reflected in cooling of the Levantine Intermediate Water between the late 1970s and mid-1980s (Brankart and Pinardi, 2001). The WMDW warming is in agreement with recent atmospheric temperature changes over the Mediterranean (Luterbacher et al., 2004). The salt content of the WMDW has also been steadily increasing during the last 50 years, mainly attributed to decreasing precipitation over the region since the 1940s (Krahmann and Schott, 1998; Mariotti et al., 2002) and to anthropogenic reduction in the freshwater inflow (Rohling and Bryden, 1992). These changes in water properties and circulation are linked to the long-term variability of surface fluxes (Krahmann and Schott, 1998) with contributions from the NAO (Vignudelli et al., 1999) that produce consistent changes in surface heat fluxes and a net warming of the Mediterranean Sea (Rixen et al., 2005).

These changes in the temperature and salinity within the Mediterranean have affected the outflow of water into the North Atlantic at Gibraltar (see also Section 5.3.2.3). Part of this shift in Mediterranean outflow properties has been traced to the Eastern Mediterranean. During 1987 to 1991, the Eastern Mediterranean Deep Water became warmer and saltier due to the switch of its source water from the Adriatic to the Aegean (Klein et al., 2000; Gertman et al., 2006), most likely related to changes in the heat and freshwater flux anomalies in the Aegean Sea (Tsimplis and Rixen, 2002; Josey, 2003; Rupolo et al., 2003). This 1987 to 1991 switch of source waters has continued and increased its impact, with density of the westward outflow in Sicily Strait now denser (Gasparini et al., 2005). While there are strong natural variations in the Mediterranean, overall there is a discernible trend of increased salinity and warmer temperature in key water masses over the last 50 years and this signal is observable in the North Atlantic.

5.3.3 Pacific Ocean

The upper Pacific Ocean has been warming and freshening overall, as revealed in global heat and freshwater analyses (Section 5.2, Figure 5.5). The subtropical North and South Pacific have been warming. In the SH, the major warming footprint is associated with the thick mode waters north of the Antarctic Circumpolar Current. The North Pacific has cooled along 40°N. Long-term trends are rather difficult to discern in the upper Pacific Ocean because of the strong interannual and decadal variability (ENSO and the PDO) and the relatively short length of the observational records. Changes associated with ENSO are described in Section 3.6.2 and are not included here. Overall, the Pacific is freshening but there are embedded salinity increases in the subtropical upper ocean, where strong evaporation dominates.

5.3.3.1 Pacific Upper Ocean Changes

In the North Pacific, the zonally averaged temperature warming trend from 1955 to 2003 (Figure 5.3) is dominated by the PDO increase in the mid-1970s. The strong cooling between 50 and 200 m is due to relaxation and subsequent shallowing of the tropical thermocline, resulting from a decrease in the shallow tropical MOC and a relaxation of the equatorial thermocline (McPhaden and Zhang, 2002), although after 1998 this shallow overturning circulation returned to levels almost as high as in the 1970s (McPhaden and Zhang, 2004).

Warming in the North Pacific subtropics, cooling around 40°N and slight warming farther north is the pattern associated with a positive PDO (strengthened Aleutian Low; Miller and Douglas, 2004; see Figure 3.28). Within the North Pacific Ocean, a positive PDO state such as occurred after 1976 is characterised by a strengthened Kuroshio Extension. After 1976, the Kuroshio Extension and North Pacific Current transport increased by 8% and expanded southward (Parrish et al., 2000). The Kuroshio's advection of temperature anomalies has been shown to be of similar importance to variations in ENSO and the strength of the Aleutian Low in maintaining the positive PDO (Schneider and Cornuelle, 2005). The Oyashio penetrated farther southward along the coast of Japan during the 1980s than during the preceding two decades, consistent with a stronger Aleutian Low (Sekine, 1988; Hanawa, 1995; Sekine, 1999). A shoaling of the halocline in the centre of the western subarctic gyre and a concurrent southward shift of the Oyashio extension front during 1976 to 1998 vs. 1945 to 1975 has been detected (Joyce and Dunworth-Baker, 2003). Similarly, mixed layer depth decreased throughout the eastern subarctic gyre, with a distinct trend over 50 years (Freeland et al., 1997; Li et al., 2005).

Temperature changes in upper-ocean water masses in response to the more positive phase of the PDO after 1976 are well documented. The thick water mass just south of the Kuroshio Extension in the subtropical gyre (Subtropical Mode Water) warmed by 0.8°C from the mid-1970s to the late 1980s, associated with stronger Kuroshio advection, and the thick water mass along the subtropical-subpolar boundary near 40°N

(North Pacific Central Mode Water) cooled by 1°C following the shift in the PDO after 1976 (Yasuda et al., 2000; Hanawa and Kamada, 2001).

Trends towards increased heat content include a major signal in the subtropical South Pacific, within the thick mixed layers just north of the Antarctic Circumpolar Current (Willis et al., 2004; Section 5.3.5). The strength of the South Pacific subtropical gyre circulation increased more than 20% after 1993, peaking in 2003, and subsequently declined. This spin up is linked to an increase of Ekman pumping over the gyre due to an increase in the SAM index (Roemmich et al., 2007).

The marginal seas of the Pacific Ocean are also subject to climate variability and change. Like the Mediterranean in the North Atlantic, the Japan (or East) Sea is nearly completely isolated from the adjacent ocean basin, and forms all of its own waters beneath the shallow pycnocline. Because of this sea's limited size, it responds quickly through its entire depth to surface forcing changes. The warming evident through the global ocean is clearly apparent in this isolated basin, which warmed by 0.1°C at 1,000 m and 0.05°C below 2,500 m since the 1960s. Salinity at these depths also changed, by 0.06 psu per century for depths of 300 to 1,000 m and by –0.02 psu per century below 1,500 m (Kwon et al., 2004). These changes have been attributed to reduced surface heat loss and increased surface salinity, which have changed the mode of ventilation (Kim et al., 2004). Deep water production in the Japan (East) Sea slowed for many decades, with a marked decrease in dissolved oxygen from the 1930s to 2000 at a rate of about 0.8 μmol kg^{-1} yr^{-1} (Gamo et al., 1986; Minami et al., 1998). However, possibly because of weakened vertical stratification at mid-depths associated with the decades-long warming, deep-water production reappeared after the 2000–2001 severe winter (e.g., Kim et al., 2002; Senjyu et al., 2002; Talley et al., 2003b). Nevertheless, the overall trend has continued with lower deep-water production in subsequent years.

5.3.3.2 Intermediate and Deep Circulation and Water Property Changes

Since the 1970s, the major mid-depth water mass in the North Pacific, North Pacific Intermediate Water (NPIW), has been freshening and has become less ventilated, as measured by oxygen content (see Section 5.4.3). The NPIW is formed in the subpolar North Pacific, with most influence from the Okhotsk Sea, and reflects changes in northern North Pacific surface conditions. The salinity of NPIW decreased by 0.1 and 0.02 psu in the subpolar and subtropical gyres, respectively (Wong et al., 2001; Joyce and Dunworth-Baker, 2003). An oxygen decrease and nutrient increase in the NPIW south of Hokkaido from 1970 to 1999 was reported (Ono et al., 2001), along with a subpolar basin-wide oxygen decrease from the mid-1980s to the late 1990s (Watanabe et al., 2001). Warming and freshening occurred in the Okhotsk Sea in the latter half of the 20th century (Hill et al., 2003). The Okhotsk Sea intermediate water thickness was reduced and its density decreased in the 1990s (Yasuda et al., 2001).

In the southwest Pacific, in the deepest waters originating from the North Atlantic and Antarctica, cooling and freshening of 0.07°C and 0.01 psu from 1968 to 1991 was observed (Johnson and Orsi, 1997) and attributed to a change in the relative importance of Antarctic and North Atlantic source waters and weakening bottom transport. Bottom waters in the North Pacific are farther from the surface sources than any other of the world's deep waters. They are also the most uniform, in terms of spatial temperature and salinity variations. A large-scale, significant warming of the bottom 1,000 m across the entire North Pacific of the order of 0.002°C occurred between 1985 and 1999, measurable because of the high accuracy of modern instruments (Fukasawa et al., 2004). The cause of this warming is uncertain, but could have resulted from warming of the deep waters in the South Pacific and Southern Ocean, where mid-depth changes since the 1950s are as high as 0.17°C (Gille, 2002; see Figure 5.8), and/or from the declining bottom water transport into the deep North Pacific (Johnson et al., 1994).

5.3.4 Indian Ocean

The upper Indian Ocean has been warming everywhere except in a band centred at about 12°S (South Equatorial Current), as seen in Section 5.2 (Figure 5.3). In the tropical and eastern subtropical Indian Ocean (north of 10°S), warming in the upper 100 m (Qian et al., 2003) is consistent with the significant warming of the sea surface from 1900 to 1999 (see Section 3.2.2 and Figure 3.9). The surface warming trend during the period 1900 to 1970 was relatively weak, but increased significantly in the 1970 to 1999 period, with some regions exceeding 0.2°C per decade.

The global-scale circulation includes transport of warm, relatively fresh waters from the Pacific passing through the Indonesian Seas to the Indian Ocean and then onward into the South Atlantic. Much of this throughflow occurs in the tropics south of the equator, and is strongly affected by ENSO and the Indian Ocean Dipole (see Section 3.6.7.2). The latter causes pronounced thermocline variability (Qian et al., 2003) and includes propagation of upper-layer thickness anomalies by Rossby waves (Xie et al., 2002; Feng and Meyers, 2003; Yamagata et al., 2004) in the 3°S to 15°S latitude band that includes the westward-flowing throughflow water.

Long-term trends in transport and properties of the throughflow have not been reported. The mean transport into the Indonesian Seas measured at Makassar Strait from 1996 to 1998 was 9 to 10 Sv (Vranes et al., 2002), matching transports exiting the Indonesian Seas (e.g., Sprintall et al., 2004). Large variability in this transport is associated with varying tropical Pacific and Indian winds (Wijffels and Meyers, 2004), including a strong ENSO response (e.g., Meyers, 1996), and may be associated with changes in SST in the tropical Indian Ocean.

Models suggest that upper-ocean warming in the south Indian Ocean can be attributed to a reduction in the southeast trade winds and associated decrease in the southward transport of heat from the tropics to the subtropics (Lee, 2004). The export of heat from the northern Indian Ocean to the south

across the equator is accomplished by a wind-driven, shallow cross-equatorial cell; data assimilation analysis has shown a significant decadal reduction in the mass exchange during 1950 to 1990 but little change in heat transport (Schoenefeldt and Schott, 2006).

Changes in Indian subtropical gyre circulation since the 1960s include a 20% slowdown from 1962 to 1987 (Bindoff and McDougall, 2000) and a 20% speedup from 1987 to 2002 (Bryden et al., 2003; McDonagh et al., 2005), with the speedup mainly between 1995 and 2002 (Palmer et al., 2004). The upper thermocline warmed during the slowdown, and then cooled during speedup. Simulations of this region and the analysis of climate change scenarios show that the slowdown and speedup were part of an oscillatory pattern in the upper part of this gyre over periods of decades (Murray et al., 2007; Stark et al., 2006). On the other hand, the lower thermocline (<10°C) freshened and warmed from 1936 to 2002 (Bryden et al., 2003), consistent with heat content increases discussed in Section 5.2 and earlier results.

5.3.5 Southern Ocean

The Southern Ocean, which is the region south of 30°S, connects the Atlantic, Indian and Pacific Oceans together, allowing inter-ocean exchange. This region is active in the formation and subduction of waters that contributed strongly to the storage of anthropogenic carbon and heat (see Section 5.2). It is also the location of the densest part of the global overturning circulation, through formation of bottom waters around Antarctica, fed by deep waters from all of the oceans to the north. Note that some observed changes found in the Atlantic, Indian and Pacific Oceans are related to changes in the Southern Ocean waters but have largely been described in those sections.

5.3.5.1 Upper-Ocean Property Changes

The upper ocean in the SH has warmed since the 1960s, dominated by changes in the thick near-surface layers called Subantarctic Mode Water (SAMW), located just north of the Antarctic Circumpolar Current (ACC) that encircles Antarctica. The observed warming of SAMW is consistent with the subduction of warmer surface waters from south of the ACC (Wong et al., 2001; Aoki et al., 2003). In the Upper Circumpolar Deep Water (UCDW) in the Indian and Pacific sectors of the Southern Ocean, temperature and salinity have been increasing (on density surfaces) and oxygen has been decreasing between the Subantarctic Front near 45°S and the Antarctic Divergence near 60°S (Aoki et al., 2005a). These changes just below the mixed layer (~100 to 300 m) are consistent with the mixing of warmer and fresher surface waters with UCDW, suggesting an increase in stratification in the surface layer of this polar region.

Mid-depth waters of the Southern Ocean have also warmed in recent decades. As shown in Figure 5.8, temperatures increased near 900 m depth between the 1950s and the 1980s throughout most of the Southern Ocean (Aoki et al., 2003; Gille, 2004).

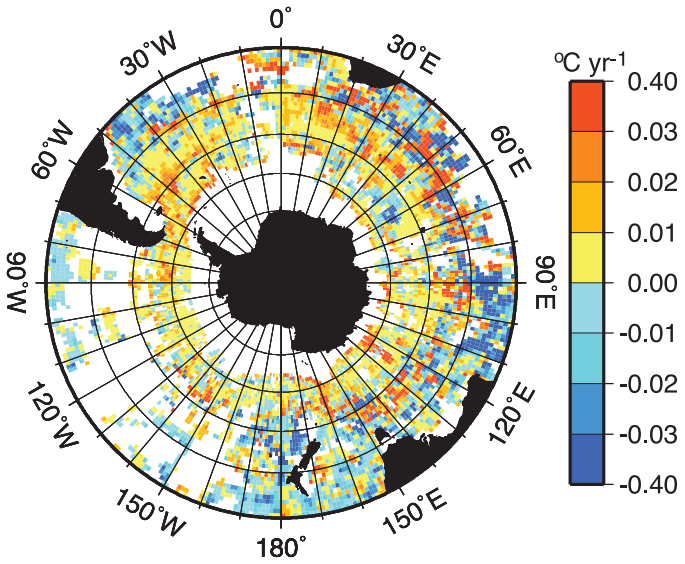


Figure 5.8. *Temperature trends (°C yr^{-1}) at 900 m depth using data collected from the 1930s to 2000, including shipboard profile and Autonomous LAgrangian Current Explorer float data. The largest warming occurs in subantarctic regions, and a slight cooling occurs to the north. From Gille (2002).*

The largest changes are found near the Antarctic Circumpolar Current, where the warming at 900 m depth is similar in magnitude to the increase in regional surface air temperatures. Analysis of altimeter and Argo float profile data suggests that, over the last 10 years, the zonally averaged warming in the upper 400 m of the ocean near 40°S (Willis et al. 2004) is much larger than that seen in long-term trends (see Section 5.2, Figure 5.3 World). The warming results from these analyses have been attributed to a southward shift and increased intensity of the SH westerlies, which would shift the ACC slightly southward and intensify the subtropical gyres (e.g., Cai, 2006).

The major mid-depth water mass in the SH, Antarctic Intermediate Water (AAIW), has also been freshening since the 1960s (Wong et al., 1999; Bindoff and McDougall, 2000; see Figure 5.6). The Atlantic freshening of AAIW is also supported by direct observations of a freshening of southern surface waters (Curry et al., 2003).

5.3.5.2. Antarctic Regions and Antarctic Circumpolar Current

The ACC, the longest current system in the world, has a transport through Drake Passage of about 130 Sv, with significant interannual variability. Measurements over 25 years across Drake Passage show no evidence for a systematic trend in total volume transport between the 1970s and the present (Cunningham et al., 2003), although continuous subsurface pressure measurements suggest that trends in seasonality of transport are highly correlated with similar trends in the SAM index (Meredith and King, 2005).

There is growing evidence for the changes in the AABW and intermediate depth waters around Antarctica. In the Weddell Sea, the deep and bottom water properties varied in the 1990s

(Robertson et al., 2002; Fahrbach et al., 2004). Changes in bottom water properties have also been observed downstream of these source regions (Hogg, 2001; Andrie et al., 2003) and in the South Atlantic (Section 5.3.2.3). The upper ocean adjacent to the West Antarctic Peninsula warmed by more than 1°C and became more saline by 0.25 psu from 1951 to 1994 (Meredith and King, 2005). The warming is likely to have resulted from large regional atmospheric warming (Vaughan et al., 2003) and reduced winter sea ice observed in this region.

In the Ross Sea and near the Ross Ice Shelf, significant decreases in salinity of 0.003 psu yr^{-1} (and density decreases) over the last four decades (Jacobs et al., 2002) have been observed. Downstream of the Ross Ice Shelf in the Australian-Antarctic Basin, AABW has also cooled and freshened (Aoki et al., 2005b). These observed decreases are significantly greater than earlier reports of AABW variability (Whitworth, 2002) and suggest that changes in the antarctic shelf waters can be quite quickly communicated to deep waters. Jacobs et al. (2002) concluded that the freshening appears to have resulted from a combination of factors including increased precipitation, reduced sea ice production and increased melting of the West Antarctic Ice Sheet.

5.3.6 Relation of Regional to Global Changes

5.3.6.1 Changes in Global Water Mass Properties

The regional analyses described in the previous sections have global organisation, as described partially in Section 5.3.1 (Figure 5.6), and as reflected in the global trend analyses in Section 5.2. The data sets used for the largest-scale descriptions over the last 30 to 50 years are reliable; different types of data and widely varying methods yield similar results, increasing confidence in the reality of the changes found in both the global and regional analyses.

The regional and global analyses of ocean warming generally show a pattern of increased ocean temperature in the regions of very thick surface mixed layer (mode water) formation. This is clearest in the North Atlantic and North Pacific and in all sectors of the Southern Ocean (Figure 5.3). There are also regions of decreased ocean temperature in both the global and regional analyses in parts of the subpolar and equatorial regions.

Both the global and regional analyses show long-term freshening in the subpolar waters in the North Atlantic and North Pacific and a salinity increase in the upper ocean (<100 m deep) at low to mid-latitudes. This is consistent with an increase in the atmospheric hydrological cycle over the oceans and could result in changes in ocean advection (Section 5.3.2). In the North Atlantic, the subpolar freshening occurred throughout the entire water column, from the 1960s to the mid-1990s (Figure 5.5 and Figure 5.6a). Increased salinity and temperature in the upper water column in the subpolar North Atlantic after 1994 are not apparent from the linear trend applied to the full time series in Figure 5.5, but are clear in all regional time series (Section 5.3.2). Freshening in the North Pacific subpolar gyre north of 45°N is apparent in both regional analyses (Section 5.3.3.2) and global analyses (Figure 5.5). Freshening of intermediate depth waters (>300 m) from Southern Ocean sources (Section 5.3.5) is apparent in both the global and regional analyses (e.g., Figure 5.5 World).

Many of the observed changes in the temperature and salinity fields have been linked to atmospheric forcing through correlations with atmospheric indices associated with the NAO, PDO and SAM. Indeed, most of the few time series of ocean measurements or repeat measurements of long sections (see Sections 5.3.2 and 5.3.4) show evidence of decadal variability. Because of the long time scales of these natural climate patterns, it is difficult to discern if observed decadal oceanic variability is natural or a climate change signal; indeed, changes in these natural patterns themselves might be related to climate change. In the North Atlantic, freshening at high latitudes and increased evaporation at subtropical latitudes prior to the mid-1990s might have been associated with an increasing NAO index, and the reversal towards higher salinity at high latitudes thereafter with a decreasing NAO index after 1990 (see Figure 3.31). Likewise in the Pacific, freshening at high latitudes and increased evaporation in the subtropics, cooling in the central North Pacific, warming in the eastern and tropical Pacific and reduced ventilation in the Kuroshio region, Japan and Okhotsk Seas could be associated with the extended positive phase of the PDO. The few detection and attribution studies of ocean changes are discussed in Section 9.5.1.

At a global scale, the observed long-term patterns of zonal temperature and salinity changes tend to be approximately symmetric around the equator (Figure 5.6) and occur simultaneously in different ocean basins (Figures 5.3 and 5.5). The scale of these patterns, which extends beyond the regions of influence normally associated with the NAO, PDO and SAM, suggests that these coherent changes between both hemispheres are associated with a global phenomenon.

5.3.6.2 Consistency with the Large-Scale Ocean Circulation

The observed changes are broadly consistent with scientific understanding of the circulation of the global oceans. The North Atlantic and antarctic regions, where the oceans ventilate the deep waters over short time scales (<50 years), show strong evidence of change over the instrumental record. For example, the North Atlantic shows evidence of a deep warming and freshening. There is evidence of change in the Southern Ocean bottom waters consistent with the sinking of fresher antarctic shelf waters. Deep waters that are far from the North Atlantic and Antarctic, remote from interaction with the atmosphere, and with replenishment rates that are long compared with the instrumental record, typically show no significant changes. Mode waters, key global water masses found in every ocean basin equatorward of major oceanic frontal systems or separated boundary currents, have a relatively rapid formation and ventilation rate (<20 years) and provide a pathway for heat (and salinity) to be transported into the main subtropical gyres of the global oceans as observed.

5.4 Ocean Biogeochemical Changes

5.4.1 Introduction

The observed increase in atmospheric carbon dioxide (CO_2; see Chapter 2) and the observed changes in the physical properties of the ocean reported in this chapter can affect marine biogeochemical cycles (here mainly carbon, oxygen, and nutrients). The increase in atmospheric CO_2 causes additional CO_2 to dissolve in the ocean. Changes in temperature and salinity affect the solubility and chemical equilibration of gases. Changes in circulation affect the supply of carbon and nutrients from below, the ventilation of oxygen-depleted waters and the downward penetration of anthropogenic carbon. The combined physical and biogeochemical changes also affect biological activity, with further consequences for the biogeochemical cycles.

The increase in surface ocean CO_2 has consequences for the chemical equilibrium of the ocean. As CO_2 increases, surface waters become more acidic and the concentration of carbonate ions decreases. This change in chemical equilibrium causes a reduction of the capacity of the ocean to take up additional CO_2. However, the response of marine organisms to ocean acidification is poorly known and could cause further changes in the marine carbon cycle with consequences that are difficult to estimate (see Section 7.3.4 and Chapter 4 of the Working Group II contribution to the IPCC Fourth Assessment Report).

Dissolved oxygen (O_2) in the ocean is affected by the same physical processes that affect CO_2, but in contrast to CO_2, O_2 is not affected by changes in its atmospheric concentration (which are only of the order of 10^{-4} of its mean concentration). Changes in oceanic O_2 concentration thus provide information on the changes in the physical or biological processes that occur within the ocean, such as ventilation (here used to describe the rate of renewal of thermocline waters), mode water formation, upwelling or biological export and respiration. Furthermore, changes in the oceanic O_2 content are needed to estimate the CO_2 budget from atmospheric O_2/molecular nitrogen (N_2) ratio measurements. However, the method currently estimates the change in air-sea fluxes of O_2 indirectly based on heat flux changes (see Section 7.3.2).

This section reports observed changes in biogeochemical cycles and assesses their consistency with observed changes in physical properties. Changes in oceanic nitrous oxide (N_2O) and methane (CH_4) have not been assessed because of the lack of large-scale observations. Observations of the mean fluxes of N_2O and CH_4 (including CH_4 hydrates) are discussed in Chapter 7.

5.4.2 Carbon

5.4.2.1 Total Change in Dissolved Inorganic Carbon and Air-Sea Carbon Dioxide Flux

Direct observations of oceanic dissolved inorganic carbon (DIC; i.e., the sum of CO_2 plus carbonate and bicarbonate) reflect changes in both the natural carbon cycle and the uptake of anthropogenic CO_2 from the atmosphere. Links between the main modes of climate variability and the marine carbon cycle have been observed on interannual time scales in several regions of the world (see Section 7.3.2.4 for quantitative estimates). In the equatorial Pacific, the reduced upwelling associated with El Niño events decreases the regional outgas of natural CO_2 to the atmosphere (Feely et al., 1999). In the subtropical North Atlantic, reduced mode water formation and reduced deep winter mixing during the positive NAO phase increase the storage of carbon in the intermediate ocean (Bates et al., 2002). These observations show that variability in the content of natural DIC in the ocean has occurred in association with climate variability.

Longer observations exist for the partial pressure of CO_2 (pCO_2) at the surface only. Over more than two decades, the oceanic pCO_2 increase has generally followed the atmospheric CO_2 within the given uncertainty, although regional differences have been observed (Feely et al., 1999; Takahashi et al., 2006). The three stations with the longest time series, all in the northern subtropics, show pCO_2 increases at a rate varying between 1.6 and 1.9 µatm yr^{-1} (Figure 5.9), indistinguishable from the atmospheric increase of 1.5 to 1.9 µatm yr^{-1}. Variability on the order of 20 µatm over periods of five years was observed in the three time series, as well as in other data sets, and has been associated with regional changes in the natural carbon cycle driven by changes in ocean circulation and by climate variability (Gruber et al., 2002; Dore et al., 2003) or with variations in biological activity (Lefèvre et al., 2004).

Direct surface pCO_2 observations have been used to compute a global air-sea CO_2 flux of 1.6 ± 1 GtC yr^{-1} for the year 1995 (Takahashi et al., 2002; Section 7.3.2.3.2, Figure 7.8). It is not yet possible to detect large-scale changes in the global air-sea CO_2 flux from direct observations because of the large influence of climate variability. However, estimates from inverse methods of the air-sea CO_2 flux from the spatio-temporal distribution of atmospheric CO_2 suggest that the global air-sea CO_2 flux increased by 0.1 to 0.6 GtC yr^{-1} between the 1980s and 1990s, consistent with results from ocean models (Le Quéré et al., 2003).

5.4.2.2 Anthropogenic Carbon Change

The recent uptake of anthropogenic carbon in the ocean is well constrained by observations to a decadal mean of 2.2 ± 0.4 GtC yr^{-1} for the 1990s (see Section 7.3.2, Table 7.1). The uptake of anthropogenic carbon over longer time scales can be estimated from oceanic measurements. Changes in DIC between two time periods reflect the anthropogenic carbon uptake plus the changes in DIC concentration due to changes in water masses and biological activity. To estimate the contribution of anthropogenic carbon alone, several corrections must be applied. From observed DIC changes between surveys in the 1970s and the 1990s, an increase in anthropogenic carbon has been inferred down to depths of 1,100 m in the North Pacific (Peng et al., 2003; Sabine et al., 2004a), 200 to 1,200 m in the Indian Ocean (Peng et al., 1998; Sabine et al., 1999) and 1,900 m in the Southern Ocean (McNeil et al., 2003).

An indirect method was used to estimate anthropogenic carbon from observations made at a single time period based on well-known processes that control the distribution of natural DIC in the ocean. The method corrects the observed DIC concentration for organic matter decomposition and dissolution of carbonate minerals, and removes an estimate of the DIC concentration of the water when it was last in contact with the atmosphere (Gruber et al., 1996). With this method, a global DIC increase of 118 ± 19 GtC between pre-industrial times (roughly 1750) and 1994 has been estimated, using 9,618 profiles from the 1990s (Sabine et al., 2004b; see Figure 5.10). The uncertainty of ±19 GtC in this estimate is based on uncertainties in the anthropogenic DIC estimates and mapping errors, which have characteristics of random error, and on an estimate of potential biases, which are not necessarily centred on the mean value. Potential biases of up to 7% in the technique have been identified, mostly caused by assumptions about the time evolution of CO_2, the age or the identification of water masses (Matsumoto and Gruber, 2005), and the recent changes in surface warming and stratification (Keeling, 2005). Potential biases from assumptions of constant carbon and nutrient uptake ratios for biological activity have not been assessed. While the magnitude and direction of all potential biases are not yet clear, the given uncertainty of ±16% appears realistic compared to the biases already identified.

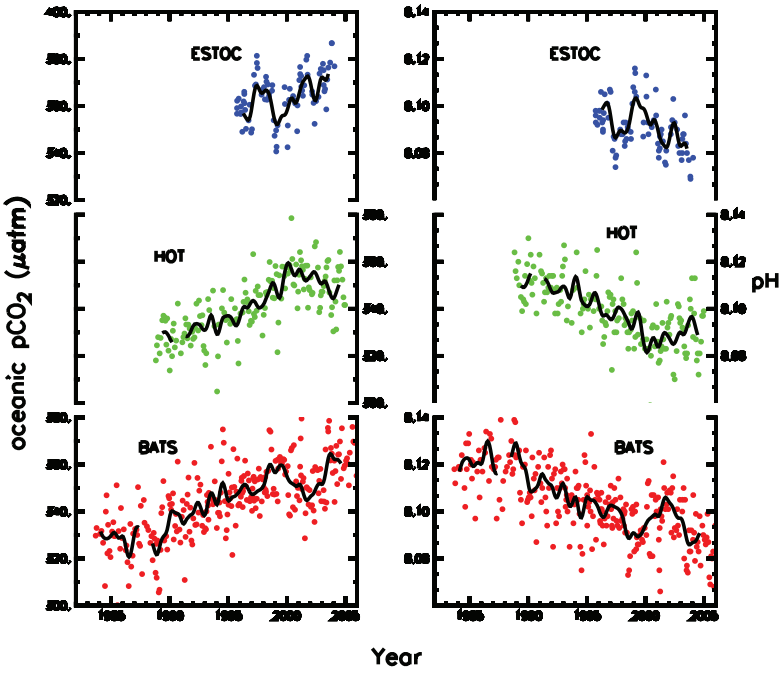


Figure 5.9. *Changes in surface oceanic pCO_2 (left; in µatm) and pH (right) from three time series stations: Blue: European Station for Time-series in the Ocean (ESTOC, 29°N, 15°W; Gonzalez-Dávila et al., 2003); green: Hawaii Ocean Time-Series (HOT, 23°N, 158°W; Dore et al., 2003); red: Bermuda Atlantic Time-series Study (BATS, 31/32°N, 64°W; Bates et al., 2002; Gruber et al., 2002). Values of pCO_2 and pH were calculated from DIC and alkalinity at HOT and BATS; pH was directly measured at ESTOC and pCO_2 was calculated from pH and alkalinity. The mean seasonal cycle was removed from all data. The thick black line is smoothed and does not contain variability less than 0.5 years period.*

Because of the limited rate of vertical transport in the ocean, more than half of the anthropogenic carbon can still be found in the upper 400 m, and it is undetectable in most of the deep ocean (Figure 5.11). The vertical penetration of anthropogenic carbon is consistent with the DIC changes observed between two cruises (Peng et al., 1998, 2003). Anthropogenic carbon has penetrated deeper in the North Atlantic and subantarctic Southern Ocean compared to other basins, due to a combination of: i) high surface alkalinity (in the Atlantic) which favours the uptake of CO_2, and ii) more active vertical exchanges caused by intense winter mixing and by the formation of deep waters (Sabine et al., 2004b). The deeper penetration of anthropogenic carbon in these regions is consistent with similar features observed in the oceanic distribution of chlorofluorocarbons (CFCs) of atmospheric origin (Willey et al., 2004), confirming that it takes decades to many centuries to transport carbon from the surface into the thermocline and the deep ocean. Deeper penetration in the North Atlantic and subantarctic Southern Ocean is also observed in the changes in heat content shown in Figure 5.3. The large storage of anthropogenic carbon observed in the subtropical gyres is caused by the lateral transport of carbon from the region of mode water formation towards the lower latitudes (Figure 5.10).

The fraction of the net CO_2 emissions taken up by the ocean (the uptake fraction) was possibly lower during 1980 to 2005 (37% ± 7%) compared to 1750 to 1994 (42% ± 7%); however the uncertainty in the estimates is larger than the difference between the estimates (Table 5.1). The net CO_2 emissions

Table 5.1. *Fraction of CO_2 emissions taken up by the ocean for different time periods.*

Time Period	Oceanic Increase (GtC)	Net CO_2 Emissions[a] (GtC)	Uptake Fraction (%)	Reference
1750–1994	118 ± 19	283 ± 19	42 ± 7	Sabine et al., 2004b
1980–2005[b]	53 ± 9	143 ± 10	37 ± 7	Chapter 7[c]

Notes:
[a] Sum of emissions from fossil fuel burning, cement production, land use change and the terrestrial biosphere response.
[b] The longest possible time period was used for the recent decades to minimise the effect of the variability in atmospheric CO_2.
[c] Sum of the estimates for the 1980s, 1990s and 2000 to 2005 from Table 7.1.

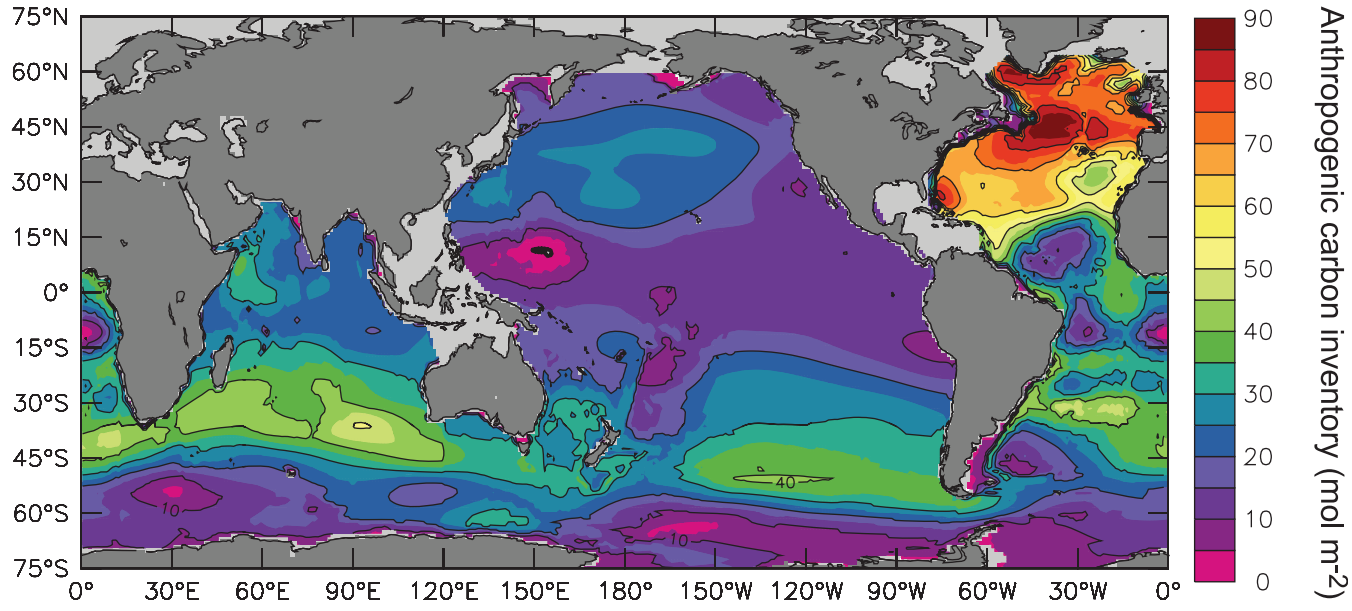


Figure 5.10. *Column inventory of anthropogenic carbon (mol m^{-2}) as of 1994 from Sabine et al. (2004b). Anthropogenic carbon is estimated indirectly by correcting the measured DIC for the contributions of organic matter decomposition and dissolution of carbonate minerals, and taking into account the DIC concentration the water had in the pre-industrial ocean when it was last in contact with the atmosphere. The global inventory of anthropogenic carbon taken up by the ocean between 1750 and 1994 is estimated to be 118 ± 19 GtC.*

include all emissions that have an influence on the atmospheric CO_2 concentration (i.e., emissions from fossil fuel burning, cement production, land use change and the terrestrial biosphere response). It is equivalent to the sum of the atmospheric and oceanic CO_2 increase. Because the atmospheric CO_2 is well constrained by observations, the uncertainty in the net CO_2 emissions is nearly equal to the uncertainty in the oceanic CO_2 increase. The decrease in oceanic uptake fraction would be consistent with the understanding that the ocean CO_2 sink is limited by the transport rate of anthropogenic carbon from the surface to the deep ocean, and also with the nonlinearity in carbon chemistry that reduces the CO_2 uptake capacity of water as its CO_2 concentration increases (Sarmiento et al., 1995).

5.4.2.3 Ocean Acidification by Carbon Dioxide

The uptake of anthropogenic carbon by the ocean changes the chemical equilibrium of the ocean. Dissolved CO_2 forms a weak acid.[1] As CO_2 increases, pH decreases, that is, the ocean becomes more acidic. Ocean pH can be computed from measurements of DIC and alkalinity. A decrease in surface pH of 0.1 over the global ocean was calculated from the estimated uptake of anthropogenic carbon between 1750 and 1994 (Sabine et al., 2004b; Raven et al., 2005), with the lowest decrease (0.06) in the tropics and subtropics, and the highest decrease (0.12) at high latitudes, consistent with the lower buffer capacity of the high latitudes compared to the low latitudes. The mean pH of surface waters ranges between 7.9 and 8.3 in the open

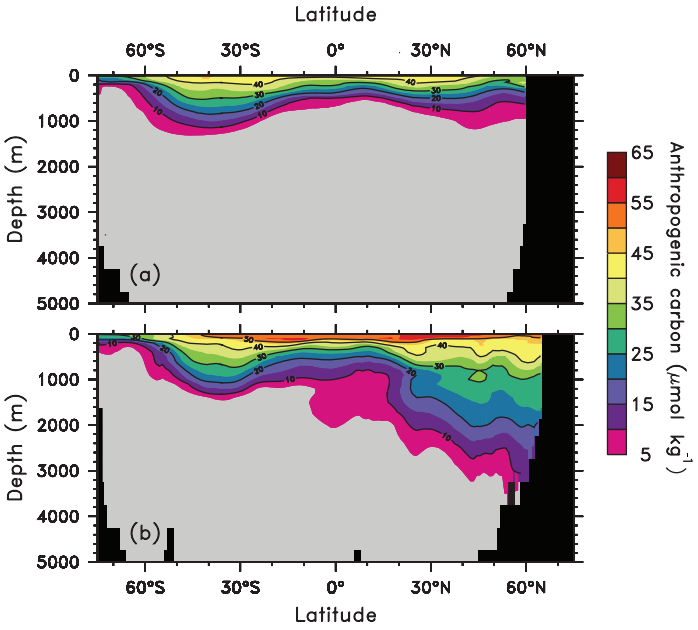


Figure 5.11. *Mean concentration of anthropogenic carbon as of 1994 in μmol kg^{-1} from Sabine et al. (2004b) averaged over (a) the Pacific and Indian Oceans and (b) the Atlantic Ocean. The calculation of anthropogenic carbon is described in the caption of Figure 5.10 and in the text (Section 5.4).*

[1] Acidity is a measure of the concentration of H^+ ions and is reported in pH units, where pH = $-\log_{10}(H^+)$. A pH decrease of 1 unit means a 10-fold increase in the concentration of H^+, or acidity.

ocean, so the ocean remains alkaline (pH > 7) even after these decreases. For comparison, pH was higher by 0.1 unit during glaciations, and there is no evidence of pH values more than 0.6 units below the pre-industrial pH during the past 300 million years (Caldeira and Wickett, 2003). A decrease in ocean pH of 0.1 units corresponds to a 30% increase in the concentration of H^+ in seawater, assuming that alkalinity and temperature remain constant. Changes in surface temperature may have induced an additional decrease in pH of <0.01. The calculated anthropogenic impact on pH is consistent with results from time series stations where a decrease in pH of 0.02 per decade was observed (Figure 5.9). Results from time series stations include not only the increase in anthropogenic carbon, but also other changes due to local physical and biological variability. The consequences of changes in pH on marine organisms are poorly known (see Section 7.3.4 and Box 7.3).

5.4.2.4 Change in Carbonate Species

The uptake of anthropogenic carbon occurs through the injection of CO_2 and causes a shift in the distribution of carbon species (i.e., the balance between CO_2, carbonate and bicarbonate). The availability of carbonate is particularly important because it controls the maximum amount of CO_2 that the ocean is able to absorb. Marine organisms use carbonate to produce shells of calcite and aragonite (both consisting of calcium carbonate; $CaCO_3$). Currently, the surface ocean is super-saturated with respect to both calcite and aragonite, but undersaturated below a depth called the 'saturation horizon'. The undersaturation starts at a depth varying between 200 m in parts of the high-latitude and the Indian Ocean and 3,500 m in the Atlantic. Calcium carbonate dissolves either when it sinks below the calcite or aragonite saturation horizons or under the action of biological activity.

Shoaling of the aragonite saturation horizon has been observed in all ocean basins based on alkalinity, DIC and oxygen measurements (Feely and Chen, 1982; Feely et al., 2002; Sabine et al., 2002; Sarma et al., 2002). The amplitude and direction of the signal was everywhere consistent with the uptake of anthropogenic carbon, with potentially smaller contributions from changes in circulation, temperature and biology. Feely et al. (2004) calculated that the uptake of anthropogenic carbon alone has caused a shoaling of the aragonite saturation horizon between 1750 and 1994 by 30 to 200 m in the eastern Atlantic (50°S–15°N), the North Pacific and the North Indian Ocean, and a shoaling of the calcite saturation horizon by 40 to 100 m in the Pacific (north of 20°N). This calculation is based on the anthropogenic DIC increase estimated by Sabine et al. (2004a), on a global compilation of biogeochemical data and on carbonate chemistry equations. Furthermore, an increase in total alkalinity (primarily controlled by carbonate and bicarbonate) at the depth of the aragonite saturation horizon between 1970 and 1990 has been reported (Sarma et al., 2002). These results are consistent with the calculated increase in $CaCO_3$ dissolution as a result of the shoaling of the aragonite saturation horizon, but with large uncertainty. Carbonate decreases at high latitudes and particularly in the Southern Ocean may have consequences for marine ecosystems because the current saturation horizon is closer to the surface than in other basins (Orr et al., 2005; see Section 7.3.4).

5.4.3 Oxygen

In the thermocline (~100 to 1,000 m), a decrease in the O_2 concentration has been observed between about the early 1970s and the late 1990s or later in several repeated hydrographic sections in the North and South Pacific, North Atlantic, and Southern Indian Oceans (Figure 5.12; see summary table in Emerson et al., 2004, and Section 5.3). Section 5.3 reports on a number of O_2 decreases that fit the overall message of Section 5.4. The reported O_2 decreases range from 0.1 to 6 μmol kg^{-1} yr^{-1}, superposed on decadal variations of ±2 μmol kg^{-1} yr^{-1} (Ono et al., 2001; Andreev and Watanabe, 2002). In all published studies, the observed O_2 decrease appeared to be driven primarily by changes in ocean circulation, and less by changes in the rate of O_2 demand from downward settling of organic matter. A few studies have quantified the contribution of the change in ocean circulation using estimates of changes in apparent CFC ages (Doney et al., 1998; Watanabe et al., 2001; Mecking et al., 2006). In nearly all cases, the decrease in O_2 could entirely be accounted for by the increased apparent CFC age that resulted from reduced rate of renewal of intermediate waters. Changes in biological processes were only significant at the coast of California and may result from assumptions in the method (Mecking et al., 2006).

It is unclear whether the recent changes in O_2 are indicative of trends or of variability. Recent data in the Indian Ocean have shown a reversal of the O_2 decrease between 1987 and 2002 in the South Indian Ocean of similar amplitude to the decrease observed during the previous decades (McDonagh et al., 2005). Variability has been observed on decadal time scales in the North Atlantic large enough to mask any potential trends (Johnson and Gruber, 2007).

In the upper 100 m of the global ocean surface, decadal variations of ±0.5 μmol kg^{-1} in O_2 concentration were observed for the period 1956 to 1998 based on a global analysis of 530,000 oxygen profiles, with no clear trends (Garcia et al., 2005). However, the near-surface changes in O_2 concentration are difficult to interpret. They can be caused by changes in biological activity, by changes in the physical transport of O_2 from intermediate waters or by changes in temperature and salinity. Because there is less confidence in the early measurements and the reported changes cannot be explained by known processes, it cannot be said whether the absence of a long-term trend in surface O_2 is realistic or not.

5.4.4 Nutrients

Changes in nutrient concentrations can provide information on changes in the physical and biological processes that affect the carbon cycle and could potentially be used as indicators for large-scale changes in marine biology. However, only a

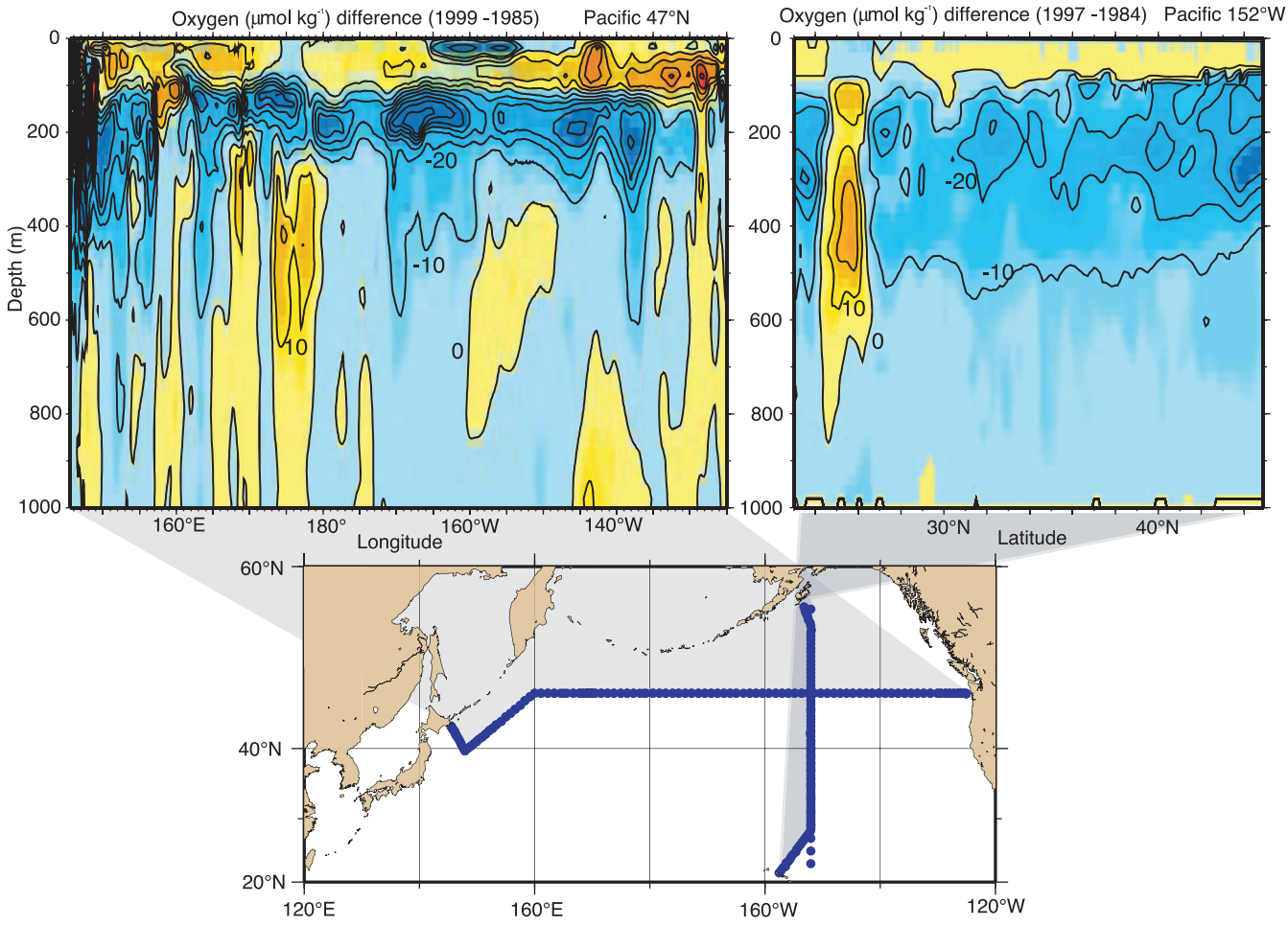


Figure 5.12. *Changes in oxygen concentration (µmol kg^{-1}) along two sections in the North Pacific (see map, bottom panel). Top left panel: Difference (1999 minus 1985) along 47°N. Top right panel: Difference (1997 minus 1984) at 152°W. Blue colours indicate a decrease and yellow colours indicate an increase in oxygen over time. The differences were calculated using density as the vertical coordinate. After Deutsch et al. (2005).*

few studies reported decadal changes in inorganic nutrient concentrations. In the North Pacific, the concentration of nitrate plus nitrite (N) and phosphate decreased at the surface (Freeland et al., 1997; Watanabe et al., 2005) and increased below the surface (Emerson et al., 2001; Ono et al., 2001; Keller et al., 2002) in the past two decades. Nutrient changes were observed in the deep ocean of all basins but no clear pattern emerges from available observations. Pahlow and Riebesell (2000) found changes in the ratio of nutrients in the North Pacific and Atlantic Oceans, and no significant changes in the South Pacific. In the North Pacific, Keller et al. (2002) observed a decrease in N associated with the increase in O_2 between 1970 and 1990 at 1,050 m, opposite to the results of Pahlow and Riebesell's longer study. Using the same data set extended to the world, large regional changes in nutrient ratios were observed (Li and Peng, 2002) but no consistent basin-scale patterns. Uncertainties in deep ocean nutrient observations may be responsible for the lack of coherence in the nutrient changes. Sources of inaccuracy include the limited number of observations and the lack of compatibility between measurements from different laboratories at different times.

In some cases, the observed trends in nutrients can be explained by either a change in thermocline ventilation or a change in biological activity (Pahlow and Riebesell, 2000; Emerson et al., 2001), but in other cases are mostly consistent with a reduction in thermocline ventilation (Freeland et al., 1997; Ono et al., 2001; Watanabe et al., 2005). Thus, all of the reported trends are consistent with a physical explanation of the observed changes, although changes in biological activity cannot be ruled out.

The concentration of surface nutrients can also be influenced by surface mixing, as a reduction in mixing leads to a decreased concentration of surface nutrients. The observed changes in surface temperature and salinity (see Sections 5.2.3 and 5.3) are indicative of changes in the surface mixing (see Section 7.3.4.3). In most of the Pacific Ocean, surface warming and freshening act in the same direction and contribute to reduced mixing (Figures 5.2 and 5.5), consistent with regional observations (Freeland et al., 1997; Watanabe et al., 2005). In the Atlantic and Indian Oceans, temperature and salinity trends generally act in opposite directions and changes in mixing have not been quantified regionally.

5.4.5 Biological Changes Relevant to Ocean Biogeochemistry

Changes in biological activity are an important part of the carbon cycle but are difficult to quantify at the global scale. Marine export production (the fraction of primary production that is not respired at the ocean surface and thus sinks to depth) is the biological process that has the largest influence on element cycles. There are no global observations on changes in export production or respiration. However, estimates of changes in primary production provide partial information. A reduction in global oceanic primary production by about 6% between the early 1980s and the late 1990s was estimated based on the comparison of chlorophyll data from two satellites (Gregg et al., 2003). The errors in this estimate are potentially large because it is based on the comparison of data from two different sensors. Nevertheless, a change in biological fluxes of this order of magnitude is plausible considering that biological production is controlled primarily by nutrient input from intermediate waters, and that a decrease in intermediate water renewal has been observed during that period as indicated by the decrease in O_2. Shifts and trends in plankton biomass have been observed for instance in the North Atlantic (Beaugrand and Reid, 2003), the North Pacific (Karl, 1999; Chavez et al., 2003) and in the Southern Indian Ocean (Hirawake et al., 2005), but the spatial and temporal coverage is limited. The potential impacts of changes in marine ecosystems or dissolved organic matter on climate are discussed in Section 7.3.4, and the impact of climate on marine ecosystems in Chapter 4 of the Working Group II contribution to the IPCC Fourth Assessment Report.

5.4.6 Consistency with Physical Changes

It is clearly established that climate variability affects the oceanic content of natural and anthropogenic DIC and the air-sea flux of CO_2, although the amplitude and physical processes responsible for the changes are less well known. Variability in the marine carbon cycle has been observed in response to physical changes associated with the dominant modes of climate variability such as El Niño events and the PDO (Feely et al., 1999; Takahashi et al., 2006), and the NAO (Bates et al., 2002; Johnson and Gruber, 2007). The regional patterns of anthropogenic CO_2 storage are consistent with those of CFCs and with changes in heat content. The observed trends in CO_2, DIC, pH and carbonate species can be primarily explained by the response of the ocean to the increase in atmospheric CO_2.

Large-scale changes in the O_2 content of the thermocline have been observed between the 1970s and the late 1990s. These changes are everywhere consistent with the local changes in ocean ventilation as identified either by changes in density gradients or by changes in apparent CFC ages. Nevertheless, an influence of changes in marine biology cannot be ruled out. The available data are insufficient to say if the changes in O_2 are caused by natural variability or are trends that are likely to persist in the future, but they do indicate that large-scale changes in ocean physics influence natural biogeochemical cycles, and thus the cycles of O_2 and CO_2 are likely to undergo changes if ocean circulation changes persist in the future.

5.5 Changes in Sea Level

5.5.1 Introductory Remarks

Present-day sea level change is of considerable interest because of its potential impact on human populations living in coastal regions and on islands. This section focuses on global and regional sea level variations, over time spans ranging from the last decade to the past century; a brief discussion of sea level change in previous centuries is given in Section 5.5.2.4. Changes over previous millennia are discussed in Section 6.4.3.

Processes in several nonlinearly coupled components of the Earth system contribute to sea level change, and understanding these processes is therefore a highly interdisciplinary endeavour. On decadal and longer time scales, global mean sea level change results from two major processes, mostly related to recent climate change, that alter the volume of water in the global ocean: i) thermal expansion (Section 5.5.3), and ii) the exchange of water between oceans and other reservoirs (glaciers and ice caps, ice sheets, other land water reservoirs - including through anthropogenic change in land hydrology, and the atmosphere; Section 5.5.5). All these processes cause geographically non-uniform sea level change (Section 5.5.4) as well as changes in the global mean; some oceanographic factors (e.g., changes in ocean circulation or atmospheric pressure) also affect sea level at the regional scale, while contributing negligibly to changes in the global mean. Vertical land movements such as resulting from glacial isostatic adjustment (GIA), tectonics, subsidence and sedimentation influence local sea level measurements but do not alter ocean water volume; nonetheless, they affect global mean sea level through their alteration of the shape and hence the volume of the ocean basins containing the water.

Measurements of present-day sea level change rely on two different techniques: tide gauges and satellite altimetry (Section 5.5.2). Tide gauges provide sea level variations with respect to the land on which they lie. To extract the signal of sea level change due to ocean water volume and other oceanographic change, land motions need to be removed from the tide gauge measurement. Land motions related to GIA can be simulated in global geodynamic models. The estimation of other land motions is not generally possible unless there are adequate nearby geodetic or geological data, which is usually not the case. However, careful selection of tide gauge sites such that records reflecting major tectonic activity are rejected, and averaging over all selected gauges, results in a small uncertainty for global sea level estimates (Appendix 5.A.4). Sea level change based on satellite altimetry is measured with respect to the Earth's centre of mass, and thus is not distorted by land motions, except for a small component due to large-scale deformation of ocean basins from GIA.

Frequently Asked Question 5.1

Is Sea Level Rising?

Yes, there is strong evidence that global sea level gradually rose in the 20th century and is currently rising at an increased rate, after a period of little change between AD 0 and AD 1900. Sea level is projected to rise at an even greater rate in this century. The two major causes of global sea level rise are thermal expansion of the oceans (water expands as it warms) and the loss of land-based ice due to increased melting.

Global sea level rose by about 120 m during the several millennia that followed the end of the last ice age (approximately 21,000 years ago), and stabilised between 3,000 and 2,000 years ago. Sea level indicators suggest that global sea level did not change significantly from then until the late 19th century. The instrumental record of modern sea level change shows evidence for onset of sea level rise during the 19th century. Estimates for the 20th century show that global average sea level rose at a rate of about 1.7 mm yr^{-1}.

Satellite observations available since the early 1990s provide more accurate sea level data with nearly global coverage. This decade-long satellite altimetry data set shows that since 1993, sea level has been rising at a rate of around 3 mm yr^{-1}, significantly higher than the average during the previous half century. Coastal tide gauge measurements confirm this observation, and indicate that similar rates have occurred in some earlier decades.

In agreement with climate models, satellite data and hydrographic observations show that sea level is not rising uniformly around the world. In some regions, rates are up to several times the global mean rise, while in other regions sea level is falling. Substantial spatial variation in rates of sea level change is also inferred from hydrographic observations. Spatial variability of the rates of sea level rise is mostly due to non-uniform changes in temperature and salinity and related to changes in the ocean circulation.

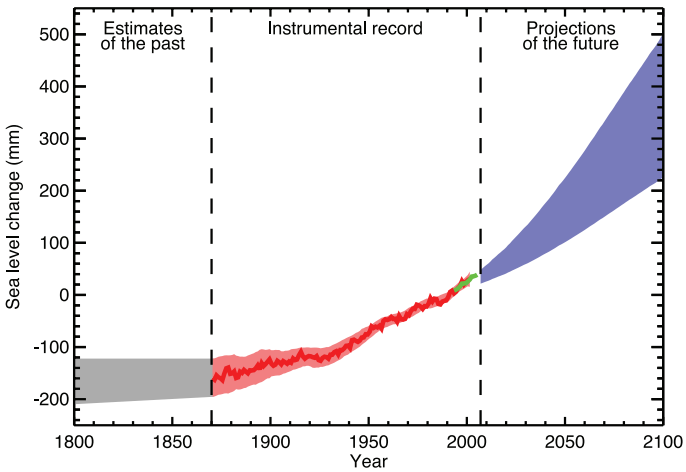
Near-global ocean temperature data sets made available in recent years allow a direct calculation of thermal expansion. It is believed that on average, over the period from 1961 to 2003, thermal expansion contributed about one-quarter of the observed sea level rise, while melting of land ice accounted for less than half. Thus, the full magnitude of the observed sea level rise during that period was not satisfactorily explained by those data sets, as reported in the IPCC Third Assessment Report.

During recent years (1993–2003), for which the observing system is much better, thermal expansion and melting of land ice each account for about half of the observed sea level rise, although there is some uncertainty in the estimates.

The reasonable agreement in recent years between the observed rate of sea level rise and the sum of thermal expansion and loss of land ice suggests an upper limit for the magnitude of change in land-based water storage, which is relatively poorly known. Model results suggest no net trend in the storage of water over land due to climate-driven changes but there are large interannual and decadal fluctuations. However, for the recent period 1993 to 2003, the small discrepancy between observed sea level rise and the sum of known contributions might be due to unquantified human-induced processes (e.g., groundwater extraction, impoundment in reservoirs, wetland drainage and deforestation).

Global sea level is projected to rise during the 21st century at a greater rate than during 1961 to 2003. Under the IPCC Special Report on Emission Scenarios (SRES) A1B scenario by the mid-2090s, for instance, global sea level reaches 0.22 to 0.44 m above 1990 levels, and is rising at about 4 mm yr^{-1}. As in the past, sea level change in the future will not be geographically uniform, with regional sea level change varying within about ±0.15 m of the mean in a typical model projection. Thermal expansion is projected to contribute more than half of the average rise, but land ice will lose mass increasingly rapidly as the century progresses. An important uncertainty relates to whether discharge of ice from the ice sheets will continue to increase as a consequence of accelerated ice flow, as has been observed in recent years. This would add to the amount of sea level rise, but quantitative projections of how much it would add cannot be made with confidence, owing to limited understanding of the relevant processes.

Figure 1 shows the evolution of global mean sea level in the past and as projected for the 21st century for the SRES A1B scenario.



FAQ 5.1, Figure 1. *Time series of global mean sea level (deviation from the 1980-1999 mean) in the past and as projected for the future. For the period before 1870, global measurements of sea level are not available. The grey shading shows the uncertainty in the estimated long-term rate of sea level change (Section 6.4.3). The red line is a reconstruction of global mean sea level from tide gauges (Section 5.5.2.1), and the red shading denotes the range of variations from a smooth curve. The green line shows global mean sea level observed from satellite altimetry. The blue shading represents the range of model projections for the SRES A1B scenario for the 21st century, relative to the 1980 to 1999 mean, and has been calculated independently from the observations. Beyond 2100, the projections are increasingly dependent on the emissions scenario (see Chapter 10 for a discussion of sea level rise projections for other scenarios considered in this report). Over many centuries or millennia, sea level could rise by several metres (Section 10.7.4).*

The TAR chapter on sea level change provided estimates of climate and other anthropogenic contributions to 20th-century sea level rise, based mostly on models (Church et al., 2001). The sum of these contributions ranged from –0.8 to 2.2 mm yr^{-1}, with a mean value of 0.7 mm yr^{-1}, and a large part of this uncertainty was due to the lack of information on anthropogenic land water change. For observed 20th-century sea level rise, based on tide gauge records, Church et al. (2001) adopted as a best estimate a value in the range of 1 to 2 mm yr^{-1}, which was more than twice as large as the TAR's estimate of climate-related contributions. It thus appeared that either the processes causing sea level rise had been underestimated or the rate of sea level rise observed with tide gauges was biased towards higher values.

Since the TAR, a number of new results have been published. The global coverage of satellite altimetry since the early 1990s (TOPography EXperiment (TOPEX)/Poseidon and Jason) has improved the estimate of global sea level rise and has revealed the complex geographical patterns of sea level change in open oceans. Near-global ocean temperature data for the last 50 years have been recently made available, allowing the first observationally based estimate of the thermal expansion contribution to sea level rise in past decades. For recent years, better estimates of the land ice contribution to sea level are available from various observations of glaciers, ice caps and ice sheets.

In this section, we summarise the current knowledge of present-day sea level rise. The observational results are assessed, followed by our current interpretation of these observations in terms of climate change and other processes, and ending with a discussion of the sea level budget (Section 5.5.6).

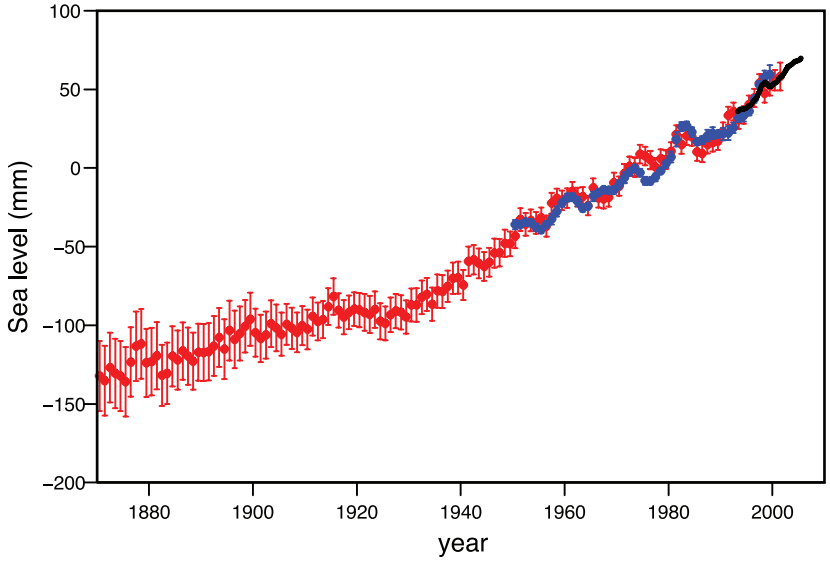


Figure 5.13. *Annual averages of the global mean sea level (mm). The red curve shows reconstructed sea level fields since 1870 (updated from Church and White, 2006); the blue curve shows coastal tide gauge measurements since 1950 (from Holgate and Woodworth, 2004) and the black curve is based on satellite altimetry (Leuliette et al., 2004). The red and blue curves are deviations from their averages for 1961 to 1990, and the black curve is the deviation from the average of the red curve for the period 1993 to 2001. Error bars show 90% confidence intervals.*

5.5.2 Observations of Sea Level Changes

5.5.2.1 20th-Century Sea Level Rise from Tide Gauges

Table 11.9 of the TAR listed several estimates for global and regional 20th-century sea level trends based on the Permanent Service for Mean Sea Level (PSMSL) data set (Woodworth and Player, 2003). The concerns about geographical bias in the PSMSL data set remain, with most long sea level records stemming from the NH, and most from continental coastlines rather than ocean interiors. Based on a small number (~25) of high-quality tide gauge records from stable land regions, the rate of sea level rise has been estimated as 1.8 mm yr^{-1} for the past 70 years (Douglas, 2001; Peltier, 2001), and Miller and Douglas (2004) find a range of 1.5 to 2.0 mm yr^{-1} for the 20th century from 9 stable tide gauge sites. Holgate and Woodworth (2004) estimated a rate of 1.7 ± 0.4 mm yr^{-1} sea level change averaged along the global coastline during the period 1948 to 2002, based on data from 177 stations divided into 13 regions. Church et al. (2004) (discussed further below) determined a global rise of 1.8 ± 0.3 mm yr^{-1} during 1950 to 2000, and Church and White (2006) determined a change of 1.7 ± 0.3 mm yr^{-1} for the 20th century. Changes in global sea level as derived from analyses of tide gauges are displayed in Figure 5.13. Considering the above results, and allowing for the ongoing higher trend in recent years shown by altimetry (see Section 5.5.2.2), we assess the rate for 1961 to 2003 as 1.8 ± 0.5 mm yr^{-1} and for the 20th century as 1.7 ± 0.5 mm yr^{-1}.

While the recently published estimates of sea level rise over the last decades remain within the range of the TAR values (i.e., 1–2 mm yr^{-1}), there is an increasing opinion that the best estimate lies closer to 2 mm yr^{-1} than to 1 mm yr^{-1}. The lower bound reported in the TAR resulted from local and regional studies; local and regional rates may differ from the global mean, as discussed below (see Section 5.5.2.5).

A critical issue concerns how the records are adjusted for vertical movements of the land upon which the tide gauges are located and of the oceans. Trends in tide gauge records are corrected for GIA using models, but not for other land motions. The GIA correction ranges from about 1 mm yr^{-1} (or more) near to former ice sheets to a few tenths of a millimetre per year in the far field (e.g., Peltier, 2001); the error in tide-gauge based global average sea level change resulting from GIA is assessed as 0.15 mm yr^{-1}. The TAR mentioned the developing geodetic technologies (especially the Global Positioning System; GPS) that hold the promise of measuring rates of vertical land movement at tide gauges, no matter if those movements are due to GIA or to other geological processes. Although there has been some model validation, especially for GIA models, systematic problems with such techniques, including short data spans, have yet to be fully resolved.

5.5.2.2 Sea Level Change during the Last Decade from Satellite Altimetry

Since 1992, global mean sea level can be computed at 10-day intervals by averaging the altimetric measurements from the TOPEX/Poseidon (T/P) and Jason satellites over the area of coverage (66°S to 66°N) (Nerem and Mitchum, 2001). Each 10-day estimate of global mean sea level has an accuracy of approximately 5 mm. Numerous papers on the altimetry results (see Cazenave and Nerem, 2004, for a review) show a current rate of sea level rise of 3.1 ± 0.7 mm yr^{-1} over 1993 to 2003 (Cazenave and Nerem, 2004; Leuliette et al., 2004; Figure 5.14). A significant fraction of the 3 mm yr^{-1} rate of change has been shown to arise from changes in the Southern Ocean (Cabanes et al., 2001).

The accuracy needed to compute mean sea level change pushes the altimeter measurement system to its performance limits, and thus care must be taken to ensure that the instrument is precisely calibrated (see Appendix 5.A.4.1). The tide gauge calibration method (Mitchum, 2000) provides diagnoses of problems in the altimeter instrument, the orbits, the measurement corrections and ultimately the final sea level data. Errors in determining the altimeter instrument drift using the tide gauge calibration, currently estimated to be about 0.4 mm yr^{-1}, are almost entirely driven by errors in knowledge of vertical land motion at the gauges (Mitchum, 2000).

Altimetry-based sea level measurements include variations in the global ocean basin volume due to GIA. Averaged over the oceanic regions sampled by the altimeter satellites, this effect yields a value close to –0.3 mm yr^{-1} in sea level (Peltier, 2001), with possible uncertainty of 0.15 mm yr^{-1}. This number is subtracted from altimetry-derived global mean sea level in order to obtain the contribution due to ocean (water) volume change.

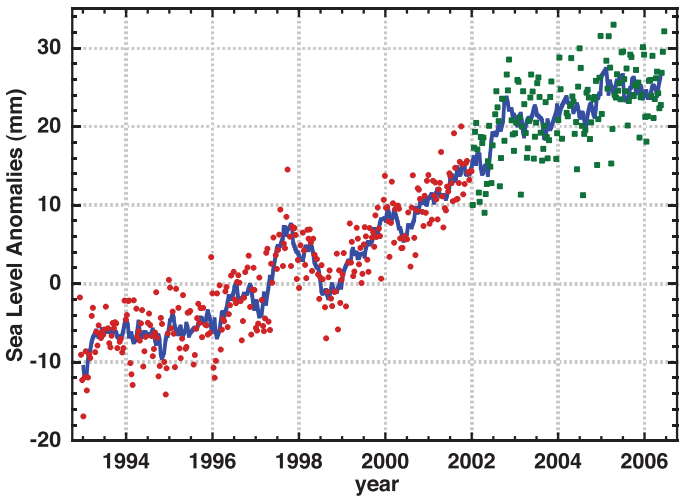


Figure 5.14. *Variations in global mean sea level (difference to the mean 1993 to mid-2001) computed from satellite altimetry from January 1993 to October 2005, averaged over 65°S to 65°N. Dots are 10-day estimates (from the TOPEX/Poseidon satellite in red and from the Jason satellite in green). The blue solid curve corresponds to 60-day smoothing. Updated from Cazenave and Nerem (2004) and Leuliette et al. (2004).*

Altimetry from T/P allows the mapping of the geographical distribution of sea level change (Figure 5.15a). Although regional variability in coastal sea level change had been reported from tide gauge analyses (e.g., Douglas, 1992; Lambeck, 2002), the global coverage of satellite altimetry provides unambiguous evidence of non-uniform sea level change in open oceans, with some regions exhibiting rates of sea level change about five times the global mean. For the past decade, sea level rise shows the highest magnitude in the western Pacific and eastern Indian oceans, regions that exhibit large interannual variability associated with ENSO. Except for the Gulf Stream region, most of the Atlantic Ocean shows sea level rise during the past decade. Despite the global mean rise, Figure 5.15a shows that sea level has been dropping in some regions (eastern Pacific and western Indian Oceans). These spatial patterns likely reflect decadal fluctuations rather than long-term trends. Empirical Orthogonal Functions (EOF) analyses of altimetry-based sea level maps over 1993 to 2003 show a strong influence of the 1997–1998 El Niño, with the geographical patterns of the dominant mode being very similar to those of the sea level trend map (e.g., Nerem et al., 1999).

5.5.2.3 Reconstructions of Sea Level Change during the Last 50 Years Based on Satellite Altimetry and Tide Gauges

Attempts have been made to reconstruct historical sea level fields by combining the near-global coverage from satellite altimeter data with the longer but spatially sparse tide gauge records (Chambers et al., 2002; Church et al., 2004). These sea level reconstructions use the short altimeter record to determine the principal EOF of sea level variability, and the tide gauge data to estimate the evolution of the amplitude of the EOFs over time. The method assumes that the geographical patterns of decadal sea level trends can be represented by a superposition of the patterns of variability that are manifest in interannual variability. The sea level for the period 1870 to 2000 (Church and White, 2006) shown in Figure 5.13 is based on this approach. As a caveat, note that variability on different time scales may have different characteristic patterns (see Section 5.5.4.1).

The trends in the EOF amplitudes (and the implied global correlations) allow the reconstruction of a spatially variable rate of sea level rise. Figure 5.16a (updated from Church et al., 2004) shows the geographical distribution of linear sea level trends for 1955 to 2003 based on this reconstruction technique. Comparison with the altimetry-based trend map for the shorter period (1993 to 2003) indicates quite different geographical patterns. These differences mainly arise from thermal expansion changes through time (see Section 5.5.3)

Changes in spatial sea level patterns through time may help reconcile apparently inconsistent estimates of regional variations in tide-gauge based sea level rise. For example, the minimum in rise along the northwest Australian coast is consistent with the results of Lambeck (2002) in having smaller rates of sea level rise and indeed sea level fall off north-western Australia over the last few decades. In addition, for the North Atlantic Ocean,

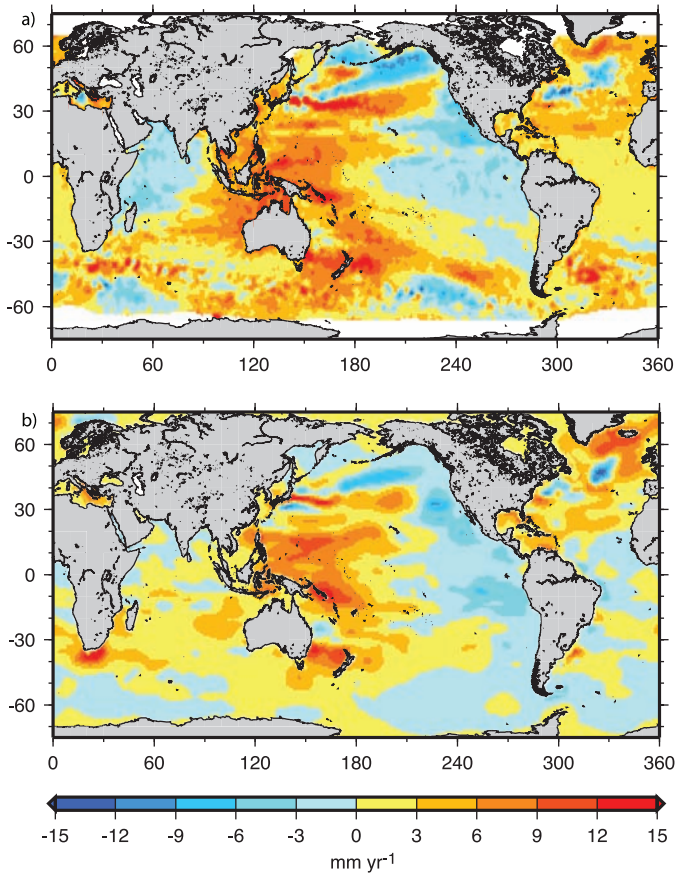


Figure 5.15. *(a) Geographic distribution of short-term linear trends in mean sea level (mm yr^{-1}) for 1993 to 2003 based on TOPEX/Poseidon satellite altimetry (updated from Cazenave and Nerem, 2004) and (b) geographic distribution of linear trends in thermal expansion (mm yr^{-1}) for 1993 to 2003 (based on temperature data down to 700 m from Ishii et al., 2006).*

the rate of rise reaches a maximum (over 2 mm yr^{-1}) in a band running east-northeast from the US east coast. The trends are lower in the eastern than in the western Atlantic (Lambeck et al., 1998; Woodworth et al., 1999; Mitrovica et al., 2001).

5.5.2.4 Interannual and Decadal Variability and Long-Term Changes in Sea Level

Sea level records contain a considerable amount of interannual and decadal variability, the existence of which is coherent throughout extended parts of the ocean. For example, the global sea level curve in Figure 5.13 shows an approximately 10 mm rise and fall of global mean sea level accompanying the 1997–1998 ENSO event. Over the past few decades, the time series of the first EOF of Church et al. (2004) represents ENSO variability, as shown by a significant (negative) correlation with the Southern Oscillation Index. The signature of the 1997–1998 El Niño is also clear in the altimetric maps of sea level anomalies (see Section 5.5.2.2). Model results suggest that large volcanic eruptions produce interannual to decadal fluctuations in the global mean sea level (see Section 9.5.2).

Holgate and Woodworth (2004) concluded that the 1990s had one of the fastest recorded rates of sea level rise averaged along the global coastline (~4 mm yr^{-1}), slightly higher than the altimetry-based open ocean sea level rise (3 mm yr^{-1}). However, their analysis also shows that some previous decades had comparably large rates of coastal sea level rise (e.g., around 1980; Figure 5.17). White et al. (2005) confirmed the larger sea level rise during the 1990s around coastlines compared to the open ocean but found that in some previous periods the coastal rate was smaller than the open ocean rate, and concluded that over the last 50 years the coastal and open ocean rates of change were the same on average. The global reconstruction of Church et al. (2004) and Church and White (2006) also exhibits large decadal variability in the rate of global mean sea level rise, and the 1993 to 2003 rate has been exceeded in some previous decades (Figure 5.17). The variability is smaller in the global reconstruction (standard deviation of overlapping 10-year rates is 1.1 mm yr^{-1}) than in the Holgate and Woodworth (2004) coastal time series (standard deviation 1.7 mm yr^{-1}). The rather

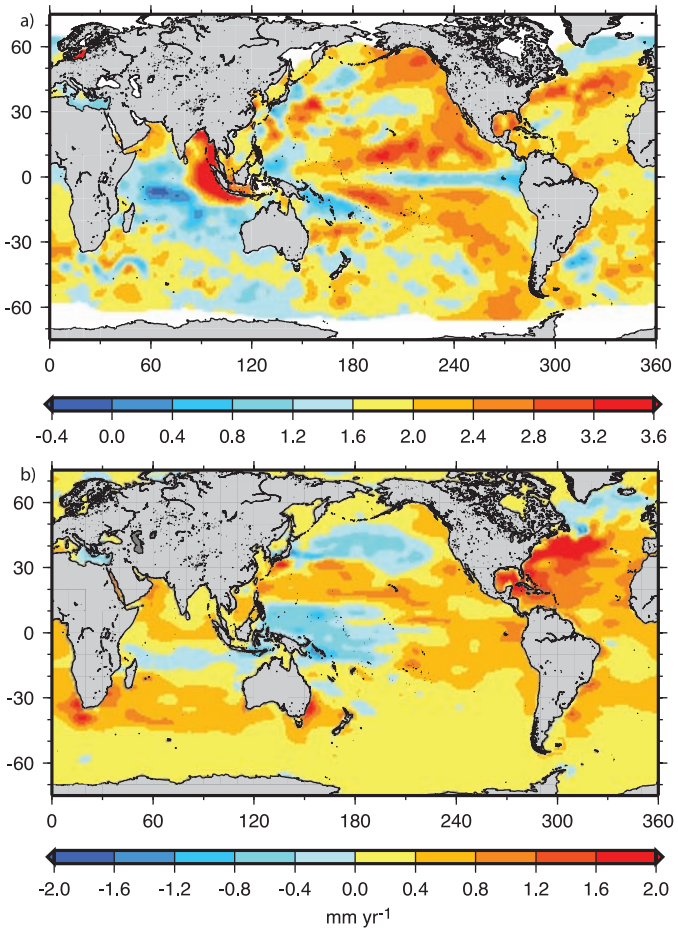


Figure 5.16. *(a) Geographic distribution of long-term linear trends in mean sea level (mm yr^{-1}) for 1955 to 2003 based on the past sea level reconstruction with tide gauges and altimetry data (updated from Church et al., 2004) and (b) geographic distribution of linear trends in thermal expansion (mm yr^{-1}) for 1955 to 2003 (based on temperature data down to 700 m from Ishii et al., 2006). Note that colours in (a) denote 1.6 mm yr^{-1} higher values than those in (b).*

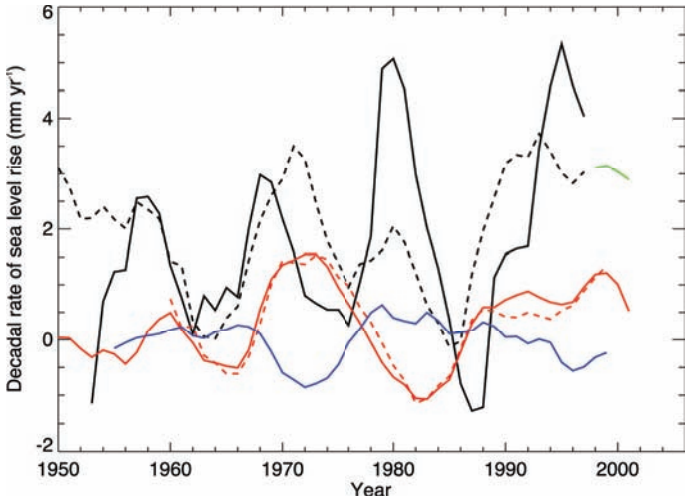


Figure 5.17. *Overlapping 10-year rates of global sea level change from tide gauge data sets (Holgate and Woodworth, 2004, in solid black; Church and White, 2006, in dashed black) and satellite altimetry (updated from Cazenave and Nerem, 2004, in green), and contributions to global sea level change from thermal expansion (Ishii et al., 2006, in solid red; Antonov et al., 2005, in dashed red) and climate-driven land water storage (Ngo-Duc et al., 2005, in blue). Each rate is plotted against the middle of its 10-year period.*

low temporal correlation (r = 0.44) between the two time series suggests that the statistical uncertainty in the linear trends calculated from either data set probably underestimates the systematic uncertainty in the results (Section 5.5.6).

Interannual or longer variability is a major reason why no long-term acceleration of sea level has been identified using 20th-century data alone (Woodworth, 1990; Douglas, 1992). Another possibility is that the sparse tide gauge network may have been inadequate to detect it if present (Gregory et al., 2001). The longest records available from Europe and North America contain accelerations of the order of 0.4 mm yr^{-1} per century between the 19th and 20th century (Ekman, 1988; Woodworth et al., 1999). For the reconstruction shown in Figure 5.13, Church and White (2006) found an acceleration of 1.3 ± 0.5 mm yr^{-1} per century over the period 1870 to 2000. These data support an inference that the onset of acceleration occurred during the 19th century (see Section 9.5.2).

Geological observations indicate that during the last 2,000 years (i.e., before the recent rise recorded by tide gauges), sea level change was small, with an average rate of only 0.0 to 0.2 mm yr^{-1} (see Section 6.4.3). The use of proxy sea level data from archaeological sources is well established in the Mediterranean. Oscillations in sea level from 2,000 to 100 yr before present did not exceed ±0.25 m, based on the Roman-Byzantine-Crusader well data (Sivan et al., 2004). Many Roman and Greek constructions are relatable to the level of the sea. Based on sea level data derived from Roman fish ponds, which are considered to be a particularly reliable source of such information, together with nearby tide gauge records, Lambeck et al. (2004) concluded that the onset of the modern sea level rise occurred between 1850 and 1950. Donnelly et al. (2004) and Gehrels et al. (2004), employing geological data from Connecticut, Maine and Nova Scotia salt-marshes together with nearby tide gauge records, demonstrated that the sea level rise observed during the 20th century was in excess of that averaged over the previous several centuries.

The joint interpretation of the geological observations, the longest instrumental records and the current rate of sea level rise for the 20th century gives a clear indication that the rate of sea level rise has increased between the mid-19th and the mid-20th centuries.

5.5.2.5 Regional Sea Level Change

Two regions are discussed here to give examples of local variability in sea level: the northeast Atlantic and small Pacific Islands.

Interannual variability in northeast Atlantic sea level records exhibits a clear relationship to the air pressure and wind changes associated with the NAO, with the magnitude and sign of the response depending primarily upon latitude (Andersson, 2002; Wakelin et al., 2003; Woolf et al., 2003). The signal of the NAO can also be observed to some extent in ocean temperature records, suggesting a possible, smaller NAO influence on regional mean sea level via steric (density) changes (Tsimplis et al., 2006). In the Russian Arctic Ocean, sea level time series for recent decades also have pronounced decadal variability that correlates with the NAO index. In this region, wind stress and atmospheric pressure loading contribute nearly half of the observed sea level rise of 1.85 mm yr^{-1} (Proshutinsky et al., 2004).

Small Pacific Islands are the subject of much concern in view of their vulnerability to sea level rise. The Pacific Ocean region is the centre of the strongest interannual variability of the climate system, the coupled ocean-atmosphere ENSO mode. There are only a few Pacific Island sea level records extending back to before 1950. Mitchell et al. (2001) calculated rates of relative sea level rise for the stations in the Pacific region. Using their results (from their Table 1) and focusing on only the island stations with more than 50 years of data (only 4 locations), the average rate of sea level rise (relative to the Earth's crust) is 1.6 mm yr^{-1}. For island stations with record lengths greater than 25 years (22 locations), the average rate of relative sea level rise is 0.7 mm yr^{-1}. However, these data sets contain a large range of rates of relative sea level change, presumably as a result of poorly quantified vertical land motions.

An example of the large interannual variability in sea level is Kwajalein (8°44'N, 167°44'E) (Marshall Archipelago). As shown in Figure 5.18, the local tide gauge data, the sea level reconstructions of Church et al. (2004) and Church and White (2006) and the shorter satellite altimeter record all agree and indicate that interannual variations associated with ENSO events are greater than 0.2 m. The Kwajalein data also suggest increased variability in sea level after the mid-1970s, consistent with the trend towards more frequent, persistent and intense ENSO events since the mid-1970s (Folland et al., 2001). For the Kwajalein record, the rate of sea level rise, after correction for GIA land motions and isostatic response to atmospheric pressure changes, is 1.9 ± 0.7 mm yr^{-1}. However,

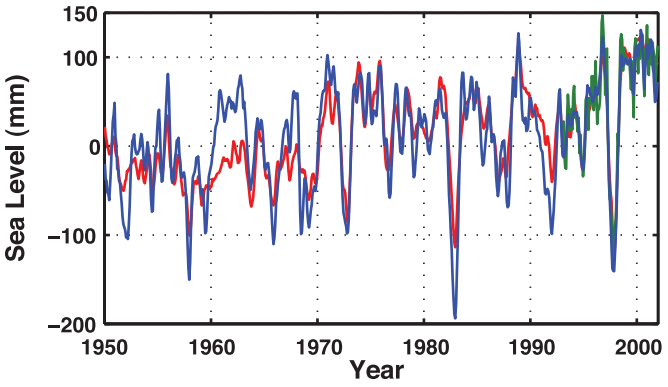


Figure 5.18. *Monthly mean sea level curve for 1950 to 2000 at Kwajalein (8°44'N, 167°44'E). The observed sea level (from tide gauge measurements) is in blue, the reconstructed sea level in red and the satellite altimetry record in green. Annual and semi-annual signals have been removed from each time series and the tide gauge data have been smoothed. The figure was drawn using techniques in Church et al. (2004) and Church and White (2006).*

the uncertainties in rates of sea level change increase rapidly with decreasing record length and can be several mm yr^{-1} for decade-long records (depending on the magnitude of the interannual variability). Sea level change on the atolls of Tuvalu (western Pacific) has been the subject of intense interest as a result of their low-lying nature and increasing incidence of flooding. There are two records available at Funafuti, Tuvalu; the first record commences in 1977 and the second (with rigorous datum control) in 1993. After allowing for subsidence affecting the first record, Church et al. (2006) estimate sea level rise at Tuvalu to be 2.0 ± 1.7 mm yr^{-1}, in agreement with the reconstructed rate of sea level rise.

5.5.2.6 Changes in Extreme Sea Level

Societal impacts of sea level change primarily occur via the extreme levels rather than as a direct consequence of mean sea level changes. Apart from non-climatic events such as tsunamis, extreme sea levels occur mainly in the form of storm surges generated by tropical or extra tropical cyclones. Secular changes and decadal variability in storminess are discussed in Chapter 3. Studies of variations in extreme sea levels during the 20th century based on tide gauge data are fewer than studies of changes in mean sea level for several reasons. A study on changes in extremes, which are caused by changes in mean sea level as well as changes in surges, is more complex than the study of mean sea level changes. Moreover, the hourly sampling interval normally used in tide gauge records is not always sufficient to accurately capture the true extreme. Among the different parameters often used to describe extremes, annual maximum surge is a good indicator of climatic trends. For study of long records extending back to the 19th century or before, annual maximum surge-at-high-water (defined as the maximum of the difference between observed high water and the predicted tide at high water) is a better-suited parameter because during that period high waters and not the full tidal curve were recorded.

Studies of the longest records of extremes are inevitably restricted to a small number of locations. From observed sea level extremes at Liverpool since 1768, Woodworth and Blackman (2002) concluded that the annual maximum surge-at-high-water was larger in the late 18th, late 19th and late 20th centuries than for most of the 20th century, qualitatively consistent with the long-term variability in storminess from meteorological data. From the tide gauge record at Brest from 1860 to 1994, Bouligand and Pirazzoli (1999) found an increasing trend in annual maxima and 99th percentile of surges; however, a decreasing trend was found during the period 1953 to 1994. From non-tidal residuals ('surges') at San Francisco since 1858, Bromirski et al. (2003) concluded that extreme winter residuals have exhibited a significant increasing trend since about 1950, a trend that is attributed to an increase in storminess during this period. Zhang et al. (2000) concluded from records at 10 stations along the east coast of the USA since 1900 that the rise in extreme sea level closely followed the rise in mean sea level. A similar conclusion can be drawn from a recent study of Firing and Merrifield (2004), who found long-term increases in the number and height of daily extremes at Honolulu (interestingly, the highest-ever value being due an anticyclonic oceanic eddy system in 2003), but no evidence for an increase relative to the underlying upward mean sea level trend.

An analysis of 99th percentiles of hourly sea level at 141 stations over the globe for recent decades (Woodworth and Blackman, 2004) showed that there is evidence for an increase in extreme high sea level worldwide since 1975. In many cases, the secular changes in extremes were found to be similar to those in mean sea level. Likewise, interannual variability in extremes was found to be correlated with regional mean sea level, as well as to indices of regional climate patterns.

5.5.3 Ocean Density Changes

Sea level will rise if the ocean warms and fall if it cools, since the density of the water column will change. If the thermal expansivity were constant, global sea level change would parallel the global ocean heat content discussed in Section 5.2. However, since warm water expands more than cold water (with the same input of heat), and water at higher pressure expands more than at lower pressure, the global sea level change depends on the three-dimensional distribution of ocean temperature change.

Analysis of the last half century of temperature observations indicates that the ocean has warmed in all basins (see Section 5.2). The average rate of thermosteric sea level rise caused by heating of the global ocean is estimated to be 0.40 ± 0.09 mm yr^{-1} over 1955 to 1995 (Antonov et al., 2005), based on five-year mean temperature data down to 3,000 m. For the 0 to 700 m layer and the 1955 to 2003 period, the averaged thermosteric trend, based on annual mean temperature data from Levitus et al. (2005a), is 0.33 ± 0.07 mm yr^{-1} (Antonov et al., 2005). For the same period and depth range, the mean thermosteric rate based on monthly ocean temperature data from Ishii et al. (2006) is 0.36 ± 0.12 mm yr^{-1}. Figure 5.19

shows the thermosteric sea level curve over 1955 to 2003 for both the Levitus and Ishii data sets. The rate of thermosteric sea level rise is clearly not constant in time and shows considerable fluctuations (Figure 5.17). A rise of more than 20 mm occurred from the late 1960s to the late 1970s (giving peak 10-year rates in the early 1970s) with a smaller drop afterwards. Another large rise began in the 1990s, but after 2003, the steric sea level is decreasing in both estimates (peak rates in the late 1990s). Overlapping 10-year rates from these two estimates have a very high temporal correlation (r = 0.97) and the standard deviation of the rates is 0.7 mm yr^{-1}.

The Levitus and Ishii data sets both give 0.32 ± 0.09 mm yr^{-1} for the upper 700 m during 1961 to 2003, but the Levitus data set of temperature down to 3,000 m ends in 1998. From the results of Antonov et al. (2005) for thermal expansion, the difference between the trends in the upper 3,000 m and the upper 700 m for 1961 to 1998 is about 0.1 mm yr^{-1}. Assuming that the ocean below 700 m continues to contribute beyond 1998 at a similar rate, with an uncertainty similar to that of the upper-ocean contribution, we assess the thermal expansion of the ocean down to 3,000 m during 1961 to 2003 as 0.42 ± 0.12 mm yr^{-1}.

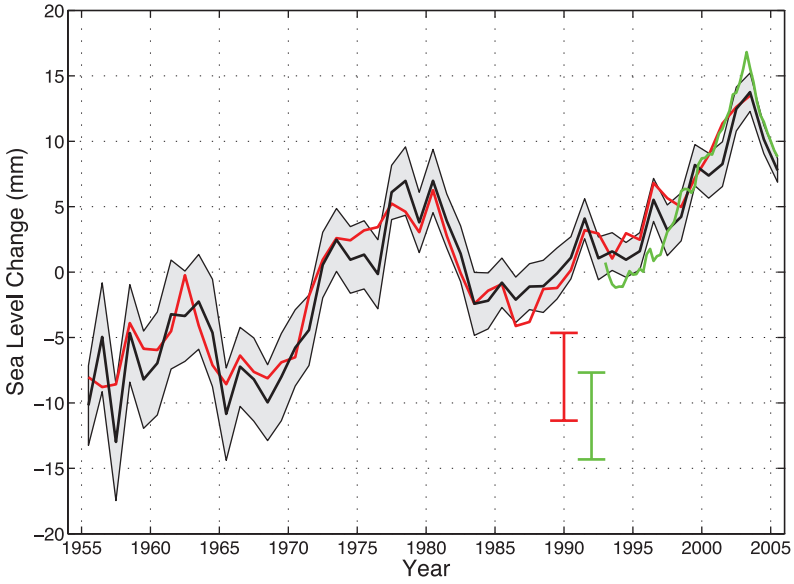


Figure 5.19. *Global sea level change due to thermal expansion for 1955 to 2003, based on Levitus et al. (2005a; black line) and Ishii et al. (2006; red line) for the 0 to 700 m layer, and based on Willis et al. (2004; green line) for the upper 750 m. The shaded area and the vertical red and green error bars represent the 90% confidence interval. The black and red curves denote the deviation from their 1961 to 1990 average, the shorter green curve the deviation from the average of the black curve for the period 1993 to 2003.*

For the recent period 1993 to 2003, a value of 1.2 ± 0.5 mm yr^{-1} for thermal expansion in the upper 700 m is estimated both by Antonov et al. (2005) and Ishii et al. (2006). Willis et al. (2004) estimate thermal expansion to be 1.6 ± 0.5 mm yr^{-1}, based on combined *in situ* temperature profiles down to 750 m and satellite measurements of altimetric height. Including the satellite data reduces the error caused by the inadequate sampling of the profile data. Error bars were estimated to be about 2 mm for individual years in the time series, with most of the remaining error due to inadequate profile availability. A close result (1.8 ± 0.4 mm yr^{-1} steric sea level rise for 1993 to 2003) was recently obtained by Lombard et al. (2006), based on a combined analysis of *in situ* hydrographic data and satellite sea surface height and SST data (Guinehut et al., 2004). It is presently unclear why the latter two estimates are significantly larger than the thermosteric rates based on temperature data alone. It is possible that the *in situ* data underestimate thermal expansion because of poor coverage in Southern Oceans, and it is interesting to note that a model based on assimilation of hydrographic data yields a somewhat higher estimate of 2.3 mm yr^{-1} (Carton et al., 2005). Published estimates of the steric sea level rates for 1955 to 2003 and 1993 to 2003 are shown in Table 5.2.

We assess the thermal expansion of the upper 700 m during 1993 to 2003 as 1.5 ± 0.5 mm yr^{-1}, and that of the upper 3,000 m as 1.6 ± 0.5 mm yr^{-1}, allowing for the ocean below 700 m as for the earlier period (see also Section 5.5.6, Table 5.3).

Table 5.2. *Recent estimates for steric sea level trends from different studies.*

Reference	Steric sea level change with errors (mm yr^{-1})	Period	Depth range (m)	Data Source
Antonov et al. (2005)	0.40 ± 0.09	1955–1998	0–3,000	Levitus et al. (2005b)
Antonov et al. (2005)	0.33 ± 0.07	1955–2003	0–700	Levitus et al. (2005b)
Ishii et al. (2006)	0.36 ± 0.06	1955–2003	0–700	Ishii et al. (2006)
Antonov et al. (2005)	1.2 ± 0.5	1993–2003	0–700	Levitus et al. (2005b)
Ishii et al. (2006)	1.2 ± 0.5	1993–2003	0–700	Ishii et al. (2006)
Willis et al. (2004)	1.6 ± 0.5	1993–2003	0–750	Willis et al. (2004)
Lombard et al. (2006)	1.8 ± 0.4	1993-2003	0-700	Guinehut et al. (2004)

Antonov et al. (2002) attributed about 10% of the global average steric sea level rise during recent decades to halosteric expansion (i.e., the volume increase caused by freshening of the water column). A similar result was obtained by Ishii et al. (2006) who estimated a halosteric contribution to 1955 to 2003 sea level rise of 0.04 ± 0.02 mm yr^{-1}. While it is of interest to quantify this effect, only about 1% of the halosteric expansion contributes to the global sea level rise budget. This is because the halosteric expansion is nearly compensated by a decrease in volume of the added freshwater when its salinity is raised (by mixing) to the mean ocean value; the compensation would be exact for a linear state equation (Gille, 2004; Lowe and Gregory, 2006). Hence, for global sums of sea level change, halosteric expansion cannot be counted separately from the volume of added land freshwater (which Antonov et al., 2002, also calculate; see Section 5.5.5.1). However, for regional changes in sea level, thermosteric and halosteric contributions can be comparably important (see, e.g., Section 5.5.4.1).

5.5.4 Interpretation of Regional Variations in the Rate of Sea Level Change

Sea level observations show that whatever the time span considered, rates of sea level change display considerable regional variability (see Sections 5.5.2.2 and 5.5.2.3). A number of processes can cause regional sea level variations.

5.5.4.1 Steric Sea Level Changes

Like the sea level trends observed by satellite altimetry (see Section 5.5.2.3), the global distribution of thermosteric sea level trends is not spatially uniform. This is illustrated by Figure 5.15b and Figure 5.16b, which show the geographical distribution of thermosteric sea level trends over two different periods, 1993 to 2003 and 1955 to 2003 respectively (updated from Lombard et al., 2005). Some regions experienced sea level rise while others experienced a fall, often with rates that are several times the global mean. However, the patterns of thermosteric sea level rise over the approximately 50-year period are different from those seen in the 1990s. This occurs because the spatial patterns, like the global average, are also subject to decadal variability. In other words, variability on different time scales may have different characteristic patterns.

An EOF analysis of gridded thermosteric sea level time series since 1955 (updated from Lombard et al., 2005) displays a spatial pattern that is similar to the spatial distribution of thermosteric sea level trends over the same time span (compare Figure 5.20 with Figure 5.16b). In addition, the first principal component is negatively correlated with the Southern Oscillation Index. Thus, it appears that ENSO-related ocean variability accounts for the largest fraction of variance in spatial patterns of thermosteric sea level. Similarly, decadal thermosteric sea level in the North Pacific and North Atlantic appears strongly influenced by the PDO and NAO respectively.

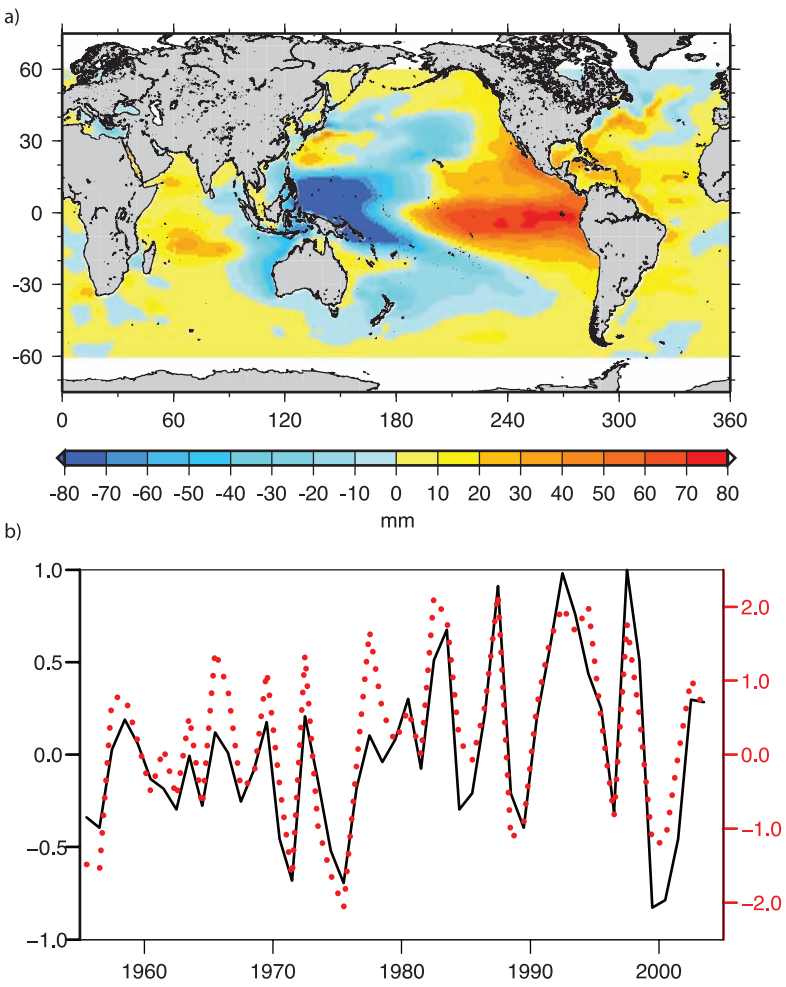


Figure 5.20. *(a) First mode of the EOF decomposition of the gridded thermosteric sea level time series of yearly temperature data down to 700 m from Ishii et al. (2006). (b) The normalised principal component (black solid curve) is highly correlated with the negative Southern Oscillation Index (dotted red curve).*

For the recent years (1993–2003), the geographic distribution of observed sea level trends (Figure 5.15a) shows correlation with the spatial patterns of thermosteric sea level change (Figure 5.15b). This suggests that at least part of the non-uniform pattern of sea level rise observed in the altimeter data over the past decade can be attributed to changes in the ocean's thermal structure, which is itself driven by surface heating effects and ocean circulation. Note that the steric changes due to salinity changes have not been included in these figures due to insufficient salinity data in parts of the World Ocean.

Ocean salinity changes, while unimportant for sea level at the global scale, can have an effect on regional sea level (e.g., Antonov et al., 2002; Ishii et al., 2006; Section 5.5.3). For example, in the subpolar gyre of the North Atlantic, especially in the Labrador Sea, the halosteric contribution nearly

counteracts the thermosteric contribution. This observational result is supported by results from data assimilation into models (e.g., Stammer et al., 2003). Since density changes can result not only from surface buoyancy fluxes but also from the wind, a simple attribution of density changes to buoyancy forcing is not possible.

While much of the non-uniform pattern of sea level change can be attributed to thermosteric volume changes, the difference between observed and thermosteric spatial trends show a high residual signal in a number of regions, especially in the southern oceans. Part of these residuals is likely due to the lack of ocean temperature coverage in remote oceans as well as in deep layers (below 700 m), and to regional salinity change.

5.5.4.2 Ocean Circulation Changes

The highly non-uniform geographical distribution of steric sea level trends is closely connected, through geostrophic balance, with changes in ocean surface circulation. Density and circulation changes result from changes in atmospheric forcing that is primarily by surface wind stress and buoyancy flux (i.e., heat and freshwater fluxes). The wind alone can therefore cause local (but not global) changes in steric sea level. Ocean general circulation models based on the assimilation of ocean data satisfactorily reproduce the spatial structure of sea level trends for the past decade, and show in particular that the tropical Pacific pattern results from decadal fluctuations in the depth of the tropical thermocline and change in equatorial trade winds (Carton et al., 2005; Köhl et al., 2006). The similarity of the patterns of steric and actual sea level change indicates that density changes are the dominant influence. Discrepancies may indicate a significant contribution from changes in the wind-driven barotropic circulation, especially at high latitudes.

5.5.4.3 Surface Atmospheric Pressure Changes

Surface atmospheric pressure also causes regional sea level variations. Over time scales longer than a few days, the ocean adjusts nearly isostatically to changes in atmospheric pressure (inverted barometer effect), that is, for each 1 hPa sea level pressure increase the ocean is depressed by approximately 10 mm, shifting the underlying mass sideways to other regions. For the temporal average, regional changes in sea level caused by atmospheric pressure loading reach about 0.2 m (e.g., between the subtropical Atlantic and the subpolar Atlantic). Such effects are generally corrected for in tide gauge and altimetry-based sea level analyses. The inverted barometer effect has a negligible effect on global mean sea level, because water is nearly incompressible, but is significant when averaged over the area of T/P and Jason-1 altimetry, which does not cover the whole World Ocean (Ponte, 2006). For that reason, the altimetry-based mean sea level curve is corrected for the inverted barometer effect.

5.5.4.4 Solid Earth and Geoid Changes

Geodynamical processes related to the solid Earth's elastic and viscoelastic response to spatially variable ice melt loading (due to the last deglaciation and present-day land ice melt) also cause non-uniform sea level change (e.g., Mitrovica et al., 2001; Peltier, 2001, 2004; Plag, 2006). The solid Earth and oceans continue to respond to the ice and complementary water loads associated with the late Pleistocene and early Holocene glacial cycles through GIA. This process not only drives large crustal uplift near the location of former ice complexes, but also produces a worldwide signature in sea level that results from gravitational, deformational and rotational effects: as the viscous mantle material flows to restore isostasy during and after the last deglaciation, uplift occurs under the former centres of the ice sheets while the surrounding peripheral bulges experience a subsidence. The return of the melt water to the oceans produces an ongoing geoid change resulting in subsidence of the ocean basins and an upward warping of the continents, while the flow of water into the subsiding peripheral bulges contributes a broad scale sea level fall in the far field of the ice complexes. The combined gravitational and deformational effects also perturb the rotation vector of the planet, and this perturbation feeds back into variations in the position of the crust and the geoid (an equipotential surface of the Earth's gravity field that coincides with the mean surface of the oceans). Corrections for GIA effects are made to both tide gauge and altimeter estimates of global sea level change (see Sections 5.5.2.1 and 5.5.2.2).

Self-gravitation and deformation of the Earth's surface in response to the ongoing change in loading by glaciers and ice sheets is another cause of regional sea level variations. Model predictions show quite different patterns of non-uniform sea level change depending on the source of the ice melt (Mitrovica et al., 2001; Plag, 2006), and associated regional sea level variations reach up to a few 0.1 mm yr^{-1}.

5.5.5 Ocean Mass Change

Global mean sea level will rise if water is added to the ocean from other reservoirs in the climate system. Water storage in the atmosphere is equivalent to only about 35 mm of global mean sea level, and the observed atmospheric storage trend of about 0.04 mm yr^{-1} in recent decades (Section 3.4.2.1) is unimportant compared with changes in ice and water stored on land, described in this subsection. Variations in land water storage result from variations in climatic conditions, direct human intervention in the water cycle and human modification of the land surface.

5.5.5.1 Ocean Mass Change Estimated from Salinity Change

Global salinity changes can be caused by changes in the global sea ice volume (which do not influence sea level) and by ocean mass changes (which do). Thus in principle, global salinity

changes can be used to estimate the global average sea level change due to fresh water input (Antonov et al., 2002; Munk, 2003; Wadhams and Munk, 2004). However, the accuracy of these estimates depends on the accuracy of the estimates for both sea ice volume (Hilmer and Lemke, 2000; Wadhams and Munk, 2004; see also Section 4.4) and global salinity change (Section 5.2.3). We assess that the error in estimates of ocean mass changes derived from salinity changes and sea ice melt is too large to provide useful constraints on the sea level change budget (Section 5.5.6).

5.5.5.2 Land Ice

During the 20th century, glaciers and ice caps have experienced considerable mass losses, with strong retreats in response to global warming after 1970. For 1961 to 2003, their contribution to sea level is assessed as 0.50 ± 0.18 mm yr^{-1} and for 1993 to 2003 as 0.77 ± 0.22 mm yr^{-1} (see Section 4.5.2).

As discussed in Section 4.6.2.2 and Table 4.6, the Greenland Ice Sheet has also been losing mass in recent years, contributing 0.05 ± 0.12 mm yr^{-1} to sea level rise during 1961 to 2003 and 0.21 ± 0.07 mm yr^{-1} during 1993 to 2003. Assessments of contributions to sea level rise from the Antarctic Ice Sheet are less certain, especially before the advent of satellite measurements, and are 0.14 ± 0.41 mm yr^{-1} for 1961 to 2003 and 0.21 ± 0.35 mm yr^{-1} for 1993 to 2003. Geodetic data on Earth rotation and polar wander allow a late-20th century sea level contribution of up to about 1 mm yr^{-1} from land ice (Mitrovica et al., 2006). However, recent estimates of ice sheet mass change exclude the large contribution inferred for Greenland by Mitrovica et al. (2001) from the geographical pattern of sea level change, confirming the lower rates reported above.

5.5.5.3 Climate-Driven Change in Land Water Storage

Continental water storage includes water (both liquid and solid) stored in subsurface saturated (groundwater) and unsaturated (soil water) zones, in the snowpack, and in surface water bodies (lakes, artificial reservoirs, rivers, floodplains and wetlands). Changes in concentrated stores, most notably very large lakes, are relatively well known from direct observation. In contrast, global estimates of changes in distributed surface stores (soil water, groundwater, snowpack and small areas of surface water) rely on computations with detailed hydrological models coupled to global ocean-atmosphere circulation models or forced by observations. Such models estimate the variation in land water storage by solving the water balance equation. The Land Dynamics (LaD) model developed by Milly and Shmakin (2002) provides global 1° by 1° monthly gridded time series of root zone soil water, groundwater and snowpack for the last two decades. With these data, the contributions of time-varying land water storage to sea level rise in response to climate change have been estimated, resulting in a small positive sea level trend of about 0.12 mm yr^{-1} for the last two decades, with larger interannual and decadal fluctuations (Milly et al., 2003). From a land surface model forced by a global climatic data set based on standard reanalysis products and on observations, land water changes during the past five decades were found to have low-frequency (decadal) variability of about 2 mm in amplitude but no significant trend (Ngo-Duc et al., 2005). These decadal variations are related to groundwater and are caused by precipitation variations. They are strongly negatively correlated with the de-trended thermosteric sea level (Figure 5.17). This suggests that the land water contribution to sea level and thermal expansion partly compensate each other on decadal time scales. However, this conclusion depends on the accuracy of the precipitation in reanalysis products.

5.5.5.4 Anthropogenic Change in Land Water Storage

The amount of anthropogenic change in land water storage systems cannot be estimated with much confidence, as already discussed by Church et al. (2001). A number of factors can contribute to sea level rise. First, natural groundwater systems typically are in a condition of dynamic equilibrium where, over long time periods, recharge and discharge are in balance. When the rate of groundwater pumping greatly exceeds the rate of recharge, as is often the case in arid or even semi-arid regions, water is removed permanently from storage. The water that is lost from groundwater storage eventually reaches the ocean through the atmosphere or surface flow, resulting in sea level rise. Second, wetlands contain standing water, soil moisture and water in plants equivalent to water roughly 1 m deep. Hence, wetland destruction contributes to sea level rise. Over time scales shorter than a few years, diversion of surface waters for irrigation in the internally draining basins of arid regions results in increased evaporation. The water lost from the basin hydrologic system eventually reaches the ocean. Third, forests store water in living tissue both above and below ground. When a forest is removed, transpiration is eliminated so that runoff is favoured in the hydrologic budget.

On the other hand, impoundment of water behind dams removes water from the ocean and lowers sea level. Dams have led to a sea level drop over the past few decades of –0.5 to –0.7 mm yr^{-1} (Chao, 1994; Sahagian et al., 1994). Infiltration from dams and irrigation may raise the water table, storing more water. Gornitz (2001) estimated –0.33 to –0.27 mm yr^{-1} sea level change equivalent held by dams (not counting additional potential storage due to subsurface infiltration).

It is very difficult to provide accurate estimates of the net anthropogenic contribution, given the lack of worldwide information on each factor, although the effect caused by dams is possibly better known than other effects. According to Sahagian (2000), the sum of the above effects could be of the order of 0.05 mm yr^{-1} sea level rise over the past 50 years, with an uncertainty several times as large.

In summary, our assessment of the land hydrology contribution to sea level change has not led to a reduction in the uncertainty compared to the TAR, which estimated the rather wide ranges of –1.1 to +0.4 mm yr^{-1} for 1910 to 1990

and –1.9 to +1.0 mm yr^{-1} for 1990. However, indirect evidence from considering other contributions to the sea level budget (see Section 5.5.6) suggests that the land contribution either is small (<0.5 mm yr^{-1}) or is compensated for by unaccounted or underestimated contributions.

5.5.6 Total Budget of the Global Mean Sea Level Change

The various contributions to the budget of sea level change are summarised in Table 5.3 and Figure 5.21 for 1961 to 2003 and 1993 to 2003. Some terms known to be small have been omitted, including changes in atmospheric water vapour and climate-driven change in land water storage (Section 5.5.5), permafrost and sedimentation (see, e.g., Church et al., 2001), which very likely total less than 0.2 mm yr^{-1}. The poorly known anthropogenic contribution from terrestrial water storage (see Section 5.5.5.4) is also omitted.

For 1961 to 2003, thermal expansion accounts for only 23 ± 9% of the observed rate of sea level rise. Miller and Douglas (2004) reached a similar conclusion by computing steric sea level change over the past 50 years in three oceanic regions (northeast Pacific, northeast Atlantic and western Atlantic); they found it to be too small by about a factor of three to account for the observed sea level rise based on nine tide gauges in these regions. They concluded that sea level rise in the second half of the 20th century was mostly due to water mass added to the oceans. However, Table 5.3 shows that the sum of thermal expansion and contributions from land ice is smaller by 0.7 ± 0.7 mm yr^{-1} than the observed global average sea level rise. This is likely to be a significant difference. The assessment of Church et al. (2001) could allow this difference to be explained by positive anthropogenic terms (especially groundwater mining) but these are expected to have been outweighed by negative terms (especially impoundment). We conclude that the budget has not yet been closed satisfactorily.

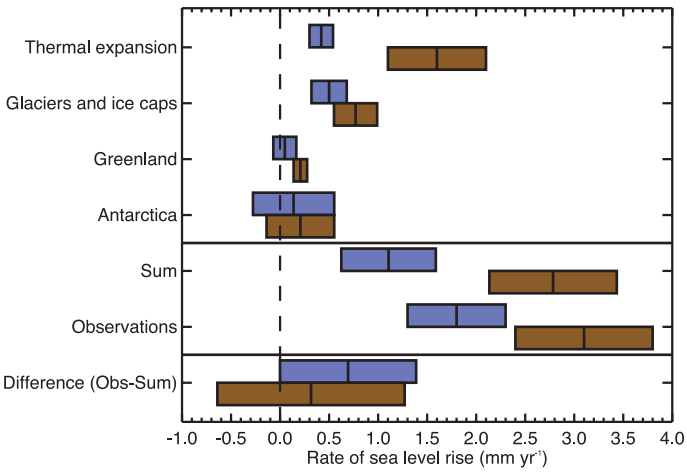


Figure 5.21. *Estimates of the various contributions to the budget of the global mean sea level change (upper four entries), the sum of these contributions and the observed rate of rise (middle two), and the observed rate minus the sum of contributions (lower), all for 1961 to 2003 (blue) and 1993 to 2003 (brown). The bars represent the 90% error range. For the sum, the error has been calculated as the square root of the sum of squared errors of the contributions. Likewise the errors of the sum and the observed rate have been combined to obtain the error for the difference.*

Given the large temporal variability in the rate of sea level rise evaluated from tide gauges (Section 5.5.2.4 and Figure 5.17), the budget is rather problematic on decadal time scales. The thermosteric contribution has smaller variability (though still substantial; Section 5.5.3) and there is only moderate temporal correlation between the thermosteric rate and the tide gauge rate. The difference between them has to be explained by ocean mass change. Because the thermosteric and climate-driven land water contributions are negatively correlated (Section 5.5.5.3.),

Table 5.3. *Estimates of the various contributions to the budget of global mean sea level change for 1961 to 2003 and 1993 to 2003 compared with the observed rate of rise. Ice sheet mass loss of 100 Gt yr^{-1} is equivalent to 0.28 mm yr^{-1} of sea level rise. A GIA correction has been applied to observations from tide gauges and altimetry. For the sum, the error has been calculated as the square root of the sum of squared errors of the contributions. The thermosteric sea level changes are for the 0 to 3,000 m layer of the ocean.*

Source	Sea Level Rise (mm yr^{-1}) 1961–2003	1993–2003	Reference
Thermal Expansion	0.42 ± 0.12	1.6 ± 0.5	Section 5.5.3
Glaciers and Ice Caps	0.50 ± 0.18	0.77 ± 0.22	Section 4.5
Greenland Ice Sheet	0.05 ± 0.12	0.21 ± 0.07	Section 4.6.2
Antarctic Ice Sheet	0.14 ± 0.41	0.21 ± 0.35	Section 4.6.2
Sum	1.1 ± 0.5	2.8 ± 0.7	
Observed	1.8 ± 0.5		Section 5.5.2.1
		3.1 ± 0.7	Section 5.5.2.2
Difference (Observed –Sum)	0.7 ± 0.7	0.3 ± 1.0	

the apparent difference implies contributions during some 10-year periods from land ice, the only remaining term, exceeding 2 mm yr^{-1} (Figure 5.17). Since it is unlikely that the land ice contributions of 1993 to 2003 were exceeded in earlier decades (Figure 4.14 and Section 4.6.2.2), we conclude that the maximum 10-year rates of global sea level rise are likely overestimated from tide gauges, indicating that the estimated variability is excessive.

For 1993 to 2003, thermal expansion is much larger and land ice contributes 1.2 ± 0.4 mm yr^{-1}. These increases may partly reflect decadal variability rather than an acceleration (Section 5.5.3; attribution of changes in rates and comparison with model results are discussed in Section 9.5.2). The sum is still less than the observed trend but the discrepancy of 0.3 ± 1.0 mm yr^{-1} is consistent with zero. It is interesting to note that the difference between the observed total and thermal expansion (assumed to be due to ocean mass change) is about the same in the two periods. The more satisfactory assessment for recent years, during which individual terms are better known and satellite altimetry is available, indicates progress since the TAR.

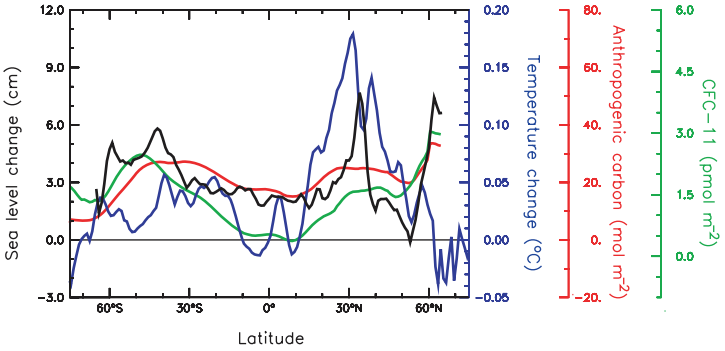


Figure 5.22. *Averages of temperature change (blue, from Levitus et al., 2005a), anthropogenic carbon (red, from Sabine et al., 2004b) and CFC-11 (green, from Willey et al., 2004) along lines of constant latitude over the top 700-m layer of the upper ocean. Also shown is sea level change averaged along lines of constant latitude (black, from Cazenave and Nerem, 2004). The temperature changes are for the 1955 to 2003 period, the anthropogenic carbon is since pre-industrial times (i.e., 1750), CFC-11 concentrations are for the period 1930 to 1994 and sea level for the period 1993 to 2003.*

5.6 Synthesis

The patterns of observed changes in global heat content and salinity, sea level, steric sea level, water mass evolution and biogeochemical cycles described in the previous four sections are broadly consistent with known characteristics of the large-scale ocean circulation (e.g., ENSO, NAO and SAM).

There is compelling evidence that the heat content of the World Ocean has increased since 1955 (Section 5.2). In the North Atlantic, the warming is penetrating deeper than in the Pacific, Indian and Southern Oceans (Figure 5.3), consistent with the strong convection, subduction and deep overturning circulation cell that occurs in the North Atlantic Ocean. The overturning cell in the North Atlantic region (carrying heat and water downwards through the water column) also suggests that there should be a higher anthropogenic carbon content as observed (Figure 5.11). Subduction of SAMW (and to a lesser extent AAIW) also carries anthropogenic carbon into the ocean, which is observed to be higher in the formation areas of these subantarctic water masses (Figure 5.10). The transfer of heat into the ocean also leads to sea level rise through thermal expansion, and the geographical pattern of sea level change since 1955 is largely consistent with thermal expansion and with the change in heat content (Figure 5.2).

Although salinity measurements are relatively sparse compared with temperature measurements, the salinity data also show significant changes. In global analyses, the waters at high latitudes (poleward of 50°N and 70°S) are fresher in the upper 500 m (Figure 5.5 World). In the upper 500 m, the subtropical latitudes in both hemispheres are characterised by an increase in salinity. The regional analyses of salinity also show a similar distributional change with a freshening of key high-latitude water masses such as LSW, AAIW and NPIW, and increased salinity in some of the subtropical gyres such as that at 24°N. The North Atlantic (and other key ocean water masses) also shows significant decadal variations, such as the recent increase in surface salinity in the North Atlantic subpolar gyre. At high latitudes (particularly in the NH), there is an observed increase in melting of perennial sea ice, precipitation, and glacial melt water (see Chapter 4), all of which act to freshen high-latitude surface waters. At mid-latitudes it is likely that evaporation minus precipitation has increased (i.e., the transport of freshwater from the ocean to the atmosphere has increased). The pattern of salinity change suggests an intensification in the Earth's hydrological cycle over the last 50 years. These trends are consistent with changes in precipitation and inferred greater water transport in the atmosphere from low latitudes to high latitudes and from the Atlantic to the Pacific.

Figure 5.22 shows zonal means of changes in temperature, anthropogenic carbon, sea level rise and a passive tracer (CFC). It is remarkable that these independent variables (albeit with widely varying reference periods) show a common pattern of change in the ocean. Specifically, the close similarity of higher levels of warming, sea level rise, anthropogenic carbon and CFC-11 at mid-latitudes and near the equator strongly suggests that these changes are the result of changes in ocean ventilation and circulation. Warming of the upper ocean should lead to a decrease in ocean ventilation and subduction rates, for which there is some evidence from observed decreases in O_2 concentrations.

In the equatorial Pacific, the pattern of steric sea level rise also shows that strong west to east gradients in the Pacific have weakened (i.e., it is now cooler in the western Pacific and warmer in the eastern Pacific). This decrease in the equatorial temperature gradient is consistent with a tendency towards more prolonged and stronger El Niños over this same period (see Section 3.6.2).

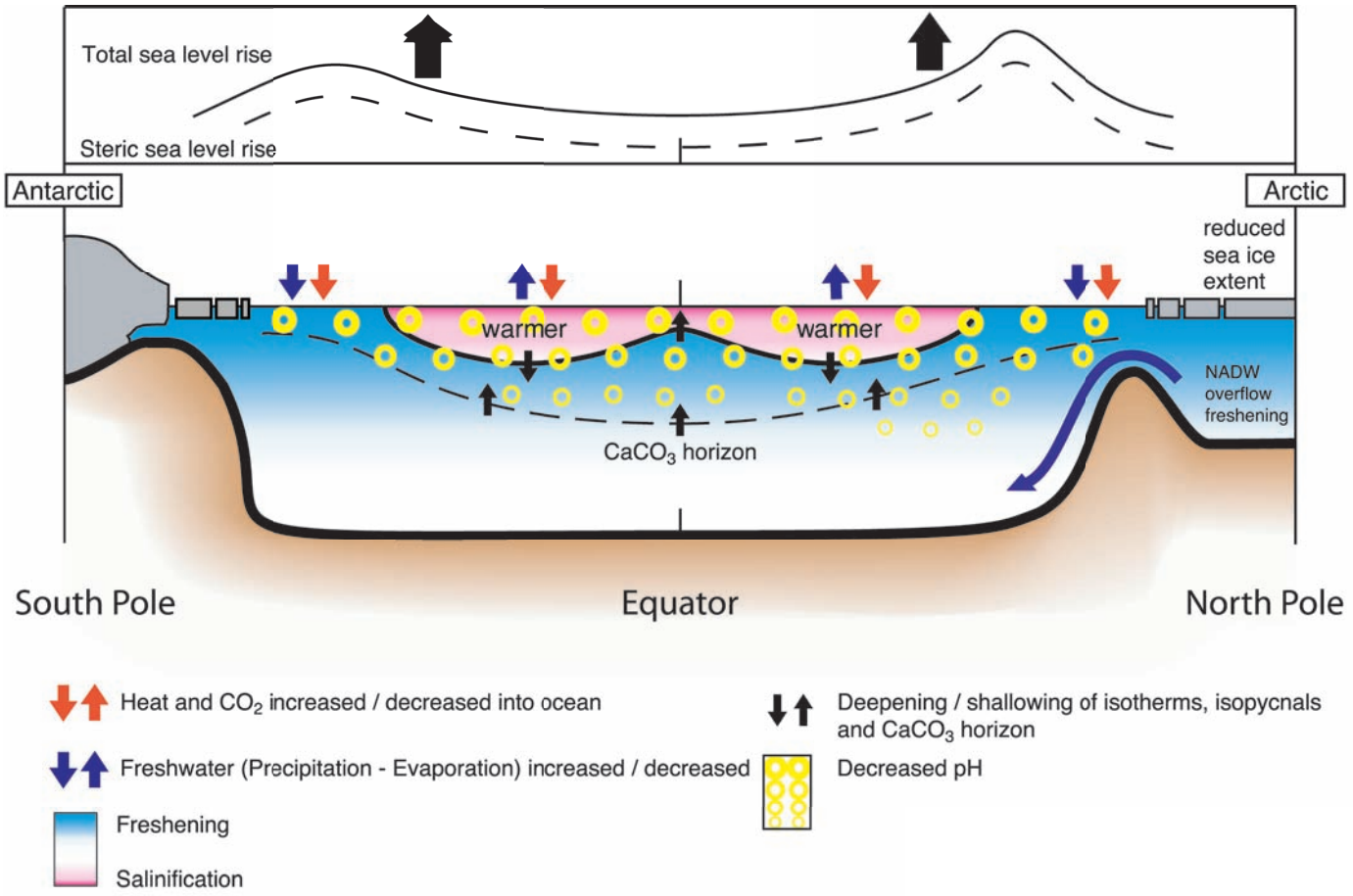


Figure 5.23. *Schematic of the observed changes in the ocean state, including ocean temperature, ocean salinity, sea level, sea ice and biogeochemical cycles. The legend identifies the direction of the changes in these variables.*

The subduction of carbon into the ocean has resulted in calcite and aragonite saturation horizons generally becoming shallower and pH decreasing primarily in the surface and near-surface ocean causing the ocean to become more acidic.

Since the TAR, the capability to measure most of the processes that contribute to sea level has been developed. In the 1990s, the observed sea level rise that was not explained through steric sea level rise could largely be explained by the transfer of mass from glaciers, ice sheets and river runoff (see Section 5.5). Figure 5.23 is a schematic that summarises the observed changes.

All of these observations taken together give high confidence that the ocean state has changed, that the spatial distribution of the changes is consistent with the large-scale ocean circulation and that these changes are in response to changed ocean surface conditions.

While there are many robust findings regarding the changed ocean state, key uncertainties still remain. Limitations in ocean sampling (particularly in the SH) mean that decadal variations in global heat content, regional salinity patterns, and rates of global sea level rise can only be evaluated with moderate confidence. Furthermore, there is low confidence in the evidence for trends in the MOC and the global ocean freshwater budget. Finally, the global average sea level rise for the last 50 years is likely to be larger than can be explained by thermal expansion and loss of land ice due to increased melting, and thus for this period it is not possible to satisfactorily quantify the known processes causing sea level rise.

References

AchutaRao, K.M. et al., 2006: Variability of ocean heat uptake: Reconciling observations and models, *J. Geophys. Res.,* **111**, C05019, doi:10.1029/2005JC003136.

Andersson, H.C., 2002: Influence of long-term regional and large-scale atmospheric circulation on the Baltic sea level. *Tellus*, **A54**, 76–88.

Andreev, A., and S. Watanabe, 2002: Temporal changes in dissolved oxygen of the intermediate water in the subarctic North Pacific. *Geophys. Res. Lett.*, **29**(14), 1680, doi:10.1029/2002GL015021.

Andrie, C., et al., 2003: Variability of AABW properties in the equatorial channel at 35 degrees W. *Geophys. Res. Lett.*, **30**(5), 8007, doi:10.1029/2002GL015766.

Antonov, J.I., S. Levitus, and T.P. Boyer, 2002: Steric sea level variations during 1957-1994: Importance of salinity. *J. Geophys. Res.*, **107**(C12), 8013, doi:10.1029/2001JC000964.

Antonov, J.I., S. Levitus, and T.P. Boyer, 2005: Steric variability of the world ocean, 1955-2003. *Geophys. Res. Lett.*, **32**(12), L12602, doi:10.1029/2005GL023112.

Aoki, S., M. Yoritaka, and A. Masuyama, 2003: Multidecadal warming of subsurface temperature in the Indian sector of the Southern Ocean. *J. Geophys. Res.*, **108**(C4), 8081, doi:10.1029/JC000307.

Aoki, S., N.L. Bindoff, and J.A. Church, 2005a: Interdecadal water mass changes in the Southern Ocean between 30E and 160E. *Geophys. Res. Lett.*, **32**, L07607, doi:10.1029/2004GL022220.

Aoki, S., S.R. Rintoul, S. Ushio, and S. Watanabe, 2005b: Freshening of the Adélie Land Bottom water near 140°E. *Geophys. Res. Lett.*, **32**, L23601, doi:10.1029/2005GL024246.

Baringer, M.O., and J.C. Larsen, 2001: Sixteen years of Florida Current transport at 27° N. *Geophys. Res. Lett.*, **28**(16), 3179–3182.

Bates, N.R., A.C. Pequignet, R.J. Johnson, and N. Gruber, 2002: A short-term sink for atmospheric CO_2 in subtropical mode water of the North Atlantic Ocean. *Nature*, **420**(6915), 489–493.

Beaugrand, G., and P.C. Reid, 2003: Long-term changes in phytoplankton, zooplankton and salmon related to climate. *Global Change Biol.*, **9**(6), 801–817.

Belkin, I.M., 2004: Propagation of the "Great Salinity Anomaly" of the 1990s around the northern North. *Geophys. Res. Lett.*, **31**, L08306, doi:10.1029/2003GL019334.

Beltrami, H., J.E. Smerdon, H.N. Pollack, and S. Huang, 2002: Continental heat gain in the global climate system. *Geophys. Res. Lett.*, **29**, doi:10.1029/2001GL014310.

Bersch, M., 2002: North Atlantic Oscillation-induced changes of the upper layer circulation in the northern North Atlantic Ocean. *J. Geophys. Res.*, **107**(C10), 3156, doi:10.1029/JC000901.

Bi, D.H., W.F. Budd, A.C. Hirst, and X.R. Wu, 2001: Collapse and reorganisation of the Southern Ocean overturning under global warming in a coupled model. *Geophys. Res. Lett.*, **28**(20), 3927–3930.

Biasutti, M., D.S. Battisti, and E.S. Sarachik, 2003: The annual cycle over the tropical Atlantic, South America, and Africa. *J. Clim.*, **16**(15), 2491–2508.

Bindoff, N.L., and T.J. McDougall, 2000: Decadal changes along an Indian Ocean section at 32 degrees S and their interpretation. *J. Phys. Oceanogr.*, **30**(6), 1207–1222.

Björk, G., et al., 2002: Return of the cold halocline layer to the Amundsen Basin of the Arctic Ocean: Implications for the sea ice mass balance. *Geophys. Res. Lett.*, **29**(11), 1513, doi:10.1029/2001GL014157.

Bouligand, R., and P.A. Pirazzoli, 1999: Les surcotes et les décotes marines à Brest, étude statistique et évolution. *Oceanol. Acta*, **22**(2), 153–166.

Boyer, T.P., J.I. Antonov, S. Levitus, and R. Locarnini, 2005: Linear trends of salinity for the world ocean, 1955-1998. *Geophys. Res. Lett.*, **32**, L01604, doi:1029/2004GL021791.

Boyer, T.P., et al., 2002: World ocean database 2001, Volume 2: Temporal distribution of bathythermograph profiles. In: *NOAA Atlas NESDIS 43* [Levitus, S. (ed.)]. Vol. 2. U.S. Government Printing Office, Washington, DC, 119 pp, CD-ROMs.

Brankart, J.M., and N. Pinardi, 2001: Abrupt cooling of the Mediterranean Levantine Intermediate Water at the beginning of the 1980s: Observational evidence and model simulation. *J. Phys. Oceanogr.*, **31**(8), 2307–2320.

Bromirski, P.D., R.E. Flick, and D.R. Cayan, 2003: Storminess variability along the California coast: 1858-2000. *J. Clim.*, **16**, 982–993.

Bryden, H.L., E.L. McDonagh, and B.A. King, 2003: Changes in ocean water mass properties: Oscillations or trends? *Science*, **300**, 2086–2088.

Bryden, H.L., H.R. Longworth, and S.A. Cunningham, 2005: Slowing of the Atlantic meridional overturning circulation at 25°N. *Nature*, **438**, 655–657, doi:10.1038/nature04385.

Bryden, H.L., et al., 1996: Decadal changes in water mass characteristics at 24 degrees N in the subtropical North Atlantic Ocean. *J. Clim.*, **9**(12), 3162–3186.

Cabanes, C., A. Cazenave, and C. Le Provost, 2001: Sea level change from Topex-Poseidon altimetry for 1993-1999 and possible warming of the southern oceans. *Geophys. Res. Lett.*, **28**(1), 9–12.

Cai, W., 2006: Antarctic ozone depletion causes an intensification of the Southern Ocean super-gyre circulation. *Geophys. Res. Lett.*, **33**, doi:1029/2005GL024911.

Caldeira, K., and M.E. Wickett, 2003: Anthropogenic carbon and ocean pH. *Nature*, **425**(6956), 365.

Carmack, E.C., et al., 1995: Evidence for warming of Atlantic Water in the southern Canadian Basin of the Arctic-Ocean - Results from the Larsen-93 Expedition. *Geophys. Res. Lett.*, **22**(9), 1061–1064.

Carton, J., B. Giese, and S. Grodsky, 2005: Sea level rise and the warming of the oceans in the Simple Ocean Data Assimilation (SODA) ocean reanalysis. *J. Geophys. Res.*, **110**, C09006, doi:1029/2004JC002817.

Cazenave, A., and R.S. Nerem, 2004: Present-day sea level change: observations and causes. *Rev. Geophys.*, **42**(3), RG3001, doi:10.1029/2003RG000139.

Chambers, D., J.C. Ries, C.K. Shum, and B.D. Tapley, 1998: On the use of tide gauges to determine altimeter drift. *J. Geophys. Res.*, **103**(C6), 12885–12890.

Chambers, D.P., et al., 2002: Low-frequency variations in global mean sea level: 1950-2000. *J. Geophys. Res.*, **107**(C4), doi:10.1029/2001JC001089.

Chao, B., 1994: Man-made lakes and global sea level. *Nature*, **370**, 258.

Chavez, F.P., J. Ryan, S.E. Lluch-Cota, and M. Niquen, 2003: From anchovies to sardines and back: Multidecadal change in the Pacific Ocean. *Science*, **299**(5604), 217–221.

Chelton, B., et al., 2001: Satellite altimetry. In: *Satellite Altimetry and Earth Sciences: A Handbook of Techniques and Applications* [Fu, L.-L., and A. Cazenave (eds.)]. Academic Press, San Diego, pp. 1–131.

Church, J.A., and N.J. White, 2006: A 20th century acceleration in global sea-level rise. *Geophys. Res. Lett.*, **33**, L01602, doi:10.1029/2005GL024826.

Church, J.A., N.J. White, and J.R. Hunter, 2006: Sea-level rise at tropical Pacific and Indian Ocean islands. *Global Planet. Change*, **53**, 155–168.

Church, J.A., et al., 2001: Changes in sea level. In: *Climate Change 2001: The Scientific Basis. Contribution of Working Group I to the Third Assessment Report of the Intergovernmental Panel on Climate Change* [Houghton, J.T., et al. (eds.)]. Cambridge University Press, Cambridge, United Kingdom and New York, NY, USA, pp. 639–693.

Church, J.A., et al., 2004: Estimates of the regional distribution of sea-level rise over the 1950 to 2000 period. *J. Clim.*, **17**(13), 2609–2625.

Clark, P.U., N.G. Pisias, T.F. Stocker, and A.J. Weaver, 2002: The role of the thermohaline circulation in abrupt climate change. *Nature*, **415**, 863–869.

Comiso, J.C., 2002: A rapidly declining perennial sea ice cover in the Arctic. *Geophys. Res. Lett.*, **29**, 1956–1959.

Comiso, J.C., 2003: Warming trends in the Arctic from clear sky satellite observations. *J. Clim.*, **16**(21), 3498–3510.

Conkright, M.E., et al., 2002: World ocean database 2001, Volume 1: Introduction. In: *NOAA Atlas NESDIS 42* [Levitus, S. (ed.). Vol. 1. U.S. Government Printing Office, Washington, DC, 159 pp, CD-ROMs.

Cunningham, S.A., S.G. Alderson, B.A. King, and M.A. Brandon, 2003: Transport and variability of the Antarctic Circumpolar Current in Drake Passage. *J. Geophys. Res.*, **108**(C5), 8084, doi:10.1029/2001JC001147.

Curry, R., and C. Mauritzen, 2005: Dilution of the northern North Atlantic Ocean in recent decades. *Science*, **308**(5729), 1772–1774.

Curry, R., B. Dickson, and I. Yashayaev, 2003: A change in the freshwater balance of the Atlantic Ocean over the past four decades. *Nature*, **426**(6968), 826–829.

Deutsch, C., S. Emerson, and L. Thompson, 2005: Fingerprints of climate change in North Pacific oxygen. *Geophys. Res. Lett.*, **32**, L16604, doi:10.1029/2005GL023190.

Dickson, B., et al., 2002: Rapid freshening of the deep North Atlantic Ocean over the past four decades. *Nature*, **416**(6883), 832–837.

Dickson, R., et al., 1996: Long-term coordinated changes in the convective activity of the North Atlantic. *Prog. Oceanogr.*, **38**, 241–295.

Dickson, R.R., R. Curry, and I. Yashayaev, 2003: Recent changes in the North Atlantic. *Philos. Trans. R. Soc. London Ser. A*, **361**(1810), 1917–1933.

Dickson, R.R., J. Meincke, S.A. Malmberg, and A.J. Lee, 1988: The Great Salinity Anomaly in the Northern North Atlantic 1968-1982. *Prog. Oceanogr.*, **20**(2), 103–151.

Doney, S.C., J.L. Bullister, and R. Wanninkhof, 1998: Climatic variability in upper ocean ventilation rates diagnosed using chlorofluorocarbons. *Geophys. Res. Lett.*, **25**(9), 1399–1402.

Donnelly, J.P., P. Cleary, P. Newby, and R. Ettinger, 2004: Coupling instrumental and geological records of sea-level change: Evidence from southern New England of an increase in the rate of sea-level rise in the late 19th century. *Geophys. Res. Lett.*, **31**(5), L05203, doi:10.1029/2003GL018933.

Dore, J.E., R. Lukas, D.W. Sadler, and D.M. Karl, 2003: Climate-driven changes to the atmospheric CO_2 sink in the subtropical North Pacific Ocean. *Nature*, **424**(6950), 754–757.

Douglas, B.C., 1992: Global sea level acceleration. *J. Geophys. Res.*, **97**(C8), 12699–12706.

Douglas, B.C., 2001: Sea level change in the era of the recording tide gauges. In: *Sea Level Rise: History and Consequences* [Douglas, B.C., Kearney, M.S., and S.P. Leatherman (eds.)]. Academic Press, New York, pp. 37–64.

Ekman, M., 1988: The world's longest continued series of sea level observations. *Pure Appl. Geophys.*, **127**, 73–77.

Emerson, S., S. Mecking, and J. Abell, 2001: The biological pump in the subtropical North Pacific Ocean: Nutrient sources, Redfield ratios, and recent changes. *Global Biogeochem. Cycles*, **15**(3), 535–554.

Emerson, S., Y.W. Watanabe, T. Ono, and S. Mecking, 2004: Temporal trends in apparent oxygen utilization in the upper pycnocline of the North Pacific: 1980-2000. *J. Oceanogr.*, **60**(1), 139–147.

Fahrbach, E., et al., 2004: Decadal-scale variations of water mass properties in the deep Weddell Sea. *Ocean Dyn.*, **54**(1), 77–91.

Feely, R.A., and C.T.A. Chen, 1982: The effect of excess CO_2 on the calculated calcite and aragonite saturation horizons in the northeast Pacific. *Geophys. Res. Lett.*, **9**(11), 1294–1297.

Feely, R.A., R. Wanninkhof, T. Takahashi, and P. Tans, 1999: Influence of El Niño on the equatorial Pacific contribution to atmospheric CO_2 accumulation. *Nature*, **398**(6728), 597–601.

Feely, R.A., et al., 2002: In situ calcium carbonate dissolution in the Pacific Ocean. *Global Biogeochem. Cycles*, **16**(4), 1144, doi:10.1029/2002GB001866.

Feely, R.A., et al., 2004: Impact of anthropogenic CO_2 on the $CaCO_3$ system in the oceans. *Science*, **305**(5682), 362–366.

Feng, M., and G. Meyers, 2003: Interannual variability in the tropical Indian Ocean: A two-year time-scale of Indian Ocean Dipole. *Deep-Sea Res. II*, **50**, 2263–2284.

Firing, Y.L., and M.A. Merrifield, 2004: Extreme sea level events at Hawaii: the influence of mesoscale eddies. *Geophys. Res. Lett.*, **31**(24), L24306, doi:10.1029/2004GL021539.

Folland, C.K., et al., 2001: Observed climate variability and change. In: *Climate Change 2001: The Scientific Basis. Contribution of Working Group I to the Third Assessment Report of the Intergovernmental Panel on Climate Change* [Houghton, J.T., et al. (eds.)]. Cambridge University Press, Cambridge, United Kingdom and New York, NY, pp. 99–181.

Freeland, H., et al., 1997: Evidence of change in the winter mixed layer in the Northeast Pacific Ocean. *Deep-Sea Res. I*, **44**(12), 2117–2129.

Fu, L.L., and A. Cazenave, 2001: *Satellite Altimetry and Earth Sciences: A Handbook of Techniques and Applications.* International Geophysics Series Vol. 69, Academic Press, San Diego, 457 pp.

Fukasawa, M., et al., 2004: Bottom water warming in the North Pacific Ocean. *Nature*, **427**(6977), 825–827.

Gamo, T., et al., 1986: Spatial and temporal variations of water characteristics in the Japan Sea bottom layer. *J. Mar. Res.*, **44**(4), 781–793.

Ganachaud, A., and C. Wunsch, 2003: Large-scale ocean heat and freshwater transports during the World Ocean Circulation Experiment. *J. Clim.*, **16**(4), 696–705.

Garcia, H.E., et al., 2005: On the variability of dissolved oxygen and apparent oxygen utilization content for the upper world ocean: 1955 to 1998. *Geophys. Res. Lett.*, **32**, L09604, doi:10.1029/GL022286.

Gasparini, G.P., et al., 2005: The effect of the Eastern Mediterranean Transient on the hydrographic characteristics in the Strait of Sicily and in the Tyrrhenian Sea. *Deep-Sea Res. I*, **52**(6), 915–935.

Gehrels, W.R., et al., 2004: Late Holocene sea-level changes and isostatic crustal movements in Atlantic Canada. *Quat. Int.*, **120**, 79–89.

Gertman, I., N. Pinardi, Y. Popov, and A. Hecht, 2006: Aegean sea water masses during the early stages of the eastern Mediterranean climatic transient (1988-1990). *J. Phys. Oceanogr.*, **36**(9), 1841–1859.

Gille, S.T., 2002: Warming of the Southern Ocean since the 1950s. *Science*, **295**(5558), 1275–1277.

Gille, S.T., 2004: How nonlinearities in the equation of state of seawater can confound estimates of steric sea level change. *J. Geophys. Res.*, **109**(3), C03005, doi:10.1029/2003JC002012.

Gonzalez-Dávila, M., et al., 2003: Seasonal and interannual variability of sea-surface carbon dioxide species at the European Station for Time Series in the Ocean at the Canary Islands (ESTOC) between 1996 and 2000. *Global Biogeochem. Cycles*, **17**(3), 1076, doi:10.1029/2002GB001993.

González-Pola, C., A. Lavin, and M. Vargas-Yanez, 2005: Intense warming and salinity modification of intermediate water masses in the southeastern corner of the Bay of Biscay for the period 1992-2003. *J. Geophys. Res.*, **110**, C05020, doi:10.1029/2004JC002367.

Gornitz, V., 2001: Impoundment, groundwater mining, and other hydrologic transformations: Impacts on global sea level rise. In: *Sea Level Rise: History and Consequences* [Douglas, B.C., M.S. Kearney, and S.P. Leatherman (eds.)]. Academic Press, San Diego, pp. 97–119.

Gregg, W.W., et al., 2003: Ocean primary production and climate: Global decadal changes. *Geophys. Res. Lett.*, **30**(15), 1809, doi:10.1029/2003GL016889.

Gregory, J.M., et al., 2001: Comparison of results from several AOGCMs for global and regional sea-level changes 1900-2100. *Clim. Dyn.*, **18**, 225–240.

Gregory, J.M., et al., 2004: Simulated and observed decadal variability in ocean heat content. *Geophys. Res. Lett.*, **31**, L15312, doi:10.1029/2004/GL020258.

Gregory, J.M., et al., 2005: A model intercomparison of changes in the Atlantic thermohaline circulation in response to increasing atmospheric CO_2 concentration. *Geophys. Res. Lett.*, **32**, L12703, doi:10.1029/2005GL023209.

Grist, J.P., and S.A. Josey, 2003: Inverse analysis adjustment of the SOC air-sea flux climatology using ocean heat transport constraints. *J. Clim.*, **16**(20), 3274–3295.

Gruber, N., J.L. Sarmiento, and T.F. Stocker, 1996: An improved method for detecting anthropogenic CO_2 in the oceans. *Global Biogeochem. Cycles*, **10**(4), 809–837.

Gruber, N., C.D. Keeling, and N.R. Bates, 2002: Interannual variability in the North Atlantic Ocean carbon sink. *Science*, **298**(5602), 2374–2378.

Guinehut, S., P.-Y. Le Traon, G. Larnicol, and S. Phillips, 2004: Combining ARGO and remote-sensing data to estimate the ocean three-dimensional temperature fields. *J. Mar. Syst.*, **46**, 85–98.

Gulev, S.K., T. Jung, and E. Ruprecht, 2006: Estimation of the sampling errors in global surface flux fields based on VOS data. *J. Clim.*, **20**(2), 279-301.

Häkkinen, S., 2002: Surface salinity variability in the northern North Atlantic during recent decades. *J. Geophys. Res.*, **107**(C12), doi:10.1029/2001JC000812.

Häkkinen, S., and P.B. Rhines, 2004: Decline of subpolar North Atlantic circulation during the 1990s. *Science*, **304**, 555–559.

Hanawa, K., 1995: Southward penetration of the Oyashio water system and the wintertime condition of midlatitude westerlies over the North Pacific. *Bull. Hokkaido Natl. Fish. Res. Inst.*, **59**, 103–119.

Hanawa, K., and J. Kamada, 2001: Variability of core layer temperature (CLT) of the North Pacific subtropical mode water. *Geophys. Res. Lett.*, **28**(11), 2229–2232.

Hanawa, K., and L.D. Talley, 2001: Mode waters. In: *Ocean Circulation and Climate* [Siedler, G., J.A. Church, and J. Gould (eds.)]. Academic Press, San Diego, pp. 373–386.

Harrison, D.E., and M. Carson, 2006: Is the World Ocean warming? Upper ocean temperature trends, 1950-2000. *J. Phys. Oceanogr.*, **37** (2), 174–187.

Hátún, H., et al., 2005: Influence of the Atlantic Subpolar Gyre on the thermohaline circulation. *Science*, **309**, 1841–1844.

Hazeleger, W., and S.S. Drijfhout, 1998: Mode water variability in a model of the subtropical gyre: Response to anomalous forcings. *J. Phys. Oceanogr.*, **28**, 266–288.

Hazeleger, W., P. de Vries, and Y. Friocourt, 2003: Sources of the Equatorial Undercurrent in the Atlantic in a high-resolution ocean model. *J. Phys. Oceanogr.*, **33**, 677–693.

Hill, K.L., A.J. Weaver, H.J. Freeland, and A. Bychkov, 2003: Evidence of change in the Sea of Okhotsk: Implications for the North Pacific. *Atmos.-Ocean*, **41**(1), 49–63.

Hilmer, M., and P. Lemke, 2000: On the decrease of Arctic sea ice volume. *Geophys. Res. Lett.*, **27**(22), 3751–3754.

Hirawake, T., T. Odate, and M. Fukuchi, 2005: Long-term variation of surface phytoplankton chlorophyll a in the Southern Ocean during 1965-2002. *Geophys. Res. Lett.*, **32**(5), L05606, doi:10.1029/2004GL021394.

Hogg, N.G., 2001: Quantification of the deep circulation. In: *Ocean Circulation and Climate* [Siedler, G., J.A. Church, and J. Gould (eds.)]. Academic Press, San Diego, pp. 259–270.

Hogg, N.G., and W. Zenk, 1997: Long-period changes in the bottom water flowing through Vema Channel. *J. Geophys. Res.*, **102**, 15639–15646.

Holgate, S.J., and P.L. Woodworth, 2004: Evidence for enhanced coastal sea level rise during the 1990s. *Geophys. Res. Lett.*, **31**, L07305, doi:10.1029/2004GL019626.

Houghton, R.W., and M. Visbeck, 2002: Quasi-decadal salinity fluctuations in the Labrador Sea. *J. Phys. Oceanogr.*, **32**, 687–701.

ICES, 2005: *The Annual ICES Ocean Climate Status Summary 2004/2005.* ICES Cooperative Research Report No.275, International Council for the Exploration of the Sea, Copenhagen, Denmark, 37 pp.

IOC, 2002: *Manual on Sea-Level Measurement and Interpretation. Volume 3 - Reappraisals and Recommendations as of the Year 2000.* Manuals and Guides No. 14, Intergovernmental Oceanographic Commission, Paris, 47 pp.

IPCC, 2001: *Climate Change 2001: The Scientific Basis. Contribution of Working Group I to the Third Assessment Report of the Intergovernmental Panel on Climate Change* [Houghton, J.T., et al. (eds.)]. Cambridge University Press, Cambridge, United Kingdom and New York, NY, USA, 881 pp.

Ishii, M., M. Kimoto, K. Sakamoto, and S.I. Iwasaki, 2006: Steric sea level changes estimated from historical ocean subsurface temperature and salinity analyses. *J. Oceanogr.*, **62**(2), 155–170.

Jacobs, S.S., C.F. Giulivi, and P.A. Mele, 2002: Freshening of the Ross Sea during the late 20th century. *Science*, **297**(5580), 386–389.

Johnson, G.C., and A.H. Orsi, 1997: Southwest Pacific Ocean water-mass changes between 1968/69 and 1990/91. *J. Clim.*, **10**(2), 306–316.

Johnson, G.C., and N. Gruber, 2007: Decadal water mass variations along 20°W in the northeastern Atlantic Ocean. *Prog. Oceanogr.*, in press.

Johnson, G.C., D.L. Rudnick, and B.A. Taft, 1994: Bottom water variability in the Samoa Passage. *J. Mar. Res.*, **52**, 177–196.

Josey, S.A., 2003: Changes in the heat and freshwater forcing of the eastern Mediterranean and their influence on deep water formation. *J. Geophys. Res.*, **108**(C7), 3237, doi:10.1029/2003JC001778.

Josey, S.A., and R. Marsh, 2005: Surface freshwater flux variability and recent freshening of the North Atlantic in the eastern Subpolar Gyre. *J. Geophys. Res.*, **110**, C05008, doi:10.1029/2004JC002521.

Joyce, T.M., and P.E. Robbins, 1996: The long-term hydrographic record at Bermuda. *J. Clim.*, **9**, 3121–3131.

Joyce, T.M., and J. Dunworth-Baker, 2003: Long-term hydrographic variability in the Northwest Pacific Ocean. *Geophys. Res. Lett.*, **30**(2), 1043, doi:10.1029/2002GL015225.

Joyce, T.M., R.S. Pickart, and R.C. Millard, 1999: Long-term hydrographic changes at 52 and 66 degrees W in the North Atlantic Subtropical Gyre & Caribbean. *Deep-Sea Res. II*, **46**(1–2), 245–278.

Joyce, T.M., C. Deser, and M.A. Spall, 2000: The relation between decadal variability of subtropical mode water and the North Atlantic Oscillation. *J. Clim.*, **13**(14), 2550–2569.

Karl, D.M., 1999: A sea of change: Biogeochemical variability in the North Pacific Subtropical Gyre. *Ecosystems*, **2**(3), 181–214.

Keeling, R.F., 2005: Comment on "The ocean sink for anthropogenic CO_2". *Science*, **308**(5729), 1743c.

Keigwin, L.D., W.B. Curry, S.J. Lehman, and S. Johnsen, 1994: The role of the deep ocean in North Atlantic climate change between 70 and 130 kyr ago. *Nature*, **371**, 323–326.

Keller, K., R.D. Slater, M. Bender, and R.M. Key, 2002: Possible biological or physical explanations for decadal scale trends in North Pacific nutrient concentrations and oxygen utilization. *Deep-Sea Res. II*, **49**(1–3), 345–362.

Kieke, D., et al., 2006: Changes in the CFC inventories and formation rates of Upper Labrador Sea water. *J. Phys. Oceanogr.*, **36**, 64–86.

Kim, K., et al., 2004: Water masses and decadal variability in the East Sea (Sea of Japan). *Prog. Oceanogr.*, **61**(2–4), 157–174.

Kim, K.R., et al., 2002: A sudden bottom-water formation during the severe winter 2000-2001: The case of the East/Japan Sea. *Geophys. Res. Lett.*, **29**(8), doi:10.1029/2001GL014498.

Klein, B., et al., 2000: Is the Adriatic returning to dominate the production of Eastern Mediterranean Deep Water? *Geophys. Res. Lett.*, **27**(20), 3377–3380.

Knight, J.R., et al., 2005: A signature of persistent natural thermohaline circulation cycles in observed climate. *Geophys. Res. Lett.*, **32**, L20708, doi:1029/2005GL024233.

Köhl, A., D. Stammer, and B. Cornuelle, 2006: Interannual to decadal changes in the ECCO global synthesis. *J. Phys. Oceanogr.*, **37**(2), 313-337.

Krahmann, G., and F. Schott, 1998: Long-term increases in Western Mediterranean salinities and temperatures: anthropogenic and climatic sources. *Geophys. Res. Lett.*, **25**(22), 4209–4212.

Kwon, Y.O., and S.C. Riser, 2004: North Atlantic Subtropical Mode Water: A history of ocean-atmosphere interaction 1961-2000. *Geophys. Res. Lett.*, **31**(19), L19307, doi:10.1029/2004GL021116.

Kwon, Y.O., K. Kim, Y.G. Kim, and K.R. Kim, 2004: Diagnosing long-term trends of the water mass properties in the East Sea (Sea of Japan). *Geophys. Res. Lett.*, **31**(20), L20306, doi:10.1029/2004GL020881.

Lambeck, K., 2002: Sea-level change from mid-Holocene to recent time: An Australian example with global implications. In: *Ice Sheets, Sea Level and the Dynamic Earth* [Mitrovica, J.X., and B. L.A. Vermeersen (eds.)]. Geodynamics Series Vol. 29, American Geophysical Union, Washington, DC, doi:10.1029/029GD03. 33–50.

Lambeck, K., C. Smither, and M. Ekman, 1998: Tests of glacial rebound models for Fennoscandinavia based on instrumental sea- and lake-level records. *Geophys. J. Int.*, **135**, 375–387.

Lambeck, K., et al., 2004: Sea level in Roman time in the Central Mediterranean and implications for recent change. *Earth Planet. Sci. Lett.*, **224**, 563–575.

Latif, M., et al., 2006: Is the thermohaline circulation changing? *J. Clim.*, **19**, 4631–4637.

Lazar, A., et al., 2002: Seasonality of the ventilation of the tropical Atlantic thermocline in an ocean general circulation mode. *J. Geophys. Res.*, **107**(C8), doi:10.1029/2000JC000667.

Lazier, J.R.N., 1995: The salinity decrease in the Labrador Sea over the past thirty years. In: *Natural Climate Variability on Decade-to-Century Time Scales* [Martinson, D.G., et al. (eds.)]. National Academy Press, Washington, DC, pp. 295–304.

Lazier, J.R.N., et al., 2002: Convection and restratification in the Labrador Sea, 1990-2000. *Deep-Sea Res. I*, **49**(10), 1819–1835.

Le Quéré, C., et al., 2003: Two decades of ocean CO_2 sink and variability. *Tellus*, **B55**(2), 649–656.

Lee, T., 2004: Decadal weakening of the shallow overturning circulation of the South Indian Ocean. *Geophys. Res. Lett.*, **31**, L18305, doi:10.1029/2004GL020884.

Lefèvre, N., et al., 2004: A decrease in the sink for atmospheric CO_2 in the North Atlantic. *Geophys. Res. Lett.*, **31**(7), L07306, doi:10.1029/2003GL018957.

Leuliette, E.W., R.S. Nerem, and G.T. Mitchum, 2004: Calibration of TOPEX/Poseidon and Jason altimeter data to construct a continuous record of mean sea level change. *Mar. Geodesy*, **27**(1–2), 79–94.

Levitus, S., 1989: Interpentadal variability of salinity in the upper 150m of the North-Atlantic Ocean, 1970-1974 versus 1955-1959. *J. Geophys. Res.*, **94**(C7), 9679–9685.

Levitus, S., J.I. Antonov, and T.P. Boyer, 2005a: Warming of the World Ocean, 1955-2003. *Geophys. Res. Lett.*, **32**, L02604, doi:10.1029/2004GL021592.

Levitus, S., J. Antonov, T.P. Boyer, and C. Stephens, 2000: Warming of the World Ocean. *Science*, **287**, 2225–2229.

Levitus, S., et al., 2005b: *Building Ocean Profile-Plankton Databases for Climate and Ecosystem System Research.* NOAA Technical Report NESDIS 117, U.S. Government Printing Office, Washington, DC, 29 pp.

Levitus, S., et al., 2005c: EOF analysis of upper ocean heat content, 1956-2003. *Geophys. Res. Lett.*, **32**, L18607, doi:10.1029/2005GL023606.

Li, M., P.G. Myers, and H. Freeland, 2005: An examination of historical mixed layer depths along Line-P in the Gulf of Alaska. *Geophys. Res. Lett.*, **32**, L05613, doi:10.1029/2004GL021911.

Li, Y.-H., and T.-H. Peng, 2002: Latitudinal change of remineralization ratios in the oceans and its implication for nutrient cycles. *Global Biogeochem. Cycles*, **16**(4), 1130, doi:10.1029/2001GB001828.

Locarnini, R.A., et al., 2002: World ocean database 2001. In: *NOAA Atlas NESDIS 45. Vol. 4: Temporal Distribution of Temperature, Salinity and Oxygen Profiles* [Levitus, S. (ed.)]. U.S. Government Printing Office, Washington, DC, 332 pp, CD-ROMs.

Lombard, A., et al., 2005: Thermosteric sea level rise for the past 50 years; comparison with tide gauges and inference on water mass contribution. *Global Planet. Change*, **48**, 303–312.

Lombard, A., et al., 2006: Perspectives on present-day sea level change: a tribute to Christian le Provost. *Ocean Dyn.*, **56**(5-6), doi:10.1007/s10236-005-0046-x.

Lowe, J.A., and J.M. Gregory, 2006: Understanding projections of sea level rise in a Hadley Centre coupled climate model. *J. Geophys. Res.*, **111**, C11014, doi:10.1029/2005JC003421.

Luterbacher, J., et al., 2004: European seasonal and annual temperature variability, trends, and extremes since 1500. *Science*, **303**(5663), 1499–1503.

Lyman, J.M., J.K. Willis, and G.C. Johnson, 2006: Recent cooling of the upper ocean. *Geophys. Res. Lett.*, **33**, L18604, doi:10.1029/2006GL027033.

Macrander, A., et al., 2005: Interannual changes in the overflow from the Nordic Seas into the Atlantic Ocean through Denmark Strait. *Geophys. Res. Lett.*, **32**, L06606, doi:10.1029/2004GL021463.

Manca, B.B., V. Kovacevic, M. Gacic, and D. Viezzoli, 2002: Dense water formation in the Southern Adriatic Sea and spreading into the Ionian Sea in the period 1997-1999. *J. Mar. Syst.*, **33**, 133–154.

Mariotti, A., et al., 2002: The hydrological cycle in the Mediterranean region and implications for the water budget of the Mediterranean Sea. *J. Clim.*, **15**(13), 1674.

Marsh, R., 2000: Recent variability of the North Atlantic thermohaline circulation inferred from surface heat and freshwater fluxes. *J. Clim.*, **13**(18), 3239–3260.

Matsumoto, K., and N. Gruber, 2005: How accurate is the estimation of anthropogenic carbon in the ocean? An evaluation of the delta C* method. *Global Biogeochem. Cycles*, **19**, GB3014, doi:10.1029/2004GB002397.

McDonagh, E.L., et al., 2005: Decadal changes in the south Indian Ocean thermocline. *J. Clim.*, **18**, 1575–1590.

McLaughlin, F.A., E.C. Carmack, R.W. Macdonald, and J.K.B. Bishop, 1996: Physical and geochemical properties across the Atlantic Pacific water mass front in the southern Canadian Basin. *J. Geophys. Res.*, **101**(C1), 1183–1197.

McNeil, B.I., et al., 2003: Anthropogenic CO_2 uptake by the ocean based on the global chlorofluorocarbon data set. *Science*, **299**(5604), 235–239.

McPhaden, M.J., and D.X. Zhang, 2002: Slowdown of the meridional overturning circulation in the upper Pacific Ocean. *Nature*, **415**(6872), 603–608.

McPhaden, M.J., and D.X. Zhang, 2004: Pacific Ocean circulation rebounds. *Geophys. Res. Lett.*, **31**(18), L18301, doi:10.1029/2004GL020727.

Mecking, S., M.J. Warner, and J.L. Bullister, 2006: Temporal changes in pCFC-12 ages and AOU along two hydrographic sections in the eastern subtropical North Pacific. *Deep-Sea Res.*, **53**(1), 169–187.

Meredith, M.P., and J.C. King, 2005: Rapid climate change in the ocean west of the Antarctic Peninsula during the second half of the 20th century. *Geophys. Res. Lett.*, **32**, L19604, doi:1029/2005GL024042.

Meyers, G., 1996: Variation of the Indonesian throughflow and the El Nino-Southern Oscillation. *J. Geophys. Res.*, **101**, 12255–12263.

Miller, L., and B.C. Douglas, 2004: Mass and volume contributions to 20th century global sea level rise. *Nature*, **428**, 406–409.

Millot, C., J.-L. Fuda, J. Candela, and Y. Tber, 2006: Large warming and salinification of the Mediterranean outflow due to changes in its composition. *Deep-Sea Res. I*, **53**, 656–666.

Milly, P.C.D., and A.B. Shmakin, 2002: Global modeling of land water and energy balances: 1. The land dynamics (LaD) model. *J. Hydrometeorol.*, **3**, 283–299.

Milly, P.C.D., A. Cazenave, and M.C. Gennero, 2003: Contribution of climate-driven change in continental water storage to recent sea-level rise. *Proc. Natl. Acad. Sci. U.S.A.*, **100**(213), 13158–13161.

Minami, H., Y. Kano, and K. Ogawa, 1998: Long-term variations of potential temperature and dissolved oxygen of the Japan Sea Water. *J. Oceanogr.*, **55**, 197–205.

Mitchell, T.P., and J.M. Wallace, 1992: The annual cycle in equatorial convection and sea-surface temperature. *J. Clim.*, **5**(10), 1140–1156.

Mitchell, W., J. Chittleborough, B. Ronai, and G.W. Lennon, 2001: Sea level rise in Australia and the Pacific. In: *Pacific Islands Conference on Climate Change, Climate Variability and Sea Level Rise, National Tidal Facility Australia, Rarotonga, Cook Islands, 3-7 April 2000*. Flinders Press, Adelaide, Australia, pp. 47–57.

Mitchum, G.T., 1994: Comparison of Topex sea surface heights and tide gauge sea levels. *J. Geophys. Res.*, **99**(C12), 24541–24554.

Mitchum, G.T., 2000: An improved calibration of satellite altimetric heights using tide gauge sea levels with adjustment for land motion. *Mar. Geodesy*, **23**, 145–166.

Mitrovica, J.X., M. Tamisiea, J.L. Davis, and G.A. Milne, 2001: Recent mass balance of polar ice sheets inferred from patterns of global sea-level change. *Nature*, **409**, 1026–1029.

Mitrovica, J.X., et al., 2006: Reanalysis of ancient eclipses, astronomic and geodetic data: a possible route to resolving the enigma of global sea level rise. *Earth Planet. Sci. Lett.*, **243**, 390–399.

Molinari, R.L., 2004: Annual and decadal variability in the western subtropical North Atlantic: signal characteristics and sampling methodologies. *Prog. Oceanogr.*, **62**(1), 33–66.

Morison, J., M. Steele, and R. Andersen, 1998: Hydrography of the upper Arctic Ocean measured from the nuclear submarine USS Pargo. *Deep-Sea Res. I*, **45**(1), 15–38.

Munk, W., 2003: Ocean freshening, sea level rising. *Science*, **300**, 2041–2043.

Murray, R.J., N.L. Bindoff, and C.J.C. Reason, 2007: Modelling decadal changes on the Indian Ocean Section I5 at 32°S. *J. Clim.*, in press.

Nerem, R.S., and G.T. Mitchum, 2001: Observations of sea level change from satellite altimetry. In: *Sea Level Rise: History and Consequences* [Douglas, B.C., M.S. Kearney, and S.P. Leatherman (eds.)]. Academic Press, San Diego, pp. 121–163.

Nerem, R.S., et al., 1999: Variations in global mean sea level associated with the 1997-1998 ENSO event: Implications for measuring long term sea level change. *Geophys. Res. Lett.*, **26**, 3005–3008.

Ngo-Duc, T., et al., 2005: Effects of land water storage on the global mean sea level over the last half century. *Geophys. Res. Lett.*, **32**, L09704, doi:10.1029/2005GL022719.

Ono, T., et al., 2001: Temporal increases of phosphate and apparent oxygen utilization in the subsurface waters of western subarctic Pacific from 1968 to 1998. *Geophys. Res. Lett.*, **28**(17), 3285–3288.

Orr, J.C., et al., 2005: 21st century decline in ocean carbonate and high latitude aragonitic organisms. *Nature*, **437**, 681–686.

Orsi, A.H., W.M. Smethie, and J.L. Bullister, 2002: On the total input of Antarctic waters to the deep ocean: A preliminary estimate from chlorofluorocarbon measurements. *J. Geophys. Res.*, **107**(C8), 3122, doi:10.1029/2001JC000976.

Østerhus, S., W.R. Turrell, S. Jónsson, and B. Hansen, 2005: Measured volume, heat, and salt fluxes from the Atlantic to the Arctic Mediterranean. *Geophys. Res. Lett.*, **32**, L07603, doi:10.1029/2004GL022188.

Pahlow, M., and U. Riebesell, 2000: Temporal trends in deep ocean Redfield ratios. *Science*, **287**(5454), 831–833.

Palmer, M.H., H.L. Bryden, J.L. Hirschi, and J. Marotzke, 2004: Observed changes in the South Indian Ocean gyre circulation, 1987-2002. *Geophys. Res. Lett.*, **31**(15), L15303, doi:15310.11029/12004GL020506.

Parrish, R.H., F.B. Schwing, and R. Mendelssohn, 2000: Midlatitude wind stress: the energy source for climatic regimes in the North Pacific Ocean. *Fish. Oceanogr.*, **9**, 224–238.

Peltier, W.R., 2001: Global glacial isostatic adjustment and modern instrumental records of relative sea level history. In: *Sea Level Rise: History and Consequences* [Douglas, B.C., M.S. Kearney, and S.P. Leatherman (eds.)]. Academic Press, San Diego, pp. 65–95.

Peltier, W.R., 2004: Global glacial isostasy and the surface of the ice-age earth: the ICE-5G (VM2) model and GRACE. *Annu. Rev. Earth Planet. Sci.*, **32**, 111–149.

Penduff, T., B. Barnier, W.K. Dewar, and J.J. O'Brien, 2004: Dynamical response of the oceanic eddy field to the North Atlantic Oscillation: A model-data comparison. *J. Phys. Oceanogr.*, **34**, 2615–2629.

Peng, T.-H., R. Wanninkhof, and R.A. Feely, 2003: Increase of anthropogenic CO_2 in the Pacific Ocean over the last two decades. *Deep-Sea Res. II*, **50**, 3065–3082.

Peng, T.-H., et al., 1998: Quantification of decadal anthropogenic CO_2 uptake in the ocean based on dissolved inorganic carbon measurements. *Nature*, **396**(6711), 560–563.

Plag, H.-P., 2006: Recent relative sea level trends: an attempt to quantify the forcing factors. *Philos. Trans. R. Soc. London A*, **364**(1841), 821–844.

Polyakov, I.V., et al., 2004: Variability of the intermediate Atlantic water of the Arctic Ocean over the last 100 years. *J. Clim.*, **17**(23), 4485–4497.

Polyakov, I.V., et al., 2005: One more step toward a warmer Arctic. *Geophys. Res. Lett.*, **32**, L17605, doi:10.1029/2005GL023740.

Ponte, R.M., 2006: Low frequency sea level variability and the inverted barometer effect. *J. Atmos. Ocean. Technol.*, **23**(4), 619–629.

Potter, R.A., and M.S. Lozier, 2004: On the warming and salinification of the Mediterranean outflow waters in the North Atlantic. *Geophys. Res. Lett.*, **31**(1), L01202, doi:10.1029/2003GL018161.

Prentice, I.C., et al., 2001: The carbon cycle and atmospheric carbon dioxide. In: *Climate Change 2001: The Scientific Basis. Contribution of Working Group I to the Third Assessment Report of the Intergovernmental Panel on Climate Change* [Houghton, J.T., et al. (eds.)]. Cambridge University Press, Cambridge, United Kingdom and New York, NY, USA, pp. 183–237.

Proshutinsky, A.Y., and M.A. Johnson, 1997: Two circulation regimes of the wind-driven Arctic Ocean. *J. Geophys. Res.*, **102**(C6), 12493–12514.

Proshutinsky, A., et al., 2004: Secular sea level change in the Russian sector of the Arctic Ocean. *J. Geophys. Res.*, **109**(C3), C03042, doi:10.1029/2003JC002007.

Qian, H., Y. Yin, and Y. Ni, 2003: Tropical Indian Ocean subsurface dipole mode and diagnostic analysis of dipole event in 1997-1998. *J. Appl. Meteorol. Sci.*, **14**, 129–139 (in Chinese).

Quadfasel, D., A. Sy, D. Wells, and A. Tunik, 1991: Warming in the Arctic. *Nature*, **350**(6317), 385.

Raven, J., et al., 2005: *Ocean Acidification due to Increasing Atmospheric Carbon Dioxide.* The Royal Society, London, 59 pp.

Reverdin, G., D. Cayan, and Y. Kushnir, 1997: Decadal variability of hydrography in the upper northern North Atlantic in 1948-1990. *J. Geophys. Res.*, **102**(C4), 8505–8531.

Rigor, I.G., J.M. Wallace, and R.L. Colony, 2002: Response of sea ice to the Arctic Oscillation. *J. Clim.*, **15**, 2648–2663.

Rixen, M., et al., 2005: The Western Mediterranean Deep Water: A new proxy for global climate change. *Geophys. Res. Lett.*, **32**, L12608, doi:10.1029/2005GL022702.

Robertson, R., M. Visbeck, A.L. Gordon, and E. Fahrbach, 2002: Long-term temperature trends in the deep waters of the Weddell Sea. *Deep-Sea Res. II*, **49**(21), 4791–4806.

Roemmich, et al., 2007: Decadal spin-up of the South Pacific Subtropical Gyre. *J. Phys. Oceanogr.*, 37, 162-173.

Roether, W., et al., 1996: Recent changes in eastern Mediterranean deep waters. *Science*, **271**(5247), 333–335.

Rohling, E.J., and H.L. Bryden, 1992: Man-induced salinity and temperature increases in western Mediterranean deep-water. *J. Geophys. Res.*, **97**(C7), 11191–11198.

Rupolo, V., S. Marullo, and D. Iudicone, 2003: Eastern Mediterranean transient studied with Lagrangian diagnostics applied to a Mediterranean OGCM forced by satellite SST and ECMWF wind stress for the years 1988-1993. *J. Geophys. Res.*, **108**(C9), 8121.

Sabine, C.L., R.M. Key, R.A. Feely, and D. Greeley, 2002: Inorganic carbon in the Indian Ocean: Distribution and dissolution processes. *Global Biogeochem. Cycles*, **16**(4), 1067, doi:10.1029/2002GB001869.

Sabine, C.L., R.A. Feely, Y.W. Watanabe, and M. Lamb, 2004a: Temporal evolution of the North Pacific CO_2 uptake rate. *J. Oceanogr.*, **60**(1), 5–15.

Sabine, C.L., et al., 1999: Anthropogenic CO_2 inventory of the Indian Ocean. *Global Biogeochem. Cycles*, **13**, 179–198.

Sabine, C.L., et al., 2004b: The oceanic sink for anthropogenic CO_2. *Science*, **305**(5682), 367–371.

Sahagian, D.L., 2000: Global physical effects of anthropogenic hydrological alterations: sea level and water redistribution. *Global Planet. Change*, **25**, 39–48.

Sahagian, D.L., F.W. Schwartz, and D.K. Jacobs, 1994: Direct anthropogenic contributions to sea level rise in the twentieth century. *Nature*, **367**, 54–56.

Sarma, V.V.S.S., T. Ono, and T. Saino, 2002: Increase of total alkalinity due to shoaling of aragonite saturation horizon in the Pacific and Indian Oceans: Influence of anthropogenic carbon inputs. *Geophys. Res. Lett.*, **29**(20), 1971, doi:10.1029/2002GL015135.

Sarmiento, J.L., C. Le Quéré, and S.W. Pacala, 1995: Limiting future atmospheric carbon dioxide. *Global Biogeochem. Cycles*, **9**(1), 121–137.

Schauer, U., E. Fahrbach, and S. Østerhus, 2004: Arctic warming through the Fram Strait - Oceanic heat transport from three years of measurements. *J. Geophys. Res.*, **109**, C06026, doi:10.1029/2003JC001823.

Schneider, N., and B.D. Cornuelle, 2005: The forcing of the Pacific Decadal Oscillation. *J. Clim.*, **18**(21), 4355–4373.

Schoenefeldt, R., and F. Schott, 2006: Decadal variability of the Indian Ocean cross-equatorial exchange in SODA. *Geophys. Res. Lett.*, **33**, L08602, doi:10.1029/2006GL025891.

Schott, F.A., et al., 2004: Circulation and deep-water export at the western exit of the subpolar North Atlantic. *J. Phys. Oceanogr.*, **34**, 817–843.

Seager, R., et al., 2001: Wind-driven shifts in the latitude of the Kuroshio-Oyashio Extension and generation of SST anomalies on decadal timescales. *J. Clim.*, **14**(22), 4249–4265.

Sekine, Y., 1988: Anomalous southward intrusion of the Oyashio east of Japan.1. Influence of the seasonal and interannual variations in the wind stress over the North Pacific. *J. Geophys. Res.*, **93**(C3), 2247–2255.

Sekine, Y., 1999: On variations in the subarctic circulation in the North Pacific. *Prog. Oceanogr.*, **43**(2–4), 193–203.

Senjyu, T., et al., 2002: Renewal of the bottom water after the winter 2000-2001 may spin-up the thermohaline circulation in the Japan Sea. *Geophys. Res. Lett.*, **29**(7), 1149, doi:10.1029/2001GL014093.

Sivan, D., et al., 2004: Ancient coastal wells of Caesarea Maritima, Israel, an indicator for sea level changes during the last 2000 years. *Earth Planet. Sci. Lett.*, **222**, 315–330.

Smith, T.M., and R.W. Reynolds, 2003: Extended reconstructions of global sea surface temperatures based on COADS Data (1854-1997). *J. Clim.*, **16**, 1495–1510.

Sprintall, J., et al., 2004: INSTANT: A new international array to measure the Indonesian Throughflow. *EOS*, **85**(39), 369.

Stammer, D., et al., 2003: Volume, heat and freshwater transports of the global ocean circulation 1993-2000. *J. Geophys. Res.*, **108**(C1), doi:10.1029/2001JC001115.

Stark, S., R.A. Wood, and H.T. Banks, 2006: Re-evaluating the causes of observed changes in Indian Ocean water masses. *J. Clim.*, **19**(16), 4075–4086.

Steele, M., and T. Boyd, 1998: Retreat of the cold halocline layer in the Arctic Ocean. *J. Geophys. Res.*, **103**(C5), 10419–10435.

Stephens, C., S. Levitus, J. Antonov, and T. Boyer, 2001: On the Pacific Ocean regime shift. *Geophys. Res. Lett.*, **28**, 3721–3724.

Stephens, C., et al., 2002: World ocean database 2001, Volume 3: Temporal distribution of conductivity-temperature-depth profiles. In: *NOAA Atlas NESDIS 44* [Levitus, S. (ed.)]. U.S. Government Printing Office, Washington, DC, pp. 47, CD-ROMs.

Sterl, A., and W. Hazeleger, 2003: Coupled variability and air-sea interaction in the South Atlantic Ocean. *J. Clim.*, **21**, 559–571.

Stramma, L., J. Fischer, P. Brandt, and F. Schott, 2003: Circulation, variability and near-equatorial meridional flow in the central tropical Atlantic. In: *Interhemispheric Water Exchange in the Atlantic Ocean* [Goni, G., and P. Malanotte-Rizzoli (eds.)]. Elsevier, Amsterdam, pp. 1–22.

Stramma, L., et al., 2004: Deep water changes at the western boundary of the subpolar North Atlantic during 1996 to 2001. *Deep-Sea Res.*, **51A**, 1033–1056.

Sy, A., et al., 1997: Surprisingly rapid spreading of newly formed intermediate waters across the North Atlantic Ocean. *Nature*, **386**(6626), 675–679.

Takahashi, T., S.C. Sutherland, R.A. Feely, and R. Wanninkhof, 2006: Decadal change of the surface water pCO_2 in the North Pacific: A synthesis of 35 years of observations. *J. Geophys. Res.*, **111**, C07S05, doi:10.1029/2005JC003074.

Takahashi, T., et al., 2002: Global sea-air CO_2 flux based on climatological surface ocean pCO_2, and seasonal biological and temperature effects. *Deep-Sea Res. II*, **49**(9–10), 1601–1622.

Talley, L.D., 1996: North Atlantic circulation and variability, reviewed for the CNLS conference. *Physica D*, **98**(2–4), 625–646.

Talley, L.D., and M.S. McCartney, 1982: Distribution and circulation of Labrador Sea-water. *J. Phys. Oceanogr.*, **12**(11), 1189–1205.

Talley, L.D., J.L. Reid, and P.E. Robbins, 2003a: Data-based meridional overturning streamfunctions for the global ocean. *J. Clim.*, **16**, 3213–3226.

Talley, L.D., et al., 2003b: Deep convection and brine rejection in the Japan Sea. *Geophys. Res. Lett.*, **30**(4), 1159, doi:10.1029/2002GL0165451.

Trenberth, K.E., and J.M. Caron, 2001: Estimates of meridional atmosphere and ocean heat transports. *J. Clim.*, **14**(16), 3433–3443.

Trenberth, K.E., J.M. Caron, and D.P. Stepaniak, 2001: The atmospheric energy budget and implications for surface fluxes and ocean heat transports. *Clim. Dyn.*, **17**, 259–276.

Tsimplis, M.N., and M. Rixen, 2002: Sea level in the Mediterranean Sea: The contribution of temperature and salinity changes. *Geophys. Res. Lett.*, **29**(23), 2136, doi:10.1029/2002GL015870.

Tsimplis, M.N., A.G.P. Shaw, R.A. Flather, and D.K. Woolf, 2006: The influence of the North Atlantic Oscillation on the sea level around the northern European coasts reconsidered: the thermosteric effects. *Phil. Trans. R. Soc.London A*, **364**(1841), 845–856, doi:10.1098/rsta.2006.1740.

Vargas-Yáñez, M., et al., 2004: Temperature and salinity increase in the eastern North Atlantic along the 24.5°N in the last ten years. *Geophys. Res. Lett.*, **31**, L06210, doi:10.1029/2003GL019308.

Vaughan, D., et al., 2003: Recent rapid regional climate warming on the Antarctic Peninsula. *Clim. Change*, **60**, 243–274.

Vellinga, M., and R.A. Wood, 2002: Global climatic impacts of a collapse of the Atlantic thermohaline circulation. *Clim. Change*, **54**, 251–267.

Venegas, S.A., L.A. Mysak, and D.N. Straub, 1998: An interdecadal climate cycle in the South Atlantic and its links to other ocean basins. *J. Geophys. Res.*, **103**(C11), 24723–24736.

Vignudelli, S., G.P. Gasparini, M. Astraldi, and M.E. Schiano, 1999: A possible influence of the North Atlantic Oscillation on the circulation of the Western Mediterranean Sea. *Geophys. Res. Lett.*, **26**(5), 623–626.

Vranes, K., A.L. Gordon, and A. Ffield, 2002: The heat transport of the Indonesian Throughflow and implications for the Indian Ocean heat budget. *Deep-Sea Res. I*, **49**, 1391–1410.

Wadhams, P., and W. Munk, 2004: Ocean freshening, sea level rising, sea ice melting. *Geophys. Res. Lett.*, **31**(11), L11311, doi:10.1029/2004GL020039.

Wakelin, S.L., P.L. Woodworth, R.A. Flather, and J.A. Williams, 2003: Sea-level dependence on the NAO over the NW European continental shelf. *Geophys. Res. Lett.*, **30**(7), 1403, doi:10.1029/2003GL017041.

Watanabe, Y.W., H. Ishida, T. Nakano, and N. Nagai, 2005: Spatiotemporal decreases of nutrients and chlorophyll-a in the surface mixed layer of the western North Pacific from 1971 to 2000. *J. Oceanogr.*, **61**, 1011–1016.

Watanabe, Y.W., et al., 2001: Probability of a reduction in the formation rate of the subsurface water in the North Pacific during the 1980s and 1990s. *Geophys. Res. Lett.*, **28**(17), 3289–3292.

White, N.J., J.A. Church, and J.M. Gregory, 2005: Coastal and global averaged sea-level rise for 1950 to 2000. *Geophys. Res. Lett.*, **32**(1), L01601, doi:10.1029/2004GL021391.

Whitworth, T., 2002: Two modes of bottom water in the Australian-Antarctic Basin. *Geophys. Res. Lett.*, **29**(5), 1973, doi:10.1029/2001GL014282.

Wijffels, S., and G.A. Meyers, 2004: An intersection of oceanic wave guides: Variability in the Indonesian Throughflow region. *J. Phys. Oceanogr.*, **34**, 1232–1253.

Willey, D.A., et al., 2004: Global oceanic chlorofluorocarbon inventory. *Geophys. Res. Lett.*, **31**, L01303, doi:10.1029/2003GL018816.

Willis, J.K., D. Roemmich, and B. Cornuelle, 2004: Interannual variability in upper-ocean heat content, temperature and thermosteric expansion on global scales. *J. Geophys. Res.*, **109**, C12036, doi:10.1029/2003JC002260.

Wong, A.P.S., N.L. Bindoff, and J.A. Church, 1999: Large-scale freshening of intermediate waters in the Pacific and Indian oceans. *Nature*, **400**(6743), 440–443.

Wong, A.P.S., N.L. Bindoff, and J.A. Church, 2001: Freshwater and heat changes in the North and South Pacific Oceans between the 1960s and 1985-94. *J. Clim.*, **14**(7), 1613–1633.

Woodworth, P.L., 1990: A search for accelerations in records of European mean sea level. *Int. J. Climatol.*, **10**, 129–143.

Woodworth, P.L., and D.L. Blackman, 2002: Changes in extreme high waters at Liverpool since 1768. *Int. J. Climatol.*, **22**, 697–714.

Woodworth, P.L., and R. Player, 2003: The Permanent Service for Mean Sea Level: An update to the 21st century. *J. Coastal Res.*, **19**, 287–295.

Woodworth, P.L., and D.L. Blackman, 2004: Evidence for systematic changes in extreme high waters since the mid-1970s. *J. Clim.*, **17**, 1190–1197.

Woodworth, P.L., M.N. Tsimplis, R.A. Flather, and I. Shennan, 1999: A review of the trends observed in British Isles mean sea level data measured by tide gauges. *Geophys. J. Int.*, **136**, 651–670.

Woolf, D., A. Shaw, and M.N. Tsimplis, 2003: The influence of the North Atlantic Oscillation on sea level variability in the North Atlantic Region. *Global Atmos. Ocean System*, **9**(4), 145–167.

Xie, S.P., H. Annamalai, F.A. Schott, and J.P. McCreary, 2002: Structure and mechanisms of South Indian Ocean climate variability. *J. Clim.*, **15**(8), 864–878.

Yamagata, T., et al., 2004: Coupled ocean-atmosphere variability in the tropical Indian Ocean. In: *Earth Climate: The Ocean-Atmosphere Interaction* [Wang, C., S.-P. Xie, and J.A. Carton (eds.)]. American Geophysical Union, Washington, DC, pp. 189–212.

Yashayaev, I., J.R.N. Lazier, and R.A. Clarke, 2003: Temperature and salinity in the central Labrador Sea. *ICES Marine Symposia Series*, **219**, 32–39.

Yasuda, I., T. Tozuka, M. Noto, and S. Kouketsu, 2000: Heat balance and regime shifts of the mixed layer in the Kuroshio Extension. *Prog. Oceanogr.*, **47**(2–4), 257–278.

Yasuda, I., et al., 2001: Hydrographic structure and transport of the Oyashio south of Hokkaido and the formation of North Pacific Intermediate Water. *J. Geophys. Res.*, **106**(C4), 6931–6942.

Zhang, K., B.C. Douglas, and S.P. Leatherman, 2000: Twentieth-century storm activity along the U.S. east coast. *J. Clim.*, **13**, 1748–1761.

Appendix 5.A: Techniques, Error Estimation and Measurement Systems

5.A.1 Ocean Temperature and Salinity

Sections 5.2 and 5.3 report on the changes in the oceans using two different approaches to the oceanic part of the climate system. Section 5.2 documents the changes found in the most comprehensive ocean data sets that exist for temperature and salinity. These data sets are collected from a wide range of organisations and are a composite of heterogeneous measurement systems, including mechanical and expendable bathythermographs, research ship measurements, voluntary observing ships, moored and drifting buoys and Argo floats for recent years. The advantage of these composite data sets is the greater spatial and temporal coverage that they offer for climate studies. The main disadvantage of these composite data sets, relative to the research data sets used in Section 5.3, is that they can have more problems related to the quality and heterogeneity of the measurements systems. This heterogeneity can lead to subtle biases and artificial noise and consequently difficulties in estimating trends at small regional scales (Harrison and Carson, 2006). On the other hand, Section 5.3 described the changes found in detailed analyses of very specific research voyages that consist mainly of very tightly calibrated and monitored temperature and salinity measurements (and other variables). The internal consistency of these research data sets is much higher than the composite data sets, and as a consequence they have significant advantages in their ease of interpretation and analysis. However, research quality oceanographic data sets are only collected occasionally and are focussed more frequently on regional rather than global issues. This means that in the poorly sampled oceans, such as the Indian, South Pacific and Southern Oceans, observational records only cover a relatively short period of time (e.g., the 1960s to present) with some decades poorly covered and highly heterogeneous in space (see Figure 5.A.1).

An example of the distribution of ocean temperature observations in both space and time is shown in Figure 5.A.1. This figure shows the *in situ* temperature data distribution for two five-year periods used to create estimates of global heat content change (e.g., Figure 5.1), one with a low (a) and one with a high (b) density of observations. It is clear that parts of the ocean, in particular in the SH, are not well sampled even in periods of high observation density. Hence, sampling errors resulting from the lack of data are potentially important but cannot easily be quantified.

Several different objective analysis techniques have been used to produce the gridded fields of temperature anomalies used to compute ocean heat content and steric sea level rise presented in this chapter. The technique used by Levitus et al. (2005b), Garcia et al. (2005) and Antonov et al. (2005) in their estimates of temperature (heat content), oxygen and the thermosteric component of sea level change is based on the construction of gridded (1° latitude by 1° longitude grid) fields at standard depth measurement levels. The objective analysis procedure used for interpolation (filling in data-void areas and smoothing the entire field) is described by Boyer et al. (2002). At each standard depth level, all data are averaged within each 1° square, and the deviation from climatology yields the observed anomaly. From all observations within the surrounding region of diameter 888 km, the analysed value is computed. Features with a wavelength of less than 500 to 600 km are substantially reduced in amplitude; in regions without sufficient data, it is essentially the climatological information that is used. Ishii et al. (2006) employed similar techniques, with a smaller de-correlation length scale of 300 km and a least-squares technique for estimating corrections to the climatological field. Willis et al. (2004) used a two-scale covariance function, but also used altimetric data in areas where ocean observations were lacking.

There are some differences in the data used in these studies. In addition to ocean temperature profile data, Ishii et al. (2006) also used the product of climatological mixed layer depth and individual SST measurements in their estimates of ocean heat content. Southern Hemisphere World Ocean Circulation Experiment profiling float temperature profiles for the 1990s were used by Willis et al. (2004) that were not used by Levitus et al. (2005a) and Ishii et al. (2006). The similarity of the three independently estimated heat content time series shown in Figure 5.1 to within confidence intervals indicates that the differences between analysis techniques and data sources do not substantially influence the estimates of the three global ocean heat content time series.

All analyses are subject to statistical errors and sampling errors. Statistical errors are estimated in a straightforward way. For example, for the Levitus et al. (2005a) fields, the uncertainty at any grid point is estimated from the variability of observations that contributed to the analysed value. In this way, 90% errors for all analysed variables are computed as a function of depth and horizontal position, and correspondingly for integrated variables such as heat content. Both Ishii et al. (2006) and Willis et al. (2004) used the interannual variability of heat content as the basis for error analyses.

5.A.2 Heat Transports

Estimates of meridional heat transport (MHT) derived from the surface heat balance involve the integration of the zonally averaged balances in the longitudinal direction. This integration also implies the integration of uncertainties in the zonally averaged estimates. For instance, an uncertainty in zonally averaged estimates of ±10 W m^{-2} results in an uncertainty of 0.5×10^{15} W in MHT in the Atlantic and nearly twice that value in the Pacific. Thus, all climatological estimates of MHT based on the surface heat balance have considerable uncertainties, and estimates of MHT variability are unlikely to be significant when derived from the surface heat balance.

In addition to the uncertainties in diagnostic computations of transports from vertical sections, estimates of MHT based on oceanic cross sections are largely influenced by sparse sampling of these sections during continuous time periods. As a result, there is no way to discriminate between the long-term signals and interannual variability using the estimates of MHT for individual years.

5.A.3 Estimates of Oxygen Changes

Estimates of changes in O_2 in the surface 100 m of the ocean between 1955 and 1998 were made for each pentad using a total of 530,000 O_2 profiles (Garcia et al., 2005). The measurement method was not reported for all the cruises. Only the Winkler titration was reported, with only manual titrations prior to 1990. The Carpenter method to improve accuracy was reported for some cruises after 1970. An automated titration gives a significant improvement for measurement reproducibility but is not the essential solution for accuracy. Problems of O_2 leakage were reported from the older samples using Nansen bottles (generally before 1970). The Niskin bottles more widely used after 1970 are thought to be more reliable. There are no agreed standards for O_2 measurements because of reagent impurity and the difficulty in preparing a stable solution, which limits accuracy of these measurements to typically less than 10 μmol kg^{-1} for modern methods.

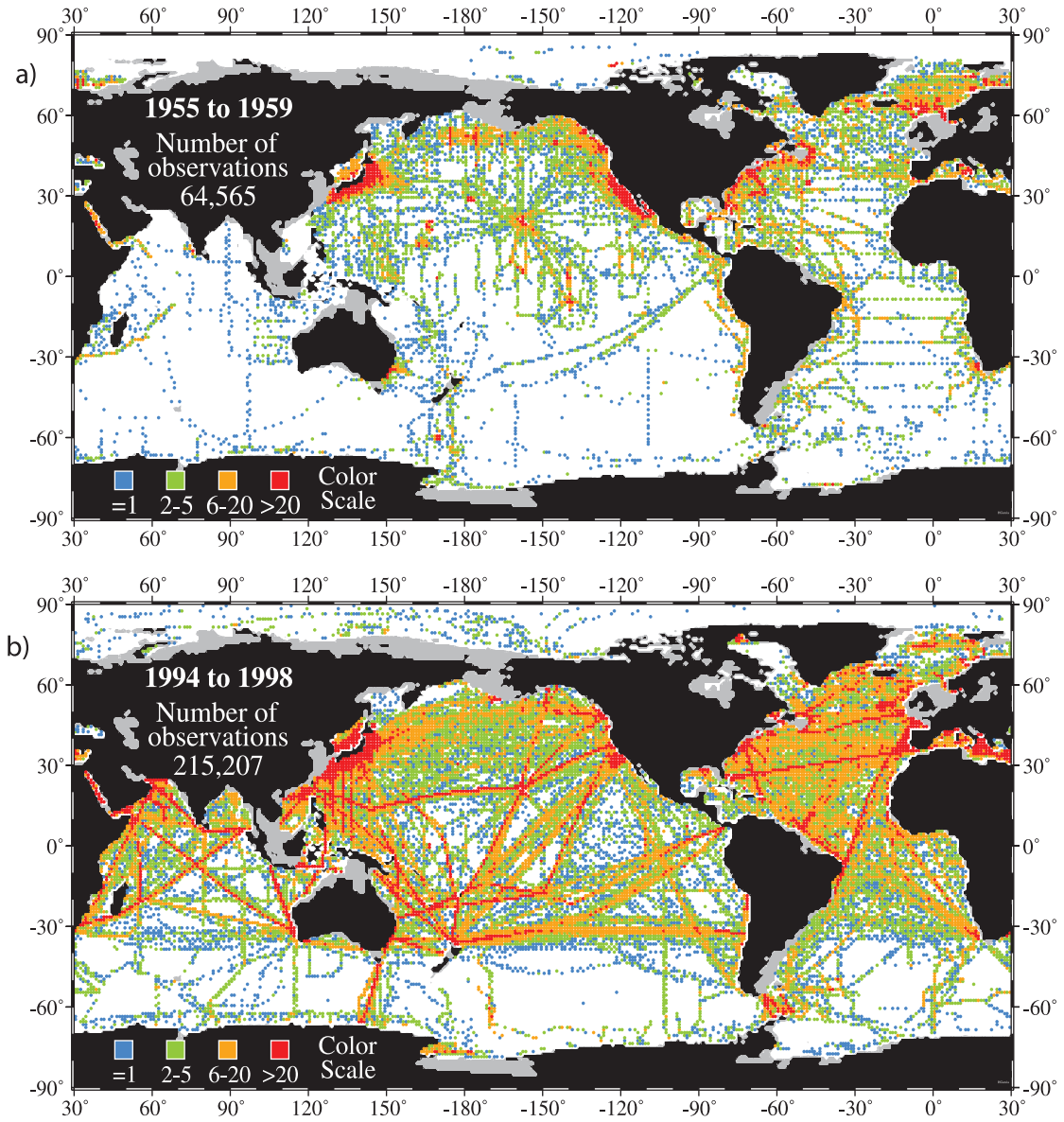


Figure 5.A.1 *The number of ocean temperature observations in each 1° grid box at 250 m depth for two periods: (a) 1955 to 1959, with a low density of observations, and (b) 1994 to 1998, with a high density of observations. A blue dot indicates a 1° grid box containing 1 observation, a green dot 2 to 5 observations, an orange dot 6 to 20 observations, and a red dot more than 20 observations.*

5.A.4 Estimation of Sea Level Change

5.A.4.1 Satellite Altimetry: Measurement Principle and Associated Errors

The concept of satellite altimetry measurement is rather straightforward. The onboard radar altimeter transmits a short pulse of microwave radiation with known power towards the nadir. Part of the incident radiation reflects back to the altimeter. Measurement of the round-trip travel time provides the height of the satellite above the instantaneous sea surface. The quantity of interest in oceanography is the height of the instantaneous sea surface above a fixed reference surface, which is computed as the difference between the altitude of the satellite above the reference ellipsoid and the altimeter range. The satellite position is computed through precise orbit determination, combining accurate modelling of the satellite motion and tracking measurements between the satellite and observing stations on Earth or other observing satellites. A number of corrections must be applied to obtain the correct sea surface height. These include instrumental corrections, ionospheric correction, dry and wet tropospheric corrections, electromagnetic bias correction, ocean and solid Earth tidal corrections, ocean loading correction, pole tide correction and an inverted barometer correction that has to be applied since the altimeter does not cover the global ocean completely. The total measurement accuracy for the TOPEX/Poseidon altimetry-based sea surface height is about 80 mm (95% error) for a single measurement based on one-second along-track averages (Chelton et al., 2001).

The above error estimates concern instantaneous sea surface height measurements. For estimating the mean sea level variations, the procedure consists of simply averaging over the ocean the point-to-point measurements collected by the satellite during a complete orbital cycle (10 days for TOPEX/Poseidon and Jason-1), accounting for the spatial distribution of the data using an equal area weighting. In effect, during this time interval, the satellite realises an almost complete coverage of the oceanic domain. The 95% error associated with a 10-day mean sea level estimate is approximately 8 mm.

When computing global mean sea level variations through time, proper account of instrumental bias and drifts (including the terrestrial reference frame) is of considerable importance. These effects (e.g., the radiometer drift onboard TOPEX/Poseidon used to correct for the wet tropospheric delay) are of the same order of magnitude as the sea level signal. Studies by Chambers et al. (1998) and Mitchum (1994; 2000) have demonstrated that comparing the altimeter sea level measurements to tide gauge sea level measurements produces the most robust way of correcting for instrumental bias and drifts. This approach uses a network of high-quality tide gauges, well distributed over the ocean domain. Current results indicate that the residual error in the mean sea level variation using the tide gauge calibration is about 0.8 mm yr^{-1} (a value resulting mainly from the uncertainties in vertical land motion at the tide gauges). The current altimeter-inferred sea level measurements do not include modelling of the geocenter or mitigating the effect resulting from the potential drift of the terrestrial reference frame.

Detailed information about satellite altimetry, uncertainty and applications can be found in Fu and Cazenave (2001).

5.A.4.2 Sea Level from Tide Gauge Observations

Tide gauges are based on a number of different technologies (float, pressure, acoustic, radar), each of which has its advantages in particular applications. The Global Sea Level Observing System (GLOSS) specifies that a gauge must be capable of measuring sea level to centimetre accuracy (or better) in all weather conditions (i.e., in all wave conditions). The most important consideration is the need to maintain the gauge datum relative to the level of the Tide Gauge Bench Mark (TGBM), which provides the land reference level for the sea level measurements. The specifications for GLOSS require that local levelling must be repeated at least annually between the reference mark of the gauge, TGBM and a set of approximately five ancillary marks in the area, in order to maintain the geodetic integrity of the measurements. In practice, this objective is easier to meet if the area around the gauge is hard rock, rather than reclaimed land, for example. The question of whether the TGBM is moving vertically within a global reference frame (for whatever reason) is being addressed by advanced geodetic methods (GPS, Determination d'Orbite et Radiopositionnement Intégrés par Satellite (DORIS), Absolute Gravity). With typical rates of sea and land level change of order of 1 mm yr^{-1}, it is necessary to maintain the accuracy of the overall gauge system at the centimetre level over many decades. This demanding requirement has been met in many countries for many years (see IOC, 2002 for more information). The tide gauge observation system for three periods is shown in Figure 5.A.2, together with the evolution over time of the number of stations in both hemispheres. The distribution of tide gauge stations was particularly sparse in space at the beginning of the 20th century, but rapidly improved in the 1950s through to the current network of GLOSS standard instruments. This distribution of instruments through time means that confidence in the estimates of sea level rise has been improving and this certainty is reflected in the shrinking confidence intervals (Figure 5.13).

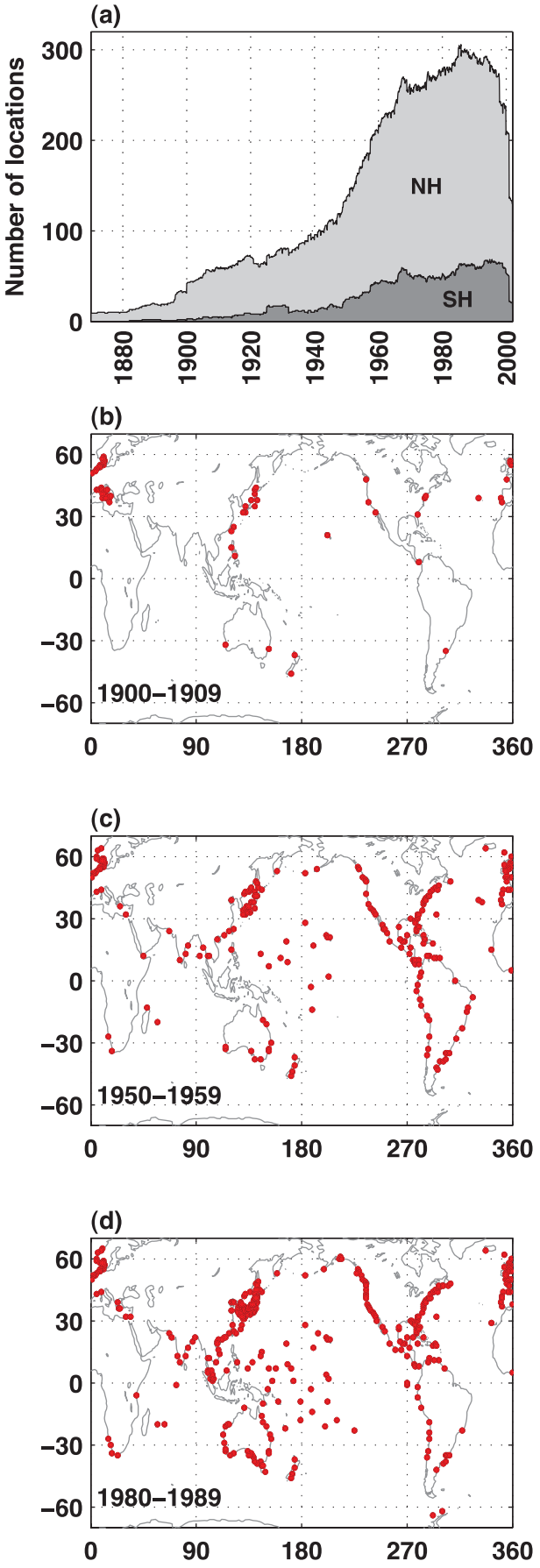


Figure 5.A.2. *(a) Number of tide gauge stations in the Northern Hemisphere (NH) and Southern Hemisphere (SH) used to derive the global sea level curve (red and blue curves in Figure 5.13) as a function of time. Lower panels show the spatial distribution of tide gauge stations (denoted by red dots) for the periods (b) 1900 to 1909, (c) 1950 to 1959 and (d) 1980 to 1989.*

6

Palaeoclimate

Coordinating Lead Authors:

Eystein Jansen (Norway), Jonathan Overpeck (USA)

Lead Authors:

Keith R. Briffa (UK), Jean-Claude Duplessy (France), Fortunat Joos (Switzerland), Valérie Masson-Delmotte (France), Daniel Olago (Kenya), Bette Otto-Bliesner (USA), W. Richard Peltier (Canada), Stefan Rahmstorf (Germany), Rengaswamy Ramesh (India), Dominique Raynaud (France), David Rind (USA), Olga Solomina (Russian Federation), Ricardo Villalba (Argentina), De'er Zhang (China)

Contributing Authors:

J.-M. Barnola (France), E. Bauer (Germany), E. Brady (USA), M. Chandler (USA), J. Cole (USA), E. Cook (USA), E. Cortijo (France), T. Dokken (Norway), D. Fleitmann (Switzerland, Germany), M. Kageyama (France), M. Khodri (France), L. Labeyrie (France), A. Laine (France), A. Levermann (Germany), Ø. Lie (Norway), M.-F. Loutre (Belgium), K. Matsumoto (USA), E. Monnin (Switzerland), E. Mosley-Thompson (USA), D. Muhs (USA), R. Muscheler (USA), T. Osborn (UK), Ø. Paasche (Norway), F. Parrenin (France), G.-K. Plattner (Switzerland), H. Pollack (USA), R. Spahni (Switzerland), L.D. Stott (USA), L. Thompson (USA), C. Waelbroeck (France), G. Wiles (USA), J. Zachos (USA), G. Zhengteng (China)

Review Editors:

Jean Jouzel (France), John Mitchell (UK)

This chapter should be cited as:

Jansen, E., J. Overpeck, K.R. Briffa, J.-C. Duplessy, F. Joos, V. Masson-Delmotte, D. Olago, B. Otto-Bliesner, W.R. Peltier, S. Rahmstorf, R. Ramesh, D. Raynaud, D. Rind, O. Solomina, R. Villalba and D. Zhang, 2007: Palaeoclimate. In: *Climate Change 2007: The Physical Science Basis. Contribution of Working Group I to the Fourth Assessment Report of the Intergovernmental Panel on Climate Change* [Solomon, S., D. Qin, M. Manning, Z. Chen, M. Marquis, K.B. Averyt, M. Tignor and H.L. Miller (eds.)]. Cambridge University Press, Cambridge, United Kingdom and New York, NY, USA.

Table of Contents

Executive Summary 435

6.1 Introduction 438

6.2 Palaeoclimatic Methods 438

6.2.1 Methods – Observations of Forcing and Response 438

6.2.2 Methods – Palaeoclimate Modelling 439

6.3 The Pre-Quaternary Climates 440

6.3.1 What is the Relationship Between Carbon Dioxide and Temperature in this Time Period? 440

6.3.2 What Does the Record of the Mid-Pliocene Show? 440

6.3.3 What Does the Record of the Palaeocene-Eocene Thermal Maximum Show? 442

6.4 Glacial-Interglacial Variability and Dynamics 444

6.4.1 Climate Forcings and Responses Over Glacial-Interglacial Cycles 444

Box 6.1: Orbital Forcing 445

Box 6.2: What Caused the Low Atmospheric Carbon Dioxide Concentrations During Glacial Times? 446

6.4.2 Abrupt Climatic Changes in the Glacial-Interglacial Record 454

6.4.3 Sea Level Variations Over the Last Glacial-Interglacial Cycle 457

6.5 The Current Interglacial 459

6.5.1 Climate Forcing and Response During the Current Interglacial 459

Box 6.3: Holocene Glacier Variability 461

6.5.2 Abrupt Climate Change During the Current Interglacial 463

6.5.3 How and Why Has the El Niño-Southern Oscillation Changed Over the Present Interglacial? 464

6.6 The Last 2,000 Years 466

6.6.1 Northern Hemisphere Temperature Variability 466

Box 6.4: Hemispheric Temperatures in the 'Medieval Warm Period' 468

6.6.2 Southern Hemisphere Temperature Variability 474

6.6.3 Comparisons of Millennial Simulations with Palaeodata 476

6.6.4 Consistency Between Temperature, Greenhouse Gas and Forcing Records; and Compatibility of Coupled Carbon Cycle-Climate Models with the Proxy Records 481

6.6.5 Regional Variability in Quantities Other than Temperature 481

6.7 Concluding Remarks on Key Uncertainties 483

Frequently Asked Questions

FAQ 6.1: *What Caused the Ice Ages and Other Important Climate Changes Before the Industrial Era?* 449

FAQ 6.2: *Is the Current Climate Change Unusual Compared to Earlier Changes in Earth's History?* 465

References 484

Supplementary Material

The following supplementary material is available on CD-ROM and in on-line versions of this report.

Appendix 6.A: *Glossary of Terms Specific to Chapter 6*

Executive Summary

What is the relationship between past greenhouse gas concentrations and climate?

- The sustained rate of increase over the past century in the combined radiative forcing from the three well-mixed greenhouse gases carbon dioxide (CO_2), methane (CH_4), and nitrous oxide (N_2O) is *very likely* unprecedented in at least the past 16 kyr. Pre-industrial variations of atmospheric greenhouse gas concentrations observed during the last 10 kyr were small compared to industrial era greenhouse gas increases, and were *likely* mostly due to natural processes.

- It is *very likely* that the current atmospheric concentrations of CO_2 (379 ppm) and CH_4 (1,774 ppb) exceed by far the natural range of the last 650 kyr. Ice core data indicate that CO_2 varied within a range of 180 to 300 ppm and CH_4 within 320 to 790 ppb over this period. Over the same period, antarctic temperature and CO_2 concentrations co-vary, indicating a close relationship between climate and the carbon cycle.

- It is *very likely* that glacial-interglacial CO_2 variations have strongly amplified climate variations, but it is *unlikely* that CO_2 variations have triggered the end of glacial periods. Antarctic temperature started to rise several centuries before atmospheric CO_2 during past glacial terminations.

- It is *likely* that earlier periods with higher than present atmospheric CO_2 concentrations were warmer than present. This is the case both for climate states over millions of years (e.g., in the Pliocene, about 5 to 3 Ma) and for warm events lasting a few hundred thousand years (i.e., the Palaeocene-Eocene Thermal Maximum, 55 Ma). In each of these two cases, warming was *likely* strongly amplified at high northern latitudes relative to lower latitudes.

What is the significance of glacial-interglacial climate variability?

- Climate models indicate that the Last Glacial Maximum (about 21 ka) was 3°C to 5°C cooler than the present due to changes in greenhouse gas forcing and ice sheet conditions. Including the effects of atmospheric dust content and vegetation changes gives an additional 1°C to 2°C global cooling, although scientific understanding of these effects is very low. It is *very likely* that the global warming of 4°C to 7°C since the Last Glacial Maximum occurred at an average rate about 10 times slower than the warming of the 20th century.

- For the Last Glacial Maximum, proxy records for the ocean indicate cooling of tropical sea surface temperatures (average *likely* between 2°C and 3°C) and much greater cooling and expanded sea ice over the high-latitude oceans. Climate models are able to simulate the magnitude of these latitudinal ocean changes in response to the estimated Earth orbital, greenhouse gas and land surface changes for this period, and thus indicate that they adequately represent many of the major processes that determine this past climate state.

- Last Glacial Maximum land data indicate significant cooling in the tropics (up to 5°C) and greater magnitudes at high latitudes. Climate models vary in their capability to simulate these responses.

- It is *virtually certain* that global temperatures during coming centuries will not be significantly influenced by a natural orbitally induced cooling. It is *very unlikely* that the Earth would naturally enter another ice age for at least 30 kyr.

- During the last glacial period, abrupt regional warmings (likely up to 16°C within decades over Greenland) and coolings occurred repeatedly over the North Atlantic region. They *likely* had global linkages, such as with major shifts in tropical rainfall patterns. It is *unlikely* that these events were associated with large changes in global mean surface temperature, but instead *likely* involved a redistribution of heat within the climate system associated with changes in the Atlantic Ocean circulation.

- Global sea level was *likely* between 4 and 6 m higher during the last interglacial period, about 125 ka, than in the 20th century. In agreement with palaeoclimatic evidence, climate models simulate arctic summer warming of up to 5°C during the last interglacial. The inferred warming was largest over Eurasia and northern Greenland, whereas the summit of Greenland was simulated to be 2°C to 5°C higher than present. This is consistent with ice sheet modelling suggestions that large-scale retreat of the south Greenland Ice Sheet and other arctic ice fields *likely* contributed a maximum of 2 to 4 m of sea level rise during the last interglacial, with most of any remainder *likely* coming from the Antarctic Ice Sheet.

What does the study of the current interglacial climate show?

- Centennial-resolution palaeoclimatic records provide evidence for regional and transient pre-industrial warm periods over the last 10 kyr, but it is *unlikely* that any of these commonly cited periods were globally synchronous. Similarly, although individual decadal-resolution interglacial palaeoclimatic records support the existence of regional quasi-periodic climate variability, it is *unlikely*

that any of these regional signals were coherent at the global scale, or are capable of explaining the majority of global warming of the last 100 years.

- Glaciers in several mountain regions of the Northern Hemisphere retreated in response to orbitally forced regional warmth between 11 and 5 ka, and were smaller (or even absent) at times prior to 5 ka than at the end of the 20th century. The present day near-global retreat of mountain glaciers cannot be attributed to the same natural causes, because the decrease of summer insolation during the past few millennia in the Northern Hemisphere should be favourable to the growth of the glaciers.

- For the mid-Holocene (about 6 ka), GCMs are able to simulate many of the robust qualitative large-scale features of observed climate change, including mid-latitude warming with little change in global mean temperature (<0.4°C), as well as altered monsoons, consistent with the understanding of orbital forcing. For the few well-documented areas, models tend to underestimate hydrological change. Coupled climate models perform generally better than atmosphere-only models, and reveal the amplifying roles of ocean and land surface feedbacks in climate change.

- Climate and vegetation models simulate past northward shifts of the boreal treeline under warming conditions. Palaeoclimatic results also indicated that these treeline shifts *likely* result in significant positive climate feedback. Such models are also capable of simulating changes in the vegetation structure and terrestrial carbon storage in association with large changes in climate boundary conditions and forcings (i.e., ice sheets, orbital variations).

- Palaeoclimatic observations indicate that abrupt decadal- to centennial-scale changes in the regional frequency of tropical cyclones, floods, decadal droughts and the intensity of the African-Asian summer monsoon *very likely* occurred during the past 10 kyr. However, the mechanisms behind these abrupt shifts are not well understood, nor have they been thoroughly investigated using current climate models.

How does the 20th-century climate change compare with the climate of the past 2,000 years?

- It is *very likely* that the average rates of increase in CO_2, as well as in the combined radiative forcing from CO_2, CH_4 and N_2O concentration increases, have been at least five times faster over the period from 1960 to 1999 than over any other 40-year period during the past two millennia prior to the industrial era.

- Ice core data from Greenland and Northern Hemisphere mid-latitudes show a *very likely* rapid post-industrial era increase in sulphate concentrations above the pre-industrial background.

- Some of the studies conducted since the Third Assessment Report (TAR) indicate greater multi-centennial Northern Hemisphere temperature variability over the last 1 kyr than was shown in the TAR, demonstrating a sensitivity to the particular proxies used, and the specific statistical methods of processing and/or scaling them to represent past temperatures. The additional variability shown in some new studies implies mainly cooler temperatures (predominantly in the 12th to 14th, 17th and 19th centuries), and only one new reconstruction suggests slightly warmer conditions (in the 11th century, but well within the uncertainty range indicated in the TAR).

- The TAR pointed to the 'exceptional warmth of the late 20th century, relative to the past 1,000 years'. Subsequent evidence has strengthened this conclusion. It is *very likely* that average Northern Hemisphere temperatures during the second half of the 20th century were higher than for any other 50-year period in the last 500 years. It is also *likely* that this 50-year period was the warmest Northern Hemisphere period in the last 1.3 kyr, and that this warmth was more widespread than during any other 50-year period in the last 1.3 kyr. These conclusions are most robust for summer in extratropical land areas, and for more recent periods because of poor early data coverage.

- The small variations in pre-industrial CO_2 and CH_4 concentrations over the past millennium are consistent with millennial-length proxy Northern Hemisphere temperature reconstructions; climate variations larger than indicated by the reconstructions would *likely* yield larger concentration changes. The small pre-industrial greenhouse gas variations also provide indirect evidence for a limited range of decadal- to centennial-scale variations in global temperature.

- Palaeoclimate model simulations are broadly consistent with the reconstructed NH temperatures over the past 1 kyr. The rise in surface temperatures since 1950 *very likely* cannot be reproduced without including anthropogenic greenhouse gases in the model forcings, and it is *very unlikely* that this warming was merely a recovery from a pre-20th century cold period.

- Knowledge of climate variability over the last 1 kyr in the Southern Hemisphere and tropics is very limited by the low density of palaeoclimatic records.

- Climate reconstructions over the past millennium indicate with *high confidence* more varied spatial climate teleconnections related to the El Niño-Southern Oscillation than are represented in the instrumental record of the 20th century.

- The palaeoclimate records of northern and eastern Africa, as well as the Americas, indicate with *high confidence* that droughts lasting decades or longer were a recurrent feature of climate in these regions over the last 2 kyr.

What does the palaeoclimatic record reveal about feedback, biogeochemical and biogeophysical processes?

- The widely accepted orbital theory suggests that glacial-interglacial cycles occurred in response to orbital forcing. The large response of the climate system implies a strong positive amplification of this forcing. This amplification has *very likely* been influenced mainly by changes in greenhouse gas concentrations and ice sheet growth and decay, but also by ocean circulation and sea ice changes, biophysical feedbacks and aerosol (dust) loading.

- It is *virtually certain* that millennial-scale changes in atmospheric CO_2 associated with individual antarctic warm events were less than 25 ppm during the last glacial period. This suggests that the associated changes in North Atlantic Deep Water formation and in the large-scale deposition of wind-borne iron in the Southern Ocean had limited impact on CO_2.

- It is *very likely* that marine carbon cycle processes were primarily responsible for the glacial-interglacial CO_2 variations. The quantification of individual marine processes remains a difficult problem.

- Palaeoenvironmental data indicate that regional vegetation composition and structure are *very likely* sensitive to climate change, and in some cases can respond to climate change within decades.

6.1 Introduction

This chapter assesses palaeoclimatic data and knowledge of how the climate system changes over interannual to millennial time scales, and how well these variations can be simulated with climate models. Additional palaeoclimatic perspectives are included in other chapters.

Palaeoclimate science has made significant advances since the 1970s, when a primary focus was on the origin of the ice ages, the possibility of an imminent future ice age, and the first explorations of the so-called Little Ice Age and Medieval Warm Period. Even in the first IPCC assessment (IPCC, 1990), many climatic variations prior to the instrumental record were not that well known or understood. Fifteen years later, understanding is much improved, more quantitative and better integrated with respect to observations and modelling.

After a brief overview of palaeoclimatic methods, including their strengths and weaknesses, this chapter examines the palaeoclimatic record in chronological order, from oldest to youngest. This approach was selected because the climate system varies and changes over all time scales, and it is instructive to understand the contributions that lower-frequency patterns of climate change might make in influencing higher-frequency patterns of variability and change. In addition, an examination of how the climate system has responded to large changes in climate forcing in the past is useful in assessing how the same climate system might respond to the large anticipated forcing changes in the future.

Cutting across this chronologically based presentation are assessments of climate forcing and response, and of the ability of state-of-the-art climate models to simulate the responses. Perspectives from palaeoclimatic observations, theory and modelling are integrated wherever possible to reduce uncertainty in the assessment. Several sections also assess the latest developments in the rapidly advancing area of abrupt climate change, that is, forced or unforced climatic change that involves crossing a threshold to a new climate regime (e.g., new mean state or character of variability), often where the transition time to the new regime is short relative to the duration of the regime (Rahmstorf, 2001; Alley et al., 2003; Overpeck and Trenberth, 2004).

6.2 Palaeoclimatic Methods

6.2.1 Methods – Observations of Forcing and Response

The field of palaeoclimatology has seen significant methodological advances since the Third Assessment Report (TAR), and the purpose of this section is to emphasize these advances while giving an overview of the methods underlying the data used in this chapter. Many critical methodological details are presented in subsequent sections where needed. Thus, this methods section is designed to be more general, and to give readers more insight to and confidence in the findings of the chapter. Readers are referred to several useful books and special issues of journals for additional methodological detail (Bradley, 1999; Cronin, 1999; Fischer and Wefer, 1999; Ruddiman and Thomson, 2001; Alverson et al., 2003; Mackay et al., 2003; Kucera et al., 2005; NRC, 2006).

6.2.1.1 How are Past Climate Forcings Known?

Time series of astronomically driven insolation change are well known and can be calculated from celestial mechanics (see Section 6.4, Box 6.1). The methods behind reconstructions of past solar and volcanic forcing continue to improve, although important uncertainties still exist (see Section 6.6).

6.2.1.2 How are Past Changes in Global Atmospheric Composition Known?

Perhaps one of the most important aspects of modern palaeoclimatology is that it is possible to derive time series of atmospheric trace gases and aerosols for the period from about 650 kyr to the present from air trapped in polar ice and from the ice itself (see Sections 6.4 to 6.6 for more methodological citations). As is common in palaeoclimatic studies of the Late Quaternary, the quality of forcing and response series are verified against recent (i.e., post-1950) measurements made by direct instrumental sampling. Section 6.3 cites several papers that reveal how atmospheric CO_2 concentrations can be inferred back millions of years, with much lower precision than the ice core estimates. As is common across all aspects of the field, palaeoclimatologists seldom rely on one method or proxy, but rather on several. This provides a richer and more encompassing view of climatic change than would be available from a single proxy. In this way, results can be cross-checked and uncertainties understood. In the case of pre-Quaternary carbon dioxide (CO_2), multiple geochemical and biological methods provide reasonable constraints on past CO_2 variations, but, as pointed out in Section 6.3, the quality of the estimates is somewhat limited.

6.2.1.3 How Precisely Can Palaeoclimatic Records of Forcing and Response be Dated?

Much has been researched and written on the dating methods associated with palaeoclimatic records, and readers are referred to the background books cited above for more detail. In general, dating accuracy gets weaker farther back in time and dating methods often have specific ranges where they can be applied. Tree ring records are generally the most accurate, and are accurate to the year, or season of a year (even back thousands of years). There are a host of other proxies that also have annual layers or bands (e.g., corals, varved sediments, some cave deposits, some ice cores) but the age models associated with these are not always exact to a specific year. Palaeoclimatologists strive to generate age information from multiple sources to

reduce age uncertainty, and palaeoclimatic interpretations must take into account uncertainties in time control.

There continue to be significant advances in radiometric dating. Each radiometric system has ranges over which the system is useful, and palaeoclimatic studies almost always publish analytical uncertainties. Because there can be additional uncertainties, methods have been developed for checking assumptions and cross verifying with independent methods. For example, secular variations in the radiocarbon clock over the last 12 kyr are well known, and fairly well understood over the last 35 kyr. These variations, and the quality of the radiocarbon clock, have both been well demonstrated via comparisons with age models derived from precise tree ring and varved sediment records, as well as with age determinations derived from independent radiometric systems such as uranium series. However, for each proxy record, the quality of the radiocarbon chronology also depends on the density of dates, the material available for dating and knowledge about the radiocarbon age of the carbon that was incorporated into the dated material.

6.2.1.4 How Can Palaeoclimatic Proxy Methods Be Used to Reconstruct Past Climate Dynamics?

Most of the methods behind the palaeoclimatic reconstructions assessed in this chapter are described in some detail in the aforementioned books, as well as in the citations of each chapter section. In some sections, important methodological background and controversies are discussed where such discussions help assess palaeoclimatic uncertainties.

Palaeoclimatic reconstruction methods have matured greatly in the past decades, and range from direct measurements of past change (e.g., ground temperature variations, gas content in ice core air bubbles, ocean sediment pore-water change and glacier extent changes) to proxy measurements involving the change in chemical, physical and biological parameters that reflect – often in a quantitative and well-understood manner – past change in the environment where the proxy carrier grew or existed. In addition to these methods, palaeoclimatologists also use documentary data (e.g., in the form of specific observations, logs and crop harvest data) for reconstructions of past climates. While a number of uncertainties remain, it is now well accepted and verified that many organisms (e.g., trees, corals, plankton, insects and other organisms) alter their growth and/or population dynamics in response to changing climate, and that these climate-induced changes are well recorded in the past growth of living and dead (fossil) specimens or assemblages of organisms. Tree rings, ocean and lake plankton and pollen are some of the best-known and best-developed proxy sources of past climate going back centuries and millennia. Networks of tree ring width and density chronologies are used to infer past temperature and moisture changes based on comprehensive calibration with temporally overlapping instrumental data. Past distributions of pollen and plankton from sediment cores can be used to derive quantitative estimates of past climate (e.g., temperatures, salinity and precipitation) via statistical methods calibrated against their modern distribution and associated climate parameters. The chemistry of several biological and physical entities reflects well-understood thermodynamic processes that can be transformed into estimates of climate parameters such as temperature. Key examples include: oxygen (O) isotope ratios in coral and foraminiferal carbonate to infer past temperature and salinity; magnesium/calcium (Mg/Ca) and strontium/calcium (Sr/Ca) ratios in carbonate for temperature estimates; alkenone saturation indices from marine organic molecules to infer past sea surface temperature (SST); and O and hydrogen isotopes and combined nitrogen and argon isotope studies in ice cores to infer temperature and atmospheric transport. Lastly, many physical systems (e.g., sediments and aeolian deposits) change in predictable ways that can be used to infer past climate change. There is ongoing work on further development and refinement of methods, and there are remaining research issues concerning the degree to which the methods have spatial and seasonal biases. Therefore, in many recent palaeoclimatic studies, a combination of methods is applied since multi-proxy series provide more rigorous estimates than a single proxy approach, and the multi-proxy approach may identify possible seasonal biases in the estimates. No palaeoclimatic method is foolproof, and knowledge of the underlying methods and processes is required when using palaeoclimatic data.

The field of palaeoclimatology depends heavily on replication and cross-verification between palaeoclimate records from independent sources in order to build confidence in inferences about past climate variability and change. In this chapter, the most weight is placed on those inferences that have been made with particularly robust or replicated methodologies.

6.2.2 Methods – Palaeoclimate Modelling

Climate models are used to simulate episodes of past climate (e.g., the Last Glacial Maximum, the last interglacial period or abrupt climate events) to help understand the mechanisms of past climate changes. Models are key to testing physical hypotheses, such as the Milankovitch theory (Section 6.4, Box 6.1), quantitatively. Models allow the linkage of cause and effect in past climate change to be investigated. Models also help to fill the gap between the local and global scale in palaeoclimate, as palaeoclimatic information is often sparse, patchy and seasonal. For example, long ice core records show a strong correlation between local temperature in Antarctica and the globally mixed gases CO_2 and methane, but the causal connections between these variables are best explored with the help of models. Developing a quantitative understanding of mechanisms is the most effective way to learn from past climate for the future, since there are probably no direct analogues of the future in the past.

At the same time, palaeoclimate reconstructions offer the possibility of testing climate models, particularly if the climate forcing can be appropriately specified, and the response is sufficiently well constrained. For earlier climates (i.e., before the current 'Holocene' interglacial), forcing and responses cover a much larger range, but data are more sparse and uncertain, whereas for recent millennia more records are

available, but forcing and response are much smaller. Testing models with palaeoclimatic data is important, as not all aspects of climate models can be tested against instrumental climate data. For example, good performance for present climate is not a conclusive test for a realistic sensitivity to CO_2 – to test this, simulation of a climate with a very different CO_2 level can be used. In addition, many parametrizations describing sub-grid scale processes (e.g., cloud parameters, turbulent mixing) have been developed using present-day observations; hence climate states not used in model development provide an independent benchmark for testing models. Palaeoclimate data are key to evaluating the ability of climate models to simulate realistic climate change.

In principle the same climate models that are used to simulate present-day climate, or scenarios for the future, are also used to simulate episodes of past climate, using differences in prescribed forcing and (for the deep past) in configuration of oceans and continents. The full spectrum of models (see Chapter 8) is used (Claussen et al., 2002), ranging from simple conceptual models, through Earth System Models of Intermediate Complexity (EMICs) and coupled General Circulation Models (GCMs). Since long simulations (thousands of years) can be required for some palaeoclimatic applications, and computer power is still a limiting factor, relatively 'fast' coupled models are often used. Additional components that are not standard in models used for simulating present climate are also increasingly added for palaeoclimate applications, for example, continental ice sheet models or components that track the stable isotopes in the climate system (LeGrande et al., 2006). Vegetation modules as well as terrestrial and marine ecosystem modules are increasingly included, both to capture biophysical and biogeochemical feedbacks to climate, and to allow for validation of models against proxy palaeoecological (e.g., pollen) data. The representation of biogeochemical tracers and processes is a particularly important new advance for palaeoclimatic model simulations, as a rich body of information on past climate has emerged from palaeoenvironmental records that are intrinsically linked to the cycling of carbon and other nutrients.

6.3 The Pre-Quaternary Climates

6.3.1 What is the Relationship Between Carbon Dioxide and Temperature in this Time Period?

Pre-Quaternary climates prior to 2.6 Ma (e.g., Figure 6.1) were mostly warmer than today and associated with higher CO_2 levels. In that sense, they have certain similarities with the anticipated future climate change (although the global biology and geography were increasingly different further back in time). In general, they verify that warmer climates are to be expected with increased greenhouse gas concentrations. Looking back in time beyond the reach of ice cores, that is, prior to about 1 Ma, data on greenhouse gas concentrations in the atmosphere become much more uncertain. However, there are ongoing efforts to obtain quantitative reconstructions of the warm climates over the past 65 Myr and the following subsections discuss two particularly relevant climate events of this period.

How accurately is the relationship between CO_2 and temperature known? There are four primary proxies used for pre-Quaternary CO_2 levels (Jasper and Hayes, 1990; Royer et al., 2001; Royer, 2003). Two proxies apply the fact that biological entities in soils and seawater have carbon isotope ratios that are distinct from the atmosphere (Cerling, 1991; Freeman and Hayes, 1992; Yapp and Poths, 1992; Pagani et al., 2005). The third proxy uses the ratio of boron isotopes (Pearson and Palmer, 2000), while the fourth uses the empirical relationship between stomatal pores on tree leaves and atmospheric CO_2 content (McElwain and Chaloner, 1995; Royer, 2003). As shown in Figure 6.1 (bottom panel), while there is a wide range of reconstructed CO_2 values, magnitudes are generally higher than the interglacial, pre-industrial values seen in ice core data. Changes in CO_2 on these long time scales are thought to be driven by changes in tectonic processes (e.g., volcanic activity source and silicate weathering drawdown; e.g., Ruddiman, 1997). Temperature reconstructions, such as that shown in Figure 6.1 (middle panel), are derived from O isotopes (corrected for variations in the global ice volume), as well as Mg/Ca in forams and alkenones. Indicators for the presence of continental ice on Earth show that the planet was mostly ice-free during geologic history, another indication of the general warmth. Major expansion of antarctic glaciations starting around 35 to 40 Ma was likely a response, in part, to declining atmospheric CO_2 levels from their peak in the Cretaceous (~100 Ma) (DeConto and Pollard, 2003). The relationship between CO_2 and temperature can be traced further back in time as indicated in Figure 6.1 (top panel), which shows that the warmth of the Mesozoic Era (230–65 Ma) was likely associated with high levels of CO_2 and that the major glaciations around 300 Ma likely coincided with low CO_2 concentrations relative to surrounding periods.

6.3.2 What Does the Record of the Mid-Pliocene Show?

The Mid-Pliocene (about 3.3 to 3.0 Ma) is the most recent time in Earth's history when mean global temperatures were substantially warmer for a sustained period (estimated by GCMs to be about 2°C to 3°C above pre-industrial temperatures; Chandler et al., 1994; Sloan et al., 1996; Haywood et al., 2000; Jiang et al., 2005), providing an accessible example of a world that is similar in many respects to what models estimate could be the Earth of the late 21st century. The Pliocene is also recent enough that the continents and ocean basins had nearly reached their present geographic configuration. Taken together, the average of the warmest times during the middle Pliocene presents a view of the equilibrium state of a globally warmer world, in which atmospheric CO_2 concentrations (estimated

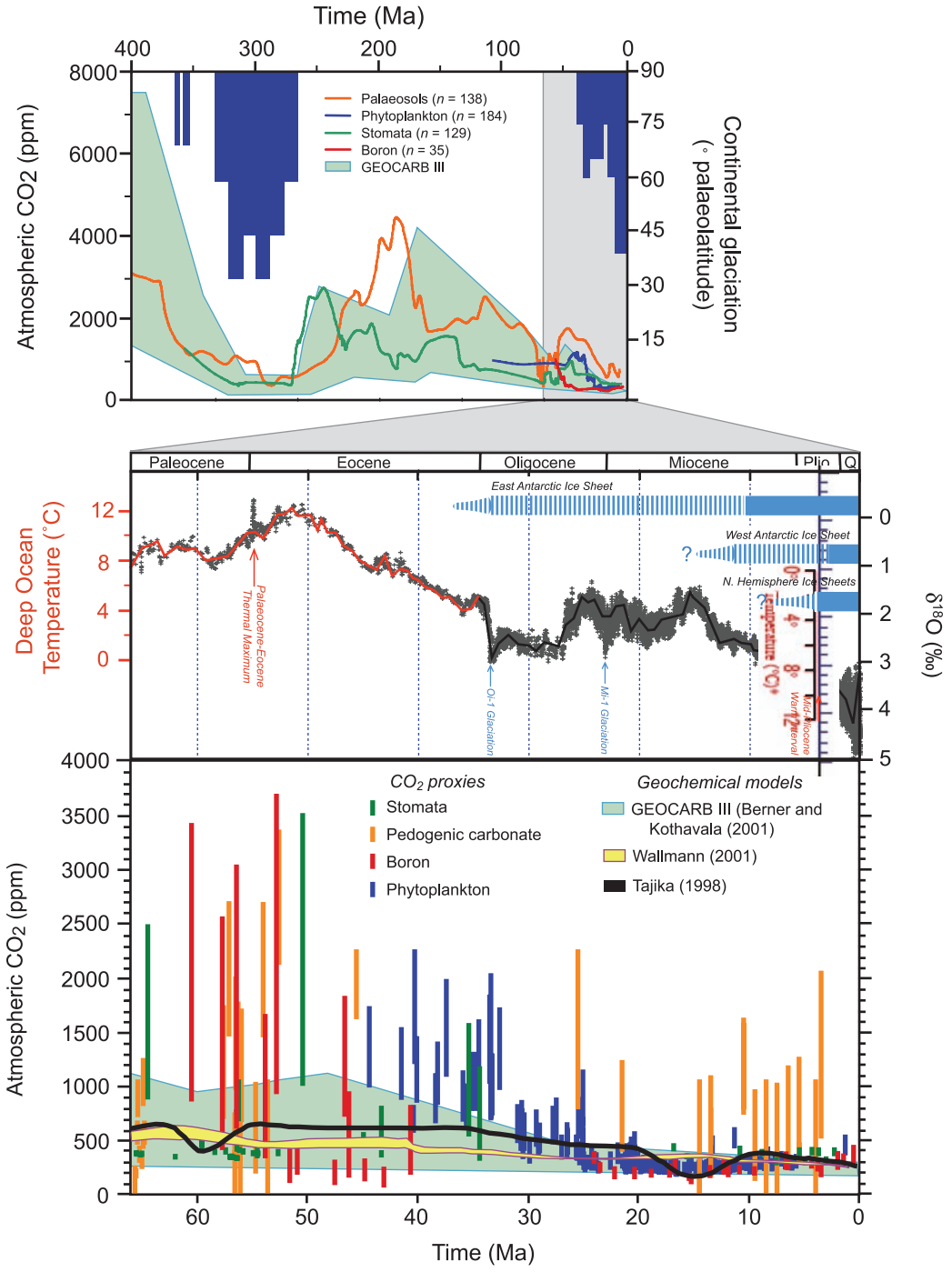


Figure 6.1. *(Top) Atmospheric CO_2 and continental glaciation 400 Ma to present. Vertical blue bars mark the timing and palaeolatitudinal extent of ice sheets (after Crowley, 1998). Plotted CO_2 records represent five-point running averages from each of the four major proxies (see Royer, 2006 for details of compilation). Also plotted are the plausible ranges of CO_2 from the geochemical carbon cycle model GEOCARB III (Berner and Kothavala, 2001). All data have been adjusted to the Gradstein et al. (2004) time scale. (Middle) Global compilation of deep-sea benthic foraminifera ^{18}O isotope records from 40 Deep Sea Drilling Program and Ocean Drilling Program sites (Zachos et al., 2001) updated with high-resolution records for the Eocene through Miocene interval (Billups et al., 2002; Bohaty and Zachos, 2003; Lear et al., 2004). Most data were derived from analyses of two common and long-lived benthic taxa,* Cibicidoides *and* Nuttallides. *To correct for genus-specific isotope vital effects, the ^{18}O values were adjusted by +0.64 and +0.4 (Shackleton et al., 1984), respectively. The ages are relative to the geomagnetic polarity time scale of Berggren et al. (1995). The raw data were smoothed using a five-point running mean, and curve-fitted with a locally weighted mean. The ^{18}O temperature values assume an ice-free ocean (–1.0‰ Standard Mean Ocean Water), and thus only apply to the time preceding large-scale antarctic glaciation (~35 Ma). After the early Oligocene much of the variability (~70%) in the ^{18}O record reflects changes in antarctic and Northern Hemisphere ice volume, which is represented by light blue horizontal bars (e.g., Hambrey et al., 1991; Wise et al., 1991; Ehrmann and Mackensen, 1992). Where the bars are dashed, they represent periods of ephemeral ice or ice sheets smaller than present, while the solid bars represent ice sheets of modern or greater size. The evolution and stability of the West Antarctic Ice Sheet (e.g., Lemasurier and Rocchi, 2005) remains an important area of uncertainty that could affect estimates of future sea level rise. (Bottom) Detailed record of CO_2 for the last 65 Myr. Individual records of CO_2 and associated errors are colour-coded by proxy method; when possible, records are based on replicate samples (see Royer, 2006 for details and data references). Dating errors are typically less than ±1 Myr. The range of error for each CO_2 proxy varies considerably, with estimates based on soil nodules yielding the greatest uncertainty. Also plotted are the plausible ranges of CO_2 from three geochemical carbon cycle models.*

to be between 360 to 400 ppm) were likely higher than pre-industrial values (Raymo and Rau, 1992; Raymo et al., 1996), and in which geologic evidence and isotopes agree that sea level was at least 15 to 25 m above modern levels (Dowsett and Cronin, 1990; Shackleton et al., 1995), with correspondingly reduced ice sheets and lower continental aridity (Guo et al., 2004).

Both terrestrial and marine palaeoclimate proxies (Thompson, 1991; Dowsett et al., 1996; Thompson and Fleming, 1996) show that high latitudes were significantly warmer, but that tropical SSTs and surface air temperatures were little different from the present. The result was a substantial decrease in the lower-tropospheric latitudinal temperature gradient. For example, atmospheric GCM simulations driven by reconstructed SSTs from the Pliocene Research Interpretations and Synoptic Mapping Group (Dowsett et al., 1996; Dowsett et al., 2005) produced winter surface air temperature warming of 10°C to 20°C at high northern latitudes with 5°C to 10°C increases over the northern North Atlantic (~60°N), whereas there was essentially no tropical surface air temperature change (or even slight cooling) (Chandler et al., 1994; Sloan et al., 1996; Haywood et al., 2000, Jiang et al., 2005). In contrast, a coupled atmosphere-ocean experiment with an atmospheric CO_2 concentration of 400 ppm produced warming relative to pre-industrial times of 3°C to 5°C in the northern North Atlantic, and 1°C to 3°C in the tropics (Haywood et al., 2005), generally similar to the response to higher CO_2 discussed in Chapter 10.

The estimated lack of tropical warming is a result of basing tropical SST reconstructions on marine microfaunal evidence. As in the case of the Last Glacial Maximum (see Section 6.4), it is uncertain whether tropical sensitivity is really as small as such reconstructions suggest. Haywood et al. (2005) found that alkenone estimates of tropical and subtropical temperatures do indicate warming in these regions, in better agreement with GCM simulations from increased CO_2 forcing (see Chapter 10). As in the study noted above, climate models cannot produce a response to increased CO_2 with large high-latitude warming, and yet minimal tropical temperature change, without strong increases in ocean heat transport (Rind and Chandler, 1991).

The substantial high-latitude response is shown by both marine and terrestrial palaeodata, and it may indicate that high latitudes are more sensitive to increased CO_2 than model simulations suggest for the 21st century. Alternatively, it may be the result of increased ocean heat transports due to either an enhanced thermohaline circulation (Raymo et al., 1989; Rind and Chandler, 1991) or increased flow of surface ocean currents due to greater wind stresses (Ravelo et al., 1997; Haywood et al., 2000), or associated with the reduced extent of land and sea ice (Jansen et al., 2000; Knies et al., 2002; Haywood et al., 2005). Currently available proxy data are equivocal concerning a possible increase in the intensity of the meridional overturning cell for either transient or equilibrium climate states during the Pliocene, although an increase would contrast with the North Atlantic transient deep-water production decreases that are found in most coupled model simulations for the 21st century (see Chapter 10). The transient response is likely to be different from an equilibrium response as climate warms. Data are just beginning to emerge that describe the deep ocean state during the Pliocene (Cronin et al., 2005). Understanding the climate distribution and forcing for the Pliocene period may help improve predictions of the likely response to increased CO_2 in the future, including the ultimate role of the ocean circulation in a globally warmer world.

6.3.3 What Does the Record of the Palaeocene-Eocene Thermal Maximum Show?

Approximately 55 Ma, an abrupt warming (in this case of the order of 1 to 10 kyr) by several degrees celsius is indicated by changes in ^{18}O isotope and Mg/Ca records (Kennett and Stott, 1991; Zachos et al., 2003; Tripati and Elderfield, 2004). The warming and associated environmental impact was felt at all latitudes, and in both the surface and deep ocean. The warmth lasted approximately 100 kyr. Evidence for shifts in global precipitation patterns is present in a variety of fossil records including vegetation (Wing et al., 2005). The climate anomaly, along with an accompanying carbon isotope excursion, occurred at the boundary between the Palaeocene and Eocene epochs, and is therefore often referred to as the Palaeocene-Eocene Thermal Maximum (PETM). The thermal maximum clearly stands out in high-resolution records of that time (Figure 6.2). At the same time, ^{13}C isotopes in marine and continental records show that a large mass of carbon with low ^{13}C concentration must have been released into the atmosphere and ocean. The mass of carbon was sufficiently large to lower the pH of the ocean and drive widespread dissolution of seafloor carbonates (Zachos et al., 2005). Possible sources for this carbon could have been methane (CH_4) from decomposition of clathrates on the sea floor, CO_2 from volcanic activity, or oxidation of sediments rich in organic matter (Dickens et al., 1997; Kurtz et al., 2003; Svensen et al., 2004). The PETM, which altered ecosystems worldwide (Koch et al., 1992; Bowen et al., 2002; Bralower, 2002; Crouch et al., 2003; Thomas, 2003; Bowen et al., 2004; Harrington et al., 2004), is being intensively studied as it has some similarity with the ongoing rapid release of carbon into the atmosphere by humans. The estimated magnitude of carbon release for this time period is of the order of 1 to 2×10^{18} g of carbon (Dickens et al., 1997), a similar magnitude to that associated with greenhouse gas releases during the coming century. Moreover, the period of recovery through natural carbon sequestration processes, about 100 kyr, is similar to that forecast for the future. As in the case of the Pliocene, the high-latitude warming during this event was substantial (~20°C; Moran et al., 2006) and considerably higher than produced by GCM simulations for the event (Sluijs et al., 2006) or in general for increased greenhouse gas experiments (Chapter 10). Although there is still too much uncertainty in the data to derive a quantitative estimate of climate sensitivity from the PETM, the event is a striking example of massive carbon release and related extreme climatic warming.

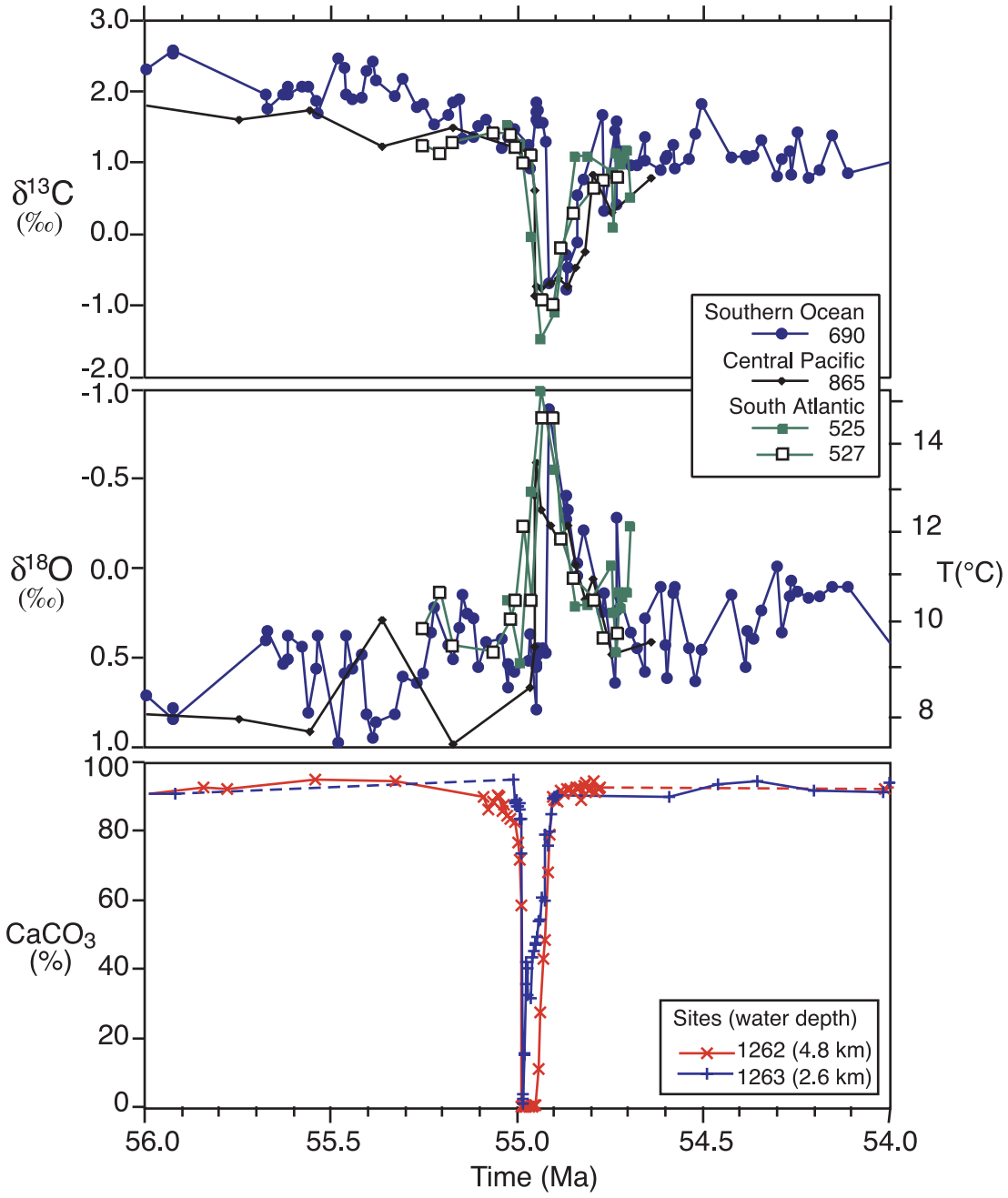


Figure 6.2. *The Palaeocene-Eocene Thermal Maximum as recorded in benthic (bottom dwelling) foraminifer* (Nuttallides truempyi) *isotopic records from sites in the Antarctic, south Atlantic and Pacific (see* Zachos *et al.,* 2003 for details*). The rapid decrease in carbon isotope ratios in the top panel is indicative of a large increase in atmospheric greenhouse gases CO_2 and CH_4 that was coincident with an approximately 5°C global warming (centre panel). Using the carbon isotope records, numerical models show that CH_4 released by the rapid decomposition of marine hydrates might have been a major component (~2,000 GtC) of the carbon flux (Dickens and Owen, 1996). Testing of this and other models requires an independent constraint on the carbon fluxes. In theory, much of the additional greenhouse carbon would have been absorbed by the ocean, thereby lowering seawater pH and causing widespread dissolution of seafloor carbonates. Such a response is evident in the lower panel, which shows a transient reduction in the carbonate ($CaCO_3$) content of sediments in two cores from the south Atlantic (Zachos et al., 2004, 2005). The observed patterns indicate that the ocean's carbonate saturation horizon rapidly shoaled more than 2 km, and then gradually recovered as buffering processes slowly restored the chemical balance of the ocean. Initially, most of the carbonate dissolution is of sediment deposited prior to the event, a process that offsets the apparent timing of the dissolution horizon relative to the base of the benthic foraminifer carbon isotope excursion. Model simulations show that the recovery of the carbonate saturation horizon should precede the recovery in the carbon isotopes by as much as 100 kyr (Dickens and Owen, 1996), another feature that is evident in the sediment records.*

6.4 Glacial-Interglacial Variability and Dynamics

6.4.1 Climate Forcings and Responses Over Glacial-Interglacial Cycles

Palaeoclimatic records document a sequence of glacial-interglacial cycles covering the last 740 kyr in ice cores (EPICA community members, 2004), and several million years in deep oceanic sediments (Lisiecki and Raymo, 2005) and loess (Ding et al., 2002). The last 430 kyr, which are the best documented, are characterised by 100-kyr glacial-interglacial cycles of very large amplitude, as well as large climate changes corresponding to other orbital periods (Hays et al., 1976; Box 6.1), and at millennial time scales (McManus et al., 2002; NorthGRIP, 2004). A minor proportion (20% on average) of each glacial-interglacial cycle was spent in the warm interglacial mode, which normally lasted for 10 to 30 kyr (Figure 6.3). There is evidence for longer interglacial periods between 430 and 740 ka, but these were apparently colder than the typical interglacials of the latest Quaternary (EPICA community members, 2004). The Holocene, the latest of these interglacials, extends to the present.

The ice core record indicates that greenhouse gases co-varied with antarctic temperature over glacial-interglacial cycles, suggesting a close link between natural atmospheric greenhouse gas variations and temperature (Box 6.2). Variations in CO_2 over the last 420 kyr broadly followed antarctic temperature, typically by several centuries to a millennium (Mudelsee, 2001). The sequence of climatic forcings and responses during deglaciations (transitions from full glacial conditions to warm interglacials) are well documented. High-resolution ice core records of temperature proxies and CO_2 during deglaciation indicates that antarctic temperature starts to rise several hundred years before CO_2 (Monnin et al., 2001; Caillon et al., 2003). During the last deglaciation, and likely also the three previous ones, the onset of warming at both high southern and northern

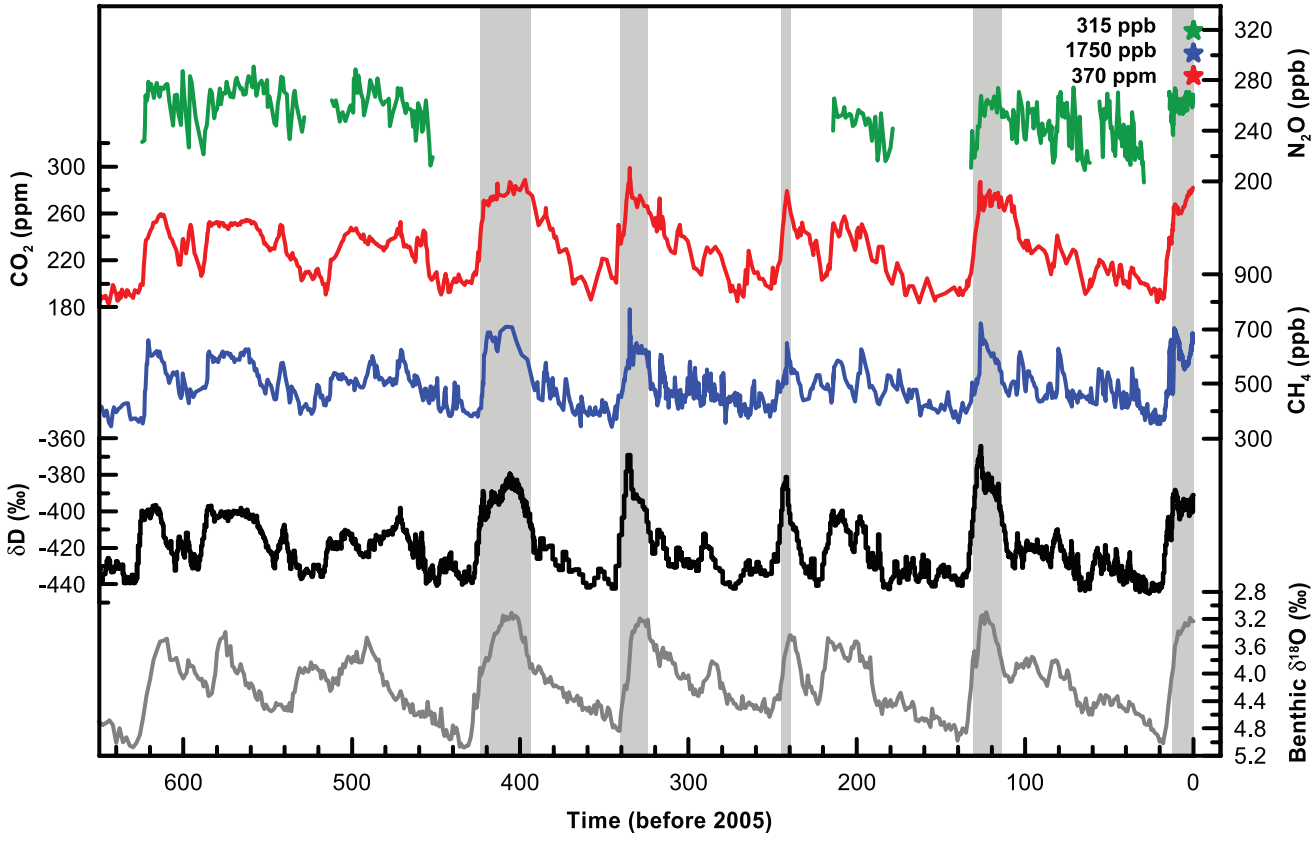


Figure 6.3. *Variations of deuterium (δD; black), a proxy for local temperature, and the atmospheric concentrations of the greenhouse gases CO_2 (red), CH_4 (blue), and nitrous oxide (N_2O; green) derived from air trapped within ice cores from Antarctica and from recent atmospheric measurements (Petit et al., 1999; Indermühle et al., 2000; EPICA community members, 2004; Spahni et al., 2005; Siegenthaler et al., 2005a,b). The shading indicates the last interglacial warm periods. Interglacial periods also existed prior to 450 ka, but these were apparently colder than the typical interglacials of the latest Quaternary. The length of the current interglacial is not unusual in the context of the last 650 kyr. The stack of 57 globally distributed benthic $\delta^{18}O$ marine records (dark grey), a proxy for global ice volume fluctuations (Lisiecki and Raymo, 2005), is displayed for comparison with the ice core data. Downward trends in the benthic $\delta^{18}O$ curve reflect increasing ice volumes on land. Note that the shaded vertical bars are based on the ice core age model (EPICA community members, 2004), and that the marine record is plotted on its original time scale based on tuning to the orbital parameters (Lisiecki and Raymo, 2005). The stars and labels indicate atmospheric concentrations at year 2000.*

Box 6.1: Orbital Forcing

It is well known from astronomical calculations (Berger, 1978) that periodic changes in parameters of the orbit of the Earth around the Sun modify the seasonal and latitudinal distribution of incoming solar radiation at the top of the atmosphere (hereafter called 'insolation'). Past and future changes in insolation can be calculated over several millions of years with a high degree of confidence (Berger and Loutre, 1991; Laskar et al., 2004). This box focuses on the time period from the past 800 kyr to the next 200 kyr.

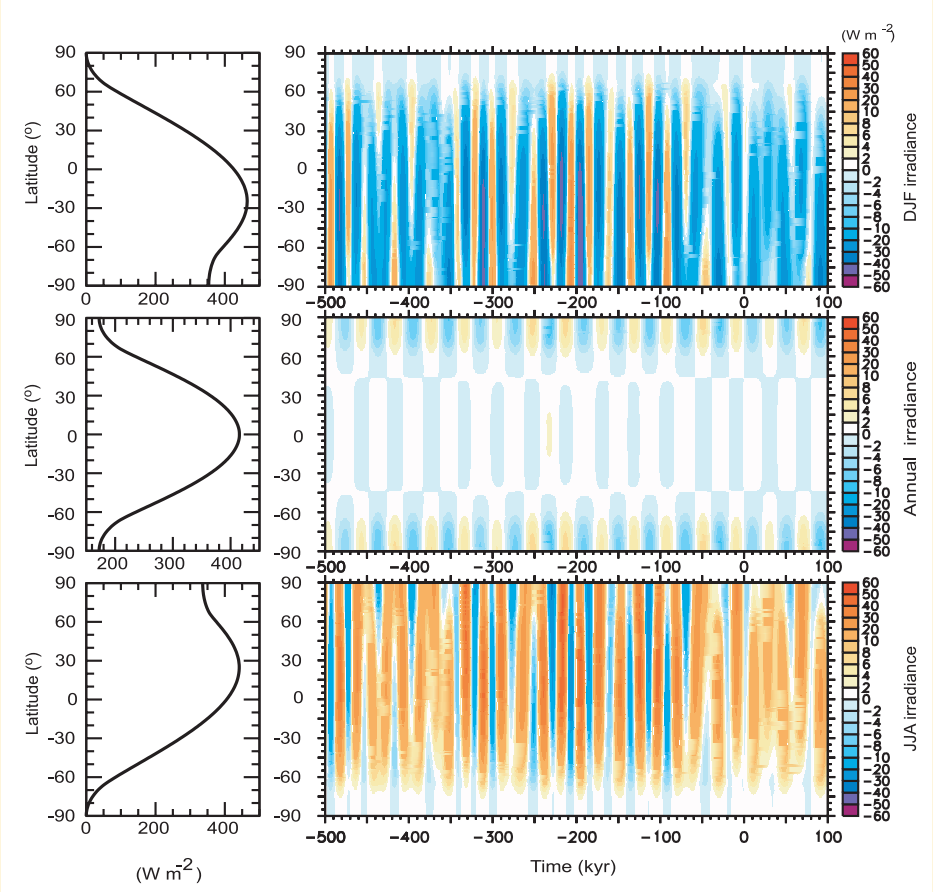
Over this time interval, the obliquity (tilt) of the Earth axis varies between 22.05° and 24.50° with a strong quasi-periodicity around 41 kyr. Changes in obliquity have an impact on seasonal contrasts. This parameter also modulates annual mean insolation changes with opposite effects in low vs. high latitudes (and therefore no effect on global average insolation). Local annual mean insolation changes remain below 6 W m^{-2}.

The eccentricity of the Earth's orbit around the Sun has longer quasi-periodicities at 400 and around 100 kyr, and varies between values of about 0.002 and 0.050 during the time period from 800 ka to 200 kyr in the future. Changes in eccentricity alone modulate the Sun-Earth distance and have limited impacts on global and annual mean insolation. However, changes in eccentricity affect the intra-annual changes in the Sun-Earth distance and thereby modulate significantly the seasonal and latitudinal effects induced by obliquity and climatic precession.

Associated with the general precession of the equinoxes and the longitude of perihelion, periodic shifts in the position of solstices and equinoxes on the orbit relative to the perihelion occur, and these modulate the seasonal cycle of insolation with periodicities of about 19 and about 23 kyr. As a result, changes in the position of the seasons on the orbit strongly modulate the latitudinal and seasonal distribution of insolation. When averaged over a season, insolation changes can reach 60 W m^{-2} (Box 6.1, Figure 1). During periods of low eccentricity, such as about 400 ka and during the next 100 kyr, seasonal insolation changes induced by precession are less strong than during periods of larger eccentricity (Box 6.1, Figure 1). High-frequency variations of orbital variations appear to be associated with very small insolation changes (Bertrand et al., 2002a).

The Milankovitch theory proposes that ice ages are triggered by minima in summer insolation near 65°N, enabling winter snowfall to persist all year and therefore accumulate to build NH glacial ice sheets. For example, the onset of the last ice age, about 116 ± 1 ka (Stirling et al., 1998), corresponds to a 65°N mid-June insolation about 40 W m^{-2} lower than today (Box 6.1, Figure 1).

Studies of the link between orbital parameters and past climate changes include spectral analysis of palaeoclimatic records and the identification of orbital periodicities; precise dating of specific climatic transitions; and modelling of the climate response to orbital forcing, which highlights the role of climatic and biogeochemical feedbacks. Sections 6.4 and 6.5 describe some aspects of the state-of-the-art understanding of the relationships between orbital forcing, climate feedbacks and past climate changes.



Box 6.1, Figure 1. *(Left) December to February (top), annual mean (middle) and June to August (bottom) latitudinal distribution of present-day (year 1950) incoming mean solar radiation (W m^{-2}). (Right) Deviations with respect to the present of December to February (top), annual mean (middle) and June to August (bottom) latitudinal distribution of incoming mean solar radiation (W m^{-2}) from the past 500 kyr to the future 100 kyr (Berger and Loutre, 1991; Loutre et al., 2004).*

Box 6.2: What Caused the Low Atmospheric Carbon Dioxide Concentrations During Glacial Times?

Ice core records show that atmospheric CO_2 varied in the range of 180 to 300 ppm over the glacial-interglacial cycles of the last 650 kyr (Figure 6.3; Petit et al., 1999; Siegenthaler et al., 2005a). The quantitative and mechanistic explanation of these CO_2 variations remains one of the major unsolved questions in climate research. Processes in the atmosphere, in the ocean, in marine sediments and on land, and the dynamics of sea ice and ice sheets must be considered. A number of hypotheses for the low glacial CO_2 concentrations have emerged over the past 20 years, and a rich body of literature is available (Webb et al., 1997; Broecker and Henderson, 1998; Archer et al., 2000; Sigman and Boyle, 2000; Kohfeld et al., 2005). Many processes have been identified that could potentially regulate atmospheric CO_2 on glacial-interglacial time scales. However, the existing proxy data with which to test hypotheses are relatively scarce, uncertain, and their interpretation is partly conflicting.

Most explanations propose changes in oceanic processes as the cause for low glacial CO_2 concentrations. The ocean is by far the largest of the relatively fast-exchanging (<1 kyr) carbon reservoirs, and terrestrial changes cannot explain the low glacial values because terrestrial storage was also low at the Last Glacial Maximum (see Section 6.4.1). On glacial-interglacial time scales, atmospheric CO_2 is mainly governed by the interplay between ocean circulation, marine biological activity, ocean-sediment interactions, seawater carbonate chemistry and air-sea exchange. Upon dissolution in seawater, CO_2 maintains an acid/base equilibrium with bicarbonate and carbonate ions that depends on the acid-titrating capacity of seawater (i.e., alkalinity). Atmospheric CO_2 would be higher if the ocean lacked biological activity. CO_2 is more soluble in colder than in warmer waters; therefore, changes in surface and deep ocean temperature have the potential to alter atmospheric CO_2. Most hypotheses focus on the Southern Ocean, where large volume-fractions of the cold deep-water masses of the world ocean are currently formed, and large amounts of biological nutrients (phosphate and nitrate) upwelling to the surface remain unused. A strong argument for the importance of SH processes is the co-evolution of antarctic temperature and atmospheric CO_2.

One family of hypotheses regarding low glacial atmospheric CO_2 values invokes an increase or redistribution in the ocean alkalinity as a primary cause. Potential mechanisms are (i) the increase of calcium carbonate ($CaCO_3$) weathering on land, (ii) a decrease of coral reef growth in the shallow ocean, or (iii) a change in the export ratio of $CaCO_3$ and organic material to the deep ocean. These mechanisms require large changes in the deposition pattern of $CaCO_3$ to explain the full amplitude of the glacial-interglacial CO_2 difference through a mechanism called carbonate compensation (Archer et al., 2000). The available sediment data do not support a dominant role for carbonate compensation in explaining low glacial CO_2 levels. Furthermore, carbonate compensation may only explain slow CO_2 variation, as its time scale is multi-millennial.

Another family of hypotheses invokes changes in the sinking of marine plankton. Possible mechanisms include (iv) fertilization of phytoplankton growth in the Southern Ocean by increased deposition of iron-containing dust from the atmosphere after being carried by winds from colder, drier continental areas, and a subsequent redistribution of limiting nutrients; (v) an increase in the whole ocean nutrient content (e.g., through input of material exposed on shelves or nitrogen fixation); and (vi) an increase in the ratio between carbon and other nutrients assimilated in organic material, resulting in a higher carbon export per unit of limiting nutrient exported. As with the first family of hypotheses, this family of mechanisms also suffers from the inability to account for the full amplitude of the reconstructed CO_2 variations when constrained by the available information. For example, periods of enhanced biological production and increased dustiness (iron supply) are coincident with CO_2 concentration changes of 20 to 50 ppm (see Section 6.4.2, Figure 6.7). Model simulations consistently suggest a limited role for iron in regulating past atmospheric CO_2 concentration (Bopp et al., 2002).

Physical processes also likely contributed to the observed CO_2 variations. Possible mechanisms include (vii) changes in ocean temperature (and salinity), (viii) suppression of air-sea gas exchange by sea ice, and (ix) increased stratification in the Southern Ocean. The combined changes in temperature and salinity increased the solubility of CO_2, causing a depletion in atmospheric CO_2 of perhaps 30 ppm. Simulations with general circulation ocean models do not fully support the gas exchange-sea ice hypothesis. One explanation (ix) conceived in the 1980s invokes more stratification, less upwelling of carbon and nutrient-rich waters to the surface of the Southern Ocean and increased carbon storage at depth during glacial times. The stratification may have caused a depletion of nutrients and carbon at the surface, but proxy evidence for surface nutrient utilisation is controversial. Qualitatively, the slow ventilation is consistent with very saline and very cold deep waters reconstructed for the last glacial maximum (Adkins et al., 2002), as well as low glacial stable carbon isotope ratios ($^{13}C/^{12}C$) in the deep South Atlantic.

In conclusion, the explanation of glacial-interglacial CO_2 variations remains a difficult attribution problem. It appears likely that a range of mechanisms have acted in concert (e.g., Köhler et al., 2005). The future challenge is not only to explain the amplitude of glacial-interglacial CO_2 variations, but the complex temporal evolution of atmospheric CO_2 and climate consistently.

latitudes preceded by several thousand years the first signals of significant sea level increase resulting from the melting of the northern ice sheets linked with the rapid warming at high northern latitudes (Petit et al., 1999; Shackleton, 2000; Pépin et al., 2001). Current data are not accurate enough to identify whether warming started earlier in the Southern Hemisphere (SH) or Northern Hemisphere (NH), but a major deglacial feature is the difference between North and South in terms of the magnitude and timing of strong reversals in the warming trend, which are not in phase between the hemispheres and are more pronounced in the NH (Blunier and Brook, 2001).

Greenhouse gas (especially CO_2) feedbacks contributed greatly to the global radiative perturbation corresponding to the transitions from glacial to interglacial modes (see Section 6.4.1.2). The relationship between antarctic temperature and CO_2 did not change significantly during the past 650 kyr, indicating a rather stable coupling between climate and the carbon cycle during the late Pleistocene (Siegenthaler et al., 2005a). The rate of change in atmospheric CO_2 varied considerably over time. For example, the CO_2 increase from about 180 ppm at the Last Glacial Maximum to about 265 ppm in the early Holocene occurred with distinct rates over different periods (Monnin et al., 2001; Figure 6.4).

6.4.1.1 How Do Glacial-Interglacial Variations in the Greenhouse Gases Carbon Dioxide, Methane and Nitrous Oxide Compare with the Industrial Era Greenhouse Gas Increase?

The present atmospheric concentrations of CO_2, CH_4 and nitrous oxide (N_2O) are higher than ever measured in the ice core record of the past 650 kyr (Figures 6.3 and 6.4). The measured concentrations of the three greenhouse gases fluctuated only slightly (within 4% for CO_2 and N_2O and within 7% for CH_4) over the past millennium prior to the industrial era, and also varied within a restricted range over the late Quaternary. Within the last 200 years, the late Quaternary natural range has been exceeded by at least 25% for CO_2, 120% for CH_4 and 9% for N_2O. All three records show effects of the large and increasing growth in anthropogenic emissions during the industrial era.

Variations in atmospheric CO_2 dominate the radiative forcing by all three gases (Figure 6.4). The industrial era increase in CO_2, and in the radiative forcing (Section 2.3) by all three gases, is similar in magnitude to the increase over the transitions from glacial to interglacial periods, but started from an interglacial level and occurred one to two orders of magnitude faster (Stocker and Monnin, 2003). There is no indication in the ice core record that an increase comparable in magnitude and rate to the industrial era has occurred in the past 650 kyr. The data resolution is sufficient to exclude with very high confidence a peak similar to the anthropogenic rise for the past 50 kyr for CO_2, for the past 80 kyr for CH_4 and for the past 16 kyr for N_2O. The ice core records show that during the industrial era, the average rate of increase in the radiative forcing from CO_2, CH_4 and N_2O is greater than at any time during the past 16 kyr (Figure 6.4). The smoothing of the atmospheric signal (Schwander et al., 1993; Spahni et al., 2003) is small at Law Dome, a high-accumulation site in Antarctica, and decadal-scale rates of change can be computed from the Law Dome record spanning the past two millennia (Etheridge et al., 1996; Ferretti et al., 2005; MacFarling Meure et al., 2006). The average rate of increase in atmospheric CO_2 was at least five times larger over the period from 1960 to 1999 than over any other 40-year period during the two millennia before the industrial era. The average rate of increase in atmospheric CH_4 was at least six times larger, and that for N_2O at least two times larger over the past four decades, than at any time during the two millennia before the industrial era. Correspondingly, the recent average rate of increase in the combined radiative forcing by all three greenhouse gases was at least six times larger than at any time during the period AD 1 to AD 1800 (Figure 6.4d).

6.4.1.2 What Do the Last Glacial Maximum and the Last Deglaciation Show?

Past glacial cold periods, sometimes referred to as 'ice ages', provide a means for evaluating the understanding and modelling of the response of the climate system to large radiative perturbations. The most recent glacial period started about 116 ka, in response to orbital forcing (Box 6.1), with the growth of ice sheets and fall of sea level culminating in the Last Glacial Maximum (LGM), around 21 ka. The LGM and the subsequent deglaciation have been widely studied because the radiative forcings, boundary conditions and climate response are relatively well known.

The response of the climate system at the LGM included feedbacks in the atmosphere and on land amplifying the orbital forcing. Concentrations of well-mixed greenhouse gases at the LGM were reduced relative to pre-industrial values (Figures 6.3 and 6.4), amounting to a global radiative perturbation of –2.8 W m^{-2} – approximately equal to, but opposite from, the radiative forcing of these gases for the year 2000 (see Section 2.3). Land ice covered large parts of North America and Europe at the LGM, lowering sea level and exposing new land. The radiative perturbation of the ice sheets and lowered sea level, specified as a boundary condition for some LGM simulations, has been estimated to be about –3.2 W m^{-2}, but with uncertainties associated with the coverage and height of LGM continental ice (Mangerud et al., 2002; Peltier, 2004; Toracinta et al., 2004; Masson-Delmotte et al., 2006) and the parametrization of ice albedo in climate models (Taylor et al., 2000). The distribution of vegetation was altered, with tundra expanded over the northern continents and tropical rain forest reduced (Prentice et al., 2000), and atmospheric aerosols (primarily dust) were increased (Kohfeld and Harrison, 2001), partly as a consequence of reduced vegetation cover (Mahowald et al., 1999). Vegetation and atmospheric aerosols are treated as specified conditions in some LGM simulations, each contributing about –1 W m^{-2} of radiative perturbation, but with very low scientific understanding of their radiative influence at the LGM (Claquin et al., 2003;

Crucifix and Hewitt, 2005). Changes in biogeochemical cycles thus played an important role and contributed, through changes in greenhouse gas concentration, dust loading and vegetation cover, more than half of the known radiative perturbation during the LGM. Overall, the radiative perturbation for the changed greenhouse gas and aerosol concentrations and land surface was approximately –8 W m^{-2} for the LGM, although with significant uncertainty in the estimates for the contributions of aerosol and land surface changes (Figure 6.5).

Understanding of the magnitude of tropical cooling over land at the LGM has improved since the TAR with more records, as well as better dating and interpretation of the climate signal associated with snow line elevation and vegetation change. Reconstructions of terrestrial climate show strong spatial

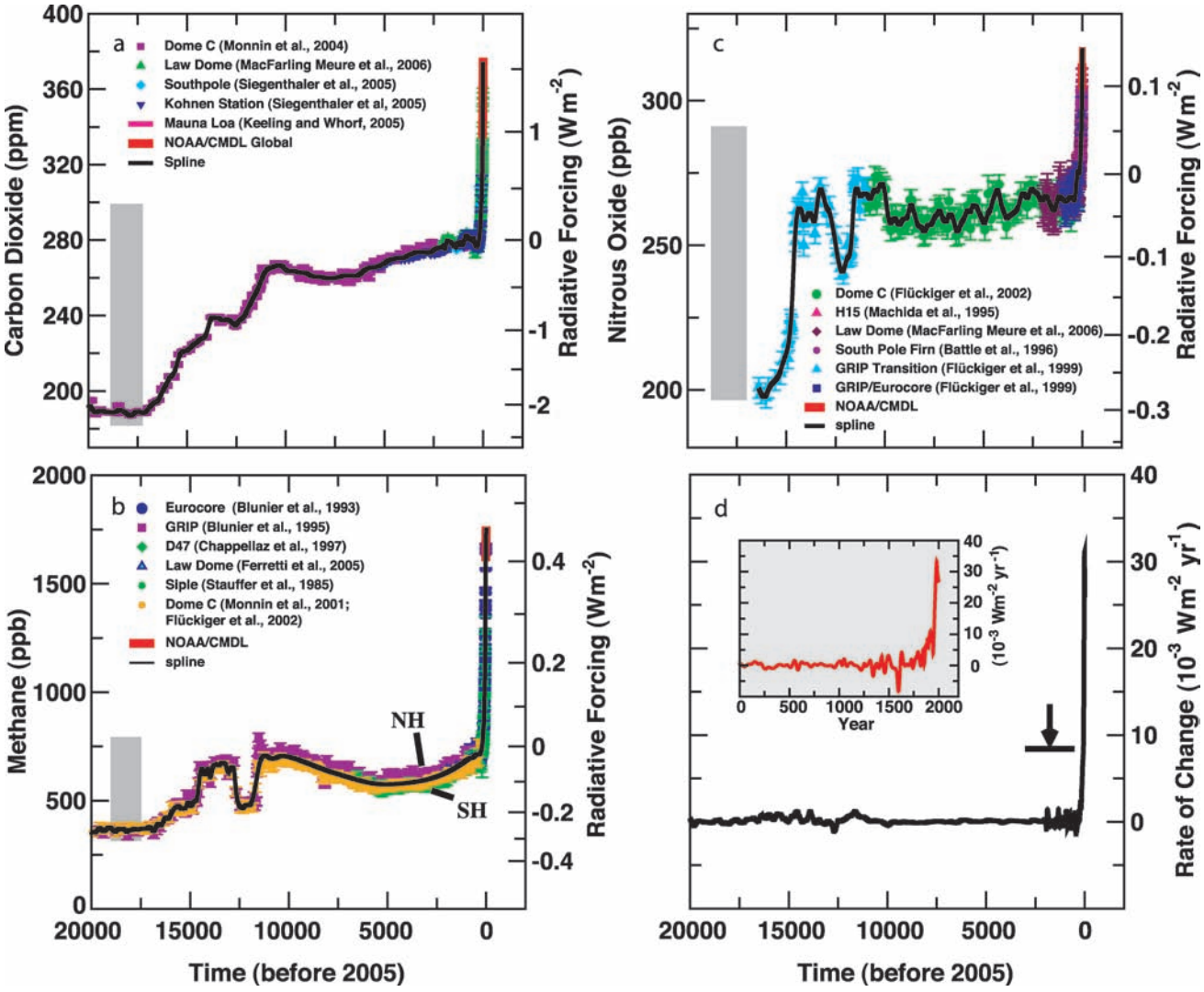


Figure 6.4. *The concentrations and radiative forcing by (a) CO_2, (b) CH_4 and (c) nitrous oxide (N_2O), and (d) the rate of change in their combined radiative forcing over the last 20 kyr reconstructed from antarctic and Greenland ice and firn data (symbols) and direct atmospheric measurements (red and magenta lines). The grey bars show the reconstructed ranges of natural variability for the past 650 kyr (Siegenthaler et al., 2005a; Spahni et al., 2005). Radiative forcing was computed with the simplified expressions of Chapter 2 (Myhre et al., 1998). The rate of change in radiative forcing (black line) was computed from spline fits (Enting, 1987) of the concentration data (black lines in panels a to c). The width of the age distribution of the bubbles in ice varies from about 20 years for sites with a high accumulation of snow such as Law Dome, Antarctica, to about 200 years for low-accumulation sites such as Dome C, Antarctica. The Law Dome ice and firn data, covering the past two millennia, and recent instrumental data have been splined with a cut-off period of 40 years, with the resulting rate of change in radiative forcing shown by the inset in (d). The arrow shows the peak in the rate of change in radiative forcing after the anthropogenic signals of CO_2, CH_4 and N_2O have been smoothed with a model describing the enclosure process of air in ice (Spahni et al., 2003) applied for conditions at the low accumulation Dome C site for the last glacial transition. The CO_2 data are from Etheridge et al. (1996); Monnin et al. (2001); Monnin et al. (2004); Siegenthaler et al. (2005b; South Pole); Siegenthaler et al. (2005a; Kohnen Station); and MacFarling Meure et al. (2006). The CH_4 data are from Stauffer et al. (1985); Steele et al. (1992); Blunier et al. (1993); Dlugokencky et al. (1994); Blunier et al. (1995); Chappellaz et al. (1997); Monnin et al. (2001); Flückiger et al. (2002); and Ferretti et al. (2005). The N_2O data are from Machida et al. (1995); Battle et al. (1996); Flückiger et al. (1999, 2002); and MacFarling Meure et al. (2006). Atmospheric data are from the National Oceanic and Atmospheric Administration's global air sampling network, representing global average concentrations (dry air mole fraction; Steele et al., 1992; Dlugokencky et al., 1994; Tans and Conway, 2005), and from Mauna Loa, Hawaii (Keeling and Whorf, 2005). The globally averaged data are available from http://www.cmdl.noaa.gov/.*

Frequently Asked Question 6.1

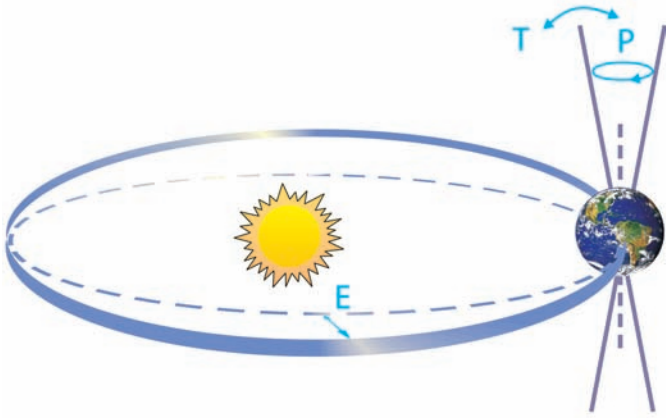
What Caused the Ice Ages and Other Important Climate Changes Before the Industrial Era?

Climate on Earth has changed on all time scales, including long before human activity could have played a role. Great progress has been made in understanding the causes and mechanisms of these climate changes. Changes in Earth's radiation balance were the principal driver of past climate changes, but the causes of such changes are varied. For each case – be it the Ice Ages, the warmth at the time of the dinosaurs or the fluctuations of the past millennium – the specific causes must be established individually. In many cases, this can now be done with good confidence, and many past climate changes can be reproduced with quantitative models.

Global climate is determined by the radiation balance of the planet (see FAQ 1.1). There are three fundamental ways the Earth's radiation balance can change, thereby causing a climate change: (1) changing the incoming solar radiation (e.g., by changes in the Earth's orbit or in the Sun itself), (2) changing the fraction of solar radiation that is reflected (this fraction is called the albedo – it can be changed, for example, by changes in cloud cover, small particles called aerosols or land cover), and (3) altering the long-wave energy radiated back to space (e.g., by changes in greenhouse gas concentrations). In addition, local climate also depends on how heat is distributed by winds and ocean currents. All of these factors have played a role in past climate changes.

Starting with the ice ages that have come and gone in regular cycles for the past nearly three million years, there is strong evidence that these are linked to regular variations in the Earth's orbit around the Sun, the so-called Milankovitch cycles (Figure 1). These cycles change the amount of solar radiation received at each latitude in each season (but hardly affect the global annual mean), and they can be calculated with astronomical precision. There is still some discussion about how exactly this starts and ends ice ages, but many studies suggest that the amount of summer sunshine on northern continents is crucial: if it drops below a critical value, snow from the past winter does not melt away in summer and an ice sheet starts to grow as more and more snow accumulates. Climate model simulations confirm that an Ice Age can indeed be started in this way, while simple conceptual models have been used to successfully 'hindcast' the onset of past glaciations based on the orbital changes. The next large reduction in northern summer insolation, similar to those that started past Ice Ages, is due to begin in 30,000 years.

Although it is not their primary cause, atmospheric carbon dioxide (CO_2) also plays an important role in the ice ages. Antarctic ice core data show that CO_2 concentration is low in the cold glacial times (~190 ppm), and high in the warm interglacials (~280 ppm); atmospheric CO_2 follows temperature changes in Antarctica with a lag of some hundreds of years. Because the climate changes at the beginning and end of ice ages take several thousand years,



FAQ 6.1, Figure 1. *Schematic of the Earth's orbital changes (Milankovitch cycles) that drive the ice age cycles. 'T' denotes changes in the tilt (or obliquity) of the Earth's axis, 'E' denotes changes in the eccentricity of the orbit (due to variations in the minor axis of the ellipse), and 'P' denotes precession, that is, changes in the direction of the axis tilt at a given point of the orbit. Source: Rahmstorf and Schellnhuber (2006).*

most of these changes are affected by a positive CO_2 feedback; that is, a small initial cooling due to the Milankovitch cycles is subsequently amplified as the CO_2 concentration falls. Model simulations of ice age climate (see discussion in Section 6.4.1) yield realistic results only if the role of CO_2 is accounted for.

During the last ice age, over 20 abrupt and dramatic climate shifts occurred that are particularly prominent in records around the northern Atlantic (see Section 6.4). These differ from the glacial-interglacial cycles in that they probably do not involve large changes in global mean temperature: changes are not synchronous in Greenland and Antarctica, and they are in the opposite direction in the South and North Atlantic. This means that a major change in global radiation balance would not have been needed to cause these shifts; a redistribution of heat within the climate system would have sufficed. There is indeed strong evidence that changes in ocean circulation and heat transport can explain many features of these abrupt events; sediment data and model simulations show that some of these changes could have been triggered by instabilities in the ice sheets surrounding the Atlantic at the time, and the associated freshwater release into the ocean.

Much warmer times have also occurred in climate history – during most of the past 500 million years, Earth was probably completely free of ice sheets (geologists can tell from the marks ice leaves on rock), unlike today, when Greenland and Antarctica are ice-covered. Data on greenhouse gas abundances going back beyond a million years, that is, beyond the reach of antarctic ice cores, are still rather uncertain, but analysis of geological

(continued)

samples suggests that the warm ice-free periods coincide with high atmospheric CO_2 levels. On million-year time scales, CO_2 levels change due to tectonic activity, which affects the rates of CO_2 exchange of ocean and atmosphere with the solid Earth. See Section 6.3 for more about these ancient climates.

Another likely cause of past climatic changes is variations in the energy output of the Sun. Measurements over recent decades show that the solar output varies slightly (by close to 0.1%) in an 11-year cycle. Sunspot observations (going back to the 17th century), as well as data from isotopes generated by cosmic radiation, provide evidence for longer-term changes in solar activity. Data correlation and model simulations indicate that solar variability and volcanic activity are likely to be leading reasons for climate variations during the past millennium, before the start of the industrial era.

These examples illustrate that different climate changes in the past had different causes. The fact that natural factors caused climate changes in the past does not mean that the current climate change is natural. By analogy, the fact that forest fires have long been caused naturally by lightning strikes does not mean that fires cannot also be caused by a careless camper. FAQ 2.1 addresses the question of how human influences compare with natural ones in their contributions to recent climate change.

differentiation, regionally and with elevation. Pollen records with their extensive spatial coverage indicate that tropical lowlands were on average 2°C to 3°C cooler than present, with strong cooling (5°C–6°C) in Central America and northern South America and weak cooling (<2°C) in the western Pacific Rim (Farrera et al., 1999). Tropical highland cooling estimates derived from snow-line and pollen-based inferences show similar spatial variations in cooling although involving substantial uncertainties from dating and mapping, multiple climatic causes of treeline and snow line changes during glacial periods (Porter, 2001; Kageyama et al., 2004), and temporal asynchroneity between different regions of the tropics (Smith et al., 2005). These new studies give a much richer regional picture of tropical land cooling, and stress the need to use more than a few widely scattered proxy records as a measure of low-latitude climate sensitivity (Harrison, 2005).

The Climate: Long-range Investigation, Mapping, and Prediction (CLIMAP) reconstruction of ocean surface temperatures produced in the early 1980s indicated about 3°C cooling in the tropical Atlantic, and little or no cooling in the tropical Pacific. More pronounced tropical cooling for the LGM tropical oceans has since been proposed, including 4°C to 5°C based on coral skeleton records from off Barbados (Guilderson et al., 1994) and up to 6°C in the cold tongue off western South America based on foraminiferal assemblages (Mix et al., 1999). New data syntheses from multiple proxy types using carefully defined chronostratigraphies and new calibration data sets are now available from the Glacial Ocean Mapping (GLAMAP) and Multiproxy Approach for the Reconstruction of the Glacial Ocean surface (MARGO) projects, although with caveats including selective species dissolution, dating precision, non-analogue situations, and environmental preferences of the organisms (Sarnthein et al., 2003b; Kucera et al., 2005; and references therein). These recent reconstructions confirm moderate cooling, generally 0°C to 3.5°C, of tropical SST at the LGM, although with significant regional variation, as well as greater cooling in eastern boundary currents and equatorial upwelling regions. Estimates of cooling show notable differences among the different proxies. Faunal-based proxies argue for an intensification of the eastern equatorial Pacific cold tongue in contrast to Mg/Ca-based SST estimates that suggest a relaxation of SST gradients within the cold tongue (Mix et al., 1999; Koutavas et al., 2002; Rosenthal and Broccoli, 2004). Using a Bayesian approach to combine different proxies, Ballantyne et al. (2005) estimated a LGM cooling of tropical SSTs of 2.7°C ± 0.5°C (1 standard deviation).

These ocean proxy synthesis projects also indicate a colder glacial winter North Atlantic with more extensive sea ice than present, whereas summer sea ice only covered the glacial Arctic Ocean and Fram Strait with the northern North Atlantic and Nordic Seas largely ice free and more meridional ocean surface circulation in the eastern parts of the Nordic Seas (Sarnthein et al., 2003a; Meland et al., 2005; de Vernal et al., 2006). Sea ice around Antarctica at the LGM also responded with a large expansion of winter sea ice and substantial seasonal variation (Gersonde et al., 2005). Over mid- and high-latitude northern continents, strong reductions in temperatures produced southward displacement and major reductions in forest area (Bigelow et al., 2003), expansion of permafrost limits over northwest Europe (Renssen and Vandenberghe, 2003), fragmentation of temperate forests (Prentice et al., 2000; Williams et al., 2000) and predominance of steppe-tundra in Western Europe (Peyron et al., 2005). Temperature reconstructions from polar ice cores indicate strong cooling at high latitudes of about 9°C in Antarctica (Stenni et al., 2001) and about 21°C in Greenland (Dahl-Jensen et al., 1998).

The strength and depth extent of the LGM Atlantic overturning circulation have been examined through the application of a variety of new marine proxy indicators (Rutberg et al., 2000; Duplessy et al., 2002; Marchitto et al., 2002; McManus et al., 2004). These tracers indicate that the boundary between North Atlantic Deep Water (NADW) and Antarctic Bottom Water was much shallower during the LGM, with a reinforced pycnocline between intermediate and particularly

cold and salty deep water (Adkins et al., 2002). Most of the deglaciation occurred over the period about 17 to 10 ka, the same period of maximum deglacial atmospheric CO_2 increase (Figure 6.4). It is thus very likely that the global warming of 4°C to 7°C since the LGM occurred at an average rate about 10 times slower than the warming of the 20th century.

In summary, significant progress has been made in the understanding of regional changes at the LGM with the development of new proxies, many new records, improved understanding of the relationship of the various proxies to climate variables and syntheses of proxy records into reconstructions with stricter dating and common calibrations.

6.4.1.3 How Realistic Are Results from Climate Model Simulations of the Last Glacial Maximum?

Model intercomparisons from the first phase of the Paleoclimate Modelling Intercomparison Project (PMIP-1), using atmospheric models (either with prescribed SST or with simple slab ocean models), were featured in the TAR. There are now six simulations of the LGM from the second phase (PMIP-2) using Atmosphere-Ocean General Circulation Models (AOGCMs) and EMICs, although only a few regional comparisons were completed in time for this assessment. The radiative perturbation for the PMIP-2 LGM simulations available for this assessment, which do not yet include the effects of vegetation or aerosol changes, is –4 to –7 W m^{-2}.

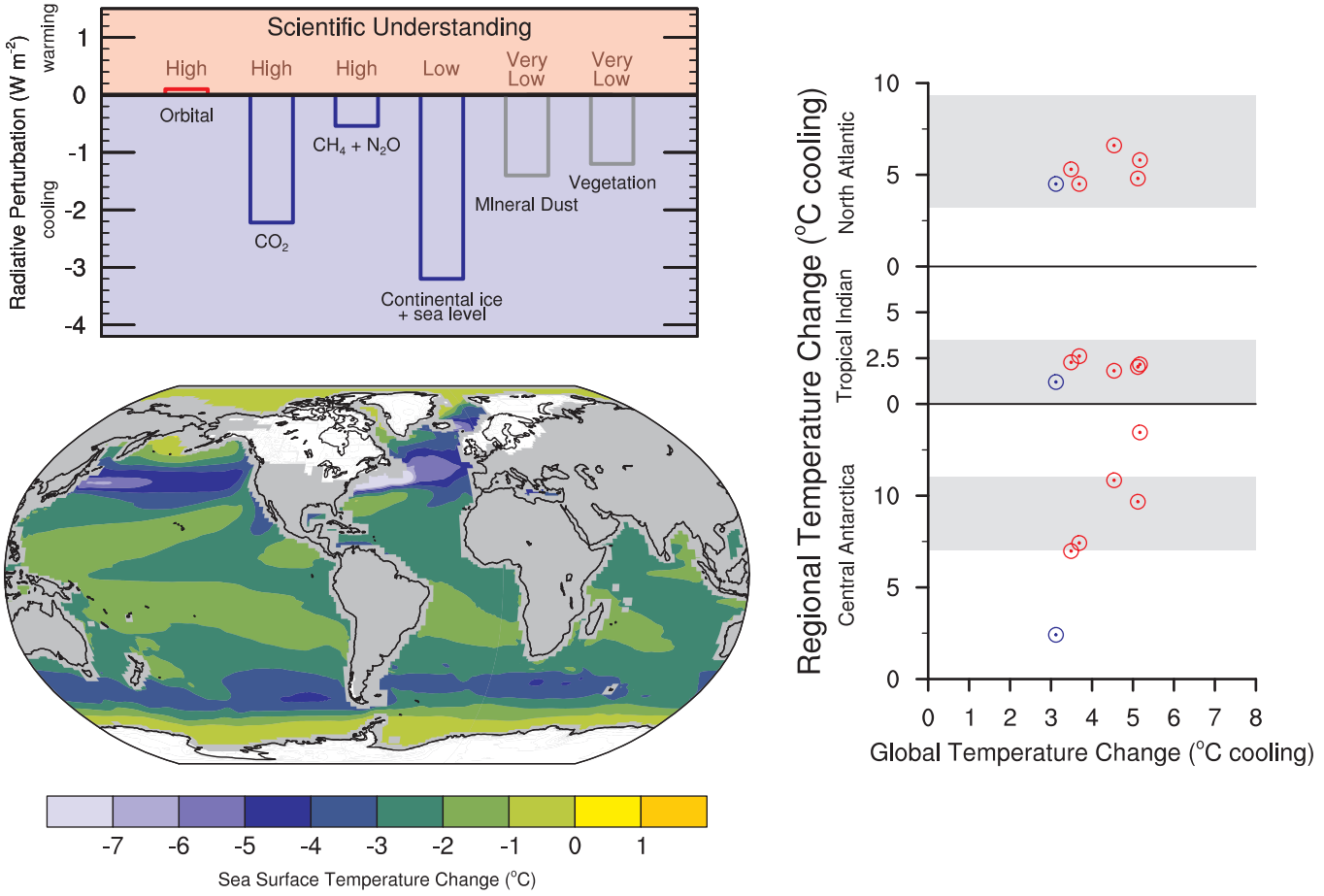


Figure 6.5. *The Last Glacial Maximum climate (approximately 21 ka) relative to the pre-industrial (1750) climate. (Top left) Global annual mean radiative influences (W m^{-2}) of LGM climate change agents, generally feedbacks in glacial-interglacial cycles, but also specified in most Atmosphere-Ocean General Circulation Model (AOGCM) simulations for the LGM. The heights of the rectangular bars denote best estimate values guided by published values of the climate change agents and conversion to radiative perturbations using simplified expressions for the greenhouse gas concentrations and model calculations for the ice sheets, vegetation and mineral dust. References are included in the text. A judgment of each estimate's reliability is given as a level of scientific understanding based on uncertainties in the climate change agents and physical understanding of their radiative effects. Paleoclimate Modelling Intercomparison Project 2 (PMIP-2) simulations shown in bottom left and right panels do not include the radiative influences of LGM changes in mineral dust or vegetation. (Bottom left) Multi-model average SST change for LGM PMIP-2 simulations by five AOGCMs (Community Climate System Model (CCSM), Flexible Global Ocean-Atmosphere-Land System (FGOALS), Hadley Centre Coupled Model (HadCM), Institut Pierre Simon Laplace Climate System Model (IPSL-CM), Model for Interdisciplinary Research on Climate (MIROC)). Ice extent over continents is shown in white. (Right) LGM regional cooling compared to LGM global cooling as simulated in PMIP-2, with AOGCM results shown as red circles and EMIC (ECBilt-CLIO) results shown as blue circles. Regional averages are defined as: Antarctica, annual for inland ice cores; tropical Indian Ocean, annual for 15°S to 15°N, 50°E to 100°E; and North Atlantic Ocean, July to September for 42°N to 57°N, 35°W to 20°E. Grey shading indicates the range of observed proxy estimates of regional cooling: Antarctica (Stenni et al., 2001; Masson-Delmotte et al., 2006), tropical Indian Ocean (Rosell-Mele et al., 2004; Barrows and Juggins, 2005), and North Atlantic Ocean (Rosell-Mele et al., 2004; Kucera et al., 2005; de Vernal et al., 2006; Kageyama et al., 2006).*

These simulations allow an assessment of the response of a subset of the models presented in Chapters 8 and 10 to very different conditions at the LGM.

The PMIP-2 multi-model LGM SST change shows a modest cooling in the tropics, and greatest cooling at mid- to high latitudes in association with increases in sea ice and changes in ocean circulation (Figure 6.5). The PMIP-2 modelled strengthening of the SST meridional gradient in the LGM North Atlantic, as well as cooling and expanded sea ice, agrees with proxy indicators (Kageyama et al., 2006). Polar amplification of global cooling, as recorded in ice cores, is reproduced for Antarctica (Figure 6.5), but the strong LGM cooling over Greenland is underestimated, although with caveats about the heights of these ice caps in the PMIP-2 simulations (Masson-Delmotte et al., 2006).

The PMIP-2 AOGCMs give a range of tropical ocean cooling between 15°S to 15°N of 1.7°C to 2.4°C. Sensitivity simulations with models indicate that this tropical cooling can be explained by the reduced glacial greenhouse gas concentrations, which had direct effects on the tropical radiative forcing (Shin et al., 2003; Otto-Bliesner et al., 2006b) and indirect effects through LGM cooling by positive sea ice-albedo feedback in the Southern Ocean contributing to enhanced ocean ventilation of the tropical thermocline and the intermediate waters (Liu et al., 2002). Regional variations in simulated tropical cooling are much smaller than indicated by MARGO data, partly related to models at current resolutions being unable to simulate the intensity of coastal upwelling and eastern boundary currents. Simulated cooling in the Indian Ocean (Figure 6.5), a region with important present-day teleconnections to Africa and the North Atlantic, compares favourably to proxy estimates from alkenones (Rosell-Mele et al., 2004) and foraminifera assemblages (Barrows and Juggins, 2005).

Considering changes in vegetation appears to improve the realism of simulations of the LGM, and points to important climate-vegetation feedbacks (Wyputta and McAvaney, 2001; Crucifix and Hewitt, 2005). For example, extension of the tundra in Asia during the LGM contributes to the local surface cooling, while the tropics warm where savannah replaces tropical forest (Wyputta and McAvaney, 2001). Feedbacks between climate and vegetation occur locally, with a decrease in the tree fraction in central Africa reducing precipitation, and remotely with cooling in Siberia (tundra replacing trees) altering (diminishing) the Asian summer monsoon. The physiological effect of CO_2 concentration on vegetation needs to be included to properly represent changes in global forest (Harrison and Prentice, 2003), as well as to widen the climatic range where grasses and shrubs dominate. The biome distribution simulated with dynamic global vegetation models reproduces the broad features observed in palaeodata (e.g., Harrison and Prentice, 2003).

In summary, the PMIP-2 LGM simulations confirm that current AOGCMs are able to simulate the broad-scale spatial patterns of regional climate change recorded by palaeodata in response to the radiative forcing and continental ice sheets of the LGM, and thus indicate that they adequately represent the primary feedbacks that determine the climate sensitivity of this past climate state to these changes. The PMIP-2 AOGCM simulations using glacial-interglacial changes in greenhouse gas forcing and ice sheet conditions give a radiative perturbation in reference to pre-industrial conditions of –4.6 to –7.2 W m^{-2} and mean global temperature change of –3.3°C to –5.1°C, similar to the range reported in the TAR for PMIP-1 (IPCC, 2001). The climate sensitivity inferred from the PMIP-2 LGM simulations is 2.3°C to 3.7°C for a doubling of atmospheric CO_2 (see Section 9.6.3.2). When the radiative perturbations of dust content and vegetation changes are estimated, climate models yield an additional cooling of 1°C to 2°C (Crucifix and Hewitt, 2005; Schneider et al., 2006), although scientific understanding of these effects is very low.

6.4.1.4 How Realistic Are Simulations of Terrestrial Carbon Storage at the Last Glacial Maximum?

There is evidence that terrestrial carbon storage was reduced during the LGM compared to today. Mass balance calculations based on ^{13}C measurements on shells of benthic foraminifera yield a reduction in the terrestrial biosphere carbon inventory (soil and living vegetation) of about 300 to 700 GtC (Shackleton, 1977; Bird et al., 1994) compared to the pre-industrial inventory of about 3,000 GtC. Estimates of terrestrial carbon storage based on ecosystem reconstructions suggest an even larger difference (e.g., Crowley, 1995). Simulations with carbon cycle models yield a reduction in global terrestrial carbon stocks of 600 to 1,000 GtC at the LGM compared to pre-industrial time (Francois et al., 1998; Beerling, 1999; Francois et al., 1999; Kaplan et al., 2002; Liu et al., 2002; Kaplan et al., 2003; Joos et al., 2004). The majority of this simulated difference is due to reduced simulated growth resulting from lower atmospheric CO_2. A major regulating role for CO_2 is consistent with the model-data analysis of Bond et al. (2003), who suggested that low atmospheric CO_2 could have been a significant factor in the reduction of trees during glacial times, because of their slower regrowth after disturbances such as fire. In summary, results of terrestrial models, also used to project future CO_2 concentrations, are broadly compatible with the range of reconstructed differences in glacial-interglacial carbon storage on land.

6.4.1.5 How Long Did the Previous Interglacials Last?

The four interglacials of the last 450 kyr preceding the Holocene (Marine Isotope Stages 5, 7, 9 and 11) were all different in multiple aspects, including duration (Figure 6.3). The shortest (Stage 7) lasted a few thousand years, and the longest (Stage 11; ~420 to 395 ka) lasted almost 30 kyr. Evidence for an unusually long Stage 11 has been recently reinforced by new ice core and marine sediment data. The European Programme for Ice Coring in Antarctica (EPICA) Dome C antarctic ice core record suggests that antarctic temperature remained approximately as warm as the Holocene

for 28 kyr (EPICA community members, 2004). A new stack of 57 globally distributed benthic $\delta^{18}O$ records presents age estimates at Stage 11 nearly identical to those provided by the EPICA results (Lisiecki and Raymo, 2005).

It has been suggested that Stage 11 was an extraordinarily long interglacial period because of its low orbital eccentricity, which reduces the effect of climatic precession on insolation (Box 6.1) (Berger and Loutre, 2003). In addition, the EPICA Dome C and the recently revisited Vostok records show CO_2 concentrations similar to pre-industrial Holocene values throughout Stage 11 (Raynaud et al., 2005). Thus, both the orbital forcing and the CO_2 feedback were providing favourable conditions for an unusually long interglacial. Moreover, the length of Stage 11 has been simulated by conceptual models of the Quaternary climate, based on threshold mechanisms (Paillard, 1998). For Stage 11, these conceptual models show that the deglaciation was triggered by the insolation maximum at about 427 ka, but that the next insolation minimum was not sufficiently low to start another glaciation. The interglacial thus lasts an additional precessional cycle, yielding a total duration of 28 kyr.

6.4.1.6 How Much Did the Earth Warm During the Previous Interglacial?

Globally, there was less glacial ice on Earth during the Last Interglacial, also referred to as "Last Interglaciation" (LIG, 130 ± 1 to 116 ± 1 ka; Stirling et al., 1998) than now. This suggests significant reduction in the size of the Greenland and possibly Antarctic Ice Sheets (see Section 6.4.3). The climate of the LIG has been inferred to be warmer than present (Kukla et al., 2002), although the evidence is regional and not necessarily synchronous globally, consistent with understanding of the primary forcing. For the first half of this interglacial (~130–123 ka), orbital forcing (Box 6.1) produced a large increase in NH summer insolation. Proxy data indicate warmer-than-present coastal waters in parts of the Pacific, Atlantic, and Indian Oceans as well as in the Mediterranean Sea, greatly reduced sea ice in the coastal waters around Alaska, extension of boreal forest into areas now occupied by tundra in interior Alaska and Siberia and a generally warmer Arctic (Brigham-Grette and Hopkins, 1995; Lozhkin and Anderson, 1995; Muhs et al., 2001, CAPE Last Interglacial Project Members, 2006). Ice core data indicate a large response over Greenland and Antarctica with early LIG temperatures 3°C to 5°C warmer than present (Watanabe et al., 2003; NGRIP, 2004; Landais et al., 2006). Palaeofauna evidence from New Zealand indicates LIG warmth during the late LIG consistent with the latitudinal dependence of orbital forcing (Marra, 2003).

There are AOGCM simulations available for the LIG, but no standardised intercomparison simulations have been performed. When forced with orbital forcing of 130 to 125 ka (Box 6.1), with over 10% more summer insolation in the NH than today, AOGCMs produce a summer arctic warming of up to 5°C, with greatest warming over Eurasia and in the Baffin Island/northern Greenland region (Figure 6.6) (Montoya et al., 2000; Kaspar et al., 2005; Otto-Bliesner et al., 2006a). Simulations generally match proxy reconstructions of the maximum arctic summer warmth (Kaspar and Cubasch, 2006; CAPE Last Interglacial Project Members, 2006) although may still underestimate warmth in Siberia because vegetation feedbacks are not included in current simulations. Simulated LIG annual average global temperature is not notably higher than present, consistent with the orbital forcing.

6.4.1.7 What Is Known About the Mechanisms of Transitions Into Ice Ages?

Successful simulation of glacial inception has been a key target for models simulating climate change. The Milankovitch theory proposes that ice ages were triggered by reduced summer insolation at high latitudes in the NH, enabling winter snowfall to persist all year and accumulate to build NH glacial ice sheets (Box 6.1). Continental ice sheet growth and associated sea level lowering took place at about 116 ka (Waelbroeck et al., 2002) when the summer incoming solar radiation in the NH at high latitudes reached minimum values. The inception took place while the continental ice volume was minimal and stable, and low and mid-latitudes of the North Atlantic continuously warm (Cortijo et al., 1999; Goni et al., 1999; McManus et al., 2002; Risebrobakken et al., 2005). When forced with orbital insolation changes, atmosphere-only models failed in the past to find the proper magnitude of response to allow for perennial snow cover. Models and data now show that shifts in the northern treeline, expansion of sea ice at high latitudes and warmer low-latitude oceans as a source of moisture for the ice sheets provide feedbacks that amplify the local insolation forcing over the high-latitude continents and allow for growth of ice sheets (Pons et al., 1992; Cortijo et al., 1999; Goni et al., 1999; Crucifix and Loutre, 2002; McManus et al., 2002; Jackson and Broccoli, 2003; Khodri et al., 2003; Meissner et al., 2003; Vettoretti and Peltier, 2003; Khodri et al., 2005; Risebrobakken et al., 2005). The rapid growth of ice sheets after inception is captured by EMICs that include models for continental ice, with increased Atlantic Meridional Overturning Circulation (MOC) allowing for increased snowfall. Increasing ice sheet altitude and extent is also important, although the ice volume-equivalent drop in sea level found in data records (Waelbroeck et al., 2002; Cutler et al., 2003) is not well reproduced in some EMIC simulations (Wang and Mysak, 2002; Kageyama et al., 2004; Calov et al., 2005).

6.4.1.8 When Will the Current Interglacial End?

There is no evidence of mechanisms that could mitigate the current global warming by a natural cooling trend. Only a strong reduction in summer insolation at high northern latitudes, along with associated feedbacks, can end the current interglacial. Given that current low orbital eccentricity will persist over the next tens of thousand years, the effects of

precession are minimised, and extremely cold northern summer orbital configurations like that of the last glacial initiation at 116 ka will not take place for at least 30 kyr (Box 6.1). Under a natural CO_2 regime (i.e., with the global temperature-CO_2 correlation continuing as in the Vostok and EPICA Dome C ice cores), the next glacial period would not be expected to start within the next 30 kyr (Loutre and Berger, 2000; Berger and Loutre, 2002; EPICA Community Members, 2004). Sustained high atmospheric greenhouse gas concentrations, comparable to a mid-range CO_2 stabilisation scenario, may lead to a complete melting of the Greenland Ice Sheet (Church et al., 2001) and further delay the onset of the next glacial period (Loutre and Berger, 2000; Archer and Ganopolski, 2005).

6.4.2 Abrupt Climatic Changes in the Glacial-Interglacial Record

6.4.2.1 What Is the Evidence for Past Abrupt Climate Changes?

Abrupt climate changes have been variously defined either simply as large changes within less than 30 years (Clark et al., 2002), or in a physical sense, as a threshold transition or a response that is rapid compared to forcing (Rahmstorf, 2001; Alley et al., 2003). Overpeck and Trenberth (2004) noted that not all abrupt changes need to be externally forced. Numerous terrestrial, ice and oceanic climatic records show that large, widespread, abrupt climate changes have occurred repeatedly throughout the past glacial interval (see review by Rahmstorf,

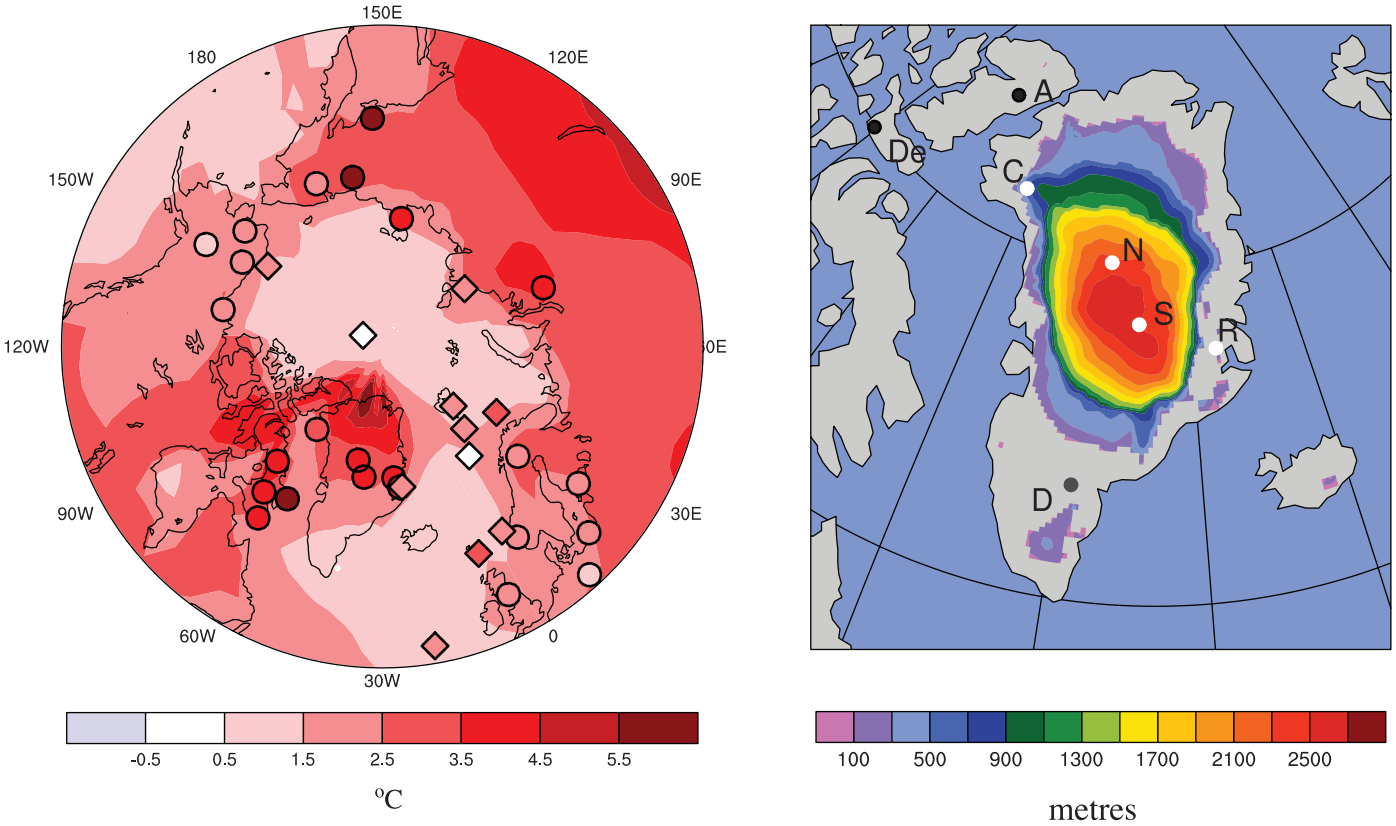


Figure 6.6. *Summer surface air temperature change over the Arctic (left) and annual minimum ice thickness and extent for Greenland and western arctic glaciers (right) for the LIG from a multi-model and a multi-proxy synthesis. The multi-model summer warming simulated by the National Center for Atmospheric Research (NCAR) Community Climate System Model (CCSM), 130 ka minus present (Otto-Bliesner et al., 2006b), and the ECHAM4 HOPE-G (ECHO-G) model, 125 ka minus pre-industrial (Kaspar et al., 2005), is contoured in the left panel and is overlain by proxy estimates of maximum summer warming from terrestrial (circles) and marine (diamonds) sites as compiled in the syntheses published by the CAPE Project Members (2006) and Kaspar et al. (2005). Extents and thicknesses of the Greenland Ice Sheet and eastern Canadian and Iceland glaciers are shown at their minimum extent for the LIG as a multi-model average from three ice models (Tarasov and Peltier, 2003; Lhomme et al., 2005a; Otto-Bliesner et al., 2006a). Ice core observations (Koerner, 1989; NGRIP, 2004) indicate LIG ice (white dots) at Renland (R), North Greenland Ice Core Project (N), Summit (S, Greenland Ice Core Project and Greenland Ice Sheet Project 2) and possibly Camp Century (C), but no LIG ice (black dots) at Devon (De) and Agassiz (A) in the eastern Canadian Arctic. Evidence for LIG ice at Dye-3 (D) in southern Greenland is equivocal (grey dot; see text for detail).*

2002). High-latitude records show that ice age abrupt temperature events were larger and more widespread than were those of the Holocene. The most dramatic of these abrupt climate changes were the Dansgaard-Oeschger (D-O) events, characterised by a warming in Greenland of 8°C to 16°C within a few decades (see Severinghaus and Brook, 1999; Masson-Delmotte et al., 2005a for a review) followed by much slower cooling over centuries. Another type of abrupt change were the Heinrich events; characterised by large discharges of icebergs into the northern Atlantic leaving diagnostic drop-stones in the ocean sediments (Hemming, 2004). In the North Atlantic, Heinrich events were accompanied by a strong reduction in sea surface salinity (Bond et al., 1993), as well as a sea surface cooling on a centennial time scale. Such ice age cold periods lasted hundreds to thousands of years, and the warming that ended them took place within decades (Figure 6.7; Cortijo et al., 1997; Voelker, 2002). At the end of the last glacial, as the climate warmed and ice sheets melted, climate went through a number of abrupt cold phases, notably the Younger Dryas and the 8.2 ka event.

The effects of these abrupt climate changes were global, although out-of-phase responses in the two hemispheres (Blunier et al., 1998; Landais et al., 2006) suggest that they were not primarily changes in global mean temperature. The highest amplitude of the changes, in terms of temperature, appears centred around the North Atlantic. Strong and fast changes are found in the global CH_4 concentration (of the order of 100 to 150 ppb within decades), which may point to changes in the extent or productivity of tropical wetlands (see Chappellaz et al., 1993; Brook et al., 2000 for a review; Masson-Delmotte et al., 2005a), and in the Asian monsoon (Wang et al., 2001). The NH cold phases were linked with a reduced northward flow of warm waters in the Nordic Seas (Figure 6.7), southward shift of the Inter-Tropical Convergence Zone (ITCZ) and thus the location of the tropical rainfall belts (Peterson et al., 2000; Lea et al., 2003). Cold, dry and windy conditions with low CH_4 and high dust aerosol concentrations generally occurred together in the NH cold events. The accompanying changes in atmospheric CO_2 content were relatively small (less than 25 ppm; Figure 6.7) and parallel to the antarctic counterparts of Greenland D-O events. The record in N_2O is less complete and shows an increase of about 50 ppb and a decrease of about 30 ppb during warm and cold periods, respectively (Flückiger et al., 2004).

A southward shift of the boreal treeline and other rapid vegetation responses were associated with past cold events (Peteet, 1995; Shuman et al., 2002; Williams et al., 2002). Decadal-scale changes in vegetation have been recorded in annually laminated sequences at the beginning and the end of the Younger Dryas and the 8.2 ka event (Birks and Ammann, 2000; Tinner and Lotter, 2001; Veski et al., 2004). Marine pollen records with a typical sampling resolution of 200 years provide unequivocal evidence of the immediate response of vegetation in Southern Europe to the climate fluctuations during glacial times (Sánchez Goñi et al., 2002; Tzedakis, 2005). The same holds true for the vegetation response in northern South America during the last deglaciation (Hughen et al., 2004).

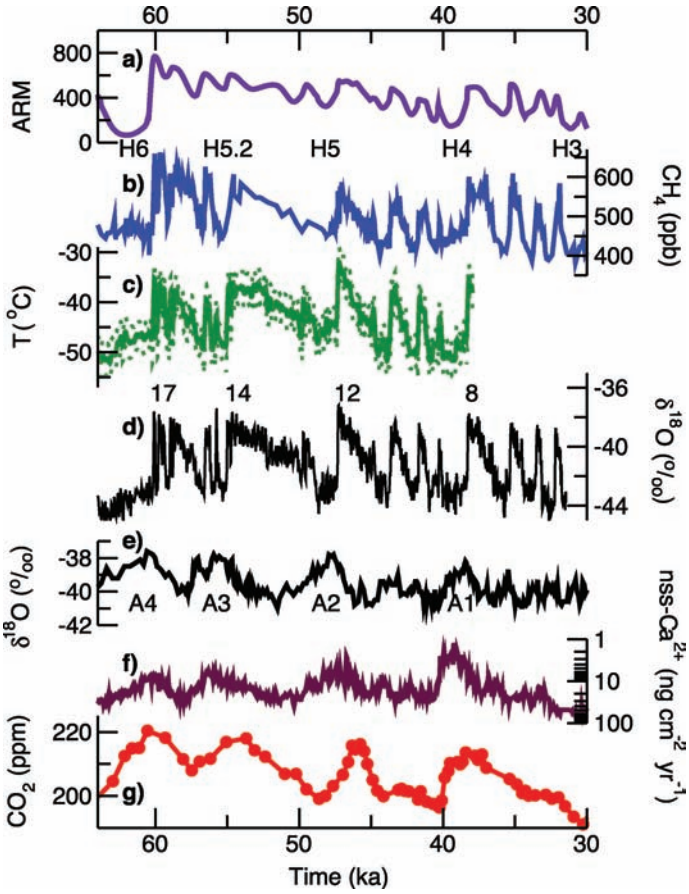


Figure 6.7. *The evolution of climate indicators from the NH (panels a to d), and from Antarctica (panels e to g), over the period 64 to 30 ka. (a) Anhysteretic remanent magnetisation (ARM), here a proxy of the northward extent of Atlantic MOC, from an ocean sediment core from the Nordic Seas (Dokken and Jansen, 1999); (b) CH_4 as recorded in Greenland ice cores at the Greenland Ice Core Project (GRIP), Greenland Ice Sheet Project (GISP) and North GRIP (NGRIP) sites (Blunier and Brook, 2001; Flückiger et al., 2004; Huber et al., 2006); CH_4 data for the period 40 to 30 ka were selected for the GRIP site and for 64 to 40 ka for the GISP site when sample resolution is highest in the cores; (c) surface temperature estimated from nitrogen isotope ratios that are influenced by thermal diffusion (Huber et al., 2006); (d) $\delta^{18}O$, a proxy for surface temperature, from NGRIP (2004) with the D-O NH warm events 8, 12, 14 and 17 indicated; (e) $\delta^{18}O$ from Byrd, Antarctica (Blunier and Brook, 2001) with A1 to A4 denoting antarctic warm events; (f) nss-Ca^{2+}, a proxy of dust and iron deposition, from Dome C, Antarctica (Röthlisberger et al., 2004); and (g) CO_2 as recorded in ice from Taylor Dome, Antarctica (Indermühle et al., 2000). The Heinrich events (periods of massive ice-rafted debris recorded in marine sediments) H3, H4, H5, H5.2, and H6, are shown. All data are plotted on the Greenland SS09sea time scale (Johnsen et al., 2001). CO_2 and CH_4 are well mixed in the atmosphere. CH_4 variations are synchronous within the resolution of ±50 years with variations in Greenland temperature, but a detailed analysis suggests that CH_4 rises lag temperature increases at the onset of the D-O events by 25 to 70 years (Huber et al., 2006). CO_2 co-varied with the antarctic temperature, but the exact synchronisation between Taylor Dome and Byrd is uncertain, thus making the determination of leads or lags between temperature and CO_2 elusive. The evolution of Greenland and antarctic temperature is consistent with a reorganisation of the heat transport and the MOC in the Atlantic (Knutti et al., 2004).*

6.4.2.2 What Is Known About the Mechanism of these Abrupt Changes?

There is good evidence now from sediment data for a link between these glacial-age abrupt changes in surface climate and ocean circulation changes (Clark et al., 2002). Proxy data show that the South Atlantic cooled when the north warmed (with a possible lag), and vice versa (Voelker, 2002), a seesaw of NH and SH temperatures that indicates an ocean heat transport change (Crowley, 1992; Stocker and Johnsen 2003). During D-O warming, salinity in the Irminger Sea increased strongly (Elliot et al., 1998; van Kreveld et al., 2000) and northward flow of temperate waters increased in the Nordic Seas (Dokken and Jansen, 1999), indicative of saline Atlantic waters advancing northward. Abrupt changes in deep water properties of the Atlantic have been documented from proxy data (e.g., ^{13}C, $^{231}Pa/^{230}Th$), which reconstruct the ventilation of the deep water masses and changes in the overturning rate and flow speed of the deep waters (Vidal et al., 1998; Dokken and Jansen, 1999; McManus et al., 2004; Gherardi et al., 2005). Despite this evidence, many features of the abrupt changes are still not well constrained due to a lack of precise temporal control of the sequencing and phasing of events between the surface, the deep ocean and ice sheets.

Heinrich events are thought to have been caused by ice sheet instability (MacAyeal, 1993). Iceberg discharge would have provided a large freshwater forcing to the Atlantic, which can be estimated from changes in the abundance of the isotope ^{18}O. These yield a volume of freshwater addition typically corresponding to a few (up to 15) metres of global sea level rise occurring over several centuries (250–750 years), that is, a flux of the order of 0.1 Sv (Hemming, 2004). For Heinrich event 4, Roche et al. (2004) have constrained the freshwater amount to 2 ±1 m of sea level equivalent provided by the Laurentide Ice Sheet, and the duration of the event to 250 ±150 years. Volume and timing of freshwater release is still controversial, however.

Freshwater influx is the likely cause for the cold events at the end of the last ice age (i.e., the Younger Dryas and the 8.2 ka event). Rather than sliding ice, it is the inflow of melt water from melting ice due to the climatic warming at this time that could have interfered with the MOC and heat transport in the Atlantic – a discharge into the Arctic Ocean of the order 0.1 Sv may have triggered the Younger Dryas (Tarasov and Peltier, 2005), while the 8.2 ka event was probably linked to one or more floods equal to 11 to 42 cm of sea level rise within a few years (Clarke et al., 2004; see Section 6.5.2). This is an important difference relative to the D-O events, for which no large forcing of the ocean is known; model simulations suggest that a small forcing may be sufficient if the ocean circulation is close to a threshold (Ganopolski and Rahmstorf, 2001). The exact cause and nature of these ocean circulation changes, however, are not universally agreed. Some authors have argued that some of the abrupt climate shifts discussed could have been triggered from the tropics (e.g., Clement and Cane, 1999), but a more specific and quantitative explanation for D-O events building on this idea is yet to emerge.

Atmospheric CO_2 changes during the glacial antarctic warm events, linked to changes in NADW (Knutti et al., 2004), were small (less than 25 ppm; Figure 6.7). A relatively small positive feedback between atmospheric CO_2 and changes in the rate of NADW formation is found in palaeoclimate and global warming simulations (Joos et al., 1999; Marchal et al., 1999). Thus, palaeodata and available model simulations agree that possible future changes in the NADW formation rate would have only modest effects on atmospheric CO_2. This finding does not, however, preclude the possibility that circulation changes in other ocean regions, in particular in the Southern Ocean, could have a larger impact on atmospheric CO_2 (Greenblatt and Sarmiento, 2004).

6.4.2.3 Can Climate Models Simulate these Abrupt Changes?

Modelling the ice sheet instabilities that are the likely cause of Heinrich events is a difficult problem because the physics are not sufficiently understood, although recent results show some promise (Calov et al., 2002). Many model studies have been performed in which an influx of freshwater from an ice sheet instability (Heinrich event) or a melt water release (8.2 ka event; see Section 6.5.2) has been assumed and prescribed, and its effects on ocean circulation and climate have been simulated. These experiments suggest that freshwater input of the order of magnitude deduced from palaeoclimatic data could indeed have caused the Atlantic MOC to shut down, and that this is a physically viable explanation for many of the climatic repercussions found in the data (e.g., the high-latitude northern cooling, the shift in the ITCZ and the hemispheric seesaw; Vellinga and Wood, 2002; Dahl et al., 2005; Zhang and Delworth, 2005). The phase relation between temperature in Greenland and Antarctic has been explained by a reduction in the NADW formation rate and oceanic heat transport into the North Atlantic region, producing cooling in the North Atlantic and a lagged warming in the SH (Ganopolski and Rahmstorf, 2001; Stocker and Johnsen, 2003). In freshwater simulations where the North Atlantic MOC is forced to collapse, the consequences also include an increase in nutrient-rich water in the deep Atlantic Ocean, higher $^{231}Pa/^{230}Th$ ratios in North Atlantic sediments (Marchal et al., 2000), a retreat of the northern treeline (Scholze et al., 2003; Higgins, 2004; Köhler et al., 2005), a small (10 ppm) temporary increase in atmospheric CO_2 in response to a reorganisation of the marine carbon cycle (Marchal et al., 1999) and CO_2 changes of a few parts per million due to carbon stock changes in the land biosphere (Köhler et al., 2005). A 10 ppb reduction in atmospheric N_2O is found in one ocean-atmosphere model (Goldstein et al., 2003), suggesting that part of the measured N_2O variation (up to 50 ppb) is of terrestrial origin. In summary, model simulations broadly reproduce the observed variations during abrupt events of this type.

Dansgaard-Oeschger events appear to be associated with latitudinal shifts in oceanic convection between the Nordic Seas and the open mid-latitude Atlantic (Alley and Clark, 1999). Models suggest that the temperature evolution in Greenland, the

seesaw response in the South Atlantic, the observed Irminger Sea salinity changes and other observed features of the events may be explained by such a mechanism (Ganopolski and Rahmstorf, 2001), although the trigger for the ocean circulation changes remains undetermined. Alley et al. (2001) showed evidence for a stochastic resonance process at work in the timing of these events, which means that a regular cycle together with random 'noise' could have triggered them. This can be reproduced in models (e.g., the above), as long as a threshold mechanism is involved in causing the events.

Some authors have argued that climate models tend to underestimate the size and extent of past abrupt climate changes (Alley et al., 2003), and hence may underestimate the risk of future ones. However, such a general conclusion is probably too simple, and a case-by-case evaluation is required to understand which effects may be misinterpreted in the palaeoclimatic record and which mechanisms may be underestimated in current models. This issue is important for an assessment of risks for the future: the expected rapid warming in the coming centuries could approach the amount of warming at the end of the last glacial, and would occur at a much faster rate. Hence, melt water input from ice sheets could again become an important factor influencing the ocean circulation, as for the Younger Dryas and 8.2 ka events. A melting of the Greenland Ice Sheet (equivalent to 7 m of global sea level) over 1 kyr would contribute an average freshwater flux of 0.1 Sv; this is a comparable magnitude to the estimated freshwater fluxes associated with past abrupt climate events. Most climate models used for future scenarios have thus far not included melt water runoff from melting ice sheets. Intercomparison experiments subjecting different models to freshwater influx have revealed that while responses are qualitatively similar, the amount of freshwater needed for a shutdown of the Atlantic circulation can differ greatly between models; the reasons for this model dependency are not yet fully understood (Rahmstorf et al., 2005; Stouffer et al., 2006). Given present knowledge, future abrupt climate changes due to ocean circulation changes cannot be ruled out.

6.4.3 Sea Level Variations Over the Last Glacial-Interglacial Cycle

6.4.3.1 What Is the Influence of Past Ice Volume Change on Modern Sea Level Change?

Palaeorecords of sea level history provide a crucial basis for understanding the background variations upon which the sea level rise related to modern processes is superimposed. Even if no anthropogenic effect were currently operating in the climate system, measurable and significant changes in relative sea level (RSL) would still be occurring. The primary cause of this natural variability in sea level has to do with the planet's memory of the last deglaciation event. Through the so-called glacial isostatic adjustment (GIA) process, gravitational equilibrium is restored following deglaciation, not only by crustal 'rebound', but also through the horizontal redistribution of water in the ocean basins required to maintain the ocean surface at gravitational equipotential.

Models of the global GIA process have enabled isolation of a contribution to the modern rate of global sea level rise being measured by the TOPography EXperiment (TOPEX)/Poseidon (T/P) satellite of –0.28 mm yr^{-1} for the ICE-4G(VM2) model of Peltier (1996) and –0.36 mm yr^{-1} for the ICE-5G(VM2) model of Peltier (2004). These analyses (Peltier, 2001) imply that the impact of modern climate change on the global rate of sea level rise is larger than implied by the uncorrected T/P measurements (see also Chapter 5).

By employing the same theory to predict the impact upon Earth's rotational state due to both the Late Pleistocene glacial cycle and the influence of present-day melting of the great polar ice sheets on Greenland and Antarctica, it has also proven possible to estimate the extent to which these ice sheets may have been losing mass over the past century. In Peltier (1998), such analysis led to an upper-bound estimate of approximately 0.5 mm yr^{-1} for the rate of global sea level rise equivalent to the mass loss. This suggests the plausibility of the notion that polar ice sheet and glacier melting may provide the required closure of the global sea level rise budget (see Chapters 4 and 5).

6.4.3.2 What Was the Magnitude of Glacial-Interglacial Sea Level Change?

Model-based palaeo-sea level analysis also helps to refine estimates of the eustatic (globally averaged) sea level rise that occurred during the most recent glacial-interglacial transition from the LGM to the Holocene. The extended coral-based RSL curve from the island of Barbados in the Caribbean Sea (Fairbanks, 1989; Peltier and Fairbanks, 2006) is especially important, as the RSL history from this site has been shown to provide a good approximation to the ice-equivalent eustatic curve itself (Peltier, 2002). The fit of the prediction of the ICE-5G(VM2) model to the Fairbanks data set, as shown in Figure 6.8b, constrains the net ice-equivalent eustatic rise subsequent to 21 ka to a value of 118.7 m, very close to the value of approximately 120 m conventionally inferred (e.g., Shackleton, 2000) on the basis of deep-sea O isotopic information (Figure 6.8b). Waelbroeck et al. (2002) produced a sea level reconstruction based upon coral records and deep-sea O isotopes corrected for the influence of abyssal ocean temperature changes for the entire glacial-interglacial cycle. This record (Figure 6.8a) is characterised by a best estimate of the LGM depression of ice-equivalent eustatic sea level that is also near 120 m. The analysis of the Red Sea O isotopic record by Siddal et al. (2003) further supports the validity of the interpretation of the extended Barbados record by Peltier and Fairbanks (2006).

The ice-equivalent eustatic sea level curve of Lambeck and Chappell (2001), based upon data from a variety of different

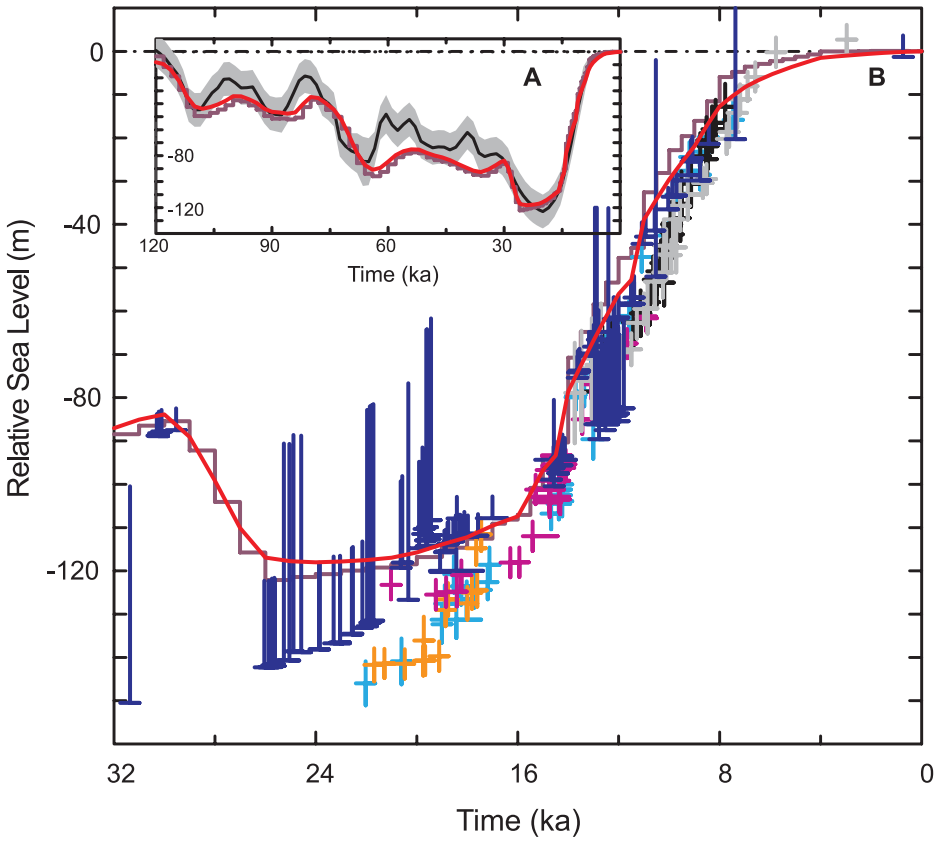


Figure 6.8. *(A) The ice-equivalent eustatic sea level history over the last glacial-interglacial cycle according to the analysis of Waelbroeck et al. (2002). The smooth black line defines the mid-point of their estimates for each age and the surrounding hatched region provides an estimate of error. The red line is the prediction of the ICE-5G(VM2) model for the Barbados location for which the RSL observations themselves provide an excellent approximation to the ice-equivalent eustatic sea level curve. (B) The fit of the ICE-5G(VM2) model prediction (red line) to the extended coral-based record of RSL history from the island of Barbados in the Caribbean Sea (Fairbanks, 1989; Peltier and Fairbanks, 2006) over the age range from 32 ka to present. The actual ice-equivalent eustatic sea level curve for this model is shown as the step-discontinuous brown line. The individual coral-based estimates of RSL (blue) have an attached error bar that depends upon the coral species. The estimates denoted by the short error bars are derived from the* Acropora palmata *species, which provide the tightest constraints upon relative sea level as this species is found to live within approximately 5 m of sea level in the modern ecology. The estimates denoted by the longer error bars are derived either from the* Montastrea annularis *species of coral (error bars of intermediate 20 m length) or from further species that are found over a wide range of depths with respect to sea level (longest error bars). These additional data are most useful in providing a lower bound for the sea level depression. The data denoted by the coloured crosses are from the ice-equivalent eustatic sea level reconstruction of Lambeck and Chappell (2001) for Barbados (cyan), Tahiti (grey), Huon (black), Bonaparte Gulf (orange) and Sunda Shelf (magenta).*

sources, including the Barbados coral record, measurements from the Sunda Shelf of Indonesia (Hanebuth et al., 2000) and observations from the Bonaparte Gulf of northern Australia (Yokoyama et al., 2000), is also shown in Figure 6.8b. This suggests an ice-equivalent eustatic sea level history that conflicts with that based upon the extended Barbados record. First, the depth of the low stand of the sea at the LGM is approximately 140 m below present sea level rather than the value of approximately 120 m required by the Barbados data set. Second, the Barbados data appear to rule out the possibility of the sharp rise of sea level at 19 ka suggested by Yokoyama et al. (2000). That the predicted RSL history at Barbados using the ICE-5G(VM2) model is essentially identical to the ice-equivalent eustatic curve for the same model is shown explicitly in Figure 6.8, where the red curve is the model prediction and the step-discontinuous purple curve is the ice-equivalent eustatic curve.

6.4.3.3 What Is the Significance of Higher than Present Sea Levels During the Last Interglacial Period?

The record of eustatic sea level change can be extended into the time of the LIG. Direct sea level measurements based upon coastal sedimentary deposits and tropical coral sequences (e.g., in tectonically stable settings) have clearly established that eustatic sea level was higher than present during this last interglacial by approximately 4 to 6 m (e.g., Rostami et al., 2000; Muhs et al., 2002). The undisturbed ice core record of the North Greenland Ice Core Project (NGRIP) to 123 ka, and older but disturbed LIG ice in the Greenland Ice Core Project (GRIP) and Greenland Ice Sheet Project 2 (GISP2) cores, indicate that the Greenland Summit region remained ice-covered during the LIG (Raynaud et al., 1997; NGRIP, 2004). Similar isotopic value differences found in the Camp Century and Renland cores (Johnsen et al., 2001) suggest that relative elevation differences during the LIG in northern Greenland were not large

(NGRIP, 2004). Interpretation of the Dye-3 ice core in southern Greenland is equivocal. The presence of isotopically enriched ice, possibly LIG ice, at the bottom of the Dye-3 core has been interpreted as substantial reduction in southern Greenland ice thickness during the LIG (NGRIP, 2004). Equally plausible interpretations suggest that the Greenland Ice Sheet's southern dome did not survive the peak interglacial warmth and that Dye-3 is recording the growth of late-LIG ice when the ice sheet re-established itself in southern Greenland (Koerner and Fisher, 2002), or ice that flowed into the region from central Greenland or from a surviving but isolated southern dome (Lhomme et al., 2005a). The absence of pre-LIG ice in the larger ice caps in the eastern Canadian Arctic indicates that they melted completely during the LIG (Koerner, 1989).

Most of the global sea level rise during the LIG must have been the result of polar ice sheet melting. Greenland Ice Sheet models forced with Greenland temperature scenarios derived from data (Cuffey and Marshall, 2000; Tarasov and Peltier, 2003; Lhomme et al., 2005a), or temperatures and precipitation produced by an AOGCM (Otto-Bliesner et al., 2006a), simulate the minimal LIG Greenland Ice Sheet as a steep-sided ice sheet in central and northern Greenland (Figure 6.6). This inferred ice sheet, combined with the change in other arctic ice fields, likely generated no more than 2 to 4 m of early LIG sea level rise over several millennia. The simulated contribution of Greenland to this sea level rise was likely driven by orbitally forced summer warming in the Arctic (see Section 6.4.1). The evidence that sea level was 4 to 6 m above present implies there may also have been a contribution from Antarctica (Scherer et al., 1998; Overpeck et al., 2006). Overpeck et al. (2006) argued that since the circum-arctic LIG warming was very similar to that expected in a future doubled CO_2 climate, significant retreat of the Greenland Ice Sheet can be expected to occur under this future condition. Since not all of the LIG increment of sea level appears to be explained by the melt-back of the Greenland Ice Sheet, it is possible that parts of the Antarctic Ice Sheet might also retreat under this future condition (see also Scherer et al., 1998; Tarasov and Peltier, 2003; Domack et al., 2005 and Oppenheimer and Alley, 2005).

6.4.3.4 *What Is the Long-Term Contribution of Polar Ice-sheet Derived Melt Water to the Observed Globally Averaged Rate of Sea Level Rise?*

Models of postglacial RSL history together with Holocene observations can be employed to assess whether or not a significant fraction of the observed globally averaged rate of sea level rise of about 2 mm yr^{-1} during the 20th century can be explained as a long term continuing influence of the most recent partial deglaciation of the polar ice sheets. Based upon post-TAR estimates derived from geological observations of Holocene sea level from 16 equatorial Pacific islands (Peltier, 2002; Peltier et al., 2002), it appears likely that the average rate of sea level rise due to this hypothetical source over the last 2 kyr was zero and at most in the range 0 to 0.2 mm yr^{-1} (Lambeck, 2002).

6.5 The Current Interglacial

A variety of proxy records provide detailed temporal and spatial information concerning climate change during the current interglacial, the Holocene, an approximately 11.6 kyr period of increasingly intense anthropogenic modifications of the local (e.g., land use) to global (e.g., atmospheric composition) environment. The well-dated reconstructions of the past 2 kyr are covered in Section 6.6. In the context of both climate forcing and response, the Holocene is far better documented in terms of spatial coverage, dating and temporal resolution than previous interglacials. The evidence is clear that significant changes in climate forcing during the Holocene induced significant and complex climate responses, including long-term and abrupt changes in temperature, precipitation, monsoon dynamics and the El Niño-Southern Oscillation (ENSO). For selected periods such as the mid-Holocene, about 6 ka, intensive efforts have been dedicated to the synthesis of palaeoclimatic observations and modelling intercomparisons. Such extensive data coverage provides a sound basis to evaluate the capacity of climate models to capture the response of the climate system to the orbital forcing.

6.5.1 Climate Forcing and Response During the Current Interglacial

6.5.1.1 *What Were the Main Climate Forcings During the Holocene?*

During the current interglacial, changes in the Earth's orbit modulated the latitudinal and seasonal distribution of insolation (Box 6.1). Ongoing efforts to quantify Holocene changes in stratospheric aerosol content recorded in the chemical composition of ice cores from both poles (Zielinski, 2000; Castellano et al., 2005) confirm that volcanic forcing amplitude and occurrence varied significantly during the Holocene (see also Section 6.6.3). Fluctuations of cosmogenic isotopes (ice core ^{10}Be and tree ring ^{14}C) have been used as proxies for Holocene changes in solar activity (e.g., Bond et al., 2001), although the quantitative link to solar irradiance remains uncertain and substantial work is needed to disentangle solar from non-solar influences on these proxies over the full Holocene (Muscheler et al., 2006). Residual continental ice sheets formed during the last ice age were retreating during the first half of the current interglacial period (Figure 6.8). The associated ice sheet albedo is thought to have locally modulated the regional climate response to the orbital forcing (e.g., Davis et al., 2003).

The evolution of atmospheric trace gases during the Holocene is well known from ice core analyses (Figure 6.4). A first decrease in atmospheric CO_2 of about 7 ppm from 11 to 8 ka was followed by a 20 ppm CO_2 increase until the onset of the industrial revolution (Monnin et al., 2004). Atmospheric CH_4 decreased from a NH value of about 730 ppb around 10 ka to about 580 ppb around 6 ka, and increased again slowly to 730

ppb in pre-industrial times (Chappellaz et al., 1997; Flückiger et al., 2002). Atmospheric N_2O largely followed the evolution of atmospheric CO_2 and shows an early Holocene decrease of about 10 ppb and an increase of the same magnitude between 8 and 2 ka (Flückiger et al., 2002). Implied radiative forcing changes from Holocene greenhouse gas variations are 0.4 W m^{-2} (CO_2) and 0.1 W m^{-2} (N_2O and CH_4), relative to pre-industrial forcing.

6.5.1.2 Why Did Holocene Atmospheric Greenhouse Gas Concentrations Vary Before the Industrial Period?

Recent transient carbon cycle-climate model simulations with a predictive global vegetation model have attributed the early Holocene CO_2 decrease to forest regrowth in areas of the waning Laurentide Ice Sheet, partly counteracted by ocean sediment carbonate compensation (Joos et al., 2004). Carbonate compensation of terrestrial carbon uptake during the glacial-interglacial transition and the early Holocene, as well as coral reef buildup during the Holocene, likely contributed to the subsequent CO_2 rise (Broecker and Clark, 2003; Ridgwell et al., 2003; Joos et al., 2004), whereas recent carbon isotope data (Eyer, 2004) and model results (Brovkin et al., 2002; Kaplan et al., 2002; Joos et al., 2004) suggest that the global terrestrial carbon inventory has been rather stable over the 7 kyr preceding industrialisation. Variations in carbon storage in northern peatlands may have contributed to the observed atmospheric CO_2 changes. Such natural mechanisms cannot account for the much more significant industrial trace gas increases; atmospheric CO_2 would be expected to remain well below 290 ppm in the absence of anthropogenic emissions (Gerber et al., 2003).

It has been hypothesised, based on Vostok ice core CO_2 data (Petit et al., 1999), that atmospheric CO_2 would have dropped naturally by 20 ppm during the past 8 kyr (in contrast with the observed 20 ppm increase) if prehistoric agriculture had not caused a release of terrestrial carbon and CH_4 during the Holocene (Ruddiman, 2003; Ruddiman et al., 2005). This hypothesis also suggests that incipient late-Holocene high-latitude glaciation was prevented by these pre-industrial greenhouse gas emissions. However, this hypothesis conflicts with several, independent lines of evidence, including the lack of orbital similarity of the three previous interglacials with the Holocene and the recent finding that CO_2 concentrations were high during the entire Stage 11 (Siegenthaler et al., 2005a; Figure 6.3), a long (~28 kyr) interglacial (see Section 6.4.1.5). This hypothesis also requires much larger changes in the Holocene atmospheric stable carbon isotope ratio ($^{13}C/^{12}C$) than found in ice cores (Eyer, 2004), as well as a carbon release by anthropogenic land use that is larger than estimated by comparing carbon storage for natural vegetation and present day land cover (Joos et al., 2004).

6.5.1.3 Was Any Part of the Current Interglacial Period Warmer than the Late 20th Century?

The temperature evolution over the Holocene has been established for many different regions, often with centennial-resolution proxy records more sensitive to specific seasons (see Section 6.1). At high latitudes of the North Atlantic and adjacent Arctic, there was a tendency for summer temperature maxima to occur in the early Holocene (10 to 8 ka), pointing to the direct influence of the summer insolation maximum on sea ice extent (Kim et al., 2004; Kaplan and Wolfe, 2006). Climate reconstructions for the mid-northern latitudes exhibit a long-term decline in SST from the warmer early to mid-Holocene to the cooler pre-industrial period of the late Holocene (Johnsen et al., 2001; Marchal et al., 2002; Andersen et al., 2004; Kim et al., 2004; Kaplan and Wolfe 2006), most likely in response to annual mean and summer orbital forcings at these latitudes (Renssen et al., 2005). Near ice sheet remnants in northern Europe or North America, peak warmth was locally delayed, probably as a result of the interplay between ice elevation, albedo, atmospheric and oceanic heat transport and orbital forcing (MacDonald et al., 2000; Davis et al., 2003; Kaufman et al., 2004). The warmest period in northern Europe and north-western North America occurs from 7 to 5 ka (Davis et al., 2003; Kaufman et al., 2004). During the mid-Holocene, global pollen-based reconstructions (Prentice and Webb, 1998; Prentice et al., 2000) and macrofossils (MacDonald et al., 2000) show a northward expansion of northern temperate forest (Bigelow et al., 2003; Kaplan et al., 2003), as well as substantial glacier retreat (see Box 6.3). Warmer conditions at mid- and high latitudes of the NH in the early to mid-Holocene are consistent with deep borehole temperature profiles (Huang et al., 1997). Other early warm periods were identified in the equatorial west Pacific (Stott et al., 2004), China (He et al., 2004), New Zealand (Williams et al., 2004), southern Africa (Holmgren et al., 2003) and Antarctica (Masson et al., 2000). At high southern latitudes, the early warm period cannot be explained by a linear response to local summer insolation changes (see Box 6.1), suggesting large-scale reorganisation of latitudinal heat transport. In contrast, tropical temperature reconstructions, only available from marine records, show that Mediterranean, tropical Atlantic, Pacific and Indian Ocean SSTs exhibit a progressive warming from the beginning of the current interglacial onwards (Kim et al., 2004; Rimbu et al., 2004; Stott et al., 2004), possibly a reflection of tropical annual mean insolation increase (Box 6.1, Figure 1).

Extratropical centennial-resolution records therefore provide evidence for local multi-centennial periods warmer than the last decades by up to several degrees in the early to mid-Holocene. These local warm periods were very likely not globally synchronous and occurred at times when there is evidence that some areas of the tropical oceans were cooler than today (Figure 6.9) (Lorenz et al., 2006). When forced by 6 ka orbital parameters, state-of-the-art coupled climate models and EMICs capture reconstructed regional temperature and precipitation

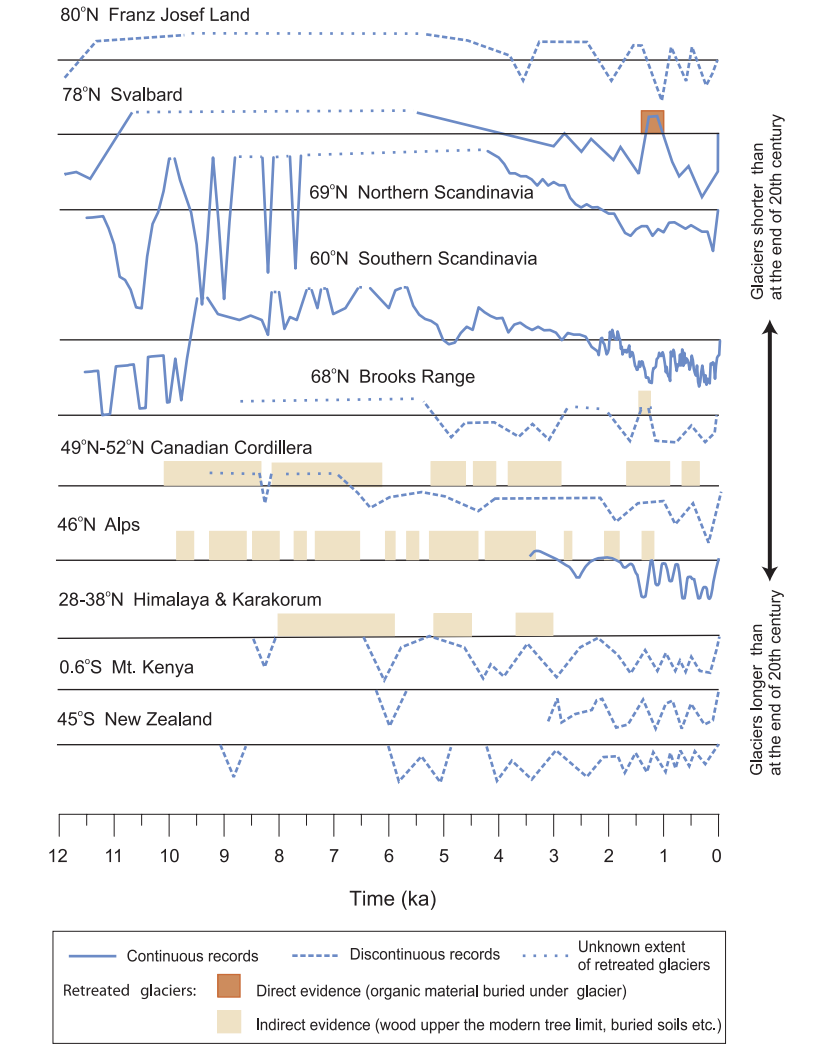
Box 6.3: Holocene Glacier Variability

The near-global retreat of mountain glaciers is among the most visible evidence of 20th- and 21st-century climate change (see Chapter 4), and the question arises as to the significance of this current retreat within a longer time perspective. The climatic conditions that cause an advance or a retreat may be different for glaciers located in different climate regimes (see Chapter 4). This distinction is crucial if reconstructions of past glacier activity are to be understood properly.

Records of Holocene glacier fluctuations provide a necessary backdrop for evaluating the current global retreat. However, in most mountain regions, records documenting past glacier variations exist as discontinuous low-resolution series (see Box 6.3, Figure 1), whereas continuous records providing the most coherent information for the whole Holocene are available so far only in Scandinavia (e.g., Nesje et al., 2005; see Box 6.3, Figure 1).

What do glaciers reveal about climate change during the Holocene?

Most archives from the NH and the tropics indicate short, or in places even absent, glaciers between 11 and 5 ka, whereas during the second half of the Holocene, glaciers reformed and expanded. This tendency is most probably related to changes in summer insolation due to the configuration of orbital forcing (see Box 6.1). Long-term changes in solar insolation, however, cannot explain the shorter, regionally diverse glacier responses, driven by complex glacier and climate (mainly precipitation and temperature) interactions. On these shorter time scales, climate phenomena such as the North Atlantic Oscillation (NAO) and ENSO affected glaciers' mass balance, explaining some of the discrepancies found between regions. This is exemplified in the anti-phasing between glacier mass balance variations from the Alps and Scandinavia (Reichert et al., 2001; Six et al., 2001). Comparing the ongoing retreat of glaciers with the reconstruction of glacier variations during the Holocene, no period analogous to the present with a globally homogenous trend of retreating glaciers over centennial and shorter time scales could be identified in the past, although account must be taken of the large gaps in the data coverage on retreated glaciers in most regions. This is in line with model experiments suggesting that present-day glacier retreat exceed any variations simulated by the GCM control experiments and must have an external cause, with anthropogenic forcing the most likely candidate (Reichert et al., 2002).



Box 6.3, Figure 1. *Timing and relative scale of selected glacier records from both hemispheres. The different records show that Holocene glacier patterns are complex and that they should be interpreted regionally in terms of precipitation and temperature. In most cases, the scale of glacier retreat is unknown and indicated on a relative scale. Lines upper the horizontal line indicate glaciers smaller than at the end of the 20th century and lines below the horizontal line denote periods with larger glaciers than at the end of the 20th century. The radiocarbon dates are calibrated and all curves are presented in calendar years. Franz Josef Land (Lubinski et al., 1999), Svalbard from Svendsen and Mangerud (1997) corrected with Humlum et al. (2005), Northern Scandinavia (Bakke et al., 2005a,b; Nesje et al., 2005), Southern Scandinavia (Dahl and Nesje, 1996; Matthews et al., 2000, 2005; Lie et al., 2004), Brooks Range (Ellis and Calkin, 1984), Canadian Cordillera (Luckman and Kearney, 1986; Osborn and Luckman, 1988; Koch et al., 2004; Menounos et al., 2004), Alps (Holzhauser et al., 2005; Jörin et al., 2006), Himalaya and Karakorum (Röthlisberger and Geyh, 1985; Bao et al., 2003), Mt. Kenya (Karlén et al., 1999), New Zealand (Gellatly et al., 1988).*

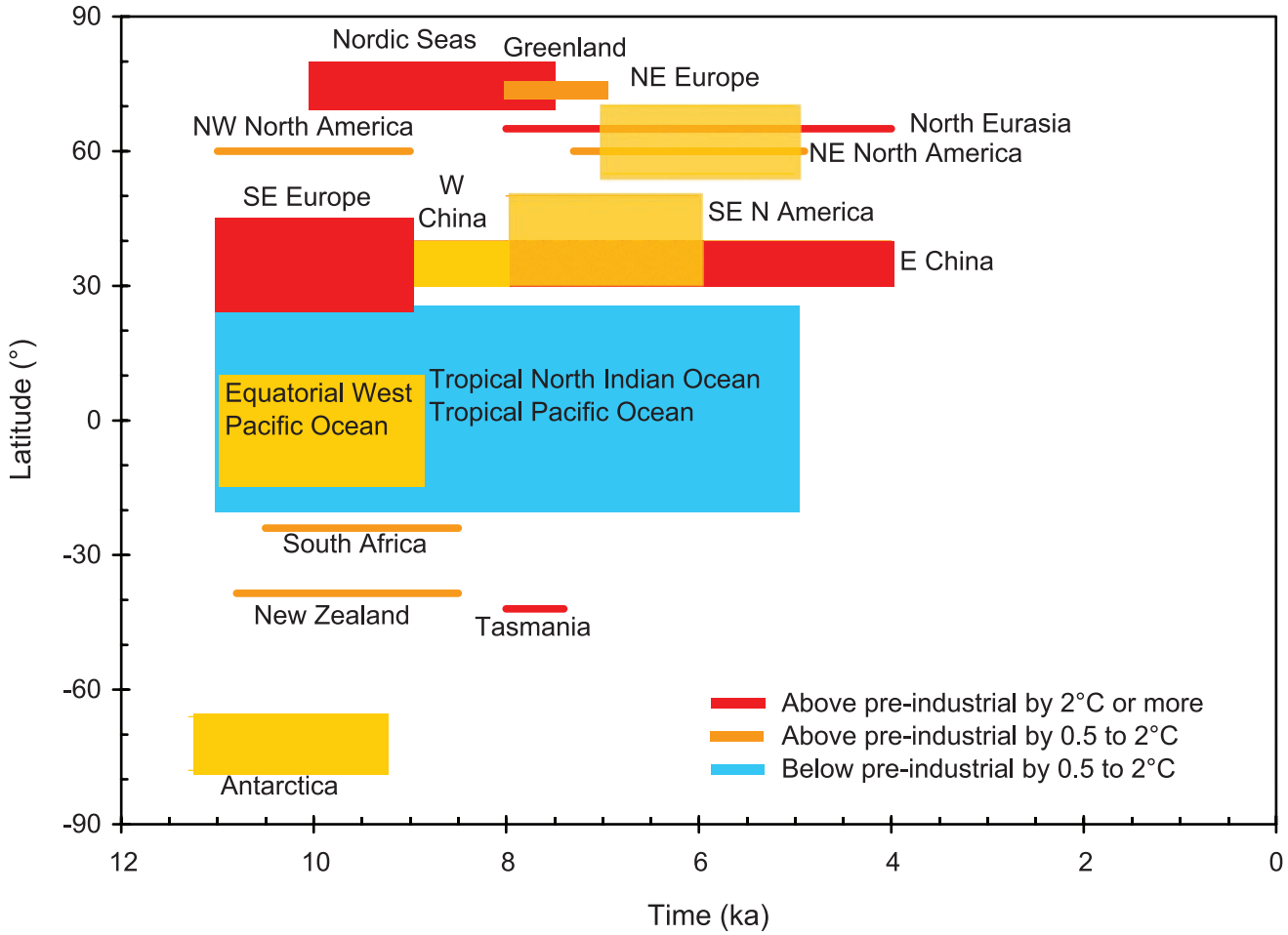


Figure 6.9. *Timing and intensity of maximum temperature deviation from pre-industrial levels, as a function of latitude (vertical axis) and time (horizontal axis, in thousands of years before present). Temperatures above pre-industrial levels by 0.5°C to 2°C appear in orange (above 2°C in red). Temperatures below pre-industrial levels by 0.5°C to 2°C appear in blue. References for data sets are: Barents Sea (Duplessy et al., 2001), Greenland (Johnsen et al., 2001), Europe (Davis et al., 2003), northwest and northeast America (MacDonald et al., 2000; Kaufman et al., 2004), China (He et al., 2004), tropical oceans (Rimbu et al., 2004; Stott et al., 2004; Lorentz et al., 2006), north Atlantic (Marchal et al., 2002; Kim et al., 2004), Tasmania (Xia et al., 2001), East Antarctica (Masson et al., 2000), southern Africa (Holmgren et al., 2003) and New Zealand (Williams et al., 2004).*

changes (Sections 6.5.1.4 and 6.5.1.5), whereas simulated global mean temperatures remain essentially unchanged (<0.4°C; Masson-Delmotte et al., 2005b), just as expected from the seasonality of the orbital forcing (see Box 6.1). Due to different regional temperature responses from the tropics to high latitudes, as well as between hemispheres, commonly used concepts such as 'mid-Holocene thermal optimum', 'altithermal', etc. are not globally relevant and should only be applied in a well-articulated regional context. Current spatial coverage, temporal resolution and age control of available Holocene proxy data limit the ability to determine if there were multi-decadal periods of global warmth comparable to the last half of 20th century.

6.5.1.4 What Are the Links Between Orbital Forcing and Mid-Holocene Monsoon Intensification?

Lake levels and vegetation changes reconstructed for the early to mid-Holocene indicate large precipitation increases in North Africa (Jolly et al., 1998). Simulating this intensification of the African monsoon is widely used as a benchmark for climate models within PMIP. When forced by mid-Holocene insolation resulting from changes in the Earth's orbit (see Box 6.1), but fixed present-day vegetation and ocean temperatures, atmospheric models simulate NH summer continental warming and a limited enhancement of summer monsoons but underestimate the reconstructed precipitation increase and extent over the Sahara (Joussaume et al., 1999; Coe and Harrison., 2002; Braconnot et al., 2004). Differences among simulations appear related to atmospheric model characteristics together with the mean tropical temperature of the control simulation (Braconnot et al., 2002). As already noted in the TAR, the vegetation and surface albedo feedbacks play a major role in the enhancement of the African monsoon (e.g., Claussen and Gayler, 1997; de Noblet-Ducoudre et al., 2000; Levis et al., 2004). New coupled ocean-atmosphere simulations show that the ocean feedback strengthens the inland monsoon flow and the length of the monsoon season, due to robust changes in late summer dipole SST patterns and in mixed layer depth (Braconnot et al., 2004; Zhao et al., 2005). When combined,

vegetation, soil characteristics and ocean feedbacks produce nonlinear interactions resulting in simulated precipitation in closer agreement with data (Braconnot et al., 2000; Levis et al., 2004). Transient simulations of Holocene climate performed with EMICs have further shown that land surface feedbacks are possibly involved in abrupt monsoon fluctuations (see Section 6.5.2). The mid-Holocene intensification of the North Australian, Indian and southwest American monsoons is captured by coupled ocean-atmosphere climate models in response to orbital forcing, again with amplifying ocean feedbacks (Harrison et al., 2003; Liu et al., 2004; Zhao et al., 2005).

6.5.1.5 What Are the Links Between Orbital Forcing and mid-Holocene Climate at Middle and High Latitudes?

Terrestrial records of the mid-Holocene indicate an expansion of forest at the expense of tundra at mid- to high latitudes of the NH (MacDonald et al., 2000; Prentice et al., 2000). Since the TAR, coupled atmosphere-ocean models, including the recent PMIP-2 simulations, have investigated the response of the climate system to orbital forcing at 6 ka during the mid-Holocene (Section 6.6.1, Box 6.1). Fully coupled atmosphere-ocean-vegetation models do produce the northward shift in the position of the northern limit of boreal forest, in response to simulated summer warming, and the northward expansion of temperate forest belts in North America, in response to simulated winter warming (Wohlfahrt et al., 2004). At high latitudes, the vegetation-snow albedo and ocean feedbacks enhance the warming in spring and autumn, respectively and transform the seasonal orbital forcing into an annual response (Crucifix et al., 2002; Wohlfahrt et al., 2004). Ocean changes simulated for this period are generally small and difficult to quantify from data due to uncertainties in the way proxy methods respond to the seasonality and stratification of the surface waters (Waelbroeck et al., 2005). Simulations with atmosphere and slab ocean models indicate that a change in the mean tropical Pacific SSTs in the mid-Holocene to conditions more like La Niña conditions can explain North American drought conditions at mid-Holocene (Shin et al., 2006). Based on proxies of SST in the North Atlantic, it has been suggested that trends from early to late Holocene are consistent with a shift from a more meridional regime over northern Europe to a positive North Atlantic Oscillation (NAO)-like mean state in the early to mid-Holocene (Rimbu et al., 2004). A PMIP2 intercomparison shows that three of nine models support a positive NAO-like atmospheric circulation in the mean state for the mid-Holocene as compared to the pre-industrial period, without significant changes in simulated NAO variability (Gladstone et al., 2005).

6.5.1.6 Are There Long-Term Modes of Climate Variability Identified During the Holocene that Could Be Involved in the Observed Current Warming?

An increasing number of Holocene proxy records are of sufficiently high resolution to describe the climate variability on centennial to millennial time scales, and to identify possible natural quasi-periodic modes of climate variability at these time scales (Haug et al., 2001; Gupta et al., 2003). Although earlier studies suggested that Holocene millennial variability could display similar frequency characteristics as the glacial variability in the North Atlantic (Bond et al., 1997), this assumption is being increasingly questioned (Risebrobakken et al., 2003; Schulz et al., 2004). In many records, there is no apparent consistent pacing at specific centennial to millennial frequencies through the Holocene period, but rather shifts between different frequencies (Moros et al., 2006). The suggested synchroneity of tropical and North Atlantic centennial to millennial variability (de Menocal et al., 2000; Mayewski et al., 2004; Y.J. Wang et al., 2005) is not common to the SH (Masson et al., 2000; Holmgren et al., 2003), suggesting that millennial scale variability cannot account for the observed 20th-century warming trend. Based on the correlation between changes in cosmogenic isotopes (^{10}Be or ^{14}C) – related to solar activity changes – and climate proxy records, some authors argue that solar activity may be a driver for centennial to millennial variability (Karlén and Kuylenstierna, 1996; Bond et al., 2001; Fleitmann et al., 2003; Y.J. Wang et al., 2005). The possible importance of (forced or unforced) modes of variability within the climate system, for instance related to the deep ocean circulation, have also been highlighted (Bianchi and McCave, 1999; Duplessy et al., 2001; Marchal et al., 2002; Oppo et al., 2003). The current lack of consistency between various data sets makes it difficult, based on current knowledge, to attribute the millennial time scale large-scale climate variations to external forcings (solar activity, episodes of intense volcanism), or to variability internal to the climate system.

6.5.2 Abrupt Climate Change During the Current Interglacial

6.5.2.1 What Do Abrupt Changes in Oceanic and Atmospheric Circulation at Mid- and High-Latitudes Show?

An abrupt cooling of 2°C to 6°C identified as a prominent feature of Greenland ice cores at 8.2 ka (Alley et al., 1997; Alley and Agustsdottir, 2005) is documented in Europe and North America by high-resolution continental proxy records (Klitgaard-Kristensen et al., 1998; von Grafenstein et al., 1998; Barber et al., 1999; Nesje et al., 2000; Rohling and Palike, 2005). A large decrease in atmospheric CH_4 concentrations (several tens of parts per billion; Spahni et al., 2003) reveals the widespread signature of the abrupt '8.2 ka event' associated

with large-scale atmospheric circulation change recorded from the Arctic to the tropics with associated dry episodes (Hughen et al., 1996; Stager and Mayewski, 1997; Haug et al., 2001; Fleitmann et al., 2003; Rohling and Palike, 2005). The 8.2 ka event is interpreted as resulting from a brief reorganisation of the North Atlantic MOC (Bianchi and McCave, 1999; Risebrobakken et al., 2003; McManus et al., 2004), however, without a clear signature identified in deep water formation records. Significant volumes of freshwater were released in the North Atlantic and Arctic at the beginning of the Holocene by the decay of the residual continental ice (Nesje et al., 2004). A likely cause for the 8.2 ka event is an outburst flood during which pro-glacial Lake Agassiz drained about 10^{14} m^3 of freshwater into Hudson Bay extremely rapidly (possibly 5 Sv over 0.5 year; Clarke et al., 2004). Climate models have been used to test this hypothesis and assess the vulnerability of the ocean and atmospheric circulation to different amounts of freshwater release (see Alley and Agustsdottir, 2005 for a review; Section 6.4.2.2). Ensemble simulations conducted with EMICs (Renssen et al., 2002; Bauer et al., 2004) and coupled ocean-atmosphere GCMs (Alley and Agustsdottir, 2005; LeGrande et al., 2006) with different boundary conditions and freshwater forcings show that climate models are capable of simulating the broad features of the observed 8.2 ka event (including shifts in the ITCZ).

The end of the first half of the Holocene – between about 5 and 4 ka – was punctuated by rapid events at various latitudes, such as an abrupt increase in NH sea ice cover (Jennings et al., 2001); a decrease in Greenland deuterium excess, reflecting a change in the hydrological cycle (Masson-Delmotte et al., 2005b); abrupt cooling events in European climate (Seppa and Birks, 2001; Lauritzen, 2003); widespread North American drought for centuries (Booth et al., 2005); and changes in South American climate (Marchant and Hooghiemstra, 2004). The processes behind these observed abrupt shifts are not well understood. As these particular events took place at the end of a local warm period caused by orbital forcing (see Box 6.1 and Section 6.5.1), these observations suggest that under gradual climate forcings (e.g., orbital) the climate system can change abruptly.

6.5.2.2 What Is the Understanding of Abrupt Changes in Monsoons?

In the tropics, precipitation-sensitive records and models indicate that summer monsoons in Africa, India and Southeast Asia were enhanced in the early to mid-Holocene due to orbital forcing, a resulting increase in land-sea temperature gradients and displacement of the ITCZ. All high-resolution precipitation-sensitive records reveal that the local transitions from wetter conditions in the early Holocene to drier modern conditions occurred in one or more steps (Guo et al., 2000; Fleitmann et al., 2003; Morrill et al., 2003; Y.J.Wang et al., 2005). In the early Holocene, large increases in monsoon-related northern African runoff and/or wetter conditions over the Mediterranean are associated with dramatic changes in Mediterranean Sea ventilation, as evidenced by sapropel layers (Ariztegui et al., 2000).

Transient simulations of the Holocene, although usually after the final disappearance of ice sheets, have been performed with EMICs and forced by orbital parameters (Box 6.1). These models have pointed to the operation of mechanisms that can generate rapid events in response to orbital forcing, such as changes in African monsoon intensity due to nonlinear interactions between vegetation and monsoon dynamics (Claussen et al., 1999; Renssen et al., 2003).

6.5.3 How and Why Has the El Niño-Southern Oscillation Changed Over the Present Interglacial?

High-resolution palaeoclimate records from diverse sources (corals, archaeological middens, lake and ocean sediments) consistently indicate that the early to mid-Holocene likely experienced weak ENSO variability, with a transition to a stronger modern regime occurring in the past few thousand years (Shulmeister and Lees, 1995; Gagan et al., 1998; Rodbell et al., 1999; Tudhope et al., 2001; Moy et al., 2002; McGregor and Gagan, 2004). Most data sources are discontinuous, providing only snapshots of mean conditions or interannual variability, and making it difficult to precisely characterise the rate and timing of the transition to the modern regime.

A simple model of the coupled Pacific Ocean and atmosphere, forced with orbital insolation variations, suggests that seasonal changes in insolation can produce systematic changes in ENSO behaviour (Clement et al., 1996, 2000; Cane, 2005). This model simulates a progressive, somewhat irregular increase in both event frequency and amplitude throughout the Holocene, due to the Bjerknes feedback mechanism (Bjerknes, 1969) and ocean dynamical thermostat (Clement and Cane, 1999; Clement et al., 2001; Cane, 2005). Snapshot experiments conducted with some coupled GCMs also reproduce an intensification of ENSO between the early Holocene and the present, although with some disagreement as to the magnitude of change. Both model results and data syntheses suggest that before the mid-Holocene, the tropical Pacific exhibited a more La Niña-like background state (Clement et al., 2000; Liu et al., 2000; Kitoh and Murakami, 2002; Otto-Bliesner et al., 2003; Liu, 2004). In palaeoclimate simulations with GCMs, ENSO teleconnections robust in the modern system show signs of weakening under mid-Holocene orbital forcing (Otto-Bliesner, 1999; Otto-Bliesner et al., 2003).

Frequently Asked Question 6.2

Is the Current Climate Change Unusual Compared to Earlier Changes in Earth's History?

Climate has changed on all time scales throughout Earth's history. Some aspects of the current climate change are not unusual, but others are. The concentration of CO_2 in the atmosphere has reached a record high relative to more than the past half-million years, and has done so at an exceptionally fast rate. Current global temperatures are warmer than they have ever been during at least the past five centuries, probably even for more than a millennium. If warming continues unabated, the resulting climate change within this century would be extremely unusual in geological terms. Another unusual aspect of recent climate change is its cause: past climate changes were natural in origin (see FAQ 6.1), whereas most of the warming of the past 50 years is attributable to human activities.

When comparing the current climate change to earlier, natural ones, three distinctions must be made. First, it must be clear which variable is being compared: is it greenhouse gas concentration or temperature (or some other climate parameter), and is it their absolute value or their rate of change? Second, local changes must not be confused with global changes. Local climate changes are often much larger than global ones, since local factors (e.g., changes in oceanic or atmospheric circulation) can shift the delivery of heat or moisture from one place to another and local feedbacks operate (e.g., sea ice feedback). Large changes in global mean temperature, in contrast, require some global forcing (such as a change in greenhouse gas concentration or solar activity). Third, it is necessary to distinguish between time scales. Climate changes over millions of years can be much larger and have different causes (e.g., continental drift) compared to climate changes on a centennial time scale.

The main reason for the current concern about climate change is the rise in atmospheric carbon dioxide (CO_2) concentration (and some other greenhouse gases), which is very unusual for the Quaternary (about the last two million years). The concentration of CO_2 is now known accurately for the past 650,000 years from antarctic ice cores. During this time, CO_2 concentration varied between a low of 180 ppm during cold glacial times and a high of 300 ppm during warm interglacials. Over the past century, it rapidly increased well out of this range, and is now 379 ppm (see Chapter 2). For comparison, the approximately 80-ppm rise in CO_2 concentration at the end of the past ice ages generally took over 5,000 years. Higher values than at present have only occurred many millions of years ago (see FAQ 6.1).

Temperature is a more difficult variable to reconstruct than CO_2 (a globally well-mixed gas), as it does not have the same value all over the globe, so that a single record (e.g., an ice core) is only of limited value. Local temperature fluctuations, even those over just a few decades, can be several degrees celsius, which is larger than the global warming signal of the past century of about 0.7°C.

More meaningful for global changes is an analysis of large-scale (global or hemispheric) averages, where much of the local variation averages out and variability is smaller. Sufficient coverage of instrumental records goes back only about 150 years. Further back in time, compilations of proxy data from tree rings, ice cores, etc., go back more than a thousand years with decreasing spatial coverage for earlier periods (see Section 6.5). While there are differences among those reconstructions and significant uncertainties remain, all published reconstructions find that temperatures were warm during medieval times, cooled to low values in the 17th, 18th and 19th centuries, and warmed rapidly after that. The medieval level of warmth is uncertain, but may have been reached again in the mid-20th century, only to have likely been exceeded since then. These conclusions are supported by climate modelling as well. Before 2,000 years ago, temperature variations have not been systematically compiled into large-scale averages, but they do not provide evidence for warmer-than-present global annual mean temperatures going back through the Holocene (the last 11,600 years; see Section 6.4). There are strong indications that a warmer climate, with greatly reduced global ice cover and higher sea level, prevailed until around 3 million years ago. Hence, current warmth appears unusual in the context of the past millennia, but not unusual on longer time scales for which changes in tectonic activity (which can drive natural, slow variations in greenhouse gas concentration) become relevant (see Box 6.1).

A different matter is the current rate of warming. Are more rapid global climate changes recorded in proxy data? The largest temperature changes of the past million years are the glacial cycles, during which the global mean temperature changed by 4°C to 7°C between ice ages and warm interglacial periods (local changes were much larger, for example near the continental ice sheets). However, the data indicate that the global warming at the end of an ice age was a gradual process taking about 5,000 years (see Section 6.3). It is thus clear that the current rate of global climate change is much more rapid and very unusual in the context of past changes. The much-discussed abrupt climate shifts during glacial times (see Section 6.3) are not counter-examples, since they were probably due to changes in ocean heat transport, which would be unlikely to affect the global mean temperature.

Further back in time, beyond ice core data, the time resolution of sediment cores and other archives does not resolve changes as rapid as the present warming. Hence, although large climate changes have occurred in the past, there is no evidence that these took place at a faster rate than present warming. If projections of approximately 5°C warming in this century (the upper end of the range) are realised, then the Earth will have experienced about the same amount of global mean warming as it did at the end of the last ice age; there is no evidence that this rate of possible future global change was matched by any comparable global temperature increase of the last 50 million years.

6.6 The Last 2,000 Years

6.6.1 Northern Hemisphere Temperature Variability

6.6.1.1 What Do Reconstructions Based on Palaeoclimatic Proxies Show?

Figure 6.10 shows the various instrumental and proxy climate evidence of the variations in average large-scale surface temperatures over the last 1.3 kyr. Figure 6.10a shows two instrumental compilations representing the mean annual surface temperature of the NH since 1850, one based on land data only, and one using land and surface ocean data combined (see Chapter 3). The uncertainties associated with one of these series are also shown (30-year smoothed combined land and marine). These arise primarily from the incomplete spatial coverage of instrumentation through time (Jones et al., 1997) and, whereas these uncertainties are larger in the 19th compared to the 20th century, the prominence of the recent warming, especially in the last two to three decades of the record, is clearly apparent in this 150-year context. The land-only record shows similar variability, although the rate of warming is greater than in the combined record after about 1980. The land-only series can be extended back beyond the 19th century, and is shown plotted from 1781 onwards. The early section is based on a much sparser network of available station data, with at least 23 European stations, but only one North American station, spanning the first two decades, and the first Asian station beginning only in the 1820s. Four European records (Central England, De Bilt, Berlin and Uppsala) provide an even longer, though regionally restricted, indication of the context for the warming observed in the last approximately 20 to 30 years, which is even greater in this area than is observed over the NH land as a whole.

The instrumental temperature data that exist before 1850, although increasingly biased towards Europe in earlier periods, show that the warming observed after 1980 is unprecedented compared to the levels measured in the previous 280 years, even allowing for the greater variance expected in an average of so few early data compared to the much greater number in the 20th century. Recent analyses of instrumental, documentary and proxy climate records, focussing on European temperatures, have also pointed to the unprecedented warmth of the 20th century and shown that the extreme summer of 2003 was very likely warmer than any that has occurred in at least 500 years (Luterbacher et al., 2004; Guiot et al., 2005; see Box 3.6).

If the behaviour of recent temperature change is to be understood, and the mechanisms and causes correctly attributed, parallel efforts are needed to reconstruct the longer and more widespread pre-instrumental history of climate variability, as well as the detailed changes in various factors that might influence climate (Bradley et al., 2003b; Jones and Mann, 2004).

The TAR discussed various attempts to use proxy data to reconstruct changes in the average temperature of the NH for the period after AD 1000, but focused on three reconstructions (included in Figure 6.10), all with yearly resolution. The first (Mann et al., 1999) represents mean annual temperatures, and is based on a range of proxy types, including data extracted from tree rings, ice cores and documentary sources; this reconstruction also incorporates a number of instrumental (temperature and precipitation) records from the 18th century onwards. For 900 years, this series exhibits multi-decadal fluctuations with amplitudes up to 0.3°C superimposed on a negative trend of 0.15°C, followed by an abrupt warming (~0.4°C) matching that observed in the instrumental data during the first half of the 20th century. Of the other two reconstructions, one (Jones et al., 1998) was based on a much smaller number of proxies, whereas the other (Briffa et al., 2001) was based solely on tree ring density series from an expansive area of the extratropics, but reached back only to AD 1400. These two reconstructions emphasise warm season rather than annual temperatures, with a geographical focus on extratropical land areas. They indicate a greater range of variability on centennial time scales prior to the 20th century, and also suggest slightly cooler conditions during the 17th century than those portrayed in the Mann et al. (1998, 1999) series.

The 'hockey stick' reconstruction of Mann et al. (1999) has been the subject of several critical studies. Soon and Baliunas (2003) challenged the conclusion that the 20th century was the warmest at a hemispheric average scale. They surveyed regionally diverse proxy climate data, noting evidence for relatively warm (or cold), or alternatively dry (or wet) conditions occurring at any time within pre-defined periods assumed to bracket the so-called 'Medieval Warm Period' (and 'Little Ice Age'). Their qualitative approach precluded any quantitative summary of the evidence at precise times, limiting the value of their review as a basis for comparison of the relative magnitude of mean hemispheric 20th-century warmth (Mann and Jones, 2003; Osborn and Briffa, 2006). Box 6.4 provides more information on the 'Medieval Warm Period'.

McIntyre and McKitrick (2003) reported that they were unable to replicate the results of Mann et al. (1998). Wahl and Ammann (2007) showed that this was a consequence of differences in the way McIntyre and McKitrick (2003) had implemented the method of Mann et al. (1998) and that the original reconstruction could be closely duplicated using the original proxy data. McIntyre and McKitrick (2005a,b) raised further concerns about the details of the Mann et al. (1998) method, principally relating to the independent verification of the reconstruction against 19th-century instrumental temperature data and to the extraction of the dominant modes of variability present in a network of western North American tree ring chronologies, using Principal Components Analysis. The latter may have some theoretical foundation, but Wahl and Amman (2006) also show that the impact on the amplitude of the final reconstruction is very small (~0.05°C; for further discussion of these issues see also Huybers, 2005; McIntyre and McKitrick, 2005c,d; von Storch and Zorita, 2005).

Since the TAR, a number of additional proxy data syntheses based on annually or near-annually resolved data, variously representing mean NH temperature changes over the last

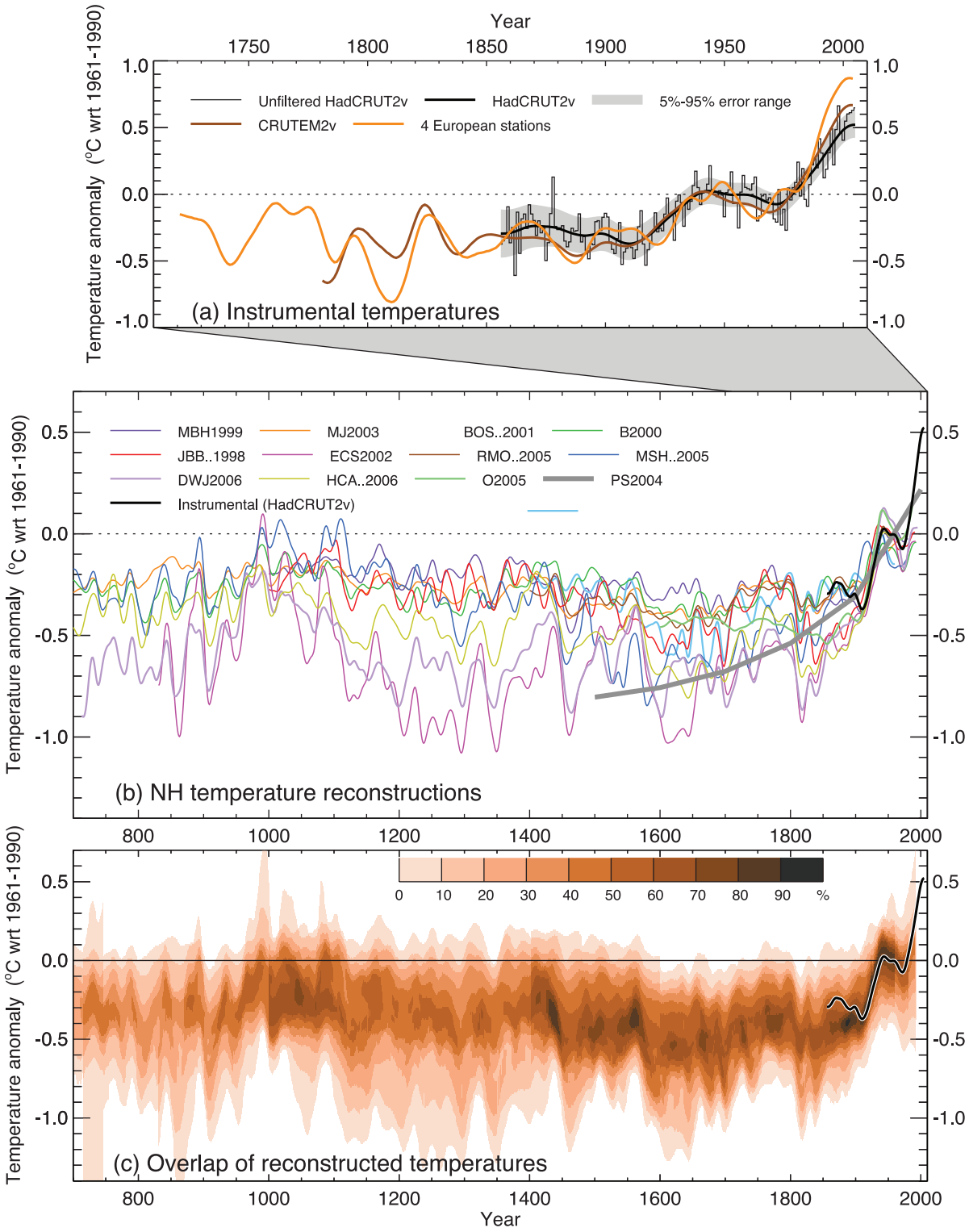


Figure 6.10. *Records of NH temperature variation during the last 1.3 kyr. (a) Annual mean instrumental temperature records, identified in Table 6.1. (b) Reconstructions using multiple climate proxy records, identified in Table 6.1, including three records (JBB..1998, MBH..1999 and BOS..2001) shown in the TAR, and the HadCRUT2v instrumental temperature record in black. (c) Overlap of the published multi-decadal time scale uncertainty ranges of all temperature reconstructions identified in Table 6.1 (except for RMO..2005 and PS2004), with temperatures within ±1 standard error (SE) of a reconstruction 'scoring' 10%, and regions within the 5 to 95% range 'scoring' 5% (the maximum 100% is obtained only for temperatures that fall within ±1 SE of all 10 reconstructions). The HadCRUT2v instrumental temperature record is shown in black. All series have been smoothed with a Gaussian-weighted filter to remove fluctuations on time scales less than 30 years; smoothed values are obtained up to both ends of each record by extending the records with the mean of the adjacent existing values. All temperatures represent anomalies (°C) from the 1961 to 1990 mean.*

Box 6.4: Hemispheric Temperatures in the 'Medieval Warm Period'

At least as early as the beginning of the 20th century, different authors were already examining the evidence for climate changes during the last two millennia, particularly in relation to North America, Scandinavia and Eastern Europe (Brooks, 1922). With regard to Iceland and Greenland, Pettersson (1914) cited evidence for considerable areas of Iceland being cultivated in the 10th century. At the same time, Norse settlers colonised areas of Greenland, while a general absence of sea ice allowed regular voyages at latitudes far to the north of what was possible in the colder 14th century. Brooks (1922) described how, after some amelioration in the 15th and 16th centuries, conditions worsened considerably in the 17th century; in Iceland, previously cultivated land was covered by ice. Hence, at least for the area of the northern North Atlantic, a picture was already emerging of generally warmer conditions around the centuries leading up to the end of the first millennium, but framed largely by comparison with strong evidence of much cooler conditions in later centuries, particularly the 17th century.

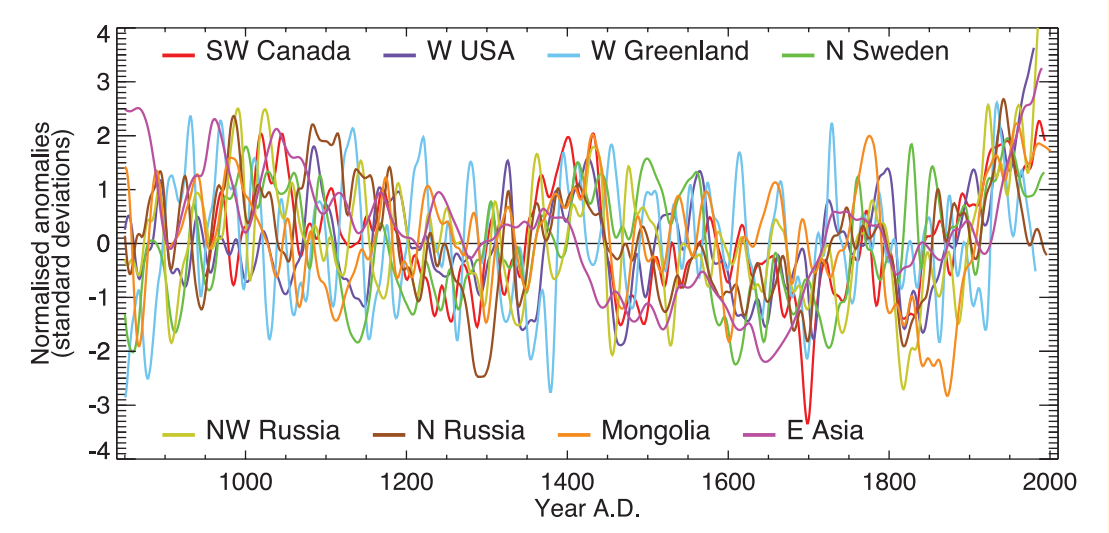
Lamb (1965) seems to have been the first to coin the phrase 'Medieval Warm Epoch' or 'Little Optimum' to describe the totality of multiple strands of evidence principally drawn from western Europe, for a period of widespread and generally warmer temperatures which he put at between AD 1000 and 1200 (Lamb, 1982). It is important to note that Lamb also considered the warmest conditions to have occurred at different times in different areas: between 950 and 1200 in European Russia and Greenland, but somewhat later, between 1150 and 1300 (though with notable warmth also in the later 900s) in most of Europe (Lamb, 1977).

Much of the evidence used by Lamb was drawn from a very diverse mixture of sources such as historical information, evidence of treeline and vegetation changes, or records of the cultivation of cereals and vines. He also drew inferences from very preliminary analyses of some Greenland ice core data and European tree ring records. Much of this evidence was difficult to interpret in terms of accurate quantitative temperature influences. Much was not precisely dated, representing physical or biological systems that involve complex lags between forcing and response, as is the case for vegetation and glacier changes. Lamb's analyses also predate any formal statistical calibration of much of the evidence he considered. He concluded that 'High Medieval' temperatures were probably 1.0°C to 2.0°C above early 20th-century levels at various European locations (Lamb, 1977; Bradley et al., 2003a).

A later study, based on examination of more quantitative evidence, in which efforts were made to control for accurate dating and specific temperature response, concluded that it was not possible to say anything other than '… in some areas of the Globe, for some part of the year, relatively warm conditions may have prevailed' (Hughes and Diaz, 1994).

In medieval times, as now, climate was unlikely to have changed in the same direction, or by the same magnitude, everywhere (Box 6.4, Figure 1). At some times, some regions may have experienced even warmer conditions than those that prevailed throughout the 20th century (e.g., see Bradley et al., 2003a). Regionally restricted evidence by itself, especially when the dating is imprecise, is of little practical relevance to the question of whether climate in medieval times was globally as warm or warmer than today. Local climate variations can be dominated by internal climate variability, often the result of the redistribution of heat by regional climate processes. Only very large-scale climate averages can be expected to reflect global forcings over recent millennia (Mann and Jones, 2003; Goosse

(continued)



Box 6.4, Figure 1. *The heterogeneous nature of climate during the 'Medieval Warm Period' is illustrated by the wide spread of values exhibited by the individual records that have been used to reconstruct NH mean temperature. These consist of individual, or small regional averages of, proxy records collated from those used by Mann and Jones (2003), Esper et al. (2002) and Luckman and Wilson (2005), but exclude shorter series or those with no evidence of sensitivity to local temperature. These records have not been calibrated here, but each has been smoothed with a 20-year filter and scaled to have zero mean and unit standard deviation over the period 1001 to 1980.*

et al., 2005a). To define medieval warmth in a way that has more relevance for exploring the magnitude and causes of recent large-scale warming, widespread and continuous palaeoclimatic evidence must be assimilated in a homogeneous way and scaled against recent measured temperatures to allow a meaningful quantitative comparison against 20th-century warmth (Figure 6.10).

A number of studies that have attempted to produce very large spatial-scale reconstructions have come to the same conclusion: that medieval warmth was heterogeneous in terms of its precise timing and regional expression (Crowley and Lowery, 2000; Folland et al., 2001; Esper et al., 2002; Bradley et al., 2003a; Jones and Mann, 2004; D'Arrigo et al., 2006).

The uncertainty associated with present palaeoclimate estimates of NH mean temperatures is significant, especially for the period prior to 1600 when data are scarce (Mann et al., 1999; Briffa and Osborn, 2002; Cook et al., 2004a). However, Figure 6.10 shows that the warmest period prior to the 20th century very likely occurred between 950 and 1100, but temperatures were probably between 0.1°C and 0.2°C below the 1961 to 1990 mean and significantly below the level shown by instrumental data after 1980.

In order to reduce the uncertainty, further work is necessary to update existing records, many of which were assembled up to 20 years ago, and to produce many more, especially early, palaeoclimate series with much wider geographic coverage. There are far from sufficient data to make any meaningful estimates of *global* medieval warmth (Figure 6.11). There are very few long records with high temporal resolution data from the oceans, the tropics or the SH.

The evidence currently available indicates that NH mean temperatures during medieval times (950–1100) were indeed warm in a 2-kyr context and even warmer in relation to the less sparse but still limited evidence of widespread average cool conditions in the 17th century (Osborn and Briffa, 2006). However, the evidence is not sufficient to support a conclusion that hemispheric mean temperatures were as warm, or the extent of warm regions as expansive, as those in the 20th century as a whole, during any period in medieval times (Jones et al., 2001; Bradley et al., 2003a,b; Osborn and Briffa, 2006).

Table 6.1. *Records of Northern Hemisphere temperature shown in Figure 6.10.*

Instrumental temperatures			
Series	**Period**	**Description**	**Reference**
HadCRUT2v[a]	1856–2005	Land and marine temperatures for the NH	Jones and Moberg, 2003; errors from Jones et al., 1997
CRUTEM2v[b]	1781–2004	Land-only temperatures for the NH	Jones and Moberg, 2003; extended using data from Jones et al., 2003
4 European Stations	1721–2004	Average of central England, De Bilt, Berlin and Uppsala	Jones et al., 2003

Proxy-based reconstructions of temperature								
		Reconstructed		Location Of Proxies[c]				
Series	**Period**	**Season**	**Region**	**H**	**M**	**L**	**O**	**Reference**
JBB..1998	1000–1991	Summer	Land, 20°N–90°N	◢	◢	☐	☐	Jones et al., 1998; calibrated by Jones et al., 2001
MBH1999	1000–1980	Annual	Land + marine, 0–90°N	■	■	◢	◢	Mann et al., 1999
BOS..2001	1402–1960	Summer	Land, 20°N–90°N	■	◢	☐	☐	Briffa et al., 2001
ECS2002	831–1992	Annual	Land, 20°N–90°N	◢	◢	☐	☐	Esper et al., 2002; recalibrated by Cook et al., 2004a
B2000	1–1993	Summer	Land, 20°N–90°N	◢	☐	☐	☐	Briffa, 2000; calibrated by Briffa et al., 2004
MJ2003	200–1980	Annual	Land + marine, 0–90°N	◢	◢	☐	☐	Mann and Jones, 2003
RMO..2005	1400–1960	Annual	Land + marine, 0–90°N	■	■	◢	◢	Rutherford et al., 2005
MSH..2005	1–1979	Annual	Land + marine, 0–90°N	◢	◢	◢	◢	Moberg et al., 2005
DWJ2006	713–1995	Annual	Land, 20°N–90°N	■	◢	☐	☐	D'Arrigo et al., 2006
HCA..2006	558–1960	Annual	Land, 20°N–90°N	◢	◢	☐	☐	Hegerl et al., 2006
PS2004	1500–2000	Annual	Land, 0–90°N	◢	■	☐	☐	Pollack and Smerdon, 2004; reference level adjusted following Moberg et al., 2005
O2005	1600–1990	Summer	Global land	◢	■	☐	☐	Oerlemans, 2005

Notes:
[a] Hadley Centre/Climatic Research Unit gridded surface temperature data set, version 2 variance adjusted.
[b] Climatic Research Unit gridded land surface air temperature, version 2 variance corrected.
[c] Location of proxies from H = high-latitude land, M = mid-latitude land, L = low-latitude land, O = oceans is indicated by ☐ (none or very few), ◢ (limited coverage) or ■ (moderate or good coverage).

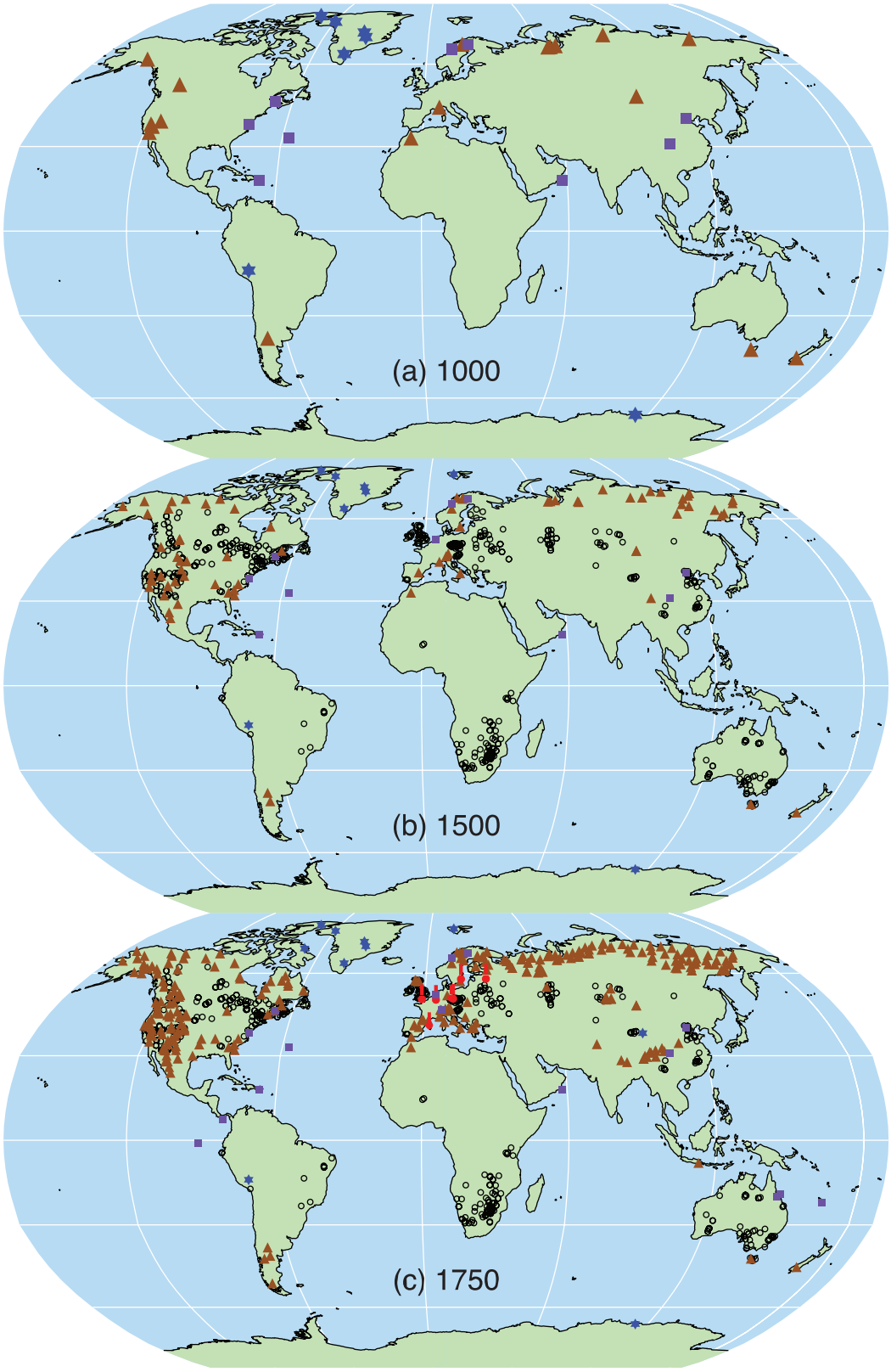


Figure 6.11. *Locations of proxy records with data back to AD 1000, 1500 and 1750 (instrumental: red thermometers; tree ring: brown triangles; borehole: black circles; ice core/ice borehole: blue stars; other including low-resolution records: purple squares) that have been used to reconstruct NH or SH temperatures by studies shown in Figure 6.10 (see Table 6.1, excluding O2005) or used to indicate SH regional temperatures (Figure 6.12).*

1 or 2 kyr, have been published (Esper et al., 2002; Crowley et al., 2003; Mann and Jones, 2003; Cook et al., 2004a; Moberg et al., 2005; Rutherford et al., 2005; D'Arrigo et al., 2006). These are shown, plotted from AD 700 in Figure 6.10b, along with the three series from the TAR. As with the original TAR series, these new records are not entirely independent reconstructions inasmuch as there are some predictors (most often tree ring data and particularly in the early centuries) that are common between them, but in general, they represent some expansion in the length and geographical coverage of the previously available data (Figures 6.10 and 6.11).

Briffa (2000) produced an extended history of interannual tree ring growth incorporating records from sites across northern Fennoscandia and northern Siberia, using a statistical technique to construct the tree ring chronologies that is capable of preserving multi-centennial time scale variability. Although ostensibly representative of northern Eurasian summer conditions, these data were later scaled using simple linear regression against a mean NH land series to provide estimates of summer temperature over the past 2 kyr (Briffa et al., 2004). Esper et al. (2002) took tree ring data from 14 sites in Eurasia and North America, and applied a variant of the same statistical technique designed to produce ring width chronologies in which evidence of long time scale climate forcing is better represented compared with earlier tree ring processing methods. The resulting series were averaged, smoothed and then scaled so that the multi-decadal variance matched that in the Mann et al. (1998) reconstruction over the period 1900 to 1977. This produced a reconstruction with markedly cooler temperatures during the 12th to the end of the 14th century than are apparent in any other series. The relative amplitude of this reconstruction is reduced somewhat when recalibrated directly against smoothed instrumental temperatures (Cook et al., 2004a) or by using annually resolved temperature data (Briffa and Osborn, 2002), but even then, this reconstruction remains at the coldest end of the range defined by all currently available reconstructions.

Mann and Jones (2003) selected only eight normalised series (all screened for temperature sensitivity) to represent annual mean NH temperature change over the last 1.8 kyr. Four of these eight represent integrations of multiple proxy site records or reconstructions, including some O isotope records from ice cores and documentary information as well tree ring records. A weighted average of these decadally smoothed series was scaled so that its mean and standard deviation matched those of the NH decadal mean land and marine record over the period 1856 to 1980. Moberg et al. (2005) used a mixture of tree ring and other proxy-based climate reconstructions to represent changes at short and longer time scales, respectively, across the NH. Seven tree ring series provided information on time scales shorter than 80 years, while 11 far less accurately dated records with lower resolution (including ice melt series, lake diatoms and pollen data, chemistry of marine shells and foraminifera, and one borehole temperature record from the Greenland Ice Sheet) were combined and scaled to match the mean and standard deviation of the instrumental record between 1856 and 1979. This reconstruction displays the warmest temperatures of any reconstruction during the 10th and early 11th centuries, although still below the level of warmth observed since 1980.

Many of the individual annually resolved proxy series used in the various reconstruction studies cited above have been combined in a new reconstruction (only back to AD 1400) based on a climate field reconstruction technique (Rutherford et al., 2005). This study also involved a methodological exploration of the sensitivity of the results to the precise specification of the predictor set, as well as the predictand target region and seasonal window. It concluded that the reconstructions were reasonably robust to differences in the choice of proxy data and statistical reconstruction technique.

D'Arrigo et al. (2006) used only tree ring data, but these include a substantial number not used in other reconstructions, particularly in northern North America. Their reconstruction, similar to that of Esper et al. (2002), displays a large amplitude of change during the past 1 kyr, associated with notably cool excursions during most of the 9th, 13th and 14th centuries, clearly below those of most other reconstructions. Hegerl et al. (2006) used a mixture of 14 regional series, of which only 3 were not made up from tree ring data (a Greenland ice O isotope record and two composite series, from China and Europe, including a mixture of instrumental, documentary and other data). Many of these are common to the earlier reconstructions. However, these series were combined and scaled using a regression approach (total least squares) intended to prevent the loss of low-frequency variance inherent in some other regression approaches. The reconstruction produced lies close to the centre of the range defined by the other reconstructions.

Various statistical methods are used to convert the various sets of original palaeoclimatic proxies into the different estimates of mean NH temperatures shown in Figure 6.10 (see discussions in Jones and Mann, 2004; Rutherford et al., 2005). These range from simple averaging of regional data and scaling of the resulting series so that its mean and standard deviation match those of the observed record over some period of overlap (Jones et al., 1998; Crowley and Lowery, 2000), to complex climate field reconstruction, where large-scale modes of spatial climate variability are linked to patterns of variability in the proxy network via a multivariate transfer function that explicitly provides estimates of the spatio-temporal changes in past temperatures, and from which large-scale average temperature changes are derived by averaging the climate estimates across the required region (Mann et al., 1998; Rutherford et al., 2003, 2005). Other reconstructions can be considered to represent what are essentially intermediate applications between these two approaches, in that they involve regionalisation of much of the data prior to the use of a statistical transfer function, and so involve fewer, but potentially more robust, regional predictors (Briffa et al., 2001; Mann and Jones, 2003; D'Arrigo et al., 2006). Some of these studies explicitly or implicitly reconstruct tropical temperatures based on data largely from the extratropics, and assume stability in the patterns of climate association between these regions. This assumption has been

questioned on the basis of both observational and model-simulated data suggesting that tropical to extratropical climate variability can be decoupled (Rind et al., 2005), and also that extratropical teleconnections associated with ENSO may vary through time (see Section 6.5.6).

Oerlemans (2005) constructed a temperature history for the globe based on 169 glacier length records. He used simplified glacier dynamics that incorporate specific response time and climate sensitivity estimates for each glacier. The reconstruction suggests that moderate global warming occurred after the middle of the 19th century, with about 0.6°C warming by the middle of the 20th century. Following a 25-year cooling, temperatures rose again after 1970, though much regional and high-frequency variability is superimposed on this overall interpretation. However, this approach does not allow for changing glacier sensitivity over time, which may limit the information before 1900. For example, analyses of glacier mass balances, volume changes and length variations along with temperature records in the western European Alps (Vincent et al., 2005) indicate that between 1760 and 1830, glacier advance was driven by precipitation that was 25% above the 20th century average, while there was little difference in average temperatures. Glacier retreat after 1830 was related to reduced winter precipitation and the influence of summer warming only became effective at the beginning of the 20th century. In southern Norway, early 18th-century glacier advances can be attributed to increased winter precipitation rather than cold temperatures (Nesje and Dahl, 2003).

Changes in proxy records, either physical (such as the isotopic composition of various elements in ice) or biological (such as the width of a tree ring or the chemical composition of a growth band in coral), do not respond precisely or solely to changes in any specific climate parameter (such as mean temperature or total rainfall), or to the changes in that parameter as measured over a specific 'season' (such as June to August or January to December). For this reason, the proxies must be 'calibrated' empirically, by comparing their measured variability over a number of years with available instrumental records to identify some optimal climate association, and to quantify the statistical uncertainty associated with scaling proxies to represent this specific climate parameter. All reconstructions, therefore, involve a degree of compromise with regard to the specific choice of 'target' or dependent variable. Differences between the temperature reconstructions shown in Figure 6.10b are to some extent related to this, as well as to the choice of different predictor series (including differences in the way these have been processed). The use of different statistical scaling approaches (including whether the data are smoothed prior to scaling, and differences in the period over which this scaling is carried out) also influences the apparent spread between the various reconstructions. Discussions of these issues can also be found in Harris and Chapman (2001), Beltrami (2002), Briffa and Osborn (2002), Esper et al. (2002), Trenberth and Otto-Bliesner (2003), Zorita et al. (2003), Jones and Mann (2004), Pollack and Smerdon (2004), Esper et al. (2005) and Rutherford et al. (2005).

The considerable uncertainty associated with individual reconstructions (2-standard-error range at the multi-decadal time scale is of the order of ±0.5°C) is shown in several publications, calculated on the basis of analyses of regression residuals (Mann et al., 1998; Briffa et al., 2001; Jones et al., 2001; Gerber et al., 2003; Mann and Jones, 2003; Rutherford et al., 2005; D'Arrigo et al., 2006). These are often calculated from the error apparent in the calibration of the proxies. Hence, they are likely to be minimum uncertainties, as they do not take into account other sources of error not apparent in the calibration period, such as any reduction in the statistical robustness of the proxy series in earlier times (Briffa and Osborn, 1999; Esper et al., 2002; Bradley et al., 2003b; Osborn and Briffa, 2006).

All of the large-scale temperature reconstructions discussed in this section, with the exception of the borehole and glacier interpretations, include tree ring data among their predictors so it is pertinent to note several issues associated with them. The construction of ring width and ring density chronologies involves statistical processing designed to remove non-climate trends that could obscure the evidence of climate that they contain. In certain situations, this process may restrict the extent to which a chronology portrays the evidence of long time scale changes in the underlying variability of climate that affected the growth of the trees; in effect providing a high-pass filtered version of past climate. However, this is generally not the case for chronologies used in the reconstructions illustrated in Figure 6.10. Virtually all of these used chronologies or tree ring climate reconstructions produced using methods that preserve multi-decadal and centennial time scale variability. As with all biological proxies, the calibration of tree ring records using linear regression against some specific climate variable represents a simplification of what is inevitably a more complex and possibly time-varying relationship between climate and tree growth. That this is a defensible simplification, however, is shown by the general strength of many such calibrated relationships, and their significant verification using independent instrumental data. There is always a possibility that non-climate factors, such as changing atmospheric CO_2 or soil chemistry, might compromise the assumption of uniformity implicit in the interpretation of regression-based climate reconstructions, but there remains no evidence that this is true for any of the reconstructions referred to in this assessment. A group of high-elevation ring width chronologies from the western USA that show a marked growth increase during the last 100 years, attributed by LaMarche et al. (1984) to the fertilizing effect of increasing atmospheric CO_2, were included among the proxy data used by Mann et al. (1998, 1999). However, their tree ring data from the western USA were adjusted specifically in an attempt to mitigate this effect. Several analyses of ring width and ring density chronologies, with otherwise well-established sensitivity to temperature, have shown that they do not emulate the general warming trend evident in instrumental temperature records over recent decades, although they do track the warming that occurred during the early part of the 20th century and they continue to maintain a good correlation with observed temperatures over the full instrumental period at the

interannual time scale (Briffa et al., 2004; D'Arrigo, 2006). This 'divergence' is apparently restricted to some northern, high-latitude regions, but it is certainly not ubiquitous even there. In their large-scale reconstructions based on tree ring density data, Briffa et al. (2001) specifically excluded the post-1960 data in their calibration against instrumental records, to avoid biasing the estimation of the earlier reconstructions (hence they are not shown in Figure 6.10), implicitly assuming that the 'divergence' was a uniquely recent phenomenon, as has also been argued by Cook et al. (2004a). Others, however, argue for a breakdown in the assumed linear tree growth response to continued warming, invoking a possible threshold exceedance beyond which moisture stress now limits further growth (D'Arrigo et al., 2004). If true, this would imply a similar limit on the potential to reconstruct possible warm periods in earlier times at such sites. At this time there is no consensus on these issues (for further references see NRC, 2006) and the possibility of investigating them further is restricted by the lack of recent tree ring data at most of the sites from which tree ring data discussed in this chapter were acquired.

Figure 6.10b illustrates how, when viewed together, the currently available reconstructions indicate generally greater variability in centennial time scale trends over the last 1 kyr than was apparent in the TAR. It should be stressed that each of the reconstructions included in Figure 6.10b is shown scaled as it was originally published, despite the fact that some represent seasonal and others mean annual temperatures. Except for the borehole curve (Pollack and Smerdon, 2004) and the interpretation of glacier length changes (Oerlemans, 2005), they were originally also calibrated against different instrumental data, using a variety of statistical scaling approaches. For all these reasons, these reconstructions would be expected to show some variation in relative amplitude.

Figure 6.10c is a schematic representation of the most likely course of hemispheric mean temperature change during the last 1.3 kyr based on all of the reconstructions shown in Figure 6.10b, and taking into account their associated statistical uncertainty. The envelopes that enclose the two standard error confidence limits bracketing each reconstruction have been overlain (with greater emphasis placed on the area within the 1 standard error limits) to show where there is most agreement between the various reconstructions. The result is a picture of relatively cool conditions in the 17th and early 19th centuries and warmth in the 11th and early 15th centuries, but the warmest conditions are apparent in the 20th century. Given that the confidence levels surrounding all of the reconstructions are wide, virtually all reconstructions are effectively encompassed within the uncertainty previously indicated in the TAR. The major differences between the various proxy reconstructions relate to the magnitude of past cool excursions, principally during the 12th to 14th, 17th and 19th centuries. Several reconstructions exhibit a short-lived maximum just prior to AD 1000 but only one (Moberg et al., 2005) indicates persistent hemispheric-scale conditions (i.e., during AD 990 to 1050 and AD 1080 to 1120) that were as warm as those in the 1940s and 50s. However, the long time scale variability in this reconstruction is determined by low-resolution proxy records that cannot be rigorously calibrated against recent instrumental temperature data (Mann et al., 2005b). None of the reconstructions in Fig. 6.10 show pre-20th century temperatures reaching the levels seen in the instrumental temperature record for the last two decades of the 20th century.

It is important to recognise that in the NH as a whole there are few long and well-dated climate proxies, particularly for the period prior to the 17th century (Figure 6.11). Those that do exist are concentrated in extratropical, terrestrial locations, and many have greatest sensitivity to summer rather than winter (or annual) conditions. Changes in seasonality probably limit the conclusions that can be drawn regarding annual temperatures derived from predominantly summer-sensitive proxies (Jones et al., 2003). There are very few strongly temperature-sensitive proxies from tropical latitudes. Stable isotope data from high-elevation ice cores provide long records and have been interpreted in terms of past temperature variability (Thompson, 2000), but recent calibration and modelling studies in South America and southern Tibet (Hoffmann et al., 2003; Vuille and Werner, 2005; Vuille et al., 2005) indicate a dominant sensitivity to precipitation changes, at least on seasonal to decadal time scales, in these regions. Very rapid and apparently unprecedented melting of tropical ice caps has been observed in recent decades (Thompson et al., 2000; Thompson, 2001; see Box 6.3), likely associated with enhanced warming at high elevations (Gaffen et al., 2000; see Chapter 4). Coral O isotopes and Sr/Ca ratios reflect SSTs, although the former are also influenced by salinity changes associated with precipitation variability (Lough, 2004). Unfortunately, these records are invariably short, of the order of centuries at best, and can be associated with age uncertainties of 1 or 2%. Virtually all coral records currently available from the tropical Indo-Pacific indicate unusual warmth in the 20th century (Cole, 2003), and in the tropical Indian Ocean many isotope records show a trend towards warmer conditions (Charles et al., 1997; Kuhnert et al., 1999; Cole et al., 2000). In most multi-centennial length coral series, the late 20th century is warmer than any time in the last 100 to 300 years.

Using pseudo-proxy networks extracted from GCM simulations of global climate for the last millennium, von Storch et al. (2004) suggested that temperature reconstructions may not fully represent variance on long time scales. This would represent a bias, as distinct from the random error represented by published reconstruction uncertainty ranges. At present, the extent of any such biases in specific reconstructions and as indicated by pseudo-proxy studies is uncertain (being dependent on the choice of statistical regression model and climate model simulation used to provide the pseudo-proxies). It is very unlikely, however, that any bias would be as large as the factor of two suggested by von Storch et al. (2004) with regard to the reconstruction by Mann et al. (1998), as discussed by Burger and Cubash (2005) and Wahl et al. (2006). However, the bias will depend on the degree to which past climate departs from the range of temperatures encompassed within the calibration period data (Mann et al., 2005b; Osborn and Briffa, 2006) and on the proportions of temperature variability

occurring on short and long time scales (Osborn and Briffa, 2004). In any case, this bias would act to damp the amplitude of reconstructed departures that are further from the calibration period mean, so that temperatures during cooler periods may have been colder than estimated by some reconstructions, while periods with comparable temperatures (e.g., possible portions of the period between AD 950 and 1150, Figure 6.10) would be largely unbiased. As only one reconstruction (Moberg et al., 2005) shows an early period that is noticeably warmer than the mean for the calibration period, the possibility of a bias does not affect the general conclusion about the relative warmth of the 20th century based on these data.

The weight of current multi-proxy evidence, therefore, suggests greater 20th-century warmth, in comparison with temperature levels of the previous 400 years, than was shown in the TAR. On the evidence of the previous and four new reconstructions that reach back more than 1 kyr, it is likely that the 20th century was the warmest in at least the past 1.3 kyr. Considering the recent instrumental and longer proxy evidence together, it is very likely that average NH temperatures during the second half of the 20th century were higher than for any other 50-year period in the last 500 years. Greater uncertainty associated with proxy-based temperature estimates for individual years means that it is more difficult to gauge the significance, or precedence, of the extreme warm years observed in the recent instrumental record, such as 1998 and 2005, in the context of the last millennium.

6.6.1.2 What Do Large-Scale Temperature Histories from Subsurface Temperature Measurements Show?

Hemispheric or global ground surface temperature (GST) histories reconstructed from measurements of subsurface temperatures in continental boreholes have been presented by several geothermal research groups (Huang et al., 2000; Harris and Chapman, 2001; Beltrami, 2002; Beltrami and Bourlon, 2004; Pollack and Smerdon, 2004); see Pollack and Huang (2000) for a review of this methodology. These borehole reconstructions have been derived using the contents of a publicly available database of borehole temperatures and climate reconstructions (Huang and Pollack, 1998) that in 2004 included 695 sites in the NH and 166 in the SH (Figure 6.11). Because the solid Earth acts as a low-pass filter on downward-propagating temperature signals, borehole reconstructions lack annual resolution; accordingly they typically portray only multi-decadal to centennial changes. These geothermal reconstructions provide independent estimates of surface temperature history with which to compare multi-proxy reconstructions. Figure 6.10b shows a reconstruction of average NH GST by Pollack and Smerdon (2004). This reconstruction, very similar to that presented by Huang et al. (2000), shows an overall warming of the ground surface of about 1.0°C over the past five centuries. The two standard error uncertainties for their series (not shown here) are 0.20°C (in 1500), 0.10°C (1800) and 0.04°C (1900). These are errors associated with various scales of areal weighting and consequent suppression of site-specific noise through aggregation (Pollack and Smerdon, 2004). The reconstruction is similar to the cooler multi-proxy reconstructions in the 16th and 17th centuries, but sits in the middle of the multi-proxy range in the 19th and early 20th centuries. A geospatial analysis by Mann et al. (2003; see correction by Rutherford and Mann, 2004) of the results of Huang et al. (2000) argued for significantly less overall warming, a conclusion contested by Pollack and Smerdon (2004) and Beltrami and Bourlon (2004). Geothermal reconstructions based on the publicly available database generally yield somewhat muted estimates of the 20th-century trend, because of a relatively sparse representation of borehole data north of 60°N. About half of the borehole sites at the time of measurement had not yet been exposed to the significant warming of the last two decades of the 20th century (Taylor et al., 2006; Majorowicz et al., 2004).

The assumption that the reconstructed GST history is a good representation of the surface air temperature (SAT) history has been examined with both observational data and model studies. Observations of SAT and GST display differences at daily and seasonal time scales, and indicate that the coupling of SAT and GST over a single year is complex (Sokratov and Barry, 2002; Stieglitz et al., 2003; Bartlett et al., 2004; Smerdon et al., 2006). The mean annual GST differs from the mean annual SAT in regions where there is snow cover and/or seasonal freezing and thawing (Gosnold et al., 1997; Smerdon et al., 2004; Taylor et al., 2006), as well as in regions without those effects (Smerdon et al., 2006). Observational time series of ground temperatures are not long enough to establish whether the mean annual differences are stable over long time scales. The long-term coupling between SAT and GST has been addressed by simulating both air and soil temperatures in global three-dimensional coupled climate models. Mann and Schmidt (2003), in a 50-year experiment using the GISS Model E, suggested that GST reconstructions may be biased by seasonal influences and snow cover variability, an interpretation contested by Chapman et al (2004). Thousand-year simulations by González-Rouco et al. (2003, 2006) using the ECHO-G model suggest that seasonal differences in coupling are of little significance over long time scales. They also indicate that deep soil temperature is a good proxy for the annual SAT on continents and that the spatial array of borehole locations is adequate to reconstruct the NH mean SAT. Neither of these climate models included time-varying vegetation cover.

6.6.2 Southern Hemisphere Temperature Variability

There are markedly fewer well-dated proxy records for the SH compared to the NH (Figure 6.11), and consequently little evidence of how large-scale average surface temperatures have changed over the past few thousand years. Mann and Jones (2003) used only three series to represent annual mean SH temperature change over the last 1.5 kyr. A weighted combination of the individual standardised series was scaled to match (at decadal time scales) the mean and the standard deviation of SH annual

mean land and marine temperatures over the period 1856 to 1980. The recent proxy-based temperature estimates, up to the end of the reconstruction in 1980, do not capture the full magnitude of the warming seen in the instrumental temperature record. Earlier periods, around AD 700 and 1000, are reconstructed as warmer than the estimated level in the 20th century, and may have been as warm as the measured values in the last 20 years. The paucity of SH proxy data also means that uncertainties associated with hemispheric temperature estimates are much greater than for the NH, and it is more appropriate at this time to consider the evidence in terms of limited regional indicators of temperature change (Figure 6.12).

The long-term oscillations in warm-season temperatures shown in a tree ring reconstruction for Tasmania (Cook et al., 2000) suggest that the last 30 years was the warmest multi-decadal period in the last 1 kyr, but only by a marginal degree. Conditions were generally warm over a longer period from 1300 to 1500 (Figure 6.12). Another tree ring reconstruction, of austral summer temperatures based on data from South Island, New Zealand, spans the past 1.1 kyr and is the longest yet produced for the region (Cook et al., 2002a). Disturbance at the site from which the trees were sampled restricts the calibration of this record to the 70 years up until 1950, but both tree rings and instrumental data indicate that the 20th century was not anomalously warm when compared to several warm periods reconstructed in the last 1 kyr (around the mid-12th and early 13th centuries and around 1500).

Tree-ring based temperature reconstructions across the Southern Andes (37°S to 55°S) of South America indicate that the annual temperatures during the 20th century have been anomalously high in the context of the past four centuries. The mean annual temperatures for northern and southern Patagonia during the interval 1900 to 1990 are 0.53°C and 0.86°C above the 1640 to 1899 means, respectively (Figure 6.12). In Northern Patagonia, the highest temperatures occurred in the 1940s. In Southern Patagonia, the year 1998 was the warmest of the past four centuries. The rate of temperature increase from 1850 to 1920 was the highest over the past 360 years (Villalba et al., 2003).

Figure 6.12 also shows the evidence of GST changes over the last 500 years, provided by regionally aggregated borehole temperature inversions (Figure 6.11) from southern Africa (92 records) and Australia (57 records) described in Huang et al. (2000). The instrumental records for these areas show warmer conditions that postdate the time when the boreholes were logged; thus, the most recent warming is not registered in these borehole curves. A more detailed analysis of the Australian geothermal reconstruction (Pollack et al., 2006), indicates that the warming of Australia in the past five centuries was apparently only half that experienced over the continents of the NH during the same period and shows good correspondence with the tree-ring based reconstructions for Tasmania and New Zealand (Cook et al., 2000, 2002a). Contrasting evidence of past temperature variations at Law Dome, Antarctica has been derived from ice core isotope measurements and from the inversion of a subsurface temperature profile (Dahl-Jensen et al., 1999; Goosse et al., 2004; Jones and Mann, 2004). The borehole analysis indicates colder intervals at around 1250 and 1850, followed by a gradual warming of 0.7°C to the present. The isotope record indicates a relatively cold 20th century and warmer conditions throughout the period 1000 to 1750.

Taken together, the very sparse evidence for SH temperatures prior to the period of instrumental records indicates that unusual warming is occurring in some regions. However, more proxy data are required to verify the apparent warm trend.

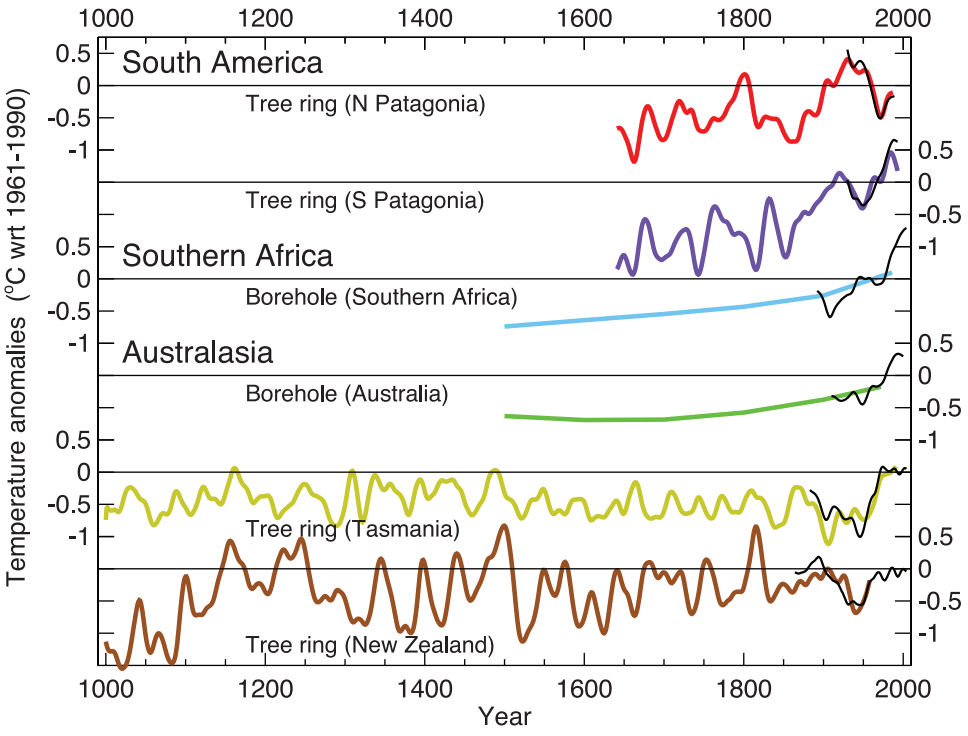


Figure 6.12. *Temperature reconstructions for regions in the SH: two annual temperature series from South American tree ring data (Villalba et al., 2003); annual temperature estimates from borehole inversions for southern Africa and Australia (Huang et al, 2000); summer temperature series from Tasmania and New Zealand tree ring data (Cook et al., 2000, 2002a). The black curves show summer or annual instrumental temperatures for each region. All tree ring and instrumental series were smoothed with a 25-year filter and represent anomalies (°C) from the 1961 to 1990 mean (indicated by the horizontal lines).*

6.6.3 Comparisons of Millennial Simulations with Palaeodata

A range of increasingly complex climate models has been used to simulate NH temperatures over the last 500 to 1,000 years using both natural and anthropogenic forcings (Figure 6.13). These models include an energy balance formulation (Crowley et al., 2003, Gerber et al., 2003), two- and three-dimensional reduced complexity models (Bertrand et al., 2002b; Bauer et al., 2003), and three fully coupled AOGCMs (Ammann et al., 2003; Von Storch et al., 2004; Tett et al., 2007).

Comparison and evaluation of the output from palaeoclimate simulations is complicated by their use of different historical forcings, as well as by the way indirect evidence of the history of various forcings is translated into geographically and seasonally specific radiative inputs within the models. Some factors, such as orbital variations of the Earth in relation to the Sun, can be calculated accurately (e.g., Berger, 1977; Bradley et al., 2003b) and directly implemented in terms of latitudinal and seasonal changes in incoming shortwave radiation at the top of the atmosphere. For the last 2 kyr, although this forcing is incorporated in most models, its impact on climate can be neglected compared to the other forcings (Bertrand et al., 2002b).

Over recent millennia, the analysis of the gas bubbles in ice cores with high deposition rates provides good evidence of greenhouse gas changes at near-decadal resolution (Figure 6.4). Other factors, such as land use changes (Ramankutty and Foley, 1999) and the concentrations and distribution of tropospheric aerosols and ozone, are not as well known (Mickley et al., 2001). However, because of their magnitude, uncertainties in the history of solar irradiance and volcanic effects are more significant for the pre-industrial period.

6.6.3.1 Solar Forcing

The direct measurement of solar irradiance by satellite began less than 30 years ago, and over this period only very small changes are apparent (0.1% between the peak and trough of recent sunspot cycles, which equates to only about 0.2 W m^{-2} change in radiative forcing; Fröhlich and Lean (2004); see Section 2.7). Earlier extensions of irradiance change used in most model simulations are estimated by assuming a direct correlation with evidence of changing sunspot numbers and cosmogenic isotope production as recorded in ice cores (^{10}Be) and tree rings (^{14}C) (Lean et al., 1995; Crowley, 2000).

There is general agreement in the evolution of the different proxy records of solar activity such as cosmogenic isotopes, sunspot numbers or aurora observations, and the annually resolved records clearly depict the well-known 11-year solar cycle (Muscheler et al., 2006). For example, palaeoclimatic ^{10}Be and ^{14}C values are higher during times of low or absent sunspot numbers. During these periods, their production is high as the shielding of the Earth's atmosphere from cosmic rays provided by the Sun's open magnetic field is weak (Beer et al., 1998). However, the relationship between the isotopic records indicative of the Sun's open magnetic field, sunspot numbers and the Sun's closed magnetic field or energy output are not fully understood (Wang and Sheeley, 2003).

Table 6.2. *Climate model simulations shown in Figure 6.13.*

Series	Model[a]	Model type	Forcings[b]	Reference
GSZ2003	ECHO-G	GCM	SV -G - - - -	González-Rouco et al., 2003
ORB2006	ECHO-G/MAGICC	GCM adj. using EBM[c]	SV -G -A -Z	Osborn et al., 2006
TBC..2006	HadCM3	GCM	SVOG -ALZ	Tett et al., 2007
AJS..2006	NCAR CSM	GCM	SV -G -A -Z	Mann et al., 2005b
BLC..2002	MoBiDiC	EMIC	SV -G -AL -	Bertrand et al., 2002b
CBK..2003	-	EBM[c]	SV -G -A - -	Crowley et al., 2003
GRT..2005	ECBilt-CLIO	EMIC	SV -G -A - -	Goosse et al., 2005b
GJB..2003	Bern CC	EBM[c]	SV -G -A -Z	Gerber et al., 2003
B..03-14C	Climber2	EMIC (solar from ^{14}C)	SV - -C -L -	Bauer et al., 2003
B..03-10Be	Climber2	EMIC (solar from ^{10}Be)	SV - -C -L -	Bauer et al., 2003
GBZ..2006	ECHO-G	GCM	SV -G - - - -	González-Rouco et al., 2006
SMC2006	ECHAM4/OPYC3	GCM	SV -G -A -Z	Stendel et al., 2006

Notes:
[a] Models: ECHO-G = ECHAM4 atmospheric GCM/HOPE-G ocean GCM, MAGICC = Model for the Assessment of Greenhouse-gas Induced Climate Change, HadCM3 = Hadley Centre Coupled Model 3; NCAR CSM = National Center for Atmospheric Research Climate System Model, MoBiDiC = Modèle Bidimensionnel du Climat , ECBilt-CLIO = ECBilt-Coupled Large-scale Ice Ocean, Bern CC = Bern Carbon Cycle-Climate Model, CLIMBER2 = Climate Biosphere Model 2, ECHAM4/OPYC3 = ECHAM4 atmospheric GCM/Ocean Isopycnal GCM 3.
[b] Forcings: S = solar, V = volcanic, O = orbital, G = well-mixed greenhouse gases, C = CO_2 but not other greenhouse gases, A = tropospheric sulphate aerosol, L = land use change, Z=tropospheric and/or stratospheric ozone changes and/or halocarbons.
[c] EBM = Energy Balance Model.

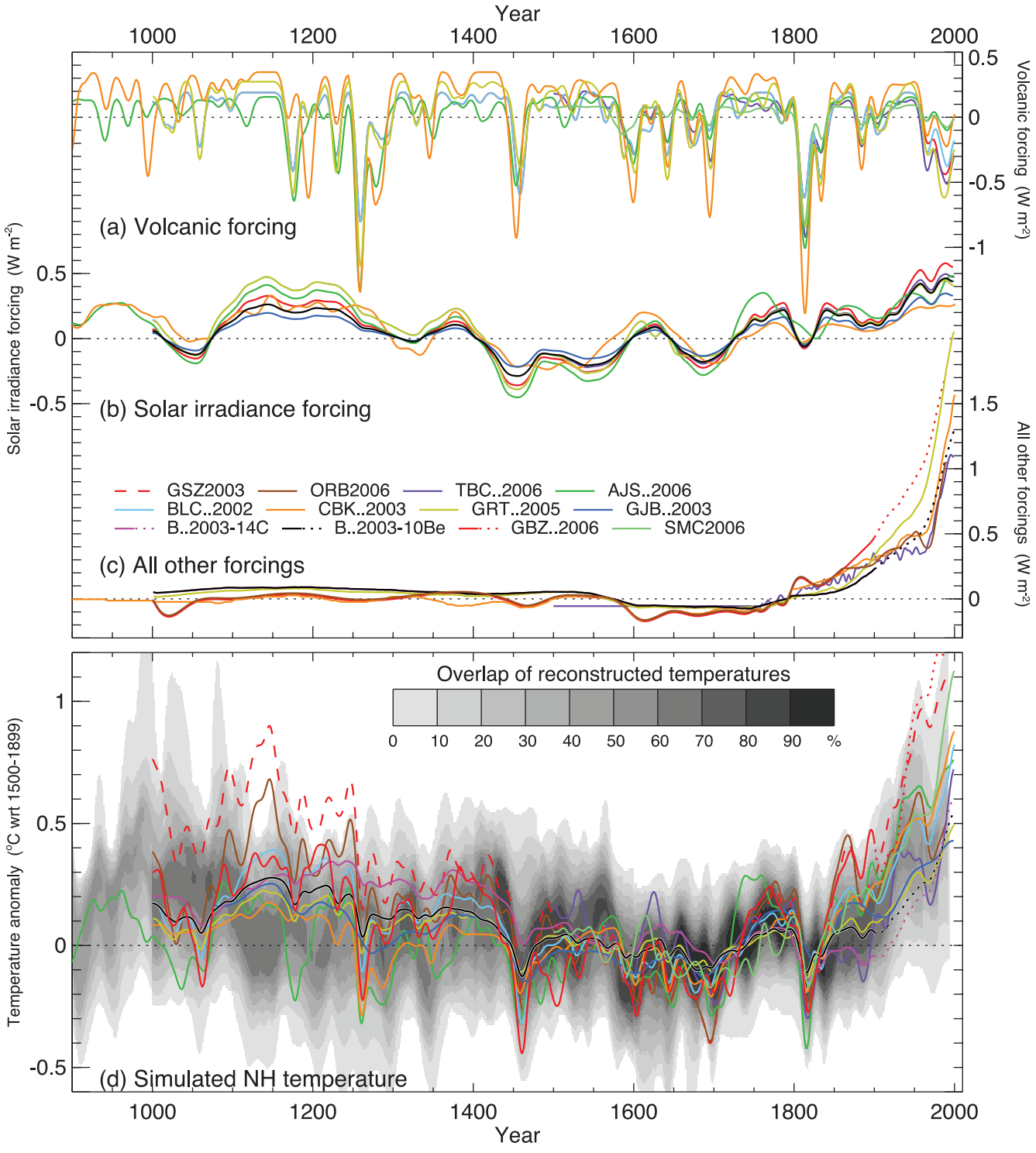


Figure 6.13. *Radiative forcings and simulated temperatures during the last 1.1 kyr. Global mean radiative forcing (W m^{-2}) used to drive climate model simulations due to (a) volcanic activity, (b) solar irradiance variations and (c) all other forcings (which vary between models, but always include greenhouse gases, and, except for those with dotted lines after 1900, tropospheric sulphate aerosols). (d) Annual mean NH temperature (°C) simulated under the range of forcings shown in (a) to (c), compared with the concentration of overlapping NH temperature reconstructions (shown by grey shading, modified from Figure 6.10c to account for the 1500 to 1899 reference period used here). All forcings and temperatures are expressed as anomalies from their 1500 to 1899 means and then smoothed with a Gaussian-weighted filter to remove fluctuations on time scales less than 30 years; smoothed values are obtained up to both ends of each record by extending the records with the mean of the adjacent existing values. The individual series are identified in Table 6.2.*

The cosmogenic isotope records have been linearly scaled to estimate solar energy output (Bard et al., 2000) in many climate simulations. More recent studies utilise physics-based models to estimate solar activity from the production rate of cosmogenic isotopes taking into account nonlinearities between isotope production and the Sun's open magnetic flux and variations in the geomagnetic field (Solanki et al., 2004; Muscheler et al., 2005). Following this approach, Solanki et al. (2004) suggested that the current level of solar activity has been without precedent over the last 8 kyr. This is contradicted by a more recent analysis linking the isotope proxy records to instrumental data that identifies, for the last millennium, three periods (around AD 1785, 1600 and 1140) when solar activity was as high, or higher, than in the satellite era (Muscheler et al., 2006).

The magnitude of the long-term trend in solar irradiance remains uncertain. A reassessment of the stellar data (Hall and Lockwood, 2004) has been unable to confirm or refute the analysis by Baliunas and Jastrow (1990) that implied significant long-term solar irradiance changes, and also underpinned some of the earlier reconstructions (see Section 2.7). Several new studies (Lean et al., 2002; Foster, 2004; Foukal et al., 2004; Y.M. Wang et al., 2005) suggest that long-term irradiance changes were notably less than in earlier reconstructions (Hoyt and Schatten, 1993; Lean et al., 1995; Lockwood and Stamper, 1999; Bard et al., 2000; Fligge and Solanki, 2000; Lean, 2000) that were employed in a number of TAR climate change simulations and in many of the simulations shown in Figure 6.13d.

In the previous reconstructions, the 17th-century 'Maunder Minimum' total irradiance was 0.15 to 0.65% (irradiance change about 2.0 to 8.7 W m^{-2}; radiative forcing about 0.36 to 1.55 W m^{-2}) below the present-day mean (Figure 6.13b). Most of the recent studies (with the exception of Solanki and Krivova, 2003) calculate a reduction of only around 0.1% (irradiance change of the order of –1 W m^{-2}, radiative forcing of –0.2 W m^{-2}; section 2.7). Following these results, the magnitude of the radiative forcing used in Chapter 9 for the Maunder Minimum period is relatively small (–0.2 W m^{-2} relative to today).

6.6.3.2 Volcanic Forcing

There is also uncertainty in the estimates of volcanic forcing during recent millennia because of the necessity to infer atmospheric optical depth changes (including geographic details as well as temporal accuracy and persistence), where there is only indirect evidence in the form of levels of acidity and sulphate measured in ice cores (Figures 6.14 and 6.15). All of the volcanic histories used in current model-based palaeoclimate simulations are based on analyses of polar ice cores containing minor dating uncertainty and obvious geographical bias.

The considerable difficulties in calculating hemispheric and regional volcanic forcing changes (Robock and Free, 1995; Robertson et al., 2001; Crowley et al., 2003) result from sensitivity to the choice of which ice cores are considered, assumptions as to the extent of stratosphere penetration by eruption products, and the radiative properties of different volcanic aerosols and their residence time in the stratosphere. Even after producing some record of volcanic activity, there are major differences in the way models implement this. Some use a direct reduction in global radiative forcing with no spatial discrimination (von Storch et al., 2004), while other models prescribe geographical changes in radiative forcing (Crowley et al., 2003; Goosse et al., 2005a; Stendel et al., 2006). Models with more sophisticated radiative schemes are able to incorporate prescribed aerosol optical depth changes, and interactively calculate the perturbed (longwave and shortwave) radiation budgets (Tett et al., 2007). The effective level of (prescribed or diagnosed) volcanic forcing therefore varies considerably between the simulations (Figure 6.13a).

6.6.3.3 Industrial Era Sulphate Aerosols

Ice core data from Greenland and the mid-latitudes of the NH (Schwikowski et al., 1999; Bigler et al., 2002) provide evidence of the rapid increase in sulphur dioxide emissions (Stern, 2005) and tropospheric sulphate aerosol loading, above the pre-industrial background, during the modern industrial era but they also show a very recent decline in these emissions (Figure 6.15). Data from ice cores show that sulphate aerosol deposition has not changed on Antarctica, remote from anthropogenic sulphur dioxide sources. The ice records are indicative of the regional-to-hemispheric scale atmospheric loading of sulphate aerosols that varies regionally as aerosols have a typical lifetime of only weeks in the troposphere. In recent years, sulphur dioxide emissions have decreased globally and in many regions of the NH (Stern, 2005; see Chapter 2). In general, tropospheric sulphate aerosols exert a negative temperature forcing that will be less if sulphur dioxide emissions and the sulphate loading in the atmosphere continue to decrease.

6.6.3.4 Comparing Simulations of Northern Hemisphere Mean Temperatures with Palaeoclimatic Observations

Various simulations of NH (mean land and marine) surface temperatures produced by a range of climate models, and the forcings that were used to drive them, are shown in Figure 6.13. Despite differences in the detail and implementation of the different forcing histories, there is generally good qualitative agreement between the simulations regarding the major features: warmth during much of the 12th through 14th centuries, with lower temperatures being sustained during the 17th, mid 15th and early 19th centuries, and the subsequent sharp rise to unprecedented levels of warmth at the end of the 20th century. The spread of this multi-model ensemble is constrained to be small during the 1500 to 1899 reference period (selected following Osborn et al., 2006), but the model spread also remains small back to 1000, with the exception of the ECHO-G simulation (Von Storch et al., 2004). The implications of the greater model spread in the rates

of warming after 1840 will be clear only after determining the extent to which it can be attributed to differences in prescribed forcings and individual model sensitivities (Goosse et al., 2005b). The ECHO-G simulation (dashed red line in Figure 6.13d) is atypical compared to the ensemble as a whole, being notably warmer in the pre-1300 and post-1900 periods. Osborn et al. (2006) showed that these anomalies are likely the result of a large initial disequilibrium and the lack of anthropogenic tropospheric aerosols in that simulation (see Figure 6.13c). One other simulation (González-Rouco et al., 2006) also exhibits greater early 20th-century warming in comparison to the other simulations but, similarly, does not include tropospheric aerosols among the forcings. All of these simulations, therefore, appear to be consistent with the reconstructions of past NH temperatures, for which the evidence (taken from Figure 6.10c) is shown by the grey shading underlying the simulations in Figure 6.13d.

It is important to note that many of the simulated temperature variations during the pre-industrial period shown in Figure 6.13 have been driven by assumed solar forcing, the magnitude of which is currently in doubt. Therefore, although the data and simulations appear consistent at this hemispheric scale, they are not a powerful test of the models because of the large uncertainty in both the reconstructed NH changes and the total radiative forcing. The influence of solar irradiance variability and anthropogenic forcings on simulated NH surface temperature is further illustrated in Figure 6.14. A range of EMICs (Petoukhov et al., 2000; Plattner et al., 2001; Montoya et al., 2005) were forced with two different reconstructions of solar irradiance (Bard et al., 2000; Y.M. Wang et al., 2005) to compare the

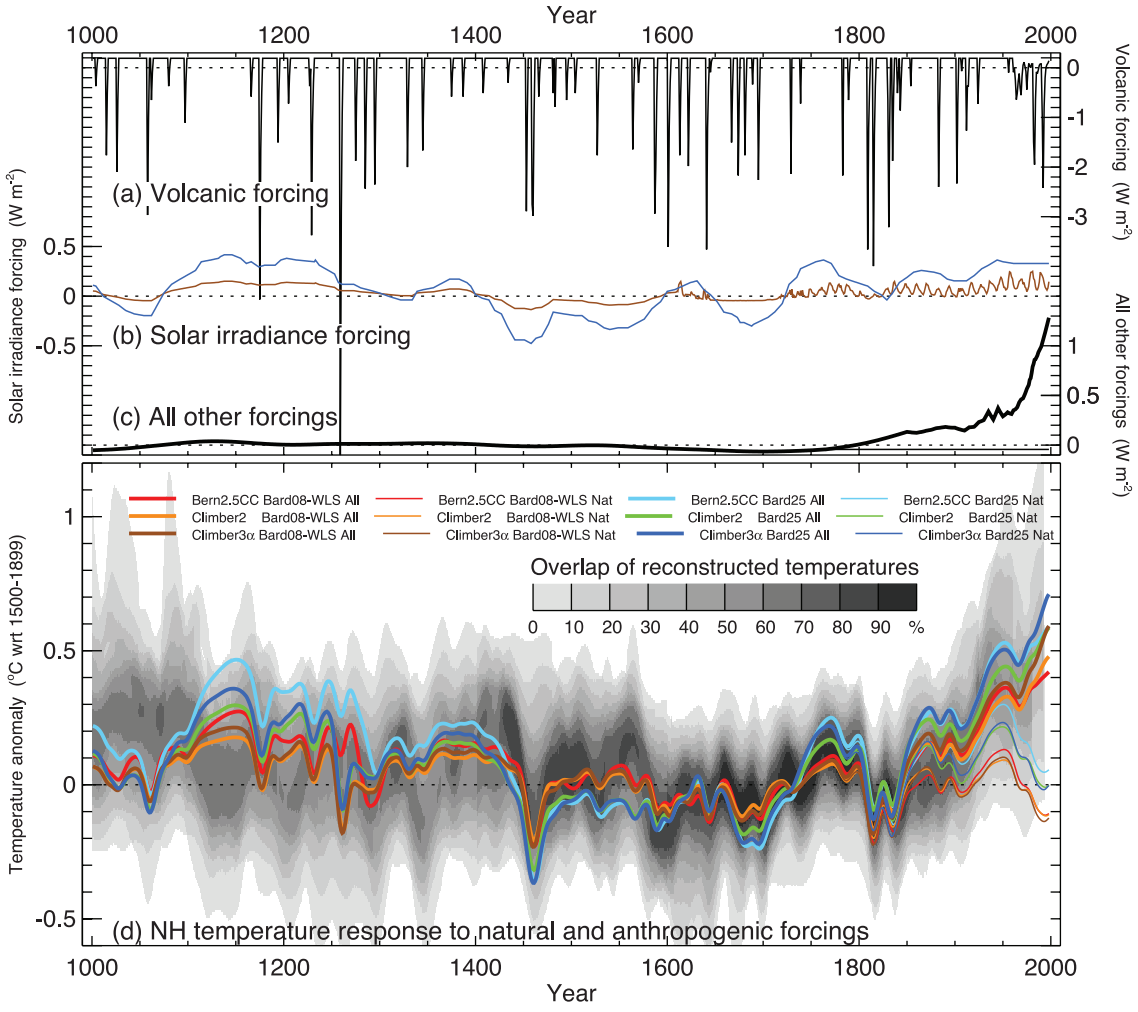


Figure 6.14. *Simulated temperatures during the last 1 kyr with and without anthropogenic forcing, and also with weak or strong solar irradiance variations. Global mean radiative forcing (W m^{-2}) used to drive climate model simulations due to (a) volcanic activity, (b) strong (blue) and weak (brown) solar irradiance variations, and (c) all other forcings, including greenhouse gases and tropospheric sulphate aerosols (the thin flat line after 1765 indicates the fixed anthropogenic forcing used in the 'Nat' simulations). (d) Annual mean NH temperature (°C) simulated by three climate models under the forcings shown in (a) to (c), compared with the concentration of overlapping NH temperature reconstructions (shown by grey shading, modified from Figure 6.10c to account for the 1500 to 1899 reference period used here). 'All' (thick lines) used anthropogenic and natural forcings; 'Nat' (thin lines) used only natural forcings. All forcings and temperatures are expressed as anomalies from their 1500 to 1899 means; the temperatures were then smoothed with a Gaussian-weighted filter to remove fluctuations on time scales less than 30 years. Note the different vertical scale used for the volcanic forcing compared with the other forcings. The individual series are identified in Table 6.3.*

influence of large versus small changes in the long-term strength of solar irradiance over the last 1 kyr (Figure 6.14b). Radiative forcing related to explosive volcanism (Crowley, 2000), atmospheric CO_2 and other anthropogenic agents (Joos et al., 2001) were identically prescribed within each model simulation. Additional simulations, in which anthropogenic forcings were not included, enable a comparison to be made between 'natural' versus 'all' (i.e., natural plus anthropogenic) forcings on the evolution of hemispheric temperatures before and during the 20th century.

The alternative solar irradiance histories used in the simulations differ in their low-frequency amplitudes by a factor of about three. The 'high-amplitude' case (strong solar irradiance forcing) corresponds roughly with the level of irradiance change assumed in many of the simulations shown in Figure 6.13b, whereas the 'low-amplitude' case (weaker solar irradiance forcing) is representative of the more recent reconstructions of solar irradiance changes (as discussed in Section 6.6.3). The high-amplitude forcing history ('Bard25', Table 6.3) is based on an ice core record of ^{10}Be scaled to give an average reduction in solar irradiance of 0.25% during the Maunder Minimum, as compared to today (Bard et al., 2000). The low-amplitude history ('Bard08-WLS') is estimated using sunspot data and a model of the Sun's closed magnetic flux for the period from 1610 to the present (Y.M. Wang et al., 2005), with an earlier extension based on the Bard et al. (2000) record scaled to a Maunder Minimum reduction of 0.08% compared to today. The low-frequency evolution of these two reconstructions is very similar (Figure 6.14) even though they are based on completely independent sources of observational data (sunspots versus cosmogenic isotopes) and are produced differently (simple linear scaling versus modelled Sun's magnetic flux) after 1610.

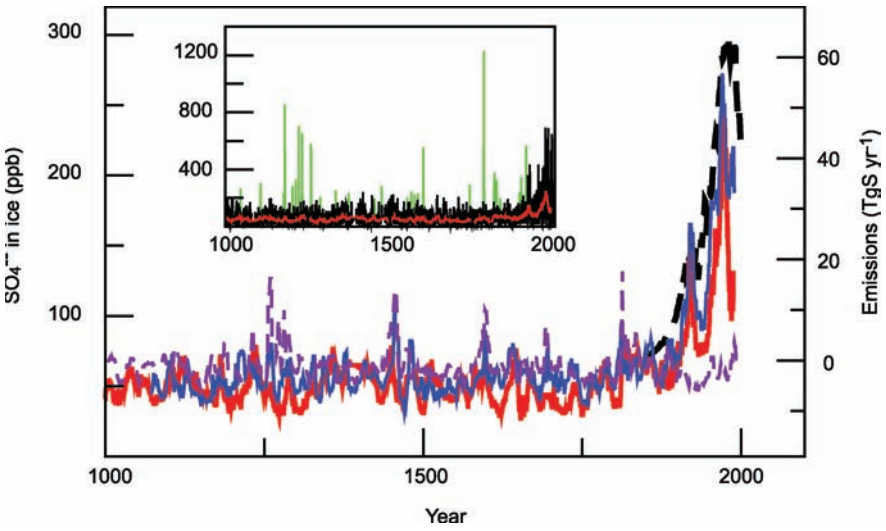


Figure 6.15. *Sulphate (SO_4^{2-}) concentrations in Greenland (Bigler et al., 2002, red line; Mieding, 2005, blue) and antarctic (Traufetter et al., 2004, dash, violet) ice cores during the last millennium. Also shown are the estimated anthropogenic sulphur (S) emissions for the NH (Stern, 2005; dashed black). The ice core data have been smoothed with a 10-year running median filter, thereby removing the peaks of major volcanic eruptions. The inset illustrates the influence of volcanic emissions over the last millennium and shows monthly sulphate data in ppm as measured (green), with identified volcanic spikes removed (black, most recent volcanic events were not assigned nor removed), and results from the 10-year filter (red) (Bigler et al., 2002). The records represent illustrative examples and can be influenced by local deposition events.*

The EMIC simulations shown in Figure 6.14, like those in Figure 6.13d, fall within the range of proxy-based NH temperature reconstructions shown in Figure 6.10c and are compatible with reconstructed and observed 20th-century warming only when anthropogenic forcings are incorporated. The standard deviation of multi-decadal variability in NH SAT is greater by 0.04°C to 0.07°C for the stronger solar forcing (Bard25, Table 6.3) compared to the weaker solar forcing (Bard08-WLS). The uncertainty associated with the proxy-

Table 6.3. *Simulations with intermediate complexity climate models shown in Figure 6.14.*

Models[a]:	
Bern2.5CC	Plattner et al., 2001
Climber2	Petoukhov et al., 2000
Climber3α	Montoya et al., 2005
Forcings:	
Volcanic	Forcing from Crowley (2000) used in all runs
Solar	'Bard25' runs used strong solar irradiance changes, based on ^{10}Be record scaled to give a Maunder Minimum irradiance 0.25% lower than today, from Bard et al. (2000) 'Bard08-WLS' runs used weak solar irradiance changes, using sunspot records and a model of the Sun's magnetic flux for the period since 1610, from Y.M. Wang et al. (2005), and extended before this by the ^{10}Be record scaled to give a Maunder Minimum irradiance 0.08% lower than today
Anthropogenic	'All' runs included anthropogenic forcings after 1765, from Joos et al. (2001) 'Nat' runs did not include any anthropogenic forcings

Notes:
[a] Models: Bern2.5CC = Bern 2.5D Carbon Cycle-Climate Model, CLIMBER = Climate Biosphere Model.

based temperature reconstructions and climate sensitivity of the models is too large to establish, based on these simulations, which of the two solar irradiance histories is the most likely. However, in the simulations that do not include anthropogenic forcing, NH temperatures reach a peak in the middle of the 20th century, and decrease afterwards, for both the strong and weak solar irradiance cases. This suggests that the contribution of natural forcing to observed 20th-century warming is small, and that solar and volcanic forcings are not responsible for the degree of warmth that occurred in the second half of the 20th century, consistent with the evidence of earlier work based on simple and more complex climate models (Crowley and Lowery, 2000; Bertrand et al., 2002b; Gerber et al., 2003; Hegerl et al., 2006; Tett et al., 2007; see also Chapter 9).

An overall conclusion can be drawn from the available instrumental and proxy evidence for the history of hemispheric average temperature change over the last 500 to 2,000 years, as well as the modelling studies exploring the possible roles of various causal factors: that is, greenhouse gases must be included among the forcings in order to simulate hemispheric mean temperatures that are compatible with the evidence of unusual warmth observed in the second half of the 20th century. It is very unlikely that this warming was merely a recovery from a pre-20th century cold period.

6.6.4 Consistency Between Temperature, Greenhouse Gas and Forcing Records; and Compatibility of Coupled Carbon Cycle-Climate Models with the Proxy Records

It is difficult to constrain the climate sensitivity from the proxy records of the last millennium (see Chapter 9). As noted above, the evidence for hemispheric temperature change as interpreted from the different proxy records, and for atmospheric trace greenhouse gases, inferred solar forcing and reconstructed volcanic forcing, is to varying degrees uncertain. The available temperature reconstructions suggest that decadally averaged NH temperatures varied within 1°C or less during the two millennia preceding the 20th century (Figure 6.10), but the magnitude of the reconstructed low-frequency variations differs by up to about a factor of two for different reconstructions. The reconstructions of natural forcings (solar and volcanic) are uncertain for this period. If they produced substantial negative energy balances (reduced solar, increased volcanic activity), then low-to-medium estimates of climate sensitivity are compatible with the reconstructed temperature variations (Figure 6.10); however, if solar and volcanic forcing varied only weakly, then moderate-to-high climate sensitivity would be consistent with the temperature reconstructions, especially those showing larger cooling (see also Chapter 9), assuming that the sensitivity of the climate system to solar irradiance changes and explosive volcanism is not different than the sensitivity to changes in greenhouse gases or other forcing agents.

The greenhouse gas record provides indirect evidence for a limited range of low-frequency hemispheric-scale climate variations over the last two millennia prior to the industrial period (AD 1–1750). The greenhouse gas histories of CO_2, CH_4 and N_2O show only small changes over this time period (MacFarling Meure et al., 2006; Figure 6.4), although there is evidence from the ice core record (Figures 6.3 and 6.7), as well as from models, that greenhouse gas concentrations react sensitively to climatic changes.

The sensitivity of atmospheric CO_2 to climatic changes as simulated by coupled carbon cycle-climate models is broadly consistent with the ice core CO_2 record and the amplitudes of the pre-industrial, decadal-scale NH temperature changes in the proxy-based reconstructions (Joos and Prentice, 2004). The CO_2 climate sensitivity can be formally defined as the change in atmospheric CO_2 relative to a nominal change in NH temperature in units of ppm per °C. Its strength depends on several factors, including the change in solubility of CO_2 in seawater, and the responses of productivity and heterotrophic respiration on land to temperature and precipitation (see Section 7.3). The sensitivity was estimated for modest (NH temperature change less than about 1°C) temperature variations from simulations with the Bern Carbon Cycle-Climate model driven with solar and volcanic forcing over the last millennium (Gerber et al., 2003) and from simulations with the range of models participating in the Coupled Carbon Cycle-Climate Model Intercomparison Project (C^4MIP) over the industrial period (Friedlingstein et al., 2006). The range of the CO_2 climate sensitivity is 4 to 16 ppm per °C for the 10 models participating in the C^4MIP intercomparison (evaluated as the difference in atmospheric CO_2 for the 1990 decade between a simulation with, and without, climate change, divided by the increase in NH temperature from the 1860 decade to the 1990 decade). This is comparable to a range of 10 to 17 ppm per °C obtained for CO_2 variations in the range of 6 to 10 ppm (Etheridge et al., 1996; Siegenthaler et al., 2005b) and the illustrative assumption that decadally averaged NH temperature varied within 0.6°C.

6.6.5 Regional Variability in Quantities Other than Temperature

6.6.5.1 Changes in the El Niño-Southern Oscillation System

Considerable interest in the ENSO system has encouraged numerous attempts at its palaeoclimatic reconstruction. These include a boreal winter (December–February) reconstruction of the Southern Oscillation Index (SOI) based on ENSO-sensitive tree ring indicators (Stahle et al., 1998), two multi-proxy reconstructions of annual and October to March Niño 3 index (average SST anomalies over 5°N to 5°S, 150°W to 90°W; Mann et al., 2005a,b), and a tropical coral-based Niño 3.4 SST reconstruction (Evans et al., 2002). Fossil coral records from Palmyra Island in the tropical Pacific also provide 30- to 150-year windows of ENSO variability within the last 1.1 kyr (Cobb et al., 2003). Finally, a new 600-year reconstruction of December to February Niño-3 SST has recently been developed (D'Arrigo et al., 2005), which is considerably longer than previous series. Although not totally independent (i.e., the

reconstructions share a number of common predictors), these palaeorecords display significant common variance (typically more than 30% during their respective cross-validation periods), suggesting a relatively consistent history of El Niño in past centuries (Jones and Mann, 2004). In most coral records from the western Pacific and the Indian Ocean, late 20th-century warmth is unprecedented over the past 100 to 300 years (Bradley et al., 2003b). However, reliable and consistent interpretation of geochemical records from corals is still problematic (Lough, 2004). Reconstructions of extratropical temperatures and atmospheric circulation features (e.g., the North Pacific Index) correlate significantly with tropical estimates, supporting evidence for tropical/high-latitude Pacific links during the past three to four centuries (Evans et al., 2002; Linsley et al., 2004; D'Arrigo et al., 2006).

The El Niño-Southern Oscillation may have responded to radiative forcing induced by solar and volcanic variations over the past millennium (Adams et al., 2003; Mann et al., 2005a). Model simulations support a statistically significant response of ENSO to radiative changes such that during higher radiative inputs, La Niña-like conditions result from an intensified zonal SST gradient that drives stronger trade winds, and vice versa (Mann et al., 2005a). Comparing data and model results over the past millennium suggests that warmer background conditions are associated with higher variability (Cane, 2005). Numerical experiments suggest that the dynamics of ENSO may have played an important role in the climatic response to past changes in radiative forcing (Mann et al., 2005b). Indeed, the low-frequency changes in both amplitude of variability and mean state indicated by ENSO reconstructions from Palmyra corals (Cobb et al., 2003) were found to correspond well with the model responses to changes in tropical volcanic radiative forcing over the past 1 kyr, with solar forcing playing a secondary role.

Proxy records suggest that ENSO's global climate imprint evolves over time, complicating predictions. Comparisons of ENSO and drought indices clearly show changes in the linkage between ENSO and moisture balance in the USA over the past 150 years. Significant ENSO-drought correlations occur consistently in the southwest USA, but the strength of moisture penetration into the continent varies substantially over time (Cole and Cook, 1998; Cook et al., 2000). Comparing reconstructed Niño 3 SST with global temperature patterns suggests that some features are robust through time, such as the warming in the eastern tropical Pacific and western coasts of North and South America, whereas teleconnections into North America, the Atlantic and Eurasia are variable (Mann et al., 2000). The spatial correlation pattern for the period 1801 to 1850 provides striking evidence of non-stationarity in ENSO teleconnections, showing a distinct absence of the typical pattern of tropical Pacific warming (Mann et al., 2000).

6.6.5.2 The Record of Past Atlantic Variability

Climate variations over the North Atlantic are related to changes in the NAO (Hurrell, 1995) and the Atlantic Multidecadal Oscillation (Delworth and Mann, 2000; Sutton and Hodson, 2005). From 1980 to 1995, the NAO tended to remain in one extreme phase and accounted for a substantial part of the winter warming over Europe and northern Eurasia. The North Atlantic region has a unique combination of long instrumental observations, many documentary records and multiple sources of proxy records. However, it remains difficult to document past variations in the dominant modes of climate variability in the region, including the NAO, due to problems of establishing proxies for atmospheric pressure, as well as the lack of stationarity in the NAO frequency and in storm tracks. Several reconstructions of NAO have been proposed (Cook et al., 2002b; Cullen et al., 2002; Luterbacher et al., 2002). Although the reconstructions differ in many aspects, there is a general tendency for more negative NAO indices during the 17th and 18th centuries than in the 20th century, thus indicating that the colder mean climate was characterised by a more zonal atmospheric pattern than in the 20th century. The coldest reconstructed European winter in 1708/1709, and the strong warming trend between 1684 and 1738 (+0.32°C per decade), have been related to a negative NAO index and the NAO response to increasing radiative forcing, respectively (Luterbacher et al., 2004). Some spatially resolved simulations employing GCMs indicate that solar and volcanic forcings lead to continental warming associated with a shift towards a high NAO index (Shindell et al., 2001, 2003, 2004; Stendel et al., 2006). Increased solar irradiance at the end of the 17th century and through the first half of the 18th century might have induced such a shift towards a high NAO index (Shindell et al., 2001; Luterbacher et al., 2004; Xoplanki et al., 2005).

It is well known that the NAO exerts a dominant influence on winter temperature and precipitation over Europe, but the strength of the relationship can change over time and region (Jones et al., 2003). The strong trend towards a more positive NAO index in the early part of the 18th century in the Luterbacher et al. (2002) NAO reconstruction appears connected with positive winter precipitation anomalies over northwest Europe and marked expansions of maritime glaciers in a manner similar to the effect of positive winter precipitation anomalies over recent decades for the same glaciers (Nesje and Dahl, 2003; Pauling et al., 2006).

6.6.5.3 Asian Monsoon Variability

Fifteen severe (three years or longer) droughts have occurred in a region of China dominated by the East Asian Monsoon over the last 1 kyr (Zhang, 2005). These palaeodroughts were generally more severe than droughts in the same region within the last 50 years. In contrast, the South Asian (Indian) monsoon, in the drier areas of its influence, has recently reversed its millennia-long orbitally driven low-frequency trend towards less rainfall. This recent reversal in monsoon rainfall also appears to coincide with a synchronous increase in inferred monsoon winds over the western Arabian Sea (Anderson et al., 2002), a change that could be related to increased summer heating over and around the Tibetan Plateau (Braüning and Mantwill, 2004; Morrill et al., 2006).

6.6.5.4 Northern and Eastern Africa Hydrologic Variability

Lake sediment and historical documentary evidence indicate that northern Africa and the Sahel region have for a long time experienced substantial droughts lasting from decades to centuries (Kadomura, 1992; Verschuren, 2001; Russell et al., 2003; Stager et al., 2003; Nguetsop et al., 2004; Brooks et al., 2005; Stager et al., 2005). Although there have been attempts to link these dry periods to solar variations, the evidence is not conclusive (Stager et al., 2005), particularly given that the relationship between hypothesised solar proxies and variation in total solar irradiance remains unclear (see Section 6.6.3). The palaeoclimate record indicates that persistent droughts have been a common feature of climate in northern and eastern Africa. However, it has not been demonstrated that these droughts can be simulated with coupled ocean-atmosphere models.

6.6.5.5 The Record of Hydrologic Variability and Change in the Americas

Multiple proxies, including tree rings, sediments, historical documents and lake sediment records make it clear that the past 2 kyr included periods with more frequent, longer and/or geographically more extensive droughts in North America than during the 20th century (Stahle and Cleaveland, 1992; Stahle et al., 1998; Woodhouse and Overpeck, 1998; Forman et al., 2001; Cook et al., 2004b; Hodell et al., 2005; MacDonald and Case, 2005). Past droughts, including decadal-length 'megadroughts' (Woodhouse and Overpeck, 1998), are most likely due to extended periods of anomalous SST (Hoerling and Kumar, 2003; Schubert et al., 2004; MacDonald and Case, 2005; Seager et al., 2005), but remain difficult to simulate with coupled ocean-atmosphere models. Thus, the palaeoclimatic record suggests that multi-year, decadal and even centennial-scale drier periods are likely to remain a feature of future North American climate, particularly in the area west of the Mississippi River.

There is some evidence that North American drought was more regionally extensive, severe and frequent during past intervals that were characterised by warmer than average NH summer temperatures (e.g., during medieval times and the mid-Holocene; Forman et al., 2001; Cook et al., 2004b). There is evidence that changes in the North American hydrologic regime can occur abruptly relative to the rate of change in climate forcing and duration of the subsequent climate regime. Abrupt shifts in drought frequency and duration have been found in palaeohydrologic records from western North America (Cumming et al., 2002; Laird et al., 2003; Cook et al., 2004b). Similarly, the upper Mississippi River Basin and elsewhere have seen abrupt shifts in the frequency and size of the largest flood events (Knox, 2000). Recent investigations of past large-hurricane activity in the southeast USA suggest that changes in the regional frequency of large hurricanes can shift abruptly in response to more gradual forcing (Liu, 2004). Although the palaeoclimatic record indicates that hydrologic shifts in drought, floods and tropical storms have occurred abruptly (i.e., within years), this past abrupt change has not been simulated with coupled atmosphere ocean models. Decadal variability of Central Chilean precipitation was greater before the 20th century, with more intense and prolonged dry episodes in the past. Tree-ring based precipitation reconstructions for the past eight centuries reveal multi-year drought episodes in the 14th and 16th to 18th centuries that exceed the estimates of decadal drought during the 20th century (LeQuesne et al., 2006).

6.7 Concluding Remarks on Key Uncertainties

Each palaeoclimatic time scale covered in this chapter contributes to the understanding of how the climate system varies naturally and also responds to changes in climate forcing. The existing body of knowledge is sufficient to support the assertions of this chapter. At the same time, key uncertainties remain, and greater confidence would result if these uncertainties were reduced.

Even though a great deal is known about glacial-interglacial variations in climate and greenhouse gases, a comprehensive mechanistic explanation of these variations remains to be articulated. Similarly, the mechanisms of abrupt climate change (for example, in ocean circulation and drought frequency) are not well enough understood, nor are the key climate thresholds that, when crossed, could trigger an acceleration in sea level rise or regional climate change. Furthermore, the ability of climate models to simulate realistic abrupt change in ocean circulation, drought frequency, flood frequency, ENSO behaviour and monsoon strength is uncertain. Neither the rates nor the processes by which ice sheets grew and disintegrated in the past are known well enough.

Knowledge of climate variability over the last 1 to 2 kyr in the SH and tropics is severely limited by the lack of palaeoclimatic records. In the NH, the situation is better, but there are important limitations due to a lack of tropical records and ocean records. Differing amplitudes and variability observed in available millennial-length NH temperature reconstructions, and the extent to which these differences relate to choice of proxy data and statistical calibration methods, need to be reconciled. Similarly, the understanding of how climatic extremes (i.e., in temperature and hydro-climatic variables) varied in the past is incomplete. Lastly, this assessment would be improved with extensive networks of proxy data that run right up to the present day. This would help measure how the proxies responded to the rapid global warming observed in the last 20 years, and it would also improve the ability to investigate the extent to which other, non-temperature, environmental changes may have biased the climate response of proxies in recent decades.

References

Adams, J.B., M.E. Mann, and C.M. Ammann, 2003: Proxy evidence for an El Niño-like response to volcanic forcing. *Nature*, **426**(6964), 274–278.

Adkins, J.F., K. McIntyre, and D.P. Schrag, 2002: The salinity, temperature, and $\delta^{18}O$ of the glacial deep ocean. *Science*, **298**, 1769–1773.

Alley, R.B., and P.U. Clark, 1999: The deglaciation of the northern hemisphere: A global perspective. *Annu. Rev. Earth Planet. Sci.*, **27**, 149–182.

Alley, R.B., and A.M. Agustsdottir, 2005: The 8k event: cause and consequences of a major Holocene abrupt climate change. *Quat. Sci. Rev.*, **24**, 1123–1149.

Alley, R.B., S. Anandakrishnan, and P. Jung, 2001: Stochastic resonance in the North Atlantic. *Paleoceanography*, **16**, 190–198.

Alley, R.B., et al., 1997: Holocene climatic instability: A large, widespread event 8200 years ago. *Geology*, **25**, 483–486.

Alley, R.B., et al., 2003: Abrupt climate change. *Science*, **299**(5615), 2005–2010.

Alverson, K.D., R.S. Bradley, and T.F. Pedersen (eds.), 2003: *Paleoclimate, Global Change and the Future.* International Geosphere Biosphere Programme Book Series, Springer-Verlag, Berlin, 221 pp.

Ammann, C.M., G.A. Meehl, W.M. Washington, and C.S. Zender, 2003: A monthly and latitudinally varying volcanic forcing dataset in simulations of 20th century climate. *Geophys. Res. Lett.*, **30**(12), 1657, doi:10.1029/2003GL016875.

Andersen, C., N. Koç, A. Jennings, and J.T. Andrews, 2004: Non uniform response of the major surface currents in the Nordic Seas to insolation forcing: implications for the Holocene climate variability. *Paleoceanography*, **19**, 1–16.

Anderson, D.M., J.T. Overpeck, and A.K. Gupta, 2002: Increase in the Asian southwest monsoon during the past four centuries. *Science*, **297**(5581), 596–599.

Archer, D., and A. Ganopolski, 2005: A movable trigger: Fossil fuel CO_2 and the onset of the next glaciation. *Geochem. Geophys. Geosystems*, **6**, Q05003.

Archer, D.A., A. Winguth, D. Lea, and N. Mahowald, 2000: What caused the glacial/interglacial atmospheric pCO_2 cycles? *Rev. Geophys.*, **12**, 159–189.

Ariztegui, D., et al., 2000: Paleoclimate and the formation of sapropel S1: inferences from Late Quaternary lacustrine and marine sequences in the central Mediterranean region. *Palaeogeogr. Palaeoclimatol. Palaeoecol.*, **158**, 215–240.

Bakke, J., S.O. Dahl, and A. Nesje, 2005a: Late glacial and early Holocene palaeoclimatic reconstruction based on glacier fluctuations and equilibrium-line altitudes at northern Folgefonna, Hardanger, western Norway. *J. Quat. Sci.*, **20**(2), 179–198.

Bakke, J., et al., 2005b: Glacier fluctuations, equilibrium-line altitudes and palaeoclimate in Lyngen, northern Norway, during the Late glacial and Holocene. *The Holocene*, **15**(4), 518–540.

Baliunas, S., and R. Jastrow, 1990: Evidence for long-term brightness changes of solar-type stars. *Nature*, **348**, 520–522.

Ballantyne, A.P., et al., 2005: Meta-analysis of tropical surface temperatures during the Last Glacial Maximum. *Geophys. Res. Lett.*, **32**, L05712, doi:10.1029/2004GL021217.

Bao, Y., A. Brauning, and S. Yafeng, 2003: Late Holocene temperature fluctuations on the Tibetan Plateau. *Quat. Sci. Rev.*, **22**(21), 2335–2344.

Barber, D.C., et al., 1999: Forcing of the cold event of 8,200 years ago by catastrophic drainage of Laurentide lakes. *Nature*, **400**, 344–347.

Bard, E., G. Raisbeck, F. Yiou, and J. Jouzel, 2000: Solar irradiance during the last millennium based on cosmogenic nucleides. *Tellus*, **52B**, 985–992.

Barrows, T.T., and S. Juggins, 2005: Sea-surface temperatures around the Australian margin and Indian Ocean during the Last Glacial Maximum. *Quat. Sci. Rev.*, **24**, 1017–1047.

Bartlett, M.G., D.S. Chapman, and R.N. Harris, 2004: Snow and the ground temperature record of climate change. *J. Geophys Res.*, **109**, F04008, doi:10.1029/2004JF000224.

Battle, M., et al., 1996: Atmospheric gas concentrations over the past century measured in air from firn at the South Pole. *Nature*, **383**(6597), 231–235.

Bauer, E., A. Ganopolski, and M. Montoya, 2004: Simulation of the cold climate event 8200 years ago by meltwater outburst from Lake Agassiz. *Paleoceanography*, **19**, PA3014, doi:10.1029/2004PA001030.

Bauer, E., M. Claussen, V. Brovkin, and A. Huenerbein, 2003: Assessing climate forcings of the Earth system for the past millennium. *Geophys. Res. Lett.*, **30**(6), 1276, doi:10.1029/2002GL016639.

Beer, J., S. Tobias, and N. Weiss, 1998: An active sun throughout the Maunder Minimum. *Sol. Phys.*, **181**(1), 237–249.

Beerling, D.J., 1999: New estimates of carbon transfer to terrestrial ecosystems between the last glacial maximum and the Holocene. *Terra Nova*, **11**(4), 162–167.

Beltrami, H., 2002: Paleoclimate: Earth's long-term memory. *Science*, **297**(5579), 206–207.

Beltrami, H., and E. Bourlon, 2004: Ground warming patterns in the Northern Hemisphere during the last five centuries. *Earth Planet. Sci. Lett.*, **227**(3–4), 169–177.

Berger, A., 1977: Long-term variations of earth's orbital elements. *Celestial Mechanics*, **15**(1), 53–74.

Berger, A., 1978: Long-term variation of caloric solar radiation resulting from the earth's orbital elements. *Quat. Res.*, **9**, 139–167.

Berger, A.L., and M.F. Loutre, 1991: Insolation values for the climate of the last 10 million years. *Quat. Sci. Rev.*, **10**, 297–317.

Berger, A.L., and M.F. Loutre, 2002: An exceptionally long interglacial ahead? *Science*, **297**, 1287–1288.

Berger, A.L., and M.F. Loutre, 2003: Climate 400,000 years ago, a key to the future? In: *Earth's Climate and Orbital Eccentricity* [Droxler, A.W., R.Z. Poore, and L.H. Burckle (eds.)]. American Geophysical Union, Washington, DC, pp. 17–26.

Berggren, W.A., D.V. Kent, C.C.I. Swisher, and M.P. Aubry, 1995: *Geochronology, Time Scales and Global Stratigraphic Correlation* [W.A. Berggren (ed)]. Special Publication No. 54, Society for Sedimentary Geology, Tulsa, OK, 386 pp.

Berner, R.A., and Z. Kothavala, 2001: GEOCARB III: A revised model of atmospheric CO_2 over phanerozoic time. *Am. J. Sci.*, **301**(2), 182–204.

Bertrand, C., M.F. Loutre, and A. Berger, 2002a: High frequency variations of the Earth's orbital parameters and climate change. *Geophys. Res. Lett.*, **29**, doi:10.1029/2002GL015622.

Bertrand, C., M.F. Loutre, M. Crucifix, and A. Berger, 2002b: Climate of the last millennium: a sensitivity study. *Tellus*, **54A**(3), 221–244.

Bianchi, G., and I.N. McCave, 1999: Holocene periodicity in north Atlantic climate and deep ocean flow south of Iceland. *Nature*, **397**, 515–518.

Bigelow, N., et al., 2003: Climate change and Arctic ecosystems: 1. Vegetation changes north of 55 degrees N between the last glacial maximum, mid-Holocene, and present. *J. Geophys. Res.*, **108**, doi:10.1029/2002JD002558.

Bigler, M., et al., 2002: Sulphate record from a northeast Greenland ice core over the last 1200 years based on continuous flow analysis. *Ann. Glaciol.*, **35**, 250–256.

Billups, K., J.E.T. Channell, and J. Zachos, 2002: Late Oligocene to early Miocene geochronology and paleoceanography from the subantarctic South Atlantic. *Paleoceanography*, **17**(1), 1004, doi:10.1029/2000PA000568.

Bird, M.I., J. Lloyd, and G.D. Farquhar, 1994: Terrestrial carbon storage at the LGM. *Nature*, **371**(6498), 566–566.

Birks, H.H., and B. Ammann, 2000: Two terrestrial records of rapid climatic change during the glacial-Holocene transition (14,000-9,000 calendar years B.P.) from Europe. *Proc. Natl. Acad. Sci. U.S.A.*, **97**, 1390–1394.

Bjerknes, J., 1969: Atmospheric teleconnections from equatorial pacific. *Mon. Weather Rev.*, **97**(3), 163–172

Blunier, T., and E.J. Brook, 2001: Timing of millennial-scale climate change in Antarctica and Greenland during the last glacial period. *Science*, **291**, 109–112.

Blunier, T., et al., 1993: Atmospheric methane record from a Greenland ice core over the last 1000 years. *Geophys. Res. Lett.*, **20**(20), 2219–2222.

Blunier, T., et al., 1995: Variations in atmospheric methane concentration during the Holocene epoch. *Nature*, **374**(6517), 46–49.

Blunier, T., et al., 1998: Asynchrony of Antarctic and Greenland climate change during the last glacial period. *Nature*, **394**, 739–743.

Bohaty, S.M., and J.C. Zachos, 2003: Significant Southern Ocean warming event in the late middle Eocene. *Geology*, **31**(11), 1017–1020.

Bond, G., et al., 1993: Correlations between climate records from North Atlantic sediments and Greenland ice. *Nature*, **365**, 143–147.

Bond, G., et al., 1997: A pervasive millennial-scale cycle in the North Atlantic Holocene and glacial climates. *Science*, **278**, 1257–1266.

Bond, G., et al., 2001: Persistent solar influence on North Atlantic climate during the Holocene. *Science*, **294**, 2130–2136.

Bond, W.J., G.F. Midgley, and F.I. Woodward, 2003: The importance of low atmospheric CO_2 and fire in promoting the spread of grasslands and savannas. *Global Change Biol.*, **9**(7), 973–982.

Booth, R.K., et al., 2005: A severe centennial-scale drought in mid-continental North America 4200 years ago and apparent global linkages. *The Holocene*, **15**, 321–328.

Bopp, L., K.E. Kohlfeld, C. Le Quéré, and O.O. Aumont, 2002: Dust impact on marine biota and atmospheric CO_2 in glacial periods. *Geochim. Cosmochim. Acta*, **66**(15A), A91, Suppl. 1, Aug. 2002.

Bowen, G.J., et al., 2002: Mammalian dispersal at the Paleocene/Eocene boundary. *Science*, **295**(5562), 2062–2065.

Bowen, G.J., et al., 2004: A humid climate state during the Palaeocene/Eocene thermal maximum. *Nature*, **432**(7016), 495–499.

Braconnot, P., O. Marti, S. Joussaume, and Y. Leclaninche, 2000: Ocean feedbacks in response to 6 kyr insolation. *J. Clim.*, **13**, 1537–1553.

Braconnot, P., et al., 2002: How the simulated change in monsoon at 6 ka BP is related to the simulation of the modern climate: results from the Paleoclimate Modeling Intercomparison Project. *Clim. Dyn.*, **19**(2), 107–121.

Braconnot, P., et al., 2004: Evaluation of PMIP coupled ocean-atmosphere simulations of the Mid-Holocene. In: *Past Climate Variability through Europe and Africa*, Vol. 6 [Battarbee, R.W., F. Gasse, and C.E. Stickley (eds)], Springer, Dordrecht, The Netherlands, 515–534.

Bradley, R.S., 1999: Climatic variability in sixteenth-century Europe and its social dimension - Preface. *Clim. Change*, **43**(1), 1–2.

Bradley, R.S., M.K. Hughes, and H.F. Diaz, 2003a: Climate in Medieval time. *Science*, **302**(5644), 404–405.

Bradley, R.S., K.R. Briffa, J. Cole, and T.J. Osborn, 2003b: The climate of the last millennium. In: *Paleoclimate, Global Change and the Future* [Alverson, K.D., R.S. Bradley, and T.F. Pedersen (eds.)]. Springer, Berlin, pp. 105–141.

Bralower, T.J., 2002: Evidence of surface water oligotrophy during the Paleocene-Eocene thermal maximum: Nannofossil assemblage data from Ocean Drilling Program Site 690, Maud Rise, Weddell Sea. *Paleoceanography*, **17**(2), 1023, doi:10.1029/2001PA000662.

Bräuning, A., and B. Mantwill, 2004: Summer temperature and summer monsoon history on the Tibetan plateau during the last 400 years recorded by tree rings. *Geophys. Res. Lett.*, **31**(24), L24205, doi:10.1029/2004GL020793.

Briffa, K.R., 2000: Annual climate variability in the Holocene: interpreting the message of ancient trees. *Quat. Sci. Rev.*, **19**(1–5), 87–105.

Briffa, K.R., and T.J. Osborn, 1999: Perspectives: Climate warming - Seeing the wood from the trees. *Science*, **284**(5416), 926–927.

Briffa, K.R., and T.J. Osborn, 2002: Paleoclimate - Blowing hot and cold. *Science*, **295**(5563), 2227–2228.

Briffa, K.R., T.J. Osborn, and F.H. Schweingruber, 2004: Large-scale temperature inferences from tree rings: a review. *Global Planet. Change*, **40**(1–2), 11–26.

Briffa, K.R., et al., 2001: Low-frequency temperature variations from a northern tree ring density network. *J. Geophys. Res.*, **106**(D3), 2929–2941.

Brigham-Grette, J., and D.M. Hopkins, 1995: Emergent marine record and paleoclimate of the last interglaciation along the northwest Alaskan coast. *Quat. Res.*, **43**, 159–173.

Broecker, W.S., and G.M. Henderson, 1998: The sequence of events surrounding Termination II and their implications for the cause of glacial-interglacial CO_2 changes. *Paleoceanography*, **13**, 352–364.

Broecker, W.S., and E. Clark, 2003: Holocene atmospheric CO_2 increase as viewed from the seafloor. *Global Biogeochem. Cycles*, **17**(2), doi:10.1029/2002GB001985.

Brook, E.J., et al., 2000: On the origin and timing of rapid changes in atmospheric methane during the last glacial period. *Global Biogeochem. Cycles*, **14**(2), 559–572.

Brooks, C.E.P., 1922: *The Evolution of Climate*. [Preface by Simpson, G.C.] Benn Brothers, London, 173 pp.

Brooks, K., et al., 2005: Late-Quaternary lowstands of Lake Bosumtwi, Ghana: evidence from high-resolution seismic-reflection and sediment-core data. *Palaeogeogr. Palaeoclimatol. Palaeoecol.*, **216**(3–4), 235–249.

Brovkin, V., et al., 2002: Carbon cycle, vegetation and climatic dynamics in the Holocene: Experiments with the CLIMBER-2 model. *Global Biogeochem. Cycles*, **16**, 1139, doi:10.1029/2001GB001662.

Burger, G., and U. Cubasch, 2005: Are multiproxy climate reconstructions robust? *Geophys. Res. Lett.*, **32**(23), doi:10.1029/2005GL024155.

Caillon, N., et al., 2003: Timing of atmospheric CO_2 and Antarctic temperature changes across Termination III. *Science*, **299**, 1728–1731.

Calov, R., A. Ganopolski, V. Petoukhov, and M. Claussen, 2002: Large-scale instabilities of the Laurentide ice sheet simulated in a fully coupled climate-system model. *Geophys. Res. Lett.*, **29**, 2216, doi:10.1029/2002GL016078.

Calov, R., et al., 2005: Transient simulation of the last glacial inception. Part II: Sensitivity and feedback analysis. *Clim. Dyn.*, **24**, 563–576.

Cane, M.A., 2005: The evolution of El Niño, past and future. *Earth Planet. Sci. Lett.*, **230**(3–4), 227–240.

CAPE Last Interglacial Project Members, 2006: Last Interglacial Arctic warmth confirms polar amplification of climate change. *Quat. Sci. Rev.*, **25**(13–14), 1383–1400.

Castellano, E., et al., 2005: Holocene volcanic history as recorded in the sulfate stratigraphy of the European Project for Ice Coring in Antarctica Dome C (EDC96) ice core. *J. Geophys. Res.*, **110**, D06114, doi:10.1029/2004JD005259.

Cerling, T.E., 1991: Carbon dioxide in the atmosphere: Evidence from Cenozoic and Mesozoic paleosols. *Am. J. Sci.*, **291**, 377–400.

Chandler, M.A., D. Rind, and R.S. Thompson, 1994: Joint investigations of the middle Pliocene climate II: GISS GCM Northern Hemisphere results. *Global Planet. Change*, **9**, 197–219.

Chapman, D.S., M.G. Bartlett, and R.N. Harris, 2004: Comment on "Ground vs. surface air temperature trends: Implications for borehole surface temperature reconstructions" by M. E. Mann and G. Schmidt. *Geophys. Res. Lett.*, **31**(7), L07205, doi:10.1029/2003GL019054.

Chappellaz, J.A., I.Y. Fung, and A.M. Thompson, 1993: The atmospheric CH_4 increase since the last glacial maximum. *Tellus*, **B45**(3), 228–241.

Chappellaz, J., et al., 1997: Changes in the atmospheric CH_4 gradient between Greenland and Antarctica during the Holocene. *J. Geophys. Res.*, **102**(D13), 15987–15997.

Charles, C.D., D.E. Hunter, and R.G. Fairbanks, 1997: Interaction between the ENSO and the Asian monsoon in a coral record of tropical climate. *Science*, **277**(5328), 925–928.

Church, J.A., et al., 2001: Changes in sea level. In: *Climate Change 2001: The Scientific Basis. Contribution of Working Group I to the Third Assessment Report of the Intergovernmental Panel on Climate Change* [Houghton, J.T. et al. (eds.)]. Cambridge University Press, Cambridge, United Kingdom and New York, NY, USA, pp. 639–693.

Claquin, T., et al., 2003: Radiative forcing of climate by ice-age atmospheric dust. *Clim. Dyn.*, **20**, 193–202.

Clark, P.U., N.G. Pisias, T.F. Stocker, and A.J. Weaver, 2002: The role of the thermohaline circulation in abrupt climate change. *Nature*, **415**, 863–869.

Clarke, G.K.C., D.W. Leverington, J.T. Teller, and A.S. Dyke, 2004: Paleohydraulics of the last outburst flood from glacial Lake Agassiz and the 8200 BP cold event. *Quat. Sci. Rev.*, **23**, 389–407.

Claussen, M., and Gayler, V., 1997: The greening of Sahara during the mid-Holocene: results of an interactive atmosphere-biome model. *Global Ecol. Biogeogr. Lett.*, **6**, 369–377.

Claussen, M., et al., 1999: Simulation of an abrupt change in Saharan vegetation in the mid-Holocene. *Geophys. Res. Lett.*, **26**(14), 2037–2040.

Claussen, M., et al., 2002: Earth system models of intermediate complexity: closing the gap in the spectrum of climate system models. *Clim. Dyn.*, **18**(7), 579–586.

Clement, A.C., and M.A. Cane, 1999: A role for the tropical Pacific coupled ocean-atmosphere system on Milankovitch and millennial timescales. Part I: A modeling study of tropical Pacific variability. In: *Mechanisms of Global Climate Change at Millennial Time Scales* [Clark, P.U., R.S. Webb, and L.D. Keigwin (eds.)]. American Geophysical Union, Washington, DC, pp. 363–371.

Clement, A.C., R. Seager, and M.A. Cane, 2000: Suppression of El Niño during the mid-Holocene by changes in the earth's orbit. *Paleoceanography*, **15**(6), 731–737.

Clement, A.C., M.A. Cane, and R. Seager, 2001: An orbitally driven tropical source for abrupt climate change. *J. Clim.*, **14**(11), 2369–2375.

Clement, A.C., R. Seager, M.A. Cane, and S.E. Zebiak, 1996: An ocean dynamical thermostat. *J. Clim.*, **9**(9), 2190–2196.

Cobb, K.M., C.D. Charles, H. Cheng, and R.L. Edwards, 2003: El Niño/Southern Oscillation and tropical Pacific climate during the last millennium. *Nature*, **424**(6946), 271–276.

Coe, M.T., and S.P. Harrison 2002: The water balance of northern Africa during the mid-Holocene: an evaluation of the 6 ka BPPMIP simulations. *Clim. Dyn.*, **19**(2), 155–166.

Cole, J., 2003: Global change - Dishing the dirt on coral reefs. *Nature*, **421**(6924), 705–706.

Cole, J.E., and E.R. Cook, 1998: The changing relationship between ENSO variability and moisture balance in the continental United States. *Geophys. Res. Lett.*, **25**(24), 4529–4532.

Cole, J.E., R.B. Dunbar, T.R. McClanahan, and N.A. Muthiga, 2000: Tropical Pacific forcing of decadal SST variability in the western Indian Ocean over the past two centuries. *Science*, **287**(5453), 617–619.

Cook, E.R., J.G. Palmer, and R.D. D'Arrigo, 2002a: Evidence for a 'Medieval Warm Period' in a 1,100 year tree-ring reconstruction of past austral summer temperatures in New Zealand. *Geophys. Res. Lett.*, **29**(14), 1667, doi:10.1029/2001GL014580.

Cook, E.R., R.D. D'Arrigo, and M.E. Mann, 2002b: A well-verified, multiproxy reconstruction of the winter North Atlantic Oscillation index since AD 1400. *J. Clim.*, **15**(13), 1754–1764.

Cook, E.R., J. Esper, and R.D. D'Arrigo, 2004a: Extra-tropical Northern Hemisphere land temperature variability over the past 1000 years. *Quat. Sci. Rev.*, **23**(20–22), 2063–2074.

Cook, E.R., B.M. Buckley, R.D. D'Arrigo, and M.J. Peterson, 2000: Warm-season temperatures since 1600 BC reconstructed from Tasmanian tree rings and their relationship to large-scale sea surface temperature anomalies. *Clim. Dyn.*, **16**(2–3), 79–91.

Cook, E.R., et al., 2004b: Long-term aridity changes in the western United States. *Science*, **306**(5698), 1015–1018.

Cortijo, E., et al., 1997: Changes in the sea surface hydrology associated with Heinrich event 4 in the North Atlantic Ocean (40-60°N). *Earth Planet. Sci. Lett.*, **146**, 29–45.

Cortijo, E., et al., 1999: Changes in meridional temperature and salinity gradients in the North Atlantic Ocean (30°-72°N) during the last interglacial period. *Paleoceanography*, **14**(1), 23–33.

Cronin, T.M., 1999: *Principles of Paleoclimatology.* Perspectives in Paleobiology and Earth History. Columbia University Press, New York, NY, 560 pp.

Cronin, T.M., et al., 2005: Mid-Pliocene deep-sea bottom-water temperatures based on ostracode Mg/Ca ratios. *Mar. Micropaleontol.*, **54**(3–4), 249–261.

Crouch, E.M., et al., 2003: The Apectodinium acme and terrestrial discharge during the Paleocene-Eocene thermal maximum: new palynological, geochemical and calcareous nannoplankton observations at Tawanui, New Zealand. *Palaeogeogr. Palaeoclimatol. Palaeoecol.*, **194**(4), 387–403.

Crowley, T.J., 1992: North Atlantic deep water cools the Southern Hemisphere. *Paleoceanography*, **7**, 489–497.

Crowley, T.J., 1995: Ice-age terrestrial carbon changes revisited. *Global Biogeochem. Cycles*, **9**(3), 377–389.

Crowley, T.J., 1998: Significance of tectonic boundary conditions for paleoclimate simulations. In: *Tectonic Boundary Conditions for Climate Reconstructions* [Crowley, T.J., and K.C. Burke (eds.)]. Oxford University Press, New York, pp. 3–17.

Crowley, T.J., 2000: Causes of climate change over the past 1000 years. *Science*, **289**(5477), 270–277.

Crowley, T.J., and T.S. Lowery, 2000: How warm was the medieval warm period? *Ambio*, **29**(1), 51–54.

Crowley, T.J., et al., 2003: Modeling ocean heat content changes during the last millennium. *Geophys. Res. Lett.*, **30**(18), 1932, doi:10.1029/2003GL017801.

Crucifix, M., and M.F. Loutre, 2002: Transient simulations over the last interglacial period (126-115 kyr BP). *Clim. Dyn.*, **19**, 417–433.

Crucifix, M., and C.D. Hewitt, 2005: Impact of vegetation changes on the dynamics of the atmosphere at the Last Glacial Maximum. *Clim. Dyn.*, **25**(5), 447–459.

Crucifix, M., et al., 2002: Climate evolution during the Holocene, a study with an Earth System model of intermediate complexity. *Clim. Dyn.*, **19**, 43–60.

Cuffey, K.M., and S.J. Marshall, 2000: Substantial contribution to sea-level rise during the last interglacial from the Greenland ice sheet. *Nature*, **404**, 591–594.

Cullen, H.M., A. Kaplan, P.A. Arkin, and P.B. Demenocal, 2002: Impact of the North Atlantic Oscillation on Middle Eastern climate and streamflow. *Clim. Change*, **55**(3), 315–338.

Cumming, B.F., et al., 2002: Persistent millennial-scale shifts in moisture regimes in western Canada during the past six millennia. *Proc. Natl. Acad. Sci. U.S.A.*, **99**(25), 16117–16121.

Cutler, K.B., et al., 2003: Rapid sea-level fall and deep-ocean temperature change since the last interglacial period, *Earth Planet. Sci. Lett.*, **206**, 253–271.

Dahl, K., A. Broccoli, and R. Stouffer, 2005: Assessing the role of North Atlantic freshwater forcing in millennial scale climate variability: a tropical Atlantic perspective. *Clim. Dyn.*, **24**(4), 325–346.

Dahl, S.O., and A. Nesje, 1996: A new approach to calculating Holocene winter precipitation by combining glacier equilibrium-line altitudes and pine-tree limits: A case study from Hardangerjøkulen, central southern Norway. *The Holocene*, **6**(4), 381–398.

Dahl-Jensen, D., V.I. Morgan, and A. Elcheikh, 1999: Monte Carlo inverse modelling of the Law Dome (Antarctica) temperature profile. *Ann. Glaciol.*, **29**, 145–150.

Dahl-Jensen, D., et al., 1998: Past temperature directly from the Greenland Ice Sheet. *Science*, **282**, 268–271.

D'Arrigo, R., R. Wilson, and G. Jacoby, 2006: On the long-term context for late twentieth century warming. *J. Geophys. Res.*, **111**(D3), doi:10.1029/2005JD006352.

D'Arrigo, R.D., et al., 2004: Thresholds for warming-induced growth decline at elevational tree line in the Yukon Territory, Canada. *Global Biogeochem. Cycles*, **18**(3), GB3021, doi:10.1029/2004GB002249.

D'Arrigo, R., et al., 2005: On the variability of ENSO over the past six centuries. *Geophys. Res. Lett.*, **32**(3), L03711, doi:10.1029/2004GL022055.

Davis, B.A.S., et al., 2003: The temperature of Europe during the Holocene reconstructed from pollen data. *Quat. Sci. Rev.*, **22**, 1701–1716.

de Menocal, P., J. Ortiz, T. Guilderson, and M. Sarnthein, 2000: Coherent high- and low-latitude climate variability during the Holocene warm period. *Science*, **288**(5474), 2198–2202.

de Noblet-Ducoudre, N., R. Claussen, and C. Prentice, 2000: Mid-Holocene greening of the Sahara: first results of the GAIM 6000 year BP experiment with two asynchronously coupled atmosphere/biome models. *Clim. Dyn.*, **16**(9), 643–659.

de Vernal, A., et al., 2006: Comparing proxies for the reconstruction of LGM sea-surface conditions in the northern North Atlantic. *Quat. Sci. Rev*., **25**(21–22), 2820–2834.

DeConto, R.M., and D. Pollard, 2003: Rapid Cenozoic glaciation of Antarctica induced by declining atmospheric CO_2. *Nature*, **421**(6920), 245–249.

Delworth, T.L., and M.E. Mann, 2000: Observed and simulated multidecadal variability in the Northern Hemisphere. *Clim. Dyn.*, **16**(9), 661–676.

Dickens, G.R., and R.M. Owen, 1996: Sediment geochemical evidence for an early-middle Gilbert (early Pliocene) productivity peak in the North Pacific Red Clay Province. *Mar. Micropaleontol.*, **27**(1–4), 107–120.

Dickens, G.R., M.M. Castillo, and J.C.G. Walker, 1997: A blast of gas in the latest Paleocene: Simulating first-order effects of massive dissociation of oceanic methane hydrate. *Geology*, **25**(3), 259–262.

Ding, Z.L., et al., 2002: Stacked 2.6-Ma grain size record from the Chinese loess based on five sections and correlation with the deep-sea $\delta^{18}O$ record. *Paleoceanography*, **17**(3), 1033, doi:10.1029/2001PA000725.

Dlugokencky, E.J., L.P. Steele, P.M. Lang, and K.A. Masarie, 1994: The growth rate and distribution of atmospheric methane. *J. Geophys. Res.*, **99**, 17021–17043.

Dokken, T.M., and E. Jansen, 1999: Rapid changes in the mechanism of ocean convection during the last glacial period. *Nature*, **401**, 458–461.

Domack, E., et al., 2005: Stability of the Larsen B ice shelf on the Antarctic Peninsula during the Holocene epoch. *Nature*, **436**, 681–685.

Dowsett, H.J., and T.M. Cronin, 1990: High eustatic sea level during the middle Pliocene: evidence from southeastern U.S. Atlantic coastal plain. *Geology*, **18**, 435–438.

Dowsett, H., J. Barron, and R. Poore, 1996: Middle Pliocene sea surface temperatures: A global reconstruction. *Mar. Micropaleontol.*, **27**(1–4), 13–25.

Dowsett, H.J., M.A. Chandler, T.M. Cronin, and G.S. Dwyer, 2005: Middle Pliocene sea surface temperature variability. *Paleoceanography*, **20**(2), doi:10.1029/2005PA001133.

Duplessy, J.C., L. Labeyrie, and C. Waelbroeck, 2002: Constraints on the ocean oxygen isotopic enrichment between the Last Glacial Maximum and the Holocene: Paleoceanographic implications. *Quat. Sci. Rev.*, **21**, 315–330.

Duplessy, J.C., et al., 2001: Holocene paleoceanography of the northern Barents Sea and variations of the northward heat transport by the Atlantic Ocean. *Boreas*, **30**, 2–16.

Ehrmann, W.U., and A. Mackensen, 1992: Sedimentological evidence for the formation of an East Antarctic ice-sheet in Eocene Oligocene time. *Palaeogeogr. Palaeoclimatol. Palaeoecol.*, **93**(1–2), 85–112.

Elliot, M., et al., 1998: Millennial scale iceberg discharges in the Irminger Basin during the last glacial period: relationship with the Heinrich events and environmental settings. *Paleoceanography*, **13**, 433–446.

Ellis, J.M., and Calkin, P.E., 1984: Chronology of Holocene glaciation, central Brooks Range, Alaska. *Geol. Soc. Am. Bull.*, **95**, 897–912.

Enting, I.G., 1987: On the use of smoothing splines to filter CO_2 data. *J. Geophys. Res.*, **92**, 10977–10984.

EPICA community members, 2004: Eight glacial cycles from an Antarctic ice core. *Nature*, **429**(6992), 623–628.

Esper, J., E.R. Cook, and F.H. Schweingruber, 2002: Low-frequency signals in long tree-ring chronologies for reconstructing past temperature variability. *Science*, **295**(5563), 2250–2253.

Esper, J., D.C. Frank, R.J.S. Wilson, and K.R. Briffa, 2005: Effect of scaling and regression on reconstructed temperature amplitude for the past millennium. *Geophys. Res. Lett.*, **32**(7), doi:10.1029/2004GL021236.

Etheridge, D.M., et al., 1996: Natural and anthropogenic changes in atmospheric CO_2 over the last 1000 years from air in Antarctic ice and firn. *J. Geophys. Res.*, **101**(D2), 4115–4128.

Evans, M.N., A. Kaplan, and M.A. Cane, 2002: Pacific sea surface temperature field reconstruction from coral $\delta^{18}O$ data using reduced space objective analysis. *Paleoceanography*, **17**(1), 1007, doi:10.1029/2000PA000590.

Eyer, M., 2004: *Highly Resolved $\delta^{13}C$ Measurements on CO_2 in Air from Antarctic Ice Cores*. PhD Thesis, University of Bern, 113 pp.

Fairbanks, R.G., 1989: A 17,000 year glacio-eustatic sea level record: Influence of glacial melting rates on the Younger Dryas event and deep-ocean circulation. *Paleoceanography*, **342**, 637–642.

Farrera, I., et al., 1999: Tropical climates at the Last Glacial Maximum: a new synthesis of terrestrial palaeoclimate data. I. Vegetation, lake-levels and geochemistry. *Clim. Dyn.*, **15**, 823–856.

Ferretti, D.F., et al., 2005: Unexpected changes to the global methane budget over the past 2000 years. *Science*, **309**, 1714–1717.

Fischer, G., and G. Wefer (eds.), 1999: *Use of Proxies in Paleoceanography: Examples from the South Atlantic*. Springer, Berlin, 735 pp.

Fleitmann, D., et al., 2003: Holocene forcing of the Indian monsoon recorded in a stalagmite from southern Oman. *Science*, **300**, 1737–1740.

Fligge, M., and S.K. Solanki, 2000: The solar spectral irradiance since 1700. *Geophys. Res. Lett.*, **27**, 2157–2160.

Flückiger, J., et al., 1999: Variations in atmospheric N_2O concentration during abrupt climatic changes. *Science*, **285**(5425), 227–230.

Flückiger, J., et al., 2002: High resolution Holocene N_2O ice core record and its relationship with CH_4 and CO_2. *Global Biogeochem. Cycles*, **16**, doi:10.1029/2001GB001417.

Flückiger, J., et al., 2004: N_2O and CH_4 variations during the last glacial epoch: Insight into global processes. *Global Biogeochem. Cycles*, **18**, doi:10.1029/2003GB002122.

Folland, C.K., et al., 2001: Observed climate variability and change. In: *Climate Change 2001: The Scientific Basis. Contribution of Working Group I to the Third Assessment Report of the Intergovernmental Panel on Climate Change* [Houghton, J.T. et al. (eds.)]. Cambridge University Press, Cambridge, United Kingdom and New York, NY, USA, pp. 99–181.

Forman, S.L., R. Oglesby, and R.S. Webb, 2001: Temporal and spatial patterns of Holocene dune activity on the Great Plains of North America: megadroughts and climate links. *Global Planet. Change*, **29**(1–2), 1–29.

Foster, S., 2004: *Reconstruction of Solar Irradiance Variations for Use in Studies of Global Climate Change: Application of Recent SOHO Observations with Historic Data from the Greenwich Observatory*. Ph.D. Thesis, University of Southampton, Southampton, UK.

Foukal, P., G. North, and T. Wigley, 2004: A stellar view on solar variations and climate. *Science*, **306**(5693), 68–69.

Francois, L.M., C. Delire, P. Warnant, and G. Munhoven, 1998: Modelling the glacial-interglacial changes in the continental biosphere. *Global Planet. Change*, **17**, 37–52.

Francois, L.M., et al., 1999: Carbon stocks and isotopic budgets of the terrestrial biosphere at mid-Holocene and last glacial maximum times. *Chem. Geol.*, **159**, 163–189.

Freeman, K.H., and J.M. Hayes, 1992: Fractionation of carbon isotopes by phytoplankton and estimates of ancient CO2 levels. *Global Biogeochem. Cycles*, **6**, 185–198.

Friedlingstein, P., et al., 2006: Climate-carbon cycle feedback analysis, results from the C^4MIP model intercomparison. *J. Clim*., **19** (14), 3337–3353.

Fröhlich, C., and J. Lean, 2004: Solar radiative output and its variability: evidence and mechanisms. *Astron. Astrophys. Rev.*, **12**, 273–320.

Gaffen, D.J., et al., 2000: Multidecadal changes in the vertical temperature structure of the tropical troposphere. *Science*, **287**(5456), 1242–1245.

Gagan, M.K., et al., 1998: Temperature and surface-ocean water balance of the mid-Holocene tropical western Pacific. *Science*, **279**, 1014–1018.

Ganopolski, A., and S. Rahmstorf, 2001: Rapid changes of glacial climate simulated in a coupled climate model. *Nature*, **409**, 153–158.

Gellatly, A.F., T.J. Chinn, and F. Röthlisberger, 1988: Holocene glacier variations in New Zealand: a review. *Quat. Sci. Rev.*, **7**, 227–242.

Gerber, S., et al., 2003: Constraining temperature variations over the last millennium by comparing simulated and observed atmospheric CO_2. *Clim. Dyn.*, **20**(2–3), 281–299.

Gersonde, R., X. Crosta, A. Abelmann, and L. Armand, 2005: Sea-surface temperature and sea ice distribution of the Southern Ocean at the EPILOG Last Glacial Maximum - a circum-Antarctic view based on siliceous microfossil records. *Quat. Sci. Rev.*, **24** (7–9), 869–896

Gherardi, J.M., et al., 2005: Evidence from the North Eastern Atlantic Basin for variability of the Meridional Overturning Circulation through the last deglaciation. *Earth Planet. Sci. Lett.*, **240**, 710–723.

Gladstone, R.M., et al., 2005: Mid-Holocene NAO: a PMIP2 model intercomparison. *Geophys. Res. Lett.*, **32**, L16707, doi:10.1029/2005GL023596.

Goldstein, B., F. Joos, and T.F. Stocker, 2003: A modeling study of oceanic nitrous oxide during the Younger Dryas cold period. *Geophys. Res. Lett.*, **30**, doi:10.1029/2002GL016418.

Goni, M.F.S., F. Eynaud, J.L. Turon, and N.J. Shackleton, 1999: High resolution palynological record off the Iberian margin: direct land-sea correlation for the Last Interglacial complex. *Earth Planet. Sci. Lett.*, **171**(1), 123–137.

González-Rouco, F., H. von Storch, and E. Zorita, 2003: Deep soil temperature as proxy for surface air-temperature in a coupled model simulation of the last thousand years. *Geophys. Res. Lett.*, **30**(21), 2116, doi:10.1029/2003GL018264.

González-Rouco, J.F., H. Beltrami, E. Zorita, and H. von Storch, 2006: Simulation and inversion of borehole temperature profiles in surrogate climates: Spatial distribution and surface coupling. *Geophys. Res. Lett.*, **33**(1), L01703, doi:10.1029/2005GL024693.

Goosse, H., H. Renssen, A. Timmermann, and R.S. Bradley, 2005a: Internal and forced climate variability during the last millennium: a model-data comparison using ensemble simulations. *Quat. Sci. Rev.*, **24**, 1345–1360.

Goosse, H., et al., 2004: A late medieval warm period in the Southern Ocean as a delayed response to external forcing? *Geophys. Res. Lett.*, **31**, L06203, doi:10.1029/2003GL019140.

Goosse, H., et al., 2005b: Modelling the climate of the last millennium: what causes the differences between simulations? *Geophys. Res. Lett.*, **32**, L06710, doi:10.1029/2005GL022368.

Gosnold, W.D., P.E. Todhunter, and W. Schmidt, 1997: The borehole temperature record of climate warming in the mid- continent of North America. *Global Planet. Change*, **15**(1–2), 33–45.

Gradstein, F.M., J.G. Ogg, and A.G. Smith (eds.), 2004: *A Geologic Time Scale*. Cambridge University Press, Cambridge, 589 pp.

Greenblatt, J.B., and J.L. Sarmiento, 2004: Variability and climate feedback mechanisms in ocean uptake of CO_2. In: *The Global Carbon Cycle* [Field, C.B., and M.R. Raupach (eds)]. Island Press, Washington, DC, pp. 257–275.

Guilderson, T.P., R.G. Fairbanks, and J.L. Rubenstone, 1994: Tropical temperature variations since 20,000 years ago: modulating interhemispheric climate change. *Science*, **263**, 663–665.

Guiot, J., et al., 2005: Last-millennium summer-temperature variations in Western Europe based on proxy data. *The Holocene*, **15**(4), 489–500.

Guo, Z.T., N. Petit-Maire, and S. Kropelin, 2000: Holocene non-orbital climatic events in present-day arid areas of Northern Africa and China. *Global Planet. Change*, **26**(1–3), 97–103.

Guo, Z.T., et al., 2004: Late Miocene-Pliocene development of Asian aridification as recorded in the Red-Earth formation in northern China. *Global Planet. Change*, **41**(3–4), 135–145.

Gupta, A.K., D.M. Anderson, and J.T. Overpeck, 2003: Abrupt changes in the Asian southwest monsoon during the Holocene and their links to the North Atlantic Ocean. *Nature*, **421**, 354–357.

Hall, J.C., and G.M. Lockwood, 2004: The chromospheric activity and variability of cycling and flat activity solar-analog stars. *Astrophys. J.*, **614**, 942–946.

Hambrey, M.J., W.U. Ehrmann, and B. Larsen, 1991: Cenozoic glacial record of the Prydz Bay continental shelf, East Antarctica. In: *Proceedings of the Ocean Drilling Program: Scientific Results*, Vol. 119. Ocean Drilling Program, College Station, TX, pp. 77–131.

Hanebuth, T., K. Stattegger, and P.M. Grootes, 2000: Rapid flooding of the Sunda Shelf: A late-glacial sea-level record. *Science*, **288**(5468), 1033–1035.

Harrington, G.J., S.J. Kemp, and P.L. Koch, 2004: Palaeocene-Eocene paratropical floral change in North America: responses to climate change and plant immigration. *J. Geol. Soc. London*, **161**, 173–184.

Harris, R.N., and D.S. Chapman, 2001: Mid-latitude (30°-60° N) climatic warming inferred by combining borehole temperatures with surface air temperatures. *Geophys. Res. Lett.*, **28**(5), 747–750.

Harrison, S.P., 2005: Snowlines at the last glacial maximum and tropical cooling. *Quat. Int.*, **138**, 5–7.

Harrison, S.P., and I.C. Prentice, 2003: Climate and CO_2 controls on global vegetation distribution at the last glacial maximum: analysis based on palaeovegetation data, biome modelling and paleoclimate simulations. *Global Change Biol.*, **9**, 983–1004.

Harrison, S.P., et al., 2003: Mid-Holocene climates of the Americas: a dynamical response to changed seasonality. *Clim. Dyn.*, **20**(7–8), 663–688.

Haug, G.H., et al., 2001: Southward migration of the Intertropical Convergence Zone through the Holocene. *Science*, **17**(293), 1304–1308.

Hays, J.D., J. Imbrie, and N.J. Shackleton, 1976: Variations in the earth's orbit: pacemaker of the ice ages. *Science*, **194**, 1121–1132.

Haywood, A.M., P.J. Valdes, and B.W. Sellwood, 2000: Global scale paleoclimate reconstruction of the middle Pliocene climate using the UKMO GCM: initial results. *Global Planet. Change*, **25**, 239–256.

Haywood, A.M., P. Dekens, A.C. Ravelo, and M. Williams, 2005: Warmer tropics during the mid-Pliocene? Evidence from alkenone paleothermometry and a fully coupled ocean-atmosphere GCM. *Geochem. Geophys. Geosystems*, **6**, Q03010, doi:10.1029/2004GC000799.

He, Y., et al., 2004: Asynchronous Holocene climatic change across China. *Quat. Res.*, **61**, 52–63.

Hegerl, G.C., T.J. Crowley, W.T. Hyde, and D.J. Frame, 2006: Climate sensitivity constrained by temperature reconstructions over the past seven centuries. *Nature*, **440**, 1029–1032.

Hemming, S.R., 2004: Heinrich events: Massive late Pleistocene detritus layers of the North Atlantic and their global climate imprint. *Rev. Geophys.*, **42**(1), RG1005, doi:10.1029/2003RG000128.

Higgins, P.A.T., 2004: Biogeochemical and biophysical responses of the land surface to a sustained thermohaline circulation weakening. *J. Clim.*, **17**, 4135–4142.

Hodell, D.A., M. Brenner, and J.H. Curtis, 2005: Terminal classic drought in the northern Maya lowlands inferred from multiple sediment cores in Lake Chichancanab (Mexico). *Quat. Sci. Rev.*, **24**(12–13), 1413–1427.

Hoerling, M., and A. Kumar, 2003: The perfect ocean for drought. *Science*, **299**(5607), 691–694.

Hoffmann, G., et al., 2003: Coherent isotope history of Andean ice cores over the last century. *Geophys. Res. Lett.*, **30**(4), doi:10.1029/2002GL014870.

Holmgren, K., et al., 2003: Persistent millennial-scale climate variability over the past 25,000 years in Southern Africa. *Quat. Sci. Rev.*, **22**, 2311–2326.

Holzhauser, H., M.J. Magny, and H.J. Zumbuhl, 2005: Glacier and lake-level variations in west-central Europe over the last 3500 years. *The Holocene*, **15**(6), 789–801.

Hoyt, D.V., and K.H. Schatten, 1993: A discussion of plausible solar irradiance variations. *J. Geophys. Res.*, **98**, 18895–18906.

Huang, S.P., and H.N. Pollack, 1998: *Global Borehole Temperature Database for Climate Reconstruction.* IGBP PAGES/World Data Center-A for Paleoclimatology Data Contribution Series #1998-044, NOAA/NGDC Paleoclimatology Program, Boulder, CO.

Huang, S.P., H.N. Pollack, and P.Y. Shen, 1997: Late Quaternary temperature changes seen in the world-wide continental heat flow measurements. *Geophys. Res. Lett.*, **24**, 1947–1950.

Huang, S.P., H.N. Pollack, and P.Y. Shen, 2000: Temperature trends over the past five centuries reconstructed from borehole temperatures. *Nature*, **403**(6771), 756–758.

Huber, C., et al., 2006: Isotope calibrated Greenland temperature record over Marine Isotope Stage 3 and its relation to CH_4. *Earth Planet. Sci. Lett.*, **243**(3–4), 504–519.

Hughen, K.A., J.T. Overpeck, L.C. Peterson, and S. Trumbore, 1996: Rapid climate changes in the tropical Atlantic region during the last deglaciation. *Nature*, **380**(6569), 51–54.

Hughen, K.A., T.I. Eglinton, L. Xu, and M. Makou, 2004: Abrupt tropical vegetation response to rapid climate changes. *Science*, **304**(5679), 1955–1959.

Hughes, M.K., and H.F. Diaz, 1994: Was there a Medieval Warm Period, and if so, where and when? *Clim. Change*, **26**(2–3), 109–142.

Humlum, O., et al., 2005: Late-Holocene glacier growth in Svalbard, documented by subglacial relict vegetation and living soil microbes. *The Holocene*, **15**(3), 396–407.

Hurrell, J.W., 1995: Decadal trends in the North-Atlantic Oscillation - regional temperatures and precipitation. *Science*, **269**(5224), 676–679.

Huybers, P., 2005: Comment on "Hockey sticks, principal components, and spurious significance" by S. McIntyre and R. McKitrick. *Geophys. Res. Lett.*, **32**(20), doi:10.1029/2005GL023395.

Indermühle, A., et al., 2000: Atmospheric CO_2 concentration from 60 to 20 kyr BP from the Taylor Dome ice core, Antarctica. *Geophys. Res. Lett.*, **27**(5), 735–738.

IPCC, 1990: *Climate Change: The IPCC Scientific Assessment* [Houghton, J.T., G.J. Jenkins, and J.J. Ephraums (eds.)]. Cambridge University Press, Cambridge, United Kingdom and New York, NY, USA, 362 pp.

IPCC, 2001: *Climate Change 2001: The Scientific Basis. Contribution of Working Group I to the Third Assessment Report of the Intergovernmental Panel on Climate Change* [Houghton, J.T., et al. (eds.)]. Cambridge University Press, Cambridge, United Kingdom and New York, NY, USA, 881 pp.

Jackson, S.C., and A.J. Broccoli, 2003: Orbital forcing of Arctic climate: mechanisms of climate response and implications for continental glaciation. *Clim. Dyn.*, **21**, 539–557.

Jansen, E., T. Fronval, F. Rack, and J.E.T. Channell, 2000: Pliocene-Pleistocene ice rafting history and cyclicity in the Nordic Seas during the last 3.5 Myr. *Paleoceanography*, **15**(6), 709–721.

Jasper, J.P., and J.M. Hayes, 1990: A carbon isotope record of CO_2 levels during the late Quaternary. *Nature*, **347**, 462–464.

Jennings, A.E., et al., 2001: A mid-Holocene shift in Arctic sea-ice variability on the East Greenland Shelf. *The Holocene*, **12**, 49–58.

Jiang, D., et al., 2005: Modeling the middle Pliocene climate with a global atmospheric general circulation model. *J. Geophys. Res.*, **110**, D14107, doi:10.1029/2004JD005639.

Jörin, U.E., T.F. Stocker, and C. Schlüchter, 2006: Multi-century glacier fluctuations in the Swiss Alps during the Holocene. *The Holocene*, **16**(5), 697–704.

Johnsen, S.J., et al., 2001: Oxygen isotope and palaeotemperature records from six Greenland ice-core stations: Camp Century, Dye-3, GRIP, GISP2, Renland and NorthGRIP. *J. Quat. Sci.*, **16**, 299–307.

Jolly, D., S.P. Harrison, B. Damnati, and R. Bonnefille, 1998: Simulated climate and biomes of Africa during the Late Quaternary: comparison with pollen and lake status data. *Quat. Sci. Rev.*, **17**, 629–657.

Jones, P.D., and A. Moberg, 2003: Hemispheric and large-scale surface air temperature variations: An extensive revision and an update to 2001. *J. Clim.*, **16**(2), 206–223.

Jones, P.D., and M.E. Mann, 2004: Climate over past millennia. *Rev. Geophys.*, **42**(2), RG2002, doi:10.1029/2003RG000143.

Jones, P.D., T.J. Osborn, and K.R. Briffa, 1997: Estimating sampling errors in large-scale temperature averages. *J. Clim.*, **10**(10), 2548–2568.

Jones, P.D., T.J. Osborn, and K.R. Briffa, 2001: The evolution of climate over the last millennium. *Science*, **292**(5517), 662–667.

Jones, P.D., K.R. Briffa, and T.J. Osborn, 2003: Changes in the Northern Hemisphere annual cycle: Implications for paleoclimatology? *J. Geophys. Res.*, **108**(D18), 4588, doi:10.1029/2003JD003695.

Jones, P.D., K.R. Briffa, T.P. Barnett, and S.F.B. Tett, 1998: High-resolution palaeoclimatic records for the last millennium: interpretation, integration and comparison with General Circulation Model control-run temperatures. *The Holocene*, **8**(4), 455–471.

Joos, F., and I.C. Prentice, 2004: A paleo-perspective on changes in atmospheric CO_2 and climate. In: *The Global Carbon Cycle: Integrating Humans, Climate and the Natural World* [Field, C.B., and M.R. Raupach (eds.)]. Island Press, Washington DC, pp. 165–186.

Joos, F., et al., 1999: Global warming and marine carbon cycle feedbacks on future atmospheric CO2. *Science*, **284**, 464–467.

Joos, F., et al., 2001: Global warming feedbacks on terrestrial carbon uptake under the Intergovernmental Panel on Climate Change (IPCC) emission scenarios. *Global Biogeochem. Cycles*, **15**(4), 891–907.

Joos, F., et al., 2004: Transient simulations of Holocene atmospheric carbon dioxide and terrestrial carbon since the Last Glacial Maximum. *Global Biogeochem. Cycles*, **18**, doi:10.1029/2003GB002156.

Joussaume, S., et al., 1999: Monsoon changes for 6000 years ago: Results of 18 simulations from the Paleoclimate Modeling Intercomparison Project (PMIP). *Geophys. Res. Lett.*, **26**(7), 859–862.

Kadomura, H., 1992: Climate change in the West African Sahel-Sudan zone since the Little Ice Age. In: *Symposium on the Little Ice Age* [Mikami, T. (ed.)]. Tokyo Metropolitan University, Tokyo, pp. 40–45.

Kageyama, M., et al., 2004: Quantifying ice-sheet feedbacks during the last glacial inception. *Geophys. Res. Lett.*, **31**, doi:10.1029/2004GL021339.

Kageyama, M., et al., 2006: Last Glacial Maximum temperatures over the North Atlantic, Europe, and western Siberia: a comparison between PMIP models, MARGO sea-surface temperatures and pollen-base reconstructions. *Quat. Sci. Rev.*, **25**, 2082–2102.

Kaplan, J.O., I.C. Prentice, W. Knorr, and P.J. Valdes, 2002: Modeling the dynamics of terrestrial carbon storage since the Last Glacial Maximum. *Geophys. Res. Lett.*, **29**, doi:10.1029/2002GL015230.

Kaplan, J.O, et al., 2003: Climate change and Arctic ecosystems: 2. Modeling, paleodata-model comparisons, and future projections. *J. Geophys. Res.*, **108,** doi:10.1029/2002JD002559.

Kaplan, M.R., and A.P. Wolfe, 2006: Spatial and temporal variability of Holocene temperature in the North Atlantic region. *Quat. Res.*, **65**, 223–231.

Karlén, W. and J. Kuylenstierna, 1996: On solar forcing of Holocene climate: evidence from Scandinavia. *The Holocene*, **6**, 359–365.

Karlén, W., et al., 1999: Glacier fluctuations on Mount Kenya since ca 6000 cal. years BP: implications for Holocene climatic change in Africa. *Ambio*, **28**(5), 409–418.

Kaspar, F., and U. Cubasch, 2006: Simulations of the Eemian interglacial and the subsequent glacial inception with a coupled ocean-atmosphere general circulation model. In: *The Climate of Past Interglacials* [Sirocko, F., M. Claussen, M.F. Sánchez-Goñi and T. Litt (eds.)], Elsevier Science, Amsterdam, pp. 499-516.

Kaspar, F., N. Kuhl, U. Cubasch, and T. Litt, 2005: A model-data comparison of European temperatures in the Eemian interglacial. *Geophys. Res. Lett.*, **32**, L11703, doi:10.1029/2005GL022456.

Kaufman, D.S., et al., 2004: Holocene thermal maximum in the western Arctic (0-180°W). *Quat. Sci. Rev.*, **23**, 529–560.

Keeling, C.D., and T.P. Whorf, 2005: Atmospheric CO_2 records from sites in the SiO air sampling network. In: *Trends: A Compendium of Data on Global Change*. Carbon Dioxide Information Analysis Center, Oak Ridge National Laboratory, U.S. Department of Energy, Oak Ridge, TN.

Kennett, J.P., and L.D. Stott, 1991: Abrupt deep-sea warming, palaeoceanographic changes and benthic extinctions at the end of the Palaeocene. *Nature*, **353**, 225–229.

Khodri, M., G. Ramstein, N. De Noblet, and M. Kageyama, 2003: Sensitivity of the northern extratropics hydrological cycle to the changing insolation forcing at 126 and 115 ky BP. *Clim. Dyn.*, **21**, 273–287.

Khodri, M., et al., 2005: The impact of precession changes on the Arctic climate during the last interglacial glacial transition. *Earth Planet. Sci. Lett.*, **236**, 285–304.

Kim, J.H., et al., 2004: North Pacific and North Atlantic sea-surface temperature variability during the Holocene. *Quat. Sci. Rev.*, **23**, 2141–2154.

Kitoh, A., and S. Murakami, 2002: Tropical Pacific climate at the mid-Holocene and the Last Glacial Maximum simulated by a coupled ocean-atmosphere general circulation model. *Paleoceanography*, **17**, 1047, doi:10.1029/2001PA000724.

Klitgaard-Kristensen, D., et al., 1998: The short cold period 8,200 years ago documented in oxygen isotope records of precipitation in Europe and Greenland. *J. Quat. Sci.*, **13**(2), 165–169.

Knies, J., J. Matthiessen, C. Vogt, and R. Stein, 2002: Evidence of 'Mid-Pliocene (similar to 3 Ma) global warmth' in the eastern Arctic Ocean and implications for the Svalbard/Barents Sea ice sheet during the late Pliocene and early Pleistocene (similar to 3-1.7 Ma). *Boreas*, **31**(1), 82–93.

Knox, J.C., 2000: Sensitivity of modern and Holocene floods to climate change. *Quat. Sci. Rev.*, **19**(1–5), 439–457.

Knutti, R., J. Flückiger, T.F. Stocker, and A. Timmermann, 2004: Strong hemispheric coupling of glacial climate through freshwater discharge and ocean circulation. *Nature*, **430**(7002), 851–856.

Koch, J., B. Menounos, J. Clague, and G.D. Osborn, 2004: Environmental change in Garibaldi Provincial Park, Southern Coast Mountains, British Columbia. *Geoscience Canada*, **31**(3), 127–135.

Koch, P.L., J.C. Zachos, and P.D. Gingerich, 1992: Correlation between isotope records in marine and continental carbon reservoirs near the Paleocene Eocene boundary. *Nature*, **358**(6384), 319–322.

Koerner, R.M., 1989: Ice core evidence for extensive melting of the Greenland Ice-sheet in the last interglacial. *Science*, **244**(4907), 964–968.

Koerner, R.M., and D.A. Fisher, 2002: Ice-core evidence for widespread Arctic glacier retreat in the Last Interglacial and the early Holocene. *Ann. Glaciol.*, **35**, 19–24.

Kohfeld, K., and S.P. Harrison, 2001: DIRTMAP: the geological record of dust. *Earth Sci. Rev.*, **54**, 81–114.

Kohfeld, K.E., C. LeQuéré, S.P. Harrison, and R.F. Anderson, 2005: Role of marine biology in glacial-interglacial CO_2 cycles. *Science*, **308**, 74–78.

Köhler, P., F. Joos, S. Gerber, and R. Knutti, 2005: Simulating changes in vegetation distribution, land carbon storage, and atmospheric CO_2 in response to a collapse of the North Atlantic thermohaline circulation. *Clim. Dyn.*, **25** (7–8), 689–708.

Koutavas, A., J. Lynch-Stieglitz, T.M. Marchitto Jr., and J.P. Sachs, 2002: El Niño-like pattern in ice age tropical Pacific sea surface temperature. *Science*, **297**, 226–230.

Kucera, M., et al., 2005: Multiproxy approach for the reconstruction of the glacial ocean surface (MARGO). *Quat. Sci. Rev.*, **24**, 813–819.

Kuhnert, H., et al., 1999: A 200-year coral stable oxygen isotope record from a high-latitude reef off western Australia. *Coral Reefs*, **18**(1), 1–12.

Kukla, G.J., et al., 2002: Last interglacial climates. *Quat. Res.*, **58**, 2–13.

Kurtz, A.C., et al., 2003: Early Cenozoic decoupling of the global carbon and sulphur cycles. *Paleoceanography*, **18**(4), doi:10.1029/2003PA000908.

Laird, K.R., et al., 2003: Lake sediments record large-scale shifts in moisture regimes across the northern prairies of North America during the past two millennia. *Proc. Natl. Acad. Sci. U.S.A.*, **100**(5), 2483–2488.

LaMarche, V.C., D.A. Graybill, H.C. Fritts, and M.R. Rose, 1984: Increasing atmospheric carbon dioxide: Tree ring evidence for growth enhancement in natural vegetation. *Science*, **225**, 1019–1021.

Lamb, H.H., 1965. The early medieval warm epoch and its sequel. *Palaeogeogr. Palaeoclimatol. Palaeoecol.*, **1**(13), 13–37.

Lamb, H.H., 1977: *Climates of the Past, Present and Future*. Vol. I and II. Metheun, London.

Lamb, H.H., 1982: *Climate History and the Modern World*. Routledge, London and New York, 433 pp.

Lambeck, K., 2002: Sea-level change from mid-Holocene to recent time: An Australian example with global implications. In: *Ice Sheets, Sea Level and the Dynamic Earth* [Mitrovica, J.X., and L.A. Vermeersen (eds.)]. Geodynamic Series Vol. 29, American Geophysical Union, Washington, DC, pp. 33–50.

Lambeck, K., and J. Chappell, 2001: Sea level change through the last glacial cycle. *Science*, **292**(5517), 679–686.

Landais, A., et al., 2006: The glacial inception as recorded in the NorthGRIP Greenland ice core: timing, structure and associated abrupt temperature changes. *Clim. Dyn.*, **26**(2–3), 273–284.

Laskar, J., et al., 2004: A long-term numerical solution for the insolation quantities of the Earth. *Astron. Astrophys.*, **428**(1), 261–285.

Lauritzen, S.E., 2003: Reconstruction of Holocene climate records from speleothems. In: *Global Change in the Holocene* [Mackay, A., R. Battarbee, J. Birks, and F. Oldfield (eds)]. Arnold, London, pp. 242–263.

Le Quesne, C., et al., 2006: Ancient *Austrocedrus* tree-ring chronologies used to reconstruct Central Chile precipitation variability from AD 1200 to 2000. *J. Clim.*, **19**(22), 5731–5744.

Lea, D.W., D.K. Pak, L.C. Peterson, and K.A. Hughen, 2003: Synchroneity of tropical and high-latitude Atlantic temperatures over the last glacial termination. *Science*, **301**(5638), 1361–1364.

Lean, J., 2000: Evolution of the sun's spectral irradiance since the Maunder Minimum. *Geophys. Res. Lett.*, **27**(16), 2425–2428.

Lean, J.L., Y.M. Wang, and N.R. Sheeley, 2002: The effect of increasing solar activity on the sun's total and open magnetic flux during multiple cycles: Implications for solar forcing of climate. *Geophys. Res. Lett.*, **29**(24), 2224, doi:10.1029/2002GL015880.

Lean, J.L., et al., 1995: Correlated brightness variations in solar radiative output from the photosphere to the corona. *Geophys. Res. Lett.*, **22**(5), 655–658.

Lear, C.H., Y. Rosenthal, H.K. Coxall, and P.A. Wilson, 2004: Late Eocene to early Miocene ice sheet dynamics and the global carbon cycle. *Paleoceanography*, **19**(4), PA4015, doi:10.1029/2004PA001039.

LeGrande, A.N., et al., 2006: Consistent simulations of multiple proxy responses to an abrupt climate change event. *Proc. Natl. Acad. Sci. U.S.A.*, **103**(4), 837–842.

Lemasurier, W.E., and S. Rocchi, 2005: Terrestrial record of post-Eocene climate history in Marie Byrd Land, West Antarctica. *Geografiska Annaler*, **87A**(1), 51–66.

Levis, S., G. B. Bonan, and C. Bonfils 2004: Soil feedback drives the mid-Holocene North African monsoon northward in fully coupled CCSM2 simulations with a dynamic vegetation model. *Clim. Dyn.*, **23**, 791–802.

Lhomme, N., G.K.C. Clarke, and S.J. Marshall, 2005: Tracer transport in the Greenland Ice Sheet: constraints on ice cores and glacial history. *Quat. Sci. Rev.*, **24**, 173–194.

Lie, Ø., et al., 2004: Holocene fluctuations of a polythermal glacier in high-alpine eastern Jotunheimen, central-southern Norway. *Quat. Sci. Rev.*, **23**(18–19), 1925–1945.

Linsley, B.K., et al., 2004: Geochemical evidence from corals for changes in the amplitude and spatial pattern of South Pacific interdecadal climate variability over the last 300 years. *Clim. Dyn.*, **22**(1), 1–11.

Lisiecki, L.E., and M.E. Raymo, 2005: A Pliocene-Pleistocene stack of 57 globally distributed benthic $\delta^{18}O$ records. *Paleoceanography*, **20**, PA1003, doi:10.1029/2004PA001071.

Liu, K.B., 2004: Paleotempestology: Principles, methods, and examples from Gulf coast lake-sediments. In: *Hurricanes and Typhoons: Past, Present and Future* [Murnane, R., and K. Liu (eds.)]. Columbia University Press, New York, pp. 13–57.

Liu, Z., J.E. Kutzbach, and L. Wu, 2000: Modeling climate shift of El Niño variability in the Holocene. *Geophys. Res. Lett.*, **27**, 2265–2268.

Liu, Z., S.P. Harrison, J.E. Kutzbach, and B. Otto-Bleisner, 2004: Global monsoons in the mid-Holocene and oceanic feedback. *Clim. Dyn.*, **22**, 157–182.

Liu, Z., et al., 2002: Tropical cooling at the last glacial maximum and extratropical ocean ventilation. *Geophys. Res. Lett.*, **29**, 1409, doi:10.1029/2001GL013938.

Lockwood, M., and R. Stamper, 1999: Long-term drift of the coronal source magnetic flux and the total solar irradiance. *Geophys. Res. Lett.*, **26**, 2461–2464.

Lorentz, S.J., et al., 2006: Orbitally driven insolation forcing on Holocene climate trends: evidence from alkenone data and climate modeling. *Paleoceanography*, **21**, doi:10.1029/2005PA001152.

Lough, J.M., 2004: A strategy to improve the contribution of coral data to high-resolution paleoclimatology. *Palaeogeogr. Paleoclimatol. Palaeoecol.*, **204**, 115–143.

Loutre, M.F., and A.L. Berger, 2000: Future climate changes: Are we entering an exceptionally long interglacial? *Clim. Change*, **46**, 61–90.

Loutre, M.F., D. Paillard, F. Vimeux, and E. Cortijo, 2004: Does mean annual insolation have the potential to change the climate? *Earth Planet. Sci. Lett.*, **221**(1–4), 1–14.

Lozhkin, A.V., and P.M. Anderson, 1995: The last interglaciation in northeast Siberia. *Quat. Res.*, **43**, 147–158.

Lubinski, D.J., S.L. Forman, and G.H. Miller, 1999: Holocene glacier and climate fluctuations on Franz Josef Land, Arctic Russia, 80° N. *Quat. Sci. Rev.*, **18**(1), 85–108.

Luckman, B.H., and M.S. Kearney, 1986: Reconstruction of Holocene changes in alpine vegetation and climate in the Maligne Range, Jasper National Park, Alberta. *Quat. Res.*, **26**(2), 244–261.

Luckman, B.H., and R.J.S. Wilson, 2005: Summer temperatures in the Canadian Rockies during the last millennium: a revised record. *Clim. Dyn.*, **24**(2–3), 131–144.

Luterbacher, J., et al., 2002: Reconstruction of sea level pressure fields over the Eastern North Atlantic and Europe back to 1500. *Clim. Dyn.*, **18**(7), 545–561.

Luterbacher, J., et al., 2004: European seasonal and annual temperature variability, trends, and extremes since 1500. *Science*, **303**(5663), 1499–1503.

MacAyeal, D.R., 1993: Binge/Purge oscillations of the Laurentide Ice-Sheet as a cause of the North-Atlantics Heinrich Events. *Paleoceanography*, **8**(6), 775–784.

MacDonald, G.M., and R.A. Case, 2005: Variations in the Pacific Decadal Oscillation over the past millennium. *Geophys. Res. Lett.*, **32**(8), doi:10.1029/2005GL022478.

MacDonald, G.M., et al., 2000: Holocene treeline history and climate change across northern Eurasia. *Quat. Res.*, **53**, 302–311.

MacFarling Meure, C., et al., 2006: The Law Dome CO_2, CH_4 and N_2O ice core records extended to 2000 years BP. *Geophys. Res. Lett.*, **33**, L14810, doi:10.1029/2006GL026152.

Machida, T., et al., 1995: Increase in the atmospheric nitrous oxide concentration during the last 250 years. *Geophys. Res. Lett.*, **22**, 2921–2924.

Mackay, A., R. Battarbee, J. Birks, and F.E. Oldfield (eds.), 2003: *Global Change in the Holocene*. Hodder Arnold, London, 480 pp.

Mahowald, N., et al., 1999: Dust sources and deposition during the Last Glacial Maximum and current climate: A comparison of model results with paleodata from ice cores and marine sediments. *J. Geophys. Res.*, **104**, 15859–15916.

Majorowicz, J.A., W.R., Skinner, and J. Safanda, 2004: Large ground warming in the Canadian Arctic inferred from inversions of temperature logs. *Earth Planet. Sci. Lett.*, **221**, 15–25.

Mangerud, J., V. Astakhov, and J.I. Svendsen, 2002: The extent of the Barents-Kara Ice Sheet during the Last Glacial Maximum. *Quat. Sci. Rev.*, **21**, 111–119.

Mann, M.E., and P.D. Jones, 2003: Global surface temperatures over the past two millennia. *Geophys. Res. Lett.*, **30**(15), 1820, doi:10.1029/2003GL017814.

Mann, M.E., and G.A. Schmidt, 2003: Ground vs. surface air temperature trends: Implications for borehole surface temperature reconstructions. *Geophys. Res. Lett.*, **30**(12), 1607, doi:10.1029/2003GL017170.

Mann, M.E., R.S. Bradley, and M.K. Hughes, 1998: Global-scale temperature patterns and climate forcing over the past six centuries. *Nature*, **392**(6678), 779–787.

Mann, M.E., R.S. Bradley, and M.K. Hughes, 1999: Northern hemisphere temperatures during the past millennium: Inferences, uncertainties, and limitations. *Geophys. Res. Lett.*, **26**(6), 759–762.

Mann, M.E., R. Bradley, and M.K. Hughes, 2000: Long-term variability in the El Niño/Southern Oscillation and associated teleconnections. In: *El Niño and the Southern Oscillation: Multiscale Variability and Global and Regional Impacts* [Diaz, H.F., and V. Markgraf (eds.)]. Cambridge University Press, Cambridge, pp. 357–412.

Mann, M.E., M.A. Cane, S.E. Zebiak, and A. Clement, 2005a: Volcanic and solar forcing of the tropical Pacific over the past 1000 years. *J. Clim.*, **18**(3), 447–456.

Mann, M.E., S. Rutherford, E. Wahl, and C.M. Ammann, 2005b: Testing the fidelity of methods used in 'proxy-based' reconstructions of past climate. *J. Clim.*, **18**(20), 4097–4107.

Mann, M.E., et al., 2003: Optimal surface temperature reconstructions using terrestrial borehole data. *J. Geophys. Res.*, **108**(D7), doi:10.1029/2002JD002532.

Marchal, O., R. Francois, T.F. Stocker, and F. Joos, 2000: Ocean thermohaline circulation and sedimentary $^{231}Pa/^{230}Th$ ratio. *Paleoceanography*, **6**, 625–641.

Marchal, O., et al., 1999: Modelling the concentration of atmospheric CO_2 during the Younger Dryas climate event. *Clim. Dyn.*, **15**, 341–354.

Marchal, O., et al., 2002: Apparent long-term cooling of the sea surface in the northeast Atlantic and Mediterranean during the Holocene. *Quat. Sci. Rev.*, **21** (4–6), 455–483.

Marchant, R., and H. Hooghiemstra, 2004: Rapid environmental change in African and South American tropics around 4000 years before present : a review. *Earth Sci. Rev.*, **66**, 217–260.

Marchitto, T.N.J., D.W. Oppo, and W.B. Curry, 2002: Paired benthic foraminiferal Cd/Ca and Zn/Ca evidence for a greatly increased presence of Southern Ocean Water in the glacial North Atlantic. *Paleoceanography*, **17**, 1038, doi:10.1029/2000PA000598.

Marra, M.J., 2003: Last interglacial beetle fauna from New Zealand. *Quart. Res.*, **59**, 122–131.

Masson, V., et al., 2000: Holocene climate variability in Antarctica based on 11 ice cores isotopic records. *Quat. Res.*, **54**, 348–358.

Masson-Delmotte, V., et al., 2005a: Rapid climate variability during warm and cold periods in polar regions and Europe. *Comptes Rendus Geoscience*, **337**(10–11), 935–946.

Masson-Delmotte, V., et al., 2005b: GRIP deuterium excess reveals rapid and orbital-scale changes in Greenland moisture origin. *Science*, **309**(5731), 118–121.

Masson-Delmotte, V., et al., 2006: Past and future polar amplification of climate change: climate model intercomparisons and ice-core constraints. *Clim. Dyn.*, **26** (5), 513–529.

Matthews, J.A., et al., 2000: Holocene glacier variations in central Jotunheimen, southern Norway based on distal glaciolacustrine sediment cores. *Quat. Sci. Rev.*, **19**, 1625–1647.

Matthews, J.A., et al., 2005: Holocene glacier history of Bjørnbreen and climatic reconstruction in central Jotunheimen, Norway, based on proximal glaciofluvial stream-bank mires. *Quat. Sci. Rev.*, **24**(1–2), 67–90.

Mayewski, P.A., et al., 2004: Holocene climate variability. *Quat. Res.*, **62** (3), 243–255.

McElwain, J.C., and W.G. Chaloner, 1995: Stomatal density and index of fossil plants track atmospheric carbon dioxide in the Palaeozoic. *Ann. Bot.(London)*, **76**, 389–395.

McGregor, H.V., and M.K. Gagan, 2004: Western Pacific coral $\delta^{18}O$ records of anomalous Holocene variability in the El Niño-Southern Oscillation. *Geophys. Res. Lett.*, **31**(11), doi:10.1029/2004GL019972.

McIntyre, S., and R. McKitrick, 2003: Corrections to the Mann et al. (1998) proxy database and northern hemispheric average temperature series. *Energy Environ.*, **14**, 751–771.

McIntyre, S., and R. McKitrick, 2005a: Hockey sticks, principal components, and spurious significance. *Geophys. Res. Lett.*, **32**(3), L03710, doi:10.1029/2004GL021750.

McIntyre, S., and R. McKitrick, 2005b: The M&M critique of the MBH98 Northern Hemisphere climate index: Update and implications. *Energy Environ.*, **16**, 69–99.

McIntyre, S., and R. McKitrick, 2005c: Reply to comment by von Storch and Zorita on "Hockey sticks, principal components, and spurious significance". *Geophys. Res. Lett.*, **32**(20), L20714, doi:10.1029/2005GL023089.

McIntyre, S., and R. McKitrick, 2005d: Reply to comment by von Huybers on "Hockey sticks, principal components, and spurious significance". *Geophys. Res. Lett.*, **32**(20), L20713, doi:10.1029/2005GL023586.

McManus, J.F., et al., 2002: Thermohaline circulation and prolonged interglacial warmth in the North Atlantic. *Quat. Res.*, **58**, 17–21.

McManus, J.F., et al., 2004: Collapse and rapid resumption of Atlantic meridional circulation linked to deglacial climate changes. *Nature*, **428**, 834–837.

Meissner, K.J., A.J. Weaver, H.D. Matthews, and P.M. Cox, 2003: The role of land surface dynamics in glacial inception: a study with the UVic Earth System Model. *Clim. Dyn.*, **21**, 7–8.

Meland, M.Y., E. Jansen, and H. Elderfield, 2005: Constraints on SST estimates for the northern North Atlantic/Nordic Seas during the LGM. *Quat. Sci. Rev.*, **24**(7–9), 835–852.

Menounos, B., et al., 2004: Early Holocene glacier advance, southern Coast Mountains, British Columbia, Canada. *Quat. Sci. Rev.*, **23**(14–15), 1543–1550.

Mickley, L.J., D.J. Jacob, and D. Rind, 2001: Uncertainty in preindustrial abundance of tropospheric ozone: Implications for radiative forcing calculations. *J. Geophys. Res.*, **106**(D4), 3389–3399.

Mieding, B., 2005: *Reconstruction of Millennial Aerosol-Chemical Ice Core Records from the Northeast Greenland: Quantification of Temporal Changes in the Atmospheric Circulation, Emission and Deposition.* Reports on Polar and Marine Research No. 513, Alfred Wegener Institute for Polar and Marine Research, Bremerhaven, 119 pp.

Mix, A.C., A.E. Morey, N.G. Pisias, and S.W. Hostetler, 1999: Foraminiferal faunal estimates of paleotemperature: Circumventing the no-analog problem yields cool ice age tropics. *Paleoceanography*, **14**, 350–359.

Moberg, A., et al., 2005: Highly variable Northern Hemisphere temperatures reconstructed from low- and high-resolution proxy data. *Nature*, **433**(7026), 613–617.

Monnin, E., et al., 2001: Atmospheric CO_2 concentrations over the last glacial termination. *Science*, **291**(5501), 112–114.

Monnin, E., et al., 2004: Evidence for substantial accumulation rate variability in Antarctica during the Holocene, through synchronization of CO_2 in the Taylor Dome, Dome C and DML ice cores. *Earth Planet. Sci. Lett.*, **224**(1–2), 45–54.

Montoya, M., H. von Storch, and T.J. Crowley, 2000: Climate simulation for 125 kyr BP with a coupled ocean-atmosphere general circulation model. *J. Clim.*, **13**, 1057–1072.

Montoya, M., et al., 2005: The Earth System Model of Intermediate Complexity CLIMBER-3α Part I: description and performance for present day conditions. *Clim. Dyn.*, **25**, 237–263.

Moran, K., et al., 2006: The Cenozoic palaeoenvironment of the Arctic Ocean. *Nature*, **441**, 601–605.

Moros, M., J.T. Andrews, D.E. Eberl, and E. Jansen, 2006: Holocene history of drift ice in the northern North Atlantic: Evidence for different spatial and temporal modes. *Paleoceanography*, **21**, PA2017, doi:10.1029/2005PA001214.

Morrill, C., J.T. Overpeck, and J.E. Cole, 2003: A synthesis of abrupt changes in the Asian summer monsoon since the last deglaciation. *The Holocene*, **13**, 465–476.

Morrill, C., et al., 2006: Holocene variations in the Asian monsoon inferred from the geochemistry of lake sediments in central Tibet. *Quat. Res.*, **65**(2), 232–243.

Moy, C.M., G.O. Seltzer, D.T. Rodbell, and D.M. Anderson, 2002: Variability of El Niño/Southern Oscillation activity at millennial timescales during the Holocene epoch. *Nature*, **420**, 162–165.

Mudelsee, M., 2001: The phase relations among atmospheric CO_2 content, temperature and global ice volume over the past 420 ka. *Quat. Sci. Rev.*, **20**, 583–589.

Muhs, D.R., T.A. Ager, and J.E. Beget, 2001: Vegetation and paleoclimate of the last interglacial period, central Alaska. *Quat. Sci. Rev.*, **20**, 41–61.

Muhs, D.R., K.R. Simmons, and B. Steinke, 2002: Timing and warmth of the last interglacial period: New U-series evidence from Hawaii and Bermuda and a new fossil compilation for North America. *Quat. Sci. Rev.*, **21**, 1355–1383.

Muscheler, R., F. Joos, S.A. Müller, and I. Snowball, 2005: Climate - How unusual is today's solar activity? *Nature*, **436**(7050), E3–E4.

Muscheler, R., et al., 2007: Solar activity during the last 1000 years inferred from radionuclide records. *Quat. Sci. Rev.,* **26**, 82-97.

Myhre, G., E.J. Highwood, K.P. Shine, and F. Stordal, 1998: New estimates of radiative forcing due to well mixed greenhouse gases. *Geophys. Res. Lett.*, **25**, 2715–1718.

Nesje, A., and S.O. Dahl, 2003: The 'Little Ice Age' - only temperature? *The Holocene*, **13**(1), 139–145.

Nesje, A., S.O. Dahl, and J. Bakke, 2004: Were abrupt late glacial and early-Holocene climate changes in northwest Europe linked to freshwater outbursts to the North Atlantic and Arctic oceans? *The Holocene*, **14**, 299–310.

Nesje, A., S.O. Dahl, C. Andersson, and J.A. Matthews, 2000: The lacustrine sedimentary sequence in Sygneskardvatnet, western Norway: a continuous, high-resolution record of the Jostedalsbreen ice cap during the Holocene. *Quat. Sci. Rev.*, **19**, 1047–1065.

Nesje, A., et al., 2005: Holocene climate variability in the Northern North Atlantic region: A review of terrestrial and marine evidence. In: *The Nordic Seas: An Integrated Perspective* [Drange, H., et al. (eds.)]. Geophysical Monographs Vol. 158, American Geophysical Union, Washington, DC, pp. 289–322.

NGRIP (North Greenland Ice Core Project), 2004: High-resolution record of Northern Hemisphere climate extending into the last interglacial period. *Nature*, **431**, 147–151.

Nguetsop, V.F., S. Servant-Vildary, and M. Servant, 2004: Late Holocene climate changes in west Africa, a high resolution diatom record from equatorial Cameroon. *Quat. Sci. Rev.*, **23**(5–6), 591–609.

NRC (National Research Council), 2006: *Surface Temperature Reconstructions for the Last 2,000 Years*. National Academies Press, Washington, DC, 196 pp.

Oerlemans, J., 2005: Extracting a climate signal from 169 glacier records. *Science*, **308**(5722), 675–677.

Oppenheimer, M., and R.B. Alley, 2005: Ice sheets, global warming, and Article 2 of the UNFCCC. *Clim. Change*, **68**(3), 257–267.

Oppo, D.W., J.F. McManus, and J.L. Cullen, 2003: Deepwater variability in Holocene epoch. *Nature*, **422**, 277–278.

Osborn, G., and B.H. Luckman, 1988: Holocene glacier fluctuations in the Canadian Cordillera (Alberta and British Columbia). *Quat. Sci. Rev.*, **7**(2), 115–128.

Osborn, T.J., and K.R. Briffa, 2004: The real color of climate change? *Science*, **306**(5296), 621–622.

Osborn, T.J., and K.R. Briffa, 2006: The spatial extent of 20th-century warmth in the context of the past 1200 years. *Science*, **311**(5762), 841–844.

Osborn, T.J., S.C.B. Raper, and K.R. Briffa, 2006: Simulated climate change during the last 1,000 years: comparing the ECHO-G general circulation model with the MAGICC simple climate model. *Clim. Dyn*., **27** (2–3), 185–197, doi:10.1007/s00382-006-0129-5.

Otto-Bliesner, B.L., 1999: El Niño La Niña and Sahel precipitation during the middle Holocene. *Geophys. Res. Lett.*, **26**, 87–90.

Otto-Bliesner, B.L., S.J. Marshall, J.T. Overpeck, and G. Miller, 2006a: Simulating Arctic climate warmth and icefield retreat in the Last Interglaciation. *Science*, **311**, 1751–1753.

Otto-Bliesner, B.L., et al., 2003: Modeling El Niño and its tropical teleconnections during the last glacial-interglacial cycle. *Geophys. Res. Lett.*, **30**(23), doi:10.1029/2003GL018553.

Otto-Bliesner, B.L., et al., 2006b: Last Glacial Maximum and Holocene climate in CCSM3. *J. Clim.*, **19**, 2567–2583.

Overpeck, J., and K.E. Trenberth, 2004: *A Multi-Millennia Perspective on Drought and Implications for the Future.* Proceedings of a joint CLIVAR/PAGES/IPCC Workshop, 18-21 Nov. 2003, Tucson, AZ. University Corporation for Atmospheric Research, Boulder CO, 30 pp.

Overpeck, J.T., et al., 2006: Paleoclimatic evidence for future ice sheet instability and rapid sea level rise. *Science*, **311**(5768), 1747–1750.

Pagani, M., et al., 2005: Marked decline in atmospheric carbon dioxide concentrations during the Paleogene. *Science*, **309**(5734), 600–603.

Paillard, D., 1998: The timing of Pleistocene glaciations from a simple multiple-state climate model. *Nature*, **391**, 378–381.

Pauling, A., J. Luterbacher, C. Casty, and H. Wanner, 2006: 500 years of gridded high-resolution precipitation reconstructions over Europe and the connection to large-scale circulation. *Clim. Dyn.*, **26**, 387–405.

Pearson, P.N., and M.R. Palmer, 2000: Atmospheric carbon dioxide concentrations over the past 60 million years. *Nature*, **406**, 695–699.

Peltier, W.R., 1996: Mantle viscosity and ice age ice sheet topography. *Science*, **273**, 1359–1364.

Peltier, W.R., 1998: Postglacial variations in the level of the sea: Implications for climate dynamics and solid-earth geophysics. *Rev. Geophys.*, **36**(4), 603–689.

Peltier, W.R., 2001: Global glacial isostatic adjustment and modern instrumental records of relative sea level history. In: *Sea Level Rise: History and Consequences* [Douglas, B.C., M.S. Kearney, and S.P. Leatherman (eds.)]. Academic Press, San Diego, CA, pp. 65–95.

Peltier, W.R., 2002: On eustatic sea level history: Last Glacial Maximum to Holocene. *Quat. Sci. Rev.*, **21**(1–3), 377–396.

Peltier, W.R., 2004: Global glacial isostasy and the surface of the ice-age Earth: The ICE-5G (VM2) model and GRACE. *Annu. Rev. Earth Planet. Sci.*, **32**, 111–149.

Peltier, W.R., and R.G. Fairbanks, 2006: Global glacial ice volume and last glacial maximum duration from an extended Barbados sea level record. *Quat. Sci. Rev*., **25**, 3322-3337.

Peltier, W.R., I. Shennan, R. Drummond, and B. Horton, 2002: On the postglacial isostatic adjustment of the British Isles and the shallow viscoelastic structure of the earth. *Geophys. J. Int.*, **148**(3), 443–475.

Pépin, L., D. Raynaud, J.-M. Barnola, and M.F. Loutre, 2001: Hemispheric roles of climate forcings during glacial-interglacial transitions, as deduced from the Vostok record and LLN-2D model experiments. *J. Geophys. Res.*, **106**(D23), 31885–31892.

Peteet, D., 1995: Global Younger Dryas. *Quat. Int.*, **28**, 93–104.

Peterson, L.C., G.H. Haug, K.A. Hughen, and U. Röhl, 2000: Rapid changes in the hydrologic cycle of the tropical Atlantic during the last glacial. *Science*, **290**, 1947–1951.

Petit, J.R., et al., 1999: Climate and atmospheric history of the past 420,000 years from the Vostok ice core, Antarctica. *Nature*, **399**, 429–436.

Petoukhov, V., et al., 2000: CLIMBER-2: a climate system model of intermediate complexity. Part I: model description and performance for present climate. *Clim. Dyn.*, **16**(1), 1–17.

Pettersson, O., 1914: Climate variations in historic and prehistoric time. *Svenska Hydrogr. - Biol. Komm. Skriften*, **5**, 1–26.

Peyron, O., et al., 2005: Lateglacial climate in the Jura Mountains (France) based on different quantitative reconstruction approaches from pollen, lake-levels, and chironomids. *Quat. Res.*, **62**(2), 197–211.

Plattner, G.K., F. Joos, T.F. Stocker, and O. Marchal, 2001: Feedback mechanisms and sensitivities of ocean carbon uptake under global warming. *Tellus*, **53B**(5), 564–592.

Pollack, H.N., and S.P. Huang, 2000: Climate reconstruction from subsurface temperatures. *Annu. Rev. Earth Planet. Sci.*, **28**, 339–365.

Pollack, H.N., and J.E. Smerdon, 2004: Borehole climate reconstructions: Spatial structure and hemispheric averages. *J. Geophys. Res.*, **109**(D11), D11106, doi:10.1029/2003JD004163.

Pollack, H.N., S. Huang, and J.E. Smerdon, 2006: Five centuries of climate change in Australia: The view from underground. *J. Quat. Sci*, **21**(7), 701–706.

Pons, A., J. Guiot, J.L. Debeaulieu, and M. Reille, 1992: Recent contributions to the climatology of the last glacial interglacial cycle based on French pollen sequences. *Quat. Sci. Rev.*, **11**(4), 439–448.

Porter, S.C., 2001: Snowline depression in the tropics during the last glaciation. *Quat. Sci. Rev.*, **20**, 1067–1091.

Prentice, I.C., and T. Webb, 1998: BIOME 6000: reconstructing global mid-Holocene vegetation patterns from palaeoecological records. *J. Biogeogr.*, **25** (6), 997–1005.

Prentice, I.C., D. Jolly, and BIOME 6000 participants, 2000: Mid-Holocene and glacial-maximum vegetation geography of the northern continents and Africa. *J. Biogeogr.*, **27**, 507–519.

Rahmstorf, S., 2001: Abrupt climate change. In: *Encyclopedia of Ocean Sciences*, Vol.1 [Steele, J., S. Thorpe, and K. Turekian (eds.)]. Academic Press, London, pp. 1–6.

Rahmstorf, S., 2002: Ocean circulation and climate during the past 120,000 years. *Nature*, **419**, 207–214.

Rahmstorf, S., and H.J. Schellnhuber, 2006: *Der Klimawandel*. Beck Verlag, Munich, 144 pp.

Rahmstorf, S., et al., 2005: Thermohaline circulation hysteresis: A model intercomparison. *Geophys. Res. Lett.*, **32**(23), doi:10.1029/2005GL023655.

Ramankutty, N., and J.A. Foley, 1999: Estimating historical changes in global land cover: Croplands from 1700 to 1992. *Global Biogeochem. Cycles*, **13**(4), 997–1027.

Ravelo, A.C., et al., 1997: Pliocene carbonate accumulation along the California margin. *Paleoceanography*, **12**, 729–741.

Raymo, M.E., and G.H. Rau, 1992: Plio-Pleistocene atmospheric CO_2 levels inferred from POM $\delta^{13}C$ at DSDP Site 607. *Eos*, **73**, 95.

Raymo, M.E., B. Grant, M. Horowitz, and G.H. Rau, 1996: Mid-Pliocene warmth: Stronger greenhouse and stronger conveyor. *Mar. Micropaleontol.*, **27**(1–4), 313–326.

Raymo, M.E., et al., 1989: Late Pliocene variation in northern hemisphere ice sheets and North Atlantic deep water circulation. *Paleoceanography*, **4**, 413–446.

Raynaud, D., J. Chappellaz, C. Ritz, and P. Martinerie, 1997: Air content along the Greenland Ice Core Project core: A record of surface climatic parameters and elevation in central Greenland. *J. Geophys. Res.*, **102**, 26607–26614.

Raynaud, D., et al., 2005: The record for marine isotopic stage 11. *Nature*, **436**(7047), 39–40.

Reichert, B.K., L. Bengtsson, and J. Oerlemans, 2001: Midlatitude forcing mechanisms for glacier mass balance investigated using general circulation models. *J. Clim.*, **14**(17), 3767–3784.

Reichert, B.K., L. Bengtsson, and J. Oerlemans, 2002: Recent glacier retreat exceeds internal variability. *J. Clim.*, **15**(21), 3069–3081.

Renssen, H., and J. Vandenberghe, 2003: Investigation of the relationship between permafrost distribution in NW Europe and extensive winter sea-ice cover in the North Atlantic Ocean during the cold phases of the last glaciation. *Quat. Sci. Rev.*, **22**, 209–223.

Renssen, H., H. Goosse, and T. Fichefet, 2002: Modeling the effect of freshwater pulses on the early Holocene climate: the influence of high frequency climate variability. *Paleoceanography*, **17**, 1020, doi:10.1029/2001PA000649.

Renssen, H., V. Brovkin, T. Fichefet, and H. Goosse, 2003: Holocene climate instability during the termination of the African humid period. *Geophys. Res. Lett.*, **30**, 1184, doi:10.1029/2002GL016636.

Renssen, H., et al., 2005: Simulating the Holocene climate evolution at northern high latitudes using a coupled atmosphere-sea ice-ocean-vegetation model. *Clim. Dyn.*, **24**(1), 23–43.

Ridgwell, A.J., A.J. Watson, M.A. Maslin, and J.O. Kaplan, 2003: Implications of coral reef buildup for the controls on atmospheric CO_2 since the Last Glacial Maximum *Paleoceanography*, **18**(4), doi:10.1029/2003PA000893.

Rimbu, N., et al., 2004: Holocene climate variability as derived from alkenone sea surface temperature and coupled ocean-atmosphere model experiments. *Clim. Dyn.*, **23**, 215–227.

Rind, D., and M.A. Chandler, 1991: Increased ocean heat transports and warmer climate. *J. Geophys. Res.*, **96**, 7437–7461.

Rind, D., J. Perlwitz, and P. Lonergan, 2005: AO/NAO response to climate change: 1. Respective influences of stratospheric and tropospheric climate changes. *J. Geophys. Res.*, **110**(D12), doi:10.1029/2004JD005103.

Risebrobakken, B., T.M. Dokken, and E. Jansen, 2005: Extent and variability of the meridional Atlantic circulation in the eastern Nordic seas during marine isotope stage 5 and its influence on the inception of the last glacial. In: *The Nordic Seas: An Integrated Perspective* [Drange, H., et al. (eds.)]. Geophysical Monographs Vol. 158, American Geophysical Union, Washington, DC, pp. 323–340.

Risebrobakken, B., et al., 2003: A high resolution study of Holocene paleoclimatic and paleoceanographic changes in the Nordic Seas. *Paleoceanography*, **18**, 1–14.

Robertson, A., et al., 2001: Hypothesized climate forcing time series for the last 500 years. *J. Geophys. Res.*, **106**(D14), 14783–14803.

Robock, A., and M.P. Free, 1995: Ice cores as an index of global volcanism from 1850 to the present. *J. Geophys. Res.*, **100**(D6), 11549–11567.

Roche, D., D. Paillard, and E. Cortijo, 2004: Constraints on the duration and freshwater release of Heinrich event 4 through isotope modelling. *Nature*, **432**, 379–382.

Rodbell, D.T., et al., 1999: An ~15,000-year record of El Niño-driven alluviation in southwestern Ecuador. *Science*, **283**, 516–520.

Rohling, E.J., and H. Palike, 2005: Centennial-scale climate cooling with a sudden cold event around 8,200 years ago. *Nature*, **434**, 975–979.

Rosell-Mele, A., et al., 2004: Sea surface temperature anomalies in the oceans at the LGM estimated from the alkenone-$U^{K'}_{37}$ index: comparison with GCMs. *Geophys. Res. Lett.*, **31**, L03208, doi:10.1029/2003GL018151.

Rosenthal, Y., and A.J. Broccoli, 2004: In search of Paleo-ENSO. *Science*, **304**, 219–221.

Rostami, K., W.R. Peltier, and A. Mangini, 2000: Quaternary marine terraces, sea-level changes and uplift history of Patagonia, Argentina. Comparisons with predictions of ICE-4G (VM2) model of the global process of glacial isostatic adjustment. *Quat. Sci. Rev.*, **19**, 1495–1525.

Röthlisberger, F., and M.A. Geyh, 1985: Glacier variations in Himalayas and Karakorum. *Z. Gletscherkunde Glazialgeologie*, **21**, 237–249.

Röthlisberger, R., et al., 2004: Ice core evidence for the extent of past atmospheric CO_2 change due to iron fertilisation. *Geophys. Res. Lett.*, **31**(16), L16207, doi:10.1029/2004GL020338.

Royer, D., 2003: Estimating latest Cretaceous and Tertiary atmospheric CO_2 from stomatal indices. In: *Causes and Consequences of Globally Warm Climates in the Early Paleogene* [Wing, S.L., P.D. Gingerich, B. Schmitz, and E. Thomas (eds.)]. Special Paper Vol. 369, Geological Society of America, Boulder, CO, pp. 79–93.

Royer, D.L., 2006: CO_2-forced climate thresholds during the Phanerozoic. *Geochim. Cosmochim. Acta*, **70**(23), 5665–5675.

Royer, D.L., et al., 2001: Paleobotanical evidence for near present-day levels of atmospheric CO_2 during part of the tertiary. *Science*, **292**(5525), 2310–2313.

Ruddiman, W.F. (ed.), 1997: *Tectonic Uplift and Climate Change.* Plenum Press, New York, 535 pp.

Ruddiman, W.F., 2003: Orbital insolation, ice volume and greenhouse gases. *Quat. Sci. Rev.*, **15–17**, 1597–1629.

Ruddiman, W.F., and J.S. Thomson, 2001: The case for human causes of increased atmospheric CH_4. *Quat. Sci. Rev.*, **20**(18), 1769–1777.

Ruddiman, W.F., S.J. Vavrus, and J.E. Kutzbach, 2005: A test of the overdue-glaciation hypothesis. *Quat. Sci. Rev.*, **24**, 1–10.

Russell, J.M., T.C. Johnson, and M.R. Talbot, 2003: A 725 yr cycle in the climate of central Africa during the late Holocene. *Geology*, **31**(8), 677–680.

Rutberg, R.L., S.R. Hemming, and S.L. Goldstein, 2000: Reduced North Atlantic deep water flux to the glacial Southern Ocean inferred from neodymium isotope ratios. *Nature*, **405**, 935–938.

Rutherford, S., and M.E. Mann, 2004: Correction to "Optimal surface temperature reconstructions using terrestrial borehole data" by Mann et al. *J. Geophys. Res.*, **109**, D11107, doi:10.1029/2003JD004163.

Rutherford, S., M.E. Mann, T.L. Delworth, and R.J. Stouffer, 2003: Climate field reconstruction under stationary and nonstationary forcing. *J. Clim.*, **16**(3), 462–479.

Rutherford, S., et al., 2005: Proxy-based Northern Hemisphere surface temperature reconstructions: Sensitivity to method, predictor network, target season, and target domain. *J. Clim.*, **18**(13), 2308–2329.

Sànchez Goñi, M.F., et al., 2002: Synchroneity between marine and terrestrial responses to millennial scale climatic variability during the last glacial period in the Mediterranean region. *Clim. Dyn.*, **19**, 95–105.

Sarnthein, M., U. Pflaumann, and M. Weinelt, 2003a: Past extent of sea ice in the northern North Atlantic inferred from foraminiferal paleotemperature estimates. *Paleoceanography*, **18**, doi:10.1029/2002PA000771.

Sarnthein, M., et al., 2003b: Overview of the Glacial Atlantic Ocean Mapping (GLAMAP 2000). *Paleoceanography*, **18**, 1030, doi:10.1029/2002PA000769.

Scherer, R.P., et al., 1998: Pleistocene collapse of the West Antarctic ice sheet. *Science*, **281**(5373), 82–85.

Schneider von Deimling, T., A. Ganopolski, H. Held, and S. Rahmstorf, 2006: How cold was the Last Glacial Maximum? *Geophys. Res. Lett.*, **33**, doi: 10.1029/2006GL026484.

Scholze, M., W. Knorr, and M. Heimann, 2003: Modelling terrestrial vegetation dynamics and carbon cycling for an abrupt climate change event. *The Holocene*, **13**, 327–333.

Schubert, S.D., et al., 2004: Causes of long-term drought in the US Great Plains. *J. Clim.*, **17**(3), 485–503.

Schulz, M., A. Paul, and A. Timmermann, 2004: Glacial-interglacial contrast in climate variability at centennial-to-millennial timescales: observations and conceptual model. *Quat. Sci. Rev.*, **23**, 2219–2230.

Schwander, J., et al., 1993: The age of the air in the firn and the ice at Summit, Greenland. *J. Geophys. Res.*, **98**(D2), 2831–2838.

Schwikowski, M., A. Döscher, H.W. Gäggeler, and U. Schotterer, 1999: Anthropogenic versus natural sources of atmospheric sulphate from an Alpine ice core. *Tellus*, **51B**, 938–951.

Seager, R., et al., 2005: Modeling of tropical forcing of persistent droughts and pluvials over western North America: 1856-2000. *J. Clim.*, **18**(19), 4065–4088.

Seppa, H., and H.J.B. Birks, 2001: July mean temperature and annual precipitation trends during Holocene in the Fennoscandian tree-line area: pollen-based climate reconstructions. *The Holocene*, **11**, 527–539.

Severinghaus, J.P., and E.J. Brook, 1999: Abrupt climate change at the end of the last glacial period inferred from trapped air in polar ice. *Science*, **286**(5441), 930–934.

Shackleton, N.J., 1977: Carbon-13 in Uvigerina: Tropical rainforest history and the equatorial Pacific carbonate dissolution cycles. In: *The Fate of Fossil Fuel CO_2 in the Ocean* [Andersen, N., and A. Malahoff (eds.)]. Plenum, New York, pp. 401–428.

Shackleton, N.J., 2000: The 100,000-year ice-age cycle identified and found to lag temperature, carbon dioxide, and orbital eccentricity. *Science*, **289**, 1897–1902.

Shackleton, N.J., M.A. Hall, and A. Boersma, 1984: Oxygen and carbon isotope data from Leg-74 foraminifers. In: *Initial Reports of the Deep Sea Drilling Project*, Vol. 74. Ocean Drilling Program, College Station, TX, pp. 599–612.

Shackleton, N.J., J.C. Hall, and D. Pate, 1995: Pliocene stable isotope stratigraphy of ODP Site 846. In: *Proceedings of the Ocean Drilling Program, Scientific Results*. Vol. 138. Ocean Drilling Program, College Station, TX, pp. 337–356.

Shin, S.I., et al., 2003: A simulation of the Last Glacial Maximum climate using the NCAR CSM. *Clim. Dyn.*, **20**, 127–151.

Shin, S.I., et al., 2006: Understanding the mid-Holocene climate. *J. Clim.*, **19**(12), 2801–2818.

Shindell, D.T., G.A. Schmidt, R.L. Miller, and M.E. Mann, 2003: Volcanic and solar forcing of climate change during the preindustrial era. *J. Clim.*, **16**(24), 4094–4107.

Shindell, D.T., G.A. Schmidt, M.E. Mann, and G. Faluvegi, 2004: Dynamic winter climate response to large tropical volcanic eruptions since 1600. *J. Geophys. Res.*, **109**(D5), D05104, doi:10.1029/2003JD004151.

Shindell, D.T., et al., 2001: Solar forcing of regional climate change during the Maunder Minimum. *Science*, **294**(5549), 2149–2152.

Shulmeister, J., and B.G. Lees, 1995: Pollen evidence from tropical Australia for the onset of an ENSO-dominated climate at c. 4000 BP. *The Holocene*, **5**, 10–18.

Shuman, B., W. Thompson, P. Bartlein, and J.W. Williams, 2002: The anatomy of a climatic oscillation: vegetation change in eastern North America during the Younger Dryas chronozone. *Quat. Sci. Rev.*, **21**(16–17), 1777–1791.

Siddall, M., et al., 2003: Sea-level fluctuations during the last glacial cycle. *Nature*, **423**, 853–858.

Siegenthaler, U., et al., 2005a: Stable carbon cycle-climate relationship during the late Pleistocene. *Science*, **310**(5752), 1313–1317.

Siegenthaler, U., et al., 2005b: Supporting evidence from the EPICA Dronning Maud Land ice core for atmospheric CO_2 changes during the past millennium. *Tellus*, **57B**(1), 51–57.

Sigman, D.M., and E.A. Boyle, 2000: Glacial/interglacial variations in atmospheric carbon dioxide. *Nature*, **407**, 859–869.

Six, D., L. Reynaud, and A. Letréguilly, 2001: Bilans de masse des glaciers alpins et scandinaves, leurs relations avec l oscillation du climat de l Atlantique nord. *C. R. Acad. Sci. Paris*, *Sciences de la Terre et des planètes/Earth and Planetary Sciences*, **333**, 693–698.

Sloan, L.C., T.J. Crowley, and D. Pollard, 1996: Modeling of middle Pliocene climate with the NCAR GENESIS general circulation model. *Mar. Micropaleontol.*, **27**, 51–61.

Sluijs, A., et al., 2006: Subtropical Arctic Ocean temperatures during the Palaeocene/Eocene thermal maximum. *Nature*, **441**, 610–613.

Smerdon, J.E., et al., 2004: Air-ground temperature coupling and subsurface propagation of annual temperature signals. *J. Geophys. Res.*, **109**(D21), D21107, doi:10.1029/2004JD005056.

Smerdon, J.E., et al., 2006: Daily, seasonal and annual relationships between air and subsurface temperatures. *J. Geophys. Res.*, **111**, D07101, doi:10.1029/2004JD005578.

Smith, J.A., et al., 2005: Early local last glacial maximum in the tropical Andes. *Science*, **308**, 678–681.

Sokratov, S.A., and R.G. Barry, 2002: Intraseasonal variation in the thermoinsulation effect of snow cover on soil temperatures and energy balance. *J. Geophys. Res.*, **107**(D19), 4374, doi:10.1029/2001JD000489.

Solanki, S.K., and N.S. Krivova, 2003: Can solar variability explain global warming since 1970? *J. Geophys. Res.*, **108**, 1200, doi:10.1029/2002JA009753.

Solanki, S.K., et al., 2004: Unusual activity of the sun during recent decades compared to the previous 11,000 years. *Nature*, **431**, 1084–1087.

Soon, W., and S. Baliunas, 2003: Proxy climatic and environmental changes of the past 1000 years. *Clim. Res.*, **23**(2), 89–110.

Spahni, R., et al., 2003: The attenuation of fast atmospheric CH_4 variations recorded in polar ice cores. *Geophys. Res. Lett.*, **30**(11), doi:10.1029/2003GL017093.

Spahni, R., et al., 2005: Atmospheric methane and nitrous oxide of the late Pleistocene from Antarctic ice cores. *Science*, **310**(5752), 1317–1321.

Stager, J.C., and P.A. Mayewski, 1997: Abrupt early to Mid-Holocene climatic transition registered at the equator and the poles. *Science*, **276**, 1834–1836.

Stager, J.C., B.F. Cumming, and L.D. Meeker, 2003: A 10,000-year high-resolution diatom record from Pilkington Bay, Lake Victoria, East Africa. *Quat. Res.*, **59**(2), 172–181.

Stager, J.C., et al., 2005: Solar variability and the levels of Lake Victoria, East Africa, during the last millennium. *J. Paleolimnol.*, **33**(2), 243–251.

Stahle, D.W., and M.K. Cleaveland, 1992: Reconstruction and analysis of spring rainfall over southeastern U.S. for the past 1000 years. *Bull. Am. Meteorol. Soc.*, **73**, 1947–1961.

Stahle, D.W., et al., 1998: Experimental dendroclimatic reconstruction of the Southern Oscillation. *Bull. Am. Meteorol. Soc.*, **79**(10), 2137–2152.

Stauffer, B., G. Fischer, A. Neftel, and H. Oeschger, 1985: Increase of atmospheric methane recorded in Antarctic ice core. *Science*, **229**(4720), 1386–1388.

Steele, L.P., et al., 1992: Slowing down of the accumulation of atmospheric methane during the 1980s. *Nature*, **358**, 313–316.

Stendel, M., I.A. Mogensen, and J.H. Christensen, 2006: Influence of various forcings on global climate in historical times using a coupled atmosphere-ocean general circulation model. *Clim. Dyn.*, **26**(1), 1–15.

Stenni, B., et al., 2001: An oceanic cold reversal during the last deglaciation. *Science*, **293**, 2074–2077.

Stern, D.I., 2005: Global sulfur emissions from 1850 to 2000. *Chemosphere*, **58**, 163–175.

Stieglitz, M., S.J. Dery, V.E. Romanovsky, and T.E. Osterkamp, 2003: The role of snow cover in the warming of arctic permafrost. *Geophys. Res. Lett.*, **30**(13), 1721, doi:10.1029/2003GL017337.

Stirling C.H., T.M. Esat, K. Lambeck, and M.T. McCulloch, 1998: Timing and duration of the last interglacial: evidence for a restricted interval of widespread coral reef growth. *Earth Planet. Sci. Lett.*, **160**, 745–762.

Stocker, T.F., and S.J. Johnsen, 2003: A minimum thermodynamic model for the bipolar seesaw. *Paleoceanography*, **18**(4), doi:10.1029/2003PA000920.

Stocker, T.F., and E. Monnin, 2003: Past rates of carbon dioxide changes and their relevance for future climate. *Pages News*, **11**(1), 6–8.

Stott, L., et al., 2004: Decline in surface temperature and salinity in the western tropical Pacific Ocean in Holocene epoch. *Nature*, **431**, 56–59.

Stouffer, R.J., et al., 2006: Investigating the causes of the response of the thermohaline circulation to past and future climate changes. *J. Clim.*, **19**(8), 1365–1386.

Sutton, R.T., and D.L.R. Hodson, 2005: Atlantic Ocean forcing of North American and European summer climate. *Science*, **309**(5731), 115–118.

Svendsen, J.I., and J. Mangerud, 1997: Holocene glacial and climatic variations on Spitsbergen, Svalbard. *The Holocene*, **7**, 45–57.

Svensen, H., et al., 2004: Release of methane from a volcanic basin as a mechanism for initial Eocene global warming. *Nature*, **429**, 542–545.

Tajika, E., 1998: Climate change during the last 150 million years: reconstruction from a carbon cycle. *Earth Planet. Sci. Lett.*, **160**(3–4), 695–707.

Tans, P.P., and T.J. Conway, 2005: Monthly atmospheric CO_2 mixing ratios from the NOAA CMDL Carbon Cycle Cooperative Global Air Sampling Network, 1968-2002. In: *Trends: A Compendium of Data on Global Change*. Carbon Dioxide Information Analysis Center, Oak Ridge National Laboratory, U.S. Department of Energy, Oak Ridge, TN.

Tarasov, L., and W.R. Peltier, 2003: Greenland glacial history, borehole constraints, and Eemian extent. *J. Geophys. Res.*, **108**, 2143, doi:10.1029/2001JB001731.

Tarasov, L., and W.R. Peltier, 2005: Arctic freshwater forcing of the Younger Dryas cold reversal. *Nature*, **435**(7042), 662–665.

Taylor, A.E., et al., 2006: Canadian arctic permafrost observatories: detecting contemporary climate change through inversion of subsurface temperature time-series. *J. Geophys. Res.*, **111**, B02411, doi:10.1029/2004JB003208.

Taylor, K.E., et al., 2000: Analysis of forcing, response, and feedbacks in a paleoclimate modeling experiment. In: *Proceedings of the Third Paleoclimate Modelling Intercomparison Project (PMIP) Workshop, 4-8 Oct. 1999, La Huardière, Canada* [Braconnot, P. (ed.)]. WCRP-111, WMO/TD-No. 1007, World Meteorological Organization, Geneva, pp. 43–49.

Tett, S.F.B., et al., 2007: The impact of natural and anthropogenic forcings on climate and hydrology since 1550. *Clim. Dyn.*, **28**(1), 3–34.

Thomas, E., 2003: Extinction and food at the sea floor: a high-resolution benthic foraminiferal record across the Initial Eocene Thermal Maximum, Southern Ocean Site 690. In: *Causes and Consequences of Globally Warm Climates of the Paleogene* [Wing, S., Gingerich, P., Schmitz, B., and Thomas, E., (eds.)]. Special Paper Vol. 369, Geological Society of America, Boulder, CO, pp. 319–332.

Thompson, L.G., 2000: Ice core evidence for climate change in the Tropics: implications for our future. *Quat. Sci. Rev.*, **19**(1–5), 19–35.

Thompson, L.G., 2001: Stable isotopes and their relationship to temperature as recorded in low latitude ice cores. In: *Geological Perspectives of Global Climate Change* [Gerhard, L.C., W.E. Harrison, and B.M. Hanson (eds.)]. Studies in Geology No. 47, American Association of Petroleum Geologists, Tulsa, OK, pp. 99–119.

Thompson, L.G., et al., 2000: A high-resolution millennial record of the South Asian Monsoon from Himalayan ice cores. *Science*, **289**(5486), 1916–1919.

Thompson, R.S., 1991: Pliocene environments and climates in the Western United States. *Quat. Sci. Rev.*, **10**, 115–132.

Thompson, R.S., and R.F. Fleming, 1996: Middle Pliocene vegetation: Reconstructions, paleoclimate inferences, and boundary conditions for climate modeling. *Mar. Micropaleontol.*, **27**, 27–49.

Tinner, W., and A.F. Lotter, 2001: Central European vegetation response to abrupt climate change at 8.2 ka. *Geology*, **29**, 551–554.

Toracinta, E.R., R.J. Oglesby, and D.H. Bromwich, 2004: Atmospheric response to modified CLIMAP ocean boundary conditions during the Last Glacial Maximum. *J. Clim.*, **17**, 504–522.

Traufetter, F., et al., 2004: Spatio-temporal variability in volcanic sulphate deposition over the past 2 kyr in snow pits and firn cores from Amundsenisen, Dronning Maud Land, Antarctica. *J. Glaciol.*, **50**, 137–146.

Trenberth, K.E., and B.L. Otto-Bliesner, 2003: Toward integrated reconstruction of past climates. *Science*, **300**(5619), 589–591.

Tripati, A.K., and H. Elderfield, 2004: Abrupt hydrographic changes in the equatorial Pacific and subtropical Atlantic from foraminiferal Mg/Ca indicate greenhouse origin for the thermal maximum at the Paleocene-Eocene Boundary. *Geochem. Geophys. Geosystems*, **5**, doi:10.1029/2003GC000631.

Tudhope, A.W., et al., 2001: Variability in the El Niño-Southern Oscillation through a glacial-interglacial cycle. *Science*, **291**, 1511–1517.

Tzedakis, P.C., 2005: Towards an understanding of the response of southern European vegetation to orbital and suborbital climate variability. *Quat. Sci. Rev.*, **24**, 1585–1599.

van Kreveld, S., et al., 2000: Potential links between surging ice sheets, circulation changes, and the Dansgaard-Oeschger cycles in the Irminger Sea, 60-18 kyr. *Paleoceanography*, **15**, 425–442.

Vellinga, M., and R.A. Wood, 2002: Global climatic impacts of a collapse of the Atlantic thermohaline circulation. *Clim. Change*, **54**(3), 251–267.

Verschuren, D., 2001: Reconstructing fluctuations of a shallow East African lake during the past 1800 yrs from sediment stratigraphy in a submerged crater basin. *J. Paleolimnol.*, **25**(3), 297–311.

Veski, S., H. Seppa, and A.E.K. Ojala, 2004: Cold event at 8200 yr BP recorded in annually laminated lake sediments in eastern Europe. *Geology*, **32**(8), 681–684.

Vettoretti, G., and W.R. Peltier, 2003: Post-Eemian glacial inception. Part II: Elements of a cryospheric moisture pump. *J. Clim.*, **16**(6), 912–927.

Vidal, L., L. Labeyrie, and T.C.E. van Weering, 1998: Benthic $\delta^{18}O$ records in the North Atlantic over the last glacial period (60-10 kyr): Evidence for brine formation. *Paleoceanography*, **13**(3), 245–251.

Villalba, R., et al., 2003: Large-scale temperature changes across the southern Andes: 20th-century variations in the context of the past 400 years. *Clim. Change*, **59**(1–2), 177–232.

Vincent, C., et al., 2005: Glacier fluctuations in the Alps and in the tropical Andes. *Comptes Rendus Geoscience*, **337**(1–2), 97–106.

Voelker, A.H.L., 2002: Global distribution of centennial-scale records for Marine Isotope Stage (MIS) 3: a database. *Quat. Sci. Rev.*, **21**(10), 1185–1212.

von Grafenstein, U., et al., 1998: The cold event 8,200 years ago documented in oxygen isotope records of precipitation in Europe and Greenland. *Clim. Dyn.*, **14**, 73–81.

von Storch, H., and E. Zorita, 2005: Comment on "Hockey sticks, principal components, and spurious significance" by S. McIntyre and R. McKitrick. *Geophys. Res. Lett.*, **32**(20), doi:10.1029/2005GL022753.

von Storch, H., et al., 2004: Reconstructing past climate from noisy data. *Science*, **306**(5296), 679–682.

Vuille, M., and M. Werner, 2005: Stable isotopes in precipitation recording South American summer monsoon and ENSO variability: observations and model results. *Clim. Dyn.*, **25**(4), 401–413.

Vuille, M., M. Werner, R.S. Bradley, and F. Keimig, 2005: Stable isotopes in precipitation in the Asian monsoon region. *J. Geophys. Res.*, **110**(D23), doi:10.1029/2005JD006022.

Waelbroeck, C., et al., 2002: Sea-level and deep water temperature changes derived from benthic foraminifera isotopic records. *Quat. Sci. Rev.*, **21**(1–3), 295–305.

Waelbroeck, C., et al., 2005: A global compilation of late Holocene planktonic foraminiferal $\delta^{18}O$: Relationship between surface water temperature and $\delta^{18}O$. *Quat. Sci. Rev.*, **24**, 853–858.

Wahl, E.R., and C.M. Ammann, 2007: Robustness of the Mann, Bradley, Hughes reconstruction of Northern Hemisphere surface temperatures: Examination of criticisms based on the nature and processing of proxy climate evidence. *Clim. Change*, in press.

Wahl, E.R., D.M. Ritson and C.M. Ammann, 2006: Comment on "Reconstructing past climate from noisy data". *Science*, **312**, 529.

Wallmann, K., 2001: Controls on the Cretaceous and Cenozoic evolution of seawater composition, atmospheric CO_2 and climate. *Geochim. Cosmochim. Acta.*, **65**(18), 3005–3025.

Wang, Y.J., et al., 2001: A high-resolution absolute-dated late Pleistocene monsoon record from Hulu Cave, China. *Science*, **294**, 2345–2348.

Wang, Y.J., et al., 2005: Holocene Asian monsoon: Links to solar changes and North Atlantic climate. *Science*, **308**, 854–857.

Wang, Y.M., and N.R. Sheeley, 2003: Modeling the sun's large-scale magnetic field during the Maunder minimum. *Astrophys. J.*, **591**(2), 1248–1256.

Wang, Y.M., J.L. Lean, and N.R. Sheeley, 2005: Modeling the sun's magnetic field and irradiance since 1713. *Astrophys. J.*, **625**, 522–538.

Wang, Z., and L.A. Mysak, 2002: Simulation of the last glacial inception and rapid ice sheet growth in the McGill paleoclimate model. *Geophys. Res. Lett.*, **29**, doi:10.1029/2002GL015120.

Watanabe, O., et al., 2003: Homogeneous climate variability across East Antarctica over the past three glacial cycles. *Nature*, **422**, 509–512.

Webb, R.S., et al., 1997: Influence of ocean heat transport on the climate of the Last Glacial Maximum. *Nature*, **385**, 695–699.

Williams, J.W., T.I. Webb, P.H. Richard, and P. Newby, 2000: Late Quaternary biomes of Canada and the eastern United States. *J. Biogeogr.*, **27**, 585–607.

Williams, J.W., et al., 2002: Rapid and widespread vegetation responses to past climate change in the North Atlantic region. *Geology*, **30**(11), 971–974.

Williams, P.W., D.N.T. King, J.-X. Zhao, and K.D. Collerson, 2004: Speleotherm master chronologies : combined Holocene ^{18}O and ^{13}C records from the north Island of New Zealand and their palaeoenvironmental interpretation. *The Holocene*, **14**, 194–208.

Wing, S.L., et al., 2005: Transient floral change and rapid global warming at the Paleocene-Eocene boundary. *Science*, **310**(5750), 993–996.

Wise, S.W.J., J.R. Breza, D.M. Harwood, and W. Wei, 1991: Paleogene glacial history of Antarctica. In: *Controversies in Modern Geology: Evolution of Geological Theories in Sedimentology, Earth History and Tectonics* [Müller, D.W., J.A. McKenzie, and H. Weissert (eds.)]. Cambridge University Press, Cambridge, pp. 133–171.

Wohlfahrt, J., S.P. Harrison, and P. Braconnot, 2004: Synergistic feedbacks between ocean and vegetation on mid- and high- latitude climates during the mid-Holocene. *Clim. Dyn.*, **22**, 223–238.

Woodhouse, C.A., and J.T. Overpeck, 1998: 2000 years of drought variability in the central United States. *Bull. Am. Meteorol. Soc.*, **79**(12), 2693–2714.

Wyputta, U., and B.J. McAvaney, 2001: Influence of vegetation changes during the Last Glacial Maximum using the BMRC atmospheric general circulation model. *Clim. Dyn.*, **17**, 923–932.

Xia, Q.K., H.X. Zhao, and K.D. Collerson, 2001: Early-Mid Holocene climatic variations in Tasmania, Australia: multi-proxy records in a stalagmite from Lynds Cave. *Earth Planet. Sci. Lett.*, **194**(1–2), 177–187.

Xoplaki, E., et al., 2005: European spring and autumn temperature variability and change of extremes over the last half millennium. *Geophys. Res. Lett.*, **32**, L15713, doi:10.1029/2005GL023424.

Yapp, C.J., and H. Poths, 1992: Ancient atmospheric CO_2 pressures inferred from natural goethites. *Nature*, **355**, 342–344.

Yokoyama, Y., et al., 2000: Timing of the Last Glacial Maximum from observed sea-level minima. *Nature*, **406**(6797), 713–716.

Zachos, J., et al., 2001: Trends, rhythms, and aberrations in global climate 65 Ma to present. *Science*, **292**(5517), 686–693.

Zachos, J.C., et al., 2003: A transient rise in tropical sea surface temperature during the Paleocene-Eocene Thermal Maximum. *Science*, **302**(5650), 1551–1554.

Zachos, J.C., et al., 2004*: Early Cenozoic Extreme Climates: The Walvis Ridge Transect, Sites 1262-1267.* Proceedings of the Ocean Drilling Program, Initial Reports Vol. 208, Ocean Drilling Program, College Station, TX.

Zachos, J.C., et al., 2005: Rapid acidification of the ocean during the Paleocene-Eocene thermal maximum. *Science*, **308**(5728), 1611–1615.

Zhang, D.E., 2005: Severe drought events as revealed in the climate record of China and their temperature situations over the last 1000 years. *Acta Meteorol. Sin.*, **19**(4), 485–491.

Zhang, R., and T.L. Delworth, 2005: Simulated tropical response to a substantial weakening of the Atlantic thermohaline circulation. *J. Clim.*, **18**(12), 1853–1860.

Zhao, Y., et al., 2005: A multi-model analysis of the role of the ocean on the African and Indian monsoon during the mid-Holocene. *Clim. Dyn.*, **25**, (7–8), 777–800.

Zielinski, G.A., 2000: Use of paleo-records in determining variability within the volcanism-climate system. *Quat. Sci. Rev.*, **19**(1), 417–438.

Zorita, E., F. Gonzalez-Rouco, and S. Legutke, 2003: Testing the Mann et al. (1998) approach to paleoclimate reconstructions in the context of a 1000-yr control simulation with the ECHO-G coupled climate model. *J. Clim.*, **16**(9), 1378–1390.

7

Couplings Between Changes in the Climate System and Biogeochemistry

Coordinating Lead Authors:

Kenneth L. Denman (Canada), Guy Brasseur (USA, Germany)

Lead Authors:

Amnat Chidthaisong (Thailand), Philippe Ciais (France), Peter M. Cox (UK), Robert E. Dickinson (USA), Didier Hauglustaine (France), Christoph Heinze (Norway, Germany), Elisabeth Holland (USA), Daniel Jacob (USA, France), Ulrike Lohmann (Switzerland), Srikanthan Ramachandran (India), Pedro Leite da Silva Dias (Brazil), Steven C. Wofsy (USA), Xiaoye Zhang (China)

Contributing Authors:

D. Archer (USA), V. Arora (Canada), J. Austin (USA), D. Baker (USA), J.A. Berry (USA), R. Betts (UK), G. Bonan (USA), P. Bousquet (France), J. Canadell (Australia), J. Christian (Canada), D.A. Clark (USA), M. Dameris (Germany), F. Dentener (EU), D. Easterling (USA), V. Eyring (Germany), J. Feichter (Germany), P. Friedlingstein (France, Belgium), I. Fung (USA), S. Fuzzi (Italy), S. Gong (Canada), N. Gruber (USA, Switzerland), A. Guenther (USA), K. Gurney (USA), A. Henderson-Sellers (Switzerland), J. House (UK), A. Jones (UK), C. Jones (UK), B. Kärcher (Germany), M. Kawamiya (Japan), K. Lassey (New Zealand), C. Le Quéré (UK, France, Canada), C. Leck (Sweden), J. Lee-Taylor (USA, UK), Y. Malhi (UK), K. Masarie (USA), G. McFiggans (UK), S. Menon (USA), J.B. Miller (USA), P. Peylin (France), A. Pitman (Australia), J. Quaas (Germany), M. Raupach (Australia), P. Rayner (France), G. Rehder (Germany), U. Riebesell (Germany), C. Rödenbeck (Germany), L. Rotstayn (Australia), N. Roulet (Canada), C. Sabine (USA), M.G. Schultz (Germany), M. Schulz (France, Germany), S.E. Schwartz (USA), W. Steffen (Australia), D. Stevenson (UK), Y. Tian (USA, China), K.E. Trenberth (USA), T. Van Noije (Netherlands), O. Wild (Japan, UK), T. Zhang (USA, China), L. Zhou (USA, China)

Review Editors:

Kansri Boonpragob (Thailand), Martin Heimann (Germany, Switzerland), Mario Molina (USA, Mexico)

This chapter should be cited as:

Denman, K.L., G. Brasseur, A. Chidthaisong, P. Ciais, P.M. Cox, R.E. Dickinson, D. Hauglustaine, C. Heinze, E. Holland, D. Jacob, U. Lohmann, S Ramachandran, P.L. da Silva Dias, S.C. Wofsy and X. Zhang, 2007: Couplings Between Changes in the Climate System and Biogeochemistry. In: *Climate Change 2007: The Physical Science Basis. Contribution of Working Group I to the Fourth Assessment Report of the Intergovernmental Panel on Climate Change* [Solomon, S., D. Qin, M. Manning, Z. Chen, M. Marquis, K.B. Averyt, M.Tignor and H.L. Miller (eds.)]. Cambridge University Press, Cambridge, United Kingdom and New York, NY, USA.

Table of Contents

Executive Summary 501

7.1 Introduction 503

7.1.1 Terrestrial Ecosystems and Climate 503

7.1.2 Ocean Ecosystems and Climate 503

7.1.3 Atmospheric Chemistry and Climate 504

7.1.4 Aerosol Particles and Climate 504

7.1.5 Coupling the Biogeochemical Cycles with the Climate System 504

7.2 The Changing Land Climate System 504

7.2.1 Introduction to Land Climate 504

7.2.2 Dependence of Land Processes and Climate on Scale 505

Box 7.1: Surface Energy and Water Balance 505

Box 7.2: Urban Effects on Climate 506

7.2.3 Observational Basis for the Effects of Land Surface on Climate 507

7.2.4 Modelling the Coupling of Vegetation, Moisture Availability, Precipitation and Surface Temperature 509

7.2.5 Evaluation of Models Through Intercomparison 510

7.2.6 Linking Biophysical to Biogeochemical and Ecohydrological Components 511

7.3 The Carbon Cycle and the Climate System 511

7.3.1 Overview of the Global Carbon Cycle 511

7.3.2 The Contemporary Carbon Budget 517

7.3.3 Terrestrial Carbon Cycle Processes and Feedbacks to Climate 526

7.3.4 Ocean Carbon Cycle Processes and Feedbacks to Climate 528

Box 7.3: Marine Carbon Chemistry and Ocean Acidification 529

7.3.5 Coupling Between the Carbon Cycle and Climate 533

7.4 Reactive Gases and the Climate System 539

7.4.1 Methane 539

Box 7.4: Effects of Climate Change on Air Quality 540

7.4.2 Nitrogen Compounds 544

7.4.3. Molecular Hydrogen 547

7.4.4 Global Tropospheric Ozone 547

7.4.5. The Hydroxyl Radical 550

7.4.6 Stratospheric Ozone and Climate 553

7.5 Aerosol Particles and the Climate System 555

7.5.1 Aerosol Emissions and Burdens Affected by Climatic Factors 555

7.5.2 Indirect Effects of Aerosols on Clouds and Precipitation 559

7.5.3 Effects of Aerosols and Clouds on Solar Radiation at the Earth's Surface 563

7.5.4 Effects of Aerosols on Circulation Patterns 564

7.6 Concluding Remarks 566

Frequently Asked Question

FAQ 7.1: *Are the Increases in Atmospheric Carbon Dioxide and Other Greenhouse Gases During the Industrial Era Caused by Human Activities?* 512

References 568

Executive Summary

Emissions of carbon dioxide, methane, nitrous oxide and of reactive gases such as sulphur dioxide, nitrogen oxides, carbon monoxide and hydrocarbons, which lead to the formation of secondary pollutants including aerosol particles and tropospheric ozone, have increased substantially in response to human activities. As a result, biogeochemical cycles have been perturbed significantly. Nonlinear interactions between the climate and biogeochemical systems could amplify (positive feedbacks) or attenuate (negative feedbacks) the disturbances produced by human activities.

The Land Surface and Climate

- Changes in the land surface (vegetation, soils, water) resulting from human activities can affect regional climate through shifts in radiation, cloudiness and surface temperature.

- Changes in vegetation cover affect surface energy and water balances at the regional scale, from boreal to tropical forests. Models indicate increased boreal forest reduces the effects of snow albedo and causes regional warming. Observations and models of tropical forests also show effects of changing surface energy and water balance.

- The impact of land use change on the energy and water balance may be very significant for climate at regional scales over time periods of decades or longer.

The Carbon Cycle and Climate

- Atmospheric carbon dioxide (CO_2) concentration has continued to increase and is now almost 100 ppm above its pre-industrial level. The annual mean CO_2 growth rate was significantly higher for the period from 2000 to 2005 (4.1 ± 0.1 GtC yr^{-1}) than it was in the 1990s (3.2 ± 0.1 GtC yr^{-1}). Annual emissions of CO_2 from fossil fuel burning and cement production increased from a mean of 6.4 ± 0.4 GtC yr^{-1} in the 1990s to 7.2 ± 0.3 GtC yr^{-1} for 2000 to 2005.[1]

- Carbon dioxide cycles between the atmosphere, oceans and land biosphere. Its removal from the atmosphere involves a range of processes with different time scales. About 50% of a CO_2 increase will be removed from the atmosphere within 30 years, and a further 30% will be removed within a few centuries. The remaining 20% may stay in the atmosphere for many thousands of years.

- Improved estimates of ocean uptake of CO_2 suggest little change in the ocean carbon sink of 2.2 ± 0.5 GtC yr^{-1} between the 1990s and the first five years of the 21st century. Models indicate that the fraction of fossil fuel and cement emissions of CO_2 taken up by the ocean will decline if atmospheric CO_2 continues to increase.

- Interannual and inter-decadal variability in the growth rate of atmospheric CO_2 is dominated by the response of the land biosphere to climate variations. Evidence of decadal changes is observed in the net land carbon sink, with estimates of 0.3 ± 0.9, 1.0 ± 0.6, and 0.9 ± 0.6 GtC yr^{-1} for the 1980s, 1990s and 2000 to 2005 time periods, respectively.

- A combination of techniques gives an estimate of the flux of CO_2 to the atmosphere from land use change of 1.6 (0.5 to 2.7) GtC yr^{-1} for the 1990s. A revision of the Third Assessment Report (TAR) estimate for the 1980s downwards to 1.4 (0.4 to 2.3) GtC yr^{-1} suggests little change between the 1980s and 1990s, and continuing uncertainty in the net CO_2 emissions due to land use change.

- Fires, from natural causes and human activities, release to the atmosphere considerable amounts of radiatively and photochemically active trace gases and aerosols. If fire frequency and extent increase with a changing climate, a net increase in CO_2 emissions is expected during this fire regime shift.

- There is yet no statistically significant trend in the CO_2 growth rate as a fraction of fossil fuel plus cement emissions since routine atmospheric CO_2 measurements began in 1958. This 'airborne fraction' has shown little variation over this period.

- Ocean CO_2 uptake has lowered the average ocean pH (increased acidity) by approximately 0.1 since 1750. Consequences for marine ecosystems may include reduced calcification by shell-forming organisms, and in the longer term, the dissolution of carbonate sediments.

- The first-generation coupled climate-carbon cycle models indicate that global warming will increase the fraction of anthropogenic CO_2 that remains in the atmosphere. This positive climate-carbon cycle feedback leads to an additional increase in atmospheric CO_2 concentration of 20 to 224 ppm by 2100, in models run under the IPCC (2000) Special Report on Emission Scenarios (SRES) A2 emissions scenario.

Reactive Gases and Climate

- Observed increases in atmospheric methane concentration, compared with pre-industrial estimates, are directly linked to human activity, including agriculture, energy production,

[1] The uncertainty ranges given here and especially in Tables 7.1 and 7. 2 are the authors' estimates of the *likely* (66%) range for each term based on their assessment of the currently available studies. There are not enough comparable studies to enable estimation of a *very likely* (90%) range for all the main terms in the carbon cycle budget.

waste management and biomass burning. Constraints from methyl chloroform observations show that there have been no significant trends in hydroxyl radical (OH) concentrations, and hence in methane removal rates, over the past few decades (see Chapter 2). The recent slowdown in the growth rate of atmospheric methane since about 1993 is thus *likely* due to the atmosphere approaching an equilibrium during a period of near-constant total emissions. However, future methane emissions from wetlands are *likely* to increase in a warmer and wetter climate, and to decrease in a warmer and drier climate.

- No long-term trends in the tropospheric concentration of OH are expected over the next few decades due to offsetting effects from changes in nitric oxides (NO_x), carbon monoxide, organic emissions and climate change. Interannual variability of OH may continue to affect the variability of methane.

- New model estimates of the global tropospheric ozone budget indicate that input of ozone from the stratosphere (approximately 500 Tg yr^{-1}) is smaller than estimated in the TAR (770 Tg yr^{-1}), while the photochemical production and destruction rates (approximately 5,000 and 4,500 Tg yr^{-1} respectively) are higher than estimated in the TAR (3,400 and 3,500 Tg yr^{-1}). This implies greater sensitivity of ozone to changes in tropospheric chemistry and emissions.

- Observed increases in NO_x and nitric oxide emissions, compared with pre-industrial estimates, are *very likely* directly linked to 'acceleration' of the nitrogen cycle driven by human activity, including increased fertilizer use, intensification of agriculture and fossil fuel combustion.

- Future climate change may cause either an increase or a decrease in background tropospheric ozone, due to the competing effects of higher water vapour and higher stratospheric input; increases in regional ozone pollution are expected due to higher temperatures and weaker circulation.

- Future climate change may cause significant air quality degradation by changing the dispersion rate of pollutants, the chemical environment for ozone and aerosol generation and the strength of emissions from the biosphere, fires and dust. The sign and magnitude of these effects are highly uncertain and will vary regionally.

- The future evolution of stratospheric ozone, and therefore its recovery following its destruction by industrially manufactured halocarbons, will be influenced by stratospheric cooling and changes in the atmospheric circulation resulting from enhanced CO_2 concentrations. With a possible exception in the polar lower stratosphere where colder temperatures favour ozone destruction by chlorine activated on polar stratospheric cloud particles, the expected cooling of the stratosphere should reduce ozone depletion and therefore enhance the ozone column amounts.

Aerosol Particles and Climate

- Sulphate aerosol particles are responsible for globally averaged temperatures being lower than expected from greenhouse gas concentrations alone.

- Aerosols affect radiative fluxes by scattering and absorbing solar radiation (direct effect, see Chapter 2). They also interact with clouds and the hydrological cycle by acting as cloud condensation nuclei (CCN) and ice nuclei. For a given cloud liquid water content, a larger number of CCN increases cloud albedo (indirect cloud albedo effect) and reduces the precipitation efficiency (indirect cloud lifetime effect), both of which are *likely* to result in a reduction of the global, annual mean net radiation at the top of the atmosphere. However, these effects may be partly offset by evaporation of cloud droplets due to absorbing aerosols (semi-direct effect) and/or by more ice nuclei (glaciation effect).

- The estimated total aerosol effect is lower than in TAR mainly due to improvements in cloud parametrizations, but large uncertainties remain.

- The radiative forcing resulting from the indirect cloud albedo effect was estimated in Chapter 2 as –0.7 W m^{-2} with a 90% confidence range of –0.3 to –1.8 W m^{-2}. Feedbacks due to the cloud lifetime effect, semi-direct effect or aerosol-ice cloud effects can either enhance or reduce the cloud albedo effect. Climate models estimate the sum of all aerosol effects (total indirect plus direct) to be –1.2 W m^{-2} with a range from –0.2 to –2.3 W m^{-2} in the change in top-of-the-atmosphere net radiation since pre-industrial times, whereas inverse estimates constrain the indirect aerosol effect to be between –0.1 and –1.7 W m^{-2} (see Chapter 9).

- The magnitude of the total aerosol effect on precipitation is more uncertain, with model results ranging from almost no change to a decrease of 0.13 mm day^{-1}. Decreases in precipitation are larger when the atmospheric General Circulation Models are coupled to mixed-layer ocean models where the sea surface temperature and, hence, the evaporation is allowed to vary.

- Deposition of dust particles containing limiting nutrients can enhance photosynthetic carbon fixation on land and in the oceans. Climate change is likely to affect dust sources.

- Since the TAR, advances have been made to link the marine and terrestrial biospheres with the climate system via the aerosol cycle. Emissions of aerosol precursors from vegetation and from the marine biosphere are expected to respond to climate change.

7.1 Introduction

The Earth's climate is determined by a number of complex connected physical, chemical and biological processes occurring in the atmosphere, land and ocean. The radiative properties of the atmosphere, a major controlling factor of the Earth's climate, are strongly affected by the biophysical state of the Earth's surface and by the atmospheric abundance of a variety of trace constituents. These constituents include long-lived greenhouse gases (LLGHGs) such as carbon dioxide (CO_2), methane (CH_4) and nitrous oxide (N_2O), as well as other radiatively active constituents such as ozone and different types of aerosol particles. The composition of the atmosphere is determined by processes such as natural and anthropogenic emissions of gases and aerosols, transport at a variety of scales, chemical and microphysical transformations, wet scavenging and surface uptake by the land and terrestrial ecosystems, and by the ocean and its ecosystems. These processes and, more generally the rates of biogeochemical cycling, are affected by climate change, and involve interactions between and within the different components of the Earth system. These interactions are generally nonlinear and may produce negative or positive feedbacks to the climate system.

An important aspect of climate research is to identify potential feedbacks and assess if such feedbacks could produce large and undesired responses to perturbations resulting from human activities. Studies of past climate evolution on different time scales can elucidate mechanisms that could trigger nonlinear responses to external forcing. The purpose of this chapter is to identify the major biogeochemical feedbacks of significance to the climate system, and to assess current knowledge of their magnitudes and trends. Specifically, this chapter will examine the relationships between the physical climate system and the land surface, the carbon cycle, chemically reactive atmospheric gases and aerosol particles. It also presents the current state of knowledge on budgets of important trace gases. Large uncertainties remain in many issues discussed in this chapter, so that quantitative estimates of the importance of the coupling mechanisms discussed in the following sections are not always available. In addition, regional differences in the role of some cycles and the complex interactions between them limit our present ability to provide a simple quantitative description of the interactions between biogeochemical processes and climate change.

7.1.1 Terrestrial Ecosystems and Climate

The terrestrial biosphere interacts strongly with the climate, providing both positive and negative feedbacks due to biogeophysical and biogeochemical processes. Some of these feedbacks, at least on a regional basis, can be large. Surface climate is determined by the balance of fluxes, which can be changed by radiative (e.g., albedo) or non-radiative (e.g., water cycle related processes) terms. Both radiative and non-radiative terms are controlled by details of vegetation. High-latitude climate is strongly influenced by snow albedo feedback, which is drastically reduced by the darkening effect of vegetation. In semi-arid tropical systems, such as the Sahel or northeast Brazil, vegetation exerts both radiative and hydrological feedbacks. Surface climate interacts with vegetation cover, biomes, productivity, respiration of vegetation and soil, and fires, all of which are important for the carbon cycle. Various processes in terrestrial ecosystems influence the flux of carbon between land and the atmosphere. Terrestrial ecosystem photosynthetic productivity changes in response to changes in temperature, precipitation, CO_2 and nutrients. If climate becomes more favourable for growth (e.g., increased rainfall in a semi-arid system), productivity increases, and carbon uptake from the atmosphere is enhanced. Organic carbon compounds in soils, originally derived from plant material, are respired (i.e., oxidized by microbial communities) at different rates depending on the nature of the compound and on the microbial communities; the aggregate rate of respiration depends on soil temperature and moisture. Shifts in ecosystem structure in response to a changing climate can alter the partitioning of carbon between the atmosphere and the land surface. Migration of boreal forest northward into tundra would initially lead to an increase in carbon storage in the ecosystem due to the larger biomass of trees than of herbs and shrubs, but over a longer time (e.g., centuries), changes in soil carbon would need to be considered to determine the net effect. A shift from tropical rainforest to savannah, on the other hand, would result in a net flux of carbon from the land surface to the atmosphere.

7.1.2 Ocean Ecosystems and Climate

The functioning of ocean ecosystems depends strongly on climatic conditions including near-surface density stratification, ocean circulation, temperature, salinity, the wind field and sea ice cover. In turn, ocean ecosystems affect the chemical composition of the atmosphere (e.g. CO_2, N_2O, oxygen (O_2), dimethyl sulphide (DMS) and sulphate aerosol). Most of these components are expected to change with a changing climate and high atmospheric CO_2 conditions. Marine biota also influence the near-surface radiation budget through changes in the marine albedo and absorption of solar radiation (bio-optical heating). Feedbacks between marine ecosystems and climate change are complex because most involve the ocean's physical responses and feedbacks to climate change. Increased surface temperatures and stratification should lead to increased photosynthetic fixation of CO_2, but associated reductions in vertical mixing and overturning circulation may decrease the return of required nutrients to the surface ocean and alter the vertical export of carbon to the deeper ocean. The sign of the cumulative feedback to climate of all these processes is still unclear. Changes in the supply of micronutrients required for photosynthesis, in particular iron, through dust deposition to the ocean surface can modify marine biological production patterns. Ocean acidification due to uptake of anthropogenic CO_2 may lead to shifts in ocean ecosystem structure and dynamics, which may alter the biological production and export from the surface ocean of organic carbon and calcium carbonate ($CaCO_3$).

7.1.3 Atmospheric Chemistry and Climate

Interactions between climate and atmospheric oxidants, including ozone, provide important coupling mechanisms in the Earth system. The concentration of tropospheric ozone has increased substantially since the pre-industrial era, especially in polluted areas of the world, and has contributed to radiative warming. Emissions of chemical ozone precursors (carbon monoxide, CH_4, non-methane hydrocarbons, nitrogen oxides) have increased as a result of larger use of fossil fuel, more frequent biomass burning and more intense agricultural practices. The atmospheric concentration of pre-industrial tropospheric ozone is not accurately known, so that the resulting radiative forcing cannot be accurately determined, and must be estimated from models. The decrease in concentration of stratospheric ozone in the 1980s and 1990s due to manufactured halocarbons (which produced a slight cooling) has slowed down since the late 1990s. Model projections suggest a slow steady increase over the next century, but continued recovery could be affected by future climate change. Recent changes in the growth rate of atmospheric CH_4 and in its apparent lifetime are not well understood, but indications are that there have been changes in source strengths. Nitrous oxide continues to increase in the atmosphere, primarily as a result of agricultural activities. Changes in atmospheric chemical composition that could result from climate changes are even less well quantified. Photochemical production of the hydroxyl radical (OH), which efficiently destroys many atmospheric compounds, occurs in the presence of ozone and water vapour, and should be enhanced in an atmosphere with increased water vapour, as projected under future global warming. Other chemistry-related processes affected by climate change include the frequency of lightning flashes in thunderstorms (which produce nitrogen oxides), scavenging mechanisms that remove soluble species from the atmosphere, the intensity and frequency of convective transport events, the natural emissions of chemical compounds (e.g., biogenic hydrocarbons by the vegetation, nitrous and nitric oxide by soils, DMS from the ocean) and the surface deposition on molecules on the vegetation and soils. Changes in the circulation and specifically the more frequent occurrence of stagnant air events in urban or industrial areas could enhance the intensity of air pollution events. The importance of these effects is not yet well quantified.

7.1.4 Aerosol Particles and Climate

Atmospheric aerosol particles modify Earth's radiation budget by absorbing and scattering incoming solar radiation. Even though some particle types may have a warming effect, most aerosol particles, such as sulphate (SO_4) aerosol particles, tend to cool the Earth surface by scattering some of the incoming solar radiation back to space. In addition, by acting as cloud condensation nuclei, aerosol particles affect radiative properties of clouds and their lifetimes, which contribute to additional surface cooling. A significant natural source of sulphate is DMS, an organic compound whose production by phytoplankton and release to the atmosphere depends on climatic factors. In many areas of the Earth, large amounts of SO_4 particles are produced as a result of human activities (e.g., coal burning). With an elevated atmospheric aerosol load, principally in the Northern Hemisphere (NH), it is likely that the temperature increase during the last century has been smaller than the increase that would have resulted from radiative forcing by greenhouse gases alone. Other indirect effects of aerosols on climate include the evaporation of cloud particles through absorption of solar radiation by soot, which in this case provides a positive warming effect. Aerosols (i.e., dust) also deliver nitrogen (N), phosphorus and iron to the Earth's surface; these nutrients could increase uptake of CO_2 by marine and terrestrial ecosystems.

7.1.5 Coupling the Biogeochemical Cycles with the Climate System

Models that attempt to perform reliable projections of future climate changes should account explicitly for the feedbacks between climate and the processes that determine the atmospheric concentrations of greenhouse gases, reactive gases and aerosol particles. An example is provided by the interaction between the carbon cycle and climate. It is well established that the level of atmospheric CO_2, which directly influences the Earth's temperature, depends critically on the rates of carbon uptake by the ocean and the land, which are also dependent on climate. Climate models that include the dynamics of the carbon cycle suggest that the overall effect of carbon-climate interactions is a positive feedback. Hence predicted future atmospheric CO_2 concentrations are therefore higher (and consequently the climate warmer) than in models that do not include these couplings. As understanding of the role of the biogeochemical cycles in the climate system improves, they should be explicitly represented in climate models. The present chapter assesses the current understanding of the processes involved and highlights the role of biogeochemical processes in the climate system.

7.2 The Changing Land Climate System

7.2.1 Introduction to Land Climate

The land surface relevant to climate consists of the terrestrial biosphere, that is, the fabric of soils, vegetation and other biological components, the processes that connect them and the carbon, water and energy they store. This section addresses from a climate perspective the current state of understanding of the land surface, setting the stage for consideration of carbon and other biogenic processes linked to climate. The land climate consists of 'internal' variables and 'external' drivers, including the various surface energy, carbon and moisture stores, and their response to precipitation, incoming radiation and near-surface atmospheric variables. The drivers and response variables change over various temporal and spatial scales.

This variation in time and space can be at least as important as averaged quantities. The response variables and drivers for the terrestrial system can be divided into biophysical, biological, biogeochemical and human processes. The present biophysical viewpoint emphasizes the response variables that involve the stores of energy and water and the mechanisms coupling these terms to the atmosphere. The exchanges of energy and moisture between the atmosphere and land surface (Boxes 7.1 and 7.2) are driven by radiation, precipitation and the temperature, humidity and winds of the overlying atmosphere. Determining how much detail to include to achieve an understanding of the system is not easy: many choices can be made and more detail becomes necessary when more processes are to be addressed.

7.2.2 Dependence of Land Processes and Climate on Scale

7.2.2.1 Multiple Scales are Important

Temporal variability ranges from the daily and weather time scales to annual, interannual, and decadal or longer scales: the amplitudes of shorter time scales change with long-term changes from global warming. The land climate system has controls on amplitudes of variables on all these time scales, varying with season and geography. For example, Trenberth and Shea (2005) evaluate from climatic observations the correlation between surface air temperature and precipitation, and find a strong $r > 0.3$) positive correlation over most winter land areas (i.e., poleward of 40°N) but a strong ($|r| > 0.3$) negative correlation over much of summer and tropical land. These differences result from competing feedbacks with the water cycle. On scales large enough that surface temperatures control atmospheric temperatures, the atmosphere will hold more water vapour and may provide more precipitation with warmer temperatures. Low clouds strongly control surface temperatures, especially in cold regions where they make the surface warmer. In warm regions without precipitation, the land surface can become warmer because of lack of evaporation, or lack of clouds. Although a drier surface will become warmer from lack of evaporative cooling, more water can evaporate from a moist surface if the temperature is warmer (see Box 7.1).

7.2.2.2 Spatial Dependence

Drivers of the land climate system have larger effects at regional and local scales than on global climate, which is controlled primarily by processes of global radiation balance. Myhre et al. (2005) point out that the albedo of agricultural systems may be only slightly higher than that of forests and estimate that the impact since pre-agricultural times of land use

Box 7.1: Surface Energy and Water Balance

The land surface on average is heated by net radiation balanced by exchanges with the atmosphere of sensible and latent heat, known as the 'surface energy balance'. Sensible heat is the energy carried by the atmosphere in its temperature and latent heat is the energy lost from the surface by evaporation of surface water. The latent heat of the water vapour is converted to sensible heat in the atmosphere through vapour condensation and this condensed water is returned to the surface through precipitation.

The surface also has a 'surface water balance'. Water coming to the surface from precipitation is eventually lost either through water vapour flux or by runoff. The latent heat flux (or equivalently water vapour flux) under some conditions can be determined from the energy balance. For a fixed amount of net surface radiation, if the sensible heat flux goes up, the latent flux will go down by the same amount. Thus, if the ratio of sensible to latent heat flux depends only on air temperature, relative humidity and other known factors, the flux of water vapour from the surface can be found from the net radiative energy at the surface. Such a relationship is most readily obtained when water removal (evaporation from soil or transpiration by plants) is not limited by availability of water. Under these conditions, the increase of water vapour concentration with temperature increases the relative amount of the water flux as does low relative humidity. Vegetation can prolong the availability of soil water through the extent of its roots and so increase the latent heat flux but also can resist movement through its leaves, and so shift the surface energy fluxes to a larger fraction carried by the sensible heat flux. Fluxes to the atmosphere modify atmospheric temperatures and humidity and such changes feed back to the fluxes. Storage and the surface can also be important at short time scales, and horizontal transports can be important at smaller spatial scales.

If a surface is too dry to exchange much water with the atmosphere, the water returned to the atmosphere should be on average not far below the incident precipitation, and radiative energy beyond that needed for evaporating this water will heat the surface. Under these circumstances, less precipitation and hence less water vapour flux will make the surface warmer. Reduction of cloudiness from the consequently warmer and drier atmosphere may act as a positive feedback to provide more solar radiation. A locally moist area (such as an oasis or pond), however, would still evaporate according to energy balance with no water limitation and thus should increase its evaporation under such warmer and drier conditions.

Various feedbacks coupling the surface to the atmosphere may work in opposite directions and their relative importance may depend on season and location as well as on temporal and spatial scales. A moister atmosphere will commonly be cloudier making the surface warmer in a cold climate and cooler in a warm climate. The warming of the atmosphere by the surface may reduce its relative humidity and reduce precipitation as happens over deserts. However, it can also increase the total water held by the atmosphere, which may lead to increased precipitation as happens over the tropical oceans.

conversion to agriculture on global radiative forcing has been only –0.09 W m^{-2}, that is, about 5% of the warming contributed by CO_2 since pre-industrial times (see Chapter 2 for a more comprehensive review of recent estimates of land surface albedo change). Land comprises only about 30% of the Earth's surface, but it can have the largest effects on the reflection of global solar radiation in conjunction with changes in ice and snow cover, and the shading of the latter by vegetation.

At a regional scale and at the surface, additional more localised and shorter time-scale processes besides radiative forcing can affect climate in other ways, and possibly be of comparable importance to the effects of the greenhouse gases. Changes over land that modify its evaporative cooling can cause large changes in surface temperature, both locally and regionally (see Boxes 7.1, 7.2). How this change feeds back to precipitation remains a major research question. Land has a strong control on the vertical distribution of atmospheric heating. It determines how much of the radiation delivered to land goes into warming the near-surface atmosphere compared with how much is released as latent heat fuelling precipitation at higher levels. Low clouds are normally closely coupled to the surface and over land can be significantly changed by modifications of surface temperature or moisture resulting from changes in land properties. For example, Chagnon et al. (2004) find a large increase in boundary layer clouds in the Amazon in areas of partial deforestation (also, e.g., Durieux et al., 2003; Ek and Holtslag, 2004). Details of surface properties at scales as small as a few kilometres can be important for larger scales. Over some fraction of moist soils, water tables can be high enough to be hydrologically connected to the rooting zone, or reach the surface as in wetlands (e.g., Koster et al., 2000; Marani et al., 2001; Milly and Shmakin, 2002; Liang et al., 2003; Gedney and Cox, 2003).

The consequences of changes in atmospheric heating from land changes at a regional scale are similar to those from ocean temperature changes such as from El Niño, potentially producing patterns of reduced or increased cloudiness and precipitation elsewhere to maintain global energy balance. Attempts have been made to find remote adjustments (e.g., Avissar and Werth, 2005). Such adjustments may occur in multiple ways, and are part of the dynamics of climate models. The locally warmer temperatures can lead to more rapid vertical decreases of atmospheric temperature so that at some level overlying temperature is lower and radiates less. The net effect of such compensations is that averages over larger areas or longer time scales commonly will give smaller estimates of change. Thus, such regional changes are better described by local and regional metrics or at larger scales by measures of change in spatial and temporal variability rather than simply in terms of a mean global quantity.

7.2.2.3 Daily and Seasonal Variability

Diurnal and seasonal variability result directly from the temporal variation of the solar radiation driver. Large-scale changes in climate variables are of interest as part of the observational record of climate changes (Chapter 3). Daytime during the warm season produces a thick layer of mixed air with temperature relatively insensitive to perturbations in daytime radiative forcing. Nighttime and high-latitude winter surface temperatures, on the other hand, are coupled by mixing to only a thin layer of atmosphere, and can be more readily altered by changes in atmospheric downward thermal radiation. Thus, land is more sensitive to changes in radiative drivers under cold stable conditions and weak winds than under warm unstable conditions. Winter or nighttime temperatures (hence diurnal temperature range) are strongly correlated with downward longwave radiation (e.g., Betts, 2006; Dickinson et al., 2006); consequently, average surface temperatures may change (e.g., Pielke and Matsui, 2005) with a change in downward longwave radiation.

Modification of downward longwave radiation by changes in clouds can affect land surface temperatures. Qian and Giorgi (2000) discussed regional aerosol effects, and noted a reduction in the diurnal temperature range of –0.26°C per decade over Sichuan China. Huang et al. (2006) model the growth of sulphate aerosols and their interactions with clouds in the context of a RCM, and find over southern China a decrease in the diurnal temperature range comparable with that observed by Zhou et al. (2004) and Qian and Giorgi. They show the nighttime temperature change to be a result of increased nighttime cloudiness and hence downward longwave radiation connected to the increase in aerosols.

Box 7.2: Urban Effects on Climate

If the properties of the land surface are changed locally, the surface net radiation and the partitioning between latent and sensible fluxes (Box 7.1) may also change, with consequences for temperatures and moisture storage of the surface and near-surface air. Such changes commonly occur to meet human needs for agriculture, housing, or commerce and industry. The consequences of urban development may be especially significant for local climates. However, urban development may have different features in different parts of an urban area and between geographical regions.

Some common modifications are the replacement of vegetation by impervious surfaces such as roads or the converse development of dry surfaces into vegetated surfaces by irrigation, such as lawns and golf courses. Buildings cover a relatively small area but in urban cores may strongly modify local wind flow and surface energy balance (Box 7.1). Besides the near-surface effects, urban areas can provide high concentrations of aerosols with local or downwind impacts on clouds and precipitation. Change to dark dry surfaces such as roads will generally increase daytime temperatures and lower humidity while irrigation will do the opposite. Changes at night may depend on the retention of heat by buildings and can be exacerbated by the thinness of the layer of atmosphere connected to the surface by mixing of air. Chapter 3 further addresses urban effects.

In moist warm regions, large changes are possible in the fraction of energy going into water fluxes, for example, by changes in vegetation cover or precipitation, and hence in soil moisture. Bonan (2001) and Oleson et al. (2004) indicate that conversion of mid-latitude forests to agriculture could cause a daytime cooling. This cooling is apparently a result of higher albedo and increased transpiration. Changes in reflected solar radiation due to changing vegetation, hence feedbacks, are most pronounced in areas with vegetation underlain by snow or light-coloured soil. Seasonal and diurnal precipitation cycles can be pronounced. Climate models simulate the diurnal precipitation cycle but apparently not yet very well (e.g., Collier and Bowman, 2004). Betts (2004) reviews how the diurnal cycle of tropical continental precipitation is linked to land surface fluxes and argues that errors in a model can feed back to model dynamics with global impacts.

7.2.2.4 Coupling of Precipitation Intensities to Leaf Water – An Issue Involving both Temporal and Spatial Scales

The bulk of the water exchanged with the atmosphere is stored in the soil until taken up by plant roots, typically weeks later. However, the rapidity of evaporation of the near-surface stores allows plant uptake and evaporation to be of comparable importance for surface water and energy balances. (Dickinson et al., 2003, conclude that feedbacks between surface moisture and precipitation may act differently on different time scales). Evaporation from the fast reservoirs acts primarily as a surface energy removal mechanism. Leaves initially intercept much of the precipitation over vegetation, and a significant fraction of this leaf water re-evaporates in an hour or less. This loss reduces the amount of water stored in the soil for use by plants. Its magnitude depends inversely on the intensity of the precipitation, which can be larger at smaller temporal and spatial scales. Modelling results can be wrong either through neglect of or through exaggeration of the magnitude of the fast time-scale moisture stores.

Leaf water evaporation may have little effect on the determination of monthly evapotranspiration (e.g., as found in the analysis of Desborough, 1999) but may still produce important changes in temperature and precipitation. Pitman et al. (2004), in a coupled study with land configurations of different complexity, were unable to find any impacts on atmospheric variability, but Bagnoud et al. (2005) found that precipitation and temperature extremes were affected. Some studies that change the intensity of precipitation find a very large impact from leaf water. For example, Wang and Eltahir (2000) studied the effect of including more realistic precipitation intensity compared to the uniform intensity of a climate model. Hahmann (2003) used another model to study this effect. Figure 7.1 compares their tropical results (Wang and Eltahir over equatorial Africa and Hahmann over equatorial Amazon). The model of Wang and Eltahir shows that more realistic precipitation greatly increases runoff whereas Hahmann shows that it reduces runoff. It has not been determined whether these contradictory results are more a consequence of model differences or of differences between the climates of the two continents, as Hahmann suggests.

7.2.3 Observational Basis for the Effects of Land Surface on Climate

7.2.3.1 Vegetative Controls on Soil Water and its Return Flux to the Atmosphere

Scanlon et al. (2005) provide an example of how soil moisture can depend on vegetation. They monitored soil moisture in the Nevada desert with lysimeters either including or excluding vegetation and for a multi-year period that included times of anomalously strong precipitation. Without vegetation, much of the moisture penetrated deeply, had a long lifetime and became available for recharge of deep groundwater, whereas for the vegetated plot, the soil moisture was all transpired. In the absence of leaves, forests in early spring also appear as especially dry surfaces with consequent large sensible fluxes that mix the atmosphere to a great depth (e.g., Betts et al., 2001). Increased water fluxes with spring green-up are observed in terms of a reduction in temperature. Trees in the Amazon can have the largest water fluxes in the dry season by development of deep roots (Da Rocha et al., 2004; Quesada et al., 2004). Forests can also retard fluxes through control by their leaves. Such control by vegetation of water fluxes is most pronounced for taller or sparser vegetation in cooler or drier climates, and from leaves that are sparse or exert the strongest resistance to water movement. The boreal forest, in particular, has been characterised as a 'green desert' because of its small release of water to the atmosphere (Gamon et al., 2003).

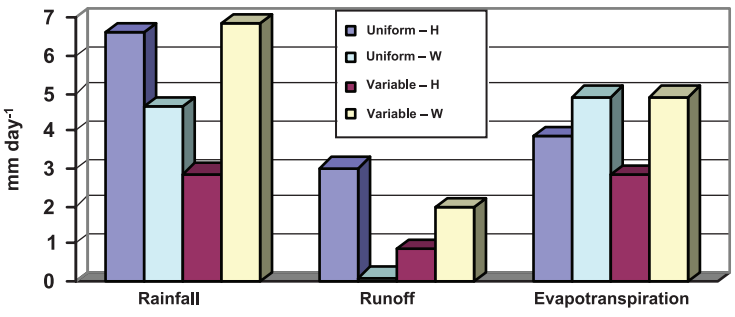


Figure 7.1. *Rainfall, runoff and evapotranspiration derived from climate simulation results of Hahmann (H; 2004) and Wang and Eltahir (W; 2000). Hahmann's results are for the Amazon centred on the equator, and Wang and Eltahir's for Africa at the equator. Both studies examined the differences between 'uniform' precipitation over a model grid square and 'variable' precipitation (added to about 10% of the grid square). Large differences are seen between the two cases in the two studies: a large reduction in precipitation is seen in the Hahmann variable case relative to the uniform case, whereas an increase is seen for the Wang and Eltahir variable case. The differences are even greater for runoff: Hahmann's uniform case runoff is three times as large as the variable case, whereas Wang and Eltahir have almost no runoff for their uniform case.*

7.2.3.2 Land Feedback to Precipitation

Findell and Eltahir (2003) examine the correlation between early morning near-surface humidity over the USA and an index of the likelihood of precipitation occurrence. They identify different geographical regions with positive, negative or little correlation. Koster et al. (2003) and Koster and Suarez (2004) show during summer over the USA, and all land 30°N to 60°N, respectively, a significant correlation of monthly precipitation with that of prior months. They further show that their model only reproduces this correlation if soil moisture feedback is allowed to affect precipitation. Additional observational evidence for such feedback is noted by D'Odorico and Porporato (2004) in support of a simplified model of precipitation soil moisture coupling (see, e.g., Salvucci et al., 2002, for support of the null hypothesis of no coupling). Liebmann and Marengo (2001) point out that the interannual variation of precipitation over the Amazon is largely controlled by the timing of the onset and end of the rainy season. Li and Fu (2004) provide evidence that onset time of the rainy season is strongly dependent on transpiration by vegetation during the dry season. Previous modelling and observational studies have also suggested that Amazon deforestation should lead to a longer dry season. Fu and Li (2004) further argue from observations that removal of tropical forest reduces surface moisture fluxes, and that such land use changes should contribute to a lengthening of the Amazon dry season. Durieux et al. (2003) find more rainfall in the deforested area in the wet season and a reduction of the dry season precipitation over deforested regions compared with forested areas. Negri et al. (2004) obtain an opposite result (although their result is consistent with Durieux during the wet season).

7.2.3.3 Properties Affecting Radiation

Albedo (the fraction of reflected solar radiation) and emissivity (the ratio of thermal radiation to that of a black body) are important variables for the radiative balance. Surfaces that have more or taller vegetation are commonly darker than are those with sparse or shorter vegetation. With sparse vegetation, the net surface albedo also depends on the albedo of the underlying surfaces, especially if snow or a light-coloured soil. A large-scale transformation of tundra to shrubs, possibly connected to warmer temperatures over the last few decades, has been observed (e.g., Chapin et al., 2005). Sturm et al. (2005) report on winter and melt season observations of how varying extents of such shrubs can modify surface albedo. New satellite data show the importance of radiation heterogeneities at the plot scale for the determination of albedo and the solar radiation used for photosynthesis, and appropriate modelling concepts to incorporate the new data are being advanced (e.g., Yang and Friedl, 2003; Niu and Yang, 2004; Wang, 2005; Pinty et al., 2006).

7.2.3.4 Improved Global and Regional Data

Specification of land surface properties has improved through new, more accurate global satellite observations. In particular, satellite observations have provided albedos of soils in non-vegetated regions (e.g., Tsvetsinskaya et al., 2002; Ogawa and Schmugge, 2004; Z. Wang, et al., 2004; Zhou et al., 2005) and their emissivities (Zhou et al., 2003a,b). They also constrain model-calculated albedos in the presence of vegetation (Oleson et al., 2003) and vegetation underlain by snow (Jin et al., 2002), and help to define the influence of leaf area on albedo (Tian et al., 2004). Precipitation data sets combining rain gauge and satellite observations (Chen et al., 2002; Adler et al., 2003) are providing diagnostic constraints for climate modelling, as are observations of runoff (Dai and Trenberth, 2002; Fekete et al., 2002).

7.2.3.5 Field Observational Programs

New and improved local site observational constraints collectively describe the land processes that need to be modelled. The largest recent such activity has been the Large-Scale Biosphere-Atmosphere Experiment in Amazonia (LBA) project (Malhi et al., 2002; Silva Dias et al., 2002). Studies within LBA have included physical climate at all scales, carbon and nutrient dynamics and trace gas fluxes. The physical climate aspects are reviewed here. Goncalves et al. (2004) discuss the importance of incorporating land cover heterogeneity. Da Rocha et al. (2004) and Quesada et al. (2004) quantify water and energy budgets for a forested and a savannah site, respectively. Dry season evapotranspiration for the savannah averaged 1.6 mm day^{-1} compared with 4.9 mm day^{-1} for the forest. Both ecosystems depend on deep rooting to sustain evapotranspiration during the dry season, which may help control the length of the dry season (see, e.g., Section 7.2.3.2). Da Rocha et al. (2004) also observed that hydraulic lift recharged the forest upper soil profiles each night. At Tapajós, the forest showed no signs of drought stress allowing uniformly high carbon uptake throughout the dry season (July through December 2000; Da Rocha et al., 2004; Goulden et al., 2004). Tibet, another key region, continues to be better characterised from observational studies (e.g., Gao et al., 2004; Hong et al., 2004). With its high elevation, hence low air densities, heating of the atmosphere by land mixes air to a much higher altitude than elsewhere, with implications for vertical exchange of energy. However, the daytime water vapour mixing ratio in this region decreases rapidly with increasing altitude (Yang et al., 2004), indicating a strong insertion of dry air from above or by lateral transport.

7.2.3.6 Connecting Changing Vegetation to Changing Climate

Only large-scale patterns are assessed here. Analysis of satellite-sensed vegetation greenness and meteorological station data suggest an enhanced plant growth and lengthened growing season duration at northern high latitudes since the 1980s (Zhou

et al., 2001, 2003c). This effect is further supported by modelling linked to observed climate data (Lucht et al., 2002). Nemani et al. (2002, 2003) suggest that increased rainfall and humidity spurred plant growth in the USA and that climate changes may have eased several critical climatic constraints to plant growth and thus increased terrestrial net primary production.

7.2.4 Modelling the Coupling of Vegetation, Moisture Availability, Precipitation and Surface Temperature

7.2.4.1 How do Models of Vegetation Control Surface Water Fluxes?

Box 7.1 provides a general description of water fluxes from surface to atmosphere. The most important factors affected by vegetation are soil water availability, leaf area and surface roughness. Whether water has been intercepted on the surface of the leaves or its loss is only from the leaf interior as controlled by stomata makes a large difference. Shorter vegetation with more leaves has the most latent heat flux and the least sensible flux. Replacement of forests with shorter vegetation together with the normally assumed higher albedo could then cool the surface. However, if the replacement vegetation has much less foliage or cannot access soil water as successfully, a warming may occur. Thus, deforestation can modify surface temperatures by up to several degrees celsius in either direction depending on what type of vegetation replaces the forest and the climate regime. Drier air can increase evapotranspiration, but leaves may decrease their stomatal conductance to counter this effect.

7.2.4.2 Feedbacks Demonstrated Through Simple Models

In semi-arid systems, the occurrence and amounts of precipitation can be highly variable from year to year. Are there mechanisms whereby the growth of vegetation in times of adequate precipitation can act to maintain the precipitation? Various analyses with simple models have demonstrated how this might happen (Zeng et al., 2002; Foley et al., 2003; G. Wang, et al., 2004; X. Zeng et al., 2004). Such models demonstrate how assumed feedbacks between precipitation and surface fluxes generated by dynamic vegetation may lead to the possibility of transitions between multiple equilibria for two soil moisture and precipitation regimes. That is, the extraction of water by roots and shading of soil by plants can increase precipitation and maintain the vegetation, but if the vegetation is removed, it may not be able to be restored for a long period. The Sahel region between the deserts of North Africa and the African equatorial forests appears to most readily generate such an alternating precipitation regime.

7.2.4.3 Consequences of Changing Moisture Availability and Land Cover

Soil moisture control of the partitioning of energy between sensible and latent heat flux is very important for local and regional temperatures, and possibly their coupling to precipitation. Oglesby et al. (2002) carried out a study starting with dry soil where the dryness of the soil over the US Great Plains for at least the first several summer months of their integration produced a warming of about 10°C to 20°C. Williamson et al. (2005), have shown that flaws in model formulation of thunderstorms can cause excessive evapotranspiration that lowers temperatures by more than 1°C. Many modelling studies have demonstrated that changing land cover can have local and regional climate impacts that are comparable in magnitude to temperature and precipitation changes observed over the last several decades as reported in Chapter 3. However, since such regional changes can be of both signs, the global average impact is expected to be small. Current literature has large disparities in conclusions. For example, Snyder et al. (2004) found that removal of northern temperate forests gave a summer warming of 1.3°C and a reduction in precipitation of 1.5 mm day^{-1}. Conversely, Oleson et al. (2004) found that removal of temperate forests in the USA would cool summer temperatures by 0.4°C to 1.5°C and probably increase precipitation, depending on the details of the model and prescription of vegetation. The discrepancy between these two studies may be largely an artefact of different assumptions. The first study assumes conversion of forest to desert and the second to crops. Such studies collectively demonstrate a potentially important impact of human activities on climate through land use modification.

Other recent such studies illustrate various aspects of this issue. Maynard and Royer (2004) address the sensitivity to different parameter changes in African deforestation experiments and find that changes in roughness, soil depth, vegetation cover, stomatal resistance, albedo and leaf area index all could make significant contributions. Voldoire and Royer (2004) find that such changes may affect temperature and precipitation extremes more than means, in particular the daytime maximum temperature and the drying and temperature responses associated with El Niño events. Guillevic et al. (2002) address the importance of interannual leaf area variability as inferred from Advanced Very High Resolution Radiometer (AVHRR) satellite data, and infer a sensitivity of climate to this variation. In contrast, Lawrence and Slingo (2004) find little difference in climate simulations that use annual mean vegetation characteristics compared with those that use a prescribed seasonal cycle. However, they do suggest model modifications that would give a much larger sensitivity. Osborne et al. (2004) examine effects of changing tropical soils and vegetation: variations in vegetation produce variability in surface fluxes and their coupling to precipitation. Thus, interactive vegetation can promote additional variability of surface temperature and precipitation as analysed by Crucifix et al. (2005). Marengo and Nobre (2001) found that removal of vegetation led to a decrease in precipitation and evapotranspiration and a decrease in moisture convergence in central and northern Amazonia. Oyama and Nobre (2004) show that removal of vegetation in northeast Brazil would substantially decrease precipitation.

7.2.4.4 *Mechanisms for Modification of Precipitation by Spatial Heterogeneity*

Clark et al. (2004) show an example of a 'squall-line' simulation where soil moisture variation at the scale of the rainfall modifies the rainfall pattern. Pielke (2001), Weaver et al. (2002) and S. Roy et al. (2003) also address various aspects of small-scale precipitation coupling to land surface heterogeneity. If deforestation occurs in patches rather than uniformly, the consequences for precipitation could be different. Avissar et al. (2002) and Silva Dias et al. (2002) suggest that there may be a small increase in precipitation (of the order of 10%) resulting from partial deforestation as a consequence of the mesoscale circulations triggered by the deforestation.

7.2.4.5 *Interactive Vegetation Response Variables*

Prognostic approaches estimate leaf cover based on physiological processes (e.g., Arora and Boer, 2005). Levis and Bonan (2004) discuss how spring leaf emergence in mid-latitude forests provides a negative feedback to rapid increases in temperature. The parametrization of water uptake by roots contributes to the computed soil water profile (Feddes et al., 2001; Barlage and Zeng, 2004), and efforts are being made to make the roots interactive (e.g., Arora and Boer, 2003). Dynamic vegetation models have advanced and now explicitly simulate competition between plant functional types (e.g., Bonan et al., 2003; Sitch et al., 2003; Arora and Boer, 2006). New coupled climate-carbon models (Betts et al., 2004; Huntingford et al., 2004) demonstrate the possibility of large feedbacks between future climate change and vegetation change, discussed further in Section 7.3.5 (i.e., a die back of Amazon vegetation and reductions in Amazon precipitation). They also indicate that the physiological forcing of stomatal closure by rising atmospheric CO_2 levels could contribute 20% to the rainfall reduction. Levis et al. (2004) demonstrate how African rainfall and dynamic vegetation could change each other.

7.2.5 Evaluation of Models Through Intercomparison

Intercomparison of vegetation models usually involves comparing surface fluxes and their feedbacks. Henderson-Sellers et al. (2003), in comparing the surface fluxes among 20 models, report over an order of magnitude range among sensible fluxes of different models. However, recently developed models cluster more tightly. Irannejad et al. (2003) developed a statistical methodology to fit monthly fluxes from a large number of climate models to a simple linear statistical model, depending on factors such as monthly net radiation and surface relative humidity. Both the land and atmosphere models are major sources of uncertainty for feedbacks. Irannejad et al. find that coupled models agree more closely due to offsetting differences in the atmospheric and land models. Modelling studies have long reported that soil moisture can influence precipitation. Only recently, however, have there been attempts to quantify this coupling from a statistical viewpoint (Dirmeyer, 2001; Koster and Suarez, 2001; Koster et al., 2002; Reale and Dirmeyer, 2002; Reale et al., 2002; Koster et al., 2003; Koster and Suarez, 2004). Koster et al. (2004, 2006) and Guo et al. (2006) report on a new model intercomparison activity, the Global Land Atmosphere Coupling Experiment (GLACE), which compares among climate models differences in precipitation variability caused by interaction with soil moisture. Using an experimental protocol to generate ensembles of simulations with soil moisture that is either prescribed or interactive as it evolves in time, they report a wide range of differences between models (Figure 7.2). Lawrence and Slingo (2005) show that the relatively weak coupling strength of the Hadley Centre model results from its atmospheric component. There is yet little confidence in this feedback component of climate models and therefore its possible contribution to global warming (see Chapter 8).

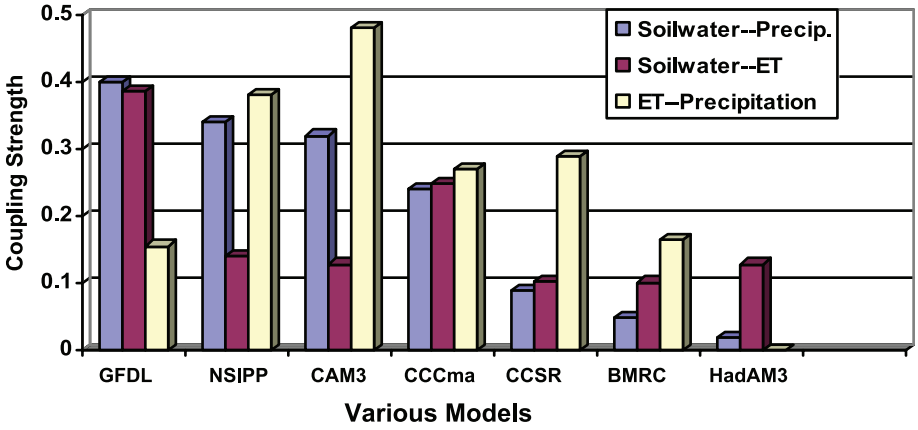


Figure 7.2. *Coupling strength (a nondimensional pattern similarity diagnostic defined in Koster et al., 2006) between summer rainfall and soil water in models assessed by the GLACE study (Guo et al., 2006), divided into how strongly soil water causes evaporation (including from plants) and how strongly this evaporation causes rainfall. The soil water-precipitation coupling is scaled up by a factor of 10, and the two indices for evaporation to precipitation coupling given in the study are averaged. Models include the Geophysical Fluid Dynamics Laboratory (GFDL) model, the National Aeronautics and Space Administration (NASA) Seasonal to Interannual Prediction Program (NSIPP) model, the National Center for Atmospheric Research Community Atmosphere Model (CAM3), the Canadian Centre for Climate Modelling and Analysis (CCCma) model, the Centre for Climate System Research (CCSR) model, the Bureau of Meteorology Research Centre (BMRC) model and the Hadley Centre Atmospheric Model version 3 (HadAM3).*

7.2.6 Linking Biophysical to Biogeochemical and Ecohydrological Components

Soil moisture and surface temperatures work together in response to precipitation and radiative inputs. Vegetation influences these terms through its controls on energy and water fluxes, and through these fluxes, precipitation. It also affects the radiative heating. Clouds and precipitation are affected through modifications of the temperature and water vapour content of near-surface air. How the feedbacks of land to the atmosphere work remains difficult to quantify from either observations or modelling (as addressed in Sections 7.2.3.2 and 7.2.5.1). Radiation feedbacks depend on vegetation or cloud cover that has changed because of changing surface temperatures or moisture conditions. How such conditions may promote or discourage the growth of vegetation is established by various ecological studies. The question of how vegetation will change its distribution at large scales and the consequent changes in absorbed radiation is quantified through remote sensing studies. At desert margins, radiation and precipitation feedbacks may act jointly with vegetation. Radiation feedbacks connected to vegetation may be most pronounced at the margins between boreal forests and tundra and involve changes in the timing of snowmelt. How energy is transferred from the vegetation to underlying snow surfaces is understood in general terms but remains problematic in modelling and process details. Dynamic vegetation models (see Section 7.2.4.5) synthesize current understanding.

Changing soil temperatures and snow cover affect soil microbiota and their processing of soil organic matter. How are nutrient supplies modified by these surface changes or delivery from the atmosphere? In particular, the treatment of carbon fluxes (addressed in more detail in Section 7.3) may require comparable or more detail in the treatment of N cycling (as attempted by S. Wang, et al., 2002; Dickinson et al., 2003). The challenge is to establish better process understanding at local scales and appropriately incorporate this understanding into global models. The Coupled Carbon-Cycle Climate Model Intercomparison Project (C^4MIP) simulations described in Section 7.3.5 are a first such effort.

Biomass burning is a major mechanism for changing vegetation cover and generation of atmospheric aerosols and is directly coupled to the land climate variables of moisture and near-surface winds, as addressed for the tropics by Hoffman et al. (2002). The aerosol plume produced by biomass burning at the end of the dry season contains black carbon that absorbs radiation. The combination of a cooler surface due to lack of solar radiation and a warmer boundary layer due to absorption of solar radiation increases the thermal stability and reduces cloud formation, and thus can reduce rainfall. Freitas et al. (2005) indicate the possibility of rainfall decrease in the Plata Basin as a response to the radiative effect of the aerosol load transported from biomass burning in the Cerrado and Amazon regions. Aerosols and clouds reduce the availability of visible light needed by plants for photosynthesis. However, leaves in full sun may be light saturated, that is, they do not develop sufficient enzymes to utilise that level of light. Leaves that are shaded, however, are generally light limited. They are only illuminated by diffuse light scattered by overlying leaves or by atmospheric constituents. Thus, an increase in diffuse light at the expense of direct light may promote leaf carbon assimilation and transpiration (Roderick et al., 2001; Cohan et al., 2002; Gu et al., 2002, 2003). Yamasoe et al. (2006) report the first observational tower evidence for this effect in the tropics. Diffuse radiation resulting from the Mt. Pinatubo eruption may have created an enhanced terrestrial carbon sink (Roderick et al., 2001; Gu et al., 2003). Angert et al. (2004) provide an analysis that rejects this hypothesis relative to other possible mechanisms.

7.3 The Carbon Cycle and the Climate System

7.3.1 Overview of the Global Carbon Cycle

7.3.1.1 The Natural Carbon Cycle

Over millions of years, CO_2 is removed from the atmosphere through weathering by silicate rocks and through burial in marine sediments of carbon fixed by marine plants (e.g., Berner, 1998). Burning fossil fuels returns carbon captured by plants in Earth's geological history to the atmosphere. New ice core records show that the Earth system has not experienced current atmospheric concentrations of CO_2, or indeed of CH_4, for at least 650 kyr – six glacial-interglacial cycles. During that period the atmospheric CO_2 concentration remained between 180 ppm (glacial maxima) and 300 ppm (warm interglacial periods) (Siegenthaler et al., 2005). It is generally accepted that during glacial maxima, the CO_2 removed from the atmosphere was stored in the ocean. Several causal mechanisms have been identified that connect astronomical changes, climate, CO_2 and other greenhouse gases, ocean circulation and temperature, biological productivity and nutrient supply, and interaction with ocean sediments (see Box 6.2).

Prior to 1750, the atmospheric concentration of CO_2 had been relatively stable between 260 and 280 ppm for 10 kyr (Box 6.2). Perturbations of the carbon cycle from human activities were insignificant relative to natural variability. Since 1750, the concentration of CO_2 in the atmosphere has risen, at an increasing rate, from around 280 ppm to nearly 380 ppm in 2005 (see Figure 2.3 and FAQ 2.1, Figure 1). The increase in atmospheric CO_2 concentration results from human activities: primarily burning of fossil fuels and deforestation, but also cement production and other changes in land use and management such as biomass burning, crop production and conversion of grasslands to croplands (see FAQ 7.1). While human activities contribute to climate change in many direct and indirect ways, CO_2 emissions from human activities are considered the single largest anthropogenic factor contributing to climate change (see FAQ 2.1, Figure 2). Atmospheric CH_4

Frequently Asked Question 7.1

Are the Increases in Atmospheric Carbon Dioxide and Other Greenhouse Gases During the Industrial Era Caused by Human Activities?

Yes, the increases in atmospheric carbon dioxide (CO_2) and other greenhouse gases during the industrial era are caused by human activities. In fact, the observed increase in atmospheric CO_2 concentrations does not reveal the full extent of human emissions in that it accounts for only 55% of the CO_2 released by human activity since 1959. The rest has been taken up by plants on land and by the oceans. In all cases, atmospheric concentrations of greenhouse gases, and their increases, are determined by the balance between sources (emissions of the gas from human activities and natural systems) and sinks (the removal of the gas from the atmosphere by conversion to a different chemical compound). Fossil fuel combustion (plus a smaller contribution from cement manufacture) is responsible for more than 75% of human-caused CO_2 emissions. Land use change (primarily deforestation) is responsible for the remainder. For methane, another important greenhouse gas, emissions generated by human activities exceeded natural emissions over the last 25 years. For nitrous oxide, emissions generated by human activities are equal to natural emissions to the atmosphere. Most of the long-lived halogen-containing gases (such as chlorofluorcarbons) are manufactured by humans, and were not present in the atmosphere before the industrial era. On average, present-day tropospheric ozone has increased 38% since pre-industrial times, and the increase results from atmospheric reactions of short-lived pollutants emitted by human activity. The concentration of CO_2 is now 379 parts per million (ppm) and methane is greater than 1,774 parts per billion (ppb), both very likely much higher than any time in at least 650 kyr (during which CO_2 remained between 180 and 300 ppm and methane between 320 and 790 ppb). The recent rate of change is dramatic and unprecedented; increases in CO_2 never exceeded 30 ppm in 1 kyr – yet now CO_2 has risen by 30 ppm in just the last 17 years.

Carbon Dioxide

Emissions of CO_2 (Figure 1a) from fossil fuel combustion, with contributions from cement manufacture, are responsible for more than 75% of the increase in atmospheric CO_2 concentration since pre-industrial times. The remainder of the increase comes from land use changes dominated by deforestation (and associated biomass burning) with contributions from changing agricultural practices. All these increases are caused by human activity. The natural carbon cycle cannot explain the observed atmospheric increase of 3.2 to 4.1 GtC yr^{-1} in the form of CO_2 over the last 25 years. (One GtC equals 10^{15} grams of carbon, i.e., one billion tonnes.)

Natural processes such as photosynthesis, respiration, decay and sea surface gas exchange lead to massive exchanges, sources and sinks of CO_2 between the land and atmosphere (estimated at ~120 GtC yr^{-1}) and the ocean and atmosphere (estimated at ~90 GtC yr^{-1}; see figure 7.3). The natural sinks of carbon produce a small net uptake of CO_2 of approximately 3.3 GtC yr^{-1} over the last 15 years, partially offsetting the human-caused emissions. Were it not for the natural sinks taking up nearly half the human-produced CO_2 over the past 15 years, atmospheric concentrations would have grown even more dramatically.

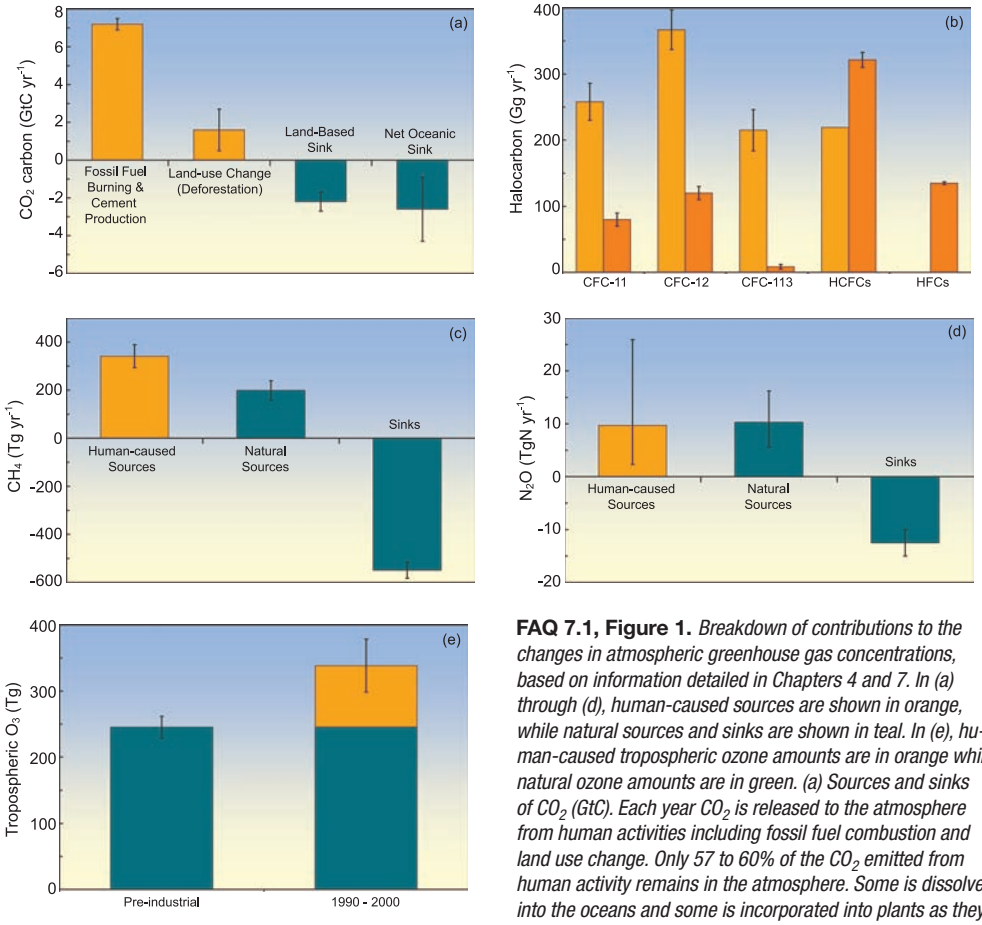
The increase in atmospheric CO_2 concentration is known to be caused by human activities because the character of CO_2 in the atmosphere, in particular the ratio of its heavy to light carbon atoms, has changed in a way that can be attributed to addition of fossil fuel carbon. In addition, the ratio of oxygen to nitrogen in the atmosphere has declined as CO_2 has increased; this is as expected because oxygen is depleted when fossil fuels are burned. A heavy form of carbon, the carbon-13 isotope, is less abundant in vegetation and in fossil fuels that were formed from past vegetation, and is more abundant in carbon in the oceans and in volcanic or geothermal emissions. The relative amount of the carbon-13 isotope in the atmosphere has been declining, showing that the added carbon comes from fossil fuels and vegetation. Carbon also has a rare radioactive isotope, carbon-14, which is present in atmospheric CO_2 but absent in fossil fuels. Prior to atmospheric testing of nuclear weapons, decreases in the relative amount of carbon-14 showed that fossil fuel carbon was being added to the atmosphere.

Halogen-Containing Gases

Human activities are responsible for the bulk of long-lived atmospheric halogen-containing gas concentrations. Before industrialisation, there were only a few naturally occurring halogen-containing gases, for example, methyl bromide and methyl chloride. The development of new techniques for chemical synthesis resulted in a proliferation of chemically manufactured halogen-containing gases during the last 50 years of the 20th century. Emissions of key halogen-containing gases produced by humans are shown in Figure 1b. Atmospheric lifetimes range from 45 to 100 years for the chlorofluorocarbons (CFCs) plotted here, from 1 to 18 years for the hydrochlorofluorocarbons (HCFCs), and from 1 to 270 years for the hydrofluorocarbons (HFCs). The perfluorocarbons (PFCs, not plotted) persist in the atmosphere for thousands of years. Concentrations of several important halogen-containing gases, including CFCs, are now stabilising or decreasing at the Earth's surface as a result of the Montreal Protocol on Substances that Deplete the Ozone Layer and its Amendments. Concentrations of HCFCs, production of which is to be phased out by 2030, and of the Kyoto Protocol gases HFCs and PFCs, are currently increasing. *(continued)*

Methane

Methane (CH_4) sources to the atmosphere generated by human activities exceed CH_4 sources from natural systems (Figure 1c). Between 1960 and 1999, CH_4 concentrations grew an average of at least six times faster than over any 40-year period of the two millennia before 1800, despite a near-zero growth rate since 1980. The main natural source of CH_4 to the atmosphere is wetlands. Additional natural sources include termites, oceans, vegetation and CH_4 hydrates. The human activities that produce CH_4 include energy production from coal and natural gas, waste disposal in landfills, raising ruminant animals (e.g., cattle and sheep), rice agriculture and biomass burning. Once emitted, CH_4 remains in the atmosphere for approximately 8.4 years before removal, mainly by chemical oxidation in the troposphere. Minor sinks for CH_4 include uptake by soils and eventual destruction in the stratosphere.



FAQ 7.1, Figure 1. *Breakdown of contributions to the changes in atmospheric greenhouse gas concentrations, based on information detailed in Chapters 4 and 7. In (a) through (d), human-caused sources are shown in orange, while natural sources and sinks are shown in teal. In (e), human-caused tropospheric ozone amounts are in orange while natural ozone amounts are in green. (a) Sources and sinks of CO_2 (GtC). Each year CO_2 is released to the atmosphere from human activities including fossil fuel combustion and land use change. Only 57 to 60% of the CO_2 emitted from human activity remains in the atmosphere. Some is dissolved into the oceans and some is incorporated into plants as they grow. Land-related fluxes are for the 1990s; fossil fuel and cement fluxes and net ocean uptake are for the period 2000 to 2005. All values and uncertainty ranges are from Table 7.1. (b) Global emissions of CFCs and other halogen-containing compounds for 1990 (light orange) and 2002 (dark orange). These chemicals are exclusively human-produced. Here, 'HCFCs' comprise HCFC-22, -141b and -142b, while 'HFCs' comprise HFC-23, -125, -134a and -152a. One Gg = 10^9 g (1,000 tonnes). Most data are from reports listed in Chapter 2. (c) Sources and sinks of CH_4 for the period 1983 to 2004. Human-caused sources of CH_4 include energy production, landfills, ruminant animals (e.g., cattle and sheep), rice agriculture and biomass burning. One Tg = 10^{12} g (1 million tonnes). Values and uncertainties are the means and standard deviations for CH_4 of the corresponding aggregate values from Table 7.6. (d) Sources and sinks of N_2O. Human-caused sources of N_2O include the transformation of fertilizer nitrogen into N_2O and its subsequent emission from agricultural soils, biomass burning, cattle and some industrial activities including nylon manufacture. Source values and uncertainties are the midpoints and range limits from Table 7.7. N_2O losses are from Chapter 7.4. (e) Tropospheric ozone in the 19th and early 20th centuries and the 1990 to 2000 period. The increase in tropospheric ozone formation is human-induced, resulting from atmospheric chemical reactions of pollutants emitted by burning of fossil fuels or biofuels. The pre-industrial value and uncertainty range are from Table 4.9 of the IPCC Third Assessment Report (TAR), estimated from reconstructed observations. The present-day total and its uncertainty range are the average and standard deviation of model results quoted in Table 7.9 of this report, excluding those from the TAR.*

Nitrous Oxide

Nitrous oxide (N_2O) sources to the atmosphere from human activities are approximately equal to N_2O sources from natural systems (Figure 1d). Between 1960 and 1999, N_2O concentrations grew an average of at least two times faster than over any 40-year period of the two millennia before 1800. Natural sources of N_2O include oceans, chemical oxidation of ammonia in the atmosphere, and soils. Tropical soils are a particularly important source of N_2O to the atmosphere. Human activities that emit N_2O include transformation of fertilizer nitrogen into N_2O and its subsequent emission from agricultural soils, biomass burning, raising cattle and some industrial activities, including nylon manufacture. Once emitted, N_2O remains in the atmosphere for approximately 114 years before removal, mainly by destruction in the stratosphere.

Tropospheric Ozone

Tropospheric ozone is produced by photochemical reactions in the atmosphere involving forerunner chemicals such as carbon monoxide, CH_4, volatile organic compounds and nitrogen oxides. These chemicals are emitted by natural biological processes and by human activities including land use change and fuel combustion. Because tropospheric ozone is relatively short-lived, lasting for a few days to weeks in the atmosphere, its distributions are highly variable and tied to the abundance of its forerunner compounds, water vapour and sunlight. Tropospheric ozone concentrations are significantly higher in urban air, downwind of urban areas and in regions of biomass burning. The increase of 38% (20–50%) in tropospheric ozone since the pre-industrial era (Figure 1e) is human-caused.

It is very likely that the increase in the combined radiative forcing from CO_2, CH_4 and N_2O was at least six times faster between 1960 and 1999 than over any 40-year period during the two millennia prior to the year 1800.

concentrations have similarly experienced a rapid rise from about 700 ppb in 1750 (Flückiger et al., 2002) to about 1,775 ppb in 2005 (see Section 2.3.2): sources include fossil fuels, landfills and waste treatment, peatlands/wetlands, ruminant animals and rice paddies. The increase in CH_4 radiative forcing is slightly less than one-third that of CO_2, making it the second most important greenhouse gas (see Chapter 2). The CH_4 cycle is presented in Section 7.4.1.

Both CO_2 and CH_4 play roles in the natural cycle of carbon, involving continuous flows of large amounts of carbon among the ocean, the terrestrial biosphere and the atmosphere, that maintained stable atmospheric concentrations of these gases for 10 kyr prior to 1750. Carbon is converted to plant biomass by photosynthesis. Terrestrial plants capture CO_2 from the atmosphere; plant, soil and animal respiration (including decomposition of dead biomass) returns carbon to the atmosphere as CO_2, or as CH_4 under anaerobic conditions. Vegetation fires can be a significant source of CO_2 and CH_4 to the atmosphere on annual time scales, but much of the CO_2 is recaptured by the terrestrial biosphere on decadal time scales if the vegetation regrows.

Carbon dioxide is continuously exchanged between the atmosphere and the ocean. Carbon dioxide entering the surface ocean immediately reacts with water to form bicarbonate (HCO_3^-) and carbonate (CO_3^{2-}) ions. Carbon dioxide, HCO_3^- and CO_3^{2-} are collectively known as dissolved inorganic carbon (DIC). The residence time of CO_2 (as DIC) in the surface ocean, relative to exchange with the atmosphere and physical exchange with the intermediate layers of the ocean below, is less than a decade. In winter, cold waters at high latitudes, heavy and enriched with CO_2 (as DIC) because of their high solubility, sink from the surface layer to the depths of the ocean. This localised sinking, associated with the Meridional Overturning Circulation (MOC; Box 5.1) is termed the 'solubility pump'. Over time, it is roughly balanced by a distributed diffuse upward transport of DIC primarily into warm surface waters.

Phytoplankton take up carbon through photosynthesis. Some of that sinks from the surface layer as dead organisms and particles (the 'biological pump'), or is transformed into dissolved organic carbon (DOC). Most of the carbon in sinking particles is respired (through the action of bacteria) in the surface and intermediate layers and is eventually recirculated to the surface as DIC. The remaining particle flux reaches abyssal depths and a small fraction reaches the deep ocean sediments, some of which is re-suspended and some of which is buried. Intermediate waters mix on a time scale of decades to centuries, while deep waters mix on millennial time scales. Several mixing times are required to bring the full buffering capacity of the ocean into effect (see Section 5.4 for long-term observations of the ocean carbon cycle and their consistency with ocean physics).

Together the solubility and biological pumps maintain a vertical gradient in CO_2 (as DIC) between the surface ocean (low) and the deeper ocean layers (high), and hence regulate exchange of CO_2 between the atmosphere and the ocean. The strength of the solubility pump depends globally on the strength of the MOC, surface ocean temperature, salinity, stratification and ice cover. The efficiency of the biological pump depends on the fraction of photosynthesis exported from the surface ocean as sinking particles, which can be affected by changes in ocean circulation, nutrient supply and plankton community composition and physiology.

In Figure 7.3 the natural or unperturbed exchanges (estimated to be those prior to 1750) among oceans, atmosphere and land are shown by the black arrows. The gross natural fluxes between the terrestrial biosphere and the atmosphere and between the oceans and the atmosphere are (circa 1995) about 120 and 90 GtC yr^{-1}, respectively. Just under 1 GtC yr^{-1} of carbon is transported from the land to the oceans via rivers either dissolved or as suspended particles (e.g., Richey, 2004). While these fluxes vary from year to year, they are approximately in balance when averaged over longer time periods. Additional small natural fluxes that are important on longer geological time scales include conversion of labile organic matter from terrestrial plants into inert organic carbon in soils, rock weathering and sediment accumulation ('reverse weathering'), and release from volcanic activity. The net fluxes in the 10 kyr prior to 1750, when averaged over decades or longer, are assumed to have been less than about 0.1 GtC yr^{-1}. For more background on the carbon cycle, see Prentice et al. (2001), Field and Raupach (2004) and Sarmiento and Gruber (2006).

7.3.1.2 Perturbations of the Natural Carbon Cycle from Human Activities

The additional burden of CO_2 added to the atmosphere by human activities, often referred to as 'anthropogenic CO_2' leads to the current 'perturbed' global carbon cycle. Figure 7.3 shows that these 'anthropogenic emissions' consist of two fractions: (i) CO_2 from fossil fuel burning and cement production, newly released from hundreds of millions of years of geological storage (see Section 2.3) and (ii) CO_2 from deforestation and agricultural development, which has been stored for decades to centuries. Mass balance estimates and studies with other gases indicate that the net land-atmosphere and ocean-atmosphere fluxes have become significantly different from zero, as indicated by the red arrows in Figure 7.3 (see also Section 7.3.2). Although the anthropogenic fluxes of CO_2 between the atmosphere and both the land and ocean are just a few percent of the gross natural fluxes, they have resulted in measurable changes in the carbon content of the reservoirs since pre-industrial times as shown in red. These perturbations to the natural carbon cycle are the dominant driver of climate change because of their persistent effect on the atmosphere. Consistent with the response function to a CO_2 pulse from the Bern Carbon Cycle Model (see footnote (a) of Table 2.14), about 50% of an increase in atmospheric CO_2 will be removed within 30 years, a further 30% will be removed within a few centuries and the remaining 20% may remain in the atmosphere for many thousands of years (Prentice et al., 2001; Archer, 2005; see also Sections 7.3.4.2 and 10.4)

About 80% of anthropogenic CO_2 emissions during the 1990s resulted from fossil fuel burning, with about 20% from land use

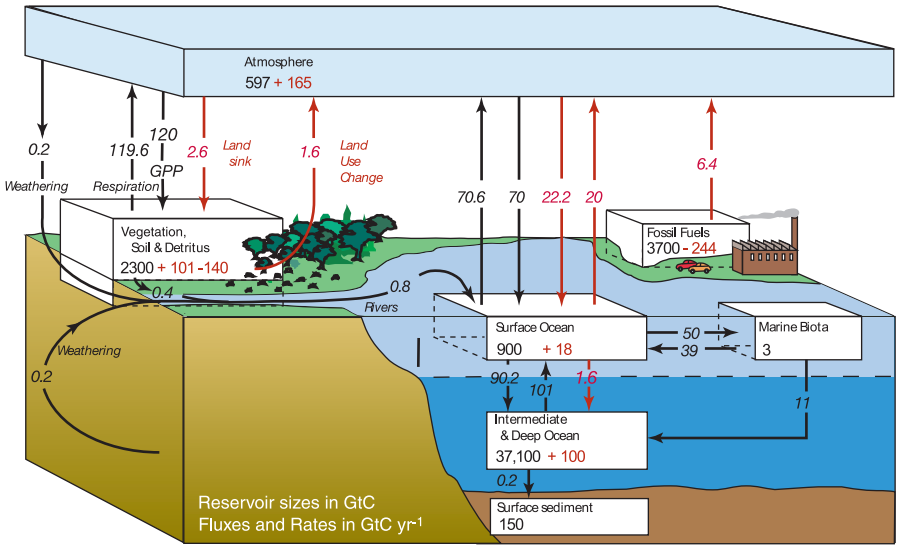


Figure 7.3. *The global carbon cycle for the 1990s, showing the main annual fluxes in GtC yr^{-1}: pre-industrial 'natural' fluxes in black and 'anthropogenic' fluxes in red (modified from Sarmiento and Gruber, 2006, with changes in pool sizes from Sabine et al., 2004a). The net terrestrial loss of –39 GtC is inferred from cumulative fossil fuel emissions minus atmospheric increase minus ocean storage. The loss of –140 GtC from the 'vegetation, soil and detritus' compartment represents the cumulative emissions from land use change (Houghton, 2003), and requires a terrestrial biosphere sink of 101 GtC (in Sabine et al., given only as ranges of –140 to –80 GtC and 61 to 141 GtC, respectively; other uncertainties given in their Table 1). Net anthropogenic exchanges with the atmosphere are from Column 5 'AR4' in Table 7.1. Gross fluxes generally have uncertainties of more than ±20% but fractional amounts have been retained to achieve overall balance when including estimates in fractions of GtC yr^{-1} for riverine transport, weathering, deep ocean burial, etc. 'GPP' is annual gross (terrestrial) primary production. Atmospheric carbon content and all cumulative fluxes since 1750 are as of end 1994.*

change (primarily deforestation) (Table 7.1). Almost 45% of combined anthropogenic CO_2 emissions (fossil fuel plus land use) have remained in the atmosphere. Oceans are estimated to have taken up approximately 30% (about 118 ± 19 GtC: Sabine et al., 2004a; Figure 7.3), an amount that can be accounted for by increased atmospheric concentration of CO_2 without any change in ocean circulation or biology. Terrestrial ecosystems have taken up the rest through growth of replacement vegetation on cleared land, land management practices and the fertilizing effects of elevated CO_2 and N deposition (see Section 7.3.3).

Because CO_2 does not limit photosynthesis significantly in the ocean, the biological pump does not take up and store anthropogenic carbon directly. Rather, marine biological cycling of carbon may undergo changes due to high CO_2 concentrations, via feedbacks in response to a changing climate. The speed with which anthropogenic CO_2 is taken up effectively by the ocean, however, depends on how quickly surface waters are transported and mixed into the intermediate and deep layers of the ocean. A considerable amount of anthropogenic CO_2 can be buffered or neutralized by dissolution of $CaCO_3$ from surface sediments in the deep sea, but this process requires many thousands of years.

The increase in the atmospheric CO_2 concentration relative to the emissions from fossil fuels and cement production only is defined here as the 'airborne fraction'.[2] Land emissions, although significant, are not included in this definition due to the difficulty of quantifying their contribution, and to the complication that much land emission from logging and clearing of forests may be compensated a few years later by uptake associated with regrowth. The 'airborne fraction of total emissions' is thus defined as the atmospheric CO_2 increase as a fraction of total anthropogenic CO_2 emissions, including the net land use fluxes. The airborne fraction varies from year to year mainly due to the effect of interannual variability in land uptake (see Section 7.3.2).

7.3.1.3 New Developments in Knowledge of the Carbon Cycle Since the Third Assessment Report

Sections 7.3.2 to 7.3.5 describe where knowledge and understanding have advanced significantly since the Third Assessment Report (TAR). In particular, the budget of anthropogenic CO_2 (shown by the red fluxes in Figure 7.3) can be calculated with improved accuracy. In the ocean, newly available high-quality data on the ocean carbon system have been used to construct robust estimates of the cumulative ocean burden of anthropogenic carbon (Sabine et al., 2004a) and associated changes in the carbonate system (Feely et al., 2004). The pH in the surface ocean is decreasing, indicating the need to understand both its interaction with a changing climate and the potential impact on organisms in the ocean (e.g., Orr et al., 2005; Royal Society, 2005). On land, there is a better understanding of the contribution to the buildup of CO_2 in the atmosphere since 1750 associated with land use and of how the land surface and the terrestrial biosphere interact with a changing climate. Globally, inverse techniques used to infer the magnitude and location of major fluxes in the global carbon

[2] This definition follows the usage of C. Keeling, distinct from that of Oeschger et al. (1980).

Table 7.1. *The global carbon budget (GtC yr^{-1}); errors represent ±1 standard deviation uncertainty estimates and not interannual variability, which is larger. The atmospheric increase (first line) results from fluxes to and from the atmosphere: positive fluxes are inputs to the atmosphere (emissions); negative fluxes are losses from the atmosphere (sinks); and numbers in parentheses are ranges. Note that the total sink of anthropogenic CO_2 is well constrained. Thus, the ocean-to-atmosphere and land-to-atmosphere fluxes are negatively correlated: if one is larger, the other must be smaller to match the total sink, and vice versa.*

	1980s		1990s		2000–2005c
	TAR	TAR revised[a]	TAR	AR4	AR4
Atmospheric Increase[b]	3.3 ± 0.1	3.3 ± 0.1	3.2 ± 0.1	3.2 ± 0.1	4.1 ± 0.1
Emissions (fossil + cement)[c]	5.4 ± 0.3	5.4 ± 0.3	6.4 ± 0.4	6.4 ± 0.4	7.2 ± 0.3
Net ocean-to-atmosphere flux[d]	–1.9 ± 0.6	–1.8 ± 0.8	–1.7 ± 0.5	–2.2 ± 0.4	–2.2 ± 0.5
Net land-to-atmosphere flux[e]	–0.2 ± 0.7	–0.3 ± 0.9	–1.4 ± 0.7	–1.0 ± 0.6	–0.9 ± 0.6
Partitioned as follows					
Land use change flux	1.7 (0.6 to 2.5)	1.4 (0.4 to 2.3)	n.a.	1.6 (0.5 to 2.7)	n.a.
Residual terrestrial sink	–1.9 (–3.8 to –0.3)	–1.7 (–3.4 to 0.2)	n.a.	–2.6 (–4.3 to –0.9)	n.a.

Notes:

[a] TAR values revised according to an ocean heat content correction for ocean oxygen fluxes (Bopp et al., 2002) and using the Fourth Assessment Report (AR4) best estimate for the land use change flux given in Table 7.2.

[b] Determined from atmospheric CO_2 measurements (Keeling and Whorf, 2005, updated by S. Piper until 2006) at Mauna Loa (19°N) and South Pole (90°S) stations, consistent with the data shown in Figure 7.4, using a conversion factor of 2.12 GtC yr^{-1} = 1 ppm.

[c] Fossil fuel and cement emission data are available only until 2003 (Marland et al., 2006). Mean emissions for 2004 and 2005 were extrapolated from energy use data with a trend of 0.2 GtC yr^{-1}.

[d] For the 1980s, the ocean-to-atmosphere and land-to-atmosphere fluxes were estimated using atmospheric O_2:N_2 and CO_2 trends, as in the TAR. For the 1990s, the ocean-to-atmosphere flux alone is estimated using ocean observations and model results (see Section 7.3.2.2.1), giving results identical to the atmospheric O_2:N_2 method (Manning and Keeling, 2006), but with less uncertainty. The net land-to-atmosphere flux then is obtained by subtracting the ocean-to-atmosphere flux from the total sink (and its errors estimated by propagation). For 2000 to 2005, the change in ocean-to-atmosphere flux was modelled (Le Quéré et al., 2005) and added to the mean ocean-to-atmosphere flux of the 1990s. The error was estimated based on the quadratic sum of the error of the mean ocean flux during the 1990s and the root mean square of the five-year variability from three inversions and one ocean model presented in Le Quéré et al. (2003).

[e] Balance of emissions due to land use change and a residual land sink. These two terms cannot be separated based on current observations.

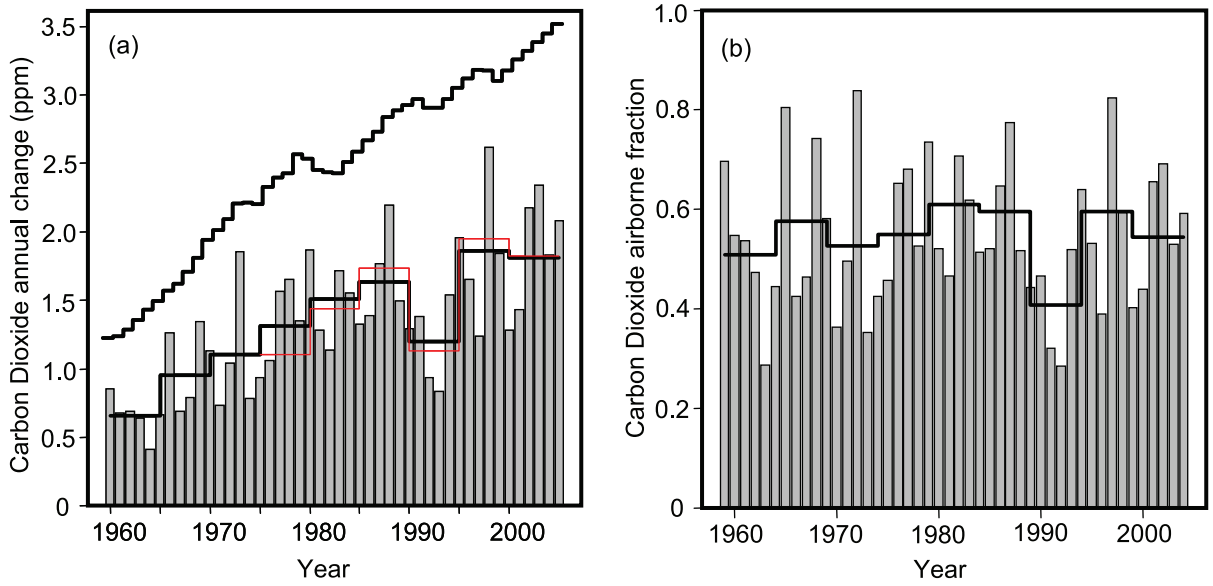


Figure 7.4. *Changes in global atmospheric CO_2 concentrations. (a) Annual (bars) and five-year mean (lower black line) changes in global CO_2 concentrations, from Scripps Institution of Oceanography observations (mean of South Pole and Mauna Loa; Keeling and Whorf, 2005, updated). The upper stepped line shows annual increases that would occur if 100% of fossil fuel emissions (Marland et al., 2006, updated as described in Chapter 2) remained in the atmosphere, and the red line shows five-year mean annual increases from National Oceanic and Atmospheric Administration (NOAA) data (mean of Samoa and Mauna Loa; Tans and Conway, 2005, updated). (b) Fraction of fossil fuel emissions remaining in the atmosphere ('airborne fraction') each year (bars), and five-year means (solid black line) (Scripps data) (mean since 1958 is 0.55). Note the anomalously low airborne fraction in the early 1990s.*

cycle have continued to mature, reflecting both refinement of the techniques and the availability of new observations. During preparation of the TAR, inclusion of the carbon cycle in climate models was new. Now, results from the first C⁴MIP are available: when the carbon cycle is included, the models consistently simulate climate feedbacks to land and ocean carbon cycles that tend to reduce uptake of CO_2 by land and ocean from 1850 to 2100 (see Section 7.3.5).

7.3.2 The Contemporary Carbon Budget

7.3.2.1 Atmospheric Increase

The atmospheric CO_2 increase is measured with great accuracy at various monitoring stations (see Chapter 2; and Keeling and Whorf, 2005 updated by S. Piper through 2006). The mean yearly increase in atmospheric CO_2 (the CO_2 'growth rate') is reported in Table 7.1. Atmospheric CO_2 has continued to increase since the TAR (Figure 7.4), and the rate of increase appears to be higher, with the average annual increment rising from 3.2 ± 0.1 GtC yr^{-1} in the 1990s to 4.1 ± 0.1 GtC yr^{-1} in the period 2000 to 2005. The annual increase represents the net effect of several processes that regulate global land-atmosphere and ocean-atmosphere fluxes, examined below. The 'airborne fraction' (atmospheric increase in CO_2 concentration/fossil fuel emissions) provides a basic benchmark for assessing short- and long-term changes in these processes. From 1959 to the present, the airborne fraction has averaged 0.55, with remarkably little variation when block-averaged into five-year bins (Figure 7.4). Thus, the terrestrial biosphere and the oceans together have consistently removed 45% of fossil CO_2 for the last 45 years, and the recent higher rate of atmospheric CO_2 increase largely reflects increased fossil fuel emissions. Year-to-year fluctuations in the airborne fraction are associated with major climatic events (see Section 7.3.2.4). The annual increase in 1998, 2.5 ppm, was the highest ever observed, but the airborne fraction (0.82) was no higher than values observed several times in prior decades. The airborne fraction dropped significantly below the average in the early 1990s, and preliminary data suggest it may have risen above the average in 2000 to 2005.

The inter-hemispheric gradient of CO_2 provides additional evidence that the increase in atmospheric CO_2 is caused primarily by NH sources. The excess atmospheric CO_2 in the NH compared with the Southern Hemisphere (SH), $\Delta CO_2^{N\text{-}S}$, has increased in proportion to fossil fuel emission rates (which are predominantly in the NH) at about 0.5 ppm per (GtC yr^{-1}) (Figure 7.5). The intercept of the best-fit line indicates that, without anthropogenic emissions, atmospheric CO_2 would be 0.8 ppm higher in the SH than in the NH, presumably due to transport of CO_2 by the ocean circulation. The consistency of the airborne fraction and the relationship between $\Delta CO_2^{N\text{-}S}$ and fossil fuel emissions suggest broad consistency in the functioning of the carbon cycle over the period. There are interannual fluctuations in $\Delta CO_2^{N\text{-}S}$ as large as ±0.4 ppm, at least some of which may be attributed to changes in atmospheric circulation (Dargaville et al., 2000), while others may be due to shifts in sources and sinks, such as large forest fires.

7.3.2.1.1 Fossil fuel and cement emissions

Fossil fuel and cement emissions rose from 5.4 ± 0.3 GtC yr^{-1} in the 1980s to 6.4 ± 0.4 GtC yr^{-1} in the 1990s (Marland et al., 2006). They have continued to increase between the 1990s and 2000 to 2005, climbing to 7.2 ± 0.3 GtC yr^{-1}. These numbers are estimated based upon international energy statistics for the 1980 to 2003 period (Marland et al., 2006) with extrapolated trends for 2004 to 2005 (see Table 7.1). The error (±1 standard deviation) for fossil fuel and cement emissions is of the order of 5% globally. Cement emissions are small compared with fossil fuel emissions (roughly 3% of the total).

7.3.2.1.2 Land use change

During the past two decades, the CO_2 flux caused by land use changes has been dominated by tropical deforestation. Agriculture and exploitation of forest resources have reached into formerly remote areas of old growth forest in the tropics, in contrast to mid-latitudes where exploitation previously eliminated most old growth forests. The land use change fluxes reported in this section include explicitly some accumulation of carbon by regrowing vegetation (e.g., Houghton et al., 2000). In the TAR, the global land use flux, adapted from Houghton (1999), was estimated to be 1.7 (0.6–2.5) GtC yr^{-1} for the 1980s. No estimate was available at the time for the 1990s. This estimate is based on a 'bookkeeping' carbon model prescribed with deforestation statistics (Houghton, 1999). A markedly lower estimate of the land use flux in the 1980s (Table 7.2) was obtained by McGuire et al. (2001) from four process-driven

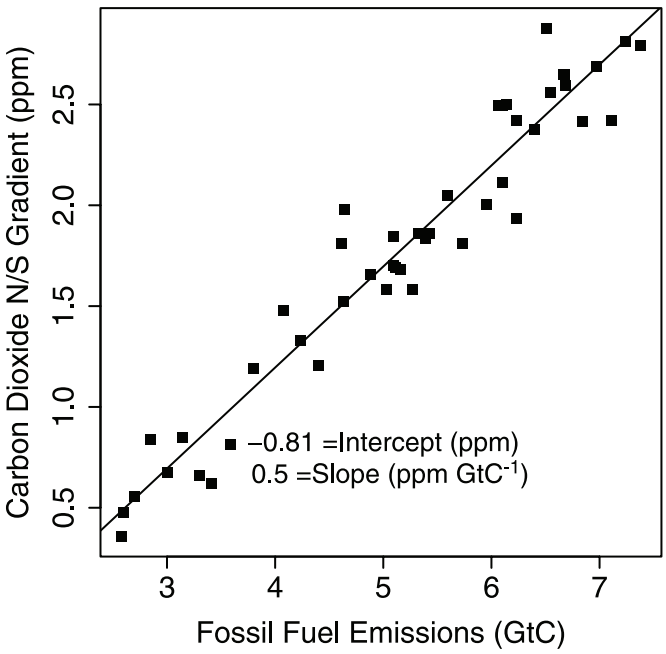


Figure 7.5. *The difference between CO_2 concentration in the NH and SH (y axis), computed as the difference between annual mean concentrations (ppm) at Mauna Loa and the South Pole (Keeling and Whorf, 2005, updated), compared with annual fossil fuel emissions (x axis; GtC; Marland, et al., 2006), with a line showing the best fit. The observations show that the north-south difference in CO_2 increases proportionally with fossil fuel use, verifying the global impact of human-caused emissions.*

terrestrial carbon models, prescribed with changes in cropland area from Ramankutty and Foley (1999). The higher land use emissions of Houghton (2003a) may reflect both the additional inclusion of conversion of forest to pasture and the use of a larger cropland expansion rate than the one of Ramankutty and Foley (1999), as noted by Jain and Yang (2005). Houghton (2003a) updated the land use flux to 2.0 ± 0.8 GtC yr^{-1} for the 1980s and 2.2 ± 0.8 GtC yr^{-1} for the 1990s (see Table 7.2). This update gives higher carbon losses from tropical deforestation than those in the TAR (Houghton 2003b).

In addition, DeFries et al. (2002) estimated a tropical land use flux of 0.7 (0.4–1.0) GtC yr^{-1} for the 1980s and 1.0 (0.5–1.6) GtC yr^{-1} for the 1990s, using the same bookkeeping approach as Houghton (1999) but driven by remotely sensed data on deforested areas. A similar estimate was independently produced by Achard et al. (2004) for the 1990s, also based on remote sensing. These different land use emissions estimates are reported in Table 7.2. Although the two recent satellite-based estimates point to a smaller source than that of Houghton (2003a), it is premature to say that Houghton's numbers are overestimated. The land use carbon source has the largest uncertainties in the global carbon budget. If a high value for the land use source is adopted in the global budget, then the residual land uptake over undisturbed ecosystems should be a large sink, and vice versa. For evaluating the global carbon budget, the mean of DeFries et al. (2002) and Houghton (2003a), which both cover the 1980s and the 1990s (Table 7.2), was chosen and the full range of uncertainty is reported. The fraction of carbon emitted by fossil fuel burning, cement production and land use changes that does not accumulate in the atmosphere must be taken up by land ecosystems and by the oceans.

Table 7.2. *Land to atmosphere emissions resulting from land use changes during the 1990s and the 1980s (GtC yr^{-1}). The Fourth Assessment Report (AR4) estimates used in the global carbon budget (Table 7.1) are shown in bold. Positive values indicate carbon losses from land ecosystems. Uncertainties are reported as ±1 standard deviation. Numbers in parentheses are ranges of uncertainty.*

	Tropical Americas	Tropical Africa	Tropical Asia	Pan-Tropical	Non-tropics	Total Globe
1990s						
Houghton (2003a)[a]	0.8 ± 0.3	0.4 ± 0.2	1.1 ± 0.5	2.2 ± 0.6	–0.02 ± 0.5	2.2 ± 0.8
DeFries et al. (2002)[b]	0.5 (0.2 to 0.7)	0.1 (0.1 to 0.2)	0.4 (0.2 to 0.6)	1.0 (0.5 to 1.6)	n.a.	n.a.
Achard et al. (2004)[c]	0.3 (0.3 to 0.4)	0.2 (0.1 to 0.2)	0.4 (0.3 to 0.5)	0.9 (0.5 to 1.4)	n.a.	n.a.
AR4[d]	0.7 (0.4 to 0.9)	0.3 (0.2 to 0.4)	0.8 (0.4 to 1.1)	1.6 (1.0 to 2.2)	–0.02 (–0.5 to +0.5)	**1.6 (0.5 to 2.7)**
1980s						
Houghton (2003a)[a]	0.8 ± 0.3	0.3 ± 0.2	0.9 ± 0.5	1.9 ± 0.6	0.06 ± 0.5	2.0 ± 0.8
DeFries et al. (2002)[b]	0.4 (0.2 to 0.5)	0.1 (0.08 to 0.14)	0.2 (0.1 to 0.3)	0.7 (0.4 to 1.0)	n.a.	n.a.
McGuire et al. (2001)[e]				0.6 to 1.2	–0.1 to +0.4	(0.6 to 1.0)
Jain and Yang (2005)[f]	0.22 to 0.24	0.08 to 0.48	0.58 to 0.34	-	-	1.33 to 2.06
TAR[g]						1.7 (0.6 to 2.5)
AR4[d]	0.6 (0.3 to 0.8)	0.2 (0.1 to 0.3)	0.6 (0.3 to 0.9)	1.3 (0.9 to 1.8)	0.06 (–0.4 to +0.6)	**1.4 (0.4 to 2.3)**

Notes:

[a] His Table 2.

[b] Their Table 3.

[c] Their Table 2 for mean estimates with the range indicated in parentheses corresponding to their reported minimum and maximum estimates.

[d] Best estimate calculated from the mean of Houghton (2003a) and DeFries et al. (2002), the only two studies covering both the 1980s and the 1990s. For non-tropical regions where DeFries et al. have no estimate, Houghton has been used.

[e] Their Table 5; range is obtained from four terrestrial carbon models.

[f] The range indicated in parentheses corresponds to two simulations using the same model, but forced with different land cover change datasets from Houghton (2003a) and DeFries et al. (2002).

[g] In the TAR estimate, no values were available for the 1990s.

7.3.2.2 Uptake of CO_2 by Natural Reservoirs and Global Carbon Budget

7.3.2.2.1 Ocean-atmosphere flux

To assess the mean ocean sink, seven methods have been used. The methods are based on: (1) observations of the partial pressure of CO_2 at the ocean surface and gas-exchange estimates (Takahashi et al., 2002); (2) atmospheric inversions based upon diverse observations of atmospheric CO_2 and atmospheric transport modelling (see Section 7.2.3.4); (3) observations of carbon, oxygen, nutrients and chlorofluorocarbons (CFCs) in seawater, from which the concentration of anthropogenic CO_2 is estimated (Sabine et al., 2004a) combined with estimates of oceanic transport (Gloor et al., 2003; Mikaloff Fletcher et al., 2006); (4) estimates of the distribution of water age based on CFC observations combined with the atmospheric CO_2 history (McNeil et al., 2003); (5) the simultaneous observations of the increase in atmospheric CO_2 and decrease in atmospheric O_2 (Manning and Keeling, 2006); (6) various methods using observations of change in ^{13}C in the atmosphere (Ciais et al., 1995) or the oceans (Gruber and Keeling, 2001; Quay et al., 2003); and (7) ocean General Circulation Models (Orr et al., 2001). The ocean uptake estimates obtained with methods (1) and (2) include in part a flux component due to the outgassing of river-supplied inorganic and organic carbon (Sarmiento and Sundquist, 1992). The magnitude of this necessary correction to obtain the oceanic uptake flux of anthropogenic CO_2 is not well known, as these estimates pertain to the open ocean, whereas a substantial fraction of the river-induced outgassing likely occurs in coastal regions. These estimates of the net oceanic sink are shown in Figure 7.3.

With these corrections, estimates from all methods are consistent, resulting in a well-constrained global oceanic sink for anthropogenic CO_2 (see Table 7.1). The uncertainty around the different estimates is more difficult to judge and varies considerably with the method. Four estimates appear better constrained than the others. The estimate for the ocean uptake of atmospheric CO_2 of -2.2 ± 0.5 GtC yr^{-1} centred around 1998 based on the atmospheric O_2/N_2 ratio needs to be corrected for the oceanic O_2 changes (Manning and Keeling, 2006). The estimate of -2.0 ± 0.4 GtC yr^{-1} centred around 1995 based on CFC observations provides a constraint from observed physical transport in the ocean. These estimates of the ocean sink are shown in Figure 7.6. The mean estimates of -2.2 ± 0.25 and -2.2 ± 0.2 GtC yr^{-1} centred around 1995 and 1994 provide constraints based on a large number of ocean carbon observations. These well-constrained estimates all point to a decadal mean ocean CO_2 sink of -2.2 ± 0.4 GtC yr^{-1} centred around 1996, where the uncertainty is the root mean square of all errors. See Section 5.4 for a discussion of changes in the ocean CO_2 sink.

7.3.2.2.2 Land-atmosphere flux

The land-atmosphere CO_2 flux is the sum of the land use change CO_2 flux (see Section 7.3.2.1) plus sources and sinks due for instance to legacies of prior land use, climate, rising CO_2 or N deposition (see Section 7.3.3 for a review of processes). For assessing the global land-atmosphere flux, more than just direct terrestrial observations must be used, because observations of land ecosystem carbon fluxes are too sparse and the ecosystems are too heterogeneous to allow global assessment of the net land flux with sufficient accuracy. For instance, large-scale biomass inventories (Goodale et al., 2002; UN-ECE/FAO, 2000) are limited to forests with commercial value, and they do not adequately survey tropical forests. Direct flux observations by the eddy covariance technique are only available at point locations, most do not yet have long-term coverage and they require considerable upscaling to obtain global estimates (Baldocchi et al., 2001). As a result, two methods can be used to quantify the net global land-atmosphere flux: (1) deducing that quantity as a residual between the fossil fuel and cement emissions and the sum of ocean uptake and atmospheric increase (Table 7.1), or (2) inferring the land-atmosphere flux simultaneously with the ocean sink by inverse analysis or mass balance computations using atmospheric CO_2 data, with terrestrial and marine processes distinguished using O_2/N_2 and/or ^{13}C observations. Individual estimates of the land-atmosphere flux deduced using either method 1 or method 2

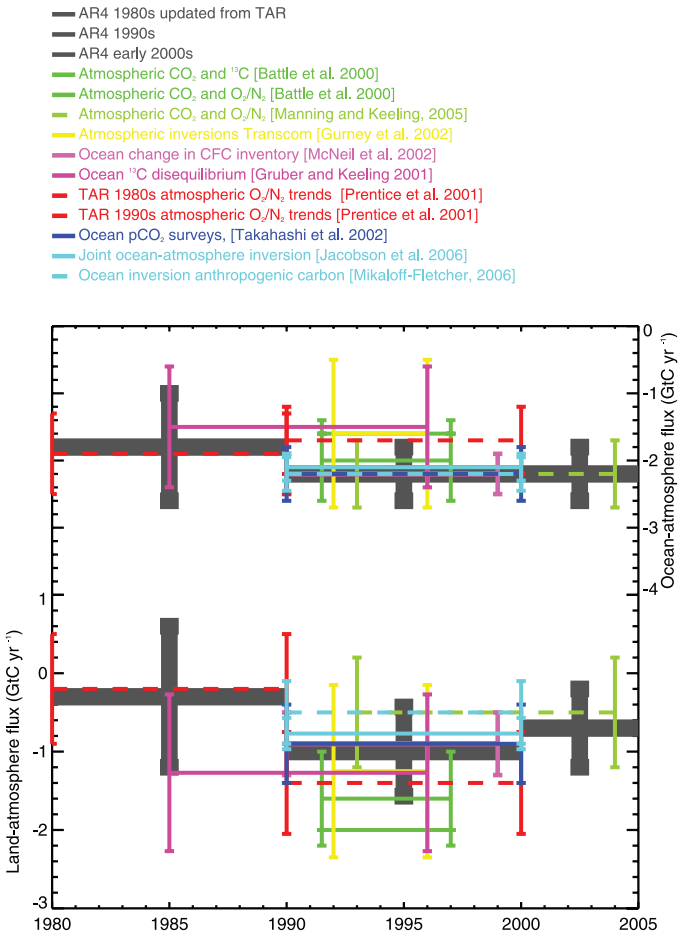


Figure 7.6. *Individual estimates of the ocean-atmosphere flux reported in Chapter 5 and of the related land-atmosphere flux required to close the global carbon budget. The dark thick lines are the revised budget estimates in the AR4 for the 1980s, the 1990s and the early 2000s, respectively.*

are shown in Figure 7.6. Method 2 was used in the TAR, based upon O_2/N_2 data (Langenfelds et al., 1999; Battle et al., 2000). Corrections have been made to the results of method 2 to account for the effects of thermal O_2 fluxes by the ocean (Le Quéré et al., 2003). This chapter includes these corrections to update the 1980s budget, resulting in a land net flux of –0.3 ± 0.9 GtC yr^{-1} during the 1980s. For the 1990s and after, method 1 was adopted for assessing the ocean sink and the land-atmosphere flux. Unlike in the TAR, method 1 is preferred for the 1990s and thereafter (i.e., estimating first the ocean uptake, and then deducing the land net flux) because the ocean uptake is now more robustly determined by various oceanographic approaches (see 7.3.2.2.1) than by the atmospheric O_2 trends. The numbers are reported in Table 7.1. The land-atmosphere flux evolved from a small sink in the 1980s of –0.3 ± 0.9 GtC yr^{-1} to a large sink during the 1990s of –1.0 ± 0.6 GtC yr^{-1}, and returned to an intermediate value of –0.9 ± 0.6 GtC yr^{-1} over the past five years. A recent weakening of the land-atmosphere uptake has also been suggested by other independent studies of the flux variability over the past decades (Jones and Cox, 2005). The global CO_2 budget is summarised in Table 7.1.

7.3.2.2.3 Residual land sink

In the context of land use change, deforestation dominates over forest regrowth (see Section 7.3.2.1), and the observed net uptake of CO_2 by the land biosphere implies that there must be an uptake by terrestrial ecosystems elsewhere, called the 'residual land sink' (formerly the 'missing sink'). Estimates of the residual land sink necessarily depend on the land use change flux, and its uncertainty reflects predominantly the (large) errors associated with the land use change term. With the high land use source of Houghton (2003a), the residual land sink equals –2.3 (–4.0 to –0.3) and –3.2 (–4.5 to –1.9) GtC yr^{-1} respectively for the 1980s and the 1990s. With the smaller land use source of DeFries et al. (2002), the residual land sink is –0.9 (–2.0 to –0.3) and –1.9 (–2.9 to –1.0) GtC yr^{-1} for the 1980s and the 1990s. Using the mean value of the land use source from Houghton (2003a) and DeFries et al. (2002) as reported in Table 7.2, a mean residual land sink of –1.7 (–3.4 to 0.2) and –2.6 (–4.3 to –0.9) GtC yr^{-1} for the 1980s and 1990s respectively is obtained. Houghton (2003a) and DeFries et al. (2002) give different estimates of the land use source, but they robustly indicate that deforestation emissions were 0.2 to 0.3 GtC yr^{-1} higher in the 1990s than in the 1980s (see Table 7.2). To compensate for that increase and to match the larger land-atmosphere uptake during the 1990s, the inferred residual land sink must have increased by 1 GtC yr^{-1} between the 1980s and the 1990s. This finding is insensitive to the method used to determine the land use flux, and shows considerable decadal variability in the residual land sink.

7.3.2.2.4 Undisturbed tropical forests: are they a carbon dioxide sink?

Despite expanding areas of deforestation and degradation, there are still large areas of tropical forests that are among the world's great wilderness areas, with fairly light human impact, especially in Amazonia. A major uncertainty in the carbon budget relates to possible net change in the carbon stocks in these forests. Old growth tropical forests contain huge stores of organic matter, and are very dynamic, accounting for a major fraction of global net primary productivity (and about 46% of global biomass; Brown and Lugo, 1982). Changes in the carbon balance of these regions could have significant effects on global CO_2.

Recent studies of the carbon balance of study plots in mature, undisturbed tropical forests (Phillips et al., 1998; Baker et al., 2004) report accumulation of carbon at a mean rate of 0.7 ± 0.2 MgC ha^{-1} yr^{-1}, implying net carbon uptake into global Neotropical biomass of 0.6 ± 0.3 GtC yr^{-1}. An intriguing possibility is that rising CO_2 levels could stimulate this uptake by accelerating photosynthesis, with ecosystem respiration lagging behind. Atmospheric CO_2 concentration has increased by about 1.5 ppm (0.4%) yr^{-1}, suggesting incremental stimulation of photosynthesis of about 0.25% (e.g., next year's photosynthesis should be 1.0025 times this year's) (Lin et al., 1999; Farquhar et al., 2001). For a mean turnover rate of about 10 years for organic matter in tropical forests, the present imbalance between uptake of CO_2 and respiration might be 2.5% (1.0025^{10}), consistent with the reported rates of live biomass increase (~3%).

But the recent pan-tropical warming, about 0.26°C per decade (Malhi and Wright, 2004), could increase water stress and respiration, and stimulation by CO_2 might be limited by nutrients (Chambers and Silver, 2004; Koerner, 2004; Lewis et al., 2005; see below), architectural constraints on how much biomass a forest can hold, light competition, or ecological shifts favouring short lived trees or agents of disturbance (insects, lianas) (Koerner, 2004). Indeed, Baker et al. (2004) note higher mortality rates and increased prevalence of lianas, and, since dead organic pools were not measured, effects of increased disturbance may give the opposite sign of the imbalance inferred from live biomass only (see, e.g., Rice et al., 2004). Methodological bias associated with small plots, which under-sample natural disturbance and recovery, might also lead to erroneous inference of net growth (Koerner, 2004). Indeed, studies involving large-area plots (9–50 ha) have indicated either no net long-term change or a long-term net decline in above ground live biomass (Chave et al., 2003; Baker et al., 2004; Clark, 2004; Laurance et al., 2004), and a five-year study of a 20 ha plot in Tapajos, Brazil show increasing live biomass offset by decaying necromass (Fearnside, 2000; Saleska et al., 2003).

Koerner (2004) argues that accurate assessment of trends in forest carbon balance requires long-term monitoring of many replicate plots or very large plots; lacking these studies, the net carbon balance of undisturbed tropical forests cannot be authoritatively assessed based on *in situ* studies. If the results from the plots are extrapolated for illustration, the mean above ground carbon sink would be 0.89 ± 0.32 MgC ha^{-1} yr^{-1} (Baker et al., 2004), or 0.54 ± 0.19 GtC yr^{-1} (Malhi and Phillips 2004) extrapolated to all Neotropical moist forest area (6.0×10^6 km^2). If the uncompiled data from the African and Asian tropics (50% of global moist tropical forest area) were to show a similar trend, the associated tropical live biomass sink would be about

1.2 ± 0.4 GtC yr^{-1}, close to balancing the net source due to deforestation inferred by DeFries et al. (2002) and Achard et al. (2004) (Table 7.2).

7.3.2.2.5 New findings on the carbon budget

The revised carbon budget in Table 7.1 shows new estimates of two key numbers. First, the flux of CO_2 released to the atmosphere from land use change is estimated to be 1.6 (0.5 to 2.7) GtC yr^{-1} for the 1990s. A revision of the TAR estimate for the 1980s (see TAR, Chapter 3) downwards to 1.4 (0.4 to 2.3) GtC yr^{-1} suggests little change between the 1980s and 1990s, but there continues to be considerable uncertainty in these estimates. Second, the net residual terrestrial sink seems to have been larger in the 1990s than in the periods before and after. Thus, a transient increase in terrestrial uptake during the 1990s explains the lower airborne fraction observed during that period. The ocean uptake has increased by 22% between the 1980s and the 1990s, but the fraction of emissions (fossil plus land use) taken up by the ocean has remained constant.

7.3.2.3 Regional Fluxes

Quantifying present-day regional carbon sources and sinks and understanding the underlying carbon mechanisms are needed to inform policy decisions. Furthermore, by analysing spatial and temporal detail, mechanisms can be isolated.

7.3.2.3.1 The top-down view: atmospheric inversions

The atmosphere mixes and integrates surface fluxes that vary spatially and temporally. The distribution of regional fluxes over land and oceans can be retrieved using observations of atmospheric CO_2 and related tracers within models of atmospheric transport. This is called the 'top-down' approach to estimating fluxes. Atmospheric inversions belong to that approach, and determine an optimal set of fluxes that minimise the mismatch between modelled and observed concentrations, accounting for measurement and model errors. Fossil fuel emissions have small uncertainties that are often ignored and, when considered (e.g., Enting et al., 1995; Rodenbeck et al., 2003a), are found to have little influence on the inversion. Fossil fuel emissions are generally considered perfectly known in inversions, so that their effect can be easily modelled and subtracted from atmospheric CO_2 data to solve for regional land-atmosphere and ocean-atmosphere fluxes, although making such an assumption biases the results (Gurney et al., 2005). Input data for inversions come from a global network of about 100 CO_2 concentration measurement sites,[3] with mostly discrete flask sampling, and a smaller number of *in situ* continuous measurement sites. Generally, regional fluxes derived from inverse models have smaller uncertainties upwind of regions with denser data coverage. Measurement and modelling errors and uneven and sparse coverage of the network generate random errors in inversion results. In addition, inverse methodological details, such as the choice of transport model, can introduce systematic errors. A number of new inversion ensembles, with different methodological details, have been produced since the TAR (Gurney et al., 2003; Rödenbeck et al., 2003a,b; Peylin et al., 2005; Baker et al., 2006). Generally, confidence in the long-term mean inverted regional fluxes is lower than confidence in the year-to-year anomalies (see Section 7.3.2.4). For individual regions, continents or ocean basins, the errors of inversions increase and the significance can be lost. Because of this, Figure 7.7 reports the oceans and land fluxes aggregated into large latitude bands, as well as a breakdown of five land and ocean regions in the NH, which is constrained by denser atmospheric stations. Both random and systematic errors are reported in Figure 7.7.

7.3.2.3.2 The bottom-up view: land and ocean observations and models

The range of carbon flux and inventory data enables quantification of the distribution and variability of CO_2 fluxes between the Earth's surface and the atmosphere. This is called the 'bottom-up' approach. The fluxes can be determined by measuring carbon stock changes at repeated intervals, from which time-integrated fluxes can be deduced, or by direct observations of the fluxes. The stock change approach includes basin-scale *in situ* measurements of dissolved and particulate organic and inorganic carbon or tracers in the ocean (e.g., Sabine et al., 2004a), extensive forest biomass inventories (e.g., UN-ECE/FAO, 2000; Fang et al., 2001; Goodale et al., 2002; Nabuurs et al., 2003; Shvidenko and Nilsson, 2003) and soil carbon inventories and models (e.g., Ogle et al., 2003; Bellamy et al., 2005; van Wesemael et al., 2005; Falloon et al., 2006). The direct flux measurement approach includes surveys of ocean CO_2 partial pressure (pCO_2) from ship-based measurements, drifters and time series (e.g., Lefèvre et al., 1999; Takahashi et al., 2002), and ecosystem flux measurements via eddy covariance flux networks (e.g., Valentini et al., 2000; Baldocchi et al., 2001).

The air-sea CO_2 fluxes consist of a superposition of natural and anthropogenic CO_2 fluxes, with the former being globally nearly balanced (except for a small net outgassing associated with the input of carbon by rivers). Takahashi et al. (2002) present both surface ocean pCO_2 and estimated atmosphere-ocean CO_2 fluxes (used as prior knowledge in many atmospheric inversions) normalised to 1995 using National Centers for Environmental Prediction (NCEP)/National Center for Atmospheric Research (NCAR) 41-year mean monthly winds. Large annual CO_2 fluxes to the ocean occur in the Southern Ocean subpolar regions (40°S–60°S), in the North Atlantic poleward of 30°N and in the North Pacific poleward of 30°N (see Figure 7.8). Ocean inversions calculate natural and anthropogenic air-sea fluxes (Gloor et al., 2003; Mikaloff Fletcher et al., 2006), by optimising ocean carbon model results against vertical profiles of DIC data. These studies indicate that the Southern Ocean is the largest sink of anthropogenic CO_2, together with mid- to high-latitude regions in the North Atlantic. This is consistent with global ocean hydrographic surveys (Sabine et al., 2004a

[3] Data can be accessed for instance via the World Data Centre for Greenhouse Gases (http://gaw.kishou.go.jp/wdcgg.html) or the NOAA ESRL Global Monitoring Division (http://www.cmdl.noaa.gov/ccgg/index.html)

and Figure 5.10). However, only half of the anthropogenic CO_2 absorbed by the Southern Ocean is stored there, due to strong northward transport (Mikaloff Fletcher et al., 2006). The tropical Pacific is a broad area of natural CO_2 outgassing to the atmosphere, but this region is a sink of anthropogenic CO_2.

Models are used to extrapolate flux observations into regional estimates, using remote-sensing properties and knowledge of the processes controlling the CO_2 fluxes and their variability. Rayner et al. (2005) use inverse process-based models, where observations are 'assimilated' to infer optimised fluxes. Since the TAR, the global air-sea flux synthesis has been updated (Takahashi et al., 2002 and Figure 7.8), and new syntheses have been made of continental-scale carbon budgets of the NH continents (Pacala et al., 2001; Goodale et al., 2002; Janssens et al., 2003; Shvidenko and Nilsson, 2003; Ciais et al., 2005a), and of tropical forests (Malhi and Grace, 2000). These estimates are shown in Figure 7.7 and compared with inversion results.

Comparing bottom-up regional fluxes with inversion results is not straightforward because: (1) inversion fluxes may contain a certain amount of prior knowledge of bottom-up fluxes so that the two approaches are not fully independent; (2) the time period for which inversion models and bottom-up estimates are compared is often not consistent, in the presence of interannual variations in fluxes[4] (see Section 7.3.2.4); and (3) inversions of CO_2 data produce estimates of CO_2 fluxes, so the results will differ from budgets for carbon fluxes (due to the emission of reduced carbon compounds that get oxidized into CO_2 in the atmosphere and are subject to transport and chemistry) and carbon storage changes (due to lateral carbon transport, e.g., by rivers) (Sarmiento and Sundquist, 1992). Some of these effects can be included by 'off-line' conversion of inversion results (Enting and Mansbridge, 1991; Suntharalingam et al., 2005). Reduced carbon compounds such as volatile organic compounds (VOCs), carbon monoxide (CO) and CH_4 emitted by ecosystems and human activities are transported and oxidized into CO_2 in the atmosphere (Folberth et al., 2005). Trade of forest and crop products displaces carbon from ecosystems (Imhoff et al., 2004). Rivers displace dissolved and particulate inorganic and organic carbon from land to ocean (e.g., Aumont et al., 2001). A summary of the main results of inversion and bottom-up estimates of regional CO_2 fluxes is given below.

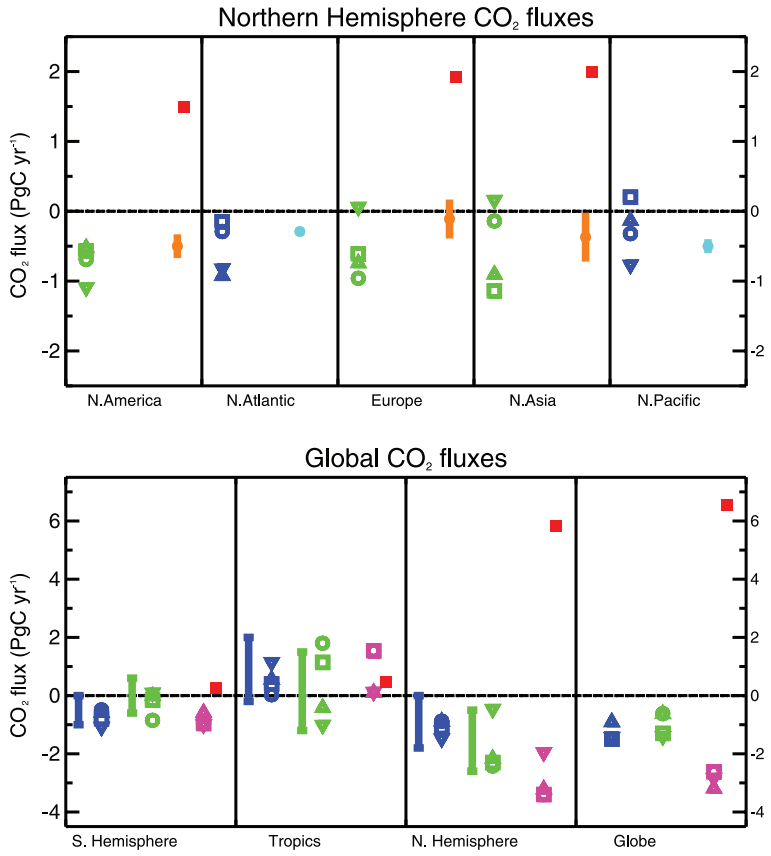


Figure 7.7. *Regional ocean-atmosphere and land-atmosphere CO_2 fluxes for the NH (top) and the globe (bottom) from inversion ensembles and bottom-up studies. Fluxes to the atmosphere are positive and uptake has a negative sign. Inversion results all correspond to the post-Pinatubo period 1992 to 1996. Orange: Bottom-up terrestrial fluxes from Pacala et al. (2001) and Kurz and Apps (1999) for North America, from Janssens et al. (2003) for Europe and from Shvidenko and Nilsson (2003) plus Fang et al. (2001) for North Asia (Asian Russia and China). Cyan (filled circles): Bottom-up ocean flux estimates from Takahashi, et al. (2002). Blue: ocean fluxes from atmospheric inversions. Green: terrestrial fluxes from inversion models. Magenta: total inversion fluxes. Red: fossil fuel emissions. The mean flux of different inversion ensembles is reported. Inversion errors for regional fluxes are not reported here; their values usually range between 0.5 and 1 GtC yr^{-1}. Error bar: range of atmospheric inversion fluxes from the TAR. Squares: Gurney et al. (2002) inversions using annual mean CO_2 observations and 16 transport models. Circles: Gurney et al. (2003) inversions using monthly CO_2 observations and 13 transport models. Triangles: Peylin et al. (2005) inversions with three transport models, three regional breakdowns and three inversion settings. Inverted triangles: Rödenbeck et al. (2003a) inversions where the fluxes are solved on the model grid using monthly flask data.*

7.3.2.3.3 *Robust findings of regional land-atmosphere flux*

- Tropical lands are found in inversions to be either carbon neutral or sink regions, despite widespread deforestation, as is apparent in Figure 7.7, where emissions from land include deforestation. This implies carbon uptake by undisturbed tropical ecosystems, in agreement with limited forest inventory data in the Amazon (Phillips et al., 1998; Malhi and Grace, 2000).
- Inversions place a substantial land carbon sink in the NH. The inversion estimate is –1.7 (–0.4 to –2.3) GtC yr^{-1} (from data in Figure 7.7). A bottom-up value of the NH land sink of –0.98 (–0.38 to –1.6) GtC yr^{-1} was also estimated,

[4] For instance, the chosen 1992 to 1996 time period for assessing inversion fluxes, dictated by the availability of the Atmospheric Tracer Transport Model Intercomparison Project (TransCom 3) intercomparison results (Gurney et al., 2002, 2003, 2004), corresponds to a low growth rate and to a stronger terrestrial carbon sink, likely due to the eruption of Mt. Pinatubo.

based upon regional synthesis studies (Kurz and Apps, 1999; Fang et al., 2001; Pacala et al., 2001; Janssens et al., 2003; Nilsson et al., 2003; Shvidenko and Nilsson, 2003). The inversion sink value is on average higher than the bottom-up value. Part of this discrepancy could be explained by lateral transport of carbon via rivers, crop trade and emission of reduced carbon compounds.

- The longitudinal partitioning of the northern land sink between North America, Europe and Northern Asia has large uncertainties (see Figure 7.7). Inversions give a very large spread over Europe (–0.9 to +0.2 GtC yr^{-1}), and Northern Asia (–1.2 to +0.3 GtC yr^{-1}) and a large spread over North America (–0.6 to –1.1 GtC yr^{-1}). Within the uncertainties of each approach, continental-scale carbon fluxes from bottom-up and top-down methods over Europe, North America and Northern Asia are mutually consistent (Pacala et al., 2001; Janssens et al., 2003). The North American carbon sink estimated by recent inversions is on average lower than an earlier widely cited study by Fan et al. (1998). Nevertheless, the Fan et al. (1998) estimate remains within the range of inversion uncertainties. In addition, the fluxes calculated in Fan et al. (1998) coincide with the low growth rate post-Pinatubo period, and hence are not necessarily representative of long-term behaviour.

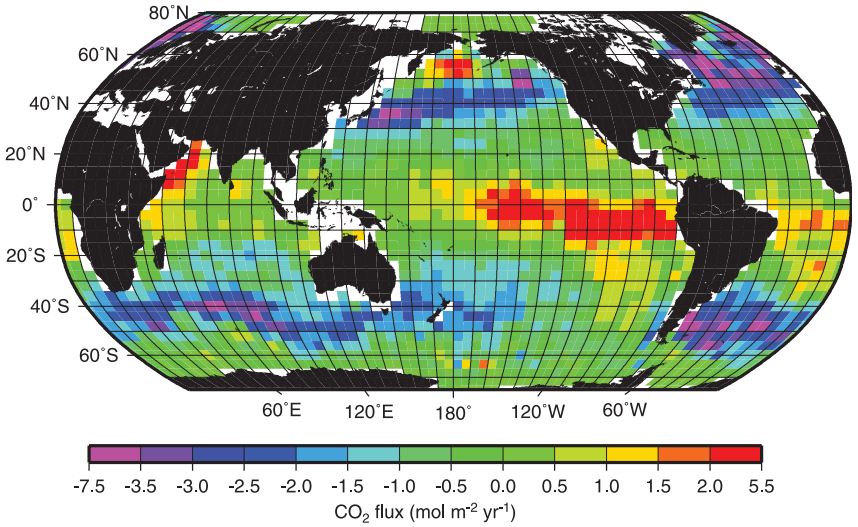


Figure 7.8. *Estimates (4° × 5°) of sea-to-air flux of CO_2, computed using 940,000 measurements of surface water pCO_2 collected since 1956 and averaged monthly, together with NCEP/NCAR 41-year mean monthly wind speeds and a (10-m wind speed)^2 dependence on the gas transfer rate (Wanninkhof, 1992). The fluxes were normalised to the year 1995 using techniques described in Takahashi et al. (2002), who used wind speeds taken at the 0.995 standard deviation level (about 40 m above the sea surface). The annual flux of CO_2 for 1995 with 10-m winds is –1.6 GtC yr^{-1}, with an approximate uncertainty (see Footnote 1) of ±1 GtC yr^{-1}, mainly due to uncertainty in the gas exchange velocity and limited data coverage. This estimated global flux consists of an uptake of anthropogenic CO_2 of –2.2 GtC yr^{-1} (see text) plus an outgassing of 0.6 GtC yr^{-1}, corresponding primarily to oxidation of organic carbon borne by rivers (Figure 7.3). The monthly flux values with 10-m winds used here are available from T. Takahashi at http://www.ldeo.columbia.edu/res/pi/CO2/carbondioxide/pages/air_sea_flux_rev1.html.*

7.3.2.3.4 *Robust findings of regional ocean-atmosphere flux*

- The regional air-sea CO_2 fluxes consist of a superposition of natural and anthropogenic CO_2 fluxes, with the former being globally nearly balanced (except for a small net outgassing associated with the input of carbon by rivers), and the latter having a global integral uptake of 2.2 ± 0.5 GtC yr^{-1} (see Table 7.1).
- The tropical oceans are outgassing CO_2 to the atmosphere (see Figure 7.8), with a mean flux of the order of 0.7 GtC yr^{-1}, estimated from an oceanic inversion (Gloor et al., 2003), in good agreement with atmospheric inversions (0 to 1.5 GtC yr^{-1}), and estimates based on oceanic pCO_2 observations (0.8 GtC yr^{-1}; Takahashi et al., 2002).
- The extratropical NH ocean is a net sink for anthropogenic and natural CO_2, with a magnitude of the order of 1.2 GtC yr^{-1}, consistent among various estimates.
- The Southern Ocean is a large sink of atmospheric CO_2 (Takahashi et al., 2002; Gurney et al., 2002) and of anthropogenic CO_2 (Gloor et al., 2003; Mikaloff Fletcher et al., 2006). Its magnitude has been estimated to be about 1.5 GtC yr^{-1}. This estimate is consistent among the different methods at the scale of the entire Southern Ocean. However, differences persist with regard to the Southern Ocean flux distribution between subpolar and polar latitudes (T. Roy et al., 2003). Atmospheric inversions and oceanic inversions indicate a larger sink in subpolar regions (Gurney et al., 2002; Gloor et al., 2003), consistent with the distribution of CO_2 fluxes based on available ΔpCO_2 observations (Figure 7.8 and Takahashi, 2002).

7.3.2.4 Interannual Changes in the Carbon Cycle

7.3.2.4.1 *Interannual changes in global fluxes*

The atmospheric CO_2 growth rate exhibits large interannual variations (see Figure 3.3, the TAR and http://lgmacweb.env.uea.ac.uk/lequere/co2/carbon_budget). The variability of fossil fuel emissions and the estimated variability in net ocean uptake are too small to account for this signal, which must be caused by year-to-year fluctuations in land-atmosphere fluxes. Over the past two decades, higher than decadal-mean CO_2 growth rates occurred in 1983, 1987, 1994 to 1995, 1997 to 1998 and 2002 to 2003. During such episodes, the net uptake of anthropogenic CO_2 (sum of land and ocean sinks) is temporarily weakened. Conversely, small growth rates occurred in 1981, 1992 to 1993 and 1996 to 1997, associated with enhanced uptake. Generally, high CO_2 growth rates correspond to El Niño climate conditions, and low growth rates to La Niña (Bacastow and Keeling, 1981; Lintner, 2002). However, two episodes of CO_2 growth rate variations during the past two decades did not reflect such an El Niño forcing. In 1992 to 1993, a marked reduction in growth rate occurred, coincident with the cooling and radiation

anomaly caused by the eruption of Mt. Pinatubo in June 1991. In 2002 to 2003, an increase in growth rate occurred, larger than expected based on the very weak El Niño event (Jones and Cox, 2005). It coincided with droughts in Europe (Ciais et al., 2005b), in North America (Breshears et al., 2005) and in Asian Russia (IFFN, 2003).

Since the TAR, many studies have confirmed that the variability of CO_2 fluxes is mostly due to land fluxes, and that tropical lands contribute strongly to this signal (Figure 7.9). A predominantly terrestrial origin of the growth rate variability can be inferred from (1) atmospheric inversions assimilating time series of CO_2 concentrations from different stations (Bousquet et al., 2000; Rödenbeck et al., 2003b; Baker et al., 2006), (2) consistent relationships between $\delta^{13}C$ and CO_2 (Rayner et al., 1999), (3) ocean model simulations (e.g., Le Quéré et al., 2003; McKinley et al., 2004a) and (4) terrestrial carbon cycle and coupled model simulations (e.g., C. Jones et al., 2001; McGuire et al., 2001; Peylin et al., 2005; Zeng et al., 2005). Currently, there is no evidence for basin-scale interannual variability of the air-sea CO_2 flux exceeding ±0.4 GtC yr^{-1}, but there are large ocean regions, such as the Southern Ocean, where interannual variability has not been well observed.

7.3.2.4.2 Interannual variability in regional fluxes, atmospheric inversions and bottom-up models

Year-to-year flux anomalies can be more robustly inferred by atmospheric inversions than mean fluxes. Yet, at the scale of continents or ocean basins, the inversion errors increase and the statistical significance of the inferred regional fluxes decreases.[5] This is why Figure 7.9 shows the land-atmosphere and ocean-atmosphere flux anomalies over broad latitude bands only for the inversion ensembles of Baker et al. (2006), Bousquet et al. (2000) and Rödenbeck et al. (2003b). An important finding of these studies is that differences in transport models have little impact on the interannual variability of fluxes. Interannual variability of global land-atmosphere fluxes (±4 GtC yr^{-1} between extremes) is larger than that of air-sea fluxes and dominates the global fluxes. This result is also true over large latitude bands (Figure 7.9). Tropical land fluxes exhibit on average a larger variability than temperate and boreal fluxes. Inversions give tropical land flux anomalies of the order of ±1.5 to 2 GtC yr^{-1}, which compare well in timing and magnitude with terrestrial model results (Tian et al., 1998; Peylin et al., 2005; Zeng et al., 2005). In these studies, enhanced sources occur during El Niño episodes and abnormal sinks during La Niña. In addition to the influence of these climate variations on ecosystem processes (Gérard et al., 1999; C. Jones et al., 2001), regional droughts during El Niño events promote large biomass fires, which appear to contribute to high CO_2 growth rates during the El Niño episodes (Barbosa et al., 1999; Langenfelds et al., 2002; Page et al., 2002; van der Werf et al., 2003, 2004; Patra et al., 2005).

Inversions robustly attribute little variability to ocean-atmosphere CO_2 flux (±0.5 GtC yr^{-1} between extremes), except for the recent work of Patra et al. (2005). This is in agreement with ocean model and ocean observations (Lee et al., 1998; Le Quéré et al., 2003; Obata and Kitamura, 2003; McKinley et al., 2004b). However, inversions and ocean models differ on the dominant geographic contributions to the variability. Inversions estimate similar variability in both hemispheres, whereas ocean models estimate more variability in the Southern Ocean (Bousquet et al., 2000; Rödenbeck et al., 2003b; Baker et al., 2006). Over the North Atlantic, Gruber et al. (2002) suggest a regional CO_2 flux variability (extremes of ±0.3 GtC yr^{-1}) by extrapolating data from a single ocean station, but McKinley et al. (2004a,b) model a small variability (extremes of ±0.1 GtC yr^{-1}). The equatorial Pacific is the ocean region of the world where the variability is constrained with repeated ΔpCO_2 observations (variations of about ±0.4 GtC yr^{-1}; Feely et al., 2002), with a reduced source of CO_2 during El Niño associated with decreased upwelling of CO_2-rich waters. Over this region, some inversion results (e.g., Bousquet et al., 2000) compare well in magnitude and timing with ocean and coupled model results (Le Quéré et al., 2000; C. Jones et al., 2001; McKinley et al., 2004a,b) and with ΔpCO_2 observations (Feely et al., 1999, 2002).

7.3.2.4.3 Slowdown in carbon dioxide growth rates during the early 1990s

The early 1990s had anomalously strong global sinks for atmospheric CO_2, compared with the decadal mean (Table 7.1). Although a weak El Niño from 1991 to 1995 may have helped to enhance ocean uptake at that time, inversions and O_2:N_2 and $\delta^{13}C$-CO_2 atmospheric data (Battle et al., 2000) indicate that the enhanced uptake was of predominantly terrestrial origin. The regions where the 1992 to 1993 abnormal sink is projected to be are not robustly estimated by inversions. Both Bousquet et al. (2000) and Rödenbeck et al. (2003b) project a large fraction of that sink in temperate North America, while Baker et al. (2006) place it predominantly in the tropics. Model results suggest that cooler temperatures caused by the Mt. Pinatubo eruption reduced soil respiration and enhanced NH carbon uptake (Jones and Cox, 2001b; Lucht et al., 2002), despite lower productivity as indicated by remote sensing of vegetation activity. In addition, aerosols from the volcanic eruption scattered sunlight and increased its diffuse fraction, which is used more efficiently by plant canopies in photosynthesis than direct light (Gu et al., 2003). It has been hypothesised that a transient increase in the diffuse fraction of radiation enhanced CO_2 uptake by land ecosystems in 1992 to 1993, but the global significance and magnitude of this effect remains unresolved (Roderick et al., 2001; Krakauer and Randerson, 2003; Angert et al., 2004; Robock, 2005).

[5] In other words, the model bias has only a small influence on inversions of interannual variability. These interannual inversion studies all report a random error and a systematic error range derived from sensitivity tests with different settings. Bousquet et al. (2000) used large regions and different inversion settings for the period 1980 to 1998. Rödenbeck et al. (2003) used one transport model and inverted fluxes at the resolution of the model grid for the period 1982 to 2002, with different inversion settings. Baker et al. (2006) used large regions but 13 different transport models for the period 1988 to 2002.

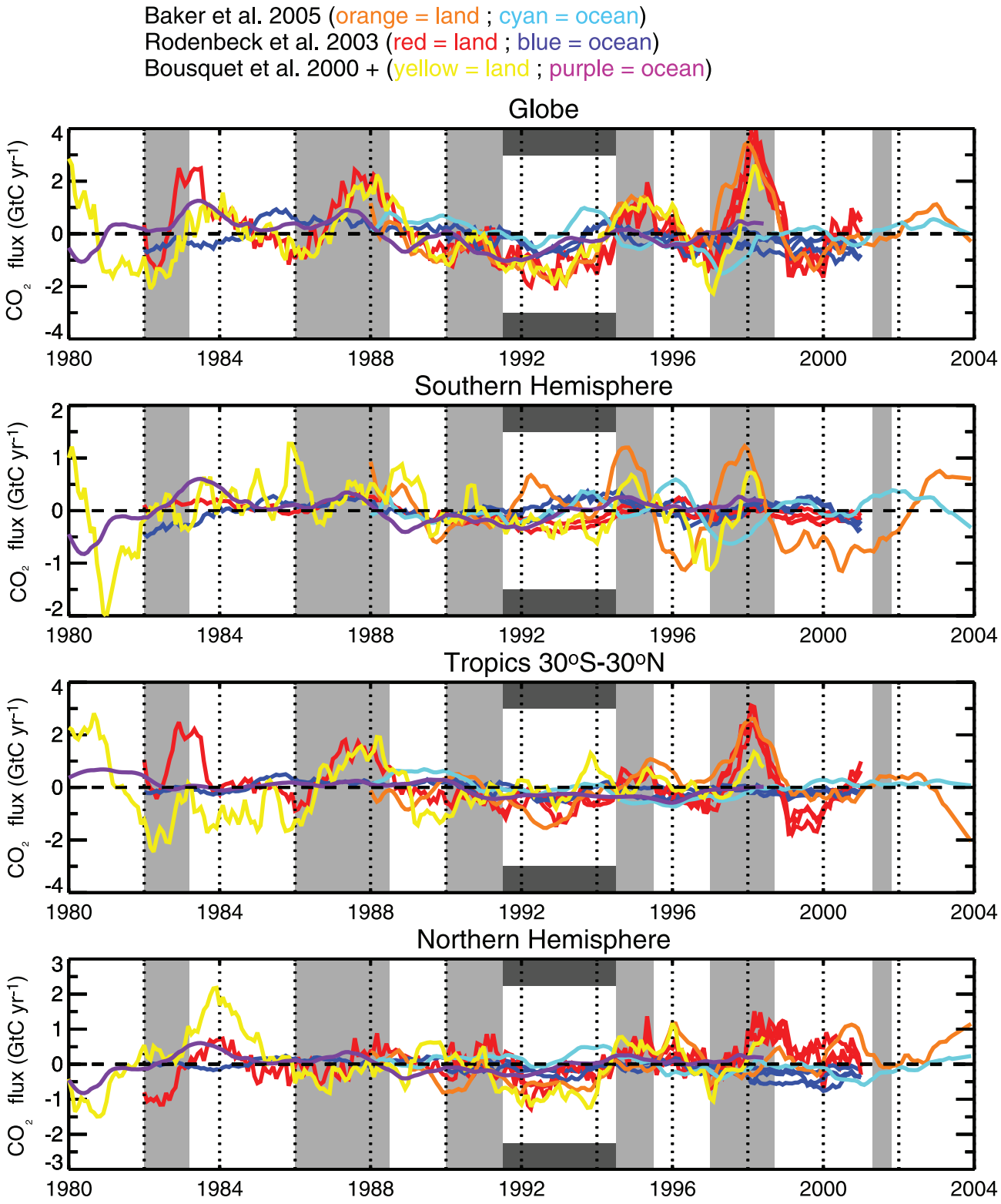


Figure 7.9. *Year-to-year anomalies in ocean-atmosphere and land-atmosphere CO_2 fluxes (GtC yr^{-1}) from interannual inversion ensembles covering the past 20 years or so, grouped into large latitude bands, and over the globe. Three different inversion ensembles from Bousquet et al. (2000), Rödenbeck et al. (2003a) and Baker et al. (2006) are shown. For each flux and each region, the anomalies were obtained by subtracting the long-term mean flux and removing the seasonal signal. Grey shaded regions indicate El Niño episodes, and the black bars indicate the cooling period following the Mt. Pinatubo eruption.*

7.3.2.4.4 Speed-up in carbon dioxide growth rates during the late 1990s

The high CO_2 growth in 1998 coincided with a global increase in CO concentrations attributable to wildfires (Yurganov et al., 2005) in Southeast Asia (60%), South America (30%) and Siberia (van der Werf et al., 2004). Langenfelds et al. (2002) analyse the correlations in the interannual growth rate of CO_2 and other species at 10 stations and link the 1997 to 1998 (and the 1994 to 1995) anomalies to high fire emissions as a single process. Achard et al. (2004) estimate a source of 0.88 ± 0.07 GtC emitted from the burning of 2.4×10^6 ha of peatland in the Indonesian forest fires in 1997 to 1998, and Page et al. (2002) estimate a source of +0.8 to +2.6 GtC. During the 1997 to 1998 high CO_2 growth rate episode, inversions place an abnormal source over tropical Southeast Asia, in good agreement with such bottom-up evidence. The relationship between El Niño and CO_2 emissions from fires is not uniform: fire emissions from low productivity ecosystems in Africa and northern Australia are limited by fuel load density and thus decrease during drier periods, in contrast to the response in tropical forests (Barbosa et al., 1999; Randerson et al., 2005). In addition, co-varying processes such as reduced productivity caused by drought in tropical forests during El Niño episodes may be superimposed on fire emissions. From 1998 to 2003, extensive drought in mid-latitudes of the NH (Hoerling and Kumar, 2003), accompanied by more wildfires in some regions (Balzter et al., 2005; Yurganov et al., 2005) may have led to decreased photosynthesis and carbon uptake (Angert et al., 2005; Ciais et al., 2005b), helping to increase the atmospheric CO_2 growth rate.

7.3.3 Terrestrial Carbon Cycle Processes and Feedbacks to Climate

The net exchange of carbon between the terrestrial biosphere and the atmosphere is the difference between carbon uptake by photosynthesis and release by plant respiration, soil respiration and disturbance processes (fire, windthrow, insect attack and herbivory in unmanaged systems, together with deforestation, afforestation, land management and harvest in managed systems). Over at least the last 30 years, the net result of all these processes has been uptake of atmospheric CO_2 by terrestrial ecosystems (Table 7.1, 'land-atmosphere flux' row). It is critical to understand the reasons for this uptake and its likely future course. Will uptake by the terrestrial biosphere grow or diminish with time, or even reverse so that the terrestrial biosphere becomes a net source of CO_2 to the atmosphere? To answer this question it is necessary to understand the underlying processes and their dependence on the key drivers of climate, atmospheric composition and human land management.

Drivers that affect the carbon cycle in terrestrial ecosystems can be classified as (1) direct climate effects (changes in precipitation, temperature and radiation regime); (2) atmospheric composition effects (CO_2 fertilization, nutrient deposition, damage by pollution); and (3) land use change effects (deforestation, afforestation, agricultural practices, and their legacies over time). This section first summarises current knowledge of the processes by which each of these drivers influence the terrestrial carbon balance, and then examines knowledge of the integrative consequences of all these processes in the key case of tropical forests.

7.3.3.1 Processes Driven by Climate, Atmospheric Composition and Land Use Change

7.3.3.1.1 Climatic regulation of terrestrial carbon exchange

Ecosystem responses to environmental drivers (sunlight, temperature, soil moisture) and to ecological factors (e.g., forest age, nutrient supply, organic substrate availability; see, e.g., Clark, 2002; Ciais et al., 2005b; Dunn et al., 2007) are complex. For example, elevated temperature and higher soil water content enhance rates for heterotrophic respiration in well-aerated soils, but depress these rates in wet soils. Soil warming experiments typically show marked soil respiration increases at elevated temperature (Oechel et al., 2000; Rustad et al., 2001; Melillo et al., 2002), but CO_2 fluxes return to initial levels in a few years as pools of organic substrate re-equilibrate with inputs (Knorr et al., 2005). However, in dry soils, decomposition may be limited by moisture and not respond to temperature (Luo et al., 2001). Carbon cycle simulations need to capture both the short- and long-term responses to changing climate to predict carbon cycle responses.

Current models of terrestrial carbon balance have difficulty simulating measured carbon fluxes over the full range of temporal and spatial scales, including instantaneous carbon exchanges at the leaf, plot or ecosystem level, seasonal and annual carbon fluxes at the stand level and decadal to centennial accumulation of biomass and organic matter at stand or regional scales (Melillo et al., 1995; Thornton et al., 2002). Moreover, projections of changes in land carbon storage are tied not only to ecosystem responses to climate change, but also to the modelled projections of climate change itself. As there are strong feedbacks between these components of the Earth system (see Section 7.3.5), future projections must be considered cautiously.

7.3.3.1.2 Effects of elevated carbon dioxide

On physiological grounds, almost all models predict stimulation of carbon assimilation and sequestration in response to rising CO_2, called 'CO_2 fertilization' (Cramer et al., 2001; Oren et al., 2001; Luo et al., 2004; DeLucia et al., 2005). Free Air CO_2 Enrichment (FACE) and chamber studies have been used to examine the response of ecosystems to large (usually about 50%) step increases in CO_2 concentration. The results have been variable (e.g., Oren et al., 2001; Nowak et al., 2004; Norby et al., 2005). On average, net CO_2 uptake has been stimulated, but not as much as predicted by some models. Other factors (e.g., nutrients or genetic limitations on growth) can limit plant growth and reduce response to CO_2. Eleven FACE experiments, encompassing bogs, grasslands, desert and young temperate tree stands report an average increased net primary productivity (NPP) of 12% when compared to ambient CO_2 levels (Nowak et al., 2004). There is a large range of responses, with woody

plants consistently showing NPP increases of 23 to 25% (Norby et al., 2005), but much smaller increases for grain crops (Ainsworth and Long, 2005), reflecting differential allocation of the incremental organic matter to shorter- vs. longer-lived compartments. Overall, about two-thirds of the experiments show positive response to increased CO_2 (Ainsworth and Long, 2005; Luo et al., 2005). Since saturation of CO_2 stimulation due to nutrient or other limitations is common (Dukes et al., 2005; Koerner et al., 2005), it is not yet clear how strong the CO_2 fertilization effect actually is.

7.3.3.1.3 Nutrient and ozone limitations to carbon sequestration

The basic biochemistry of photosynthesis implies that stimulation of growth will saturate under high CO_2 concentrations and be further limited by nutrient availability (Dukes et al., 2005; Koerner et al., 2005) and by possible acclimation of plants to high CO_2 levels (Ainsworth and Long, 2005). Carbon storage by terrestrial plants requires net assimilation of nutrients, especially N, a primary limiting nutrient at middle and high latitudes and an important nutrient at lower latitudes (Vitousek et al., 1998). Hungate et al. (2003) argue that 'soil C sequestration under elevated CO_2 is constrained both directly by N availability and indirectly by nutrients needed to support N_2 fixation', and Reich et al. (2006) conclude that 'soil N supply is probably an important constraint on global terrestrial responses to elevated CO_2'. This view appears to be consistent with other recent studies (e.g., Finzie et al., 2006; Norby et al., 2006; van Groenigen et al., 2006) and with at least some of the FACE data, further complicating estimation of the current effects of rising CO_2 on carbon sequestration globally.

Additional N supplied through atmospheric deposition or direct fertilization can stimulate plant growth (Vitousek, 2004) and in principle could relieve the nutrient constraint on CO_2 fertilization. Direct canopy uptake of atmospheric N may be particularly effective (Sievering et al., 2000). Overall, the effectiveness of N inputs appears to be limited by immobilisation and other mechanisms. For example, when labelled nitrogen (^{15}N) was added to soil and litter in a forest over seven years, only a small fraction became available for tree growth (Nadelhoffer et al., 2004). Moreover, atmospheric N deposition is spatially correlated with air pollution, including elevated atmospheric ozone. Ozone and other pollutants may have detrimental effects on plant growth, possibly further limiting the stimulation of carbon uptake by anthropogenic N emissions (Ollinger and Aber, 2002; Holland and Carroll, 2003). Indeed, Felzer et al. (2004) estimate that surface ozone increases since 1950 may have reduced CO_2 sequestration in the USA by 18 to 20 TgC yr^{-1}. The current generation of coupled carbon-climate models (see Section 7.3.5) does not include nutrient limitations or air pollution effects.

7.3.3.1.4 Fire

Fire is a major agent for conversion of biomass and soil organic matter to CO_2 (Randerson et al., 2002a–d; Cochrane, 2003; Nepstad et al., 2004; Jones and Cox, 2005; Kasischke et al., 2005; Randerson et al., 2005). Globally, wildfires (savannah and forest fires, excluding biomass burning for fuel and land clearing) oxidize 1.7 to 4.1 GtC yr^{-1} (Mack et al., 1996; Andreae and Merlet, 2001), or about 3 to 8% of total terrestrial NPP. There is an additional large enhancement of CO_2 emissions associated with fires stimulated by human activities, such as deforestation and tropical agricultural development. Thus, there is a large potential for future alteration in the terrestrial carbon balance through altered fire regimes. A striking example occurred during the 1997 to 1998 El Niño, when large fires in the Southeast Asian archipelago are estimated to have released 0.8 to 2.6 GtC (see Section 7.3.2.4). Fire frequency and intensity are strongly sensitive to climate change and variability, and to land use practices. Over the last century, trends in burned area have been largely driven by land use practices, through fire suppression policies in mid-latitude temperate regions and increased use of fire to clear forest in tropical regions (Mouillot and Field, 2005). However, there is also evidence that climate change has contributed to an increase in fire frequency in Canada (Gillett et al., 2004). The decrease in fire frequency in regions like the USA and Europe has contributed to the land carbon sink there, while increased fire frequency in regions like Amazonia, Southeast Asia and Canada has contributed to the carbon source. At high latitudes, the role of fire appears to have increased in recent decades: fire disturbance in boreal forests was higher in the 1980s than in any previous decade on record (Kurz et al., 1995; Kurz and Apps, 1999; Moulliot and Field, 2005). Flannigan et al. (2005) estimate that in the future, the CO_2 source from fire will increase.

7.3.3.1.5 Direct effects of land use and land management

Evolution of landscape structure, including woody thickening: Changes in the structure and distribution of ecosystems are driven in part by changes in climate and atmospheric CO_2, but also by human alterations of landscapes through land management and the introduction of invasive species and exotic pathogens. The single most important process in the latter category is woody encroachment or vegetation thickening, the increase in woody biomass occurring in (mainly semi-arid) grazing lands. In many regions, this increase arises from fire suppression and associated grazing management practices, but there is also a possibility that increases in CO_2 are giving C_3 woody plants a competitive advantage over C_4 grasses (Bond et al., 2003). Woody encroachment could account for as much as 22 to 40% of the regional carbon sink in the USA (Pacala et al., 2001), and a high proportion in northeast Australia (Burrows et al., 2002). Comprehensive data are lacking to define this effect accurately.

Deforestation: Forest clearing (mainly in the tropics) is a large contributor to the land use change component of the current atmospheric CO_2 budget, accounting for up to one-third of total anthropogenic emissions (see Table 7.2; Section 7.3.2.1; also Table 7.1, row 'land use change flux'). The future evolution of this term in the CO_2 budget is therefore of critical importance. Deforestation in Africa, Asia and the tropical Americas is expected to decrease towards the end of the 21st century to a

small fraction of the levels in 1990 (IPCC, 2000). The declines in Asia and Africa are driven by the depletion of forests, while trends in the Americas have the highest uncertainty given the extent of the forest resource.

Afforestation: Recent (since 1970) afforestation and reforestation as direct human-induced activities have not yet had much impact on the global terrestrial carbon sink. However, regional sinks have been created in areas such as China, where afforestation since the 1970s has sequestered 0.45 GtC (Fang et al., 2001). The largest effect of afforestation is not immediate but through its legacy.

Agricultural practices: Improvement of agricultural practices on carbon-depleted soils has created a carbon sink. For instance, the introduction of conservation tillage in the USA is estimated to have increased soil organic matter (SOM) stocks by about 1.4 GtC over the last 30 years. However, yearly increases in SOM can be sustained only for 50 to 100 years, after which the system reaches a new equilibrium (Cole et al., 1996; Smith et al., 1997). Moreover, modern conservation tillage often entails large inputs of chemicals and fertilizer, which are made using fossil fuels, reducing the CO_2 benefit from carbon sequestration in agricultural soils. The increase in soil carbon stocks under low-tillage systems may also be mostly a topsoil effect with little increase in total profile carbon storage observed, confounded by the fact that most studies of low-tillage systems have only sampled the uppermost soil layers.

7.3.3.1.6 Forest regrowth

Some studies suggest that forest regrowth could be a major contributor to the global land carbon sink (e.g., Pacala et al., 2001; Schimel et al., 2001; Hurtt et al., 2002). Forest areas generally increased during the 20th century at middle and high latitudes (unlike in the tropics). This surprising trend reflects the intensification of agriculture and forestry. Globally, more food is being grown on less land, reflecting mechanisation of agriculture, increased fertilizer use and adoption of high-yield cultivars, although in parts of Africa and Asia the opposite is occurring. Likewise, intensive forest management and agroforestry produce more fibre on less land; improved forest management favours more rapid regrowth of forests after harvest. These trends have led to carbon sequestration by regrowing forests. It should be noted, however, that industrialised agriculture and forestry require high inputs of fossil energy, so it is difficult to assess the net global effects of agricultural intensification on atmospheric greenhouse gases and radiative forcing.

Regional studies have confirmed the plausibility of strong mid-latitude sinks due to forest regrowth. Data from the eddy flux tower network show that forests on long-abandoned former agricultural lands (Curtis et al., 2002) and in industrial managed forests (Hollinger et al., 2002) take up significant amounts of carbon every year. Analysis of forest inventory data shows that, in aggregate, current forest lands are significant sinks for atmospheric CO_2 (Pacala et al., 2001). Few old growth forests remain at mid-latitudes (most forests are less than 70 years old), in part due to forest management. Therefore, forests in these areas are accumulating biomass because of their ages and stages of succession. Within wide error bands (see Section 7.3.2.3), the uptake rates inferred from flux towers are generally consistent with those inferred from inverse methods (e.g., Hurtt et al., 2002). Stocks of soil carbon are also likely increasing due to replenishment of soil organic matter and necromass depleted during the agricultural phase, and changes in soil microclimate associated with reforestation; these effects might add 30 to 50% to the quantity of CO_2 sequestered (e.g., Barford et al., 2001). It is important to note that at least some of this sequestration is 'refilling' the deficits in biomass and soil organic matter, accumulated in previous epochs (see Figure 7.3), and the associated CO_2 uptake should be expected to decline in the coming decades unless sustained by careful management strategies designed to accomplish that purpose.

7.3.4 Ocean Carbon Cycle Processes and Feedbacks to Climate

7.3.4.1 Overview of the Ocean Carbon Cycle

Oceanic carbon exists in several forms: as DIC, DOC, and particulate organic carbon (POC) (living and dead) in an approximate ratio DIC:DOC:POC = 2000:38:1 (about 37,000 GtC DIC: Falkowski et al., 2000 and Sarmiento and Gruber, 2006; 685 GtC DOC: Hansell and Carlson, 1998; and 13 to 23 GtC POC: Eglinton and Repeta, 2004). Before the industrial revolution, the ocean contained about 60 times as much carbon as the atmosphere and 20 times as much carbon as the terrestrial biosphere/soil compartment.

Seawater can, through inorganic processes, absorb large amounts of CO_2 from the atmosphere, because CO_2 is a weakly acidic gas and the minerals dissolved in the ocean have over geologic time created a slightly alkaline ocean (surface pH 7.9 to 8.25: Degens et al., 1984; Royal Society, 2005). The air-sea exchange of CO_2 is determined largely by the air-sea gradient in pCO_2 between atmosphere and ocean. Equilibration of surface ocean and atmosphere occurs on a time scale of roughly one year. Gas exchange rates increase with wind speed (Wanninkhof and McGillis, 1999; Nightingale et al., 2000) and depend on other factors such as precipitation, heat flux, sea ice and surfactants. The magnitudes and uncertainties in local gas exchange rates are maximal at high wind speeds. In contrast, the equilibrium values for partitioning of CO_2 between air and seawater and associated seawater pH values are well established (Zeebe and Wolf-Gladrow, 2001; see Box 7.3).

In addition to changes in advection and mixing, the ocean can alter atmospheric CO_2 concentration through three mechanisms (Volk and Hoffert, 1985), illustrated in Figure 7.10: (1) absorption or release of CO_2 due to changes in solubility of gaseous CO_2 ('solubility pump'); (2) changes in carbon fixation to POC in surface waters by photosynthesis and export of this carbon through sinking of organic particles out of the surface layer ('organic carbon pump') – this process is limited to first order by availability of light and nutrients (phosphate, nitrate, silicic acid and micronutrients such as iron); and (3) changes in

Box 7.3: Marine Carbon Chemistry and Ocean Acidification

The marine carbonate buffer system allows the ocean to take up CO_2 far in excess of its potential uptake capacity based on solubility alone, and in doing so controls the pH of the ocean. This control is achieved by a series of reactions that transform carbon added as CO_2 into HCO_3^- and CO_3^{2-}. These three dissolved forms (collectively known as DIC) are found in the approximate ratio CO_2:HCO_3^-:CO_3^{2-} of 1:100:10 (Equation (7.1)). CO_2 is a weak acid and when it dissolves, it reacts with water to form carbonic acid, which dissociates into a hydrogen ion (H^+) and a HCO_3^- ion, with some of the H^+ then reacting with CO_3^{2-} to form a second HCO_3^- ion (Equation (7.2)).

$$CO_2 + H_2O \rightarrow H^+ + HCO_3^- \rightarrow 2H^+ + CO_3^{2-} \quad (7.1)$$

$$CO_2 + H_2O + CO_3^{2-} \rightarrow HCO_3^- + H^+ + CO_3^{2-} \rightarrow 2HCO_3^- \quad (7.2)$$

Therefore, the net result of adding CO_2 to seawater is an increase in H^+ and HCO_3^-, but a reduction in CO_3^{2-}. The decrease in the CO_3^{2-} ion reduces the overall buffering capacity as CO_2 increases, with the result that proportionally more H^+ ions remain in solution and increase acidity.

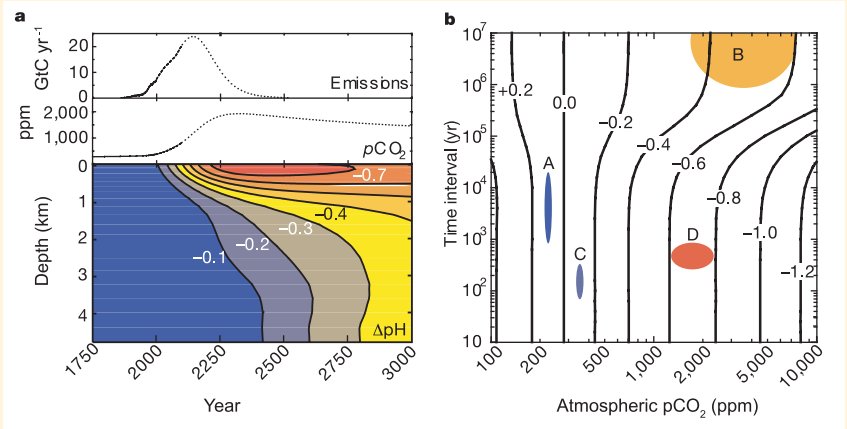
This ocean acidification is leading to a decrease in the saturation state of $CaCO_3$ in the ocean. Two primary effects are expected: (1) the biological production of corals as well as calcifying phytoplankton and zooplankton within the water column may be inhibited or slowed down (Royal Society, 2005), and (2) the dissolution of $CaCO_3$ at the ocean floor will be enhanced (Archer, 2005). Aragonite, the meta-stable form of $CaCO_3$ produced by corals and pteropods (planktonic snails; Lalli and Gilmer, 1989), will be particularly susceptible to a pH reduction (Kleypas et al., 1999b; Hughes et al., 2003; Orr et al., 2005). Laboratory experiments under high ambient CO_2 with the coccolithophore species *Emiliania huxleyi* and *Gephyrocapsa oceanica* produce a significant reduction in $CaCO_3$ production and a stimulation of POC production (Riebesell et al., 2000; Zondervan et al., 2001). Other species and growth under other conditions may show different responses, so that no conclusive quantification of the $CaCO_3$ feedback is possible at present (Tortell et al., 2002; Sciandra et al., 2003).

The sinking speed of marine particle aggregates depends on their composition: $CaCO_3$ may act as an efficient ballast component, leading to high sinking speeds of aggregates (Armstrong et al., 2002; Klaas and Archer, 2002). The relatively small negative feedback of reduced $CaCO_3$ production to atmospheric pCO_2 may be compensated for by a change in the ballast for settling biogenic particles and the associated shallowing of re-mineralization depth levels in the water column for organic carbon (Heinze, 2004). On the other hand, production of extracellular organic carbon could increase under high CO_2 levels and lead to an increase in export (Engel et al., 2004).

Ecological changes due to expected ocean acidification may be severe for corals in tropical and cold waters (Gattuso et al., 1999; Kleypas et al., 1999a; Langdon et al., 2003; Buddemeier et al., 2004; Roberts et al., 2006) and for pelagic ecosystems (Tortell et al., 2002; Royal Society, 2005). Acidification can influence the marine food web at higher trophic levels (Langenbuch and Pörtner, 2003; Ishimatsu et al., 2004).

Since the beginning of the industrial revolution, sea surface pH has dropped by about 0.1 pH units (corresponding to a 30% increase in the H ion concentration). The expected continued decrease may lead within a few centuries to an ocean pH estimated to have occurred most recently a few hundred million years before present (Caldeira and Wickett, 2003; Key et al., 2004; Box 7.3, Figure 1).

According to a model experiment based on the IPCC Scenarios 1992a (IS92a) emission scenario, bio-calcification will be reduced by 2100, in particular within the Southern Ocean (Orr et al., 2005), and by 2050 for aragonite-producing organisms (see also Figure 10.24). It is important to note that ocean acidification is not a direct consequence of climate change but a consequence of fossil fuel CO_2 emissions, which are the main driver of the anticipated climate change.



Box 7.3, Figure 1. *(a) Atmospheric CO_2 emissions, historical atmospheric CO_2 levels and predicted CO_2 concentrations from the given emission time series, together with changes in ocean pH based on horizontally averaged chemistry. The emission time series is based on the mid-range IS92a emission scenario (solid line) prior to 2100 and then assumes that emissions continue until fossil fuel reserves decline. (b) Estimated maximum change in surface ocean pH as a function of final atmospheric CO_2 pressure, and the transition time over which this CO_2 pressure is linearly approached from 280 ppm. A: Glacial-interglacial CO_2 changes; B: slow changes over the past 300 Myr; C: historical changes in ocean surface waters; D: unabated fossil fuel burning over the next few centuries. Source: Caldeira and Wickett (2003). Reprinted with permission from Macmillan Publishers Ltd: Nature, Caldeira and Wickett (2003), copyright (2003).*

the release of CO_2 in surface waters during formation of $CaCO_3$ shell material by plankton ('$CaCO_3$ counter pump').

Organic particles are re-mineralized (oxidized to DIC and other inorganic compounds through the action of bacteria) primarily in the upper 1,000 m of the oceanic water column, with an accompanying decrease in dissolved O. On the average, $CaCO_3$ particles sink deeper before they undergo dissolution: deep waters are undersaturated with respect to $CaCO_3$. The remainder of the particle flux enters marine sediments and is subject to either re-dissolution within the water column or accumulation within the sediments. Although the POC reservoir is small, it plays an important role in keeping DIC concentrations low in surface waters and high in deep waters. The loop is closed through the three-dimensional ocean circulation: upwelling water brings inorganic carbon and nutrients to the surface again, leading to outgassing and biogenic particle production. Dissolved organic carbon enters the ocean water column from rivers and marine metabolic processes. A large fraction of DOC has a long ocean residence time (1–10 kyr), while other fractions are more short-lived (days to hundreds of years; Loh et al., 2004). The composition of dissolved organic matter is still largely unknown.

In conjunction with the global ocean mixing or overturning time of the order of 1 kyr (Broecker and Peng, 1982), small changes in the large ocean carbon reservoir can induce significant changes in atmospheric CO_2 concentration. Likewise, perturbations in the atmospheric pCO_2 can be buffered by the ocean. Glacial-interglacial changes in the atmospheric CO_2 content can potentially be attributed to a change in functioning of the marine carbon pump (see Chapter 6). The key role for the timing of the anthropogenic carbon uptake by the ocean is played by the downward transport of surface water, with a high burden of anthropogenic carbon, into the ocean's interior. The organic carbon cycle and the $CaCO_3$ counter pump modulate, but do not dominate, the net marine uptake of anthropogenic carbon.

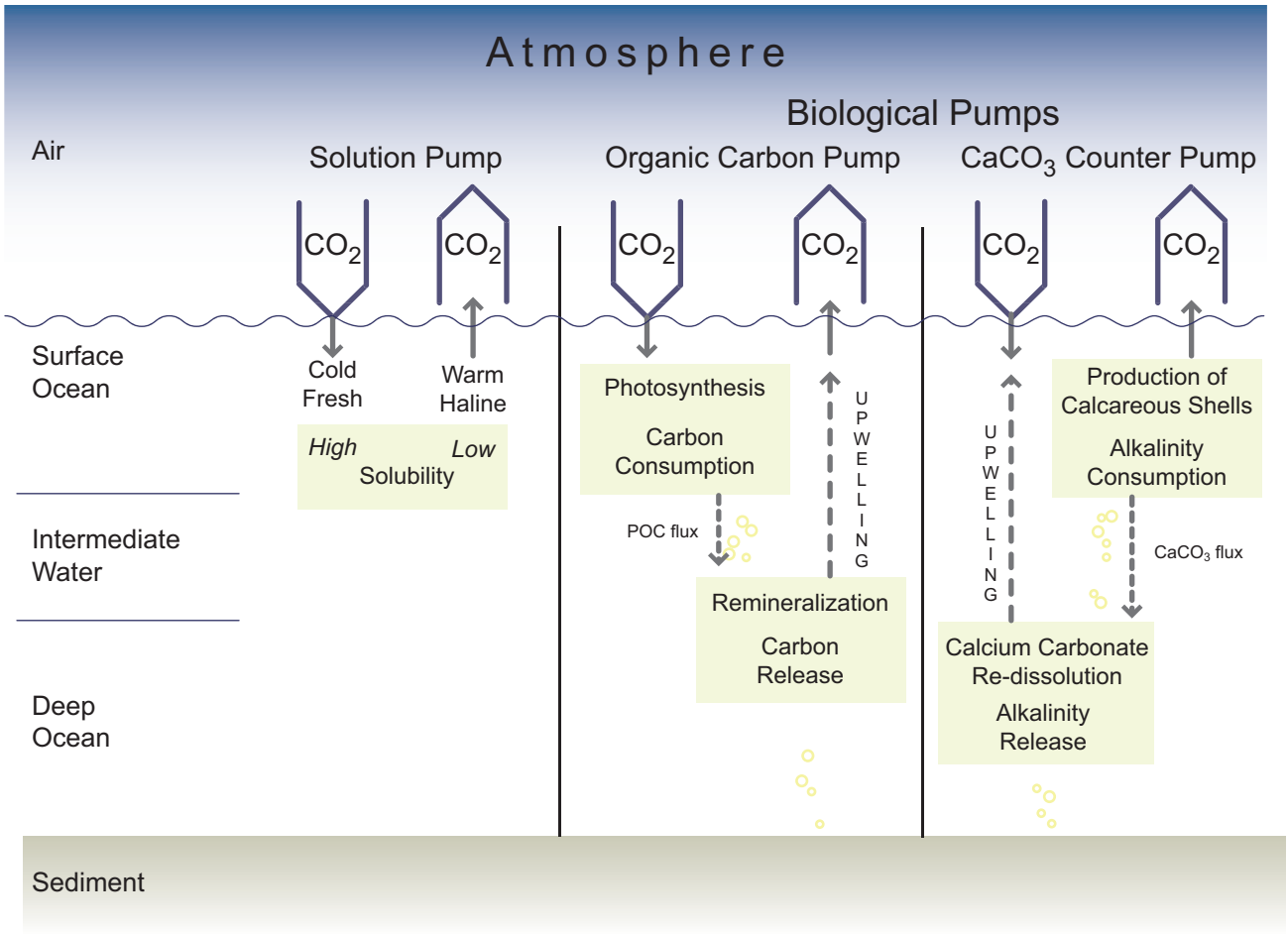


Figure 7.10. *Three main ocean carbon pumps govern the regulation of natural atmospheric CO_2 changes by the ocean (Heinze et al., 1991): the solubility pump, the organic carbon pump and the $CaCO_3$ 'counter pump'. The oceanic uptake of anthropogenic CO_2 is dominated by inorganic carbon uptake at the ocean surface and physical transport of anthropogenic carbon from the surface to deeper layers. For a constant ocean circulation, to first order, the biological carbon pumps remain unaffected because nutrient cycling does not change. If the ocean circulation slows down, anthropogenic carbon uptake is dominated by inorganic buffering and physical transport as before, but the marine particle flux can reach greater depths if its sinking speed does not change, leading to a biologically induced negative feedback that is expected to be smaller than the positive feedback associated with a slower physical downward mixing of anthropogenic carbon. Reprinted with permission, copyright 1991 American Geophysical Union.*

7.3.4.2 Carbon Cycle Feedbacks to Changes in Atmospheric Carbon Dioxide

Chemical buffering of anthropogenic CO_2 is the quantitatively most important oceanic process acting as a carbon sink. Carbon dioxide entering the ocean is buffered due to scavenging by the CO_3^{2-} ions and conversion to HCO_3^-, that is, the resulting increase in gaseous seawater CO_2 concentration is smaller than the amount of CO_2 added per unit of seawater volume. Carbon dioxide buffering in seawater is quantified by the Revelle factor ('buffer factor', Equation (7.3)), relating the fractional change in seawater pCO_2 to the fractional change in total DIC after re-equilibration (Revelle and Suess, 1957; Zeebe and Wolf-Gladrow, 2001):

$$\text{Revelle factor (or buffer factor)} = (\Delta[CO_2] / [CO_2]) / (\Delta[DIC] / [DIC]) \quad (7.3)$$

The lower the Revelle factor, the larger the buffer capacity of seawater. Variability of the buffer factor in the ocean depends mainly on changes in pCO_2 and the ratio of DIC to total alkalinity. In the present-day ocean, the buffer factor varies between 8 and 13 (Sabine et al., 2004a; Figure 7.11). With respect to atmospheric pCO_2 alone, the inorganic carbon system of the ocean reacts in two ways: (1) seawater re-equilibrates, buffering a significant amount of CO_2 from the atmosphere depending on the water volume exposed to equilibration; and (2) the Revelle factor increases with pCO_2 (positive feedback; Figure 7.11). Both processes are quantitatively important. While the first is generally considered as a system response, the latter is a feedback process.

The ocean will become less alkaline (seawater pH will decrease) due to CO_2 uptake from the atmosphere (see Box 7.3). The ocean's capacity to buffer increasing atmospheric CO_2 will decline in the future as ocean surface pCO_2 increases (Figure 7.11a). This anticipated change is certain, with potentially severe consequences.

Increased carbon storage in the deep ocean leads to the dissolution of calcareous sediments below their saturation depth (Broecker and Takahashi, 1978; Feely et al., 2004). The feedback of $CaCO_3$ sediment dissolution to atmospheric pCO_2 increase is negative and quantitatively significant on a 1 to 100 kyr time scale, where $CaCO_3$ dissolution will account for a 60 to 70% absorption of the anthropogenic CO_2 emissions, while the ocean water column will account for 22 to 33% on a time scale of 0.1 to 1 kyr. In addition, the remaining 7 to 8% may be compensated by long-term terrestrial weathering cycles involving silicate carbonates (Archer et al., 1998). Due to the slow $CaCO_3$ buffering mechanism (and the slow silicate weathering), atmospheric pCO_2 will approach a new equilibrium asymptotically only after several tens of thousands of years (Archer, 2005; Figure 7.12).

Elevated ambient CO_2 levels appear to also influence the production rate of POC by marine calcifying planktonic organisms (e.g., Zondervan et al., 2001). This increased carbon fixation under higher CO_2 levels was also observed for three diatom (siliceous phytoplankton) species (Riebesell et al., 1993). It is critical to know whether these increased carbon fixation rates translate into increased export production rates (i.e., removal of carbon to greater depths). Studies of the nutrient to carbon ratio in marine phytoplankton have not yet shown any significant changes related to CO_2 concentration of the nutrient utilisation efficiency (expressed through the 'Redfield ratio' – carbon:nitrogen:phosphorus:silicon) in organic tissue (Burkhardt et al., 1999).

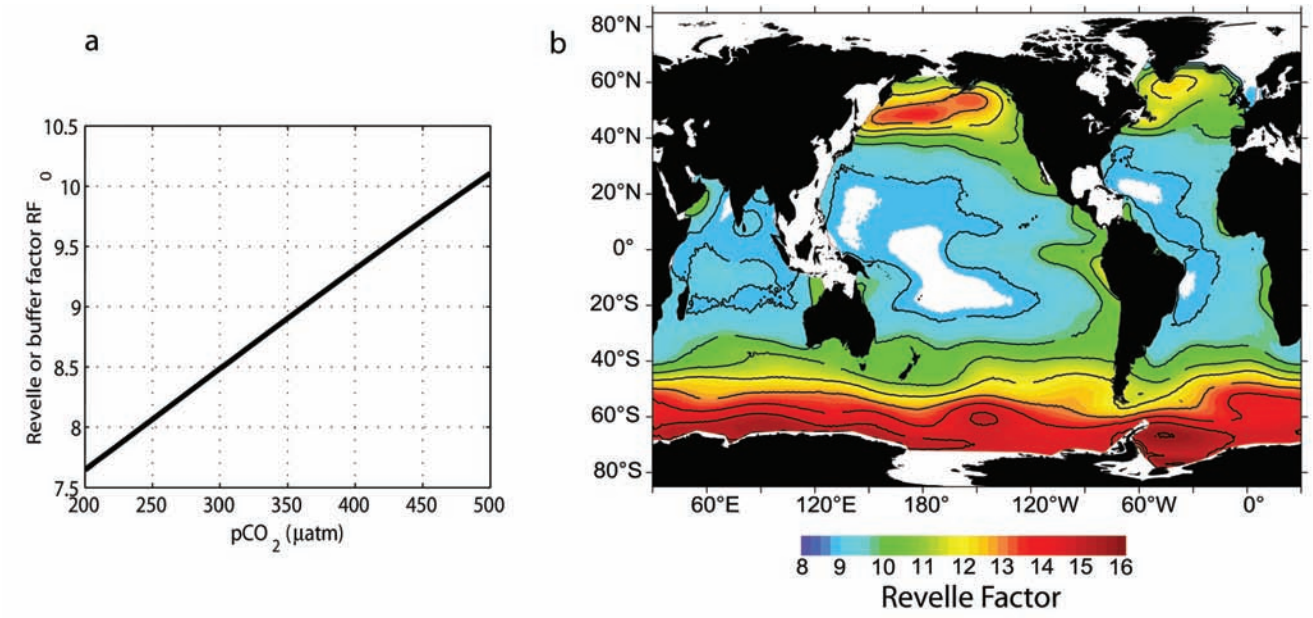


Figure 7.11. *(a) The Revelle factor (or buffer factor) as a function of CO_2 partial pressure (for temperature 25°C, salinity 35 psu, and total alkalinity 2,300 µmol kg^{-1}) (Zeebe and Wolf-Gladrow, 2001, page 73; reprinted with permission, copyright 2001 Elsevier). (b) The geographical distribution of the buffer factor in ocean surface waters in 1994 (Sabine et al., 2004a; reprinted with permission, copyright 2004 American Association for the Advancement of Science). High values indicate a low buffer capacity of the surface waters.*

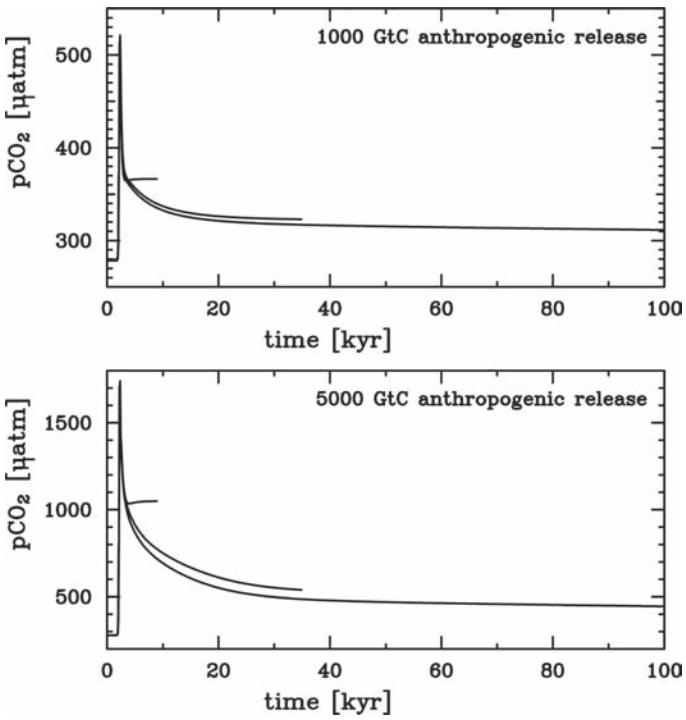


Figure 7.12. *Model projections of the neutralization of anthropogenic CO_2 for an ocean-only model, a model including dissolution of $CaCO_3$ sediment and a model including weathering of silicate rocks, (top) for a total of 1,000 GtC of anthropogenic CO_2 emissions and (bottom) for a total of 5,000 GtC of anthropogenic CO_2. Note that the y-axis is different for the two diagrams. Without $CaCO_3$ dissolution from the sea-floor, the buffering of anthropogenic CO_2 is limited. Even after 100 kyr, the remaining pCO_2 is substantially higher than the pre-industrial value. Source: Archer (2005).*

7.3.4.3 Carbon Cycle Feedbacks to Changes in Physical Forcing

A more sluggish ocean circulation and increased density stratification, both expected in a warmer climate, would slow down the vertical transport of carbon, alkalinity and nutrients, and the replenishment of the ocean surface with water that has not yet been in contact with anthropogenic CO_2. This narrowing of the 'bottleneck' for anthropogenic CO_2 invasion into the ocean would provide a significant positive feedback to atmospheric greenhouse gas concentrations (Bolin and Eriksson, 1959; see also the carbon cycle climate model simulations by Cox et al., 2000; Friedlingstein et al., 2001, 2006). As long as the vertical transfer rates for marine biogenic particles remain unchanged, in a more sluggish ocean the biological carbon pump will be more efficient (Boyle, 1988; Heinze et al., 1991), thus inducing a negative feedback, which is expected to be smaller than the physical transport feedback (Broecker, 1991; Maier-Reimer et al., 1996; Plattner et al., 2001; see Figure 7.10). However, a modelling study by Bopp et al. (2005) predicts a decrease in vertical particle transfer and hence shallower depths of re-mineralization of particulate organic carbon resulting in a positive CO_2 feedback. Further changes in plankton community structure including the role of N_2-fixing organisms can feed back to the carbon cycle (Sarmiento et al., 2004; Mahaffey et al., 2005). Changes in ocean circulation can affect the regional circulation of shelf and coastal seas, leading either to increased export of nutrients plus carbon from the shallow seas into the open ocean or to increased upwelling of nutrients plus carbon onto the shelf and towards coastal areas (Walsh, 1991; Smith and Hollibaugh, 1993; Chen et al., 2003; Borges, 2005). A reduction in sea ice cover may increase the uptake area for anthropogenic CO_2 and act as a minor negative carbon feedback (ACIA, 2005). The physical 'bottleneck' feedback dominates over biological feedbacks induced by circulation change, resulting in an anticipated overall positive feedback to climate change. Both feedbacks depend on details of the future ocean circulation and model projections show a large range.

The solubility of CO_2 gas in seawater and the two dissociation constants of carbonic acid in seawater depend on temperature and salinity (Weiss, 1974; Millero et al., 2002). A 1°C increase in sea surface temperature produces an increase in pCO_2 of 6.9 to 10.2 ppm after 100 to 1,000 years (Heinze et al., 2003; see also Broecker and Peng, 1986; Plattner et al., 2001). Warming may increase the biological uptake rate of nutrients and carbon from surface waters, but the net effect on export and DIC is uncertain. Laws et al. (2000) proposed that export efficiency increases with net photosynthesis at low temperatures, which implies a positive feedback to warming. In addition, DOC may be degraded more quickly at higher temperatures.

7.3.4.4 Carbon Cycle Feedbacks Induced by Nutrient Cycling and Land Ocean Coupling

Rivers deliver carbon (DIC, DOC) and nutrients to the ocean. Rising CO_2 levels in the atmosphere and land use may lead to increased chemical and physical weathering, resulting in increased carbon and alkalinity loads in rivers (Clair et al., 1999; Hejzlar et al., 2003; Raymond and Cole, 2003; Freeman et al., 2004). Depending on the lithology and soil composition of the catchment areas, increased levels of alkalinity, DIC or DOC can lead to local positive or negative feedbacks. Mobilisation of silicate carbonates from soils and transfer to the ocean would lead to a negative feedback to atmospheric CO_2 on long time scales (Dupre et al., 2003). Variations in nutrient supply can lead to species shifts and to deviations from the large-scale average Redfield ratios mainly in coastal waters, but also in the open ocean (Pahlow and Riebesell, 2000). Nutrient supply to the ocean has been changed through increased nitrate release from land due to fertilizer use as well as nitrogen deposition from the atmosphere in highly polluted areas (De Leeuw et al., 2001; Green et al., 2004).

Dust deposition to the ocean provides an important source of micronutrients (iron, zinc and others, e.g., Frew et al., 2001; Boyd et al., 2004) and ballast material to the ocean. Areas where iron is not supplied by aeolian dust transport in sufficient amounts tend to be iron-limited. A warmer climate may result on the average in a decrease of dust mobilisation and transport (Werner et al., 2002; Mahowald and Luo, 2003) although increased dust loads may result as well due to changes in land

use (Tegen et al., 2004) and in vegetation cover (Woodward et al., 2005). A decrease in dust loads could result in a net positive feedback, further increasing CO_2 through a weakening of marine biological production and export of aggregates due to clay ballast (Haake and Ittekkot, 1990; Ittekkot, 1993). Changes in plankton species composition and regional shifts of high production zones due to a changing climate could lead to a series of further feedbacks. Light absorption due to changes in bio-optical heating may change and induce a respective temperature change in ocean surface water (Sathyendranath et al., 1991; Wetzel et al., 2006). An increase in blooms involving calcifying organisms as indicated for the high northern latitudes (Broerse et al., 2003; Smyth et al., 2004) can temporarily increase surface ocean albedo, though the effect on the radiation budget is small (Tyrell et al., 1999).

7.3.4.5 Summary of Marine Carbon Cycle Climate Couplings

Couplings between the marine carbon cycle and climate are summarised in Table 7.3 and below.

7.3.4.5.1 Robust findings

- A potential slowing down of the ocean circulation and the decrease of seawater buffering with rising CO_2 concentration will suppress oceanic uptake of anthropogenic CO_2.
- Ocean CO_2 uptake has lowered the average ocean pH (increased acidity) by approximately 0.1 since 1750. Ocean acidification will continue and is directly and inescapably coupled to the uptake of anthropogenic CO_2 by the ocean.
- Inorganic chemical buffering and dissolution of marine $CaCO_3$ sediments are the main oceanic processes for neutralizing anthropogenic CO_2. These processes cannot prevent a temporary buildup of a large atmospheric CO_2 pool because of the slow large-scale overturning circulation.

7.3.4.5.2 Key uncertainties

- Future changes in ocean circulation and density stratification are still highly uncertain. Both the physical uptake of CO_2 by the ocean and changes in the biological cycling of carbon depend on these factors.
- The overall reaction of marine biological carbon cycling (including processes such as nutrient cycling as well as ecosystem changes including the role of bacteria and viruses) to a warm and high-CO_2 world is not yet well understood. Several small feedback mechanisms may add up to a significant one.
- The response of marine biota to ocean acidification is not yet clear, both for the physiology of individual organisms and for ecosystem functioning as a whole. Potential impacts are expected especially for organisms that build $CaCO_3$ shell material ('bio-calcification'). Extinction thresholds will likely be crossed for some organisms in some regions in the coming century.

7.3.5 Coupling Between the Carbon Cycle and Climate

7.3.5.1 Introduction

Atmospheric CO_2 is increasing at only about half the rate implied by fossil fuel plus land use emissions, with the remainder being taken up by the ocean, and vegetation and soil on land. Therefore, the land and ocean carbon cycles are currently helping to mitigate CO_2-induced climate change. However, these carbon cycle processes are also sensitive to climate. The glacial-interglacial cycles are an example of tight coupling between climate and the carbon cycle over long time scales, but there is also clear evidence of the carbon cycle responding to short-term climatic anomalies such as the El Niño-Southern Oscillation (ENSO) and Arctic Oscillation (Rayner et al., 1999; Bousquet et al., 2000; C. Jones et al., 2001; Lintner, 2002; Russell and Wallace, 2004) and the climate perturbation arising from the Mt. Pinatubo volcanic eruption (Jones and Cox, 2001a; Lucht et al., 2002; Angert et al., 2004).

Previous IPCC reports have used simplified or 'reduced-form' models to estimate the impact of climate change on the carbon cycle. However, detailed climate projections carried out with Atmosphere-Ocean General Circulation Models (AOGCMs) have typically used a prescribed CO_2 concentration scenario, neglecting two-way coupling between climate and the carbon cycle. This section discusses the first generation of coupled climate-carbon cycle AOGCM simulations, using the results to highlight a number of critical issues in the interaction between climate change and the carbon cycle.

7.3.5.2 Coupled Climate-Carbon Cycle Projections

The TAR reported two initial climate projections using AOGCMs with interactive carbon cycles. Both indicated positive feedback due largely to the impacts of climate warming on land carbon storage (Cox et al., 2000; Friedlingstein et al., 2001), but the magnitude of the feedback varied markedly between the models (Friedlingstein et al., 2003). Since the TAR a number of other climate modelling groups have completed climate-carbon cycle projections (Brovkin et al., 2004; Thompson et al., 2004; N. Zeng et al., 2004, Fung et al., 2005; Kawamiya et al., 2005; Matthews et al., 2005; Sitch et al., 2005) as part of C^{4}MIP. The 11 models involved in C^{4}MIP differ in the complexity of their components (Friedlingstein et al., 2006), including both Earth System Models of Intermediate Complexity and AOGCMs.

The models were forced by historical and Special Report on Emission Scenarios (SRES; IPCC, 2000) A2 anthropogenic CO_2 emissions for the 1850 to 2100 time period. Each modelling group carried out at least two simulations: one 'coupled' in which climate change affects the carbon cycle, and one 'uncoupled' in which atmospheric CO_2 increases do not influence climate (so that the carbon cycle experiences no CO_2-induced climate change). A comparison of the runs defines the climate-carbon cycle feedback, quantified by the feedback factor:

Table 7.3. *Couplings between climate change (increased atmospheric pCO_2, warming) and ocean carbon cycle processes. The response in terms of direct radiative forcing is considered (furthering or counteracting uptake of anthropogenic CO_2 from the atmosphere). The two quantitatively most important marine processes for neutralization of anthropogenic CO_2 work on long time scales only and are virtually certain to be in effect.*

Marine Carbon Cycle Process	Major Forcing Factors	Response + = positive feedback – = negative feedback and Quantitative Potential	Start	Re-equilibration Time Scale (kyr)	Likelihood	Comment
Biological export production of organic carbon and changes in organic carbon cycling	Warming, ocean circulation, nutrient supply, radiation, atmospheric CO_2, pH value	(Sum of effects not clear) +/– medium	immediate	0.001–10	*Likely*	Complex feedback chain, reactions can be fast for surface ocean, nutrient supply from land works on longer time scales, patterns of biodiversity and ecosystem functioning may be affected
Biological export production of calcium carbonate	Warming, atmospheric CO_2, pH value	(Sum of effects not clear) +/– small	immediate	0.001–1	*Likely*	Complex feedback chain, extinction of species likely, patterns of biodiversity and ecosystem functioning may be affected
Seawater buffering	Atmospheric CO_2, ocean circulation	– high	immediate	5–10	*Virtually certain*	System response, leads to ocean acidification
Changes in inorganic carbon chemistry (solubility, dissociation, buffer factor)	Warming, atmospheric CO_2, ocean circulation	+ medium	immediate	5–10	*Virtually certain*	Positive feedback dependent on 'bottleneck' ocean mixing
Dissolution of calcium carbonate sediments	pH value, ocean circulation	– high	immediate	40	*Virtually certain*	Patterns of biodiversity and ecosystem functioning in deep sea may be affected
Weathering of silicate carbonates	Atmospheric CO_2, warming	– medium	immediate	100	*Likely*	Very long-term negative feedback

Table 7.4. *Impact of carbon cycle feedbacks in the C⁴MIP models. Column 2 shows the impact of climate change on the CO_2 concentration by 2100, and column 3 shows the related amplification of the atmospheric CO_2 increase (i.e., the climate-carbon cycle feedback factor). Columns 4 to 8 list effective sensitivity parameters of the models: transient sensitivity of mean global temperature to CO_2, and the sensitivities of land and ocean carbon storage to CO_2 and climate (Friedlingstein et al., 2006). These parameters were calculated by comparison of the coupled and uncoupled runs over the entire period of the simulations (typically 1860 to 2100). Model details are given in Friedlingstein et al. (2006).*

Model[a]	Impact of Climate Change on the CO_2 Concentration by 2100 (ppm)	Climate-Carbon Feedback Factor	Transient Climate Sensitivity to Doubling CO_2 (°C)	Land Carbon Storage Sensitivity to CO_2 (GtC ppm^{-1})	Ocean Carbon Storage Sensitivity to CO_2 (GtC ppm^{-1})	Land Carbon Storage Sensitivity to Climate (GtC °C^{-1})	Ocean Carbon Storage Sensitivity to Climate (GtC °C^{-1})
A. HadCM3LC	224	1.44	2.3	1.3	0.9	–175	–24
B. IPSL-CM2C	74	1.18	2.3	1.6	1.6	–97	–30
C. MPI-M	83	1.18	2.6	1.4	1.1	–64	–22
D. LLNL	51	1.13	2.5	2.5	0.9	–81	–14
E. NCAR CSM-1	20	1.04	1.2	1.1	0.9	–24	–17
F. FRCGC	128	1.26	2.3	1.4	1.2	–111	–47
G. Uvic-2.7	129	1.25	2.3	1.2	1.1	–97	–43
H. UMD	98	1.17	2.0	0.2	1.5	–36	–60
I. BERN-CC	65	1.15	1.5	1.6	1.3	–104	–38
J. CLIMBER2-LPJ	59	1.11	1.9	1.2	0.9	–64	–22
K. IPSL-CM4-LOOP	32	1.07	2.7	1.2	1.1	–19	–17
Mean	**87**	**1.18**	**2.1**	**1.4**	**1.1**	**–79**	**–30**
Standard Deviation	±57	±0.11	±0.4	±0.5	±0.3	±45	±15

Notes:

[a] HadCM3LC: Hadley Centre coupled climate-carbon cycle general circulation model; IPSL-CM2C: Institut Pierre-Simon Laplace; MPI-M: Max Planck Institute for Meteorology; LLNL: Lawrence Livermore National Laboratory; NCAR CSM-1: NCAR Climate System Model version 1; FRCGC: Frontier Research Center for Global Change; Uvic-2.7: University of Victoria Earth System Climate Model; UMD: University of Maryland; BERN-CC: Bern Carbon Cycle Model; CLIMBER2-LPJ: Climate Biosphere Model 2 - Lund Potsdam Jena Terrestrial Carbon Model; IPSL-CM4-LOOP: Institute Pierre-Simon Laplace.

$F = \Delta C_A{}^c / \Delta C_A{}^u$, where $\Delta C_A{}^c$ is the change in CO_2 in the coupled run, and $\Delta C_A{}^u$ is the change in CO_2 in the uncoupled run. All of the eleven C⁴MIP models produce a positive climate-carbon cycle feedback, but with feedback factors varying from 1.04 (Model E) to 1.44 (Model A). This translates into an additional CO_2 concentration of between 20 and 224 ppm by 2100, with a mean of 87 ppm (Table 7.4).

All C⁴MIP models predict that an increasing fraction of total anthropogenic CO_2 emissions will remain airborne through the 21st century. Figure 7.13 shows the simulated partitioning of anthropogenic CO_2 for the entire simulation period to 2100 from each of the coupled models, and compares this with the partitioning simulated by the same models over the historical period to 1999. The dashed box shows observational constraints on the historical CO_2 partitioning, based on estimates of changes in ocean carbon storage (Sabine et al., 2004a) and total anthropogenic CO_2 emissions. The area of this box is largely due to uncertainties in the net land use emissions. The majority of the models sit within or very close to the historical constraints, but they differ in the magnitude of the changes projected for the 21st century. However, all models produce an increase in the fraction of total emissions that remain in the atmosphere, and most also indicate a decline in the fraction of emissions absorbed by the ocean (9 out of 11 models) and the land (10 out of 11 models). In the case of the oceanic uptake, this is largely a consequence of the reduced buffering capacity as CO_2 increases, and therefore also occurs in the uncoupled C⁴MIP models.

7.3.5.3 Sensitivity Analysis

The coupled and uncoupled model experiments can be used to separate the effects of climate change and CO_2 increase on land and ocean carbon storage (Friedlingstein et al., 2003). Table 7.4 also shows the linear sensitivity parameters diagnosed from each of the C⁴MIP models (Friedlingstein et al., 2006).

7.3.5.3.1 *Increase in ocean carbon uptake with increasing atmospheric carbon dioxide*

The ocean takes up CO_2 at a rate that depends on the difference between pCO_2 in the atmosphere and in the surface ocean. Model estimates of uptake differ primarily because of differences in the rate at which carbon is exported from the surface ocean to depth by the large-scale circulation (Doney et al., 2004; Section 7.3.4.1; Box 7.3) and the biological pump (Sarmiento et al., 2004). Ocean carbon cycle model intercomparisons have shown that the simulated circulation in the Southern Ocean can have a large impact on the efficiency with which CO_2, and other anthropogenic tracers such as CFCs,

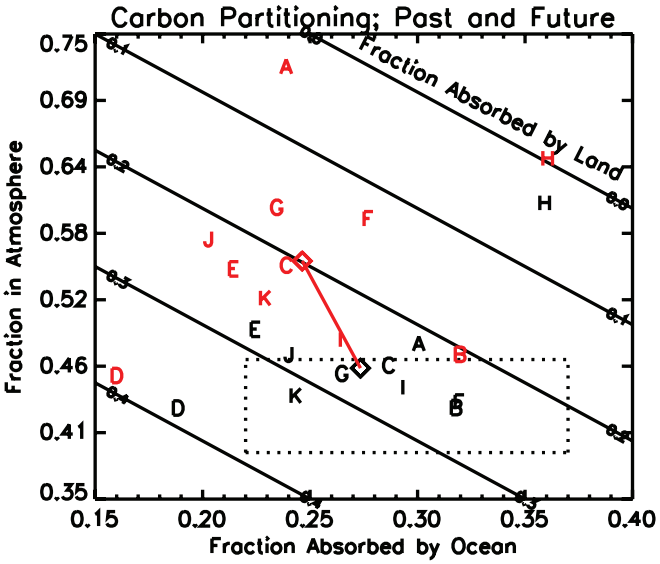


Figure 7.13. *Predicted increase in the fraction of total emissions that add to atmospheric CO_2. Changes in the mean partitioning of emissions as simulated by the C⁴MIP models up to 2000 (black symbols) and for the entire simulation period to 2100 (red symbols). The letters represent the models as given in Table 7.4. The box shown by the dotted line is a constraint on the historical carbon balance based on records of atmospheric CO_2 increase, and estimates of total emissions (fossil fuel plus land use emissions) and the oceanic uptake of anthropogenic CO_2 (Sabine et al., 2004a). The black and red diamonds show the model-mean carbon partitioning for the historical period and the entire simulation period, respectively. The red line shows the mean tendency towards an increasing airborne fraction through the 21st century, which is common to all models.*

are drawn down (Orr et al., 2001; Dutay et al., 2002). The C⁴MIP models show ocean carbon storage increases ranging from 0.9 to 1.6 GtC ppm^{-1}, which is equivalent to ocean uptake increasing at between 42 and 75% of the rate of atmospheric CO_2 increase. Basic ocean carbonate chemistry suggests that the ocean-borne fraction of emissions will fall in the future, even in the absence of climate change, because of an increasing ocean buffer factor (Section 7.3.4.2).

7.3.5.3.2 *Increase in land carbon uptake with increasing atmospheric carbon dioxide*

In the absence of land use change and forest fires, land carbon storage depends on the balance between the input of carbon as NPP, and the loss of carbon as heterotrophic (soil) respiration (Section 7.3.3). There is an ongoing debate concerning the importance of CO_2 fertilization at the patch scale where other constraints such as N limitation may dominate; recent surveys indicate a wide range of possible responses to a CO_2 increase of around 50%, with average increases of 12 to 23% (Norby et al., 2005; see Section 7.3.3.1).

The C⁴MIP models show increases in global NPP of between 6 and 33% when CO_2 increases over the same range. These figures are not directly comparable: some C⁴MIP models include vegetation dynamics, which are likely to increase the vegetation cover as well as the NPP per unit of vegetation area, and therefore lead to higher overall sensitivity of global NPP to CO_2. The FACE experiments also typically involve an instantaneous increase in CO_2. However, most C⁴MIP models are within the range of the CO_2 sensitivities measured.

The overall response of land carbon storage to CO_2 is given by the fifth column of Table 7.4. The C⁴MIP models show time-mean land carbon storage increases ranging from 0.2 to 2.5 GtC ppm^{-1}, with all but two models between 1.1 and 1.6 GtC ppm^{-1}. This response is driven by the CO_2 fertilization of NPP in each model, with a counteracting tendency for the mean soil carbon turnover rate (i.e., the heterotrophic respiration by unit soil carbon) to increase even in the absence of climate change. This somewhat surprising effect of CO_2 is seen to varying degrees in all C⁴MIP models. It appears to arise because CO_2 fertilization of NPP acts particularly to increase vegetation carbon, and therefore litter fall and soil carbon, in productive tropical regions that have high intrinsic decomposition rates. This increases the average turnover rate of the global soil carbon pool even though local turnover rates are unchanged. In some models (e.g., model C) this acts to offset a significant fraction of the land carbon increase arising from CO_2 fertilization. Models with large responses of ocean or land carbon storage to CO_2 tend to have weaker climate-carbon cycle feedbacks because a significant fraction of any carbon released through climate change effects is reabsorbed through direct CO_2 effects (Thompson et al., 2004).

7.3.5.3.3 *Transient climate sensitivity to carbon dioxide*

The strength of the climate-carbon cycle feedback loop depends on both the sensitivity of the carbon cycle to climate, and the sensitivity of climate to CO_2. The equilibrium climate sensitivity to a doubling of atmospheric CO_2 concentration remains a critical uncertainty in projections of future climate change, but also has a significant bearing on future CO_2 concentrations, with higher climate sensitivities leading to larger climate-carbon cycle feedbacks (Andreae et al., 2005). The fourth column of Table 7.4 shows the transient global climate sensitivity (i.e., the global climate warming that results when the transient simulation passes doubled atmospheric CO_2) for each of the C⁴MIP models. All but two models (models E and I) have transient climate sensitivities in the range 1.9°C to 2.7°C. However, differences in carbon cycle responses are likely to occur because of potentially large differences in regional climate change, especially where this affects water availability on the land.

7.3.5.3.4 *Dependence of ocean carbon uptake on climate.*

Climate change can reduce ocean uptake through reductions in CO_2 solubility, suppression of vertical mixing by thermal stratification and decreases in surface salinity. On longer time scales (>70 years) the ocean carbon sink may also be affected by climate-driven changes in large-scale circulation (e.g., a slowing down of the thermohaline circulation). The last column of Table 7.4 shows the sensitivity of ocean carbon storage to climate change as diagnosed from the C⁴MIP models. All models indicate a reduction in the ocean carbon sink by climate change of between –14 and –60 GtC °C^{-1}, implying a positive climate-CO_2 feedback.

7.3.5.3.5 Dependence of land carbon storage on climate.

The major land-atmosphere fluxes of CO_2 are strongly climate dependent. Heterotrophic respiration and NPP are both very sensitive to water availability and ambient temperatures. Changes in water availability depend critically on uncertain regional aspects of climate change projections and are therefore likely to remain a dominant source of uncertainty (see Chapter 11). The overall sensitivity of land carbon storage to climate (Table 7.4, seventh column) is negative in all models, implying a positive climate-CO_2 feedback, but the range is large: –19 to –175 GtC °C^{-1}. These values are determined by the combined effects of climate change on NPP and the soil carbon turnover (or decomposition) rate, as shown in Table 7.5.

The C^{4}MIP models utilise different representations of soil carbon turnover, ranging from single-pool models (model A) to nine-pool models (model E). However, most soil models assume a similar acceleration of decay with temperature, approximately equivalent to a doubling of the specific respiration rate for every 10°C warming. This temperature sensitivity is broadly consistent with a long history of lab and field measurements of soil efflux (Raich and Schlesinger, 1992), although there is an ongoing difficulty in separating root and soil respiration. Note, however, that the expected dependence on temperature was not found at the whole ecosystem level for decadal time scales, in forest soils (Giardina and Ryan, 2000; Melillo et al., 2002), grasslands (Luo et al., 2001) or boreal forests (Dunn et al., 2007). These apparent discrepancies may reflect the rapid depletion of labile pools of organic matter, with strong temperature responses likely so long as litter inputs are maintained (Knorr et al., 2005). Nevertheless, the temperature sensitivity of the slow carbon pools is still poorly known.

Table 7.5 shows that all C^{4}MIP models simulate an overall increase in soil carbon turnover rate as the climate warms, ranging from 2 to 10% per °C. The use of a single soil carbon pool in the Hadley model (A) cannot completely account for the relatively large sensitivity of soil respiration to temperature in this model (Jones et al., 2005), as evidenced by the lower effective sensitivity diagnosed from the UVic model (model G), which uses the same soil-vegetation component. It seems more likely that differences in soil moisture simulations are playing the key part in determining the effective sensitivity of soil turnover rate to climate. Table 7.5 also shows the effective sensitivities of NPP to climate, ranging from a significant reduction of 6% per °C to smaller climate-change driven increases of 2% per °C under climate change. This variation may reflect different time scales for boreal forest response to warming (leading to a positive impact on global NPP), as well as different regional patterns of climate change (Fung et al., 2005). The models with the largest negative responses of NPP to climate (models A, B and C) also show the tendency for tropical regions to dry under climate change, in some cases significantly (Cox et al., 2004).

7.3.5.4 Summary of Coupling Between the Carbon Cycle and Climate

7.3.5.4.1 Robust findings

Results from the coupled climate-carbon cycle models participating in the C^{4}MIP project support the following statements:

Table 7.5. *Effective sensitivities of land processes in the C^{4}MIP models: percent change of vegetation NPP to a doubling of atmospheric CO_2 concentration (Column 2), and sensitivities of vegetation NPP and specific heterotrophic soil respiration to a 1°C global temperature increase (Columns 3 and 4).*

Model[a]	Sensitivity of Vegetation NPP to CO_2: % change for a CO_2 doubling	Sensitivity of Vegetation NPP to Climate: % change for a 1°C increase	Sensitivity of Specific Heterotrophic Respiration Rate to Climate: % change for a 1°C increase
A. HadCM3LC	57	–5.8	10.2
B. IPSL-CM2C	50	–4.5	2.3
C. MPI-M	76	–4.0	2.8
D. LLNL	73	–0.4	7.0
E. NCAR CSM-1	34	0.8	6.2
F. FRCGC	21	1.2	7.2
G. UVic-2.7	47	–2.3	6.5
H. UMC	12	–1.6	4.8
I. BERN-CC	46	1.2	8.7
J. CLIMBER2-LPJ	44	1.9	9.4
K. IPSL-CM4-LOOP	64	–0.3	2.9
Mean	48	–1.3	6.2
Std Dev	±20	±2.6	±2.7

Notes:
[a] See Table 7.4 for model descriptions.

- All C4MIP models project an increase in the airborne fraction of total anthropogenic CO_2 emissions through the 21st century.
- The CO_2 increase alone will lead to continued uptake by the land and the ocean, although the efficiency of this uptake will decrease through the carbonate buffering mechanism in the ocean, and through saturation of the land carbon sink.
- Climate change alone will tend to suppress both land and ocean carbon uptake, increasing the fraction of anthropogenic CO_2 emissions that remain airborne and producing a positive feedback to climate change. The magnitude of this feedback varies among the C4MIP models, ranging from a 4 to 44% increase in the rate of increase of CO_2, with a mean (± standard deviation) of 18 ± 11%.

7.3.5.4.2 Key uncertainties

The C4MIP models also exhibit uncertainties in the evolution of atmospheric CO_2 for a given anthropogenic emissions scenario. Figure 7.14 shows how uncertainties in the sensitivities of ocean and land carbon processes contribute to uncertainties in the fraction of emissions that remain in the atmosphere. The confidence limits were produced by spanning the range of sensitivities diagnosed from the 11 C4MIP models (Tables 7.4 and 7.5). In the absence of climate change effects (lowest three bars), models simulate increased uptake by ocean and land (primarily as a result of CO_2 enhancement of NPP), with a slight offset of the land uptake by enhancement of the specific heterotrophic respiration rate (see Section 7.3.5.3.2). However, there is a wide range of response to CO_2, even in the absence of climate change effects on the carbon cycle. Climate change increases the fraction of emissions that remain airborne by suppressing ocean uptake, enhancing soil respiration and reducing plant NPP. The sensitivity of NPP to climate change is especially uncertain because it depends on changing soil water availability, which varies significantly between General Circulation Models (GCMs), with some models suggesting major drying and reduced productivity in tropical ecosystems (Cox et al., 2004). The transient climate sensitivity to CO_2 is also a major contributor to the overall uncertainty in the climate-carbon cycle feedback (top bar).

Other potentially important climate-carbon cycle interactions were not included in these first generation C4MIP experiments. The ocean ecosystem models used in C4MIP are at an early stage of development. These models have simple representations of the biological fluxes, which include the fundamental response to changes in internal nutrients, temperature and light availability, but for most models do not include the more complex responses

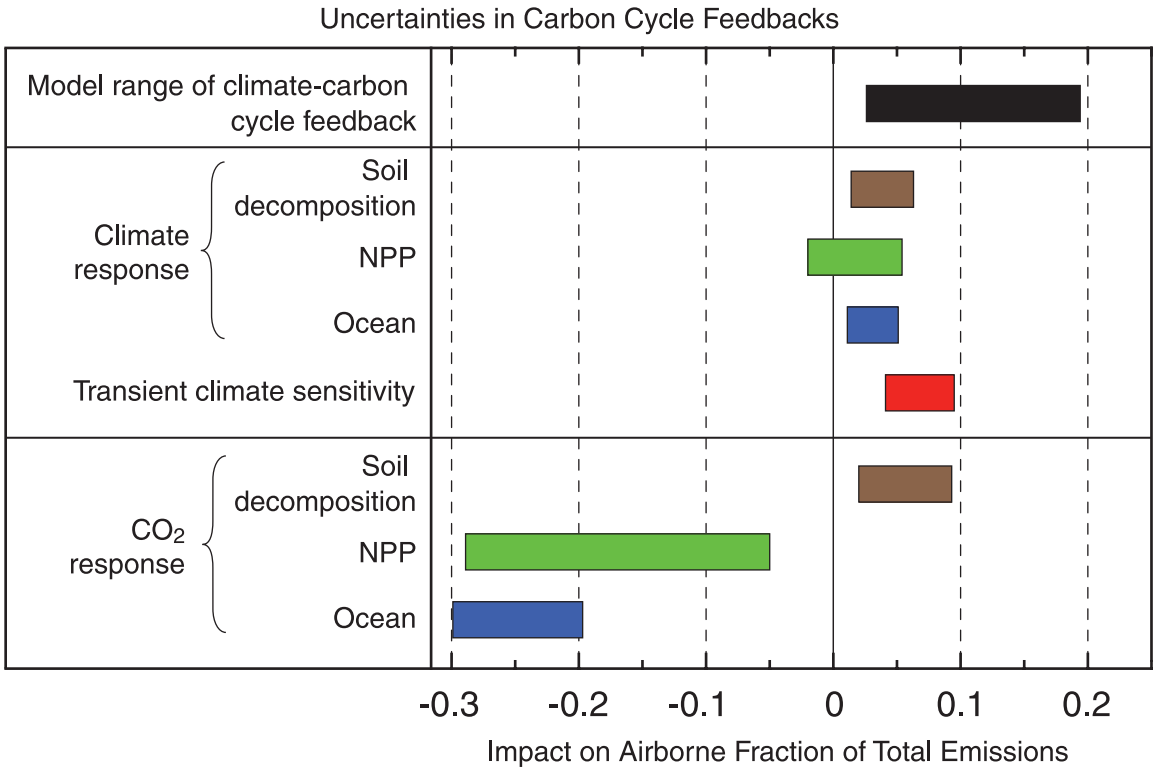


Figure 7.14. *Uncertainties in carbon cycle feedbacks estimated from analysis of the results from the C4MIP models. Each effect is given in terms of its impact on the mean airborne fraction over the simulation period (typically 1860 to 2100), with bars showing the uncertainty range based on the ranges of effective sensitivity parameters given in Tables 7.4 and 7.5. The lower three bars are the direct response to increasing atmospheric CO_2 (see Section 7.3.5 for details), the middle four bars show the impacts of climate change on the carbon cycle, and the top black bar shows the range of climate-carbon cycle feedbacks given by the C4MIP models.*

to changes in ecosystem structure. Changes in ecosystem structure can occur when specific organisms respond to surface warming, acidification, changes in nutrient ratios resulting from changes in external sources of nutrients (atmosphere or rivers) and changes in upper trophic levels (fisheries). Shifts in the structure of ocean ecosystems can influence the rate of CO_2 uptake by the ocean (Bopp et al., 2005).

The first-generation C^{4}MIP models also currently exclude, by design, the effects of forest fires and prior land use change. Forest regrowth may account for a large part of the land carbon sink in some regions (e.g., Pacala et al., 2001; Schimel et al., 2001; Hurtt et al., 2002; Sitch et al., 2005), while combustion of vegetation and soil organic matter may be responsible for a significant fraction of the interannual variability in CO_2 (Cochrane, 2003; Nepstad et al., 2004; Kasischke et al., 2005; Randerson et al., 2005). Other important processes were excluded in part because modelling these processes is even less straightforward. Among these are N cycling on the land (which could enhance or suppress CO_2 uptake by plants) and the impacts of increasing ozone concentrations on plants (which could suppress CO_2 uptake).

7.4 Reactive Gases and the Climate System

The atmospheric concentration of many reactive gases has increased substantially during the industrial era as a result of human activities. Some of these compounds (CH_4, N_2O, halocarbons, ozone, etc.) interact with longwave (infrared) solar radiation and, as a result, contribute to 'greenhouse warming'. Ozone also efficiently absorbs shortwave (ultraviolet and visible) solar energy, so that it protects the biosphere (including humans) from harmful radiation and plays a key role in the energy budget of the middle atmosphere. Many atmospheric chemical species are emitted at the surface as a result of biological processes (soils, vegetation, oceans) or anthropogenic activities (fossil fuel consumption, land use changes) before being photochemically destroyed in the atmosphere and converted to compounds that are eventually removed by wet and dry deposition. The oxidizing power (or capacity) of the atmosphere is determined primarily by the atmospheric concentration of the OH radical (daytime) and to a lesser extent the concentrations of the nitrate radical (NO_3; nighttime), ozone and hydrogen peroxide (H_2O_2). The coupling between chemical processes in the atmosphere and the climate system (Figure 7.15) are complex because they involve a large number of physical, chemical and biological processes that are not always very well quantified. An important issue is to determine to what extent predicted climate change could affect air quality (see Box 7.4). The goal of this section is assess recent progress made in the understanding of the two-way interactions between reactive gases and the climate system.

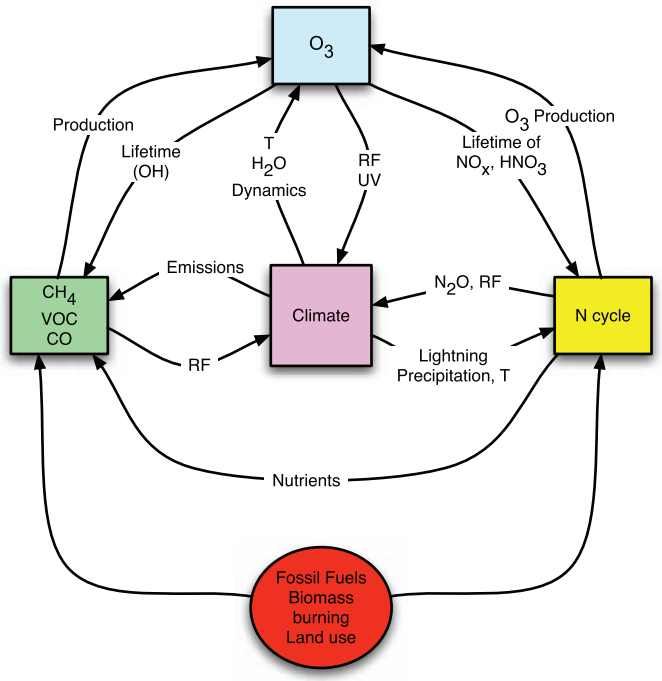


Figure 7.15. *Schematic representation of the multiple interactions between tropospheric chemical processes, biogeochemical cycles and the climate system. RF represents radiative forcing, UV ultraviolet radiation, T temperature and HNO_3 nitric acid.*

7.4.1 Methane

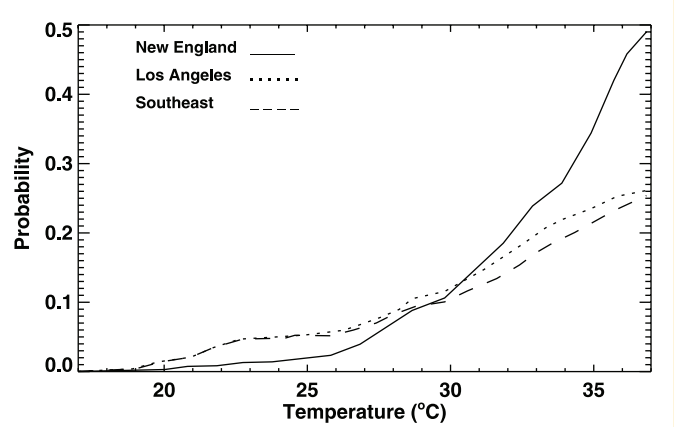
7.4.1.1 Biogeochemistry and Budgets of Methane

Atmospheric CH_4 originates from both non-biogenic and biogenic sources. Non-biogenic CH_4 includes emissions from fossil fuel mining and burning (natural gas, petroleum and coal), biomass burning, waste treatment and geological sources (fossil CH_4 from natural gas seepage in sedimentary basins and geothermal/volcanic CH_4). However, emissions from biogenic sources account for more than 70% of the global total. These sources include wetlands, rice agriculture, livestock, landfills, forests, oceans and termites. Emissions of CH_4 from most of these sources involve ecosystem processes that result from complex sequences of events beginning with primary fermentation of organic macromolecules to acetic acid (CH_3COOH), other carboxylic acids, alcohols, CO_2 and hydrogen (H_2), followed by secondary fermentation of the alcohols and carboxylic acids to acetate, H_2 and CO_2, which are finally converted to CH_4 by the so-called methanogenic Archaea: $CH_3COOH \rightarrow CH_4 + CO_2$ and $CO_2 + 4H_2 \rightarrow CH_4 + 2H_2O$ (Conrad, 1996). Alternatively, CH_4 sources can be divided into anthropogenic and natural. The anthropogenic sources include rice agriculture, livestock, landfills and waste treatment, some biomass burning, and fossil fuel combustion. Natural CH_4 is emitted from sources such as wetlands, oceans, forests, fire, termites and geological sources (Table 7.6).

Box 7.4: Effects of Climate Change on Air Quality

Weather is a key variable affecting air quality. Surface air concentrations of pollutants are highly sensitive to boundary layer ventilation, winds, temperature, humidity and precipitation. Anomalously hot and stagnant conditions in the summer of 1988 were responsible for the highest ozone year on record in the north-eastern USA (Lin et al., 2001). The summer heat wave in Europe in 2003 was associated with exceptionally high ozone (Ordonez et al., 2005). Such high interannual variability of surface ozone correlated with temperature demonstrates the potential air quality implications of climate change over the next century.

A few GCM studies have investigated how air pollution meteorology might respond to future climate change. Rind et al. (2001) found that increased continental ventilation as a result of more vigorous convection should decrease surface concentrations, while Holzer and Boer (2001) found that weaker winds should result in slower dilution of pollution plumes and hence higher concentrations. A focused study by Mickley et al. (2004) for the eastern USA found an increase in the severity and persistence of regional pollution episodes due to the reduced frequency of ventilation by cyclones tracking across Canada. This effect more than offsets the dilution associated with the small rise in mixing depths. A decrease in cyclone frequency at northern mid-latitudes and a shift to higher latitudes has been noted in observations from the past few decades (McCabe et al., 2001). An urban air quality model study by Jacobson (1999) pointed out that decreasing soil moisture or increasing surface temperature would decrease mixing depths and reduce near-surface pollutant concentrations.



Box 7.4, Figure 1. *Probability that the daily maximum eight-hour average ozone concentration will exceed the US National Ambient Air Quality Standard of 0.08 ppm for a given daily maximum temperature based on 1980 to 1998 data. Values are shown for New England (bounded by 36°N, 44°N, 67.5°W and 87.5°W), the Los Angeles Basin (bounded by 32°N, 40°N, 112.5°W and 122.5°W) and the southeastern USA (bounded by 32°N, 36°N, 72.5°W and 92.5°W). Redrawn from Lin et al. (2001).*

A number of studies in the USA have shown that summer daytime ozone concentrations correlate strongly with temperature (NRC, 1991). This correlation appears to reflect contributions of comparable magnitude from (1) temperature-dependent biogenic VOC emissions, (2) thermal decomposition of peroxyacetylnitrate, which acts as a reservoir for NO_x and (3) association of high temperatures with regional stagnation (Jacob et al., 1993; Sillman and Samson, 1995; Hauglustaine et al., 2005). Empirical relationships between ozone air quality standard exceedances and temperature, as shown in Figure 1, integrate all of these effects and could be used to estimate how future regional changes in temperature would affect ozone air quality. Changes in the global ozone background would also have to be accounted for (Stevenson et al., 2005).

A few GCM studies have examined more specifically the effect of changing climate on regional ozone air quality, assuming constant emissions. Knowlton et al. (2004) use a GCM coupled to a Regional Climate Model (RCM) to investigate the impact of 2050 climate change (compared with 1990) on ozone concentrations in the New York City metropolitan area. They found a significant ozone increase that they translated into a 4.5% increase in ozone-related acute mortality. Langner et al. (2005) use an RCM driven by two different GCMs to examine changes in the Accumulated Ozone concentration above a Threshold of 40 ppb (AOT40) statistic (ozone-hours above 40 ppb) over Europe in 2050 to 2070 relative to the present. They found an increase in southern and central Europe and a decrease in northern Europe that they attributed to different regional trends in cloudiness and precipitation. Dentener et al. (2006) synthesise the results of 10 global model simulations for 2030 driven by future compared with present climate. They find that climate change caused mean decreases in surface ozone of 0.5 to 1 ppb over continents and 1 to 2 ppb over the oceans, although some continental regions such as the Eastern USA experienced slight increases.

There has been less work on the sensitivity of aerosols to meteorological conditions. Regional model simulations by Aw and Kleeman (2003) find that increasing temperatures should increase surface aerosol concentrations due to increased production of aerosol precursors (in particular semi-volatile organic compounds and HNO_3) although this is partly compensated by the increasing vapour pressure of these compounds at higher temperatures. Perturbations of precipitation frequencies and patterns might be expected to have a major impact on aerosol concentrations, but the GCM study by Mickley et al. (2004) for 2000 to 2050 climate change finds little effect in the USA.

The net rate of CH_4 emissions is generally estimated from three approaches: (1) extrapolation from direct flux measurements and observations, (2) process-based modelling (bottom-up approach) and (3) inverse modelling that relies on spatially distributed, temporally continuous observations of concentration, and in some cases isotopic composition in the atmosphere (top-down approach). The top-down method also includes aircraft and satellite observations (Xiao et al., 2004; Frankenberg et al., 2005, 2006). When the bottom-up approach is used to extrapolate the emissions to larger scales, uncertainty results from the inherent large temporal and spatial variations of fluxes and the limited range of observational conditions. The top-down approach helps to overcome the weaknesses in bottom-up methods. However, obstacles to extensive application of the top-down approach include inadequate observations, and insufficient capabilities of the models to account for error amplification in the inversion process and to simulate complex topography and meteorology (Dentener et al., 2003a; Mikaloff Fletcher et al., 2004a, 2004b; Chen and Prinn, 2005, 2006). Measurements of isotopes of CH_4 (^{13}C, ^{14}C, and ^{2}H) provide additional constraints on CH_4 budgets and specific sources, but such data are even more limited (Bergamaschi et al., 2000; Lassey et al., 2000; Mikaloff Fletcher et al., 2004a, 2004b).

Since the TAR, availability of new data from various measurement networks and from national reporting documents has enabled re-estimates of CH_4 source magnitudes and insights into individual source strengths. Total global pre-industrial emissions of CH_4 are estimated to be 200 to 250 $Tg(CH_4)$ yr^{-1} (Chappellaz et al., 1993; Etheridge et al., 1998; Houweling et al., 2000; Ferretti et al., 2005; Valdes et al., 2005). Of this, natural CH_4 sources emitted between 190 and 220 $Tg(CH_4)$ yr^{-1}, and anthropogenic sources (rice agriculture, livestock, biomass burning and waste) accounted for the rest (Houweling et al., 2000; Ruddiman and Thomson, 2001). In contrast, anthropogenic emissions dominate present-day CH_4 budgets, accounting for more than 60% of the total global budget (Table 7.6).

The single largest CH_4 source is natural wetlands. Recent estimates combine bottom-up and top-down fluxes, and global observations of atmospheric CH_4 concentrations in a three-dimensional Atmospheric Transport and Chemical Model (ATCM) simulation (Chen and Prinn, 2005, 2006). In these estimates, southern and tropical regions account for more than 70% of total global wetland emissions. Other top-down studies that include both direct observations and $^{13}C/^{12}C$ ratios of CH_4 suggest greater emissions in tropical regions compared with previously estimates (Mikaloff Fletcher et al., 2004a, 2004b; Xiao et al., 2004; Frankenberg et al., 2006). However, several bottom-up studies indicate fewer emissions from tropical rice agriculture (Li et al., 2002; Yan et al., 2003; Khalil and Shearer 2006). Frankenberg et al. (2005, 2006) and Keppler et al. (2006) suggest that tropical trees emit CH_4 via an unidentified process. The first estimate of this source was 10 to 30% (62–236 $Tg(CH_4)$ yr^{-1}) of the global total, but Kirschbaum et al. (2006) revise this estimate downwards to 10 to 60 $Tg(CH_4)$ yr^{-1}. Representative $^{13}C/^{12}C$ ratios ($\delta^{13}C$ values) of CH_4 emitted from individual sources are included in Table 7.6. Due to isotope fractionation associated with CH_4 production and consumption processes, CH_4 emitted from each source exhibits a measurably different $\delta^{13}C$ value. Therefore, it is possible, using mixing models, to constrain further the sources of atmospheric CH_4.

Geological sources of CH_4 are not included in Table 7.6. However, several studies suggest that significant amounts of CH_4, produced within the Earth's crust (mainly by bacterial and thermogenic processes), are released into the atmosphere through faults and fractured rocks, mud volcanoes on land and the seafloor, submarine gas seepage, microseepage over dry lands and geothermal seeps (Etiope and Klusman, 2002; Etiope, 2004; Kvenvolden and Rogers, 2005). Emissions from these sources are estimated to be as large as 40 to 60 $Tg(CH_4)$ yr^{-1}.

The major CH_4 sinks are oxidation by OH in the troposphere, biological CH_4 oxidation in drier soil, and loss to the stratosphere (Table 7.6). Oxidation by chlorine (Cl) atoms in the marine atmospheric boundary layer is suggested as an additional sink for CH_4, possibly constituting an additional loss of about 19 $Tg(CH_4)$ yr^{-1} (Gupta et al., 1997; Tyler et al., 2000; Platt et al., 2004; Allan et al., 2005). However, the decline in the growth rate of atmospheric CH_4 concentration since the TAR shows no clear correlation with change in sink strengths over the same period (Prinn et al., 2001, 2005; Allan et al., 2005). This trend has continued since 1993, and the reduction in the CH_4 growth rate has been suggested to be a consequence of source stabilisation and the approach of the global CH_4 budget towards steady state (Dlugokencky et al., 1998, 2003). Thus, total emissions are likely not increasing but partitioning among the different sources may have changed (see Section 2.3). Consequently, in the Fourth Assessment Report (AR4) the sink strength is treated as in the TAR (576 $Tg(CH_4)$ yr^{-1}). However, the AR4 estimate has been increased by 1% (to 581 $Tg(CH_4)$ yr^{-1}) to take into account the recalibration of the CH_4 scale explained in Chapter 2. The main difference between TAR and AR4 estimates is the source-sink imbalance inferred from the annual increment in concentration. The TAR used 8 ppb yr^{-1} for a period centred on 1998 when there was clearly an anomalously high growth rate. The present assessment uses 0.2 ppb yr^{-1}, the average over 2000 to 2005 (see Section 2.3 and Figure 2.4). Thus, using the CH_4 growth rate for a single anomalous year, as in the TAR, gives an anomalously high top-down value relative to the longer-term average source. For a conversion factor of 2.78 $Tg(CH_4)$ per ppb and an atmospheric concentration of 1,774 ppb, the atmospheric burden of CH_4 in 2005 was 4,932 Tg, with an annual average increase (2000–2005) of about 0.6 Tg yr^{-1}. Total average annual emissions during the period considered here are approximately 582 $Tg(CH_4)$ yr^{-1}.

Uncertainty in this estimate may arise from several sources. Uncertainty in the atmospheric concentration measurement, given in Chapter 2 as 1,774 ± 1.8 ppb in 2005, is small (about 0.1%). Uncertainty ranges for individual sink estimates are ±103 $Tg(CH_4)$ (20%), ±15 $Tg(CH_4)$ (50%), ±8 $Tg(CH_4)$ (20%) for OH, soil and stratospheric loss, respectively (as reported in the Second Assessment Report). The use of a different lifetime for CH_4 (8.7 ± 1.3 years) leads to an uncertainty in overall sink strength of ±15%. Thus, the top-down method used in AR4 is

Table 7.6 *Sources, sinks and atmospheric budgets of CH_4 ($Tg(CH_4)$ yr^{-1}).*[a]

References	Indicative ^{13}C, ‰[b]	Hein et al., 1997[c]	Houweling et al., 2000[c]	Olivier et al., 2005	Wuebbles and Hayhoe, 2002	Scheehle et al., 2002	J. Wang et al., 2004[c]	Mikaloff Fletcher et al., 2004a[c]	Chen and Prinn, 2006[c]	TAR	AR4
Base year		1983–1989		2000		1990	1994	1999	1996–2001	1998	2000–2004
Natural sources			**222**		**145**		**200**	**260**	**168**		
Wetlands	–58	231	163		100		176	231	145		
Termites	–70		20		20		20	29	23		
Ocean	–60		15		4						
Hydrates	–60				5		4				
Geological sources	–40		4		14						
Wild animals	–60		15								
Wildfires	–25		5		2						
Anthropogenic sources		**361**		**320**	**358**	**264**	**307**	**350**	**428**		
Energy						74	77				
Coal mining	–37	32		34	46			30	48[d]		
Gas, oil, industry	–44	68		64	60			52	36[e]		
Landfills & waste	–55	43		66	61	69	49	35			
Ruminants	–60	92		80	81	76	83	91	189[f]		
Rice agriculture	–63	83		39	60	31	57	54	112		
Biomass burning	–25	43			50	14	41	88	43[e]		
C3 vegetation	–25			27							
C4 vegetation	–12			9							
Total sources		**592**			**503**		**507**	**610**	**596**	**598**	**582**
Imbalance		+33								+22	+1
Sinks											
Soils	–18	26			30		34	30		30	30[g]
Tropospheric OH	–3.9	488			445		428	507		506	511[g]
Stratospheric loss		45			40		30	40		40	40[g]
Total sink		**559**			**515**		**492**	**577**		**576**	**581**[g]

Notes:

[a] Table shows the best estimate values.

[b] Indicative ^{13}C values for sources are taken mainly from Mikaloff Fletcher et al. (2004a). Entries for sinks are the fractionation, (k_{13}/k_{12}–1) where k_n is the removal rate of $^nCH_4$; the fractionation for OH is taken from Saueressig et al. (2001) and that for the soil sink from Snover and Quay (2000) as the most recent determinations.

[c] Estimates from global inverse modelling (top-down method).

[d] Includes natural gas emissions.

[e] Biofuel emissions are included under Industry.

[f] Includes emissions from landfills and wastes.

[g] Numbers are increased by 1% from the TAR according to recalibration described in Chapter 2.

constrained mainly by uncertainty in sink estimates and the choice of lifetime used in the mass balance calculation.

7.4.1.2 Effects of Climate

Effects of climate on CH_4 biogeochemistry are investigated by examining records of the past and from model simulations under various climate change scenarios. Ice core records going back 650 ka (Petit et al., 1999; Spahni et al., 2005) reveal that the atmospheric concentration of CH_4 is closely tied to atmospheric temperature, falling and rising in phase with temperature at the inception and termination of glacial episodes (Wuebbles and Hayhoe, 2002). Brook et al. (2000) show that, following each transition, temperature increased more rapidly than CH_4 concentration. Since biogenic CH_4 production and emission from major sources (wetlands, landfills, rice agriculture and biomass burning) are influenced by climate variables such as temperature and moisture, the effect of climate on emissions from these sources is significant.

Several studies indicate a high sensitivity of wetland CH_4 emissions to temperature and water table. Before the 1990s, elevated surface temperature and emissions from wetlands were believed to contribute to the increase in global CH_4 emissions (Walter and Heimann, 2001a,b; Christensen et al., 2003; Zhuang et al., 2004). Observations indicate substantial increases in CH_4 released from northern peatlands that are experiencing permafrost melt (Christensen et al., 2004; Wickland et al., 2006). Based on the relationship between emissions and temperature at two wetland sites in Scotland, Chapman and Thurlow (1996) predicted that CH_4 emissions would increase by 17, 30 and 60% for warmings of 1.5°C, 2.5°C and 4.5°C (warming above the site's mean temperature during 1951 to 1980), respectively. A model simulation by Cao et al. (1998) yielded a 19% emission increase under a uniform 2°C warming. The combined effects of a 2°C warming and a 10% increase in precipitation yielded an increase of 21% in emissions. In most cases, the net emission depends on how an increase in temperature affects net ecosystem production (NEP), as this is the source of methanogenic substrates (Christensen et al., 2003), and on the moisture regime of wetlands, which determines if decomposition is aerobic or anaerobic. Emissions increase under a scenario where an increase in temperature is associated with increases in precipitation and NEP, but emissions decrease if elevated temperature results in either reduced precipitation or reduced NEP.

For a doubling in atmospheric CO_2 concentration, the GCM of Shindell et al. (2004) simulates a 3.4°C warming. Changes in the hydrological cycle due to this CO_2 doubling cause CH_4 emissions from wetlands to increase by 78%. Gedney et al. (2004) also simulate an increase in CH_4 emissions from northern wetlands due to an increase in wetland area and an increase in CH_4 production due to higher temperatures. Zhuang et al. (2004) use a terrestrial ecosystem model based on emission data for the 1990s to study how rates of CH_4 emission and consumption in high-latitude soils of the NH (north of 45°N) have changed over the past century (1900–2000) in response to observed change in the region's climate. They estimate that average net emissions of CH_4 increased by 0.08 Tg yr^{-1} over the 20th century. Their decadal net CH_4 emission rate correlates with soil temperature and water table depth.

In rice agriculture**,** climate factors that will likely influence CH_4 emission are those associated with plant growth. Plant growth controls net emissions by determining how much substrate will be available for either methanogenesis or methanotrophy (Matthews and Wassmann, 2003). Sass et al. (2002) show that CH_4 emissions correlate strongly with plant growth (height) in a Texas rice field. Any climate change scenario that results in an increase in plant biomass in rice agriculture is likely to increase CH_4 emissions (Xu et al., 2004). However, the magnitude of increased emission depends largely on water management. For example, field drainage could significantly reduce emission due to aeration of the soil (i.e., influx of air into anaerobic zones that subsequently suppresses methanogenesis, Li et al., 2002).

Past observations indicate large interannual variations in CH_4 growth rates (Dlugokencky et al., 2001). The mechanisms causing these variations are poorly understood and the role of climate is not well known. Emissions from wetlands and biomass burning may have contributed to emission peaks in 1993 to 1994 and 1997 to 1998 (Langenfelds et al., 2002; Butler et al., 2004). Unusually warm and dry conditions in the NH during ENSO periods increase biomass burning. Kasischke and Bruhwiler (2002) attribute CH_4 releases of 3 to 5 Tg in 1998 to boreal forest fires in Eastern Siberia resulting from unusually warm and dry conditions.

Meteorological conditions can affect global mean removal rates (Warwick et al., 2002; Dentener et al., 2003a). Dentener et al. find that over the period 1979 to 1993, the primary effect resulted from changes in OH distribution caused by variations in tropical tropospheric water vapour. Johnson et al. (2001) studied predictions of the CH_4 evolution over the 21st century and found that there is also a substantial increase in CH_4 destruction due to increases in the CH_4 + OH rate coefficient in a warming climate. There also appear to be significant interannual variations in the active Cl sink, but a climate influence has yet to be identified (Allan et al., 2005). On the other hand, several model studies indicate that CH_4 oxidation in soil is relatively insensitive to temperature increase (Ridgwell at al., 1999; Zhuang et al., 2004). A doubling of atmospheric CO_2 would likely change the sink strength only marginally (in the range of –1 to +3 Tg(CH_4) yr^{-1}; Ridgwell et al., 1999). However, any change in climate that alters the amount and pattern of precipitation may significantly affect the CH_4 oxidation capacity of soils. A process-based model simulation indicated that CH_4 oxidation strongly depends on soil gas diffusivity, which is a function of soil bulk density and soil moisture content (Bogner et al., 2000; Del Grosso et al., 2000).

Climate also affects the stability of CH_4 hydrates beneath the ocean, where large amounts of CH_4 are stored (~4×10^6 Tg; Buffett and Archer, 2004). The $\delta^{13}C$ values of ancient seafloor carbonates reveal several hydrate dissociation events that appear to have occurred in connection with rapid warming episodes in the Earth's history (Dickens et al., 1997; Dickens, 2001). Model

results indicate that these hydrate decomposition events occurred too fast to be controlled by the propagation of the temperature change into the sediments (Katz et al., 1999; Paull et al., 2003). Additional studies infer other indirect and inherently more rapid mechanisms such as enhanced migration of free gas, or reordering of gas hydrates due to slump slides (Hesselbo et al., 2000; Jahren et al., 2001; Kirschvink et al., 2003; Ryskin, 2003). Recent modelling suggests that today's seafloor CH_4 inventory would be diminished by 85% with a warming of bottom water temperatures by 3°C (Buffett and Archer, 2004). Based on this inventory, the time-dependent feedback of hydrate destabilisation to global warming has been addressed using different assumptions for the time constant of destabilisation: an anthropogenic release of 2,000 GtC to the atmosphere could cause an additional release of CH_4 from gas hydrates of a similar magnitude (~2,000 Gt(CH_4)) over a period of 1 to 100 kyr (Archer and Buffett, 2005). Thus, gas hydrate decomposition represents an important positive CH_4 feedback to be considered in global warming scenarios on longer time scales.

In summary, advances have been made since the TAR in constraining estimates of CH_4 source strengths and in understanding emission variations. These improvements are attributed to increasing availability of worldwide observations and improved modelling techniques. Emissions from anthropogenic sources remain the major contributor to atmospheric CH_4 budgets. Global emissions are likely not to have increased since the time of the TAR, as nearly zero growth rates in atmospheric CH_4 concentrations have been observed with no significant change in the sink strengths.

7.4.2 Nitrogen Compounds

The N cycle is integral to functioning of the Earth system and to climate (Vitousek et al., 1997; Holland et al., 2005a). Over the last century, human activities have dramatically increased emissions and removal of reactive N to the global atmosphere by as much as three to five fold. Perturbations of the N cycle affect the atmosphere climate system through production of three key N-containing trace gases: N_2O, ammonia (NH_3) and NO_x (nitric oxide (NO) + nitrogen dioxide (NO_2)). Nitrous oxide is the fourth largest single contributor to positive radiative forcing, and serves as the only long-lived atmospheric tracer of human perturbations of the global N cycle (Holland et al., 2005a). Nitrogen oxides have short atmospheric lifetimes of hours to days (Prather et al., 2001). The dominant impact of NO_x emissions on the climate is through the formation of tropospheric ozone, the third largest single contributor to positive radiative forcing (Sections 2.3.6, 7.4.4). Emissions of NO_x generate indirect negative radiative forcing by shortening the atmospheric lifetime of CH_4 (Prather 2002). Ammonia contributes to the formation of sulphate and nitrate aerosols, thereby contributing to aerosol cooling and the aerosol indirect effect (Section 7.5), and to increased nutrient supply for the carbon cycle (Section 7.5). Ammonium and NO_x are removed from the atmosphere by deposition, thus affecting the carbon cycle through increased nutrient supply (Section 7.3.3.1.3).

Atmospheric concentrations of N_2O have risen 16%, from about 270 ppb during the pre-industrial era to 319 ppb in 2005 (Figure 7.16a). The average annual growth rate for 1999 to 2000 was 0.85 to 1.1 ppb yr^{-1}, or about 0.3% per year (WMO, 2003). The main change in the global N_2O budget since the TAR is quantification of the substantial human-driven emission of N_2O (Table 7.7; Naqvi et al., 2000; Nevison et al., 2004; Kroeze et al., 2005; Hirsch et al., 2006). The annual source of N_2O from the Earth's surface has increased by about 40 to 50% over pre-industrial levels as a result of human activity (Hirsch et al., 2006). Human activity has increased N supply to coastal and open oceans, resulting in decreased O_2 availability and N_2O emissions (Naqvi et al., 2000; Nevison et al., 2004).

Since the TAR, both top-down and bottom-up estimates of N_2O have been refined. Agriculture remains the single biggest anthropogenic N_2O source (Bouwman et al., 2002; Smith and Conen, 2004; Del Grosso et al., 2005). Land use change continues to affect N_2O and NO emissions (Neill et al., 2005): logging is estimated to increase N_2O and NO emissions by 30 to 350% depending on conditions (Keller et al., 2005). Both studies underscore the importance of N supply, temperature and moisture as regulators of trace gas emissions. The inclusion of several minor sources (human excreta, landfills and atmospheric deposition) has increased the total bottom-up budget to 20.6 TgN yr^{-1} (Bouwman et al., 2002). Sources of N_2O now estimated since the TAR include coastal N_2O fluxes of 0.2 TgN yr^{-1} (±70%; Nevison et al., 2004) and river and estuarine N_2O fluxes of 1.5 TgN yr^{-1} (Kroeze et al., 2005). Box model calculations show the additional river and estuarine sources to be consistent with the observed rise in atmospheric N_2O (Kroeze et al., 2005).

Top-down estimates of surface sources use observed concentrations to constrain total sources and their spatial distributions. A simple calculation, using the present-day N_2O burden divided by its atmospheric lifetime, yields a global stratospheric loss of about 12.5 ± 2.5 TgN yr^{-1}. Combined with the atmospheric increase, this loss yields a surface source of 16 TgN yr^{-1}. An inverse modelling study of the surface flux of N_2O yields a global source of 17.2 to 17.4 TgN yr^{-1} with an estimated uncertainty of 1.4 (1 standard deviation; Hirsch et al., 2006). The largest sources of N_2O are from land at tropical latitudes, the majority located north of the equator. The Hirsch et al. inversion results further suggest that N_2O source estimates from agriculture and fertilizer may have increased markedly over the last three decades when compared with an earlier inverse model estimate (Prinn et al., 1990). Bottom-up estimates, which sum individual source estimates, are more evenly distributed with latitude and lack temporal variability. However, there is clear consistency between top-down and bottom-up global source estimates, which are 17.3 (15.8–18.4) and 17.7 (8.5–27.7) TgN yr^{-1}, respectively.

Concentrations of NO_x and reduced nitrogen (NH_x = NH_3 + ammonium ion (NH_4^+)) are difficult to measure because the atmospheric lifetimes of hours to days instead of years generate pronounced spatial and temporal variations in their distributions. Atmospheric concentrations of NO_x and NH_x

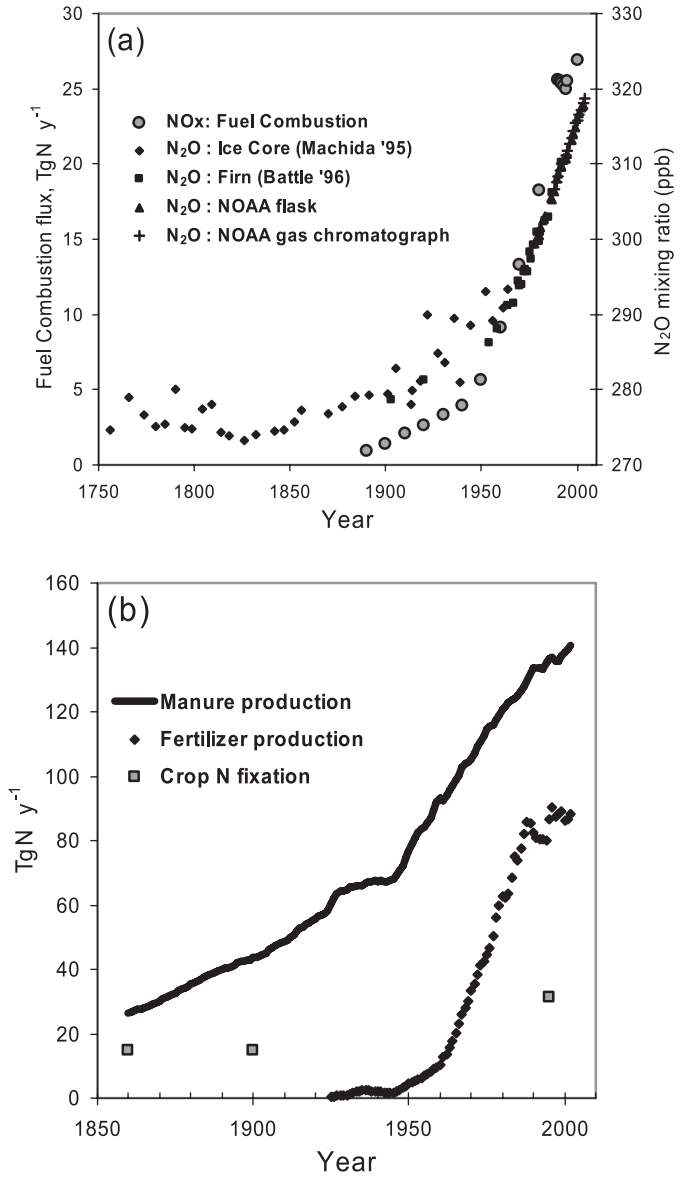


Figure 7.16. *(a) Changes in the emissions of fuel combustion NO_x and atmospheric N_2O mixing ratios since 1750. Mixing ratios of N_2O provide the atmospheric measurement constraint on global changes in the N cycle. (b) Changes in the indices of the global agricultural N cycle since 1850: the production of manure, fertilizer and estimates of crop N fixation. For data sources see http://www-eosdis.ornl.gov/ (Holland et al., 2005b) and http://www.cmdl.noaa.gov/. Figure adapted from Holland et al. (2005c).*

vary more regionally and temporally than concentrations of N_2O. Total global NO_x emissions have increased from an estimated pre-industrial value of 12 TgN yr^{-1} (Holland et al., 1999; Galloway et al., 2004) to between 42 and 47 TgN yr^{-1} in 2000 (Table 7.7). Lamarque et al. (2005a) forecast them to be 105 to 131 TgN yr^{-1} by 2100. The range of surface NO_x emissions (excluding lightning and aircraft) used in the current generation of global models is 33 to 45 TgN yr^{-1} with small ranges for individual sources. The agreement reflects the use of similar inventories and parametrizations. Current estimates of NO_x emissions from fossil fuel combustion are smaller than in the TAR.

Since the TAR, estimates of tropospheric NO_2 columns from space by the Global Ozone Monitoring Experiment (GOME, launched in 1995) and the SCanning Imaging Absorption SpectroMeter for Atmospheric CHartographY (SCIAMACHY, launched in 2002) (Richter and Burrows, 2002; Heue et al., 2005) provide constraints on estimates of NO_x emissions (Leue et al., 2001). Martin et al. (2003a) use GOME data to estimate a global surface source of NO_x of 38 TgN yr^{-1} for 1996 to 1997 with an uncertainty factor of 1.6. Jaeglé et al. (2005) partition the surface NO_x source inferred from GOME into 25.6 TgN yr^{-1} from fuels, 5.9 TgN yr^{-1} from biomass burning and 8.9 TgN yr^{-1} from soils. Interactions between soil emissions and scavenging by plant canopies have a significant impact on soil NO_x emissions to the free troposphere: the impact may be greatest in subtropical and tropical regions where emissions from fuel combustion are rising (Ganzeveld et al., 2002). Boersma et al. (2005) find that GOME data constrain the global lightning NO_x source for 1997 to the range 1.1 to 6.4 TgN yr^{-1}. Comparison of the tropospheric NO_2 column of three state-of-the-art retrievals from GOME for the year 2000 with model results from 17 global atmospheric chemistry models highlights significant differences among the various models and among the three GOME retrievals (Figure 7.17, van Noije et al., 2006). The discrepancies among the retrievals (10 to 50% in the annual mean over polluted regions) indicate that the previously estimated retrieval uncertainties have a large systematic component. Top-down estimates of NO_x emissions from satellite retrievals of tropospheric NO_2 are strongly dependent on the choice of model and retrieval.

Knowledge of the spatial distribution of NO_x emissions has evolved significantly since the TAR. An Asian increase in emissions has been compensated by a European decrease over the past decade (Naja et al., 2003). Richter et al. (2005; see also Irie et al., 2005) use trends for 1996 to 2004 observed by GOME and SCIAMACHY to deduce a 50% increase in NO_x emissions over industrial areas of China. Observations of NO_2 in shipping lanes from GOME (Beirle et al., 2004) and SCIAMACHY (Richter et al., 2004) give values at the low end of emission inventories. Data from GOME and SCIAMACHY further reveal large pulses of soil NO_x emissions associated with rain (Jaeglé et al., 2004) and fertilizer application (Bertram et al., 2005).

All indices show an increase since pre-industrial times in the intensity of agricultural nitrogen cycling, the primary source of NH_3 emissions (Figure 7.16b and Table 7.7; Bouwman et al., 2002). Total global NH_3 emissions have increased from an estimated pre-industrial value of 11 TgN yr^{-1} to 54 TgN yr^{-1} for 2000 (Holland et al., 1999; Galloway et al., 2004), and are projected to increase to 116 TgN yr^{-1} by 2050.

The primary sink for NH_x and NO_x and their reaction products is wet and dry deposition. Estimates of the removal rates of both NH_x and NO_x are provided by measurements of

wet deposition over the USA and Western Europe to quantify acid rain inputs (Hauglustaine et al., 2004; Holland et al., 2005a; Lamarque et al., 2005a). Chemical transport models represent the wet and dry deposition of NO_x and NH_x and their reaction products. A study of 29 simulations with 6 different tropospheric chemistry models, focusing on present-day and 2100 conditions for NO_x and its reaction products, projects an average increase in N deposition over land by a factor of 2.5 by 2100 (Lamarque et al., 2005b), mostly due to increases in NO_x emissions. Nitrogen deposition rates over Asia are projected to increase by a factor of 1.4 to 2 by 2030. Climate contributions to the changes in oxidized N deposition are limited by the models' ability to represent changes in precipitation patterns. An intercomparison of 26 global atmospheric chemistry models demonstrates that current scenarios and projections are not sufficient to stabilise or reduce N deposition or ozone pollution before 2030 (Dentener et al., 2006).

Table 7.7. *Global sources (TgN yr^{-1}) of NO_x, NH_3 and N_2O for the 1990s.*

Source	NO_x		NH_3		N_2O	
	TAR[a]	AR4[b]	TAR[a]	AR4[a]	TAR[c]	AR4
Anthropogenic sources						
Fossil fuel combustion & industrial processes	33 (20–24)	25.6 (21–28)	0.3 (0.1–0.5)	2.5[d]	1.3/0.7 (0.2–1.8)	0.7 (0.2–1.8)[d]
Aircraft	0.7 (0.2–0.9)	– [e] (0.5–0.8)	-	-	-	-
Agriculture	2.3[f] (0–4)	1.6[g]	34.2 (16–48)	35[g] (16–48)	6.3/2.9 (0.9–17.9)	2.8 (1.7–4.8)[g]
Biomass and biofuel burning	7.1 (2–12)	5.9 (6–12)	5.7 (3–8)	5.4[d] (3–8)	0.5 (0.2–1.0)	0.7 (0.2–1.0)[g]
Human excreta	–	–	2.6 (1.3–3.9)	2.6[g] (1.3–3.9)	–	0.2[g] (0.1–0.3)[h]
Rivers, estuaries, coastal zones	–	–	–	–	–	1.7 (0.5–2.9)[i]
Atmospheric deposition	–	0.3[g]	–	–	–	0.6[j] (0.3–0.9)[h]
Anthropogenic total	**43.1**	**33.4**	**42.8**	**45.5**	**8.1/4.1**	**6.7**
Natural sources						
Soils under natural vegetation	3.3[f] (3–8)	7.3[j] (5–8)	2.4 (1–10)	2.4[g] (1–10)	6.0/6.6 (3.3–9.9)	6.6 (3.3–9.0)[g]
Oceans	–	–	8.2 (3–16)	8.2[g] (3–6)	3.0/3.6 (1.0–5.7)	3.8 (1.8–5.8)[k]
Lightning	5 (2–12)	1.1–6.4 (3–7)	–	–	–	–
Atmospheric chemistry	<0.5	–	–	–	0.6 (0.3–1.2)	0.6 (0.3–1.2)[c]
Natural total	**8.8**	**8.4–13.7**	**10.6**	**10.6**	**9.6/10.8**	**11.0**
Total sources	**51.9** (27.2–60.9)	**41.8–47.1** (37.4–57.7)	**53.4** (40–70)	**56.1** (26.8–78.4)	**17.7/14.9** (5.9–37.5)	**17.7** (8.5–27.7)

Notes:

[a] Values from the TAR: NO_x from Table 4.8 with ranges from Tables 4.8 and 5.2; NH_3 from Table 5.2, unless noted.

[b] Parentheses show the range of emissions used in the model runs described in Table 7.9. See text for explanation. Where possible, the best estimate NO_x emission is based on satellite observations. None of the model studies includes the NO_x source from oxidation of NH_3, which could contribute up to 3 TgN yr^{-1}. The source of NO_x from stratosphere-troposphere exchange is less than 1 TgN yr^{-1} in all models, which is well constrained from observations of N_2O-NO_x correlations in the lower stratosphere (Olsen et al., 2001).

[c] Values are from the TAR, Table 4.4; Mosier et al. (1998); Kroeze et al. (1999)/Olivier et al. (1998): a single value indicates agreement between the sources and methodologies of the different studies.

[d] Van Aardenne et al. (2001), range from the TAR.

[e] The aircraft source is included in the total for industrial processes. The parentheses indicate values used in model runs.

[f] The total soil NO_x emissions estimate of 5.6 provided in Table 4.8 of the TAR was distributed between agriculture and soil NO_x according to the proportions provided in the TAR, Table 5.2.

[g] Bouwman et al. (2001, Table 1); Bouwman et al. (2002) for the 1990s; range from the TAR or calculated as ±50%.

[h] Estimated as ±50%.

[i] Kroeze et al. (2005); Nevison et al. (2004); estimated uncertainty is ±70% from Nevison et al. (2004).

[j] All soils, minus the fertilized agricultural soils indicated above.

[k] Nevison et al. (2003, 2004), combining the uncertainties in ocean production and oceanic exchange.

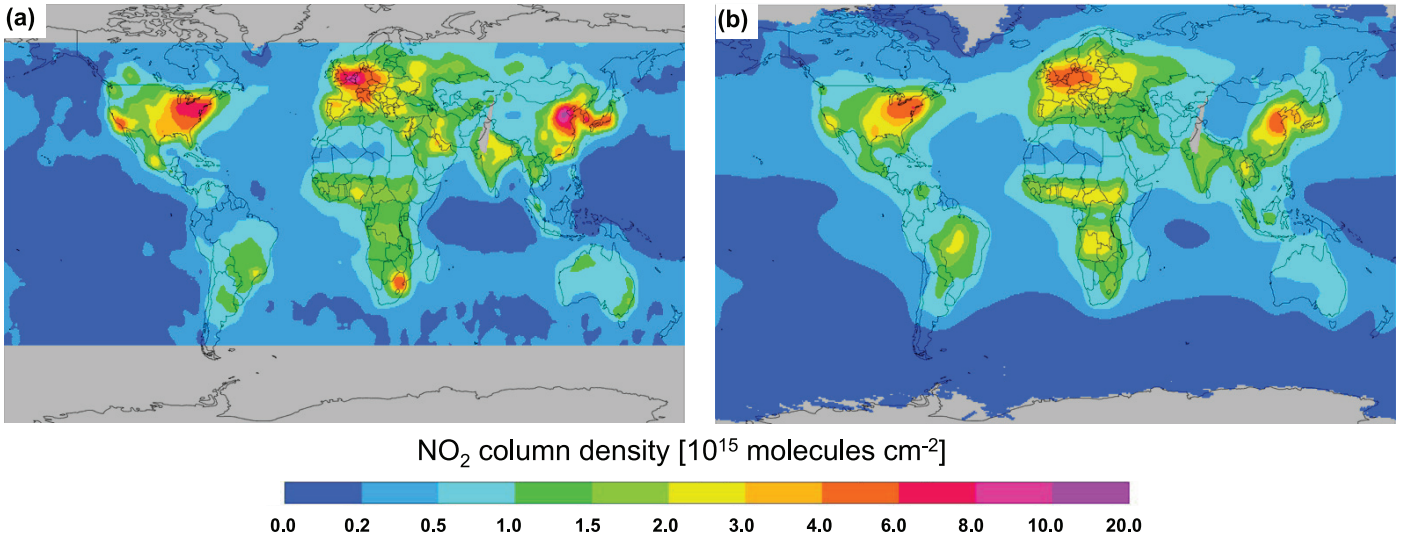


Figure 7.17. *Tropospheric column NO_2 from (a) satellite measurements and (b) atmospheric chemistry models. The maps represent ensemble average annual mean tropospheric NO_2 column density maps for the year 2000. The satellite retrieval ensemble comprises three state-of-the-art retrievals from GOME; the model ensemble includes 17 global atmospheric chemistry models. These maps were obtained after smoothing the data to a common horizontal resolution of 5° × 5° (adapted from van Noije et al., 2006).*

7.4.3. Molecular Hydrogen

Increased interest in atmospheric H_2 is due to its potential role as an indirect greenhouse gas (Derwent et al., 2001) and expected perturbations of its budget in a prospective 'hydrogen economy' (Schultz et al., 2003; Tromp et al., 2003; Warwick et al., 2004). Potential consequences of increased H_2 emissions include a reduction of global oxidizing capacity (presently H_2 constitutes 5 to 10% of the global average OH sink, Schultz et al., 2003) and increased formation of water vapour, which could lead to increased cirrus formation in the troposphere and increased polar stratospheric clouds (PSCs) and additional cooling in the stratosphere, thereby leading to more efficient ozone depletion (Tromp et al., 2003).

Studies of the global tropospheric H_2 budget (see Table 7.8) generally agree on a total source strength of between 70 and 90 Tg(H_2) yr^{-1}, which is approximately balanced by its sinks. About half of the H_2 is produced in the atmosphere via photolysis of formaldehyde (CH_2O), which itself originates from the oxidation of CH_4 and other volatile organic compounds. The other half stems mostly from the combustion of fossil fuels (e.g., car exhaust) and biomass burning. About 10% of the global H_2 source is due to ocean biochemistry and N fixation in soils. Presently, about 50 Tg(H_2) yr^{-1} are produced in the industrial sector, mostly for the petrochemical industry (e.g., refineries) (Lovins, 2003). Evaporative losses of industrial H_2 are generally assumed to be negligible (Zittel and Altmann, 1996). The dominant sink of atmospheric H_2 is deposition with catalytic destruction by soil microorganisms and possibly enzymes (Conrad and Seiler, 1981). The seasonal cycle of observed H_2 concentrations implies an atmospheric lifetime of about 2 years (Novelli et al., 1999; Simmonds et al., 2000; Hauglustaine and Ehhalt, 2002), whereas the lifetime with respect to OH oxidation is 9 to 10 years, which implies that the deposition sink is about three to four times as large as the oxidation. Loss of H_2 to the stratosphere and its subsequent escape to space is negligible for the tropospheric H_2 budget, because the budgets of the troposphere and stratosphere are largely decoupled (Warneck, 1988).

Estimates of H_2 required to fuel a future carbon-free energy system are highly uncertain and depend on the technology as well as the fraction of energy that might be provided by H_2. In the future, H_2 emissions could at most double: the impact on global oxidizing capacity and stratospheric temperatures and ozone concentrations is estimated to be small (Schultz et al., 2003; Warwick et al., 2004). According to Schultz et al. (2003), the side effects of a global H_2 economy could have a stronger impact on global climate and air pollution. Global oxidizing capacity is predominantly controlled by the concentration of NO_x. Large-scale introduction of H_2-powered vehicles would lead to a significant decrease in global NO_x emissions, leading to a reduction in OH of the order of 5 to 10%. Reduced NO_x levels could also significantly reduce tropospheric ozone concentrations in urban areas. Despite the expected large-scale use of natural gas for H_2 production, the impact of a H_2 economy on the global CH_4 budget is likely to be small, except for the feedback between reduced oxidizing capacity (via NO_x reduction) and CH_4 lifetime.

7.4.4 Global Tropospheric Ozone

7.4.4.1 Present-Day Budgets of Ozone and its Precursors

Tropospheric ozone is (after CO_2 and CH_4) the third most important contributor to greenhouse radiative forcing. Trends over the 20th century are discussed in Chapter 2. Ozone is produced in the troposphere by photochemical oxidation of CO, CH_4 and non-methane VOCs (NMVOCs) in the presence

Table 7.8. *Summary of global budget studies of atmospheric H_2 ($Tg(H_2)$ yr^{-1}).*

	Sanderson et al. (2003a)	Hauglustaine and Ehhalt (2002)	Novelli et al. (1999)	Ehhalt (1999)	Warneck (1988)	Seiler and Conrad (1987)
Sources						
Oxidation of CH_4 and VOC	30.2	31	40 ± 16	35 ± 15	50	40 ± 15
Fossil fuel combustion	20	16	15 ± 10	15 ± 10	17	20 ± 10
Biomass burning	20	13	16 ± 11	16 ± 5	15	20 ± 10
N_2 fixation	4	5	3 ± 1	3 ± 2	3	3 ± 2
Ocean release	4	5	3 ± 2	3 ± 2	4	4 ± 2
Volcanoes	–	–	–	–	0.2	–
Total	78.2	70	77 ± 16	71 ± 20	89	87
Sinks						
Deposition	58.3	55	56 ± 41	40 ± 30	78	90 ± 20
Oxidation by OH	17.1	15	19 ± 5	25 ± 5	11	8 ± 3
Total	74.4	70	75 ± 41	65 ± 30	89	98

of NO_x. Stratosphere-troposphere exchange (STE) is another source of ozone to the troposphere. Loss of tropospheric ozone takes place through chemical reactions and dry deposition. Understanding of tropospheric ozone and its relationship to sources requires three-dimensional tropospheric chemistry models that describe the complex nonlinear chemistry involved and its coupling to transport.

The past decade has seen considerable development in global models of tropospheric ozone, and the current generation of models can reproduce most climatological features of ozone observations. The TAR reported global tropospheric ozone budgets from 11 models in the 1996 to 2000 literature. Table 7.9 presents an update to the post-2000 literature, including a recent intercomparison of 25 models (Stevenson et al., 2006). Models concur that chemical production and loss are the principal terms in the global budget. Although STE is only a minor term in the global budget, it delivers ozone to the upper troposphere where its lifetime is particularly long (about one month, limited by transport to the lower troposphere) and where it is of most importance from a radiative forcing perspective.

The post-2000 model budgets in Table 7.9 show major differences relative to the older generation TAR models: on average a 34% weaker STE, a 35% stronger chemical production, a 10% larger tropospheric ozone burden, a 16% higher deposition velocity and a 10% shorter chemical lifetime. It is now well established that many of the older studies overestimated STE, as observational constraints in the lower stratosphere impose an STE ozone flux of 540 ± 140 Tg yr^{-1} (Gettelman et al., 1997; Olsen et al., 2001). Overestimation of the STE flux appears to be most serious in models using assimilated meteorological data, due to the effect of assimilation on vertical motions (Douglass et al., 2003; Schoeberl et al., 2003; Tan et al., 2004; Van Noije et al., 2004). The newer models correct for this effect by using dynamic flux boundary conditions in the tropopause region (McLinden et al., 2000) or by relaxing model results to observed climatology (Horowitz et al., 2003). Such corrections, although matching the global STE flux constraints, may still induce errors in the location of the transport (Hudman et al., 2004) with implications for the degree of stratospheric influence on tropospheric concentrations (Fusco and Logan, 2003).

The faster chemical production and loss of ozone in the current generation of models could reflect improved treatment of NMVOC sources and chemistry (Houweling et al., 1998), ultraviolet (UV) actinic fluxes (Bey et al., 2001) and deep convection (Horowitz et al., 2003), as well as higher NO_x emissions (Stevenson et al., 2006). Subtracting ozone chemical production and loss terms in Table 7.9 indicates that the current generation of models has net production of ozone in the troposphere, while the TAR models had net loss, reflecting the decrease in STE. Net production is not a useful quantity in analysing the ozone budget because (1) it represents only a small residual between production and loss and (2) it reflects a balance between STE and dry deposition, both of which are usually parametrized in models.

Detailed budgets of ozone precursors were presented in the TAR. The most important precursors are CH_4 and NO_x (Wang et al., 1998; Grenfell et al., 2003; Dentener et al., 2005). Methane is in general not simulated explicitly in ozone models and is instead constrained from observations. Nitrogen oxides are explicitly simulated and proper representation of sources and chemistry is critical for the ozone simulation. The lightning source is particularly uncertain (Nesbitt et al., 2000; Tie et al., 2002), yet is of great importance because of the high production efficiency of ozone in the tropical upper troposphere. The range of the global lightning NO_x source presently used in models (3–7 TgN yr^{-1}) is adjusted to match atmospheric observations of ozone and NO_x, although large model uncertainties in deep

Table 7.9. *Global budgets of tropospheric ozone (Tg yr^{-1}) for the present-day atmosphere*[a].

Reference	Model[b]	Stratosphere-Troposphere Exchange	Chemical Production[c]	Chemical Loss[c]	Dry Deposition	Burden (Tg)	Lifetime[d] (days)
TAR[e]	11 models	770 ± 400	3420 ± 770	3470 ± 520	770 ± 180	300 ± 30	24 ± 2
Lelieveld and Dentener (2000)	TM3	570	3310	3170	710	350	33
Bey et al. (2001)	GEOS-Chem	470	4900	4300	1070	320	22
Sudo et al. (2002b)	CHASER	593	4895	4498	990	322	25
Horowitz et al. (2003)	MOZART-2	340	5260	4750	860	360	23
Von Kuhlmann et al. (2003)	MATCH-MPIC	540	4560	4290	820	290	21
Shindell et al. (2003)	GISS	417	NR[f]	NR	1470	349	NR
Hauglustaine et al. (2004)	LMDz-INCA	523	4486	3918	1090	296	28
Park et al. (2004)	UMD-CTM	480	NR	NR	1290	340	NR
Rotman et al. (2004)	IMPACT	660	NR	NR	830	NR	NR
Wong et al. (2004)	SUNY/UiO GCCM	600	NR	NR	1100	376	NR
Stevenson et al. (2004)	STOCHEM	395	4980	4420	950	273	19
Wild et al. (2004)	FRSGC/UCI	520	4090	3850	760	283	22
Folberth et al. (2006)	LMDz-INCA	715	4436	3890	1261	303	28
Stevenson et al. (2006)	25 models	520 ± 200	5060 ± 570	4560 ± 720	1010 ± 220	340 ± 40	22 ± 2

Notes:

[a] From global model simulations describing the atmosphere of the last decade of the 20th century.

[b] TM3: Royal Netherlands Meteorological Institute (KNMI) chemistry transport model; GEOS-Chem: atmospheric composition model driven by observations from the Goddard Earth Observing System; CHASER: Chemical AGCM for Study of Atmospheric Environment and Radiative Forcing; MOZART-2: Model for (tropospheric) Ozone and Related Tracers; MATCH-MPIC: Model of Atmospheric Transport and Chemistry – Max Planck Institute for Chemistry; GISS: Goddard Institute for Space Studies chemical transport model; LMDz-INCA: Laboratoire de Météorologie Dynamique GCM-Interactive Chemistry and Aerosols model; UMD-CTM: University of Maryland Chemical Transport Model; IMPACT: Integrated Massively Parallel Atmospheric Chemistry Transport model; SUNY/UiO GCCM: State University of New York/University of Oslo Global Tropospheric Climate-Chemistry Model; STOCHEM: Hadley Centre global atmospheric chemistry model; FRSGC/UCI: Frontier Research System for Global Change/University of California at Irvine chemical transport model.

[c] Chemical production and loss rates are calculated for the odd oxygen family, usually defined as O_x = ozone + O + NO_2 + 2NO_3 + 3 dinitrogen pentoxide (N_2O_5) + pernitric acid (HNO_4) + peroxyacylnitrates (and sometimes nitric acid; HNO_3), to avoid accounting for rapid cycling of ozone with short-lived species that have little implication for its budget. Chemical production is mainly contributed by reactions of NO with peroxy radicals, while chemical loss is mainly contributed by the oxygen radical in the 1D excited state ($O(^1D)$) plus water (H_2O) reaction and by the reactions of ozone with the hydroperoxyl radical (HO_2), OH, and alkenes.

[d] Calculated as the ratio of the burden to the sum of chemical and deposition losses.

[e] Means and standard deviations for 11 global model budgets from the 1996 to 2000 literature reported in the TAR. The mean budget does not balance exactly because only nine chemical transport models reported their chemical production and loss statistics.

[f] Not reported.

convection and lightning vertical distributions detract from the strength of this constraint. Process-based models tend to predict higher lightning emissions (5–20 TgN yr^{-1}; Price et al., 1997).

Other significant precursors for tropospheric ozone are CO and NMVOCs, the most important of which is biogenic isoprene. Satellite measurements of CO from the Measurements of Pollution in the Troposphere (MOPITT) instrument launched in 1999 (Edwards et al., 2004) have provided important new constraints for CO emissions, pointing in particular to an underestimate of Asian sources in current inventories (Kasibhatla et al., 2002; Arellano et al., 2004; Heald et al., 2004; Petron et al., 2004), as confirmed also by aircraft observations of Asian outflow (Palmer et al., 2003a; Allen et al., 2004). Satellite measurements of formaldehyde columns from the GOME instrument (Chance et al., 2000) have been used to place independent constraints on isoprene emissions and indicate values generally consistent with current inventories, although with significant regional discrepancies (Palmer et al., 2003b; Shim et al., 2005).

A few recent studies have examined the effect of aerosols on global tropospheric ozone involving both heterogeneous chemistry and perturbations to actinic fluxes. Jacob (2000) reviewed the heterogeneous chemistry involved. Hydrolysis of dinitrogen pentoxide (N_2O_5) in aerosols is a well-known sink for NO_x, but other processes involving reactive uptake of the hydroperoxyl radical (HO_2), NO_2 and ozone itself could also be significant. Martin et al. (2003b) find that including these processes along with effects of aerosols on UV radiation in

a global Chemical Transport Model (CTM) reduced ozone production rates by 6% globally, with larger effects over aerosol source regions.

Although the current generation of tropospheric ozone models is generally successful in describing the principal features of the present-day global ozone distribution, there is much less confidence in the ability to reproduce the changes in ozone associated with perturbations of emissions or climate. There are major discrepancies with observed long-term trends in ozone concentrations over the 20th century (Hauglustaine and Brasseur, 2001; Mickley et al., 2001; Shindell and Favulegi, 2002; Shindell et al., 2003; Lamarque et al., 2005c), including after 1970 when the reliability of observed ozone trends is high (Fusco and Logan, 2003). Resolving these discrepancies is needed to establish confidence in the models.

7.4.4.2 Effects of Climate Change

Climate change can affect tropospheric ozone by modifying emissions of precursors, chemistry, transport and removal (European Commission, 2003). These and other effects are discussed below. They could represent positive or negative feedbacks to climate change.

7.4.4.2.1 Effects on emissions

Climate change affects the sources of ozone precursors through physical response (lightning), biological response (soils, vegetation, biomass burning) and human response (energy generation, land use, agriculture). It is generally expected that lightning will increase in a warmer climate (Price and Rind, 1994a; Brasseur et al., 2005; Hauglustaine et al., 2005), although a GCM study by Stevenson et al. (2006) for the 2030 climate finds no global increase but instead a shift from the tropics to mid-latitudes. Perturbations to lightning could have a large effect on ozone in the upper troposphere (Toumi et al., 1996; Thompson et al., 2000; Martin et al., 2002; Wong et al., 2004). Mickley et al. (2001) find that observed long-term trends in ozone over the past century might be explainable by an increase in lightning.

Biomass burning in the tropics and at high latitudes is likely to increase with climate change, both as a result of increased lightning and as a result of increasing temperatures and dryness (Price and Rind, 1994b; Stocks et al., 1998; A. Williams et al., 2001; Brown et al., 2004). Biomass burning is known to make a large contribution to the budget of ozone in the tropical troposphere (Thompson et al., 1996), and there is evidence that boreal forest fires can enhance ozone throughout the extratropical NH (Jaffe et al., 2004). With climate warming, it is likely that boreal fires will increase due to a shorter duration of the seasonal snowpack and decreased soil moisture (Kasischke et al., 1995).

Biogenic VOC emissions may be highly sensitive to climate change. The most important global ozone precursors are CH_4 and isoprene. The effect of climate change on CH_4 is discussed in Section 7.4.1. The effect on NMVOCs was examined by Constable et al. (1999), Sanderson et al. (2003b), and Lathière et al. (2005). Although biogenic NMVOC emissions increase with increasing temperature, all three studies concur that climate-driven changes in vegetation types unfavourable to isoprene emissions (notably the recession of tropical forests) would partly compensate for the effect of warming in terms of ozone generation.

7.4.4.2.2 Effects on chemistry

Changes in temperature, humidity and UV radiation intensity brought about by climate change could affect ozone significantly. Simulations with GCMs by Stevenson et al. (2000) and Grewe et al. (2001) for the 21st century indicate a decrease in the lifetime of tropospheric ozone as increasing water vapour enhances the dominant ozone sink from the oxygen radical in the 1D excited state ($O(^1D)$) plus water (H_2O) reaction. Stevenson et al. (2006) find similar results in an intercomparison of nine models for 2030 compared with 2000 climate. However, regional ozone pollution may increase in the future climate as a result of higher temperatures (see Section 7.6, Box 7.4).

7.4.4.2.3 Effects on transport

Changes in atmospheric circulation could have a major effect on tropospheric ozone. Studies using GCMs concur that STE should increase in the future climate because of the stronger Brewer-Dobson stratospheric circulation (Sudo et al., 2002a; Collins et al., 2003; Zeng and Pyle, 2003; Hauglustaine et al., 2005; Stevenson et al., 2005). Changes in vertical transport within the troposphere are also important, in view of the rapid increase in both ozone production efficiency and ozone lifetime with altitude. Convection is expected to intensify as climate warms (Rind et al., 2001), although this might not be the case in the tropics (Stevenson et al., 2005). The implications are complex, as recently discussed by Pickering et al. (2001), Lawrence et al. (2003), Olivié et al. (2004), Doherty et al. (2005) and Li et al. (2005). On the one hand, convection brings down ozone-rich air from the upper troposphere to the lower troposphere where it is rapidly destroyed, and replaces it with low-ozone air. On the other hand, injection of NO_x to the upper troposphere greatly increases its ozone production efficiency.

7.4.5 The Hydroxyl Radical

The hydroxyl radical (OH) is the primary cleansing agent of the lower atmosphere, providing the dominant sink for many greenhouse gases (e.g., CH_4, hydrochlorofluorocarbons (HCFCs), hydrofluorocarbons) and pollutants (e.g., CO, non-methane hydrocarbons). Steady-state lifetimes of these trace gases are determined by the morphology of their atmospheric distribution, the kinetics of their reaction with OH and the OH distribution. Local abundance of OH is controlled mainly by local abundances of NO_x, CO, CH_4 and higher hydrocarbons, ozone, water vapour, as well as the intensity of solar UV radiation at wavelengths shorter than 0.310 µm. New laboratory and field work also shows significant formation of $O(^1D)$ from ozone photolysis in the wavelength range between

0.310 µm and 0.350 µm (Matsumi et al., 2002; Hofzumahaus et al., 2004). The primary source of tropospheric OH is a pair of reactions starting with the photodissociation of ozone by solar UV radiation.

Additionally, in the remote, and in particular upper, troposphere, photodissociation of oxygenated volatile organic chemicals such as peroxides, acetone and other ketones, alcohols, and aldehydes may be the dominant sources of OH radical (e.g., Müller and Brasseur, 1999; Collins et al., 1999; Jaeglé et al., 2001; Tie et al., 2003; Singh et al., 2004). Over continents, measurements in the lower troposphere suggest that processing of unsaturated hydrocarbons or photolysis of carbonyls can also sustain a large pool of radicals (e.g., Handisides et al., 2003; Heard et al., 2004). Furthermore, the net formation of OH by photolysis of nitrous acid (HONO) was found to be the dominant OH radical source in urban atmospheres (e.g., Ren et al., 2003) and in a forest canopy (Kleffmann et al., 2005). The hydroxyl radical reacts with many atmospheric trace gases, in most cases as the first and rate-determining step of a reaction chain that leads to more or less complete oxidation of the compound. These chains often lead to formation of HO_2, which then reacts with ozone or NO to recycle back to OH. Tropospheric OH and HO_2 are lost through radical-radical reactions leading to the formation of peroxides or with NO_2 to form nitric acid (HNO_3). Sources and sinks of OH involve most of the fast photochemistry of the troposphere.

7.4.5.1 Changes in the Hydroxyl Radical Over Time

7.4.5.1.1 Impact of emissions

Because of its dependence on CH_4 and other pollutants, tropospheric OH is also expected to have changed since the pre-industrial era and to change in the future. Pre-industrial OH is likely to have been different than today, but because of the counteracting effects of higher CO and CH_4 (decreasing OH) and increased NO_x and ozone (increasing OH) there is still little consensus on the magnitude of this change. Several model studies suggest a decline in weighted global mean OH from pre-industrial time to the present of less than 10% (Shindell et al., 2001; Lelieveld et al., 2002a; Lamarque et al., 2005a). Other studies have reported larger decreases in global OH of 16% (Mickley et al., 1999), 25% (Wong et al., 2004) and 33% (Hauglustaine and Brasseur, 2001). The model study by Lelieveld et al. (2002b) suggests that during the past century, OH concentration decreased substantially in the marine troposphere through reaction with CH_4 and CO. However, on a global scale it has been compensated by an increase over the continents associated with strong emissions of NO_x.

Karlsdottir and Isaksen (2000) used a three-dimensional CTM accounting for varying NO_x, CO and NMVOC emissions and found a positive trend in OH of 0.43% yr^{-1} over the period 1980 to 1996. Dentener et al. (2003a,b), with a three-dimensional CTM accounting for varying emissions of ozone precursors and CH_4, meteorology and column ozone, derive a positive trend of 0.26% yr^{-1} over the 1979 to 1993 period. J. Wang et al. (2004) also use a three-dimensional CTM accounting for interannual variations in CH_4 and CO emissions, transport and column ozone to analyse the trend in CH_4 from 1988 to 1997. They do not account for interannual variability of a number of other variables that affect OH such as concentrations of NO_x, tropospheric ozone and NMVOCs. They also derive a positive trend in OH over the period considered of 0.63% yr^{-1}. Their calculated trend in OH is associated primarily with the negative trend in the overhead column ozone over the period considered and the trend is reduced to 0.16% yr^{-1} when the total ozone column is held constant.

Future changes in OH depend on relative changes in hydrocarbons compared with NO_x abundances. In the TAR, Prather et al. (2001), using scenarios reported in the IPCC SRES (IPCC, 2000) and on the basis of a comparison of results from 14 models, predicted that global OH could decrease by 10 to 18% by 2100 for five emission scenarios and increase by 5% for one scenario (which assumes large decreases in CH_4 and other ozone precursor emissions). Based on a different emission scenario for future emissions, Wang and Prinn (1999) also predicted an OH decrease of 16 ± 3% in 2100.

7.4.5.1.2 Effects of climate change

In addition to the emission changes, future increases in greenhouse gases could also induce changes in OH, arising through direct participation in OH-controlling chemistry and indirectly through stratospheric ozone changes that could increase solar UV radiation in the troposphere. OH will also be affected by changes in temperature, humidity and clouds or climate change effects on biogenic emissions of CH_4 and other ozone precursors. Changes in tropospheric water could have important chemical repercussions. The reaction between water vapour and electronically excited oxygen atoms constitutes the major source of tropospheric OH. So, in a warmer climate characterised by increased specific humidity, the abundance of OH is expected to increase. This effect was proposed by Pinto and Khalil (1991) to explain the variation of OH during the cold dry Last Glacial Maximum (LGM). It was quantified by Martinerie et al. (1995) who calculated that the global mean OH concentration during the LGM was 7% lower than at present because the atmospheric water vapour concentration was lower during that period. Valdes et al. (2005) estimate that the cold and dry LGM climate was responsible for a 7% decrease in global OH. Brasseur et al. (1998) and Johnson et al. (1999) estimated that in a warmer (doubled atmospheric CO_2) climate, the global and annual mean OH concentration would increase by 7% and 12.5%, respectively. More recently, Hauglustaine et al. (2005) use a climate-chemistry three-dimensional model to estimate a 16% reduction in global OH from the present day to 2100 accounting solely for changes in surface emissions. The effect of climate change and mainly of increased water vapour in this model is to increase global OH by 13%. In this study, the competing effects of emissions and climate change maintain the future global average OH concentration close to its present-day value. The importance of the water vapour distribution to global OH is illustrated by Lamarque et al. (2005a), who show that under reduced aerosol emissions, a warmer and moister climate significantly increases global OH concentration.

Changes in lightning NO_x emissions in a warmer climate may also affect OH. Labrador et al. (2004) show that global OH is sensitive to the magnitude of lightning NO_x emissions, and increases by 10% and 23% when global lightning is increased by a factor of 2 and 4, respectively, from a 5 TgN yr^{-1} best estimate. Similar sensitivity of global OH to the lightning source was estimated by Wang et al. (1998), who calculated a 10.6% increase in OH for a doubling of the source (from 3 to 6 TgN yr^{-1}). Regarding the large uncertainty about lightning emissions and the sensitivity of OH to the total amount of N emitted, an improved understanding of this source appears important for the ability to simulate OH accurately over time.

7.4.5.2 Consequences for Lifetimes

7.4.5.2.1 Lifetime definition

The global instantaneous atmospheric lifetime of a trace gas in the atmosphere is obtained by integrating the loss frequency l over the atmospheric domain considered. The integral must be weighted by the distribution of the trace gas on which the sink processes act. Considering a distribution of the trace gas $C(x,y,z,t)$, a global instantaneous lifetime derived from the budget can be defined as:

$$\tau_{global} = \int C \, dv \, / \int C \, l \, dv \qquad (7.4)$$

where dv is an atmospheric volume element. This expression can be averaged over one year to determine the global and annual mean lifetime. The global atmospheric lifetime (also called 'burden lifetime' or 'turnover lifetime') characterises the time required to turn over the global atmospheric burden.

The global atmospheric lifetime characterises the time to achieve an e-fold decrease of the global atmospheric burden. Unfortunately τ_{global} is a constant only in very limited circumstances. In the case where the loss rate depends on the burden, the perturbation or pulse decay lifetime (τ_{pert}) is introduced (see Velders et al., 2005). The perturbation lifetime is used to determine how a one-time pulse emission may decay as a function of time as needed for the calculation of Global Warming Potentials (GWPs). The perturbation lifetime can be distinctly different from the global atmospheric lifetime. For example, if the CH_4 abundance increases above its present-day value due to a one-time emission, the time it takes for CH_4 to decay back to its background value is longer than its global unperturbed atmospheric lifetime. This delay occurs because the added CH_4 will cause a suppression of OH, in turn increasing the background CH_4. Such feedbacks cause the decay time of a perturbation (τ_{pert}) to differ from the global atmospheric lifetime (τ_{global}). In the limit of small perturbations, the relation between the perturbation lifetime of a gas and its global atmospheric lifetime can be derived from a simple budget relationship as $\tau_{pert} = \tau_{global} / (1 - f)$, where the sensitivity coefficient $f = d\ln(\tau_{global}) / d\ln(B)$. Prather et al. (2001) estimated the feedback of CH_4 to tropospheric OH and its lifetime and determined a sensitivity coefficient $f = 0.28$, giving a ratio $\tau_{pert} / \tau_{global}$ of 1.4. Stevenson et al. (2006), from 25 CTMs, calculate an ensemble mean and 1 standard deviation uncertainty in present-day CH_4 global lifetime τ_{global} of 8.7 ± 1.3 years, which is the AR4 updated value. The corresponding perturbation lifetime that should be used in the GWP calculation is 12 ± 1.8 years.

Perturbation lifetimes can be estimated from global models by simulating the injection of a pulse of gas and tracking the decay of the added amount. The pulse of added CO, HCFCs or hydrocarbons, by causing the concentration of OH to decrease and thus the lifetime of CH_4 to increase temporarily, causes a buildup of CH_4 while the added burden of the gas persists. Thus, changes in the emissions of short-lived gases can generate long-lived perturbations as shown in global models (Derwent et al., 2001; Wild et al., 2001; Collins et al., 2002). Changes in tropospheric ozone accompany the CH_4 decay on a 12-year time scale as an inherent component of this mode, a key example of chemical coupling in the troposphere. Any chemically reactive gas, whether a greenhouse gas or not, will produce some level of indirect greenhouse effect through its impact on atmospheric chemistry.

7.4.5.2.2 Changes in lifetime

Since OH is the primary oxidant in the atmosphere of many greenhouse gases including CH_4 and hydrogenated halogen species, changes in OH will directly affect their lifetime in the atmosphere and hence their impact on the climate system. Recent studies show that interannual variations in the chemical removal of CH_4 by OH have an important impact on the variability of the CH_4 growth rate (Johnson et al., 2002; Warwick et al., 2002; J. Wang et al., 2004). Variations in CH_4 oxidation by OH contribute to a significant fraction of the observed variations in the annual accumulation rate of CH_4 in the atmosphere. In particular, the 1992 to 1993 anomaly in the CH_4 growth rate can be explained by fluctuations in OH and wetland emissions after the eruption of Mt. Pinatubo (J. Wang et al., 2004). CH_4 variability simulated by Johnson et al. (2002), resulting only from OH sink processes, also indicates that the ENSO cycle is the largest component of that variability. These findings are consistent with the variability of global OH reconstructed by Prinn et al. (2005), Manning and Keeling (2006) and Bousquet et al. (2005), which is strongly affected by large-scale wildfires as in 1997 to 1998, by El Niño events and by the Mt. Pinatubo eruption.

The effect of climate change on tropospheric chemistry has been investigated in several studies. In most cases, the future CH_4 lifetime increases when emissions increase and climate change is ignored (Brasseur et al., 1998; Stevenson et al., 2000; Hauglustaine and Brasseur, 2001; Prather et al., 2001; Hauglustaine et al., 2005). This reflects the fact that increased levels of CH_4 and CO depress OH, reducing the CH_4 sink. However, climate warming increases the temperature-dependent CH_4 oxidation rate coefficient (Johnson et al., 1999), and increases in water vapour and NO_x concentrations tend to increase OH. In most cases, these effects partly offset or exceed the CH_4 lifetime increase due to emissions. As a consequence, the future CH_4 lifetime calculated by Brasseur et al. (1998), Stevenson et al. (2000) and Hauglustaine et al.

(2005) remains relatively constant (within a few percent) over the 21st century. In their transient simulation over the period 1990 to 2100, Johnson et al. (2001) find a dominant effect of climate change on OH in the free troposphere so that the global CH_4 lifetime declines from about 9 years in 1990 to about 8.3 years by 2025 but does not change significantly thereafter. Hence the evolution of the CH_4 lifetime depends on the relative timing of NO_x and hydrocarbon emission changes in the emission scenarios, causing the calculated CH_4 increase in 2100 to be reduced by 27% when climate change is considered. Stevenson et al. (2006) reach a similar conclusion about the relatively constant CH_4 lifetime. As a result of future changes in emissions, the CH_4 steady-state lifetime simulated by 25 state-of-the-art CTMs increases by 2.7 ± 2.3% in 2030 from an ensemble mean of 8.7 ± 1.3 years for the present day (mean ± 1 standard deviation) for a current legislation scenario of future emissions of ozone precursors. Under the 2030 warmer climate scenario, the lifetime is reduced by 4.0 ± 1.8%: the total effect of both emission and climate changes reduces the CH_4 lifetime by only 1.3%.

7.4.6 Stratospheric Ozone and Climate

From about 1980 to the mid-1990s a negative trend in globally averaged total ozone occurred, due primarily to an increase in Cl and bromine loading (Montzka et al., 1999). A reduction in halogen loading appears to have occurred recently (Montzka et al., 2003) as well as the beginning of ozone recovery (e.g., Newchurch et al., 2003; Huck et al., 2005; Reinsel et al., 2005; Yang et al., 2005). Evidence suggests that a sustainable recovery of ozone is not expected before the end of the current decade (e.g., Steinbrecht et al., 2004; Dameris et al., 2006). Atmospheric concentrations of LLGHGs have increased (see Chapter 2) and are expected to continue to increase, with consequences for the ozone layer. This section assesses current understanding of interactions and feedbacks between stratospheric ozone and climate. More detailed discussions can be found in recent reports (European Commission, 2003; IPCC/TEAP, 2005).

7.4.6.1 Interactions

Stratospheric ozone is affected by climate change through changes in dynamics and in the chemical composition of the troposphere and stratosphere. An increase in the concentrations of LLGHGs, especially CO_2, cools the stratosphere, allowing the possibility of more PSCs, and alters the ozone distribution (Rosenlof et al., 2001; Rosenfield et al., 2002; Randel et al., 2004, 2006; Fueglistaler and Haynes, 2005). With the possible exception of the polar lower stratosphere, a decrease in temperature reduces ozone depletion leading to higher ozone column amounts and a positive correction to the LLGHG-induced radiative cooling of the stratosphere. Moreover, ozone itself is a greenhouse gas and absorbs UV radiation in the stratosphere. Absorption of UV radiation provides the heating responsible for the observed temperature increase with height above the tropopause. Changes in stratospheric temperatures, induced by changes in ozone or LLGHG concentration, alter the Brewer-Dobson circulation (Butchart and Scaife, 2001; Butchart et al., 2006), controlling the rate at which long-lived molecules, such as LLGHGs, CFCs, HCFCs and halogens are transported from the troposphere to various levels in the stratosphere**.** Furthermore, increases in the Brewer-Dobson circulation increase temperatures adiabatically in the polar regions and decrease temperatures adiabatically in the tropics.

Climate is affected by changes in stratospheric ozone, which radiates infrared radiation down to the troposphere. For a given percentage change in the vertical structure of ozone, the largest dependence of the radiative forcing is in the upper troposphere and ozone layer regions (e.g., TAR, Figure 6.1). Past ozone depletion has induced surface cooling (Chapter 2). The observed decrease in stratospheric ozone and the resultant increase in UV irradiance (e.g., Zerefos et al., 1998; McKenzie et al., 1999) have affected the biosphere and biogenic emissions (Larsen, 2005). Such UV radiation increases lead to an enhanced OH production, reducing the lifetime of CH_4 and influencing tropospheric ozone, both important greenhouse gases (European Commission, 2003). In addition to global mean equilibrium surface temperature changes, local surface temperature changes have been identified by Gillett and Thompson (2003) as a result of ozone loss from the lower stratosphere. Observational (e.g., Baldwin and Dunkerton, 1999, 2001; Thompson et al., 2005) and modelling (Polvani and Kushner, 2002; Norton, 2003; Song and Robinson, 2004; Thompson et al., 2005) evidence exists for month-to-month changes to the stratospheric flow feedback to the troposphere, affecting its circulation. Model results show that trends in the SH stratosphere can affect high-latitude surface climate (Gillett and Thompson, 2003).

7.4.6.2 Past Changes in Stratospheric Ozone

Ozone losses have been largest in the polar lower stratosphere during later winter and spring. For example, the ozone hole over Antarctica has occurred every spring since the early 1980s (Fioletov et al., 2002). Antarctic ozone destruction is driven by climatologically low temperatures combined with high Cl and bromine amounts produced from photochemical breakdown of primarily anthropogenic CFCs and halons. Similar losses, smaller in magnitude, have occurred over the Arctic due to the same processes during cold winters. During warm winters, arctic ozone has been relatively unaffected (Tilmes et al., 2004). The antarctic lower stratosphere is nearly always cold enough to produce substantial ozone loss, but in the year 2002, a sudden stratospheric warming split the early ozone hole into two separate regions (e.g., Simmons et al., 2005). Temperatures were subsequently too high to produce further ozone loss. Following the later merging of the two separate regions back into a single vortex, the dynamical conditions were unsuitable for further ozone loss. This is not an indication of recovery in ozone amounts, but rather the result of a dynamical disturbance (e.g., Newman et al., 2004). A summary of recent stratospheric ozone changes is given in Chapter 2.

7.4.6.3 *Future Changes in Stratospheric Ozone*

The evolution of stratospheric ozone over the next few decades will depend on natural, including solar and volcanic activity (e.g., Steinbrecht et al., 2004; Dameris et al., 2005), and human-caused factors such as stratospheric halogen loading, which is expected to decrease over future decades (WMO, 2003; IPCC/TEAP, 2005). The evolution of ozone will also depend on changes in many stratospheric constituents: it is expected that the reduction of ozone-depleting substances in the 21st century will cause ozone to increase via chemical processes (Austin et al., 2003). However, this increase could be strongly affected by temperature changes (due to LLGHGs), other chemical changes (e.g., due to water vapour) and transport changes. Coupled Chemistry-Climate Models (CCMs) provide tools to simulate future atmospheric composition and climate. For this purpose, a set of consistent model forcings has been prescribed as part of the CCM Validation Activity for Stratospheric Processes and their Role in Climate (SPARC CCMVal; Eyring et al., 2005). Forcings include natural and anthropogenic emissions based on existing scenarios, atmospheric observations and the Kyoto and Montreal Protocols and Amendments. The simulations follow the IPCC SRES scenario A1B (IPCC, 2000) and changes in halocarbons as prescribed in Table 4B-2 of WMO (2003). Figure 7.18 shows the late winter minimum total column ozone poleward of 60° for various transient CCM reference simulations compared with observations. Antarctic ozone follows mainly the behaviour of Cl and bromine in the models. The peak depletion simulated by the CCMs occurs around the year 2000 followed by a slow increase with minimum values remaining constant between 2000 and 2010 in many models. Most models predict that antarctic ozone amounts will increase to 1980 values close to the time when modelled halogen amounts decrease to 1980 values, lagging the recovery in mid-latitudes due to the delay associated with transport of stratospheric air to polar regions. The late return to pre-1980 values by about 2065 in the Atmospheric Model with Transport and Chemistry (AMTRAC) model (Austin and Wilson, 2006) is consistent with an empirical model study based on observations (Newman et al., 2006). Moreover, increased atmospheric fluxes of CFCs have recently been reported (Hurst et al., 2006), which may point to a still later recovery. The CCMs do not predict consistent values for minimum arctic column ozone, with some models showing large discrepancies with observations. In all CCMs that have been run long enough, arctic ozone increases to 1980 values before antarctic ozone does, by as much as 30 years (e.g., Austin and Wilson 2006). This delay in the Antarctic arises from an increased Brewer-Dobson circulation (Butchart and Scaife, 2001; Butchart et al., 2006) combined with a reduction in stratospheric temperatures.

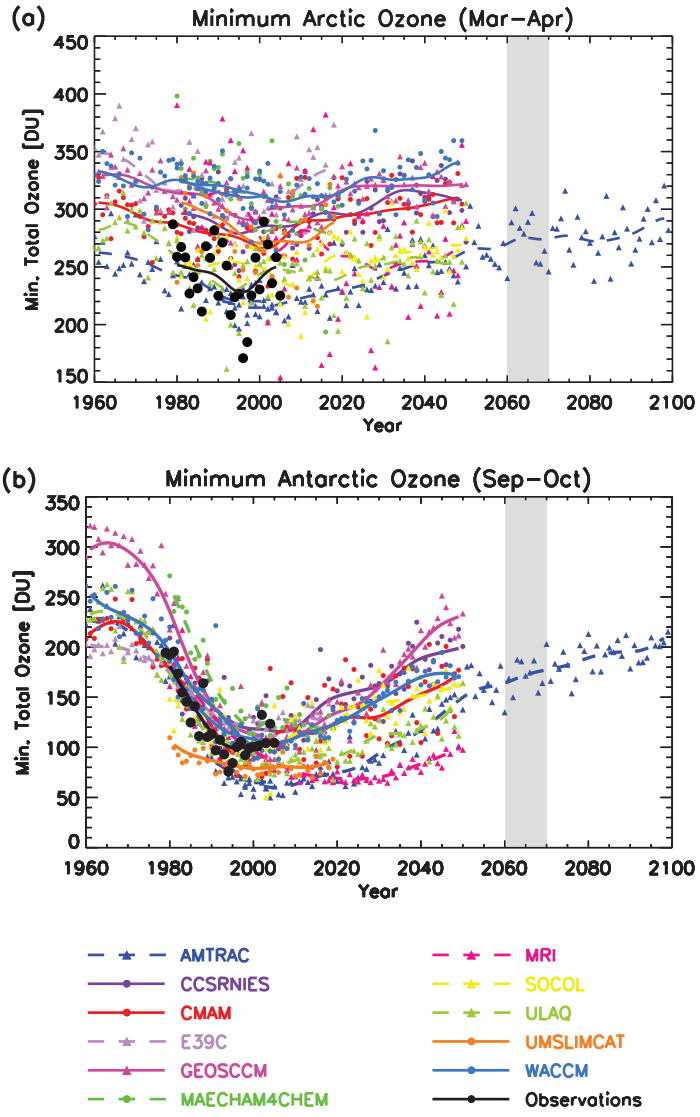


Figure 7.18. *(a) Minimum arctic total column ozone for March to April and (b) minimum antarctic total column ozone for September to October (both poleward of 60°) in Dobson Units (DU). Simulations of future evolution of ozone were performed by 11 CCMs analysed as part of the CCM Validation Activity for SPARC (http://www.pa.op.dlr.de/CCMVal/). Model results are compared with values calculated from the National Institute of Water and Atmospheric Research (NIWA) assimilated total column ozone database shown as black dots (Bodeker et al., 2005). The light grey shading between 2060 and 2070 shows the period when halogen amounts in the polar lower stratosphere are expected to return to 1980 values. Models include AMTRAC: Atmospheric Model with Transport and Chemistry; CCSRNIES: Center for Climate System Research - National Institute for Environmental Studies; CMAM: Canadian Middle Atmosphere Model; E39C: German Aerospace Center (DLR) version of ECHAM4 with chemistry and 39 levels; GEOSCCM: Goddard Earth Observing System Chemistry-Climate Model; MAECHAM4/CHEM: Middle Atmosphere ECHAM4 with Chemistry; MRI: Meteorological Research Institute; SOCOL: Solar Climate Ozone Links; ULAQ: University of L'Aquila; UMSLIMCAT: Unified Model SLIMCAT; WACCM: Whole Atmosphere Community Climate Model.*

7.4.6.4 Uncertainties Due to Atmospheric Dynamics

Changes in atmospheric dynamics could affect ozone. For example, sub-grid scale processes such as gravity wave propagation (e.g., Warner and McIntyre, 2001), prescribed for past and present conditions, may change in the future. Tropospheric climate changes will also alter planetary-scale waves. Together with changes in orographic gravity waves, these waves give rise to the increase in the Brewer-Dobson circulation seen in most models (Butchart et al., 2006). The magnitude of this effect varies from model to model and leads to increased adiabatic heating of the polar regions, compensating in part the increased radiative cooling from CO_2 increases. Hence, the net heating or cooling is subject to large uncertainty, and available model simulations do not give a consistent picture of future development of ozone, particularly in the Arctic (Figure 7.18).

7.5 Aerosol Particles and the Climate System

Aerosols are an integral part of the atmospheric hydrological cycle and the atmosphere's radiation budget, with many possible feedback mechanisms that are not yet fully understood. This section assesses (1) the impact of meteorological (climatic) factors like wind, temperature and precipitation on the natural aerosol burden and (2) possible effects of aerosols on climate parameters and biogeochemistry. The most easily understood interaction between aerosols and climate is the direct effect (scattering and absorption of shortwave and thermal radiation), which is discussed in detail in Chapter 2. Interactions with the hydrological cycle, and additional impacts on the radiation budget, occur through the role of aerosols in cloud microphysical processes, as aerosol particles act as cloud condensation nuclei (CCN) and ice nuclei (IN). The suite of possible impacts of aerosols through the modification of cloud properties is called 'indirect effects'. The forcing aspect of the indirect effect at the top of the atmosphere is discussed in Chapter 2, while the processes that involve feedbacks or interactions, like the 'cloud lifetime effect'[6], the 'semi-direct effect' and aerosol impacts on the large-scale circulation, convection, the biosphere through nutrient supply and the carbon cycle, are discussed here.

7.5.1 Aerosol Emissions and Burdens Affected by Climatic Factors

Most natural aerosol sources are controlled by climatic parameters like wind, moisture and temperature. Hence, human-induced climate change is also expected to affect the natural aerosol burden. The sections below give a systematic overview of the major natural aerosol sources and their relations to climate parameters while anthropogenic aerosol emissions and combined aerosols are the subject of Chapter 2.

7.5.1.1 Dust

Estimates of the global source strength of bulk dust aerosols with diameters below 10 µm of between 1,000 and 3,000 Tg yr^{-1} agree well with a wide range of observations (Duce, 1995; Textor et al., 2005; Cakmur et al., 2006). Seven to twenty percent of the dust emissions are less than 1 µm in diameter (Cakmur et al., 2006; Schulz et al., 1998). Zhang et al. (1997) estimated that about 800 Tg yr^{-1} of Asian dust emissions are injected into the atmosphere annually, about 30% of which is re-deposited onto the deserts and 20% is transported over regional scales, while the remaining approximately 50% is subject to long-range transport to the Pacific Ocean and beyond. Asian dust appears to be a continuous source that dominates background dust aerosol concentrations on the west coast of the USA (Duce, 1995; Perry et al., 2004). Uncertainties in the estimates of global dust emissions are greater than a factor of two (Zender et al., 2004) due to problems in validating and modelling the global emissions. The representation of the high wind tail of the wind speed distribution alone, responsible for most of the dust flux, leads to differences in emissions of more then 30% (Timmreck and Schulz, 2004). Observations suggest that annual mean African dust may have varied by a factor of four during 1960 to 2000 (Prospero and Lamb, 2003), possibly due to rainfall variability in the Sahel zone. Likewise, simulations of dust emissions in 2100 are highly uncertain, ranging from a 60% decrease to a factor of 3.8 increase as compared to present-day dust emissions (Mahowald and Luo, 2003; Tegen et al., 2004; Woodward et al., 2005; Stier et al., 2006a). Reasons for these discrepancies include different treatments of climate-biosphere interactions and the climate model used to drive the vegetation and dust models. The potentially large impact of climate change on dust emissions shows up in particular when comparing present-day with LGM conditions for dust erosion (e.g., Werner et al., 2002).

The radiative effect of dust, which, for example, could intensify the African Easterly Waves, may be a feedback mechanism between climate and dust (Jones et al., 2004). It also alters the atmospheric circulation, which feeds back to dust emission from natural sources (see Section 7.5.4). Perlwitz et al. (2001) estimate that this feedback reduces the global dust load by roughly 15%, as dust radiative forcing reduces the downward mixing of momentum within the planetary boundary layer, the surface wind speed, and thus dust emission (Miller et al., 2004a). In addition to natural dust production, human activities have created another potential source for dust mobilisation through desertification. The contribution to global dust emission of desertification through human activities is uncertain: estimates vary from 50% (Tegen et al., 1996; Mahowald et al., 2004) to less than 10% (Tegen et al., 2004) to insignificant values (Ginoux et al., 2001; Prospero et al., 2002). A 43-year estimate of Asian dust emissions reveals that meteorology and climate have a greater influence on Asian

[6] The processes involved are more complex than can be encompassed in a single expression. The term 'cloud lifetime effect' thus should be understood to mean that aerosols can change precipitation efficiency in addition to increasing cloud albedo.

dust emissions and associated Asian dust storm occurrences than does desertification (Figure 7.19; Zhang et al., 2003).

In addition, aerosol deposition affects global ecosystems. Deposition of mineral dust plays an important role in the biogeochemical cycle of the oceans, by providing the nutrient iron, which affects ocean biogeochemistry with feedbacks to climate and dust production (Jickells et al., 2005; Section 7.3.4.4). Conversely, water-soluble particulate iron over the Pacific Ocean is linked to elemental carbon emissions resulting from anthropogenic activity in Asia (Chuang et al., 2005). The input of trace elements by dust deposition is also of importance to terrestrial ecosystems. For example, it has been proposed that the vegetation of the Amazon basin is highly dependent on Saharan dust deposition, which provides phosphorus, necessary for maintenance of long-term productivity (Okin et al., 2004; Section 7.3). The Hawaiian Islands also depend on phosphorus from Asian dust transport (Chadwick et al., 1999). Moreover, mineral dust can act as a sink for acidic trace gases, such as sulphur dioxide (SO_2) and HNO_3, and thereby interact with the sulphur and N cycles (e.g., Dentener et al., 1996; Umann et al., 2005). Coatings with soluble substances, such as sulphate or nitrate, will change the ability of mineral dust aerosols to nucleate cloud droplets (Levin et al., 1996; Section 7.5.2.1).

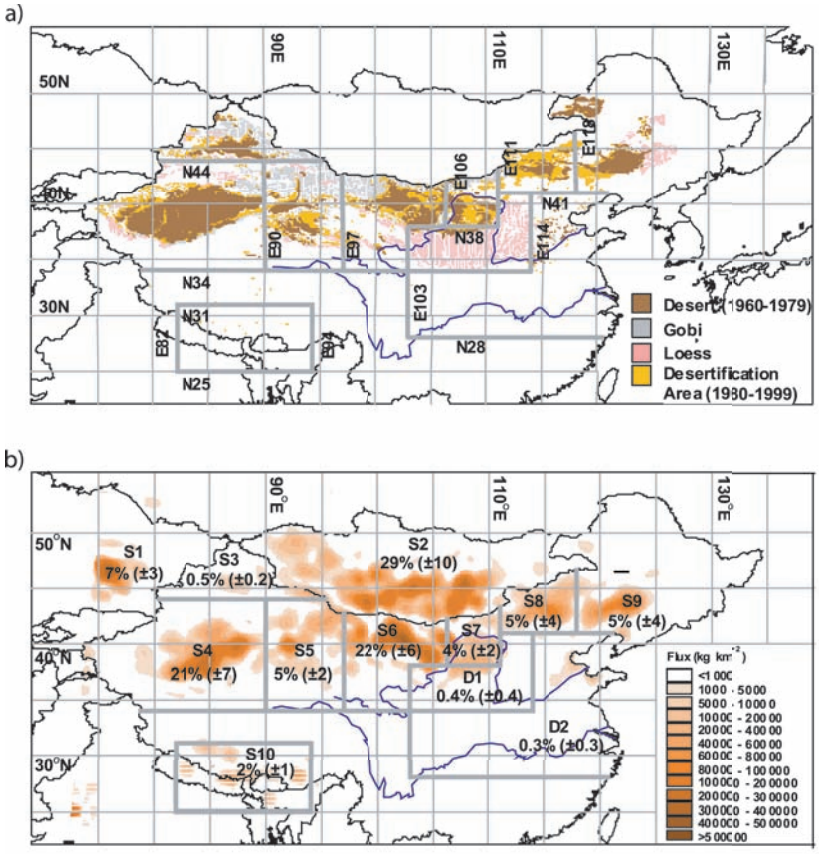


Figure 7.19. *(a) Chinese desert distributions from 1960 to 1979 and desert plus desertification areas from 1980 to 1999. (b) Sources (S1 to S10) and typical depositional areas (D1 and D2) for Asian dust indicated by spring average dust emission flux (kg km^{-2} per month) averaged over 1960 to 2002. The percentages with standard deviations in parentheses denote the average amount of dust production in each source region and the total amount of emissions between 1960 and 2002. The deserts in Mongolia (S2) and in western (S4) and northern (S6) China (mainly the Taklimakan and Badain Juran, respectively) can be considered the major sources of Asian dust emissions. Several areas with more expansions of deserts (S7, S8, S9 and S5) are not key sources. Adapted from Zhang et al. (2003).*

7.5.1.2 Sea Salt

Sea salt aerosol is a key aerosol constituent of the marine atmosphere. Sea salt aerosol particles affect the formation of clouds and rain. They serve as sinks for reactive gases and small particles and possibly suppress new particle formation. Sea salt is also responsible for a large fraction of the non-sea salt sulphate formation (e.g., Sievering et al., 1992). The major meteorological and environmental factors that affect sea salt formation are wind speed, atmospheric stability and wind friction velocity, sea surface and air temperatures, present and prior rain or snow and the amount and nature of surface-active materials in the near-surface ocean waters (Lewis and Schwartz, 2005). The average annual global sea salt flux from 12 models is estimated to be 16,300 Tg ± 200% (Textor et al., 2005) of which 15% is emitted into the submicron mode.

7.5.1.3 Natural Organic Carbon

Biogenic organic material is both directly emitted into the atmosphere and produced by VOCs. Primary emissions from the continents have been thought to be a relatively minor source but some studies suggest that these emissions could be much higher than previously estimated (Folberth et al., 2005; Jaenicke, 2005). Kanakidou et al. (2005) estimate a global biogenic secondary organic aerosol production of about 30 Tg yr^{-1} and recognise the potentially large, but uncertain, flux of primary biogenic particles. Annual global biogenic VOC emission estimates range from 500 to 1,200 Tg yr^{-1} (Guenther et al., 1995). There is a large range (less than 5 to greater than 90%) of organic aerosol yield for individual compounds and atmospheric conditions resulting in estimates of global annual secondary organic aerosol production from biogenic VOCs that range from 2.5 to 44.5 Tg of organic matter per year (Tsigaridis and Kanakidou, 2003). All biogenic VOC emissions are highly sensitive to changes in temperature, and some emissions respond to changes in solar radiation and precipitation (Guenther et al., 1995). In addition to the direct response to climatic changes, biogenic VOC emissions are also highly sensitive to climate-induced changes in plant species composition and biomass distributions.

Global biogenic VOC emissions respond to climate change (e.g., Turner et al., 1991; Adams et al., 2001; Penner et al., 2001; Sanderson et al., 2003b). These model studies predict that solar radiation and climate-induced vegetation change can affect emissions, but they do not agree on the sign of the change. Emissions are predicted to increase by 10% per °C (Guenther et al., 1993). There is evidence of physiological adaptation to higher temperatures that would lead to a greater response for long-term temperature changes (Guenther et al., 1999). The response of biogenic secondary organic carbon aerosol production to a temperature change, however, could be considerably lower than the response of biogenic VOC emissions since aerosol yields can decrease with increasing temperature. A potentially important feedback among forest ecosystems, greenhouse gases, aerosols and climate exists through increased photosynthesis and forest growth due to increasing temperatures and CO_2 fertilization (Kulmala et al., 2004). Increased forest biomass would increase VOC emissions and thereby organic aerosol production. This couples the climate effect of CO_2 with that of aerosols.

New evidence shows that the ocean also acts as a source of organic matter from biogenic origin (O'Dowd et al., 2004; Leck and Bigg, 2005b). O'Dowd et al. (2004) show that during phytoplankton blooms (summer conditions), the organic aerosols can constitute up to 63% of the total aerosol. Surface-active organic matter of biogenic origin (such as lipidic and proteinaceous material and humic substances), enriched in the oceanic surface layer and transferred to the atmosphere by bubble-bursting processes, are the most likely candidates to contribute to the observed organic fraction in marine aerosol. Insoluble heat-resistant organic sub-micrometre particles (peaking at 40 to 50 nm in diameter), mostly combined into chains or aggregated balls of 'marine microcolloids' linked by an amorphous electron-transparent material with properties entirely consistent with exopolymer secretions (Decho, 1990; Verdugo et al., 2004), are found in near-surface water of lower-latitude oceans (Benner et al., 1992; Wells and Goldberg, 1994), in leads between ice floes (Bigg et al., 2004), above the arctic pack ice (Leck and Bigg, 2005a) and over lower-latitude oceans (Leck and Bigg, 2005b). This aerosol formation pathway may constitute an ice (microorganisms)-ocean-aerosol-cloud feedback.

7.5.1.4 Aerosols from Dimethyl Sulphide

Dimethyl sulphide produced by phytoplankton is the most abundant form in which the ocean releases gaseous sulphur. Sea-air fluxes of DMS vary by orders of magnitude depending mainly on DMS sea surface concentration and on wind speed. Estimates of the global DMS flux vary widely depending mainly on the DMS sea surface climatology utilised, sea-air exchange parametrization and wind speed data, and range from 16 to 54 Tg yr^{-1} of sulphur (see Kettle and Andreae, 2000 for a review). According to model studies (Gondwe et al., 2003; Kloster et al., 2006), 18 to 27% of the DMS is converted into sulphate aerosols. Penner et al. (2001) show a small increase in DMS emissions between 2000 and 2100 (from 26.0 to 27.7 Tg yr^{-1} of sulphur) using constant DMS sea surface concentrations together with a constant monthly climatological ice cover. Gabric et al. (2004) predict an increase of the globally integrated DMS flux perturbation of 14% for a tripling of the pre-industrial atmospheric CO_2 concentration.

Bopp et al. (2004) estimate the feedback of DMS to cloud albedo with a coupled atmosphere-ocean-biogeochemical climate model that includes phytoplankton species in the ocean and a sulphur cycle in the atmospheric climate model. They obtain an increase in the sea-air DMS flux of 3% for doubled atmospheric CO_2 conditions, with large spatial heterogeneities (–15 to +30%). The mechanisms affecting those fluxes are marine biology, relative abundance of phytoplankton types and wind intensity. The simulated increase in fluxes causes an increase in sulphate aerosols and, hence, cloud droplets resulting in a radiative perturbation of cloud albedo of –0.05 W m^{-2}, which represents a small negative climate feedback to global warming.

7.5.1.5 Aerosols from Iodine Compounds

Intense new aerosol particle formation has been frequently observed in the coastal environment (O'Dowd et al., 2002a). Simultaneous coastal observations of reactive iodine species (Saiz-Lopez et al., 2005), chamber studies using iodocarbon precursors and laboratory characterisation of iodine oxide particles formed from exposure of *Laminaria* macroalgae to ozone (McFiggans et al., 2004) have demonstrated that coastal particle formation is linked to iodine compound precursor released from abundant infralittoral beds of macroalgae. The particle bursts overwhelmingly occur during daytime low tides (O'Dowd et al., 2002b; Saiz-Lopez et al., 2005). Tidal exposure of kelp leads to the well-documented release of significant fluxes of iodocarbons (Carpenter et al., 2003), the most photolabile of which, di-iodomethane (CH_2I_2), may yield a high iodine atom flux. However, the iodine monoxide (IO) and iodine dioxide (OIO) radicals, and new particles are thought more likely to result from emissions of molecular iodine (McFiggans et al., 2004), which will yield a much greater iodine atom flux (Saiz-Lopez and Plane, 2004). It is unclear whether such particles grow sufficiently to act as CCN (O'Dowd, 2002; Saiz-Lopez et al., 2005). Thus, a hitherto undiscovered remote ocean source of iodine atoms (such as molecular iodine) must be present if iodine-mediated particle formation is to be important in the remote marine boundary layer (McFiggans, 2005).

7.5.1.6 Climatic Factors Controlling Aerosol Burdens and Cycling

As discussed above, near-surface wind speed determines the source strength for primary aerosols (sea salt, dust, primary organic particles) and precursors of secondary aerosols (mainly DMS). Progress has been made in the development of source functions (in terms of wind speed) for sea salt and desert dust (e.g., Tegen et al., 2002; Gong, 2003; Balkanski et al., 2004).

Wind speed also affects dry deposition velocities and hence the lifetime of aerosols. In addition, biogenic emissions are strongly dependent on temperature (together with humidity/moisture; e.g., Guenther et al., 1995). Temperature also is a key factor in the gas-aerosol partitioning of semi-volatile secondary organics (Kanakidou et al., 2005).

Precipitation directly affects the wet removal and hence the lifetime of atmospheric aerosols. More aerosols decrease the precipitation formation rate, which in turn increases the lifetime of aerosols and results in more long-range aerosol transport to remote regions where wet removal is less efficient. At the same time, precipitating boundary layer clouds maintain themselves by keeping aerosol concentrations low (e.g., Baker and Charlson, 1990; Stevens et al., 2005; Sharon et al., 2006). Precipitation also affects soil moisture, with impacts on dust source strength and on stomatal opening/closure of plant leaves, hence affecting biogenic emissions. Cloud processing is an important pathway in the gas-to-particle conversion. It is the most important oxidation pathway for sulphate aerosols and shifts the aerosol size distribution to larger sizes, such that aerosols are more easily activated in subsequent cloud events (e.g., Hoppel et al., 1990; Kerkweg et al., 2003; Yin et al., 2005). It is also important in the conversion of hydrophobic to hydrophilic carbon.

Aerosol burden and lifetime are also affected by microphysical interactions among the different aerosol compounds as well as by changes in the spatial and seasonal distribution of the emissions. Sea salt aerosols, for example, provide surfaces for conversion of SO_2 into sulphate aerosols (Sievering et al., 1992) with consequences for cloud formation (Gong and Barrie, 2003; Section 7.5.2.1). A future reduction in SO_2 emissions and the associated reduced conversion of hydrophobic to hydrophilic soot could lead to a prolonged residence time of soot (Cooke et al., 2002; Stier et al., 2006b) and increased ammonium nitrate (Liao and Seinfeld, 2005). However, in a transient AOGCM climate simulation with an embedded microphysical aerosol module, Stier et al. (2006a) show that the effect on the hydrophobic to hydrophilic conversion can be outweighed by a general shift to low-latitude dry-season soot emissions. Consequently, soot lifetime increases in a future climate despite an enhanced conversion of hydrophobic to hydrophilic soot.

Table 7.10a. *Overview of the different aerosol indirect effects and their sign of the net radiative flux change at the top of the atmosphere (TOA).*

Effect	Cloud Types Affected	Process	Sign of Change in TOA Radiation	Potential Magnitude	Scientific Understanding
Cloud albedo effect	All clouds	For the same cloud water or ice content more but smaller cloud particles reflect more solar radiation	Negative	Medium	Low
Cloud lifetime effect	All clouds	Smaller cloud particles decrease the precipitation efficiency thereby presumably prolonging cloud lifetime	Negative	Medium	Very low
Semi-direct effect	All clouds	Absorption of solar radiation by absorbing aerosols affects static stability and the surface energy budget, and may lead to an evaporation of cloud particles	Positive or negative	Small	Very low
Glaciation indirect effect	Mixed-phase clouds	An increase in IN increases the precipitation efficiency	Positive	Medium	Very low
Thermodynamic effect	Mixed-phase clouds	Smaller cloud droplets delay freezing causing super-cooled clouds to extend to colder temperatures	Positive or negative	Medium	Very low

Table 7.10b. *Overview of the different aerosol indirect effects and their implications for the global mean net shortwave radiation at the surface, F_{sfc} (Columns 2-4) and for precipitation (Columns 5-7).*

Effect	Sign of Change in F_{sfc}	Potential Magnitude	Scientific Understanding	Sign of Change in Precipitation	Potential Magnitude	Scientific Understanding
Cloud albedo effect	Negative	Medium	Low	n.a.	n.a.	n.a.
Cloud lifetime effect	Negative	Medium	Very low	Negative	Small	Very low
Semi-direct effect	Negative	Large	Very low	Negative	Large	Very low
Glaciation indirect effect	Positive	Medium	Very low	Positive	Medium	Very low
Thermodynamic effect	Positive or negative	Medium	Very low	Positive or negative	Medium	Very low

7.5.2 Indirect Effects of Aerosols on Clouds and Precipitation

Aerosols can interact with clouds and precipitation in many ways, acting either as CCN or IN, or as absorbing particles, redistributing solar energy as thermal energy inside cloud layers. These indirect effects (in contrast to the direct interaction with radiation, see Chapter 2) are the subject of this subsection. They can be subdivided into different contributing processes, as summarised in Table 7.10 and shown in Figure 7.20. Cloud feedbacks remain the largest source of uncertainty in climate sensitivity estimates and the relatively poor simulation of boundary layer clouds in the present climate is a reason for some concern (see Chapter 8). Therefore the results discussed below need to be considered with caution.

The cloud-albedo effect, that is, the distribution of the same cloud liquid water content over more, hence smaller, cloud droplets leading to higher cloud reflectivity, is a purely radiative forcing and is therefore treated in Chapter 2. The other effects involve feedbacks in the climate system and are discussed here. The albedo effect cannot be easily separated from the other effects; in fact, the processes that decrease the cloud droplet size per given liquid water content also decrease precipitation formation, presumably prolonging cloud lifetime (cloud lifetime effect, Section 7.5.2.1 and Figure 7.20). In turn, an increase in cloud lifetime also contributes to a change in the time-averaged cloud albedo. The semi-direct effect refers to the absorption of solar radiation by soot, re-emitted as thermal radiation, hence heating the air mass and increasing static stability relative to the surface. It may also cause evaporation of cloud droplets (see Sections 2.4 and 7.5.4.1 and Figure 7.20). The glaciation effect refers to an increase in IN resulting in a rapid glaciation of a super-cooled liquid water cloud due to the difference in vapour pressure over ice and water. Unlike cloud droplets, these ice crystals grow in an environment of high super-saturation with respect to ice, quickly reaching precipitation size, with the potential to turn a non-precipitating cloud into a precipitating cloud (Section 7.5.2.2 and Figure 7.20). The thermodynamic effect refers to a delay in freezing by the smaller droplets causing super-cooled clouds to extend to colder temperatures (Section 7.5.2.2 and Figure 7.20). In addition to aerosol-induced changes at the top of the atmosphere (TOA), aerosols affect the surface energy budget (Table 7.10b; Section 7.5.2) with consequences for convection, evaporation and precipitation (Figure 7.20).

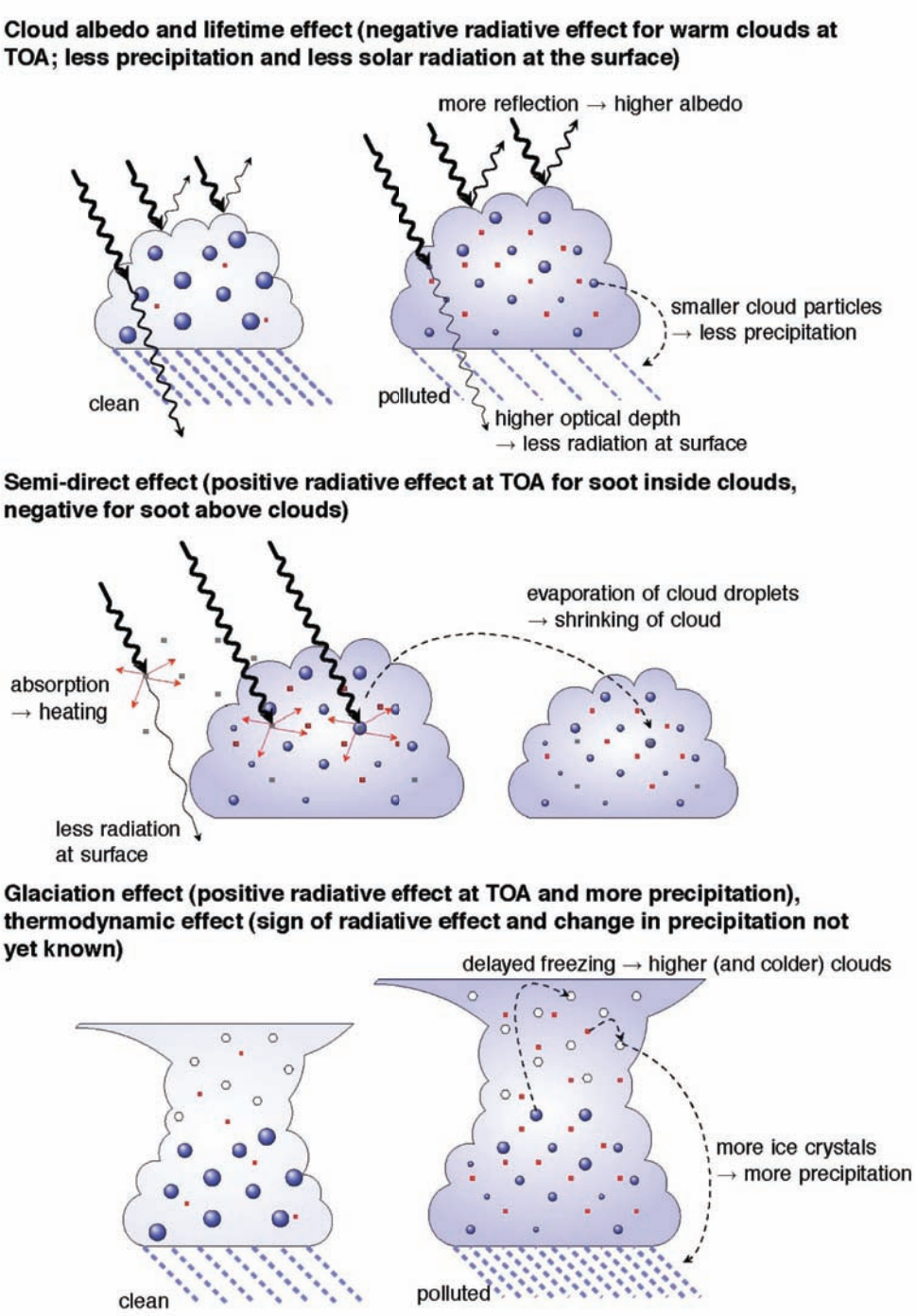


Figure 7.20. *Schematic diagram of the aerosol effects discussed in Table 7.10. TOA refers to the top-of-the-atmosphere.*

7.5.2.1 Aerosol Effects on Water Clouds and Warm Precipitation

Aerosols are hypothesised to increase the lifetime of clouds because increased concentrations of smaller droplets lead to decreased drizzle production and reduced precipitation efficiency (Albrecht, 1989). It is difficult to devise observational studies that can separate the cloud lifetime from the cloud albedo effect (see Section 2.4). Thus, observational studies usually provide estimates of the combined effects. Similarly, climate models cannot easily separate the cloud lifetime indirect effect once the aerosol scheme is fully coupled to a cloud microphysics scheme, but also predict the combined cloud albedo, lifetime and semi-direct effect.

Evidence for the absence of a drizzle mode due to anthropogenic emissions of aerosols and their precursors comes, for instance, from ship tracks perturbing marine stratus cloud decks off the coast of California (Ferek et al., 1998) as well as from analysing polluted compared with clean clouds off the Atlantic coast of Canada (Peng et al., 2002). One problem is that most climate models suggest an increase in liquid water when adding anthropogenic aerosols, whereas newer ship track studies show that polluted marine water clouds can have less liquid water than clean clouds (Platnick et al., 2000; Coakley and Walsh, 2002). Ackerman et al. (2004) attribute this effect to enhanced entrainment of dry air in polluted clouds in these instances with subsequent evaporation of cloud droplets. Similarly, when cloud lifetime is analysed, an increase in aerosol concentration from very clean to very polluted does not increase cloud lifetime, even though precipitation is suppressed (Jiang et al., 2006). This effect is due to competition between precipitation suppression and enhanced evaporation of the more numerous smaller cloud droplets in polluted clouds. Observed lower aerosol concentrations in pockets of open cells (Stevens et al., 2005) and in rifts of broken clouds surrounded by solid decks of stratocumulus with higher aerosol concentrations (Sharon et al., 2006) are manifestations of two stable aerosol regimes (Baker and Charlson, 1990). The low aerosol concentration regimes maintain themselves by higher drizzle rates. However, it is hard to disentangle cause and effect from these studies.

Smoke from burning vegetation reduces cloud droplet sizes and delays the onset of precipitation (Warner and Twomey, 1967; Rosenfeld, 1999; Andreae et al., 2004). In addition, desert dust suppresses precipitation in thin low-altitude clouds (Rosenfeld et al., 2001; Mahowald and Kiehl, 2003). Contradictory results have been found regarding the suppression of precipitation by aerosols downwind of urban areas (Givati and Rosenfeld, 2004; Jin et al., 2005) and in Australia (Rosenfeld, 2000; Ayers, 2005).

Models suggest that anthropogenic aerosols suppress precipitation in the absence of giant CCN and aerosol-induced changes in ice microphysics (e.g., Lohmann, 2002; Menon and DelGenio, 2007) as well as in mixed-phase clouds where the ice phase only plays a minor role (Phillips et al., 2002). A reduction in precipitation formation leads to increased cloud processing of aerosols. Feingold et al. (1998) and Wurzler et al. (2000) showed that cloud processing could either lead to an increase or decrease in precipitation formation in subsequent cloud cycles, depending on the size and concentration of activated CCN. Giant sea salt nuclei, on the other hand, may override the precipitation suppression effect of the large number of small pollution nuclei (Johnson, 1982; Feingold et al., 1999; Rosenfeld et al., 2002). Likewise, Gong and Barrie (2003) predict a reduction of 20 to 60% in marine cloud droplet number concentrations and an increase in precipitation when interactions of sulphate with sea salt aerosols are considered. When aerosol effects on warm convective clouds are included in addition to their effect on warm stratiform clouds, the overall indirect aerosol effect and the change in surface precipitation can be larger or smaller than if just the aerosol effect on stratiform clouds is considered (Nober et al., 2003; Menon and Rotstayn, 2006). Besides changes in the distribution of precipitation, the frequency of extreme events may also be reduced by the presence of aerosols (Paeth and Feichter, 2006).

Observations show that aerosols can decrease or increase cloud cover. Kaufman et al. (2005) conclude from satellite observations that the aerosol indirect effect is likely primarily due to an increase in cloud cover, rather than an increase in cloud albedo. In contrast, model results of Lohmann et al. (2006) associate the increase in cloud cover with differing dynamic regimes and higher relative humidities that maintain higher aerosol optical depths. On the other hand, the semi-direct effect of absorbing aerosols can cause evaporation of cloud droplets and/or inhibit cloud formation. In a large area with absorbing biomass-burning aerosol, few low-lying clouds were observed when the aerosol optical depth exceeded 1.2 (Koren et al., 2004). Increasing emissions of absorbing aerosols from the late 1980s to the late 1990s in China also reduced cloud amount leading to a decrease in local planetary albedo, as deduced from satellite data (Krüger and Grassl, 2004). When the combined effect of pollution and smoke aerosols is considered from ground-based observations, the net effect seems to be an increase in cloud cover with increasing aerosol column concentrations (Kaufman and Koren, 2006).

7.5.2.2 Aerosol Impacts on Mixed-Phase Clouds

As satellite observations of aerosol effects on mixed-phase clouds are not conclusive (Mahowald and Kiehl, 2003), this section only refers to model results and field studies. Studies with GCMs suggest that if, in addition to mineral dust, hydrophilic black carbon aerosols are assumed to act as IN at temperatures between 0°C and –35°C, then increases in aerosol concentration from pre-industrial to present times may cause a glaciation indirect effect (Lohmann, 2002). Increases in IN can result in more frequent glaciation of super-cooled stratiform clouds and increase the amount of precipitation via the ice phase, which could decrease the global mean cloud cover leading to more absorption of solar radiation. Whether the glaciation effect or warm cloud lifetime effect is larger depends on the chemical

nature of the dust (Lohmann and Diehl, 2006). Likewise, the number and size of ice particles in convective mixed-phase clouds is sensitive to the chemical composition of the insoluble fraction (e.g., dust, soot, biological particles) of the aerosol particles (Diehl and Wurzler, 2004).

Rosenfeld (1999) and Rosenfeld and Woodley (2000) analysed aircraft data together with satellite data suggesting that pollution aerosols suppress deep convective precipitation by decreasing cloud droplet size and delaying the onset of freezing. This hypothesis was supported by a cloud-resolving model study (Khain et al., 2001) showing that super-cooled cloud droplets down to –37.5°C could only be simulated if the cloud droplets were small and numerous. Precipitation from single-cell mixed-phase convective clouds is reduced under continental and maritime conditions when aerosol concentrations are increased (Yin et al., 2000; Khain et al., 2004; Seifert and Beheng, 2006). In the modelling study by Cui et al. (2006), this is caused by drops evaporating more rapidly in the high aerosol case (see also Jiang et al., 2006), which eventually reduces ice mass and hence precipitation. Khain et al. (2005) postulate that smaller cloud droplets, such as those originating from human activity, would change the thermodynamics of convective clouds. More, smaller droplets would reduce the production of rain in convective clouds. When these droplets freeze, the associated latent heat release would then result in more vigorous convection and more precipitation. In a clean cloud, on the other hand, rain would have depleted the cloud so that less latent heat is released when the cloud glaciates, resulting in less vigorous convection and less precipitation. Similar results were obtained by Koren et al. (2005), Zhang et al. (2005) and for the multi-cell cloud systems studied by Seifert and Beheng (2006). For a thunderstorm in Florida in the presence of Saharan dust, the simulated precipitation enhancement only lasted two hours after which precipitation decreased as compared with clean conditions (van den Heever et al., 2006). Cloud processing of dust particles, sulphate particles and trace gases can lead to an acceleration of precipitation formation in continental mixed-phase clouds, whereas in maritime clouds, which already form on rather large CCN, the simulated effect on precipitation is small (Yin et al., 2002). This highlights the complexity of the system and indicates that the sign of the global change in precipitation due to aerosols is not yet known. Note that microphysical processes can only change the temporal and spatial distribution of precipitation while the total amount of precipitation can only change if evaporation from the surface changes.

7.5.2.3 Aerosol Impacts on Cirrus Clouds

Cirrus clouds can form by homogeneous and heterogeneous ice nucleation mechanisms at temperatures below 235 K. While homogeneous freezing of super-cooled aqueous phase aerosol particles is rather well understood, understanding of heterogeneous ice nucleation is still in its infancy. A change in the number of ice crystals in cirrus clouds could exert a cloud albedo effect in the same way that the cloud albedo effect acts for water clouds. In addition, a change in the cloud ice water content could exert a radiative effect in the infrared. The magnitude of these effects in the global mean has not yet been fully established, but the development of physically based parametrization schemes of cirrus formation for use in global models led to significant progress in understanding underlying mechanisms of aerosol-induced cloud modifications (Kärcher and Lohmann, 2002; Liu and Penner, 2005; Kärcher et al., 2006).

A global climate model study concluded that a cloud albedo effect based solely on ubiquitous homogeneous freezing is small globally (Lohmann and Kärcher, 2002). This is expected to also hold in the presence of heterogeneous IN that cause cloud droplets to freeze at relative humidities over ice close to homogeneous values (above 130–140%) (Kärcher and Lohmann, 2003). Efficient heterogeneous IN, however, would be expected to lower the relative humidity over ice, so that the climate effect may be larger (Liu and Penner, 2005). *In situ* measurements reveal that organic-containing aerosols are less abundant than sulphate aerosols in ice cloud particles, suggesting that organics do not freeze preferentially (Cziczo et al., 2004). A model study explains this finding by the disparate water uptake of organic aerosols, and suggests that organics are unlikely to significantly modify cirrus formation unless they are present in very high concentrations (compared with sulphate-rich particles) at low temperatures (Kärcher and Koop, 2004).

With regard to aerosol effects on cirrus clouds, a strong link has been established between gravity wave induced, mesoscale variability in vertical velocities and climate forcing by cirrus (Kärcher and Ström, 2003; Hoyle et al., 2005). Hemispheric-scale studies of aerosol-cirrus interactions using ensemble trajectories suggest that changes in upper-tropospheric cooling rates and ice-forming aerosols in a future climate may induce changes in cirrus occurrence and optical properties that are comparable in magnitude with observed decadal trends in global cirrus cover (Haag and Kärcher, 2004). Optically thin and sub-visible cirrus are particularly susceptible to IN and therefore likely affected by anthropogenic activities.

Radiative forcing estimates and observed trends of aviation-induced cloudiness are discussed in Section 2.6. In terms of indirect effects of aircraft-induced aerosols on cirrus clouds, Lohmann and Kärcher (2002) show that the impact of aircraft sulphur emissions on cirrus properties via homogeneous freezing is small. The contribution from air traffic to the global atmospheric black carbon cycle was assessed by Hendricks et al. (2004). Assuming that black carbon particles from aviation serve as efficient IN, maximum increases or decreases in ice crystal number concentrations of more than 40% are simulated in a climate model study assuming that the 'background' (no aviation impact) cirrus cloud formation is dominated by heterogeneous or homogeneous nucleation, respectively (Hendricks et al., 2005). Progress in assessing the impact of aircraft black carbon on cirrus is hampered by the poor knowledge of natural freezing modes in cirrus conditions and the inability to describe the full complexity of cirrus processes in global models.

7.5.2.4 Global Climate Model Estimates of the Total Anthropogenic Aerosol Effect

The total anthropogenic aerosol effect as defined here includes estimates of the direct effect, semi-direct effect, indirect cloud albedo and cloud lifetime effect for warm clouds from several climate models. The total anthropogenic aerosol effect is obtained as the difference between a multi-year simulation with present-day aerosol emissions and a simulation representative for pre-industrial conditions, where anthropogenic emissions are turned off. It should be noted that the representation of the cloud lifetime effect in GCMs is essentially one of changing the auto-conversion of cloud water to rainwater.

The global mean total anthropogenic aerosol effect on net radiation at TOA from pre-industrial times to the present day is shown in Figure 7.21. Whereas Chapter 2 only considers the radiative forcing of the cloud albedo effect, here feedbacks are included in the radiative flux change. In most simulations shown in Figures 7.21 to 7.23, the total aerosol effect is restricted to warm clouds except for the simulations by Jacobson (2006) and Lohmann and Diehl (2006), who also include aerosol effects on mixed-phase and ice clouds. The total aerosol effect ranges from –0.2 W m^{-2} in the combined GCM plus satellite simulations (Quaas et al., 2006) to –2.3 W m^{-2} in the simulations by Ming et al. (2005), with an average forcing of –1.2 W m^{-2}. The total aerosol effect is larger when sulphate aerosols are used as surrogates for all anthropogenic aerosols than if multiple

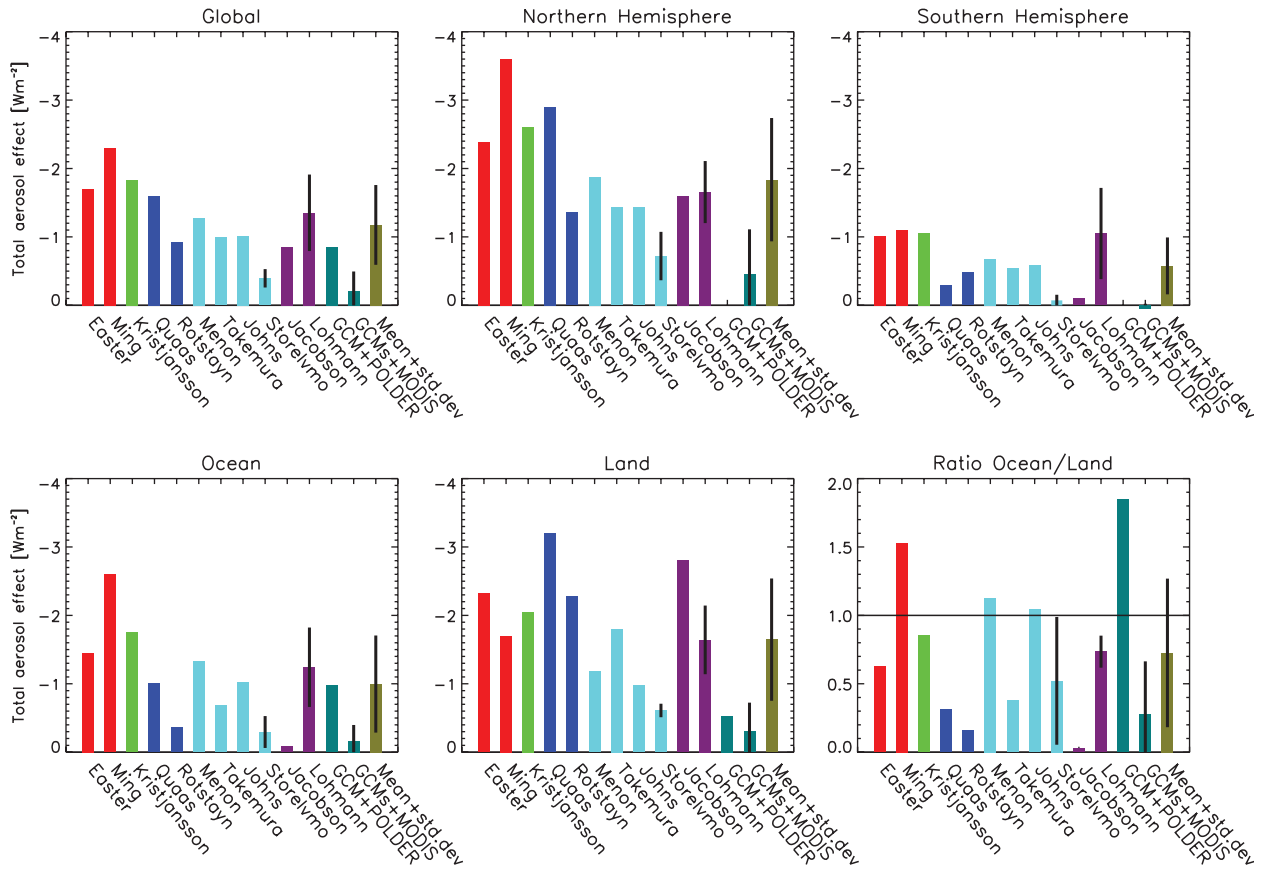


Figure 7.21. *Global mean total anthropogenic aerosol effect (direct, semi-direct and indirect cloud albedo and lifetime effects) defined as the response in net radiation at TOA from pre-industrial times to the present day and its contribution over the NH and SH, over oceans and over land, and the ratio over oceans/land. Red bars refer to anthropogenic sulphate (Easter et al., 2004; Ming et al., 2005^{+}), green bars refer to anthropogenic sulphate and black carbon (Kristjánsson, 2002$^{*,+}$), blue bars to anthropogenic sulphate and organic carbon (Quaas et al., 2004; Rotstayn and Liu, 2005^{+}), cyan bars to anthropogenic sulphate and black and organic carbon (Menon and Del Genio, 2005; Takemura et al., 2005; Johns et al., 2006; Storelvmo et al., 2006), dark purple bars to anthropogenic sulphate and black and organic carbon effects on water and ice clouds (Jacobson, 2006; Lohmann and Diehl, 2006), teal bars refer to a combination of GCM and satellite results (European Centre for Medium Range Weather Forecasts/Max-Planck Institute for Meteorology Atmospheric GCM (ECHAM) plus Polarisation and Directionality of the Earth's Reflectance (POLDER), Lohmann and Lesins, 2002; Laboratoire de Météorologie Dynamique GCM (LMDZ)/ECHAM plus Moderate Resolution Imaging Spectroradiometer (MODIS), Quaas et al., 2006) and olive bars to the mean and standard deviation from all simulations. Vertical black lines for individual results refer to ±1 standard deviation in cases of multiple simulations and/or results.*

** refers to estimates of the aerosol effect deduced from the shortwave radiative flux only*
$^{+}$ refers to estimates solely from the indirect effects

aerosol types are considered (Figure 7.21). Although most model estimates also include the direct and semi-direct effects, their contribution to the TOA radiation is generally small compared with the indirect effect, ranging from +0.1 to –0.5 W m^{-2} due to variations in the locations of black carbon with respect to the cloud (Lohmann and Feichter, 2005). The simulated cloud lifetime effect in a subset of models displayed in Figure 7.21 varies between –0.3 and –1.4 W m^{-2} (Lohmann and Feichter, 2005), which highlights some of the differences among models. The importance of the cloud albedo effect compared with the cloud lifetime effect varies even when the models use the same aerosol fields (Penner et al., 2006). Other differences among the simulations include an empirical treatment of the relationship between aerosol mass and cloud droplet number concentration vs. a mechanistic relationship, the dependence of the indirect aerosol effect on the assumed background aerosol or cloud droplet number concentration, and the competition between natural and anthropogenic aerosols as CCN (Ghan et al., 1998; O'Dowd et al., 1999). Likewise, differences in the cloud microphysics scheme, especially in the auto-conversion rate, cause different cloud responses (e.g., A. Jones et al., 2001; Menon et al., 2002a, 2003; Penner et al., 2006).

All models agree that the total aerosol effect is larger over the NH than over the SH (Figure 7.21). The values of the NH total aerosol effect vary between –0.5 and –3.6 W m^{-2} and in the SH between slightly positive and –1.1 W m^{-2}, with an average SH to NH ratio of 0.3. Estimates of the ocean/land partitioning of the total indirect effect vary from 0.03 to 1.8 with an average value of 0.7. While the combined European Centre for Medium Range Weather Forecasts/Max-Planck Institute for Meteorology Atmospheric GCM (ECHAM4) plus Polarisation and Directionality of the Earth's Reflectance (POLDER) satellite estimate suggests that the total aerosol effect should be larger over oceans (Lohmann and Lesins, 2002), combined estimates of the Laboratoire de Météorologie Dynamique (LMD) and ECHAM4 GCMs with Moderate Resolution Imaging Spectroradiometer (MODIS) satellite data reach the opposite conclusion (Quaas et al., 2006). The average total aerosol effect over the ocean of –1 W m^{-2} agrees with estimates of between –1 and –1.6 W m^{-2} from the Advanced Very High Resolution Radiometer (AVHRR)/POLDER (Sekiguchi et al., 2003). Estimates from GCMs of the total aerosol effect are generally larger than those from inverse models (Anderson et al., 2003 and Chapter 9).

As compared with the estimates of the total aerosol effect in Lohmann and Feichter (2005), some new estimates (Chen and Penner, 2005; Rotstayn and Liu, 2005; Lohmann and Diehl, 2006) now also include the influence of aerosols on the cloud droplet size distribution (dispersion effect; Liu and Daum, 2002). The dispersion effect refers to a widening of the size distribution in the polluted clouds that partly counteracts the reduction in the effective cloud droplet radius in these clouds. Thus, if the dispersion effect is taken into account, the indirect cloud albedo aerosol effect is reduced by 12 to 42% (Peng and Lohmann, 2003; Rotstayn and Liu, 2003; Chen and Penner, 2005). The global mean total indirect aerosol effect in the simulation by Rotstayn and Liu (2005) has also been reduced due to a smaller cloud lifetime effect resulting from a new treatment of auto-conversion.

Global climate model estimates of the change in global mean precipitation due to the total aerosol effects are summarised in Figure 7.22. Consistent with the conflicting results from detailed cloud system studies, the change in global mean precipitation varies between 0 and –0.13 mm day^{-1}. These differences are amplified over the SH, ranging from –0.06 mm day^{-1} to 0.12 mm day^{-1}. In general, the decreases in precipitation are larger when the atmospheric GCMs are coupled to mixed-layer ocean models (green bars), where the sea surface temperature and, hence, evaporation are allowed to vary.

7.5.3 Effects of Aerosols and Clouds on Solar Radiation at the Earth's Surface

By increasing aerosol and cloud optical depth, anthropogenic emissions of aerosols and their precursors contribute to a reduction of solar radiation at the surface. As such, worsening air quality contributes to regional aerosol effects. The partially conflicting observations on solar dimming/brightening are discussed in detail in Section 3.4 and Box 3.2. This section focuses on the possible contribution by aerosols. The decline in solar radiation from 1961 to 1990 affects the partitioning between direct and diffuse solar radiation: Liepert and Tegen (2002) concluded that over Germany, both aerosol absorption and scattering must have declined from 1975 to 1990 in order to explain the simultaneously weakened aerosol forcing and increased direct/diffuse solar radiation ratio. The direct/diffuse solar radiation ratio over the USA also increased from 1975 to 1990, likely due to increases in absorbing aerosols. Increasing aerosol optical depth associated with scattering aerosols alone in otherwise clear skies produces a larger fraction of diffuse radiation at the surface, which results in larger carbon assimilation into vegetation (and therefore greater transpiration) without a substantial reduction in the total surface solar radiation (Niyogi et al., 2004; Section 7.2.6.2).

For the tropical Indian Ocean, Ramanathan et al. (2001) estimate an indirect aerosol effect of –5 W m^{-2} at TOA and –6 W m^{-2} at the surface. While the direct effect is negligible at TOA, its surface forcing amounts to –14 W m^{-2} as a consequence of large atmospheric absorption in this region. In South Asia, absorbing aerosols may have masked up to 50% of the surface warming due to the global increase in greenhouse gases (Ramanathan et al., 2005). Global climate model estimates of the mean decrease in surface shortwave radiation in response to all aerosol effects vary between –1.3 and –3.3 W m^{-2} (Figure 7.23). It is larger than the TOA radiation flux change because some aerosols like black carbon absorb solar radiation within the atmosphere (see also Jacobson, 2001; Lohmann and Feichter, 2001; Ramanathan et al., 2001; Liepert et al., 2004). As for the TOA net radiation, the decrease is largest over land, with values approaching –9 W m^{-2}. Consistent with the above-mentioned regional studies, most models predict larger decreases over land than over the oceans.

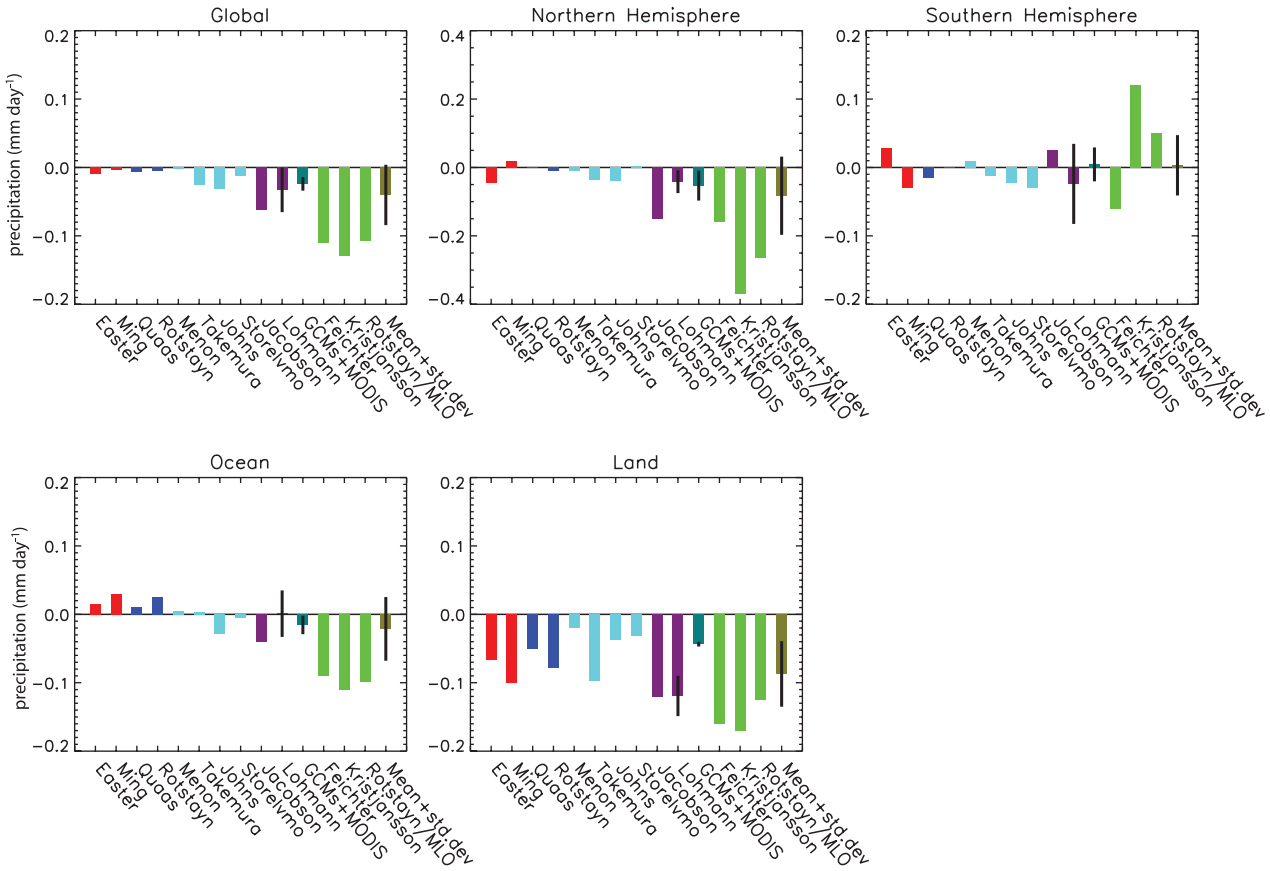


Figure 7.22. *Global mean change in precipitation due to the total anthropogenic aerosol effect (direct, semi-direct and indirect cloud albedo and lifetime effects) from pre-industrial times to the present day and its contribution over the NH and SH, over oceans and over land. Red bars refer to anthropogenic sulphate (Easter et al., 2004; Ming et al., 2005+), blue bars to anthropogenic sulphate and organic carbon (Quaas et al., 2004; Rotstayn and Liu, 2005+), cyan bars to anthropogenic sulphate, and black and organic carbon (Menon and Del Genio, 2005; Takemura et al., 2005; Johns et al., 2006; Storelvmo et al., 2006), dark purple bars to anthropogenic sulphate and black and organic carbon effects on water and ice clouds (Jacobson, 2006; Lohmann and Diehl, 2006), teal bars refer to a combination of GCM and satellite results (LMDZ/ECHAM plus MODIS, Quaas et al., 2006), green bars refer to results from coupled atmosphere/mixed-layer ocean (MLO) experiments (Feichter et al., 2004: sulphate and black and organic carbon; Kristjansson et al., 2005: sulphate and black carbon; Rotstayn and Lohmann, 2002+: sulphate only) and olive bars to the mean from all simulations. Vertical black lines refer to ±1 standard deviation.*

+ refers to estimates solely from the indirect effects

Transient simulations (Roeckner et al., 1999) and coupled GCM-mixed-layer ocean equilibrium simulations (Feichter et al., 2004; Liepert et al., 2004) suggest that the decrease in solar radiation at the surface resulting from increases in optical depth due to the direct and indirect anthropogenic aerosol effects is more important for controlling the surface energy budget than the greenhouse-gas induced increase in surface temperature. There is a slight increase in downwelling longwave radiation due to aerosols, which in the global mean is small compared to the decrease in shortwave radiation at the surface. The other components of the surface energy budget (thermal radiative flux, sensible and latent heat fluxes) decrease in response to the reduced input of solar radiation. As global mean evaporation must equal precipitation, a reduction in the latent heat flux in the model leads to a reduction in precipitation (Liepert et al., 2004). This is in contrast to the observed precipitation evolution in the last century (see Section 3.3) and points to an overestimation of aerosol influences on precipitation. The simulated decrease in global mean precipitation from pre-industrial times to the present may reverse into an increase of about 1% in 2031 to 2050 as compared to 1981 to 2000, because the increased warming due to black carbon and greenhouse gases then dominates over the sulphate cooling (Roeckner et al., 2006).

7.5.4 Effects of Aerosols on Circulation Patterns

7.5.4.1 Effects on Stability

Changes in the atmospheric lapse rate modify the longwave emission and affect the water vapour feedback (Hu, 1996) and the formation of clouds (see, e.g., Section 8.6). Observations and model studies show that an increase in the lapse rate produces an amplification of the water vapour feedback (Sinha, 1995). As aerosols cool the Earth's surface and warm the aerosol layer, the lapse rate will decrease globally and suppress the water vapour feedback (e.g., Feichter et al., 2004). The local change

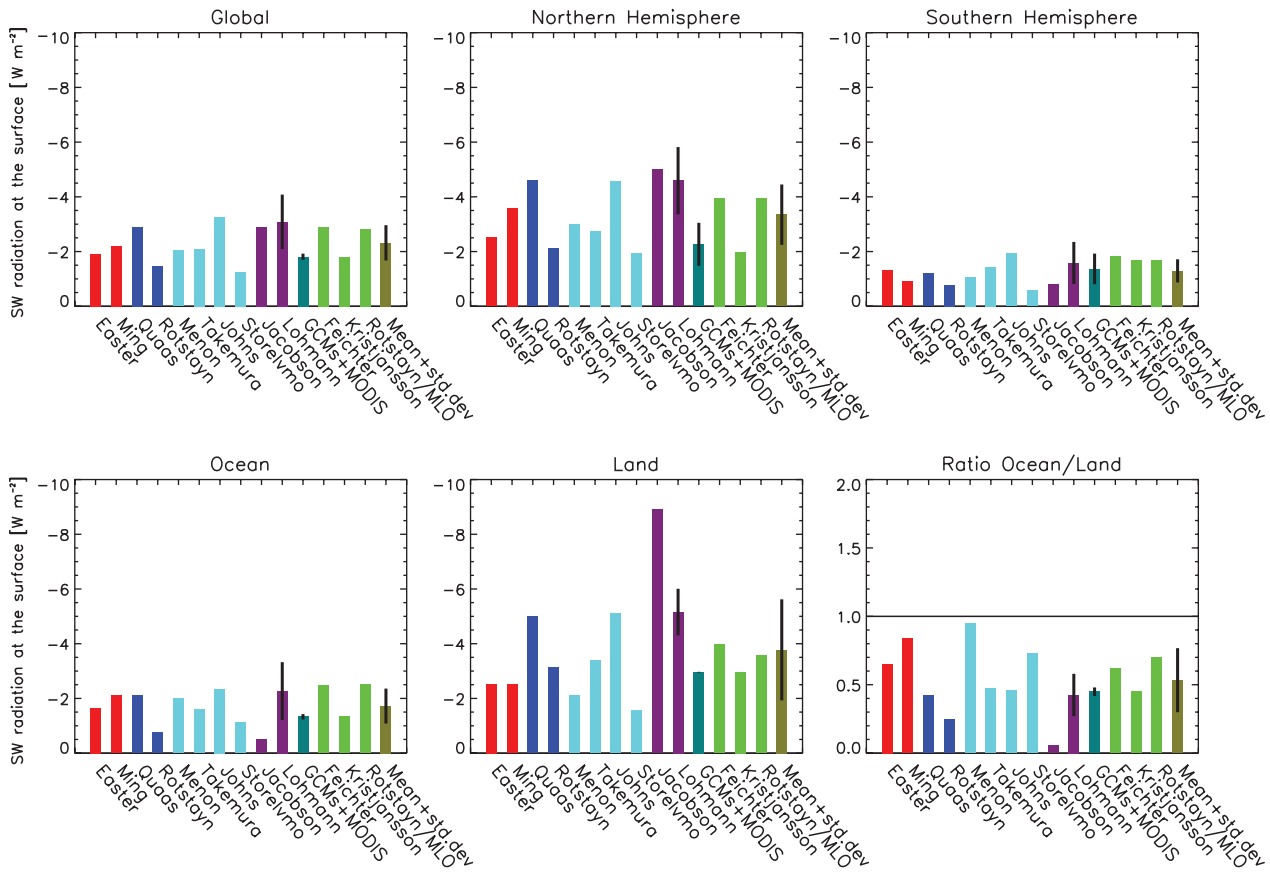


Figure 7.23. *Global mean change in net solar radiation at the surface due to the total anthropogenic aerosol effect (direct, semi-direct and indirect cloud albedo and lifetime effects) from pre-industrial times to the present day and its contribution over the NH and SH, over oceans and over land and the ratio over oceans/land. Red bars refer to anthropogenic sulphate (Easter et al., 2004; Ming et al., 2005+), blue bars to anthropogenic sulphate and organic carbon (Quaas et al., 2004; Rotstayn and Liu, 2005+), cyan bars to anthropogenic sulphate and black and organic carbon (Menon and Del Genio, 2005; Takemura et al., 2005; Johns et al., 2006; Storelvmo et al., 2006), dark purple bars to anthropogenic sulphate and black and organic carbon effects on water and ice clouds (Jacobson, 2006; Lohmann and Diehl, 2006), teal bars refer to a combination of GCM and satellite results (LMDZ/ECHAM plus MODIS, Quaas et al., 2006), green bars refer to results from coupled atmosphere/mixed-layer ocean (MLO) experiments (Feichter et al., 2004: sulphate and black and organic carbon; Kristjansson et al., 2005: sulphate and black carbon; Rotstayn and Lohmann, 2002+: sulphate only) and olive bars to the mean from all simulations. Vertical black lines refer to ±1 standard deviation.*

+ refers to estimates solely from the indirect effects

in atmospheric stability strongly depends on the altitude of the black carbon heating (Penner et al., 2003).

Absorption of solar radiation by aerosols can change the cloud amount (semi-direct effect; Grassl, 1975; Hansen et al., 1997; Ackerman et al., 2000; Ramanathan et al., 2001; Jacobson, 2006; Figure 7.20). The semi-direct effect has been simulated with GCMs and high-resolution cloud-resolving models, since it is implicitly accounted for whenever absorbing aerosols coupled to the radiation scheme are included (Hansen et al., 1997; Lohmann and Feichter, 2001; Jacobson, 2002; Menon et al., 2002b; Penner et al., 2003; Cook and Highwood, 2004; Hansen et al., 2005). Aerosol heating within cloud layers reduces cloud fractions, whereas aerosol heating above the cloud layer tends to increase cloud fractions. When diagnosed within a GCM framework, the semi-direct effect can also include cloud changes due to circulation effects and/or surface albedo effects. Moreover, the semi-direct effect is not exclusive to absorbing aerosol, as potentially any radiative heating of the mid-troposphere can produce a similar response in a GCM (Hansen et al., 2005; see also Section 2.8). Cloud-resolving models of cumulus and stratocumulus case studies also diagnose semi-direct effects indicating a similar relationship between the height of the aerosol layer relative to the cloud and the sign of the semi-direct effect (Ackerman et al., 2000; Ramanathan et al., 2001; Johnson et al., 2004; Johnson, 2005). Using a large eddy simulation, Feingold et al. (2005) show that the reduction in net surface radiation and in surface latent and sensible heat fluxes is the most simple explanation of the reduction in cloudiness associated with absorbing aerosols.

7.5.4.2 *Effects on the Large-Scale Circulation*

Several studies have considered the response of a GCM with a mixed-layer ocean to indirect aerosol effects (Rotstayn et al., 2000; K. Williams et al., 2001; Rotstayn and Lohmann, 2002) or to a combination of direct and indirect aerosol effects

(Feichter et al., 2004; Kristjansson et al., 2005; Takemura et al., 2005). All of these, and recent transient simulations (Held et al., 2005; Paeth and Feichter, 2006), found a substantial cooling that was strongest in the NH, with a consequent southward shift of the Inter-Tropical Convergence Zone (ITCZ) and the associated tropical rainfall belt. Rotstayn and Lohmann (2002) even suggest that aerosol effects might have contributed to the Sahelian droughts of the 1970s and 1980s (see Sections 9.5 and 11.2). If in turn the NH is warmed, for instance due to the direct forcing by black carbon aerosols, the ITCZ is found to shift northward (Chung and Seinfeld, 2005).

Menon et al. (2002b) and Wang (2004) found that circulation changes could be caused by aerosols in southeast China. In India and China, where absorbing aerosols have been added, increased rising motions are seen as well as increased subsidence to the south and north (Menon et al., 2002b). However, Ramanathan et al. (2005) found that convection was suppressed due to increased stability resulting from black carbon heating. Drier conditions resulting from suppressed rainfall can induce more dust and smoke due to the burning of drier vegetation (Ramanathan et al., 2001), thus affecting both regional and global hydrological cycles (Wang, 2004). Heating of a lofted dust layer could increase the occurrence of deep convection (Stephens et al., 2004). It can also strengthen the Asian summer monsoon circulation and cause a local increase in precipitation, despite the global reduction of evaporation that compensates aerosol radiative heating at the surface (Miller et al., 2004b). The dust-induced thermal contrast changes between the Eurasian continent and the surrounding oceans are found to trigger or modulate a rapidly varying or unstable Asian winter monsoon circulation, with a feedback to reduce the dust emission from its sources (Zhang et al., 2002).

In summary, an increase in atmospheric aerosol load decreases air quality and reduces the amount of solar radiation reaching the surface. This negative radiative forcing competes with the greenhouse gas warming for determining the change in evaporation and precipitation. At present, no transient climate simulation accounts for all aerosol-cloud interactions, so that the net aerosol effect on clouds deduced from models is not conclusive.

7.6 Concluding Remarks

Biogeochemical cycles interact closely with the climate system over a variety of temporal and spatial scales. On geological time scales, this interaction is illustrated by the Vostok ice core record, which provides dramatic evidence of the coupling between the carbon cycle and the climate system. The dynamics of the Earth system inferred from this record result from a combination of external forcing (in this case long-term periodic changes in the orbital parameters of the Earth and hence solar forcing) and an array of feedback mechanisms within the Earth environment (see Chapter 6). On shorter time scales, a range of forcings originating from human activities (conversion and fragmentation of natural ecosystems, emissions of greenhouse gases, nitrogen fixation, degradation of air quality, stratospheric ozone depletion) is expected to produce planet-wide effects and perturb numerous feedback mechanisms that characterise the dynamics of the Earth system.

A number of feedbacks that amplify or attenuate the climate response to radiative forcing have been identified. In addition to the well-known positive water vapour and ice-albedo feedbacks, a feedback between the carbon cycle and the climate system could produce substantial effects on climate. The reduction in surface carbon uptake expected in future climate should produce an additional increase in the atmospheric CO_2 concentration and therefore enhance climate forcing. Large differences between models, however, make the quantitative estimate of this feedback uncertain. Other feedbacks (involving, for example, atmospheric chemical and aerosol processes) are even less well understood. Their magnitude and even their sign remain uncertain. Potentially important aerosol-cloud interactions such as changes in cloud lifetime and aerosol effects on ice clouds can influence the hydrologic cycle and the radiative budget; however, the scientific understanding of these processes is low. The response of the climate system to anthropogenic forcing is expected to be more complex than simple cause and effect relationships would suggest; rather, it could exhibit chaotic behaviour with cascades of effects across the different scales and with the potential for abrupt and perhaps irreversible transitions.

This chapter has assessed how processes related to vegetation dynamics, carbon exchanges, gas-phase chemistry and aerosol microphysics could affect the climate system. These processes, however, cannot be considered in isolation because of the potential interactions that exist between them. Air quality and climate change, for example, are intimately coupled (Dentener et al., 2006). Brasseur and Roeckner (2005) estimate that the hypothetical removal from the atmosphere of the entire burden of anthropogenic sulphate aerosol particles (in an effort to improve air quality) would produce a rather immediate increase of about 0.8°C in the globally averaged temperature, with geographical patterns that bear a resemblance to the temperature changes found in greenhouse gas scenario experiments (Figure 7.24). Thus, environmental strategies

aimed at maintaining 'global warming' below a prescribed threshold must therefore account not only for CO_2 emissions but also for measures implemented to improve air quality. To cope with the complexity of Earth system processes and their interactions, and particularly to evaluate sophisticated models of the Earth system, observations and long-term monitoring of climate and biogeochemical quantities will be essential. Climate models will have to reproduce accurately the important processes and feedback mechanisms discussed in this chapter.

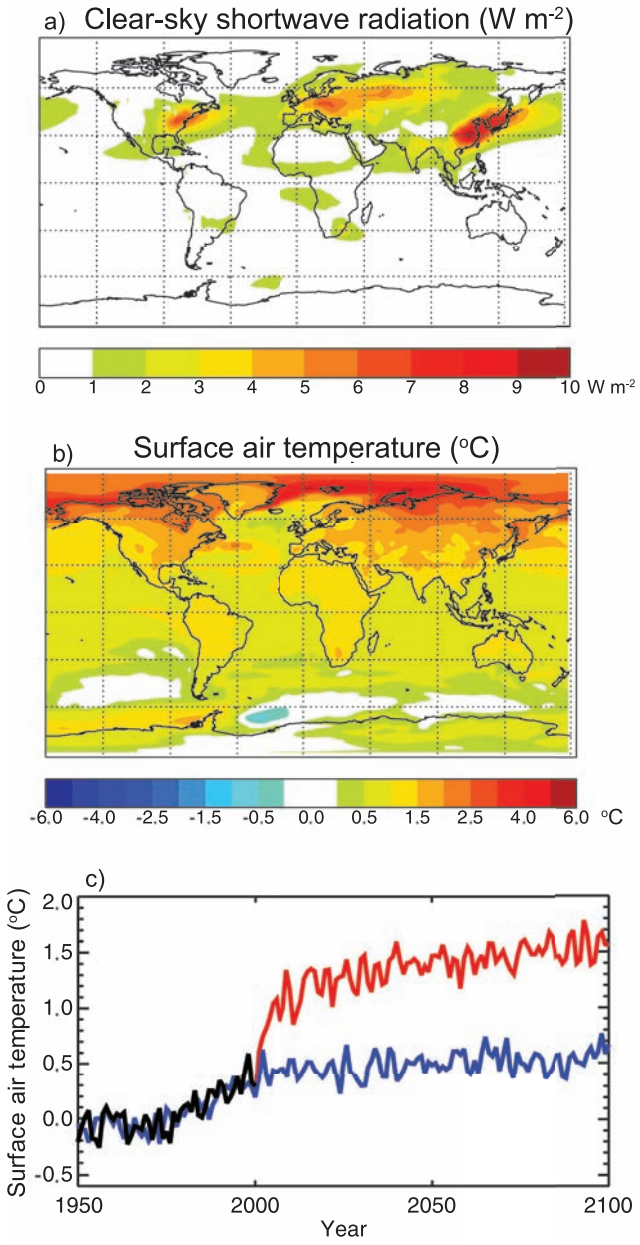


Figure 7.24. *Effect of removing the entire burden of sulphate aerosols in the year 2000 on (a) the annual mean clear sky TOA shortwave radiation (W m^{-2}) calculated by Brasseur and Roeckner (2005) for the time period 2071 to 2100 and (b) on the annual mean surface air temperature (°C) calculated for the same time period. (c) temporal evolution of global and annual mean surface air temperature anomalies (°C) with respect to the mean 1961 to 1990 values. The evolution prior to the year 2000 is driven by observed atmospheric concentrations of greenhouse gases and aerosols as adopted by IPCC (see Chapter 10). After 2000, the concentration of greenhouse gases remains constant while the aerosol burden is unchanged (blue line) or set to zero (red line). The black curve shows observations (A. Jones et al., 2001; Jones et al., 2006).*

References

Achard, F., et al., 2004: Improved estimates of net carbon emissions from land cover change in the tropics for the 1990s. *Global Biogeochem. Cycles*, **18**, GB2008, doi:10.1029/2003GB002142.

ACIA, 2005: *Arctic Climate Impact Assessment*. Cambridge University Press, Cambridge, 1042 pp.

Ackerman, A.S., M.P. Kirkpatrick, D.E. Stevens, and O.B. Toon, 2004: The impact of humidity above stratiform clouds on indirect climate forcing. *Nature*, **432**, 1014–1017.

Ackerman, A.S., et al., 2000: Reduction of tropical cloudiness by soot. *Science*, **288**, 1042–1047.

Adams, J., J. Constable, A. Guenther, and P. Zimmerman, 2001: An estimate of natural volatile organic compound emissions from vegetation since the last glacial maximum. *Chemosphere*, **3**, 73–91.

Adler, R.F., et al., 2003: The version-2 Global Precipitation Climatology Project (GPCP) monthly precipitation analysis (1979-present). *J. Hydrometeorol.*, **4**, 1147–1167.

Ainsworth, E.A., and S.P. Long, 2005: What have we learned from 15 years of free-air CO_2 enrichment (FACE)? A meta-analytic review of the responses of photosynthesis, canopy. *New Phytol.*, **165**(2), 351–371.

Albrecht, B., 1989: Aerosols, cloud microphysics, and fractional cloudiness. *Science*, **245**, 1227–1230.

Allan, W., et al., 2005: Interannual variations of ^{13}C in tropospheric methane: Implications for a possible atomic chlorine sink in the marine boundary layer. *J. Geophys. Res.*, **110**, doi:10.1029/2004JD005650.

Allen, D., K. Pickering, and M. Fox-Rabinovitz, 2004: Evaluation of pollutant outflow and CO sources during TRACE-P using model-calculated, aircraft-based, and Measurements of Pollution in the Troposphere (MOPITT)-derived CO concentrations. *J. Geophys. Res.*, **109**, D15S03, doi:10.1029/2003JD004250.

Anderson, T.L., et al., 2003: Climate forcing by aerosols - a hazy picture. *Science*, **300**, 1103–1104.

Andreae, M.O., and P. Merlet, 2001: Emission of trace gases and aerosols from biomass burning. *Global Biogeochem. Cycles*, **15**, 955–966.

Andreae, M.O., C.D. Jones, and P.M. Cox, 2005: Strong present-day aerosol cooling implies a hot future. *Nature*, **435**(7046), 1187–1190.

Andreae, M.O., et al., 2004: Smoking rain clouds over the Amazon. *Science*, **303**, 1337–1342.

Angert, A., et al., 2004: CO_2 seasonality indicates origins of post-Pinatubo sink. *Geophys. Res. Lett.*, **31**(11), L11103, doi:10.1029/2004GL019760.

Angert, A., et al., 2005: Drier summers cancel out the CO_2 uptake enhancement induced by warmer springs. *Proc. Natl. Acad. Sci. U.S.A.*, **102**, 10823–10827.

Archer, D., 2005: The fate of fossil fuel CO_2 in geologic time. *J. Geophys. Res.*, **110**(C9), C09S05, doi:10.1029/2004JC002625.

Archer, D., and B. Buffett, 2005: Time-dependent response of the global ocean clathrate reservoir to climatic and anthropogenic forcing. *Geochem. Geophys. Geosystems*, **6**, Q03002, doi:10.1029/2004GC000854.

Archer, D., H. Kheshgi, and E. Maier-Reimer, 1998: Dynamics of fossil fuel CO_2 neutralization by marine $CaCO_3$. *Global Biogeochem. Cycles*, **12**(2), 259–276.

Arellano, A.F. Jr., et al., 2004: Top-down estimates of global CO sources using MOPITT measurements. *Geophys. Res. Lett.*, **31**, L01104, doi:10.1029/ 2003GL018609.

Armstrong, R.A., et al., 2002: A new, mechanistic model for organic carbon fluxes in the ocean based on the quantitative association of POC with ballast minerals. *Deep-Sea Res. II*, **49**, 219–236.

Arora, V.K., and G.J. Boer, 2003: A representation of variable root distribution in dynamic vegetation models. *Earth Interactions*, **7**(6), 1–19.

Arora, V.K., and G.J. Boer, 2005: A parameterization of leaf phenology for the terrestrial ecosystem component of climate models. *Global Change Biol.*, **11**(1), 39–59.

Arora, V.K., and G.J. Boer, 2006: Simulating competition and coexistence between plant functional types in a dynamic vegetation model. *Earth Interactions*, **10**, Paper 10, 30 pp., doi:10.1175/EI170.1.

Aumont, O., et al., 2001: Riverine-driven interhemispheric transport of carbon. *Global Biogeochem. Cycles*, **15**, 393–405.

Austin, J., and R.J. Wilson, 2006: Ensemble simulations of the decline and recovery of stratospheric ozone. *J. Geophys. Res.*, **111**, D16314, doi:10.1029/2005JD006907.

Austin, J., et al., 2003: Uncertainties and assessments of chemistry-climate models of the stratosphere. *Atmos. Chem. Phys.*, **3**, 1–27.

Avissar, R., and D. Werth, 2005: Global hydroclimatological teleconnections resulting from tropical deforestation. *J. Hydrometeorol.*, **6**(2), 134–145.

Avissar, R., P.L. Silva Dias, M.A.F. Silva Dias, and C. Nobre, 2002: The Large-scale Biosphere-Atmosphere Experiment in Amazonia (LBA): Insights and future research needs. *J. Geophys. Res.*, **107**(D20), 8034, doi:10.1029/2002JD002507.

Aw, J., and M.J. Kleeman, 2003: Evaluating the first-order effect of intraannual air pollution on urban air pollution. *J. Geophys. Res.*, **108**, 4365, doi:10.1029/2002JD002688.

Ayers, G.P., 2005: "Air pollution and climate change: has air pollution suppressed rainfall over Australia?" *Clean Air and Environmental Quality*, **39**, 51–57.

Bacastow, R.B., and C.D. Keeling, 1981: Atmospheric carbon dioxide concentration and the observed airborne fraction. In: *Carbon Cycle Modelling* [Bolin, B. (ed.)]. SCOPE 16. John Wiley and Sons, New York, pp. 103–112.

Bagnoud, N., A.J. Pitman, B.J. McAvaney, and N.J. Holbrook, 2005: The contribution of the land surface energy balance complexity to differences in means, variances and extremes using the AMIP-II methodology. *Clim. Dyn.*, **25**, 171–188. doi:10.1007/S00382-005-0004-9.

Baker, D.F., et al., 2006: TransCom 3 inversion intercomparison: impact of transport model errors on the interannual variability of regional CO_2 fluxes, 1988-2003. *Global Biogeochem. Cycles*, **20**, GB1002, doi:1010.1029/2004GB002439.

Baker, M., and R.J. Charlson, 1990: Bistability of CCN concentrations and thermodynamics in the cloud-topped boundary layer. *Nature*, **345**, 142–145.

Baker, T.R., et al., 2004: Increasing biomass in Amazonian forest plots. *Philos. Trans. R. Soc. London Ser. B*, **359**, 353–365.

Baldocchi, D., et al., 2001: FLUXNET: A new tool to study the temporal and spatial variability of ecosystem-scale carbon dioxide, water vapor, and energy flux densities. *Bull. Am. Meteorol. Soc.*, **82**, 2415–2434.

Baldwin, M.P., and T.J. Dunkerton, 1999: Downward propagation of the Arctic Oscillation from the stratosphere to the troposphere. *J. Geophys. Res*., **104**, 30937–30946.

Baldwin, M.P., and T.J. Dunkerton, 2001: Stratospheric harbingers of anomalous weather regimes. *Science*, **244**, 581–584.

Balkanski, Y., et al., 2004: Global emissions of mineral aerosol: formulation and validation using satellite imagery. In: *Emission of Atmospheric Trace Compounds* [Granier, C., P. Artaxo, and C.E. Reeves (eds.)]. Kluwer, Dordrecht, pp. 239–267.

Balzter H., et al., 2005: Impact of the Arctic Oscillation pattern on interannual forest fire variability in Central Siberia. *Geophys. Res. Lett*., **32**, L14709, doi:10.1029/2005GL022526.

Barbosa, P.M., et al., 1999: An assessment of vegetation fire in Africa (1981–1991): Burned areas, burned biomass, and atmospheric emissions. *Global Biogeochem. Cycles*, **13**, 933–950.

Barford, C.C., et al., 2001: Factors controlling long and short term sequestration of atmospheric CO_2 in a mid-latitude forest. *Science*, **294**(5547), 1688–1691.

Barlage, M., and X. Zeng, 2004: Impact of observed vegetation root distribution on seasonal global simulations of land surface processes. *J. Geophys. Res.*, **109**, D09101, doi:10.1029/2003JD003847.

Battle, M., et al., 2000: Global carbon sinks and their variability inferred from atmospheric O_2 and $\delta^{13}C$. *Science*, **287**(5462), 2467–2470.

Beirle, S., et al., 2004: Estimate of nitrogen oxide emissions from shipping by satellite remote sensing. *Geophys. Res. Lett.*, **31**, L18102, doi:10.1029/2004GL020312.

Bellamy, P.H., et al., 2005: Carbon losses from all soils across England and Wales 1978–2003. *Nature*, **437**, 245248.

Benner R., et al., 1992: Bulk chemical characteristics of dissolved organic matter in the ocean. *Science*, **255**, 1561–1564.

Bergamaschi, P., M. Braeunlich, T. Marik, and C.A.M. Brenninkmeijer. 2000: Measurements of the carbon and hydrogen isotopes of atmospheric methane at Izana, Tenerife: Seasonal cycles and synoptic-scale variations. *J. Geophys. Res*., **105**, 14531–14546.

Berner, R.A., 1998: The carbon cycle and CO_2 over Phanerozoic time: the role of land plants. *Philos. Trans. R. Soc. London Ser. B*, **353**(1365), 75–81.

Bertram, T.H., et al., 2005: Satellite measurements of daily variations in soil NO_x emissions. *Geophys. Res. Lett.*, **32**, L24812, doi:10.1029/2005GL024640.

Betts, A.K., 2004: Understanding hydrometeorology using global models. *Bull. Am. Meteorol. Soc.*, **85**, 1673–1688.

Betts, A.K., 2006: Radiative scaling of the nocturnal boundary layer and the diurnal temperature range. *J. Geophys. Res.*, **111**, D07105, doi:10.1029/2005JD006560.

Betts, A.K., J. Ball, and J. McCaughey, 2001: Near-surface climate in the boreal forest. *J. Geophys. Res.*, **106**, 33529–33541.

Betts, R., et al., 2004: The role of ecosystem-atmosphere interactions in simulated Amazonian precipitation decrease and forest dieback under global change warming. *Theor. Appl. Climatol.*, **78**(1–3), 157–175.

Bey, I., et al., 2001: Global modeling of tropospheric chemistry with assimilated meteorology: model description and evaluation. *J. Geophys. Res.*, **106**(D19), 23073–23096.

Bigg, E.K., C. Leck, and L. Tranvik, 2004: Particulates of the surface microlayer of open water in the central Arctic Ocean in summer. *Mar. Chem.*, **91**(1–4), 131–141.

Bodeker, G.E., H. Shiona, and H. Eskes, 2005: Indicators of Antarctic ozone depletion. *Atmos. Chem. Phys.*, **5**, 2603–2615.

Boersma, K.F., H.J. Eskes, E.W. Meijer, and H.M. Keider, 2005: Estimates of lightning NO_x production from GOME satellite observations. *Atmos. Chem. Phys. Discussions*, **5**, 3047–3104.

Bogner, J.E., R.L. Sass, and B.P. Walter, 2000: Model comparisons of methane oxidation across a management gradient: Wetlands, rice production systems, and landfill. *Global Biogeochem. Cycles.*, **14**, 1021–1033.

Bolin, B., and E. Eriksson, 1959: Changes in the carbon dioxide content of the atmosphere and sea due to fossil fuel combustion. In: *The Atmosphere and Sea in Motion* [Bolin, B. (ed.)]. Rossby Memorial Volume. Rockefeller Institute, New York, NY, pp. 130–142.

Bonan, G.B., 2001: Observational evidence for reduction of daily maximum temperature by croplands in the midwest United States. *J. Clim.*, **14**, 2430–2442.

Bonan, G.B., et al., 2003: A dynamic global vegetation model for use with climate models: concepts and description of simulated vegetation dynamics. *Global Change Biol.*, **9**, 1543–1566.

Bond, W.J., G.F. Midgley, and F.I. Woodward, 2003: The importance of low atmospheric CO_2 and fire in promoting the spread of grasslands and savannas. *Global Change Biol.*, **9**, 973–982.

Bopp, L., et al., 2002: Climate-induced oceanic oxygen fluxes: Implications for the contemporary carbon budget. *Global Biogeochem. Cycles*, **16**, doi:10.1029/2001GB001445.

Bopp, L., et al., 2004: Will marine dimethyl sulfide emissions amplify or alleviate global warming? A model study. *Can. J. Fish Aquat. Sci.*, **61**(5), 826–835.

Bopp, L., et al., 2005: Response of diatoms distribution to global warming and potential implications – a global model study. *Geophys. Res. Lett.*, **32**(19), L19606, doi:10.1029/2005GL023653.

Borges, A.V., 2005: Do we have enough pieces of the jigsaw to integrate CO_2 fluxes in the coastal ocean? *Estuaries*, **28**, 3–27.

Bousquet, P., et al., 2000: Regional changes in carbon dioxide fluxes of land and oceans since 1980. *Science*, **290**(5495), 1342–1346.

Bousquet, P., et al., 2005: Two decades of OH variability as inferred by an inversion of atmospheric transport and chemistry of methyl chloroform, *Atmos. Chem. Phys*., **5**, 2635–2656.

Bouwman, A.F., L.J.M. Boumans, and N.H. Batjes, 2001*: Global Estimates of Gaseous Emission of NH_3, NO and N_2O from Agricultural Land*. Food and Agriculture Organisation, Rome, 57 pp.

Bouwman, A.F., L.J.M. Boumans, and N.H. Batjes, 2002: Modeling global annual N_2O and NO emissions from fertilized fields. *Global Biogeochem. Cycles*, **16**(4), 1080, doi:10.1029/2001GB001812.

Boyd, P.W., et al., 2004: The decline and fate of an iron-induced subarctic phytoplankton bloom. *Nature*, **428**, 549–553.

Boyle, E.D., 1988: The role of vertical chemical fractionation in controlling late quaternary atmospheric carbon dioxide. *J. Geophys. Res.*, **93**(C12), 15701–15714.

Brasseur, G.P, and E. Roeckner, 2005: Impact of improved air quality on the future evolution of climate. *Geophys. Res. Lett*., **32**, L23704, doi:10.1029/2005GL023902.

Brasseur, G.P., et al., 1998: Past and future changes in global tropospheric ozone: impact on radiative forcing. *Geophys. Res. Lett.*, **25**(20), 3807–3810.

Brasseur, G.P, et al., 2005: Impact of climate change on the future chemical composition of the global troposphere. *J. Clim.*, **19**, 3932–3951

Breshears, D.D., et al., 2005: Regional vegetation die-off in response to global-change-type drought. *Proc. Natl. Acad. Sci. U.S.A.*, **102**(42), 15144–15148.

Broecker, W.S., 1991: Keeping global change honest. *Global Biogeochem. Cycles*, **5**, 191–195.

Broecker, W.S., and T. Takahashi, 1978: Neutralization of fossil fuel CO_2 by marine calcium carbonate. In: *The Fate of Fossil Fuel CO_2 in the Ocean* [Andersen, N.R., and A. Malahoff (eds.)]. Plenum Press, New York, NY, pp. 213–248.

Broecker, W.S., and T.-H. Peng, 1982: *Tracers in the Sea*. ELDIGIO Press, New York, NY, 689 pp.

Broecker, W.S., and T.-H. Peng, 1986: Carbon cycle: 1985 – glacial to interglacial changes in the operation of the global carbon cycle. *Radiocarbon*, **28**, 309–327.

Broerse, A.T.C., et al., 2003: The cause of bright waters in the Bering Sea in winter. *Continental Shelf Res.*, **23**, 1579–1596.

Brook, E., et al., 2000: On the origin and timing of rapid changes in atmospheric methane during the last glacial period. *Global Biogeochem. Cycles*, **14**, 559–572.

Brovkin, V., et al., 2004: Role of land cover changes for atmospheric CO_2 increase and climate change during the last 150 years. *Global Change Biol.*, **10**, 1253–1266, doi:10.1111/j.1365-2486.2004.00812.

Brown, S., and A.E. Lugo, 1982: The storage and production of organic-matter in tropical forests and their role in the global carbon-cycle. *Biotropica*, **14**(3), 161–187.

Brown, T.J., B.L. Hall, and A.L. Westerling, 2004: The impact of twenty-first century climate change on wildland fire danger in the western United States: an applications perspective. *Clim. Change*, **62**, 365–388.

Buddemeier, R.W., J.A. Kleypas, and R.B. Aronson, 2004: *Coral Reefs and Global Climate Change*. Pew Centre on Global Climate Change, Arlington, VA, 44 pp.

Buffett, B., and D. Archer, 2004: Global inventory of methane clathrate: sensitivity to changes in the deep ocean. *Earth Planet. Sci. Lett.*, **227**, 185–199.

Burkhardt, S., I. Zondervan, and U. Riebesell, 1999: Effect of CO_2 concentration on C:N:P ratio in marine phytoplankton: a species comparison. *Limnol. Oceanogr.*, **44**(3), 683–690.

Burrows, W.H., et al., 2002: Growth and carbon stock change in eucalypt woodlands in northeast Australia: ecological and greenhouse sink implications. *Global Change Biol*., **8**, 769–784.

Butchart, N., and A.A. Scaife, 2001: Removal of chlorofluorocarbons by increased mass exchange between the stratosphere and troposphere in a changing climate. *Nature*, **410**, 799–802.

Butchart, N., et al., 2006: Simulations of anthropogenic change in the strength of the Brewer–Dobson circulation. *Clim. Dyn.*, **27**, doi:10.1007/s00382-006-0162-4.

Butler, T.M., I. Simmonds, and P.J. Rayner, 2004: Mass balance inverse modeling of methane in the 1990s using a chemistry transport model. *Atmos. Chem. Phys*., **4**, 2561–2580.

Cakmur, R.V., et al., 2006: Constraining the magnitude of the global dust cycle by minimizing the difference between a model and observations. *J. Geophys. Res*., **111**, doi:10.1029/2005JD005791

Caldeira, K., and M.E. Wickett, 2003: Anthropogenic carbon and ocean pH. *Nature*, **425**(6956), 365–368.

Cao, M., K. Gregson, and S. Marshall, 1998: Global methane emission from wetlands and its sensitivity to climate change. *Atmos. Environ.*, **32**, 3291–3299.

Carpenter, L.J., 2003: Iodine in the marine boundary layer. *Chem. Rev*., 103, 4953–4962.

Chadwick, O.A., et al., 1999: Changing sources of nutrients during four million years of ecosystem development. *Nature*, **397**(6719), 491.

Chagnon, F.J.F., R.L. Bras, and J. Wang, 2004: Climatic shift in patterns of shallow clouds over the Amazon. *Geophys. Res. Lett.*, **31**(24), L24212, doi:10.1029/2004GL021188.

Chambers, J.Q., and S.E. Trumbore, 1999: An age-old problem. *Trends Plant Sci.*, **4**(10), 385–386.

Chambers, J.Q., and W.L. Silver, 2004: Some aspects of ecophysiological and biogeochemical responses of tropical forests to atmospheric change. *Philos. Trans. R. Soc. London Ser. B*, **359**(1443), 463–476.

Chance, K., et al., 2000: Satellite observations of formaldehyde over North America from GOME. *Geophys. Res. Lett.*, **27**, 3461–3464.

Chapin, F.S. III, et al., 2005: Role of land-surface changes in arctic summer warming. *Science*, **310**, 657–660.

Chapman, S.J., and M. Thurlow, 1996: The influence of climate on CO_2 and CH_4 emissions from organic soils. *J. Agric. For. Meteorol.*, **79**, 205–217.

Chappellaz, J.A., I.Y. Fung, and A.M. Thompson, 1993: The atmospheric CH_4 increase since the last Glacial Maximum (1) Source estimates. *Tellus*, **45B**, 228–241.

Chave, J., et al., 2003: Spatial and temporal variation of biomass in a tropical forest: results from a large census plot in Panama. *J. Ecol.*, **91**, 240–252.

Chen, C.-T.A., K.-K. Liu, and R. MacDonald, 2003: Continental margin exchanges. In: *Ocean Biogeochemistry* [Fasham, M.J.R. (ed.)]. Springer-Verlag, Berlin, pp. 53–97.

Chen, M., P. Xie, and J.E. Janowiak, 2002: Global land precipitation: a 50-yr monthly analysis based on gauge observations. *J. Hydrometeorol.*, **3**, 249–266.

Chen, Y., and J.E. Penner, 2005: Uncertainty analysis for estimates of the first indirect effect. *Atmos. Chem. Phys*., **5**, 2935–2948.

Chen, Y-H., and R.G. Prinn, 2005: Atmospheric modeling of high- and low-frequency methane observations: Importance of interannually varying transport. *J. Geophys. Res.*, **110**, D10303, doi:10.1029/2004JD005542.

Chen, Y-H., and R.G. Prinn, 2006: Estimation of atmospheric methane emission between 1996-2001 using a 3-D global chemical transport model. *J. Geophys. Res.*, **111**, D10307, doi:10.1029/2005JD006058.

Christensen, T.R., A. Ekberg, L. Ström, and M. Mastepanov, 2003: Factors controlling large scale variations in methane emission from wetlands. *Geophys. Res. Lett*., **30**, 1414, doi:10.1029/2002GL016848.

Christensen, T.R., et al., 2004: Thawing sub-arctic permafrost: Effects on vegetation and methane emissions. *Geophys. Res. Lett.*, **31**, doi:10.1029/2003GL018680.

Chuang, P.Y., R.M. Duvall, M.M. Shafer, and J.J. Schauer, 2005: The origin of water soluble particulate iron in the Asian atmospheric outflow. *Geophys. Res. Lett*., **32**, doi:10.1029/2004GL021946.

Chung, S.H., and J.H. Seinfeld, 2005: Climate response of direct radiative forcing of anthropogenic black carbon. *J. Geophys. Res*., **110**, D11102, doi:10.1029/2004JD005441.

Ciais, P., et al., 1995: Partitioning of ocean and land uptake of CO_2 as inferred by $\delta^{13}C$ measurements from the NOAA Climate Monitoring and Diagnostics Laboratory Global Air Sampling Network. *J. Geophys. Res.*, **100**(D3), 5051–5070.

Ciais, P., et al., 2005a: The potential for rising CO_2 to account for the observed uptake of carbon by tropical, temperate, and boreal forest biomes. In: *The Carbon Balance of Forest Biomes* [Griffiths, H., and P. G. Jarvis (eds.)]. Taylor and Francis, New York, pp. 109–150.

Ciais, P., et al., 2005b: Europe-wide reduction in primary productivity caused by the heat and drought in 2003. *Nature*, **437**(7058), 529–533.

Clair, T.A., J.M. Ehrman, and K. Higuchi, 1999: Changes in freshwater carbon exports from Canadian terrestrial basins to lakes and estuaries under 2xCO_2 atmospheric scenario. *Global Biogeochem. Cycles*, **13**(4), 1091–1097.

Clark, D.A., 2002: Are tropical forests an important carbon sink? Reanalysis of the long-term plot data. *Ecol. Appl.*, **12**, 3–7.

Clark, D.A., 2004: Sources or sinks? The responses of tropical forests to current and future climate and atmospheric composition. *Philos. Trans. R. Soc. London Ser. B*, **359**, 477–491.

Clark, D.B., C.M. Taylor, and A.J. Thorpe, 2004: Feedback between the land surface and rainfall at convective length scales. *J. Hydrometeorol.*, **5**(4), 625–639.

Coakley, J.A. Jr., and C.D. Walsh, 2002: Limits to the aerosol indirect radiative forcing derived from observations of ship tracks. *J. Atmos. Sci.*, **59**, 668–680.

Cochrane, M.A., 2003: Fire science for rainforests. *Nature*, **421**(6926), 913–919.

Cohan, D.S., et al., 2002: Impact of atmospheric aerosol light scattering and absorption on terrestrial net primary productivity. *Global Biogeochem. Cycles*, **16**(4), 25–34, 1090, doi:10.1029/2001GB001441.

Cole, V., et al., 1996: Agricultural options for mitigation of greenhouse gas emissions. In: *Climate Change 1995. Impacts, Adaptations and Mitigation of Climate Change: Scientific-Technical Analyses* [Watson, R.T, M.C. Zinyowera, R.H. Moss, and D.J. Dokken (eds)]. Cambridge University Press, Cambridge, United Kingdom and New York, NY, USA, pp 745–771.

Collier, J.C., and K.P. Bowman, 2004: Diurnal cycle of tropical precipitation in a general circulation model. *J. Geophys. Res.*, **109**, D17105, doi:10.1029/2004JD004818.

Collins, W.J., D.S. Stevenson, C.E. Johnson, and R.G. Derwent, 1999: Role of convection in determining the budget of odd hydrogen in the upper troposphere. *J. Geophys. Res*., **104**(D21), 26927–26942.

Collins, W.J., R.G. Derwent, C.E. Johnson, and D.S. Stevenson, 2002: The oxidation of organic compounds in the troposphere and their global warming potentials. *Clim. Change*, **52**(4), 453–479.

Collins, W.J., et al., 2003: Effect of stratosphere-troposphere exchange on the future tropospheric ozone trend. *J. Geophys.Res.*, **108**(D12), 8528, doi:10.1029/2002JD002617.

Conrad, R., 1996: Soil microorganisms as controllers of atmospheric trace gases (H_2, CO, CH_4, OCS, N_2O, and NO). *Microbiol. Rev.*, **60**, 609–640.

Conrad, R., and W. Seiler, 1981: Decomposition of atmospheric hydrogen by soil-microorganisms and soil enzymes. *Soil Biol. Biochem.*, **13**, 43–49.

Constable, J.V.H., A.B. Guenther, D.S. Schimel, and R.K. Monson, 1999: Modeling changes in VOC emission in response to climate change in the continental United States. *Global Change Biol.*, **5**, 791–806.

Cook, J., and E.J. Highwood, 2004: Climate response to tropospheric absorbing aerosols in an intermediate general circulation model. *Q. J. R. Meteorol. Soc.*, **130**, 175–191.

Cooke, W.F., V. Ramaswamy, and P. Kasibhatla, 2002: A general circulation model study of the global carbonaceous aerosol distribution. *J. Geophys. Res.*, **107**, 4279, doi:10.1029/2001JD001274.

Cox, P.M., et al., 2000: Acceleration of global warming due to carbon-cycle feedbacks in a coupled climate model. *Nature*, **408**(6809), doi:10.1038/35041539.

Cox, P.M., et al., 2004: Amazonian forest dieback under climate-carbon cycle projections for the 21st century. *Theor. Appl. Climatol.*, **78**, 137–156.

Cramer, W., et al., 2001: Global response of terrestrial ecosystem structure and function to CO_2 and climate change: results from six dynamic global vegetation models. *Global Change Biol.*, **7**(4), 357–374.

Crucifix, M., R.A. Betts, and P.M. Cox, 2005: Vegetation and climate variability: a GCM modeling study. *Clim. Dyn.*, **24**, 457–467, doi:10.1007/S00382-004-0504-z.

Cui, Z.Q., K.S. Carslaw, Y. Yin, and S. Davies, 2006: A numerical study of aerosol effects on the dynamics and microphysics of a deep convective cloud in a continental environment. *J. Geophys. Res.,* **111**, D05201, doi:10.1029/2005JD005981.

Curtis, P.S., et al., 2002: Biometric and eddy-covariance based estimates of annual carbon storage in five eastern North American deciduous forests. *Agric. For. Meteorol.*, **113**, 3–19.

Cziczo, D.J., et al., 2004: Observations of organic species and atmospheric ice formation. *Geophys. Res. Lett.*, **31**, doi:10.1029/2004GL019822.

Da Rocha, H.R., et al., 2004: Seasonality of water and heat fluxes over a tropical forest in eastern Amazonia. *Ecol. Appl.*, **14**, S114–S126.

Dai, A., and K.E. Trenberth, 2002: Estimates of freshwater discharge from continents: latitudinal and seasonal variations. *J. Hydrometeorol.*, **3**, 660–687.

Dameris, M., et al., 2005: Long-term changes and variability in a transient simulation with a chemistry-climate model employing realistic forcing. *Atmos. Chem. Phys.*, **5**, 2121–2145.

Dameris, M., et al., 2006: Impact of solar cycle for onset of ozone recovery. *Geophys. Res. Lett.*, **33**, L03806, doi:10.1029/2005GL024741.

Dargaville, R.J., et al., 2000: Implications of interannual variability in atmospheric circulation on modeled CO_2 concentrations and source estimates. *Global Biogeochem. Cycles*, **14**, 931–943.

De Leeuw, G., et al., 2001: Atmospheric input of nitrogen into the North Sea: ANICE project overview. *Continental Shelf Res.*, **21**(18–19), 2073–2094.

Decho, A.W., 1990: Microbial exopolymer secretions in ocean environments: their role(s) in food webs and marine processes. *Oceanogr. Mar. Biol. Annu. Rev.*, **28**, 73–153.

DeFries, R.S., et al., 2002: Carbon emissions from tropical deforestation and regrowth based on satellite observations for the 1980s and 1990s. *Proc. Natl. Acad. Sci. U.S.A.*, **99**(22), 14256–14261.

Degens, E.T., S. Kempe, and A. Spitzy, 1984: Carbon dioxide: A biogeochemical portrait. In: *The Handbook of Environmental Chemistry* [Hutzinger, O. (ed.)]. Vol. 1, Part C, Springer-Verlag, Berlin, Heidelberg, pp. 127–215.

Del Grosso, S.J., A.R. Mosier, W.J. Parton, and D.S. Ojima, 2005: DAYCENT model analysis of past and contemporary soil N_2O and net greenhouse gas flux for major crops in the USA. *Soil Tillage Res.*, **83**(1), 9–24.

Del Grosso, S.J., et al., 2000: General CH_4 oxidation model and comparison of CH_4 oxidation in natural and managed systems. *Global Biogeochem. Cycles*, **14**, 999–1019.

DeLucia, E.H., D.J. Moore, and R.J. Norby, 2005: Contrasting responses of forest ecosystems to rising atmospheric CO_2: implications for the global C cycle. *Global Biogeochem. Cycles*, **19**, G3006, doi:10.1029/2004GB002346.

Dentener, F., et al., 1996: Role of mineral aerosol as a reactive surface in the global troposphere. *J. Geophys. Res*., **101**, 22869–22889.

Dentener, F., et al., 2003a: Interannual variability and trend of CH_4 lifetime as a measure for OH changes in the 1979–1993 time period. *J. Geophys. Res.*, **108**(D15), 4442, doi:10.1029/2002JD002916.

Dentener, F., et al., 2003b: Trends and inter-annual variability of methane emissions derived from 1979–1993 global CTM simulations. *Atmos. Chem. Phys.*, **3**, 73–88.

Dentener, F., et al., 2005: The impact of air pollutant and methane emission controls on tropospheric ozone and radiative forcing: CTM calculations for the period 1990–2030. *Atmos. Chem. Phys.*, **5**, 1731–1755.

Dentener, F., et al., 2006: The global atmospheric environment for the next generation. *Environ. Sci. Technol.*, **40**(11), 3586–3594.

Derwent, R.G., W.J. Collins, C.E. Johnson, and D.S. Stevenson, 2001: Transient behaviour of tropospheric ozone precursors in a global 3-D CTM and their indirect greenhouse effects. *Clim. Change*, **49**(4), 463–487.

Desborough, C.E., 1999: Surface energy balance complexity in GCM land surface models. *Clim. Dyn.*, **15**, 389–403.

Dickens, G.R., 2001: Modeling the global carbon cycle with gas hydrate capacitor: Significance for the latest Paleocene thermal maximum. In: *Natural Gas Hydrates: Occurrence, Distribution, and Detection* [Paull, C.K., and W.P. Dillon (eds.)]. Geophysical Monographs Vol. 124, American Geophysical Union, Washington, DC, pp. 19–38.

Dickens, G.R., M.M. Castillo, and J.G.C. Walker, 1997: A blast of gas in the latest Paleocene: Simulating first-order effects of massive dissociation of oceanic methane hydrate. *Geology*, **25**, 259–262.

Dickinson, R.E., G. Wang, X. Zeng, and Q.-C. Zeng, 2003: How does the partitioning of evapotranspiration and runoff between different processes affect the variability and predictability of soil moisture and precipitation? *Adv. Atmos. Sci.*, **20**(3), 475–478.

Dickinson, R.E., et al., 2006: The community land model and its climate statistics as a component of the community climate system model. *J. Clim.*, **19**, 2302–2324.

Diehl, K., and S. Wurzler, 2004: Heterogeneous drop freezing in the immersion mode: Model calculations considering soluble and insoluble particles in the drops. *J. Atmos. Sci.,* **61**, 2063–2072.

Dirmeyer, P.A., 2001: An evaluation of the strength of land-atmosphere coupling. *J. Hydrometeorol.*, **2**(4), 329–344.

Dlugokencky, E.J., K.A. Masarie, P.M. Lang, and P.P. Tans, 1998: Continuing decline in the growth rate of the atmospheric methane burden. *Nature*, **393**, 447–450.

Dlugokencky, E.J., et al., 2001: Measurements of an anomalous global methane increase during 1998. *Geophys. Res. Lett.*, **28**, 499–502.

Dlugokencky, E.J., et al., 2003: Atmospheric methane levels off: Temporary pause or a new steady state. *Geophys. Res. Lett.*, **30**, doi:10.1029/2003GL018126.

D'Odorico, P., and A. Porporato, 2004: Preferential states in soil moisture and climate dynamics. *Proc. Natl. Acad. Sci. U.S.A.*, **101**(24), 8848–8851.

Doherty, R.M., D.S. Stevenson, W.J. Collins, and M.G. Sanderson, 2005: Influence of convective transport on tropospheric ozone and its precursors in a chemistry-climate model. *Atmos. Chem. Phys.*, **5**, 3747–3771.

Doney, S.C., et al., 2004: Evaluating global ocean carbon models: the importance of realistic physics. *Global Biogeochem. Cycles*, **18**(3), GB3017, doi:10.1029/2003GB002150.

Douglass, A.R., M.R. Schoeberl, R.B. Rood, and S. Pawson, 2003: Evaluation of transport in the lower tropical stratosphere in a global chemistry and transport model. *J. Geophys. Res.*, **108**(D9), 4259, doi:10.1029/2002JD002696.

Duce, R.A., 1995: Sources, distributions and fluxes of mineral aerosols and their relationship to climate. In: *Aerosol Forcing of Climate* [Charlson, R.J. and J. Heintzenberg (eds.)]. John Wiley & Sons Ltd., Chichester, New York, pp. 43–72.

Dukes, J.S., et al., 2005: Responses of grassland production to single and multiple global environmental changes. *PLoS Biol.*, **3**(10), 1829–1836.

Dunn, A.L, et al., 2007: A long-term record of carbon exchange in a boreal black spruce forest: means, responses to interannual variability, and decadal trends. *Global Change Biol.*, **13**, 577-590, doi:10.1111/j.1365-2486.2006.01221.x.

Dupre, B., et al., 2003: Rivers, chemical weathering and Earth's climate. *Comptes Rendus Geoscience*, **335**(16), 1141–1160.

Durieux, L., L.A.T. Machado, and H. Laurent, 2003: The impact of deforestation on cloud cover over the Amazon arc of deforestation. *Remote Sens. Environ*., **86**(1), 132–140.

Dutay, J.C., et al., 2002: Evaluation of ocean model ventilation with CFC-11: comparison of 13 global ocean models. *Ocean Modelling*, **4**(2), 89–102.

Easter, R.C., et al., 2004: MIRAGE: Model description and evaluation of aerosols and trace gases. *J. Geophys. Res.*, **109**, doi:10.1029/2004JD004571.

Edwards, D.P., et al., 2004: Observations of carbon monoxide and aerosols from the Terra satellite: Northern Hemisphere variability. *J. Geophys. Res.*, **109**, D24202, doi:10.1029/2004JD004727.

Eglinton, T.I., and D.J. Repeta, 2004, Organic matter in the contemporary ocean. In: *Treatise on Geochemistry* [Holland, H.D., and K.K. Turekian (eds.)]. Volume 6, The Oceans and Marine Geochemistry, Elsevier Pergamon, Amsterdam, pp. 145–180.

Ehhalt, D.H., 1999: Gas phase chemistry of the troposphere. In: *Global Aspects of Atmospheric Chemistry* [Baumgärtl, H., W. Grünbein, and F. Hensel (eds.)]. Dr. Dietrich Steinkopf Verlag, Darmstadt, Germany, pp. 21–110.

Ek, M.B., and A.A.M. Holtslag, 2004: Influence of soil moisture on boundary layer cloud development. *J. Hydrometeorol.*, **5**, 86–99.

Engel, A., et al., 2004: Polysaccharide aggregation as a potential sink of marine dissolved organic carbon. *Nature*, **428**, 929–932.

Enting, I.G., and J.V. Mansbridge, 1991: Latitudinal distribution of sources and sinks of CO_2 - Results of an inversion study. *Tellus*, **43B**, 156–170.

Enting, I.G., C.M. Trudinger, and R.J. Francey, 1995: A synthesis inversion of the concentration and ^{13}C of atmospheric CO_2. *Tellus*, **47B**, 35–52.

Etheridge, D.M., L.P. Steel, R.J. Francey, and R.L. Langenfelds, 1998: Atmospheric methane between 1000 A.D. and present: Evidence of anthropogenic emissions and climatic variability. *J. Geophys. Res.*, **103**, 15979–15993.

Etiope, G., 2004: GEM-Geologic Emission of Methane, the missing source in the atmospheric methane budget. *Atmos. Environ.*, **38**, 3099–3100.

Etiope, G., and R.W. Klusman, 2002: Geologic emissions of methane to the atmosphere. *Chemosphere*, **49**, 777–789.

European Commission, 2003: *Ozone-Climate Interactions*. Air Pollution Research Report 81, EUR 20623, European Commission, Luxembourg, 143 pp.

Eyring, V., et al., 2005: A strategy for process-oriented validation of coupled chemistry-climate models. *Bull. Am. Meteorol. Soc.*, **86**, 1117–1133.

Falkowski, P., et al., 2000: The global carbon cycle: A test of our knowledge of Earth as a system. *Science*, **290**(5490), 291–296.

Falloon, P., et al., 2006: RothCUK – a dynamic modelling system for estimating changes in soil C at 1km scale in the UK. *Soil Use Management*, **22**, 274–288.

Fan, S., et al., 1998: A large terrestrial carbon sink in North America implied by atmospheric and oceanic carbon dioxide data and models. *Science*, **282**, 442–446.

Fang, J., et al., 2001: Changes in forest biomass carbon storage in China between 1949 and 1998. *Science*, **292**, 2320–2322.

Farquhar, G.D., S. von Caemmerer, and J.A. Berry, 2001: Models of photosynthesis. *Plant Physiol.*, **125**(1), 42–45.

Fearnside, P.M., 2000: Global warming and tropical land-use change: greenhouse gas emissions from biomass burning, decomposition and soils in forest conversion, shifting cultivation and secondary vegetation. *Clim. Change*, **46**, 115–158.

Feddes, R.A., et al., 2001: Modeling root water uptake in hydrological and climate models. *Bull. Am. Meteorol. Soc.*, **82**(12), 2797–2809.

Feely, R.A., R. Wanninkhof, T. Takahashi, and P. Tans, 1999: Influence of El Nino on the equatorial Pacific contribution to atmospheric CO_2 accumulation. *Nature*, **398**(6728), 597–601.

Feely, R.A., et al., 2002: Seasonal and interannual variability of CO_2 in the equatorial Pacific. *Deep-Sea Res. II*, **49**, 2443–2469.

Feely, R.A., et al., 2004: Impact of anthropogenic CO_2 on the $CaCO_3$ system in the oceans. *Science*, **305**, 362–366.

Feichter, J., E. Roeckner, U. Lohmann, and B. Liepert, 2004: Nonlinear aspects of the climate response to greenhouse gas and aerosol forcing. *J. Clim.*, **17**(12), 2384–2398.

Feingold, G., S.M. Kreidenweis, and Y.P. Zhang, 1998: Stratocumulus processing of gases and cloud condensation nuclei - 1. Trajectory ensemble model. *J. Geophys. Res.,* **103**(D16), 19527–19542.

Feingold, G., H. Jiang, and J. Y. Harrington, 2005: On smoke suppression of clouds in Amazonia. *Geophys. Res. Lett.*, **32**, L02804, doi:10.1029/2004GL021369.

Feingold, G., W.R. Cotton, S.M. Kreidenweis, and J.T. Davis, 1999: The impact of giant cloud condensation nuclei on drizzle formation in stratocumulus: Implications for cloud radiative properties. *J. Atmos. Sci.*, **56**, 4100–4117.

Fekete, B.M., C.J. Vorosmarty, and W. Grabs, 2002: High-resolution fields of global runoff combining observed river discharge and simulated water balances. *Global Biogeochem. Cycles*, **16**, doi:10.1029/1999GB001254.

Felzer, B., et al., 2004: Effects of ozone on net primary production and carbon sequestration in the conterminous United States using a biogeochemistry model. *Tellus*, **56B**, 230–248.

Ferek, R.J., et al., 1998: Measurements of ship-induced tracks in clouds off the Washington coast. *J. Geophys. Res.*, **103**, 23199–23206.

Ferretti, D.F., et al., 2005: Unexpected changes to the global methane budget over the past 2000 years. *Science*, **309**, 1714–1717.

Field, C.B., and M.R. Raupach (eds.), 2004: *The Global Carbon Cycle: Integrating Humans, Climate, and the Natural World*. SCOPE 62, Island Press, Washington, DC, 526 pp.

Finzi, A.C., et al., 2006: Progressive nitrogen limitation of ecosystem processes under elevated CO_2 in a warm-temperate forest. *Ecology*, 87, 15–25.

Findell, K.L., and E.A.B. Eltahir, 2003: Atmospheric controls on soil moisture–boundary layer interactions. Part II: Feedbacks within the continental United States. *J. Hydrometeorol.*, **4**, 570–583.

Fioletov, V.E., et al., 2002: Global and zonal total ozone variations estimated from ground-based and satellite measurements: 1964–2000. *J. Geophys. Res.*, **107**(D22), 4647, doi:10.1029/2001JD001350.

Flannigan, M.D., B.J. Stocks, and B.M. Wotton, 2000: Climate change and forest fires. *Sci. Total Environ.*, **262**, 221–229.

Flückiger, J., et al., 2002: High resolution Holocene N_2O ice core record and its relationship with CH_4 and CO_2. *Global Biogeochem. Cycles*, **16**, doi: 10.1029/2001GB001417.

Folberth, G., D.A. Hauglustaine, P. Ciais, and J. Lathière, 2005: On the role of atmospheric chemistry in the global CO_2 budget. *Geophys. Res. Lett.*, **32**, L08801, doi:10.1029/2004GL021812.

Folberth, G.A., D.A. Hauglustaine, J. Lathière, and F. Brocheton, 2006: Interactive chemistry in the Laboratoire de Météorologie Dynamique general circulation model: model description and impact of biogenic hydrocarbons on tropospheric chemistry. *Atmos. Chem. Phys.*, **6**, 2273–2319.

Foley, J.A., et al., 2003: Green Surprise? How terrestrial ecosystems could affect Earth's climate. *Frontiers Ecol. Environ.*, **1**(1), 38–44.

Frankenberg, C., et al., 2005: Assessing methane emission from global space-borne observation. *Science*, **308**, 1010–1014.

Frankenberg, C., et al., 2006: Satellite chartography of atmospheric methane from SCIAMACHY on board EMVISAT: Analysis of the years 2003 and 2004. *J. Geophys. Res.*, **111**, doi:10.1029/2005JD006235.

Freeman, C., et al., 2004: Export of dissolved organic carbon from peatlands under elevated carbon dioxide levels. *Nature*, **430**, 195–198.

Freitas, S.R., et al., 2005: Monitoring the transport of biomass burning emissions in South America. *Environ. Fluid Mech.*, **5**, 135–167.

Frew, R., A. Bowie, P. Croot, and S. Pickmere, 2001: Macronutrient and trace-metal geochemistry of an in situ iron-induced Southern Ocean bloom. *Deep-Sea Res. II*, **48**(11–12), 2467–2481.

Friedlingstein, P., J.-L. Dufresne, P.M. Cox, and P. Rayner, 2003: How positive is the feedback between climate change and the carbon cycle? *Tellus*, **55B**(2), 692–700.

Friedlingstein, P., et al., 2001: Positive feedback between future climate change and the carbon cycle. *Geophys. Res. Lett.*, **28**, 1543–1546, doi:10.1029/2000GL012015.

Friedlingstein, P., et al., 2006: Climate-carbon cycle feedback analysis: results from the C4MIP model intercomparison. *J. Clim.*, **19**, 3337–3353.

Fu, R., and W. Li, 2004: The influence of the land surface on the transition from dry to wet season in Amazonia. *Theor. Appl. Climatol.*, **78**, 97–110, doi:10.1007/s00704-004-0046-7.

Fueglistaler, S., and P.H. Haynes, 2005: Control of interannual and longer-term variability of stratospheric water vapor. *J. Geophys. Res*., **110**, D24108, doi:10.1029/2005JD006019.

Fung, I., S.C. Doney, K. Lindsay, and J. John, 2005: Evolution of carbon sinks in a changing climate. *Proc. Natl. Acad. Sci. U.S.A.*, **102**(32), 11201–11206.

Fusco, A.C., and J.A. Logan, 2003: Analysis of 1970-1995 trends in tropospheric ozone at northern hemisphere midlatitudes with the GEOS-CHEM model. *J. Geophys. Res.*, **108**(D15), 4449, doi:10.1029/2002JD002742.

Gabric, A.J., et al., 2004: Modeling estimates of the global emission of dimethylsulfide under enhanced greenhouse conditions. *Global Biogeochem. Cycles*, **18**(2), GB2014, doi:10.1029/2003GB002183.

Galloway, J.N., et al., 2004: Nitrogen cycles: past, present, and future. *Biogeochemistry*, **70**(2), 153–226.

Gamon, J.A., et al., 2003. Remote sensing in BOREAS: Lessons learned. *Remote Sens. Environ.*, **89**, 139–162.

Ganzeveld, L.N., et al., 2002: Global soil-biogenic NO_x emissions and the role of canopy processes. *J. Geophys. Res.*, **107**(D16), 4298, doi:10.1029/2001JD001289.

Gao, Z., et al., 2004: Modeling of surface energy partitioning, surface temperature, and soil wetness in the Tibetan prairie using the Simple Biosphere Model 2 (SiB2). *J. Geophys. Res.*, **109**, D06102, doi:10.1029/2003JD004089.

Gattuso, J.-P., D. Allemand, and M. Frankignoulle, 1999: Photosynthesis and calcification at cellular, organismal and community levels in coral reefs: a review on interactions and control by carbonate chemistry. *Am. Zool.*, **39**, 160–183.

Gedney, N., and P. Cox, 2003: The sensitivity of global climate model simulations to the representation of soil moisture heterogeneity. *J. Hydrometeorol.*, **4**, 1265–1275.

Gedney, N., P.M. Cox, and C. Huntingford, 2004: Climate feedback from wetland methane emissions. *Geophys. Res. Lett.*, **31**, L20503, doi:10.1029/2004GL020919.

Gérard, J.C., et al., 1999: The interannual change of atmospheric CO_2: contribution of subtropical ecosystems. *Geophys. Res. Lett.*, **26**, 243–246.

Gettelman, A., J.R. Holton, and K.H. Rosenlof, 1997: Mass fluxes of O_3, CH_4, N_2O, and CF_2Cl_2 in the lower stratosphere calculated from observational data. *J. Geophys. Res.*, **102**, 19149–19159.

Ghan, S.J., G. Guzman, and H. Abdul-Razzak, 1998: Competition between sea salt and sulphate particles as cloud condensation nuclei. *J. Atmos. Sci.*, **55**, 3340–3347.

Giardina, C.P., and M.G. Ryan, 2000: Evidence that decomposition rates of organic carbon in mineral soil do not vary with temperature. *Nature*, **404**, 858–861.

Gillett, N.P., and D.W.J. Thompson, 2003: Simulation of recent Southern Hemisphere climate change. *Science*, **302**, 273–275.

Gillett, N.P., A.J. Weaver, F.W. Zwiers, and M.D. Flannigan, 2004: Detecting the effect of climate change on Canadian forest fires. *Geophys. Res. Lett.*, **31**(18), L18211, doi:10.1029/2004GL020876.

Ginoux, P., et al., 2001: Sources and distributions of dust aerosols simulated with the GOCART model. *J. Geophys. Res.*, **16**, 20255–20274.

Givati, A., and D. Rosenfeld, 2004: Quantifying precipitation suppression due to air pollution. *J. Appl. Meteorol.*, **43**(7), 1038–1056.

Gloor, M., et al., 2003: A first estimate of present and preindustrial air-sea CO_2 flux patterns based on ocean interior carbon measurements and models. *Geophys. Res. Lett.*, **30**(1), 1010, doi:10.1029/2002GL015594.

Goncalves, L.G.G., E.J. Burke, and W.J. Shuttleworth, 2004: Application of improved ecosystem aerodynamics in regional weather forecasts. *Ecol. Appl.*, **14**, S17–S21.

Gondwe, M., et al., 2003: Correction to ''The contribution of ocean-leaving DMS to the global atmospheric burdens of DMS, MSA, SO, and NSS SO=''. *Global Biogeochem. Cycles*, **17**, 1106, doi:10.1029/2003GB002153.

Gong, S.L., 2003: A parameterization of sea-salt aerosol source function for sub- and super-micron particles. *Global Biogeochem. Cycles*, **17**(4), 1097, doi:10.1029/2003GB002079.

Gong, S.L., and L.A. Barrie, 2003: Simulating the impact of sea salt on global nss sulphate aerosols. *J. Geophys. Res.*, **108**(D16), 4516, doi:10.1029/2002JD003181.

Goodale, C.L., et al., 2002: Forest carbon sinks in the northern hemisphere. *Ecol. Appl.*, **12**(3), 891–899.

Goulden, M.L., et al., 2004: Diel and seasonal patterns of tropical forest CO_2 exchange. *Ecol. Appl.*, **14**, S42–S54.

Grassl, H., 1975: Albedo reduction and radiative heating of clouds by absorbing aerosol particles. *Contrib. Atmos. Phys.*, **48**, 199–210.

Green, P.A., et al., 2004: Pre-industrial and contemporary fluxes of nitrogen through rivers: a global assessment based on typology. *Biogeochemistry*, **68**(1), 71–105.

Grenfell, J.L., D.T. Shindell, and V. Grewe, 2003: Sensitivity studies of oxidative changes in the troposphere in 2100 using the GISS GCM. *Atmos. Chem. Phys.*, **3**, 1267–1283.

Grewe, V., et al., 2001: Future changes of the atmospheric composition and the impact on climate change. *Tellus*, **53B**(2), 103–121.

Gruber, N., and C.D. Keeling, 2001: An improved estimate of the isotopic air-sea disequilibrium of CO_2: Implications for the oceanic uptake of anthropogenic CO_2. *Geophys. Res. Lett*., **28**, 555–558.

Gruber, N., N. Bates, and C.D. Keeling, 2002: Interannual variability in the North Atlantic Ocean carbon sink. *Science*, **298**(5602), 2374–2378.

Gu, L., et al., 2002: Advantages of diffuse radiation for terrestrial ecosystem productivity. *J. Geophys. Res.*, **107**(6), 4050, doi:10.1029/2001JD001242.

Gu, L., et al., 2003: Response of a deciduous forest to the Mt. Pinatubo eruption: enhanced photosynthesis. *Science*, **299**(5615), 2035–2038.

Guenther, A.B., et al., 1993: Isoprene and monoterpene emission rate variability - model evaluations and sensitivity analyses. *J. Geophys. Res.*, **98**(D7), 12609–12617.

Guenther, A.B., et al., 1995: A global-model of natural volatile organic-compound emissions. *J. Geophys. Res.*, **100**(D5), 8873–8892.

Guenther, A.B., et al., 1999: Isoprene emission estimates and uncertainties for the Central African EXPRESSO study domain. *J. Geophys. Res.*, **104**(D23), 30625–30639.

Guillevic, P., et al., 2002: Influence of the interannual variability of vegetation on the surface energy balance - a global sensitivity study. *J. Hydrometeorol.*, **3**, 617–629.

Guo, Z., et al., 2006. GLACE: The Global Land-Atmosphere Coupling Experiment. 2. Analysis. *J. Hydrometeorol.*, **7**, 611–625.

Gupta, M., et al., 1997: $^{12}C/^{13}C$ kinetic isotope effects in the reactions of CH_4 with OH and Cl. *Geophys. Res. Lett.*, **24**, 2761–2764.

Gurney, K.R., et al., 2002: Towards robust regional estimates of CO_2 sources and sinks using atmospheric transport models. *Nature*, **415**(6872), 626–630.

Gurney, K.R., et al., 2003: TransCom 3 CO_2 inversion intercomparison: 1. Annual mean control results and sensitivity to transport and prior flux information. *Tellus*, **55B**(2), 555–579.

Gurney, K.R., et al., 2004: Transcom 3 inversion intercomparison: model mean results for the estimation of seasonal carbon sources and sinks. *Global Biogeochem. Cycles*, **18**(1), GB1010, doi:10.1029/2003GB002111.

Gurney, K.R., et al., 2005: Sensitivity of atmospheric CO_2 inversions to seasonal and interannual variations in fossil fuel emissions. *J. Geophys. Res.*, **110**, D10308, doi:10.1029/2004JD005373.

Haag, W., and B. Kärcher, 2004: The impact of aerosols and gravity waves on cirrus clouds at midlatitudes. *J. Geophys. Res.*, **109**, doi:10.1029/2004JD004579.

Haake, B., and V. Ittekkot, 1990: The wind-driven biological pump and carbon removal in the ocean. *Naturwissenschaften*, **77**(2), 75–79.

Hahmann, A.N., 2003: Representing spatial sub-grid precipitation variability in a GCM. *J. Hydrometeorol.*, **4**(5), 891–900.

Handisides, G.M., et al., 2003: Hohenpeissenberg photochemical experiment (HOPE 2000): measurements and photostationary state calculations of OH and peroxy radicals. *Atmos. Chem. Phys.*, **3**, 1565–1588.

Hansell, D.A., and C.A. Carlson, 1998: Deep-ocean gradients in the concentration of dissolved organic carbon. *Nature*, **395**, 263–266.

Hansen, J., M. Sato, and R. Ruedy, 1997: Radiative forcing and climate response. *J. Geophys. Res.*, **102**, 6831–6864.

Hansen, J., et al., 2005: Efficacy of climate forcings. *J. Geophys. Res.,* **110**(D18), D18104, doi:10.1029/2005JD005776.

Hauglustaine, D.A., and G.P. Brasseur, 2001: Evolution of tropospheric ozone under anthropogenic activities and associated radiative forcing of climate. *J. Geophys. Res.*, **106**(D23), 32337–32360.

Hauglustaine, D., and D.H. Ehhalt, 2002: A three-dimensional model of molecular hydrogen in the troposphere. *J. Geophys. Res.*, **107**(D17), doi:10.1029/2001JD001156.

Hauglustaine, D.A., J. Lathière, S. Szopa, and G. Folberth, 2005: Future tropospheric ozone simulated with a climate-chemistry-biosphere model. *Geophys. Res. Lett.*, **32**, L24807, doi:10.1029/2005GL024031.

Hauglustaine, D.A., et al., 2004: Interactive chemistry in the laboratoire de meteorologie dynamique general circulation model: description and background tropospheric chemistry. *J. Geophys. Res.*, **109**, D04314, doi:10.1029/2003JD003957.

Heald, C.L., et al., 2004: Comparative inverse analysis of satellite (MOPITT) and aircraft (TRACE-P) observations to estimate Asian sources of carbon monoxide. *J. Geophys. Res.*, **109**(D23), D23306, doi:10.1029/2004JD005185.

Heard, D.E., et al., 2004: High levels of the hydroxyl radical in the winter urban troposphere. *Geophys. Res. Lett.*, **31**, L18112, doi:10.1029/2004GL020544.

Hein, R., P.J. Crutzen, and M. Heimann, 1997: An inverse modeling approach to investigate the global atmospheric methane cycle. *Global Biogeochem. Cycles*, **11**, 43–76.

Heinze, C., 2004: Simulating oceanic $CaCO_3$ export production in the greenhouse. *Geophys. Res. Lett.*, **31**, L16308, doi:10.1029/2004GL020613.

Heinze, C., E. Maier-Reimer, and K. Winn, 1991: Glacial pCO_2 reduction by the World Ocean: experiments with the Hamburg carbon cycle model. *Paleoceanography*, **6**(4), 395–430.

Heinze, C., et al., 2003: Sensitivity of the marine biospheric Si cycle for biogeochemical parameter variations. *Global Biogeochem. Cycles*, **17**(3), 1086, doi:10.1029/2002GB001943.

Hejzlar, J., M. Dubrovsky, J. Buchtele, and M. Ruzicka, 2003: The apparent and potential effects of climate change on the inferred concentration of dissolved organic matter in a temperate stream (the Malse River, South Bohemia). *Sci. Total Environ.*, **310**(1–3), 143–152.

Held, I.M., et al., 2005: Simulation of Sahel drought in the 20th and 21st centuries. *Proc. Natl. Acad. Sci. U.S.A.*, **102**(50), 17891–17896

Henderson-Sellers, A., P. Irannejad, K. McGuffie, and A.J. Pitman, 2003: Predicting land-surface climates - better skill or moving targets? *Geophys. Res. Lett.*, **30**(14), 1777, doi:10.1029/2003GL017387.

Hendricks, J., B. Kärcher, M. Ponater, and U. Lohmann, 2005: Do aircraft black carbon emissions affect cirrus clouds on a global scale? *Geophys. Res. Lett.*, **32**, L12814, doi:10.1029/2005GL022740.

Hendricks, J., et al., 2004: Simulating the global atmospheric black carbon cycle: A revisit to the contribution of aircraft emissions. *Atmos. Chem. Phys.* **4**, 2521–2541.

Hesselbo, S.P., et al., 2000: Massive dissociation of gas hydrate during a Jurassic oceanic anoxic event. *Nature*, **406**, 392–395.

Heue, K.-P., et al., 2005: Validation of SCIAMACHY tropospheric NO_2 columns with AMAXDOAS measurements. *Atmos. Chem. Phys.*, **5**, 1039–1051.

Hirsch, A.I., et al., 2006: Inverse modeling estimates of the global nitrous oxide surface flux from 1998–2001. *Global Biogeochem. Cycles*, **20**, GB1008, doi:10.1029/2004GB002443.

Hoerling, M., and A. Kumar, 2003: The perfect ocean for drought. *Science*, **299**(5607), 691–694.

Hoffman, W.A., W. Schroeder, and R.B. Jackson, 2002: Positive feedbacks of fire, climate, and vegetation and the conversion of tropical savanna. *Geophys. Res. Lett.*, **15**, doi:10.1029/2002G0152.

Hofzumahaus, A., et al., 2004: Photolysis frequency of O_3 to O(1D): Measurements and modeling during the International Photolysis Frequency Measurement and Modeling Intercomparison (IPMMI). *J. Geophys. Res*., **109**, D08S90, doi:10.1029/2003JD004333.

Holland, E.A., and M.A. Carroll, 2003: Atmospheric chemistry and the bio-atmospheric carbon and nitrogen cycles. In: *Interactions of the Major Biogeochemical Cycles*, *Global Change and Human Impacts* [Melillo, J.M., C.B. Field, and B. Moldan (eds.)]. SCOPE 61, Island Press, Washington, DC, pp. 273–294.

Holland, E.A., F.J. Dentener, B.H. Braswell, and J.M. Sulzman, 1999: Contemporary and pre-industrial reactive nitrogen budgets. *Biogeochemistry*, **46**, 7–43.

Holland, E.A., B.H. Braswell, J. Sulzman, and J.F. Lamarque, 2005a: Nitrogen deposition onto the United States and Western Europe: synthesis of observations and models. *Ecol. Appl.*, **15**, 38–57.

Holland, E.A., J. Lee-Taylor, C. Nevison, and J. Sulzman, 2005b: Global N Cycle: Fluxes and N_2O mixing ratios originating from human activity. Data set. Available online from Oak Ridge National Laboratory Distributed Active Archive Center, Oak Ridge, TN, http://www.daac.ornl.gov.

Holland, E.A., et al., 2005c: U.S. nitrogen science plan focuses collaborative efforts. *Eos*, **86**(27), 253–260.

Hollinger, D.Y., et al., 1999: Seasonal patterns and environmental control of carbon dioxide and water vapour exchange in an ecotonal boreal forest. *Global Change Biol*., **5**, 891–902.

Holzer, M., and G.J. Boer, 2001: Simulated changes in atmospheric transport climate. *J. Clim.*, **14**, 4398–4420.

Hong, J., T. Choi, H. Ishikawa, and J. Kim, 2004: Turbulence structures in the near-neutral surface layer on the Tibetan Plateau. *Geophys. Res. Lett.*, **31**, L15106, doi:10.1029/2004GL019935.

Hoppel, W.A., J.W. Fitzgerald, G.M. Frick, and R.E. Larson, 1990: Aerosol size distributions and optical properties found in the marine boundary layer over the Atlantic Ocean. *J. Geophys. Res.*, **95**, 3659–3686.

Horowitz, L.W., et al., 2003: A global simulation of tropospheric ozone and related tracers: description and evaluation of MOZART, version 2. *J. Geophys. Res.*, **108**, 4784, doi:10.1029/2002JD002853.

Houghton, R.A., 1999: The annual net flux of carbon to the atmosphere from changes in land use 1850-1990. *Tellus*, **51B**, 298–313.

Houghton, R.A., 2003a: Revised estimates of the annual net flux of carbon to the atmosphere from changes in land use and land management 1850-2000. *Tellus*, **55B**(2), 378–390.

Houghton, R.A., 2003b: Why are estimates of the terrestrial carbon balance so different? *Global Change Biol.*, **9**, 500–509.

Houghton, R.A., et al., 2000: Annual fluxes of carbon from deforestation and regrowth in the Brazilian Amazon. *Nature*, **403**, 301–304.

Houweling, S., F. Dentener, and J. Lelieveld, 1998: The impact of nonmethane hydrocarbon compounds on tropospheric photochemistry. *J. Geophys. Res.*, **103**, 10673–10696.

Houweling, S., F. Dentener, and J. Lelieveld, 2000: Simulation of preindustrial atmospheric methane to constrain the global source strength of natural wetlands. *J. Geophys. Res.*, **105**, 17243–17255.

Hoyle, C.R., B.P. Luo, and T. Peter, 2005: The origin of high ice crystal number densities in cirrus clouds. *J. Atmos. Sci*., **62**, 2568–2579.

Hu, H., 1996: Water vapour and temperature lapse rate feedbacks in the mid-latitude seasonal cycle. *Geophys. Res. Lett.*, **23**, 1761–1764.

Huang, Y., R.E. Dickinson, and W.L. Chameides, 2006: Impact of aerosol indirect effect on climate over East Asia. *Proc. Natl. Acad. Sci. U.S.A.*, **103**, 4371–4376.

Huck, P.E., A.J. McDonald, G.E. Bodeker, and H. Struthers, 2005: Interannual variability in Antarctic ozone depletion controlled by planetary waves and polar temperatures. *Geophys. Res. Lett.*, **32**, L13819, doi:10.1029/2005GL022943.

Hudman, R.C., et al., 2004: Ozone production in transpacific Asian pollution plumes and implications for ozone air quality in California. *J. Geophys. Res.*, **109**, D23S10, doi:10.1029/2004JD004974.

Hughes, T.P., et al., 2003: Climate change, human impacts, and the resilience of coral reefs. *Science*, **301**, 929–933.

Hungate, B., et al., 2003: Nitrogen and climate change. *Science*, **302**(5650), 1512–1513.

Huntingford, C., et al., 2004: Using a GCM analogue model to investigate the potential for Amazonian forest dieback. *Theor. Appl. Climatol.*, **78**(1–3), 177–185.

Hurst, D.F., et al., 2006: Continuing global significance of emissions of Montreal Protocol-restricted halocarbons in the USA and Canada. *J. Geophys. Res.*, **111**, D15302, doi:10.1029/2005JD006785.

Hurtt, G.C., et al., 2002: Projecting the future of the U.S. carbon sink. *Proc. Natl. Acad. Sci. U.S.A.*, **99**(3), 1389–1394.

IFFN, 2003: Russian Federation Fire 2002 Special. Part III: The 2002 fire season in the Asian part of the Russian Federation: A view from space. *International Forest Fire News (IFFN)*, **28**, 18–28.

Imhoff, M.L., et al., 2004: Global patterns in human consumption of net primary production. *Nature*, **429**(6994), 870–873.

IPCC, 2000: *Special Report on Emission Scenarios. A Special Report of Working Group III of the Intergovernmental Panel on Climate Change* [Nakićenović, N., et al. (eds.)]. Cambridge University Press, Cambridge, United Kingdom and New York, NY, USA, 599 pp.

IPCC/TEAP, 2005: *IPCC/TEAP Special Report on Safeguarding the Ozone Layer and the Global Climate System: Issues related to Hydrofluorocarbons and Perfluorocarbons. Prepared by Working Group I and III of the Intergovernmental Panel on Climate Change and the Technology and Economic Assessment Panel* [Metz, B., et al. (eds.)]. Cambridge University Press, Cambridge, United Kingdom and New York, NY, USA, 488 pp.

Irannejad, P., A. Henderson-Sellers, and S. Sharmeen, 2003: Importance of land-surface parameterisation for latent heat simulation in global atmospheric models. *Geophys. Res. Lett.*, **30**(17), 1904, doi:10.1029/2003GL018044.

Irie, H., et al., 2005: Evaluation of long-term tropospheric NO_2 data obtained by GOME over East Asia in 1996-2002. *Geophys. Res. Lett.*, **32**, L11810, doi:10.1029/2005GL022770.

Ishimatsu, A., et al., 2004: Effects of CO_2 on marine fish: larvae and adults. *J. Oceanogr.*, **60**, 731–741.

Ittekkot, V., 1993: The abiotically driven biological pump in the ocean and short-term fluctuations in atmospheric CO_2 contents. *Global Planet. Change*, **8**(1–2), 17–25.

Jacob, D.J., 2000: Heterogeneous chemistry and tropospheric ozone. *Atmos. Environ.*, **34**, 2131–2159.

Jacob, D.J., et al., 1993: Factors regulating ozone over the United States and its export to the global atmosphere. *J. Geophys. Res.*, **98**, 14817–14826.

Jacobson, M.Z., 1999: Effects of soil moisture on temperatures, winds, and pollutant concentrations in Los Angeles. *J. Appl. Meteorol.*, **38**(5), 607–616.

Jacobson, M.Z., 2001: Global direct radiative forcing due to multicomponent anthropogenic and natural aerosols. *J. Geophys. Res*., **106**, 1551–1568.

Jacobson, M.Z., 2002: Control of fossil-fuel particulate black carbon and organic matter, possibly the most effective method of slowing global warming. *J. Geophys. Res.*, **107**, doi:10.1029/2001JD001376.

Jacobson, M.Z., 2006: Effects of externally-through-internally-mixed soot inclusions within clouds and precipitation on global climate. *J. Phys. Chem. A*, **110**, 6860–6873.

Jaeglé, L., D.J. Jacob, W.H. Brune, and P.O. Wenberg, 2001: Chemistry of HO_x radicals in the upper troposphere. *Atmos. Environ.*, **35**, 469–489.

Jaeglé, L., L. Steinberger, R.V. Martin, and K. Chance, 2005: Global partitioning of NO_x sources using satellite observations: Relative roles of fossil fuel combustion, biomass burning and soil emissions. *Faraday Discuss.*, **130**, 407–423.

Jaeglé, L., et al., 2004: Satellite mapping of rain-induced nitric oxide emissions from soils. *J. Geophys. Res.*, **109**, D21310, doi:10.1029/2004JD004787.

Jaenicke, R., 2005: Abundance of cellular material and proteins in the atmosphere. *Science*, **308**(5718), doi:10.1126/science.1106335.

Jaffe, D., et al., 2004: Long-range transport of Siberian biomass burning emissions and impact on surface ozone in western North America. *Geophys. Res. Lett.*, **31**, L16106, doi:10.1029/2004GL020093.

Jahren, A.H., et al., 2001: Terrestrial record of methane hydrate dissociation in the Early Cretaceous. *Geology*, **29**(2), 159–162.

Jain, A.K., and X. Yang, 2005: Modeling the effects of two different land cover change data sets on the carbon stocks of plants and soils in concert in CO_2 and climate change. *Global Biogeochem. Cycles*, **19**, doi:10.1029/2004GB002349.

Janssens, I.A., et al., 2003: Europe's terrestrial biosphere absorbs 7 to 12% of European anthropogenic CO_2 emissions. *Science*, **300**(5625), 1538–1542.

Jiang, H., et al., 2006: Aerosol effects on the lifetime of shallow cumulus. *Geophys. Res. Lett*., **33**, doi:10.1029/2006GL026024.

Jickells, T.D., et al., 2005: Global iron connections between desert dust, ocean biogeochemistry, and climate. *Science*, **308**(5718), 67–71.

Jin, M.L., J.M. Shepherd, and M.D. King, 2005: Urban aerosols and their variations with clouds and rainfall: a case study for New York and Houston. *J. Geophys. Res.*, **110**, doi:10.1029/2004JD005081.

Jin, Y., et al., 2002: How does snow impact the albedo of vegetated land surfaces as analyzed with MODIS data? *Geophys. Res. Lett.*, **29**, doi:10.1029/2001GLO14132.

Johns, T.C., et al., 2006: The new Hadley Centre climate model HadGEM1: Evaluation of coupled simulations. *J. Clim.*, **19**, 1327–1353.

Johnson, B.T., 2005: The semidirect aerosol effect: Comparison of a single-column model with large eddy simulation for marine stratocumulus. *J. Clim.*, **18**, 119–130.

Johnson, B.T., K.P. Shine, and P.M. Forster, 2004: The semi-direct aerosol effect: Impact of absorbing aerosols on marine stratocumulus. *Q. J .R. Meteorol. Soc.*, **130**, 1407–1422.

Johnson, C.E., W.J. Collins, D.S. Stevenson, and R.G. Derwent, 1999: Relative roles of climate and emissions changes on future tropospheric oxidant concentrations. *J. Geophys. Res.*, **104**(D15), 18631–18645.

Johnson, C.E., D.S. Stevenson, W.J. Collins, and R.G. Derwent, 2001: Role of climate feedback on methane and ozone studied with a coupled ocean-atmosphere-chemistry model. *Geophys. Res. Lett.*, **28**(9), 1723–1726.

Johnson, C.E., D.S. Stevenson, W.J. Collins, and R.G. Derwent, 2002: Interannual variability in methane growth rate simulated with a coupled ocean-atmosphere-chemistry model. *Geophys. Res. Lett.*, **29**(19), 1903, doi:10.1029/2002GL015269.

Johnson, D.B., 1982: The role of giant and ultragiant aerosol particles in warm rain initiation. *J. Atmos. Sci*., **39**, 448–460.

Jones, A., D.L. Roberts, M.J. Woodage, and C. E. Johnson, 2001: Indirect sulphate aerosol forcing in a climate model with an interactive sulphur cycle. *J. Geophys. Res.*, **106**, 20293–20310.

Jones, C., N. Mahowald, and C. Luo, 2004: Observational evidence of African desert dust intensification of easterly waves. *Geophys. Res. Lett.*, **31**, doi:10.1029/2004GL020107.

Jones, C.D., and P.M. Cox, 2001a: Modelling the volcanic signal in the atmospheric CO_2 record. *Global Biogeochem. Cycles*, **15**(2), 453–466.

Jones, C.D., and P.M. Cox, 2001b: Constraints on the temperature sensitivity of global soil respiration from the observed interannual variability in atmospheric CO_2. *Atmos. Sci. Lett.*, **1**, doi:10.1006/asle.2001.0041.

Jones, C.D., and P.M. Cox, 2005: On the significance of atmospheric CO_2 growth rate anomalies in 2002–2003. *Geophys. Res. Lett.*, **32**, L14816, doi:10.1029/2005GL023027.

Jones, C.D., M. Collins, P.M. Cox, and S.A. Spall, 2001: The carbon cycle response to ENSO: a coupled climate-carbon cycle model study. *J. Clim.*, **14**, 4113–4129.

Jones, C.D., et al., 2005: Global climate change and soil carbon stocks: predictions from two contrasting models for the turnover of organic carbon in soil. *Global Change Biol.*, **11**(1), 154–166.

Jones, P.D., D.E. Parker, T.J. Osborn, and K.R. Briffa, 2006: Global and hemispheric temperature anomalies--land and marine instrumental records. In: *Trends: A Compendium of Data on Global Change.* Carbon Dioxide Information Analysis Center, Oak Ridge National Laboratory, U.S. Department of Energy, Oak Ridge, TN.

Kanakidou, M., et al., 2005: Organic aerosol and global climate modelling: a review. *Atmos. Chem. Phys.*, **5**, 1053–1123.

Kärcher, B., and U. Lohmann, 2002: A parameterization of cirrus cloud formation: homogeneous freezing of supercooled aerosols. *J. Geophys. Res.*, **107**, doi:10.1029/2001JD000470.

Kärcher, B., and U. Lohmann, 2003: A parameterization of cirrus cloud formation: heterogeneous freezing. *J. Geophys. Res.*, **108**, doi:10.1029/2002JD003220.

Kärcher, B., and J. Ström, 2003: The roles of dynamical variability and aerosols in cirrus cloud formation. *Atmos. Chem. Phys.*, **3**, 823–838.

Kärcher, B., and T. Koop, 2004: The role of organic aerosols in homogeneous ice formation. *Atmos. Chem. Phys.*, **4**, 6719–6745.

Kärcher, B., J. Hendricks, and U. Lohmann, 2006: Physically-based parameterization of cirrus cloud formation for use in global atmospheric models. *J. Geophys. Res*., **111**, doi:10.1029/2005JD006219.

Karlsdottir, S., and I.S.A. Isaksen, 2000: Changing methane lifetime: Possible cause for reduced growth. *Geophys. Res. Lett.*, **27**(1), 93–96.

Kasibhatla, P., et al., 2002: Top-down estimate of a large source of atmospheric carbon monoxide associated with fuel combustion in Asia. *Geophys. Res. Lett.*, **29**(19), 1900, doi:10.1029/2002GL015581.

Kasischke, E.S., and L.P. Bruhwiler, 2002: Emissions of carbon dioxide, carbon monoxide, and methane from boreal forest fires in 1998. *J. Geophys. Res.*, **107**, 8146, doi:10.1029/2001JD000461.

Kasischke, E.S., N.L. Christensen, and B.J. Stocks, 1995: Fire, global warming and the carbon balance of boreal forests. *Ecol. Appl.*, **5**(2), 437–451.

Kasischke, E.S., et al., 2005: Influences of boreal fire emissions on Northern Hemisphere atmospheric carbon and carbon monoxide. *Global Biogeochem. Cycles*, **19**(1), GB1012, doi:10.1029/2004GB002300.

Katz, M.E., D.K. Pak, G.R. Dickens, and K.G. Miller. 1999: The source and fate of massive carbon input during the Latest Paleocene Thermal Maximum. *Science*, **286**, 1531–1533.

Kaufman, Y.J., and I. Koren, 2006: Smoke and pollution aerosol effect on cloud cover. *Science*, **313**, 655–658, doi:10.1126/science.1126232.

Kaufman, Y.J., et al., 2005: The effect of smoke, dust, and pollution aerosol on shallow cloud development over the Atlantic Ocean. *Proc. Natl. Acad. Sci. U.S.A.*, **102**(32), 11207–11212.

Kawamiya, M., et al., 2005: Development of an integrated Earth system model on the Earth Simulator. *J. Earth Simulator*, **4**, 18–30.

Keeling, C.D., and T.P. Whorf, 2005: Atmospheric CO_2 records from sites in the SIO air sampling network. In: *Trends: A Compendium of Data on Global Change*. Carbon Dioxide Information Analysis Center, Oak Ridge National Laboratory, U.S. Department of Energy, Oak Ridge, TN, http://cdiac.esd.ornl.gov/trends/co2/sio-keel-flask/sio-keel-flask.html.

Keller, M., et al., 2005: Soil-atmosphere exchange for nitrous oxide, nitric oxide, methane, and carbon dioxide in logged and undisturbed forest in the Tapajos National Forest, Brazil. *Earth Interactions*, **9**, 1–28, doi:10.1175/EI125.1.

Keppler, F., J.T.G. Hamilton, M. Brass, and T. Roeckmann, 2006: Methane emissions from terrestrial plants under aerobic conditions. *Nature*, **439**, 187–191.

Kerkweg, A., S. Wurzler, T. Reisin, and A. Bott, 2003: On the cloud processing of aerosol particles: An entraining air-parcel model with two-dimensional spectral cloud microphysics and a new formulation of the collection kernel. *Q. J. R. Meteorol. Soc.*, **129**(587), 1–18.

Kettle, A., and M. Andreae, 2000: Flux of the dimethylsulfide from the oceans: A comparison of updated data sets and flux models. *J. Geophys. Res.*, **105**, 26793–26808.

Key, R.M., et al., 2004: A global ocean carbon climatology: Results from Global Data Analysis Project (GLODAP). *Global Biogeochem. Cycles*, **18**(4), GB4031, doi:10.1029/2004GB002247.

Khain, A.P., D. Rosenfeld, and A. Pokrovsky, 2001: Simulating convective clouds with sustained supercooled liquid water down to –37.5°C using a spectral microphysics model. *Geophys. Res. Lett.*, **28**, 3887–3890.

Khain, A.P., D. Rosenfeld, and A. Pokrovsky, 2005: Aerosol impact on the dynamics and microphysics of convective clouds. *Q. J. R. Meteorol. Soc.*, **131**(611), 2639–2663.

Khain, A.P., et al., 2004: Simulation of effects of atmospheric aerosols on deep turbulent convective using a spectral microphysics mixed-phase cumulus cloud model. 1. Model description and possible applications. *J. Atmos. Sci.*, **61**, 2963–2982.

Khalil, M.A.K., and M.J. Shearer, 2006: Decreasing emissions of methane from rice agriculture. *Int. Congress Ser.*, **1293**, 33–41.

Kirschbaum, M.U.F., et al., 2006: A comment on the quantitative significance of aerobic methane release by plants. *Funct. Plant Biol.*, **33**, 521–530.

Kirschvink, J.L., and T.D. Raub, 2003: A methane fuse for the Cambrian explosion: carbon cycles and true polar wander. *Comptes Rendus Geoscience*, **335**, 65–78.

Klaas, C., and D.E. Archer, 2002: Association of sinking organic matter with various types of mineral ballast in the deep sea: Implications for the rain ratio. *Global Biogeochem. Cycles*, **16**(4), 1116, doi:10.1029/2001GB001765.

Kleffmann, J., et al., 2005: Daytime formation of nitrous acid: a major source of OH radicals in a forest. *Geophys. Res. Lett*., **32**, L05818, doi:10.1029/2005GL022524.

Kleypas, J.A., J. McManus, and L. Menez, 1999a: Using environmental data to define reef habitat: where do we draw the line? *Am. Zool.*, **39**, 146–159.

Kleypas, J.A., et al., 1999b: Geochemical consequences of increased atmospheric carbon dioxide on coral reefs. *Science*, **284**, 118–120.

Kloster, S., et al., 2006: DMS cycle in the marine ocean-atmosphere system - a global model study. *Biogeosciences*, **3**, 29–51.

Knorr, W., I.C. Prentice, J.I. House, and E.A. Holland, 2005: Long-term sensitivity of soil carbon turnover to warming. *Nature*, **433**, 298–301.

Knowlton, K., et al., 2004: Assessing ozone-related health impacts under a changing climate. *Environ. Health Perspect.*, **112**, 1557–1563.

Koerner, C., 2004: Through enhanced tree dynamics carbon dioxide enrichment may cause tropical forests to lose carbon. *Philos. Trans. R. Soc. London Ser. B*, **359**, 493–498.

Koerner, C., et al., 2005: Carbon flux and growth in mature deciduous forest trees exposed to elevated CO_2. *Science*, **309**(5739), 1360–1362.

Koren, I., Y.J. Kaufman, L.A. Remer, and J.V. Martins, 2004: Measurements of the effect of smoke aerosol on inhibition of cloud formation. *Science*, **303**, 1342–1345.

Koren, I., et al., 2005: Aerosol invigoration and restructuring of Atlantic convective clouds. *Geophys. Res. Lett.*, **32**(14), L14828, doi:10.1029/2005GL023187.

Koster, R.D., and M.J. Suarez, 2001: Soil moisture memory in climate models. *J. Hydrometeorol.*, **2**(6), 558–570.

Koster, R.D., and M.J. Suarez, 2004: Suggestions in the observational record of land-atmosphere feedback operating at seasonal time scales. *J. Hydrometeorol.*, **5**(3), doi: 10.1175/1525.

Koster, R.D., M.J. Suarez, R.W. Higgins, and H.M. Van den Dool, 2003: Observational evidence that soil moisture variations affect precipitation. *Geophys. Res. Lett.*, **30**(5), 1241. doi:10.1029/2002GL016571.

Koster, R.D., et al., 2000: A catchment-based approach to modeling land surface processes in a general circulation model. 1. Model structure. *J. Geophys. Res.*, **105**, 24809–24822.

Koster, R.D., et al., 2002: Comparing the degree of land-atmosphere interaction in four atmospheric general circulation models. *J. Hydrometeorol.*, **3**(3), 363–375.

Koster, R.D., et al., 2004: Regions of strong coupling between soil moisture and precipitation. *Science*, **305**, 1138–1140.

Koster, R.D., et al., 2006: GLACE: The Global Land-Atmosphere Coupling Experiment. 1. Overview. *J. Hydrometeorol.*, **7**, 590–610.

Krakauer, N.Y., and J.T. Randerson, 2003: Do volcanic eruptions enhance or diminish net primary production? Evidence from tree rings. *Global Biogeochem. Cycles*, **17**(4), 1118, doi:10.1029/2003GB002076.

Kristjánsson, J.E., 2002: Studies of the aerosol indirect effect from sulphate and black carbon aerosols. *J. Geophys. Res.*, **107**, doi:10.1029/2001JD000887.

Kristjánsson, J.E., et al., 2005: Response of the climate system to aerosol direct and indirect forcing: Role of cloud feedbacks. *J. Geophys. Res.*, **110**, D24206, doi:10.1029/2005JD006299.

Kroeze, C., A. Mosier, and L. Bouwman, 1999: Closing the N_2O budget: A retrospective analysis. *Global Biogeochem. Cycles*, **13**, 1–8.

Kroeze, C., E. Dumont, and S.P. Seitzinger, 2005: New estimates of global emissions of N_2O from rivers and estuaries. *Environ. Sci.*, **2**, 159–165.

Krüger, O., and H. Grassl, 2004: Albedo reduction by absorbing aerosols over China. *Geophys. Res. Lett.*, **31**, doi:10.1029/2003GL019111.

Kulmala, M., et al., 2004: A new feedback mechanism linking forests, aerosols, and climate. *Atmos. Chem. Phys.*, **4**, 557–562.

Kurz, W.A., and M. Apps, 1999: A 70-years retrospective analysis of carbon fluxes in the Canadian forest sector. *Ecol. Appl.*, **9**, 526–547.

Kurz, W.A., M.J. Apps, S.J. Beukema, and T. Lekstrum, 1995: 20th-century carbon budget of Canadian forests. *Tellus*, **47B**(1–2), 170–177.

Kvenvolden, K.A., and B.W. Rogers, 2005: Gaia's breath - global methane exhalations. *Mar. Petrol. Geol.*, **22**, 579–590.

Labrador, L.J., R. von Kuhlmann, and M.G. Lawrence, 2004: Strong sensitivity of the global mean OH concentration and the tropospheric oxidizing efficiency to the source of NO_x from lightning. *Geophys. Res. Lett.*, **31**, L06102, doi:10.1029/2003GL019229.

Lalli, C.M., and R.W. Gilmer, 1989: *Pelagic Snails: The Biology of Holoplanktonic Gastropod Mollusks*. Stanford University Press, Palo Alto, CA, 259 pp.

Lamarque, J.-F., et al., 2005a: Coupled chemistry-climate response to changes in aerosol emissions: global impact on the hydrological cycle and the tropospheric burdens of OH, ozone and NO_x. *Geophys. Res. Lett.*, **32**, L16809, doi:10.1029/2005GL023419.

Lamarque J.-F., et al., 2005b: Assessing future nitrogen deposition and carbon cycle feedback using a multimodel approach: Part 1. Analysis of nitrogen deposition. *J. Geophys. Res.*, **110**, D19303, doi:10.1029/2005JD005825.

Lamarque, J.-F., et al., 2005c: Tropospheric ozone evolution between 1890 and 1990. *J. Geophys. Res.*, **110**, D08304, doi:10.1029/2004JD005537.

Langdon, C., et al., 2003: Effect of elevated CO_2 on the community metabolism of an experimental coral reef. *Global Biogeochem. Cycles*, **17**, 1011, doi:10.1029/2002GB001941.

Langenbuch, H., and H.O. Pörtner, 2003: Energy budget of heptocytes from Antarctic fish (*Pachycara brachycephalum* and *Lepidonotothen kempi*) as a function of ambient CO_2: pH-dependent limitations of cellular protein biosynthesis? *J. Exp. Biol.*, **206**, 3895–3903.

Langenfelds, R.L., et al., 1999: Partitioning of the global fossil CO_2 sink using a 19-year trend in atmospheric O_2. *Geophys. Res. Lett.*, **26**, 1897–1900.

Langenfelds, R.L., et al., 2002: Interannual growth rate variations of atmospheric CO_2 and its ^{13}C, H_2, CH_4, and CO between 1992 and 1999 linked to biomass burning. *Global Biogeochem. Cycles*, **16**(3), 1048, doi:10.1029/2001GB001466.

Langner, J., R. Bergstrom, and V. Foltescu, 2005: Impact of climate change on surface ozone and deposition of sulphur and nitrogen in Europe. *Atmos. Environ.*, **39**, 1129–1141.

Larsen, S.H., 2005: Solar variability, dimethyl sulphide, clouds, and climate. *Global Biogeochem. Cycles*, **19**, GB1014, doi:10.1029/2004GB002333.

Lassey, K.R., D.C Lowe, and M.R. Manning, 2000: The trend in atmospheric methane $\delta^{13}C$ and implications for isotopic constraints on the global methane budget. *Global Biogeochem. Cycles*, **14**, 41–49.

Lathière, J., et al., 2005: Past and future changes in biogenic volatile organic compound emissions simulated with a global dynamic vegetation model. *Geophys. Res. Lett.*, **32**, L20818, doi:10.1029/2005GL024164.

Laurance, W.F., et al., 2004: Pervasive alteration of tree communities in undisturbed Amazonian forests. *Nature*, **428**, 171–175.

Lawrence, D.M., and J.M. Slingo, 2004: An annual cycle of vegetation in a GCM. Part I: implementation and impact on evaporation. *Clim. Dyn.*, **22**, doi:10.1007/s0038200303669.

Lawrence, D.M., and J.M. Slingo, 2005: Weak land-atmosphere coupling strength in HadAM3: The role of soil moisture variability. *J. Hydrometeorol.*, **6**(5), 670–680, doi:10.1775/JHM445.1.

Lawrence, M.G., R. von Kuhlmann, M. Salzmann, and P.J. Rasch, 2003: The balance of effects of deep convective mixing on tropospheric ozone. *Geophys. Res. Lett.*, **30**(18), 1940, doi:10.1029/2003GL017644.

Laws, E.A., et al., 2000: Temperature effects on export production in the open ocean. *Global Biogeochem. Cycles*, **14**, 1231–1246.

Le Quéré, C., et al., 2000: Interannual variability of the oceanic sink of CO_2 from 1979 to 1997. *Global Biogeochem. Cycles*, **14**, 1247–1265.

Le Quéré, C., et al., 2003: Two decades of ocean CO_2 sink and variability. *Tellus*, **55B**(2), 649–656.

Le Quéré, C., et al., 2005: Ecosystem dynamics based on plankton functional types for global ocean biogeochemistry models. *Global Change Biol.*, **11**, doi:10.1111/j.1365-2486.2005.001004.x.

Leck, C., and E.K. Bigg, 2005a: Biogenic particles in the surface microlayer and overlaying atmosphere in the central Arctic Ocean during summer. *Tellus*, **57B**(4), 305–316.

Leck, C., and E.K. Bigg, 2005b: Source and evolution of the marine aerosol - A new perspective. *Geophys. Res. Lett.*, **32**, L19803, doi:10.1029/2005GL023651.

Lee, K., et al., 1998: Low interannual variability in recent oceanic uptake of atmospheric carbon dioxide. *Nature*, **396**, 155–159.

Lefèvre, N., et al., 1999: Assessing the seasonality of the oceanic sink for CO_2 in the northern hemisphere. *Glob. Biogeochem. Cycles*, **13**, 273–286.

Lelieveld, J., and F.J. Dentener, 2000: What controls tropospheric ozone? *J. Geophys. Res.*, **105**, 3531–3551.

Lelieveld, J., W. Peters, F.J. Dentener, and M.C. Krol, 2002a: Stability of tropospheric hydroxyl chemistry. *J. Geophys. Res.*, **107**(D23), 4715, doi:10.1029/2002JD002272.

Lelieveld, J., et al., 2002b: Global air pollution crossroads over the Mediterranean. *Science*, **298**, 794–799.

Leue, C., et al., 2001: Quantitative analysis of NO_x emissions from GOME satellite image sequences. *J. Geophys. Res.*, **106**, 5493–5505.

Levin, Z., E. Ganor, and V. Gladstein, 1996: The effects of desert particles coated with sulfate on rain formation in the eastern Mediterranean. *J. Appl. Meteorol.*, **35**, 1511–1523.

Levis, S., and G.B. Bonan, 2004: Simulating springtime temperature patterns in the community atmosphere model coupled to the community land model using prognostic leaf area. *J. Clim.*, **17**, 4531–4540.

Levis, S., G.B. Bonan, and C. Bonfils, 2004: Soil feedback drives the mid-Holocene North African monsoon northward in fully coupled CCSM2 simulations with a dynamic vegetation model. *Clim. Dyn.*, **23**, doi:10.1007/s00382-004-0477-y.

Lewis, E.R., and S.E. Schwartz, 2005: *Sea Salt Aerosol Production: Mechanisms, Methods, Measurements, and Models: A Critical Review*. Geophysical Monograph Vol. 152, American Geophysical Union, Washington, DC, 413 pp.

Lewis, S.L., Y. Malhi, and O.L. Phillips, 2005: Fingerprinting the impacts of global change on tropical forests. *Philos. Trans. R. Soc. London Ser. B*, **359**, doi:10.1098/rstb.2003.1432.

Li, C., et al., 2002: Reduced methane emissions from large-scale changes in water management of China's rice paddies during 1980-2000. *Geophys. Res. Lett.*, **29**, doi: 10.1029/2002GL015370.

Li, Q., et al., 2005: North American pollution outflow and the trapping of convectively lifted pollution by upper-level anticyclone. *J. Geophys. Res.*, **110**, D10301, doi:10.1029/2004JD005039.

Li, W., and R. Fu, 2004: Transition of the large-scale atmospheric and land surface conditions from the dry to the wet season over Amazonia as diagnosed by the ECMWF re-analysis. *J. Clim.*, **17**, 2637–2651.

Liang X., Z. Xie, and M. Huang, 2003: A new parameterization for surface and groundwater interactions and its impact on water budgets with the variable infiltration capacity (VIC) land surface model. *J. Geophys. Res.*, **108**, 8613, doi:19.1029/2002JD003090.

Liao, H., and J.H. Seinfeld, 2005: Global impacts of gas-phase chemistry-aerosol interactions on direct radiative forcing by anthropogenic aerosols and ozone. *J. Geophys. Res.*, **110**, D18208, doi:10.1029/2005JD005907.

Liebmann, B., and J.A. Marengo, 2001: Interannual variability of the rainy season and rainfall in the Brazilian Amazon basin. *J. Clim.*, **14**(22), 4308–4318.

Liepert, B.G., and I. Tegen, 2002: Multidecadal solar radiation trends in the United States and Germany and direct tropospheric aerosol forcing. *J. Geophys. Res.*, **107**, doi:10.1029/2001JD000760.

Liepert, B.G., J. Feichter, U. Lohmann, and E. Roeckner, 2004: Can aerosols spin down the water cycle in a warmer and moister world. *Geophys. Res. Lett.*, **31**, L06207, doi:10.1029/2003GL019060.

Lin, C.-Y.C., D.J. Jacob, and A.M. Fiore, 2001: Trends in exceedances of the ozone air quality standard in the continental United States, 1980-1998. *Atmos. Environ.*, **35**, 3217–3228.

Lin, G.H., et al., 1999: Ecosystem carbon exchange in two terrestrial ecosystem mesocosms under changing atmospheric CO_2 concentrations. *Oecologia*, **119**(1), 97–108.

Lintner, B.R., 2002: Characterizing global CO_2 interannual variability with empirical orthogonal function/principal component (EOF/PC) analysis. *Geophys. Res. Lett.*, **29**(19), 1921, doi:10.1029/2001GL014419.

Liu, X., and J.E. Penner, 2005: Ice nucleation parameterization for a global model. *Meteorol. Z.*, **14**(4), 499–514.

Liu, Y., and P.H. Daum, 2002: Indirect warming effect from dispersion forcing. *Nature*, **419**, 580–581.

Loh, A.N., J.E. Bauer, and E.R.M. Druffel, 2004: Variable ageing and storage of dissolved organic components in the open ocean. *Nature*, **430**, 877–881.

Lohmann, U., 2002: A glaciation indirect aerosol effect caused by soot aerosols. *Geophys. Res. Lett.*, **29**, doi:10.1029/2001GL014357.

Lohmann, U., and J. Feichter, 2001: Can the direct and semi-direct aerosol effect compete with the indirect effect on a global scale? *Geophys. Res. Lett.*, **28**(1), 159–161, doi:10.1029/2000GL012051.

Lohmann, U., and B. Kärcher, 2002: First interactive simulations of cirrus clouds formed by homogeneous freezing in the ECHAM GCM. *J. Geophys. Res.*, **107**, doi:10.1029/2001JD000767.

Lohmann, U., and G. Lesins, 2002: Stronger constraints on the anthropogenic indirect aerosol effect. *Science*, **298**, 1012–1016.

Lohmann, U., and J. Feichter, 2005: Global indirect aerosol effects: a review. *Atmos. Chem. Phys.*, **5**, 715–737.

Lohmann, U., and K. Diehl, 2006: Sensitivity studies of the importance of dust ice nuclei for the indirect aerosol effect on stratiform mixed-phase clouds. *J. Atmos. Sci.*, **63**, 1338–1347.

Lohmann, U., I. Koren, and Y.J. Kaufman, 2006: Disentangling the role of microphysical and dynamical effects in determining cloud properties over the Atlantic. *Geophys. Res. Lett.*, **33,** L09802, doi:10.1029/2005GL024625.

Lovins, A.B., 2003: Hydrogen primer. *RMI Solutions Newsletter*, **19**(2), 1–4; 36–39.

Lucht, W., et al., 2002: Climatic control of the high-latitude vegetation greening trend and Pinatubo effect. *Science*, **296**(5573), 1687–1689.

Luo, Y., S.Q. Wan, D.F. Hui, and L.L. Wallace, 2001: Acclimatization of soil respiration to warming in a tall grass prairie. *Nature*, **413**, 622–625.

Luo, Y., et al., 2004: Progressive nitrogen limitation of ecosystem responses to rising atmospheric carbon dioxide. *Bioscience*, **54**, 731–739.

Mack, F., J. Hoffstadt, G. Esser, and J.G. Goldammer, 1996: Modeling the influence of vegetation fires on the global carbon cycle. In: *Biomass Burning and Global Change* [Levine, J.S. (ed)]. MIT Press, Cambridge, MA, pp. 149–159.

Mahaffey, C., A.F. Michaels, and D.G. Capone, 2005: The conundrum of marine N_2 fixation. *Am. J. Sci.*, **305**(6–8): 546–595.

Mahowald, N.M., and L.M. Kiehl, 2003: Mineral aerosol and cloud interactions. *Geophys. Res. Lett.*, **30**, doi:10.1029/2002GL016762.

Mahowald, N.M., and C. Luo, 2003: A less dusty future? *Geophys. Res. Lett.*, **30**(7), 1903, doi:10.1029/2003GL017880.

Mahowald, N.M., G.D.R. Rivera, and C. Luo, 2004: Comment on "Relative importance of climate and land use in determining present and future global soil dust emission" by I. Tegen et al. *Geophys. Res. Lett.*, **31**(24), L24105, doi:10.1029/2004GL021272.

Maier-Reimer, E., U. Mikolajewicz, and A.Winguth, 1996: Future ocean uptake of CO_2: interaction between ocean circulation and biology. *Clim. Dyn.*, **12**, 711–721.

Malhi, Y., and J. Grace, 2000: Tropical forests and atmospheric carbon dioxide. *Trends Ecol. Evol.*, **15**(8), 332–337.

Malhi, Y., and O.L. Phillips, 2004: Tropical forests and global atmospheric change: a synthesis. *Philos. Trans. R. Soc. London Ser. B*, **359**, doi:10.1098/rstb.2003.1449.

Malhi, Y., and J. Wright, 2004: Spatial patterns and recent trends in the climate of tropical rainforest regions. *Philos. Trans. R. Soc. London Ser. B*, **359**, doi:10.1098/rstb.2003.1433.

Malhi, Y., et al., 2002: An international network to understand the biomass and dynamics of Amazonian forests (RAINFOR). *J. Veg. Sci.*, **13**, 439–450.

Manning, A.C., and R.F. Keeling, 2006: Global oceanic and land biotic carbon sinks from the Scripps atmospheric oxygen flask sampling network. *Tellus*, **58B**(2), 95–116.

Marani, M., E. Eltahir, and A. Rinaldo, 2001: Geomorphic controls on regional base flow. *Water Resour. Res.*, **37**, 2619–2630.

Marengo, J., and C.A. Nobre, 2001: The hydroclimatological framework in Amazonia. In: *Biogeochemistry of the Amazon Basin* [McClaine, M., R. Victoria, and J. Richey (eds.)]. Oxford University Press, Oxford, UK, pp. 17–42.

Marland, G., T.A. Boden, and R.J. Andres, 2006: Global, regional, and national CO_2 emissions. In: *Trends: A Compendium of Data on Global Change*. Carbon Dioxide Information Analysis Center, Oak Ridge National Laboratory, U.S. Department of Energy, Oak Ridge, TN, http://cdiac.esd.ornl.gov/trends/emis/tre_glob.htm.

Martin, R.V., et al., 2002: Interpretation of TOMS observations of tropical tropospheric ozone with a global model and in-situ observations. *J. Geophys. Res.*, **107**(D18), 4351, doi:10.1029/2001JD001480.

Martin, R.V., et al., 2003a: Global inventory of nitrogen oxide emissions constrained by space-based observations of NO_2 columns. *J. Geophys. Res.*, **108**(D17), 4537, doi:10.1029/2003JD003453.

Martin, R.V., et al., 2003b: Global and regional decreases in tropospheric oxidants from photochemical effects of aerosols. *J. Geophys. Res.*, **108**(D3), 4097, doi:10.1029/2002JD002622.

Martinerie, P., G.P. Brasseur, and C. Granier, 1995: The chemical composition of ancient atmospheres: a model study constrained by ice core data. *J. Geophys. Res.*, **100**, 14291–14304.

Matsumi, Y., et al., 2002: Quantum yields for production of O(1D) in the ultraviolet photolysis of ozone: Recommendation based on evaluation of laboratory data. *J. Geophys. Res.*, **104**(D3), doi:10.1029/2001JD000510.

Matthews, H.D., M. Eby, A.J. Weaver, and B.J. Hawkins, 2005: Primary productivity control of simulated carbon cycle-climate feedbacks. *Geophys. Res. Lett.*, **32**, L14708, doi:10.1029/2005GL022941.

Matthews, R., and R. Wassmann, 2003: Modelling the impacts of climate change and methane emission reductions on rice production: a review. *Eur. J. Agron.*, **19**, 573–598.

Maynard, K., and J.-F. Royer, 2004: Sensitivity of a general circulation model to land surface parameters in African tropical deforestation experiments. *Clim. Dyn.*, **22**, doi:10.1007/s0038200403989.

McCabe, G.J., M.P. Clark, and M.C. Serreze, 2001: Trends in northern hemisphere surface cyclone frequency and intensity. *J. Clim.*, **14**, 2763–2768.

McFiggans, G., 2005: Marine aerosols and iodine emissions. *Nature*, **433**, E13.

McFiggans, G., et al., 2004: Direct evidence for coastal iodine particles from Laminaria macroalgae - linkage to emissions of molecular iodine. *Atmos. Chem. Phys.*, **4**, 701–713.

McGuire, A.D. III, et al., 2001: Carbon balance of the terrestrial biosphere in the twentieth century: Analyses of CO_2, climate and land use effects with four process-based ecosystem models. *Global Biogeochem. Cycles*, **15**, 183–206.

McKenzie, R.L., B.J. Connor, and G.E. Bodeker, 1999: Increased summertime UV observed in New Zealand in response to ozone loss. *Science*, **285**, 1709–1711.

McKinley, G.A., M.J. Follows, and J. Marshall, 2004a: Mechanisms of air-sea CO_2 flux variability in the equatorial Pacific and the North Atlantic. *Global Biogeochem. Cycles*, **18**, GB2011, doi:10.1029/2003GB002179.

McKinley, G.A., et al., 2004b: Pacific dominance to global air-sea CO_2 flux variability: A novel atmospheric inversion agrees with ocean models. *Geophys. Res. Lett.*, **31**, L22308, doi:10.1029/2004GL021069.

McLinden, C., et al., 2000: Stratospheric ozone in 3-D models: a simple chemistry and the cross-tropopause flux. *J. Geophys. Res.*, **105**, 14653–14665.

McNeil, B.I., et al., 2003: Anthropogenic CO_2 uptake by the ocean based on the global chlorofluorocarbon data set. *Science*, **299**(5604), 235–239.

Melillo, J.M., et al., 1995: Vegetation/ecosystem modeling and analysis project: Comparing biogeography and biogeochemistry models in a continental-scale study of terrestrial ecosystem responses to climate change and CO_2 doubling. *Global Biogeochem. Cycles*, **9**, 407–437.

Melillo, J.M., et al., 2002: Soil warming and carbon-cycle feedbacks to the climate system. *Science*, **298**, 2173–2176.

Menon, S., and A. Del Genio, 2007: Evaluating the impacts of carbonaceous aerosols on clouds and climate. In: *An Interdisciplinary Assessment: Human-Induced Climate Change* [Schlesinger, M., et al. (eds.)]. Cambridge University Press, Cambridge, UK, in press.

Menon, S., and L. Rotstayn, 2006: The radiative influence of aerosol effects on liquid-phase cumulus and stratiform clouds based on sensitivity studies with two climate models. *Clim. Dyn.*, **27**, 345–356.

Menon, S., A.D. Del Genio, D. Koch, and G. Tselioudis, 2002a: GCM Simulations of the aerosol indirect effect: sensitivity to cloud parameterization and aerosol burden. *J. Atmos. Sci.*, **59**, 692–713.

Menon, S., J. Hansen, L. Nazarenko, and Y. Luo, 2002b: Climate effects of black carbon aerosols in China and India. *Science*, **297**, 2250–2252.

Menon, S., et al., 2003: Evaluating aerosol/cloud/radiation process parameterizations with single-column models and Second Aerosol Characterization Experiment (ACE-2) cloudy column observations. *J. Geophys. Res.*, **108**, doi:10.1029/2003JD003902.

Mickley, L.J., D.J. Jacob, and D. Rind, 2001: Uncertainty in preindustrial abundance of tropospheric ozone: implications for radiative forcing calculations. *J. Geophys. Res.*, **106**, 3389–3399.

Mickley, L.J., D.J. Jacob, B.D. Field, and D. Rind, 2004: Effects of future climate change on regional air pollution episodes in the United States. *Geophys. Res. Lett.*, **30**, 1862, doi:10.1029/2003GL017933.

Mickley, L.J., et al., 1999: Radiative forcing from tropospheric ozone calculated with a unified chemistry–climate model. *J. Geophys. Res.*, **104**(D23), 30153–30172.

Mikaloff Fletcher, S.E., et al., 2004a: CH_4 sources estimated from atmospheric observations of CH_4 and its $^{13}C/^{12}C$ isotopic ratios: 1. Inverse modeling of source processes. *Global Biogeochem. Cycles*, **18**, GB4004, doi:10.1029/2004GB002223.

Mikaloff Fletcher, S.E., et al., 2004b: CH_4 sources estimated from atmospheric observations of CH_4 and its $^{13}C/^{12}C$ isotopic ratios: 2. Inverse modeling of CH_4 fluxes from geographical regions. *Global Biogeochem. Cycles*, **18**, doi:10.1029/2004GB002224.

Mikaloff Fletcher, S.E., et al., 2006: Inverse estimates of anthropogenic CO_2 uptake, transport, and storage by the ocean. *Global Biogeochem. Cycles*, **18**, doi:10.1029/2005GB002530.

Miller, R.L., J. Perlwitz, and I. Tegen, 2004a: Feedback upon dust emission by dust radiative forcing through the planetary boundary layer. *J. Geophys. Res.*, **109**, D24209, doi:10.1029/2004JD004912.

Miller, R.L., I. Tegen, and J. Perlwitz, 2004b: Surface radiative forcing by soil dust aerosols and the hydrologic cycle. *J. Geophys. Res.*, **109**, D04203, doi:10.1029/2003JD004085.

Millero, F.J., et al., 2002: Dissociation constants for carbonic acid determined from field measurements. *Deep-Sea Res. I*, **49**, 1705–1723.

Milly, P.C.D, and A.B. Schmakin, 2002: Global modeling of land water and energy balances, Part I: The Land Dynamics (LaD) model. *J. Hydrometeorol.*, **3**, 301–310.

Ming, Y., et al., 2005: Geophysical Fluid Dynamics Laboratory general circulation model investigation of the indirect radiative effects of anthropogenic sulfate aerosol. *J. Geophys. Res.*, **110**, D22206, doi:10.1029/2005JD006161.

Montzka, S.A., et al., 1999: Present and future trends in the atmospheric burden of ozone depleting halogens. *Nature*, **398**, 690–694.

Montzka, S.A., et al., 2003: A decline in tropospheric bromine. *Geophys. Res. Lett.*, **30**(15), 1826, doi:10.1029/2003GL017745.

Mosier, A., et al., 1998: Closing the global N_2O budget: N_2O emissions through the agricultural nitrogen cycle-OECD/IPCC.IEA phase II development of IPCC guidelines for national greenhouse gas inventory methodology. *Nutrient Cycling in Agroecosystems*, **52**, 225–248.

Mouillot, F., and C.B. Field, 2005: Fire history and the global carbon budget: a 1° x 1° fire history reconstruction for the 20th century. *Global Change Biol.*, **11**, 398–420.

Müller, J., and G. Brasseur, 1999: Sources of upper tropospheric HO_x: A three-dimensional study. *J. Geophys. Res.*, **104**(D1), 1705–1716.

Myhre, G., M.M. Kvalevag, and C.B. Schaaf, 2005: Radiative forcing due to anthropogenic vegetation change based on MODIS surface albedo data. *Geophys. Res. Lett.*, **32**, L21410, doi: 10.1029/2005GLO24004.

Nabuurs, G.J., et al., 2003: Temporal evolution of the European forest sector carbon sink from 1950 to 1999. *Global Change Biol.*, **9**, 152–160.

Nadelhoffer, K., et al., 2004: Decadal-scale fates of N-15 tracers added to oak and pine stands under ambient and elevated N inputs at the Harvard Forest (USA). *For. Ecol. Manage.*, **196**, 89–107.

Naja, M., H. Akimoto, and J. Staehelin, 2003: Ozone in background and photochemically aged air over central Europe: analysis of long-term ozonesonde data from Hohenpeissenberg and Payerne. *J. Geophys. Res.*, **108**(D2), 4063, doi:10.1029/2002JD002477.

Naqvi, S.W.A., et al., 2000: Increased marine production of N_2O due to intensifying anoxia on the Indian continental shelf. *Nature*, **408**(6810), 346–349.

Negri, A.J., R.F. Adler, L.M. Xu, and J. Surratt, 2004: The impact of Amazonian deforestation on dry season rainfall. *J. Clim.*, **17**(6), 1306–1319.

Neill, C., et al., 2005: Rates and controls of nitrous oxide and nitric oxide emissions following conversion of forest to pasture in Rondônia. *Nutrient Cycling in Agroecosystems*, **71**, 1–15.

Nemani, R., et al., 2002: Recent trends in hydrologic balance have enhanced the terrestrial carbon sink in the United States. *Geophys. Res. Lett.*, **29**(10), 1468, doi:10.1029/2002GL014867.

Nemani, R.R., et al., 2003: Climate-driven increases in global terrestrial net primary production from 1982 to 1999. *Science*, **300**, 1560–1563.

Nepstad, D., et al., 2004: Amazon drought and its implications for forest flammability and tree growth: a basin-wide analysis. *Global Change Biol.*, **10**(5), 704–717.

Nesbitt, S.W., R.Y. Zhang, and R.E. Orville, 2000: Seasonal and global NO_x production by lightning estimated from the Optical Transient Detector (OTD). *Tellus*, **52B**, 1206–1215.

Nevison, C.D., J.H. Butler, and J.W. Elkins, 2003: Global distribution of N_2O and the N_2O/AOU yield in the subsurface ocean. *Global Biogeochem. Cycles*, **17**(4), 1119, doi:10.1029/2003GB002068.

Nevison, C.D., T. Lueker, and R.F. Weiss, 2004: Quantifying the nitrous oxide source from coastal upwelling. *Global Biogeochem. Cycles*, **18**, GB1018, doi:10.1029/2003GB002110.

Newchurch, M.J., et al., 2003: Evidence for slowdown in stratospheric ozone loss: first stage of ozone recovery. *J. Geophys. Res.*, **108**(D16), 4507, doi:10.1029/2003jd003471.

Newman, P.A., S.R. Kawa, and E.R. Nash, 2004: On the size of the Antarctic ozone hole. *Geophys. Res. Lett.*, **31**, L21104, doi:10.1029/2004GL020596.

Newman, P.A., et al., 2006: When will the Antarctic ozone hole recover? *Geophys. Res. Lett.*, **33**, L12814, doi:10.1029/2005GL025232.

Nightingale, P.D., et al., 2000: In situ evaluation of air-sea gas exchange parameterisations using novel conservative and volatile tracers. *Global Biogeochem. Cycles*, **14**(1), 373–387.

Nilsson, S., et al., 2003: The missing "missing sink". *Forestry Chronicle*, **79**(6), 1071–1074.

Niu, G.-Y., and Z.-L. Yang, 2004: Effects of vegetation canopy processes on snow surface energy and mass balances. *J. Geophys. Res.*, **109**, D23111, doi:10.1029/2004JD004884.

Niyogi, D., et al., 2004: Direct observations of the effects of aerosol loading on net ecosystem CO_2 exchanges over different landscapes. *Geophys. Res. Lett.*, **31**, L20506, doi:10.1029/2004GL020915.

Nober, F.J., H.-F. Graf, and D. Rosenfeld, 2003: Sensitivity of the global circulation to the suppression of precipitation by anthropogenic aerosols. *Global Planet. Change*, **37**, 57–80.

Norby, R.J., and C.M. Iversen, 2006: Nitrogen uptake, distribution, turnover, and efficiency of use in a CO_2-enriched sweetgum forest. *Ecology*, **87**, 5–14.

Norton, W.A., 2003: Sensitivity of northern hemisphere surface climate to simulation of the stratospheric polar vortex. *Geophys. Res. Lett.*, **30**(12), doi:10.1029/2003GL016958.

Novelli, P.C., et al., 1999: Molecular hydrogen in the troposphere: global distribution and budget. *J. Geophys. Res.*, **104**(D23), 30427–30444.

Nowak, R.S., D.S. Ellsworth, and S.D. Smith, 2004: Functional responses of plants to elevated atmospheric CO_2 – do photosynthetic and productivity data from FACE experiments support early predictions? *New Phytol.*, **162**, 253–280.

NRC (National Research Council), 1991: *Rethinking the Ozone Problem in Urban and Regional Air Pollution*. National Academy Press, Washington, DC, 524 pp.

Obata, A., and Y. Kitamura, 2003: Interannual variability of the sea-air exchange of CO_2 from 1961 to 1998 simulated with a global ocean circulation-biogeochemistry model. *J. Geophys. Res.*, **108**, 3337, doi:10.1029/2001JC001088.

O'Dowd, C.D., 2002: On the spatial extent and evolution of coastal aerosol plumes. *J. Geophys. Res.*, **107**(D19), 8105, doi:10.1029/2001JD000422.

O'Dowd, C.D., J.A. Lowe, and M.H. Smith, 1999: Coupling sea-salt and sulphate interactions and its impact on cloud droplet concentration predictions. *Geophys. Res. Lett.*, **26**, 1311–1314.

O'Dowd, C.D., et al., 2002a: Coastal new particle formation: Environmental conditions and aerosol physicochemical characteristics during nucleation bursts. *J. Geophys. Res.*, **107**(D19), 8107, doi:10.1029/2000JD000206.

O'Dowd, C.D., et al., 2002b: A dedicated study of New Particle Formation and Fate in the Coastal Environment (PARFORCE): Overview of objectives and achievements. *J. Geophys. Res.*, **107**(D19), 8108, doi:10.1029/2001JD000555.

O'Dowd, C.D., et al., 2004: Biogenically driven organic contribution to marine aerosols. *Nature*, **431**, 676–680.

Oechel, W.C, et al., 2000: Acclimation of ecosystem CO_2 exchange in the Alaskan Arctic in response to decadal climate warming. *Nature*, **406**, 978–981.

Ogawa, K., and T. Schmugge, 2004: Mapping surface broadband emissivity of the Sahara desert using ASTER and MODIS data. *Earth Interactions*, **8**(7), 1–14.

Ogle, S.M., M.D. Eve, F.J. Breidt, and K. Paustian, 2003: Uncertainty in estimating land use and management impacts on soil organic carbon storage for US agroecosystems between 1982 and 1997. *Global Change Biol.*, **9**, 1521–1542.

Oglesby, R.J., et al., 2002: Thresholds in atmosphere-soil moisture interactions: results from climate model studies. *J. Geophys. Res.*, **107**(14), doi:10.1029/2001JD001045.

Okin, G.S., N. Mahowald, O.A. Chadwick, and P. Artaxo, 2004: Impact of desert dust on the biogeochemistry of phosphorus in terrestrial ecosystems. *Global Biogeochem. Cycles*, **18**, GB2005, doi:10.1029/2003GB002145.

Oleson, K.W., G.B. Bonan, S. Levis, and M. Vertenstein, 2004: Effects of land use change on North American climate: impact of surface datasets and model biogeophysics. *Clim. Dyn.*, **23**, 117–132, doi:10.1007/s00382-004-0426-9.

Oleson, K.W., et al., 2003: Assessment of global climate model land surface albedo using MODIS data. *Geophys. Res. Lett.*, **30**(8), 1443, doi:10.1029/2002GL016749.

Olivié, D.J.L., P.F.J. van Velthoven, A.C.M. Beliaars, and H.M. Kelder, 2004: Comparison between archived and off-line diagnosed convective mass fluxes in the chemistry transport model TM3. *J. Geophys. Res.*, **109**, D11303, doi:10.1029/2003JD004036.

Olivier, J.G.J., A.F. Bouwman, K.W. Van Der Hoek, and J.J.M. Berdowski, 1998: Global air emission inventories for anthropogenic sources of NO_x, NH_3 and N_2O in 1990. *Environ. Pollut.*, **102**(1, S1), 135–148.

Olivier, J.G.J., et al., 2005: Recent trends in global greenhouse emissions: regional trends 1970–2000 and spatial distribution of key sources in 2000. *Environ. Sci.*, **2**, 81–99.

Ollinger, S.V., and J.D. Aber, 2002: The interactive effects of land use, carbon dioxide, ozone, and N deposition. *Global Change Biol.*, **8**, 545–562

Olsen, S.C., C.A. McLinden, and M.J. Prather, 2001: Stratospheric N_2O-NO_y system: testing uncertainties in a three-dimensional framework. *J. Geophys. Res.*, **106**, 28771–28784.

Ordóñez, C., et al., 2005: Changes of daily surface ozone maxima in Switzerland in all seasons from 1992 to 2002 and discussion of summer 2003. *Atmos. Chem. Phys.*, **5**, 1187–1203.

Oren, R., et al., 2001: Soil fertility limits carbon sequestration by forest ecosystems in a CO_2-enriched atmosphere. *Nature*, **411**(6836), 469–472.

Orr, J.C., et al., 2001: Estimates of anthropogenic carbon uptake from four three-dimensional global ocean models. *Global Biogeochem. Cycles*, **15**(1), 43–60, doi:10.1029/1999GB001256.

Orr, J.C., et al., 2005: Anthropogenic ocean acidification over the twenty-first century and its impact on calcifying organisms. *Nature*, **437**(7059), 681–686.

Osborne, T.M., et al., 2004: Influence of vegetation on the local climate and hydrology in the tropics: sensitivity to soil parameters. *Clim. Dyn.*, **23**, 45–61.

Oyama, M.D., and C.A. Nobre, 2004: Climatic consequences of a large-scale desertification in northeast Brazil: a GCM simulation study. *J. Clim.*, **17**(16), 3203–3213.

Pacala, S.W., et al., 2001: Consistent land- and atmosphere-based US carbon sink estimates. *Science*, **292**, 2316–2320.

Paeth, H., and J. Feichter, 2006: Greenhouse-gas versus aerosol forcing and African climate response. *Clim Dyn*., **26**(1), 35–54.

Page, S., et al., 2002: The amount of carbon released from peat and forest fires in Indonesia during 1997. *Nature*, **320**, 61–65.

Pahlow, M., and U. Riebesell, 2000, Temporal trends in deep ocean Redfield ratios. *Science*, **287**, 831–833.

Palmer, P.I., et al., 2003a: Inverting for emissions of carbon monoxide from Asia using aircraft observations over the western Pacific. *J. Geophys. Res.*, **108**(D21), 8828, doi:10.1029/2003JD003397.

Palmer, P.I., et al., 2003b: Mapping isoprene emissions over North America using formaldehyde column observations from space. *J. Geophys. Res.*, **108**, 4180, doi:10.1029/2002JD002153.

Park, R.J., et al., 2004: Global simulation of tropospheric ozone using the University of Maryland Chemical Transport Model (UMD-CTM): 1. Model description and evaluation. *J. Geophys. Res.*, **109**, D09301, doi:10.1029/2003JD004266.

Patra, P.K., et al., 2005: Role of biomass burning and climate anomalies for land-atmosphere carbon fluxes based on inverse modeling of atmospheric CO_2. *Global Biogeochem. Cycles*, **19**, GB3005, doi:10.1029/2004GB002258 .

Paull, C.K., et al., 2003: An experiment demonstrating that marine slumping is a mechanism to transfer methane from seafloor gas-hydrate deposits into the upper ocean and atmosphere. *Geo.-Marine Lett.*, **22**, 198–203.

Peng, Y., and U. Lohmann, 2003: Sensitivity study of the spectral dispersion of the cloud droplet size distribution on the indirect aerosol effect. *Geophys. Res. Lett.*, **30**(10), 1507, doi:10.1029/2003GL017192.

Peng, Y., et al., 2002: The cloud albedo-cloud droplet effective radius relationship for clean and polluted clouds from ACE and FIRE. *J. Geophys. Res.*, **107**(D11), doi:10.1029/2002JD000281.

Penner, J., et al., 2001: Aerosols, their direct and indirect effects. In: *Climate Change 2001: The Scientific Basis. Contribution of Working Group I to the Third Assessment Report of the Intergovernmental Panel on Climate Change* [Houghton, J.T., et al. (eds.)]. Cambridge University Press, Cambridge, United Kingdom and New York, NY, USA, pp. 289–348.

Penner, J.E., S.Y. Zhang, and C.C. Chuang, 2003: Soot and smoke aerosol may not warm climate. *J. Geophys. Res.*, **108**(21), 4657, doi:10.1029/2003JD003409.

Penner., J.E., et al., 2006: Model intercomparison of indirect aerosol effects. *Atmos. Chem. Phys. Discuss.*, **6**, 1579–1617.

Perlwitz, J., I. Tegen, and R.L. Miller, 2001: Interactive soil dust aerosol model in the GISS GCM 1. Sensitivity of the soil dust cycle to radiative properties of soil dust aerosols. *J. Geophys. Res.*, **106**(D16), doi:10.1029/2000JD900668.

Perry, K.D., S.S. Cliff, and M.P. Jimenez-Cruz, 2004: Evidence for hygroscopic mineral dust particles from the Intercontinental Transport and Chemical Transformation Experiment. *J. Geophys. Res.*, **109,** D23S28, doi:10.1029/2004JD004979.

Petit, J., et al., 1999: Climate and atmospheric history of the past 420,000 years from the Vostok ice core, Antarctica. *Nature*, **399**, 429–436.

Pétron, G., et al., 2004: Monthly CO surface sources inventory based on the 2000-2001 MOPITT data. *Geophys. Res. Lett.*, **31**, L21107, doi:10.1029/2004GL020560.

Peylin, P., et al., 2005: Multiple constraints on regional CO_2 flux variations over land and oceans. *Global Biogeochem. Cycles*, **19**, GB1011, doi:10.1029/2003GB002214.

Phillips, O.L., et al., 1998: Changes in the carbon balance of tropical forests: evidence from long-term plots. *Science*, **282**(5388), 439–442.

Phillips, V.T.J., T.W. Choularton, A.M. Blyth, and J. Latham, 2002: The influence of aerosol concentrations on the glaciation and precipitation of a cumulus cloud. *Q. J. R. Meteorol. Soc.*, **128**(581), 951–971.

Pickering, K.E., et al., 2001: Trace gas transport and scavenging in PEM-Tropics B South Pacific convergence zone convection. *J. Geophys. Res.*, **106**(D23), doi:10.1029/2001JD000328.

Pielke, R.A. Sr., 2001: Influence of the spatial distribution of vegetation and soils on the prediction of cumulus convective rainfall. *Rev. Geophys.*, **39**(2), 151–177.

Pielke, R.A. Sr., and T. Matsui, 2005: Should light wind and windy nights have the same temperature trends at individual levels even if the boundary layer averaged heat content change is the same? *Geophys. Res. Lett.*, **32**, L21813, doi:10.1029/2005GL024407.

Pinto, J.P., and M.A.K. Khalil, 1991: The stability of tropospheric OH during ice ages, inter-glacial epochs and modern times. *Tellus*, **43B**, 347–352.

Pinty, B., et al., 2006: Simplifying the interaction of land surfaces with radiation for relating remote sensing products to climate models. *J. Geophys. Res.*, **111**, D02116, doi:10.1029/2005JD005952.

Pitman, A.J., B.J. McAvaney, N. Bagnound, and B. Chemint, 2004: Are inter-model differences in AMIP-II near surface air temperature means and extremes explained by land surface energy balance complexity. *Geophys. Res. Lett.*, **31**, L05205, doi:10.1029/2003GL019233.

Platnick, S., et al., 2000: The role of background cloud microphysics in the radiative formation of ship tracks. *J. Atmos. Sci.*, **57**, 2607–2624.

Platt, U., W. Allan, and D. Lowe. 2004: Hemispheric average Cl atom concentration from $^{12}C/^{13}C$ ratios in atmospheric methane. *Atmos. Chem. Phys.*, **4**, 2393–2399.

Plattner, G.-K., F. Joos, T.F. Stocker, and O. Marchal, 2001: Feedback mechanisms and sensitivities of ocean carbon uptake under global warming. *Tellus*, **53B**, 564–592.

Polvani, L.M. and P.J. Kushner, 2002: Tropospheric response to stratospheric perturbations in a relatively simple general circulation model. *Geophys. Res. Lett.*, **29**, doi:10.1029/2001GL014284.

Prather, M.J., 2002: Lifetimes of atmospheric species: integrating environmental impacts. *Geophys. Res. Lett.*, **29**(22), 2063, doi:10.1029/2002GL016299

Prather, M.J., et al., 2001: Atmospheric chemistry and greenhouse gases. In: *Climate Change 2001: The Scientific Basis. Contribution of Working Group I to the Third Assessment Report of the Intergovernmental Panel on Climate Change* [Houghton, J.T., et al. (eds.)]. Cambridge University Press, Cambridge, United Kingdom and New York, NY, USA, pp. 239–287.

Prentice, I.C., et al., 2001: The Carbon Cycle and Atmospheric Carbon Dioxide. In: *Climate Change 2001: The Scientific Basis. Contribution of Working Group I to the Third Assessment Report of the Intergovernmental Panel on Climate Change* [Houghton, J.T., et al. (eds.)]. Cambridge University Press, Cambridge, United Kingdom and New York, NY, USA, pp. 99–181.

Price, C., and D. Rind, 1994a: Possible implications of global climate change on global lightning distributions and frequencies. *J. Geophys. Res.*, **99**(D5), doi:10.1029/94JD00019.

Price, C., and D. Rind, 1994b: The impact of a $2xCO_2$ climate on lightning-caused fires. *J. Clim.*, **7**, 1484–1494.

Price, C., J. Penner, and M. Prather, 1997: NO_x from lightning 1. Global distribution based on lightning physics. *J. Geophys. Res.*, **102**(D5), doi:10.1029/96JD03504.

Prinn, R.G., et al., 1990: Atmospheric emissions and trends of nitrous-oxide deduced from 10 years of ALE-gauge data. *J. Geophys. Res.*, **95**(D11), 18369–18385.

Prinn, R.G., et al., 2001: Evidence for substantial variations of atmospheric hydroxyl radicals in the past two decades. *Science*, **292**(5523), 1882–1888.

Prinn, R.G., et al., 2005: Evidence for variability of atmospheric hydroxyl radicals over the past quarter century. *Geophys.Res.Lett.*, **32**, L07809, doi:10.1029/2004GL022228.

Prospero, J.M., and P.J. Lamb, 2003: African droughts and dust transport to the Caribbean: Climate change implications. *Science*, **302**, 1024–1027.

Prospero, J.M., et al., 2002: Environmental characterization of global sources of atmospheric soil dust identified with the NIMBUS 7 total ozone mapping spectrometer (TOMS) absorbing aerosol product. *Rev. Geophys.*, **40**, doi:10.1029/2000RG000095.

Qian, Y., and F. Giorgi, 2000: Regional climatic effects of anthropogenic aerosols? The case of Southwestern China. *Geophys. Res. Lett.*, **27**(21), doi:10.1029/2000GL011942.

Quaas, J., O. Boucher, and F.-M. Bréon, 2004: Aerosol indirect effects in POLDER satellite data and the Laboratoire de Météorologie Dynamique-Zoom (LMDZ) general circulation model. *J. Geophys. Res.*, **109**, doi:10.1029/2003JD004317.

Quaas, J., O. Boucher, and U. Lohmann, 2006: Constraining the total aerosol indirect effect in the LMDZ and ECHAM4 GCMs using MODIS satellite data. *Atmos. Chem. Phys.*, **6**, 947-955.

Quay, P., et al., 2003: Changes in the $^{13}C/^{12}C$ of dissolved inorganic carbon in the ocean as a tracer of anthropogenic CO_2 uptake. *Global Biogeochem. Cycles*, **17**(1), 1004, doi:10.1029/2001GB001817.

Quesada, C.A., et al., 2004: Seasonal and depth variation of soil moisture in a burned open savanna (campo sujo) in central Brazil. *Ecol. Appl.*, **14**, S33–41.

Raich, J., and W. Schlesinger, 1992: The global carbon dioxide flux in soil respiration and its relationship to vegetation and climate. *Tellus*, **44B**, 81–99.

Ramanathan, V., P.J. Crutzen, J.T. Kiehl, and D. Rosenfeld, 2001: Aerosols, climate, and the hydrological cycle. *Science*, **294**, 2119–2123.

Ramanathan, V., et al., 2005: Atmospheric brown clouds: impacts on South Asian climate and hydrological cycle. *Proc. Natl. Acad. Sci. U.S.A.*, **102**, 5326–5333.

Ramankutty, N., and J.A. Foley, 1999: Estimating historical changes in global land cover: Croplands from 1700 to 1992. *Global Biogeochem. Cycles*, **13**, 997–1028.

Randel, W.J., et al., 2004: Interannual changes of stratospheric water vapor and correlations with tropical tropopause temperatures. *J. Atmos. Sci.*, **61**, 2133–2148.

Randel, W.J., et al., 2006: Decreases in stratospheric water vapor after 2001: Links to changes in the tropical tropopause and the Brewer-Dobson circulation. *J. Geophys. Res.*, **111**, D12312, doi:10.1029/2005JD006744.

Randerson, J.T., et al., 2002a: Net ecosystem production: A comprehensive measure of net carbon accumulation by ecosystems. *Ecol. Appl.*, **12**(4), 937–947.

Randerson, J.T., et al., 2002b: Seasonal and latitudinal variability of troposphere $\Delta^{14}CO_2$: Post bomb contributions from fossil fuels, oceans, the stratosphere, and the terrestrial biosphere. *Global Biogeochem. Cycles*, **16**(4), 1112, doi:10.1029/2002GB001876.

Randerson, J.T., et al., 2002c: A possible global covariance between terrestrial gross primary production and ^{13}C discrimination: Consequences for the atmospheric ^{13}C budget and its response to ENSO. *Global Biogeochem. Cycles*, **16**(4), 1136, doi:10.1029/2001GB001845.

Randerson, J.T., et al., 2002d: Carbon isotope discrimination of arctic and boreal biomes inferred from remote atmospheric measurements and a biosphere-atmosphere model. *Global Biogeochem. Cycles*, **16**(3), doi:10.1029/2001GB001435.

Randerson, J.T., et al., 2005: Fire emissions from C-3 and C-4 vegetation and their influence on interannual variability of atmospheric CO_2 and $\Delta^{13}CO_2$. *Global Biogeochem. Cycles*, **19**(2), GB2019, doi:10.1029/2004GB002366.

Raymond, P.A., and J.J. Cole, 2003: Increase in the export of alkalinity from North America's largest river. *Science*, **301**, 88–91.

Rayner, P.J., I.G. Enting, R.J. Francey, and R. Langenfelds, 1999: Reconstructing the recent carbon cycle from atmospheric CO_2, $\delta^{13}C$ and O_2/N_2 observations. *Tellus*, **51B**(2), 213–232.

Rayner, P.J., et al., 2005: Two decades of terrestrial carbon fluxes from a Carbon Cycle Data Assimilation System (CCDAS). *Global Biogeochem. Cycles*, **19**, doi:10.1029/2004GB002254.

Reale, O., and P. Dirmeyer, 2002: Modeling the effect of land surface evaporation variability on precipitation variability. I: General response. *J. Hydrometeorol.*, **3**(4), 433–450.

Reale, O., P. Dirmeyer, and A. Schlosser, 2002: Modeling the effect of land surface evaporation variability on precipitation variability. II: Time- and space-scale structure. *J. Hydrometeorol.*, **3**(4), 451–466.

Reich, P.B., et al., 2006: Nitrogen limitation constrains sustainability of ecosystem response to CO_2. *Nature,* **440**, 922–925, doi:10.1038/nature04486.

Reinsel, G.C., et al., 2005: Trend analysis of total ozone data for turnaround and dynamical contributions. *J. Geophys. Res.*, **110**, D16306, doi:10.1029/2004JD004662.

Ren, X., et al., 2003: OH and HO_2 chemistry in the urban atmosphere of New York City. *Atmos. Environ.*, **37**, 3639–3651.

Revelle, R., and H.E. Suess, 1957: Carbon dioxide exchange between atmosphere and ocean and the question of an increase of atmospheric CO_2 during past decades. *Tellus*, **9**, 18–27.

Rice, A.H., et al., 2004: Carbon balance and vegetation dynamics in an old-growth Amazonian Forest. *Ecol. Appl.*, **14**(4), S55–S71.

Richey, J.E., 2004: Pathways of atmospheric CO_2 through fluvial systems. In: *The Global Carbon Cycle: Integrating Humans, Climate, and the Natural World* [Field, C., and M. Raupach (eds)]. SCOPE 62, Island Press, Washington, DC, pp. 329–340.

Richter, A., and J.P. Burrows, 2002: Tropospheric NO_2 from GOME measurements. *Adv. Space Res.*, **29**, 1673–1683.

Richter, A., et al., 2004: Satellite measurements of NO_2 from international shipping emissions. *Geophys. Res. Lett.*, **31**, doi:10.1029/2004GL020822.

Richter, A., et al., 2005: Increase in tropospheric nitrogen dioxide over China observed from space. *Nature*, **437**, 129–132.

Ridgwell, A.J., S.J. Marshall, and K. Gregson, 1999: Consumption of atmospheric methane by soils: A process-based model. *Global Biogeochem. Cycles*, **13**, 59–70.

Riebesell, U., D.A. Wolf-Gladrow, and V. Smetacek, 1993: Carbon dioxide limitation of marine phytoplankton growth rates. *Nature*, **361**, 249–251.

Riebesell, U., et al., 2000: Reduced calcification of marine plankton in response to increased atmospheric CO_2. *Nature*, **407**, 364–367.

Rind, D., J. Lerner, and C. McLinden, 2001: Changes of tracer distribution in the doubled CO_2 climate. *J. Geophys. Res.*, **106**(D22), doi:10.1029/2001JD000439.

Roberts, J.M., A.J. Wheeler, and A. Freiwald, 2006: Reefs of the deep: The biology and geology of cold-water coral ecosystems. *Science*, **312**, 543–547.

Robock, A., 2005: Cooling following large volcanic eruptions corrected for the effect of diffuse radiation on tree rings. *Geophys. Res. Lett*., **32**, L06702, doi:10.1029/2004GL022116.

Rödenbeck, C., S. Houweling, M. Gloor, and M. Heimann, 2003a: Time-dependent atmospheric CO_2 inversions based on interannually varying tracer transport. *Tellus*, **55B**, 488–497.

Rödenbeck, C., S. Houweling, M. Gloor, and M. Heimann, 2003b: CO_2 flux history 1982–2001 inferred from atmospheric data using a global inversion of atmospheric transport. *Atmos. Chem. Phys.*, **3**, 2575–2659.

Roderick, M.L., G.D. Farquhar, S.L. Berry, and I.R. Noble, 2001: On the direct effect of clouds and atmospheric particles on the productivity and structure of vegetation. *Oecologia*, **129**, 21–30.

Roeckner, E., et al., 1999: Transient climate change simulations with a coupled atmosphere-ocean GCM including the tropospheric sulphur cycle. *J. Clim.*, **12**, 3004–3032.

Roeckner, E., et al., 2006: Impact of carbonaceous aerosol emissions on regional climate change. *Clim. Dyn.*, **27**, 553–571.

Rosenfeld, D., 1999: TRMM observed first direct evidence of smoke from forest fires inhibiting rainfall. *Geophys. Res. Lett.*, **26**(20), doi:10.1029/1999GL006066.

Rosenfeld, D., 2000: Suppression of rain and snow by urban and industrial air pollution. *Science*, **287**, 1793–1796.

Rosenfeld, D., and W.L. Woodley, 2000: Deep convective clouds with sustained supercooled liquid water down to –37.5 °C. *Nature*, **405**, 440–442.

Rosenfeld, D., Y. Rudich, and R. Lahav, 2001: Desert dust suppressing precipitation: a possible desertification feedback loop. *Proc. Natl. Acad. Sci. U.S.A.*, **98**, 5975–5980.

Rosenfeld, D., R. Lahav, A. Khain, and M. Pinsky, 2002: The role of sea spray in cleansing air pollution over ocean via cloud processes. *Science*, **297**, 1667–1670.

Rosenfield, J.E., A.R. Douglass, and D.B. Considine, 2002: The impact of increasing carbon dioxide on ozone recovery. *J. Geophys. Res.*, **107**(D6), 4049, doi:10.1029/2001JD000824.

Rosenlof, K.H., et al., 2001. Stratospheric water vapor increase over the past half-century. *Geophys. Res. Lett.*, **28**, 1195–1198.

Rotman, D.A., et al., 2004: IMPACT, the LLNL 3-D global atmospheric chemical transport model for the combined troposphere and stratosphere: Model description and analysis of ozone and other trace gases. *J. Geophys. Res.*, **109**, D04303, doi:10.1029/2002JD003155.

Rotstayn, L.D., and U. Lohmann, 2002: Tropical rainfall trends and the indirect aerosol effect. *J. Clim.*, **15**, 2103–2116.

Rotstayn, L.D., and Y. Liu, 2003: Sensitivity of the first indirect aerosol effect to an increase of cloud droplet spectral dispersion with droplet number concentration. *J. Clim.*, **16**, 3476–3481.

Rotstayn, L.D., and Y. Liu, 2005: A smaller global estimate of the second indirect aerosol effect. *Geophys. Res. Lett.*, **32**, L05708, doi:10.1029/2004GL021922.

Rotstayn, L.D., B.F. Ryan, and J.E. Penner, 2000: Precipitation changes in a GCM resulting from the indirect effects of anthropogenic aerosols. *Geophys. Res. Lett.*, **27**, 3045–3048.

Roy, S.B., G.C. Hurtt, C.P. Weaver, and S.W. Pacala, 2003: Impact of historical land cover change on the July climate of the United States. *J. Geophys. Res.*, **108**(D24), 4793, doi:10.1029/2003JD003565.

Roy, T., P. Rayner, R. Matear, and R. Francey, 2003: Southern hemisphere ocean CO_2 uptake: reconciling atmospheric and oceanic estimates. *Tellus*, **55B**(2), 701–710.

Royal Society, 2005: *Ocean Acidification Due to Increasing Atmospheric Carbon Dioxide*. Policy document 12/05, June 2005, The Royal Society, London, 60 pp., http://www.royalsoc.ac.uk/document.asp?tip=0&id=3249.

Ruddiman, W.F., and J.S. Thomson, 2001: The case for human causes of increased atmospheric CH_4 over the last 5000 years. *Quat. Sci. Rev.*, **20**, 1769–1777.

Russell, J.L., and J.M. Wallace, 2004: Annual carbon dioxide drawdown and the Northern Annular Mode. *Global Biogeochem. Cycles*, **18**(1), GB1012, doi:10.1029/2003GB002044.

Rustad, L.E., et al., 2001: A meta-analysis of the response of soil respiration, net nitrogen mineralization, and above ground plant growth to experimental ecosystem warming. *Oecologia*, **126**, 543–562.

Ryskin, G., 2003: Methane-driven oceanic eruptions and mass extinctions. *Geology*, **31**(9), 741–744.

Sabine, C.L., et al., 2004a: The oceanic sink for anthropogenic CO_2. *Science*, **305**(5682), 367–371.

Sabine, C.L., et al., 2004b: Current status and past trends of the global carbon cycle. In: *The Global Carbon Cycle: Integrating Humans, Climate and the Natural World* [Field, C., and M. Raupach (eds.)]. SCOPE 62, Island Press, Washington, DC, pp. 17–44.

Saiz-Lopez, A., and J.M.C. Plane, 2004: Novel iodine chemistry in the marine boundary layer. *Geophys. Res. Lett.*, **31**, L04112, doi:10.1029/2003GL019215.

Saiz-Lopez, A., et al., 2005: Modelling molecular iodine emissions in a coastal marine environment: the link to new particle formation. *Atmos. Chem. Phys. Discuss.*, **5**, 5405–5439.

Saleska, S.R., et al., 2003: Carbon in Amazon forests: Unexpected seasonal fluxes and disturbance–induced losses. *Science*, **302**(5650), 1554–1557.

Salvucci, G.D., J.A. Saleem, and R. Kaufmann, 2002: Investigating soil moisture feedbacks on precipitation with tests of Granger causality. *Adv. Water Resour.*, **25**, 1305–1312.

Sanderson, M.G., W.J. Collins, R.G. Derwent, and C.E. Johnson, 2003a: Simulation of global hydrogen levels using a Lagrangian three-dimensional model. *J. Atmos. Chem.*, **46**(1), 15–28.

Sanderson, M.G., et al., 2003b: Effect of climate change on isoprene emissions and surface ozone levels. *Geophys. Res. Lett.*, **30**(18), 1936, doi:10.1029/2003GL017642.

Sarmiento, J.L., and E.T. Sundquist, 1992: Revised budget for the oceanic uptake of anthropogenic carbon dioxide. *Nature*, **356**, 589–593.

Sarmiento, J.L., and N. Gruber, 2006: *Ocean Biogeochemical Dynamics*. Princeton University Press, Princeton, NJ, 503 pp.

Sarmiento, J.L., et al., 2004: Response of ocean ecosystems to climate warming. *Global Biogeochem. Cycles*, **18**(3), GB3003, doi:10.1029/2003GB002134.

Sass, R.L., J.A. Andrews, A.J. Ding, and F.M. Fisher, 2002: Spatial and temporal variability in methane emissions from rice paddies: implications for assessing regional methane budgets. *Nutrient Cycling in Agroecosystems*, **64**(1–2), 3–7.

Sathyendranath, S., et al., 1991: Biological control of surface temperature in the Arabian Sea. *Nature*, **349**, 54–56.

Saueressig, G., et al., 2001: Carbon 13 and D kinetic isotope effects in the reaction of CH_4 with $O(^1D)$ and OH: New laboratory measurements and their implications for the isotopic composition of stratospheric methane. *J. Geophys. Res.*, **106**, 23127–23138.

Scanlon, B.R., et al., 2005: Ecological controls on water-cycle response to climate variability in deserts. *Proc. Natl. Acad. Sci. U.S.A.*, **102**, 6033–6038.

Scheehle, E.A., W.N. Irving, and D. Kruger, 2002: Global anthropogenic methane emission. In: *Non-CO_2 Greenhouse Gases* [Van Ham, J., A.P. Baede, R. Guicherit, and J.Williams-Jacobse (eds)]. Millpress, Rotterdam, pp. 257–262.

Schimel, D.S., et al., 2001: Recent patterns and mechanisms of carbon exchange by terrestrial ecosystems. *Nature*, **414**, 169–172.

Schoeberl, M.R., A.R. Douglass, Z. Zhu, and S. Pawson, 2003: A comparison of the lower stratospheric age-spectra derived from a general circulation model and two data assimilation systems. *J. Geophys. Res.*, **108**(D3), doi:10.1029/2002JD002652.

Schultz, M.G., T. Diehl, G.P. Brasseur, and W. Zittel, 2003: Air pollution and climate-forcing impacts of a global hydrogen economy. *Science*, **302**, 624–627.

Schulz, M., Y. Balkanski, F. Dulac, and W. Guelle, 1998: Role of aerosol size distribution and source location in a three-dimensional simulation of a Saharan dust episode tested against satellite-derived optical thickness. *J. Geophys Res*, **103**, 10579–10592.

Sciandra, A., et al., 2003: Response of the coccolithophorid *Emiliana huxleyi* to elevated partial pressure of CO_2 under nitrogen limitation. *Mar. Ecol. Prog. Ser.*, **261**, 111–122.

Seifert, A., and K.D. Beheng, 2006: A two-moment cloud microphysics parameterization for mixed-phase clouds. Part II: Deep convective storms. *Meteorol. Atmos. Phys.*, **92**, doi:10.1007/s00703-005-0113-3.

Seiler, W., and R. Conrad, 1987: Contribution of tropical ecosystems to the global budget of trace gases, especially CH_4, H_2, CO, and N_2O. In: *The Geophysiology of Amazonia: Vegetation and Climate Interactions* [Dickinson, R.E. (ed.)]. John Wiley, New York, pp. 33–62.

Sekiguchi, M., et al., 2003: A study of the direct and indirect effects of aerosols using global satellite data sets of aerosol and cloud parameters. *J. Geophys. Res.*, **108**, 4699, doi:10.1029/2002JD003359.

Sharon, T.M., et al., 2006: Aerosol and cloud microphysical characteristics of rifts and gradients in maritime stratocumulus clouds. *J. Atmos. Sci.*, **63**(3), 983–997.

Shim, C., et al., 2005: Constraining global isoprene emissions with Global Ozone Monitoring Experiment (GOME) formaldehyde column measurements. *J. Geophys. Res.*, **110**, D24301, doi:10.1029/2004JD005629.

Shindell, D.T., and G. Faluvegi, 2002: An exploration of ozone changes and their radiative forcing prior to the chlorofluorocarbon era. *Atmos. Chem. Phys.*, **2**, 363–374.

Shindell, D.T., G. Faluvegi, and N. Bell, 2003: Preindustrial-to-present-day radiative forcing by tropospheric ozone from improved simulations with the GISS chemistry-climate GCM. *Atmos. Chem. Phys.*, **3**, 1675–1702.

Shindell, D.T., B.P. Walter, and G. Faluvegi, 2004: Impacts of climate change on methane emissions from wetlands. *Geophys. Res. Lett.*, **31**, L21202, doi:10.1029/2004GL021009.

Shindell, D.T., et al., 2001: Chemistry-climate interactions in the Goddard Institute for Space Studies general circulation model 1. Tropospheric chemistry model description and evaluation. *J. Geophys. Res.*, **106**(D8), doi:10.1029/2000JD900704.

Shvidenko, A.Z., and S. Nilsson, 2003: A synthesis of the impact of Russian forests on the global carbon budget for 1961-1998. *Tellus*, **55B**, 391–415.

Siegenthaler, U., et al., 2005: Stable carbon cycle-climate relationship during the late Pleistocene. *Science*, **310**(5752), 1313–1317.

Sievering, H., et al., 1992: Removal of sulphur from the marine boundary layer by ozone oxidation in sea-salt aerosols. *Nature*, **360**, 571–573.

Sievering, H., et al., 2000: Forest canopy uptake of atmospheric nitrogen deposition at eastern U.S. conifer sites: Carbon storage implications. *Global Biogeochem. Cycles*, **14**(4), doi:10.1029/1999GB001250.

Sillman, S., and P.J. Samson, 1995: Impact of temperature on oxidant photochemistry in urban, polluted rural, and remote environments. *J. Geophys. Res.*, **100**(D6), 11497–11508, doi:10.1029/94JD02146.

Silva Dias, M.A.F., et al., 2002: Clouds and rain processes in a biosphere atmosphere interaction context. *J. Geophys. Res.*, **107**(D20), 8072, doi:10.1029/2001JD000335.

Simmonds, P.G., et al., 2000: Continuous high-frequency observations of hydrogen at the Mace Head baseline atmospheric monitoring station over the 1994-1998 period. *J. Geophys. Res.*, **105**(D10), 12105–12121, doi:10.1029/2000JD900007.

Simmons, A.J., et al., 2005: ECMWF analyses and forecasts of stratospheric winter polar vortex breakup: September 2002 in the southern hemisphere and related events. *J. Atmos. Sci*., **62**, 668–689.

Singh, H.B., et al., 2004: Analysis of the atmospheric distribution, sources, and sinks of oxygenated volatile organic chemicals based on measurements over the Pacific during TRACE-P. *J. Geophys. Res.*, **109**, D15S07, doi:10.1029/2003JD003883.

Sinha, A., 1995: Relative influence of lapse rate and water vapour on the greenhouse effect. *J. Geophys. Res.*, **100**(D3), 5095–5103, doi:10.1029/94JD03248.

Sitch, S., et al., 2003: Evaluation of ecosystem dynamics, plant geography and terrestrial carbon cycling in the LPJ dynamic global vegetation model. *Global Change Biol.*, **9**, 161–185.

Sitch, S., et al., 2005: Impacts of future land cover changes on atmospheric CO_2 and climate. *Global Biogeochem. Cycles*, **19**, doi:10.1029/2004GB002311.

Smith, K.A., and F. Conen, 2004: Impacts of land management on fluxes of trace greenhouse gases. *Soil Use Management*, **20**, 255–263.

Smith, P., D.S. Powlson, M.J. Glendining, and J.U. Smith, 1997: Potential for carbon sequestration in European soils: preliminary estimates for five scenarios using results from long-term experiments. *Global Change Biol*., **3**, 67–79.

Smith, S.V., and J.T. Hollibaugh, 1993: Coastal metabolism and the oceanic organic carbon balance. *Rev. Geophys.*, **31**(1), 75–89.

Smyth, T.J., T. Tyrrell, and B. Tarrant, 2004: Time series coccolithophore activity in the Barents Sea, from twenty years of satellite imagery. *Geophys. Res. Lett.*, **31**, L11302, doi:10.1029/2004GL019735.

Snover, A.K., and P.D. Quay, 2000: Hydrogen and carbon kinetic effects during soil uptake of atmospheric methane. *Global Biogeochem. Cycles*, **14**, 25–39.

Snyder, P.K., C. Delire, and J.A. Foley, 2004: Evaluating the influence of different vegetation biomes on the global climate. *Clim. Dyn.*, **23**, 279–302, doi:10.1007/s00382-004-0430-0.

Song, Y., and W.A. Robinson, 2004: Dynamical mechanisms for stratospheric influences on the troposphere. *J. Atmos. Sci*., **61**, 1711–1725.

Spahni, R., et al., 2005: Atmospheric methane and nitrous oxide of the Late Pleistocene from Antarctic ice cores. *Science*, **310**(5752), 1317–1321.

Steinbrecht, W., H. Claude, and P. Winkler, 2004: Enhanced upper stratospheric ozone: Sign of recovery or solar cycle effect? *J. Geophys. Res.*, **109**, D02308, doi:10.1029/2003JD004284.

Stephens, G.L., N.B. Wood, and L.A. Pakula, 2004: On the radiative effects of dust on tropical convection. *Geophys. Res. Lett.*, **31**, L23112, doi:10.1029/2004GL021342.

Stevens, B., et al., 2005: Pockets of open cells and drizzle in marine stratocumulus. *Bull. Am. Meteorol. Soc.*, **86**, 51–57.

Stevenson, D.S., et al., 2000: Future estimates of tropospheric ozone radiative forcing and methane turnover - the impact of climate change. *Geophys. Res. Lett.*, **105**(14), doi:10.1029/1999GL010887.

Stevenson, D.S., et al., 2004: Radiative forcing from aircraft NO_x emissions: mechanisms and seasonal dependence. *J. Geophys. Res.*, **109**, D17307, doi:10.1029/2004JD004759.

Stevenson, D.S., et al., 2005: Impacts of climate change and variability on tropospheric ozone and its precursors. *Faraday Discuss.*, **130**, doi:10.1039/b417412g.

Stevenson, D.S., et al., 2006: Multi-model ensemble of present-day and near-future tropospheric ozone. *J. Geophys. Res.*, **111**, D8301, doi:10.1029/2005JD006338.

Stier, P., et al., 2006a: The evolution of the global aerosol system in a transient climate simulation from 1860 to 2100. *Atmos. Chem. Phys.*, **6**, 3059–3076.

Stier, P., et al., 2006b: Emission-induced nonlinearities in the global aerosol system - results from the ECHAM5-HAM aerosol-climate model. *J. Clim.*, **19**, 3845–3862.

Stocks, B.J., et al., 1998: Climate change and forest fire potential in Russian and Canadian boreal forests. *Clim. Change*, **38**, 1–13.

Storelvmo T., et al., 2006: Predicting cloud droplet number concentration in Community Atmosphere Model (CAM)-Oslo, *J. Geophys. Res.*, **111**, D24208, doi:10.1029/2005JD006300.

Sturm, M., T. Douglas, C. Racine, and G. Liston, 2005: Changing snow and shrub conditions affect albedo with global implications. *J. Geophys. Res.*, **110**, G01004, doi:10.1029/2005JG000013.

Sudo, K., M. Takahashi, and H. Akimoto, 2002a: CHASER: A global chemical model of the troposphere 2. Model results and evaluation. *J. Geophys. Res.*, **107**, 4586, doi:10.1029/2001JD001114.

Sudo, K., M. Takahashi, J. Kurokawa, and H. Akimoto, 2002b: CHASER: A global chemical model of the troposphere 1. Model description. *J. Geophys. Res.*, **107**, 4339, doi:10.1029/2001JD001113.

Suntharalingam, P., et al., 2005: Influence of reduced carbon emissions and oxidation on the distribution of atmospheric CO_2: Implications for inversion analyses. *Global Biogeochem. Cycles*, **19**, GB4003, doi:10.1029/2005GB002466.

Takahashi, T., et al., 2002: Global sea-air CO_2 flux based on climatological surface ocean pCO_2, and seasonal biological and temperature effects. *Deep-Sea Res. II*, **49**(9–10), 1601–1622.

Takemura, T., et al., 2005: Simulation of climate response to aerosol direct and indirect effects with aerosol transport-radiation model. *J. Geophys. Res*, **110**, doi:10.1029/2004JD00502.

Tan, W.W., M.A. Geller, S. Pawson, and A. da Silva, 2004: A case study of excessive subtropical transport in the stratosphere of a data assimilation system. *J. Geophys. Res.*, **109**, D11102, doi:10.1029/2003JD004057.

Tans, P. P., and T.J. Conway, 2005: Monthly atmospheric CO_2 mixing ratios from the NOAA CMDL Carbon Cycle Cooperative Global Air Sampling Network, 1968-2002. In: *Trends: A Compendium of Data on Global Change*. Carbon Dioxide Information Analysis Center, Oak Ridge National Laboratory, U.S. Department of Energy, Oak Ridge, TN, http://cdiac.ornl.gov/trends/co2/cmdl-flask/cmdl-flask.html.

Tegen, I., A.A. Lacis, and I. Fung, 1996: The influence of mineral aerosols from disturbed soils on the global radiation budget. *Nature*, **380**, 419–422.

Tegen, I., M. Werner, S.P. Harrison, and K.E. Kohfeld, 2004: Relative importance of climate and land use in determining present and future global soil dust emission. *Geophys. Res. Lett.*, **31**, L05105, doi:10.1029/2003GL019216.

Tegen, I., et al., 2002. Impact of vegetation and preferential source areas on global dust aerosol: results from a model study. *J. Geophys. Res.*, **107**(D21), 4576, doi:10.1029/2001JD000963.

Textor, C., et al., 2005: Analysis and quantification of the diversities of aerosol life cycles within AEROCOM. *Atmos. Chem. Phys. Discuss.*, **5**, 8331–8420.

Thompson, A.M., et al., 1996: Where did tropospheric ozone over southern Africa and the tropical Atlantic come from in October 1992? Insights from TOMS, GTE TRACE A, and SAFARI 1992. *J. Geophys. Res.*, **101**(D19), doi:10.1029/96JD01463.

Thompson, A.M., et al., 2000: A tropical Atlantic paradox: shipboard and satellite views of a tropospheric ozone maximum and wave-one in January–February 1999. *Geophys. Res. Lett.*, **27**(20), doi:10.1029/1999GL011273.

Thompson, D.W.J., M.P. Baldwin, and S. Solomon, 2005: Stratosphere/troposphere coupling in the Southern Hemisphere. *J. Atmos. Sci.*, **62**, 708–715.

Thompson, S.L., et al., 2004: Quantifying the effects of CO_2-fertilized vegetation on future global climate and carbon dynamics. *Geophys. Res. Lett.*, **31**, L23211, doi:10.1029/2004GL021239.

Thornton, P.E., et al., 2002: Modeling and measuring the effects of disturbance history and climate on carbon and water budgets in evergreen needleleaf forests. *Agric. For. Meteorol*., **113**, 185–222.

Tian, H., et al., 1998: Effect of interannual climate variability on carbon storage in Amazonian ecosystems. *Nature*, **396**, 664–667.

Tian, Y., et al., 2004: Comparison of seasonal and spatial variations of leaf area index and fraction of absorbed photosynthetically active radiation from Moderate Resolution Imaging Spectroradiometer (MODIS) and common land model. *J. Geophys. Res.*, **109**, doi:10.1029/2003JD003777.

Tie, X.X., A. Guenther, and E. Holland, 2003: Biogenic methanol and its impact on tropospheric oxidants. *Geophys. Res. Lett.*, **30**(17), 1881, doi:10.1029/2003GL017167.

Tie, X.X., R.Y. Zhang, G. Brasseur, and W.F. Lei, 2002: Global NO_x production by lightning. *J. Atmos. Chem.*, **43**(1), 61–74.

Tilmes, S., R. Müller, J.-U. Grooß, and J.M. Russell III, 2004: Ozone loss and chlorine activation in the Arctic winters 1991–2003 derived with the TRAC method. *Atmos. Chem. Phys.*, **4**, 2181–2213.

Timmreck, C., and M. Schulz, 2004: Significant dust simulation differences in nudged and climatological operation mode of the AGCM ECHAM. *J. Geophys. Res.*, **109**, D13202, doi:10.1029/2003JD004381.

Tortell, P.D., G.R. DiTullio, D.M. Sigman, and F.M.M. Morel, 2002: CO_2 effects on taxonomic composition and nutrient utilization in an Equatorial Pacific phytoplankton assemblage. *Mar. Ecol. Prog. Ser.*, **236**, 37–43.

Toumi, R., J.D. Haigh, and K.S. Law, 1996: A tropospheric ozone-lightning climate feedback. *Geophys. Res. Lett.*, **23**(9), doi:10.1029/96GL00944.

Trenberth, K.E., and D.J. Shea, 2005: Relationships between precipitation and surface temperature. *Geophys. Res. Lett.*, **32**, L14703, doi:10.1029/2005GL022760.

Tromp, T.K., et al., 2003: Potential environmental impact of a hydrogen economy on the stratosphere. *Science*, **300**, 1740–1742.

Tsigaridis, K., and M. Kanakidou, 2003: Global modelling of secondary organic aerosol in the troposphere: a sensitivity analysis. *Atmos. Chem. Phys.*, **3**, 1849–1869.

Tsvetsinskaya, E.A., et al., 2002: Relating MODIS-derived surface albedo to soils and rock types over Northern Africa and the Arabia Peninsula. *Geophys. Res. Lett.*, **29**(9), doi:10.1029/2001GLO14096.

Turner, D.P., et al., 1991: Climate change and isoprene emissions from vegetation. *Chemosphere*, **23**, 37–56.

Tyler, S.C., et al., 2000: Experimentally determined kinetic isotope effects in the reaction of CH_4 with Cl: Implications for atmospheric CH_4. *Geophys. Res. Lett.*, **27**, 1715–1718.

Tyrrell, T., P.M. Holligan, and C.D. Mobley, 1999: Optical impacts of oceanic coccolithophore blooms. *J. Geophys. Res.*, **104**(C2), 3223–3241.

Umann, B., et al., 2005: Interaction of mineral dust with gas phase nitric acid and sulfur dioxide during the MINATROC II field campaign: First estimate of the uptake coefficient gamma(HNO_3) from atmospheric data. *J. Geophys. Res., 110,* D22306, doi:10.1029/2005JD005906.

UN-ECE/FAO (ed.), 2000: *Forest Resources of Europe, CIS, North America, Australia, Japan and New Zealand*. UN-ECE/FAO Contribution to the Global Forest Resources Assessment 2000, United Nations, New York and Geneva, 445 pp.

Valdes, P.J., D.J. Beeling, and C.E. Johnson, 2005: The ice age methane budget. *Geophys. Res. Lett.*, **32**, doi:10.1029/2004GL021004.

Valentini, R., et al., 2000: Respiration as the main determinant of carbon balance in European forests. *Nature*, **404**(6780), 861–865.

Van Aardenne, J.A., et al., 2001: A 1°×1° resolution data set of historical anthropogenic trace gas emissions for the period 1890–1990. *Global Biogeochem. Cycles*, **15**, 909– 928.

Van den Heever, S.C., et al., 2006: Impacts of nucleating aerosol on Florida storms, Part I: Mesoscale simulations. *J. Atmos. Sci.*, **63**, 1752–1775.

van der Werf, G.R., J.T. Randerson, G.J. Collatz, and L. Giglio, 2003: Carbon emissions from fires in tropical and subtropical ecosystems. *Global Change Biol.*, **9**, 547–562.

van der Werf, G.R., et al., 2004: Continental-scale partitioning of fire emissions during the 1997 to 2001 El Niño/La Niña period. *Science*, **303**(5654), 73–76.

van Groenigen, K.J., et al., 2006: Element interactions limit soil carbon storage. *Proc. Natl. Acad. Sci. U.S.A.*, **103**, 6571–6574.

van Noije, T.P.C., H.J. Eskes, M. Van Weele, and P.F.J. van Velthoven, 2004: Implications of enhanced Brewer-Dobson circulation in European Centre for Medium-Range Weather Forecasts reanalysis for the stratosphere-troposphere exchange of ozone in global chemistry transport models. *J. Geophys. Res.*, **109**, D19308, doi:10.1029/2004JD004586.

van Noije, T.P.C., et al., 2006: Multi-model ensemble simulations of tropospheric NO_2 compared with GOME retrievals for the year 2000. *Atmos. Chem. Phys.*, **6**, 2943–2979.

van Wesemael, B., S. Lettens, C. Roelandt, and J. Van Orshoven, 2005: Modelling the evolution of regional carbon stocks in Belgian 19 cropland soils. *Can. J. Soil Sci*., **85**(4), 511–521.

Velders, G.J.M., et al., 2005: Chemical and radiative effects of halocarbons and their replacement compounds. In: *IPCC/TEAP Special Report on Safeguarding the Ozone Layer and the Global Climate System: Issues related to Hydrofluorocarbons and Perfluorocarbons. Prepared by Working Group I and III of the Intergovernmental Panel on Climate Change and the Technology and Economic Assessment Panel* [Metz, B., et al. (eds.)]. Cambridge University Press, Cambridge, United Kingdom and New York, NY, USA, pp. 133–180.

Verdugo, P., et al., 2004: The oceanic gel phase: a bridge in the DOM-POM continuum. *Mar. Chem*., **92**, 67–85.

Vitousek, P.M., 2004: *Nutrient Cycling and Limitations: Hawai'i as a Model Ecosystem*. Princeton University Press, Princeton, NJ, 232 pp.

Vitousek, P.M., et al., 1997: Human alteration of the global nitrogen cycle: sources and consequences. *Ecol. Appl.*, **7**, 737–750.

Vitousek, P.M., et al., 1998: Within-system element cycles, input-output budgets, and nutrient limitations. In: *Successes, Limitations, and Frontiers in Ecosystem Science* [Pace, M., and P. Groffman (eds.)]. Springer-Verlag, New York, pp. 432–451.

Voldoire, A., and J.-F. Royer, 2004: Tropical deforestation and climate variability. *Clim. Dyn.*, **22**, 857–874, doi:10.1007/s00382-004-0423-z.

Volk, T., and M.I. Hoffert, 1985: Ocean carbon pumps: Analysis of relative strengths and efficiencies in ocean-driven atmospheric CO_2 changes. In: *The Carbon Cycle and Atmospheric CO_2: Natural Variations Archean to Present* [Sundquist, E.T., and W.S. Broecker (eds.)]. Geophysical Monograph Vol. 32, American Geophysical Union, Washington, DC, pp. 99–110.

Von Kuhlmann, R., M.G. Lawrence, P.J. Crutzen, and P.J. Rasch, 2003: A model for studies of tropospheric ozone and nonmethane hydrocarbons: model description and ozone results. *J. Geophys. Res.*, **108**, 4294, doi:10.1029/2002JD002893.

Walsh, J.J., 1991: Importance of continental margins in the marine biogeochemical cycling of carbon and nitrogen. *Nature*, **350**, 53–55.

Walter, B.P., and M. Heimann, 2001a: Modeling modern methane emission from natural wetlands, 1. Model description and results. *J. Geophys. Res*., **106**, 34189–34206.

Walter, B.P., and M. Heimann, 2001b: Modeling modern methane emission from natural wetlands, 2. Interannual variations 1982-1993. *J. Geophys. Res*., **106**, 34207–37219.

Wang, C., 2004: A modeling study on the climate impacts of black carbon aerosols. *J. Geophys. Res.*, **109**, doi:10.1029/2003JD004084.

Wang, C., and R. Prinn, 1999: Impact of emissions, chemistry and climate on atmospheric carbon monoxide: 100 year predictions from a global chemistry model. *Chemosphere*, **1**, 73–81.

Wang, G., and E. Eltahir, 2000: Modeling the biosphere-atmosphere system: the impact of the subgrid variability in rainfall interception. *J. Clim.*, **13**, 2887–3078.

Wang, G., et al., 2004: Decadal variability of rainfall in the Sahel: results from the coupled GENESIS-IBIS atmosphere-biosphere model. *Clim. Dyn.*, **22**, doi:10.1007/s00382-004-0411-3.

Wang, J.S., M.B. McElroy, C.M. Spivakovsky, and D.B.A. Jones, 2002: On the contribution of anthropogenic Cl to the increase in $\delta^{13}C$ of atmospheric methane. *Global Biogeochem. Cycles*, **16**, doi:10.1029/2001GB001572.

Wang, J.S., et al., 2004: A 3-D model analysis of the slowdown and interannual variability in the methane growth rate from 1988 to 1997. *Global Biogeochem. Cycles*, **18**, GB3011, doi:10.1029/3003GB002180.

Wang, S.S., 2005: Dynamics of surface albedo of a boreal forest and its simulation. *Ecol. Model.*, **183**, 477–494.

Wang, S.S., et al., 2002: Modelling carbon dynamics of boreal forest ecosystems using the Canadian Land Surface Scheme. *Clim. Change*, **55**(4), 451–477.

Wang, Y., D.J. Jacob, and J.A. Logan, 1998: Global simulation of tropospheric O_3-NO_x-hydrocarbon chemistry, 3. Origin of tropospheric ozone and effects of non-methane hydrocarbons. *J. Geophys. Res.*, **103**(D9), 10757–10768.

Wang, Z., et al., 2004: Using MODIS BRDF and albedo data to evaluate global model land surface albedo. *J. Hydrometeorol.*, **5**, 3–14.

Wanninkhof, R., and W.R. McGillis, 1999: A cubic relationship between air-sea CO_2 exchange and wind speed. *Geophys. Res. Lett.*, **26**(13), 1889–1892.

Warneck, P., 1988: *Chemistry of the Natural Atmosphere*. Academic Press, London, 757 pp.

Warner, C.D., and M.E. McIntyre, 2001: An ultrasimple spectral parameterization for nonorographic gravity waves. *J. Atmos Sci.*, **58**, 1837–1857.

Warner, J., and S. Twomey, 1967: The production of cloud nuclei by cane fires and the effect on cloud droplet concentration. *J. Atmos Sci.*, **24**, 704–706.

Warwick, N.J., S. Bekki, E.G. Nisbet, and J.A. Pyle, 2004: Impact of a hydrogen economy on the stratosphere and troposphere studied in a 2-D model. *Geophys. Res. Lett.*, **31**, L05107, doi:10.1029/2003GL019224.

Warwick, N.J., et al., 2002: The impact of meteorology on the interannual growth rate of atmospheric methane. *Geophys. Res. Lett.*, **29**(20), 1947, doi:10.1029/2002GL015282.

Weaver, C.P., S.B. Roy, and R. Avissar, 2002: Sensitivity of simulated mesoscale atmospheric circulations resulting from landscape heterogeneity to aspects of model configuration. *J. Geophys. Res.*, **107**(D20), 8041, doi:10.1029/2001JD000376.

Weiss, R.F., 1974: Carbon dioxide in water and seawater: the solubility of a non-ideal gas. *Mar. Chem.*, **2**, 203–215.

Wells, M.L., and E.D. Goldberg, 1994: The distribution of colloids in the North Atlantic and Southern Oceans. *Limnol. Oceanogr.*, **39**, 286–302.

Werner, M., et al., 2002: Seasonal and interannual variability of the mineral dust cycle under present and glacial climate conditions. *J. Geophys. Res.*, **107**(D24), 4744, doi:10.1029/2002JD002365.

Wetzel, P., et al., 2006. Effects of ocean biology on the penetrative radiation in a coupled climate model. *J. Clim.*, **19**, 3973–3987.

Wickland, K., R. Striegl, J. Neff, and T. Sachs, 2006: Effects of permafrost melting on CO_2 and CH_4 exchange of a poorly drained black spruce lowland. *J. Geophys. Res.*, **111**, G02011, doi:10.1029/2005JG000099.

Wild, O., M.J. Prather, and H. Akimoto, 2001: Indirect long-term global radiative cooling from NO_x emissions. *Geophys. Res. Lett.*, **28**(9), 1719–1722.

Wild, O., P. Pochanart, and H. Akimoto, 2004: Trans-Eurasian transport of ozone and its precursors. *J. Geophys. Res.*, **109**, D11302, doi:10.1029/2003JD004501.

Williams, A.A.J., D.J. Karoly, and N. Tapper, 2001: The sensitivity of Australian fire danger to climate change. *Clim. Change*, **49**, 171–191.

Williams, K.D., et al., 2001: The response of the climate system to the indirect effects of anthropogenic sulphate aerosols. *Clim. Dyn.*, **17**, 845–856.

Williamson, D., et al., 2005: Moisture and temperature at the Atmospheric Radiation Measurement Southern Great Plains site in forecasts with the Community Atmosphere Model (CAM2). *J. Geophys. Res.*, **110**, doi:10.1029/2004JD005109.

WMO, 2003: *Scientific Assessment of Ozone Depletion: 2002*. Global Ozone Research and Monitoring Project Report No. 47, World Meteorological Organization, Geneva, 498 pp.

Wong, S., et al., 2004: A global climate-chemistry model study of present-day tropospheric chemistry and radiative forcing from changes in tropospheric O_3 since the preindustrial period. *J. Geophys. Res.*, **109**, D11309, doi:10.1029/2003JD003998.

Woodward, S., D.L. Roberts, and R.A. Betts, 2005: A simulation of the effect of climate change-induced desertification on mineral dust aerosol. *Geophys. Res. Lett.*, **32**, L18810, doi:10.1029/2005GL023482.

Wuebbles, D.J., and K. Hayhoe, 2002: Atmospheric methane and global change. *Earth Sci. Rev.*, **57**, 177–210.

Wurzler, S., T.G. Reisin, and Z. Levin, 2000: Modification of mineral dust particles by cloud processing and subsequent effects on drop size distributions. *J. Geophys. Res.*, **105**(D4), 4501–4512.

Xiao, Y., et al., 2004: Constraints on Asian and European sources of methane from CH_4-C_2H_6-Co correlation in Asian outflow. *J. Geophys. Res.*, **109**, doi:10.1029/2003JD004475.

Xu, Z., et al., 2004: Effects of elevated CO_2 and N fertilization of CH_4 emissions from paddy rice fields. *Global Biogechem. Cycles*, **18**, GB3009, doi:10.1029/2004GB002233.

Yamasoe, M.A., et al., 2006: Effect of smoke and clouds on the transmissivity of photosynthetically active radiation inside the canopy. *Atmos. Chem. Phys.*, **6**, 1645–1656.

Yan, X., T. Ohara, and H. Akimoto, 2003: Development of region-specific emission factors and estimation of methane emission from rice fields in the East, Southeast, and South Asian countries. *Global Change Biol.*, **9**, 237–254.

Yang, E.-S., D.M. Cunnold, M.J. Newchurch, and R.J. Salawitch, 2005: Change in ozone trends at southern high latitudes. *Geophys. Res. Lett.*, **32**, L12812, doi:10.1029/2004GL022296.

Yang, K., et al., 2004: The daytime evolution of the atmospheric boundary layer and convection over the Tibetan Plateau: observations and simulations. *J. Meteorol. Soc. Japan*, **82**(6), 1777–1792.

Yang, R., and M.A. Friedl, 2003: Modeling the effects of 3-D vegetation structure on surface radiation and energy balance in boreal forests. *J. Geophys. Res.*, **108**(D16), 8615, doi:10.1029/2002JD003109.

Yin, Y., K.S. Carslaw, and G. Feingold, 2005: Vertical transport and processing of aerosols in a mixed-phase convective cloud and the feedback on cloud development. *Q. J. R. Meteorol. Soc.*, **131**, 221–246.

Yin, Y., A. Levin, T.G. Reisin, and S. Tzivion, 2000: The effect of giant cloud condensation nuclei on the development of precipitation in convective clouds - a numerical study. *Atmos. Res.*, **53**, 91–116.

Yin, Y., S. Wurzler, A. Levin, and T.G. Reisin, 2002: Interactions of mineral dust particles and clouds: Effects on precipitation and cloud optical properties. *J. Geophys. Res.*, **107**, doi:10.1029/2001JD001544.

Yurganov, L.N., et al., 2005: Increased Northern Hemispheric carbon monoxide burden in the troposphere in 2002 and 2003 detected from the ground and from space. *Atm. Chem. Phys.*, **5**, 563–573.

Zeebe, R.E., and D. Wolf-Gladrow, 2001: *CO_2 in Seawater: Equilibrium, Kinetics, Isotopes*. Elsevier Oceanography Series 65, Elsevier, Amsterdam, 346 pp.

Zender, C., R.L. Miller, and I. Tegen, 2004: Quantifying mineral dust mass budgets: systematic terminology, constraints, and current estimates. *Eos*, **85**(48), 509, 512.

Zeng, G., and J.A. Pyle, 2003: Changes in tropospheric ozone between 2000 and 2100 modeled in a chemistry-climate model. *Geophys. Res. Lett.*, **30**, 1392, doi:10.1029/2002GL016708.

Zeng, N., K. Hales, and J.D. Neelin, 2002: Nonlinear dynamics in a coupled vegetation-atmosphere system and implications for desert-forest gradient. *J. Clim.*, **15**, 3474–3485.

Zeng, N., A. Mariotti, and P. Wetzel, 2005: Terrestrial mechanisms of interannual CO_2 variability, *Global Biogeochem. Cycles*, **19**, GB1016, doi:10.1029/2004GB002273.

Zeng, N., H. Qian, E. Munoz, and R. Iacono, 2004: How strong is carbon cycle-climate feedback under global warming? *Geophys. Res. Lett.*, **31**, L20203, doi:10.1029/2004GL020904.

Zeng, X.-D., S.S.P. Shen, X. Zeng, and R.E. Dickinson, 2004: Multiple equilibrium states and the abrupt transitions in a dynamical system of soil water interacting with vegetation. *Geophys. Res. Lett.*, **31**, L05501, doi:10.1029/2003GL018910.

Zerefos, C., et al., 1998: Quasi-biennial and longer-term changes in clear sky UV-B solar irradiance. *Geophys. Res. Lett.*, **25**, 4345–4348.

Zhang, J., U. Lohmann, and P. Stier, 2005: A microphysical parameterization for convective clouds in the ECHAM5 climate model, 1. Single column results evaluated at the Oklahoma ARM site. *J. Geophys. Res.*, **110**, doi:10.1029/2004JD005128.

Zhang, X.Y., R. Arimoto, and Z.S. An, 1997: Dust emission from Chinese desert sources linked to variations in atmospheric circulation. *J. Geophys. Res.*, **102**, 28041–28047.

Zhang, X.Y., H.Y. Lu, R. Arimoto, and S.L. Gong, 2002: Atmospheric dust loadings and their relationship to rapid oscillations of the Asian winter monsoon climate: two 250-kyr loess records. *Earth Planet. Sci. Lett.*, **202**, 637–643.

Zhang, X.Y., et al., 2003: Sources of Asian dust and role of climate change versus desertification in Asian dust emission. *Geophys. Res. Lett.*, **30**, 2272, doi:10.1029/2003GL018206.

Zhou, L., R.E. Dickinson, and Y. Tian, 2005: Derivation of a soil albedo dataset from MODIS using principal component analysis: Northern Africa and the Arabian Peninsula. *Geophys. Res. Lett*., **32**, L21407, doi:10.1029/205GL024448.

Zhou, L., et al., 2001: Variations in northern vegetation activity inferred from satellite data of vegetation index during 1981 to 1999. *J. Geophys. Res.*, **106**, 20069–20083.

Zhou, L., et al., 2003a: A sensitivity study of climate and energy balance simulations with use of satellite-derived emissivity data over Northern Africa and the Arabian Peninsula. *J. Geophys. Res.*, **108**(D24), 4795, doi:10.1029/2003JD004083.

Zhou, L., et al., 2003b: Relations between albedos and emissivities from MODIS and ASTER data over North African desert. *Geophys. Res. Lett.*, **30**(20), 2026, doi:10/1029/2003GL018069.

Zhou, L., et al., 2003c: Relation between interannual variations in satellite measures of northern forest greenness and climate between 1982 and 1999. *J. Geophys. Res.*, **108**(D1), 4004, doi:10.1029/2002JD002510.

Zhou, L., et al., 2004: Evidence for a significant urbanization effect on climate in China. *Proc. Natl. Acad. Sci. U.S.A.*, **101**(26), 9540–9544.

Zhuang, Q., et al., 2004: Methane fluxes between terrestrial ecosystem and the atmosphere at northern high latitudes during the past century: A retrospective analysis with a process-based biogeochemistry model. *Global Biogeochem.Cycles*, **18**, doi:10.1029/2008GB002239.

Zittel, W., and M. Altmann, 1996: Molecular hydrogen and water vapour emissions in a global hydrogen energy economy. In: *Proceedings of the 11th World Hydrogen Energy Conference, Stuttgart, Germany, June 1996*. Schön & Wetzel, Frankfurt, Germany, pp. 71–82.

Zondervan, I., R.E. Zeebe, B. Rost, and U. Riebesell, 2001: Decreasing marine biogenic calcification: a negative feedback on rising pCO_2. *Global Biogeochem. Cycles*, **15**, 507–516.

8

Climate Models and Their Evaluation

Coordinating Lead Authors:

David A. Randall (USA), Richard A. Wood (UK)

Lead Authors:

Sandrine Bony (France), Robert Colman (Australia), Thierry Fichefet (Belgium), John Fyfe (Canada), Vladimir Kattsov (Russian Federation), Andrew Pitman (Australia), Jagadish Shukla (USA), Jayaraman Srinivasan (India), Ronald J. Stouffer (USA), Akimasa Sumi (Japan), Karl E. Taylor (USA)

Contributing Authors:

K. AchutaRao (USA), R. Allan (UK), A. Berger (Belgium), H. Blatter (Switzerland), C. Bonfils (USA, France), A. Boone (France, USA), C. Bretherton (USA), A. Broccoli (USA), V. Brovkin (Germany, Russian Federation), W. Cai (Australia), M. Claussen (Germany), P. Dirmeyer (USA), C. Doutriaux (USA, France), H. Drange (Norway), J.-L. Dufresne (France), S. Emori (Japan), P. Forster (UK), A. Frei (USA), A. Ganopolski (Germany), P. Gent (USA), P. Gleckler (USA), H. Goosse (Belgium), R. Graham (UK), J.M. Gregory (UK), R. Gudgel (USA), A. Hall (USA), S. Hallegatte (USA, France), H. Hasumi (Japan), A. Henderson-Sellers (Switzerland), H. Hendon (Australia), K. Hodges (UK), M. Holland (USA), A.A.M. Holtslag (Netherlands), E. Hunke (USA), P. Huybrechts (Belgium), W. Ingram (UK), F. Joos (Switzerland), B. Kirtman (USA), S. Klein (USA), R. Koster (USA), P. Kushner (Canada), J. Lanzante (USA), M. Latif (Germany), N.-C. Lau (USA), M. Meinshausen (Germany), A. Monahan (Canada), J.M. Murphy (UK), T. Osborn (UK), T. Pavlova (Russian Federationi), V. Petoukhov (Germany), T. Phillips (USA), S. Power (Australia), S. Rahmstorf (Germany), S.C.B. Raper (UK), H. Renssen (Netherlands), D. Rind (USA), M. Roberts (UK), A. Rosati (USA), C. Schär (Switzerland), A. Schmittner (USA, Germany), J. Scinocca (Canada), D. Seidov (USA), A.G. Slater (USA, Australia), J. Slingo (UK), D. Smith (UK), B. Soden (USA), W. Stern (USA), D.A. Stone (UK), K.Sudo (Japan), T. Takemura (Japan), G. Tselioudis (USA, Greece), M. Webb (UK), M. Wild (Switzerland)

Review Editors:

Elisa Manzini (Italy), Taroh Matsuno (Japan), Bryant McAvaney (Australia)

This chapter should be cited as:

Randall, D.A., R.A. Wood, S. Bony, R. Colman, T. Fichefet, J. Fyfe, V. Kattsov, A. Pitman, J. Shukla, J. Srinivasan, R.J. Stouffer, A. Sumi and K.E. Taylor, 2007: Cilmate Models and Their Evaluation. In: *Climate Change 2007: The Physical Science Basis. Contribution of Working Group I to the Fourth Assessment Report of the Intergovernmental Panel on Climate Change* [Solomon, S., D. Qin, M. Manning, Z. Chen, M. Marquis, K.B. Averyt, M.Tignor and H.L. Miller (eds.)]. Cambridge University Press, Cambridge, United Kingdom and New York, NY, USA.

Table of Contents

Executive Summary 591

8.1 Introduction and Overview 594

8.1.1 What is Meant by Evaluation? 594
8.1.2 Methods of Evaluation 594
8.1.3 How Are Models Constructed? 596

8.2 Advances in Modelling 596

8.2.1 Atmospheric Processes 602
8.2.2 Ocean Processes 603
8.2.3 Terrestrial Processes 604
8.2.4 Cryospheric Processes 606
8.2.5 Aerosol Modelling and Atmospheric Chemistry 607
8.2.6 Coupling Advances 607
8.2.7 Flux Adjustments and Initialisation 607

8.3 Evaluation of Contemporary Climate as Simulated by Coupled Global Models 608

8.3.1 Atmosphere 608
8.3.2 Ocean 613
8.3.3 Sea Ice 616
8.3.4 Land Surface 617
8.3.5 Changes in Model Performance 618

8.4 Evaluation of Large-Scale Climate Variability as Simulated by Coupled Global Models 620

8.4.1 Northern and Southern Annular Modes 620
8.4.2 Pacific Decadal Variability 621
8.4.3 Pacific-North American Pattern 622
8.4.4 Cold Ocean-Warm Land Pattern 622
8.4.5 Atmospheric Regimes and Blocking 623
8.4.6 Atlantic Multi-decadal Variability 623
8.4.7 El Niño-Southern Oscillation 623
8.4.8 Madden-Julian Oscillation 625
8.4.9 Quasi-Biennial Oscillation 625
8.4.10 Monsoon Variability 626
8.4.11 Shorter-Term Predictions Using Climate Models 626

8.5 Model Simulations of Extremes 627

8.5.1 Extreme Temperature 627
8.5.2 Extreme Precipitation 628
8.5.3 Tropical Cyclones 628
8.5.4 Summary 629

8.6 Climate Sensitivity and Feedbacks 629

8.6.1 Introduction 629
8.6.2 Interpreting the Range of Climate Sensitivity Estimates Among General Circulation Models 629

Box 8.1: Upper-Tropospheric Humidity and Water Vapour Feedback 632

8.6.3 Key Physical Processes Involved in Climate Sensitivity 633
8.6.4 How to Assess Our Relative Confidence in Feedbacks Simulated by Different Models? 639

8.7 Mechanisms Producing Thresholds and Abrupt Climate Change 640

8.7.1 Introduction 640
8.7.2 Forced Abrupt Climate Change 640
8.7.3 Unforced Abrupt Climate Change 643

8.8 Representing the Global System with Simpler Models 643

8.8.1 Why Lower Complexity? 643
8.8.2 Simple Climate Models 644
8.8.3 Earth System Models of Intermediate Complexity 644

Frequently Asked Question

FAQ 8.1: *How Reliable Are the Models Used to Make Projections of Future Climate Change?* 600

References 648

Supplementary Material

The following supplementary material is available on CD-ROM and in on-line versions of this report.

Figures S8.1–S8.15: *Model Simulations for Different Climate Variables*

Table S8.1: *MAGICC Parameter Values*

Executive Summary

This chapter assesses the capacity of the global climate models used elsewhere in this report for projecting future climate change. Confidence in model estimates of future climate evolution has been enhanced via a range of advances since the IPCC Third Assessment Report (TAR).

Climate models are based on well-established physical principles and have been demonstrated to reproduce observed features of recent climate (see Chapters 8 and 9) and past climate changes (see Chapter 6). There is considerable confidence that Atmosphere-Ocean General Circulation Models (AOGCMs) provide credible quantitative estimates of future climate change, particularly at continental and larger scales. Confidence in these estimates is higher for some climate variables (e.g., temperature) than for others (e.g., precipitation). This summary highlights areas of progress since the TAR:

- Enhanced scrutiny of models and expanded diagnostic analysis of model behaviour have been increasingly facilitated by internationally coordinated efforts to collect and disseminate output from model experiments performed under common conditions. This has encouraged a more comprehensive and open evaluation of models. The expanded evaluation effort, encompassing a diversity of perspectives, makes it less likely that significant model errors are being overlooked.

- Climate models are being subjected to more comprehensive tests, including, for example, evaluations of forecasts on time scales from days to a year. This more diverse set of tests increases confidence in the fidelity with which models represent processes that affect climate projections.

- Substantial progress has been made in understanding the inter-model differences in equilibrium climate sensitivity. Cloud feedbacks have been confirmed as a primary source of these differences, with low clouds making the largest contribution. New observational and modelling evidence strongly supports a combined water vapour-lapse rate feedback of a strength comparable to that found in General Circulation Models (approximately 1 W m^{-2} $°C^{-1}$, corresponding to around a 50% amplification of global mean warming). The magnitude of cryospheric feedbacks remains uncertain, contributing to the range of model climate responses at mid- to high latitudes.

- There have been ongoing improvements to resolution, computational methods and parametrizations, and additional processes (e.g., interactive aerosols) have been included in more of the climate models.

- Most AOGCMs no longer use flux adjustments, which were previously required to maintain a stable climate. At the same time, there have been improvements in the simulation of many aspects of present climate. The uncertainty associated with the use of flux adjustments has therefore decreased, although biases and long-term trends remain in AOGCM control simulations.

- Progress in the simulation of important modes of climate variability has increased the overall confidence in the models' representation of important climate processes. As a result of steady progress, some AOGCMs can now simulate important aspects of the El Niño-Southern Oscillation (ENSO). Simulation of the Madden-Julian Oscillation (MJO) remains unsatisfactory.

- The ability of AOGCMs to simulate extreme events, especially hot and cold spells, has improved. The frequency and amount of precipitation falling in intense events are underestimated.

- Simulation of extratropical cyclones has improved. Some models used for projections of tropical cyclone changes can simulate successfully the observed frequency and distribution of tropical cyclones.

- Systematic biases have been found in most models' simulation of the Southern Ocean. Since the Southern Ocean is important for ocean heat uptake, this results in some uncertainty in transient climate response.

- The possibility that metrics based on observations might be used to constrain model projections of climate change has been explored for the first time, through the analysis of ensembles of model simulations. Nevertheless, a proven set of model metrics that might be used to narrow the range of plausible climate projections has yet to be developed.

- To explore the potential importance of carbon cycle feedbacks in the climate system, explicit treatment of the carbon cycle has been introduced in a few climate AOGCMs and some Earth System Models of Intermediate Complexity (EMICs).

- Earth System Models of Intermediate Complexity have been evaluated in greater depth than previously. Coordinated intercomparisons have demonstrated that these models are useful in addressing questions involving long time scales or requiring a large number of ensemble simulations or sensitivity experiments.

Developments in model formulation

Improvements in atmospheric models include reformulated dynamics and transport schemes, and increased horizontal and vertical resolution. Interactive aerosol modules have been incorporated into some models, and through these, the direct and the indirect effects of aerosols are now more widely included.

Significant developments have occurred in the representation of terrestrial processes. Individual components continue to be improved via systematic evaluation against observations and against more comprehensive models. The terrestrial processes that might significantly affect large-scale climate over the next few decades are included in current climate models. Some processes important on longer time scales are not yet included.

Development of the oceanic component of AOGCMs has continued. Resolution has increased and models have generally abandoned the 'rigid lid' treatment of the ocean surface. New physical parametrizations and numerics include true freshwater fluxes, improved river and estuary mixing schemes and the use of positive definite advection schemes. Adiabatic isopycnal mixing schemes are now widely used. Some of these improvements have led to a reduction in the uncertainty associated with the use of less sophisticated parametrizations (e.g., virtual salt flux).

Progress in developing AOGCM cryospheric components is clearest for sea ice. Almost all state-of-the-art AOGCMs now include more elaborate sea ice dynamics and some now include several sea ice thickness categories and relatively advanced thermodynamics. Parametrizations of terrestrial snow processes in AOGCMs vary considerably in formulation. Systematic evaluation of snow suggests that sub-grid scale heterogeneity is important for simulating observations of seasonal snow cover. Few AOGCMs include ice sheet dynamics; in all of the AOGCMs evaluated in this chapter and used in Chapter 10 for projecting climate change in the 21st century, the land ice cover is prescribed.

There is currently no consensus on the optimal way to divide computer resources among: finer numerical grids, which allow for better simulations; greater numbers of ensemble members, which allow for better statistical estimates of uncertainty; and inclusion of a more complete set of processes (e.g., carbon feedbacks, atmospheric chemistry interactions).

Developments in model climate simulation

The large-scale patterns of seasonal variation in several important atmospheric fields are now better simulated by AOGCMs than they were at the time of the TAR. Notably, errors in simulating the monthly mean, global distribution of precipitation, sea level pressure and surface air temperature have all decreased. In some models, simulation of marine low-level clouds, which are important for correctly simulating sea surface temperature and cloud feedback in a changing climate, has also improved. Nevertheless, important deficiencies remain in the simulation of clouds and tropical precipitation (with their important regional and global impacts).

Some common model biases in the Southern Ocean have been identified, resulting in some uncertainty in oceanic heat uptake and transient climate response. Simulations of the thermocline, which was too thick, and the Atlantic overturning and heat transport, which were both too weak, have been substantially improved in many models.

Despite notable progress in improving sea ice formulations, AOGCMs have typically achieved only modest progress in simulations of observed sea ice since the TAR. The relatively slow progress can partially be explained by the fact that improving sea ice simulation requires improvements in both the atmosphere and ocean components in addition to the sea ice component itself.

Since the TAR, developments in AOGCM formulation have improved the representation of large-scale variability over a wide range of time scales. The models capture the dominant extratropical patterns of variability including the Northern and Southern Annular Modes, the Pacific Decadal Oscillation, the Pacific-North American and Cold Ocean-Warm Land Patterns. AOGCMs simulate Atlantic multi-decadal variability, although the relative roles of high- and low-latitude processes appear to differ between models. In the tropics, there has been an overall improvement in the AOGCM simulation of the spatial pattern and frequency of ENSO, but problems remain in simulating its seasonal phase locking and the asymmetry between El Niño and La Niña episodes. Variability with some characteristics of the MJO is simulated by most AOGCMs, but the events are typically too infrequent and too weak.

Atmosphere-Ocean General Circulation Models are able to simulate extreme warm temperatures, cold air outbreaks and frost days reasonably well. Models used in this report for projecting tropical cyclone changes are able to simulate present-day frequency and distribution of cyclones, but intensity is less well simulated. Simulation of extreme precipitation is dependent on resolution, parametrization and the thresholds chosen. In general, models tend to produce too many days with weak precipitation (<10 mm day^{-1}) and too little precipitation overall in intense events (>10 mm day^{-1}).

Earth system Models of Intermediate Complexity have been developed to investigate issues in past and future climate change that cannot be addressed by comprehensive AOGCMs because of their large computational cost. Owing to the reduced resolution of EMICs and their simplified representation of some physical processes, these models only allow inferences about very large scales. Since the TAR, EMICs have been evaluated via several coordinated model intercomparisons which have revealed that, at large scales, EMIC results compare well with observational data and AOGCM results. This lends support to the view that EMICS can be used to gain understanding of processes and interactions within the climate system that evolve on time scales beyond those generally accessible to current AOGCMs. The uncertainties in long-term climate change projections can also be explored more comprehensively by using large ensembles of EMIC runs.

Developments in analysis methods

Since the TAR, an unprecedented effort has been initiated to make available new model results for scrutiny by scientists outside the modelling centres. Eighteen modelling groups performed a set of coordinated, standard experiments, and the resulting model output, analysed by hundreds of researchers worldwide, forms the basis for much of the current IPCC assessment of model results. The benefits of coordinated model intercomparison include increased communication among modelling groups, more rapid identification and correction of errors, the creation of standardised benchmark calculations and a more complete and systematic record of modelling progress.

A few climate models have been tested for (and shown) capability in initial value predictions, on time scales from weather forecasting (a few days) to seasonal forecasting (annual). The capability demonstrated by models under these conditions increases confidence that they simulate some of the key processes and teleconnections in the climate system.

Developments in evaluation of climate feedbacks

Water vapour feedback is the most important feedback enhancing climate sensitivity. Although the strength of this feedback varies somewhat among models, its overall impact on the spread of model climate sensitivities is reduced by lapse rate feedback, which tends to be anti-correlated. Several new studies indicate that modelled lower- and upper-tropospheric humidity respond to seasonal and interannual variability, volcanically induced cooling and climate trends in a way that is consistent with observations. Recent observational and modelling evidence thus provides strong additional support for the combined water vapour-lapse rate feedback being around the strength found in AOGCMs.

Recent studies reaffirm that the spread of climate sensitivity estimates among models arises primarily from inter-model differences in cloud feedbacks. The shortwave impact of changes in boundary-layer clouds, and to a lesser extent mid-level clouds, constitutes the largest contributor to inter-model differences in global cloud feedbacks. The relatively poor simulation of these clouds in the present climate is a reason for some concern. The response to global warming of deep convective clouds is also a substantial source of uncertainty in projections since current models predict different responses of these clouds. Observationally based evaluation of cloud feedbacks indicates that climate models exhibit different strengths and weaknesses, and it is not yet possible to determine which estimates of the climate change cloud feedbacks are the most reliable.

Despite advances since the TAR, substantial uncertainty remains in the magnitude of cryospheric feedbacks within AOGCMs. This contributes to a spread of modelled climate response, particularly at high latitudes. At the global scale, the surface albedo feedback is positive in all the models, and varies between models much less than cloud feedbacks. Understanding and evaluating sea ice feedbacks is complicated by the strong coupling to polar cloud processes and ocean heat and freshwater transport. Scarcity of observations in polar regions also hampers evaluation. New techniques that evaluate surface albedo feedbacks have recently been developed. Model performance in reproducing the observed seasonal cycle of land snow cover may provide an indirect evaluation of the simulated snow-albedo feedback under climate change.

Systematic model comparisons have helped establish the key processes responsible for differences among models in the response of the ocean to climate change. The importance of feedbacks from surface flux changes to the meridional overturning circulation has been established in many models. At present, these feedbacks are not tightly constrained by available observations.

The analysis of processes contributing to climate feedbacks in models and recent studies based on large ensembles of models suggest that in the future it may be possible to use observations to narrow the current spread in model projections of climate change.

8.1 Introduction and Overview

The goal of this chapter is to evaluate the capabilities and limitations of the global climate models used elsewhere in this assessment. A number of model evaluation activities are described in various chapters of this report. This section provides a context for those studies and a guide to direct the reader to the appropriate chapters.

8.1.1 What is Meant by Evaluation?

A specific prediction based on a model can often be demonstrated to be right or wrong, but the model itself should always be viewed critically. This is true for both weather prediction and climate prediction. Weather forecasts are produced on a regular basis, and can be quickly tested against what actually happened. Over time, statistics can be accumulated that give information on the performance of a particular model or forecast system. In climate change simulations, on the other hand, models are used to make projections of possible future changes over time scales of many decades and for which there are no precise past analogues. Confidence in a model can be gained through simulations of the historical record, or of palaeoclimate, but such opportunities are much more limited than are those available through weather prediction. These and other approaches are discussed below.

8.1.2 Methods of Evaluation

A climate model is a very complex system, with many components. The model must of course be tested at the system level, that is, by running the full model and comparing the results with observations. Such tests can reveal problems, but their source is often hidden by the model's complexity. For this reason, it is also important to test the model at the component level, that is, by isolating particular components and testing them independent of the complete model.

Component-level evaluation of climate models is common. Numerical methods are tested in standardised tests, organised through activities such as the quasi-biennial Workshops on Partial Differential Equations on the Sphere. Physical parametrizations used in climate models are being tested through numerous case studies (some based on observations and some idealised), organised through programs such as the Atmospheric Radiation Measurement (ARM) program, EUROpean Cloud Systems (EUROCS) and the Global Energy and Water cycle Experiment (GEWEX) Cloud System Study (GCSS). These activities have been ongoing for a decade or more, and a large body of results has been published (e.g., Randall et al., 2003).

System-level evaluation is focused on the outputs of the full model (i.e., model simulations of particular observed climate variables) and particular methods are discussed in more detail below.

8.1.2.1 Model Intercomparisons and Ensembles

The global model intercomparison activities that began in the late 1980s (e.g., Cess et al., 1989), and continued with the Atmospheric Model Intercomparison Project (AMIP), have now proliferated to include several dozen model intercomparison projects covering virtually all climate model components and various coupled model configurations (see http://www.clivar.org/science/mips.php for a summary). By far the most ambitious organised effort to collect and analyse Atmosphere-Ocean General Circulation Model (AOGCM) output from standardised experiments was undertaken in the last few years (see http://www-pcmdi.llnl.gov/ipcc/about_ipcc.php). It differed from previous model intercomparisons in that a more complete set of experiments was performed, including unforced control simulations, simulations attempting to reproduce observed climate change over the instrumental period and simulations of future climate change. It also differed in that, for each experiment, multiple simulations were performed by some individual models to make it easier to separate climate change signals from internal variability within the climate system. Perhaps the most important change from earlier efforts was the collection of a more comprehensive set of model output, hosted centrally at the Program for Climate Model Diagnosis and Intercomparison (PCMDI). This archive, referred to here as 'The Multi-Model Data set (MMD) at PCMDI', has allowed hundreds of researchers from outside the modelling groups to scrutinise the models from a variety of perspectives.

The enhancement in diagnostic analysis of climate model results represents an important step forward since the Third Assessment Report (TAR). Overall, the vigorous, ongoing intercomparison activities have increased communication among modelling groups, allowed rapid identification and correction of modelling errors and encouraged the creation of standardised benchmark calculations, as well as a more complete and systematic record of modelling progress.

Ensembles of models represent a new resource for studying the range of plausible climate responses to a given forcing. Such ensembles can be generated either by collecting results from a range of models from different modelling centres ('multi-model ensembles' as described above), or by generating multiple model versions within a particular model structure, by varying internal model parameters within plausible ranges ('perturbed physics ensembles'). The approaches are discussed in more detail in Section 10.5.

8.1.2.2 Metrics of Model Reliability

What does the accuracy of a climate model's simulation of past or contemporary climate say about the accuracy of its projections of climate change? This question is just beginning to be addressed, exploiting the newly available ensembles of models. A number of different observationally based metrics have been used to weight the reliability of contributing models when making probabilistic projections (see Section 10.5.4).

For any given metric, it is important to assess how good a test it is of model results for making projections of future climate change. This cannot be tested directly, since there are no observed periods with forcing changes exactly analogous to those expected over the 21st century. However, relationships between observable metrics and the predicted quantity of interest (e.g., climate sensitivity) can be explored across model ensembles. Shukla et al. (2006) correlated a measure of the fidelity of the simulated surface temperature in the 20th century with simulated 21st-century temperature change in a multi-model ensemble. They found that the models with the smallest 20th-century error produced relatively large surface temperature increases in the 21st century. Knutti et al. (2006), using a different, perturbed physics ensemble, showed that models with a strong seasonal cycle in surface temperature tended to have larger climate sensitivity. More complex metrics have also been developed based on multiple observables in present day climate, and have been shown to have the potential to narrow the uncertainty in climate sensitivity across a given model ensemble (Murphy et al., 2004; Piani et al., 2005). The above studies show promise that quantitative metrics for the likelihood of model projections may be developed, but because the development of robust metrics is still at an early stage, the model evaluations presented in this chapter are based primarily on experience and physical reasoning, as has been the norm in the past.

An important area of progress since the TAR has been in establishing and quantifying the feedback processes that determine climate change response. Knowledge of these processes underpins both the traditional and the metric-based approaches to model evaluation. For example, Hall and Qu (2006) developed a metric for the feedback between temperature and albedo in snow-covered regions, based on the simulation of the seasonal cycle. They found that models with a strong feedback based on the seasonal cycle also had a strong feedback under increased greenhouse gas forcing. Comparison with observed estimates of the seasonal cycle suggested that most models in the MMD underestimate the strength of this feedback. Section 8.6 discusses the various feedbacks that operate in the atmosphere-land surface-sea ice system to determine climate sensitivity, and Section 8.3.2 discusses some processes that are important for ocean heat uptake (and hence transient climate response).

8.1.2.3 Testing Models Against Past and Present Climate

Testing models' ability to simulate 'present climate' (including variability and extremes) is an important part of model evaluation (see Sections 8.3 to 8.5, and Chapter 11 for specific regional evaluations). In doing this, certain practical choices are needed, for example, between a long time series or mean from a 'control' run with fixed radiative forcing (often pre-industrial rather than present day), or a shorter, transient time series from a '20th-century' simulation including historical variations in forcing. Such decisions are made by individual researchers, dependent on the particular problem being studied. Differences between model and observations should be considered insignificant if they are within:

1. unpredictable internal variability (e.g., the observational period contained an unusual number of El Niño events);
2. expected differences in forcing (e.g., observations for the 1990s compared with a 'pre-industrial' model control run); or
3. uncertainties in the observed fields.

While space does not allow a discussion of the above issues in detail for each climate variable, they are taken into account in the overall evaluation. Model simulation of present-day climate at a global to sub-continental scale is discussed in this chapter, while more regional detail can be found in Chapter 11.

Models have been extensively used to simulate observed climate change during the 20th century. Since forcing changes are not perfectly known over that period (see Chapter 2), such tests do not fully constrain future response to forcing changes. Knutti et al. (2002) showed that in a perturbed physics ensemble of Earth System Models of Intermediate Complexity (EMICs), simulations from models with a range of climate sensitivities are consistent with the observed surface air temperature and ocean heat content records, if aerosol forcing is allowed to vary within its range of uncertainty. Despite this fundamental limitation, testing of 20th-century simulations against historical observations does place some constraints on future climate response (e.g., Knutti et al., 2002). These topics are discussed in detail in Chapter 9.

8.1.2.4 Other Methods of Evaluation

Simulations of climate states from the more distant past allow models to be evaluated in regimes that are significantly different from the present. Such tests complement the 'present climate' and 'instrumental period climate' evaluations, since 20th-century climate variations have been small compared with the anticipated future changes under forcing scenarios derived from the IPCC Special Report on Emission Scenarios (SRES). The limitations of palaeoclimate tests are that uncertainties in both forcing and actual climate variables (usually derived from proxies) tend to be greater than in the instrumental period, and that the number of climate variables for which there are good palaeo-proxies is limited. Further, climate states may have been so different (e.g., ice sheets at last glacial maximum) that processes determining quantities such as climate sensitivity were different from those likely to operate in the 21st century. Finally, the time scales of change were so long that there are difficulties in experimental design, at least for General Circulation Models (GCMs). These issues are discussed in depth in Chapter 6.

Climate models can be tested through forecasts based on initial conditions. Climate models are closely related to the models that are used routinely for numerical weather prediction, and increasingly for extended range forecasting on seasonal to interannual time scales. Typically, however, models used

for numerical weather prediction are run at higher resolution than is possible for climate simulations. Evaluation of such forecasts tests the models' representation of some key processes in the atmosphere and ocean, although the links between these processes and long-term climate response have not always been established. It must be remembered that the quality of an initial value prediction is dependent on several factors beyond the numerical model itself (e.g., data assimilation techniques, ensemble generation method), and these factors may be less relevant to projecting the long-term, forced response of the climate system to changes in radiative forcing. There is a large body of literature on this topic, but to maintain focus on the goal of this chapter, discussions here are confined to the relatively few studies that have been conducted using models that are very closely related to the climate models used for projections (see Section 8.4.11).

8.1.3 How Are Models Constructed?

The fundamental basis on which climate models are constructed has not changed since the TAR, although there have been many specific developments (see Section 8.2). Climate models are derived from fundamental physical laws (such as Newton's laws of motion), which are then subjected to physical approximations appropriate for the large-scale climate system, and then further approximated through mathematical discretization. Computational constraints restrict the resolution that is possible in the discretized equations, and some representation of the large-scale impacts of unresolved processes is required (the parametrization problem).

8.1.3.1 Parameter Choices and 'Tuning'

Parametrizations are typically based in part on simplified physical models of the unresolved processes (e.g., entraining plume models in some convection schemes). The parametrizations also involve numerical parameters that must be specified as input. Some of these parameters can be measured, at least in principle, while others cannot. It is therefore common to adjust parameter values (possibly chosen from some prior distribution) in order to optimise model simulation of particular variables or to improve global heat balance. This process is often known as 'tuning'. It is justifiable to the extent that two conditions are met:

1. Observationally based constraints on parameter ranges are not exceeded. Note that in some cases this may not provide a tight constraint on parameter values (e.g., Heymsfield and Donner, 1990).

2. The number of degrees of freedom in the tuneable parameters is less than the number of degrees of freedom in the observational constraints used in model evaluation. This is believed to be true for most GCMs – for example, climate models are not explicitly tuned to give a good representation of North Atlantic Oscillation (NAO) variability – but no studies are available that formally address the question. If the model has been tuned to give a good representation of a particular observed quantity, then agreement with that observation cannot be used to build confidence in that model. However, a model that has been tuned to give a good representation of certain key observations may have a greater likelihood of giving a good prediction than a similar model (perhaps another member of a 'perturbed physics' ensemble) that is less closely tuned (as discussed in Section 8.1.2.2 and Chapter 10).

Given sufficient computer time, the tuning procedure can in principle be automated using various data assimilation procedures. To date, however, this has only been feasible for EMICs (Hargreaves et al., 2004) and low-resolution GCMs (Annan et al., 2005b; Jones et al., 2005; Severijns and Hazeleger, 2005). Ensemble methods (Murphy et al., 2004; Annan et al., 2005a; Stainforth et al., 2005) do not always produce a unique 'best' parameter setting for a given error measure.

8.1.3.2 Model Spectra or Hierarchies

The value of using a range of models (a 'spectrum' or 'hierarchy') of differing complexity is discussed in the TAR (Section 8.3), and here in Section 8.8. Computationally cheaper models such as EMICs allow a more thorough exploration of parameter space, and are simpler to analyse to gain understanding of particular model responses. Models of reduced complexity have been used more extensively in this report than in the TAR, and their evaluation is discussed in Section 8.8. Regional climate models can also be viewed as forming part of a climate modelling hierarchy.

8.2 Advances in Modelling

Many modelling advances have occurred since the TAR. Space does not permit a comprehensive discussion of all major changes made over the past several years to the 23 AOGCMs used widely in this report (see Table 8.1). Model improvements can, however, be grouped into three categories. First, the dynamical cores (advection, etc.) have been improved, and the horizontal and vertical resolutions of many models have been increased. Second, more processes have been incorporated into the models, in particular in the modelling of aerosols, and of land surface and sea ice processes. Third, the parametrizations of physical processes have been improved. For example, as discussed further in Section 8.2.7, most of the models no longer use flux adjustments (Manabe and Stouffer, 1988; Sausen et al., 1988) to reduce climate drift. These various improvements, developed across the broader modelling community, are well represented in the climate models used in this report.

Despite the many improvements, numerous issues remain. Many of the important processes that determine a model's response to changes in radiative forcing are not resolved by

Table 8.1. *Selected model features. Salient features of the AOGCMs participating in the MMD at PCMDI are listed by IPCC identification (ID) along with the calendar year ('vintage') of the first publication of results from each model. Also listed are the respective sponsoring institutions, the pressure at the top of the atmospheric model, the horizontal and vertical resolution of the model atmosphere and ocean models, as well as the oceanic vertical coordinate type (Z: see Griffies (2004) for definitions) and upper boundary condition (BC: free surface or rigid lid). Also listed are the characteristics of sea ice dynamics/structure (e.g., rheology vs 'free drift' assumption and inclusion of ice leads), and whether adjustments of surface momentum, heat or freshwater fluxes are applied in coupling the atmosphere, ocean and sea ice components. Land features such as the representation of soil moisture (single-layer 'bucket' vs multi-layered scheme) and the presence of a vegetation canopy or a river routing scheme also are noted. Relevant references describing details of these aspects of the models are cited.*

Model ID, Vintage	Sponsor(s), Country	Atmosphere Top Resolution[a] References	Ocean Resolution[b] Z Coord., Top BC References	Sea Ice Dynamics, Leads References	Coupling Flux Adjustments References	Land Soil, Plants, Routing References
1: BCC-CM1, 2005	Beijing Climate Center, China	top = 25 hPa T63 (1.9° x 1.9°) L16 Dong et al., 2000; CSMD, 2005; Xu et al., 2005	1.9° x 1.9° L30 depth, free surface Jin et al., 1999	no rheology or leads Xu et al., 2005	heat, momentum Yu and Zhang, 2000; CSMD, 2005	layers, canopy, routing CSMD, 2005
2: BCCR-BCM2.0, 2005	Bjerknes Centre for Climate Research, Norway	top = 10 hPa T63 (1.9° x 1.9°) L31 Déqué et al., 1994	0.5°–1.5° x 1.5° L35 density, free surface Bleck et al., 1992	rheology, leads Hibler, 1979; Harder, 1996	no adjustments Furevik et al., 2003	Layers, canopy, routing Mahfouf et al., 1995; Douville et al., 1995; Oki and Sud, 1998
3: CCSM3, 2005	National Center for Atmospheric Research, USA	top = 2.2 hPa T85 (1.4° x 1.4°) L26 Collins et al., 2004	0.3°–1° x 1° L40 depth, free surface Smith and Gent, 2002	rheology, leads Briegleb et al., 2004	no adjustments Collins et al., 2006	layers, canopy, routing Oleson et al., 2004; Branstetter, 2001
4: CGCM3.1(T47), 2005	Canadian Centre for Climate Modelling and Analysis, Canada	top = 1 hPa T47 (~2.8° x 2.8°) L31 McFarlane et al., 1992; Flato, 2005	1.9° x 1.9° L29 depth, rigid lid Pacanowski et al., 1993	rheology, leads Hibler, 1979; Flato and Hibler, 1992	heat, freshwater Flato, 2005	layers, canopy, routing Verseghy et al., 1993
5: CGCM3.1(T63), 2005		top = 1 hPa T63 (~1.9° x 1.9°) L31 McFarlane et al., 1992; Flato 2005	0.9° x 1.4° L29 depth, rigid lid Flato and Boer, 2001; Kim et al., 2002	rheology, leads Hibler, 1979; Flato and Hibler, 1992	heat, freshwater Flato, 2005	layers, canopy, routing Verseghy et al., 1993
6: CNRM-CM3, 2004	Météo-France/Centre National de Recherches Météorologiques, France	top = 0.05 hPa T63 (~1.9° x 1.9°) L45 Déqué et al., 1994	0.5°–2° x 2° L31 depth, rigid lid Madec et al., 1998	rheology, leads Hunke-Dukowicz, 1997; Salas-Mélia, 2002	no adjustments Terray et al., 1998	layers, canopy,routing Mahfouf et al., 1995; Douville et al., 1995; Oki and Sud, 1998
7: CSIRO-MK3.0, 2001	Commonwealth Scientific and Industrial Research Organisation (CSIRO) Atmospheric Research, Australia	top = 4.5 hPa T63 (~1.9° x 1.9°) L18 Gordon et al., 2002	0.8° x 1.9° L31 depth, rigid lid Gordon et al., 2002	rheology, leads O'Farrell, 1998	no adjustments Gordon et al., 2002	layers, canopy Gordon et al., 2002
8: ECHAM5/MPI-OM, 2005	Max Planck Institute for Meteorology, Germany	top = 10 hPa T63 (~1.9° x 1.9°) L31 Roeckner et al., 2003	1.5° x 1.5° L40 depth, free surface Marsland et al., 2003	rheology, leads Hibler, 1979; Semtner, 1976	no adjustments Jungclaus et al., 2005	bucket, canopy, routing Hagemann, 2002; Hagemann and Dümenil-Gates, 2001
9: ECHO-G, 1999	Meteorological Institute of the University of Bonn, Meteorological Research Institute of the Korea Meteorological Administration (KMA), and Model and Data Group, Germany/Korea	top = 10 hPa T30 (~3.9° x 3.9°) L19 Roeckner et al., 1996	0.5°–2.8° x 2.8° L20 depth, free surface Wolff et al., 1997	rheology, leads Wolff et al., 1997	heat, freshwater Min et al., 2005	bucket, canopy, routing Roeckner et al., 1996; Dümenil and Todini, 1992

Table 8.1 (continued)

Model ID, Vintage	Sponsor(s), Country	Atmosphere Top Resolution[a] References	Ocean Resolution[b] Z Coord., Top BC References	Sea Ice Dynamics, Leads References	Coupling Flux Adjustments References	Land Soil, Plants, Routing References
10: FGOALS-g1.0, 2004	National Key Laboratory of Numerical Modeling for Atmospheric Sciences and Geophysical Fluid Dynamics (LASG)/Institute of Atmospheric Physics, China	top = 2.2 hPa T42 (~2.8° x 2.8°) L26 Wang et al., 2004	1.0° x 1.0° L16 eta, free surface Jin et al., 1999; Liu et al., 2004	rheology, leads Briegleb et al., 2004	no adjustments Yu et al., 2002, 2004	layers, canopy, routing Bonan et al., 2002
11: GFDL-CM2.0, 2005	U.S. Department of Commerce/ National Oceanic and Atmospheric Administration (NOAA)/Geophysical Fluid Dynamics Laboratory (GFDL), USA	top = 3 hPa 2.0° x 2.5° L24 GFDL GAMDT, 2004	0.3°–1.0° x 1.0° depth, free surface Gnanadesikan et al., 2004	rheology, leads Winton, 2000; Delworth et al., 2006	no adjustments Delworth et al., 2006	bucket, canopy, routing Milly and Shmakin, 2002; GFDL GAMDT, 2004
12: GFDL-CM2.1, 2005		top = 3 hPa 2.0° x 2.5° L24 GFDL GAMDT, 2004 with semi-Lagrangian transports	0.3°–1.0° x 1.0° depth, free surface Gnanadesikan et al., 2004	rheology, leads Winton, 2000; Delworth et al., 2006	no adjustments Delworth et al., 2006	bucket, canopy, routing Milly and Shmakin, 2002; GFDL GAMDT, 2004
13: GISS-AOM, 2004	National Aeronautics and Space Administration (NASA)/ Goddard Institute for Space Studies (GISS), USA	top = 10 hPa 3° x 4° L12 Russell et al., 1995; Russell, 2005	3° x 4° L16 mass/area, free surface Russell et al., 1995; Russell, 2005	rheology, leads Flato and Hibler, 1992; Russell, 2005	no adjustments Russell, 2005	layers, canopy, routing Abramopoulos et al., 1988; Miller et al., 1994
14: GISS-EH, 2004		top = 0.1 hPa 4° x 5° L20 Schmidt et al., 2006	2° x 2° L16 density, free surface Bleck, 2002	rheology, leads Liu et al., 2003; Schmidt et al., 2004	no adjustments Schmidt et al., 2006	layers, canopy, routing Friend and Kiang, 2005
15: GISS-ER, 2004	NASA/GISS, USA	top = 0.1 hPa 4° x 5° L20 Schmidt et al., 2006	4° x 5° L13 mass/area, free surface Russell et al., 1995	rheology, leads Liu et al., 2003; Schmidt et al., 2004	no adjustments Schmidt et al., 2006	layers, canopy, routing Friend and Kiang, 2005
16: INM-CM3.0, 2004	Institute for Numerical Mathematics, Russia	top = 10 hPa 4° x 5° L21 Alekseev et al., 1998; Galin et al., 2003	2° x 2.5° L33 sigma, rigid lid Diansky et al., 2002	no rheology or leads Diansky et al., 2002	regional freshwater Diansky and Volodin, 2002; Volodin and Diansky, 2004	layers, canopy, no routing Alekseev et al., 1998; Volodin and Lykosoff, 1998
17: IPSL-CM4, 2005	Institut Pierre Simon Laplace, France	top = 4 hPa 2.5° x 3.75° L19 Hourdin et al., 2006	2° x 2° L31 depth, free surface Madec et al., 1998	rheology, leads Fichefet and Morales Maqueda, 1997; Goosse and Fichefet, 1999	no adjustments Marti et al., 2005	layers, canopy, routing Krinner et al., 2005
18: MIROC3.2(hires), 2004	Center for Climate System Research (University of Tokyo), National Institute for Environmental Studies, and Frontier Research Center for Global Change (JAMSTEC), Japan	top = 40 km T106 (~1.1° x 1.1°) L56 K-1 Developers, 2004	0.2° x 0.3° L47 sigma/depth, free surface K-1 Developers, 2004	rheology, leads K-1 Developers, 2004	no adjustments K-1 Developers, 2004	layers, canopy, routing K-1 Developers, 2004; Oki and Sud, 1998
19: MIROC3.2(medres), 2004		top = 30 km T42 (~2.8° x 2.8°) L20 K-1 Developers, 2004	0.5°–1.4° x 1.4° L43 sigma/depth, free surface K-1 Developers, 2004	rheology, leads K-1 Developers, 2004	no adjustments K-1 Developers, 2004	layers, canopy, routing K-1 Developers, 2004; Oki and Sud, 1998

Table 8.1 (continued)

Model ID, Vintage	Sponsor(s), Country	Atmosphere Top Resolution[a] References	Ocean Resolution[b] Z Coord., Top BC References	Sea Ice Dynamics, Leads References	Coupling Flux Adjustments References	Land Soil, Plants, Routing References
20: MRI-CGCM2.3.2, 2003	Meteorological Research Institute, Japan	top = 0.4 hPa T42 (~2.8° x 2.8°) L30 Shibata et al., 1999	0.5°–2.0° x 2.5° L23 depth, rigid lid Yukimoto et al., 2001	free drift, leads Mellor and Kantha, 1989	heat, freshwater, momentum (12°S–12°N) Yukimoto et al., 2001; Yukimoto and Noda, 2003	layers, canopy, routing Sellers et al., 1986; Sato et al., 1989
21: PCM, 1998	National Center for Atmospheric Research, USA	top = 2.2 hPa T42 (~2.8° x 2.8°) L26 Kiehl et al., 1998	0.5°–0.7° x 1.1° L40 depth, free surface Maltrud et al., 1998	rheology, leads Hunke and Dukowicz 1997, 2003; Zhang et al., 1999	no adjustments Washington et al., 2000	layers, canopy, no routing Bonan, 1998
22: UKMO-HadCM3, 1997	Hadley Centre for Climate Prediction and Research/Met Office, UK	top = 5 hPa 2.5° x 3.75° L19 Pope et al., 2000	1.25° x 1.25° L20 depth, rigid lid Gordon et al., 2000	free drift, leads Cattle and Crossley, 1995	no adjustments Gordon et al., 2000	layers, canopy, routing Cox et al., 1999
23: UKMO-HadGEM1, 2004		top = 39.2 km ~1.3° x 1.9° L38 Martin et al., 2004	0.3°–1.0° x 1.0° L40 depth, free surface Roberts, 2004	rheology, leads Hunke and Dukowicz, 1997; Semtner, 1976; Lipscomb, 2001	no adjustments Johns et al., 2006	layers, canopy, routing Essery et al., 2001; Oki and Sud, 1998

Notes:

[a] Horizontal resolution is expressed either as degrees latitude by longitude or as a triangular (T) spectral truncation with a rough translation to degrees latitude and longitude. Vertical resolution (L) is the number of vertical levels.

[b] Horizontal resolution is expressed as degrees latitude by longitude, while vertical resolution (L) is the number of vertical levels.

Frequently Asked Question 8.1

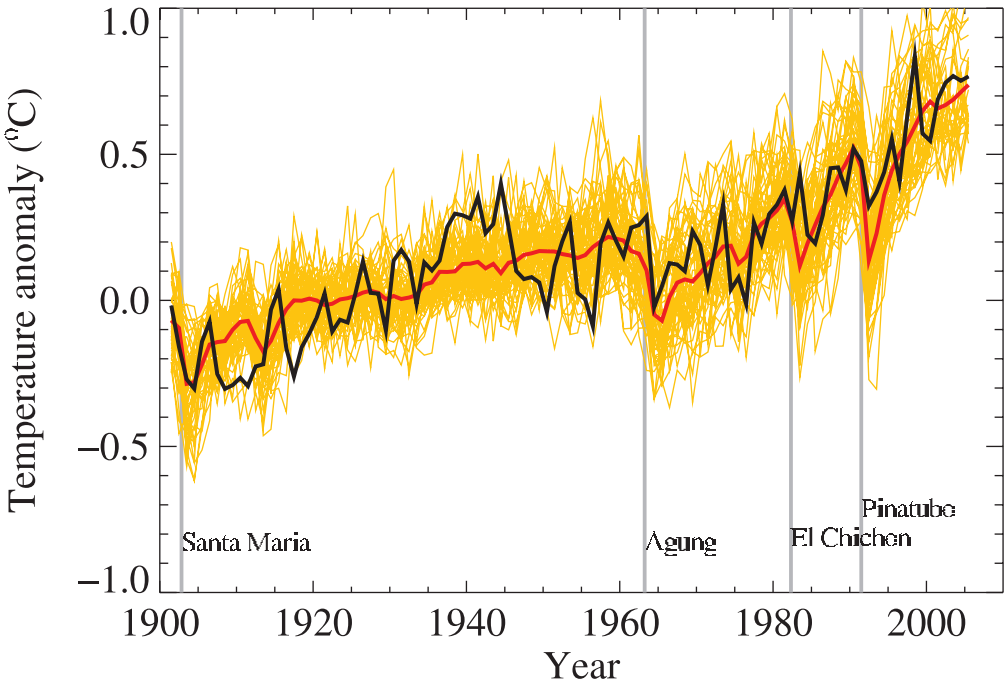
How Reliable Are the Models Used to Make Projections of Future Climate Change?

There is considerable confidence that climate models provide credible quantitative estimates of future climate change, particularly at continental scales and above. This confidence comes from the foundation of the models in accepted physical principles and from their ability to reproduce observed features of current climate and past climate changes. Confidence in model estimates is higher for some climate variables (e.g., temperature) than for others (e.g., precipitation). Over several decades of development, models have consistently provided a robust and unambiguous picture of significant climate warming in response to increasing greenhouse gases.

Climate models are mathematical representations of the climate system, expressed as computer codes and run on powerful computers. One source of confidence in models comes from the fact that model fundamentals are based on established physical laws, such as conservation of mass, energy and momentum, along with a wealth of observations.

A second source of confidence comes from the ability of models to simulate important aspects of the current climate. Models are routinely and extensively assessed by comparing their simulations with observations of the atmosphere, ocean, cryosphere and land surface. Unprecedented levels of evaluation have taken place over the last decade in the form of organised multi-model 'intercomparisons'. Models show significant and increasing skill in representing many important mean climate features, such as the large-scale distributions of atmospheric temperature, precipitation, radiation and wind, and of oceanic temperatures, currents and sea ice cover. Models can also simulate essential aspects of many of the patterns of climate variability observed across a range of time scales. Examples include the advance and retreat of the major monsoon systems, the seasonal shifts of temperatures, storm tracks and rain belts, and the hemispheric-scale seesawing of extratropical surface pressures (the Northern and Southern 'annular modes'). Some climate models, or closely related variants, have also been tested by using them to predict weather and make seasonal forecasts. These models demonstrate skill in such forecasts, showing they can represent important features of the general circulation across shorter time scales, as well as aspects of seasonal and interannual variability. Models' ability to represent these and other important climate features increases our confidence that they represent the essential physical processes important for the simulation of future climate change. (Note that the limitations in climate models' ability to forecast weather beyond a few days do not limit their ability to predict long-term climate changes, as these are very different types of prediction – see FAQ 1.2.)

(continued)



FAQ 8.1, Figure 1. *Global mean near-surface temperatures over the 20th century from observations (black) and as obtained from 58 simulations produced by 14 different climate models driven by both natural and human-caused factors that influence climate (yellow). The mean of all these runs is also shown (thick red line). Temperature anomalies are shown relative to the 1901 to 1950 mean. Vertical grey lines indicate the timing of major volcanic eruptions. (Figure adapted from Chapter 9, Figure 9.5. Refer to corresponding caption for further details.)*

A third source of confidence comes from the ability of models to reproduce features of past climates and climate changes. Models have been used to simulate ancient climates, such as the warm mid-Holocene of 6,000 years ago or the last glacial maximum of 21,000 years ago (see Chapter 6). They can reproduce many features (allowing for uncertainties in reconstructing past climates) such as the magnitude and broad-scale pattern of oceanic cooling during the last ice age. Models can also simulate many observed aspects of climate change over the instrumental record. One example is that the global temperature trend over the past century (shown in Figure 1) can be modelled with high skill when both human and natural factors that influence climate are included. Models also reproduce other observed changes, such as the faster increase in nighttime than in daytime temperatures, the larger degree of warming in the Arctic and the small, short-term global cooling (and subsequent recovery) which has followed major volcanic eruptions, such as that of Mt. Pinatubo in 1991 (see FAQ 8.1, Figure 1). Model global temperature projections made over the last two decades have also been in overall agreement with subsequent observations over that period (Chapter 1).

Nevertheless, models still show significant errors. Although these are generally greater at smaller scales, important large-scale problems also remain. For example, deficiencies remain in the simulation of tropical precipitation, the El Niño-Southern Oscillation and the Madden-Julian Oscillation (an observed variation in tropical winds and rainfall with a time scale of 30 to 90 days). The ultimate source of most such errors is that many important small-scale processes cannot be represented explicitly in models, and so must be included in approximate form as they interact with larger-scale features. This is partly due to limitations in computing power, but also results from limitations in scientific understanding or in the availability of detailed observations of some physical processes. Significant uncertainties, in particular, are associated with the representation of clouds, and in the resulting cloud responses to climate change. Consequently, models continue to display a substantial range of global temperature change in response to specified greenhouse gas forcing (see Chapter 10). Despite such uncertainties, however, models are unanimous in their prediction of substantial climate warming under greenhouse gas increases, and this warming is of a magnitude consistent with independent estimates derived from other sources, such as from observed climate changes and past climate reconstructions.

Since confidence in the changes projected by global models decreases at smaller scales, other techniques, such as the use of regional climate models, or downscaling methods, have been specifically developed for the study of regional- and local-scale climate change (see FAQ 11.1). However, as global models continue to develop, and their resolution continues to improve, they are becoming increasingly useful for investigating important smaller-scale features, such as changes in extreme weather events, and further improvements in regional-scale representation are expected with increased computing power. Models are also becoming more comprehensive in their treatment of the climate system, thus explicitly representing more physical and biophysical processes and interactions considered potentially important for climate change, particularly at longer time scales. Examples are the recent inclusion of plant responses, ocean biological and chemical interactions, and ice sheet dynamics in some global climate models.

In summary, confidence in models comes from their physical basis, and their skill in representing observed climate and past climate changes. Models have proven to be extremely important tools for simulating and understanding climate, and there is considerable confidence that they are able to provide credible quantitative estimates of future climate change, particularly at larger scales. Models continue to have significant limitations, such as in their representation of clouds, which lead to uncertainties in the magnitude and timing, as well as regional details, of predicted climate change. Nevertheless, over several decades of model development, they have consistently provided a robust and unambiguous picture of significant climate warming in response to increasing greenhouse gases.

the model's grid. Instead, sub-grid scale parametrizations are used to parametrize the unresolved processes, such as cloud formation and the mixing due to oceanic eddies. It continues to be the case that multi-model ensemble simulations generally provide more robust information than runs of any single model. Table 8.1 summarises the formulations of each of the AOGCMs used in this report.

There is currently no consensus on the optimal way to divide computer resources among finer numerical grids, which allow for better simulations; greater numbers of ensemble members, which allow for better statistical estimates of uncertainty; and inclusion of a more complete set of processes (e.g., carbon feedbacks, atmospheric chemistry interactions).

8.2.1 Atmospheric Processes

8.2.1.1 Numerics

In the TAR, more than half of the participating atmospheric models used spectral advection. Since the TAR, semi-Lagrangian advection schemes have been adopted in several atmospheric models. These schemes allow long time steps and maintain positive values of advected tracers such as water vapour, but they are diffusive, and some versions do not formally conserve mass. In this report, various models use spectral, semi-Lagrangian, and Eulerian finite-volume and finite-difference advection schemes, although there is still no consensus on which type of scheme is best.

8.2.1.2 Horizontal and Vertical Resolution

The horizontal and vertical resolutions of AOGCMs have increased relative to the TAR. For example, HadGEM1 has eight times as many grid cells as HadCM3 (the number of cells has doubled in all three dimensions). At the National Center for Atmospheric Research (NCAR), a T85 version of the Climate System Model (CSM) is now routinely used, while a T42 version was standard at the time of the TAR. The Center for Climate System Research (CCSR), National Institute for Environmental Studies (NIES) and Frontier Research Center for Global Change (FRCGC) have developed a high-resolution climate model (MIROC-hi, which consists of a T106 L56 Atmospheric GCM (AGCM) and a 1/4° by 1/6° L48 Ocean GCM (OGCM)), and The Meteorological Research Institute (MRI) of the Japan Meteorological Agency (JMA) has developed a TL959 L60 spectral AGCM (Oouchi et al., 2006), which is being used in time-slice mode. The projections made with these models are presented in Chapter 10.

Due to the increased horizontal and vertical resolution, both regional- and global-scale climate features are better simulated. For example, a far-reaching effect of the Hawaiian Islands in the Pacific Ocean (Xie et al., 2001) has been well simulated (Sakamoto et al., 2004) and the frequency distribution of precipitation associated with the Baiu front has been improved (Kimoto et al., 2005).

8.2.1.3 Parametrizations

The climate system includes a variety of physical processes, such as cloud processes, radiative processes and boundary-layer processes, which interact with each other on many temporal and spatial scales. Due to the limited resolutions of the models, many of these processes are not resolved adequately by the model grid and must therefore be parametrized. The differences between parametrizations are an important reason why climate model results differ. For example, a new boundary-layer parametrization (Lock et al., 2000; Lock, 2001) had a strong positive impact on the simulations of marine stratocumulus cloud produced by the Geophysical Fluid Dynamics Laboratory (GFDL) and the Hadley Centre climate models, but the same parametrization had less positive impact when implemented in an earlier version of the Hadley Centre model (Martin et al., 2006). Clearly, parametrizations must be understood in the context of their host models.

Cloud processes affect the climate system by regulating the flow of radiation at the top of the atmosphere, by producing precipitation, by accomplishing rapid and sometimes deep redistributions of atmospheric mass and through additional mechanisms too numerous to list here (Arakawa and Schubert, 1974; Arakawa, 2004). Cloud parametrizations are based on physical theories that aim to describe the statistics of the cloud field (e.g., the fractional cloudiness or the area-averaged precipitation rate) without describing the individual cloud elements. In an increasing number of climate models, microphysical parametrizations that represent such processes as cloud particle and raindrop formation are used to predict the distributions of liquid and ice clouds. These parametrizations improve the simulation of the present climate, and affect climate sensitivity (Iacobellis et al., 2003). Realistic parametrizations of cloud processes are a prerequisite for reliable current and future climate simulation (see Section 8.6).

Data from field experiments such as the Global Atmospheric Research Program (GARP) Atlantic Tropical Experiment (GATE, 1974), the Monsoon Experiment (MONEX, 1979), ARM (1993) and the Tropical Ocean Global Atmosphere (TOGA) Coupled Ocean-Atmosphere Response Experiment (COARE, 1993) have been used to test and improve parametrizations of clouds and convection (e.g., Emanuel and Zivkovic-Rothmann, 1999; Sud and Walker, 1999; Bony and Emanuel, 2001). Systematic research such as that conducted by the GCSS (Randall et al., 2003) has been organised to test parametrizations by comparing results with both observations and the results of a cloud-resolving model. These efforts have influenced the development of many of the recent models. For example, the boundary-layer cloud parametrization of Lock et al. (2000) and Lock (2001) was tested via the GCSS. Parametrizations of radiative processes have been improved and tested by comparing results of radiation parametrizations used in AOGCMs with those of much more detailed 'line-by-line' radiation codes (Collins et al., 2006). Since the TAR, improvements have been made in several models to the physical coupling between cloud and convection parametrizations, for example, in the Max Planck Institute (MPI) AOGCM using

Tompkins (2002), in the IPSL-CM4 AOGCM using Bony and Emanuel (2001) and in the GFDL model using Tiedtke (1993). These are examples of component-level testing.

In parallel with improvement in parametrizations, a non-hydrostatic model has been used for downscaling. A model with a 5 km grid on a domain of 4,000 x 3,000 x 22 km centred over Japan has been run by MRI/JMA, using the time-slice method for the Fourth Assessment Report (AR4) (Yoshizaki et al., 2005).

Aerosols play an important role in the climate system. Interactive aerosol parametrizations are now used in some models (HADGEM1, MIROC-hi, MIROC-med). Both the 'direct' and 'indirect' aerosol effects (Chapter 2) have been incorporated in some cases (e.g., IPSL-CM4). In addition to sulphates, other types of aerosols such as black and organic carbon, sea salt and mineral dust are being introduced as prognostic variables (Takemura et al., 2005; see Chapter 2). Further details are given in Section 8.2.5.

8.2.2 Ocean Processes

8.2.2.1 Numerics

Recently, isopycnic or hybrid vertical coordinates have been adopted in some ocean models (GISS-EH and BCCR-BCM2.0). Tests show that such models can produce solutions for complex regional flows that are as realistic as those obtained with the more common depth coordinate (e.g., Drange et al., 2005). Issues remain over the proper treatment of thermobaricity (nonlinear relationship of temperature, salinity and pressure to density), which means that in some isopycnic coordinate models the relative densities of, for example, Mediterranean and Antarctic Bottom Water masses are distorted. The merits of these vertical coordinate systems are still being established.

An explicit representation of the sea surface height is being used in many models, and real freshwater flux is used to force those models instead of a 'virtual' salt flux. The virtual salt flux method induces a systematic error in sea surface salinity prediction and causes a serious problem at large river basin mouths (Hasumi, 2002a,b; Griffies, 2004).

Generalised curvilinear horizontal coordinates with bipolar or tripolar grids (Murray, 1996) have become widely used in the oceanic component of AOGCMs. These are strategies used to deal with the North Pole coordinate singularity, as alternatives to the previously common polar filter or spherical coordinate rotation. The newer grids have the advantage that the singular points can be shifted onto land while keeping grid points aligned on the equator. The older methods of representing the ocean surface, surface water flux and North Pole are still in use in several AOGCMs.

8.2.2.2 Horizontal and Vertical Resolution

There has been a general increase in resolution since the TAR, with a horizontal resolution of order one to two degrees now commonly used in the ocean component of most climate models. To better resolve the equatorial waveguide, several models use enhanced meridional resolution in the tropics. Resolution high enough to allow oceanic eddies, eddy permitting, has not been used in a full suite of climate scenario integrations due to computational cost, but since the TAR it has been used in some idealised and scenario-based climate experiments as discussed below. A limited set of integrations using the eddy-permitting MIROC3.2 (hires) model is used here and in Chapter 10. Some modelling centres have also increased vertical resolution since the TAR.

A few coupled climate models with eddy-permitting ocean resolution (1/6° to 1/3°) have been developed (Roberts et al., 2004; Suzuki et al., 2005), and large-scale climatic features induced by local air-sea coupling have been successfully simulated (e.g., Sakamoto et al., 2004).

Roberts et al. (2004) found that increasing the ocean resolution of the HadCM3 model from about 1° to 0.33° by 0.33° by 40 levels (while leaving the atmospheric component unchanged) resulted in many improvements in the simulation of ocean circulation features. However, the impact on the atmospheric simulation was relatively small and localised. The climate change response was similar to the standard resolution model, with a slightly faster rate of warming in the Northern Europe-Atlantic region due to differences in the Atlantic Meridional Overturning Circulation (MOC) response. The adjustment time scale of the Atlantic Basin freshwater budget decreased from being of order 400 years to being of order 150 years with the higher resolution ocean, suggesting possible differences in transient MOC response on those time scales, but the mechanisms and the relative roles of horizontal and vertical resolution are not clear.

The Atlantic MOC is influenced by freshwater as well as thermal forcing. Besides atmospheric freshwater forcing, freshwater transport by the ocean itself is also important. For the Atlantic MOC, the fresh Pacific water coming through the Bering Strait could be poorly simulated on its transit to the Canadian Archipelago and the Labrador Sea (Komuro and Hasumi, 2005). These aspects have been improved since the TAR in many of the models evaluated here.

Changes around continental margins are very important for regional climate change. Over these areas, climate is influenced by the atmosphere and open ocean circulation. High-resolution climate models contribute to the improvement of regional climate simulation. For example, the location of the Kuroshio separation from the Japan islands is well simulated in the MIROC3.2 (hires) model (see Figure 8.1), which makes it possible to study a change in the Kuroshio axis in the future climate (Sakamoto et al., 2005).

Guilyardi et al. (2004) suggested that ocean resolution may play only a secondary role in setting the time scale of model El Niño-Southern Oscillation (ENSO) variability, with the dominant time scales being set by the atmospheric model provided the basic speeds of the equatorial ocean wave modes are adequately represented.

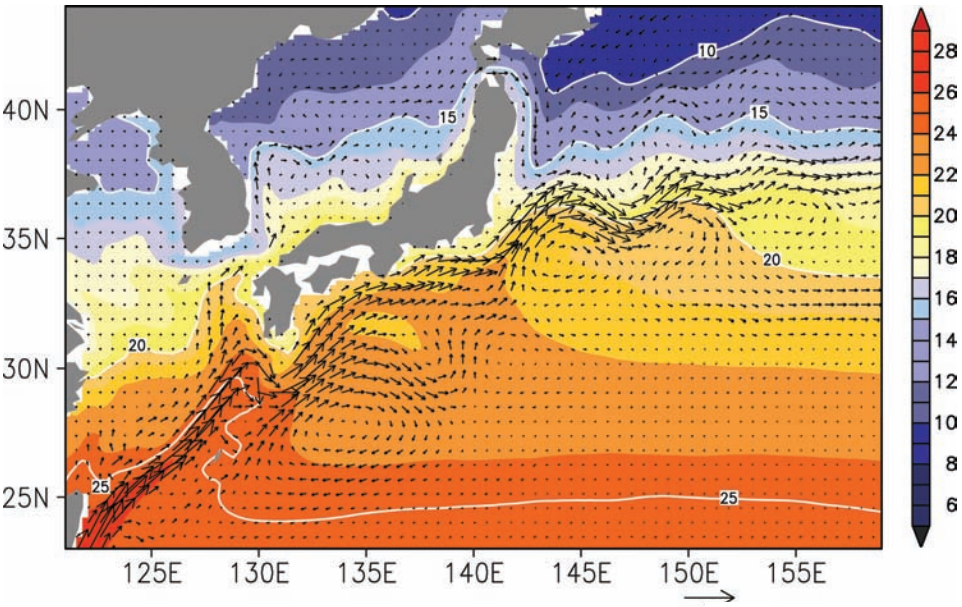


Figure 8.1. *Long-term mean ocean current velocities at 100 m depth (vectors, unit: m s^{-1}) and sea surface temperature (colours, °C) around the Kuroshio and the Kuroshio Extension obtained from a control experiment forced by pre-industrial conditions (CO_2 concentration 295.9 ppm) using MIROC3.2 (hires).*

8.2.2.3 Parametrizations

In the tracer equations, isopycnal diffusion (Redi, 1982) with isopycnal layer thickness diffusion (Gent et al., 1995), including its modification by Visbeck et al. (1997), has become a widespread choice instead of a simple horizontal diffusion. This has led to improvements in the thermocline structure and meridional overturning (Böning et al., 1995; see Section 8.3.2). For vertical mixing of tracers, a wide variety of parametrizations is currently used, such as turbulence closures (e.g., Mellor and Yamada, 1982), non-local diffusivity profiles (Large et al., 1994) and bulk mixed-layer models (e.g., Kraus and Turner, 1967). Representation of the surface mixed layer has been much improved due to developments in these parametrizations (see Section 8.3.2). Observations have shown that deep ocean vertical mixing is enhanced over rough bottoms, steep slopes and where stratification is weak (Kraus, 1990; Polzin et al., 1997; Moum et al., 2002). While there have been modelling studies indicating the significance of such inhomogeneous mixing for the MOC (e.g., Marotzke, 1997; Hasumi and Suginohara, 1999; Otterå et al., 2004; Oliver et al., 2005, Saenko and Merryfield 2005), comprehensive parametrizations of the effects and their application in coupled climate models are yet to be seen.

Many of the dense waters formed by oceanic convection, which are integral to the global MOC, must flow over ocean ridges or down continental slopes. The entrainment of ambient water around these topographic features is an important process determining the final properties and quantity of the deep waters. Parametrizations for such bottom boundary-layer processes have come into use in some AOGCMs (e.g., Winton et al., 1998; Nakano and Suginohara, 2002). However, the impact of the bottom boundary-layer representation on the coupled system is not fully understood (Tang and Roberts, 2005). Thorpe et al. (2004) studied the impact of the very simple scheme used in the HadCM3 model to control mixing of overflow waters from the Nordic Seas into the North Atlantic. Although the scheme does result in a change of the subpolar water mass properties, it appears to have little impact on the simulation of the strength of the large-scale MOC, or its response to global warming.

8.2.3 Terrestrial Processes

Few multi-model analyses of terrestrial processes included in the models in Table 8.1 have been conducted. However, significant advances since the TAR have been reported based on climate models that are similar to these models. Analysis of these models provides insight on how well terrestrial processes are included in the AR4 models.

8.2.3.1 Surface Processes

The addition of the terrestrial biosphere models that simulate changes in terrestrial carbon sources and sinks into fully coupled climate models is at the cutting edge of climate science. The major advance in this area since the TAR is the inclusion of carbon cycle dynamics including vegetation and soil carbon cycling, although these are not yet incorporated routinely into the AOGCMs used for climate projection (see Chapter 10). The inclusion of the terrestrial carbon cycle introduces a new and potentially important feedback into the climate system on time scales of decades to centuries (see Chapters 7 and 10). These feedbacks include the responses of the terrestrial biosphere to increasing carbon dioxide (CO_2), climate change and changes in climate variability (see Chapter 7). However, many issues remain to be resolved. The magnitude of the sink remains uncertain (Cox et al., 2000; Friedlingstein et al., 2001;

Dufresne et al., 2002) because it depends on climate sensitivity as well as on the response of vegetation and soil carbon to increasing CO_2 (Friedlingstein et al., 2003). The rate at which CO_2 fertilization saturates in terrestrial systems dominates the present uncertainty in the role of biospheric feedbacks. A series of studies have been conducted to explore the present modelling capacity of the response of the terrestrial biosphere rather than the response of just one or two of its components (Friedlingstein et al., 2006). This work has built on systematic efforts to evaluate the capacity of terrestrial biosphere models to simulate the terrestrial carbon cycle (Cramer et al., 2001) via intercomparison exercises. For example, Friedlingstein et al. (2006) found that in all models examined, the sink decreases in the future as the climate warms.

Other individual components of land surface processes have been improved since the TAR, such as root parametrization (Arora and Boer, 2003; Kleidon, 2004) and higher-resolution river routing (Ducharne et al., 2003). Cold land processes have received considerable attention with multi-layer snowpack models now more common (e.g., Oleson et al., 2004) as is the inclusion of soil freezing and thawing (e.g., Boone et al., 2000; Warrach et al., 2001). Sub-grid scale snow parametrizations (Liston, 2004), snow-vegetation interactions (Essery et al., 2003) and the wind redistribution of snow (Essery and Pomeroy, 2004) are more commonly considered. High-latitude organic soils are included in some models (Wang et al., 2002). A recent advance is the coupling of groundwater models into land surface schemes (Liang et al., 2003; Maxwell and Miller, 2005; Yeh and Eltahir, 2005). These have only been evaluated locally but may be adaptable to global scales. There is also evidence emerging that regional-scale projection of warming is sensitive to the simulation of processes that operate at finer scales than current climate models resolve (Pan et al., 2004). In general, the improvements in land surface models since the TAR are based on detailed comparisons with observational data. For example, Boone et al. (2004) used the Rhone Basin to investigate how land surface models simulate the water balance for several annual cycles compared to data from a dense observation network. They found that most land surface schemes simulate very similar total runoff and evapotranspiration but the partitioning between the various components of both runoff and evaporation varies greatly, resulting in different soil water equilibrium states and simulated discharge. More sophisticated snow parametrizations led to superior simulations of basin-scale runoff.

An analysis of results from the second phase of AMIP (AMIP-2) explored the land surface contribution to climate simulation. Henderson-Sellers et al. (2003) found a clear chronological sequence of land surface schemes (early models that excluded an explicit canopy, more recent biophysically based models and very recent biophysically based models). Statistically significant differences in annually averaged evaporation were identified that could be associated with the parametrization of canopy processes. Further improvements in land surface models depends on enhanced surface observations, for example, the use of stable isotopes (e.g., Henderson-Sellers et al., 2004) that allow several components of evaporation to be evaluated separately. Pitman et al. (2004) explored the impact of the level of complexity used to parametrize the surface energy balance on differences found among the AMIP-2 results. They found that quite large variations in surface energy balance complexity did not lead to systematic differences in the simulated mean, minimum or maximum temperature variance at the global scale, or in the zonal averages, indicating that these variables are not limited by uncertainties in how to parametrize the surface energy balance. This adds confidence to the use of the models in Table 8.1, as most include surface energy balance modules of more complexity than the minimum identified by Pitman et al. (2004).

While little work has been performed to assess the capability of the land surface models used in coupled climate models, the upgrading of the land surface models is gradually taking place and the inclusion of carbon in these models is a major conceptual advance. In the simulation of the present-day climate, the limitations of the standard bucket hydrology model are increasingly clear (Milly and Shmakin, 2002; Henderson-Sellers et al., 2004; Pitman et al., 2004), including evidence that it overestimates the likelihood of drought (Seneviratne et al., 2002). Relatively small improvements to the land surface model, for example, the inclusion of spatially variable water-holding capacity and a simple canopy conductance, lead to significant improvements (Milly and Shmakin, 2002). Since most models in Table 8.1 represent the continental-scale land surface more realistically than the standard bucket hydrology scheme, and include spatially variable water-holding capacity, canopy conductance, etc. (Table 8.1), most of these models likely capture the key contribution made by the land surface to current large-scale climate simulations. However, it is not clear how well current climate models can capture the impact of future warming on the terrestrial carbon balance. A systematic evaluation of AOGCMs with the carbon cycle represented would help increase confidence in the contribution of the terrestrial surface resulting from future warming.

8.2.3.2 Soil Moisture Feedbacks in Climate Models

A key role of the land surface is to store soil moisture and control its evaporation. An important process, the soil moisture-precipitation feedback, has been explored extensively since the TAR, building on regionally specific studies that demonstrated links between soil moisture and rainfall. Recent studies (e.g., Gutowski et al., 2004; Pan et al., 2004) suggest that summer precipitation strongly depends on surface processes, notably in the simulation of regional extremes. Douville (2001) showed that soil moisture anomalies affect the African monsoon while Schär et al. (2004) suggested that an active soil moisture-precipitation feedback was linked to the anomalously hot European summer in 2003.

The soil moisture-precipitation feedback in climate models had not been systematically assessed at the time of the TAR. It is associated with the strength of coupling between the land and atmosphere, which is not directly measurable at the large scale in nature and has only recently been quantified in models

(Dirmeyer, 2001). Koster et al. (2004) provided an assessment of where the soil moisture-precipitation feedback is regionally important during the Northern Hemisphere (NH) summer by quantifying the coupling strength in 12 atmospheric GCMs. Some similarity was seen among the model responses, enough to produce a multi-model average estimate of where the global precipitation pattern during the NH summer was most strongly affected by soil moisture variations. These 'hot spots' of strong coupling are found in transition regions between humid and dry areas. The models, however, also show strong disagreement in the strength of land-atmosphere coupling. A few studies have explored the differences in coupling strength. Seneviratne et al. (2002) highlighted the importance of differing water-holding capacities among the models while Lawrence and Slingo (2005) explored the role of soil moisture variability and suggested that frequent soil moisture saturation and low soil moisture variability could partially explain the weak coupling strength in the HadAM3 model (note that 'weak' does not imply 'wrong' since the real strength of the coupling is unknown).

Overall, the uncertainty in surface-atmosphere coupling has implications for the reliability of the simulated soil moisture-atmosphere feedback. It tempers our interpretation of the response of the hydrologic cycle to simulated climate change in 'hot spot' regions. Note that no assessment has been attempted for seasons other than NH summer.

Since the TAR, there have been few assessments of the capacity of climate models to simulate observed soil moisture. Despite the tremendous effort to collect and homogenise soil moisture measurements at global scales (Robock et al., 2000), discrepancies between large-scale estimates of observed soil moisture remain. The challenge of modelling soil moisture, which naturally varies at small scales, linked to landscape characteristics, soil processes, groundwater recharge, vegetation type, etc., within climate models in a way that facilitates comparison with observed data is considerable. It is not clear how to compare climate-model simulated soil moisture with point-based or remotely sensed soil moisture. This makes assessing how well climate models simulate soil moisture, or the change in soil moisture, difficult.

8.2.4 Cryospheric Processes

8.2.4.1 Terrestrial Cryosphere

Ice sheet models are used in calculations of long-term warming and sea level scenarios, though they have not generally been incorporated in the AOGCMs used in Chapter 10. The models are generally run in 'off-line' mode (i.e., forced by atmospheric fields derived from high-resolution time-slice experiments), although Huybrechts et al. (2002) and Fichefet et al. (2003) reported early efforts at coupling ice sheet models to AOGCMs. Ice sheet models are also included in some EMICs (e.g., Calov et al., 2002). Ridley et al. (2005) pointed out that the time scale of projected melting of the Greenland Ice Sheet may be different in coupled and off-line simulations. Presently available thermomechanical ice sheet models do not include processes associated with ice streams or grounding line migration, which may permit rapid dynamical changes in the ice sheets. Glaciers and ice caps, due to their relatively small scales and low likelihood of significant climate feedback at large scales, are not currently included interactively in any AOGCMs. See Chapters 4 and 10 for further detail. For a discussion of terrestrial snow, see Section 8.3.4.1.

8.2.4.2 Sea Ice

Sea ice components of current AOGCMs usually predict ice thickness (or volume), fractional cover, snow depth, surface and internal temperatures (or energy) and horizontal velocity. Some models now include prognostic sea ice salinity (Schmidt et al., 2004). Sea ice albedo is typically prescribed, with only crude dependence on ice thickness, snow cover and puddling effects.

Since the TAR, most AOGCMs have started to employ complex sea ice dynamic components. The complexity of sea ice dynamics in current AOGCMs varies from the relatively simple 'cavitating fluid' model (Flato and Hibler, 1992) to the viscous-plastic model (Hibler, 1979), which is computationally expensive, particularly for global climate simulations. The elastic-viscous-plastic model (Hunke and Dukowicz, 1997) is being increasingly employed, particularly due to its efficiency for parallel computers. New numerical approaches for solving the ice dynamics equations include more accurate representations on curvilinear model grids (Hunke and Dukowicz, 2002; Marsland et al., 2003; Zhang and Rothrock, 2003) and Lagrangian methods for solving the viscous-plastic equations (Lindsay and Stern, 2004; Wang and Ikeda, 2004).

Treatment of sea ice thermodynamics in AOGCMs has progressed more slowly: it typically includes constant conductivity and heat capacities for ice and snow (if represented), a heat reservoir simulating the effect of brine pockets in the ice, and several layers, the upper one representing snow. More sophisticated thermodynamic schemes are being developed, such as the model of Bitz and Lipscomb (1999), which introduces salinity-dependent conductivity and heat capacities, modelling brine pockets in an energy-conserving way as part of a variable-layer thermodynamic model (e.g., Saenko et al., 2002). Some AOGCMs include snow ice formation, which occurs when an ice floe is submerged by the weight of the overlying snow cover and the flooded snow layer refreezes. The latter process is particularly important in the antarctic sea ice system.

Even with fine grid scales, many sea ice models incorporate sub-grid scale ice thickness distributions (Thorndike et al., 1975) with several thickness 'categories', rather than considering the ice as a uniform slab with inclusions of open water. An ice thickness distribution enables more accurate simulation of thermodynamic variations in growth and melt rates within a single grid cell, which can have significant consequences for ice-ocean albedo feedback processes (e.g., Bitz et al., 2001; Zhang and Rothrock, 2001). A well-resolved ice thickness distribution enables a more physical formulation for ice ridging and rafting events, based on energetic principles. Although parametrizations of ridging mechanics and their relationship

with the ice thickness distribution have improved (Babko et al., 2002; Amundrud et al., 2004; Toyota et al., 2004), inclusion of advanced ridging parametrizations has lagged other aspects of sea ice dynamics (rheology, in particular) in AOGCMs. Better numerical algorithms used for the ice thickness distribution (Lipscomb, 2001) and ice strength (Hutchings et al., 2004) have also been developed for AOGCMs.

8.2.5 Aerosol Modelling and Atmospheric Chemistry

Climate simulations including atmospheric aerosols with chemical transport have greatly improved since the TAR. Simulated global aerosol distributions are better compared with observations, especially satellite data (e.g., Advanced Very High Resolution Radar (AVHRR), Moderate Resolution Imaging Spectroradiometer (MODIS), Multi-angle Imaging Spectroradiometer (MISR), Polarization and Directionality of the Earth's Reflectance (POLDER), Total Ozone Mapping Spectrometer (TOMS)), the ground-based network (Aerosol Robotic Network; AERONET) and many measurement campaigns (e.g., Chin et al., 2002; Takemura et al., 2002). The global Aerosol Model Intercomparison project, AeroCom, has also been initiated in order to improve understanding of uncertainties of model estimates, and to reduce them (Kinne et al., 2003). These comparisons, combined with cloud observations, should result in improved confidence in the estimation of the aerosol direct and indirect radiative forcing (e.g., Ghan et al., 2001a,b; Lohmann and Lesins, 2002; Takemura et al., 2005). Interactive aerosol sub-component models have been incorporated in some of the climate models used in Chapter 10 (HadGEM1 and MIROC). Some models also include indirect aerosol effects (e.g., Takemura et al., 2005); however, the formulation of these processes is still the subject of much research.

Interactive atmospheric chemistry components are not generally included in the models used in this report. However, CCSM3 includes the modification of greenhouse gas concentrations by chemical processes and conversion of sulphur dioxide and dimethyl sulphide to sulphur aerosols.

8.2.6 Coupling Advances

In an advance since the TAR, a number of groups have developed software allowing easier coupling of the various components of a climate model (e.g., Valcke et al., 2006). An example, the Ocean Atmosphere Sea Ice Soil (OASIS) coupler, developed at the Centre Europeen de Recherche et de Formation Avancee en Calcul Scientific (CERFACS) (Terray et al., 1998), has been used by many modelling centres to synchronise the different models and for the interpolation of the coupling fields between the atmosphere and ocean grids. The schemes for interpolation between the ocean and the atmosphere grids have been revised. The new schemes ensure both a global and local conservation of the various fluxes at the air-sea interface, and track terrestrial, ocean and sea ice fluxes individually.

Coupling frequency is an important issue, because fluxes are averaged during a coupling interval. Typically, most AOGCMs evaluated here pass fluxes and other variables between the component parts once per day. The K-Profile Parametrization ocean vertical scheme (Large et al., 1994), used in several models, is very sensitive to the wind energy available for mixing. If the models are coupled at a frequency lower than once per ocean time step, nonlinear quantities such as wind mixing power (which depends on the cube of the wind speed) must be accumulated over every time step before passing to the ocean. Improper averaging therefore could lead to too little mixing energy and hence shallower mixed-layer depths, assuming the parametrization is not re-tuned. However, high coupling frequency can bring new technical issues. In the MIROC model, the coupling interval is three hours, and in this case, a poorly resolved internal gravity wave is excited in the ocean so some smoothing is necessary to damp this numerical problem. It should also be noted that the AOGCMs used here have relatively thick top oceanic grid boxes (typically 10 m or more), limiting the sea surface temperature (SST) response to frequent coupling (Bernie et al., 2005).

8.2.7 Flux Adjustments and Initialisation

Since the TAR, more climate models have been developed that do not adjust the surface heat, water and momentum fluxes artificially to maintain a stable control climate. As noted by Stouffer and Dixon (1998), the use of such flux adjustments required relatively long integrations of the component models before coupling. In these models, normally the initial conditions for the coupled integrations were obtained from long spin ups of the component models.

In AOGCMs that do not use flux adjustments (see Table 8.1), the initialisation methods tend to be more varied. The oceanic components of many models are initialised using values obtained either directly from an observationally based, gridded data set (Levitus and Boyer, 1994; Levitus and Antonov, 1997; Levitus et al., 1998) or from short ocean-only integrations that used an observational analysis for their initial conditions. The initial atmospheric component data are usually obtained from atmosphere-only integrations using prescribed SSTs.

To obtain initial data for the pre-industrial control integrations discussed in Chapter 10, most AOGCMs use variants of the Stouffer et al. (2004) scheme. In this scheme, the coupled model is initialised as discussed above. The radiative forcing is then set back to pre-industrial conditions. The model is integrated for a few centuries using constant pre-industrial radiative forcing, allowing the coupled system to partially adjust to this forcing. The degree of equilibration in the real pre-industrial climate to the pre-industrial radiative forcing is not known. Therefore, it seems unnecessary to have the pre-industrial control fully equilibrated. After this spin-up integration, the pre-industrial control is started and perturbation integrations can begin. An important next step, once the start of the control integration is determined, is the assessment of the control integration climate drift. Large climate drifts can distort both the natural variability

(e.g., Inness et al., 2003) and the climate response to changes in radiative forcing (Spelman and Manabe, 1984).

In earlier IPCC reports, the initialisation methods were quite varied. In some cases, the perturbation integrations were initialised using data from control integrations where the SSTs were near present-day values and not pre-industrial. Given that many climate models now use some variant of the Stouffer et al. (2004) method, this situation has improved.

8.3 Evaluation of Contemporary Climate as Simulated by Coupled Global Models

Due to nonlinearities in the processes governing climate, the climate system response to perturbations depends to some extent on its basic state (Spelman and Manabe, 1984). Consequently, for models to predict future climatic conditions reliably, they must simulate the current climatic state with some as yet unknown degree of fidelity. Poor model skill in simulating present climate could indicate that certain physical or dynamical processes have been misrepresented. The better a model simulates the complex spatial patterns and seasonal and diurnal cycles of present climate, the more confidence there is that all the important processes have been adequately represented. Thus, when new models are constructed, considerable effort is devoted to evaluating their ability to simulate today's climate (e.g., Collins et al., 2006; Delworth et al., 2006).

Some of the assessment of model performance presented here is based on the 20th-century simulations that constitute a part of the MMD archived at PCMDI. In these simulations, modelling groups initiated the models from pre-industrial (circa 1860) 'control' simulations and then imposed the natural and anthropogenic forcing thought to be important for simulating the climate of the last 140 years or so. The 23 models considered here (see Table 8.1) are those relied on in Chapters 9 and 10 to investigate historical and future climate changes. Some figures in this section are based on results from a subset of the models because the data set is incomplete.

In order to identify errors that are systematic across models, the mean of fields available in the MMD, referred to here as the 'multi-model mean field', will often be shown. The multi-model mean field results are augmented by results from individual models available as Supplementary Material (see Figures S8.1 to S8.15). The multi-model averaging serves to filter out biases of individual models and only retains errors that are generally pervasive. There is some evidence that the multi-model mean field is often in better agreement with observations than any of the fields simulated by the individual models (see Section 8.3.1.1.2), which supports continued reliance on a diversity of modelling approaches in projecting future climate change and provides some further interest in evaluating the multi-model mean results.

Faced with the rich variety of climate characteristics that could potentially be evaluated here, this section focuses on those elements that can critically affect societies and natural ecosystems and that are most likely to respond to changes in radiative forcing.

8.3.1 Atmosphere

8.3.1.1 Surface Temperature and the Climate System's Energy Budget

For models to simulate accurately the global distribution of the annual and diurnal cycles of surface temperature, they must, in the absence of compensating errors, correctly represent a variety of processes. The large-scale distribution of annual mean surface temperature is largely determined by the distribution of insolation, which is moderated by clouds, other surface heat fluxes and transport of energy by the atmosphere and to a lesser extent by the ocean. Similarly, the annual and diurnal cycles of surface temperature are governed by seasonal and diurnal changes in these factors, respectively, but they are also damped by storage of energy in the upper layers of the ocean and to a lesser degree the surface soil layers.

8.3.1.1.1 Temperature

Figure 8.2a shows the observed time mean surface temperature as a composite of surface air temperature over regions of land and SST elsewhere. Also shown is the difference between the multi-model mean field and the observed field. With few exceptions, the absolute error (outside polar regions and other data-poor regions) is less than 2°C. Individual models typically have larger errors, but in most cases still less than 3°C, except at high latitudes (see Figure 8.2b and Supplementary Material, Figure S8.1). Some of the larger errors occur in regions of sharp elevation changes and may result simply from mismatches between the model topography (typically smoothed) and the actual topography. There is also a tendency for a slight, but general, cold bias. Outside the polar regions, relatively large errors are evident in the eastern parts of the tropical ocean basins, a likely symptom of problems in the simulation of low clouds. The extent to which these systematic model errors affect a model's response to external perturbations is unknown, but may be significant (see Section 8.6).

In spite of the discrepancies discussed here, the fact is that models account for a very large fraction of the global temperature pattern: the correlation coefficient between the simulated and observed spatial patterns of annual mean temperature is typically about 0.98 for individual models. This supports the view that major processes governing surface temperature climatology are represented with a reasonable degree of fidelity by the models.

An additional opportunity for evaluating models is afforded by the observed annual cycle of surface temperature. Figure 8.3 shows the standard deviation of monthly mean surface temperatures, which is dominated by contributions from the amplitudes of the annual and semi-annual components of the annual cycle. The difference between the mean of the model results and the observations is also shown. The absolute

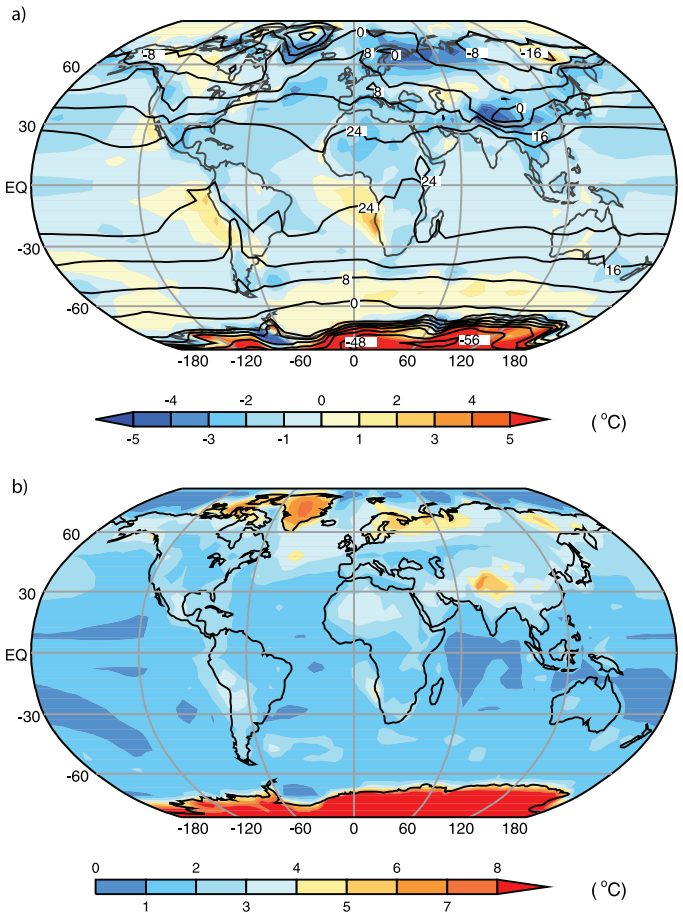


Figure 8.2. *(a) Observed climatological annual mean SST and, over land, surface air temperature (labelled contours) and the multi-model mean error in these temperatures, simulated minus observed (colour-shaded contours). (b) Size of the typical model error, as gauged by the root-mean-square error in this temperature, computed over all AOGCM simulations available in the MMD at PCMDI. The Hadley Centre Sea Ice and Sea Surface Temperature (HadISST; Rayner et al., 2003) climatology of SST for 1980 to 1999 and the Climatic Research Unit (CRU; Jones et al., 1999) climatology of surface air temperature over land for 1961 to 1990 are shown here. The model results are for the same period in the 20th-century simulations. In the presence of sea ice, the SST is assumed to be at the approximate freezing point of seawater (–1.8°C). Results for individual models can be seen in the Supplementary Material, Figure S8.1.*

differences are in most regions less than 1°C. Even over extensive land areas of the NH where the standard deviation generally exceeds 10°C, the models agree with observations within 2°C almost everywhere. The models, as a group, clearly capture the differences between marine and continental environments and the larger magnitude of the annual cycle found at higher latitudes, but there is a general tendency to underestimate the annual temperature range over eastern Siberia. In general, the largest fractional errors are found over the oceans (e.g., over much of tropical South America and off the east coasts of North America and Asia). These exceptions to the overall good agreement illustrate a general characteristic of current climate models: the largest-scale features of climate are simulated more accurately than regional- and smaller-scale features.

Like the annual range of temperature, the diurnal range (the difference between daily maximum and minimum surface air temperature) is much smaller over oceans than over land, where it is also better observed, so the discussion here is restricted to continental regions. The diurnal temperature range, zonally and annually averaged over the continents, is generally too small in the models, in many regions by as much as 50% (see Supplementary Material, Figure S8.3). Nevertheless, the models simulate the general pattern of this field, with relatively high values over the clearer, drier regions. It is not yet known why models generally underestimate the diurnal temperature range; it is possible that in some models it is in part due to shortcomings of the boundary-layer parametrizations or in the simulation of freezing and thawing soil, and it is also known that the diurnal cycle of convective cloud, which interacts strongly with surface temperature, is rather poorly simulated.

Surface temperature is strongly coupled with the atmosphere above it. This is especially evident at mid-latitudes, where migrating cold fronts and warm fronts can cause relatively large swings in surface temperature. Given the strong interactions between the surface temperature and the temperature of the air above, it is of special interest to evaluate how well models simulate the vertical profile of atmospheric temperature. The multi-model mean absolute error in the zonal mean, annual mean air temperature is almost everywhere less than 2°C (compared with the observed range of temperatures, which spans more than 100°C when the entire troposphere is considered; see Supplementary Material, Figure S8.4). It is notable, however, that near the tropopause at high latitudes the models are generally biased cold. This bias is a problem that has persisted for many years, but in general is now less severe than in earlier models. In a few of the models, the bias has been eliminated entirely, but

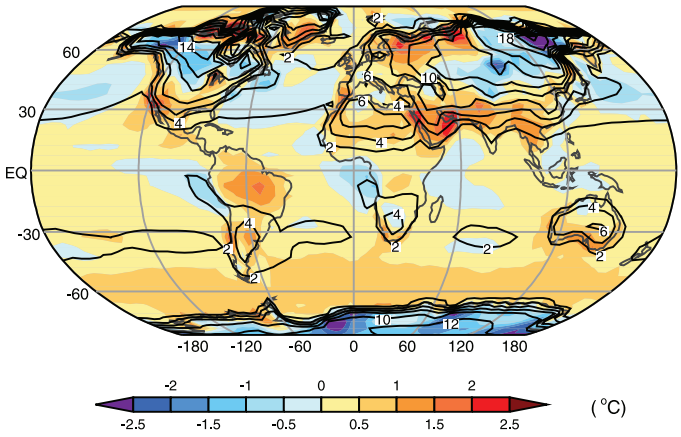


Figure 8.3. *Observed standard deviation (labelled contours) of SST and, over land, surface air temperature, computed over the climatological monthly mean annual cycle, and the multi-model mean error in the standard deviations, simulated minus observed (colour-shaded contours). In most regions, the standard deviation provides a measure of the amplitude of the seasonal range of temperature. The observational data sets, the model results and the climatological periods are as described in Figure 8.2. Results for individual models can be seen in the Supplementary Material, Figure S8.2.*

compensating errors may be responsible. It is known that the tropopause cold bias is sensitive to several factors, including horizontal and vertical resolution, non-conservation of moist entropy, and the treatment of sub-grid scale vertical convergence of momentum ('gravity wave drag'). Although the impact of the tropopause temperature bias on the model's response to radiative forcing changes has not been definitively quantified, it is almost certainly small relative to other uncertainties.

8.3.1.1.2 The balance of radiation at the top of the atmosphere

The primary driver of latitudinal and seasonal variations in temperature is the seasonally varying pattern of incident sunlight, and the fundamental driver of the circulation of the atmosphere and ocean is the local imbalance between the shortwave (SW) and longwave (LW) radiation at the top of the atmosphere. The impact on temperature of the distribution of insolation can be strongly modified by the distribution of clouds and surface characteristics.

Considering first the annual mean SW flux at the 'top' of the atmosphere (TOA)[1], the insolation is determined by well-known orbital parameters that ensure good agreement between models and observations. The annual mean insolation is strongest in the tropics, decreasing to about half as much at the poles. This largely drives the strong equator-to-pole temperature gradient. As for outgoing SW radiation, the Earth, on average, reflects about the same amount of sunlight (~100 W m^{-2} in the annual mean) at all latitudes. At most latitudes, the difference between the multi-model mean zonally averaged outgoing SW radiation and observations is in the annual mean less than 6 W m^{-2} (i.e., an error of about 6%; see Supplementary Material, Figure S8.5). Given that clouds are responsible for about half the outgoing SW radiation, these errors are not surprising, for it is known that cloud processes are among the most difficult to simulate with models (see Section 8.6.3.2.3).

There are additional errors in outgoing SW radiation due to variations with longitude and season, and these can be quantified by means of the root-mean-square (RMS) error, calculated for each latitude over all longitudes and months and plotted in Figure 8.4a (see also Supplementary Material, Figure S8.6). Errors in the complete two-dimensional fields (see Supplementary Material, Figure S8.6) tend to be substantially larger than the zonal mean errors of about 6 W m^{-2}, an example of the common result that model errors tend to increase as smaller spatial scales and shorter time scales are considered. Figure 8.4a also illustrates a common result that the errors in the multi-model average of monthly mean fields are often smaller than the errors in the individual model fields. In the case of outgoing SW radiation, this is true at nearly all latitudes. Calculation of the global mean RMS error, based on the monthly mean fields and area-weighted over all grid cells, indicates that the individual model errors are in the range 15 to 22 W m^{-2}, whereas the error in the multi-model mean climatology is only 13.1 W m^{-2}. Why the multi-model mean field turns out to be closer to the observed than the fields in any of the individual models is the subject of ongoing research; a superficial explanation is that at each location and

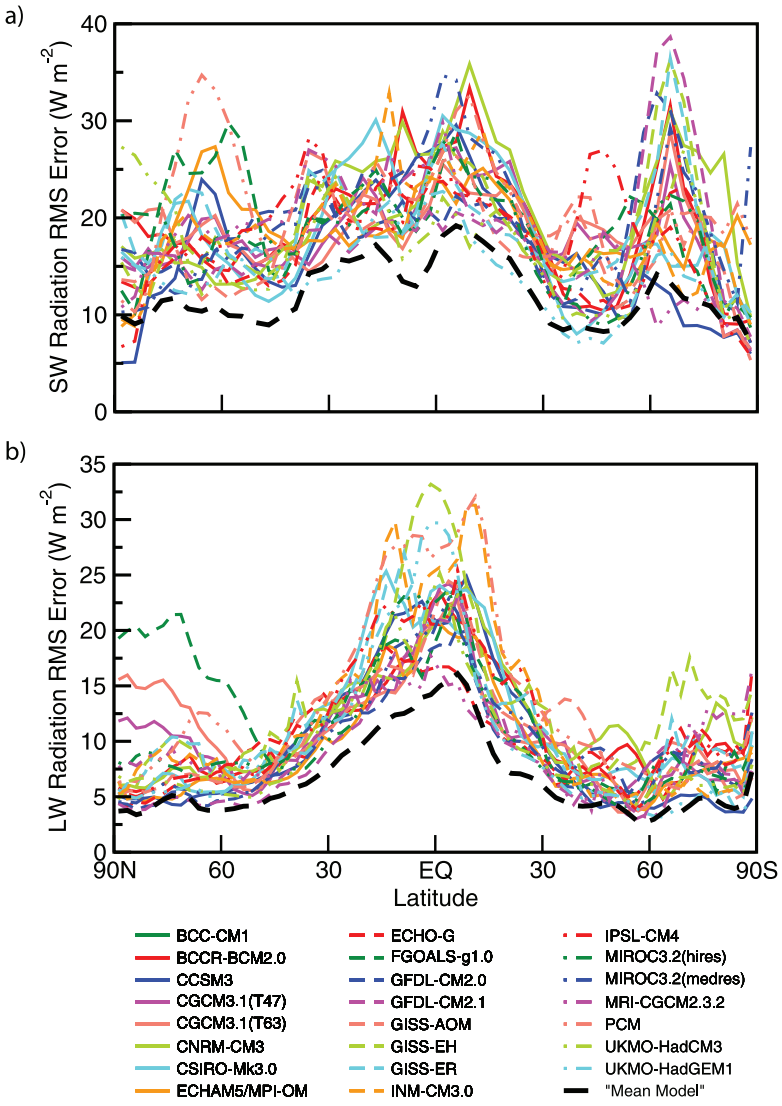


Figure 8.4. *Root-mean-square (RMS) model error, as a function of latitude, in simulation of (a) outgoing SW radiation reflected to space and (b) outgoing LW radiation. The RMS error is calculated over all longitudes and over all 12 months of a climatology formed from several years of data. The RMS statistic labelled 'Mean Model' is computed by first calculating the multi-model monthly mean fields, and then calculating the RMS error (i.e., it is not the mean of the individual model RMS errors). The Earth Radiation Budget Experiment (ERBE; Barkstrom et al., 1989) observational estimates used here are for the period 1985 to 1989 from satellite-based radiometers, and the model results are for the same period in the 20th-century simulations in the MMD at PCMDI. See Table 8.1 for model descriptions. Results for individual models can be seen in the Supplementary Material, Figures S8.5 to S8.8.*

[1] The atmosphere clearly has no identifiable 'top', but the term is used here to refer to an altitude above which the absorption of SW and LW radiation is negligibly small.

for each month, the model estimates tend to scatter around the correct value (more or less symmetrically), with no single model consistently closest to the observations. This, however, does not explain why the results should scatter in this way.

At the TOA, the net SW radiation is everywhere partially compensated by outgoing LW radiation (i.e., infrared emissions) emanating from the surface and the atmosphere. Globally and annually averaged, this compensation is nearly exact. The pattern of LW radiation emitted by earth to space depends most critically on atmospheric temperature, humidity, clouds and surface temperature. With a few exceptions, the models can simulate the observed zonal mean of the annual mean outgoing LW within 10 W m^{-2} (an error of around 5%; see Supplementary Material, Figure S8.7). The models reproduce the relative minimum in this field near the equator where the relatively high humidity and extensive cloud cover in the tropics raises the effective height (and lowers the effective temperature) at which LW radiation emanates to space.

The seasonal cycle of the outgoing LW radiation pattern is also reasonably well simulated by models (see Figure 8.4b). The RMS error for most individual models varies from about 3% of the outgoing LW radiation (OLR) near the poles to somewhat less than 10% in the tropics. The errors for the multi-model mean simulation, ranging from about 2 to 6% across all latitudes, are again generally smaller than those in the individual models.

For a climate in equilibrium, any local annual mean imbalance in the net TOA radiative flux (SW plus LW) must be balanced by a vertically integrated net horizontal divergence of energy carried by the ocean and atmosphere. The fact that the TOA SW and LW fluxes are well simulated implies that the models must also be properly accounting for poleward transport of total energy by the atmosphere and ocean. This proves to be the case, with most models correctly simulating poleward energy transport within about 10%. Although superficially this would seem to provide an important check on models, it is likely that in current models compensating errors improve the agreement of the simulations with observations. There are theoretical and model studies that suggest that if the atmosphere fails to transport the observed portion of energy, the ocean will tend to largely compensate (e.g., Shaffrey and Sutton, 2004).

8.3.1.2 Moisture and Precipitation

Water is fundamental to life, and if regional seasonal precipitation patterns were to change, the potential impacts could be profound. Consequently, it is of real practical interest to evaluate how well models can simulate precipitation, not only at global scales, but also regionally. Unlike seasonal variation in temperature, which at large scales is strongly determined by the insolation pattern and configuration of the continents, precipitation variations are also strongly influenced by vertical movement of air due to atmospheric instabilities of various kinds and by the flow of air over orographic features. For models to simulate accurately the seasonally varying pattern of precipitation, they must correctly simulate a number of processes (e.g., evapotranspiration, condensation, transport) that are difficult to evaluate at a global scale. Some of these are discussed further in Sections 8.2 and 8.6. In this subsection, the focus is on the distribution of precipitation and water vapour.

Figure 8.5a shows observation-based estimates of annual mean precipitation and Figure 8.5b shows the multi-model mean field. At the largest scales, the lower precipitation rates at higher latitudes reflect both reduced local evaporation at lower temperatures and a lower saturation vapour pressure of cooler air, which tends to inhibit the transport of vapour from other regions. In addition to this large-scale pattern, captured well by models, is a local minimum in precipitation near the equator in the Pacific, due to a tendency for the Inter-Tropical Convergence Zone (ITCZ)[2] to reside off the equator. There are local maxima at mid-latitudes, reflecting the tendency for subsidence to suppress precipitation in the subtropics and for storm systems to enhance precipitation at mid-latitudes. The models capture these large-scale zonal mean precipitation differences, suggesting that they can adequately represent these features of atmospheric circulation. Moreover, there is some evidence provided in Section 8.3.5 that models have improved over the last several years in simulating the annual cycle of the precipitation patterns.

Models also simulate some of the major regional characteristics of the precipitation field, including the major convergence zones and the maxima over tropical rain forests, although there is a tendency to underestimate rainfall over the Amazon. When considered in more detail, however, there are deficiencies in the multi-model mean precipitation field. There is a distinct tendency for models to orient the South Pacific convergence zone parallel to latitudes and to extend it too far eastward. In the tropical Atlantic, the precipitation maximum is too weak in most models with too much rain south of the equator. There are also systematic east-west positional errors in the precipitation distribution over the Indo-Pacific Warm Pool in most models, with an excess of precipitation over the western Indian Ocean and over the Maritime Continent. These lead to systematic biases in the location of the major rising branches of the Walker Circulation and can compromise major teleconnection[3] pathways, in particular those associated with El Niño (e.g., Turner et al., 2005). Systematic dry biases over the Bay of Bengal are related to errors in the monsoon simulations.

Despite the apparent skill suggested by the multi-model mean (Figure 8.5), many models individually display substantial precipitation biases, especially in the tropics, which often approach the magnitude of the mean observed climatology (e.g., Johns et al., 2006; see also the Supplementary Material, Figures S8.9 and S8.10). Although some of these biases can be attributed to errors in the SST field of the coupled model, even

[2] The ITCZ is manifested as a band of relatively intense convective precipitation, accompanied by surface convergence of moisture, which tends to locate seasonally over the warmest surface temperatures and circumnavigates the earth in the tropics (though not continuously).

[3] Teleconnection describes the process through which changes in one part of the climate system affect a remote location via changes in atmospheric circulation patterns.

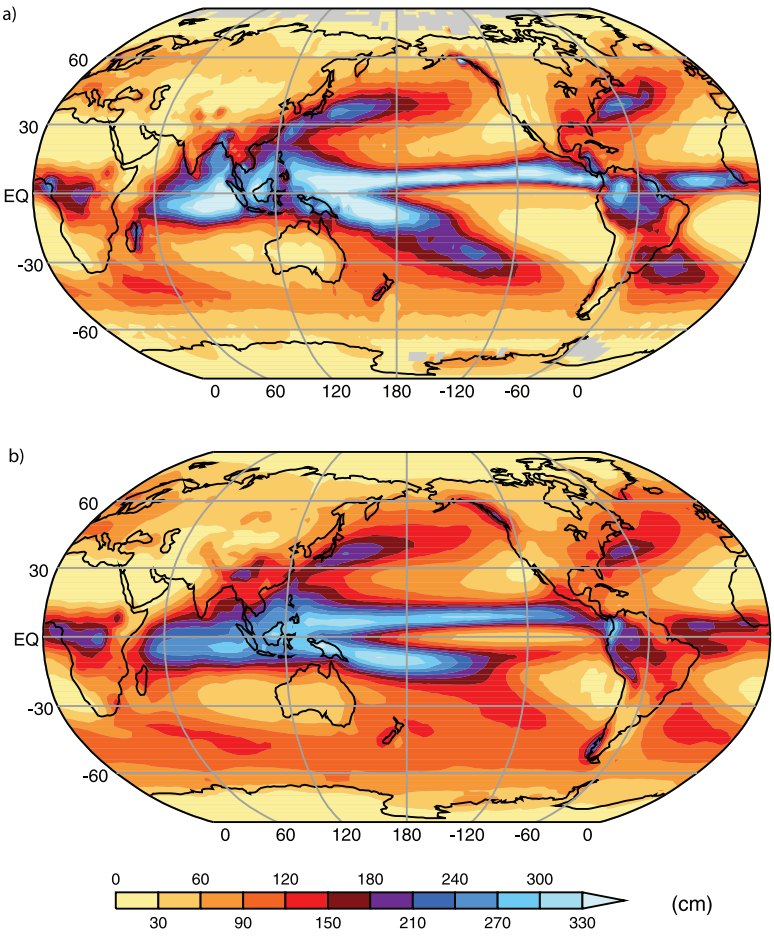


Figure 8.5. *Annual mean precipitation (cm), observed (a) and simulated (b), based on the multi-model mean. The Climate Prediction Center Merged Analysis of Precipitation (CMAP; Xie and Arkin, 1997) observation-based climatology for 1980 to 1999 is shown, and the model results are for the same period in the 20th-century simulations in the MMD at PCMDI. In (a), observations were not available for the grey regions. Results for individual models can be seen in Supplementary Material, Figure S8.9.*

atmosphere-only versions of the models show similarly large errors (e.g., Slingo et al., 2003). This may be one factor leading to a lack of consensus among models even as to the sign of future regional precipitation changes predicted in parts of the tropics (see Chapter 10).

At the heart of understanding what determines the regional distribution of precipitation over land and oceans in the tropics is atmospheric convection and its interaction with large-scale circulation. Convection occurs on a wide range of spatial and temporal scales, and there is increasing evidence that interactions across all scales may be crucial for determining the mean tropical climate and its regional rainfall distributions (e.g., Khairoutdinov et al., 2005). Over tropical land, the diurnal cycle dominates, and yet many models have difficulty simulating the early evening maximum in rainfall. Instead, they systematically tend to simulate rain before noon (Yang and Slingo, 2001; Dai, 2006), which compromises the energy budget of the land surface. Similarly, the land-sea breezes around the complex system of islands in Indonesia have been implicated in the failure of models to capture the regional rainfall patterns across the Indo-Pacific Warm Pool (Neale and Slingo, 2003). Over the oceans, the precipitation distribution along the ITCZ results from organised convection associated with weather systems occurring on synoptic and intra-seasonal time scales (e.g., the Madden-Julian Oscillation (MJO); see Section 8.4.8). These systems are frequently linked to convectively coupled equatorial wave structures (e.g., Yang et al., 2003), but these are poorly represented in models (e.g., Lin et al., 2006; Ringer et al., 2006). Thus the rain-bearing systems, which establish the mean precipitation climatology, are not well simulated, contributing also to the poor temporal characteristics of daily rainfall (e.g., Dai, 2006) in which many models simulate rain too frequently but with reduced intensity.

Precipitation patterns are intimately linked to atmospheric humidity, evaporation, condensation and transport processes. Good observational estimates of the global pattern of evaporation are not available, and condensation and vertical transport of water vapour can often be dominated by sub-grid scale convective processes which are difficult to evaluate globally. The best prospect for assessing water vapour transport processes in humid regions, especially at annual and longer time scales, may be to compare modelled and observed streamflow, which must nearly balance atmospheric transport since terrestrial water storage variations on longer time scales are small (Milly et al., 2005; see Section 8.3.4.2).

Although an analysis of runoff in the MMD at PCMDI has not yet been performed, the net result of evaporation, transport and condensation processes can be seen in the atmospheric humidity distribution. Models reproduce the large-scale decrease in humidity with both latitude and altitude (see Supplementary Material, Figure S8.11), although this is not truly an independent check of models, since it is almost a direct consequence of their reasonably realistic simulation of temperature. The multi-model mean bias in humidity, zonally and annually averaged, is less than 10% throughout most of the lower troposphere compared with reanalyses, but model evaluation in the upper troposphere is considerably hampered by observational uncertainty.

Any errors in the water vapour distribution should affect the outgoing LW radiation (see Section 8.3.1.1.2), which was seen to be free of systematic zonal mean biases. In fact, the observed differences in outgoing LW radiation between the moist and dry regions are reproduced by the models, providing some confidence that any errors in humidity are not critically affecting the net fluxes at the TOA. However, the strength of water vapour feedback, which strongly affects global climate sensitivity, is primarily determined by fractional changes in water vapour in response to warming, and the ability of models to correctly represent this feedback is perhaps better assessed with process studies (see Section 8.6).

8.3.1.3 Extratropical Storms

The impact of extratropical cyclones on global climate derives primarily from their role in transporting heat, momentum and humidity. Regionally and individually, these mid-latitude storms often provide beneficial precipitation, but also occasionally produce destructive flooding and high winds. For these reasons, the effect of climate change on extratropical cyclones is of considerable importance and interest.

Among the several approaches used to characterise cyclone activity (e.g., Paciorek et al., 2002), analysis methods that identify and track extratropical cyclones can provide the most direct information concerning their frequency and movement (Hoskins and Hodges, 2002, 2005). Climatologies for the distribution and properties of cyclones found in models can be compared with reanalysis products (Chapter 3), which provide the best observation-constrained data.

Results from a systematic analysis of AMIP-2 simulations (Hodges, 2004; Stratton and Pope, 2004) indicate that models run with observed SSTs are capable of producing storm tracks located in about the right locations, but nearly all show some deficiency in the distribution and level of cyclone activity. In particular, simulated storm tracks are often more zonally oriented than is observed. A study by Lambert and Fyfe (2006), based on the MMD at PCMDI, finds that as a group, the recent models, which include interactive oceans, tend to underestimate slightly the total number of cyclones in both hemispheres. However, the number of intense storms is slightly overestimated in the NH, but underestimated in the Southern Hemisphere (SH), although observations are less certain there.

Increases in model resolution (characteristic of models over the last several years) appear to improve some aspects of extratropical cyclone climatology (Bengtsson et al., 2006), particularly in the NH where observations are most reliable (Hodges et al., 2003; Hanson et al., 2004; Wang et al., 2006). Improvements to the dynamical core and physics of models have also led to better agreement with reanalyses (Ringer et al., 2006; Watterson, 2006).

Our assessment is that although problems remain, climate models are improving in their simulation of extratropical cyclones.

8.3.2 Ocean

As noted earlier, this chapter focuses only on those variables important in determining the transient response of climate models (see Section 8.6). Due to space limitations, much of the analysis performed for this section is found in the Supplementary Material (Figures S8.12 to S8.15). An assessment of the modes of natural, internally generated variability can be found in Section 8.4. Comparisons of the type performed here need to be made with an appreciation of the uncertainties in the historical estimates of radiative forcing and various sampling issues in the observations (see Chapters 2 and 5). Unless otherwise noted, all results discussed here are based on the MMD at PCMDI.

8.3.2.1 Simulation of Mean Temperature and Salinity Structure

Before discussing the oceanic variables directly involved in determining the climatic response, it is important to discuss the fluxes between the ocean and atmosphere. Modelling experience shows that the surface fluxes play a large part in determining the fidelity of the oceanic simulation. Since the atmosphere and ocean are coupled, the fidelity of the oceanic simulation feeds back to the atmospheric simulation, affecting the surface fluxes.

Unfortunately, the total surface heat and water fluxes (see Supplementary Material, Figure S8.14) are not well observed. Normally, they are inferred from observations of other fields, such as surface temperature and winds. Consequently, the uncertainty in the observational estimate is large – of the order of tens of watts per square metre for the heat flux, even in the zonal mean. An alternative way of assessing the surface fluxes is by looking at the horizontal transports in the ocean. In the long-term average, the heat and water storage in the ocean are small so that the horizontal transports have to balance the surface fluxes. Since the heat transport seems better constrained by the available observations, it is presented here.

North of 45°N, most model simulations transport too much heat northward when compared to the observational estimates used here (Figure 8.6), but there is uncertainty in the observations. At 45°N, for example, the model simulations lie much closer to the estimate of 0.6×10^{15} W obtained by Ganachaud and Wunsch (2003). From 45°N to the equator, most model estimates lie near or between the observational estimates shown. In the tropics and subtropical zone of the SH, most models underestimate the southward heat transport away from the equator. At middle

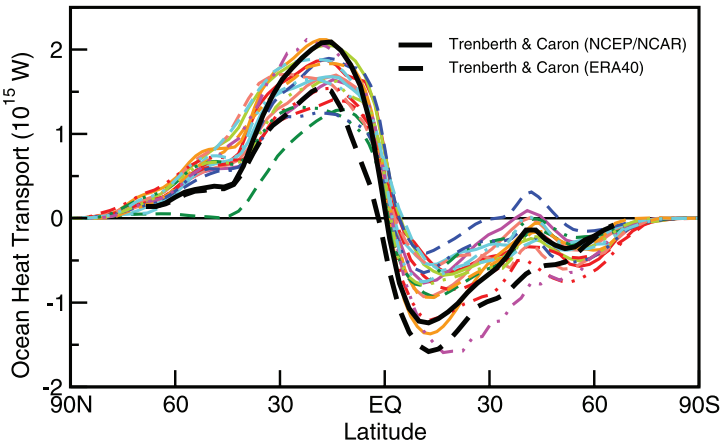


Figure 8.6. *Annual mean, zonally averaged oceanic heat transport implied by net heat flux imbalances at the sea surface, under an assumption of negligible changes in oceanic heat content. The observationally based estimate, taken from Trenberth and Caron (2001) for the period February 1985 to April 1989, derives from reanalysis products from the National Centers for Environmental Prediction (NCEP)/NCAR (Kalnay et al., 1996) and European Centre for Medium Range Weather Forecasts 40-year reanalysis (ERA40; Uppala et al., 2005). The model climatologies are derived from the years 1980 to 1999 in the 20th-century simulations in the MMD at PCMDI. The legend identifying individual models appears in Figure 8.4.*

and high latitudes of the SH, the observational estimates are more uncertain and the model-simulated heat transports tend to surround the observational estimates.

The oceanic heat fluxes have large seasonal variations which lead to large variations in the seasonal storage of heat by the oceans, especially in mid-latitudes. The oceanic heat storage tends to damp and delay the seasonal cycle of surface temperature. The model simulations evaluated here agree well with the observations of seasonal heat storage by the oceans (Gleckler et al., 2006a). The most notable problem area for the models is in the tropics, where many models continue to have biases in representing the flow of heat from the tropics into middle and high latitudes.

The annually averaged zonal component of surface wind stress, zonally averaged over the oceans, is reasonably well simulated by the models (Figure 8.7). At most latitudes, the reanalysis estimates (based on atmospheric models constrained by observations) lie within the range of model results. At middle to low latitudes, the model spread is relatively small and all the model results lie fairly close to the reanalysis. At middle to high latitudes, the model-simulated wind stress maximum tends to lie equatorward of the reanalysis. This error is particularly large in the SH, a region where there is more uncertainty in the reanalysis. Almost all model simulations place the SH wind stress maximum north of the reanalysis estimate. The Southern Ocean wind stress errors in the control integrations may adversely affect other aspects of the simulation and possibly the oceanic heat uptake under climate change, as discussed below.

The largest individual model errors in the zonally averaged SST (Figure 8.8) are found at middle and high latitudes, particularly the mid-latitudes of the NH where the model-simulated temperatures are too cold. Almost every model has some tendency for this cold bias. This error seems to be associated with poor simulation of the path of the North Atlantic Current and seems to be due to an ocean component problem rather than a problem with the surface fluxes. In the zonal averages near 60°S, there is a warm bias in the multi-model mean results. Many models suffer from a too-warm bias in the Southern Ocean SSTs.

In the individual model SST error maps (see Supplementary Material, Figure S8.1), it is apparent that most models have a large warm bias in the eastern parts of the tropical ocean basins, near the continental boundaries. This is also evident in the multi-model mean result (Figure 8.2a) and is associated with insufficient resolution, which leads to problems in the simulation of the local wind stress, oceanic upwelling and under-prediction of the low cloud amounts (see Sections 8.2 and 8.3.1). These are also regions where there is a relatively large spread among the model simulations, indicating a relatively wide range in the magnitude of these errors. Another area where the model error spread is relatively large is found in the North Atlantic Ocean. As noted above, this is an area where many models have problems properly locating the North Atlantic Current, a region of large SST gradients.

In spite of the errors, the model simulation of the SST field is fairly realistic overall. Over all latitudes, the multi-model mean

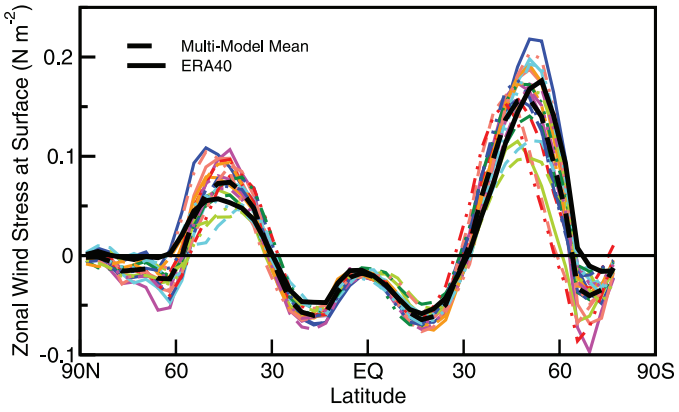


Figure 8.7. *Annual mean east-west component of wind stress zonally averaged over the oceans. The observationally constrained estimate is from the years 1980 to 1999 in the European Centre for Medium Range Weather Forecasts 40-year re-analysis (ERA40; Uppala et al., 2005), and the model climatologies are calculated for the same period in the 20th-century simulations in the MMD at PCMDI. The legend identifying individual models appears in Figure 8.4.*

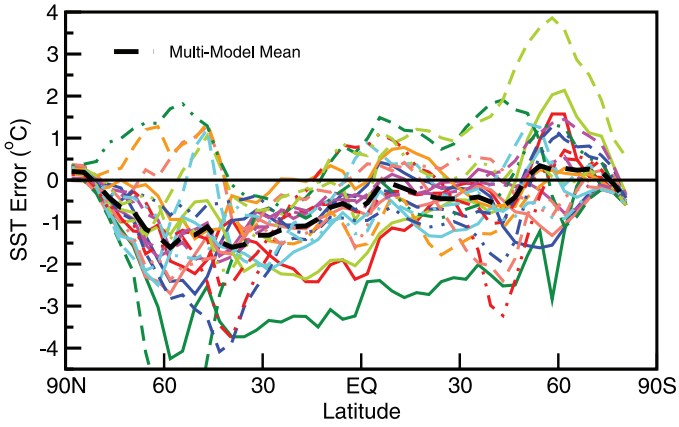


Figure 8.8. *Annual mean, zonally averaged SST error, simulated minus observed climatology. The Hadley Centre Sea Ice and Sea Surface Temperature (HadISST; Rayner et al., 2003) observational climatology for 1980 to 1999 is the reference used here, and the model results are for the same period in the 20th-century simulations in the MMD at PCMDI. In the presence of sea ice, the SST is assumed to be at the freezing point of seawater. The legend identifying individual models appears in Figure 8.4.*

zonally averaged SST error is less than 2°C, which is fairly small considering that most models do not use flux adjustments in these simulations. The model mean local SST errors are also less than 2°C over most regions, with only relatively small areas exceeding this value. Even relatively small SST errors, however, can adversely affect the simulation of variability and teleconnections (Section 8.4).

Over most latitudes, at depths ranging from 200 to 3,000 m, the multi-model mean zonally averaged ocean temperature is too warm (see Figure 8.9). The maximum warm bias (about 2°C) is located in the region of the North Atlantic Deep Water (NADW) formation. Above 200 m, however, the multi-model mean is too cold, with maximum cold bias (more than 1°C) near the surface at mid-latitudes of the NH, as discussed above. Most models generally have an error pattern similar to the

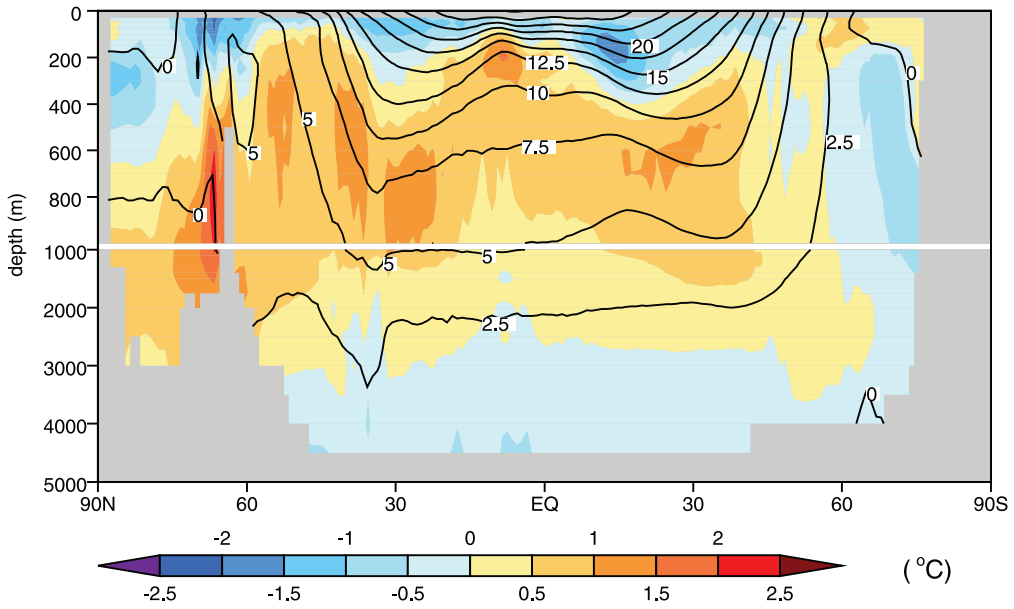


Figure 8.9. *Time-mean observed potential temperature (°C), zonally averaged over all ocean basins (labelled contours) and multi-model mean error in this field, simulated minus observed (colour-filled contours). The observations are from the 2004 World Ocean Atlas compiled by Levitus et al. (2005) for the period 1957 to 1990, and the model results are for the same period in the 20th-century simulations in the MMD at PCMDI. Results for individual models can be seen in the Supplementary Material, Figure S8.12.*

multi-model mean (see Supplementary Material, Figure S8.12) except for CNRM-CM3 and MRI-CGCM2.3.2, which are too cold throughout most of the mid- and low-latitude ocean (see Supplementary Material, Figure S8.12). The GISS-EH model is much too cold throughout the subtropical thermocline and only the NH part of the FGOALS-g1.0 error pattern is similar to the model mean error described here. The magnitude of these errors, especially in the deeper parts of the ocean, depends on the AOGCM initialisation method (Section 8.2.7).

The error pattern, in which the upper 200 m of the ocean tend to be too cold while the layers below are too warm, indicates that the thermocline in the multi-model mean is too diffuse. This error, which was also present at the time of the TAR, seems partly related to the wind stress errors in the SH noted above and possibly to errors in formation and mixing of NADW. The multi-model mean errors in temperature (too warm) and salinity (too salty; see Supplementary Material, Figure S8.13) at middle and low latitudes near the base of the thermocline tend to cancel in terms of a density error and appear to be associated with the problems in the formation of Antarctic Intermediate Water (AAIW), as discussed below.

8.3.2.2 Simulation of Circulation Features Important for Climate Response

8.3.2.2.1 Meridional overturning circulation

The MOC is an important component of present-day climate and many models indicate that it will change in the future (Chapter 10). Unfortunately, many aspects of this circulation are not well observed. The MOC transports large amounts of heat and salt into high latitudes of the North Atlantic Ocean, where the relatively warm, salty surface waters are cooled by the atmosphere, making the water dense enough to sink to depth. These waters then flow southward towards the Southern Ocean where they mix with the rest of the World Ocean waters (see Supplementary Material, Figure S8.15).

The models simulate this major aspect of the MOC and also simulate a number of distinct wind-driven surface cells (see Supplementary Material, Figure S8.15). In the tropics and subtropics, these cells are quite shallow, but at the latitude of the Drake Passage (55°S) the wind-driven cell extends to a much greater depth (2 to 3 km). Most models in the multi-model data set have some manifestation of the wind-driven cells. The strength and pattern of the overturning circulation varies greatly from model to model (see Supplementary Material, Figure S8.15). The GISS-AOM exhibits the strongest overturning circulation, almost 40 to 50 Sv (10^6 m^3 s^{-1}). The CGCM (T47 and T63) and FGOALS have the weakest overturning circulations, about 10 Sv. The observed value is about 18 Sv (Ganachaud and Wunsch 2000).

In the Atlantic, the MOC, extending to considerable depth, is responsible for a large fraction of the northward oceanic heat transport in both observations and models (e.g., Hall and Bryden, 1982; Gordon et al., 2000). Figure 10.15 contains an index of the Atlantic MOC at 30°N for the suite of AOGCM 20th-century simulations. While the majority of models show an MOC strength that is within observational uncertainty, some show higher and lower values and a few show substantial drifts which could make interpretation of MOC projections using those models very difficult.

Overall, some aspects of the simulation of the MOC have improved since the TAR. This is due in part to improvements in mixing schemes, the use of higher resolution ocean models (see Section 8.2) and better simulation of the surface fluxes. This improvement can be seen in the individual model MOC sections (see Supplementary Material, Figure S8.15) by the

fact that (1) the location of the deep-water formation is more realistic, with more sinking occurring in the Greenland-Iceland-Norwegian and Labrador Seas as evidenced by the larger stream function values north of the sill located at 60°N (e.g., Wood et al., 1999) and (2) deep waters are subjected to less spurious mixing, resulting in better water mass properties (Thorpe et al., 2004) and a larger fraction of the water that sinks in the northern part of the North Atlantic Ocean exiting the Atlantic Ocean near 30°S (Danabasoglu et al., 1995). There is still room for improvement in the models' simulation of these processes, but there is clear evidence of improvement in many of the models analysed here.

8.3.2.2.2 Southern Ocean circulation

The Southern Ocean wind stress error has a particularly large detrimental impact on the Southern Ocean simulation by the models. Partly due to the wind stress error identified above, the simulated location of the Antarctic Circumpolar Current (ACC) is also too far north in most models (Russell et al., 2006). Since the AAIW is formed on the north side of the ACC, the water mass properties of the AAIW are distorted (typically too warm and salty: Russell et al., 2006). The relatively poor AAIW simulation contributes to the multi-model mean error identified above where the thermocline is too diffuse, because the waters near the base of thermocline are too warm and salty.

It is likely that the relatively poor Southern Ocean simulation will influence the transient climate response to increasing greenhouse gases by affecting the oceanic heat uptake. When forced by increases in radiative forcing, models with too little Southern Ocean mixing will probably underestimate the ocean heat uptake; models with too much mixing will likely exaggerate it. These errors in oceanic heat uptake will also have a large impact on the reliability of the sea level rise projections. See Chapter 10 for more discussion of this subject.

8.3.2.3 Summary of Oceanic Component Simulation

Overall, the improvements in the simulation of the observed time mean ocean state noted in the TAR (McAvaney et al., 2001) have continued in the models evaluated here. It is notable that this improvement has continued in spite of the fact that nearly all models no longer use flux adjustments. This suggests that the improvements in the physical parametrizations, increased resolution (see Section 8.2) and improved surface fluxes are together having a positive impact on model simulations. The temperature and salinity errors in the thermocline, while still large, have been reduced in many models. In the NH, many models still suffer from a cold bias in the upper ocean which is at a maximum near the surface and may distort the ice-albedo feedback in some models (see Section 8.3.3). In the Southern Ocean, the equatorward bias of the westerly wind stress maximum found in most model simulations is a problem that may affect the models' response to increasing radiative forcing.

8.3.3 Sea Ice

The magnitude and spatial distribution of the high-latitude climate changes can be strongly affected by sea ice characteristics, but evaluation of sea ice in models is hampered by insufficient observations of some key variables (e.g., ice thickness) (see Section 4.4). Even when sea ice errors can be quantified, it is difficult to isolate their causes, which might arise from deficiencies in the representation of sea ice itself, but could also be due to flawed simulation of the atmospheric and oceanic fields at high latitudes that drive ice movement (see Sections 8.3.1, 8.3.2 and 11.3.8).

Although sea ice treatment in AOGCMs has become more sophisticated, including better representation of both the dynamics and thermodynamics (see Section 8.2.4), improvement in simulating sea ice in these models, as a group, is not obvious (compare Figure 8.10 with TAR Figure 8.10; or Kattsov and Källén, 2005, Figure 4.11). In some models, however, the geographic distribution and seasonality of sea ice is now better reproduced.

For the purposes of model evaluation, the most reliably measured characteristic of sea ice is its seasonally varying extent (i.e., the area enclosed by the ice edge, operationally defined as the 15% contour; see Section 4.4). Despite the wide differences among the models, the multi-model mean of sea ice extent is in reasonable agreement with observations. Based on 14 of the 15 AOGCMs available at the time of analysis (one model was excluded because of unrealistically large ice extents; Arzel et al., 2006), the mean extent of simulated sea ice exceeds that observed in the NH by up to roughly 1×10^6 km^2 throughout the year, whereas in the SH the annual cycle is exaggerated, with too much sea ice in September (~2×10^6 km^2) and too little in March by a lesser amount. In many models the regional distribution of sea ice is poorly simulated, even if the hemispheric areal extent is approximately correct (Arzel et al., 2006; Holland and Raphael, 2006; Zhang and Walsh, 2006). The spread of simulated sea ice extents, measured as the multi-model standard deviation from the model mean, is generally narrower in the NH than in the SH (Arzel et al., 2006). Even in the best case (NH winter), the range of simulated sea ice extent exceeds 50% of the mean, and ice thickness also varies considerably, suggesting that projected decreases in sea ice cover remain rather uncertain. The model sea ice biases may influence global climate sensitivity (see Section 8.6). There is a tendency for models with relatively large sea ice extent in the present climate to have higher sensitivity. This is apparently especially true of models with low to moderate polar amplification (Holland and Bitz, 2003).

Among the primary causes of biases in simulated sea ice (especially its distribution) are biases in the simulation of high-latitude winds (Bitz et al., 2002; Walsh et al., 2002; Chapman and Walsh, 2007), as well as vertical and horizontal mixing in the ocean (Arzel et al., 2006). Also important are surface heat flux errors, which in particular may result from inadequate parametrizations of the atmospheric boundary layer (under stable conditions commonly occurring at night and in the winter over sea ice) and generally from poor simulation

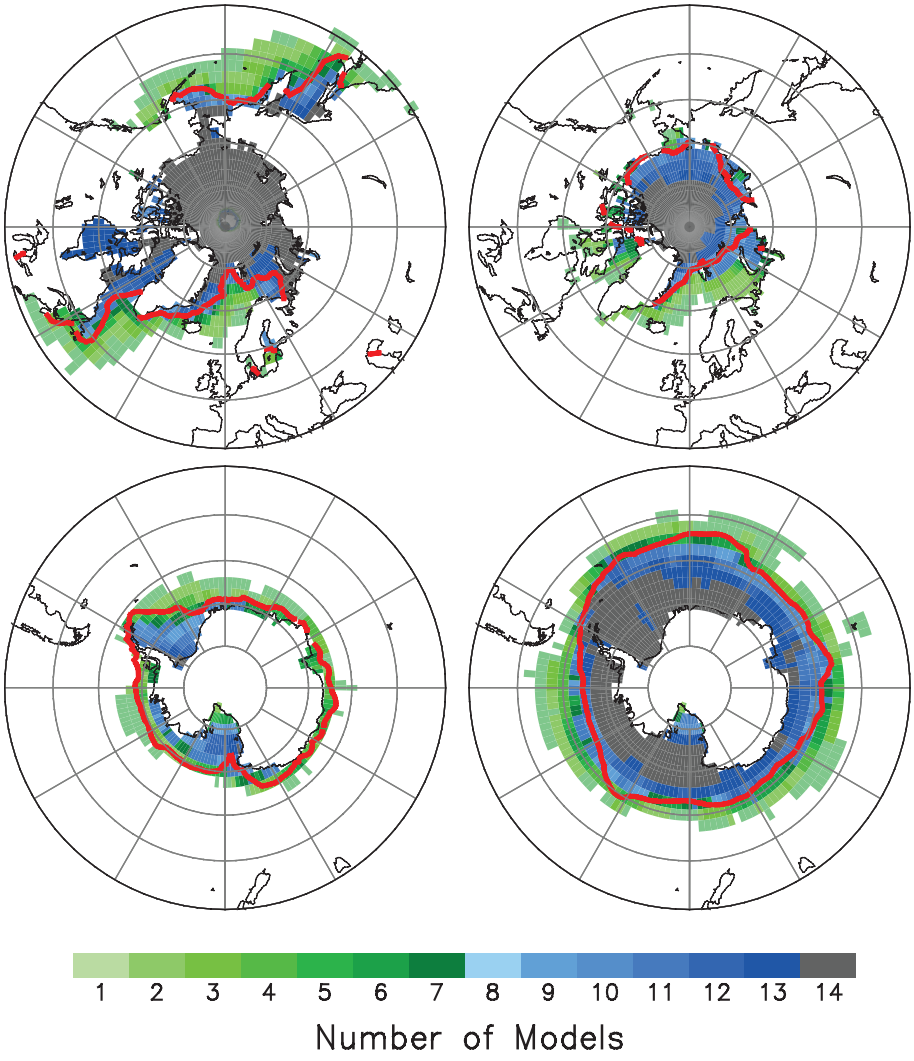


Figure 8.10. *Baseline climate (1980–1999) sea ice distribution in the Northern Hemisphere (upper panels) and Southern Hemisphere (lower panels) simulated by 14 of the AOGCMs listed in Table 8.1 for March (left) and September (right), adapted from Arzel et al. (2006). For each 2.5° x 2.5° longitude-latitude grid cell, the figure indicates the number of models that simulate at least 15% of the area covered by sea ice. The observed 15% concentration boundaries (red line) are based on the Hadley Centre Sea Ice and Sea Surface Temperature (HadISST; Rayner et al., 2003) data set.*

of high-latitude cloudiness, which is evident from the striking inter-model scatter (e.g., Kattsov and Källén, 2005).

8.3.4 Land Surface

Evaluation of the land surface component in coupled models is severely limited by the lack of suitable observations. The terrestrial surface plays key climatic roles in influencing the partitioning of available energy between sensible and latent heat fluxes, determining whether water drains or remains available for evaporation, determining the surface albedo and whether snow melts or remains frozen, and influencing surface fluxes of carbon and momentum. Few of these can be evaluated at large spatial or long temporal scales. This section therefore evaluates those quantities for which some observational data exist.

8.3.4.1 Snow Cover

Analysis and comparison of AMIP-2 results, available at the time of the TAR, and more recent AOGCM results in the present MMD at PCMDI, show that models are now more consistent in their simulation of snow cover. Problems remain, however, and Roesch (2006) showed that the recent models predict excessive snow water equivalent (SWE) in spring, likely because of excessive winter precipitation. Frei et al. (2005) found that AMIP-2 models simulate the seasonal timing and the relative spatial patterns of SWE over North America fairly well, but identified a tendency to overestimate ablation during spring. At the continental scale, the highest monthly SWE integrated over the North American continent in AMIP-2 models varies within ±50% of the observed value of about 1,500 km^3. The magnitude of these model errors is large enough to affect continental water balances. Snow cover area (SCA) is well captured by the recent models, but interannual variability is too low during melt. Frei et al. (2003) showed where observations were within the inter-quartile range of AMIP-2 models for all months at the hemispheric and continental scale. Encouragingly, there was significant improvement over earlier AMIP-1 simulations for seasonal and interannual variability of SCA (Frei et al., 2005). Both the recent AOGCMs and AMIP models reproduced the observed decline in annual SCA over the period 1979 to 1995 and most models captured the observed decadal-scale variability over the 20th century. Despite these improvements, a minority of models still exaggerate SCA.

Large discrepancies remain in albedo for forested areas under snowy conditions, due to difficulties in determining the extent of masking of snow by vegetation (Roesch, 2006). The ability of terrestrial models to simulate snow under observed meteorological forcing has been evaluated via several intercomparisons. At the scale of individual grid cells, for mid-latitude (Slater et al., 2001) and alpine (Etchevers et al., 2004) locations, the spread of model simulations usually encompasses observations. However, grid-box scale simulations of snow over high-latitude river basins identified significant limitations (Nijssen et al., 2003), due to difficulties relating to calculating net radiation, fractional snow cover and interactions with vegetation.

8.3.4.2 Land Hydrology

The evaluation of the hydrological component of climate models has mainly been conducted uncoupled from AOGCMs (Bowling et al., 2003; Nijssen et al., 2003; Boone et al., 2004). This is due in part to the difficulties of evaluating runoff simulations across a range of climate models due to variations in rainfall, snowmelt and net radiation. Some attempts have, however, been made. Arora (2001) used the AMIP-2 framework to show that the Canadian Climate Model's simulation of the global hydrological cycle compared well to observations, but regional variations in rainfall and runoff led to differences at the basin scale. Gerten et al. (2004) evaluated the hydrological performance of the Lund-Potsdam-Jena (LPJ) model and showed that the model performed well in the simulation of runoff and evapotranspiration compared to other global hydrological models, although the version of LPJ assessed had been enhanced to improve the simulation of hydrology over the versions used by Sitch et al. (2003).

Milly et al. (2005) made use of the MMD, which contains results from recent models, to investigate whether observed 20th-century trends in regional land hydrology could be attributed to variations in atmospheric composition and solar irradiance. Their analysis, based on an ensemble of 26 integrations of 20th-century climate from nine climate models, showed that at regional scales these models simulated observed streamflow measurements with good qualitative skill. Further, the models demonstrated highly significant quantitative skill in identifying the regional runoff trends indicated by 165 long-term stream gauges. They concluded that the impact of changes in atmospheric composition and solar irradiance on observed streamflow was, at least in part, predictable. This is an important scientific advance: it suggests that despite limitations in the hydrological parametrizations included in climate models, these models can capture observed changes in 20th-century streamflow associated with atmospheric composition and solar irradiance changes. This enhances confidence in the use of these models for future projection.

8.3.4.3 Surface Fluxes

Despite considerable effort since the TAR, uncertainties remain in the representation of solar radiation in climate models (Potter and Cess, 2004). The AMIP-2 results and the recent model results in the MMD provide an opportunity for a major systematic evaluation of model ability to simulate solar radiation. Wild (2005) and Wild et al. (2006) evaluated these models and found considerable differences in the global annual mean solar radiation absorbed at the Earth's surface. In comparison to global surface observations, Wild (2005) concluded that many climate models overestimate surface absorption of solar radiation partly due to problems in the parametrizations of atmospheric absorption, clouds and aerosols. Similar uncertainties exist in the simulation of downwelling infrared radiation (Wild et al., 2001). Difficulties in simulating absorbed solar and infrared radiation at the surface leads inevitably to uncertainty in the simulation of surface sensible and latent heat fluxes.

8.3.4.4 Carbon

A major advance since the TAR is some systematic assessments of the capability of land surface models to simulate carbon. Dargaville et al. (2002) evaluated the capacity of four global vegetation models to simulate the seasonal dynamics and interannual variability of atmospheric CO_2 between 1980 and 1991. Using off-line forcing, they evaluated the capacity of these models to simulate carbon fluxes, via an atmospheric transport model, using observed atmospheric CO_2 concentration. They found that the terrestrial models tended to underestimate the amplitude of the seasonal cycle and simulated the spring uptake of CO_2 approximately one to two months too early. Of the four models, none was clearly superior in its capacity to simulate the global carbon budget, but all four reproduced the main features of the observed seasonal cycle in atmospheric CO_2. A further off-line evaluation of the LPJ global vegetation model by Sitch et al. (2003) provided confidence that the model could replicate the observed vegetation pattern, seasonal variability in net ecosystem exchange and local soil moisture measurements when forced by observed climatologies.

The only systematic evaluation of carbon models that were interactively coupled to climate models occurred as part of the Coupled Climate-Carbon Cycle Model Intercomparison Project (C^4MIP), where Friedlingstein et al. (2006) compared the ability of a suite of models to simulate historical atmospheric CO_2 concentration forced by observed emissions. Issues relating to the magnitude of the fertilization effect and the partitioning between land and ocean uptake were identified in individual models, but it is only under increasing CO_2 in the future (see Chapter 10) that the differences become large. Several other groups have evaluated the impact of coupling specific models of carbon to climate models but clear results are difficult to obtain because of inevitable biases in both the terrestrial and atmospheric modules (e.g., Delire et al., 2003).

8.3.5 Changes in Model Performance

Standard experiments, agreed upon by the climate modelling community to facilitate model intercomparison (see Section 8.1.2.2), have produced archives of model output that make it easier to track historical changes in model performance. Most of the modelling groups that contributed output to the current MMD at PCMDI also archived simulations from their earlier models (circa 2000) as part of the Coupled Model Intercomparison Project (CMIP1&2). The TAR largely relied on the earlier generation of models in its assessment.

Based on the archived model output, it is possible to quantify changes in performance of evolving models.[4] This can be done most straightforwardly by only considering the 14 modelling

[4] One modelling group participating in CMIP1&2 did not contribute to the MMD, and four groups providing output to the MMD did not do so for CMIP1&2. Results from these five groups are therefore not considered in this subsection. Some modelling groups contributed results from more than one version of their model (sometimes, simply running it at two different resolutions), and in these cases the mean of the two model results is considered here.

groups that contributed output from both their earlier and more recent models. One important aspect of model skill is how well the models simulate the seasonally varying global pattern of climatically important fields. The only monthly mean fields available in the CMIP1&2 archive are surface air temperature, precipitation and mean sea level pressure, so these are the focus of this analysis. Although the simulation conditions in the MMD 20th-century simulations were not identical to those in the CMIP1&2 control runs, the differences do not alter the conclusions summarised below because the large-scale climatological features dominate, not the relatively small perturbations resulting from climate change.

A summary of the ability of AOGCMs to simulate the seasonally varying climate state is provided by Figure 8.11, which displays error measures that gauge how well recent models simulate precipitation, sea level pressure and surface temperature, compared with their predecessors. The normalised RMS error shown is a so-called space-time statistic, computed from squared errors, summed over all 12 climatological months and over the entire globe, with grid cell values weighted by the corresponding grid cell area. This statistic can be used to assess the combined contributions of both spatial pattern errors and seasonal cycle errors. The RMS error is divided by the corresponding observed standard deviation of the field to provide a relative measure of the error. In Figure 8.11 this scaling implies that pressure is better simulated than precipitation, and that surface temperature is simulated best of all.

The models in Figure 8.11 are categorised based on whether or not flux adjustments were applied (see Section 8.2.7). Of the earlier generation models, 8 of the 14 models were flux adjusted, but only two of these groups continue this practice. Several conclusions can be drawn from the figure: 1) although flux-adjusted models on average have smaller errors than those without (in both generations), the smallest errors in simulating sea level pressure and surface temperature are found in models without flux adjustment; 2) despite the elimination of flux adjustment in all but two of the recent models, the mean error obtained from the recent suite of 14 models is smaller than errors found in the corresponding earlier suite of models; and 3) models without flux adjustment have improved on average, as have the flux-adjusted models. An exception to this last statement is the slight increase in mean RMS error for sea level pressure found in non-flux-adjusted models. Despite no apparent improvement in the mean in this case, three of the recent generation models have smaller sea level pressure errors than any of the earlier models.

These results demonstrate that the models now being used in applications by major climate modelling groups better simulate seasonally varying patterns of precipitation, mean sea level pressure and surface air temperature than the models relied on by these same groups at the time of the TAR.

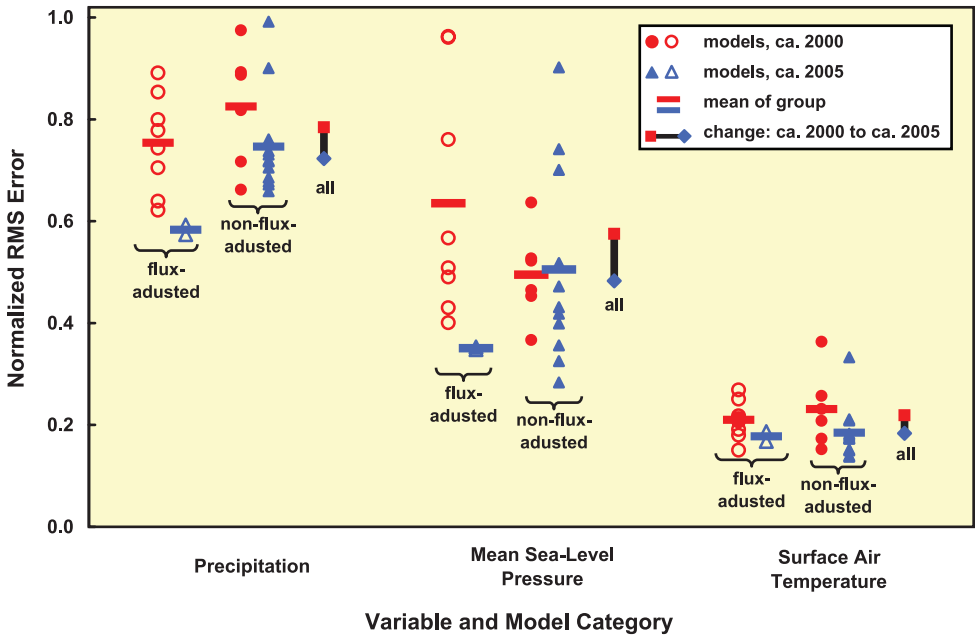


Figure 8.11. *Normalised RMS error in simulation of climatological patterns of monthly precipitation, mean sea level pressure and surface air temperature. Recent AOGCMs (circa 2005) are compared to their predecessors (circa 2000 and earlier). Models are categorised based on whether or not any flux adjustments were applied. The models are gauged against the following observation-based datasets: Climate Prediction Center Merged Analysis of Precipitation (CMAP; Xie and Arkin, 1997) for precipitation (1980–1999), European Centre for Medium Range Weather Forecasts 40-year reanalysis (ERA40; Uppala et al., 2005) for sea level pressure (1980–1999) and Climatic Research Unit (CRU; Jones et al., 1999) for surface temperature (1961–1990). Before computing the errors, both the observed and simulated fields were mapped to a uniform 4° x 5° latitude-longitude grid. For the earlier generation of models, results are based on the archived output from control runs (specifically, the first 30 years, in the case of temperature, and the first 20 years for the other fields), and for the recent generation models, results are based on the 20th-century simulations with climatological periods selected to correspond with observations. (In both groups of models, results are insensitive to the period selected.)*

8.4 Evaluation of Large-Scale Climate Variability as Simulated by Coupled Global Models

The atmosphere-ocean coupled climate system shows various modes of variability that range widely from intra-seasonal to inter-decadal time scales. Successful simulation and prediction over a wide range of these phenomena increase confidence in the AOGCMs used for climate predictions of the future.

8.4.1 Northern and Southern Annular Modes

There is evidence (e.g., Fyfe et al., 1999; Shindell et al., 1999) that the simulated response to greenhouse gas forcing in AOGCMs has a pattern that resembles the models' Northern Annular Mode (NAM), and thus it would appear important that the NAM (see Chapters 3 and 9) is realistically simulated. Analyses of individual AOGCMs (e.g., Fyfe et al., 1999; Shindell et al., 1999) have demonstrated that they are capable of simulating many aspects of the NAM and NAO patterns including linkages between circulation and temperature. Multi-model comparisons of winter atmospheric pressure (Osborn, 2004), winter temperature (Stephenson and Pavan, 2003) and atmospheric pressure across all months of the year (AchutaRao et al., 2004), including assessments of the MMD at PCMDI (Miller et al., 2006) confirm the overall skill of AOGCMs but also identify that teleconnections between the Atlantic and Pacific Oceans are stronger in many models than is observed (Osborn, 2004). In some models this is related to a bias towards a strong polar vortex in all winters so that their simulations nearly always reflect behaviour that is only observed at times with strong vortices (when a stronger Atlantic-Pacific correlation is observed; Castanheira and Graf, 2003).

Most AOGCMs organise too much sea level-pressure variability into the NAM and NAO (Miller et al., 2006). The year-to-year variance of the NAM or NAO is correctly simulated by some AOGCMs, while other simulations are significantly too variable (Osborn, 2004); for the models that simulate stronger variability, the persistence of anomalous states is greater than is observed (AchutaRao et al., 2004). The magnitude of multi-decadal variability (relative to sub-decadal variability) is lower in AOGCM control simulations than is observed, and cannot be reproduced in current model simulations with external forcings (Osborn, 2004; Gillett, 2005). However, Scaife et al. (2005) show that the observed multi-decadal trend in the surface NAM and NAO can be reproduced in an AOGCM if observed trends in the lower stratospheric circulation are prescribed in the model. Troposphere-stratosphere coupling processes may therefore need to be included in models to fully simulate NAM variability. The response of the NAM and NAO to volcanic aerosols (Stenchikov et al., 2002), sea surface temperature variability (Hurrell et al., 2004) and sea ice anomalies (Alexander et al., 2004) demonstrate some compatibility with observed variations, though the difficulties in determining cause and effect in the coupled system limit the conclusions that can be drawn with regards to the trustworthiness of model behaviour.

Like its NH counterpart, the NAM, the Southern Annular Mode (SAM; see Chapters 3 and 9) has signatures in the tropospheric circulation, the stratospheric polar vortex, mid-latitude storm tracks, ocean circulation and sea ice. AOGCMs generally simulate the SAM realistically (Fyfe et al., 1999; Cai et al., 2003; Miller et al., 2006). For example, Figure 8.12 compares the austral winter SAM simulated in the MMD at PCMDI to the observed SAM as represented in the National Centers for Environmental Prediction (NCEP) reanalysis. The main elements of the pattern, the low-pressure anomaly over Antarctica and the high-pressure anomalies equatorward of 60°S are captured well by the AOGCMs. In all but two AOGCMs, the spatial correlation between the observed and simulated SAM is greater than 0.95. Further analysis shows that the SAM signature in surface temperature, such as the surface warm anomaly over the Antarctic Peninsula associated with a positive SAM event, is also captured by some AOGCMs (e.g., Delworth et al., 2006; Otto-Bliesner et al., 2006). This follows from the realistic simulation of the SAM-related circulation shown in Figure 8.12, because the surface temperature signatures of the SAM typically reflect advection of the climatological temperature distribution by the SAM-related circulation (Thompson and Wallace, 2000).

Although the spatial structure of the SAM is well simulated by the AOGCMs in the MMD at PCMDI, other features of the SAM, such as the amplitude, the detailed zonal structure and the temporal spectra, do not always compare well with the NCEP reanalysis SAM (Miller et al., 2006; Raphael and Holland, 2006). For example, Figure 8.12 shows that the simulated SAM variance (the square of the SAM amplitude) ranges between 0.9 and 2.4 times the NCEP reanalysis SAM variance. However, such features vary considerably among different realisations of multiple-member ensembles (Raphael and Holland, 2006), and the temporal variability of the NCEP reanalysis SAM does not compare well to station data (Marshall, 2003). Thus, it is difficult to assess whether these discrepancies between the simulated SAM and the NCEP reanalysis SAM point to shortcomings in the models or to shortcomings in the observed analysis.

Resolving these issues may require a better understanding of SAM dynamics. Although the SAM exhibits clear signatures in the ocean and stratosphere, its tropospheric structure can be simulated, for example, in atmospheric GCMs with a poorly resolved stratosphere and driven by prescribed SSTs (e.g., Limpasuvan and Hartmann, 2000; Cai et al., 2003). Even much simpler atmospheric models with one or two vertical levels produce SAM-like variability (Vallis et al., 2004). These relatively simple models capture the dynamics that underlie SAM variability – namely, interactions between the tropospheric jet stream and extratropical weather systems (Limpasuvan and Hartmann, 2000; Lorenz and Hartmann, 2001). Nevertheless, the ocean and stratosphere might still influence SAM variability in important ways. For example, AOGCM simulations suggest strong SAM-related impacts on ocean temperature, ocean heat transport and sea ice distribution (Watterson, 2001; Hall and Visbeck, 2002), suggesting a potential for air-sea interactions to influence SAM dynamics. Furthermore, observational

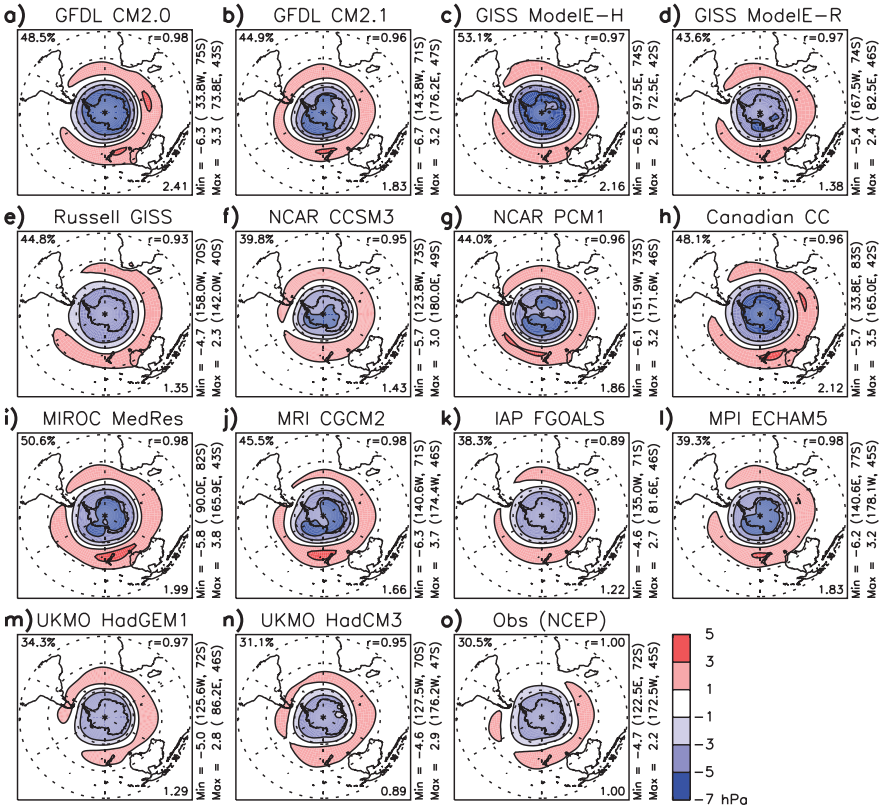


Figure 8.12. *Ensemble mean leading Empirical Orthogonal Function (EOF) of summer (November through February) Southern Hemisphere sea level pressure (hPa) for 1950 to 1999. The EOFs are scaled so that the associated principal component has unit variance over this period. The percentage of variance accounted for by the leading mode is listed at the upper left corner of each panel. The spatial correlation (r) with the observed pattern is given at the upper right corner. At the lower right is the ratio of the EOF spatial variance to the observed value. "Canadian CC" refers to CGCM3.1 (T47), and "Russell GISS" refers to the GISS AOM. Adapted from Miller et al. (2006).*

and modelling studies (e.g., Thompson and Solomon, 2002; Baldwin et al., 2003; Gillett and Thompson, 2003) suggest that the stratosphere might also influence the tropospheric SAM, at least in austral spring and summer. Thus, an accurate simulation of stratosphere-troposphere and ocean-atmosphere coupling may still be necessary to accurately simulate the SAM.

8.4.2 Pacific Decadal Variability

Recent work suggests that the Pacific Decadal Oscillation (PDO, see Chapters 3 and 9) is the North Pacific expression of a near-global ENSO-like pattern of variability called the Inter-decadal Pacific Oscillation or IPO (Power et al., 1999; Deser et al., 2004). The appearance of the IPO as the leading Empirical Orthogonal Function (EOF) of SST in AOGCMs that do not include inter-decadal variability in natural or external forcing indicates that the IPO is an internally generated, natural form of variability. Note, however, that some AOGCMs exhibit an El Niño-like response to global warming (Cubasch et al., 2001) that can take decades to emerge (Cai and Whetton, 2000). Therefore some, though certainly not all, of the variability seen in the IPO and PDO indices might be anthropogenic in origin (Shiogama et al., 2005). The IPO and PDO can be partially understood as the residual of random inter-decadal changes in ENSO activity (e.g., Power et al., 2006), with their spectra reddened (i.e., increasing energy at lower frequencies) by the integrating effect of the upper ocean mixed layer (Newman et al., 2003; Power and Colman, 2006) and the excitation of low frequency off-equatorial Rossby waves (Power and Colman, 2006). Some of the inter-decadal variability in the tropics also has an extratropical origin (e.g., Barnett et al., 1999; Hazeleger et al., 2001) and this might give the IPO a predictable component (Power et al., 2006).

Atmosphere-Ocean General Circulation Models do not seem to have difficulty in simulating IPO-like variability (e.g., Yeh and Kirtman, 2004; Meehl and Hu, 2006), even AOGCMs that are too coarse to properly resolve equatorially trapped waves important for ENSO dynamics. Some studies have provided objective measures of the realism of the modelled decadal variability. For example, Pierce et al. (2000) found that the ENSO-like decadal SST mode in the Pacific Ocean of their AOGCM had a pattern that gave a correlation of 0.56 with its observed counterpart. This compared with a correlation coefficient of 0.79 between the modelled and observed interannual ENSO mode. The reduced agreement on decadal time scales was attributed to lower than observed variability in the North Pacific subpolar gyre, over the southwest Pacific and along the western coast of North America. The latter was attributed to poor resolution of the coastal waveguide in the AOGCM. The importance of properly resolving coastally trapped waves in the context of simulating decadal variability in the Pacific has been raised in a number studies (e.g., Meehl and Hu, 2006). Finally, there has been little work evaluating the amplitude of Pacific decadal variability in AOGCMs. Manabe and Stouffer (1996) showed that the variability has roughly the right magnitude in their AOGCM, but a more detailed investigation using recent AOGCMs with a specific focus on IPO-like variability would be useful.

8.4.3 Pacific-North American Pattern

The Pacific-North American (PNA) pattern (see Chapter 3) is commonly associated with the response to anomalous boundary forcing. However, PNA-like patterns have been simulated in atmospheric GCM experiments subjected to constant boundary conditions. Hence, both external and internal processes may contribute to the formation of this pattern. Particular attention has been paid to the external influences due to SST anomalies related to ENSO episodes in the tropical Pacific, as well as those situated in the extratropical North Pacific. Internal mechanisms that might play a role in the formation of the PNA pattern include interactions between the slowly varying component of the circulation and high-frequency transient disturbances, and instability of the climatological flow pattern. Trenberth et al. (1998) reviewed the myriad observational and modelling studies on various processes contributing to the PNA pattern.

The ability of GCMs to replicate various aspects of the PNA pattern has been tested in coordinated experiments. Until several years ago, such experiments were conducted by prescribing observed SST anomalies as lower boundary conditions for atmospheric GCMs. Particularly noteworthy are the ensembles of model runs performed under the auspices of the European Prediction of Climate Variations on Seasonal to Interannual Time Scales (PROVOST) and the US Dynamical Seasonal Prediction (DSP) projects. The skill of seasonal hindcasts of the participating models' atmospheric anomalies in different regions of the globe (including the PNA sector) was summarised in a series of articles edited by Palmer and Shukla (2000). These results demonstrate that the prescribed SST forcing exerts a notable impact on the model atmospheres. The hindcast skill for the winter extratropical NH is particularly high during the largest El Niño and La Niña episodes. However, these experiments indicate considerable variability of the responses in individual models, and among ensemble members of a given model. This large scatter of model responses suggests that atmospheric changes in the extratropics are only weakly constrained by tropical SST forcing.

The performance of the dynamical seasonal forecast system at the US NCEP in predicting the atmospheric anomalies given prescribed anomalous SST forcing (in the PNA sector) was assessed by Kanamitsu et al. (2002). During the large El Niño event of 1997 to 1998, the forecasts based on this system with one-month lead time are in good agreement with the observed changes in the PNA sector, with anomaly correlation scores of 0.8 to 0.9 (for 200 mb height), 0.6 to 0.8 (surface temperature) and 0.4 to 0.5 (precipitation). More recently, hindcast experiments have been launched using AOGCMs. The European effort was supported by the Development of a European Multimodel Ensemble System for Seasonal to Interannual Prediction (DEMETER) programme (Palmer et al., 2004). For the boreal winter season, and with hindcasts initiated in November, the model-generated PNA indices exhibit statistically significant temporal correlations with the corresponding observations. The fidelity of the PNA simulations is evident in both the multi-model ensemble means, as well as in the output from individual member models. However, the strength of the ensemble mean signal remains low when compared with the statistical spread due to sampling fluctuations among different models, and among different realisations of a given model. The model skill is notably lower for other seasons and longer lead times. Empirical Orthogonal Function analyses of the geopotential height data produced by individual member models confirm that the PNA pattern is a leading spatial mode of atmospheric variability in these models.

Multi-century integrations have also been conducted at various institutions using the current generation of AOGCMs. Unlike the hindcasting or forecasting experiments mentioned above, these climate simulations are not aimed at reproducing specific ENSO events in the observed system. Diagnosis of the output from one such AOGCM integration indicates that the modelled ENSO events are linked to a PNA-like pattern in the upper troposphere (Wittenberg et al., 2006). The centres of action of the simulated patterns are systematically displaced 20 to 30 degrees of longitude west of the observed positions. This discrepancy is evidently linked to a corresponding spatial shift in the ENSO-related SST and precipitation anomaly centres simulated in the tropical Pacific. This finding illustrates that the spatial configuration of the PNA pattern in AOGCMs is crucially dependent on the accuracy of ENSO simulations in the tropics.

8.4.4 Cold Ocean-Warm Land Pattern

The Cold Ocean-Warm Land (COWL) pattern indicates that the oceans are relatively cold and the continents are relatively warm poleward of 40°N when the NH is relatively warm. The COWL pattern results from the contrast in thermal inertia between the continents and oceans, which allows continental temperature anomalies to have greater amplitude, and thus more strongly influence hemispheric mean temperature. The COWL pattern has been simulated in climate models of varying degrees of complexity (e.g., Broccoli et al., 1998), and similar patterns have been obtained from cluster analysis (Wu and Straus, 2004a) and EOF analysis (Wu and Straus, 2004b) of reanalysis data. In a number of studies, cold season trends in NH temperature and sea level pressure during the late 20th century have been associated with secular trends in indices of the COWL pattern (Wallace et al., 1996; Lu et al., 2004).

In their analysis of AOGCM simulations, Broccoli et al. (1998) found that the original method for extracting the COWL pattern could yield potentially misleading results when applied to a simulation forced by past and future variations in anthropogenic forcing (as is the case with most other patterns, or modes, of climate variability). The resulting spatial pattern was a mixture of the patterns associated with unforced climate variability and the anthropogenic fingerprint. Broccoli et al. (1998) also noted that temperature anomalies in the two continental centres of the COWL pattern are virtually uncorrelated, suggesting that different atmospheric teleconnections are involved in producing this pattern. Quadrelli and Wallace (2004) recently showed that the COWL pattern can be reconstructed as a linear combination of the first two EOFs of monthly mean December to March sea level pressure.

These two EOFs are the NAM and a mode closely resembling the PNA pattern. A linear combination of these two fundamental patterns can also account for a substantial fraction of the winter trend in NH sea level pressure during the late 20th century.

8.4.5 Atmospheric Regimes and Blocking

Weather, or climate, regimes are important factors in determining climate at various locations around the world and they can have a large impact on day-to-day variability (e.g., Plaut and Simonnet, 2001; Trigo et al., 2004; Yiou and Nogaj, 2004). General Circulation Models have been found to simulate hemispheric climate regimes quite similar to those found in observations (Robertson, 2001; Achatz and Opsteegh, 2003; Selten and Branstator, 2004). Simulated regional climate regimes over the North Atlantic strongly similar to the observed regimes were reported by Cassou et al. (2004), while the North Pacific regimes simulated by Farrara et al. (2000) were broadly consistent with those in observations. Since the TAR, agreement between different studies has improved regarding the number and structure of both hemispheric and sectoral atmospheric regimes, although this remains a subject of research (e.g., Wu and Straus, 2004a) and the statistical significance of the regimes has been discussed and remains an unresolved issue (e.g., Hannachi and O'Neill, 2001; Hsu and Zwiers, 2001; Stephenson et al., 2004; Molteni et al., 2006).

Blocking events are an important class of sectoral weather regimes (see Chapter 3), associated with local reversals of the mid-latitude westerlies. The most recent systematic intercomparison of atmospheric GCM simulations of NH blocking (D'Andrea et al., 1998) was reported in the TAR. Consistent with the conclusions of this earlier study, recent studies have found that GCMs tend to simulate the location of NH blocking more accurately than frequency or duration: simulated events are generally shorter and rarer than observed events (e.g., Pelly and Hoskins, 2003b). An analysis of one of the AOGCMs from the MMD at the PCMDI found that increased horizontal resolution combined with better physical parametrizations has led to improvements in simulations of NH blocking and synoptic weather regimes over Europe. Finally, both GCM simulations and analyses of long data sets suggest the existence of considerable interannual to inter-decadal variability in blocking frequency (e.g., Stein, 2000; Pelly and Hoskins, 2003a), highlighting the need for caution when assessing blocking climatologies derived from short records (either observed or simulated). Blocking events also occur in the SH mid-latitudes (Sinclair, 1996); no systematic intercomparison of observed and simulated SH blocking climatologies has been carried out. There is also evidence of connections between North and South Pacific blocking and ENSO variability (e.g., Renwick, 1998; Chen and Yoon, 2002), and between North Atlantic blocks and sudden stratospheric warmings (e.g., Kodera and Chiba, 1995; Monahan et al., 2003) but these connections have not been systematically explored in AOGCMs.

8.4.6 Atlantic Multi-decadal Variability

The Atlantic Ocean exhibits considerable multi-decadal variability with time scales of about 50 to 100 years (see Chapter 3). This multi-decadal variability appears to be a robust feature of the surface climate in the Atlantic region, as shown by tree ring reconstructions for the last few centuries (e.g., Mann et al., 1998). Atlantic multi-decadal variability has a unique spatial pattern in the SST anomaly field, with opposite changes in the North and South Atlantic (e.g., Mestas-Nunez and Enfield, 1999; Latif et al., 2004), and this dipole pattern has been shown to be significantly correlated with decadal changes in Sahelian rainfall (Folland et al., 1986). Decadal variations in hurricane activity have also been linked to the multi-decadal SST variability in the Atlantic (Goldenberg et al., 2001). Atmosphere-Ocean General Circulation Models simulate Atlantic multi-decadal variability (e.g., Delworth et al., 1993; Latif, 1998 and references therein; Knight et al., 2005), and the simulated space-time structure is consistent with that observed (Delworth and Mann, 2000). The multi-decadal variability simulated by the AOGCMs originates from variations in the MOC (see Section 8.3). The mechanisms, however, that control the variations in the MOC are fairly different across the ensemble of AOGCMs. In most AOGCMs, the variability can be understood as a damped oceanic eigenmode that is stochastically excited by the atmosphere. In a few other AOGCMs, however, coupled interactions between the ocean and the atmosphere appear to be more important. The relative roles of high- and low-latitude processes differ also from model to model. The variations in the Atlantic SST associated with the multi-decadal variability appear to be predictable a few decades ahead, which has been shown by potential (diagnostic) and classical (prognostic) predictability studies. Atmospheric quantities do not exhibit predictability at decadal time scales in these studies, which supports the picture of stochastically forced variability.

8.4.7 El Niño-Southern Oscillation

During the last decade, there has been steady progress in simulating and predicting ENSO (see Chapters 3 and 9) and the related global variability using AOGCMs (Latif et al., 2001; Davey et al., 2002; AchutaRao and Sperber, 2002). Over the last several years the parametrized physics have become more comprehensive (Gregory et al., 2000; Collins et al., 2001; Kiehl and Gent, 2004), the horizontal and vertical resolutions, particularly in the atmospheric component models, have markedly increased (Guilyardi et al., 2004) and the application of observations in initialising forecasts has become more sophisticated (Alves et al., 2004). These improvements in model formulation have led to a better representation of the spatial pattern of the SST anomalies in the eastern Pacific (AchutaRao and Sperber, 2006). In fact, as an indication of recent model improvements, some IPCC class models are being used for ENSO prediction (Wittenberg et al., 2006). Despite this progress, serious systematic errors in both the simulated mean climate and the natural variability persist. For example, the

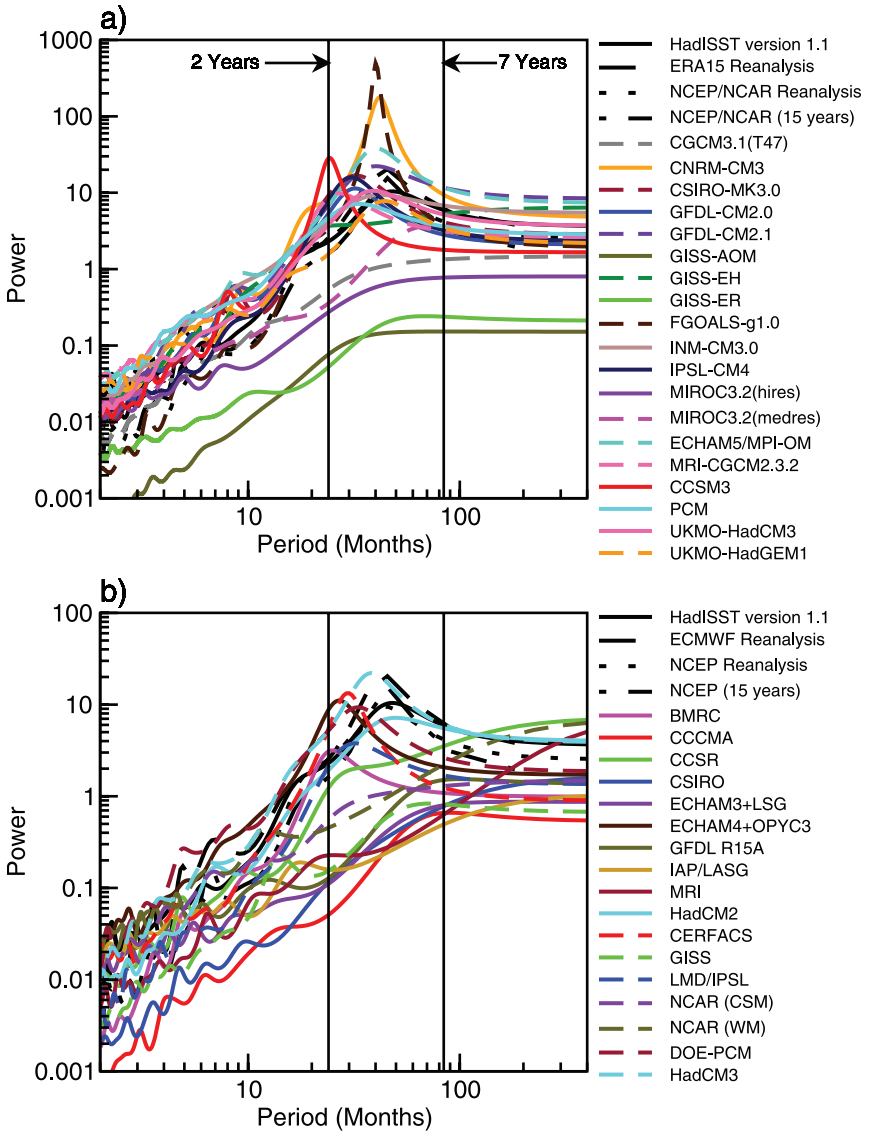


Figure 8.13. *Maximum entropy power spectra of surface air temperature averaged over the $NINO_3$ region (i.e., 5°N to 5°S, 150°W to 90° W) for (a) the MMD at the PCMDI and (b) the CMIP2 models. Note the differing scales on the vertical axes and that ECMWF reanalysis in (b) refers to the European Centre for Medium Range Weather Forecasts (ECMWF) 15-year reanalysis (ERA15) as in (a). The vertical lines correspond to periods of two and seven years. The power spectra from the reanalyses and for SST from the Hadley Centre Sea Ice and Sea Surface Temperature (HadISST) version 1.1 data set are given by the series of solid, dashed and dotted black curves. Adapted from AchutaRao and Sperber (2006).*

so-called 'double ITCZ' problem noted by Mechoso et al. (1995; see Section 8.3.1) remains a major source of error in simulating the annual cycle in the tropics in most AOGCMs, which ultimately affects the fidelity of the simulated ENSO. Along the equator in the Pacific the models fail to adequately capture the zonal SST gradient, the equatorial cold tongue structure is equatorially confined and extends too far too to the west (Cai et al., 2003), and the simulations typically have thermoclines that are far too diffuse (Davey et al., 2002). Most AOGCMs fail to capture the meridional extent of the anomalies in the eastern Pacific and tend to produce anomalies that extend too far into the western tropical Pacific. Most, but not all, AOGCMs produce ENSO variability that occurs on time scales considerably faster than observed (AchutaRao and Sperber, 2002), although there has been some notable progress in this regard over the last decade (AchutaRao and Sperber, 2006) in that more models are consistent with the observed time scale for ENSO (see Figure 8.13). The models also have difficulty capturing the correct phase locking between the annual cycle and ENSO. Further, some AOGCMs fail to represent the spatial and temporal structure of the El Niño-La Niña asymmetry (Monahan and Dai, 2004). Other weaknesses in the simulated amplitude and structure of ENSO variability are discussed in Davey et al. (2002) and van Oldenborgh et al. (2005).

Current research points to some promise in addressing some of the above problems. For example, increasing the atmospheric resolution in both the horizontal (Guilyardi et al., 2004) and vertical (NCEP Coupled Forecast System) may improve the simulated spectral characteristics of the variability, ocean parametrized physics have also been shown to significantly influence the coupled variability (Meehl et al., 2001) and continued methodical numerical experimentation into the sources of model error (e.g., Schneider, 2001) will ultimately suggest model improvement strategies.

In terms of ENSO prediction, the two biggest recent advances are: (i) the recognition that forecasts must include quantitative information regarding uncertainty (i.e., probabilistic prediction) and that verification must include skill measures for probability forecasts (Kirtman, 2003); and (ii) that a multi-model ensemble strategy may be the best current approach for adequately dealing with forecast uncertainty, for example, Palmer et al. (2004), in which Figure 2 demonstrates that a multi-model ensemble forecast has better skill than a comparable ensemble based on a single model. Improvements in the use of data, particularly in the ocean, for initialising forecasts continues to yield enhancements in forecast skill (Alves et al., 2004); moreover, other research indicates that forecast initialisation strategies that are implemented within the framework of the coupled system as opposed to the individual component models may also lead to substantial improvements in skill (Chen et al., 1995). However, basic questions regarding the predictability of SST in the tropical Pacific remain open challenges in the forecast community. For instance, it is unclear how westerly wind bursts, intra-seasonal variability or atmospheric weather noise in general limit the predictability of ENSO (e.g., Thompson and Battisti, 2001; Kleeman et al., 2003; Flugel et

al., 2004; Kirtman et al., 2005). There are also apparent decadal variations in ENSO forecast skill (Balmaseda et al., 1995; Ji et al., 1996; Kirtman and Schopf, 1998), and the sources of these variations are the subject of some debate. Finally, it remains unclear how changes in the mean climate will ultimately affect ENSO predictability (Collins et al., 2002).

8.4.8 Madden-Julian Oscillation

The MJO (Madden and Julian, 1971) refers to the dominant mode of intra-seasonal variability in the tropical troposphere. It is characterised by large-scale regions of enhanced and suppressed convection, coupled to a deep baroclinic, primarily zonal circulation anomaly. Together, they propagate slowly eastward along the equator from the western Indian Ocean to the central Pacific and exhibit local periodicity in a broad 30- to 90-day range. Simulation of the MJO in contemporary coupled and uncoupled climate models remains unsatisfactory (e.g., Zhang, 2005; Lin et al., 2006), partly because more is now demanded from the model simulations, as understanding of the role of the MJO in the coupled atmosphere-ocean climate system expands. For instance, simulations of the MJO in models at the time of the TAR were judged using gross metrics (e.g., Slingo et al., 1996). The spatial phasing of the associated surface fluxes, for instance, are now recognised as critical for the development of the MJO and its interaction with the underlying ocean (e.g., Hendon, 2005; Zhang, 2005). Thus, while a model may simulate some gross characteristics of the MJO, the simulation may be deemed unsuccessful when the detailed structure of the surface fluxes is examined (e.g., Hendon, 2000).

Variability with MJO characteristics (e.g., convection and wind anomalies of the correct spatial scale that propagate coherently eastward with realistic phase speeds) is simulated in many contemporary models (e.g., Sperber et al., 2005; Zhang, 2005), but this variability is typically not simulated to occur often enough or with sufficient strength so that the MJO stands out realistically above the broadband background variability (Lin et al., 2006). This underestimation of the strength and coherence of convection and wind variability at MJO temporal and spatial scales means that contemporary climate models still simulate poorly many of the important climatic effects of the MJO (e.g., its impact on rainfall variability in the monsoons or the modulation of tropical cyclone development). Simulation of the spatial structure of the MJO as it evolves through its life cycle is also problematic, with tendencies for the convective anomaly to split into double ITCZs in the Pacific and for erroneously strong convective signals to sometimes develop in the eastern Pacific ITCZ (e.g., Inness and Slingo, 2003). It has also been suggested that inadequate representation in climate models of cloud-radiative interactions and/or convection-moisture interactions may explain some of the difficulties in simulating the MJO (e.g., Lee et al., 2001; Bony and Emanuel, 2005).

Even though the MJO is probably not fundamentally a coupled ocean-atmosphere mode (e.g., Waliser et al., 1999), air-sea coupling does appear to promote more coherent eastward, and, in northern summer, northward propagation at MJO temporal and spatial scales. The interaction with an active ocean is important especially in the suppressed convective phase when SSTs are warming and the atmospheric boundary layer is recovering (e.g., Hendon, 2005). Thus, the most realistic simulation of the MJO is anticipated to be with AOGCMs. However, coupling, in general, has not been a panacea. While coupling in some models improves some aspects of the MJO, especially eastward propagation and coherence of convective anomalies across the Indian and western Pacific Oceans (e.g., Kemball-Cook et al., 2002; Inness and Slingo, 2003), problems with the horizontal structure and seasonality remain. Typically, models that show the most beneficial impact of coupling on the propagation characteristics of the MJO are also the models that possess the most unrealistic seasonal variation of MJO activity (e.g., Zhang, 2005). Unrealistic simulation of the seasonal variation of MJO activity implies that the simulated MJO will improperly interact with climate phenomena that are tied to the seasonal cycle (e.g., the monsoons and ENSO).

Simulation of the MJO is also adversely affected by biases in the mean state (see Section 8.4.7). These biases include the tendency for coupled models to exaggerate the double ITCZ in the Indian and western Pacific Oceans, under-predict the eastward extent of surface monsoonal westerlies into the western Pacific, and over-predict the westward extension of the Pacific cold tongue. Together, these flaws limit development, maintenance and the eastward extent of convection associated with the MJO, thereby reducing its overall strength and coherence (e.g., Inness et al., 2003). To date, simulation of the MJO has proven to be most sensitive to the convective parametrization employed in climate models (e.g., Wang and Schlesinger, 1999; Maloney and Hartmann, 2001; Slingo et al., 2005). A consensus, although with exceptions (e.g., Liu et al., 2005), appears to be emerging that convective schemes based on local vertical stability and that include some triggering threshold produce more realistic MJO variability than those that convect too readily. However, some sophisticated models, with arguably the most physically based convective parametrizations, are unable to simulate reasonable MJO activity (e.g., Slingo et al., 2005).

8.4.9 Quasi-Biennial Oscillation

The Quasi-Biennial Oscillation (QBO; see Chapter 3) is a quasi-periodic wave-driven zonal mean wind reversal that dominates the low-frequency variability of the lower equatorial stratosphere (3 to 100 hPa) and affects a variety of extratropical phenomena including the strength and stability of the winter polar vortex (e.g., Baldwin et al., 2001). Theory and observations indicate that a broad spectrum of vertically propagating waves in the equatorial atmosphere must be considered to explain the QBO. Realistic simulation of the QBO in GCMs therefore depends on three important conditions: (i) sufficient vertical resolution in the stratosphere to allow the representation of equatorial waves at the horizontally resolved scales of a GCM, (ii) a realistic excitation of resolved equatorial waves by simulated tropical weather and (iii) parametrization of the

effects of unresolved gravity waves. Due to the computational cost associated with the requirement of a well-resolved stratosphere, the models employed for the current assessment do not generally include the QBO.

The inability of resolved wave driving to induce a spontaneous QBO in GCMs has been a long-standing issue (Boville and Randel, 1992). Only recently (Takahashi, 1996, 1999; Horinouchi and Yoden, 1998; Hamilton et al., 2001) have two necessary conditions been identified that allow resolved waves to induce a QBO: high vertical resolution in the lower stratosphere (roughly 0.5 km), and a parametrization of deep cumulus convection with sufficiently large temporal variability. However, recent analysis of satellite and radar observations of deep tropical convection (Horinouchi, 2002) indicates that the forcing of a QBO by resolved waves alone requires a parametrization of deep convection with an unrealistically large amount of temporal variability. Consequently, it is currently thought that a combination of resolved and parametrized waves is required to properly model the QBO. The utility of parametrized non-orographic gravity wave drag to force a QBO has now been demonstrated by a number of studies (Scaife et al., 2000; Giorgetta et al., 2002, 2006). Often an enhancement of input momentum flux in the tropics relative to that needed in the extratropics is required. Such an enhancement, however, depends implicitly on the amount of resolved waves and in turn, the spatial and temporal properties of parametrized deep convection employed in each model (Horinouchi et al., 2003; Scinocca and McFarlane, 2004).

8.4.10 Monsoon Variability

Monsoon variability (see Chapters 3, 9 and 11) occurs over a range of temporal scales from intra-seasonal to inter-decadal. Since the TAR, the ability of AOGCMs to simulate monsoon variability on intra-seasonal as well as interannual time scales has been examined. Lambert and Boer (2001) compared the AOGCMs that participated in CMIP, finding large errors in the simulated precipitation in the equatorial regions and in the Asian monsoon region. Lin et al. (2006) evaluated the intra-seasonal variation of precipitation in the MMD at PCMDI. They found that the intra-seasonal variance of precipitation simulated by most AOGCMs was smaller than observed. The space-time spectra of most model simulations have much less power than is observed, especially at periods shorter than six days. The speed of the equatorial waves is too fast, and the persistence of the precipitation is too long, in most of the AOGCM simulations. Annamalai et al (2004) examined the fidelity of precipitation simulation in the Asian monsoon region in the MMD at PCMDI. They found that just 6 of the 18 AOGCMs considered realistically simulated climatological monsoon precipitation for the 20th century. For the former set of models, the spatial correlation of the patterns of monsoon precipitation between the models exceeded 0.6, and the seasonal cycle of monsoon rainfall was simulated well. Among these models, only four exhibited a robust ENSO-monsoon contemporaneous teleconnection. Cook and Vizy (2006) evaluated the simulation of the 20th-century climate in North Africa in the MMD at PCMDI. They found that the simulation of North African summer precipitation was less realistic than the simulation of summer precipitation over North America or Europe. In short, most AOGCMs do not simulate the spatial or intra-seasonal variation of monsoon precipitation accurately. See Chapter 11 for a more detailed regional evaluation of simulated monsoon variability.

8.4.11 Shorter-Term Predictions Using Climate Models

This subsection focuses on the few results of initial value predictions made using models that are identical, or very close to, the models used in other chapters of this report for understanding and predicting climate change.

Weather prediction

Since the TAR, it has been shown that climate models can be integrated as weather prediction models if they are initialised appropriately (Phillips et al., 2004). This advance appears to be due to: (i) improvements in the forecast model analyses and (ii) increases in the climate model spatial resolution. An advantage of testing a model's ability to predict weather is that some of the sub-grid scale physical processes that are parametrized in models (e.g., cloud formation, convection) can be evaluated on time scales characteristic of those processes, without the complication of feedbacks from these processes altering the underlying state of the atmosphere (Pope and Stratton, 2002; Boyle et al., 2005; Williamson et al., 2005; Martin et al., 2006). Full use can be made of the plentiful meteorological data sets and observations from specialised field experiments. According to these studies, some of the biases found in climate simulations are also evident in the analysis of their weather forecasts. This suggests that ongoing improvements in model formulation driven primarily by the needs of weather forecasting may lead also to more reliable climate predictions.

Seasonal prediction

Verification of seasonal-range predictions provides a direct test of a model's ability to represent the physical and dynamical processes controlling (unforced) fluctuations in the climate system. Satisfactory prediction of variations in key climate signals such as ENSO and its global teleconnections provides evidence that such features are realistically represented in long-term forced climate simulations.

A version of the HadCM3 AOGCM (known as GloSea) has been assessed for skill in predicting observed seasonal climate variations (Davey et al., 2002; Graham et al., 2005). Graham et al. (2005) analysed 43 years of retrospective six-month forecasts ('hindcasts') with GloSea, run from observed ocean-land-atmosphere initial conditions. A nine-member ensemble was used to sample uncertainty in the initial conditions. Conclusions relevant to HadCM3 include: (i) the model is able to reproduce observed large-scale lagged responses to ENSO events in the tropical Atlantic and Indian Ocean SSTs; and (ii) the model can realistically predict anomaly patterns in North

Atlantic SSTs, shown to have important links with the NAO and seasonal temperature anomalies over Europe.

The GFDL-CM2.0 AOGCM has also been assessed for seasonal prediction. Twelve-month retrospective and contemporaneous forecasts were produced using a six-member ensemble over 15 years starting in 1991. The forecasts were initialised using global ocean data assimilation (Derber and Rosati, 1989; Rosati et al., 1997) and observed atmospheric forcing, combined with atmospheric initial conditions derived from the atmospheric component of the model forced with observed SSTs. Results indicated considerable model skill out to 12 months for ENSO prediction (see http://www.gfdl.noaa.gov/~rgg/si_workdir/Forecasts.html). Global teleconnections, as diagnosed from the NCEP reanalysis (GFDL GAMDT, 2004), were evident throughout the 12-month forecasts.

8.5 Model Simulations of Extremes

Society's perception of climate variability and climate change is largely formed by the frequency and the severity of extremes. This is especially true if the extreme events have large and negative impacts on lives and property. As climate models' resolution and the treatment of physical processes have improved, the simulation of extremes has also improved. Mainly because of increased data availability (e.g., daily data, various indices, etc.), the modelling community has now examined the model simulations in greater detail and presented a comprehensive description of extreme events in the coupled models used for climate change projections.

Some extreme events, by their very nature of being smaller in scale and shorter in duration, are manifestations of either a rapid amplification, or an equilibration at a higher amplitude, of naturally occurring local instabilities. Large-scale and long-duration extreme events are generally due to persistence of weather patterns associated with air-sea and air-land interactions. A reasonable hypothesis might be that the coarse-resolution AOGCMs might not be able to simulate local short-duration extreme events, but that is not the case. Our assessment of the recent scientific literature shows, perhaps surprisingly, that the global statistics of the extreme events in the current climate, especially temperature, are generally well simulated by the current models (see Section 8.5.1). These models have been more successful in simulating temperature extremes than precipitation extremes.

The assessment of extremes, especially for temperature, has been done by examining the amplitude, frequency and persistence of the following quantities: daily maximum and minimum temperature (e.g., hot days, cold days, frost days), daily precipitation intensity and frequency, seasonal mean temperature and precipitation and frequency and tracks of tropical cyclones. For precipitation, the assessment has been done either in terms of return values or extremely high rates of precipitation.

8.5.1 Extreme Temperature

Kiktev et al. (2003) compared station observations of extreme events with the simulations of an atmosphere-only GCM (Hadley Centre Atmospheric Model version 3; HadAM3) forced by prescribed oceanic forcing and anthropogenic radiative forcing during 1950 to 1995. The indices of extreme events they used were those proposed by Frich et al. (2002). They found that inclusion of anthropogenic radiative forcing was required to reproduce observed changes in temperature extremes, particularly at large spatial scales. The decrease in the number of frost days in Southern Australia simulated by HadAM3 with anthropogenic forcing is in good agreement with the observations. The increase in the number of warm nights over Eurasia is poorly simulated when anthropogenic forcing is not included, but the inclusion of anthropogenic forcing improves the modelled trend patterns over western Russia and reproduces the general increase in the occurrence of warm nights over much of the NH.

Meehl et al. (2004) compared the number of frost days simulated by the PCM model with observations. The 20th-century simulations include the variations in solar, volcano, sulphate aerosol, ozone and greenhouse gas forcing. Both model simulations and observations show that the number of frost days decreased by two days per decade in the western USA during the 20th century. The model simulations do not agree with observations in the southeastern USA, where the model simulates a decrease in the number of frost days in this region in the 20th century, while observations indicate an increase in this region. Meehl et al. (2004) argue that this discrepancy could be due to the model's inability to simulate the impact of El Niño events on the number of frost days in the southeastern USA. Meehl and Tebaldi (2004) compared the heat waves simulated by the PCM with observations. They defined a heat wave as the three consecutive warmest nights during the year. During the period 1961 to 1990, there is good agreement between the model and observations (NCEP reanalysis).

Kharin et al. (2005) examined the simulations of temperature and precipitation extremes for AMIP-2 models, some of which are atmospheric components of coupled models used in this assessment. They found that models simulate the temperature extremes, especially the warm extremes, reasonably well. Models have serious deficiencies in simulating precipitation extremes, particularly in the tropics. Vavrus et al. (2006) used daily values of 20th-century integrations from seven models. They defined a cold air outbreak as 'an occurrence of two or more consecutive days during which the local mean daily surface air temperature is at least two standard deviations below the local winter mean temperature'. They found that the climate models reproduce the location and magnitude of cold air outbreaks in the current climate.

Researchers have also established relationships between large-scale circulation features and cold air outbreaks or heat waves. For example, Vavrus et al. (2006) found that 'the favored regions of cold air outbreaks are located near and downstream

from preferred locations of atmosphere blocking'. Likewise, Meehl and Tebaldi (2004) found that heat waves over Europe and North America were associated with changes in the 500 hPa circulation pattern.

8.5.2 Extreme Precipitation

Sun et al. (2006) investigated the intensity of daily precipitation simulated by 18 AOGCMs, including several used in this report. They found that most of the models produce light precipitation (<10 mm day^{-1}) more often than observed, too few heavy precipitation events and too little precipitation in heavy events (>10 mm day^{-1}). The errors tend to cancel, so that the seasonal mean precipitation is fairly realistic (see Section 8.3).

Since the TAR, many simulations have been made with high-resolution GCMs. Iorio et al. (2004) examined the impact of model resolution on the simulation of precipitation in the USA using the Community Climate Model version 3 (CCM3). They found that the high-resolution simulation produces more realistic daily precipitation statistics. The coarse-resolution model had too many days with weak precipitation and not enough with intense precipitation. This tendency was partially eliminated in the high-resolution simulation, but, in the simulation at the highest resolution (T239), the high-percentile daily precipitation was still too low. This problem was eliminated when a cloud-resolving model was embedded in every grid point of the GCM.

Kimoto et al. (2005) compared the daily precipitation over Japan in an AOGCM with two different resolutions (high res. and med res. of MIROC 3.2) and found more realistic precipitation distributions with the higher resolution. Emori et al. (2005) showed that a high-resolution AGCM (the atmospheric part of high res. MIROC 3.2) can simulate the extreme daily precipitation realistically if there is provision in the model to suppress convection when the ambient relative humidity is below 80%, suggesting that modelled extreme precipitation can be strongly parametrization dependent. Kiktev et al. (2003) compared station observations of rainfall with the simulations of the atmosphere-only GCM HadAM3 forced by prescribed oceanic forcing and anthropogenic radiative forcing. They found that this model shows little skill in simulating changing precipitation extremes. May (2004) examined the variability and extremes of daily rainfall in the simulation of present day climate by the ECHAM4 GCM. He found that this model simulates the variability and extremes of rainfall quite well over most of India when compared to satellite-derived rainfall, but has a tendency to overestimate heavy rainfall events in central India. Durman et al. (2001) compared the extreme daily European precipitation simulated by the HadCM2 GCM with station observations. They found that the GCM's ability to simulate daily precipitation events exceeding 15 mm per day was good but its ability to simulate events exceeding 30 mm per day was poor. Kiktev et al. (2003) showed that HadAM3 was able to simulate the natural variability of the precipitation intensity index (annual mean precipitation divided by number of days with precipitation less than 1 mm) but was not able to simulate accurately the variability in the number of wet days (the number of days in a year with precipitation greater than 10 mm).

Using the Palmer Drought Severity Index (PDSI), Dai at al. (2004) concluded that globally very dry or wet areas (PDSI above +3 or below –3) have increased from 20% to 38% since 1972. In addition to simulating the short-duration events like heat waves, frost days and cold air outbreaks, models have also shown success in simulating long time-scale anomalies. For example, Burke et al. (2006) showed that the HadCM3 model, on a global basis and at decadal time scales, 'reproduces the observed drying trend' as defined by the PDSI if the anthropogenic forcing is included, although the model does not always simulate correctly the regional distributions of wet and dry areas.

8.5.3 Tropical Cyclones

The spatial resolution of the coupled ocean-atmosphere models used in the IPCC assessment is generally not high enough to resolve tropical cyclones, and especially to simulate their intensity. A common approach to investigate the effects of global warming on tropical cyclones has been to utilise the SST boundary conditions from a global change scenario run to force a high-resolution AGCM. That model run is then compared with a control run using the high-resolution AGCM forced with specified observed SST for the current climate (Sugi et al., 2002; Camargo et al., 2005; McDonald et al., 2005; Bengtsson et al., 2006; Oouchi et al., 2006; Yoshimura et al., 2006). There are also several idealised model experiments in which a high-resolution AGCM is integrated with and without a fixed global warming or cooling of SST. Another method is to embed a high-resolution regional model in the lower-resolution climate model (Knutson and Tuleya, 1999; Walsh et al., 2004). Projections using these methods are discussed in Chapter 10.

Bengtsson et al. (2006) showed that the global metrics of tropical cyclones (tropical or hemispheric averages) are broadly reproduced by the ECHAM5 model, even as a function of intensity. However, varying degrees of errors (in some cases substantial) in simulated tropical storm frequency and intensity have been noted in some models (e.g., GFDL GAMDT, 2004; Knutson and Tuleya, 2004; Camargo et al., 2005). The tropical cyclone simulation has been shown to be sensitive to the choice of convection parametrization in some cases.

Oouchi et al. (2006) used one of the highest-resolution (20 km) atmospheric models to simulate the frequency, distribution and intensity of tropical cyclones in the current climate. Although there were some deficiencies in simulating the geographical distribution of tropical cyclones (over-prediction of tropical cyclones between 0° to 10°S in the Indian Ocean, and under-prediction between 0° to 10°N in the western Pacific), the overall simulation of geographical distribution and frequency was remarkably good. The model could not simulate the strongest observed maximum wind speeds, and central pressures were not as low as observed, suggesting that even higher resolution may be required to simulate the most intense tropical cyclones.

8.5.4 Summary

Because most AOGCMs have coarse resolution and large-scale systematic errors, and extreme events tend to be short lived and have smaller spatial scales, it is somewhat surprising how well the models simulate the statistics of extreme events in the current climate, including the trends during the 20th century (see Chapter 9 for more detail). This is especially true for the temperature extremes, but intensity, frequency and distribution of extreme precipitation are less well simulated. The higher-resolution models used for projections of tropical cyclone changes (Chapter 10) produce generally good simulation of the frequency and distribution of tropical cyclones, but less good simulation of their intensity. Improvements in the simulation of the intensity of precipitation and tropical cyclones with increases in the resolution of AGCMs (Oouchi et al., 2006) suggest that when climate models have sufficient resolution to explicitly resolve at least the large convective systems without using parametrizations for deep convection, it is likely that simulation of precipitation and intensity of tropical cyclones will improve.

8.6 Climate Sensitivity and Feedbacks

8.6.1 Introduction

Climate sensitivity is a metric used to characterise the response of the global climate system to a given forcing. It is broadly defined as the equilibrium global mean surface temperature change following a doubling of atmospheric CO_2 concentration (see Box 10.2). Spread in model climate sensitivity is a major factor contributing to the range in projections of future climate changes (see Chapter 10) along with uncertainties in future emission scenarios and rates of oceanic heat uptake. Consequently, differences in climate sensitivity between models have received close scrutiny in all four IPCC reports. Climate sensitivity is largely determined by internal feedback processes that amplify or dampen the influence of radiative forcing on climate. To assess the reliability of model estimates of climate sensitivity, the ability of climate models to reproduce different climate changes induced by specific forcings may be evaluated. These include the Last Glacial Maximum and the evolution of climate over the last millennium and the 20th century (see Section 9.6). The compilation and comparison of climate sensitivity estimates derived from models and from observations are presented in Box 10.2. An alternative approach, which is followed here, is to assess the reliability of key climate feedback processes known to play a critical role in the models' estimate of climate sensitivity.

This section explains why the estimates of climate sensitivity and of climate feedbacks differ among current models (Section 8.6.2), summarises understanding of the role of key radiative feedback processes associated with water vapour and lapse rate, clouds, snow and sea ice in climate sensitivity, and assesses the treatment of these processes in the global climate models used to make projections of future climate change (Section 8.6.3). Finally we discuss how we can assess our relative confidence in the different climate sensitivity estimates derived from climate models (Section 8.6.4). Note that climate feedbacks associated with chemical or biochemical processes are not discussed in this section (they are addressed in Chapters 7 and 10), nor are local-scale feedbacks (e.g., between soil moisture and precipitation; see Section 8.2.3.2).

8.6.2 Interpreting the Range of Climate Sensitivity Estimates Among General Circulation Models

8.6.2.1 Definition of Climate Sensitivity

As defined in previous assessments (Cubasch et al., 2001) and in the Glossary, the global annual mean surface air temperature change experienced by the climate system after it has attained a new equilibrium in response to a doubling of atmospheric CO_2 concentration is referred to as the 'equilibrium climate sensitivity' (unit is °C), and is often simply termed the 'climate sensitivity'. It has long been estimated from numerical experiments in which an AGCM is coupled to a simple non-dynamic model of the upper ocean with prescribed ocean heat transports (usually referred to as 'mixed-layer' or 'slab' ocean models) and the atmospheric CO_2 concentration is doubled. In AOGCMs and non-steady-state (or transient) simulations, the 'transient climate response' (TCR; Cubasch et al., 2001) is defined as the global annual mean surface air temperature change (with respect to a 'control' run) averaged over a 20-year period centred at the time of CO_2 doubling in a 1% yr^{-1} compound CO_2 increase scenario. That response depends both on the sensitivity and on the ocean heat uptake. An estimate of the equilibrium climate sensitivity in transient climate change integrations is obtained from the 'effective climate sensitivity' (Murphy, 1995). It corresponds to the global temperature response that would occur if the AOGCM was run to equilibrium with feedback strengths held fixed at the values diagnosed at some point of the transient climate evolution. It is computed from the oceanic heat storage, the radiative forcing and the surface temperature change (Cubasch et al., 2001; Gregory et al., 2002).

The climate sensitivity depends on the type of forcing agents applied to the climate system and on their geographical and vertical distributions (Allen and Ingram, 2002; Sausen et al., 2002; Joshi et al., 2003). As it is influenced by the nature and the magnitude of the feedbacks at work in the climate response, it also depends on the mean climate state (Boer and Yu, 2003). Some differences in climate sensitivity will also result simply from differences in the particular radiative forcing calculated by different radiation codes (see Sections 10.2.1 and 8.6.2.3). The global annual mean surface temperature change thus presents limitations regarding the description and the understanding of the climate response to an external forcing. Indeed, the regional temperature response to a uniform forcing (and even more to a vertically or geographically distributed forcing) is highly inhomogeneous. In addition, climate sensitivity only considers

the surface mean temperature and gives no indication of the occurrence of abrupt changes or extreme events. Despite its limitations, however, the climate sensitivity remains a useful concept because many aspects of a climate model scale well with global average temperature (although not necessarily across models), because the global mean temperature of the Earth is fairly well measured, and because it provides a simple way to quantify and compare the climate response simulated by different models to a specified perturbation. By focusing on the global scale, climate sensitivity can also help separate the climate response from regional variability.

8.6.2.2 Why Have the Model Estimates Changed Since the TAR?

The current generation of GCMs[5] covers a range of equilibrium climate sensitivity from 2.1°C to 4.4°C (with a mean value of 3.2°C; see Table 8.2 and Box 10.2), which is quite similar to the TAR. Yet most climate models have undergone substantial developments since the TAR (probably more than between the Second Assessment Report and the TAR) that generally involve improved parametrizations of specific processes such as clouds, boundary layer or convection (see Section 8.2). In some cases, developments have also concerned numerics, dynamical cores or the coupling to new components (ocean, carbon cycle, etc.). Developing new versions of a model to improve the physical basis of parametrizations or the simulation of the current climate is at the heart of modelling group activities. The rationale for these changes is generally based upon a combination of process-level tests against observations or against cloud-resolving or large-eddy simulation models (see Section 8.2), and on the overall quality of the model simulation (see Sections 8.3 and 8.4). These developments can, and do, affect the climate sensitivity of models.

The equilibrium climate sensitivity estimates from the latest model version used by modelling groups have increased (e.g., CCSM3 vs CSM1.0, ECHAM5/MPI-OM vs ECHAM3/LSG, IPSL-CM4 vs IPSL-CM2, MRI-CGCM2.3.2 vs MRI2, UKMO-HadGEM1 vs UKMO-HadCM3), decreased (e.g., CSIRO-MK3.0 vs CSIRO-MK2, GFDL-CM2.0 vs GFDL_R30_c, GISS-EH and GISS-ER vs GISS2, MIROC3.2(hires) and MIROC3.2(medres) vs CCSR/NIES2) or remained roughly unchanged (e.g., CGCM3.1(T47) vs CGCM1, GFDL-CM2.1 vs GFDL_R30_c) compared to the TAR. In some models, changes in climate sensitivity are primarily ascribed to changes in the cloud parametrization or in the representation of cloud-radiative properties (e.g., CCSM3, MRI-CGCM2.3.2, MIROC3.2(medres) and MIROC3.2(hires)). However, in most models the change in climate sensitivity cannot be attributed to a specific change in the model. For instance, Johns et al. (2006) showed that most of the individual changes made during the development of HadGEM1 have a small impact on the climate sensitivity, and that the global effects of the individual changes largely cancel each other. In addition, the parametrization changes can interact nonlinearly with each other so that the sum of change A and change B does not produce the same as the change in A plus B (e.g., Stainforth et al., 2005). Finally, the interaction among the different parametrizations of a model explains why the influence on climate sensitivity of a given change is often model dependent (see Section 8.2). For instance, the introduction of the Lock boundary-layer scheme (Lock et al., 2000) to HadCM3 had a minimal impact on the climate sensitivity, in contrast to the introduction of the scheme to the GFDL atmospheric model (Soden et al., 2004; Johns et al., 2006).

8.6.2.3 What Explains the Current Spread in Models' Climate Sensitivity Estimates?

As discussed in Chapter 10 and throughout the last three IPCC assessments, climate models exhibit a wide range of climate sensitivity estimates (Table 8.2). Webb et al. (2006), investigating a selection of the slab versions of models in Table 8.1, found that differences in feedbacks contribute almost three times more to the range in equilibrium climate sensitivity estimates than differences in the models' radiative forcings (the spread of models' forcing is discussed in Section 10.2).

Several methods have been used to diagnose climate feedbacks in GCMs, whose strengths and weaknesses are reviewed in Stephens (2005) and Bony et al. (2006). These methods include the 'partial radiative perturbation' approach and its variants (e.g., Colman, 2003a; Soden and Held, 2006), the use of radiative-convective models and the 'cloud radiative forcing' method (e.g., Webb et al., 2006). Since the TAR, there has been progress in comparing the feedbacks produced by climate models in doubled atmospheric CO_2 equilibrium experiments (Colman, 2003a; Webb et al., 2006) and in transient climate change integrations (Soden and Held, 2006). Water vapour, lapse rate, cloud and surface albedo feedback parameters, as estimated by Colman (2003a), Soden and Held (2006) and Winton (2006a) are shown in Figure 8.14.

In AOGCMs, the water vapour feedback constitutes by far the strongest feedback, with a multi-model mean and standard deviation for the MMD at PCMDI of 1.80 ± 0.18 W m^{-2} $°C^{-1}$, followed by the (negative) lapse rate feedback (–0.84 ± 0.26 W m^{-2} $°C^{-1}$) and the surface albedo feedback (0.26 ± 0.08 W m^{-2} $°C^{-1}$). The cloud feedback mean is 0.69 W m^{-2} $°C^{-1}$ with a very large inter-model spread of ±0.38 W m^{-2} $°C^{-1}$ (Soden and Held, 2006).

A substantial spread is apparent in the strength of water vapour feedback that is smaller in Soden and Held (2006) than in Colman (2003a). It is not known whether this smaller spread indicates a closer consensus among current AOGCMs than among older models, differences in the methodology or differences in the nature of climate change integrations between the two studies. In both studies, the lapse rate feedback also shows a substantial spread among models, which is explained

[5] Unless explicitly stated, GCM here refers both to AOGCM (used to estimate TCR) and AGCM coupled to a slab ocean (used to estimate equilibrium climate sensitivity).

Table 8.2. *Climate sensitivity estimates from the AOGCMs assessed in this report (see Table 8.1 for model details). Transient climate response (TCR) and equilibrium climate sensitivity (ECS) were calculated by the modelling groups (using atmosphere models coupled to slab ocean for equilibrium climate sensitivity), except those in italics, which were calculated from simulations in the MMD at PCMDI. The ocean heat uptake efficiency (W m^{-2} °C^{-1}), discussed in Chapter 10, may be roughly estimated as F_{2x} x (TCR^{-1} – ECS^{-1}), where F_{2x} is the radiative forcing for doubled atmospheric CO_2 concentration (see Supplementary Material, Table 8.SM.1)*

AOGCM	Equilibrium climate sensitivity (°C)	Transient climate response (°C)
1: BCC-CM1	n.a.	n.a.
2: BCCR-BCM2.0	n.a.	n.a.
3: CCSM3	2.7	1.5
4: CGCM3.1(T47)	3.4	*1.9*
5: CGCM3.1(T63)	*3.4*	n.a.
6: CNRM-CM3	n.a.	1.6
7: CSIRO-MK3.0	3.1	1.4
8: ECHAM5/MPI-OM	3.4	2.2
9: ECHO-G	3.2	1.7
10: FGOALS-g1.0	*2.3*	*1.2*
11: GFDL-CM2.0	2.9	1.6
12: GFDL-CM2.1	3.4	1.5
13: GISS-AOM	n.a.	n.a.
14: GISS-EH	2.7	1.6
15: GISS-ER	2.7	1.5
16: INM-CM3.0	2.1	1.6
17: IPSL-CM4	4.4	2.1
18: MIROC3.2(hires)	4.3	2.6
19: MIROC3.2(medres)	4.0	2.1
20: MRI-CGCM2.3.2	3.2	2.2
21: PCM	2.1	1.3
22: UKMO-HadCM3	3.3	2.0
23: UKMO-HadGEM1	4.4	1.9

by inter-model differences in the relative surface warming of low and high latitudes (Soden and Held, 2006). Because the water vapour and temperature responses are tightly coupled in the troposphere (see Section 8.6.3.1), models with a larger (negative) lapse rate feedback also have a larger (positive) water vapour feedback. These act to offset each other (see Box 8.1). As a result, it is more reasonable to consider the sum of water vapour and lapse rate feedbacks as a single quantity when analysing the causes of inter-model variability in climate sensitivity. This makes inter-model differences in the combination of water vapour and lapse rate feedbacks a substantially smaller contributor to the spread in climate sensitivity estimates than differences in cloud feedback (Figure 8.14). The source of the difference in mean lapse rate feedback between the two studies is unclear, but may relate to inappropriate inclusion of stratospheric temperature response in some feedback analyses (Soden and Held, 2006).

The three studies, using different methodologies to estimate the global surface albedo feedback associated with snow and sea ice changes, all suggest that this feedback is positive in all the models, and that its range is much smaller than that of cloud feedbacks. Winton (2006a) suggests that about three-quarters of the global surface albedo feedback arises from the NH (see Section 8.6.3.3).

The diagnosis of global radiative feedbacks allows better understanding of the spread of equilibrium climate sensitivity estimates among current GCMs. In the idealised situation that the climate response to a doubling of atmospheric CO_2 consisted of a uniform temperature change only, with no feedbacks operating (but allowing for the enhanced radiative cooling resulting from the temperature increase), the global warming from GCMs would be around 1.2°C (Hansen et al., 1984; Bony et al., 2006). The water vapour feedback, operating alone on top of this, would at least double the response.[6] The water vapour feedback is, however, closely related to the lapse rate feedback (see above), and the two combined result in a feedback parameter of approximately 1 W m^{-2} °C^{-1}, corresponding to an amplification of the basic temperature response by approximately 50%. The

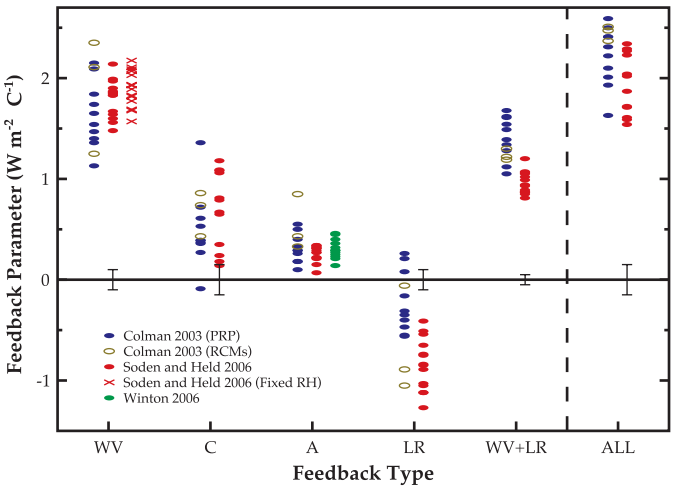


Figure 8.14. *Comparison of GCM climate feedback parameters for water vapour (WV), cloud (C), surface albedo (A), lapse rate (LR) and the combined water vapour plus lapse rate (WV + LR) in units of W m^{-2} °C^{-1}. 'ALL' represents the sum of all feedbacks. Results are taken from Colman (2003a; blue, black), Soden and Held (2006; red) and Winton (2006a; green). Closed blue and open black symbols from Colman (2003a) represent calculations determined using the partial radiative perturbation (PRP) and the radiative-convective method (RCM) approaches respectively. Crosses represent the water vapour feedback computed for each model from Soden and Held (2006) assuming no change in relative humidity. Vertical bars depict the estimated uncertainty in the calculation of the feedbacks from Soden and Held (2006).*

[6] Under these simplifying assumptions the amplification of the global warming from a feedback parameter λ (in W m^{-2} °C^{-1}) with no other feedbacks operating is $\frac{1}{1+\lambda/\lambda_P}$, where λ_P is the 'uniform temperature' radiative cooling response (of value approximately –3.2 W m^{-2} °C^{-1}; Bony et al., 2006). If *n* independent feedbacks operate, λ is replaced by ($\lambda_1 + \lambda_2 + ... \lambda_n$).

Box 8.1: Upper-Tropospheric Humidity and Water Vapour Feedback

Water vapour is the most important greenhouse gas in the atmosphere. Tropospheric water vapour concentration diminishes rapidly with height, since it is ultimately limited by saturation-specific humidity, which strongly decreases as temperature decreases. Nevertheless, these relatively low upper-tropospheric concentrations contribute disproportionately to the 'natural' greenhouse effect, both because temperature contrast with the surface increases with height, and because lower down the atmosphere is nearly opaque at wavelengths of strong water vapour absorption.

In the stratosphere, there are potentially important radiative impacts due to anthropogenic sources of water vapour, such as from methane oxidation (see Section 2.3.7). In the troposphere, the radiative forcing due to direct anthropogenic sources of water vapour (mainly from irrigation) is negligible (see Section 2.5.6). Rather, it is the response of tropospheric water vapour to warming itself – the water vapour feedback – that matters for climate change. In GCMs, water vapour provides the largest positive radiative feedback (see Section 8.6.2.3): alone, it roughly doubles the warming in response to forcing (such as from greenhouse gas increases). There are also possible stratospheric water vapour feedback effects due to tropical tropopause temperature changes and/or changes in deep convection (see Sections 3.4.2 and 8.6.3.1.1).

The radiative effect of absorption by water vapour is roughly proportional to the logarithm of its concentration, so it is the fractional change in water vapour concentration, not the absolute change, that governs its strength as a feedback mechanism. Calculations with GCMs suggest that water vapour remains at an approximately constant fraction of its saturated value (close to unchanged relative humidity (RH)) under global-scale warming (see Section 8.6.3.1). Under such a response, for uniform warming, the largest fractional change in water vapour, and thus the largest contribution to the feedback, occurs in the upper troposphere. In addition, GCMs find enhanced warming in the tropical upper troposphere, due to changes in the lapse rate (see Section 9.4.4). This further enhances moisture changes in this region, but also introduces a partially offsetting radiative response from the temperature increase, and the net effect of the combined water vapour/lapse rate feedback is to amplify the warming in response to forcing by around 50% (Section 8.6.2.3). The close link between these processes means that water vapour and lapse rate feedbacks are commonly considered together. The strength of the combined feedback is found to be robust across GCMs, despite significant inter-model differences, for example, in the mean climatology of water vapour (see Section 8.6.2.3).

Confidence in modelled water vapour feedback is thus affected by uncertainties in the physical processes controlling upper-tropospheric humidity, and confidence in their representation in GCMs. One important question is what the relative contribution of large-scale advective processes (in which confidence in GCMs' representation is high) is compared with microphysical processes (in which confidence is much lower) for determining the distribution and variation in water vapour. Although advection has been shown to establish the general distribution of tropical upper-tropospheric humidity in the present climate (see Section 8.6.3.1), a significant role for microphysics in humidity response to climate change cannot yet be ruled out.

Difficulties in observing water vapour in the upper troposphere have long hampered both observational and modelling studies, and significant limitations remain in coverage and reliability of observational humidity data sets (see Section 3.4.2). To reduce the impact of these problems, in recent years there has been increased emphasis on the use of satellite data (such as 6.3 to 6.7 μm thermal radiance measurements) for inferring variations or trends in humidity, and on direct simulation of satellite radiances in models as a basis for model evaluation (see Sections 3.4.2 and 8.6.3.1.1).

Variations in upper-tropospheric water vapour have been observed across time scales from seasonal and interannual to decadal, as well as in response to external forcing (see Section 3.4.2.2). At tropics-wide scales, they correspond to roughly unchanged RH (see Section 8.6.3.1), and GCMs are generally able to reproduce these observed variations. Both column-integrated (see Section 3.4.2.1) and upper-tropospheric (see Section 3.4.2.2) specific humidity have increased over the past two decades, also consistent with roughly unchanged RH. There remains substantial disagreement between different observational estimates of lapse rate changes over recent decades, but some of these are consistent with GCM simulations (see Sections 3.4.1 and 9.4.4).

Overall, since the TAR, confidence has increased in the conventional view that the distribution of RH changes little as climate warms, particularly in the upper troposphere. Confidence has also increased in the ability of GCMs to represent upper-tropospheric humidity and its variations, both free and forced. Together, upper-tropospheric observational and modelling evidence provide strong support for a combined water vapour/lapse rate feedback of around the strength found in GCMs (see Section 8.6.3.1.2).

surface albedo feedback amplifies the basic response by about 10%, and the cloud feedback does so by 10 to 50% depending on the GCM. Note, however, that because of the inherently nonlinear nature of the response to feedbacks, the final impact on sensitivity is not simply the sum of these responses. The effect of multiple positive feedbacks is that they mutually amplify each other's impact on climate sensitivity.

Using feedback parameters from Figure 8.14, it can be estimated that in the presence of water vapour, lapse rate and surface albedo feedbacks, but in the absence of cloud feedbacks, current GCMs would predict a climate sensitivity (±1 standard deviation) of roughly 1.9°C ± 0.15°C (ignoring spread from radiative forcing differences). The mean and standard deviation of climate sensitivity estimates derived from current GCMs are larger (3.2°C ± 0.7°C) essentially because the GCMs all predict a positive cloud feedback (Figure 8.14) but strongly disagree on its magnitude.

The large spread in cloud radiative feedbacks leads to the conclusion that differences in cloud response are the primary source of inter-model differences in climate sensitivity (see discussion in Section 8.6.3.2.2). However, the contributions of water vapour/lapse rate and surface albedo feedbacks to sensitivity spread are non-negligible, particularly since their impact is reinforced by the mean model cloud feedback being positive and quite strong.

8.6.3 Key Physical Processes Involved in Climate Sensitivity

The traditional approach in assessing model sensitivity has been to consider water vapour, lapse rate, surface albedo and cloud feedbacks separately. Although this division can be regarded as somewhat artificial because, for example, water vapour, clouds and temperature interact strongly, it remains conceptually useful, and is consistent in approach with previous assessments. Accordingly, and because of the relationship between lapse rate and water vapour feedbacks, this subsection separately addresses the water vapour/lapse rate feedbacks and then the cloud and surface albedo feedbacks.

8.6.3.1 Water Vapour and Lapse Rate

Absorption of LW radiation increases approximately with the logarithm of water vapour concentration, while the Clausius-Clapeyron equation dictates a near-exponential increase in moisture-holding capacity with temperature. Since tropospheric and surface temperatures are closely coupled (see Section 3.4.1), these constraints predict a strongly positive water vapour feedback if relative humidity (RH) is close to unchanged. Furthermore, the combined water vapour-lapse rate feedback is relatively insensitive to changes in lapse rate for unchanged RH (Cess, 1975) due to the compensating effects of water vapour and temperature on the OLR (see Box 8.1). Understanding processes determining the distribution and variability in RH is therefore central to understanding of the water vapour-lapse rate feedback. To a first approximation, GCM simulations indeed maintain a roughly unchanged distribution of RH under greenhouse gas forcing. More precisely, a small but widespread RH decrease in GCM simulations typically reduces feedback strength slightly compared with a constant RH response (Colman, 2004; Soden and Held, 2006; Figure 8.14).

In the planetary boundary layer, humidity is controlled by strong coupling with the surface, and a broad-scale quasi-unchanged RH response is uncontroversial (Wentz and Schabel, 2000; Trenberth et al., 2005; Dai, 2006). Confidence in GCMs' water vapour feedback is also relatively high in the extratropics, because large-scale eddies, responsible for much of the moistening throughout the troposphere, are explicitly resolved, and keep much of the atmosphere at a substantial fraction of saturation throughout the year (Stocker et al., 2001). Humidity changes in the tropical middle and upper troposphere, however, are less well understood and have more TOA radiative impact than do other regions of the atmosphere (e.g., Held and Soden, 2000; Colman, 2001). Therefore, much of the research since the TAR has focused on the RH response in the tropics with emphasis on the upper troposphere (see Bony et al., 2006 for a review), and confidence in the humidity response of this region is central to confidence in modelled water vapour feedback.

The humidity distribution within the tropical free troposphere is determined by many factors, including the detrainment of vapour and condensed water from convective systems and the large-scale atmospheric circulation. The relatively dry regions of large-scale descent play a major role in tropical LW cooling, and changes in their area or humidity could potentially have a significant impact on water vapour feedback strength (Pierrehumbert, 1999; Lindzen et al., 2001; Peters and Bretherton, 2005). Given the complexity of processes controlling tropical humidity, however, simple convincing physical arguments about changes under global-scale warming are difficult to sustain, and a combination of modelling and observational studies are needed to assess the reliability of model water vapour feedback.

In contrast to cloud feedback, a strong positive water vapour feedback is a robust feature of GCMs (Stocker et al., 2001), being found across models with many different schemes for advection, convection and condensation of water vapour. High-resolution mesoscale (Larson and Hartmann, 2003) and cloud-resolving models (Tompkins and Craig, 1999) run on limited tropical domains also display humidity responses consistent with strong positive feedback, although with differences in the details of upper-tropospheric RH (UTRH) trends with temperature. Experiments with GCMs have found water vapour feedback strength to be insensitive to large changes in vertical resolution, as well as convective parametrization and advection schemes (Ingram, 2002). These modelling studies provide evidence that the free-tropospheric RH response of global coupled models under climate warming is not simply an artefact of GCMs or of coarse GCM resolution, since broadly similar changes are found in a range of models of different complexity and scope. Indirect supporting evidence for model water vapour

feedback strength also comes from experiments which show that suppressing humidity variation from the radiation code in an AOGCM produces unrealistically low interannual variability (Hall and Manabe, 1999).

Confidence in modelled water vapour feedback is dependent upon understanding of the physical processes important for controlling UTRH, and confidence in their representation in GCMs. The TAR noted a sensitivity of UTRH to the representation of cloud microphysical processes in several simple modelling studies. However, other evidence suggests that the role of microphysics is limited. The observed RH field in much of the tropics can be well simulated without microphysics, but simply by observed winds while imposing an upper limit of 100% RH on parcels (Pierrehumbert and Roca, 1998; Gettelman et al., 2000; Dessler and Sherwood, 2000), or by determining a detrainment profile from clear-sky radiative cooling (Folkins et al., 2002). Evaporation of detrained cirrus condensate also does not play a major part in moistening the tropical upper troposphere (Soden, 2004; Luo and Rossow, 2004), although cirrus might be important as a water vapour sink (Luo and Rossow, 2004). Overall, these studies increase confidence in GCM water vapour feedback, since they emphasise the importance of large-scale advective processes, or radiation, in which confidence in representation by GCMs is high, compared with microphysical processes, in which confidence is much lower. However, a significant role for microphysics in determining the distribution of changes in water vapour under climate warming cannot yet be ruled out.

Observations provide ample evidence of regional-scale increases and decreases in tropical UTRH in response to changes in convection (Zhu et al., 2000; Bates and Jackson, 2001; Blankenship and Wilheit, 2001; Wang et al., 2001; Chen et al., 2002; Chung et al., 2004; Sohn and Schmetz, 2004). Such changes, however, provide little insight into large-scale thermodynamic relationships (most important for the water vapour feedback) unless considered over entire circulation systems. Recent observational studies of the tropical mean UTRH response to temperature have found results consistent with that of near-unchanged RH at a variety of time scales (see Section 3.4.2.2). These include responses from interannual variability (Bauer et al., 2002; Allan et al., 2003; McCarthy and Toumi, 2004), volcanic forcing (Soden et al., 2002; Forster and Collins, 2004) and decadal trends (Soden et al., 2005), although modest RH decreases are noted at high levels on interannual time scales (Minschwaner and Dessler, 2004; Section 3.4.2.3). Seasonal variations in observed global LW radiation trapping are also consistent with a strong positive water vapour feedback (Inamdar and Ramanathan, 1998; Tsushima et al., 2005). Note, however, that humidity responses to variability or shorter time-scale forcing must be interpreted cautiously, as they are not direct analogues to that from greenhouse gas increases, because of differences in patterns of warming and circulation changes.

8.6.3.1.1 Evaluation of water vapour/lapse rate feedback processes in models

Evaluation of the humidity distribution and its variability in GCMs, while not directly testing their climate change feedbacks, can assess their ability to represent key physical processes controlling water vapour and therefore affect confidence in their water vapour feedback. Limitations in coverage or accuracy of radiosonde measurements or reanalyses have long posed a problem for UTRH evaluation in models (Trenberth et al., 2001; Allan et al., 2004), and recent emphasis has been on assessments using satellite measurements, along with increasing efforts to directly simulate satellite radiances in models (so as to reduce errors in converting to model-level RH) (e.g., Soden et al., 2002; Allan et al., 2003; Iacono et al., 2003; Brogniez et al., 2005; Huang et al., 2005).

Major features of the mean humidity distribution are reasonably simulated by GCMs, along with the consequent distribution of OLR (see Section 8.3.1). In the important subtropical subsidence regions, models show a range of skill in representing the mean UTRH. Some large regional biases have been found (Iacono et al., 2003; Chung et al., 2004), although good agreement of distribution and variability with satellite data has also been noted in some models (Allan et al., 2003; Brogniez et al., 2005). Uncertainties in satellite-derived data sets further complicate such comparisons, however. Skill in the reproduction of 'bimodality' in the humidity distribution at different time scales has also been found to differ between models (Zhang et al., 2003; Pierrehumbert et al., 2007), possibly associated with mixing processes and resolution. Note, however, that given the near-logarithmic dependence of LW radiation on humidity, errors in the control climate humidity have little direct effect on climate sensitivity: it is the fractional change of humidity as climate changes that matters (Held and Soden, 2000).

A number of new tests of large-scale variability of UTRH have been applied to GCMs since the TAR, and have generally found skill in model simulations. Allan et al. (2003) found that an AGCM forced by observed SSTs simulated interannual changes in tropical mean 6.7 μm radiance (sensitive to UTRH and temperature) in broad agreement with High Resolution Infrared Radiation Sounder (HIRS) observations over the last two decades. Minschwaner et al. (2006) analysed the interannual response of tropical mean 250 hPa RH to the mean SST of the most convectively active region in 16 AOGCMs from the MMD at PCMDI. The mean model response (a small decrease in RH) was statistically consistent with the 215 hPa response inferred from satellite observations, when uncertainties from observations and model spread were taken into account. AGCMs have been able to reproduce global or tropical mean variations in clear sky OLR (sensitive to water vapour and temperature distributions) over seasonal (Tsushima et al., 2005) as well as interannual and decadal (Soden, 2000; Allan and Slingo, 2002) time scales (although aerosol or greenhouse gas uncertainties and sampling differences can affect these latter comparisons; Allan et al., 2003). In the lower

troposphere, GCMs can simulate global-scale interannual moisture variability well (e.g., Allan et al., 2003). At a smaller scale, a number of GCMs have also shown skill in reproducing regional changes in UTRH in response to circulation changes such as from seasonal or interannual variability (e.g., Soden, 1997; Allan et al., 2003; Brogniez et al., 2005).

A further test of the response of free tropospheric temperature and humidity to surface temperature in models is how well they can reproduce interannual correlations between surface temperature and vertical humidity profiles. Although GCMs are only partially successful in reproducing regional (Ross et al., 2002) and mean tropical (Bauer et al., 2002) correlations, the marked disagreement found in previous studies (Sun and Held, 1996; Sun et al., 2001) has been shown to be in large part an artefact of sampling techniques (Bauer et al., 2002).

There have also been efforts since the TAR to test GCMs' water vapour response against that from global-scale temperature changes of recent decades. One recent study used a long period of satellite data (1982–2004) to infer trends in UTRH, and found that an AGCM, forced by observed SSTs, was able to capture the observed global and zonal humidity trends well (Soden et al., 2005). A second approach uses the cooling following the eruption of Mt Pinatubo. Using estimated aerosol forcing, Soden et al. (2002) found a model-simulated response of HIRS 6.7 μm radiance consistent with satellite observations. They also found a model global temperature response similar to that observed, but not if the water vapour feedback was switched off (although the study neglected changes in cloud cover and potential heat uptake by the deep ocean). Using radiation calculations based on humidity observations, Forster and Collins (2004) found consistency in inferred water vapour feedback strength with an ensemble of coupled model integrations, although the latitude-height pattern of the observed humidity response did not closely match any single realisation. They deduced a water vapour feedback of 0.9 to 2.5 W m^{-2} $°C^{-1}$, a range which covers that of models under greenhouse gas forcing (see Figure 8.14). An important caveat to these studies is that the climate perturbation from Mt Pinatubo was small, not sitting clearly above natural variability (Forster and Collins, 2004). Caution is also required when comparing with feedbacks from increased greenhouse gases, because radiative forcing from volcanic aerosol is differently distributed and occurs over shorter time scales, which can induce different changes in circulation and bias the relative land/ocean response (although a recent AOGCM study found similar global LW radiation clear sky feedbacks between the two forcings; Yokohata et al., 2005). Nevertheless, comparing observed and modelled water vapour response to the eruption of Mt. Pinatubo constitutes one way to test model ability to simulate humidity changes induced by an external global-scale forcing.

At low latitudes, GCMs show negative lapse rate feedback because of their tendency towards a moist adiabatic lapse rate, producing amplified warming aloft. At middle to high latitudes, enhanced low-level warming, particularly in winter, contributes a positive feedback (e.g., Colman, 2003b), and global feedback strength is dependent upon the meridional warming gradient (Soden and Held, 2006). There has been extensive testing of GCM tropospheric temperature response against observational trends for climate change detection purposes (see Section 9.4.4). Although some recent studies have suggested consistency between modelled and observed changes (e.g., Fu et al., 2004; Santer et al., 2005), debate continues as to the level of agreement, particularly in the tropics (Section 9.4.4). Regardless, if RH remains close to unchanged, the combined lapse rate and water vapour feedback is relatively insensitive to differences in lapse rate response (Cess, 1975; Allan et al., 2002; Colman, 2003a).

In the stratosphere, GCM water vapour response is sensitive to the location of initial radiative forcing (Joshi et al., 2003; Stuber et al., 2005). Forcing concentrated in the lower stratosphere, such as from ozone changes, invoked a positive feedback involving increased stratospheric water vapour and tropical cold point temperatures in one study (Stuber et al., 2005). However, for more homogenous forcing, such as from CO_2, the stratospheric water vapour contribution to model sensitivity appears weak (Colman, 2001; Stuber et al., 2001, 2005). There is observational evidence of possible long-term increases in stratospheric water vapour (Section 3.4.2.3), although it is not yet clear whether this is a feedback process. If there is a significant global mean trend associated with feedback mechanisms, however, this could imply a significant stratospheric water vapour feedback (Forster and Shine, 2002).

8.6.3.1.2 Summary of water vapour and lapse fate feedbacks

Significant progress has been made since the TAR in understanding and evaluating water vapour and lapse rate feedbacks. New tests have been applied to GCMs, and have generally found skill in the representation of large-scale free tropospheric humidity responses to seasonal and interannual variability, volcano-induced cooling and climate trends. New evidence from both observations and models has reinforced the conventional view of a roughly unchanged RH response to warming. It has also increased confidence in the ability of GCMs to simulate important features of humidity and temperature response under a range of different climate perturbations. Taken together, the evidence strongly favours a combined water vapour-lapse rate feedback of around the strength found in global climate models.

8.6.3.2 Clouds

By reflecting solar radiation back to space (the albedo effect of clouds) and by trapping infrared radiation emitted by the surface and the lower troposphere (the greenhouse effect of clouds), clouds exert two competing effects on the Earth's radiation budget. These two effects are usually referred to as the SW and LW components of the cloud radiative forcing (CRF). The balance between these two components depends on many factors, including macrophysical and microphysical cloud properties. In the current climate, clouds exert a cooling effect on climate (the global mean CRF is negative). In response to

global warming, the cooling effect of clouds on climate might be enhanced or weakened, thereby producing a radiative feedback to climate warming (Randall et al., 2006; NRC, 2003; Zhang, 2004; Stephens, 2005; Bony et al., 2006).

In many climate models, details in the representation of clouds can substantially affect the model estimates of cloud feedback and climate sensitivity (e.g., Senior and Mitchell, 1993; Le Treut et al., 1994; Yao and Del Genio, 2002; Zhang, 2004; Stainforth et al., 2005; Yokohata et al., 2005). Moreover, the spread of climate sensitivity estimates among current models arises primarily from inter-model differences in cloud feedbacks (Colman, 2003a; Soden and Held, 2006; Webb et al., 2006; Section 8.6.2, Figure 8.14). Therefore, cloud feedbacks remain the largest source of uncertainty in climate sensitivity estimates.

This section assesses the evolution since the TAR in the understanding of the physical processes involved in cloud feedbacks (see Section 8.6.3.2.1), in the interpretation of the range of cloud feedback estimates among current climate models (see Section 8.6.3.2.2) and in the evaluation of model cloud feedbacks using observations (see Section 8.6.3.2.3).

8.6.3.2.1 Understanding of the physical processes involved in cloud feedbacks

The Earth's cloudiness is associated with a large spectrum of cloud types, ranging from low-level boundary-layer clouds to deep convective clouds and anvils. Understanding cloud feedbacks requires an understanding of how a change in climate may affect the spectrum and the radiative properties of these different clouds, and an estimate of the impact of these changes on the Earth's radiation budget. Moreover, since cloudy regions are also moist regions, a change in the cloud fraction matters for both the water vapour and the cloud feedbacks (Pierrehumbert, 1995; Lindzen et al., 2001). Since the TAR, there have been some advances in the analysis of physical processes involved in cloud feedbacks, thanks to the combined analysis of observations, simple conceptual models, cloud-resolving models, mesoscale models and GCMs (reviewed in Bony et al., 2006). Major issues are presented below.

Several climate feedback mechanisms involving convective anvil clouds have been examined. Hartmann and Larson (2002) proposed that the emission temperature of tropical anvil clouds is essentially independent of the surface temperature (Fixed Anvil Temperature hypothesis), and that it will thus remain unchanged during climate change. This suggestion is consistent with cloud-resolving model simulations showing that in a warmer climate, the vertical profiles of mid- and upper-tropospheric cloud fraction, condensate and RH all tend to be displaced upward in height together with the temperature (Tompkins and Craig, 1999). However, this hypothesis has not yet been tested with observations or with cloud-resolving model simulations having a fine vertical resolution in the upper troposphere. The response of the anvil cloud fraction to a change in temperature remains a subject of debate. Assuming that an increase with temperature in the precipitation efficiency of convective clouds could decrease the amount of water detrained in the upper troposphere, Lindzen et al. (2001) speculated that the tropical area covered by anvil clouds could decrease with rising temperature, and that would lead to a negative climate feedback (iris hypothesis). Numerous objections have been raised about various aspects of the observational evidence provided so far (Chambers et al., 2002; Del Genio and Kovari, 2002; Fu et al., 2002; Harrison, 2002; Hartmann and Michelsen, 2002; Lin et al., 2002, 2004), leading to a vigorous debate with the authors of the hypothesis (Bell et al., 2002; Chou et al., 2002; Lindzen et al., 2002). Other observational studies (Del Genio and Kovari, 2002; Del Genio et al., 2005b) suggest an increase in the convective cloud cover with surface temperature.

Boundary-layer clouds have a strong impact on the net radiation budget (e.g., Harrison et al., 1990; Hartmann et al., 1992) and cover a large fraction of the global ocean (e.g., Norris, 1998a,b). Understanding how they may change in a perturbed climate is thus a vital part of the cloud feedback problem. The observed relationship between low-level cloud amount and a particular measure of lower tropospheric stability (Klein and Hartmann, 1993), which has been used in some simple climate models and in some GCMs' parametrizations of boundary-layer cloud amount (e.g., CCSM3, FGOALS), led to the suggestion that a global climate warming might be associated with an increased low-level cloud cover, which would produce a negative cloud feedback (e.g., Miller, 1997; Zhang, 2004). However, variants of the lower-tropospheric stability measure, which may predict boundary-layer cloud amount as well as the Klein and Hartmann (1993) measure, would not necessarily predict an increase in low-level clouds in a warmer climate (e.g., Williams et al., 2006). Moreover, observations indicate that in regions covered by low-level clouds, the cloud optical depth decreases and the SW CRF weakens as temperature rises (Tselioudis and Rossow, 1994; Greenwald et al., 1995; Bony et al., 1997; Del Genio and Wolf, 2000; Bony and Dufresne, 2005), but the different factors that may explain these observations are not well established. Therefore, understanding of the physical processes that control the response of boundary-layer clouds and their radiative properties to a change in climate remains very limited.

At mid-latitudes, the atmosphere is organised in synoptic weather systems, with prevailing thick, high-top frontal clouds in regions of synoptic ascent and low-level or no clouds in regions of synoptic descent. In the NH, several climate models report a decrease in overall extratropical storm frequency and an increase in storm intensity in response to climate warming (e.g., Carnell and Senior, 1998; Geng and Sugi, 2003) and a poleward shift of the storm tracks (Yin, 2005). Using observations and reanalyses to investigate the impact that dynamical changes such as those found by Carnell and Senior (1998) would have on the NH radiation budget, Tselioudis and Rossow (2006) suggested that the increase in storm strength would have a larger radiative impact than the decrease in storm frequency, and that this would produce increased reflection of SW radiation and decreased emission of LW radiation. However, the poleward shift of the storm tracks may decrease the amount of SW radiation reflected (Tsushima et al., 2006). In addition, several

studies have used observations to investigate the dependence of mid-latitude cloud radiative properties on temperature. Del Genio and Wolf (2000) showed that the physical thickness of low-level continental clouds decreases with rising temperature, resulting in a decrease in the cloud water path and optical thickness as temperature rises, and Norris and Iacobellis (2005) suggested that over the NH ocean, a uniform change in surface temperature would result in decreased cloud amount and optical thickness for a large range of dynamical conditions. The sign of the climate change radiative feedback associated with the combined effects of dynamical and temperature changes on extratropical clouds is still unknown.

The role of polar cloud feedbacks in climate sensitivity has been emphasized by Holland and Bitz (2003) and Vavrus (2004). However, these feedbacks remain poorly understood.

8.6.3.2.2 *Interpretation of the range of cloud feedbacks among climate models*

In doubled atmospheric CO_2 equilibrium experiments performed by mixed-layer ocean-atmosphere models as well as in transient climate change integrations performed by fully coupled ocean-atmosphere models, models exhibit a large range of global cloud feedbacks, with roughly half of the climate models predicting a more negative CRF in response to global warming, and half predicting the opposite (Soden and Held, 2006; Webb et al., 2006). Several studies suggest that the sign of cloud feedbacks may not be necessarily that of CRF changes (Zhang et al., 1994; Colman, 2003a; Soden et al., 2004), due to the contribution of clear-sky radiation changes (i.e., of water vapour, temperature and surface albedo changes) to the change in CRF. The Partial Radiative Perturbation (PRP) method, that excludes clear-sky changes from the definition of cloud feedbacks, diagnoses a positive global net cloud feedback in virtually all the models (Colman, 2003a; Soden and Held, 2006). However, the cloud feedback estimates diagnosed from either the change in CRF or the PRP method are well correlated (i.e., their relative ranking is similar), and they exhibit a similar spread among GCMs.

By decomposing the GCM feedbacks into regional components or dynamical regimes, substantial progress has been made in the interpretation of the range of climate change cloud feedbacks. The comparison of coupled AOGCMs used for the climate projections presented in Chapter 10 (Bony and Dufresne, 2005), of atmospheric or slab ocean versions of current GCMs (Webb et al., 2006; Williams et al., 2006; Wyant et al., 2006), or of slightly older models (Williams et al., 2003; Bony et al., 2004; Volodin, 2004; Stowasser et al.; 2006) show that inter-model differences in cloud feedbacks are mostly attributable to the SW cloud feedback component, and that the responses to global warming of both deep convective clouds and low-level clouds differ among GCMs. Recent analyses suggest that the response of boundary-layer clouds constitutes the largest contributor to the range of climate change cloud feedbacks among current GCMs (Bony and Dufresne, 2005; Webb et al., 2006; Wyant et al., 2006). It is due both to large discrepancies in the radiative response simulated by models in regions dominated by low-level cloud cover (Figure 8.15), and to the large areas of the globe covered by these regions. However, the response of other cloud types is also important because for each model it either reinforces or partially cancels the radiative response from low-level clouds. The spread of model cloud feedbacks is substantial at all latitudes, and tends to be larger in the tropics (Bony et al., 2006; Webb et al., 2006). Differences in the representation of mixed-phase clouds and in the degree of latitudinal shift of the storm tracks predicted by the models also contribute to inter-model differences in the CRF response to climate change, particularly in the extratropics (Tsushima et al., 2006).

8.6.3.2.3 *Evaluation of cloud feedbacks produced by climate models*

The evaluation of clouds in climate models has long been based on comparisons of observed and simulated climatologies of TOA radiative fluxes and total cloud amount (see Section 8.3.1).

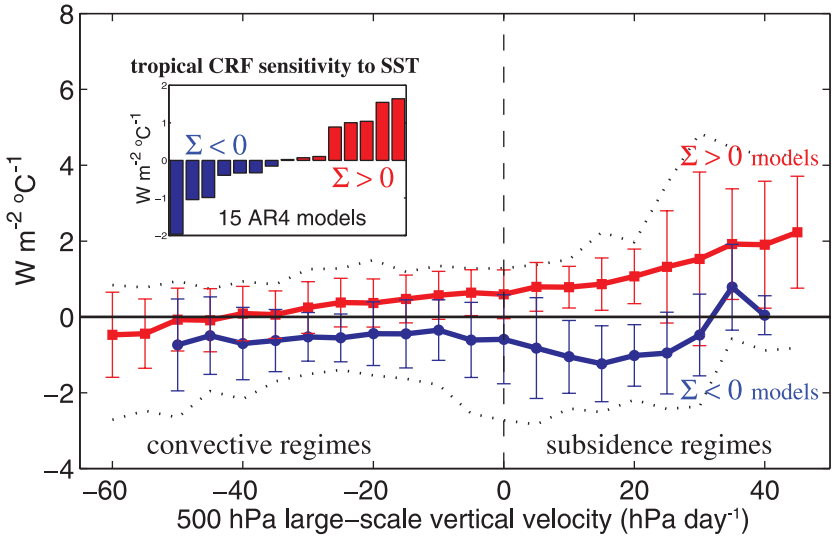


Figure 8.15. *Sensitivity (in W m^{-2} °C^{-1}) of the tropical net cloud radiative forcing (CRF) to SST changes associated with global warming (simulations in which CO_2 increases by 1% yr^{-1}). The inset shows the tropically averaged sensitivity Σ predicted by 15 AOGCMs used in this report: 7 models predict Σ < 0 and 8 models predict Σ > 0. The main panel compares the CRF sensitivity to SST predicted by the two groups of models in different regimes of the large-scale tropical circulation (the 500 hPa vertical pressure velocity is used as a proxy for large-scale motions, with negative values corresponding to large-scale ascending motions, and positive values to sinking motions).Thick lines and vertical lines represent the mean and the standard deviation of model sensitivities within each group; dotted lines represent the minimum and maximum values of model sensitivities within each dynamical regime. The discrepancy between the two groups of models is greatest in regimes of large-scale subsidence. These regimes, which have a large statistical weight in the tropics, are primarily covered by boundary-layer clouds. As a result, the spread of tropical cloud feedbacks among the models (inset) primarily arises from inter-model differences in the radiative response of low-level clouds in regimes of large-scale subsidence. Adapted from Bony and Dufresne (2005).*

However, a good agreement with these observed quantities may result from compensating errors. Since the TAR, and partly due to the use of an International Satellite Cloud Climatology Project (ISCCP) simulator (Klein and Jakob, 1999; Webb et al., 2001), the evaluation of simulated cloud fields is increasingly done in terms of cloud types and cloud optical properties (Klein and Jakob, 1999; Webb et al., 2001; Williams et al., 2003; Lin and Zhang, 2004; Weare, 2004; Zhang et al., 2005; Wyant et al., 2006). It has thus become more powerful and constrains the models more. In addition, a new class of observational tests has been applied to GCMs, using clustering or compositing techniques, to diagnose errors in the simulation of particular cloud regimes or in specific dynamical conditions (Tselioudis et al., 2000; Norris and Weaver, 2001; Jakob and Tselioudis, 2003; Williams et al., 2003; Bony et al., 2004; Lin and Zhang, 2004; Ringer and Allan, 2004; Bony and Dufresne, 2005; Del Genio et al., 2005a; Gordon et al., 2005; Bauer and Del Genio, 2006; Williams et al., 2006; Wyant et al., 2006). An observational test focused on the global response of clouds to seasonal variations has been proposed to evaluate model cloud feedbacks (Tsushima et al., 2005), but has not yet been applied to current models.

These studies highlight some common biases in the simulation of clouds by current models (e.g., Zhang et al., 2005). This includes the over-prediction of optically thick clouds and the under-prediction of optically thin low and middle-top clouds. However, uncertainties remain in the observational determination of the relative amounts of the different cloud types (Chang and Li, 2005). For mid-latitudes, these biases have been interpreted as the consequence of the coarse resolution of climate GCMs and their resulting inability to simulate the right strength of ageostrophic circulations (Bauer and Del Genio, 2006) and the right amount of sub-grid scale variability (Gordon et al., 2005). Although the errors in the simulation of the different cloud types may eventually compensate and lead to a prediction of the mean CRF in agreement with observations (see Section 8.3), they cast doubts on the reliability of the model cloud feedbacks. For instance, given the nonlinear dependence of cloud albedo on cloud optical depth, the overestimate of the cloud optical thickness implies that a change in cloud optical depth, even of the right sign and magnitude, would produce a too small radiative signature. Similarly, the under-prediction of low- and mid-level clouds presumably affects the magnitude of the radiative response to climate warming in the widespread regions of subsidence. Modelling assumptions controlling the cloud water phase (liquid, ice or mixed) are known to be critical for the prediction of climate sensitivity. However, the evaluation of these assumptions is just beginning (Doutriaux-Boucher and Quaas, 2004; Naud et al., 2006). Tsushima et al. (2006) suggested that observations of the distribution of each phase of cloud water in the current climate would provide a substantial constraint on the model cloud feedbacks at middle and high latitudes.

As an attempt to assess some components of the cloud response to a change in climate, several studies have investigated the ability of GCMs to simulate the sensitivity of clouds and CRF to interannual changes in environmental conditions. When examining atmosphere-mixed-layer ocean models, Williams et al. (2006) found for instance that by considering the CRF response to a change in large-scale vertical velocity and in lower-tropospheric stability, a component of the local mean climate change cloud response can be related to the present-day variability, and thus evaluated using observations. Bony and Dufresne (2005) and Stowasser and Hamilton (2006) examined the ability of the AOGCMs of Chapter 10 to simulate the change in tropical CRF to a change in SST, in large-scale vertical velocity and in lower-tropospheric RH. They showed that the models are most different and least realistic in regions of subsidence, and to a lesser extent in regimes of deep convective activity. This emphasizes the necessity to improve the representation and the evaluation of cloud processes in climate models, and especially those of boundary-layer clouds.

8.6.3.2.4 Conclusion on cloud feedbacks

Despite some advances in the understanding of the physical processes that control the cloud response to climate change and in the evaluation of some components of cloud feedbacks in current models, it is not yet possible to assess which of the model estimates of cloud feedback is the most reliable. However, progress has been made in the identification of the cloud types, the dynamical regimes and the regions of the globe responsible for the large spread of cloud feedback estimates among current models. This is likely to foster more specific observational analyses and model evaluations that will improve future assessments of climate change cloud feedbacks.

8.6.3.3 Cryosphere Feedbacks

A number of feedbacks that significantly contribute to the global climate sensitivity are due to the cryosphere. A robust feature of the response of climate models to increases in atmospheric concentrations of greenhouse gases is the poleward retreat of terrestrial snow and sea ice, and the polar amplification of increases in lower-tropospheric temperature. At the same time, the high-latitude response to increased greenhouse gas concentrations is highly variable among climate models (e.g., Holland and Bitz, 2003) and does not show substantial convergence in the latest generation of AOGCMs (Chapman and Walsh, 2007; see also Section 11.8). The possibility of threshold behaviour also contributes to the uncertainty of how the cryosphere may evolve in future climate scenarios.

Arguably, the most important simulated feedback associated with the cryosphere is an increase in absorbed solar radiation resulting from a retreat of highly reflective snow or ice cover in a warmer climate. Since the TAR, some progress has been made in quantifying the surface albedo feedback associated with the cryosphere. Hall (2004) found that the albedo feedback was responsible for about half the high-latitude response to a doubling of atmospheric CO_2. However, an analysis of long control simulations showed that it accounted for surprisingly little internal variability. Hall and Qu (2006) show that biases of a number of MMD models in reproducing the observed seasonal cycle of land snow cover (especially the spring melt) are tightly related to the large variations in snow albedo feedback strength

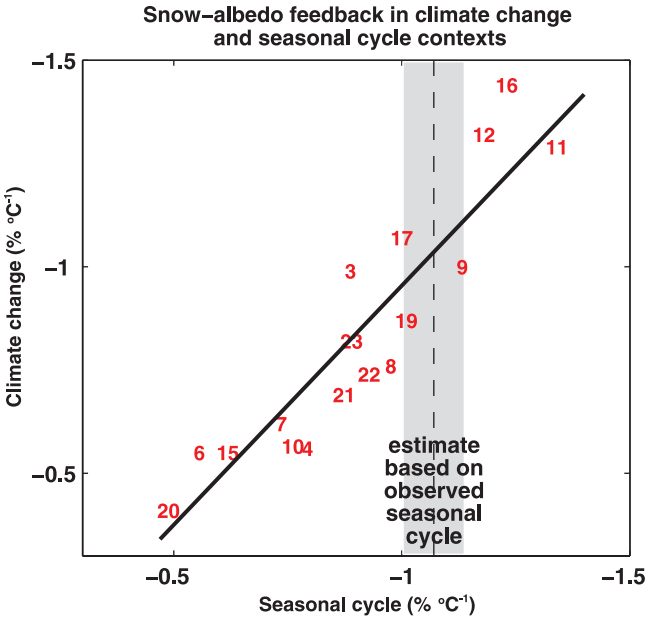


Figure 8.16. *Scatter plot of simulated springtime $\Delta\alpha_s/\Delta T_s$ values in climate change (ordinate) vs simulated springtime $\Delta\alpha_s/\Delta T_s$ values in the seasonal cycle (abscissa) in transient climate change experiments with 17 AOGCMs used in this report ($\Delta\alpha_s$ and T_s are surface albedo and surface air temperature, respectively). The climate change $\Delta\alpha_s/\Delta T_s$ values are the reduction in springtime surface albedo averaged over Northern Hemisphere continents between the 20th and 22nd centuries divided by the increase in surface air temperature in the region over the same time period. Seasonal cycle $\Delta\alpha_s/\Delta T_s$ values are the difference between 20th-century mean April and May α_s averaged over Northern Hemisphere continents divided by the difference between April and May T_s averaged over the same area and time period. A least-squares fit regression line for the simulations (solid line) and the observed seasonal cycle $\Delta\alpha_s/\Delta T_s$ value based on ISCCP and ERA40 reanalysis (dashed vertical line) are also shown. The grey bar gives an estimate of statistical error, according to a standard formula for error in the estimate of the mean of a time series (in this case the observed time series of $\Delta\alpha_s/\Delta T_s$) given the time series' length and variance. If this statistical error only is taken into account, the probability that the actual observed value lies outside the grey bar is 5%. Each number corresponds to a particular AOGCM (see Table 8.1). Adapted from Hall and Qu (2006).*

simulated by the same models in climate change scenarios. Addressing the seasonal cycle biases would therefore provide a constraint that would reduce divergence in simulations of snow albedo feedback under climate change. However, possible use of seasonal snow albedo feedback to evaluate snow albedo feedback under climate change conditions is of course dependent upon the realism of the correlation between the two feedbacks suggested by GCMs (Figure 8.16). A new result found independently by Winton (2006a) and Qu and Hall (2005) is that surface processes are the main source of divergence in climate simulations of surface albedo feedback, rather than simulated differences in cloud fields in cryospheric regions.

Understanding of other feedbacks associated with the cryosphere (e.g., ice insulating feedback, MOC/SST-sea ice feedback, ice thickness/ice growth feedback) has improved since the TAR (NRC, 2003; Bony et al., 2006). However, the relative influence on climate sensitivity of these feedbacks has not been quantified.

Understanding and evaluating sea ice feedbacks is complicated by their strong coupling to processes in the high-latitude atmosphere and ocean, particularly to polar cloud processes and ocean heat and freshwater transport. Additionally, while impressive advances have occurred in developing sea ice components of the AOGCMs since the TAR, particularly by the inclusion of more sophisticated dynamics in most of them (see Section 8.2.4), evaluation of cryospheric feedbacks through the testing of model parametrizations against observations is hampered by the scarcity of observational data in the polar regions. In particular, the lack of sea ice thickness observations is a considerable problem.

The role of sea ice dynamics in climate sensitivity has remained uncertain for years. Some recent results with AGCMs coupled to slab ocean models (Hewitt et al., 2001; Vavrus and Harrison, 2003) support the hypothesis that a representation of sea ice dynamics in climate models has a moderating impact on climate sensitivity. However, experiments with full AOGCMs (Holland and Bitz, 2003) show no compelling relationship between the transient climate response and the presence or absence of ice dynamics, with numerous model differences presumably overwhelming whatever signal might be due to ice dynamics. A substantial connection between the initial (i.e., control) simulation of sea ice and the response to greenhouse gas forcing (Holland and Bitz, 2003; Flato, 2004) further hampers 'clean' experiments aimed at identifying or quantifying the role of sea ice dynamics.

A number of processes, other than surface albedo feedback, have been shown to also contribute to the polar amplification of warming in models (Alexeev, 2003, 2005; Holland and Bitz, 2003; Vavrus, 2004; Cai, 2005; Winton, 2006b). An important one is additional poleward energy transport, but contributions from local high-latitude water vapour, cloud and temperature feedbacks have also been found. The processes and their interactions are complex, however, with substantial variation between models (Winton, 2006b), and their relative importance contributing to or dampening high-latitude amplification has not yet been properly resolved.

8.6.4 How to Assess Our Relative Confidence in Feedbacks Simulated by Different Models?

Assessments of our relative confidence in climate projections from different models should ideally be based on a comprehensive set of observational tests that would allow us to quantify model errors in simulating a wide variety of climate statistics, including simulations of the mean climate and variability and of particular climate processes. The collection of measures that quantify how well a model performs in an ensemble of tests of this kind are referred to as 'climate metrics'. To have the ability to constrain future climate projections, they would ideally have strong connections with one or several aspects of climate change: climate sensitivity, large-scale patterns of climate change (inter-hemispheric symmetry, polar amplification, vertical patterns of temperature change, land-sea contrasts), regional patterns or transient aspects of climate change. For example, to assess confidence in model projections of the Australian climate, the metrics would need to include

some measures of the quality of ENSO simulation because the Australian climate depends much on this variability (see Section 11. 7).

To better assess confidence in the different model estimates of climate sensitivity, two kinds of observational tests are available: tests related to the global climate response associated with specified external forcings (discussed in Chapters 6, 9 and 10; Box 10.2) and tests focused on the simulation of key feedback processes.

Based on the understanding of both the physical processes that control key climate feedbacks (see Section 8.6.3), and also the origin of inter-model differences in the simulation of feedbacks (see Section 8.6.2), the following climate characteristics appear to be particularly important: (i) for the water vapour and lapse rate feedbacks, the response of upper-tropospheric RH and lapse rate to interannual or decadal changes in climate; (ii) for cloud feedbacks, the response of boundary-layer clouds and anvil clouds to a change in surface or atmospheric conditions and the change in cloud radiative properties associated with a change in extratropical synoptic weather systems; (iii) for snow albedo feedbacks, the relationship between surface air temperature and snow melt over northern land areas during spring and (iv) for sea ice feedbacks, the simulation of sea ice thickness.

A number of diagnostic tests have been proposed since the TAR (see Section 8.6.3), but few of them have been applied to a majority of the models currently in use. Moreover, it is not yet clear which tests are critical for constraining future projections. Consequently, a set of model metrics that might be used to narrow the range of plausible climate change feedbacks and climate sensitivity has yet to be developed.

8.7 Mechanisms Producing Thresholds and Abrupt Climate Change

8.7.1 Introduction

This discussion of thresholds and abrupt climate change is based on the definitions of 'threshold' and 'abrupt' proposed by Alley et al. (2002). The climate system tends to respond to changes in a gradual way until it crosses some threshold: thereafter any change that is defined as abrupt is one where the change in the response is much larger than the change in the forcing. The changes at the threshold are therefore abrupt relative to the changes that occur before or after the threshold and can lead to a transition to a new state. The spatial scales for these changes can range from global to local. In this definition, the magnitude of the forcing and response are important. In addition to the magnitude, the time scale being considered is also important. This section focuses mainly on decadal to centennial time scales.

Because of the somewhat subjective nature of the definitions of threshold and abrupt, there have been efforts to develop quantitative measures to identify these points in a time series of a given variable (e.g., Lanzante, 1996; Seidel and Lanzante, 2004; Tomé and Miranda, 2004). The most common way to identify thresholds and abrupt changes is by linearly de-trending the input time series and looking for large deviations from the trend line. More statistically rigorous methods are usually based on Bayesian statistics.

This section explores the potential causes and mechanisms for producing thresholds and abrupt climate change and addresses the issue of how well climate models can simulate these changes. The following discussion is split into two main areas: forcing changes that can result in abrupt changes and abrupt climate changes that result from large natural variability on long time scales. Formally, the latter abrupt changes do not fit the definition of thresholds and abrupt changes, because the forcing (at least radiative forcing – the external boundary condition) is not changing in time. However these changes have been discussed in the literature and popular press and are worthy of assessment here.

8.7.2 Forced Abrupt Climate Change

8.7.2.1 Meridional Overturning Circulation Changes

As the radiative forcing of the planet changes, the climate system responds on many different time scales. For the physical climate system typically simulated in coupled models (atmosphere, ocean, land, sea ice), the longest response time scales are found in the ocean (Stouffer, 2004). In terms of thresholds and abrupt climate changes on decadal and longer time scales, the ocean has also been a focus of attention. In particular, the ocean's Atlantic MOC (see Box 5.1 for definition and description) is a main area of study.

The MOC transports large amounts of heat (order of 10^{15} Watts) and salt into high latitudes of the North Atlantic. There, the heat is released to the atmosphere, cooling the surface waters. The cold, relatively salty waters sink to depth and flow southward out of the Atlantic Basin. The complete set of climatic drivers of this circulation remains unclear but it is likely that both density (e.g., Stommel 1961; Rooth 1982) and wind stress forcings (e.g., Wunsch, 2002; Timmermann and Goosse, 2004) are important. Both palaeoclimate studies (e.g., Broecker, 1997; Clark et al., 2002) and modelling studies (e.g., Manabe and Stouffer, 1988, 1997; Vellinga and Wood, 2002) suggest that disruptions in the MOC can produce abrupt climate changes. A systematic model intercomparison study (Rahmstorf et al., 2005) found that all 11 participating EMICs had a threshold where the MOC shuts down (see Section 8.8.3). Due to the high computational cost, such a search for thresholds has not yet been performed with AOGCMs.

It is important to note the distinction between the equilibrium and transient or time-dependent responses of the MOC to changes in forcing. Due to the long response time scales found in the ocean (some longer than 1 kyr), it is possible that the short-term response to a given forcing change may be very different from the equilibrium response. Such behaviour of the coupled

system has been documented in at least one AOGCM (Stouffer and Manabe, 2003) and suggested in the results of a few other AOGCM studies (e.g., Hirst, 1999; Senior and Mitchell, 2000; Bryan et al., 2006). In these AOGCM experiments, the MOC weakens as the greenhouse gases increase in the atmosphere. When the CO_2 concentration is stabilised, the MOC slowly returns to its unperturbed value.

As discussed in section 10.3.4, the MOC typically weakens as greenhouse gases increase due to the changes in surface heat and freshwater fluxes at high latitudes (Manabe et al., 1991). The surface flux changes reduce the surface density, hindering the vertical movement of water and slowing the MOC. As the MOC slows, it could approach a threshold where the circulation can no longer sustain itself. Once the MOC crosses this threshold, it could rapidly change states, causing abrupt climate change where the North Atlantic and surrounding land areas would cool relative to the case where the MOC is active. This cooling is the result of the loss of heat transport from low latitudes in the Atlantic and the feedbacks associated with the reduction in the vertical mixing of high-latitude waters.

A common misunderstanding is that the MOC weakening could cause the onset of an ice age. However, no model has supported this speculation when forced with realistic estimates of future climate forcings (see Section 10.3.4). In addition, in idealised modelling studies where the MOC was forced to shut down through very large sources of freshwater (not changes in greenhouse gases), the surface temperature changes do not support the idea that an ice age could result from a MOC shut down, although the impacts on climate would be large (Manabe and Stouffer, 1988, 1997; Schiller et al., 1997; Vellinga and Wood, 2002; Stouffer et al., 2006). In a recent intercomparison involving 11 coupled atmosphere-ocean models (Gregory et al., 2005), the MOC decreases by only 10 to 50% during a 140-year period (as atmospheric CO_2 quadruples), and in no model is there a land cooling anywhere (as the global-scale heating due to increasing CO_2 overwhelms the local cooling effect due to reduced MOC).

Because of the large amount of heat and salt transported northward and its sensitivity to surface fluxes, the changes in the MOC are able to produce abrupt climate change on decadal to centennial time scales (e.g., Manabe and Stouffer, 1995; Stouffer et al., 2006). Idealised studies using present-day simulations have shown that models can simulate many of the variations seen in the palaeoclimate record on decadal to centennial time scales when forced by fluxes of freshwater water at the ocean surface. However, the quantitative response to freshwater inputs varies widely among models (Stouffer et al., 2006), which led the CMIP and Paleoclimate Modelling Intercomparison Project (PMIP) panels to design and support a set of coordinated experiments to study this issue (http://www.gfdl.noaa.gov/~kd/CMIP.html and http://www.pmip2.cnrs-gif.fr/pmip2/design/experiments/waterhosing.shtml).

In addition to the amount of the freshwater input, the exact location of that input may also be important (Rahmstorf 1996, Manabe and Stouffer, 1997; Rind et al., 2001). Designing experiments and determining the realistic past forcings needed to test the models' response on decadal to centennial time scales remains to be accomplished.

The processes determining MOC response to increasing greenhouse gases have been studied in a number of models. In many models, initial MOC response to increasing greenhouse gases is dominated by thermal effects. In most models, this is enhanced by changes in salinity driven by, among other things, the expected strengthening of the hydrological cycle (Gregory et al., 2005; Chapter 10). Melt water runoff from a melting of the Greenland Ice Sheet is a potentially major source of freshening not yet included in the models found in the MMD (see Section 8.7.2.2). More complex feedbacks, associated with wind and hydrological changes, are also important in many models. These include local surface flux anomalies in deep-water formation regions (Gent, 2001) and oceanic teleconnections driven by changes to the freshwater budget of the tropical and South Atlantic (e.g., Latif et al., 2000; Thorpe et al., 2001; Vellinga et al., 2002; Hu et al., 2004). The magnitudes of the climate factors causing the MOC to weaken, along with the feedbacks and the associated restoring factors, are all uncertain at this time. Evaluation of these processes in AOGCMs is mainly restricted by lack of observations, but some early progress has been made in individual studies (e.g., Schmittner et al., 2000; Pardaens et al., 2003; Wu et al., 2005; Chapter 9). Model intercomparison studies (e.g., Gregory et al., 2005; Rahmstorf et al., 2005; Stouffer et al., 2006) were developed to identify and understand the causes for the wide range of MOC responses in the coupled models used here (see Chapters 4, 6 and 10).

8.7.2.2 Rapid West Antarctic and/or Greenland Ice Sheet Collapse and Meridional Overturning Circulation Changes

Increased influx of freshwater to the ocean from the ice sheets is a potential forcing for abrupt climate changes. For Antarctica in the present climate, these fluxes chiefly arise from melting below the ice shelves and from melting of icebergs transported by the ocean; both fluxes could increase significantly in a warmer climate. Ice sheet runoff and iceberg calving, in roughly equal shares, currently dominate the freshwater flux from the Greenland Ice Sheet (Church et al., 2001; Chapter 4). In a warming climate, runoff is expected to quickly increase and become much larger than the calving rate, the latter of which in turn is likely to decrease as less and thinner ice borders the ocean; basal melting from below the grounded ice will remain several orders of magnitude smaller than the other fluxes (Huybrechts et al., 2002). For a discussion of the likelihood of these ice sheet changes and the effects on sea level, see the discussion in Chapter 10.

Changes in the surface forcing near the deep-water production areas seem to be most capable of producing rapid climate changes on decadal and longer time scales due to changes in the ocean circulation and mixing. If there are large changes in the ice volume over Greenland, it is likely that much of this melt water will freshen the surface waters in the

high-latitude North Atlantic, slowing down the MOC (see Section 8.7.2.1; Chapter 10). Rind et al. (2001) found that changes in the NADW formation rate could instigate changes in the deep-water formation around Antarctica.

The response of the Atlantic MOC to changes in the Antarctic Ice Sheet is less well understood. Experiments with ocean-only models where the melt water changes are imposed as surface salinity changes indicate that the Atlantic MOC will intensify as the waters around Antarctica become less dense (Seidov et al., 2001). Weaver et al. (2003) showed that by adding freshwater in the Southern Ocean, the MOC could change from an 'off' state to a state similar to present day. However, in an experiment with an AOGCM, Seidov et al. (2005) found that an external source of freshwater in the Southern Ocean resulted in a surface freshening throughout the world ocean, weakening the Atlantic MOC. In these model results, the SH MOC associated with Antarctic Bottom Water (AABW) formation weakened, causing a cooling around Antarctica. See Chapters 4, 6 and 10 for more discussion about the likelihood of large melt water fluxes from the ice sheets affecting the climate.

In summary, there is a potential for rapid ice sheet changes to produce rapid climate change both through sea level changes and ocean circulation changes. The ocean circulation changes result from increased freshwater flux over the particularly sensitive deep-water production sites. In general, the possible climate changes associated with future evolution of the Greenland Ice Sheet are better understood than are those associated with changes in the Antarctic Ice Sheets.

8.7.2.3 Volcanoes

Volcanoes produce abrupt climate responses on short time scales. The surface cooling effect of the stratospheric aerosols, the main climatic forcing factor, decays in one to three years after an eruption due to the lifetime of the aerosols in the stratosphere. It is possible for one large volcano or a series of large volcanic eruptions to produce climate responses on longer time scales, especially in the subsurface region of the ocean (Delworth et al., 2005; Gleckler et al., 2006b).

The models' ability to simulate any possible abrupt response of the climate system to volcanic eruptions seems conceptually similar to their ability to simulate the climate response to future changes in greenhouse gases in that both produce changes in the radiative forcing of the planet. However, mechanisms involved in the exchange of heat between the atmosphere and ocean may be different in response to volcanic forcing when compared to the response to increase greenhouse gases. Therefore, the feedbacks involved may be different (see Section 9.6.2.2 for more discussion).

8.7.2.4 Methane Hydrate Instability/Permafrost Methane

Methane hydrates are stored on the seabed along continental margins where they are stabilised by high pressures and low temperatures, implying that ocean warming may cause hydrate instability and release of methane into the atmosphere (see Section 4.7.2.4). Methane is also stored in the soils in areas of permafrost and warming increases the likelihood of a positive feedback in the climate system via permafrost melting and the release of trapped methane into the atmosphere. The likelihood of methane release from methane hydrates found in the oceans or methane trapped in permafrost layers is assessed in Chapter 7.

This subsection considers the potential usefulness of models in determining if those releases could trigger an abrupt climate change. Both forms of methane release represent a potential threshold in the climate system. As the climate warms, the likelihood of the system crossing a threshold for a sudden release increases (see Chapters 4, 7 and 10). Since these changes produce changes in the radiative forcing through changes in the greenhouse gas concentrations, the climatic impacts of such a release are the same as an increase in the rate of change in the radiative forcing. Therefore, the models' ability to simulate any abrupt climate change should be similar to their ability to simulate future abrupt climate changes due to changes in the greenhouse gas forcing.

8.7.2.5 Biogeochemical

Two questions concerning biogeochemical aspects of the climate system are addressed here. First, can biogeochemical changes lead to abrupt climate change? Second, can abrupt changes in the MOC further affect radiative forcing through biogeochemical feedbacks?

Abrupt changes in biogeochemical systems of relevance to our capacity to simulate the climate of the 21st century are not well understood (Friedlingstein et al., 2003). The potential for major abrupt change exists in the uptake and storage of carbon by terrestrial systems. While abrupt change within the climate system is beginning to be seriously considered (Rial et al., 2004; Schneider, 2004), the potential for abrupt change in terrestrial systems, such as loss of soil carbon (Cox et al., 2000) or die back of the Amazon forests (Cox et al., 2004) remains uncertain. In part this is due to lack of understanding of processes (see Friedlingstein et al., 2003; Chapter 7) and in part it results from the impact of differences in the projected climate sensitivities in the host climate models (Joos et al., 2001; Govindasamy et al., 2005; Chapter 10) where changes in the physical climate system affect the biological response.

There is some evidence of multiple equilibria within vegetation-soil-climate systems. These include North Africa and Central East Asia where Claussen (1998), using an EMIC with a land vegetation component, showed two stable equilibria for rainfall, dependent on initial land surface conditions. Kleidon et al. (2000), Wang and Eltahir (2000) and Renssen et al. (2003) also found evidence for multiple equilibria. These are preliminary assessments using relatively simple physical climate models that highlight the possibility of irreversible change in the Earth system but require extensive further research to assess the reliability of the phenomena found.

There have only been a few preliminary studies of the impact of abrupt climate changes such as the shutdown of the MOC on the carbon cycle. The findings of these studies indicate that the

shutdown of the MOC would tend to increase the amount of greenhouse gases in the atmosphere (Joos et al., 1999; Plattner et al., 2001; Chapter 6). In both of these studies, only the effect of the oceanic component of the carbon cycle changes was considered.

8.7.3 Unforced Abrupt Climate Change

Formally, as noted above, the changes discussed here do not fall into the definition of abrupt climate change. In the literature, unforced abrupt climate change falls into two general categories. One is just a red noise time series, where there is power at decadal and longer time scales. A second category is a bimodal or multi-modal distribution. In practice, it can be very difficult to distinguish between the two categories unless the time series are very long – long enough to eliminate sampling as an issue – and the forcings are fairly constant in time. In observations, neither of these conditions is normally met.

Models, both AOGCMs and less complex models, have produced examples of large abrupt climate change (e.g., Hall and Stouffer 2001; Goosse et al., 2002) without any changes in forcing. Typically, these events are associated with changes in the ocean circulation, mainly in the North Atlantic. An abrupt event can last for several years to a few centuries. They bear some similarities with the conditions observed during a relatively cold period in the recent past in the Arctic (Goosse et al., 2003)

Unfortunately, the probability of such an event is difficult to estimate as it requires a very long experiment and is certainly dependent on the mean state simulated by the model. Furthermore, comparison with observations is nearly impossible since it would require a very long period with constant forcing which does not exist in nature. Nevertheless, if an event such as the one of those mentioned above were to occur in the future, it would make the detection and attribution of climate changes very difficult.

8.8 Representing the Global System with Simpler Models

8.8.1 Why Lower Complexity?

An important concept in climate system modelling is that of a spectrum of models of differing levels of complexity, each being optimum for answering specific questions. It is not meaningful to judge one level as being better or worse than another independently of the context of analysis. What is important is that each model be asked questions appropriate for its level of complexity and quality of its simulation.

The most comprehensive models available are AOGCMs. These models, which include more and more components of the climate system (see Section 8.2), are designed to provide the best representation of the system and its dynamics, thereby serving as the most realistic laboratory of nature. Their major limitation is their high computational cost. To date, unless modest-resolution models are executed on an exceptionally large-scale distributed computed system, as in the climate*prediction*.net project (http://climateprediction.net; Stainforth et al., 2005), only a limited number of multi-decadal experiments can be performed with AOGCMs, which hinders a systematic exploration of uncertainties in climate change projections and prevents studies of the long-term evolution of climate.

At the other end of the spectrum of climate system model complexity are the so-called simple climate models (see Harvey et al., 1997 for a review of these models). The most advanced simple climate models contain modules that calculate in a highly parametrized way (1) the abundances of atmospheric greenhouse gases for given future emissions, (2) the radiative forcing resulting from the modelled greenhouse gas concentrations and aerosol precursor emissions, (3) the global mean surface temperature response to the computed radiative forcing and (4) the global mean sea level rise due to thermal expansion of sea water and the response of glaciers and ice sheets. These models are much more computationally efficient than AOGCMs and thus can be utilised to investigate future climate change in response to a large number of different scenarios of greenhouse gas emissions. Uncertainties from the modules can also be concatenated, potentially allowing the climate and sea level results to be expressed as probabilistic distributions, which is harder to do with AOGCMs because of their computational expense. A characteristic of simple climate models is that climate sensitivity and other subsystem properties must be specified based on the results of AOGCMs or observations. Therefore, simple climate models can be tuned to individual AOGCMs and employed as a tool to emulate and extend their results (e.g., Cubasch et al., 2001; Raper et al., 2001). They are useful mainly for examining global-scale questions.

To bridge the gap between AOGCMs and simple climate models, EMICs have been developed. Given that this gap is quite large, there is a wide range of EMICs (see the reviews of Saltzman, 1978 and Claussen et al., 2002). Typically, EMICs use a simplified atmospheric component coupled to an OGCM or simplified atmospheric and oceanic components. The degree of simplification of the component models varies among EMICs.

Earth System Models of Intermediate Complexity are reduced-resolution models that incorporate most of the processes represented by AOGCMs, albeit in a more parametrized form. They explicitly simulate the interactions between various components of the climate system. Similar to AOGCMs, but in contrast to simple climate models, the number of degrees of freedom of an EMIC exceeds the number of adjustable parameters by several orders of magnitude. However, these models are simple enough to permit climate simulations over several thousand of years or even glacial cycles (with a period of some 100 kyr), although not all are suitable for this purpose. Moreover, like simple climate models, EMICs can explore the parameter space with some completeness and are thus appropriate for assessing uncertainty. They can also be utilised to screen the phase space of climate or the history of climate in order to identify interesting time slices, thereby

providing guidance for more detailed studies to be undertaken with AOGCMs. In addition, EMICs are invaluable tools for understanding large-scale processes and feedbacks acting within the climate system. Certainly, it would not be sensible to apply an EMIC to studies that require high spatial and temporal resolution. Furthermore, model assumptions and restrictions, hence the limit of applicability of individual EMICs, must be carefully studied. Some EMICs include a zonally averaged atmosphere or zonally averaged oceanic basins. In a number of EMICs, cloudiness and/or wind fields are prescribed and do not evolve with changing climate. In still other EMICs, the atmospheric synoptic variability is not resolved explicitly, but diagnosed by using a statistical-dynamical approach. *A priori*, it is not obvious how the reduction in resolution or dynamics/physics affects the simulated climate. As shown in Section 8.8.3 and in Chapters 6, 9 and 10, at large scales most EMIC results compare well with observational or proxy data and AOGCM results. Therefore, it is argued that there is a clear advantage in having available a spectrum of climate system models.

8.8.2 Simple Climate Models

As in the TAR, a simple climate model is utilised in this report to emulate the projections of future climate change conducted with state-of-the-art AOGCMs, thus allowing the investigation of the temperature and sea level implications of all relevant emission scenarios (see Chapter 10). This model is an updated version of the Model for the Assessment of Greenhouse-Gas Induced Climate Change (MAGICC) model (Wigley and Raper, 1992, 2001; Raper et al., 1996). The calculation of the radiative forcings from emission scenarios closely follows that described in Chapter 2, and the feedback between climate and the carbon cycle is treated consistently with Chapter 7. The atmosphere-ocean module consists of an atmospheric energy balance model coupled to an upwelling-diffusion ocean model. The atmospheric energy balance model has land and ocean boxes in each hemisphere, and the upwelling-diffusion ocean model in each hemisphere has 40 layers with inter-hemispheric heat exchange in the mixed layer.

This simple climate model has been tuned to outputs from 19 of the AOGCMs described in Table 8.1, with resulting parameter values as given in the Supplementary Material, Table S8.1. The applied tuning procedure involves an iterative optimisation to derive least-square optimal fits between the simple model results and the AOGCM outputs for temperature time series and net oceanic heat uptake. This procedure attempts to match not only the global mean temperature but also the hemispheric land and ocean surface temperature changes of the AOGCM results by adjusting the equilibrium land-ocean warming ratio. Where data availability allowed, the tuning procedure took simultaneous account of low-pass filtered AOGCM data for two scenarios, namely a 1% per year compounded increase in atmospheric CO_2 concentration to twice and quadruple the pre-industrial level, with subsequent stabilisation. Before tuning, the AOGCM temperature and heat uptake data was de-drifted by subtracting the respective low-pass filtered pre-industrial control run segments. The three tuned parameters in the simple climate model are the effective climate sensitivity, the ocean effective vertical diffusivity, and the equilibrium land-ocean warming ratio. Values specific to each AOGCM for the radiative forcing for CO_2 doubling were used in the tuning procedure where available (from Forster and Taylor, 2006, supplemented with values provided directly from the modelling groups). Otherwise, a default value of 3.71 W m^{-2} was chosen (Myhre et al., 1998). Default values of 1 W m^{-2} $°C^{-1}$, 1 W m^{-2} $°C^{-1}$ and 8°C were used for the land-ocean heat exchange coefficient, the inter-hemispheric heat exchange coefficient and the magnitude of the warming that would result in a collapse of the MOC, respectively (see Appendix 9.1 of the TAR).

The obtained best-fit climate sensitivity estimates differ for various reasons from other estimates that were derived with alternative methods. Such alternative methods include, for example, regression estimates that use a global energy balance equation around the year of atmospheric CO_2 doubling or the analysis of slab ocean equilibrium warmings. The resulting differences in climate sensitivity estimates can be partially explained by the non-time constant effective climate sensitivities in many of the AOGCM runs. Furthermore, tuning results of a simple climate model will be affected by the model structure, although simple, and other default parameter settings that affect the simple model transient response.

8.8.3 Earth System Models of Intermediate Complexity

Pictorially, EMICs can be defined in terms of the components of a three-dimensional vector (Claussen et al., 2002): the number of interacting components of the climate system explicitly represented in the model, the number of processes explicitly simulated and the detail of description. Some basic information on the EMICs used in Chapter 10 of this report is presented in Table 8.3. A comprehensive description of all EMICs in operation can be found in Claussen (2005). Actually, there is a broad range of EMICs, reflecting the differences in scope. In some EMICs, the number of processes and the detail of description are reduced to simulate feedbacks between as many components of the climate system as feasible. Others, with fewer interacting components, are utilised in long-term ensemble experiments to investigate specific aspects of climate variability. The gap between some of the most complicated EMICs and AOGCMs is not very large. In fact, this particular class of EMICs is derived from AOGCMs. On the other hand, EMICs and simple climate models differ much more. For instance, EMICs as well as AOGCMs realistically represent the large-scale geographical structures of the Earth, like the shape of continents and ocean basins, which is certainly not the case for simple climate models.

Since the TAR, EMICs have intensively been used to study past and future climate changes (see Chapters 6, 9 and 10). Furthermore, a great deal of effort has been devoted to the evaluation of those models through coordinated intercomparisons.

Figure 8.17 compares the results from some of the EMICs utilised in Chapter 10 (see Table 8.3) with observation-based estimates and results of GCMs that took part in AMIP and CMIP1 (Gates et al., 1999; Lambert and Boer, 2001). The EMIC results refer to simulations in which climate is in equilibrium with an atmospheric CO_2 concentration of 280 ppm. Figures 8.17a and 8.17b show that the simulated latitudinal distributions of the zonally averaged surface air temperature for boreal winter and boreal summer are in good agreement with observations, except at northern and southern high latitudes. Interestingly, the GCM results also exhibit a larger scatter in these regions, and they somewhat deviate from data there. Figures 8.17c and 8.17d indicate that EMICs satisfactorily reproduce the general structure of the observed zonally averaged precipitation. Here again, at most latitudes, the scatter in the EMIC results seems to be as large as the scatter in the GCM results, and both EMIC and GCM results agree with observational estimates. When these EMICs are allowed to adjust to a doubling of atmospheric CO_2 concentration, they all simulate an increase in globally averaged annual mean surface temperature and precipitation that falls largely within the range of GCM results (Petoukhov et al., 2005).

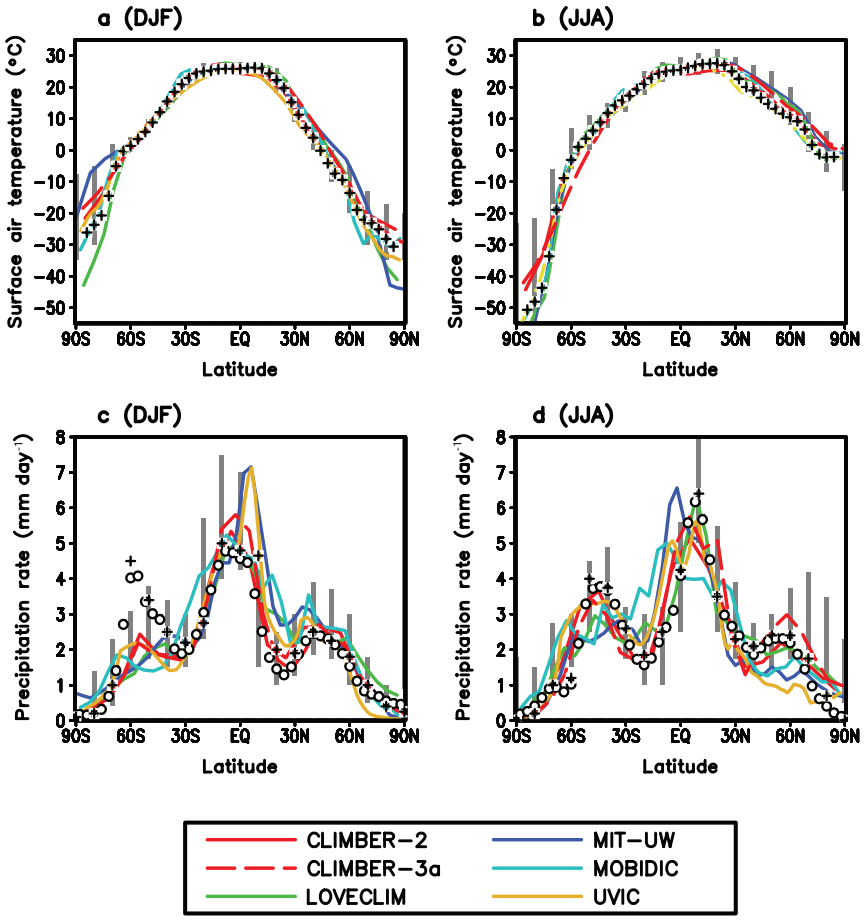


Figure 8.17. *Latitudinal distributions of the zonally averaged surface air temperature (a, b) and precipitation rate (c, d) for boreal winter (DJF) (a, c) and boreal summer (JJA) (b, d) as simulated at equilibrium by some of the EMICs used in Chapter 10 (see Table 8.3) for an atmospheric CO_2 concentration of 280 ppm. In (a) and (b), observational data merged from Jennings (1975), Jones (1988), Schubert et al. (1992), da Silva et al. (1994) and Fiorino (1997) are shown by crosses. In (c) and (d), observation-based estimates from Jaeger (1976; crosses) and Xie and Arkin (1997; open circles) are shown. The vertical grey bars indicate the range of GCM results from AMIP and CMIP1 (see text). Note that the model versions used in this intercomparison have no interactive biosphere and ice sheet components. The MIT-UW model is an earlier version of MIT-IGSM2.3. Adapted from Petoukhov et al., 2005.*

The responses of the North Atlantic MOC to increasing atmospheric CO_2 concentration and idealised freshwater perturbations as simulated by EMICs have also been compared to those obtained by AOGCMs (Gregory et al., 2005; Petoukhov et al., 2005; Stouffer et al., 2006). These studies reveal no systematic difference in model behaviour, which gives added confidence to the use of EMICs.

In a further intercomparison, Rahmstorf et al. (2005) compared results from 11 EMICs in which the North Atlantic Ocean was subjected to a slowly varying change in freshwater input. All the models analysed show a characteristic hysteresis response of the North Atlantic MOC to freshwater forcing, which can be explained by Stommel's (1961) salt advection feedback. The width of the hysteresis curve varies between 0.2 and 0.5 Sv in the models. Major differences are found in the location of the present-day climate on the hysteresis diagram. In seven of the models, the present-day climate for standard parameter choices is found in the bi-stable regime, while in the other four models, this climate is situated in the mono-stable regime. The proximity of the present-day climate to Stommel's bifurcation point, beyond which NADW formation cannot be sustained, varies from less than 0.1 Sv to over 0.5 Sv.

A final example of EMIC intercomparison is discussed in Brovkin et al. (2006). Earth System Models of Intermediate Complexity that explicitly simulate the interactions between atmosphere, ocean and land surface were forced by a reconstruction of land cover changes during the last millennium. In response to historical deforestation of about 18 x 10^6 km^2, all models exhibited a decrease in globally averaged annual mean surface temperature in the range of 0.13°C to 0.25°C, mainly due to the increase in land surface albedo. Further experiments with the models forced by the historical atmospheric CO_2 trend reveal that, for the whole last millennium, the biogeophysical cooling due to land cover changes is less pronounced than the warming induced by the elevated atmospheric CO_2 level (0.27°C–0.62°C). During the 19th century, the cooling effect of deforestation appears to counterbalance, albeit not completely, the warming effect of increasing CO_2 concentration.

Table 8.3. *Description of the EMICs used in Chapter 10. The naming convention for the models is as agreed by all modelling groups involved. An asterisk after a component or parametrization means that this component or parametrization was not activated in the experiments discussed in Chapter 10.*

Name	Atmosphere[a]	Ocean[b]	Sea Ice[c]	Coupling/Flux Adjustments[d]	Land Surface[e]	Biosphere[f]	Ice Sheets[g]
E1: BERN2.5CC (Plattner et al., 2001; Joos et al., 2001)	EMBM, 1-D (φ), NCL, 7.5° x 15° (Schmittner and Stocker, 1999)	FG with parametrized zonal pressure gradient, 2-D (φ, z), 3 basins, RL, ISO, MESO, 7.5°x15°, L14 (Wright and Stocker, 1992)	0-LT, 2-LIT (Wright and Stocker, 1993)	PM, NH, NW (Stocker et al., 1992; Schmittner and Stocker, 1999)	NST, NSM (Schmittner and Stocker, 1999)	BO (Marchal et al., 1998), BT (Sitch et al., 2003; Gerber et al., 2003), BV (Sitch et al., 2003; Gerber et al., 2003)	
E2: C-GOLDSTEIN (Edwards and Marsh, 2005)	EMBM, 2-D (φ, λ), NCL, 5° x 10° (Edwards and Marsh, 2005)	FG, 3-D, RL, ISO, MESO, 5° x 10°, L8 (Edwards and Marsh, 2005)	0-LT, DOC, 2-LIT (Edwards and Marsh, 2005)	GM, NH, RW (Edwards and Marsh, 2005)	NST, NSM, RIV (Edwards and Marsh, 2005)		
E3: CLIMBER-2 (Petoukhov et al., 2000)	SD, 3-D, CRAD, ICL, 10° x 51°, L10 (Petoukhov et al., 2000)	FG with parametrized zonal pressure gradient, 2-D (φ, z), 3 basins, RL, 2.5°, L21 (Wright and Stocker, 1992)	0-LT, DOC, 2-LIT (Petoukhov et al., 2000)	NM, NH, NW (Petoukhov et al., 2000)	1-LST, CSM, RIV (Petoukhov et al., 2000)	BO (Brovkin et al., 2002), BT (Brovkin et al., 2002), BV (Brovkin et al., 2002)	TM, 3-D, 0.75° x 1.5°, L20* (Calov et al., 2005)
E4: CLIMBER-3a (Montoya et al., 2005)	SD, 3-D, CRAD, ICL, 7.5° x 22.5°, L10 (Petoukhov et al., 2000)	PE, 3-D, FS, ISO, MESO, TCS, DC*, 3.75° x 3.75°, L24 (Montoya et al., 2005)	2-LT, R, 2-LIT (Fichefet and Morales Maqueda, 1997)	AM, NH, RW (Montoya et al., 2005)	1-LST, CSM, RIV (Petoukhov et al., 2000)	BO* (Six and Maier-Reimer, 1996), BT* (Brovkin et al., 2002), BV* (Brovkin et al., 2002)	
E5: LOVECLIM (Driesschaert, 2005)	QG, 3-D, LRAD, NCL, T21 (5.6° x 5.6°), L3 (Opsteegh et al., 1998)	PE, 3-D, FS, ISO, MESO, TCS, DC, 3° x 3°, L30 (Goosse and Fichefet, 1999)	3-LT, R, 2-LIT (Fichefet and Morales Maqueda, 1997)	NM, NH, RW (Driesschaert., 2005)	1-LST, BSM, RIV (Opsteegh et al., 1998)	BO (Mouchet and François, 1996), BT (Brovkin et al., 2002), BV (Brovkin et al., 2002)	TM, 3-D, 10 km x 10 km, L30 (Huybrechts, 2002)
E6: MIT-IGSM2.3 (Sokolov et al., 2005)	SD, 2-D (φ, z), CRAD, ICL, 4°, L11 (Sokolov and Stone, 1998), CHEM* (Mayer et al., 2000)	PE, 3-D, FS, ISO, MESO, 4° x 4°, L15 (Marshall et al., 1997)	3-LT, 2-LIT (Winton, 2000)	AM, GH, GW (Sokolov et al., 2005)	10-LST, CSM (Bonan et al., 2002)	BO (Parekh et al., 2005), BT (Felzer et al., 2005), BV* (Felzer et al., 2005)	
E7: MOBIDIC (Crucifix et al., 2002)	QG, 2-D (φ, z), CRAD, NCL, 5°, L2 (Gallée et al., 1991)	PE with parametrized zonal pressure gradient, 2-D (φ, z), 3 basins, RL, DC, 5°, L15 (Hovine and Fichefet, 1994)	0-LT, PD, 2-LIT (Crucifix et al., 2002)	NM, NH, NW (Crucifix et al., 2002)	1-LST, BSM (Gallée et al., 1991)	BO* (Crucifix, 2005), BT* (Brovkin et al., 2002), BV (Brovkin et al., 2002)	M, 1-D (φ), 0.5° (Crucifix and Berger, 2002)
E8: UVIC (Weaver et al., 2001)	DEMBM, 2-D (φ, λ), NCL, 1.8° x 3.6° (Weaver et al., 2001)	PE, 3-D, RG, ISO, MESO, 1.8° x 3.6° (Weaver et al., 2001)	0-LT, R, 2-LIT (Weaver et al., 2001)	AM, NH, NW (Weaver et al., 2001)	1-LST, CSM, RIV (Meissner et al., 2003)	BO (Weaver et al., 2001), BT (Cox, 2001), BV (Cox, 2001)	M, 2-D (φ, λ), 1.8° x 3.6°* (Weaver et al., 2001)

Notes:

[a] EMBM = energy-moisture balance model; DEMBM = energy-moisture balance model including some dynamics; SD = statistical-dynamical model; QG = quasi-geostrophic model; 1-D (φ) = zonally and vertically averaged; 2-D(φ, λ) = vertically averaged; 2-D(φ, z) = zonally averaged; 3-D = three-dimensional; LRAD = linearized radiation scheme; CRAD = comprehensive radiation scheme; NCL = non-interactive cloudiness; ICL = interactive cloudiness; CHEM = chemistry module; horizontal and vertical resolutions: the horizontal resolution is expressed either as degrees latitude x longitude or as spectral truncation with a rough translation to degrees latitude x longitude; the vertical resolution is expressed as 'Lm', where m is the number of vertical levels.

[b] FG = frictional geostrophic model; PE = primitive equation model; 2-D (φ, z) = zonally averaged; 3-D = three-dimensional; RL = rigid lid; FS = free surface; ISO = isopycnal diffusion; MESO = parametrization of the effect of mesoscale eddies on tracer distribution; TCS = complex turbulence closure scheme; DC = parametrization of density-driven down-sloping currents; horizontal and vertical resolutions: the horizontal resolution is expressed as degrees latitude x longitude; the vertical resolution is expressed as 'Lm', where m is the number of vertical levels.

[c] n-LT = n-layer thermodynamic scheme; PD = prescribed drift; DOC = drift with oceanic currents; R = viscous-plastic or elastic-viscous-plastic rheology; 2-LIT = two-level ice thickness distribution (level ice and leads).

Notes (continued):

[d] PM = prescribed momentum flux; GM = global momentum flux adjustment; AM = momentum flux anomalies relative to the control run are computed and added to climatological data; NM = no momentum flux adjustment; GH = global heat flux adjustment; NH = no heat flux adjustment; GW = global freshwater flux adjustment; RW = regional freshwater flux adjustment; NW = no freshwater flux adjustment.

[e] NST = no explicit computation of soil temperature; n-LST = n-layer soil temperature scheme; NSM = no moisture storage in soil; BSM = bucket model for soil moisture; CSM = complex model for soil moisture; RIV = river routing scheme.

[f] BO = model of oceanic carbon dynamics; BT = model of terrestrial carbon dynamics; BV = dynamical vegetation model.

[g] TM = thermomechanical model; M = mechanical model (isothermal); 1-D (φ) = vertically averaged with east-west parabolic profile; 2-D (φ, λ) = vertically averaged; 3-D = three-dimensional; horizontal and vertical resolutions: the horizontal resolution is expressed either as degrees latitude x longitude or kilometres x kilometres; the vertical resolution is expressed as 'Lm', where m is the number of vertical levels.

References

Abramopoulos, F., C. Rosenzweig, and B. Choudhury, 1988: Improved ground hydrology calculations for global climate models (GCMs): Soil water movement and evapotranspiration. *J. Clim.*, **1**, 921–941.

Achatz, U., and J.D. Opsteegh, 2003: Primitive-equation-based low-order models with seasonal cycle, Part II: Application to complexity and nonlinearity of large-scale atmospheric dynamics. *J. Atmos. Sci.*, **60**, 478–490.

AchutaRao, K., and K.R. Sperber, 2002: Simulation of the El Niño Southern Oscillation: Results from the coupled model intercomparison project. *Clim. Dyn.*, **19**, 191–209.

AchutaRao, K., and K.R. Sperber, 2006: ENSO simulation in coupled ocean-atmosphere models: Are the current models better? *Clim. Dyn.*, **27**, 1–15.

AchutaRao, K., et al., 2004: *An Appraisal of Coupled Climate Model Simulations*. UCRL-TR-202550, Lawrence Livermore National Laboratory, Livermore, CA, 197 pp.

Alexander, M.A., et al., 2004: The atmospheric response to realistic Arctic sea ice anomalies in an AGCM during winter. *J. Clim.*, **17**, 890–905.

Alexeev, V.A., 2003: Sensitivity to CO_2 doubling of an atmospheric GCM coupled to an oceanic mixed layer: a linear analysis. *Clim. Dyn.*, **20**, 775–787.

Alexeev, V.A., P.L. Langen, and J.R. Bates, 2005: Polar amplification of surface warming on an aquaplanet in "ghost forcing" experiments without sea ice feedbacks. *Clim. Dyn.*, **24**, 655–666.

Alexeev, V.A., et al., 1998: *Modelling of the present-day climate by the INM RAS atmospheric model "DNM GCM"*. Institute of Numerical Mathematics, Moscow, Russia, 200 pp.

Allan, R.P., and A. Slingo, 2002: Can current climate forcings explain the spatial and temporal signatures of decadal OLR variations? *Geophys. Res. Lett.*, **29**(7), 1141, doi:10.1029/2001GL014620.

Allan, R.P., V. Ramaswamy, and A. Slingo, 2002: A diagnostic analysis of atmospheric moisture and clear-sky radiative feedback in the Hadley Centre and Geophysical Fluid Dynamics Laboratory (GFDL) climate models. *J. Geophys. Res.*, **107**(D17), 4329, doi:10.1029/2001JD001131.

Allan, R.P., M.A. Ringer, and A. Slingo, 2003: Evaluation of moisture in the Hadley Centre Climate Model using simulations of HIRS water vapour channel radiances. *Q. J. R. Meteorol. Soc.*, **129**, 3371–3389.

Allan, R.P., M.A. Ringer, J.A. Pamment, and A. Slingo, 2004: Simulation of the Earth's radiation budget by the European Centre for Medium Range Weather Forecasts 40-year Reanalysis (ERA40). *J. Geophys. Res.*, **109**, D18107, doi:10.1029/2004JD004816.

Allen, M.R., and W.J. Ingram, 2002: Constraints on future changes in climate and the hydrologic cycle. *Nature*, **419**, 224–231.

Alley, R.B., et al., 2002: *Abrupt Climate Changes: Inevitable Surprises*. National Research Council, National Academy Press, Washington, DC, 221 pp.

Alves, O., M.A. Balmaseda, D. Anderson, and T. Stockdale, 2004: Sensitivity of dynamical seasonal forecast to ocean initial conditions. *Q. J. R. Meteorol. Soc.*, **130**, 647–667.

Amundrud, T.L., H. Mailing, and R.G. Ingram, 2004: Geometrical constraints on the evolution of ridged sea ice. *J. Geophys. Res.*, **109**, C06005, doi:10.1029/2003JC002251.

Annamalai, H., K. Hamilton, and K.R. Sperber, 2007: South Asian summer monsoon and its relationship with ENSO in the IPCC AR4 simulations. *J. Clim.*, **20**, 1071-1083.

Annan, J.D., J.C. Hargreaves, N.R. Edwards, and R. Marsh, 2005a: Parameter estimation in an intermediate complexity Earth System Model using an ensemble Kalman filter. *Ocean Modelling*, **8**, 135–154.

Annan, J.D., et al., 2005b: Efficiently constraining climate sensitivity with palaeoclimate observations. *Scientific Online Letters on the Atmosphere*, **1**, 181–184.

Arakawa, A., 2004: The cumulus parameterization problem: Past, present, and future. *J. Clim.*, **17**, 2493–2525.

Arakawa, A., and W.H. Schubert, 1974: Interaction of a cumulus cloud ensemble with the large-scale environment, Part I. *J. Atmos. Sci.*, **31**, 674–701.

Arora, V.K., 2001: Assessment of simulated water balance for continental-scale river basins in an AMIP 2 simulation. *J. Geophys. Res.*, **106**, 14827–14842.

Arora, V.K., and G.J. Boer, 2003: A representation of variable root distribution in dynamic vegetation models. *Earth Interactions*, **7**, 1–19.

Arzel, O., T. Fichefet, and H. Goosse, 2006: Sea ice evolution over the 20th and 21st centuries as simulated by the current AOGCMs. *Ocean Modelling*, **12**, 401–415.

Babko, O., D.A. Rothrock, and G.A. Maykut, 2002: Role of rafting in the mechanical redistribution of sea ice thickness. *J. Geophys. Res.*, **107**, 3113, doi:10.1029/1999JC000190.

Baldwin, M.P., et al., 2001: The quasi-biennial oscillation. *Rev. Geophys.*, **39**, 179–229.

Baldwin, M.P., et al., 2003: Stratospheric memory and skill of extended-range weather forecasts. *Science*, **301**, 636–640.

Balmaseda, M.A., M.K. Davey, and D.L.T. Anderson, 1995: Decadal and seasonal dependence of ENSO prediction skill. *J. Clim.*, **8**, 2705–2715.

Barkstrom, B., et al., 1989: Earth Radiation Budget Experiment (ERBE) archival and April 1985 results. *Bull. Am. Meteorol. Soc.*, **70**, 1254–1262.

Barnett, T.P., et al., 1999: Origins of midlatitude Pacific decadal variability. *Geophys. Res. Lett.*, **26**, 1453–1456.

Bates, J.J., and D.L. Jackson, 2001: Trends in upper-tropospheric humidity. *Geophys. Res. Lett.*, **28**, 1695–1698.

Bauer, M., and A.D. Del Genio, 2006: Composite analysis of winter cyclones in a GCM: Influence on climatological humidity. *J. Clim.*, **19**, 1652–1672. .

Bauer, M., A.D. Del Genio, and J.R. Lanzante, 2002: Observed and simulated temperature humidity relationships: sensitivity to sampling and analysis. *J. Clim.*, **15**, 203–215.

Bell, T.L., M.-D. Chou, R.S. Lindzen, and A.Y. Hou, 2002: Comments on "Does the Earth have an adaptive infrared iris?" Reply. *Bull. Am. Meteorol. Soc.*, **83**, 598–600.

Bengtsson, L.K., I. Hodges, and E. Roeckner, 2006: Storm tracks and climate change. *J. Clim.*, **19**, 3518–3543.

Bernie, D., S.J. Woolnough, J.M. Slingo, and E. Guilyardi, 2005: Modelling diurnal and intraseasonal variability of the ocean mixed layer. *J. Clim.*, **15**, 1190–1202.

Bitz, C.M., and W.H. Lipscomb, 1999: An energy-conserving thermodynamic sea ice model for climate study. *J. Geophys. Res.*, **104**, 15669–15677.

Bitz, C.M., G. Flato, and J. Fyfe, 2002: Sea ice response to wind forcing from AMIP models. *J. Clim.*, **15**, 523–535.

Bitz, C.M., M.M., Holland, A.J. Weaver, and M. Eby, 2001: Simulating the ice-thickness distribution in a coupled climate model. *J. Geophys. Res.*, **106**, 2441–2463.

Blankenship, C.B., and T.T Wilheit, 2001: SSM/T-2 measurements of regional changes in three-dimensional water vapour fields during ENSO events. *J. Geophys. Res.*, **106**, 5239–5254.

Bleck, R., 2002: An oceanic general circulation model framed in hybrid isopycnic-Cartesian coordinates. *Ocean Modelling*, **4**, 55–88.

Bleck, R., C. Rooth, D. Hu, and L.T. Smith, 1992: Salinity-driven thermocline transients in a wind- and thermohaline-forced isopycnic coordinate model of the North Atlantic. *J. Phys. Oceanogr.*, **22**, 1486–1505.

Boer, G.J., and B. Yu, 2003: Climate sensitivity and climate state. *Clim. Dyn.*, **21**, 167–176.

Bonan, G.B., 1998: The land surface climatology of the NCAR land surface model (LSM 1.0) coupled to the NCAR Community Climate Model (CCM3). *J. Clim.*, **11**, 1307–1326.

Bonan, G.B., K.W. Oleson, M. Vertenstein, and S. Levis, 2002: The land surface climatology of the Community Land Model coupled to the NCAR Community Climate Model. *J. Clim.*, **15**, 3123–3149.

Böning, C.W., et al., 1995: An overlooked problem in model simulations of the thermohaline circulation and heat transports in the Atlantic Ocean. *J. Clim.*, **8**, 515–523.

Bony, S., and K.A. Emanuel, 2001: A parameterization of the cloudiness associated with cumulus convection: Evaluation using TOGA COARE data. *J. Atmos. Sci.*, **58**, 3158–3183.

Bony, S., and J.-L. Dufresne, 2005: Marine boundary-layer clouds at the heart of tropical cloud feedback uncertainties in climate models. *Geophys. Res. Lett.*, **32**(20), L20806, doi:10.1029/2005GL023851.

Bony, S., and K.A. Emanuel, 2005: On the role of moist processes in tropical intraseasonal variability: cloud-radiation and moisture-convection feedbacks. *J. Atmos. Sci.*, **62**, 2770–2789.

Bony, S., K.-M. Lau, and Y.C. Sud, 1997: Sea surface temperature and large-scale circulation influences on tropical greenhouse effect and cloud radiative forcing. *J. Clim.*, **10**, 2055–2077.

Bony, S., et al., 2004: On dynamic and thermodynamic components of cloud changes. *Clim. Dyn.*, **22**, 71–86.

Bony, S., et al., 2006: How well do we understand and evaluate climate change feedback processes? *J. Clim.*, **19**, 3445–3482.

Boone, A., V. Masson, T. Meyers, and J. Noilhan, 2000: The influence of the inclusion of soil freezing on simulations by a soil-vegetation-atmosphere transfer scheme. *J. Appl. Meteorol.*, **39**(9), 1544–1569.

Boone, A., et al., 2004: The Rhone-Aggregation land surface scheme intercomparison project: An overview. *J. Clim.*, **17**, 187–208.

Boville, B.A., and W.J. Randel, 1992: Equatorial waves in a stratospheric GCM: Effects of resolution. *J. Atmos. Sci.*, **49**, 785–801.

Bowling, L.C., et al., 2003: Simulation of high latitude hydrological processes in the Torne-Kalix basin: PILPS Phase 2(e) 1: Experiment description and summary intercomparisons. *Global Planet. Change*, **38**, 1–30.

Boyle, J.S., et al., 2005: Diagnosis of Community Atmospheric Model 2 (CAM2) in numerical weather forecast configuration at Atmospheric Radiation Measurement (ARM) sites. *J. Geophys. Res.*, **110**, doi:10.1029/2004JD005042.

Branstetter, M.L., 2001: *Development of a Parallel River Transport Algorithm and Application to Climate Studies*. PhD Dissertation, University of Texas, Austin, TX.

Briegleb, B.P., et al., 2004: *Scientific Description of the Sea Ice Component in the Community Climate System Model*, *Version Three*. Technical Note TN-463STR, NTIS #PB2004-106574, National Center for Atmospheric Research, Boulder, CO, 75 pp.

Broccoli, A.J., N.-C. Lau, and M.J. Nath, 1998: The cold ocean-warm land pattern: Model simulation and relevance to climate change detection. *J. Clim.*, **11**, 2743–2763.

Broecker, W.S., 1997: Thermohaline circulation, the Achilles heel of our climate system: will man-made CO_2 upset the current balance? *Science*, **278**, 1582–1588.

Brogniez, H., R. Roca, and L. Picon, 2005: Evaluation of the distribution of subtropical free tropospheric humidity in AMIP-2 simulations using METEOSAT water vapour channel data. *Geophys. Res. Lett.*, **32**, L19708, doi:10.1029/2005GL024341.

Brovkin, V., et al., 2002: Carbon cycle, vegetation and climate dynamics in the Holocene: Experiments with the CLIMBER-2 model. *Global Biogeochem. Cycles*, **16**(4), 1139, doi:10.1029/2001GB001662.

Brovkin, V., et al., 2006: Biogeophysical effects of historical land cover changes simulated by six Earth system models of intermediate complexity. *Clim. Dyn.*, **26**, 587–600, doi:10.1007/s00382-005-0092-6.

Bryan, F.O., et al., 2006: Response of the North Atlantic thermohaline circulation and ventilation to increasing carbon dioxide in CCSM3. *J. Clim.*, **19**, 2382–2397.

Burke, E.J., S.J. Brown, and N. Christidis, 2006: Modelling the recent evolution of global drought and projections for the 21st century with the Hadley Centre climate model. *J. Hydrometeorol.*, **7**, 1113–1125.

Cai, M., 2005: Dynamical amplification of polar warming. *Geophys. Res. Lett.*, **32**, L22710, doi:10.1029/2005GL024481.

Cai, W.J., and P.H. Whetton, 2000: Evidence for a time-varying pattern of greenhouse warming in the Pacific Ocean. *Geophys. Res. Lett.*, **27**(16), 2577–2580.

Cai, W.J., P.H. Whetton, and D.J. Karoly, 2003: The response of the Antarctic Oscillation to increasing and stabilized atmospheric CO_2. *J. Clim.*, **16**, 1525–1538.

Calov, R., et al., 2002: Large-scale instabilities of the Laurentide ice sheet simulated in a fully coupled climate-system model. *Geophys. Res. Lett.*, **29**(24), 2216, doi:10.1029/2002GL016078.

Calov, R., et al., 2005: Transient simulation of the last glacial inception. Part I: Glacial inception as a bifurcation of the climate system. *Clim. Dyn.*, **24**(6), 545–561.

Camargo, S., A.G. Barnston, and S.E. Zebiak, 2005: A statistical assessment of tropical cyclone activity in atmospheric general circulation models. *Tellus*, **57A**, 589–604.

Carnell, R., and C. Senior, 1998: Changes in mid-latitude variability due to increasing greenhouse gases and sulphate aerosols. *Clim. Dyn.*, **14**, 369–383.

Cassou, C., L. Terray, J.W. Hurrell, and C. Deser, 2004: North Atlantic winter climate regimes: Spatial asymmetry, stationarity with time, and oceanic forcing. *J. Clim.*, **17**, 1055–1068.

Castanheira, J.M., and H.-F. Graf, 2003: North Pacific–North Atlantic relationships under stratospheric control? *J. Geophys. Res.*, **108**, 4036, doi:10.1029/2002JD002754.

Cattle, H., and J. Crossley, 1995: Modelling Arctic climate change. *Philos. Trans. R. Soc. London Ser. A*, **352**, 201–213.

Cess, R.D., 1975: Global climate change: an investigation of atmospheric feedback mechanisms. *Tellus*, **27**, 193–198.

Cess, R.D., et al., 1989: Interpretation of cloud-climate feedback as produced by 14 atmospheric general circulation models. *Science*, **245**, 513–516.

Chambers, L.H., B. Lin, and D.F. Young, 2002: Examination of new CERES data for evidence of tropical Iris feedback. *J. Clim.*, **15**, 3719–3726.

Chang, F.-L., and Z. Li, 2005: A comparison of the global surveys of high, mid and low clouds from satellite and general circulation models. In: *Proceedings of the Fifteenth Atmospheric Radiation Measurement (ARM) Science Team Meeting, Daytona Beach, Florida, 14–18 March 2005*. Atmospheric Radiation Measurement Program, US Department of Energy, Washington, DC, http://www.arm.gov/publications/proceedings/conf15/

Chapman, W.L., and J. E. Walsh, 2007: Simulations of arctic temperature and pressure by global coupled models. *J. Clim.*, **20**, 609-632.

Chen, D., S.E. Zebiak, A.J. Busalacchi, and M.A. Cane, 1995: An improved procedure for El Niño forecasting. *Science*, **269**, 1699–1702.

Chen, J., B.E. Carlson, and A.D. Del Genio, 2002: Evidence for strengthening of the tropical general circulation in the 1990s. *Science*, **295**, 838–841.

Chen, T.-C., and J.-H. Yoon, 2002: Interdecadal variation of the North Pacific wintertime blocking. *Mon. Weather Rev.*, **130**, 3136–3143.

Chin, M., et al., 2002: Tropospheric aerosol optical thickness from GOCART model and comparisons with satellite and sun photometer measurements. *J. Atmos. Sci.*, **59**, 461–483.

Chou, M.-D., R.S. Lindzen, and A.Y. Hou, 2002: Reply to: "Tropical cirrus and water vapor: An effective Earth infrared iris feedback?". *Atmos. Chem. Phys.*, **2**, 99–101.

Chung, E.S., B.J. Sohn, and V. Ramanathan, 2004: Moistening processes in the upper troposphere by deep convection: a case study over the tropical Indian Ocean. *J. Meteorol. Soc. Japan*, **82**, 959–965.

Church, J.A., et al., 2001: Changes in sea level. In: *Climate Change 2001: The Scientific Basis. Contribution of Working Group I to the Third Assessment Report of the Intergovernmental Panel on Climate Change* [Houghton, J.T., et al. (eds.)]. Cambridge University Press, Cambridge, United Kingdom and New York, NY, USA, pp. 663–693.

Clark, P.U., N.G. Pisias, T.F. Stocker, and A.J. Weaver, 2002: The role of the thermohaline circulation in abrupt climate change. *Nature*, **415**, 863–869.

Claussen, M., 1998: On multiple solutions of the atmosphere-vegetation system in present-day climate. *Global Change Biol.*, **4**, 549–559.

Claussen, M., 2005: *Table of EMICs (Earth System Models of Intermediate Complexity)*. PIK Report 98, Potsdam-Institut für Klimafolgenforschung, Potsdam, Germany, 55 pp, http://www.pik-potsdam.de/emics.

Claussen, M., et al., 2002: Earth system models of intermediate complexity: closing the gap in the spectrum of climate system models. *Clim. Dyn.*, **18**, 579–586.

Collins, M., S.F.B. Tett, and C. Cooper, 2001: The internal climate variability of HadCM3, a version of the Hadley Centre coupled model without flux adjustments. *Clim. Dyn.*, **17**, 61–81.

Collins, M., D. Frame, B. Sinha, and C. Wilson, 2002: How far ahead could we predict El Niño? *Geophys. Res. Lett.*, **29**(10), 1492, doi:10.1029/2001GL013919.

Collins, W.D., et al., 2004: *Description of the NCAR Community Atmosphere Model (CAM3.0)*. Technical Note TN-464+STR, National Center for Atmospheric Research, Boulder, CO, 214 pp.

Collins, W.D., et al., 2006: The Community Climate System Model: CCSM3. *J. Clim.*, **19**, 2122–2143.

Colman, R.A., 2001: On the vertical extent of atmospheric feedbacks. *Clim. Dyn.*, **17**, 391–405.

Colman, R.A., 2003a: A comparison of climate feedbacks in general circulation models. *Clim. Dyn.*, **20**, 865–873.

Colman, R.A., 2003b: Seasonal contributions to climate feedbacks. *Clim. Dyn.*, **20**, 825–841.

Colman, R.A., 2004: On the structure of water vapour feedbacks in climate models. *Geophys. Res. Lett.*, **31**, L21109, doi:10.1029/2004GL020708.

Cook, K.H., and E.K. Vizy, 2006: Coupled model simulations of the West African monsoon system: 20th century simulations and 21st century predictions. *J. Clim.*, **19**, 3681–3703.

Cox, P., 2001: *Description of the "TRIFFID" Dynamic Global Vegetation Model*. Technical Note 24, Hadley Centre, United Kingdom Meteorological Office, Bracknell, UK.

Cox, P.M., et al., 1999: The impact of new land surface physics on the GCM simulation of climate and climate sensitivity. *Clim. Dyn.*, **15**, 183–203.

Cox, P.M., et al., 2000: Acceleration of global warming due to carbon-cycle feedbacks in a coupled climate model. *Nature*, **408**, 184–187.

Cox, P.M., et al., 2004: Amazonian forest dieback under climate-carbon cycle projections for the 21st century. *Theor. Appl. Climatol.*, **78**, 137–156, doi:10.1007/s00704-004-0049-4.

Cramer, W., et al., 2001: Global response of terrestrial ecosystem structure and function to CO_2 and climate change: results from six dynamic global vegetation models. *Global Change Biol.*, **7**, 357–373.

Crucifix, M., 2005: Carbon isotopes in the glacial ocean: A model study. *Paleoceanography*, **20**, PA4020, doi:10.1029/2005PA001131.

Crucifix, M., and A. Berger, 2002: Simulation of ocean–ice sheet interactions during the last deglaciation. *Paleoceanography*, **17**(4), 1054, doi:10.1029/2001PA000702.

Crucifix, M., et al., 2002: Climate evolution during the Holocene: A study with an Earth system model of intermediate complexity. *Clim. Dyn.*, **19**, 43–60, doi:10.10007/s00382-001-0208-6.

CSMD (Climate System Modeling Division), 2005: An introduction to the first general operational climate model at the National Climate Center. *Advances in Climate System Modeling*, 1, National Climate Center, China Meteorological Administration, 14 pp (in English and Chinese).

Cubasch, U., et al., 2001: Projections of future climate changes. In: *Climate Change 2001: The Scientific Basis. Contribution of Working Group I to the Third Assessment Report of the Intergovernmental Panel on Climate Change* [Houghton, J.T., et al. (eds.)]. Cambridge University Press, Cambridge, United Kingdom and New York, NY, USA, pp. 525–582.

da Silva, A.M., C.C. Young, and S. Levitus, 1994: *Atlas of Surface Marine Data 1994, NOAA Atlas NESDIS 6*. NOAA/NESDIS E/OC21 (6 Volumes). US Department of Commerce, National Oceanographic Data Center, User Services Branch, Washington, DC.

Dai, A., 2006: Precipitation characteristics in eighteen coupled climate models. *J. Clim.*, **19**, 4605–4630.

Dai, A., K.E. Trenberth, and T. Qian, 2004: A global data set of Palmer Drought Severity Index for 1870-2002: Relationship with soil moisture and effects of surface warming. *J. Hydrometeorol.*, **5**, 1117–1130. PDSI data: http://www.cgd.ucar.edu/cas/catalog/climind/pdsi.html.

Danabasoglu, G., J.C. McWilliams, and P.R. Gent, 1995: The role of mesoscale tracer transports in the global ocean circulation. *Science*, **264**, 1123–1126.

D'Andrea, F., et al., 1998: Northern Hemisphere atmospheric blocking as simulated by 15 atmospheric general circulation models in the period 1979–1988. *Clim. Dyn.*, **14**(6), 385–407.

Dargaville, R.J., et al., 2002: Evaluation of terrestrial carbon cycle models with atmospheric CO_2 measurements: Results from transient simulations considering increasing CO_2, climate, and land-use effects. *Global Biogeochem. Cycles*, **16**, 1092, doi:10.1029/2001GB001426.

Davey, M., et al., 2002: STOIC: A study of coupled GCM climatology and variability in tropical ocean regions. *Clim. Dyn.*, **18**, 403–420, doi:10.1007/s00382-001-0188-6.

Del Genio, A.D., and A.B. Wolf, 2000: The temperature dependence of the liquid water path of low clouds in the southern great plains. *J. Clim.*, **13**, 3465 3486.

Del Genio, A.D., and W. Kovari, 2002: Climatic properties of tropical precipitating convection under varying environmental conditions. *J. Clim.*, **15**, 2597–2615.

Del Genio, A.D., A. Wolf, and M.-S. Yao, 2005a: Evaluation of regional cloud feedbacks using single-column models. *J. Geophys. Res.*, **110**, D15S13, doi:10.1029/2004JD005011.

Del Genio, A.D., W. Kovari, M.-S. Yao, and J. Jonas, 2005b: Cumulus microphysics and climate sensitivity. *J. Clim.*, **18**, 2376–2387, doi:10.1175/JCLI3413.1.

Delire, C., J.A. Foley, and S. Thompson, 2003: Evaluating the carbon cycle of a coupled atmosphere–biosphere model. *Global Biogeochem. Cycles*, **17**, 1012, doi:10.1029/2002GB001870.

Delworth, T.L., and M.E. Mann, 2000: Observed and simulated multidecadal variability in the Northern Hemisphere. *Clim. Dyn.*, **16**(9), 661–676.

Delworth, T., S. Manabe, and R.J. Stouffer, 1993: Interdecadal variations of the thermohaline circulation in a coupled ocean-atmosphere model. *J. Clim.*, **6**, 1993–2011.

Delworth, T.L., V. Ramaswamy, and G.L. Stenchikov, 2005: The impact of aerosols on simulated ocean temperature and heat content in the 20th century. *Geophys. Res. Lett.*, **32**, L24709, doi:10.1029/2005GL024457.

Delworth, T., et al., 2006: GFDL's CM2 global coupled climate models – Part 1: Formulation and simulation characteristics. *J. Clim.*, **19**, 643–674.

Déqué, M., C. Dreveton, A. Braun, and D. Cariolle, 1994: The ARPEGE/IFS atmosphere model: A contribution to the French community climate modeling. *Clim. Dyn.*, **10**, 249–266.

Derber, J., and A. Rosati, 1989: A global oceanic data assimilation system. *J. Phys. Oceanogr.*, **19**(9), 1333–1347.

Deser, C., A.S. Phillips, and J.W. Hurrell, 2004: Pacific interdecadal climate variability: Linkages between the tropics and North Pacific during boreal winter since 1900. *J. Clim.*, **17**, 3109–3124.

Dessler, A.E., and S.C. Sherwood, 2000: Simulations of tropical upper tropospheric humidity. *J. Geophys. Res.*, **105**, 20155–20163.

Diansky, N.A., and E.M. Volodin, 2002: Simulation of the present-day climate with a coupled atmosphere-ocean general circulation model. *Izv. Atmos. Ocean. Phys.*, **38**, 732–747 (English translation).

Diansky, N.A., A.V. Bagno, and V.B. Zalesny, 2002: Sigma model of global ocean circulation and its sensitivity to variations in wind stress. *Izv. Atmos. Ocean. Phys.*, **38**, 477–494 (English translation).

Dirmeyer, P.A., 2001: An evaluation of the strength of land-atmosphere coupling. *J. Hydrometeorol.*, **2**, 329–344.

Dong, M., et al., 2000: Developments and implications of the atmospheric general circulation model. In: *Investigations on the Model System of the Short-Term Climate Predictions* [Ding, Y., et al. (eds.)]. China Meteorological Press, Beijing, China, pp. 63–69 (in Chinese).

Doutriaux-Boucher, M., and J. Quaas, 2004: Evaluation of cloud thermodynamic phase parametrizations in the LMDZ GCM by using POLDER satellite data. *Geophys. Res. Lett.*, **31**, L06126, doi:10.1029/2003GL019095.

Douville, H., 2001: Influence of soil moisture on the Asian and African Monsoons. Part II: interannual variability. *J. Clim.*, **15**, 701–720.

Douville, H., J.-F. Royer, and J.-F. Mahfouf, 1995: A new snow parameterization for the Meteo-France climate model. *Clim. Dyn.*, **12**, 21–35.

Drange, H., et al., 2005: Ocean general circulation modelling of the Nordic Seas. In: *The Nordic Seas: An Integrated Perspective* [Drange, H., et al. (eds.)]. Geophysical Monograph 158, American Geophysical Union, Washington, DC, pp. 199–220.

Driesschaert, E., 2005: *Climate Change over the Next Millennia Using LOVECLIM, a New Earth System Model Including Polar Ice Sheets*. PhD Thesis, Université Catholique de Louvain, Louvain-la-Neuve, Belgium, 214 pp, http://edoc.bib.ucl.ac.be:81/ETD-db/collection/available/BelnUcetd-10172005-185914/.

Ducharne, A., et al., 2003: Development of a high resolution runoff routing model, calibration and application to assess runoff from the LMD GCM. *J. Hydrol.*, **280**, 207–228.

Dufresne, J.-L., et al., 2002: On the magnitude of positive feedback between future climate change and the carbon cycle. *Geophys. Res. Lett.*, **29**(10), doi:10.1029/2001GL013777.

Dümenil, L., and E. Todini, 1992: A rainfall-runoff scheme for use in the Hamburg climate model. In: *Advances in Theoretical Hydrology: A Tribute to James Dooge. European Geophysical Society Series on Hydrological Sciences, Vol. 1* [O'Kane, J.P. (ed.)]. Elsevier Press, Amsterdam, pp. 129–157.

Durman, C.F., et al., 2001: A comparison of extreme European daily precipitation simulated by a global model and regional climate model for present and future climates. *Q. J. R. Meteorol. Soc.*, **127**, 1005–1015.

Edwards, N.R., and R.J. Marsh, 2005: Uncertainties due to transport-parameter sensitivity in an efficient 3-D ocean-climate model. *Clim. Dyn.*, **24**, 415–433, doi:10.1007/s00382-004-0508-8.

Emanuel, K.A., and M. Zivkovic-Rothman, 1999: Development and evaluation of a convection scheme for use in climate models. *J. Atmos. Sci.*, **56**, 1766–1782.

Emori, S., A. Hasegawa, T. Suzuki, and K. Dairaku, 2005: Validation, parameterization dependence and future projection of daily precipitation simulated with an atmospheric GCM. *Geophys. Res. Lett.*, **32**, L06708, doi:10.1029/2004GL022306.

Essery, R.H., and J. Pomeroy, 2004: Vegetation and topographic control of wind-blown snow distributions in distributed and aggregated simulations. *J. Hydrometeorol.*, **5**(5), 735–744.

Essery, R., M. Best, and P. Cox, 2001: *MOSES 2.2 Technical Documentation*. Hadley Centre Technical Note No. 30, Hadley Centre for Climate Prediction and Research, UK Met Office, Exeter, UK, http://www.metoffice.gov.uk/research/hadleycentre/pubs/HCTN/index.html.

Essery, R.H., J. Pomeroy, J. Parvianen, and P. Storck, 2003: Sublimation of snow from boreal forests in a climate model. *J. Clim.*, **16**, 1855–1864.

Etchevers, P., et al., 2004: Validation of the energy budget of an alpine snowpack simulated by several snow models (SnowMIP project). *Ann. Glaciol.*, **38**, 150–158.

Farrara, J.D., C.R. Mechoso, and A.W. Robertson, 2000: Ensembles of AGCM two-tier predictions and simulations of the circulation anomalies during winter 1997–1998. *Mon. Weather Rev.*, **128**, 3589–3604.

Felzer, B., et al., 2005: Global and future implications of ozone on net primary production and carbon sequestration using a biogeochemical model. *Clim. Change*, **73**, 345–373.

Fichefet, T., and M.A. Morales Maqueda, 1997: Sensitivity of a global sea ice model to the treatment of ice thermodynamics and dynamics. *J. Geophys. Res.*, **102**, 12609–12646.

Fichefet, T., et al., 2003: Implications of changes in freshwater flux from the Greenland ice sheet for the climate of the 21st century. *Geophys. Res. Lett.*, **30**(17), 1911, doi:10.1029/2003GL017826.

Fiorino, M., 1997: *PCMDI IPCC '95 AMIP Analysis: Observations used in the analysis*. PCMDI Web. Rep., Program for Climate Model Diagnosis and Intercomparison, Lawrence Livermore National Laboratory, Livermore, CA, http://www-pcmdi.llnl.gov/obs/ipcc/ipcc.obs.dat.htm.

Flato, G.M., 2004: Sea-ice and its response to CO_2 forcing as simulated by global climate models. *Clim. Dyn.*, **23**, 229–241, doi:10.1007/s00382-004-0436-7.

Flato, G.M., 2005: *The Third Generation Coupled Global Climate Model (CGCM3)* (and included links to the description of the AGCM3 atmospheric model). http://www.cccma.bc.ec.gc.ca/models/cgcm3.shtml.

Flato, G.M., and W.D. Hibler, 1992: Modeling pack ice as a cavitating fluid. *J. Phys. Oceanogr.*, **22**, 626–651.

Flato, G.M., and G.J. Boer, 2001: Warming asymmetry in climate change simulations. *Geophys. Res. Lett.*, **28**, 195–198.

Flugel, M., P. Chang, and C. Penland, 2004: The role of stochastic forcing in modulating ENSO predictability. *J. Clim.*, **17**(16), 3125–3140.

Folkins, I., K.K. Kelly, and E.M. Weinstock, 2002: A simple explanation of the increase in relative humidity between 11 and 14 km in the tropics. *J. Geophys. Res.*, **107**, doi:10.1029/2002JD002185.

Folland, C.K., T.K. Palmer, and D.E. Parker, 1986: Sahel rainfall and worldwide sea temperatures. *Nature*, **320**, 602–607.

Forster, P.M. de F., and K.P. Shine, 2002: Assessing the climate impact of trends in stratospheric water vapour. *Geophys. Res. Lett.*, **6**, doi:10.1029/2001GL013909.

Forster, P.M. de F., and M. Collins, 2004: Quantifying the water vapour feedback associated with post-Pinatubo cooling. *Clim. Dyn.*, **23**, 207–214.

Forster, P.M. de F., and K.E. Taylor, 2006: Climate forcings and climate sensitivities diagnosed from coupled climate model integrations. *J. Clim.*, **19**, 6181–6194.

Frei, A., J. Miller, and D. Robinson, 2003: Improved simulations of snow extent in the second phase of the Atmospheric Model Intercomparison Project (AMIP-2). *J. Geophys. Res.*, **108**(D12), 4369, doi:10.1029/2002JD003030.

Frei, A., J.A. Miller, R. Brown, and D.A. Robinson, 2005: Snow mass over North America: observations and results from the second phase of the Atmospheric Model Intercomparison Project (AMIP-2). *J. Hydrometeorol.*, **6**, 681–695.

Frich, P., et al., 2002: Observed coherent changes in climatic extremes during the second half of the twentieth century. *Clim. Res.*, **19**, 193–212.

Friedlingstein, P., et al., 2001: Positive feedback between future climate change and the carbon cycle. *Geophys. Res. Lett.*, **28**(8), 1543–1546.

Friedlingstein, P., J.-L. Dufresne, P.M Cox, and P. Rayner, 2003: How positive is the feedback between climate change and the carbon cycle? *Tellus*, **55B**, 692–700.

Friedlingstein, P., et al., 2006: Climate–carbon cycle feedback analysis, results from the C4MIP model intercomparison. *J. Clim.*, **19**, 3337–3353.

Friend, A.D., and N.Y. Kiang, 2005: Land surface model development for the GISS GCM: Effects of improved canopy physiology on simulated climate. *J. Clim.*, **18**, 2883–2902.

Fu, Q., M. Baker, and D.L. Hartmann, 2002: Tropical cirrus and water vapour: an effective Earth infrared iris? *Atmos. Chem. Phys.*, **2**, 31–37.

Fu, Q., C.M. Johanson, S.G. Warren, and D.J. Seidel, 2004: Contribution of stratospheric cooling to satellite-inferred tropospheric temperature trends. *Nature*, **429**, 55–58.

Furevik, T., et al., 2003: Description and evaluation of the Bergen climate model: ARPEGE coupled with MICOM. *Clim. Dyn.*, **21**, 27–51.

Fyfe, J.C., G.J. Boer, and G.M. Flato, 1999: The Arctic and Antarctic Oscillations and their projected changes under global warming. *Geophys. Res. Lett.*, **11**, 1601–1604.

Galin, V. Ya., E.M. Volodin, and S.P. Smyshliaev, 2003: Atmospheric general circulation model of INM RAS with ozone dynamics. *Russ. Meteorol. Hydrol.*, **5**, 13–22.

Gallée, H., et al., 1991: Simulation of the last glacial cycle by a coupled, sectorally averaged climate–ice sheet model. Part I: The climate model. *J. Geophys. Res.*, **96**, 13139–13161.

Ganachaud, A., and C. Wunsch, 2000: Improved estimates of global ocean circulation, heat transport and mixing from hydrographic data. *Nature*, **408**, 453–457.

Ganachaud, A., and C. Wunsch, 2003: Large-scale ocean heat and freshwater transports during the World Ocean Circulation Experiment. *J. Clim.*, **16**, 696–705.

Gates, W.L., et al., 1999: An overview of the results of the Atmospheric Model Intercomparison Project (AMIP I). *Bull. Am. Meteorol. Soc.*, **80**, 29–55.

Geng, Q., and M. Sugi, 2003: Possible change of extratropical cyclone activity due to enhanced greenhouse gases and sulfate aerosols–Study with a high-resolution AGCM. *J. Clim.*, **16**, 2262–2274.

Gent, P.R., 2001: Will the North Atlantic Ocean thermohaline circulation weaken during the 21st century? *Geophys. Res. Lett.*, **28**, 1023–1026.

Gent, P.R., J. Willebrand, T.J. McDougall, and J.C. McWilliams, 1995: Parameterizing eddy-induced tracer transports in ocean circulation models. *J. Phys. Oceanogr.*, **25**, 463–474.

Gerber, S., et al., 2003: Constraining temperature variations over the last millennium by comparing simulated and observed atmospheric CO_2. *Clim. Dyn.*, **20**, 281–299.

Gerten, D., et al., 2004: Terrestrial vegetation and water balance–hydrological evaluation of a dynamic global vegetation model. *J. Hydrol.*, **286**, 249–270.

Gettelman, A., J.R. Holton, and A.R. Douglass, 2000: Simulations of water vapor in the lower stratosphere and upper troposphere. *J. Geophys. Res.*, **105**, 9003–9023.

GFDL GAMDT (The GFDL Global Atmospheric Model Development Team), 2004: The new GFDL global atmosphere and land model AM2-LM2: Evaluation with prescribed SST simulations. *J. Clim.*, **17**, 4641–4673.

Ghan, S.J., R. Easter, J. Hudson, and F.-M. Bréon, 2001a: Evaluation of aerosol indirect radiative forcing in MIRAGE. *J. Geophys. Res.*, **106**, 5317–5334.

Ghan, S.J., et al., 2001b: Evaluation of aerosol direct radiative forcing in MIRAGE. *J. Geophys. Res.*, **106**, 5295–5316.

Gillett, N.P., 2005: Northern Hemisphere circulation. *Nature*, **437**, 496.

Gillett, N.P., and D.W.J. Thompson, 2003: Simulation of recent Southern Hemisphere climate change. *Science*, **302**, 273–275.

Giorgetta, M.A., E. Manzini, and E. Roeckner, 2002: Forcing of the quasi-biennial oscillation from a broad spectrum of atmospheric waves. *Geophys. Res. Lett.*, **29**, 1245, doi:10.1029/2002GL014756.

Giorgetta M.A., et al., 2006: Climatology and forcing of the quasi-biennial oscillation in the MAECHAM5 model. *J. Clim.*, **19**, 3882–3901.

Gleckler, P.J., K.R. Sperber, and K. AchutaRao, 2006a: The annual cycle of global ocean heat content: observed and simulated. *J. Geophys. Res.*, **111**, C06008, doi:10.1029/2005JC003223.

Gleckler, P.J., et al., 2006b: Krakatoa's signature persists in the ocean. *Nature*, **439**, 675, doi:10.1038/439675a.

Gnanadesikan, A., et al., 2004: GFDL's CM2 global coupled climate models–Part 2: The baseline ocean simulation. *J. Clim.*, **19**, 675–697.

Goldenberg, S.B., C.W. Landsea, A.M. Mestas-Nunez, and W.M. Gray, 2001: The recent increase in Atlantic hurricane activity: Causes and implications. *Science*, **293**, 474–479.

Goosse, H., and T. Fichefet, 1999: Importance of ice-ocean interactions for the global ocean circulation: A model study. *J. Geophys. Res.*, **104**, 23337–23355.

Goosse, H., F.M. Selten, R.J. Haarsma, and J.D. Opsteegh, 2003: Large sea-ice volume anomalies simulated in a coupled climate model. *Clim. Dyn.*, **20**, 523–536, doi:10.1007/s00382-002-0290-4.

Goosse, H., et al., 2002: Potential causes of abrupt climate events: a numerical study with a three-dimensional climate model. *Geophys. Res. Lett.*, **29**(18), 1860, doi:10.1029/2002GL014993.

Gordon, C., et al., 2000: The simulation of SST, sea ice extents and ocean heat transports in a version of the Hadley Centre coupled model without flux adjustments. *Clim. Dyn.*, **16**, 147–168.

Gordon, H.B., et al., 2002: *The CSIRO Mk3 Climate System Model*. CSIRO Atmospheric Research Technical Paper No. 60, Commonwealth Scientific and Industrial Research Organisation Atmospheric Research, Aspendale, Victoria, Australia, 130 pp, http://www.cmar.csiro.au/e-print/open/gordon_2002a.pdf.

Gordon, N.D., J.R. Norris, C.P. Weaver, and S.A. Klein, 2005: Cluster analysis of cloud regimes and characteristic dynamics of midlatitude synoptic systems in observations and a model. *J. Geophys. Res.*, **110**, D15S17, doi:10.1029/2004JD005027.

Govindasamy, B., et al., 2005: Increase of the carbon cycle feedback with climate sensitivity: results from a coupled and carbon climate and carbon cycle model. *Tellus*, **57B**, 153–163.

Graham, R.J., et al., 2005: A performance comparison of coupled and uncoupled versions of the Met Office seasonal prediction general circulation model. *Tellus*, **57A**, 320–339.

Greenwald, T.J., G.L. Stephens, S.A. Christopher, and T.H.V. Haar, 1995: Observations of the global characteristics and regional radiative effects of marine cloud liquid water. *J. Clim.*, **8**, 2928–2946.

Gregory, D., et al., 2000: Revision of convection, radiation and cloud schemes in the ECMWF Integrated Forecasting System. *Q. J. R. Meteorol. Soc.*, **126**, 1685–1710.

Gregory, J.M., et al., 2002: An observationally based estimate of the climate sensitivity. *J. Clim.*, **15**, 3117–3121.

Gregory, J.M., et al., 2005: A model intercomparison of changes in the Atlantic thermohaline circulation in response to increasing atmospheric CO_2 concentration. *Geophys. Res. Lett.*, **32**, L12703, doi:10.1029/2005GL023209.

Griffies, S.M., 2004: *Fundamentals of Ocean Climate Models.* Princeton University Press, Princeton, NJ, 496 pp.

Guilyardi, E., et al., 2004: Representing El Niño in coupled ocean-atmosphere GCMs: the dominant role of the atmospheric component. *J. Clim.*, **17**, 4623–4629.

Gutowski, W.J., et al., 2004: Diagnosis and attribution of a seasonal precipitation deficit in a US regional climate simulation. *J. Hydrometeorol.*, **5**(1), 230–242.

Hagemann, S., 2002: *An Improved Land Surface Parameter Dataset for Global and Regional Climate Models*. Max Planck Institute for Meteorology Report 162, MPI for Meteorology, Hamburg, Germany, 21 pp.

Hagemann, S., and L. Dümenil-Gates, 2001: Validation of the hydrological cycle of ECMWF and NCEP reanalyses using the MPI hydrological discharge model. *J. Geophys. Res.*, **106**, 1503–1510.

Hall, A., 2004: The role of surface albedo feedback in climate. *J. Clim.*, **17**, 1550–1568.

Hall, A., and S. Manabe, 1999: The role of water vapour feedback in unperturbed climate variability and global warming. *J. Clim.*, **12**, 2327–2346.

Hall, A., and R.J. Stouffer, 2001: An abrupt climate event in a coupled ocean-atmosphere simulation without external forcing. *Nature*, **409**(6817), 171–174.

Hall, A., and M. Visbeck, 2002: Synchronous variability in the Southern Hemisphere atmosphere, sea ice and ocean resulting from the annular mode. *J. Clim.*, **15**, 3043–3057.

Hall, A., and X. Qu, 2006: Using the current seasonal cycle to constrain snow albedo feedback in future climate change. *Geophys. Res. Lett.*, **33**, L03502, doi:10.1029/2005GL025127.

Hall, M.M., and H.L. Bryden, 1982: Direct estimates and mechanisms of ocean heat transport. *Deep Sea Res.*, **29**, 339–359.

Hamilton, K., R.J. Wilson, and R.S. Hemler, 2001: Spontaneous stratospheric QBO-like oscillations simulated by the GFDL SKYHI general circulation model. *J. Atmos. Sci.*, **58**, 3271–3292.

Hannachi, A., and A. O'Neill, 2001: Atmospheric multiple equilibria and non-Gaussian behaviour in model simulations. *Q. J. R. Meteorol. Soc.*, **127**, 939–958.

Hansen, J., et al., 1984: Climate sensitivity: analysis of feedback mechanisms. *Meteorol. Monogr.*, **29**, 130–163.

Hanson, C.E., J.P. Palutikof, and T.D. Davies, 2004: Objective cyclone climatologies of the North Atlantic - a comparison between the ECMWF and NCEP Reanalyses. *Clim. Dyn.*, **22**, 757–769.

Harder, M., 1996: *Dynamik, Rauhigkeit und Alter des Meereises in der Arktis*. PhD Thesis, Alfred-Wegener-Institut für Polar und Meeresforschung, Bremerhaven, Germany, 124 pp.

Hargreaves, J.C., J.D. Annan, N.R. Edwards, and R. Marsh, 2004: An efficient climate forecasting method using an intermediate complexity Earth System Model and the ensemble Kalman filter. *Clim. Dyn.*, **23**, 745–760.

Harrison, E.F., et al., 1990: Seasonal variation of cloud radiative forcing derived from the Earth Radiation Budget Experiment. *J. Geophys. Res.*, **95**, 18687–18703.

Harrison, H., 2002: Comments on "Does the Earth have an adaptive infrared iris?". *Bull. Am. Meteorol. Soc.*, **83**, 597.

Hartmann, D.L., and K. Larson, 2002: An important constraint on tropical cloud-climate feedback. *Geophys. Res. Lett.*, **29**(20), 1951–1954.

Hartmann, D.L., and M.L. Michelsen, 2002: No evidence for iris. *Bull. Am. Meteorol. Soc.*, **83**, 249–254.

Hartmann, D.L., M.E. Ockert-Bell, and M.L. Michelsen, 1992: The effect of cloud type on Earth's energy balance: Global analysis. *J. Clim.*, **5**, 1281–1304.

Harvey, D., et al., 1997: *An Introduction to Simple Climate Models Used in the IPCC Second Assessment Report*. IPCC Technical Paper 2 [Houghton, J.T., L.G. Meira Filho, D.J. Griggs, and K. Maskell (eds.)]. IPCC, Geneva, Switzerland, 51 pp.

Hasumi, H., 2002a: Sensitivity of the global thermohaline circulation to interbasin freshwater transport by the atmosphere and the Bering Strait throughflow. *J. Clim.*, **15**, 2516–2526.

Hasumi, H., 2002b: Modeling the global thermohaline circulation. *J. Oceanogr.*, **58**, 25–33.

Hasumi, H., and N. Suginohara, 1999: Effects of locally enhanced vertical diffusivity over rough bathymetry on the world ocean circulation. *J. Geophys. Res.*, **104**, 23367–23374.

Hazeleger, W., et al., 2001: Decadal upper ocean temperature variability in the tropical Pacific. *J. Geophys. Res.*, **106**(C5), 8971–8988.

Held, I.M., and B.J. Soden, 2000: Water vapour feedback and global warming. *Annu. Rev. Energy Environ.*, **25**, 441– 475.

Henderson-Sellers, A., P. Irannejad, K. McGuffie, and A.J. Pitman, 2003: Predicting land-surface climates - better skill or moving targets? *Geophys. Res. Lett.*, **30**(14), 1777–1780.

Henderson-Sellers, A., K. McGuffie, D. Noone, and P. Irannejad, 2004: Using stable water isotopes to evaluate basin-scale simulations of surface water budgets. *J. Hydrometeorol.*, **5**(5), 805–822.

Hendon, H.H., 2000: Impact of air–sea coupling on the Madden–Julian oscillation in a general circulation model. *J. Atmos. Sci.*, **57**, 3939–3952.

Hendon, H.H., 2005: Air sea interaction. In: *Intraseasonal Variability in the Atmosphere-Ocean Climate System* [Lau, W.K.M., and D.E. Waliser (eds.)]. Praxis Publishing, 436 pp.

Hewitt, C.D., C.S. Senior, and J.F.B. Mitchell, 2001: The impact of dynamic sea-ice on the climate sensitvity of a GCM: a study of past, present and future climates. *Clim. Dyn.*, **17**, 655–668.

Heymsfield, A.J., and L. Donner, 1990: A scheme for parameterizing ice-cloud water content in general circulation models. *J. Atmos. Sci.*, **47**, 1865–1877.

Hibler, W.D., 1979: A dynamic thermodynamic sea ice model. *J. Phys. Oceanogr.*, **9**, 817–846.

Hirst, A.C., 1999: The Southern Ocean response to global warming in the CSIRO coupled ocean-atmosphere model. *Environ. Model. Software*, **14**, 227–241.

Hodges, K.I., B.J. Hoskins, J. Boyle, and C. Thorncroft, 2003: A comparison of recent reanalysis data sets using objective feature tracking: storm tracks and tropical easterly waves. *Mon. Weather Rev.*, **131**, 2012–2037.

Hodges, K.: Feature based diagnostics from ECMWF/NCEP Analyses and AMIP II: Model Climatologies. In: *The Second Phase of the Atmospheric Model Intercomparison Project (AMIP2)* [Gleckler, P. (ed.)]. Proceedings of the WCRP/WGNE Workshop, Toulouse, France, pp. 201-204.

Holland, M.M., and C.M. Bitz, 2003: Polar amplification of climate change in coupled models. *Clim. Dyn.*, **21**, 221–232, doi:10.1007/s00382-003-0332-6.

Holland, M.M., and M. Raphael, 2006: Twentieth century simulation of the Southern Hemisphere climate in coupled models. Part II: sea ice conditions and variability. *Clim. Dyn.*, **26**, 229–245, doi:10.1007/s00382-005-0087-3.

Horinouchi, T., 2002: Mesoscale variability of tropical precipitation: Validation of satellite estimates of wave forcing using TOGA COARE radar data. *J. Atmos. Sci.*, **59**, 2428–2437.

Horinouchi, T., and S. Yoden, 1998: Wave-mean flow interaction associated with a QBO-like oscillation simulated in a simplified GCM. *J. Atmos. Sci.*, **55**, 502–526.

Horinouchi, T., et al., 2003: Tropical cumulus convection and upward-propagating waves in middle-atmospheric GCMs. *J. Atmos. Sci.*, **60**, 2765–2782.

Hoskins, B.J., and K.I. Hodges, 2002: New perspectives on the Northern Hemisphere winter storm tracks. *J. Atmos. Sci.*, **59**, 1041–1061.

Hoskins, B.J., and K.I. Hodges, 2005: New perspectives on the Southern Hemisphere storm tracks. *J. Clim.*, **18**, 4108–4129.

Hourdin, F., et al., 2006: The LMDZ4 general circulation model: Climate performance and sensitivity to parameterized physics with emphasis on tropical convection. *Clim. Dyn.*, **27**, 787–813.

Hovine, S., and T. Fichefet, 1994: A zonally averaged, three-basin ocean circulation model for climate studies. *Clim. Dyn.*, **15**, 1405–1413.

Hsu, C.J., and F. Zwiers, 2001: Climate change in recurrent regimes and modes of atmospheric variability. *J. Geophys. Res.*, **106**, 20145–20160.

Hu, A.X., G.A. Meehl, W.M. Washington, and A. Dai, 2004: Response of the Atlantic thermohaline circulation to increased atmospheric CO_2 in a coupled model. *J. Clim.*, **17**, 4267–4279.

Huang, X., B.J. Soden, and D.L. Jackson, 2005: Interannual co-variability of tropical temperature and humidity: A comparison of model, reanalysis data and satellite observation. *Geophys. Res. Lett.*, **32**, L17808, doi:10.1029/2005GL023375.

Hunke, E.C., and J.K. Dukowicz, 1997: An elastic-viscous-plastic model for sea ice dynamics. *J. Phys. Oceanogr.*, **27**, 1849–1867.

Hunke, E.C., and J.K. Dukowicz, 2002: The Elastic-Viscous-Plastic sea ice dynamics model in general orthogonal curvilinear coordinates on a sphere–Effect of metric terms. *Mon. Weather Rev.*, **130**, 1848–1865.

Hunke, E.C., and J.K. Dukowicz, 2003: *The Sea Ice Momentum Equation in the Free Drift Regime*. Technical Report LA-UR-03-2219, Los Alamos National Laboratory, Los Alamos, NM.

Hurrell, J.W., M.P. Hoerling, A.S. Phillips, and T. Xu, 2004: Twentieth century North Atlantic climate change. Part I: assessing determinism. *Clim. Dyn.*, **23**, 371–389.

Hutchings, J.K., H. Jasak, and S.W. Laxon, 2004: A strength implicit correction scheme for the viscous-plastic sea ice model. *Ocean Modelling*, **7**, 111–133.

Huybrechts, P., 2002: Sea-level changes at the LGM from ice-dynamics reconstructions of the Greenland and Antarctic ice sheets during the glacial cycles. *Quat. Sci. Rev.*, **21**, 203–231.

Huybrechts, P., I. Janssens, C. Poncin, and T. Fichefet, 2002: The response of the Greenland ice sheet to climate changes in the 21st century by interactive coupling of an AOGCM with a thermomechanical ice sheet model. *Ann. Glaciol.*, **35**, 409–415.

Iacobellis, S.F., G.M. McFarquhar, D.L. Mitchell, and R.C.J. Somerville, 2003: The sensitivity of radiative fluxes to parameterized cloud microphysics. *J. Clim.*, **16**, 2979–2996.

Iacono, M.J., J.S. Delamere, E.J. Mlawer, and S.A. Clough, 2003: Evaluation of upper tropospheric water vapor in the NCAR Community Climate Model, CCM3, using modeled and observed HIRS radiances. *J. Geophys. Res.*, **108**(D2), 4037, doi:10.1029/2002JD002539.

Inamdar, A.K., and V. Ramanathan, 1998: Tropical and global scale interactions among water vapour, atmospheric greenhouse effect, and surface temperature. *J. Geophys. Res.*, **103**, 32177–32194.

Ingram, W.J., 2002: On the robustness of the water vapor feedback: GCM vertical resolution and formulation. *J. Clim.*, **15**, 917–921.

Inness, P.M., and J.M. Slingo, 2003: Simulation of the MJO in a coupled GCM. I: Comparison with observations and atmosphere-only GCM. *J. Clim.*, **16**, 345–364.

Inness, P.M., J.M. Slingo, E. Guilyardi, and J. Cole, 2003: Simulation of the MJO in a coupled GCM. II: The role of the basic state. *J. Clim.*, **16**, 365–382.

Iorio, J.P., et al., 2004: Effects of model resolution and subgrid scale physics on the simulation of precipitation in the continental United States. *Clim. Dyn.*, **23**, 243–258, doi:10.1007/s00382-004-0440-y.

Jaeger, L., 1976: *Monatskarten des Niederschlags für die Ganze Erde*. Ber. Deutsche Wetterdienstes 139, Germany, 38 pp.

Jakob, C., and G. Tselioudis, 2003: Objective identification of cloud regimes in the tropical western pacific. *Geophys. Res. Lett.*, **30**, doi:10.1029/2003GL018367.

Jennings, R.L., 1975: *Data Sets for Meteorological Research*. NCAR-TN/1A, National Center for Atmospheric Research, Boulder, CO, 156 pp.

Ji, M., A. Leetmaa, and V.E. Kousky, 1996: Coupled model predictions of ENSO during the 1980s and the 1990s at the National Centers for Environmental Prediction. *J. Clim.*, **9**, 3105–3120.

Jin, X.Z., X.H. Zhang, and T.J. Zhou, 1999: Fundamental framework and experiments of the third generation of the IAP/LASG World Ocean General Circulation Model. *Adv. Atmos. Sci.*, **16**, 197–215.

Johns, T.C., et al., 2006: The new Hadley Centre climate model HadGEM1: Evaluation of coupled simulations. *J. Clim.*, **19**, 1327–1353.

Jones, C.D., et al., 2005: Systematic optimisation and climate simulation of FAMOUS, a fast version of HadCM3. *Clim. Dyn.*, **25**, 189–204.

Jones, P.D., 1988: Hemispheric surface air temperature variations: Recent trends and an update to 1987. *J. Clim.*, **1**, 654–660.

Jones, P.D., et al., 1999: Surface air temperature and its variations over the last 150 years. *Rev. Geophys.*, **37**, 173–199.

Joos, F., et al., 1999: Global warming and marine carbon cycle feedbacks on future atmospheric CO_2. *Science*, **284**, 464–467.

Joos, F., et al., 2001: Global warming feedbacks on terrestrial carbon uptake under the IPCC emission scenarios. *Global Biogeochem. Cycles*, **15**, 891–907.

Joshi, M., et al., 2003: A comparison of climate response to different radiative forcings in three general circulation models: towards an improved metric of climate change. *Clim. Dyn.*, **20**, 843–854.

Jungclaus, J.H., et al., 2006: Ocean circulation and tropical variability in the AOGCM ECHAM5/MPI-OM. *J. Clim.*, **19**, 3952–3972.

K-1 Model Developers, 2004: *K-1 Coupled Model (MIROC) Description*. K-1 Technical Report 1 [Hasumi, H., and S. Emori (eds.)]. Center for Climate System Research, University of Tokyo, Tokyo, Japan, 34 pp., http://www.ccsr.u-tokyo.ac.jp/kyosei/hasumi/MIROC/tech-repo.pdf.

Kalnay, E., et al., 1996: The NCEP/NCAR 40-year reanalysis project. *Bull. Am. Meteorol. Soc.*, **77**, 437–471.

Kanamitsu, M., et al., 2002: NCEP dynamical seasonal forecast system 2000. *Bull. Am. Meteorol. Soc.*, **83**, 1019–1037.

Kattsov, V., and E. Källén, 2005: Future climate change: Modeling and scenarios for the Arctic. In: *Arctic Climate Impact Assessment (ACIA)*. Cambridge University Press, Cambridge, UK, pp. 99–150.

Kemball-Cook, S., B. Wang, and X. Fu, 2002: Simulation of the intraseasonal oscillation in ECHAM-4 model: The impact of coupling with an ocean model. *J. Atmos. Sci.*, **59**, 1433–1453.

Khairoutdinov, M., D. Randall, and C. DeMott, 2005: Simulations of the atmospheric general circulation using a cloud-resolving model as a superparameterization of physical processes. *J. Atmos. Sci.*, **62**, 2136–2154.

Kharin, V.V., F.W. Zwiers, and X. Zhang, 2005: Intercomparison of near surface temperature and precipitation extremes in AMIP-2 simulations, reanalyses and observations. *J. Clim.*, **18**(24), 5201–5223.

Kiehl, J.T., and P.R. Gent, 2004: The Community Climate System Model, Version 2. *J. Clim.*, **17**, 3666–3682.

Kiehl, J.T., et al., 1998: The National Center for Atmospheric Research Community Climate Model: CCM3. *J. Clim.*, **11**, 1131–1149.

Kiktev, D., D.M.H. Sexton, L. Alexander, and C.K. Folland, 2003: Comparison of modeled and observed trends in indices of daily climate extremes. *J. Clim.*, **16**(22), 3560–3571.

Kim, S.-J., G.M. Flato, G.J. Boer, and N.A. McFarlane, 2002: A coupled climate model simulation of the Last Glacial Maximum, Part 1: Transient multi-decadal response. *Clim. Dyn.*, **19**, 515–537.

Kimoto, M., N. Yasutomi, C. Yokoyama, and S. Emori, 2005: Projected changes in precipitation characteristics near Japan under the global warming. *Scientific Online Letters on the Atmosphere*, **1**, 85–88, doi:10.2151/sola.2005-023.

Kinne, S., et al., 2003: Monthly averages of aerosol properties: A global comparison among models, satellite, and AERONET ground data. *J. Geophys. Res.*, **108**(D20), 4634, doi:10.1029/2001JD001253.

Kirtman, B.P., 2003: The COLA anomaly coupled model: Ensemble ENSO prediction. *Mon. Weather Rev.*, **131**, 2324–2341.

Kirtman, B.P., and P.S. Schopf, 1998: Decadal variability in ENSO predictability and prediction. *J. Clim.*, **11**, 2804–2822.

Kirtman, B.P., K. Pegion, and S. Kinter, 2005: Internal atmospheric dynamics and tropical indo-pacific climate variability. *J. Atmos. Sci.*, **62**, 2220–2233.

Kleeman, R., Y. Tang, and A.M. Moore, 2003: The calculation of climatically relevant singular vectors in the presence of weather noise as applied to the ENSO problem. *J. Atmos. Sci.*, **60**, 2856–2868.

Kleidon, A., 2004: Global datasets of rooting zone depth inferred from inverse methods. *J. Clim.*, **17**, 2714–2722.

Kleidon, A., K. Fraedrich, and M. Heimann, 2000: A green planet versus a desert world: estimating the maximum effect of vegetation on the land surface climate. *Clim. Change*, **44**, 471–493.

Klein, S.A., and D.L. Hartmann, 1993: The seasonal cycle of low stratiform clouds. *J. Clim.*, **6**, 1587–1606.

Klein, S.A., and C. Jakob, 1999: Validation and sensitivities of frontal clouds simulated by the ECMWF model. *Mon. Weather Rev.*, **127**, 2514–2531.

Knight, J.R, et al., 2005: A signature of persistent natural thermohaline circulation cycles in observed climate. *Geophys. Res. Lett.*, **32**, L20708, doi:10.1029/2005GL024233.

Knutson, T.R., and R.E. Tuleya, 1999: Increased hurricane intensities with CO_2-induced global warming as simulated using the GFDL hurricane prediction system. *Clim. Dyn.*, **15**(7), 503–519.

Knutson, T.R., and R.E. Tuleya, 2004: Impact of CO_2-induced warming on simulated hurricane intensity and precipitation: Sensitivity to the choice of climate model and convective parameterization. *J. Clim.*, **17**, 3477–3495.

Knutti, R., T.F. Stocker, F. Joos, and G.K. Plattner, 2002: Constraints on radiative forcing and future climate change from observations and climate model ensembles. *Nature*, **416**, 719–723.

Knutti, R., G.A. Meehl, M.R. Allen and D.A. Stainforth, 2006: Constraining climate sensitivity from the seasonal cycle in surface temperature. *J. Clim.*, **19**, 4224–4233.

Kodera, K., and M. Chiba, 1995: Tropospheric circulation changes associated with stratospheric sudden warmings: A case study. *J. Geophys. Res.*, **100**, 11055–11068.

Komuro, Y., and H. Hasumi, 2005: Intensification of the Atlantic deep circulation by the Canadian Archipelago throughflow. *J. Phys. Oceanogr.*, **35**, 775–789.

Koster, R.D., et al., 2004: Regions of coupling between soil moisture and precipitation. *Science*, **305**, 1138–1140.

Kraus, E.B., 1990: Diapycnal mixing. In: *Climate-Ocean Interaction* [Schlesinger, M.E. (ed.)]. Kluwer, Amsterdam, pp. 269–293.

Kraus, E.B., and J.S. Turner, 1967: A one-dimensional model of the seasonal thermocline. II. The general theory and its consequences. *Tellus*, **19**, 98–105.

Krinner, G., et al., 2005: A dynamic global vegetation model for studies of the coupled atmosphere-biosphere system. *Global Biogeochem. Cycles*, **19**, GB1015, doi:10.1029/2003GB002199.

Lambert, S.J., and G.J. Boer, 2001: CMIP1 evaluation and intercomparison of coupled climate models. *Clim. Dyn.*, **17**, 83–106.

Lambert, S.J., and J. Fyfe, 2006: Changes in winter cyclone frequencies and strengths simulated in enhanced greenhouse gas simulations: Results from the models participating in the IPCC diagnostic exercise. *Clim. Dyn.*, **26**, 713–728.

Lanzante, J.R., 1996: Resistant, robust and nonparametric techniques for analysis of climate data: Theory and examples, including applications to historical radiosonde station data. *Int. J. Climatol.*, **16**, 1197–1226.

Large, W.G., J.C. McWilliams, and S.C. Doney, 1994: Oceanic vertical mixing: a review and a model with a nonlocal boundary layer parameterization. *Rev. Geophys.*, **32**, 363–403.

Larson, K., and D.L. Hartmann, 2003: Interactions among cloud, water vapour, radiation and large-scale circulation in the tropical climate. Part 1: sensitivity to uniform sea surface temperature changes. *J. Clim.*, **15**, 1425–1440.

Latif, M., 1998: Dynamics of interdecadal variability in coupled ocean-atmosphere models. *J. Clim.*, **11**, 602–624.

Latif, M., E. Roeckner, U. Mikolajewicz, and R. Voss, 2000: Tropical stabilisation of the thermohaline circulation in a greenhouse warming simulation. *J. Clim.*, **13**, 1809–1813.

Latif, M., et al., 2001: ENSIP: The El Niño simulation intercomparison project. *Clim. Dyn.*, **18**, 255–276.

Latif, M., et al., 2004: Reconstructing, monitoring, and predicting multidecadal scale changes in the North Atlantic thermohaline circulation with sea surface temperatures. *J. Clim.*, **17**, 1605–1614.

Lawrence, D.M., and J.M. Slingo, 2005: Weak land–atmosphere coupling strength in HadAM3: The role of soil moisture variability. *J. Hydrometeorol.*, **6**, 670–680.

Le Treut, H., Z.X. Li, and M. Forichon, 1994: Sensitivity of the LMD general circulation model to greenhouse forcing associated with two different cloud water parametrizations. *J. Clim.*, **7**, 1827–1841.

Lee, M.-I., I.-S. Kang, J.-K. Kim, and B. E. Mapes, 2001: Influence of cloud-radiation interaction on simulating tropical intraseasonal oscillation with an atmospheric general circulation model. *J. Geophys. Res.*, **106**, 14219–14233.

Levitus, S., and T.P. Boyer, 1994: *World Ocean Atlas 1994, Volume 4: Temperature*. NOAA NESDIS E/OC21, Washington, DC, 117 pp.

Levitus, S., and J. Antonov, 1997: *Variability of Heat Storage of and the Rate of Heat Storage of the World Ocean*. NOAA NESDIS Atlas 16, US Government Printing Office, Washington, DC, 6 pp., 186 figures.

Levitus, S., J. Antonov, and T. Boyer, 2005: Warming of the world ocean, 1955-2003. *Geophys. Res. Lett.*, **32**, L02604, doi:10.1029/2004GLO21592.

Levitus, S., et al., 1998: *World Ocean Database 1998, Volume 1: Introduction*. NOAA Atlas NESDIS 18, US Government Printing Office, Washington, DC.

Liang, X., Z. Xie, and M. Huang, 2003: A new parameterization for surface and groundwater interactions and its impact on water budgets with the variable infiltration capacity (VIC) land surface model. *J. Geophys. Res.*, **108**, 8613, doi:10.1029/2002JD003090.

Limpasuvan, V., and D.L. Hartmann, 2000: Wave-maintained annular modes of climate variability. *J. Clim.*, **13**, 4414–4429.

Lin, B., T. Wong, B.A. Wielicki, and Y. Hu, 2004: Examination of the decadal tropical mean ERBS nonscanner radiation data for the iris hypothesis. *J. Clim.*, **17**, 1239–1246.

Lin, B., et al., 2002: The iris hypothesis: A negative or positive cloud feedback? *J. Clim.*, **15**, 3–7.

Lin, J.L., et al., 2006: Tropical intraseasonal variability in 14 IPCC AR4 climate models. Part I: Convective signals. *J. Clim.*, **19**, 2665–2690.

Lin, W.Y., and M.H. Zhang, 2004: Evaluation of clouds and their radiative effects simulated by the NCAR Community Atmospheric Model against satellite observations. *J. Clim.*, **17**, 3302–3318.

Lindsay, R.W., and H.L. Stern, 2004: A new Lagrangian model of Arctic sea ice. *J. Phys. Oceanogr.*, **34**, 272–283.

Lindzen, R.S., M.-D. Chou, and A.Y. Hou, 2001: Does the Earth have an adaptative infrared iris? *Bull. Am. Meteorol. Soc.*, **82**, 417–432.

Lindzen, R.S., M.-D. Chou, and A.Y. Hou, 2002: Comment on "No evidence for iris". *Bull. Am. Meteorol. Soc.*, **83**, 1345–1349.

Lipscomb, W.H., 2001: Remapping the thickness distribution in sea ice models. *J. Geophys. Res.*, **106**, 13989–14000.

Liston, G., 2004: Representing subgrid snow cover heterogeneities in regional and global models. *J. Clim.*, **17**, 1381–1397.

Liu, H., et al., 2004: An eddy-permitting oceanic general circulation model and its preliminary evaluations. *Adv. Atmos. Sci.*, **21**, 675–690.

Liu, J., et al., 2003: Sensitivity of sea ice to physical parameterizations in the GISS global climate model. *J. Geophys. Res.*, **108**, 3053, doi:10.1029/2001JC001167.

Liu, P., et al., 2005: MJO in the NCAR CAM2 with the Tiedtke convective scheme. *J. Clim.*, **18**, 3007–3020.

Lock, A.P., 2001: The numerical representation of entrainment in parameterizations of boundary layer turbulent mixing. *Mon. Weather Rev.*, **129**, 1148–1163.

Lock, A.P., et al., 2000: A new boundary layer mixing scheme. Part I: Scheme description and SCM tests. *Mon. Weather Rev.*, **128**, 3187–3199.

Lohmann, U., and G. Lesins, 2002: Stronger constraints on the anthropogenic indirect aerosol effect. *Science*, **298**, 1012–1015.

Lorenz, D.J., and D.L. Hartmann, 2001: Eddy–zonal flow feedback in the Southern Hemisphere. *J. Atmos. Sci.*, **58**, 3312–3327.

Lu, J., R.J. Greatbatch, and K.A. Peterson, 2004: Trend in Northern Hemisphere winter atmospheric circulation during the last half of the twentieth century. *J. Clim.*, **17**, 3745–3760.

Luo, Z., and W.B. Rossow, 2004: Characterising tropical cirrus life cycle, evolution and interaction with upper tropospheric water vapour using a Lagrangian trajectory analysis of satellite observations. *J. Clim.*, **17**, 4541–4563.

Madden, R.A., and P.R. Julian, 1971: Detection of a 40-50 day oscillation in the zonal wind in the tropical Pacific. *J. Atmos. Sci.*, **28**, 702–708.

Madec, G., P. Delecluse, M. Imbard, and C. Lévy, 1998: *OPA Version 8.1 Ocean General Circulation Model Reference Manual*. Notes du Pôle de Modélisation No. 11, Institut Pierre-Simon Laplace, Paris, 91 pp., http://www.lodyc.jussieu.fr/opa/Docu_Free/Doc_models/Doc_OPA8.1.pdf.

Mahfouf, J.-F., et al., 1995: The land surface scheme ISBA within the Meteo-France climate model ARPEGE. Part 1: Implementation and preliminary results. *J. Clim.*, **8**, 2039–2057.

Maloney, E.D., and D.L. Hartmann, 2001: The sensitivity of the intraseasonal variability in the NCAR CCM3 to changes in convective parameterization. *J. Clim.*, **14**, 2015–2034.

Maltrud, M.E., R.D. Smith, A.J. Semtner, and R.C. Malone, 1998: Global eddy-resolving ocean simulations driven by 1985–1995 atmospheric winds. *J. Geophys. Res.*, **103**, 30825–30853.

Manabe, S., and R.J. Stouffer, 1988: Two stable equilibria of a coupled ocean-atmosphere model. *J. Clim.*, **1**(9), 841–866.

Manabe, S., and R.J. Stouffer, 1995: Simulation of abrupt climate change induced by fresh water input to the North Atlantic Ocean. *Nature*, **378**, 165–167.

Manabe, S., and R.J. Stouffer, 1996: Low-frequency variability of surface air temperature in a 1000-year integration of a coupled atmosphere-ocean-land surface model. *J. Clim.*, **9**, 376–393.

Manabe, S., and R.J. Stouffer, 1997: Coupled ocean-atmosphere model response to freshwater input: Comparison to Younger Dryas event. *Paleoceanography*, **12**, 321–336.

Manabe, S., R.J. Stouffer, M.J. Spelman, and K. Bryan, 1991: Transient responses of a coupled ocean atmosphere model to gradual changes of atmospheric CO_2. I: Annual mean response. *J. Clim.*, **4**, 785–818.

Mann, M.E., R.S. Bradley, and M.K. Hughes, 1998: Global-scale temperature patterns and climate forcing over the past six centuries. *Nature*, **392**, 779–787.

Marchal, O., T.F. Stocker, and F. Joos, 1998: A latitude-depth, circulation-biogeochemical ocean model for paleoclimate studies. *Tellus*, **50B**, 290–316.

Marotzke, J., 1997: Boundary mixing and the dynamics of three-dimensional thermohaline circulation. *J. Phys. Oceanogr.*, **27**, 1713–1728.

Marshall, G.J., 2003: Trends in the Southern Annular Mode from observations and reanalyses. *J. Clim.*, **16**, 4134–4143.

Marshall, J.C., C. Hill, L. Perelman, and A. Adcroft, 1997: Hydrostatic, quasi-hydrostatic and non-hydrostatic ocean modeling. *J. Geophys. Res.*, **102**, 5733–5752.

Marsland, S.J., et al., 2003: The Max-Planck-Institute global ocean/sea ice model with orthogonal curvilinear coordinates. *Ocean Modelling*, **5**, 91–127.

Marti, O., et al., 2005: *The New IPSL Climate System Model: IPSL-CM4*. Note du Pôle de Modélisation No. 26, Institut Pierre Simon Laplace des Sciences de l'Environnement Global, Paris, http://dods.ipsl.jussieu.fr/omamce/IPSLCM4/DocIPSLCM4/FILES/DocIPSLCM4.pdf.

Martin, G.M., et al., 2004: *Evaluation of the Atmospheric Performance of HadGAM/GEM1*. Hadley Centre Technical Note No. 54, Hadley Centre for Climate Prediction and Research/Met Office, Exeter, UK, http://www.metoffice.gov.uk/research/hadleycentre/pubs/HCTN/index.html.

Martin, G.M., et al., 2006: The physical properties of the atmosphere in the new Hadley Centre Global Environmental Model, HadGEM1. Part I: Model description and global climatology. *J. Clim.*, **19**, 1274–1301.

Maxwell, R.M., and N.L. Miller, 2005: Development of a coupled land surface and groundwater model. *J. Hydrometeorol.*, **6**, 233–247.

May, W., 2004: Simulation of the variability and extremes of daily rainfall during the Indian summer monsoon for present and future times in a global time-slice experiment. *Clim. Dyn.*, **22**, 183–204.

Mayer, M., C. Wang, M. Webster, and R. Prinn, 2000: Linking air pollution to global chemistry and climate. *J. Geophys. Res.*, **105**, 22869–22896.

McAvaney, B.J., et al., 2001: Model evaluation. In: *Climate Change 2001: The Scientific Basis. Contribution of Working Group I to the Third Assessment Report of the Intergovernmental Panel on Climate Change* [Houghton, J.T., et al. (eds.)]. Cambridge University Press, Cambridge, United Kingdom and New York, NY, USA, pp. 471–523.

McCarthy, M.P., and R. Toumi, 2004: Observed interannual variability of tropical troposphere relative humidity. *J. Clim.*, **17**, 3181–3191.

McDonald, R.E., et al., 2005: Tropical storms: representation and diagnosis in climate models and the impacts of climate change. *Clim. Dyn.*, **25**, 19–36.

McFarlane, N.A., G.J. Boer, J.-P. Blanchet, and M. Lazare, 1992: The Canadian Climate Centre second-generation general circulation model and its equilibrium climate. *J. Clim.*, **5**, 1013–1044.

Mechoso, C.R., et al., 1995: The seasonal cycle over the tropical Pacific in general circulation model. *Mon. Weather Rev.*, **123**, 2825–2838.

Meehl, G.A., and C. Tebaldi, 2004: More intense, more frequent, and longer lasting heat waves in the 21st century. *Science*, **305**, 994–997.

Meehl, G.A., and A. Hu, 2006: Mega droughts in the Indian monsoon and southwest North America and a mechanism for associated multi-decadal sea surface temperature anomalies. *J. Clim.*, **19**, 1605–1623.

Meehl, G.A., C. Tebaldi, and D. Nychka, 2004: Changes in frost days in simulations of twenty-first century climate. *Clim. Dyn.*, **23**, 495–511.

Meehl, G.A., et al., 2001: Factors that affect the amplitude of El Niño in global coupled climate models. *Clim. Dyn.*, **17**, 515–526.

Meissner, K.J., A.J. Weaver, H.D. Matthews, and P.M. Cox, 2003: The role of land surface dynamics in glacial inception: A study with the UVic Earth System Model. *Clim. Dyn.*, **21**, 515–537, doi:10.1007/s00382-003-0352-2.

Mellor, G.L., and T. Yamada, 1982: Development of a turbulence closure model for geophysical fluid problems. *Rev. Geophys.*, **20**, 851–875.

Mellor, G.L., and L. Kantha, 1989: An ice-ocean coupled model. *J. Geophys. Res.*, **94**, 10937–10954.

Mestas-Nunez, A.M., and D.B. Enfield, 1999: Rotated global modes of non-ENSO sea surface temperature variability. *J. Clim.*, **12**, 2734–2745.

Miller, J.R., G.L. Russell, and G. Caliri, 1994: Continental-scale river flow in climate models. *J. Clim.*, **7**, 914–928.

Miller, R.L., 1997: Tropical thermostats and low cloud cover. *J. Clim.*, **10**, 409–440.

Miller, R.L., G.A. Schmidt, and D.T. Shindell, 2006: Forced variations of annular modes in the 20th century IPCC AR4 simulations. *J. Geophys. Res.*, **111**, D18101, doi:10.1029/2005JD006323.

Milly, P.C.D., and A.B. Shmakin, 2002: Global modeling of land water and energy balances, Part I: The Land Dynamics (LaD) model. *J. Hydrometeorol.*, **3**, 283–299.

Milly, P.C.D., K.A. Dunne, and A.V. Vecchia, 2005: Global pattern of trends in streamflow and water availability in a changing climate. *Nature*, **438**, 347–350, doi:10.1038/nature04312.

Min, S.-K., S. Legutke, A. Hense, and W.-T. Kwon, 2005: Climatology and internal variability in a 1000-year control simulation with the coupled climate model ECHO-G—I. Near-surface temperature, precipitation and mean sea level pressure. *Tellus*, **57A**, 605–621.

Minschwaner, K., and A.E. Dessler, 2004: Water vapor feedback in the tropical upper troposphere: model results and observations. *J. Clim.*, **17**, 1272–1282.

Minschwaner, K., A.E. Dessler, and S. Parnchai, 2006: Multi-model analysis of the water vapour feedback in the tropical upper troposphere. *J. Clim.*, **19**, 5455–5464.

Mitchell, T.D., and P.D. Jones, 2005: An improved method of constructing a database of monthly climate observations and associated high-resolution grids. *Int. J. Climatol.*, **25**, 693712.

Molteni, F., Kuchraski, F., and Corti, S., 2006: On the predictability of flow-regime properties on interannual to interdecadal timescales. In: *Predictability of Weather and Climate* [Palmer, T. and R. Hagedorn (eds.)]. Cambridge University Press, Cambridge, UK.

Monahan, A.H., and A. Dai, 2004: The spatial and temporal structure of ENSO nonlinearity. *J. Clim.*, **17**, 3026–3036.

Monahan, A.H., J.C. Fyfe, and L. Pandolfo, 2003: The vertical structure of wintertime climate regimes of the Northern Hemisphere extratropical atmosphere. *J. Clim.*, **16**, 2005–2021.

Montoya, M., et al., 2005: The Earth System Model of Intermediate Complexity CLIMBER-3α. Part I: Description and performance for present day conditions. *Clim. Dyn.*, **25**, 237–263, doi:10.1007/s00382-005-0044-1.

Mouchet, A., and L. François, 1996: Sensitivity of a global oceanic carbon cycle model to the circulation and to the fate of organic matter: Preliminary results. *Phys. Chem. Earth*, **21**, 511–516.

Moum, J.N., D.R. Caldwell, J.D. Nash, and G.D. Gunderson, 2002: Observations of boundary mixing over the continental slope. *J. Phys. Oceanogr.*, **32**, 2113–2130.

Murphy, J.M., 1995: Transient response of the Hadley Centre coupled ocean-atmosphere model to increasing carbon dioxide. Part III: analysis of global-mean response using simple models. *J. Clim.*, **8**, 496–514.

Murphy, J.M., et al., 2004: Quantification of modelling uncertainties in a large ensemble of climate change simulations. *Nature*, **430**, 768–772.

Murray, R.J., 1996: Explicit generation of orthogonal grids for ocean models. *J. Comput. Phys.*, **126**, 251–273.

Myhre, G., E.J. Highwood, K.P. Shine, and F. Stordal, 1998: New estimates of radiative forcing due to well mixed greenhouse gases. *Geophys. Res. Lett.*, **25**, 2715–2718.

Nakano, H., and N. Suginohara, 2002: Effects of bottom boundary layer parameterization on reproducing deep and bottom waters in a World Ocean model. *J. Phys. Oceanogr.*, **32**, 1209–1227.

Naud, C.M., A.D. Del Genio, and M. Bauer, 2006: Observational constraints on cloud thermodynamic phase in midlatitude storms. *J. Clim.*, **19**, 5273–5288.

Neale, R., and J. Slingo, 2003: The maritime continent and its role in the global climate: A GCM study. *J. Clim.*, **16**, 834–848.

Newman, M., G.P. Compo, and M.A. Alexander, 2003: ENSO-forced variability of the PDO. *J. Clim.*, **16**, 3853–3857.

Nijssen, B., et al., 2003: Simulation of high latitude hydrological processes in the Torne-Kalix basin: PILPS Phase 2(e) 2: Comparison of model results with observations. *Global Planet. Change*, **38**, 31–53.

Norris, J.R., 1998a: Low cloud type over the ocean from surface observations. Part I: relationship to surface meteorology and the vertical distribution of temperature and moisture. *J. Clim.*, **11**, 369–382.

Norris, J.R., 1998b: Low cloud type over the ocean from surface observations. Part II: geographical and seasonal variations. *J. Clim.*, **11**, 383–403.

Norris, J.R., and C.P. Weaver, 2001: Improved techniques for evaluating GCM cloudiness applied to the NCAR CCM3. *J. Clim.*, **14**, 2540–2550.

Norris, J.R., and S.F. Iacobellis, 2005: North pacific cloud feedbacks inferred from synoptic-scale dynamic and thermodynamic relationships. *J. Clim.*, **18**, 4862–4878.

NRC (National Research Council), 2003: *Understanding Climate Change Feedbacks*. National Academies Press, Washington, DC, 152 pp.

O'Farrell, S.P., 1998: Investigation of the dynamic sea ice component of a coupled atmosphere sea-ice general circulation model. *J. Geophys. Res.*, **103**, 15751–15782.

Oki, T., and Y.C. Sud, 1998: Design of total runoff integrating pathways (TRIP)—A global river channel network. *Earth Interactions*, **2**, 1–37.

Oleson, K.W., et al., 2004: *Technical Description of the Community Land Model (CLM)*. NCAR Technical Note NCAR/TN-461+STR, National Center for Atmospheric Research, Boulder, CO, 173 pp.

Oliver, K.I.C., A.J. Watson, and D.P. Stevens, 2005: Can limited ocean mixing buffer rapid climate change? *Tellus*, **57A**, 676–690.

Oouchi, K., et al., 2006: Tropical cyclone climatology in a global-warming climate as simulated in a 20 km-mesh global atmospheric model: Frequency and wind intensity analyses. *J. Meteorol. Soc. Japan*, **84**, 259–276.

Opsteegh, J.D., R.J. Haarsma, F.M. Selten, and A. Kattenberg, 1998: ECBILT: A dynamic alternative to mixed boundary conditions in ocean models. *Tellus*, **50A**, 348–367.

Osborn, T.J., 2004: Simulating the winter North Atlantic Oscillation: the roles of internal variability and greenhouse gas forcing. *Clim. Dyn.*, **22**, 605–623.

Otterå, O.H., et al., 2004: Transient response of the Atlantic meridional overturning circulation to enhanced freshwater input to the Nordic Seas-Arctic Ocean in the Bergen Climate Model. *Tellus*, **56A**, 342–361.

Otto-Bliesner, B.L., et al., 2006: Climate sensitivity of moderate- and low-resolution versions of CCSM3 to preindustrial forcings. *J. Clim.*, **19**, 2567–2583.

Pacanowski, R.C., K. Dixon, and A. Rosati, 1993: *The GFDL Modular Ocean Model Users Guide, Version 1.0*. GFDL Ocean Group Technical Report No. 2, Geophysical Fluid Dynamics Laboratory, Princeton, NJ.

Paciorek, C.J., J.S. Risbey, V. Ventura, and R.D. Rosen, 2002: Multiple indices of Northern Hemisphere cyclone activity, winters 1949-99. *J. Clim.*, **15**, 1573–1590.

Palmer, T.N., and J. Shukla, 2000: Editorial (for special issue on DSP/PROVOST). *Q. J. R. Meteorol. Soc.*, **126**, 1989–1990.

Palmer, T.N., et al., 2004: Development of a European multimodel ensemble system for seasonal to interannual prediction (DEMETER). *Bull. Am. Meteorol. Soc.*, **85**, 853–872.

Pan, Z., et al., 2004: Evaluation of uncertainties in regional climate change simulations. *J. Geophys. Res.*, **106**, 17735–17752.

Pardaens, A.K., H.T. Banks, J.M. Gregory, and P.R. Rowntree, 2003: Freshwater transports in HadCM3. *Clim. Dyn.*, **21**, 177–195.

Parekh, P., M.J. Follows, and E. Boyle, 2005: Decoupling of iron and phosphate in the global ocean. *Global Biogeochem. Cycles*, **19**, doi:10.1029/2004GB002280.

Pelly, J.L., and B.J. Hoskins, 2003a: A new perspective on blocking. *J. Atmos. Sci.*, **60**, 743–755.

Pelly, J.L., and B.J. Hoskins, 2003b: How well does the ECMWF Ensemble Prediction System predict blocking? *Q. J. R. Meteorol. Soc.*, **129**, 1683–1702.

Peters, M.E., and C.S. Bretherton, 2005: A simplified model of the Walker circulation with an interactive ocean mixed layer and cloud-radiative feedbacks. *J. Clim.*, **18**, 4216–4234.

Petoukhov, V., et al., 2000: CLIMBER-2: A climate system model of intermediate complexity. Part I: Model description and performance for present climate. *Clim. Dyn.*, **16**, 1–17.

Petoukhov, V., et al., 2005: EMIC Intercomparison Project (EMIP-CO_2): Comparative analysis of EMIC simulations of current climate and equilibrium and transient responses to atmospheric CO_2 doubling. *Clim. Dyn.*, **25**, 363–385, doi:10.1007/s00382-005-0042-3.

Phillips, T.J., et al., 2004: Evaluating parameterizations in general circulation models: Climate simulation meets weather prediction. *Bull. Am. Meteorol. Soc.*, **85**, 1903–1915.

Piani, C., D.J. Frame, D.A. Stainforth, and M.R. Allen, 2005: Constraints on climate change from a multi-thousand member ensemble of simulations. *Geophys. Res. Lett.*, **32**, L23825, doi:10.1029/2005GL024452.

Pierce, D.W., T.P. Barnett, and M. Latif, 2000: Connections between the Pacific Ocean tropics and midlatitudes on decadal time scales. *J. Clim.*, **13**, 1173–1194.

Pierrehumbert, R.T., 1995: Thermostats, radiator fins, and the local runaway greenhouse. *J. Atmos. Sci.*, **52**, 1784–180.

Pierrehumbert, R.T., 1999: Subtropical water vapour as a mediator of rapid global climate change. In: *Mechanisms of Global Climate Change at Millennial Timescales*. Geophysical Monograph 112, American Geophysical Union, Washington, DC, pp. 339–361.

Pierrehumbert, R.T., and R. Roca, 1998: Evidence for control of Atlantic subtropical humidity by large scale advection. *Geophys. Res. Lett.*, **25**, 4537–4540.

Pierrehumbert, R.T., H. Brogniez, and R. Roca, 2007: On the relative humidity of the Earth's atmosphere. In: *The General Circulation* [Schneider, T., and A. Sobel (eds.)]. Princeton University Press, Princeton, NJ, in press.

Pitman, A.J., B.J. McAvaney, N. Bagnoud, and B. Cheminat, 2004: Are inter-model differences in AMIP-II near surface air temperature means and extremes explained by land surface energy balance complexity? *Geophys. Res. Lett.*, **31**, L05205, doi:10.1029/2003GL019233.

Plattner, G.-K., F. Joos, T.F. Stocker, and O. Marchal, 2001: Feedback mechanisms and sensitivities of ocean carbon uptake under global warming. *Tellus*, **53B**, 564–592.

Plaut, G., and E. Simonnet, 2001: Large–scale circulation classification, weather regimes, and local climate over France, the Alps, and Western Europe. *Clim. Res.*, **17**, 303–324.

Polzin, K.L., J.M. Toole, J.R. Redwell, and R.W. Schmitt, 1997: Spatial variability of turbulent mixing in the abyssal ocean. *Science*, **276**, 93–96.

Pope, V.D., and R.A. Stratton, 2002: The processes governing horizontal resolution sensitivity in a climate model. *Clim. Dyn.*, **19**, 211–236.

Pope, V.D., M.L. Gallani, P.R. Rowntree, and R.A. Stratton, 2000: The impact of new physical parametrizations in the Hadley Centre climate model: HadAM3. *Clim. Dyn.*, **16**, 123–146.

Potter, G.L., and R.D. Cess, 2004: Testing the impact of clouds on the radiation budgets of 19 atmospheric general circulation models. *J. Geophys. Res.*, **109**, doi:10.1029/2003JD004018.

Power, S.B., and R. Colman, 2006: Multi-decadal predictability in a coupled GCM. *Clim. Dyn.*, **26**, 247–272.

Power, S.B., M.H. Haylock, R. Colman, and X. Wang, 2006: The predictability of interdecadal changes in ENSO activity and ENSO teleconnections. *J. Clim.*, **19**, 4755–4771.

Power, S., et al., 1999: Interdecadal modulation of the impact of ENSO on Australia. *Clim. Dyn.*, **15**, 319–324.

Qu, X., and A. Hall, 2005: Surface contribution to planetary albedo variability in cryosphere regions. *J. Clim.*, **18**, 5239–5252.

Quadrelli, R., and J.M. Wallace, 2004: A simplified linear framework for interpreting patterns of northern hemisphere wintertime climate variability. *J. Clim.*, **17**, 3728–3744.

Rahmstorf, S., 1996: On the freshwater forcing and transport of the Atlantic thermohaline circulation. *Clim. Dyn.*, **12**, 799–811.

Rahmstorf, S., et al., 2005: Thermohaline circulation hysteresis: A model intercomparison. *Geophys. Res. Lett.*, **32**, L23605, doi:10.1029/2005GL023655.

Randall, D.A., et al., 2003: Confronting models with data: The GEWEX Cloud Systems Study. *Bull. Am. Meteorol. Soc.*, **84**, 455–469.

Randall, D.A., et al., 2006: Cloud feedbacks. In: *Frontiers in the Science of Climate Modeling* [Kiehl, J.T., and V. Ramanathan (eds.)]. Proceedings of a symposium in honor of Professor Robert D. Cess.

Raper, S.C.B., T.M.L. Wigley, and R.A. Warrick, 1996: Global sea-level rise: past and future. In: *Sea-Level Rise and Coastal Subsidence: Causes, Consequences and Strategies* [Milliman, J.D., and B.U. Haq (eds.)]. Kluwer Academic Publishers, Dordrecht, The Netherlands, pp. 11–46.

Raper, S.C.B., J.M. Gregory, and T.J. Osborn, 2001: Use of an upwelling-diffusion energy balance model to simulate and diagnose A/OGCM results. *Clim. Dyn.*, **17**, 601–613.

Raphael, M.N., and M.M. Holland, 2006: Twentieth century simulation of the Southern Hemisphere climate in coupled models. Part 1: Large scale circulation variability. *Clim. Dyn.*, **26**, 217–228, doi:10.1007/s00382-005-0082-8.

Rayner, N.A., et al., 2003: Global analyses of sea surface temperature, sea ice, and night marine air temperature since the late nineteenth century. *J. Geophys. Res.*, **108**(D14), doi:10.1029/2002JD002670.

Redi, M.H., 1982: Oceanic isopycnal mixing by coordinate rotation. *J. Phys. Oceanogr.*, **12**, 1154–1158.

Renssen, H., V. Brovkin, T. Fichefet, and H. Goosse, 2003: Holocene climate instability during the termination of the African Humid Period. *Geophys. Res. Lett.*, **30**(4), 1184, doi:10.1029/2002GL016636.

Renwick, J.A., 1998: ENSO-related variability in the frequency of South Pacific blocking. *Mon. Weather Rev.*, **126**, 3117–3123.

Rial, J.A., 2004: Abrupt climate change: chaos and order at orbital and millennial scales. *Global Planet. Change*, **41**, 95–109.

Ridley, J.K., P. Huybrechts, J.M. Gregory, and J.A. Lowe, 2005: Elimination of the Greenland ice sheet in a high CO_2 climate. *J. Clim.*, **18**, 3409–3427.

Rind, D.G., et al., 2001: Effects of glacial meltwater in the GISS Coupled Atmosphere-Ocean model: Part II. A bipolar seesaw in deep water production. *J. Geophys. Res.*, **106**, 27355–27365.

Ringer, M.A., and R.P. Allan, 2004: Evaluating climate model simulations of tropical clouds. *Tellus*, **56A**, 308–327.

Ringer, M.A., et al., 2006: The physical properties of the atmosphere in the new Hadley Centre Global Environmental Model (HadGEM1). Part II: Aspects of variability and regional climate. *J. Clim.*, **19**, 1302–1326.

Roberts, M.J., 2004: *The Ocean Component of HadGEM1*. GMR Report Annex IV.D.3, Met Office, Exeter, UK.

Roberts, M., et al., 2004: Impact of an eddy-permitting ocean resolution on control and climate change simulations with a global coupled GCM. *J. Clim.*, **17**, 3–20.

Robertson, A.W., 2001: Influence of ocean-atmosphere interaction on the Arctic Oscillation in two general circulation models. *J. Clim.*, **14**, 3240–3254.

Robock, A., et al., 2000: The global soil moisture data bank. *Bull. Am. Meteorol. Soc.*, **81**, 1281–1299.

Roeckner, E., et al., 1996: *The Atmospheric General Circulation Model ECHAM4: Model Description and Simulation of Present-Day Climate*. MPI Report No. 218, Max-Planck-Institut für Meteorologie, Hamburg, Germany, 90 pp.

Roeckner, E., et al., 2003: *The Atmospheric General Circulation Model ECHAM5. Part I: Model Description*. MPI Report 349, Max Planck Institute for Meteorology, Hamburg, Germany, 127 pp.

Roesch, A., 2006: Evaluation of surface albedo and snow cover in AR4 coupled climate models. *J. Geophys. Res.*, **111**, D15111, doi:10.1029/2005JD006473.

Rooth, C., 1982: Hydrology and ocean circulation. *Prog. Oceanogr.*, **11**, 131–149.

Rosati, A., K. Miyakoda, and R. Gudgel, 1997: The impact of ocean initial conditions on ENSO forecasting with a coupled model. *Mon. Weather Rev.*, **125**(5), 754–772.

Ross, R.J., W.P. Elliott, D.J. Seidel, and participating AMIP-II modelling groups, 2002: Lower tropospheric humidity-temperature relationships in radiosonde observations and atmospheric general circulation models. *J. Hydrometeorol.*, **3**, 26–38.

Russell, G.L., 2005: *4x3 Atmosphere-Ocean Model Documentation*. http://aom.giss.nasa.gov/doc4x3.html.

Russell, G.L., J.R. Miller, and D. Rind, 1995: A coupled atmosphere-ocean model for transient climate change studies. *Atmos.-Ocean*, **33**, 683–730.

Russell, J.L., R.J. Stouffer, and K.W. Dixon, 2006: Intercomparison of the Southern Ocean circulations in IPCC coupled model control simulations. *J. Clim.*, **19**, 4560–4575.

Saenko, O.A., and W.J. Merryfield, 2005: On the effect of topographically-enhanced mixing on the global ocean circulation. *J. Phys. Oceanogr.*, **35**, 826–834.

Saenko, O.A., G.M. Flato, and A.J. Weaver, 2002: Improved representation of sea-ice processes in climate models. *Atmos.-Ocean*, **40**, 21–43.

Sakamoto, T.T., et al., 2004: Far-reaching effects of the Hawaiian Islands in the CCSR/NIES/FRCGC high-resolution climate model. *Geophys. Res. Lett.*, **31**, doi:10.1029/2004GL020907.

Sakamoto, T., et al., 2005: Responses of the Kuroshio and the Kuroshio Extension to global warming in a high-resolution climate model. *Geophys. Res. Lett.*, **32**, L14617, doi:10.1029/2005GL023384.

Salas-Mélia, D., 2002: A global coupled sea ice-ocean model. *Ocean Modelling*, **4**, 137–172.

Saltzman, B., 1978: A survey of statistical-dynamical models of the terrestrial climate. *Adv. Geophys.*, **20**, 183–295.

Santer, B.D., et al., 2005: Amplification of surface temperature trends and variability in the tropical atmosphere. *Science*, **309**, 1551–1556.

Sato, N., et al., 1989: Effects of implementing the simple biosphere model in a general circulation model. *J. Atmos. Sci.*, **46**, 2757–2782.

Sausen, R., K. Barthel, and K. Hasselmann, 1988: Coupled ocean-atmosphere models with flux correction. *Clim. Dyn.*, **2**, 145–163.

Sausen, R., et al., 2002: Climate response to inhomogeneously distributed forcing agents. In: *Non-CO_2 Greenhouse Gases: Scientific Understanding, Control Options and Policy Aspects* [van Ham, J., A.P.M. Baede, R. Guicherit, and J.G.F.M. Williams-Jacobse (eds.)]. Millpress, Rotterdam, Netherlands, pp. 377–381.

Schär, C., et al., 2004: The role of increasing temperature variability for European summer heat waves. *Nature*, **427**, 332–336, doi:10.1038/nature02300.

Scaife, A.A., J.R. Knight, C.K. Folland, and G.K. Vallis, 2005: A stratospheric influence on the winter NAO and North Atlantic surface climate. *Geophys. Res. Lett.*, **32**, L18715.

Scaife, A.A., et al., 2000: Realistic quasi-biennial oscillations in a simulation of the global climate. *Geophys. Res. Lett.*, **27**, 3481–3484.

Schiller, A., U. Mikolajewicz, and R. Voss, 1997: The stability of the North Atlantic thermohaline circulation in a coupled ocean-atmosphere general circulation model. *Clim. Dyn.*, **13**, 325–347.

Schmidt, G.A., C.M. Bitz, U. Mikolajewicz, and L.B. Tremblay, 2004: Ice-ocean boundary conditions for coupled models. *Ocean Modelling*, **7**, 59–74.

Schmidt, G.A., et al., 2006: Present day atmospheric simulations using GISS ModelE: Comparison to in-situ, satellite and reanalysis data. *J. Clim.*, **19**, 153–192, http://www.giss.nasa.gov/tools/modelE/.

Schmittner, A., and T.F. Stocker, 1999: The stability of the thermohaline circulation in global warming experiments. *J. Clim.*, **12**, 1117–1133.

Schmittner, A., C. Appenzeller, and T.F. Stocker, 2000: Enhanced Atlantic freshwater export during El Niño. *Geophys. Res. Lett.*, **27**, 1163–1166.

Schneider, E.K., 2001: Causes of differences between the equatorial Pacific as simulated by two coupled GCM's. *J. Clim.*, **15**, 2301–2320.

Schneider, S.H., 2004: Abrupt non-linear climate change, irreversibility and surprise. *Global Environ. Change*, **14**, 245–258.

Schubert, S., et al., 1992: *Monthly Means of Selected Climate Variables for 1985–1989*. NASA Technical Memorandum, Goddard Space Flight Center, Greenbelt, MD, 376 pp. Available from the NASA Technical Report Server, Accession Number: 92N29653; Document ID: 19920020410; Report Number: NAS 1.15104565, NASA-TM-104565, REPT-92B00088.

Scinocca, J.F., and N.A. McFarlane, 2004: The variability of modelled tropical precipitation. *J. Atmos. Sci.*, **61**, 1993–2015.

Seidel, D.J., and J.R. Lanzante, 2004: An assessment of three alternatives to linear trends for characterizing global atmospheric temperature changes. *J. Geophys. Res.*, **109**, D14108, doi:10.1029/2003JD004414.

Seidov, D., E.J. Barron, and B.J. Haupt, 2001: Meltwater and the global ocean conveyor: Northern versus southern connections. *Global Planet. Change*, **30**, 253–266.

Seidov, D., R.J. Stouffer, and B.J. Haupt, 2005: Is there a simple bi-polar ocean seesaw? *Global Planet. Change*, **49**, 19–27.

Sellers, P.J., Y. Mintz, Y.C. Sud, and A. Dalcher, 1986: A simple biosphere model (SiB) for use within general circulation models. *J. Atmos. Sci.*, **43**, 505–531.

Selten, F.M., and G. Branstator, 2004: Preferred regime transition routes and evidence for an unstable periodic orbit in a baroclinic model. *J. Atmos. Sci.*, **61**, 2267–2268.

Semtner, A.J., 1976: A model for the thermodynamic growth of sea ice in numerical investigations of climate. *J. Phys. Oceanogr.*, **6**, 379–389.

Seneviratne, S.I., J.S. Pal, E.A.B. Eltahir, and C. Schär, 2002: Summer dryness in a warmer climate: A process study with a regional climate model. *Clim. Dyn.*, **20**, 69–85.

Senior, C.A., and J.F.B. Mitchell, 1993: Carbon dioxide and climate: The impact of cloud parameterization. *J. Clim.*, **6**, 393–418.

Senior, C.A., and J.F.B. Mitchell, 2000: The time dependence of climate sensitivity. *Geophys. Res. Lett.*, **27**, 2685–2688.

Severijns, C.A., and W. Hazeleger, 2005: Optimising parameters in an atmospheric general circulation model. *J. Clim.*, **18**, 3527–3535.

Shaffrey, L., and R. Sutton, 2004: The interannual variability of energy transports within and over the Atlantic Ocean in a coupled climate model. *J. Clim.*, **17**, 1433–1448.

Shibata, K., et al., 1999: A simulation of troposphere, stratosphere and mesosphere with an MRI/JMA98 GCM. *Papers in Meteorology and Geophysics*, **50**, 15–53.

Shindell, D.T., R.L. Miller, G.A. Schmidt, and L. Pandolfo, 1999: Simulation of recent northern winter climate trends by greenhouse-gas forcing. *Nature*, **399**, 452–455.

Shiogama, H., M. Watanabe, M. Kimoto, and T. Nozawa, 2005: Anthropogenic and natural forcing impacts on the Pacific Decadal Oscillation during the second half of the 20th century. *Geophys. Res. Lett.*, **32**, L21714, doi:10.1029/2005GL023871.

Shukla, J., et al., 2006: Climate model fidelity and projections of climate change. *Geophys. Res. Lett.*, **33**, L07702, doi:10.1029/2005GL025579.

Sinclair, M.R., 1996: A climatology of anticyclones and blocking for the Southern Hemisphere. *Mon. Weather Rev.*, **124**, 245–263.

Sitch, S., et al., 2003: Evaluation of ecosystem dynamics, plant geography and terrestrial carbon cycling in the LPJ dynamic global vegetation model. *Global Change Biol.*, **9**, 161–185.

Six, K.D., and E. Maier-Reimer, 1996: Effects of plankton dynamics on seasonal carbon fluxes in an ocean general circulation model. *Global Biogeochem. Cycles*, **10**, 559–583.

Slater, A.G., et al., 2001: The representation of snow in land-surface schemes: Results from PILPS 2(d). *J. Hydrometeorol.*, **2**, 7–25.

Slingo, J.M., P.M. Inness, and K.R. Sperber, 2005: Modelling the Madden Julian Oscillation. In: *Intraseasonal Variability of the Atmosphere-Ocean Climate System* [Lau, W.K.-M., and D.E. Waliser (eds.)]. Praxis Publishing.

Slingo, J.M., et al., 1996: Intraseasonal oscillations in 15 atmospheric general circulation models: Results from an AMIP Diagnostic Subproject. *Clim. Dyn.*, **12**, 325–357.

Slingo, J., et al., 2003: Scale interactions on diurnal to seasonal timescales and their relevance to model systematic errors. *Ann. Geophys.*, **46**, 139–155.

Smith, R.D., and P.R. Gent, 2002: *Reference Manual for the Parallel Ocean Program (POP), Ocean Component of the Community Climate System Model (CCSM2.0 and 3.0)*. Technical Report LA-UR-02-2484, Los Alamos National Laboratory, Los Alamos, NM, http://www.ccsm.ucar.edu/models/ccsm3.0/pop/.

Soden, B.J., 1997: Variations in the tropical greenhouse effect during El Niño. *J. Clim.*, **10**(5), 1050–1055.

Soden, B.J., 2000: The sensitivity of the tropical hydrological cycle to ENSO. *J. Clim.*, **13**, 538–549.

Soden, B.J., 2004: The impact of tropical convection and cirrus on upper tropospheric humidity: A Lagrangian analysis of satellite measurements. *Geophys. Res. Lett.*, **31**, L20104, doi:10.1029/2004GL020980.

Soden, B.J., and I.M. Held, 2006: An assessment of climate feedbacks in coupled ocean-atmosphere models. *J. Clim.*, **19**, 3354–3360.

Soden, B.J., A.J. Broccoli, and R.S. Hemler, 2004: On the use of cloud forcing to estimate cloud feedback. *J. Clim.*, **17**, 3661–3665.

Soden, B.J., R.T. Wetherald, G.L. Stenchikov, and A. Robock, 2002: Global cooling after the eruption of Mount Pinatubo: A test of climate feedback by water vapour. *Science*, **296**, 727–730.

Soden, B.J., et al., 2005: The radiative signature of upper tropospheric moistening. *Science*, **310**(5749), 841–844.

Sohn, B.-J., and J. Schmetz, 2004: Water vapor-induced OLR variations associated with high cloud changes over the tropics: a study from Meteosat-5 observations. *J. Clim.*, **17**, 1987–1996.

Sokolov, A., and P. Stone, 1998: A flexible climate model for use in integrated assessments. *Clim. Dyn.*, **14**, 291–303.

Sokolov, A.P., et al., 2005: *The MIT Integrated Global System Model (IGSM), Version 2: Model Description And Baseline Evaluation*. Report No. 124, Joint Program on the Science and Policy of Global Change, Massachusetts Institute of Technology, Cambridge, MA, http://web.mit.edu/globalchange/www/MITJPSPGC_Rpt124.pdf.

Spelman, M.J., and S. Manabe, 1984: Influence of oceanic heat transport upon the sensitivity of a model climate. *J. Geophys. Res.*, **89**, 571–586.

Sperber, K.R., S. Gualdi, S. Legutke, and V. Gayler, 2005: The Madden-Julian Oscillation in ECHAM4 coupled and uncoupled GCMs. *Clim. Dyn.*, **25**, doi:10.1007/s00382-005-0026-3.

Stainforth, D.A., et al., 2005: Uncertainty in predictions of the climate response to rising levels of greenhouse gases. *Nature*, **433**, 403–406.

Stein, O., 2000: The variability of Atlantic-European blocking as derived from long SLP time series. *Tellus*, **52A**, 225–236.

Stenchikov, G., et al., 2002: Arctic Oscillation response to the 1991 Mount Pinatubo eruption: Effects of volcanic aerosols and ozone depletion. *J. Geophys. Res.*, **107**(D24), 4803.

Stephens, G.L., 2005: Cloud feedbacks in the climate system: a critical review. *J. Clim.*, **18**, 237–273.

Stephenson, D.B., and V. Pavan, 2003: The North Atlantic Oscillation in coupled climate models: a CMIP1 evaluation. *Clim. Dyn.*, **20**, 381–399.

Stephenson, D.B., A. Hannachi, and A. O'Neill, 2004: On the existence of multiple climate regimes. *Q. J. R. Meteorol. Soc.*, **130**, 583–605.

Stocker, T.F., D.G. Wright, and L.A. Mysak, 1992: A zonally averaged, coupled atmosphere-ocean model for paleoclimate studies. *J. Clim.*, **5**, 773–797.

Stocker, T.F., et al., 2001: Physical climate processes and feedbacks. In: *Climate Change 2001: The Scientific Basis. Contribution of Working Group I to the Third Assessment Report of the Intergovernmental Panel on Climate Change* [Houghton, J.T., et al. (eds.)]. Cambridge University Press, Cambridge, United Kingdom and New York, NY, USA, pp. 419–470.

Stommel, H., 1961: Thermohaline convection with two stable regimes of flow. *Tellus*, **13**, 224–230.

Stouffer, R.J., 2004: Time scales of climate response. *J. Clim.*, **17**(1), 209–217.

Stouffer, R.J., and K.W. Dixon, 1998: *Initialization of Coupled Models for Use in Climate Studies: A Review*. Research Activities in Atmospheric and Oceanic Modelling, Report No. 27, WMO/TD-No. 865, World Meteorological Organization, Geneva, Switzerland, I.1–I.8.

Stouffer, R.J., and S. Manabe, 2003: Equilibrium response of thermohaline circulation to large changes in atmospheric CO_2 concentration. *Clim. Dyn.*, **20**(7/8), 759–773.

Stouffer, R.J., A.J. Weaver, and M. Eby, 2004: A method for obtaining pre-twentieth century initial conditions for use in climate change studies. *Clim. Dyn.*, **23**, 327–339.

Stouffer, R.J., et al., 2006: Investigating the causes of the response of the thermohaline circulation to past and future climate changes. *J. Clim.*, **19**, 1365–1387.

Stowasser, M., and K. Hamilton, 2006: Relationship between shortwave cloud radiative forcing and local meteorological variables compared in observations and several global climate models. *J. Clim.*, **19**, 4344–4359.

Stowasser, M., K. Hamilton, and G.J. Boer, 2006: Local and global climate feedbacks in models with differing climate sensitivity. *J. Clim.*, **19**, 193–209.

Stratton, R.A., and V.D. Pope, 2004: Modelling the climatology of storm tracks - Sensitivity to resolution. In: *The Second Phase of the Atmospheric Model Intercomparison Project (AMIP2)* [Gleckler, P. (ed.)]. Proceedings of the WCRP/WGNE Workshop, Toulouse, pp. 207-210.

Stuber, N., M. Ponater, and R. Sausen, 2001: Is the climate sensitivity to ozone perturbations enhanced by stratospheric water vapor feedback? *Geophys. Res. Lett.*, **28**, doi:10.1029/2001GL013000.

Stuber, N., M. Ponater, and R. Sausen, 2005: Why radiative forcing might fail as a predictor of climate change. *Clim. Dyn.*, **24**, 497–510.

Sud, Y.C., and G.K. Walker, 1999: Microphysics of clouds with the relaxed Arakawa-Schubert Cumulus Scheme (McRAS). Part I: Design and evaluation with GATE Phase III data. *J. Atmos. Sci.*, **56**, 3196–3220.

Sugi, M., A. Noda, and N. Sato, 2002: Influence of the global warming on tropical cyclone climatology: An experiment with the JMA global model. *J. Meteorol. Soc. Japan*, **80**, 249–272.

Sun, D.-Z., and I.M. Held, 1996: A comparison of modeled and observed relationships between interannual variations of water vapor and temperature. *J. Clim.*, **9**, 665–675.

Sun, D.-Z., C. Covey, and R.S. Lindzen, 2001: Vertical correlations of water vapor in GCMs. *Geophys. Res. Lett.*, **28**, 259–262.

Sun, Y., S. Solomon, A. Dai, and R. Portmann, 2006: How often does it rain? *J. Clim.*, **19**, 916–934.

Suzuki, T., et al., 2005: Projection of future sea level and its variability in a high-resolution climate model: Ocean processes and Greenland and Antarctic ice-melt contributions. *Geophys. Res. Lett.*, **32**, L19706, doi:10.1029/2005GL023677.

Takahashi, M., 1996: Simulation of the stratospheric quasi-biennial oscillation using a general circulation model. *Geophys. Res. Lett.*, **23**, 661–664.

Takahashi, M., 1999: The first realistic simulation of the stratospheric quasi-biennial oscillation in a general circulation model. *Geophys. Res. Lett.*, **26**, 1307–1310.

Takemura, T., et al., 2002: Single scattering albedo and radiative forcing of various aerosol species with a global three-dimensional model. *J. Clim.*, **15**, 333–352.

Takemura, T., et al., 2005: Simulation of climate response to aerosol direct and indirect effects with aerosol transport-radiation model. *J. Geophys. Res.*, **110**, D02202, doi:10.1029/2004JD005029.

Tang, Y.M., and M.J. Roberts, 2005: The impact of a bottom boundary layer scheme on the North Atlantic Ocean in a global coupled climate model. *J. Phys. Oceanogr.*, **35**(2), 202–217.

Terray, L., S. Valcke, and A. Piacentini, 1998: *OASIS 2.2 Guide and Reference Manual*. Technical Report TR/CMGC/98-05, Centre Europeen de Recherche et de Formation Avancée en Calcul Scientifique, Toulouse, France.

Thompson, C.J., and D.S. Battisti, 2001: A linear stochastic dynamical model of ENSO. Part II: Analysis. *J. Clim.*, **14**, 445–466.

Thompson, D.W.J., and J.M. Wallace, 2000: Annular modes in the extratropical circulation. Part I: Month-to-month variability. *J. Clim.*, **13**, 1000–1016.

Thompson, D.W.J., and S. Solomon, 2002: Interpretation of recent Southern Hemisphere climate change. *Science*, **296**, 895–899.

Thorndike, A.S., D.A. Rothrock, G.A. Maykut, and R. Colony, 1975: The thickness distribution of sea ice. *J. Geophys. Res.*, **80**, 4501–4513.

Thorpe, R.B., R.A. Wood, and J.F.B. Mitchell, 2004: The sensitivity of the thermohaline circulation response to preindustrial and anthropogenic greenhouse gas forcing to the parameterisation of mixing across the Greenland-Scotland ridge. *Ocean Modelling*, **7**, 259–268.

Thorpe, R.B., et al., 2001: Mechanisms determining the Atlantic thermohaline circulation response to greenhouse gas forcing in a non-flux-adjusted coupled climate model. *J. Clim.*, **14**, 3102–3116.

Tiedtke, M., 1993: Representation of clouds in large-scale models. *Mon. Weather Rev.*, **121**, 3040–3061

Timmermann, A., and H. Goosse, 2004: Is the wind stress forcing essential for the meridional overturning circulation? *Geophys. Res. Lett.*, **31**(4), L04303, doi:10.1029/2003GL018777.

Tomé, A., and P.M.A. Miranda, 2004: Piecewise linear fitting and trend changing points of climate parameters. *Geophys. Res. Lett.*, **31**, L02207, doi:10.1029/2003GL019100.

Tompkins, A., 2002: A prognostic parameterization for the subgrid-scale variability of water vapor and clouds in large-scale models and its use to diagnose cloud cover. *J. Atmos. Sci.*, **59**, 1917–1942.

Tompkins, A.M., and G.C. Craig, 1999: Sensitivity of tropical convection to sea surface temperature in the absence of large-scale flow. *J. Clim.*, **12**, 462–476.

Toyota, T., et al., 2004: Thickness distribution, texture and stratigraphy, and a simple probabilistic model for dynamical thickening of sea ice in the southern Sea of Okhotsk. *J. Geophys. Res.*, **109**, C06001, doi:10.1029/2003JC002090.

Trenberth, K.E., and J.M. Caron, 2001: Estimates of meridional atmosphere and ocean heat transports. *J. Clim.*, **14**, 3433–3443.

Trenberth, K.E., J. Fasullo, and L. Smith, 2005: Trends and variability in column-integrated atmospheric water vapour. *Clim. Dyn.*, **24**, 741–758.

Trenberth, K.E., D.P. Stepaniak, J.W. Hurrel, and M. Fiorino, 2001: Quality of re-analyses in the tropics. *J. Clim.*, **14**, 1499–1510.

Trenberth, K.E., et al., 1998: Progress during TOGA in understanding and modeling global teleconnection associated with tropical sea surface temperatures. *J. Geophys. Res.*, **103**, 14291–14324.

Trigo, R.M., I.F. Trigo, C.C. DaCamra, and T.J. Osborn, 2004: Climate impact of the European winter blocking episodes from the NCEP/NCAR reanalyses. *Clim. Dyn.*, **23**, 17–28.

Tselioudis, G., and W.B. Rossow, 1994: Global, multiyear variations of optical-thickness with temperature in low and cirrus clouds. *Geophys. Res. Lett.*, **21**, 2211–2214

Tselioudis, G., and W.B. Rossow, 2006: Climate feedback implied by observed radiation and precipitation changes with midlatitude storm strength and frequency. *Geophys. Res. Lett.*, **33**, L02704, doi:10.1029/2005GL024513.

Tselioudis, G., Y.-C. Zhang, and W.R. Rossow, 2000: Cloud and radiation variations associated with northern midlatitude low and high sea level pressure regimes. *J. Clim.*, **13**, 312–327.

Tsushima, Y., A. Abe-Ouchi, and S. Manabe, 2005: Radiative damping of annual variation in global mean surface temperature: Comparison between observed and simulated feedback. *Clim. Dyn.*, **24**, 591–597, doi:10.1007/s00382-005-0002-y.

Tsushima, Y., et al., 2006: Importance of the mixed-phase cloud distribution in the control climate for assessing the response of clouds to carbon dioxide increase: a multi-model study. *Clim. Dyn.*, **27**, 113–126, doi:10.1007/s00382-006-0127-7.

Turner, A.G., P.M. Inness and J.M. Slingo, 2005: The role of the basic state in monsoon prediction. *Q. J. R. Meteorol. Soc.*, **131**, 781–804.

Uppala, S.M., et al., 2005: The ERA-40 Reanalysis. *Q. J. R. Meteorol. Soc.*, **131**, 2961–3012, doi:10.1256/qj.04.176.

Valcke, S., E. Guilyardi, and C. Larsson, 2006: PRISM and ENES: A European approach to Earth system modelling. *Concurrency and Computation: Practice and Experience*, **18**(2), 247–262.

Van Oldenborgh, G.J., S.Y. Philip, and M. Collins, 2005: El Nino in a changing climate: a multi-model study. *Ocean Sci.*, **1**, 81–95.

Vallis, G.K., E.P. Gerber, P.J. Kushner, and B.A. Cash, 2004: A mechanism and simple dynamical model of the North Atlantic Oscillation and Annular Modes. *J. Atmos. Sci.*, **61**, 264–280.

Vavrus, S., 2004: The impact of cloud feedbacks on Arctic climate under greenhouse forcing. *J. Clim.*, **17**, 603–615.

Vavrus, S., and S.P. Harrison, 2003: The impact of sea-ice dynamics on the Arctic climate system. *Clim. Dyn.*, **20**, 741–757.

Vavrus, S., J.E. Walsh, W.L. Chapman, and D. Portis, 2006: The behavior of extreme cold air outbreaks under greenhouse warming. *Int. J. Climatol.*, **26**, 1133–1147.

Vellinga, M., and R.A. Wood, 2002: Global climate impacts of a collapse of the Atlantic thermohaline circulation. *Clim. Change*, **54**, 251–267.

Vellinga, M., R.A.Wood, and J.M. Gregory, 2002: Processes governing the recovery of a perturbed thermohaline circulation in HadCM3. *J. Clim.*, **15**, 764–780.

Verseghy, D.L., N.A. McFarlane, and M. Lazare, 1993: A Canadian land surface scheme for GCMs: II. Vegetation model and coupled runs. *Int. J. Climatol.*, **13**, 347–370.

Visbeck, M., J. Marshall, T. Haine, and M. Spall, 1997: Specification of eddy transfer coefficients in coarse-resolution ocean circulation models. *J. Phys. Oceanogr.*, **27**, 381–402.

Volodin, E.M., 2004: Relation between the global-warming parameter and the heat balance on the Earth's surface at increased contents of carbon dioxide. *Izv. Atmos. Ocean. Phys.*, **40**, 269–275.

Volodin, E.M., and V.N. Lykossov, 1998: Parameterization of heat and moisture processes in the soil-vegetation system: 1. Formulation and simulations based on local observational data. *Izv. Atmos. Ocean. Phys.*, **34**(4), 453–465.

Volodin, E.M., and N.A. Diansky, 2004: El-Niño reproduction in a coupled general circulation model of atmosphere and ocean. *Russ. Meteorol. Hydrol.*, **12**, 5–14.

Waliser, D.E., K.M. Lau, and J.H. Lim, 1999: The influence of coupled sea surface temperatures on the Madden–Julian oscillation: A model perturbation experiment. *J. Atmos. Sci.*, **56**, 333–358.

Wallace, J.M., Y. Zhang, and L. Bajuk, 1996: Interpretation of interdecadal trends in Northern Hemisphere surface air temperature. *J. Clim.*, **9**, 249–259.

Walsh, J.E., et al., 2002: Comparison of Arctic climate simulations by uncoupled and coupled global models. *J. Clim.*, **15**, 1429–1446.

Walsh, K.J.E., K.C. Nguyen and J.L. McGregor, 2004: Fine-resolution regional climate model simulations of the impact of climate change on tropical cyclones near Australia. *Clim. Dyn.*, **22**, 47–56.

Wang, B., et al., 2004: Design of a new dynamical core for global atmospheric models based on some efficient numerical methods. *Science in China*, *Ser. A*, **47** Suppl., 4–21.

Wang, G.L., and E.A.B. Eltahir, 2000: Ecosystem dynamics and the Sahel drought. *Geophys. Res. Lett.*, **27**, 795–798.

Wang, J., H.L. Cole, and D.J. Carlson, 2001: Water vapor variability in the tropical western Pacific from 20-year radiosonde data. *Adv. Atmos. Sci.*, **18**(5), 752–766.

Wang, L.R., and M. Ikeda, 2004: A Lagrangian description of sea ice dynamics using the finite element method. *Ocean Modelling*, **7**, 21–38.

Wang, S., R.F. Grant, D.L. Verseghy, and T.A. Black, 2002: Modelling carbon dynamics of boreal forest ecosystems using the Canadian land surface scheme. *Clim. Change*, **55**, 451–477.

Wang, W., and M. Schlesinger, 1999: The dependence on convection parameterization of the tropical intraseasonal oscillation simulated by the UIUC 11-layer atmospheric GCM. *J. Clim.*, **12**, 1423–1457.

Wang, X.L.L., V.R. Swai, and F.W. Zwiers, 2006: Climatology and changes of extratropical cyclone activity: Comparison of ERA-40 with NCEP-NCAR reanalysis for 1958-2001. *J. Clim.*, **19**, 3145–3166.

Warrach, K., H.T. Mengelkamp, and E. Raschke, 2001: Treatment of frozen soil and snow cover in the land surface model SEWAB. *Theor. Appl. Climatol.*, **69**(1–2), 23–37.

Washington, W.M., et al., 2000: Parallel Climate Model (PCM) control and transient simulations. *Clim. Dyn.*, **16**, 755–774.

Watterson, I.G., 2001: Zonal wind vacillation and its interaction with the ocean: Implications for interannual variability and predictability. *J. Geophys. Res.*, **106**, 23965–23975.

Watterson, I.G., 2006: The intensity of precipitation during extratropical cyclones in global warming simulations: a link to cyclone intensity? *Tellus*, **58A**, 82–97.

Weare, B.C., 2004: A comparison of AMIP II model cloud layer properties with ISCCP D2 estimates. *Clim. Dyn.*, **22**, 281–292.

Weaver, A.J., O.A. Saenko, P.U. Clark, and J.X. Mitrovica, 2003: Meltwater pulse 1A from Antarctica as a trigger of the Bølling-Allerød warm interval. *Science*, **299**, 1709–1713.

Weaver, A.J., et al., 2001: The UVic Earth System Climate Model: Model description, climatology and application to past, present and future climates. *Atmos.-Ocean*, **39**, 361–428.

Webb, M., C. Senior, S. Bony, and J.-J. Morcrette, 2001: Combining ERBE and ISCCP data to assess clouds in the Hadley Centre ECMWF and LMD atmospheric climate models. *Clim. Dyn.*, **17**, 905–922.

Webb, M.J., et al., 2006: On the contribution of local feedback mechanisms to the range of climate sensitivity in two GCM ensembles. *Clim. Dyn.*, **27,** 17–38.

Wentz, F.J., and M. Schabel, 2000: Precise climate monitoring using complementary satellite data sets. *Nature*, **403**, 414–416.

Wigley, T.M.L., and S.C.B. Raper, 1992: Implications for climate and sea level of revised IPCC emissions scenarios. *Nature*, **357**, 293–300.

Wigley, T.M.L., and S.C.B. Raper, 2001: Interpretation of high projections for global-mean warming. *Science*, **293**, 451–454.

Wild, M., 2005: Solar radiation budgets in atmospheric model intercomparisons from a surface perspective. *Geophys. Res. Lett.*, **32**, doi:10.1029/2005GL022421.

Wild, M., C.N. Long, and A. Ohmura, 2006: Evaluation of clear-sky solar fluxes in GCMs participating in AMIP and IPCC-AR4 from a surface perspective. *J. Geophys. Res*., **111**, D01104, doi:10.1029/2005JD006118.

Wild, M., et al., 2001: Downward longwave radiation in General Circulation Models. *J. Clim.*, **14**, 3227–3239.

Williams, K.D., M.A. Ringer, and C.A. Senior, 2003: Evaluating the cloud response to climate change and current climate variability. *Clim. Dyn.*, **20**(7–8), 705–721.

Williams, K.D., et al., 2006: Evaluation of a component of the cloud response to climate change in an intercomparison of climate models. *Clim. Dyn.*, **26**, 145–165.

Williamson, D.L., et al., 2005: Moisture and temperature balances at the Atmospheric Radiation Measurement Southern Great Plains Site in forecasts with the Community Atmosphere Model (CAM2). *J. Geophys. Res.*, **110**, D15S16, doi:10.1029/2004JD00510.

Winton, M., 2000: A reformulated three-layer sea ice model. *J. Atmos. Ocean. Technol.*, **17**(4), 525–531.

Winton, M., 2006a: Surface albedo feedback estimates for the AR4 climate models. *J. Clim.*, **19**, 359–365.

Winton, M., 2006b: Amplified Arctic climate change: what does surface albedo feedback have to do with it? *Geophys. Res. Lett.*, **33**, L03701, doi:10.1029/2005GL025244.

Winton, M., R. Hallberg, and A. Gnanadesikan, 1998: Simulation of density-driven frictional downslope flow in z-coordinate ocean models. *J. Phys. Oceanogr.*, **28**, 2163–2174.

Wittenberg, A.T., A. Rosati, N.-C. Lau, and J.J. Ploshay, 2006: GFDL's CM2 global coupled climate models, Part 3: Tropical Pacific climate and ENSO. *J. Clim.*, **19**, 698–722.

Wolff, J.-O., E. Maier-Reimer, and S. Lebutke, 1997: *The Hamburg Ocean Primitive Equation Model*. DKRZ Technical Report No. 13, Deutsches KlimaRechenZentrum, Hamburg, Germany, 100 pp., http://www.mad.zmaw.de/Pingo/reports/ReportNo.13.pdf.

Wood, R.A., A.B. Keen, J.F.B. Mitchell, and J.M. Gregory, 1999: Changing spatial structure of the thermohaline circulation in response to atmospheric CO_2 forcing in a climate model. *Nature*, **399**, 572–575.

Wright, D.G., and T.F. Stocker, 1992: Sensitivities of a zonally averaged global ocean circulation model. *J. Geophys. Res.*, **97**, 12707–12730.

Wright, D.G., and T.F. Stocker, 1993: Younger Dryas experiments. In: *Ice in the Climate System, NATO ASI Series, I12* [Peltier, R. (ed.)]. Springer-Verlag, London, pp. 395–416.

Wu, P., R.A. Wood, and P. Stott, 2005: Human influence on increasing Arctic river discharges. *Geophys. Res. Lett.*, **32**, L02703, doi:10.1029/2004GL021570.

Wu, Q., and D.M. Straus, 2004a: On the existence of hemisphere-wide climate variations. *J. Geophys. Res.*, **109**, D06118, doi:10.1029/2003JD004230.

Wu, Q., and D.M. Straus, 2004b: AO, COWL, and observed climate trends. *J. Clim.*, **17**, 2139–2156.

Wunsch, C., 2002: What is the thermohaline circulation? *Science*, **298**, 1179–1180.

Wyant, M.C., et al., 2006: A comparison of low-latitude cloud properties and their response to climate change in three US AGCMs sorted into regimes using mid-tropospheric vertical velocity. *Clim. Dyn.*, **27**, 261–279.

Xie, P., and P.A. Arkin, 1997: Global precipitation: A 17-year monthly analysis based on gauge observations, satellite estimates, and numerical model outputs. *Bull. Am. Meteorol. Soc.*, **78**, 2539–2558.

Xie, S.-P., W.T. Liu, Q. Liu and M. Nonaka, 2001: Far-reaching effects of the Hawaiian Islands on the Pacific ocean-atmosphere system. *Science*, **292**, 2057–2060.

Xu, Y., et al., 2005: Detection of climate change in the 20th century by the NCC T63. *Acta Meteorol. Sin.*, Special Report on Climate Change, **4**, 1–15.

Yang, G.Y., and J. Slingo, 2001: The diurnal cycle in the tropics. *Mon. Weather Rev.*, **129**, 784–801.

Yang, G.Y., B. Hoskins, and J. Slingo, 2003: Convectively coupled equatorial waves: A new methodology for identifying wave structures in observational data. *J. Atmos. Sci.*, **60**, 1637–1654.

Yao, M.-S., and A. Del Genio, 2002: Effects of cloud parameterization on the simulation of climate changes in the GISS GCM. Part II: Sea surface temperature and cloud feedbacks. *J. Clim.*, **15**, 2491–2503.

Yeh, P. J.-F., and E.A.B. Eltahir, 2005: Representation of water table dynamics in a land surface scheme. Part 1. Model development. *J. Clim.*, **18**, 1861–1880.

Yeh, S.-W., and B.P. Kirtman, 2004: Decadal North Pacific sea surface temperature variability and the associated global climate anomalies in a coupled GCM. *J. Geophys. Res.*, **109**, D20113, doi:10.1029/2004JD004785.

Yin, H., 2005: A consistent poleward shift of the storm tracks in simulations of 21st century climate. *Geophys. Res. Lett.*, **32**, L18701, doi:10.1029/2005GL023684.

Yiou, P., and M. Nogaj, 2004: Extreme climatic events and weather regimes over the North Atlantic: When and where? *Geophys. Res. Lett.*, **31**, doi:10.1029/2003GL019119.

Yokohata, T., et al., 2005: Climate response to volcanic forcing: Validation of climate sensitivity of a coupled atmosphere-ocean general circulation model. *Geophys. Res. Lett.*, **32**, L21710, doi:10.1029/2005GL023542.

Yoshimura, J., M. Sugi, and A. Noda, 2006: Influence of greenhouse warming on tropical cyclone frequency. *J. Meteorol. Soc. Japan*, **84**, 405–428.

Yoshizaki, M., et al., 2005: Changes of Baui (Mei-yu) frontal activity in the global warming climate simulated by a non-hydrostatic regional model. *Scientific Online Letters on the Atmosphere*, **1**, 25–28.

Yu, Y., and X. Zhang, 2000: Coupled schemes of flux adjustments of the air and sea. In: *Investigations on the Model System of the Short-Term Climate Predictions* [Ding, Y., et al. (eds.)]. China Meteorological Press, Beijing, China, pp. 201–207 (in Chinese).

Yu, Y., Z. Zhang, and Y. Guo, 2004: Global coupled ocean-atmosphere general circulation models in LASG/IAP. *Adv. Atmos. Sci.*, **21**, 444–455.

Yu, Y., R. Yu, X. Zhang, and H. Liu, 2002: A flexible global coupled climate model. *Adv. Atmos. Sci.*, **19**(1), 169–190.

Yukimoto, S., and A. Noda, 2003: *Improvements of the Meteorological Research Institute Global Ocean-Atmosphere Coupled GCM (MRI-GCM2) and its Climate Sensitivity*. CGER's Supercomputing Activity Report, National Institute for Environmental Studies, Ibaraki, Japan.

Yukimoto, S., et al., 2001: The new Meteorological Research Institute global ocean-atmosphere coupled GCM (MRI-CGCM2)--Model climate and variability. *Papers in Meteorology and Geophysics*, **51**, 47–88.

Zhang, C., 2005: Madden-Julian Oscillation. *Rev. Geophys.*, **43**, RG2003, doi:10.1029/2004RG000158.

Zhang, C., B. Mapes, and B.J. Soden, 2003: Bimodality of water vapour. *Q. J. R. Meteorol. Soc.*, **129**, 2847–2866.

Zhang, J., and D. Rothrock, 2001: A thickness and enthalpy distribution sea-ice model. *J. Phys. Oceanogr.*, **31**, 2986–3001.

Zhang, J., and D. Rothrock, 2003: Modeling global sea ice with a thickness and enthalpy distribution model in generalized curvilinear coordinates. *Mon. Weather Rev.*, **131**, 845–861.

Zhang, M., 2004: Cloud-climate feedback: how much do we know? In: *Observation, Theory, and Modeling of Atmospheric Variability, World Scientific Series on Meteorology of East Asia, Vol. 3* [Zhu et al. (eds.)]. World Scientific Publishing Co., Singapore, 632 pp.

Zhang, M.H., R.D. Cess, J.J. Hack, and J.T. Kiehl, 1994: Diagnostic study of climate feedback processed in atmospheric general circulation models. *J. Geophys. Res.*, **99**, 5525–5537.

Zhang, M.H., et al., 2005: Comparing clouds and their seasonal variations in 10 atmospheric general circulation models with satellite measurements. *J. Geophys. Res.*, **110**, D15S02, doi:10.1029/2004JD005021.

Zhang, X., and J.E. Walsh, 2006: Toward a seasonally ice-covered Arctic Ocean: scenarios from the IPCC AR4 model simulations. *J. Clim.*, **19**, 1730–1747.

Zhang, Y., W. Maslowski, and A.J. Semtner, 1999: Impacts of mesoscale ocean currents on sea ice in high-resolution Arctic ice and ocean simulations. *J. Geophys. Res.*, **104**(C8), 18409–18429.

Zhu, Y., R.E. Newell, and W.G. Read, 2000: Factors controlling upper-troposphere water vapour. *J. Clim.*, **13**, 836–848.

9

Understanding and Attributing Climate Change

Coordinating Lead Authors:

Gabriele C. Hegerl (USA, Germany), Francis W. Zwiers (Canada)

Lead Authors:

Pascale Braconnot (France), Nathan P. Gillett (UK), Yong Luo (China), Jose A. Marengo Orsini (Brazil, Peru), Neville Nicholls (Australia), Joyce E. Penner (USA), Peter A. Stott (UK)

Contributing Authors:

M. Allen (UK), C. Ammann (USA), N. Andronova (USA), R.A. Betts (UK), A. Clement (USA), W.D. Collins (USA), S. Crooks (UK), T.L. Delworth (USA), C. Forest (USA), P. Forster (UK), H. Goosse (Belgium), J.M. Gregory (UK), D. Harvey (Canada), G.S. Jones (UK), F. Joos (Switzerland), J. Kenyon (USA), J. Kettleborough (UK), V. Kharin (Canada), R. Knutti (Switzerland), F.H. Lambert (UK), M. Lavine (USA), T.C.K. Lee (Canada), D. Levinson (USA), V. Masson-Delmotte (France), T. Nozawa (Japan), B. Otto-Bliesner (USA), D. Pierce (USA), S. Power (Australia), D. Rind (USA), L. Rotstayn (Australia), B. D. Santer (USA), C. Senior (UK), D. Sexton (UK), S. Stark (UK), D.A. Stone (UK), S. Tett (UK), P. Thorne (UK), R. van Dorland (The Netherlands), M. Wang (USA), B. Wielicki (USA), T. Wong (USA), L. Xu (USA, China), X. Zhang (Canada), E. Zorita (Germany, Spain)

Review Editors:

David J. Karoly (USA, Australia), Laban Ogallo (Kenya), Serge Planton (France)

This chapter should be cited as:

Hegerl, G.C., F. W. Zwiers, P. Braconnot, N.P. Gillett, Y. Luo, J.A. Marengo Orsini, N. Nicholls, J.E. Penner and P.A. Stott, 2007: Understanding and Attributing Climate Change. In: *Climate Change 2007: The Physical Science Basis. Contribution of Working Group I to the Fourth Assessment Report of the Intergovernmental Panel on Climate Change* [Solomon, S., D. Qin, M. Manning, Z. Chen, M. Marquis, K.B. Averyt, M. Tignor and H.L. Miller (eds.)]. Cambridge University Press, Cambridge, United Kingdom and New York, NY, USA.

Table of Contents

Executive Summary 665

9.1 Introduction 667

9.1.1 What are Climate Change and Climate Variability? 667

9.1.2 What are Climate Change Detection and Attribution? 667

9.1.3 The Basis from which We Begin 669

9.2 Radiative Forcing and Climate Response 670

9.2.1 Radiative Forcing Estimates Used to Simulate Climate Change 671

9.2.2 Spatial and Temporal Patterns of the Response to Different Forcings and their Uncertainties 674

9.2.3 Implications for Understanding 20th-Century Climate Change 678

9.2.4 Summary 678

9.3 Understanding Pre-Industrial Climate Change 679

9.3.1 Why Consider Pre-Industrial Climate Change? 679

9.3.2 What can be Learned from the Last Glacial Maximum and the Mid-Holocene? 679

9.3.3 What can be Learned from the Past 1,000 Years? 680

9.3.4 Summary 683

9.4 Understanding of Air Temperature Change During the Industrial Era 683

9.4.1 Global-Scale Surface Temperature Change 683

9.4.2 Continental and Sub-continental Surface Temperature Change 693

9.4.3 Surface Temperature Extremes 698

9.4.4 Free Atmosphere Temperature 699

9.4.5 Summary 704

9.5 Understanding of Change in Other Variables during the Industrial Era 705

9.5.1 Ocean Climate Change 705

9.5.2 Sea Level 707

9.5.3 Atmospheric Circulation Changes 709

9.5.4 Precipitation 712

9.5.5 Cryosphere Changes 716

9.5.6 Summary 717

9.6 Observational Constraints on Climate Sensitivity 718

9.6.1 Methods to Estimate Climate Sensitivity 718

9.6.2 Estimates of Climate Sensitivity Based on Instrumental Observations 719

9.6.3 Estimates of Climate Sensitivity Based on Palaeoclimatic Data 724

9.6.4 Summary of Observational Constraints for Climate Sensitivity 725

9.7 Combining Evidence of Anthropogenic Climate Change 727

Frequently Asked Questions

FAQ 9.1: *Can Individual Extreme Events be Explained by Greenhouse Warming?* 696

FAQ 9.2: *Can the Warming of the 20th Century be Explained by Natural Variability?* 702

References 733

Appendix 9.A: Methods Used to Detect Externally Forced Signals 744

Supplementary Material

The following supplementary material is available on CD-ROM and in on-line versions of this report.

Appendix 9.B: *Methods Used to Estimate Climate Sensitivity and Aerosol Forcing*

Appendix 9.C: *Notes and technical details on Figures displayed in Chapter 9*

Appendix 9.D: *Additional Figures and Tables*

References for Appendices 9.B to 9.D

Executive Summary

Evidence of the effect of external influences on the climate system has continued to accumulate since the Third Assessment Report (TAR). The evidence now available is substantially stronger and is based on analyses of widespread temperature increases throughout the climate system and changes in other climate variables.

Human-induced warming of the climate system is widespread. Anthropogenic warming of the climate system can be detected in temperature observations taken at the surface, in the troposphere and in the oceans. Multi-signal detection and attribution analyses, which quantify the contributions of different natural and anthropogenic forcings to observed changes, show that greenhouse gas forcing alone during the past half century would *likely* have resulted in greater than the observed warming if there had not been an offsetting cooling effect from aerosol and other forcings.

It is *extremely unlikely* (<5%) that the global pattern of warming during the past half century can be explained without external forcing, and *very unlikely* that it is due to known natural external causes alone. The warming occurred in both the ocean and the atmosphere and took place at a time when natural external forcing factors would *likely* have produced cooling.

Greenhouse gas forcing has *very likely* caused most of the observed global warming over the last 50 years. This conclusion takes into account observational and forcing uncertainty, and the possibility that the response to solar forcing could be underestimated by climate models. It is also robust to the use of different climate models, different methods for estimating the responses to external forcing and variations in the analysis technique.

Further evidence has accumulated of an anthropogenic influence on the temperature of the free atmosphere as measured by radiosondes and satellite-based instruments. The observed pattern of tropospheric warming and stratospheric cooling is *very likely* due to the influence of anthropogenic forcing, particularly greenhouse gases and stratospheric ozone depletion. The combination of a warming troposphere and a cooling stratosphere has *likely* led to an increase in the height of the tropopause. It is *likely* that anthropogenic forcing has contributed to the general warming observed in the upper several hundred meters of the ocean during the latter half of the 20th century. Anthropogenic forcing, resulting in thermal expansion from ocean warming and glacier mass loss, has *very likely* contributed to sea level rise during the latter half of the 20th century. It is difficult to quantify the contribution of anthropogenic forcing to ocean heat content increase and glacier melting with presently available detection and attribution studies.

It is *likely* that there has been a substantial anthropogenic contribution to surface temperature increases in every continent except Antarctica since the middle of the 20th century. Anthropogenic influence has been detected in every continent except Antarctica (which has insufficient observational coverage to make an assessment), and in some sub-continental land areas. The ability of coupled climate models to simulate the temperature evolution on continental scales and the detection of anthropogenic effects on each of six continents provides stronger evidence of human influence on the global climate than was available at the time of the TAR. No climate model that has used natural forcing only has reproduced the observed global mean warming trend or the continental mean warming trends in all individual continents (except Antarctica) over the second half of the 20th century.

Difficulties remain in attributing temperature changes on smaller than continental scales and over time scales of less than 50 years. Attribution at these scales, with limited exceptions, has not yet been established. Averaging over smaller regions reduces the natural variability less than does averaging over large regions, making it more difficult to distinguish between changes expected from different external forcings, or between external forcing and variability. In addition, temperature changes associated with some modes of variability are poorly simulated by models in some regions and seasons. Furthermore, the small-scale details of external forcing, and the response simulated by models are less credible than large-scale features.

Surface temperature extremes have *likely* been affected by anthropogenic forcing. Many indicators of climate extremes and variability, including the annual numbers of frost days, warm and cold days, and warm and cold nights, show changes that are consistent with warming. An anthropogenic influence has been detected in some of these indices, and there is evidence that anthropogenic forcing may have substantially increased the risk of extremely warm summer conditions regionally, such as the 2003 European heat wave.

There is evidence of anthropogenic influence in other parts of the climate system. Anthropogenic forcing has *likely* contributed to recent decreases in arctic sea ice extent and to glacier retreat. The observed decrease in global snow cover extent and the widespread retreat of glaciers are consistent with warming, and there is evidence that this melting has *likely* contributed to sea level rise.

Trends over recent decades in the Northern and Southern Annular Modes, which correspond to sea level pressure reductions over the poles, are *likely* related in part to human activity, affecting storm tracks, winds and temperature patterns in both hemispheres. Models reproduce the sign of the Northern Annular Mode trend, but the simulated response is smaller than observed. Models including both greenhouse gas and stratospheric ozone changes simulate a realistic trend in the Southern Annular Mode, leading to a detectable human influence on global sea level pressure patterns.

The response to volcanic forcing simulated by some models is detectable in global annual mean land precipitation during the latter half of the 20th century. The latitudinal pattern of change in land precipitation and observed increases in heavy

precipitation over the 20th century appear to be consistent with the anticipated response to anthropogenic forcing. It is *more likely than not* that anthropogenic influence has contributed to increases in the frequency of the most intense tropical cyclones. Stronger attribution to anthropogenic factors is not possible at present because the observed increase in the proportion of such storms appears to be larger than suggested by either theoretical or modelling studies and because of inadequate process knowledge, insufficient understanding of natural variability, uncertainty in modelling intense cyclones and uncertainties in historical tropical cyclone data.

Analyses of palaeoclimate data have increased confidence in the role of external influences on climate. Coupled climate models used to predict future climate have been used to understand past climatic conditions of the Last Glacial Maximum and the mid-Holocene. While many aspects of these past climates are still uncertain, key features have been reproduced by climate models using boundary conditions and radiative forcing for those periods. A substantial fraction of the reconstructed Northern Hemisphere inter-decadal temperature variability of the seven centuries prior to 1950 is *very likely* attributable to natural external forcing, and it is *likely* that anthropogenic forcing contributed to the early 20th-century warming evident in these records.

Estimates of the climate sensitivity are now better constrained by observations. Estimates based on observational constraints indicate that it is *very likely* that the equilibrium climate sensitivity is larger than 1.5°C with a most likely value between 2°C and 3°C. The upper 95% limit remains difficult to constrain from observations. This supports the overall assessment based on modelling and observational studies that the equilibrium climate sensitivity is *likely* 2°C to 4.5°C with a most likely value of approximately 3°C (Box 10.2). The transient climate response, based on observational constraints, is *very likely* larger than 1°C and *very unlikely* to be greater than 3.5°C at the time of atmospheric CO_2 doubling in response to a 1% yr^{-1} increase in CO_2, supporting the overall assessment that the transient climate response is *very unlikely* greater than 3°C (Chapter 10).

Overall consistency of evidence. Many observed changes in surface and free atmospheric temperature, ocean temperature and sea ice extent, and some large-scale changes in the atmospheric circulation over the 20th century are distinct from internal variability and consistent with the expected response to anthropogenic forcing. The simultaneous increase in energy content of all the major components of the climate system as well as the magnitude and pattern of warming within and across the different components supports the conclusion that the cause of the warming is *extremely unlikely* (<5%) to be the result of internal processes. Qualitative consistency is also apparent in some other observations, including snow cover, glacier retreat and heavy precipitation.

Remaining uncertainties. Further improvements in models and analysis techniques have led to increased confidence in the understanding of the influence of external forcing on climate since the TAR. However, estimates of some radiative forcings remain uncertain, including aerosol forcing and inter-decadal variations in solar forcing. The net aerosol forcing over the 20th century from inverse estimates based on the observed warming likely ranges between –1.7 and –0.1 W m^{-2}. The consistency of this result with forward estimates of total aerosol forcing (Chapter 2) strengthens confidence in estimates of total aerosol forcing, despite remaining uncertainties. Nevertheless, the robustness of surface temperature attribution results to forcing and response uncertainty has been evaluated with a range of models, forcing representations and analysis procedures. The potential impact of the remaining uncertainties has been considered, to the extent possible, in the overall assessment of every line of evidence listed above. There is less confidence in the understanding of forced changes in other variables, such as surface pressure and precipitation, and on smaller spatial scales.

Better understanding of instrumental and proxy climate records, and climate model improvements, have increased confidence in climate model-simulated internal variability. However, uncertainties remain. For example, there are apparent discrepancies between estimates of ocean heat content variability from models and observations. While reduced relative to the situation at the time of the TAR, uncertainties in the radiosonde and satellite records still affect confidence in estimates of the anthropogenic contribution to tropospheric temperature change. Incomplete global data sets and remaining model uncertainties still restrict understanding of changes in extremes and attribution of changes to causes, although understanding of changes in the intensity, frequency and risk of extremes has improved.

9.1 Introduction

The objective of this chapter is to assess scientific understanding about the extent to which the observed climate changes that are reported in Chapters 3 to 6 are expressions of natural internal climate variability and/or externally forced climate change. The scope of this chapter includes 'detection and attribution' but is wider than that of previous detection and attribution chapters in the Second Assessment Report (SAR; Santer et al., 1996a) and the Third Assessment Report (TAR; Mitchell et al., 2001). Climate models, physical understanding of the climate system and statistical tools, including formal climate change detection and attribution methods, are used to interpret observed changes where possible. The detection and attribution research discussed in this chapter includes research on regional scales, extremes and variables other than temperature. This new work is placed in the context of a broader understanding of a changing climate. However, the ability to interpret some changes, particularly for non-temperature variables, is limited by uncertainties in the observations, physical understanding of the climate system, climate models and external forcing estimates. Research on the impacts of these observed climate changes is assessed by Working Group II of the IPCC.

9.1.1 What are Climate Change and Climate Variability?

'Climate change' refers to a change in the state of the climate that can be identified (e.g., using statistical tests) by changes in the mean and/or the variability of its properties, and that persists for an extended period, typically decades or longer (see Glossary). Climate change may be due to internal processes and/or external forcings. Some external influences, such as changes in solar radiation and volcanism, occur naturally and contribute to the total natural variability of the climate system. Other external changes, such as the change in composition of the atmosphere that began with the industrial revolution, are the result of human activity. A key objective of this chapter is to understand climate changes that result from anthropogenic and natural external forcings, and how they may be distinguished from changes and variability that result from internal climate system processes.

Internal variability is present on all time scales. Atmospheric processes that generate internal variability are known to operate on time scales ranging from virtually instantaneous (e.g., condensation of water vapour in clouds) up to years (e.g., troposphere-stratosphere or inter-hemispheric exchange). Other components of the climate system, such as the ocean and the large ice sheets, tend to operate on longer time scales. These components produce internal variability of their own accord and also integrate variability from the rapidly varying atmosphere (Hasselmann, 1976). In addition, internal variability is produced by coupled interactions between components, such as is the case with the El-Niño Southern Oscillation (ENSO; see Chapters 3 and 8).

Distinguishing between the effects of external influences and internal climate variability requires careful comparison between observed changes and those that are expected to result from external forcing. These expectations are based on physical understanding of the climate system. Physical understanding is based on physical principles. This understanding can take the form of conceptual models or it might be quantified with climate models that are driven with physically based forcing histories. An array of climate models is used to quantify expectations in this way, ranging from simple energy balance models to models of intermediate complexity to comprehensive coupled climate models (Chapter 8) such as those that contributed to the multi-model data set (MMD) archive at the Program for Climate Model Diagnosis and Intercomparison (PCMDI). The latter have been extensively evaluated by their developers and a broad investigator community. The extent to which a model is able to reproduce key features of the climate system and its variations, for example the seasonal cycle, increases its credibility for simulating changes in climate.

The comparison between observed changes and those that are expected is performed in a number of ways. Formal detection and attribution (Section 9.1.2) uses objective statistical tests to assess whether observations contain evidence of the expected responses to external forcing that is distinct from variation generated within the climate system (internal variability). These methods generally do not rely on simple linear trend analysis. Instead, they attempt to identify in observations the responses to one or several forcings by exploiting the time and/or spatial pattern of the expected responses. The response to forcing does not necessarily evolve over time as a linear trend, either because the forcing itself may not evolve in that way, or because the response to forcing is not necessarily linear.

The comparison between model-simulated and observed changes, for example, in detection and attribution methods (Section 9.1.2), also carefully accounts for the effects of changes over time in the availability of climate observations to ensure that a detected change is not an artefact of a changing observing system. This is usually done by evaluating climate model data only where and when observations are available, in order to mimic the observational system and avoid possible biases introduced by changing observational coverage.

9.1.2 What are Climate Change Detection and Attribution?

The concepts of climate change 'detection' and 'attribution' used in this chapter remain as they were defined in the TAR (IPCC, 2001; Mitchell et al., 2001). 'Detection' is the process of demonstrating that climate has changed in some defined statistical sense, without providing a reason for that change (see Glossary). In this chapter, the methods used to identify change in observations are based on the expected responses to external forcing (Section 9.1.1), either from physical understanding or as simulated by climate models. An identified change is 'detected' in observations if its likelihood of occurrence by chance due to internal variability alone is determined to be small. A failure to

detect a particular response might occur for a number of reasons, including the possibility that the response is weak relative to internal variability, or that the metric used to measure change is insensitive to the expected change. For example, the annual global mean precipitation may not be a sensitive indicator of the influence of increasing greenhouse concentrations given the expectation that greenhouse forcing would result in moistening at some latitudes that is partially offset by drying elsewhere (Chapter 10; see also Section 9.5.4.2). Furthermore, because detection studies are statistical in nature, there is always some small possibility of spurious detection. The risk of such a possibility is reduced when corroborating lines of evidence provide a physically consistent view of the likely cause for the detected changes and render them less consistent with internal variability (see, for example, Section 9.7).

Many studies use climate models to predict the expected responses to external forcing, and these predictions are usually represented as patterns of variation in space, time or both (see Chapter 8 for model evaluation). Such patterns, or 'fingerprints', are usually derived from changes simulated by a climate model in response to forcing. Physical understanding can also be used to develop conceptual models of the anticipated pattern of response to external forcing and the consistency between responses in different variables and different parts of the climate system. For example, precipitation and temperature are ordinarily inversely correlated in some regions, with increases in temperature corresponding to drying conditions. Thus, a warming trend in such a region that is not associated with rainfall change may indicate an external influence on the climate of that region (Nicholls et al., 2005; Section 9.4.2.3). Purely diagnostic approaches can also be used. For example, Schneider and Held (2001) use a technique that discriminates between slow changes in climate and shorter time-scale variability to identify in observations a pattern of surface temperature change that is consistent with the expected pattern of change from anthropogenic forcing.

The spatial and temporal scales used to analyse climate change are carefully chosen so as to focus on the spatio-temporal scale of the response, filter out as much internal variability as possible (often by using a metric that reduces the influence of internal variability, see Appendix 9.A) and enable the separation of the responses to different forcings. For example, it is expected that greenhouse gas forcing would cause a large-scale pattern of warming that evolves slowly over time, and thus analysts often smooth data to remove small-scale variations. Similarly, when fingerprints from Atmosphere-Ocean General Circulation Models (AOGCMs) are used, averaging over an ensemble of coupled model simulations helps separate the model's response to forcing from its simulated internal variability.

Detection does not imply attribution of the detected change to the assumed cause. 'Attribution' of causes of climate change is the process of establishing the most likely causes for the detected change with some defined level of confidence (see Glossary). As noted in the SAR (IPCC, 1996) and the TAR (IPCC, 2001), unequivocal attribution would require controlled experimentation with the climate system. Since that is not possible, in practice attribution of anthropogenic climate change is understood to mean demonstration that a detected change is 'consistent with the estimated responses to the given combination of anthropogenic and natural forcing' and 'not consistent with alternative, physically plausible explanations of recent climate change that exclude important elements of the given combination of forcings' (IPCC, 2001).

The consistency between an observed change and the estimated response to a hypothesised forcing is often determined by estimating the amplitude of the hypothesised pattern of change from observations and then assessing whether this estimate is statistically consistent with the expected amplitude of the pattern. Attribution studies additionally assess whether the response to a key forcing, such as greenhouse gas increases, is distinguishable from that due to other forcings (Appendix 9.A). These questions are typically investigated using a multiple regression of observations onto several fingerprints representing climate responses to different forcings that, ideally, are clearly distinct from each other (i.e., as distinct spatial patterns or distinct evolutions over time; see Section 9.2.2). If the response to this key forcing can be distinguished, and if even rescaled combinations of the responses to other forcings do not sufficiently explain the observed climate change, then the evidence for a causal connection is substantially increased. For example, the attribution of recent warming to greenhouse gas forcing becomes more reliable if the influences of other external forcings, for example solar forcing, are explicitly accounted for in the analysis. This is an area of research with considerable challenges because different forcing factors may lead to similar large-scale spatial patterns of response (Section 9.2.2). Note that another key element in attribution studies is the consideration of the physical consistency of multiple lines of evidence.

Both detection and attribution require knowledge of the internal climate variability on the time scales considered, usually decades or longer. The residual variability that remains in instrumental observations after the estimated effects of external forcing have been removed is sometimes used to estimate internal variability. However, these estimates are uncertain because the instrumental record is too short to give a well-constrained estimate of internal variability, and because of uncertainties in the forcings and the estimated responses. Thus, internal climate variability is usually estimated from long control simulations from coupled climate models. Subsequently, an assessment is usually made of the consistency between the residual variability referred to above and the model-based estimates of internal variability; analyses that yield implausibly large residuals are not considered credible (for example, this might happen if an important forcing is missing, or if the internal variability from the model is too small). Confidence is further increased by systematic intercomparison of the ability of models to simulate the various modes of observed variability (Chapter 8), by comparisons between variability in observations and climate model data (Section 9.4) and by comparisons between proxy reconstructions and climate simulations of the last millennium (Chapter 6 and Section 9.3).

Studies where the estimated pattern amplitude is substantially different from that simulated by models can still provide some understanding of climate change but need to be treated with caution (examples are given in Section 9.5). If this occurs for variables where confidence in the climate models is limited, such a result may simply reflect weaknesses in models. On the other hand, if this occurs for variables where confidence in the models is higher, it may raise questions about the forcings, such as whether all important forcings have been included or whether they have the correct amplitude, or questions about uncertainty in the observations.

Model and forcing uncertainties are important considerations in attribution research. Ideally, the assessment of model uncertainty should include uncertainties in model parameters (e.g., as explored by multi-model ensembles), and in the representation of physical processes in models (structural uncertainty). Such a complete assessment is not yet available, although model intercomparison studies (Chapter 8) improve the understanding of these uncertainties. The effects of forcing uncertainties, which can be considerable for some forcing agents such as solar and aerosol forcing (Section 9.2), also remain difficult to evaluate despite advances in research. Detection and attribution results based on several models or several forcing histories do provide information on the effects of model and forcing uncertainty. Such studies suggest that while model uncertainty is important, key results, such as attribution of a human influence on temperature change during the latter half of the 20th century, are robust.

Detection of anthropogenic influence is not yet possible for all climate variables for a variety of reasons. Some variables respond less strongly to external forcing, or are less reliably modelled or observed. In these cases, research that describes observed changes and offers physical explanations, for example, by demonstrating links to sea surface temperature changes, contributes substantially to the understanding of climate change and is therefore discussed in this chapter.

The approaches used in detection and attribution research described above cannot fully account for all uncertainties, and thus ultimately expert judgement is required to give a calibrated assessment of whether a specific cause is responsible for a given climate change. The assessment approach used in this chapter is to consider results from multiple studies using a variety of observational data sets, models, forcings and analysis techniques. The assessment based on these results typically takes into account the number of studies, the extent to which there is consensus among studies on the significance of detection results, the extent to which there is consensus on the consistency between the observed change and the change expected from forcing, the degree of consistency with other types of evidence, the extent to which known uncertainties are accounted for in and between studies, and whether there might be other physically plausible explanations for the given climate change. Having determined a particular likelihood assessment, this was then further downweighted to take into account any remaining uncertainties, such as, for example, structural uncertainties or a limited exploration of possible forcing histories of uncertain forcings. The overall assessment also considers whether several independent lines of evidence strengthen a result.

While the approach used in most detection studies assessed in this chapter is to determine whether observations exhibit the expected response to external forcing, for many decision makers a question posed in a different way may be more relevant. For instance, they may ask, 'Are the continuing drier-than-normal conditions in the Sahel due to human causes?' Such questions are difficult to respond to because of a statistical phenomenon known as 'selection bias'. The fact that the questions are 'self selected' from the observations (only large observed climate anomalies in a historical context would be likely to be the subject of such a question) makes it difficult to assess their statistical significance from the same observations (see, e.g., von Storch and Zwiers, 1999). Nevertheless, there is a need for answers to such questions, and examples of studies that attempt to do so are discussed in this chapter (e.g., see Section 9.4.3.3).

9.1.3 The Basis from which We Begin

Evidence of a human influence on the recent evolution of the climate has accumulated steadily during the past two decades. The first IPCC Assessment Report (IPCC, 1990) contained little observational evidence of a detectable anthropogenic influence on climate. However, six years later the IPCC Working Group I SAR (IPCC, 1996) concluded that 'the balance of evidence' suggested there had been a 'discernible' human influence on the climate of the 20th century. Considerably more evidence accumulated during the subsequent five years, such that the TAR (IPCC, 2001) was able to draw a much stronger conclusion, not just on the detectability of a human influence, but on its contribution to climate change during the 20th century.

The evidence that was available at the time of the TAR was considerable. Using results from a range of detection studies of the instrumental record, which was assessed using fingerprints and estimates of internal climate variability from several climate models, it was found that the warming over the 20th century was 'very unlikely to be due to internal variability alone as estimated by current models'.

Simulations of global mean 20th-century temperature change that accounted for anthropogenic greenhouse gases and sulphate aerosols as well as solar and volcanic forcing were found to be generally consistent with observations. In contrast, a limited number of simulations of the response to known natural forcings alone indicated that these may have contributed to the observed warming in the first half of the 20th century, but could not provide an adequate explanation of the warming in the second half of the 20th century, nor the observed changes in the vertical structure of the atmosphere.

Attribution studies had begun to use techniques to determine whether there was evidence that the responses to several different forcing agents were simultaneously present in observations, mainly of surface temperature and of temperature in the free atmosphere. A distinct greenhouse gas signal was found to be detectable whether or not other external influences were explicitly considered, and the amplitude of the

simulated greenhouse gas response was generally found to be consistent with observationally based estimates on the scales that were considered. Also, in most studies, the estimated rate and magnitude of warming over the second half of the 20th century due to increasing greenhouse gas concentrations alone was comparable with, or larger than, the observed warming. This result was found to be robust to attempts to account for uncertainties, such as observational uncertainty and sampling error in estimates of the response to external forcing, as well as differences in assumptions and analysis techniques.

The TAR also reported on a range of evidence of qualitative consistencies between observed climate changes and model responses to anthropogenic forcing, including global temperature rise, increasing land-ocean temperature contrast, diminishing arctic sea ice extent, glacial retreat and increases in precipitation at high northern latitudes.

A number of uncertainties remained at the time of the TAR. For example, large uncertainties remained in estimates of internal climate variability. However, even substantially inflated (doubled or more) estimates of model-simulated internal variance were found unlikely to be large enough to nullify the detection of an anthropogenic influence on climate. Uncertainties in external forcing were also reported, particularly in anthropogenic aerosol, solar and volcanic forcing, and in the magnitude of the corresponding climate responses. These uncertainties contributed to uncertainties in detection and attribution studies. Particularly, estimates of the contribution to the 20th-century warming by natural forcings and anthropogenic forcings other than greenhouse gases showed some discrepancies with climate simulations and were model dependent. These results made it difficult to attribute the observed climate change to one specific combination of external influences.

Based on the available studies and understanding of the uncertainties, the TAR concluded that 'in the light of new evidence and taking into account the remaining uncertainties, most of the observed warming over the last 50 years is likely to have been due to the increase in greenhouse gas concentrations'. Since the TAR, a larger number of model simulations using more complete forcings have become available, evidence on a wider range of variables has been analysed and many important uncertainties have been further explored and in many cases reduced. These advances are assessed in this chapter.

9.2 Radiative Forcing and Climate Response

This section briefly summarises the understanding of radiative forcing based on the assessment in Chapter 2, and of the climate response to forcing. Uncertainties in the forcing and estimates of climate response, and their implications for understanding and attributing climate change are also discussed. The discussion of radiative forcing focuses primarily on the period since 1750, with a brief reference to periods in the more distant past that are also assessed in the chapter, such as the last millennium, the Last Glacial Maximum and the mid-Holocene.

Two basic types of calculations have been used in detection and attribution studies. The first uses best estimates of forcing together with best estimates of modelled climate processes to calculate the effects of external changes in the climate system (forcings) on the climate (the response). These 'forward calculations' can then be directly compared to the observed changes in the climate system. Uncertainties in these simulations result from uncertainties in the radiative forcings that are used, and from model uncertainties that affect the simulated response to the forcings. Forward calculations are explored in this chapter and compared to observed climate change.

Results from forward calculations are used for formal detection and attribution analyses. In such studies, a climate model is used to calculate response patterns ('fingerprints') for individual forcings or sets of forcings, which are then combined linearly to provide the best fit to the observations. This procedure assumes that the amplitude of the large-scale pattern of response scales linearly with the forcing, and that patterns from different forcings can be added to obtain the total response. This assumption may not hold for every forcing, particularly not at smaller spatial scales, and may be violated when forcings interact nonlinearly (e.g., black carbon absorption decreases cloudiness and thereby decreases the indirect effects of sulphate aerosols). Generally, however, the assumption is expected to hold for most forcings (e.g., Penner et al., 1997; Meehl et al., 2004). Errors or uncertainties in the magnitude of the forcing or the magnitude of a model's response to the forcing should not affect detection results provided that the space-time pattern of the response is correct. However, for the linear combination of responses to be considered consistent with the observations, the scaling factors for individual response patterns should indicate that the model does not need to be rescaled to match the observations (Sections 9.1.2, 9.4.1.4 and Appendix 9.A) given uncertainty in the amplitude of forcing, model response and estimate due to internal climate variability. For detection studies, if the space-time pattern of response is incorrect, then the scaling, and hence detection and attribution results, will be affected.

In the second type of calculation, the so-called 'inverse' calculations, the magnitude of uncertain parameters in the forward model (including the forcing that is applied) is varied in order to provide a best fit to the observational record. In general, the greater the degree of *a priori* uncertainty in the parameters of the model, the more the model is allowed to adjust. Probabilistic posterior estimates for model parameters and uncertain forcings are obtained by comparing the agreement between simulations and observations, and taking into account prior uncertainties (including those in observations; see Sections 9.2.1.2, 9.6 and Supplementary Material, Appendix 9.B).

9.2.1 Radiative Forcing Estimates Used to Simulate Climate Change

9.2.1.1 Summary of 'Forward' Estimates of Forcing for the Instrumental Period

Estimates of the radiative forcing (see Section 2.2 for a definition) since 1750 from forward model calculations and observations are reviewed in detail in Chapter 2 and provided in Table 2.12. Chapter 2 describes estimated forcing resulting from increases in long-lived greenhouse gases (carbon dioxide (CO_2), methane, nitrous oxide, halocarbons), decreases in stratospheric ozone, increases in tropospheric ozone, sulphate aerosols, nitrate aerosols, black carbon and organic matter from fossil fuel burning, biomass burning aerosols, mineral dust aerosols, land use change, indirect aerosol effects on clouds, aircraft cloud effects, solar variability, and stratospheric and tropospheric water vapour increases from methane and irrigation. An example of one model's implemented set of forcings is given in Figure 2.23. While some members of the MMD at PCMDI have included a nearly complete list of these forcings for the purpose of simulating the 20th-century climate (see Supplementary Material, Table S9.1), most detection studies to date have used model runs with a more limited set of forcings. The combined anthropogenic forcing from the estimates in Section 2.9.2 since 1750 is 1.6 W m^{-2}, with a 90% range of 0.6 to 2.4 W m^{-2}, indicating that it is extremely likely that humans have exerted a substantial warming influence on climate over that time period. The combined forcing by greenhouse gases plus ozone is 2.9 ± 0.3 W m^{-2} and the total aerosol forcing (combined direct and indirect 'cloud albedo' effect) is virtually certain to be negative and estimated to be –1.3 (90% uncertainty range of –2.2 to –0.5 W m^{-2}; see Section 2.9). In contrast, the direct radiative forcing due to increases in solar irradiance is estimated to be +0.12 (90% range from 0.06 to 0.3) W m^{-2}. In addition, Chapter 2 concludes that it is exceptionally unlikely that the combined natural (solar and volcanic) radiative forcing has had a warming influence comparable to that of the combined anthropogenic forcing over the period 1950 to 2005. As noted in Chapter 2, the estimated global average surface temperature response from these forcings may differ for a particular magnitude of forcing since all forcings do not have the same 'efficacy' (i.e., effectiveness at changing the surface temperature compared to CO_2; see Section 2.8). Thus, summing these forcings does not necessarily give an adequate estimate of the response in global average surface temperature.

9.2.1.2 Summary of 'Inverse' Estimates of Net Aerosol Forcing

Forward model approaches to estimating aerosol forcing are based on estimates of emissions and models of aerosol physics and chemistry. They directly resolve the separate contributions by various aerosol components and forcing mechanisms. This must be borne in mind when comparing results to those from inverse calculations (see Section 9.6 and Supplementary Material, Appendix 9.B for details), which, for example, infer the net aerosol forcing required to match climate model simulations with observations. These methods can be applied using a global average forcing and response, or using the spatial and temporal patterns of the climate response in order to increase the ability to distinguish between responses to different external forcings. Inverse methods have been used to constrain one or several uncertain radiative forcings (e.g., by aerosols), as well as climate sensitivity (Section 9.6) and other uncertain climate parameters (Wigley, 1989; Schlesinger and Ramankutty, 1992; Wigley et al., 1997; Andronova and Schlesinger, 2001; Forest et al., 2001, 2002; Harvey and Kaufmann, 2002; Knutti et al., 2002, 2003; Andronova et al., 2007; Forest et al., 2006; see Table 9.1 – Stott et al., 2006c). The reliability of the spatial and temporal patterns used is discussed in Sections 9.2.2.1 and 9.2.2.2.

In the past, forward calculations have been unable to rule out a total net negative radiative forcing over the 20th century (Boucher and Haywood, 2001). However, Section 2.9 updates the Boucher and Haywood analysis for current radiative forcing estimates since 1750 and shows that it is extemely likely that the combined anthropogenic RF is both positive and substantial (best estimate: +1.6 W m^{-2}). A net forcing close to zero would imply a very high value of climate sensitivity, and would be very difficult to reconcile with the observed increase in temperature (Sections 9.6 and 9.7). Inverse calculations yield only the 'net forcing', which includes all forcings that project on the fingerprint of the forcing that is estimated. For example, the response to tropospheric ozone forcing could project onto that for sulphate aerosol forcing. Therefore, differences between forward estimates and inverse estimates may have one of several causes, including (1) the magnitude of the forward model calculation is incorrect due to inadequate physics and/or chemistry, (2) the forward calculation has not evaluated all forcings and feedbacks or (3) other forcings project on the fingerprint of the forcing that is estimated in the inverse calculation.

Studies providing inverse estimates of aerosol forcing are compared in Table 9.1. One type of inverse method uses the ranges of climate change fingerprint scaling factors derived from detection and attribution analyses that attempt to separate the climate response to greenhouse gas forcing from the response to aerosol forcing and often from natural forcing as well (Gregory et al., 2002a; Stott et al., 2006c; see also Section 9.4.1.4). These provide the range of fingerprint magnitudes (e.g., for the combined temperature response to different aerosol forcings) that are consistent with observed climate change, and can therefore be used to infer the likely range of forcing that is consistent with the observed record. The separation between greenhouse gas and aerosol fingerprints exploits the fact that the forcing from well-mixed greenhouse gases is well known, and that errors in the model's transient sensitivity can therefore be separated from errors in aerosol forcing in the model (assuming that there are similar errors in a model's sensitivity to greenhouse gas and aerosol

Table 9.1. *Inverse estimates of aerosol forcing from detection and attribution studies and studies estimating equilibrium climate sensitivity (see Section 9.6 and Table 9.3 for details on studies). The 5 to 95% estimates for the range of aerosol forcing relate to total or net fossil-fuel related aerosol forcing (in W m^{-2}).*

	Forest et al. (2006)	Andronova and Schlesinger (2001)	Knutti et al. (2002, 2003)	Gregory et al. (2002a)	Stott et al. (2006c)	Harvey and Kaufmann (2002)
Observational data used to constrain aerosol forcing	Upper air, surface and deep ocean space-time temperature, latter half of 20th century	Global mean and hemispheric difference in surface air temperature 1856 to 1997	Global mean ocean heat uptake 1955 to 1995, global mean surface air temperature increase 1860 to 2000	Surface air temperature space-time patterns, one AOGCM	Surface air temperature space-time patterns, three AOGCMs	Global mean and hemispheric difference in surface air temperature 1856 to 2000
Forcings considered[a]	G, Sul, Sol, Vol, OzS, land surface changes	G, OzT, Sul, Sol, Vol	G, Sul, Suli, OzT, OzS, BC+OM, stratospheric water vapour, Vol, Sol	G, Sul, Suli, Sol, Vol	G, Sul, Suli, OzT, OzS, Sol, Vol	G, Sul, biomass aerosol, Sol, Vol
Year[b]	1980s	1990	2000	2000	2000	1990
Aerosol forcing (W m^{-2})[c]	–0.14 to –0.74 –0.07 to –0.65 with expert prior	–0.54 to –1.3	0 to –1.2 indirect aerosol –0.6 to –1.7 total aerosol	–0.4 to –1.6 total aerosol	–0.4 to –1.4 total aerosol	Fossil fuel aerosol unlikely < –1, biomass plus dust unlikely < –0.5[d]

Notes:

[a] G: greenhouse gases; Sul: direct sulphate aerosol effect; Suli: (first) indirect sulphate aerosol effect; OzT: tropospheric ozone; OzS: stratospheric ozone; Vol: volcanic forcing; Sol: solar forcing; BC+OM: black carbon and organic matter from fossil fuel and biomass burning.

[b] Year(s) for which aerosol forcing is calculated, relative to pre-industrial conditions.

[c] 5 to 95% inverse estimate of the total aerosol forcing in the year given relative to pre-industrial forcing. The aerosol range refers to the net fossil-fuel related aerosol range, which tends to be all forcings not directly accounted for that project onto the pattern associated with fossil fuel aerosols, and includes all unknown forcings and those not explicitly considered (for example, OzT and BC+OM in several of the studies).

[d] Explores IPCC TAR range of climate sensitivity (i.e., 1.5°C to 4.5°C), while other studies explore wider ranges

forcing; see Gregory et al., 2002a; Table 9.1). By scaling spatio-temporal patterns of response up or down, this technique takes account of gross model errors in climate sensitivity and net aerosol forcing but does not fully account for modelling uncertainty in the patterns of temperature response to uncertain forcings.

Another approach uses the response of climate models, most often simple climate models or Earth System Models of Intermediate Complexity (EMICs, Table 8.3**)** to explore the range of forcings and climate parameters that yield results consistent with observations (Andronova and Schlesinger, 2001; Forest et al., 2002; Harvey and Kaufmann, 2002; Knutti et al., 2002, 2003; Forest et al., 2006). Like detection methods, these approaches seek to fit the space-time patterns, or spatial means in time, of observed surface, atmospheric or ocean temperatures. They determine the probability of combinations of climate sensitivity and net aerosol forcing based on the fit between simulations and observations (see Section 9.6 and Supplementary Material, Appendix 9.B for further discussion). These are often based on Bayesian approaches, where prior assumptions about ranges of external forcing are used to constrain the estimated net aerosol forcing and climate sensitivity. Some of these studies use the difference between Northern and Southern Hemisphere mean temperature to separate the greenhouse gas and aerosol forcing effects (e.g., Andronova and Schlesinger, 2001; Harvey and Kaufmann, 2002). In these analyses, it is necessary to accurately account for hemispheric asymmetry in tropospheric ozone forcing in order to infer the hemispheric aerosol forcing. Additionally, aerosols from biomass burning could cause an important fraction of the total aerosol forcing although this forcing shows little hemispheric asymmetry. Since it therefore projects on the greenhouse gas forcing, it is difficult to separate in an inverse calculation. Overall, results will be only as good as the spatial or temporal pattern that is assumed in the analysis. Missing forcings or lack of knowledge about uncertainties, and the highly parametrized spatial distribution of response in some of these models may hamper the interpretation of results.

Aerosol forcing appears to have grown rapidly during the period from 1945 to 1980, while greenhouse gas forcing

grew more slowly (Ramaswamy et al., 2001). Global sulphur emissions (and thus sulphate aerosol forcing) appear to have decreased after 1980 (Stern, 2005), further rendering the temporal evolution of aerosols and greenhouse gases distinct. As long as the temporal pattern of variation in aerosol forcing is approximately correct, the need to achieve a reasonable fit to the temporal variation in global mean temperature and the difference between Northern and Southern Hemisphere temperatures can provide a useful constraint on the net aerosol radiative forcing (as demonstrated, e.g., by Harvey and Kaufmann, 2002; Stott et al., 2006c).

The inverse estimates summarised in Table 9.1 suggest that to be consistent with observed warming, the net aerosol forcing over the 20th century should be negative with likely ranges between –1.7 and –0.1 W m^{-2}. This assessment accounts for the probability of other forcings projecting onto the fingerprints. These results typically provide a somewhat smaller upper limit for the total aerosol forcing than the estimates given in Chapter 2, which are derived from forward calculations and range between –2.2 and –0.5 W m^{-2} (5 to 95% range, median –1.3 W m^{-2}). Note that the uncertainty ranges from inverse and forward calculations are different due to the use of different information, and that they are affected by different uncertainties. Nevertheless, the similarity between results from inverse and forward estimates of aerosol forcing strengthens confidence in estimates of total aerosol forcing, despite remaining uncertainties. Harvey and Kaufmann (2002), who use an approach that focuses on the TAR range of climate sensitivity, further conclude that global mean forcing from fossil-fuel related aerosols was probably less than –1.0 W m^{-2} in 1990 and that global mean forcing from biomass burning and anthropogenically enhanced soil dust aerosols is 'unlikely' to have exceeded –0.5 W m^{-2} in 1990.

9.2.1.3 Radiative Forcing of Pre-Industrial Climate Change

Here we briefly discuss the radiative forcing estimates used for understanding climate during the last millennium, the mid-Holocene and the Last Glacial Maximum (LGM) (Section 9.3) and in estimates of climate sensitivity based on palaeoclimatic records (Section 9.6.3).

Regular variation in the Earth's orbital parameters has been identified as the pacemaker of climate change on the glacial to interglacial time scale (see Berger, 1988 for a review). These orbital variations, which can be calculated from astronomical laws (Berger, 1978), force climate variations by changing the seasonal and latitudinal distribution of solar radiation (Chapter 6).

Insolation at the time of the LGM (21 ka) was similar to today. Nonetheless, the LGM climate remained cold due to the presence of large ice sheets in the Northern Hemisphere (Peltier, 1994, 2004) and reduced atmospheric CO_2 concentration (185 ppm according to recent ice core estimates, see Monnin et al., 2001). Most modelling studies of this period do not treat ice sheet extent and elevation or CO_2 concentration prognostically, but specify them as boundary conditions. The LGM radiative forcing from the reduced atmospheric concentrations of well-mixed greenhouse gases is likely to have been about –2.8 W m^{-2} (see Figure 6.5). Ice sheet albedo forcing is estimated to have caused a global mean forcing of about –3.2 W m^{-2} (based on a range of several LGM simulations) and radiative forcing from increased atmospheric aerosols (primarily dust and vegetation) is estimated to have been about –1 W m^{-2} each. Therefore, the total annual and global mean radiative forcing during the LGM is likely to have been approximately –8 W m^{-2} relative to 1750, with large seasonal and geographical variations and significant uncertainties (see Section 6.4.1).

The major mid-Holocene forcing relative to the present was due to orbital perturbations that led to large changes in the seasonal cycle of insolation. The Northern Hemisphere (NH) seasonal cycle was about 27 W m^{-2} greater, whereas there was only a negligible change in NH annual mean solar forcing. For the Southern Hemisphere (SH), the seasonal forcing was –6.5 W m^{-2}. In contrast, the global and annual mean net forcing was only 0.011 W m^{-2}.

Changes in the Earth's orbit have had little impact on annual mean insolation over the past millennium. Summer insolation decreased by 0.33 W m^{-2} at 45°N over the millennium, winter insolation increased by 0.83 W m^{-2} (Goosse et al., 2005), and the magnitude of the mean seasonal cycle of insolation in the NH decreased by 0.4 W m^{-2}. Changes in insolation are also thought to have arisen from small variations in solar irradiance, although both timing and magnitude of past solar radiation fluctuations are highly uncertain (see Chapters 2 and 6; Lean et al., 2002; Gray et al., 2005; Foukal et al., 2006). For example, sunspots were generally missing from approximately 1675 to 1715 (the so-called Maunder Minimum) and thus solar irradiance is thought to have been reduced during this period. The estimated difference between the present-day solar irradiance cycle mean and the Maunder Minimum is 0.08% (see Section 2.7.1.2.2), which corresponds to a radiative forcing of about 0.2 W m^{-2}, which is substantially lower than estimates used in the TAR (Chapter 2).

Natural external forcing also results from explosive volcanism that introduces aerosols into the stratosphere (Section 2.7.2), leading to a global negative forcing during the year following the eruption. Several reconstructions are available for the last two millennia and have been used to force climate models (Section 6.6.3). There is close agreement on the timing of large eruptions in the various compilations of historic volcanic activity, but large uncertainty in the magnitude of individual eruptions (Figure 6.13). Different reconstructions identify similar periods when eruptions happened more frequently. The uncertainty in the overall amplitude of the reconstruction of volcanic forcing is also important for quantifying the influence of volcanism on temperature reconstructions over longer periods, but is difficult to quantify and may be a substantial fraction of the best estimate (e.g., Hegerl et al., 2006a).

9.2.2 Spatial and Temporal Patterns of the Response to Different Forcings and their Uncertainties

9.2.2.1 Spatial and Temporal Patterns of Response

The ability to distinguish between climate responses to different external forcing factors in observations depends on the extent to which those responses are distinct (see, e.g., Section 9.4.1.4 and Appendix 9.A). Figure 9.1 illustrates the zonal average temperature response in the PCM model (see Table 8.1 for model details) to several different forcing agents over the last 100 years, while Figure 9.2 illustrates the zonal average temperature response in the Commonwealth Scientific and Industrial Research Organisation (CSIRO) atmospheric model (when coupled to a simple mixed layer ocean model) to fossil fuel black carbon and organic matter, and to the combined effect of these forcings together with biomass burning aerosols (Penner et al., 2007). These figures indicate that the modelled vertical and zonal average signature of the temperature response should depend on the forcings. The major features shown in Figure 9.1 are robust to using different climate models. On the other hand, the response to black carbon forcing has not been widely examined and therefore the features in Figure 9.2 may be model dependent. Nevertheless, the response to black carbon forcings appears to be small.

Greenhouse gas forcing is expected to produce warming in the troposphere, cooling in the stratosphere, and, for transient simulations, somewhat more warming near the surface in the NH due to its larger land fraction, which has a shorter surface response time to the warming than do ocean regions (Figure 9.1c). The spatial pattern of the transient surface temperature response to greenhouse gas forcing also typically exhibits a land-sea pattern of stronger warming over land, for the same reason (e.g., Cubasch et al., 2001). Sulphate aerosol forcing results in cooling throughout most of the globe, with greater cooling in the NH due to its higher aerosol loading (Figure 9.1e; see Chapter 2), thereby partially offsetting the greater NH greenhouse-gas induced warming. The combined effect of tropospheric and stratospheric ozone forcing (Figure 9.1d) is expected to warm the troposphere, due to increases in tropospheric ozone, and cool the stratosphere, particularly at high latitudes where stratospheric ozone loss has been greatest. Greenhouse gas forcing is also expected to change the hydrological cycle worldwide, leading to disproportionately greater increases in heavy precipitation (Chapter 10 and Section 9.5.4), while aerosol forcing can influence rainfall regionally (Section 9.5.4).

The simulated responses to natural forcing are distinct from those due to the anthropogenic forcings described above. Solar forcing results in a general warming of the atmosphere (Figure 9.1a) with a pattern of surface warming that is similar to that expected from greenhouse gas warming, but in contrast to the response to greenhouse warming, the simulated solar-forced warming extends throughout the atmosphere (see, e.g., Cubasch et al., 1997). A number of independent analyses have identified tropospheric changes that appear to be associated with the solar cycle (van Loon and Shea, 2000; Gleisner and Thejll, 2003; Haigh, 2003; White et al., 2003; Coughlin and Tung, 2004; Labitzke, 2004; Crooks and Gray, 2005), suggesting an overall warmer and moister troposphere during solar maximum. The peak-to-trough amplitude of the response to the solar cycle globally is estimated to be approximately 0.1°C near the surface. Such variations over the 11-year solar cycle make it is necessary to use several decades of data in detection and attribution studies. The solar cycle also affects atmospheric ozone concentrations with possible impacts on temperatures and winds in the stratosphere, and has been hypothesised to influence clouds through cosmic rays (Section 2.7.1.3). Note that there is substantial uncertainty in the identification of climate response to solar cycle variations because the satellite period is short relative to the solar cycle length, and because the response is difficult to separate from internal climate variations and the response to volcanic eruptions (Gray et al., 2005).

Volcanic sulphur dioxide (SO_2) emissions ejected into the stratosphere form sulphate aerosols and lead to a forcing that causes a surface and tropospheric cooling and a stratospheric warming that peak several months after a volcanic eruption and last for several years. Volcanic forcing also likely leads to a response in the atmospheric circulation in boreal winter (discussed below) and a reduction in land precipitation (Robock and Liu, 1994; Broccoli et al., 2003; Gillett et al., 2004b). The response to volcanic forcing causes a net cooling over the 20th century because of variations in the frequency and intensity of volcanic eruptions. This results in stronger volcanic forcing towards the end of the 20th century than early in the 20th century. In the PCM, this increase results in a small warming in the lower stratosphere and near the surface at high latitudes, with cooling elsewhere (Figure 9.1b).

The net effect of all forcings combined is a pattern of NH temperature change near the surface that is dominated by the positive forcings (primarily greenhouse gases), and cooling in the stratosphere that results predominantly from greenhouse gas and stratospheric ozone forcing (Figure 9.1f). Results obtained with the CSIRO model (Figure 9.2) suggest that black carbon, organic matter and biomass aerosols would slightly enhance the NH warming shown in Figure 9.1f. On the other hand, indirect aerosol forcing from fossil fuel aerosols may be larger than the direct effects that are represented in the CSIRO and PCM models, in which case the NH warming could be somewhat diminished. Also, while land use change may cause substantial forcing regionally and seasonally, its forcing and response are expected to have only a small impact at large spatial scales (Sections 9.3.3.3 and 7.2.2; Figures 2.20 and 2.23).

The spatial signature of a climate model's response is seldom very similar to that of the forcing, due in part to the strength of the feedbacks relative to the initial forcing. This comes about because climate system feedbacks vary spatially and because the atmospheric and ocean circulation cause a redistribution of energy over the globe. For example, sea ice albedo feedbacks

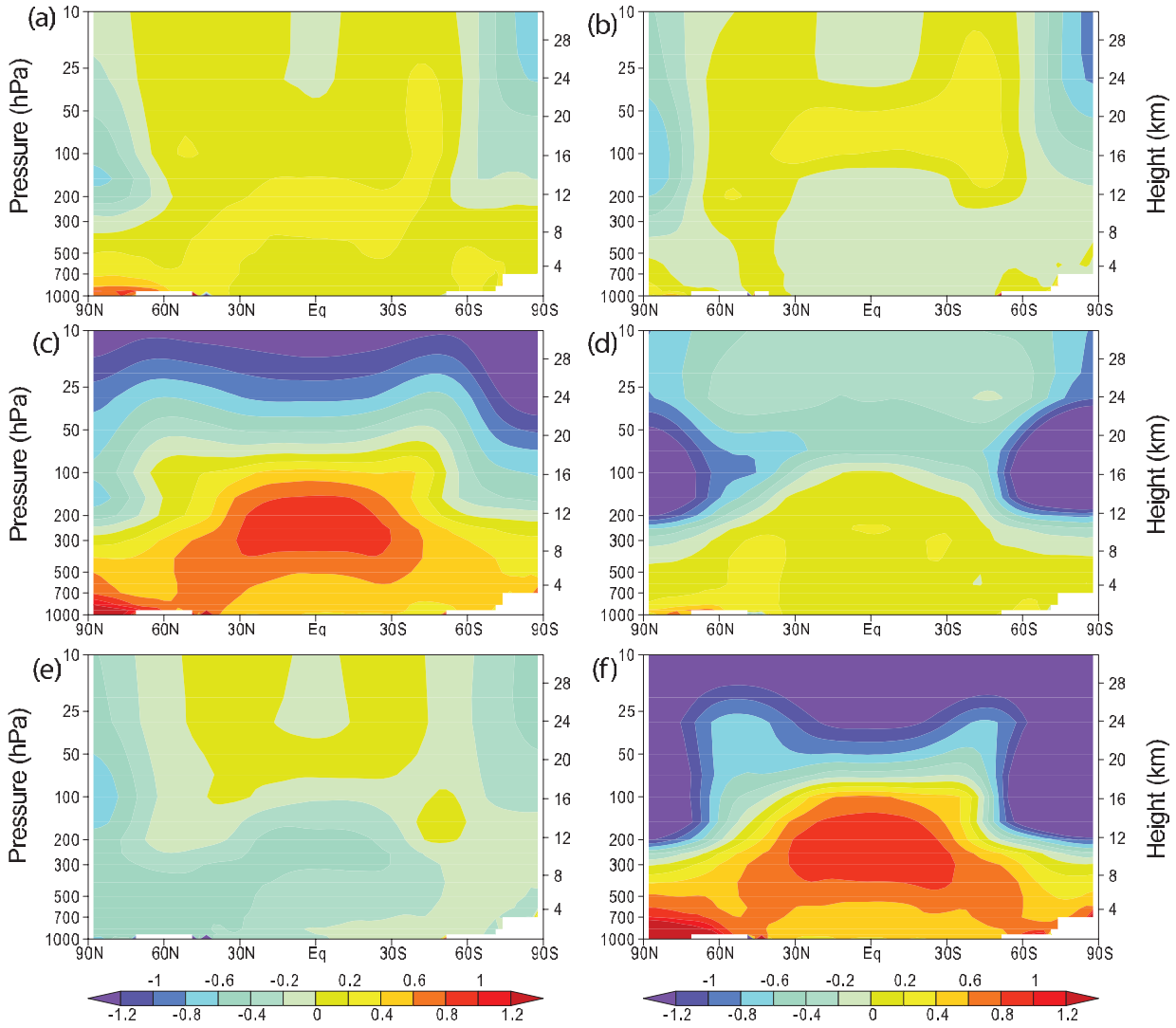


Figure 9.1. *Zonal mean atmospheric temperature change from 1890 to 1999 (°C per century) as simulated by the PCM model from (a) solar forcing, (b) volcanoes, (c) well-mixed greenhouse gases, (d) tropospheric and stratospheric ozone changes, (e) direct sulphate aerosol forcing and (f) the sum of all forcings. Plot is from 1,000 hPa to 10 hPa (shown on left scale) and from 0 km to 30 km (shown on right). See Appendix 9.C for additional information. Based on Santer et al. (2003a).*

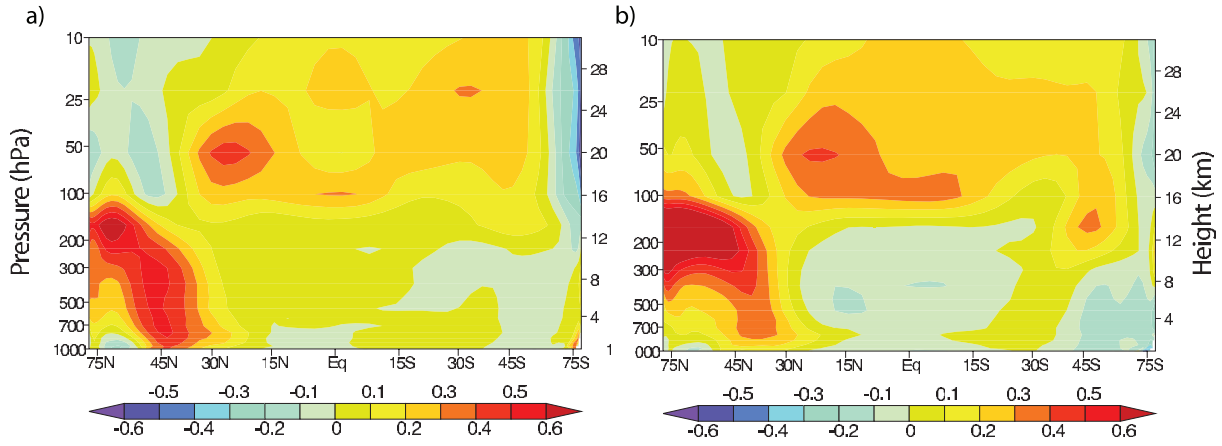


Figure 9.2. *The zonal mean equilibrium temperature change (°C) between a present day minus a pre-industrial simulation by the CSIRO atmospheric model coupled to a mixed-layer ocean model from (a) direct forcing from fossil fuel black carbon and organic matter (BC+OM) and (b) the sum of fossil fuel BC+OM and biomass burning. Plot is from 1,000 hPa to 10 hPa (shown on left scale) and from 0 km to 30 km (shown on right). Note the difference in colour scale from Figure 9.1. See Supplementary Material, Appendix 9.C for additional information. Based on Penner et al. (2007).*

tend to enhance the high-latitude response of both a positive forcing, such as that of CO_2, and a negative forcing such as that of sulphate aerosol (e.g., Mitchell et al., 2001; Rotstayn and Penner, 2001). Cloud feedbacks can affect both the spatial signature of the response to a given forcing and the sign of the change in temperature relative to the sign of the radiative forcing (Section 8.6). Heating by black carbon, for example, can decrease cloudiness (Ackerman et al., 2000). If the black carbon is near the surface, it may increase surface temperatures, while at higher altitudes it may reduce surface temperatures (Hansen et al., 1997; Penner et al., 2003). Feedbacks can also lead to differences in the response of different models to a given forcing agent, since the spatial response of a climate model to forcing depends on its representation of these feedbacks and processes. Additional factors that affect the spatial pattern of response include differences in thermal inertia between land and sea areas, and the lifetimes of the various forcing agents. Shorter-lived agents, such as aerosols, tend to have a more distinct spatial pattern of forcing, and can therefore be expected to have some locally distinct response features.

The pattern of response to a radiative forcing can also be altered quite substantially if the atmospheric circulation is affected by the forcing. Modelling studies and data comparisons suggest that volcanic aerosols (e.g., Kirchner et al., 1999; Shindell et al., 1999; Yang and Schlesinger, 2001; Stenchikov et al., 2006) and greenhouse gas changes (e.g., Fyfe et al., 1999; Shindell et al., 1999; Rauthe et al., 2004) can alter the North Atlantic Oscillation (NAO) or the Northern Annular Mode (NAM). For example, volcanic eruptions, with the exception of high-latitude eruptions, are often followed by a positive phase of the NAM or NAO (e.g., Stenchikov et al., 2006) leading to Eurasian winter warming that may reduce the overall cooling effect of volcanic eruptions on annual averages, particularly over Eurasia (Perlwitz and Graf, 2001; Stenchikov et al., 2002; Shindell et al., 2003; Stenchikov et al., 2004; Oman et al., 2005; Rind et al., 2005a; Miller et al., 2006; Stenchikov et al., 2006). In contrast, NAM or NAO responses to solar forcing vary between studies, some indicating a response, perhaps with dependence of the response on season or other conditions, and some finding no changes (Shindell et al., 2001a,b; Ruzmaikin and Feynman, 2002; Tourpali et al., 2003; Egorova et al., 2004; Palmer et al., 2004; Stendel et al., 2006; see also review in Gray et al., 2005).

In addition to the spatial pattern, the temporal evolution of the different forcings (Figure 2.23) generally helps to distinguish between the responses to different forcings. For example, Santer et al. (1996b,c) point out that a temporal pattern in the hemispheric temperature contrast would be expected in the second half of the 20th century with the SH warming more than the NH for the first two decades of this period and the NH subsequently warming more than the SH, as a result of changes in the relative strengths of the greenhouse gas and aerosol forcings. However, it should be noted that the integrating effect of the oceans (Hasselmann, 1976) results in climate responses that are more similar in time between different forcings than the forcings are to each other, and that there are substantial uncertainties in the evolution of the hemispheric temperature contrasts associated with sulphate aerosol forcing.

9.2.2.2 *Aerosol Scattering and Cloud Feedback in Models and Observations*

One line of observational evidence that reflective aerosol forcing has been changing over time comes from satellite observations of changes in top-of-atmosphere outgoing shortwave radiation flux. Increases in the outgoing shortwave radiation flux can be caused by increases in reflecting aerosols, increases in clouds or a change in the vertical distribution of clouds and water vapour, or increases in surface albedo. Increases in aerosols and clouds can cause decreases in surface radiation fluxes and decreases in surface warming. There has been continuing interest in this possibility (Gilgen et al., 1998; Stanhill and Cohen, 2001; Liepert, 2002). Sometimes called 'global dimming', this phenomena has reversed since about 1990 (Pinker et al., 2005; Wielicki et al., 2005; Wild et al., 2005; Section 3.4.3), but over the entire period from 1984 to 2001, surface solar radiation has increased by about 0.16 W m^{-2} yr^{-1} on average (Pinker et al., 2005). Figure 9.3 shows the top-of-

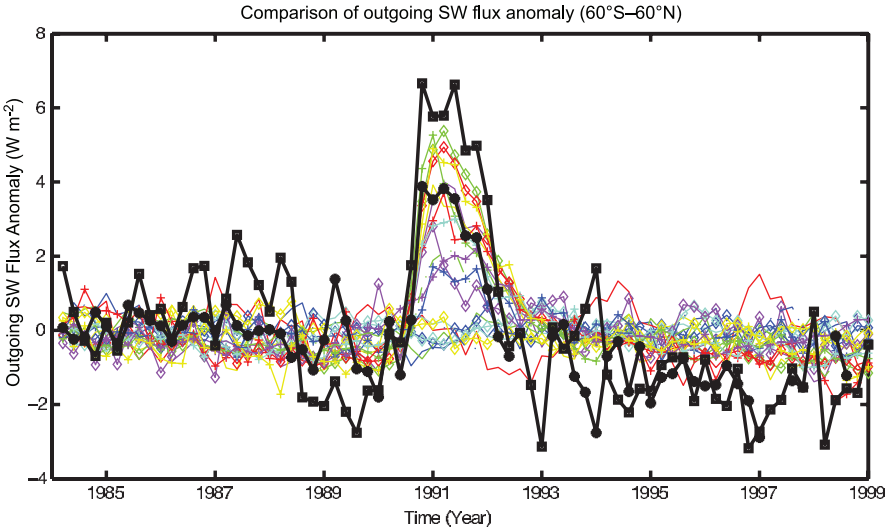


Figure 9.3. *Comparison of outgoing shortwave radiation flux anomalies (in W m^{-2}, calculated relative to the entire time period) from several models in the MMD archive at PCMDI (coloured curves) with ERBS satellite data (black with stars; Wong et al., 2006) and with the ISCCP flux data set (black with squares; Zhang et al., 2004). Models shown are CCSM3, CGCM3.1(T47), CGCM3.1(T63), CNRM-CM3, CSIRO-MK3.0, FGOALS-g1.0, GFDL-CM2.0, GFDL-CM2.1, GISS-AOM, GISS-EH, GISS-ER, INM-CM3.0, IPSL-CM4, and MRI-CGCM2.3.2 (see Table 8.1 for model details). The comparison is restricted to 60°S to 60°N because the ERBS data are considered more accurate in this region. Note that not all models included the volcanic forcing from Mt. Pinatubo (1991–1993) and so do not predict the observed increase in outgoing solar radiation. See Supplementary Material, Appendix 9.C for additional information.*

atmosphere outgoing shortwave radiation flux anomalies from the MMD at PCMDI, compared to that measured by the Earth Radiation Budget Satellite (ERBS; Wong et al., 2006) and inferred from International Satellite Cloud Climatology Project (ISCCP) flux data (FD) (Zhang et al., 2004). The downward trend in outgoing solar radiation is consistent with the long-term upward trend in surface radiation found by Pinker et al. (2005). The effect of the eruption of Mt. Pinatubo in 1991 results in an increase in the outgoing shortwave radiation flux (and a corresponding dimming at the surface) and its effect has been included in most (but not all) models in the MMD. The ISCCP flux anomaly for the Mt. Pinatubo signal is almost 2 W m^{-2} larger than that for ERBS, possibly due to the aliasing of the stratospheric aerosol signal into the ISCCP cloud properties. Overall, the trends from the ISCCP FD (–0.18 with 95% confidence limits of ±0.11 W m^{-2} yr^{-1}) and the ERBS data (–0.13 ± 0.08 W m^{-2} yr^{-1}) from 1984 to 1999 are not significantly different from each other at the 5% significance level, and are in even better agreement if only tropical latitudes are considered (Wong et al., 2006). These observations suggest an overall decrease in aerosols and/or clouds, while estimates of changes in cloudiness are uncertain (see Section 3.4.3). The model-predicted trends are also negative over this time period, but are smaller in most models than in the ERBS observations (which are considered more accurate than the ISCCP FD). Wielicki et al. (2002) explain the observed downward trend by decreases in cloudiness, which are not well represented in the models on these decadal time scales (Chen et al., 2002; Wielicki et al., 2002).

9.2.2.3 Uncertainty in the Spatial Pattern of Response

Most detection methods identify the magnitude of the space-time patterns of response to forcing (sometimes called 'fingerprints') that provide the best fit to the observations. The fingerprints are typically estimated from ensembles of climate model simulations forced with reconstructions of past forcing. Using different forcing reconstructions and climate models in such studies provides some indication of forcing and model uncertainty. However, few studies have examined how uncertainties in the spatial pattern of forcing explicitly contribute to uncertainties in the spatial pattern of the response. For short-lived components, uncertainties in the spatial pattern of forcing are related to uncertainties in emissions patterns, uncertainties in the transport within the climate model or chemical transport model and, especially for aerosols, uncertainties in the representation of relative humidities or clouds. These uncertainties affect the spatial pattern of the forcing. For example, the ratio of the SH to NH indirect aerosol forcing associated with the total aerosol forcing ranges from –0.12 to 0.63 (best guess 0.29) in different studies, and that between ocean and land forcing ranges from 0.03 to 1.85 (see Figure 7.21; Rotstayn and Penner, 2001; Chuang et al., 2002; Kristjansson, 2002; Lohmann and Lesins, 2002; Menon et al., 2002a; Rotstayn and Liu, 2003; Lohmann and Feichter, 2005).

9.2.2.4 Uncertainty in the Temporal Pattern of Response

Climate model studies have also not systematically explored the effect of uncertainties in the temporal evolution of forcings. These uncertainties depend mainly on the uncertainty in the spatio-temporal expression of emissions, and, for some forcings, fundamental understanding of the possible change over time.

The increasing forcing by greenhouse gases is relatively well known. In addition, the global temporal history of SO_2 emissions, which have a larger overall forcing than the other short-lived aerosol components, is quite well constrained. Seven different reconstructions of the temporal history of global anthropogenic sulphur emissions up to 1990 have a relative standard deviation of less than 20% between 1890 and 1990, with better agreement in more recent years. This robust temporal history increases confidence in results from detection and attribution studies that attempt to separate the effects of sulphate aerosol and greenhouse gas forcing (Section 9.4.1).

In contrast, there are large uncertainties related to the anthropogenic emissions of other short-lived compounds and their effects on forcing. For example, estimates of historical emissions from fossil fuel combustion do not account for changes in emission factors (the ratio of the emitted gas or aerosol to the fuel burned) of short-lived species associated with concerns over urban air pollution (e.g., van Aardenne et al., 2001). Changes in these emission factors would have slowed the emissions of nitrogen oxides as well as carbon monoxide after about 1970 and slowed the accompanying increase in tropospheric ozone compared to that represented by a single emission factor for fossil fuel use. In addition, changes in the height of SO_2 emissions associated with the implementation of tall stacks would have changed the lifetime of sulphate aerosols and the relationship between emissions and effects. Another example relates to the emissions of black carbon associated with the burning of fossil fuels. The spatial and temporal emissions of black carbon by continent reconstructed by Ito and Penner (2005) are significantly different from those reconstructed using the methodology of Novakov et al. (2003). For example, the emissions in Asia grow significantly faster in the inventory based on Novakov et al. (2003) compared to those based on Ito and Penner (2005). In addition, before 1988 the growth in emissions in Eastern Europe using the Ito and Penner (2005) inventory is faster than the growth based on the methodology of Novakov et al. (2003). Such spatial and temporal uncertainties will contribute to both spatial and temporal uncertainties in the net forcing and to spatial and temporal uncertainties in the distribution of forcing and response.

There are also large uncertainties in the magnitude of low-frequency changes in forcing associated with changes in total solar radiation as well as its spectral variation, particularly on time scales longer than the 11-year cycle. Previous estimates of change in total solar radiation have used sunspot numbers to calculate these slow changes in solar irradiance over the last few centuries, but these earlier estimates are not necessarily supported by current understanding and the estimated

magnitude of low-frequency changes has been substantially reduced since the TAR (Lean et al., 2002; Foukal et al., 2004, 2006; Sections 6.6.3.1 and 2.7.1.2). In addition, the magnitude of radiative forcing associated with major volcanic eruptions is uncertain and differs between reconstructions (Sato et al., 1993; Andronova et al., 1999; Ammann et al., 2003), although the timing of the eruptions is well documented.

9.2.3 Implications for Understanding 20th-Century Climate Change

Any assessment of observed climate change that compares simulated and observed responses will be affected by errors and uncertainties in the forcings prescribed in a climate model and its corresponding responses. As noted above, detection studies scale the response patterns to different forcings to obtain the best match to observations. Thus, errors in the magnitude of the forcing or in the magnitude of the model response to a forcing (which is approximately, although not exactly, a function of climate sensitivity), should not affect detection results provided that the large-scale space-time pattern of the response is correct. Attribution studies evaluate the consistency between the model-simulated amplitude of response and that inferred from observations. In the case of uncertain forcings, scaling factors provide information about the strength of the forcing (and response) needed to reproduce the observations, or about the possibility that the simulated pattern or strength of response is incorrect. However, for a model simulation to be considered consistent with the observations given forcing uncertainty, the forcing used in the model should remain consistent with the uncertainty bounds from forward model estimates of forcing.

Detection and attribution approaches that try to distinguish the response to several external forcings simultaneously may be affected by similarities in the pattern of response to different forcings and by uncertainties in forcing and response. Similarities between the responses to different forcings, particularly in the spatial patterns of response, make it more difficult to distinguish between responses to different external forcings, but also imply that the response patterns will be relatively insensitive to modest errors in the magnitude and distribution of the forcing. Differences between the temporal histories of different kinds of forcing (e.g., greenhouse gas versus sulphate aerosol) ameliorate the problem of the similarity between the spatial patterns of response considerably. For example, the spatial response of surface temperature to solar forcing resembles that due to anthropogenic greenhouse gas forcing (Weatherall and Manabe, 1975; Nesme-Ribes et al., 1993; Cubasch et al., 1997; Rind et al., 2004; Zorita et al., 2005). Distinct features of the vertical structure of the responses in the atmosphere to different types of forcing further help to distinguish between the different sources of forcing. Studies that interpret observed climate in subsequent sections use such strategies, and the overall assessment in this chapter uses results from a range of climate variables and observations.

Many detection studies attempt to identify in observations both temporal and spatial aspects of the temperature response to a given set of forcings because the combined space-time responses tend to be more distinct than either the space-only or the time-only patterns of response. Because the emissions and burdens of different forcing agents change with time, the net forcing and its rate of change vary with time. Although explicit accounting for uncertainties in the net forcing is not available (see discussion in Sections 9.2.2.3 and 9.2.2.4), models often employ different implementations of external forcing. Detection and attribution studies using such simulations suggest that results are not very sensitive to moderate forcing uncertainties. A further problem arises due to spurious temporal correlations between the responses to different forcings that arise from sampling variability. For example, spurious correlation between the climate responses to solar and volcanic forcing over parts of the 20th century (North and Stevens, 1998) can lead to misidentification of one as the other, as in Douglass and Clader (2002).

The spatial pattern of the temperature response to aerosol forcing is quite distinct from the spatial response pattern to CO_2 in some models and diagnostics (Hegerl et al., 1997), but less so in others (Reader and Boer, 1998; Tett et al., 1999; Hegerl et al., 2000; Harvey, 2004). If it is not possible to distinguish the spatial pattern of greenhouse warming from that of fossil-fuel related aerosol cooling, the observed warming over the last century could be explained by large greenhouse warming balanced by large aerosol cooling or alternatively by small greenhouse warming with very little or no aerosol cooling. Nevertheless, estimates of the amplitude of the response to greenhouse forcing in the 20th century from detection studies are quite similar, even though the simulated responses to aerosol forcing are model dependent (Gillett et al., 2002a; Hegerl and Allen, 2002). Considering three different climate models, Stott et al. (2006c) conclude that an important constraint on the possible range of responses to aerosol forcing is the temporal evolution of the global mean and hemispheric temperature contrast as was suggested by Santer et al. (1996a; see also Section 9.4.1.5).

9.2.4 Summary

The uncertainty in the magnitude and spatial pattern of forcing differs considerably between forcings. For example, well-mixed greenhouse gas forcing is relatively well constrained and spatially homogeneous. In contrast, uncertainties are large for many non-greenhouse gas forcings. Inverse model studies, which use methods closely related to those used in climate change detection research, indicate that the magnitude of the total net aerosol forcing has a likely range of –1.7 to –0.1 W m^{-2}. As summarised in Chapter 2, forward calculations of aerosol radiative forcing, which do not depend on knowledge of observed climate change or the ability of climate models to simulate the transient response to forcings, provide results (–2.2 to –0.5 W m^{-2}; 5 to 95%) that are quite consistent with inverse estimates; the uncertainty ranges from inverse and forward calculations are different due to the use of different information. The large uncertainty in total aerosol forcing makes it more difficult to accurately infer the climate sensitivity from observations (Section 9.6). It also increases uncertainties in

results that attribute cause to observed climate change (Section 9.4.1.4), and is in part responsible for differences in probabilistic projections of future climate change (Chapter 10). Forcings from black carbon, fossil fuel organic matter and biomass burning aerosols, which have not been considered in most detection studies performed to date, are likely small but with large uncertainties relative to the magnitudes of the forcings.

Uncertainties also differ between natural forcings and sometimes between different time scales for the same forcing. For example, while the 11-year solar forcing cycle is well documented, lower-frequency variations in solar forcing are highly uncertain. Furthermore, the physics of the response to solar forcing and some feedbacks are still poorly understood. In contrast, the timing and duration of forcing due to aerosols ejected into the stratosphere by large volcanic eruptions is well known during the instrumental period, although the magnitude of that forcing is uncertain.

Differences in the temporal evolution and sometimes the spatial pattern of climate response to external forcing make it possible, with limitations, to separate the response to these forcings in observations, such as the responses to greenhouse gas and sulphate aerosol forcing. In contrast, the climate response and temporal evolution of other anthropogenic forcings is more uncertain, making the simulation of the climate response and its detection in observations more difficult. The temporal evolution, and to some extent the spatial and vertical pattern, of the climate response to natural forcings is also quite different from that of anthropogenic forcing. This makes it possible to separate the climate response to solar and volcanic forcing from the response to anthropogenic forcing despite the uncertainty in the history of solar forcing noted above.

9.3 Understanding Pre-Industrial Climate Change

9.3.1 Why Consider Pre-Industrial Climate Change?

The Earth system has experienced large-scale climate changes in the past (Chapter 6) that hold important lessons for the understanding of present and future climate change. These changes resulted from natural external forcings that, in some instances, triggered strong feedbacks as in the case of the LGM (see Chapter 6). Past periods offer the potential to provide information not available from the instrumental record, which is affected by anthropogenic as well as natural external forcings and is too short to fully understand climate variability and major climate system feedbacks on inter-decadal and longer time scales. Indirect indicators ('proxy data' such as tree ring width and density) must be used to infer climate variations (Chapter 6) prior to the instrumental era (Chapter 3). A complete description of these data and of their uncertainties can be found in Chapter 6.

The discussion here is restricted to several periods in the past for which modelling and observational evidence can be compared to test understanding of the climate response to external forcings. One such period is the last millennium, which places the recent instrumental record in a broader context (e.g., Mitchell et al., 2001). The analysis of the past 1 kyr focuses mainly on the climate response to natural forcings (changes in solar radiation and volcanism) and on the role of anthropogenic forcing during the most recent part of the record. Two time periods analysed in the Paleoclimate Modelling Intercomparison Project (PMIP, Joussaume and Taylor, 1995; PMIP2, Harrison et al., 2002) are also considered, the mid-Holocene (6 ka) and the LGM (21 ka). Both periods had a substantially different climate compared to the present, and there is relatively good information from data synthesis and model simulation experiments (Braconnot et al., 2004; Cane et al., 2006). An increased number of simulations using EMICs or Atmosphere-Ocean General Circulation Models (AOGCMs) that are the same as, or related to, the models used in simulations of the climates of the 20th and 21st centuries are available for these periods.

9.3.2 What Can be Learned from the Last Glacial Maximum and the Mid-Holocene?

Relatively high-quality global terrestrial climate reconstructions exist for the LGM and the mid-Holocene and as part of the Global Palaeovegetation Mapping (BIOME 6000) project (Prentice and Webb, 1998; Prentice and Jolly, 2000). The Climate: Long-range Investigation, Mapping and Prediction (CLIMAP, 1981) reconstruction of LGM sea surface temperatures has also been improved (Chapter 6). The LGM climate was colder and drier than at present as is indicated by the extensive tundra and steppe vegetation that existed during this period. Most LGM proxy data suggest that the tropical oceans were colder by about 2°C than at present, and that the frontal zones in the SH and NH were shifted equatorward (Kucera et al., 2005), even though large differences are found between temperature estimates from the different proxies in the North Atlantic.

Several new AOGCM simulations of the LGM have been produced since the TAR. These simulations show a global cooling of approximately 3.5°C to 5.2°C when LGM greenhouse gas and ice sheet boundary conditions are specified (Chapter 6), which is within the range (–1.8°C to –6.5°C) of PMIP results from simpler models that were discussed in the TAR (McAvaney et al., 2001). Only one simulation exhibits a very strong response with a cooling of approximately 10°C (Kim et al., 2002). All of these simulations exhibit a strongly damped hydrological cycle relative to that of the modern climate, with less evaporation over the oceans and continental-scale drying over land. Changes in greenhouse gas concentrations may account for about half of the simulated tropical cooling (Shin et al., 2003), and for the production of colder and saltier water found at depth in the Southern Ocean (Liu et al., 2005). Most LGM simulations with coupled models shift the deep-water formation in the North

Atlantic southward, but large differences exist between models in the intensity of the Atlantic meridional overturning circulation. Including vegetation changes appears to improve the realism of LGM simulations (Wyputta and McAvaney, 2001). Furthermore, including the physiological effect of the atmospheric CO_2 concentration on vegetation has a non-negligible impact (Levis et al., 1999) and is necessary to properly represent changes in global forest (Harrison and Prentice, 2003) and terrestrial carbon storage (e.g., Kaplan et al., 2002; Joos et al., 2004; see also Chapter 6). To summarise, despite large uncertainties, LGM simulations capture the broad features found in palaeoclimate data, and better agreement is obtained with new coupled simulations using more recent models and more complete feedbacks from ocean, sea ice and land surface characteristics such as vegetation and soil moisture (Chapter 6).

Closer to the present, during the mid-Holocene, one of the most noticeable indications of climate change is the northward extension of northern temperate forest (Bigelow et al., 2003), which reflects warmer summers than at present. In the tropics the more vegetated conditions inferred from pollen records in the now dry sub-Saharan regions indicate wetter conditions due to enhanced summer monsoons (see Braconnot et al., 2004 for a review). Simulations of the mid-Holocene with AOGCMs (see Section 9.2.1.3 for forcing) produce an amplification of the mean seasonal cycle of temperature of approximately 0.5°C to 0.7°C. This range is slightly smaller than that obtained using atmosphere-only models in PMIP1 (~0.5°C to ~1.2°C) due to the thermal response of the ocean (Braconnot et al., 2000). Simulated changes in the ocean circulation have strong seasonal features with an amplification of the sea surface temperature (SST) seasonal cycle of 1°C to 2°C in most places within the tropics (Zhao et al., 2005), influencing the Indian and African monsoons. Over West Africa, AOGCM-simulated changes in annual mean precipitation are about 5 to 10% larger than for atmosphere-only simulations, and in better agreement with data reconstructions (Braconnot et al., 2004). Results for the Indian and Southwest Asian monsoon are less consistent between models.

As noted in the TAR (McAvaney et al., 2001), vegetation change during the mid-Holocene likely triggered changes in the hydrological cycle, explaining the wet conditions that prevailed in the Sahel region that were further enhanced by ocean feedbacks (Ganopolski et al., 1998; Braconnot et al., 1999), although soil moisture may have counteracted some of these feedbacks (Levis et al., 2004). Wohlfahrt et al. (2004) show that at middle and high latitudes the vegetation and ocean feedbacks enhanced the warming in spring and autumn by about 0.8°C. However, models have a tendency to overestimate the mid-continental drying in Eurasia, which is further amplified when vegetation feedbacks are included (Wohlfahrt et al., 2004).

A wide range of proxies containing information about ENSO variability during the mid-Holocene is now also available (Section 6.5.3). These data suggest that ENSO variability was weaker than today prior to approximately 5 kyr before present (Moy et al., 2002 and references therein; Tudhope and Collins, 2003). Several studies have attempted to analyse these changes in interannual variability from model simulations. Even though some results are controversial, a consistent picture has emerged for the mid-Holocene, for which simulations produce reduced variability in precipitation over most ocean regions in the tropics (Liu et al., 2000; Braconnot et al., 2004; Zhao et al., 2005). Results obtained with the Cane-Zebiak model suggest that the Bjerknes (1969) feedback mechanism may be a key element of the ENSO response in that model. The increased mid-Holocene solar heating in boreal summer leads to more warming in the western than in the eastern Pacific, which strengthens the trade winds and inhibits the development of ENSO (Clement et al., 2000, 2004). Atmosphere-Ocean General Circulation Models also tend to simulate less intense ENSO events, in qualitative agreement with data, although there are large differences in magnitude and proposed mechanisms, and inconsistent responses of the associated teleconnections (Otto-Bliesner, 1999; Liu et al., 2000; Kitoh and Murakami, 2002; Otto-Bliesner et al., 2003).

9.3.3 What Can be Learned from the Past 1,000 Years?

External forcing relative to the present is generally small for the last millennium when compared to that for the mid-Holocene and LGM. Nonetheless, there is evidence that climatic responses to forcing, together with natural internal variability of the climate system, produced several well-defined climatic events, such as the cool conditions during the 17th century or relatively warm periods early in the millennium.

9.3.3.1 Evidence of External Influence on the Climate Over the Past 1,000 Years

A substantial number of proxy reconstructions of annual or decadal NH mean surface temperature are now available (see Figure 6.11, and the reviews by Jones et al., 2001 and Jones and Mann, 2004). Several new reconstructions have been published, some of which suggest larger variations over the last millennium than assessed in the TAR, but uncertainty remains in the magnitude of inter-decadal to inter-centennial variability. This uncertainty arises because different studies rely on different proxy data or use different reconstruction methods (Section 6.6.1). Nonetheless, NH mean temperatures in the second half of the 20th century were likely warmer than in any other 50-year period in the last 1.3 kyr (Chapter 6), and very likely warmer than any such period in the last 500 years. Temperatures subsequently decreased, and then rose rapidly during the most recent 100 years. This long-term tendency is punctuated by substantial shorter-term variability (Figure 6.10). For example, cooler conditions with temperatures 0.5°C to 1°C below the 20th-century mean value are found in the 17th and early 18th centuries.

A number of simulations of the last millennium (Figure 6.13) have been performed using a range of models, including some simulations with AOGCMs (e.g., Crowley, 2000; Goosse and Renssen, 2001; Bertrand et al., 2002; Bauer et al., 2003; Gerber

et al., 2003; see also Gonzalez-Rouco et al., 2003; Jones and Mann, 2004; Zorita et al., 2004; Weber, 2005; Tett et al., 2007). These simulations use different reconstructions of external forcing, particularly solar, volcanic and greenhouse gas forcing, and often include land use changes (e.g., Bertrand et al., 2002; Stendel et al., 2006; Tett et al., 2007). While the use of different models and forcing reconstructions leads to differences, the simulated evolution of the NH annual mean surface temperature displays some common characteristics between models that are consistent with the broad features of the data (Figures 6.13 and 9.4). For example, all simulations show relatively cold conditions during the period around 1675 to 1715 in response to natural forcing, which is in qualitative agreement with the proxy reconstructions. In all simulations shown in Figure 6.13, the late 20th century is warmer than any other multi-decadal period during the last millennium. In addition, there is significant correlation between simulated and reconstructed variability (e.g., Yoshimori et al., 2005). By comparing simulated and observed atmospheric CO_2 concentration during the last 1 kyr, Gerber et al. (2003) suggest that the amplitude of the temperature evolution simulated by simple climate models and EMICs is consistent with the observed evolution of CO_2. Since reconstructions of external forcing are virtually independent from the reconstructions of past temperatures, this broad consistency increases confidence in the broad features of the reconstructions and the understanding of the role of external forcing in recent climate variability. The simulations also show that it is not possible to reproduce the large 20th-century warming without anthropogenic forcing regardless of which solar or volcanic forcing reconstruction is used (Crowley, 2000; Bertrand et al., 2002; Bauer et al., 2003; Hegerl et al., 2003, 2007), stressing the impact of human activity on the recent warming.

While there is broad qualitative agreement between simulated and reconstructed temperatures, it is difficult to fully assess model-simulated variability because of uncertainty in the magnitude of historical variations in the reconstructions and differences in the sensitivity to external forcing (Table 8.2). The role of internal variability has been found to be smaller than that of the forced variability for hemispheric temperature means at decadal or longer time scales (Crowley, 2000; Hegerl et al., 2003; Goosse et al., 2004; Weber et al., 2004; Hegerl et al., 2007; Tett et al., 2007), and thus internal variability is a relatively small contributor to differences between different simulations of NH mean temperature. Other sources of uncertainty in simulations include model ocean initial conditions, which, for example, explain the warm conditions found in the Zorita et al. (2004) simulation during the first part of the millennium (Goosse et al., 2005; Osborn et al., 2006).

9.3.3.2 Role of Volcanism and Solar Irradiance

Volcanic eruptions cause rapid decreases in hemispheric and global mean temperatures followed by gradual recovery over several years (Section 9.2.2.1) in climate simulations driven by volcanic forcing (Figure 6.13; Crowley, 2000; Bertrand et al., 2002; Weber, 2005; Yoshimori et al., 2005; Tett et al., 2007). These simulated changes appear to correspond to cool episodes in proxy reconstructions (Figure 6.13). This suggestive correspondence has been confirmed in comparisons between composites of temperatures following multiple volcanic eruptions in simulations and reconstructions (Hegerl et al., 2003; Weber, 2005). In addition, changes in the frequency of large eruptions result in climate variability on decadal and possibly longer time scales (Crowley, 2000; Briffa et al., 2001; Bertrand et al., 2002; Bauer et al., 2003; Weber, 2005). Hegerl et al. (2003; 2007), using a multi-regression approach based on Energy Balance Model (EBM) simulated fingerprints of solar, volcanic and greenhouse gas forcing (Appendix 9.A.1; see also Section 9.4.1.4 for the 20th century), simultaneously detect the responses to volcanic and greenhouse gas forcing in a number of proxy reconstructions of average NH mean annual and growing season temperatures (Figure 9.4) with high significance. They find that a high percentage of decadal variance in the reconstructions used can be explained by external forcing (between 49 and 70% of decadal variance depending upon the reconstruction).

There is more uncertainty regarding the influence of solar forcing. In addition to substantial uncertainty in the timing and amplitude of solar variations on time scales of several decades to centuries, which has increased since the TAR although the estimate of solar forcing has been revised downwards (Sections 9.2.1.3 and 2.7.1), uncertainty also arises because the spatial response of surface temperature to solar forcing resembles that due to greenhouse gas forcing (Section 9.2.3). Analyses that make use of differences in the temporal evolution of solar and volcanic forcings are better able to distinguish between the two (Section 9.2.3; see also Section 9.4.1.5 for the 20th century). In such an analysis, solar forcing can only be detected and distinguished from the effect of volcanic and greenhouse gas forcing over some periods in some reconstructions (Hegerl et al., 2003, 2007), although the effect of solar forcing has been detected over parts of the 20th century in some time-space analyses (Section 9.4.1.5) and there are similarities between regressions of solar forcing on model simulations and several proxy reconstructions (Weber, 2005; see also Waple, 2002). A model simulation (Shindell et al., 2003) suggests that solar forcing may play a substantial role in regional anomalies due to dynamical feedbacks. These uncertainties in the contribution of different forcings to climatic events during the last millennium reflect substantial uncertainty in knowledge about past solar and volcanic forcing, as well as differences in the way these effects are taken into account in model simulations.

Overall, modelling and detection and attribution studies confirm a role of volcanic, greenhouse gas and probably solar forcing in explaining the broad temperature evolution of the last millennium, although the role of solar forcing has recently been questioned (Foukal et al., 2006). The variability that remains in proxy reconstructions after estimates of the responses to external forcing have been removed is broadly consistent with AOGCM-simulated internal variability (e.g., Hegerl et al., 2003, 2007), providing a useful check on AOGCMs even though

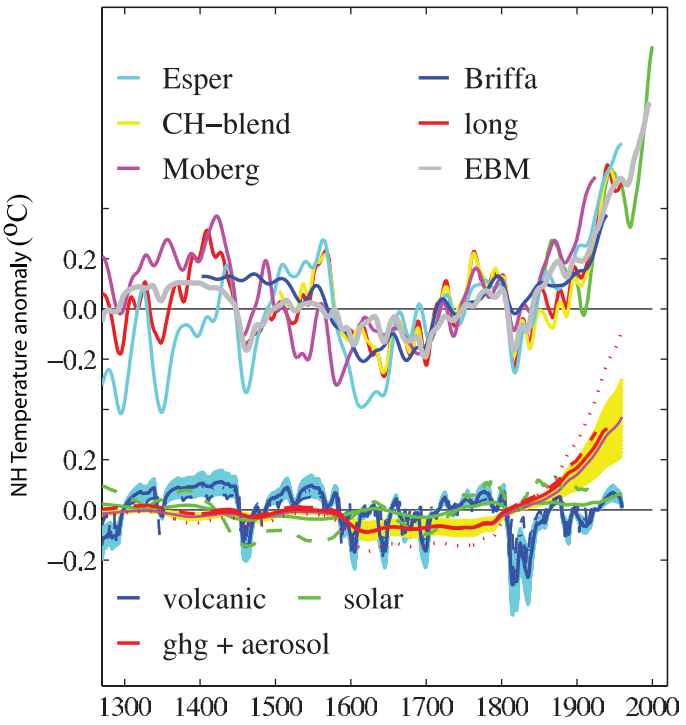


Figure 9.4. *Contribution of external forcing to several high-variance reconstructions of NH temperature anomalies, (Esper et al., 2002; Briffa et al., 2001; Hegerl et al., 2007, termed CH-blend and CH-blend long; and Moberg et al., 2005). The top panel compares reconstructions to an EBM simulation (equilibrium climate sensitivity of 2.5°C) of NH 30°N to 90°N average temperature, forced with volcanic, solar and anthropogenic forcing. All timeseries are centered on the 1500-1925 average. Instrumental temperature data are shown by a green line (centered to agree with CH-blend average over the period 1880-1960). The displayed data are low-pass filtered (20-year cutoff) for clarity. The bottom panel shows the estimated contribution of the response to volcanic (blue lines with blue uncertainty shade), solar (green) and greenhouse gas (GHG) and aerosol forcing (red line with yellow shades, aerosol only in 20th century) to each reconstruction (all timeseries are centered over the analysis period). The estimates are based on multiple regression of the reconstructions on fingerprints for individual forcings. The contributions to different reconstructions are indicated by different line styles (Briffa et al.: solid, fat; Esper et al.: dotted; Moberg: dashed; CH-blend: solid, thin; with shaded 90% confidence limits around best estimates for each detectable signal). All reconstructions show a highly significant volcanic signal, and all but Moberg et al. (which ends in 1925) show a detectable greenhouse gas signal at the 5% significance level. The latter shows a detectable greenhouse gas signal with less significance. Only Moberg et al. contains a detectable solar signal (only shown for these data and CH-blend, where it is not detectable). All data are decadally averaged. The reconstructions represent slightly different regions and seasons: Esper et al. (2002) is calibrated to 30°N to 90°N land temperature, CH-blend and CH-blend long (Hegerl et al., 2007) to 30°N to 90°N mean temperature and Moberg et al. (2005) to 0° to 90°N temperature. From Hegerl et al. (2007).*

uncertainties are large. Such studies also help to explain episodes during the climate of the last millennium. For example, several modelling studies suggest that volcanic activity has a dominant role in explaining the cold conditions that prevailed from 1675 to 1715 (Andronova et al., 2007; Yoshimori et al., 2005). In contrast, Rind et al. (2004) estimate from model simulations that the cooling relative to today was primarily associated with reduced greenhouse gas forcing, with a substantial contribution from solar forcing.

There is also some evidence from proxy data that the response to external forcing may influence modes of climate variability. For example, Cobb et al. (2003), using fossil corals, attempt to extend the ENSO record back through the last millennium. They find that ENSO events may have been as frequent and intense during the mid-17th century as during the instrumental period, with events possibly rivalling the strong 1997–1998 event. On the other hand, there are periods during the 12th and 14th centuries when there may have been significantly less ENSO variability, a period during which there were also cooler conditions in the northeast Pacific (MacDonald and Case, 2005) and evidence of droughts in central North America (Cook et al., 2004). Cobb et al. (2003) find that fluctuations in reconstructed ENSO variability do not appear to be correlated in an obvious way with mean state changes in the tropical Pacific or global mean climate, while Adams et al. (2003) find statistical evidence for an El Niño-like anomaly during the first few years following explosive tropical volcanic eruptions. The Cane-Zebiak model simulates changes similar to those in the Cobb et al. (2003) data when volcanism and solar forcing are accounted for, supporting the link with volcanic forcing over the past millennium (Mann et al., 2005). However, additional studies with different models are needed to fully assess this relationship, since previous work was less conclusive (Robock, 2000).

Extratropical variability also appears to respond to volcanic forcing. During the winter following a large volcanic eruption, the zonal circulation may be more intense, causing a relative warming over the continents during the cold season that could partly offset the direct cooling due to the volcanic aerosols (Sections 9.2.2.1 and 8.4.1; Robock, 2000; Shindell et al., 2003). A tendency towards the negative NAO state during periods of reduced solar input is found in some reconstructions of this pattern for the NH (Shindell et al., 2001b; Luterbacher et al., 2002, 2004; Stendel et al., 2006), possibly implying a solar forcing role in some long-term regional changes, such as the cooling over the NH continents around 1700 (Shindell et al., 2001b; Section 9.2.2). Indications of changes in ENSO variability during the low solar irradiance period of the 17th to early 18th centuries are controversial (e.g., D'Arrigo et al., 2005).

9.3.3.3 Other Forcings and Sources of Uncertainties

In addition to forcing uncertainties discussed above, a number of other uncertainties affect the understanding of pre-industrial climate change. For example, land cover change may have influenced the pre-industrial climate (Bertrand et al., 2002; Bauer et al., 2003), leading to a regional cooling of 1°C to 2°C in winter and spring over the major agricultural regions of North America and Eurasia in some model simulations, when pre-agriculture vegetation was replaced by present-day vegetation (Betts, 2001). The largest anthropogenic land cover changes involve deforestation (Chapter 2). The greatest proportion of deforestation has occurred in the temperate regions of the NH (Ramankutty and Foley, 1999; Goldewijk, 2001). Europe had cleared about 80% of its agricultural area by 1860, but over

half of the forest removal in North America took place after 1860 (Betts, 2001), mainly in the late 19th century (Stendel et al., 2006). During the past two decades, the CO_2 flux caused by land use changes has been dominated by tropical deforestation (Section 7.3.2.1.2). Climate model simulations suggest that the effect of land use change was likely small at hemispheric and global scales, estimated variously as –0.02°C relative to natural pre-agricultural vegetation (Betts, 2001), less than –0.1°C since 1700 (Stendel et al., 2006) and about –0.05°C over the 20th century and too small to be detected statistically in observed trends (Matthews et al., 2004). However, the latter authors did find a larger cooling effect since 1700 of between –0.06°C and –0.22°C when they explored the sensitivity to different representations of land cover change.

Oceanic processes and ocean-atmosphere interaction may also have played a role in the climate evolution during the last millennium (Delworth and Knutson, 2000; Weber et al., 2004; van der Schrier and Barkmeijer, 2005). Climate models generally simulate a weak to moderate increase in the intensity of the oceanic meridional overturning circulation in response to a decrease in solar irradiance (Cubasch et al., 1997; Goosse and Renssen, 2004; Weber et al., 2004). A delayed response to natural forcing due to the storage and transport of heat anomalies by the deep ocean has been proposed to explain the warm Southern Ocean around the 14th to 15th centuries (Goosse et al., 2004).

9.3.4 Summary

Considerable progress has been made since the TAR in understanding the response of the climate system to external forcings. Periods like the mid-Holocene and the LGM are now used as benchmarks for climate models that are used to simulate future climate (Chapter 6). While considerable uncertainties remain in the climate reconstructions for these periods, and in the boundary conditions used to force climate models, comparisons between simulated and reconstructed conditions in the LGM and mid-Holocene demonstrate that models capture the broad features of changes in the temperature and precipitation patterns. These studies have also increased understanding of the roles of ocean and vegetation feedbacks in determining the response to solar and greenhouse gas forcing. Moreover, although proxy data on palaeoclimatic interannual to multi-decadal variability during these periods remain very uncertain, there is an increased appreciation that external forcing may, in the past, have affected climatic variability such as that associated with ENSO.

The understanding of climate variability and change, and its causes during the past 1 kyr, has also improved since the TAR (IPCC, 2001). There is consensus across all millennial reconstructions on the timing of major climatic events, although their magnitude remains somewhat uncertain. Nonetheless, the collection of reconstructions from palaeodata, which is larger and more closely scrutinised than that available for the TAR, indicates that it is likely that NH average temperatures during the second half of the 20th century were warmer than any other 50-year period during the past 1.3 kyr (Chapter 6). While uncertainties remain in temperature and forcing reconstructions, and in the models used to estimate the responses to external forcings, the available detection studies, modelling and other evidence support the conclusion that volcanic and possibly solar forcings have very likely affected NH mean temperature over the past millennium and that external influences explain a substantial fraction of inter-decadal temperature variability in the past. The available evidence also indicates that natural forcing may have influenced the climatic conditions of individual periods, such as the cooler conditions around 1700. The climate response to greenhouse gas increases can be detected in a range of proxy reconstructions by the end of the records.

When driven with estimates of external forcing for the last millennium, AOGCMs simulate changes in hemispheric mean temperature that are in broad agreement with proxy reconstructions (given their uncertainties), increasing confidence in the forcing reconstructions, proxy climate reconstructions and models. In addition, the residual variability in the proxy climate reconstructions that is not explained by forcing is broadly consistent with AOGCM-simulated internal variability. Overall, the information on temperature change over the last millennium is broadly consistent with the understanding of climate change in the instrumental era.

9.4 Understanding of Air Temperature Change During the Industrial Era

9.4.1 Global-Scale Surface Temperature Change

9.4.1.1 Observed Changes

Six additional years of observations since the TAR (Chapter 3) show that temperatures are continuing to warm near the surface of the planet. The annual global mean temperature for every year since the TAR has been among the 10 warmest years since the beginning of the instrumental record. The global mean temperature averaged over land and ocean surfaces warmed by 0.76°C ± 0.19°C between the first 50 years of the instrumental record (1850–1899) and the last 5 years (2001–2005) (Chapter 3; with a linear warming trend of 0.74°C ± 0.18°C over the last 100 years (1906–2005)). The rate of warming over the last 50 years is almost double that over the last 100 years (0.13°C ± 0.03°C vs 0.07°C ± 0.02°C per decade; Chapter 3). The larger number of proxy reconstructions from palaeodata than were available for the TAR indicate that it is very likely that average NH temperatures during the second half of the 20th century were warmer than any other 50-year period in the last 500 years and it is likely that this was the warmest period in the past 1.3 kyr (Chapter 6). Global mean temperature has not increased smoothly since 1900 as would be expected if it were influenced only by forcing from increasing greenhouse gas concentrations (i.e., if natural variability and other forcings did not have a role; see Section 9.2.1; Chapter 2). A rise in near-surface temperatures

also occurred over several decades during the first half of the 20th century, followed by a period of more than three decades when temperatures showed no pronounced trend (Figure 3.6). Since the mid-1970s, land regions have warmed at a faster rate than oceans in both hemispheres (Figure 3.8) and warming over the SH was smaller than that over the NH during this period (Figure 3.6), while warming rates during the early 20th century were similar over land and ocean.

9.4.1.2 Simulations of the 20th Century

There are now a greater number of climate simulations from AOGCMs for the period of the global surface instrumental record than were available for the TAR, including a greater variety of forcings in a greater variety of combinations. These simulations used models with different climate sensitivities, rates of ocean heat uptake and magnitudes and types of forcings (Supplementary Material, Table S9.1). Figure 9.5 shows that simulations that incorporate anthropogenic forcings, including increasing greenhouse gas concentrations and the effects of aerosols, and that also incorporate natural external forcings provide a consistent explanation of the observed temperature record, whereas simulations that include only natural forcings do not simulate the warming observed over the last three decades. A variety of different forcings is used in these simulations. For example, some anthropogenically forced simulations include both the direct and indirect effects of sulphate aerosols whereas others include just the direct effect, and the aerosol forcing that is calculated within models differs due to differences in the representation of physics. Similarly, the effects of tropospheric and stratospheric ozone changes are included in some simulations but not others, and a few simulations include the effects of carbonaceous aerosols and land use changes, while the naturally forced simulations include different representations of changing solar and volcanic forcing. Despite this additional uncertainty, there is a clear separation in Figure 9.5 between the simulations with anthropogenic forcings and those without.

Global mean and hemispheric-scale temperatures on multi-decadal time scales are largely controlled by external forcings (Stott et al., 2000). This external control is demonstrated by ensembles of model simulations with identical forcings (whether anthropogenic or natural) whose members exhibit very similar simulations of global mean temperature on multi-decadal time scales (e.g., Stott et al., 2000; Broccoli et al., 2003; Meehl et al., 2004). Larger interannual variations are seen in the observations than in the ensemble mean model simulation of the 20th century because the ensemble averaging process filters out much of the natural internal interannual variability that is simulated by the models. The interannual variability in the individual simulations that is evident in Figure 9.5 suggests that current models generally simulate large-scale natural internal variability quite well, and also capture the cooling associated with volcanic eruptions on shorter time scales. Section 9.4.1.3 assesses the variability of near surface temperature observations and simulations.

The fact that climate models are only able to reproduce observed global mean temperature changes over the 20th century when they include anthropogenic forcings, and that they fail to do so when they exclude anthropogenic forcings, is evidence for the influence of humans on global climate. Further evidence is provided by spatial patterns of temperature change. Figure 9.6 compares observed near-surface temperature trends over the

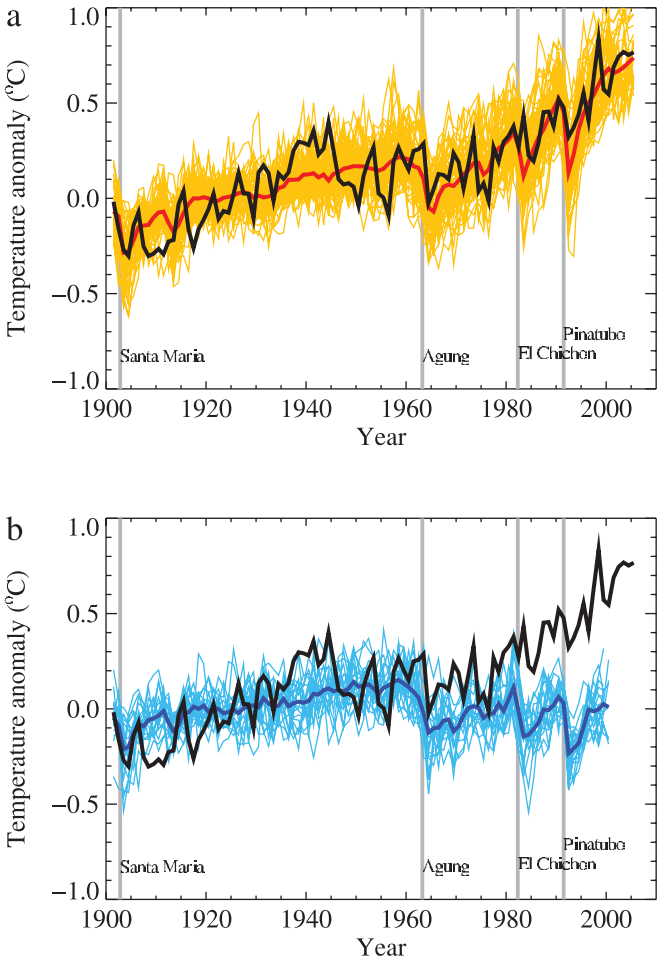


Figure 9.5. *Comparison between global mean surface temperature anomalies (°C) from observations (black) and AOGCM simulations forced with (a) both anthropogenic and natural forcings and (b) natural forcings only. All data are shown as global mean temperature anomalies relative to the period 1901 to 1950, as observed (black, Hadley Centre/Climatic Research Unit gridded surface temperature data set (HadCRUT3); Brohan et al., 2006) and, in (a) as obtained from 58 simulations produced by 14 models with both anthropogenic and natural forcings. The multi-model ensemble mean is shown as a thick red curve and individual simulations are shown as thin yellow curves. Vertical grey lines indicate the timing of major volcanic events. Those simulations that ended before 2005 were extended to 2005 by using the first few years of the IPCC Special Report on Emission Scenarios (SRES) A1B scenario simulations that continued from the respective 20th-century simulations, where available. The simulated global mean temperature anomalies in (b) are from 19 simulations produced by five models with natural forcings only. The multi-model ensemble mean is shown as a thick blue curve and individual simulations are shown as thin blue curves. Simulations are selected that do not exhibit excessive drift in their control simulations (no more than 0.2°C per century). Each simulation was sampled so that coverage corresponds to that of the observations. Further details of the models included and the methodology for producing this figure are given in the Supplementary Material, Appendix 9.C. After Stott et al. (2006b).*

globe (top row) with those simulated by climate models when they include anthropogenic and natural forcing (second row) and the same trends simulated by climate models when only natural forcings are included (third row). The observed trend over the entire 20th century (Figure 9.6, top left panel) shows warming almost everywhere with the exception of the southeastern USA, northern North Atlantic, and isolated grid boxes in Africa and South America (see also Figure 3.9). Such a pattern of warming is not associated with known modes of internal climate variability. For example, while El Niño or El Niño-like decadal variability results in unusually warm annual temperatures, the spatial pattern associated with such a warming is more structured, with cooling in the North Pacific and South Pacific (see, e.g., Zhang et al., 1997). In contrast, the trends in climate model simulations that include anthropogenic and natural forcing (Figure 9.6, second row) show a pattern of spatially near-uniform warming similar to that observed. There is much greater similarity between the general evolution of the warming in observations and that simulated by models when anthropogenic and natural forcings are included than when only natural forcing is included (Figure 9.6, third row). Figure 9.6 (fourth row) shows that climate models are only able to reproduce the observed patterns of zonal mean near-surface temperature trends over the 1901 to 2005 and 1979 to 2005 periods when they include anthropogenic forcings and fail to do so when they exclude anthropogenic forcings. Although there is less warming at low latitudes than at high northern latitudes, there is also less internal variability at low latitudes, which results in a greater separation of the climate simulations with and without anthropogenic forcings.

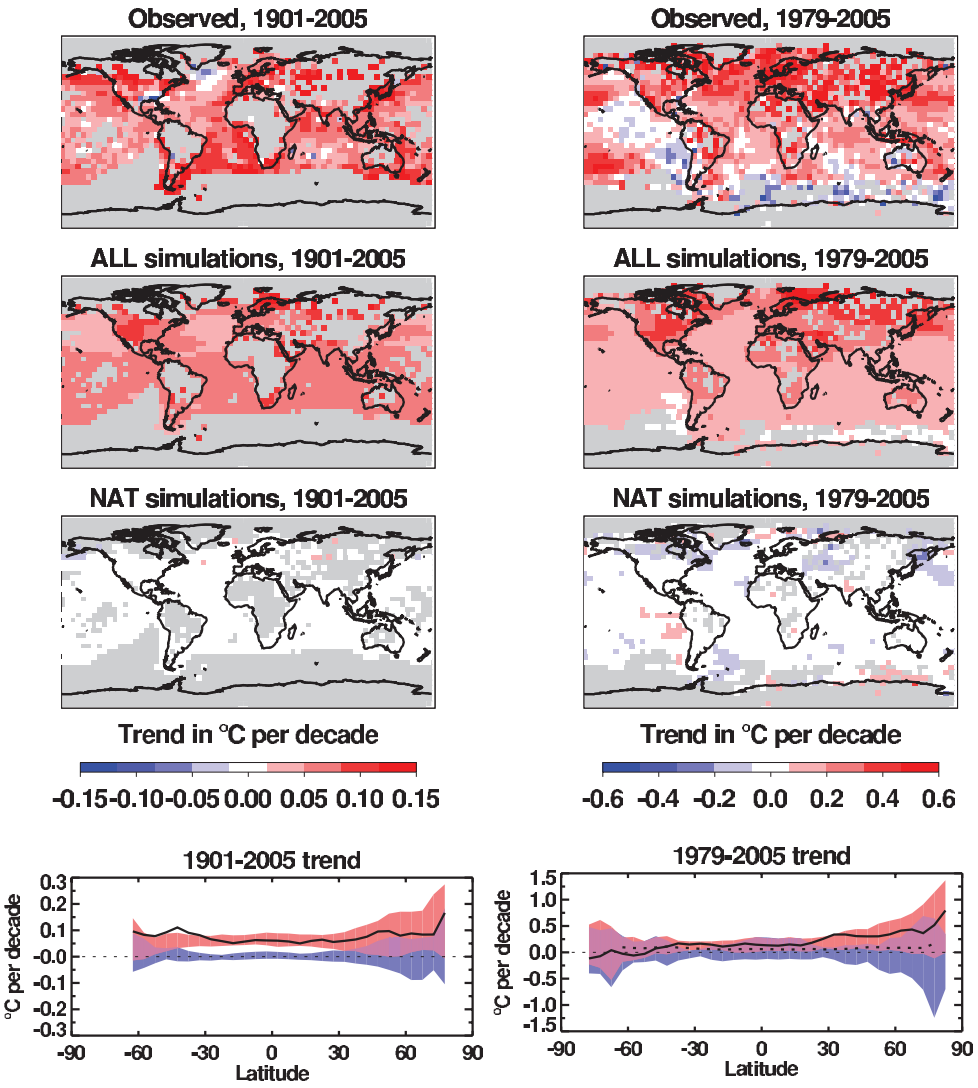


Figure 9.6. *Trends in observed and simulated temperature changes (°C) over the 1901 to 2005 (left column) and 1979 to 2005 (right column) periods. First row: trends in observed temperature changes (Hadley Centre/Climatic Research Unit gridded surface temperature data set (HadCRUT3), Brohan et al., 2006). Second row: average trends in 58 historical simulations from 14 climate models including both anthropogenic and natural forcings. Third row: average trends in 19 historical simulations from five climate models including natural forcings only. Grey shading in top three rows indicates regions where there are insufficient observed data to calculate a trend for that grid box (see Supplementary Material, Appendix 9.C for further details of data exclusion criteria). Fourth row: average trends for each latitude; observed trends are indicated by solid black curves. Red shading indicates the middle 90% range of trend estimates from the 58 simulations including both anthropogenic and natural forcings (estimated as the range between 4th and 55th of the 58 ranked simulations); blue shading indicates the middle 90% range of trend estimates from the 19 simulations with natural forcings only (estimated as the range between 2nd and 18th of the 19 ranked simulations); for comparison, the dotted black curve in the right-hand plot shows the observed 1901 to 2005 trend. Note that scales are different between columns. The 'ALL' simulations were extended to 2005 by adding their IPCC Special Report on Emission Scenarios (SRES) A1B continuation runs where available. Where not available, and in the case of the 'NAT' simulations, the mean for the 1996 to 2005 decade was estimated using model output from 1996 to the end of the available runs. In all plots, each climate simulation was sampled so that coverage corresponds to that of the observations. Further details of the models included and the methodology for producing this figure are given in the Supplementary Material, Appendix 9.C.*

Climate simulations are consistent in showing that the global mean warming observed since 1970 can only be reproduced when models are forced with combinations of external forcings that include anthropogenic forcings (Figure 9.5). This conclusion holds despite a variety of different anthropogenic forcings and processes being included in these models (e.g., Tett et al., 2002; Broccoli et al., 2003; Meehl et al., 2004; Knutson et al., 2006). In all cases, the response to forcing from well-mixed greenhouse gases dominates the anthropogenic warming in the model. No

climate model using natural forcings alone has reproduced the observed global warming trend in the second half of the 20th century. Therefore, modelling studies suggest that late 20th-century warming is much more likely to be anthropogenic than natural in origin, a finding which is confirmed by studies relying on formal detection and attribution methods (Section 9.4.1.4).

Modelling studies are also in moderately good agreement with observations during the first half of the 20th century when both anthropogenic and natural forcings are considered, although assessments of which forcings are important differ, with some studies finding that solar forcing is more important (Meehl et al., 2004) while other studies find that volcanic forcing (Broccoli et al., 2003) or internal variability (Delworth and Knutson, 2000) could be more important. Differences between simulations including greenhouse gas forcing only and those that also include the cooling effects of sulphate aerosols (e.g., Tett et al., 2002) indicate that the cooling effects of sulphate aerosols may account for some of the lack of observational warming between 1950 and 1970, despite increasing greenhouse gas concentrations, as was proposed by Schwartz (1993). In contrast, Nagashima et al. (2006) find that carbonaceous aerosols are required for the MIROC model (see Table 8.1 for a description) to provide a statistically consistent representation of observed changes in near-surface temperature in the middle part of the 20th century. The mid-century cooling that the model simulates in some regions is also observed, and is caused in the model by regional negative surface forcing from organic and black carbon associated with biomass burning. Variations in the Atlantic Multi-decadal Oscillation (see Section 3.6.6 for a more detailed discussion) could account for some of the evolution of global and hemispheric mean temperatures during the instrumental period (Schlesinger and Ramankutty, 1994; Andronova and Schlesinger, 2000; Delworth and Mann, 2000); Knight et al. (2005) estimate that variations in the Atlantic Multi-decadal Oscillation could account for up to 0.2°C peak-to-trough variability in NH mean decadal temperatures.

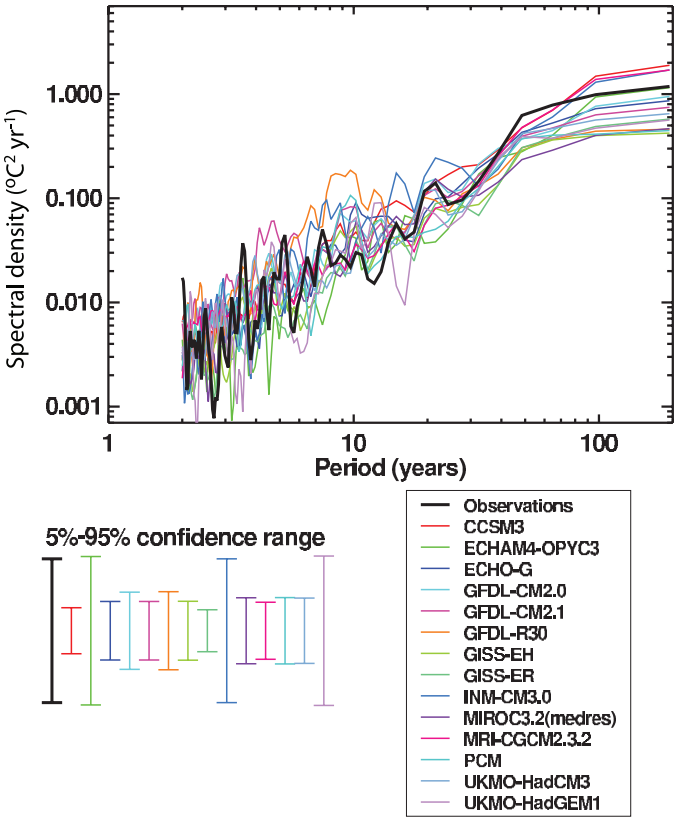


Figure 9.7. *Comparison of variability as a function of time scale of annual global mean temperatures (°C² yr⁻¹) from the observed record (Hadley Centre/Climatic Research Unit gridded surface temperature data set (HadCRUT3), Brohan et al., 2006) and from AOGCM simulations including both anthropogenic and natural forcings. All power spectra are estimated using a Tukey-Hanning filter of width 97 years. The model spectra displayed are the averages of the individual spectra estimated from individual ensemble members. The same 58 simulations and 14 models are used as in Figure 9.5a. All models simulate variability on decadal time scales and longer that is consistent with observations at the 10% significance level. Further details of the method of calculating the spectra are given in the Supplementary Material, Appendix 9.C.*

9.4.1.3 Variability of Temperature from Observations and Models

Year-to-year variability of global mean temperatures simulated by the most recent models compares reasonably well with that of observations, as can be seen by comparing observed and modelled variations in Figure 9.5a. A more quantitative evaluation of modelled variability can be carried out by comparing the power spectra of observed and modelled global mean temperatures. Figure 9.7 compares the power spectrum of observations with the power spectra of transient simulations of the instrumental period. This avoids the need to compare variability estimated from long control runs of models with observed variability, which is difficult because observations are likely to contain a response to external forcings that cannot be reliably removed by subtracting a simple linear trend. The simulations considered contain both anthropogenic and natural forcings, and include most 20th Century Climate in Coupled Models (20C3M) simulations in the MMD at PCMDI. Figure 9.7 shows that the models have variance at global scales that is consistent with the observed variance at the 5% significance level on the decadal to inter-decadal time scales important for detection and attribution. Figure 9.8 shows that this is also generally the case at continental scales, although model uncertainty is larger at smaller scales (Section 9.4.2.2).

Detection and attribution studies routinely assess if the residual variability unexplained by forcing is consistent with the estimate of internal variability (e.g., Allen and Tett, 1999; Tett et al., 1999; Stott et al., 2001; Zwiers and Zhang, 2003). Furthermore, there is no evidence that the variability in palaeoclimatic reconstructions that is not explained by forcing is stronger than that in models, and simulations of the last 1 kyr show similar variability to reconstructions (Section 9.3.3.2). Chapter 8 discusses the simulation of major modes of variability and the extent to which they are simulated by models (including on decadal to inter-decadal time scales).

9.4.1.4 The Influence of Greenhouse Gas and Total Anthropogenic Forcing on Global Surface Temperature

Since the TAR, a large number of studies based on the longer observational record, improved models and stronger signal-to-noise ratio have increased confidence in the detection of an anthropogenic signal in the instrumental record (see, e.g., the recent review by IDAG, 2005). Many more detection and attribution studies are now available than were available for the TAR, and these have used more recent climate data than previous studies and a much greater variety of climate simulations with more sophisticated treatments of a greater number of both anthropogenic and natural forcings.

Fingerprint studies that use climate change signals estimated from an array of climate models indicate that detection of an anthropogenic contribution to the observed warming is a result that is robust to a wide range of model uncertainty, forcing uncertainties and analysis techniques (Hegerl et al., 2001; Gillett et al., 2002c; Tett et al., 2002; Zwiers and Zhang, 2003; IDAG, 2005; Stone and Allen, 2005b; Stone et al., 2007a,b; Stott et al., 2006b,c; Zhang et al., 2006). These studies account for the possibility that the agreement between simulated and observed global mean temperature changes could be fortuitous as a result of, for example, balancing too great (or too small) a model sensitivity with a too large (or too small) negative aerosol forcing (Schwartz, 2004; Hansen et al., 2005) or a too small (or too large) warming due to solar changes. Multi-signal detection and attribution analyses do not rely on such agreement because they seek to explain the observed temperature changes in terms of the responses to individual forcings, using model-derived patterns of response and a noise-reducing metric (Appendix 9.A) but determining their amplitudes from observations. As discussed in Section 9.2.2.1, these approaches make use of differences in the temporal and spatial responses to forcings to separate their effect in observations.

Since the TAR, there has also been an increased emphasis on quantifying the greenhouse gas contribution to observed warming, and distinguishing this contribution from other factors, both anthropogenic, such as the cooling effects of aerosols, and natural, such as from volcanic eruptions and changes in solar radiation.

A comparison of results using four different models (Figure 9.9) shows that there is a robust identification of a significant greenhouse warming contribution to observed warming that is likely greater than the observed warming over the last 50 years

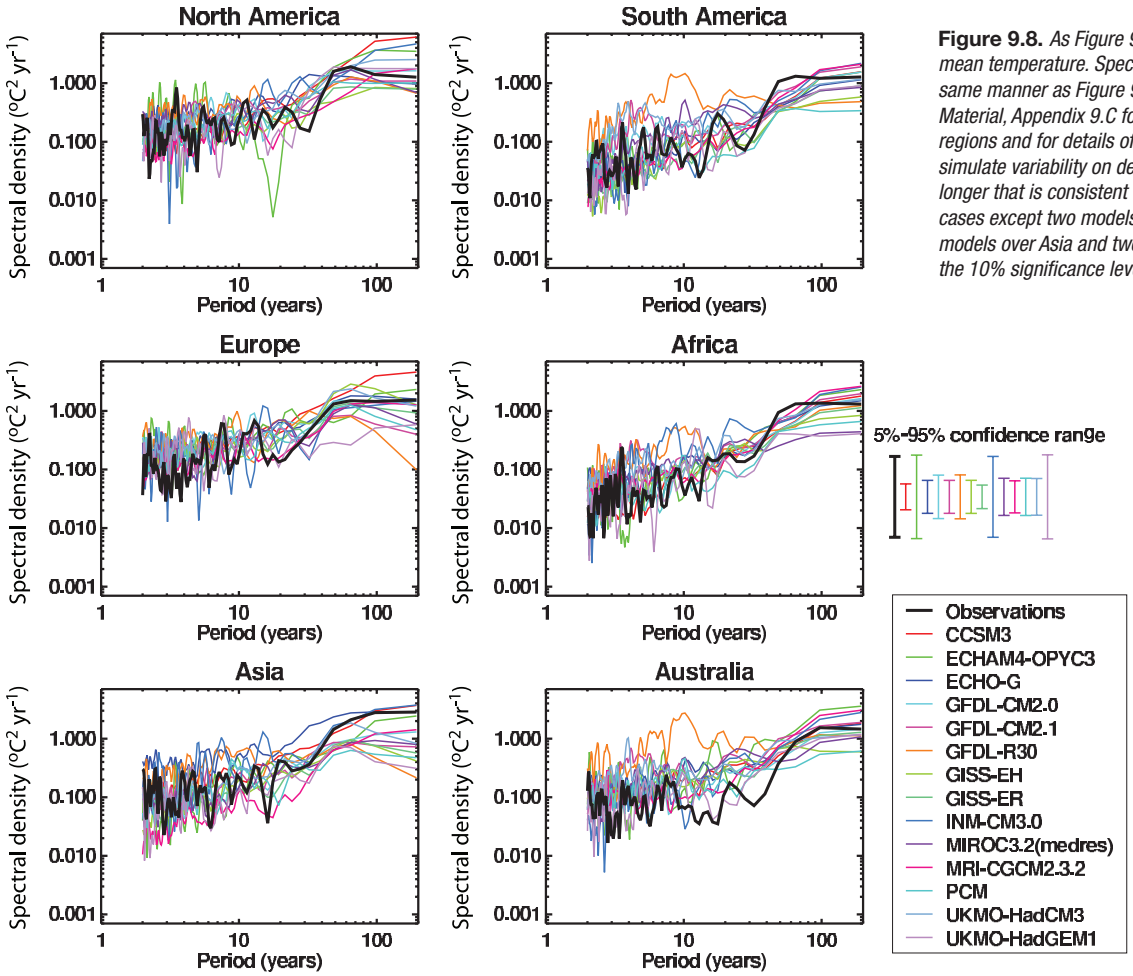


Figure 9.8. *As Figure 9.7, except for continental mean temperature. Spectra are calculated in the same manner as Figure 9.7. See the Supplementary Material, Appendix 9.C for a description of the regions and for details of the method used. Models simulate variability on decadal time scales and longer that is consistent with observations in all cases except two models over South America, five models over Asia and two models over Australia (at the 10% significance level).*

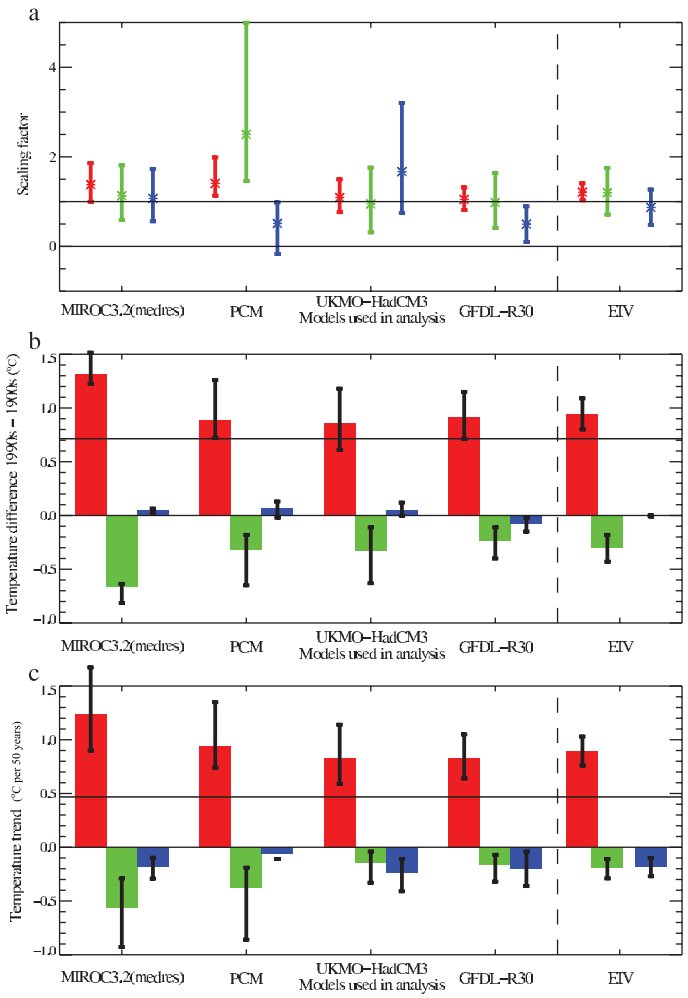


Figure 9.9. *Estimated contribution from greenhouse gas (red), other anthropogenic (green) and natural (blue) components to observed global mean surface temperature changes, based on 'optimal' detection analyses (Appendix 9.A). (a) 5 to 95% uncertainty limits on scaling factors (dimensionless) based on an analysis over the 20th century, (b) the estimated contribution of forced changes to temperature changes over the 20th century, expressed as the difference between 1990 to 1999 mean temperature and 1900 to 1909 mean temperature (°C) and (c) estimated contribution to temperature trends over 1950 to 1999 (°C per 50 years). The horizontal black lines in (b) and (c) show the observed temperature changes from the Hadley Centre/Climatic Research Unit gridded surface temperature data set (HadCRUT2v; Parker et al., 2004). The results of full space-time optimal detection analyses (Nozawa et al., 2005; Stott et al., 2006c) using a total least squares algorithm (Allen and Stott, 2003) from ensembles of simulations containing each set of forcings separately are shown for four models, MIROC3.2(medres), PCM, UKMO-HadCM3 and GFDL-R30. Also shown, labelled 'EIV', is an optimal detection analysis using the combined spatio-temporal patterns of response from three models (PCM, UKMO-HadCM3 and GFDL-R30) for each of the three forcings separately, thus incorporating inter-model uncertainty (Huntingford et al., 2006).*

with a significant net cooling from other anthropogenic forcings over that period, dominated by aerosols. Stott et al. (2006c) compare results over the 20th century obtained using the UKMO-HadCM3, PCM (see Table 8.1 for model descriptions) and Geophysical Fluid Dynamics Laboratory (GFDL) R30 models. They find consistent estimates for the greenhouse gas attributable warming over the century, expressed as the difference between temperatures in the last and first decades of the century, of 0.6°C to 1.3°C (5 to 95%) offset by cooling from other anthropogenic factors associated mainly with cooling from aerosols of 0.1°C to 0.7°C and a small net contribution from natural factors over the century of –0.1°C to 0.1°C (Figure 9.9b). Scaling factors for the model response to three forcings are shown in Figure 9.9a. A similar analysis for the MIROC3.2 model (see Table 8.1 for a description) finds a somewhat larger warming contribution from greenhouse gases of 1.2°C to 1.5°C offset by a cooling of 0.6°C to 0.8°C from other anthropogenic factors and a very small net natural contribution (Figure 9.9b). In all cases, the fifth percentile of the warming attributable to greenhouse gases is greater than the observed warming over the last 50 years of the 20th century (Figure 9.9c).

The detection and estimation of a greenhouse gas signal is also robust to accounting more fully for model uncertainty. An analysis that combines results from three climate models and thereby incorporates uncertainty in the response of these three models (by including an estimate of the inter-model covariance structure in the regression method; Huntingford et al., 2006), supports the results from each of the models individually that it is likely that greenhouse gases would have caused more warming than was observed over the 1950 to 1999 period (Figure 9.9, results labelled 'EIV'). These results are consistent with the results of an earlier analysis, which calculated the mean response patterns from five models and included a simpler estimate of model uncertainty (obtained by a simple rescaling of the variability estimated from a long control run, thereby assuming that inter-model uncertainty has the same covariance structure as internal variability; Gillett et al., 2002c). Both the results of Gillett et al. (2002c) and Huntingford et al. (2006) indicate that inter-model differences do not greatly increase detection and attribution uncertainties and that averaging fingerprints improves detection results.

A robust anthropogenic signal is also found in a wide range of climate models that do not have the full range of simulations required to directly estimate the responses to individual forcings required for the full multi-signal detection and attribution analyses (Stone et al., 2007a,b). In these cases, an estimate of the model's pattern of response to each individual forcing can be diagnosed by fitting a series of EBMs, one for each forcing, to the mean coupled model response to all the forcings to diagnose the time-dependent response in the global mean for each individual forcing. The magnitude of these time-only signals can then be inferred from observations using detection methods (Stone et al., 2007a,b). When applied to 13 different climate models that had transient simulations of 1901 to 2005 temperature change, Stone et al. (2007a) find a robust detection across the models of greenhouse gas warming over this period, although uncertainties in attributable temperature changes due to the different forcings are larger than when considering spatio-temporal patterns. By tuning an EBM to the observations, and using an AOGCM solely to estimate internal variability, Stone and Allen (2005b) detect the effects of greenhouse gases and tropospheric sulphate aerosols in the observed 1900 to 2004 record, but not the effects of volcanic and solar forcing.

The detection of an anthropogenic signal is also robust to using different methods. For example, Bayesian detection analyses (Appendix 9.A.2) robustly detect anthropogenic influence on near-surface temperature changes (Smith et al., 2003; Schnur and Hasselmann, 2005; Min and Hense, 2006a,b). In these studies, Bayes Factors (ratios of posterior to prior odds) are used to assess evidence supporting competing hypotheses (Kass and Raftery, 1995; see Appendix 9.A.2). A Bayesian analysis of seven climate models (Schnur and Hasselman, 2005) and Bayesian analyses of MMD 20C3M simulations (Min and Hense, 2006a,b) find decisive evidence for the influence of anthropogenic forcings. Lee et al. (2005), using an approach suggested by Berliner et al. (2000), evaluate the evidence for the presence of the combined greenhouse gas and sulphate aerosol (GS) signal, estimated from CGCM1 and CGCM2 (Table 8.1; McAvaney et al., 2001), in observations for several five-decade windows, beginning with 1900 to 1949 and ending with 1950 to 1999. Very strong evidence was found in support of detection of the forced response during both halves of the 20th century regardless of the choice of prior distribution. However, evidence for attribution in that approach is based on the extent to which observed data narrow the prior uncertainty on the size of the anthropogenic signal. That evidence was not found to be very strong, although Lee et al. (2005) estimate that strong evidence for attribution as defined in their approach may emerge within the next two decades as the anthropogenic signal strengthens.

In a further study, Lee et al. (2006) assess whether anthropogenic forcing has enhanced the predictability of decadal global-scale temperature changes; a forcing-related enhancement in predictability would give a further indication of its role in the evolution of the 20th-century climate. Using an ensemble of simulations of the 20th century with GS forcing, they use Bayesian tools similar to those of Lee et al. (2005) to produce, for each decade beginning with 1930 to 1939, a forecast of the probability of above-normal temperatures where 'normal' is defined as the mean temperature of the preceding three decades. These hindcasts become skilful during the last two decades of the 20th century as indicated both by their Brier skill scores, a standard measure of the skill of probabilistic forecasts, and by the confidence bounds on hindcasts of global mean temperature anomalies (Figure 9.10). This indicates that greenhouse gas forcing contributes to predictability of decadal temperature changes during the latter part of the 20th century.

Another type of analysis is a Granger causality analysis of the lagged covariance structure of observed hemispheric temperatures (Kaufmann and Stern, 2002), which also provides evidence for an anthropogenic signal, although such

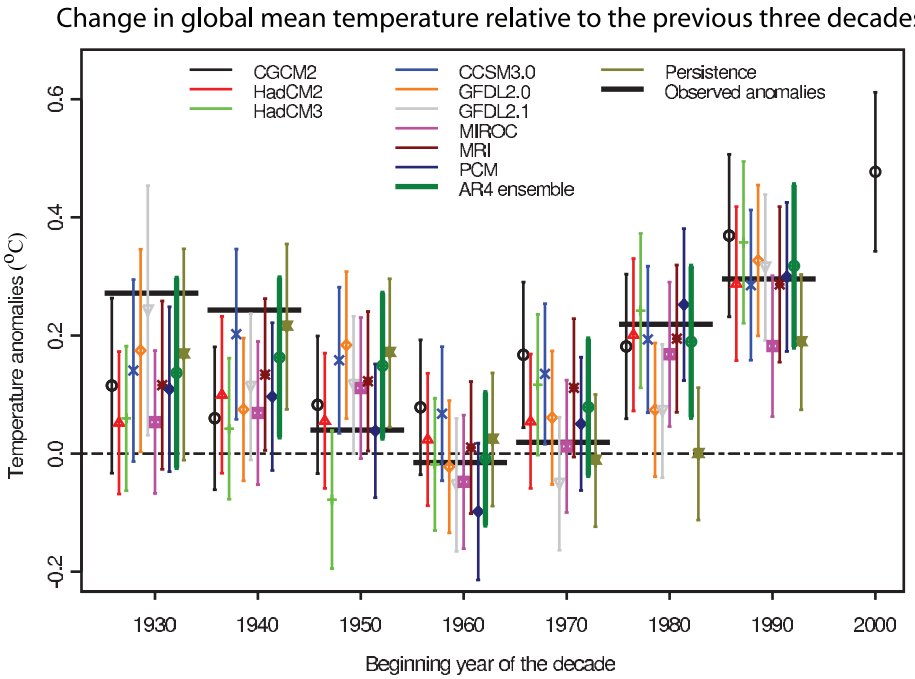


Figure 9.10. *Observed and hindcast decadal mean surface temperature anomalies (°C) expressed, for each decade, relative to the preceding three decades. Observed anomalies are represented by horizontal black lines. Hindcast decadal anomalies and their uncertainties (5 to 95% confidence bounds) are displayed as vertical bars. Hindcasts are based on a Bayesian detection analysis using the estimated response to historical external forcing. Hindcasts made with CGCM2, HadCM2 (see Table 8.1 of the TAR) and HadCM3 (see Table 8.1, this report) use the estimated response to anthropogenic forcing only (left hand column of legend) while those made with selected MMD 20C3M models used anthropogenic and natural forcings (centre column of legend; see Table 8.1 for model descriptions). Hindcasts made with the ensemble mean of the selected 20C3M models are indicated by the thick green line. A hindcast based on persisting anomalies from the previous decade is also shown. The hindcasts agree well with observations from the 1950s onward. Hindcasts for the decades of the 1930s and 1940s are sensitive to the details of the hindcast procedure. A forecast for the decadal global mean anomaly for the decade 2000 to 2009, relative to the 1970 to 1999 climatology, based on simulations performed with the Canadian Centre for Climate Modelling and Analysis Coupled Global Climate Model (CGCM2) is also displayed. From Lee et al. (2006).*

evidence may not be conclusive on its own without additional information from climate models (Triacca, 2001). Consistently, a neural network model is unable to reconstruct the observed global temperature record from 1860 to 2000 if anthropogenic forcings are not taken into account (Pasini et al., 2006). Further, an assessment of recent climate change relative to the long-term persistence of NH mean temperature as diagnosed from a range of reconstructed temperature records (Rybski et al., 2006) suggests that the recent warming cannot be explained solely in terms of natural factors, regardless of the reconstruction used. Similarly, Fomby and Vogelsang (2002), using a test of trend that accounts for the effects of serial correlation, find that the increase in global mean temperature over the 20th century is statistically significant even if it is assumed that natural climate variability has strong serial correlation.

9.4.1.5 The Influence of Other Anthropogenic and Natural Forcings

A significant cooling due to other anthropogenic factors, dominated by aerosols, is a robust feature of a wide range of detection analyses. These analyses indicate that it is likely that greenhouse gases alone would have caused more than the observed warming over the last 50 years of the 20th century, with some warming offset by cooling from natural and other anthropogenic factors, notably aerosols, which have a very short residence time in the atmosphere relative to that of well-mixed greenhouse gases (Schwartz, 1993). A key factor in identifying the aerosol fingerprint, and therefore the amount of aerosol cooling counteracting greenhouse warming, is the change through time of the hemispheric temperature contrast, which is affected by the different evolution of aerosol forcing in the two hemispheres as well as the greater thermal inertia of the larger ocean area in the SH (Santer et al., 1996b,c; Hegerl et al., 2001; Stott et al., 2006c). Regional and seasonal aspects of the temperature response may help to distinguish further the response to greenhouse gas increases from the response to aerosols (e.g., Ramanathan et al., 2005; Nagashima et al., 2006).

Results on the importance and contribution from anthropogenic forcings other than greenhouse gases vary more between different approaches. For example, Bayesian analyses differ in the strength of evidence they find for an aerosol effect. Schnur and Hasselman (2005), for example, fail to find decisive evidence for the influence of aerosols. They postulate that this could be due to taking account of modelling uncertainty in the response to aerosols. However, two other studies using frequentist methods that also include modelling uncertainty find a clear detection of sulphate aerosols, suggesting that the use of multiple models helps to reduce uncertainties and improves detection of a sulphate aerosol effect (Gillett et al., 2002c; Huntingford et al., 2006). Similarly, a Bayesian study of hemispheric mean temperatures from 1900 to 1996 finds decisive evidence for an aerosol cooling effect (Smith et al., 2003). Differences in the separate detection of sulphate aerosol influences in multi-signal approaches can also reflect differences in the diagnostics applied (e.g., the space-time analysis of Tett et al. (1999) versus the space-only analysis of Hegerl et al. (1997, 2000)) as was shown by Gillett et al. (2002a).

Recent estimates (Figure 9.9) indicate a relatively small combined effect of natural forcings on the global mean temperature evolution of the second half of the 20th century, with a small net cooling from the combined effects of solar and volcanic forcings. Coupled models simulate much less warming over the 20th century in response to solar forcing alone than to greenhouse gas forcing (Cubasch et al., 1997; Broccoli et al., 2003; Meehl et al., 2004), independent of which solar forcing reconstruction is used (Chapter 2). Several studies have attempted to estimate the individual contributions from solar and volcanic forcings separately, thus allowing for the possibility of enhancement of the solar response in observations due to processes not represented in models. Optimal detection studies that attempt to separate the responses to solar and other forcings in observations can also account for gross errors in the overall magnitude of past solar forcing, which remains uncertain (Chapter 2), by scaling the space-time patterns of response (Section 9.2.2.1). Using such a method, Tett et al. (1999) estimate that the net anthropogenic warming in the second half of the 20th century was much greater than any possible solar warming, even when using the solar forcing reconstruction by Hoyt and Schatten (1993), which indicates larger solar forcing and a different evolution over time than more recent reconstructions (Section 2.7.1). However, Stott et al. (2003b), using the same solar reconstruction but a different model, are not able to completely rule out the possibility that solar forcing might have caused more warming than greenhouse gas forcing over the 20th century due to difficulties in distinguishing between the patterns of response to solar and greenhouse forcing. This was not the case when using the response to solar forcing based on the alternative reconstruction of Lean et al. (1995), in which case they find a very small likelihood (less than 1%, as opposed to approximately 10%) that solar warming could be greater than greenhouse warming since 1950. Note that recent solar forcing reconstructions show a substantially decreased magnitude of low-frequency variations in solar forcing (Section 2.7.1) compared to Lean et al. (1995) and particularly Hoyt and Schatten (1993).

The conclusion that greenhouse warming dominates over solar warming is supported further by a detection and attribution analysis using 13 models from the MMD at PCMDI (Stone et al., 2007a) and an analysis of the National Center for Atmospheric Research (NCAR) Community Climate System Model (CCSM1.4; Stone et al., 2007b). In both these analyses, the response to solar forcing in the model was inferred by fitting a series of EBMs to the mean coupled model response to the combined effects of anthropogenic and natural forcings. In addition, a combined analysis of the response at the surface and through the depth of the atmosphere using HadCM3 and the solar reconstruction of Lean et al. (1995) concluded that the near-surface temperature response to solar forcing over 1960 to 1999 is much smaller than the response to greenhouse gases (Jones et al., 2003). This conclusion is also supported by the vertical

pattern of climate change, which is more consistent with the response to greenhouse gas than to solar forcing (Figure 9.1). Further evidence against a dominant solar role arises from older analyses targeted at detecting the solar response (e.g., North and Stevens, 1998). Based on these detection results, which allow for possible amplification of the solar influence by processes not represented in climate models, we conclude that it is very likely that greenhouse gases caused more global warming over the last 50 years than changes in solar irradiance.

Detection and attribution as well as modelling studies indicate more uncertainty regarding the causes of early 20th-century warming than the recent warming. A number of studies detect a significant natural contribution to early 20th-century warming (Tett et al., 2002; Stott et al., 2003b; Nozawa et al., 2005; Shiogama et al., 2006). Some studies find a greater role for solar forcing than other forcings before 1950 (Stott et al., 2003b), although one detection study finds a roughly equal role for solar and volcanic forcing (Shiogama et al., 2006), and others find that volcanic forcing (Hegerl et al., 2003, 2007) or a substantial contribution from natural internal variability (Tett et al., 2002; Hegerl et al., 2007) could be important. There could also be an early expression of greenhouse warming in the early 20th century (Tett et al., 2002; Hegerl et al., 2003, 2007).

9.4.1.6 Implications for Transient Climate Response

Quantification of the likely contributions of greenhouse gases and other forcing factors to past temperature change (Section 9.4.1.4) in turn provides observational constraints on the transient climate response, which determines the rapidity and strength of a global temperature response to external forcing (see Glossary and Sections 9.6.2.3 and 8.6.2.1 for detailed definitions) and therefore helps to constrain likely future rates of warming. Scaling factors derived from detection analyses can be used to scale predictions of future change by assuming that the fractional error in model predictions of global mean temperature change is constant (Allen et al., 2000, 2002; Allen and Stainforth, 2002; Stott and Kettleborough, 2002). This linear relationship between past and future fractional error in temperature change has been found to be sufficiently robust over a number of realistic forcing scenarios to introduce little additional uncertainty (Kettleborough et al., 2007). In this approach based on detection and attribution methods, which is compared with other approaches for producing probabilistic projections in Section 10.5.4.5, different scaling factors are applied to the greenhouse gases and to the response to other anthropogenic forcings (notably aerosols); these separate scaling factors are used to account for possible errors in the models and aerosol forcing. Uncertainties calculated in this way are likely to be more reliable than uncertainty ranges derived from simulations by coupled AOGCMs that happen to be available. Such ensembles could provide a misleading estimate of forecast uncertainty because they do not systematically explore modelling uncertainty (Allen et al., 2002; Allen and Stainforth, 2002). Stott et al. (2006c) compare observationally constrained predictions from three coupled climate models with a range of sensitivities and show that predictions made in this way are relatively insensitive to the particular choice of model used to produce them. The robustness to choice of model of such observationally constrained predictions was also demonstrated by Stone et al. (2007a) for the MMD ensemble. The observationally constrained transient climate response at the time of doubling of atmospheric CO_2 following a 1% per year increase in CO_2 was estimated by Stott et al. (2006c) to lie between 1.5°C and 2.8°C (Section 9.6.2, Figure 9.21). Such approaches have also been used to provide observationally constrained predictions of global mean (Stott and Kettleborough, 2002; Stone et al., 2007a) and continental-scale temperatures (Stott et al., 2006a) following the IPCC Special Report on Emission Scenarios (SRES) emissions scenarios, and these are discussed in Sections 10.5.4.5 and 11.10.

9.4.1.7 Studies of Indices of Temperature Change

Another method for identifying fingerprints of climate change in the observational record is to use simple indices of surface air temperature patterns that reflect features of the anticipated response to anthropogenic forcing (Karoly and Braganza, 2001; Braganza et al., 2003). By comparing modelled and observed changes in such indices, which include the global mean surface temperature, the land-ocean temperature contrast, the temperature contrast between the NH and SH, the mean magnitude of the annual cycle in temperature over land and the mean meridional temperature gradient in the NH mid-latitudes, Braganza et al. (2004) estimate that anthropogenic forcing accounts for almost all of the warming observed between 1946 and 1995 whereas warming between 1896 and 1945 is explained by a combination of anthropogenic and natural forcing and internal variability. These results are consistent with the results from studies using space-time detection techniques (Section 9.4.1.4).

Diurnal temperature range (DTR) has decreased over land by about 0.4°C over the last 50 years, with most of that change occurring prior to 1980 (Section 3.2.2.1). This decreasing trend has been shown to be outside the range of natural internal variability estimated from models. Hansen et al. (1995) demonstrate that tropospheric aerosols plus increases in continental cloud cover, possibly associated with aerosols, could account for the observed decrease in DTR. However, although models simulate a decrease in DTR when they include anthropogenic changes in greenhouse gases and aerosols, the observed decrease is larger than the model-simulated decrease (Stone and Weaver, 2002, 2003; Braganza et al., 2004). This discrepancy is associated with simulated increases in daily maximum temperature being larger than observed, and could be associated with simulated increases in cloud cover being smaller than observed (Braganza et al., 2004; see Section 3.4.3.1 for observations), a result supported by other analyses (Dai et al., 1999; Stone and Weaver, 2002, 2003).

9.4.1.8 Remaining Uncertainties

A much larger range of forcing combinations and climate model simulations has been analysed in detection studies than was available for the TAR (Supplementary Material, Table S9.1). Detection and attribution analyses show robust evidence for an anthropogenic influence on climate. However, some forcings are still omitted by many models and uncertainties remain in the treatment of those forcings that are included by the majority of models.

Most studies omit two forcings that could have significant effects, particularly at regional scales, namely carbonaceous aerosols and land use changes. However, detection and attribution analyses based on climate simulations that include these forcings, (e.g., Stott et al., 2006b), continue to detect a significant anthropogenic influence in 20th-century temperature observations even though the near-surface patterns of response to black carbon aerosols and sulphate aerosols could be so similar at large spatial scales (although opposite in sign) that detection analyses may be unable to distinguish between them (Jones et al., 2005). Forcing from surface albedo changes due to land use change is expected to be negative globally (Sections 2.5.3, 7.3.3 and 9.3.3.3) although tropical deforestation could increase evaporation and warm the climate (Section 2.5.5), counteracting cooling from albedo change. However, the albedo-induced cooling effect is expected to be small and was not detected in observed trends in the study by Matthews et al. (2004).

For those forcings that have been included in attribution analyses, uncertainties associated with the temporal and spatial pattern of the forcing and the modelled response can affect the results. Large uncertainties associated with estimates of past solar forcing (Section 2.7.1) and omission of some chemical and dynamical response mechanisms (Gray et al., 2005) make it difficult to reliably estimate the contribution of solar forcing to warming over the 20th century. Nevertheless, as discussed above, results generally indicate that the contribution is small even if allowance is made for amplification of the response in observations, and simulations used in attribution analyses use several different estimates of solar forcing changes over the 20th century (Supplementary Material, Table S9.1). A number of different volcanic reconstructions are included in the modelling studies described in Section 9.4.1.2 (e.g., Sato et al., 1993; Andronova et al., 1999; Ammann et al., 2003; Supplementary Material, Table S9.1). Some models include volcanic effects by simply perturbing the incoming shortwave radiation at the top of the atmosphere, while others simulate explicitly the radiative effects of the aerosols in the stratosphere. In addition, some models include the indirect effects of tropospheric sulphate aerosols on clouds (e.g., Tett et al., 2002), whereas others consider only the direct radiative effect (e.g., Meehl et al., 2004). In models that include indirect effects, different treatments of the indirect effect are used, including changing the albedo of clouds according to an off-line calculation (e.g., Tett et al., 2002) and a fully interactive treatment of the effects of aerosols on clouds (e.g., Stott et al., 2006b). The overall level of consistency between attribution results derived from different models (as shown in Figure 9.9), and the ability of climate models to simulate large-scale temperature changes during the 20th century (Figures 9.5 and 9.6), indicate that such model differences are likely to have a relatively small impact on attribution results of large-scale temperature change at the surface.

There have also been methodological developments that have resulted in attribution analyses taking uncertainties more fully into account. Attribution analyses normally directly account for errors in the magnitude of the model's pattern of response to different forcings by the inclusion of factors that scale the model responses up or down to best match observed climate changes. These scaling factors compensate for under- or overestimates of the amplitude of the model response to forcing that may result from factors such as errors in the model's climate sensitivity, ocean heat uptake efficiency or errors in the imposed external forcing. Older analyses (e.g., Tett et al., 2002) did not take account of uncertainty due to sampling signal estimates from finite-member ensembles. This can lead to a low bias, particularly for weak forcings, in the scaling factor estimates (Appendix 9.A.1; Allen and Stott, 2003; Stott et al., 2003a). However, taking account of sampling uncertainty (as most more recent detection and attribution studies do, including those shown in Figure 9.9) makes relatively little difference to estimates of attributable warming rates, particularly those due to greenhouse gases; the largest differences occur in estimates of upper bounds for small signals, such as the response to solar forcing (Allen and Stott, 2003; Stott et al., 2003a). Studies that compare results between models and analysis techniques (e.g., Hegerl et al., 2000; Gillett et al., 2002a; Hegerl and Allen, 2002), and more recently, that use multiple models to determine fingerprints of climate change (Gillett et al., 2002c; Huntingford et al., 2006; Stott et al., 2006c; Zhang et al., 2006) find a robust detection of an anthropogenic signal in past temperature change.

A common aspect of detection analyses is that they assume the response in models to combinations of forcings to be additive. This was shown to be the case for near-surface temperatures in the PCM (Meehl et al., 2004), in the Hadley Centre Climate Model version 2 (HadCM2; Gillett et al., 2004c) and in the GFDL CM2.1 (see Table 8.1) model (Knutson et al., 2006), although none of these studies considered the indirect effects of sulphate aerosols. Sexton et al. (2003) did find some evidence for a nonlinear interaction between the effects of greenhouse gases and the indirect effect of sulphate aerosols in the atmosphere-only version of HadCM3 forced by observed SSTs; the additional effect of combining greenhouse gases and indirect aerosol effects together was much smaller than each term separately but was found to be comparable to the warming due to increasing tropospheric ozone. In addition, Meehl et al. (2003) found that additivity does not hold so well for regional responses to solar and greenhouse forcing in the PCM. Linear additivity was found to hold in the PCM model for changes in tropopause height and synthetic satellite-borne Microwave Sounding Unit (MSU) temperatures (Christy et al., 2000; Mears et al., 2003; Santer et al., 2003b).

A further source of uncertainty derives from the estimates of internal variability that are required for all detection analyses. These estimates are generally model-based because of difficulties in obtaining reliable internal variability estimates from the observational record on the spatial and temporal scales considered in detection studies. However, models would need to underestimate variability by factors of over two in their standard deviation to nullify detection of greenhouse gases in near-surface temperature data (Tett et al., 2002), which appears unlikely given the quality of agreement between models and observations at global and continental scales (Figures 9.7 and 9.8) and agreement with inferences on temperature variability from NH temperature reconstructions of the last millennium. The detection of the effects of other forcings, including aerosols, is likely to be more sensitive (e.g., an increase of 40% in the estimate of internal variability is enough to nullify detection of aerosol and natural forcings in HadCM3; Tett et al., 2002)

Few detection studies have explicitly considered the influence of observational uncertainty on near-surface temperature changes. However, Hegerl et al. (2001) show that inclusion of observational sampling uncertainty has relatively little effect on detection results and that random instrumental error has even less effect. Systematic instrumental errors, such as changes in measurement practices or urbanisation, could be more important, especially earlier in the record (Chapter 3), although these errors are calculated to be relatively small at large spatial scales. Urbanisation effects appear to have negligible effects on continental and hemispheric average temperatures (Chapter 3). Observational uncertainties are likely to be more important for surface temperature changes averaged over small regions (Section 9.4.2) and for analyses of free atmosphere temperature changes (Section 9.4.4).

9.4.2 Continental and Sub-continental Surface Temperature Change

9.4.2.1 Observed Changes

Over the 1901 to 2005 period there has been warming over most of the Earth's surface with the exception of an area south of Greenland and parts of North and South America (Figure 3.9 and Section 3.2.2.7, see also Figure 9.6). Warming has been strongest over the continental interiors of Asia and north-western North America and some mid-latitude ocean regions of the SH as well as south-eastern Brazil. Since 1979, almost all land areas with observational data coverage show warming (Figure 9.6). Warming is smaller in the SH than in the NH, with cooling over parts of the mid-latitude oceans. There have been widespread decreases in continental DTR since the 1950s which coincide with increases in cloud amounts (Section 3.4.3.1).

9.4.2.2 Studies Based on Space-Time Patterns

Global-scale analyses using space-time detection techniques (Section 9.4.1.4) have robustly identified the influence of anthropogenic forcing on the 20th-century global climate. A number of studies have now extended these analyses to consider sub-global scales. Two approaches have been used; one to assess the extent to which global studies can provide information at sub-global scales, the other to assess the influence of external forcing on the climate in specific regions. Limitations and problems in using smaller spatial scales are discussed at the end of this section.

The approach taken by IDAG (2005) was to compare analyses of full space-time fields with results obtained after removing the globally averaged warming trend, or after removing the annual global mean from each year in the analysis. They find that the detection of anthropogenic climate change is driven by the pattern of the observed warming in space and time, not just by consistent global mean temperature trends between models and observations. These results suggest that greenhouse warming should also be detectable at sub-global scales (see also Barnett et al., 1999). It was also shown by IDAG (2005) that uncertainties increase, as expected, when global mean information, which has a high signal-to-noise ratio, is disregarded (see also North et al., 1995).

Another approach for assessing the regional influence of external forcing is to apply detection and attribution analyses to observations in specific continental- or sub-continental scale regions. A number of studies using a range of models and examining various continental- or sub-continental scale land areas find a detectable human influence on 20th-century temperature changes, either by considering the 100-year period from 1900 or the 50-year period from 1950. Stott (2003) detects the warming effects of increasing greenhouse gas concentrations in six continental-scale regions over the 1900 to 2000 period, using HadCM3 simulations. In most regions, he finds that cooling from sulphate aerosols counteracts some of the greenhouse warming. However, the separate detection of a sulphate aerosol signal in regional analyses remains difficult because of lower signal-to-noise ratios, loss of large-scale spatial features of response such as hemispheric asymmetry that help to distinguish different signals, and greater modelling and forcing uncertainty at smaller scales. Zwiers and Zhang (2003) also detect human influence using two models (CGCM1 and CGCM2; see Table 8.1, McAvaney et al., 2001) over the 1950 to 2000 period in a series of nested regions, beginning with the full global domain and descending to separate continental domains for North America and Eurasia. Zhang et al. (2006) update this study using additional models (HadCM2 and HadCM3). They find evidence that climates in both continental domains have been influenced by anthropogenic emissions during 1950 to 2000, and generally also in the sub-continental domains (Figure 9.11). This finding is robust to the exclusion of NAO/Arctic Oscillation (AO) related variability, which is associated with part of the warming in Central Asia and could itself be related to anthropogenic forcing (Section 9.5.3). As the spatial scales considered become smaller, the uncertainty in estimated signal amplitudes (as demonstrated by the size of the vertical bars in Figure 9.11) becomes larger, reducing the signal-to-noise ratio (see also Stott and Tett, 1998). The signal-to-noise ratio, however, also depends on the strength of the climate change

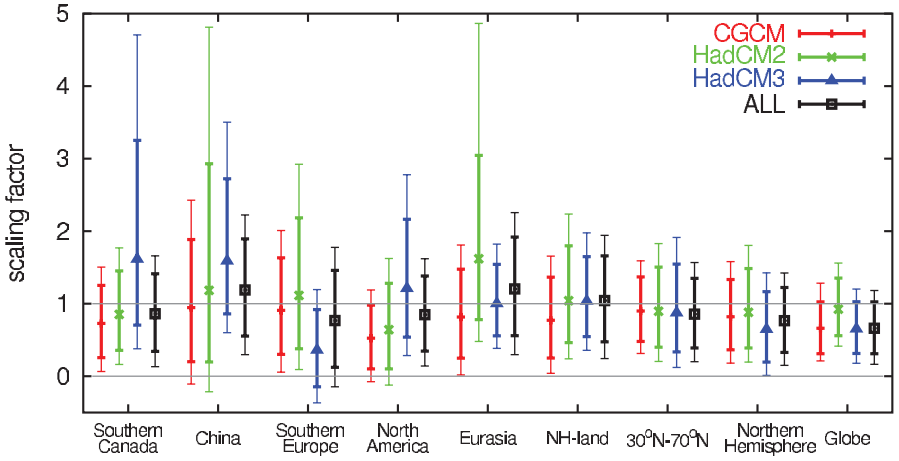


Figure 9.11. *Scaling factors indicating the match between observed and simulated decadal near-surface air temperature change (1950–1999) when greenhouse gas and aerosol forcing responses (GS) are taken into account in 'optimal' detection analyses (Appendix 9.A), at a range of spatial scales from global to sub-continental. Thick bars indicate 90% confidence intervals on the scaling factors, and the thin extensions indicate the increased width of these confidence intervals when estimates of the variance due to internal variability are doubled. Scaling factors and uncertainties are provided for different spatial domains including Canada (Canadian land area south of 70°N), China, Southern Europe (European land area bounded by 10°W to 40°E, 35° to 50°N), North America (North American land area between 30°N and 70°N), Eurasia (Eurasian land area between 30°N and 70°N), mid-latitude land area between 30°N and 70°N (labelled NH-land), the NH mid-latitudes (30°N to 70°N including land and ocean), the NH, and the globe. The GS signals are obtained from CGCM1 and CGCM2 combined (labelled CGCM, see Table 8.1 of the TAR), HadCM2 (see Table 8.1 of the TAR), and HadCM3 (see Table 8.1, this report), and these four models combined ('ALL'). After Zhang et al. (2006) and Hegerl et al. (2006b).*

and the local level of natural variability, and therefore differs between regions. Most of the results noted above hold even if the estimate of internal climate variability from the control simulation is doubled.

The ability of models to simulate many features of the observed temperature changes and variability at continental and sub-continental scales and the detection of anthropogenic effects on each of six continents provides stronger evidence of human influence on climate than was available to the TAR. A comparison between a large ensemble of 20th-century simulations of regional temperature changes made with the MMD at PCMDI (using the same simulations for which the global mean temperatures are plotted in Figure 9.5) shows that the spread of the multi-model ensembles encompasses the observed changes in regional temperature changes in almost all sub-continental regions (Figure 9.12; see also FAQ 9.2, Figure 1 and related figures in Chapter 11). In many of the regions, there is a clear separation between the ensembles of simulations that include only natural forcings and those that contain both anthropogenic and natural forcings. A more detailed analysis of one particular model, HadCM3, shows that it reproduces many features of the observed temperature changes and variability in the different regions (IDAG, 2005). The GFDL-CM2 model (see Table 8.1) is also able to reproduce many features of the evolution of temperature change in a number of regions of the globe (Knutson et al., 2006). Other studies show success at simulating regional temperatures when models include anthropogenic and natural forcings. Wang et al. (2007) showed that all MMD 20C3M simulations replicated the late 20th-century arctic warming to various degrees, while both forced and control simulations reproduce multi-year arctic warm anomalies similar in magnitude to the observed mid 20th-century warming event.

There is some evidence that an anthropogenic signal can now be detected in some sub-continental scale areas using formal detection methods (Appendix 9.A.1), although this evidence is weaker than at continental scales. Zhang et al. (2006) detect anthropogenic fingerprints in China and southern Canada. Spagnoli et al. (2002) find some evidence for a human influence on 30-year trends of summer daily minimum temperatures in France, but they use a fingerprint estimated from a simulation of future climate change and do not detect an anthropogenic influence on the other indices they consider, including summer maximum daily temperatures and winter temperatures. Min et al. (2005) find an anthropogenic influence on East Asian temperature changes in a Bayesian framework, but they do not consider anthropogenic aerosols or natural forcings in their analysis. Atmosphere-only general circulation model (AGCM) simulations forced with observed SSTs can potentially detect anthropogenic influence at smaller spatial and temporal scales than coupled model analyses, but have the weakness that they do not explain the observed SST changes (Sexton et al., 2003). Two studies have applied attribution analysis to sub-continental temperatures to make inferences about changes in related variables. Stott et al. (2004) detect an anthropogenic influence on southern European summer mean temperature changes of the past 50 years and then infer the likelihood of exceeding an extreme temperature threshold (Section 9.4.3.3). Gillett et al. (2004a) detect an anthropogenic contribution to summer season warming in Canada and demonstrate a statistical link with area burned in forest fires. However, the robustness of these results to factors such as the choice of model or analysis method remains to be established given the limited number of studies at sub-continental scales.

Knutson et al. (2006) assess temperature changes in regions of the world covering between 0.3 and 7.4% of the area of the globe and including tropical and extratropical land and ocean regions. They find much better agreement between climate simulations and observations when the models include rather than exclude anthropogenic forcings, which suggests a detectable anthropogenic warming signal over many of the regions they examine. This would indicate the potential for formal detection studies to detect anthropogenic warming in many of these regions, although Knutson et al. (2006) also note that in some regions the climate simulations they examined were not very realistic and showed that some of these discrepancies are associated with modes of variability such as the AO.

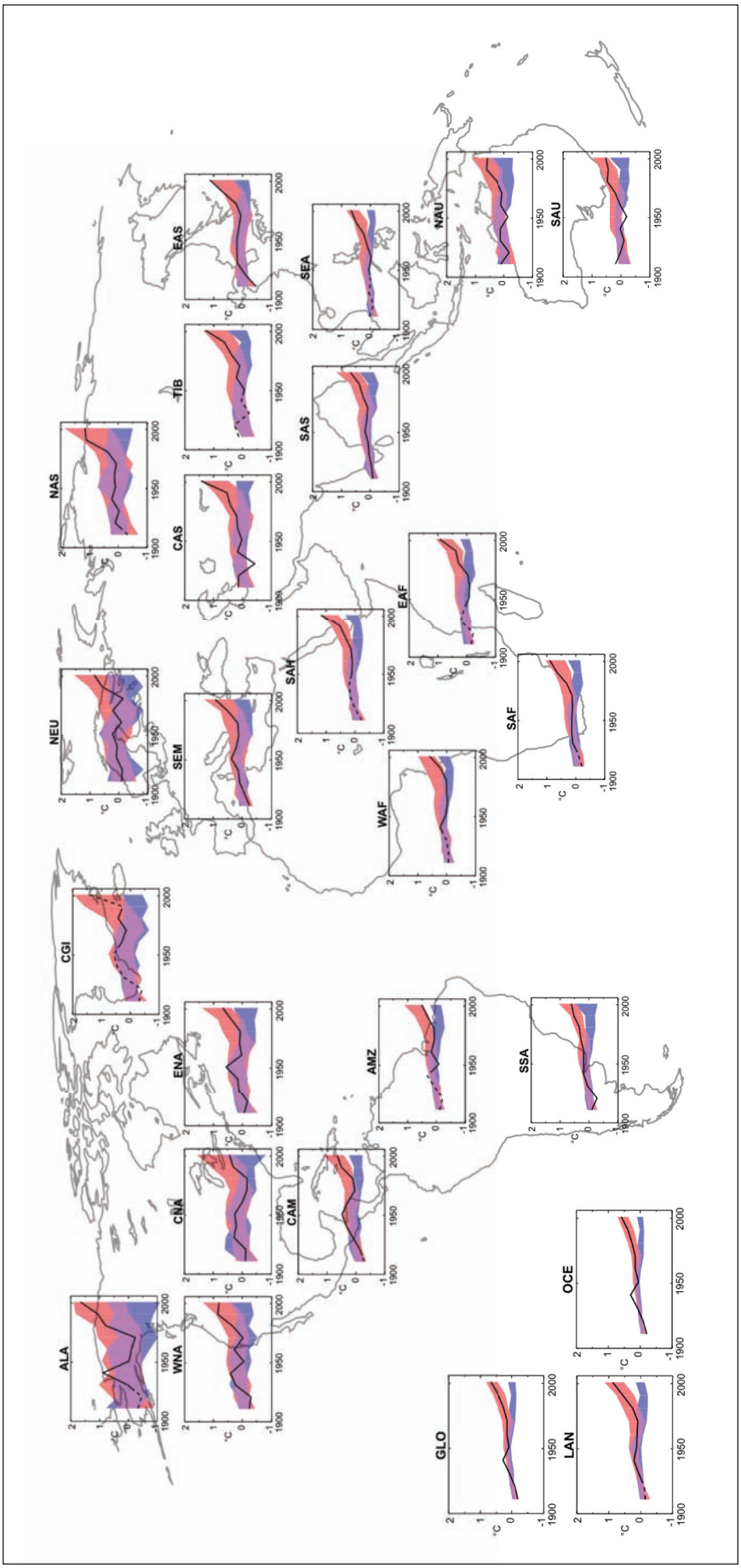


Figure 9.12. *Comparison of multi-model data set 20C3M model simulations containing all forcings (red shaded regions) and containing natural forcings only (blue shaded regions) with observed decadal mean temperature changes (°C) from 1906 to 2005 from the Hadley Centre/Climatic Research Unit gridded surface temperature data set (HadCRUT3; Brohan et al., 2006). The panel labelled GLO shows comparison for global mean; LAN, global land; and OCE, global ocean data. Remaining panels display results for 22 sub-continental scale regions (see the Supplementary Material, Appendix 9.C for a description of the regions). This figure is produced identically to FAQ 9.2, Figure 1 except sub-continental regions were used; a full description of the procedures for producing FAQ 9.2, Figure 1 is given in the Supplementary Material, Appendix 9.C. Shaded bands represent the middle 90% range estimated from the multi-model ensemble. Note that the model simulations have not been scaled in any way. The same simulations are used as in Figure 9.5 (58 simulations using all forcings from 14 models, and 19 simulations using natural forcings only from 5 models). Each simulation was sampled so that coverage corresponds to that of the observations, and was centred relative to the 1901 to 1950 mean obtained by that simulation in the region of interest. Observations in each region were centred relative to the same period. The observations in each region are generally consistent with model simulations that include anthropogenic and natural forcings, whereas in many regions the observations are inconsistent with model simulations that include natural forcings only. Lines are dashed where spatial coverage is less than 50%.*

Frequently Asked Question 9.1

Can Individual Extreme Events be Explained by Greenhouse Warming?

Changes in climate extremes are expected as the climate warms in response to increasing atmospheric greenhouse gases resulting from human activities, such as the use of fossil fuels. However, determining whether a specific, single extreme event is due to a specific cause, such as increasing greenhouse gases, is difficult, if not impossible, for two reasons: 1) extreme events are usually caused by a combination of factors and 2) a wide range of extreme events is a normal occurrence even in an unchanging climate. Nevertheless, analysis of the warming observed over the past century suggests that the likelihood of some extreme events, such as heat waves, has increased due to greenhouse warming, and that the likelihood of others, such as frost or extremely cold nights, has decreased. For example, a recent study estimates that human influences have more than doubled the risk of a very hot European summer like that of 2003.

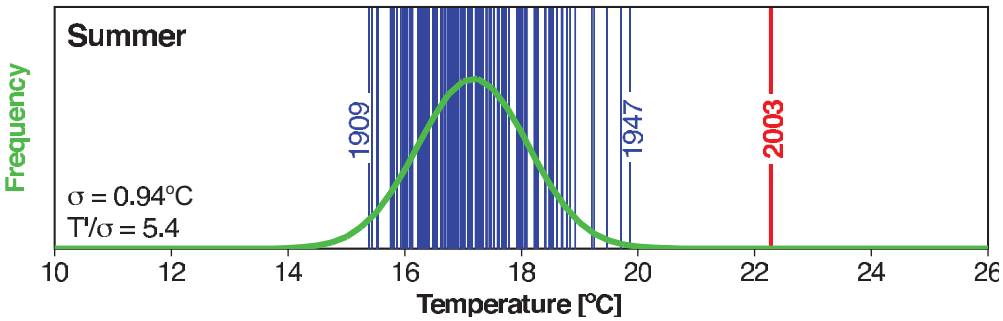
People affected by an extreme weather event often ask whether human influences on the climate could be held to some extent responsible. Recent years have seen many extreme events that some commentators have linked to increasing greenhouse gases. These include the prolonged drought in Australia, the extremely hot summer in Europe in 2003 (see Figure 1), the intense North Atlantic hurricane seasons of 2004 and 2005 and the extreme rainfall events in Mumbai, India in July 2005. Could a human influence such as increased concentrations of greenhouse gases in the atmosphere have 'caused' any of these events?

Extreme events usually result from a combination of factors. For example, several factors contributed to the extremely hot European summer of 2003, including a persistent high-pressure system that was associated with very clear skies and dry soil, which left more solar energy available to heat the land because less energy was consumed to evaporate moisture from the soil. Similarly, the formation of a hurricane requires warm sea surface temperatures and specific atmospheric circulation conditions. Because some factors may be strongly affected by human activities, such as sea surface temperatures, but others may not, it is not simple to detect a human influence on a single, specific extreme event.

Nevertheless, it may be possible to use climate models to determine whether human influences have changed the likelihood of certain types of extreme events. For example, in the case of the 2003 European heat wave, a climate model was run including only historical changes in natural factors that affect the climate, such as volcanic activity and changes in solar output. Next, the model was run again including both human and natural factors, which produced a simulation of the evolution of the European climate that was much closer to that which had actually occurred. Based on these experiments, it was estimated that over the 20th century, human influences more than doubled the risk of having a summer in Europe as hot as that of 2003, and that in the absence of human influences, the risk would probably have been one in many hundred years. More detailed modelling work will be required to estimate the change in risk for specific high-impact events, such as the occurrence of a series of very warm nights in an urban area such as Paris.

The value of such a probability-based approach – 'Does human influence change the likelihood of an event?' – is that it can be used to estimate the influence of external factors, such as increases in greenhouse gases, on the frequency of specific types of events, such as heat waves or frost. Nevertheless, careful statistical analyses are required, since the likelihood of individual extremes, such as a late-spring frost, could change due to changes in climate variability as well as changes in average climate conditions. Such analyses rely on climate-model based estimates of climate variability, and thus the climate models used should adequately represent that variability.

The same likelihood-based approach can be used to examine changes in the frequency of heavy rainfall or floods. Climate models predict that human influences will cause an increase in many types of extreme events, including extreme rainfall. There is already evidence that, in recent decades, extreme rainfall has increased in some regions, leading to an increase in flooding.



FAQ 9.1, Figure 1. *Summer temperatures in Switzerland from 1864 to 2003 are, on average, about 17°C, as shown by the green curve. During the extremely hot summer of 2003, average temperatures exceeded 22°C, as indicated by the red bar (a vertical line is shown for each year in the 137-year record). The fitted Gaussian distribution is indicated in green. The years 1909, 1947 and 2003 are labelled because they represent extreme years in the record. The values in the lower left corner indicate the standard deviation (σ) and the 2003 anomaly normalised by the 1864 to 2000 standard deviation (T'/σ). From Schär et al. (2004).*

Karoly and Wu (2005) compare observed temperature trends in 5° × 5° grid boxes globally over 30-, 50- and 100-year periods ending in 2002 with 1) internal variability as simulated by three models (GFDL R30, HadCM2, PCM) and 2) the simulated response to greenhouse gas and sulphate aerosol forcing in those models (see also Knutson et al., 1999). They find that a much higher percentage of grid boxes show trends that are inconsistent with model-estimated internal variability than would be expected by chance and that a large fraction of grid boxes show changes that are consistent with the forced simulations, particularly over the two shorter periods. This assessment is essentially a global-scale detection result because its interpretation relies upon a global composite of grid-box scale statistics. As discussed in the paper, this result does not rule out the possibility that individual grid box trends may be explained by different external forcing combinations, particularly since natural forcings and forcings that could be important at small spatial scales, such as land use change or black carbon aerosols, are missing from these models. The demonstration of local consistency between models and observations in this study does not necessarily imply that observed changes can be attributed to anthropogenic forcing in a specific grid box, and it does not allow confident estimates of the anthropogenic contribution to change at those scales.

Models do not reproduce the observed temperature changes equally well in all regions. Areas where temperature changes are not particularly well simulated by some models include parts of North America (Knutson et al., 2006) and mid-Asia (IDAG, 2005). This could be due to a regional trend or variation that was caused by internal variability (a result that models would not be expected to reproduce), uncertain forcings that are locally important, or model errors. Examples of uncertain forcings that play a small role globally, but could be more important regionally, are the effects of land use changes (Sections 9.2 and 9.3) or atmospheric brown clouds. The latter could be important in explaining observed temperature trends in South Asia and the northern Indian Ocean (Ramanathan et al., 2005; see Chapter 2).

An analysis of the MMD 20C3M experiments indicates that multi-decadal internal variability could be responsible for some of the rapid warming seen in the central USA between 1901 and 1940 and rapid cooling between 1940 and 1979 (Kunkel et al., 2006). Also, regional temperature is more strongly influenced by variability and changes in climate dynamics, such as temperature changes associated with the NAO, which may itself show an anthropogenic influence (Section 9.5.3.2), or the Atlantic Multi-decadal Oscillation (AMO), which could in some regions and seasons be poorly simulated by models and could be confounded with the expected temperature response to external forcings. Thus the anthropogenic signal is likely to be more easy to identify in some regions than in others, with temperature changes in those regions most affected by multi-decadal scale variability being the most difficult to attribute, even if those changes are inconsistent with model estimated internal variability and therefore detectable.

The extent to which temperature changes at sub-continental scales can be attributed to anthropogenic forcings, and the extent to which it is possible to estimate the contribution of greenhouse gas forcing to regional temperature trends, remains a topic for further research. Idealised studies (e.g., Stott and Tett, 1998) suggest that surface temperature changes are detectable mainly at large spatial scales of the order of several thousand kilometres (although they also show that as the signal of climate change strengthens in the 21st century, surface temperature changes are expected to become detectable at increasingly smaller scales). Robust detection and attribution are inhibited at the grid box scales because it becomes difficult to separate the effects of the relatively well understood large-scale external influences on climate, such as greenhouse gas, aerosols, solar and volcanic forcing, from each other and from local influences that may not be related to these large-scale forcings. This occurs because the contribution from internal climate variability increases at smaller scales, because the spatial details that can help to distinguish between different forcings at large scales are not available or unreliable at smaller scales, and because forcings that could be important at small spatial scales, such as land use change or black carbon aerosols, are uncertain and may not have been included in the models used for detection. Although models do not typically underestimate natural internal variability of temperature at continental scales over land (Figure 9.8), even at a grid box scale (Karoly and Wu, 2005), the credibility of small-scale details of climate simulated by models is lower than for large-scale features. While the large-scale coherence of temperatures means that temperatures at a particular grid box should adequately represent a substantial part of the variability of temperatures averaged over the area of that grid box, the remaining variability from local-scale processes and the upward cascades from smaller to larger scales via nonlinear interactions may not be well represented in models at the grid box scale. Similarly, the analysis of shorter temporal scales also decreases the signal-to-noise ratio and the ability to use temporal information to distinguish between different forcings. This is why most detection and attribution studies use temporal scales of 50 or more years.

9.4.2.3 Studies Based on Indices of Temperature Change and Temperature-Precipitation Relationships

Studies based on indices of temperature change support the robust detection of human influence on continental-scale land areas. Observed trends in indices of North American continental-scale temperature change, (including the regional mean, the mean land-ocean temperature contrast and the annual cycle) were found by Karoly et al. (2003) to be generally consistent with simulated trends under historical forcing from greenhouse gases and sulphate aerosols during the second half of the 20th century. In contrast, they find only a small likelihood of agreement with trends driven by natural forcing only during this period. An analysis of changes in Australian mean, daily maximum and daily minimum temperatures and diurnal temperature range using six coupled climate models showed that it is likely that

there has been a significant contribution to observed warming in Australia from increasing greenhouse gases and sulphate aerosols (Karoly and Braganza, 2005a). An anomalous warming has been found over all Australia (Nicholls, 2003) and in New South Wales (Nicholls et al., 2005) since the early 1970s, associated with a changed relationship between annual mean maximum temperature and rainfall. Whereas interannual rainfall and temperature variations in this region are strongly inversely correlated, in recent decades temperatures have tended to be higher for a given rainfall than in previous decades. By removing the rainfall-related component of Australian temperature variations, thereby enhancing the signal-to-noise ratio, Karoly and Braganza (2005b) detect an anthropogenic warming signal in south-eastern Australia, although their results are affected by some uncertainty associated with their removal of rainfall-related temperature variability. A similar technique applied to the Sudan and Sahel region improved the agreement between model simulations and observations of temperature change over the last 60 years in this region (Douville, 2006) and could improve the detectability of regional temperature signals over other regions where precipitation is likely to affect the surface energy budget (Trenberth and Shea, 2005).

9.4.3 Surface Temperature Extremes

9.4.3.1 Observed Changes

Observed changes in temperature extremes are consistent with the observed warming of the climate (Alexander et al., 2006) and are summarised in Section 3.8.2.1. There has been a widespread reduction in the number of frost days in mid-latitude regions in recent decades, an increase in the number of warm extremes, particularly warm nights, and a reduction in the number of cold extremes, particularly cold nights. A number of regional studies all show patterns of changes in extremes consistent with a general warming, although the observed changes in the tails of the temperature distributions are generally not consistent with a simple shift of the entire distribution alone.

9.4.3.2 Global Assessments

Evidence for observed changes in short-duration extremes generally depends on the region considered and the analysis method (IPCC, 2001). Global analyses have been restricted by the limited availability of quality-controlled and homogenised daily station data. Indices of temperature extremes have been calculated from station data, including some indices from regions where daily station data are not released (Frich et al., 2002; Klein Tank and Können, 2003; Alexander et al., 2006). Kiktev et al. (2003) analyse a subset of such indices by using fingerprints from atmospheric model simulations driven by prescribed SSTs. They find significant decreases in the number of frost days and increases in the number of very warm nights over much of the NH. Comparisons of observed and modelled trend estimates show that inclusion of anthropogenic effects in the model integrations improves the simulation of these changing temperature extremes, indicating that human influences are probably an important contributor to changes in the number of frost days and warm nights. Tebaldi et al. (2006) find that changes simulated by eight MMD models agreed well with observed trends in heat waves, warm nights and frost days over the last four decades.

Christidis et al. (2005) analyse a new gridded data set of daily temperature data (Caesar et al., 2006) using the indices shown by Hegerl et al. (2004) to have a potential for attribution, namely the average temperature of the most extreme 1, 5, 10 and 30 days of the year. Christidis et al. (2005) detect robust anthropogenic changes in indices of extremely warm nights using signals estimated with the HadCM3 model, although with some indications that the model overestimates the observed warming of warm nights. They also detect human influence on cold days and nights, but in this case the model underestimates the observed changes, significantly so in the case of the coldest day of the year. Anthropogenic influence was not detected in observed changes in extremely warm days.

9.4.3.3 Attributable Changes in the Risk of Extremes

Many important impacts of climate change may manifest themselves through a change in the frequency or likelihood of occurrence of extreme events. While individual extreme events cannot be attributed to external influences, a change in the probability of such events might be attributable to external influences (Palmer, 1999; Palmer and Räisänen, 2002). One study estimates that anthropogenic forcings have significantly increased the risk of extremely warm summer conditions over southern Europe, as was observed during the 2003 European heat wave. Stott et al. (2004) apply a methodology for making quantitative statements about change in the likelihood of such specific types of climatic events (Allen, 2003; Stone and Allen, 2005a), by expressing the contribution of external forcing to the risk of an event exceeding a specific magnitude. If P_1 is the probability of a climatic event (such as a heat wave) occurring in the presence of anthropogenic forcing of the climate system, and P_0 is the probability of it occurring if anthropogenic forcing had not been present, then the fraction of the current risk that is attributable to past greenhouse gas emissions (fraction of attributable risk; FAR) is given by $\text{FAR} = 1 - P_0 / P_1$ (Allen, 2003). Stott et al. (2004) apply the FAR concept to mean summer temperatures of a large part of continental Europe and the Mediterranean. Using a detection and attribution analysis, they determine that regional summer mean temperature has likely increased due to anthropogenic forcing, and that the observed change is inconsistent with natural forcing. They then use the HadCM3 model to estimate the FAR associated with a particular extreme threshold of regional summer mean temperature that was exceeded in 2003, but in no other year since the beginning of the record in 1851. Stott et al. (2004) estimate that it is very likely that human influence has more than doubled the risk of the regional summer mean temperature exceeding this threshold (Figure 9.13).

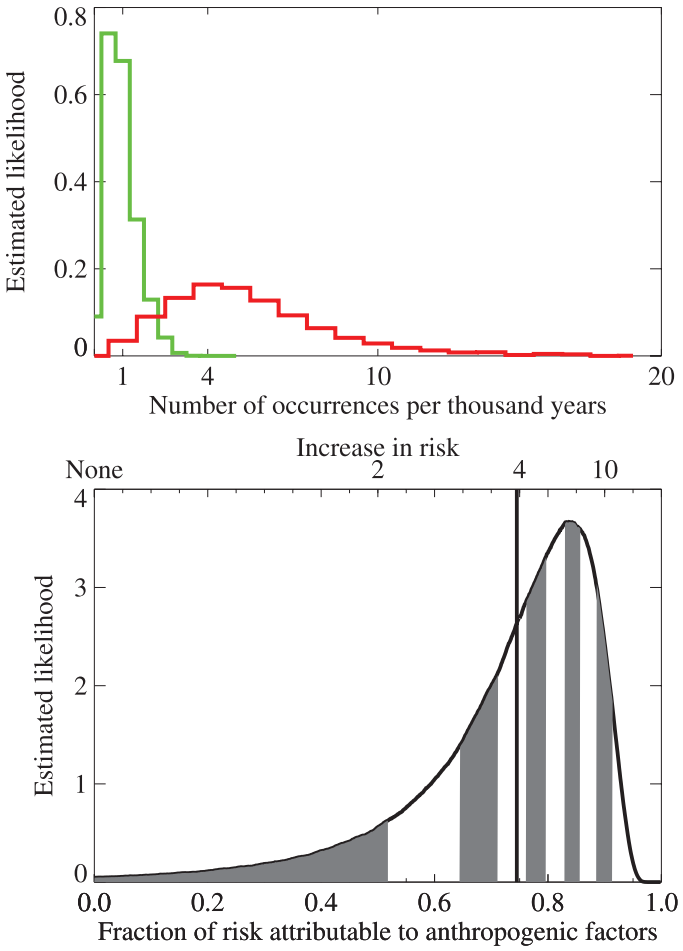


Figure 9.13. *Change in risk of mean European summer temperatures exceeding a threshold of 1.6°C above 1961 to 1990 mean temperatures, a threshold that was exceeded in 2003 but in no other year since the start of the instrumental record in 1851. (Top) Frequency histograms of the estimated likelihood of the risk (probability) of exceeding a 1.6°C threshold (relative to the 1961–1990 mean) in the 1990s in the presence (red curve) and absence (green curve) of anthropogenic change, expressed as an occurrence rate. (Bottom) Fraction of attributable risk (FAR). The vertical line indicates the 'best estimate' FAR, the mean risk attributable to anthropogenic factors averaged over the distribution. The alternation between grey and white bands indicates the deciles of the estimated FAR distribution. The shift from the green to the red distribution in (a) implies a FAR distribution with mean 0.75, corresponding to a four-fold increase in the risk of such an event (b). From Stott et al. (2004).*

This study considered only continental mean seasonally averaged temperatures. Consideration of shorter-term and smaller-scale heat waves will require higher resolution modelling and will need to take complexities such as land surface processes into account (Schär and Jendritzky, 2004). Also, Stott et al. (2004) assume no change in internal variability in the region they consider (which was the case in HadCM3 21st-century climate projections for summer mean temperatures in the region they consider), thereby ascribing the increase in risk only to an increase in mean temperatures (i.e., as shown in Box TS.5, Figure 1, which illustrates how a shift in the mean of a distribution can cause a large increase in the frequency of extremes). However, there is some evidence for a weak increase in European temperature variability in summer (and a decrease in winter) for the period 1961 to 2004 (Scherrer et al., 2005), which could contribute to an increase in the likelihood of extremes. Schär et al. (2004) show that the central European heat wave of 2003 could also be consistent with model-predicted increases in temperature variability due to soil moisture and vegetation feedbacks. In addition, multi-decadal scale variability, associated with basin-scale changes in the Atlantic Ocean related to the Meridional Overturning Circulation (MOC) could have contributed to changes in European summer temperatures (Sutton and Hodson, 2005), although Klein Tank et al. (2005) show evidence that patterns of change in European temperature variance in spring and summer are not consistent with patterns of change in temperature variance expected from natural variability. Meteorological aspects of the summer 2003 European heat wave are discussed in Box 3.6.

9.4.4 Free Atmosphere Temperature

9.4.4.1 Observed Changes

Observed free atmosphere temperature changes are discussed in Section 3.4.1 and Karl et al. (2006) provide a comprehensive review. Radiosonde-based observations (with near global coverage since 1958) and satellite-based temperature measurements (beginning in late 1978) show warming trends in the troposphere and cooling trends in the stratosphere. All data sets show that the global mean and tropical troposphere has warmed from 1958 to the present, with the warming trend in the troposphere slightly greater than at the surface. Since 1979, it is likely that there is slightly greater warming in the troposphere than at the surface, although uncertainties remain in observed tropospheric warming trends and whether these are greater or less than the surface trend. The range (due to different data sets) of the global mean tropospheric temperature trend since 1979 is 0.12°C to 0.19°C per decade based on satellite-based estimates (Chapter 3) compared to a range of 0.16°C to 0.18°C per decade for the global surface warming. While all data sets show that the stratosphere has cooled considerably from 1958 and from 1979 to present, there are large differences in the linear trends estimated from different data sets. However, a linear trend is a poor fit to the data in the stratosphere and the tropics at all levels (Section 3.4.1). The uncertainties in the observational records are discussed in detail in Section 3.4.1 and by Karl et al. (2006). Uncertainties remain in homogenised radiosonde data sets which could result in a spurious inference of net cooling in the tropical troposphere. Differences between temperature trends measured from different versions of tropospheric satellite data result primarily from differences in how data from different satellites are merged.

9.4.4.2 Changes in Tropopause Height

The height of the lapse rate tropopause (the boundary between the stratosphere and the troposphere) is sensitive to bulk changes in the thermal structure of the stratosphere and the troposphere, and may also be affected by changes in surface temperature gradients

(Schneider, 2004). Analyses of radiosonde data have documented increases in tropopause height over the past 3 to 4 decades (Highwood et al., 2000; Seidel et al., 2001). Similar increases have been inferred from three different reanalysis products, the European Centre for Medium Range Weather Forecasts (ECMWF) 15- and 40-year reanalyses (ERA-15 and ERA-40) and the NCAR- National Center for Environmental Prediction (NCEP) reanalysis (Kalnay et al., 1996; Gibson et al., 1997; Simmons and Gibson, 2000; Kistler et al., 2001), and from model simulations with combined anthropogenic and natural forcing (Santer et al., 2003a,b, 2004; see Figure 9.14). In both models and reanalyses, changes in tropopause height over the satellite and radiosonde eras are smallest in the tropics and largest over Antarctica (Santer et al., 2003a,b, 2004). Model simulations with individual forcings indicate that the major drivers of the model tropopause height increases are ozone-induced stratospheric cooling and the tropospheric warming caused by greenhouse gas increases (Santer et al., 2003a). However, earlier model studies have found that it is difficult to alter tropopause height through stratospheric ozone changes alone (Thuburn and Craig, 2000). Santer et al. (2003c) found that the model-simulated response to combined anthropogenic and natural forcing is robustly detectable in different reanalysis products, and that solar and volcanic forcing alone could not explain the tropopause height increases (Figure 9.14). Climate data from reanalyses, especially the 'first generation' reanalysis analysed by Santer et al. (2003a), are subject to some deficiencies, notably inhomogeneities related to changes over time in the availability and quality of input data, and are subject to a number of specific technical choices in the reanalysis scheme (see Santer et al., 2004, for a discussion). Also, the NCEP reanalysis detection results could be due to compensating errors because of excessive stratospheric cooling in the reanalysis (Santer et al., 2004), since the stratosphere cools more relative to the troposphere in the NCEP reanalysis while models warm the troposphere. In contrast, the finding of a significant anthropogenic influence on tropopause height in the 'second generation' ERA-40 reanalysis is driven by similar large-scale changes in both models and the reanalysis. Detection results there are robust to removing global mean tropopause height increases.

9.4.4.3 Overall Atmospheric Temperature Change

Anthropogenic influence on free atmosphere temperatures has been detected in analyses of satellite data since 1979, although this finding has been found to be sensitive to which analysis of satellite data is used. Satellite-borne MSUs, beginning in 1978, estimate the temperature of thick layers of the atmosphere. The main layers represent the lower troposphere ($T2_{LT}$), the mid-troposphere (T2) and the lower stratosphere (T4) (Section 3.4.1.2.1). Santer et al. (2003c) compare T2 and T4 temperature changes simulated by the PCM model including anthropogenic and natural forcings with the University of Alabama in Huntsville (UAH; Christy et al., 2000) and Remote Sensing Systems (RSS; Mears and Wentz, 2005) satellite data sets (Section 3.4.1.2.2). They find that the model fingerprint of the T4 response to combined anthropogenic and natural forcing is consistently detected in both satellite data sets, whereas the T2 response is detected only in the RSS data set. However, when the global mean changes are removed, the T2 fingerprint is detected in both data sets, suggesting a common spatial pattern of response overlain by a systematic global mean difference.

Anthropogenic influence on free atmosphere temperatures has been robustly detected in a number of different studies analysing various versions of the Hadley Centre Radiosonde Temperature (HadRT2) data set (Parker et al., 1997) by means of a variety of different diagnostics and fingerprints estimated with the HadCM2 and HadCM3 models (Tett et al., 2002; Thorne et al., 2002, 2003; Jones et al., 2003). Whereas an analysis of spatial

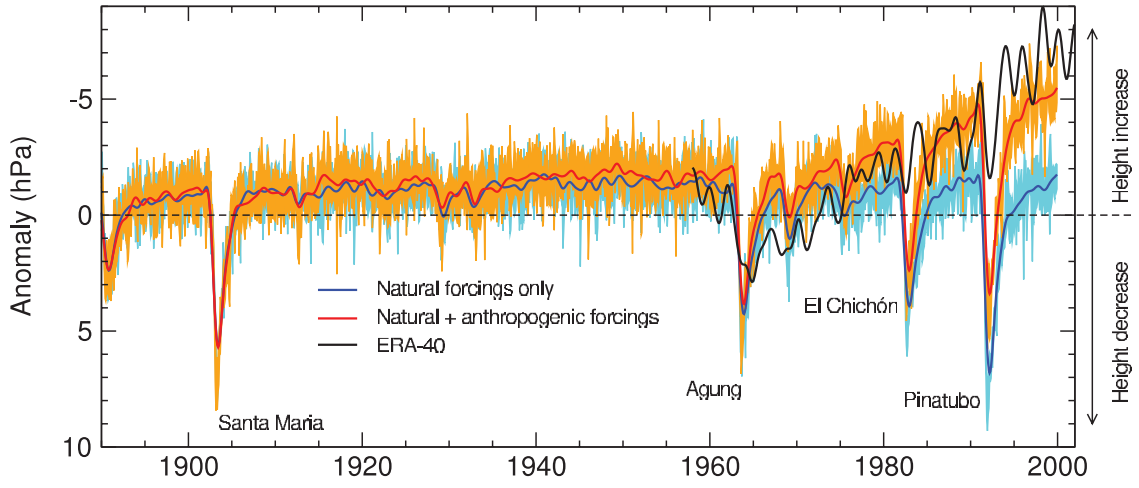


Figure 9.14. *Comparison between reanalysis and climate-model simulated global monthly mean anomalies in tropopause height. Model results are from two different PCM (Table 8.1) ensemble experiments using either natural forcings, or natural and anthropogenic forcings (ALL). There are four realisations of each experiment. Both the low-pass filtered ensemble mean and the unfiltered range between the highest and lowest values of the realisations are shown. All model anomalies are defined relative to climatological monthly means computed over 1890 to 1999. Reanalysis-based tropopause height anomalies estimated from ERA-40 were filtered in the same way as model data. The ERA-40 record spans 1957 to 2002 and was forced to have the same mean as ALL over 1960 to 1999. After Santer et al. (2003a) and Santer et al. (2004).*

patterns of zonal mean free atmosphere temperature changes was unable to detect the response to natural forcings (Tett et al., 2002), an analysis of spatio-temporal patterns detected the influence of volcanic aerosols and (less convincingly) solar irradiance changes, in addition to detecting the effects of greenhouse gases and sulphate aerosols (Jones et al., 2003). In addition, Crooks (2004) detects a solar signal in atmospheric temperature changes as seen in the HadRT2.1s radiosonde data set when a diagnostic chosen to extract the solar signal from other signals is used. The models used in these studies have poor vertical resolution in the stratosphere and they significantly underestimate stratospheric variability, thus possibly overestimating the significance of these detected signals (Tett et al., 2002). However, a sensitivity study (Thorne et al., 2002) showed that detection of human influence on free atmosphere temperature changes does not depend on the inclusion of stratospheric temperatures. An analysis of spatial patterns of temperature change, represented by large-scale area averages at the surface, in broad atmospheric layers and in lapse rates between layers, showed robust detection of an anthropogenic influence on climate when a range of uncertainties were explored relating to the choice of fingerprints and the radiosonde and model data sets (Thorne et al., 2003). However, Thorne et al. were not able to attribute recent observed tropospheric temperature changes to any particular combination of external forcing influences because the models analysed (HadCM2 and HadCM3) overestimate free atmosphere warming as estimated by the radiosonde data sets, an effect also seen by Douglass et al. (2004) during the satellite era. However, there is evidence that radiosonde data during the satellite era are contaminated by spurious cooling trends (Sherwood et al., 2005; Randel and Wu, 2006; Section 3.4.1), and since structural uncertainty arising from the choice of techniques used to analyse radiosonde data has not yet been quantified (Thorne et al., 2005), it is difficult to assess, based on these analyses alone, whether model-data discrepancies are due to model or observational deficiencies. However further information is provided by an analysis of modelled and observed tropospheric lapse rates, discussed in Section 9.4.4.4.

A different approach is to assess detectability of observed temperature changes through the depth of the atmosphere with AGCM simulations forced with observed SSTs, although the vertical profile of the atmospheric temperature change signal estimated in this way can be quite different from the same signal estimated by coupled models with the same external forcings (Hansen et al., 2002; Sun and Hansen, 2003; Santer et al., 2005). Sexton et al. (2001) find that inclusion of anthropogenic effects improves the simulation of zonally averaged upper air temperature changes from the HadRTt1.2 data set such that an anthropogenic signal is detected at the 5% significance level in patterns of seasonal mean temperature change calculated as overlapping eight-year means over the 1976 to 1994 period and expressed as anomalies relative to the 1961 to 1975 base period. In addition, analysing patterns of annual mean temperature change for individual years shows that an anthropogenic signal is also detected on interannual time scales for a number of years towards the end of the analysis period.

9.4.4.4 Differential Temperature Trends

Subtracting temperature trends at the surface from those in the free atmosphere removes much of the common variability between these layers and tests whether the model-predicted trends in tropospheric lapse rate are consistent with those observed by radiosondes and satellites (Karl et al., 2006). Since 1979, globally averaged modelled trends in tropospheric lapse rates are consistent with those observed. However, this is not the case in the tropics, where most models have more warming aloft than at the surface while most observational estimates show more warming at the surface than in the troposphere (Karl et al., 2006). Karl et al. (2006) carried out a systematic review of this issue. There is greater consistency between simulated and observed differential warming in the tropics in some satellite measurements of tropospheric temperature change, particularly when the effect of the cooling stratosphere on tropospheric retrievals is taken into account (Karl et al., 2006). External forcing other than greenhouse gas changes can also help to reconcile some of the differential warming, since both volcanic eruptions and stratospheric ozone depletion are expected to have cooled the troposphere more than the surface over the last several decades (Santer et al., 2000, 2001; IPCC, 2001; Free and Angell, 2002; Karl et al., 2006). There are, however, uncertainties in quantifying the differential cooling caused by these forcings, both in models and observations, arising from uncertainties in the forcings and model response to the forcings. Differential effects of natural modes of variability, such as ENSO and the NAM, on observed surface and tropospheric temperatures, which arise from differences in the amplitudes and spatial expression of these modes at the surface and in the troposphere, make only minor contributions to the overall differences in observed surface and tropospheric warming rates (Santer et al., 2001; Hegerl and Wallace, 2002; Karl et al., 2006).

A systematic intercomparison between radiosonde-based (Radiosonde Atmospheric Temperature Products for Assessing Climate (RATPAC); Free et al., 2005, and Hadley Centre Atmospheric Temperature (HadAT), Thorne et al., 2005) and satellite-based (RSS, UAH) observational estimates of tropical lapse rate trends with those simulated by 19 MMD models shows that on monthly and annual time scales, variations in temperature at the surface are amplified aloft in both models and observations by consistent amounts (Santer et al., 2005; Karl et al., 2006). It is only on longer time scales that disagreement between modelled and observed lapse rates arises (Hegerl and Wallace, 2002), that is, on the time scales over which discrepancies would arise from inhomogeneities in the observational record. Only one observational data set (RSS) was found to be consistent with the models on both short and long time scales. While Vinnikov et al. (2006) have not produced a lower-tropospheric retrieval, their estimate of the T2 temperature trend (Figure 3.18) is consistent with model simulations (Karl et al., 2006). One possibility is that amplification effects are controlled by different physical mechanisms on short and long time scales, although a more probable explanation is that some observational records are contaminated by errors that affect their long-term trends (Section 3.4.1; Karl et al., 2006).

Frequently Asked Question 9.2

Can the Warming of the 20th Century be Explained by Natural Variability?

It is very unlikely that the 20th-century warming can be explained by natural causes. The late 20th century has been unusually warm. Palaeoclimatic reconstructions show that the second half of the 20th century was likely the warmest 50-year period in the Northern Hemisphere in the last 1300 years. This rapid warming is consistent with the scientific understanding of how the climate should respond to a rapid increase in greenhouse gases like that which has occurred over the past century, and the warming is inconsistent with the scientific understanding of how the climate should respond to natural external factors such as variability in solar output and volcanic activity. Climate models provide a suitable tool to study the various influences on the Earth's climate. When the effects of increasing levels of greenhouse gases are included in the models, as well as natural external factors, the models produce good simulations of the warming that has occurred over the past century. The models fail to reproduce the observed warming when run using only natural factors. When human factors are included, the models also simulate a geographic pattern of temperature change around the globe similar to that which has occurred in recent decades. This spatial pattern, which has features such as a greater warming at high northern latitudes, differs from the most important patterns of natural climate variability that are associated with internal climate processes, such as El Niño.

Variations in the Earth's climate over time are caused by natural internal processes, such as El Niño, as well as changes in external influences. These external influences can be natural in origin, such as volcanic activity and variations in solar output, or caused by human activity, such as greenhouse gas emissions, human-sourced aerosols, ozone depletion and land use change. The role of natural internal processes can be estimated by studying observed variations in climate and by running climate models without changing any of the external factors that affect climate. The effect of external influences can be estimated with models by changing these factors, and by using physical understanding of the processes involved. The combined effects of natural internal variability and natural external factors can also be estimated from climate information recorded in tree rings, ice cores and other types of natural 'thermometers' prior to the industrial age.

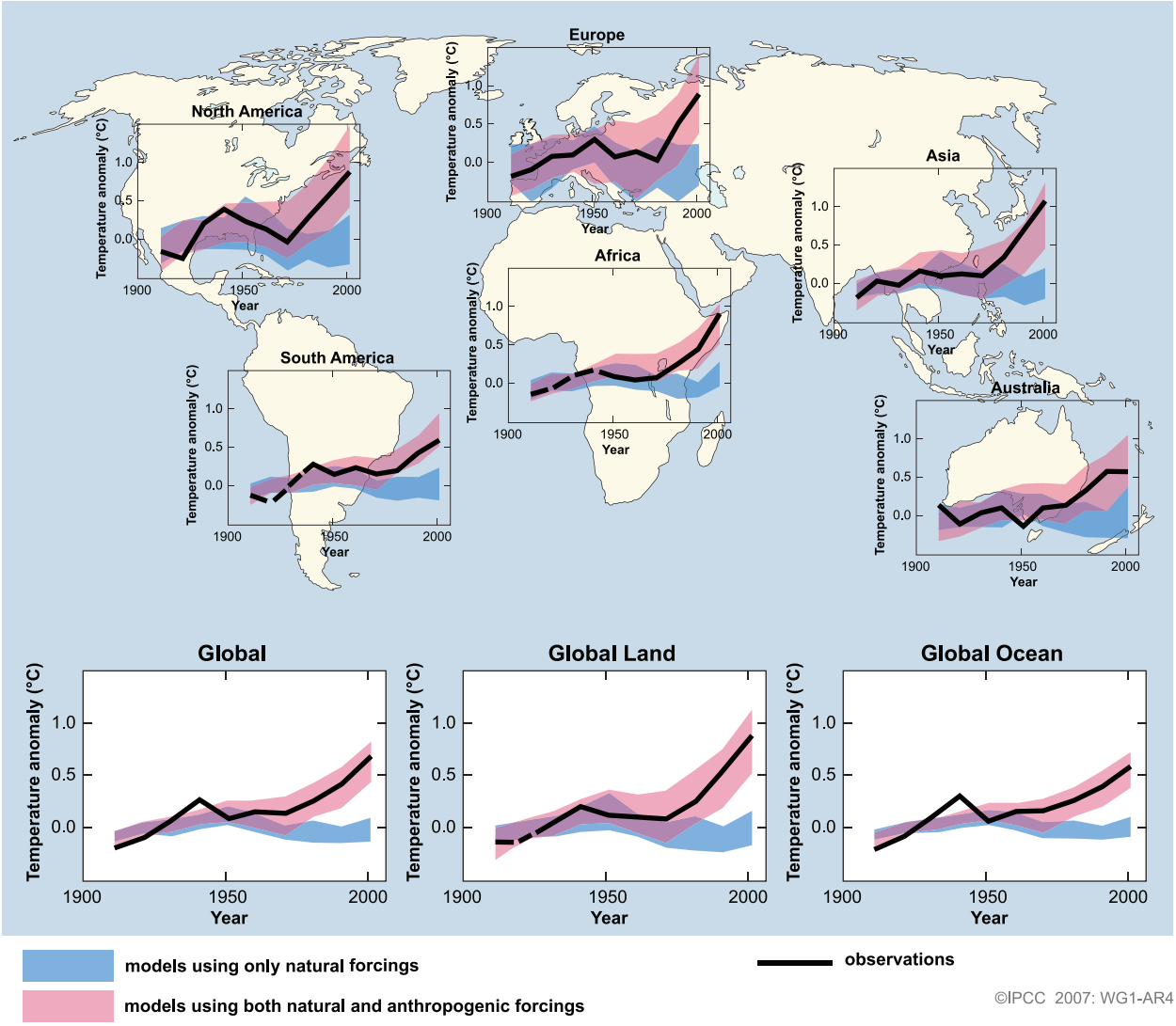
The natural external factors that affect climate include volcanic activity and variations in solar output. Explosive volcanic eruptions occasionally eject large amounts of dust and sulphate aerosol high into the atmosphere, temporarily shielding the Earth and reflecting sunlight back to space. Solar output has an 11-year cycle and may also have longer-term variations. Human activities over the last 100 years, particularly the burning of fossil fuels, have caused a rapid increase in carbon dioxide and other greenhouse gases in the atmosphere. Before the industrial age, these gases had remained at near stable concentrations for thousands of years. Human activities have also caused increased concentrations of fine reflective particles, or 'aerosols', in the atmosphere, particularly during the 1950s and 1960s.

Although natural internal climate processes, such as El Niño, can cause variations in global mean temperature for relatively short periods, analysis indicates that a large portion is due to external factors. Brief periods of global cooling have followed major volcanic eruptions, such as Mt. Pinatubo in 1991. In the early part of the 20th century, global average temperature rose, during which time greenhouse gas concentrations started to rise, solar output was probably increasing and there was little volcanic activity. During the 1950s and 1960s, average global temperatures levelled off, as increases in aerosols from fossil fuels and other sources cooled the planet. The eruption of Mt. Agung in 1963 also put large quantities of reflective dust into the upper atmosphere. The rapid warming observed since the 1970s has occurred in a period when the increase in greenhouse gases has dominated over all other factors.

Numerous experiments have been conducted using climate models to determine the likely causes of the 20th-century climate change. These experiments indicate that models cannot reproduce the rapid warming observed in recent decades when they only take into account variations in solar output and volcanic activity. However, as shown in Figure 1, models are able to simulate the observed 20th-century changes in temperature when they include all of the most important external factors, including human influences from sources such as greenhouse gases and natural external factors. The model-estimated responses to these external factors are detectable in the 20th-century climate globally and in each individual continent except Antarctica, where there are insufficient observations. The human influence on climate very likely dominates over all other causes of change in global average surface temperature during the past half century.

An important source of uncertainty arises from the incomplete knowledge of some external factors, such as human-sourced aerosols. In addition, the climate models themselves are imperfect. Nevertheless, all models simulate a pattern of response to greenhouse gas increases from human activities that is similar to the observed pattern of change. This pattern includes more warming over land than over the oceans. This pattern of change, which differs from the principal patterns of temperature change associated with natural internal variability, such as El Niño, helps to distinguish the response to greenhouse gases from that of natural external factors. Models and observations also both show warming in the lower part of

(continued)



FAQ 9.2, Figure 1. *Temperature changes relative to the corresponding average for 1901-1950 (°C) from decade to decade from 1906 to 2005 over the Earth's continents, as well as the entire globe, global land area and the global ocean (lower graphs). The black line indicates observed temperature change, while the coloured bands show the combined range covered by 90% of recent model simulations. Red indicates simulations that include natural and human factors, while blue indicates simulations that include only natural factors. Dashed black lines indicate decades and continental regions for which there are substantially fewer observations. Detailed descriptions of this figure and the methodology used in its production are given in the Supplementary Material, Appendix 9.C.*

the atmosphere (the troposphere) and cooling higher up in the stratosphere. This is another 'fingerprint' of change that reveals the effect of human influence on the climate. If, for example, an increase in solar output had been responsible for the recent climate warming, both the troposphere and the stratosphere would have warmed. In addition, differences in the timing of the human and natural external influences help to distinguish the climate responses to these factors. Such considerations increase confidence that human rather than natural factors were the dominant cause of the global warming observed over the last 50 years.

Estimates of Northern Hemisphere temperatures over the last one to two millennia, based on natural 'thermometers' such as tree rings that vary in width or density as temperatures change, and historical weather records, provide additional evidence that the 20th-century warming cannot be explained by only natural internal variability and natural external forcing factors. Confidence in these estimates is increased because prior to the industrial era, much of the variation they show in Northern Hemisphere average temperatures can be explained by episodic cooling caused by large volcanic eruptions and by changes in the Sun's output. The remaining variation is generally consistent with the variability simulated by climate models in the absence of natural and human-induced external factors. While there is uncertainty in the estimates of past temperatures, they show that it is likely that the second half of the 20th century was the warmest 50-year period in the last 1300 years. The estimated climate variability caused by natural factors is small compared to the strong 20th-century warming.

9.4.5 Summary

Since the TAR, the evidence has strengthened that human influence has increased global temperatures near the surface of the Earth. Every year since the publication of the TAR has been in the top ten warmest years in the instrumental global record of near-surface temperatures. Many climate models are now available which simulate global mean temperature changes that are consistent with those observed over the last century when they include the most important forcings of the climate system. The fact that no coupled model simulation so far has reproduced global temperature changes over the 20th century without anthropogenic forcing is strong evidence for the influence of humans on global climate. This conclusion is robust to variations in model formulation and uncertainties in forcings as far as they have been explored in the large multi-model ensemble now available (Figure 9.5).

Many studies have detected a human influence on near-surface temperature changes, applying a variety of statistical techniques and using many different climate simulations. Comparison with observations shows that the models used in these studies appear to have an adequate representation of internal variability on the decadal to inter-decadal time scales important for detection (Figure 9.7). When evaluated in a Bayesian framework, very strong evidence is found for a human influence on global temperature change regardless of the choice of prior distribution.

Since the TAR, there has been an increased emphasis on partitioning the observed warming into contributions from greenhouse gas increases and other anthropogenic and natural factors. These studies lead to the conclusion that greenhouse gas forcing has very likely been the dominant cause of the observed global warming over the last 50 years, and account for the possibility that the agreement between simulated and observed temperature changes could be reproduced by different combinations of external forcing. This is because, in addition to detecting the presence of model-simulated spatio-temporal response patterns in observations, such analyses also require consistency between the model-simulated and observational amplitudes of these patterns.

Detection and attribution analyses indicate that over the past century there has likely been a cooling influence from aerosols and natural forcings counteracting some of the warming influence of the increasing concentrations of greenhouse gases (Figure 9.9). Spatial information is required in addition to temporal information to reliably detect the influence of aerosols and distinguish them from the influence of increased greenhouse gases. In particular, aerosols are expected to cause differential warming and cooling rates between the NH and SH that change with time depending on the evolution of the aerosol forcing, and this spatio-temporal fingerprint can help to constrain the possible range of cooling from aerosols over the century. Despite continuing uncertainties in aerosol forcing and the climate response, it is likely that greenhouse gases alone would have caused more warming than observed during the last 50 years, with some warming offset by cooling from aerosols and other natural and anthropogenic factors. The overall evidence from studies using instrumental surface temperature and free atmospheric temperature data, along with evidence from analysis of temperature over the last few hundred years (Section 9.3.3.2), indicates that it is very unlikely that the contribution from solar forcing to the warming of the last 50 years was larger than that from greenhouse gas forcing.

An important development since the TAR has been the detection of an anthropogenic signal in surface temperature changes since 1950 over continental and sub-continental scale land areas. The ability of models to simulate many aspects of the temperature evolution at these scales (Figure 9.12) and the detection of significant anthropogenic effects on each of six continents provides stronger evidence of human influence on the global climate than was available to the TAR. Difficulties remain in attributing temperature changes at smaller than continental scales and over time scales of less than 50 years. Attribution at these scales has, with limited exceptions, not yet been established. Temperature changes associated with some modes of variability, which could be wholly or partly naturally caused, are poorly simulated by models in some regions and seasons and could be confounded with the expected temperature response to external forcings. Averaging over smaller regions reduces the natural variability less than averaging over large regions, making it more difficult to distinguish changes expected from external forcing. In addition, the small-scale details of external forcing and the response simulated by models are less credible than large-scale features. Overall, uncertainties in observed and model-simulated climate variability and change at smaller spatial scales make it difficult at present to estimate the contribution of anthropogenic forcing to temperature changes at scales smaller than continental and on time scales shorter than 50 years.

There is now some evidence that anthropogenic forcing has affected extreme temperatures. There has been a significant decrease in the frequency of frost days and an increase in the incidence of warm nights. A detection and attribution analysis has shown a significant human influence on patterns of changes in extremely warm nights and evidence for a human-induced warming of the coldest nights and days of the year. Many important impacts of climate change are likely to manifest themselves through an increase in the frequency of heat waves in some regions and a decrease in the frequency of extremely cold events in others. Based on a single study, and assuming a model-based estimate of temperature variability, past human influence may have more than doubled the risk of European mean summer temperatures as high as those recorded in 2003 (Figure 9.13).

Since the TAR, further evidence has accumulated that there has been a significant anthropogenic influence on free atmosphere temperature since widespread measurements became available from radiosondes in the late 1950s. The influence of greenhouse gases on tropospheric temperatures has been detected, as has the influence of stratospheric ozone depletion on stratospheric temperatures. The combination of a warming troposphere and a cooling stratosphere has likely

led to an increase in the height of the tropopause and model-data comparisons show that greenhouse gases and stratospheric ozone changes are likely largely responsible (Figure 9.14).

Whereas, on monthly and annual time scales, variations of temperature in the tropics at the surface are amplified aloft in both the MMD simulations and observations by consistent amounts, on longer time scales, simulations of differential tropical warming rates between the surface and the free atmosphere are inconsistent with some observational records. One possible explanation for the discrepancies on multi-annual but not shorter time scales is that amplification effects are controlled by different physical mechanisms, but a more probable explanation is that some observational records are contaminated by errors that affect their long-term trends.

9.5 Understanding of Change in Other Variables during the Industrial Era

The objective of this section is to assess large-scale climate change in variables other than air temperature, including changes in ocean climate, atmospheric circulation, precipitation, the cryosphere and sea level. This section draws heavily on Chapters 3, 4, 5 and 8. Where possible, it attempts to identify links between changes in different variables, such as those that associate some aspects of SST change with precipitation change. It also discusses the role of external forcing, drawing where possible on formal detection studies.

9.5.1 Ocean Climate Change

9.5.1.1 Ocean Heat Content Changes

Since the TAR, evidence of climate change has accumulated within the ocean, both at regional and global scales (Chapter 5). The overall heat content in the World Ocean is estimated to have increased by 14.2×10^{22} J during the period 1961 to 2003 (Section 5.2.2). This overall increase has been superimposed on strong interannual and inter-decadal variations. The fact that the entire ocean, which is by far the system's largest heat reservoir (Levitus et al., 2005; see also Figure 5.4) gained heat during the latter half of the 20th century is consistent with a net positive radiative forcing of the climate system. Late 20th-century ocean heat content changes were at least one order of magnitude larger than the increase in energy content of any other component of the Earth's ocean-atmosphere-cryosphere system (Figure 5.4; Levitus et al., 2005).

All analyses indicate a large anthropogenic component of the positive trend in global ocean heat content. Levitus et al. (2001) and Gregory et al (2004) analyse simulations from the GFDL R30 and HadCM3 models respectively and show that climate simulations agree best with observed changes when the models include anthropogenic forcings from increasing greenhouse gas concentrations and sulphate aerosols. Gent and Danabasoglu (2004) show that the observed trend cannot be explained by natural internal variability as simulated by a long control run of the Community Climate System Model (CCSM2). Barnett et al. (2001) and Reichert et al. (2002b) use detection analyses similar to those described in Section 9.4 to detect model-simulated ocean climate change signals in the observed spatio-temporal patterns of ocean heat content across the ocean basins.

Barnett et al. (2005) extend previous detection and attribution analyses of ocean heat content changes to a basin by basin analysis of the temporal evolution of temperature changes in the upper 700 m of the ocean (see also Pierce et al., 2006). They report that whereas the observed change is not consistent with internal variability and the response to natural external forcing as simulated by two climate models (PCM and HadCM3), the simulated ocean warming due to anthropogenic factors (including well-mixed greenhouse gases and sulphate aerosols) is consistent with the observed changes and reproduces many of the different responses seen in the individual ocean basins (Figure 9.15), indicating a human-induced warming of the world's oceans with a complex vertical and geographical structure that is simulated quite well by the two AOGCMs. Barnett et al. (2005) find that the earlier conclusions of Barnett et al. (2001) were not affected by the Levitus et al. (2005) revisions to the Levitus et al. (2000) ocean heat content data.

In contrast, changes in solar forcing can potentially explain only a small fraction of the observationally based estimates of the increase in ocean heat content (Crowley et al., 2003), and the cooling influence of natural (volcanic) and anthropogenic aerosols would have slowed ocean warming over the last half century. Delworth et al. (2005) find a delay of several decades and a reduction in the magnitude of the warming of approximately two-thirds in simulations with the GFDL-CM2 model that included these forcings compared to the response to increasing greenhouse gases alone, consistent with results based on an upwelling diffusion EBM (Crowley et al., 2003). Reductions in ocean heat content are found following volcanic eruptions in climate simulations (Church et al., 2005), including a persistent centennial time-scale signal of ocean cooling at depth following the eruption of Krakatoa (Gleckler et al., 2006).

Although the heat uptake in the ocean cannot be explained without invoking anthropogenic forcing, there is some evidence that the models have overestimated how rapidly heat has penetrated below the ocean's mixed layer (Forest et al., 2006; see also Figure 9.15). In simulations that include natural forcings in addition to anthropogenic forcings, eight coupled climate models simulate heat uptake of 0.26 ± 0.06 W m^{-2} (± 1 standard deviation) for 1961 to 2003, whereas observations of ocean temperature changes indicate a heat uptake of 0.21 ± 0.04 W m^{-2} (Section 5.2.2.1). These could be consistent within their uncertainties but might indicate a tendency of climate models to overestimate ocean heat uptake.

In addition, the interannual to decadal variability seen in Levitus et al. (2000, 2005) (Section 5.2.2) is underestimated by models; Gregory et al. (2004) show significant differences between observed and modelled interannual deviations from a linear trend in five-year running means of world ocean heat content above 3,000 m for 1957 to 1994. While some studies

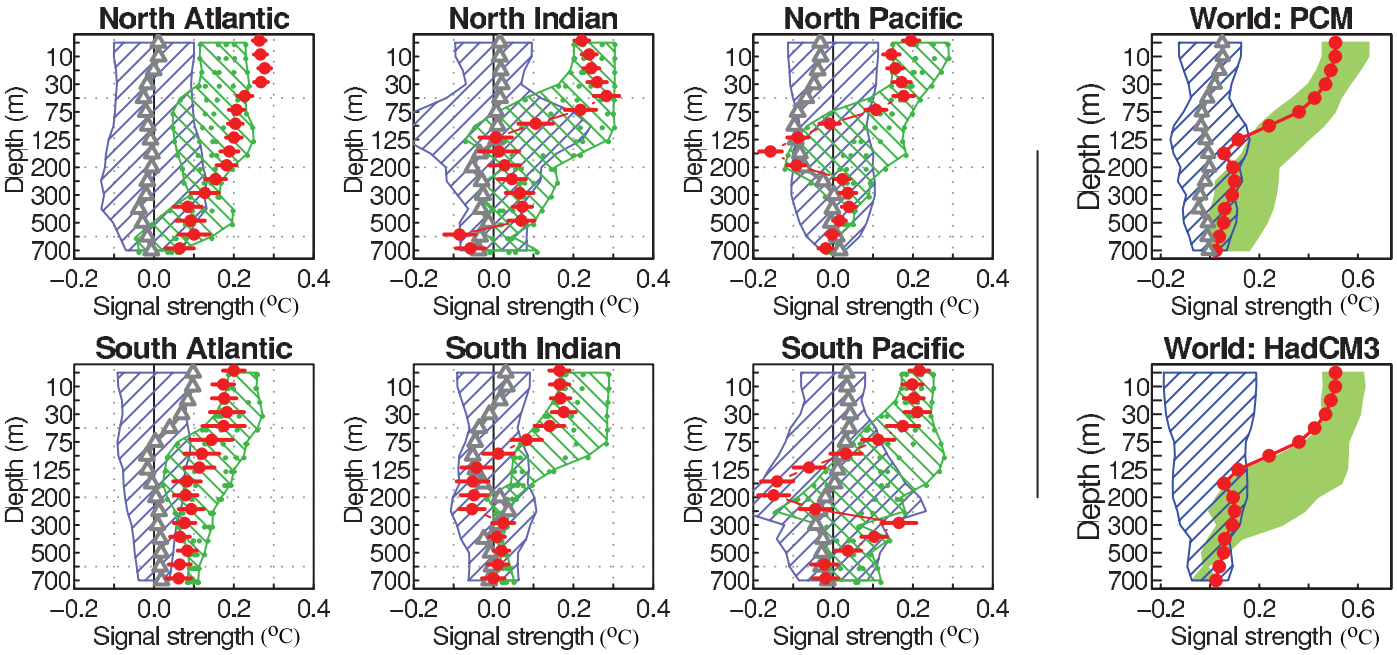


Figure 9.15. *Strength of observed and model-simulated warming signal by depth for the World Ocean and for each ocean basin individually (in °C, see Barnett et al., 2005 and Pierce et al., 2006 for calculation of signal strength). For ocean basins, the signal is estimated from PCM (Table 8.1) while for the World Ocean it is estimated from both PCM and HadCM3 (Table 8.1). Red dots represent the projection of the observed temperature changes onto the normalised model-based pattern of warming. They show substantial basin-to-basin differences in how the oceans have warmed over the past 40 years, although all oceans have experienced net warming over that interval. The red bars represent the ±2 standard deviation limits associated with sampling uncertainty. The blue crosshatched swaths represent the 90% confidence limits of the natural internal variability strength. The green crosshatched swaths represent the range of the anthropogenically forced signal estimates from different realisations of identically forced simulations with the PCM model for each ocean basin (the smaller dots within the green swaths are the individual realisations) and the green shaded regions represent the range of anthropogenically forced signal estimates from different realisations of identically forced simulations with the PCM and HadCM3 models for the World Ocean (note that PCM and HadCM3 use different representations of anthropogenic forcing). The ensemble-averaged strength of the warming signal in four PCM simulations with solar and volcanic forcing is also shown (grey triangles). From Barnett et al. (2005) and Pierce et al. (2006).*

note the potential importance of the choice of infilling method in poorly sampled regions (Gregory et al., 2004; AchutaRao et al., 2006), the consistency of the differently processed data from the Levitus et al. (2005), Ishii et al. (2006) and Willis et al. (2004) analyses adds confidence to their use for analysing trends in climate change studies (Chapter 5). Gregory et al. (2004) show that agreement between models and observations is better in the well-observed upper ocean (above 300 m) in the NH and that there is large sensitivity to the method of infilling the observational data set outside this well-observed region. They find a strong maximum in variability in the Levitus data set at around 500 m depth that is not seen in HadCM3 simulations, a possible indication of model deficiency or an artefact in the Levitus data. AchutaRao et al. (2006) also find that observational estimates of temperature variability over much of the oceans may be substantially affected by sparse observational coverage and the method of infilling.

9.5.1.2 Water Mass Properties

Interior water masses, which are directly ventilated at the ocean surface, act to integrate highly variable surface changes in heat and freshwater, and could therefore provide indicators of global change (Stark et al., 2006). Some studies have attempted to investigate changes in three-dimensional water mass properties (Section 5.3). Sub-Antarctic Mode Water (SAMW) and the subtropical gyres have warmed in the Indian and Pacific basins since the 1960s, waters at high latitudes have freshened in the upper 500 m and salinity has increased in some of the subtropical gyres. These changes are consistent with an increase in meridional moisture flux over the oceans over the last 50 years leading to increased precipitation at high latitudes (Section 5.2.3; Wong et al., 1999) and a reduction in the difference between precipitation and evaporation at mid-latitudes (Section 5.6). This suggests that the ocean might integrate rainfall changes to produce detectable salinity changes. Boyer et al. (2005) estimated linear trends in salinity for the global ocean from 1955 to 1998 that indicate salinification in the Antarctic Polar Frontal Zone around 40°S and in the subtropical North Atlantic, and freshening in the sub-polar Atlantic (Figures 5.5 and 5.7). However, variations in other terms (e.g., ocean freshwater transport) may be contributing substantially to the observed salinity changes and have not been quantified.

An observed freshening of SAMW in the South Indian Ocean between the 1960s and 1990s has been shown to be consistent with anthropogenically forced simulations from HadCM3 (Banks et al., 2000) but care should be taken in interpreting sparse hydrographic data, since apparent trends could reflect

natural variability or the aliased effect of changing observational coverage. Although SAMW was fresher along isopycnals in 1987 than in the 1960s, in 2002 the salinity was again near the 1960s values (Bindoff and McDougall, 2000; Bryden et al., 2003). An analysis of an ocean model forced by observed atmospheric fluxes and SSTs indicates that this is likely associated with natural variability (Murray et al., 2007), a result supported by an analysis of 20th-century simulations with HadCM3 which shows that it is not possible to reject the null hypothesis that the observed differences are due to internal variability (Stark et al., 2006), although this model does project a long-term freshening trend in the 21st century due to the large-scale response to surface heating and hydrological changes (Banks et al., 2000).

9.5.1.3 Changes in the Meridional Overturning Circulation

It is possible that anthropogenic and natural forcing may have influenced the MOC in the Atlantic (see also Box 5.1). One possible oceanic consequence of climate change is a slowing down or even halting of the MOC. An estimate of the overturning circulation and associated heat transport based on a trans-Atlantic section along latitude 25°N indicates that the Atlantic MOC has slowed by about 30% over five samples taken between 1957 and 2004 (Bryden et al., 2005), although given the infrequent sampling and considerable variability it is not clear whether the trend estimate is robust (Box 5.1). Freshening of North East Atlantic Deep Water has been observed (Dickson et al., 2002; Curry et al., 2003; Figure 5.6) and has been interpreted as being consistent with an enhanced difference between precipitation and evaporation at high latitudes and a possible slowing down of the MOC. Wu et al. (2004) show that the observed freshening trend is well reproduced by an ensemble of HadCM3 simulations that includes both anthropogenic and natural forcings, but this freshening coincides with a strengthening rather than a weakening trend in the MOC. Therefore, this analysis is not consistent with an interpretation of the observed freshening trends in the North Atlantic as an early signal of a slowdown of the thermohaline circulation. Dickson et al. (2002) propose a possible role for the Arctic in driving the observed freshening of the subpolar North Atlantic. Wu et al. (2005) show that observed increases in arctic river flow (Peterson et al., 2002) are well simulated by HadCM3 including anthropogenic and natural forcings and propose that this increase is anthropogenic, since it is not seen in HadCM3 simulations including just natural forcing factors. However, the relationship between this increased source of freshwater and freshening in the Labrador Sea is not clear in the HadCM3 simulations, since Wu et al. (2007) find that recent freshening in the Labrador Sea is simulated by the model when it is driven by natural rather than anthropogenic forcings. Importantly, freshening is also associated with decadal and multi-decadal variability, with links to the NAO (Box 5.1) and the AMO (Box 5.1; Vellinga and Wu, 2004; Knight et al., 2005).

9.5.2 Sea Level

A precondition for attributing changes in sea level rise to anthropogenic forcing is that model-based estimates of historical global mean sea level rise should be consistent with observational estimates. Although AOGCM simulations of global mean surface air temperature trends are generally consistent with observations (Section 9.4.1, Figure 9.5), consistency with surface air temperature alone does not guarantee a realistic simulation of thermal expansion, as there may be compensating errors among climate sensitivity, ocean heat uptake and radiative forcing (see, e.g., Raper et al., 2002, see also Section 9.6). Model simulations also offer the possibility of attributing past sea level changes to particular forcing factors. The observational budget for sea level (Section 5.5.6) assesses the periods 1961 to 2003 and 1993 to 2003. Table 9.2 evaluates the same terms from 20C3M simulations in the MMD at PCMDI, although most 20C3M simulations end earlier (between 1999 and 2002), so the comparison is not quite exact.

Simulations including natural as well as anthropogenic forcings (the 'ALL' models in Table 9.2) generally have smaller ocean heat uptake during the period 1961 to 2003 than those without volcanic forcing, since several large volcanic eruptions cooled the climate during this period (Gleckler et al., 2006). This leads to a better agreement of those simulations with

Table 9.2. *Components of the rate of global mean sea level rise (mm yr^{-1}) from models and observations. All ranges are 5 to 95% confidence intervals. The observational components and the observed rate of sea level rise ('Obs' column) are repeated from Section 5.5.6 and Table 5.3. The 'ALL' column is computed (following the methods of Gregory and Huybrechts, 2006 and Section 10.6.3.1) from eight 20C3M simulations that include both natural and anthropogenic forcings (models 3, 9, 11, 12, 14, 15, 19 and 21; see Table 8.1), and the 'ALL/ANT' column from 16 simulations: the eight ALL and eight others that have anthropogenic forcings only (models 4, 6, 7, 8, 13, 16, 20 and 22; see Table 8.1).*

	1961–2003			1993–2003		
	Obs	ALL	ALL/ANT	Obs	ALL	ALL/ANT
Thermal expansion	0.42 ± 0.12	0.5 ± 0.2	0.7 ± 0.4	1.60 ± 0.50	1.5 ± 0.7	1.2 ± 0.9
Glaciers and ice caps	0.50 ± 0.18	0.5 ± 0.2	0.5 ± 0.3	0.77 ± 0.22	0.7 ± 0.3	0.8 ± 0.3
Ice sheets (observed)	0.19 ± 0.43			0.41 ± 0.35		
Sum of components	1.1 ± 0.5	1.2 ± 0.5	1.4 ± 0.7	2.8 ± 0.7	2.6 ± 0.8	2.4 ± 1.0
Observed rate of rise	1.8 ± 0.5			3.1 ± 0.7		

thermal expansion estimates based on observed ocean warming (Section 5.5.3) than for the complete set of model simulations ('ALL/ANT' in Table 9.2). For 1993 to 2003, the models that include natural forcings agree well with observations. Although this result is somewhat uncertain because the simulations end at various dates from 1999 onwards, it accords with results obtained by Church et al. (2005) using the PCM and Gregory et al. (2006) using HadCM3, which suggest that 0.5 mm yr^{-1} of the trend in the last decade may result from warming as a recovery from the Mt. Pinatubo eruption of 1991. Comparison of the results for 1961 to 2003 and 1993 to 2003 shows that volcanoes influence the ocean differently over shorter and longer periods. The rapid expansion of 1993 to 2003 was caused, in part, by rapid warming of the upper ocean following the cooling due to the Mt. Pinatubo eruption, whereas the multi-decadal response is affected by the much longer persistence in the deep ocean of cool anomalies caused by volcanic eruptions (Delworth et al., 2005; Gleckler et al., 2006; Gregory et al., 2006).

Both observations and model results indicate that the global average mass balance of glaciers and ice caps depends linearly on global average temperature change, but observations of accelerated mass loss in recent years suggest a greater sensitivity than simulated by models. The global average temperature change simulated by AOGCMs gives a good match to the observational estimates of the contribution of glaciers and ice caps to sea level change in 1961 to 2003 and 1993 to 2003 (Table 9.2) with the assumptions that the global average mass balance sensitivity is 0.80 mm yr^{-1} $°C^{-1}$ (sea level equivalent) and that the climate of 1900 to 1929 was 0.16°C warmer than the temperature required to maintain the steady state for glaciers (see discussion in Section 10.6.3.1 and Appendix 10.A).

Calculations of ice sheet surface mass balance changes due to climate change (following the methods of Gregory and Huybrechts, 2006 and Section 10.6.3.1) indicate small but uncertain contributions during 1993 to 2003 of 0.1 ± 0.1 mm yr^{-1} (5 to 95% range) from Greenland and –0.2 ± 0.4 mm yr^{-1} from Antarctica, the latter being negative because rising temperature in AOGCM simulations leads to greater snow accumulation (but negligible melting) at present. The observational estimates (Sections 4.6.2 and 5.5.6) are 0.21 ± 0.07 mm yr^{-1} for Greenland and 0.21 ± 0.35 mm yr^{-1} for Antarctica. For both ice sheets, there is a significant contribution from recent accelerations in ice flow leading to greater discharge of ice into the sea, an effect that is not included in the models because its causes and mechanisms are not yet properly understood (see Sections 4.6.2 and 10.6.4 for discussion). Hence, the surface mass balance model underestimates the sea level contribution from ice sheet melting. Model-based and observational estimates may also differ because the model-based estimates are obtained using estimates of the correlation between global mean climate change and local climate change over the ice sheets in the 21st century under SRES scenarios. This relationship may not represent recent changes over the ice sheets.

Summing the modelled thermal expansion, global glacier and ice cap contributions and the observational estimates of the ice sheet contributions results in totals that lie below the observed rates of global mean sea level rise during 1961 to 2003 and 1993 to 2003. As shown by Table 9.2, the terms are reasonably well reproduced by the models. Nevertheless, the discrepancy in the total, especially for 1961 to 2003, indicates the lack of a satisfactory explanation of sea level rise. This is also a difficulty for the observational budget (discussed in Section 5.5.6).

A discrepancy between model and observations could also be partly explained by the internally generated variability of the climate system, which control simulations suggest could give a standard deviation in the thermal expansion component of ~0.2 mm yr^{-1} in 10-year trends. This variability may be underestimated by models, since observations give a standard deviation in 10-year trends of 0.7 mm yr^{-1} in thermal expansion (see Sections 5.5.3 and Section 9.5.1.1; Gregory et al., 2006).

Since recent warming and thermal expansion are likely largely anthropogenic (Section 9.5.1.1), the model results suggest that the greater rate of rise in 1993 to 2003 than in 1961 to 2003 could have been caused by rising anthropogenic forcing. However, tide gauge estimates suggests larger variability than models in 10-year trends, and that rates as large as that observed during 1993 to 2003 occurred in previous decades (Section 5.5.2.4).

Overall, it is very likely that the response to anthropogenic forcing contributed to sea level rise during the latter half of the 20th century. Models including anthropogenic and natural forcing simulate the observed thermal expansion since 1961 reasonably well. Anthropogenic forcing dominates the surface temperature change simulated by models, and has likely contributed to the observed warming of the upper ocean and widespread glacier retreat. It is very unlikely that the warming during the past half century is due only to known natural causes. Lack of studies quantifying the contribution of anthropogenic forcing to ocean heat content increase and glacier melting, and the fact that the observational budget is not closed, make it difficult to estimate the anthropogenic contribution. Nevertheless, an expert assessment based on modelling and ocean heat content studies suggests that anthropogenic forcing has likely contributed at least one-quarter to one-half of the sea level rise during the second half of the 20th century (see also Woodworth et al., 2004).

Anthropogenic forcing is also expected to produce an accelerating rate of sea level rise (Woodworth et al., 2004). On the other hand, natural forcings could have increased the rate of sea level rise in the early 20th century and decreased it later in the 20th century, thus producing a steadier rate of rise during the 20th century when combined with anthropogenic forcing (Crowley et al., 2003; Gregory et al., 2006). Observational evidence for acceleration during the 20th century is equivocal, but the rate of sea level rise was greater in the 20th than in the 19th century (Section 5.5.2.4). An onset of higher rates of rise in the early 19th century could have been caused by natural factors, in particular the recovery from the Tambora eruption of 1815 (Crowley et al., 2003; Gregory et al., 2006), with anthropogenic forcing becoming important later in the 19th century.

9.5.3 Atmospheric Circulation Changes

Natural low-frequency variability of the climate system is dominated by a small number of large-scale circulation patterns such as ENSO, the Pacific Decadal Oscillation (PDO), and the NAM and Southern Annular Mode (SAM) (Section 3.6 and Box 3.4). The impact of these modes on terrestrial climate on annual to decadal time scales can be profound, but the extent to which they can be excited or altered by external forcing remains uncertain. While some modes might be expected to change as a result of anthropogenic effects such as the enhanced greenhouse effect, there is little *a priori* expectation about the direction or magnitude of such changes.

9.5.3.1 El Niño-Southern Oscillation/Pacific Decadal Oscillation

The El Niño-Southern Oscillation is the leading mode of variability in the tropical Pacific, and it has impacts on climate around the globe (Section 3.6.2). There have been multi-decadal oscillations in the ENSO index (conventionally defined as a mean SST anomaly in the eastern equatorial Pacific) throughout the 20th century, with more intense El Niño events since the late 1970s, which may reflect in part a mean warming of the eastern equatorial Pacific (Mendelssohn et al., 2005). Model projections of future climate change generally show a mean state shift towards more El-Niño-like conditions, with enhanced warming in the eastern tropical Pacific and a weakened Walker Circulation (Section 10.3.5.3); there is some evidence that such a weakening has been observed over the past 140 years (Vecchi et al., 2006). While some simulations of the response to anthropogenic influence have shown an increase in ENSO variability in response to greenhouse gas increases (Timmermann, 1999; Timmermann et al., 1999; Collins, 2000b), others have shown no change (e.g., Collins, 2000a) or a decrease in variability (Knutson et al., 1997). A recent survey of the simulated response to atmospheric CO_2 doubling in 15 MMD AOGCMs (Merryfield, 2006) finds that three of the models exhibited significant increases in ENSO variability, five exhibited significant decreases and seven exhibited no significant change. Thus, as yet there is no detectable change in ENSO variability in the observations, and no consistent picture of how it might be expected to change in response to anthropogenic forcing (Section 10.3.5.3).

Decadal variability in the North Pacific is characterised by variations in the strength of the Aleutian Low coupled to changes in North Pacific SST (Sections 3.6.3 and 8.4.2). The leading mode of decadal variability in the North Pacific is usually referred to as the PDO, and has a spatial structure in the atmosphere and upper North Pacific Ocean similar to the pattern that is associated with ENSO. One recent study showed a consistent tendency towards the positive phase of the PDO in observations and simulations with the MIROC model that included anthropogenic forcing (Shiogama et al., 2005), although differences between the observed and simulated PDO patterns, and the lack of additional studies, limit confidence in these findings.

9.5.3.2 North Atlantic Oscillation/Northern Annular Mode

The NAM is an approximately zonally symmetric mode of variability in the NH (Thompson and Wallace, 1998), and the NAO (Hurrell, 1996) may be viewed as its Atlantic counterpart (Section 3.6.4). The NAM index exhibited a pronounced trend towards its positive phase between the 1960s and the 1990s, corresponding to a decrease in surface pressure over the Arctic and an increase over the subtropical North Atlantic (see Section 3.6.4; see also Hurrell, 1996; Thompson et al., 2000; Gillett et al., 2003a). Several studies have shown this trend to be inconsistent with simulated internal variability (Osborn et al., 1999; Gillett et al., 2000, 2002b; Osborn, 2004; Gillett, 2005). Although the NAM index has decreased somewhat since its peak in the mid-1990s, the trend calculated over recent decades remains significant at the 5% significance level compared to simulated internal variability in most models (Osborn, 2004; Gillett, 2005), although one study found that the NAO index trend was marginally consistent with internal variability in one model (Selten et al., 2004).

Most climate models simulate some increase in the NAM index in response to increased concentrations of greenhouse gases (Fyfe et al., 1999; Paeth et al., 1999; Shindell et al., 1999; Gillett et al., 2003a,b; Osborn, 2004; Rauthe et al., 2004), although the simulated trend is generally smaller than that observed (Gillett et al., 2002b, 2003b; Osborn, 2004; Gillett, 2005; and see Figure 9.16). Simulated sea level pressure changes are generally found to project more strongly onto the hemispheric NAM index than onto a two-station NAO index (Gillett et al., 2002b; Osborn, 2004; Rauthe et al., 2004). Some studies have postulated an influence of ozone depletion (Volodin and Galin, 1999; Shindell et al., 2001a), changes in solar irradiance (Shindell et al., 2001a) and volcanic eruptions (Kirchner et al., 1999; Shindell et al., 2001a; Stenchikov et al., 2006) on the NAM. Stenchikov et al. (2006) examine changes in sea level pressure following nine volcanic eruptions in the MMD 20C3M ensemble of 20th-century simulations, and find that the models simulated a positive NAM response to the volcanoes, albeit one that was smaller than that observed. Nevertheless, ozone, solar and volcanic forcing changes are generally not found to have made a large contribution to the observed NAM trend over recent decades (Shindell et al., 2001a; Gillett et al., 2003a). Simulations incorporating all the major anthropogenic and natural forcings from the MMD 20C3M ensemble generally showed some increase in the NAM over the latter part of the 20th century (Gillett, 2005; Miller et al., 2006; and see Figure 9.16), although the simulated trend is in all cases smaller than that observed, indicating inconsistency between simulated and observed trends at the 5% significance level (Gillett, 2005).

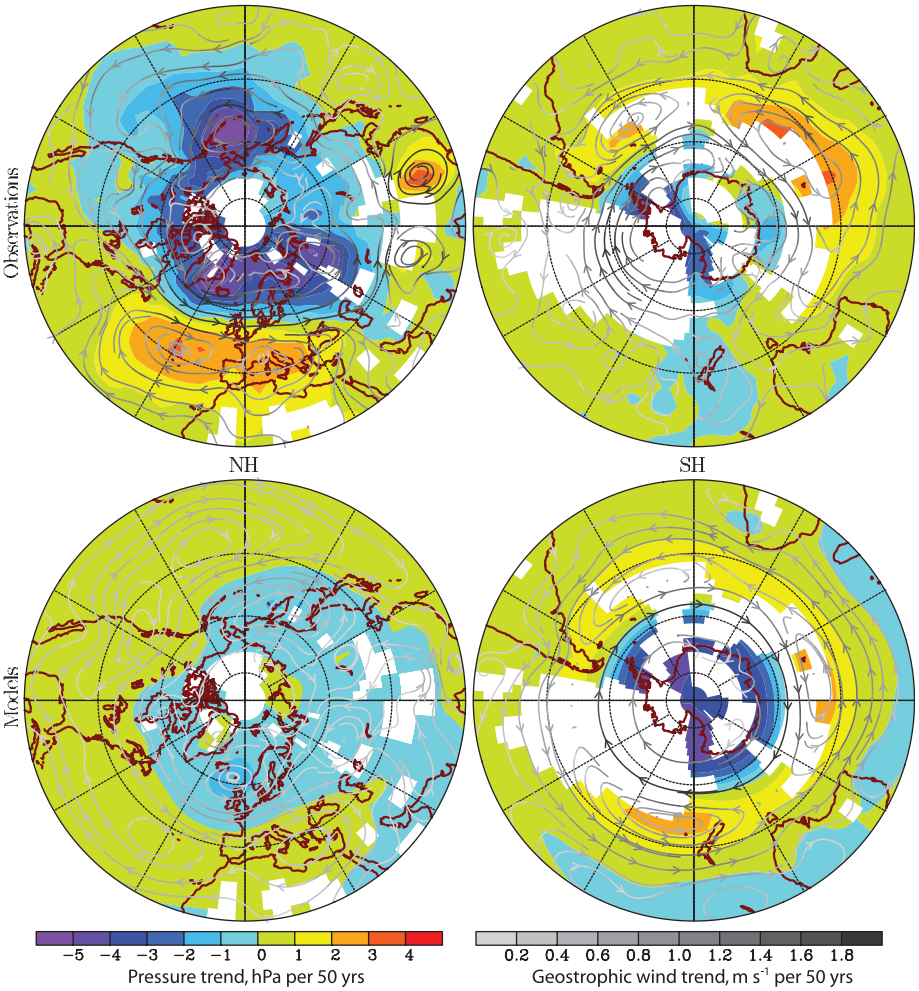


Figure 9.16. *Comparison between observed (top) and model-simulated (bottom) December to February sea-level pressure trends (hPa per 50 years) in the NH (left panels) and SH (right panels) based on decadal means for the period 1955 to 2005. Observed trends are based on the Hadley Centre Mean Sea Level Pressure data set (HadSLP2r, an infilled observational data set; Allan and Ansell, 2006). Model-simulated trends are the mean simulated response to greenhouse gas, sulphate aerosol, stratospheric ozone, volcanic aerosol and solar irradiance changes from eight coupled models (CCSM3, GFDL-CM2.0, GFDL-CM2.1, GISS-EH, GISS-ER, MIROC3.2(medres), PCM, UKMO-HadCM3; see Table 8.1 for model descriptions). Streamlines indicate the direction of the trends (m s^{-1} per 50 years) in the geostrophic wind velocity derived from the trends in sea level pressure, and the shading of the streamlines indicates the magnitude of the change, with darker streamlines corresponding to larger changes in geostrophic wind. White areas in all panels indicate regions with insufficient station-based measurements to constrain analysis. Further explanation of the construction of this figure is provided in the Supplementary Material, Appendix 9.C. Updated after Gillett et al. (2005).*

The mechanisms underlying NH circulation changes remain open to debate. Simulations in which observed SST changes, which may in part be externally forced, were prescribed either globally or in the tropics alone were able to capture around half of the recent trend towards the positive phase of the NAO (Hoerling et al., 2005; Hurrell et al., 2005), suggesting that the trend may in part relate to SST changes, particularly over the Indian Ocean (Hoerling et al., 2005). Another simulation in which a realistic trend in stratospheric winds was prescribed was able to reproduce the observed trend in the NAO (Scaife et al., 2005). Rind et al. (2005a,b) find that both stratospheric changes and changes in SST can force changes in the NAM and NAO, with changes in SSTs being the dominant forcing mechanism.

Over the period 1968 to 1997, the trend in the NAM was associated with approximately 50% of the winter surface warming in Eurasia, due to increased advection of maritime air onto the continent, but only a small fraction (16%) of the NH extratropical annual mean warming trend (Thompson et al., 2000; Section 3.6.4 and Figure 3.30). It was also associated with a decrease in winter precipitation over southern Europe and an increase over northern Europe, due the northward displacement of the storm track (Thompson et al., 2000).

9.5.3.3 Southern Annular Mode

The SAM is more zonally symmetric than its NH counterpart (Thompson and Wallace, 2000; Section 3.6.5). It too has exhibited a pronounced upward trend over the past 30 years, corresponding to a decrease in surface pressure over the Antarctic and an increase over the southern mid-latitudes (Figure 9.16), although the mean SAM index since 2000 has been below the mean in the late 1990s, but above the long term mean (Figure 3.32). An upward trend in the SAM has occurred in all seasons, but the largest trend has been observed during the southern summer (Thompson et al., 2000; Marshall, 2003). Marshall et al. (2004) show that observed trends in the SAM are not consistent with simulated internal variability in HadCM3, suggesting an external cause. On the other hand, Jones and Widmann (2004) develop a 95-year reconstruction of the summer SAM index based largely on mid-latitude pressure measurements, and find that their reconstructed SAM index was as high in the early 1960s as in the late 1990s. However, a more reliable reconstruction from 1958, using more Antarctic data and a different method, indicates that the summer SAM index was higher at the end of the 1990s than at any other time in the observed record (Marshall et al., 2004).

Based on an analysis of the structure and seasonality of the observed trends in SH circulation, Thompson and Solomon (2002) suggest that they have been largely induced by stratospheric ozone depletion. Several modelling studies simulate an upward trend in the SAM in response to stratospheric ozone depletion (Sexton, 2001; Gillett and Thompson, 2003; Marshall et al., 2004; Shindell and Schmidt, 2004; Arblaster and Meehl, 2006; Miller et al., 2006), particularly in the southern summer. Stratospheric ozone depletion cools and strengthens

the antarctic stratospheric vortex in spring, and observations and models indicate that this strengthening of the stratospheric westerlies can be communicated downwards into the troposphere (Thompson and Solomon, 2002; Gillett and Thompson, 2003). While ozone depletion may be the dominant cause of the trends, other studies have indicated that greenhouse gas increases have also likely contributed (Fyfe et al., 1999; Kushner et al., 2001; Stone et al., 2001; Cai et al., 2003; Marshall et al., 2004; Shindell and Schmidt, 2004; Stone and Fyfe, 2005; Arblaster and Meehl, 2006). During the southern summer, the trend in the SAM has been associated with the observed increase of about 3 m s^{-1} in the circumpolar westerly winds over the Southern Ocean. This circulation change is estimated to explain most of the summer surface cooling over the Antarctic Plateau, and about one-third to one-half of the warming of the Antarctic Peninsula (Thompson and Solomon, 2002; Carril et al., 2005; Section 3.6.5), with the largest influence on the eastern side of the Peninsula (Marshall et al., 2006), although other factors are also likely to have contributed to this warming (Vaughan et al., 2001).

9.5.3.4 Sea Level Pressure Detection and Attribution

Global December to February sea level pressure changes observed over the past 50 years have been shown to be inconsistent with simulated internal variability (Gillett et al., 2003b, 2005), but are consistent with the simulated response to greenhouse gas, stratospheric ozone, sulphate aerosol, volcanic aerosol and solar irradiance changes based on 20C3M simulations by eight MMD coupled models (Gillett et al., 2005; Figure 9.16). This result is dominated by the SH, where the inclusion of stratospheric ozone depletion leads to consistency between simulated and observed sea level pressure changes. In the NH, simulated sea level pressure trends are much smaller than those observed (Gillett, 2005). Global mean sea level pressure changes associated with increases in atmospheric water vapour are small in comparison to the spatial variations in the observed change in sea level pressure, and are hard to detect because of large observational uncertainties (Trenberth and Smith, 2005).

9.5.3.5 Monsoon Circulation

The current understanding of climate change in the monsoon regions remains one of considerable uncertainty with respect to circulation and precipitation (Sections 3.7, 8.4.10 and 10.3.5.2). The Asian monsoon circulation in the MMD models was found to decrease by 15% by the late 21st century under the SRES A1B scenario (Tanaka et al., 2005; Ueda et al., 2006), but trends during the 20th century were not examined. Ramanathan et al. (2005) simulate a pronounced weakening of the Asian monsoon circulation between 1985 and 2000 in response to black carbon aerosol increases. Chase et al. (2003) examine changes in several indices of four major tropical monsoonal circulations (Southeastern Asia, western Africa, eastern Africa and the Australia/Maritime Continent) for the period 1950 to 1998. They find significantly diminished monsoonal circulation in each region, although this result is uncertain due to changes in the observing system affecting the NCEP reanalysis (Section 3.7). These results are consistent with simulations (Ramanathan et al., 2005; Tanaka et al., 2005) of weakening monsoons due to anthropogenic factors, but further model and empirical studies are required to confirm this.

9.5.3.6 Tropical Cyclones

Several recent events, including the active North Atlantic hurricane seasons of 2004 and 2005, the unusual development of a cyclonic system in the subtropical South Atlantic that hit the coast of southern Brazil in March 2004 (e.g., Pezza and Simmonds, 2005) and a hurricane close to the Iberian Peninsula in October 2005, have raised public and media interest in the possible effects of climate change on tropical cyclone activity. The TAR concluded that there was 'no compelling evidence to indicate that the characteristics of tropical and extratropical storms have changed', but that an increase in tropical peak wind intensities was likely to occur in some areas with an enhanced greenhouse effect (see also Box 3.5 and Trenberth, 2005). The spatial resolution of most climate models limits their ability to realistically simulate tropical cyclones (Section 8.5.3), therefore, most studies of projected changes in hurricanes have either used time slice experiments with high-resolution atmosphere models and prescribed SSTs, or embedded hurricane models in lower-resolution General Circulation Models (GCMs) (Section 10.3.6.3). While results vary somewhat, these studies generally indicate a reduced frequency of tropical cyclones in response to enhanced greenhouse gas forcing, but an increase in the intensity of the most intense cyclones (Section 10.3.6.3). It has been suggested that the simulated frequency reduction may result from a decrease in radiative cooling associated with increased CO_2 concentration (Sugi and Yoshimura, 2004; Yoshimura and Sugi, 2005; Section 10.3.6.3; Box 3.5), while the enhanced atmospheric water vapour concentration under greenhouse warming increases available potential energy and thus cyclone intensity (Trenberth, 2005).

There continues to be little evidence of any trend in the observed total frequency of global tropical cyclones, at least up until the late 1990s (e.g., Solow and Moore, 2002; Elsner et al., 2004; Pielke et al., 2005; Webster et al., 2005). However, there is some evidence that tropical cyclone intensity may have increased. Globally, Webster et al. (2005) find a strong increase in the number and proportion of the most intense tropical cyclones over the past 35 years. Emanuel (2005) reports a marked increase since the mid-1970s in the Power Dissipation Index (PDI), an index of the destructiveness of tropical cyclones (essentially an integral, over the lifetime of the cyclone, of the cube of the maximum wind speed), in the western North Pacific and North Atlantic, reflecting the apparent increases in both the duration of cyclones and their peak intensity. Several studies have shown that tropical cyclone activity was also high in the 1950 to 1970 period in the North Atlantic (Landsea, 2005) and North Pacific (Chan, 2006), although recent values of the PDI may be

higher than those recorded previously (Emanuel, 2005; Section 3.8.3). Emanuel (2005) and Elsner et al. (2006) report a strong correlation between the PDI and tropical Atlantic SSTs, although Chan and Liu (2004) find no analogous relationship in the western North Pacific. While changes in Atlantic SSTs have been linked in part to the AMO, the recent warming appears to be mainly associated with increasing global temperatures (Section 3.8.3.2; Mann and Emanuel, 2006; Trenberth and Shea, 2006). Tropical cyclone development is also strongly influenced by vertical wind shear and static stability (Box 3.5). While increasing greenhouse gas concentrations have likely contributed to a warming of SSTs, effects on static stability and wind shear may have partly opposed this influence on tropical cyclone formation (Box 3.5). Thus, detection and attribution of observed changes in hurricane intensity or frequency due to external influences remains difficult because of deficiencies in theoretical understanding of tropical cyclones, their modelling and their long-term monitoring (e.g., Emanuel, 2005; Landsea, 2005; Pielke, 2005). These deficiencies preclude a stronger conclusion than an assessment that anthropogenic factors more likely than not have contributed to an increase in tropical cyclone intensity.

9.5.3.7 Extratropical Cyclones

Simulations of 21st-century climate change in the MMD 20C3M model ensemble generally exhibit a decrease in the total number of extratropical cyclones in both hemispheres, but an increase in the number of the most intense events (Lambert and Fyfe, 2006), although this behaviour is not reproduced by all models (Bengtsson et al., 2006; Section 10.3.6.4). Many 21st-century simulations also show a poleward shift in the storm tracks in both hemispheres (Bengtsson et al., 2006; Section 10.3.6.4). Recent observational studies of winter NH storms have found a poleward shift in storm tracks and increased storm intensity, but a decrease in total storm numbers, in the second half of the 20th century (Section 3.5.3). Analysis of observed wind and significant wave height suggests an increase in storm activity in the NH. In the SH, the storm track has also shifted poleward, with increases in the radius and depth of storms, but decreases in their frequency. These features appear to be associated with the observed trends in the SAM and NAM. Thus, simulated and observed changes in extratropical cyclones are broadly consistent, but an anthropogenic influence has not yet been detected, owing to large internal variability and problems due to changes in observing systems (Section 3.5.3).

9.5.4 Precipitation

9.5.4.1 Changes in Atmospheric Water Vapour

The amount of moisture in the atmosphere is expected to increase in a warming climate (Trenberth et al., 2005) because saturation vapour pressure increases with temperature according to the Clausius-Clapeyron equation. Satellite-borne Special Sensor Microwave/Imager (SSM/I) measurements of water vapour since 1988 are of higher quality than either radiosonde or reanalysis data (Trenberth et al., 2005) and show a statistically significant upward trend in precipitable (column-integrated) water of 1.2 ± 0.3 % per decade averaged over the global oceans (Section 3.4.2.1). Soden et al. (2005) demonstrate that the observed changes, including the upward trend, are well simulated in the GFDL atmospheric model when observed SSTs are prescribed (Figure 9.17). The simulation and observations show common low-frequency variability, which is largely associated with ENSO. Soden et al. (2005) also demonstrate that upper-tropospheric changes in water vapour are realistically simulated by the model. Observed warming over the global oceans is likely largely anthropogenic (Figure 9.12), suggesting that anthropogenic influence has contributed to the observed increase in atmospheric water vapour over the oceans.

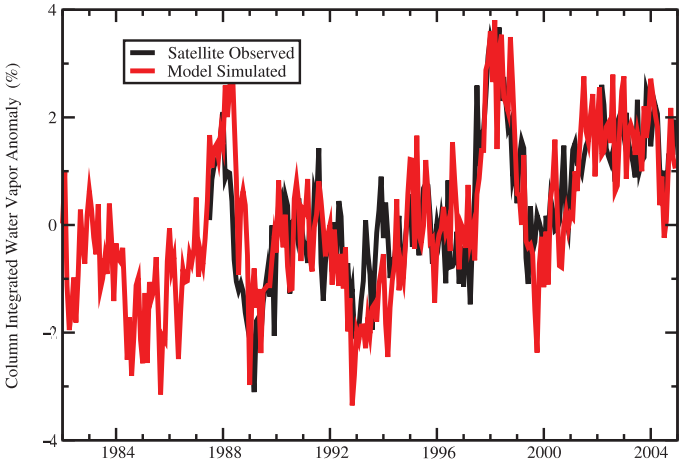


Figure 9.17. *Global mean (ocean-only) anomalies relative to 1987 to 2000 in column-integrated water vapour (%) from simulations with the GFDL AM2-LM2 AGCM forced with observed SSTs (red), and satellite observations from SSM/I (black, Wentz and Schabel, 2000). From Soden et al. (2005).*

9.5.4.2 Global Precipitation Changes

The increased atmospheric moisture content associated with warming might be expected to lead to increased global mean precipitation (Section 9.5.4.1). Global annual land mean precipitation showed a small, but uncertain, upward trend over the 20th century of approximately 1.1 mm per decade (Section 3.3.2.1 and Table 3.4). However, the record is characterised by large inter-decadal variability, and global annual land mean precipitation shows a non-significant decrease since 1950 (Figure 9.18; see also Table 3.4).

9.5.4.2.1 Detection of external influence on precipitation

Mitchell et al. (1987) argue that global mean precipitation changes should be controlled primarily by the energy budget of the troposphere where the latent heat of condensation is balanced by radiative cooling. Warming the troposphere enhances the cooling rate, thereby increasing precipitation, but this may be partly offset by a decrease in the efficiency of

radiative cooling due to an increase in atmospheric CO_2 (Allen and Ingram, 2002; Yang et al., 2003; Lambert et al., 2004; Sugi and Yoshimura, 2004). This suggests that global mean precipitation should respond more to changes in shortwave forcing than CO_2 forcing, since shortwave forcings, such as volcanic aerosol, alter the temperature of the troposphere without affecting the efficiency of radiative cooling. This is consistent with a simulated decrease in precipitation following large volcanic eruptions (Robock and Liu, 1994; Broccoli et al., 2003), and may explain why anthropogenic influence has not been detected in measurements of global land mean precipitation (Ziegler et al., 2003; Gillett et al., 2004b), although Lambert et al. (2004) urge caution in applying the energy budget argument to land-only data. Greenhouse-gas induced increases in global precipitation may have also been offset by decreases due to anthropogenic aerosols (Ramanathan et al., 2001).

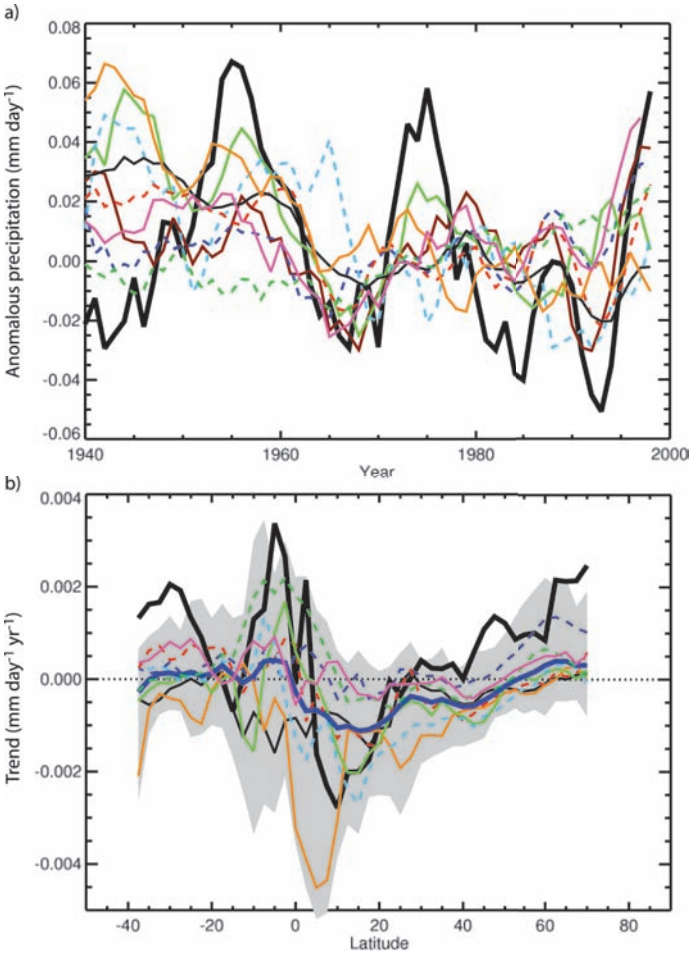


Figure 9.18. *Simulated and observed anomalies (with respect to 1961-1990) in terrestrial mean precipitation (a), and zonal mean precipitation trends 1901-1998 (b). Observations (thick black line) are based on a gridded data set of terrestrial rain gauge measurements (Hulme et al., 1998). Model data are from 20th-century MMD integrations with anthropogenic, solar and volcanic forcing from the following coupled climate models (see Table 8.1 for model details): UKMO-HadCM3 (brown), CCSM3 (dark blue), GFDL-CM2.0 (pale green), GFDL-CM2.1 (pale blue), GISS-EH (red), GISS-ER (thin black), MIROC3.2(medres) (orange), MRI-CGCM2.3.2 (dashed green) and PCM (pink). Coloured curves are ensemble means from individual models. In (a), a five-year running mean was applied to suppress other sources of natural variability, such as ENSO. In (b), the grey band indicates the range of trends simulated by individual ensemble members, and the thick dark blue line indicates the multi-model ensemble mean. External influence in observations on global terrestrial mean precipitation is detected with those precipitation simulations shown by continuous lines in the top panel. Adapted from Lambert et al. (2005).*

Several studies have demonstrated that simulated land mean precipitation in climate model integrations including both natural and anthropogenic forcings is significantly correlated with that observed (Allen and Ingram, 2002; Gillett et al., 2004b; Lambert et al., 2004), thereby detecting external influence in observations of precipitation (see Section 8.3.1.2 for an evaluation of model-simulated precipitation). Lambert et al. (2005) examine precipitation changes in simulations of nine MMD 20C3M models including anthropogenic and natural forcing (Figure 9.18a), and find that the responses to combined anthropogenic and natural forcing simulated by five of the nine models are detectable in observed land mean precipitation (Figure 9.18a). Lambert et al. (2004) detect the response to shortwave forcing, but not longwave forcing, in land mean precipitation using HadCM3, and Gillett et al. (2004b) similarly detect the response to volcanic forcing using the PCM. Climate models appear to underestimate the variance of land mean precipitation compared to that observed (Gillett et al., 2004b; Lambert et al., 2004, 2005), but it is unclear whether this discrepancy results from an underestimated response to shortwave forcing (Gillett et al., 2004b), underestimated internal variability, errors in the observations, or a combination of these.

Greenhouse gas increases are also expected to cause enhanced horizontal transport of water vapour that is expected to lead to a drying of the subtropics and parts of the tropics (Kumar et al., 2004; Neelin et al., 2006), and a further increase in precipitation in the equatorial region and at high latitudes (Emori and Brown, 2005; Held and Soden, 2006). Simulations of 20th-century zonal mean land precipitation generally show an increase at high latitudes and near the equator, and a decrease in the subtropics of the NH (Hulme et al., 1998; Held and Soden, 2006; Figure 9.18b). Projections for the 21st century show a similar effect (Figure 10.12). This simulated drying of the northern subtropics and southward shift of the Inter-Tropical Convergence Zone may relate in part to the effects of sulphate aerosol (Rotstayn and Lohmann, 2002), although simulations without aerosol effects also show drying in the northern subtropics (Hulme et al., 1998). This pattern of zonal mean precipitation changes is broadly consistent with that observed over the 20th century (Figure 9.18b; Hulme et al., 1998; Allen and Ingram, 2002; Rotstayn and Lohmann, 2002), although the observed record is characterised by large inter-decadal variability (Figure 3.15). The agreement between the simulated and observed zonal mean precipitation trends is not sensitive to the inclusion of forcing by volcanic eruptions in the simulations, suggesting that anthropogenic influence may be evident in this diagnostic.

Changes in runoff have been observed in many parts of the world, with increases or decreases corresponding to changes in precipitation (Section 3.3.4). Climate models suggest that runoff

will increase in regions where precipitation increases faster than evaporation, such as at high northern latitudes (Section 10.3.2.3 and Figure 10.12; see also Milly et al., 2005; Wu et al., 2005). Gedney et al. (2006) attribute increased continental runoff in the latter decades of the 20th century in part to suppression of transpiration due to CO_2-induced stomatal closure. They find that observed climate changes (including precipitation changes) alone are insufficient to explain the increased runoff, although their result is subject to considerable uncertainty in the runoff data. In addition, Qian et al. (2006) simulate observed runoff changes in response to observed temperature and precipitation alone, and Milly et al. (2005) demonstrate that 20th-century runoff trends simulated by the MMD models are significantly correlated with observed runoff trends. Wu et al. (2005) demonstrate that observed increases in arctic river discharge are reproduced in coupled model simulations with anthropogenic forcing, but not in simulations with natural forcings only.

Mid-latitude summer drying is another anticipated response to greenhouse gas forcing (Section 10.3.6.1), and drying trends have been observed in the both the NH and SH since the 1950s (Section 3.3.4). Burke et al. (2006), using the HadCM3 model with all natural and anthropogenic external forcings and a global Palmer Drought Severity Index data set compiled from observations by Dai et al. (2004), are able to formally detect the observed global trend towards increased drought in the second half of the 20th century, although the model trend is weaker than observed and the relative contributions of natural external forcings and anthropogenic forcings are not assessed. The model also simulates some aspects of the spatial pattern of observed drought trends, such as the trends across much of Africa and southern Asia, but not others, such as the trend to wetter conditions in Brazil and northwest Australia.

9.5.4.2.2 Changes in extreme precipitation

Allen and Ingram (2002) suggest that while global annual mean precipitation is constrained by the energy budget of the troposphere, extreme precipitation is constrained by the atmospheric moisture content, as predicted by the Clausius-Clapeyron equation. For a given change in temperature, they therefore predict a larger change in extreme precipitation than in mean precipitation, which is consistent with the HadCM3 response. Consistent with these findings, Emori and Brown (2005) discuss physical mechanisms governing changes in the dynamic and thermodynamic components of mean and extreme precipitation and conclude that changes related to the dynamic component (i.e., that due to circulation change) are secondary factors in explaining the greater percentage increase in extreme precipitation than in mean precipitation that is seen in models. Meehl et al. (2005) demonstrate that tropical precipitation intensity increases are related to water vapour increases, while mid-latitude intensity increases are related to circulation changes that affect the distribution of increased water vapour.

Climatological data show that the most intense precipitation occurs in warm regions (Easterling et al., 2000) and diagnostic analyses have shown that even without any change in total precipitation, higher temperatures lead to a greater proportion of total precipitation in heavy and very heavy precipitation events (Karl and Trenberth, 2003). In addition, Groisman et al. (1999) demonstrate empirically, and Katz (1999) theoretically, that as total precipitation increases a greater proportion falls in heavy and very heavy events if the frequency remains constant. Similar characteristics are anticipated under global warming (Cubasch et al., 2001; Semenov and Bengtsson, 2002; Trenberth et al., 2003). Trenberth et al. (2005) point out that since the amount of moisture in the atmosphere is likely to rise much faster as a consequence of rising temperatures than the total precipitation, this should lead to an increase in the intensity of storms, offset by decreases in duration or frequency of events.

Model results also suggest that future changes in precipitation extremes will likely be greater than changes in mean precipitation (Section 10.3.6.1; see Section 8.5.2 for an evaluation of model-simulated precipitation extremes). Simulated changes in globally averaged annual mean and extreme precipitation appear to be quite consistent between models. The greater and spatially more uniform increases in heavy precipitation as compared to mean precipitation may allow extreme precipitation change to be more robustly detectable (Hegerl et al., 2004).

Evidence for changes in observations of short-duration precipitation extremes varies with the region considered (Alexander et al., 2006) and the analysis method employed (Folland et al., 2001; Section 3.8.2.2). Significant increases in observed extreme precipitation have been reported over some parts of the world, for example over the USA, where the increase is similar to changes expected under greenhouse warming (e.g., Karl and Knight, 1998; Semenov and Bengtsson, 2002; Groisman et al., 2005). However, a quantitative comparison between area-based extreme events simulated in models and station data remains difficult because of the different scales involved (Osborn and Hulme, 1997). A first attempt based on Frich et al. (2002) indices used fingerprints from atmospheric model simulations with prescribed SST (Kiktev et al., 2003) and found little similarity between patterns of simulated and observed rainfall extremes, in contrast to the qualitative similarity found in other studies (Semenov and Bengtsson, 2002; Groisman et al., 2005). Tebaldi et al. (2006) report that eight MMD 20C3M models show a general tendency towards a greater frequency of heavy precipitation events over the past four decades, most coherently at high latitudes of the NH, broadly consistent with observed changes (Groisman et al., 2005).

9.5.4.3 Regional Precipitation Changes

Observed trends in annual precipitation during the period 1901 to 2003 are shown in Figure 3.13 for regions in which data is available. Responses to external forcing in regional precipitation trends are expected to exhibit low signal-to-noise ratios and are likely to exhibit strong spatial variations because of the dependence of precipitation on atmospheric circulation and on geographic factors such as orography. There have been some suggestions, for specific regions, of a possible anthropogenic influence on precipitation, which are discussed below.

9.5.4.3.1 *Sahel drought*

Rainfall decreased substantially across the Sahel from the 1950s until at least the late 1980s (Dai et al., 2004; Figure 9.19, see also Figure 3.37). There has been a partial recovery since about 1990, although rainfall has not returned to levels typical of the period 1920 to 1965. Zeng (2003) note that two main hypotheses have been proposed as a cause of the extended drought: overgrazing and conversion of woodland to agriculture increasing surface albedo and reducing moisture supply to the atmosphere, and large-scale atmospheric circulation changes related to decadal global SST changes that could be of anthropogenic or natural origin (Nicholson, 2001). Black carbon has also been suggested as a contributor (Menon et al., 2002b). Taylor et al. (2002) examine the impact of land use change with an atmospheric GCM forced only by estimates of Sahelian land use change since 1961. They simulate a small decrease in Sahel rainfall (around 5% by 1996) and conclude that the impacts of recent land use changes are not large enough to have been the principal cause of the drought.

Several recent studies have demonstrated that simulations with a range of atmospheric models using prescribed observed SSTs are able to reproduce observed decadal variations in Sahel rainfall (Bader and Latif, 2003; Giannini et al., 2003; Rowell, 2003; Haarsma et al., 2005; Held et al., 2005; Lu and Delworth, 2005; see also Figure 9.19; Hoerling et al., 2006), consistent with earlier findings (Folland, 1986; Rowell, 1996). Hoerling et al. (2006) show that AGCMs with observed SST changes typically underestimate the magnitude of the observed precipitation changes, although the models and observations are not inconsistent. These studies differ somewhat in terms of which ocean SSTs they find to be most important: Giannini et al. (2003) and Bader and Latif (2003) emphasize the role of tropical Indian Ocean warming, Hoerling et al. (2006) attribute the drying trend to a progressive warming of the South Atlantic relative to the North Atlantic, and Rowell (2003) finds that Mediterranean SSTs are an additional important contributor to decadal variations in Sahel rainfall. Based on a multi-model ensemble of coupled model simulations Hoerling et al. (2006) conclude that the observed drying trend in the Sahel is not consistent with simulated internal variability alone.

Thus, recent research indicates that changes in SSTs are probably the dominant influence on rainfall in the Sahel, although land use changes possibly also contribute (Taylor et al., 2002). But what has caused the differential SST changes? Rotstayn and Lohmann (2002) propose that spatially varying, anthropogenic sulphate aerosol forcing (both direct and indirect) can alter low-latitude atmospheric circulation leading to a decline in Sahel rainfall. They find a southward shift of tropical rainfall due to a hemispheric asymmetry in the SST response to changes in cloud albedo and lifetime in a climate simulation forced with recent anthropogenic changes in sulphate aerosol. Williams et al. (2001) also find a southward shift of tropical rainfall as a response to the indirect effect of sulphate aerosol. These results suggest that sulphate aerosol changes may have led to reduced warming of the northern tropical oceans, which in turn led to the decrease in Sahel rainfall, possibly enhanced through land-atmosphere interaction, although a full attribution analysis has yet to be conducted. Held et al. (2005) show that historical climate simulations with the both the GFDL-CM2.0 and CM2.1 models (see Table 8.1 for details) exhibit drying trends over the Sahel in the second half of the 20th century, which they ascribe to a combination of greenhouse gas and sulphate aerosol changes. The spatial pattern of the trends in simulated rainfall also shows some agreement with observations. However, Hoerling et al. (2006) find that eight other coupled climate models with prescribed anthropogenic forcing do not simulate significant trends in Sahel rainfall over the 1950 to 1999 period.

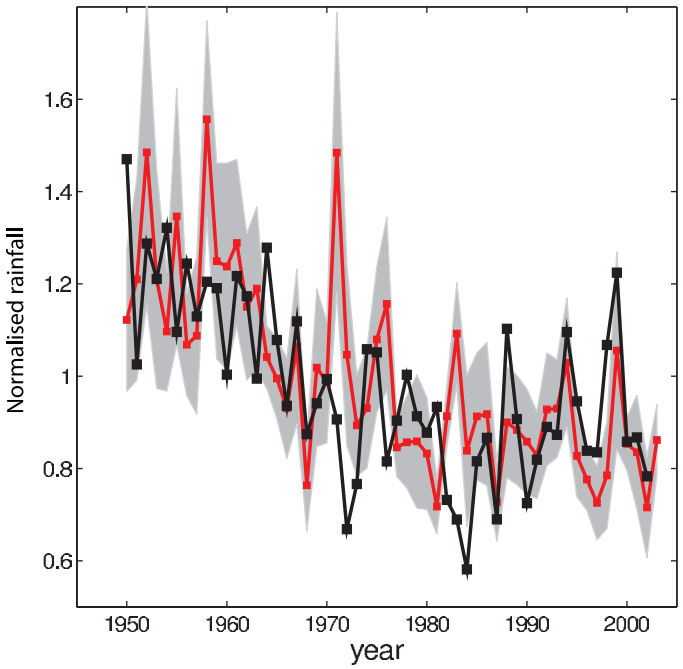


Figure 9.19. *Observed (Climatic Research Unit TS 2.1; Mitchell and Jones, 2005) Sahel July to September rainfall for each year (black), compared to an ensemble mean of 10 simulations of the atmospheric/land component of the GFDL-CM2.0 model (see Table 8.1 for model details) forced with observed SSTs (red). Both model and observations are normalized to unit mean over 1950-2000. The grey band represents ±1 standard deviation of intra-ensemble variability. After Held et al. (2005), based on results in Lu and Delworth (2005).*

9.5.4.3.2 *Southwest Australian drought*

Early winter (May–July) rainfall in the far southwest of Australia declined by about 15% in the mid-1970s (IOCI, 2002) and remained low subsequently. The rainfall decrease was accompanied by a change in large-scale atmospheric circulation in the surrounding region (Timbal, 2004). The circulation and precipitation changes are somewhat consistent with, but larger than, those simulated by climate models in response to greenhouse gas increases. The Indian Ocean Climate Initiative (IOCI, 2005) concludes that land cover change could not be the primary cause of the rainfall decrease because of the link between the rainfall decline and changes in large-scale atmospheric circulation, and re-affirms the conclusion of IOCI

(2002) that both natural variability and greenhouse forcing likely contributed. Timbal et al. (2005) demonstrate that climate change signals downscaled from the PCM show some similarity to observed trends, although the significance of this finding is uncertain.

Some authors (e.g., Karoly, 2003) have suggested that the decrease in rainfall is related to anthropogenic changes in the SAM (see Section 9.5.3.3). However, the influence of changes in circulation on southwest Australian drought remains unclear as the largest SAM trend has occurred during the SH summer (December–March; Thompson et al., 2000; Marshall et al., 2004), while the largest rainfall decrease has occurred in early winter (May–July).

9.5.4.3.3 Monsoon precipitation

Decreasing trends in precipitation over the Indonesian Maritime Continent, equatorial western and central Africa, Central America, Southeast Asia and eastern Australia have been observed over the period 1948 to 2003, while increasing trends were found over the USA and north-western Australia (Section 3.7). The TAR (IPCC, 2001, pp. 568) concluded that an increase in Southeast Asian summer monsoon precipitation is simulated in response to greenhouse gas increases in climate models, but that this effect is reduced by an increase in sulphate aerosols, which tend to decrease monsoon precipitation. Since then, additional modelling studies have come to conflicting conclusions regarding changes in monsoon precipitation (Lal and Singh, 2001; Douville et al., 2002; Maynard et al., 2002; May, 2004; Wardle and Smith, 2004; see also Section 9.5.3.5). Ramanathan et al. (2005) were able to simulate realistic changes in Indian monsoon rainfall, particularly a decrease that occurred between 1950 and 1970, by including the effects of black carbon aerosol. In both the observations and model, these changes were associated with a decreased SST gradient over the Indian Ocean and an increase in tropospheric stability, and they were not reproduced in simulations with greenhouse gas and sulphate aerosol changes only.

9.5.5 Cryosphere Changes

9.5.5.1 Sea Ice

Widespread warming would, in the absence of other countervailing effects, lead to declines in sea ice, snow, and glacier and ice sheet extent and thickness. The annual mean area of arctic sea ice cover has decreased in recent decades, with stronger declines in summer than in winter, and some thinning (Section 4.4). Gregory et al. (2002b) show that a four-member ensemble of HadCM3 integrations with all major anthropogenic and natural forcing factors simulates a decline in arctic sea ice extent of about 2.5% per decade over the period 1970 to 1999, which is close to the observed decline of 2.7% per decade over the satellite period 1978 to 2004. This decline is inconsistent with simulated internal climate variability and the response to natural forcings alone (Vinnikov et al., 1999; Gregory et al., 2002b; Johannssen et al., 2004), indicating that anthropogenic forcing has likely contributed to the trend in NH sea ice extent. Models such as those described by Rothrock et al. (2003) and references therein are able to reproduce the observed interannual variations in ice thickness, at least when averaged over fairly large regions. Simulations of historical arctic ice thickness or volume (Goeberle and Gerdes, 2003; Rothrock et al., 2003) show a marked reduction in ice thickness starting in the late 1980s, but disagree somewhat with respect to trends and/or variations earlier in the century. Although some of the dramatic change inferred may be a consequence of a spatial redistribution of ice volume over time (e.g., Holloway and Sou, 2002), thermodynamic changes are also believed to be important. Low-frequency atmospheric variability (such as interannual changes in circulation connected to the NAM) appears to be important in flushing ice out of the Arctic Basin, thus increasing the amount of summer open water and enhancing thermodynamic thinning through the ice-albedo feedback (e.g., Lindsay and Zhang, 2005). Large-scale modes of variability affect both wind driving and heat transport in the atmosphere, and therefore contribute to interannual variations in ice formation, growth and melt (e.g., Rigor et al., 2002; Dumas et al., 2003). Thus, the decline in arctic sea ice extent and its thinning appears to be largely, but not wholly, due to greenhouse gas forcing.

Unlike in the Arctic, a strong decline in sea ice extent has not been observed in the Antarctic during the period of satellite observations (Section 4.4.2.2). Fichefet et al. (2003) conducted a simulation of Antarctic ice thickness using observationally based atmospheric forcing covering the period 1958 to 1999. They note pronounced decadal variability, with area average ice thickness varying by ±0.1 m (compared to a mean thickness of roughly 0.9 m), but no long-term trend. However, Gregory et al. (2002b) find a decline in antarctic sea ice extent in their model, contrary to observations. They suggest that the lack of consistency between the observed and modelled changes in sea ice extent might reflect an unrealistic simulation of regional warming around Antarctica, rather than a deficiency in the ice model. Holland and Raphael (2006) examine sea ice variability in six MMD 20C3M simulations that include stratospheric ozone depletion. They conclude that the observed weak increase in antarctic sea ice extent is not inconsistent with simulated internal variability, with some simulations reproducing the observed trend over 1979 to 2000, although the models exhibit larger interannual variability in sea ice extent than satellite observations.

9.5.5.2 Snow and Frozen Ground

Snow cover in the NH, as measured from satellites, has declined substantially in the past 30 years, particularly from early spring through summer (Section 4.2). Trends in snow depth and cover can be driven by precipitation or temperature trends. The trends in recent decades have generally been driven by warming at lower and middle elevations. Evidence for this includes: (a) interannual variations in NH April snow-covered area are strongly correlated ($r = -0.68$) with April

40°N to 60°N temperature; (b) interannual variations in snow (water equivalent, depth or duration) are strongly correlated with temperature at lower- and middle-elevation sites in North America (Mote et al., 2005), Switzerland (Scherrer et al., 2004) and Australia (Nicholls, 2005); (c) trends in snow water equivalent or snow depth show strong dependence on elevation or equivalently mean winter temperature, both in western North America and Switzerland (with stronger decreases at lower, warmer elevations where a warming is more likely to affect snowfall and snowmelt); and (d) the trends in North America, Switzerland and Australia have been shown to be well explained by warming and cannot be explained by changes in precipitation. In some very cold places, increases in snow depth have been observed and have been linked to higher precipitation.

Widespread permafrost warming and degradation appear to be the result of increased summer air temperatures and changes in the depth and duration of snow cover (Section 4.7.2). The thickness of seasonally frozen ground has decreased in response to winter warming and increases in snow depth (Section 4.7.3).

9.5.5.3 Glaciers, Ice Sheets and Ice Shelves

During the 20th century, glaciers generally lost mass with the strongest retreats in the 1930s and 1940s and after 1990 (Section 4.5). The widespread shrinkage appears to imply widespread warming as the probable cause (Oerlemans, 2005), although in the tropics changes in atmospheric moisture might be contributing (Section 4.5.3). Over the last half century, both global mean winter accumulation and summer melting have increased steadily (Ohmura, 2004; Dyurgerov and Meier, 2005; Greene, 2005), and at least in the NH, winter accumulation and summer melting correlate positively with hemispheric air temperature (Greene, 2005); the negative correlation of net balance with temperature indicates the primary role of temperature in forcing the respective glacier fluctuations.

There have been a few studies for glaciers in specific regions examining likely causes of trends. Mass balances for glaciers in western North America are strongly correlated with global mean winter (October–April) temperatures and the decline in glacier mass balance has paralleled the increase in temperature since 1968 (Meier et al., 2003). Reichert et al. (2002a) forced a glacier mass balance model for the Nigardsbreen and Rhône glaciers with downscaled data from an AOGCM control simulation and conclude that the rate of glacier advance during the 'Little Ice Age' could be explained by internal climate variability for both glaciers, but that the recent retreat cannot, implying that the recent retreat of both glaciers is probably due to externally forced climate change. As well, the thinning and acceleration of some polar glaciers (e.g., Thomas et al., 2004) appear to be the result of ice sheet calving driven by oceanic and atmospheric warming (Section 4.6.3.4).

Taken together, the ice sheets of Greenland and Antarctica are shrinking. Slight thickening in inland Greenland is more than compensated for by thinning near the coast (Section 4.6.2.2). Warming is expected to increase low-altitude melting and high-altitude precipitation in Greenland; altimetry data suggest that the former effect is dominant. However, because some portions of ice sheets respond only slowly to climate changes, past forcing may be influencing ongoing changes, complicating attribution of recent trends (Section 4.6.3.2).

9.5.6 Summary

In the TAR, quantitative evidence for human influence on climate was based almost exclusively on atmospheric and surface temperature. Since then, anthropogenic influence has also been identified in a range of other climate variables, such as ocean heat content, atmospheric pressure and sea ice extent, thereby contributing further evidence of an anthropogenic influence on climate, and improving confidence in climate models.

Observed changes in ocean heat content have now been shown to be inconsistent with simulated natural climate variability, but consistent with a combination of natural and anthropogenic influences both on a global scale, and in individual ocean basins. Models suggest a substantial anthropogenic contribution to sea level rise, but underestimate the actual rise observed. While some studies suggest that an anthropogenic increase in high-latitude rainfall may have contributed to a freshening of the Arctic Ocean and North Atlantic deep water, these results are still uncertain.

There is no evidence that 20th-century ENSO behaviour is distinguishable from natural variability. By contrast, there has been a detectable human influence on global sea level pressure. Both the NAM and SAM have shown significant trends. Models reproduce the sign but not magnitude of the NAM trend, and models including both greenhouse gas and ozone simulate a realistic trend in the SAM. Anthropogenic influence on either tropical or extratropical cyclones has not been detected, although the apparent increased frequency of intense tropical cyclones, and its relationship to ocean warming, is suggestive of an anthropogenic influence.

Simulations and observations of total atmospheric water vapour averaged over oceans agree closely when the simulations are constrained by observed SSTs, suggesting that anthropogenic influence has contributed to an increase in total atmospheric water vapour. However, global mean precipitation is controlled not by the availability of water vapour, but by a balance between the latent heat of condensation and radiative cooling in the troposphere. This may explain why human influence has not been detected in global precipitation, while the influence of volcanic aerosols has been detected. However, observed changes in the latitudinal distribution of land precipitation are suggestive of a possible human influence as is the observed increased incidence of drought as measured by the Palmer Drought Severity Index. Observational evidence indicates that the frequency of the heaviest rainfall events has likely increased within many land regions in general agreement with model simulations that indicate that rainfall in the heaviest events is likely to increase in line with atmospheric water vapour concentration. Many AGCMs capture the observed

decrease in Sahel rainfall when constrained by observed SSTs, although this decrease is not simulated by most AOGCMs. One study found that an observed decrease in Asian monsoon rainfall could only be simulated in response to black carbon aerosol, although conclusions regarding the monsoon response to anthropogenic forcing differ.

Observed decreases in arctic sea ice extent have been shown to be inconsistent with simulated internal variability, and consistent with the simulated response to human influence, but SH sea ice extent has not declined. The decreasing trend in global snow cover and widespread melting of glaciers is consistent with a widespread warming. Anthropogenic forcing has likely contributed substantially to widespread glacier retreat during the 20th century.

9.6 Observational Constraints on Climate Sensitivity

This section assesses recent research that infers equilibrium climate sensitivity and transient climate response from observed changes in climate. 'Equilibrium climate sensitivity' (ECS) is the equilibrium annual global mean temperature response to a doubling of equivalent atmospheric CO_2 from pre-industrial levels and is thus a measure of the strength of the climate system's eventual response to greenhouse gas forcing. 'Transient climate response' (TCR) is the annual global mean temperature change at the time of CO_2 doubling in a climate simulation with a 1% yr^{-1} compounded increase in CO_2 concentration (see Glossary and Section 8.6.2.1 for detailed definitions). TCR is a measure of the strength and rapidity of the climate response to greenhouse gas forcing, and depends in part on the rate at which the ocean takes up heat. While the direct temperature change that results from greenhouse gas forcing can be calculated in a relatively straightforward manner, uncertain atmospheric feedbacks (Section 8.6) lead to uncertainties in estimates of future climate change. The objective here is to assess estimates of ECS and TCR that are based on observed climate changes, while Chapter 8 assesses feedbacks individually. Inferences about climate sensitivity from observed climate *changes* complement approaches in which uncertain parameters in climate models are varied and assessed by evaluating the resulting skill in reproducing observed *mean* climate (Section 10.5.4.4). While observed climate changes have the advantage of being most clearly related to future climate change, the constraints they provide on climate sensitivity are not yet very strong, in part because of uncertainties in both climate forcing and the estimated response (Section 9.2). An overall summary assessment of ECS and TCR, based on the ability of models to simulate climate change and mean climate and on other approaches, is given in Box 10.2. Note also that this section does not assess regional climate sensitivity or sensitivity to forcings other than CO_2.

9.6.1 Methods to Estimate Climate Sensitivity

The most straightforward approach to estimating climate sensitivity would be to relate an observed climate change to a known change in radiative forcing. Such an approach is strictly correct only for changes between equilibrium climate states. Climatic states that were reasonably close to equilibrium in the past are often associated with substantially different climates than the pre-industrial or present climate, which is probably not in equilibrium (Hansen et al., 2005). An example is the climate of the LGM (Chapter 6 and Section 9.3). However, the climate's sensitivity to external forcing will depend on the mean climate state and the nature of the forcing, both of which affect feedback mechanisms (Chapter 8). Thus, an estimate of the sensitivity directly derived from the ratio of response to forcing cannot be readily compared to the sensitivity of climate to a doubling of CO_2 under idealised conditions. An alternative approach, which has been pursued in most work reported here, is based on varying parameters in climate models that influence the ECS in those models, and then attaching probabilities to the different ECS values based on the realism of the corresponding climate change simulations. This ameliorates the problem of feedbacks being dependent on the climatic state, but depends on the assumption that feedbacks are realistically represented in models and that uncertainties in all parameters relevant for feedbacks are varied. Despite uncertainties, results from simulations of climates of the past and recent climate change (Sections 9.3 to 9.5) increase confidence in this assumption.

The ECS and TCR estimates discussed here are generally based on large ensembles of simulations using climate models of varying complexity, where uncertain parameters influencing the model's sensitivity to forcing are varied. Studies vary key climate and forcing parameters in those models, such as the ECS, the rate of ocean heat uptake, and in some instances, the strength of aerosol forcing, within plausible ranges. The ECS can be varied directly in simple climate models and in some EMICs (see Chapter 8), and indirectly in more complex EMICs and AOGCMs by varying model parameters that influence the strength of atmospheric feedbacks, for example, in cloud parametrizations. Since studies estimating ECS and TCR from observed climate changes require very large ensembles of simulations of past climate change (ranging from several hundreds to thousands of members), they are often, but not always, performed with EMICs or EBMs.

The idea underlying this approach is that the plausibility of a given combination of parameter settings can be determined from the agreement of the resulting simulation of historical climate with observations. This is typically evaluated by means of Bayesian methods (see Supplementary Material, Appendix 9.B for methods). Bayesian approaches constrain parameter values by combining prior distributions that account for uncertainty in the knowledge of parameter values with information about the parameters estimated from data (Kennedy and O'Hagan, 2001). The uniform distribution has been used widely as a prior distribution, which enables comparison of constraints obtained from the data in different approaches. ECS ranges

encompassed by the uniform prior distribution must be limited due to computer time limiting the size of model ensembles, but generally cover the range considered possible by experts, such as from 0°C to 10°C. Note that uniform prior distributions for ECS, which only require an expert assessment of possible range, generally assign a higher prior belief to high sensitivity than, for example, non-uniform prior distributions that depend more heavily on expert assessments (e.g., Forest et al., 2006). In addition, Frame et al. (2005) point out that care must be taken when specifying the uniform prior distribution. For example, a uniform prior distribution for the climate feedback parameter (see Glossary) implies a non-uniform prior distribution for ECS due to the nonlinear relationship between the two parameters.

Since observational constraints on the upper bound of ECS are still weak (as shown below), these prior assumptions influence the resulting estimates. Frame et al. (2005) advocate sampling a flat prior distribution in ECS if this is the target of the estimate, or in TCR if future temperature trends are to be constrained. In contrast, statistical research on the design and interpretation of computer experiments suggests the use of prior distributions for model input parameters (e.g., see Kennedy and O'Hagan, 2001; Goldstein and Rougier, 2004). In such Bayesian studies, it is generally good practice to explore the sensitivity of results to different prior beliefs (see, for example, Tol and Vos, 1998; O'Hagan and Forster, 2004). Furthermore, as demonstrated by Annan and Hargreaves (2005) and Hegerl et al. (2006a), multiple and independent lines of evidence about climate sensitivity from, for example, analysis of climate change at different times, can be combined by using information from one line of evidence as prior information for the analysis of another line of evidence. The extent to which the different lines of evidence provide complete information on the underlying physical mechanisms and feedbacks that determine the climate sensitivity is still an area of active research. In the following, uniform prior distributions for the target of the estimate are used unless otherwise specified.

Methods that incorporate a more comprehensive treatment of uncertainty generally produce wider uncertainty ranges for the inferred climate parameters. Methods that do not vary uncertain parameters, such as ocean diffusivity, in the course of the uncertainty analysis will yield probability distributions for climate sensitivity that are conditional on these values, and therefore are likely to underestimate the uncertainty in climate sensitivity. On the other hand, approaches that do not use all available evidence will produce wider uncertainty ranges than estimates that are able to use observations more comprehensively.

9.6.2 Estimates of Climate Sensitivity Based on Instrumental Observations

9.6.2.1 Estimates of Climate Sensitivity Based on 20th-Century Warming

A number of recent studies have used instrumental records of surface, ocean and atmospheric temperature changes to estimate climate sensitivity. Most studies use the observed surface temperature changes over the 20th century or the last 150 years (Chapter 3). In addition, some studies also use the estimated ocean heat uptake since 1955 based on Levitus et al. (2000, 2005) (Chapter 5), and temperature changes in the free atmosphere (Chapter 3; see also Table 9.3). For example, Frame et al. (2005) and Andronova and Schlesinger (2000) use surface air temperature alone, while Forest et al. (2002, 2006), Knutti et al. (2002, 2003) and Gregory et al. (2002a) use both surface air temperature and ocean temperature change to constrain climate sensitivity. Forest et al. (2002, 2006) and Lindzen and Giannitsis (2002) use free atmospheric temperature data from radiosondes in addition to surface air temperature. Note that studies using radiosonde data may be affected by recently discovered inhomogeneities (Section 3.4.1.1), although Forest et al. (2006) illustrate that the impact of the radiosonde atmospheric temperature data on their climate sensitivity estimate is smaller than that of surface and ocean warming data. A further recent study uses Earth Radiation Budget Experiment (ERBE) data (Forster and Gregory, 2006) in addition to surface temperature changes to estimate climate feedbacks (and thus ECS) from observed changes in forcing and climate.

Wigley et al. (1997) pointed out that uncertainties in forcing and response made it impossible to use observed global temperature changes to constrain ECS more tightly than the range explored by climate models at the time (1.5°C to 4.5°C), and particularly the upper end of the range, a conclusion confirmed by subsequent studies. A number of subsequent publications qualitatively describe parameter values that allow models to reproduce features of observed changes, but without directly estimating a climate sensitivity probability density function (PDF). For example, Harvey and Kaufmann (2002) find a best-fit ECS of 2.0°C out of a range of 1°C to 5°C, and constrain fossil fuel and biomass aerosol forcing (Section 9.2.1.2). Lindzen and Giannitsis (2002) pose the hypothesis that the rapid change in tropospheric (850–300 hPa) temperatures around 1976 triggered a delayed response in surface temperature that is best modelled with a climate sensitivity of less than 1°C. However, their estimate does not account for substantial uncertainties in the analysis of such a short time period, most notably those associated with the role of internal climate variability in the rapid tropospheric warming of 1976. The 1976–1977 climate shift occurred along with a phase shift of the PDO, and a concurrent change in the ocean (Section 3.6.3) that appears to contradict the Lindzen and Giannitsis (2002) assumption that the change was initiated by tropospheric forcing. In addition, the authors do not account for uncertainties in the simple model whose sensitivity is fitted. The finding of Lindzen and Giannitsis is in contrast with that of Forest et al. (2002, 2006) who consider the joint evolution of surface and upper air temperatures on much longer time scales.

Several recent studies have derived probability estimates for ECS using a range of models and diagnostics. The diagnostics, which are used to compare model-simulated and observed changes, are often simple temperature indices such as the global mean surface temperature and ocean mean warming

(Knutti et al., 2002, 2003) or the differential warming between the SH and NH (together with the global mean; Andronova and Schlesinger, 2001). Results that use more detailed information about the space-time evolution of climate may be able to provide tighter constraints than those that use simpler indices. Forest et al. (2002, 2006) use a so-called 'optimal' detection method (Section 9.4.1.4 and Appendix 9.A.1) to diagnose the fit between model-simulated and observed patterns of zonal mean temperature change. Frame et al. (2005) use detection results from an analysis based on several multi-model AOGCM fingerprints (Section 9.4.1.4) that separate the greenhouse gas response from that to other anthropogenic and natural forcings (Stott et al., 2006c). Similarly, Gregory et al. (2002a) apply an inverse estimate of the range of aerosol forcing based on fingerprint detection results. Note that while results from fingerprint detection approaches will be affected by uncertainty in separation between greenhouse gas and aerosol forcing, the resulting uncertainty in estimates of the near-surface temperature response to greenhouse gas forcing is relatively small (Sections 9.2.3 and 9.4.1.4).

A further consideration in assessing these results is the extent to which realistic forcing estimates were used, and whether forcing uncertainty was included. Most studies consider a range of anthropogenic forcing factors, including greenhouse gases and sulphate aerosol forcing, sometimes directly including the indirect forcing effect, such as Knutti et al. (2002, 2003), and sometimes indirectly accounting for the indirect effect by using a wide range of direct forcing (e.g., Andronova and Schlesinger, 2001; Forest et al., 2002, 2006). Many studies also consider tropospheric ozone (e.g., Andronova and Schlesinger, 2001; Knutti et al., 2002, 2003). Forest et al. (2006) demonstrate that the inclusion of natural forcing affects the estimated PDF of climate sensitivity since net negative natural forcing in the second half of the 20th century favours higher sensitivities than earlier results that disregarded natural forcing (Forest et al., 2002; see Figure 9.20), particularly if the same ocean warming estimates were used. Note that some of the changes due to inclusion of natural forcing are offset by using recently revised ocean warming data (Levitus et al., 2005), which favour somewhat smaller ocean heat uptakes than earlier data (Levitus et al., 2001; Forest et al., 2006). Only a few estimates account for uncertainty in forcings other than from aerosols (e.g., Gregory et al., 2002a; Knutti et al., 2002, 2003); some other studies perform some sensitivity testing to assess the effect of forcing uncertainty not accounted for, for example, in natural forcing (e.g., Forest et al., 2006; see Table 9.1 for an overview).

The treatment of uncertainty in the ocean's uptake of heat varies, from assuming a fixed value for a model's ocean diffusivity (Andronova and Schlesinger, 2001) to trying to allow for a wide range of ocean mixing parameters (Knutti et al., 2002, 2003) or systematically varying the ocean's effective diffusivity (e.g., Forest et al., 2002, 2006; Frame et al., 2005). Furthermore, all approaches that use the climate's time evolution attempt to account for uncertainty due to internal climate variability, either by bootstrapping (Andronova and Schlesinger, 2001), by using a noise model in fingerprint studies whose results are used (Frame et al., 2005) or directly (Forest et al., 2002, 2006).

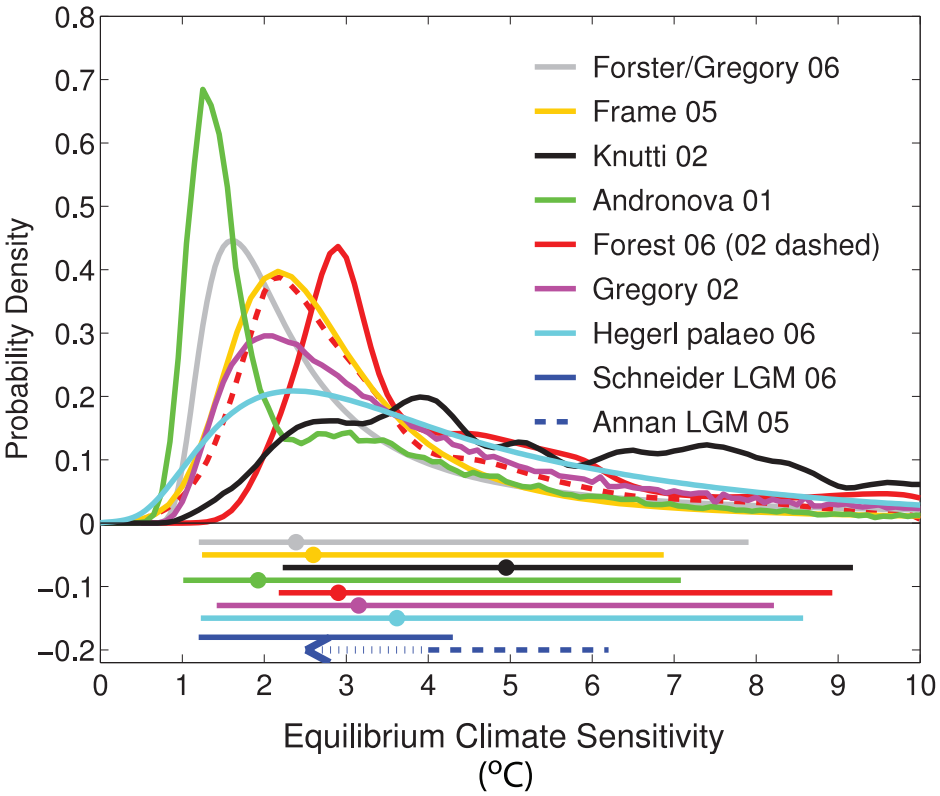


Figure 9.20. *Comparison between different estimates of the PDF (or relative likelihood) for ECS (°C). All PDFs/likelihoods have been scaled to integrate to unity between 0°C and 10°C ECS. The bars show the respective 5 to 95% ranges, dots the median estimate. The PDFs/likelihoods based on instrumental data are from Andronova and Schlesinger (2001), Forest et al. (2002; dashed line, considering anthropogenic forcings only), Forest et al. (2006; solid, anthropogenic and natural forcings), Gregory et al. (2002a), Knutti et al. (2002), Frame et al. (2005), and Forster and Gregory (2006), transformed to a uniform prior distribution in ECS using the method after Frame et al. (2005). Hegerl et al. (2006a) is based on multiple palaeoclimatic reconstructions of NH mean temperatures over the last 700 years. Also shown are the 5 to 95% approximate ranges for two estimates from the LGM (dashed, Annan et al., 2005; solid, Schneider von Deimling et al., 2006) which are based on models with different structural properties. Note that ranges extending beyond the published range in Annan et al. (2005), and beyond that sampled by the climate model used there, are indicated by dots and an arrow, since Annan et al. only provide an upper limit. For details of the likelihood estimates, see Table 9.3. After Hegerl et al. (2006a).*

Figure 9.20 compares results from many of these studies. All PDFs shown are based on a uniform prior distribution of ECS and have been rescaled to integrate to unity for all positive sensitivities up to 10°C to enable comparisons of results using different ranges of uniform prior distributions (this affects both median and upper 95th percentiles if original estimates were based on a wider uniform range). Thus, zero prior probability is assumed for sensitivities exceeding 10°C, since many results do not consider those, and for negative sensitivities. Negative climate sensitivity would lead to cooling in response to a positive forcing and is inconsistent with understanding of the energy balance of the system (Stouffer et al., 2000; Gregory et al., 2002a; Lindzen and Giannitsis, 2002). This figure shows that best estimates of the ECS (mode of the estimated PDFs) typically range between 1.2°C and 4°C when inferred from constraints provided by historical instrumental data, in agreement with estimates derived from more comprehensive climate models. Most studies suggest a 5th percentile for climate sensitivity of 1°C or above. The upper 95th percentile is not well constrained, particularly in studies that account conservatively for uncertainty in, for example, 20th-century radiative forcing and ocean heat uptake. The upper tail is particularly long in studies using diagnostics based on large-scale mean data because separation of the greenhouse gas response from that to aerosols or climate variability is more difficult with such diagnostics (Andronova and Schlesinger, 2001; Gregory et al., 2002a; Knutti et al., 2002, 2003). Forest et al. (2006) find a 5 to 95% range of 2.1°C to 8.9°C for climate sensitivity (Table 9.3), which is a wider range than their earlier result based on anthropogenic forcing only (Forest et al., 2002). Frame et al. (2005) infer a 5 to 95% uncertainty range for the ECS of 1.2°C to 11.8°C, using a uniform prior distribution that extends well beyond 10°C sensitivity. Studies generally do not find meaningful constraints on the rate at which the climate system mixes heat into the deep ocean (e.g., Forest et al., 2002, 2006). However, Forest et al. (2006) find that many coupled AOGCMs mix heat too rapidly into the deep ocean, which is broadly consistent with comparisons based on heat uptake (Section 9.5.1.1,). However the relevance of this finding is unclear because most MMD AOGCMs were not included in the Forest et al. comparison, and because they used a relatively simple ocean model. Knutti et al. (2002) also determine that strongly negative aerosol forcing, as has been suggested by several observational studies (Anderson et al., 2003), is incompatible with the observed warming trend over the last century (Section 9.2.1.2 and Table 9.1).

Table 9.3. *Results from key studies on observational estimates of ECS (in °C) from instrumental data, individual volcanic eruptions, data for the last millennium, and simulations of the LGM . The final three rows list some studies using non-uniform prior distributions, while the other studies use uniform prior distributions of ECS.*

Study	Observational Data Used to Constrain Study[a]	Model[b]	External Forcings Included[c]	Treatment of uncertainties[d]	Estimated ECS Range 5 to 95% (°C)
From Instrumental Data					
Forest et al. (2006)	Upper air, surface and deep ocean space-time 20th-century temperatures Prior 0°C to 10°C	2-D EMIC (~E6)	G, Sul, Sol, Vol, OzS, land surface changes (2002: G, Sul, OzS)	ε_{obs}, noise, κ, ε_{aer}, sensitivity tests for solar/volcanic. forcing uncertainty	2.1 to 8.9 (1.4 to 7.7 without natural forcings)
Andronova and Schlesinger (2001)	Global mean and hemispheric difference in surface air temperature 1856 to 1997	EBM	G, OzT, Sul, Sol, Vol	Noise (bootstrap residual), choice of radiative forcing factors	1.0 to 9.3 prob ~ 54% that ECS outside 1.5 to 4.5
Knutti et al. (2002; 2003)	Global mean ocean heat uptake 1955 to 1995, mean surface air temperature 1860 to 2000 Prior 0°C to 10°C	EMIC (~E1) plus neural net	G, OzT, OzS, fossil fuel and biomass burning BC+OM, stratospheric water vapour, Vol, Sol, Sul, Suli	ε_{obs}, ε_{forc} for multiple forcings from IPCC (2001), κ, different ocean mixing schemes	2.2 to 9.2 prob ~ 50% that ECS outside 1.5 to 4.5
Gregory et al. (2002a)	Global mean change in surface air temperature and ocean heat change between 1861 to 1900 and 1957 to 1994	1-Box	G, Sul and Suli (top down via Stott et al., 2001), Sol, Vol	ε_{obs}, ε_{forc}	1.1 to ∞
Frame et al. (2005)	Global change in surface temperature	EBM	G, accounted for other anthropogenic and natural forcing by fingerprints, Sul, Nat	Noise, uncertainty in amplitude but not pattern of natural and anthropogenic. forcings and response (scaling factors), κ (range consistent with ocean warming)	1.2 to 11.8

(continued)

Table 9.3 (continued)

Study	Observational Data Used to Constrain Study[a]	Model[b]	External Forcings Included[c]	Treatment of uncertainties[d]	Estimated ECS Range 5 to 95% (°C)
Forster and Gregory (2006)	1985 to 1996 ERBE data 60°N to 60°S, global surface temperature Prior 0°C to 18.5°C, transformed after Frame et al. (2005)	1-Box	G, Vol, Sol, Sul	ε_{obs}, ε_{forc}	1.2 to 14.2
From individual volcanic eruptions					
Wigley et al. (2005a)	Global mean surface temperature	EBM	From volcanic forcing only	El Niño	Agung: 1.3 to 6.3; El Chichon: 0.3 to 7.7; Mt. Pinatubo: 1.8 to 5.2
From last millenium					
Hegerl et al. (2006a)	NH mean surface air temperature pre-industrial (1270/1505 to 1850) from multiple reconstructions Prior 0°C to 10°C	2D EBM	G, Sul, Sol, Vol	Noise (from residual), κ, uncertainty in magnitude of reconstructions and solar and volcanic forcing	1.2 to 8.6
From LGM					
Schneider von Deimling et al. (2006)	LGM tropical SSTs and other LGM data	EMIC (~E3)	LGM forcing: greenhouse gases, dust, ice sheets, vegetation, insolation	uncertainty of proxy-based ice age SSTs (one type of data); attempt to account for structural uncertainty, estimate of forcing uncertainty	1.2 to 4.3 (based on encompassing several ranges given)
Annan et al. (2005)	LGM tropical SSTs, present-day seasonal cycle of a number of variables for sampling prior distribution of model parameters	AGCM with mixed-layer ocean	PMIP2 LGM forcing	Observational uncertainty in tropical SST estimates (one type of data)	<7% chance of sensitivity >6
Using non-uniform prior distributions					
Forest et al. (2002, 2006)	Expert prior, 20th-century temperature change (see above)	See Forest et al.	see above	See individual estimates	1.9 to 4.7
Annan et al. (2006)	Estimates from LGM, 20th-century change, volcanism combined	See Annan et al.	see above	See individual estimates	> 1.7 to 4.5
Hegerl et al. (2006a)	1950 to 2000 surface temperature change (Frame et al., 2005), NH mean pre-industrial surface air temperature from last millennium	See Hegerl et al. and Frame et al. (2005)	see above	See individual estimates	1.5 to 6.2

Notes:

[a] Range covered by uniform prior distribution if narrower than 0°C to 20°C.

[b] Energy Balance Model (EBM), often with upwelling-diffusive ocean; 1-box energy balance models; EMIC (numbers refer to related EMICs described in Table 8.3).

[c] G: greenhouse gases; Sul: direct sulphate aerosol effect; Suli: (first) indirect sulphate effect; OzT: tropospheric ozone; OzS: stratospheric ozone; Vol: volcanism; Sol: solar; BC+OM: black carbon and organic matter.).

[d] Uncertainties taken into account (e.g., uncertainty in ocean diffusivity $\mathcal{K}$, or total aerosol forcing ε_{forc}). Ideally, studies account for model uncertainty, forcing uncertainty (for example, in aerosol forcing ε_{aer} or natural forcing ε_{nat}), uncertainty in observations, ε_{obs}, and internal climate variability ('noise').

Some studies have further attempted to use non-uniform prior distributions. Forest et al. (2002, 2006) obtained narrower uncertainty ranges when using expert prior distributions (Table 9.3). While they reflect credible prior ranges of ECS, expert priors may also be influenced by knowledge about observed climate change, and thus may yield overly confident estimates when combined with the same data (Supplementary Material, Appendix 9.B). Frame et al. (2005) find that sampling uniformly in TCR results in an estimated ECS of 1.2°C to 5.2°C with a median value of 2.3°C. In addition, several approaches have been based on a uniform prior distribution of climate feedback. Translating these results into ECS estimates is equivalent to using a prior distribution that favours smaller sensitivities, and hence tends to result in narrower ECS ranges (Frame et al., 2005). Forster and Gregory (2006) estimate ECS based on radiation budget data from the ERBE combined with surface temperature observations based on a regression approach, using the observation that there was little change in aerosol forcing

over that time. They find a climate feedback parameter of 2.3 ± 1.4 W m^{-2} $°C^{-1}$, which corresponds to a 5 to 95% ECS range of 1.0°C to 4.1°C if using a prior distribution that puts more emphasis on lower sensitivities as discussed above, and a wider range if the prior distribution is reformulated so that it is uniform in sensitivity (Table 9.3). The climate feedback parameter estimated from the MMD AOGCMs ranges from about 0.7 to 2.0 W m^{-2} $°C^{-1}$ (Supplementary Material, Table S8.1).

9.6.2.2 Estimates Based on Individual Volcanic Eruptions

Some recent analyses have attempted to derive insights into ECS from the well-observed forcing and response to the eruption of Mt. Pinatubo, or from other major eruptions during the 20th century. Such events allow for the study of physical mechanisms and feedbacks and are discussed in detail in Section 8.6. For example, Soden et al. (2002) demonstrate agreement between observed and simulated responses based on an AGCM with a climate sensitivity of 3.0°C coupled to a mixed-layer ocean, and that the agreement breaks down if the water vapour feedback in the model is switched off. Yokohata et al. (2005) find that a version of the MIROC climate model with a sensitivity of 4.0°C yields a much better simulation of the Mt. Pinatubo eruption than a model version with sensitivity of 6.3°C, concluding that the cloud feedback in the latter model appears inconsistent with data. Note that both results may be specific to the model analysed.

Constraining ECS from the observed responses to individual volcanic eruptions is difficult because the response to short-term volcanic forcing is strongly nonlinear in ECS, yielding only slightly enhanced peak responses and substantially extended response times for very high sensitivities (Frame et al., 2005; Wigley et al., 2005a). The latter are difficult to distinguish from a noisy background climate. A further difficulty arises from uncertainty in the rate of heat taken up by the ocean in response to a short, strong forcing. Wigley et al. (2005a) find that the lower boundary and best estimate obtained by comparing observed and simulated responses to major eruptions in the 20th century are consistent with the TAR range of 1.5°C to 4.5°C, and that the response to the eruption of Mt. Pinatubo suggests a best fit sensitivity of 3.0°C and an upper 95% limit of 5.2°C. However, as pointed out by the authors, this estimate does not account for forcing uncertainties. In contrast, an analysis by Douglass and Knox (2005) based on a box model suggests a very low climate sensitivity (under 1°C) and negative climate feedbacks based on the eruption of Mt. Pinatubo. Wigley et al. (2005b) demonstrate that the analysis method of Douglass and Knox (2005) severely underestimates (by a factor of three) climate sensitivity if applied to a model with known sensitivity. Furthermore, as pointed out by Frame et al. (2005), the effect of noise on the estimate of the climatic background level can lead to a substantial underestimate of uncertainties if not taken into account.

In summary, the responses to individual volcanic eruptions provide a useful test for feedbacks in climate models (Section 8.6). However, due to the physics involved in the response, such individual events cannot provide tight constraints on ECS. Estimates of the most likely sensitivity from most such studies are, however, consistent with those based on other analyses.

9.6.2.3 Constraints on Transient Climate Response

While ECS is the equilibrium global mean temperature change that eventually results from atmospheric CO_2 doubling, the smaller TCR refers to the global mean temperature change that is realised at the time of CO_2 doubling under an idealised scenario in which CO_2 concentrations increase by 1% yr^{-1} (Cubasch et al., 2001; see also Section 8.6.2.1). The TCR is therefore indicative of the temperature trend associated with external forcing, and can be constrained by an observable quantity, the observed warming trend that is attributable to greenhouse gas forcing. Since external forcing is likely to continue to increase through the coming century, TCR may be more relevant to determining near-term climate change than ECS.

Stott et al. (2006c) estimate TCR based on scaling factors for the response to greenhouse gases only (separated from aerosol and natural forcing in a three-pattern optimal detection analysis) using fingerprints from three different model simulations (Figure 9.21) and find a relatively tight constraint. Using three model simulations together, their estimated median TCR is 2.1°C at the time of CO_2 doubling (based on a 1% yr^{-1} increase in CO_2), with a 5 to 95% range of 1.5°C to 2.8°C. Note that since TCR scales linearly with the errors in the estimated scaling factors, estimates do not show a tendency for a long upper tail, as is the case for ECS. However, the separation of greenhouse gas response from the responses to other external forcing in a multi-fingerprint analysis introduces a small uncertainty, illustrated by small differences in results between three models (Figure 9.21). The TCR does not scale linearly with ECS because the transient response is strongly influenced by the speed with which the ocean transports heat into its interior, while the equilibrium sensitivity is governed by feedback strengths (discussion in Frame et al., 2005).

Estimates of a likely range for TCR can also be inferred directly from estimates of attributable greenhouse warming obtained in optimal detection analyses since there is a direct linear relationship between the two (Frame et al., 2005). The attributable greenhouse warming rates inferred from Figure 9.9 generally support the TCR range shown in Figure 9.21, although the lowest 5th percentile (1.3°C) and the highest 95th percentile (3.3°C) estimated in this way from detection and attribution analyses based on individual models lie outside the 5% to 95% range of 1.5°C to 2.8°C obtained from Figure 9.21.

Choosing lower and upper limits that encompass the range of these results and deflating significance levels in order to account for structural uncertainty in the estimate leads to the conclusion that it is very unlikely that TCR is less than 1°C and very unlikely that TCR is greater than 3.5°C. Information based on the models discussed in Chapter 10 provides additional information that can help constrain TCR further (Section 10.5.4.5).

9.6.3 Estimates of Climate Sensitivity Based on Palaeoclimatic Data

The palaeoclimate record offers a range of opportunities to assess the response of climate models to changes in external forcing. This section discusses estimates from both the palaeoclimatic record of the last millennium, and from the climate of the LGM. The latter gives a different perspective on feedbacks than anticipated with greenhouse warming, and thus provides a test bed for the physics in climate models. There also appears to be a likely positive relationship between temperature and CO_2 prior to the 650 kyr period covered by ice core measurements of CO_2 (Section 6.3).

As with analyses of the instrumental record discussed in Section 9.6.2, some studies using palaeoclimatic data have also estimated PDFs for ECS by varying model parameters. Inferences about ECS made through direct comparisons between radiative forcing and climate response, without using climate models, show large uncertainties since climate feedbacks, and thus sensitivity, may be different for different climatic background states and for different seasonal characteristics of forcing (e.g., Montoya et al., 2000). Thus, sensitivity to forcing during these periods cannot be directly compared to that for atmospheric CO_2 doubling.

9.6.3.1 Estimates of Climate Sensitivity Based on Data for the Last Millennium

The relationship between forcing and response based on a long time horizon can be studied using palaeoclimatic reconstructions of temperature and radiative forcing, particularly volcanism and solar forcing, for the last millennium. However, both forcing and temperature reconstructions are subject to large uncertainties (Chapter 6). To account for the uncertainty in reconstructions, Hegerl et al. (2006a) use several proxy data reconstructions of NH extratropical temperature for the past millennium (Briffa et al., 2001; Esper et al., 2002; Mann and Jones, 2003; Hegerl et al., 2007) to constrain ECS estimates for the pre-industrial period up to 1850. This study used a large ensemble of simulations of the last millennium performed with an energy balance model forced with reconstructions of volcanic (Crowley, 2000, updated), solar (Lean et al., 2002) and greenhouse gas forcing (see Section 9.3.3 for results on the detection of these external influences). Their estimated PDFs for ECS incorporate an estimate of uncertainty in the overall amplitude (including an attempt to account for uncertainty in efficacy), but not the time evolution, of volcanic and solar forcing. They also attempt to account for uncertainty in the amplitude of reconstructed temperatures in one reconstruction (Hegerl et al., 2007), and assess the sensitivity of their results to changes in amplitude for others. All reconstructions combined yield a median climate sensitivity of 3.4°C and a 5 to 95% range of 1.2°C to 8.6°C (Figure 9.20). Reconstructions with a higher amplitude of past climate variations (e.g., Esper et al., 2002; Hegerl et al., 2007) are found to support higher ECS estimates than reconstructions with lower amplitude (e.g., Mann and Jones, 2003). Note that the constraint on ECS originates mainly from low-frequency temperature variations associated with changes in the frequency and intensity of volcanism which lead to a highly significant detection of volcanic response (Section 9.3.3) in all records used in the study.

The results of Andronova et al. (2004) are broadly consistent with these estimates. Andronova et al. (2004) demonstrate that climate sensitivities in the range of 2.3°C to 3.4°C yield reasonable simulations of both the NH mean temperature from 1500 onward when compared to the Mann and Jones (2003) reconstruction, and for the instrumental period. The agreement is less good for reconstructed SH temperature, where reconstructions are substantially more uncertain (Chapter 6).

Rind et al. (2004) studied the period from about 1675 to 1715 to attempt a direct estimate of climate sensitivity. This period has reduced radiative forcing relative to the present due to decreased solar radiation, decreased greenhouse gas and possibly increased volcanic forcing (Section 9.2.1.3). Different NH temperature reconstructions (Figure 6.10) have a wide range of cooling estimates relative to the late 20th century that

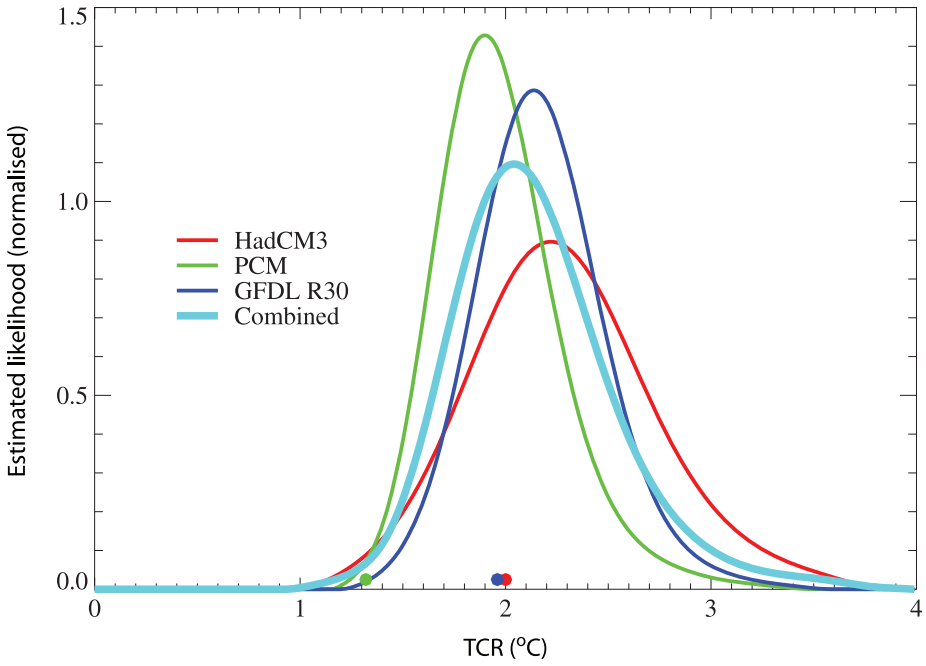


Figure 9.21. *Probability distributions of TCR (expressed as warming at the time of CO_2 doubling), as constrained by observed 20th-century temperature change, for the HadCM3 (Table 8.1, red), PCM (Table 8.1, green) and GFDL R30 (Delworth et al., 2002, blue) models. The average of the PDFs derived from each model is shown in cyan. Coloured circles show each model's TCR. (After Stott et al., 2006c).*

is broadly reproduced by climate model simulations. While climate in this cold period may have been close to radiative balance (Rind et al., 2004), some of the forcing during the present period is not yet realised in the system (estimated as 0.85 W m^{-2}; Hansen et al., 2005). Thus, ECS estimates based on a comparison between radiative forcing and climate response are subject to large uncertainties, but are broadly similar to estimates discussed above. Again, reconstructions with stronger cooling in this period imply higher climate sensitivities than those with weaker cooling (results updated from Rind et al., 2004).

9.6.3.2 *Inferences About Climate Sensitivity Based on the Last Glacial Maximum*

The LGM is one of the key periods used to estimate ECS (Hansen et al., 1984; Lorius et al., 1990; Hoffert and Covey, 1992), since it represents a quasi-equilibrium climate response to substantially altered boundary conditions. When forced with changes in greenhouse gas concentrations and the extent and height of ice sheet boundary conditions, AOGCMs or EMICs identical or similar to those used for 20th- and 21st-century simulations produce a 3.3°C to 5.1°C cooling for this period in response to radiative perturbations of 4.6 to 7.2 W m^{-2} (Sections 6.4.1.3; see also Section 9.3.2; see also Masson-Delmotte et al., 2006). The simulated cooling in the tropics ranges from 1.7°C to 2.4°C. The ECS of the models used in PMIP2 ranges from 2.3°C to 3.7°C (Table 8.2), and there is some tendency for models with larger sensitivity to produce larger tropical cooling for the LGM, but this relationship is not very tight. Comparison between simulated climate change and reconstructed climate is affected by substantial uncertainties in forcing and data (Chapter 6 and Section 9.2.1.3). For example, the PMIP2 forcing does not account for changes in mineral dust, since the level of scientific understanding for this forcing is very low (Figure 6.5). The range of simulated temperature changes is also affected by differences in the radiative influence of the ice-covered regions in different models (Taylor et al., 2000). Nevertheless, the PMIP2 models simulate LGM climate changes that are approximately consistent with proxy information (Chapter 6).

Recent studies (Annan et al., 2005; Schneider von Deimling et al., 2006) attempt to estimate the PDF of ECS from ensemble simulations of the LGM by systematically exploring model uncertainty. Both studies investigate the relationship between climate sensitivity and LGM tropical SSTs, which are influenced strongly by CO_2 changes. In a perturbed physics ensemble, Schneider von Deimling et al. (2006) vary 11 ocean and atmospheric parameters in a 1,000-member ensemble simulation of the LGM with the CLIMBER-2 EMIC (Table 8.3). They find a close relationship between ECS and tropical SST cooling in their model, implying a 5 to 95% range of ECS of 1.2°C to 4.3°C when attempting to account for model parameter, forcing and palaeoclimate data uncertainties. Similar constraints on climate sensitivity are found when proxy reconstructions of LGM antarctic temperatures are used instead of tropical SSTs (Schneider von Deimling et al., 2006). In contrast, Annan et al. (2005) use a perturbed physics ensemble based on a low-resolution version of the atmospheric component of the MIROC3.2 model, perturbing a range of model parameters over prior distributions determined from the ability of the model to reproduce seasonal mean climate in a range of climate variables. They find a best-fit sensitivity of about 4.5°C, and their results suggest that sensitivities in excess of 6°C are unlikely given observational estimates of LGM tropical cooling and the relationship between tropical SST and sensitivity in their model. Since the perturbed physics ensemble based on that atmospheric model does not produce sensitivities less than 4°C, this result cannot provide a lower limit or a PDF for ECS.

The discrepancy between the inferred upper limits in the two studies probably arises from both different radiative forcing and structural differences between the models used. Forcing from changes in vegetation cover and dust is not included in the simulations done by Annan et al. (2005), which according to Schneider von Deimling et al. (2006) would reduce the Annan et al. ECS estimates and yield better agreement between the results of the two studies. However, the effect of these forcings and their interaction with other LGM forcings is very uncertain, limiting confidence in such estimates of their effect (Figure 6.5). Structural differences in models are also likely to play a role. The Annan et al. (2005) estimate shows a weaker association between simulated tropical SST changes and ECS than the Schneider von Deimling et al. (2006) result. Since Annan et al. use a mixed-layer ocean model, and Schneider von Deimling a simplified ocean model, both models may not capture the full ocean response affecting tropical SSTs. The atmospheric model used in Schneider von Deimling is substantially simpler than that used in the Annan et al. (2005) study. Overall, estimates of climate sensitivity from the LGM are broadly consistent with other estimates of climate sensitivity derived, for example, from the instrumental period.

9.6.4 Summary of Observational Constraints for Climate Sensitivity

Any constraint of climate sensitivity obtained from observations must be interpreted in light of the underlying assumptions. These assumptions include (i) the choice of prior distribution for each of the model parameters (Section 9.6.1 and Supplementary Material, Appendix 9.B), including the parameter range explored, (ii) the treatment of other parameters that influence the estimate, such as effective ocean diffusivity, and (iii) the methods used to account for uncertainties, such as structural and forcing uncertainties, that are not represented by the prior distributions. Neglecting important sources of uncertainty in these estimates will result in overly narrow ranges that overstate the certainty with which the ECS or TCR is known. Errors in assumptions about forcing or model response will also result in unrealistic features of model simulations, which can result in erroneous modes (peak probabilities) and shapes of the PDF. On the other hand, using less than all available information will yield results that are less constrained than they could be under optimal use of available data.

While a variety of important uncertainties (e.g., radiative forcing, mixing of heat into the ocean) have been taken into account in most studies (Table 9.3), some caveats remain. Some processes and feedbacks might be poorly represented or missing, particularly in simple and many intermediate complexity models. Structural uncertainties in the models, for example, in the representation of cloud feedback processes (Chapter 8) or the physics of ocean mixing, will affect results for climate sensitivity and are very difficult to quantify. In addition, differences in efficacy between forcings are not directly represented in simple models, so they may affect the estimate (e.g., Tett et al., 2007), although this uncertainty may be folded into forcing uncertainty (e.g., Hegerl et al., 2003, 2007). The use of a single value for the ECS further assumes that it is constant in time. However, some authors (e.g., Senior and Mitchell, 2000; Boer and Yu, 2003) have shown that ECS varies in time in the climates simulated by their models. Since results from instrumental data and the last millennium are dominated primarily by decadal- to centennial-scale changes, they will therefore only represent climate sensitivity at an equilibrium that is not too far from the present climate. There is also a small uncertainty in the radiative forcing due to atmospheric CO_2 doubling (<10%; see Chapter 2), which is not accounted for in most studies that derive observational constraints on climate sensitivity.

Despite these uncertainties, which are accounted for to differing degrees in the various studies, confidence is increased by the similarities between individual ECS estimates (Figure 9.20). Most studies find a lower 5% limit of between 1°C and 2.2°C, and studies that use information in a relatively complete manner generally find a most likely value between 2°C and 3°C (Figure 9.20). Constraints on the upper end of the likely range of climate sensitivities are also important, particularly for probabilistic forecasts of future climate with constant radiative forcing. The upper 95% limit for ECS ranges from 5°C to 10°C, or greater in different studies depending upon the approach taken, the number of uncertainties included and specific details of the prior distribution that was used. This wide range is largely caused by uncertainties and nonlinearities in forcings and response. For example, a high sensitivity is difficult to rule out because a high aerosol forcing could nearly cancel greenhouse gas forcing over the 20th century. This problem can be addressed, at least to some extent, if the differences in the spatial and temporal patterns of response between aerosol and greenhouse gas forcing are used for separating these two responses in observations (as, for example, in Gregory et al., 2002a; Harvey and Kaufmann, 2002; Frame et al., 2005). In addition, nonlinearities in the response to transient forcing make it more difficult to constrain the upper limit on ECS based on observed transient forcing responses (Frame et al., 2005). The TCR, which may be more relevant for near-term climate change, is easier to constrain since it relates more linearly to observables. For the pre-instrumental part of the last millennium, uncertainties in temperature and forcing reconstructions, and the nonlinear connection between ECS and the response to volcanism, prohibit tighter constraints. Estimates of climate sensitivity based on the ability of climate models to reproduce climatic conditions of the LGM broadly support the ranges found from the instrumental period, although a tight constraint is also difficult to obtain from this period alone because of uncertainties in tropical temperature changes, forcing uncertainties and the effect of structural model uncertainties. In addition, the number of studies providing estimates of PDFs from palaeoclimatic data, using independent approaches and complementary sources of proxy data, are limited.

Thus, most studies that use a simple uniform prior distribution of ECS are not able to exclude values beyond the traditional IPCC First Assessment Report range of 1.5°C to 4.5°C (IPCC, 1990). However, considering all available evidence on ECS together provides a stronger constraint than individual lines of evidence. Bayesian methods can be used to incorporate multiple lines of evidence to sharpen the posterior distribution of ECS, as in Annan and Hargreaves (2006) and Hegerl et al. (2006a). Annan and Hargreaves (2006) demonstrate that using three lines of evidence, namely 20th-century warming, the response to individual volcanic eruptions and the LGM response, results in a tighter estimate of ECS, with a probability of less than 5% that ECS exceeds 4.5°C. The authors find a similar constraint using five lines of evidence under more conservative assumptions about uncertainties (adding cooling during the Little Ice Age and studies based on varying model parameters to match climatological means, see Box 10.2). However, as discussed in Annan and Hargreaves (2006), combining multiple lines of evidence may produce overly confident estimates unless every single line of evidence is entirely independent of others, or dependence is explicitly taken into account. Hegerl et al. (2006a) argue that instrumental temperature change during the second half of the 20th century is essentially independent of the palaeoclimate record of the last millennium and of the instrumental data from the first half of the 20th century that is used to calibrate the palaeoclimate records. Hegerl et al. (2006a) therefore base their prior probability distribution for the climate sensitivity on results from the late 20th century (Frame et al., 2005), which reduces the 5 to 95% ECS range from all proxy reconstructions analysed to 1.5°C to 6.2°C compared to the previous range of 1.2°C to 8.6°C. Both results demonstrate that independent estimates, when properly combined in a Bayesian analysis, can provide a tighter constraint on climate sensitivity, even if they individually provide only weak constraints. These studies also find a 5% lower limit of 1.5°C or above, consistent with several studies based on the 20th-century climate change alone (Knutti et al., 2002; Forest et al., 2006) and estimates that greenhouse warming contributes substantially to observed temperature changes (Section 9.4.1.4).

Overall, several lines of evidence strengthen confidence in present estimates of ECS, and new results based on objective analyses make it possible to assign probabilities to ranges of climate sensitivity previously assessed from expert opinion alone. This represents a significant advance. Results from studies of observed climate change and the consistency of estimates from different time periods indicate that ECS is very likely larger than 1.5°C with a most likely value between 2°C

and 3°C. The lower bound is consistent with the view that the sum of all atmospheric feedbacks affecting climate sensitivity is positive. Although upper limits can be obtained by combining multiple lines of evidence, remaining uncertainties that are not accounted for in individual estimates (such as structural model uncertainties) and possible dependencies between individual lines of evidence make the upper 95% limit of ECS uncertain at present. Nevertheless, constraints from observed climate change support the overall assessment that the ECS is likely to lie between 2°C and 4.5°C with a most likely value of approximately 3°C (Box 10.2).

9.7 Combining Evidence of Anthropogenic Climate Change

The widespread change detected in temperature observations of the surface (Sections 9.4.1, 9.4.2, 9.4.3), free atmosphere (Section 9.4.4) and ocean (Section 9.5.1), together with consistent evidence of change in other parts of the climate system (Section 9.5), strengthens the conclusion that greenhouse gas forcing is the dominant cause of warming during the past several decades. This combined evidence, which is summarised in Table 9.4, is substantially stronger than the evidence that is available from observed changes in global surface temperature alone (Figure 3.6).

The evidence from surface temperature observations is strong: The observed warming is highly significant relative to estimates of internal climate variability which, while obtained from models, are consistent with estimates obtained from both instrumental data and palaeoclimate reconstructions. It is extremely unlikely (<5%) that recent global warming is due to internal variability alone such as might arise from El Niño (Section 9.4.1). The widespread nature of the warming (Figures 3.9 and 9.6) reduces the possibility that the warming could have resulted from internal variability. No known mode of internal variability leads to such widespread, near universal warming as has been observed in the past few decades. Although modes of internal variability such as El Niño can lead to global average warming for limited periods of time, such warming is regionally variable, with some areas of cooling (Figures 3.27 and 3.28). In addition, palaeoclimatic evidence indicates that El Niño variability during the 20th century is not unusual relative to earlier periods (Section 9.3.3.2; Chapter 6). Palaeoclimatic evidence suggests that such a widespread warming has not been observed in the NH in at least the past 1.3 kyr (Osborn and Briffa, 2006), further strengthening the evidence that the recent warming is not due to natural internal variability. Moreover, the response to anthropogenic forcing is detectable on all continents individually except Antarctica, and in some sub-continental regions. Climate models only reproduce the observed 20th-century global mean surface warming when both anthropogenic and natural forcings are included (Figure 9.5). No model that has used natural forcing only has reproduced the observed global mean warming trend or the continental mean warming trends in all individual continents (except Antarctica) over the second half of the 20th century. Detection and attribution of external influences on 20th-century and palaeoclimatic reconstructions, from both natural and anthropogenic sources (Figure 9.4 and Table 9.4), further strengthens the conclusion that the observed changes are very unusual relative to internal climate variability.

The energy content change associated with the observed widespread warming of the atmosphere is small relative to the energy content change of the ocean, and also smaller than that associated with other components such as the cryosphere. In addition, the solid Earth also shows evidence for warming in boreholes (Huang et al., 2000; Beltrami et al., 2002; Pollack and Smerdon, 2004). It is theoretically feasible that the warming of the near surface could have occurred due to a reduction in the heat content of another component of the system. However, all parts of the cryosphere (glaciers, small ice caps, ice sheets and sea ice) have decreased in extent over the past half century, consistent with anthropogenic forcing (Section 9.5.5, Table 9.4), implying that the cryosphere consumed heat and thus indicating that it could not have provided heat for atmospheric warming. More importantly, the heat content of the ocean (the largest reservoir of heat in the climate system) also increased, much more substantially than that of the other components of the climate system (Figure 5.4; Hansen et al., 2005; Levitus et al., 2005). The warming of the upper ocean during the latter half of the 20th century was likely due to anthropogenic forcing (Barnett et al., 2005; Section 9.5.1.1; Table 9.4). While the statistical evidence in this research is very strong that the warming cannot be explained by ocean internal variability as estimated by two different climate models, uncertainty arises since there are discrepancies between estimates of ocean heat content variability from models and observations, although poor sampling of parts of the World Ocean may explain this discrepancy. However, the spatial pattern of ocean warming with depth is very consistent with heating of the ocean resulting from net positive radiative forcing, since the warming proceeds downwards from the upper layers of the ocean and there is deeper penetration of heat at middle to high latitudes and shallower penetration at low latitudes (Barnett et al., 2005; Hansen et al., 2005). This observed ocean warming pattern is inconsistent with a redistribution of heat between the surface and the deep ocean.

Thus, the evidence appears to be inconsistent with the ocean or land being the source of the warming at the surface. In addition, simulations forced with observed SST changes cannot fully explain the warming in the troposphere without increases in greenhouse gases (e.g., Sexton et al., 2001), further strengthening the evidence that the warming does not originate from the ocean. Further evidence for forced changes arises from widespread melting of the cryosphere (Section 9.5.5), increases in water vapour in the atmosphere (Section 9.5.4.1) and changes in top-of-the atmosphere radiation that are consistent with changes in forcing.

The simultaneous increase in energy content of all the major components of the climate system and the pattern and amplitude of warming in the different components, together with evidence that the second half of the 20th century was likely the warmest in 1.3 kyr (Chapter 6) indicate that the cause of the warming is extremely unlikely to be the result of internal processes alone. The consistency across different lines of evidence makes a strong case for a significant human influence on observed warming at the surface. The observed rates of surface temperature and ocean heat content change are consistent with the understanding of the likely range of climate sensitivity and net climate forcings. Only with a net positive forcing, consistent with observational and model estimates of the likely net forcing of the climate system (as used in Figure 9.5), is it possible to explain the large increase in heat content of the climate system that has been observed (Figure 5.4).

Table 9.4. *A synthesis of climate change detection results: (a) surface and atmospheric temperature evidence and (b) evidence from other variables. Note that our likelihood assessments are reduced compared to individual detection studies in order to take into account remaining uncertainties (see Section 9.1.2), such as forcing and model uncertainty not directly accounted for in the studies. The likelihood assessment is indicated in percentage terms, in parentheses where the term is not from the standard IPCC likelihood levels.*

a)

Result	Region	Likelihood	Factors contributing to likelihood assessment
Surface temperature			
Warming during the past half century cannot be explained without external radiative forcing	Global	Extremely likely (>95%)	Anthropogenic change has been detected in surface temperature with very high significance levels (less than 1% error probability). This conclusion is strengthened by detection of anthropogenic change in the upper ocean with high significance level. Upper ocean warming argues against the surface warming being due to natural internal processes. Observed change is very large relative to climate-model simulated internal variability. Surface temperature variability simulated by models is consistent with variability estimated from instrumental and palaeorecords. Main uncertainty from forcing and internal variability estimates (Sections 9.4.1.2, 9.4.1.4, 9.5.1.1, 9.3.3.2, 9.7).
Warming during the past half century is not solely due to known natural causes	Global	Very Likely	This warming took place at a time when non-anthropogenic external factors would likely have produced cooling. The combined effect of known sources of forcing would have been extremely likely to produce a warming. No climate model that has used natural forcing only has reproduced the observed global warming trend over the 2nd half of the 20th century. Main uncertainties arise from forcing, including solar, model-simulated responses and internal variability estimates (Sections 2.9.2, 9.2.1, 9.4.1.2, 9.4.1.4; Figures 9.5, 9.6, 9.9).
Greenhouse gas forcing has been the dominant cause of the observed global warming over the last 50 years.	Global	Very likely	All multi-signal detection and attribution studies attribute more warming to greenhouse gas forcing than to a combination of all other sources considered, including internal variability, with a very high significance. This conclusion accounts for observational, model and forcing uncertainty, and the possibility that the response to solar forcing could be underestimated by models. Main uncertainty from forcing and internal variability estimates (Section 9.4.1.4; Figure 9.9).
Increases in greenhouse gas concentrations alone would have caused more warming than observed over the last 50 years because volcanic and anthropogenic aerosols have offset some warming that would otherwise have taken place.	Global	Likely	Estimates from different analyses using different models show consistently more warming than observed over the last 50 years at the 5% significance level. However, separation of the response to non-greenhouse gas (particularly aerosol) forcing from greenhouse gas forcing varies between models (Section 9.4.1.4; Figure 9.9).
There has been a substantial anthropogenic contribution to surface temperature increases in every continent except Antarctica since the middle of the 20th century	Africa, Asia, Australia, Europe, North America and South America	Likely	Anthropogenic change has been estimated using detection and attribution methods on every individual continent (except Antarctica). Greater variability compared to other continental regions makes detection more marginal in Europe. No climate model that used natural forcing only reproduced the observed continental mean warming trend over the second half of the 20th century. Uncertainties arise because sampling effects result in lower signal-to-noise ratio at continental than at global scales. Separation of the response to different forcings is more difficult at these spatial scales (Section 9.4.2; FAQ 9.2, Figure 1).
Early 20th-century warming is due in part to external forcing.	Global	Very Likely	A number of studies detect the influence of external forcings on early 20th-century warming, including a warming from anthropogenic forcing. Both natural forcing and response are uncertain, and different studies find different forcings dominant. Some studies indicate that internal variability could have made a large contribution to early 20th-century warming. Some observational uncertainty in early 20th-century trend (Sections 9.3.3.2, 9.4.1.4; Figures 9.4, 9.5).

(continued)

Table 9.4 (continued)

Result	Region	Likelihood	Factors contributing to likelihood assessment
Surface temperature			
Pre-industrial temperatures were influenced by natural external forcing (period studied is past 7 centuries)	NH (mostly extratropics)	Very Likely	Detection studies indicate that external forcing explains a substantial fraction of inter-decadal variability in NH temperature reconstructions. Simulations in response to estimates of pre-industrial forcing reproduce broad features of reconstructions. Substantial uncertainties in reconstructions and past forcings are unlikely to lead to a spurious agreement between temperature reconstructions and forcing reconstructions as they are derived from independent proxies (Section 9.3.3; Figures 9.4, 6.13).
Temperature extremes have changed due to anthropogenic forcing	NH land areas and Australia combined.	Likely	A range of observational evidence indicates that temperature extremes are changing. An anthropogenic influence on the temperatures of the 1, 5, 10 and 30 warmest nights, coldest days and coldest nights annually has been formally detected and attributed in one study, but observed change in the temperature of the warmest day annually is inconsistent with simulated change. The detection of changes in temperature extremes is supported by other comparisons between models and observations. Model uncertainties in changes in temperature extremes are greater than for mean temperatures and there is limited observational coverage and substantial observational uncertainty (Section 9.4.3).
Free atmosphere changes			
Tropopause height increases are detectable and attributable to anthropogenic forcing (latter half of the 20th century)	Global	Likely	There has been robust detection of anthropogenic influence on increasing tropopause height. Simulated tropopause height increases result mainly from greenhouse gas increases and stratospheric ozone decreases. Detection and attribution studies rely on reanalysis data, which are subject to inhomogeneities related to differing availability and quality of input data, although tropopause height increases have also been identified in radiosonde observations. Overall tropopause height increases in recent model and one reanalysis (ERA-40) appear to be driven by similar large-scale changes in atmospheric temperature, although errors in tropospheric warming and stratospheric cooling could lead to partly spurious agreement in other data sets (Section 9.4.4.2; Figure 9.14).
Tropospheric warming is detectable and attributable to anthropogenic forcing (latter half of the 20th century)	Global	Likely	There has been robust detection and attribution of anthropogenic influence on tropospheric warming, which does not depend on including stratospheric cooling in the fingerprint pattern of response. There are observational uncertainties in radiosonde and satellite records. Models generally predict a relative warming of the free troposphere compared to the surface in the tropics since 1979, which is not seen in the radiosonde record (possibly due to uncertainties in the radiosonde record) but is seen in one version of the satellite record, although not others (Section 9.4.4).
Simultaneous tropospheric warming and stratospheric cooling due to the influence of anthropogenic forcing has been observed (latter half of the 20th century)	Global	Very Likely	Simultaneous warming of the troposphere and cooling of the stratosphere due to natural factors is less likely than warming of the troposphere or cooling of the stratosphere alone. Cooling of the stratosphere is in part related to decreases in stratospheric ozone. Modelled and observational uncertainties as discussed under entries for tropospheric warming with additional uncertainties due to stratospheric observing systems and the relatively poor representations of stratospheric processes and variability in climate models (Section 9.4.4).

b)

Result	Region	Likelihood	Factors contributing to likelihood assessment
Ocean changes			
Anthropogenic forcing has warmed the upper several hundred metres of the ocean during the latter half of the 20th century	Global (but with limited sampling in some regions)	Likely	Robust detection and attribution of anthropogenic fingerprint from three different models in ocean temperature changes, and in ocean heat content data, suggests high likelihood, but observational and modelling uncertainty remains. 20th-century simulations with MMD models simulate comparable ocean warming to observations only if anthropogenic forcing is included. Simulated and observed variability appear inconsistent, either due to sampling errors in the observations or under-simulated internal variability in the models. Limited geographical coverage in some ocean basins (Section 9.5.1.1; Figure 9.15).
Anthropogenic forcing contributed to sea level rise during the latter half 20th century	Global	Very likely	Natural factors alone do not satisfactorily explain either the observed thermal expansion of the ocean or the observed sea level rise. Models including anthropogenic and natural forcing simulate the observed thermal expansion since 1961 reasonably well. Anthropogenic forcing dominates the surface temperature change simulated by models, and has likely contributed to the observed warming of the upper ocean and widespread glacier retreat. It is very unlikely that the warming during the past half century is due only to known natural causes. It is therefore very likely that anthropogenic forcing contributed to sea level rise associated with ocean thermal expansion and glacier retreat. However, it remains difficult to estimate the anthropogenic contribution to sea level rise because suitable studies quantifying the anthropogenic contribution to sea level rise and glacier retreat are not available, and because the observed sea level rise budget is not closed (Table 9.2; Section 9.5.2).
Circulation			
Sea level pressure shows a detectable anthropogenic signature during the latter half of the 20th century	Global	Likely	Changes of similar nature are observed in both hemispheres and are qualitatively, but not quantitatively consistent with model simulations. Uncertainty in models and observations. Models underestimate the observed NH changes for reasons that are not understood, based on a small number of studies. Simulated response to 20th century forcings is consistent with observations in SH if effect of stratospheric ozone depletion is included (Section 9.5.3.4; Figure 9.16).
Anthropogenic forcing contributed to the increase in frequency of the most intense tropical cyclones since the 1970s	Tropical regions	More likely than not (>50%)	Recent observational evidence suggests an increase in frequency of intense storms. Increase in intensity is consistent with theoretical expectations. Large uncertainties due to models and observations. Modelling studies generally indicate a reduced frequency of tropical cyclones in response to enhanced greenhouse gas forcing, but an increase in the intensity of the most intense cyclones. Observational evidence, which is affected by substantial inhomogeneities in tropical cyclone data sets for which corrections have been attempted, suggests that increases in cyclone intensity since the 1970s are associated with SST and atmospheric water vapour increases (Section 3.8.3, Box 3.5 and Section 9.5.2.6).
Precipitation, Drought, Runoff			
Volcanic forcing influences total rainfall	Global land areas	More likely than not (>50%)	Model response detectable in observations for some models and result supported by theoretical understanding. However, uncertainties in models, forcings and observations. Limited observational sampling, particularly in the SH (Section 9.5.4.2; Figure 9.18).
Increases in heavy rainfall are consistent with anthropogenic forcing during latter half 20th century	Global land areas (limited sampling)	More likely than not (>50%)	Observed increases in heavy precipitation appear to be consistent with expectations of response to anthropogenic forcing. Models may not represent heavy rainfall well; observations suffer from sampling inadequacies (Section 9.5.4.2).

(continued)

Table 9.4 (continued)

Result	Region	Likelihood	Factors contributing to likelihood assessment
Precipitation, Drought, Runoff			
Increased risk of drought due to anthropogenic forcing during latter half 20th century	Global land areas	More likely than not (>50%)	One detection study has identified an anthropogenic fingerprint in a global Palmer Drought Severity Index data set with high significance, but the simulated response to anthropogenic and natural forcing combined is weaker than observed, and the model appears to have less inter-decadal variability than observed. Studies of some regions indicate that droughts in those regions are linked either to SST changes that, in some instances, may be linked to anthropogenic aerosol forcing (e.g., Sahel) or to a circulation response to anthropogenic forcing (e.g., southwest Australia). Models, observations and forcing all contribute uncertainty (Section 9.5.3.2).
Cryosphere			
Anthropogenic forcing has contributed to reductions in NH sea ice extent during the latter half of the 20th century	Arctic	Likely	The observed change is qualitatively consistent with model-simulated changes for most models and expectation of sea ice melting under arctic warming. Sea ice extent change detected in one study. The model used has some deficiencies in arctic sea ice annual cycle and extent. The conclusion is supported by physical expectations and simulations with another climate model. Change in SH sea ice probably within range explained by internal variability (Section 9.5.5.1).
Anthropogenic forcing has contributed to widespread glacier retreat during the 20th century	Global	Likely	Observed changes are qualitatively consistent with theoretical expectations and temperature detection. Anthropogenic contribution to volume change difficult to estimate. Few detection and attribution studies, but retreat in vast majority of glaciers consistent with expected reaction to widespread warming (Section 9.5.5.3).

References

AchutaRao, K.M., et al., 2006: Variability of ocean heat uptake: Reconciling observations and models. *J. Geophys. Res.*, **111**, C05019.

Ackerman, A.S., et al., 2000: Reduction of tropical cloudiness by soot. *Science*, **288**, 1042–1047.

Adams, J.B., M.E. Mann, and C.M. Ammann, 2003: Proxy evidence for an El Nino-like response to volcanic forcing. *Nature*, **426**(6964), 274–278.

Alexander, L.V., et al., 2006: Global observed changes in daily climate extremes of temperature and precipitation. *J. Geophys. Res.*, **111**, D05109, doi:10.1029/2005JD006290.

Allan, R.J., and T.J. Ansell, 2006: A new globally-complete monthly historical gridded mean sea level pressure data set (HadSLP2): 1850-2004. *J. Clim.*, **19**, 5816–5842.

Allen, M.R., 2003: Liability for climate change. *Nature*, **421**, 891–892.

Allen, M.R., and S.F.B. Tett, 1999: Checking for model consistency in optimal fingerprinting. *Clim. Dyn.*, **15**, 419–434.

Allen, M.R., and W.J. Ingram, 2002: Constraints on future changes in climate and the hydrologic cycle. *Nature*, **419**, 224–232.

Allen, M.R., and D.A. Stainforth, 2002: Towards objective probabilistic climate forecasting. *Nature*, **419**, 228–228.

Allen, M.R., and P.A. Stott, 2003: Estimating signal amplitudes in optimal fingerprinting, Part I: Theory. *Clim. Dyn.*, **21**, 477–491.

Allen, M.R., J.A. Kettleborough, and D.A. Stainforth, 2002: Model error in weather and climate forecasting. In: *ECMWF Predictability of Weather and Climate Seminar* [Palmer, T.N. (ed.)]. European Centre for Medium Range Weather Forecasts, Reading, UK, http://www.ecmwf.int/publications/library/do/references/list/209.

Allen, M.R., et al., 2000: Quantifying the uncertainty in forecasts of anthropogenic climate change. *Nature*, **407**, 617–620.

Ammann, C.M., G.A. Meehl, W.M. Washington, and C. Zender, 2003: A monthly and latitudinally varying volcanic forcing dataset in simulations of 20th century climate. *Geophys. Res. Lett.*, **30**(12), 1657.

Anderson, T.L., et al., 2003: Climate forcing by aerosols: A hazy picture. *Science*, **300**, 1103–1104.

Andronova, N.G., and M.E. Schlesinger, 2000: Causes of global temperature changes during the 19th and 20th centuries. *Geophys. Res. Lett.*, **27**(14), 2137–2140.

Andronova, N.G., and M.E. Schlesinger, 2001: Objective estimation of the probability density function for climate sensitivity. *J. Geophys. Res.*, **106**(D19), 22605–22611.

Andronova, N.G., M.E. Schlesinger, and M.E. Mann, 2004: Are reconstructed pre-instrumental hemispheric temperatures consistent with instrumental hemispheric temperatures? *Geophys. Res. Lett.*, **31**, L12202, doi:10.1029/2004GL019658.

Andronova, N.G., et al., 1999: Radiative forcing by volcanic aerosols from 1850 to 1994. *J. Geophys. Res.*, **104**, 16807–16826.

Andronova, N.G., et al., 2007: The concept of climate sensitivity: History and development. In: *Human-Induced Climate Change: An Interdisciplinary Assessment* [Schlesinger, M., et al. (eds.)]. Cambridge University Press, Cambridge, UK, in press.

Annan, J.D., and J.C. Hargreaves, 2006: Using multiple observationally-based constraints to estimate climate sensitivity. *Geophys. Res. Lett.*, **33**, L06704, doi:10.1029/2005GL025259.

Annan, J.D., et al., 2005: Efficiently constraining climate sensitivity with paleoclimate simulations. *Scientific Online Letters on the Atmosphere*, **1**, 181–184.

Arblaster, J.M., and G.A. Meehl, 2006: Contributions of external forcing to Southern Annular Mode trends. *J. Clim.*, **19**, 2896–2905.

Bader, J., and M. Latif, 2003: The impact of decadal-scale Indian Ocean sea surface temperature anomalies on Sahelian rainfall and the North Atlantic Oscillation. *Geophys. Res. Lett.*, **30**(22), 2169.

Banks, H.T., et al., 2000: Are observed decadal changes in intermediate water masses a signature of anthropogenic climate change? *Geophys. Res. Lett.*, **27**, 2961–2964.

Barnett, T.P., D.W. Pierce, and R. Schnur, 2001: Detection of anthropogenic climate change in the world's oceans. *Science*, **292**, 270–274.

Barnett, T.P., et al., 1999: Detection and attribution of recent climate change. *Bull. Am. Meteorol. Soc.*, **80**, 2631–2659.

Barnett, T.P., et al., 2005: Penetration of a warming signal in the world's oceans: human impacts. *Science*, **309**, 284–287.

Bauer, E., M. Claussen, V. Brovkin, and A. Huenerbein, 2003: Assessing climate forcings of the Earth system for the past millennium. *Geophys. Res. Lett.*, **30**(6), 1276.

Beltrami, H., J.E. Smerdon, H.N. Pollack, and S. Huang, 2002: Continental heat gain in the global climate system. *Geophys. Res. Lett.*, **29**, 1167.

Bengtsson, L., K.I. Hodges, and E. Roechner, 2006: Storm tracks and climate change. *J. Clim.*, **19**, 3518–3543.

Berger, A., 1978: Long-term variations of caloric solar radiation resulting from the earth's orbital elements. *Quat. Res.*, **9**, 139–167.

Berger, A., 1988: Milankovitch theory and climate. *Rev. Geophys.*, **26**, 624–657.

Berliner, L.M., R.A. Levine, and D.J. Shea, 2000: Bayesian climate change assessment. *J. Clim.*, **13**, 3805–3820.

Bertrand, C., M.F. Loutre, M. Crucifix, and A. Berger, 2002: Climate of the last millennium: a sensitivity study. *Tellus*, **54A**(3), 221–244.

Betts, R.A., 2001: Biogeophysical impacts of land use on present-day climate: near surface temperature and radiative forcing. *Atmos. Sci. Lett.*, **2**, 39–51.

Bigelow, N.H., et al., 2003: Climate change and Arctic ecosystems: 1. Vegetation changes north of 55 degrees N between the last glacial maximum, mid-Holocene, and present. *J. Geophys. Res.*, **108**(D19), 8170, doi:10.1029/2002JD002558.

Bindoff, N.L., and T.J. McDougall, 2000: Decadal changes along an Indian Ocean section at 32S and their interpretation. *J. Phys. Oceanogr.*, **30**(6), 1207–1222.

Bjerknes, J., 1969: Atmospheric teleconnections from the equatorial Pacific. *Mon. Weather Rev.*, **97**, 163–172.

Boer, G.J., and B. Yu, 2003: Climate sensitivity and climate state. *Clim. Dyn.*, **21**, 167–176.

Boucher, O., and J. Haywood, 2001: On summing the components of radiative forcing of climate change. *Clim. Dyn.*, **18**, 297–302.

Boyer, T.P., et al., 2005: Linear trends in salinity for the World Ocean, 1955-1998. *Geophys. Res. Lett.*, **32**, L01604.

Braconnot, P., S. Joussaume, O. Marti, and N. de Noblet, 1999: Synergistic feedbacks from ocean and vegetation on the African monsoon response to mid-Holocene insolation. *Geophys. Res. Lett.*, **26**, 2481–2484.

Braconnot, P., O. Marti, S. Joussaume, and Y. Leclainche, 2000: Ocean feedback in response to 6 kyr BP insolation. *J. Clim.*, **13**(9), 1537–1553.

Braconnot, P., et al., 2004: Evaluation of PMIP coupled ocean-atmosphere simulations of the Mid-Holocene. In: *Past Climate Variability through Europe and Africa* [Battarbee, R.W., F. Gasse, and C.E. Stickley (eds.)]. Springer, London, UK, pp. 515-533.

Braganza, K., et al., 2003: Simple indices of global climate variability and change: Part I - Variability and correlation structure. *Clim. Dyn.*, **20**, 491–502.

Braganza, K., et al., 2004: Simple indices of global climate variability and change: Part II - Attribution of climate change during the 20th century. *Clim. Dyn.*, **22**, 823–838.

Briffa, K.R., et al., 2001: Low-frequency temperature variations from a northern tree ring density network. *J. Geophys. Res.*, **106**(D3), 2929–2941.

Broccoli, A.J., et al., 2003: Twentieth-century temperature and precipitation trends in ensemble climate simulations including natural and anthropogenic forcing. *J. Geophys. Res.*, **108**(D24), 4798.

Brohan, P., et al., 2006: Uncertainty estimates in regional and global observed temperature changes: a new dataset from 1850. *J. Geophys. Res.*, **111**, D12106, doi:10.1029/2005JD006548.

Bryden, H.L., E. McDonagh, and B.A. King, 2003: Changes in ocean water mass properties: oscillations of trends? *Science*, **300**, 2086–2088.

Bryden, H.L., H.R. Longworth, and S.A. Cunningham, 2005: Slowing of the Atlantic meridional overturning circulation at 25° N. *Nature*, **438**, 655–657.

Burke, E.J., S.J. Brown, and N. Christidis, 2006: Modelling the recent evolution of global drought and projections for the 21st century with the Hadley Centre climate model. *J. Hydrometeorol.*, **7**, 1113–1125.

Caesar, J., L. Alexander, and R. Vose, 2006: Large-scale changes in observed daily maximum and minimum temperatures, 1946-2000. *J. Geophys. Res.*, **111**, D05101, doi:10.1029/2005JD006280.

Cai, W., P.H. Whetton, and D.J. Karoly, 2003: The response of the Antarctic Oscillation to increasing and stabilized atmospheric CO_2. *J. Clim.*, **16**, 1525–1538.

Cane, M., et al., 2006: Progress in paleoclimate modeling. *J. Clim.*, **19**, 5031–5057.

Carril, A.F., C.G. Menéndez, and A. Navarra, 2005: Climate response associated with the Southern Annular Mode in the surroundings of Antarctic Peninsula: A multimodel ensemble analysis. *Geophys. Res. Lett.*, **32**, L16713, doi:10.1029/2005GL023581.

Chan, J.C.L., 2006: Comment on "Changes in tropical cyclone number, duration, and intensity in a warming environment". *Science*, **311**, 1713.

Chan, J.C.L., and K.S. Liu, 2004: Global warming and western North Pacific typhoon activity from an observational perspective. *J. Clim.*, **17**, 4590–4602.

Chase, T.N., J.A. Knaff, R.A. Pielke, and E. Kalnay, 2003: Changes in global monsoon circulations since 1950. *Natural Hazards*, **29**, 229–254.

Chen, J., B.E. Carlson, and A.D. Del Genio, 2002: Evidence for strengthening of the tropical general circulation in the 1990s. *Science*, **295**, 838–841.

Christidis, N., et al., 2005: Detection of changes in temperature extremes during the second half of the 20th century. *Geophys. Res. Lett.*, **32**, L20716, doi:10.1029/2005GL023885.

Christy, J.R., R.W. Spencer, and W.D. Braswell, 2000: MSU tropospheric temperatures: Dataset construction and radiosonde comparison. *J. Atmos. Ocean. Technol.*, **17**, 1153–1170.

Chuang, C.C., et al., 2002: Cloud susceptibility and the first aerosol indirect forcing: Sensitivity to black carbon and aerosol concentrations. *J. Geophys. Res.*, **107**(D21), 4564, doi:10.1029/2000JD000215.

Church, J.A., N.J. White, and J.M. Arblaster, 2005: Volcanic eruptions: their impact on sea level and oceanic heat content. *Nature*, **438**, 74–77.

Clement, A.C., R. Seager, and M.A. Cane, 2000: Suppression of El Nino during the mid-Holocene by changes in the Earth's orbit. *Paleoceanography*, **15**(6), 731–737.

Clement, A.C., A. Hall, and A.J. Broccoli, 2004: The importance of precessional signals in the tropical climate. *Clim. Dyn.*, **22**, 327–341.

CLIMAP (Climate: Long-range Investigation, Mapping and Prediction), 1981: *Seasonal Reconstructions of the Earth's Surface at the Last Glacial Maximum.* Map Series Technical Report MC-36, Geological Society of America, Boulder, CO.

Cobb, K.M., C.D. Charles, H. Cheng, and R.L. Edwards, 2003: El Nino/Southern Oscillation and tropical Pacific climate during the last millennium. *Nature*, **424**(6946), 271–276.

Collins, M., 2000a: The El-Nino Southern Oscillation in the second Hadley Centre coupled model and its response to greenhouse warming. *J. Clim.*, **13**, 1299–1312.

Collins, M., 2000b: Understanding uncertainties in the response of ENSO to greenhouse warming. *Geophys. Res. Lett.*, **27**, 3509–3513.

Cook, E.R., et al., 2004: Long-term aridity changes in the western United States. *Science*, **306**(5698), 1015–1018.

Coughlin, K., and K.K. Tung, 2004: Eleven-year solar cycle signal throughout the lower atmosphere. *J. Geophys. Res.*, **109**, D21105, doi:10.1029/2004JD004873.

Crooks, S., 2004: *Solar Influence On Climate.* PhD Thesis, University of Oxford.

Crooks, S.A., and L.J. Gray, 2005: Characterization of the 11-year solar signal using a multiple regression analysis of the ERA-40 dataset. *J. Clim.*, **18**(7), 996–1015.

Crowley, T.J., 2000: Causes of climate change over the past 1000 years. *Science*, **289**(5477), 270–277.

Crowley, T.J., et al., 2003: Modeling ocean heat content changes during the last millennium. *Geophys. Res. Lett.*, **30**(18), 1932.

Cubasch, U., et al., 1997: Simulation of the influence of solar radiation variations on the global climate with an ocean-atmosphere general circulation model. *Clim. Dyn.*, **13**(11), 757–767.

Cubasch, U., et al., 2001: Projections of future climate change. In: *Climate Change 2001: The Scientific Basis. Contribution of Working Group I to the Third Assessment Report of the Intergovernmental Panel on Climate Change* [Houghton, J.T., et al. (eds.)]. Cambridge University Press, Cambridge, United Kingdom and New York, NY, USA, pp. 99–181.

Curry, R., B. Dickson, and I. Yashayaev, 2003: A change in the freshwater balance of the Atlantic Ocean over the past four decades. *Nature*, **426**, 826–829.

Dai, A., K.E. Trenberth, and T.R. Karl, 1999: Effects of clouds, soil, moisture, precipitation and water vapour on diurnal temperature range. *J. Clim.*, **12**, 2451–2473.

Dai, A., et al., 2004: The recent Sahel drought is real. *Int. J. Climatol.*, **24**, 1323–1331.

D'Arrigo, R., et al., 2005: On the variability of ENSO over the past six centuries. *Geophys. Res. Lett.*, **32**(3), L03711, doi:10.1029/2004GL022055.

Delworth, T.L., and T.R. Knutson, 2000: Simulation of early 20th century global warming. *Science*, **287**, 2246–2250.

Delworth, T.L., and M.E. Mann, 2000: Observed and simulated multidecadal variability in the Northern Hemisphere. *Clim. Dyn.*, **16**(9), 661–676.

Delworth, T.L., V. Ramaswamy, and G.L. Stenchikov, 2005: The impact of aerosols on simulated ocean temperature and heat content in the 20th century. *Geophys. Res. Lett.*, **32**, L24709, doi:10.1029/2005GL024457.

Delworth, T., et al., 2002: Review of simulations of climate variability and change with the GFDL R30 coupled climate model. *Clim. Dyn.*, **19**, 555–574.

Dickson, R.R., et al., 2002: Rapid freshening of the deep North Atlantic Ocean over the past four decades. *Nature*, **416**, 832–837.

Douglass, D.H., and B.D. Clader, 2002: Climate sensitivity of the Earth to solar irradiance. *Geophys. Res. Lett.*, **29**(16), 1786.

Douglass, D.H., and R.S. Knox, 2005: Climate forcing by volcanic eruption of Mount Pinatubo. *Geophys. Res. Lett.*, **32**, L05710, doi:10.1029/2004GL022119.

Douglass, D.H., B.D. Pearson, and S.F. Singer, 2004: Altitude dependence of atmospheric temperature trends: Climate models versus observation. *Geophys. Res. Lett.*, **31**, doi:10.1029/2004GL020103.

Douville, H., 2006: Detection-attribution of global warming at the regional scale: How to deal with precipitation variability. *Geophys. Res. Lett.*, **33**, L02701, doi:10.1029/2005GL024967.

Douville, H., et al., 2002: Sensitivity of the hydrological cycle to increasing amounts of greenhouse gases and aerosols. *Clim. Dyn.*, **20**, 45–68.

Dumas, J.A., G.M. Flato, and A.J. Weaver, 2003: The impact of varying atmospheric forcing on the thickness of Arctic multi-year sea ice. *Geophys. Res. Lett.*, **30**, 1918.

Dyurgerov, M.B., and M.F. Meier, 2005: *Glaciers and the Changing Earth System: A 2004 Snapshot*. Institute of Arctic and Alpine Research, University of Colorado, Boulder, CO, 117 pp.

Easterling, D.R., et al., 2000: Climate extremes: Observations, modeling and impacts. *Science*, **289**, 2068–2074.

Egorova, T., et al., 2004: Chemical and dynamical response to the 11-year variability of the solar irradiance simulated with a chemistry-climate model. *Geophys. Res. Lett.*, **31**, L06119, doi:10.1029/2003GL019294.

Elsner, J.B., X. Niu, and T.H. Jagger, 2004: Detecting shifts in hurricane rates using a Markov chain Monte Carlo approach. *J. Clim.*, **17**, 2652–2666.

Elsner, J.B., A.A. Tsonis, and T.H. Jagger, 2006: High-frequency variability in hurricane power dissipation and its relationship to global temperature. *Bull. Am. Meteorol. Soc.*, **87**, 763–768.

Emanuel, K., 2005: Increasing destructiveness of tropical cyclones over the past 30 years. *Nature*, **436**, 686–688.

Emori, S., and S.J. Brown, 2005: Dynamic and thermodynamic changes in mean and extreme precipitation under changed climate. *Geophys. Res. Lett.*, **32**, L17706, doi:10.1029/2005GL023272.

Esper, J., E.R. Cook, and F.H. Schweingruber, 2002: Low-frequency signals in long tree-ring chronologies for reconstructing past temperature variability. *Science*, **295**(5563), 2250–2253.

Fichefet, T., B. Tartinville, and H. Goosse, 2003: Antarctic sea ice variability during 1958-1999: A simulation with a global ice-ocean model. *J. Geophys. Res.*, **108**(C3), 3102–3113.

Folland, C.K., T. N. Palmer, and D. E. Parker, 1986: Sahel rainfall and worldwide sea temperatures 1901-85. *Nature*, **320**, 602–607.

Folland, C.K., et al., 2001: Observed variability and change. In: *Climate Change 2001: The Scientific Basis. Contribution of Working Group I to the Third Assessment Report of the Intergovernmental Panel on Climate Change* [Houghton, J.T., et al. (eds.)]. Cambridge University Press, Cambridge, United Kingdom and New York, NY, USA, pp. 881pp.

Fomby, T.B., and T.J. Vogelsang, 2002: The application of size-robust trend statistics to global-warming temperature series. *J. Clim.*, **15**, 117–123.

Forest, C.E., M.R. Allen, A.P. Sokolov, and P.H. Stone, 2001: Constraining climate model properties using optimal fingerprint detection methods. *Clim. Dyn.*, **18**, 277–295.

Forest, C.E., et al., 2002: Quantifying uncertainties in climate system properties with the use of recent observations. *Science*, **295**, 113.

Forest, D.J., P.H. Stone, and A.P. Sokolov, 2006: Estimated PDFs of climate system properties including natural and anthropogenic forcings. *Geophys. Res. Lett.*, **33**, L01705, doi:10.1029/2005GL023977.

Forster, P.M.D.F., and J.M. Gregory, 2006: The climate sensitivity and its components diagnosed from Earth radiation budget data. *J. Clim.*, **19**, 39–52.

Foukal, P., G. North, and T. Wigley, 2004: A stellar view on solar variations and climate. *Science*, **306**, 68–69.

Foukal, P., C. Froehlich, H. Sruit, and T.M.L. Wigley, 2006: Variations in solar luminosity and their effect on Earth's climate. *Nature*, **443**, 161–166, doi:10.1038/nature05072.

Frame, D.J., et al., 2005: Constraining climate forecasts: The role of prior assumptions. *Geophys. Res. Lett.*, **32**, L09702, doi:10.1029/2004GL022241.

Free, M., and J.K. Angell, 2002: Effect of volcanoes on the vertical temperature profile in radiosonde data. *J. Geophys. Res.*, **107**, doi:10.1029/2001JD001128.

Free, M., et al., 2005: Radiosonde Atmospheric Temperature Products for Assessing Climate (RATPAC): A new dataset of large-area anomaly time series. *J. Geophys. Res.*, **110**, D22101, doi:10.1029/2005JD006169.

Frich, P., et al., 2002: Observed coherent changes in climatic extremes during the second half of the twentieth century. *Clim. Res.*, **19**, 193–212.

Fyfe, J.C., G.J. Boer, and G.M. Flato, 1999: The Arctic and Antarctic Oscillations and their projected changes under global warming. *Geophys. Res. Lett.*, **26**, 1601–1604.

Ganopolski, A., et al., 1998: The influence of vegetation-atmosphere-ocean interaction on climate during the mid-Holocene. *Science*, **280**, 1916–1919.

Gedney, N., et al., 2006: Detection of a direct carbon dioxide effect in continental river runoff records. *Nature*, **439**, 835–838.

Gent, P.R., and G. Danabasoglu, 2004: Heat uptake and the thermohaline circulation in the Coummunity Climate System Model, Version 2. *J. Clim.*, **17**, 4058–4069.

Gerber, S., et al., 2003: Constraining temperature variations over the last millennium by comparing simulated and observed atmospheric CO_2. *Clim. Dyn.*, **20**(2–3), 281–299.

Giannini, A., R. Saravanan, and P. Chang, 2003: Oceanic forcing of Sahel rainfall on interannual to interdecadal time scales. *Science*, **302**, 1027–1030.

Gibson, J.K., et al., 1997: *ERA Description.* ECMWF Reanalysis Project Report Series Vol. 1. European Centre for Medium-Range Weather Forecasts, Reading, UK, 66 pp.

Gilgen, H., M. Wild, and A. Ohmura, 1998: Means and trends of shortwave irradiance at the surface estimated from global energy balance archive data. *J. Clim.*, **11**, 2042–2061.

Gillett, N.P., 2005: Northern Hemisphere circulation. *Nature*, **437**, 496.

Gillett, N.P., and D.W.J. Thompson, 2003: Simulation of recent Southern Hemisphere climate change. *Science*, **302**, 273–275.

Gillett, N.P., H.F. Graf, and T.J. Osborn, 2003a: Climate change and the North Atlantic Oscillation. In: *The North Atlantic Oscillation: Climate Significance and Environmental Impact* [Hurrell, Y.K.J., G. Ottersen, and M. Visbeck (eds.)]. Geophysical Monograph Vol. 134, American Geophysical Union, Washington, DC, pp. 193-209.

Gillett, N.P., R.J. Allan, and T.J. Ansell, 2005: Detection of external influence on sea level pressure with a multi-model ensemble. *Geophys. Res. Lett.*, **32**(19), L19714, doi:10.1029/2005GL023640.

Gillett, N.P., G.C. Hegerl, M.R. Allen, and P.A. Stott, 2000: Implications of changes in the Northern Hemispheric circulation for the detection of anthropogenic climate change. *Geophys. Res. Lett.*, **27**, 993–996.

Gillett, N.P., F.W. Zwiers, A.J. Weaver, and P.A. Stott, 2003b: Detection of human influence on sea level pressure. *Nature*, **422**, 292–294.

Gillett, N.P., A.J. Weaver, F.W. Zwiers, and M.D. Flannigan, 2004a: Detecting the effect of climate change on Canadian forest fires. *Geophys. Res. Lett.*, **31**(18), L18211, doi:10.1029/2004GL020876.

Gillett, N.P., A.J. Weaver, F.W. Zwiers, and M.F. Wehner, 2004b: Detection of volcanic influence on global precipitation. *Geophys. Res. Lett.*, **31**(12), L12217, doi:10.1029/2004GL020044.

Gillett, N.P., M.F. Wehner, S.F.B. Tett, and A.J. Weaver, 2004c: Testing the linearity of the response to combined greenhouse gas and sulfate aerosol forcing. *Geophys. Res. Lett.*, **31**, L14201, doi:10.1029/2004GL020111.

Gillett, N.P., et al., 2002a: Reconciling two approaches to the detection of anthropogenic influence on climate. *J. Clim.*, **15**, 326–329.

Gillett, N.P., et al., 2002b: How linear is the Arctic Oscillation response to greenhouse gases? *J. Geophys. Res.*, **107**, doi: 10.1029/2001JD000589.

Gillett, N.P., et al., 2002c: Detecting anthropogenic influence with a multi-model ensemble. *Geophys. Res. Lett.*, **29**, doi:10.1029/2002GL015836.

Gleckler, P.J., et al., 2006: Krakatoa's signature persists in the ocean. *Nature*, **439**, 675.

Gleisner, H., and P. Thejll, 2003: Patterns of tropospheric response to solar variability. *Geophys. Res. Lett.*, **30**, 44–47.

Goeberle, C., and R. Gerdes, 2003: Mechanisms determining the variability of Arctic sea ice conditions and export. *J. Clim.*, **16**, 2843–2858.

Goldewijk, K.K., 2001: Estimating global land use change over the past 300 years: The HYDE Database. *Global Biogeochem. Cycles*, **15**(2), 417–433.

Goldstein, M., and J. Rougier, 2004: Probabilistic formulations for transferring inferences from mathematical models to physical systems. *SIAM J. Sci. Computing*, **26**(2), 467–487.

Gonzalez-Rouco, F., H. von Storch, and E. Zorita, 2003: Deep soil temperature as proxy for surface air-temperature in a coupled model simulation of the last thousand years. *Geophys. Res. Lett.*, **30**(21), 2116, doi:10.1029/2003GL018264.

Goosse, H., and H. Renssen, 2001: A two-phase response of the Southern Ocean to an increase in greenhouse gas concentrations. *Geophys. Res. Lett.*, **28**(18), 3469–3472.

Goosse, H., and H. Renssen, 2004: Exciting natural modes of variability by solar and volcanic forcing: idealized and realistic experiments. *Clim. Dyn.*, **23**(2), 153–163.

Goosse, H., et al., 2004: A late medieval warm period in the Southern Ocean as a delayed response to external forcing? *Geophys. Res. Lett.*, **31**(6), L06203, doi:10.1029/2003GL19140.

Goosse, H., et al., 2005: Modelling the climate of the last millennium: What causes the differences between simulations? *Geophys. Res. Lett.*, **32**(6), L06710, doi:10.1029/2005GL022368.

Gray, L.J., R.G. Harrison, and J.D. Haigh, 2005: *The Influence of Solar Changes on the Earth's Climate.* Hadley Centre Technical Note 62, The UK Met Office.

Greene, A.M., 2005: A time constant for hemispheric glacier mass balance. *J. Glaciol.*, **51**(174), 353–362.

Gregory, J.M., and P. Huybrechts, 2006: Ice-sheet contributions to future sea-level change. *Philos. Trans. R. Soc. London Ser. A*, **364**, 1709–1731.

Gregory, J.M., J.A. Lowe, and S.F.B. Tett, 2006: Simulated global-mean sea-level changes over the last half-millennium. *J. Clim.*, **19**, 4576–4591.

Gregory, J.M., et al., 2002a: An observationally based estimate of the climate sensitivity. *J. Clim.*, **15**(22), 3117–3121.

Gregory, J.M., et al., 2002b: Recent and future changes in Arctic sea ice simulated by the HadCM3 AOGCM. *Geophys. Res. Lett.*, **29**, 2175.

Gregory, J.M., et al., 2004: Simulated and observed decadal variability in ocean heat content. *Geophys. Res. Lett.*, **31**, L15312.

Groisman, P.Y., et al., 1999: Changes in the probability of heavy precipitation: Important indicators of climatic change. *Clim. Change*, **42**, 243–283.

Groisman, P.Y., et al., 2005: Trends in intense precipitation in the climate record. *J. Clim.*, **18**, 1326–1350.

Haarsma, R.J., F. Selten, N. Weber, and M. Kliphuis, 2005: Sahel rainfall variability and response to greenhouse warming. *Geophys. Res. Lett.*, **32**, L17702, doi:10.1029/2005GL023232.

Haigh, J.D., 2003: The effects of solar variability on the Earth's climate. *Philos. Trans. R. Soc. London Ser. A*, **361**, 95–111.

Hansen, J.E., M. Sato, and R. Ruedy, 1995: Long-term changes of the diurnal temperature cycle: implications about mechanisms of global climate change. *Atmos. Res.*, **37**, 175–209.

Hansen, J.E., M. Sato, and R. Ruedy, 1997: Radiative forcing and climate response. *J. Geophys. Res.*, **102**, 6831–6864.

Hansen, J., et al., 1984: Climate sensitivity: Analysis of feedback mechanisms. In: *Climate Processes and Climate Sensitivity* [Hansen, J.E., and T. Takahashi (eds.)]. Geophysical Monographs Vol. 29, American Geophysical Union, Washington, DC, pp. 130–163.

Hansen, J., et al., 2002: Climate forcings in Goddard Institute for Space Studies SI2000 simulations. *J. Geophys. Res.*, **107**(D18), 4347.

Hansen, J., et al., 2005: Earth's energy imbalance: Confirmation and implications. *Science*, **308**, 1431–1435.

Harrison, S., and C. Prentice, 2003: Climate and CO_2 controls on global vegetation distribution at the last glacial maximum: analysis based on palaeovegetation data, biome modelling and palaeoclimate simulations. *Global Change Biol.*, **9**, 983–1004.

Harrison, S., P. Braconnot, C. Hewitt, and R.J. Stouffer, 2002: Fourth international workshop of The Palaeoclimate Modelling Intercomparison Project (PMIP): launching PMIP Phase II. *Eos*, **83**, 447.

Harvey, L.D.D., 2004: Characterizing the annual-mean climatic effect of anthropogenic CO_2 and aerosol emissions in eight coupled atmosphere-ocean GCMs. *Clim. Dyn.*, **23**, 569–599.

Harvey, L.D.D., and R.K. Kaufmann, 2002: Simultaneously constraining climate sensitivity and aerosol radiative forcing. *J. Clim.*, **15** (20), 2837–2861.

Hasselmann, K., 1976: Stochastic climate models. Part 1. Theory. *Tellus*, **28**, 473–485.

Hasselmann, K., 1979: On the signal-to-noise problem in atmospheric response studies. In: *Meteorology of Tropical Oceans* [Shaw, D.B. (ed.)]. Royal Meteorological Society, Bracknell, UK, pp. 251–259.

Hasselmann, K., 1997: Multi-pattern fingerprint method for detection and attribution of climate change. *Climate Dyn.*, **13**, 601–612.

Hasselmann, K., 1998: Conventional and Bayesian approach to climate-change detection and attribution. *Q. J. R. Meteorol. Soc.*, **124**, 2541–2565.

Hegerl, G.C., and M.R. Allen, 2002: Origins of model-data discrepancies in optimal fingerprinting. *J. Clim.*, **15**, 1348–1356.

Hegerl, G.C., and J.M. Wallace, 2002: Influence of patterns of climate variability on the difference between satellite and surface temperature trends. *J. Clim.*, **15**, 2412–2428.

Hegerl, G.C., P.D. Jones, and T.P. Barnett, 2001: Effect of observational sampling error on the detection and attribution of anthropogenic climate change. *J. Clim.*, **14**, 198–207.

Hegerl, G.C., F.W. Zwiers, V.V. Kharin, and P.A. Stott, 2004: Detectability of anthropogenic changes in temperature and precipitation extremes. *J. Clim.*, **17**, 3683–3700.

Hegerl, G.C., T. Crowley, W.T. Hyde, and D. Frame, 2006a: Constraints on climate sensitivity from temperature reconstructions of the past seven centuries. *Nature*, **440**, doi:10.1038/nature04679.

Hegerl, G.C., et al., 1996: Detecting greenhouse gas induced climate change with an optimal fingerprint method. *J. Clim.*, **9**, 2281–2306.

Hegerl, G.C., et al., 1997: Multi-fingerprint detection and attribution of greenhouse-gas and aerosol-forced climate change. *Clim. Dyn.*, **13**, 613–634.

Hegerl, G.C., et al., 2000: Detection and attribution of climate change: Sensitivity of results to climate model differences. *Clim. Dyn.*, **16**, 737–754.

Hegerl, G.C., et al., 2003: Detection of volcanic, solar and greenhouse gas signals in paleo-reconstructions of Northern Hemispheric temperature. *Geophys. Res. Lett.*, **30**(5), 1242.

Hegerl, G.C., et al., 2006b: Climate change detection and attribution: beyond mean temperature signals. *J. Clim.*, **19**, 5058–5077.

Hegerl, G.C., et al., 2007: Detection of human influence on a new 1500yr climate reconstruction. *J. Clim.*, **20**, 650-666.

Held, I.M., and B.J. Soden, 2006: Robust responses of the hydrological cycle to global warming. *J. Clim.*, **19**, 5686–5699.

Held, I.M., et al., 2005: Simulation of Sahel drought in the 20th and 21st centuries. *Proc. Natl. Acad. Sci. U.S.A.*, **102**(50), 17891–17896.

Highwood, E.J., B.J. Hoskins, and P. Berrisford, 2000: Properties of the Arctic tropopause. *Q. J. R. Meteorol. Soc.*, **126**, 1515–1532.

Hoerling, M.P., J.W. Hurrell, J. Eischeid, and A. Phillips, 2006: Detection and attribution of twentieth-century northern and southern African rainfall change. *J. Clim.*, **19**, 3989–4008.

Hoerling, M.P., et al., 2005: Twentieth century North Atlantic climate change. Part II: Understanding the effect of Indian Ocean warming. *Clim. Dyn.*, **23**, 391–405.

Hoffert, M.I., and C. Covey, 1992: Deriving global climate sensitivity from paleoclimate reconstructions. *Nature*, **360**, 573–576.

Holland, M.M., and M.N. Raphael, 2006: Twentieth century simulation of the southern hemisphere climate in coupled models. Part II: sea ice conditions and variability. *Clim. Dyn.*, **26**, 229–245.

Holloway, G., and T. Sou, 2002: Has Arctic sea ice rapidly thinned? *J. Clim.*, **15**, 1691–1701.

Hoyt, D.V., and K.H. Schatten, 1993: A discussion of plausible solar irradiance variations, 1700-1992. *J. Geophys. Res.*, **98**, 18895–18906.

Huang, S.P., H.N. Pollack, and P.Y. Shen, 2000: Temperature trends ever the past five centuries reconstructed from borehole temperatures. *Nature*, **403**(6771), 756–758.

Hulme, M., T.J. Osborn, and T.C. Johns, 1998: Precipitation sensitivity to global warming: Comparison of observations with HadCM2 simulations. *Geophys. Res. Lett.*, **25**, 3379–3382.

Huntingford, C., P.A. Stott, M.R. Allen, and F.H. Lambert, 2006: Incorporating model uncertainty into attribution of observed temperature change. *Geophys. Res. Lett.*, **33**, L05710, doi:10.1029/2005GL024831.

Hurrell, J.W., 1996: Influence of variations in extratropical wintertime teleconnections on Northern Hemisphere temperature. *Geophys. Res. Lett.*, **23**, 665–668.

Hurrell, J.W., M.P. Hoerling, A.S. Phillips, and T. Xu, 2005: Twentieth century North Atlantic climate change. Part I: Assessing determinism. *Clim. Dyn.*, **23**, 371–389.

IDAG (International Ad Hoc Detection and Attribution Group), 2005: Detecting and attributing external influences on the climate system: A review of recent advances. *J. Clim.*, **18**, 1291–1314.

IOCI, 2002: *Climate Variability And Change In South West Western Australia, September 2002*. Indian Ocean Climate Initiative, Perth, Australia, 34 pp.

IOCI, 2005: *Indian Ocean Climate Initiative Stage 2: Report of Phase 1 Activity*. Indian Ocean Climate Initiative, Perth, Australia, 42 pp.

IPCC, 1990: *Climate Change: The Intergovernmental Panel on Climate Change Scientific Assessment* [Houghton, J.T., G.J. Jenkins, and J.J. Ephraums (eds.)]. Cambridge University Press, Cambridge, United Kingdom and New York, NY, USA, 365 pp.

IPCC, 1996: *Climate Change 1995: The Science of Climate Change. Contribution of the Working Group I to the Second Assessment Report of the Intergovernmental Panel on Climate Change* [Houghton, J.T., et al. (eds.)]. Cambridge University Press, Cambridge, United Kingdom and New York, NY, USA, 572 pp.

IPCC, 2001: *Climate Change 2001: The Scientific Basis. Contribution of Working Group I to the Third Assessment Report of the Intergovernmental Panel on Climate Change* [Houghton, J.T., et al. (eds.)]. Cambridge University Press, Cambridge, United Kingdom and New York, NY, USA, 881 pp.

Ishii, M., M. Kimoto, K. Sakamoto, and S.-I. Iwasaki, 2006: Steric sea level changes estimated from historical ocean subsurface temperature and salinity analyses. *J. Oceanogr.*, **62**, 155–170.

Ito, A., and J.E. Penner, 2005: Historical emissions of carbonaceous aerosols from biomass and fossil fuel burning for the period 1870-2000. *Global Biogeochem. Cycles*, **19**(2), GB2028, doi:10.1029/2004GB002374.

Johannssen, O.M., et al., 2004: Arctic climate change: observed and modeled temperature and sea-ice variability. *Tellus*, **56A**, 328–341.

Jones, G.S., S.F.B. Tett, and P.A. Stott, 2003: Causes of atmospheric temperature change 1960-2000: A combined attribution analysis. *Geophys. Res. Lett.*, **30**, 1228.

Jones, G.S., et al., 2005: Sensitivity of global scale attribution results to inclusion of climatic response to black carbon. *Geophys. Res. Lett.*, **32**, L14701, doi:10.1029/2005GL023370.

Jones, J.M., and M. Widmann, 2004: Early peak in Antarctic Oscillation index. *Nature*, **432**, 290–291.

Jones, P.D., and M.E. Mann, 2004: Climate over past millennia. *Rev. Geophys.*, **42**(2), RG2002, doi:10.1029/2003RG000143.

Jones, P.D., T.J. Osborn, and K.R. Briffa, 2001: The evolution of climate over the last millennium. *Science*, **292**(5517), 662–667.

Joos, F., et al., 2004: Transient simulations of Holocene atmospheric carbon dioxide and terrestrial carbon since the Last Glacial Maximum. *Global Biogeochem. Cycles*, **18**, 1–18.

Joussaume, S., and K.E. Taylor, 1995: Status of the Paleoclimate Modeling Intercomparison Project. In: *Proceedings of the First International AMIP Scientific Conference, WCRP-92, Monterey, USA*. WMO/TD-No. 732, Geneva, Switzerland, pp. 425–430.

Kalnay, E., et al., 1996: The NCEP/NCAR Reanalysis Project. *Bull. Am. Meteorol. Soc.*, **77**, 437–471.

Kaplan, J.O., I.C. Prentice, W. Knorr, and P.J. Valdes, 2002: Modeling the dynamics of terrestrial carbon storage since the Last Glacial Maximum. *Geophys. Res. Lett.*, **29**(22), 2074.

Karl, T.R., and R.W. Knight, 1998: Secular trends of precipitation amount, frequency, and intensity in the USA. *Bull. Am. Meteorol. Soc.*, **79**, 231–241.

Karl, T.R., and K.E. Trenberth, 2003: Modern global climate change. *Science*, **302**, 1719–1723.

Karl, T.R., S.J. Hassol, C.D. Miller, and W.L. Murray (eds.), 2006: *Temperature Trends in the Lower Atmosphere: Steps for Understanding and Reconciling Differences*. A Report by the Climate Change Science Program and Subcommittee on Global Change Research, Washington, DC, 180pp, http://www.climatescience.gov/Library/sap/sap1-1/finalreport/default.htm.

Karoly, D.J., 2003: Ozone and climate change. *Science*, **302**, 236–237.

Karoly, D.J., and K. Braganza, 2001: Identifying global climate change using simple indices. *Geophys. Res. Lett.*, **28**, 2205–2208.

Karoly, D.J., and K. Braganza, 2005a: Attribution of recent temperature changes in the Australian region. *J. Clim.*, **18**, 457–464.

Karoly, D.J., and K. Braganza, 2005b: A new approach to detection of anthropogenic temperature changes in the Australian region. *Meteorol. Atmos. Phys.*, **89**, 57–67.

Karoly, D.J., and Q. Wu, 2005: Detection of regional surface temperature trends. *J. Clim.*, **18**, 4337–4343.

Karoly, D.J., et al., 2003: Detection of a human influence on North American climate. *Science*, **302**, 1200–1203.

Kass, R.E., and A.E. Raftery, 1995: Bayes Factors. *J. Am. Stat. Assoc.*, **90**, 773–795.

Katz, R.W., 1999: Extreme value theory for precipitation: Sensitivity analysis for climate change. *Adv. Water Resour.*, **23**, 133–139.

Kaufmann, R.K., and D.L. Stern, 2002: Cointegration analysis of hemispheric temperature relations. *J. Geophys. Res.*, **107**, 4012.

Kennedy, M.C., and A. O'Hagan, 2001: Bayesian calibration of computer models. *J. Roy. Stat. Soc. Ser. B*, **63**(3), 425–464.

Kettleborough, J.A., B.B.B. Booth, P.A. Stott, and M.R. Allen, 2007: Estimates of uncertainty in predictions of global mean surface temperature. *J. Clim.*, **20**, 843-855.

Kiktev, D., D. Sexton, L. Alexander, and C. Folland, 2003: Comparison of modelled and observed trends in indices of daily climate extremes. *J. Clim.*, **16**, 3560–3571.

Kim, S.J., G.M. Flato, G.J. Boer, and N.A. McFarlane, 2002: A coupled climate model simulation of the Last Glacial Maximum, part 1: Transient multi-decadal response. *Clim. Dyn.*, **19**(5–6), 515–537.

Kirchner, I., et al., 1999: Climate model simulation of winter warming and summer cooling following the 1991 Mount Pinatubo volcanic eruption. *J. Geophys. Res.*, **104**, 19039–19055.

Kistler, R., et al., 2001: The NCEP-NCAR 50-year reanalysis: Monthly means CD-ROM and documentation. *Bull. Am. Meteorol. Soc.*, **82**, 247–267.

Kitoh, A., and S. Murakami, 2002: Tropical Pacific climate at the mid-Holocene and the Last Glacial Maximum simulated by a coupled ocean-atmosphere general circulation model. *Paleoceanography*, **17**(3), 1047, doi:10.1029/2001PA000724.

Klein Tank, A.M.G., and G.P. Können, 2003: Trends in indices of daily temperature and precipitation extremes in Europe, 1946-99. *J. Clim.*, **16**, 3665–3680.

Klein Tank, A.M.G., G.P. Können, and F.M. Selten, 2005: Signals of anthropogenic influence on European warming as seen in the trend patterns of daily temperature variance. *Int. J. Climatol.*, **25**, 1–16.

Knight, J.R., et al., 2005: A signature of persistent natural thermohaline circulation cycles in observed climate. *Geophys. Res. Lett.*, **32**, L20708, doi:10.1029/2005GL024233.

Knutson, T.R., S. Manabe, and D. Gu, 1997: Simulated ENSO in a global coupled ocean-atmosphere model: Multidecadal amplitude modulation and CO_2 sensitivity. *J. Clim.*, **10**(1), 138–161.

Knutson, T.R., T.L. Delworth, K.W. Dixon, and R.J. Stouffer, 1999: Model assessment of regional surface temperature trends (1949-1997). *J. Geophys. Res.*, **104**, 30981–30996.

Knutson, T.R., et al., 2006: Assessment of twentieth-century regional surface temperature trends using the GFDL CM2 coupled models. *J. Clim.*, **19**, 1624–1651.

Knutti, R., T.F. Stocker, F. Joos, and G.-K. Plattner, 2002: Constraints on radiative forcing and future climate change from observations and climate model ensembles. *Nature*, **416**, 719–723.

Knutti, R., T.F. Stocker, F. Joos, and G.-K. Plattner, 2003: Probabilistic climate change projections using neural networks. *Clim. Dyn.*, **21**, 257–272.

Kristjansson, J.E., 2002: Studies of the aerosol indirect effect from sulfate and black carbon aerosols. *J. Geophys. Res.*, **107**, doi: 10.1029/2001JD000887.

Kucera, M., et al., 2005: Reconstruction of sea-surface temperatures from assemblages of planktonic foraminifera: multi-technique approach based on geographically constrained calibration data sets and its application to glacial Atlantic and Pacific Oceans. *Quat. Sci. Rev.*, **24**(7–9), 951–998.

Kumar, A., F. Yang, L. Goddard, and S. Schubert, 2004: Differing trends in the tropical surface temperatures and precipitation over land and oceans. *J. Clim.*, **17**, 653–664.

Kunkel, K.E., X.-Z. Liang, J. Zhu, and Y. Lin, 2006: Can CGCMS simulate the twentieth century "warming hole" in the central United States? *J. Clim.*, **19**, 4137–4153.

Kushner, P.J., I.M. Held, and T.L. Delworth, 2001: Southern Hemisphere atmospheric circulation response to global warming. *J. Clim.*, **14**, 2238–3349.

Labitzke, K., 2004: On the signal of the 11-year sunspot cycle in the stratosphere and its modulation by the quasi, biennial oscillation. *J. Atmos. Solar Terr. Phys.*, **66**, 1151–1157.

Lal, M., and S.K. Singh, 2001: Global warming and monsoon climate. *Mausam*, **52**, 245–262.

Lambert, F.H., P.A. Stott, M.R. Allen, and M.A. Palmer, 2004: Detection and attribution of changes in 20th century land precipitation. *Geophys. Res. Lett.*, **31**(10), L10203, doi:10.1029/2004GL019545.

Lambert, F.H., N.P. Gillett, D.A. Stone, and C. Huntingford, 2005: Attribution studies of observed land precipitation changes with nine coupled models. *Geophys. Res. Lett.*, **32**, L18704, doi:10.1029/2005GL023654.

Lambert, S.J., and J.C. Fyfe, 2006: Changes in winter cyclone frequencies and strengths simulated in enhanced greenhouse warming experiments: Results from the models participating in the IPCC diagnostic exercise. *Clim. Dyn.*, **26**, 713–728.

Landsea, C.W., 2005: Hurricanes and global warming. *Nature*, **438**, E11–E12.

Lean, J.L., J. Beer, and R. Bradley, 1995: Reconstruction of solar irradiance changes since 1610: Implications for climate change. *Geophys. Res. Lett.*, **22**, 3195.

Lean, J.L., Y.M. Wang, and N.R. Sheeley, 2002: The effect of increasing solar activity on the Sun's total and open magnetic flux during multiple cycles: Implications for solar forcing of climate. *Geophys. Res. Lett.*, **29**(24), 2224, doi:10.1029/2002GL015880.

Lee, T.C.K., F.W. Zwiers, X. Zhang, and M. Tsao, 2006: Evidence of decadal climate prediction skill resulting from changes in anthropogenic forcing. *J. Clim.*, **19**, 5305–5318.

Lee, T.C.K., et al., 2005: A Bayesian approach to climate change detection and attribution. *J. Clim.*, **18**, 2429–2440.

Leroy, S.S., 1998: Detecting climate signals: Some Bayesian aspects. *J. Clim.*, **11**, 640–651.

Levis, S., J.A. Foley, and D. Pollard, 1999: CO_2, climate, and vegetation feedbacks at the Last Glacial Maximum. *J. Geophys. Res.*, **104**(D24), 31191–31198.

Levis, S., G.B. Bonan, and C. Bonfils, 2004: Soil feedback drives the mid-Holocene North African monsoon northward in fully coupled CCSM2 simulations with a dynamic vegetation model. *Clim. Dyn.*, **23**(7–8), 791–802.

Levitus, S., J. Antonov, and T. Boyer, 2005: Warming of the world ocean, 1955–2003. *Geophys. Res. Lett.*, **32**, L02604, doi:10.1029/2004GL021592.

Levitus, S., J. Antonov, T.P. Boyer, and C. Stephens, 2000: Warming of the world ocean. *Science*, **287**, 2225–2229.

Levitus, S., et al., 2001: Anthropogenic warming of the Earth's climate system. *Science*, **292**, 267–270.

Liepert, B., 2002: Observed reductions of surface solar radiation at sites in the United States and worldwide from 1961 to 1990. *Geophys. Res. Lett.*, **29**, 1421.

Lindsay, R.W., and J. Zhang, 2005: The thinning of arctic sea ice, 1988-2003: Have we passed a tipping point? *J. Clim.*, **18**, 4879–4894.

Lindzen, R.S., and C. Giannitsis, 2002: Reconciling observations of global temperature change. *Geophys. Res. Lett.*, **29**, doi:10.1029/2001GL014074.

Liu, Z.Y., J. Kutzbach, and L.X. Wu, 2000: Modeling climate shift of El Nino variability in the Holocene. *Geophys. Res. Lett.*, **27**(15), 2265–2268.

Liu, Z.Y., et al., 2005: Atmospheric CO_2 forcing on glacial thermohaline circulation and climate. *Geophys. Res. Lett.*, **32**(2), L02706, doi:10.1029/2004GL021929.

Lohmann, U., and G. Lesins, 2002: Stronger constraints on the anthropogenic indirect aerosol effect. *Science*, **298**, 1012–1016.

Lohmann, U., and J. Feichter, 2005: Global indirect aerosol effects: A review. *Atmos. Chem. Phys.*, **5**, 715–737.

Lorius, C., et al., 1990: The ice-core record: climate sensitivity and future greenhouse warming. *Nature*, **347**, 139–145.

Lu, J., and T.L. Delworth, 2005: Oceanic forcing of the late 20th century Sahel drought. *Geophys. Res. Lett.*, **32**, L22706, doi:10.1029/2005GL023316.

Luterbacher, J., et al., 2002: Extending North Atlantic Oscillation reconstructions back to 1500. *Atmos. Sci. Lett.*, **2**(114–124).

Luterbacher, J., et al., 2004: European seasonal and annual temperature variability, trends, and extremes since 1500. *Science*, **303**(5663), 1499–1503.

MacDonald, G.M., and R.A. Case, 2005: Variations in the Pacific Decadal Oscillation over the past millennium. *Geophys. Res. Lett.*, **32**(8), L08703, doi:10.1029/2005GL022478.

Mann, M.E., and P.D. Jones, 2003: Global surface temperature over the past two millennia. *Geophys. Res. Lett.*, **30**, 1820.

Mann, M.E., and K.A. Emanuel, 2006: Atlantic hurricane trends linked to climate change. *Eos*, **87**, 233–241.

Mann, M.E., M.A. Cane, S.E. Zebiak, and A. Clement, 2005: Volcanic and solar forcing of the tropical Pacific over the past 1000 years. *J. Clim.*, **18**(3), 447–456.

Marshall, G.J., 2003: Trends in the Southern Annular Mode from observations and reanalyses. *J. Clim.*, **16**, 4134–4143.

Marshall, G.J., A. Orr, N.P.M. van Lipzig, and J.C. King, 2006: The impact of a changing Southern Hemisphere Annular Mode on Antarctic Peninsula summer temperatures. *J. Clim.*, **19**, 5388–5404.

Marshall, G.J., et al., 2004: Causes of exceptional atmospheric circulation changes in the Southern Hemisphere. *Geophys. Res. Lett.*, **31**, L14205, doi:10.1029/2004GL019952.

Masson-Delmotte, V., et al., 2006: Past and future polar amplification of climate change: climate model intercomparisons and ice-core constraints. *Clim. Dyn.*, **26**, 513–529.

Matthews, H.D., et al., 2004: Natural and anthropogenic climate change: incorporating historical land cover change, vegetation dynamics and the global carbon cycle. *Clim. Dyn.*, **22**(5), 461–479.

May, W., 2004: Potential future changes in the Indian summer monsoon due to greenhouse warming: analysis of mechanisms in a global time-slice experiment. *Clim. Dyn.*, **22**, 389–414.

Maynard, K., J.F. Royer, and F. Chauvin, 2002: Impact of greenhouse warming on the West African summer monsoon. *Clim. Dyn.*, **19**, 499–514.

McAvaney, B.J., et al., 2001: Model evaluation. In: *Climate Change 2001: The Scientific Basis. Contribution of Working Group I to the Third Assessment Report of the Intergovernmental Panel on Climate Change* [Houghton, J.T., et al. (eds.)]. Cambridge University Press, Cambridge, United Kingdom and New York, NY, USA, pp. 471–525.

Mears, C.A., and F.J. Wentz, 2005: The effect of diurnal correction on satellite-derived lower tropospheric temperature. *Science*, **309**, 1548–1551.

Mears, C.A., M.C. Schabel, and F.J. Wentz, 2003: A reanalysis of the MSU channel 2 tropospheric temperature record. *J. Clim.*, **16**, 3650–3664.

Meehl, G.A., J.M. Arblaster, and C. Tebaldi, 2005: Understanding future patterns of precipitation extremes in climate model simulations. *Geophys. Res. Lett.*, **32**, L18719, doi:10.1029/2005GL023680.

Meehl, G.A., et al., 2003: Solar and greenhouse gas forcing and climate response in the 20th century. *J. Clim.*, **16**, 426–444.

Meehl, G.A., et al., 2004: Combinations of natural and anthropogenic forcings in 20th century climate. *J. Clim.*, **17**, 3721–3727.

Meier, M.F., M.B. Dyurgerov, and G.J. McCabe, 2003: The health of glaciers: Recent changes in glacier regime. *Clim. Change*, **59**, 123–135.

Mendelssohn, R., S.J. Bograd, F.B. Schwing, and D.M. Palacios, 2005: Teaching old indices new tricks: A state-space analysis of El Niño related climate indices. *Geophys. Res. Lett.*, **32**, L07709, doi:10.1029/2005GL022350.

Menon, S., A.D. Del Genio, D. Koch, and G. Tselioudis, 2002a: GCM Simulations of the aerosol indirect effect: Sensitivity to cloud parameterization and aerosol burden. *J. Atmos. Sci.*, **59**, 692–713.

Menon, S., J.E. Hansen, L. Nazarenko, and Y. Luo, 2002b: Climate effects of black carbon aerosols in China and India. *Science*, **297**, 2250–2253.

Merryfield, W.J., 2006: Changes to ENSO under CO_2 doubling in a multimodel ensemble. *J. Clim.*, **19**, 4009–4027.

Miller, R.L., G.A. Schmidt, and D.T. Shindell, 2006: Forced variations in the annular modes in the 20th century IPCC AR4 simulations. *J. Geophys. Res.*, **111**, D18101, doi:10.1029/2005JD006323.

Milly, P.C.D., K.A. Dunne, and A.V. Vecchia, 2005: Global patterns of trends in streamflow and water availability in a changing climate. *Nature*, **438**, 347–350.

Min, S.-K., and A. Hense, 2006a: A Bayesian approach to climate model evaluation and multi-model averaging with an application to global mean surface temperatures from IPCC AR4 coupled climate models. *Geophys. Res. Lett.*, **33**, L08708, doi:10.1029/2006GL025779.

Min, S.-K., and A. Hense, 2006b: A Bayesian assessment of climate change using multi-model ensembles. Part I: Global mean surface temperature. *J. Clim.*, **19**, 3237–3256.

Min, S.-K., A. Hense, and W.-T. Kwon, 2005: Regional-scale climate change detection using a Bayesian decision method. *Geophys. Res. Lett.*, **32**, L03706, doi:10.1029/2004GL021028.

Min, S.-K., A. Hense, H. Paeth, and W.-T. Kwon, 2004: A Bayesian decision method for climate change signal analysis. *Meteorol. Z.*, **13**, 421–436.

Mitchell, J.F.B., C.A. Wilson, and W.M. Cunningham, 1987: On CO_2 climate sensitivity and model dependence of results. *Q. J. R. Meteorol. Soc.*, **113**, 293–322.

Mitchell, J.F.B., et al., 2001: Detection of climate change and attribution of causes. In: *Climate Change 2001: The Scientific Basis. Contribution of Working Group I to the Third Assessment Report of the Intergovernmental Panel on Climate Change* [Houghton, J.T., et al. (eds.)]. Cambridge University Press, Cambridge, United Kingdom and New York, NY, USA, pp. 695–738.

Mitchell, T.D., and P.D. Jones, 2005: An improved method of constructing a database of monthly climatological observations and associated high-resolution grids. *Int. J. Climatol.*, **25**, 693–712.

Moberg, A., et al., 2005: Highly variable Northern Hemisphere temperatures reconstructed from low- and high-resolution proxy data. *Nature*, **433**, 613–617.

Monnin, E., et al., 2001: Atmospheric CO_2 concentrations over the last glacial termination. *Science*, **291**(5501), 112–114.

Montoya, M., H. von Storch, and T.J. Crowley, 2000: Climate simulation for 125,000 years ago with a coupled ocean-atmosphere General Circulation Model. *J. Clim.*, **13**, 1057–1070.

Mote, P.W., A.F. Hamlet, M.P. Clark, and D.P. Lettenmaier, 2005: Declining mountain snowpack in western North America. *Bull. Am. Meteorol. Soc.*, **86**, 39–49.

Moy, C.M., G.O. Seltzer, D.T. Rodbell, and D.M. Anderson, 2002: Variability of El Nino/Southern Oscillation activity at millennial timescales during the Holocene epoch. *Nature*, **420**(6912), 162–165.

Murray, R.J., N.L. Bindoff, and C.J.C. Reason, 2007: Modelling decadal changes on the Indian Ocean Section I5 at 32°S. *J. Clim.*, accepted.

Nagashima, T., et al., 2006: The effect of carbonaceous aerosols on surface temperature in the mid twentieth century. *Geophys. Res. Lett.*, **33**, L04702, doi:10.1029/2005GL024887.

Neelin, J.D., et al., 2006: Tropical drying trends in global warming models and observations. *Proc. Natl. Acad. Sci. U.S.A.*, **103**, 6110–6115.

Nesme-Ribes, E., et al., 1993: Solar dynamics and its impact on solar irradiance and the terrestrial climate. *J. Geophys. Res.*, **98**, 18923–18935.

New, M.G., M. Hulme, and P.D. Jones, 2000: Representing twentieth-century space-time climate variability. Part II: development of 1901-96 monthly grids of terrestrial surface climate. *J. Clim.*, **13**, 2217–2238.

Nicholls, N., 2003: Continued anomalous warming in Australia. *Geophys. Res. Lett.*, **30**, doi:10.1029/2003GL017037.

Nicholls, N., 2005: Climate variability, climate change, and the Australian snow season. *Aust. Meteorol. Mag.*, **54**, 177–185.

Nicholls, N., P. Della-Marta, and D. Collins, 2005: 20th century changes in temperature and rainfall in New South Wales. *Aust. Meteorol. Mag.*, **53**, 263–268.

Nicholson, S.E., 2001: Climatic and environmental change in Africa during the last two centuries. *Clim. Res.*, **17**, 123–144.

North, G.R., and M. Stevens, 1998: Detecting climate signals in the surface temperature record. *J. Clim.*, **11**, 563–577.

North, G.R., K.-Y. Kim, S.S.P. Shen, and J.W. Hardin, 1995: Detection of forced climate signals. Part 1: Filter theory. *J. Climate*, **8**, 401–408.

Novakov, T., et al., 2003: Large historical changes of fossil-fuel black carbon aerosols. *Geophys. Res. Lett.*, **30**(6), 1324.

Nozawa, T., T. Nagashima, H. Shiogama, and S. Crooks, 2005: Detecting natural influence on surface air temperature in the early twentieth century. *Geophys. Res. Lett.*, **32**, L20719, doi:10.1029/2005GL023540.

Oerlemans, J., 2005: Extracting a climate signal from 169 glacier records. *Science*, **308**, 675–677.

O'Hagan, A., and J. Forster, 2004: *Kendall's Advanced Theory of Statistics. Volume 2b, Bayesian Inference.* Arnold, London, 480 pp.

Ohmura, A., 2004: Cryosphere during the twentieth century, the state of the planet. In: *The State of the Planet: Frontiers and Challenges in Geophysics* [Sparks, R.S.J., and C.J. Hawkesworth (eds.)]. International Union of Geodesy and Geophysics, Washington, DC, pp. 239–257.

Oman, L., et al., 2005: Climatic response to high latitude volcanic eruptions. *J. Geophys. Res.*, **110**, D13103, doi:10.1029/2004JD005487.

Osborn, T.J., 2004: Simulating the winter North Atlantic Oscillation: the roles of internal variability and greenhouse gas forcing. *Clim. Dyn.*, **22**, 605–623.

Osborn, T.J., and M. Hulme, 1997: Development of a relationship between station and grid-box rainday frequencies for climate model evaluation. *J. Clim.*, **10**, 1885–1908.

Osborn, T.J., and K.R. Briffa, 2006: The spatial extent of 20th-century warmth in the context of the past 1200 years. *Science*, **311**, 841–844.

Osborn, T.J., S. Raper, and K.R. Briffa, 2006: Simulated climate change during the last 1000 years: comparing the ECHO-G general circulation model with the MAGICC simple climate model. *Clim. Dyn.*, **27**, 185–197.

Osborn, T.J., et al., 1999: Evaluation of the North Atlantic Oscillation as simulated by a coupled climate model. *Clim. Dyn.*, **15**, 685–702.

Otto-Bliesner, B.L., 1999: El Nino La Nina and Sahel precipitation during the middle Holocene. *Geophys. Res. Lett.*, **26**(1), 87–90.

Otto-Bliesner, B.L., et al., 2003: Modeling El Nino and its tropical teleconnections during the last glacial-interglacial cycle. *Geophys. Res. Lett.*, **30**(23), 2198, doi:10.1029/2003GL018553.

Paeth, H., A. Hense, R. Glowienka-Hense, and R. Voss, 1999: The North Atlantic Oscillation as an indicator for greenhouse-gas induced regional climate change. *Clim. Dyn.*, **15**, 953–960.

Palmer, M.A., L.J. Gray, M.R. Allen, and W.A. Norton, 2004: Solar forcing of climate: model results. *Adv. Space Res.*, **34**, 343–348.

Palmer, T.N., 1999: Predicting uncertainty in forecasts of weather and climate. *Rep. Prog. Phys.*, **63**, 71–116.

Palmer, T.N., and J. Räisänen, 2002: Quantifying the risk of extreme seasonal precipitation events in a changing climate. *Nature*, **415**, 512–514.

Parker, D.E., L.V. Alexander, and J. Kennedy, 2004: Global and regional climate in 2003. *Weather*, **59**, 145–152.

Parker, D.E., et al., 1997: A new global gridded radiosonde temperature database and recent temperature trends. *Geophys. Res. Lett.*, **24**, 1499–1452.

Pasini, A., M. Lorè, and F. Ameli, 2006: Neural network modelling for the analysis of forcings/temperatures relationships at different scales in the climate system. *Ecol. Model.*, **191**, 58–67.

Peltier, W.R., 1994: Ice age paleotopography. *Science*, **265**, 195–201.
Peltier, W.R., 2004: Global glacial isostasy and the surface of the ice-age Earth: the ICE-5G(VM2) model and GRACE. *Annu. Rev. Earth Planet. Sci.*, **32**, 111–149.
Penner, J.E., S.Y. Zhang, and C.C. Chuang, 2003: Soot and smoke aerosol may not warm climate. *J. Geophys. Res.*, **108**(D21), 4657, doi:10.1029/2003JD003409.
Penner, J.E., et al., 1997: Anthropogenic aerosols and climate change: A method for calibrating forcing. In: *Assessing Climate Change: Results from the Model Evaluation Consortium for Climate Assessment* [Howe, W., and A. Henderson-Sellers (eds.)]. Gordon & Breach Science Publishers, Sydney, Australia, pp. 91–111.
Penner, J.E., et al., 2007: Effect of black carbon on mid-troposphere and surface temperature trends. In: *Human-Induced Climate Change: An Interdisciplinary Assessment* [Schlesinger, M., et al. (eds.)]. Cambridge University Press, Cambridge, UK, in press.
Perlwitz, J., and H.-F. Graf, 2001: Troposphere-stratosphere dynamic coupling under strong and weak polar vortex conditions. *Geophys. Res. Lett.*, **28**, 271–274.
Peterson, B.J., et al., 2002: Increasing river discharge to the Arctic Ocean. *Science*, **298**, 2171–2173.
Pezza, A.B., and I. Simmonds, 2005: The first South Atlantic hurricane: Unprecedented blocking, low shear and climate change. *Geophys. Res. Lett.*, **32**, L15712, doi:10.1029/2005GL023390.
Pielke, R.A. Jr., 2005: Are there trends in hurricane destruction? *Nature*, **438**, E11.
Pielke, R.A. Jr., et al., 2005: Hurricanes and global warming. *Bull. Am. Meteorol. Soc.*, **86**, 1571–1575.
Pierce, D.W., et al., 2006: Anthropogenic warming of the oceans: observations and model results. *J. Clim.*, **19**, 1873–1900.
Pinker, R.T., B. Zhang, and E.G. Dutton, 2005: Do satellites detect trends in surface solar radiation? *Science*, **308**, 850–854.
Pollack, H.N., and J.E. Smerdon, 2004: Borehole climate reconstructions: Spatial structure and hemispheric averages. *J. Geophys. Res.*, **109**, D11106, doi:10.1029/2003JD004163.
Prentice, I.C., and T. Webb, 1998: BIOME 6000: reconstructing global mid-Holocene vegetation patterns from palaeoecological records. *J. Biogeogr.*, **25**(6), 997–1005.
Prentice, I.C., and D. Jolly, 2000: Mid-Holocene and glacial-maximum vegetation geography of the northern continents and Africa. *J. Biogeogr.*, **27**(3), 507–519.
Qian, T., A. Dai, K.E. Trenberth, and K.W. Oleson, 2006: Simulation of global land surface conditions from 1948 to 2002: Part I: Forcing data and evaluations. *J. Hydrometeorol.*, **7**, 953–975.
Ramanathan, V., P.J. Crutzen, J.T. Kiehl, and D. Rosenfeld, 2001: Aerosols, climate, and the hydrological cycle. *Science*, **294**, 2119–2124.
Ramanathan, V., et al., 2005: Atmospheric brown clouds: Impacts on South Asian climate and hydrological cycle. *Proc. Natl. Acad. Sci. U.S.A.*, **102**, 5326–5333.
Ramankutty, N., and J.A. Foley, 1999: Estimating historical changes in global land cover: Croplands from 1700 to 1992. *Global Biogeochem. Cycles*, **13**(4), 997–1027.
Ramaswamy, V., et al., 2001: Radiative forcing of climate change. In: *Climate Change 2001: The Scientific Basis. Contribution of Working Group I to the Third Assessment Report of the Intergovernmental Panel on Climate Change* [Houghton, J.T., et al. (eds.)]. Cambridge University Press, Cambridge, United Kingdom and New York, NY, USA, pp. 349–416.
Randel, W.J., and F. Wu, 2006: Biases in stratospheric temperature trends derived from historical radiosonde data. *J. Clim.*, **19**, 2094–2104.
Raper, S.C.B., J.M. Gregory, and R.J. Stouffer, 2002: The role of climate sensitivity and ocean heat uptake on AOGCM transient temperature response. *J. Clim.*, **15**, 124–130.
Rauthe, M., A. Hense, and H. Paeth, 2004: A model intercomparison study of climate change-signals in extratropical circulation. *Int. J. Climatol.*, **24**, 643–662.
Reader, M., and G. Boer, 1998: The modification of greenhouse gas warming by the direct effect of sulphate aerosols. *Clim. Dyn.*, **14**, 593–607.
Reichert, B.K., L. Bengtsson, and J. Oerlemans, 2002a: Recent glacier retreat exceeds internal variability. *J. Clim.*, **15**, 3069–3081.
Reichert, B.K., R. Schnur, and L. Bengtsson, 2002b: Global ocean warming tied to anthropogenic forcing. *Geophys. Res. Lett.*, **29**(11), 1525.
Rigor, I.G., J.M. Wallace, and R.L. Colony, 2002: Response of sea ice to the Arctic Oscillation. *J. Clim.*, **15**, 2648–2668.
Rind, D., J. Perlwitz, and P. Lonergan, 2005a: AO/NAO response to climate change. Part I: The respective influences of stratospheric and tropospheric climate changes. *J. Geophys. Res.*, **110**, D12107, doi:10.1029/2004JD005103.
Rind, D., J. Perlwitz, and P. Lonergan, 2005b: AO/NAO response to climate change. Part II: The relative importance of low and high latitude temperature changes. *J. Geophys. Res.*, **110**, D12108, doi:10.1029/2004JD005686.
Rind, D., et al., 2004: The relative importance of solar and anthropogenic forcing of climate change between the Maunder Minimum and the present. *J. Clim.*, **17**(5), 906–929.
Robock, A., 2000: Volcanic eruptions and climate. *Rev. Geophys.*, **38**(2), 191–219.
Robock, A., and Y. Liu, 1994: The volcanic signal in Goddard Institute for Space Studies three-dimensional model simulations. *J. Clim.*, **7**, 44–55.
Rothrock, D.A., J. Zhang, and Y. Yu, 2003: The arctic ice thickness anomaly of the 1990s: A consistent view from observations and models. *J. Geophys. Res.*, **108**(C3), 3083, doi:10.1029/2001JC001208.
Rotstayn, L.D., and J.E. Penner, 2001: Forcing, quasi-forcing and climate response. *J. Clim.*, **14**, 2960–2975.
Rotstayn, L.D., and U. Lohmann, 2002: Tropical rainfall trends and the indirect aerosol effect. *J. Clim.*, **15**, 2103–2116.
Rotstayn, L.D., and Y. Liu, 2003: Sensitivity of the first indirect aerosol effect to an increase of cloud droplet spectral dispersion with droplet number concentration. *J. Clim.*, **16**, 3476–3481.
Rowell, D.P., 1996: Reply to comments by Y.C. Sud and W.K.-M. Lau. *Q. J. R. Meteorol. Soc.*, **122**, 1007–1013.
Rowell, D.P., 2003: The Impact of Mediterranean SSTs on the Sahelian rainfall season. *J. Clim.*, **16**, 849–862.
Ruzmaikin, A., and J. Feynman, 2002: Solar influence on a major mode of atmospheric variability. *J. Geophys. Res.*, **107**(D14), doi:10.1029/2001JD001239.
Rybski, D., A. Bunde, S. Havlin, and H. von Storch, 2006: Long-term persistence in climate and the detection problem. *Geophys. Res. Lett.*, **33**, L06718, doi:10.1029/2005GL025591.
Santer, B.D., T.M.L. Wigley, T. Barnett, and E. Anyamba, 1996a: Detection of climate change and attribution of causes. In: *Climate Change 1995: The Science of Climate Change. Contribution of Working Group I to the Second Assessment Report of the Intergovernmental Panel on Climate Change* [Houghton, J.T. et al. (eds.)]. Cambridge University Press, Cambridge, United Kingdom and New York, NY, USA, pp. 407–444.
Santer, B.D., et al., 1996b: A search for human influences on the thermal structure of the atmosphere. *Nature*, **382**, 39–46.
Santer, B.D., et al., 1996c: Reply to "Human effect on global climate?" *Nature*, **384**, 522–525.
Santer, B.D., et al., 2000: Interpreting differential temperature trends at the surface and in the lower troposphere. *Science*, **287**, 1227–1231.
Santer, B.D., et al., 2001: Accounting for the effects of volcanoes and ENSO in comparisons of modeled and observed temperature trends. *J. Geophys. Res.*, **106**, 28033–28059.
Santer, B.D., et al., 2003a: Contributions of anthropogenic and natural forcing to recent tropopause height changes. *Science*, **301**, 479–483.
Santer, B.D., et al., 2003b: Behavior of tropopause height and atmospheric temperature in models, reanalyses, and observations: Decadal changes. *J. Geophys. Res.*, **108**(D1), 4002.
Santer, B.D., et al., 2003c: Influence of satellite data uncertainties on the detection of externally-forced climate change. *Science*, **300**, 1280–1284.

Santer, B.D., et al., 2004: Identification of anthropogenic climate change using a second-generation reanalysis. *J. Geophys. Res.*, **109**, doi:10.1029/2004JD005075.

Santer, B.D., et al., 2005: Amplification of surface temperature trends and variability in the tropical atmosphere. *Science*, **309**, 1551–1556.

Sato, M., J.E. Hansen, M.P. McCormick, and J.B. Pollack, 1993: Stratospheric aerosol optical depths, 1850-1990. *J. Geophys. Res.*, **98**, 22987–22994.

Scaife, A.A., J.R. Knight, G.K. Vallis, and C.K. Folland, 2005: A stratospheric influence on the winter NAO and North Atlantic surface climate. *Geophys. Res. Lett.*, **32**, L18715, doi:10.1029/2005GL023226.

Schär, C., and G. Jendritzky, 2004: Hot news for summer 2003. *Nature*, **432**, 559–560.

Schär, C., et al., 2004: The role of increasing temperature variability in European summer heat waves. *Nature*, **427**, 332–336

Scherrer, S.C., C. Appenzeller, and M. Laternser, 2004: Trends in Swiss alpine snow days – the role of local and large scale climate variability. *Geophys. Res. Lett.*, **31**, doi:10.1029/2004GL020255.

Scherrer, S.C., C. Appenzeller, M. A. Linger and C. Schär, 2005: European temperature distribution changes in observations and climate change scenarios. *Geophys. Res. Lett.*, **32**, doi:10.1029/2005GL024108.

Schlesinger, M.E., and N. Ramankutty, 1992: Implications for global warming of intercycle solar irradiance variations. *Nature*, **360**, 330–333.

Schlesinger, M.E., and N. Ramankutty, 1994: An oscillation in the global climate system of period 65-70 years. *Nature*, **367**, 723–726.

Schneider, T., 2004: The tropopause and the thermal stratification in the extratropics of a dry atmosphere. *J. Atmos. Sci.*, **61**, 1317–1340.

Schneider, T., and I.M. Held, 2001: Discriminants of twentieth-century changes in Earth surface temperatures. *J. Clim.*, **14**, 249–254.

Schneider von Deimling, T., H. Held, A. Ganopolski, and S. Rahmstorf, 2006: Climate sensitivity estimated from ensemble simulations of glacial climate. *Clim. Dyn.*, **27**, 149–163.

Schnur, R., and K. Hasselmann, 2005: Optimal filtering for Bayesian detection of climate change. *Clim. Dyn.*, **24**, 45–55.

Schwartz, S.E., 1993: Does fossil fuel combustion lead to global warming? *Energy Int. J.*, **18**, 1229–1248.

Schwartz, S.E., 2004: Uncertainty requirements in radiative forcing of climate change. *J. Air Waste Manage. Assoc.*, **54**, 1351–1359.

Seidel, D.J., R.J. Ross, J.K. Angell, and G.C. Reid, 2001: Climatological characteristics of the tropical tropopause as revealed by radiosondes. *J. Geophys. Res.*, **106**, 7857–7878.

Selten, F.M., G.W. Branstator, H.A. Dijkstra, and M. Kliphuis, 2004: Tropical origins for recent and future Northern Hemisphere climate change. *Geophys. Res. Lett.*, **31**, L21205, doi:10.1029/2004GL020739.

Semenov, V.A., and L. Bengtsson, 2002: Secular trends in daily precipitation characteristics: Greenhouse gas simulation with a coupled AOGCM. *Clim. Dyn.*, **19**, 123–140.

Senior, C.A., and J.F.B. Mitchell, 2000: The time dependence of climate sensitivity. *Geophys. Res. Lett.*, **27**, 2685–2689.

Sexton, D.M.H., 2001: The effect of stratospheric ozone depletion on the phase of the Antarctic Oscillation. *Geophys. Res. Lett.*, **28**, 3697–3700.

Sexton, D.M.H., D.P. Rowell, C.K. Folland, and D.J. Karoly, 2001: Detection of anthropogenic climate change using an atmospheric GCM. *Clim. Dyn.*, **17**, 669–685.

Sexton, D.M.H., H. Grubb, K.P. Shine, and C.K. Folland, 2003: Design and analysis of climate model experiments for the efficient estimation of anthropogenic signals. *J. Clim.*, **16**, 1320–1336.

Sherwood, S., J. Lanzante, and C. Meyer, 2005: Radiosonde daytime biases and late-20th century warming. *Science*, **309**, 1156–1159.

Shin, S.I., et al., 2003: A simulation of the last glacial maximum climate using the NCAR-CCSM. *Clim. Dyn.*, **20**(2–3), 127–151.

Shindell, D.T., and G.A. Schmidt, 2004: Southern Hemisphere climate response to ozone changes and greenhouse gas increases. *Geophys. Res. Lett.*, **31**, L18209, doi:10.1029/2004GL020724.

Shindell, D.T., R.L. Miller, G.A. Schmidt, and L. Pandolfo, 1999: Simulation of recent northern winter climate trends by greenhouse-gas forcing. *Nature*, **399**, 452–455.

Shindell, D.T., G.A. Schmidt, R.L. Miller, and D. Rind, 2001a: Northern Hemispheric climate response to greenhouse gas, ozone, solar and volcanic forcing. *J. Geophys. Res.*, **106**, 7193–7210.

Shindell, D.T., G.A. Schmidt, R.L. Miller, and M.E. Mann, 2003: Volcanic and solar forcing of climate change during the preindustrial era. *J. Clim.*, **16**(24), 4094–4107.

Shindell, D.T., et al., 2001b: Solar forcing of regional climate change during the Maunder Minimum. *Science*, **294**(5549), 2149–2152.

Shiogama, H., M. Watanabe, M. Kimoto, and T. Nozawa, 2005: Anthropogenic and natural forcing impacts on ENSO-like decadal variability during the second half of the 20th century. *Geophys. Res. Lett.*, **32**, L21714, doi:10.1029/2005GL023871.

Shiogama, H., et al., 2006: Influence of volcanic activity and changes in solar irradiance on surface air temperatures in the early twentieth century. *Geophys. Res. Lett.*, **33**, L09702, doi:10.1029/2005GL025622.

Simmons, A.J., and J.K. Gibson, 2000: *The ERA-40 Project Plan.* ERA-40 Project Report Series, Vol. 1, European Centre for Medium-Range Weather Forecasts, Reading, UK, 62 pp.

Smith, R.L., T.M.L. Wigley, and B.D. Santer, 2003: A bivariate time series approach to anthropogenic trend detection in hemispheric mean temperatures. *J. Clim.*, **16**, 1228–1240.

Soden, B.J., R.T. Wetherald, G.L. Stenchikov, and A. Robock, 2002: Global cooling after the eruption of Mount Pinatubo: A test of climate feedback by water vapor. *Science*, **296**(5568), 727–730.

Soden, B.J., et al., 2005: The radiative signature of upper tropospheric moistening. *Science*, **310**(5749), 841–844.

Solow, A.R., and L.J. Moore, 2002: Testing for trend in North Atlantic hurricane activity, 1900-98. *J. Clim.*, **15**, 3111–3114.

Spagnoli, B., et al., 2002: Detecting climate change at a regional scale: the case of France. *Geophys. Res. Lett.*, **29**, doi:10.1029/2001GL014619.

Stanhill, G., and S. Cohen, 2001: Global dimming, a review of the evidence for a widespread and significant reduction in global radiation with a discussion of its probable causes and possible agricultural consequences. *Agric. Forest Meteorol.*, **107**, 255–278.

Stark, S., R.A. Wood, and H.T. Banks, 2006: Reevaluating the causes of observed changes in Indian Ocean water masses. *J. Clim.*, **19**, 4075–4086.

Stenchikov, G.L., et al., 2002: Arctic Oscillation response to the 1991 Mount Pinatubo eruption: Effects of volcanic aerosols and ozone depletion. *J. Geophys. Res.*, **107**, 4803.

Stenchikov, G., et al., 2004: Arctic Oscillation response to the 1991 Pinatubo eruption in the SKYHI GCM with a realistic Quasi-Biennial Oscillation. *J. Geophys. Res.*, **109**, D03112, doi:10.1029/2003JD003699.

Stenchikov, G., et al., 2006: Arctic Oscillation response to volcanic eruptions in the IPCC AR4 climate models. *J. Geophys. Res.*, **111**, D07107, doi:10.1029/2005JD006286.

Stendel, M., I.A. Mogensen, and J.H. Christensen, 2006: Influence of various forcings on global climate in historical times using a coupled atmosphere–ocean general circulation model. *Clim. Dyn.*, **26**, 1–15.

Stern, D.I., 2005: Global sulfur emissions from 1850 to 2000. *Chemosphere*, **58**, 163–175.

Stone, D.A., and A.J. Weaver, 2002: Daily minimum and maximum temperature trends in a climate model. *Geophys. Res. Lett.*, **29**, doi:10.1029/2001GL014556.

Stone, D.A., and A.J. Weaver, 2003: Factors contributing to diurnal temperature trends in twentieth and twenty-first century simulations of the CCCma coupled model. *Clim. Dyn.*, **20**, 435–445.

Stone, D.A., and M.R. Allen, 2005a: The end-to-end attribution problem: From emissions to impacts. *Clim. Change*, **71**, 303–318.

Stone, D.A., and M.R. Allen, 2005b: Attribution of global surface warming without dynamical models. *Geophys. Res. Lett.*, **32**, L18711, doi:10.1029/2005GL023682.

Stone, D.A., and J.C. Fyfe, 2005: The effect of ocean mixing parameterisation on the enhanced CO_2 response of the Southern Hemisphere mid-latitude jet. *Geophys. Res. Lett.*, **32**, L06811, doi:10.1029/2004GL022007.

Stone, D.A., A.J. Weaver, and R.J. Stouffer, 2001: Projection of climate change onto modes of atmospheric variability. *J. Clim.*, **14**, 3551–3565.

Stone, D.A., M.R. Allen, and P.A. Stott, 2007a: A multi-model update on the detection and attribution of global surface warming. *J. Clim.*, **20**, 517-530.

Stone, D.A., M.R. Allen, F. Selten, and M. Kilphuis, 2007b: The detection and attribution of climate change using an ensemble of opportunity. *J. Clim.*, **20**, 504-516.

Stott, P.A., 2003: Attribution of regional-scale temperature changes to anthropogenic and natural causes. *Geophys. Res. Lett.*, **30**, doi:10.1029/2003GL017324.

Stott, P.A., and S.F.B. Tett, 1998: Scale-dependent detection of climate change. *J. Clim.*, **11**, 3282–3294.

Stott, P.A., and J.A. Kettleborough, 2002: Origins and estimates of uncertainty in predictions of 21st century temperature rise. *Nature*, **416**, 723–726.

Stott, P.A., M.R. Allen, and G.S. Jones, 2003a: Estimating signal amplitudes in optimal fingerprinting, Part II: Application to general circulation models. *Clim. Dyn.*, **21**, doi:10.1007/s00382-003-0314-8.

Stott, P.A., G.S. Jones, and J.F.B. Mitchell, 2003b: Do models underestimate the solar contribution to recent climate change? *J. Clim.*, **16**, 4079–4093.

Stott, P.A., D.A. Stone, and M.R. Allen, 2004: Human contribution to the European heatwave of 2003. *Nature*, **432**, 610–614.

Stott, P.A., J.A. Kettleborough, and M.R. Allen, 2006a: Uncertainty in predictions of continental scale temperature rise. *Geophys. Res. Lett.*, **33**, doi:10.1029/GL024423.

Stott, P.A., et al., 2000: External control of 20th century temperature by natural and anthropogenic forcings. *Science*, **290**, 2133–2137.

Stott, P.A., et al., 2001: Attribution of twentieth century temperature change to natural and anthropogenic causes. *Clim. Dyn.*, **17**, 1–21.

Stott, P.A., et al., 2006b: Transient climate simulations with the HadGEM1 model: causes of past warming and future climate change. *J. Clim.*, **19**, 2763–2782.

Stott, P.A., et al., 2006c: Observational constraints on past attributable warming and predictions of future global warming. *J. Clim.*, **19**, 3055–3069.

Stouffer, R.J., G.C. Hegerl, and S.F.B. Tett, 2000: A comparison of surface air temperature variability in three 1000-year coupled ocean-atmosphere model integrations. *J. Clim.*, **13**, 513–547.

Sugi, M., and J. Yoshimura, 2004: A mechanism of tropical precipitation change due to CO_2 increase. *J. Clim.*, **17**, 238–243.

Sun, S., and J. Hansen, 2003: Climate simulations for 1951-2050 with a coupled atmosphere-ocean model. *J. Clim.*, **16**, 2807–2826.

Sutton, R.T., and L.R. Hodson, 2005: Atlantic ocean forcing of North American and European summer climate. *Science*, **309**, 115–118.

Tanaka, H.L., N. Ishizaki, and N. Nohara, 2005: Intercomparison of the intensities and trends of Hadley, Walker and Monsoon Circulations in the global warming predictions. *Scientific Online Letters on the Atmosphere*, **1**, 77–80.

Taylor, C.M., et al., 2002: The influence of land use change on climate in the Sahel. *J. Clim.*, **15**, 3615–3629.

Taylor, K.E., et al., 2000: Analysis of forcing, response, and feedbacks in a paleoclimate modeling experiment. In: *Paleoclimate Modeling Intercomparison Project (PMIP): Proceedings of the Third PMIP Workshop, La Huardière, Canada, 4-8 October 1999* [P. Braconnot (ed.)]. WCRP-111, WMO/TD-1007, World Meteorological Organization, Geneva, Switzerland, pp. 271.

Tebaldi, C., K. Hayhoe, J.M. Arblaster, and G.A. Meehl, 2006: Going to extremes: An intercomparison of model-simulated historical and future changes in extreme events. *Clim. Change*, **79**, 185–211.

Tett, S.F.B., et al., 1999: Causes of twentieth-century temperature change near the Earth's surface. *Nature*, **399**, 569–572.

Tett, S.F.B., et al., 2002: Estimation of natural and anthropogenic contributions to twentieth century temperature change. *J. Geophys. Res.*, **107**(D16), 4306, doi:10.1029/2000JD000028.

Tett, S.F.B., et al., 2007: The impact of natural and anthropogenic forcings on climate and hydrology since 1550. *Clim. Dyn.*, **28**, 3–34, doi:10.1007/s00382-006-0165-1.

Thomas, R., et al., 2004: Accelerated sea level rise from West Antarctica. *Science*, **306**, 255–258.

Thompson, D.W.J., and J.M. Wallace, 1998: The Arctic Oscillation signature in the wintertime geopotential height and temperature fields. *Geophys. Res. Lett.*, **25**, 1297–1300.

Thompson, D.W.J., and J.M. Wallace, 2000: Annular modes in the extratropical circulation. Part I: Month-to-month variability. *J. Clim.*, **13**, 1000–1016.

Thompson, D.W.J., and S. Solomon, 2002: Interpretation of recent Southern Hemisphere climate change. *Science*, **296**, 895–899.

Thompson, D.W.J., J.M. Wallace, and G.C. Hegerl, 2000: Annular modes in the extratropical circulation: Part II, Trends. *J. Clim.*, **13**, 1018–1036.

Thorne, P.W., et al., 2002: Assessing the robustness of zonal mean climate change detection. *Geophys. Res. Lett.*, **29**, doi:10.1029/2002GL015717.

Thorne, P.W., et al., 2003: Probable causes of late twentieth century tropospheric temperature trends. *Clim. Dyn.*, **21**, 573–591.

Thorne, P.W., et al., 2005: Revisiting radiosonde upper air temperatures from 1958 to 2002. *J. Geophys. Res.*, **110**, D18105, doi:10.1029/2004JD005753.

Thuburn, J., and G.C. Craig, 2000: Stratospheric influence on tropopause height: The radiative constraint. *J. Atmos. Sci.*, **57**, 17–28.

Timbal, B., 2004: Southwest Australia past and future rainfall trends. *Clim. Res.*, **26**, 233–249.

Timbal, B., J.M. Arblaster, and S. Power, 2005: Attribution of late 20th century rainfall decline in South-West Australia. *J. Clim.*, **19**, 2046–2062.

Timmermann, A., 1999: Detecting the nonstationary response of ENSO to greenhouse warming. *J. Atmos. Sci.*, **56**, 2313–2325.

Timmermann, A., et al., 1999: Increased El Niño frequency in a climate model forced by future greenhouse warming. *Nature*, **398**, 694–696.

Tol, R.S.J., and A.F. De Vos, 1998: A Bayesian statistical analysis of the enhanced greenhouse effect. *Clim. Change*, **38**, 87–112.

Tourpali, K., et al., 2003: Stratospheric and tropospheric response to enhanced solar UV radiation: A model study. *Geophys. Res. Lett.*, **30**(5), doi:10.1029/2002GL016650.

Trenberth, K.E., 2005: Uncertainty in hurricanes and global warming. *Science*, **308**, 1753–1754.

Trenberth, K.E., and D.J. Shea, 2005: Relationships between precipitation and surface temperature. *Geophys. Res. Lett.*, **32**, L14703, doi:10.1029/2005GL022760.

Trenberth, K.E., and L. Smith, 2005: The mass of the atmosphere: A constraint on global analyses. *J. Clim.*, **18**, 864–875.

Trenberth, K.E., and D. Shea, 2006: Atlantic hurricanes and natural variability in 2005. *Geophys. Res. Lett.*, **33**, L12704, doi:10.1029/2006GL026894.

Trenberth, K.E., J. Fasullo, and L. Smith, 2005: Trends and variability in column-integrated water vapour. *Clim. Dyn.*, **24**, 741–758.

Trenberth, K.E., A. Dai, R.M. Rasmussen, and D.B. Parsons, 2003: The changing character of precipitation. *Bull. Am. Meteorol. Soc.*, **84**, 1205–1217.

Triacca, U., 2001: On the use of Granger causality to investigate the human influence on climate. *Theor. Appl. Climatol.*, **69**, 137–138.

Tudhope, S., and M. Collins, 2003: Global change – The past and future of El Nino. *Nature*, **424**(6946), 261–262.

Ueda, H., A. Iwai, K. Kuwako, and M.E. Hori, 2006: Impact of anthropogenic forcing on the Asian summer monsoon simulated by 8 GCMs. *Geophys. Res. Lett.*, **33**, L06703, doi:10.1029/2005GL025336.

van Aardenne, J.A., et al., 2001: A 1° x 1° resolution data set of historical anthropogenic trace gas emissions for the period 1890-1990. *Global Biogeochem. Cycles*, **15**, 909–928.

van der Schrier, G., and J. Barkmeijer, 2005: Bjerknes' hypothesis on the coldness during AD 1790-1820 revisited. *Clim. Dyn.*, **24**(4), 355–371.
van Loon, H., and D.J. Shea, 2000: The global 11-year solar signal in July-August. *Geophys. Res. Lett.*, **27**, 2965–2968.
Vaughan, D.G., et al., 2001: Devil in the detail. *Science*, **293**, 1777–1779.
Vecchi, G.A., et al., 2006: Weakening of tropical Pacific atmospheric circulation due to anthropogenic forcing. *Nature*, **44**, 73–76.
Vellinga, M., and P. Wu, 2004: Low-latitude freshwater influence on centennial variability of the thermohaline circulation. *J. Clim.*, **17**, 4498–4511.
Vinnikov, K.Y., et al., 1999: Global warming and Northern Hemisphere sea ice extent. *Science*, **286**(5446), 1934–1937.
Vinnikov, K.Y., et al., 2006: Trends at the surface and in the troposphere. *J. Geophys. Res.*, **111**, D03106, doi:10.1029/2005JD006392.
Volodin, E.M., and V.Y. Galin, 1999: Interpretation of winter warming on Northern Hemisphere continents in 1977-1994. *J. Clim.*, **12**, 2947–2955.
von Storch, H., and F.W. Zwiers, 1999: *Statistical Analysis in Climate Research.* Cambridge University Press, Cambridge, UK, 484 pp.
Wang, M., et al., 2007: Intrinsic versus forced variation in coupled climate model simulations over the Arctic during the 20th century. *J. Clim.*, **20**, 1084-1098.
Waple, A.M., M.E. Mann, and R.S. Bradley, 2002: Long-term patterns of solar irradiance forcing in model experiments and proxy based surface temperature reconstructions. *Clim. Dyn.*, **18**, 563–578.
Wardle, R., and I. Smith, 2004: Modeled response of the Australian monsoon to changes in land surface temperatures. *Geophys. Res. Lett.*, **31**, L16205, doi:10.1029/2004GL020157.
Weatherall, R.T., and S. Manabe, 1975: The effects of changing the solar constant on the climate of a general circulation model. *J. Atmos. Sci.*, **32**, 2044–2059.
Weber, S.L., 2005: A timescale analysis of the NH temperature response to volcanic and solar forcing in the past millennium. *Climate of the Past*, **1**, 9–17.
Weber, S.L., T.J. Crowley, and G. van der Schrier, 2004: Solar irradiance forcing of centennial climate variability during the Holocene. *Clim. Dyn.*, **22**(5), 539–553.
Webster, P.J., G.J. Holland, J.A. Curry, and H.-R. Chang, 2005: Changes in tropical cyclone number, duration, and intensity in a warming environment. *Science*, **309**(5742), 1844–1846.
Wentz, F.J., and M. Schabel, 2000: Precise climate monitoring using complementary satellite data sets. *Nature*, **403**, 414–416.
White, W.B., M.D. Dettinger, and D.R. Cayan, 2003: Sources of global warming of the upper ocean on decadal period scales. *J. Geophys. Res.*, **108**, 3248, doi:10.1029/2002JC001396.
Wielicki, B.A., et al., 2002: Evidence of large decadal variability in tropical mean radiative energy budget. *Science*, **295**, 841–844.
Wielicki, B.A., et al., 2005: Changes in Earth's albedo measured by satellite. *Science*, **308**, 825.
Wigley, T.M.L., 1989: Climate variability on the 10-100-year time scale: Observations and possible causes. In: *Global Changes of the Past: Papers Arising from the 1989 OIES Global Change Institute* [Bradley, R.S. (ed.)]. University Corporation for Atmospheric Research, Boulder, CO, pp. 83–101.
Wigley, T.M.L., P.D. Jones, and S.C.B. Raper, 1997: The observed global warming record: What does it tell us? *Proc. Natl. Acad. Sci. U.S.A.*, **94**, 8314–8320.
Wigley, T.M.L., C.M. Ammann, B.D. Santer, and S.C.B. Raper, 2005a: Effect of climate sensitivity on the response to volcanic forcing. *J. Geophys. Res.*, **110**, D09107, doi:10.1029/2004JD005557.
Wigley, T.M.L., C.M. Ammann, B.D. Santer, and K.E. Taylor, 2005b: Comment on "Climate forcing by the volcanic eruption of Mount Pinatubo" by David H. Douglass and Robert S. Knox. *Geophys. Res. Lett.*, **32**, L20709, doi:10.1029/2005GL023312.
Wild, M., et al., 2005: From dimming to brightening: Decadal changes in solar radiation at Earth's surface. *Science*, **308**, 847–850.
Williams, K.D., et al., 2001: The response of the climate system to the indirect effects of anthropogenic aerosol. *Clim. Dyn.*, **17**, 845–856.
Willis, J.K., D. Roemmich, and B. Cornuelle, 2004: Interannual variability in upper ocean heat content, temperature and thermosteric expansion on global scales. *J. Geophys. Res.*, **109**, C12036, doi:10.1029/2003JC002260.
Wohlfahrt, J., S.P. Harrison, and P. Braconnot, 2004: Synergistic feedbacks between ocean and vegetation on mid- and high-latitude climates during the mid-Holocene. *Clim. Dyn.*, **22**(2–3), 223–238.
Wong, A.P.S., N.L. Bindoff, and J. Church, 1999: Large-scale freshening of intermediate waters in the Pacific and Indian Oceans. *Nature*, **400**, 440–444.
Wong, T., et al., 2006: Reexamination of the observed decadal variability of the Earth Radiation Budget using altitude-corrected ERBE/ERBS nonscanner WFOV data. *J. Clim.*, **19**, 4028–4040.
Woodworth, P.L., J.M. Gregory, and R.J. Nicholls, 2004: Long term sea level changes and their impacts. In: *The Sea* [Robinson, A.R. and K.H. Brink (eds.)]. Harvard University Press, Cambridge, MA, pp. 715–753.
Wu, P., R. Wood, and P.A. Stott, 2004: Does the recent freshening trend in the North Atlantic indicate a weakening thermohaline circulation? *Geophys. Res. Lett.*, **31**, doi:10.1029/2003GL018584.
Wu, P., R. Wood, and P.A. Stott, 2005: Human influence on increasing Arctic river discharges. *Geophys. Res. Lett.*, **32**, L02703, doi:10.1029/2004GL021570.
Wu, P., R. Wood, P.A. Stott, and G.S. Jones, 2007: Deep North Atlantic freshening simulated in a coupled model. *Progr. Oceanogr.*, accepted.
Wyputta, U., and B.J. McAvaney, 2001: Influence of vegetation changes during the Last Glacial Maximum using the BMRC atmospheric general circulation model. *Clim. Dyn.*, **17**(12), 923–932.
Yang, F., and M. Schlesinger, 2001: Identification and separation of Mount Pinatubo and El Nino-Southern Oscillation land surface temperature anomalies. *J. Geophys. Res.*, **106**, 14757–14770.
Yang, F., A. Kumar, M.E. Schlesinger, and W. Wang, 2003: Intensity of hydrological cycles in warmer climates. *J. Clim.*, **16**, 2419–2423.
Yokohata, T., et al., 2005: Climate response to volcanic forcing: Validation of climate sensitivity of a coupled atmosphere-ocean general circulation model. *Geophys. Res. Lett.*, **32**, L21710, doi:10.1029/2005GL023542.
Yoshimori, M., T. Stocker, C.C. Raible, and M. Renold, 2005: Externally forced and internal variability in ensemble climate simulations of the Maunder Minimum. *J. Clim.*, **18**, 4253–4270.
Yoshimura, J., and M. Sugi, 2005: Tropical cyclone climatology in a high-resolution AGCM -Impacts of SST warming and CO2 increase. *Scientific Online Letters on the Atmosphere*, **1**, 133–136.
Zeng, N., 2003: Drought in the Sahel. *Science*, **302**, 999–1000.
Zhang, X., F.W. Zwiers, and P.A. Stott, 2006: Multi-model multi-signal climate change detection at regional scale. *J. Clim.*, **19**, 4294–4307.
Zhang, Y., J.M. Wallace, and D.S. Battisti, 1997: ENSO-like interdecadal variability: 1900-93. *J. Clim.*, **10**, 1004–1020.
Zhang, Y.-C., et al., 2004: Calculation of radiative flux profiles from the surface to top-of-atmosphere based on ISCCP and other global data sets: Refinements of the radiative transfer model and the input data. *J. Geophys. Res.*, **109**, D19105, doi:10.1029/2003JD004457.
Zhao, Y., et al., 2005: A multi-model analysis of the role of the ocean on the African and Indian monsoon during the mid-Holocene. *Clim. Dyn.*, **25**, 777–800.
Ziegler, A.D., et al., 2003: Detection of intensification in global- and continental-scale hydrological cycles: Temporal scale of evaluation. *J. Clim.*, **16**, 535–547.
Zorita, E., et al., 2004: Climate evolution in the last five centuries simulated by an atmosphere-ocean model: Global temperatures, the North Atlantic Oscillation and the Late Maunder Minimum. *Meteorol. Z.*, **13**(4), 271–289.
Zorita, E., et al., 2005: Natural and anthropogenic modes of surface temperature variations in the last thousand years. *Geophys. Res. Lett.*, **32**(8), L08707, doi:10.1029/2004GL021563.
Zwiers, F.W., and X. Zhang, 2003: Toward regional scale climate change detection. *J. Clim.*, **16**, 793–797.

Appendix 9.A: Methods Used to Detect Externally Forced Signals

This appendix very briefly reviews the statistical methods that have been used in most recent detection and attribution work. Standard 'frequentist' methods (methods based on the relative frequency concept of probability) are most often used, but there is also increasing use of Bayesian methods of statistical inference. The following sections briefly describe the optimal fingerprinting technique followed by a short discussion on the differences between the standard and Bayesian approaches to statistical inferences that are relevant to detection and attribution.

9.A.1 Optimal Fingerprinting

Optimal fingerprinting is generalised multivariate regression adapted to the detection of climate change and the attribution of change to externally forced climate change signals (Hasselmann, 1979, 1997; Allen and Tett, 1999). The regression model has the form $\mathbf{y} = \mathbf{X}\mathbf{a} + \mathbf{u}$, where vector $\mathbf{y}$ is a filtered version of the observed record, matrix $\mathbf{X}$ contains the estimated response patterns to the external forcings (signals) that are under investigation, $\mathbf{a}$ is a vector of scaling factors that adjusts the amplitudes of those patterns and $\mathbf{u}$ represents internal climate variability. Vector $\mathbf{u}$ is usually assumed to be a Gaussian random vector with covariance matrix $\mathbf{C}$. Vector $\mathbf{a}$ is estimated with $\hat{\mathbf{a}} = (\mathbf{X}^T\mathbf{C}^{-1}\mathbf{X})^{-1}\mathbf{X}^T\mathbf{C}^{-1}\mathbf{y}$, which is equivalent to $(\tilde{\mathbf{X}}^T\tilde{\mathbf{X}})^{-1}\tilde{\mathbf{X}}^T\tilde{\mathbf{y}}$, where matrix $\tilde{\mathbf{X}}$ and vector $\tilde{\mathbf{y}}$ represent the signal patterns and observations after normalisation by the climate's internal variability. This normalisation, standard in linear regression, is used in most detection and attribution approaches to improve the signal-to-noise ratio (see, e.g., Hasselmann, 1979; Allen and Tett, 1999; Mitchell et al., 2001).

The matrix $\mathbf{X}$ typically contains signals that are estimated with either an AOGCM, an AGCM (see Sexton et al., 2001, 2003) or a simplified climate model such as an EBM. Because AOGCMs simulate natural internal variability as well as the response to specified anomalous external forcing, AOGCM-simulated climate signals are typically estimated by averaging across an ensemble of simulations (for a discussion of optimal ensemble size and composition, see Sexton et al., 2003). If an observed response is to be attributed to anthropogenic influence, $\mathbf{X}$ should at a minimum contain separate natural and anthropogenic responses. In order to relax the assumption that the relative magnitudes of the responses to individual forcings are correctly simulated, $\mathbf{X}$ may contain separate responses to all the main forcings, including greenhouse gases, sulphate aerosol, solar irradiance changes and volcanic aerosol. The vector $\mathbf{a}$ accounts for possible errors in the amplitude of the external forcing and the amplitude of the climate model's response by scaling the signal patterns to best match the observations.

Fitting the regression model requires an estimate of the covariance matrix $\mathbf{C}$ (i.e., the internal variability), which is usually obtained from unforced variation simulated by AOGCMs (e.g., from long control simulations) because the instrumental record is too short to provide a reliable estimate and may be affected by external forcing. Atmosphere-Ocean General Circulation Models may not simulate natural internal climate variability accurately, particularly at small spatial scales, and thus a residual consistency test (Allen and Tett, 1999) is typically used to assess the model-simulated variability at the scales that are retained in the analysis. To avoid bias (Hegerl et al., 1996, 1997), uncertainty in the estimate of the vector of scaling factors $\mathbf{a}$ is usually assessed with a second, statistically independent estimate of the covariance matrix $\mathbf{C}$ which is ordinarily obtained from an additional, independent sample of simulated unforced variation.

Signal estimates are obtained by averaging across an ensemble of forced climate change simulations, but contain remnants of the climate's natural internal variability because the ensembles are finite. When ensembles are small or signals weak, these remnants may bias ordinary least-squares estimates of $\mathbf{a}$ downward. This is avoided by estimating $\mathbf{a}$ with the total least-squares algorithm (Allen and Stott 2003).

9.A.2 Methods of Inference

Detection and attribution questions are assessed through a combination of physical reasoning (to determine, for example, by assessing consistency of possible responses, whether other mechanisms of change not included in the climate model could plausibly explain the observed change) and by evaluating specific hypotheses about the scaling factors contained in $\mathbf{a}$. Most studies evaluate these hypotheses using standard frequentist methods (Hasselmann, 1979, 1997; Hegerl et al., 1997; Allen and Tett, 1999). Several recent studies have also used Bayesian methods (Hasselmann, 1998; Leroy, 1998; Min et al., 2004, 2005; Lee et al., 2005, 2006; Schnur and Hasselmann, 2005; Min and Hense, 2006a,b).

In the standard approach, detection of a postulated climate change signal occurs when its amplitude in observations is shown to be significantly different from zero (i.e., when the null hypothesis H_D : $\mathbf{a} = \mathbf{0}$ where $\mathbf{0}$ is a vector of zeros, is rejected) with departure from zero in the physically plausible direction. Subsequently, the second attribution requirement (consistency with a combination of external forcings and natural internal variability) is assessed with the 'attribution consistency test' (Hasselmann, 1997; see also Allen and Tett, 1999) that evaluates the null hypothesis H_A : $\mathbf{a} = \mathbf{1}$ where $\mathbf{1}$ denotes a vector of units. This test does not constitute a complete attribution assessment, but contributes important evidence to such assessments (see Mitchell et al., 2001). Attribution studies usually also test whether the response to a key forcing, such as greenhouse gas increases, is distinguishable from that to other forcings, usually based on the results of multiple regression (see above) using the most important forcings simultaneously in $\mathbf{X}$. If the response to a key forcing (e.g., due to greenhouse gas increases) is detected by rejecting the hypothesis that its amplitude $a_{GHG} = 0$ in such a multiple regression, this provides strong attribution information

because it demonstrates that the observed climate change is 'not consistent with alternative, physically plausible explanations of recent climate change that exclude important elements of the given combination of forcings' (Mitchell et al., 2001).

Bayesian approaches are of interest because they can be used to integrate information from multiple lines of evidence, and can incorporate independent prior information into the analysis. Essentially two approaches (described below) have been taken to date. In both cases, inferences are based on a posterior distribution that blends evidence from the observations with the independent prior information, which may include information on the uncertainty of external forcing estimates, climate models and their responses to forcing. In this way, all information that enters into the analysis is declared explicitly.

Schnur and Hasselmann (2005) approach the problem by developing a filtering technique that optimises the impact of the data on the prior distribution in a manner similar to the way in which optimal fingerprints maximise the ratio of the anthropogenic signal to natural variability noise in the conventional approach. The optimal filter in the Bayesian approach depends on the properties of both the natural climate variability and model errors. Inferences are made by comparing evidence, as measured by Bayes Factors (Kass and Raftery, 1995), for competing hypotheses. Other studies using similar approaches include Min et al. (2004) and Min and Hense (2006a,b). In contrast, Berliner et al. (2000) and Lee et al. (2005) use Bayesian methods only to make inferences about the estimate of **a** that is obtained from conventional optimal fingerprinting.

10

Global Climate Projections

Coordinating Lead Authors:

Gerald A. Meehl (USA), Thomas F. Stocker (Switzerland)

Lead Authors:

William D. Collins (USA), Pierre Friedlingstein (France, Belgium), Amadou T. Gaye (Senegal), Jonathan M. Gregory (UK), Akio Kitoh (Japan), Reto Knutti (Switzerland), James M. Murphy (UK), Akira Noda (Japan), Sarah C.B. Raper (UK), Ian G. Watterson (Australia), Andrew J. Weaver (Canada), Zong-Ci Zhao (China)

Contributing Authors:

R.B. Alley (USA), J. Annan (Japan, UK), J. Arblaster (USA, Australia), C. Bitz (USA), P. Brockmann (France), V. Brovkin (Germany, Russian Federation), L. Buja (USA), P. Cadule (France), G. Clarke (Canada), M. Collier (Australia), M. Collins (UK), E. Driesschaert (Belgium), N.A. Diansky (Russian Federation), M. Dix (Australia), K. Dixon (USA), J.-L. Dufresne (France), M. Dyurgerov (Sweden, USA), M. Eby (Canada), N.R. Edwards (UK), S. Emori (Japan), P. Forster (UK), R. Furrer (USA, Switzerland), P. Gleckler (USA), J. Hansen (USA), G. Harris (UK, New Zealand), G.C. Hegerl (USA, Germany), M. Holland (USA), A. Hu (USA, China), P. Huybrechts (Belgium), C. Jones (UK), F. Joos (Switzerland), J.H. Jungclaus (Germany), J. Kettleborough (UK), M. Kimoto (Japan), T. Knutson (USA), M. Krynytzky (USA), D. Lawrence (USA), A. Le Brocq (UK), M.-F. Loutre (Belgium), J. Lowe (UK), H.D. Matthews (Canada), M. Meinshausen (Germany), S.A. Müller (Switzerland), S. Nawrath (Germany), J. Oerlemans (Netherlands), M. Oppenheimer (USA), J. Orr (Monaco, USA), J. Overpeck (USA), T. Palmer (ECMWF, UK), A. Payne (UK), G.-K. Plattner (Switzerland), J. Räisänen (Finland), A. Rinke (Germany), E. Roeckner (Germany), G.L. Russell (USA), D. Salas y Melia (France), B. Santer (USA), G. Schmidt (USA, UK), A. Schmittner (USA, Germany), B. Schneider (Germany), A. Shepherd (UK), A. Sokolov (USA, Russian Federation), D. Stainforth (UK), P.A. Stott (UK), R.J. Stouffer (USA), K.E. Taylor (USA), C. Tebaldi (USA), H. Teng (USA, China), L. Terray (France), R. van de Wal (Netherlands), D. Vaughan (UK), E. M. Volodin (Russian Federation), B. Wang (China), T. M. L. Wigley (USA), M. Wild (Switzerland), J. Yoshimura (Japan), R. Yu (China), S. Yukimoto (Japan)

Review Editors:

Myles Allen (UK), Govind Ballabh Pant (India)

This chapter should be cited as:

Meehl, G.A., T.F. Stocker, W.D. Collins, P. Friedlingstein, A.T. Gaye, J.M. Gregory, A. Kitoh, R. Knutti, J.M. Murphy, A. Noda, S.C.B. Raper, I.G. Watterson, A.J. Weaver and Z.-C. Zhao, 2007: Global Climate Projections. In: *Climate Change 2007: The Physical Science Basis. Contribution of Working Group I to the Fourth Assessment Report of the Intergovernmental Panel on Climate Change* [Solomon, S., D. Qin, M. Manning, Z. Chen, M. Marquis, K.B. Averyt, M. Tignor and H.L. Miller (eds.)]. Cambridge University Press, Cambridge, United Kingdom and New York, NY, USA.

Table of Contents

Executive Summary 749

10.1 Introduction 753

10.2 Projected Changes in Emissions, Concentrations and Radiative Forcing 755

10.2.1 Emissions Scenarios and Radiative Forcing in the Multi-Model Climate Projections 755

10.2.2 Recent Developments in Projections of Radiative Species and Forcing for the 21st Century 759

10.3 Projected Changes in the Physical Climate System 760

10.3.1 Time-Evolving Global Change 762

10.3.2 Patterns of Change in the 21st Century 764

10.3.3 Changes in Ocean/Ice and High-Latitude Climate? 770

10.3.4 Changes in the Atlantic Meridional Overturning Circulation 772

Box 10.1: Future Abrupt Climate Change, 'Climate Surprises', and Irreversible Changes 775

10.3.5 Changes in Properties of Modes of Variability 778

10.3.6 Future Changes in Weather and Climate Extremes 782

10.4 Changes Associated with Biogeochemical Feedbacks and Ocean Acidification 789

10.4.1 Carbon Cycle/Vegetation Feedbacks 789

10.4.2 Ocean Acidification Due to Increasing Atmospheric Carbon Dioxide 793

10.4.3 Simulations of Future Evolution of Methane, Ozone and Oxidants 793

10.4.4 Simulations of Future Evolution of Major Aerosol Species 796

10.5 Quantifying the Range of Climate Change Projections 797

10.5.1 Sources of Uncertainty and Hierarchy of Models 797

Box 10.2: Equilibrium Climate Sensitivity 798

10.5.2 Range of Responses from Different Models 800

10.5.3 Global Mean Responses from Different Scenarios 802

10.5.4 Sampling Uncertainty and Estimating Probabilities 805

10.6 Sea Level Change in the 21st Century 812

10.6.1 Global Average Sea Level Rise Due to Thermal Expansion 812

10.6.2 Local Sea Level Change Due to Change in Ocean Density and Dynamics 812

10.6.3 Glaciers and Ice Caps 814

10.6.4 Ice Sheets 816

10.6.5 Projections of Global Average Sea Level Change for the 21st Century 820

10.7 Long Term Climate Change and Commitment 822

10.7.1 Climate Change Commitment to Year 2300 Based on AOGCMs 822

10.7.2 Climate Change Commitment to Year 3000 and Beyond to Equilibrium 823

10.7.3 Long-Term Integrations: Idealised Overshoot Experiments 827

10.7.4 Commitment to Sea Level Rise 828

Frequently Asked Questions

FAQ 10.1: *Are Extreme Events, Like Heat Waves, Droughts or Floods, Expected to Change as the Earth's Climate Changes?* 783

FAQ 10.2: *How Likely are Major or Abrupt Climate Changes, such as Loss of Ice Sheets or Changes in Global Ocean Circulation?* 818

FAQ 10.3: *If Emissions of Greenhouse Gases are Reduced, How Quickly do Their Concentrations in the Atmosphere Decrease?* 824

References 832

Appendix 10.A: Methods for Sea Level Projections for the 21st Century 844

Supplementary Material

The following Supplementary Material is available on CD-ROM and in on-line versions of this report.

Supplementary Figures S10.1 to S10.4

Figures Showing Individual Model Results for Different Climate Variables

Executive Summary

The future climate change results assessed in this chapter are based on a hierarchy of models, ranging from Atmosphere-Ocean General Circulation Models (AOGCMs) and Earth System Models of Intermediate Complexity (EMICs) to Simple Climate Models (SCMs). These models are forced with concentrations of greenhouse gases and other constituents derived from various emissions scenarios ranging from non-mitigation scenarios to idealised long-term scenarios. In general, we assess non-mitigated projections of future climate change at scales from global to hundreds of kilometres. Further assessments of regional and local climate changes are provided in Chapter 11. Due to an unprecedented, joint effort by many modelling groups worldwide, climate change projections are now based on multi-model means, differences between models can be assessed quantitatively and in some instances, estimates of the probability of change of important climate system parameters complement expert judgement. New results corroborate those given in the Third Assessment Report (TAR). Continued greenhouse gas emissions at or above current rates will cause further warming and induce many changes in the global climate system during the 21st century that would *very likely* be larger than those observed during the 20th century.

Mean Temperature

All models assessed here, for all the non-mitigation scenarios considered, project increases in global mean surface air temperature (SAT) continuing over the 21st century, driven mainly by increases in anthropogenic greenhouse gas concentrations, with the warming proportional to the associated radiative forcing. There is close agreement of globally averaged SAT multi-model mean warming for the early 21st century for concentrations derived from the three non-mitigated IPCC Special Report on Emission Scenarios (SRES: B1, A1B and A2) scenarios (including only anthropogenic forcing) run by the AOGCMs (warming averaged for 2011 to 2030 compared to 1980 to 1999 is between +0.64°C and +0.69°C, with a range of only 0.05°C). Thus, this warming rate is affected little by different scenario assumptions or different model sensitivities, and is consistent with that observed for the past few decades (see Chapter 3). Possible future variations in natural forcings (e.g., a large volcanic eruption) could change those values somewhat, but about half of the early 21st-century warming is committed in the sense that it would occur even if atmospheric concentrations were held fixed at year 2000 values. By mid-century (2046–2065), the choice of scenario becomes more important for the magnitude of multi-model globally averaged SAT warming, with values of +1.3°C, +1.8°C and +1.7°C from the AOGCMs for B1, A1B and A2, respectively. About a third of that warming is projected to be due to climate change that is already committed. By late century (2090–2099), differences between scenarios are large, and only about 20% of that warming arises from climate change that is already committed.

An assessment based on AOGCM projections, probabilistic methods, EMICs, a simple model tuned to the AOGCM responses, as well as coupled climate carbon cycle models, suggests that for non-mitigation scenarios, the future increase in global mean SAT is *likely* to fall within –40 to +60% of the multi-model AOGCM mean warming simulated for a given scenario. The greater uncertainty at higher values results in part from uncertainties in the carbon cycle feedbacks. The multi-model mean SAT warming and associated uncertainty ranges for 2090 to 2099 relative to 1980 to 1999 are B1: +1.8°C (1.1°C to 2.9°C), B2: +2.4°C (1.4°C to 3.8°C), A1B: +2.8°C (1.7°C to 4.4°C), A1T: 2.4°C (1.4°C to 3.8°C), A2: +3.4°C (2.0°C to 5.4°C) and A1FI: +4.0°C (2.4°C to 6.4°C). It is not appropriate to compare the lowest and highest values across these ranges against the single range given in the TAR, because the TAR range resulted only from projections using an SCM and covered all SRES scenarios, whereas here a number of different and independent modelling approaches are combined to estimate ranges for the six illustrative scenarios separately. Additionally, in contrast to the TAR, carbon cycle uncertainties are now included in these ranges. These uncertainty ranges include only anthropogenically forced changes.

Geographical patterns of projected SAT warming show greatest temperature increases over land (roughly twice the global average temperature increase) and at high northern latitudes, and less warming over the southern oceans and North Atlantic, consistent with observations during the latter part of the 20th century (see Chapter 3). The pattern of zonal mean warming in the atmosphere, with a maximum in the upper tropical troposphere and cooling throughout the stratosphere, is notable already early in the 21st century, while zonal mean warming in the ocean progresses from near the surface and in the northern mid-latitudes early in the 21st century, to gradual penetration downward during the course of the 21st century.

An expert assessment based on the combination of available constraints from observations (assessed in Chapter 9) and the strength of known feedbacks simulated in the models used to produce the climate change projections in this chapter indicates that the equilibrium global mean SAT warming for a doubling of atmospheric carbon dioxide (CO_2), or 'equilibrium climate sensitivity', is *likely* to lie in the range 2°C to 4.5°C, with a most likely value of about 3°C. Equilibrium climate sensitivity is *very likely* larger than 1.5°C. For fundamental physical reasons, as well as data limitations, values substantially higher than 4.5°C still cannot be excluded, but agreement with observations and proxy data is generally worse for those high values than for values in the 2°C to 4.5°C range. The 'transient climate response' (TCR, defined as the globally averaged SAT change at the time of CO_2 doubling in the 1% yr^{-1} transient CO_2 increase experiment) is better constrained than equilibrium climate sensitivity. The TCR is *very likely* larger than 1°C and *very unlikely* greater than 3°C based on climate models, in agreement with constraints from the observed surface warming.

Temperature Extremes

It is *very likely* that heat waves will be more intense, more frequent and longer lasting in a future warmer climate. Cold episodes are projected to decrease significantly in a future warmer climate. Almost everywhere, daily minimum temperatures are projected to increase faster than daily maximum temperatures, leading to a decrease in diurnal temperature range. Decreases in frost days are projected to occur almost everywhere in the middle and high latitudes, with a comparable increase in growing season length.

Mean Precipitation

For a future warmer climate, the current generation of models indicates that precipitation generally increases in the areas of regional tropical precipitation maxima (such as the monsoon regimes) and over the tropical Pacific in particular, with general decreases in the subtropics, and increases at high latitudes as a consequence of a general intensification of the global hydrological cycle. Globally averaged mean water vapour, evaporation and precipitation are projected to increase.

Precipitation Extremes and Droughts

Intensity of precipitation events is projected to increase, particularly in tropical and high latitude areas that experience increases in mean precipitation. Even in areas where mean precipitation decreases (most subtropical and mid-latitude regions), precipitation intensity is projected to increase but there would be longer periods between rainfall events. There is a tendency for drying of the mid-continental areas during summer, indicating a greater risk of droughts in those regions. Precipitation extremes increase more than does the mean in most tropical and mid- and high-latitude areas.

Snow and Ice

As the climate warms, snow cover and sea ice extent decrease; glaciers and ice caps lose mass owing to a dominance of summer melting over winter precipitation increases. This contributes to sea level rise as documented for the previous generation of models in the TAR. There is a projected reduction of sea ice in the 21st century in both the Arctic and Antarctic with a rather large range of model responses. The projected reduction is accelerated in the Arctic, where some models project summer sea ice cover to disappear entirely in the high-emission A2 scenario in the latter part of the 21st century. Widespread increases in thaw depth over much of the permafrost regions are projected to occur in response to warming over the next century.

Carbon Cycle

There is unanimous agreement among the coupled climate-carbon cycle models driven by emission scenarios run so far that future climate change would reduce the efficiency of the Earth system (land and ocean) to absorb anthropogenic CO_2. As a result, an increasingly large fraction of anthropogenic CO_2 would stay airborne in the atmosphere under a warmer climate. For the A2 emission scenario, this positive feedback leads to additional atmospheric CO_2 concentration varying between 20 and 220 ppm among the models by 2100. Atmospheric CO_2 concentrations simulated by these coupled climate-carbon cycle models range between 730 and 1,020 ppm by 2100. Comparing these values with the standard value of 836 ppm (calculated beforehand by the Bern carbon cycle-climate model without an interactive carbon cycle) provides an indication of the uncertainty in global warming due to future changes in the carbon cycle. In the context of atmospheric CO_2 concentration stabilisation scenarios, the positive climate-carbon cycle feedback reduces the land and ocean uptake of CO_2, implying that it leads to a reduction of the compatible emissions required to achieve a given atmospheric CO_2 stabilisation. The higher the stabilisation scenario, the larger the climate change, the larger the impact on the carbon cycle, and hence the larger the required emission reduction.

Ocean Acidification

Increasing atmospheric CO_2 concentrations lead directly to increasing acidification of the surface ocean. Multi-model projections based on SRES scenarios give reductions in pH of between 0.14 and 0.35 units in the 21st century, adding to the present decrease of 0.1 units from pre-industrial times. Southern Ocean surface waters are projected to exhibit undersaturation with regard to calcium carbonate for CO_2 concentrations higher than 600 ppm, a level exceeded during the second half of the century in most of the SRES scenarios. Low-latitude regions and the deep ocean will be affected as well. Ocean acidification would lead to dissolution of shallow-water carbonate sediments and could affect marine calcifying organisms. However, the net effect on the biological cycling of carbon in the oceans is not well understood.

Sea Level

Sea level is projected to rise between the present (1980–1999) and the end of this century (2090–2099) under the SRES B1 scenario by 0.18 to 0.38 m, B2 by 0.20 to 0.43 m, A1B by 0.21 to 0.48 m, A1T by 0.20 to 0.45 m, A2 by 0.23 to 0.51 m, and A1FI by 0.26 to 0.59 m. These are 5 to 95% ranges based on the spread of AOGCM results, not including uncertainty in carbon cycle feedbacks. For each scenario, the midpoint of the range is within 10% of the TAR model average for 2090-2099. The ranges are narrower than in the TAR mainly because of improved information about some uncertainties in the projected contributions. In all scenarios, the average rate of rise during

the 21st century *very likely* exceeds the 1961 to 2003 average rate (1.8 ± 0.5 mm yr^{-1}). During 2090 to 2099 under A1B, the central estimate of the rate of rise is 3.8 mm yr^{-1}. For an average model, the scenario spread in sea level rise is only 0.02 m by the middle of the century, and by the end of the century it is 0.15 m.

Thermal expansion is the largest component, contributing 70 to 75% of the central estimate in these projections for all scenarios. Glaciers, ice caps and the Greenland Ice Sheet are also projected to contribute positively to sea level. General Circulation Models indicate that the Antarctic Ice Sheet will receive increased snowfall without experiencing substantial surface melting, thus gaining mass and contributing negatively to sea level. Further accelerations in ice flow of the kind recently observed in some Greenland outlet glaciers and West Antarctic ice streams could substantially increase the contribution from the ice sheets. For example, if ice discharge from these processes were to scale up in future in proportion to global average surface temperature change (taken as a measure of global climate change), it would add 0.1 to 0.2 m to the upper bound of sea level rise by 2090 to 2099. In this example, during 2090 to 2099 the rate of scaled-up Antarctic discharge would roughly balance the expected increased rate of Antarctic accumulation, being under A1B a factor of 5 to 10 greater than in recent years. Understanding of these effects is too limited to assess their likelihood or to give a best estimate.

Sea level rise during the 21st century is projected to have substantial geographical variability. The model median spatial standard deviation is 0.08 m under A1B. The patterns from different models are not generally similar in detail, but have some common features, including smaller than average sea level rise in the Southern Ocean, larger than average in the Arctic, and a narrow band of pronounced sea level rise stretching across the southern Atlantic and Indian Oceans.

Mean Tropical Pacific Climate Change

Multi-model averages show a weak shift towards average background conditions which may be described as 'El Niño-like', with sea surface temperatures in the central and east equatorial Pacific warming more than those in the west, weakened tropical circulations and an eastward shift in mean precipitation.

El Niño

All models show continued El Niño-Southern Oscillation (ENSO) interannual variability in the future no matter what the change in average background conditions, but changes in ENSO interannual variability differ from model to model. Based on various assessments of the current multi-model data set, in which present-day El Niño events are now much better simulated than in the TAR, there is no consistent indication at this time of discernible changes in projected ENSO amplitude or frequency in the 21st century.

Monsoons

An increase in precipitation is projected in the Asian monsoon (along with an increase in interannual season-averaged precipitation variability) and the southern part of the west African monsoon with some decrease in the Sahel in northern summer, as well as an increase in the Australian monsoon in southern summer in a warmer climate. The monsoonal precipitation in Mexico and Central America is projected to decrease in association with increasing precipitation over the eastern equatorial Pacific through Walker Circulation and local Hadley Circulation changes. However, the uncertain role of aerosols in general, and carbon aerosols in particular, complicates the nature of future projections of monsoon precipitation, particularly in the Asian monsoon.

Sea Level Pressure

Sea level pressure is projected to increase over the subtropics and mid-latitudes, and decrease over high latitudes (order several millibars by the end of the 21st century) associated with a poleward expansion and weakening of the Hadley Circulation and a poleward shift of the storm tracks of several degrees latitude with a consequent increase in cyclonic circulation patterns over the high-latitude arctic and antarctic regions. Thus, there is a projected positive trend of the Northern Annular Mode (NAM) and the closely related North Atlantic Oscillation (NAO) as well as the Southern Annular Mode (SAM). There is considerable spread among the models for the NAO, but the magnitude of the increase for the SAM is generally more consistent across models.

Tropical Cyclones (Hurricanes and Typhoons)

Results from embedded high-resolution models and global models, ranging in grid spacing from 100 km to 9 km, project a *likely* increase of peak wind intensities and notably, where analysed, increased near-storm precipitation in future tropical cyclones. Most recent published modelling studies investigating tropical storm frequency simulate a decrease in the overall number of storms, though there is less confidence in these projections and in the projected decrease of relatively weak storms in most basins, with an increase in the numbers of the most intense tropical cyclones.

Mid-latitude Storms

Model projections show fewer mid-latitude storms averaged over each hemisphere, associated with the poleward shift of the storm tracks that is particularly notable in the Southern Hemisphere, with lower central pressures for these poleward-shifted storms. The increased wind speeds result in more extreme wave heights in those regions.

Atlantic Ocean Meridional Overturning Circulation

Based on current simulations, it is *very likely* that the Atlantic Ocean Meridional Overturning Circulation (MOC) will slow down during the course of the 21st century. A multi-model ensemble shows an average reduction of 25% with a broad range from virtually no change to a reduction of over 50% averaged over 2080 to 2099. In spite of a slowdown of the MOC in most models, there is still warming of surface temperatures around the North Atlantic Ocean and Europe due to the much larger radiative effects of the increase in greenhouse gases. Although the MOC weakens in most model runs for the three SRES scenarios, none shows a collapse of the MOC by the year 2100 for the scenarios considered. No coupled model simulation of the Atlantic MOC shows a mean increase in the MOC in response to global warming by 2100. It is *very unlikely* that the MOC will undergo a large abrupt transition during the course of the 21st century. At this stage, it is too early to assess the likelihood of a large abrupt change of the MOC beyond the end of the 21st century. In experiments with the low (B1) and medium (A1B) scenarios, and for which the atmospheric greenhouse gas concentrations are stabilised beyond 2100, the MOC recovers from initial weakening within one to several centuries after 2100 in some of the models. In other models the reduction persists.

Radiative Forcing

The radiative forcings by long-lived greenhouse gases computed with the radiative transfer codes in twenty of the AOGCMs used in the Fourth Assessment Report have been compared against results from benchmark line-by-line (LBL) models. The mean AOGCM forcing over the period 1860 to 2000 agrees with the mean LBL value to within 0.1 W m^{-2} at the tropopause. However, there is a range of 25% in longwave forcing due to doubling atmospheric CO_2 from its concentration in 1860 across the ensemble of AOGCM codes. There is a 47% relative range in longwave forcing in 2100 contributed by all greenhouse gases in the A1B scenario across the ensemble of AOGCM simulations. These results imply that the ranges in climate sensitivity and climate response from models discussed in this chapter may be due in part to differences in the formulation and treatment of radiative processes among the AOGCMs.

Climate Change Commitment (Temperature and Sea Level)

Results from the AOGCM multi-model climate change commitment experiments (concentrations stabilised for 100 years at year 2000 for 20th-century commitment, and at 2100 values for B1 and A1B commitment) indicate that if greenhouse gases were stabilised, then a further warming of 0.5°C would occur. This should not be confused with 'unavoidable climate change' over the next half century, which would be greater because forcing cannot be instantly stabilised. In the very long term, it is plausible that climate change could be less than in a commitment run since forcing could be reduced below current levels. Most of this warming occurs in the first several decades after stabilisation; afterwards the rate of increase steadily declines. The globally averaged precipitation commitment 100 years after stabilising greenhouse gas concentrations amounts to roughly an additional increase of 1 to 2% compared to the precipitation values at the time of stabilisation.

If concentrations were stabilised at A1B levels in 2100, sea level rise due to thermal expansion in the 22nd century would be similar to that in the 21st, and would amount to 0.3 to 0.8 m (relative to 1980 to 1999) above present by 2300. The ranges of thermal expansion overlap substantially for stabilisation at different levels, since model uncertainty is dominant; A1B is given here because most model results are available for that scenario. Thermal expansion would continue over many centuries at a gradually decreasing rate, reaching an eventual level of 0.2 to 0.6 m per °C of global warming relative to present. Under sustained elevated temperatures, some glacier volume may persist at high altitudes, but most could disappear over centuries.

If greenhouse gas concentrations could be reduced, global temperatures would begin to decrease within a decade, although sea level would continue to rise due to thermal expansion for at least another century. Earth System Models of Intermediate Complexity with coupled carbon cycle model components show that for a reduction to zero emissions at year 2100 the climate would take of the order of 1 kyr to stabilise. At year 3000, the model range for temperature increase is 1.1°C to 3.7°C and for sea level rise due to thermal expansion is 0.23 to 1.05 m. Hence, they are projected to remain well above their pre-industrial values.

The Greenland Ice Sheet is projected to contribute to sea level after 2100, initially at a rate of 0.03 to 0.21 m per century for stabilisation in 2100 at A1B concentrations. The contribution would be greater if dynamical processes omitted from current models increased the rate of ice flow, as has been observed in recent years. Except for remnant glaciers in the mountains, the Greenland Ice Sheet would largely be eliminated, raising sea level by about 7 m, if a sufficiently warm climate were maintained for millennia; it would happen more rapidly if ice flow accelerated. Models suggest that the global warming required lies in the range 1.9°C to 4.6°C relative to the pre-industrial temperature. Even if temperatures were to decrease later, it is possible that the reduction of the ice sheet to a much smaller extent would be irreversible.

The Antarctic Ice Sheet is projected to remain too cold for widespread surface melting, and to receive increased snowfall, leading to a gain of ice. Loss of ice from the ice sheet could occur through increased ice discharge into the ocean following weakening of ice shelves by melting at the base or on the surface. In current models, the net projected contribution to sea level rise is negative for coming centuries, but it is possible that acceleration of ice discharge could become dominant, causing a net positive contribution. Owing to limited understanding of the relevant ice flow processes, there is presently no consensus on the long-term future of the ice sheet or its contribution to sea level rise.

10.1 Introduction

Since the Third Assessment Report (TAR), the scientific community has undertaken the largest coordinated global coupled climate model experiment ever attempted in order to provide the most comprehensive multi-model perspective on climate change of any IPCC assessment, the World Climate Research Programme (WCRP) Coupled Model Intercomparison Project phase three (CMIP3), also referred to generically throughout this report as the 'multi-model data set' (MMD) archived at the Program for Climate Model Diagnosis and Intercomparison (PCMDI). This open process involves experiments with idealised climate change scenarios (i.e., 1% yr^{-1} carbon dioxide (CO_2) increase, also included in the earlier WCRP model intercomparison projects CMIP2 and CMIP2+ (e.g., Covey et al., 2003; Meehl et al., 2005b), equilibrium 2 × CO_2 experiments with atmospheric models coupled to non-dynamic slab oceans, and idealised stabilised climate change experiments at 2 × CO_2 and 4 × atmospheric CO_2 levels in the 1% yr^{-1} CO_2 increase simulations).

In the idealised 1% yr^{-1} CO_2 increase experiments, there is no actual real year time line. Thus, the rate of climate change is not the issue in these experiments, but what is studied are the types of climate changes that occur at the time of doubling or quadrupling of atmospheric CO_2 and the range of, and difference in, model responses. Simulations of 20th-century climate have been completed that include temporally evolving natural and anthropogenic forcings. For projected climate change in the 21st century, a subset of three IPCC Special Report on Emission Scenarios (SRES; Nakićenović and Swart, 2000) scenario simulations have been selected from the six commonly used marker scenarios. With respect to emissions, this subset (B1, A1B and A2) consists of a 'low', 'medium' and 'high' scenario among the marker scenarios, and this choice is solely made by the constraints of available computer resources that did not allow for the calculation of all six scenarios. This choice, therefore, does not imply a qualification of, or preference over, the six marker scenarios. In addition, it is not within the scope of the Working Group I contribution to the Fourth Assessment Report (AR4) to assess the plausibility or likelihood of emission scenarios.

In addition to these non-mitigation scenarios, a series of idealised model projections is presented, each of which implies some form and level of intervention: (i) stabilisation scenarios in which greenhouse gas concentrations are stabilised at various levels, (ii) constant composition commitment scenarios in which greenhouse gas concentrations are fixed at year 2000 levels, (iii) zero emission commitment scenarios in which emissions are set to zero in the year 2100 and (iv) overshoot scenarios in which greenhouse gas concentrations are reduced after year 2150.

The simulations with the subset A1B, B1 and A2 were performed to the year 2100. Three different stabilisation scenarios were run, the first with all atmospheric constituents fixed at year 2000 values and the models run for an additional 100 years, and the second and third with constituents fixed at year 2100 values for A1B and B1, respectively, for another 100 to 200 years. Consequently, the concept of climate change commitment (for details and definitions see Section 10.7) is addressed in much wider scope and greater detail than in any previous IPCC assessment. Results based on this Atmosphere-Ocean General Circulation Model (AOGCM) multi-model data set are featured in Section 10.3.

Uncertainty in climate change projections has always been a subject of previous IPCC assessments, and a substantial amount of new work is assessed in this chapter. Uncertainty arises in various steps towards a climate projection (Figure 10.1). For

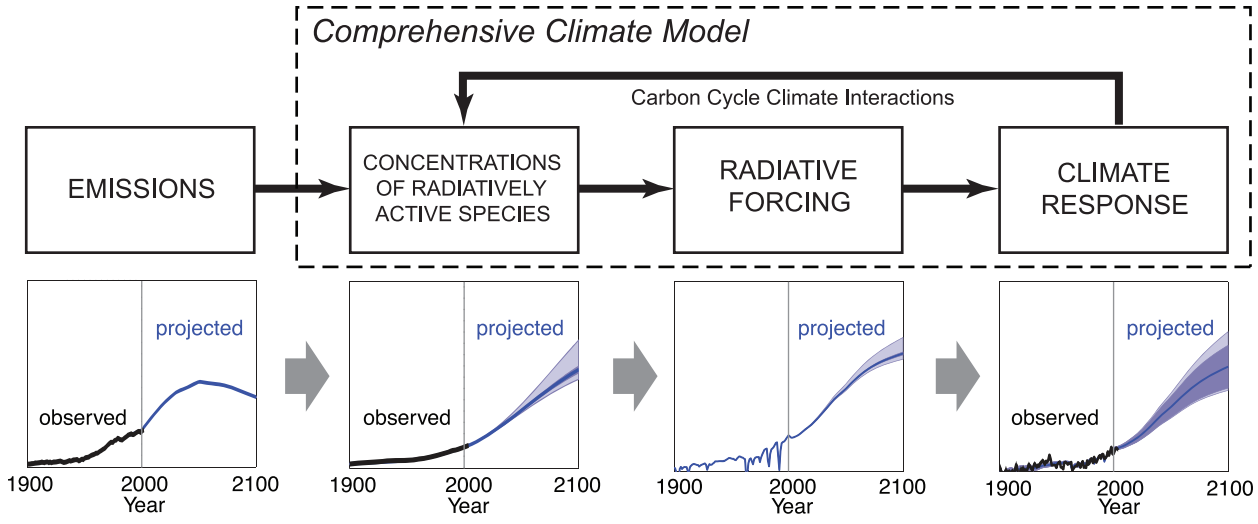


Figure 10.1. *Several steps from emissions to climate response contribute to the overall uncertainty of a climate model projection. These uncertainties can be quantified through a combined effort of observation, process understanding, a hierarchy of climate models, and ensemble simulations. In a comprehensive climate model, physical and chemical representations of processes permit a consistent quantification of uncertainty. Note that the uncertainty associated with the future emission path is of an entirely different nature and not addressed in Chapter 10. Bottom row adapted from Figure 10.26, A1B scenario, for illustration only.*

a given emissions scenario, various biogeochemical models are used to calculate concentrations of constituents in the atmosphere. Various radiation schemes and parametrizations are required to convert these concentrations to radiative forcing. Finally, the response of the different climate system components (atmosphere, ocean, sea ice, land surface, chemical status of atmosphere and ocean, etc.) is calculated in a comprehensive climate model. In addition, the formulation of, and interaction with, the carbon cycle in climate models introduces important feedbacks which produce additional uncertainties. In a comprehensive climate model, physical and chemical representations of processes permit a consistent quantification of uncertainty. Note that the uncertainties associated with the future emission path are of an entirely different nature and not considered in this chapter.

Many of the figures in Chapter 10 are based on the mean and spread of the multi-model ensemble of comprehensive AOGCMs. The reason to focus on the multi-model mean is that averages across structurally different models empirically show better large-scale agreement with observations, because individual model biases tend to cancel (see Chapter 8). The expanded use of multi-model ensembles of projections of future climate change therefore provides higher quality and more quantitative climate change information compared to the TAR. Even though the ability to simulate present-day mean climate and variability, as well as observed trends, differs across models, no weighting of individual models is applied in calculating the mean. Since the ensemble is strictly an 'ensemble of opportunity', without sampling protocol, the spread of models does not necessarily span the full possible range of uncertainty, and a statistical interpretation of the model spread is therefore problematic. However, attempts are made to quantify uncertainty throughout the chapter based on various other lines of evidence, including perturbed physics ensembles specifically designed to study uncertainty within one model framework, and Bayesian methods using observational constraints.

In addition to this coordinated international multi-model experiment, a number of entirely new types of experiments have been performed since the TAR to quantify uncertainty regarding climate model response to external forcings. The extent to which uncertainties in parametrizations translate into the uncertainty in climate change projections is addressed in much greater detail. New calculations of future climate change from the larger suite of SRES scenarios with simple models and Earth System Models of Intermediate Complexity (EMICs) provide additional information regarding uncertainty related to the choice of scenario. Such models also provide estimates of long-term evolution of global mean temperature, ocean heat uptake and sea level rise due to thermal expansion beyond the 21st century, and thus allow climate change commitments to be better constrained.

Climate sensitivity has always been a focus in the IPCC assessments, and this chapter assesses more quantitative estimates of equilibrium climate sensitivity and transient climate response (TCR) in terms of not only ranges but also probabilities within these ranges. Some of these probabilities are now derived from ensemble simulations subject to various observational constraints, and no longer rely solely on expert judgement. This permits a much more complete assessment of model response uncertainties from these sources than ever before. These are now standard benchmark calculations with the global coupled climate models, and are useful to assess model response in the subsequent time-evolving climate change scenario experiments.

With regard to these time-evolving experiments simulating 21st-century climate, since the TAR increased computing capabilities now allow routine performance of multi-member ensembles in climate change scenario experiments with global coupled climate models. This provides the capability to analyse more multi-model results and multi-member ensembles, and yields more probabilistic estimates of time-evolving climate change in the 21st century.

Finally, while future changes in some weather and climate extremes (e.g., heat waves) were addressed in the TAR, there were relatively few studies on this topic available for assessment at that time. Since then, more analyses have been performed regarding possible future changes in a variety of extremes. It is now possible to assess, for the first time, multi-model ensemble results for certain types of extreme events (e.g., heat waves, frost days, etc.). These new studies provide a more complete range of results for assessment regarding possible future changes in these important phenomena with their notable impacts on human societies and ecosystems. A synthesis of results from studies of extremes from observations and model is provided in Chapter 11.

The use of multi-model ensembles has been shown in other modelling applications to produce simulated climate features that are improved over single models alone (see discussion in Chapters 8 and 9). In addition, a hierarchy of models ranging from simple to intermediate to complex allows better quantification of the consequences of various parametrizations and formulations. Very large ensembles (order hundreds) with single models provide the means to quantify parametrization uncertainty. Finally, observed climate characteristics are now being used to better constrain future climate model projections.

10.2 Projected Changes in Emissions, Concentrations and Radiative Forcing

The global projections discussed in this chapter are extensions of the simulations of the observational record discussed in Chapter 9. The simulations of the 19th and 20th centuries are based upon changes in long-lived greenhouse gases (LLGHGs) that are reasonably constrained by the observational record. Therefore, the models have qualitatively similar temporal evolutions of their radiative forcing time histories for LLGHGs (e.g., see Figure 2.23). However, estimates of future concentrations of LLGHGs and other radiatively active species are clearly subject to significant uncertainties. The evolution of these species is governed by a variety of factors that are difficult to predict, including changes in population, energy use, energy sources and emissions. For these reasons, a range of projections of future climate change has been conducted using coupled AOGCMs. The future concentrations of LLGHGs and the anthropogenic emissions of sulphur dioxide (SO_2), a chemical precursor of sulphate aerosol, are obtained from several scenarios considered representative of low, medium and high emission trajectories. These basic scenarios and other forcing agents incorporated in the AOGCM projections, including several types of natural and anthropogenic aerosols, are discussed in Section 10.2.1. Developments in projecting radiatively active species and radiative forcing for the early 21st century are considered in Section 10.2.2.

10.2.1 Emissions Scenarios and Radiative Forcing in the Multi-Model Climate Projections

The temporal evolution of the LLGHGs, aerosols and other forcing agents are described in Sections 10.2.1.1 and 10.2.1.2. Typically, the future projections are based upon initial conditions extracted from the end of the simulations of the 20th century. Therefore, the radiative forcing at the beginning of the model projections should be approximately equal to the radiative forcing for present-day concentrations relative to pre-industrial conditions. The relationship between the modelled radiative forcing for the year 2000 and the estimates derived in Chapter 2 is evaluated in Section 10.2.1.3. Estimates of the radiative forcing in the multi-model integrations for one of the standard scenarios are also presented in this section. Possible explanations for the range of radiative forcings projected for 2100 are discussed in Section 10.2.1.4, including evidence for systematic errors in the formulations of radiative transfer used in AOGCMs. Possible implications of these findings for the range of global temperature change and other climate responses are summarised in Section 10.2.1.5.

10.2.1.1 The Special Report on Emission Scenarios and Constant-Concentration Commitment Scenarios

The future projections discussed in this chapter are based upon the standard A2, A1B and B2 SRES scenarios (Nakićenović and Swart, 2000). The emissions of CO_2, methane (CH_4) and SO_2, the concentrations of CO_2, CH_4 and nitrous oxide (N_2O) and the total radiative forcing for the SRES scenarios are illustrated in Figure 10.26 and summarised for the A1B scenario in Figure 10.1. The models have been integrated to year 2100 using the projected concentrations of LLGHGs and emissions of SO_2 specified by the A1B, B1 and A2 emissions scenarios. Some of the AOGCMs do not include sulphur chemistry, and the simulations from these models are based upon concentrations of sulphate aerosols from Boucher and Pham (2002; see Section 10.2.1.2). The simulations for the three scenarios were continued for another 100 to 200 years with all anthropogenic forcing agents held fixed at values applicable to the year 2100. There is also a new constant-concentration commitment scenario that assumes concentrations are held fixed at year 2000 levels (Section 10.7.1). In this idealised scenario, models are initialised from the end of the simulations for the 20th century, the concentrations of radiatively active species are held constant at year 2000 values from these simulations, and the models are integrated to 2100.

For comparison with this constant composition case, it is useful to note that constant emissions would lead to much larger radiative forcing. For example, constant CO_2 emissions at year 2000 values would lead to concentrations reaching about 520 ppm by 2100, close to the B1 case (Friedlingstein and Solomon, 2005; Hare and Munschausen, 2006; see also FAQ 10.3).

10.2.1.2 Forcing by Additional Species and Mechanisms

The forcing agents applied to each AOGCM used to make climate projections are summarised in Table 10.1. The radiatively active species specified by the SRES scenarios are CO_2, CH_4, N_2O, chlorofluorocarbons (CFCs) and SO_2, which is listed in its aerosol form as sulphate (SO_4) in the table. The inclusion, magnitude and temporal evolution of the remaining forcing agents listed in Table 10.1 were left to the discretion of the individual modelling groups. These agents include tropospheric and stratospheric ozone, all of the non-sulphate aerosols, the indirect effects of aerosols on cloud albedo and lifetime, the effects of land use and solar variability.

The scope of the treatments of aerosol effects in AOGCMs has increased markedly since the TAR. Seven of the AOGCMs include the first indirect effects and five include the second indirect effects of aerosols on cloud properties (Section 2.4.5). Under the more emissions-intensive scenarios considered in this chapter, the magnitude of the first indirect (Twomey) effect can saturate. Johns et al. (2003) parametrize the first indirect effect of anthropogenic sulphur (S) emissions as perturbations to the effective radii of cloud drops in simulations of the B1, B2, A2 and A1FI scenarios using UKMO-HadCM3. At 2100, the first indirect forcing ranges from –0.50 to

Table 10.1. *Radiative forcing agents in the multi-model global climate projections. See Table 8.1 for descriptions of the models. Entries mean Y: forcing agent is included; C: forcing agent varies with time during the 20th Century Climate in Coupled Models (20C3M) simulations and is set to constant or annually cyclic distribution for scenario integrations; E: forcing agent represented using equivalent CO_2; and n.a.: forcing agent is not specified in either the 20th-century or scenario integrations. Numeric codes indicate that the forcing agent is included using data described at 1: http://www.cnrm.meteo.fr/ensembles/public/results/results.html; 2: Boucher and Pham (2002); 3: Yukimoto et al. (2006); 4: Meehl, et al., 2006b; 5: http://aom.giss.nasa.gov/IN/GHGA1B.LP; and 6: http://sres.ciesin.org/final_data.html.*

Model	Forcing Agents																	
	Greenhouse Gases						Aerosols										Other	
	CO_2	CH_4	N_2O	Stratospheric Ozone	Tropospheric Ozone	CFCs	SO_4	Urban	Black carbon	Organic carbon	Nitrate	1st Indirect	2nd Indirect	Dust	Volcanic	Sea Salt	Land Use	Solar
BCC-CM1	Y	Y	Y	Y	C	4	4	n.a.	n.a.	n.a.	n.a.	n.a.	n.a.	n.a.	C	n.a.	C	C
BCCR-BCM2.0	1	1	1	C	C	1	2	C	n.a.	n.a.	n.a.	n.a.	n.a.	C	n.a.	C	C	C
CCSM3	4	4	4	4	4	4	4	n.a.	4	4	n.a.	n.a.	n.a.	Y	C	Y	n.a.	C
CGCM3.1(T47)	Y	Y	Y	C	C	Y	2	n.a.	n.a.	n.a.	n.a.	n.a.	n.a.	C	C	C	C	C
CGCM3.1(T63)	Y	Y	Y	C	C	Y	2	n.a.	n.a.	n.a.	n.a.	n.a.	n.a.	C	C	C	C	C
CNRM-CM3	1	1	1	Y	Y	1	2	C	n.a.	n.a.	n.a.	n.a.	n.a.	C	n.a.	C	n.a.	n.a.
CSIRO-MK3.0	Y	E	E	Y	Y	E	Y	n.a.	n.a.	n.a.	n.a.	n.a.	n.a.	n.a.	n.a.	n.a.	n.a.	n.a.
ECHAM5/MPI-OM	1	1	1	Y	C	1	2	n.a.	n.a.	n.a.	n.a.	Y	n.a.	n.a.	n.a.	n.a.	n.a.	n.a.
ECHO-G	1	1	1	C	Y	1	6	n.a.	n.a.	n.a.	n.a.	Y	n.a.	n.a.	C	n.a.	n.a.	C
FGOALS-g1.0	4	4	4	C	C	4	4	n.a.	n.a.	n.a.	n.a.	n.a.	n.a.	n.a.	n.a.	n.a.	n.a.	C
GFDL-CM2.0	Y	Y	Y	Y	Y	Y	Y	n.a.	Y	Y	n.a.	n.a.	n.a.	C	C	C	C	C
GFDL-CM2.1	Y	Y	Y	Y	Y	Y	Y	n.a.	Y	Y	n.a.	n.a.	n.a.	C	C	C	C	C
GISS-AOM	5	5	5	C	C	5	2	n.a.	n.a.	n.a.	n.a.	n.a.	n.a.	n.a.	n.a.	Y	n.a.	n.a.
GISS-EH	Y	Y	Y	Y	Y	Y	Y	n.a.	Y	Y	Y	n.a.	Y	C	Y	C	Y	Y
GISS-ER	Y	Y	Y	Y	Y	Y	Y	n.a.	Y	Y	Y	n.a.	Y	C	Y	C	Y	Y
INM-CM3.0	4	4	4	C	C	n.a.	4	n.a.	n.a.	n.a.	n.a.	n.a.	n.a.	n.a.	C	n.a.	n.a.	C
IPSL-CM4	1	1	1	n.a.	n.a.	1	2	n.a.	n.a.	n.a.	n.a.	Y	n.a.	n.a.	n.a.	n.a.	n.a.	n.a.
MIROC3.2(H)	Y	Y	Y	Y	Y	Y	Y	n.a.	Y	Y	n.a.	Y	Y	Y	C	Y	C	C
MIROC3.2(M)	Y	Y	Y	Y	Y	Y	Y	n.a.	Y	Y	n.a.	Y	Y	Y	C	Y	C	C
MRI-CGCM2.3.2	3	3	3	C	C	3	3	n.a.	n.a.	n.a.	n.a.	n.a.	n.a.	n.a.	C	n.a.	n.a.	C
PCM	Y	Y	Y	Y	Y	Y	Y	n.a.	n.a.	n.a.	n.a.	n.a.	n.a.	n.a.	C	n.a.	n.a.	C
UKMO-HadCM3	Y	Y	Y	Y	Y	Y	Y	n.a.	n.a.	n.a.	n.a.	Y	n.a.	n.a.	C	n.a.	n.a.	C
UKMO-HadGEM1	Y	Y	Y	Y	Y	Y	Y	n.a.	Y	Y	n.a.	Y	Y	n.a.	C	Y	Y	C

–0.79 W m^{-2}. The normalised indirect forcing (the ratio of the forcing (W m^{-2}) to the mass burden of a species (mg m^{-2}), leaving units of W mg^{-1}) decreases by a factor of four, from approximately –7 W mgS^{-1} in 1860 to between –1 and –2 W mgS^{-1} by the year 2100. Boucher and Pham (2002) and Pham et al. (2005) find a comparable projected decrease in forcing efficiency of the indirect effect, from –9.6 W mgS^{-1} in 1860 to between –2.1 and –4.4 W mgS^{-1} in 2100. Johns et al. (2003) and Pham et al. (2005) attribute the projected decline to the decreased sensitivity of clouds to greater sulphate concentrations at sufficiently large aerosol burdens.

10.2.1.3 Comparison of Modelled Forcings to Estimates in Chapter 2

The forcings used to generate climate projections for the standard SRES scenarios are not necessarily uniform across the multi-model ensemble. Differences among models may be caused by different projections for radiatively active species (see Section 10.2.1.2) and by differences in the formulation of radiative transfer (see Section 10.2.1.4). The AOGCMs in the ensemble include many species that are not specified or constrained by the SRES scenarios, including ozone, tropospheric non-sulphate aerosols, and stratospheric volcanic aerosols. Other types of forcing that vary across the ensemble include solar variability, the indirect effects of aerosols on clouds and the effects of land use change on land surface albedo and other land surface properties (Table 10.1). While the time series of LLGHGs for the future scenarios are mostly identical across the ensemble, the concentrations of these gases in the 19th and early 20th centuries were left to the discretion of individual modelling groups. The differences in radiatively active species and the formulation of radiative transfer affect both the 19th- and 20th-century simulations and the scenario integrations initiated from these historical simulations. The resulting differences in the forcing complicate the separation of forcing and response across the multi-model ensemble. These differences can be quantified by comparing the range of shortwave and longwave forcings across the multi-model ensemble against standard estimates of radiative forcing over the historical record. Shortwave and longwave forcing refer to modifications of the solar and infrared atmospheric radiation fluxes, respectively, that are caused by external changes to the climate system (Section 2.2).

The longwave radiative forcings for the SRES A1B scenario from climate model simulations are compared against estimates using the TAR formulae (see Chapter 2) in Figure 10.2a. The graph shows the longwave forcings from the TAR and 20 AOGCMs in the multi-model ensemble from 2000 to 2100. The forcings from the models are diagnosed from changes in top-of-atmosphere fluxes and the forcing for doubled atmospheric CO_2 (Forster and Taylor, 2006). The TAR and median model estimates of the longwave forcing are in very good agreement over the 21st century, with differences ranging from –0.37 to +0.06 W m^{-2}. For the year 2000, the global mean values from the TAR and median model differ by only –0.13 W m^{-2}. However, the 5th to 95th percentile range of the models for the period 2080 to 2099 is approximately 3.1 W m^{-2}, or approximately 47% of the median longwave forcing for that time period.

The corresponding time series of shortwave forcings for the SRES A1B scenario are plotted in Figure 10.2b. It is evident that the relative differences among the models and between the models and the TAR estimates are larger for the shortwave band. The TAR value is larger than the median model forcing by 0.2 to 0.3 W m^{-2} for individual 20-year segments of the integrations. For the year 2000, the TAR estimate is larger by 0.42 W m^{-2}. In addition, the range of modelled forcings is sufficiently large that it includes positive and negative values

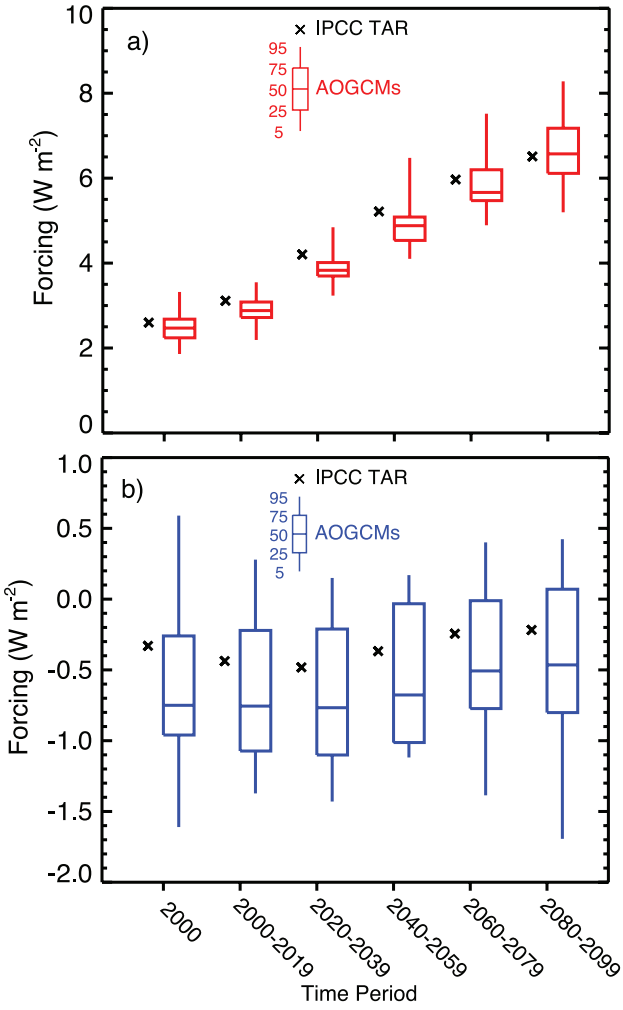


Figure 10.2. *Radiative forcings for the period 2000 to 2100 for the SRES A1B scenario diagnosed from AOGCMs and from the TAR (IPCC, 2001) forcing formulas (Forster and Taylor, 2006). (a) Longwave forcing; (b) shortwave forcing. The AOGCM results are plotted with box-and-whisker diagrams representing percentiles of forcings computed from 20 models in the AR4 multi-model ensemble. The central line within each box represents the median value of the model ensemble. The top and bottom of each box shows the 75th and 25th percentiles, and the top and bottom of each whisker displays the 95th and 5th percentile values in the ensemble, respectively. The models included are CCSM3, CGCM3.1 (T47 and T63), CNRM-CM3, CSIRO-MK3, ECHAM5/MPI-OM, ECHO-G, FGOALS-g1.0, GFDL-CM2.0, GFDL-CM2.1, GISS-EH, GISS-ER, INM-CM3.0, IPSL-CM4, MIROC3.2 (medium and high resolution), MRI-CGCM2.3.2, PCM1, UKMO-HadCM3 and UKMO-HadGEM1 (see Table 8.1 for model details).*

Table 10.2. *All-sky radiative forcing for doubled atmospheric CO_2. See Table 8.1 for model details.*

Model[Source]	Longwave (W m^{-2})	Shortwave (W m^{-2})
CGCM 3.1 (T47/T63)[a]	3.39	–0.07
CSIRO-MK3.0[b]	3.42	0.05
GISS-EH/ER[a]	4.21	–0.15
GFDL-CM2.0/2.1[b]	3.62	–0.12
IPSL-CM4[c]	3.50	–0.02
MIROC 3.2-hires[d]	3.06	0.08
MIROC 3.2-medres[d]	2.99	0.10
ECHAM5/MPI-OM[a]	3.98	0.03
MRI-CGCM2.3.2[b]	3.75	–0.28
CCSM3[a]	4.23	–0.28
UKMO-HadCM3[a]	4.03	–0.22
UKMO-HadGEM1[a]	4.02	–0.24
Mean ± standard deviation[e]	3.80 ± 0.33	–0.13 ± 0.11

Notes:
[a] Forster and Taylor (2006) based upon forcing data from PCMDI for 200 hPa. Longwave forcing accounts for stratospheric adjustment; shortwave forcing does not.
[b] Forcings derived by individual modelling groups using the method of Gregory et al. (2004b).
[c] Based upon forcing data from PCMDI for 200 hPa. Longwave and shortwave forcing account for stratospheric adjustment.
[d] Forcings at diagnosed tropopause.
[e] Mean and standard deviation are calculated just using forcings at 200 hPa, with each model and model version counted once.

for every 20-year period. For the year 2100, the shortwave forcing from individual AOGCMs ranges from approximately –1.7 W m^{-2} to +0.4 W m^{-2} (5th to 95th percentile). The reasons for this large range include the variety of the aerosol treatments and parametrizations for the indirect effects of aerosols in the multi-model ensemble.

Since the large range in both longwave and shortwave forcings may be caused by a variety of factors, it is useful to determine the range caused just by differences in model formulation for a given (identical) change in radiatively active species. A standard metric is the global mean, annually averaged all-sky forcing at the tropopause for doubled atmospheric CO_2. Estimates of this forcing for 15 of the models in the ensemble are given in Table 10.2. The shortwave forcing is caused by absorption in the near-infrared bands of CO_2. The range in the longwave forcing at 200 mb is 0.84 W m^{-2}, and the coefficient of variation, or ratio of the standard deviation to mean forcing, is 0.09. These results suggest that up to 35% of the range in longwave forcing in the ensemble for the period 2080 to 2099 is due to the spread in forcing estimates for the specified increase in CO_2. The findings also imply that it is not appropriate to use a single best value of the forcing from doubled atmospheric CO_2 to relate forcing and response (e.g., climate sensitivity) across a multi-model ensemble. The relationships for a given model should be derived using the radiative forcing produced by the radiative parametrizations in that model. Although the shortwave forcing has a coefficient of variation close to one, the range across the ensemble explains less than 17% of the range in shortwave forcing at the end of the 21st-century simulations. This suggests that species and forcing agents other than CO_2 cause the large variation among modelled shortwave forcings.

10.2.1.4 Results from the Radiative-Transfer Model Intercomparison Project: Implications for Fidelity of Forcing Projections

Differences in radiative forcing across the multi-model ensemble illustrated in Table 10.2 have been quantified in the Radiative-Transfer Model Intercomparison Project (RTMIP, W.D. Collins et al., 2006). The basis of RTMIP is an evaluation of the forcings computed by 20 AOGCMs using five benchmark line-by-line (LBL) radiative transfer codes. The comparison is focused on the instantaneous clear-sky radiative forcing by the LLGHGs CO_2, CH_4, N_2O, CFC-11, CFC-12 and the increased water vapour expected in warmer climates. The results of this intercomparison are not directly comparable to the estimates of forcing at the tropopause (Chapter 2), since the latter include the effects of stratospheric adjustment. The effects of adjustment on forcing are approximately –2% for CH_4, –4% for N_2O, +5% for CFC-11, +8% for CFC-12 and –13% for CO_2 (IPCC, 1995; Hansen et al., 1997). The total (longwave plus shortwave) radiative forcings at 200 mb, a surrogate for the tropopause, are shown in Table 10.3 for climatological mid-latitude summer conditions.

Table 10.3. *Total instantaneous forcing at 200 hPa (W m^{-2}) from AOGCMs and LBL codes in RTMIP (W.D. Collins et al., 2006). Calculations are for cloud-free climatological mid-latitude summer conditions.*

Radiative Species	CO_2	CO_2	N_2O + CFCs	CH_4 + CFCs	All LLGHGs	Water Vapour
Forcing[a]	2000–1860	2x–1x	2000–1860	2000–1860	2000–1860	1.2x–1x
AOGCM mean	1.56	4.28	0.47	0.95	2.68	4.82
AOGCM std. dev.	0.23	0.66	0.15	0.30	0.30	0.34
LBL mean	1.69	4.75	0.38	0.73	2.58	5.08
LBL std. dev.	0.02	0.04	0.12	0.12	0.11	0.16

Notes:
[a] 2000–1860 is the forcing due to an increase in the concentrations of radiative species between 1860 and 2000. 2x–1x$^{\times}$ and 1.2x–1x are forcings from increases in radiative species by 100% and 20% relative to 1860 concentrations.

Total forcings calculated from the AOGCM and LBL codes due to the increase in LLGHGs from 1860 to 2000 differ by less than 0.04, 0.49 and 0.10 W m^{-2} at the top of model, surface and pseudo-tropopause at 200mb, respectively (Table 10.3). Based upon the Student t-test, none of the differences in mean forcings shown in Table 10.3 is statistically significant at the 0.01 level. This indicates that the ensemble mean forcings are in reasonable agreement with the LBL codes. However, the forcings from individual models, for example from doubled atmospheric CO_2, span a range at least 10 times larger than that exhibited by the LBL models.

The forcings from doubling atmospheric CO_2 from its concentration at 1860 AD are shown in Figure 10.3a at the top of the model (TOM), 200 hPa (Table 10.3), and the surface. The AOGCMs tend to underestimate the longwave forcing at these three levels. The relative differences in the mean forcings are less than 8% for the pseudo-tropopause at 200 hPa but increase to approximately 13% at the TOM and to 33% at the surface. In general, the mean shortwave forcings from the LBL and AOGCM codes are in good agreement at all three surfaces. However, the range in shortwave forcing at the surface from individual AOGCMs is quite large. The coefficient of variation (the ratio of the standard deviation to the mean) for the surface shortwave forcing from AOGCMs is 0.95. In response to a doubling in atmospheric CO_2, the specific humidity increases by approximately 20% through much of the troposphere. The changes in shortwave and longwave fluxes due to a 20% increase in water vapour are illustrated in Figure 10.3b. The mean longwave forcing from increasing water vapour is quite well simulated with the AOGCM codes. In the shortwave, the only significant difference between the AOGCM and LBL calculations occurs at the surface, where the AOGCMs tend to underestimate the magnitude of the reduction in insolation. In general, the biases in the AOGCM forcings are largest at the surface level.

10.2.1.5 Implications for Range in Climate Response

The results from RTMIP imply that the spread in climate response discussed in this chapter is due in part to the diverse representations of radiative transfer among the members of the multi-model ensemble. Even if the concentrations of LLGHGs were identical across the ensemble, differences in radiative transfer parametrizations among the ensemble members would lead to different estimates of radiative forcing by these species. Many of the climate responses (e.g., global mean temperature) scale linearly with the radiative forcing to first approximation. Therefore, systematic errors in the calculations of radiative forcing should produce a corresponding range in climate responses. Assuming that the RTMIP results (Table 10.3) are globally applicable, the range of forcings for 1860 to 2000 in the AOGCMs should introduce a ±18% relative range (the 5 to 95% confidence interval) for 2000 in the responses that scale with forcing. The corresponding relative range for doubled atmospheric CO_2, which is comparable to the change in CO_2 in the B1 scenario by 2100, is ± 25%.

10.2.2 Recent Developments in Projections of Radiative Species and Forcing for the 21st Century

Estimation of ozone forcing for the 21st century is complicated by the short chemical lifetime of ozone compared to atmospheric transport time scales and by the sensitivity of the radiative forcing to the vertical distribution of ozone. Gauss et al. (2003) calculate the forcing by anthropogenic increases

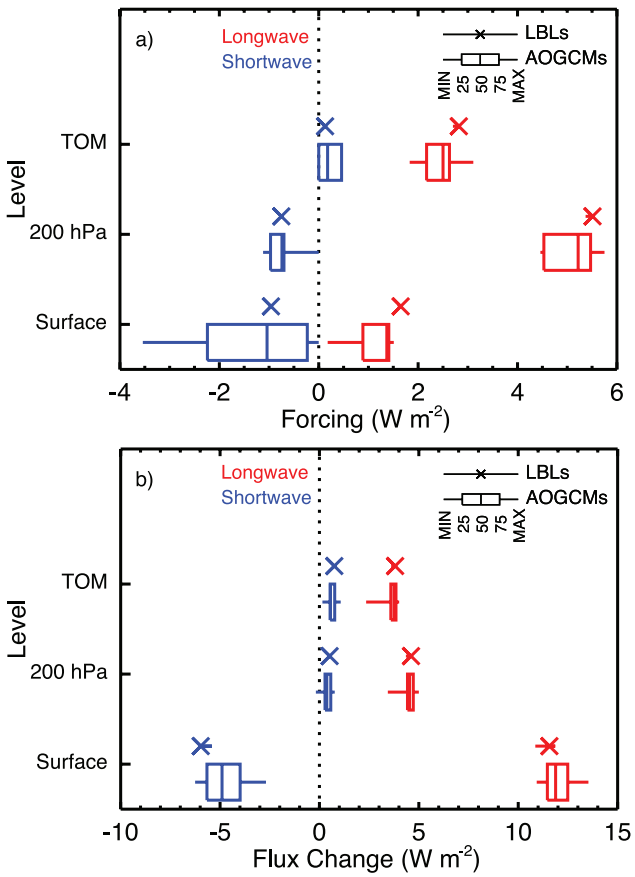


Figure 10.3. *Comparison of shortwave and longwave instantaneous radiative forcings and flux changes computed from AOGCMs and line-by-line (LBL) radiative transfer codes (W.D. Collins et al., 2006). (a) Instantaneous forcing from doubling atmospheric CO_2 from its concentration in 1860; b) changes in radiative fluxes caused by the 20% increase in water vapour expected in the climate produced from doubling atmospheric CO_2. The forcings and flux changes are computed for clear-sky conditions in mid-latitude summer and do not include effects of stratospheric adjustment. No other well-mixed greenhouse gases are included. The minimum-to-maximum range and median are plotted for five representative LBL codes. The AOGCM results are plotted with box-and-whisker diagrams (see caption for Figure 10.2) representing percentiles of forcings from 20 models in the AR4 multi-model ensemble. The AOGCMs included are BCCR-BCM2.0, CCSM3, CGCM3.1(T47 and T63), CNRM-CM3, ECHAM5/MPI-OM, ECHO-G, FGOALS-g1.0, GFDL-CM2.0, GFDL-CM2.1, GISS-EH, GISS-ER, INM-CM3.0, IPSL-CM4, MIROC3.2 (medium and high resolution), MRI-CGCM2.3.2, PCM, UKMO-HadCM3, and UKMO-HadGEM1 (see Table 8.1 for model details). The LBL codes are the Geophysical Fluid Dynamics Laboratory (GFDL) LBL, the Goddard Institute for Space Studies (GISS) LBL3, the National Center for Atmospheric Research (NCAR)/Imperial College of Science, Technology and Medicine (ICSTM) general LBL GENLN2, the National Aeronautics and Space Administration (NASA) Langley Research Center MRTA and the University of Reading Reference Forward Model (RFM).*

of tropospheric ozone through 2100 from 11 different chemical transport models integrated with the SRES A2p scenario. The A2p scenario is the preliminary version of the marker A2 scenario and has nearly identical time series of LLGHGs and forcing. Since the emissions of CH_4, carbon monoxide (CO), reactive nitrogen oxides (NO_x) and volatile organic compounds (VOCs), which strongly affect the formation of ozone, are maximised in the A2p scenario, the modelled forcings should represent an upper bound for the forcing produced under more constrained emissions scenarios. The 11 models simulate an increase in tropospheric ozone of 11.4 to 20.5 Dobson units (DU) by 2100, corresponding to a range of radiative forcing from 0.40 to 0.78 W m^{-2}. Under this scenario, stratospheric ozone increases by between 7.5 and 9.3 DU, which raises the radiative forcing by an additional 0.15 to 0.17 W m^{-2}.

One aspect of future direct aerosol radiative forcing omitted from all but 2 (the GISS-EH and GISS-ER models) of the 23 AOGCMS analysed in AR4 (see Table 8.1 for list) is the role of nitrate aerosols. Rapid increases in NO_x emissions could produce enough nitrate aerosol to offset the expected decline in sulphate forcing by 2100. Adams et al. (2001) compute the radiative forcing by sulphate and nitrate accounting for the interactions among sulphate, nitrate and ammonia. For 2000, the sulphate and nitrate forcing are –0.95 and –0.19 W m^{-2}, respectively. Under the SRES A2 scenario, by 2100 declining SO_2 emissions cause the sulphate forcing to drop to –0.85 W m^{-2}, while the nitrate forcing rises to –1.28 W m^{-2}. Hence, the total sulphate-nitrate forcing increases in magnitude from –1.14 W m^{-2} to –2.13 W m^{-2} rather than declining as models that omit nitrates would suggest. This projection is consistent with the large increase in coal burning forecast as part of the A2 scenario.

Recent field programs focused on Asian aerosols have demonstrated the importance of black carbon (BC) and organic carbon (OC) for regional climate, including potentially significant perturbations of the surface energy budget and hydrological cycle (Ramanathan et al., 2001). Modelling groups have developed a multiplicity of projections for the concentrations of these aerosol species. For example, Takemura et al. (2001) use data sets for BC released by fossil fuel and biomass burning (Cooke and Wilson, 1996) under current conditions and scale them by the ratio of future to present-day CO_2. The emissions of OC are derived using OC:BC ratios estimated for each source and fuel type. Koch (2001) models the future radiative forcing of BC by scaling a different set of present-day emission inventories by the ratio of future to present-day CO_2 emissions. There are still large uncertainties associated with current inventories of BC and OC (Bond et al., 2004), the ad hoc scaling methods used to produce future emissions, and considerable variation among estimates of the optical properties of carbonaceous aerosols (Kinne et al., 2006). Given these uncertainties, future projections of forcing by BC and OC should be quite model dependent.

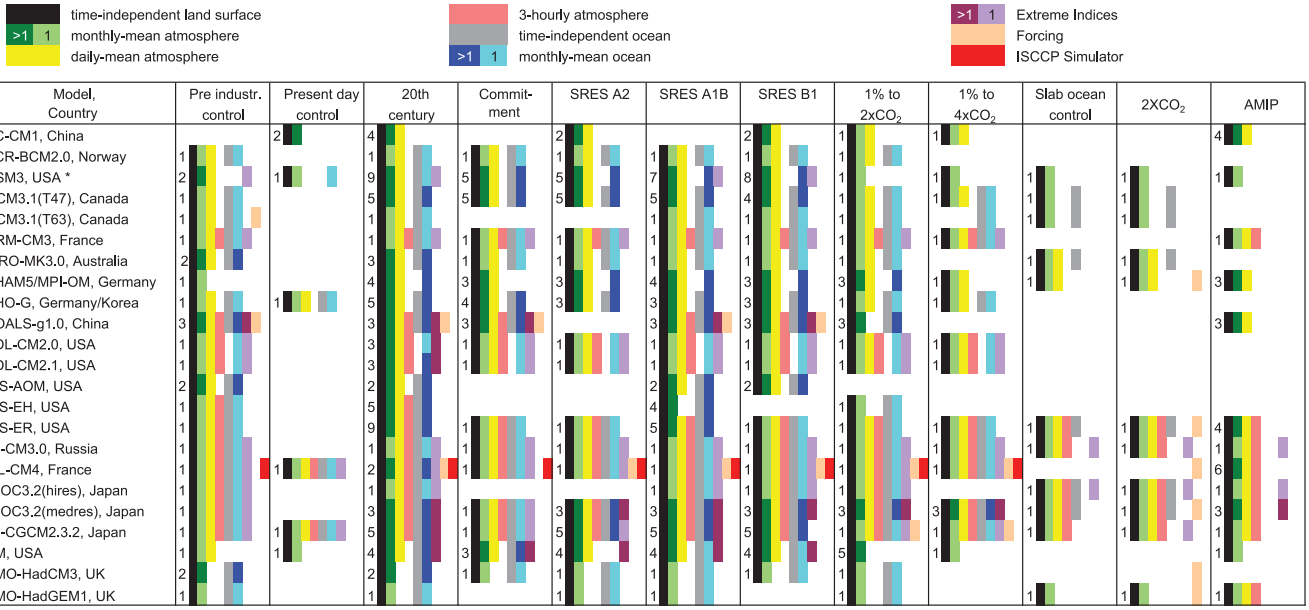
Recent evidence suggests that there are detectable anthropogenic increases in stratospheric sulphate (e.g., Myhre et al., 2004), water vapour (e.g., Forster and Shine, 2002), and condensed water in the form of aircraft contrails. However, recent modelling studies suggest that these forcings are relatively minor compared to the major LLGHGs and aerosol species. Marquart et al. (2003) estimate that the radiative forcing by contrails will increase from 0.035 W m^{-2} in 1992 to 0.094 W m^{-2} in 2015 and to 0.148 W m^{-2} in 2050. The rise in forcing is due to an increase in subsonic aircraft traffic following estimates of future fuel consumption (Penner et al., 1999). These estimates are still subject to considerable uncertainties related to poor constraints on the microphysical properties, optical depths and diurnal cycle of contrails (Myhre and Stordal, 2001, 2002; Marquart et al., 2003). Pitari et al. (2002) examine the effect of future emissions under the A2 scenario on stratospheric concentrations of sulphate aerosol and ozone. By 2030, the mass of stratospheric sulphate increases by approximately 33%, with the majority of the increase contributed by enhanced upward fluxes of anthropogenic SO_2 through the tropopause. The increase in direct shortwave forcing by stratospheric aerosols in the A2 scenario during 2000 to 2030 is –0.06 W m^{-2}.

Some recent studies have suggested that the global atmospheric burden of soil dust aerosols could decrease by between 20 and 60% due to reductions in desert areas associated with climate change (Mahowald and Luo, 2003). Tegen et al. (2004a,b) compared simulations by the European Centre for Medium Range Weather Forecasts/Max Planck Institute for Meteorology Atmospheric GCM (ECHAM4) and UKMO-HadCM3 that included the effects of climate-induced changes in atmospheric conditions and vegetation cover and the effects of increased CO_2 concentrations on vegetation density. These simulations are forced with identical (IS92a) time series for LLGHGs. Their findings suggest that future projections of changes in dust loading are quite model dependent, since the net changes in global atmospheric dust loading produced by the two models have opposite signs. They also conclude that dust from agriculturally disturbed soils is less than 10% of the current burden, and that climate-induced changes in dust concentrations would dominate land use changes under both minimum and maximum estimates of increased agricultural area by 2050.

10.3 Projected Changes in the Physical Climate System

The context for the climate change results presented here is set in Chapter 8 (evaluation of simulation skill of the control runs and inherent natural variability of the global coupled climate models), and in Chapter 9 (evaluation of the simulations of 20th-century climate using the global coupled climate models). Table 8.1 describes the characteristics of the models, and Table 10.4 summarises the climate change experiments that have been performed with the AOGCMs and other models that are assessed in this chapter.

Table 10.4. *Summary of climate change model experiments produced with AOGCMs. Numbers in each scenario column indicate how many ensemble members were produced for each model. Coloured fields indicate that some but not necessarily all variables of the specific data type (separated by climate system component and time interval) were available for download at the PCMDI to be used in this report; ISCCP is the International Satellite Cloud Climatology Project. Additional data has been submitted for some models and may subsequently become available. Where different colour shadings are given in the legend, the colour indicates whether data from a single or from multiple ensemble members is available. Details on the scenarios, variables and models can be found at the PCMDI webpage (http://www-pcmdi.llnl.gov/ipcc/about_ipcc.php). Model IDs are the same as in Table 8.1, which provides details of the models.*



Model ID	Model, Country	Pre industr. control	Present day control	20th century	Commit-ment	SRES A2	SRES A1B	SRES B1	1% to 2xCO$_2$	1% to 4xCO$_2$	Slab ocean control	2XCO$_2$	AMIP
1	BCC-CM1, China		2	4		2		2	1	1			4
2	BCCR-BCM2.0, Norway	1		1	1	1	1	1	1				
3	CCSM3, USA *	2	1	9	5	5	7	8	1	1	1	1	1
4	CGCM3.1(T47), Canada	1		5	5	5	5	4	1	1	1	1	
5	CGCM3.1(T63), Canada	1		1			1	1	1		1		
6	CNRM-CM3, France	1		1	1	1	1	1	1	1			1
7	CSIRO-MK3.0, Australia	2		3	1	1	1	1	1		1	1	
8	ECHAM5/MPI-OM, Germany	1		4	3	3	4	3	3	1	1	1	3
9	ECHO-G, Germany/Korea	1	1	5	4	3	3	3	1	1			
10	FGOALS-g1.0, China	3		3	3		3	3	3				3
11	GFDL-CM2.0, USA	1		3	1	1	1	1	1	1			
12	GFDL-CM2.1, USA	1		3	1	1	1	1	1	1			
13	GISS-AOM, USA	2		2			2	2					
14	GISS-EH, USA	1		5			4		1				
15	GISS-ER, USA	1		9	1	1	5	1	1	1	1	1	4
16	INM-CM3.0, Russia	1		1	1	1	1	1	1	1	1	1	1
17	IPSL-CM4, France	1	1	2	1	1	1	1	1	1			6
18	MIROC3.2(hires), Japan	1		1			1	1	1		1	1	1
19	MIROC3.2(medres), Japan	1		3	1	3	3	3	3	3	1	1	3
20	MRI-CGCM2.3.2, Japan	1	1	5	1	5	5	5	1	1	1	1	1
21	PCM, USA	1	1	4	3	4	4	4	5	1			1
22	UKMO-HadCM3, UK	2		2	1	1	1	1	1				
23	UKMO-HadGEM1, UK	1		1		1	1		1		1	1	1

** Some of the ensemble members using the CCSM3 were run on the Earth Simulator in Japan in collaboration with the Central Research Institute of Electric Power Industry (CRIEPI).*

The TAR showed multi-model results for future changes in climate from simple 1% yr^{-1} CO_2 increase experiments, and from several scenarios including the older IS92a, and, new to the TAR, two SRES scenarios (A2 and B2). For the latter, results from nine models were shown for globally averaged temperature change and regional changes. As noted in Section 10.1, since the TAR, an unprecedented internationally coordinated climate change experiment has been performed by 23 models from around the world, listed in Table 10.4 along with the results submitted. This larger number of models running the same experiments allows better quantification of the multi-model signal as well as uncertainty regarding spread across the models (in this section), and also points the way to probabilistic estimates of future climate change (Section 10.5). The emission scenarios considered here include one of the SRES scenarios from the TAR, scenario A2, along with two additional scenarios, A1B and B1 (see Section 10.2 for details regarding the scenarios). This is a subset of the SRES marker scenarios used in the TAR, and they represent 'low' (B1), 'medium' (A1B) and 'high' (A2) scenarios with respect to the prescribed concentrations and the resulting radiative forcing, relative to the SRES range. This choice was made solely due to the limited computational resources for multi-model simulations using comprehensive AOGCMs and does not imply any preference or qualification of these three scenarios over the others. Qualitative conclusions derived from those three scenarios are in most cases also valid for other SRES scenarios.

Additionally, three climate change commitment experiments were performed, one where concentrations of greenhouse gases were held fixed at year 2000 values (constant composition commitment) and the models were run to 2100 (termed 20th-century stabilisation here), and two where concentrations were held fixed at year 2100 values for A1B and B1, and the models were run for an additional 100 to 200 years (see Section 10.7). The span of the experiments is shown in Figure 10.4.

This section considers the basic changes in climate over the next hundred years simulated by current climate models under non-mitigation anthropogenic forcing scenarios. While we assess all studies in this field, the focus is on results derived by the authors from the new data set for the three SRES scenarios. Following the TAR, means across the multi-model ensemble are used to illustrate representative changes. Means are able to simulate the contemporary climate more accurately than individual models, due to biases tending to compensate each other (Phillips and Gleckler, 2006). It is anticipated that this holds for changes in climate also (Chapter 9). The mean temperature trends from the 20th-century simulations are included in Figure 10.4. While the range of model results is indicated here, the consideration of uncertainty resulting from this range is addressed more completely in Section 10.5. The use of means has the additional advantage of reducing the 'noise' associated with internal or unforced variability in the simulations. Models are equally weighted here, but other options are noted in Section 10.5. Lists of the models used in the results are provided in the Supplementary Material for this Chapter.

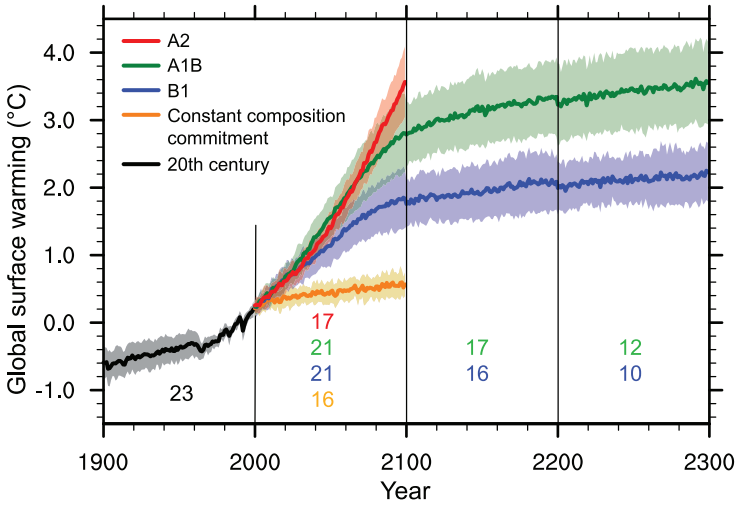


Figure 10.4. *Multi-model means of surface warming (relative to 1980–1999) for the scenarios A2, A1B and B1, shown as continuations of the 20th-century simulation. Values beyond 2100 are for the stabilisation scenarios (see Section 10.7). Linear trends from the corresponding control runs have been removed from these time series. Lines show the multi-model means, shading denotes the ±1 standard deviation range of individual model annual means. Discontinuities between different periods have no physical meaning and are caused by the fact that the number of models that have run a given scenario is different for each period and scenario, as indicated by the coloured numbers given for each period and scenario at the bottom of the panel. For the same reason, uncertainty across scenarios should not be interpreted from this figure (see Section 10.5.4.6 for uncertainty estimates).*

Standard metrics for response of global coupled models are the equilibrium climate sensitivity, defined as the equilibrium globally averaged surface air temperature change for a doubling of CO_2 for the atmosphere coupled to a non-dynamic slab ocean, and the TCR, defined as the globally averaged surface air temperature change at the time of CO_2 doubling in the 1% yr^{-1} transient CO_2 increase experiment. The TAR showed results for these 1% simulations, and Section 10.5.2 discusses equilibrium climate sensitivity, TCR and other aspects of response. Chapter 8 includes processes and feedbacks involved with these metrics.

10.3.1 Time-Evolving Global Change

The globally averaged surface warming time series from each model in the MMD is shown in Figure 10.5, either as a single member (if that was all that was available) or a multi-member ensemble mean, for each scenario in turn. The multi-model ensemble mean warming is also plotted for each case. The surface air temperature is used, averaged over each year, shown as an anomaly relative to the 1980 to 1999 period and offset by any drift in the corresponding control runs in order to extract the forced response. The base period was chosen to match the contemporary climate simulation that is the focus of previous chapters. Similar results have been shown in studies of these models (e.g., Xu et al., 2005; Meehl et al., 2006b; Yukimoto et al., 2006). Interannual variability is evident in each single-model series, but little remains in the ensemble mean because most of this is unforced and is a result of internal variability, as was presented in detail in Section 9.2.2 of TAR. Clearly, there is a range of model results for each year, but over time this range due to internal variability becomes smaller as a fraction of the mean warming. The range is somewhat smaller than the range of warming at the end of the 21st century for the A2 scenario in the comparable Figure 9.6 of the TAR, despite the larger number of models here (the ensemble mean warming is comparable, +3.0°C in the TAR for 2071 to 2100 relative to 1961 to 1990, and +3.13°C here for 2080 to 2099 relative to 1980 to 1999, Table 10.5). Consistent with the range of forcing presented in Section 10.2, the warming by 2100 is largest in the high greenhouse gas growth scenario A2, intermediate in the moderate growth A1B, and lowest in the low growth B1. Naturally, models with high sensitivity tend to simulate above-average warming in each scenario. The trends of the multi-model mean temperature vary somewhat over the century because of the varying forcings, including that of aerosols (see Section 10.2). This is illustrated in Figure 10.4, which shows the mean for A1B exceeding that for A2 around 2040. The time series beyond 2100 are derived from the extensions of the simulations (those available) under the idealised constant composition commitment experiments (Section 10.7.1).

Internal variability in the model response is reduced by averaging over 20-year time periods. This span is shorter than the traditional 30-year climatological period, in recognition of the transient nature of the simulations, and of the larger size of the ensemble. This analysis focuses on three periods over the coming century: an early-century period 2011 to 2030, a mid-century period 2046 to 2065 and the late-century period 2080 to 2099, all relative to the 1980 to 1999 means. The multi-model ensemble mean warmings for the three future periods in the different experiments are given in Table 10.5, among other results. The close agreement of warming for the early century, with a range of only 0.05°C among the SRES cases, shows that no matter which of these non-mitigation scenarios is followed, the warming is similar on the time scale of the next decade or two. Note that the precision given here is only relevant for comparison between these means. As evident in Figure 10.4 and discussed in Section 10.5, uncertainties in the projections are larger. It is also worth noting that half of the early-century climate change arises from warming that is already committed to under constant composition (0.37°C for the early century). By mid-century, the choice of scenario becomes more important for the magnitude of warming, with a range of 0.46°C, and with about one-third of that warming due to climate change that is already committed to. By the late century, there are clear consequences for which scenario is followed, with a range of 1.3°C in these results, with as little as 18% of that warming coming from climate change that is already committed to.

Global mean precipitation increases in all scenarios (Figure 10.5, right column), indicating an intensification of the hydrological cycle. Douville et al. (2002) show that this is associated with increased water-holding capacity of the atmosphere in addition to other processes. The multi-model

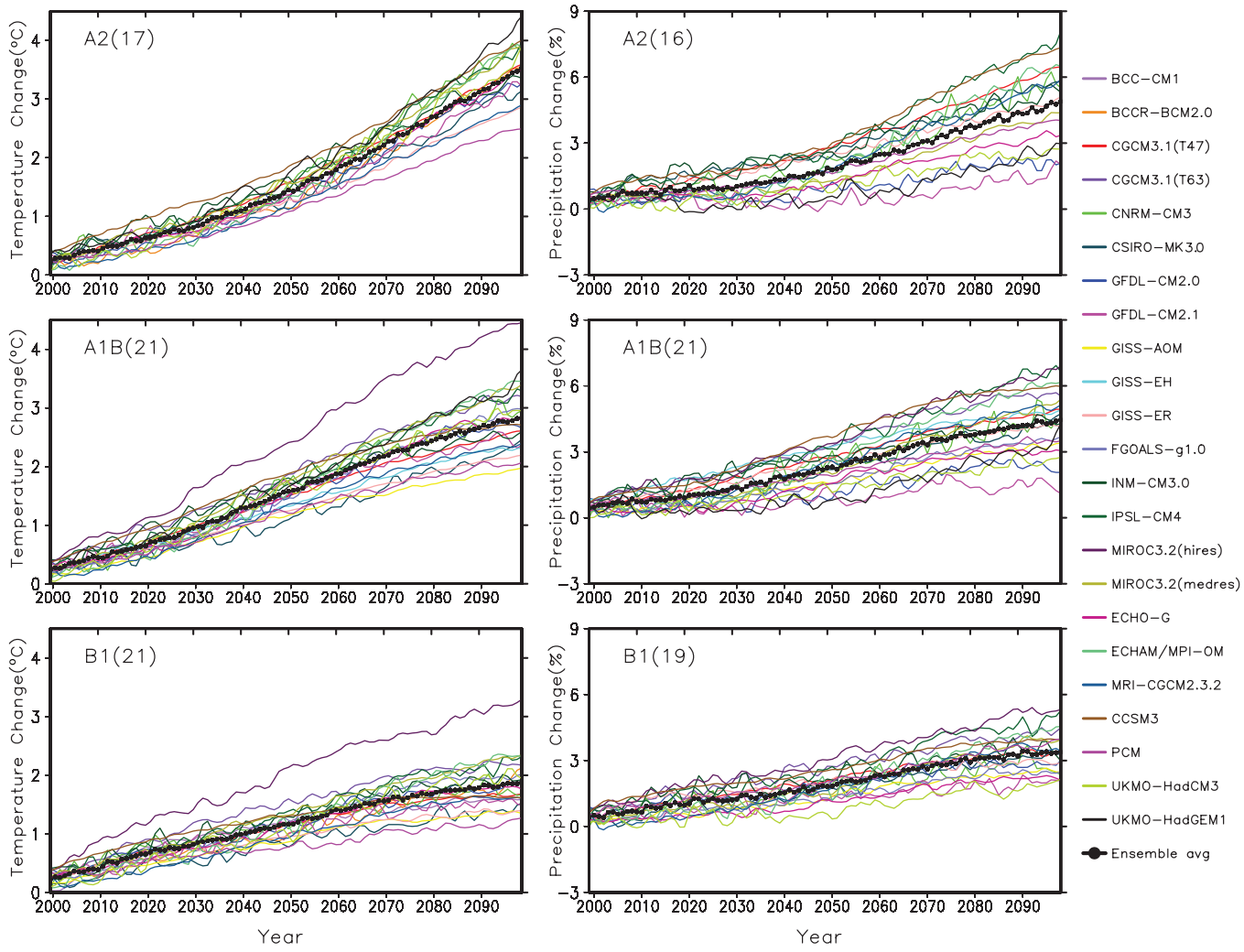


Figure 10.5. *Time series of globally averaged (left) surface warming (surface air temperature change, °C) and (right) precipitation change (%) from the various global coupled models for the scenarios A2 (top), A1B (middle) and B1 (bottom). Numbers in parentheses following the scenario name represent the number of simulations shown. Values are annual means, relative to the 1980 to 1999 average from the corresponding 20th-century simulations, with any linear trends in the corresponding control run simulations removed. A three-point smoothing was applied. Multi-model (ensemble) mean series are marked with black dots. See Table 8.1 for model details.*

Table 10.5. *Global mean warming (annual mean surface air temperature change) from the multi-model ensemble mean for four time periods relative to 1980 to 1999 for each of the available scenarios. (The mean for the base period is 13.6°C). Also given are two measures of agreement of the geographic scaled patterns of warming (the fields in Figure 10.8 normalised by the global mean), relative to the A1B 2080 to 2099 case. First the non-dimensional M value (see Section 10.3.2.1) and second (in italics) the global mean absolute error (*mae*, or difference, in °C/°C) between the fields, both multiplied by 100 for brevity. Here* $M = (2/\pi)\ \arcsin[1 - \text{mse} / (V_X + V_Y + (G_X - G_Y)^2)]$, *with* mse *the mean square error between the two fields X and Y, and V and G are variance and global mean of the fields (as subscripted). Values of 1 for M and 0 for* mae *indicate perfect agreement with the standard pattern. 'Commit' refers to the constant composition commitment experiment. Note that warming values for the end of the 21st century, given here as the average of years 2080 to 2099, are for a somewhat different averaging period than used in Figure 10.29 (2090–2099); the longer averaging period here is consistent with the comparable averaging period for the geographic plots in this section and is intended to smooth spatial noise.*

	Global mean warming (°C)				Measures of agreement (M × 100, *mae* × 100)			
	2011–2030	2046–2065	2080–2099	2180–2199	2011–2030	2046–2065	2080–2099	2180–2199
A2	0.64	1.65	3.13		83, *8*	91, *4*	93, *3*	
A1B	0.69	1.75	2.65	3.36	88, *5*	94, *4*	100, *0*	90, *5*
B1	0.66	1.29	1.79	2.10	86, *6*	89, *4*	92, *3*	86, *6*
Commit[a]	0.37	0.47	0.56		74, *11*	66, *13*	68, *13*	

Notes:
[a] Committed warming values are given relative to the 1980 to 1999 base period, whereas the commitment experiments started with stabilisation at year 2000. The committed warming trend is about 0.1°C per decade over the next two decades with a reduced rate after that (see Figure 10.4).

mean varies approximately in proportion to the mean warming, though uncertainties in future hydrological cycle behaviour arise due in part to the different responses of tropical precipitation across models (Douville et al., 2005). Expressed as a percentage of the mean simulated change for 1980 to 1999 (2.83 mm day^{-1}), the rate varies from about 1.4% °C^{-1} in A2 to 2.3% °C^{-1} in the constant composition commitment experiment (for a table corresponding to Table 10.5 but for precipitation, see the Supplementary Material, Table S10.1). These increases are less than increases in extreme precipitation events, consistent with energetic constraints (see Sections 9.5.4.2 and 10.3.6.1)

10.3.2 Patterns of Change in the 21st Century

10.3.2.1 Warming

The TAR noted that much of the regional variation of the annual mean warming in the multi-model means is associated with high- to low-latitude contrast. This can be better quantified from the new multi-model mean in terms of zonal averages. A further contrast is provided by partitioning the land and ocean values based on model data interpolated to a standard grid. Figure 10.6 illustrates the late-century A2 case, with all values shown both in absolute terms and relative to the global mean warming. Warming over land is greater than the mean except in the southern mid-latitudes, where the warming over ocean is a minimum. Warming over ocean is smaller than the mean except at high latitudes, where sea ice changes have an influence. This pattern of change illustrated by the ratios is quite similar across the scenarios. The commitment case (shown), discussed in Section 10.7.1, has relatively smaller warming of land, except in the far south, which warms closer to the global rate. At nearly all latitudes, the A1B and B1 warming ratios lie between A2 and commitment, with A1B particularly close to the A2 results. Aside from the commitment case, the ratios for the other time periods are also quite similar to those for A2. Regional patterns and precipitation contrasts are discussed in Section 10.3.2.3.

Figure 10.7 shows the zonal mean warming for the A1B scenario at each latitude from the bottom of the ocean to the top of the atmosphere for the three 21st-century periods used in Table 10.5. To produce this ensemble mean, the model data were first interpolated to standard ocean depths and atmospheric pressures. Consistent with the global transfer of excess heat from the atmosphere to the ocean, and the difference between warming over land and ocean, there is some discontinuity between the plotted means of the lower atmosphere and the upper ocean. The relatively uniform warming of the troposphere and cooling of the stratosphere in this multi-model mean are consistent with the changes shown in Figure 9.8 of the TAR, but now its evolution during the 21st century under this scenario can also be seen. Upper-tropospheric warming reaches a maximum in the tropics and is seen even in the early-century

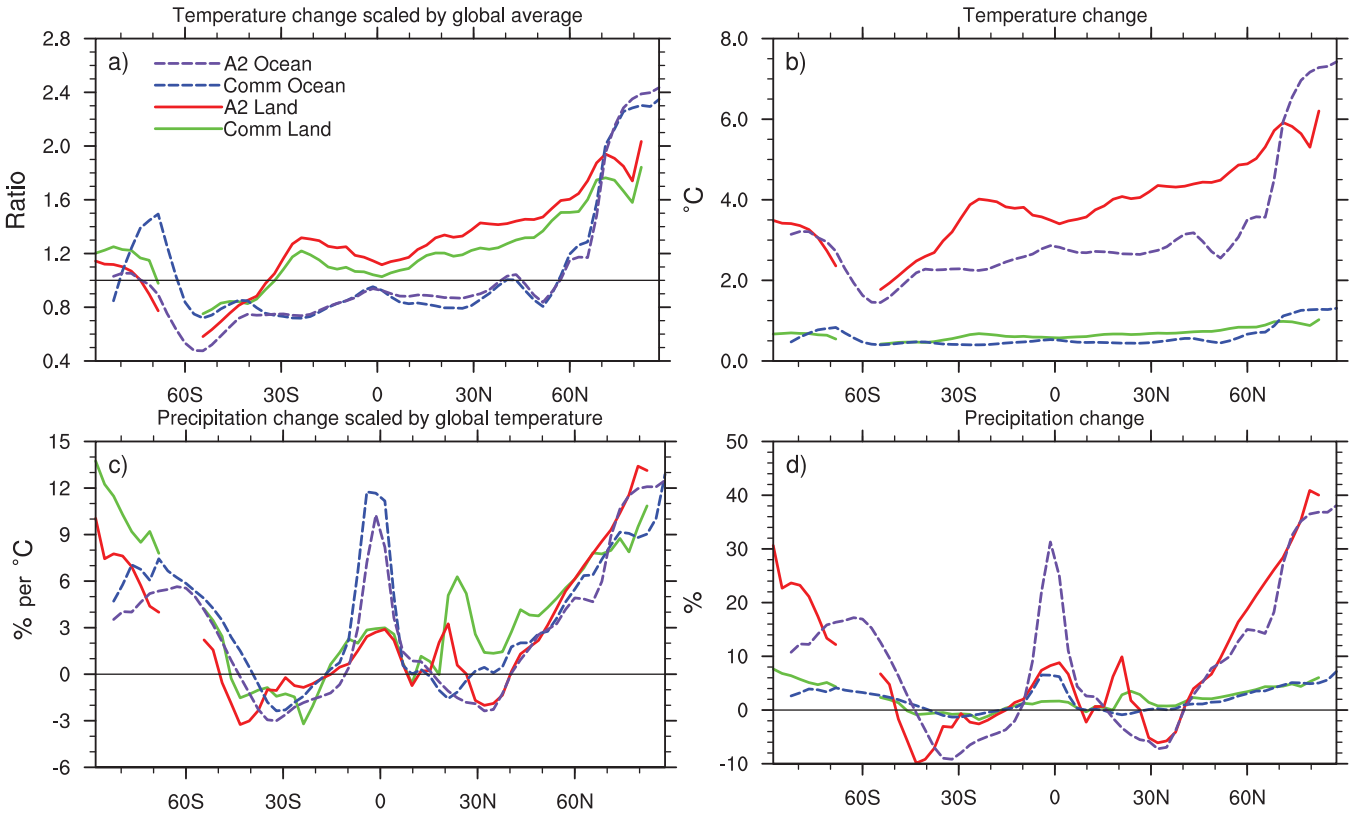


Figure 10.6. *Zonal means over land and ocean separately, for annual mean surface warming (a, b) and precipitation (c, d), shown as ratios scaled with the global mean warming (a, c) and not scaled (b, d). Multi-model mean results are shown for two scenarios, A2 and Commitment (see Section 10.7), for the period 2080 to 2099 relative to the zonal means for 1980 to 1999. Results for individual models can be seen in the Supplementary Material for this chapter.*

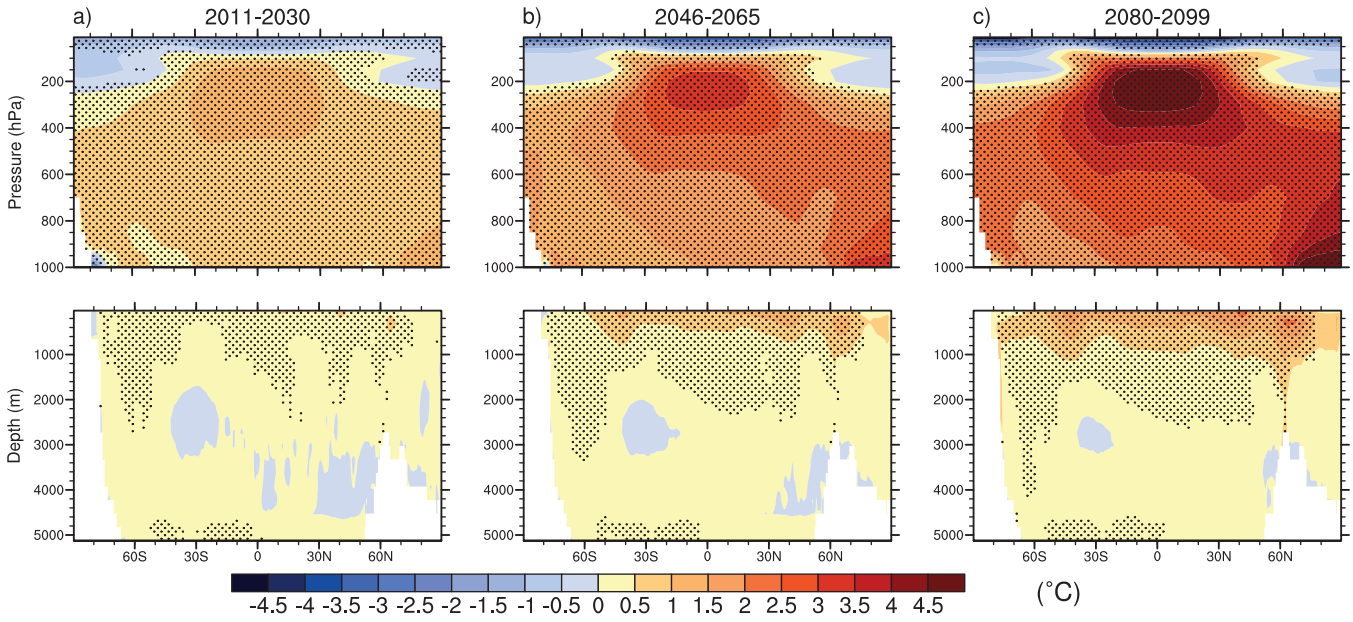


Figure 10.7. *Zonal means of change in atmospheric (top) and oceanic (bottom) temperatures (°C), shown as cross sections. Values are the multi-model means for the A1B scenario for three periods (a–c). Stippling denotes regions where the multi-model ensemble mean divided by the multi-model standard deviation exceeds 1.0 (in magnitude). Anomalies are relative to the average of the period 1980 to 1999. Results for individual models can be seen in the Supplementary Material for this chapter.*

time period. The pattern is very similar over the three periods, consistent with the rapid adjustment of the atmosphere to the forcing. These changes are simulated with good consistency among the models. The larger values of both signs are stippled, indicating that the ensemble mean is larger in magnitude than the inter-model standard deviation. The ratio of mean to standard deviation can be related to formal tests of statistical significance and confidence intervals, if the individual model results were to be considered a sample.

The ocean warming evolves more slowly. There is initially little warming below the mixed layer, except at some high latitudes. Even as a ratio with mean surface warming, later in the century the temperature increases more rapidly in the deep ocean, consistent with results from individual models (e.g., Watterson, 2003; Stouffer, 2004). This rapid warming of the atmosphere and the slow penetration of the warming into the ocean has implications for the time scales of climate change commitment (Section 10.7). It has been noted in a five-member multi-model ensemble analysis that, associated with the changes in temperature of the upper ocean in Figure 10.7, the tropical Pacific Ocean heat transport remains nearly constant with increasing greenhouse gases due to the compensation of the subtropical cells and the horizontal gyre variations, even as the subtropical cells change in response to changes in the trade winds (Hazeleger, 2005). Additionally, a southward shift of the Antarctic Circumpolar Current is projected to occur in a 15-member multi-model ensemble, due to changes in surface winds in a future warmer climate (Fyfe and Saenko, 2005). This is associated with a poleward shift of the westerlies at the surface (see Section 10.3.6) and in the upper troposphere particularly notable in the Southern Hemisphere (SH) (Stone and Fyfe, 2005), and increased relative angular momentum from stronger westerlies (Räisänen, 2003) and westerly momentum flux in the lower stratosphere particularly in the tropics and southern mid-latitudes (Watanabe et al., 2005). The surface wind changes are associated with corresponding changes in wind stress curl and horizontal mass transport in the ocean (Saenko et al., 2005).

Global-scale patterns for each of the three scenarios and time periods are given in Figure 10.8. In each case, greater warming over most land areas is evident (e.g., Kunkel and Liang, 2005). Over the ocean, warming is relatively large in the Arctic and along the equator in the eastern Pacific (see Sections 10.3.5.2 and 10.3.5.3), with less warming over the North Atlantic and the Southern Ocean (e.g., Xu et al., 2005). Enhanced oceanic warming along the equator is also evident in the zonal means of Figure 10.6, and can be associated with oceanic heat flux changes (Watterson, 2003) and forced by the atmosphere (Liu et al., 2005).

Fields of temperature change have a similar structure, with the linear correlation coefficient as high as 0.994 between the late-century A2 and A1B cases. As for the zonal means, the fields normalised by the mean warming are very similar. The strict agreement between the A1B field, as a standard, and the others is quantified in Table 10.5, by the absolute measure M (Watterson, 1996; a transformation of a measure of Mielke, 1991), with unity meaning identical fields and zero meaning no similarity (the expected value under random rearrangement of the data on the grid of the measure prior to the arcsin transformation). Values of M become progressively larger later in the 21st century, with values of 0.9 or larger for the late 21st century, thus confirming the closeness of the scaled patterns in the late-century cases. The deviation from unity is approximately proportional to the mean absolute difference. The earlier warming patterns are also similar to the standard case,

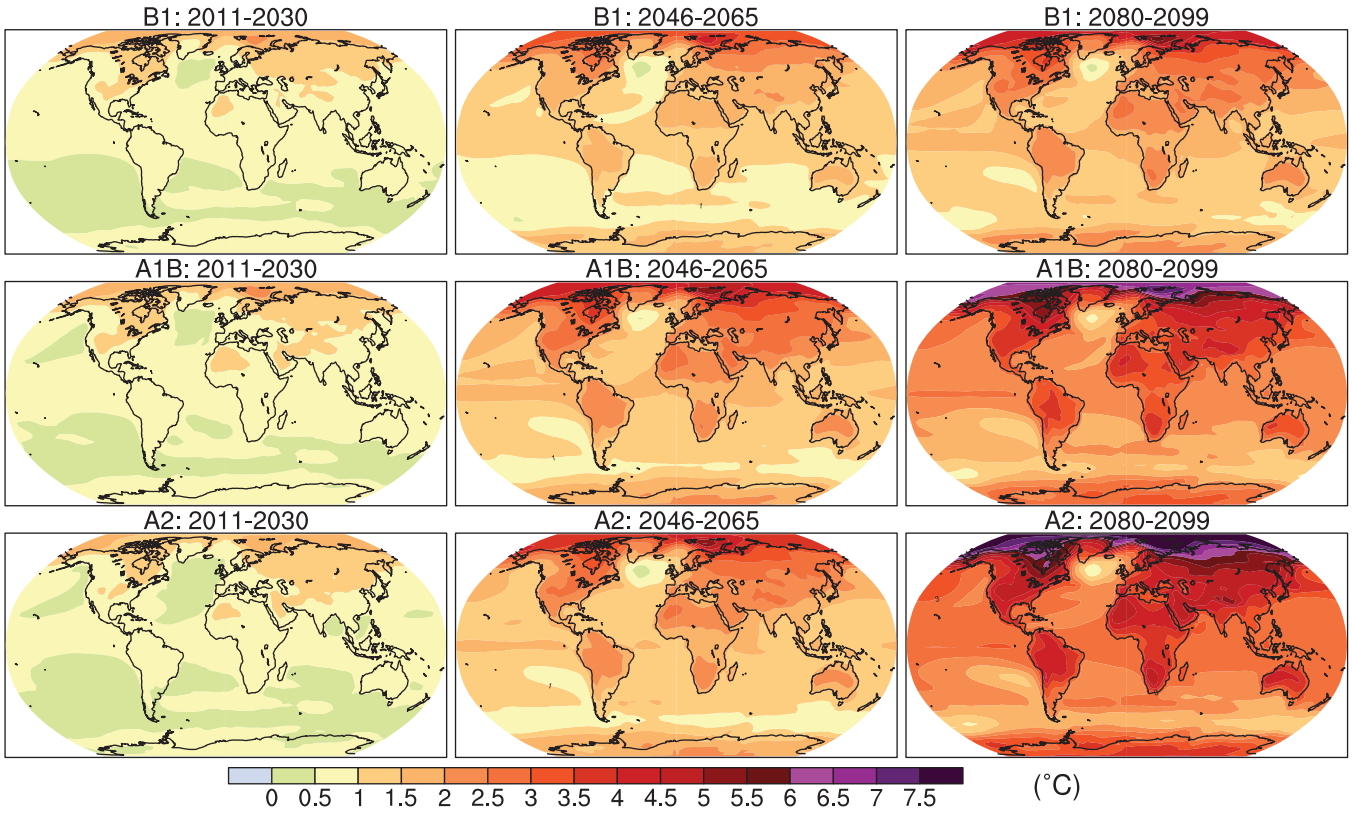


Figure 10.8. *Multi-model mean of annual mean surface warming (surface air temperature change, °C) for the scenarios B1 (top), A1B (middle) and A2 (bottom), and three time periods, 2011 to 2030 (left), 2046 to 2065 (middle) and 2080 to 2099 (right). Stippling is omitted for clarity (see text). Anomalies are relative to the average of the period 1980 to 1999. Results for individual models can be seen in the Supplementary Material for this chapter.*

particularly for the same scenario A1B. Furthermore, the zonal means over land and ocean considered above are representative of much of the small differences in warming ratio. While there is some influence of differences in forcing patterns among the scenarios, and of effects of oceanic uptake and heat transport in modifying the patterns over time, there is also support for the role of atmospheric heat transport in offsetting such influences (e.g., Boer and Yu, 2003b; Watterson and Dix, 2005). Dufresne et al. (2005) show that aerosol contributes a modest cooling of the Northern Hemisphere (NH) up to the mid-21st century in the A2 scenario.

Such similarities in patterns of change have been described by Mitchell (2003) and Harvey (2004). They aid the efficient presentation of the broad scale multi-model results, as patterns depicted for the standard A1B 2080 to 2099 case are usually typical of other cases. This largely applies to other seasons and also other variables under consideration here. Where there is similarity of normalised changes, values for other cases can be estimated by scaling by the appropriate ratio of global means from Table 10.5. Note that for some quantities like variability and extremes, such scaling is unlikely to work. The use of such scaled results in combination with global warmings from simple models is discussed in Section 11.10.1.

As for the zonal means (aside from the Arctic Ocean), consistency in local warmings among the models is high (stippling is omitted in Figure 10.8 for clarity). Only in the central North Atlantic and the far south Pacific in 2011 to 2030 is the mean change less than the standard deviation, in part a result of ocean model limitations there (Section 8.3.2). Some regions of high-latitude surface cooling occur in individual models.

The surface warming fields for the extratropical winter and summer seasons, December to February (DJF) and June to August (JJA), are shown for scenario A1B in Figure 10.9. The high-latitude warming is rather seasonal, being larger in winter as a result of sea ice and snow, as noted in Chapter 9 of the TAR. However, the relatively small warming in southern South America is more extensive in southern winter. Similar patterns of change in earlier model simulations are described by Giorgi et al. (2001).

10.3.2.2 Cloud and Diurnal Cycle

In addition to being an important link to humidity and precipitation, cloud cover plays an important role for the sensitivity of the general circulation models (GCMs; e.g., Soden and Held, 2006) and for the diurnal temperature range (DTR) over land (e.g., Dai and Trenberth, 2004 and references therein) so this section considers the projection of these variables now made possible by multi-model ensembles. Cloud radiative feedbacks to greenhouse gas forcing are sensitive to the elevation, latitude and hence temperature of the clouds, in addition to their optical

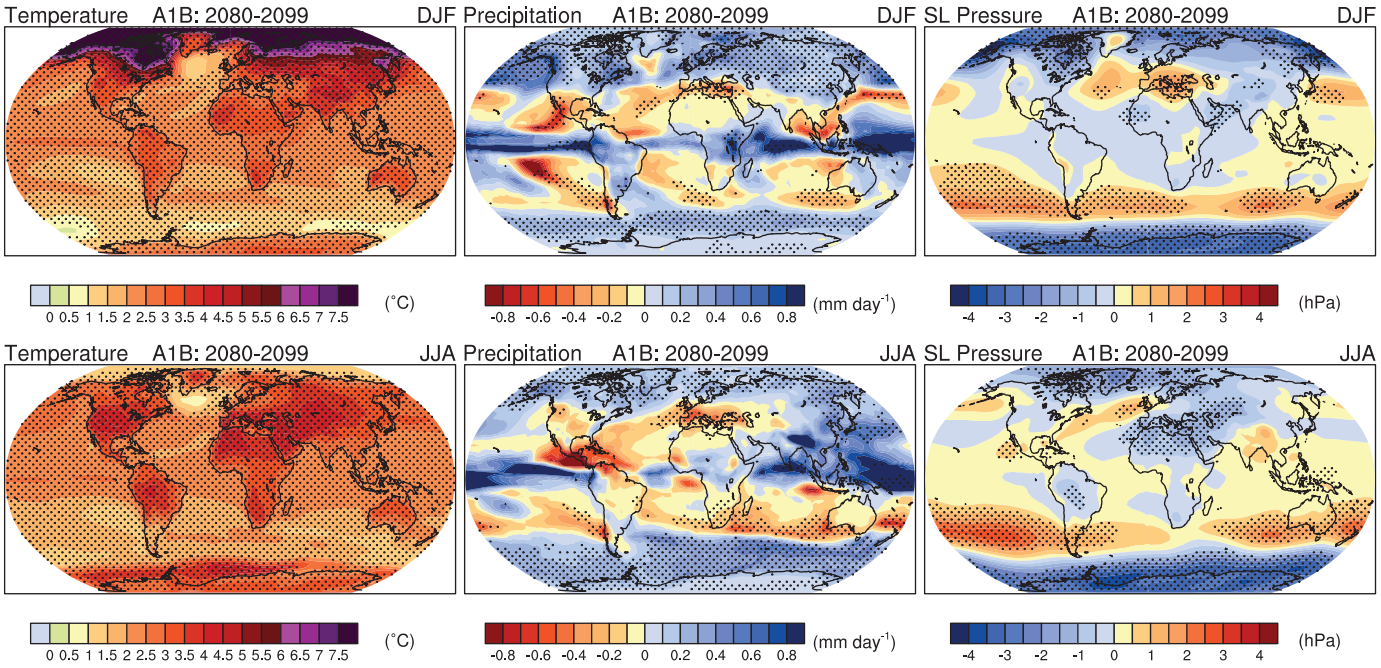


Figure 10.9. *Multi-model mean changes in surface air temperature (°C, left), precipitation (mm day^{-1}, middle) and sea level pressure (hPa, right) for boreal winter (DJF, top) and summer (JJA, bottom). Changes are given for the SRES A1B scenario, for the period 2080 to 2099 relative to 1980 to 1999. Stippling denotes areas where the magnitude of the multi-model ensemble mean exceeds the inter-model standard deviation. Results for individual models can be seen in the Supplementary Material for this chapter.*

depth and their atmospheric environment (see Section 8.6.3.2). Current GCMs simulate clouds through various complex parametrizations (see Section 8.2.1.3) to produce cloud cover quantified by an area fraction within each grid square and each atmospheric layer. Taking multi-model ensemble zonal means of this quantity interpolated to standard pressure levels and latitudes shows increases in cloud cover at all latitudes in the vicinity of the tropopause, and mostly decreases below, indicating an increase in the altitude of clouds overall (Figure 10.10a). This shift occurs consistently across models. Outside the tropics the increases aloft are rather consistent, as indicated by the stippling in the figure. Near-surface amounts increase at some latitudes. The mid-level mid-latitude decreases are very consistent, amounting to as much as one-fifth of the average cloud fraction simulated for 1980 to 1999.

The total cloud area fraction from an individual model represents the net coverage over all the layers, after allowance for the overlap of clouds, and is an output included in the data set. The change in the ensemble mean of this field is shown in Figure 10.10b. Much of the low and middle latitudes experience a decrease in cloud cover, simulated with some consistency. There are a few low-latitude regions of increase, as well as substantial increases at high latitudes. The larger changes relate well to changes in precipitation discussed in Section 10.3.2.3. While clouds need not be precipitating, moderate spatial correlation between cloud cover and precipitation holds for seasonal means of both the present climate and future changes.

The radiative effect of clouds is represented by the cloud radiative forcing diagnostic (see Section 8.6.3.2). This can be

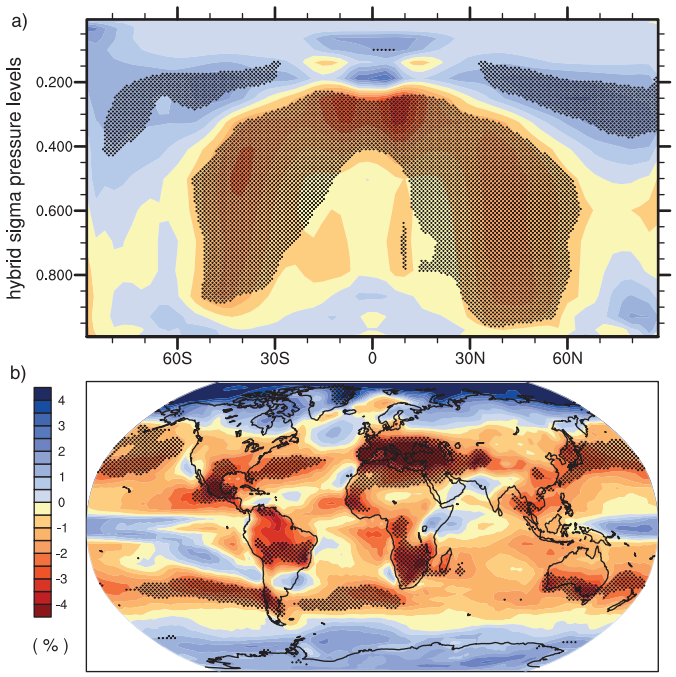


Figure 10.10. *Multi-model mean changes in (a) zonal mean cloud fraction (%), shown as a cross section though the atmosphere, and (b) total cloud area fraction (percent cover from all models). Changes are given as annual means for the SRES A1B scenario for the period 2080 to 2099 relative to 1980 to 1999. Stippling denotes areas where the magnitude of the multi-model ensemble mean exceeds the inter-model standard deviation. Results for individual models can be seen in the Supplementary Material for this chapter.*

evaluated from radiative fluxes at the top of the atmosphere calculated with or without the presence of clouds that are output by the GCMs. In the multi-model mean (not shown) values vary in sign over the globe. The global and annual mean averaged over the models, for 1980 to 1999, is –22.3 W m^{-2}. The change in mean cloud radiative forcing has been shown to have different signs in a limited number of previous modelling studies (Meehl et al., 2004b; Tsushima et al., 2006). Figure 10.11a shows globally averaged cloud radiative forcing changes for 2080 to 2099 under the A1B scenario for individual models of the data set, which have a variety of different magnitudes and even signs. The ensemble mean change is –0.6 W m^{-2}. This range indicates that cloud feedback is still an uncertain feature of the global coupled models (see Section 8.6.3.2.2).

The DTR has been shown to be decreasing in several land areas of the globe in 20th-century observations (see Section 3.2.2.7), together with increasing cloud cover (see also Section 9.4.2.3). In the multi-model mean of present climate, DTR over land is indeed closely spatially anti-correlated with the total cloud cover field. This is true also of the 21st-century changes in the fields under the A1B scenario, as can be seen by comparing the change in DTR shown in Figure 10.11b with the cloud area fraction shown in Figure 10.10b. Changes in DTR reach a magnitude of 0.5°C in some regions, with some consistency among the models. Smaller widespread decreases are likely due to the radiative effect of the enhanced greenhouse gases including water vapour (see also Stone and Weaver, 2002). Further discussion of DTR is provided in Section 10.3.6.2.

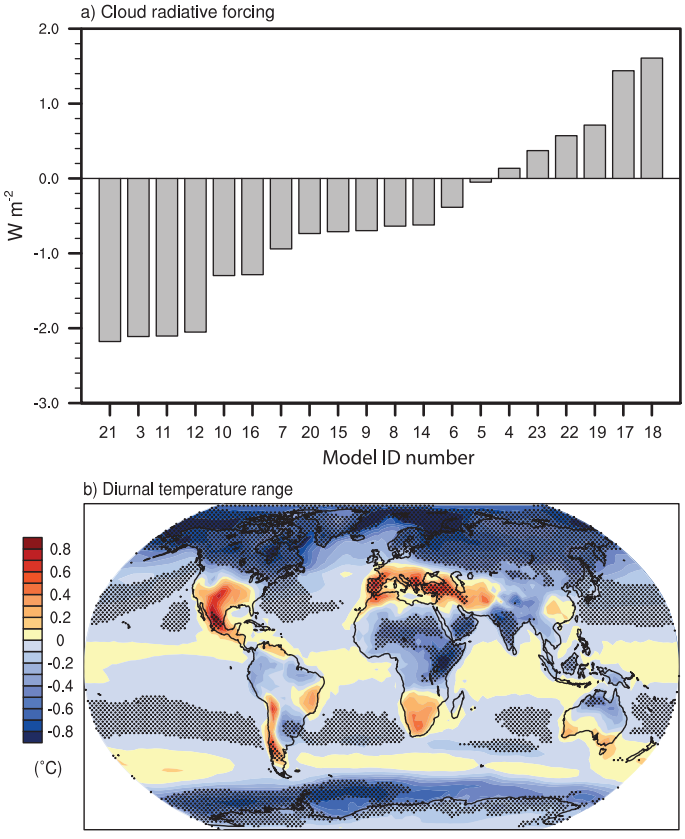


Figure 10.11. *Changes in (a) global mean cloud radiative forcing (W m^{-2}) from individual models (see Table 10.4 for the list of models) and (b) multi-model mean diurnal temperature range (°C). Changes are annual means for the SRES A1B scenario for the period 2080 to 2099 relative to 1980 to 1999. Stippling denotes areas where the magnitude of the multi-model ensemble mean exceeds the inter-model standard deviation. Results for individual models can be seen in the Supplementary Material for this chapter.*

In addition to the DTR, Kitoh and Arakawa (2005) document changes in the regional patterns of diurnal precipitation over the Indonesian region, and show that over ocean, nighttime precipitation decreases and daytime precipitation increases, while over land the opposite is the case, thus producing a decrease in the diurnal precipitation amplitude over land and ocean. They attribute these changes to a larger nighttime temperature increase over land due to increased greenhouse gases.

10.3.2.3 Precipitation and Surface Water

Models simulate that global mean precipitation increases with global warming. However, there are substantial spatial and seasonal variations in this field even in the multi-model means depicted in Figure 10.9. There are fewer areas stippled for precipitation than for the warming, indicating more variation in the magnitude of change among the ensemble of models. Increases in precipitation at high latitudes in both seasons are very consistent across models. The increases in precipitation over the tropical oceans and in some of the monsoon regimes (e.g., South Asian monsoon in JJA, Australian monsoon in DJF) are notable, and while not as consistent locally, considerable agreement is found at the broader scale in the tropics (Neelin et al., 2006). There are widespread decreases in mid-latitude summer precipitation, except for increases in eastern Asia. Decreases in precipitation over many subtropical areas are evident in the multi-model ensemble mean, and consistency in the sign of change among the models is often high (Wang, 2005), particularly in some regions like the tropical Central American-Caribbean (Neelin et al., 2006). Further discussion of regional changes is presented in Chapter 11.

The global map of the A1B 2080 to 2099 change in annual mean precipitation is shown in Figure 10.12, along with other hydrological quantities from the multi-model ensemble. Emori and Brown (2005) show percentage changes of annual precipitation from the ensemble. Increases of over 20% occur at most high latitudes, as well as in eastern Africa, central Asia and the equatorial Pacific Ocean. The change over the ocean between 10°S and 10°N accounts for about half the increase in the global mean (Figure 10.5). Substantial decreases, reaching 20%, occur in the Mediterranean region (Rowell and Jones, 2006), the Caribbean region (Neelin et al., 2006) and the subtropical western coasts of each continent. Overall, precipitation over land increases by about 5%, while precipitation over ocean increases 4%, but with regional changes of both signs. The net change over land accounts for 24% of the global mean increase in precipitation, a little less than the areal proportion of land (29%). In Figure 10.12, stippling indicates that the sign of the

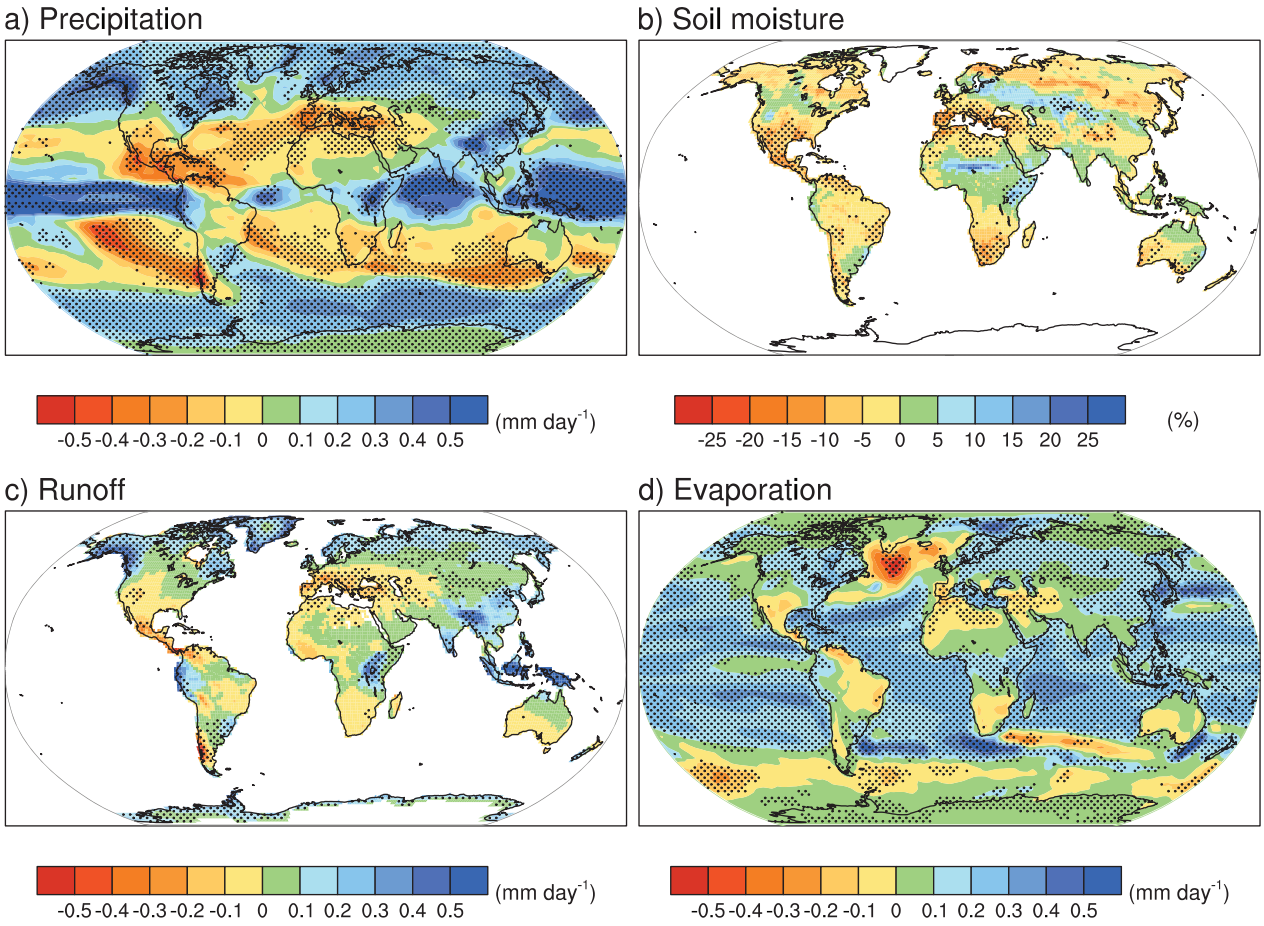


Figure 10.12. *Multi-model mean changes in (a) precipitation (mm day–1), (b) soil moisture content (%), (c) runoff (mm day–1) and (d) evaporation (mm day–1). To indicate consistency in the sign of change, regions are stippled where at least 80% of models agree on the sign of the mean change. Changes are annual means for the SRES A1B scenario for the period 2080 to 2099 relative to 1980 to 1999. Soil moisture and runoff changes are shown at land points with valid data from at least 10 models. Details of the method and results for individual models can be found in the Supplementary Material for this chapter.*

local change is common to at least 80% of the models (with the alternative test shown in the Supplementary Material). This simpler test for consistency is of particular interest for quantities where the magnitudes for the base climate vary across models.

These patterns of change occur in the other scenarios, although with agreement (by the metric M) a little lower than for the warming. The predominance of increases near the equator and at high latitudes, for both land and ocean, is clear from the zonal mean changes of precipitation included in Figure 10.6. The results for change scaled by global mean warming are rather similar across the four scenarios, an exception being a relatively large increase over the equatorial ocean for the commitment case. As with surface temperature, the A1B and B1 scaled values are always close to the A2 results. The zonal means of the percentage change map (shown in Figure 10.6) feature substantial decreases in the subtropics and lower mid-latitudes of both hemispheres in the A2 case, even if increases occur over some regions.

Wetherald and Manabe (2002) provide a good description of the mechanism of hydrological change simulated by GCMs. In GCMs, the global mean evaporation changes closely balance the precipitation change, but not locally because of changes in the atmospheric transport of water vapour. Annual average evaporation (Figure 10.12) increases over much of the ocean, with spatial variations tending to relate to those in the surface warming (Figure 10.8). As found by Kutzbach et al. (2005) and Bosilovich et al. (2005), atmospheric moisture convergence increases over the equatorial oceans and over high latitudes. Over land, rainfall changes tend to be balanced by both evaporation and runoff. Runoff (Figure 10.12) is notably reduced in southern Europe and increased in Southeast Asia and at high latitudes, where there is consistency among models in the sign of change (although less consistency in the magnitude of change). The larger changes reach 20% or more of the simulated 1980 to 1999 values, which range from 1 to 5 mm day–1 in wetter regions to below 0.2 mm day–1 in deserts. Runoff from the melting of ice sheets (Section 10.3.3) is not included here. Nohara et al. (2006) and Milly et al. (2005) assess the impacts of these changes in terms of river flow, and find that discharges from high-latitude rivers increase, while those from major rivers in the Middle East, Europe and Central America tend to decrease.

Models simulate the moisture in the upper few metres of the land surface in varying ways, and evaluation of the soil moisture content is still difficult (See Section 8.2.3.2; Wang, 2005; Gao and Dirmeyer, 2006 for multi-model analyses). The average of the total soil moisture content quantity submitted to the data set is presented here to indicate typical trends. In the annual mean (Figure 10.12), decreases are common in the subtropics and the Mediterranean region. There are increases in east Africa, central Asia, and some other regions with increased precipitation. Decreases also occur at high latitudes, where snow cover diminishes (Section 10.3.3). While the magnitudes of change are quite uncertain, there is good consistency in the signs of change in many of these regions. Similar patterns of change occur in seasonal results (Wang, 2005). Regional hydrological changes are considered in Chapter 11 and in the IPCC Working Group II report.

10.3.2.4 Sea Level Pressure and Atmospheric Circulation

As a basic component of the mean atmospheric circulations and weather patterns, projections of the mean sea level pressure for the medium scenario A1B are considered. Seasonal mean changes for DJF and JJA are shown in Figure 10.9 (matching results in Wang and Swail, 2006b). Sea level pressure differences show decreases at high latitudes in both seasons in both hemispheres. The compensating increases are predominantly over the mid-latitude and subtropical ocean regions, extending across South America, Australia and southern Asia in JJA, and the Mediterranean in DJF. Many of these increases are consistent across the models. This pattern of change, discussed further in Section 10.3.5.3, has been linked to an expansion of the Hadley Circulation and a poleward shift of the mid-latitude storm tracks (Yin, 2005). This helps explain, in part, the increases in precipitation at high latitudes and decreases in the subtropics and parts of the mid-latitudes. Further analysis of the regional details of these changes is given in Chapter 11. The pattern of pressure change implies increased westerly flows across the western parts of the continents. These contribute to increases in mean precipitation (Figure 10.9) and increased precipitation intensity (Meehl et al., 2005a).

10.3.3 Changes in Ocean/Ice and High-Latitude Climate

10.3.3.1 Changes in Sea Ice Cover

Models of the 21st century project that future warming is amplified at high latitudes resulting from positive feedbacks involving snow and sea ice, and other processes (Section 8.6.3.3). The warming is particularly large in autumn and early winter (Manabe and Stouffer, 1980; Holland and Bitz, 2003) when sea ice is thinnest and the snow depth is insufficient to blur the relationship between surface air temperature and sea ice thickness (Maykut and Untersteiner, 1971). As shown by Zhang and Walsh (2006), the coupled models show a range of responses in NH sea ice areal extent ranging from very little change to a strong and accelerating reduction over the 21st century (Figure 10.13a,b).

An important characteristic of the projected change is for summer ice area to decline far more rapidly than winter ice area (Gordon and O'Farrell, 1997), and hence sea ice rapidly approaches a seasonal ice cover in both hemispheres (Figures 10.13b and 10.14). Seasonal ice cover is, however, rather robust and persists to some extent throughout the 21st century in most (if not all) models. Bitz and Roe (2004) note that future projections show that arctic sea ice thins fastest where it is initially thickest, a characteristic that future climate projections share with sea ice thinning observed in the late 20th century (Rothrock et al., 1999). Consistent with these results, a projection by Gregory et al. (2002b) shows that arctic sea ice volume decreases more quickly than sea ice area (because trends in winter ice area are low) in the 21st century.

In 20th- and 21st-century simulations, antarctic sea ice cover is projected to decrease more slowly than in the Arctic (Figures 10.13c,d and 10.14), particularly in the vicinity of the Ross Sea where most models predict a local minimum in surface warming. This is commensurate with the region with the greatest reduction in ocean heat loss, which results from reduced vertical mixing in the ocean (Gregory, 2000). The ocean stores much of its increased heat below 1 km depth in the Southern Ocean. In contrast, horizontal heat transport poleward of about 60°N increases in many models (Holland and Bitz, 2003), but much of this heat remains in the upper 1 km of the northern subpolar seas and Arctic Ocean (Gregory, 2000; Bitz et al., 2006). Bitz et al. (2006) argue that these differences in the depth where heat is accumulating in the high-latitude oceans have consequences for the relative rates of sea ice decay in the Arctic and Antarctic.

While most climate models share these common characteristics (peak surface warming in autumn and early winter, sea ice rapidly becomes seasonal, arctic ice decays faster than antarctic ice, and northward ocean heat transport increases into the northern high latitudes), models have poor agreement on the amount of thinning of sea ice (Flato and Participating CMIP Modeling Groups, 2004; Arzel et al., 2006) and the overall climate change in the polar regions (IPCC, 2001; Holland and Bitz, 2003). Flato (2004) shows that the basic state of the sea ice and the reduction in thickness and/or extent have little to do with sea ice model physics among CMIP2 models. Holland and Bitz (2003) and Arzel et al. (2006) find serious biases in the basic state of simulated sea ice thickness and extent. Further, Rind et al. (1995), Holland and Bitz (2003) and Flato (2004) show that the basic state of the sea ice thickness and extent have a significant influence on the projected change in sea ice thickness in the Arctic and extent in the Antarctic.

10.3.3.2 Changes in Snow Cover and Frozen Ground

Snow cover is an integrated response to both temperature and precipitation and exhibits strong negative correlation with air temperature in most areas with a seasonal snow cover (see Section 8.6.3.3 for an evaluation of model-simulated

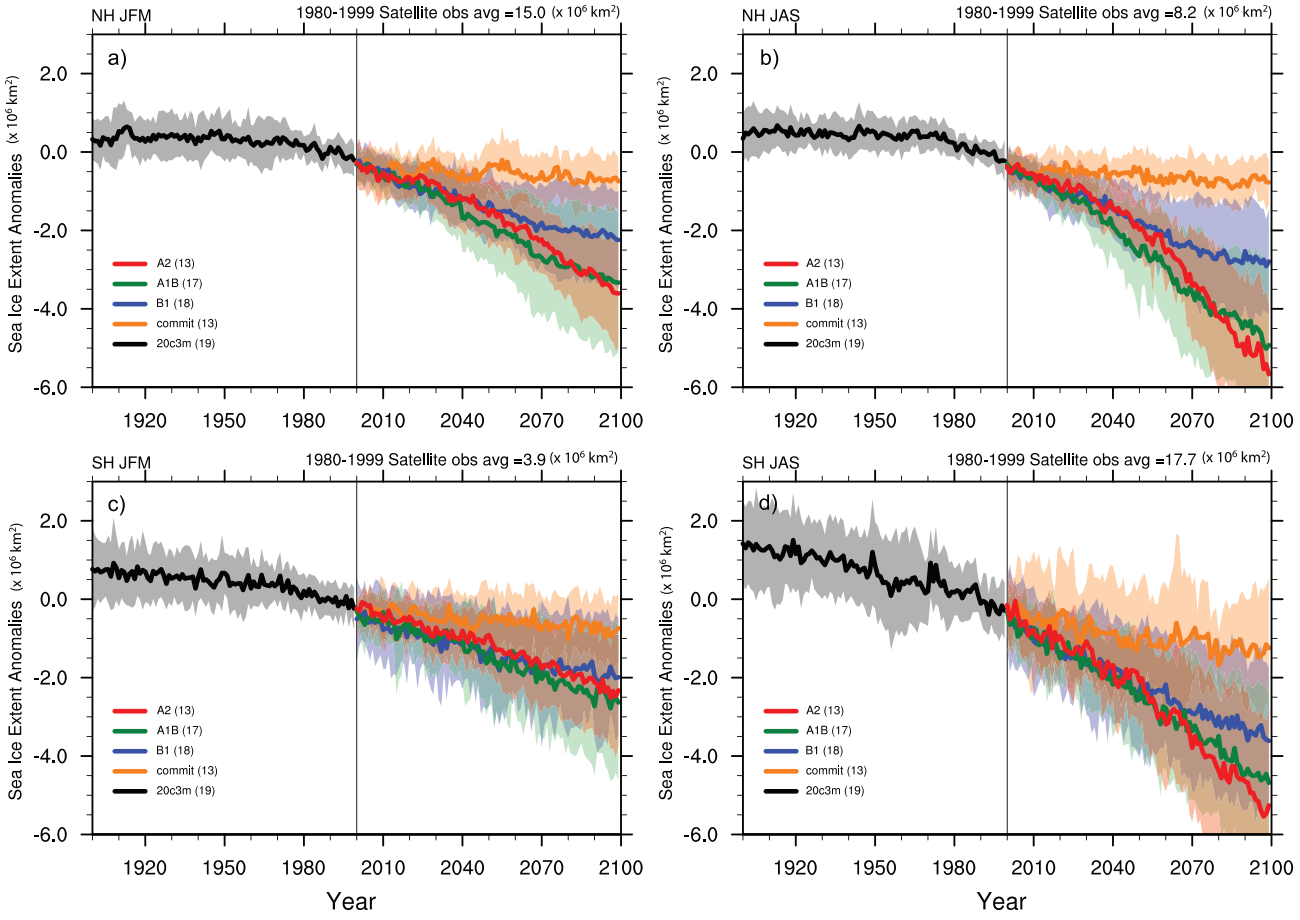


Figure 10.13. *Multi-model simulated anomalies in sea ice extent for the 20th century (20c3m) and 21st century using the SRES A2, A1B and B1 as well as the commitment scenario for (a) Northern Hemisphere January to March (JFM), (b) Northern Hemisphere July to September (JAS). Panels (c) and (d) are as for (a) and (b) but for the Southern Hemisphere. The solid lines show the multi-model mean, shaded areas denote ±1 standard deviation. Sea ice extent is defined as the total area where sea ice concentration exceeds 15%. Anomalies are relative to the period 1980 to 2000. The number of models is given in the legend and is different for each scenario.*

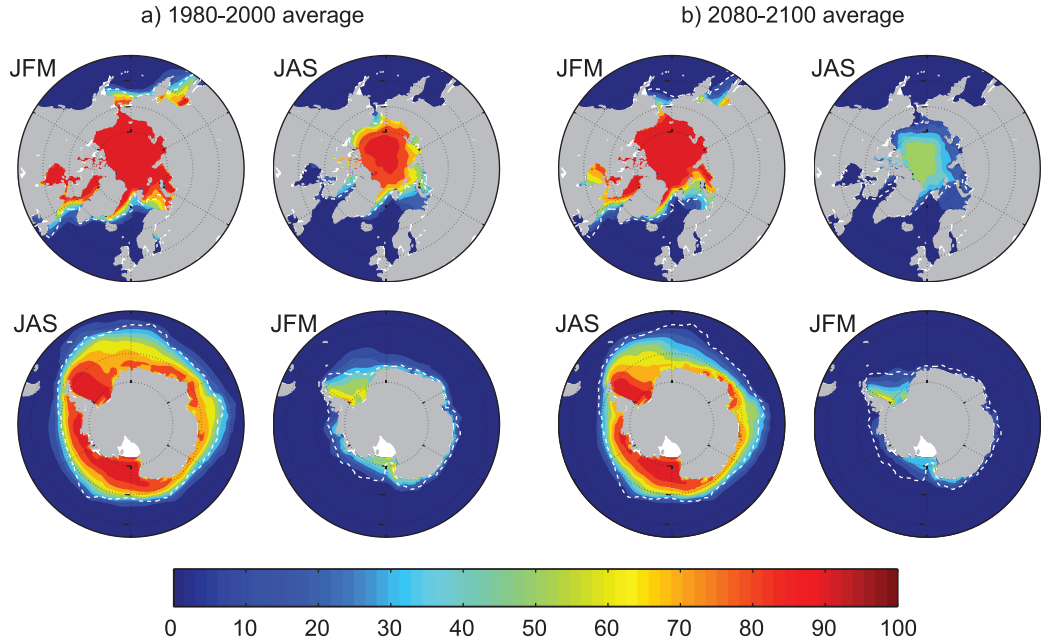


Figure 10.14. *Multi-model mean sea ice concentration (%) for January to March (JFM) and June to September (JAS), in the Arctic (top) and Antarctic (bottom) for the periods (a) 1980 to 2000 and b) 2080 to 2100 for the SRES A1B scenario. The dashed white line indicates the present-day 15% average sea ice concentration limit. Modified from Flato et al. (2004).*

present-day snow cover). Because of this temperature association, the simulations project widespread reductions in snow cover over the 21st century (Supplementary Material, Figure S10.1). For the Arctic Climate Impact Assessment (ACIA) model mean, at the end of the 21st century the projected reduction in the annual mean NH snow cover is 13% under the B2 scenario (ACIA, 2004). The individual model projections range from reductions of 9 to 17%. The actual reductions are greatest in spring and late autumn/early winter, indicating a shortened snow cover season (ACIA, 2004). The beginning of the snow accumulation season (the end of the snowmelt season) is projected to be later (earlier), and the fractional snow coverage is projected to decrease during the snow season (Hosaka et al., 2005).

Warming at high northern latitudes in climate model simulations is also associated with large increases in simulated thaw depth over much of the permafrost regions (Lawrence and Slater, 2005; Yamaguchi et al., 2005; Kitabata et al., 2006). Yamaguchi et al. (2005) show that initially soil moisture increases during the summer. In the late 21st century when the thaw depth has increased substantially, a reduction in summer soil moisture eventually occurs (Kitabata et al., 2006). Stendel and Christensen (2002) show poleward movement of permafrost extent, and a 30 to 40% increase in active layer thickness for most of the permafrost area in the NH, with the largest relative increases concentrated in the northernmost locations.

Regionally, the changes are a response to both increased temperature and increased precipitation (changes in circulation patterns) and are complicated by the competing effects of warming and increased snowfall in those regions that remain below freezing (see Section 4.2 for a further discussion of processes that affect snow cover). In general, snow amount and snow coverage decreases in the NH (Supplementary Material, Figure S10.1). However, in a few regions (e.g., Siberia), snow amount is projected to increase. This is attributed to the increase in precipitation (snowfall) from autumn to winter (Meleshko et al., 2004; Hosaka et al., 2005).

10.3.3.3 Changes in Greenland Ice Sheet Mass Balance

As noted in Section 10.6, modelling studies (e.g., Hanna et al., 2002; Kiilsholm et al., 2003; Wild et al., 2003) as well as satellite observations, airborne altimeter surveys and other studies (Abdalati et al., 2001; Thomas et al., 2001; Krabill et al., 2004; Johannessen et al., 2005; Zwally et al., 2005; Rignot and Kanagaratnam, 2006) suggest a slight inland thickening and strong marginal thinning resulting in an overall negative Greenland Ice Sheet mass balance which has accelerated recently (see Section 4.6.2.2.). A consistent feature of all climate models is that projected 21st-century warming is amplified in northern latitudes. This suggests continued melting of the Greenland Ice Sheet, since increased summer melting dominates over increased winter precipitation in model projections of future climate. Ridley et al. (2005) coupled UKMO-HadCM3 to an ice sheet model to explore the melting of the Greenland Ice Sheet under elevated (four times pre-industrial) levels of atmospheric CO_2 (see Section 10.7.4.3, Figure 10.38). While the entire Greenland Ice Sheet eventually completely ablated (after 3 kyr), the peak rate of melting was 0.06 Sv (1 Sv = 10^6 m^3 s^{-1}) corresponding to about 5.5 mm yr^{-1} global sea level rise (see Sections 10.3.4 and 10.6.6). Toniazzo et al. (2004) further show that in UKMO-HadCM3, the complete melting of the Greenland Ice sheet is an irreversible process even if pre-industrial levels of atmospheric CO_2 are re-established after it melts.

10.3.4 Changes in the Atlantic Meridional Overturning Circulation

A feature common to all climate model projections is the increase in high-latitude temperature as well as an increase in high-latitude precipitation. This was reported in the TAR and is confirmed by the projections using the latest versions of comprehensive climate models (see Section 10.3.2). Both of these effects tend to make the high-latitude surface waters less dense and hence increase their stability, thereby inhibiting convective processes. As more coupled models have become available since the TAR, the evolution of the Atlantic Meridional Overturning Circulation (MOC) can be more thoroughly assessed. Figure 10.15 shows simulations from 19 coupled models integrated from 1850 to 2100 under SRES A1B atmospheric CO_2 and aerosol scenarios up to year 2100, and constant concentrations thereafter (see Figure 10.5). All of the models, except CGCM3.1, INM-CM3.0 and MRI-CGCM2.3.2, were run without flux adjustments (see Table 8.1). The MOC is influenced by the density structure of the Atlantic Ocean, small-scale mixing and the surface momentum and buoyancy fluxes. Some models simulate a MOC strength that is inconsistent with the range of present-day estimates (Smethie and Fine, 2001; Ganachaud, 2003; Lumpkin and Speer, 2003; Talley, 2003). The MOC for these models is shown for completeness but is not used in assessing potential future changes in the MOC in response to various emissions scenarios.

Fewer studies have focused on projected changes in the Southern Ocean resulting from future climate warming. A common feature of coupled model simulations is the projected poleward shift and strengthening of the SH westerlies (Yin, 2005; Fyfe and Saenko, 2006). This in turn leads to a strengthening, poleward shift and narrowing of the Antarctic Circumpolar Current. Fyfe and Saenko (2006) further note that the enhanced equatorward surface Ekman transport, associated with the intensified westerlies, is balanced by an enhanced deep geostrophic poleward return flow below 2,000 m.

Generally, the simulated late-20th century Atlantic MOC shows a spread ranging from a weak MOC of about 12 Sv to over 20 Sv (Figure 10.15; Schmittner et al., 2005). When forced with the SRES A1B scenario, the models show a reduction in the MOC of up to 50% or more, but in one model, the changes are not distinguishable from the simulated natural variability. The reduction in the MOC proceeds on the time scale of the simulated warming because it is a direct response to the increase in buoyancy at the ocean surface. A positive North Atlantic Oscillation (NAO) trend might delay this response by a few decades but not prevent it (Delworth and Dixon, 2000). Such

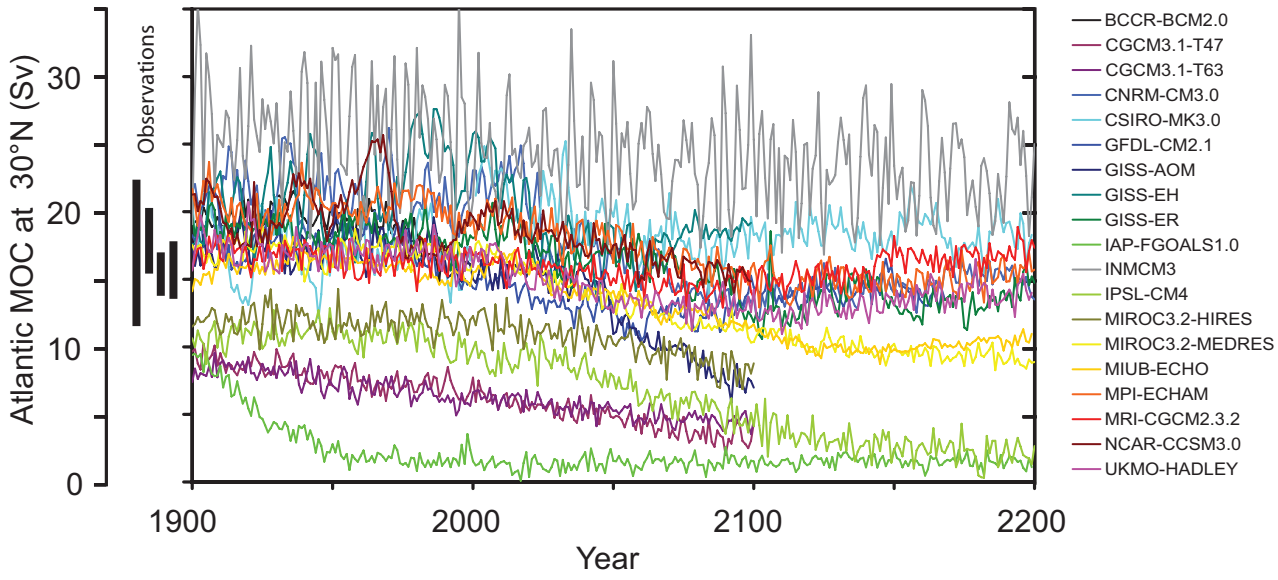


Figure 10.15. *Evolution of the Atlantic meridional overturning circulation (MOC) at 30°N in simulations with the suite of comprehensive coupled climate models (see Table 8.1 for model details) from 1850 to 2100 using 20th Century Climate in Coupled Models (20C3M) simulations for 1850 to 1999 and the SRES A1B emissions scenario for 1999 to 2100. Some of the models continue the integration to year 2200 with the forcing held constant at the values of year 2100. Observationally based estimates of late-20th century MOC are shown as vertical bars on the left. Three simulations show a steady or rapid slow down of the MOC that is unrelated to the forcing; a few others have late-20th century simulated values that are inconsistent with observational estimates. Of the model simulations consistent with the late-20th century observational estimates, no simulation shows an increase in the MOC during the 21st century; reductions range from indistinguishable within the simulated natural variability to over 50% relative to the 1960 to 1990 mean; and none of the models projects an abrupt transition to an off state of the MOC. Adapted from Schmittner et al. (2005) with additions.*

a weakening of the MOC in future climate causes reduced sea surface temperature (SST) and salinity in the region of the Gulf Stream and North Atlantic Current (Dai et al., 2005). This can produce a decrease in northward heat transport south of 60°N, but increased northward heat transport north of 60°N (A. Hu et al., 2004). No model shows an increase in the MOC in response to the increase in greenhouse gases, and no model simulates an abrupt shut-down of the MOC within the 21st century. One study suggests that inherent low-frequency variability in the Atlantic region, the Atlantic Multidecadal Oscillation, may produce a natural weakening of the MOC over the next few decades that could further accentuate the decrease due to anthropogenic climate change (Knight et al., 2005; see Section 8.4.6).

In some of the older models (e.g., Dixon et al., 1999), increased high-latitude precipitation dominates over increased high-latitude warming in causing the weakening, while in others (e.g., Mikolajewicz and Voss, 2000), the opposite is found. In a recent model intercomparison, Gregory et al. (2005) find that for all 11 models analysed, the MOC reduction is caused more by changes in surface heat flux than changes in surface freshwater flux. In addition, simulations using models of varying complexity (Stocker et al., 1992b; Saenko et al., 2003; Weaver et al., 2003) show that freshening or warming in the Southern Ocean acts to increase or stabilise the Atlantic MOC. This is likely a consequence of the complex coupling of Southern Ocean processes with North Atlantic Deep Water production.

A few simulations using coupled models are available that permit the assessment of the long-term stability of the MOC (Stouffer and Manabe, 1999; Voss and Mikolajewicz, 2001; Stouffer and Manabe, 2003; Wood et al., 2003; Yoshida et al., 2005; Bryan et al., 2006). Most of these simulations assume an idealised increase in atmospheric CO_2 by 1% yr^{-1} to various levels ranging from two to four times pre-industrial levels. One study also considers slower increases (Stouffer and Manabe, 1999), or a reduction in CO_2 (Stouffer and Manabe, 2003). The more recent models are not flux adjusted and have higher resolution (about 1.0°) (Yoshida et al., 2005; Bryan et al., 2006). A common feature of all simulations is a reduction in the MOC in response to the warming and a stabilisation or recovery of the MOC when the concentration is kept constant after achieving a level of two to four times the pre-industrial atmospheric CO_2 concentration. None of these models shows a shutdown of the MOC that continues after the forcing is kept constant. But such a long-term shutdown cannot be excluded if the amount of warming and its rate exceed certain thresholds as shown using an EMIC (Stocker and Schmittner, 1997). Complete shut-downs, although not permanent, were also simulated by a flux-adjusted coupled model (Manabe and Stouffer, 1994; Stouffer and Manabe, 2003; see also Chan and Motoi, 2005). In none of these AOGCM simulations were the thresholds, as determined by the EMIC, passed (Stocker and Schmittner, 1997). As such, the long-term stability of the MOC found in the present AOGCM simulations is consistent with the results from the simpler models.

The reduction in MOC strength associated with increasing greenhouse gases represents a negative feedback for the warming in and around the North Atlantic. That is, through reducing the transport of heat from low to high latitudes, SSTs are cooler than they would otherwise be if the MOC was unchanged. As

such, warming is reduced over and downstream of the North Atlantic. It is important to note that in models where the MOC weakens, warming still occurs downstream over Europe due to the overall dominant role of the radiative forcing associated with increasing greenhouse gases (Gregory et al., 2005). Many future projections show that once the radiative forcing is held fixed, re-establishment of the MOC occurs to a state similar to that of the present day. The partial or complete re-establishment of the MOC is slow and causes additional warming in and around the North Atlantic. While the oceanic meridional heat flux at low latitudes is reduced upon a slowdown of the MOC, many simulations show increasing meridional heat flux into the Arctic which contributes to accelerated warming and sea ice melting there. This is due to both the advection of warmer water and an intensification of the influx of North Atlantic water into the Arctic (A. Hu et al., 2004).

Climate models that simulated a complete shutdown of the MOC in response to sustained warming were flux-adjusted coupled GCMs or EMICs. A robust result from such simulations is that the shutdown of the MOC takes several centuries after the forcing is kept fixed (e.g., at 4 × atmospheric CO_2 concentration). Besides the forcing amplitude and rate (Stocker and Schmittner, 1997), the amount of mixing in the ocean also appears to determine the stability of the MOC: increased vertical and horizontal mixing tends to stabilise the MOC and to eliminate the possibility of a second equilibrium state (Manabe and Stouffer, 1999; Knutti and Stocker, 2000; Longworth et al., 2005). Random internal variability or noise, often not present in simpler models, may also be important in determining the effective MOC stability (Knutti and Stocker, 2002; Monahan, 2002).

The MOC is not necessarily a comprehensive indicator of ocean circulation changes in response to global warming. In a transient 2 × atmospheric CO_2 experiment using a coupled AOGCM, the MOC changes were small, but convection in the Labrador Sea stopped due to warmer and hence less dense waters that inflow from the Greenland-Iceland-Norwegian Sea (GIN Sea) (Wood et al., 1999; Stouffer et al., 2006a). Similar results were found by A. Hu et al. (2004), who also report an increase in convection in the GIN Sea due to the influx of more saline waters from the North Atlantic. Various simulations using coupled models of different complexity find significant reductions in convection in the GIN Sea in response to warming (Schaeffer et al., 2004; Bryan et al., 2006). Presumably, a delicate balance exists in the GIN Sea between the circum-arctic river runoff, sea ice production and advection of saline waters from the North Atlantic, and on a longer time scale, the inflow of freshwater through Bering Strait. The projected increases in circum-arctic river runoff (Wu et al., 2005) may enhance the tendency towards a reduction in GIN Sea convection (Stocker and Raible, 2005; Wu et al., 2005). Cessation of convection in the Labrador Sea in the next few decades is also simulated in a high-resolution model of the Atlantic Ocean driven by surface fluxes from two AOGCMs (Schweckendiek and Willebrand, 2005). The large-scale responses of the high-resolution ocean model (e.g., MOC, Labrador Seas) agree with those from the AOGCMs. The grid resolution of the ocean components in the coupled AOGCMs has significantly increased since the TAR, and some consistent patterns of changes in convection and water mass properties in the Atlantic Ocean emerge in response to the warming, but models still show a variety of responses in the details.

The best estimate of sea level from 1993 to 2003 (see Section 5.5.5.2) associated with the slight net negative mass balance from Greenland is 0.1 to 0.3 mm yr^{-1} over the total ocean surface. This converts to only about 0.002 to 0.003 Sv of freshwater forcing. Such an amount, even when added directly and exclusively to the North Atlantic, has been suggested to be too small to affect the North Atlantic MOC (see Weaver and Hillaire-Marcel, 2004a). While one model exhibits a MOC weakening in the later part of the 21st century due to Greenland Ice Sheet melting (Fichefet et al., 2003), this same model had a very large downward drift of its overturning in the control climate, making it difficult to actually attribute the model MOC changes to the ice sheet melting. As noted in Section 10.3.3.3, Ridley et al. (2005) find the peak rate of Greenland Ice Sheet melting is about 0.1 Sv when they instantaneously elevate greenhouse gas levels in UKMO-HadCM3. They further note that this has little effect on the North Atlantic meridional overturning, although 0.1 Sv is sufficiently large to cause more dramatic transient changes in the strength of the MOC in other models (Stouffer et al., 2006b).

Taken together, it is very likely that the MOC, based on currently available simulations, will decrease, perhaps associated with a significant reduction in Labrador Sea Water formation, but very unlikely that the MOC will undergo an abrupt transition during the course of the 21st century. At this stage, it is too early to assess the likelihood of an abrupt change of the MOC beyond the end of the 21st century, but the possibility cannot be excluded (see Box 10.1). The few available simulations with models of different complexity instead suggest a centennial slowdown. Recovery of the MOC is simulated in some models if the radiative forcing is stabilised but would take several centuries; in other models, the reduction persists.

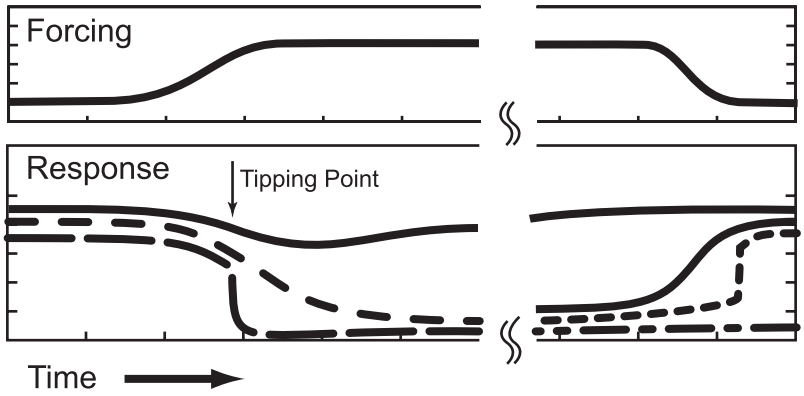
Box 10.1: Future Abrupt Climate Change, 'Climate Surprises', and Irreversible Changes

Theory, models and palaeoclimatic reconstructions (see Chapter 6) have established the fact that changes in the climate system can be abrupt and widespread. A working definition of 'abrupt climate change' is given in Alley et al. (2002): 'Technically, an abrupt climate change occurs when the climate system is forced to cross some threshold, triggering a transition to a new state at a rate determined by the climate system itself and faster than the cause'. More generally, a gradual change in some determining quantity of the climate system (e.g., radiation balance, land surface properties, sea ice, etc.) can cause a variety of structurally different responses (Box 10.1, Figure 1). The response of a purely linear system scales with the forcing, and at stabilisation of the forcing, a new equilibrium is achieved which is structurally similar, but not necessarily close to the original state. However, if the system contains more than one equilibrium state, transitions to structurally different states are possible. Upon the crossing of a tipping point (bifurcation point), the evolution of the system is no longer controlled by the time scale of the forcing, but rather determined by its internal dynamics, which can either be much faster than the forcing, or significantly slower. Only the former case would be termed 'abrupt climate change', but the latter case is of equal importance. For the long-term evolution of a climate variable one must distinguish between reversible and irreversible changes. The notion of 'climate surprises' usually refers to abrupt transitions and temporary or permanent transitions to a different state in parts of the climate system such as, for example, the 8.2 kyr event (see Section 6.5.2.1).

Atlantic Meridional Overturning Circulation and other ocean circulation changes:

The best-documented type of abrupt climate change in the palaeoclimatic archives is that associated with changes in the ocean circulation (Stocker, 2000). Since the TAR, many new results from climate models of different complexity have provided a more detailed view on the anticipated changes in the Atlantic MOC in response to global warming. Most models agree that the MOC weakens over the next 100 years and that this reduction ranges from indistinguishable from natural variability to over 50% by 2100 (Figure 10.15). None of the AOGCM simulations shows an abrupt change when forced with the SRES emissions scenarios until 2100, but some long-term model simulations suggest that a complete cessation can result for large forcings (Stouffer and Manabe, 2003). Models of intermediate complexity indicate that thresholds in the MOC may be present but that they depend on the amount and rate of warming for a given model (Stocker and Schmittner, 1997). The few long-term simulations from AOGCMs indicate that even complete shutdowns of the MOC may be reversible (Stouffer and Manabe, 2003; Yoshida et al., 2005; Stouffer et al., 2006b). However, until millennial simulations with AOGCMs are available, the important question of potential irreversibility of an MOC shutdown remains unanswered. Both simplified models and AOGCMs agree, however, that a potentially complete shut-down of the MOC, induced by global warming, would take many decades to more than a century. There is no direct model evidence that the MOC could collapse within a few decades in response to global warming. However, a few studies do show the potential for rapid changes in the MOC (Manabe and Stouffer, 1999), and the processes concerned are poorly understood (see Section 8.7). This is not inconsistent with the palaeoclimate records. The cooling events during the last ice ages registered in the Greenland ice cores developed over a couple of centuries to millennia. In contrast, there were also a number of very rapid warmings, the so-called Dansgaard-Oeschger events (NorthGRIP Members, 2004), or rapid cooling (LeGrande et al., 2006), which evolved over decades or less, most probably associated with rapid latitudinal shifts in ocean convection sites and changes in strength of the MOC (see Section 6.3.2).

(continued)



Box 10.1, Figure 1. *Schematic illustration of various responses of a climate variable to forcing. The forcing (top panels) reaches a new stable level (left part of figure), and later approaches the original level on very long time scales (right part of the figure). The response of the climate variable (bottom panels) can be smooth (solid line) or cross a tipping point inducing a transition to a structurally different state (dashed lines). That transition can be rapid (abrupt change, long-dashed), or gradual (short-dashed), but is usually dictated by the internal dynamics of the climate system rather than the forcing. The long-term behaviour (right part) also exhibits different possibilities. Changes can be irreversible (dash-dotted) with the system settling at a different stable state, or reversible (solid, dotted) when the forcing is set back to its original value. In the latter case, the transition again can be gradual or abrupt. An example for illustration, but not the only one, is the response of the Atlantic meridional overturning circulation to a gradual change in radiative forcing.*

Recent simulations with models with ocean components that resolve topography in sufficient detail obtain a consistent pattern of a strong to complete reduction of convection in the Labrador Sea (Wood et al., 1999; Schweckendiek and Willebrand, 2005). Such changes in the convection, with implications for the atmospheric circulation, can develop within a few years (Schaeffer et al., 2002). The long-term and regional-to-hemispheric scale effects of such changes in water mass properties have not yet been investigated.

With a reduction in the MOC, the meridional heat flux also decreases in the subtropical and mid-latitudes with large-scale effects on the atmospheric circulation. In consequence, the warming of the North Atlantic surface proceeds more slowly. Even for strong reductions in MOC towards the end of the 21st century, no cooling is observed in the regions around the North Atlantic because it is overcompensated by the radiative forcing that caused the ocean response in the first place.

At high latitudes, an increase in the oceanic meridional heat flux is simulated by these models. This increase is due to both an increase in the overturning circulation in the Arctic and the advection of warmer waters from lower latitudes and thus contributes significantly to continuing sea ice reduction in the Atlantic sector of the Arctic (A. Hu et al., 2004). Few simulations have also addressed the changes in overturning in the South Atlantic and Southern Ocean. In addition to water mass modifications, this also has an effect on the transport by the Antarctic Circumpolar Current, but results are not yet conclusive.

Current understanding of the processes responsible for the initiation of an ice age indicate that a reduction or collapse of the MOC in response to global warming could not start an ice age (Berger and Loutre, 2002; Crucifix and Loutre, 2002; Yoshimori et al., 2002; Weaver and Hillaire-Marcel, 2004b).

Arctic sea ice:

Arctic sea ice is responding sensitively to global warming. While changes in winter sea ice cover are moderate, late summer sea ice is projected to disappear almost completely towards the end of the 21st century. A number of positive feedbacks in the climate system accelerate the melt back of sea ice. The ice-albedo feedback allows open water to receive more heat from the Sun during summer, and the increase in ocean heat transport to the Arctic through the advection of warmer waters and stronger circulation further reduces ice cover. Minimum arctic sea ice cover is observed in September. Model simulations indicate that the September sea ice cover decreases substantially in response to global warming, generally evolving on the time scale of the warming. With sustained warming, the late summer disappearance of a major fraction of arctic sea ice is permanent.

Glaciers and ice caps:

Glaciers and ice caps are sensitive to changes in temperature and precipitation. Observations point to a reduction in volume over the last 20 years (see Section 4.5.2), with a rate during 1993 to 2003 corresponding to 0.77 ± 0.22 mm yr^{-1} sea level equivalent, with a larger mean central estimate than that for 1961 to 1998 (corresponding to 0.50 ± 0.18 mm yr^{-1} sea level equivalent). Rapid changes are therefore already underway and enhanced by positive feedbacks associated with the surface energy balance of shrinking glaciers and newly exposed land surface in periglacial areas. Acceleration of glacier loss over the next few decades is likely (see Section 10.6.3). Based on simulations of 11 glaciers in various regions, a volume loss of 60% of these glaciers is projected by the year 2050 (Schneeberger et al., 2003). Glaciated areas in the Americas are also affected. A comparative study including seven GCM simulations at $2 \times$ atmospheric CO_2 conditions inferred that many glaciers may disappear completely due to an increase in the equilibrium line altitude (Bradley et al., 2004). The disappearance of these ice bodies is much faster than a potential re-glaciation several centuries hence, and may in some areas be irreversible.

Greenland and West Antarctic Ice Sheets:

Satellite and *in situ* measurement networks have demonstrated increasing melting and accelerated ice flow around the periphery of the Greenland Ice Sheet (GIS) over the past 25 years (see Section 4.6.2). The few simulations of long-term ice sheet simulations suggest that the GIS will significantly decrease in volume and area over the coming centuries if a warmer climate is maintained (Gregory et al., 2004a; Huybrechts et al., 2004; Ridley et al., 2005). A threshold of annual mean warming of 1.9°C to 4.6°C in Greenland has been estimated for elimination of the GIS (Gregory and Huybrechts, 2006; see section 10.7.3.3), a process which would take many centuries to complete. Even if temperatures were to decrease later, the reduction of the GIS to a much smaller extent might be irreversible, because the climate of an ice-free Greenland could be too warm for accumulation; however, this result is model dependent (see Section 10.7.3.3). The positive feedbacks involved here are that once the ice sheet gets thinner, temperatures in the accumulation region are higher, increasing the melting and causing more precipitation to fall as rain rather than snow; that the lower albedo of the exposed ice-free land causes a local climatic warming; and that surface melt water might accelerate ice flow (see Section 10.6.4.2).

A collapse of the West Antarctic Ice Sheet (WAIS) has been discussed as a potential response to global warming for many years (Bindschadler, 1998; Oppenheimer, 1998; Vaughan, 2007). A complete collapse would cause a global sea level rise of about 5 m. The observed acceleration of ice streams in the Amundsen Sea sector of the WAIS, the rapidity of propagation of this signal upstream and the acceleration of glaciers that fed the Larsen B Ice Shelf after its collapse have renewed these concerns (see Section 10.6.4.2).

(continued)

It is possible that the presence of ice shelves tends to stabilise the ice sheet, at least regionally. Therefore, a weakening or collapse of ice shelves, caused by melting on the surface or by melting at the bottom by a warmer ocean, might contribute to a potential destabilisation of the WAIS, which could proceed through the positive feedback of grounding-line retreat. Present understanding is insufficient for prediction of the possible speed or extent of such a collapse (see Box 4.1 and Section 10.7.3.4).

Vegetation cover:

Irreversible and relatively rapid changes in vegetation cover and composition have occurred frequently in the past. The most prominent example is the desertification of the Sahara region about 4 to 6 ka (Claussen et al., 1999). The reason for this behaviour is believed to lie in the limits of plant communities with respect to temperature and precipitation. Once critical levels are crossed, certain species can no longer compete within their ecosystem. Areas close to vegetation boundaries will experience particularly large and rapid changes due to the slow migration of these boundaries induced by global warming. A climate model simulation into the future shows that drying and warming in South America leads to a continuous reduction in the forest of Amazonia (Cox et al., 2000, 2004). While evolving continuously over the 21st century, such a change and ultimate disappearance could be irreversible, although this result could be model dependent since an analysis of 11 AOGCMs shows a wide range of future possible rainfall changes over the Amazon (Li et al., 2006).

One of the possible 'climate surprises' concerns the role of the soil in the global carbon cycle. As the concentration of CO_2 is increasing, the soil is acting, in the global mean, as a carbon sink by assimilating carbon due to accelerated growth of the terrestrial biosphere (see also Section 7.3.3.1.1). However, by about 2050, a model simulation suggests that the soil changes to a source of carbon by releasing previously accumulated carbon due to increased respiration (Cox et al., 2000) induced by increasing temperature and precipitation. This represents a positive feedback to the increase in atmospheric CO_2. While different models agree regarding the sign of the feedback, large uncertainties exist regarding the strength (Cox et al., 2000; Dufresne et al., 2002; Friedlingstein et al., 2006). However, the respiration increase is caused by a warmer and wetter climate. The switch from moderate sink to strong source of atmospheric carbon is rather rapid and occurs within two decades (Cox et al., 2004), but the timing of the onset is uncertain (Huntingford et al., 2004). A model intercomparison reveals that once set in motion, the increase in respiration continues even after the CO_2 levels are held constant (Cramer et al., 2001). Although considerable uncertainties still exist, it is clear that feedback mechanisms between the terrestrial biosphere and the physical climate system exist which can qualitatively and quantitatively alter the response to an increase in radiative forcing.

Atmospheric and ocean-atmosphere regimes:

Changes in weather patterns and regimes can be abrupt processes that might occur spontaneously due to dynamical interactions in the atmosphere-ice-ocean system, or manifest as the crossing of a threshold in the system due to slow external forcing. Such shifts have been reported in SST in the tropical Pacific, leading to a more positive ENSO phase (Trenberth, 1990), in the stratospheric polar vortex (Christiansen, 2003), in a shut-down of deep convection in the Greenland Sea (Bönisch et al., 1997; Ronski and Budeus, 2005) and in an abrupt freshening of the Labrador Sea (Dickson et al., 2002). In the latter, the freshening evolved throughout the entire depth but the shift in salinity was particularly rapid: the 34.87 psu isohaline plunged from seasonally surface to 1,600 metres within 2 years with no return since 1973.

In a long, unforced model simulation, a period of a few decades with anomalously cold temperatures (up to 10 standard deviations below average) in the region south of Greenland was found (Hall and Stouffer, 2001). It was caused by persistent winds that changed the stratification of the ocean and inhibited convection, thereby reducing heat transfer from the ocean to the atmosphere. Similar results were found in a different model in which the major convection site in the North Atlantic spontaneously switched to a more southerly location for several decades to centuries (Goosse et al., 2002). Other simulations show that the slowly increasing radiative forcing is able to cause transitions in the convective activity in the Greenland-Iceland-Norwegian Sea that have an influence on the atmospheric circulation over Greenland and Western Europe (Schaeffer et al., 2002). The changes unfold within a few years and indicate that the system has crossed a threshold.

A multi-model analysis of regimes of polar variability (NAO, Arctic and Antarctic Oscillations) reveals that the simulated trends in the 21st century influence the Arctic and Antarctic Oscillations and point towards more zonal circulation (Rauthe et al., 2004). Temperature changes associated with changes in atmospheric circulation regimes such as the NAO can exceed in certain regions (e.g., Northern Europe) the long-term global warming that causes such inter-decadal regime shifts (Dorn et al., 2003).

10.3.5 Changes in Properties of Modes of Variability

10.3.5.1 Interannual Variability in Surface Air Temperature and Precipitation

Future changes in anthropogenic forcing will result not only in changes in the mean climate state but also in the variability of climate. Addressing the interannual variability in monthly mean surface air temperature and precipitation of 19 AOGCMs in CMIP2, Räisänen (2002) finds a decrease in temperature variability during the cold season in the extratropical NH and a slight increase in temperature variability in low latitudes and in warm season northern mid-latitudes. The former is likely due to the decrease of sea ice and snow with increasing temperature. The summer decrease in soil moisture over the mid-latitude land surfaces contributes to the latter. Räisänen (2002) also finds an increase in monthly mean precipitation variability in most areas, both in absolute value (standard deviation) and in relative value (coefficient of variation). However, the significance level of these variability changes is markedly lower than that for time mean climate change. Similar results were obtained from 18 AOGCM simulations under the SRES A2 scenario (Giorgi and Bi, 2005).

10.3.5.2 Monsoons

In the tropics, an increase in precipitation is projected by the end of the 21st century in the Asian monsoon and the southern part of the West African monsoon with some decreases in the Sahel in northern summer (Cook and Vizy, 2006), as well as increases in the Australian monsoon in southern summer in a warmer climate (Figure 10.9). The monsoonal precipitation in Mexico and Central America is projected to decrease in association with increasing precipitation over the eastern equatorial Pacific that affects Walker Circulation and local Hadley Circulation changes (Figure 10.9). A more detailed assessment of regional monsoon changes is provided in Chapter 11.

As a projected global warming will be more rapid over land than over the oceans, the continental-scale land-sea thermal contrast will become larger in summer and smaller in winter. Based on this, a simple idea is that the summer monsoon will be stronger and the winter monsoon will be weaker in the future than the present. However, model results are not as straightforward as this simple consideration. Tanaka et al. (2005) define the intensities of Hadley, Walker and monsoon circulations using the velocity potential fields at 200 hPa. Using 15 AOGCMs, they show a weakening of these tropical circulations by 9%, 8% and 14%, respectively, by the late 21st century compared to the late 20th century. Using eight AOGCMs, Ueda et al. (2006) demonstrate that pronounced warming over the tropics results in a weakening of the Asian summer monsoon circulations in relation to a reduction in the meridional thermal gradients between the Asian continent and adjacent oceans.

Despite weakening of the dynamical monsoon circulation, atmospheric moisture buildup due to increased greenhouse gases and consequent temperature increase results in a larger moisture flux and more precipitation for the Indian monsoon (Douville et al., 2000; IPCC, 2001; Ashrit et al., 2003; Meehl and Arblaster, 2003; May, 2004; Ashrit et al., 2005). For the South Asian summer monsoon, models suggest a northward shift of lower-tropospheric monsoon wind systems with a weakening of the westerly flow over the northern Indian Ocean (Ashrit et al., 2003, 2005). Over Africa in northern summer, multi-model analysis projects an increase in rainfall in East and Central Africa, a decrease in the Sahel, and increases along the Gulf of Guinea coast (Figure 10.9). However, some individual models project an increase of rainfall in more extensive areas of West Africa related to a projected northward movement of the Sahara and the Sahel (Liu et al., 2002; Haarsma et al., 2005). Whether the Sahel will be more or less wet in the future is thus uncertain, although a multi-model assessment of the West African monsoon indicates that the Sahel could become marginally more dry (Cook and Vizy, 2006). This inconsistency of the rainfall projections may be related to AOGCM biases, or an unclear relationship between Gulf of Guinea and Indian Ocean warming, land use change and the West African monsoon. Nonlinear feedbacks that may exist within the West African climate system should also be considered (Jenkins et al., 2005).

Most model results project increased interannual variability in season-averaged Asian monsoon precipitation associated with an increase in its long-term mean value (e.g., Hu et al., 2000b; Räisänen, 2002; Meehl and Arblaster, 2003). Hu et al. (2000a) relate this to increased variability in the tropical Pacific SST (El Niño variability) in their model. Meehl and Arblaster (2003) relate the increased monsoon precipitation variability to increased variability in evaporation and precipitation in the Pacific due to increased SSTs. Thus, the South Asian monsoon variability is affected through the Walker Circulation such that the role of the Pacific Ocean dominates and that of the Indian Ocean is secondary.

Atmospheric aerosol loading affects regional climate and its future changes (see Chapter 7). If the direct effect of the aerosol increase is considered, surface temperatures will not get as warm because the aerosols reflect solar radiation. For this reason, land-sea temperature contrast becomes smaller than in the case without the direct aerosol effect, and the summer monsoon becomes weaker. Model simulations of the Asian monsoon project that the sulphate aerosols' direct effect reduces the magnitude of precipitation change compared with the case of only greenhouse gas increases (Emori et al., 1999; Roeckner et al., 1999; Lal and Singh, 2001). However, the relative cooling effect of sulphate aerosols is dominated by the effects of increasing greenhouse gases by the end of the 21st century in the SRES marker scenarios (Figure 10.26), leading to the increased monsoon precipitation at the end of the 21st century in these scenarios (see Section 10.3.2.3). Furthermore, it is suggested that aerosols with high absorptivity such as black carbon absorb solar radiation in the lower atmosphere, cool the surface, stabilise the atmosphere and reduce precipitation (Ramanathan et al., 2001). The solar

radiation reaching the surface decreases as much as 50% locally, which could reduce the surface warming by greenhouse gases (Ramanathan et al., 2005). These atmospheric brown clouds could cause precipitation to increase over the Indian Ocean in winter and decrease in the surrounding Indonesia region and the western Pacific Ocean (Chung et al., 2002), and could reduce the summer monsoon precipitation in South and East Asia (Menon et al., 2002; Ramanathan et al., 2005). However, the total influence on monsoon precipitation of temporally varying direct and indirect effects of various aerosol species is still not resolved and the subject of active research.

10.3.5.3 Mean Tropical Pacific Climate Change

This subsection assesses changes in mean tropical Pacific climate. Enhanced greenhouse gas concentrations result in a general increase in SST, which will not be spatially uniform in association with a general reduction in tropical circulations in a warmer climate (see Section 10.3.5.2). Figures 10.8 and 10.9 indicate that SST increases more over the eastern tropical Pacific than over the western tropical Pacific, together with a decrease in the sea level pressure (SLP) gradient along the equator and an eastward shift of the tropical Pacific rainfall distribution. These background tropical Pacific changes can be called an El Niño-like mean state change (upon which individual El Niño-Southern Oscillation (ENSO) events occur). Although individual models show a large scatter of 'ENSO-ness' (Collins and The CMIP Modelling Groups, 2005; Yamaguchi and Noda, 2006), an ENSO-like global warming pattern with positive polarity (i.e., El Niño-like mean state change) is simulated based on the spatial anomaly patterns of SST, SLP and precipitation (Figure 10.16; Yamaguchi and Noda, 2006). The El Niño-like change may be attributable to the general reduction in tropical circulations resulting from the increased dry static stability in the tropics in a warmer climate (Knutson and Manabe, 1995; Sugi et al., 2002; Figure 10.7). An eastward displacement of precipitation in the tropical Pacific accompanies an intensified and south-westward displaced subtropical anticyclone in the western Pacific, which can be effective in transporting moisture from the low latitudes to the Meiyu/Baiu region, thus generating more precipitation in the East Asian summer monsoon (Kitoh and Uchiyama, 2006).

In summary, the multi-model mean projects a weak shift towards conditions which may be described as 'El Niño-like', with SSTs in the central and eastern equatorial Pacific warming more than those in the west, and with an eastward shift in mean precipitation, associated with weaker tropical circulations.

10.3.5.4 El Niño

This subsection addresses the projected change in the amplitude, frequency and spatial pattern of El Niño. Guilyardi (2006) assessed mean state, coupling strength and modes (SST mode resulting from local SST-wind interaction or thermocline mode resulting from remote wind-thermocline feedbacks), using the pre-industrial control and stabilised 2 × and 4 × atmospheric

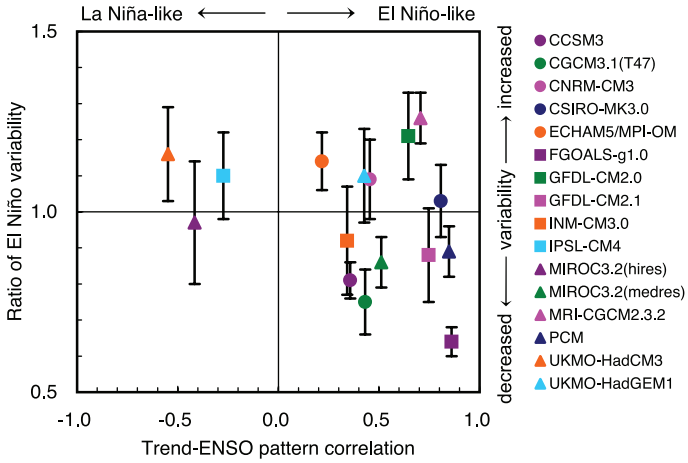


Figure 10.16. *Base state change in average tropical Pacific SSTs and change in El Niño variability simulated by AOGCMs (see Table 8.1 for model details). The base state change (horizontal axis) is denoted by the spatial anomaly pattern correlation coefficient between the linear trend of SST in the 1% yr^{-1} CO_2 increase climate change experiment and the first Empirical Orthogonal Function (EOF) of SST in the control experiment over the area 10°S to 10°N, 120°E to 80°W (reproduced from Yamaguchi and Noda, 2006). Positive correlation values indicate that the mean climate change has an El Niño-like pattern, and negative values are La Niña-like. The change in El Niño variability (vertical axis) is denoted by the ratio of the standard deviation of the first EOF of sea level pressure (SLP) between the current climate and the last 50 years of the SRES A2 experiments (2051–2100), except for FGOALS-g1.0 and MIROC3.2(hires), for which the SRES A1B was used, and UKMO-HadGEM1 for which the 1% yr^{-1} CO_2 increase climate change experiment was used, in the region 30°S to 30°N, 30°E to 60°W with a five-month running mean (reproduced from van Oldenborgh et al., 2005). Error bars indicate the 95% confidence interval. Note that tropical Pacific base state climate changes with either El Niño-like or La Niña-like patterns are not permanent El Niño or La Niña events, and all still have ENSO inter-annual variability superimposed on that new average climate state in a future warmer climate.*

CO_2 simulations in a multi-model ensemble. The models that exhibit the largest El Niño amplitude change in scenario experiments are those that shift towards a thermocline mode. The observed 1976 climate shift in the tropical Pacific actually involved such a mode shift (Fedorov and Philander, 2001). The mean state change, through change in the sensitivity of SST variability to surface wind stress, plays a key role in determining the ENSO variance characteristics (Z. Hu et al., 2004; Zelle et al., 2005). For example, a more stable ENSO system is less sensitive to changes in the background state than one that is closer to instability (Zelle et al., 2005). Thus, GCMs with an improper simulation of present-day climate mean state and air-sea coupling strength are not suitable for ENSO amplitude projections. Van Oldenborgh et al. (2005) calculate the change in ENSO variability by the ratio of the standard deviation of the first Empirical Orthogonal Function (EOF) of SLP between the current climate and in the future (Figure 10.16), which shows that changes in ENSO interannual variability differ from model to model. They categorised 19 models based on their skill in the present-day ENSO simulations. Using the most realistic 6 out of 19 models, they find no statistically significant changes in the amplitude of ENSO variability in the future. Large uncertainty in the skewness of the variability limits the assessment of the future relative strength of El Niño and La Niña events.

Merryfield (2006) also analysed a multi-model ensemble and finds a wide range of behaviour for future El Niño amplitude, ranging from little change to larger El Niño events to smaller El Niño events, although several models that simulated some observed aspects of present-day El Niño events showed future increases in El Niño amplitude. However, significant multi-decadal fluctuations in El Niño amplitude in observations and in long coupled model control runs add another complicating factor to attempting to discern whether any future changes in El Niño amplitude are due to external forcing or are simply a manifestation of internal multi-decadal variability (Meehl et al., 2006a). Even with the larger warming scenario under 4 × atmospheric CO_2 climate, Yeh and Kirtman (2005) find that despite the large changes in the tropical Pacific mean state, the changes in ENSO amplitude are highly model dependent. Therefore, there are no clear indications at this time regarding future changes in El Niño amplitude in a warmer climate. However, as first noted in the TAR, ENSO teleconnections over North America appear to weaken due at least in part to the mean change of base state mid-latitude atmospheric circulation (Meehl et al., 2006a).

In summary, all models show continued ENSO interannual variability in the future no matter what the change in average background conditions, but changes in ENSO interannual variability differ from model to model. Based on various assessments of the current multi-model archive, in which present-day El Niño events are now much better simulated than in the TAR, there is no consistent indication at this time of discernible future changes in ENSO amplitude or frequency.

10.3.5.5 ENSO-Monsoon Relationship

The El Niño-Southern Oscillation affects interannual variability throughout the tropics through changes in the Walker Circulation. Analysis of observational data finds a significant correlation between ENSO and tropical circulation and precipitation such that there is a tendency for less Indian summer monsoon rainfall in El Niño years and above normal rainfall in La Niña years. Recent analyses have revealed that the correlation between ENSO and the Indian summer monsoon has decreased recently, and many hypotheses have been put forward (see Chapter 3). With respect to global warming, one hypothesis is that the Walker Circulation (accompanying ENSO) shifted south-eastward, reducing downward motion in the Indian monsoon region, which originally suppressed precipitation in that region at the time of El Niño, but now produces normal precipitation as a result (Krishna Kumar et al., 1999). Another explanation is that as the ground temperature of the Eurasian continent has risen in the winter-spring season, the temperature difference between the continent and the ocean has increased, thereby causing more precipitation, and the Indian monsoon is normal in spite of the occurrence of El Niño (Ashrit et al., 2001).

An earlier version of an AOGCM developed at the Max Planck Institute (MPI) (Ashrit et al., 2001) and the Action de Recherche Petite Echelle Grande Echelle/Océan Parallélisé (ARPEGE/OPA) model (Ashrit et al., 2003) simulated no global-warming related change in the ENSO-monsoon relationship, although a decadal-scale fluctuation is seen, suggesting that a weakening of the relationship might be part of the natural variability. However, Ashrit et al. (2001) show that while the impact of La Niña does not change, the influence of El Niño on the monsoon becomes small, suggesting the possibility of asymmetric behaviour of the changes in the ENSO-monsoon relationship. On the other hand, the MRI-CGCM2 (see Table 8.1 for model details) indicates a weakening of the correlation into the 21st century, particularly after 2050 (Ashrit et al., 2005). The MRI-CGCM2 model results support the above hypothesis that the Walker Circulation shifts eastward and no longer influences India at the time of El Niño in a warmer climate. Camberlin et al. (2004) and van Oldenborgh and Burgers (2005) find decadal fluctuations in the effect of ENSO on regional precipitation. In most cases, these fluctuations may reflect natural variability in the ENSO teleconnection, and long-term correlation trends may be comparatively weaker.

The Tropospheric Biennial Oscillation (TBO) has been suggested as a fundamental set of coupled interactions in the Indo-Pacific region that encompasses ENSO and the Asian-Australian monsoon, and the TBO has been shown to be simulated by current AOGCMs (see Chapter 8). Nanjundiah et al. (2005) analyse a multi-model data set to show that, for models that successfully simulate the TBO for present-day climate, the TBO becomes more prominent in a future warmer climate due to changes in the base state climate, although, as with ENSO, there is considerable inherent decadal variability in the relative dominance of TBO and ENSO.

In summary, the ENSO-monsoon relationship can vary due to natural variability. Model projections suggest that a future weakening of the ENSO-monsoon relationship could occur in a future warmer climate.

10.3.5.6 Annular Modes and Mid-Latitude Circulation Changes

Many simulations project some decrease in the arctic surface pressure in the 21st century, as seen in the multi-model average (see Figure 10.9). This contributes to an increase in indices of the Northern Annular Mode (NAM) or the Arctic Oscillation (AO), as well as the NAO, which is closely related to the NAM in the Atlantic sector (see Chapter 8). In the recent multi-model analyses, more than half of the models exhibit a positive trend in the NAM (Rauthe et al., 2004; Miller et al., 2006) and/or NAO (Osborn, 2004; Kuzmina et al., 2005). Although the magnitude of the trends shows a large variation among different models, Miller et al. (2006) find that none of the 14 models exhibits a trend towards a lower NAM index and higher arctic SLP. In another multi-model analysis, Stephenson et al. (2006) show that of the 15 models able to simulate the NAO pressure dipole, 13 predict a positive increase in the NAO index with increasing CO_2 concentrations, although the magnitude of the response is generally small and model dependent. However, the multi-model average from the larger number (21) of models shown in

Figure 10.9 indicates that it is likely that the NAM index would not notably decrease in a future warmer climate. The average of IPCC-AR4 simulations from 13 models suggests the increase of the NAM index becomes statistically significant early in the 21st century (Figure 10.17a, Miller et al., 2006).

The spatial patterns of the simulated SLP trends vary among different models, in spite of close correlations of the models' leading patterns of interannual (or internal) variability with the observations (Osborn, 2004; Miller et al., 2006). However, at the hemispheric scale of SLP change, the reduction in the Arctic is seen in the multi-model mean (Figure 10.9), although the change is smaller than the inter-model standard deviation. Besides the decrease in the arctic region, increases over the North Pacific and the Mediterranean Sea exceed the inter-model standard deviation; the latter suggests an association with a north-eastward shift of the NAO's centre of action (Hu and Wu, 2004). The diversity of the patterns seems to reflect different responses in the Aleutian Low (Rauthe et al., 2004) in the North Pacific. Yamaguchi and Noda (2006) discuss the modelled response of ENSO versus AO, and find that many models project a positive AO-like change. In the North Pacific at high latitudes, however, the SLP anomalies are incompatible between the El Niño-like change and the positive AO-like change, because models that project an El Niño-like change over the Pacific simulate a non-AO-like pattern in the polar region. As a result, the present models cannot fully determine the relative importance of the mechanisms inducing the positive AO-like change and those inducing the ENSO-like change, leading to scatter in global warming patterns at regional scales over the North Pacific. Rauthe et al. (2004) suggest that the effects of sulphate aerosols contribute to a deepening of the Aleutian Low resulting in a slower or smaller increase in the AO index.

Analyses of results from various models indicate that the NAM can respond to increasing greenhouse gas concentrations through tropospheric processes (Fyfe et al., 1999; Gillett et al., 2003; Miller et al., 2006). Greenhouse gases can also drive a positive NAM trend through changes in the stratospheric circulation, similar to the mechanism by which volcanic aerosols in the stratosphere force positive annular changes (Shindell et al., 2001). Models with their upper boundaries extending farther into the stratosphere exhibit, on average, a relatively larger increase in the NAM index and respond consistently to the observed volcanic forcing (Figure 10.17a, Miller et al., 2006), implying the importance of the connection between the troposphere and the stratosphere.

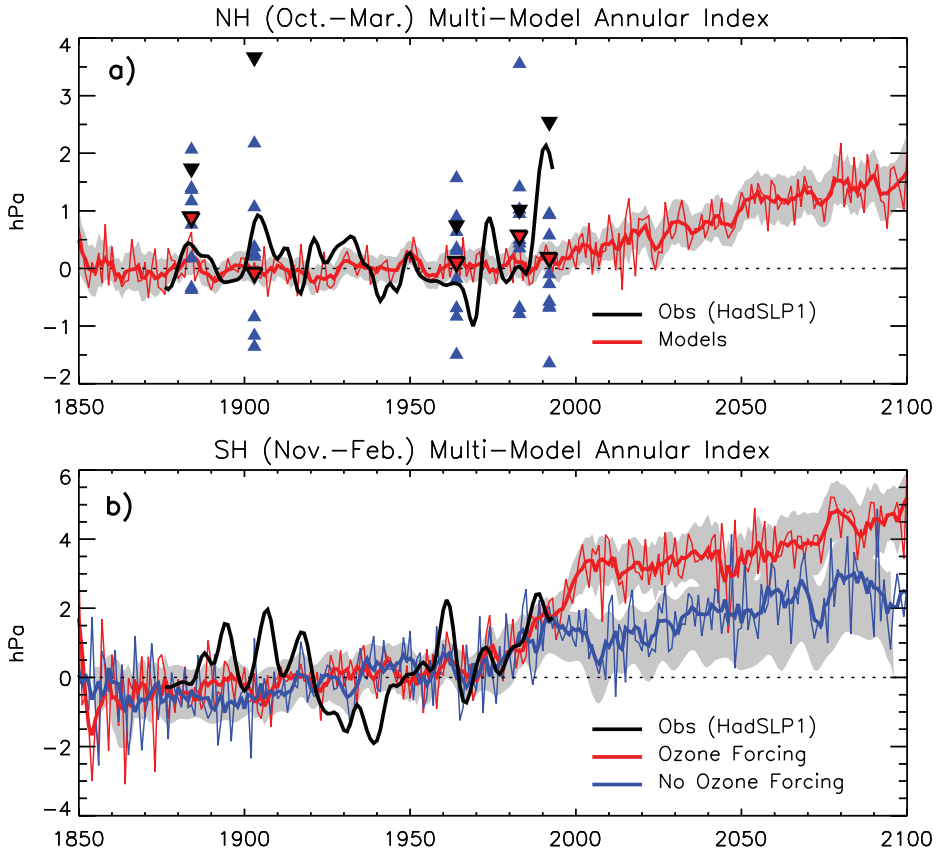


Figure 10.17. *(a) Multi-model mean of the regression of the leading EOF of ensemble mean Northern Hemisphere sea level pressure (NH SLP, thin red line). The time series of regression coefficients has zero mean between year 1900 and 1970. The thick red line is a 10-year low-pass filtered version of the mean. The grey shading represents the inter-model spread at the 95% confidence level and is filtered. A filtered version of the observed SLP from the Hadley Centre (HadSLP1) is shown in black. The regression coefficient for the winter following a major tropical eruption is marked by red, blue and black triangles for the multi-model mean, the individual model mean and observations, respectively. (b) As in (a) for Southern Hemisphere SLP for models with (red) and without (blue) ozone forcing. Adapted from Miller et al. (2006).*

A plausible explanation for the cause of the upward NAM trend simulated by the models is an intensification of the polar vortex resulting from both tropospheric warming and stratospheric cooling mainly due to the increase in greenhouse gases (Shindell et al., 2001; Sigmond et al., 2004; Rind et al., 2005a). The response may not be linear with the magnitude of radiative forcing (Gillett et al., 2002) since the polar vortex response is attributable to an equatorward refraction of planetary waves (Eichelberger and Holton, 2002) rather than radiative forcing itself. Since the long-term variation in the NAO is closely related to SST variations (Rodwell et al., 1999), it is considered essential that the projection of the changes in the tropical SST (Hoerling et al., 2004; Hurrell et al., 2004) and/or meridional gradient of the SST change (Rind et al., 2005b) is reliable.

The future trend in the Southern Annular Mode (SAM) or the Antarctic Oscillation (AAO) has been projected in a number of model simulations (Gillett and Thompson, 2003; Shindell and Schmidt, 2004; Arblaster and Meehl, 2006; Miller et al., 2006). According to the latest multi-model analysis (Miller et al., 2006), most models indicate a positive trend in the SAM index, and a declining trend in the antarctic SLP (as seen in Figure 10.9), with a higher likelihood than for the future NAM trend. On average, a larger positive trend is projected during the late 20th century by models that include stratospheric ozone changes than those that do not (Figure 10.17b), although during the 21st century, when ozone changes are smaller, the SAM trends of models with and without ozone are similar. The cause of the positive SAM trend in the second half of the 20th century is mainly attributed to stratospheric ozone depletion, evidenced by the fact that the signal is largest in the lower stratosphere in austral spring through summer (Thompson and Solomon, 2002; Arblaster and Meehl, 2006). However, increases in greenhouse gases are also important factors (Shindell and Schmidt, 2004; Arblaster and Meehl, 2006) for the year-round positive SAM trend induced by meridional temperature gradient changes (Brandefelt and Källén, 2004). During the 21st century, although the ozone amount is expected to stabilise or recover, the polar vortex intensification is likely to continue due to the increases in greenhouse gases (Arblaster and Meehl, 2006).

It is implied that the future change in the annular modes leads to modifications of the future change in various fields such as surface temperatures, precipitation and sea ice with regional features similar to those for the modes of natural variability (e.g., Hurrell et al., 2003). For instance, the surface warming in winter would be intensified in northern Eurasia and most of North America while weakened in the western North Atlantic, and winter precipitation would increase in northern Europe while decreasing in southern Europe. The atmospheric circulation change would also affect the ocean circulations. Sakamoto et al. (2005) simulate an intensification of the Kuroshio Current but no shift in the Kuroshio Extension in response to an AO-like circulation change for the 21st century. However, Sato et al. (2006) simulate a northward shift of the Kuroshio Extension, which leads to a strong warming off the eastern coast of Japan.

In summary, the future changes in the extratropical circulation variability are likely to be characterised by increases in positive phases of both the NAM and the SAM. The response in the NAM to anthropogenic forcing might not be distinct from the larger multi-decadal internal variability in the first half of the 21st century. The change in the SAM would appear earlier than in the NAM since stratospheric ozone depletion acts as an additional forcing. The positive trends in annular modes would influence the regional changes in temperature, precipitation and other fields, similar to those that accompany the NAM and the SAM in the present climate, but would be superimposed on the global-scale changes in a future warmer climate.

10.3.6 Future Changes in Weather and Climate Extremes

Projections of future changes in extremes rely on an increasingly sophisticated set of models and statistical techniques. Studies assessed in this section rely on multi-member ensembles (three to five members) from single models, analyses of multi-model ensembles ranging from 8 to 15 or more AOGCMs, and a perturbed physics ensemble with a single mixed-layer model with over 50 members. The discussion here is intended to identify general characteristics of changes in extremes in a global context. Chapter 3 provides a definition of weather and climate extremes, and Chapter 11 addresses changes in extremes for specific regions.

10.3.6.1 Precipitation Extremes

A long-standing result from global coupled models noted in the TAR is a projected increase in the chance of summer drying in the mid-latitudes in a future warmer climate with associated increased risk of drought. This is shown in Figure 10.12, and has been documented in the more recent generation of models (Burke et al., 2006; Meehl et al., 2006b; Rowell and Jones, 2006). For example, Wang (2005) analyse 15 recent AOGCMs and show that in a future warmer climate, the models simulate summer dryness in most parts of the northern subtropics and mid-latitudes, but with a large range in the amplitude of summer dryness across models. Droughts associated with this summer drying could result in regional vegetation die-offs (Breshears et al., 2005) and contribute to an increase in the percentage of land area experiencing drought at any one time, for example, extreme drought increasing from 1% of present-day land area to 30% by the end of the century in the A2 scenario (Burke et al., 2006). Drier soil conditions can also contribute to more severe heat waves as discussed in Section 10.3.6.2 (Brabson et al., 2005).

Associated with the risk of drying is a projected increase in the chance of intense precipitation and flooding. Although somewhat counter-intuitive, this is because precipitation is projected to be concentrated into more intense events, with longer periods of little precipitation in between. Therefore, intense and heavy episodic rainfall events with high runoff amounts are interspersed with longer relatively dry periods with increased evapotranspiration, particularly in the subtropics

Frequently Asked Question 10.1

Are Extreme Events, Like Heat Waves, Droughts or Floods, Expected to Change as the Earth's Climate Changes?

Yes; the type, frequency and intensity of extreme events are expected to change as Earth's climate changes, and these changes could occur even with relatively small mean climate changes. Changes in some types of extreme events have already been observed, for example, increases in the frequency and intensity of heat waves and heavy precipitation events (see FAQ 3.3).

In a warmer future climate, there will be an increased risk of more intense, more frequent and longer-lasting heat waves. The European heat wave of 2003 is an example of the type of extreme heat event lasting from several days to over a week that is likely to become more common in a warmer future climate. A related aspect of temperature extremes is that there is likely to be a decrease in the daily (diurnal) temperature range in most regions. It is also likely that a warmer future climate would have fewer frost days (i.e., nights where the temperature dips below freezing). Growing season length is related to number of frost days, and has been projected to increase as climate warms. There is likely to be a decline in the frequency of cold air outbreaks (i.e., periods of extreme cold lasting from several days to over a week) in NH winter in most areas. Exceptions could occur in areas with the smallest reductions of extreme cold in western North America, the North Atlantic and southern Europe and Asia due to atmospheric circulation changes.

In a warmer future climate, most Atmosphere-Ocean General Circulation Models project increased summer dryness and winter wetness in most parts of the northern middle and high latitudes. Summer dryness indicates a greater risk of drought. Along with the risk of drying, there is an increased chance of intense precipitation and flooding due to the greater water-holding capacity of a warmer atmosphere. This has already been observed and is projected to continue because in a warmer world, precipitation tends to be concentrated into more intense events, with longer periods of little precipitation in between. Therefore, intense and heavy downpours would be interspersed with longer relatively dry periods. Another aspect of these projected changes is that wet extremes are projected to become more severe in many areas where mean precipitation is expected to increase, and dry extremes are projected to become more severe in areas where mean precipitation is projected to decrease.

In concert with the results for increased extremes of intense precipitation, even if the wind strength of storms in a future climate did not change, there would be an increase in extreme rainfall intensity. In particular, over NH land, an increase in the likelihood of very wet winters is projected over much of central and northern Europe due to the increase in intense precipitation during storm events, suggesting an increased chance of flooding over Europe and other mid-latitude regions due to more intense rainfall and snowfall events producing more runoff. Similar results apply for summer precipitation, with implications for more flooding in the Asian monsoon region and other tropical areas. The increased risk of floods in a number of major river basins in a future warmer climate has been related to an increase in river discharge with an increased risk of future intense storm-related precipitation events and flooding. Some of these changes would be extensions of trends already underway.

There is evidence from modelling studies that future tropical cyclones could become more severe, with greater wind speeds and more intense precipitation. Studies suggest that such changes may already be underway; there are indications that the average number of Category 4 and 5 hurricanes per year has increased over the past 30 years. Some modelling studies have projected a decrease in the number of tropical cyclones globally due to the increased stability of the tropical troposphere in a warmer climate, characterised by fewer weak storms and greater numbers of intense storms. A number of modelling studies have also projected a general tendency for more intense but fewer storms outside the tropics, with a tendency towards more extreme wind events and higher ocean waves in several regions in association with those deepened cyclones. Models also project a poleward shift of storm tracks in both hemispheres by several degrees of latitude.

as discussed in Section 10.3.6.2 in relation to Figure 10.19 (Frei et al., 1998; Allen and Ingram, 2002; Palmer and Räisänen, 2002; Christensen and Christensen, 2003; Beniston, 2004; Christensen and Christensen, 2004; Pal et al., 2004; Meehl et al., 2005a). However, increases in the frequency of dry days do not necessarily mean a decrease in the frequency of extreme high rainfall events depending on the threshold used to define such events (Barnett et al., 2006). Another aspect of these changes has been related to the mean changes in precipitation, with wet extremes becoming more severe in many areas where mean precipitation increases, and dry extremes where the mean precipitation decreases (Kharin and Zwiers, 2005; Meehl et al., 2005a; Räisänen, 2005a; Barnett et al., 2006). However, analysis of the 53-member perturbed physics ensemble indicates that the change in the frequency of extreme precipitation at an individual location can be difficult to estimate definitively due to model parametrization uncertainty (Barnett et al., 2006). Some specific regional aspects of these changes in precipitation extremes are discussed further in Chapter 11.

Climate models continue to confirm the earlier results that in a future climate warmed by increasing greenhouse gases, precipitation intensity (e.g., proportionately more precipitation per precipitation event) is projected to increase over most regions (Wilby and Wigley, 2002; Kharin and Zwiers, 2005; Meehl et al., 2005a; Barnett et al., 2006), and the increase in precipitation extremes is greater than changes in mean precipitation (Kharin and Zwiers, 2005). As discussed in Chapter 9, this is related to the fact that the energy budget of the atmosphere constrains increases in large-scale mean precipitation, but extreme precipitation relates to increases in moisture content and thus the nonlinearities involved with the Clausius-Clapeyron relationship such that, for a given increase in temperature, increases in extreme precipitation can be more than the mean precipitation increase (e.g., Allen and Ingram, 2002). Additionally, time scale can play a role whereby increases in the frequency of seasonal mean rainfall extremes can be greater than the increases in the frequency of daily extremes (Barnett et al., 2006). The increase in mean and extreme precipitation in various regions has been attributed to contributions from both dynamic and thermodynamic processes associated with global warming (Emori and Brown, 2005). The greater increase in extreme precipitation compared to the mean is attributed to the greater thermodynamic effect on the extremes due to increases in water vapour, mainly over subtropical areas. The thermodynamic effect is important nearly everywhere, but changes in circulation also contribute to the pattern of precipitation intensity changes at middle and high latitudes (Meehl et al., 2005a). Kharin and Zwiers (2005) show that changes in both the location and scale of the extreme value distribution produce increases in precipitation extremes substantially greater than increases in annual mean precipitation. An increase in the scale parameter from the gamma distribution represents an increase in precipitation intensity, and various regions such as the NH land areas in winter showed particularly high values of increased scale parameter (Semenov and Bengtsson, 2002; Watterson and Dix, 2003). Time-slice simulations with a higher-resolution model (~1°) show similar results using changes in the gamma distribution, namely increased extremes in the hydrological cycle (Voss et al., 2002). However, some regional decreases are also projected such as over the subtropical oceans (Semenov and Bengtsson, 2002).

A number of studies have noted the connection between increased rainfall intensity and an implied increase in flooding. McCabe et al. (2001) and Watterson (2005) show a projected increase in extreme rainfall intensity with the extra-tropical surface lows, particularly over NH land, with an implied increase in flooding. In a multi-model analysis of the CMIP models, Palmer and Räisänen (2002) show an increased likelihood of very wet winters over much of central and northern Europe due to an increase in intense precipitation associated with mid-latitude storms, suggesting more floods across Europe (see also Chapter 11). They found similar results for summer precipitation with implications for greater flooding in the Asian monsoon region in a future warmer climate. Similarly, Milly et al. (2002), Arora and Boer (2001) and Voss et al. (2002) relate the increased risk of floods in a number of major river basins in a future warmer climate to an increase in spring river discharge related to increased winter snow depth in some regions. Christensen and Christensen (2003) conclude that there could be an increased risk of summer flooding in Europe.

Globally averaged time series of the Frich et al. (2002) indices in the multi-model analysis of Tebaldi et al. (2006) show simulated increases in precipitation intensity during the 20th century continuing through the 21st century (Figure 10.18a,b), along with a somewhat weaker and less consistent trend of increasing dry periods between rainfall events for all scenarios (Figure 10.18c,d). Part of the reason for these results is shown in the geographic maps for these quantities, where precipitation intensity increases almost everywhere, but particularly at middle and high latitudes where mean precipitation also increases (Meehl et al., 2005a; compare Figure 10.18b to Figure 10.9). However, in Figure 10.18d, there are regions of increased runs of dry days between precipitation events in the subtropics and lower mid-latitudes, but decreased runs of dry days at higher mid-latitudes and high latitudes where mean precipitation increases (compare Figure 10.9 with Figure 10.18d). Since there are areas of both increases and decreases in consecutive dry days between precipitation events in the multi-model average (Figure 10.9), the global mean trends are smaller and less consistent across models as shown in Figure 10.18. Consistency of response in a perturbed physics ensemble with one model shows only limited areas of increased frequency of wet days in July, and a larger range of changes in precipitation extremes relative to the control ensemble mean in contrast to the more consistent response of temperature extremes (Section 10.6.3.2), indicating a less consistent response for precipitation extremes in general compared to temperature extremes (Barnett et al., 2006). Analysis of the Frich et al. (2002) precipitation indices in a 20-km resolution global model shows similar results to those in Figure 10.18, with particularly large increases in precipitation intensity in South Asia and West Africa (Kamiguchi et al., 2005).

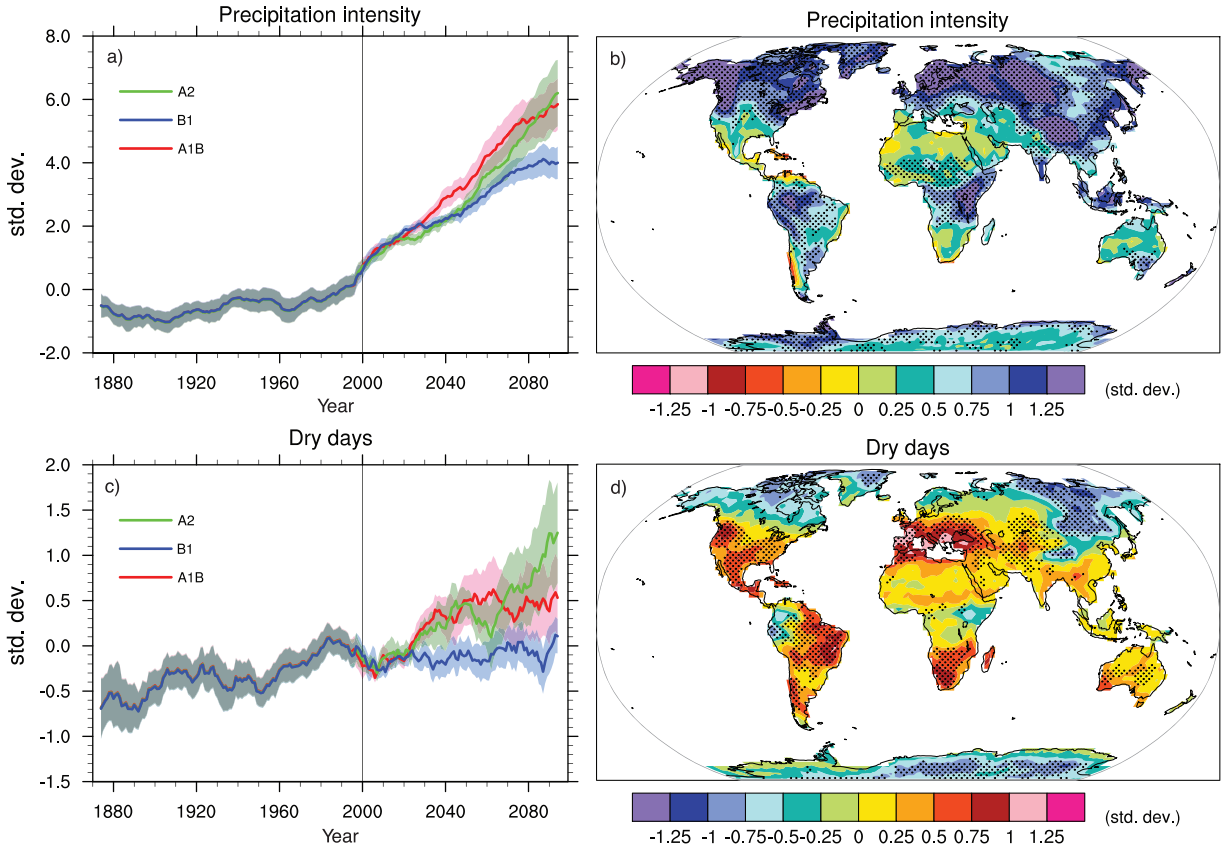


Figure 10.18. *Changes in extremes based on multi-model simulations from nine global coupled climate models, adapted from Tebaldi et al. (2006). (a) Globally averaged changes in precipitation intensity (defined as the annual total precipitation divided by the number of wet days) for a low (SRES B1), middle (SRES A1B) and high (SRES A2) scenario. (b) Changes in spatial patterns of simulated precipitation intensity between two 20-year means (2080–2099 minus 1980–1999) for the A1B scenario. (c) Globally averaged changes in dry days (defined as the annual maximum number of consecutive dry days). (d) Changes in spatial patterns of simulated dry days between two 20-year means (2080–2099 minus 1980–1999) for the A1B scenario. Solid lines in (a) and (c) are the 10-year smoothed multi-model ensemble means; the envelope indicates the ensemble mean standard deviation. Stippling in (b) and (d) denotes areas where at least five of the nine models concur in determining that the change is statistically significant. Extreme indices are calculated only over land following Frich et al. (2002). Each model's time series was centred on its 1980 to 1999 average and normalised (rescaled) by its standard deviation computed (after de-trending) over the period 1960 to 2099. The models were then aggregated into an ensemble average, both at the global and at the grid-box level. Thus, changes are given in units of standard deviations.*

10.3.6.2 Temperature Extremes

The TAR concluded that there was a very likely risk of increased high temperature extremes (and reduced risk of low temperature extremes) with more extreme heat episodes in a future climate. The latter result has been confirmed in subsequent studies (Yonetani and Gordon, 2001). Kharin and Zwiers (2005) show in a single model that future increases in temperature extremes follow increases in mean temperature over most of the world except where surface properties change (melting snow, drying soil). Furthermore, they show that in most instances warm extremes correspond to increases in daily maximum temperature, but cold extremes warm up faster than daily minimum temperatures, although this result is less consistent when model parameters are varied in a perturbed physics ensemble where there are increased daily temperature maxima for nearly the entire land surface. However, the range in magnitude of increases was substantial indicating a sensitivity to model formulations (Clark et al., 2006).

Weisheimer and Palmer (2005) examine changes in extreme seasonal (DJF and JJA) temperatures in 14 models for three scenarios. They show that by the end of 21st century, the probability of such extreme warm seasons is projected to rise in many areas. This result is consistent with the perturbed physics ensemble where, for nearly all land areas, extreme JJA temperatures were at least 20 times and in some areas 100 times more frequent compared to the control ensemble mean, making these changes greater than the ensemble spread.

Since the TAR, possible future cold air outbreaks have been studied. Vavrus et al. (2006) analyse seven AOGCMs run with the A1B scenario, and define a cold air outbreak as two or more consecutive days when the daily temperatures are at least two standard deviations below the present-day winter mean. For a future warmer climate, they document a 50 to 100% decline in the frequency of cold air outbreaks in NH winter in most areas compared to the present, with the smallest reductions occurring in western North America, the North Atlantic and southern Europe and Asia due to atmospheric circulation changes associated with the increase in greenhouse gases.

No studies at the time of the TAR specifically documented changes in heat waves (very high temperatures over a sustained period of days, see Chapter 3). Several recent studies address possible future changes in heat waves explicitly, and find an increased risk of more intense, longer-lasting and more frequent heat waves in a future climate (Meehl and Tebaldi, 2004; Schär et al., 2004; Clark et al., 2006). Meehl and Tebaldi (2004) show that the pattern of future changes in heat waves, with greatest intensity increases over western Europe, the Mediterranean and the southeast and western USA, is related in part to base state circulation changes due to the increase in greenhouse gases. An additional factor leading to extreme heat is drier soils in a future warmer climate (Brabson et al., 2005; Clark et al., 2006). Schär et al. (2004), Stott et al. (2004) and Beniston (2004) use the European 2003 heat wave as an example of the types of heat waves that are likely to become more common in a future warmer climate. Schär et al. (2004) note that the increase in the frequency of extreme warm conditions is also associated with a change in interannual variability, such that the statistical distribution of mean summer temperatures is not merely shifted towards warmer conditions but also becomes wider. A multi-model ensemble shows that heat waves are simulated to have been increasing over the latter part of the 20th century, and are projected to increase globally and over most regions (Figure 10.19; Tebaldi et al., 2006), although different model parameters can contribute to the range in the magnitude of this response (Clark et al., 2006).

A decrease in DTR in most regions in a future warmer climate was reported in the TAR, and is substantiated by more recent studies (e.g., Stone and Weaver, 2002; also discussed in relation to Figure 10.11b and in Chapter 11). For a quantity related to the DTR, the TAR concluded that it would be likely that a future warmer climate would also be characterised by a decrease in the number of frost days, although there were no studies at that time from global coupled climate models that addressed this issue explicitly. It has since been shown that there would indeed be decreases in frost days in a future warmer climate in the extratropics (Meehl et al., 2004a), with the pattern of the decreases dictated by the changes in atmospheric circulation due to the increase in greenhouse gases (Meehl et al., 2004a). Results from a nine-member multi-model ensemble show simulated decreases in frost days for the 20th century continuing into the 21st century globally and in most regions (Figure 10.19). A quantity related to frost days in many mid- and high-latitude areas, particularly in the NH, is growing season length as defined by Frich et al. (2002), and this has been projected to increase in future climate (Tebaldi et al., 2006). This result is also shown in a nine-member multi-model ensemble where the simulated increase in growing season length in the 20th century continues into the 21st century globally and in most regions (Figure 10.19). The globally averaged extremes indices in Figures 10.18 and 10.19 have non-uniform changes across the scenarios compared to the more consistent relative increases in Figure 10.5 for globally averaged temperature. This indicates that patterns that scale well by radiative forcing for temperature (e.g., Figure 10.8) would not scale for extremes.

10.3.6.3 Tropical Cyclones (Hurricanes)

Earlier studies assessed in the TAR showed that future tropical cyclones would likely become more severe with greater wind speeds and more intense precipitation. More recent modelling experiments have addressed possible changes in tropical cyclones in a warmer climate and generally confirmed those earlier results. These studies fall into two categories: those with model grid resolutions that only roughly represent some aspects of individual tropical cyclones, and those with model grids of sufficient resolution to reasonably simulate individual tropical cyclones.

In the first category, a number of climate change experiments with global models have started to simulate some characteristics of individual tropical cyclones, although classes of models with 50 to 100 km resolution or lower cannot accurately simulate observed tropical cyclone intensities due to the limitations of the relatively coarse grid spacing (e.g., Yoshimura et al., 2006). A study with roughly 100-km grid spacing shows a decrease in tropical cyclone frequency globally and in the North Pacific but a regional increase over the North Atlantic and no significant changes in maximum intensity (Sugi et al., 2002). Yoshimura et al. (2006) use the same model but different SST patterns and two different convection schemes, and show a decrease in the global frequency of relatively weak tropical cyclones but no significant change in the frequency of intense storms. They also show that the regional changes are dependent on the SST pattern, and precipitation near the storm centres could increase in the future. Another study using a 50 km resolution model confirms this dependence on SST pattern, and also shows a consistent increase in precipitation intensity in future tropical cyclones (Chauvin et al., 2006). Another global modelling study with roughly a 100-km grid spacing finds a 6% decrease in tropical storms globally and a slight increase in intensity, with both increases and decreases regionally related to the El Niño-like base state response in the tropical Pacific to increased greenhouse gases (McDonald et al., 2005). Another study with the same resolution model indicates decreases in tropical cyclone frequency and intensity but more mean and extreme precipitation from the tropical cyclones simulated in the future in the western north Pacific (Hasegawa and Emori, 2005). An AOGCM analysis with a coarser-resolution atmospheric model (T63, or about 200-km grid spacing) shows little change in overall numbers of tropical storms in that model, but a slight decrease in medium-intensity storms in a warmer climate (Bengtsson et al., 2006). In a global warming simulation with a coarse-resolution atmospheric model (T42, or about 300-km grid spacing), the frequency of global tropical cyclone occurrence did not change significantly, but the mean intensity of the global tropical cyclones increased significantly (Tsutsui, 2002). Thus, from this category of coarser-grid models that can only represent rudimentary aspects of tropical cyclones, there is no consistent evidence for large changes in either frequency or intensity of these models' representation of tropical cyclones, but there is a consistent response of more intense precipitation from future storms in a warmer climate. Also note that the

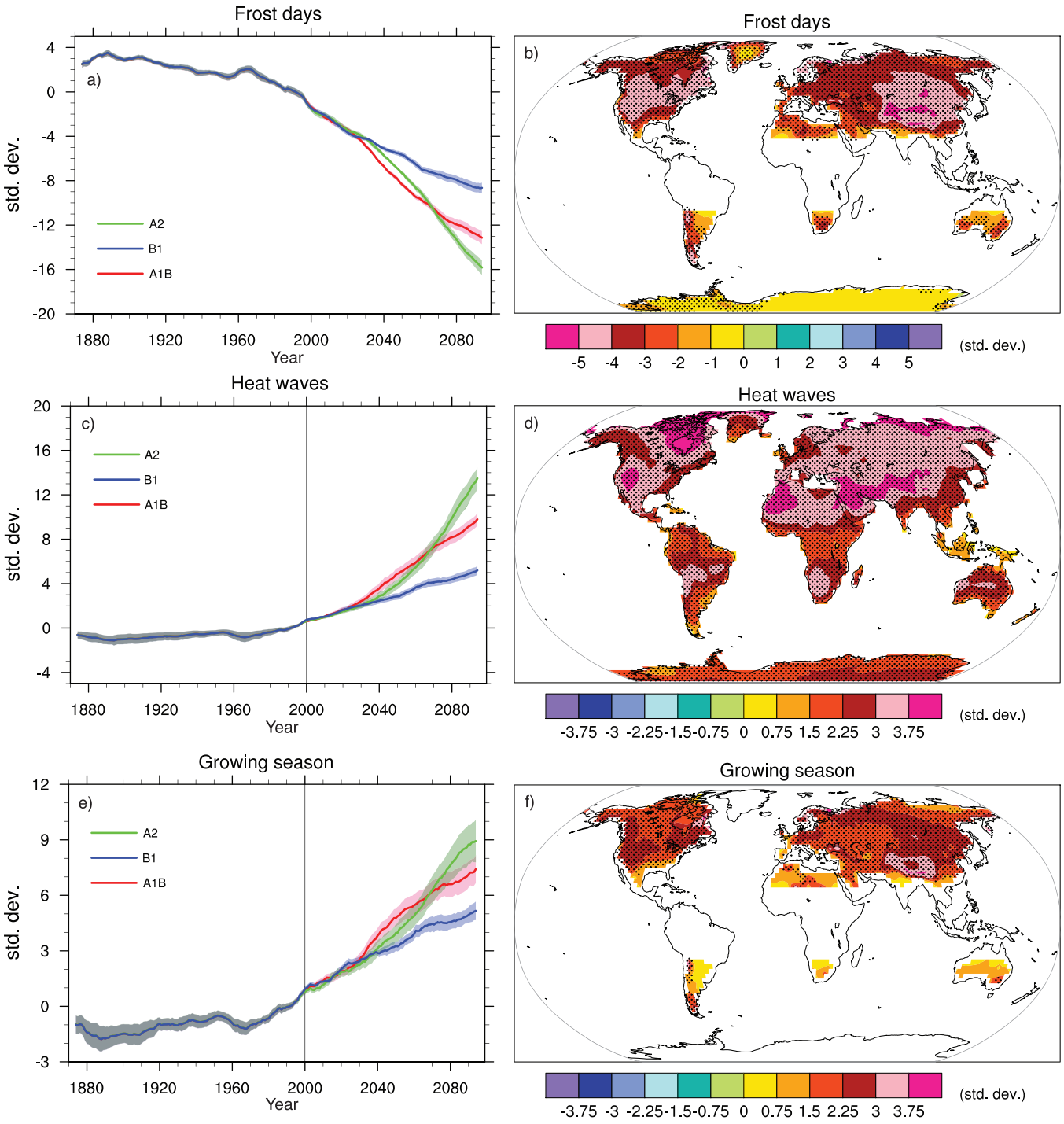


Figure 10.19. *Changes in extremes based on multi-model simulations from nine global coupled climate models, adapted from Tebaldi et al. (2006). (a) Globally averaged changes in the frost day index (defined as the total number of days in a year with absolute minimum temperature below 0°C) for a low (SRES B1), middle (SRES A1B) and high (SRES A2) scenario. (b) Changes in spatial patterns of simulated frost days between two 20-year means (2080–2099 minus 1980–1999) for the A1B scenario. (c) Globally averaged changes in heat waves (defined as the longest period in the year of at least five consecutive days with maximum temperature at least 5°C higher than the climatology of the same calendar day). (d) Changes in spatial patterns of simulated heat waves between two 20-year means (2080–2099 minus 1980–1999) for the A1B scenario. (e) Globally averaged changes in growing season length (defined as the length of the period between the first spell of five consecutive days with mean temperature above 5°C and the last such spell of the year). (f) Changes in spatial patterns of simulated growing season length between two 20-year means (2080–2099 minus 1980–1999) for the A1B scenario. Solid lines in (a), (c) and (e) show the 10-year smoothed multi-model ensemble means; the envelope indicates the ensemble mean standard deviation. Stippling in (b), (d) and (f) denotes areas where at least five of the nine models concur in determining that the change is statistically significant. Extreme indices are calculated only over land. Frost days and growing season are only calculated in the extratropics. Extremes indices are calculated following Frich et al. (2002). Each model's time series was centred around its 1980 to 1999 average and normalised (rescaled) by its standard deviation computed (after de-trending) over the period 1960 to 2099. The models were then aggregated into an ensemble average, both at the global and at the grid-box level. Thus, changes are given in units of standard deviations.*

decreasing tropical precipitation in future climate in Yoshimura et al. (2006) is for SSTs held fixed as atmospheric CO_2 is increased, a situation that does not occur in any global coupled model.

In the second category, studies have been performed with models that have been able to credibly simulate many aspects of tropical cyclones. For example, Knutson and Tuleya (2004) use a high-resolution (down to 9 km) mesoscale hurricane model to simulate hurricanes with intensities reaching about 60 to 70 m s^{-1}, depending on the treatment of moist convection in the model. They use mean tropical conditions from nine global climate models with increased CO_2 to simulate tropical cyclones with 14% more intense central pressure falls, 6% higher maximum surface wind speeds and about 20% greater near-storm rainfall after an idealised 80-year buildup of CO_2 at 1% yr^{-1} compounded (warming given by TCR shown for models in Chapter 8). Using a multiple nesting technique, an AOGCM was used to force a regional model over Australasia and the western Pacific with 125-km grid resolution, with an embedded 30-km resolution model over the south-western Pacific (Walsh et al., 2004). At that 30-km resolution, the model is able to closely simulate the climatology of the observed tropical cyclone lower wind speed threshold of 17 m s^{-1}. Tropical cyclone occurrence (in terms of days of tropical cyclone activity) is slightly greater than observed, and the somewhat weaker than observed pressure gradients near the storm centres are associated with lower than observed maximum wind speeds, likely due to the 30-km grid spacing that is too coarse to capture extreme pressure gradients and winds. For 3 × atmospheric CO_2 in that model configuration, the simulated tropical cyclones experienced a 56% increase in the number of storms with maximum wind speed greater than 30 m s^{-1} and a 26% increase in the number of storms with central pressures less than 970 hPa, with no large changes in frequency and movement of tropical cyclones for that southwest Pacific region. It should also be noted that ENSO fluctuations have a strong impact on patterns of tropical cyclone occurrence in the southern Pacific (Nguyen and Walsh, 2001), and that uncertainty with respect future ENSO behaviour (Section 10.3.5.1) contributes to uncertainty with respect to tropical cyclones (Walsh, 2004).

In another experiment with a high resolution global model that is able to generate tropical cyclones that begin to approximate real storms, a global 20-km grid atmospheric model was run in time slice experiments for a present-day 10-year period and a 10-year period at the end of the 21st century for the A1B scenario to examine changes in tropical cyclones. Observed climatological SSTs were used to force the atmospheric model for the 10-year period at the end of the 20th century, time-mean SST anomalies from an AOGCM simulation for the future climate were added to the observed SSTs and atmospheric composition was changed in the model to be consistent with the A1B scenario. At that resolution, tropical cyclone characteristics, numbers and tracks were relatively well simulated for present-day climate, although simulated wind speed intensities were somewhat weaker than observed intensities (Oouchi et al., 2006). In that study, tropical cyclone frequency decreased 30% globally (but increased about 34% in the North Atlantic). The strongest tropical cyclones with extreme surface winds increased in number while weaker storms decreased. The tracks were not appreciably altered, and maximum peak wind speeds in future simulated tropical cyclones increased by about 14% in that model, although statistically significant increases were not found in all basins. As noted above, the competing effects of greater stabilisation of the tropical troposphere (less storms) and greater SSTs (the storms that form are more intense) likely contribute to these changes except for the tropical North Atlantic where there are greater SST increases than in the other basins in that model. Therefore, the SST warming has a greater effect than the vertical stabilisation in the Atlantic and produces not only more storms but also more intense storms there. However, these regional changes are largely dependent on the spatial pattern of future simulated SST changes (Yoshimura et al., 2006).

Sugi et al. (2002) show that the global-scale reduction in tropical cyclone frequency is closely related to weakening of tropospheric circulation in the tropics in terms of vertical mass flux. They note that a significant increase in dry static stability in the tropical troposphere and little increase in tropical precipitation (or convective heating) are the main factors contributing to the weakening of the tropospheric circulation. Sugi and Yoshimura (2004) investigate a mechanism of this tropical precipitation change. They show that the effect of CO_2 enhancement (without changing SST conditions, which is not realistic as noted above) is a decrease in mean precipitation (Sugi and Yoshimura, 2004) and a decrease in the number of tropical cyclones as simulated in an atmospheric model with about 100 km resolution (Yoshimura and Sugi, 2005). Future changes in the large-scale steering flow as a mechanism to deduce possible changes in tropical cyclone tracks in the western North Pacific (Wu and Wang, 2004) were analysed to show different shifts at different times in future climate change experiments along with a dependence of such shifts on the degree of El Niño-like mean climate change in the Pacific (see Section 10.3.5).

A synthesis of the model results to date indicates that, for a future warmer climate, coarse-resolution models show few consistent changes in tropical cyclones, with results dependent on the model, although those models do show a consistent increase in precipitation intensity in future storms. Higher-resolution models that more credibly simulate tropical cyclones project some consistent increase in peak wind intensities, but a more consistent projected increase in mean and peak precipitation intensities in future tropical cyclones. There is also a less certain possibility of a decrease in the number of relatively weak tropical cyclones, increased numbers of intense tropical cyclones and a global decrease in total numbers of tropical cyclones.

10.3.6.4 Extratropical Storms and Ocean Wave Height

The TAR noted that there could be a future tendency for more intense extratropical storms, although the number of storms could be less. A more consistent result that has emerged more

recently, in agreement with earlier results (e.g., Schubert et al., 1998), is a tendency for a poleward shift of several degrees latitude in mid-latitude storm tracks in both hemispheres (Geng and Sugi, 2003; Fischer-Bruns et al., 2005; Yin, 2005; Bengtsson et al., 2006). Consistent with these shifts in storm track activity, Cassano et al. (2006), using a 10-member multi-model ensemble, show a future change to a more cyclonically dominated circulation pattern in winter and summer over the Arctic, and increasing cyclonicity and stronger westerlies in the same multi-model ensemble for the Antarctic (Lynch et al., 2006).

Some studies have shown little change in extratropical cyclone characteristics (Kharin and Zwiers, 2005; Watterson, 2005). But a regional study showed a tendency towards more intense systems, particularly in the A2 scenario in another global coupled climate model analysis (Leckebusch and Ulbrich, 2004), with more extreme wind events in association with those deepened cyclones for several regions of Western Europe, with similar changes in the B2 simulation although less pronounced in amplitude. Geng and Sugi (2003) use a higher-resolution (about 100 km resolution) atmospheric GCM (AGCM) with time-slice experiments and find a decrease in cyclone density (number of cyclones in a 4.5° by 4.5° area per season) in the mid-latitudes of both hemispheres in a warmer climate in both the DJF and JJA seasons, associated with the changes in the baroclinicity in the lower troposphere, in general agreement with earlier results and coarser GCM results (e.g., Dai et al., 2001b). They also find that the density of strong cyclones increases while the density of weak and medium-strength cyclones decreases. Several studies have shown a possible reduction in mid-latitude storms in the NH but a decrease in central pressures in these storms (Lambert and Fyfe, 2006, for a 15-member multi-model ensemble) and in the SH (Fyfe, 2003, with a possible 30% reduction in sub-antarctic cyclones). The latter two studies did not definitively identify a poleward shift of storm tracks, but their methodologies used a relatively coarse grid that may not have been able to detect shifts of several degrees latitude and they used only identification of central pressures which could imply an identification of semi-permanent features like the sub-antarctic trough. More regional aspects of these changes were addressed for the NH in a single model study by Inatsu and Kimoto (2005), who show a more active storm track in the western Pacific in the future but weaker elsewhere. Fischer-Bruns et al. (2005) document storm activity increasing over the North Atlantic and Southern Ocean and decreasing over the Pacific Ocean.

By analysing stratosphere-troposphere exchanges using time-slice experiments with the middle atmosphere version of ECHAM4, Land and Feichter (2003) suggest that cyclonic and blocking activity becomes weaker poleward of 30°N in a warmer climate at least in part due to decreased baroclinicity below 400 hPa, while cyclonic activity becomes stronger in the SH associated with increased baroclinicity above 400 hPa. The atmospheric circulation variability on inter-decadal time scales may also change due to increasing greenhouse gases and aerosols. One model result (Hu et al., 2001) showed that inter-decadal variability of the SLP and 500 hPa height fields increased over the tropics and decreased at high latitudes due to global warming.

In summary, the most consistent results from the majority of the current generation of models show, for a future warmer climate, a poleward shift of storm tracks in both hemispheres that is particularly evident in the SH, with greater storm activity at higher latitudes.

A new feature that has been studied related to extreme conditions over the oceans is wave height. Studies by Wang et al. (2004), Wang and Swail (2006a,b) and Caires et al. (2006) have shown that for many regions of the mid-latitude oceans, an increase in extreme wave height is likely to occur in a future warmer climate. This is related to increased wind speed associated with mid-latitude storms, resulting in higher waves produced by these storms, and is consistent with the studies noted above that showed decreased numbers of mid-latitude storms but more intense storms.

10.4 Changes Associated with Biogeochemical Feedbacks and Ocean Acidification

10.4.1 Carbon Cycle/Vegetation Feedbacks

As a parallel activity to the standard IPCC AR4 climate projection simulations described in this chapter, the Coupled Climate-Carbon Cycle Model Intercomparison Project (C^4MIP) supported by WCRP and the International Geosphere-Biosphere Programme (IGBP) was initiated. Eleven climate models with a representation of the land and ocean carbon cycle (see Chapter 7) performed simulations where the model was driven by an anthropogenic CO_2 emissions scenario for the 1860 to 2100 time period (instead of an atmospheric CO_2 concentration scenario as in the standard IPCC AR4 simulations). Each C^4MIP model performed two simulations, a 'coupled' simulation where the growth of atmospheric CO_2 induces a climate change which affects the carbon cycle, and an 'uncoupled' simulation, where atmospheric CO_2 radiative forcing is held fixed at pre-industrial levels, in order to estimate the atmospheric CO_2 growth rate that would occur if the carbon cycle was unperturbed by the climate. Emissions were taken from the observations for the historical period (Houghton and Hackler, 2000; Marland et al., 2005) and from the SRES A2 scenario for the future (Leemans et al., 1998).

Chapter 7 describes the major results of the C^4MIP models in terms of climate impact on the carbon cycle. This section starts from these impacts to infer the feedback effect on atmospheric CO_2 and therefore on the climate system. There is unanimous agreement among the models that future climate change will reduce the efficiency of the land and ocean carbon cycle to absorb anthropogenic CO_2, essentially owing to a reduction in land carbon uptake. The latter is driven by a combination of

reduced net primary productivity and increased soil respiration of CO_2 under a warmer climate. As a result, a larger fraction of anthropogenic CO_2 will stay airborne if climate change controls the carbon cycle. By the end of the 21st century, this additional CO_2 varies between 20 and 220 ppm for the two extreme models, with most of the models lying between 50 and 100 ppm (Friedlingstein et al., 2006). This additional CO_2 leads to an additional radiative forcing of between 0.1 and 1.3 W m^{-2} and hence an additional warming of between 0.1°C and 1.5°C.

All of the C⁴MIP models simulate a higher atmospheric CO_2 growth rate in the coupled runs than in the uncoupled runs. For the A2 emission scenario, this positive feedback leads to a greater atmospheric CO_2 concentration (Friedlingstein et al., 2006) as noted above, which is in addition to the concentrations in the standard coupled models assessed in the AR4 (e.g., Meehl et al., 2005b). By 2100, atmospheric CO_2 varies between 730 and 1,020 ppm for the C⁴MIP models, compared with 836 ppm for the standard SRES A2 concentration in the multi-model data set (e.g., Meehl et al., 2005b). This uncertainty due to future changes in the carbon cycle is illustrated in Figure 10.20a where the CO_2 concentration envelope of the C⁴MIP uncoupled simulations is centred on the standard SRES A2 concentration value. The range reflects the uncertainty in the carbon cycle. It should be noted that the standard SRES A2 concentration value of 836 ppm was calculated in the TAR with the Bern carbon cycle-climate model (BERN-CC; Joos et al., 2001) that accounted for the climate-carbon cycle feedback. Parameter sensitivity studies were performed with the BERN-CC model at that time and gave a range of 735 ppm to 1,080 ppm, comparable to the range of the C⁴MIP study. The effects of climate feedback uncertainties on the carbon cycle have also been considered probabilistically by Wigley and Raper (2001). A later paper (Wigley, 2004) considers individual emissions scenarios, accounting for carbon cycle feedbacks in the same way as Wigley and Raper (2001). The results of these studies are consistent with the more recent C⁴MIP results. For the A2 scenario considered in C⁴MIP, the CO_2 concentration range in 2100 using the Wigley and Raper model is 769 to 1,088 ppm, compared with 730 to 1,020 ppm in the C⁴MIP study (which ignored the additional warming effect due to non-CO_2 gases). Similarly, using neural networks, Knutti et al. (2003) show that the climate-carbon cycle feedback leads to an increase of about 0.6°C over the central estimate for the SRES A2 scenario and an increase of about 1.5°C for the upper bound of the uncertainty range.

Further uncertainties regarding carbon uptake were addressed with a 14-member multi-model ensemble using the CMIP2 models to quantify contributions to uncertainty from inter-model variability as opposed to internal variability (Berthelot et al., 2002). They found that the AOGCMs with the largest climate sensitivity also had the largest drying of soils in the tropics and thus the largest reduction in carbon uptake.

The C⁴MIP protocol did not account for the evolution of non-CO_2 greenhouse gases and aerosols. In order to compare the C⁴MIP simulated warming with the IPCC AR4 climate models, the SRES A2 radiative forcings of CO_2 alone and total forcing (CO_2 plus non-CO_2 greenhouse gases and aerosols) as given in Appendix II of the TAR were used. Using these numbers and knowing the climate sensitivity of each C⁴MIP model, the warming that would have been simulated by the C⁴MIP models if they had included the non-CO_2 greenhouse gases and aerosols can be estimated. For the SRES A2 scenario, these estimates show that the C⁴MIP range of global temperature increase by the end of the 21st century would be 2.4°C to 5.6°C, compared with 2.6°C to 4.1°C for standard IPCC-AR4 climate models (Figure 10.20b). As a result of a much larger CO_2 concentration by 2100 in most of the C⁴MIP models, the upper estimate of the global warming by 2100 is up to 1.5°C higher than for the standard SRES A2 simulations.

The C⁴MIP results highlight the importance of coupling the climate system and the carbon cycle in order to simulate, for a

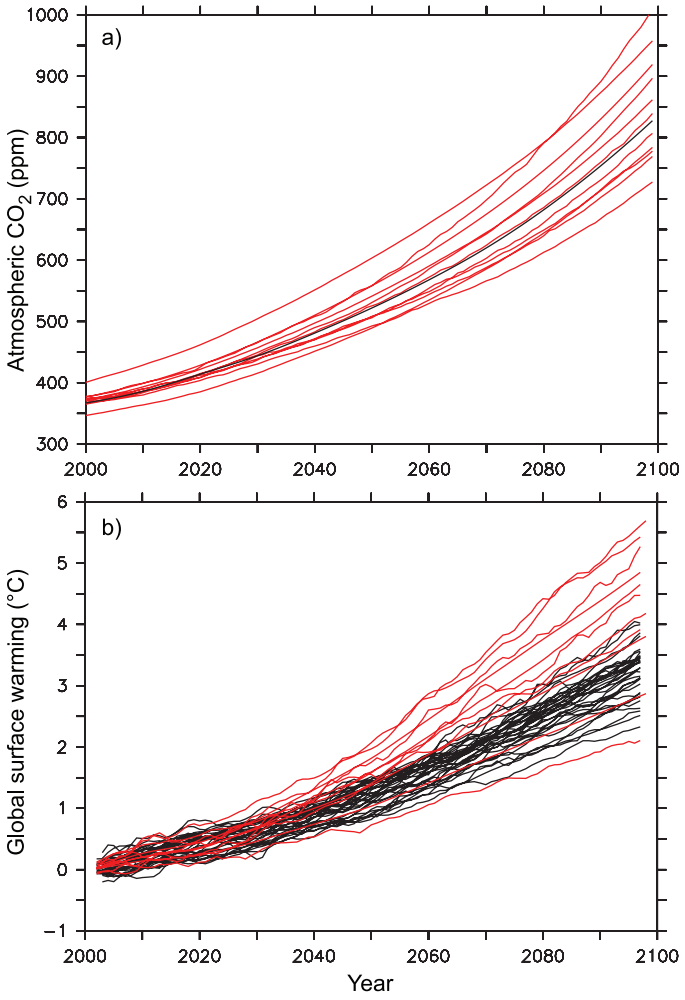


Figure 10.20. *(a) 21st-century atmospheric CO_2 concentration as simulated by the 11 C⁴MIP models for the SRES A2 emission scenario (red) compared with the standard atmospheric CO_2 concentration used as a forcing for many IPCC AR4 climate models (black). The standard CO_2 concentration values were calculated by the BERN-CC model and are identical to those used in the TAR. For some IPCC-AR4 models, different carbon cycle models were used to convert carbon emissions to atmospheric concentrations. (b) Globally averaged surface temperature change (relative to 2000) simulated by the C⁴MIP models forced by CO_2 emissions (red) compared to global warming simulated by the IPCC AR4 models forced by CO_2 concentration (black). The C⁴MIP global temperature change has been corrected to account for the non-CO_2 radiative forcing used by the standard IPCC AR4 climate models.*

given scenario of CO_2 emissions, a climate change that takes into account the dynamic evolution of the Earth's capacity to absorb the CO_2 perturbation.

Conversely, the climate-carbon cycle feedback will have an impact on the estimate of the projected CO_2 emissions leading to stabilisation of atmospheric CO_2 at a given level. The TAR showed the range of future emissions for the Wigley, Richels and Edmonds (WRE; Wigley et al., 1996) stabilisation concentration scenarios, using different model parametrizations (including the climate-carbon feedback, Joos et al., 2001; Kheshgi and Jain, 2003). However, the emission reduction due to this feedback was not quantified. Similar to the C⁴MIP protocol, coupled and uncoupled simulations have been recently performed in order to specifically evaluate the impact of climate change on the future CO_2 emissions required to achieve stabilisation (Matthews, 2005; Jones et al., 2006). Figure 10.21 shows the emissions required to achieve CO_2 stabilisation for the stabilisation profiles SP450, SP550, SP750 and SP1000 (SP450 refers to stabilisation at a CO_2 concentration of 450 ppm, etc.) as simulated by three climate-carbon cycle models. As detailed above, the climate-carbon cycle feedback reduces the land and ocean uptake of CO_2, leading to a reduction in the emissions compatible with a given atmospheric CO_2 stabilisation pathway. The higher the stabilisation scenario, the larger the climate change, the larger the impact on the carbon cycle, and hence the larger the emission reduction relative to the case without climate-carbon cycle feedback. For example, stabilising atmospheric CO_2 at 450 ppm, which will likely result in a global equilibrium warming of 1.4°C to 3.1°C, with a best guess of about 2.1°C, would require a reduction of current annual greenhouse gas emissions by 52 to 90% by 2100. Positive carbon cycle feedbacks (i.e., reduced ocean and terrestrial carbon uptake caused by the warming) reduce the total (cumulative) emissions over the 21st century compatible with a stabilisation of CO_2 concentration at 450 ppm by 105 to 300 GtC relative to a hypothetical case where the carbon cycle does not respond to temperature. The uncertainty regarding the strength of the climate-carbon cycle feedback highlighted in the C⁴MIP analysis is also evident in Figure 10.21. For higher stabilisation scenarios such as SP550, SP750 and SP1000, the larger warming (2.9°C, 4.3°C and 5.5°C, respectively) requires an increasingly larger reduction (130 to 425 GtC, 160 to 500 GtC and 165 to 510 GtC, respectively) in the cumulated compatible emissions.

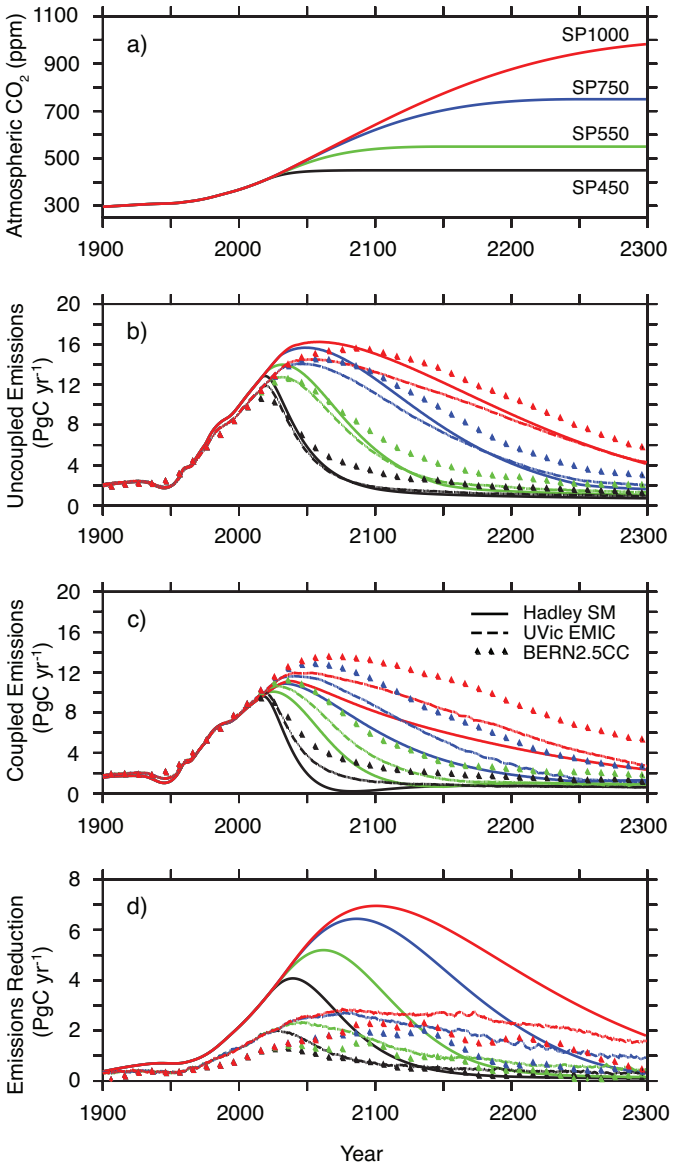


Figure 10.21. *(a) Atmospheric CO_2 stabilisation scenarios SP1000 (red), SP750 (blue), SP550 (green) and SP450 (black). (b) Compatible annual emissions calculated by three models, the Hadley simple model (Jones et al., 2006; solid), the UVic EMIC (Matthews, 2005; dashed) and the BERN2.5CC EMIC (Joos et al., 2001; Plattner et al., 2001; triangles) for the three stabilisation scenarios without accounting for the impact of climate on the carbon cycle (see Table 8.3 for details of the latter two models). (c) As for (b) but with the climate impact on the carbon cycle accounted for. (d) The difference between (b) and (c) showing the impact of the climate-carbon cycle feedback on the calculation of compatible emissions.*

The current uncertainty involving processes driving the land and ocean carbon uptake will translate into an uncertainty in the future emissions of CO_2 required to achieve stabilisation. In Figure 10.22, the carbon-cycle related uncertainty is addressed using the BERN2.5CC carbon cycle EMIC (Joos et al., 2001; Plattner et al., 2001; see Table 8.3 for model details) and the series of S450 to SP1000 CO_2 stabilisation scenarios. The range of emission uncertainty was derived using identical assumptions as made in the TAR, varying ocean transport parameters and parametrizations describing the cycling of carbon through the terrestrial biosphere. Results are thus very closely comparable, and the small differences can be largely explained by the different CO_2 trajectories and the use of a dynamic ocean model here compared to the TAR.

The model results confirm that for stabilisation of atmospheric CO_2, emissions need to be reduced well below year 2000 values in all scenarios. This is true for the full range of simulations covering carbon cycle uncertainty, even including the upper bound, which is based on rather extreme assumptions of terrestrial carbon cycle processes.

Cumulative emissions for the period from 2000 to 2100 (to 2300) range between 596 GtC (933 GtC) for SP450, and 1,236 GtC (3,052 GtC) for SP1000. The emission uncertainty varies

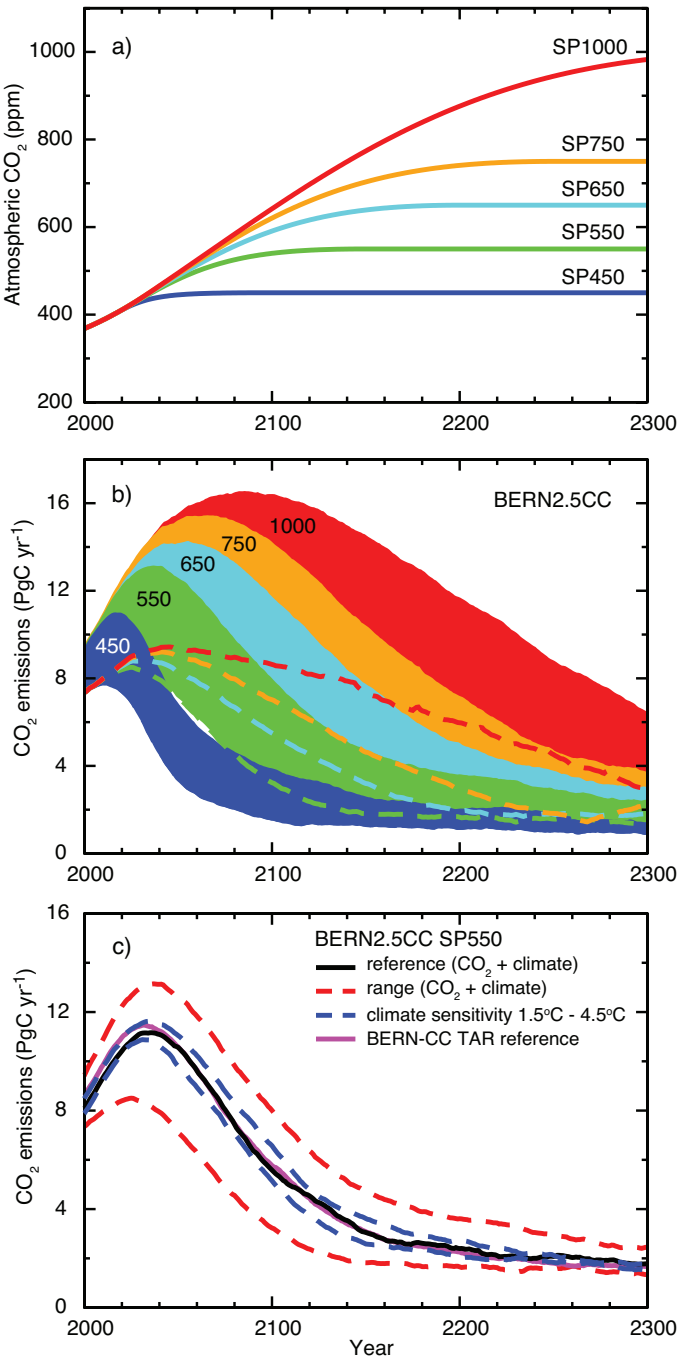


Figure 10.22. *Projected CO_2 emissions leading to stabilisation of atmospheric CO_2 concentrations at different levels and the effect of uncertainty in carbon cycle processes on calculated emissions. Panel (a) shows the assumed trajectories of CO_2 concentration (SP scenarios)(Knutti et al., 2005); (b) and (c) show the implied CO_2 emissions, as projected with the Bern2.5CC EMIC (Joos et al., 2001; Plattner et al., 2001). The ranges given in (b) for each of the SP scenarios represent effects of different model parametrizations and assumptions illustrated for scenario SP550 in panel (c) (range for 'CO_2 + climate'). The upper and lower bounds in (b) are indicated by the top and bottom of the shaded areas. Alternatively, the lower bound (where hidden) is indicated by a dashed line. Panel (c) illustrates emission ranges and sensitivities for scenario SP550.*

between –26 and +28% about the reference cases in year 2100 and between –26 and +34% in year 2300, increasing with time. The range of uncertainty thus depends on the magnitude of the CO_2 stabilisation level and the induced climate change. The additional uncertainty in projected emissions due to uncertainty in climate sensitivity is illustrated by two additional simulations with 1.5°C and 4.5°C climate sensitivities (see Box 10.2). The resulting emissions for this range of climate sensitivities lie within the range covered by the uncertainty in processes driving the carbon cycle.

Both the standard IPCC-AR4 and the C^{4}MIP models ignore the effect of land cover change in future projections. However, as described in Chapters 2 and 7, past and future changes in land cover may affect the climate through several processes. First, they may change surface characteristics such as albedo. Second, they may affect the ratio of latent to sensible heat and therefore affect surface temperature. Third, they may induce additional CO_2 emissions from the land. Fourth, they can affect the capacity of the land to take up atmospheric CO_2. So far, no comprehensive coupled AOGCM has addressed these four components all together. Using AGCMs, DeFries et al. (2004) studied the impact of future land cover change on the climate, while Maynard and Royer (2004) performed a similar experiment on Africa only. DeFries et al. (2002) forced the Colorado State University GCM (Randall et al., 1996) with Atmospheric Model Intercomparison Project (AMIP) climatological sea surface temperatures and with either the present-day vegetation cover or a 2050 vegetation map adapted from a low-growth scenario of the Integrated Model to Assess the Global Environment (IMAGE-2; Leemans et al., 1998). The study finds that in the tropics and subtropics, replacement of forests by grassland or cropland leads to a reduction in carbon assimilation, and therefore in latent heat flux. The latter reduction leads to a surface warming of up to 1.5°C in deforested tropical regions. Using the ARPEGE-Climat AGCM (Déqué et al., 1994) with a higher resolution over Africa, Maynard et al. (2002) performed two experiments, one simulation with 2 × atmospheric CO_2 SSTs taken from a previous ARPEGE transient SRES B2 simulation and present-day vegetation, and one with the same SSTs but the vegetation taken from a SRES B2 simulation of the IMAGE-2 model (Leemans et al., 1998). Similar to DeFries et al. (2002), they find that future deforestation in tropical Africa leads to a redistribution of latent and sensible heat that leads to a warming of the surface. However, this warming is relatively small (0.4°C) and represents about 20% of the warming due to the atmospheric CO_2 doubling.

Two recent studies further investigated the relative roles of future changes in greenhouse gases compared with future changes in land cover. Using a similar model design as Maynard and Royer (2004), Voldoire (2006) compared the climate change simulated under a 2050 SRES B2 greenhouse gases scenario to the one under a 2050 SRES B2 land cover change scenario. They show that the relative impact of vegetation change compared to greenhouse gas concentration increase is of the order of 10%, and can reach 30% over localised tropical regions. In a more comprehensive study, Feddema et al. (2005) applied the same

methodology for the SRES A2 and B1 scenario over the 2000 to 2100 period. Similarly, they find no significant effect at the global scale, but a potentially large effect at the regional scale, such as a warming of 2°C by 2100 over the Amazon for the A2 land cover change scenario, associated with a reduction in the DTR. The general finding of these studies is that the climate change due to land cover changes may be important relative to greenhouse gases at the regional level, where intense land cover change occurs. Globally, the impact of greenhouse gas concentrations dominates over the impact of land cover change.

10.4.2 Ocean Acidification Due to Increasing Atmospheric Carbon Dioxide

Increasing atmospheric CO_2 concentrations lower oceanic pH and carbonate ion concentrations, thereby decreasing the saturation state with respect to calcium carbonate (Feely et al., 2004). The main driver of these changes is the direct geochemical effect due to the addition of anthropogenic CO_2 to the surface ocean (see Box 7.3). Surface ocean pH today is already 0.1 unit lower than pre-industrial values (Section 5.4.2.3). In the multi-model median shown in Figure 10.23, pH is projected to decrease by another 0.3 to 0.4 units under the IS92a scenario by 2100. This translates into a 100 to 150% increase in the concentration of H^+ ions (Orr et al., 2005). Simultaneously, carbonate ion concentrations will decrease. When water is undersaturated with respect to calcium carbonate, marine organisms can no longer form calcium carbonate shells (Raven et al., 2005).

Under scenario IS92a, the multi-model projection shows large decreases in pH and carbonate ion concentrations throughout the world oceans (Orr et al., 2005; Figures 10.23 and 10.24). The decrease in surface carbonate ion concentrations is found to be largest at low and mid-latitudes, although undersaturation is projected to occur at high southern latitudes first (Figure 10.24). The present-day surface saturation state is strongly influenced by temperature and is lowest at high latitudes, with minima in the Southern Ocean. The model simulations project that undersaturation will be reached in a few decades. Therefore, conditions detrimental to high-latitude ecosystems could develop within decades, not centuries as suggested previously (Orr et al., 2005).

While the projected changes are largest at the ocean surface, the penetration of anthropogenic CO_2 into the ocean interior will alter the chemical composition over the 21st century down to several thousand metres, albeit with substantial regional differences (Figure 10.23). The total volume of water in the ocean that is undersaturated with regard to calcite (not shown) or aragonite, a meta-stable form of calcium carbonate, increases substantially as atmospheric CO_2 concentrations continue to rise (Figure 10.23). In the multi-model projections, the aragonite saturation horizon (i.e., the 100% line separating over- and undersaturated regions) reaches the surface in the Southern Ocean by about 2050 and substantially shoals by 2100 in the South Pacific (by >1,000 m) and throughout the Atlantic (between 800 m and 2,200 m).

Ocean acidification could thus conceivably lead to undersaturation and dissolution of calcium carbonate in parts of the surface ocean during the 21st century, depending on the evolution of atmospheric CO_2 (Orr et al., 2005). Southern Ocean surface water is projected to become undersaturated with respect to aragonite at a CO_2 concentration of approximately 600 ppm. This concentration threshold is largely independent of emission scenarios.

Uncertainty in these projections due to potential future climate change effects on the ocean carbon cycle (mainly through changes in temperature, ocean stratification and marine biological production and re-mineralization; see Box 7.3) are small compared to the direct effect of rising atmospheric CO_2 from anthropogenic emissions. Orr et al. (2005) estimate that 21st century climate change could possibly counteract less than 10% of the projected direct geochemical changes. By far the largest uncertainty in the future evolution of these ocean interior changes is thus associated with the future pathway of atmospheric CO_2.

10.4.3 Simulations of Future Evolution of Methane, Ozone and Oxidants

Simulations using coupled chemistry-climate models indicate that the trend in upper-stratospheric ozone changes sign sometime between 2000 and 2005 due to the gradual reduction in halocarbons. While ozone concentrations in the upper stratosphere decreased at a rate of 400 ppb (–6%) per decade during 1980 to 2000, they are projected to increase at a rate of 100 ppb (1 to 2%) per decade from 2000 to 2020 (Austin and Butchart, 2003). On longer time scales, simulations show significant changes in ozone and CH_4 relative to current concentrations. The changes are related to a variety of factors, including increased emissions of chemical precursors, changes in gas-phase and heterogeneous chemistry, altered climate conditions due to global warming and greater transport and mixing across the tropopause. The impacts on CH_4 and ozone from increased emissions are a direct effect of anthropogenic activity, while the impacts of different climate conditions and stratosphere-troposphere exchange represent indirect effects of these emissions (Grewe et al., 2001).

The projections for ozone based upon scenarios with high emissions (IS92a; Leggett et al., 1992) and SRES A2 (Nakićenović and Swart, 2000) indicate that concentrations of tropospheric ozone might increase throughout the 21st century, primarily as a result of these emissions. Simulations for the period 2015 through 2050 project increases in ozone of 20 to 25% (Grewe et al., 2001; Hauglustaine and Brasseur, 2001), and simulations through 2100 indicate that ozone below 250 mb may grow by 40 to 60% (Stevenson et al., 2000; Grenfell et al., 2003; Zeng and Pyle, 2003; Hauglustaine et al., 2005; Yoshimura et al., 2006). The primary species contributing to the increase in tropospheric ozone are anthropogenic emissions of NO_x, CH_4, CO and compounds from fossil fuel combustion. The photochemical reactions that produce smog are accelerated by increases of 2.6 times the present flux of NO_x, 2.5 times the

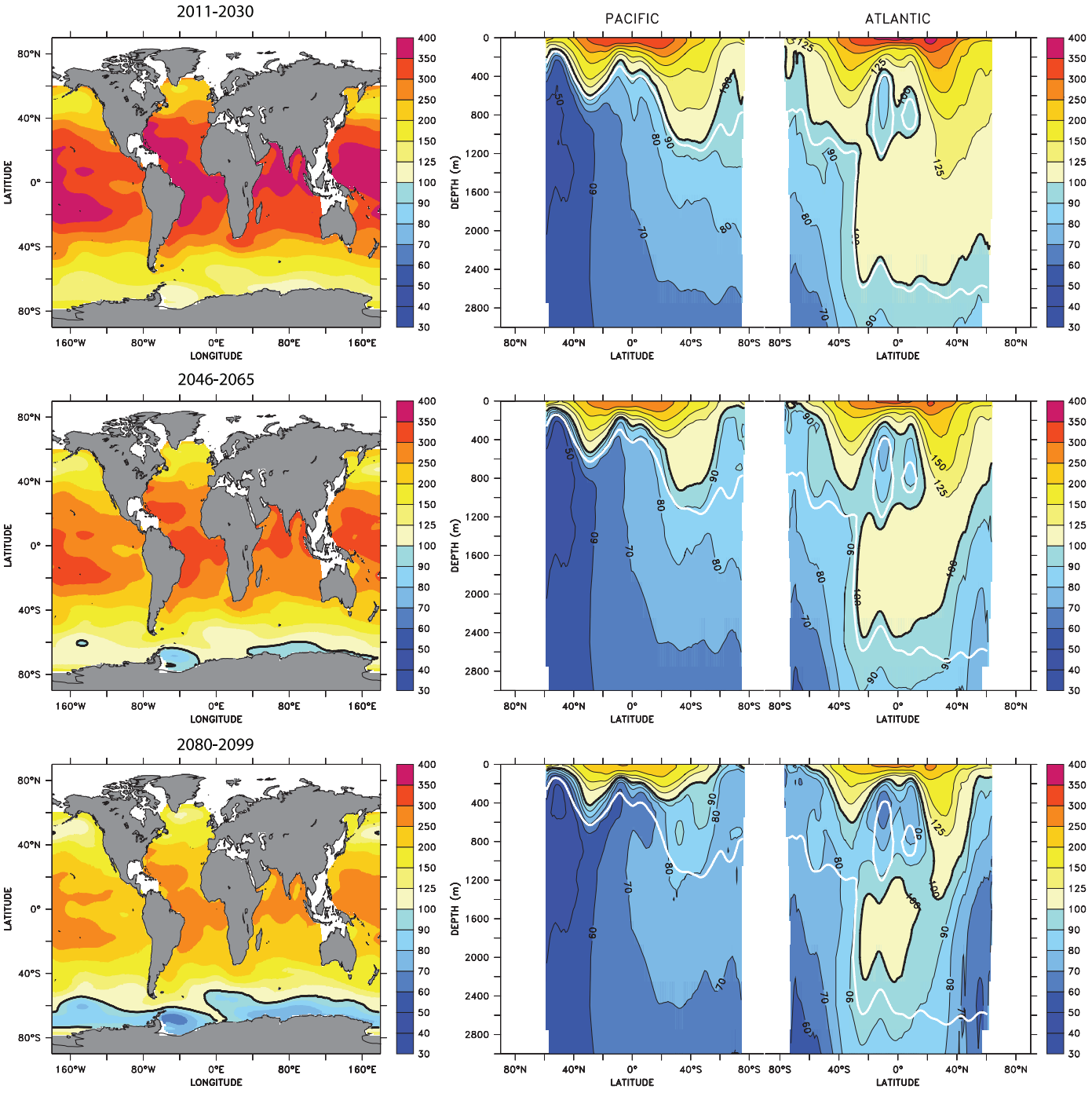


Figure 10.23. *Multi-model median for projected levels of saturation (%) with respect to aragonite, a meta-stable form of calcium carbonate, over the 21st century from the Ocean Carbon-Cycle Model Intercomparison Project (OCMIP-2) models (adapted from Orr et al., 2005). Calcium carbonate dissolves at levels below 100%. Surface maps (left) and combined Pacific/Atlantic zonal mean sections (right) are given for scenario IS92a as averages over three time periods: 2011 to 2030 (top), 2045 to 2065 (middle) and 2080 to 2099 (bottom). Atmospheric CO_2 concentrations for these three periods average 440, 570 and 730 ppm, respectively. Latitude-depth sections start in the North Pacific (at the left border), extend to the Southern Ocean Pacific section and return through the Southern Ocean Atlantic section to the North Atlantic (right border). At 100%, waters are saturated (solid black line - the aragonite saturation horizon); values larger than 100% indicate super-saturation; values lower than 100% indicate undersaturation. The observation-based (Global Ocean Data Analysis Project; GLODAP) 1994 saturation horizon (solid white line) is also shown to illustrate the projected changes in the saturation horizon compared to the present.*

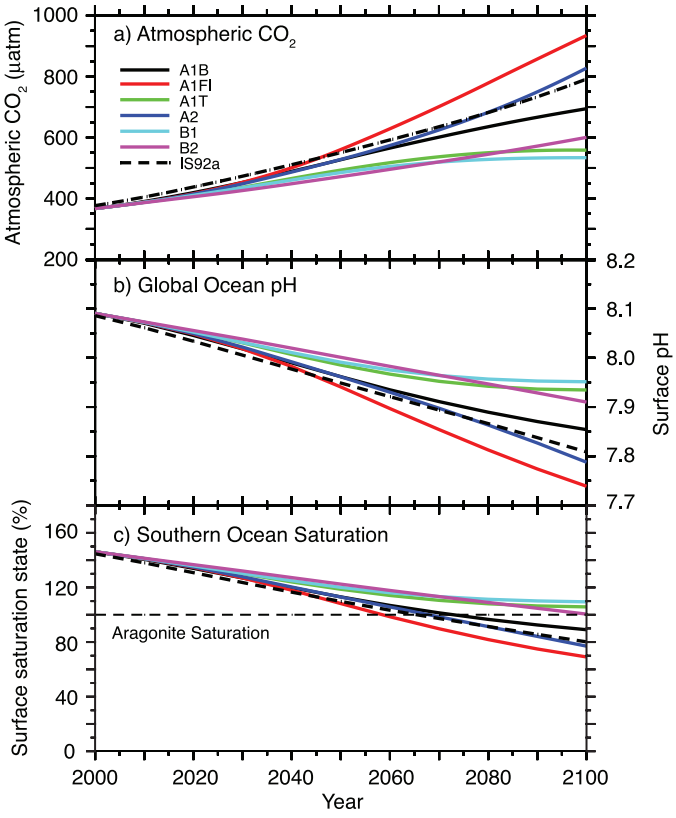


Figure 10.24. *Changes in global average surface pH and saturation state with respect to aragonite in the Southern Ocean under various SRES scenarios. Time series of (a) atmospheric CO_2 for the six illustrative SRES scenarios, (b) projected global average surface pH and (c) projected average saturation state in the Southern Ocean from the BERN2.5D EMIC (Plattner et al., 2001). The results for the SRES scenarios A1T and A2 are similar to those for the non-SRES scenarios S650 and IS92a, respectively. Modified from Orr et al. (2005).*

present flux of CH_4 and 1.8 times the present flux of CO in the A2 scenario. Between 91 and 92% of the higher concentrations in ozone are related to direct effects of these emissions, with the remainder of the increase attributable to secondary effects of climate change (Zeng and Pyle, 2003) combined with biogenic precursor emissions (Hauglustaine et al., 2005). These emissions may also lead to higher concentrations of oxidants including the hydroxyl radical (OH), possibly leading to an 8% reduction in the lifetime of tropospheric CH_4 (Grewe et al., 2001).

Since the projected growth in emissions occurs primarily in low latitudes, the ozone increases are largest in the tropics and subtropics (Grenfell et al., 2003). In particular, the concentrations in Southeast Asia, India and Central America increase by 60 to 80% by 2050 under the A2 scenario. However, the effects of tropical emissions are not highly localised, since the ozone spreads throughout the lower atmosphere in plumes emanating from these regions. As a result, the ozone in remote marine regions in the SH may grow by 10 to 20% over present-day levels by 2050. The ozone may also be distributed through vertical transport in tropical convection followed by lateral transport on isentropic surfaces. Ozone concentrations can also be increased by emissions of biogenic hydrocarbons (e.g., Hauglustaine et al., 2005), in particular isoprene emitted by broadleaf forests. Under the A2 scenario, biogenic hydrocarbons are projected to increase by between 27% (Sanderson et al., 2003) and 59% (Hauglustaine et al., 2005) contributing to a 30 to 50% increase in ozone formation over northern continental regions.

Developing countries have begun reducing emissions from mobile sources through stricter standards. New projections of the evolution of ozone precursors that account for these reductions have been developed with the Regional Air Pollution Information and Simulation (RAINS) model (Amann et al., 2004). One set of projections is consistent with source strengths permitted under the Current Legislation (CLE) scenario. A second set of projections is consistent with lower emissions under a Maximum Feasible Reduction (MFR) scenario. The concentrations of ozone and CH_4 have been simulated for the MFR, CLE and A2 scenarios for the period 2000 through 2030 using an ensemble of 26 chemical transport models (Dentener et al., 2006; Stevenson et al., 2006). The changes in NO_x emissions for these three scenarios are –27%, +12% and +55%, respectively, relative to year 2000. The corresponding changes in ensemble-mean burdens in tropospheric ozone are –5%, +6% and +18% for the MFR, CLE and A2 scenarios, respectively. There are substantial inter-model differences of order ±25% in these results. The ozone decreases throughout the troposphere in the MFR scenario, but the zonal annual mean concentrations increase by up to 6 ppb in the CLE scenario and by typically 6 to 10 ppb in the A2 scenario (Supplementary Material, Figure S10.2).

The radiative forcing by the combination of ozone and CH_4 changes by –0.05, 0.18, and 0.30 W m^{-2} for the MFR, CLE and A2 scenarios, respectively. These projections indicate that the growth in tropospheric ozone between 2000 and 2030 could be reduced or reversed depending on emission controls.

The major issues in the fidelity of these simulations for future tropospheric ozone are the sensitivities to the representation of the stratospheric production, destruction and transport of ozone and the exchange of species between the stratosphere and troposphere. Few of the models include the effects of non-methane hydrocarbons (NMHCs), and the sign of the effects of NMHCs on ozone are not consistent among the models that do (Hauglustaine and Brasseur, 2001; Grenfell et al., 2003).

The effect of more stratosphere-troposphere exchange (STE) in response to climate change is projected to increase the concentrations of ozone in the upper troposphere due to the much greater concentrations of ozone in the lower stratosphere than in the upper troposphere. While the sign of the effect is consistent in recent simulations, the magnitude of the change in STE and its effects on ozone are very model dependent. In a simulation forced by the SRES A1FI scenario, Collins et al. (2003) project that the downward flux of ozone increases by 37% from the 1990s to the 2090s. As a result, the concentration of ozone in the upper troposphere at mid-latitudes increases by 5 to 15%. For the A2 scenarios, projections of the increase in ozone by 2100 due to STE range from 35% (Hauglustaine et al., 2005) to 80% (Sudo et al., 2003; Zeng and Pyle, 2003). The increase in STE is driven by increases in the descending

branches of the Brewer-Dobson Circulation at mid-latitudes and is caused by changes in meridional temperature gradients in the upper troposphere and lower stratosphere (Rind et al., 2001). The effects of the enhanced STE are sensitive to the simulation of processes in the stratosphere, including the effects of lower temperatures and the evolution of chlorine, bromine and NO_x concentrations. Since the greenhouse effect of ozone is largest in the upper troposphere, the treatment of STE remains a significant source of uncertainty in the calculation of the total greenhouse effect of tropospheric ozone.

The effects of climate change, in particular increased tropospheric temperatures and water vapour, tend to offset some of the increase in ozone driven by emissions. The higher water vapour is projected to offset the increase in ozone by between 10% (Hauglustaine et al., 2005) and 17% (Stevenson et al., 2000). The water vapour both decelerates the chemical production and accelerates the chemical destruction of ozone. The photochemical production depends on the concentrations of NO_y (reactive odd nitrogen), and the additional water vapour causes a larger fraction of NO_y to be converted to nitric acid, which can be efficiently removed from the atmosphere in precipitation (Grewe et al., 2001). The water vapour also increases the concentrations of OH through reaction with the oxygen radical in the 1D excited state ($O(^1D)$), and the removal of $O(^1D)$ from the atmosphere slows the formation of ozone. The increased concentrations of OH and the increased rates of CH_4 oxidation with higher temperature further reduce the lifetime of tropospheric CH_4 by 12% by 2100 (Stevenson et al., 2000; Johnson et al., 2001). Decreases in CH_4 concentrations also tend to reduce tropospheric ozone (Stevenson et al., 2000).

Recent measurements show that CH_4 growth rates have declined and were negative for several years in the early 21st century (see Section 2.3.2). The observed rate of increase of 0.8 ppb yr^{-1} for the period 1999 to 2004 is considerably less than the rate of 6 ppb yr^{-1} assumed in all the SRES scenarios for the period 1990 to 2000 (Nakićenović and Swart, 2000; TAR Appendix II). Recent studies (Dentener et al., 2005) have considered lower emission scenarios (see above) that take account of new pollution control techniques adopted in major developing countries. In the CLE scenario, emissions of CH_4 are comparable to the B2 scenario and increase from 340 Tg yr^{-1} in 2000 to 450 Tg yr^{-1} in 2030. The CH_4 concentrations increase from 1,750 ppb in 2000 to between 2,090 and 2,200 ppb in 2030 under this scenario. In the MFR scenario, the emissions are sufficiently low that the concentrations in 2030 are unchanged at 1,750 ppb. Under these conditions, the changes in radiative forcing due to CH_4 between the 1990s and 2020s are less than 0.01 W m^{-2}.

Current understanding of the magnitude and variation of CH_4 sources and sinks is covered in Section 7.4, where it is noted that there are substantial uncertainties although the modelling has progressed. There is some evidence for a coupling between climate and wetland emissions. For example, calculations using atmospheric concentrations and small-scale emission measurements as input differ by 60% (Shindell and Schmidt, 2004). Concurrent changes in natural sources of CH_4 are now being estimated to first order using simple models of the biosphere coupled to AOGCMs. Simulations of the response of wetlands to climate change from doubling atmospheric CO_2 show that wetland emissions increase by 78% (Shindell and Schmidt, 2004). Most of this effect is caused by growth in the flux of CH_4 from existing tropical wetlands. The increase would be equivalent to approximately 20% of current inventories and would contribute an additional 430 ppb to atmospheric concentrations. Global radiative forcing would increase by approximately 4 to 5% from the effects of wetland emissions by 2100 (Gedney et al., 2004).

10.4.4 Simulations of Future Evolution of Major Aerosol Species

The time-dependent evolution of major aerosol species and the interaction of these species with climate represent some of the major sources of uncertainty in projections of climate change. An increasing number of AOGCMs have included multiple types of tropospheric aerosols including sulphates, nitrates, black and organic carbon, sea salt and soil dust. Of the 23 models represented in the multi-model ensemble of climate-change simulations for IPCC AR4, 13 include other tropospheric species besides sulphates. Of these, seven have the non-sulphate species represented with parametrizations that interact with the remainder of the model physics. Nitrates are treated in just two of the models in the ensemble. Recent projections of nitrate and sulphate loading under the SRES A2 scenario suggest that forcing by nitrates may exceed forcing by sulphates by the end of the 21st century (Adams et al., 2001). This result is of course strongly dependent upon the evolution of precursor emissions for these aerosol species.

The black and organic carbon aerosols in the atmosphere include a very complex system of primary organic aerosols (POA) and secondary organic aerosols (SOA), which are formed by oxidation of biogenic VOCs. The models used for climate projections typically use highly simplified bulk parametrizations for POA and SOA. More detailed parametrizations for the formation of SOA that trace oxidation pathways have only recently been developed and used to estimate the direct radiative forcing by SOA for present-day conditions (Chung and Seinfeld, 2002). The forcing by SOA is an emerging issue for simulations of present-day and future climate since the rate of chemical formation of SOA may be 60% or more of the emissions rate for primary carbonaceous aerosols (Kanakidou et al., 2005). In addition, two-way coupling between reactive chemistry and tropospheric aerosols has not been explored comprehensively in climate change simulations. Unified models that treat tropospheric ozone-NO_x-hydrocarbon chemistry, aerosol formation, heterogeneous processes in clouds and on aerosols, and gas-phase photolysis have been developed and applied to the current climate (Liao et al., 2003). However, these unified models have not yet been used extensively to study the evolution of the chemical state of the atmosphere under future scenarios.

The interaction of soil dust with climate is under active investigation. Whether emissions of soil dust aerosols increase or decrease in response to changes in atmospheric state and circulation is still unresolved (Tegen et al., 2004a). Several recent studies have suggested that the total surface area where dust can be mobilised will decrease in a warmer climate with higher concentrations of CO_2 (e.g., Harrison et al., 2001). The net effects of reductions in dust emissions from natural sources combined with land use change could potentially be significant but have not been systematically modelled as part of climate change assessment.

Uncertainty regarding the scenario simulations is compounded by inherently unpredictable natural forcings from future volcanic eruptions and solar variability. The eruptions that produce climatologically significant forcing represent just the extremes of global volcanic activity (Naveau and Ammann, 2005). Global simulations can account for the effects of future natural forcings using stochastic representations based upon prior eruptions and variations in solar luminosity. The relative contribution of these forcings to the projections of global mean temperature anomalies are largest in the period up to 2030 (Stott and Kettleborough, 2002).

10.5 Quantifying the Range of Climate Change Projections

10.5.1 Sources of Uncertainty and Hierarchy of Models

Uncertainty in predictions of anthropogenic climate change arises at all stages of the modelling process described in Section 10.1. The specification of future emissions of greenhouse gases, aerosols and their precursors is uncertain (e.g., Nakićenović and Swart, 2000). It is then necessary to convert these emissions into concentrations of radiatively active species, calculate the associated forcing and predict the response of climate system variables such as surface temperature and precipitation (Figure 10.1). At each step, uncertainty in the true signal of climate change is introduced both by errors in the representation of Earth system processes in models (e.g., Palmer et al., 2005) and by internal climate variability (e.g., Selten et al., 2004). The effects of internal variability can be quantified by running models many times from different initial conditions, provided that simulated variability is consistent with observations. The effects of uncertainty in the knowledge of Earth system processes can be partially quantified by constructing ensembles of models that sample different parametrizations of these processes. However, some processes may be missing from the set of available models, and alternative parametrizations of other processes may share common systematic biases. Such limitations imply that distributions of future climate responses from ensemble simulations are themselves subject to uncertainty (Smith, 2002), and would be wider were uncertainty due to structural model errors accounted for. These distributions may be modified to reflect observational constraints expressed through metrics of the agreement between the observed historical climate and the simulations of individual ensemble members, for example through Bayesian methods (see Chapter 9 Supplementary Material, Appendix 9.B). In this case, the choice of observations and their associated errors introduce further sources of uncertainty. In addition, some sources of future radiative forcing are yet to be accounted for in the ensemble projections, including those from land use change, variations in solar and volcanic activity (Kettleborough et al., 2007), and CH_4 release from permafrost or ocean hydrates (see Section 8.7).

A spectrum or hierarchy of models of varying complexity has been developed (Claussen et al., 2002; Stocker and Knutti, 2003) to assess the range of future changes consistent with the understanding of known uncertainties. Simple climate models (SCMs) typically represent the ocean-atmosphere system as a set of global or hemispheric boxes, predicting global surface temperature using an energy balance equation, a prescribed value of climate sensitivity and a basic representation of ocean heat uptake (see Section 8.8.2). Their role is to perform comprehensive analyses of the interactions between global variables, based on prior estimates of uncertainty in their controlling parameters obtained from observations, expert judgement and from tuning to complex models. By coupling SCMs to simple models of biogeochemical cycles they can be used to extrapolate the results of AOGCM simulations to a wide range of alternative forcing scenarios (e.g., Wigley and Raper, 2001; see Section 10.5.3).

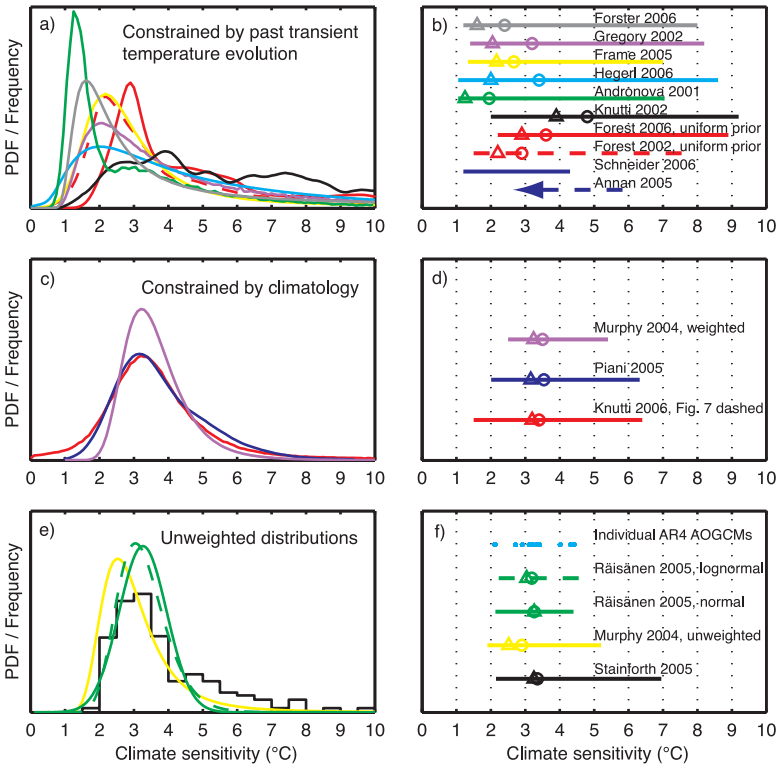
Compared to SCMs, EMICs include more of the processes simulated in AOGCMs, but in a less detailed, more highly parametrized form (see Section 8.8.3), and at coarser resolution. Consequently, EMICs are not suitable for quantifying uncertainties in regional climate change or extreme events, however they can be used to investigate the large-scale effects of coupling between multiple Earth system components in large ensembles or long simulations (e.g., Forest et al., 2002; Knutti et al., 2002), which is not yet possible with AOGCMs due to their greater computational expense. Some EMICs therefore include modules such as vegetation dynamics, the terrestrial and ocean carbon cycles and atmospheric chemistry (Plattner et al., 2001; Claussen et al., 2002), filling a gap in the spectrum of models between AOGCMs and SCMs. Thorough sampling of parameter space is computationally feasible for some EMICs (e.g., Stocker and Schmittner, 1997; Forest et al., 2002; Knutti et al., 2002), as for SCMs (Wigley and Raper, 2001), and is used to obtain probabilistic projections (see Section 10.5.4.5). In some EMICs, climate sensitivity is an adjustable parameter, as in SCMs. In other EMICs, climate sensitivity is dependent on multiple model parameters, as in AOGCMs. Probabilistic estimates of climate sensitivity and TCR from SCMs and EMICs are assessed in Section 9.6 and compared with estimates from AOGCMs in Box 10.2.

The high resolution and detailed parametrizations in AOGCMs enable them to simulate more comprehensively the

Box 10.2: Equilibrium Climate Sensitivity

The likely range[1] for equilibrium climate sensitivity was estimated in the TAR (Technical Summary, Section F.3; Cubasch et al., 2001) to be 1.5°C to 4.5°C. The range was the same as in an early report of the National Research Council (Charney, 1979), and the two previous IPCC assessment reports (Mitchell et al., 1990; Kattenberg et al., 1996). These estimates were expert assessments largely based on equilibrium climate sensitivities simulated by atmospheric GCMs coupled to non-dynamic slab oceans. The mean ±1 standard deviation values from these models were 3.8°C ± 0.78°C in the SAR (17 models), 3.5°C ± 0.92°C in the TAR (15 models) and in this assessment 3.26°C ± 0.69°C (18 models).

Considerable work has been done since the TAR (IPCC, 2001) to estimate climate sensitivity and to provide a better quantification of relative probabilities, including a most likely value, rather than just a subjective range of uncertainty. Since climate sensitivity of the real climate system cannot be measured directly, new methods have been used since the TAR to establish a relationship between sensitivity and some observable quantity (either directly or through a model), and to estimate a range or probability density function (PDF) of climate sensitivity consistent with observations. These methods are summarised separately in Chapters 9 and 10, and here we synthesize that information into an assessment. The information comes from two main categories: constraints from past climate change on various time scales, and the spread of results for climate sensitivity from ensembles of models.



Box 10.2, Figure 1. *(a) PDFs or frequency distributions constrained by the transient evolution of the atmospheric temperature, radiative forcing and ocean heat uptake, (b) as in (a) and (b) but 5 to 95% ranges, medians (circles) and maximum probabilities (triangles), (c) and (d) as in (a) but using constraints from present-day climatology, and (e) and (f) unweighted or fitted distributions from different models or from perturbing parameters in a single model. Distributions in (e) and (f) should not be strictly interpreted as PDFs. See Chapter 9 text, Figure 9.20 and Table 9.3 for details. Note that Annan et al. (2005b) only provide an upper but no lower bound. All PDFs are truncated at 10°C for consistency, some are shown for different prior distributions than in the original studies, and ranges may differ from numbers reported in individual studies.*

The first category of methods (see Section 9.6) uses the historical transient evolution of surface temperature, upper air temperature, ocean temperature, estimates of the radiative forcing, satellite data, proxy data over the last millennium, or a subset thereof to calculate ranges or PDFs for sensitivity (e.g., Wigley et al., 1997b; Tol and De Vos, 1998; Andronova and Schlesinger, 2001; Forest et al., 2002; Gregory et al., 2002a; Harvey and Kaufmann, 2002; Knutti et al., 2002, 2003; Frame et al., 2005; Forest et al., 2006; Forster and Gregory, 2006; Hegerl et al., 2006). A summary of all PDFs of climate sensitivity from those methods is shown in Figure 9.20 and in Box 10.2, Figure 1a. Median values, most likely values (modes) and 5 to 95% uncertainty ranges are shown in Box 10.2, Figure 1b for each PDF. Most of the results confirm that climate sensitivity is very unlikely below 1.5°C. The upper bound is more difficult to constrain because of a nonlinear relationship between climate sensitivity and the observed transient response, and is further hampered by the limited length of the observational record and uncertainties in the observations, which are particularly large for ocean heat uptake and for the magnitude of the aerosol radiative forcing. Studies that take all the important known uncertainties in observed historical trends into account cannot rule out the possibility that the climate sensitivity exceeds 4.5°C, although such high values are consistently found to be less likely than values of around 2.0°C to 3.5°C. Observations of transient climate change provide better constraints for the TCR (see Section 9.6.1.3).

Two recent studies use a modelled relation between climate sensitivity and tropical SSTs in the Last Glacial Maximum (LGM) and proxy records of the latter to estimate ranges of climate sensitivity (Annan et al., 2005b; Schneider von Deimling et al., 2006; see

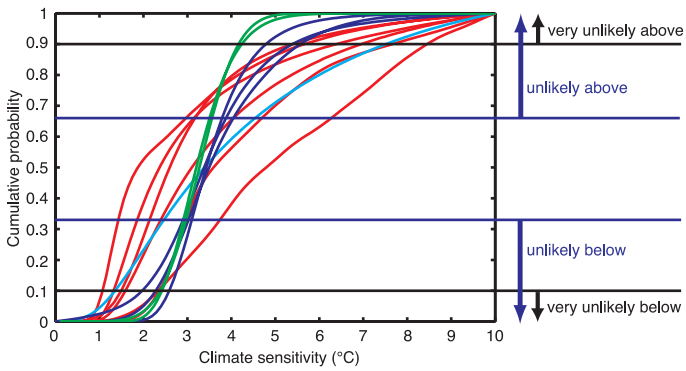
(continued)

[1] Though the TAR Technical Summary attached 'likely' to the 1.5°C - 4.5°C range, the word 'likely' was used there in a general sense rather than in a specific calibrated sense. No calibrated confidence assessment was given in either the Summary for Policymakers or in Chapter 9 of the TAR, and no probabilistic studies on climate sensitivity were cited in Chapter 9 where the range was assessed.

Section 9.6). While both of these estimates overlap with results from the instrumental period and results from other AOGCMS, the results differ substantially due to different forcings and the different relationships between LGM SSTs and sensitivity in the models used. Therefore, LGM proxy data provide support for the range of climate sensitivity based on other lines of evidence.

Studies comparing the observed transient response of surface temperature after large volcanic eruptions with results obtained from models with different climate sensitivities (see Section. 9.6) do not provide PDFs, but find best agreement with sensitivities around 3°C, and reasonable agreement within the 1.5°C to 4.5°C range (Wigley et al., 2005). They are not able to exclude sensitivities above 4.5°C.

The second category of methods examines climate sensitivity in GCMs. Climate sensitivity is not a single tuneable parameter in these models, but depends on many processes and feedbacks. Three PDFs of climate sensitivity were obtained by comparing different variables of the simulated present-day climatology and variability against observations in a perturbed physics ensemble (Murphy et al., 2004; Piani et al., 2005; Knutti et al., 2006, Box 10.2, Figure 1c,d; see Section 10.5.4.2). Equilibrium climate sensitivity is found to be most likely around 3.2°C, and very unlikely to be below about 2°C. The upper bound is sensitive to how model parameters are sampled and to the method used to compare with observations.



Box 10.2, Figure 2. *Individual cumulative distributions of climate sensitivity from the observed 20th-century warming (red), model climatology (blue) and proxy evidence (cyan), taken from Box 10.2, Figure 1a, c (except LGM studies and Forest et al. (2002), which is superseded by Forest et al. (2006)) and cumulative distributions fitted to the AOGCMs' climate sensitivities (green) from Box 10.2, Figure 1e. Horizontal lines and arrows mark the edges of the likelihood estimates according to IPCC guidelines.*

Box 10.2, Figure 1e,f show the frequency distributions obtained by different methods when perturbing parameters in the Hadley Centre Atmospheric Model (HadAM3) but before weighting with observations (Section10.5.4). Murphy et al. (2004; unweighted) sampled 29 parameters and assumed individual effects to combine linearly. Stainforth et al. (2005) found nonlinearities when simulating multiple combinations of a subset of key parameters. The most frequently occurring climate sensitivity values are grouped around 3°C, but this could reflect the sensitivity of the unperturbed model. Some, but not all, of the simulations by high-sensitivity models have been found to agree poorly with observations and are therefore unlikely, hence even very high values are not excluded. This inability to rule out very high values is common to many methods, since for well-understood physical reasons, the rate of change (against sensitivity) of most quantities that can be observed tends to zero as the sensitivity increases (Hansen et al., 1985; Knutti et al., 2005; Allen et al., 2006b).

There is no well-established formal way of estimating a single PDF from the individual results, taking account of the different assumptions in each study. Most studies do not account for structural uncertainty, and thus probably tend to underestimate the uncertainty. On the other hand, since several largely independent lines of evidence indicate similar most likely values and ranges, climate sensitivity values are likely to be better constrained than those found by methods based on single data sets (Annan and Hargreaves, 2006; Hegerl et al., 2006).

The equilibrium climate sensitivity values for the AR4 AOGCMs coupled to non-dynamic slab ocean models are given for comparison (Box 10.2, Figure 1e,f; see also Table 8.2). These estimates come from models that represent the current best efforts from the international global climate modelling community at simulating climate. A normal fit yields a 5 to 95% range of about 2.1°C to 4.4°C with a mean value of equilibrium climate sensitivity of about 3.3°C (2.2°C to 4.6°C for a lognormal distribution, median 3.2°C) (Räisänen, 2005b). A probabilistic interpretation of the results is problematic, because each model is assumed to be equally credible and the results depend upon the assumed shape of the fitted distribution. Although the AOGCMs used in IPCC reports are an 'ensemble of opportunity' not designed to sample modelling uncertainties systematically or randomly, the range of sensitivities covered has been rather stable over many years. This occurs in spite of substantial model developments, considerable progress in simulating many aspects of the large-scale climate, and evaluation of those models against observations. Progress has been made since the TAR in diagnosing and understanding inter-model differences in climate feedbacks and equilibrium climate sensitivity. Confidence has increased in the strength of water vapour-lapse rate feedbacks, whereas cloud feedbacks (particularly from low-level clouds) have been confirmed as the primary source of climate sensitivity differences (see Section 8.6).

Since the TAR, the levels of scientific understanding and confidence in quantitative estimates of equilibrium climate sensitivity have increased substantially. Basing our assessment on a combination of several independent lines of evidence, as summarised in Box 10.2 Figures 1 and 2, including observed climate change and the strength of known feedbacks simulated in GCMs, we conclude that the global mean equilibrium warming for doubling CO_2, or 'equilibrium climate sensitivity', is likely to lie in the range 2°C to 4.5°C, with a most likely value of about 3°C. Equilibrium climate sensitivity is very likely larger than 1.5°C.

For fundamental physical reasons as well as data limitations, values substantially higher than 4.5°C still cannot be excluded, but agreement with observations and proxy data is generally worse for those high values than for values in the 2°C to 4.5°C range.

processes giving rise to internal variability (see Section 8.4), extreme events (see Section 8.5) and climate change feedbacks, particularly at the regional scale (Boer and Yu, 2003a; Bony and Dufresne, 2005; Bony et al., 2006; Soden and Held, 2006). Given that ocean dynamics influence regional feedbacks (Boer and Yu, 2003b), quantification of regional uncertainties in time-dependent climate change requires multi-model ensemble simulations with AOGCMs containing a full, three-dimensional dynamic ocean component. However, downscaling methods (see Chapter 11) are required to obtain credible information at spatial scales near or below the AOGCM grid scale (125 to 400 km in the AR4 AOGCMs, see Table 8.1).

10.5.2 Range of Responses from Different Models

10.5.2.1 Comprehensive AOGCMs

The way a climate model responds to changes in external forcing, such as an increase in anthropogenic greenhouse gases, is characterised by two standard measures: (1) 'equilibrium climate sensitivity' (the equilibrium change in global surface temperature following a doubling of the atmospheric equivalent CO_2 concentration; see Glossary), and (2) 'transient climate response' (the change in global surface temperature in a global coupled climate model in a 1% yr^{-1} CO_2 increase experiment at the time of atmospheric CO_2 doubling; see Glossary). The first measure provides an indication of feedbacks mainly residing in the atmospheric model but also in the land surface and sea ice components, and the latter quantifies the response of the fully coupled climate system including aspects of transient ocean heat uptake (e.g., Sokolov et al., 2003). These two measures have become standard for quantifying how an AOGCM will react to more complicated forcings in scenario simulations.

Historically, the equilibrium climate sensitivity has been given in the range from 1.5°C to 4.5°C. This range was reported in the TAR with no indication of a probability distribution within this range. However, considerable recent work has addressed the range of equilibrium climate sensitivity, and attempted to assign probabilities to climate sensitivity.

Equilibrium climate sensitivity and TCR are not independent (Figure 10.25a). For a given AOGCM, the TCR is smaller than the equilibrium climate sensitivity because ocean heat uptake delays the atmospheric warming. A large ensemble of the BERN2.5D EMIC has been used to explore the relationship of TCR and equilibrium sensitivity over a wide range of ocean heat uptake parametrizations (Knutti et al., 2005). Good agreement with the available results from AOGCMs is found, and the BERN2.5D EMIC covers almost the entire range of structurally different models. The percent change in precipitation is closely related to the equilibrium climate sensitivity for the current generation of AOGCMs (Figure 10.25b), with values from the current models falling within the range of the models from the TAR. Figure 10.25c shows the percent change in globally averaged precipitation as a function of TCR at the time of atmospheric CO_2 doubling, as simulated by 1% yr^{-1} transient CO_2 increase experiments with AOGCMs. The figure suggests

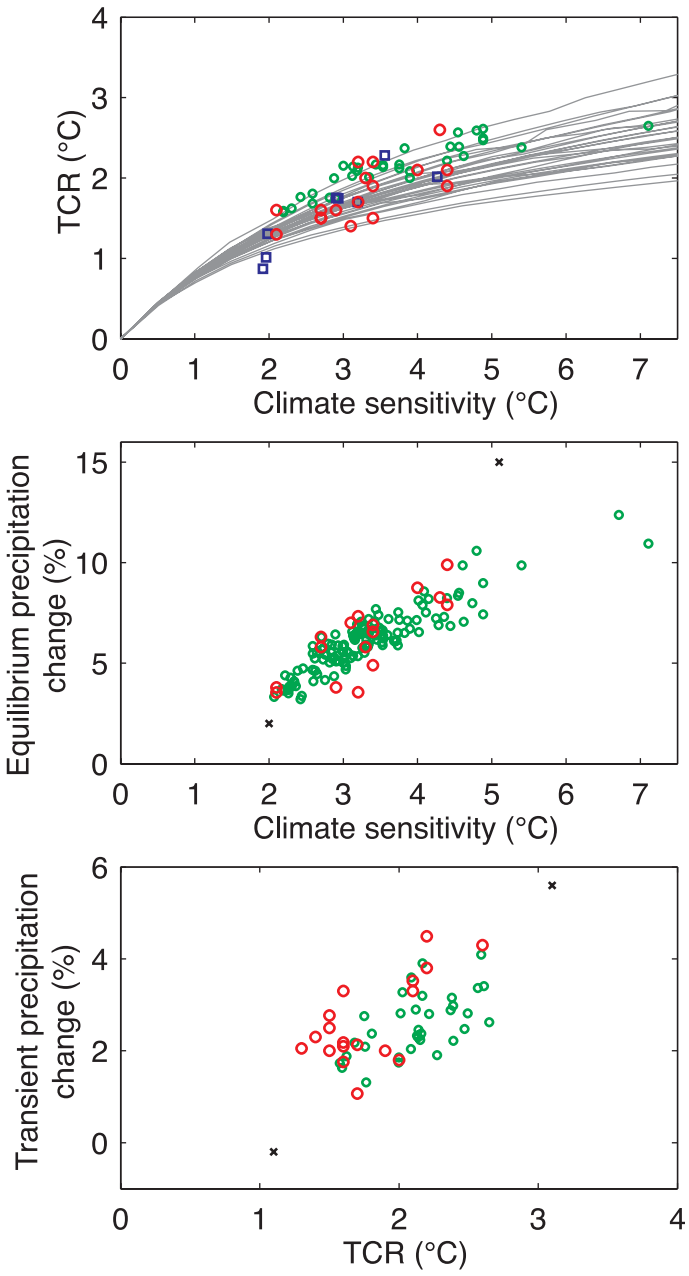


Figure 10.25. *(a) TCR versus equilibrium climate sensitivity for all AOGCMs (red), EMICs (blue), a perturbed physics ensemble of the UKMO-HadCM3 AOGCM (green; an updated ensemble based on M. Collins et al., 2006) and from a large ensemble of the Bern2.5D EMIC (Knutti et al., 2005) using different ocean vertical diffusivities and mixing parametrizations (grey lines). (b) Global mean precipitation change (%) as a function of global mean temperature change at equilibrium for doubled CO_2 in atmospheric GCMs coupled to a non-dynamic slab ocean (red all AOGCMS, green from a perturbed physics ensemble of the atmosphere-slab ocean version of UKMO-HadCM3 (Webb et al., 2006)). (c) Global mean precipitation change (%) as a function of global mean temperature change (TCR) at the time of CO_2 doubling in a transient 1% yr^{-1} CO_2 increase scenario, simulated by coupled AOGCMs (red) and the UKMO-HadCM3 perturbed physics ensemble (green). Black crosses in (b) and (c) mark ranges covered by the TAR AOGCMs (IPCC, 2001) for each quantity.*

a broadly positive correlation between these two quantities similar to that for equilibrium climate sensitivity, with these values from the new models also falling within the range of the previous generation of AOGCMs assessed in the TAR. Note that the apparent relationships may not hold for other forcings or at smaller scales. Values for an ensemble with perturbations made to parameters in the atmospheric component of UKMO-HadCM3 (M. Collins et al., 2006) cover similar ranges and are shown in Figure 10.25 for comparison.

Fitting normal distributions to the results, the 5 to 95% uncertainty range for equilibrium climate sensitivity from the AOGCMs is approximately 2.1°C to 4.4°C and that for TCR is 1.2°C to 2.4°C (using the method of Räisänen, 2005b). The mean for climate sensitivity is 3.26°C and that for TCR is 1.76°C. These numbers are practically the same for both the normal and the lognormal distribution (see Box 10.2). The assumption of a (log) normal fit is not well supported by the limited sample of AOGCM data. In addition, the AOGCMs represent an 'ensemble of opportunity' and are by design not sampled in a random way. However, most studies aiming to constrain climate sensitivity with observations do indeed indicate a similar to lognormal probability distribution of climate sensitivity and an approximately normal distribution of the uncertainty in future warming and thus TCR (see Box 10.2). Those studies also suggest that the current AOGCMs may not cover the full range of uncertainty for climate sensitivity. An assessment of all the evidence on equilibrium climate sensitivity is provided in Box 10.2. The spread of the AOGCM climate sensitivities is discussed in Section 8.6 and the AOGCM values for climate sensitivity and TCR are listed in Table 8.2.

The nonlinear relationship between TCR and equilibrium climate sensitivity shown in Figure 10.25a also indicates that on time scales well short of equilibrium, the model's TCR is not particularly sensitive to the model's climate sensitivity. The implication is that transient climate change is better constrained than the equilibrium climate sensitivity, that is, models with different sensitivity might still show good agreement for projections on decadal time scales. Therefore, in the absence of unusual solar or volcanic activity, climate change is well constrained for the coming few decades, because differences in some feedbacks will only become important on long time scales (see also Section 10.5.4.5) and because over the next few decades, about half of the projected warming would occur as a result of radiative forcing being held constant at year 2000 levels (constant composition commitment, see Section 10.7).

Comparing observed thermal expansion with those AR4 20th-century simulations that have natural forcings indicates that ocean heat uptake in the models may be 25% larger than observed, although both could be consistent within their uncertainties. This difference is possibly due to a combination of overestimated ocean heat uptake in the models, observational uncertainties and limited data coverage in the deep ocean (see Sections 9.5.1.1, 9.5.2, and 9.6.2.1). Assigning this difference solely to overestimated ocean heat uptake, the TCR estimates could increase by 0.6°C at most. This is in line with evidence for a relatively weak dependence of TCR on ocean mixing based on SCMs and EMICS (Allen et al., 2000; Knutti et al., 2005). The range of TCR covered by an ensemble with perturbations made to parameters in the atmospheric component of UKMO-HadCM3 is 1.5 to 2.6°C (M. Collins et al., 2006), similar to the AR4 AOGCM range. Therefore, based on the range covered by AOGCMs, and taking into account structural uncertainties and possible biases in transient heat uptake, TCR is assessed as very likely larger than 1°C and very unlikely greater than 3°C (i.e., 1.0°C to 3.0°C is a 10 to 90% range). Because the dependence of TCR on sensitivity becomes small as sensitivity increases, uncertainties in the upper bound on sensitivity only weakly affect the range of TCR (see Figure 10.25; Chapter 9; Knutti et al., 2005; Allen et al., 2006b). Observational constraints based on detection and attribution studies provide further support for this TCR range (see Section 9.6.2.3).

10.5.2.2 Earth System Models of Intermediate Complexity

Over the last few years, a range of climate models has been developed that are dynamically simpler and of lower resolution than comprehensive AOGCMs, although they might well be more 'complete' in terms of climate system components that are included. The class of such models, usually referred to as EMICs (Claussen et al., 2002), is very heterogeneous, ranging from zonally averaged ocean models coupled to energy balance models (Stocker et al., 1992a) or to statistical-dynamical models of the atmosphere (Petoukhov et al., 2000), to low resolution three-dimensional ocean models, coupled to energy balance or simple dynamical models of the atmosphere (Opsteegh et al., 1998; Edwards and Marsh, 2005; Müller et al., 2006). Some EMICs have a radiation code and prescribe greenhouse gases, while others use simplified equations to project radiative forcing from projected concentrations and abundances (Joos et al., 2001; see Chapter 2 and the TAR, Appendix II, Table II.3.11). Compared to comprehensive models, EMICs have hardly any computational constraints, and therefore many simulations can be performed. This allows for the creation of large ensembles, or the systematic exploration of long-term changes many centuries hence. However, because of the reduced resolution, only results at the largest scales (continental to global) are to be interpreted (Stocker and Knutti, 2003). Table 8.3 lists all EMICs used in this section, including their components and resolution.

A set of simulations is used to compare EMICs with AOGCMs for the SRES A1B scenario with stable atmospheric concentrations after year 2100 (see Section 10.7.2). For global mean temperature and sea level, the EMICs generally reproduce the AOGCM behaviour quite well. Two of the EMICs have values for climate sensitivity and transient response below the AOGCM range. However, climate sensitivity is a tuneable parameter in some EMICs, and no attempt was made here to match the range of response of the AOGCMs. The transient reduction of the MOC in most EMICs is also similar to the AOGCMs (see also Sections 10.3.4 and 10.7.2 and Figure 10.34), providing support that this class of models can be used for both long-term commitment projections (see Section 10.7) and probabilistic projections involving hundreds to thousands

of simulations (see Section 10.5.4.5). If the forcing is strong enough, and lasts long enough (e.g., 4 × CO_2), a complete and irreversible collapse of the MOC can be induced in a few models. This is in line with earlier results using EMICs (Stocker and Schmittner, 1997; Rahmstorf and Ganopolski, 1999) or a coupled model (Stouffer and Manabe, 1999).

10.5.3 Global Mean Responses from Different Scenarios

The TAR projections with an SCM presented a range of warming over the 21st century for 35 SRES scenarios. The SRES emission scenarios assume that no climate policies are implemented (Nakićenović and Swart, 2000). The construction of Figure 9.14 of the TAR was pragmatic. It used a simple model tuned to AOGCMs that had a climate sensitivity within the long-standing range of 1.5°C to 4.5°C (e.g., Charney, 1979; and stated in earlier IPCC Assessment Reports). Models with climate sensitivity outside that range were discussed in the text and allowed the statement that the presented range was not the extreme range indicated by AOGCMs. The figure was based on a single anthropogenic-forcing estimate for 1750 to 2000, which is well within the range of values recommended by TAR Chapter 6, and is also consistent with that deduced from model simulations and the observed temperature record (TAR Chapter 12.). To be consistent with TAR Chapter 3, climate feedbacks on the carbon cycle were included. The resulting range of global mean temperature change from 1990 to 2100 given by the full set of SRES scenarios was 1.4°C to 5.8°C.

Since the TAR, several studies have examined the TAR projections and attempted probabilistic assessments. Allen et al. (2000) show that the forcing and simple climate model tunings used in the TAR give projections that are in agreement with the observationally constrained probabilistic forecast, reported in TAR Chapter 12.

As noted by Moss and Schneider (2000), giving only a range of warming results is potentially misleading unless some guidance is given as to what the range means in probabilistic terms. Wigley and Raper (2001) interpret the warming range in probabilistic terms, accounting for uncertainties in emissions, the climate sensitivity, the carbon cycle, ocean mixing and aerosol forcing. They give a 90% probability interval for 1990 to 2100 warming of 1.7°C to 4°C. As pointed out by Wigley and Raper (2001), such results are only as realistic as the assumptions upon which they are based. Key assumptions in this study were that each SRES scenario was equally likely, that 1.5°C to 4.5°C corresponds to the 90% confidence interval for the climate sensitivity, and that carbon cycle feedback uncertainties can be characterised by the full uncertainty range of abundance in 2100 of 490 to 1,260 ppm given in the TAR. The aerosol probability density function (PDF) was based on the uncertainty estimates given in the TAR together with constraints based on fitting the SCM to observed global and hemispheric mean temperatures.

The most controversial assumption in the Wigley and Raper (2001) probabilistic assessment was the assumption that each SRES scenario was equally likely. The *Special Report on Emissions Scenarios* (Nakićenović and Swart, 2000) states that 'No judgment is offered in this report as to the preference for any of the scenarios and they are not assigned probabilities of occurrence, neither must they be interpreted as policy recommendations.'

Webster et al. (2003) use the probabilistic emissions projections of Webster et al. (2002), which consider present uncertainty in SO_2 emissions, and allow the possibility of continuing increases in SO_2 emissions over the 21st century, as well as the declining emissions consistent with SRES scenarios. Since their climate model parameter PDFs were constrained by observations and are mutually dependent, the effect of the lower present-day aerosol forcing on the projections is not easy to separate, but there is no doubt that their projections tend to be lower where they admit higher and increasing SO_2 emissions.

Irrespective of the question of whether it is possible to assign probabilities to specific emissions scenarios, it is important to distinguish different sources of uncertainties in temperature projections up to 2100. Different emission scenarios arise because future greenhouse gas emissions are largely dependent on key socioeconomic drivers, technological development and political decisions. Clearly, one factor leading to different temperature projections is the choice of scenario. On the other hand, the 'response uncertainty' is defined as the range in projections for a particular emission scenario and arises from the limited knowledge of how the climate system will react to the anthropogenic perturbations. In the following, all given uncertainty ranges reflect the response uncertainty of the climate system and should therefore be seen as conditional on a specific emission scenario.

The following paragraphs describe the construction of the AR4 temperature projections for the six illustrative SRES scenarios, using the SCM tuned to 19 models from the MMD (see Section 8.8). These 19 tuned simple model versions have effective climate sensitivities in the range 1.9°C to 5.9°C. The simple model sensitivities are derived from the fully coupled 2 × and 4 × CO_2 1% yr^{-1} CO_2 increase AOGCM simulations and in some cases differ from the equilibrium slab ocean model sensitivities given in Table 8.2.

The SRES emission scenarios used here were designed to represent plausible futures assuming that no climate policies will be implemented. This chapter does not analyse any scenarios with explicit climate change mitigation policies. Still, there is a wide variation across these SRES scenarios in terms of anthropogenic emissions, such as those of fossil CO_2, CH_4 and SO_2 (Nakićenović and Swart, 2000) as shown in the top three panels of Figure 10.26. As a direct consequence of the different emissions, the projected concentrations vary widely for the six illustrative SRES scenarios (see panel rows four to six in Figure 10.26 for the concentrations of the main greenhouse gases, CO_2, CH_4 and N_2O). These results incorporate the effect of carbon cycle uncertainties (see Section 10.4.1), which were not explored with the SCM in the TAR. Projected CH_4 concentrations are influenced by the temperature-dependent water vapour feedback on the lifetime of CH_4.

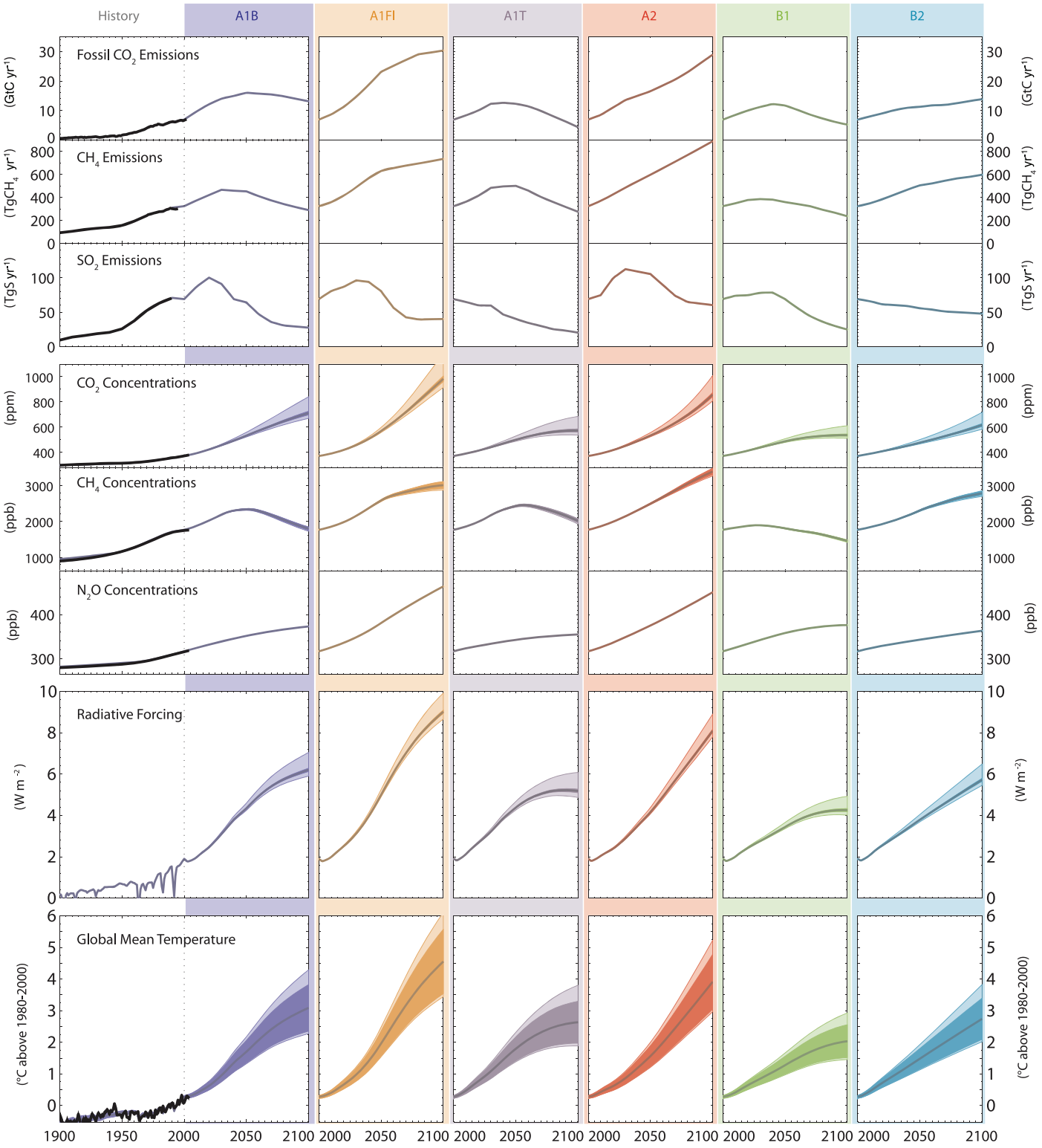


Figure 10.26. *Fossil CO_2, CH_4 and SO_2 emissions for six illustrative SRES non-mitigation emission scenarios, their corresponding CO_2, CH_4 and N_2O concentrations, radiative forcing and global mean temperature projections based on an SCM tuned to 19 AOGCMs. The dark shaded areas in the bottom temperature panel represent the mean ±1 standard deviation for the 19 model tunings. The lighter shaded areas depict the change in this uncertainty range, if carbon cycle feedbacks are assumed to be lower or higher than in the medium setting. Mean projections for mid-range carbon cycle assumptions for the six illustrative SRES scenarios are shown as thick coloured lines. Historical emissions (black lines) are shown for fossil and industrial CO_2 (Marland et al., 2005), for SO_2 (van Aardenne et al., 2001) and for CH_4 (van Aardenne et al., 2001, adjusted to Olivier and Berdowski, 2001). Observed CO_2, CH_4 and N_2O concentrations (black lines) are as presented in Chapter 6. Global mean temperature results from the SCM for anthropogenic and natural forcing compare favourably with 20th-century observations (black line) as shown in the lower left panel (Folland et al., 2001; Jones et al., 2001; Jones and Moberg, 2003).*

In Figure 10.26, the plumes of CO_2 concentration reflect high and low carbon cycle feedback settings of the applied SCM. Their derivation is described as follows. The carbon cycle model in the SCM used here (Model for the Assessment of Greenhouse-gas Induced Climate Change: MAGICC) includes a number of climate-related carbon cycle feedbacks driven by global mean temperature. The parametrization of the overall effect of carbon cycle feedbacks is tuned to the more complex and physically realistic carbon cycle models of the C^{4}MIP (Friedlingstein et al, 2006; see also Section 10.4) and the results are comparable to the BERN-CC model results across the six illustrative scenarios. This allows the SCM to produce projections of future CO_2 concentration change that are consistent with state-of-the-art carbon cycle model results. Specifically, the C^{4}MIP range of CO_2 concentrations for the A2 emission scenario in 2100 is 730 to 1,020 ppm, while the SCM results presented here show an uncertainty range of 806 ppm to 1,008 ppm. The lower bound of this SCM uncertainty range is the mean minus one standard deviation for low carbon cycle feedback settings and the 19 AOGCM tunings, while the upper bound represents the mean plus one standard deviation for high carbon cycle settings. For comparison, the 90% confidence interval from Wigley and Raper (2001) is 770 to 1,090 ppm. The simple model CO_2 concentration projections can be slightly higher than under the C^{4}MIP because the SCM's carbon cycle is driven by the full temperature changes in the A2 scenario, while the C^{4}MIP values are driven by the component of A2 climate change due to CO_2 alone.

The radiative forcing projections in Figure 10.26 combine anthropogenic and natural (solar and volcanic) forcing. The forcing plumes reflect primarily the sensitivity of the forcing to carbon cycle uncertainties. Results are based on a forcing of 3.71 W m^{-2} for a doubling of the atmospheric CO_2 concentration. The anthropogenic forcing is based on Table 2.12 but uses a value of –0.8 W m^{-2} for the present-day indirect aerosol forcing. Solar forcing for the historical period is prescribed according to Lean et al. (1995) and volcanic forcing according to Ammann et al. (2003). The historical solar forcing series is extended into the future using its average over the most recent 22 years. The volcanic forcing is adjusted to have a zero mean over the past 100 years and the anomaly is assumed to be zero for the future. In the TAR, the anthropogenic forcing was used alone even though the projections started in 1765. There are several advantages of using both natural and anthropogenic forcing for the past. First, this was done by most of the AOGCMs the simple models are emulating. Second, it allows the simulations to be compared with observations. Third, the warming commitments accrued over the instrumental period are reflected in the projections. The disadvantage of including natural forcing is that the warming projections in 2100 are dependent to a few tenths of a degree on the necessary assumptions made about the natural forcing (Bertrand et al., 2002). These assumptions include how the natural forcing is projected into the future and whether to reference the volcanic forcing to a past reference period mean value. In addition, the choice of data set for both solar and volcanic forcing affects the results (see Section 2.7 for discussion about uncertainty in natural forcings).

The temperature projections for the six illustrative scenarios are shown in the bottom panel of Figure 10.26. Model results are shown as anomalies from the mean of observations (Folland et al., 2001; Jones et al., 2001; Jones and Moberg, 2003) over the 1980 to 2000 period and the corresponding observed temperature anomalies are shown for comparison. The inner (darker) plumes show the ±1 standard deviation uncertainty due to the 19 model tunings and the outer (lighter) plumes show results for the corresponding high and low carbon cycle settings. Note that the asymmetry in the carbon cycle uncertainty causes global mean temperature projections to be skewed towards higher warming.

Considering only the mean of the SCM results with mid-range carbon cycle settings, the projected global mean temperature rise above 1980 to 2000 levels for the lower-emission SRES scenario B1 is 2.0°C in 2100. For a higher-emission scenario, for example, the SRES A2 scenario, the global mean temperature is projected to rise by 3.9°C above 1980 to 2000 levels in 2100. This clear difference in projected mean warming highlights the importance of assessing different emission scenarios separately. As mentioned above, the 'response uncertainty' is defined as the range in projections for a particular emission scenario. For the A2 emission scenario, the temperature change projections with the SCM span a ±1 standard deviation range of about 1.8°C, from 3.0°C to 4.8°C above 1980 to 2000 levels in 2100. If carbon cycle feedbacks are considered to be low, the lower end of this range decreases only slightly and is unchanged to one decimal place. For the higher carbon cycle feedback settings, the upper bound of the ±1 standard deviation range increases to 5.2°C. For lower-emission scenarios, this uncertainty range is smaller. For example, the B1 scenario projections span a range of about 1.4°C, from 1.5°C to 2.9°C, including carbon cycle uncertainties. The corresponding results for the medium-emission scenario A1B are 2.3°C to 4.3°C, and for the higher-emission scenario A1FI, they are 3.4°C to 6.1°C. Note that these uncertainty ranges are not the minimum to maximum bounds of the projected warming across all SCM runs, which are higher, namely 2.7°C to 7.1°C for the A2 scenario and 1.3°C to 4.2°C for the B1 scenario (not shown).

The SCM results presented here are a sensitivity study with different model tunings and carbon cycle feedback parameters. Note that forcing uncertainties have not been assessed and that the AOGCM model results available for SCM tuning may not span the full range of possible climate response. For example, studies that constrain forecasts based on model fits to historic or present-day observations generally allow for a somewhat wider 'response uncertainty' (see Section 10.5.4). The concatenation of all such uncertainties would require a probabilistic approach because the extreme ranges have low probability. A synthesis of the uncertainty in global temperature increase by the year 2100 is provided in Section 10.5.4.6.

10.5.4 Sampling Uncertainty and Estimating Probabilities

Uncertainty in the response of an AOGCM arises from the effects of internal variability, which can be sampled in isolation by creating ensembles of simulations of a single model using alternative initial conditions, and from modelling uncertainties, which arise from errors introduced by the discretization of the equations of motion on a finite resolution grid, and the parametrization of sub-grid scale processes (radiative transfer, cloud formation, convection, etc). Modelling uncertainties are manifested in alternative structural choices (for example, choices of resolution and the basic physical assumptions on which parametrizations are based), and in the values of poorly constrained parameters within parametrization schemes. Ensemble approaches are used to quantify the effects of uncertainties arising from variations in model structure and parameter settings. These are assessed in Sections 10.5.4.1 to 10.5.4.3, followed by a discussion of observational constraints in Section 10.5.4.4 and methods used to obtain probabilistic predictions in Sections 10.5.4.5 to 10.5.4.7.

While ensemble projections carried out to date give a wide range of responses, they do not sample all possible sources of modelling uncertainty. For example, the AR4 multi-model ensemble relies on specified concentrations of CO_2, thus neglecting uncertainties in carbon cycle feedbacks (see Section 10.4.1), although this can be partially addressed by using less detailed models to extrapolate the AOGCM results (see Section 10.5.3). More generally, the set of available models may share fundamental inadequacies, the effects of which cannot be quantified (Kennedy and O'Hagan, 2001). For example, climate models currently implement a restricted approach to the parametrization of sub-grid scale processes, using deterministic bulk formulae coupled to the resolved flow exclusively at the grid scale. Palmer et al. (2005) argue that the outputs of parametrization schemes should be sampled from statistical distributions consistent with a range of possible sub-grid scale states, following a stochastic approach that has been tried in numerical weather forecasting (e.g., Buizza et al., 1999; Palmer, 2001). The potential for missing or inadequately parametrized processes to broaden the simulated range of future changes is not clear, however, this is an important caveat for the results discussed below.

10.5.4.1 The Multi-Model Ensemble Approach

The use of ensembles of AOGCMs developed at different modelling centres has become established in climate prediction/projection on both seasonal-to-interannual and centennial time scales. To the extent that simulation errors in different AOGCMs are independent, the mean of the ensemble can be expected to outperform individual ensemble members, thus providing an improved 'best estimate' forecast. Results show this to be the case, both in verification of seasonal forecasts (Palmer et al., 2004; Hagedorn et al., 2005) and of the present-day climate from long term simulations (Lambert and Boer, 2001). By sampling modelling uncertainties, ensembles of AOGCMs should provide an improved basis for probabilistic projections compared with ensembles of a single model sampling only uncertainty in the initial state (Palmer et al., 2005). However, members of a multi-model ensemble share common systematic errors (Lambert and Boer, 2001), and cannot span the full range of possible model configurations due to resource constraints. Verification of future climate change projections is not possible, however, Räisänen and Palmer (2001) used a 'perfect model approach' (treating one member of an ensemble as truth and predicting its response using the other members) to show that the hypothetical economic costs associated with climate events can be reduced by calculating the probability of the event across the ensemble, rather than using a deterministic prediction from an individual ensemble member.

An additional strength of multi-model ensembles is that each member is subjected to careful testing in order to obtain a plausible and stable control simulation, although the process of tuning model parameters to achieve this (Section 8.1.3.1) involves subjective judgement, and is not guaranteed to identify the optimum location in the model parameter space.

10.5.4.2 Perturbed Physics Ensembles

The AOGCMs featured in Section 10.5.2 are built by selecting components from a pool of alternative parametrizations, each based on a given set of physical assumptions and including a number of uncertain parameters. In principle, the range of predictions consistent with these components could be quantified by constructing very large ensembles with systematic sampling of multiple options for parametrization schemes and parameter values, while avoiding combinations likely to double-count the effect of perturbing a given physical process. Such an approach has been taken using simple climate models and EMICs (Wigley and Raper, 2001; Knutti et al., 2002), and Murphy et al. (2004) and Stainforth et al. (2005) describe the first steps in this direction using AOGCMs, constructing large ensembles by perturbing poorly constrained parameters in the atmospheric component of UKMO-HadCM3 coupled to a mixed layer ocean. These experiments quantify the range of equilibrium responses to doubled atmospheric CO_2 consistent with uncertain parameters in a single GCM. Murphy et al. (2004) perturbed 29 parameters one at a time, assuming that effects of individual parameters were additive but making a simple allowance for additional uncertainty introduced by nonlinear interactions. They find a probability distribution for climate sensitivity with a 5 to 95% range of 2.4°C to 5.4°C when weighting the models with a broadly based metric of the agreement between simulated and observed climatology, compared to 1.9°C to 5.3°C when all model versions are assumed equally reliable (Box 10.2, Figure 1c).

Stainforth et al. (2005) deployed a distributed computing approach (Allen, 1999) to run a very large ensemble of 2,578 simulations sampling combinations of high, intermediate and low values of six parameters known to affect climate sensitivity. They find climate sensitivities ranging from 2°C to

11°C, with 4.2% of model versions exceeding 8°C, and show that the high-sensitivity models cannot be ruled out, based on a comparison with surface annual mean climatology. By utilising multivariate linear relationships between climate sensitivity and spatial fields of several present-day observables, the 5 to 95% range of climate sensitivity is estimated at 2.2°C to 6.8°C from the same data set (Piani et al., 2005; Box 10.2 Figure 1c). In this ensemble, Knutti et al. (2006) find a strong relationship between climate sensitivity and the amplitude of the seasonal cycle in surface temperature in the present-day simulations. Most of the simulations with high sensitivities overestimate the observed amplitude. Based on this relationship, the 5 to 95% range of climate sensitivity is estimated at 1.5°C to 6.4°C (Box 10.2, Figure 1c). The differences between the PDFs in Box 10.2, Figure 1c, which are all based on the same climate model, reflect uncertainties in methodology arising from choices of uncertain parameters, their expert-specified prior distributions and alternative applications of observational constraints. They do not account for uncertainties associated with changes in ocean circulation, and do not account for structural model errors (Smith, 2002; Goldstein and Rougier, 2004)

Annan et al. (2005a) use an ensemble Kalman Filter technique to obtain uncertainty ranges for model parameters in an EMIC subject to the constraint of minimising simulation errors with respect to a set of climatological observations. Using this method, Hargreaves and Annan (2006) find that the risk of a collapse in the Atlantic MOC (in response to increasing CO_2) depends on the set of observations to which the EMIC parameters are tuned. Section 9.6.3 assesses perturbed physics studies of the link between climate sensitivity and cooling during the Last Glacial Maximum (Annan et al., 2005b; Schneider von Deimling et al., 2006).

10.5.4.3 Diagnosing Drivers of Uncertainty from Ensemble Results

Figure 10.27a shows the agreement between annual changes simulated by members of the AR4 multi-model ensemble for 2080 to 2099 relative to 1980 to 1999 for the A1B scenario, calculated as in Räisänen (2001). For precipitation, the agreement increases with spatial scale. For surface temperature, the agreement is high even at local scales, indicating the robustness of the simulated warming (see also Figure 10.8, discussed in Section 10.3.2.1). Differences in model formulation are the dominant contributor to ensemble spread, though the role of internal variability increases at smaller scales (Figure 10.27b). The agreement between AR4 ensemble members is slightly higher compared with the earlier CMIP2 ensemble of Räisänen (2001) (also reported in the TAR), and internal variability explains a smaller fraction of the ensemble spread. This is expected, given the larger forcing and responses in the A1B scenario for 2080 to 2099 compared to the transient response to doubled CO_2 considered by Räisänen (2001), although the use of an updated set of models may also contribute. For seasonal changes, internal variability is found to be comparable with model differences as a source of

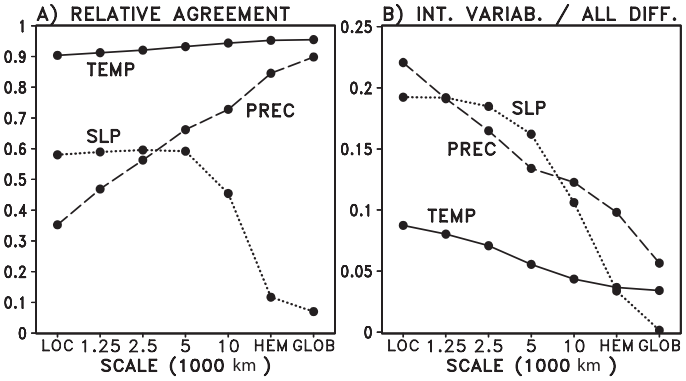


Figure 10.27. *Statistics of annual mean responses to the SRES A1B scenario, for 2080 to 2099 relative to 1980 to 1999, calculated from the 21-member AR4 multi-model ensemble using the methodology of Räisänen (2001). Results are expressed as a function of horizontal scale on the x axis ('Loc': grid box scale; 'Hem': hemispheric scale; 'Glob': global mean) plotted against the y axis showing (a) the relative agreement between ensemble members, a dimensionless quantity defined as the square of the ensemble-mean response (corrected to avoid sampling bias) divided by the mean squared response of individual ensemble members, and (b) the dimensionless fraction of internal variability relative to the ensemble variance of responses. Values are shown for surface air temperature, precipitation and sea level pressure. The low agreement of SLP changes at hemispheric and global scales reflects problems with the conservation of total atmospheric mass in some of the models, however, this has no practical significance because SLP changes at these scales are extremely small.*

uncertainty in local precipitation and SLP changes (although not for surface temperature) in both multi-model and perturbed physics ensembles (Räisänen, 2001; Murphy et al., 2004). Consequently the local seasonal changes for precipitation and SLP are not consistent in the AR4 ensemble over large areas of the globe (i.e., the multi-model mean change does not exceed the ensemble standard deviation; see Figure 10.9), whereas the surface temperature changes are consistent almost everywhere, as discussed in Section 10.3.2.1.

Wang and Swail (2006b) examine the relative importance of internal variability, differences in radiative forcing and model differences in explaining the transient response of ocean wave height using three AOGCMs each run for three plausible forcing scenarios, and find model differences to be the largest source of uncertainty in the simulated changes.

Selten et al. (2004) report a 62-member initial condition ensemble of simulations of 1940 to 2080 including natural and anthropogenic forcings. They find an individual member that reproduces the observed trend in the NAO over the past few decades, but no trend in the ensemble mean, and suggest that the observed change can be explained through internal variability associated with a mode driven by increases in precipitation over the tropical Indian Ocean. Terray et al. (2004) find that the ARPEGE coupled ocean-atmosphere model shows small increases in the residence frequency of the positive phase of the NAO in response to SRES A2 and B2 forcing, whereas larger increases are found when SST changes prescribed from the coupled experiments are used to drive a version of the atmosphere model with enhanced resolution over the North Atlantic and Europe (Gibelin and Déqué, 2003).

Figure 10.25 compares global mean transient and equilibrium changes simulated by the AR4 multi-model ensembles against perturbed physics ensembles (M. Collins et al., 2006; Webb et al., 2006) designed to produce credible present-day simulations while sampling a wide range of multiple parameter perturbations and climate sensitivities. The AR4 ensembles partially sample structural variations in model components, whereas the perturbed physics ensembles sample atmospheric parameter uncertainties for a fixed choice of model structure. The results show similar relationships between TCR, climate sensitivity and precipitation change in both types of ensemble. The perturbed physics ensembles contain several members with sensitivities higher than the multi-model range, while some of the multi-model transient simulations give TCR values slightly below the range found in the perturbed physics ensemble (Figure 10.25a,b).

Soden and Held (2006) find that differences in cloud feedback are the dominant source of uncertainty in the transient response of surface temperature in the AR4 ensemble (see also Section 8.6.3.2), as in previous IPCC assessments. Webb et al. (2006) compare equilibrium radiative feedbacks in a 9-member multi-model ensemble against those simulated in a 128-member perturbed physics ensemble with multiple parameter perturbations. They find that the ranges of climate sensitivity in both ensembles are explained mainly by differences in the response of shortwave cloud forcing in areas where changes in low-level clouds predominate. Bony and Dufresne (2005) find that marine boundary layer clouds in areas of large-scale subsidence provide the largest source of spread in tropical cloud feedbacks in the AR4 ensemble. Narrowing the uncertainty in cloud feedback may require both improved parametrizations of cloud microphysical properties (e.g., Tsushima et al., 2006) and improved representations of cloud macrophysical properties, through improved parametrizations of other physical processes (e.g., Williams et al., 2001) and/or increases in resolution (Palmer, 2005).

10.5.4.4 Observational Constraints

A range of observables has been used since the TAR to explore methods for constraining uncertainties in future climate change in studies using simple climate models, EMICs and AOGCMs. Probabilistic estimates of global climate sensitivity have been obtained from the historical transient evolution of surface temperature, upper-air temperature, ocean temperature, estimates of the radiative forcing, satellite data, proxy data over the last millennium, or a subset thereof (Wigley et al., 1997a; Tol and De Vos, 1998; Andronova and Schlesinger, 2001; Forest et al., 2002; Gregory et al., 2002a; Knutti et al., 2002, 2003; Frame et al., 2005; Forest et al., 2006; Forster and Gregory, 2006; Hegerl et al., 2006; see Section 9.6). Some of these studies also constrain the transient response to projected future emissions (see section 10.5.4.5). For climate sensitivity, further probabilistic estimates have been obtained using statistical measures of the correspondence between simulated and observed fields of present-day climate (Murphy et al., 2004; Piani et al., 2005), the climatological seasonal cycle of surface temperature (Knutti et al., 2006) and the response to palaeoclimatic forcings (Annan et al., 2005b; Schneider von Deimling et al., 2006). For the purpose of constraining regional climate projections, spatial averages or fields of time-averaged regional climate have been used (Giorgi and Mearns, 2003; Tebaldi et al., 2004, 2005; Laurent and Cai, 2007), as have past regional- or continental-scale trends in surface temperature (Greene et al., 2006; Stott et al., 2006a).

Further observables have been suggested as potential constraints on future changes, but are not yet used in formal probabilistic estimates. These include measures of climate variability related to cloud feedbacks (Bony et al., 2004; Bony and Dufresne, 2005; Williams et al., 2005), radiative damping of the seasonal cycle (Tsushima et al., 2005), the relative entropy of simulated and observed surface temperature variations (Shukla et al., 2006), major volcanic eruptions (Wigley et al., 2005; Yokohata et al., 2005; see Section 9.6) and trends in multiple variables derived from reanalysis data sets (Lucarini and Russell, 2002).

Additional constraints could also be found, for example, from evaluation of ensemble climate prediction systems on shorter time scales for which verification data exist. These could include assessment of the reliability of seasonal to interannual probabilistic forecasts (Palmer et al., 2004; Hagedorn et al., 2005) and the evaluation of model parametrizations in short-range weather predictions (Phillips et al., 2004; Palmer, 2005). Annan and Hargreaves (2006) point out the potential for narrowing uncertainty by combining multiple lines of evidence. This will require objective quantification of the impact of different constraints and their degree of independence, estimation of the effects of structural modelling errors and the development of comprehensive probabilistic frameworks in which to combine these elements (e.g., Rougier, 2007).

10.5.4.5 Probabilistic Projections - Global Mean

A number of methods for providing probabilistic climate change projections, both for global means (discussed in this section) and geographical depictions (discussed in the following section) have emerged since the TAR.

Methods of constraining climate sensitivity using observations of present-day climate are discussed in Section 10.5.4.2. Results from both the AR4 multi-model ensemble and from perturbed physics ensembles suggest a very low probability for a climate sensitivity below 2°C, despite exploring the effects of a wide range of alternative modelling assumptions on the global radiative feedbacks arising from lapse rate, water vapour, surface albedo and cloud (Bony et al., 2006; Soden and Held, 2006; Webb et al., 2006; Box 10.2). However, exclusive reliance on AOGCM ensembles can be questioned on the basis that models share components, and therefore errors, and may not sample the full range of possible outcomes (e.g., Allen and Ingram, 2002).

Observationally constrained probability distributions for climate sensitivity have also been derived from physical

relationships based on energy balance considerations, and from instrumental observations of historical changes during the past 50 to 150 years or proxy reconstructions of surface temperature during the past millennium (Section 9.6). The results vary according to the choice of verifying observations, the forcings considered and their specified uncertainties, however, all these studies report a high upper limit for climate sensitivity, with the 95th percentile of the distributions invariably exceeding 6°C (Box 10.2). Frame et al. (2005) demonstrate that uncertainty ranges for sensitivity are dependent on the choices made about prior distributions of uncertain quantities before the observations are applied. Frame et al. (2005) and Piani et al. (2005) show that many observable variables are likely to scale inversely with climate sensitivity, implying that projections of quantities that are inversely related to sensitivity will be more strongly constrained by observations than climate sensitivity itself, particularly with respect to the estimated upper limit (Allen et al., 2006b).

In the case of transient climate change, optimal detection techniques have been used to determine factors by which hindcasts of global surface temperature from AOGCMs can be scaled up or down while remaining consistent with past changes, accounting for uncertainty due to internal variability (Section 9.4.1.6). Uncertainty is propagated forward in time by assuming that the fractional error found in model hindcasts of global mean temperature change will remain constant in projections of future changes. Using this approach, Stott and Kettleborough (2002) find that probabilistic projections of global mean temperature derived from UKMO-HadCM3 simulations were insensitive to differences between four representative SRES emissions scenarios over the first few decades of the 21st century, but that much larger differences emerged between the response to different SRES scenarios by the end of the 21st century (see also Section 10.5.3 and Figure 10.28). Stott et al. (2006b) show that scaling the responses of three models with different sensitivities brings their projections into better agreement. Stott et al. (2006a) extend their approach to obtain probabilistic projections of future warming averaged over continental-scale regions under the SRES A2 scenario. Fractional errors in the past continental warming simulated by UKMO-HadCM3 are used to scale future changes, yielding wide uncertainty ranges, notably for North America and Europe where the 5 to 95% ranges for warming during the 21st century are 2°C to 12°C and 2°C to 11°C respectively. These estimates do not account for potential constraints arising from regionally differentiated warming rates. Tighter ranges of 4°C to 8°C for North America and 4°C to 7°C for Europe are obtained if fractional errors in past global mean temperature are used to scale the future continental changes, although this neglects uncertainty in the relationship between global and regional temperature changes.

Allen and Ingram (2002) suggest that probabilistic projections for some variables may be made by searching for 'emergent constraints'. These are relationships between variables that can be directly constrained by observations, such as global surface temperature, and variables that may be indirectly constrained by establishing a consistent, physically based relationship which holds across a wide range of models. They present an example in which future changes in global mean precipitation are constrained using a probability distribution for global temperature obtained from a large EMIC ensemble (Forest et al., 2002) and a relationship between precipitation and temperature obtained from multi-model ensembles of the response to doubled atmospheric CO_2. These methods are designed to produce distributions constrained by observations, and are relatively model independent (Allen and Stainforth, 2002; Allen et al., 2006a). This can be achieved provided the inter-variable relationships are robust to alternative modelling assumptions Piani et al. (2005) and Knutti et al. (2006) (described in Section 10.5.4.2) follow this approach, noting that in these cases the inter-variable relationships are derived from perturbed versions of a single model, and need to be confirmed using other models.

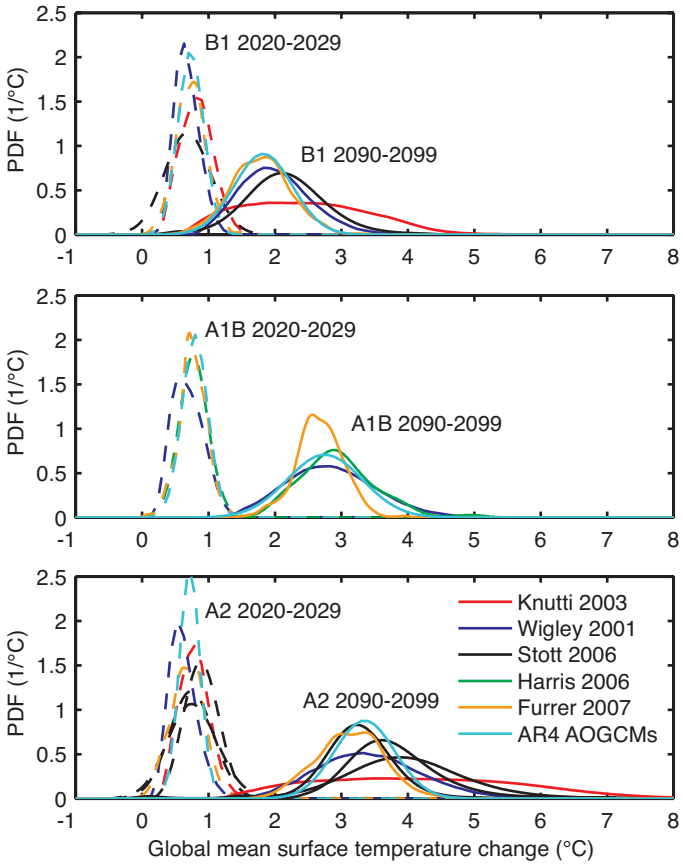


Figure 10.28. *Probability density functions from different studies for global mean temperature change for the SRES scenarios B1, A1B and A2 and for the decades 2020 to 2029 and 2090 to 2099 relative to the 1980 to 1999 average (Wigley and Raper, 2001; Knutti et al., 2002; Furrer et al., 2007; Harris et al., 2006; Stott et al., 2006b). A normal distribution fitted to the multi-model ensemble is shown for comparison.*

A synthesis of published probabilistic global mean projections for the SRES scenarios B1, A1B and A2 is given in Figure 10.28. Probability density functions are given for short-term projections (2020–2030) and the end of the century (2090–2100). For comparison, normal distributions fitted to results from AOGCMs in the multi-model archive (see Section

10.3.1) are also given, although these curve fits should not be regarded as PDFs. The five methods of producing PDFs are all based on different models and/or techniques, described in Section 10.5. In short, Wigley and Raper (2001) use a large ensemble of a simple model with expert prior distributions for climate sensitivity, ocean heat uptake, sulphate forcing and the carbon cycle, without applying constraints. Knutti et al. (2002, 2003) use a large ensemble of EMIC simulations with non-informative prior distributions, consider uncertainties in climate sensitivity, ocean heat uptake, radiative forcing and the carbon cycle, and apply observational constraints. Neither method considers natural variability explicitly. Stott et al. (2006b) apply the fingerprint scaling method to AOGCM simulations to obtain PDFs which implicitly account for uncertainties in forcing, climate sensitivity and internal unforced as well as forced natural variability. For the A2 scenario, results obtained from three different AOGCMs are shown, illustrating the extent to which the Stott et al. PDFs depend on the model used. Harris et al. (2006) obtain PDFs by boosting a 17-member perturbed physics ensemble of the UKMO-HadCM3 model using scaled equilibrium responses from a larger ensemble of simulations. Furrer et al. (2007) use a Bayesian method described in Section 10.5.4.7 to calculate PDFs from the AR4 multi-model ensemble. The Stott et al. (2006b), Harris et al. (2006) and Furrer et al. (2007) methods neglect carbon cycle uncertainties.

Two key points emerge from Figure 10.28. For the projected short-term warming (i) there is more agreement among models and methods (narrow width of the PDFs) compared to later in the century (wider PDFs), and (ii) the warming is similar across different scenarios, compared to later in the century where the choice of scenario significantly affects the projections. These conclusions are consistent with the results obtained with SCMs (Section 10.5.3).

Additionally, projection uncertainties increase close to linearly with temperature in most studies. The different methods show relatively good agreement in the shape and width of the PDFs, but with some offsets due to different methodological choices. Only Stott et al. (2006b) account for variations in future natural forcing, and hence project a small probability of cooling over the next few decades not seen in the other PDFs. The results of Knutti et al. (2003) show wider PDFs for the end of the century because they sample uniformly in climate sensitivity (see Section 9.6.2 and Box 10.2). Resampling uniformly in observables (Frame et al., 2005) would bring their PDFs closer to the others. In sum, probabilistic estimates of uncertainties for the next few decades seem robust across a variety of models and methods, while results for the end of the century depend on the assumptions made.

10.5.4.6 Synthesis of Projected Global Temperature at Year 2100

All available estimates for projected warming by the end of the 21st century are summarised in Figure 10.29 for the six SRES non-intervention marker scenarios. Among the various techniques, the AR4 AOGCM ensemble provides the most

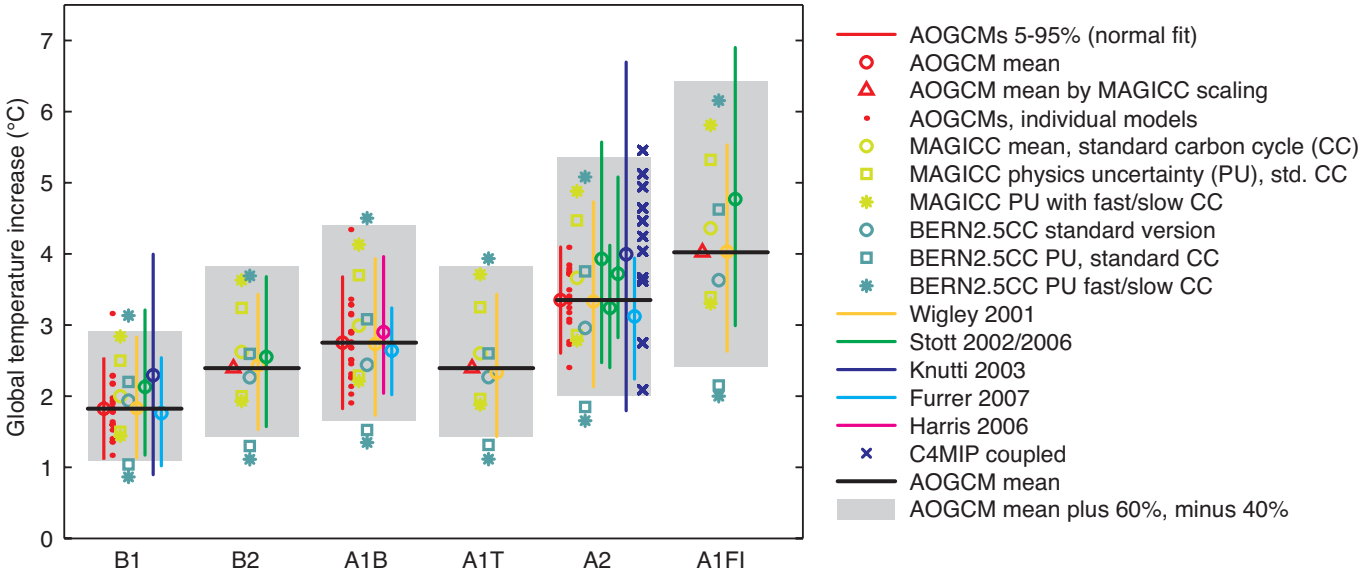


Figure 10.29. *Projections and uncertainties for global mean temperature increase in 2090 to 2099 (relative to the 1980 to 1999 average) for the six SRES marker scenarios. The AOGCM means and the uncertainty ranges of the mean –40% to +60% are shown as black horizontal solid lines and grey bars, respectively. For comparison, results are shown for the individual models (red dots) of the multi-model AOGCM ensemble for B1, A1B and A2, with a mean and 5 to 95% range (red line and circle) from a fitted normal distribution. The AOGCM mean estimates for B2, A1T and A1FI (red triangles) are obtained by scaling the A1B AOGCM mean with ratios obtained from the SCM (see text). The mean (light green circle) and one standard deviation (light green square) of the MAGICC SCM tuned to all AOGCMs (representing the physics uncertainty) are shown for standard carbon cycle settings, as well as for a slow and fast carbon cycle assumption (light green stars). Similarly, results from the BERN2.5CC EMIC are shown for standard carbon cycle settings and for climate sensitivities of 3.2°C (AOGCM average, dark green circle), 1.5°C and 4.5°C (dark green squares). High climate sensitivity/low carbon cycle and low climate sensitivity/high carbon cycle combinations are shown as dark green stars. The 5 to 95% ranges (vertical lines) and medians (circles) are shown from probabilistic methods (Wigley and Raper, 2001; Stott and Kettleborough, 2002; Knutti et al., 2003; Furrer et al., 2007; Harris et al., 2006; Stott et al., 2006b). Individual model results are shown for the C⁴MIP models (blue crosses, see Figure 10.20).*

sophisticated set of models in terms of the range of processes included and consequent realism of the simulations compared to observations (see Chapters 8 and 9). On average, this ensemble projects an increase in global mean surface air temperature of 1.8°C, 2.8°C and 3.4°C in the B1, A1B and A2 scenarios, respectively, by 2090 to 2099 relative to 1980 to 1999 (note that in Table 10.5, the years 2080 to 2099 were used for those globally averaged values to be consistent with the comparable averaging period for the geographic plots in Section 10.3; this longer averaging period smoothes spatial noise in the geographic plots). A scaling method is used to estimate AOGCM mean results for the three missing scenarios B2, A1T and A1FI. The ratio of the AOGCM mean values for B1 relative to A1B and A2 relative to A1B are almost identical to the ratios obtained with the MAGICC SCM, although the absolute values for the SCM are higher. Thus, the AOGCM mean response for the scenarios B2, A1T and A1FI can be estimated as 2.4°C, 2.4°C and 4.0°C by multiplying the AOGCM A1B mean by the SCM-derived ratios B2/A1B, A1T/A1B and A1FI/A1B, respectively (for details see Appendix 10.A.1).

The AOGCMs cannot sample the full range of possible warming, in particular because they do not include uncertainties in the carbon cycle. In addition to the range derived directly from the AR4 multi-model ensemble, Figure 10.29 depicts additional uncertainty estimates obtained from published probabilistic methods using different types of models and observational constraints: the MAGICC SCM and the BERN2.5CC coupled climate-carbon cycle EMIC tuned to different climate sensitivities and carbon cycle settings, and the C^{4}MIP coupled climate-carbon cycle models. Based on these results, the future increase in global mean temperature is likely to fall within –40 to +60% of the multi-model AOGCM mean warming simulated for each scenario. This range results from an expert judgement of the multiple lines of evidence presented in Figure 10.29, and assumes that the models approximately capture the range of uncertainties in the carbon cycle. The range is well constrained at the lower bound since climate sensitivity is better constrained at the low end (see Box 10.2), and carbon cycle uncertainty only weakly affects the lower bound. The upper bound is less certain as there is more variation across the different models and methods, partly because carbon cycle feedback uncertainties are greater with larger warming. The uncertainty ranges derived from the above percentages for the warming by 2090 to 2099 relative to 1980 to 1999 are 1.1°C to 2.9°C, 1.4°C to 3.8°C, 1.7°C to 4.4°C, 1.4°C to 3.8°C, 2.0°C to 5.4°C and 2.4°C to 6.4°C for the scenarios B1, B2, A1B, A1T, A2 and A1FI, respectively. It is not appropriate to compare the lowest and highest values across these ranges against the single range given in the TAR, because the TAR range resulted only from projections using an SCM and covered all SRES scenarios, whereas here a number of different and independent modelling approaches are combined to estimate ranges for the six illustrative scenarios separately. Additionally, in contrast to the TAR, carbon cycle uncertainties are now included in these ranges. These uncertainty ranges include only anthropogenically forced changes.

10.5.4.7 Probabilistic Projections - Geographical Depictions

Tebaldi et al. (2005) present a Bayesian approach to regional climate prediction, developed from the ideas of Giorgi and Mearns (2002, 2003). Non-informative prior distributions for regional temperature and precipitation are updated using observations and results from AOGCM ensembles to produce probability distributions of future changes. Key assumptions are that each model and the observations differ randomly and independently from the true climate, and that the weight given to a model prediction should depend on the bias in its present-day simulation and its degree of convergence with the weighted ensemble mean of the predicted future change. Lopez et al. (2006) apply the Tebaldi et al. (2005) method to a 15-member multi-model ensemble to predict future changes in global surface temperature under a 1% yr^{-1} increase in atmospheric CO_2. They compare it with the method developed by Allen et al. (2000) and Stott and Kettleborough (2002) (ASK), which aims to provide relatively model independent probabilities consistent with observed changes (see Section 10.5.4.5). The Bayesian method predicts a much narrower uncertainty range than ASK. However its results depend on choices made in its design, particularly the convergence criterion for up-weighting models close to the ensemble mean, relaxation of which substantially reduces the discrepancy with ASK.

Another method by Furrer et al. (2007) employs a hierarchical Bayesian model to construct PDFs of temperature change at each grid point from a multi-model ensemble. The main assumptions are that the true climate change signal is a common large-scale structure represented to some degree in each of the model simulations, and that the signal unexplained by climate change is AOGCM-specific in terms of small-scale structure, but can be regarded as noise when averaged over all AOGCMs. In this method, spatial fields of future minus present temperature difference from each ensemble member are regressed upon basis functions. One of the basis functions is a map of differences of observed temperatures from late- minus mid-20th century, and others are spherical harmonics. The statistical model then estimates the regression coefficients and their associated errors, which account for the deviation in each AOGCM from the (assumed) true pattern of change. By recombining the coefficients with the basis functions, an estimate is derived of the true climate change field and its associated uncertainty, thus providing joint probabilities for climate change at all grid points around the globe.

Estimates of uncertainty derived from multi-model ensembles of 10 to 20 members are potentially sensitive to outliers (Räisänen, 2001). Harris et al. (2006) therefore augment a 17-member ensemble of AOGCM transient simulations by scaling the equilibrium response patterns of a large perturbed physics ensemble. Transient responses are emulated by scaling equilibrium response patterns according to global temperature (predicted from an energy balance model tuned to the relevant climate sensitivities). For surface temperature, the scaled equilibrium patterns correspond well to the transient response patterns, while scaling errors for precipitation vary more

widely with location. A correction field is added to account for ensemble-mean differences between the equilibrium and transient patterns, and uncertainty is allowed for in the emulated result. The correction field and emulation errors are determined by comparing the responses of model versions for which both transient and equilibrium simulations exist. Results are used to obtain frequency distributions of transient regional changes in surface temperature and precipitation in response to increasing atmospheric CO_2, arising from the combined effects of atmospheric parameter perturbations and internal variability in UKMO-HadCM3.

Figure 10.30 shows probabilities of a temperature change larger than 2°C by the end of the 21st century under the A1B scenario, comparing values estimated from the 21-member AR4 multi-model ensemble (Furrer et al., 2007) against values estimated by combining transient and equilibrium perturbed physics ensembles of 17 and 128 members, respectively (Harris et al., 2006). Although the methods use different ensembles and different statistical approaches, the large-scale patterns are similar in many respects. Both methods show larger probabilities (typically 80% or more) over land, and at high latitudes in the winter hemisphere, with relatively low values (typically less than 50%) over the southern oceans. However, the plots also reveal some substantial differences at a regional level, notably over the North Atlantic Ocean, the sub-tropical Atlantic and Pacific Oceans in the SH, and at high northern latitudes during June to August.

10.5.4.8 Summary

Significant progress has been made since the TAR in exploring ensemble approaches to provide uncertainty ranges and probabilities for global and regional climate change. Different methods show consistency in some aspects of their results, but differ significantly in others (see Box 10.2; Figures 10.28 and 10.30), because they depend to varying degrees on the nature and use of observational constraints, the nature and design of model ensembles and the specification of prior distributions for uncertain inputs (see, e.g., Table 11.3). A preferred method cannot yet be recommended, but the assumptions and limitations underlying the various approaches, and the sensitivity of the results to them, should be communicated to users. A good example concerns the treatment of model error in Bayesian methods, the uncertainty in which affects the calculation of the likelihood of different model versions, but is difficult to specify (Rougier, 2007). Awareness of this issue is growing in the field of climate prediction (Annan et al., 2005b; Knutti et al., 2006), however, it is yet to be thoroughly addressed. Probabilistic depictions, particularly at the regional level, are new to climate change science and are being facilitated by the recently available multi-model ensembles. These are discussed further in Section 11.10.2.

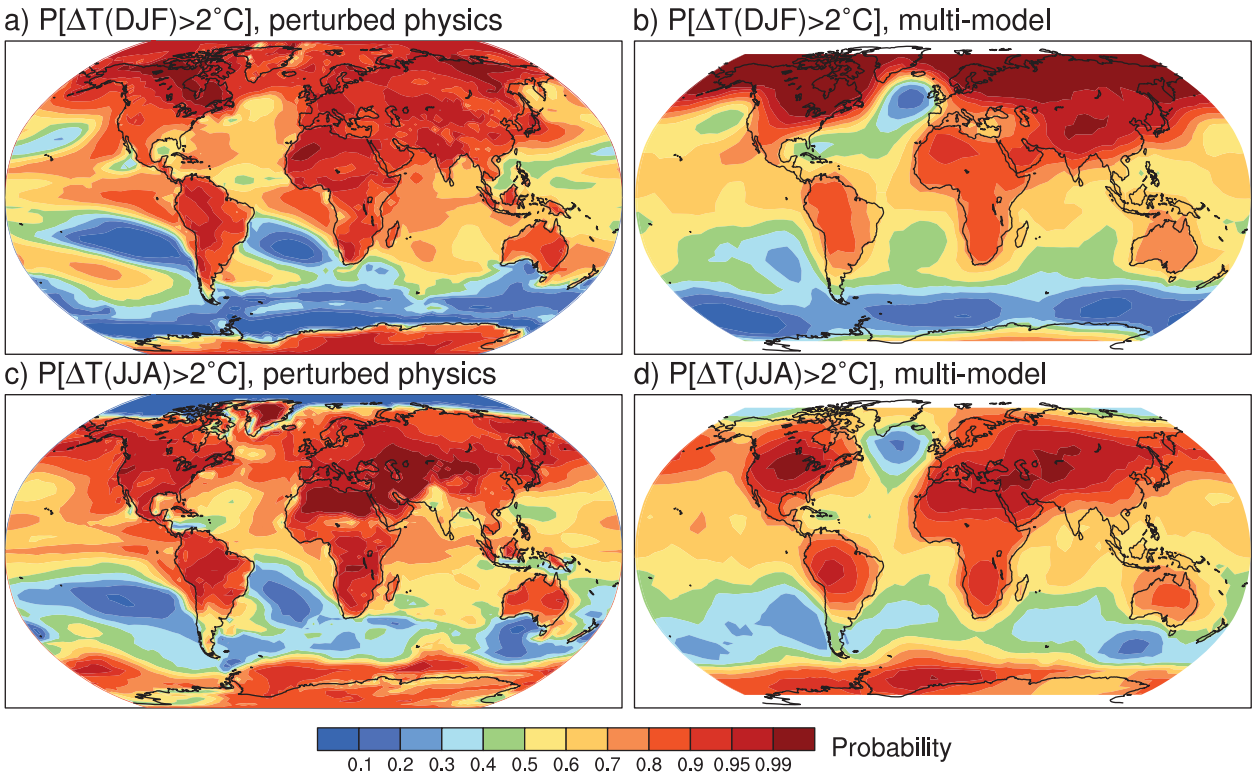


Figure 10.30. *Estimated probabilities for a mean surface temperature change exceeding 2°C in 2080 to 2099 relative to 1980 to 1999 under the SRES A1B scenario. Results obtained from a perturbed physics ensemble of a single model (a, c), based on Harris et al. (2006), are compared with results from the AR4 multi-model ensemble (b, d), based on Furrer et al. (2007), for December to February (DJF, a, b) and June to August (JJA, c, d).*

10.6 Sea Level Change in the 21st Century

10.6.1 Global Average Sea Level Rise Due to Thermal Expansion

As seawater warms up, it expands, increasing the volume of the global ocean and producing thermosteric sea level rise (see Section 5.5.3). Global average thermal expansion can be calculated directly from simulated changes in ocean temperature. Results are available from 17 AOGCMs for the 21st century for SRES scenarios A1B, A2 and B1 (Figure 10.31), continuing from simulations of the 20th century. One ensemble member was used for each model and scenario. The time series are rather smooth compared with global average temperature time series, because thermal expansion reflects heat storage in the entire ocean, being approximately proportional to the time integral of temperature change (Gregory et al., 2001).

During 2000 to 2020 under scenario SRES A1B in the ensemble of AOGCMs, the rate of thermal expansion is 1.3 ± 0.7 mm yr^{-1}, and is not significantly different under A2 or B1. This rate is more than twice the observationally derived rate of 0.42 ± 0.12 mm yr^{-1} during 1961 to 2003. It is similar to the rate of 1.6 ± 0.5 mm yr^{-1} during 1993 to 2003 (see Section 5.5.3), which may be larger than that of previous decades partly because of natural forcing and internal variability (see Sections 5.5.2.4, 5.5.3 and 9.5.2). In particular, many of the AOGCM experiments do not include the influence of Mt. Pinatubo, the omission of which may reduce the projected rate of thermal expansion during the early 21st century.

During 2080 to 2100, the rate of thermal expansion is projected to be 1.9 ± 1.0, 2.9 ± 1.4 and 3.8 ± 1.3 mm yr^{-1} under scenarios SRES B1, A1B and A2 respectively in the AOGCM ensemble (the width of the range is affected by the different numbers of models under each scenario). The acceleration is caused by the increased climatic warming. Results are shown for all SRES marker scenarios in Table 10.7 (see Appendix 10.A for methods). In the AOGCM ensemble, under any given SRES scenario, there is some correlation of the global average temperature change across models with thermal expansion and its rate of change, suggesting that the spread in thermal expansion for that scenario is caused both by the spread in surface warming and by model-dependent ocean heat uptake efficiency (Raper et al., 2002; Table 8.2) and the distribution of added heat within the ocean (Russell et al., 2000).

10.6.2 Local Sea Level Change Due to Change in Ocean Density and Dynamics

The geographical pattern of mean sea level relative to the geoid (the dynamic topography) is an aspect of the dynamical balance relating the ocean's density structure and its circulation, which are maintained by air-sea fluxes of heat, freshwater and momentum. Over much of the ocean on multi-annual time scales, a good approximation to the pattern of dynamic topography change is given by the steric sea level change, which can be calculated straightforwardly from local temperature and salinity change (Gregory et al., 2001; Lowe and Gregory, 2006). In much of the world, salinity changes are as important as temperature changes in determining the pattern of dynamic topography change in the future, and their contributions can be opposed (Landerer et al., 2007; and as in the past, Section 5.5.4.1). Lowe and Gregory (2006) show that in the UKMO-HadCM3 AOGCM, changes in heat fluxes are the cause of many of the large-scale features of sea level change, but freshwater

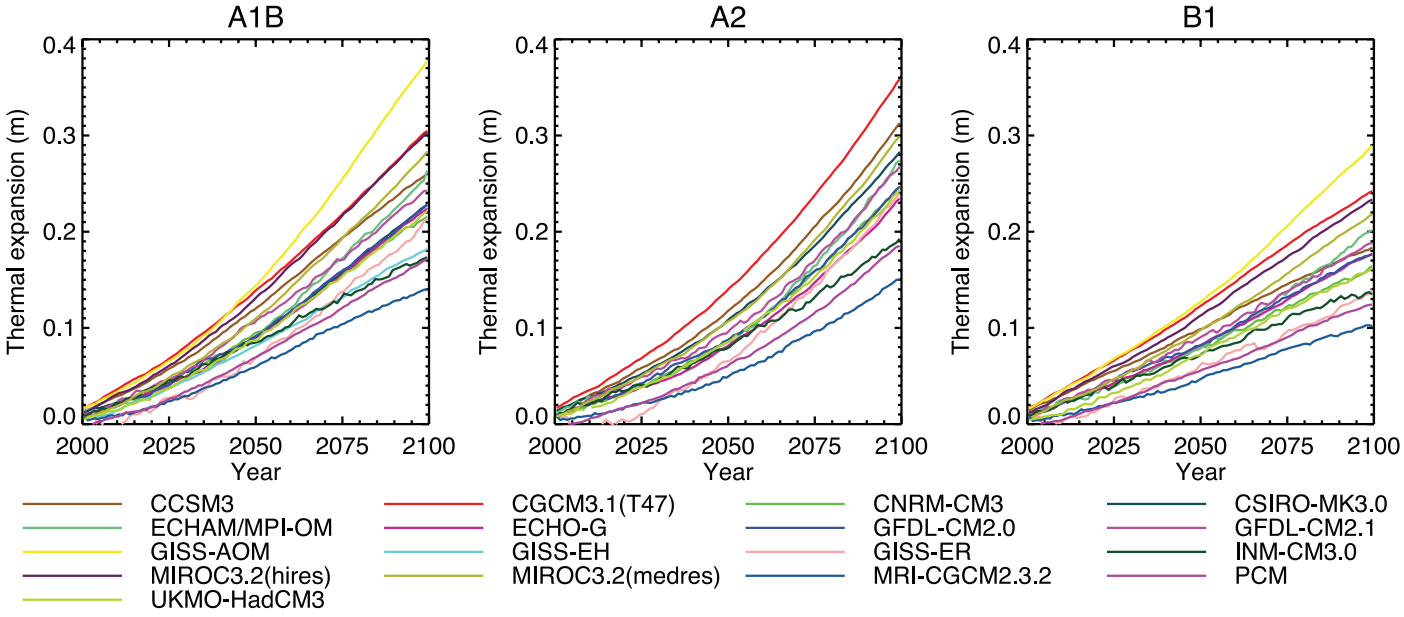


Figure 10.31. *Projected global average sea level rise (m) due to thermal expansion during the 21st century relative to 1980 to 1999 under SRES scenarios A1B, A2 and B1. See Table 8.1 for model descriptions.*

flux change dominates the North Atlantic and momentum flux change has a signature in the north and low-latitude Pacific and the Southern Ocean.

Results are available for local sea level change due to ocean density and circulation change from AOGCMs in the multi-model ensemble for the 20th century and the 21st century. There is substantial spatial variability in all models (i.e., sea level change is not uniform), and as the geographical pattern of climate change intensifies, the spatial standard deviation of local sea level change increases (Church et al., 2001; Gregory et al., 2001). Suzuki et al. (2005) show that, in their high-resolution model, enhanced eddy activity contributes to this increase, but across models there is no significant correlation of the spatial standard deviation with model spatial resolution. This section evaluates sea level change between 1980 to 1999 and 2080 to 2099 projected by 16 models forced with SRES scenario A1B. (Other scenarios are qualitatively similar, but fewer models are available.) The ratio of spatial standard deviation to global average thermal expansion varies among models, but is mostly within the range 0.3 to 0.4. The model median spatial standard deviation of thermal expansion is 0.08 m, which is about 25% of the central estimate of global average sea level rise during the 21st century under A1B (Table 10.7).

The geographical patterns of sea level change from different models are not generally similar in detail, although they have more similarity than those analysed in the TAR by Church et al. (2001). The largest spatial correlation coefficient between any pair is 0.75, but only 25% of correlation coefficients exceed 0.5. To identify common features, an ensemble mean (Figure 10.32) is examined. There are only limited areas where the model ensemble mean change exceeds the inter-model standard deviation, unlike for surface air temperature change (Section 10.3.2.1).

Like Church et al. (2001) and Gregory et al. (2001), Figure 10.32 shows smaller than average sea level rise in the Southern Ocean and larger than average in the Arctic, the former possibly due to wind stress change (Landerer et al., 2007) or low thermal expansivity (Lowe and Gregory, 2006) and the latter due to freshening. Another obvious feature is a narrow band of pronounced sea level rise stretching across the southern Atlantic and Indian Oceans and discernible in the southern Pacific. This could be associated with a southward shift in the circumpolar front (Suzuki et al., 2005) or subduction of warm anomalies in the region of formation of sub antarctic mode water (Banks et al., 2002). In the zonal mean, there are maxima of sea level rise in 30°S to 45°S and 30°N to 45°N. Similar indications are present in the altimetric and thermosteric patterns of sea level change for 1993 to 2003 (Figure 5.15). The model projections do not share other aspects of the observed pattern of sea level rise, such as in the western Pacific, which could be related to interannual variability.

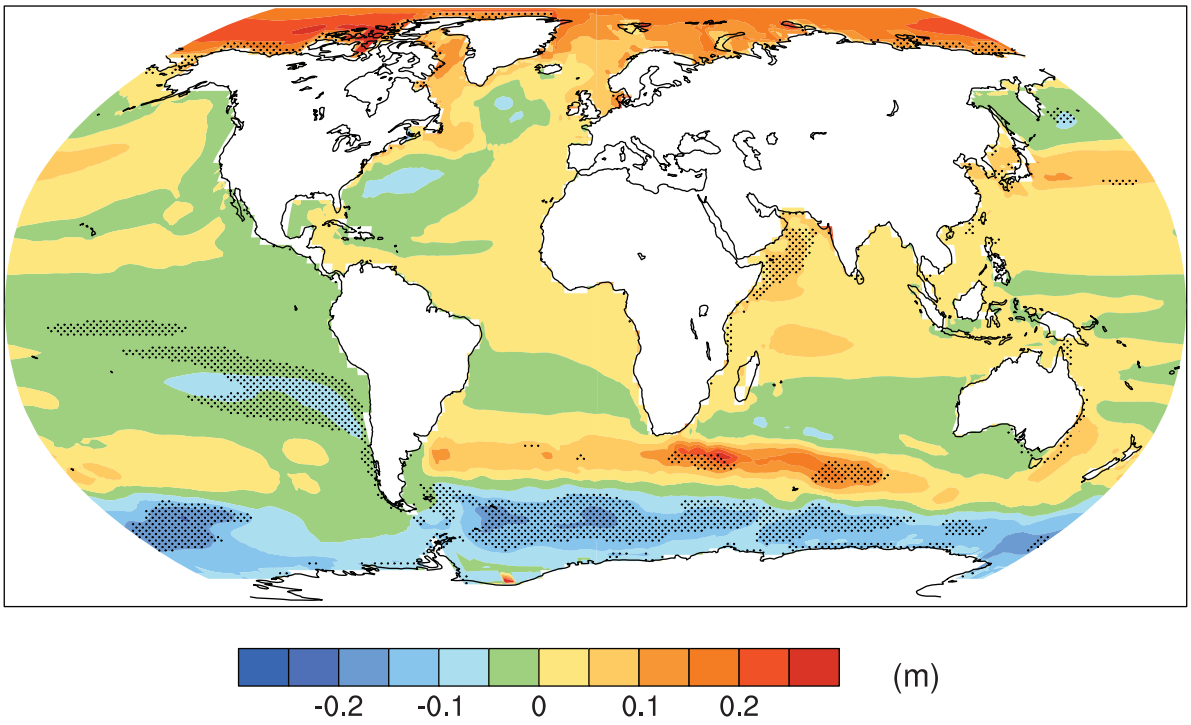


Figure 10.32. *Local sea level change (m) due to ocean density and circulation change relative to the global average (i.e., positive values indicate greater local sea level change than global) during the 21st century, calculated as the difference between averages for 2080 to 2099 and 1980 to 1999, as an ensemble mean over 16 AOGCMs forced with the SRES A1B scenario. Stippling denotes regions where the magnitude of the multi-model ensemble mean divided by the multi-model standard deviation exceeds 1.0.*

The North Atlantic dipole pattern noted by Church et al. (2001), that is, reduced rise to the south of the Gulf Stream extension, enhanced to the north, consistent with a weakening of the circulation, is present in some models; a more complex feature is described by Landerer et al. (2007). The reverse is apparent in the north Pacific, which Suzuki et al. (2005) associate with a wind-driven intensification of the Kuroshio Current. Using simplified models, Hsieh and Bryan (1996) and Johnson and Marshall (2002) show how upper-ocean velocities and sea level would be affected in North Atlantic coastal regions within months of a cessation of sinking in the North Atlantic as a result of propagation by coastal and equatorial Kelvin waves, but would take decades to adjust in the central regions and the south Atlantic. Levermann et al. (2005) show that a sea level rise of several tenths of a metre could be realised in coastal regions of the North Atlantic within a few decades (i.e., tens of millimetres per year) of a collapse of the MOC. Such changes to dynamic topography would be much more rapid than global average sea level change. However, it should be emphasized that these studies are sensitivity tests, not projections; the Atlantic MOC does not collapse in the SRES scenario runs evaluated here (see Section 10.3.4).

The geographical pattern of sea level change is affected also by changes in atmospheric surface pressure, but this is a relatively small effect given the projected pressure changes (Figure 10.9; a pressure increase of 1 hPa causes a drop in local sea level of 0.01 m; see Section 5.5.4.3). Land movements and changes in the gravitational field resulting from the changing loading of the crust by water and ice also have effects which are small over most of the ocean (see Section 5.5.4.4).

10.6.3 Glaciers and Ice Caps

Glaciers and ice caps (G&IC, see also Section 4.5.1) comprise all land ice except for the ice sheets of Greenland and Antarctica (see Sections 4.6.1 and 10.6.4). The mass of G&IC can change because of changes in surface mass balance (Section 10.6.3.1). Changes in mass balance cause changes in area and thickness (Section 10.6.3.2), with feedbacks on surface mass balance.

10.6.3.1 Mass Balance Sensitivity to Temperature and Precipitation

Since G&IC mass balance depends strongly on their altitude and aspect, use of data from climate models to make projections requires a method of downscaling, because individual G&IC are much smaller than typical AOGCM grid boxes. Statistical relations for meteorological quantities can be developed between the GCM and local scales (Reichert et al., 2002), but they may not continue to hold in future climates. Hence, for projections the approach usually adopted is to use GCM simulations of changes in climate parameters to perturb the observed climatology or mass balance (Gregory and Oerlemans, 1998; Schneeberger et al., 2003).

Change in ablation (mostly melting) of a glacier or ice cap is modelled using b_T (in m yr^{-1} °C^{-1}), the sensitivity of the mean specific surface mass balance to temperature (refer to Section 4.5 for a discussion of the relation of mass balance to climate). One approach determines b_T by energy balance modelling, including evolution of albedo and refreezing of melt water within the firn (Zuo and Oerlemans, 1997). Oerlemans and Reichert (2000), Oerlemans (2001) and Oerlemans et al. (2006) refine this approach to include dependence on monthly temperature and precipitation changes. Another approach uses a degree-day method, in which ablation is proportional to the integral of mean daily temperature above the freezing point (Braithwaite et al., 2003). Braithwaite and Raper (2002) show that there is excellent consistency between the two approaches, which indicates a similar relationship between b_T and climatological precipitation. Schneeberger et al. (2000, 2003) use a degree-day method for ablation modified to include incident solar radiation, again obtaining similar results. De Woul and Hock (2006) find somewhat larger sensitivities for arctic G&IC from the degree-day method than the energy balance method. Calculations of b_T are estimated to have an uncertainty of ±15% (standard deviation) (Gregory and Oerlemans, 1998; Raper and Braithwaite, 2006).

The global average sensitivity of G&IC surface mass balance to temperature is estimated by weighting the local sensitivities by land ice area in various regions. For a geographically and seasonally uniform rise in global temperature, Oerlemans and Fortuin (1992) derive a global average G&IC surface mass balance sensitivity of –0.40 m yr^{-1} °C^{-1}, Dyurgerov and Meier (2000) –0.37 m yr^{-1} °C^{-1} (from observations), Braithwaite and Raper (2002) –0.41 m yr^{-1} °C^{-1} and Raper and Braithwaite (2005) –0.35 m yr^{-1} °C^{-1}. Applying the scheme of Oerlemans (2001) and Oerlemans et al. (2006) worldwide gives a smaller value of –0.32 m yr^{-1} °C^{-1}, the reduction being due to the modified treatment of albedo by Oerlemans (2001).

These global average sensitivities for uniform temperature change are given only for scenario-independent comparison of the various methods; they cannot be used for projections, which require regional and seasonal temperature changes (Gregory and Oerlemans, 1998; van de Wal and Wild, 2001). Using monthly temperature changes simulated in G&IC regions by 17 AR4 AOGCMs for scenarios A1B, A2 and B1, the global total surface mass balance sensitivity to global average temperature change for all G&IC outside Greenland and Antarctica is 0.61 ± 0.12 mm yr^{-1} °C^{-1} (sea level equivalent) with the b_T of Zuo and Oerlemans (1997) or 0.49 ± 0.13 mm yr^{-1} °C^{-1} with those of Oerlemans (2001) and Oerlemans et al. (2006), subject to uncertainty in G&IC area (see Section 4.5.2 and Table 4.4).

Hansen and Nazarenko (2004) collate measurements of soot (fossil fuel black carbon) in snow and estimate consequent reductions in snow and ice albedo of between 0.001 for the pristine conditions of Antarctica and over 0.10 for polluted NH land areas. They argue that glacial ablation would be increased by this effect. While it is true that soot has not been explicitly considered in existing sensitivity estimates, it may already be included because the albedo and degree-day parametrizations have been empirically derived from data collected in affected regions.

For seasonally uniform temperature rise, Oerlemans et al. (1998) find that an increase in precipitation of 20 to 50% °C^{-1} is required to balance increased ablation, while Braithwaite et al. (2003) report a required precipitation increase of 29 to 41% °C^{-1}, in both cases for a sample of G&IC representing a variety of climatic regimes. Oerlemans et al. (2006) require a precipitation increase of 20 to 43% °C^{-1} to balance ablation increase, and de Woul and Hock (2006) approximately 20% °C^{-1} for Arctic G&IC. Although AOGCMs generally project larger than average precipitation change in northern mid- and high-latitude regions, the global average is 1 to 2% °C^{-1} (Section 10.3.1), so ablation increases would be expected to dominate worldwide. However, precipitation changes may sometimes dominate locally (see Section 4.5.3).

Regressing observed global total mass balance changes of all G&IC outside Greenland and Antarctica against global average surface temperature change gives a global total mass balance sensitivity which is greater than model results (see Appendix 10.A). The current state of knowledge does not permit a satisfactory explanation of the difference. Giving more weight to the observational record but enlarging the uncertainty to allow for systematic error, a value of 0.80 ± 0.33 mm yr^{-1} °C^{-1} (5 to 95% range) is adopted for projections. The regression indicates that the climate of 1865 to 1895 was 0.13°C warmer globally than the climate that gives a steady state for G&IC (cf., Zuo and Oerlemans, 1997; Gregory et al., 2006). Model results for the 20th century are sensitive to this value, but the projected temperature change in the 21st century is large by comparison, making the effect relatively less important for projections (see Appendix 10.A).

10.6.3.2 Dynamic Response and Feedback on Mass Balance

As glacier volume is lost, glacier area declines so the ablation decreases. Oerlemans et al. (1998) calculate that omitting this effect leads to overestimates of ablation of about 25% by 2100. Church et al. (2001), following Bahr et al. (1997) and Van de Wal and Wild (2001), make some allowance for it by diminishing the area A of a glacier of volume V according to $V \propto A^{1.375}$. This is a scaling relation derived for glaciers in a steady state, which may hold only approximately during retreat. For example, thinning in the ablation zone will steepen the surface slope and tend to increase the flow. Comparison with a simple flow model suggests the deviations do not exceed 20% (van de Wal and Wild, 2001). Schneeberger et al. (2003) find that the scaling relation produced a mixture of over- and underestimates of volume loss for their sample of glaciers compared with more detailed dynamic modelling. In some regions where G&IC flow into the sea or lakes there is accelerated dynamic discharge (Rignot et al., 2003) that is not included in currently available glacier models, leading to an underestimate of G&IC mass loss.

The mean specific surface mass balance of the glacier or ice cap will change as volume is lost: lowering the ice surface as the ice thins will tend to make it more negative, but the predominant loss of area at lower altitude in the ablation zone will tend to make it less negative (Braithwaite and Raper, 2002). For rapid thinning rates in the ablation zone, of several metres per year, lowering the surface will give enhanced local warmings comparable to the rate of projected climatic warming. However, those areas of the ablation zone of valley glaciers that thin most rapidly will soon be removed altogether, resulting in retreat of the glacier. The enhancement of ablation by surface lowering can only be sustained in glaciers with a relatively large, thick and flat ablation area. On multi-decadal time scales, for the majority of G&IC, the loss of area is more important than lowering of the surface (Schneeberger et al., 2003).

The dynamical approach (Oerlemans et al., 1998; Schneeberger et al., 2003) cannot be applied to all the world's glaciers individually as the required data are unknown for the vast majority of them. Instead, it might be applied to a representative ensemble derived from statistics of size distributions of G&IC. Raper et al. (2000) developed a geometrical approach, in which the width, thickness and length of a glacier are reduced as its volume and area declines. When applied statistically to the world population of glaciers and individually to ice caps, this approach shows that the reduction of area of glaciers strongly reduces the ablation during the 21st century (Raper and Braithwaite, 2006), by about 45% under scenario SRES A1B for the GFDL-CM2.0 and PCM AOGCMs (see Table 8.1 for model details). For the same cases, using the mass-balance sensitivities to temperature of Oerlemans (2001) and Oerlemans et al. (2006), G&IC mass loss is reduced by about 35% following the area scaling of Van de Wal and Wild (2001), suggesting that the area scaling and the geometrical model have a similar effect in reducing estimated ablation for the 21st century. The effect is greater when using the observationally derived mass balance sensitivity (Section 10.6.3.1), which is larger, implying faster mass loss for fixed area. The uncertainty in present-day glacier volume (Table 4.4) introduces a 5 to 10% uncertainty into the results of area scaling. For projections, the area scaling of Van de Wal and Wild (2001) is applied, using three estimates of world glacier volume (see Table 4.4 and Appendix 10.A). The scaling reduces the projections of the G&IC contribution up to the mid-21st century by 25% and over the whole century by 40 to 50% with respect to fixed G&IC area.

10.6.3.3 Glaciers and Ice Caps on Greenland and Antarctica

The G&IC on Greenland and Antarctica (apart from the ice sheets) have been less studied and projections for them are consequently more uncertain. A model estimate for the G&IC on Greenland indicates an addition of about 6% to the G&IC sea level contribution in the 21st century (van de Wal and Wild, 2001). Using a degree-day scheme, Vaughan (2006) estimates that ablation of glaciers in the Antarctic Peninsula presently amounts to 0.008 to 0.055 mm yr^{-1} of sea level, 1 to 9% of the contribution from G&IC outside Greenland and Antarctica (Table 4.4). Morris and Mulvaney (2004) find that accumulation increases on the Antarctic Peninsula were larger than ablation increases during 1972 to 1998, giving a small net *negative* sea

level contribution from the region. However, because ablation increases nonlinearly with temperature, they estimate that for future warming the contribution would become positive, with a sensitivity of 0.07 ± 0.03 mm yr^{-1} $°C^{-1}$ to uniform temperature change in Antarctica, that is, about 10% of the global sensitivity of G&IC outside Greenland and Antarctica (Section 10.6.3.1).

These results suggest that the Antarctic and Greenland G&IC will together give 10 to 20% of the sea level contribution of other G&IC in future decades. In recent decades, the G&IC on Greenland and Antarctica have together made a contribution of about 20% of the total of other G&IC (see Section 4.5.2). On these grounds, the global G&IC sea level contribution is increased by a factor of 1.2 to include those in Greenland and Antarctica in projections for the 21st century (see Section 10.6.5 and Table 10.7). Dynamical acceleration of glaciers in Greenland and Antarctica following removal of ice shelves, as has recently happened on the Antarctic Peninsula (Sections 4.6.2.2 and 10.6.4.2), would add further to this, and is included in projections of that effect (Section 10.6.4.3).

10.6.4 Ice Sheets

The mass of ice grounded on land in the Greenland and Antarctic Ice Sheets (see also Section 4.6.1) can change as a result of changes in surface mass balance (the sum of accumulation and ablation; Section 10.6.4.1) or in the flux of ice crossing the grounding line, which is determined by the dynamics of the ice sheet (Section 10.6.4.2). Surface mass balance and dynamics together both determine and are affected by the change in surface topography.

10.6.4.1 Surface Mass Balance

Surface mass balance (SMB) is immediately influenced by climate change. A good simulation of the ice sheet SMB requires a resolution exceeding that of AGCMs used for long climate experiments, because of the steep slopes at the margins of the ice sheet, where the majority of the precipitation and all of the ablation occur. Precipitation over ice sheets is typically overestimated by AGCMs, because their smooth topography does not present a sufficient barrier to inland penetration (Ohmura et al., 1996; Glover, 1999; Murphy et al., 2002). Ablation also tends to be overestimated because the area at low altitude around the margins of the ice sheet, where melting preferentially occurs, is exaggerated (Glover, 1999; Wild et al., 2003). In addition, AGCMs do not generally have a representation of the refreezing of surface melt water within the snowpack and may not include albedo variations dependent on snow ageing and its conversion to ice.

To address these issues, several groups have computed SMB at resolutions of tens of kilometres or less, with results that compare acceptably well with observations (e.g., van Lipzig et al., 2002; Wild et al., 2003). Ablation is calculated either by schemes based on temperature (degree-day or other temperature index methods) or by energy balance modelling. In the studies listed in Table 10.6, changes in SMB have been calculated from climate change simulations with high-resolution AGCMs or by perturbing a high-resolution observational climatology with climate model output, rather than by direct use of low-resolution GCM results. The models used for projected SMB changes are similar in kind to those used to study recent SMB changes (Section 4.6.3.1).

All the models show an increase in accumulation, but there is considerable uncertainty in its size (Table 10.6; van de Wal et al., 2001; Huybrechts et al., 2004). Precipitation increase could be determined by atmospheric radiative balance, increase in saturation specific humidity with temperature, circulation changes, retreat of sea ice permitting greater evaporation or a combination of these (van Lipzig et al., 2002). Accumulation also depends on change in local temperature, which strongly affects whether precipitation is solid or liquid (Janssens and Huybrechts, 2000), tending to make the accumulation increase smaller than the precipitation increase for a given temperature rise. For Antarctica, accumulation increases by 6 to 9% $°C^{-1}$ in the high-resolution AGCMs. Precipitation increases somewhat less in AR4 AOGCMs (typically of lower resolution), by 3 to 8% $°C^{-1}$. For Greenland, accumulation derived from the high-resolution AGCMs increases by 5 to 9% $°C^{-1}$. Precipitation increases by 4 to 7% $°C^{-1}$ in the AR4 AOGCMs.

Kapsner et al. (1995) do not find a relationship between precipitation and temperature variability inferred from Greenland ice cores for the Holocene, although both show large changes from the Last Glacial Maximum (LGM) to the Holocene. In the UKMO-HadCM3 AOGCM, the relationship is strong for climate change forced by greenhouse gases and the glacial-interglacial transition, but weaker for naturally forced variability (Gregory et al., 2006). Increasing precipitation in conjunction with warming has been observed in recent years in Greenland (Section 4.6.3.1).

All studies for the 21st century project that antarctic SMB changes will contribute negatively to sea level, owing to increasing accumulation exceeding any ablation increase (see Table 10.6). This tendency has not been observed in the average over Antarctica in reanalysis products for the last two decades (see Section 4.6.3.1), but during this period Antarctica as a whole has not warmed; on the other hand, precipitation has increased on the Antarctic Peninsula, where there has been strong warming.

In projections for Greenland, ablation increase is important but uncertain, being particularly sensitive to temperature change around the margins. Climate models project less warming in these low-altitude regions than the Greenland average, and less warming in summer (when ablation occurs) than the annual average, but greater warming in Greenland than the global average (Church et al., 2001; Huybrechts et al., 2004; Chylek and Lohmann, 2005; Gregory and Huybrechts, 2006). In most studies, Greenland SMB changes represent a net positive contribution to sea level in the 21st century (Table 10.6; Kiilsholm et al., 2003) because the ablation increase is larger than the precipitation increase. Only Wild et al. (2003) find the opposite, so that the net SMB change contributes negatively to sea level in the 21st century. Wild et al. (2003) attribute this

Table 10.6. *Comparison of ice sheet (grounded ice area) SMB changes calculated from high-resolution climate models. $\Delta P/\Delta T$ is the change in accumulation divided by change in temperature over the ice sheet, expressed as sea level equivalent (positive for falling sea level), and $\Delta R/\Delta T$ the corresponding quantity for ablation (positive for rising sea level). Note that ablation increases more rapidly than linearly with ΔT (van de Wal et al., 2001; Gregory and Huybrechts, 2006). To convert from mm yr^{-1} °C^{-1} to kg yr^{-1} °C^{-1}, multiply by 3.6 × 10^{14} m^2. To convert mm yr^{-1} °C^{-1} of sea level equivalent to mm yr^{-1} °C^{-1} averaged over the ice sheet, multiply by –206 for Greenland and –26 for Antarctica. $\Delta P/(P\Delta T)$ is the fractional change in accumulation divided by the change in temperature.*

Study	Climate model[a]	Model resolution and SMB source[b]	Greenland			Antarctica	
			$\Delta P/\Delta T$ (mm yr^{-1} °C^{-1})	$\Delta P/(P\Delta T)$ (% °C^{-1})	$\Delta R/\Delta T$ (mm yr^{-1} °C^{-1})	$\Delta P/\Delta T$ (mm yr^{-1} °C^{-1})	$\Delta P/(P\Delta T)$ (% °C^{-1})
Van de Wal et al. (2001)	ECHAM4	20 km EB	0.14	8.5	0.16	n.a.	n.a.
Wild and Ohmura (2000)	ECHAM4	T106 ≈ 1.1° EB	0.13	8.2	0.22	0.47	7.4
Wild et al. (2003)	ECHAM4	2 km TI	0.13	8.2	0.04	0.47	7.4
Bugnion and Stone (2002)	ECHAM4	20 km EB	0.10	6.4	0.13	n.a.	n.a.
Huybrechts et al. (2004)	ECHAM4	20 km TI	0.13[c]	7.6[c]	0.14	0.49[c]	7.3[c]
Huybrechts et al. (2004)	HadAM3H	20 km TI	0.09[c]	4.7[c]	0.23	0.37[c]	5.5[c]
Van Lipzig et al. (2002)	RACMO	55 km EB	n.a.	n.a.	n.a.	0.53	9.0
Krinner et al. (2007)	LMDZ4	60 km EB	n.a.	n.a.	n.a.	0.49	8.4

Notes:
[a] ECHAM4: Max Planck Institute for Meteorology AGCM; HadAM3H: high-resolution Met Office Hadley Centre AGCM; RACMO: Regional Atmospheric Climate Model (for Antarctica); LMDZ4: Laboratoire de Météorologie Dynamique AGCM (with high resolution over Antarctica).
[b] EB: SMB calculated from energy balance; TI: SMB calculated from temperature index.
[c] In these cases *P* is precipitation rather than accumulation.

difference to the reduced ablation area in their higher-resolution grid. A positive SMB change is not consistent with analyses of recent changes in Greenland SMB (see Section 4.6.3.1).

For an average temperature change of 3°C over each ice sheet, a combination of four high-resolution AGCM simulations and 18 AR4 AOGCMs (Huybrechts et al., 2004; Gregory and Huybrechts, 2006) gives SMB changes of 0.3 ± 0.3 mm yr^{-1} for Greenland and –0.9 ± 0.5 mm yr^{-1} for Antarctica (sea level equivalent), that is, sensitivities of 0.11 ± 0.09 mm yr^{-1} °C^{-1} for Greenland and –0.29 ± 0.18 mm yr^{-1} °C^{-1} for Antarctica. These results generally cover the range shown in Table 10.6, but tend to give more positive (Greenland) or less negative (Antarctica) sea level rise because of the smaller precipitation increases projected by the AOGCMs than by the high-resolution AGCMs. The uncertainties are from the spatial and seasonal patterns of precipitation and temperature change over the ice sheets, and from the ablation calculation. Projections under SRES scenarios for the 21st century are shown in Table 10.7.

10.6.4.2 Dynamics

Ice sheet flow reacts to changes in topography produced by SMB change. Projections for the 21st century are given in Section 10.6.5 and Table 10.7, based on the discussion in this section. In Antarctica, topographic change tends to increase ice flow and discharge. In Greenland, lowering of the surface tends to increase the ablation, while a steepening slope in the ablation zone opposes the lowering, and thinning of outlet glaciers reduces discharge. Topographic and dynamic changes simulated by ice flow models (Huybrechts and De Wolde, 1999; van de Wal et al., 2001; Huybrechts et al., 2002, 2004; Gregory and Huybrechts, 2006) can be roughly represented as modifying the sea level changes due to SMB change with fixed topography by –5% ± 5% from Antarctica, and 0% ±10% from Greenland (± one standard deviation) during the 21st century.

The TAR concluded that accelerated sea level rise caused by rapid dynamic response of the ice sheets to climate change is very unlikely during the 21st century (Church et al., 2001). However, new evidence of recent rapid changes in the Antarctic Peninsula, West Antarctica and Greenland (see Section 4.6.3.3) has again raised the possibility of larger dynamical changes in the future than are projected by state-of-the-art continental models, such as cited above, because these models do not incorporate all the processes responsible for the rapid marginal thinning currently taking place (Box 4.1; Alley et al., 2005a; Vaughan, 2007).

The main uncertainty is the degree to which the presence of ice shelves affects the flow of inland ice across the grounding

Frequently Asked Question 10.2

How Likely are Major or Abrupt Climate Changes, such as Loss of Ice Sheets or Changes in Global Ocean Circulation?

Abrupt climate changes, such as the collapse of the West Antarctic Ice Sheet, the rapid loss of the Greenland Ice Sheet or large-scale changes of ocean circulation systems, are not considered likely to occur in the 21st century, based on currently available model results. However, the occurrence of such changes becomes increasingly more likely as the perturbation of the climate system progresses.

Physical, chemical and biological analyses from Greenland ice cores, marine sediments from the North Atlantic and elsewhere and many other archives of past climate have demonstrated that local temperatures, wind regimes and water cycles can change rapidly within just a few years. The comparison of results from records in different locations of the world shows that in the past major changes of hemispheric to global extent occurred. This has led to the notion of an unstable past climate that underwent phases of abrupt change. Therefore, an important concern is that the continued growth of greenhouse gas concentrations in the atmosphere may constitute a perturbation sufficiently strong to trigger abrupt changes in the climate system. Such interference with the climate system could be considered dangerous, because it would have major global consequences.

Before discussing a few examples of such changes, it is useful to define the terms 'abrupt' and 'major'. 'Abrupt' conveys the meaning that the changes occur much faster than the perturbation inducing the change; in other words, the response is nonlinear. A 'major' climate change is one that involves changes that exceed the range of current natural variability and have a spatial extent ranging from several thousand kilometres to global. At local to regional scales, abrupt changes are a common characteristic of natural climate variability. Here, isolated, short-lived events that are more appropriately referred to as 'extreme events' are not considered, but rather large-scale changes that evolve rapidly and persist for several years to decades. For instance, the mid-1970s shift in sea surface temperatures in the Eastern Pacific, or the salinity reduction in the upper 1,000 m of the Labrador Sea since the mid-1980s, are examples of abrupt events with local to regional consequences, as opposed to the larger-scale, longer-term events that are the focus here.

One example is the potential collapse, or shut-down of the Gulf Stream, which has received broad public attention. The Gulf Stream is a primarily horizontal current in the north-western Atlantic Ocean driven by winds. Although a stable feature of the general circulation of the ocean, its northern extension, which feeds deep-water formation in the Greenland-Norwegian-Iceland Seas and thereby delivers substantial amounts of heat to these seas and nearby land areas, is influenced strongly by changes in the density of the surface waters in these areas. This current constitutes the northern end of a basin-scale meridional overturning circulation (MOC) that is established along the western boundary of the Atlantic basin. A consistent result from climate model simulations is that if the density of the surface waters in the North Atlantic decreases due to warming or a reduction in salinity, the strength of the MOC is decreased, and with it, the delivery of heat into these areas. Strong sustained reductions in salinity could induce even more substantial reduction, or complete shut-down of the MOC in all climate model projections. Such changes have indeed happened in the distant past.

The issue now is whether the increasing human influence on the atmosphere constitutes a strong enough perturbation to the MOC that such a change might be induced. The increase in greenhouse gases in the atmosphere leads to warming and an intensification of the hydrological cycle, with the latter making the surface waters in the North Atlantic less salty as increased rain leads to more freshwater runoff to the ocean from the region's rivers. Warming also causes land ice to melt, adding more freshwater and further reducing the salinity of ocean surface waters. Both effects would reduce the density of the surface waters (which must be dense and heavy enough to sink in order to drive the MOC), leading to a reduction in the MOC in the 21st century. This reduction is predicted to proceed in lockstep with the warming: none of the current models simulates an abrupt (nonlinear) reduction or a complete shut-down in this century. There is still a large spread among the models' simulated reduction in the MOC, ranging from virtually no response to a reduction of over 50% by the end of the 21st century. This cross-model variation is due to differences in the strengths of atmosphere and ocean feedbacks simulated in these models.

Uncertainty also exists about the long-term fate of the MOC. Many models show a recovery of the MOC once climate is stabilised. But some models have thresholds for the MOC, and they are passed when the forcing is strong enough and lasts long enough. Such simulations then show a gradual reduction of the MOC that continues even after climate is stabilised. A quantification of the likelihood of this occurring is not possible at this stage. Nevertheless, even if this were to occur, Europe would still experience warming, since the radiative forcing caused by increasing greenhouse gases would overwhelm the cooling associated with the MOC reduction. Catastrophic scenarios suggesting the beginning of an ice age triggered by a shutdown of the MOC are thus mere speculations, and no climate model has produced such an outcome. In fact, the processes leading to an ice age are sufficiently well understood and so completely different from those discussed here, that we can confidently exclude this scenario.

(continued)

Irrespective of the long-term evolution of the MOC, model simulations agree that the warming and resulting decline in salinity will significantly reduce deep and intermediate water formation in the Labrador Sea during the next few decades. This will alter the characteristics of the intermediate water masses in the North Atlantic and eventually affect the deep ocean. The long-term effects of such a change are unknown.

Other widely discussed examples of abrupt climate changes are the rapid disintegration of the Greenland Ice Sheet, or the sudden collapse of the West Antarctic Ice Sheet. Model simulations and observations indicate that warming in the high latitudes of the Northern Hemisphere is accelerating the melting of the Greenland Ice Sheet, and that increased snowfall due to the intensified hydrological cycle is unable to compensate for this melting. As a consequence, the Greenland Ice Sheet may shrink substantially in the coming centuries. Moreover, results suggest that there is a critical temperature threshold beyond which the Greenland Ice Sheet would be committed to disappearing completely, and that threshold could be crossed in this century. However, the total melting of the Greenland Ice Sheet, which would raise global sea level by about seven metres, is a slow process that would take many hundreds of years to complete.

Recent satellite and *in situ* observations of ice streams behind disintegrating ice shelves highlight some rapid reactions of ice sheet systems. This raises new concern about the overall stability of the West Antarctic Ice Sheet, the collapse of which would trigger another five to six metres of sea level rise. While these streams appear buttressed by the shelves in front of them, it is currently unknown whether a reduction or failure of this buttressing of relatively limited areas of the ice sheet could actually trigger a widespread discharge of many ice streams and hence a destabilisation of the entire West Antarctic Ice Sheet. Ice sheet models are only beginning to capture such small-scale dynamical processes that involve complicated interactions with the glacier bed and the ocean at the perimeter of the ice sheet. Therefore, no quantitative information is available from the current generation of ice sheet models as to the likelihood or timing of such an event.

line. A strong argument for enhanced flow when the ice shelf is removed is yielded by the acceleration of Jakobshavn Glacier (Greenland) following the loss of its floating tongue, and of the glaciers supplying the Larsen B Ice Shelf (Antarctic Peninsula) after it collapsed (see Section 4.6.3.3). The onset of disintegration of the Larsen B Ice Shelf has been attributed to enhanced fracturing by crevasses promoted by surface melt water (Scambos et al., 2000). Large portions of the Ross and Filchner-Ronne Ice Shelves (West Antarctica) currently have mean summer surface temperatures of around –5°C (Comiso, 2000, updated). Four high-resolution GCMs (Gregory and Huybrechts, 2006) project summer surface warming in these major ice shelf regions of between 0.2 and 1.3 times the antarctic annual average warming, which in turn will be a factor 1.1 ± 0.3 greater than global average warming according to AOGCM simulations using SRES scenarios. These figures indicate that a local mean summer warming of 5°C is unlikely for a global warming of less than 5°C (see Appendix 10.A). This suggests that ice shelf collapse due to surface melting is unlikely under most SRES scenarios during the 21st century, but we have low confidence in the inference because there is evidently large systematic uncertainty in the regional climate projections, and it is not known whether episodic surface melting might initiate disintegration in a warmer climate while mean summer temperatures remain below freezing.

In the Amundsen Sea sector of West Antarctica, ice shelves are not so extensive and the cause of ice shelf thinning is not surface melting, but bottom melting at the grounding line (Rignot and Jacobs, 2002). Shepherd et al. (2004) find an average ice-shelf thinning rate of 1.5 ± 0.5 m yr^{-1}. At the same time as the basal melting, accelerated inland flow has been observed for Pine Island, Thwaites and other glaciers in the sector (Rignot, 1998, 2001; Thomas et al., 2004). The synchronicity of these changes strongly implies that their cause lies in oceanographic change in the Amundsen Sea, but this has not been attributed to anthropogenic climate change and could be connected with variability in the SAM.

Because the acceleration took place in only a few years (Rignot et al., 2002; Joughin et al., 2003) but appears up to about 150 km inland, it implies that the dynamical response to changes in the ice shelf can propagate rapidly up the ice stream. This conclusion is supported by modelling studies of Pine Island Glacier by Payne et al. (2004) and Dupont and Alley (2005), in which a single and instantaneous reduction of the basal or lateral drag at the ice front is imposed in idealised ways, such as a step retreat of the grounding line. The simulated acceleration and inland thinning are rapid but transient; the rate of contribution to sea level declines as a new steady state is reached over a few decades. In the study of Payne et al. (2004) the imposed perturbations were designed to resemble loss of drag in the 'ice plain', a partially grounded region near the ice front, and produced a velocity increase of about 1 km yr^{-1} there. Thomas et al. (2005) suggest the ice plain will become ungrounded during the next decade and obtain a similar velocity increase using a simplified approach.

Most of inland ice of West Antarctica is grounded below sea level and so it could float if it thinned sufficiently; discharge therefore promotes inland retreat of the grounding line, which

represents a positive feedback by further reducing basal traction. Unlike the one-time change in the idealised studies, this would represent a sustained dynamical forcing that would prolong the contribution to sea level rise. Grounding line retreat of the ice streams has been observed recently at rates of up to about 1 km yr^{-1} (Rignot, 1998, 2001; Shepherd et al., 2002), but a numerical model formulation is difficult to construct (Vieli and Payne, 2005).

The majority of West Antarctic ice discharge is through the ice streams that feed the Ross and Ronne-Filchner ice shelves, but in these regions no accelerated flow causing thinning is currently observed; on the contrary, they are thickening or near balance (Zwally et al., 2005). Excluding these regions, and likewise those parts of the East Antarctic Ice Sheet that drain into the large Amery ice shelf, the total area of ice streams (areas flowing faster than 100 m yr^{-1}) discharging directly into the sea or via a small ice shelf is 270,000 km^2. If all these areas thinned at 2 m yr^{-1}, the order of magnitude of the larger rates observed in fast-flowing areas of the Amundsen Sea sector (Shepherd et al., 2001, 2002), the contribution to sea level rise would be about 1.5 mm yr^{-1}. This would require sustained retreat simultaneously on many fronts, and should be taken as an indicative upper limit for the 21st century (see also Section 10.6.5).

The observation in west-central Greenland of seasonal variation in ice flow rate and of a correlation with summer temperature variation (Zwally et al., 2002) suggest that surface melt water may join a sub-glacially routed drainage system lubricating the ice flow (although this implies that it penetrates more than 1,200 m of subfreezing ice). By this mechanism, increased surface melting during the 21st century could cause acceleration of ice flow and discharge; a sensitivity study (Parizek and Alley, 2004) indicated that this might increase the sea level contribution from the Greenland Ice Sheet during the 21st century by up to 0.2 m, depending on the warming and other assumptions. However, other studies (Echelmeyer and Harrison, 1990; Joughin et al., 2004) found no evidence of seasonal fluctuations in the flow rate of nearby Jakobshavn Glacier despite a substantial supply of surface melt water.

10.6.5 Projections of Global Average Sea Level Change for the 21st Century

Table 10.7 and Figure 10.33 show projected changes in global average sea level under the SRES marker scenarios for the 21st century due to thermal expansion and land ice changes based on AR4 AOGCM results (see Sections 10.6.1, 10.6.3 and 10.6.4 for discussion). The ranges given are 5 to 95% intervals characterising the spread of model results, but we are not able to assess their likelihood in the way we have done for temperature change (Section 10.5.4.6), for two main reasons. First, the observational constraint on sea level rise projections is weaker, because records are shorter and subject to more uncertainty. Second, current scientific understanding leaves poorly known uncertainties in the methods used to make projections for land ice (Sections 10.6.3 and 10.6.4). Since the AOGCMs are integrated with scenarios of CO_2 concentration, uncertainties in carbon cycle feedbacks are not included in the results. The carbon cycle uncertainty in projections of temperature change cannot be translated into sea level rise because thermal expansion is a major contributor and its relation to temperature change is uncertain (Section 10.6.1).

Table 10.7. *Projected global average sea level rise during the 21st century and its components under SRES marker scenarios. The upper row in each pair gives the 5 to 95% range (m) of the rise in sea level between 1980 to 1999 and 2090 to 2099. The lower row in each pair gives the range of the rate of sea level rise (mm yr^{-1}) during 2090 to 2099. The land ice sum comprises G&IC and ice sheets, including dynamics, but excludes the scaled-up ice sheet discharge (see text). The sea level rise comprises thermal expansion and the land ice sum. Note that for each scenario the lower/upper bound for sea level rise is larger/smaller than the total of the lower/upper bounds of the contributions, since the uncertainties of the contributions are largely independent. See Appendix 10.A for methods.*

		B1		B2		A1B		A1T		A2		A1FI	
Thermal expansion	m	0.10	0.24	0.12	0.28	0.13	0.32	0.12	0.30	0.14	0.35	0.17	0.41
	mm yr^{-1}	1.1	2.6	1.6	4.0	1.7	4.2	1.3	3.2	2.6	6.3	2.8	6.8
G&IC	m	0.07	0.14	0.07	0.15	0.08	0.15	0.08	0.15	0.08	0.16	0.08	0.17
	mm yr^{-1}	0.5	1.3	0.5	1.5	0.6	1.6	0.5	1.4	0.6	1.9	0.7	2.0
Greenland Ice Sheet SMB	m	0.01	0.05	0.01	0.06	0.01	0.08	0.01	0.07	0.01	0.08	0.02	0.12
	mm yr^{-1}	0.2	1.0	0.2	1.5	0.3	1.9	0.2	1.5	0.3	2.8	0.4	3.9
Antarctic Ice Sheet SMB	m	-0.10	-0.02	-0.11	-0.02	-0.12	-0.02	-0.12	-0.02	-0.12	-0.03	-0.14	-0.03
	mm yr^{-1}	-1.4	-0.3	-1.7	-0.3	-1.9	-0.4	-1.7	-0.3	-2.3	-0.4	-2.7	-0.5
Land ice sum	m	0.04	0.18	0.04	0.19	0.04	0.20	0.04	0.20	0.04	0.20	0.04	0.23
	mm yr^{-1}	0.0	1.8	-0.1	2.2	-0.2	2.5	-0.1	2.1	-0.4	3.2	-0.8	4.0
Sea level rise	m	0.18	0.38	0.20	0.43	0.21	0.48	0.20	0.45	0.23	0.51	0.26	0.59
	mm yr^{-1}	1.5	3.9	2.1	5.6	2.1	6.0	1.7	4.7	3.0	8.5	3.0	9.7
Scaled-up ice sheet discharge	m	0.00	0.09	0.00	0.11	-0.01	0.13	-0.01	0.13	-0.01	0.13	-0.01	0.17
	mm yr^{-1}	0.0	1.7	0.0	2.3	0.0	2.6	0.0	2.3	-0.1	3.2	-0.1	3.9

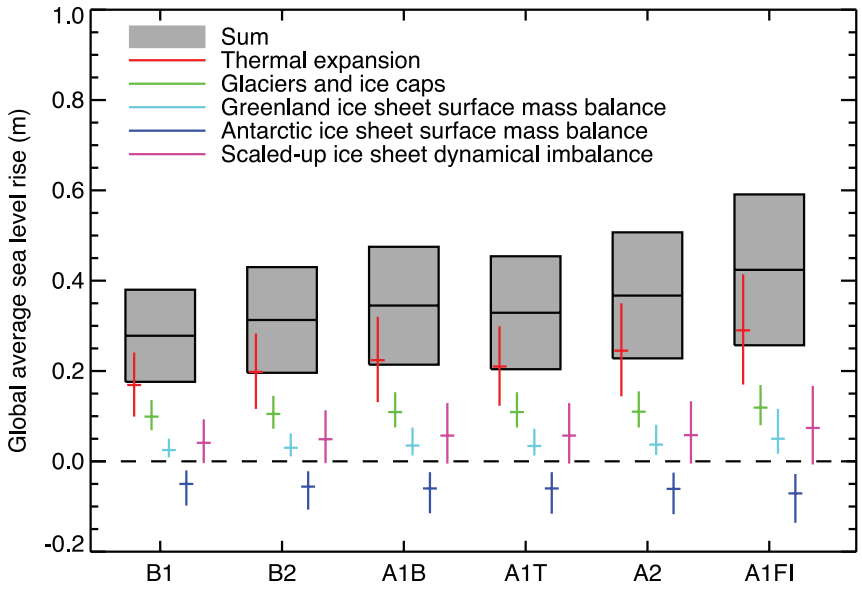


Figure 10.33. *Projections and uncertainties (5 to 95% ranges) of global average sea level rise and its components in 2090 to 2099 (relative to 1980 to 1999) for the six SRES marker scenarios. The projected sea level rise assumes that the part of the present-day ice sheet mass imbalance that is due to recent ice flow acceleration will persist unchanged. It does not include the contribution shown from scaled-up ice sheet discharge, which is an alternative possibility. It is also possible that the present imbalance might be transient, in which case the projected sea level rise is reduced by 0.02 m. It must be emphasized that we cannot assess the likelihood of any of these three alternatives, which are presented as illustrative. The state of understanding prevents a best estimate from being made.*

In all scenarios, the average rate of rise during the 21st century is very likely to exceed the 1961 to 2003 average rate of 1.8 ± 0.5 mm yr^{-1} (see Section 5.5.2.1). The central estimate of the rate of sea level rise during 2090 to 2099 is 3.8 mm yr^{-1} under A1B, which exceeds the central estimate of 3.1 mm yr^{-1} for 1993 to 2003 (see Section 5.5.2.2). The 1993 to 2003 rate may have a contribution of about 1 mm yr^{-1} from internally generated or naturally forced decadal variability (see Sections 5.5.2.4 and 9.5.2). These sources of variability are not predictable and not included in the projections; the actual rate during any future decade might therefore be more or less than the projected rate by a similar amount. Although simulated and observed sea level rise agree reasonably well for 1993 to 2003, the observed rise for 1961 to 2003 is not satisfactorily explained (Section 9.5.2), as the sum of observationally estimated components is 0.7 ± 0.7 mm yr^{-1} less than the observed rate of rise (Section 5.5.6). This indicates a deficiency in current scientific understanding of sea level change and may imply an underestimate in projections.

For an average model (the central estimate for each scenario), the scenario spread (from B1 to A1FI) in sea level rise is only 0.02 m by the middle of the century. This is small because of the time-integrating effect of sea level rise, on which the divergence among the scenarios has had little effect by then. By 2090 to 2099 it is 0.15 m.

In all scenarios, the central estimate for thermal expansion by the end of the century is 70 to 75% of the central estimate for the sea level rise. In all scenarios, the average rate of expansion during the 21st century is larger than central estimate of 1.6 mm yr^{-1} for 1993 to 2003 (Section 5.5.3). Likewise, in all scenarios the average rate of mass loss by G&IC during the 21st century is greater than the central estimate of 0.77 mm yr^{-1} for 1993 to 2003 (Section 4.5.2). By the end of the century, a large fraction of the present global G&IC mass is projected to have been lost (see, e.g., Table 4.3). The G&IC projections are rather insensitive to the scenario because the main uncertainties come from the G&IC model.

Further accelerations in ice flow of the kind recently observed in some Greenland outlet glaciers and West Antarctic ice streams could increase the ice sheet contributions substantially, but quantitative projections cannot be made with confidence (see Section 10.6.4.2). The land ice sum in Table 10.7 includes the effect of dynamical changes in the ice sheets that can be simulated with a continental ice sheet model (Section 10.6.4.2). It also includes a scenario-independent term of 0.32 ± 0.35 mm yr^{-1} (0.035 ± 0.039 m in 110 years). This is the central estimate for 1993 to 2003 of the sea level contribution from the Antarctic Ice Sheet, plus half of that from Greenland (Sections 4.6.2.2 and 5.5.5.2). We take this as an estimate of the part of the present ice sheet mass imbalance that is due to recent ice flow acceleration (Section 4.6.3.2), and assume that this contribution will persist unchanged.

We also evaluate the contribution of rapid dynamical changes under two alternative assumptions (see, e.g., Alley et al., 2005b). First, the present imbalance might be a rapid short-term adjustment, which will diminish during coming decades. We take an e-folding time of 100 years, on the basis of an idealised model study (Payne et al., 2004). This assumption reduces the sea level rise in Table 10.7 by 0.02 m. Second, the present imbalance might be a response to recent climate change, perhaps through oceanic or surface warming (Section 10.6.4.2). No models are available for such a link, so we assume that the imbalance might scale up with global average surface temperature change, which we take as a measure of the magnitude of climate change (see Appendix 10.A). This assumption adds 0.1 to 0.2 m to the estimated upper bound for sea level rise depending on the scenario (Table 10.7). During 2090 to 2099, the rate of scaled-up antarctic discharge roughly balances the increased rate of antarctic accumulation (SMB). The central estimate for the increased antarctic discharge under the SRES scenario A1FI is about 1.3 mm yr^{-1}, a factor of 5 to 10 greater than in recent years, and similar to the order-of-magnitude upper limit of Section 10.6.4.2. It must be emphasized that we cannot assess the likelihood of any of these three alternatives, which are presented as illustrative. The state of understanding prevents a best estimate from being made.

The central estimates for sea level rise in Table 10.7 are smaller than the TAR model means (Church et al., 2001) by 0.03 to 0.07 m, depending on scenario, for two reasons. First, these projections are for 2090-2099, whereas the TAR projections were for 2100. Second, the TAR included some small constant additional contributions to sea level rise which are omitted here (see below regarding permafrost). If the TAR model means are adjusted for this, they are within 10% of the central estimates from Table 10.7. (See Appendix 10.A for further information.) For each scenario, the upper bound of sea level rise in Table 10.7 is smaller than in the TAR, and the lower bound is larger than in the TAR. This is because the uncertainty on the sea level projection has been reduced, for a combination of reasons (see Appendix 10.A for details). The TAR would have had similar ranges to those shown here if it had treated the uncertainties in the same way.

Thawing of permafrost is projected to contribute about 5 mm during the 21st century under the SRES scenario A2 (calculated from Lawrence and Slater, 2005). The mass of the ocean will also be changed by climatically driven alteration in other water storage, in the forms of atmospheric water vapour, seasonal snow cover, soil moisture, groundwater, lakes and rivers. All of these are expected to be relatively small terms, but there may be substantial contributions from anthropogenic change in terrestrial water storage, through extraction from aquifers and impounding in reservoirs (see Sections 5.5.5.3 and 5.5.5.4).

10.7 Long Term Climate Change and Commitment

10.7.1 Climate Change Commitment to Year 2300 Based on AOGCMs

Building on Wigley (2005), we use three specific definitions of climate change commitment: (i) the 'constant composition commitment', which denotes the further change of temperature ('constant composition temperature commitment' or 'committed warming'), sea level ('constant composition sea level commitment') or any other quantity in the climate system, since the time the composition of the atmosphere, and hence the radiative forcing, has been held at a constant value; (ii) the 'constant emission commitment', which denotes the further change of, for example, temperature ('constant emission temperature commitment') since the time the greenhouse gas emissions have been held at a constant value; and (iii) the 'zero emission commitment', which denotes the further change of, for example, temperature ('zero emission temperature commitment') since the time the greenhouse gas emissions have been set to zero.

The concept that the climate system exhibits commitment when radiative forcing has changed is mainly due to the thermal inertia of the oceans, and was discussed independently by Wigley (1984), Hansen et al. (1984) and Siegenthaler and Oeschger (1984). The term 'commitment' in this regard was introduced by Ramanathan (1988). In the TAR, this was illustrated in idealised scenarios of doubling and quadrupling atmospheric CO_2, and stabilisation at 2050 and 2100 after an IS92a forcing scenario. Various temperature commitment values were reported (about 0.3°C per century with much model dependency), and EMIC simulations were used to illustrate the long-term influence of the ocean owing to long mixing times and the MOC. Subsequent studies have confirmed this behaviour of the climate system and ascribed it to the inherent property of the climate system that the thermal inertia of the ocean introduces a lag to the warming of the climate system after concentrations of greenhouse gases are stabilised (Mitchell et al., 2000; Wetherald et al., 2001; Wigley and Raper, 2003; Hansen et al., 2005b; Meehl et al., 2005c; Wigley, 2005). Climate change commitment as discussed here should not be confused with 'unavoidable climate change' over the next half century, which would surely be greater because forcing cannot be instantly stabilised. Furthermore, in the very long term it is plausible that climate change could be less than in a commitment run since forcing could plausibly be reduced below current levels as illustrated in the overshoot simulations and zero emission commitment simulations discussed below.

Three constant composition commitment experiments have recently been performed by the global coupled climate modelling community: (1) stabilising concentrations of greenhouse gases at year 2000 values after a 20th-century climate simulation, and running the model for an additional 100 years; (2) stabilising concentrations of greenhouse gases at year 2100 values after a 21st-century B1 experiment (e.g., CO_2 near 550 ppm) and running the model for an additional 100 years (with some models run to 200 years); and (3) stabilising concentrations of greenhouse gases at year 2100 values after a 21st-century A1B experiment (e.g., CO_2 near 700 ppm), and running the model for an additional 100 years (and some models to 200 years). Multi-model mean warming in these experiments is depicted in Figure 10.4. Time series of the globally averaged surface temperature and percent precipitation change after stabilisation are shown for all the models in the Supplementary Material, Figure S10.3.

The multi-model average warming for all radiative forcing agents held constant at year 2000 (reported earlier for several of the models by Meehl et al., 2005c), is about 0.6°C for the period 2090 to 2099 relative to the 1980 to 1999 reference period. This is roughly the magnitude of warming simulated in the 20th century. Applying the same uncertainty assessment as for the SRES scenarios in Fig. 10.29 (–40 to +60%), the likely uncertainty range is 0.3°C to 0.9°C. Hansen et al. (2005a) calculate the current energy imbalance of the Earth to be 0.85 W m^{-2}, implying that the unrealised global warming is about 0.6°C without any further increase in radiative forcing. The committed warming trend values show a rate of warming averaged over the first two decades of the 21st century of about 0.1°C per decade, due mainly to the slow response of the oceans. About twice as much warming (0.2°C per decade) would be expected if emissions are within the range of the SRES scenarios.

For the B1 constant composition commitment run, the additional warming after 100 years is also about 0.5°C, and roughly the same for the A1B constant composition commitment (Supplementary Material, Figure S10.3). These new results quantify what was postulated in the TAR in that the warming commitment after stabilising concentrations is about 0.5°C for the first century, and considerably smaller after that, with most of the warming commitment occurring in the first several decades of the 22nd century.

Constant composition precipitation commitment for the multi-model ensemble average is about 1.1% by 2100 for the 20th-century constant composition commitment experiment, and for the B1 constant composition commitment experiment it is 0.8% by 2200 and 1.5% by 2300, while for the A1B constant composition commitment experiment it is 1.5% by 2200 and 2% by 2300.

The patterns of change in temperature in the B1 and A1B experiments, relative to the pre-industrial period, do not change greatly after stabilisation (Table 10.5). Even the 20th-century stabilisation case warms with some similarity to the A1B pattern (Table 10.5). However, there is some contrast in the land and ocean warming rates, as seen from Figure 10.6. Mid- and low-latitude land warms at rates closer to the global mean of that of A1B, while high-latitude ocean warming is larger.

10.7.2 Climate Change Commitment to Year 3000 and Beyond to Equilibrium

Earth System Models of Intermediate Complexity are used to extend the projections for a scenario that follows A1B to 2100 and then keeps atmospheric composition, and hence radiative forcing, constant to the year 3000 (see Figure 10.34). By 2100, the projected warming is between 1.2°C and 4.1°C, similar to the range projected by AOGCMs. A large constant composition temperature and sea level commitment is evident in the simulations and is slowly realised over coming centuries. By the year 3000, the warming range is 1.9°C to 5.6°C. While surface temperatures approach equilibrium relatively quickly, sea level continues to rise for many centuries.

Five of these EMICs include interactive representations of the marine and terrestrial carbon cycle and, therefore, can be used to assess carbon cycle-climate feedbacks and effects of

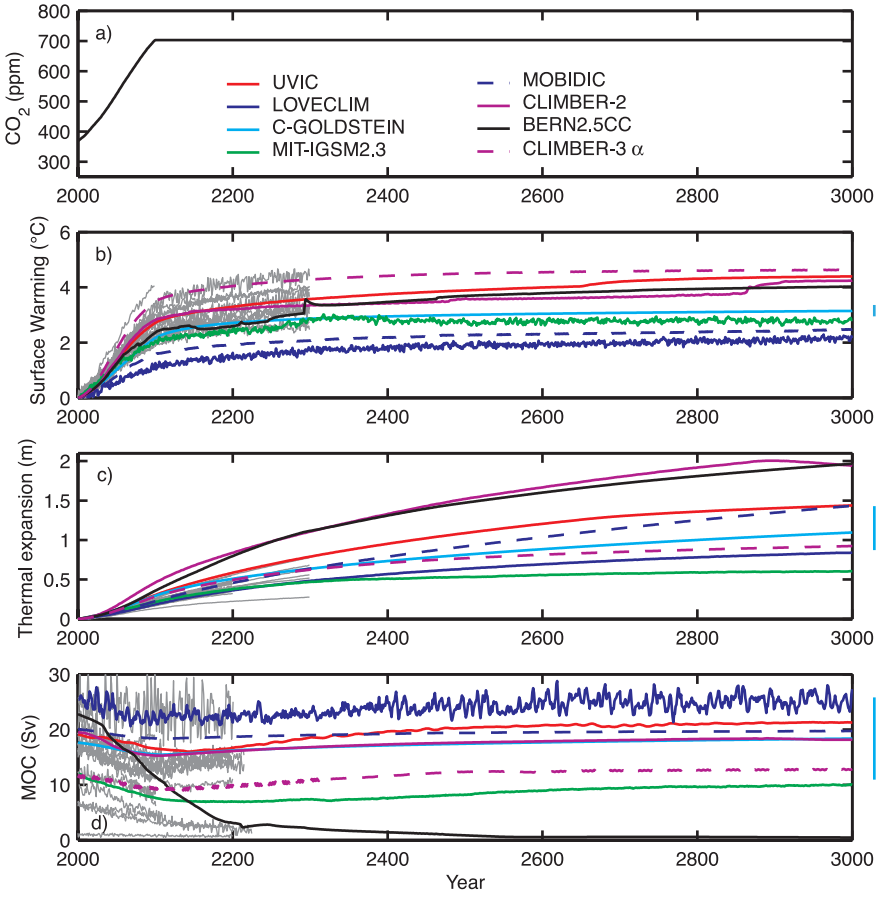


Figure 10.34. *(a) Atmospheric CO_2, (b) global mean surface warming, (c) sea level rise from thermal expansion and (d) Atlantic meridional overturning circulation (MOC) calculated by eight EMICs for the SRES A1B scenario and stable radiative forcing after 2100, showing long-term commitment after stabilisation. Coloured lines are results from EMICs, grey lines indicate AOGCM results where available for comparison. Anomalies in (b) and (c) are given relative to the year 2000. Vertical bars indicate ±2 standard deviation uncertainties due to ocean parameter perturbations in the C-GOLDSTEIN model. The MOC shuts down in the BERN2.5CC model, leading to an additional contribution to sea level rise. Individual EMICs (see Table 8.3 for model details) treat the effect from non-CO_2 greenhouse gases and the direct and indirect aerosol effects on radiative forcing differently. Despite similar atmospheric CO_2 concentrations, radiative forcing among EMICs can thus differ within the uncertainty ranges currently available for present-day radiative forcing (see Chapter 2).*

Frequently Asked Question 10.3

If Emissions of Greenhouse Gases are Reduced, How Quickly do Their Concentrations in the Atmosphere Decrease?

The adjustment of greenhouse gas concentrations in the atmosphere to reductions in emissions depends on the chemical and physical processes that remove each gas from the atmosphere. Concentrations of some greenhouse gases decrease almost immediately in response to emission reduction, while others can actually continue to increase for centuries even with reduced emissions.

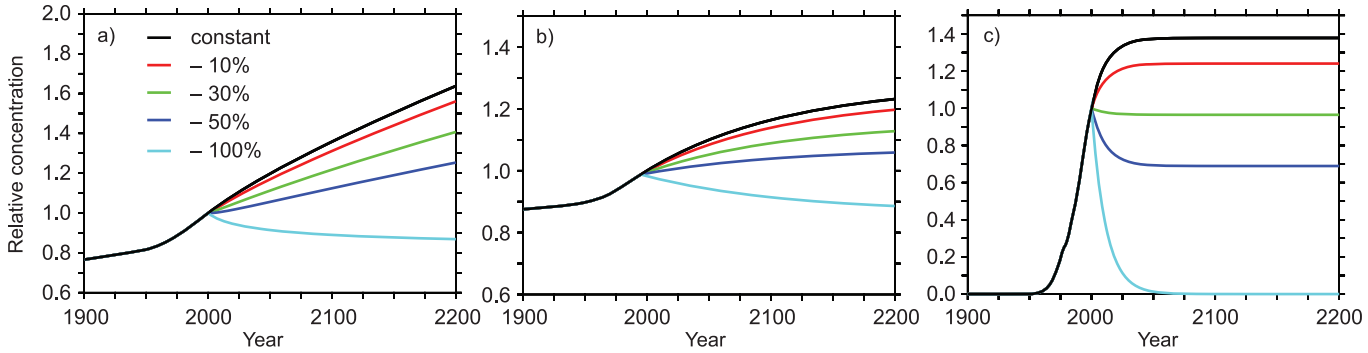
The concentration of a greenhouse gas in the atmosphere depends on the competition between the rates of emission of the gas into the atmosphere and the rates of processes that remove it from the atmosphere. For example, carbon dioxide (CO_2) is exchanged between the atmosphere, the ocean and the land through processes such as atmosphere-ocean gas transfer and chemical (e.g., weathering) and biological (e.g., photosynthesis) processes. While more than half of the CO_2 emitted is currently removed from the atmosphere within a century, some fraction (about 20%) of emitted CO_2 remains in the atmosphere for many millennia. Because of slow removal processes, atmospheric CO_2 will continue to increase in the long term even if its emission is substantially reduced from present levels. Methane (CH_4) is removed by chemical processes in the atmosphere, while nitrous oxide (N_2O) and some halocarbons are destroyed in the upper atmosphere by solar radiation. These processes each operate at different time scales ranging from years to millennia. A measure for this is the lifetime of a gas in the atmosphere, defined as the time it takes for a perturbation to be reduced to 37% of its initial amount. While for CH_4, N_2O, and other trace gases such as hydrochlorofluorocarbon-22 (HCFC-22), a refrigerant fluid, such lifetimes can be reasonably determined (for CH_4 it is about 12 yr, for N_2O about 110 yr and for HCFC-22 about 12 yr), a lifetime for CO_2 cannot be defined.

The change in concentration of any trace gas depends in part on how its emissions evolve over time. If emissions increase with time, the atmospheric concentration will also increase with time, regardless of the atmospheric lifetime of the gas. However, if actions are taken to reduce the emissions, the fate of the trace gas concentration will depend on the relative changes not only of emissions but also of its removal processes. Here we show how the lifetimes and removal processes of different gases dictate the evolution of concentrations when emissions are reduced.

As examples, FAQ 10.3, Figure 1 shows test cases illustrating how the future concentration of three trace gases would respond to illustrative changes in emissions (represented here as a response to an imposed pulse change in emission). We consider CO_2, which has no specific lifetime, as well as a trace gas with a well-defined long lifetime on the order of a century (e.g., N_2O), and a trace gas with a well-defined short lifetime on the order of decade (such as CH_4, HCFC-22 or other halocarbons). For each gas, five illustrative cases of future emissions are presented: stabilisation of emissions at present-day levels, and immediate emission reduction by 10%, 30%, 50% and 100%.

The behaviour of CO_2 (Figure 1a) is completely different from the trace gases with well-defined lifetimes. Stabilisation of CO_2 emissions at current levels would result in a continuous increase of atmospheric CO_2 over the 21st century and beyond, whereas for a gas with a lifetime on the order of a century (Figure 1b) or a decade (Figure 1c), stabilisation of emissions at current levels would lead to a stabilisation of its concentration at a level higher than today within a couple of centuries, or decades, respectively. In fact, only in the case of essentially complete elimination of

(continued)



FAQ 10.3, Figure 1. *(a) Simulated changes in atmospheric CO_2 concentration relative to the present-day for emissions stabilised at the current level (black), or at 10% (red), 30% (green), 50% (dark blue) and 100% (light blue) lower than the current level; (b) as in (a) for a trace gas with a lifetime of 120 years, driven by natural and anthropogenic fluxes; and (c) as in (a) for a trace gas with a lifetime of 12 years, driven by only anthropogenic fluxes.*

emissions can the atmospheric concentration of CO_2 ultimately be stabilised at a constant level. All other cases of moderate CO_2 emission reductions show increasing concentrations because of the characteristic exchange processes associated with the cycling of carbon in the climate system.

More specifically, the rate of emission of CO_2 currently greatly exceeds its rate of removal, and the slow and incomplete removal implies that small to moderate reductions in its emissions would not result in stabilisation of CO_2 concentrations, but rather would only reduce the rate of its growth in coming decades. A 10% reduction in CO_2 emissions would be expected to reduce the growth rate by 10%, while a 30% reduction in emissions would similarly reduce the growth rate of atmospheric CO_2 concentrations by 30%. A 50% reduction would stabilise atmospheric CO_2, but only for less than a decade. After that, atmospheric CO_2 would be expected to rise again as the land and ocean sinks decline owing to well-known chemical and biological adjustments. Complete elimination of CO_2 emissions is estimated to lead to a slow decrease in atmospheric CO_2 of about 40 ppm over the 21st century.

The situation is completely different for the trace gases with a well-defined lifetime. For the illustrative trace gas with a lifetime of the order of a century (e.g., N_2O), emission reduction of more than 50% is required to stabilise the concentrations close to present-day values (Figure 1b). Constant emission leads to a stabilisation of the concentration within a few centuries.

In the case of the illustrative gas with the short lifetime, the present-day loss is around 70% of the emissions. A reduction in emissions of less than 30% would still produce a short-term increase in concentration in this case, but, in contrast to CO_2, would lead to stabilisation of its concentration within a couple of decades (Figure 1c). The decrease in the level at which the concentration of such a gas would stabilise is directly proportional to the emission reduction. Thus, in this illustrative example, a reduction in emissions of this trace gas larger than 30% would be required to stabilise concentrations at levels significantly below those at present. A complete cut-off of the emissions would lead to a return to pre-industrial concentrations within less than a century for a trace gas with a lifetime of the order of a decade.

carbon emission reductions on atmospheric CO_2 and climate. Although carbon cycle processes in these models are simplified, global-scale quantities are in good agreement with more complex models (Doney et al., 2004).

Results for one carbon emission scenario are shown in Figure 10.35, where anthropogenic emissions follow a path towards stabilisation of atmospheric CO_2 at 750 ppm but at year 2100 are reduced to zero. This permits the determination of the zero emission climate change commitment. The prescribed emissions were calculated from the SP750 profile (Knutti et al., 2005) using the BERN-CC model (Joos et al., 2001). Although unrealistic, such a scenario permits the calculation of zero emission commitment, i.e., climate change due to 21st-century emissions. Even though emissions are instantly reduced to zero at year 2100, it takes about 100 to 400 years in the different models for the atmospheric CO_2 concentration to drop from the maximum (ranges between 650 to 700 ppm) to below the level of doubled pre-industrial CO_2 (~560 ppm) owing to a continuous transfer of carbon from the atmosphere into the terrestrial and oceanic reservoirs. Emissions during the 21st century continue to have an impact even at year 3000 when both surface temperature and sea level rise due to thermal expansion are still substantially higher than pre-industrial. Also shown are atmospheric CO_2 concentrations and ocean/terrestrial carbon inventories at year 3000 versus total emitted carbon for similar emission pathways targeting (but not actually reaching) 450, 550, 750 and 1,000 ppm atmospheric CO_2 and with carbon emissions reduced to zero at year 2100. Atmospheric CO_2 at year 3000 is approximately linearly related to the total amount of carbon emitted in each model, but with a substantial spread among the models in both slope and absolute values, because the redistribution of carbon between the different reservoirs is model dependent. In summary, the model results show that 21st-century emissions represent a minimum commitment of climate change for several centuries, irrespective of later emissions. A reduction of this 'minimum' commitment is possible only if, in addition to avoiding CO_2 emissions after 2100, CO_2 were actively removed from the atmosphere.

Using a similar approach, Friedlingstein and Solomon (2005) show that even if emissions were immediately cut to zero, the system would continue to warm for several more decades before starting to cool. It is important also to note that ocean heat content and changes in the cryosphere evolve on time scales extending over centuries.

On very long time scales (order several thousand years as estimated by AOGCM experiments, Bi et al., 2001; Stouffer, 2004), equilibrium climate sensitivity is a useful concept to characterise the ultimate response of climate models to different future levels of greenhouse gas radiative forcing. This concept can be applied to climate models irrespective of their complexity. Based on a global energy balance argument, equilibrium climate sensitivity S and global mean surface temperature increase ΔT at equilibrium relative to pre-industrial for an equivalent stable CO_2 concentration are linearly related according to $\Delta T = S \times \log(CO_2 / 280 \text{ ppm}) / \log(2)$, which follows from the definition of climate sensitivity and simplified expressions for the radiative forcing of CO_2 (Section 6.3.5 of the TAR). Because the combination of various lines of modelling results and expert judgement yields a quantified range of climate sensitivity S (see Box 10.2), this can be carried over to equilibrium temperature increase. Most likely values, and the likely range, as well as a very likely lower bound for the warming, all consistent with the quantified range of S, are given in Table 10.8.

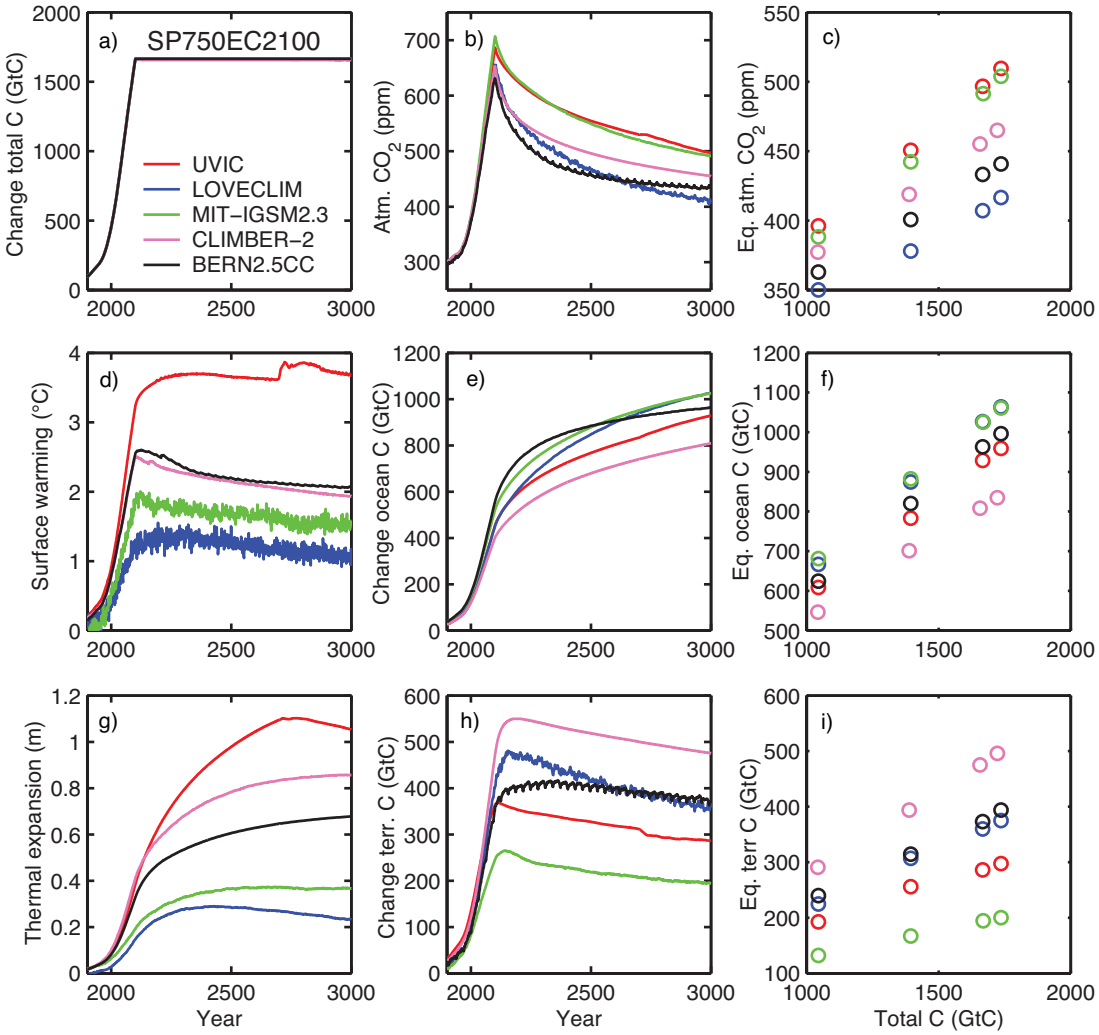


Figure 10.35. *Changes in carbon inventories and climate response relative to the pre-industrial period simulated by five different intermediate complexity models (see Table 8.3 for model descriptions) for a scenario where emissions follow a pathway leading to stabilisation of atmospheric CO_2 at 750 ppm, but before reaching this target, emissions are reduced to zero instantly at year 2100. (a) Change in total carbon, (b) atmospheric CO_2, (d) change in surface temperature, (e) change in ocean carbon, (g) sea level rise from thermal expansion and (h) change in terrestrial carbon. Right column: (c) atmospheric CO_2 and the change in (f) oceanic and (i) terrestrial carbon inventories at year 3000 relative to the pre-industrial period for several emission scenarios of similar shape but with different total carbon emissions.*

Table 10.8. *Best guess (i.e. most likely), likely and very likely bounds/ranges of global mean equilibrium surface temperature increase ΔT(°C) above pre-industrial temperatures for different levels of CO_2 equivalent concentrations (ppm), based on the assessment of climate sensitivity given in Box 10.2.*

Equivalent CO_2	Best Guess	Very Likely Above	Likely in the Range
350	1.0	0.5	0.6–1.4
450	2.1	1.0	1.4–3.1
550	2.9	1.5	1.9–4.4
650	3.6	1.8	2.4–5.5
750	4.3	2.1	2.8–6.4
1,000	5.5	2.8	3.7–8.3
1,200	6.3	3.1	4.2–9.4

It is emphasized that this table does not contain more information than the best knowledge of S and that the numbers are not the result of any climate model simulation. Rather it is assumed that the above relationship between temperature increase and CO_2 holds true for the entire range of equivalent CO_2 concentrations. There are limitations to the concept of radiative forcing and climate sensitivity (Senior and Mitchell, 2000; Joshi et al., 2003; Shine et al., 2003; Hansen et al., 2005b). Only a few AOGCMs have been run to equilibrium under elevated CO_2 concentrations, and some results show that nonlinearities in the feedbacks (e.g., clouds, sea ice and snow cover) may cause a time dependence of the effective climate sensitivity and substantial deviations from the linear relation assumed above (Manabe and Stouffer, 1994; Senior and Mitchell, 2000; Voss and Mikolajewicz, 2001; Gregory et al., 2004b), with effective climate sensitivity tending to grow with time in some of the AR4 AOGCMs. Some studies suggest

that climate sensitivities larger than the likely estimate given below (which would suggest greater warming) cannot be ruled out (see Box 10.2 on climate sensitivity).

Another way to address eventual equilibrium temperature for different CO_2 concentrations is to use the projections from the AOGCMs in Figure 10.4, and an idealised 1% yr^{-1} CO_2 increase to 4 × CO_2. The equivalent CO_2 concentrations in the AOGCMs can be estimated from the forcings given in Table 6.14 in the TAR. The actual CO_2 concentrations for A1B and B1 are roughly 715 ppm and 550 ppm (depending on which model is used to convert emissions to concentrations), and equivalent CO_2 concentrations are estimated to be about 835 ppm and 590 ppm, respectively. Using the equation above for an equilibrium climate sensitivity of 3.0°C, eventual equilibrium warming in these experiments would be 4.8°C and 3.3°C, respectively. The multi-model average warming in the AOGCMs at the end of the 21st century (relative to pre-industrial temperature) is 3.1°C and 2.3°C, or about 65 to 70% of the eventual estimated equilibrium warming. Given rates of CO_2 increase of between 0.5 and 1.0% yr^{-1} in these two scenarios, this can be compared to the calculated fraction of eventual warming of around 50% in AOGCM experiments with those CO_2 increase rates (Stouffer and Manabe, 1999). The Stouffer and Manabe (1999) model has somewhat higher equilibrium climate sensitivity, and was actually run to equilibrium in a 4-kyr integration to enable comparison of transient and equilibrium warming. Therefore, the AOGCM results combined with the estimated equilibrium warming seem roughly consistent with earlier AOGCM experiments of transient warming rates. Additionally, similar numbers for the 4 × CO_2 stabilisation experiments performed with the AOGCMs can be computed. In that case, the actual and equivalent CO_2 concentrations are the same, since there are no other radiatively active species changing in the models, and the multi-model CO_2 concentration at quadrupling would produce an eventual equilibrium warming of 6°C, where the multi-model average warming at the time of quadrupling is about 4.0°C or 66% of eventual equilibrium. This is consistent with the numbers for the A1B and B1 scenario integrations with the AOGCMs.

It can be estimated how much closer to equilibrium the climate system is 100 years after stabilisation in these AOGCM experiments. After 100 years of stabilised concentrations, the warming relative to pre-industrial temperature is 3.8°C in A1B and 2.6°C in B1, or about 80% of the estimated equilibrium warming. For the stabilised 4 × CO_2 experiment, after 100 years of stabilised CO_2 concentrations the warming is 4.7°C, or 78% of the estimated equilibrium warming. Therefore, about an additional 10 to 15% of the eventual equilibrium warming is achieved after 100 years of stabilised concentrations (Stouffer, 2004). This emphasizes that the approach to equilibrium takes a long time, and even after 100 years of stabilised atmospheric concentrations, only about 80% of the eventual equilibrium warming is realised.

10.7.3 Long-Term Integrations: Idealised Overshoot Experiments

The concept of mitigation related to overshoot scenarios has implications for IPCC Working Groups II and III and was addressed in the Second Assessment Report. A new suite of mitigation scenarios is currently being assessed for the AR4. Working Group I does not have the expertise to assess such scenarios, so this section assesses the processes and response of the physical climate system in a very idealised overshoot experiment. Plausible new mitigation and overshoot scenarios will be run subsequently by modelling groups and assessed in the next IPCC report.

An idealised overshoot scenario has been run in an AOGCM where the CO_2 concentration decreases from the A1B stabilised level to the B1 stabilised level between 2150 and 2250, followed by 200 years of integration with that constant B1 level (Figure 10.36a). This reduction in CO_2 concentration would require large reductions in emissions, but such an idealised experiment illustrates the processes involved in how the climate system would respond to such a large change in emissions and concentrations. Yoshida et al. (2005) and Tsutsui et al. (2007) show that there is a relatively fast response in the surface and upper ocean, which start to recover to temperatures at the B1 level after several decades, but a much more sluggish response with more commitment in the deep ocean. As shown in Figure 10.36b and c, the overshoot scenario temperatures only slowly decrease to approach the lower temperatures of the B1 experiment, and continue a slow convergence that has still not cooled to the B1 level at the year 2350, or 100 years after the CO_2 concentration in the overshoot experiment was reduced to equal the concentration in the B1 experiment. However, Dai et al. (2001a) show that reducing emissions to achieve a stabilised CO_2 concentration in the 21st century reduces warming moderately (less than 0.5°C) by the end of the 21st century in comparison to a business-as-usual scenario, but the warming reduction is about 1.5°C by the end of the 22nd century in that experiment. Other climate system responses include the North Atlantic MOC and sea ice volume that almost recover to the B1 level in the overshoot scenario experiment, except for a significant hysteresis effect that is shown in the sea level change due to thermal expansion (Yoshida et al., 2005; Nakashiki et al., 2006).

Such stabilisation and overshoot scenarios have implications for risk assessment as suggested by Yoshida et al. (2005) and others. For example, in a probabilistic study using an SCM and multi-gas scenarios, Meinshausen (2006) estimated that the probability of exceeding a 2°C warming is between 68 and 99% for a stabilisation of equivalent CO_2 at 550 ppm. They also considered scenarios with peaking CO_2 and subsequent stabilisation at lower levels as an alternative pathway and found that if the risk of exceeding a warming of 2°C is not to be greater than 30%, it is necessary to peak equivalent CO_2 concentrations around 475 ppm before returning to lower concentrations of about 400 ppm. These overshoot and targeted climate change estimations take into account the climate change commitment

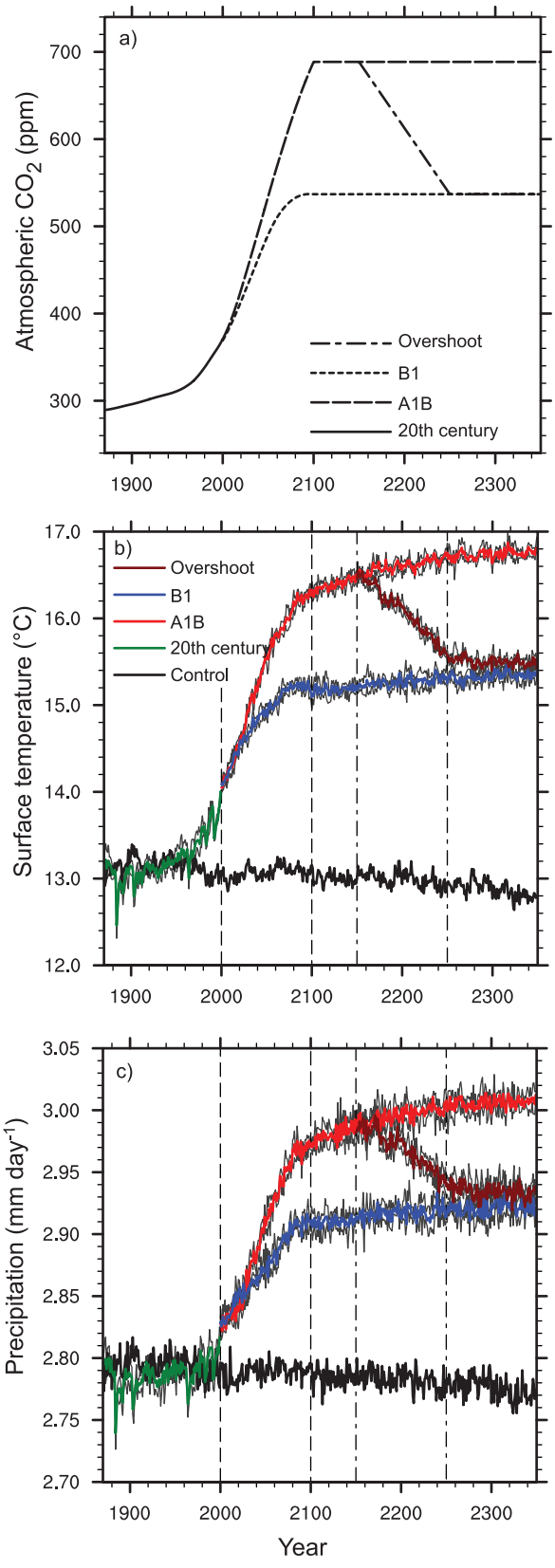


Figure 10.36. *(a) Atmospheric CO_2 concentrations for several experiments simulated with an AOGCM; (b) globally averaged surface air temperatures for the overshoot scenario and the A1B and B1 experiments; (c) same as in (b) but for globally averaged precipitation rate. Modified from Yoshida et al. (2005).*

in the system that must be overcome on the time scale of any overshoot or emissions target calculation. The probabilistic studies also show that when certain thresholds of climate change are to be avoided, emission pathways depend on the certainty requested of not exceeding the threshold.

Earth System Models of Intermediate Complexity have been used to calculate the long-term climate response to stabilisation of atmospheric CO_2, although EMICs have not been adjusted to take into account the full range of AOGCM sensitivities. The newly developed stabilisation profiles were constructed following Enting et al. (1994) and Wigley et al. (1996) using the most recent atmospheric CO_2 observations, CO_2 projections with the BERN-CC model (Joos et al., 2001) for the A1T scenario over the next few decades, and a ratio of two polynomials (Enting et al., 1994) leading to stabilisation at levels of 450, 550, 650, 750 and 1,000 ppm atmospheric CO_2 equivalent. Other forcings are not considered. Supplementary Material, Figure S10.4a shows the equilibrium surface warming for seven different EMICs and six stabilisation levels. Model differences arise mainly from the models having different climate sensitivities.

Knutti et al. (2005) explore this further with an EMIC using several published PDFs of climate sensitivity and different ocean heat uptake parametrizations and calculate probabilities of not overshooting a certain temperature threshold given an equivalent CO_2 stabilisation level (Supplementary Material, Figure S10.4b). This plot illustrates, for example, that for low values of stabilised CO_2, the range of response of possible warming is smaller than for high values of stabilised CO_2. This is because with greater CO_2 forcing, there is a greater spread of outcomes as illustrated in Figure 10.26. Figure S10.4b also shows that for any given temperature threshold, the smaller the desired probability of exceeding the target is, the lower the stabilisation level that must be chosen. Stabilisation of atmospheric greenhouse gases below about 400 ppm CO_2 equivalent is required to keep the global temperature increase likely less than 2°C above pre-industrial temperature (Knutti et al., 2005).

10.7.4 Commitment to Sea Level Rise

10.7.4.1 Thermal Expansion

The sea level rise commitment due to thermal expansion has much longer time scales than the surface warming commitment, owing to the slow processes that mix heat into the deep ocean (Church et al., 2001). If atmospheric composition were stabilised at A1B levels in 2100, thermal expansion in the 22nd century would be similar to in the 21st (see, e.g., Section 10.6.1; Meehl et al., 2005c), reaching 0.3 to 0.8 m by 2300 (Figure 10.37). The ranges of thermal expansion overlap substantially for stabilisation at different levels, since model uncertainty is dominant; A1B is given here because results are available from more models for this scenario than for other scenarios. Thermal expansion would continue over many centuries at a gradually decreasing rate (Figure 10.34). There is a wide spread among

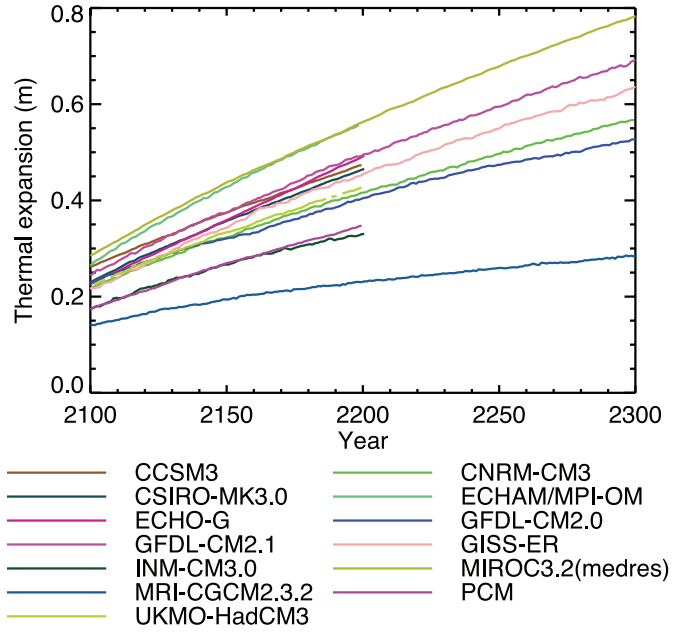


Figure 10.37. *Globally averaged sea level rise from thermal expansion relative to the period 1980 to 1999 for the A1B commitment experiment calculated from AOGCMs. See Table 8.1 for model details.*

the models for the thermal expansion commitment at constant composition due partly to climate sensitivity, and partly to differences in the parametrization of vertical mixing affecting ocean heat uptake (e.g., Weaver and Wiebe, 1999). If there is deep-water formation in the final steady state as in the present day, the ocean will eventually warm up fairly uniformly by the amount of the global average surface temperature change (Stouffer and Manabe, 2003), which would result in about 0.5 m of thermal expansion per degree celsius of warming, calculated from observed climatology; the EMICs in Figure 10.34 indicate 0.2 to 0.6 m °C^{-1} for their final steady state (year 3000) relative to 2000. If deep-water formation is weakened or suppressed, the deep ocean will warm up more (Knutti and Stocker, 2000). For instance, in the 3 × CO_2 experiment of Bi et al. (2001) with the CSIRO AOGCM, both North Atlantic Deep Water and Antarctic Bottom Water formation cease, and the steady-state thermal expansion is 4.5 m. Although these commitments to sea level rise are large compared with 21st-century changes, the eventual contributions from the ice sheets could be larger still.

10.7.4.2 Glaciers and Ice Caps

Steady-state projections for G&IC require a model that evolves their area-altitude distribution (see, e.g., Section 10.6.3.3). Little information is available on this. A comparative study including seven GCM simulations at 2 × CO_2 conditions inferred that many glaciers may disappear completely due to an increase of the equilibrium line altitude (Bradley et al., 2004), but even in a warmer climate, some glacier volume may persist at high altitude. With a geographically uniform warming relative to 1900 of 4°C maintained after 2100, about 60% of G&IC volume would vanish by 2200 and practically all by 3000 (Raper and Braithwaite, 2006). Nonetheless, this commitment to sea level rise is relatively small (<1 m; Table 4.4) compared with those from thermal expansion and ice sheets.

10.7.4.3 Greenland Ice Sheet

The present SMB of Greenland is a net accumulation estimated as 0.6 mm yr^{-1} of sea level equivalent from a compilation of studies (Church et al., 2001) and 0.47 mm yr^{-1} for 1988 to 2004 (Box et al., 2006). In a steady state, the net accumulation would be balanced by calving of icebergs. General Circulation Models suggest that ablation increases more rapidly than accumulation with temperature (van de Wal et al., 2001; Gregory and Huybrechts, 2006), so warming will tend to reduce the SMB, as has been observed in recent years (see Section 4.6.3), and is projected for the 21st century (Section 10.6.4.1). Sufficient warming will reduce the SMB to zero. This gives a threshold for the long-term viability of the ice sheet because negative SMB means that the ice sheet must contract even if ice discharge has ceased owing to retreat from the coast. If a warmer climate is maintained, the ice sheet will eventually be eliminated, except perhaps for remnant glaciers in the mountains, raising sea level by about 7 m (see Table 4.1). Huybrechts et al. (1991) evaluated the threshold as 2.7°C of seasonally and geographically uniform warming over Greenland relative to a steady state (i.e. pre-industrial temperature). Gregory et al. (2004a) examine the probability of this threshold being reached under various CO_2 stabilisation scenarios for 450 to 1000 ppm using TAR projections, and find that it was exceeded in 34 out of 35 combinations of AOGCM and CO_2 concentration considering seasonally uniform warming, and 24 out of 35 considering summer warming and using an upper bound on the threshold.

Assuming the warming to be uniform underestimates the threshold, because warming is projected by GCMs to be weaker in the ablation area and in summer, when ablation occurs. Using geographical and seasonal patterns of simulated temperature change derived from a combination of four high-resolution AGCM simulations and 18 AR4 AOGCMs raises the threshold to 3.2°C to 6.2°C in annual- and area-average warming in Greenland, and 1.9°C to 4.6°C in the global average (Gregory and Huybrechts, 2006), relative to pre-industrial temperatures. This is likely to be reached by 2100 under the SRES A1B scenario, for instance (Figure 10.29). These results are supported by evidence from the last interglacial, when the temperature in Greenland was 3°C to 5°C warmer than today and the ice sheet survived, but may have been smaller by 2 to 4 m in sea level equivalent (including contributions from arctic ice caps, see Section 6.4.3). However, a lower threshold of 1°C (Hansen, 2005) in global warming above present-day temperatures has also been suggested, on the basis that global mean (rather than Greenland) temperatures during previous interglacials exceeded today's temperatures by no more than that.

For stabilisation in 2100 with SRES A1B atmospheric composition, Greenland would initially contribute 0.3 to

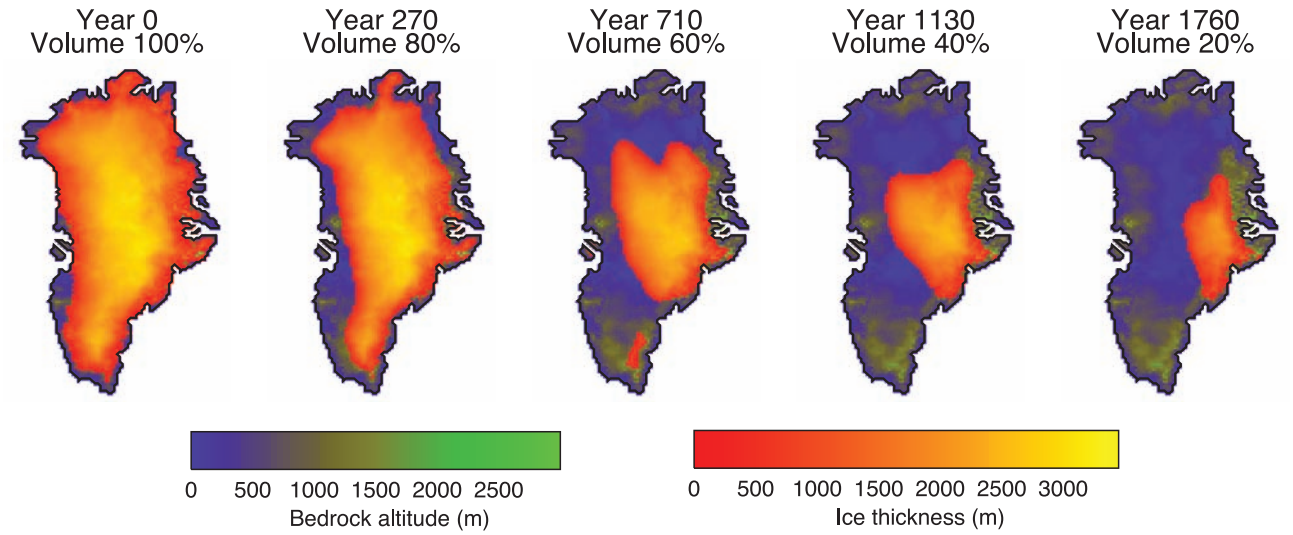


Figure 10.38. *Evolution of Greenland surface elevation and ice sheet volume versus time in the experiment of Ridley et al. (2005) with the UKMO-HadCM3 AOGCM coupled to the Greenland Ice Sheet model of Huybrechts and De Wolde (1999) under a climate of constant quadrupled pre-industrial atmospheric CO_2.*

2.1 mm yr^{-1} to sea level (Table 10.7). The greater the warming, the faster the loss of mass. Ablation would be further enhanced by the lowering of the surface, which is not included in the calculations in Table 10.7. To include this and other climate feedbacks in calculating long-term rates of sea level rise requires coupling an ice sheet model to a climate model. Ridley et al. (2005) couple the Greenland Ice Sheet model of Huybrechts and De Wolde (1999) to the UKMO-HadCM3 AOGCM. Under constant $4 \times CO_2$, the sea level contribution is 5.5 mm yr^{-1} over the first 300 years and declines as the ice sheet contracts; after 1 kyr only about 40% of the original volume remains and after 3 kyr only 4% (Figure 10.38). The rate of deglaciation would increase if ice flow accelerated, as in recent years (Section 4.6.3.3). Basal lubrication due to surface melt water might cause such an effect (see Section 10.6.4.2). The best estimate of Parizek and Alley (2004) is that this could add an extra 0.15 to 0.40 m to sea level by 2500, compared with 0.4 to 3.2 m calculated by Huybrechts and De Wolde (1999) without this effect. The processes whereby melt water might penetrate through subfreezing ice to the bed are unclear and only conceptual models exist at present (Alley et al., 2005b).

Under pre-industrial or present-day atmospheric CO_2 concentrations, the climate of Greenland would be much warmer without the ice sheet, because of lower surface altitude and albedo, so it is possible that Greenland deglaciation and the resulting sea level rise would be irreversible. Toniazzo et al. (2004) find that snow does not accumulate anywhere on an ice-free Greenland with pre-industrial atmospheric CO_2, whereas Lunt et al. (2004) obtain a substantial regenerated ice sheet in east and central Greenland using a higher-resolution model.

10.7.4.4 Antarctic Ice Sheet

With rising global temperature, GCMs indicate increasingly positive SMB for the Antarctic Ice Sheet as a whole because of greater accumulation (Section 10.6.4.1). For stabilisation in 2100 with SRES A1B atmospheric composition, antarctic SMB would contribute 0.4 to 2.0 mm yr^{-1} of sea level fall (Table 10.7). Continental ice sheet models indicate that this would be offset by tens of percent by increased ice discharge (Section 10.6.4.2), but still give a negative contribution to sea level, of –0.8 m by 3000 in one simulation with antarctic warming of about 4.5°C (Huybrechts and De Wolde, 1999).

However, discharge could increase substantially if buttressing due to the major West Antarctic ice shelves were reduced (see Sections 4.6.3.3 and 10.6.4.2), and could outweigh the accumulation increase, leading to a net positive antarctic sea level contribution in the long term. If the Amundsen Sea sector were eventually deglaciated, it would add about 1.5 m to sea level, while the entire West Antarctic Ice Sheet (WAIS) would account for about 5 m (Vaughan, 2007). Contributions could also come in this manner from the limited marine-based portions of East Antarctica that discharge into large ice shelves.

Weakening or collapse of the ice shelves could be caused either by surface melting or by thinning due to basal melting. In equilibrium experiments with mixed-layer ocean models, the ratio of antarctic to global annual warming is 1.4 ± 0.3. Following reasoning in Section 10.6.4.2 and Appendix 10.A, it appears that mean summer temperatures over the major West Antarctic ice shelves are about as likely as not to pass the melting point if global warming exceeds 5°C, and disintegration might be initiated earlier by surface melting. Observational and modelling studies indicate that basal melt rates depend on water temperature near to the base, with a constant of proportionality of about 10 m yr^{-1} $°C^{-1}$ indicated for the Amundsen Sea ice shelves (Rignot and Jacobs, 2002; Shepherd et al., 2004) and 0.5 to 10 m yr^{-1} $°C^{-1}$ for the Amery ice shelf (Williams et al., 2002). If this order of magnitude applies to future changes, a warming of about 1°C under the major ice shelves would eliminate them within centuries. We are not able to relate this

quantitatively to global warming with any confidence, because the issue has so far received little attention, and current models may be inadequate to treat it because of limited resolution and poorly understood processes. Nonetheless, it is reasonable to suppose that sustained global warming would eventually lead to warming in the seawater circulating beneath the ice shelves.

Because the available models do not include all relevant processes, there is much uncertainty and no consensus about what dynamical changes could occur in the Antarctic Ice Sheet (see, e.g., Vaughan and Spouge, 2002; Alley et al., 2005a). One line of argument is to consider an analogy with palaeoclimate (see Box 4.1). Palaeoclimatic evidence that sea level was 4 to 6 m above present during the last interglacial may not all be explained by reduction in the Greenland Ice Sheet, implying a contribution from the Antarctic Ice Sheet (see Section 6.4.3). On this basis, using the limited available evidence, sustained global warming of 2°C (Oppenheimer and Alley, 2005) above present-day temperatures has been suggested as a threshold beyond which there will be a commitment to a large sea level contribution from the WAIS. The maximum rates of sea level rise during previous glacial terminations were of the order of 10 mm yr^{-1} (Church et al., 2001). We can be confident that future accelerated discharge from WAIS will not exceed this size, which is roughly an order of magnitude increase in present-day WAIS discharge, since no observed recent acceleration has exceeded a factor of ten.

Another line of argument is that there is insufficient evidence that rates of dynamical discharge of this magnitude could be sustained over long periods. The WAIS is 20 times smaller than the LGM NH ice sheets that contributed most of the melt water during the last deglaciation at rates that can be explained by surface melting alone (Zweck and Huybrechts, 2005). In the study of Huybrechts and De Wolde (1999), the largest simulated rate of sea level rise from the Antarctic Ice Sheet over the next 1 kyr is 2.5 mm yr^{-1}. This is dominated by dynamical discharge associated with grounding line retreat. The model did not simulate ice streams, for which widespread acceleration would give larger rates. However, the maximum loss of ice possible from rapid discharge of existing ice streams is the volume in excess of flotation in the regions occupied by these ice streams (defined as regions of flow exceeding 100 m yr^{-1}; see Section 10.6.4.2). This volume (in both West and East Antarctica) is 230,000 km^3, equivalent to about 0.6 m of sea level, or about 1% of the mass of the Antarctic Ice Sheet, most of which does not flow in ice streams. Loss of ice affecting larger portions of the ice sheet could be sustained at rapid rates only if new ice streams developed in currently slow-moving ice. The possible extent and rate of such changes cannot presently be estimated, since there is only very limited understanding of controls on the development and variability of ice streams. In this argument, rapid discharge may be transient and the long-term sign of the antarctic contribution to sea level depends on whether increased accumulation is more important than large-scale retreat of the grounding line.

References

Abdalati, W., et al., 2001: Outlet glacier and margin elevation changes: Near-coastal thinning of the Greenland ice sheet. *J. Geophys. Res.*, **106**, 33729–33741.

ACIA, 2004: *Arctic Climate Impact Assessment (ACIA): Impacts of a Warming Arctic*. Cambridge University Press, New York, NY, 140 pp.

Adams, P.J., et al., 2001: General circulation model assessment of direct radiative forcing by the sulfate-nitrate-ammonium-water inorganic aerosol system. *J. Geophys. Res.*, **106**, 1097–1111.

Allen, M.R., 1999: Do-it-yourself climate prediction. *Nature*, **401**, 627.

Allen, M.R., and W.J. Ingram, 2002: Constraints on future changes in climate and the hydrologic cycle. *Nature*, **419**, 224–232.

Allen, M.R., and D.A. Stainforth, 2002: Towards objective probabilistic climate forecasting. *Nature*, **419**, 228.

Allen, M.R., D.J. Frame, J.A. Kettleborough, and D.A. Stainforth, 2006a: Model error in weather and climate forecasting. In: *Predictability of Weather and Climate* [Palmer, T., and R. Hagedorn (eds.)]. Cambridge University Press, New York, NY, pp. 391–427.

Allen, M.R., et al., 2000: Quantifying the uncertainty in forecasts of anthropogenic climate change. *Nature*, **407**, 617–620.

Allen, M.R., et al., 2006b: Observational constraints on climate sensitivity. In: *Avoiding Dangerous Climate Change* [Schellnhuber, H.J., et al. (eds.)]. Cambridge University Press, New York, NY, pp. 281–289.

Alley, R.B., P.U. Clark, P. Huybrechts, and I. Joughin, 2005a: Ice-sheet and sea-level changes. *Science*, **310**, 456–460.

Alley, R.B., T.K. Dupont, B.R. Parizek, and S. Anandakrishnan, 2005b: Access of surface meltwater to beds of sub-freezing glaciers: Preliminary insights. *Ann. Glaciol.*, **40**, 8–14.

Alley, R.B., et al., 2002: *Abrupt Climate Change: Inevitable Surprises*. US National Research Council Report, National Academy Press, Washington, DC, 230 pp.

Amann, M., et al., 2004: *The RAINS Model. Documentation of the Model Approach Prepared for the RAINS Peer Review 2004*. International Institute for Applied Systems Analysis, Laxenburg, Austria, 156 pp.

Ammann, C.M., G.A. Meehl, W.M. Washington, and C.S. Zender, 2003: A monthly and latitudinally varying volcanic forcing dataset in simulations of 20th century climate. *Geophys. Res. Lett.*, **30**, 1657.

Andronova, N.G., and M.E. Schlesinger, 2001: Objective estimation of the probability density function for climate sensitivity. *J. Geophys. Res.*, **106**, 22605–22612.

Annan, J.D., and J.C. Hargreaves, 2006: Using multiple observationally-based constraints to estimate climate sensitivity. *Geophys. Res. Lett.*, **33**, L06704, doi:10.1029/2005GL025259.

Annan, J.D., J.C. Hargreaves, N.R. Edwards, and R. Marsh, 2005a: Parameter estimation in an intermediate complexity earth system model using an ensemble Kalman filter. *Ocean Modelling*, **8**, 135–154.

Annan, J.D., et al., 2005b: Efficiently constraining climate sensitivity with ensembles of paleoclimate simulations. *Scientific Online Letters on the Atmosphere*, **1**, 181–184.

Arblaster, J.M., and G.A. Meehl, 2006: Contributions of external forcings to Southern Annular Mode trends. *J. Clim.*, **19**, 2896–2905.

Arora, V.K., and G.J. Boer, 2001: Effects of simulated climate change on the hydrology of major river basins. *J. Geophys. Res.*, **106**, 3335–3348.

Arzel, O., T. Fichefet, and H. Goosse, 2006: Sea ice evolution over the 20th and 21st centuries as simulated by current AOGCMs. *Ocean Modelling*, **12**, 401–415.

Ashrit, R.G., K. Rupa Kumar, and K. Krishna Kumar, 2001: ENSO-monsoon relationships in a greenhouse warming scenario. *Geophys. Res. Lett.*, **28**, 1727–1730.

Ashrit, R.G., H. Douville, and K. Rupa Kumar, 2003: Response of the Indian monsoon and ENSO-monsoon teleconnection to enhanced greenhouse effect in the CNRM coupled model. *J. Meteorol. Soc. Japan*, **81**, 779–803.

Ashrit, R.G., A. Kitoh, and S. Yukimoto, 2005: Transient response of ENSO-monsoon teleconnection in MRI.CGCM2 climate change simulations. *J. Meteorol. Soc. Japan*, **83**, 273–291.

Austin, J., and N. Butchart, 2003: Coupled chemistry-climate model simulations for the period 1980 to 2020: Ozone depletion and the start of ozone recovery. *Q. J. R. Meteorol. Soc.*, **129**, 3225–3249.

Bahr, D.B., M.F. Meier, and S.D. Peckham, 1997: The physical basis of glacier volume-area scaling. *J. Geophys. Res.*, **102**, 20355–20362.

Banks, H., R.A. Wood, and J.M. Gregory, 2002: Changes to Indian Ocean subantarctic mode water in a coupled climate model as CO_2 forcing increases. *J. Phys. Oceanogr.*, **32**, 2816–2827.

Barnett, D.N., et al., 2006: Quantifying uncertainty in changes in extreme event frequency in response to doubled CO_2 using a large ensemble of GCM simulations. *Clim. Dyn.*, **26**, 489–511.

Bengtsson, L., K.I. Hodges, and E. Roeckner, 2006: Storm tracks and climate change. *J. Clim.*, **19**, 3518–3543.

Beniston, M., 2004: The 2003 heat wave in Europe: A shape of things to come? An analysis based on Swiss climatological data and model simulations. *Geophys. Res. Lett.*, **31**, L02202.

Berger, A., and M.F. Loutre, 2002: An exceptionally long interglacial ahead? *Science*, **297**, 1287–1288.

Berthelot, M., et al., 2002: Global response of the terrestrial biosphere to CO_2 and climate change using a coupled climate-carbon cycle model. *Global Biogeochem. Cycles*, **16**, 1084.

Bertrand, C., J.P. Van Ypersele, and A. Berger, 2002: Are natural climate forcings able to counteract the projected global warming. *Clim. Change*, **55**, 413–427.

Bi, D.H., W.F. Budd, A.C. Hirst, and X.R. Wu, 2001: Collapse and reorganisation of the Southern Ocean overturning under global warming in a coupled model. *Geophys. Res. Lett.*, **28**, 3927–3930.

Bindschadler, R., 1998: Future of the West Antarctic ice sheet. *Science*, **282**, 428–429.

Bitz, C.M., and G.H. Roe, 2004: A mechanism for the high rate of sea-ice thinning in the Arctic Ocean. *J. Clim.*, **18**, 3622–3631.

Bitz, C.M., et al., 2006: The influence of sea ice on ocean heat uptake in response to increasing CO_2. *J. Clim.*, **19**, 2437–2450.

Boer, G.J., and B. Yu, 2003a: Climate sensitivity and response. *Clim. Dyn.*, **20**, 415–429.

Boer, G.J., and B. Yu, 2003b: Dynamical aspects of climate sensitivity. *Geophys. Res. Lett.*, **30**, 1135.

Bond, T.C., et al., 2004: A technology-based global inventory of black and organic carbon emissions from combustion. *J. Geophys. Res.*, **109**, D14203, doi:10.1029/2003JD003697.

Bönisch, G., et al., 1997: Long-term trends of temperature, salinity, density, and transient tracers in the central Greenland Sea. *J. Geophys. Res.*, **102**, 18553–18571.

Bony, S., and J.-L. Dufresne, 2005: Marine boundary layer clouds at the heart of cloud feedback uncertainties in climate models. *Geophys. Res. Lett.*, **32**, L20806, doi:10.1029/2005GL023851.

Bony, S., et al., 2004: On dynamic and thermodynamic components of cloud changes. *Clim. Dyn.*, **22**, 71–86.

Bony, S., et al., 2006: How well do we understand and evaluate climate change feedback processes? *J. Clim.*, **19**, 3445–3482.

Bosilovich, M.G., S.D. Schubert, and G.K. Walker, 2005: Global changes of the water cycle intensity. *J. Clim.*, **18**, 1591–1608.

Boucher, O., and M. Pham, 2002: History of sulfate aerosol radiative forcings. *Geophys. Res. Lett.*, **29**, L1308, doi:10.1029/2001GL014048.

Box, J.E., et al., 2006: Greenland ice sheet surface mass balance variability (1988-2004) from calibrated Polar MM5 output. *J. Clim.*, **19**, 2783–2800.

Brabson, B.B., D.H. Lister, P.D. Jones, and J.P. Palutikof, 2005: Soil moisture and predicted spells of extreme temperatures in Britain. *J. Geophys. Res.*, **110**, D05104, doi:10.1029/2004JD005156.

Bradley, R.S., F.T. Keimig, and H.F. Diaz, 2004: Projected temperature changes along the American cordillera and the planned GCOS network. *Geophys. Res. Lett.*, **31**, L16210, doi:10.1029/2004GL020229.

Braithwaite, R.J., and S.C.B. Raper, 2002: Glaciers and their contribution to sea level change. *Phys. Chem. Earth*, **27**, 1445–1454.

Braithwaite, R.J., Y. Zhang, and S.C.B. Raper, 2003: Temperature sensitivity of the mass balance of mountain glaciers and ice caps as a climatological characteristic. *Z. Gletscherk. Glazialgeol.*, **38**, 35–61.

Brandefelt, J., and E. Källén, 2004: The response of the Southern Hemisphere atmospheric circulation to an enhanced greenhouse gas forcing. *J. Clim.*, **17**, 4425–4442.

Breshears, D.D., et al., 2005: Regional vegetation die-off in response to global-change-type drought. *Proc. Natl. Acad. Sci. U.S.A.*, **102**, 15144–15148.

Bryan, F.O., et al., 2006: Response of the North Atlantic thermohaline circulation and ventilation to increasing carbon dioxide in CCSM3. *J. Clim.*, **19**, 2382–2397.

Bugnion, V., and P.H. Stone, 2002: Snowpack model estimates of the mass balance of the Greenland ice sheet and its changes over the twenty-first century. *Clim. Dyn.*, **20**, 87–106.

Buizza, R., M. Miller, and T.N. Palmer, 1999: Stochastic representation of model uncertainties in the ECMWF ensemble prediction system. *Q. J. R. Meteorol. Soc.*, **125**, 2887–2908.

Burke, E.J., S.J. Brown, and N. Christidis, 2006: Modelling the recent evolution of global drought and projections for the twenty-first century with the Hadley Centre climate model. *J. Hydrometeorol.*, **7**, 1113–1125.

Caires, S., V.R. Swail, and X.L. Wang, 2006: Projection and analysis of extreme wave climate. *J. Clim.*, **19**, 5581–5605.

Camberlin, P., F. Chauvin, H. Douville, and Y. Zhao, 2004: Simulated ENSO-tropical rainfall teleconnections in present-day and under enhanced greenhouse gases conditions. *Clim. Dyn.*, **23**, 641–657.

Cassano, J.J., P. Uotila, and A. Lynch, 2006: Changes in synoptic weather patterns in the polar regions in the twentieth and twenty-first centuries, Part 1: Arctic. *Int. J. Climatol.*, **26**, 1027–1049.

Chan, W.L., and T. Motoi, 2005: Response of thermohaline circulation and thermal structure to removal of ice sheets and high atmospheric CO_2 concentration. *Geophys. Res. Lett.*, **32**, L07601, doi:10.1029/2004GL021951.

Charney, J.G., 1979: *Carbon Dioxide and Climate: A Scientific Assessment.* National Academy of Science, Washington, DC, 22 pp.

Chauvin, F., J.-F. Royer, and M. Déqué, 2006: Response of hurricane-type vortices to global warming as simulated by ARPEGE-Climat at high resolution. *Clim. Dyn.*, **27**, 377–399.

Christensen, J.H., and O.B. Christensen, 2003: Severe summertime flooding in Europe. *Nature*, **421**, 805–806.

Christensen, O.B., and J.H. Christensen, 2004: Intensification of extreme European summer precipitation in a warmer climate. *Global Planet. Change*, **44**, 107–117.

Christiansen, B., 2003: Evidence for nonlinear climate change: Two stratospheric regimes and a regime shift. *J. Clim.*, **16**, 3681–3690.

Chung, C.E., V. Ramanathan, and J.T. Kiehl, 2002: Effects of the South Asian absorbing haze on the northeast monsoon and surface-air heat exchange. *J. Clim.*, **15**, 2462–2476.

Chung, S.H., and J.H. Seinfeld, 2002: Global distribution and climate forcing of carbonaceous aerosols. *J. Geophys. Res.*, **107**, 4407.

Church, J.A., et al., 2001: Changes in sea level. In: *Climate Change 2001: The Scientific Basis. Contribution of Working Group I to the Third Assessment Report of the Intergovernmental Panel on Climate Change* [Houghton, J.T., et al. (eds.)]. Cambridge University Press, Cambridge, United Kingdom and New York, NY, USA, pp. 639–693.

Chylek, P., and U. Lohmann, 2005: Ratio of the Greenland to global temperature change: Comparison of observations and climate modeling results. *Geophys. Res. Lett.*, **32**, L14705, doi:10.1029/2005GL023552.

Clark, R., S. Brown, and J. Murphy, 2006: Modelling northern hemisphere summer heat extreme changes and their uncertainties using a physics ensemble of climate sensitivity experiments. *J. Clim.*, **19**, 4418–4435.

Claussen, M., et al., 1999: Simulation of an abrupt change in Saharan vegetation in the mid-Holocene. *Geophys. Res. Lett.*, **26**, 2037–2040.

Claussen, M., et al., 2002: Earth system models of intermediate complexity: closing the gap in the spectrum of climate system models. *Clim. Dyn.*, **18**, 579–586.

Collins, M., and The CMIP Modelling Groups, 2005: El Niño- or La Niña-like climate change? *Clim. Dyn.*, **24**, 89–104.

Collins, M., et al., 2006: Towards quantifying uncertainty in transient climate change. *Clim. Dyn.*, **27**, 127–147.

Collins, W.D., et al., 2006: Radiative forcing by well-mixed greenhouse gases: Estimates from climate models in the Intergovernmental Panel on Climate Change (IPCC) Fourth Assessment Report (AR4). *J. Geophys. Res.*, **111**, D14317, doi:10.1029/2005JD006713.

Collins, W.J., et al., 2003: Effect of stratosphere-troposphere exchange on the future tropospheric ozone trend. *J. Geophys. Res.*, **108**, 8528.

Comiso, J.C., 2000: Variability and trends in Antarctic surface temperatures from in situ and satellite infrared measurements. *J. Clim.*, **13**, 1675–1696.

Cook, K.H., and E.K. Vizy, 2006: Coupled model simulations of the West African Monsoon system: Twentieth- and twenty-first-century simulations. *J. Clim.*, **19**, 3681–3703.

Cooke, W.F., and J.J.N. Wilson, 1996: A global black carbon aerosol model. *J. Geophys. Res.*, **101**, 19395–19409.

Covey, C., et al., 2003: An overview of results from the Coupled Model Intercomparison Project. *Global Planet. Change*, **37**, 103–133.

Cox, P.M., et al., 2000: Acceleration of global warming due to carbon-cycle feedbacks in a coupled climate model. *Nature*, **408**, 184–187.

Cox, P.M., et al., 2004: Amazonian forest dieback under climate-carbon cycle projections for the 21st century. *Theor. Appl. Climatol.*, **78**, 137–156.

Cramer, W., et al., 2001: Global response of terrestrial ecosystem structure and function to CO_2 and climate change: results from six dynamic global vegetation models. *Global Change Biol.*, **7**, 357–373.

Crucifix, M., and M.F. Loutre, 2002: Transient simulations over the last interglacial period (126-115 kyr BP): feedback and forcing analysis. *Clim. Dyn.*, **19**, 417–433.

Cubasch, U., et al., 2001: Projections of future climate change. In: *Climate Change 2001: The Scientific Basis. Contribution of Working Group I to the Third Assessment Report of the Intergovernmental Panel on Climate Change* [Houghton, J.T., et al. (eds.)]. Cambridge University Press, Cambridge, United Kingdom and New York, NY, USA, pp. 525–582.

Dai, A.G., and K.E. Trenberth, 2004: The diurnal cycle and its depiction in the Community Climate System Model. *J. Clim.*, **17**, 930–951.

Dai, A.G., T.M.L. Wigley, G.A. Meehl, and W.M. Washington, 2001a: Effects of stabilizing atmospheric CO_2 on global climate in the next two centuries. *Geophys. Res. Lett.*, **28**, 4511–4514.

Dai, A., et al., 2001b: Climates of the twentieth and twenty-first centuries simulated by the NCAR Climate System Model. *J. Clim.*, **14**, 485–519.

Dai, A., et al., 2005: Atlantic thermohaline circulation in a coupled general circulation model: Unforced variations versus forced changes. *J. Clim.*, **18**, 3270–3293.

de Woul, M., and R. Hock, 2006: Static mass balance sensitivity of Arctic glaciers and ice caps using a degree-day approach. *Ann. Glaciol.*, **42**, 217–224.

DeFries, R.S., L. Bouboua, and G.J. Collatz, 2002: Human modification of the landscape and surface climate in the next fifty years. *Global Change Biol.*, **8**, 438–458.

DeFries, R.S., J.A. Foley, and G.P. Asner, 2004: Land-use choices: balancing human needs and ecosystem function. *Frontiers Ecol. Environ.*, **2**, 249–257.

Delworth, T.L., and K.W. Dixon, 2000: Implications of the recent trend in the Arctic/North Atlantic Oscillation for the North Atlantic thermohaline circulation. *J. Clim.*, **13**, 3721–3727.

Dentener, F., et al., 2005: The impact of air pollutant and methane emission controls on tropospheric ozone and radiative forcing: CTM calculations for the period 1990-2030. *Atmos. Chem. Phys.*, **5**, 1731–1755.

Dentener, F., et al., 2006: The global atmospheric environment for the next generation. *Environ. Sci. Technol.*, **40**, 3586–3594.

Déqué, M., C. Dreveton, A. Braun, and D. Cariolle, 1994: The ARPEGE/IFS atmosphere model: a contribution to the French community climate modelling. *Clim. Dyn.*, **10**, 249–266.

Dickson, B., et al., 2002: Rapid freshening of the deep North Atlantic Ocean over the past four decades. *Nature*, **416**, 832–837.

Dixon, K.W., T.L. Delworth, M.J. Spelman, and R.J. Stouffer, 1999: The influence of transient surface fluxes on North Atlantic overturning in a coupled GCM climate change experiment. *Geophys. Res. Lett.*, **26**, 2749–2752.

Doney, S.C., et al., 2004: Evaluating global ocean carbon models: The importance of realistic physics. *Global Biogeochem. Cycles*, **18**, GB3017, doi:10.1029/2003GB002150.

Dorn, W., K. Dethloff, A. Rinke, and E. Roeckner, 2003: Competition of NAO regime changes and increasing greenhouse gases and aerosols with respect to Arctic climate projections. *Clim. Dyn.*, **21**, 447–458.

Douville, H., D. Salas-Mélia, and S. Tyteca, 2005: On the tropical origin of uncertainties in the global land precipitation response to global warming. *Clim. Dyn.*, **26**, 367–385.

Douville, H., et al., 2000: Impact of CO_2 doubling on the Asian summer monsoon: Robust versus model-dependent responses. *J. Meteorol. Soc. Japan*, **78**, 421–439.

Douville, H., et al., 2002: Sensitivity of the hydrological cycle to increasing amounts of greenhouse gases and aerosols. *Clim. Dyn.*, **20**, 45–68.

Dufresne, J.L., et al., 2002: On the magnitude of positive feedback between future climate change and the carbon cycle. *Geophys. Res. Lett.*, **29**, 1405.

Dufresne, J.L., et al., 2005: Contrasts in the effects on climate of anthropogenic sulfate aerosols between the 20th and the 21st century. *Geophys. Res. Lett.*, **32**, L21703, doi:10.1029/2005GL023619.

Dupont, T.K., and R.B. Alley, 2005: Assessment of the importance of ice-shelf buttressing to ice-sheet flow. *Geophys. Res. Lett.*, **32**, L04503, doi:10.1029/2004GL022024.

Dyurgerov, M.B., and M.F. Meier, 2000: Twentieth century climate change: evidence from small glaciers. *Proc. Natl. Acad. Sci. U.S.A.*, **97**, 1406–1411.

Echelmeyer, K., and W.D. Harrison, 1990: Jakobshavn Isbræ, West Greenland: Seasonal variations in velocity - or lack thereof. *J. Glaciol.*, **36**, 82–88.

Edwards, N., and R. Marsh, 2005: Uncertainties due to transport-parameter sensitivity in an efficient 3-D ocean-climate model. *Clim. Dyn.*, **24**, 415–433.

Eichelberger, S.J., and J.R. Holton, 2002: A mechanistic model of the northern annular mode. *J. Geophys. Res.*, **107**, 4388.

Emori, S., and S.J. Brown, 2005: Dynamic and thermodynamic changes in mean and extreme precipitation under changed climate. *Geophys. Res. Lett.*, **32**, L17706, doi:10.1029/2005GL023272.

Emori, S., et al., 1999: Coupled ocean-atmosphere model experiments of future climate with an explicit representation of sulphate aerosol scattering. *J. Meteorol. Soc. Japan*, **77**, 1299–1307.

Enting, I.G., T.M.L. Wigley, and M. Heimann, 1994: *Future Emissions and Concentrations of Carbon Dioxide: Key Ocean/ Atmosphere/ Land Analyses.* Technical Report 31, Commonwealth Scientific and Industrial Research Organisation, Div. of Atmospheric Research, Melbourne, Australia.

Feddema, J.J., et al., 2005: The importance of land-cover change in simulating future climates. *Science*, **310**, 1674–1678.

Fedorov, A.V., and S.G. Philander, 2001: A stability analysis of tropical ocean-atmosphere interactions: Bridging measurements and theory for El Niño. *J. Clim.*, **14**, 3086–3101.

Feely, R.A., et al., 2004: Impact of anthropogenic CO_2 on the $CaCO_3$ system in the oceans. *Science*, **305**, 362–366.

Fichefet, T., et al., 2003: Implications of changes in freshwater flux from the Greenland ice sheet for the climate of the 21st century. *Geophys. Res. Lett.*, **30**, 1911.

Fischer-Bruns, I., H. Von Storch, J.F. Gonzalez-Rouco, and E. Zorita, 2005: Modelling the variability of midlatitude storm activity on decadal to century time scales. *Clim. Dyn.*, **25**, 461–476.

Flato, G.M., and Participating CMIP Modeling Groups, 2004: Sea-ice and its response to CO_2 forcing as simulated by global climate change studies. *Clim. Dyn.*, **23**, 220–241.

Folland, C.K., et al., 2001: Global temperature change and its uncertainties since 1861. *Geophys. Res. Lett.*, **28**, 2621–2624.

Forest, C.E., P.H. Stone, and A.P. Sokolov, 2006: Estimated PDFs of climate system properties including natural and anthropogenic forcings. *Geophys. Res. Lett.*, **33**, L01705, doi:10.1029/2005GL023977.

Forest, C.E., et al., 2002: Quantifying uncertainties in climate system properties with the use of recent climate observations. *Science*, **295**, 113–117.

Forster, P.M.D., and K.P. Shine, 2002: Assessing the climate impact of trends in stratospheric water vapor. *Geophys. Res. Lett.*, **29**, 1086.

Forster, P.M.D., and J.M. Gregory, 2006: The climate sensitivity and its components diagnosed from Earth radiation budget data. *J. Clim.*, **19**, 39–52.

Forster, P.M.D., and K.E. Taylor, 2006: Climate forcings and climate sensitivities diagnosed from coupled climate model integrations. *J. Clim.*, **19**, 6181–6194.

Frame, D.J., et al., 2005: Constraining climate forecasts: The role of prior assumptions. *Geophys. Res. Lett.*, **32**, L09702, doi:10.1029/2004GL022241.

Frei, C., C. Schär, D. Lüthi, and H.C. Davies, 1998: Heavy precipitation processes in a warmer climate. *Geophys. Res. Lett.*, **25**, 1431–1434.

Frich, P., et al., 2002: Observed coherent changes in climatic extremes during the second half of the twentieth century. *Clim. Res.*, **19**, 193–212.

Friedlingstein, P., and S. Solomon, 2005: Contributions of past and present human generations to committed warming caused by carbon dioxide. *Proc. Natl. Acad. Sci. U.S.A.*, **102**, 10832–10836.

Friedlingstein, P., et al., 2006: Climate-carbon cycle feedback analysis: Results from the C^4MIP model intercomparison. *J. Clim.*, **19**, 3337–3353.

Furrer, R., S.R. Sain, D. Nychka, and G.A. Meehl, 2007: Multivariate Bayesian analysis of atmosphere-ocean general circulation models. *Environ. Ecol. Stat.*, in press.

Fyfe, J.C., 2003: Extratropical southern hemisphere cyclones: Harbingers of climate change? *J. Clim.*, **16**, 2802–2805.

Fyfe, J.C., and O.A. Saenko, 2005: Human-induced change in the Antarctic Circumpolar Current. *J. Clim.*, **18**, 3068–3073.

Fyfe, J.C., and O.A. Saenko, 2006: Simulated changes in the extratropical Southern Hemisphere winds and currents. *Geophys. Res. Lett.*, **33**, L06701, doi:10.1029/2005GL025332.

Fyfe, J.C., G.J. Boer, and G.M. Flato, 1999: The Arctic and Antarctic oscillations and their projected changes under global warming. *Geophys. Res. Lett.*, **26**, 1601–1604.

Ganachaud, A., 2003: Large-scale mass transports, water mass formation, and diffusivities estimated from World Ocean Circulation Experiment (WOCE) hydrographic data. *J. Geophys. Res.*, **108**, 3213.

Gao, X., and P.A. Dirmeyer, 2006: A multimodel analysis, validation and transferability study of global soil wetness products. *J. Hydrometeorol.*, **7**, 1218–1236.

Gauss, M., et al., 2003: Radiative forcing in the 21st century due to ozone changes in the troposphere and the lower stratosphere. *J. Geophys. Res.*, **108**, 4292.

Gedney, N., P.M. Cox, and C. Huntingford, 2004: Climate feedback from wetland methane emissions. *Geophys. Res. Lett.*, **31**, L20503, doi:10.1029/2004GL020919.

Geng, Q.Z., and M. Sugi, 2003: Possible change of extratropical cyclone activity due to enhanced greenhouse gases and sulfate aerosols - Study with a high-resolution AGCM. *J. Clim.*, **16**, 2262–2274.

Gibelin, A.-L., and M. Déqué, 2003: Anthropogenic climate change over the Mediterranean region simulated by a global variable resolution model. *Clim. Dyn.*, **20**, 327–339.

Gillett, N.P., and D.W.J. Thompson, 2003: Simulation of recent Southern Hemisphere climate change. *Science*, **302**, 273–275.

Gillett, N.P., M.R. Allen, and K.D. Williams, 2003: Modeling the atmospheric response to doubled CO_2 and depleted stratospheric ozone using a stratosphere-resolving coupled GCM. *Q. J. R. Meteorol. Soc.*, **129**, 947–966.

Gillett, N.P., et al., 2002: How linear is the Arctic Oscillation response to greenhouse gases? *J. Geophys. Res.*, **107**, 4022.

Giorgi, F., and L.O. Mearns, 2002: Calculation of average, uncertainty range and reliability of regional climate changes from AOGCM simulations via the reliability ensemble averaging (REA) method. *J. Clim.*, **15**, 1141–1158.

Giorgi, F., and L.O. Mearns, 2003: Probability of regional climate change based on the Reliability Ensemble Averaging (REA) method. *Geophys. Res. Lett.*, **30**, 1629.

Giorgi, F., and X. Bi, 2005: Regional changes in surface climate interannual variability for the 21st century from ensembles of global model simulations. *Geophys. Res. Lett.*, **32**, L13701, doi:10.1029/2005GL023002.

Giorgi, F., et al., 2001: Emerging patterns of simulated regional climatic changes for the 21st century due to anthropogenic forcings. *Geophys. Res. Lett.*, **28**, 3317–3320.

Glover, R.W., 1999: Influence of spatial resolution and treatment of orography on GCM estimates of the surface mass balance of the Greenland ice sheet. *J. Clim.*, **12**, 551–563.

Goldstein, M., and J.C. Rougier, 2004: Probabilistic formulations for transferring inferences from mathematical models to physical systems. *SIAM J. Sci. Computing*, **26**, 467–487.

Goosse, H., et al., 2002: Potential causes of abrupt climate events: A numerical study with a three-dimensional climate model. *Geophys. Res. Lett.*, **29**, 1860.

Gordon, H.B., and S.P. O'Farrell, 1997: Transient climate change in the CSIRO coupled model with dynamic sea ice. *Mon. Weather Rev.*, **125**, 875–907.

Greene, A.M., L. Goddard, and U. Lall, 2006: Probabilistic multimodel regional temperature change projections. *J. Clim.*, **19**, 4326–4346.

Gregory, J.M., 2000: Vertical heat transports in the ocean and their effect on time-dependent climate change. *Clim. Dyn.*, **16**, 501–515.

Gregory, J.M., and J. Oerlemans, 1998: Simulated future sea-level rise due to glacier melt based on regionally and seasonally resolved temperature changes. *Nature*, **391**, 474–476.

Gregory, J.M., and P. Huybrechts, 2006: Ice-sheet contributions to future sea-level change. *Philos. Trans. R. Soc. London Ser. A*, **364**, 1709–1731.

Gregory, J.M., P. Huybrechts, and S.C.B. Raper, 2004a: Threatened loss of the Greenland ice-sheet. *Nature*, **428**, 616.

Gregory, J.M., J.A. Lowe, and S.F.B. Tett, 2006: Simulated global-mean sea-level changes over the last half-millennium. *J. Clim.*, **19**, 4576–4591.

Gregory, J.M., et al., 2001: Comparison of results from several AOGCMs for global and regional sea-level change 1900-2100. *Clim. Dyn.*, **18**, 241–253.

Gregory, J.M., et al., 2002a: An observationally based estimate of the climate sensitivity. *J. Clim.*, **15**, 3117–3121.

Gregory, J.M., et al., 2002b: Recent and future changes in Arctic sea ice simulated by the HadCM3 AOGCM. *Geophys. Res. Lett.*, **29**, 2175.

Gregory, J.M., et al., 2004b: A new method for diagnosing radiative forcing and climate sensitivity. *Geophys. Res. Lett.*, **31**, L03205, doi:10.1029/2003GL018747.

Gregory, J.M., et al., 2005: A model intercomparison of changes in the Atlantic thermohaline circulation in response to increasing atmospheric CO_2 concentration. *Geophys. Res. Lett.*, **32**, L12703, doi:10.1029/2005GL023209.

Grenfell, J.L., D.T. Shindell, and V. Grewe, 2003: Sensitivity studies of oxidative changes in the troposphere in 2100 using the GISS GCM. *Atmos. Chem. Phys.*, **3**, 1267–1283.

Grewe, V., et al., 2001: Future changes of the atmospheric composition and the impact of climate change. *Tellus*, **53B**, 103–121.

Guilyardi, E., 2006: El Niño-mean state-seasonal cycle interactions in a multi-model ensemble. *Clim. Dyn.*, **26**, 329–348.

Haarsma, R.J., F.M. Selten, S.L. Weber, and M. Kliphuis, 2005: Sahel rainfall variability and response to greenhouse warming. *Geophys. Res. Lett.*, **32**, L17702, doi:10.1029/2005GL023232.

Hagedorn, R., F.J. Doblas-Reyes, and T.N. Palmer, 2005: The rationale behind the success of multi-model ensembles in seasonal forecasting. Part I: Basic concept. *Tellus*, **57A**, 219–233.

Hall, A., and R.J. Stouffer, 2001: An abrupt climate event in a coupled ocean-atmosphere simulation without external forcing. *Nature*, **409**, 171–174.

Hanna, E., P. Huybrechts, and T.L. Mote, 2002: Surface mass balance of the Greenland ice sheet from climate-analysis data and accumulation/runoff models. *Ann. Glaciol.*, **35**, 67–72.

Hansen, J., 2005: A slippery slope: How much global warming constitutes dangerous anthropogenic interference? *Clim. Change*, **68**, 269–279.

Hansen, J., and L. Nazarenko, 2004: Soot climate forcing via snow and ice albedos. *Proc. Natl. Acad. Sci. U.S.A.*, **101**, 423–428.

Hansen, J.E., M. Sato, and R. Ruedy, 1997: Radiative forcing and climate response. *J. Geophys. Res.*, **102**, 6831–6864.

Hansen, J., et al., 1984: Climate sensitivity: Analysis of feedback mechanisms. In: *Climate Processes and Climate Sensitivity* [Hansen, J., and T. Takahashi (eds.)]. Geophysical Monograph Vol. 29, American Geophysical Union, Washington, DC, pp. 130–163.

Hansen, J., et al., 1985: Climate response-times - Dependence on climate sensitivity and ocean mixing. *Science*, **229**, 857–859.

Hansen, J., et al., 2005a: Earth's energy imbalance: Confirmation and implications. *Science*, **308**, 1431–1435.

Hansen, J., et al., 2005b: Efficacy of climate forcings. *J. Geophys. Res.*, **110**, D18104, doi:10.1029/2005JD005776.

Hare, W.L., and M. Meinshausen, 2006: How much warming are we committed to and how much can be avoided? *Clim. Change*, **75**, 111–149.

Hargreaves, J.C., and J.D. Annan, 2006: Using ensemble prediction methods to examine regional climate variation under global warming scenarios. *Ocean Modelling*, **11**, 174–192.

Harris, G., et al., 2006: Frequency distributions of transient regional climate change from perturbed physics ensembles of general circulation model simulations. *Clim. Dyn.*, **27**, 357–375.

Harrison, S.P., K.E. Kohfeld, C. Roelandt, and T. Claquin, 2001: The role of dust in climate changes today, at the last glacial maximum, and in the future. *Earth Sci. Rev.*, **54**, 43–80.

Harvey, L.D.D., 2004: Characterizing the annual-mean climatic effect of anthropogenic CO_2 and aerosol emissions in eight coupled atmosphere-ocean GCMs. *Clim. Dyn.*, **23**, 569–599.

Harvey, L.D.D., and R.K. Kaufmann, 2002: Simultaneously constraining climate sensitivity and aerosol radiative forcing. *J. Clim.*, **15**, 2837–2861.

Hasegawa, A., and S. Emori, 2005: Tropical cyclones and associated precipitation over the western North Pacific: T106 atmospheric GCM simulation for present-day and doubled CO_2 climates. *Scientific Online Letters on the Atmosphere*, **1**, 145–148.

Hauglustaine, D.A., and G.P. Brasseur, 2001: Evolution of tropospheric ozone under anthropogenic activities and associated radiative forcing of climate. *J. Geophys. Res.*, **106**, 32337–32360.

Hauglustaine, D.A., J. Lathiere, S. Szopa, and G.A. Folberth, 2005: Future tropospheric ozone simulated with a climate-chemistry-biosphere model. *Geophys. Res. Lett.*, **32**, L24807, doi:10.1029/2005GL024031.

Hazeleger, W., 2005: Can global warming affect tropical ocean heat transport? *Geophys. Res. Lett.*, **32**, L22701, doi:10.1029/2005GL023450.

Hegerl, G.C., T.J. Crowley, W.T. Hyde, and D.J. Frame, 2006: Climate sensitivity constrained by temperature reconstructions over the past seven centuries. *Nature*, **440**, 1029–1032.

Hoerling, M.P., et al., 2004: Twentieth century North Atlantic climate change. Part II: Understanding the effect of Indian Ocean warming. *Clim. Dyn.*, **23**, 391–405.

Holland, M.M., and C.M. Bitz, 2003: Polar amplification of climate change in the Coupled Model Intercomparison Project. *Clim. Dyn.*, **21**, 221–232.

Hosaka, M., D. Nohara, and A. Kitoh, 2005: Changes in snow coverage and snow water equivalent due to global warming simulated by a 20km-mesh global atmospheric model. *Scientific Online Letters on the Atmosphere*, **1**, 93–96.

Houghton, R.A., and J.L. Hackler, 2000: Changes in terrestrial carbon storage in the United States. 1: The roles of agriculture and forestry. *Global Ecol. Biogeogr.*, **9**, 125–144.

Hsieh, W.W., and K. Bryan, 1996: Redistribution of sea level rise associated with enhanced greenhouse warming: A simple model study. *Clim. Dyn.*, **12**, 535–544.

Hu, A., G.A. Meehl, W.M. Washington, and A. Dai, 2004: Response of the Atlantic thermohaline circulation to increased atmospheric CO_2 in a coupled model. *J. Clim.*, **17**, 4267–4279.

Hu, Z.-Z., and A. Wu, 2004: The intensification and shift of the annual North Atlantic Oscillation in a global warming scenario simulation. *Tellus*, **56A**, 112–124.

Hu, Z.-Z., L. Bengtsson, and K. Arpe, 2000a: Impact of the global warming on the Asian winter monsoon in a coupled GCM. *J. Geophys. Res.*, **105**, 4607–4624.

Hu, Z.-Z., M. Latif, E. Roeckner, and L. Bengtsson, 2000b: Intensified Asian summer monsoon and its variability in a coupled model forced by increasing greenhouse gas concentrations. *Geophys. Res. Lett.*, **27**, 2681–2684.

Hu, Z.-Z., E.K. Schneider, U.S. Bhatt, and B.P. Kirtman, 2004: Potential mechanism for response of El Niño-Southern Oscillation variability to change in land surface energy budget. *J. Geophys. Res.*, **109**, D21113, doi:10.1029/2004JD004771.

Hu, Z.-Z., et al., 2001: Impact of global warming on the interannual and interdecadal climate modes in a coupled GCM. *Clim. Dyn.*, **17**, 361–374.

Huntingford, C., et al., 2004: Using a GCM analogue model to investigate the potential for Amazonian forest dieback. *Theor. Appl. Climatol.*, **78**, 177–185.

Hurrell, J.W., Y. Kushnir, G. Ottersen, and M. Visbeck, 2003: An overview of the North Atlantic Oscillation. In: *The North Atlantic Oscillation: Climatic Significance and Environmental Impact* [Hurrell, J.W., et al. (eds.)]. Geophysical Monograph Vol. 134, American Geophysical Union, Washington, DC, pp. 1–35.

Hurrell, J.W., M.P. Hoerling, A. Phillips, and T. Xu, 2004: Twentieth century North Atlantic climate change. Part I: Assessing determinism. *Clim. Dyn.*, **23**, 371–389.

Huybrechts, P., and J. De Wolde, 1999: The dynamic response of the Greenland and Antarctic ice sheets to multiple-century climatic warming. *J. Clim.*, **12**, 2169–2188.

Huybrechts, P., A. Letréguilly, and N. Reeh, 1991: The Greenland ice sheet and greenhouse warming. *Palaeogeogr. Palaeoclimatol. Palaeoecol.*, **89**, 399–412.

Huybrechts, P., I. Janssens, C. Poncin, and T. Fichefet, 2002: The response of the Greenland ice sheet to climate changes in the 21st century by interactive coupling of an AOGCM with a thermomechanical ice-sheet model. *Ann. Glaciol.*, **35**, 409–415.

Huybrechts, P., J. Gregory, I. Janssens, and M. Wild, 2004: Modelling Antarctic and Greenland volume changes during the 20th and 21st centuries forced by GCM time slice integrations. *Global Planet. Change*, **42**, 83–105.

Inatsu, M., and M. Kimoto, 2005: Two types of interannual variability of the mid-winter storm-track and their relationship to global warming. *Scientific Online Letters on the Atmosphere*, **1**, 61–64.

IPCC, 1995: *Climate Change 1994: Radiative Forcing of Climate Change* [Houghton, J.T., et al. (eds.)]. Intergovernmental Panel on Climate Change, Cambridge University Press, Cambridge, United Kingdom and New York, NY, USA, 339 pp.

IPCC, 2001: *Climate Change 2001: The Scientific Basis. Contribution of Working Group I to the Third Assessment Report of the Intergovernmental Panel on Climate Change* [Houghton, J.T., et al. (eds.)]. Cambridge University Press, Cambridge, United Kingdom and New York, NY, USA, 881 pp.

Janssens, I., and P. Huybrechts, 2000: The treatment of meltwater retention in mass-balance parameterizations of the Greenland ice sheet. *Ann. Glaciol.*, **31**, 133–140.

Jenkins, G.S., A.T. Gaye, and B. Sylla, 2005: Late 20th century attribution of drying trends in the Sahel from the Regional Climate Model (RegCM3). *Geophys. Res. Lett.*, **32**, L22705, doi:10.1029/2005GL024225.

Johannessen, O.M., K. Khvorostovsky, M.W. Miles, and L.P. Bobylev, 2005: Recent ice-sheet growth in the interior of Greenland. *Science*, **310**, 1013–1016.

Johns, T.C., et al., 2003: Anthropogenic climate change for 1860 to 2100 simulated with the HadCM3 model under updated emissions scenarios. *Clim. Dyn.*, **20**, 583–612.

Johnson, C.E., D.S. Stevenson, W.J. Collins, and R.G. Derwent, 2001: Role of climate feedback on methane and ozone studied with a coupled ocean-atmosphere-chemistry model. *Geophys. Res. Lett.*, **28**, 1723–1726.

Johnson, H.L., and D.P. Marshall, 2002: A theory for surface Atlantic response to thermohaline variability. *J. Phys. Oceanogr.*, **32**, 1121–1132.

Jones, C.D., P.M. Cox, and C. Huntingford, 2006: Impact of climate-carbon cycle feedbacks on emission scenarios to achieve stabilisation. In: *Avoiding Dangerous Climate Change* [Schellnhuber, H.J., et al. (eds.)]. Cambridge University Press, New York, NY, pp. 323–331.

Jones, P.D., and A. Moberg, 2003: Hemispheric and large-scale surface air temperature variations: An extensive revision and an update to 2001. *J. Clim.*, **16**, 206–223.

Jones, P.D., et al., 2001: Adjusting for sampling density in grid box land and ocean surface temperature time series. *J. Geophys. Res.*, **106**, 3371–3380.

Joos, F., et al., 2001: Global warming feedbacks on terrestrial carbon uptake under the Intergovernmental Panel on Climate Change (IPCC) emission scenarios. *Global Biogeochem. Cycles*, **15**, 891–908.

Joshi, M., et al., 2003: A comparison of climate response to different radiative forcings in three general circulation models: towards an improved metric of climate change. *Clim. Dyn.*, **20**, 843–854.

Joughin, I., W. Abdalati, and M. Fahnestock, 2004: Large fluctuations in speed on Greenland's Jakobshavn Isbræ. *Nature*, **432**, 608–610.

Joughin, I., et al., 2003: Timing of recent accelerations of Pine Island Glacier, Antarctica. *Geophys. Res. Lett.*, **30**, 1706.

Kamiguchi, K., et al., 2005: Changes in precipitation-based extremes indices due to global warming projected by a global 20-km-mesh atmospheric model. *Scientific Online Letters on the Atmosphere*, **2**, 64–77.

Kanakidou, M., et al., 2005: Organic aerosol and global climate modelling: a review. *Atmos. Chem. Phys.*, **5**, 1053–1123.

Kapsner, W.R., et al., 1995: Dominant influence of atmospheric circulation on snow accumulation in Greenland over the past 18,000 years. *Nature*, **373**, 52–54.

Kattenberg, A., et al., 1996: Climate models – Projections of future climate. In: *Climate Change 1995: The Science of Climate Change. Contribution of Working Group I to the Second Assessment Report of the Intergovernmental Panel on Climate Change* [Houghton, J.T., et al. (eds.)]. Cambridge University Press, Cambridge United Kingdom and New York, NY, USA, pp. 285–357.

Kennedy, M., and A. O'Hagan, 2001: Bayesian calibration of computer models. *J. Roy. Stat. Soc.*, **63B**, 425–464.

Kettleborough, J.A., B.B.B. Booth, P.A. Stott, and M.R. Allen, 2007: Estimates of uncertainty in predictions of global mean surface temperature. *J. Clim.*, **20**, 843–855.

Kharin, V.V., and F.W. Zwiers, 2005: Estimating extremes in transient climate change simulations. *J. Clim.*, **18**, 1156–1173.

Kheshgi, H.S., and A.K. Jain, 2003: Projecting future climate change: Implications of carbon cycle model intercomparisons. *Global Biogeochem. Cycles*, **17**, GB001842, doi:10.1029/2001GB001842.

Kiilsholm, S., J.H. Christensen, K. Dethloff, and A. Rinke, 2003: Net accumulation of the Greenland ice sheet: High resolution modeling of climate changes. *Geophys. Res. Lett.*, **30**, 1485.

Kinne, S., et al., 2006: An AeroCom initial assessment - optical properties in aerosol component modules of global models. *Atmos. Chem. Phys.*, **6**, 1815–1834.

Kitabata, H., K. Nishizawa, Y. Yoshida, and K. Maruyama, 2006: Permafrost thawing in circum-Arctic and highland under climatic change scenarios projected by CCSM3. *Scientific Online Letters on the Atmosphere*, **2**, 53–56.

Kitoh, A., and O. Arakawa, 2005: Reduction in tropical rainfall diurnal variation by global warming simulated by a 20-km mesh climate model. *Geophys. Res. Lett.*, **32**, L18709, doi:10.1029/2005GL023350.

Kitoh, A., and T. Uchiyama, 2006: Changes in onset and withdrawal of the East Asian summer rainy season by multi-model global warming experiments. *J. Meteorol. Soc. Japan*, **84**, 247–258.

Knight, J.R., et al., 2005: A signature of persistent natural thermohaline circulation cycles in observed climate. *Geophys. Res. Lett.*, **32**, L20708, doi:10.1029/2005GL024233.

Knutson, T.R., and S. Manabe, 1995: Time-mean response over the tropical Pacific to increased CO_2 in a coupled ocean-atmosphere model. *J. Clim.*, **8**, 2181–2199.

Knutson, T.R., and R.E. Tuleya, 2004: Impact of CO_2-induced warming on simulated hurricane intensity and precipitation: Sensitivity to the choice of climate model and convective parameterization. *J. Clim.*, **17**, 3477–3495.

Knutti, R., and T.F. Stocker, 2000: Influence of the thermohaline circulation on projected sea level rise. *J. Clim.*, **13**, 1997–2001.

Knutti, R., and T.F. Stocker, 2002: Limited predictability of the future thermohaline circulation close to an instability threshold. *J. Clim.*, **15**, 179–186.

Knutti, R., T.F. Stocker, F. Joos, and G.-K. Plattner, 2002: Constraints on radiative forcing and future climate change from observations and climate model ensembles. *Nature*, **416**, 719–723.

Knutti, R., T.F. Stocker, F. Joos, and G.-K. Plattner, 2003: Probabilistic climate change projections using neural networks. *Clim. Dyn.*, **21**, 257–272.

Knutti, R., G.A. Meehl, M.R. Allen, and D.A. Stainforth, 2006: Constraining climate sensitivity from the seasonal cycle in surface temperature. *J. Clim.*, **19**, 4224–4233.

Knutti, R., et al., 2005: Probabilistic climate change projections for CO_2 stabilization profiles. *Geophys. Res. Lett.*, **32**, L20707, doi:10.1029/2005GL023294.

Koch, D., 2001: Transport and direct radiative forcing of carbonaceous and sulfate aerosols in the GISS GCM. *J. Geophys. Res.*, **106**, 20311–20332.

Krabill, W., et al., 2004: Greenland Ice Sheet: Increased coastal thinning. *Geophys. Res. Lett.*, **31**, L24402, doi:10.1029/2004GL021533.

Krinner, G., et al., 2007: Simulated Antarctic precipitation and surface mass balance at the end of the twentieth and twenty-first centuries. *Clim. Dyn.*, **28**, 215–230.

Krishna Kumar, K., B. Rajagopalan, and M.A. Cane, 1999: On the weakening relationship between the Indian monsoon and ENSO. *Science*, **284**, 2156–2159.

Kunkel, K.E., and X.Z. Liang, 2005: GCM simulations of the climate in the central United States. *J. Clim.*, **18**, 1016–1031.

Kutzbach, J.E., J.W. Williams, and S.J. Vavrus, 2005: Simulated 21st century changes in regional water balance of the Great Lakes region and links to changes in global temperature and poleward moisture transport. *Geophys. Res. Lett.*, **32**, L17707, doi:10.1029/2005GL023506.

Kuzmina, S.I., et al., 2005: The North Atlantic Oscillation and greenhouse-gas forcing. *Geophys. Res. Lett.*, **32**, L04703, doi:10.1029/2004GL021064.

Lal, M., and S.K. Singh, 2001: Global warming and monsoon climate. *Mausam*, **52**, 245–262.

Lambert, S.J., and G.J. Boer, 2001: CMIP1 evaluation and intercomparison of coupled climate models. *Clim. Dyn.*, **17**, 83–106.

Lambert, S.J., and J.C. Fyfe, 2006: Changes in winter cyclone frequencies and strengths simulated in enhanced greenhouse warming experiments: results from the models participating in the IPCC diagnostic exercise. *Clim. Dyn.*, **26**, 713–728.

Land, C., and J. Feichter, 2003: Stratosphere-troposphere exchange in a changing climate simulated with the general circulation model MAECHAM4. *J. Geophys. Res.*, **108**, 8523.

Landerer, F.W., J.H. Jungclaus, and J. Marotzke, 2007: Regional dynamic and steric sea level change in response to the IPCC-A1B scenario. *J. Phys. Oceanogr.*, in press.

Laurent, R., and X. Cai, 2007: A maximum entropy method for combining AOGCMs for regional intra-year climate change assessment. *Clim. Change*, **82**, 411–435.

Lawrence, D.M., and A.G. Slater, 2005: A projection of severe near-surface permafrost degradation during the 21st century. *Geophys. Res. Lett.*, **32**, L24401, doi:10.1029/2005GL025080.

Lean, J., J. Beer, and R.S. Bradley, 1995: Reconstruction of solar irradiance since 1610: Implications for climate change. *Geophys. Res. Lett.*, **22**, 3195–3198.

Leckebusch, G.C., and U. Ulbrich, 2004: On the relationship between cyclones and extreme windstorm events over Europe under climate change. *Global Planet. Change*, **44**, 181–193.

Leemans, R., et al., 1998: *The IMAGE User Support System: Global Change Scenarios from IMAGE 2.1.* CD-ROM 4815006, National Institute of Public Health and the Environment (RIVM), Bilthoven, The Netherlands.

Leggett, J., W.J. Pepper, and R. Swart, 1992: Emissions scenarios for IPCC: An update. In: *Climate Change 1992. The Supplementary Report to the IPCC Scientific Assessment* [Houghton, J.T., B.A. Calalnder, and S.K. Varney (eds.)]. Cambridge University Press, Cambridge, United Kingdom and New York, NY, USA, pp. 69–95.

LeGrande, A.N., et al., 2006: Consistent simulations of multiple proxy responses to an abrupt climate change event. *Proc. Natl. Acad. Sci. U.S.A.*, **103**, 837–842.

Levermann, A., et al., 2005: Dynamic sea level changes following changes in the thermohaline circulation. *Clim. Dyn.*, **24**, 347–354.

Li, W., R. Fu, and R.E. Dickinson, 2006: Rainfall and its seasonality over the Amazon in the 21st century as assessed by the coupled models for the IPCC AR4. *J. Geophys. Res.*, **111**, D02111, doi:10.1029/2005JD006355.

Liao, H., et al., 2003: Interactions between tropospheric chemistry and aerosols in a unified general circulation model. *J. Geophys. Res.*, **108**, 4001.

Liu, P., G.A. Meehl, and G. Wu, 2002: Multi-model trends in the Sahara induced by increasing CO_2. *Geophys. Res. Lett.*, **29**, 1881.

Liu, Z., et al., 2005: Rethinking tropical ocean response to global warming: The enhanced equatorial warming. *J. Clim.*, **18**, 4684–4700.

Longworth, H., J. Marotzke, and T.F. Stocker, 2005: Ocean gyres and abrupt change in the thermohaline circulation: A conceptual analysis. *J. Clim.*, **18**, 2403–2416.

Lopez, A., et al., 2006: Two approaches to quantifying uncertainty in global temperature changes. *J. Clim.*, **19**, 4785–4796.

Lowe, J.A., and J.M. Gregory, 2006: Understanding projections of sea level rise in a Hadley Centre coupled climate model. *J. Geophys. Res.*, **111**, C11014, doi:10.1029/2005JC003421.

Lucarini, V., and G.L. Russell, 2002: Comparison of mean climate trends in the northern hemisphere between National Centers for Environmental Prediction and two atmosphere-ocean model forced runs. *J. Geophys. Res.*, **107**, 4269.

Lumpkin, R., and K. Speer, 2003: Large-scale vertical and horizontal circulation in the North Atlantic Ocean. *J. Phys. Oceanogr.*, **33**, 1902–1920.

Lunt, D.J., N. de Noblet-Ducoudré, and S. Charbit, 2004: Effects of a melted Greenland ice sheet on climate, vegetation, and the cryosphere. *Clim. Dyn.*, **23**, 679–694.

Lynch, A., P. Uotila, and J.J. Cassano, 2006: Changes in synoptic weather patterns in the polar regions in the twentieth and twenty-first centuries, Part 2: Antarctic. *Int. J. Climatol.*, **26**, 1181–1199.

Mahowald, N.M., and C. Luo, 2003: A less dusty future? *Geophys. Res. Lett.*, **30**, 1903.

Manabe, S., and R.J. Stouffer, 1980: Sensitivity of a global climate model to an increase of CO_2 concentration in the atmosphere. *J. Geophys. Res.*, **85**, 5529–5554.

Manabe, S., and R.J. Stouffer, 1994: Multiple-century response of a coupled ocean-atmosphere model to an increase of atmospheric carbon dioxide. *J. Clim.*, **7**, 5–23.

Manabe, S., and R.J. Stouffer, 1999: Are two modes of the thermohaline circulation stable? *Tellus*, **51A**, 400–411.

Marland, G., T.A. Boden, and R.J. Andres, 2005: Global, regional and national fossil fuel CO_2 emissions. In: *Trends: A Compendium of Data on Global Change*. Carbon Dioxide Information Analysis Center, Oak Ridge National Laboratory, U.S. Department of Energy, Oak Ridge, TN.

Marquart, S., M. Ponater, F. Mager, and R. Sausen, 2003: Future development of contrail cover, optical depth, and radiative forcing: Impacts of increasing air traffic and climate change. *J. Clim.*, **16**, 2890–2904.

Matthews, H.D., 2005: Decrease of emissions required to stabilize atmospheric CO_2 due to positive carbon cycle-climate feedbacks. *Geophys. Res. Lett.*, **32**, L21707, doi:10.1029/2005GL023435.

May, W., 2004: Potential future changes in the Indian summer monsoon due to greenhouse warming: analysis of mechanisms in a global time-slice experiment. *Clim. Dyn.*, **22**, 389–414.

Maykut, G.A., and N. Untersteiner, 1971: Some results from a time-dependent thermodynamic model of sea ice. *J. Geophys. Res.*, **76**, 1550–1575.

Maynard, K., and J.-F. Royer, 2004: Effects of "realistic" land-cover change on a greenhouse-warmed African climate. *Clim. Dyn.*, **22**, 343–358.

Maynard, K., J.-F. Royer, and F. Chauvin, 2002: Impact of greenhouse warming on the West African summer monsoon. *Clim. Dyn.*, **19**, 499–514.

McCabe, G.J., M.P. Clark, and M.C. Serreze, 2001: Trends in Northern Hemisphere surface cyclone frequency and intensity. *J. Clim.*, **14**, 2763–2768.

McDonald, R.E., et al., 2005: Tropical storms: Representation and diagnosis in climate models and the impacts of climate change. *Clim. Dyn.*, **25**, 19–36.

Meehl, G.A., and J.M. Arblaster, 2003: Mechanisms for projected future changes in south Asian monsoon precipitation. *Clim. Dyn.*, **21**, 659–675.

Meehl, G.A., and C. Tebaldi, 2004: More intense, more frequent, and longer lasting heat waves in the 21st century. *Science*, **305**, 994–997.

Meehl, G.A., C. Tebaldi, and D. Nychka, 2004a: Changes in frost days in simulations of twenty-first century climate. *Clim. Dyn.*, **23**, 495–511.

Meehl, G.A., J.M. Arblaster, and C. Tebaldi, 2005a: Understanding future patterns of precipitation extremes in climate model simulations. *Geophys. Res. Lett.*, **32**, L18719, doi:10.1029/2005GL023680.

Meehl, G.A., H. Teng, and G.W. Branstator, 2006a: Future changes of El Niño in two global coupled climate models. *Clim. Dyn.*, **26**, 549–566.

Meehl, G.A., W.M. Washington, J.M. Arblaster, and A. Hu, 2004b: Factors affecting climate sensitivity in global coupled models. *J. Clim.*, **17**, 1584–1596.

Meehl, G.A., et al., 2005b: Overview of the coupled model intercomparison project. *Bull. Am. Meteorol. Soc.*, **86**, 89–93.

Meehl, G.A., et al., 2005c: How much more global warming and sea level rise? *Science*, **307**, 1769–1772.

Meehl, G.A., et al., 2006b: Climate change projections for the twenty-first century and climate change commitment in the CCSM3. *J. Clim.*, **19**, 2597–2616.

Meinshausen, M., 2006: What does a 2°C target mean for greenhouse gas concentrations? A brief analysis based on multi-gas emission pathways and several climate sensitivity uncertainty estimates. In: *Avoiding Dangerous Climate Change* [Schellnhuber, H.J., et al. (eds.)]. Cambridge University Press, New York, NY, pp. 265–279.

Meleshko, V.P., et al., 2004: Anthropogenic climate change in 21st century over Northern Eurasia. *Meteorol. Hydrol.*, **7**, 5–26.

Menon, S., J. Hansen, L. Nazarenko, and Y. Luo, 2002: Climate effects of black carbon aerosols in China and India. *Science*, **297**, 2250–2253.

Merryfield, W., 2006: Changes to ENSO under CO_2 doubling in a multi-model ensemble. *J. Clim.*, **19**, 4009–4027.

Mielke, P.W., 1991: The application of multivariate permutation methods based on distance functions in the earth sciences. *Earth Sci. Rev.*, **31**, 55–71.

Mikolajewicz, U., and R. Voss, 2000: The role of the individual air-sea flux components in CO_2-induced changes of the ocean's circulation and climate. *Clim. Dyn.*, **16**, 627–642.

Miller, R.L., G.A. Schmidt, and D.T. Shindell, 2006: Forced annular variations in the 20th century IPCC AR4 simulations. *J. Geophys. Res.*, **111**, D18101, doi:10.1029/2005JD006323.

Milly, P.C.D., K.A. Dunne, and A.V. Vecchia, 2005: Global pattern of trends in streamflow and water availability in a changing climate. *Nature*, **438**, 347–350.

Milly, P.C.D., R.T. Wetherald, K.A. Dunne, and T.L. Delworth, 2002: Increasing risk of great floods in a changing climate. *Nature*, **415**, 514–517.

Mitchell, J.F.B., S. Manabe, V. Meleshko, and T. Tokioka, 1990: Equilibrium climate change – and its implications for the future. In: *Climate Change. The IPCC Scientific Assessment. Contribution of Working Group 1 to the First Assessment Report of the Intergovernmental Panel on Climate Change* [Houghton, J.L., G.J. Jenkins, and J.J. Ephraums (eds.)]. Cambridge University Press, Cambridge, United Kingdom and New York, NY, USA, pp. 137–164.

Mitchell, J.F.B., T.C. Johns, W.J. Ingram, and J.A. Lowe, 2000: The effect of stabilising atmospheric carbon dioxide concentrations on global and regional climate change. *Geophys. Res. Lett.*, **27**, 2977–2980.

Mitchell, T.D., 2003: Pattern scaling - An examination of the accuracy of the technique for describing future climates. *Clim. Change*, **60**, 217–242.

Monahan, A.H., 2002: Stabilisation of climate regimes by noise in a simple model of the thermohaline circulation. *J. Phys. Oceanogr.*, **32**, 2072–2085.

Morris, E.M., and R. Mulvaney, 2004: Recent variations in surface mass balance of the Antarctic Peninsula ice sheet. *J. Glaciol.*, **50**, 257–267.

Moss, R.H., and S.H. Schneider, 2000: Uncertainties in the IPCC TAR: Recommendations to Lead Authors for more consistent assessment and reporting. In: *Guidance Papers on the Cross-Cutting Issues of the Third Assessment Report of the IPCC* [Pachauri, R., et al. (eds.)]. Intergovernmental Panel on Climate Change, Geneva, pp. 33–51.

Müller, S.A., F. Joos, N.R. Edwards, and T.F. Stocker, 2006: Water mass distribution and ventilation time scales in a cost-efficient, 3-dimensional ocean model. *J. Clim.*, **19**, 5479–5499.

Murphy, B.F., I. Marsiat, and P. Valdes, 2002: Atmospheric contributions to the surface mass balance of Greenland in the HadAM3 atmospheric model. *J. Geophys. Res.*, **107**, 4556.

Murphy, J.M., et al., 2004: Quantification of modelling uncertainties in a large ensemble of climate change simulations. *Nature*, **429**, 768–772.

Myhre, G., and F. Stordal, 2001: On the tradeoff of the solar and thermal infrared radiative impact of contrails. *Geophys. Res. Lett.*, **28**, 3119–3122.

Myhre, G., T.F. Berglen, C.E.L. Myhre, and I.S.A. Isaksen, 2004: The radiative effect of the anthropogenic influence on the stratospheric sulfate aerosol layer. *Tellus*, **56B**, 294–299.

Nakashiki, N., et al., 2006: Recovery of thermohaline circulation under CO_2 stabilization and overshoot scenarios. *Ocean Modelling*, **15**, 200–217.

Nakićenović, N., and R. Swart (eds.), 2000: *Special Report on Emissions Scenarios*. *A Special Report of Working Group III of the Intergovernmental Panel on Climate Change.* Cambridge University Press, Cambridge, United Kingdom and New York, NY, USA, 599 pp.

Nanjundiah, R.S., V. Vidyunmala, and J. Srinivasan, 2005: The impact of increase in CO_2 on the simulation of tropical biennial oscillations (TBO) in 12 coupled general circulation models. *Atmos. Sci. Lett.*, **6**, 183–191.

Naveau, P., and C.M. Ammann, 2005: Statistical distributions of ice core sulphate from climatically relevant volcanic eruptions. *Geophys. Res. Lett.*, **32**, L05711, doi:10.1029/2004GL021732.

Neelin, J.D., et al., 2006: Tropical drying trends in global warming models and observations. *Proc. Natl. Acad. Sci. U.S.A.*, **103**, 6110–6115.

Nguyen, K.C., and K.J.E. Walsh, 2001: Interannual, decadal, and transient greenhouse simulation of tropical cyclone-like vortices in a regional climate model of the South Pacific. *J. Clim.*, **14**, 3043–3054.

Nohara, D., A. Kitoh, M. Hosaka, and T. Oki, 2006: Impact of climate change on river discharge projected by multi-model ensemble. *J. Hydrometeorol.*, **7**, 1076–1089.

NorthGRIP Members, 2004: High-resolution climate record of the northern hemisphere back into the last interglacial period. *Nature*, **431**, 147–151.

Oerlemans, J., 2001: *Glaciers and Climate Change*. A. A. Balkema, Lisse, The Netherlands, 148 pp.

Oerlemans, J., and J.P.F. Fortuin, 1992: Sensitivity of glaciers and small ice caps to greenhouse warming. *Science*, **258**, 115–117.

Oerlemans, J., and B.K. Reichert, 2000: Relating glacier mass balance to meteorological data by using a seasonal sensitivity characteristic. *J. Glaciol.*, **46**, 1–6.

Oerlemans, J., et al., 1998: Modeling the response of glaciers to climate warming. *Clim. Dyn.*, **14**, 267–274.

Oerlemans, J., et al., 2006: Estimating the contribution from Arctic glaciers to sea-level change in the next hundred years. *Ann. Glaciol.*, **42**, 230–236.

Ohmura, A., M. Wild, and L. Bengtsson, 1996: Present and future mass balance of the ice sheets simulated with GCM. *Ann. Glaciol.*, **23**, 187–193.

Olivier, J.G.J., and J.J.M. Berdowski, 2001: Global emissions sources and sinks. In: *The Climate System* [Berdowski, J., R. Guicherit, and B.J. Heij (eds.)]. A. A. Balkema, Lisse, The Netherlands, pp. 33–78.

Oouchi, K., et al., 2006: Tropical cyclone climatology in a global-warming climate as simulated in a 20km-mesh global atmospheric model: Frequency and wind intensity analyses. *J. Meteorol. Soc. Japan*, **84**, 259–276.

Oppenheimer, M., 1998: Global warming and the stability of the West Antarctic Ice Sheet. *Nature*, **393**, 325–332.

Oppenheimer, M., and R.B. Alley, 2005: Ice sheets, global warming, and Article 2 of the UNFCCC. *Clim. Change*, **68**, 257–267.

Opsteegh, J.D., R.J. Haarsma, F.M. Selten, and A. Kattenberg, 1998: ECBILT: A dynamic alternative to mixed boundary conditions in ocean models. *Tellus*, **50A**, 348–367.

Orr, J.C., et al., 2005: Anthropogenic ocean acidification over the twenty-first century and its impact on calcifying organisms. *Nature*, **437**, 681–686.

Osborn, T.J., 2004: Simulating the winter North Atlantic Oscillation: The roles of internal variability and greenhouse forcing. *Clim. Dyn.*, **22**, 605–623.

Pal, J.S., F. Giorgi, and X. Bi, 2004: Consistency of recent European summer precipitation trends and extremes with future regional climate projections. *Geophys. Res. Lett.*, **31**, L13202, doi:10.1029/2004GL019836.

Palmer, T.N., 2001: A nonlinear dynamical perspective on model error: A proposal for non-local stochastic-dynamic parametrization in weather and climate prediction models. *Q. J. R. Meteorol. Soc.*, **127**, 279–303.

Palmer, T.N., 2005: Global warming in a nonlinear climate - Can we be sure? *Europhys. News*, **36**, 42–46.

Palmer, T.N., and J. Räisänen, 2002: Quantifying the risk of extreme seasonal precipitation events in a changing climate. *Nature*, **415**, 514–517.

Palmer, T.N., et al., 2004: Development of a European multimodel ensemble system for seasonal-to-interannual prediction (DEMETER). *Bull. Am. Meteorol. Soc.*, **85**, 853–872.

Palmer, T.N., et al., 2005: Representing model uncertainty in weather and climate prediction. *Annu. Rev. Earth Planet. Sci.*, **33**, 4.1–4.31.

Parizek, B.R., and R.B. Alley, 2004: Implications of increased Greenland surface melt under global-warming scenarios: Ice-sheet simulations. *Quat. Sci. Rev.*, **23**, 1013–1027.

Payne, A.J., et al., 2004: Recent dramatic thinning of largest West Antarctic ice stream triggered by oceans. *Geophys. Res. Lett.*, **31**, L23401, doi:10.1029/2004GL021284.

Penner, J.E., et al. (eds.), 1999: *Aviation and the Global Atmosphere*. Cambridge University Press, Cambridge, United Kingdom and New York, NY, USA, 373 pp.

Petoukhov, V., et al., 2000: CLIMBER-2: a climate system model of intermediate complexity. Part I: model description and performance for present climate. *Clim. Dyn.*, **16**, 1–17.

Pham, M., O. Boucher, and D. Hauglustaine, 2005: Changes in atmospheric sulfur burdens and concentrations and resulting radiative forcings under IPCC SRES emission scenarios for 1990-2100. *J. Geophys. Res.*, **110**, D06112, doi:10.1029/2004JD005125.

Phillips, T.J., and P.J. Gleckler, 2006: Evaluation of continental precipitation in 20th century climate simulations: The utility of multi-model statistics. *Water Resour. Res.*, **42**, W03202, doi:10.1029/2005WR004313.

Phillips, T.J., et al., 2004: Evaluating parameterizations in general circulation models. *Bull. Am. Meteorol. Soc.*, **85**, 1903–1915.

Piani, C., D.J. Frame, D.A. Stainforth, and M.R. Allen, 2005: Constraints on climate change from a multi-thousand member ensemble of simulations. *Geophys. Res. Lett.*, **32**, L23825, doi:10.1029/2005GL024452.

Pitari, G., E. Mancini, V. Rizi, and D.T. Shindell, 2002: Impact of future climate and emission changes on stratospheric aerosols and ozone. *J. Atmos. Sci.*, **59**, 414–440.

Plattner, G.-K., F. Joos, T.F. Stocker, and O. Marchal, 2001: Feedback mechanisms and sensitivities of ocean carbon uptake under global warming. *Tellus*, **53B**, 564–592.

Rahmstorf, S., and A. Ganopolski, 1999: Long-term global warming scenarios computed with an efficient coupled climate model. *Clim. Change*, **43**, 353–367.

Räisänen, J., 2001: CO_2-induced climate change in CMIP2 experiments: Quantification of agreement and role of internal variability. *J. Clim.*, **14**, 2088–2104.

Räisänen, J., 2002: CO_2-induced changes in interannual temperature and precipitation variability in 19 CMIP2 experiments. *J. Clim.*, **15**, 2395–2411.

Räisänen, J., 2003: CO_2-induced changes in angular momentum in CMIP2 experiments. *J. Clim.*, **16**, 132–143.

Räisänen, J., 2005a: Impact of increasing CO_2 on monthly-to-annual precipitation extremes: Analysis of the CMIP2 experiments. *Clim. Dyn.*, **24**, 309–323.

Räisänen, J., 2005b: Probability distributions of CO_2-induced global warming as inferred directly from multimodel ensemble simulations. *Geophysica*, **41**, 19–30.

Räisänen, J., and T.N. Palmer, 2001: A probability and decision-model analysis of a multimodel ensemble of climate change simulations. *J. Clim.*, **14**, 3212–3226.

Ramanathan, V., 1988: The greenhouse theory of climate change: A test by an inadvertent global experiment. *Science*, **240**, 293–299.

Ramanathan, V., P.J. Crutzen, J.T. Kiehl, and D. Rosenfeld, 2001: Aerosols, climate, and the hydrologic cycle. *Science*, **294**, 2119–2124.

Ramanathan, V., et al., 2005: Atmospheric brown clouds: Impacts on South Asian climate and hydrological cycle. *Proc. Natl. Acad. Sci. U.S.A.*, **102**, 5326–5333.

Randall, D.A., et al., 1996: A revised land surface parameterization (SiB2) for GCMs. Part III: The greening of the Colorado State University General Circulation Model. *J. Clim.*, **9**, 738–763.

Raper, S.C.B., and R.J. Braithwaite, 2005: The potential for sea level rise: New estimates from glacier and ice cap area and volume distributions. *Geophys. Res. Lett.*, **32**, L05502, doi:10.1029/2004GL021981.

Raper, S.C.B., and R.J. Braithwaite, 2006: Low sea level rise projections from mountain glaciers and icecaps under global warming. *Nature*, **439**, 311–313.

Raper, S.C.B., O. Brown, and R.J. Braithwaite, 2000: A geometric glacier model for sea-level change calculations. *J. Glaciol.*, **46**, 357–368.

Raper, S.C.B., J.M. Gregory, and R.J. Stouffer, 2002: The role of climate sensitivity and ocean heat uptake on AOGCM transient temperature response. *J. Clim.*, **15**, 124–130.

Rauthe, M., A. Hense, and H. Paeth, 2004: A model intercomparison study of climate change-signals in extratropical circulation. *Int. J. Climatol.*, **24**, 643–662.

Raven, J., et al., 2005: *Ocean Acidification Due to Increasing Atmospheric Carbon Dioxide*. The Royal Society, London, 60 pp.

Reichert, B.K., L. Bengtsson, and J. Oerlemans, 2002: Recent glacier retreat exceeds internal variability. *J. Clim.*, **15**, 3069–3081.

Ridley, J.K., P. Huybrechts, J.M. Gregory, and J.A. Lowe, 2005: Elimination of the Greenland ice sheet in a high CO_2 climate. *J. Clim.*, **17**, 3409–3427.

Rignot, E., 1998: Fast recession of a West Antarctic glacier. *Science*, **281**, 549–551.

Rignot, E., 2001: Evidence for a rapid retreat and mass loss of Thwaites Glacier, West Antarctica. *J. Glaciol.*, **47**, 213–222.

Rignot, E., and S.S. Jacobs, 2002: Rapid bottom melting widespread near Antarctic ice sheet grounding lines. *Science*, **296**, 2020–2023.

Rignot, E., and P. Kanagaratnam, 2006: Changes in the velocity structure of the Greenland ice sheet. *Science*, **311**, 986–990.

Rignot, E., A. Rivera, and G. Casassa, 2003: Contribution of the Patagonia ice fields of South America to sea level rise. *Science*, **302**, 434–437.

Rignot, E., et al., 2002: Acceleration of Pine Island and Thwaites Glaciers, West Antarctica. *Ann. Glaciol.*, **34**, 189–194.

Rind, D., J. Lerner, and C. McLinden, 2001: Changes of tracer distributions in the doubled CO_2 climate. *J. Geophys. Res.*, **106**, 28061–28079.

Rind, D., J. Perlwitz, and P. Lonergan, 2005a: AO/NAO response to climate change: 1. Respective influences of stratospheric and tropospheric climate changes. *J. Geophys. Res.*, **110**, D12107, doi:10.1029/2004JD005103.

Rind, D., R.J. Healy, C. Parkinson, and D. Martinson, 1995: The role of sea ice in $2\times CO_2$ climate model sensitivity. 1. The total influence of sea ice thickness and extent. *J. Clim.*, **8**, 449–463.

Rind, D., J. Perlwitz, P. Lonergan, and J. Lerner, 2005b: AO/NAO response to climate change: 2. Relative importance of low- and high-latitude temperature changes. *J. Geophys. Res.*, **110**, D12108, doi:10.1029/2004JD005686.

Rodwell, M.J., D.P. Rowell, and C.K. Folland, 1999: Oceanic forcing of the wintertime North Atlantic oscillation and European climate. *Nature*, **398**, 320–323.

Roeckner, E., L. Bengtsson, and J. Feichter, 1999: Transient climate change simulations with a coupled atmosphere-ocean GCM including the tropospheric sulfur cycle. *J. Clim.*, **12**, 3004–3032.

Ronski, S., and G. Budeus, 2005: Time series of winter convection in the Greenland Sea. *J. Geophys. Res.*, **110**, C04015, doi:10.1029/2004JC002318.

Rothrock, D.A., Y. Yu, and G.A. Maykut, 1999: Thinning of the Arctic sea-ice cover. *Geophys. Res. Lett.*, **26**, 3469–3472.

Rougier, J.C., 2007: Probabilistic inference for future climate using an ensemble of climate model evaluations. *Clim. Change*, **81**, 247–264.

Rowell, D.P., and R.G. Jones, 2006: Causes and uncertainty of future summer drying over Europe. *Clim. Dyn.*, **27**, 281–299.

Russell, G.L., V. Gornitz, and J.R. Miller, 2000: Regional sea-level changes projected by the NASA/GISS atmosphere-ocean model. *Clim. Dyn.*, **16**, 789–797.

Saenko, O.A., A.J. Weaver, and J.M. Gregory, 2003: On the link between the two modes of the ocean thermohaline circulation and the formation of global-scale water masses. *J. Clim.*, **16**, 2797–2801.

Saenko, O.A., J.C. Fyfe, and M.H. England, 2005: On the response of the oceanic wind-driven circulation to atmospheric CO_2 increase. *Clim. Dyn.*, **25**, 415–426.

Sakamoto, T.T., et al., 2005: Responses of the Kuroshio and the Kuroshio Extension to global warming in a high-resolution climate model. *Geophys. Res. Lett.*, **32**, L14617, doi:10.1029/2005GL023384.

Sanderson, M.G., et al., 2003: Effect of climate change on isoprene emissions and surface ozone levels. *Geophys. Res. Lett.*, **30**, 1936.

Sato, Y., et al., 2006: Response of North Pacific ocean circulation in a Kuroshio-resolving ocean model to an Arctic Oscillation (AO)-like change in Northern Hemisphere atmospheric circulation due to greenhouse-gas forcing. *J. Meteorol. Soc. Japan*, **84**, 295–309.

Scambos, T.A., C. Hulbe, M.A. Fahnestock, and J. Bohlander, 2000: The link between climate warming and break-up of ice shelves in the Antarctic Peninsula. *J. Glaciol.*, **46**, 516–530.

Schaeffer, M., F.M. Selten, J.D. Opsteegh, and H. Goosse, 2002: Intrinsic limits to predictability of abrupt regional climate change in IPCC SRES scenarios. *Geophys. Res. Lett.*, **29**, 1767.

Schaeffer, M., F.M. Selten, J.D. Opsteegh, and H. Goosse, 2004: The influence of ocean convection patterns on high-latitude climate projections. *J. Clim.*, **17**, 4316–4329.

Schär, C., et al., 2004: The role of increasing temperature variability in European summer heat waves. *Nature*, **427**, 332–336.

Schmittner, A., M. Latif, and B. Schneider, 2005: Model projections of the North Atlantic thermohaline circulation for the 21st century assessed by observations. *Geophys. Res. Lett.*, **32**, L23710, doi:10.1029/2005GL024368.

Schneeberger, C., H. Blatter, A. Abe-Ouchi, and M. Wild, 2003: Modelling changes in the mass balance of glaciers of the northern hemisphere for a transient $2\times CO_2$ scenario. *J. Hydrol.*, **282**, 145–163.

Schneeberger, C., et al., 2000: Størglacieren in doubling CO_2 climate. *Clim. Dyn.*, **17**, 825–834.

Schneider von Deimling, T., H. Held, A. Ganopolski, and S. Rahmstorf, 2006: Climate sensitivity estimated from ensemble simulations of glacial climate. *Clim. Dyn.*, **27**, 149–163.

Schubert, M., et al., 1998: North Atlantic cyclones in CO_2-induced warm climate simulations: frequency, intensity, and tracks. *Clim. Dyn.*, **14**, 827–838.

Schweckendiek, U., and J. Willebrand, 2005: Mechanisms for the overturning response in global warming simulations. *J. Clim.*, **18**, 4925–4936.

Selten, F.M., G.W. Branstator, M. Kliphuis, and H.A. Dijkstra, 2004: Tropical origins for recent and future northern hemisphere climate change. *Geophys. Res. Lett.*, **31**, L21205, doi:10.1029/2004GL020739.

Semenov, V.A., and L. Bengtsson, 2002: Secular trends in daily precipitation characteristics: Greenhouse gas simulation with a coupled AOGCM. *Clim. Dyn.*, **19**, 123–140.

Senior, C.A., and J.F.B. Mitchell, 2000: The time-dependence of climate sensitivity. *Geophys. Res. Lett.*, **27**, 2685–2688.

Shepherd, A., D.J. Wingham, and J.A.D. Mansley, 2002: Inland thinning of the Amundsen Sea sector, West Antarctica. *Geophys. Res. Lett.*, **29**, 1364.

Shepherd, A., D. Wingham, and E. Rignot, 2004: Warm ocean is eroding West Antarctic ice sheet. *Geophys. Res. Lett.*, **31**, L23402, doi:10.1029/2004GL021106.

Shepherd, A., D.J. Wingham, J.A.D. Mansley, and H.F.J. Corr, 2001: Inland thinning of Pine Island Glacier, West Antarctica. *Science*, **291**, 862–864.

Shindell, D.T., and G.A. Schmidt, 2004: Southern hemisphere climate response to ozone changes and greenhouse gas increases. *Geophys. Res. Lett.*, **31**, L18209, doi:10.1029/2004GL020724.

Shindell, D.T., G.A. Schmidt, R.L. Miller, and D. Rind, 2001: Northern hemisphere winter climate response to greenhouse gas, ozone, and volcanic forcing. *J. Geophys. Res.*, **106**, 7193–7210.

Shine, K.P., J. Cook, E.J. Highwood, and M.M. Joshi, 2003: An alternative to radiative forcing for estimating the relative importance of climate change mechanisms. *Geophys. Res. Lett.*, **30**, 2047.

Shukla, J., et al., 2006: Climate model fidelity and projections of climate change. *Geophys. Res. Lett.*, **33**, L07702, doi:10.1029/2005GL025579.

Siegenthaler, U., and H. Oeschger, 1984: Transient temperature changes due to increasing CO_2 using simple models. *Ann. Glaciol.*, **5**, 153–159.

Sigmond, M., P.C. Siegmund, E. Manzini, and H. Kelder, 2004: A simulation of the separate climate effects of middle-atmosphere and tropospheric CO_2 doubling. *J. Clim.*, **17**, 2352–2367.

Smethie, W.M., and R.A. Fine, 2001: Rates of North Atlantic Deep Water formation calculated from chlorofluorocarbon inventories. *Deep-Sea Res. I*, **48**, 189–215.

Smith, L.A., 2002: What might we learn from climate forecasts? *Proc. Natl. Acad. Sci. U.S.A.*, **99**, 2487–2492.

Soden, B.J., and I.M. Held, 2006: An assessment of climate feedbacks in coupled ocean-atmosphere models. *J. Clim.*, **19**, 3354–3360.

Sokolov, A., C.E. Forest, and P.H. Stone, 2003: Comparing oceanic heat uptake in AOGCM transient climate change experiments. *J. Clim.*, **16**, 1573–1582.

Stainforth, D.A., et al., 2005: Uncertainty in predictions of the climate response to rising levels of greenhouse gases. *Nature*, **433**, 403–406.

Stendel, M., and J.H. Christensen, 2002: Impact of global warming on permafrost conditions in a coupled GCM. *Geophys. Res. Lett.*, **29**, 1632.

Stephenson, D.B., et al., 2006: North Atlantic Oscillation response to transient greenhouse gas forcing and the impact on European winter climate: A CMIP2 multi-model assessment. *Clim. Dyn.*, **27**, 401–420.

Stevenson, D.S., et al., 2000: Future estimates of tropospheric ozone radiative forcing and methane turnover - the impact of climate change. *Geophys. Res. Lett.*, **27**, 2073–2076.

Stevenson, D.S., et al., 2006: Multi-model ensemble simulations of present-day and near-future tropospheric ozone. *J. Geophys. Res.*, **111**, D08301, doi:10.1029/2005JD006338.

Stocker, T.F., 2000: Past and future reorganisations in the climate system. *Quat. Sci. Rev.*, **19**, 301–319.

Stocker, T.F., and A. Schmittner, 1997: Influence of CO_2 emission rates on the stability of the thermohaline circulation. *Nature*, **388**, 862–865.

Stocker, T.F., and R. Knutti, 2003: Do simplified climate models have any useful skill? *CLIVAR Exchanges*, **8**, 7–10.

Stocker, T.F., and C.C. Raible, 2005: Climate change - Water cycle shifts gear. *Nature*, **434**, 830–833.

Stocker, T.F., D.G. Wright, and L.A. Mysak, 1992a: A zonally averaged, coupled ocean-atmosphere model for paleoclimate studies. *J. Clim.*, **5**, 773–797.

Stocker, T.F., D.G. Wright, and W.S. Broecker, 1992b: The influence of high-latitude surface forcing on the global thermohaline circulation. *Paleoceanogr.*, **7**, 529–541.

Stone, D.A., and A.J. Weaver, 2002: Daily maximum and minimum temperature trends in a climate model. *Geophys. Res. Lett.*, **29**, 1356.

Stone, D.A., and J.C. Fyfe, 2005: The effect of ocean mixing parametrisation on the enhanced CO_2 response of the Southern Hemisphere midlatitude jet. *Geophys. Res. Lett.*, **32**, L06811, doi:10.1029/2004GL022007.

Stott, P.A., and J.A. Kettleborough, 2002: Origins and estimates of uncertainty in predictions of twenty-first century temperature rise. *Nature*, **416**, 723–726.

Stott, P.A., D.A. Stone, and M.R. Allen, 2004: Human contribution to the European heatwave of 2003. *Nature*, **432**, 610–613.

Stott, P.A., J.A. Kettleborough, and M.R. Allen, 2006a: Uncertainty in continental-scale temperature predictions. *Geophys. Res. Lett.*, **33**, L02708, doi:10.1029/2005GL024423.

Stott, P.A., et al., 2006b: Observational constraints on past attributable warming and predictions of future global warming. *J. Clim.*, **19**, 3055–3069.

Stouffer, R.J., 2004: Time scales of climate response. *J. Clim.*, **17**, 209–217.

Stouffer, R.J., and S. Manabe, 1999: Response of a coupled ocean-atmosphere model to increasing atmospheric carbon dioxide: sensitivity to the rate of increase. *J. Clim.*, **12**, 2224–2237.

Stouffer, R.J., and S. Manabe, 2003: Equilibrium response of thermohaline circulation to large changes in atmospheric CO_2 concentration. *Clim. Dyn.*, **20**, 759–773.

Stouffer, R.J., et al., 2006a: GFDL's CM2 global coupled climate models. Part IV: Idealized climate response. *J. Clim.*, **19**, 723–740.

Stouffer, R.J., et al., 2006b: Investigating the causes of the response of the thermohaline circulation to past and future climate changes. *J. Clim.*, **19**, 1365–1387.

Sudo, K., M. Takahashi, and H. Akimoto, 2003: Future changes in stratosphere-troposphere exchange and their impacts on future tropospheric ozone simulations. *Geophys. Res. Lett.*, **30**, 2256.

Sugi, M., and J. Yoshimura, 2004: A mechanism of tropical precipitation change due to CO_2 increase. *J. Clim.*, **17**, 238–243.

Sugi, M., A. Noda, and N. Sato, 2002: Influence of the global warming on tropical cyclone climatology: An experiment with the JMA global model. *J. Meteorol. Soc. Japan*, **80**, 249–272.

Suzuki, T., et al., 2005: Projection of future sea level and its variability in a high-resolution climate model: Ocean processes and Greenland and Antarctic ice-melt contributions. *Geophys. Res. Lett.*, **32**, L19706, doi:10.1029/2005GL023677.

Takemura, T., T. Nakajima, T. Nozawa, and K. Aoki, 2001: Simulation of future aerosol distribution, radiative forcing, and long-range transport in East Asia. *J. Meteorol. Soc. Japan*, **79**, 1139–1155.

Talley, L.D., 2003: Shallow, intermediate, and deep overturning components of the global heat budget. *J. Phys. Oceanogr.*, **33**, 530–560.

Tanaka, H.L., N. Ishizaki, and D. Nohara, 2005: Intercomparison of the intensities and trends of Hadley, Walker and monsoon circulations in the global warming projections. *Scientific Online Letters on the Atmosphere*, **1**, 77–80.

Tebaldi, C., L.O. Mearns, D. Nychka, and R.L. Smith, 2004: Regional probabilities of precipitation change: A Bayesian analysis of multimodel simulations. *Geophys. Res. Lett.*, **31**, L24213, doi:10.1029/2004GL021276.

Tebaldi, C., R.W. Smith, D. Nychka, and L.O. Mearns, 2005: Quantifying uncertainty in projections of regional climate change: A Bayesian approach to the analysis of multi-model ensembles. *J. Clim.*, **18**, 1524–1540.

Tebaldi, C., K. Hayhoe, J.M. Arblaster, and G.A. Meehl, 2006: Going to the extremes: An intercomparison of model-simulated historical and future changes in extreme events. *Clim. Change*, **79**, 185-211

Tegen, I., M. Werner, S.P. Harrison, and K.E. Kohfeld, 2004a: Reply to comment by N. M. Mahowald et al. on "Relative importance of climate and land use in determining present and future global soil dust emission". *Geophys. Res. Lett.*, **31**, L24106, doi:10.1029/2004GL021560.

Tegen, I., M. Werner, S.P. Harrison, and K.E. Kohfeld, 2004b: Relative importance of climate and land use in determining present and future global soil dust emission'. *Geophys. Res. Lett.*, **31**, L05105, doi:10.1029/2003GL019216.

Terray, L., et al., 2004: Simulation of late twenty-first century changes in wintertime atmospheric circulation over Europe de to anthropogenic causes. *J. Clim.*, **17**, 4630–4635.

Thomas, R., et al., 2001: Mass balance of higher-elevation parts of the Greenland ice sheet. *J. Geophys. Res.*, **106**, 33707–33716.

Thomas, R., et al., 2004: Accelerated sea level rise from West Antarctica. *Science*, **306**, 255–258.

Thomas, R., et al., 2005: Force-perturbation analysis of Pine Island Glacier, Antarctica, suggests cause for recent acceleration. *Ann. Glaciol.*, **39**, 133–138.

Thompson, D.W., and S. Solomon, 2002: Interpretation of recent Southern Hemisphere climate change. *Science*, **296**, 895–899.

Tol, R.S.J., and A.F. De Vos, 1998: A Bayesian statistical analysis of the enhanced greenhouse effect. *Clim. Change*, **38**, 87–112.

Toniazzo, T., J.M. Gregory, and P. Huybrechts, 2004: Climatic impact of Greenland deglaciation and its possible irreversibility. *J. Clim.*, **17**, 21–33.

Trenberth, K.E., 1990: Recent observed interdecadal climate changes in the Northern Hemisphere. *Bull. Am. Meteorol. Soc.*, **71**, 988–993.

Tsushima, Y., A. Abe-Ouchi, and S. Manabe, 2005: Radiative damping of annual variation in global mean surface temperature: Comparison between observed and simulated feedback. *Clim. Dyn.*, **24**, 591–597.

Tsushima, Y., et al., 2006: Importance of the mixed-phase cloud distribution in the control climate for assessing the response of clouds to carbon dioxide increase: a multi-model study. *Clim. Dyn.*, **27**, 113–126.

Tsutsui, J., 2002: Implications of anthropogenic climate change for tropical cyclone activity: A case study with the NCAR CCM2. *J. Meteorol. Soc. Japan*, **80**, 45–65.

Tsutsui, J., et al., 2007: Long-term climate response to stabilized and overshoot anthropogenic forcings beyond the 21st century. *Clim. Dyn.*, **28**, 199–214.

Ueda, H., A. Iwai, K. Kuwako, and M.E. Hori, 2006: Impact of anthropogenic forcing on the Asian summer monsoon as simulated by eight GCMs. *Geophys. Res. Lett.*, **33**, L06703, doi:10.1029/2005GL025336.

van Aardenne, J.A., et al., 2001: A 1×1 degree resolution dataset of historical anthropogenic trace gas emissions for the period 1890-1990. *Global Biogeochem. Cycles*, **15**, 909–928.

van de Wal, R.S.W., and M. Wild, 2001: Modelling the response of glaciers to climate change by applying volume-area scaling in combination with a high resolution GCM. *Clim. Dyn.*, **18**, 359–366.

van de Wal, R.S.W., M. Wild, and J. de Wolde, 2001: Short-term volume change of the Greenland ice sheet in response to doubled CO_2 conditions. *Tellus*, **53B**, 94–102.

van der Veen, C.J., 2002: Polar ice sheets and global sea level: how well can we predict the future? *Global Planet. Change*, **32**, 165–194.

van Lipzig, N.M., E. van Meijgaard, and J. Oerlemans, 2002: Temperature sensitivity of the Antarctic surface mass balance in a regional atmospheric climate model. *J. Clim.*, **15**, 2758–2774.

van Oldenborgh, G.J., and G. Burgers, 2005: Searching for decadal variations in ENSO precipitation teleconnections. *Geophys. Res. Lett.*, **32**, L15701, doi:10.1029/2005GL023110.

van Oldenborgh, G.J., S.Y. Philip, and M. Collins, 2005: El Niño in a changing climate: a multi-model study. *Ocean Sci.*, **1**, 81–95.

Vaughan, D.G., 2006: Recent trends in melting conditions on the Antarctic Peninsula and their implications for ice-sheet mass balance and sea level. *Arctic, Antarctic, and Alpine Res.*, **38**, 147–152.

Vaughan, D.G., 2007: West Antarctic Ice Sheet collapse – the fall and rise of a paradigm. *Clim. Change*, in press.

Vaughan, D.G., and J.R. Spouge, 2002: Risk estimation of collapse of the West Antarctic Ice Sheet. *Clim. Change*, **52**, 65–91.

Vavrus, S.J., J.E. Walsh, W.L. Chapman, and D. Portis, 2006: The behavior of extreme cold air outbreaks under greenhouse warming. *Int. J. Climatol.*, **26**, 1133–1147.

Vieli, A., and A.J. Payne, 2005: Assessing the ability of numerical ice sheet models to simulate grounding line migration. *J. Geophys. Res.*, **110**, F01003, doi:10.1029/2004JF000202.

Voldoire, A., 2006: Quantifying the impact of future land-use changes against increases in GHG concentrations. *Geophys. Res. Lett.*, **33**, L04701, doi:10.1029/2005GL024354.

Voss, R., and U. Mikolajewicz, 2001: Long-term climate changes due to increased CO_2 concentration in the coupled atmosphere-ocean general circulation model ECHAM3/LSG. *Clim. Dyn.*, **17**, 45–60.

Voss, R., W. May, and E. Roeckner, 2002: Enhanced resolution modeling study on anthropogenic climate change: changes in the extremes of the hydrological cycle. *Int. J. Climatol.*, **22**, 755–777.

Walsh, K., 2004: Tropical cyclones and climate change: Unresolved issues. *Clim. Res.*, **27**, 77–84.

Walsh, K.J.E., K.C. Nguyen, and J.L. McGregor, 2004: Fine-resolution regional climate model simulations of the impact of climate change on tropical cyclones near Australia. *Clim. Dyn.*, **22**, 47–56.

Wang, G., 2005: Agricultural drought in a future climate: Results from 15 global climate models participating in the IPCC 4th Assessment. *Clim. Dyn.*, **25**, 739–753.

Wang, X.L., and V.R. Swail, 2006a: Historical and possible future changes of wave heights in northern hemisphere ocean. In: *Atmosphere-Ocean Interactions* [Perrie, W. (ed.)]. Vol. 2, Wessex Institute of Technology Press, Southampton, pp. 240.

Wang, X.L., and V.R. Swail, 2006b: Climate change signal and uncertainty in projections of ocean wave heights. *Clim. Dyn.*, **26**, 109–126.

Wang, X.L., F.W. Zwiers, and V.R. Swail, 2004: North Atlantic Ocean wave climate change scenarios for the twenty-first century. *J. Clim.*, **17**, 2368–2383.

Watanabe, S., T. Nagashima, and S. Emori, 2005: Impact of global warming on gravity wave momentum flux in the lower stratosphere. *Scientific Online Letters on the Atmosphere*, **1**, 189–192.

Watterson, I.G., 1996: Non-dimensional measures of climate model performance. *Int. J. Climatol.*, **16**, 379–391.

Watterson, I.G., 2003: Effects of a dynamic ocean on simulated climate sensitivity to greenhouse gases. *Clim. Dyn.*, **21**, 197–209.

Watterson, I.G., 2005: Simulated changes due to global warming in the variability of precipitation, and their interpretation using a gamma-distributed stochastic model. *Adv. Water Res.*, **28**, 1368–1381.

Watterson, I.G., and M.R. Dix, 2003: Simulated changes due to global warming in daily precipitation means and extremes and their interpretation using the gamma distribution. *J. Geophys. Res.*, **108**, 4379.

Watterson, I.G., and M.R. Dix, 2005: Effective sensitivity and heat capacity in the response of climate models to greenhouse gas and aerosol forcings. *Q. J. R. Meteorol. Soc.*, **131**, 259–279.

Weaver, A.J., and E.C. Wiebe, 1999: On the sensitivity of projected oceanic thermal expansion to the parameterisation of sub-grid scale ocean mixing. *Geophys. Res. Lett.*, **26**, 3461–3464.

Weaver, A.J., and C. Hillaire-Marcel, 2004a: Ice growth in the greenhouse: A seductive paradox but unrealistic scenario. *Geoscience Canada*, **31**, 77–85.

Weaver, A.J., and C. Hillaire-Marcel, 2004b: Global warming and the next ice age. *Science*, **304**, 400–402.

Weaver, A.J., O.A. Saenko, P.U. Clark, and J.X. Mitrovica, 2003: Meltwater pulse 1A from Antarctica as a trigger of the Bølling-Allerød warm interval. *Science*, **299**, 1709–1713.

Webb, M.J., et al., 2006: On the contribution of local feedback mechanisms to the range of climate sensitivity in two GCM ensembles. *Clim. Dyn.*, **27**, 17–38.

Webster, M.D., et al., 2002: Uncertainty in emissions projections for climate models. *Atmos. Environ.*, **36**, 3659–3670.

Webster, M., et al., 2003: Uncertainty analysis of climate change and policy response. *Clim. Change*, **61**, 295–320.

Weisheimer, A., and T.N. Palmer, 2005: Changing frequency of occurrence of extreme seasonal-mean temperatures under global warming. *Geophys. Res. Lett.*, **32**, L20721, doi:10.1029/2005GL023365.

Wetherald, R.T., and S. Manabe, 2002: Simulation of hydrologic changes associated with global warming. *J. Geophys. Res.*, **107**, 4379.

Wetherald, R.T., R.J. Stouffer, and K.W. Dixon, 2001: Committed warming and its implications for climate change. *Geophys. Res. Lett.*, **28**, 1535–1538.

Wigley, T.M.L., 1984: Carbon dioxide, trace gases and global warming. *Climate Monitor*, **13**, 133–148.

Wigley, T.M.L., 2004: Modeling climate change under no-policy and policy emissions pathways. In: *The Benefits of Climate Change Policies: Analytical and Framework Issues*. OECD Publications, Paris, pp. 221–248.

Wigley, T.M.L., 2005: The climate change commitment. *Science*, **307**, 1766–1769.

Wigley, T.M.L., and S.C.B. Raper, 2001: Interpretation of high projections for global-mean warming. *Science*, **293**, 451–454.

Wigley, T.M.L., and S.C.B. Raper, 2003: Future changes in global-mean temperature and sea level. In: *Climate and Sea Level Change: Observations, Projections and Implications* [Warrick, R.A., et al. (eds.)]. Cambridge University Press, Cambridge, pp. 111–133.

Wigley, T.M.L., and S.C.B. Raper, 2005: Extended scenarios for glacier melt due to anthropogenic forcing. *Geophys. Res. Lett.*, **32**, L05704, doi:10.1029/2004GL021238.

Wigley, T.M.L., R. Richels, and J.A. Edmonds, 1996: Economic and environmental choices in the stabilization of atmospheric CO_2 concentrations. *Nature*, **379**, 240–243.

Wigley, T.M.L., P.D. Jones, and S.C.B. Raper, 1997a: The observed global warming record: What does it tell us? *Proc. Natl. Acad. Sci. U.S.A.*, **94**, 8314–8320.

Wigley, T.M.L., C.M. Ammann, B.D. Santer, and S.C.B. Raper, 2005: Effect of climate sensitivity on the response to volcanic forcing. *J. Geophys. Res.*, **110**, D09107, doi:10.1029/2004JD005557.

Wigley, T.M.L., et al., 1997b: *Implications of Proposed CO_2 Emissions Limitations*. IPCC Technical Paper IV, Intergovernmental Panel on Climate Change, Geneva, 51 pp.

Wilby, R.L., and T.M.L. Wigley, 2002: Future changes in the distribution of daily precipitation totals across North America. *Geophys. Res. Lett.*, **29**, 1135.

Wild, M., and A. Ohmura, 2000: Changes in mass balance of the polar ice sheets and sea level from high resolution GCM simulations of global warming. *Ann. Glaciol.*, **30**, 197–203.

Wild, M., P. Calanca, S. Scherrer, and A. Ohmura, 2003: Effects of polar ice sheets on global sea level in high resolution greenhouse scenarios. *J. Geophys. Res.*, **108**, 4165.

Williams, K.D., C.A. Senior, and J.F.B. Mitchell, 2001: Transient climate change in the Hadley Centre models: The role of physical processes. *J. Clim.*, **14**, 2659–2674.

Williams, K.D., et al., 2005: Evaluation of a component of the cloud response to climate change in an intercomparison of climate models. *Clim. Dyn.*, **26**, 145–165.

Williams, M.J.M., R.C. Warner, and W.F. Budd, 2002: Sensitivity of the Amery ice shelf, Antarctica, to changes in the climate of the Southern Ocean. *J. Clim.*, **15**, 2740–2757.

Wood, R.A., M. Vellinga, and R. Thorpe, 2003: Global warming and thermohaline circulation stability. *Philos. Trans. R. Soc. London Ser. A*, **361**, 1961–1975.

Wood, R.A., A.B. Keen, J.F.B. Mitchell, and J.M. Gregory, 1999: Changing spatial structure of the thermohaline circulation in response to atmospheric CO_2 forcing in a climate model. *Nature*, **399**, 572–575.

Wu, L., and B. Wang, 2004: Assessing impacts of global warming on tropical cyclone tracks. *J. Clim.*, **17**, 1686–1698.

Wu, P., R. Wood, and P. Stott, 2005: Human influence on increasing Arctic river discharge. *Geophys. Res. Lett.*, **32**, L02703, doi:10.1029/2004GL021570.

Xu, Y., Z.-C. Zhao, Y. Luo, and X. Gao, 2005: Climate change projections for the 21st century by the NCC/IAP T63 with SRES scenarios. *Acta Meteorol. Sin.*, **19**, 407–417.

Yamaguchi, K., and A. Noda, 2006: Global warming patterns over the North Pacific: ENSO versus AO. *J. Meteorol. Soc. Japan*, **84**, 221–241.

Yamaguchi, K., A. Noda, and A. Kitoh, 2005: The changes in permafrost induced by greenhouse warming: A numerical study applying multiple-layer ground model. *J. Meteorol. Soc. Japan*, **83**, 799–815.

Yeh, S.-W., and B.P. Kirtman, 2005: Pacific decadal variability and decadal ENSO amplitude modulation. *Geophys. Res. Lett.*, **32**, L05703, doi:10.1029/2004GL021731.

Yin, J.H., 2005: A consistent poleward shift of the storm tracks in simulations of 21st century climate. *Geophys. Res. Lett.*, **32**, L18701, doi:10.1029/2005GL023684.

Yokohata, T., et al., 2005: Climate response to volcanic forcing: Validation of climate sensitivity of a coupled atmosphere-ocean general circulation model. *Geophys. Res. Lett.*, **32**, L21710, doi:10.1029/2005GL023542.

Yonetani, T., and H.B. Gordon, 2001: Simulated changes in the frequency of extremes and regional features of seasonal/annual temperature and precipitation when atmospheric CO_2 is doubled. *J. Clim.*, **14**, 1765–1779.

Yoshida, Y., et al., 2005: Multi-century ensemble global warming projections using the Community Climate System Model (CCSM3). *J. Earth Simulator*, **3**, 2–10.

Yoshimori, M., M.C. Reader, A.J. Weaver, and N.A. McFarlane, 2002: On the causes of glacial inception at 116 kaBP. *Clim. Dyn.*, **18**, 383–402.

Yoshimura, J., and M. Sugi, 2005: Tropical cyclone climatology in a high-resolution AGCM: Impacts of SST warming and CO_2 increase. *Scientific Online Letters on the Atmosphere*, **1**, 133–136.

Yoshimura, J., M. Sugi, and A. Noda, 2006: Influence of greenhouse warming on tropical cyclone frequency. *J. Meteorol. Soc. Japan*, **84**, 405–428.

Yukimoto, S., et al., 2006: Climate change of the twentieth through the twenty-first centuries simulated by the MRI-CGCM2.3. *Pap. Meteorol. Geophys.*, **56**, 9–24.

Zelle, H., G.J. van Oldenborgh, G. Burgers, and H.A. Dijkstra, 2005: El Niño and greenhouse warming: Results from ensemble simulations with the NCAR CCSM. *J. Clim.*, **18**, 4669–4683.

Zeng, G., and J.A. Pyle, 2003: Changes in tropospheric ozone between 2000 and 2100 modeled in a chemistry-climate model. *Geophys. Res. Lett.*, **30**, 1392.

Zhang, X.D., and J.E. Walsh, 2006: Toward a seasonally ice-covered Arctic Ocean: Scenarios from the IPCC AR4 model simulations. *J. Clim.*, **19**, 1730–1747.

Zuo, Z., and J. Oerlemans, 1997: Contribution of glacial melt to sea level rise since AD 1865: A regionally differentiated calculation. *Clim. Dyn.*, **13**, 835–845.

Zwally, H.J., et al., 2002: Surface melt-induced acceleration of Greenland ice-sheet flow. *Science*, **297**, 218-222.

Zwally, H.J., et al., 2005: Mass changes of the Greenland and Antarctic ice sheets and shelves and contributions to sea level rise: 1992-2002. *J. Glaciol.*, **175**, 509–527.

Zweck, C., and P. Huybrechts, 2005: Modeling of the northern hemisphere ice sheets during the last glacial cycle and glaciological sensitivity. *J. Geophys. Res.*, **110**, D07103, doi:10.1029/2004JD005489.

Appendix 10.A: Methods for Sea Level Projections for the 21st Century

10.A.1 Scaling MAGICC Results

The MAGICC SCM was tuned to emulate global average surface air temperature change and radiative flux at the top of the atmosphere (assumed equal to ocean heat uptake on decadal time scales; Section 5.2.2.3 and Figure 5.4) simulated by each of 19 AOGCMs in scenarios with CO_2 increasing at 1% yr^{-1} (Section 10.5.3). Under SRES scenarios for which AOGCMs have been run (B1, A1B and A2), the ensemble average of the tuned versions of MAGICC gives about 10% greater temperature rise and 25% more thermal expansion over the 21st century (2090 to 2099 minus 1980 to 1999) than the average of the corresponding AOGCMs. The MAGICC radiative forcing is close to that of the AOGCMs (as estimated for A1B by Forster and Taylor, 2006), so the mismatch suggests there may be structural limitations on the accurate emulation of AOGCMs by the SCM. We therefore do not use the tuned SCM results directly to make projections, unlike in the TAR. The TAR model means for thermal expansion were 0.06–0.10 m larger than the central estimates in Table 10.7, probably because the simple climate model used in the TAR overestimated the TAR AOGCM results.

The SCM may nonetheless be used to estimate results for scenarios that have not been run in AOGCMs, by calculating time-dependent ratios between pairs of scenarios (Section 10.5.4.6). This procedure is supported by the close match between the ratios derived from the AOGCM and MAGICC ensemble averages under the scenarios for which AOGCMs are available. Applying the MAGICC ratios to the A1B AOGCM results yields estimates of temperature rise and thermal expansion for B1 and A2 differing by less than 5% from the AOGCM ensemble averages. We have high confidence that the procedure will yield similarly accurate estimates for the results that the AOGCMs would give under scenarios B2, A1T and A1FI.

The spread of MAGICC models is much narrower than the AOGCM ensemble because the AOGCMs have internally generated climate variability and a wider range of forcings. We assume inter-model standard deviations of 20% of the model average for temperature rise and 25% for thermal expansion, since these proportions are found to be fairly time and scenario independent in the AOGCM ensemble.

10.A.2 Mass Balance Sensitivity of Glaciers and Ice Caps

A linear relationship $r_g = b_g \times (T - T_0)$ is found for the period 1961 to 2003 between the observational time series of the contribution r_g to the rate of sea level rise from the world's glaciers and ice caps (G&IC, excluding those on Antarctica and Greenland; Section 4.5.2, Figure 4.14) and global average surface air temperature T (Hadley Centre/Climatic Research Unit gridded surface temperature dataset HadCRUT3; Section 3.2.2.4, Figure 3.6), where b_g is the global total G&IC mass balance sensitivity and T_0 is the global average temperature of the climate in which G&IC are in a steady state, T and T_0 being expressed relative to the average of 1865 to 1894. The correlation coefficient is 0.88. Weighted least-squares regression gives a slope b_g = 0.84 ± 0.15 (one standard deviation) mm yr^{-1} $°C^{-1}$, with $T_0 = -0.13$°C. Surface mass balance models driven with climate change scenarios from AOGCMs (Section 10.6.3.1) also indicate such a linear relationship, but the model results give a somewhat lower b_g of around 0.5 to 0.6 mm yr^{-1} $°C^{-1}$ (Section 10.6.3.1). To cover both observations and models, we adopt a value of b_g = 0.8 ± 0.2 (one standard deviation) mm yr^{-1} $°C^{-1}$. This uncertainty of ±25% is smaller than that of ±40% used in the TAR because of the improved observational constraint now available. To make projections, we choose a set of values of b_g randomly from a normal distribution. We use $T_0 = T - r_g/b_g$, where T = 0.40 °C and r_g = 0.45 mm yr^{-1}, are the averages over the period 1961 to 2003. This choice of T_0 minimises the root mean square difference of the predicted r_g from the observed, and gives T_0 in the range −0.5°C to 0.0°C (5 to 95%). Note that a constant b_g is not expected to be a good approximation if glacier area changes substantially (see Section 10.A.3).

10.A.3 Area Scaling of Glaciers and Ice Caps

Model results using area-volume scaling of G&IC (Section 10.6.3.2) are approximately described by the relations $b_g / b_1 = (A_g / A_1)^{1.96}$ and $A_g / A_1 = (V_g / V_1)^{0.84}$, where A_g and V_g are the global G&IC area and volume (excluding those on Greenland and Antarctica) and variable X_1 is the initial value of X_g. The first relation describes how total SMB sensitivity declines as the most sensitive areas are ablated most rapidly. The second relation follows Wigley and Raper (2005) in its form, and describes how area declines as volume is lost, with $dV_g / dt = -r_g$ (expressing V as sea level equivalent, i.e., the liquid-water-equivalent volume of ice divided by the surface area of the world ocean). Projections are made starting from 1990 using T from Section 10.A.1 with initial values of the present-day b_g from Section 10.A.2 and the three recent estimates V_g = 0.15, 0.24 and 0.37 m from Table 4.4, which are assumed equally likely. We use T = 0.48°C at 1990 relative to 1865 to 1894, and choose T_0 as in Section 10.A.2. An uncertainty of 10% (one standard deviation) is assumed because of the scaling relations. The results are multiplied by 1.2 (Section 10.6.3.3) to include contributions from G&IC on Greenland and Antarctica (apart from the ice sheets). These scaling relations are expected to give a decreasingly adequate approximation as greater area and volume is lost, because they do not model hypsometry explicitly; they predict that V will tend eventually to zero in any steady-state warmer climate, for instance, although this is not necessarily the case. A similar scaling procedure was used in the TAR. Current estimates of present-day G&IC mass are smaller than those used in the TAR, leading to more rapid wastage of

area. Hence, the central estimates for the G&IC contribution to sea level rise in Table 10.7 are similar to those in the TAR, despite our use of a larger mass balance sensitivity (Section 10.A.2).

10.A.4 Changes in Ice Sheet Surface Mass Balance

Quadratic fits are made to the results of Gregory and Huybrechts (2006) (Section 10.6.4.1) for the SMB change of each ice sheet as a function of global average temperature change relative to a steady state, which is taken to be the late 19th century (1865–1894). The spread of results for the various models used by Gregory and Huybrechts represents uncertainty in the patterns of temperature and precipitation change. The Greenland contribution has a further uncertainty of 20% (one standard deviation) from the ablation calculation. The Antarctic SMB projections are similar to those of the TAR, while the Greenland SMB projections are larger by 0.01–0.04 m because of the use of a quadratic fit to temperature change rather than the constant sensitivity of the TAR, which gave an underestimate for larger warming.

10.A.5 Changes in Ice Sheet Dynamics

Topographic and dynamic changes that can be simulated by currently available ice flow models are roughly represented as modifying the sea level changes due to SMB change by –5% ± 5% from Antarctica, and 0% ± 10% from Greenland (± one standard deviation) (Section 10.6.4.2).

The contribution from scaled-up ice sheet discharge, given as an illustration of the effect of accelerated ice flow (Section 10.6.5), is calculated as $r_1 \times T / T_1$, with T and T_1 expressed relative to the 1865 to 1894 average, where $r_1 = 0.32$ mm yr^{-1} is an estimate of the contribution during 1993 to 2003 due to recent acceleration and $T_1 = 0.63$°C is the global average temperature during that period.

10.A.6 Combination of Uncertainties

For each scenario, time series of temperature rise and the consequent land ice contributions to sea level are generated using a Monte Carlo simulation (van der Veen, 2002). Temperature rise and thermal expansion have some correlation for a given scenario in AOGCM results (Section 10.6.1). In the Monte Carlo simulation, we assume them to be perfectly correlated; by correlating the uncertainties in the thermal expansion and land ice contributions, this increases the resulting uncertainty in the sea level rise projections. However, the uncertainty in the projections of the land ice contributions is dominated by the various uncertainties in the land ice models themselves (Sections 10.A.2–4) rather than in the temperature projections. We assume the uncertainties in land ice models and temperature projections to be uncorrelated. The procedure used in the TAR, however, effectively assumed the land ice model uncertainty to be correlated with the temperature and expansion projection uncertainty. This is the main reason why the TAR ranges for sea level rise under each of the scenarios are wider than those of Table 10.7. Also, the TAR gave uncertainty ranges of ±2 standard deviations, whereas the present report gives ±1.65 standard deviations (5 to 95%).

10.A.7 Change in Surface Air Temperature Over the Major West Antarctic Ice Shelves

The mean surface air temperature change over the area of the Ross and Filchner-Ronne ice shelves in December and January, divided by the mean annual antarctic surface air temperature change, is $F_1 = 0.62 \pm 0.48$ (one standard deviation) on the basis of the climate change simulations from the four high-resolution GCMs used by Gregory and Huybrechts (2006). From AR4 AOGCMs, the ratio of mean annual antarctic temperature change to global mean temperature change is $F_2 = 1.1 \pm 0.2$ (one standard deviation) under SRES scenarios with stabilisation beyond 2100 (Gregory and Huybrechts, 2006), while from AR4 AGCMs coupled to mixed-layer ocean models it is $F_2 = 1.4 \pm 0.2$ (one standard deviation) at equilibrium under doubled CO_2. To evaluate the probability of ice shelf mean summer temperature increase exceeding a particular value, given the global temperature rise, a Monte Carlo distribution of $F_1 \times F_2$ is used, generated by assuming the two factors to be normal and independent random variables. Since this procedure is based on a small number of models, and given other caveats noted in Sections 10.6.4.2 and 10.7.4.4, we have low confidence in these probabilities.

11

Regional Climate Projections

Coordinating Lead Authors:

Jens Hesselbjerg Christensen (Denmark), Bruce Hewitson (South Africa)

Lead Authors:

Aristita Busuioc (Romania), Anthony Chen (Jamaica), Xuejie Gao (China), Isaac Held (USA), Richard Jones (UK), Rupa Kumar Kolli (India), Won-Tae Kwon (Republic of Korea), René Laprise (Canada), Victor Magaña Rueda (Mexico), Linda Mearns (USA), Claudio Guillermo Menéndez (Argentina), Jouni Räisänen (Finland), Annette Rinke (Germany), Abdoulaye Sarr (Senegal), Penny Whetton (Australia)

Contributing Authors:

R. Arritt (USA), R. Benestad (Norway), M. Beniston (Switzerland), D. Bromwich (USA), D. Caya (Canada), J. Comiso (USA), R. de Elía (Canada, Argentina), K. Dethloff (Germany), S. Emori (Japan), J. Feddema (USA), R. Gerdes (Germany), J.F. González-Rouco (Spain), W. Gutowski (USA), I. Hanssen-Bauer (Norway), C. Jones (Canada), R. Katz (USA), A. Kitoh (Japan), R. Knutti (Switzerland), R. Leung (USA), J. Lowe (UK), A.H. Lynch (Australia), C. Matulla (Canada, Austria), K. McInnes (Australia), A.V. Mescherskaya (Russian Federation), A.B. Mullan (New Zealand), M. New (UK), M.H. Nokhandan (Iran), J.S. Pal (USA, Italy), D. Plummer (Canada), M. Rummukainen (Sweden, Finland), C. Schär (Switzerland), S. Somot (France), D.A. Stone (UK, Canada), R. Suppiah (Australia), M. Tadross (South Africa), C. Tebaldi (USA), W. Tennant (South Africa), M. Widmann (Germany, UK), R. Wilby (UK), B.L. Wyman (USA)

Review Editors:

Congbin Fu (China), Filippo Giorgi (Italy)

This chapter should be cited as:

Christensen, J.H., B. Hewitson, A. Busuioc, A. Chen, X. Gao, I. Held, R. Jones, R.K. Kolli, W.-T. Kwon, R. Laprise, V. Magaña Rueda, L. Mearns, C.G. Menéndez, J. Räisänen, A. Rinke, A. Sarr and P. Whetton, 2007: Regional Climate Projections. In: *Climate Change 2007: The Physical Science Basis. Contribution of Working Group I to the Fourth Assessment Report of the Intergovernmental Panel on Climate Change* [Solomon, S., D. Qin, M. Manning, Z. Chen, M. Marquis, K.B. Averyt, M. Tignor and H.L. Miller (eds.)]. Cambridge University Press, Cambridge, United Kingdom and New York, NY, USA.

Table of Contents

Executive Summary 849

11.1 Introduction 852

11.1.1 Summary of the Third Assessment Report 852

11.1.2 Introduction to Regional Projections 852

Box 11.1: Summary of Regional Responses 858

11.1.3 Some Unifying Themes 860

11.2 Africa 866

11.2.1 Key Processes 866

11.2.2 Skill of Models in Simulating Present and Past Climates 867

11.2.3 Climate Projections 867

11.3 Europe and the Mediterranean 872

11.3.1 Key Processes 872

11.3.2 Skill of Models in Simulating Present Climate 872

Box 11.2: The PRUDENCE Project 873

11.3.3 Climate Projections 873

11.4 Asia 879

11.4.1 Key Processes 879

11.4.2 Skill of Models in Simulating Present Climate 880

11.4.3 Climate Projections 881

Box 11.3: Climatic Change in Mountain Regions 886

11.5 North America 887

11.5.1 Key Processes 887

11.5.2 Skill of Models in Simulating Present Climate 888

11.5.3 Climate Projections 889

11.6 Central and South America 892

11.6.1 Key Processes 892

11.6.2 Skill of Models in Simulating Present Climate 893

11.6.3 Climate Projections 894

11.6.4 Extremes 896

11.7 Australia – New Zealand 896

Box 11.4: Land Use and Land Cover Change Experiments Related to Climate Change 897

11.7.1 Key Processes 898

11.7.2 Skill of Models in Simulating Present Climate 898

11.7.3 Climate Projections 899

11.8 Polar Regions 902

11.8.1 Arctic 903

11.8.2 Antarctic 907

11.9 Small Islands 909

11.9.1 Key Processes 910

11.9.2 Skill of Models in Simulating Present Climate 911

11.9.3 Temperature and Precipitation Projections 911

11.9.4 Sea Level Rise 914

11.9.5 Tropical Cyclones 915

Box 11.5: Coastal Zone Climate Change 916

11.10 Assessment of Regional Climate Projection Methods 918

11.10.1 Methods for Generating Regional Climate Information 918

11.10.2 Quantifying Uncertainties 921

Frequently Asked Question

FAQ 11.1: *Do Projected Changes in Climate Vary from Region to Region?* 865

References 926

Supplementary Material

The following supplementary material is available on CD-ROM and in on-line versions of this report.

Supplementary Figures S11.1–S11.37

Supplementary Tables S1.1 and S1.2

Supplementary References

Executive Summary

Increasingly reliable regional climate change projections are now available for many regions of the world due to advances in modelling and understanding of the physical processes of the climate system. A number of important themes have emerged:

- Warming over many land areas is greater than global annual mean warming due to less water availability for evaporative cooling and a smaller thermal inertia as compared to the oceans.
- Warming generally increases the spatial variability of precipitation, contributing to a reduction of rainfall in the subtropics and an increase at higher latitudes and in parts of the tropics. The precise location of boundaries between regions of robust increase and decrease remains uncertain and this is commonly where Atmosphere-Ocean General Circulation Model (AOGCM) projections disagree.
- The poleward expansion of the subtropical highs, combined with the general tendency towards reductions in subtropical precipitation, creates especially robust projections of a reduction in precipitation at the poleward edges of the subtropics. Most of the regional projections of reductions in precipitation in the 21st century are associated with areas adjacent to these subtropical highs.
- There is a tendency for monsoonal circulations to result in increased precipitation due to enhanced moisture convergence, despite a tendency towards weakening of the monsoonal flows themselves. However, many aspects of tropical climatic responses remain uncertain.

Atmosphere-Ocean General Circulation Models remain the primary source of regional information on the range of possible future climates. A clearer picture of the robust aspects of regional climate change is emerging due to improvement in model resolution, the simulation of processes of importance for regional change and the expanding set of available simulations. Advances have been made in developing probabilistic information at regional scales from the AOGCM simulations, but these methods remain in the exploratory phase. There has been less development extending this to downscaled regional information. However, downscaling methods have matured since the Third Assessment Report (TAR; IPCC, 2001) and have been more widely applied, although only in some regions has large-scale coordination of multi-model downscaling of climate change simulations been achieved.

Regional climate change projections presented here are assessed drawing on information from four potential sources: AOGCM simulations; downscaling of AOGCM-simulated data using techniques to enhance regional detail; physical understanding of the processes governing regional responses; and recent historical climate change.

Previous chapters describe observed climate change on regional scales (Chapter 3) and compare global model simulations with these changes (Chapter 9). Comparisons of model simulations of temperature change with observations can be used to help constrain future regional temperature projections. Regional assessments of precipitation change rely primarily on convergence in both global and downscaling models along with physical insights. Where there is near unanimity among models with good supporting physical arguments, as is more typical for middle and higher latitudes, these factors encourage stronger statements as to the likelihood of a regional climate change. In some circumstances, physical insights alone clearly indicate the direction of future change.

The summary likelihood statements on projected regional climate are as follows:

- ***Temperature projections:*** These are comparable in magnitude to those of the TAR and confidence in the regional projections is now higher due to a larger number and variety of simulations, improved models, a better understanding of the role of model deficiencies and more detailed analyses of the results. Warming, often greater than the global mean, is *very likely* over all landmasses.
- ***Precipitation projections:*** Overall patterns of change are comparable to those of TAR, with greater confidence in the projections for some regions. Model agreement is seen over more and larger regions. For some regions, there are grounds for stating that the projected precipitation changes are *likely* or *very likely*. For other regions, confidence in the projected change remains weak.
- ***Extremes:*** There has been a large increase in the available analyses of changes in extremes. This allows for a more comprehensive assessment for most regions. The general findings are in line with the assessment made in TAR and now have a higher level of confidence derived from multiple sources of information. The most notable improvements in confidence relate to the regional statements concerning heat waves, heavy precipitation and droughts. Despite these advances, specific analyses of models are not available for some regions, which is reflected in the robust statements on extremes. In particular, projections concerning extreme events in the tropics remain uncertain. The difficulty in projecting the distribution of tropical cyclones adds to this uncertainty. Changes in extra-tropical cyclones are dependent on details of regional atmospheric circulation response, some of which remain uncertain.

The following summarises the robust findings of the projected regional change over the 21st century. Supporting narratives are provided in Sections 11.2 to 11.9. These changes are assessed as *likely* to *very likely* taking into account the uncertainties in climate sensitivity and emission trajectories (in the Special Report on Emission Scenarios (SRES) B1/A1B/B2 scenario range) discussed in earlier chapters.

All land regions:

It is *very likely* that all land regions will warm in the 21st century.

Africa:

Warming is *very likely* to be larger than the global annual mean warming throughout the continent and in all seasons, with drier subtropical regions warming more than the moister tropics. Annual rainfall is *likely* to decrease in much of Mediterranean Africa and the northern Sahara, with a greater likelihood of decreasing rainfall as the Mediterranean coast is approached. Rainfall in southern Africa is *likely* to decrease in much of the winter rainfall region and western margins. There is *likely* to be an increase in annual mean rainfall in East Africa. It is unclear how rainfall in the Sahel, the Guinean Coast and the southern Sahara will evolve.

Mediterranean and Europe:

Annual mean temperatures in Europe are *likely* to increase more than the global mean. Seasonally, the largest warming is *likely* to be in northern Europe in winter and in the Mediterranean area in summer. Minimum winter temperatures are *likely* to increase more than the average in northern Europe. Maximum summer temperatures are *likely* to increase more than the average in southern and central Europe. Annual precipitation is *very likely* to increase in most of northern Europe and decrease in most of the Mediterranean area. In central Europe, precipitation is *likely* to increase in winter but decrease in summer. Extremes of daily precipitation are *very likely* to increase in northern Europe. The annual number of precipitation days is *very likely* to decrease in the Mediterranean area. Risk of summer drought is *likely* to increase in central Europe and in the Mediterranean area. The duration of the snow season is *very likely* to shorten, and snow depth is *likely* to decrease in most of Europe.

Asia:

Warming is *likely* to be well above the global mean in central Asia, the Tibetan Plateau and northern Asia, above the global mean in eastern Asia and South Asia, and similar to the global mean in Southeast Asia. Precipitation in boreal winter is *very likely* to increase in northern Asia and the Tibetan Plateau, and *likely* to increase in eastern Asia and the southern parts of Southeast Asia. Precipitation in summer is *likely* to increase in northern Asia, East Asia, South Asia and most of Southeast Asia, but is *likely* to decrease in central Asia. It is *very likely* that heat waves/hot spells in summer will be of longer duration, more intense and more frequent in East Asia. Fewer very cold days are *very likely* in East Asia and South Asia. There is *very likely* to be an increase in the frequency of intense precipitation events in parts of South Asia, and in East Asia. Extreme rainfall and winds associated with tropical cyclones are *likely* to increase in East Asia, Southeast Asia and South Asia.

North America:

The annual mean warming is *likely* to exceed the global mean warming in most areas. Seasonally, warming is *likely* to be largest in winter in northern regions and in summer in the southwest. Minimum winter temperatures are *likely* to increase more than the average in northern North America. Maximum summer temperatures are *likely* to increase more than the average in the southwest. Annual mean precipitation is *very likely* to increase in Canada and the northeast USA, and *likely* to decrease in the southwest. In southern Canada, precipitation is *likely* to increase in winter and spring but decrease in summer. Snow season length and snow depth are *very likely* to decrease in most of North America except in the northernmost part of Canada where maximum snow depth is *likely* to increase.

Central and South America:

The annual mean warming is *likely* to be similar to the global mean warming in southern South America but larger than the global mean warming in the rest of the area. Annual precipitation is *likely* to decrease in most of Central America and in the southern Andes, although changes in atmospheric circulation may induce large local variability in precipitation response in mountainous areas. Winter precipitation in Tierra del Fuego and summer precipitation in south-eastern South America is *likely* to increase. It is uncertain how annual and seasonal mean rainfall will change over northern South America, including the Amazon forest. However, there is qualitative consistency among the simulations in some areas (rainfall increasing in Ecuador and northern Peru, and decreasing at the northern tip of the continent and in southern northeast Brazil).

Australia and New Zealand:

Warming is *likely* to be larger than that of the surrounding oceans, but comparable to the global mean. The warming is less in the south, especially in winter, with the warming in the South Island of New Zealand *likely* to remain less than the global mean. Precipitation is *likely* to decrease in southern Australia in winter and spring. Precipitation is *very likely* to decrease in south-western Australia in winter. Precipitation is *likely* to increase in the west of the South Island of New Zealand. Changes in rainfall in northern and central Australia are uncertain. Increased mean wind speed is *likely* across the South Island of New Zealand, particularly in winter. Increased frequency of extreme high daily temperatures in Australia and New Zealand, and a decrease in the frequency of cold extremes is *very likely*. Extremes of daily precipitation are *very likely* to increase, except possibly in areas of significant decrease in mean rainfall (southern Australia in winter and spring). Increased risk of drought in southern areas of Australia is *likely*.

Polar regions:

The Arctic is *very likely* to warm during this century more than the global mean. Warming is projected to be largest in winter and smallest in summer. Annual arctic precipitation is *very likely* to increase. It is *very likely* that the relative precipitation increase will be largest in winter and smallest in summer. Arctic sea ice is *very likely* to decrease in its extent and thickness. It is uncertain how the Arctic Ocean circulation will change. The Antarctic is *likely* to warm and the precipitation is *likely* to increase over the continent. It is uncertain to what extent the frequency of extreme temperature and precipitation events will change in the polar regions.

Small Islands:

Sea levels are *likely* to rise on average during the century around the small islands of the Caribbean Sea, Indian Ocean and northern and southern Pacific Oceans. The rise will *likely* not be geographically uniform but large deviations among models make regional estimates across the Caribbean, Indian and Pacific Oceans uncertain. All Caribbean, Indian Ocean and North and South Pacific islands are *very likely* to warm during this century. The warming is *likely* to be somewhat smaller than the global annual mean. Summer rainfall in the Caribbean is *likely* to decrease in the vicinity of the Greater Antilles but changes elsewhere and in winter are uncertain. Annual rainfall is *likely* to increase in the northern Indian Ocean with increases *likely* in the vicinity of the Seychelles in December, January and February, and in the vicinity of the Maldives in June, July and August, while decreases are *likely* in the vicinity of Mauritius in June, July and August. Annual rainfall is *likely* to increase in the equatorial Pacific, while decreases are projected by most models for just east of French Polynesia in December, January and February.

11.1 Introduction

Increasingly reliable regional climate change projections are now available for many regions of the world due to advances in modelling and understanding of the physical processes of the climate system. Atmosphere-Ocean General Circulation Models (AOGCMs) remain the foundation for projections while downscaling techniques now provide valuable additional detail. Atmosphere-Ocean General Circulation Models cannot provide information at scales finer than their computational grid (typically of the order of 200 km) and processes at the unresolved scales are important. Providing information at finer scales can be achieved through using high resolution in dynamical models or empirical statistical downscaling. Development of downscaling methodologies remains an important focus. Downscaled climate change projections tailored to specific needs are only now starting to become available.

11.1.1 Summary of the Third Assessment Report

The assessment of regional climate projections in the Third Assessment Report (TAR; Chapter 10 of IPCC, 2001) was largely restricted to General Circulation Model (GCM)-derived temperature with limited precipitation statements. The major assessment of temperature change was that it is very likely all land areas will warm more than the global average (with the exception of Southeast Asia and South America in June, July and August; JJA), with amplification at high latitudes. The changes in precipitation assessed to be likely were: an increase over northern mid-latitude regions in winter and over high-latitude regions in both winter and summer; in December, January and February (DJF), an increase in tropical Africa, little change in Southeast Asia, and a decrease in Central America; an increase or little change in JJA over South Asia and a decrease over Australia and the Mediterranean region. These projections were almost entirely based on analysis of nine coarse-resolution AOGCMs that had performed transient experiments for the 20th century with the specifications for the A2 and B2 emission scenarios. Chapter 10 of the TAR noted that studies with regional models indicate that changes at finer scales may be substantially different in magnitude from these large sub-continental findings.

Information available for assessment regarding climate variability and extremes at the regional scale was too sparse for it to be meaningfully drawn together in a systematic manner. However, some statements of a more generic nature were made. It was assessed that the variability of daily to interannual temperatures is likely to decrease in winter and increase in summer for mid-latitude Northern Hemisphere (NH) land areas, daily high temperature extremes are likely to increase and future increases in mean precipitation are very likely to lead to an increase in variability. In some specifically analysed regions, it was assessed that extreme precipitation may increase and there were indications that droughts or dry spells may increase in occurrence in Europe, North America and Australia.

11.1.2 Introduction to Regional Projections

Assessments of climate change projections are provided here on a region-by-region basis. The discussion is organised according to the same continental-scale regions used by Working Group II (WGII) in the Fourth Assessment Report (AR4) and in earlier assessments: Africa, Europe and Mediterranean, Asia, North America, Central and South America, Australia-New Zealand, Polar Regions and Small Islands. While the topics covered vary somewhat from region to region, each section includes a discussion of key processes of importance for climate change in that region, relevant aspects of model skill in simulating current climate, and projections of future regional climate change based on global models and downscaling techniques.

Each of these continental-scale regions encompasses a broad range of climates and is too large to be used as a basis for conveying quantitative regional climate change information. Therefore, each is subdivided into a number of sub-continental or oceanic regions. The sub-continental regions as defined in Table 11.1 are the framework for developing specific regional or sub-continental robust statements of projected change.

Area-averaged temperature and precipitation changes are presented from the coordinated set of climate model simulations archived at the Program for Climate Model Diagnosis and Intercomparison (PCMDI; subsequently called the multi-model data set or MMD). The regions are very close to those initially devised by Giorgi and Francesco (2000) with some minor modifications similar to those of Ruosteenoja et al. (2003). They have simple shapes and are no smaller than the horizontal scales on which current AOGCMs are useful for climate simulations (typically judged to be roughly 1,000 km).

These regional averages have some deficiencies for discussion of the AOGCM projections. In several instances, the simple definition of these boxes results in spatial averaging over regions in which precipitation is projected to increase and decrease. There are also sub-regions where the case can be made for a robust and physically plausible hydrological response, information about which is lost in the regional averages. Partially to help in discussing these features, this chapter also uses maps of temperature and precipitation responses, interpolated to a grid with 128 longitudes by 64 latitudes which is typical of many of the lower-resolution atmospheric models in the MMD.

In the regional discussion to follow, the starting points are temperature and precipitation. Changes in temperature are introduced in each continental section by plotting for each of the regions the evolution of the range of projected decadal mean change for the A1B scenario through the 21st century (simulations hereafter referred to as MMD-A1B). These are put into the context of observed changes in the 20th century by plotting the observed changes and how well the models reproduce these. This summary information is displayed for continental regions in Box 11.1, which also contains details of how the figures were constructed. The equivalent figures for the individual regions of each continental-scale region are displayed in the following sections. These are constructed in

the same way as Box 11.1, Figure 1. The 20th-century parts of these figures are also displayed in Section 9.4, where more details on their construction are provided. The discussion on precipitation provides a limited view of hydrological changes. Supplementary Material Figure S11.1 expands on this issue by comparing the annual mean responses in precipitation and in precipitation minus evaporation over the 21st century in the MMD-A1B projections. Over North America and Europe, for example, the region of drying in the sense of precipitation minus evaporation is shifted poleward compared to the region of reduced precipitation. A summary of the more significant hydrological cycle changes from the regional discussions is presented in Box 11.1.

Table 11.1 provides detailed information for each region generated from the MMD-A1B models focusing on the change in climate between the 1980 to 1999 period in the 20th-century integrations and the 2080 to 2099 period. The distribution of the annual and seasonal mean surface air temperature response and percentage change in precipitation are described by the median, the 25 and 75% values (half of the models lie between these two values) and the maximum and minimum values in the model ensemble. Information on model biases in these regional averages for the 1980 to 1999 simulations is provided in Supplementary Material Table S11.1 in a similar format. Maps of biases are referred to in some of the following and are included in the Supplementary Material as well. Data sources used in these comparisons are listed in the table and figure captions where these biases are displayed.

Most of the discussion focuses on the A1B scenario. The global mean near-surface temperature responses (between the period 1980 to 1999 of the 20th-century integrations and the period 2080 to 2099) in the ensemble mean of the MMD models are in the ratio 0.69:1:1.17 for the B1:A1B:A2 scenarios. The local temperature responses in nearly all regions closely follow the same ratio, as discussed in Chapter 10 and as illustrated in Supplementary Material Figures S11.2 to S11.4. Therefore, little is gained by repeating the discussion of the A1B scenario for the other scenarios. The ensemble mean local precipitation responses also approximately scale with the global mean temperature response, although not as precisely as the temperature itself. Given the substantial uncertainties in hydrological responses, the generally smaller signal/noise ratio and the similarities in the basic structure of the AOGCM precipitation responses in the different scenarios, a focus on A1B seems justified for the precipitation as well. The overall regional assessments, however, do rely on all available scenario information.

Given the dominantly linear response of the models, the 2080 to 2099 period allows the greatest clarity of the background climate change underlying the interannual and decadal variability. In the ensemble mean AOGCM projections there is no indication of abrupt climate change, nor does the literature on individual models provide any strong suggestions of robust nonlinearities. Some local temporal nonlinearities are to be expected, for example as the sea ice boundary retreats from a particular location in the Arctic. While the possibility exists that changes of more abrupt character could happen, such as major ocean circulation or land surface/vegetation change, there is little basis to judge the plausibility of these factors (see Chapter 10). Therefore, this discussion is based on this linear picture.

Table 11.1 also provides some simple estimates of the signal-to-noise ratio. The signal is the change in 20-year means of seasonal or annual mean temperature or precipitation. The noise is an estimate of the internal variability of 20-year means of seasonal or annual mean temperature or precipitation, as generated by the models. The signal-to-noise ratio is converted into the time interval that is required before the signal is clearly discernible, assuming that the signal grows linearly over the century at the average rate in the ensemble mean A1B projection. 'Clearly discernible' is defined in this context as distinguishable with 95% confidence. As an example, the annual mean precipitation increase in northern Europe (NEU) (Table 11.1) is clearly discernible in these models after 45 years, meaning that the 20-year average from 2025 to 2044 will be greater than the 20-year mean over 1980 to 1999 with 95% confidence, accounting only for the internal variability in the models and no other sources of uncertainty. In contrast, the annual temperature response in Southeast Asia (SEA) rises above the noise by this measure after only 10 years, implying that the average temperature over the period 1990 to 2009 is clearly discernible in the models from the average over the control period 1980 to 1999. This measure is likely an overestimate of the time of emergence of the signal as compared to that obtained with more refined detection strategies (of the kind discussed in Chapter 9). This noise estimate is solely based on the models and must be treated with caution, but it would be wrong to assume that models always underestimate this internal variability. Some models overestimate and some underestimate the amplitude of the El Niño-Southern Oscillation (ENSO), for example, thereby over- or underestimating the most important source of interannual variability in the tropics. On the other hand, few models capture the range of decadal variability of rainfall in West Africa, for example (Hoerling, et al., 2006; Section 8.4).

Also included in Table 11.1 is an estimate of the probability of extremely warm, extremely wet and extremely dry seasons, for the A1B scenario and for the time period 2080 to 2099. An 'extremely warm' summer is defined as follows. Examining all of the summers simulated in a particular realisation of a model in the 1980 to 1999 control period, the warmest of these 20 summers can be computed as an estimate of the temperature of the warmest 5% of all summers in the control climate. The period 2080 to 2099 is then examined, and the fraction of the summers exceeding this warmth determined. This is referred to as the probability of extremely warm summers. The results are tabulated after averaging over models, and similarly for both extremely low and extremely high seasonal precipitation amounts. Values smaller (larger) than 5% indicate a decrease (increase) in the frequency of extremes. This follows the approach in Weisheimer and Palmer (2005) except that this chapter compares each model's future with its own 20th century to help avoid distortions due to differing biases in the different

Table 11.1. *Regional averages of temperature and precipitation projections from a set of 21 global models in the MMD for the A1B scenario. The mean temperature and precipitation responses are first averaged for each model over all available realisations of the 1980 to 1999 period from the 20th Century Climate in Coupled Models (20C3M) simulations and the 2080 to 2099 period of A1B. Computing the difference between these two periods, the table shows the minimum, maximum, median (50%), and 25 and 75% quartile values among the 21 models, for temperature (°C) and precipitation (%) change. Regions in which the middle half (25–75%) of this distribution is all of the same sign in the precipitation response are coloured light brown for decreasing and light blue for increasing precipitation. Signal-to-noise ratios for these 20-year mean responses is indicated by first computing a consensus standard deviation of 20-year means, using those models that have at least three realisations of the 20C3M simulations and using all 20-year periods in the 20th century. The signal is assumed to increase linearly in time, and the time required for the median signal to reach 2.83 ($2 \times \sqrt{2}$) times the standard deviation is displayed as an estimate of when this signal is significant at the 95% level. These estimates of the times for emergence of a clearly discernible signal are only shown for precipitation when the models are in general agreement on the sign of the response, as indicated by the colouring. The frequency (%) of extremely warm, wet and dry seasons, averaged over the models, is also presented, as described in Section 11.2.1. Values are only shown when at least 14 out of the 21 models agree on an increase (bold) or a decrease in the extremes. A value of 5% indicates no change, as this is the nominal value for the control period by construction. The regions are defined by rectangular latitude/longitude boxes and the coordinates of the bottom left-hand and top right-hand corners of these are given in degrees in the first column under the region acronym (see table notes for full names of regions). Information is provided for land areas contained in the boxes except for the Small Islands regions where sea areas are used and for Antarctica where both land and sea areas are used.*

		Temperature Response (°C)						Precipitation Response (%)						Extreme Seasons (%)		
Region[a]	Season	Min	25	50	75	Max	T yrs	Min	25	50	75	Max	T yrs	Warm	Wet	Dry
AFRICA																
WAF	DJF	2.3	2.7	3.0	3.5	4.6	10	-16	-2	6	13	23		**100**	**21**	4
	MAM	1.7	2.8	3.5	3.6	4.8	10	-11	-7	-3	5	11		**100**		
12S,20W	JJA	1.5	2.7	3.2	3.7	4.7	10	-18	-2	2	7	16		**100**	**19**	
to	SON	1.9	2.5	3.3	3.7	4.7	10	-12	0	1	10	15		**100**	**15**	
22N,18E	Annual	1.8	2.7	3.3	3.6	4.7	10	-9	-2	2	7	13		**100**	**22**	
EAF	DJF	2.0	2.6	3.1	3.4	4.2	10	-3	6	13	16	33	55	**100**	**25**	1
	MAM	1.7	2.7	3.2	3.5	4.5	10	-9	2	6	9	20	>100	**100**	**15**	4
12S,22E	JJA	1.6	2.7	3.4	3.6	4.7	10	-18	-2	4	7	16		**100**		
to	SON	1.9	2.6	3.1	3.6	4.3	10	-10	3	7	13	38	95	**100**	**21**	3
18N,52E	Annual	1.8	2.5	3.2	3.4	4.3	10	-3	2	7	11	25	60	**100**	**30**	1
SAF	DJF	1.8	2.7	3.1	3.4	4.7	10	-6	-3	0	5	10		**100**	**11**	
	MAM	1.7	2.9	3.1	3.8	4.7	10	-25	-8	0	4	12		**98**		
35S,10E	JJA	1.9	3.0	3.4	3.6	4.8	10	-43	-27	-23	-7	-3	70	**100**	1	**23**
to	SON	2.1	3.0	3.7	4.0	5.0	10	-43	-20	-13	-8	3	90	**100**	1	**20**
12S,52E	Annual	1.9	2.9	3.4	3.7	4.8	10	-12	-9	-4	2	6		**100**	4	**13**
SAH	DJF	2.4	2.9	3.2	3.5	5.0	15	-47	-31	-18	-12	31	>100	**97**		**12**
	MAM	2.3	3.3	3.6	3.8	5.2	10	-42	-37	-18	-10	13	>100	**100**	2	**21**
18N,20E	JJA	2.6	3.6	4.1	4.4	5.8	10	-53	-28	-4	16	74		**100**		
to	SON	2.8	3.4	3.7	4.3	5.4	10	-52	-15	6	23	64		**100**		
30N,65E	Annual	2.6	3.2	3.6	4.0	5.4	10	-44	-24	-6	3	57		**100**		
EUROPE																
NEU	DJF	2.6	3.6	4.3	5.5	8.2	40	9	13	15	22	25	50	**82**	**43**	0
	MAM	2.1	2.4	3.1	4.3	5.3	35	0	8	12	15	21	60	**79**	**28**	2
48N,10W	JJA	1.4	1.9	2.7	3.3	5.0	25	-21	-5	2	7	16		**88**	**11**	
to	SON	1.9	2.6	2.9	4.2	5.4	30	-5	4	8	11	13	80	**87**	**20**	2
75N,40E	Annual	2.3	2.7	3.2	4.5	5.3	25	0	6	9	11	16	45	**96**	**48**	2
SEM	DJF	1.7	2.5	2.6	3.3	4.6	25	-16	-10	-6	-1	6	>100	**93**	3	**12**
	MAM	2.0	3.0	3.2	3.5	4.5	20	-24	-17	-16	-8	-2	60	**98**	1	**31**
30N,10W	JJA	2.7	3.7	4.1	5.0	6.5	15	-53	-35	-24	-14	-3	55	**100**	1	**42**
to	SON	2.3	2.8	3.3	4.0	5.2	15	-29	-15	-12	-9	-2	90	**100**	1	**21**
48N,40E	Annual	2.2	3.0	3.5	4.0	5.1	15	-27	-16	-12	-9	-4	45	**100**	0	**46**

Table 11.1 (continued)

		Temperature Response (°C)						Precipitation Response (%)						Extreme Seasons (%)		
Region[a]	Season	Min	25	50	75	Max	T yrs	Min	25	50	75	Max	T yrs	Warm	Wet	Dry
ASIA																
NAS	DJF	2.9	4.8	6.0	6.6	8.7	20	12	20	26	37	55	30	**93**	**68**	0
	MAM	2.0	2.9	3.7	5.0	6.8	25	2	16	18	24	26	30	**89**	**66**	1
50N,40E	JJA	2.0	2.7	3.0	4.9	5.6	15	-1	6	9	12	16	40	**100**	**51**	2
to	SON	2.8	3.6	4.8	5.8	6.9	15	7	15	17	19	29	30	**99**	**65**	0
70N,180E	Annual	2.7	3.4	4.3	5.3	6.4	15	10	12	15	19	25	20	**100**	**92**	0
CAS	DJF	2.2	2.6	3.2	3.9	5.2	25	-11	0	4	9	22		**84**	**8**	
	MAM	2.3	3.1	3.9	4.5	4.9	20	-26	-14	-9	-4	3	>100	**94**		**16**
30N,40E	JJA	2.7	3.7	4.1	4.9	5.7	10	-58	-28	-13	-4	21	>100	**100**	3	**20**
to	SON	2.5	3.2	3.8	4.1	4.9	15	-18	-4	3	9	24		**99**		
50N,75E	Annual	2.6	3.2	3.7	4.4	5.2	10	-18	-6	-3	2	6		**100**		**12**
TIB	DJF	2.8	3.7	4.1	4.9	6.9	20	1	12	19	26	36	45	**95**	**40**	0
	MAM	2.5	2.9	3.6	4.3	6.3	15	-3	4	10	14	34	70	**96**	**34**	2
30N,50E	JJA	2.7	3.2	4.0	4.7	5.4	10	-11	0	4	10	28		**100**	**24**	
to	SON	2.7	3.3	3.8	4.6	6.2	15	-8	-4	8	14	21		**100**	**20**	
75N,100E	Annual	2.8	3.2	3.8	4.5	6.1	10	-1	2	10	13	28	45	**100**	**46**	1
EAS	DJF	2.1	3.1	3.6	4.4	5.4	20	-4	6	10	17	42	>100	**96**	**18**	2
	MAM	2.1	2.6	3.3	3.8	4.6	15	0	7	11	14	20	55	**98**	**35**	2
20N,100E	JJA	1.9	2.5	3.0	3.9	5.0	10	-2	5	9	11	17	45	**100**	**32**	1
to	SON	2.2	2.7	3.3	4.2	5.0	15	-13	-1	9	15	29		**100**	**20**	3
50N,145E	Annual	2.3	2.8	3.3	4.1	4.9	10	2	4	9	14	20	40	**100**	**47**	1
SAS	DJF	2.7	3.2	3.6	3.9	4.8	10	-35	-9	-5	1	15		**99**		
	MAM	2.1	3.0	3.5	3.8	5.3	10	-30	-2	9	18	26		**100**	**14**	
5N,64E	JJA	1.2	2.2	2.7	3.2	4.4	15	-3	4	11	16	23	45	**96**	**32**	1
to	SON	2.0	2.5	3.1	3.5	4.4	10	-12	8	15	20	26	50	**100**	**29**	3
50N,100E	Annual	2.0	2.7	3.3	3.6	4.7	10	-15	4	11	15	20	40	**100**	**39**	3
SEA	DJF	1.6	2.1	2.5	2.9	3.6	10	-4	3	6	10	12	80	**99**	**23**	2
	MAM	1.5	2.2	2.7	3.1	3.9	10	-4	2	7	9	17	75	**100**	**27**	1
11S,95E	JJA	1.5	2.2	2.4	2.9	3.8	10	-3	3	7	9	17	70	**100**	**24**	2
to	SON	1.6	2.2	2.4	2.9	3.6	10	-2	2	6	10	21	85	**99**	**26**	3
20N,115E	Annual	1.5	2.2	2.5	3.0	3.7	10	-2	3	7	8	15	40	**100**	**44**	1
NORTH AMERICA																
ALA	DJF	4.4	5.6	6.3	7.5	11.0	30	6	20	28	34	56	40	**80**	**39**	0
	MAM	2.3	3.2	3.5	4.7	7.7	35	2	13	17	23	38	40	**69**	**45**	0
60N,170W	JJA	1.3	1.8	2.4	3.8	5.7	25	1	8	14	20	30	45	**86**	**51**	1
to	SON	2.3	3.6	4.5	5.3	7.4	25	6	14	19	31	36	40	**86**	**51**	0
72N,103W	Annual	3.0	3.7	4.5	5.2	7.4	20	6	13	21	24	32	25	**97**	**80**	0
CGI	DJF	3.3	5.2	5.9	7.2	8.5	20	6	15	26	32	42	30	**95**	**58**	0
	MAM	2.4	3.2	3.8	4.6	7.2	20	4	13	17	20	34	35	**94**	**49**	1
50N,103W	JJA	1.5	2.1	2.8	3.7	5.6	15	0	8	11	12	19	35	**99**	**46**	1
to	SON	2.7	3.4	4.0	5.7	7.3	20	7	14	16	22	37	35	**99**	**62**	0
85N,10W	Annual	2.8	3.5	4.3	5.0	7.1	15	8	12	15	20	31	25	**100**	**90**	0

Table 11.1 (continued)

Region[a]	Season	Temperature Response (°C) Min	25	50	75	Max	T yrs	Precipitation Response (%) Min	25	50	75	Max	T yrs	Extreme Seasons (%) Warm	Wet	Dry
NORTH AMERICA (continued)																
WNA	DJF	1.6	3.1	3.6	4.4	5.8	25	-4	2	7	11	36	>100	**80**	**18**	3
	MAM	1.5	2.4	3.1	3.4	6.0	20	-7	2	5	8	14	>100	**87**	**14**	
30N,50E	JJA	2.3	3.2	3.8	4.7	5.7	10	-18	-10	-1	2	10		**100**	3	
to	SON	2.0	2.8	3.1	4.5	5.3	20	-3	3	6	12	18	>100	**95**	**17**	2
75N,100E	Annual	2.1	2.9	3.4	4.1	5.7	15	-3	0	5	9	14	70	**100**	**21**	2
CNA	DJF	2.0	2.9	3.5	4.2	6.1	30	-18	0	5	8	14		**71**	**7**	
	MAM	1.9	2.8	3.3	3.9	5.7	25	-17	2	7	12	17	>100	**81**	**19**	4
30N,103W	JJA	2.4	3.1	4.1	5.1	6.4	20	-31	-15	-3	4	20	>100	**93**		**15**
to	SON	2.4	3.0	3.5	4.6	5.8	20	-17	-4	4	11	24		**91**	**11**	
50N,85W	Annual	2.3	3.0	3.5	4.4	5.8	15	-16	-3	3	7	15		**98**		
ENA	DJF	2.1	3.1	3.8	4.6	6.0	25	2	9	11	19	28	85	**78**	**24**	
	MAM	2.3	2.7	3.5	3.9	5.9	20	-4	7	12	16	23	60	**86**	**23**	2
25N,85W	JJA	2.1	2.6	3.3	4.3	5.4	15	-17	-3	1	6	13		**98**		
to	SON	2.2	2.8	3.5	4.4	5.7	20	-7	4	7	11	17	>100	**97**	**19**	
50N,50W	Annual	2.3	2.8	3.6	4.3	5.6	15	-3	5	7	10	15	55	**100**	**29**	1
CENTRAL AND SOUTH AMERICA																
CAM	DJF	1.4	2.2	2.6	3.5	4.6	15	-57	-18	-14	-9	0	>100	**96**	2	**25**
	MAM	1.9	2.7	3.6	3.8	5.2	10	-46	-25	-16	-10	15	75	**100**	2	**18**
10N,116W	JJA	1.8	2.7	3.4	3.6	5.5	10	-44	-25	-9	-4	12	90	**100**		**24**
to	SON	2.0	2.7	3.2	3.7	4.6	10	-45	-10	-4	7	24		**100**		**15**
30N,83W	Annual	1.8	2.6	3.2	3.6	5.0	10	-48	-16	-9	-5	9	65	**100**	2	**33**
AMZ	DJF	1.7	2.4	3.0	3.7	4.6	10	-13	0	4	11	17	>100	**93**	**27**	4
	MAM	1.7	2.5	3.0	3.7	4.6	10	-13	-1	1	4	14		**100**	**18**	
20S,82W	JJA	2.0	2.7	3.5	3.9	5.6	10	-38	-10	-3	2	13		**100**		
to	SON	1.8	2.8	3.5	4.1	5.4	10	-35	-12	-2	8	21		**100**		
12N,34W	Annual	1.8	2.6	3.3	3.7	5.1	10	-21	-3	0	6	14		**100**		
SSA	DJF	1.5	2.5	2.7	3.3	4.3	10	-16	-2	1	7	10		**100**		
	MAM	1.8	2.3	2.6	3.0	4.2	15	-11	-2	1	5	7		**98**	8	
56S,76W	JJA	1.7	2.1	2.4	2.8	3.6	15	-20	-7	0	3	17		**95**		
to	SON	1.8	2.2	2.7	3.2	4.0	15	-20	-12	1	6	11		**99**		
20S,40W	Annual	1.7	2.3	2.5	3.1	3.9	10	-12	-1	3	5	7		**100**		
AUSTRALIA AND NEW ZEALAND																
NAU	DJF	2.2	2.6	3.1	3.7	4.6	20	-20	-8	1	8	27		**89**		
	MAM	2.1	2.7	3.1	3.3	4.3	20	-24	-12	1	15	40		**92**		3
30S,110E	JJA	2.0	2.7	3.0	3.3	4.3	25	-54	-20	-14	3	26		**94**	3	
to	SON	2.5	3.0	3.2	3.8	5.0	20	-58	-32	-12	2	20		**98**		
11S,155E	Annual	2.2	2.8	3.0	3.5	4.5	15	-25	-8	-4	8	23		**99**		
SAU	DJF	2.0	2.4	2.7	3.2	4.2	20	-23	-12	-2	12	30		**95**		
	MAM	2.0	2.2	2.5	2.8	3.9	20	-31	-9	-5	13	32		**90**		**6**
45S,110E	JJA	1.7	2.0	2.3	2.5	3.5	15	-37	-20	-11	-4	9	>100	**95**		**17**
to	SON	2.0	2.6	2.8	3.0	4.1	20	-42	-27	-14	-5	4	>100	**95**		**15**
30S,155E	Annual	1.9	2.4	2.6	2.8	3.9	15	-27	-13	-4	3	12		**100**		

Table 11.1 (continued)

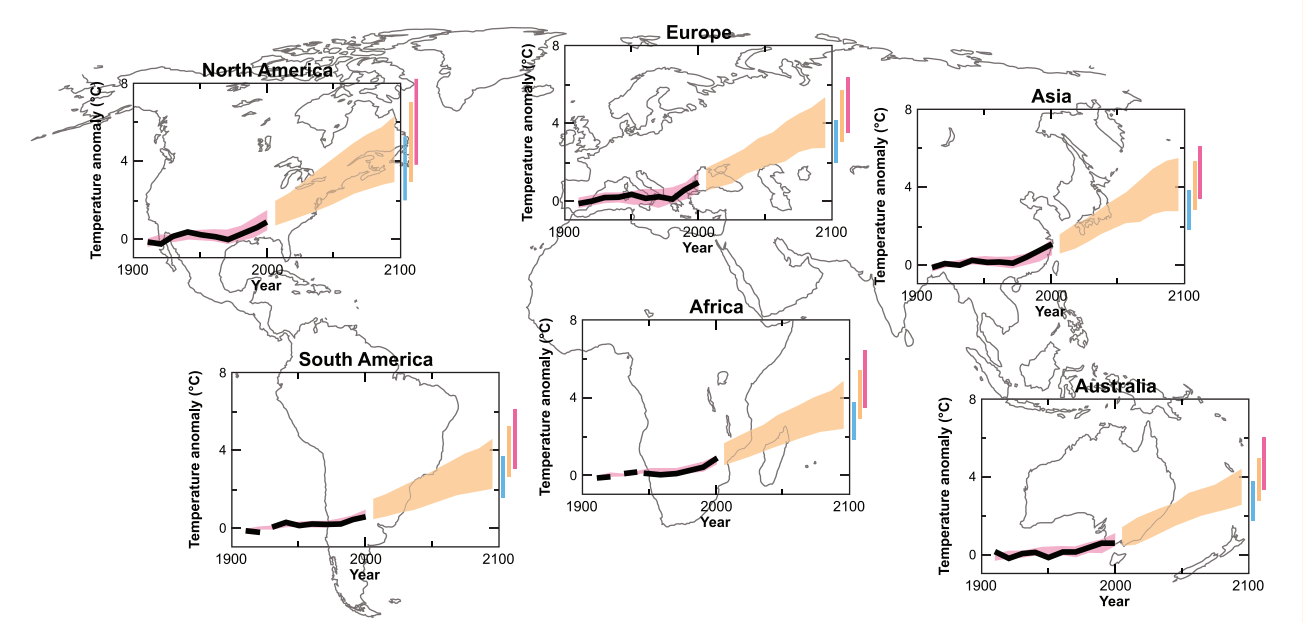
		Temperature Response (°C)						Precipitation Response (%)						Extreme Seasons (%)		
Region[a]	Season	Min	25	50	75	Max	T yrs	Min	25	50	75	Max	T yrs	Warm	Wet	Dry
POLAR REGIONS																
ARC[b]	DJF	4.3	6.0	6.9	8.4	11.4	15	11	19	26	29	39	25	**100**	**90**	0
	MAM	2.4	3.7	4.4	4.9	7.3	15	9	14	16	21	32	25	**100**	**79**	0
60N,180E	JJA	1.2	1.6	2.1	3.0	5.3	15	4	10	14	17	20	25	**100**	**85**	0
to	SON	2.9	4.8	6.0	7.2	8.9	15	9	17	21	26	35	20	**100**	**96**	0
90N,180W	Annual	2.8	4.0	4.9	5.6	7.8	15	10	15	18	22	28	20	**100**	**100**	0
ANT[c]	DJF	0.8	2.2	2.6	2.8	4.6	20	-11	5	9	14	31	50	**85**	**34**	3
	MAM	1.3	2.2	2.6	3.3	5.3	20	1	8	12	19	40	40	**88**	**54**	0
90S,180E	JJA	1.4	2.3	2.8	3.3	5.2	25	5	14	19	24	41	30	**83**	**59**	0
to	SON	1.3	2.1	2.3	3.2	4.8	25	-2	9	12	18	36	45	**79**	**42**	1
60S,180W	Annual	1.4	2.3	2.6	3.0	5.0	15	-2	9	14	17	35	25	**99**	**81**	1
SMALL ISLANDS																
CAR	DJF	1.4	1.8	2.1	2.4	3.2	10	-21	-11	-6	0	10		**100**	2	
	MAM	1.3	1.8	2.2	2.4	3.2	10	-28	-20	-13	-6	6	>100	**100**	3	**18**
10N,85W	JJA	1.3	1.8	2.0	2.4	3.2	10	-57	-35	-20	-6	8	60	**100**	2	**40**
to	SON	1.6	1.9	2.0	2.5	3.4	10	-38	-18	-6	1	19		**100**		**22**
25N,60W	Annual	1.4	1.8	2.0	2.4	3.2	10	-39	-19	-12	-3	11	60	**100**	3	**39**
IND	DJF	1.4	2.0	2.1	2.4	3.8	10	-4	2	4	9	20	>100	**100**	**19**	1
	MAM	1.5	2.0	2.2	2.5	3.8	10	0	3	5	6	20	80	**100**	**22**	1
35S,50E	JJA	1.4	1.9	2.1	2.4	3.7	10	-3	-1	3	5	20		**100**	**17**	
to	SON	1.4	1.9	2.0	2.3	3.6	10	-5	2	4	7	21	>100	**100**	**17**	2
17.5N,100E	Annual	1.4	1.9	2.1	2.4	3.7	10	-2	3	4	5	20	65	**100**	**30**	2
MED	DJF	1.5	2.0	2.3	2.7	4.2	25	-25	-16	-14	-10	-2	85	**96**	1	**18**
	MAM	1.5	2.1	2.4	2.7	3.7	20	-32	-23	-19	-16	-6	65	**99**	0	**32**
30N,5W	JJA	2.0	2.6	3.1	3.7	4.7	15	-64	-34	-29	-20	-3	60	**100**	1	**36**
to	SON	1.9	2.3	2.7	3.2	4.4	20	-33	-16	-10	-5	9	>100	**99**	2	**21**
45N,35E	Annual	1.7	2.2	2.7	3.0	4.2	15	-30	-16	-15	-10	-6	45	**100**	0	**50**
TNE	DJF	1.4	1.9	2.1	2.3	3.3	10	-35	-8	-6	3	10	>100	**100**		
	MAM	1.5	1.9	2.0	2.2	3.1	15	-16	-7	-2	6	39	>100	**100**		
0,30W	JJA	1.4	1.9	2.1	2.4	3.6	15	-8	-2	2	7	13	>100	**100**		
to	SON	1.5	2.0	2.2	2.6	3.7	15	-16	-5	-1	3	9	>100	**100**		
40N,10W	Annual	1.4	1.9	2.1	2.4	3.5	15	-7	-3	1	3	7	>100	**100**		
NPA	DJF	1.5	1.9	2.4	2.5	3.6	10	-5	1	3	6	17	>100	**100**	**20**	2
	MAM	1.4	1.9	2.3	2.5	3.5	10	-17	-1	1	3	17		**100**	**14**	
0,150E	JJA	1.4	1.9	2.3	2.7	3.9	10	1	5	8	14	25	55	**100**	**43**	1
to	SON	1.6	1.9	2.4	2.9	3.9	10	1	5	6	13	22	50	**100**	**31**	1
40N,120W	Annual	1.5	1.9	2.3	2.6	3.7	10	0	3	5	10	19	60	**100**	**35**	1
SPA	DJF	1.4	1.7	1.8	2.1	3.2	10	-6	1	4	7	15	80	**100**	**19**	4
	MAM	1.4	1.8	1.9	2.1	3.2	10	-3	3	6	8	17	35	**100**	**35**	1
55S,150E	JJA	1.4	1.7	1.8	2.0	3.1	10	-2	1	3	5	12	70	**100**	**27**	3
to	SON	1.4	1.6	1.8	2.0	3.0	10	-8	-2	2	4	5		**100**		
0,80W	Annual	1.4	1.7	1.8	2.0	3.1	10	-4	3	3	6	11	40	**100**	**40**	3

Notes:
[a] Regions are: West Africa (WAF), East Africa (EAF), South Africa (SAF), Sahara (SAH), Northern Europe (NEU), Southern Europe and Mediterranean (SEM), Northern Asia (NAS), Central Asia (CAS), Tibetan Plateau (TIB), East Asia (EAS), South Asia (SAS), Southeast Asia (SEA), Alaska (ALA), East Canada, Greenland and Iceland (CGI), Western North America (WNA), Central North America (CNA), Eastern North America (ENA), Central America (CAM), Amazonia (AMZ), Southern South America (SSA), North Australia (NAU), South Australia (SAU), Arctic (ARC), Antarctic (ANT), Caribbean (CAR), Indian Ocean (IND), Mediterrranean Basin (MED), Tropical Northeast Atlantic (TNE), North Pacific Ocean (NPA), and South Pacific Ocean (SPA).
[b] land and ocean
[c] land only

Box 11.1: Summary of Regional Responses

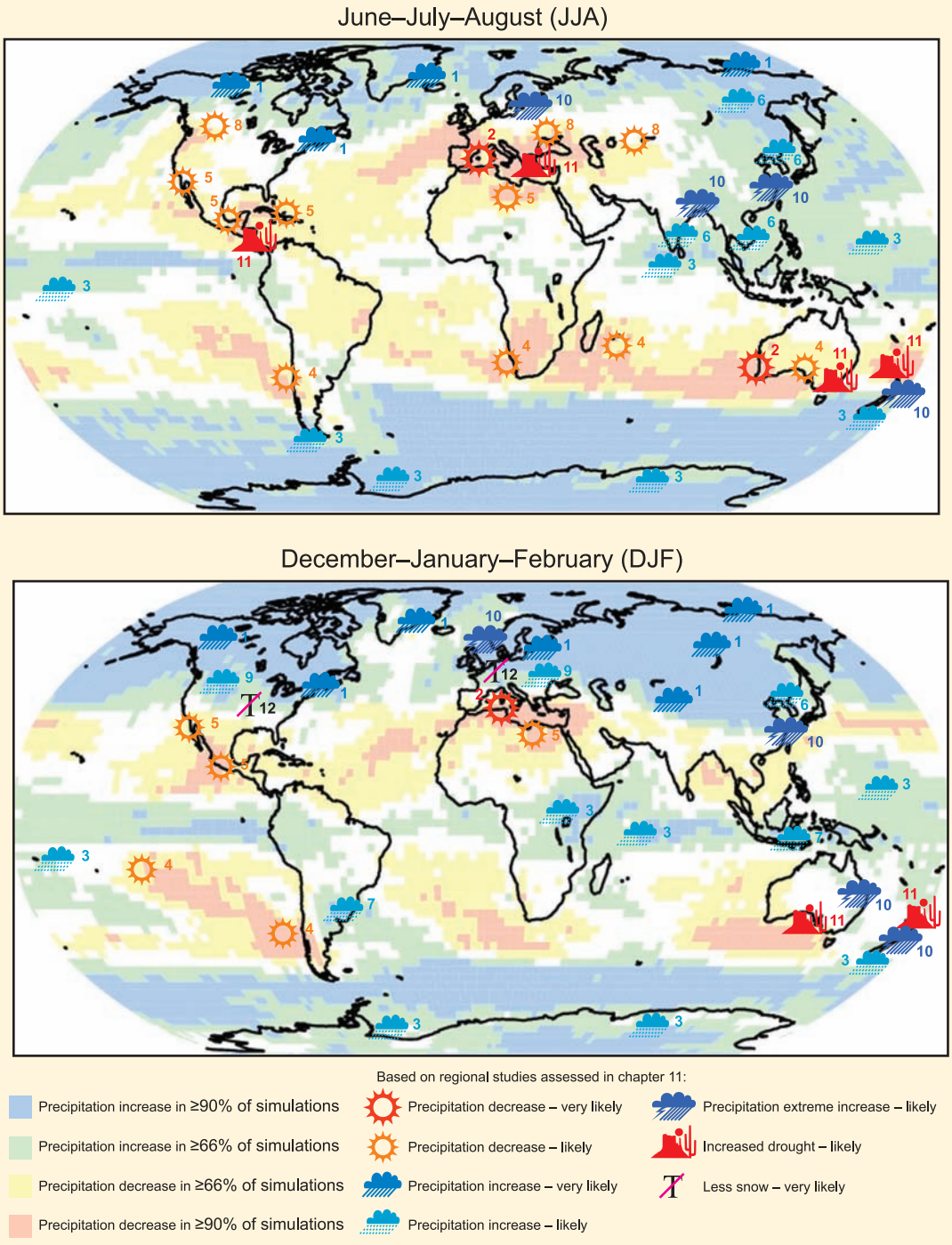
As an introduction to the more detailed regional analysis presented in this chapter, Box 11.1, Figure 1 illustrates how continental-scale warming is projected to evolve in the 21st century using the MMD models. This warming is also put into the context of the observed warming during the 20th century by comparing results from that subset of the models incorporating a representation of all known forcings with the observed evolution (see Section 9.4 for more details). Thus for the six continental regions, the figure displays: 1) the observed time series of the evolution of decadally averaged surface air temperature from 1906 to 2005 as an anomaly from the 1901 to 1950 average; 2) the range of the equivalent anomalies derived from 20th-century simulations by the MMD models that contain a full set of historical forcings; 3) the evolution of the range of this anomaly in MMD-A1B projections between 2000 and 2100; and 4) the range of the projected anomaly for the last decade of the 21st century for the B1, A1B, and A2 scenarios. For the observed part of these graphs, the decadal averages are centred on the decade boundaries (i.e., the last point is for 1996 to 2005), whereas for the future period they are centred on the decade mid-points (i.e., the first point is for 2001 to 2010). The width of the shading and the bars represents the 5 to 95% range of the model results. To construct the ranges, all simulations from the set of models involved were considered independent realisations of the possible evolution of the climate given the forcings applied. This involved 58 simulations from 14 models for the observed period and 47 simulations from 18 models for the future. Important in this representation is that the models' estimate of natural climate variability is included and thus the ranges include both the potential mitigating and amplifying effects of variability on the underlying signal. In contrast, the bars representing the range of projected change at the end of the century are constructed from ensemble mean changes from the models and thus provide a measure of the forced response. These bars were constructed from decadal mean anomalies from 21 models using A1B scenario forcings, from the 20 of these models that used the B1 forcings and the 17 that used the A2 forcings. The bars for the B1 and A2 scenarios were scaled to approximate ranges for the full set of models. The scaling factor for B1 was derived from the ratio between its range and the A1B range of the corresponding 20 models. The same procedure was used to obtain the A2 scaling factor. Only 18 models were used to display the ranges of projected temperature evolution as the control simulations for the other 3 had a drift of >0.2°C per century, which precludes clearly defining the decadal anomalies from these models. However, anomalies from all 21 models were included in calculating the bars in order to provide the fullest possible representation of projected changes in the MMD. Comparison of these different representations shows that the main messages from the MMD about projected continental temperature change are insensitive to the choices made. Finally, results are not shown here for Antarctica because the observational record is not long enough to provide the relevant information for the first part of the 20th century. Results of a similar nature to those shown here using the observations that are available are presented in Section 11.8. *(continued)*

Box 11.1, Figure 1. *Temperature anomalies with respect to 1901 to 1950 for six continental-scale regions for 1906 to 2005 (black line) and as simulated (red envelope) by MMD models incorporating known forcings; and as projected for 2001 to 2100 by MMD models for the A1B scenario (orange envelope). The bars at the end of the orange envelope represent the range of projected changes for 2091 to 2100 for the B1 scenario (blue), the A1B scenario (orange) and the A2 scenario (red). The black line is dashed where observations are present for less than 50% of the area in the decade concerned. More details on the construction of these figures are given in Section 11.1.2.*



Box 11.1, Figure 2 serves to illustrate some of the more significant hydrological changes, with the two panels corresponding to DJF and JJA. The backdrop to these figures is the fraction of the AOGCMs (out of the 21 considered for this purpose) that predict an increase in mean precipitation in that grid cell (using the A1B scenario and comparing the period 2080 to 2099 with the control period 1980 to 1999). Aspects of this pattern are examined more closely in the separate regional discussions.

Robust findings on regional climate change for mean and extreme precipitation, drought and snow are highlighted in the figure with further detail in the accompanying notes. *(continued)*



Box 11.1, Figure 2. *Robust findings on regional climate change for mean and extreme precipitation, drought, and snow. This regional assessment is based upon AOGCM based studies, Regional Climate Models, statistical downscaling and process understanding. More detail on these findings may be found in the notes below, and their full description, including sources is given in the text. The background map indicates the degree of consistency between AR4 AOGCM simulations (21 simulations used) in the direction of simulated precipitation change.*

(1) Very likely annual mean increase in most of northern Europe and the Arctic (largest in cold season), Canada, and the North-East USA; and winter (DJF) mean increase in Northern Asia and the Tibetan Plateau.
(2) Very likely annual mean decrease in most of the Mediterranean area, and winter (JJA) decrease in southwestern Australia.
(3) Likely annual mean increase in tropical and East Africa, Northern Pacific, the northern Indian Ocean, the South Pacific (slight, mainly equatorial regions), the west of the South Island of New Zealand, Antarctica and winter (JJA) increase in Tierra del Fuego.
(4) Likely annual mean decrease in and along the southern Andes, summer (DJF) decrease in eastern French Polynesia, winter (JJA) decrease for Southern Africa and in the vicinity of Mauritius, and winter and spring decrease in southern Australia.
(5) Likely annual mean decrease in North Africa, northern Sahara, Central America (and in the vicinity of the Greater Antilles in JJA) and in South-West USA.
(6) Likely summer (JJA) mean increase in Northern Asia, East Asia, South Asia and most of Southeast Asia, and likely winter (DJF) increase in East Asia.
(7) Likely summer (DJF) mean increase in southern Southeast Asia and southeastern South America
(8) Likely summer (JJA) mean decrease in Central Asia, Central Europe and Southern Canada.
(9) Likely winter (DJF) mean increase in central Europe, and southern Canada
(10) Likely increase in extremes of daily precipitation in northern Europe, South Asia, East Asia, Australia and New Zealand.
(11) Likely increase in risk of drought in Australia and eastern New Zealand; the Mediterranean, central Europe (summer drought); in Central America (boreal spring and dry periods of the annual cycle).
(12) Very likely decrease in snow season length and likely to very likely decrease in snow depth in most of Europe and North America.

models. The results are shown in Table 11.1 only when 14 out of the 21 models agree as to the sign of the change in frequency of extremes. For example, in Central North America (CNA), 15% of the summers in 2080 to 2099 in the A1B scenario are projected to be extremely dry, corresponding to a factor of three increase in the frequency of these events. In contrast, in many regions and seasons, the frequency of extreme warmth is 100%, implying that all seasons in 2080 to 2099 are warmer than the warmest season in 1980 to 1999, according to every model in this ensemble.

In each continental section, a figure is provided summarising the temperature and precipitation responses in the MMD-A1B projection for the last two decades of the 21st century. These figures portray a multi-model mean comprising individual models or model ensemble means where ensembles exist. Also shown is the simple statistic of the number of these models that show agreement in the sign of the precipitation change. The annual mean temperature and precipitation responses in each of the 21 separate AOGCMs are provided in Supplementary Material Figures S11.5 to 11.12 and S11.13 to 11.20, respectively.

Recent explorations of multi-model ensemble projections seek to develop probabilistic estimates of uncertainties and are provided in the Supplementary Material Table S11.2. This information is based on the approach of Tebaldi et al. (2004a,b; see also section 11.10.2).

11.1.3 Some Unifying Themes

The basic pattern of the projected warming as described in Chapter 10 is little changed from previous assessments. Examining the spread across the MMD models, temperature projections in many regions are strongly correlated with the global mean projections, with the most sensitive models in global mean temperature often the most sensitive locally. Differing treatments of regional processes and the dynamical interactions between a given region and the rest of the climate system are responsible for some spread. However, a substantial part of the spread in regional temperature projections is due to differences in the sum of the feedbacks that control transient climate sensitivity (see also Chapter 10).

The response of the hydrological cycle is controlled in part by fundamental consequences of warmer temperatures and the increase in water vapour in the atmosphere (Chapter 3). Water is transported horizontally by the atmosphere from regions of moisture divergence (particularly in the subtropics) to regions of convergence. Even if the circulation does not change, these transports will increase due to the increase in water vapour. The consequences of this increased moisture transport can be seen in the global response of precipitation, described in Chapter 10, where, on average, precipitation increases in the inter-tropical convergence zones, decreases in the subtropics, and increases in subpolar and polar regions. Over North America and Europe, the pattern of subpolar moistening and subtropical

drying dominates the 21st-century projections. This pattern is also described in Section 9.5.4, which assesses the extent to which this pattern is visible over land during the 20th century in precipitation observations and model simulations. Regions of large uncertainty often lie near the boundaries between these robust moistening and drying regions, with boundaries placed differently by each model.

High-resolution model results indicate that in regions with strong orographic forcing, some of these large-scale findings can be considerably altered locally. In some cases, this may result in changes in the opposite direction to the more general large-scale behaviour. In addition, large-area and grid-box average projections for precipitation are often very different from local changes within the area (Good and Lowe, 2006). These issues demonstrate the inadequacy of inferring the behaviour at fine scales from that of large-area averages.

Another important theme in the 21st-century projections is the poleward expansion of the subtropical highs, and the poleward displacement of the mid-latitude westerlies and associated storm tracks. This circulation response is often referred to as an enhanced positive phase of the Northern or Southern Annular Mode, or when focusing on the North Atlantic, the positive phase of the North Atlantic Oscillation (NAO). In regions without strong orographic forcing, superposition of the tendency towards subtropical drying and poleward expansion of the subtropical highs creates especially robust drying responses at the poleward boundaries of the five subtropical oceanic high centres in the South Indian, South Atlantic, South Pacific, North Atlantic and, less robustly, the North Pacific (where a tendency towards El-Niño like conditions in the Pacific in the models tends to counteract this expansion). Most of the regional projections of strong drying tendencies over land in the 21st century are immediately downstream of these centres (south-western Australia, the Western Cape Provinces of South Africa, the southern Andes, the Mediterranean and Mexico). The robustness of this large-scale circulation signal is discussed in Chapter 10, while Chapters 3, 8 and 9 describe the observed poleward shifts in the late 20th century and the ability of models to simulate these shifts.

The retreats of snow and ice cover are important for local climates. The difficulty of quantifying these effects in regions of substantial topographic relief is a significant limitation of global models (see Section 11.4.3.2, Box 11.3) and is improved with dynamical and statistical downscaling. The drying effect of an earlier spring snowmelt and, more generally, the earlier reduction in soil moisture (Manabe and Wetherald, 1987) is a continuing theme in discussion of summer continental climates.

The strong interactions between sea surface temperature gradients and tropical rainfall variability provides an important unifying theme for tropical climates. Models can differ in their projections of small changes in tropical ocean temperature gradients and in the simulation of the potentially large shifts in rainfall that are related to these oceanic changes. Chou and Neelin (2004) provide a guide to some of the complexity involved in diagnosing and evaluating hydrological responses in the tropics. With a few exceptions, the spread in projections of hydrological changes is still too large to make strong statements about the future of tropical climates at regional scales (see also Section 10.3). Many AOGCMs project large tropical precipitation changes, so uncertainty as to the regional pattern of these changes should not be taken as evidence that these changes are likely to be small.

Assessments of the regional and sub-regional climate change projections have primarily been based on the AOGCM projections summarised in Table 11.1 and an analysis of the biases in the AOGCM simulations, regional downscaling studies available for some regions with either physical or statistical models or both, and reference to plausible physical mechanisms.

To assist the reader in placing the various regional assessments in a global context, Box 11.1 displays many of the detailed assessments documented in the following regional sections. Likewise, an overview of projected changes in various types of extreme weather statistics is summarised in Table 11.2, which contains information from the assessments within this chapter and from Chapter 10. Thus, the details of the assessment that lead to each individual statement can all be found in either Chapter 10, or the respective regional sections, and links for each statement are identifiable from Table 11.2.

Table 11.2. *Projected changes in climate extremes. This table summarises key phenomena for which there is confidence in the direction of projected change based on the current scientific evidence. The included phenomena are those where confidence ranges between medium and very likely, and are listed with the notation of VL (very likely), L (likely), and M (medium confidence). maxTmax refers to the highest maximum temperature, maxTmin to the highest minimum temperature, minTmax to the lowest maximum temperature, and minTmin to the lowest minimum temperature. In addition to changes listed in the table, there are two phenomena of note for which there is little confidence. The issue of drying and associated risk of drought in the Sahel remains uncertain as discussed in Section 11.2.4.2. The change in mean duration of tropical cyclones cannot be assessed with confidence at this stage due to insufficient studies.*

Temperature-Related Phenomena	
Change in phenomenon	**Projected changes**
Higher monthly absolute maximum of daily maximum temperatures (maxTmax) more hot / warm summer days	**VL (consistent across model projections)** maxTmax increases at same rate as the mean or median[1] over northern Europe,[2] Australia and New Zealand[3] **L (fairly consistent across models, but sensitivity to land surface treatment)** maxTmax increases more than the median over southern and central Europe,[4] and southwest USA[5] **L (consistent with projected large increase in mean temperature)** Large increase in probability of extreme warm seasons over most parts of the world[6]
Longer duration, more intense, more frequent heat waves / hot spells in summer	**VL (consistent across model projections)** Over almost all continents[7], but particularly central Europe,[8] western USA,[9] East Asia[10] and Korea[11]
Higher monthly absolute maximum of daily minimum temperatures (maxTmin); more warm and fewer cold nights	**VL (consistent with higher mean temperatures)** Over most continents[12]
Higher monthly absolute minimum of daily minimum temperatures (minTmin)	**VL (consistent across model projections)** minTmin increases more than the mean in many mid- and high-latitude locations,[13] particularly in winter over most of Europe except the southwest[14]
Higher monthly absolute minimum of daily maximum temperatures (minTmax), fewer cold days	**L (consistent with warmer mean temperatures)** minTmin increases more than the mean in some areas[15]
Fewer frost days	**VL (consistent across model projections)** Decrease in number of days with below-freezing temperatures everywhere[16]
Fewer cold outbreaks; fewer, shorter, less intense cold spells / cold extremes in winter	**VL (consistent across model projections)** Northern Europe, South Asia, East Asia[17] **L (consistent with warmer mean temperatures)** Most other regions[18]
Reduced diurnal temperature range	**L (consistent across model projections)** Over most continental regions, night temperatures increase faster than the day temperatures[19]
Temperature variability on interannual and daily time scales	**L (general consensus across model projections)** Reduced in winter over most of Europe[20] Increase in central Europe in summer[21]

1 Kharin and Zwiers (2005)
2 §11.3.3.3, Supplementary Material Figure S11.23, PRUDENCE, Kjellström et al. (2007)
3 §11.7.3.5, CSIRO (2001)
4 §11.3.3.3, PRUDENCE, Kjellström et al. (2007)
5 §11.5.3.3, Bell et al. (2004),
6 Table 11.1
7 §11.3.3.3, Tebaldi et al. (2006), Meehl and Tebaldi (2004)
8 §11.5.3.3, Barnett et al. (2006), Clark et al. (2006), Tebaldi et al. (2006), Gregory and Mitchell (1995), Zwiers and Kharin (1998), Hegerl et al. (2004), Meehl and Tebaldi (2004)
9 §11.5.3.3, Bell et al. (2004), Leung et al. (2004)
10 §11.4.3.2, Gao et al. (2002)
11 §11.4.3.2, Kwon et al. (2005), Boo et al. (2006)
12 §11.3.3.2, §11.4.3.1
13 Kharin and Zwiers (2005)
14 §11.3.3.2, Fig. 11.3.3.3, PRUDENCE
15 §11.7.3.5, Whetton et al. (2002)
16 Tebaldi et al. (2006), Meehl and Tebaldi (2004), §11.3.3.2, PRUDENCE, §11.7.3.1, CSIRO (2001), Mullan et al. (2001b)
17 §11.3.3.2, PRUDENCE, Kjellström et al. (2007), §11.4.3.2, Gao et al. (2002), Rupa Kumar et al. (2006)
18 §11.1.3
19 §11.5.3.3, Bell et al. (2004), Leung et al. (2004), §11.4.3.2, Rupa Kumar et al. (2006), Mizuta et al. (2005)
20 §11.3.3.2, Räisänen (2001), Räisänen and Alexandersson (2003), Giorgi and Bi (2005), Zwiers and Kharin (1998), Hegerl et al. (2004), Kjellström et al. (2007)
21 §11.3.3.2, PRUDENCE, Schär et al. (2004), Vidale et al. (2007)

Table 11.2. (continued)

Moisture-Related Phenomena	
Phenomenon	**Projected changes**
Intense precipitation events	**VL (consistent across model projections; empirical evidence, generally higher precipitation extremes in warmer climates)** Much larger increase in the frequency than in the magnitude of precipitation extremes over most land areas in middle latitudes,[22] particularly over northern Europe,[23] Australia and New Zealand[24] Large increase during the Indian summer monsoon season over Arabian Sea, tropical Indian Ocean, South Asia[25] Increase in summer over south China, Korea and Japan[26]
Intense precipitation events	**L (some inconsistencies across model projections)** Increase over central Europe in winter[27] Increase associated with tropical cyclones over Southeast Asia, Japan[28] **Uncertain** Changes in summer over Mediterranean and central Europe[29] **L decrease (consistent across model projections)** Iberian Peninsula[30]
Wet days	**L (consistent across model projections)** Increase in number of days at high latitudes in winter, and over northwest China[31] Increase over the Inter-Tropical Convergence Zone[32] Decrease in South Asia[33] and the Mediterranean area[34]
Dry spells (periods of consecutive dry days)	**VL (consistent across model projections)** Increase in length and frequency over the Mediterranean area[35], southern areas of Australia, New Zealand[36] **L (consistent across model projections)** Increase in most subtropical areas[37] Little change over northern Europe[38]
Continental drying and associated risk of drought	**L (consistent across model projections; consistent change in precipitation minus evaporation, but sensitivity to formulation of land surface processes)** Increased in summer over many mid-latitude continental interiors, e.g., central[39] and southern Europe, Mediterranean area,[40] in boreal spring and dry periods of the annual cycle over Central America[41]

22 §11.3.3.4, Groisman et al. (2005), Kharin and Zwiers (2005), Hegerl et al. (2004), Semenov and Bengtsson (2002), Meehl et al. (2006)
23 §11.3.3.4, Räisänen (2002), Giorgi and Bi (2005), Räisänen (2005)
24 §11.1.3, §11.7.3.2, §11.3.3.4, Huntingford et al. (2003), Barnett et al. (2006), Frei et al. (2006), Hennessy et al. (1997), Whetton et al. (2002), Watterson and Dix (2003), Suppiah et al. (2004), McInnes et al. (2003), Hennessy et al. (2004b), Abbs (2004), Semenov and Bengtsson (2002)
25 §11.4.3.2, May (2004a), Rupa Kumar et al. (2006)
26 §11.4.3.2, Gao et al. (2002), Boo et al. (2006), Kimoto et al. (2005), Kitoh et al. (2005), Mizuta et al. (2005)
27 §11.3.3.4, PRUDENCE, Frei et al. (2006), Christensen and Christensen (2003, 2004)
28 §11.1.3, §11.4.3.2, Kimoto et al. (2005), Mizuta et al. (2005), Hasegawa and Emori (2005), Kanada et al. (2005)
29 §11.3.3.4, PRUDENCE, Frei et al. (2006), Christensen and Christensen (2004), Tebaldi et al. (2006)
30 §11.3.3.4, PRUDENCE, Frei et al. (2006)
31 §11.4.3.2, Gao et al. (2002), Hasegawa and Emori (2005)
32 Semenov and Bengtsson (2002)
33 §11.4.3.2 Krishna Kumar et al. (2003)
34 §11.3.3.4, Semenov and Bengtsson (2002), Voss et al. (2002); Räisänen et al. (2004); Frei et al. (2006)
35 §11.3.3.4, Semenov and Bengtsson, 2002; Voss et al., 2002; Hegerl et al., 2004; Wehner, 2004; Kharin and Zwiers, 2005; Tebaldi et al., 2006
36 §11.1.3, §11.7.3.2, §11.7.3.4, Whetton and Suppiah (2003), McInnes et al. (2003), Walsh et al. (2002), Hennessy et al. (2004c), Mullan et al. (2005)
37 §11.1.3
38 §11.3.3.4, Beniston et al. (2007), Tebaldi et al. (2006), Voss et al. (2002)
39 §11.3.3.2, Rowell and Jones (2006)
40 §11.1.3, §11.3.3.4, Voss et al. (2002)
41 §11.1.3

Table 11.2. (continued)

Tropical Cyclones (typhoons and hurricanes)	
Change in phenomenon	**Projected changes**
Increase in peak wind intensities	**L (high-resolution Atmospheric GCM (AGCM) and embedded hurricane model projections)** Over most tropical cyclone areas[42]
Increase in mean and peak precipitation intensities	**L (high-resolution AGCM projections and embedded hurricane model projections)** Over most tropical cyclone areas,[43] South,[44] East[45] and southeast Asia[46]
Changes in frequency of occurrence	**M (some high-resolution AGCM projections)** Decrease in number of weak storms, increase in number of strong storms[47] **M (several climate model projections)** Globally averaged decrease in number, but specific regional changes dependent on sea surface temperature change[48] Possible increase over the North Atlantic[49]
Extratropical Cyclones	
Change in phenomenon	**Projected changes**
Changes in frequency and position	**L (consistent in AOGCM projections)** Decrease in the total number of extratropical cyclones[50] Slight poleward shift of storm track and associated precipitation, particularly in winter[51]
Change in storm intensity and winds	**L (consistent in most AOGCM projections, but not explicitly analysed for all models)** Increased number of intense cyclones[52] and associated strong winds, particularly in winter over the North Atlantic,[53] central Europe[54] and Southern Island of New Zealand[55] **More likely than not** Increased windiness in northern Europe and reduced windiness in Mediterranean Europe[56]
Increased wave height	**L (based on projected changes in extratropical storms)** Increased occurrence of high waves in most mid-latitude areas analysed, particularly the North Sea[57]

42 Knutson and Tuleya (2004)
43 Knutson and Tuleya (2004)
44 §11.4.3.2, Unnikrishnan et al. (2006)
45 §11.3.4, Hasegawa and Emori (2005)
46 §11.3.4, Hasegawa and Emori (2005), Knutson and Tuleya (2004)
47 Oouchi et al. (2006)
48 Hasegawa and Emori (2005)
49 Sugi et al. (2002), Oouchi et al. (2006)
50 §11.3.3.6, Yin (2005), Lambert and Fyfe (2006), §11.3.3.5, Lionello et al. (2002), Leckebusch et al. (2006), Vérant (2004), Somot (2005)
51 §11.1.3, Yin (2005), Lambert and Fyfe (2006)
52 §11.1.2, §11.3.3.5, Yin (2005), Lambert and Fyfe (2006)
53 §11.3.3.5, Leckebusch and Ulbrich (2004)
54 §11.3.3.5, Zwiers and Kharin (1998), Knippertz et al. (2000), Leckebusch and Ulbrich (2004), Pryor et al. (2005a), Lionello et al. (2002), Leckebusch et al. (2006), Vérant (2004), Somot (2005)
55 §11.1.3, §11.7.3.7
56 §11.3.3.5, Lionello et al. (2002), Leckebusch et al. (2006), Vérant (2004), Somot (2005)
57 X.L. Wang et al. (2004)

Frequently Asked Question 11.1

Do Projected Changes in Climate Vary from Region to Region?

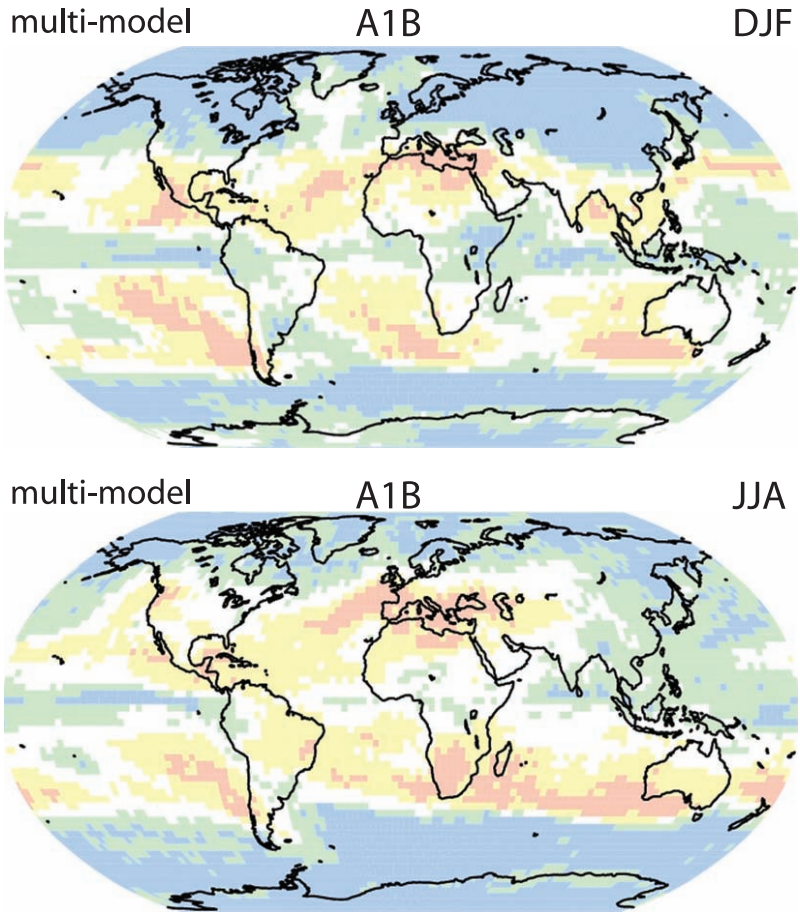
Climate varies from region to region. This variation is driven by the uneven distribution of solar heating, the individual responses of the atmosphere, oceans and land surface, the interactions between these, and the physical characteristics of the regions. The perturbations of the atmospheric constituents that lead to global changes affect certain aspects of these complex interactions. Some human-induced factors that affect climate ('forcings') are global in nature, while others differ from one region to another. For example, carbon dioxide, which causes warming, is distributed evenly around the globe, regardless of where the emissions originate, whereas sulphate aerosols (small particles) that offset some of the warming tend to be regional in their distribution. Furthermore, the response to forcings is partly governed by feedback processes that may operate in different regions from those in which the forcing is greatest. Thus, the projected changes in climate will also vary from region to region.

Latitude is a good starting point for considering how changes in climate will affect a region. For example, while warming is expected everywhere on Earth, the amount of projected warming generally increases from the tropics to the poles in the Northern Hemisphere. Precipitation is more complex, but also has some latitude-dependent features. At latitudes adjacent to the polar regions, precipitation is projected to increase, while decreases are projected in many regions adjacent to the tropics (see Figure 1). Increases in tropical precipitation are projected during rainy seasons (e.g., monsoons), and over the tropical Pacific in particular.

Location with respect to oceans and mountain ranges is also an important factor. Generally, the interiors of continents are projected to warm more than the coastal areas. Precipitation responses are especially sensitive not only to the continental geometry, but to the shape of nearby mountain ranges and wind flow direction. Monsoons, extratropical cyclones and hurricanes/typhoons are all influenced in different ways by these region-specific features.

Some of the most difficult aspects of understanding and projecting changes in regional climate relate to possible changes in the circulation of the atmosphere and oceans, and their patterns of variability. Although general statements covering a variety of regions with qualitatively similar climates can be made in some cases, nearly every region is idiosyncratic in some ways. This is true whether it is the coastal zones surrounding the subtropical Mediterranean Sea, the extreme weather in the North American interior that depends on moisture transport from the Gulf of Mexico, or the interactions between vegetation distribution, oceanic temperatures and atmospheric circulation that help control the southern limit of the Sahara Desert.

While developing an understanding of the correct balance of global and regional factors remains a challenge, the understanding of these factors is steadily growing, increasing our confidence in regional projections.



FAQ 11.1, Figure 1. *Blue and green areas on the map are by the end of the century projected to experience increases in precipitation, while areas in yellow and pink are projected to have decreases. The top panel shows projections for the period covering December, January and February, while the bottom panel shows projections for the period covering June, July and August.*

11.2 Africa

Assessment of projected climate changes for Africa:

All of Africa is very likely to warm during this century. The warming is very likely to be larger than the global, annual mean warming throughout the continent and in all seasons, with drier subtropical regions warming more than the moister tropics.

Annual rainfall is likely to decrease in much of Mediterranean Africa and northern Sahara, with the likelihood of a decrease in rainfall increasing as the Mediterranean coast is approached. Rainfall in southern Africa is likely to decrease in much of the winter rainfall region and on western margins. There is likely to be an increase in annual mean rainfall in East Africa. It is uncertain how rainfall in the Sahel, the Guinean Coast and the southern Sahara will evolve in this century.

The MMD models have significant systematic errors in and around Africa (excessive rainfall in the south, southward displacement of the Atlantic Inter-Tropical Convergence Zone (ITCZ), insufficient upwelling off the West Coast) making it difficult to assess the consequences for climate projections. The absence of realistic variability in the Sahel in most 20th-century simulations casts some doubt on the reliability of coupled models in this region. Vegetation feedbacks and feedbacks from dust aerosol production are not included in the global models. Possible future land surface modification is also not taken into account in the projections. The extent to which current regional models can successfully downscale precipitation over Africa is unclear, and limitations of empirical downscaling results for Africa are not fully understood. There is insufficient information on which to assess possible changes in the spatial distribution and frequency of tropical cyclones affecting Africa.

11.2.1 Key Processes

The bulk of the African continent is tropical or subtropical with the central phenomenon being the seasonal migration of the tropical rain belts. Small shifts in the position of these rain belts result in large local changes in rainfall. There are also regions on the northern and southern boundaries of the continent with winter rainfall regimes governed by the passage of mid-latitude fronts, which are therefore sensitive to a poleward displacement of the storm tracks. This is evident from the correlation between South African rainfall and the Southern Annular Mode (Reason and Rouault, 2005) and between North African rainfall and the NAO (Lamb and Peppler, 1987). Troughs penetrating into the tropics from mid-latitudes also influence warm season rainfall, especially in southern Africa, and can contribute to a sensitivity of warm season rains to a displacement of the circulation (Todd and Washington, 1999). Any change in tropical cyclone distribution and intensity will affect the southeast coastal regions, including Madagascar (Reason and Keibel, 2004).

The factors that determine the southern boundary of the Sahara and rainfall in the Sahel have attracted special interest because of the extended drought experienced by this region in the 1970s and 1980s. The field has moved steadily away from explanations for rainfall variations in this region as primarily due to land use changes and towards explanations based on changes in sea surface temperatures (SSTs). The early SST perturbation Atmospheric GCM (AGCM) experiments (Palmer, 1986; Rowell, et al., 1995) are reinforced by the results from the most recent models (Giannini et al., 2003; Lu and Delworth, 2005; Hoerling et al., 2006). The north-south inter-hemispheric gradient, with colder NH oceans conducive to an equatorward shift and/or a reduction in Sahel rainfall, is important. This has created interest in the possibility that aerosol cooling localised in the NH could dry the Sahel (Rotstayn and Lohmann, 2002; see also Section 9.5.4.3.1). However, temperatures over other oceanic regions, including the Mediterranean (Rowell, 2003), are also important.

In southern Africa, changing SSTs are also thought to be more important than changing land use patterns in controlling warm season rainfall variability and trends. Evidence has been presented for strong links with Indian Ocean temperatures (Hoerling et al., 2006). The warming of the troposphere over South Africa, possibly a consequence of warming of the Indo-Pacific, has been linked with the increase in days with stable inversion layers over southern Africa (Freiman and Tyson, 2000; Tadross et al., 2005a, 2006) in the late 20th century.

In addition to the importance of ocean temperatures, vegetation patterns help shape the climatic zones throughout much of Africa (e.g., Wang and Eltahir, 2000; Maynard and Royer, 2004a; Paeth and Henre, 2004; see also Section 11.7, Box 11.4). In the past, land surface changes have primarily acted as feedbacks generated by the underlying response to SST anomalies, and vegetation changes are thought to provide a positive feedback to climate change. The plausibility of this positive feedback is enhanced by recent work suggesting that land surface feedbacks may also play an important role in both intra-seasonal variability and rainy season onset in southern Africa (New et al., 2003; Anyah and Semazzi, 2004; Tadross et al., 2005a,b).

The MMD models prescribe vegetation cover; they would likely respond more strongly to large-scale forcing if they predicted vegetation, especially in semi-arid areas. The possibility of multiple stable modes of African climate due to vegetation-climate interactions has been raised, especially in the context of discussions of the very wet Sahara during the mid-Holocene 6 to 8 ka (Claussen et al., 1999; Foley et al., 2003). One implication is that centennial time-scale feedbacks associated with vegetation patterns may have the potential to make climate changes over Africa less reversible.

11.2.2 Skill of Models in Simulating Present and Past Climates

There are biases in the simulations of African climate that are systematic across the MMD models, with 90% of models overestimating precipitation in southern Africa, by more than 20% on average (and in some cases by as much as 80%) over a wide area often extending into equatorial Africa. The temperature biases over land are not considered large enough to directly affect the credibility of the model projections (see Supplementary Material Figure S11.21 and Table S11.1).

The ITCZ in the Atlantic is displaced equatorward in nearly all of these AOGCM simulations. Ocean temperatures are too warm by an average of 1°C to 2°C in the Gulf of Guinea and typically by 3°C off the southwest coast in the region of intense upwelling, which is clearly too weak in many models. In several of the models there is no West African monsoon as the summer rains fail to move from the Gulf onto land, but most of the models do have a monsoonal climate albeit with some distortion. Moderately realistic interannual variability of SSTs in the Gulf of Guinea and the associated dipolar rainfall variations in the Sahel and the Guinean Coast are, by the criteria of Cook and Vizy (2006), only present in 4 of the 18 models examined. Tennant (2003) describes biases in several AGCMs, such as the equatorward displacement of the mid-latitude jet in austral summer, a deficiency that persists in the most recent simulations (Chapter 8).

Despite these deficiencies, AGCMs can simulate the basic pattern of rainfall trends in the second half of the 20th century if given the observed SST evolution as boundary conditions, as described in the multi-model analysis of Hoerling et al. (2006) and the growing literature on the interannual variability and trends in individual models (e.g., Rowell et al., 1995; Bader and Latif, 2003; Giannini et al., 2003; Haarsma et al., 2005; Kamga et al., 2005; Lu and Delworth, 2005). However, there is less confidence in the ability of AOGCMs to generate interannual variability in the SSTs of the type known to affect African rainfall, as evidenced by the fact that very few AOGCMs produce droughts comparable in magnitude to the Sahel drought of the 1970s and 1980s (Hoerling et al., 2006). There are exceptions, but what distinguishes these from the bulk of the models is not understood.

The very wet Sahara 6 to 8 ka is thought to have been a response to the increased summer insolation due to changes in the Earth's orbital configuration. Modelling studies of this response provide background information on the quality of a model's African monsoon, but the processes controlling the response to changing seasonal insolation may be different from those controlling the response to increasing greenhouse gases. The fact that GCMs have difficulty in simulating the full magnitude of the mid-Holocene wet period, especially in the absence of vegetation feedbacks, may indicate a lack of sensitivity to other kinds of forcing (Jolly et al., 1996; Kutzbach et al., 1996).

Regional climate modelling has mostly focused on southern Africa, where the models generally improve on the climate simulated by global models but also share some of the biases in the global models. For example, Engelbrecht et al. (2002) and Arnell et al. (2003) both simulate excessive rainfall in parts of southern Africa, reminiscent of the bias in the MMD. Hewitson et al. (2004) and Tadross et al. (2006) note strong sensitivity to the choice of convective parametrization, and to changes in soil moisture and vegetative cover (New et al., 2003; Tadross et al., 2005a), reinforcing the view (Rowell et al., 1995) that land surface feedbacks enhance regional climate sensitivity over Africa's semi-arid regions. Over West Africa, the number of Regional Climate Model (RCM) investigations is even more limited (Jenkins et al., 2002; Vizy and Cook, 2002). The quality of the 25-year simulation undertaken by Paeth et al. (2005) is encouraging, emphasizing the role of regional SSTs and changes in the land surface in forcing West African rainfall anomalies. Several recent AGCM time-slice simulations focusing on tropical Africa show good simulation of the rainy season (Coppola and Giorgi, 2005; Caminade et al., 2006; Oouchi et al., 2006).

Hewitson and Crane (2005) developed empirical downscaling for point-scale precipitation at sites spanning the continent, as well as a 0.1° resolution grid over South Africa. The downscaled precipitation forced by reanalysis data provides a close match to the historical climate record, including regions such as the eastern escarpment of the sub-continent that have proven difficult for RCMs.

11.2.3 Climate Projections

11.2.3.1 Mean Temperature

The differences in near-surface temperature between the years 2080 to 2099 and the years 1980 to 1999 in the MMD-A1B projections, averaged over the West African (WAF), East African (EAF), South African (SAF) and Saharan (SAH) sub-regions, are provided in Table 11.1, with the temporal evolution displayed in Figure 11.1. The Mediterranean coast is discussed together with southern Europe in Section 11.3. In all four regions and in all seasons, the median temperature increase lies between 3°C and 4°C, roughly 1.5 times the global mean response. Half of the models project warming within about 0.5°C of these median values. The distributions estimated by Tebaldi et al. (2004a,b; see also Supplementary Material Table S11.2) have a very similar half-width, but reduce the likelihood of the extreme high limit as compared to the raw quartiles in Table 11.1. There is a strong correlation across these AOGCMs between the global mean temperature response and the response in Africa. The signal-to-noise ratio is very large for these 20-year mean temperatures and 10 years is typically adequate to obtain a clearly discernible signal, as defined in Section 11.1.2. Regionally averaged temperatures averaged over the period 1990 to 2009 are clearly discernible from the 1980 to 1999 averages.

The upper panels in Figure 11.2 show the geographical structure of the ensemble-mean projected warming for the A1B scenario in more detail. Smaller values of projected warming, near 3°C, are found in equatorial and coastal areas and larger

values, above 4°C, in the western Sahara. The largest temperature responses in North Africa are projected to occur in JJA, while the largest responses in southern Africa occur in September, October and November (SON). But the seasonal structure in the temperature response over Africa is modest as compared to extratropical regions. The basic pattern of projected warming has been robust to changes in models since the TAR, as indicated by comparison with Hulme et al. (2001).

To date there is insufficient evidence from RCMs to modify the large-scale temperature projections from GCMs, although Tadross et al. (2005a) project changes in the A2 scenario for southern Africa that are lower than those in the forcing GCM and near the low end of the spread in the MMD models, likely due to a weaker drying tendency than in most of the global models.

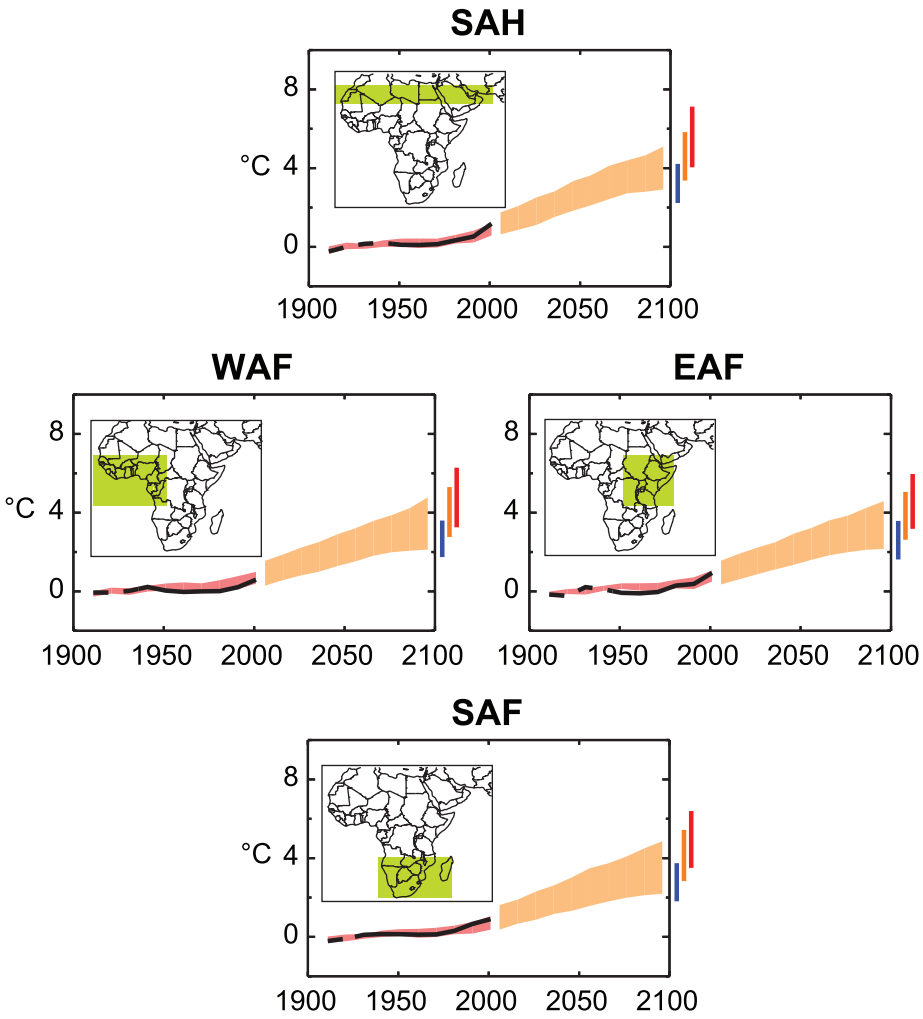


Figure 11.1. *Temperature anomalies with respect to 1901 to 1950 for four African land regions for 1906 to 2005 (black line) and as simulated (red envelope) by MMD models incorporating known forcings; and as projected for 2001 to 2100 by MMD models for the A1B scenario (orange envelope). The bars at the end of the orange envelope represent the range of projected changes for 2091 to 2100 for the B1 scenario (blue), the A1B scenario (orange) and the A2 scenario (red). The black line is dashed where observations are present for less than 50% of the area in the decade concerned. More details on the construction of these figures are given in Box 11.1 and Section 11.1.2.*

11.2.3.2 Mean Precipitation

Figure 11.2 and Table 11.1 illustrate some of the robust aspects of the precipitation response over Africa in the MMD-A1B projections. The fractional changes in annual mean precipitation in each of the 21 models are provided in Supplementary Material Figure S11.13. With respect to the most robust features (drying in the Mediterranean and much of southern Africa, and increases in rainfall in East Africa), there is qualitative agreement with the results in Hulme et al. (2001) and Ruosteenoja et al. (2003), which summarise results from the models available at the time of the TAR.

The large-scale picture is one of drying in much of the subtropics and an increase (or little change) in precipitation in the tropics, increasing the rainfall gradients. This is a plausible hydrological response to a warmer atmosphere, a consequence of the increase in water vapour and the resulting increase in vapour transport in the atmosphere from regions of moisture divergence to regions of moisture convergence (see Chapter 9 and Section 11.2.1).

The drying along Africa's Mediterranean coast is a component of a larger-scale drying pattern surrounding the Mediterranean and is discussed further in the section on Europe (Section 11.3). A 20% drying in the annual mean is typical along the African Mediterranean coast in A1B by the end of the 21st century. Drying is seen throughout the year and is generated by nearly every MMD model. The drying signal in this composite extends into the northern Sahara, and down the West Coast as far as 15°N. The processes involved include increased moisture divergence and a systematic poleward shift of the storm tracks affecting the winter rains, with positive feedback from decreasing soil moisture in summer (see Section 11.3).

In southern Africa, a similar set of processes produces drying that is especially robust in the extreme southwest in winter, a manifestation of a much broader-scale poleward shift in the circulation across the South Atlantic and Indian Oceans. However, the drying is subject to the caveat that strong orographic forcing may result in locally different changes (as discussed in Section 11.4.3.2, Box 11.3). With the exception of the winter rainfall region in the southwest, the robust drying in winter corresponds to the dry season over most of the sub-continent and does not contribute to the bulk of the annual mean

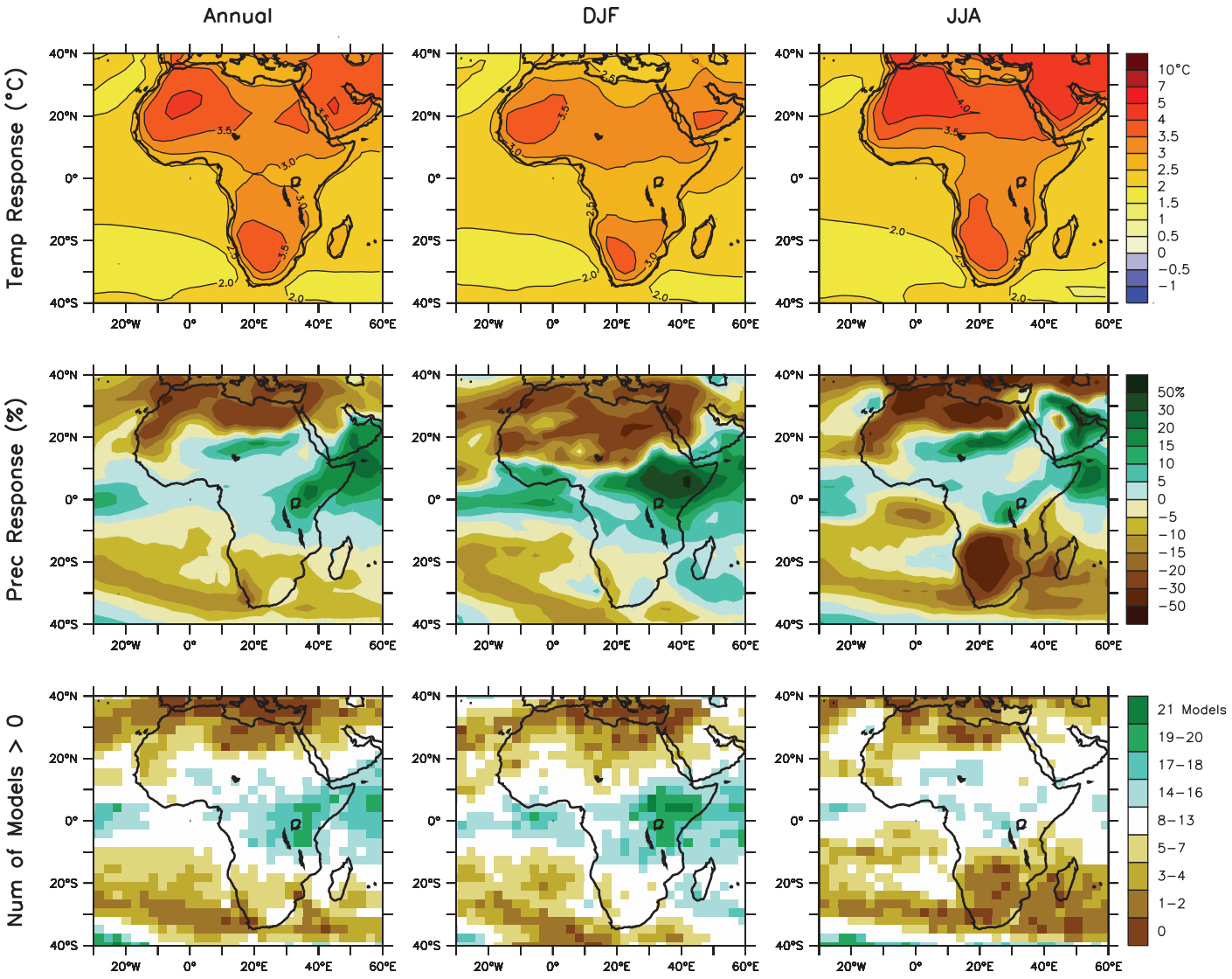


Figure 11.2. *Temperature and precipitation changes over Africa from the MMD-A1B simulations. Top row: Annual mean, DJF and JJA temperature change between 1980 to 1999 and 2080 to 2099, averaged over 21 models. Middle row: same as top, but for fractional change in precipitation. Bottom row: number of models out of 21 that project increases in precipitation.*

drying. More than half of the annual mean reduction occurs in the spring and is mirrored in some RCM simulations for this region (see below). To an extent, this can be thought of as a delay in the onset of the rainy season. This spring drying suppresses evaporation, contributing to the spring maximum in the temperature response.

The increase in rainfall in East Africa, extending into the Horn of Africa, is also robust across the ensemble of models, with 18 of 21 models projecting an increase in the core of this region, east of the Great Lakes. This East African increase is also evident in Hulme et al. (2001) and Ruosteenoja et al. (2003). The Guinean coastal rain belts and the Sahel do not show as robust a response. A straight average across the ensemble results in modest moistening in the Sahel with little change on the Guinean coast. The composite MMD simulations have a weak drying trend in the Sahel in the 20th century that does not continue in the future projections (Biasutti and Giannini, 2006; Hoerling, et al., 2006), implying that the weak 20th-century drying trend in the composite 20th-century simulations is unlikely to be forced by greenhouse gases, but is more likely forced by aerosols, as in Rotstayn and Lohmann (2002), or a result of low-frequency internal variability of the climate.

Individual models generate large, but disparate, responses in the Sahel. Two outliers are GFDL/CM2.1, which projects very strong drying in the Sahel and throughout the Sahara, and MIROC3.2_midres, which shows a very strong trend towards increased rainfall in the same region (see Supplementary Figure S11.13; and see Table 8.1 for model descriptions). Cook and Vizy (2006) find moderately realistic interannual variability in the Gulf of Guinea and Sahel in both models. While the drying in the GFDL model is extreme within the ensemble, it generates a plausible simulation of 20th-century Sahel

rainfall trends (Held et al., 2005; Hoerling et al., 2006) and an empirical downscaling from AOGCMs (Hewitson and Crane, 2006) shows a similar response (see below). More research is needed to understand the variety of modelled precipitation responses in the Sahel and elsewhere in the tropics. Progress is being made in developing new methodologies for this purpose (e.g., Chou and Neelin, 2004; Lintner and Chiang, 2005; Chou et al., 2007), leading to better appreciation of the sources of model differences. Haarsma et al. (2005) describe a plausible mechanism associated with increasing land-ocean temperature contrast and decreasing surface pressures over the Sahara, which contributes to the increase in Sahel precipitation with warming in some models.

It has been argued (e.g., Paethe and Hense, 2004) that the partial amelioration of the Sahel drought since the 1990s may be a sign of a greenhouse-gas driven increase in rainfall, providing support for those models that moisten the Sahel into the 21st century (e.g., Maynard et al., 2002; Haarsma et al., 2005; Kamga et al., 2005). However, it is premature to take this partial amelioration as evidence of a global warming signature, given the likely influence of internal variability on the inter-hemispheric SST gradients that influence Sahel rainfall, as well as the influence of aerosol variations.

Table 11.1 provides information on the spread of model-projected precipitation change in the four African sub-regions. The regions and seasons for which the central half (25 to 75%) of the projections are uniformly of one sign are: EAF where there is an increase in DJF, March, April and May (MAM), SON and in the annual mean; SAF where there is a decrease in austral winter and spring; and SAH where there is a decrease in boreal winter and spring. The Tebaldi et al. (2004a,b) Bayesian estimates (Supplementary Material Table S11.2)

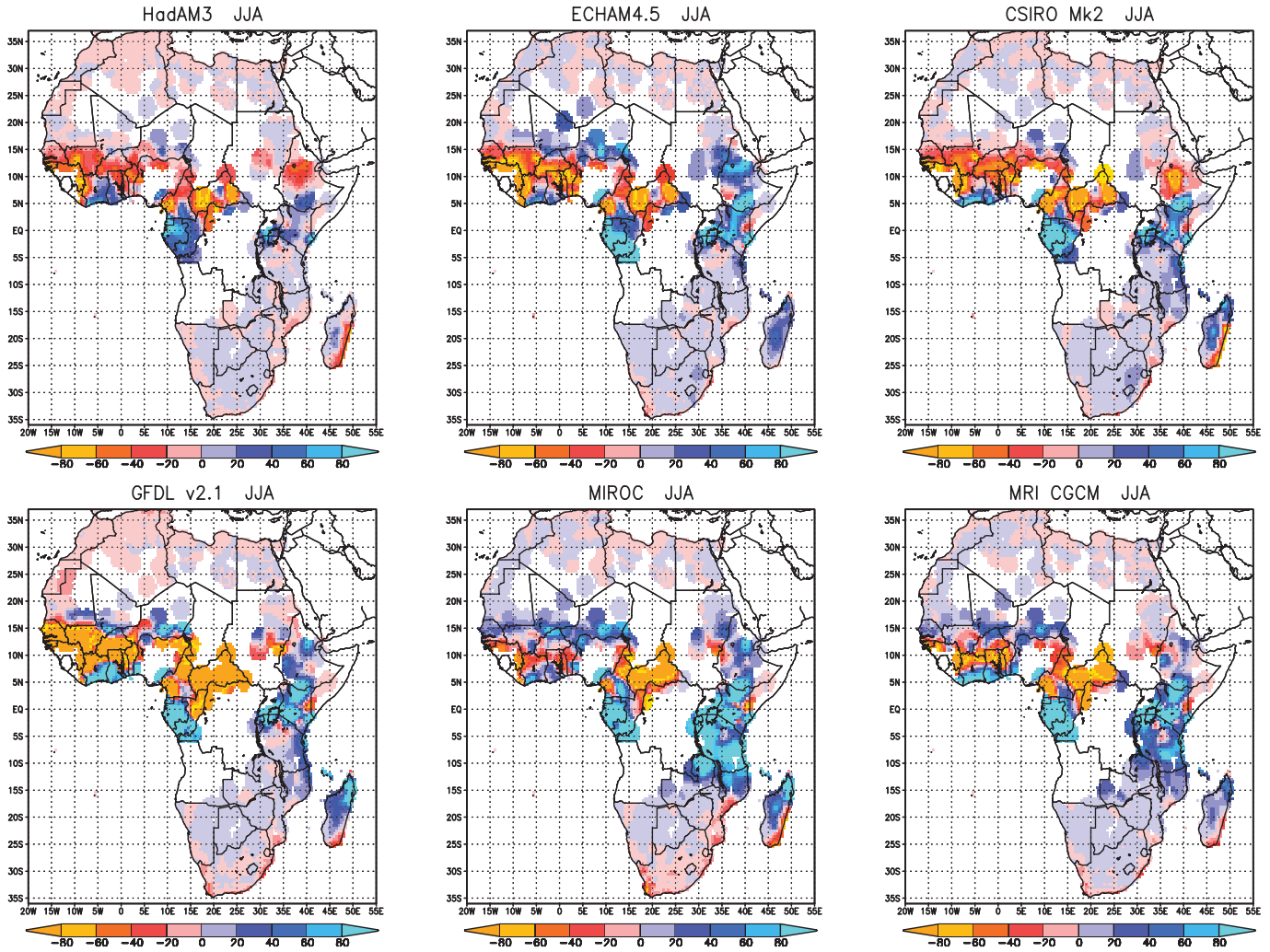


Figure 11.3. *Anomaly of mean monthly precipitation (mm) using daily data empirically downscaled from six GCMs (ECHAM4.5, Hadley Centre Atmospheric Model (HadAM3), CSIRO Mk2, GFDL 2.1, MRI, MIROC; see Table 8.1 for descriptions of most of these models) to 858 station locations. The GCMs were forced by the SRES A2 scenario. Anomalies are for the future period (2070 to 2099 for the first three models, and 2080 to 2099 for the latter three models) minus a control 30-year period (from Hewitson and Crane, 2006).*

do not change this distinction between robust and non-robust regions and seasons. The time required for emergence of a clearly discernible signal in these robust regions and seasons is typically 50 to 100 years, except in the Sahara where even longer times are required.

Land use change is a potential contributor to climate change in the 21st century (see also Section 11.7, Box 11.4). C.M. Taylor et al. (2002) project drying over the Sahel of 4% from 1996 to 2015 due to changing land use, but suggest that the potential exists for this contribution to grow substantially further into the century. Maynard and Royer (2004a) suggest that estimated land use change scenarios for the mid-21st century would have only a modest compensating effect on the greenhouse-gas induced moistening in their model. Neither of these studies includes a dynamic vegetation model.

Several climate change projections based on RCM simulations are available for southern Africa but are much scarcer for other regions. Tadross et al. (2005a) examine two RCMs, Providing Regional Impacts for Climate Studies (PRECIS) and Mesoscale Model version 5 (MM5), nested for southern Africa in a time-slice AGCM based in turn on lower-resolution Hadley Centre Coupled Model (HadCM3) coupled simulations for the Special Report on Emission Scenarios (SRES) A2 scenario. During the early summer season, October to December, both models predict drying over the tropical western side of the continent, responding to the increase in high-pressure systems entering from the west, with MM5 indicating that the drying extends further south and PRECIS further east. The drying in the west continues into late summer, but there are increases in total rainfall towards the east in January and February, a feature barely present in the ensemble mean of the MMD models. Results obtained by downscaling one global model must be assessed in the context of the variety of responses in southern Africa among the MMD models (Supplementary Material Figure S11.13).

Hewitson and Crane (2006) use empirical downscaling to provide projections for daily precipitation as a function of six GCM simulations. The degree of convergence in the downscaled results for the SRES A2 scenario near the end of the 21st century suggests more commonality in GCM-projected changes in daily circulation, on which the downscaling is based, than in the GCM precipitation responses. Figure 11.3 shows the response of mean JJA monthly total precipitation for station locations across Africa. The ensemble mean of these downscaling results shows increased precipitation in east Africa extending into southern Africa, especially in JJA, strong drying in the core Sahel in JJA with some coastal wetting, and moderate wetting in DJF. There is also drying along the Mediterranean coast, and, in most models, drying in the western portion of southern Africa. The downscaling also shows marked local-scale variation in the projected changes, for example, the contrasting changes in the west and east of Madagascar, and on the coastal and inland borders of the Sahel.

While this result is generally consistent with the underlying GCMs and the composite MMD projections, there is a tendency for greater Sahel drying than in the underlying GCMs, providing further rationale (alongside the large spread in model responses and poor coupled model performance in simulating droughts of the magnitude observed in the 20th century) for viewing with caution the projection for a modest increase in Sahel rainfall in the ensemble mean of the MMD models.

11.2.3.3 Extremes

Research on changes in extremes specific to Africa, in either models or observations, is limited. A general increase in the intensity of high-rainfall events, associated in part with the increase in atmospheric water vapour, is expected in Africa, as in other regions. Regional modelling and downscaling results (Tadross et al., 2005a) both support an increase in the rainfall intensity in southern Africa. In regions of mean drying, there is generally a proportionally larger decrease in the number of rain days, indicating compensation between intensity and frequency of rain. In the downscaling results of Hewitson and Crane (2006) and Tadross et al. (2005a), changes in the median precipitation event magnitude at the station scale do not always mirror the projected changes in seasonal totals.

There is little modelling guidance on possible changes in tropical cyclones affecting the southeast coast of Africa. Thermodynamic arguments for increases in precipitation rates and intensity of tropical storms (see Chapter 10) are applicable to these Indian Ocean storms as for other regions, but changes in frequency and spatial distribution remain uncertain. In a time-slice simulation with a 20-km resolution AGCM, Oouchi et al. (2006) obtain a significant reduction in the frequency of tropical storms in the Indian Ocean.

Using the definition of 'extreme seasons' given in Section 11.1.2, the probability of extremely warm, wet and dry seasons, as estimated by the MMD models, is provided in Table 11.1. As in most tropical regions, all seasons are extremely warm by the end of the 21st century, with very high confidence under the A1B scenario. Although the mean precipitation response in West Africa is less robust than in East Africa, the increase in the number of extremely wet seasons is comparable in both, increasing to roughly 20% (i.e., 1 in 5 of the seasons are extremely wet, as compared to 1 in 20 in the control period in the late 20th century). In southern Africa, the frequency of extremely dry austral winters and springs increases to roughly 20%, while the frequency of extremely wet austral summers doubles in this ensemble of models.

11.3 Europe and the Mediterranean

Assessments of projected climate change for Europe:

Annual mean temperatures in Europe are likely to increase more than the global mean. The warming in northern Europe is likely to be largest in winter and that in the Mediterranean area largest in summer. The lowest winter temperatures are likely to increase more than average winter temperature in northern Europe, and the highest summer temperatures are likely to increase more than average summer temperature in southern and central Europe.

Annual precipitation is very likely to increase in most of northern Europe and decrease in most of the Mediterranean area. In central Europe, precipitation is likely to increase in winter but decrease in summer. Extremes of daily precipitation are very likely to increase in northern Europe. The annual number of precipitation days is very likely to decrease in the Mediterranean area. The risk of summer drought is likely to increase in central Europe and in the Mediterranean area.

Confidence in future changes in windiness is relatively low, but it seems more likely than not that there will be an increase in average and extreme wind speeds in northern Europe.

The duration of the snow season is very likely to shorten in all of Europe, and snow depth is likely to decrease in at least most of Europe.

Although many features of the simulated climate change in Europe and the Mediterranean area are qualitatively consistent among models and qualitatively well understood in physical terms, substantial uncertainties remain. Simulated seasonal-mean temperature changes vary even at the sub-continental scale by a factor of two to three among the current generation of AOGCMs. Similarly, while agreeing on a large-scale increase in winter half-year precipitation in the northern parts of the area and a decrease in summer half-year precipitation in the southern parts of the area, models disagree on the magnitude and geographical details of precipitation change. These uncertainties reflect the sensitivity of the European climate change to the magnitude of the global warming and the changes in the atmospheric circulation and the Atlantic Meridional Overturning Circulation (MOC). Deficiencies in modelling the processes that regulate the local water and energy cycles in Europe also introduce uncertainty, for both the changes in mean conditions and extremes. Finally, the substantial natural variability of European climate is a major uncertainty, particularly for short-term climate projections in the area (e.g., Hulme et al., 1999).

11.3.1 Key Processes

In addition to global warming and its direct thermodynamic consequences such as increased water vapour transport from low to high latitudes (Section 11.1.3), several other factors may shape future climate changes in Europe and the Mediterranean area. Variations in the atmospheric circulation influence the European climate both on interannual and longer time scales. Recent examples include the central European heat wave in the summer 2003, characterised by a long period of anticyclonic weather (see Box 3.5), the severe cyclone-induced flooding in central Europe in August 2002 (see Box 3.6), and the strong warming of winters in northern Europe from the 1960s to 1990s that was affected by a trend toward a more positive phase of the NAO (Hurrell and van Loon, 1997; Räisänen and Alexandersson, 2003; Scaife et al., 2005). At fine geographical scales, the effects of atmospheric circulation are modified by topography, particularly in areas of complex terrain (Fernandez et al., 2003; Bojariu and Giorgi, 2005).

Europe, particularly its north-western parts, owes its relatively mild climate partly to the northward heat transport by the Atlantic MOC (e.g., Stouffer et al., 2006). Most models suggest increased greenhouse gas concentrations will lead to a weakening of the MOC (see Section 10.3), which will act to reduce the warming in Europe. However, in the light of present understanding, it is very unlikely to reverse the warming to cooling (see Section 11.3.3.1).

Local thermodynamic factors also affect the European climate and are potentially important for its future changes. In those parts of Europe that are presently snow-covered in winter, a decrease in snow cover is likely to induce a positive feedback, further amplifying the warming. In the Mediterranean region and at times in central Europe, feedbacks associated with the drying of the soil in summer are important even in the present climate. For example, they acted to exacerbate the heat wave of 2003 (Black et al., 2004; Fink et al., 2004).

11.3.2 Skill of Models in Simulating Present Climate

Atmosphere-Ocean General Circulation Models show a range of performance in simulating the climate in Europe and the Mediterranean area. Simulated temperatures in the MMD models vary on both sides of the observational estimates in summer but are mostly lower than observed in the winter half-year, particularly in northern Europe (Supplementary Material Table S11.1). Excluding one model that simulates extremely cold winters in northern Europe, the seasonal area mean temperature biases in the northern Europe region (NEU) vary from –5°C to 3°C and those in the southern Europe and Mediterranean region (SEM) from –5°C to 6°C, depending on model and season. The cold bias in northern Europe tends to increase towards the northeast, reaching –7°C in the ensemble mean in the northeast of European Russia in winter. This cold bias coincides with a north-south gradient in the winter mean sea level pressure that is weaker than observed, which implies

Box 11.2: The PRUDENCE Project

The Prediction of Regional scenarios and Uncertainties for Defining European Climate change risks and Effects (PRUDENCE) project involved more than 20 European research groups. The main objectives of the project were to provide dynamically downscaled high-resolution climate change scenarios for Europe at the end of the 21st century, and to explore the uncertainty in these projections. Four sources of uncertainty were studied: (i) sampling uncertainty due to the fact that model climate is estimated as an average over a finite number (30) of years, (ii) regional model uncertainty due to the fact that RCMs use different techniques to discretize the equations and to represent sub-grid effects, (iii) emission uncertainty due to choice of IPCC SRES emission scenario, and (iv) Boundary uncertainty due to the different boundary conditions obtained from different global climate models.

Each PRUDENCE experiment consisted of a control simulation representing the period 1961 to 1990 and a future scenario simulation representing 2071 to 2100. A large fraction of the simulations used the same boundary data (from the Hadley Centre Atmospheric Model (HadAM3H) for the A2 scenario) to provide a detailed understanding of the regional model uncertainty. Some simulations were also made for the B2 scenario, and by using driving data from two other GCMs and from different ensemble members from the same GCM. More details are provided in, for example, Christensen et al. (2007), Déqué et al. (2005) and http://prudence.dmi.dk.

weaker than observed westerly flow from the Atlantic Ocean to northern Europe in most models (Supplementary Material Figure S11.22).

Biases in simulated precipitation vary substantially with season and location. The average simulated precipitation in NEU exceeds that observed from autumn to spring (Supplementary Material Table S11.1), but the interpretation of the difference is complicated by the observational uncertainty associated with the undercatch of, in particular, solid precipitation (e.g., Adam and Lettenmaier, 2003). In summer, most models simulate too little precipitation, particularly in the eastern parts of the area. In SEM, the area and ensemble mean precipitation is close to observations.

Regional Climate Models capture the geographical variation of temperature and precipitation in Europe better than global models but tend to simulate conditions that are too dry and warm in southeastern Europe in summer, both when driven by analysed boundary conditions (Hagemann et al., 2004) and when driven by GCM data (e.g., Jacob et al., 2007). Most but not all RCMs also overestimate the interannual variability of summer temperatures in southern and central Europe (Jacob et al., 2007; Lenderink et al., 2007; Vidale et al., 2007). The excessive temperature variability coincides with excessive interannual variability in either shortwave radiation or evaporation, or both (Lenderink et al., 2007). A need for improvement in the modelling of soil, boundary layer and cloud processes is implied. One of the key model parameters may be the depth of the hydrological soil reservoir, which appears to be too small in many RCMs (van den Hurk et al., 2005).

The ability of RCMs to simulate climate extremes in Europe has been addressed in several studies. In the Prediction of Regional scenarios and Uncertainties for Defining European Climate change risks and Effects (PRUDENCE) simulations (Box 11.2), the biases in the tails of the temperature distribution varied substantially between models but were generally larger than the biases in average temperatures (Kjellström et al., 2007). Inspection of the individual models showed similarity between the biases in daily and interannual variability, suggesting that similar mechanisms may be affecting both.

The magnitude of precipitation extremes in RCMs is model-dependent. In a comparison of the PRUDENCE RCMs, Frei et al. (2006) find that the area-mean five-year return values of one-day precipitation in the vicinity of the European Alps vary by up to a factor of two between the models. However, except for too-low extremes in the southern parts of the area in summer, the set of models as a whole showed no systematic tendency to over- or underestimate the magnitude of the extremes when compared with gridded observations. A similar level of skill has been found in other model verification studies made for European regions (e.g., Booij, 2002; Semmler and Jacob, 2004; Fowler et al., 2005; see also Frei et al., 2003).

Evidence of model skill in simulation of wind extremes is mixed. Weisse et al. (2005) find that an RCM simulated a very realistic wind climate over the North Sea, including the number and intensity of storms, when driven by analysed boundary conditions. However, most PRUDENCE RCMs, while quite realistic over sea, severely underestimate the occurrence of very high wind speeds over land and coastal areas (Rockel and Woth, 2007). Realistic frequencies of high wind speeds were only found in the two models that used a gust parametrization to mimic the large local and temporal variability of near-surface winds over land.

11.3.3 Climate Projections

11.3.3.1 Mean Temperature

The observed evolution of European temperatures in the 20th century, characterised by a warming trend modulated by multi-decadal variability, was well within the envelope of the MMD simulations (Figure 11.4).

In this century, the warming is projected to continue at a rate somewhat greater than its global mean, with the increase in 20-year mean temperatures (from its values in 1980 to 1999) becoming clearly discernible (as defined in Section 11.1.2) within a few decades. Under the A1B scenario, the simulated area and annual mean warming from 1980 to 1999 to 2080 to 2099 varies from 2.3°C to 5.3°C in NEU and from 2.2°C to 5.1°C in SEM. The warming in northern Europe is likely to be largest in winter and that in the Mediterranean area largest

in summer (Figure 11.5). Seasonal mean temperature changes typically vary by a factor of three among the MMD models (Table 11.1); however, the upper end of the range in NEU in DJF is reduced from 8.1°C to 6.7°C when one model with an extreme cold bias in present-day winter climate is excluded. Further details are given in Table 11.1 and Supplementary Material Figures S11.2 to S11.4.

Although changes in atmospheric circulation have a significant potential to affect temperature in Europe (e.g., Dorn et al., 2003), they are not the main cause of the projected warming (e.g., Rauthe and Paeth, 2004; Stephenson et al., 2006; van Ulden et al., 2007). A regression-based study using five of the MMD models (van Ulden and van Oldenborgh, 2006) indicated that in a region comprising mainly Germany, circulation changes enhanced the warming in most models in winter (due to an increase in westerly flow) and late summer (due to a decrease in westerly flow), but reduced the warming slightly in May and June. However, the circulation contribution to the simulated temperature changes (typically –1°C to 1.5°C depending on model and month) was generally much smaller than the total simulated warming in the late 21st century.

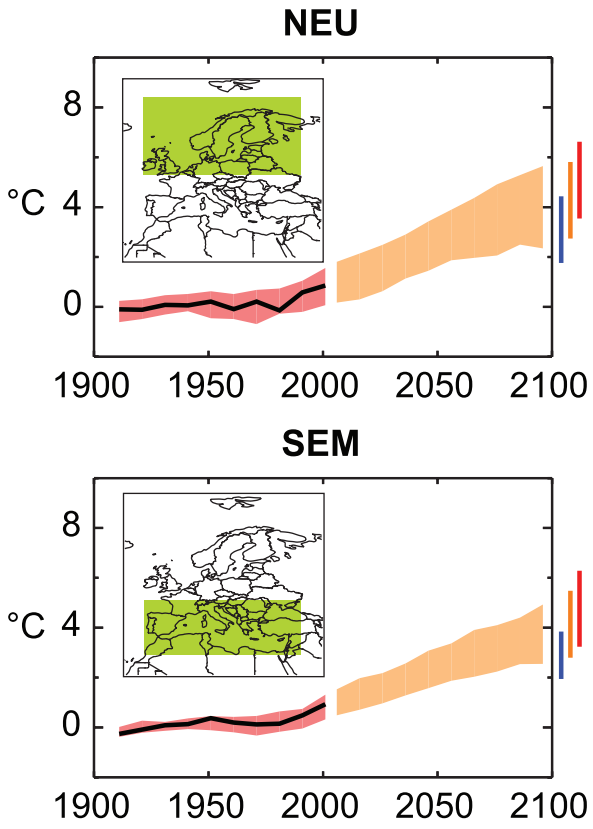


Figure 11.4. *Temperature anomalies with respect to 1901 to 1950 for two Europe land regions for 1906 to 2005 (black line) and as simulated (red envelope) by MMD models incorporating known forcings; and as projected for 2001 to 2100 by MMD models for the A1B scenario (orange envelope). The bars at the end of the orange envelope represent the range of projected changes for 2091 to 2100 for the B1 scenario (blue), the A1B scenario (orange) and the A2 scenario (red). More details on the construction of these figures are given in Box 11.1 and Section 11.1.2.*

Despite a decrease in the North Atlantic MOC in most models (see Section 10.3), all the MMD simulations show warming in Great Britain and continental Europe, as other climatic effects of increased greenhouse gases dominate over the changes in ocean circulation. The same holds for earlier simulations with increased greenhouse gas concentrations, except for a very few (Russell and Rind, 1999; Schaeffer et al., 2004) with slight cooling along the north-western coastlines of Europe but warming over the rest of the continent. The impact of MOC changes depends on the regional details of the change, being largest if ocean convection is suppressed at high latitudes where the sea ice feedback may amplify atmospheric cooling (Schaeffer et al., 2004). Sensitivity studies using AOGCMs with an artificial shutdown of the MOC and no changes in greenhouse gas concentrations typically show a 2°C to 4°C annual mean cooling in most of Europe, with larger cooling in the extreme north-western parts (e.g., Stouffer et al., 2006).

Statistical downscaling (SD) studies tend to show a large-scale warming similar to that of dynamical models but with finer-scale regional details affected by factors such as distance from the coast and altitude (e.g., Benestad, 2005; Hanssen-Bauer et al., 2005). Comparing RCM and SD projections for Norway downscaled from the same GCM, Hanssen-Bauer et al. (2003) found the largest differences between the two approaches in winter and/or spring at locations with frequent temperature inversions in the present climate. A larger warming at these locations in the SD projections was found, consistent with increased winter wind speed in the driving GCM and reduced snow cover, both of which suppress formation of ground inversions.

11.3.3.2 Mean Precipitation

A south-north contrast in precipitation changes across Europe is indicated by AOGCMs, with increases in the north and decreases in the south (Figure 11.5). The annual area-mean change from 1980 to 1999 to 2080 to 2099 in the MMD-A1B projections varies from 0 to 16% in NEU and from –4 to –27% in SEM (Table 11.1). The largest increases in northern and central Europe are simulated in winter. In summer, the NEU area mean changes vary in sign between models, although most models simulate increased (decreased) precipitation north (south) of about 55°N. In SEM, the most consistent and, in percentage terms, largest decreases, occur in summer, but the area mean precipitation in the other seasons also decreases in most or all models. More detailed statistics are given in Table 11.1. Increasing evaporation makes the simulated decreases in annual precipitation minus evaporation extend a few hundred kilometres further north in central Europe than the decreases in precipitation (Supplementary Material Figure S11.1).

Both circulation changes and thermodynamic factors appear to affect the simulated seasonal cycle of precipitation changes in Europe. Applying a regression method to five of the MMD simulations, van Ulden and van Oldenborgh (2006) found that in a region comprising mainly Germany, circulation changes played a major role in all seasons. In most models, increases

in winter precipitation were enhanced by increased westerly winds, with decreases in summer precipitation largely due to more easterly and anticyclonic flow. However, differences in the simulated circulation changes among the individual models were accompanied by large differences in precipitation change, particularly in summer. The residual precipitation change varied less with season and among models, being generally positive as expected from the increased moisture transport capacity of a warmer atmosphere. In a more detailed study of one model, HadAM3P, Rowell and Jones (2006) showed that decreases in summer precipitation in continental and southeastern Europe were mainly associated with thermodynamic factors. These included reduced relative humidity resulting from larger continental warming compared to surrounding sea areas and reduced soil moisture due mainly to spring warming causing earlier snowmelt. Given the confidence in the warming patterns driving these changes, the reliability of the simulated drying was assessed as being high.

Changes in precipitation may vary substantially on relatively small horizontal scales, particularly in areas of complex topography. Details of these variations are sensitive to changes in the atmospheric circulation, as illustrated in Figure 11.6 for two PRUDENCE simulations that only differ with respect to the driving global model. In one, an increase in westerly flow from the Atlantic Ocean (caused by a large increase in the north-south pressure gradient) is accompanied by increases of up to 70% in annual precipitation over the Scandinavian mountains. In the other, with little change in the average pressure pattern, the increase is in the range of 0 to 20%. When compared with circulation changes in the more recent MMD simulations, these two cases fall in the opposite ends of the range. Most MMD models suggest an increased north-south pressure gradient

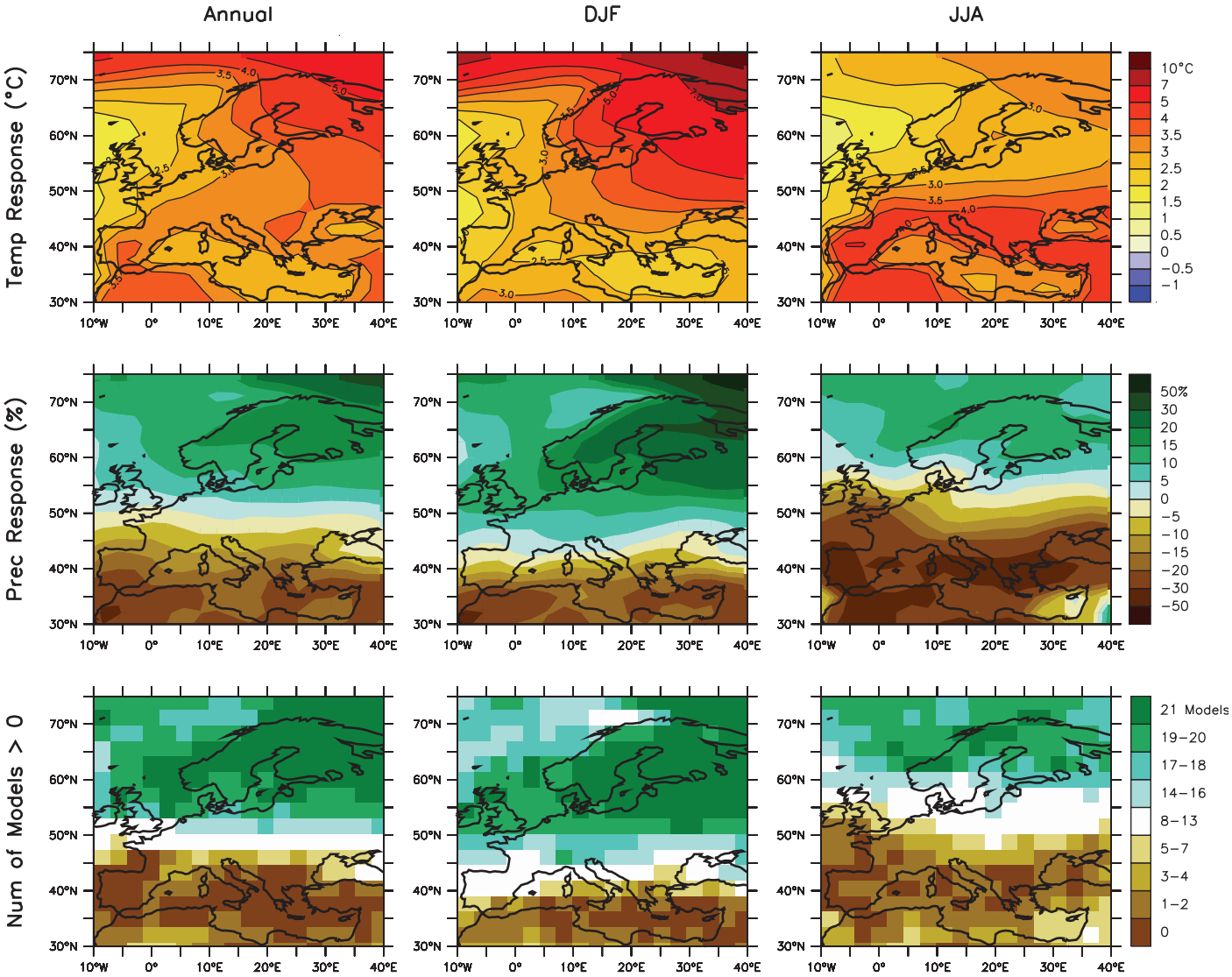


Figure 11.5. *Temperature and precipitation changes over Europe from the MMD-A1B simulations. Top row: Annual mean, DJF and JJA temperature change between 1980 to 1999 and 2080 to 2099, averaged over 21 models. Middle row: same as top, but for fractional change in precipitation. Bottom row: number of models out of 21 that project increases in precipitation.*

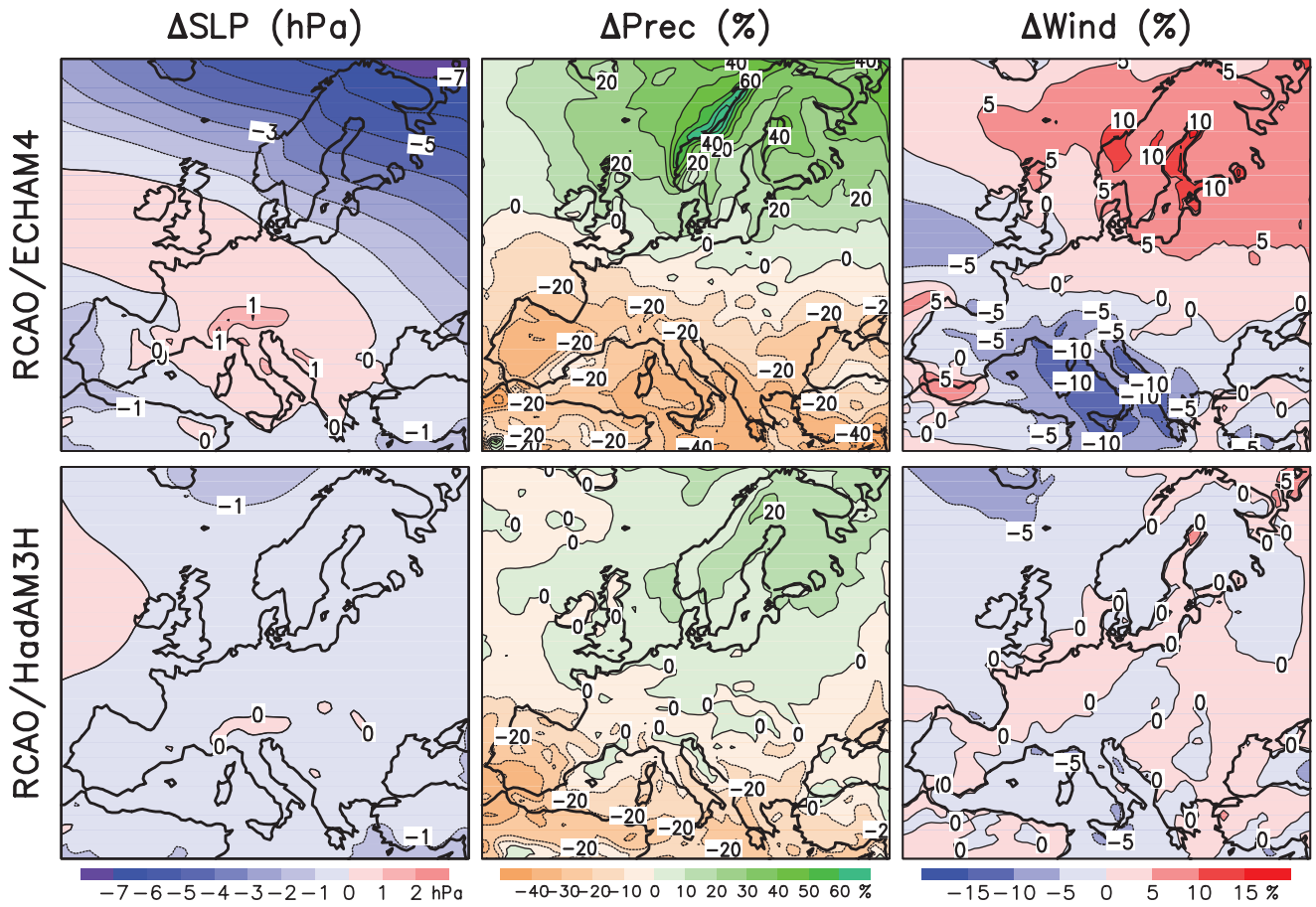


Figure 11.6. *Simulated changes in annual mean sea level pressure (ΔSLP), precipitation (ΔPrec) and mean 10-m level wind speed (ΔWind) from the years 1961 to 1990 to the years 2071 to 2100. The results are based on the SRES A2 scenario and were produced by the same RCM (Rossby Centre regional Atmosphere-Ocean model; RCAO) using boundary data from two global models: ECHAM4/OPYC3 (top) and HadAM3H (bottom) (redrawn from Rummukainen et al., 2004).*

across northern Europe, but the change is generally smaller than in the top row of Figure 11.6.

Projections of precipitation change in Europe based on SD tend to support the large-scale picture from dynamical models (e.g., Busuioc et al., 2001; Beckmann and Buishand, 2002; Hanssen-Bauer et al., 2003, 2005; Benestad, 2005; Busuioc et al., 2006), although variations between SD methods and the dependence on the GCM data sets used (see Section 11.10.1.3) make it difficult to draw quantitative conclusions. However, some SD studies have suggested a larger small-scale variability of precipitation changes than indicated by GCM and RCM results, particularly in areas of complex topography (Hellström et al., 2001).

The decrease in precipitation together with enhanced evaporation in spring and early summer is very likely to lead to reduced summer soil moisture in the Mediterranean region and parts of central Europe (Douville et al., 2002; Wang, 2005). In northern Europe, where increased precipitation competes with earlier snowmelt and increased evaporation, the MMD models disagree on whether summer soil moisture will increase or decrease (Wang, 2005).

11.3.3.3 Temperature Variability and Extremes

Based on both GCM (Giorgi and Bi, 2005; Rowell, 2005; Clark et al., 2006) and RCM simulations (Schär et al., 2004; Vidale et al., 2007), interannual temperature variability is likely to increase in summer in most areas. However, the magnitude of change is uncertain, even in central Europe where the evidence for increased variability is strongest. In some PRUDENCE simulations, interannual summer temperature variability in central Europe doubled between 1961 to 1990 and 2071 to 2100 under the A2 scenario, while other simulations showed almost no change (Vidale et al., 2007). Possible reasons for the increase in temperature variability are reduced soil moisture, which reduces the capability of evaporation to damp temperature variations, and increased land-sea contrast in average summer temperature (Rowell, 2005; Lenderink et al., 2007).

Simulated increases in summer temperature variability also extend to daily time scales. Kjellström et al. (2007) analyse the PRUDENCE simulations and find that the inter-model differences in the simulated temperature change increase towards the extreme ends of the distribution. However, a general increase in summer daily temperature variability is

evident, especially in southern and central parts of Europe, with the highest maximum temperatures increasing more than the median daily maximum temperature (Supplementary Material Figure S11.23). Similarly, Shkolnik et al. (2006) report a simulated increase in summer daily time-scale temperature variability in mid-latitude western Russia. These RCM results are supported by GCM studies of Hegerl et al. (2004), Meehl and Tebaldi (2004) and Clark et al. (2006).

In contrast with summer, models project reduced temperature variability in most of Europe in winter, both on interannual (Räisänen, 2001; Räisänen et al., 2003; Giorgi et al., 2004; Giorgi and Bi, 2005; Rowell, 2005) and daily time scales (Hegerl et al., 2004; Kjellström et al., 2007). In the PRUDENCE simulations, the lowest winter minimum temperatures increased more than the median minimum temperature especially in eastern, central and northern Europe, although the magnitude of this change was strongly model-dependent (Supplementary Material Figure S11.23). The geographical patterns of the change indicate a feedback from reduced snow cover, with a large warming of the cold extremes where snow retreats but a more moderate warming in the mostly snow-free south-western Europe (Rowell, 2005; Kjellström et al., 2007).

Along with the overall warming and changes in variability, heat waves are very likely to increase in frequency, intensity and duration (Barnett et al., 2006; Clark et al., 2006; Tebaldi et al., 2006). Conversely, the number of frost days is very likely to decrease (Tebaldi et al., 2006).

11.3.3.4 Precipitation Variability and Extremes

In northern Europe and in central Europe in winter, where time mean precipitation is simulated to increase, high extremes of precipitation are very likely to increase in magnitude and frequency. In the Mediterranean area and in central Europe in summer, where reduced mean precipitation is projected, extreme short-term precipitation may either increase (due to the increased water vapour content of a warmer atmosphere) or decrease (due to a decreased number of precipitation days, which if acting alone would also make heavy precipitation less common). These conclusions are based on several GCM (e.g., Semenov and Bengtsson, 2002; Voss et al., 2002; Hegerl et al., 2004; Wehner, 2004; Kharin and Zwiers, 2005; Tebaldi et al., 2006) and RCM (e.g., Jones and Reid, 2001; Räisänen and Joelsson, 2001; Booij, 2002; Christensen and Christensen, 2003, 2004; Pal et al., 2004; Räisänen et al., 2004; Sánchez et al., 2004; Ekström et al., 2005; Frei et al., 2006; Gao et al., 2006a; Shkolnik et al., 2006; Beniston et al., 2007) studies. However, there is still a lot of quantitative uncertainty in the changes in both mean and extreme precipitation.

Time scale also matters. Although there are some indications of increased interannual variability, particularly in summer precipitation (Räisänen, 2002; Giorgi and Bi, 2005; Rowell, 2005), changes in the magnitude of long-term (monthly to annual) extremes are expected to follow the changes in mean precipitation more closely than are those in short-term extremes (Räisänen, 2005). On the other hand, changes in the frequency of extremes tend to increase with increasing time scale even when this is not the case for the changes in the magnitude of extremes (Barnett et al., 2006).

Figure 11.7 illustrates the possible characteristics of precipitation change. The eight models in this PRUDENCE study (Frei et al., 2006) projected an increase in mean precipitation in winter in both southern Scandinavia and central Europe, due to both increased wet day frequency and increased mean precipitation for the wet days. In summer, a decrease in the number of wet days led to a decrease in mean precipitation, particularly in central Europe. Changes in extreme short-term precipitation were broadly similar to the change in average wet-day precipitation in winter. In summer, extreme daily precipitation increased in most models despite the decrease in mean precipitation, although the magnitude of the change was highly model-dependent. However, this study only covered the uncertainties associated with the choice of the RCM, not those associated with the driving GCM and the emissions scenario.

Much larger changes are expected in the recurrence frequency of precipitation extremes than in the magnitude of extremes (Huntingford et al., 2003; Barnett et al., 2006; Frei et al., 2006). For example, Frei et al. (2006) estimate that, in Scandinavia under the A2 scenario, the highest five-day winter precipitation totals occurring once in 5 years in 2071 to 2100 would be similar to those presently occurring once in 8 to 18 years (the range reflects variation between the PRUDENCE models). In the MMD simulations, large increases occur in the frequencies of both high winter precipitation in northern Europe and low summer precipitation in southern Europe and the Mediterranean area (Table 11.1).

The risk of drought is likely to increase in southern and central Europe. Several model studies have indicated a decrease in the number of precipitation days (e.g., Semenov and Bengtsson, 2002; Voss et al., 2002; Räisänen et al., 2003, 2004; Frei et al., 2006) and an increase in the length of the longest dry spells in this area (Voss et al., 2002; Pal et al., 2004; Beniston et al., 2007; Gao et al., 2006a; Tebaldi et al., 2006). By contrast, the same studies do not suggest major changes in dry-spell length in northern Europe.

11.3.3.5 Wind Speed

Confidence in future changes in windiness in Europe remains relatively low. Several model studies (e.g., Zwiers and Kharin, 1998; Knippertz et al., 2000; Leckebusch and Ulbrich, 2004; Pryor et al., 2005a; van den Hurk et al., 2006) have suggested increased average and/or extreme wind speeds in northern and/or central Europe, but some studies point in the opposite direction (e.g., Pryor et al., 2005b). The changes in both average and extreme wind speeds may be seasonally variable, but the details of this variation appear to be model-dependent (e.g., Räisänen et al., 2004; Rockel and Woth, 2007).

A key factor is the change in the large-scale atmospheric circulation (Räisänen et al., 2004; Leckebusch et al., 2006). Simulations with an increased north-south pressure gradient across northern Europe (e.g., top row of Figure 11.6) tend to

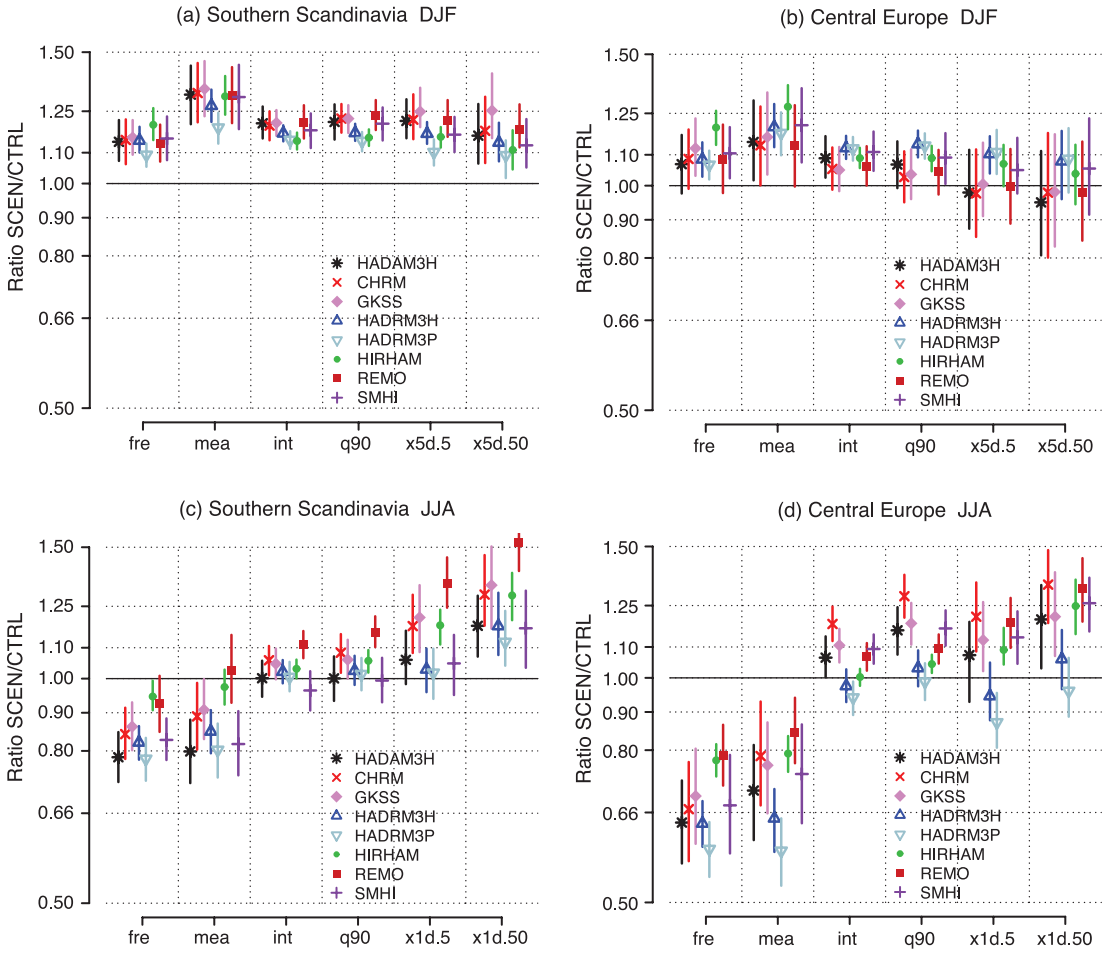


Figure 11.7. *Changes (ratio 2071–2100 / 1961–1990 for the A2 scenario) in domain-mean precipitation diagnostics in the PRUDENCE simulations in southern Scandinavia (5°E–20°E, 55°N–62°N) and central Europe (5°E–15°E, 48°N–54°N) in winter (top) and in summer (bottom). fre = wet-day frequency; mea = mean seasonal precipitation; int = mean wet-day precipitation; q90 = 90th percentile of wet-day precipitation; x1d.5 and x1d.50 = 5- and 50-year return values of one-day precipitation; x5d.5 and x5d.50 = 5- and 50-year return values of five-day precipitation. For each of the eight models, the vertical bar gives the 95% confidence interval associated with sampling uncertainty (re-drawn from Frei et al., 2006). Models are the Hadley Centre Atmospheric Model (HadAM3H), the Climate High Resolution Model (CHRM), the climate version of the 'Lokalmodell' (CLM), the Hadley Centre Regional Model (HadRM3H and HadRM3P), the combination of the High-Resolution Limited Area Model (HIRLAM) and the European Centre Hamburg (ECHAM4) GCM (HIRHAM), the regional climate model REMO, and the Rossby Centre regional Atmosphere-Ocean model (RCAO).*

indicate stronger winds in northern Europe, because of both the larger time-averaged pressure gradient and a northward shift in cyclone activity. Conversely, the northward shift in cyclone activity tends to reduce windiness in the Mediterranean area. On the other hand, simulations with little change in the pressure pattern tend to show only small changes in the mean wind speed (bottom row of Figure 11.6). Most of the MMD-projected pressure changes fall between the two PRUDENCE simulations shown in Figure 11.6, which suggests that the most likely outcome for windiness might be between these two cases.

Extreme wind speeds in Europe are mostly associated with strong winter cyclones (e.g., Leckebush and Ullbrich, 2004), the occurrence of which is only indirectly related to the time-mean circulation. Nevertheless, models suggest a general similarity between the changes in average and extreme wind speeds (Knippertz et al., 2000; Räisänen et al., 2004). A caveat to this conclusion is that, even in most RCMs, the simulated extremes of wind speed over land tend to be too low (see Section 11.3.2).

11.3.3.6 Mediterranean Cyclones

Several studies have suggested a decrease in the total number of cyclones in the Mediterranean Sea (Lionello et al., 2002; Vérant, 2004; Somot 2005; Leckebusch et al., 2006; Pinto et al., 2006; Ulbrich et al., 2006), but there is no agreement on whether the number of intense cyclones will increase or decrease (Lionello et al., 2002; Pinto et al., 2006).

11.3.3.7 Snow and Sea Ice

The overall warming is very likely to shorten the snow season in all of Europe. Snow depth is also likely to be reduced, at least in most areas, although increases in total winter precipitation may counteract the increased melting and decreased fraction of

solid precipitation associated with the warming. The changes may be large, including potentially a one-to-three month shortening of the snow season in northern Europe (Räisänen et al., 2003) and a 50 to 100% decrease in snow depth in most of Europe (Räisänen et al., 2003; Rowell, 2005) by the late 21st century. However, snow conditions in the coldest parts of Europe, such as northern Scandinavia and north-western Russia (Räisänen et al., 2003; Shkolnik et al., 2006) and the highest peaks of the Alps (Beniston et al., 2003) appear to be less sensitive to the temperature and precipitation changes projected for this century than those at lower latitudes and altitudes (see also Section 11.4.3.2, Box 11.3).

The Baltic Sea is likely to lose a large part of its seasonal ice cover during this century. Using a regional atmosphere-Baltic Sea model (Meier et al., 2004), the average winter maximum ice extent decreased by about 70% (60%) between 1961 to 1990 and 2071 to 2100 under the A2 (B2) scenario. The length of the ice season was projected to decrease by one to two months in northern parts and two to three months in the central parts. Comparable decreases in Baltic Sea ice cover were projected by earlier studies (Haapala et al., 2001; Meier, 2002).

11.4 Asia

Assessment of projected climate change for Asia:

All of Asia is very likely to warm during this century; the warming is likely to be well above the global mean in central Asia, the Tibetan Plateau and northern Asia, above the global mean in East and South Asia, and similar to the global mean in Southeast Asia. It is very likely that summer heat waves/hot spells in East Asia will be of longer duration, more intense, and more frequent. It is very likely that there will be fewer very cold days in East Asia and South Asia.

Boreal winter precipitation is very likely to increase in northern Asia and the Tibetan Plateau, and likely to increase in eastern Asia and the southern parts of Southeast Asia. Summer precipitation is likely to increase in northern Asia, East and South Asia and most of Southeast Asia, but it is likely to decrease in central Asia. An increase in the frequency of intense precipitation events in parts of South Asia, and in East Asia, is very likely.

Extreme rainfall and winds associated with tropical cyclones are likely to increase in East, Southeast and South Asia. Monsoonal flows and the tropical large-scale circulation are likely to be weakened.

While broad aspects of Asian climate change show consistency among AOGCM simulations, a number of sources of uncertainty remain. A lack of observational data in some areas limits model assessment. There has been little assessment of the projected changes in regional climatic means and extremes. There are substantial inter-model differences in representing monsoon processes, and a lack of clarity over changes in ENSO further contributes to uncertainty about future regional monsoon and tropical cyclone behaviour. Consequently, quantitative estimates of projected precipitation change are difficult to obtain. It is likely that some local climate changes will vary significantly from regional trends due to the region's very complex topography and marine influences.

11.4.1 Key Processes

As monsoons are the dominant phenomena over much of Asia, the factors that influence the monsoonal flow and precipitation are of central importance for understanding climate change in this region. Precipitation is affected both by the strength of the monsoonal flows and the amount of water vapour transported. Monsoonal flows and the tropical large-scale circulation often weaken in global warming simulations (e.g., Knutson and Manabe, 1995). This arises out of an increase in dry static stability associated with the tropical warming in these models, and the reduction in adiabatic warming/cooling needed to balance a given amount of radiative cooling/condensational heating (e.g., Betts, 1998). But there is an emerging consensus that the effect of enhanced moisture convergence in a warmer, moister atmosphere dominates over any such weakening of the circulation, resulting in increased monsoonal precipitation (e.g., Douville et al., 2000; Giorgi et al., 2001a,b; Stephenson et al., 2001; Dairaku and Emori, 2006; Ueda et al., 2006).

There is an association of the phase of ENSO with the strength of the summer monsoons (Pant and Rupa Kumar, 1997), so changes in ENSO will have an impact on these monsoons. However, such an impact can be compounded by a change in the ENSO-South Asian monsoon connection under greenhouse gas warming (Krishna Kumar et al., 1999; Ashrit et al., 2001; Sarkar et al., 2004; see Section 3.7). Moreover, there is a link between Eurasian snow cover and the strength of the monsoon (see also Section 3.7), with the monsoon strengthening if snow cover retreats. Aerosols, particularly absorbing aerosols, further modify monsoonal precipitation (e.g., Ramanathan et al., 2005 for South Asia), as do modifications of vegetation cover (e.g., Chen et al., 2004 for East Asia). However, most emission scenarios suggest that future changes in regional climate are still likely to be dominated by increasing greenhouse gas forcing rather than changes in sulphate and absorbing aerosols, at least over the South Asian region.

For South Asia, the monsoon depressions and tropical cyclones generated over the Indian seas modulate the monsoon anomalies. For East Asia, the monsoonal circulations are strengthened by extratropical cyclones energised in the lee of the Tibetan Plateau and by the strong temperature gradient along the East Coast. The influence of ENSO on the position and strength of the subtropical high in the North Pacific influences both typhoons and other damaging heavy rainfall events, and has been implicated in observed inter-decadal variations in typhoon tracks (Ho et al., 2004). This suggests that the spatial structure of warming in the Pacific will be relevant for changes

in these features. The dynamics of the Meiyu-Changma-Baiu rains in the early summer, which derive from baroclinic disturbances strongly modified by latent heat release, remain poorly understood. While an increase in rainfall in the absence of circulation shifts is expected, relatively modest shifts or changes in timing can significantly affect East Chinese, Korean and Japanese climates.

Over central and Southeast Asia and the maritime continent, interannual rainfall variability is significantly affected by ENSO (e.g., McBride et al., 2003), particularly the June to November rainfall in southern and eastern parts of the Indonesian Archipelago, which is reduced in El Niño years (Aldrian and Susanto, 2003). Consequently, the pattern of ocean temperature change across the Pacific is of central importance to climate change in this region.

In central Asia, including the Tibetan Plateau, the temperature response is strongly influenced by changes in winter and spring snow cover, the isolation from maritime influences, and the spread of the larger winter arctic warming into the region. With regard to precipitation, a key issue is related to the moisture transport from the northwest by westerlies and polar fronts. How far the projected drying of the neighbouring Mediterranean penetrates into these regions is likely to be strongly dependent on accurate simulation of these moisture transport processes. The dynamics of climate change in the Tibetan Plateau are further complicated by the high altitude of this region and its complex topography with large elevation differences.

11.4.2 Skill of Models in Simulating Present Climate

Regional mean temperature and precipitation in the MMD models show biases when compared with observed climate (Supplementary Material Table S11.1). The multi-model mean shows a cold and wet bias in all regions and in most seasons, and the bias of the annual average temperature ranges from –2.5°C over the Tibetan Plateau (TIB) to –1.4°C over South Asia (SAS). For most regions, there is a 6°C to 7°C range in the biases from individual models with a reduced bias range in Southeast Asia (SEA) of 3.6°C. The median bias in precipitation is small (less than 10%) in Southeast Asia, South Asia, and Central Asia (CAS), larger in northern Asia and East Asia (NAS and EAS, around +23%), and very large in the Tibetan Plateau (+110%). Annual biases in individual models are in the range of –50 to +60% across all regions except the Tibetan Plateau, where some models simulate annual precipitation 2.5 times that observed and even larger seasonal biases occur in winter and spring. These global models clearly have significant problems over Tibet, due to the difficulty in simulating the effects of the dramatic topographic relief, as well as the distorted albedo feedbacks due to extensive snow cover. However, with only limited observations available, predominantly in valleys, large errors in temperature and significant underestimates of precipitation are likely.

South Asia

Over South Asia, the summer is dominated by the southwest monsoon, which spans the four months from June to September and dominates the seasonal cycles of the climatic parameters. While most models simulate the general migration of seasonal tropical rain, the observed maximum rainfall during the monsoon season along the west coast of India, the north Bay of Bengal and adjoining northeast India is poorly simulated by many models (Lal and Harasawa, 2001; Rupa Kumar and Ashrit, 2001; Rupa Kumar et al., 2002, 2003). This is likely linked to the coarse resolution of the models, as the heavy rainfall over these regions is generally associated with the steep orography. However, the simulated annual cycles in South Asian mean precipitation and surface air temperature are reasonably close to the observed (Supplementary Material Figure S11.24). The MMD models capture the general regional features of the monsoon, such as the low rainfall amounts coupled with high variability over northwest India. However, there has not yet been sufficient analysis of whether finer details of regional significance are simulated more adequately in the MMD models.

Recent work indicates that time-slice experiments using an AGCM with prescribed SSTs, as opposed to a fully coupled system, are not able to accurately capture the South Asian monsoon response (Douville, 2005). Thus, neglecting the short-term SST feedback and variability seems to have a significant impact on the projected monsoon response to global warming, complicating the regional downscaling problem. However, May (2004a) notes that the high-resolution (about 1.5 degrees) European Centre-Hamburg (ECHAM4) GCM simulates the variability and extremes of daily rainfall (intensity as well as frequency of wet days) in good agreement with the observations (Global Precipitation Climatology Project, Huffman et al., 2001).

Three-member ensembles of baseline simulations (1961–1990) from an RCM (PRECIS) at 50 km resolution have confirmed that significant improvements in the representation of regional processes over South Asia can be achieved (Rupa Kumar et al., 2006). For example, the steep gradients in monsoon precipitation with a maximum along the western coast of India are well represented in PRECIS.

East Asia

Simulated temperatures in most MMD models are too low in all seasons over East Asia; the mean cold bias is largest in winter and smallest in summer. Zhou and Yu (2006) show that over China, the models perform reasonably in simulating the dominant variations of the mean temperature over China, but not the spatial distributions. The annual precipitation over East Asia exceeds the observed estimates in almost all models and the rain band in the mid-latitudes is shifted northward in seasons other than summer. This bias in the placement of the rains in central China also occurred in earlier models (e.g., Zhou and Li, 2002; Gao et al., 2004). In winter, the area-mean precipitation is overestimated by more than 50% on average due to strengthening of the rain band associated with extratropical systems over South China. The bias and inter-model differences

in precipitation are smallest in summer but the northward shift of this rain band results in large discrepancies in summer rainfall distribution over Korea, Japan and adjacent seas.

Kusunoki et al. (2006) find that the simulation of the Meiyu-Changma-Baiu rains in the East Asian monsoon is improved substantially with increasing horizontal resolution. Confirming the importance of resolution, RCMs simulate more realistic climatic characteristics over East Asia than AOGCMs, whether driven by re-analyses or by AOGCMs (e.g., Ding et al., 2003; Oh et al., 2004; Fu et al., 2005; Zhang et al., 2005a, Ding et al., 2006; Sasaki et al., 2006b). Several studies reproduce the fine-scale climatology of small areas using a multiply nested RCM (Im et al., 2006) and a very-high resolution (5 km) RCM (Yasunaga et al., 2006). Gao et al. (2006b) report that simulated East Asia large-scale precipitation patterns are significantly affected by resolution, particularly during the mid- to late-monsoon months, when smaller-scale convective processes dominate.

Southeast Asia

The broad-scale spatial distribution of temperature and precipitation in DJF and JJA averaged across the MMD models compares well with observations. Rajendran et al. (2004) examine the simulation of current climate in the MRI coupled model (see Table 8.1 for model details). Large-scale features were well simulated, but errors in the timing of peak rainfall over Indochina were considered a major shortcoming. Collier et al. (2004) assess the performance of the CCSM3 model (see Table 8.1 for model details) in simulating tropical precipitation forced by observed SST. Simulation was good over the Maritime continent compared to the simulation for other tropical regions. B. Wang et al. (2004) assess the ability of 11 AGCMs in the Asian-Australian monsoon region simulation forced with observed SST variations. They found that the models' ability to simulate observed interannual rainfall variations was poorest in the Southeast Asian portion of the domain. Since current AOGCMs continue to have some significant shortcomings in representing ENSO variability (see Section 8.4), the difficulty of projecting changes in ENSO-related rainfall in this region is compounded.

Rainfall simulation across the region at finer scales has been examined in some studies. The Commonwealth Scientific and Industrial Research Organisation (CSIRO) stretched-grid Conformal-Cubic Atmospheric Model (CCAM) at 80-km resolution shows reasonable precipitation simulation in JJA, although Indochina tended to be drier than in the observations (McGregor and Nguyen, 2003). Aldrian et al. (2004a) conducted a number of simulations with the Max-Planck Institute (MPI) regional model for an Indonesian domain, forced by reanalyses and by the ECHAM4 GCM. The model was able to represent the spatial pattern of seasonal rainfall. It was found that a resolution of at least 50 km was required to simulate rainfall seasonality correctly over Sulawesi. The formulation of a coupled regional model improves regional rainfall simulation over the oceans (Aldrian et al., 2004b). Arakawa and Kitoh (2005) demonstrate an accurate simulation of the diurnal cycle of rainfall over Indonesia with an AGCM of 20-km horizontal resolution.

Central Asia and Tibet

Due to the complex topography and the associated mesoscale weather systems of the high-altitude and arid areas, GCMs typically perform poorly over the region. Importantly, the GCMs, and to a lesser extent RCMs, tend to overestimate the precipitation over arid and semi-arid areas in the north (e.g., Small et al., 1999; Gao et al., 2001; Elguindi and Giorgi, 2006).

Over Tibet, the few available RCM simulations generally exhibit improved performance in the simulation of present-day climate compared to GCMs (e.g., Gao et al., 2003a,b; Zhang et al., 2005b). For example, the GCM simulation of Gao et al. (2003a) overestimated the precipitation over the north-western Tibetan Plateau by a factor of five to six, while in an RCM nested in this model, the overestimate was less than a factor of two.

11.4.3 Climate Projections

11.4.3.1 Temperature

The temperature projections for the 21st century based on the MMD-A1B models (Figure 11.8 and Table 11.1) represent a strong warming over the 21st century. Warming is similar to the global mean warming in Southeast Asia (mean warming between 1980 to 1999 and 2080 to 2099 of 2.5°C). Warming greater than the global mean is projected for South Asia (3.3°C) and East Asia (3.3°C), and much more than the global mean in the continental interior of Asia (3.7°C in central Asia, 3.8°C in Tibet and 4.3°C in northern Asia). In four out of the six regions, the largest warming occurs in DJF, but in central Asia, the maximum occurs in JJA. In Southeast Asia, the warming is nearly the same throughout the year. Model-to-model variation in projected warming is typically about three-quarters of the mean warming (e.g., 2.0°C to 4.7°C for annual mean warming in South Asia). The 5 to 95% ranges based on Tebaldi et al. (2004a) suggest a slightly smaller uncertainty than the full range of the model results (Supplementary Material Table S11.2). Because the projected warming is large compared to the interannual temperature variability, a large majority of individual years and seasons in the late 21st century are likely to be extremely warm by present standards (Table 11.1). The projections of changes in mean temperature and, where available, temperature extremes, are discussed below in more detail for individual Asian regions.

South Asia

For the A1B scenario, the MMD-A1B models show a median increase of 3.3°C (see Table 11.1) in annual mean temperature by the end of the 21st century. The median warming varies seasonally from 2.7°C in JJA to 3.6°C in DJF, and is likely to increase northward in the area, particularly in winter, and from sea to land (Figure 11.9). Studies based on earlier AOGCM simulations (Douville et al., 2000; Lal and Harasawa, 2001; Lal et al., 2001; Rupa Kumar and Ashrit, 2001; Rupa Kumar et al., 2002, 2003; Ashrit et al., 2003; May, 2004b) support this picture. The tendency of the warming to be more pronounced in

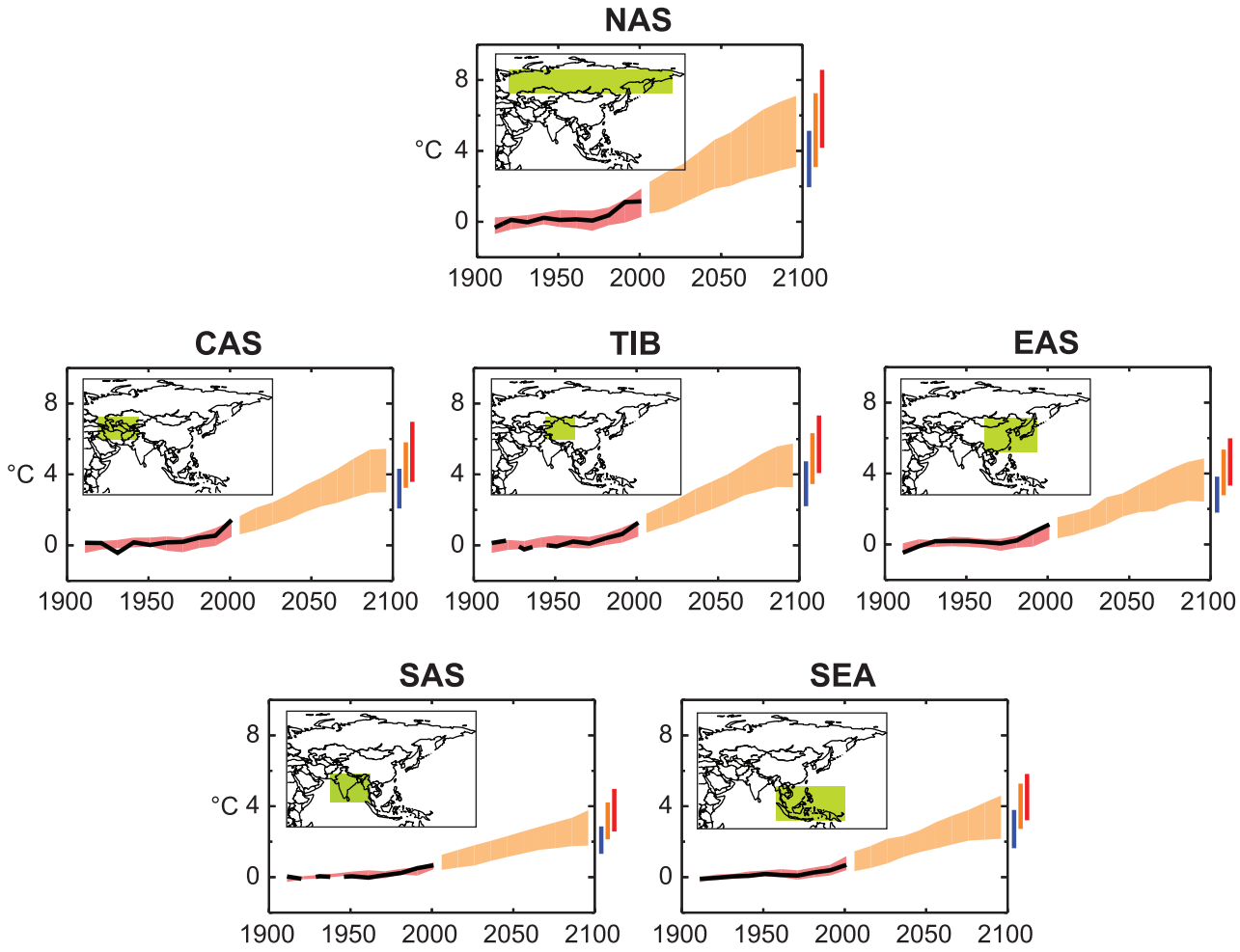


Figure 11.8. *Temperature anomalies with respect to 1901 to 1950 for six Asian land regions for 1906 to 2005 (black line) and as simulated (red envelope) by MMD models incorporating known forcings; and as projected for 2001 to 2100 by MMD models for the A1B scenario (orange envelope). The bars at the end of the orange envelope represent the range of projected changes for 2091 to 2100 for the B1 scenario (blue), the A1B scenario (orange) and the A2 scenario (red). The black line is dashed where observations are present for less than 50% of the area in the decade concerned. More details on the construction of these figures are given in Box 11.1 and Section 11.1.2.*

winter is also a conspicuous feature of the observed temperature trends over India (Rupa Kumar et al., 2002, 2003).

Downscaled projections using the Hadley Centre Regional Model (HadRM2) indicate future increases in extreme daily maximum and minimum temperatures throughout South Asia due to the increase in greenhouse gas concentrations. This projected increase is of the order of 2°C to 4°C in the mid-21st century under the IPCC Scenario IS92a in both minimum and maximum temperatures (Krishna Kumar et al., 2003). Results from a more recent RCM, PRECIS, indicate that the night temperatures increase faster than the day temperatures, with the implication that cold extremes are very likely to be less severe in the future (Rupa Kumar et al., 2006).

East Asia

The MMD-A1B models project a median warming of 3.3°C (Table 11.1) by the end of the 21st century, which varies seasonally from 3.0°C in JJA to 3.6°C in DJF. The warming tends to be largest in winter, especially in the northern inland area (Figure 11.9), but the area-mean difference from the other seasons is not large. There is no obvious relationship between model bias and the magnitude of the warming. The spatial pattern of larger warming over northwest EAS (Figure 11.9) is very similar to the ensemble mean of pre-MMD models. Regional Climate Model simulations show mean temperature increases similar to those simulated by AOGCMs (Gao et al., 2001, 2002; Kwon et al., 2003; Jiang, 2005; Kurihara et al., 2005; Y.L. Xu et al., 2005).

Daily maximum and minimum temperatures are very likely to increase in East Asia, resulting in more severe warm but less severe cold extremes (Gao et al., 2002; Mizuta et al., 2005; Y.L. Xu et al., 2005; Boo et al., 2006). Mizuta et al. (2005) analyse temperature-based extreme indices over Japan with a 20-km mesh AGCM and find the changes in the indices to be basically those expected from the mean temperature increase, with changes in the distribution around the mean not playing a large role. Boo et al. (2005) report similar results for Korea. Gao et al. (2002) and Y.L. Xu et al. (2005) find a reduced diurnal temperature range in China and larger increases in daily minimum than maximum temperatures.

Southeast Asia

In the MMD-A1B simulations, the median warming for the region is 2.5°C by the end of the 21st century, with little seasonal variation (Table 11.1). Simulations by the CSIRO Division of Atmospheric Research Limited Area Model (DARLAM; McGregor et al., 1998) and more recently by the CSIRO stretched-grid model (McGregor and Dix, 2001) centred on the Indochina Peninsula (AIACC, 2004) at a resolution of 14 km have demonstrated the potential for significant local variation in warming, particularly the tendency for warming to be significantly stronger over the interior of the landmasses than over the surrounding coastal regions. A tendency for the warming to be stronger over Indochina and the larger landmasses of the archipelago is also visible in the MMD models (Figures 10.8 and 11.9). As in other regions, the magnitude of the warming depends on the forcing scenario.

Central Asia and Tibet

In the MMD-A1B simulations, central Asia warms by a median of 3.7°C, and Tibet by 3.8°C (Table 11.1) by the end of the 21st century. The seasonal variation in the simulated warming is modest. Findings from earlier multi-model studies (Zhao et al., 2002; Xu et al., 2003a,b; Meleshko et al., 2004; Y. Xu et al., 2005) are consistent with the MMD models' results.

An RCM study by Gao et al. (2003b) indicates greater warming over the Plateau compared to surrounding areas, with the largest warming at highest altitudes, for example, over the Himalayas (see also Box 11.3). The higher temperature increase over high-altitude areas can be explained by the decrease in surface albedo associated with the melting of snow and ice (Giorgi et al., 1997). This phenomenon is found to different extents in some, although not all, of the MMD models, and it is visible in the multi-model mean changes, particularly in the winter (Figure 11.9).

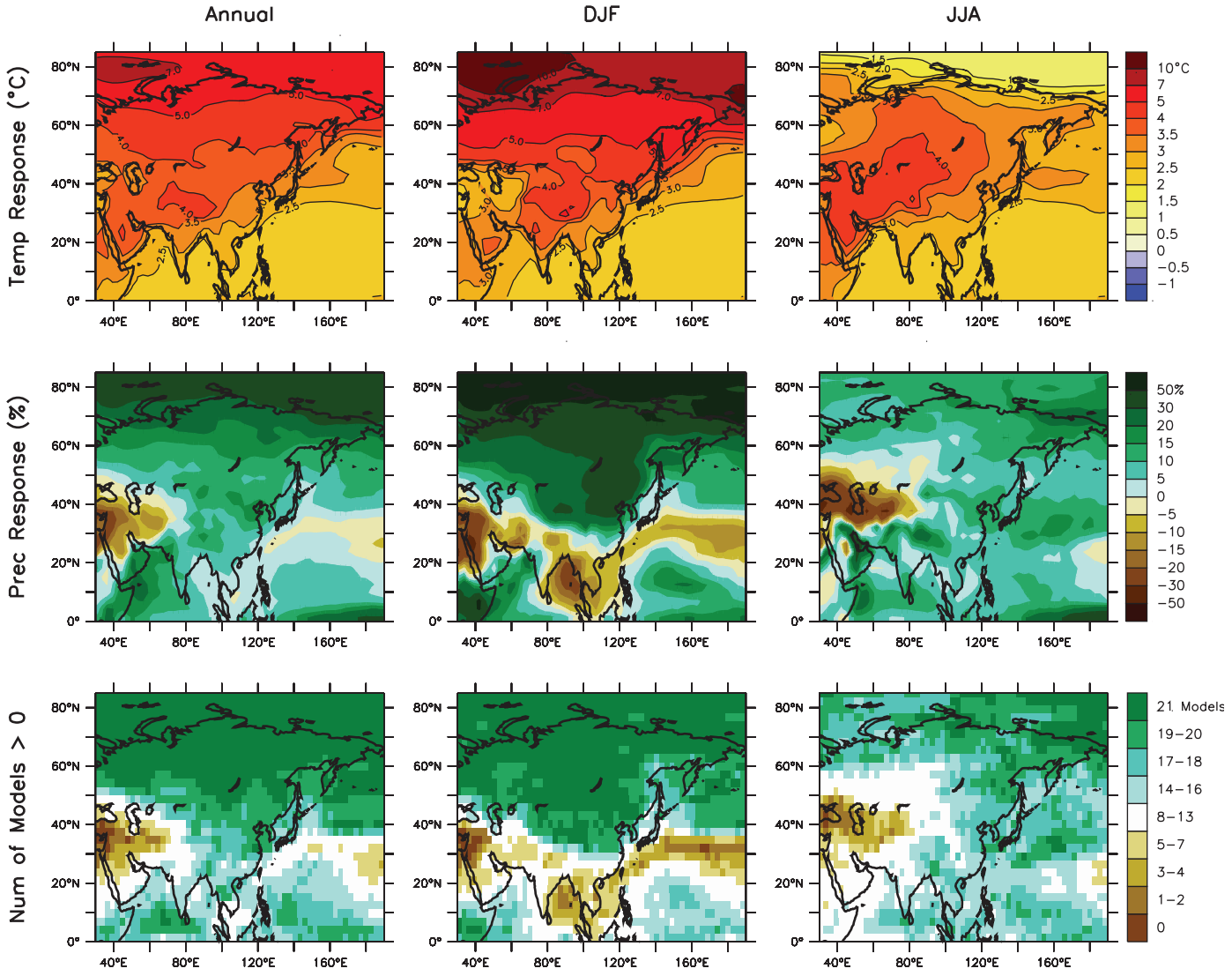


Figure 11.9. *Temperature and precipitation changes over Asia from the MMD-A1B simulations. Top row: Annual mean, DJF and JJA temperature change between 1980 to 1999 and 2080 to 2099, averaged over 21 models. Middle row: same as top, but for fractional change in precipitation. Bottom row: number of models out of 21 that project increases in precipitation.*

11.4.3.2 Precipitation and Associated Circulation Systems

The MMD models indicate an increase in annual precipitation in most of Asia during this century, the percentage increase being largest and most consistent among models in North and East Asia (Figure 11.9 and Table 11.1). The main exception is central Asia, particularly its western parts, where most models simulate reduced precipitation in the summer. Based on these simulations, sub-continental boreal winter precipitation is very likely to increase in northern Asia and the Tibetan Plateau, and likely to increase in eastern Asia. It is also likely to increase in the southern parts of Southeast Asia. Summer precipitation is likely to increase in North, South, Southeast and East Asia, but decrease in central Asia. Probability estimates from Tebaldi et al. (2004a; see Supplementary Material Table S11.2) support these judgments.

The projected decrease in mean precipitation in central Asia is accompanied by an increase in the frequency of very dry spring, summer and autumn seasons; conversely, in winter, where models project increases in the mean precipitation, very high precipitation becomes more common (Table 11.1). The projections of changes in mean precipitation and, where available, precipitation extremes, are discussed in more detail below for individual Asian regions. Where appropriate, the connection to changes in circulation systems that bring precipitation is also discussed. Smaller (slightly larger) changes are generally projected for the B1 (A2) scenario, but the inter-scenario differences are small compared with the inter-model differences.

South Asia

Most of the MMD-A1B models project a decrease in precipitation in DJF (the dry season), and an increase during the rest of the year. The median change is 11% by the end of the 21st century, and seasonally is –5% in DJF and 11% in JJA, with a large inter-model spread (Table 11.1). The probabilistic method of Tebaldi et al. (2004a) similarly shows a large spread, although only 3 of the 21 models project a decrease in annual precipitation. This qualitative agreement on increasing precipitation for most of the year is also supported by earlier AOGCM simulations (Lal and Harasawa, 2001; Lal et al., 2001; Rupa Kumar and Ashrit, 2001; Rupa Kumar et al., 2002, 2003; Ashrit et al., 2003; May, 2004b).

In a study with four GCMs, Douville et al. (2000) find a significant spread in the summer monsoon precipitation anomalies despite a general weakening of the monsoon circulation (see also May, 2004b). They conclude that the changes in atmospheric water content, precipitation and land surface hydrology under greenhouse forcing could be more important than the increase in the land-sea thermal gradient for the future evolution of monsoon precipitation. Stephenson et al. (2001) propose that the consequences of climate change could manifest in different ways in the physical and dynamical components of monsoon circulation. Douville et al. (2000) also argue that the weakening of the ENSO-monsoon correlation could be explained by a possible increase in precipitable water as a result of global warming, rather than by an increased land-sea thermal gradient. However, model diagnostics using ECHAM4 to investigate this aspect indicate that both the above mechanisms can play a role in monsoon changes in a greenhouse-gas warming scenario. Ashrit et al. (2001) show that the monsoon deficiency due to El Niño might not be as severe, while the favourable impact of La Niña seems to remain unchanged. In a later study using the Centre National de Recherches Météorologiques (CNRM) GCM, Ashrit et al. (2003) find that the simulated ENSO-monsoon teleconnection shows a strong modulation on multi-decadal time scales, but no systematic change with increasing amounts of greenhouse gases.

Time-slice experiments with ECHAM4 indicate a general increase in the intensity of heavy rainfall events in the future, with large increases over the Arabian Sea and the tropical Indian Ocean, in northern Pakistan and northwest India, as well as in northeast India, Bangladesh and Myanmar (May, 2004a). The HadRM2 RCM shows an overall decrease by up to 15 days in the annual number of rainy days over a large part of South Asia, under the IS92a scenario in the 2050s, but with an increase in the precipitation intensity as well as extreme precipitation (Krishna Kumar et al., 2003). Simulations with the PRECIS RCM also project substantial increases in extreme precipitation over a large area, particularly over the west coast of India and west central India (Rupa Kumar et al., 2006). Dairaku and Emori (2006) show from a high-resolution AGCM simulation (about 1.5 degrees) that the increased extreme precipitation over land in South Asia would arise mainly from dynamic effects, that is, enhanced upward motion due to the northward shift of monsoon circulation.

Based on regional HadRM2 simulations, Unnikrishnan et al. (2006) report increases in the frequency as well as intensities of tropical cyclones in the 2050s under the IS92a scenario in the Bay of Bengal, which will cause more heavy precipitation in the surrounding coastal regions of South Asia, during both southwest and northeast monsoon seasons.

East Asia

The MMD-A1B models project an increase in precipitation in East Asia in all seasons. The median change at the end of the 21st century is +9% in the annual mean with little seasonal difference, and a large model spread in DJF (Table 11.1). In winter, this increase contrasts with a decrease in precipitation over the ocean to the southeast, where reduced precipitation corresponds well with increased mean sea level pressure. While the projections have good qualitative agreement, there remain large quantitative differences among the models, which is consistent with previous studies (e.g., Giorgi et al., 2001a; Hu et al., 2003; Min et al., 2004).

Based on the MMD models, Kimoto (2005) projects increased Meiyu-Changma-Baiu activity associated with the strengthening of anticyclonic cells to its south and north, and Kwon et al. (2005) show increased East Asia summer precipitation due to an enhanced monsoon circulation in the decaying phase of El Niño. A 20-km mesh AGCM simulation shows that Meiyu-Changma-Baiu rainfall increases over the Yangtze River valley,

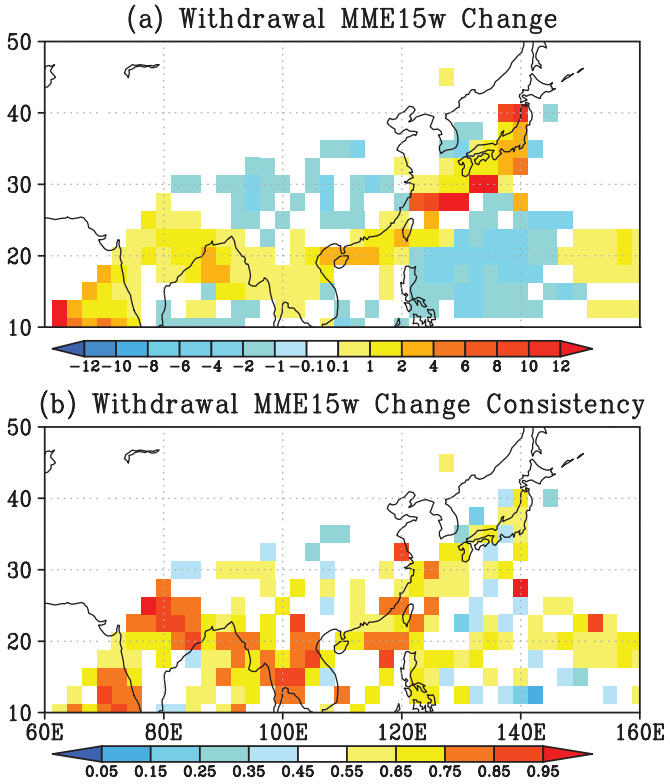


Figure 11.10. *(a) The ensemble mean change in withdrawal date of the summer rainy season between the MMD-A1B projections in 2081 to 2100 as compared with the 1981 to 2000 period in the 20C3M simulations. A positive value indicates a later withdrawal date in the A1B scenario. Units are 5 days. (b) Fraction of the models projecting a positive difference in withdrawal date. (Kitoh and Uchiyama, 2006).*

the East China Sea and western Japan, while rainfall decreases to the north of these areas mostly due to the lengthening of the Meiyu-Changma-Baiu (Kusunoki et al., 2006). Simulations by RCMs support the results from AOGCMs. For example, Kurihara et al. (2005) show an increase in precipitation over western Japan in summer.

Kitoh and Uchiyama (2006) investigated the onset and withdrawal times of the Asian summer rainfall season in 15 MMD simulations (Figure 11.10). They find a delay in early summer rain withdrawal over the region extending from Taiwan to the Ryukyu Islands to the south of Japan, but an earlier withdrawal over the Yangtze Basin, although the latter is not significant due to large inter-model variation. Changes in onset dates are smaller.

Yasunaga et al. (2006) used a 5-km mesh cloud-resolving RCM to investigate summer rainfall in Japan. They find no changes in June rainfall but increased July rainfall in a warmer climate. The increase in July can be attributed to the more frequent large-precipitation systems.

Intense precipitation events are very likely to increase in East Asia, consistent with the historical trend in this region (Fujibé et al., 2005; Zhai et al., 2005). Kanada et al. (2005) show, using a 5-km resolution RCM, that the confluence of disturbances from the Chinese continent and from the East China Sea would often cause extremely heavy precipitation over Japan's Kyushu Island in July in a warmer climate. An increase in the frequency and intensity of heavy precipitation events also occurs in Korea in the long RCM simulation of Boo et al. (2006). Similarly based on RCM simulations, Y.L. Xu et al. (2005) report more extreme precipitation events over China. Gao et al. (2002) find a simulated increase in the number of rainy days in northwest China, and a decrease in rain days but an increase in days with heavy rain over South China. Kitoh et al. (2005) report similar results in South China from an AOGCM simulation.

Kimoto et al. (2005) suggest that the frequencies of non-precipitating and heavy (≥30 mm day^{-1}) rainfall days would increase significantly at the expense of relatively weak (1–20 mm day^{-1}) rainfall days in Japan. Mizuta et al. (2005) find significantly more days with heavy precipitation and stronger average precipitation intensity in western Japan and Hokkaido Island. Hasegawa and Emori (2005) show that daily precipitation associated with tropical cyclones over the western North Pacific would increase.

The previously noted weakening of the East Asian winter monsoon (e.g., Hu et al., 2000) is further confirmed by recent studies (e.g., Kimoto, 2005; Hori and Ueda, 2005).

Southeast Asia

Area-mean precipitation over Southeast Asia increases in most MMD model simulations, with a median change of about 7% in all seasons (Table 11.1), but the projected seasonal changes vary strongly within the region. The seasonal confidence intervals based on the methods of Tebaldi et al. (2004a,b) are similar for DJF and JJA (roughly –4% to 17%). The strongest and most consistent increases broadly follow the ITCZ, lying over northern Indonesia and Indochina in JJA, and over southern Indonesia and Papua New Guinea in DJF (Figure 11.9). Away from the ITCZ, precipitation decreases are often simulated. The pattern is broadly one of wet season rainfall increase and dry season decrease.

Earlier studies of precipitation change in the area in some cases have suggested a worse inter-model agreement than found for the MMD models. Both Giorgi et al. (2001a) and Ruosteenoja et al. (2003) find inconsistency in the simulated direction of precipitation change in the region, but a relatively narrow range of possible changes; similar results were found over an Indonesian domain by Boer and Faqih (2004). Compositing the projections from a range of earlier simulations forced by the IS92a scenario, Hulme and Sheard (1999a,b) find a pattern of rainfall increase across northern Indonesia and the Philippines, and decrease over the southern Indonesian archipelago. More recently, Boer and Faqih (2004) compared patterns of change across Indonesia from five AOGCMS and obtained highly contrasting results. They conclude that 'no generalisation could be made on the impact of global warming on rainfall' in the region.

The regional high-resolution simulations of McGregor et al. (1998), McGregor and Dix (2001) and AIACC (2004) have demonstrated the potential for significant local variation in projected precipitation change. The simulations showed

considerable regional detail in the simulated patterns of change, but little consistency across the three simulations. The authors related this result to significant deficiencies in the current-climate simulations of the models for this region.

Rainfall variability will be affected by changes in ENSO and its effect on monsoon variability, but this is not well understood (see Section 10.3). However, as Boer and Faqih (2004) note, those parts of Indonesia that experience a mean rainfall decrease are likely to also experience increases in drought risk. The region is also likely to share the general tendency for daily extreme precipitation to become more intense under enhanced greenhouse conditions, particularly where the mean precipitation is projected to increase. This has been demonstrated in a range of global and regional studies (see Section 10.3), but needs explicit study for the Southeast Asian region.

The northern part of the Southeast Asian region will be affected by any change in tropical cyclone characteristics. As noted in Section 10.3, there is evidence in general of likely increases in tropical cyclone intensity, but less consistency about how occurrence will change (see also Walsh, 2004). The likely

Box 11.3: Climatic Change in Mountain Regions

Although mountains differ considerably from one region to another, one common feature is the complexity of their topography. Related characteristics include rapid and systematic changes in climatic parameters, in particular temperature and precipitation, over very short distances (Becker and Bugmann, 1997); greatly enhanced direct runoff and erosion; systematic variation of other climatic (e.g., radiation) and environmental (e.g., soil types) factors. In some mountain regions, it has been shown that temperature trends and anomalies have an elevation dependence (Giorgi et al., 1997), a feature that is not, however, systematically observed in all upland areas (e.g., Vuille and Bradley, 2000, for the Andes).

Few model simulations have attempted to directly address issues related specifically to future climatic change in mountain regions, primarily because the current spatial resolution of GCMs and even RCMs is generally too crude to adequately represent the topographic detail of most mountain regions and other climate-relevant features such as land cover that are important determinants in modulating climate in the mountains (Beniston et al., 2003). High-resolution RCM simulations (5-km and 1-km grid scales) are used for specific investigations of processes such as surface runoff, infiltration, evaporation and extreme events such as precipitation (Weisman et al., 1997; Walser and Schär, 2004; Kanada et al., 2005; Yasunaga et al., 2006) and damaging wind storms (Goyette et al., 2003), but these simulations are too costly to operate in a 'climate mode'. Because of the highly complex terrain, empirical and statistical downscaling techniques have often been seen as a very valuable tool to generate climate change information for mountainous regions (e.g., Benestad, 2005; Hanssen-Bauer et al., 2005).

Projections of changes in precipitation patterns in mountains are unreliable in most GCMs because the controls of topography on precipitation are not adequately represented. In addition, it is now recognised that the superimposed effects of natural modes of climatic variability such as ENSO or the NAO can perturb mean precipitation patterns on time scales ranging from seasons to decades (Beniston and Jungo, 2001). Even though there has been progress in reproducing some of these mechanisms in coupled ocean-atmosphere models (Osborn et al., 1999), deficiencies remain and prevent a good simulation of these large-scale modes of variability (see also Section 8.4). However, several studies indicate that the higher resolution of RCMs and GCMs can represent observed mesoscale patterns of the precipitation climate that are not resolved in coarse-resolution GCMs (Frei et al., 2003; Kanada et al., 2005; Schmidli et al., 2006; Yasunaga et al., 2006).

Snow and ice are, for many mountain ranges, a key component of the hydrological cycle, and the seasonal character and amount of runoff is closely linked to cryospheric processes. In temperate mountain regions, the snowpack is often close to its melting point, so that it may respond rapidly to minor changes in temperature. As warming increases in the future, regions where snowfall is the current norm will increasingly experience precipitation in the form of rain (e.g., Leung et al., 2004). For every degree celsius increase in temperature, the snow line will on average rise by about 150 m. Although the snow line is difficult to determine in the field, it is established that at lower elevations the snow line is very likely to rise by more than this simple average estimate (e.g., Martin et al., 1994; Vincent, 2002; Gerbaux et al., 2005; see also Section 4.2). Beniston et al. (2003) show that for a 4°C shift in mean winter temperatures in the European Alps, as projected by recent RCM simulations for climatic change in Europe under the A2 emissions scenario, snow duration is likely to be reduced by 50% at altitudes near 2,000 m and by 95% at levels below 1,000 m. Where some models predict an increase in winter precipitation, this increase does not compensate for the effect of changing temperature. Similar reductions in snow cover that will affect other mountain regions of the world will have a number of implications, in particular for early seasonal runoff (e.g., Beniston, 2003), and the triggering of the annual cycle of mountain vegetation (Cayan et al., 2001; Keller et al., 2005).

Because mountains are the source region for over 50% of the globe's rivers, the impacts of climatic change on mountain hydrology not only affect the mountains themselves but also populated lowland regions that depend on mountain water resources for domestic, agricultural, energy and industrial supply. Water resources for populated lowland regions are influenced by mountain climates and vegetation; shifts in intra-annual precipitation regimes could lead to critical water amounts resulting in greater flood or drought episodes (e.g., Barnett et al., 2005; Graham et al., 2007).

increase in intensity (precipitation and winds) is supported for the northwest Pacific (and other regions) by the recent modelling study of Knutson and Tuleya (2004). The high-resolution time-slice modelling experiment of Hasegawa and Emori (2005) also demonstrates an increase in tropical cyclone precipitation in the western North Pacific, but not an increase in tropical cyclone intensity. Wu and Wang (2004) examined possible changes in tracks in the northwest Pacific due to changes in steering flow in two Geophysical Fluid Dynamics Laboratory (GFDL) enhanced greenhouse gas experiments. Tracks moved more north-easterly, possibly reducing tropical cyclone frequency in the Southeast Asian region. Since most of the tropical cyclones form along the monsoon trough and are also influenced by ENSO, changes in the occurrence, intensity and characteristics of tropical cyclones and their interannual variability will be affected by changes in ENSO (see Section 10.3).

Central Asia and Tibet

Precipitation over central Asia increases in most MMD-A1B projections for DJF but decreases in the other seasons. The median change by the end of the 21st century is –3% in the annual mean, with +4% in DJF and –13% in JJA (the dry season) (Table 11.1). This seasonal variation in the changes is broadly consistent with the earlier multi-model study of Meleshko et al. (2004), although they find an increase in summer precipitation in the northern part of the area.

Over the Tibetan Plateau, all MMD-A1B models project increased precipitation in DJF (median 19%). Most but not all models also simulate increased precipitation in the other seasons (Table 11.1). Earlier studies both by AOGCMs and RCMs are consistent with these findings (Gao et al., 2003b; Y. Xu et al., 2003a,b, 2005).

11.5 North America

Assessment of projected climate change for North America:

All of North America is very likely to warm during this century, and the annual mean warming is likely to exceed the global mean warming in most areas. In northern regions, warming is likely to be largest in winter, and in the southwest USA largest in summer. The lowest winter temperatures are likely to increase more than the average winter temperature in northern North America, and the highest summer temperatures are likely to increase more than the average summer temperature in the southwest USA.

Annual mean precipitation is very likely to increase in Canada and the northeast USA, and likely to decrease in the southwest USA. In southern Canada, precipitation is likely to increase in winter and spring, but decrease in summer.

Snow season length and snow depth are very likely to decrease in most of North America, except in the northernmost part of Canada where maximum snow depth is likely to increase.

The uncertainties in regional climate changes over North America are strongly linked to the ability of AOGCMs to reproduce the dynamical features affecting the region (Chapter 10). Atmosphere-Ocean General Circulation Models exhibit large model-to-model differences in ENSO and NAO/Arctic Oscillation (AO) responses to climate changes. Changes in the Atlantic MOC are uncertain, and thus so is the magnitude of consequent reduced warming in the extreme north-eastern part of North America; cooling here cannot be totally excluded. The Hudson Bay and Canadian Archipelago are poorly resolved by AOGCMs, contributing to uncertainty in ocean circulation and sea ice changes and their influence on the climate of northern regions. Tropical cyclones are not resolved by the MMD models and inferred changes in the frequency, intensity and tracks of disturbances making landfall in southeast regions remain uncertain. At the coarse horizontal resolution of the MMD models, high-altitude terrain is poorly resolved, which likely results in an underestimation of warming associated with snow-albedo feedback at high elevations in western regions. Little is known about the dynamical consequences of the larger warming over land than over ocean, which may affect the northward displacement and intensification of the subtropical anticyclone off the West Coast. This could affect the subtropical North Pacific eastern boundary current, the offshore Ekman transport, the upwelling and its cooling effect on SST, the persistent marine stratus clouds and thus precipitation in the southwest USA.

The uncertainty associated with RCM projections of climate change over North America remains large despite the investments made in increasing horizontal resolution. All reported RCM projections were driven by earlier AOGCMs that exhibited larger biases than the MMD models. Coordinated ensemble RCM projections over North America are not yet available, making it difficult to compare results.

11.5.1 Key Processes

Central and northern regions of North America are under the influence of mid-latitude cyclones. Projections by AOGCMs (Chapter 10) generally indicate a slight poleward shift in storm tracks, an increase in the number of strong cyclones but a reduction in medium-strength cyclones over Canada and poleward of 70°N. Consequent with the projected warming, the atmospheric moisture transport and convergence is projected to increase, resulting in a widespread increase in annual precipitation over most of the continent except the south and south-western part of the USA and over Mexico.

The southwest region is very arid, under the general influence of a subtropical ridge of high pressure associated with the thermal contrast between land and adjacent ocean. The North American Monsoon System develops in early July (e.g., Higgins

and Mo, 1997); the prevailing winds over the Gulf of California undergo a seasonal reversal, from northerly in winter to southerly in summer, bringing a pronounced increase in rainfall over the southwest USA and ending the late spring wet period in the Great Plains (e.g., Bordoni et al., 2004). The projection of smaller warming over the Pacific Ocean than over the continent, and amplification and northward displacement of the subtropical anticyclone, is likely to induce a decrease in annual precipitation in the south-western USA and northern Mexico.

The Great Plains Low-Level Jet (LLJ) is a dynamical feature that transports considerable moisture from the Gulf of Mexico into the central USA, playing a critical role in the summer precipitation there. Several factors, including the land-sea thermal contrast, contribute to the strength of the moisture convergence during the night and early morning, resulting in prominent nocturnal maximum precipitation in the plains of the USA (such as Nebraska and Iowa; e.g., Augustine and Caracena, 1994). The projections of climate changes indicate an increased land-sea thermal contrast in summer, with anticipated repercussions on the LLJ.

Interannual variability over North America is connected to two large-scale oscillation patterns (see Chapter 3), ENSO and the NAO/AO. The MMD model projections indicate an intensification of the polar vortex and many models project a decrease in the arctic surface pressure, which contributes to an increase in the AO/NAO index; the uncertainty is large, however, due to the diverse responses of AOGCMs in simulating the Aleutian Low (Chapter 10). The MMD model projections indicate a shift towards mean El-Niño like conditions, with the eastern Pacific warming more than the western Pacific; there is a wide range of behaviour among the current models, with no clear indication of possible changes in the amplitude or period of El Niño (Chapter 10).

11.5.2 Skill of Models in Simulating Present Climate

Individual AOGCMs in the MMD vary in their ability to reproduce the observed patterns of pressure, surface air temperature and precipitation over North America (Chapter 8). The ensemble mean of MMD models reproduces very well the annual-mean mean sea level pressure distribution (Section 8.4). The maximum error is of the order of ±2 hPa, with the simulated Aleutian Low pressure extending somewhat too far north, probably due to the inability of coarse-resolution models to adequately resolve the high topography of the Rocky Mountains that blocks incoming cyclones in the Gulf of Alaska. Conversely, the pressure trough over the Labrador Sea is not deep enough. The depth of the thermal low pressure over the southwest region in summer is somewhat excessive.

The MMD models simulate successfully the overall pattern of surface air temperature over North America, with reduced biases compared to those reported in the TAR. Ensemble-mean regional mean bias ranges from –4.5°C to 1.9°C for the 25th to 75th percentile range, and medians vary from –2.4°C to +0.4°C depending on region and season (Supplementary Material Table S11.1). The ensemble mean of MMD models reproduces the overall distribution of annual mean precipitation (Supplementary Material Table S11.1), but almost all models overestimate precipitation for western and northern regions. The ensemble-mean regional mean precipitation bias medians vary from –16% to +93% depending on region and season. The ensemble-mean precipitation is excessive on the windward side of major mountain ranges, with the excess reaching 1 to 2 mm day^{-1} over high terrain in the west of the continent.

Regional Climate Models are quite successful in reproducing the overall climate of North America when driven by reanalyses. Over a 10° × 10° Southern Plains region, an ensemble of six RCMs in the North American Regional Climate Change Assessment Program (NARCCAP; Mearns et al., 2005) had 76% of all monthly temperature biases within ±2°C and 82% of all monthly precipitation biases within ±50%, based on preliminary results for a single year. RCM simulations over North America exhibit rather high sensitivity to parameters such as domain size (e.g., Juang and Hong, 2001; Pan et al., 2001; Vannitsem and Chomé, 2005) and the intensity of large-scale nudging (providing large-scale information to the interior of the model domain, see e.g., von Storch et al., 2000; Miguez-Macho et al., 2004) if used. In general, RCMs are more skilful at reproducing cold-season temperature and precipitation (e.g., Pan et al., 2001; Han and Roads, 2004; Plummer et al., 2006) because the warm-season climate is more controlled by mesoscale and convective-scale precipitation events, which are harder to simulate (Giorgi et al., 2001a; Leung et al., 2003; Liang et al., 2004; Jiao and Caya, 2006). On the other hand, Gutowski et al. (2004) find that spatial patterns of monthly precipitation for the USA, when viewed as a whole rather than broken into individual regions, are better simulated in summer than winter. Several studies point to the large sensitivity of RCMs to parametrization of moist convection, including the vertical transport of moisture from the boundary layer (Chaboureau et al., 2004; Jiao and Caya, 2006) and entrainment mixing between convective plumes and the local environment (Derbyshire et al., 2004). In a study of the simulation of the 1993 summer flood in the central USA by 13 RCMs, Anderson et al. (2003) find that all models produced a precipitation maximum that represented the flood, but most underestimated it to some degree, and 10 out of 13 of the models succeeded in reproducing the observed nocturnal maxima of precipitation. Leung et al. (2003) examined the 95th percentile of daily precipitation and find generally good agreement across many areas of the western USA.

A survey of recently published RCM current-climate simulations driven with AOGCMs data reveals that biases in surface air temperature and precipitation are two to three times larger than the simulations driven with reanalyses. The sensitivity of simulated surface air temperature to changing lateral boundary conditions from reanalyses to AOGCMs appears to be high in winter and low in summer (Han and Roads, 2004; Plummer et al., 2006). Most RCM simulations to date for North America have been made for time slices that are too short to properly sample natural variability. Some

RCMs have employed less than optimal formulations, such as outdated parametrizations (e.g., bucket land surface scheme), too few levels in the vertical (e.g., 14) or a too-low uppermost computational level (e.g., 100 hPa).

11.5.3 Climate Projections

11.5.3.1 Surface Air Temperature

The ensemble mean of the MMD models projects a generalised warming for the entire continent with the magnitude projected to increase almost linearly with time (Figure 11.11). On an annual-mean basis, projected surface air temperature warming varies from 2°C to 3°C along the western, southern and eastern continental edges (where at least 16 out of the 21 models project a warming in excess of 2°C) up to more than 5°C in the northern region (where 16 out of the 21 AOGCMs project a warming in excess of 4°C). This warming exceeds the spread among models by a factor of three to four over most of the continent. The warming in the USA is projected to exceed 2°C by nearly all the models, and to exceed 4°C by more than 5 AOGCMs out of 21. More regional and seasonal detail on ranges of projected warming is provided in Table 11.1 and Supplementary Table S11.2.

The largest warming is projected to occur in winter over northern parts of Alaska and Canada, reaching 10°C in the northernmost parts, due to the positive feedback from a reduced period of snow cover. The ensemble-mean northern warming varies from more than 7°C in winter (nearly all AOGCMs project a warming exceeding 4°C) to as little as 2°C in summer. In summer, ensemble-mean projected warming ranges between 3°C and 5°C over most of the continent, with smaller values near the coasts. In western, central and eastern regions, the projected warming has less seasonal variation and is more modest, especially near the coast, consistent with less warming over the oceans. The warming could be larger in winter over elevated areas as a result of snow-albedo feedback, an effect that is poorly modelled by AOGCMs due to insufficient horizontal resolution (see also Box 11.3). In winter, the northern part of the eastern region is projected to warm most while coastal areas are projected to warm by only 2°C to 3°C.

The climate change response of RCMs is sometimes different from that of the driving AOGCM. This appears to be the result of a combination of factors, including the use of different parametrizations (convection and land surface processes are particularly important over North America in summer) and resolution (different resolution may lead to differing behaviour of the same parametrization). For example, Chen et al. (2003) find that two RCMs project larger temperature changes in summer than their driving AOGCM. In contrast, the projected warming of an RCM compared to its driving AOGCM was found to be 1.5°C less in the central USA (Pan et al., 2004; Liang et al., 2006), a region where observations have shown a cooling trend in recent decades. This resulted in an area of little warming that may have been due to a changing pattern of the LLJ frequency and associated moisture convergence. It is argued that the improved simulation of the LLJ in the RCM is made possible owing to its increased horizontal and vertical resolution. However, other RCMs with similar resolution do not produce the same response.

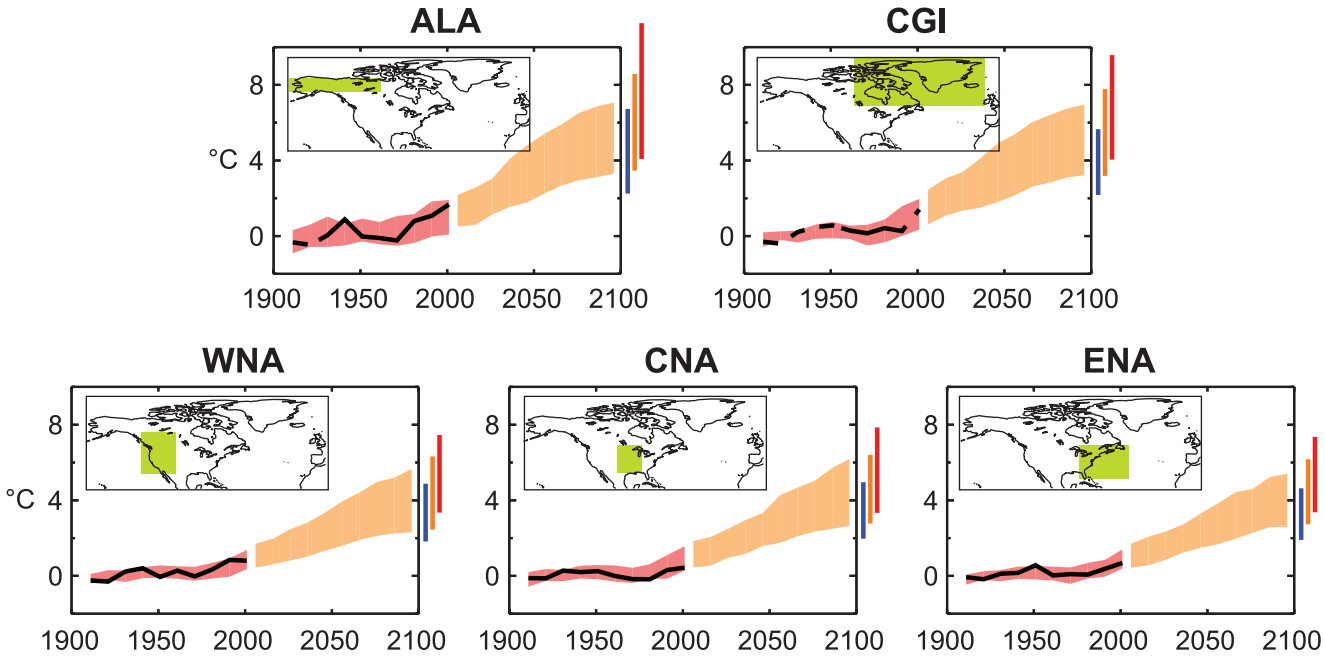


Figure 11.11. *Temperature anomalies with respect to 1901 to 1950 for five North American land regions for 1906 to 2005 (black line) and as simulated (red envelope) by MMD models incorporating known forcings; and as projected for 2001 to 2100 by MMD models for the A1B scenario (orange envelope). The bars at the end of the orange envelope represent the range of projected changes for 2091 to 2100 for the B1 scenario (blue), the A1B scenario (orange) and the A2 scenario (red). The black line is dashed where observations are present for less than 50% of the area in the decade concerned. More details on the construction of these figures are given in Box 11.1 and Section 11.1.2.*

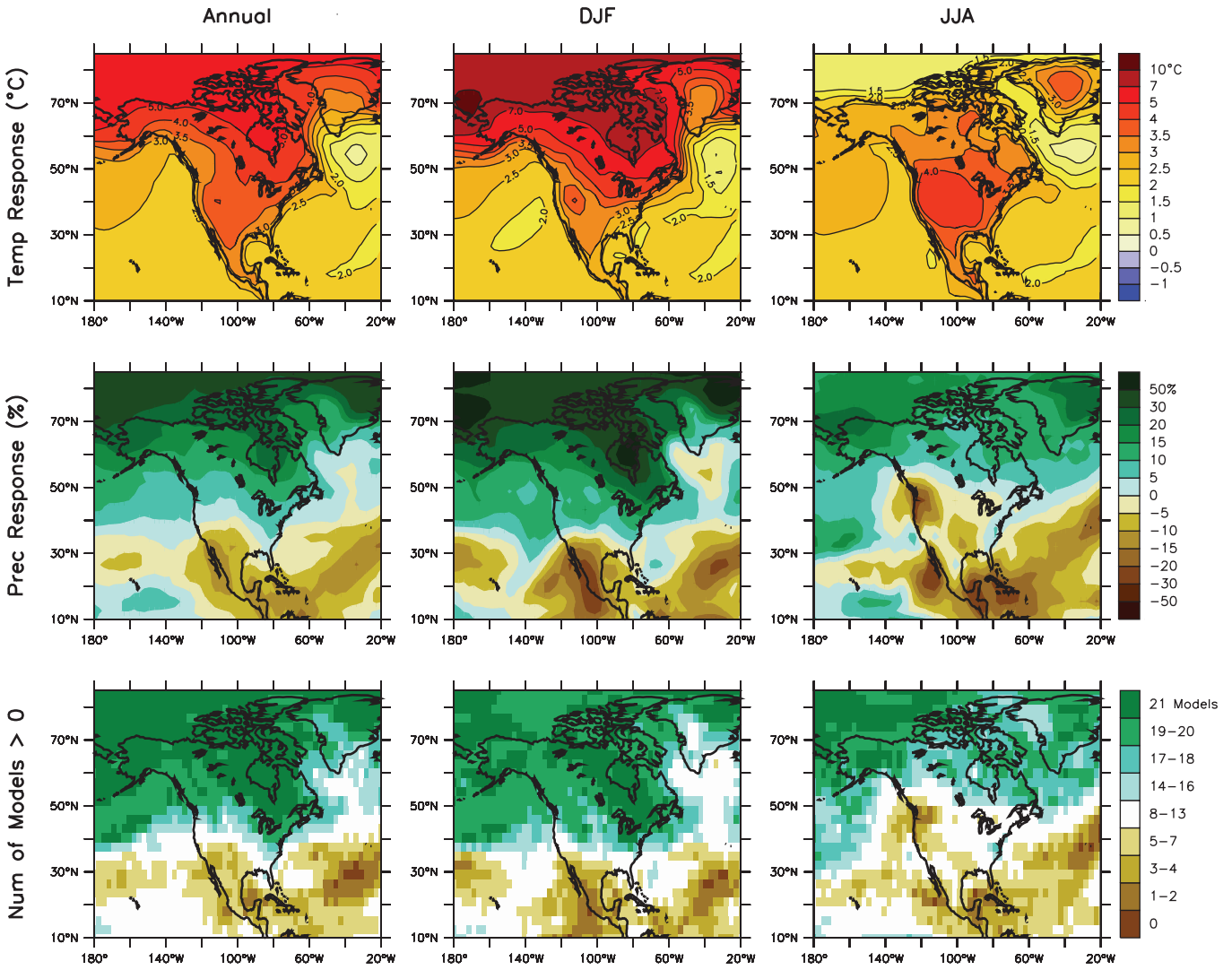


Figure 11.12. *Temperature and precipitation changes over North America from the MMD-A1B simulations. Top row: Annual mean, DJF and JJA temperature change between 1980 to 1999 and 2080 to 2099, averaged over 21 models. Middle row: same as top, but for fractional change in precipitation. Bottom row: number of models out of 21 that project increases in precipitation.*

11.5.3.2 Precipitation

As a consequence of the temperature dependence of the saturation vapour pressure in the atmosphere, the projected warming is expected to be accompanied by an increase in atmospheric moisture flux and its convergence/divergence intensity. This results in a general increase in precipitation over most of the continent except the most south-westerly part (Figure 11.12). The ensemble mean of MMD models projects an increase in annual mean precipitation in the north reaching +20%, which is twice the inter-model spread, so likely significant; the projected increase reaches as much as +30% in winter. Because the increased saturation vapour pressure can also yield greater evaporation, projected increases in annual precipitation are partially offset by increases in evaporation; regions in central North America may experience net surface drying as a result (see Supplementary Material Figure S11.1). See Table 11.1 and Supplementary Table S11.2 for more regional and seasonal details, noting that regional averaging hides important north-south differences.

In keeping with the projected northward displacement of the westerlies and the intensification of the Aleutian Low (Section 11.5.3.3), northern region precipitation is projected to increase, by the largest amount in autumn and by the largest fraction in winter. Due to the increased precipitable water, the increase in precipitation amount is likely to be larger on the windward slopes of the mountains in the west with orographic precipitation. In western regions, modest changes in annual mean precipitation are projected, but the majority of AOGCMs indicate an increase in winter and a decrease in summer. Models show greater consensus on winter increases (ensemble mean maximum of 15%) to the north and on summer decreases (ensemble mean maximum of –20%) to the south. These decreases are consistent with enhanced subsidence and flow of drier air masses in the southwest USA and northern Mexico resulting from an amplification of the subtropical anticyclone

off the West Coast due to the land-sea contrast in warming (e.g., Mote and Mantua, 2002). However, this reduction is close to the inter-model spread so it contains large uncertainty, an assessment that is reinforced by the fact that some AOGCMs project an increase in precipitation.

In central and eastern regions, projections from the MMD models show the same characteristics as in the west, with greater consensus for winter increases to the north and summer decreases to the south. The line of zero change is oriented more or less west-to-east and moves north from winter to summer. The line of zero change is also projected to lie further to the north under SRES scenarios with larger greenhouse gas amounts. However, uncertainty around the projected changes is large and the changes do not scale well across different SRES scenarios.

Govindasamy (2003) finds that, averaged over the USA, the few existing time-slice simulations with high-resolution AGCM results do not significantly differ from those obtained with AOGCMs. Available RCM simulations provide little extra information on average changes. Some RCMs project precipitation changes of different sign, either locally (Chen et al., 2003) or over the entire continental USA (Han and Roads, 2004, where in summer the AOGCM generally produced a small increase and the RCM a substantial decrease). In contrast, Plummer et al. (2006) find only small differences in precipitation responses using two sets of physical parametrizations in their RCM, despite the fact that one corrected significant summer precipitation excess present in the other.

11.5.3.3 Temperature and Precipitation Extremes

Several RCM studies focused particularly on changes in extreme temperature events. Bell et al. (2004) examine changes in temperature extremes in their simulations centred on California. They find increases in extreme temperature events, both as distribution percentiles and threshold events, prolonged hot spells and increased diurnal temperature range. Leung et al. (2004) examine changes in extremes in their RCM simulations of the western USA; in general, they find increases in diurnal temperature range in six sub-regions of their domain in summer. Diffenbaugh et al. (2005) find that the frequency and magnitude of extreme temperature events changes dramatically under SRES A2, with increases in extreme hot events and a decrease in extreme cold events.

In a study of precipitation extremes over California, Bell et al. (2004) find that changes in precipitation exceeding the 95th percentile followed changes in mean precipitation, with decreases in heavy precipitation in most areas. Leung et al. (2004) find that extremes in precipitation during the cold season increase in the northern Rockies, the Cascades, the Sierra Nevada and British Columbia by up to 10% for 2040 to 2060, although mean precipitation was mostly reduced, in accord with earlier studies (Giorgi et al., 2001a). In a large river basin in the Pacific Northwest, increases in rainfall over snowfall and rain-on-snow events increased extreme runoff by 11%, which would contribute to more severe flooding. In their 25-km RCM simulations covering the entire USA, Diffenbaugh et al. (2005) find widespread increases in extreme precipitation events under SRES A2, which they determine to be significant.

11.5.3.4 Atmospheric Circulation

In general, the projected climate changes over North America follow the overall features of those over the NH (Chapter 10). The MMD models project a northward displacement and strengthening of the mid-latitude westerly flow, most pronounced in autumn and winter. Surface pressure is projected to decrease in the north, with a northward displacement of the Aleutian low-pressure centre and a north-westward displacement of the Labrador Sea trough, and to decrease slightly in the south. The reductions in surface pressure in the north are projected to be strongest in winter, reaching –1.5 to –3 hPa, in part as a result of the warming of the continental arctic air mass. On an annual basis, the pressure decrease in the north exceeds the spread among models by a factor of 3 on an annual-mean basis and a factor of 1.5 in summer, so it is significant. The East Pacific subtropical anticyclone is projected to intensify in summer, particularly off the coast of California and Baja California, resulting in an increased air mass subsidence and drier airflow over south-western North America. The pressure increase (less than 0.5 hPa) is small compared to the spread among models, so this projection is rather uncertain.

11.5.3.5 Snowpack, Snowmelt and River Flow

The ensemble mean of the MMD models projects a general decrease in snow depth (Chapter 10) as a result of delayed autumn snowfall and earlier spring snowmelt. In some regions where winter precipitation is projected to increase, the increased snowfall can more than make up for the shorter snow season and yield increased snow accumulation. Snow depth increases are projected by some GCMs over some land around the Arctic Ocean (Figure S10.1) and by some RCMs in the northernmost part of the Northwest Territories (Figure 11.13). In principle a similar situation could arise at lower latitudes at high elevations in the Rocky Mountains, although most models project a widespread decrease of snow depth there (Kim et al., 2002; Snyder et al., 2003; Leung et al., 2004; see also Box 11.3).

Much SD research activity has focused on resolving future water resources in the complex terrain of the western USA. Studies typically point to a decline in winter snowpack and hastening of the onset of snowmelt caused by regional warming (Hayhoe et al., 2004; Salathé, 2005). Comparable trends towards increased annual mean river flows and earlier spring peak flows have also been projected by two SD techniques for the Saguenay watershed in northern Québec, Canada (Dibike and Coulibaly, 2005). Such changes in the flow regime also favour increased risk of winter flooding and lower summer soil moisture and river flows. However, differences in snowpack behaviour derived from AOGCMs depend critically on the realism of downscaled winter temperature variability and its

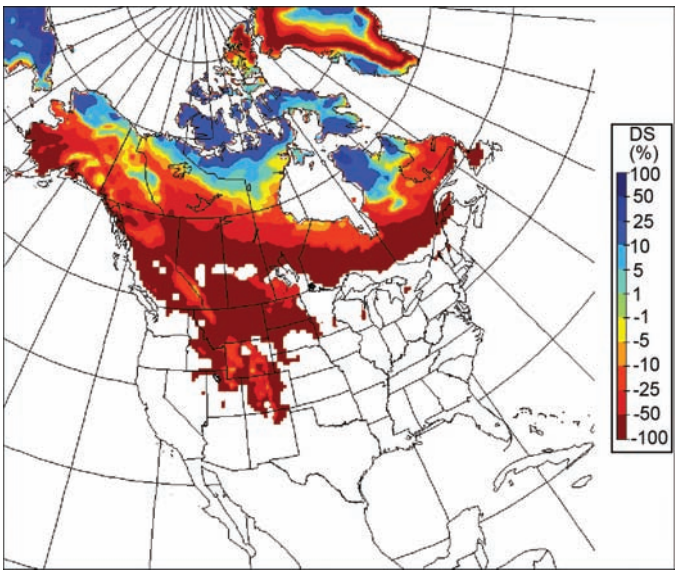


Figure 11.13. *Percent snow depth changes in March (only calculated where climatological snow amounts exceed 5 mm of water equivalent), as projected by the Canadian Regional Climate Model (CRCM; Plummer et al., 2006), driven by the Canadian General Circulation Model (CGCM), for 2041 to 2070 under SRES A2 compared to 1961 to 1990.*

interplay with precipitation and snowpack accumulation and melt (Salathé, 2005). Hayhoe et al. (2004) produced a standard set of statistically downscaled temperature and precipitation scenarios for California; under both the A1F1 and B1 scenarios, they find overall declines in snowpack.

11.6 Central and South America

Assessment of projected climate change for Central and South America:

All of Central and South America is very likely to warm during this century. The annual mean warming is likely to be similar to the global mean warming in southern South America but larger than the global mean warming in the rest of the area.

Annual precipitation is likely to decrease in most of Central America, with the relatively dry boreal spring becoming drier. Annual precipitation is likely to decrease in the southern Andes, with relative precipitation changes being largest in summer. A caveat at the local scale is that changes in atmospheric circulation may induce large local variability in precipitation changes in mountainous areas. Precipitation is likely to increase in Tierra del Fuego during winter and in south-eastern South America during summer.

It is uncertain how annual and seasonal mean rainfall will change over northern South America, including the Amazon forest. In some regions, there is qualitative consistency among the simulations (rainfall increasing in Ecuador and northern Peru, and decreasing at the northern tip of the continent and in southern northeast Brazil).

The systematic errors in simulating current mean tropical climate and its variability (Section 8.6) and the large inter-model differences in future changes in El Niño amplitude (Section10.3) preclude a conclusive assessment of the regional changes over large areas of Central and South America. Most MMD models are poor at reproducing the regional precipitation patterns in their control experiments and have a small signal-to-noise ratio, in particular over most of Amazonia (AMZ). The high and sharp Andes Mountains are unresolved in low-resolution models, affecting the assessment over much of the continent. As with all landmasses, the feedbacks from land use and land cover change are not well accommodated, and lend some degree of uncertainty. The potential for abrupt changes in biogeochemical systems in AMZ remains as a source of uncertainty (see Box 10.1). Large differences in the projected climate sensitivities in the climate models incorporating these processes and a lack of understanding of processes have been identified (Friedlingstein et al., 2003). Over Central America, tropical cyclones may become an additional source of uncertainty for regional scenarios of climate change, since the summer precipitation over this region may be affected by systematic changes in hurricane tracks and intensity.

11.6.1 Key Processes

Over much of Central and South America, changes in the intensity and location of tropical convection are the fundamental concern, but extratropical disturbances also play a role in Mexico's winter climate and throughout the year in southern South America. A continental barrier over Central America and along the Pacific coast in South America and the world's largest rainforest are unique geographical features that shape the climate in the area.

Climate over most of Mexico and Central America is characterised by a relatively dry winter and a well-defined rainy season from May through October (Magaña et al., 1999). The seasonal evolution of the rainy season is largely the result of air-sea interactions over the Americas' warm pools and the effects of topography over a dominant easterly flow, as well as the temporal evolution of the ITCZ. During the boreal winter, the atmospheric circulation over the Gulf of Mexico and the Caribbean Sea is dominated by the seasonal fluctuation of the Subtropical North Atlantic Anticyclone, with invasions of extratropical systems that affect mainly Mexico and the western portion of the Great Antilles.

A warm season precipitation maximum, associated with the South American Monsoon System (Vera et al., 2006), dominates the mean seasonal cycle of precipitation in tropical and subtropical latitudes over South America. Amazonia has had

increasing rainfall over the last 40 years, despite deforestation, due to global-scale water vapour convergence (Chen et al., 2001; see also Section 3.3). The future of the rainforest is not only of vital ecological importance, but also central to the future evolution of the global carbon cycle, and as a driver of regional climate change. The monsoon system is strongly influenced by ENSO (e.g., Lau and Zhou, 2003), and thus future changes in ENSO will induce complementary changes in the region. Displacements of the South Atlantic Convergence Zone have important regional impacts such as the large positive precipitation trend over the recent decades centred over southern Brazil (Liebmann et al., 2004). There are well-defined teleconnection patterns (the Pacific-South American modes, Mo and Nogués-Paegle, 2001) whose preferential excitation could help shape regional changes. The Mediterranean climate of much of Chile makes it sensitive to drying as a consequence of poleward expansion of the South Pacific subtropical high, in close analogy to other regions downstream of oceanic subtropical highs in the Southern Hemisphere (SH). South-eastern South America would experience an increase in precipitation from the same poleward storm track displacement.

11.6.2 Skill of Models in Simulating Present Climate

In the Central America (CAM) and AMZ regions, most models in the MMD have a cold bias of 0°C to 3°C, except in AMZ in SON (Supplementary Material Table S11.1). In southern South America (SSA) average biases are close to zero. The biases are unevenly geographically distributed (Supplementary Material Figure S11.25). The MMD mean climate shows a warm bias around 30°S (particularly in summer) and in parts of central South America (especially in SON). Over the rest of South America (central and northern Andes, eastern Brazil, Patagonia) the biases tend to be predominantly negative. The SST biases along the western coasts of South America are likely related to weakness in oceanic upwelling.

For the CAM region, the multi-model scatter in precipitation is substantial, but half of the models lie in the range of –15 to 25% in the annual mean. The largest biases occur during the boreal winter and spring seasons, when precipitation is meagre (Supplementary Material Table S11.1). For both AMZ and SSA, the ensemble annual mean climate exhibits drier than observed conditions, with about 60% of the models having a negative bias. Unfortunately, this choice of regions for averaging is particularly misleading for South America since it does not clearly bring out critical regional biases such as those related to rainfall underestimation in the Amazon and La Plata Basins (Supplementary Material Figure S11.26). Simulation of the regional climate is seriously affected by model deficiencies at low latitudes. In particular, the MMD ensemble tends to depict a relatively weak ITCZ, which extends southward of its observed position. The simulations have a systematic bias towards underestimated rainfall over the Amazon Basin. The simulated subtropical climate is typically also adversely affected by a dry bias over most of south-eastern South America and in the South Atlantic Convergence Zone, especially during the rainy season. In contrast, rainfall along the Andes and in northeast Brazil is excessive in the ensemble mean.

Some aspects of the simulation of tropical climate with AOGCMs have improved. However, in general, the largest errors are found where the annual cycle is weakest, such as over tropical South America (see, e.g., Section 8.3). Atmospheric GCMs approximate the spatial distribution of precipitation over the tropical Americas, but they do not correctly reproduce the temporal evolution of the annual cycle in precipitation, specifically the mid-summer drought (Magaña and Caetano, 2005). Tropical cyclones are important contributors to precipitation in the region. If close to the continent, they will produce large amounts of precipitation over land, and if far from the coast, moisture divergence over the continental region enhances drier conditions.

Zhou and Lau (2002) analyse the precipitation and circulation biases in a set of six AGCMs provided by the Climate Variability and Predictability Programme (CLIVAR) Asian-Australian Monsoon AGCM Intercomparison Project (Kang et al., 2002). This model ensemble captures some large-scale features of the South American monsoon system reasonably well, including the seasonal migration of monsoon rainfall and the rainfall associated with the South America Convergence Zone. However, the South Atlantic subtropical high and the Amazonia low are too strong, whereas low-level flow tends to be too strong during austral summer and too weak during austral winter. The model ensemble captures the Pacific-South American pattern quite well, but its amplitude is generally underestimated.

Regional models are still being tested and developed for this region. Relatively few studies using RCMs for Central and South America exist, and those that do are constrained by short simulation length. Some studies (Chou et al., 2000; Nobre et al., 2001; Druyan et al., 2002) examine the skill of experimental dynamic downscaling of seasonal predictions over Brazil. Results suggest that both more realistic GCM forcing and improvements in the RCMs are needed. Seth and Rojas (2003) performed seasonal integrations driven by reanalyses, with emphasis on tropical South America. The model was able to simulate the different rainfall anomalies and large-scale circulations but, as a result of weak low-level moisture transport from the Atlantic, rainfall over the western Amazon was underestimated. Vernekar et al. (2003) follow a similar approach to study the low-level jets and report that the RCM produces better regional circulation details than does the reanalysis. However, an ensemble of four RCMs did not provide a noticeable improvement in precipitation over the driving large-scale reanalyses (Roads et al., 2003).

Other studies (Misra et al., 2003; Rojas and Seth, 2003) analyse seasonal RCM simulations driven by AGCM simulations. Relative to the AGCMs, regional models generally improve the rainfall simulation and the tropospheric circulation over both tropical and subtropical South America. However, AGCM-driven RCMs degrade compared with the reanalyses-driven integrations and they could even exacerbate the dry bias over sectors of AMZ and perpetuate the erroneous ITCZ over

the neighbouring ocean basins from the AGCMs. Menéndez et al. (2001) used a RCM driven by a stretched-grid AGCM with higher resolution over the southern mid-latitudes to simulate the winter climatology of SSA. They find that both the AGCM and the regional model have similar systematic errors but the biases are reduced in the RCM. Analogously, other RCM simulations for SSA give too little precipitation over the subtropical plains and too much over elevated terrain (e.g., Nicolini et al., 2002; Menéndez et al., 2004).

11.6.3 Climate Projections

11.6.3.1 Temperature

The warming as simulated by the MMD-A1B projections increases approximately linearly with time during this century, but the magnitude of the change and the inter-model range are greater over CAM and AMZ than over SSA (Figure 11.14). The annual mean warming under the A1B scenario between 1980 to 1999 and 2080 to 2099 varies in the CAM region from 1.8°C to 5.0°C, with half of the models within 2.6°C to 3.6°C and a median of 3.2°C. The corresponding numbers for AMZ are 1.8°C to 5.1°C, 2.6°C to 3.7°C and 3.3°C, and those for SSA 1.7°C to 3.9°C, 2.3°C to 3.1°C and 2.5°C (Table 11.1). The median warming is close to the global ensemble mean in SSA but about 30% above the global mean in the other two regions. As in the rest of the tropics, the signal-to-noise ratio is large for temperature, and it requires only 10 years for a 20-year mean temperature, growing at the rate of the median A1B response, to be clearly discernible above the models' internal variability.

The simulated warming is generally largest in the most continental regions, such as inner Amazonia and northern Mexico (Figure 11.15). Seasonal variation in the regional area mean warming is relatively modest, except in CAM where there is a difference of 1°C in median values between DJF and MAM (Table 11.1). The warming in central Amazonia tends to be larger in JJA than in DJF, while the reverse is true over the Altiplano where, in other words, the seasonal cycle of temperature is projected to increase (Figure 11.15). Similar results were found by Boulanger et al. (2006), who studied the regional thermal response over South America by applying a statistical method based on neural networks and Bayesian statistics to find optimal weights for a linear combination of MMD models.

For the variation of seasonal warming between the individual models, see Table 11.1. As an alternative approach to estimating uncertainty in the magnitude of the warming, the 5th and 95th percentiles for temperature change at the end of the 21st century, assessed using the method of Tebaldi et al. (2004a), are typically within ±1°C of the median value in all three of these regions (Supplementary Material Table S11.2).

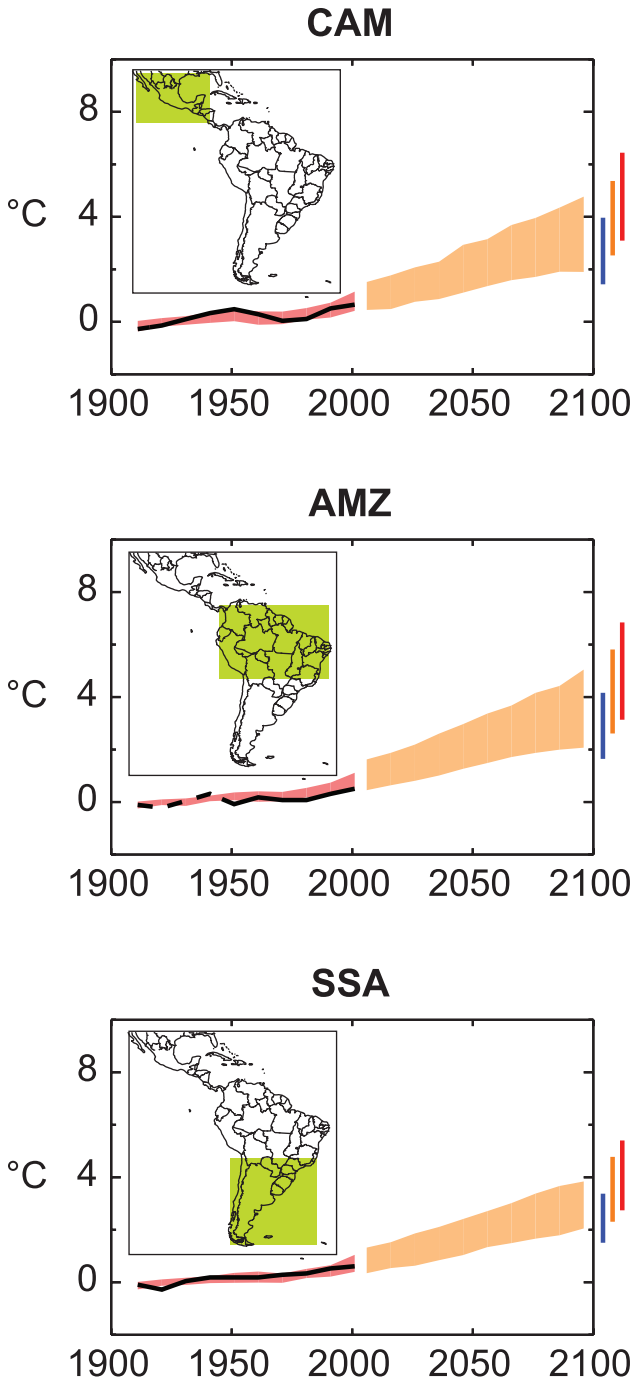


Figure 11.14. *Temperature anomalies with respect to 1901 to 1950 for three Central and South American land regions for 1906 to 2005 (black line) and as simulated (red envelope) by MMD models incorporating known forcings; and as projected for 2001 to 2100 by MMD models for the A1B scenario (orange envelope). The bars at the end of the orange envelope represent the range of projected changes for 2091 to 2100 for the B1 scenario (blue), the A1B scenario (orange) and the A2 scenario (red). The black line is dashed where observations are present for less than 50% of the area in the decade concerned. More details on the construction of these figures are given in Box 11.1 and Section 11.1.2.*

11.6.3.2 Precipitation

The MMD models suggest a general decrease in precipitation over most of Central America, consistent with Neelin et al. (2006), where the median annual change by the end of the 21st

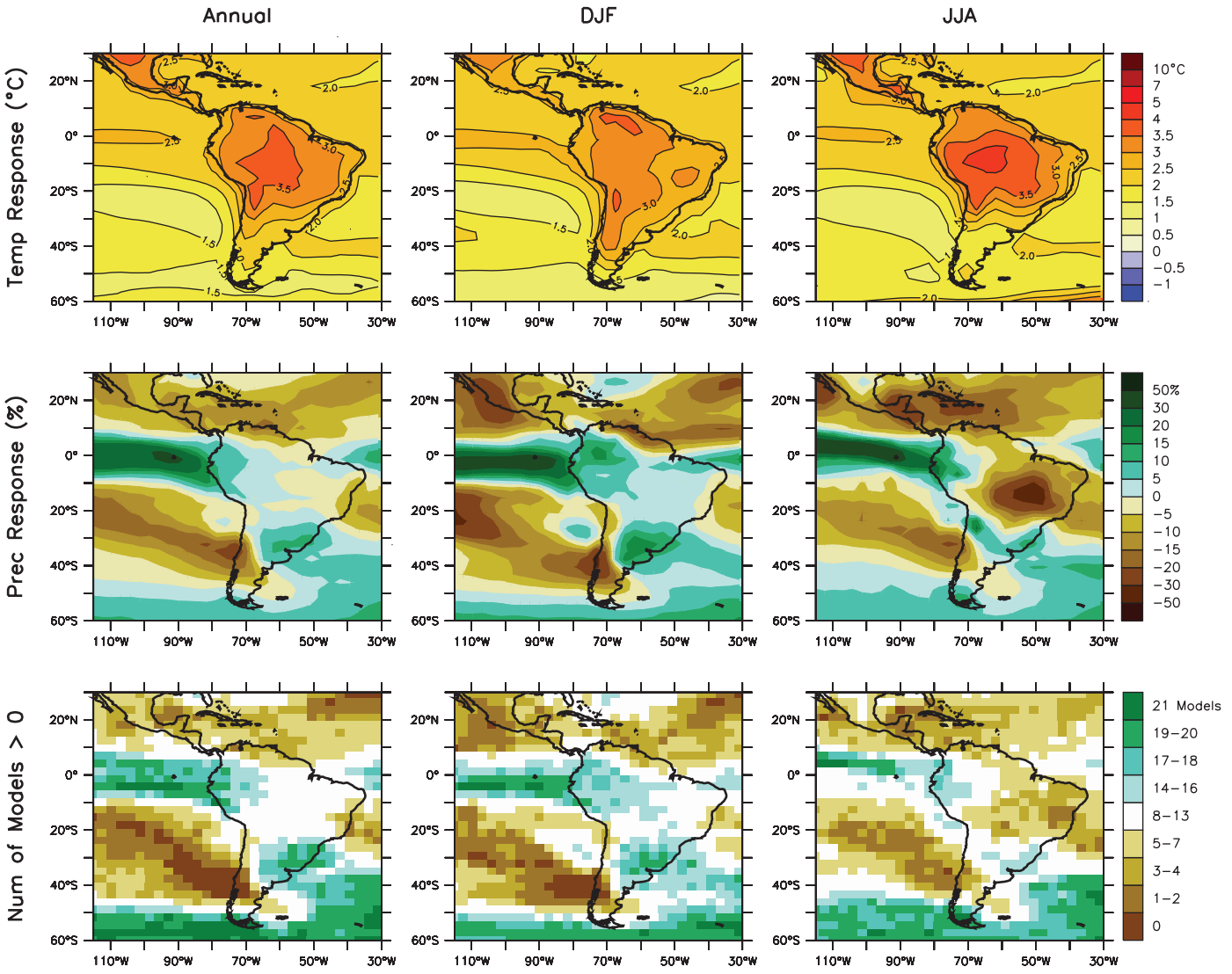


Figure 11.15. *Temperature and precipitation changes over Central and South America from the MMD-A1B simulations. Top row: Annual mean, DJF and JJA temperature change between 1980 to 1999 and 2080 to 2099, averaged over 21 models. Middle row: same as top, but for fractional change in precipitation. Bottom row: number of models out of 21 that project increases in precipitation.*

century is –9% under the A1B scenario, and half of the models project area mean changes from –16 to –5%, although the full range of the projections extends from –48 to 9%. Median changes in area mean precipitation in Amazonia and southern South America are small and the variation between the models is also more modest than in Central America, but the area means hide marked regional differences (Table 11.1, Figure 11.15).

Area mean precipitation in Central America decreases in most models in all seasons. It is only in some parts of north-eastern Mexico and over the eastern Pacific, where the ITCZ forms during JJA, that increases in summer precipitation are projected (Figure 11.15). However, since tropical storms can contribute a significant fraction of the rainfall in the hurricane season in this region, these conclusions might be modified by the possibility of increased rainfall in storms not well captured by these global models. In particular, if the number of storms does not change, Knutson and Tuleya (2004) estimate nearly a 20% increase in average precipitation rate within 100 km of the storm centre at the time of atmospheric carbon dioxide (CO_2) doubling.

For South America, the multi-model mean precipitation response (Figure 11.15) indicates marked regional variations. The annual mean precipitation is projected to decrease over northern South America near the Caribbean coasts, as well as over large parts of northern Brazil, Chile and Patagonia, while it is projected to increase in Colombia, Ecuador and Peru, around the equator and in south-eastern South America. The seasonal cycle modulates this mean change, especially over the Amazon Basin where monsoon precipitation increases in DJF and decreases in JJA. In other regions (e.g., Pacific coasts of northern South America, a region centered over Uruguay, Patagonia) the sign of the response is preserved throughout the seasonal cycle.

As seen in the bottom panels of Figure 11.15, most models project a wetter climate near the Rio de la Plata and drier conditions along much of the southern Andes, especially in DJF. However, when estimating the likelihood of this response, the qualitative consensus within this set of models should be weighed against the fact that most models show considerable biases in regional precipitation patterns in their control simulations.

The poleward shift of the South Pacific and South Atlantic subtropical anticyclones is a robust response across the models. Parts of Chile and Patagonia are influenced by the polar boundary of the subtropical anticyclone in the South Pacific and experience particularly strong drying because of the combination of the poleward shift in circulation and increase in moisture divergence. The strength and position of the subtropical anticyclone in the South Atlantic is known to influence the climate of south-eastern South America and the South Atlantic Convergence Zone (Robertson et al., 2003; Liebmann et al., 2004). The increase in rainfall in south-eastern South America is related to a corresponding poleward shift in the Atlantic storm track (Yin, 2005).

Some projected changes in precipitation (such as the drying over east-central Amazonia and northeast Brazil and the wetter conditions over south-eastern South America) could be a partial consequence of the El-Niño like response projected by the models (Section 10.3). The accompanying shift and alterations in the Walker Circulation would directly affect tropical South America (Cazes Boezio et al., 2003) and affect southern South America through extratropical teleconnections (Mo and Nogués-Paegle, 2001).

Although feedbacks from carbon cycle and dynamic vegetation are not included in MMD models, a number of coupled carbon cycle-climate projections have been performed since the TAR (see Sections 7.2 and 10.4.1). The initial carbon-climate simulations suggest that drying of the Amazon potentially contributes to acceleration of the rate of anthropogenic global warming by increasing atmospheric CO_2 (Cox et al., 2000; Friedlingstein et al., 2001; Dufresne et al., 2002; Jones et al., 2003). These models display large uncertainty in climate projections and differ in the timing and sharpness of the changes (Friedlingstein et al., 2003). Changes in CO_2 are related to precipitation changes in regions such as the northern Amazon (Zeng et al., 2004). In a version of the HadCM3 model with dynamic vegetation and an interactive global carbon cycle (Betts et al., 2004), a tendency to a more El Niño-like state contributes to reduced rainfall and vegetation dieback in the Amazon (Cox et al., 2004). But the version of HadCM3 participating in the MMD projects by far the largest reduction in annual rainfall over AMZ (–21% for the A1B scenario). This stresses the necessity of being very cautious in interpreting carbon cycle impacts on the regional climate and ecosystem change until there is more convergence among models on rainfall projections for the Amazon with fixed vegetation. Box 11.4 summarises some of the major issues related to regional land use/land changes in the context of climate change.

11.6.4 Extremes

Little research is available on extremes of temperature and precipitation for this region. Table 11.1 provides estimates on how frequently the seasonal temperature and precipitation extremes as simulated in 1980 to 1999 are exceeded in model projections using the A1B scenario. Essentially all seasons and regions are extremely warm by this criterion by the end of the century. In Central America, the projected time mean precipitation decrease is accompanied by more frequent dry extremes in all seasons. In AMZ, models project extremely wet seasons in about 27% (18%) of all DJF (MAM) seasons in the period 2080 to 2099. Significant changes are not projected in the frequency of extremely wet or dry seasons over SSA.

On the daily time scale, Hegerl et al. (2004) analyse an ensemble of simulations from two AOGCMs and find that both models simulate a temperature increase in the warmest night of the year larger than the mean response over the Amazon Basin but smaller than the mean response over parts of SSA. Concerning extreme precipitation, both models project more intense wet days per year over large parts of south-eastern South America and central Amazonia and weaker precipitation extremes over the coasts of northeast Brazil. Intensification of the rainfall amounts are consistent, given the agreement between the MMD model simulations over parts of south-eastern South America and most of AMZ but with longer periods between rainfall events, except in north-western South America, where the models project that it will rain more frequently (Meehl et al., 2005; Tebaldi et al., 2006).

11.7 Australia – New Zealand

Assessment of projected climate change for Australia and New Zealand:

All of Australia and New Zealand are very likely to warm during this century, with amplitude somewhat larger than that of the surrounding oceans, but comparable overall to the global mean warming. The warming is smaller in the south, especially in winter, with the warming in the South Island of New Zealand likely to remain smaller than the global mean. Increased frequency of extreme high daily temperatures in Australia and New Zealand, and decrease in the frequency of cold extremes is very likely.

Precipitation is likely to decrease in southern Australia in winter and spring. Precipitation is very likely to decrease in south-western Australia in winter. Precipitation is likely to increase in the west of the South Island of New Zealand. Changes in rainfall in northern and central Australia are uncertain. Extremes of daily precipitation are very likely to increase. The effect may be offset or reversed in areas of significant decrease in

Box 11.4: Land Use and Land Cover Change Experiments Related to Climate Change

Land use and land cover change significantly affect climate at the regional and local scales (e.g., Hansen et al., 1998; Bonan, 2001; Kabat et al., 2002; Foley et al., 2005). Recent modelling studies also show that in some instances these effects can extend beyond the areas where the land cover changes occur, through climate teleconnection processes (e.g., Gaertner et al., 2001; Pielke et al., 2002; Marland et al., 2003). Changes in vegetation result in alteration of surface properties, such as albedo and roughness length, and alter the efficiency of ecosystem exchange of water, energy and CO_2 with the atmosphere (for more details see Section 7.2). The effects differ widely based on the type and location of the altered ecosystem. The effects of land use and land cover change on climate can also be divided into biogeochemical and biophysical effects (Brovkin et al., 1999; see Sections 7.2 and 2.5 for discussion of these effects).

The net effect of human land cover activities increases the concentration of greenhouse gases in the atmosphere, thus increasing warming (see Sections 7.2 and 10.4 for further discussion); it has been suggested that these land cover emissions have been underestimated in the future climate projections used in the SRES scenarios (Sitch, 2005). Climate models assessed in this report incorporate various aspects of the effects of land cover change including representation of the biogeochemical flux, inclusion of dynamic land use where natural vegetation shifts as climate changes, and explicit human land cover forcing. In all cases, these efforts should be considered at early stages of development (see Chapters 2 and 7, and Table 10.1 for more details on many of these aspects).

One important impact of land cover conversion, generally not simulated in GCMs, is urbanisation. Although small in aerial extent, conversion to urban land cover creates urban heat islands associated with considerable warming (Arnfield, 2003). Since much of the world population lives in urban environments (and this proportion may increase, thus expanding urban areas), many people will be exposed to climates that combine expanded urban heat island effects and increased temperature from greenhouse gas forcing (see Box 7.2 for more details on urban land use effects).

One major shift in land use, relevant historically and in the future, is conversion of forest to agriculture and agriculture back to forest. Most areas well suited to large-scale agriculture have already been converted to this land use/cover type. Yet land cover conversion to agriculture may continue in the future, especially in parts of western North America, tropical areas of south and central America and arable regions in Africa and south and central Asia (IPCC, 2001; RIVM, 2002). In the future, mid-latitude agricultural areal expansion (especially into forested areas) could possibly result in cooling that would offset a portion of the expected warming due to greenhouse gas effects alone. In contrast, reforestation may occur in eastern North America and the eastern portion of Europe. In these areas, climate effects may include local warming associated with reforestation due to decreased albedo values (Feddema et al., 2005).

Tropical land cover change results in a very different climate response compared to mid-latitude areas. Changes in plant cover and the reduced ability of the vegetation to transpire water to the atmosphere lead to temperatures that are warmer by as much as 2°C in regions of deforestation (Costa and Foley, 2000; Gedney and Valdes, 2000; De Fries et al., 2002). The decrease in transpiration acts to reduce precipitation, but this effect may be modified by changes in atmospheric moisture convergence. Most model simulations of Amazonian deforestation suggest reduced moisture convergence, which would amplify the decrease in precipitation (e.g., McGuffie et al., 1995; Costa and Foley, 2000; Avissar and Worth, 2005). However, increased precipitation and moisture convergence in Amazonia during the last few decades contrast with this expectation, suggesting that deforestation has not been the dominant driver of the observed changes (see Section 11.6).

Tropical regions also have the potential to affect climates beyond their immediate areal extent (Chase et al., 2000; Delire et al., 2001; Voldoire and Royer, 2004; Avissar and Werth, 2005; Feddema et al., 2005; Snyder, 2006). For example, changes in convection patterns can affect the Hadley Circulation and thus propagate climate perturbations into the mid-latitudes. In addition, tropical deforestation in the Amazon has been found to affect SSTs in nearby ocean locations, further amplifying teleconnections (Avissar and Werth, 2005;Feddema et al., 2005; Neelin and Su, 2005; Voldoire and Royer, 2005). However, studies also indicate that there are significantly different responses to similar land use changes in other tropical regions and that responses are typically linked to dry season conditions (Voldoire and Royer, 2004a; Feddema et al., 2005). However, tropical land cover change in Africa and southeast Asia appears to have weaker local impacts largely due to influences of the Asian and African monsoon circulation systems (Mabuchi et al., 2005a,b; Voldoire and Royer, 2005).

Several land cover change studies have explicitly assessed the potential impacts (limited to biophysical effects) associated with specific future SRES land cover change scenarios, and the interaction between land cover change and greenhouse gas forcings (De Fries et al., 2002; Maynard and Royer, 2004a; Feddema et al., 2005; Sitch et al., 2005; Voldoire, 2006). In the A2 scenario, large-scale Amazon deforestation could double the expected warming in the region (De Fries et al., 2002; Feddema et al., 2005). Lesser local impacts are expected in tropical Africa and south Asia, in part because of the difference in regional circulation patterns (Delire et al., 2001; Maynard and Royer, 2004a,b; Feddema et al., 2005; Mabuchi et al., 2005a,b). In mid-latitude regions, land-cover induced cooling could offset some of the greenhouse-gas induced warming. Feddema et al. (2005) suggest that in the B1 scenario (where reforestation occurs in many areas and there are other low-impact tropical land cover changes) there are few local tropical climate or teleconnection effects. However, in this scenario, mid-latitude reforestation could lead to additional local warming compared to greenhouse-gas forcing scenarios alone.

(continued)

These simulations suggest that the effects of future land cover change will be a complex interaction of local land cover change impacts combined with teleconnection effects due to land cover change elsewhere, in particular the Amazon, and areas surrounding the Indian Ocean. However, projecting the potential outcomes of future climate effects due to land cover change is difficult for two reasons. First, there is considerable uncertainty regarding how land cover will change in the future. In this context, the past may not be a good indicator of the types of land transformation that may occur in the future. For example, if land cover change becomes a part of climate change mitigation (e.g., carbon trading) then a number of additional factors that include carbon sequestration in soils and additional land cover change processes will need to be incorporated in scenario development schemes. Second, current land process models cannot simulate all the potential impacts of human land cover transformation. Such processes as adequate simulation of urban systems, agricultural systems, ecosystem disturbance regimes (e.g., fire) and soil impacts are not yet well represented.

mean rainfall (southern Australian in winter and spring). An increase in potential evaporation is likely. Increased risk of drought in southern areas of Australia is likely.

Increased mean wind speed across the Southern Island of New Zealand, particularly in winter, is likely.

Significant factors contribute to uncertainty in projected climate change for the region. The El Niño-Southern Oscillation significantly influences rainfall, drought and tropical cyclone behaviour in the region and it is uncertain how ENSO will change in the future. Monsoon rainfall simulations and projections vary substantially from model to model, thus we have little confidence in model precipitation projections for northern Australia. More broadly, across the continent summer rainfall projections vary substantially from model to model, reducing confidence in their reliability. In addition, no detailed assessment of MMD model performance over Australia or New Zealand is available, which hinders efforts to establish the reliability of projections from these models. Finally, downscaling of MMD model projections are not yet available for New Zealand but are much needed because of the strong topographical control of New Zealand rainfall.

11.7.1 Key Processes

Key climate processes affecting the Australian region include the Australian monsoon (the SH counterpart of the Asian monsoon), the Southeast trade wind circulation, the subtropical high-pressure belt and the mid-latitude westerly wind circulation with its embedded disturbances. The latter two systems also predominate over New Zealand. Climatic variability in Australia and New Zealand is also strongly affected by the ENSO system (McBride and Nicholls, 1983; Mullan, 1995) modulated by the Inter-decadal Pacific Oscillation (IPO; Power et al., 1999; Salinger et al., 2001). Tropical cyclones occur in the region, and are a major source of extreme rainfall and wind events in northern coastal Australia, and, more rarely, on the North Island of New Zealand (Sinclair, 2002). Rainfall patterns in New Zealand are also strongly influenced by the interaction of the predominantly westerly circulation with its very mountainous topography.

Apart from the general increase in temperature that the region will share with most other parts of the globe, details of anthropogenic climate change in the Australia-New Zealand region will depend on the response of the Australian monsoon, tropical cyclones, the strength and latitude of the mid-latitude westerlies, and ENSO.

11.7.2 Skill of Models in Simulating Present Climate

There are relatively few studies of the quality of the MMD global model simulations in the Australia-New Zealand area. The ensemble mean of the MMD model simulations has a systematic low-pressure bias near 50°S at all longitudes in the SH, including the Australia-New Zealand sector, corresponding to an equatorward displacement of the mid-latitude westerlies (see Chapter 8). On average, mid-latitude storm track eddies are displaced equatorward (Yin, 2005) and deep winter troughs over southwest Western Australia are over-represented (Hope 2006a,b). How this bias might affect climate change simulations is unclear. It can be hypothesised that by spreading the effects of mid-latitude depressions too far inland, the consequences of a poleward displacement of the westerlies and the storm track might be exaggerated, but the studies needed to test this hypothesis are not yet available.

The simulated surface temperatures in the surrounding oceans are typically warmer than observed, but at most by 1°C in the composite. Despite this slight warm bias, the ensemble mean temperatures are biased cold over land, especially in winter in the southeast and southwest of the Australian continent, where the cold bias is larger than 2°C. At large scales, the precipitation also has some systematic biases (see Supplementary Material Table S11.1). Averaged across northern Australia, the median model error is 20% more precipitation than observed, but the range of biases in individual models is large (–71 to +131%). This is discouraging with regard to confidence in many of the individual models. Consistent with this, Moise et al. (2005) identify simulation of Australian monsoon rainfall as a major deficiency of many of the AOGCM simulations included in Phase 2 of the Coupled Model Intercomparison Project (CMIP2). The median annual bias in the southern Australian region is –6%, and the range of biases –59 to +36%. In most models, the northwest is too wet and the northeast and east coast too dry, and the central arid zone is insufficiently arid.

The Australasian simulations in the AOGCMs utilised in the TAR have recently been scrutinised more closely, in part as a component of a series of national and state-based climate change

projection studies (e.g., Whetton et al., 2001; Cai et al., 2003b; McInnes et al., 2003; Hennessy et al., 2004a,b; McInnes et al., 2004). Some high-resolution regional simulations were also considered in this process. The general conclusion is that large-scale features of Australian climate were quite well simulated. In winter, temperature patterns were more poorly simulated in the south where topographic variations have a stronger influence, although this was alleviated in the higher-resolution simulations. A set of the TAR AOGCM simulations was also assessed for the New Zealand region by Mullan et al. (2001a) with similar conclusions. The models were able to represent ENSO-related variability in the Pacific and the temperature and rainfall teleconnection patterns at the Pacific-wide scale, but there was considerable variation in model performance at finer scales (such as over the New Zealand region).

Decadal-scale variability patterns in the Australian region as simulated by the CSIRO AOGCM were considered by Walland et al. (2000) and found 'broadly consistent' with the observational studies of Power et al. (1998). At smaller scales, Suppiah et al. (2004) directly assessed rainfall-producing processes by comparing the simulated correlation between rainfall anomalies and pressure anomalies in Victoria against observations. They find that this link was simulated well by most models in winter and autumn, but less well in spring and summer. As a result of this, they warn that the spring and summer projected rainfall changes should be viewed as less reliable.

Pitman and McAvaney (2004) examine the sensitivity of GCM simulations of Australian climate to methods of representation of the surface energy balance. They find that the quality of the simulation of variability is strongly affected by the land surface model, but that simulation of climate means, and the changes in those means in global warming simulations, is less sensitive to the scheme employed.

Statistical downscaling methods have been employed in the Australian region and have demonstrated good performance at representing means, variability and extremes of station temperature and rainfall (Timbal and McAvaney, 2001; Charles et al., 2004; Timbal, 2004) based on broad-scale observational or climate model predictor fields. The method of Charles et al. (2004) is able to represent spatial coherence at the daily time scale in station rainfall, thus enhancing its relevance to hydrological applications.

11.7.3 Climate Projections

In addition to the MMD models, numerous studies have been conducted with earlier models. Recent regional average projections are provided in Giorgi et al. (2001b) and Ruosteenoja et al. (2003). The most recent national climate change projections of CSIRO (2001) were based on the results of eight AOGCMs and one higher-resolution regional simulation. The methodology (and simulations) used in these projections is described in Whetton et al. (2005) and follows closely that described for earlier projections in Whetton et al. (1996). More detailed projections for individual states and other regions have also been prepared in recent years (Whetton et al., 2001; Cai et al., 2003b; McInnes et al., 2003, 2004; Hennessy et al., 2004a,b; IOCI, 2005). This work has focused on temperature and precipitation, with additional variables such as potential evaporation and winds being included in the more recent assessments.

A range of dynamically downscaled projections have been undertaken for Australia using the DARLAM regional model (Whetton et al., 2001) and the CCAM stretched grid model (McGregor and Dix, 2001) at resolutions of 60 km across Australia and down to 14 km for Tasmania (McGregor, 2004). These projections use forcing from recent CSIRO AOGCM projections. Downscaled projected climate change using statistical methods has also been recently undertaken for parts of Australia (e.g., Timbal and McAvaney, 2001; Charles et al., 2004; Timbal, 2004) and New Zealand (Mullan et al., 2001a; Ministry for the Environment, 2004).

11.7.3.1 Mean Temperature

In both the southern and northern Australia regions, the projected MMD-A1B warming in the 21st century represents a significant acceleration of warming over that observed in the 20th century (Figure 11.16). The warming is larger than over the surrounding oceans, but only comparable to, or slightly larger than the global mean warming. Averaging over the region south of 30°S (SAU), the median 2100 warming among all of the models is 2.6°C (with an inter-quartile range of 2.4°C to 2.9°C) whereas the median warming averaged over the region north of 30°S (NAU) is 3.0°C (range of 2.8°C to 3.5°C). The seasonal cycle in the warming is weak, but with larger values (and larger spread among model projections) in summer (DJF). Across the MMD models, the warming is well correlated with the global mean warming, with a correlation coefficient of 0.79, so that more than half of the variance among models is controlled by global rather than local factors, as in many other regions. The range of responses is comparable but slightly smaller than the range in global mean temperature responses, and warming over equivalent time periods under the B1, A1B, and A2 scenarios is close to the ratios of the global mean responses The warming varies sub-regionally, with less warming in coastal regions, Tasmania and the South Island of New Zealand, and greater warming in central and northwest Australia (see Figure 10.8).

These results are broadly (and in many details) similar to those described in earlier studies, so other aspects of these earlier studies can be assumed to remain relevant. For the CSIRO (2001) projections, pattern-scaling methods were used to provide patterns of change rescaled by the range of global warming given by IPCC (2001) for 2030 and 2070 based on the SRES scenarios. By 2030, the warming is 0.4°C to 2°C over most of Australia, with slightly less warming in some coastal areas and Tasmania, and slightly more warming in the northwest. By 2070, annual average temperatures increase by 1°C to 6°C over most of Australia with spatial variations similar to those for 2030. Dynamically downscaled mean temperature change typically does not differ very significantly from the picture based on AOGCMs (e.g., see Whetton et al., 2002).

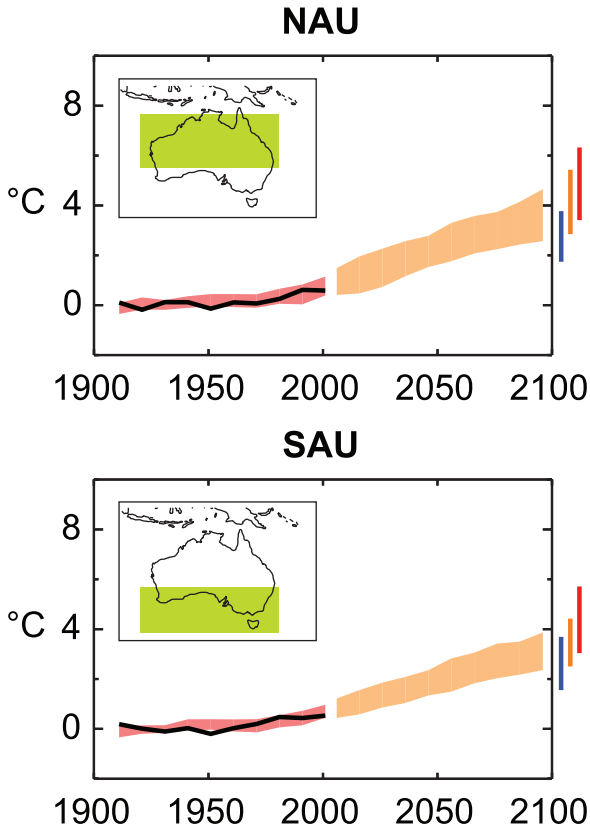


Figure 11.16. *Temperature anomalies with respect to 1901 to 1950 for two Australian land regions for 1906 to 2005 (black line) and as simulated (red envelope) by MMD models incorporating known forcings; and as projected for 2001 to 2100 by MMD models for the A1B scenario (orange envelope). The bars at the end of the orange envelope represent the range of projected changes for 2091 to 2100 for the B1 scenario (blue), the A1B scenario (orange) and the A2 scenario (red). More details on the construction of these figures are given in Box 11.1 and Section 11.1.2.*

Projected warming over New Zealand (allowing for the IPCC (2001) range of global warming and differences in the regional results of six GCMs used for downscaling) is 0.2°C to 1.3°C by the 2030s and 0.5°C to 3.5°C by the 2080s (Ministry for the Environment, 2004).

11.7.3.2 Mean Precipitation

A summary of projected precipitation changes from the MMD models is presented in Figure 11.17 and Table 11.1. The most robust feature is the reduction in rainfall along the south coast in JJA (not including Tasmania) and in the annual mean, and a decrease is also strongly evident in SON. The percentage JJA change in 2100 under the A1B scenario for southern Australia has an inter-quartile range of –26 to –7% and by comparison the same range using the probabilistic method of Tebaldi et al. (2004b) is –13 to –6% (Supplemental Material Table S11.2). There are large reductions to the south of the continent in all seasons, due to the poleward movement of the westerlies and embedded depressions (Cai et al., 2003a; Yin, 2005; Chapter 10), but this reduction extends over land during winter when the storm track is placed furthest equatorward. Due to poleward drift of the storm track as it crosses Australian longitudes, the strongest effect is in the southwest, where the ensemble mean drying is in the 15 to 20% range. Hope (2006a,b) shows a southward or longitudinal shift in storms away from south-western Australia in the MMD simulations. To the east of Australia and over New Zealand, the primary storm track is more equatorward, and the north/south drying/moistening pattern associated with the poleward displacement is shifted equatorward as well. The result is a robust projection of increased rainfall on the South Island (especially its southern half), possibly accompanied by a decrease in the north part of the North Island. The South Island increase is likely to be modulated by the strong topography (see Box 11.3) and to appear mainly upwind of the main mountain range.

Other aspects of simulated precipitation change appear less robust. On the east coast of Australia, there is a tendency in the models for an increase in rain in the summer and a decrease in winter, with a slight annual decrease. However, consistency among the models on these features is weak.

These results are broadly consistent with results based on earlier GCM simulations. In the CSIRO (2001) projections based on a range of nine simulations, projected ranges of annual average rainfall change tend towards a decrease in the southwest and south but show more mixed results elsewhere (Whetton et al., 2005). Seasonal results showed that rainfall tended to decrease in southern and eastern Australia in winter and spring, increase inland in autumn and increase along the east coast in summer. Moise et al. (2005) also find a tendency for winter rainfall decreases across southern Australia and a slight tendency for rainfall increases in eastern Australia in 18 CMIP2 simulations under a 1% yr^{-1} atmospheric CO_2 increase.

Whetton et al. (2001) demonstrate that inclusion of high-resolution topography could reverse the simulated direction of rainfall change in parts of Victoria (see Box 11.3). In a region of strong rainfall decrease as simulated directly by the GCMs, two different downscaling methods (Charles et al., 2004; Timbal, 2004) have been applied to obtain the characteristics of rainfall change at stations (IOCI, 2002, 2005; Timbal, 2004). The downscaled results continued to show the simulated decrease, although the magnitude of the changes was moderated relative to the GCM in the Timbal (2004) study. Downscaled rainfall projections for New Zealand (incorporating differing results from some six GCMs) showed a strong variation across the islands (Ministry for the Environment, 2004). The picture that emerges is that the pattern of precipitation changes described above in the global simulations is still present, but with the precipitation changes focused on the upwind sides of the islands, with the increase in rainfall in the south concentrated in the west, and the decrease in the north concentrated in the east.

11.7.3.3 Snow Cover

The likelihood that precipitation will fall as snow will decrease as temperature rises. Hennessy et al. (2003) modelled snowfall and snow cover in the Australian Alps under the

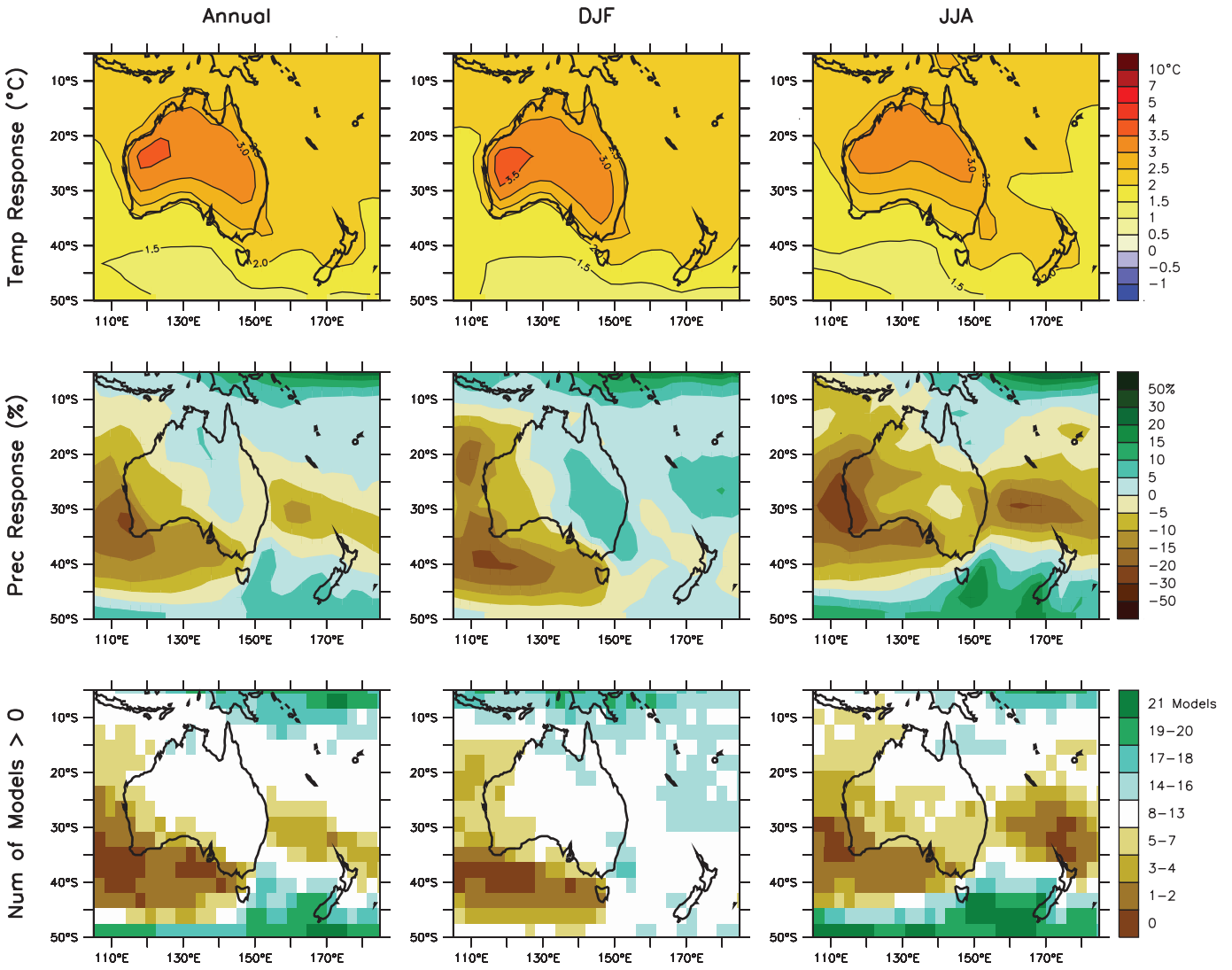


Figure 11.17. *Temperature and precipitation changes over Australia and New Zealand from the MMD-A1B simulations. Top row: Annual mean, DJF and JJA temperature change between 1980 to 1999 and 2080 to 2099, averaged over 21 models. Middle row: same as top, but for fractional change in precipitation. Bottom row: number of models out of 21 that project increases in precipitation.*

CSIRO (2001) projected temperature and precipitation changes and obtained very marked reductions in snow. The total alpine area with at least 30 days of snow cover decreases 14 to 54% by 2020, and 30 to 93% by 2050. Because of projected increased winter precipitation over the southern Alps, it is less clear that mountain snow will be reduced in New Zealand (Ministry for the Environment, 2004; see also Box 11.3). However, marked decreases in average snow water over New Zealand (60% by 2040 under the A1B scenario) have been simulated by Ghan and Shippert (2006) using a high-resolution sub-grid scale orography in a global model that simulates little change in precipitation.

11.7.3.4 Potential Evaporation

Using the method of Walsh et al. (1999), changes in potential evaporation in the Australian region have been calculated for a range of enhanced greenhouse climate model simulations (Whetton et al., 2002; Cai et al., 2003b; McInnes et al., 2003, 2004; Hennessy et al., 2004a,b). In all cases, increases in potential evaporation were simulated, and in almost all cases, the moisture balance deficit became larger. This has provided a strong indication of the Australian environment becoming drier under enhanced greenhouse conditions.

11.7.3.5 Temperature and Precipitation Extremes

Where the analysis has been done for Australia (e.g., Whetton et al., 2002), the effect on changes in extreme temperature due to simulated changes in variability is small relative to the effect of the change in the mean. Therefore, most regional assessments of changes in extreme temperatures have been based on adding a projected mean temperature change to each day of a

station-observed data set. Based on the CSIRO (2001) projected mean temperature change scenarios, the average number of days over 35°C each summer in Melbourne would increase from 8 at present to 9 to 12 by 2030 and 10 to 20 by 2070 (CSIRO, 2001). In Perth, such hot days would rise from 15 at present to 16 to 22 by 2030 and 18 to 39 by 2070 (CSIRO, 2001). On the other hand, cold days become much less frequent. For example, Canberra's current 44 winter days of minimum temperature below 0°C is projected to be 30 to 42 by 2030 and 6 to 38 by 2070 (CSIRO, 2001).

Changes in extremes in New Zealand have been assessed using a similar methodology and simulations (Mullan et al., 2001b). Decreases in the annual frequency of days below 0°C of 5 to 30 days by 2100 are projected for New Zealand, particularly for the lower North Island and the South Island. Increases in the annual number of days above 25°C of 10 to 50 days by 2100 are projected.

A range of GCM and regional modelling studies in recent years have identified a tendency for daily rainfall extremes to increase under enhanced greenhouse conditions in the Australian region (e.g., Hennessy et al., 1997; Whetton et al., 2002; McInnes et al., 2003; Watterson and Dix, 2003; Hennessy et al., 2004b; Suppiah et al., 2004; Kharin and Zwiers, 2005). Commonly, return periods of extreme rainfall events halve in late 21st-century simulations. This tendency can apply even when average rainfall is simulated to decrease, but not necessarily when this decrease is marked (see Timbal, 2004). Recently, Abbs (2004) dynamically downscaled to a resolution of 7 km current and enhanced greenhouse cases of extreme daily rainfall occurrence in northern New South Wales and southern Queensland as simulated by the CSIRO GCM. The downscaled extreme events for a range of return periods compared well with observations and the enhanced greenhouse simulations for 2040 showed increases of around 30% in magnitude, with the 1-in-40 year event becoming the 1-in-15 year event. Less work has been done on projected changes in rainfall extremes in New Zealand, although the recent analysis of Ministry for the Environment (2004) based on Semenov and Bengtsson (2002) indicates the potential for extreme winter rainfall (95th percentile) to change by between –6% and +40%.

Where GCMs simulate a decrease in average rainfall, it may be expected that there would be an increase in the frequency of dry extremes (droughts). Whetton and Suppiah (2003) examine simulated monthly frequencies of serious rainfall deficiency for Victoria, which show strong average rainfall decreases in most simulations considered. There is a marked increase in the frequency of rainfall deficiencies in most simulations, with doubling in some cases by 2050. Using a slightly different approach, likely increases in the frequency of drought have also been established for the states of South Australia, New South Wales and Queensland (Walsh et al., 2002; McInnes et al., 2003; Hennessy et al., 2004c). Mullan et al. (2005) show that by the 2080s in New Zealand there may be significant increases in drought frequency in the east of both islands.

11.7.3.6 Tropical Cyclones

A number of recent regional model-based studies of changes in tropical cyclone behaviour in the Australian region have examined aspects of number, tracks and intensities under enhanced greenhouse conditions (e.g., Walsh and Katzfey, 2000; Walsh and Ryan, 2000; Walsh et al., 2004). There is no clear picture with respect to regional changes in frequency and movement, but increases in intensity are indicated. For example, Walsh et al. (2004) obtained, under tripled CO_2 conditions, a 56% increase in storms with a maximum wind speed greater than 30 m s^{-1}. It should also be noted that ENSO fluctuations have a strong impact on patterns of tropical cyclone occurrence in the region, and therefore uncertainty with respect to future ENSO behaviour (see Section 10.3) contributes to uncertainty with respect to tropical cyclone behaviour (Walsh, 2004). See Section 10.3.6.3 for a global assessment of changes in tropical cyclone characteristics.

11.7.3.7 Winds

The MMD ensemble mean projected change in winter sea level pressure is shown in Figure 10.9. Much of Australia lies to the north of the centre of the high-pressure anomaly. With the mean latitude of maximum pressure near 30°S at this season, this corresponds to a modest strengthening of the mean wind over inland and northern areas and a slight weakening of the mean westerlies on the southern coast, consistent with Hennessy et al. (2004b). Studies of daily extreme winds in the region using high-resolution model output (McInnes et al., 2003) indicate increases of up to 10% across much of the northern half of Australia and the adjacent oceans during summer by 2030. In winter, the pressure gradient is projected to increase over the South Island of New Zealand (see Figure 10.9), implying increased windiness. This increase is present in all of the MMD-A1B projections.

11.8 Polar Regions

Assessment of projected climate change for the polar regions:

The Arctic is very likely to warm during this century in most areas, and the annual mean warming is very likely to exceed the global mean warming. Warming is projected to be largest in winter and smallest in summer.

Annual arctic precipitation is very likely to increase. It is very likely that the relative precipitation increase will be largest in the winter and smallest in summer.

Arctic sea ice is very likely to decrease in extent and thickness. It is uncertain how the Arctic Ocean circulation will change.

It is likely that the Antarctic will be warmer and that precipitation will increase over the continent.

It is uncertain to what extent the frequency of extreme temperature and precipitation events will change in the polar regions.

Polar climate involves large natural variability on interannual, decadal and longer time scales, which is an important source of uncertainty. The projections of the trends in the underlying teleconnections, such as the Northern Annular Mode (NAM) or ENSO, contain substantial uncertainty (see Chapter 10). Further, understanding of the polar climate system is still incomplete due to its complex atmosphere-land-cryosphere-ocean-ecosystem interactions involving a variety of distinctive feedbacks. Processes that are not particularly well represented in the models are clouds, planetary boundary layer processes and sea ice. Additionally, the resolution of global models is still not adequate to resolve important processes in the polar seas. All this contributes to a rather large range of present-day and future simulations, which may reduce confidence in the future projections. A serious problem is the lack of observations against which to assess models, and for developing process knowledge, particularly over Antarctica.

11.8.1 Arctic

11.8.1.1 Key Processes

Arctic climate is characterised by a distinctive complexity due to numerous nonlinear interactions between and within the atmosphere, cryosphere, ocean, land and ecosystems. Sea ice plays a crucial role in the arctic climate, particularly through its albedo. Reduction of ice extent leads to warming due to increased absorption of solar radiation at the surface. Substantial low-frequency variability is evident in various atmosphere and ice parameters (Polyakov et al., 2003a,b), complicating the detection and attribution of arctic changes. Natural multi-decadal variability has been suggested as partly responsible for the large warming in the 1920s to 1940s (Bengtsson et al., 2004; Johannessen et al., 2004) followed by cooling until the 1960s. In both models and observations, the interannual variability of monthly temperatures is at a maximum at high latitudes (Räisänen, 2002). Natural atmospheric patterns of variability on annual and decadal time scales play an important role in the arctic climate. Such patterns include the NAM, the NAO, the Pacific-North American (PNA) pattern and the Pacific Decadal Oscillation (PDO), which are associated with prominent arctic regional precipitation and temperature anomalies (see Box 3.4 and Section 3.6). For instance, the positive NAM/NAO phase is associated with warmer, wetter winters in Siberia and colder, drier winters in western Greenland and north-eastern Canada. The NAM/NAO showed a trend towards its positive phase over the last three to four decades, although it returned to near its long-term mean state in the last five years (see Section 3.6). In the future, global models project a positive trend in the NAO/NAM during the 21st century (see Section 10.3). There was substantial decadal-to-inter-decadal atmospheric variability in the North Pacific over the 20th century, associated with fluctuations in the strength of the winter Aleutian Low that co-vary with North Pacific SST in the PDO (see Section 3.6). A deeper and eastward-shifted Aleutian Low advects warmer and moister air into Alaska. While some studies have suggested that the Brooks Range effectively isolates arctic Alaska from much of the variability associated with North Pacific teleconnection patterns (e.g., L'Heureux et al., 2004), other studies find relationships between the Alaskan and Beaufort-Chukchi region's climate and North Pacific variability (Stone, 1997; Curtis et al., 1998; Lynch et al., 2004). Patterns of variability in the North Pacific, and their implications for climate change, are especially difficult to sort out due to the presence of several patterns (NAM, PDO, PNA) with potentially different underlying mechanisms (see Chapter 3).

11.8.1.2 Skill of Models in Simulating Present Climate

Many processes are still poorly understood and thus continue to pose a challenge for climate models (ACIA, 2005). In addition, evaluating simulations of the Arctic is difficult because of the uncertainty in the observations. The few available observations are sparsely distributed in space and time and different data sets often differ considerably (Serreze and Hurst, 2000; ACIA, 2005; Liu et al., 2005; Wyser and Jones, 2005). This holds especially for precipitation measurements, which are problematic in cold environments (Goodison et al., 1998; Bogdanova et al., 2002).

Few pan-arctic atmospheric RCMs are in use. When driven by analysed lateral and sea ice boundary conditions, RCMs tend to show smaller temperature and precipitation biases in the Arctic compared to GCMs, indicating that sea ice simulation biases and biases originating from lower latitudes contribute substantially to the contamination of GCM results in the Arctic (e.g., Dethloff et al., 2001; Wei et al., 2002; Lynch et al., 2003; Semmler et al., 2005). However, even under a very constrained experimental design, there can be considerable across-model scatter in RCM simulations (Tjernström et al., 2005; Rinke et al., 2006). The construction of coupled atmosphere-ice-ocean RCMs for the Arctic is a recent development (Maslanik et al., 2000; Debernard et al., 2003; Rinke et al., 2003; Mikolajewicz et al., 2005).

Temperature

The simulated spatial patterns of the MMD ensemble mean temperatures agree closely with those of the observations throughout the annual cycle. Generally, the simulations are 1°C to 2°C colder than the European Centre for Medium-Range Weather Forecasts 40-year (ERA40) reanalyses with the exception of a cold bias maximum of 6°C to 8°C in the Barents Sea (particularly in winter/spring) caused by overestimated sea ice in this region (Chapman and Walsh, 2007; see also Section 8.3). Compared with earlier model versions, the annual temperature simulations improved in the Barents and Norwegian Seas and Sea of Okhotsk, but some deterioration is noted in the central Arctic Ocean and the high terrain areas

of Alaska and northwest Canada (Chapman and Walsh, 2007). The mean model ensemble bias is relatively small compared to the across-model scatter of temperatures. The annual mean root-mean-squared error in the individual MMD models ranges from 2°C to 7°C (Chapman and Walsh, 2007). Compared with previous models, the MMD-simulated temperatures are more consistent across the models in winter, but somewhat less so in summer. There is considerable agreement between the modelled and observed interannual variability both in magnitude and spatial pattern.

Precipitation

The AOGCM-simulated monthly precipitation varies substantially among the models throughout the year but the MMD ensemble mean monthly means are within the range of different observational data sets. This is an improvement compared to earlier simulations (Walsh et al., 2002; ACIA, 2005), particularly from autumn to spring (Kattsov et al., 2007). The ensemble mean bias varies with season and remains greatest in spring and smallest in summer. The annual bias pattern (positive over most parts of the Arctic) can be partly attributed to coarse orography and to biased atmospheric storm tracks and sea ice cover (see Chapter 8). The MMD models capture the observed increase in the annual precipitation through the 20th century (see Section 3.3).

Sea Ice and Ocean

Arctic sea ice biases in present-day MMD simulations are discussed in Section 8.3. Arctic ocean-sea ice RCMs under realistic atmospheric forcing are increasingly capable of reproducing the known features of the Arctic Ocean circulation and observed sea ice drift patterns. The inflow of the two branches of Atlantic origin via the Fram Strait and the Barents Sea and their subsequent passage at mid-depths in several cyclonic circulation cells are present in most recent simulations (Karcher et al., 2003; Maslowski et al., 2004; Steiner et al., 2004). Most of the models are biased towards overly salty values in the Beaufort Gyre and thus too little freshwater storage in the arctic halocline. Several potential causes have been identified, among them a biased simulation of arctic shelf processes and wind forcing. Most hindcast simulations with these RCMs show a reduction in the arctic ice volume over recent decades (Holloway and Sou, 2002).

11.8.1.3 Climate Projections

Temperature

A northern high-latitude maximum in the warming ('polar amplification') is consistently found in all AOGCM simulations (see Section 10.3). The simulated annual mean arctic warming exceeds the global mean warming by roughly a factor of two in the MMD models, while the winter warming in the central arctic is a factor of four larger than the global annual mean when averaged over the models. These magnitudes are comparable to those obtained in previous studies (Holland and Bitz, 2003; ACIA, 2005). The consistency between observations and the ensemble mean 20th-century simulations (Figure 11.18), combined with the fact that the near-future projections (2010–2029) continue the late 20th-century trends in temperature, ice extent and thickness with little modification (Serreze and Francis, 2006), increases confidence in this basic polar-amplified warming pattern, despite the inter-model differences in the amount of polar amplification.

At the end of the 21st century, the projected annual warming in the Arctic is 5°C, estimated by the MMD-A1B ensemble mean projection (Section 11.8.2.3, Figure 11.21). There is a considerable across-model range of 2.8°C to 7.8°C (Table 11.1). Larger (smaller) mean warming is found for the A2 (B1) scenario of 5.9°C (3.4°C), with a proportional across-model range. The across-model and across-scenario variability in the projected temperatures are both considerable and of comparable amplitude (Chapman and Walsh, 2007).

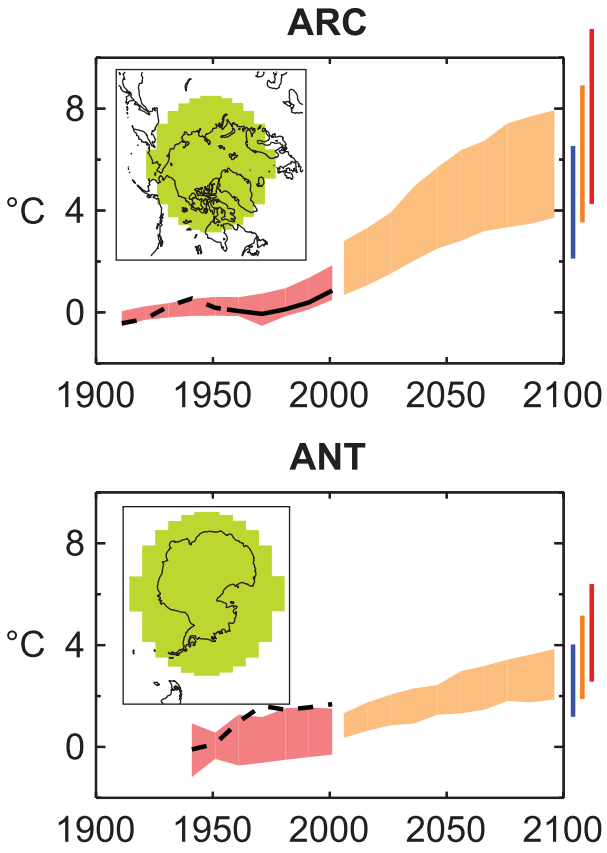


Figure 11.18. *Top panels: Temperature anomalies with respect to 1901 to 1950 for the whole Arctic for 1906 to 2005 (black line) as simulated (red envelope) by MMD models incorporating known forcings; and as projected for 2001 to 2100 by MMD models for the A1B scenario (orange envelope). The bars at the end of the orange envelope represent the range of projected changes for 2091 to 2100 for the B1 scenario (blue), the A1B scenario (orange) and the A2 scenario (red). The black line is dashed where observations are present for less than 50% of the area in the decade concerned. Bottom panels: The same for Antarctic land, but with observations for 1936 to 2005 and anomalies calculated with respect to 1951 to 2000. More details on the construction of these figures are given in Box 11.1 and Section 11.1.2.*

Over both ocean and land, the largest (smallest) warming is projected in winter (summer) (Table 11.1, Figure 11.19). But the seasonal amplitude of the temperature change is much larger over ocean than over land due the presence of melting sea ice in summer keeping the temperatures close to the freezing point. The surface air temperature over the Arctic Ocean region is generally warmed more than over arctic land areas (except in summer). The range between the individual simulated changes remains large (Figure 11.19, Table 11.1). By the end of the century, the mean warming ranges from 4.3°C to 11.4°C in winter, and from 1.2°C to 5.3°C in summer under the A1B scenario. The corresponding 5 to 95% confidence intervals are given in Supplementary Material Table S11.2. In addition to the overall differences in global warming, difficulties in simulating sea ice, partly related to biases in the surface wind fields, as well as deficiencies in cloud schemes, are likely responsible for much of the inter-model scatter. Internal variability plays a secondary role when examining these late-21st century responses.

The annual mean temperature response pattern at the end of the 21st century under the A1B scenario (Supplementary Material Figures S11.27 and S11.11) is characterised by a robust and large warming over the central Arctic Ocean (5°C to 7°C), dominated by the warming in winter/autumn associated with the reduced sea ice. The maximum warming is projected over the Barents Sea, although this could result from an overestimated albedo feedback caused by removal of the present-day simulations' excessive sea ice cover. A region of reduced warming (<2°C, even slight cooling in several models) is projected over the northern North Atlantic, which is consistent among the models. This is due to weakening of the MOC (see Section 10.3).

While the natural variability in arctic temperatures is large compared to other regions, the signals are still large enough to emerge quickly from the noise (Table 11.1). Looking more locally, as described by Chapman and Walsh (2007), Alaska is perhaps the land region with the smallest signal-to-noise ratio, and is the only arctic region in which the 20-year mean 2010 to 2029 temperature is not clearly discernible from the 1981 to 2000 mean in the MMD models. But even here the signal is clear by mid-century in all three scenarios.

The regional temperature responses are modified by changes in circulation patterns (Chapter 10). In winter, shifts in NAO phase can induce inter-decadal temperature variations of up to 5°C in the eastern Arctic (Dorn et al., 2003). The MMD models project winter circulation changes consistent with an increasingly positive NAM/NAO (see Section 10.3), which acts to enhance the warming in Eurasia and western North America. In summer, circulation changes are projected to favour warm anomalies north of Scandinavia and extending into the eastern Arctic, with cold anomalies over much of Alaska (Cassano et al., 2006). However, deficiencies in the arctic summer synoptic activity in these models reduce confidence in the detailed spatial structure. In addition, these circulation-induced temperature changes are not large enough to change the relatively uniform summer warming seen in the MMD models

The patterns of temperature changes simulated by RCMs are quite similar to those simulated by GCMs. However, they show an increased warming along the sea ice margin possibly due to a better description of the mesoscale weather systems and air-sea fluxes associated with the ice edge (ACIA, 2005). The warming over most of the central Arctic and Siberia, particularly in summer, tends to be lower in RCM simulations (by up to 2°C) probably due to more realistic present-day snowpack simulations (ACIA, 2005). The warming is modulated by the topographical height, snow cover and associated albedo feedback as shown for the region of northern Canada and Alaska (see Section 11.5.3).

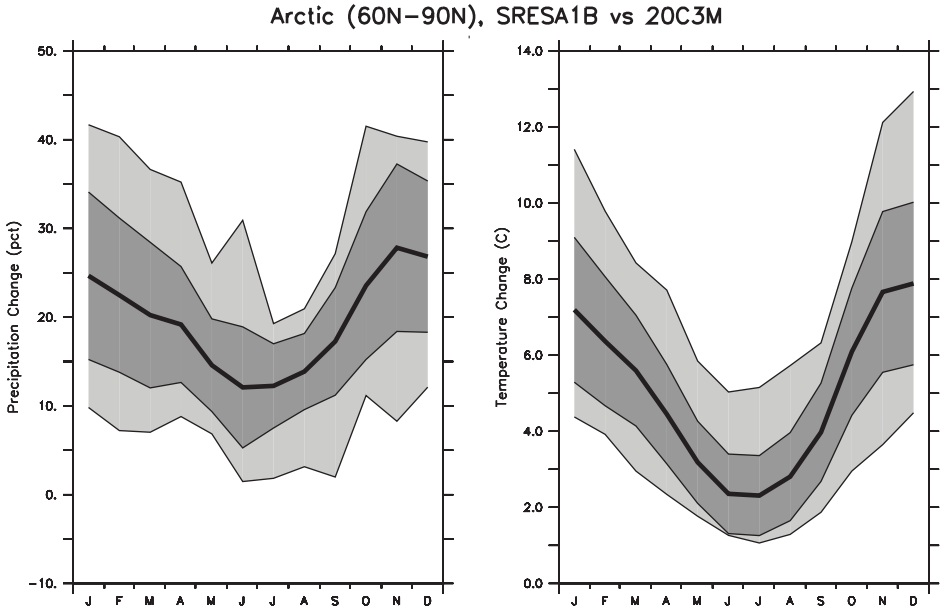


Figure 11.19. *Annual cycle of arctic area mean temperature and percentage precipitation changes (averaged over the area north of 60°N) for 2080 to 2099 minus 1980 to 1999, under the A1B scenario. Thick lines represent the ensemble median of the 21 MMD models. The dark grey area represents the 25 and 75% quartile values among the 21 models, while the light grey area shows the total range of the models.*

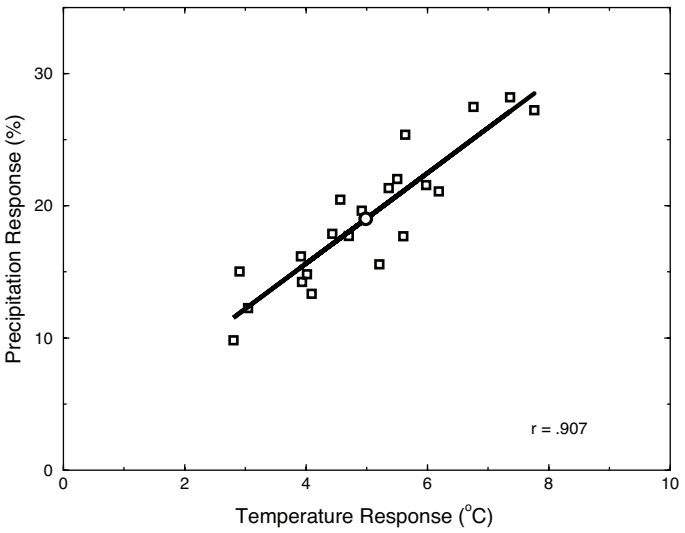


Figure 11.20. *Relationship between the change in annual precipitation (%) and temperature (°C) (2080–2099 minus 1980–1999) in the Arctic (averaged over the area north of 60°N) in the MMD-A1B projections. Each point represents one model. The model ensemble mean response is indicated by the circle.*

Precipitation

The MMD simulations show a general increase in precipitation over the Arctic at the end of the 21st century (Table 11.1; Supplementary Material Figure S11.28). The precipitation increase is robust among the models (Table 11.1; Supplementary Material Figure S11.19) and qualitatively well understood, attributed to the projected warming and related increased moisture convergence (Section 10.3). The very strong correlation between the temperature and precipitation changes (approximately a 5% precipitation increase per degree celsius warming) across the model ensemble is worth noting (Figure 11.20). Thus, both the sign and the magnitude (per degree warming) of the percentage precipitation change are robust among the models.

The spatial pattern of the projected change (Supplementary Material Figure S11.28) shows the greatest percentage increase over the Arctic Ocean (30 to 40%) and smallest (and even slight decrease) over the northern North Atlantic (<5%). By the end of the 21st century, the projected change in the annual mean arctic precipitation varies from 10 to 28%, with an MMD-A1B ensemble median of 18% (Table 11.1). Larger (smaller) mean precipitation increases are found for the A2 (B1) scenario with 22% (13%). The percentage precipitation increase is largest in winter and smallest in summer, consistent with the projected warming (Figure 11.19; Table 11.1). The across-model scatter of the precipitation projections is substantial (Figure 11.19; Table 11.1). The Tebaldi et al. (2004a) 5th to 95th percentile confidence interval of percentage precipitation change in winter is 13 to 36% and in summer 5 to 19% (Supplementary Material Table S11.2).

Differences between the projections for different scenarios are small in the first half of the 21st century but increase later. Differences among the models increase rapidly as the spatial domain becomes smaller (ACIA, 2005). The geographical variation of precipitation changes is determined largely by changes in the synoptic circulation patterns. During winter, the MMD models project a decreased (increased) frequency of strong Arctic high (Icelandic low) pressure patterns that favour precipitation increases along the Canadian west coast, southeast Alaska and North Atlantic extending into Scandinavia (Cassano et al., 2006). Projections with RCMs support the broad-scale messages while adding expected local and regional detail (ACIA, 2005).

By the end of the 21st century, the MMD-A1B ensemble-projected precipitation increase is significant (Table 11.1), particularly the annual and cold season (winter/autumn) precipitation. However, local precipitation changes in some regions and seasons (particularly in the Atlantic sector and generally in summer) remain difficult to discern from natural variability (ACIA, 2005).

Extremes of Temperature and Precipitation

Very little work has been done in analysing future changes in extreme events in the Arctic. However, the MMD simulations indicate that the increase in mean temperature and precipitation will be combined with an increase in the frequency of very warm and wet winters and summers. Using the definition of extreme season in Section 11.1.2, every DJF and JJA season, in all model projections, is 'extremely' warm in the period 2080 to 2099 (Table 11.1). The corresponding numbers for extremely wet seasons are 90 and 85% for DJF and JJA. For the other scenarios, the frequency of extremes is very similar, except that for the wet seasons under B1, which is smaller (~63%).

Cryosphere

Northern Hemisphere sea ice, snow and permafrost projections are discussed in Section 10.3; projected changes in the surface mass balance of arctic glaciers and of the Greenland Ice Sheet are discussed in Sections 10.3 and 10.7.

Arctic Ocean

A systematic analysis of future projections for the Arctic Ocean circulation is still lacking. Coarse resolution in global models prevents the proper representation of local processes that are of global importance (such as the convection in the Greenland Sea that affects the deep waters in the Arctic Ocean and the intermediate waters that form overflow waters). The MMD models project a reduction in the MOC in the Atlantic Ocean (see Section 10.3). Correspondingly, the northward oceanic heat transport decreases south of 60°N in the Atlantic. However, the CMIP2 model assessment showed a projected increase in the oceanic heat transport at higher latitudes, associated with a stronger subarctic gyre circulation in the models (Holland and Bitz, 2003). The Atlantic Ocean north of 60°N freshens during the 21st century, in pronounced contrast to the observed development in the late 20th century (Wu et al., 2003).

11.8.2 Antarctic

11.8.2.1 Key Processes

Over Antarctica, there is special interest in changes in snow accumulation expected to accompany global climate change as well as the pattern of temperature change, particularly any differences in warming over the peninsula and the interior of the ice sheet. As in the Arctic, warming of the troposphere is expected to increase precipitation. However, circulation changes in both ocean and atmosphere can alter the pattern of air masses, which would modify both precipitation and temperature patterns substantially over the region.

The dominant patterns controlling the atmospheric seasonal-to-interannual variability of the SH extratropics are the Southern Annular Mode (SAM) and ENSO (see Section 3.6). Signatures of these patterns in the Antarctic have been revealed in many studies (reviews by Carleton, 2003 and Turner, 2004). The positive phase of the SAM is associated with cold anomalies over most of Antarctica and warm anomalies over the Antarctic Peninsula (Kwok and Comiso, 2002a). Over recent decades, a drift towards the positive phase in the SAM is evident (see Section 3.6). Observational studies have presented evidence of pronounced warming over the Antarctic Peninsula, but little change over the rest of the continent during the last half of the 20th century (see Sections 3.6 and 4.6). The response of the SAM in transient warming simulations is a robust positive trend, but the response to the ozone hole in the late 20th century, which is also a positive perturbation to the SAM, makes any simple extrapolation of current trends into the future uncertain (see Section 10.3).

Compared to the SAM, the Southern Oscillation (SO) shows weaker association with surface temperature over Antarctica but the correlation with SST and sea ice variability in the Pacific sector of the Southern Ocean is significant (e.g., Kwok and Comiso, 2002b; Renwick, 2002; Bertler et al., 2004; Yuan, 2004). Correlation between the SO index and antarctic precipitation and accumulation has also been studied but the persistence of the signal is not clear (Bromwich et al., 2000, 2004a; Genthon and Cosme, 2003; Guo et al., 2004; Genthon et al., 2005). Recent work suggests that this intermittence is due to nonlinear interactions between ENSO and SAM that vary on decadal time scales (Fogt and Bromwich, 2006; L'Heureux and Thompson, 2006). The SO index has a negative trend over recent decades (corresponding to a tendency towards more El Niño-like conditions in the equatorial Pacific; see Section 3.6) associated with sea ice cover anomalies in the Pacific sector, namely negative (positive) anomalies in the Ross and Amundsen Seas (Bellingshausen and Weddell Seas) (Kwok and Comiso, 2002a). However, a definitive assessment of ENSO amplitude and frequency changes in the 21st century cannot be made (see Chapter 10).

11.8.2.2 Skill of Models in Simulating Present Climate

Evaluating temperature and precipitation simulations over Antarctica is difficult due to sparse observations and often relies on numerical weather prediction (re)analyses. However, significant differences between those have been found, and comparisons with station observations show that the surface temperature can be subject to considerable biases (Connolley and Harangozo, 2001; Bromwich and Fogt, 2004). Marked improvement in the bias is seen after the satellite era (~1978) (Simmons et al., 2004), and parts of the bias are explained by the reanalyses' smoothing of the sharp changes in the terrain near coastal stations. Satellite-derived monthly surface temperatures agree with antarctic station data with an accuracy of 3°C (Comiso, 2000). Precipitation evaluation is even more challenging and the different (re)analyses differ significantly (Connolley and Harangozo, 2001; Zou et al., 2004). Very few direct precipitation gauge and detailed snow accumulation data are available, and these are uncertain to varying degrees (see Section 4.6).

Major challenges face the simulation of the atmospheric conditions and precipitation patterns of the polar desert in the high interior of East Antarctica (Guo et al., 2003; Bromwich et al., 2004a; Pavolonis et al., 2004, Van de Berg et al., 2005). Driven by analysed boundary conditions, RCMs tend to show smaller temperature and precipitation biases in the Antarctic compared to the GCMs (Bailey and Lynch, 2000; Van Lipzig et al., 2002a,b; Van den Broeke and Van Lipzig, 2003; Bromwich et al., 2004b; Monaghan et al., 2006). Krinner et al. (1997) show the value of a stretched model grid with higher horizontal resolution over the Antarctic as compared to standard GCM formulations. Despite these promising developments, since the TAR there has been no coordinated comparison of the performance of GCMs, RCMs and other alternatives to global GCMs over Antarctica.

Temperature

Compared to National Centers for Environmental Prediction (NCEP) reanalyses, the MMD ensemble annual surface temperatures are in general slightly warmer in the Southern Ocean to the north of the sea ice region. The mean bias is predominantly less than 2°C (Carril et al., 2005), which may indicate a slight improvement compared to previous models due to better simulation of the position and depth of the Antarctic trough (Carril et al., 2005; Raphael and Holland, 2006). The temperature bias over sea ice is larger. Biases over the continent are several degrees where the model topography is erroneous (Turner et al., 2006). However, as emphasized above, the biases have to be viewed in the context of the uncertainty in the observations. Changes in cloud and radiation parametrizations have been shown to change the temperature simulation significantly (Hines et al., 2004). A lateral nudging of a stretched-grid GCM (imposing the correct synoptic cyclones from 60°S and lower latitudes) brings the model in better agreement with observations but significant biases remain (Genthon et al., 2002).

The spread in the individual MMD-simulated patterns of surface temperature trends over the past 50 years is very large, but in contrast to previous models, the multi-model composite of the MMD models qualitatively captures the observed enhanced warming trend over the Antarctic Peninsula (Chapman and Walsh, 2006). The general improvements in resolution, sea ice models and cloud-radiation packages have evidently contributed to improved simulations. The ensemble-mean temperature trends show similarity to the observed spatial pattern of the warming, for both annual and seasonal trends. For the annual trend, this includes the warming of the peninsula and near-coastal Antarctica and neutral or slight cooling over the sea-ice covered regions of the Southern Ocean. While the large spread among the models is not encouraging, this level of agreement suggests that some confidence in the ensemble mean 21st-century projection is appropriate.

Precipitation

The MMD models simulate the position of the storm tracks reasonably well but nearly all show some deficiency in the distribution and level of cyclone activity compared to reanalyses (see Section 8.3). Regional Climate Models generally capture the cyclonic events affecting the coast and the associated synoptic variability of precipitation with more fidelity (Adams, 2004; Bromwich et al., 2004a). Over the 20th century, the MMD models simulate changes in storm track position that are generally consistent with observed changes (i.e., poleward displacement of the storm tracks; see Sections 9.5 and 10.3).

The precipitation simulations by both GCMs and RCMs contain uncertainty, on all time scales (Covey et al., 2003; Bromwich et al., 2004a,b; Van de Berg et al., 2005), as a result of model physics limitations. All atmospheric models, including the models underlying the reanalyses, have incomplete parametrizations of polar cloud microphysics and ice crystal precipitation. The simulated precipitation depends, among other things, on the simulated sea ice concentrations, and is strongly affected by biases in the sea ice simulations (Weatherly, 2004). Recent RCM simulations driven by observed sea ice conditions demonstrate good precipitation skill (Van de Berg et al., 2005; Monaghan et al., 2006). However, as emphasized above, the observational uncertainty contributes to uncertainty in the differences between observations and simulations.

Sea Ice

The performance biases of SH sea ice conditions in present-day MMD simulations are discussed in Section 8.3.

11.8.2.3 Climate Projections

Very little effort has been spent to model the future climate of Antarctica at a spatial scale finer than that of GCMs.

Temperature

At the end of the 21st century, the annual warming over the Antarctic continent is moderate but significant (Figure 11.21; Table 11.1; Chapman and Walsh, 2006). It is estimated to be 2.6°C by the median of the MMD-A1B models with a range from 1.4°C to 5.0°C across the models (Table 11.1). Larger (smaller) warming is found for the A2 (B1) scenario with mean value of 3.1°C (1.8°C). These warming magnitudes are similar to previous estimates (Covey et al., 2003). The annual mean MMD model projections show a relatively uniform warming over the entire continent (with a maximum in the Weddell Sea) (Figure 11.21; Carril et al., 2005; Chapman and Walsh, 2006). They do not show a local maximum warming over the Antarctic Peninsula. This is a robust feature among the individual models (Supplementary Material Figure S11.12). Thus, the pattern of observed temperature trends in the last half of the 20th century (warming over the Antarctic Peninsula, little change over the rest of the continent) is not projected to continue throughout the 21st century, despite a projected positive SAM trend (see

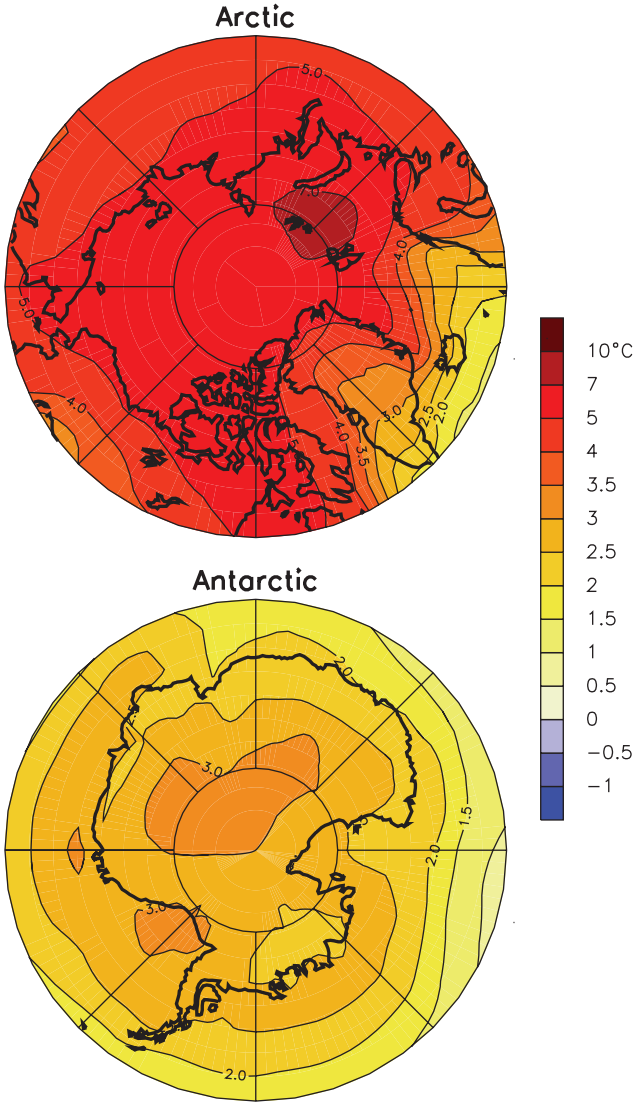


Figure 11.21. *Annual surface temperature change between 1980 to 1999 and 2080 to 2099 in the Arctic and Antarctic from the MMD-A1B projections.*

Section 10.3). It has been argued that two distinct factors have contributed to the observed SAM trend: greenhouse gas forcing and the ozone hole formation (Stone et al., 2001; Shindell and Schmidt, 2004). Their relative importance for the peninsular warming is not readily understood (see Chapter 10).

The mean antarctic temperature change does not show a strong seasonal dependency; the MMD-A1B ensemble mean winter (summer) warming is 2.8°C (2.6°C) (Table 11.1; Supplementary Material Figure S11.29; Chapman and Walsh, 2006). This is also illustrated by how close the Tebaldi et al. (2004a) 5 to 95% confidence interval for the two seasons is: 0.1°C to 5.7°C in summer and 1.0°C to 4.8°C in winter (Supplementary Material Table S11.2). However, over the Southern Oceans, the temperature change is larger in winter/autumn than in summer/spring, which can primarily be attributed to the sea ice retreat (see Section 10.3).

Precipitation

Almost all MMD models simulate a robust precipitation increase in the 21st century (Supplementary Material Figures S11.29 and S11.30; Table 11.1). However, the scatter among the individual models is considerable. By the end of the 21st century, the projected change in the annual precipitation over the Antarctic continent varies from –2% to 35%, with a MMD-A1B ensemble median of 14% (Table 11.1). Similar (smaller) mean precipitation increase is found for the A2 (B1) scenario, with values of 15% (10%). The spatial pattern of the annual change is rather uniform (Supplementary Material Figure S11.30). The projected relative precipitation change shows a seasonal dependency, and is larger in winter than in summer (Supplementary Material Figure S11.29). The Tebaldi et al. (2004a) 5 to 95% confidence interval for winter is –1 to 34% and in summer –6 to 22% (Supplementary Material Table S11.2). The projected increase in precipitation over Antarctica and thus greater accumulation of snow, without substantial surface melting, will contribute negatively to sea level rise relative to the present day (see Section 10.6). It is notable that the most recent model studies of antarctic precipitation show no significant contemporary trends (Van de Berg et al., 2005; Monaghan et al., 2006; Van den Broeke et al., 2006; see Section 4.6).

The moisture transport to the continent by synoptic activity represents a large fraction of net precipitation (Noone and Simmonds, 2002; Massom et al., 2004). During summer and winter, a systematic shift towards strong cyclonic events is projected by the MMD models (see Section 10.3). In particular, the frequency of occurrence of deep cyclones in the Ross Sea to Bellingshausen Sea sector is projected to increase by 20 to 40% (63%) in summer (winter) by the middle of the 21st century (Lynch et al., 2006). Related to this, the precipitation over the sub-antarctic seas and Antarctic Peninsula is projected to increase.

Extremes of Temperature and Precipitation

Very little work has been done in analysing future changes in extreme events in the Antarctic. However, the MMD simulations indicate that the increase in mean temperature and precipitation will be combined with an increase in the frequency of very warm and wet winters and summers. Using the definition of 'extreme' seasons provided in Section 11.1.2, the MMD models predict extremely warm seasons in about 85% of all DJF and 83% of all JJA seasons in the period 2080 to 2099, as averaged over all models (Table 11.1). The corresponding numbers for extremely wet seasons are 34% and 59%. For the B1 scenario, the frequency of extremes is smaller, with little difference between A1B and A2.

Sea Ice and Antarctic Ice Sheet

Southern Hemisphere sea ice projections are discussed in Section 10.3. The projections of the Antarctic Ice Sheet surface mass balance are discussed in Section 10.6.

11.9 Small Islands

Assessment of projected climate change for Small Islands regions:

Sea levels are likely to continue to rise on average during the century around the small islands of the Caribbean Sea, Indian Ocean and Northern and Southern Pacific Oceans. Models indicate that the rise will not be geographically uniform but large deviations among models make regional estimates across the Caribbean, Indian and Pacific Oceans uncertain.

All Caribbean, Indian Ocean and North and South Pacific islands are very likely to warm during this century. The warming is likely to be somewhat smaller than the global annual mean warming in all seasons.

Summer rainfall in the Caribbean is likely to decrease in the vicinity of the Greater Antilles but changes elsewhere and in winter are uncertain. Annual rainfall is likely to increase in the northern Indian Ocean with increases likely in the vicinity of the Seychelles in DJF, and in the vicinity of the Maldives in JJA while decreases are likely in the vicinity of Mauritius in JJA. Annual rainfall is likely to increase in the equatorial Pacific, while most models project decreases just east of French Polynesia in DJF.

Since AOGCMs do not have sufficiently fine resolution to see the islands, the projections are given over ocean surfaces rather than over land and very little work has been done in downscaling these projections to individual islands. Assessments are also difficult because some climatic processes are still not well understood, such as the midsummer drought in the Caribbean and the ocean-atmosphere interaction in the Indian Ocean. Furthermore, there is insufficient information on future SST changes to determine the regional distribution of cyclone changes. Large deviations among models make the regional distribution of sea level rise uncertain and the number of models addressing storm surges is very limited.

11.9.1 Key Processes

Climate change scenarios for small islands of the Caribbean Sea, Indian Ocean and Pacific Ocean are included in the AR4 for a number of reasons. Ocean-atmosphere interactions play a major role in determining the climate of the islands and including their climate in the projections for neighbours with larger landmasses would miss features peculiar to the islands themselves. Many small islands are sufficiently removed from large landmasses so that atmospheric circulation may be different over the smaller islands compared to their larger neighbours (e.g., in the Pacific Ocean). For the Caribbean, which is close to large landmasses in Central America and northern South America, some islands partly share climate features of one, while others partly share features of the other. At the same time, the Caribbean islands share many common features that are more important than are those shared with the larger landmasses, such as the strong relationship of their climate to SST.

11.9.1.1 Caribbean

The Caribbean region spans roughly the area between 10°N to 25°N and 85°W to 60°W. Its climate can be broadly characterised as dry winter/wet summer with orography and elevation being significant modifiers at the sub-regional scale (Taylor and Alfero, 2005). The dominant synoptic influence is the North Atlantic subtropical high (NAH). During the winter, the NAH is southernmost and the region is generally at its driest. With the onset of the spring, the NAH moves northward, the trade wind intensity decreases and the equatorial flank of the NAH becomes convergent. Concurrently, easterly waves traverse the Atlantic from the coast of Africa into the Caribbean. These waves frequently mature into storms and hurricanes under warm SSTs and low vertical wind shear, generally within a 10°N to 20°N latitudinal band. They represent the primary rainfall source and their onset in June and demise in November roughly coincide with the mean Caribbean rainy season. In the coastal zones of Venezuela and Columbia, the wet season occurs later, from October to January (Martis et al., 2002). Interannual variability of the rainfall is influenced mainly by ENSO events through their effect on SSTs in the Atlantic and Caribbean Basins. The late rainfall season tends to be drier in El Niño years and wetter in La Niña years (Giannini et al., 2000, Martis et al., 2002, M. Taylor et al., 2002) and tropical cyclone activity diminishes over the Caribbean during El Niño summers (Gray, 1984). However, the early rainfall season in the central and southern Caribbean tends to be wetter in the year after an El Niño and drier in a La Niña year (Chen and Taylor, 2002). The phase of the NAO modulates the behaviour of warm ENSO events (Giannini et al., 2001). A positive NAO phase implies a stronger than normal NAH and amplifies the drying during a warm ENSO. On the other hand, a negative NAO phase amplifies the precipitation in the early rainfall season in the year after an El Niño.

11.9.1.2 Indian Ocean

The Indian Ocean region refers to the area between 35°S to 17.5°N and 50°E to 100°E. The climate of the region is influenced primarily by the Asian monsoons (see Section 11.4.1 for processes influencing monsoons). During January, the ITCZ is located primarily in the SH. The region north of the ITCZ then experiences north-easterly trade winds (northeast monsoons) and the region to the south, the south-easterly trades. During northern summer, the ITCZ is located in the north and virtually covers the entire Bay of Bengal, the surrounding lands and the eastern Arabian Sea. The winds in the north turn into strong south-westerlies (southwest monsoons), while the south-easterlies persist in the south. Precipitation and wind stress bring about a response that is distinctly different in the northern and southern parts of the Indian Ocean (International CLIVAR Project Office, 2006). The wet (dry) season in the Maldives occurs during the southwest (northeast) monsoons. From May to October, the southeast trades dominate in the Seychelles and the climate is relatively cool and dry, and December to March is the principal wet season with winds mainly from west to northwest.

While the monsoons recur each year, their irregularity at a range of time scales from weeks to years depends on feedback from the ocean in ways that are not fully understood. Intra-seasonal variability is associated with the Monsoon Intra-Seasonal Oscillation (MISO) and the Madden-Julian Oscillation (MJO), which are long-lasting weather patterns that evolve in a systematic way for periods of four to eight weeks. On an interannual and decadal scale, statistical methods have shown that while there are periods of high correlation between ENSO and monsoon variation, there are decades where there appears to be little or no association (International CLIVAR Project Office, 2006; see also Section 10.3.5.4). A modulating factor is the Indian Ocean Dipole or Indian Ocean Zonal Mode (IOZM), a large interannual variation in zonal SST gradient (see Section 3.6). The magnitude of the secondary rainfall maximum from October to December in East Africa is strongly correlated with IOZM events, and the positive phase of IOZM, with higher SSTs in the west, counters the drying effect that ENSO has on monsoon rainfall (Ashok et al., 2001).

11.9.1.3 Pacific

The Pacific region refers to equatorial, tropical and subtropical region of the Pacific in which there is a high density of inhabited small islands. Broadly, it is the region between 20°N and 30°S and 120°E to 120°W. The major climatic processes that play a key role in the climate of this region are the easterly trade winds (both north and south of the equator), the SH high pressure belt, the ITCZ and the South Pacific Convergence Zone (SPCZ; see Vincent, 1994), which extends from the ICTZ near the equator due north of New Zealand south-eastward to at least 21°S, 130°W. The region has a warm, highly maritime climate and rainfall is abundant. The highest rainfall follows the seasonal migration of the ITCZ and SPCZ.

Year-to-year climatic variability in the region is very strongly affected by ENSO events. During El Niño conditions, rainfall increases in the zone northeast of the SPCZ (Vincent, 1994). Tropical cyclones are also a feature of the climate of the region, except within 10 degrees of the equator, and are associated with extreme rainfall, strong winds and storm surge. Many islands in the region are very low lying, but there are also many with strong topographical variations. In the case of the latter, orographic effects on rainfall amount and seasonal distribution can be strong.

11.9.2 Skill of Models in Simulating Present Climate

The ability of the MMD models to simulate present climate in the Caribbean, Indian Ocean and North and South Pacific Ocean is summarised in Supplementary Material Table S11.1. In general, the biases in about half of the temperature simulations are less than 1°C in all seasons, so that the model performances are, on the whole, satisfactory. There are, however, large spreads in precipitation simulations. During the last decade, steady progress has been made in simulating and predicting ENSO using coupled GCMs. However, serious systematic errors in both the simulated mean climate and the natural variability persist (see Section 8.4.7)

11.9.2.1 Caribbean

Simulations of the annual Caribbean temperature in the 20th century (1980–1999) by the MMD models give an average that agrees closely with climatology, differing by less than 0.1°C. The inter-quartile range difference between individual models and climatology ranged from –0.3°C to +0.3°C. Thus, the models have good skill in simulating annual temperature. The average of the MMD simulations of precipitation, however, underestimates the observed precipitation by approximately 30%. The deviations in individual models range from –64 to +20%, a much greater range than the deviations in temperature simulations. Recently the Parallel Climate Model (at T42 resolution – about 3.75 degrees), a fully coupled global climate model, was found to be capable of simulating the main climate features over the Caribbean region (Angeles et al., 2007), but it also underestimated the area average precipitation across the Caribbean. Martinez-Castro et al. (2006), in a sensitivity experiment, conclude that the Regional Climate Model (RegCM3), using the Anthes-Kuo cumulus parametrization scheme, can be used for long-term area-averaged climatology.

11.9.2.2 Indian Ocean

For annual temperature in the Indian Ocean in the 20th century (1980–1999), the mean value of the MMD outputs overestimated the climatology by 0.6°C, with 50% of deviations ranging from 0.2°C to 1.0°C. For rainfall, the multi-model ensemble average was only slightly below the mean precipitation by 3%, and the model deviations ranged from –22 to +20%. There are, however, problems with the simulation of year-to-year variation. Many of the important climatic effects of the MJO, including its impacts on rainfall variability in the monsoons, are still poorly simulated by contemporary climate models (see Section 8.4).

11.9.2.3 Pacific

Climate model simulations of current-climate means of temperature and precipitation were investigated by Jones et al. (2000, 2002) and Lal et al. (2002) for the South Pacific. The AOGCMs available at the time of these studies simulated well the broad-scale patterns of temperature and precipitation across the region, with the precipitation patterns more variable than for temperature in the models considered, and with some significantly underestimating or overestimating of the intensity of rainfall in the high-rainfall zones. All models simulated a broad rainfall maximum stretching across the SPCZ and ITCZ, but not all models resolved a rainfall minimum between these two regions. A problem of simulating the spatial structure of the MJO resulting in tendencies for the convective anomaly to split into double ITCZs in the Pacific is also discussed in Section 8.4.8.

Analysis of the MMD simulations shows that the average model value overestimated the annual mean temperature from 1980 to 1999 by 0.9°C over a southern Pacific region, with 50% of the deviations varying from 0.6°C to 1.2°C. Over the North Pacific, the simulated ensemble average temperature for the same period was only 0.7°C above the climatology, with half of the model deviations from the climatology ranging from 0.2°C to 1.0°C. Average precipitation was overestimated by 10%, but individual model values varied from –7 to 31% in the southern Pacific region, whereas in the northern Pacific the mean model output for precipitation almost agreed with the climatology, while the individual models deviated from –13 to 13%. Thus, the models are better at simulating rainfall in the northern Pacific than in the southern Pacific and the quality of the simulations, both north and south, were not much different from those for the Indian Ocean.

11.9.3 Temperature and Precipitation Projections

Scenarios of temperature change and percentage precipitation change between 1980 to 1999 and 2080 to 2099 are summarised in Table 11.1 (described in Section 11.1.3). A small value of T implies a large signal-to-noise ratio and it can be seen that, in general, the signal-to-noise ratio is greater for temperature than for precipitation change. The probability of extreme warm seasons is 100% in all cases for the small islands and the scenarios of warming are all very significant by the end of the century. Approximate results for the A2 and B1 scenarios and for other future times in this century can obtained by scaling the A1B values, as described in Section 11.1.3.

The temporal evolution of temperature as simulated by the MMD models for the 20th and 21st centuries is also shown in Figure 11.22 for oceanic regions including the Caribbean (CAR), Indian Ocean (IND), North Pacific Ocean (NPA) and South

Pacific Ocean (SPA). In general, it can be seen, by comparison with Box 11.1, Figure 1, that the temperature increases for the small islands are less than for the continental regions. The almost linear nature of the evolution is also apparent in the figure. Temperature and precipitation projections for the small island regions are discussed below in the context of Table 11.1.

11.9.3.1 Caribbean

The MMD-simulated annual temperature increases at the end of the 21st century range from 1.4°C to 3.2°C with a median of 2.0°C, somewhat below the global average. Fifty percent of the models give values differing from the median by only ±0.4°C. Statistical downscaling of HadCM3 results using the A2 and B2 emission scenarios gives around a 2°C rise in temperature by the 2080s, approximately the same as the HadCM3 model. The agreement between the AOGCMs and the downscaling analysis gives a high level of confidence in the temperature simulations. The downscaling was performed with the use of the Statistical DownScaling Model (SDSM) developed by Wilby et al. (2002) as part of an Assessments of Impacts and Adaptations to Climate Change in Multiple Regions and Sectors (AIACC) Small Island States SIS06 project (http://www.aiaccproject.org). Angeles et al. (2007) also simulate an approximately 1°C rise in SST up to the 2050s using the IS92a scenario. There were no noticeable differences in monthly changes (see Supplementary Material Figure S11.31). Observations suggest that warming is ongoing (Peterson et al., 2002).

According to Table 11.1, most models project decreases in annual precipitation and a few increases, varying from –39 to +11%, with a median of –12%. Figure 11.23 shows that the annual mean decrease is spread across the entire region. In DJF, some areas of increases are noted and in JJA, the region-wide decrease is enhanced, especially in the region of the Greater Antilles, where the model consensus is also strong. Monthly changes in the Caribbean are shown in Supplementary Material Figure S11.32, which also shows that the simulations for the Caribbean have a greater spread compared to the other oceanic regions (IND, NPA and SPA in S11.32). Results from HadCM3 downscaled for the A2 and B2 emission scenarios using the SDSM also show a near-linear decrease in summer precipitation to the 2080s for a station in Jamaica. Downscaled results from the SDSM for stations in Barbados and Trinidad, however, show increases rather than decreases. Thus, there is consensus between the MMD results and the downscaled results for the Greater Antilles in JJA but not for the other islands, and also not on an annual basis. Angeles et al. (2007) also simulate decreases up to the middle of the century in the vicinity of the Greater Antilles but not in the other islands in the late rainfall season. Table 11.1 shows that the decrease in JJA has the largest signal-to-noise ratio. The decrease is in agreement with the expected drying in the subtropics discussed in Sections 9.5 and 11.1. In the multi-model analysis, most models show shift to a more positive phase of the NAO (see Section 10.3), and consensus on temperature changes in the Pacific indicates an El Niño-like pattern with higher temperatures in the eastern Pacific (see Section 10.3). These conditions are associated with drying in the Caribbean. Observed trends in precipitation are unclear. While Peterson et al. (2002) find no statistically significant trends in mean precipitation amounts from the 1950s to 2000, Neelin et al. (2006) note a modest but statistically significant summer drying trend over recent decades in the Caribbean in several observational data sets.

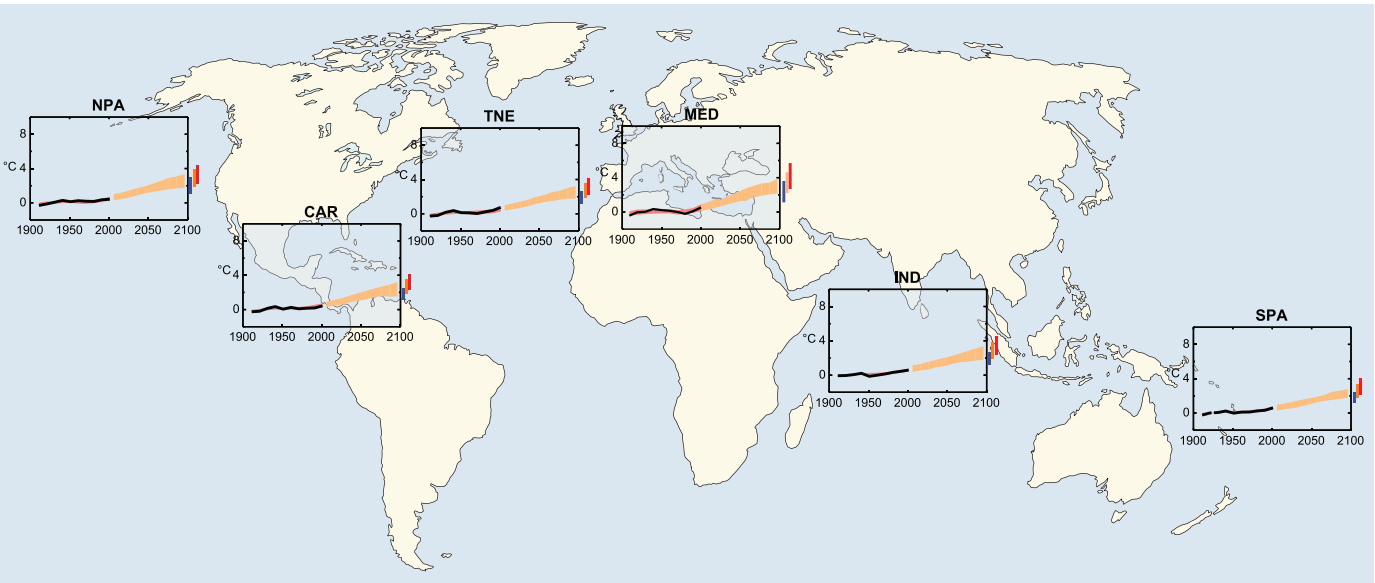


Figure 11.22. *Temperature anomalies with respect to 1901 to 1950 for six oceanic regions for 1906 to 2005 (black line) and as simulated (red envelope) by MMD models incorporating known forcings; and as projected for 2001 to 2100 by MMD models for the A1B scenario (orange envelope). The bars at the end of the orange envelope represent the range of projected changes for 2091 to 2100 for the B1 scenario (blue), the A1B scenario (orange) and the A2 scenario (red). The black line is dashed where observations are present for less than 50% of the area in the decade concerned. More details on the construction of these figures are given in Box 11.1 and Section 11.1.2.*

11.9.3.2 Indian Ocean

Based on the MMD ensemble mean the annual temperature is projected to increase by about 2.1°C, somewhat below the global average, with individual models ranging from 1.4°C to 3.7°C and at least half of the models giving values quite close to the mean. All models show temperature increases in all months with no significant seasonal variation (Supplementary Material Figure S11.31). Evidence of temperature increases from 1961 to 1990 in the Seychelles is provided by Easterling et al. (2003), who find that the percentage of time when the minimum temperature is below the 10th percentile is decreasing, and the percentage of time where the minimum temperature exceeds the 90th percentile is increasing. Similar results were obtained for the maximum temperatures. This is consistent with general patterns of warming elsewhere (see Chapter 3).

The annual precipitation changes projected by individual MMD models varied from –2 to 20% with a median of 4% and 50% of the models projecting changes between 3 and 5%. Thus, there is some level of confidence in the precipitation results although not as high as for temperature. Figure 11.24 shows that the annual increase is restricted mainly to the north Indian Ocean, where the model consensus is greatest, especially in the vicinity of the Maldives. In DJF, some increases are noted in the south. Model agreement on increases is greatest for the Seychelles in DJF and for the Maldives in JJA. There is also strong agreement on decreases in the vicinity of Mauritius in JJA. Sections 10.3.5 and 11.4 discuss changes in monsoon behaviour in a warmer climate. There is an emerging consensus that the effect of enhanced moisture convergence in a warmer atmosphere will dominate over possible weaker monsoonal flows and tropical large-scale circulation in global warming simulations, resulting in increased monsoonal precipitation. Easterling et al. (2003) find evidence that extreme rainfall tended to increase from 1961 to 1990 (see also Section 11.4.3, South Asia projections).

11.9.3.3 Pacific

Projected regional temperature changes in the South Pacific from a range of AOGCMs have been prepared by Lal et al. (2002), Lal (2004) and Ruosteenoja et al. (2003). Jones et al. (2000, 2002) and Whetton and Suppiah (2003) also consider patterns of change. Broadly, simulated warming in the South Pacific closely follows the global average warming rate. However, there is a tendency in many models for the warming to be a little stronger in the central equatorial Pacific (North Polynesia) and a little weaker to the south (South Polynesia).

The MMD-A1B projections for the period 2080 to 2099 show an increase in annual temperature of 1.8°C, somewhat below the global average over the South Pacific (Table 11.1). The individual model values vary from 1.4°C to 3.1°C and at least half of the models project values very close to the mean. All models show increases, slightly less in the second half of

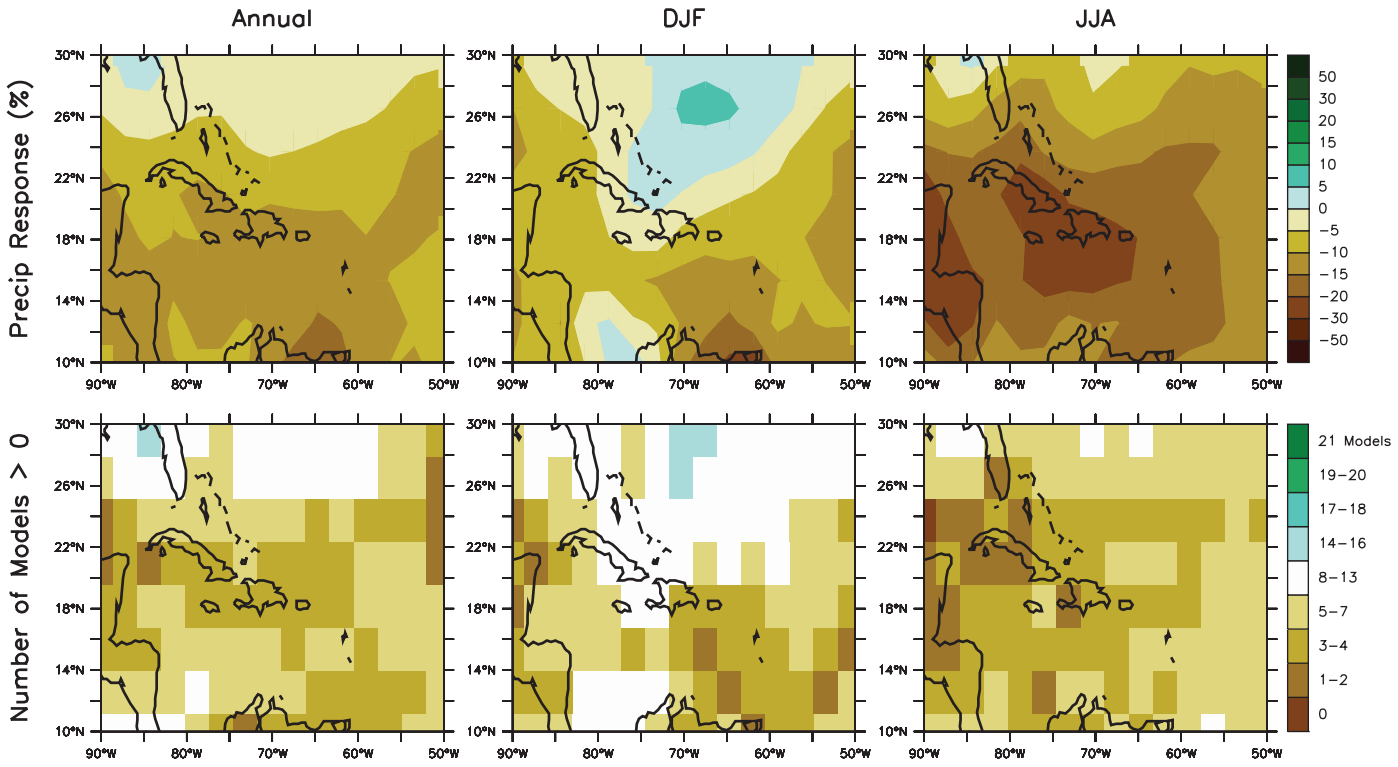


Figure 11.23. *Precipitation changes over the Caribbean from the MMD-A1B simulations. Top row: Annual mean, DJF and JJA fractional precipitation change between 1980 to 1999 and 2080 to 2099, averaged over 21 models. Bottom row: number of models out of 21 that project increases in precipitation.*

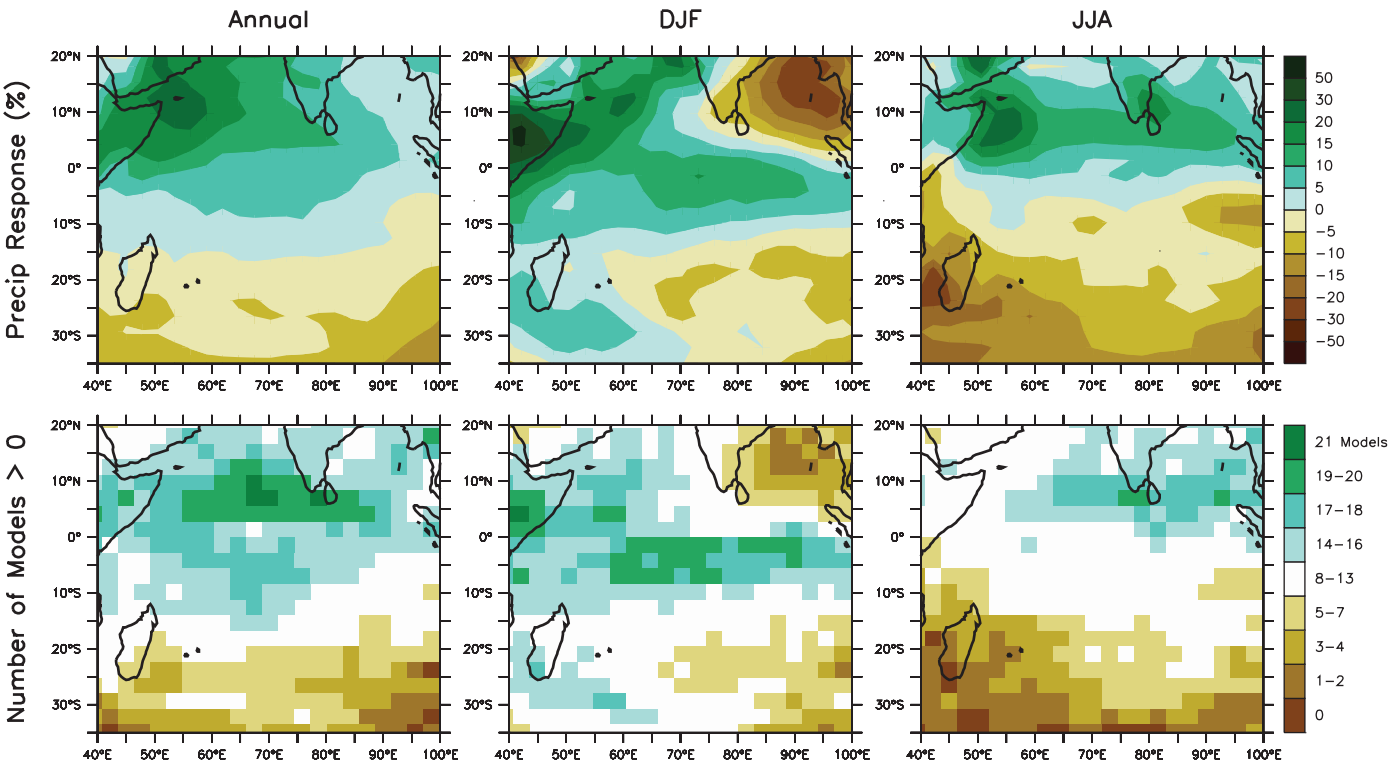


Figure 11.24. *As for Figure 11.23 but for the Indian Ocean.*

the year compared to the first (Supplementary Material Figure S11.31). Over the North Pacific, the models simulate an increase in temperature of 2.3°C, slightly below the global average, with values ranging from 1.5°C to 3.7°C and 50% of the models within ±0.4°C of the mean. All models show increases, more in the second half of the year compared to the first (Supplementary Material Figure S11.31).

For the same period, 2080 to 2099, annual precipitation increases over the southern Pacific when averaged over all MMD models are close to 3%, with individual models projecting values from –4 to +11% and 50% of the models showing increases between 3 and 6%. The time to reach a discernible signal is relatively short. (Table 11.1). Most of these increases were in the first half of the year (Supplementary Material Figure S11.32). For precipitation in the northern Pacific, an increase of 5% is found, with individual models projecting values from 0 to 19% and at least half of the models within –2 to +5% of the median. The time to reach a discernible signal is relatively long. Most of these increases were in the latter half of the year (Supplementary Material Figure S11.32). Figure 11.25 illustrates the spatial distribution of annual, DJF and JJA rainfall changes and inter-model consistency. The figure shows that the tendency for precipitation increase in the Pacific is strongest in the region of the ITCZ due to increased moisture transport described in Section 11.1.3.1. Griffiths et al. (2003) find an increasing trend from 1961 to 2000 in mean rainfall in and northeast of the SPCZ in the southern Pacific. As for the Indian Ocean, there is some level of confidence in the precipitation results for the Pacific, but not as high as for the temperature results.

Changes in rainfall variability in the South Pacific were analysed by Jones et al. (2000) using IPCC (1996) scenarios, but more recent simulations have not been examined. These changes will be strongly driven by changes in ENSO, and this is not well understood (see Section 10.3).

11.9.4 Sea Level Rise

Sea level is projected to rise between the present (1980–1999) and the end of this century (2090–2099) by 0.35 m (0.23 to 0.47 m) for the A1B scenario (see Section 10.6). Due to ocean density and circulation changes, the distribution will not be uniform and Figure 10.32 shows a distribution of local sea level change based on ensemble mean of 14 AOGCMs. A lower-than-average rise in the Southern Ocean can be seen, possibly due to increased wind stress. Also obvious is a narrow band of pronounced sea level rise stretching across the southern Atlantic and Indian Oceans at about 40°S. This is also seen in the southern Pacific at about 30°S. However, large deviations among models make estimates of distribution across the Caribbean, Indian and Pacific Oceans uncertain. Extreme sea level changes, including storm surges, are discussed in Box 11.5 in a broader context. The range of uncertainty cannot be reliably quantified due to the limited set of models addressing the problem.

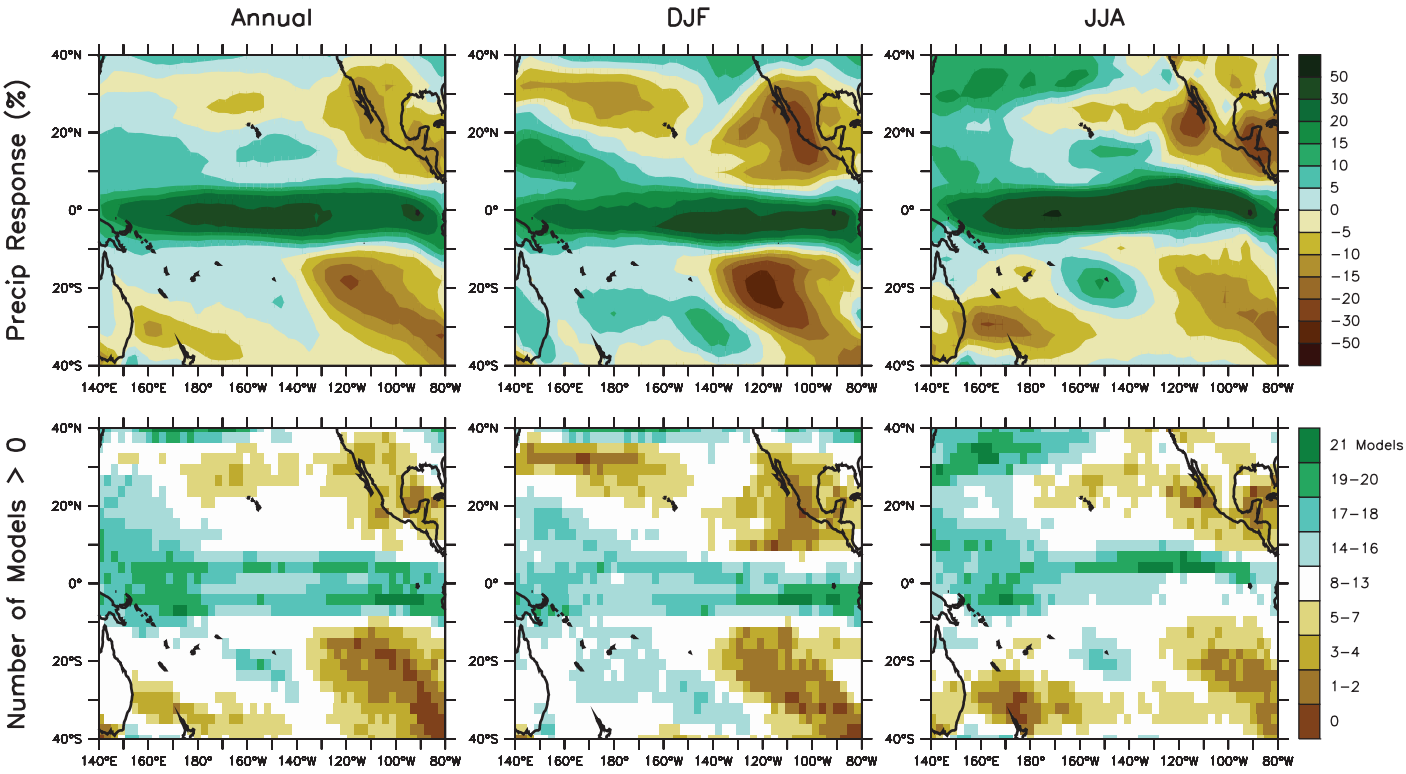


Figure 11.25. *As for Figure 11.23 but for the northern and southern Pacific Ocean.*

Global sea level rise over the 20th century is discussed in Section 5.5; the best estimate is 0.17 ± 0.05 m. From estimates of observed sea level rise from 1950 to 2000 by Church et al. (2004), the rise in the Caribbean appeared to be near the global mean. Church et al. (2006) also estimate the average rise in the region of the Indian and Pacific Ocean to be close to the global average. There have been large observed variations in sea level rise in the Pacific Ocean mainly due to ocean circulation changes associated with ENSO events. From 1993 to 2001, all the data show large rates of sea level rise over the western Pacific and eastern Indian Ocean and sea level falls in the eastern Pacific and western Indian Ocean (Church et al., 2006). Observed sea level rise in the Pacific and Indian Oceans is discussed in Chapter 5.

11.9.5 Tropical Cyclones

Fewer models have simulated tropical cyclones in the context of climate change than those simulating temperature and precipitation changes and sea level rise, mainly because of the computational burden associated with the high resolution needed to capture the characteristics of tropical cyclones. Accordingly, there is less certainty about the changes in frequency and intensity of tropical cyclones on a regional basis than for temperature and precipitation changes. An assessment of results for projected changes in tropical cyclones is presented in Section 10.3.6.3, and a synthesis is given at the end of the section. Regional model-based studies of changes in tropical cyclone behaviour in the southwest Pacific include works by Nguyen and Walsh (2001) and Walsh (2004). Walsh concludes that in general there is no clear picture with respect to regional changes in frequency and movement, but increases in intensity are indicated. It should also be noted that ENSO fluctuations have a strong impact on patterns of tropical cyclone occurrence in the southern Pacific, and that therefore uncertainty with respect to future ENSO behaviour (see Section 10.3) contributes to uncertainty with respect to tropical cyclone behaviour (Walsh, 2004).

Box 11.5: Coastal Zone Climate Change

Introduction

Climate change has the potential to interact with the coastal zone in a number of ways including inundation, erosion and salt water intrusion into the water table. Inundation and intrusion will clearly be affected by the relatively slow increases in mean sea level over the next century and beyond. Mean sea level is addressed in Chapter 10; this box concentrates on changes in extreme sea level that have the potential to significantly affect the coastal zone. There is insufficient information on changes in waves or near-coastal currents to provide an assessment of the effects of climate change on erosion.

The characteristics of extreme sea level events are dependent on the atmospheric storm intensity and movement and coastal geometry. In many locations, the risk of extreme sea levels is poorly defined under current climate conditions because of sparse tide gauge networks and relatively short temporal records. This gives a poor baseline for assessing future changes and detecting changes in observed records. Using results from 141 sites worldwide for the last four decades, Woodworth and Blackman (2004) find that at some locations extreme sea levels have increased and that the relative contribution from changes in mean sea level and atmospheric storminess depends on location.

Methods of simulating extreme sea levels

Climate-driven changes in extreme sea level will come about because of the increases in mean sea level and changes in the track, frequency or intensity of atmospheric storms. (From the perspective of coastal flooding, the vertical movement of land, for instance due to post glacial rebound, is also important when considering the contribution from mean sea level change.) To provide the large-scale context for these changes, global climate models are required, although their resolution (typically 150 to 300 km horizontally) is too coarse to represent the details of tropical cyclones or even the extreme winds associated with mid-latitude cyclones. However, some studies have used global climate model forcing to drive storm surge models in order to provide estimates of changes in extreme sea level (e.g., Flather and Williams, 2000). To obtain more realistic simulations from the large-scale drivers, three approaches are used: dynamical and statistical downscaling and a stochastic method (see Section 11.10 for general details).

As few RCMs currently have an ocean component, these are used to provide high-resolution (typically 25 to 50 km horizontally) surface winds and pressure to drive a storm surge model (e.g., Lowe et al., 2001). This sequence of one-way coupled models is usually carried out for a present-day (Debenard et al., 2003) or historical baseline (e.g., Flather et al., 1998) and a period in the future (e.g., Lowe et al., 2001; Debenard et al., 2003). In the statistical approach, relationships between large-scale synoptic conditions and local extreme sea levels are constructed. These relationships can be developed either by using analyses from weather prediction models and observed extreme sea levels, or by using global climate models and present-day simulations of extreme water level generated using the dynamic methods described above. Simulations of future extreme sea level are then derived from applying the statistical relationships to the future large-scale atmospheric synoptic conditions simulated by a global climate model (e.g., von Storch and Reichardt, 1997). The statistical and dynamical approach can be combined, using a statistical model to produce the high-resolution wind fields forcing the wave and storm surge dynamical models (Lionello et al., 2003). Similarly, the stochastic sampling method identifies the key characteristics of synoptic weather events responsible for extreme sea levels (intensity and movement) and represents these by frequency distributions. For each event, simple models are used to generate the surface wind and pressure fields and these are applied to the storm surge model (e.g., Hubbert and McInnes, 1999). Modifications to the frequency distributions of the weather events to represent changes under enhanced greenhouse conditions are derived from global climate models and then used to infer a future storm surge climatology.

Extreme sea level changes – sample projections from three regions

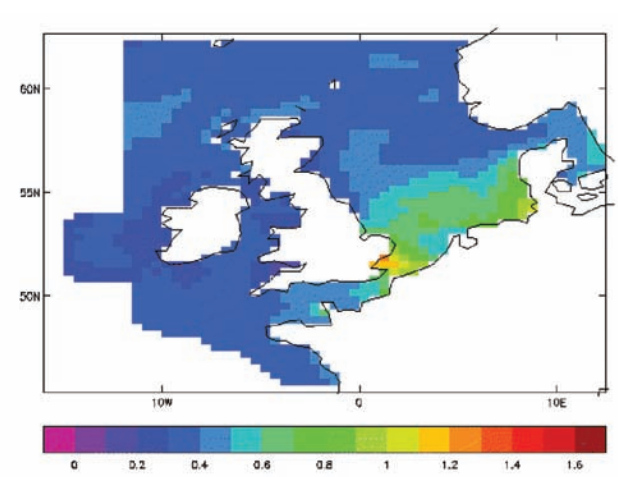
1. Australia

In a study of storm surge impacts in northern Australia, a region with only a few short sea level records, McInnes et al. (2005) used stochastic sampling and dynamical modelling to investigate the implications of climate change on extreme storm surges and inundation. Cyclones occurring in the Cairns region from 1907 to 1997 were used to develop probability distribution functions governing the cyclone characteristics of speed and direction with an extreme value distribution fitted to the cyclone intensity. Cyclone intensity distribution was then modified for enhanced greenhouse conditions based on Walsh and Ryan (2000), in which cyclones off northeast Australia were found to increase in intensity by about 10%. No changes were imposed upon cyclone frequency or direction since no reliable information is available on the future behaviour of the main influences on these, respectively ENSO or mid-level winds. Analysis of the surges resulting from 1,000 randomly selected cyclones with current and future intensities shows that the increased intensity leads to an increase in the height of the 1-in-100 year event from 2.6 m to 2.9 m with the 1-in-100 year event becoming the 1-in-70 year event. This also results in the areal extent of inundation more than doubling (from approximately 32 to 71 km^2). Similar increases for Cairns and other coastal locations were found by Hardy et al. (2004). *(continued)*

2. Europe

Several dynamically downscaled projections of climate-driven changes in extreme water levels in the European shelf region have been carried out. Woth (2005) explored the effect of two different GCMs and their projected climates changes due to two different emissions scenarios (SRES A2 and B2) on storm surges along the North Sea coast. She used data from one RCM downscaling the four GCM simulations (Woth et al., 2006) (using data from four RCMs driven by one GCM produced indistinguishable results) and demonstrates significant increases in the top 1% of events (10 to 20 cm above average sea level change) over the continental European North Sea coast. The changes projected by the different experiments were statistically indistinguishable, although those from the models incorporating the A2 emissions scenario were consistently larger. When including the effects of global mean sea level rise and vertical land movements, Lowe and Gregory (2005) find that increases in extreme sea level are projected for the entire UK coastline, using a storm surge model driven by one of the RCMs analysed by Woth et al. (2006) (Box 11.5, Figure 1). Using a Baltic Sea model driven by data from four RCM simulations, Meier (2006) finds that the changes in storm surges vary strongly between the simulations but with some tendency for larger increases in the 100-year surges than in the mean sea level.

Lionello et al. (2003) estimate the effect of atmospheric CO_2 doubling on the frequency and intensity of high wind waves and storm surge events in the Adriatic Sea. The regional surface wind fields were derived from the sea level pressure field in a 30-year long ECHAM4 high-resolution (about 1.5 degrees) time slice experiment by statistical downscaling and then used to force a wave and an ocean model. They find no statistically significant changes in the extreme surge level and a decrease in the extreme wave height with increased atmospheric CO_2. An underestimation of the observed wave heights and surge levels calls for caution in the interpretation of these results. Using AOGCM projections, X.L. Wang et al. (2004) infer an increase in winter and autumn seasonal mean and extreme wave heights in the northeast and southwest North Atlantic, but a decrease in the mid-latitudes of the North Atlantic. Not all changes were significant and in some regions (e.g., the North Sea), their sign was found to depend on the emissions scenario.



Box 11.5, Figure 1. *The change with respect to 1961-1990 in the 50-year return period extreme water level (m) in the North Sea due to changes in atmospheric storminess, mean sea level and vertical land movements for the period 2071 to 2100 under the A2 scenario (from Lowe and Gregory, 2005).*

3. Bay of Bengal

Several dynamic simulations of storm surges have been carried out for the region but these have often involved using results from a small set of historical storms with simple adjustments (such as adding on a mean sea level or increasing wind speeds by 10%) to account for future climate change (e.g., Flather and Khandker, 1993). This technique has the disadvantage that by taking a relatively small and potentially biased set of storms it may lead to a biased distribution of water levels with an unrealistic count of extreme events. In one study using dynamical models driven by RCM simulations of current and future climates, Unnikrishnan et al. (2006) show that despite no significant change in the frequency of cyclones there are large increases in the frequency of the highest storm surges.

Uncertainty

Changes in storm surges and wave heights have been addressed for only a limited set of models. Thus, we cannot reliably quantify the range of uncertainty in estimates of future coastal flooding and can only make crude estimates of the minimum values (Lowe and Gregory, 2005). There is some evidence that the dynamical downscaling step in providing data for storm surge modelling is robust (i.e., does not add to the uncertainty). However, the general low level of confidence in projected circulation changes from AOGCMs implies a substantial uncertainty in these projections.

11.10 Assessment of Regional Climate Projection Methods

The assessment of methods recognises the challenges posed by the complex interactions that occur at many spatial and temporal scales, involving the general circulation, cross-scale feedbacks and regional-scale forcing.

11.10.1 Methods for Generating Regional Climate Information

Atmosphere-Ocean General Circulation Models constitute the primary tool for capturing the global climate system behaviour. They are used to investigate the processes responsible for maintaining the general circulation and its natural and forced variability (Chapter 8), to assess the role of various forcing factors in observed climate change (Chapter 9) and to provide projections of the response of the system to scenarios of future external forcing (Chapter 10). As AOGCMs seek to represent the whole climate system, clearly they provide information on regional climate and climate change and relevant processes directly. For example, the skill in simulating the climate of the last century when accounting for all known forcings demonstrates the causes of recent climate change (Chapter 9) and this information can be used to constrain the likelihood of future regional climate change (Stott et al., 2006; see also Section 11.10.2). AOGCM projections provide plausible future regional climate scenarios, although methods to establish the reliability of the regional AOGCM scales have yet to mature. The spread within an ensemble of AOGCMs is often used to characterise the uncertainty in projected future climate changes. Some regional responses are consistent across AOGCM simulations, although for other regions the spread remains large (see Sections 11.2 to 11.9).

Because of their significant complexity and the need to provide multi-century integrations, horizontal resolutions of the atmospheric components of the AOGCMs in the MMD range from 400 to 125 km. Generating information below the grid scale of AOGCMs is referred to as downscaling. There are two main approaches, dynamical and statistical. Dynamical downscaling uses high-resolution climate models to represent global or regional sub-domains, and uses either observed or lower-resolution AOGCM data as their boundary conditions. Dynamical downscaling has the potential for capturing mesoscale nonlinear effects and providing coherent information among multiple climate variables. These models are formulated using physical principles and they can credibly reproduce a broad range of climates around the world, which increases confidence in their ability to downscale realistically future climates. The main drawbacks of dynamical models are their computational cost and that in future climates the parametrization schemes they use to represent sub-grid scale processes may be operating outside the range for which they were designed.

Empirical SD methods use cross-scale relationships that have been derived from observed data, and apply these to climate model data. Statistical downscaling methods have the advantage of being computationally inexpensive, able to access finer scales than dynamical methods and applicable to parameters that cannot be directly obtained from the RCM outputs. They require observational data at the desired scale for a long enough period to allow the method to be well trained and validated. The main drawbacks of SD methods are that they assume that the derived cross-scale relationships remain stable when the climate is perturbed, they cannot effectively accommodate regional feedbacks and, in some methods, can lack coherency among multiple climate variables.

11.10.1.1 High-Resolution Atmosphere-Only GCMs

Atmosphere-only GCMs (AGCMs) include interactive land surface schemes as in an AOGCM but require information on SST and sea ice as a lower boundary condition. Given the short time scales associated with the atmosphere and land surface components compared to those in the ocean, relatively short time slices (a few decades) can be run at high resolution. The SST and sea ice information required can be derived from observations or AOGCMs. The use of observations can improve simulations of current climate but combining these with AOGCM-derived changes for the future climate (e.g., Rowell, 2005) increases the risk of inconsistency in the projected climate. The absence of two-way feedback between the atmosphere and ocean in AGCMs can cause a significant distortion of the climatic variability (Bretherton and Battisti, 2000), as documented over regions such as the Indian Ocean and the South Asian monsoon (Douville, 2005; Inatsu and Kimoto, 2005). The large-scale climate responses of AGCMs and AOGCMs appear to be similar in many regions; when and where they differ, the consistency of the oceanic surface boundary condition may be questioned (May and Roeckner, 2001; Govindasamy et al., 2003). Further research is required to determine if the similarity is sufficient for the time-slice approach with AGCMs to be considered a robust downscaling technique.

Model grids of 100 km and finer have become feasible and 50 km will likely be the norm in the near future (Bengtsson, 1996; May and Roeckner, 2001; Déqué and Gibelin, 2002; Govindaswamy, 2003). High-performance computer systems now allow global computations at 20 km (e.g., May, 2004a; Mizuta et al., 2006), although for short time slices only. Evaluated on the scale typical of current AOGCMs, nearly all quantities simulated by high-resolution AGCMs agree better with observations, but the improvements vary significantly for different regions (Duffy et al., 2003) and specific variables, and extensive recalibration of parametrizations is often required. Notable improvements occur in orographic precipitation and dynamics of mid-latitude weather systems (see Chapter 10). The highest resolution offers the prospect of credible simulations of the climatology of tropical cyclones (e.g., May, 2004a; Mizuta et al., 2006). Coordinated multi-model experiments are needed,

however, to optimise the value of these high-resolution studies for general assessment.

An alternative to uniform high-resolution AGCMs is Variable-Resolution AGCMs (VRGCMs; e.g., Déqué and Piedelievre, 1995; Krinner et al., 1997; Fox-Rabinovitz et al., 2001; McGregor et al., 2002; Gibelin and Déqué, 2003). The VRGCM approach is attractive as it permits, within a unified modelling framework, a regional increase in resolution while retaining the interaction of all regions of the atmosphere. Numerical artefacts due to stretching have been shown to be small when using modest stretching factors (e.g., Lorant and Royer, 2001). The results from VRGCMs capture, over the high-resolution region, finer-scale details than uniform-resolution models while retaining global skill similar to uniform-resolution simulations with the same number of grid points.

11.10.1.2 Nested Regional Climate Models

The principle behind nested modelling is that, consistent with the large-scale atmospheric circulation, realistic regional climate information can be generated by integrating an RCM if the following premises are satisfied: time-varying large-scale atmospheric fields (winds, temperature and moisture) are supplied as lateral boundary conditions (LBCs) and SST and sea ice as lower boundary conditions; the control from the LBCs keeps the interior solution of the RCM consistent with the driving atmospheric circulation; and sub-grid scale physical processes are suitably parametrized, including fine-scale surface forcing such as orography, land-sea contrast and land use.

A typical RCM grid for climate change projections is around 50 km, although some climate simulations have been performed using grids of 15 or 20 km (e.g., Leung et al., 2003, 2004; Christensen and Christensen, 2004; Kleinn et al., 2005). Recently, projections of climate changes for East Asia were completed with a 5-km non-hydrostatic RCM (Kanada et al., 2005; Yoshizaki et al., 2005; Yasunaga et al., 2006), but only for short simulations. Following the trend in global modelling, RCMs are increasingly coupled interactively with other components of the climate system, such as regional ocean and sea ice (e.g., Bailey and Lynch 2000; Döscher et al., 2002; Rinke et al., 2003; Bailey et al., 2004; Meier et al., 2004; Sasaki et al., 2006a), hydrology, and with interactive vegetation (Gao and Yu, 1998; Xue et al., 2000).

Multi-decadal RCM experiments are becoming standard (e.g., Whetton et al., 2000; Kwon et al., 2003; Leung et al., 2004; Kjellström et al., 2007; Plummer et al., 2006), including the use of ensembles (Christensen et al., 2002), enabling a more thorough validation and exploration of projected changes. In multi-year ensemble simulations driven by reanalyses of atmospheric observations, Vidale et al. (2003) show that RCMs have skill in reproducing interannual variability in precipitation and surface air temperature. The use of ensemble simulations has enabled quantitative estimates regarding the sources of uncertainty in projections of regional climate changes (Rowell, 2005; Déqué et al., 2005, 2007; Beniston et al., 2007; Frei et al., 2006; Graham et al., 2007). Combining information from four RCM simulations, Christensen et al. (2001) and Rummukainen et al. (2003) demonstrate that it is feasible to explore not only uncertainties related to projections in the mean climate state, but also for higher-order statistics.

The difficulties associated with the implementation of LBCs in nested models are well documented (e.g., Davies, 1976; Warner et al., 1997). As time progresses in a climate simulation, the RCM solution gradually turns from an initial-value problem more into a boundary value problem. The mathematical interpretation is that nested models represent a fundamentally ill-posed boundary value problem (Staniforth, 1997; Laprise, 2003). The control exerted by LBCs on the internal solution generated by RCMs appears to vary with the size of the computational domain (e.g., Rinke and Dethloff, 2000), as well as location and season (e.g., Caya and Biner, 2004). In some applications, the flow developing within the RCM domain may become inconsistent with the driving LBC. This may (Jones et al., 1997) or may not (Caya and Biner, 2004) affect climate statistics. Normally, RCMs are only driven by LBCs with high time resolution to capture the temporal variations of large-scale flow. Some RCMs also use nudging or relaxation of large scales in the interior of the domain (e.g., Kida et al., 1991; Biner et al., 2000; von Storch et al., 2000). This has proved useful to minimise the distortion of the large scales in RCMs (von Storch et al., 2000; Mabuchi et al., 2002; Miguez-Macho et al., 2004), although it can also hide model biases. One-way RCM-GCM coupling is mostly used, although recently a two-way nested RCM has been developed (Lorenz and Jacob, 2005) thus achieving interaction with the global atmosphere as with variable-resolution AGCMs.

The ability of RCMs to simulate the regional climate depends strongly on the realism of the large-scale circulation that is provided by the LBCs (e.g., Pan et al., 2001). Latif et al. (2001) and Davey et al. (2002) show that strong biases in the tropical climatology of AOGCMs can negatively affect downscaling studies for several regions of the world. Nonetheless, the reliability of nested models, that is, their ability to generate meaningful fine-scale structures that are absent in the LBCs, is clear. A number of studies have shown that the climate statistics of atmospheric small scales can be re-created with the right amplitude and spatial distribution, even if these small scales are absent in the LBCs (Denis et al., 2002, 2003; Antic et al., 2005; Dimitrijevic and Laprise, 2005). This implies that RCMs can add value at small scales to climate statistics when driven by AOGCMs with accurate large scales. Overall, the skill at simulating current climate has improved with the MMD AOGCMs (Chapter 8), which will lead to higher quality LBCs for RCMs.

11.10.1.3 Empirical and Statistical Downscaling Methods

A complementary technique to RCMs is to use derived relationships linking large-scale atmospheric variables (predictors) and local/regional climate variables (predictands).

The local/regional-scale climate change information is then obtained by applying the relationships to equivalent predictors from AOGCM simulations. The guidance document (Wilby et al., 2004) from the IPCC Task Group on Data and Scenario Support for Impact and Climate Analysis (TGICA) provides a comprehensive background on this approach and covers important issues in using SD applications. Statistical downscaling methods cover regression-type models including both linear and nonlinear relationships, unconditional or conditional weather generators for generating synthetic sequences of local variables, techniques based on weather classification that draw on the more skilful attributes of models to simulate circulation patterns, and analogue methods that seek equivalent weather states from the historical record; a combination of these techniques possibly being most appropriate. An extension to SD is the statistical-dynamical downscaling technique (e.g., Fuentes and Heimann, 2000), which combines weather classification with RCM simulations. A further development is the application of SD to high-resolution climate model output (Lionello et al., 2003; Imbert and Benestad, 2005).

Research on SD has shown an extensive growth in application, and includes an increased availability of generic tools for the impact community (e.g., SDSM, Wilby et al., 2002; the clim.pact package, Benestad, 2004b; the pyclimate package, Fernández and Sáenz, 2003); applications in new regions (e.g., Asia, Chen and Chen, 2003); the use of techniques to address exotic variables such as phenological series (Matulla et al., 2003), extreme heat-related mortality (Hayhoe et al., 2004), ski season (Scott et al., 2003), land use (Solecki and Oliveri, 2004), streamflow or aquatic ecosystems (Cannon and Whitfield, 2002; Blenckner and Chen, 2003); the treatment of climate extremes (e.g., Katz et al., 2002; Seem, 2004; X.L. Wang et al., 2004; Caires et al., 2006); intercomparison studies evaluating methods (e.g., STAtistical and Regional dynamical Downscaling of EXtremes for European regions (STARDEX), Haylock et al., 2006; Schmidli et al., 2006); application to multi-model and multi-ensemble simulations in order to express model uncertainty alongside other key uncertainties (e.g., Benestad, 2002a,b; Hewitson and Crane, 2006; Wang and Swail, 2006b); assessing non-stationarity in climate relationships (Hewitson and Crane, 2006); and spatial interpolation using geographical dependencies (Benestad, 2005). In some cases SD methods have been used to project statistical attributes instead of raw values of the predictand, for example, the probability of rainfall occurrence, precipitation, wind or wave height distribution parameters and extreme event frequency (e.g., Beckmann and Buishand, 2002; Buishand et al., 2004; Busuioc and von Storch, 2003; Abaurrea and Asin, 2005; Diaz-Nieto and Wilby, 2005; Pryor et al., 2005a,b; Wang and Swail, 2006a,b).

Evaluation of SD is done most commonly through cross-validation with observational data for a period that represents an independent or different 'climate regime' (e.g., Busuioc et al. 2001; Trigo and Palutikof, 2001; Bartman et al., 2003; Hanssen-Bauer et al., 2003). Stationarity, that is, whether the statistical relationships are valid under future climate regimes, remains a concern with SD methods. This is only weakly assessed through cross-validation tests because future changes in climate are likely to be substantially larger than observed historical changes. This issue was assessed in Hewitson and Crane (2006) where, within the SD method used, the non-stationarity was shown to result in an underestimation of the magnitude of the change. In general, the most effective SD methods are those that combine elements of deterministic transfer functions and stochastic components (e.g., Hansen and Mavromatis, 2001; Palutikof et al., 2002; Beersma and Buishand, 2003; Busuioc and von Storch, 2003; Katz et al., 2003; Lionello et al., 2003; Wilby et al., 2003; X.L. Wang et al., 2004; Hewitson and Crane, 2006). Regarding the predictors, the best choice appears to combine dynamical and moisture variables, especially in cases where precipitation is the predictand (e.g., Wilby et al., 2003).

Pattern scaling is a simple statistical method for projecting regional climate change, which involves normalising AOGCM response patterns according to the global mean temperature. These normalised patterns are then rescaled using global mean temperature responses estimated for different emissions scenarios from a simple climate model (see Chapter 10). Some developments were made using various versions of scaling techniques (e.g., Christensen et al., 2001; Mitchell, 2003; Salathé, 2005; Ruosteenoja et al., 2007). For example, Ruosteenoja et al. (2007) developed a pattern-scaling method using linear regression to represent the relationship between the local AOGCM-simulated temperature and precipitation response and the global mean temperature change. Another simple statistical technique is to use the GCM output for the variable of interest (i.e., the predictand) as the predictor and then apply a simple local change factor/scaling procedure (e.g., Chapter 13 of IPCC, 2001; Hanssen-Bauer et al., 2003; Widmann et al., 2003; Diaz-Nieto and Wilby, 2005).

Many studies have been performed since the TAR comparing various SD methods. In general, conclusions about one method compared to another are dependent on region and the criteria used for comparison, and on the inherent attributes of each method. For example, Diaz-Nieto and Wilby (2005) downscale river flow and find that while two methods give comparable results, they differ in responses as a function of how the methods treat multi-decadal variability.

When comparing the merits of SD methods based on daily and monthly downscaling models, in terms of their ability to predict monthly means, daily models are better (e.g., Buishand et al., 2004). In terms of nonlinearity in downscaling relationships, Trigo and Palutikof (2001) note that complex nonlinear models may not be better than simpler linear/slightly nonlinear approaches for some applications. However, Haylock et al. (2006) find that SD methods based on nonlinear artificial neural networks are best at modelling the interannual variability of heavy precipitation but they underestimate extremes. Much downscaling work remains unreported, as SD activities are often implemented pragmatically for serving specific project needs, rather than for use by a broader scientific community; this is especially the case in developing nations. In some cases, this

work is only found within the "grey" literature, for example, the AIACC project (http://www.aiaccproject.org/), which supports impact studies in developing nations.

11.10.1.4 Intercomparison of Downscaling Methods

At the time of the TAR, SD methods were viewed as a complementary technique to RCMs for downscaling regional climate, each approach having distinctive strengths and weaknesses. The conclusion of the TAR that SD methods and RCMs are comparable for simulating current climate still holds.

Since the TAR, a few additional studies have systematically compared the SD and RCM approaches (e.g., Huth et al., 2001; Hanssen-Bauer et al., 2003, 2005; Wood et al., 2004, Busuioc et al., 2006; Haylock et al., 2006; Schmidli et al., 2006). These related mainly to the similarity of the climate change signal (e.g., Hanssen-Bauer et al., 2003). A more complex study considered additional information about the RCM skill in simulating the current regional climate features and reproducing the connection between large- and regional-scale patterns used for fitting the SD method (Busuioc et al., 2006). Other studies following the STARDEX project (e.g., Haylock et al., 2006; Schmidli et al., 2006) compared the two approaches in terms of their skill in reproducing current climate features, as well as in terms of the climate change signal derived from their outputs, focusing on climate extremes and complex topography processes over Europe.

11.10.2 Quantifying Uncertainties

11.10.2.1 Sources of Regional Uncertainty

Most sources of uncertainty at regional scales are similar to those at the global scale (Section 10.5 and Box 10.2), but there are both changes in emphasis and new issues that arise in the regional context. Spatial inhomogeneity of both land use and land cover change (De Fries et al., 2002; Chapter 2, Section 7.2 and Box 11.4) and aerosol forcing adds to regional uncertainty. When analysing studies involving models to add local detail, the full cascade of uncertainty through the chain of models has to be considered. The degree to which these uncertainties influence the regional projections of different climate variables is not uniform. An indication of this is, for example, that models agree more readily on the sign and magnitude of temperature changes than of precipitation changes.

The regional impact of these uncertainties in climate projections has been illustrated by several authors. For example, incorporating a model of the carbon cycle into a coupled AOGCM gave a dramatically enhanced response to climate change over the Amazon Basin (Cox et al., 2000; Jones et al., 2003) and Borneo (Kumagi et al., 2004). Further, the scale of the resolved processes in a climate model can significantly affect its simulation of climate over large regional scales (Pope and Stratton, 2002; Lorenz and Jacob, 2005). Frei et al. (2003) show that models with the same representation of resolved processes but different representations of sub-grid scale processes can represent the climate differently. The regional impact of changes in the representation of the land surface feedback is demonstrated by, for example, Oleson et al. (2004) and Feddema et al. (2005) (see also Box 11.4).

Evaluation of uncertainties at regional and local scales is complicated by the smaller ratio of the signal to the internal variability, especially for precipitation, which makes the detection of a response more difficult. In addition, the climate may itself be poorly known on regional scales in many data-sparse regions. Thus, evaluation of model performance as a component of an analysis of uncertainty can itself be problematic.

11.10.2.2 Characterising and Quantifying Regional Uncertainty

11.10.2.2.1 Review of regional uncertainty portrayed in the TAR

In the TAR, uncertainties in regional climate projections were discussed, but methods for quantifying them were relatively primitive. For example, in the TAR chapter on regional projections (Giorgi et al., 2001a), uncertainties in regional projections of climate change (e.g., large or small increases/decreases in precipitation) from different GCMs were qualitatively portrayed based only on simple agreement heuristics (e.g., seven of the nine models showed increases). Early examples of quantitative estimates of regional uncertainty include portraying the median and inter-model range of a variable (e.g., temperature) across a series of model projections and attaching probabilities to a group of scenarios on a regional scale (Jones, 2000; New and Hulme, 2000).

11.10.2.2.2 Using multi-model ensembles

A number of studies have taken advantage of multi-model ensembles formed by GCMs that have been driven by the same forcing scenarios to generate quantitative measures of uncertainty, particularly probabilistic information at a regional scale. Table 11.3 summarises aspects of the methods reviewed in this section and in Section 11.10.2.2.3. The results highlighted in Section 10.5 and Box 10.2 on climate sensitivity demonstrate that multi-model ensembles explore only a limited range of the uncertainty. In addition, the distribution of GCM sensitivities is not by construction a representative sample from those probability distributions and thus the regional probabilities generated using multi-model ensembles will not represent the full spread of possible regional changes.

Räisänen and Palmer (2001) used 17 GCMs forced with an idealised annual increase in atmospheric CO_2 of 1% to calculate the probability of exceedance of thresholds of temperature increase (e.g., >1°C) and precipitation change (e.g., <–10%). These were used to demonstrate that a probabilistic approach has advantages over conventional deterministic estimates by demonstrating the economic value of a probabilistic assessment of future climate change. Giorgi and Mearns (2002) developed measures of uncertainty for regional temperature

Table 11.3. *Methods for generating probabilistic information from future climate simulations at continental and sub-continental scales, SRES-scenario specific. Results from the methods of Greene et al. (2006) and Tebaldi et al. (2004a,b) are displayed in Figure 11.26.*

Reference	Experiment	Input Type Spatial Scale	Time Resolution	Methodological Assumptions Synthesis Method and Results	Model Performance Evaluation
Furrer et al. (2007)	Multi-model Ensemble	Grid points (after interpolation to common grid)	Seasonal multi-decadal averages	Bayesian approach. AOGCMs are assumed independent. Large-scale patterns projected on basis functions, small-scale modelled as an isotropic Gaussian process. Spatial dependence fully accounted for by spatial model. PDFs at grid point level, jointly derived accounting for spatial dependence	Model performance not explicitly brought to bear.
Giorgi and Mearns (2003)	Multi-model Ensemble	Regional averages (Giorgi and Francisco, 2000)	Seasonal multi-decadal averages	Cumulative Distribution Functions (CDFs) derived by counting threshold exceedances among members, and weighing the counts by the REA method. Stepwise CDFs at the regional levels	Model performance (bias and convergence) explicitly quantified in each AOGCMs' weight. Observable at same spatial scale and time resolution, for period 1961 to 1990.
Greene et al. (2006)	Multi-model Ensemble	Regional averages (Giorgi and Francisco, 2000)	Seasonal and annual averages	Bayesian approach. AOGCMs dependence is modelled. Linear regression of observed values on model's values (similar to Model-Output-Statistics approach used in weather forecasting and seasonal forecasting) with coefficients estimates applied to future simulations. PDFs at regional level	Model performance measured on 1902 to 1998 historical trend reproduction at same spatial scale and time resolution.
Harris et al. (2006)	Perturbed Physics Ensemble (PPE)	Grid points	Seasonal multi-annual averages	Scaled equilibrium response patterns from a large slab-model Perturbed Physics Ensemble (PPE), using transient responses of an Energy Balance Model driven by PPE climate feedbacks. Quantifying scaling error, against a smaller PPE of transient simulations, to include in PDFs. PDFs at arbitrary level of aggregation	All model versions assumed equally likely.
Stott et al. (2006a)	Single Model (HadCM3)	Continental averages	Annual decadal averages	Linear scaling factor estimated through optimal fingerprinting approach at continental scales or at global scale and applied to future projections, with estimated uncertainty. Natural variability estimated from control run added as additional uncertainty component. PDFs at the continental-scale level	Not applicable
Tebaldi et al. (2004a,b)	Multi-model Ensemble	Regional averages (Giorgi and Francisco, 2000)	Seasonal multi-decadal averages	Bayesian approach. AOGCMs are assumed independent. Normal likelihood for their projections, with AOGCM-specific variability. PDFs at the regional level	Model performance (bias and convergence) implicitly brought to bear through likelihood assumptions. Observable at same spatial scale and time resolution, for period 1961 to 1990 in original papers, for period 1980 to 1999 for results displayed in this report.

and precipitation change by weighting model results according to biases in their simulation of present-day climate and convergence of their projections to the ensemble's mean. Their Reliability Ensemble Average (REA) method was applied to the nine GCMs assessed in the TAR to provide uncertainty estimates separately for the SRES A2 and B2 emission scenarios for 22 large sub-continental regions.

Tebaldi et al. (2004a,b) used a Bayesian approach to define a formal statistical model for deriving probabilities from an ensemble of projections forced by a given SRES scenario. Using the Giorgi and Mearns (2002, 2003) approach, model bias and convergence criteria determine the shape and width of the posterior probability density functions (PDFs) of temperature and precipitation change signals. Expert judgement can be incorporated in the form of prior distributions that have the effect of assigning different relative weights to the two criteria (Tebaldi et al., 2004b; Lopez et al., 2006). The method developed by Furrer et al. (2007) to combine GCM output at the grid point scale into probabilistic projections is described in detail in Chapter 10. By straightforward area averaging, PDFs of climate change at the regional scale can be obtained. When this is done for the Giorgi and Francisco (2000) regions, the regional PDFs from Furrer et al. (2007) agree overall with the empirical histogram of the ensemble projections and the Tebaldi et al. (2004b) PDFs, with relatively small differences in spread and generally no clear difference in location.

Greene et al. (2006) used a Bayesian framework to model an ensemble of GCM projections under individual SRES scenarios by an extension of methods used for seasonal ensemble forecasting. The set of GCM simulations of the observed period 1902 to 1998 are individually aggregated in area-averaged annual or seasonal time series and jointly calibrated through a linear model to the corresponding observed regional trend. The calibration coefficients and their uncertainty are estimated and then applied to the future projections to provide probabilistic forecasts of future trends. Two critical assumptions are responsible for this method's results being so different from the ensemble projections or the PDFs produced by Tebaldi et al. (2004a,b) (see Figure 11.26 and Supplementary Material Figures S11.33 to S11.35). Firstly, the method attributes large uncertainty to models that are unable to reproduce historical trends despite the uncertainty in the relatively weak forcings in the historical period and the large natural variability at regional scales. Second, a strong stationarity assumption is required to extrapolate the relationship derived over the historical record to future trends, which involve a different combination of and

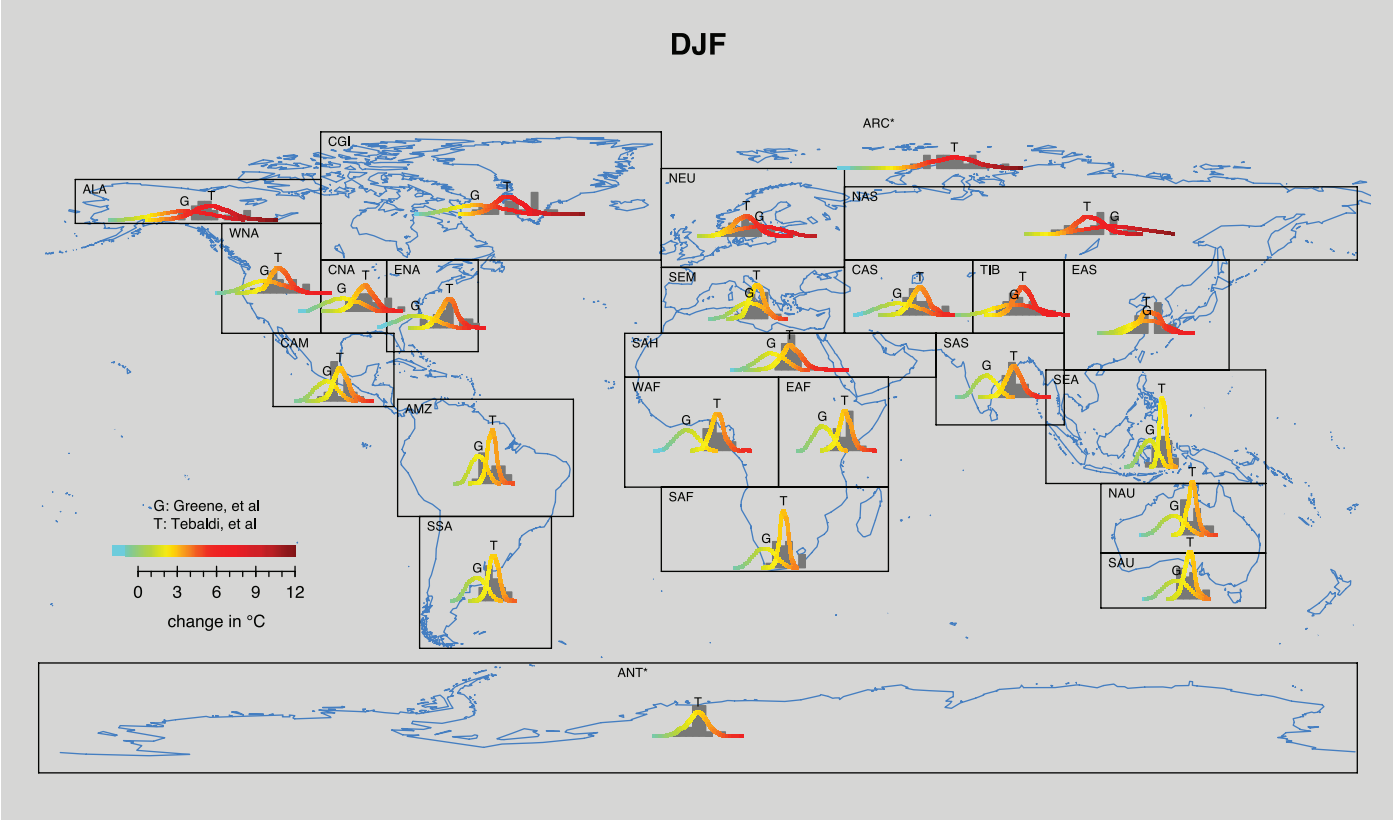


Figure 11.26. *Map comparing PDFs of change in temperature (2080 to 2099 compared to 1980 to 1999) from Tebaldi et al. (2004a,b) and Greene et al. (2006) as well as the raw model projections (represented by shaded histograms) for the Giorgi and Francisco (2000) regions. Areas under the curves and areas covered by the histograms have been scaled to equal unity. The scenario is SRES A1B and the season is NH winter (DJF). Asterisks adjacent to ARC and ANT regions indicate that only the Tebaldi et al. results were available.*

some significantly stronger forcings. The significantly smaller warming and the large width of the PDFs (at times including negative values) labelled by a 'G' in Figure 11.26 are then interpretable as a result of this stationarity constraint and the large uncertainty in the fitting of the trends. They contrast starkly with the larger warming represented in the histograms of model projections and their synthesis in the Tebaldi et al. (2004a,b) and in the Furrer et al. (2007, not shown) PDFs. This is particularly so in the lower-latitude regions of Africa, South Asia and the SH, possibly as a consequence of particularly weak trends in the observations and/or relatively worse performance of the GCMs.

Dessai et al. (2005) apply the idea of simple pattern scaling (Santer et al., 1990) to a multi-model ensemble of AOGCMs. They 'modulate' the normalised regional patterns of change by the global mean temperature changes generated under many SRES scenarios and climate sensitivities through the Model for the Assessment of Greenhouse-Gas Induced Climate Change (MAGICC), a simple probabilistic energy balance model (Wigley and Raper, 2001). Their work focuses on measuring the changes in PDFs as a function of different sources of uncertainty. In this analysis, the impact of the SRES scenarios turns out to be the most relevant for temperature changes, particularly in the upper tail of the distributions, while the GCM weighting does not produce substantial differences. This result is probably dependent on the long horizon of the projections considered (late 21st century). Arguably, the emission scenario would be less important in the short to mid-term. Climate sensitivity has an impact mainly in the lower tail of the distributions. For precipitation changes, all sources of uncertainty seem relevant but the results are very region-specific and thus difficult to generalise. More work to test the robustness of these conclusions is needed, especially when these are obviously not consistent with the results in Figure 10.29. For example, the use of pattern scaling is likely to underestimate the range of projections that would be obtained by running a larger ensemble of GCMs (Murphy et al., 2004).

The work described above has involved either large-area averages of temperature and precipitation change or statistical modelling at the grid box scale. Good and Lowe (2006) show that trends in large-area and grid-box average projections of precipitation are often very different from the local trends within the area. This demonstrates the inadequacy of inferring the behaviour at fine scales from that of large-area averages.

11.10.2.2.3 Using perturbed physics ensembles

Another method for exploring uncertainties in regional climate projections is the use of large perturbed physics ensembles (described in detail in Chapter 10). These allow a characterisation of the uncertainty due to poorly constrained parameters within the formulation of a model. Harris et al. (2006) combined the results from a 17-member ensemble (Collins et al., 2006) with a larger perturbed physics ensemble, investigating the equilibrium climate response to a doubling of atmospheric CO_2 (Webb et al., 2006). They developed a bridge between spatial patterns of the transient and equilibrium climate response by way of simple pattern scaling (Santer et al., 1990), allowing results from the large ensemble to be translated into PDFs of time-dependent regional changes. Uncertainties in surface temperature and precipitation changes are derived (Supplementary Material Figures S11.36 and S11.37), which arise from the poorly constrained atmospheric model parameters, internal variability and pattern scaling errors. The latter are quantified by comparing the scaled equilibrium response with the transient response for 17 model versions with identical parameter settings. Errors introduced by the pattern-scaling technique are largest when the transient response varies nonlinearly with global temperature, as is the case for precipitation in certain regions.

11.10.2.2.4 Other approaches to quantifying regional uncertainty

As described in Chapter 10, Stott and Kettleborough (2002) provide PDFs of future change in climate by making use of the robust observational constraints on a climate model's response to greenhouse gas and sulphate aerosol forcings that underpin the attribution of recent climate change to anthropogenic sources. The study by Stott et al. (2006a) is the first to adapt this method for continental scales. It considers two methods of constraining future continental temperature projections, one based on using observed historical changes only over the region of interest and one based on using observed changes in global temperature patterns. The first approach produces wider PDFs, since the uncertainty of detection at the regional scale is larger. The second approach incorporates more information, hence reducing the uncertainty, but assumes that the GCM represents correctly the relationship between global mean and regional temperature change. In contrast to the studies of Section 11.10.2.2.2, this work uses projections from a single GCM (HadCM3), although Stott et al. (2006b) have confirmed the results of this methodology for other models.

In general, the regional sections of this chapter assess the uncertainty in regional changes based on expert understanding of the relevant processes, rather than by formal probabilistic methods, which are still in their infancy and currently do not provide definitive results. An approach to a process-based assessment of the reliability of modelled climate change responses and thus uncertainties in its future projections has been proposed by Rowell and Jones (2006). They perform an assessment of the physical and dynamical mechanisms responsible for a specific future outcome, in their case European summer drying. Their analysis isolates the contribution of the four major mechanisms analysed: the spatial pattern of warming, other large-scale changes, reduced spring soil moisture and summer soil moisture feedbacks. In certain regions, the second process makes a minor contribution with the first and third dominating. This leads to the conclusion that the sign of the change is robust as confidence in the processes underlying these mechanisms is high.

11.10.2.2.5 Combined uncertainties: General Circulation Models, emissions and downscaling techniques

It is important to quantify the relative importance of the uncertainty arising from the downscaling step (from the RCM formulation or the assumptions underlying an empirical SD method) against the other sources of uncertainty. For example, in the application of SD methods to probabilistic scenarios, Benestad (2002b, 2004a) used a multi-model ensemble coupled to SD to derive tentative probabilistic scenarios at a regional scale for northern Europe.

The PRUDENCE project (Box 11.2) provided the first opportunity to weigh these various sources of uncertainty for simulations over Europe. Rowell (2005) evaluated a four-dimensional matrix of climate modelling experiments that included two different emissions scenarios, four different GCM experiments, multiple ensemble members within the latter to assess internal variability, and nine different RCMs, for the area of the British Isles. He found that the dynamical downscaling added a small amount of uncertainty compared to the other sources for temperature evaluated as monthly/seasonal averages. For precipitation, the relative contributions of the four sources of uncertainty are more balanced. Déqué et al. (2005, 2007) show similar results for the whole of Europe, as do Ruosteenoja et al. (2007) for subsections of Europe. Kjellström et al. (2007) find that the differences among different RCMs driven by the same GCM become comparable to those among the same RCM driven by different GCMs when evaluating daily maximum and minimum temperatures. However, mean responses in the PRUDENCE RCMs were often quite different from that of the driving GCM. This suggests that some of the spread in RCM responses may be unrealistic due to model inconsistency (Jones et al., 1997). However, it should be noted that only a few of the RCMs in PRUDENCE were driven by more than one GCM, which adds further uncertainty regarding these conclusions. Other programs similar to PRUDENCE have begun for other regions of the world, such as NARCCAP over North America (Mearns et al., 2005), Regional Climate Change Scenarios for South America (CREAS; Marengo and Ambrizzi, 2006), and the Europe-South America Network for Climate Change Assessment and Impact Studies (CLARIS; http://www.claris-eu.org) over South America.

References

Abaurrea, J., and J. Asin, 2005: Forecasting local daily precipitation patterns in a climate change scenario. *Clim. Res.*, **28**, 183–197.

Abbs, D.J., 2004: A high resolution modelling study of the effect of climate change on the intensity of extreme rainfall events. In: *Staying Afloat: Floodplain Management Authorities of NSW 44th Annual Conference: Conference Proceedings, Coffs Harbour, NSW*. Floodplain Management Authorities of New South Wales, Tamworth, pp. 17–24.

ACIA, 2005: *Arctic Climate Impact Assessment*. Cambridge University Press, New York, 1042 pp.

Adam, J.C., and D.P. Lettenmeier, 2003: Adjustment of global gridded precipitation for systematic bias. *J. Geophys. Res.*, **108**, 4257–4272.

Adams, N., 2004: A numerical modelling study of the weather in East Antarctica and the surrounding Southern Ocean. *Weather Forecasting*, **19**, 653–672.

AIACC (Assessments of Impacts and Adaptations to Climate Change in Multiple Regions and Sectors), 2004: *AIACC Regional Study AS07: Southeast Asia Regional Vulnerability to Changing Water Resource and Extreme Hydrological Events due to Climate Change. Progress Report: Period Year-end 2003*. 8 pp., http://sedac.ciesin.columbia.edu/aiacc/progress/AS07_Jan04.pdf.

Aldrian, E., and R. Dwi Susanto, 2003: Identification of three dominant rainfall regions within Indonesia and their relationship to sea surface temperature. *Int. J. Climatol.*, **23**(12), 1435–1452.

Aldrian, E., et al., 2004a: Long term simulation of the Indonesian rainfall with the MPI Regional Model. *Clim. Dyn.*, **22**(8), 794–814, doi:10.1007/s00382-004-0418-9.

Aldrian, E., et al., 2004b: Modelling Indonesian rainfall with a coupled regional model. *Clim. Dyn.*, **25**(1), 1–17, doi:10.1007/s00382-004-0483-0.

Anderson, C.J., et al., 2003: Hydrological processes in regional climate model simulations of the Central United States flood of June-July 1993. *J. Hydrometeorol.*, **4**, 584–598.

Angeles, M.E., J.E. Gonzalez, D.J. Erickson, and J.L. Hernández, 2007: Predictions of future climate change in the Caribbean region using global general circulation models. *Int. J. Climatol.*, **27**, 555-569, doi:10.1002/joc.1416.

Antic, S., R. Laprise, B. Denis, and R. de Elia, 2005: Testing the downscaling ability of a one-way nested regional climate model in regions of complex topography. *Clim. Dyn.*, **23**, 473–493.

Anyah, R., and F. Semazzi, 2004: Simulation of the sensitivity of Lake Victoria basin climate to lake surface temperatures. *Theor. Appl. Climatol.*, **79**(1–2), 55–69.

Arakawa, O., and A. Kitoh, 2005: Rainfall diurnal variation over the Indonesian Maritime Continent simulated by 20km-mesh GCM. *Scientific Online Letters on the Atmosphere*, **1**, 109–112.

Arnell, N., D. Hudson, and R. Jones, 2003: Climate change scenarios from a regional climate model: Estimating change in runoff in southern Africa. *J. Geophys. Res.*, **108**(D16), 4519, doi:10.1029/2002JD002782.

Arnfield, A.J., 2003: Two decades of urban climate research: a review of turbulence, exchanges of energy and water, and the urban heat island. *Int. J. Climatol.*, **23**, 1–26.

Ashok, K., Z.Y. Guan, and T. Yamagata, 2001: Impact of the Indian Ocean Dipole on the relationship between the Indian monsoon rainfall and ENSO. *Geophys. Res. Lett.*, **28**, 4499–4502.

Ashrit, R.G., K. Rupa Kumar, and K. Krishna Kumar, 2001: ENSO-monsoon relationships in a greenhouse warming scenario. *Geophys. Res. Lett.*, **29**, 1727–1730.

Ashrit, R.G., H. Douville, and K. Rupa Kumar, 2003: Response of the Indian monsoon and ENSO-monsoon teleconnection to enhanced greenhouse effect in the CNRM coupled model. *J. Meteorol. Soc. Japan*, **81**, 779–803.

Augustine, J.A., and F. Caracena, 1994: Lower-tropospheric precursors to nocturnal MCS development over central United States. *Weather Forecasting*, **9**, 116–135.

Avissar, R., and D. Werth, 2005: Global hydroclimatological teleconnections resulting from tropical deforestation. *J. Hydrometeorol.*, **6**, 134–145.

Bader, J., and M. Latif, 2003: The impact of decadal-scale Indian Ocean sea surface temperature anomalies on Sahelian rainfall and the North Atlantic Oscillation. *Geophys. Res. Lett.*, **30**(22), 2166–2169, doi.10.1029/2003GL018426.

Bailey, D.A., and A.H. Lynch, 2000: Development of an Antarctic regional climate system model: Part 2. Station validation and surface energy balance. *J. Clim.*, **13**, 1351–1361.

Bailey, D.A., A.H. Lynch, and T.E. Arbetter, 2004: The relationship between synoptic forcing and polynya formation in the Cosmonaut Sea, II: Polynya simulation. *J. Geophys. Res*, **109**, doi:10.1029/2003JC001838.

Barnett, D.N., et al., 2006: Quantifying uncertainty in changes in extreme event frequency in response to doubled CO_2 using a large ensemble of GCM simulations. *Clim. Dyn.*, **26**, 489–511.

Barnett, T.P., J.C. Adam, and D.P. Lettenmeier, 2005: Potential impacts of a warming climate on water availability in snow-dominated regions. *Nature*, **438**, 303–309, doi:10.1038/nature04141.82511-825179.

Bartman, A.G., W.A. Landman, and C.J. de W. Ratenbach, 2003: Recalibration of general circulation model output to Austral summer rainfall over Southern Africa. *Int. J. Climatol.*, **23**, 1407–1419.

Becker, A., and H. Bugmann (eds.), 1997: *Predicting Global Change Impacts on Mountain Hydrology and Ecology: Integrated Catchment Hydrology/Altitudinal Gradient Studies*. IGBP Report 43, International Geosphere-Biosphere Programme, Stockholm.

Beckmann, B.R., and T.A. Buishand, 2002: Statistical downscaling relationship for precipitation in the Netherlands and North Germany. *Int. J. Climatol.*, **22**, 15–32.

Beersma, J.J., and T.A. Buishand, 2003: Multi-site simulation of daily precipitation and temperature conditional on atmospheric circulation. *Clim. Res.*, **25**, 121–133.

Bell, J.L., L.C. Sloan, and M.A. Snyder, 2004: Changes in extreme climatic events: A future climate scenario. *J. Clim.*, **17**(1), 81–87.

Benestad, R.E., 2002a: Empirically downscaled temperature scenarios for Northern Europe based on a multi-model ensemble. *Clim. Res.*, **21**(2), 105–125.

Benestad, R.E., 2002b: Empirically downscaled multimodel ensemble temperature and precipitation scenarios for Norway. *J. Clim.*, **15**, 3008–3027.

Benestad, R.E., 2004a: Tentative probabilistic temperature scenarios for Northern Europe. *Tellus*, **56A**(2), 89–101.

Benestad, R.E., 2004b: Empirical-statistical downscaling in climate modeling. *Eos*, **85**(42), 417.

Benestad, R.E., 2005: Climate change scenarios for northern Europe from multi-model IPCC AR4 climate simulations. *Geophys. Res. Lett.*, **32**, L17704, doi:10.1029/2005GL023401.

Bengtsson, L., 1996: The climate response to the changing greenhouse gas concentration in the atmosphere. In: *Decadal Climate Variability, Dynamics And Variability* [Anderson, D.L.T., and J. Willebrand (eds.)]. NATO ASI Series 44, Springer, Berlin, 493 pp.

Bengtsson, L., V.A. Semenov, and O.M. Johannessen, 2004: The early twentieth-century warming in the Arctic - a possible mechanism. *J. Clim.*, **17**, 4045–4057.

Beniston, M., and P. Jungo, 2001: Shifts in the distributions of pressure, temperature and moisture in the alpine region in response to the behavior of the North Atlantic Oscillation. *Theor. Appl. Climatol.*, **71**, 29–42.

Beniston, M., F. Keller, B. Koffi, and S. Goyette, 2003: Estimates of snow accumulation and volume in the Swiss Alps under changing climatic conditions. *Theor. Appl. Climatol.*, **76**, 125–140.

Beniston, M., et al., 2007: Future extreme events in European climate: An exploration of regional climate model projections. *Clim. Change*, doi:10.1007/s10584-006-9226-z.

Bertler, N.A.N., P.J. Barrett, P.A. Mayewski, and R.L. Fogt, 2004: El Niño suppresses Antarctic warming. *Geophys. Res. Lett.*, **31**, L15207, doi:10.1029/2004GL020749.

Betts, A.K., 1998: Climate-convection feedbacks: Some further issues. *Clim. Dyn.*, **39**(1), 35–38.

Betts, R.A., et al., 2004: The role of ecosystem-atmosphere interactions in simulated Amazonian precipitation decrease and forest dieback under global climate warming. *Theor. Appl. Climatol.*, **78**, 157–175.

Biasutti, M., and A. Giannini, 2006: Robust Sahel drying in response to late 20th century forcings. *Geophys. Res. Lett.*, **33**, L11706, doi:10.1029/2006GRL026067.

Biner, S., D. Caya, R. Laprise and L. Spacek, 2000: Nesting of RCMs by imposing large scales. In: *Research Activities in Atmospheric and Oceanic Modelling*. WMO/TD No. 987, Report No. 30, World Meteorological Organization, Geneva, pp. 7.3–7.4.

Black, E., et al., 2004: Factors contributing to the summer 2003 European heatwave. *Weather*, **59**, 217–223.

Blenckner, T. and D. Chen, 2003: Comparison of the impact of regional and North-Atlantic atmospheric circulation on an aquatic ecosystem. *Clim. Res.*, **23**, 131–136.

Boer, R., and A. Faqih, 2004: *Current and Future Rainfall Variability in Indonesia*. AIACC Technical Report 021, http://sedac.ciesin.columbia.edu/aiacc/progress/AS21_Jan04.pdf.

Bogdanova, E.G, B.M. Ilyin, and I.V. Dragomilova, 2002: Application of a comprehensive bias correction model to application of a comprehensive bias correction model to stations. *J. Hydrometeorol.*, **3**, 700–713.

Bojariu, R., and F. Giorgi, 2005: The North Atlantic Oscillation signal in a regional climate simulation for the European region. *Tellus*, **57A**(4), 641–653.

Bonan, G.B., 2001: Observational evidence for reduction of daily maximum temperature by croplands in the Midwest United States. *J. Clim.*, **14**, 2430–2442.

Boo, K.-O., W.-T. Kwon, and J.-K. Kim, 2005: Vegetation changes in the regional surface climate over East Asia due to global warming using BIOME4. *Il Nuovo Cimento*, **27**(4), 317–327.

Boo, K.-O., W.-T. Kwon, and H.-J. Baek, 2006: Change of extreme events of temperature and precipitation over Korea using regional projection of future climate change. *Geophys. Res. Lett.*, **33**(1), L01701, doi:10.1029/2005GL023378.

Booij, M.J., 2002: Extreme daily precipitation in western Europe with climate change at appropriate spatial scales. *Int. J. Climatol.*, **22**, 69–85.

Bordoni, S., et al., 2004: The low-level circulation of the North American Monsoon as revealed by QuikSCAT. *Geophys. Res. Lett.*, **31**, L10109, doi:10.1029/2004GL020009.

Boulanger, J.P., F. Martinez, and E.C. Segura, 2006: Projection of future climate change conditions using IPCC simulations, neural networks and Bayesian statistics. Part 1: Temperature mean state and seasonal cycle in South America. *Clim. Dyn.*, **27**, 233–259.

Bretherton, C.S., and D.S. Battisti, 2000: An interpretation of the results from atmospheric general circulation models forced by the time history of the observed sea surface temperature distribution. *Geophys. Res. Lett.*, **27**, 767–770.

Bromwich, D.H., and R.L. Fogt, 2004: Strong trends in the skill of the ERA-40 and NCEP/NCAR Reanalyses in the high and middle latitudes of the Southern Hemisphere, 1958-2001. *J. Clim.*, **17**, 4603–4619.

Bromwich, D.H., A.J. Monaghan, and Z. Guo, 2004a: Modeling the ENSO modulation of Antarctic climate in the late 1990s with the Polar MM5. *J. Clim.*, **17**, 109–132.

Bromwich, D.H., A.J. Monaghan, K.W. Manning, and J.G. Powers, 2004b: Real-time forecasting for the Antarctic: An evaluation of the Antarctic Mesoscale Prediction System (AMPS). *Mon. Weather Rev.*, **133**, 579–603.

Bromwich, D.H., et al., 2000: ECMWF analyses and reanalyses depiction of ENSO signal in Antarctic precipitation. *J. Clim.*, **13**, 1406–1420.

Brovkin, V., et al., 1999: Modelling climate response to historical land cover change. *Global Ecol. Biogeogr.*, **8**, 509–517.

Buishand, T.A., M.V. Shabalova, and T. Brandsma, 2004: On the choice of the temporal aggregation level for statistical downscaling of precipitation. *J. Clim.*, **17**, 1816–1827.

Busuioc, A., and H. von Storch, 2003: Conditional stochastic model for generating daily precipitation time series. *Clim. Res.*, 24, 181–195.

Busuioc, A., D. Chen, and C. Hellström, 2001: Performance of statistical downscaling models in GCM validation and regional climate change estimates: application for Swedish precipitation. *Int. J. Climatol.*, **21**(5), 557–578.

Busuioc, A., F. Giorgi, X. Bi, and M. Ionita, 2006: Comparison of regional climate model and statistical downscaling simulations of different winter precipitation change scenarios over Romania. *Theor. Appl. Climatol.*, **86**, 101–120.

Cai, W., P.H. Whetton, and D.J. Karoly, 2003a: The response of the Antarctic Oscillation to increasing and stabilized atmospheric CO_2. *J. Clim.*, **16**, 1525–1538.

Cai, W., et al., 2003b: *Climate Change in Queensland under Enhanced Greenhouse Conditions*. *Annual Report, 2003*. CSIRO Atmospheric Research, Aspendale, Vic., 74 pp, http://www.longpaddock.qld.gov.au/ClimateChanges/pub/CSIRO2003.html#end.

Caires, S., V.R. Swail, and X.L. Wang, 2006: Projection and analysis of extreme wave climate. *J. Clim.*, **19**, 5581–5605.

Caminade, C., L. Teray, and E. Maisonnave, 2006: West African monsoon system response to greenhouse gase and sulphate aerosol forcing under two emission scenarios. *Clim. Dyn.*, **26**, 531–547.

Cannon, A., and P. Whitfield, 2002: Downscaling recent streamflow conditions in British Columbia, Canada using ensemble neural network models. *J. Hydrol.*, **259**(1–4), 136–151.

Carleton, A.M., 2003: Atmospheric teleconnections involving the Southern Ocean. *J. Geophys. Res.*, **108**, 8080, doi:10.1029/2000JC000379.

Carril, A.F., C.G. Menéndez, and A. Navarra, 2005: Climate response associated with the Southern Annular Mode in the surroundings of Antarctic Peninsula: a multi-model ensemble analysis. *Geophys. Res. Lett.*, **32**, L16713, doi:10.1029/2005GL023581.

Cassano, J.J., P. Uotila, and A. Lynch, 2006: Changes in synoptic weather patterns in the polar regions in the 20th and 21st centuries. Part 1: Arctic. *Int. J. Climatol.*, **26**, 1027–1049, doi:10.1002/joc.1306.

Caya, D., and S. Biner, 2004: Internal variability of RCM simulations over an annual cycle. *Clim. Dyn.*, **22**, 33–46.

Cayan, D.R., et al., 2001: Changes in the onset of spring in the western United States. *Bull. Am. Meteorol. Soc.*, **82**, 399–415.

Cazes Boezio, G., A.W. Robertson, and C.R. Mechoso, 2003: Seasonal dependence of ENSO teleconnections over South America and relationships with precipitation in Uruguay. *J. Clim.*, **16**(8), 1159–1176.

Chaboureau, J.P., F. Guichard, J.L. Redelsperger, and J.P. Lafore, 2004: The role of stability and moisture in the diurnal cycle of convection over land. *Q. J. R. Meteorol. Soc.*, **130**, 3105–3117.

Chapman, W.L., and J.E. Walsh, 2006: A synthesis of Antarctic temperatures. *J. Clim.*, **26**, 1181–2119, doi:10.1002/joc.1305.

Chapman, W.L., and J.E. Walsh, 2007: Simulations of Arctic temperature and pressure by global coupled models. *J. Clim.*, **20**, 609-632, doi: 10.1175/JCLI4026.1.

Charles, S.P., B.C. Bates, I.N. Smith, and J.P. Hughes, 2004: Statistical downscaling of daily precipitation from observed and modelled atmospheric fields. *Hydrolog. Process.*, **18**(8), 1373–1394.

Chase, T.N., et al., 2000: Simulated impacts of historical land cover changes on global climate in northern winter. *Clim. Dyn.*, **16**, 93–105.

Chen, A.A., and M.A. Taylor, 2002: Investigating the link between early season Caribbean rainfall and the El Niño +1 year. *Int. J. Climatol.*, **22**, 87–106.

Chen, D.L., and Y.M. Chen, 2003: Association between winter temperature in China and upper air circulation over East Asia revealed by canonical correlation analysis. *Global Planet. Change*, **37**, 315–325.

Chen, M., D. Pollard, and E.J. Barron, 2003: Comparison of future climate change over North America simulated by two regional climate models. *J. Geophys. Res.*, **108**(D12), 4348, doi:10.1029/2002JD002738.

Chen, T.-C., J.-H. Yoon, K.J. St. Croix, and E.S. Takle, 2001: Suppressing impacts of the Amazonian deforestation by the global circulation change. *Bull. Am. Meteorol. Soc*., **82**, 2209–2216.

Chen, T.-C., S.-Y. Wang, W.-R. Huang, and M.-C. Yen, 2004: Variation of the East Asian summer monsoon rainfall. *J. Clim.*, **17**, 744–762.

Chou, C., and J.D. Neelin, 2004: Mechanisms of global warming impacts of regional tropical precipitation. *J. Clim.*, **17**, 2688–2701.

Chou, C., J.D. Neelin, J.-Y. Tu, and C.-T. Chen, 2007: Regional tropical precipitation change mechanisms in ECHAM4/OPYC3 under global warming. *J. Clim.* **19**, 4207-4223..

Chou, S.C., A.M.B. Nunes, and I.F.A. Cavalcanti, 2000: Extended range forecasts over South America using the regional eta model. *J. Geophys. Res.*, **105**, 10147–10160.

Christensen, J.H., and O.B. Christensen, 2003. Severe summertime flooding in Europe. *Nature*, **421**, 805–806.

Christensen, J.H., T. Carter, and F. Giorgi, 2002: PRUDENCE employs new methods to assess European climate change. *Eos*, **83**, 147.

Christensen, J.H., T.R. Carter, M. Rummukainen, and G. Amanatidis, 2007: Evaluating the performance and utility of regional climate models: the PRUDENCE project. *Clim. Change*, doi:10.1007/s10584-006-9211-6.

Christensen, J.H., et al., 2001: A synthesis of regional climate change simulations – A Scandinavian perspective. *Geophys. Res. Lett.*, **28**(6), 1003–1006.

Christensen, O.B., and J.H. Christensen, 2004: Intensification of extreme European summer precipitation in a warmer climate. *Global Planet. Change*, **44**, 107–117.

Church, J.A., N.J. White, and J.R. Hunter, 2006: Sea level rise at tropical Pacific and Indian Ocean islands. *Global Planet. Change*, **53**(3), 155–168.

Church, J.A., et al., 2004: Estimates of regional distribution of sea level rise over the 1950-2000 period. *J. Clim.*, **17**, 2609–2625.

Clark, R., S. Brown, and J. Murphy, 2006: Modelling Northern Hemisphere summer heat extreme changes and their uncertainties using a physics ensemble of climate sensitivity experiments. *J. Clim.*, **19**, 4418–4435.

Claussen, M., C. Kutzbaki, V. Brovkin, and A. Ganapolski, 1999: Simulation of an abrupt change in Saharan vegetation in the mid-Holocene. *Geophys. Res. Lett.*, **26**, 2037–2040.

Collier, J.C., K.P. Bowman, and G.R. North, 2004: A comparison of tropical precipitation simulated by the community climate model with that measured by the tropical rainfall measuring mission satellite. *J. Clim.*, **17**, 3319–3333.

Collins, M., et al., 2006: Towards quantifying uncertainty in transient climate change. *Clim. Dyn*., **27**, 127–147.

Comiso, J.C., 2000: Variability and trends in Antarctic surface temperatures from in situ and satellite infrared measurements. *J. Clim.*, **13**, 1674–1696.

Connolley, W.M., and S.A. Harangozo, 2001: A comparison of five numerical weather prediction analysis climatologies in southern high latitudes. *J. Clim.*, **14**, 30–44.

Cook, K.H., and E.K. Vizy, 2006: Coupled model simulations of the West African monsoon system: twentieth-century simulations and twenty-first-century predictions. *J. Clim*., **19**, 3681–3703.

Coppola, E., and F. Giorgi, 2005: Climate change in tropical regions from high-resolution time-slice AGCM experiments. *Q. J. R. Meteorol. Soc.*, **131**(612), 3123–3145.

Costa, M.H., and J.A. Foley, 2000: Combined effects of deforestation and doubled atmospheric CO_2 concentrations on the climate of Amazonia. *J. Clim.*, **13**, 35–58.

Covey, C., et al., 2003: An overview of results from the Coupled Model Intercomparison Project (CMIP). *Global Planet. Change*, **37**, 103–133, doi:10.1016/S0921-8181(02)00193-5.

Cox, P.M., et al., 2000: Acceleration of global warming due to carbon-cycle feedbacks in a coupled climate model. *Nature*, **408**, 184–187.

Cox, P.M., et al., 2004: Amazonian forest dieback under climate-carbon cycle projections for the 21st century. *Theor. Appl. Clim.*, **78**, 137–156.

CSIRO (Commonwealth Scientific and Industrial Research Organisation), 2001: *Climate Projections for Australia*. CSIRO Atmospheric Research, Melbourne, 8 pp., http://www.dar.csiro.au/publications/projections2001.pdf.

Curtis, J., G. Wendler, R. Stone, and E. Dutton, 1998: Precipitation decrease in the western Arctic, with special emphasis on Barrow and Barter Island, Alaska. *Int. J. Climatol.*, **18**, 1687–1707.

Dairaku, K., and S. Emori, 2006: Dynamic and thermodynamic influences on intensified daily rainfall during the Asian summer monsoon under doubled atmospheric CO_2 conditions. *Geophys. Res. Lett.*, **33**, L01704, doi:10.1029/2005GL024754.

Davey, M.K., et al., 2002: STOIC: A study of coupled model climatology and variability in tropical ocean regions. *Clim. Dyn.*, **18**, 403–420.

Davies, H.C., 1976: A lateral boundary formulation for multi-levels prediction models. *Q. J. R. Meteorol. Soc.*, **102**, 405–418.

Debernard, J., M.Ø. Køltzow, J.E. Haugen, and L.P. Røed, 2003: Improvements in the sea-ice module of the regional coupled atmosphere-ice-ocean model and the strategy for the coupling of the three spheres. In: *RegClim General Technical Report No. 7* [Iversen, T., and M. Lystad (eds)]. Norwegian Meteorological Institute, Oslo, pp. 59–69.

DeFries, R.S., L. Bounoua, and G.J. Collatz, 2002: Human modification of the landscape and surface climate in the next fifty years. *Global Change Biol.*, **8**, 438–458.

Delire, C., et al., 2001: Simulated response of the atmosphere-ocean system to deforestation in the Indonesian Archipelago. *Geophys Res Lett*, **28**(10), 2081–2084.

Denis, B., R. Laprise, and D. Caya, 2003: Sensitivity of a regional climate model to the spatial resolution and temporal updating frequency of the lateral boundary conditions. *Clim. Dyn.*, **20**, 107–126.

Denis, B., R. Laprise, D. Caya, and J. Côté, 2002: Downscaling ability of one-way-nested regional climate models: The big-brother experiment. *Clim. Dyn.*, **18**, 627–646.

Déqué, M., and J.P. Piedelievre, 1995: High resolution climate simulation over Europe. *Clim. Dyn.*, **11**, 321–339.

Déqué, M., and A.L. Gibelin, 2002: High versus variable resolution in climate modelling. In: *Research Activities in Atmospheric and Oceanic Modelling* [Ritchie, H. (ed.)]. WMO/TD No. 1105, Report No. 32, World Meteorological Organization, Geneva, pp. 74–75.

Déqué, M., et al., 2005: Global high resolution versus Limited Area Model climate change scenarios over Europe: results from the PRUDENCE project. *Clim. Dyn.*, **25**, 653–670, 10.1007/s00382-005-0052-1.

Déqué, M., et al., 2007: An intercomparison of regional climate simulations for Europe: assessing uncertainties in model projections. *Clim. Change*, doi:10.1007/s10584-006-9228-x.

Derbyshire, S.H., et al., 2004: Sensitivity of moist convection to environmental humidity. *Q. J. R. Meteorol. Soc.*, **130**, 3055–3079.

Dessai, S., X. Lu, and M. Hulme, 2005: Limited sensitivity analysis of regional climate change probabilities for the 21st century. *J. Geophys. Res.*, **110**, D19108, doi:10.1029/2005JD005919.

Dethloff, K., et al., 2001: Sensitivity of Arctic climate simulations to different boundary layer parameterizations in a regional climate model. *Tellus*, **53**, 1–26.

Diaz-Nieto, J., and R.L. Wilby, 2005: A comparison of statistical downscaling and climate change factor methods: impacts on low flows in the River Thames, United Kingdom. *Clim. Change*, **69**, 245–268.

Dibike, Y.B., and P. Coulibaly, 2005: Hydrologic impact of climate change in the Saguenay watershed: Comparison of downscaling methods and hydrologic models. *J. Hydrol.*, **307**, 145–163.

Diffenbaugh, N.S., J.S. Pal, R.J. Trapp, and F. Giorgi, 2005: Fine-scale processes regulate the response of extreme events to global climate change. *Proc. Natl. Acad. Sci. U.S.A.*, **102**(44), 15774–15778, doi:10.1073/pnas.0506042102.

Dimitrijevic, M., and R. Laprise, 2005: Validation of the nesting technique in a regional climate model through sensitivity tests to spatial resolution and the time interval of lateral boundary conditions during summer. *Clim. Dyn.*, **25**, 555–580.

Ding, Y.H., Y.M. Liu, X.L. Shi, and Q.Q. Li, 2003: The experimental use of the regional climate model in the seasonal prediction in China National Climate Center. In: *Proceedings of the 2nd Workshop on Regional Climate Model, March 3-6, 2003, Yokohama, Japan,* GAME Publication No. 39, pp. 9–14.

Ding, Y.H., et al., 2006: Multi-year simulations and experimental seasonal predictions for rainy seasons in China by using a nested regional climate model (RegCM_NCC). Part I: Sensitivity study. *Adv. Atmos. Sci.*, **23**(3), 323–341.

Dorn, W., K. Dethloff, and A. Rinke, 2003: Competition of NAO regime changes and increasing greenhouse gases and aerosols with respect to Arctic climate estimate. *Clim. Dyn.*, **21**(5–6), 447–458, doi:10.1007/s00382-003-0344-2.

Döscher, R., et al., 2002: The development of the coupled ocean-atmosphere model RCAO. *Boreal Environ. Res.*, **7**, 183–192.

Douville, H., 2005: Limitations of time-slice experiments for predicting regional climate change over South Asia. *Clim. Dyn.*, **24**(4), 373–391.

Douville, H., et al., 2000: Impact of CO_2 doubling on the Asian summer monsoon: Robust versus model dependent responses. *J. Meteorol. Soc. Japan*, **78**, 1–19.

Douville, H., et al., 2002: Sensitivity of the hydrological cycle to increasing amounts of greenhouse gases and aerosols. *Clim. Dyn.*, **20**, 45–68.

Druyan, L.M., M. Fulakeza, and P. Lonergan, 2002: Dynamic downscaling of seasonal climate predictions over Brazil. *J. Clim.*, **15**, 3411–3426.

Duffy, P.B., et al., 2003: High-resolution simulations of global climate, part 1: Present climate. *Clim. Dyn.*, **21**, 371–390.

Dufresne, J.-L., et al., 2002: On the magnitude of positive feedback between future climate change and the carbon cycle, *Geophys. Res. Lett.*, **29**(10), 1405, doi:10.1029/2001GL013777.

Easterling, D.R., L.V. Alexander, A. Mokssit, and V. Detemmerman, 2003: CC1/Clivar workshop to develop priority climate indices. *Bull. Am. Meteorol. Soc.*, **84,** 1403 –1407.

Ekström, M., H.J. Fowler, C.G. Kilsby, and P.D. Jones, 2005: New estimates of future changes in extreme rainfall across the UK using regional climate model integrations. 2. Future estimates and use in impact studies. *J. Hydrol.*, **300**, 234–251.

Elguindi, N., and F. Giorgi, 2006: Simulating multi-decadal variability of Caspian Sea level changes using regional climate model outputs. *Clim. Dyn.*, **26**: 167–181.

Engelbrecht, F., C. Rautenbach, J. McGregor, and J. Katzfey, 2002: January and July climate simulations over the SADC region using the limited-area model DARLAM. *Water SA*, **28**(4), 361–374.

Feddema, J.J., et al., 2005: A comparison of a GCM response to historical anthropogenic land cover change and model sensitivity to uncertainty in present-day land cover representations. *Clim. Dyn.*, **25**, 581–609.

Fernández, J., and J. Sáenz, 2003: Improved field reconstruction with the analog method: searching the CCA space. *Clim. Res.*, **24**, 199–213.

Fernandez, J., J. Sáenz, and E. Zorita, 2003: Analysis of wintertime atmospheric moisture transport and its variability over southern Europe in the NCEP reanalyses. *Clim. Res.*, **23**, 195–215.

Fink, A.H., et al., 2004: The 2003 European summer heatwaves and drought – synoptic diagnostics and impacts. *Weather*, **59**, 209–216.

Flather, R.A., and H. Khandker, 1993: The storm surge problem and possible effects of sea level changes on coastal flooding in the Bay of Bengal. In: *Climate and Sea Level Change* [Warrick, R.A., E.M. Barrow, and T. Wigley (eds)]. Cambridge University Press, Cambridge, UK, pp. 229–245.

Flather, R.A., and J.A. Williams, 2000: Climate change effects on storm surges: methodologies and results. In: *Climate Scenarios for Water-Related and Coastal Impacts* [Beersma, J., M. Agnew, D. Viner, and M. Hulme (eds.)]. ECLAT-2 Workshop Report No. 3, KNMI, The Netherlands, pp. 66–78.

Flather, R.A., et al., 1998: Direct estimates of extreme storm surge elevations from a 40-year numerical model simulation and from observations. *Global Atmos. Ocean System*, **6**, 165–176.

Fogt, R.L., and D.H. Bromwich, 2006: Decadal variability of the ENSO teleconnection to the high latitude South Pacific governed by coupling with the Southern Annular Mode. *J. Clim.*, **19**, 979–997.

Foley, J.A., M.T. Coe, M. Scheffer, and G. Wang., 2003: Regime shifts in the Sahara and Sahel: Interactions between ecological systems in Southern Africa. *Ecosystems*, **6**, 524–539.

Foley, J.A., et al., 2005: Global consequences of land use. *Science*, **309**, 570–574.

Fowler, H.J., M. Ekström, C.G. Kilsby, and P.D. Jones, 2005: New estimates of future changes in extreme rainfall across the UK using regional climate model integrations. 1. Assessment of control climate. *J. Hydrol.*, **300**, 212–233.

Fox-Rabinovitz, M.S., L.L. Takacs, R.C. Govindaraju, and M.J. Suarez, 2001: A variable-resolution stretched-grid general circulation model: Regional climate simulation. *Mon. Weather Rev.*, **129**(3), 453–469.

Frei, C., et al., 2003: Daily precipitation statistics in regional climate models: Evaluation and intercomparison for the European Alps. *J. Geophys. Res.*, **108**(D3), 4124, doi:10.1029/2002JD002287.

Frei, C., et al., 2006: Future change of precipitation extremes in Europe: Intercomparison of scenarios from regional climate models. *J. Geophys. Res*., **111**, D06105, doi:10.1029/2005JD005965.

Freiman, M., and P. Tyson, 2000: The thermodynamic structure of the atmosphere over South Africa: Implications for water vapour transport. *Water SA*, **26**(2), 153–158.

Friedlingstein, P., J.-L. Dufresne, P.M. Cox, and P. Rayner, 2003: How positive is the feedback between climate change and the carbon cycle? *Tellus*, **55B**, 692–700.

Friedlingstein, P., et al., 2001: Positive feedback between future climate change and the carbon cycle. *Geophys. Res. Lett.*, **28**, 1543–1546.

Fu, C.B., et al., 2005: Regional Climate Model Intercomparison project for Asia. *Bull. Am. Meteorol. Soc.*, **86**(2), 257–266, doi:10.11/BAMS-86-2-257.

Fuentes, U., and D. Heimann, 2000: An improved statistical-dynamical downscaling scheme and its application to the alpine precipitation climatology. *Theor. Appl. Climatol.*, **65**, 119–135.

Fujibé, F., N. Yamazaki, M. Katsuyama, and K. Kobayashi, 2005: The increasing trend of intense precipitation in Japan based on four-hourly data for a hundred years. *Scientific Online Letters on the Atmosphere*, **1**, 41–44.

Furrer, R., S.R. Sain, D.W. Nychka, and G.A. Meehl, 2007: Multivariate Bayesian analysis of atmosphere-ocean general circulation models. *Environ. Ecol. Stat.*, in press.

Gaertner, M.A., et al., 2001: The impact of deforestation on the hydrological cycle in the western Mediterranean: an ensemble study with two regional climate models. *Clim. Dyn.*, **17**, 857-873

Gao, Q., and M. Yu, 1998: A model of regional vegetation dynamics and its application to the study of Northeast China Transect (NECT) responses to global change. *Global Biogeochem. Cycles*, **12**(2), 329–344.

Gao, X.J., Z.C. Zhao, and F. Giorgi, 2002: Changes of extreme events in regional climate simulations over East Asia. *Adv. Atmos. Sci.*, **19**, 927–942.

Gao, X.J., Z.C. Zhao, and Y.H. Ding, 2003a: Climate change due to greenhouse effects in Northwest China as simulated by a regional climate model. *J. Glaciol. Geocryol.*, **25**(2), 165–169.

Gao, X.J., J.S. Pal, and F. Giorgi, 2006a: Projected changes in mean and extreme precipitation over the Mediterranean region from a high resolution double nested RCM simulation. *Geophys. Res. Lett.*, **33**, L03706, doi:10.1029/2005GL024954.

Gao, X.J., D.L. Li, Z.C. Zhao, and F. Giorgi, 2003b: Climate change due to greenhouse effects in Qinghai-Xizang Plateau and along the Qianghai-Tibet Railway. *Plateau Meteorol.*, **22**(5), 458–463.

Gao, X.J., W.T. Lin, Z.C. Zhao, and F. Kucharsky, 2004: Simulation of climate and short-term climate prediction in China by CCM3 driven by observed SST. *Chin. J. Atmos. Sci.*, **28**, 63–76.

Gao, X.J., et al., 2001: Climate change due to greenhouse effects in China as simulated by a regional climate model. *Adv. Atmos. Sci.*, **18**, 1224–1230.

Gao, X.J., et al., 2006b: Impacts of horizontal resolution and topography on the numerical simulation of East Asia precipitation. *Chin. J. Atmos. Sci.*, **30**, 185–192.

Gedney, N., and P.J. Valdes, 2000: The effect of Amazonian deforestation on the Northern Hemisphere circulation and climate. *Geophys. Res. Lett.*, **27**(19), 3053–3056.

Genthon, C., and E. Cosme, 2003: Intermittent signature of ENSO in west-Antarctic precipitation. *Geophys. Res. Lett.*, **30**, 2081, doi:10.1029/2003GL018280.

Genthon, C., G. Krinner, and E. Cosme, 2002: Free and laterally-nudged Antarctic climate of an atmospheric general circulation model. *Mon. Weather Rev.*, **130**, 1601–1616.

Genthon, C., S. Kapari, and P.A. Mayewski, 2005: Interannual variability of the surface mass balance of West Antarctica from ITASE cores and ERA40 reanalyses. *Clim. Dyn.*, **24**, 759–770.

Gerbaux, M., et al., 2005: Surface mass balance of glaciers in the French Alps: distributed modeling and sensitivity to climate change. *J. Glaciol.*, **51**(175), 561–572.

Ghan, S.J., and T. Shippert, 2006: Physically-based global downscaling climate change projections for a full century, *J. Clim.*, **19**, 1589–1604.

Giannini, A., Y. Kushnir, and M.A. Cane, 2000: Interannual variability of Caribbean rainfall, ENSO and the Atlantic Ocean. *J. Clim.*, **13**, 297–311.

Giannini, A., M.A. Cane, and Y. Kushnir, 2001: Interdecadal changes in the ENSO teleconnection to the Caribbean region and North Atlantic Oscillation. *J. Clim.*, **14**, 2867–2879.

Giannini, A., R. Saravanan, and P. Chang, 2003: Oceanic forcing of Sahel rainfall on interannual to interdecadal time scales. *Science*, **302**, 1027–1030.

Gibelin, A.L., and Déqué, M., 2003: Anthropogenic climate change over the Mediterranean region simulated by a global variable resolution model. *Clim. Dyn.*, **20**, 327–339.

Giorgi, F., and R. Francesco, 2000: Evaluating uncertainties in the prediction of regional climate change. *Geophys. Res. Lett.*, **27**, 1295–1298.

Giorgi, F., and L.O. Mearns, 2002: Calculation of average, uncertainty range, and reliability of regional climate changes from AOGCM simulations via the reliability ensemble averaging (REA) method. *J. Clim.*, **15**, 1141–1158.

Giorgi, F., and L.O. Mearns, 2003: Probability of regional climate change based on the Reliability Ensemble Averaging (REA) method. *Geophys. Res. Lett.*, **30**(12), 1629, doi:10.1029/2003GL017130.

Giorgi, F., and X. Bi, 2005: Regional changes in surface climate interannual variability for the 21st century from ensembles of global model simulations. *Geophys. Res. Lett.*, **32**, L13701, doi:10.1029/2005GL023002.

Giorgi, F., X. Bi, and J.S. Pal, 2004: Mean, interannual variability and trends in a regional climate change experiment over Europe. II: climate change scenarios (2071-2100). *Clim. Dyn.*, **23**, 839–858.

Giorgi, F., J.W. Hurrell, M.R. Marinucci, and M. Beniston, 1997: Elevation signal in surface climate change: A model study. *J. Clim.*, **10**, 288–296.

Giorgi, F., et al., 2001a: Regional climate information – Evaluation and projections. In: *Climate Change 2001: The Scientific Basis. Contribution of Working Group I to the Third Assessment Report of the Intergovernmental Panel on Climate Change* [Houghton, J.T., et al. (eds.)]. Cambridge University Press, Cambridge, United Kingdom and New York, NY, USA, pp. 583–638.

Giorgi, F., et al., 2001b: Emerging patterns of simulated regional climatic changes for the 21st century due to anthropogenic forcings. *Geophys. Res. Lett.*, **28**(17), 3317–3320.

Good, P., and J. Lowe, 2006: Emergent behavior and uncertainty in multi-model climate projections of precipitation trends at small spatial scales. *J. Clim.*, **27**(4), 357–375.

Goodison, B.E., P.Y.T. Louie, and D. Yang, 1998: *WMO Solid Precipitation Measurement Intercomparison, Final Report*. WMO/TD No.872, World Meteorological Organization, Geneva, 212 pp.

Govindasamy, B., P.B. Duffy, and J. Coquard, 2003: High resolution simulations of global climate, part 2: Effects of increased greenhouse gases. *Clim. Dyn.*, **21**, 391–404.

Goyette, S., O. Brasseur, and M. Beniston, 2003: Application of a new wind gust parameterisation: multi-scale case studies performed with the Canadian RCM. *J. Geophys. Res.*, **108**, 4371–4389.

Graham, L.P., S. Hagemann, S. Jaun, and M. Beniston, 2007: On interpreting hydrological change from regional climate models. *Clim. Change*, doi:10.1007/s10584-006-9217-0.

Gray, W.M., 1984: Atlantic seasonal hurricane frequency. Part I: El Niño and 30 mb quasi-biennial oscillation influences. *Mon. Weather Rev.*, **112**, 1649–1668.

Greene, A.M., L. Goddard, and U. Lall, 2006: Probabilistic multimodel regional temperature change projections. *J. Clim*., **19**, 4326–4343.

Gregory, J.M., and J.F.B. Mitchell, 1995: Simulation of daily variability of surface temperature and precipitation over Europe in the current and $2\times CO_2$ climate using the UKMO climate model. *Q. J. R. Meteorol. Soc*., **121**, 1451–1476.

Griffiths, G.M., M.J. Salinger, and I. Leleu, 2003: Trends in extreme daily rainfall across the South Pacific and relationship to the South Pacific convergence zone. *Int. J. Climatol.*, **23**, 847- 869.

Groisman, P.Y., et al., 2005: Trends in intense precipitation in the climate record. *J. Clim.*, **18**, 1326–1350.

Guo, Z., D.H. Bromwich, and J.J. Cassano, 2003: Evaluation of Polar MM5 simulations of Antarctic atmospheric circulation. *Mon. Weather Rev.*, **131**, 384–411.

Guo, Z., D.H. Bromwich, and K.M. Hines, 2004: Modeled Antarctic precipitation. Part II: ENSO modulation over West Antarctica. *J. Clim.*, **17**, 448–465.

Gutowski, W.J., et al., 2004: Diagnosis and attribution of a seasonal precipitation deficit in a U.S. regional climate simulation. *J. Hydrometeorol.*, **5**(1), 230–242.

Haapala, J., H.E.M. Meier, and J. Rinne, 2001: Numerical investigations of future ice conditions in the Baltic Sea. *Ambio*, **30**, 237–244.

Haarsma, R.J., F. Selten, S. Weber, and M. Kliphuis, 2005: Sahel rainfall variability and response to greenhouse warming. *Geophys. Res. Lett.*, **32**, L17702, doi:10.1029/2005GL023232.

Hagemann, S., et al., 2004: Evaluation of water and energy budgets in regional climate models applied over Europe. *Clim. Dyn.*, **23**, 547–607.

Han, J., and J. Roads, 2004: US climate sensitivity simulated with the NCEP Regional Spectral Model. *Clim. Change*, **62**, 115–154, doi:10.1023/B:CLIM.0000013675.66917.15.

Hansen, J.E., et al., 1998: Climate forcings in the industrial era. *Proc. Natl. Acad. Sci. U.S.A.*, **95**, 12753–12758.

Hansen, J.W., and T. Mavromatis, 2001: Correcting low-frequency variability bias in stochastic weather generators. *Agr. For. Meteorol.*, **109**, 297–310.

Hanssen-Bauer, I., E.J. Førland, J.E. Haugen, and O.E. Tveito, 2003: Temperature and precipitation scenarios for Norway: comparison of results from dynamical and empirical downscaling. *Clim. Res.*, **25**(1), 15–27.

Hanssen-Bauer, I., et al., 2005: Statistical downscaling of climate scenarios over Scandinavia: A review. *Clim. Res.*, **29**, 255–268.

Hardy, T., L. Mason, A. Astorquia, and B. Harper 2004: *Queensland Climate Change and Community Vulnerability to Tropical Cyclones: Ocean Hazards Assessment*. Report to Queensland Government, 45 pp. +7 appendices, http://www.longpaddock.qld.gov.au/ClimateChanges/pub/OceanHazards/Stage2LowRes.pdf.

Harris, G.R., et al., 2006: Frequency distributions of transient regional climate change from perturbed physics ensembles of general circulation model simulations. *Clim. Dyn.*, **27**, 357–375.

Hasegawa, A., and S. Emori, 2005: Tropical cyclones and associated precipitation over the Western North Pacific: T106 atmospheric GCM simulation for present-day and doubled CO_2 climates. *Scientific Online Letters on the Atmosphere*, **1**, 145–148.

Hayhoe, K., et al., 2004: Emissions pathways, climate change, and impacts on California. *Proc. Natl. Acad. Sci. U.S.A.*, **101**, 12422–12427.

Haylock, M.R., et al., 2006: Downscaling heavy precipitation over the UK: A comparison of dynamical and statistical methods and their future scenarios. *Int. J. Climatol.*, **26**(10), 1397–1415, doi:10.1002/joc.1318.

Hegerl, G.C., F.W. Zwiers, P.A. Stott, and V.V. Kharin, 2004: Detectability of anthropogenic changes in annual temperature and precipitation extremes. *J. Clim.*, **17**, 3683–3700.

Held, I.M., et al., 2005: Simulation of Sahel drought in the 20th and 21st centuries. *Proc. Natl. Acad. Sci. U.S.A.*, **102**(50), 17891–17896.

Hellström, C., D. Chen, C. Achberger, and J. Räisänen, 2001: A comparison of climate change scenarios for Sweden based on statistical and dynamical downscaling of monthly precipitation. *Clim. Res.*, **19**, 45–55.

Hennessy, K.J., J.M. Gregory, and J.F.B. Mitchell, 1997: Changes in daily precipitation under enhanced greenhouse conditions. *Clim. Dyn.*, **13**, 667–680.

Hennessy, K.J., et al., 2003: *The Impact of Climate Change on Snow Conditions in Mainland Australia*. CSIRO Atmospheric Research, Aspendale, 47 pp., http://www.cmar.csiro.au/e-print/open/hennessy_2003a.pdf.

Hennessy, K.J., et al., 2004a: *Climate Change in the Northern Territory.* Consultancy report for the Northern Territory Department of Infrastructure, Planning and Environment by CSIRO Atmospheric Research Climate Impact Group and Melbourne University School of Earth Sciences, Northern Territory Government, Darwin, 65 pp.

Hennessy, K.J., et al., 2004b: *Climate Change in New South Wales – Part 1: Past Climate Variability and Projected Changes in Average Climate*. Consultancy report for the New South Wales Greenhouse Office by CSIRO Atmospheric Research and Australian Government Bureau of Meteorology, 46 pp., http://www.dar.csiro.au/publications/hennessy_2004b.pdf.

Hennessy, K.J., et al., 2004c: *Climate Change in New South Wales– Part 2, Projected Changes in Climate Extremes.* Consultancy report for the New South Wales Greenhouse Office. CSIRO Atmospheric Research, Aspendale, 79 pp.

Hewitson, B.C., and R.G. Crane, 2005: Gridded area-averaged daily precipitation via conditional interpolation. *J. Clim.*, **18**, 41–51.

Hewitson, B.C., and R.G. Crane, 2006: Consensus between GCM climate change projections with empirical downscaling: precipitation downscaling over South Africa. *Int. J. Climatol.*, **26**, 1315–1337

Hewitson, B.C., et al., 2004: *Dynamical Modelling of the Present and Future Climate System*. Technical Report to the Water Research Commission, Report No. 1154/1/04 , Pretoria, South Africa.

Higgins, R.W., and K.C. Mo, 1997: Persistent North Pacific circulation anomalies and the tropical intraseasonal oscillation. *J. Clim.*, **10**, 223–244.

Hines, K.M., D.H. Bromwich, P.J. Rasch, and M.J. Iacono, 2004: Antarctic clouds and radiation within the NCAR climate models. *J. Clim.*, **17**, 1198–1212.

Ho, C.-H., J.-J. Baik, J.-H. Kim, and D.Y. Gong, 2004: Interdecadal changes in summertime typhoon tracks. *J. Clim.*, **17**, 1767–1776.

Hoerling, M.P., J.W. Hurrell, and J. Eischeid, 2006: Detection and attribution of 20th century Northern and Southern African monsoon change. *J. Clim.* **19**(16), 3989–4008.

Holland, M.M., and C.M. Bitz, 2003: Polar amplification of climate change in the coupled model intercomparison project. *Clim. Dyn.*, **21**, 221–232.

Holloway, G., and T. Sou, 2002: Has Arctic sea ice rapidly thinned? *J. Clim.*, **15**, 1691–1701.

Hope, P.K., 2006a: Shifts in synoptic systems influencing southwest Western Australia. *Clim. Dyn.*, **26**, 751–764.

Hope, P.K., 2006b: Future changes in synoptic systems influencing southwest Western Australia. *Clim. Dyn.*, **26**, 765–780.

Hori, M.E., and H. Ueda, 2006: Impact of global warming on the East Asian winter monsoon as revealed by nine coupled atmosphere-ocean GCMs. *Geophys. Res. Lett.*, **33**, L03713, doi:10.1029/2005GL024961.

Hu, Z.Z., L. Bengtsson, and K. Arpe, 2000: Impact of global warming on the Asian winter monsoon in a coupled GCM. *J. Geophys. Res.*, **105**(D4), 4607–4624.

Hu, Z.Z., S. Yang, and R. Wu, 2003: Long-term climate variations in China and global warming signals. *J. Geophys. Res.*, **108**(D19), 4614, doi:10.1029/2003JD003651.

Hubbert, G.D., and K.L. McInnes, 1999: A storm surge inundation model for coastal planning and impact studies. *J. Coastal Res.*, **15**, 168–185.

Huffman, G.J., et al., 2001: Global precipitation at one-degree daily resolution from multisatellite observations. *J. Hydrometeorol.*, **2**, 36–50.

Hulme, M., and N. Sheard, 1999a: *Climate Change Scenarios for Indonesia*. Climatic Research Unit, Norwich, UK, 6 pp.

Hulme, M., and N. Sheard, 1999b: *Climate Change Scenarios for the Philippines*. Climatic Research Unit, Norwich, UK, 6 pp.

Hulme, M., R. Doherty, and T. Ngara, 2001: African climate change: 1900-2100. *Clim. Res.*, **17**, 145–168.

Hulme, M., et al., 1999: Relative impacts of human-induced climate change and natural variability. *Nature*, **397**, 688–691.

Huntingford, C., et al., 2003: Regional climate-model predictions of extreme rainfall for a changing climate. *Q. J. R.. Meteorol. Soc.*, **129**, 1607–1621.

Hurrell, J.W., and H. van Loon, 1997: Decadal variations in climate associated with the North Atlantic Oscillation. *Clim. Change*, **36**, 301–326.

Huth, R., J. Kysely, and M. Dubrovsky, 2001: Time structure of observed, GCM-simulated, downscaled, and stochastically generated daily temperature series. *J. Clim.*, **14**, 4047–4061.

Im, E.S., E-H. Park, W.-T. Kwon, and F. Giorgi, 2006: Present climate simulation over Korea with a regional climate model using a one-way double-nested system. *Theor. Appl. Climatol.* **86**, 183–196.

Imbert, A., and R.E. Benestad, 2005: An improvement of analog model strategy for more reliable local climate change scenarios. *Theor. Appl. Climatol.*, **82**, 245–255.

Inatsu, M., and M. Kimoto, 2005: Difference of boreal summer climate between coupled and atmosphere-only GCMs. *Scientific Online Letters on the Atmosphere*, **1**, 105–108.

International CLIVAR Project Office, 2006: *Understanding the Role of the Indian Ocean in the Climate System — Implementation Plan for Sustained Observations*. CLIVAR Publication Series No.100, International CLIVAR Project Office, Southampton, UK, 76 pp.

IOCI, 2002: *Climate Variability and Change in South West Western Australia*. Technical Report, Indian Ocean Climate Initiative Panel, Perth, Australia, 34 pp.

IOCI, 2005: *Indian Ocean Climate Initiative Stage 2: Report of Phase 1 Activity*. Indian Ocean Climate Initiative Panel, Perth, Australia, 42 pp., http://www.ioci.org.au/publications/pdf/2005202-IOCI%20reportvis2.pdf.

IPCC, 1996: Technical summary. In: *Climate Change 1995: The Science of Climate Change. Contribution of Working Group I to the Second Assessment Report of the Intergovernmental Panel on Climate Change* [Houghton, J.T., et al. (eds.)]. Cambridge University Press, Cambridge, United Kingdom and New York, NY, USA, pp. 9–49.

IPCC, 2001: *Climate Change 2001: The Scientific Basis. Contribution of Working Group I to the Third Assessment Report of the Intergovernmental Panel on Climate Change* [Houghton, J.T., et al. (eds.)]. Cambridge University Press, Cambridge, United Kingdom and New York, NY, USA, 881 pp.

Jacob, D., et al., 2007: An intercomparison of regional climate models for Europe: design of the experiments and model performance. *Clim. Change*, doi: 10.1007/s10584-006-9213-4.

Jenkins, G.S., G. Adamou, and S. Fongang, 2002: The challenges of modeling climate variability and change in West Africa. *Clim. Change*, **52**, 263–286.

Jiang, Y.D., 2005: *The Northward Shift of Climatic Belts in China during the Last 50 Years, and the Possible Future Changes*. PhD Thesis, Institute of Atmospheric Physics, China Academy of Science, Beijing, 137 pp.

Jiao, Y., and D. Caya, 2006: An investigation of summer precipitation simulated by the Canadian regional climate model. *Mon. Weather Rev.*, **134**, 919–932.

Johannessen, O.M., et al., 2004: Arctic climate change: observed and modelled temperature and sea-ice variability. *Tellus*, **56A**(4), 328.

Jolly, D., S.P. Harrison, B. Damnati, and E. Bonnefille, 1996: Simulated climate and biomes of Africa during the late Quaternary: comparison with pollen and lake status data. *Quat. Sci. Rev.*, **17**, 629–657.

Jones, C.D., et al., 2003: Strong carbon cycle feedbacks in a climate model with interactive CO_2 and sulphate aerosols. *Geophys. Res. Lett.*, **30**(9), 1479, doi:10.1029/2003GL016867.

Jones, P.D., and P.A. Reid, 2001: Assessing future changes in extreme precipitation over Britain using regional climate model integrations. *Int. J. Climatol.*, **21**, 1337–1356.

Jones, R.G., J.M. Murphy, M. Noguer, and A.B. Keen, 1997: Simulation of climate change over Europe using a nested regional climate model. II: Comparison of driving and regional model responses to a doubling of carbon dioxide. *Q. J. R. Meteorol. Soc.*, **123**, 265–292.

Jones, R.N., 2000: Managing uncertainty in climate change projections – issues for impact assessment. *Clim. Change*, **45**, 403–419.

Jones, R.N., et al., 2000: *An Analysis of the Effects of The Kyoto Protocol on Pacific Island Countries, Part Two: Regional Climate Change Scenarios and Risk Assessment Methods*. South Pacific Regional Environment Programme, Apia, Samoa, 68 pp., available from sprep@sprep.org.ws.

Jones, R.N., et al., 2002: Scenarios and projected ranges of change for mean climate and climate variability for the South Pacific. *Asia Pac. J. Environ. Dev.*, **9**(1–2), 1–42.

Juang, H.M.H., and S.Y. Hong, 2001: Sensitivity of the NCEP regional spectral model to domain size and nesting strategy. *Mon. Weather Rev.*, **129**, 2904–2922.

Kabat, P., et al., 2002: *Vegetation, Water, Humans and the Climate Change: A New Perspective on an Interactive System*. Springer, Heidelberg, Germany, 566 pp.

Kamga, A.F., et al., 2005: Evaluating the National Center for Atmospheric Research climate system model over West Africa: Present-day and the 21st century A1 scenario. *J. Geophys. Res.*, **110**(D03106), doi:10.1029/2004JD004689.

Kanada, S., et al., 2005: Structure of mesoscale convective systems during the late Baiu season in the global warming climate simulated by a non-hydrostatic regional model. *Scientific Online Letters on the Atmosphere*, **1**, 117–120.

Kang I.-S., et al., 2002: Intercomparison of atmospheric GCM simulated anomalies associated with the 1997/98 El Niño. *J. Clim.*, **15**, 2791–2805.

Karcher, M.J., R. Gerdes, F. Kauker, and C. Köberle, 2003: Arctic warming: Evolution and spreading of the 1990s warm event in the Nordic seas and the Arctic Ocean. *J. Geophys. Res.*, **108**(C2), 3034, doi:10.1029/2001JC001265.

Kattsov, V.M., et al., 2007: Simulation and projection of Arctic freshwater budget components by the IPCC AR4 global climate models. *J. Hydrometeorol.*, **8**, in press.

Katz, R.W., M.B. Parlange, and P. Naveau, 2002: Statistics of extremes in hydrology. *Adv. Water Resour.*, **25**, 1287–1304.

Katz, R.W., M.B. Parlange, and C. Tebaldi, 2003: Stochastic modelling of the effects of large-scale circulation on daily weather in the southeastern US. *Clim. Change*, **60**, 189–216.

Keller, F., S. Goyette, and M. Beniston, 2005: Sensitivity analysis of snow cover to climate change scenarios and their impact on plant habitats in alpine terrain. *Clim. Change*, **72**, 299–319.

Kharin, V.V., and F.W. Zwiers, 2005: Estimating extremes in transient climate change simulations. *J. Clim.*, **18**, 1156–1173.

Kida, H., T. Koide, H. Sasaki, and M. Chiba, 1991: A new approach for coupling a limited area model to a GCM for regional climate simulations. *J. Meteorol. Soc. Japan.*, **69**, 723–728.

Kim, J., T.-K. Kim, R.W. Arritt, and N.L. Miller, 2002: Impacts of increased atmospheric CO_2 on the hydroclimate of the Western United States. *J. Clim.*, **15**(14), 1926–1942.

Kimoto, M., 2005: Simulated change of the east Asian circulation under global warming scenario. *Geophys. Res. Lett.*, **32**, L16701, doi:10.1029/2005GRL023383.

Kimoto, M., N. Yasutomi, C. Yokoyama, and S. Emori, 2005: Projected changes in precipitation characteristics around Japan under the global warming. *Scientific Online Letters on the Atmosphere*, **1**, 85–88.

Kitoh, A., and T. Uchiyama, 2006: Changes in onset and withdrawal of the East Asian summer rainy season by multi-model global warming experiments. *J. Meteorol. Soc. Japan*, **84**, 247–258.

Kitoh, A., M. Hosaka, Y. Adachi and K. Kamiguchi, 2005: Future projections of precipitation characteristics in East Asia simulated by the MRI CGCM2. *Adv. Atmos. Sci.*, **22**(4), 467–478.

Kjellström, E., et al., 2007: Variability in daily maximum and minimum temperatures: recent and future changes over Europe. *Clim. Change*, doi: 10.1007/s10584-006-9220-5.

Kleinn, J., et al., 2005: Hydrological simulations in the Rhine basin, driven by a regional climate model. *J. Geophys. Res.*, **110**, D04102, doi:10.1029/2004JD005143.

Knippertz, P., U. Ulbrich, and P. Speth, 2000: Changing cyclones and surface wind speeds over the North-Atlantic and Europe in a transient GHG experiment. *Clim. Res.*, **15**, 109–122.

Knutson, T.R., and S. Manabe, 1995: Time-mean response over the tropical Pacific to increased CO_2 in a coupled ocean-atmosphere model. *J. Clim.*, **8**, 2181–2199.

Knutson, T.R., and R.E. Tuleya, 2004: Impacts of CO_2-induced warming on simulated hurricane intensities and precipitation: sensitivity to the choice of climate model and convective parameterization. *J. Clim.*, **17**, 3477–3495.

Krinner, G., C. Genthon, Z. Li, and P.L. Van, 1997: Studies of the Antarctic climate with a stretched-grid general circulation model. *J. Geophys. Res.*, **102**, 13731–13745.

Krishna Kumar, K., B. Rajagopalan, and M.A. Cane, 1999: On the weakening relationship between the Indian monsoon and ENSO. *Science*, **284**, 2156–2159.

Krishna Kumar, K., et al., 2003: Future scenarios of extreme rainfall and temperature over India. In: *Proceedings of the Workshop on Scenarios and Future Emissions, Indian Institute of Management (IIM), Ahmedabad, July 22, 2003*. NATCOM Project Management Cell, Ministry of Environment and Forests, Government of India, New Delhi, pp. 56–68.

Kumagi, T., G.G. Katul, and A. Porporato, 2004: Carbon and water cycling in a Bornean tropical rainforest under current and future climate scenarios. *Adv. Water Resour.*, **27**, 1135–1150.

Kurihara, K., et al., 2005: Projection of climatic change over Japan due to global warming by high-resolution regional climate model in MRI. *Scientific Online Letters on the Atmosphere*, **1**, 97–100.

Kusunoki, S., et al., 2006: Change of Baiu rain band in global warming projection by an atmospheric general circulation model with a 20-km grid size. *J. Meteorol. Soc. Japan*, **84**(4), 581–611

Kutzbach, J.E., G. Bonan, J. Foley, and S. Harrison, 1996: Vegetation and soil feedbacks on the response of the African monsoon to forcing in the early to middle Holocene. *Nature*, **384**, 623–626.

Kwok, R., and J.C. Comiso, 2002a: Spatial patterns of variability in Antarctic surface temperature: Connections to the Southern Hemisphere annular mode and the Southern Oscillation. *Geophys. Res. Lett.*, **29**(14), 1705, doi:10.1029/2002GL015415.

Kwok, R., and J.C. Comiso, 2002b: Southern Ocean climate and sea ice anomalies associated with the Southern Oscillation. *J. Clim.*, **15**, 487–501.

Kwon, W.-T., et al., 2003: *The Development of Regional Climate Change Scenario for the National Climate Change Report (II)*. METRI Technical Report MR030CR09, Meteorological Research Institute, Seoul, Korea, 502 pp (in Korean).

Kwon, W.-T., et al., 2005: *The Application of Regional Climate Change Scenario of the National Climate Change Report (I)*. METRI Technical Report MR050C03, Meteorological Research Institute, Seoul, Korea, 408 pp (in Korean).

Lal, M., 2004: Climate change and small island developing countries of the South Pacific. *Fijian Studies*, **2**(1), 1–15.

Lal, M., and H. Harasawa, 2001: Future climate change scenarios for Asia as inferred from selected coupled atmosphere-ocean global climate models. *J. Meteorol. Soc. Japan*, **79**, 219–227.

Lal, M., H. Harasawa, and K. Takahashi, 2002: Future climate change and it's impacts over small island states. *Clim. Res.*, **19**, 179–192.

Lal, M., et al., 2001: Future climate change: Implications for Indian summer monsoon and its variability. *Curr. Sci.*, **81**, 1196–1207.

Lamb, P.J., and R.A. Peppler, 1987: North Atlantic Oscillation: Concept and an application. *Bull. Am. Meteorol. Soc.*, **68**(10), 1218–1225.

Lambert, S.J., and J.C. Fyfe, 2006: Changes in winter cyclone frequencies and strengths simulated in enhanced greenhouse warming experiments: results from the models participating in the IPCC diagnostic exercise. *J. Clim. Dyn.*, **26**, 713–728.

Laprise, R., 2003: Resolved scales and nonlinear interactions in limited-area models. *J. Atmos. Sci.*, **60**(5), 768–779.

Latif, M., et al., 2001: ENSIP: The El Niño Simulation Intercomparison Project. *Clim. Dyn*, **18**, 255–276.

Lau, K.M., and J. Zhou, 2003: Responses of the South American Summer Monsoon climate system to ENSO during 1997–99. *Int. J. Climatol.*, **23**, 529–539.

Leckebusch, G.C., and U. Ulbrich, 2004: On the relationship between cyclones and extreme windstorm events over Europe under climate change. *Global Planet. Change*, **44**, 181–193.

Leckebusch, G.C., et al., 2007: Analysis of frequency and intensity of winter storm events in Europe on synoptic and regional scales from a multi-model perspective. *Clim. Res.* **31**, 59–74.

Lenderink, G., A. van Ulden, B. van den Hurk, and E. van Meijgaard, 2007: Summertime inter-annual temperature variability in an ensemble of regional model simulations: analysis of the surface energy budget. *Clim. Change*, doi: 10.1007/s10584-006-9229-9

Leung, L.R., L.O. Mearns, F. Giorgi, and R.L. Wilby, 2003: Regional climate research: needs and opportunities. *Bull. Am. Meteorol. Soc.*, **84**, 89–95.

Leung, L.R., et al., 2004: Mid-century ensemble regional climate change scenarios for the western United States. *Clim. Change*, **62**, 75–113.

L'Heureux, M.L., and D.W.J. Thompson, 2006: Observed relationships between the El-Niño/Southern Oscillation and the extratropical zonal mean circulation. *J. Clim.*, **19**, 276–287.

L'Heureux, M.L., et al., 2004: Atmospheric circulation influences on seasonal precipitation patterns in Alaska during the latter 20th century. *J. Geophys. Res.*, **109**(6), D06106, doi:10.1029/2003JD003845.

Liang, X.Z., et al., 2004: Regional climate model simulation of U.S. precipitation during 1982–2002. Part I: Annual cycle. *J. Clim.*, **17**(18), 3510–3529.

Liang, X.Z., et al., 2006: Regional climate model downscaling of the U.S. summer climate and future change. *J. Geophys. Res.*, **111**, D10108, doi:10.1029/2005JD006685.

Liebmann, B., et al., 2004: An observed trend in Central South American precipitation. *J. Clim.*, **17**, 4357–4367.

Lintner, B.R., and J.C.H. Chiang, 2005: Reorganization of tropical climate during El Niño: a weak temperature gradient approach. *J. Clim.*, **18**(24), 5312–5329.

Lionello, P., F. Dalan, and E. Elvini, 2002: Cyclones in the Mediterranean region: the present and the doubled CO_2 climate scenarios. *Clim. Res.*, **22**, 147–159.

Lionello, P., E. Elvini, and A. Nizzero, 2003: Ocean waves and storm surges in the Adriatic Sea: intercomparison between the present and the doubled CO_2 climate scenarios. *Clim. Res.*, **23**, 217–231.

Liu, J., et al., 2005: Comparison of surface radiative flux data sets over the Arctic Ocean. *J. Geophys. Res.*, **110**, C02015, doi:10.1029/2004JC002381.

Lopez, A., et al., 2006: Two approaches to quantifying uncertainty in global temperature changes. *J. Clim.*, **19**, 4785–4796.

Lorant, V., and J-F. Royer, 2001: Sensitivity of equatorial convection to horizontal resolution in aquaplanet simulations with a variable-resolution GCM. *Mon. Weather Rev.*, **129**(11), 2730–2745.

Lorenz, P., and D. Jacob, 2005: Influence of regional scale information on the global circulation: a two-way nested climate simulation. *Geophys. Res. Lett.*, **32**, L18706, doi:10.1029/2005GL023351.

Lowe, J.A., and J.M. Gregory, 2005: The effects of climate change on storm surges around the United Kingdom. *Philos. Trans. R. Soc. London Ser. A.*, **363**, 1313–1328.

Lowe, J.A., J.M. Gregory, and R.A. Flather, 2001: Changes in the occurrence of storm surges around the United Kingdom under a future climate scenario using a dynamic storm surge model driven by the Hadley Centre climate models. *Clim. Dyn.*, **18**(3–4), 179–188.

Lu, J., and T.L. Delworth, 2005: Oceanic forcing of late 20th century Sahel drought. *Geophys. Res. Lett.*, **32**, L22706, doi:10.1029/2005GL023316.

Lynch, A., P. Uotila, and J.J. Cassano, 2006: Changes in synoptic weather patterns in the polar regions in the 20th and 21st centuries, Part 2: Antarctic. *Int. J. Climatol.*, **26**, 1181–2119.

Lynch, A.H., E.N. Cassano, J.J. Cassano, and L. Lestak, 2003: Case studies of high wind events in Barrow, Alaska: Climatological context and development processes. *Mon. Weather Rev.*, **131**, 719–732.

Lynch, A.H., J.A. Curry, R.D. Brunner, and J.A. Maslanik, 2004: Toward an integrated assessment of the impacts of extreme wind events on Barrow, Alaska. *Bull. Am. Meteorol. Soc.*, **85**, 209–221.

Mabuchi, K., Y. Sato, and H. Kida, 2002: Verification of the climatic features of a regional climate model with BAIM. *J. Meteorol. Soc. Japan*, **80**(4), 621–644.

Mabuchi, K., Y. Sato, and H. Kida, 2005a: Climatic impact of vegetation change in the Asian tropical region. Part I: Case of the Northern Hemisphere summer. *J. Clim.*, **18**(3), 410–428.

Mabuchi, K., Y. Sato, and H. Kida, 2005b: Climatic impact of vegetation change in the Asian tropical region. Part II: Case of the Northern Hemisphere winter and impact on the extratropical circulation. *J. Clim.*, **18**(3), 429–446.

Magaña, V., and E. Caetano, 2005: Temporal evolution of summer convective activity over the Americas warm pools. *Geophys. Res. Lett.*, **32**, L02803, doi:10.1029/2004GL021033.

Magaña, V., J.A. Amador, and S. Medina, 1999: The mid-summer drought over Mexico and Central America. *J. Clim.*, **12**, 1577–1588.

Manabe, S., and R.T. Wetherald, 1987: Large-scale changes of soil wetness induced by an increase in atmospheric carbon dioxide. *J. Atmos. Sci.*, **44**, 1211–1235.

Marengo, J.A., and T. Ambrizzi, 2006: Use of regional climate models in impacts assessments and adaptation studies from continental to regional and local scales. In: *Proceedings of the 8th International Conference on Southern Hemisphere Meteorology and Oceanography (ICSHMO), Foz do Iguaçu, Brazil, 24-28 April 2006*. Brazilian Institute for Space Research (INPE), São José dos Campos, pp. 291–296.

Marland, G., et al., 2003: The climatic impacts of land surface change and carbon management, and the implications for climate-change mitigation policy. *Clim. Policy*, **3**, 149–157.

Martin E., E. Brun, and Y. Durand, 1994: Sensitivity of the French Alps snow cover to the variation of climatic variables. *Ann. Geophys.*, **12**, 469–477.

Martinez-Castro, D., et al., 2006: Sensitivity studies of the RegCM-3 simulation of summer precipitation, temperature and local wind field in the Caribbean region. *Theor. Appl. Climatol.*, **86**, 5–22.

Martis, A., G.J. van Oldenborgh, and G. Burgers, 2002: Predicting rainfall in the Dutch Caribbean – More than El Niño? *Int. J. Climatol.*, **22**, 1219–1234.

Maslanik, J.A., A.H. Lynch, M.C. Serreze, and W. Wu, 2000: A case study of regional climate anomalies in the Arctic: performance requirements for a coupled model. *J. Clim.*, **13**, 383–401.

Maslowski, W., et al., 2004: On climatological mass, heat, and salt transports through the Barents Sea and Fram Strait from a pan-Arctic coupled ice-ocean model simulation. *J. Geophys. Res.*, **109**, C03032, doi:10.1029/2001JC001039.

Massom, R.A., et al., 2004: Precipitation over the interior East Antarctic ice sheet related to midlatitude blocking-high activity. *J. Clim.*, **17**, 1914–1928.

Matulla C., H. Scheifinger, A. Menzel, and E. Koch, 2003: Exploring two methods for statistical downscaling of Central European phenological time series. *Int. J. Biometeorol.*, **48**, 56–64.

May, W., 2004a: Simulation of the variability and extremes of daily rainfall during the Indian summer monsoon for present and future times in a global time-slice experiment. *Clim. Dyn.*, **22**, 183–204.

May, W., 2004b: Potential of future changes in the Indian summer monsoon due to greenhouse warming: analysis of mechanisms in a global time-slice experiment. *Clim. Dyn.*, **22**, 389–414.

May, W., and E. Roeckner, 2001: A time-slice experiment with the ECHAM4 AGCM at high resolution: The impact of horizontal resolution on annual mean climate change. *Clim. Dyn.*, **17**, 407–420.

Maynard, K., and J.-F. Royer, 2004a: Effects of realistic land-cover change on a greenhouse-warmed African climate. *Clim. Dyn.*, **22**(4), 343–358.

Maynard, K., and J.-F. Royer, 2004b: Sensitivity of a general circulation model to land surface parameters in African tropical deforestation experiments. *Clim. Dyn.*, **22**(6/7), 555–572.

Maynard, K., J.-F. Royer, and F. Chauvin, 2002: Impact of greenhouse warming on the West African summer monsoon. *Clim. Dyn.*, **19**, 499–514.

McBride, J.L., and N. Nicholls, 1983: Seasonal relationships between Australian rainfall and the Southern Oscillation. *Mon. Weather Rev.*, **111**, 1998–2004.

McBride, J.L., M.R. Haylock, and N. Nicholls, 2003: Relationships between the Maritime Continent heat source and the El Niño-Southern Oscillation phenomenon. *J. Clim.*, **16**, 2905–2914.

McGregor, J.L., 2004: Regional climate modelling activities at CSIRO. In: *Symposium on Water Resource and its Variability in Asia in the 21st Century, 1-2 March 2004, Epochal Tsukuba (International Congress Center), Tsukuba, Ibaraki, Japan*. Meteorological Research Institute, Japan Meteorological Agency, Tsukuba, Japan, pp. 68–71.

McGregor, J.L., and M.R. Dix, 2001: The CSIRO conformal-cubic atmospheric GCM. In: *IUTAM Symposium on Advances in Mathematical Modelling of Atmosphere and Ocean Dynamics* [Hodnett, P.F. (ed.)]. Kluwer Academic, Dordrecht, pp. 307–315.

McGregor, J.L., and K.C. Nguyen, 2003: Simulations of the East Asian and Australian monsoons using a variable-resolution model. In: *Proceedings of the 2nd Workshop on Regional Climate Modeling for Monsoon System, Yokohama, Japan*. GAME Publication No. 39, FRSGC and GAME International Science Panel, Yokohama, pp.117–120.

McGregor, J.L., J.J. Katzfey, and K.C. Nguyen, 1998: *Fine Resolution Simulations of Climate Change for Southeast Asia*. Final report for a research project commissioned by Southeast Asian Regional Committee for START (SARCS), CSIRO Atmospheric Research, Aspendale, Vic., 35 pp. + 3 CD-ROMs.

McGregor, J.L., K.C. Nguyen, and J.J. Katzfey, 2002: Regional climate simulations using a stretched-grid global model. In: *Research Activities in Atmospheric and Oceanic Modelling* [Ritchie, H. (ed.)]. Report No. 32, WMO/TD-No. 1105, World Meteorological Organisation, Geneva, pp. 15–16.

McGuffie, K., et al., 1995: Global climate sensitivity to tropical deforestation. *Global Planet. Change*, **10**, 97–128.

McInnes, K.L., et al, 2003: *Assessment of climate change, impacts and possible adaptation strategies relevant to South Australia.* Consultancy report undertaken for the South Australian Government by the Climate Impact Group, CSIRO Atmospheric Research, Aspendale, VIC, Australia, 61pp. http://www.cmar.csiro.au/e-print/open/mcinnes_2003a.pdf

McInnes, K. L., et al. (2004). *Climate change in Tasmania*. A report undertaken for Hydro Tasmania by the Climate Impact GroupC/0919. CSIRO Atmospheric Research, Aspendale, Vic, 49 pp., http://www.cmar.csiro.au/e-print/open/mcinnesskl_2004a.pdf

McInnes, K. L., et al. (2005). *Climate change in Eastern Victoria*: *Stage 2 report*: *the effect of climate change on storm surges*. A project undertaken for the Gippsland Coastal Board. CSIRO Marine and Atmospheric Research, Aspendale, Vic.: 37 pp. http://www.cmar.csiro.au/e-print/open/mcinnes_2005b.pdf

Mearns, L.O., et al., 2005: NARCCAP, North American Regional Climate Change Assessment Program, A multiple AOGCM and RCM climate scenario project over North America. *Preprints of the American Meteorological Society 16th Conference on Climate Variations and Change. 9-13 January, 2005*. Paper J6.10, American Meteorological Society, Washington, DC, pp. 235–238.

Meehl, G.A., and C. Tebaldi, 2004: More intense, more frequent, and longer lasting heat waves in the 21st century. *Science*, **305**, 994–997.

Meehl, G.A., J.M. Arblaster, and C. Tebaldi, 2005: Understanding future patterns of increased precipitation intensity in climate model simulations. *Geophys. Res. Lett.*, **32**, L18719, doi:10.1029/2005GL023680.

Meehl, G.A., et al., 2006: Climate change in the 20th and 21st centuries and climate change commitment in the CCSM3. *J. Clim.*, **19**, 2597–2616.

Meier, H.E.M, 2002: Regional ocean climate simulations with a 3D ice-ocean model for the Baltic Sea. Part 2: results for sea ice. *Clim. Dyn*., **19**, 255–266.

Meier, H.E.M, 2006: Baltic Sea climate in the late twenty-first century: a dynamical downscaling approach using two global models and two emission scenarios. *Clim. Dyn*., **27**(1), 39–68, doi:10.1007/s00382-006-0124-x.

Meier, H.E.M., R. Döscher, and A. Halkka, 2004: Simulated distributions of Baltic sea-ice in warming climate and consequences for the winter habitat of the Baltic Sea ringed seal. *Ambio*, **33**, 249–256.

Meleshko, V.P., et al., 2004: Anthropogenic climate changes in Northern Eurasia in the 21st century. *Russ. Meteorol. Hydrol.*, **7**, 5–26.

Menéndez, C.G., A.C. Saulo, and Z.-X. Li, 2001: Simulation of South American wintertime climate with a nesting system. *Clim. Dyn*., **17**, 219–231.

Menéndez, C.G., M.F. Cabré, and M.N. Nuñez, 2004: Interannual and diurnal variability of January precipitation over subtropical South America simulated by a regional climate model. *CLIVAR Exchanges*, **29**, 1–3.

Miguez-Macho, G., G.L. Stenchikov, and A. Robock, 2004: Spectral nudging to eliminate the effects of domain position and geometry in regional climate model simulations. *J. Geophys. Res*., **109**, D13104, doi:10.1029/2003JD004495.

Mikolajewicz, U., et al., 2005: Simulating Arctic sea ice variability with a coupled regional atmosphere-ocean-sea ice model. *Meteorol. Z.*, **14**, 793–800.

Min, S.K., E.H. Park, and W.T. Kwon, 2004: Future projections of East Asian climate change from Multi-AOGCM ensembles of IPCC SRES scenario simulations. *J. Meteorol. Soc. Japan*, **82**(4), 1187–1211.

Ministry for the Environment, 2004: *Climate Change Effects and Impacts Assessment: A Guidance Manual for Local Government in New Zealand.* New Zealand Climate Change Office, Ministry for the Environment, Wellington, http://www.climatechange.govt.nz/resources/local-govt/effects-impacts-may04/index.html.

Misra, V., P.A. Dirmeyer, and B.P. Kirtman, 2003: Dynamic downscaling of seasonal simulations over South America. *J. Clim*., **16**, 103–117.

Mitchell, T.D., 2003: Pattern scaling: an examination of the accuracy of the technique for describing future climates. *Clim. Change*, **60**(3), 217–242.

Mizuta, R., et al., 2005: Changes in extremes indices over Japan due to global warming projected by a global 20-km-mesh atmospheric model. *Scientific Online Letters on the Atmosphere*, **1** 153–156.

Mizuta, R., et al., 2006: 20km-mesh global climate simulations using JMA-GSM model. Mean climate states. *J. Meteorol. Soc. Japan.*, **84**, 165–185.

Mo, K.C., and J. Nogués-Paegle, 2001: The Pacific-South American modes and their downstream effects. *Int. J. Climatol.*, **21**, 1211–1229.

Moise, A., R. Colman, and H. Zhang, 2005: Coupled model simulations of current Australian surface climate and its changes under greenhouse warming: An analysis of 18 CMIP2 models. *Aust. Meteorol. Mag.*, **54**, 291–307.

Monaghan, A.J., D.H. Bromwich, and S.-H. Wang, 2006: Recent trends in Antarctic snow accumulation from Polar MM5 simulations. *Philos. Trans. R. Soc. London Ser. A.*, **364**, 1683–1708.

Mote, P.W., and N.J. Mantua, 2002: Coastal upwelling in a warmer future. *Geophys. Res. Lett.*, **29**(23), 2138, doi:10.1029/2002GL016086.

Mullan, A.B., 1995: On the linearity and stability of Southern Oscillation - climate relationships for New Zealand. *Int. J. Climatol.*, **15**, 1365–1386.

Mullan, A.B., D.S. Wratt, and J.A. Renwick, 2001a: Transient model scenarios of climate changes for New Zealand. *Weather and Climate*, **21**, 3–34.

Mullan, A.B., M.J. Salinger, C.S. Thompson, and A.S. Porteous, 2001b: The New Zealand climate: present and future. In: *Effects of Climate Change and Variation in New Zealand: An Assessment using the CLIMPACTS System* [Warrick, R.A., G.J. Kenny, and J.J. Harman, (eds.)]. International Global Change Institute, University of Waikato, pp. 11–31.

Mullan, B., A. Porteous, D. Wratt, and M. Hollis, 2005: *Changes in Drought Risk with Climate Change*. NIWA Client Report WLG2005-23, National Institute for Water and Atmosphere Research, Wellington, New Zealand, 68 pp.

Murphy, J.M., et al., 2004: Quantification of modelling uncertainties in a large ensemble of climate change simulations. *Nature*, **430**, 768–772.

Neelin, J.D., and H. Su, 2005: Moist teleconnection mechanisms for the tropical South American and Atlantic sector. *J. Clim.*, **18**(18), 3928–3950.

Neelin, J.D., et al., 2006: Tropical drying trends in global warming models and observations. *Proc. Natl. Acad. Sci. U.S.A.*, **103**, 6110–6115.

New, M., and M. Hulme, 2000: Representing uncertainty in climate change scenarios: a Monte Carlo approach. *Integr. Assess. J.*, **1**, 203–213.

New, M., B.C. Hewitson, C. Jack, and R.Washington, 2003: Sensitivity of southern African rainfall to soil moisture. *CLIVAR Exchanges*, **27**, 45–47.

Nguyen, K.C., and K.J.E. Walsh, 2001: Interannual, decadal, and transient greenhouse simulation of tropical cyclone-like vortices in a regional climate model of the South Pacific. *J. Clim.*, **14**(13), 3043–3054.

Nicolini, M., et al., 2002: January and July regional climate simulation over South America. *J. Geophys. Res.*, **107**(D22), 4637, doi:10.1029/2001JD000736.

Nobre, P., A. Moura, and L. Sun, 2001: Dynamic downscaling of seasonal climate prediction over Nordeste Brazil with ECHAM3 and NCEP's regional spectral models at IRI. *Bull. Am. Meteorol. Soc.*, **82**, 2787–2796.

Noone, D., and I. Simmonds, 2002: Annular variations in moisture transport mechanisms and the abundance of delta O-18 in Antarctic snow. *J. Geophys. Res.*, **107**, 4742, doi:10.1029/2002JD002262.

Oh, J-H et al., 2004: Regional climate simulation for Korea using dynamic downscaling and statistical adjustment. *J. Meteorol. Soc. Japan*, **82**(6), 1629–1643.

Oleson, K.W., G.B. Bonan, S. Levis, and M. Vertenstein, 2004: Effects of land use change on U.S. climate: Impact of surface datasets and model biogeophysics. *Clim. Dyn.*, **23**, 117–132.

Oouchi, K., et al., 2006: Tropical cyclone climatology in a global-warming climate as simulated in a 20 km-mesh global atmospheric model: Frequency and wind intensity analyses. *J. Meteorol. Soc. Japan*, **84**, 259–276.

Osborn, T.J., et al., 1999: Evaluation of the North Atlantic Oscillation as simulated by a coupled climate model. *Clim. Dyn.*, **15**, 685–702.

Paeth, H., and A. Hense, 2004: SST versus climate change signals in West African rainfall: 20th-century variations and future projections. *Clim. Change*, **65**(1–2): 179–208.

Paeth, H., K. Born, D. Jacob, and R. Podzun, 2005: Regional dynamic downscaling over West Africa: model validation and comparison of wet and dry years. *Meteorol. Z.*, **14**(3), 349–367.

Pal, J.S., F. Giorgi, and X. Bi, 2004: Consistency of recent European summer precipitation trends and extremes with future regional climate projections. *Geophys. Res. Lett.*, **31**, L13202, doi:10.1029/2004GL019836.

Palmer, T.N., 1986: Influence of the Atlantic, Pacific and Indian Oceans on Sahel rainfall, *Nature*, **322**, 251–253.

Palutikof, J.P., C.M. Goodess, S.J. Watkins, and T. Holt, 2002: Generating rainfall and temperature scenarios at multiple sites: examples from the Mediterranean. *J. Clim.*, **15**, 3529–3548.

Pan, Z., E.S. Takle, and F. Otieno., 2001: Evaluation of uncertainties in regional climate change simulations. *J. Geophys. Res.*, **106**(D16), 17735–17752.

Pan, Z., M. Segal, R.W. Arritt, and E.S. Takle, 2004: On the potential change in solar radiation over the US due to increases of atmospheric greenhouse gases. *Renew. Energy*, **29**(11), 1923–1928.

Pant, G.B., and K. Rupa Kumar, 1997: *Climates of South Asia*. John Wiley & Sons, Chichester, 320 pp.

Pavolonis, M.J., J.R. Key, and J.J. Cassano, 2004: A study of the Antarctic surface energy budget using a polar regional atmospheric model forced with satellite-derived cloud properties. *Mon. Weather Rev.*, **132**, 654–661.

Peterson, T.C., et al., 2002: Recent changes in climate extremes in the Caribbean region. *J. Geophys. Res.*, **107**(D21), 4601, doi:10.1029/2002JD002251.

Pielke, R.A. Sr., et al., 2002: The influence of land-use change and landscape dynamics on the climate system – Relevance to climate change policy beyond the radiative effect of greenhouse gases. *Philos. Trans. R. Soc. London Ser. A*, **360**, 1705–1719.

Pinto, J.G., T. Spangehl, U. Ulbrich, and P. Speth, 2006: Assessment of winter cyclone activity in a transient ECHAM4-OPYC3 GHG experiment. *Meteorol. Z.*, **15**, 279–291.

Pitman, A.J., and B.J. McAvaney, 2004: Impact of varying the complexity of the land surface energy balance on the sensitivity of the Australian climate to increasing carbon dioxide. *Clim. Res.*, **25**(3), 191–203.

Plummer, D.A., et al., 2006: Climate and climate change over North America as simulated by the Canadian Regional Climate Model. *J. Clim.*, **19**, 3112–3132.

Polyakov, I.V., et al., 2003a: Long-term ice variability in Arctic marginal seas. *J. Clim.*, **16**, 2078–2085.

Polyakov, I.V., et al., 2003b: Variability and trends of air temperature and pressure in the maritime Arctic, 1875-2000. *J. Clim.*, **16**, 2067–2077.

Pope, V.D, and R.A. Stratton, 2002: The processes governing resolution sensitivity in a climate model. *Clim. Dyn.*, **19**, 211–236.

Power, S., C. Folland, A. Colman, and V. Mehta, 1999: Inter-decadal modulation of the impact of ENSO on Australia. *Clim. Dyn.*, **15**, 319–324.

Power, S., et al., 1998: Australian temperature, Australian rainfall, and the Southern Oscillation, 1910-1996: Coherent variability and recent changes. *Aust. Meteorol. Mag.*, **47**, 85–101.

Pryor, S.C., R.J. Barthelmie, and E. Kjellström, 2005a: Potential climate change impact on wind energy resources in northern Europe: Analyses using a regional climate model. *Clim. Dyn.*, **25**, 815–835.

Pryor, S.C., J.T. School, and R.J. Barthelmie, 2005b: Potential climate change impacts on wind speeds and wind energy density in northern Europe: Results from empirical downscaling of multiple AOGCMs. *Clim. Res.*, **29**, 183–198.

Räisänen, J., 2001: Hiilidioksidin lisääntymisen vaikutus Pohjois-Euroopan ilmastoon globaaleissa ilmastomalleissa (The impact of increasing carbon dioxide on the climate of northern Europe in global climate models). *Terra*, **113**, 139–151.

Räisänen, J., 2002: CO_2-induced changes in interannual temperature and precipitation variability in 19 CMIP2 experiments. *J. Clim.*, **15**, 2395–2411.

Räisänen, J., 2005: CO_2-induced impact of increasing CO_2 on monthly-to-annual precipitation extremes: analysis of the CMIP2 experiments. *Clim. Dyn.*, **24**, 309–323.

Räisänen, J., and R. Joelsson, 2001: Changes in average and extreme precipitation in two regional climate model experiments. *Tellus*, **53A**, 547–566.

Räisänen, J., and T.N. Palmer, 2001: A probability and decision-model analysis of a multi-model ensemble of climate change simulations. *J. Clim.*, **14**, 3212–3226.

Räisänen, J., and H. Alexandersson, 2003: A probabilistic view on recent and near future climate change in Sweden. *Tellus*, **55A**, 113–125.

Räisänen, J., et al., 2003: *GCM Driven Simulations of Recent and Future Climate with the Rossby Centre Coupled Atmosphere – Baltic Sea Regional Climate Model RCAO*. Reports Meteorology and Climatology 101, Swedish Meteorological and Hydrological Institute, Norrköping, Sweden, 61 pp.

Räisänen, J., et al., 2004: European climate in the late 21st century: regional simulations with two driving global models and two forcing scenarios. *Clim. Dyn.*, **22**, 13–31.

Rajendran, K., A. Kitoh, and S. Yukimoto, 2004: South and East Asian summer monsoon climate and variation in the MRI coupled model (MRI-CGM2). *J. Clim.*, **17**, 763–782.

Ramanathan, V., et al., 2005: Atmospheric brown clouds: Impacts on South Asian climate and hydrological cycle. *Proc. Natl. Acad. Sci. U.S.A.*, **102**(15), 5326–5333.

Raphael, M.N., and M.M. Holland, 2006: Twentieth century simulation of the Southern hemisphere climate in coupled models. Part 1: Large-scale circulation variability. *Clim. Dyn.*, **26**, 217–228, doi:10.1007/s00382-005-0082-8.

Rauthe, M., and H. Paeth, 2004: Relative importance of Northern Hemisphere circulation modes in predicting regional climate change. *J. Clim.*, **17**, 4180–4189.

Reason, C., and A. Keibel, 2004: Tropical Cyclone Eline and its unusual penetration and impacts over the southern African mainland. *Weather Forecasting*, **19**(5), 789–805.

Reason, C.J.C., and M. Rouault, 2005: Links between the Antarctic Oscillation and winter rainfall over western South Africa. *Geophys. Res. Lett.*, **32**, L07705, doi:10.1029/2005GL022419.

Renwick, J.A., 2002: Southern Hemisphere circulation and relations with sea ice and sea surface temperature. *J. Clim.*, **15**, 3058–3068.

Rinke, A., and K. Dethloff, 2000: On the sensitivity of a regional Arctic climate model to initial and boundary conditions. *Clim. Res.*, **14**(2), 101–113.

Rinke, A., et al., 2003: A case study of the anomalous Arctic sea ice conditions during 1990: Insights from coupled and uncoupled regional climate model simulations. *J. Geophys. Res.*, **108**, 4275, doi:10.1029/2002JD003146.

Rinke, A., et al., 2006: Evaluation of an ensemble of Arctic regional climate models: Spatial patterns and height profiles. *Clim. Dyn.*, **26**(5), 459–472, doi:10.1007/s00382-005-0095-3.

RIVM (Rijks Instituut voor Volksgezondheid en Milieu), 2002: *The IMAGE 2.2 Implementation of the SRES Scenarios: A Comprehensive Analysis of Emissions, Climate Change and Impacts in the 21st Century*. CD-ROM, http://www.rivm.nl/bibliotheek/rapporten/481508018.html.

Roads, J., et al., 2003: International Research Institute/Applied Research Centers (IRI/ARCs) regional model intercomparison over South America. *J. Geophys. Res.*, **108**(D14), 4425, doi:10.1029/2002jd003201.

Robertson, A.W., J.D. Farrara, and C.R. Mechoso, 2003: Simulations of the atmospheric response to South Atlantic sea surface temperature anomalies. *J. Clim.*, **16**, 2540–2551.

Rockel, B., and K. Woth, 2007: Future changes in near surface wind speed extremes over Europe from an ensemble of RCM simulations. *Clim. Change*, doi: 10.1007/s10584-006-9227-y.

Rojas, M., and A. Seth, 2003: Simulation and sensitivity in a nested modeling system for South America. Part II: GCM boundary forcing. *J. Clim.*, **16**, 2454–2471.

Rotstayn, L.D., and U. Lohmann, 2002: Tropical rainfall trends and the indirect aerosol effect. *J. Clim.*, **15** (15), 2103–2116.

Rowell, D.P., 2003: The impact of Mediterranean SSTs on the Sahelian rainfall season. *J. Clim.*, **16** (5), 849–862.

Rowell, D.P., 2005: A scenario of European climate change for the late 21st century: seasonal means and interannual variability. *Clim. Dyn.*, **25**, 837–849.

Rowell, D.P., and R.G. Jones, 2006: Causes and uncertainty of future summer drying over Europe. *Clim. Dyn.*, **27**, 281–299.

Rowell, D.P., C.K. Folland, K. Maskell, and N.M. Ward, 1995: Variability of summer rainfall over Tropical North Africa (1906-92): Observations and modelling. *Q. J. R. Meteorol. Soc.*, **121**, 669–704.

Rummukainen, M., et al., 2003: Regional climate scenarios for use in Nordic water resources studies. *Nord Hydrol.*, **34**(5), 399–412.

Rummukainen, M., et al., 2004: The Swedish Regional Climate Modelling Programme, SWECLIM: a review. *Ambio*, **33**, 176–182.

Ruosteenoja, K., H. Tuomenvirta, and K. Jylhä, 2007: GCM-based regional temperature and precipitation change estimates for Europe under four SRES scenarios applying a super-ensemble pattern-scaling method. *Clim. Change*, doi: 10.1007/s10584-006-9222-3.

Ruosteenoja, K, T.R. Carter, K. Jylhä, and H. Tuomenvirta, 2003: *Future Climate in World Regions: And Intercomparison of Model-Based Projections for the New IPCC Emissions Scenarios*. Finnish Environment Institute, Helsinki, 83 pp.

Rupa Kumar, K., and R.G. Ashrit, 2001: Regional aspects of global climate change simulations: Validation and assessment of climate response over Indian monsoon region to transient increase of greenhouse gases and sulfate aerosols. *Mausam, Special Issue on Climate Change*, **52**, 229–244.

Rupa Kumar, K., et al., 2002: Climate change in India: Observations and model projections, In: *Climate Change and India: Issues, Concerns and Opportunities* [Shukla, P.R., et al., (eds.)]. Tata McGraw-Hill Publishing Co. Ltd., New Delhi, pp. 24–75.

Rupa Kumar, K., et al., 2003: Future climate scenarios. In: *Climate Change and India: Vulnerability Assessment and Adaptation* [Shukla, P.R., et al. (eds.)]. Universities Press, Hyderabad, pp. 69–127.

Rupa Kumar, K., et al., 2006: High-resolution climate change scenarios for India for the 21st century. *Curr. Sci. India.*, **90**, 334–345.

Russell, G.L., and D. Rind, 1999: Response to CO_2 transient increase in the GISS model: regional coolings in a warming climate. *J. Clim.*, **12**, 531–539.

Salathé, E.P., 2005: Downscaling simulations of future global climate with application to hydrologic modelling. *Int. J. Climatol.*, **25**, 419–436.

Salinger, M.J., J.A. Renwick, and A.B. Mullan, 2001: Interdecadal Pacific Oscillation and South Pacific climate. *Int. J. Climatol.*, **21**, 1705–1721.

Sánchez, E., C. Gallardo, M.A. Gaertner, A. Arribas and M. Castro, 2004: Future climate extreme events in the Mediterranean simulated by a regional climate model: first approach. *Global Planet. Change*, **44**, 163-180.

Santer, B.D., T.W.L. Wigley, M.E. Schlesinger, and J.F.B. Mitchell, 1990: *Developing Climate Scenarios from Equilibrium GCM Results*. Report No. 47, Max-Plank Institute for Meteorology, Hamburg, 29 pp.

Sarkar, S., R.P. Singh, and M. Kafatos, 2004: Further evidences for the weakening relationship of Indian rainfall and ENSO over India. *Geophys. Res. Lett.*, **31**, L13209, doi:10.1029/2004GL020259.

Sasaki, H., K. Kurihara, and I. Takayabu, 2006a: Comparison of climate reproducibilities between a super-high-resolution atmosphere general circulation model and a Meteorological Institute regional climate model. *Scientific Online Letters on the Atmosphere*, **1**, 81–84.

Sasaki, H., et al., 2006b: Preliminary results from the coupled atmosphere-ocean regional climate model developed at Meteorological Research Institute. *J. Meteorol. Soc. Japan*, **84**, 389–403.

Scaife, A., J.R. Knight, G.K. Vallis, and C.K. Folland, 2005: A stratospheric influence on the winter NAO and North Atlantic surface climate. *Geophys. Res. Lett.*, **32**, L18715, doi:10.1029/2005GL023226.

Schaeffer, M., F.M. Selten, J.D. Opsteegh, and H. Goosse, 2004: The influence of ocean convection patterns on high-latitude climate projections. *J. Clim.*, **17**, 4316–4329.

Schär, C., et al., 2004: The role of increasing temperature variability in European summer heatwaves. *Nature*, **427**, 332–336.

Schmidli, J., C. Frei, and P.L. Vidale, 2006: Downscaling from GCM precipitation: A benchmark for dynamical and statistical downscaling. *Int. J. Climatol.*, **26**, 679–689.

Scott, D., G. McBoyle, and B. Mills, 2003: Climate change and the skiing industry in southern Ontario (Canada): exploring the importance of snowmaking as a technical adaptation. *Clim. Res.*, **23**, 171–181.

Seem, R., 2004: Forecasting plant disease in a changing climate: a question of scale. *Can. J. Plant Pathol.*, **26**(3), 274–283.

Semenov, V.A., and L. Bengtsson, 2002: Secular trends in daily precipitation characteristics: greenhouse gas simulation with a coupled AOGCM. *Clim. Dyn.*, **19**, 123–140.

Semmler, T., and D. Jacob, 2004: Modeling extreme precipitation events – a climate change simulation for Europe. *Global Planet. Change*, **44**, 119–127.

Semmler, T., D. Jacob, K.H. Schluenzen, and R. Podzun, 2005: The water and energy budget of the Arctic atmosphere. *J. Clim.*, **18**, 2515–2530, doi:10.1175/JCLI3414.1.

Serreze, M.C., and C.M. Hurst, 2000: Representation of mean Arctic precipitation from NCEP-NCAR and ERA reanalyses. *J. Clim.*, **13**, 182–201.

Serreze, M.C., and J. Francis, 2006: The Arctic amplification debate. *Clim. Change*, **76**, 241–264, doi:10.1007/s10584-005-9017-y.

Seth, A., and M. Rojas, 2003: Simulation and sensitivity in a nested modeling system for South America. Part I: Reanalyses boundary forcing. *J. Clim.*, **16**, 2437–2453.

Shindell, D.T., and G.A. Schmidt, 2004: Southern hemisphere climate response to ozone changes and greenhouse gas increases. *Geophys. Res. Lett.*, **31**, L18209, doi:10.1029/2004GL020724.

Shkolnik, I.M., V.P. Meleshko, and V.M. Kattsov, 2006: Climate change in the 21st century over the Western Russia: a simulation with the MGO Regional Climate Model. *Russ. Meteorol. Hydrol.*, **3**, 5–17.

Simmons, A.J., et al., 2004: Comparison of trends and low-frequency variability in CRU, ERA-40, and NCEP/ NCAR analyses of surface air temperature. *J. Geophys. Res.*, **109**, D24115, doi:10.1029/2004JD005306.

Sinclair, M.R., 2002: Extratropical transition of southwest Pacific tropical cyclones. Part I: Climatology and mean structure changes. *Mon. Weather Rev.*, **130**, 590–609.

Sitch, S., et al., 2005: Impacts of future land cover changes on atmospheric CO_2 and climate. *Global Biogeochem. Cycles*, **19**(2), GB2013, doi:10.1029/2004GB002311.

Small, E., F. Giorgi, and L.C. Sloan, 1999: Regional climate model simulation of precipitation in central Asia: Mean and interannual variability. *J. Geophys. Res.*, **104**, 6563–6582.

Snyder, M.A., L.C. Sloan, N.S. Diffenbaugh, and J.L. Bell, 2003: Future climate change and upwelling in the California Current. *Geophys. Res. Lett.*, **30**(15), 1823, doi:10.1029/2003GL017647.

Solecki, W.D., and C. Oliveri, 2004: Downscaling climate change scenarios in an urban land use change model. *J. Environ. Manage.*, **72**, 105–115.

Somot, S., 2005: *Modélisation Climatique du Bassin Méditerranéen: Variabilité et Scénarios de Changement Climatique*. PhD Thesis, Université Paul Sabatier, Toulouse, France, 333 pp.

Staniforth, A., 1997: Regional modeling: A theoretical discussion. *Meteorol. Atmos. Phys.*, **63**, 15–29.

Steiner, N., et al., 2004: Comparing modelled streamfunction, heat and freshwater content in the Arctic Ocean. *Ocean Model.*, **6**(3–4), 265–284.

Stephenson, D.B., H. Douville, and K. Rupa Kumar, 2001: Searching for a fingerprint of global warming in the Asian summer monsoon. *Mausam*, **52**, 213–220.

Stephenson, D.B., et al., 2006: North Atlantic Oscillation response to transient greenhouse gas forcing and the impact on European winter climate: A CMIP2 multi-model assessment. *Clim. Dyn.*, **27**, 401–420.

Stone, D.A., A.J. Weaver, and R.J. Stouffer, 2001: Projection of climate change onto modes of atmospheric variability. *J. Clim.*, **14**, 3551–3565.

Stone, R.S., 1997: Variations in western Arctic temperatures in response to cloud radiative and synoptic-scale influences. *J. Geophys. Res.*, **102**, 21769–21776.

Stott, P.A., and J.A. Kettleborough, 2002: Origins and estimates of uncertainty in predictions of twenty-first century temperature rise. *Nature*, **416**, 723–726.

Stott, P.A., J.A. Kettleborough, and M.R. Allen, 2006a: Uncertainty in continental-scale temperature predictions. *Geophys. Res. Lett.*, **33**, L02708, doi:10.1029/2005GL024423.

Stott, P.A., et al., 2006b: Observational constraints on past attributable warming and predictions of future global warming. *J. Clim.*, **19**, 3055–3069.

Stouffer, R.J., et al., 2006: Investigating the causes of the response of the thermohaline circulation to past and future climate changes. *J. Clim.*, **19**(8), 1365–1387.

Sugi, M., A. Noda, and N. Sato, 2002: Influence of the global warming on tropical cyclone climatology: An experiment with the JMA Global Model. *J. Meteorol. Soc. Japan*, **80**, 249–272.

Suppiah, R., P.H. Whetton, and I.G. Watterson, 2004: *Climate Change in Victoria: Assessment of Climate Change for Victoria: 2001-2002*. Undertaken for Victorian Department of Sustainability and Environment. CSIRO Atmospheric Research, Aspendale, Vic., 33 pp.

Tadross, M.A., B.C. Hewitson, and M.T. Usman, 2005a: The interannual variability of the onset of the maize growing season over South Africa and Zimbabwe. *J. Clim.*, **18**(16), 3356–3372.

Tadross M.A., C. Jack, and B. Hewitson, 2005b: On RCM-based projections of change in southern African summer climate. *Geophys. Res. Lett.*, **32**, L23713, doi:10.1029/2005GL024460.

Tadross, M.A., et al., 2006: MM5 simulations of interannual change and the diurnal cycle of southern African regional climate. *Theor. Appl. Climatol*, **86**, 63–80.

Taylor, C.M., et al., 2002: The influence of land use change on climate in the Sahel. *J. Clim.*, **15**, 3615–3629.

Taylor, M., and E. Alfero, 2005: Climate of Central America and the Caribbean. In: *The Encyclopedia of World Climatology* [Oliver, J. (ed.)]. Encyclopedia of Earth Sciences Series, Springer Press, 854 pp.

Taylor, M., D. Enfield, and A. Chen, 2002: The influence of the tropical Atlantic vs. the tropical Pacific on Caribbean rainfall. *J. Geophys. Res.*, **107** (C9), 3127, doi:10.1029/2001JC001097.

Tebaldi, C., L.O. Mearns, D. Nychka, and R. Smith, 2004a: Regional probabilities of precipitation change: A Bayesian analysis of multi-model simulations. *Geophys. Res. Lett.*, **31**, L24213, doi:10.1029/2004GL021276.

Tebaldi, C., R. Smith, D. Nychka, and L.O. Mearns, 2004b: Quantifying uncertainty in projections of regional climate change: A Bayesian Approach. *J. Clim.*, **18**(10), 1524–1540.

Tebaldi, C., K. Hayhoe, J.M. Arblaster, and G.E. Meehl, 2006: Going to the extremes: an intercomparison of model-simulated historical and future changes in extreme events. *Clim. Change*, **79**, 185–211.

Tennant, W., 2003: An assessment of intraseasonal variability from 13-yr GCM simulations. *Mon. Weather Rev.*, **131**(9), 1975–1991.

Timbal, B., 2004: Southwest Australia past and future rainfall trends. *Clim. Res.*, **26**, 233–249.

Timbal, B., and B.J. McAvaney, 2001: An analogue-based method to downscale surface air temperature: Application for Australia. *Clim. Dyn*., **17**(12), 947–963.

Tjernström, M., et al., 2005: Modeling the Arctic boundary layer: An evaluation of six ARCMIP regional-scale models with data from the SHEBA project. *Bound.-Lay. Meteorol.*, **117**, 337–381.

Todd, M., and R. Washington, 1999: Circulation anomalies associated with tropical-temperate troughs in southern Africa and the south west Indian Ocean. *Clim. Dyn.*, **15**(12), 937–951.

Trigo, R.M., and J.P. Palutikof, 2001: Precipitation scenarios over Iberia: a comparison between direct GCM output and different downscaling techniques. *J. Clim*., **14**, 4422–4446.

Turner, J., 2004: The El Niño-Southern Oscillation and Antarctica. *Int. J. Climatol*., **24**, 1–31.

Turner, J., W.M. Connolley, T.A. Lachlan-Cope, and G.J. Marshall, 2006: The performance of the Hadley Centre climate model (HadCM3) in high southern latitudes. *Int. J. Climatol*., **26**, 91–112.

Ueda, H., A. Iwai, K. Kuwako, and M.E. Hori, 2006: Impact of anthropogenic forcing on the Asian summer monsoon as simulated by eight GCMs. *Geophys. Res. Lett.*, **33**, L06703, doi:10.1029/2005GL025336.

Ulbrich, U., et al., 2006: The Mediterranean climate change under global warming. In: *Mediterranean Climate Variability* [Lionello, P., P. Malanotte, and R. Boscolo (eds.)]. Elsevier B.V, pp. 399–415.

Unnikrishnan, A.S., et al., 2006: Sea level changes along the Indian coast: Observations and projections. *Curr. Sci. India*, **90**, 362–368.

van de Berg, W.J., M.R. van den Broeke, C.H. Reijmer, and E. van Meijgaard, 2005: Characteristics of the Antarctic surface mass balance (1958-2002) using a regional atmospheric climate model. *Ann. Glaciol.*, **41**, 97–104.

van den Broeke, M.R., and N.P.M. van Lipzig, 2003: Factors controlling the near-surface wind field in Antarctica. *Mon. Weather Rev*., **131**, 733–743.

van den Broeke, M., W.J. van de Berg, and E. van Meijgaard, 2006: Snowfall in coastal West Antarctica much greater than previously assumed. *Geophys. Res. Lett*., **33**, L02505, doi:10.1029/2005GL025239.

van den Hurk, B., et al., 2005: Soil control on runoff response to climate change in regional climate model simulations. *J. Clim*., **18**, 3536–3551.

van den Hurk, B., et al., 2006: *KNMI Climate Change Scenarios 2006 for the Netherlands.* KNMI WR-2006-01, KNMI, The Netherlands, 82 pp.

van Lipzig, N.P.M., E.W. van Meijgaard, and J. Oerlemans, 2002a: The spatial and temporal variability of the surface mass balance in Antarctica: results from a regional atmospheric climate model. *Int. J. Climatol.*, **22**, 1197–1217.

van Lipzig, N.P.M., E.W. van Meijgaard, and J. Oerlemans, 2002b: Temperature sensitivity of the Antarctic surface mass balance in a regional atmospheric climate model. *J. Clim.*, **15**, 2758–2774.

van Ulden, A.P., and G.J. van Oldenborgh, 2006: Large-scale atmospheric circulation biases and changes in global climate model simulations and their importance for climate change in Central Europe. *Atmos. Chem. Phys*., **6**, 863–881.

van Ulden, A., G. Lenderink, B. van den Hurk, and E. van Meijgaard, 2007: Circulation statistics and climate change in Central Europe: Prudence simulations and observations. *Clim. Change*, doi: 10.1007/s10584-006-9212-5.

Vannitsem, S., and F. Chomé, 2005: One-way nested regional climate simulations and domain size. *J. Clim.*, **18**, 229–233.

Vera, C., et al., 2006: Towards a unified view of the American monsoon systems. *J. Clim*., **19**, 4977–5000.

Vérant, S., 2004: *Etude des Dépressions sur l'Europe de l'Ouest : Climat Actuel et Changement Climatique*. PhD thesis, Université Paris VI, Paris, France, 204 pp.

Vernekar, A.D., B.P. Kirtman, and M.J. Fennessy, 2003: Low-level jets and their effects on the South American summer climate as simulated by the NCEP Eta model. *J. Clim*., **16**, 297–311.

Vidale, P.L., D. Lüthi, R. Wegmann, and C. Schär, 2007: European climate variability in a heterogeneous multi-model ensemble. *Clim. Change*, doi: 10.1007/s10584-006-9218-z.

Vidale, P.L., et al., 2003: Predictability and uncertainty in a regional climate model. *J. Geophys. Res*., **108**(D18), 4586, doi:10.1029/2002JD002810.

Vincent, C., 2002: Influence of climate change over the 20th century on 4 French glacier mass balances. *J. Geophys. Res*., **107**, 4375, doi:10.1029/2001JD000832.

Vincent, D.G., 1994: The South Pacific Convergence Zone (SPCZ): A review. *Mon. Weather Rev*., **122**, 1949–1970.

Vizy, E.K., and K.H. Cook, 2002: Development and application of a mesoscale climate model for the tropics: Influence of sea surface temperature anomalies on the West African monsoon. *J. Geophys. Res.*, **107**(D3), 4023, doi:10.1029/2001JD000686.

Voldoire, A., 2006: Quantifying the impact of future land-use changes against increases in GHG concentrations. *Geophys. Res. Lett.*, **33**, L04701, doi:10.1029/2005GL024354.

Voldoire, A., and J.F. Royer, 2004: Tropical deforestation and climate variability. *Clim. Dyn*., **22**, 857–874.

Voldoire, A., and J.F. Royer, 2005: Climate sensitivity to tropical land surface changes with coupled versus prescribed SSTs, *Clim. Dyn*., **24**, 843–862.

von Storch, H., and H. Reichardt, 1997: A scenario of storm surge statistics for the German Bight at the expected time of doubled atmospheric carbon dioxide concentration. *J. Clim*., **10**, 2653–2662.

von Storch, H., H. Langenberg, and F. Feser, 2000: A spectral nudging technique for dynamical downscaling purposes. *Mon. Weather Rev*., **128**, 3664–3673.

Voss, R., W. May, and E. Roeckner, 2002: Enhanced resolution modelling study on anthropogenic climate change: Changes in extremes of the hydrological cycle. *Int. J. Climatol*., **22**, 755–777.

Vuille, M., and Bradley, R.S., 2000: Mean annual temperature trends and their vertical structure in the tropical Andes. *Geophys. Res. Lett*., **27**, 3885–3888.

Walland, D.J., S.B. Power, and A.C. Hirst, 2000: Decadal climate variability simulated in a coupled general circulation model. *Clim. Dyn*., **16**(2–3), 201–211.

Walser, A., and C. Schär, 2004: Convection-resolving precipitation forecasting and its predictability in Alpine river catchments. *J. Hydrol.*, **288**, 57–73.

Walsh, J.E., et al., 2002: Comparison of Arctic climate simulations by uncoupled and coupled global models. *J. Clim*., **15**, 1429–1446.

Walsh, K.J., 2004: Tropical cyclones and climate change: unresolved issues. *Clim. Res.*, **27**, 77–84.

Walsh, K.J.E., and J.J. Katzfey, 2000: The impact of climate change on the poleward movement of tropical cyclone-like vortices in a regional climate model. *J. Clim*., **13**(6), 1116–1132.

Walsh, K.J.E., and B.F. Ryan, 2000: Tropical cyclone intensity increase near Australia as a result of climate change. *J. Clim*., **13**(16), 3029–3036.

Walsh, K.J., K.C. Nguyen, and J.L. McGregor, 2004: Fine-resolution regional climate model simulations of the impact of climate change on tropical cyclones near Australia. *Clim. Dyn.*, **22**(1), 47–56.

Walsh, K., et al., 1999: *Climate Change in Queensland Under Enhanced Greenhouse Conditions: First Annual Report, 1997-1998*. CSIRO Atmospheric Research, Melbourne, 84 pp.

Wang, B., I.S. Kang, and J.Y. Lee, 2004: Ensemble simulations of Asian-Australian monsoon variability by 11 GCMs. *J. Clim*., **17**, 803–818.

Wang, G., 2005: Agricultural drought in a future climate: results from 15 global climate models participating in the IPCC 4th assessment. *Clim. Dyn*., **25**, 739–753.

Wang, G., and E.A.B. Eltahir, 2000: Role of vegetation dynamics in enhancing the low-frequency variability of the Sahel rainfall. *Water Resour. Res.*, **36**(4), 1013–1021.

Wang, X.L., and V.R. Swail, 2006a: Climate change signal and uncertainty in projections of ocean wave heights. *Clim. Dyn*., **26**, 106–126, doi:10.1007/s00382-005-0080-x.

Wang, X.L., and V.R. Swail, 2006b: Historical and possible future changes of wave heights in Northern Hemisphere oceans. In: *Atmosphere-Ocean Interactions – Vol. 2* [Perrie, W. (ed.)]. Advances in Fluid Mechanics Series, Vol 39. Wessex Institute of Technology Press, Southampton, UK, 240 pp.

Wang, X.L., F. Zwiers, and V. Swail, 2004: North Atlantic ocean wave climate change scenarios for the twenty-first century. *J. Clim*., **17**, 2368–2383.

Warner, T.T., R.A. Peterson, and R.E. Treadon, 1997: A tutorial on lateral conditions as a basic and potentially serious limitation to regional numerical weather prediction. *Bull. Am. Meteorol. Soc.*, **78**(11), 2599–2617.

Watterson, I.G., and M.R. Dix, 2003: Simulated changes due to global warming in daily precipitation means and extremes and their interpretation using the gamma distribution. *J. Geophys. Res.*, **108**(D13), 4379, doi:10.1029/2002JD002928.

Weatherly, J., 2004: Sensitivity of Antarctic precipitation to sea ice concentrations in a general circulation model. *J. Clim*., **17**, 3214–3223.

Webb, M., et al., 2006: On the contribution of local feedback mechanisms to the range of climate sensitivity in two GCM ensembles. *Clim. Dyn.*, **27**, 17–38.

Wehner, M.F., 2004: Predicted twenty-first-century changes in seasonal extreme precipitation events in the Parallel Climate Model. *J. Clim*., **17**, 4281–4290.

Wei, H., W.J. Gutowski, C.J. Vorosmarty, and B.M. Fekete, 2002: Calibration and validation of a regional climate model for pan-Arctic hydrologic simulation. *J. Clim*., **15**, 3222–3236.

Weisheimer, A., and T. Palmer, 2005: Changing frequency of occurrence of extreme seasonal temperatures under global warming. *Geophys. Res. Lett.*, **32**, L20721, doi:10.1029/2005GL023365.

Weisman, M.L., W.S. Skamarock, and J.B. Klemp, 1997: The resolution dependence of explicitly modeled convective systems. *Mon. Weather Rev*., **125**, 527–548.

Weisse, R., H. von Storch, and F. Feser, 2005: Northeast Atlantic and North Sea storminess as simulated by a regional climate model 1958-2001 and comparison with observations. *J. Clim*., **18**, 465–479.

Whetton, P.H., and R. Suppiah, 2003: Climate change projections and drought. In: *Science for Drought. Proceedings of the National Drought Forum, Carlton Crest Hotel, Brisbane* [Stone, R., and I. Partridge (eds.)]. Queensland Department of Primary Industries, Brisbane, Qld., pp. 130–136.

Whetton, P.H., A.B. Mullan, and A.B. Pittock, 1996: Climate-change scenarios for Australia and New Zealand. In: *Greenhouse: Coping with Climate Change* [Bouma, W.J., G.I. Pearman, and M.R. Manning (eds.)]. CSIRO, Collingwood, Vic., pp. 145–168.

Whetton, P.H., et al., 2000: *Climate Averages Based on a Doubled CO_2 Simulation*. Victorian Dept. of Natural Resources and Environment, Melbourne, 43 pp.

Whetton, P.H., et al., 2001: Developing scenarios of climate change for Southeastern Australia: An example using regional climate model output. *Clim. Res.*, **16**(3), 181–201.

Whetton, P. H., et al. 2002. *Climate change in Victoria : high resolution regional assessment of climate change impacts*. Undertaken for the Victorian Department of Natural Resources and Environment. Dept. of Natural Resources and Environment, East Melbourne, VIC, 44 pp., http://www.greenhouse.vic.gov.au/climatechange.pdf

Whetton, P.H., et al., 2005: *Australian Climate Change Projections for Impact Assessment and Policy Application: A Review*. CSIRO Marine and Atmospheric Research Paper 001, CSIRO Marine and Atmospheric Research, Aspendale, Vic., 34 pp.

Widmann, M., C.S. Bretherton, and E.P. Salathé Jr., 2003: Statistical precipitation downscaling over the Northwestern United States using numerically simulated precipitation as a predictor. *J. Clim*., **16**, 799–816.

Wigley, T.M.L., and S.C.B. Raper, 2001: Interpretation of high projections for global-mean warming. *Science*, **293**, 451–454.

Wilby, R.L., C.W. Dawson, and E.M. Barrow, 2002: SDSM – A decision support tool for the assessment of regional climate change impacts. *Environ. Model. Software*, **17**, 147–159.

Wilby, R.L., O.J. Tomlinson, and C.W. Dawson, 2003: Multi-site simulation of precipitation by conditional resampling. *Clim. Res.*, **23**, 183–194.

Wilby, R.L., et al., 2004: *Guidelines for Use of Climate Scenarios Developed from Statistical Downscaling Methods*. IPCC Task Group on Data and Scenario Support for Impact and Climate Analysis (TGICA), http://ipcc-ddc.cru.uea.ac.uk/guidelines/StatDown_Guide.pdf.

Wood, A.W., L.R. Leung, V. Sridhar, and D.P. Lettenmaier, 2004: Hydrologic implications of dynamical and statistical approaches to downscaling climate model outputs. *Clim. Change*, **62**, 189–216.

Woodworth, R., and D.L. Blackman, 2004: Evidence for systematic changes in extreme high waters since the mid-1970s. *J. Clim*., **17**(6), 1190–1197.

Woth, K., 2005: North Sea storm surge statistics based on projections in a warmer climate: How important are the driving GCM and the chosen emission scenario? *Geophys. Res. Lett*., **32**, L22708, doi:10.1029/2005GL023762.

Woth, K., R. Weisse, and H. von Storch, 2006: Climate change and North Sea storm surge extremes: An ensemble study of storm surge extremes expected in a changed climate projected by four different Regional Climate Models. *Ocean Dyn.*, **56**, 3–15, doi:10.1007/s10236-005-0024-3.

Wu, B., and B. Wang, 2004: Assessing impacts of global warming on tropical cyclone tracks. *J. Clim*., **17**(8), 1686–1698.

Wu, P., R. Wood, and P. Scott, 2003: Does the recent freshening trend in the North Atlantic indicate a weakening thermohaline circulation? *Geophys. Res. Lett.*, **31**, doi:10.1029/2003GL018584.

Wyser, K., and C.G. Jones, 2005: Modeled and observed clouds during Surface Heat Budget of the Arctic Ocean (SHEBA). *J. Geophys. Res.*, **110**, D09207, doi:10.1029/2004JD004751.

Xu, Y., Y.H. Ding., and L.D. Li, 2003a: Climate change projection in Qinghai-Xizang Plateau in the future 100 years. *Plateau Meteorol.*, **22**(5), 451–457.

Xu, Y., Y.H. Ding, and Z.C. Zhao, 2003b: Scenario of temperature and precipitation changes in Northwest China due to effects of human activities in 21st century. *J. Glaciol.*, **25**(3), 327–330.

Xu, Y., Z.C. Zhao, and L.D. Li, 2005: The simulated result analyses on climate changes over Qinghai-Xizang Plateau and along the Railway in the coming 50 Years, *Plateau Meteorol.*, **24**(5), 700–707.

Xu, Y.L., et al., 2005: Statistical analyses of climate change scenario over China in the 21st century. *Adv. Clim. Change Res.*, **1**, 80–83.

Xue, M., K.K. Droegemeier, and V. Wong, 2000: The Advanced Regional Prediction System (ARPS) - A multi-scale nonhydrostatic atmospheric simulation and prediction model. Part I: Model dynamics and verification. *Meteorol. Atmos. Phys.*, **75**(3 – 4), 161–193.

Yasunaga, K., et al., 2006: Changes in the Baiu frontal activity in the future climate simulated by super-high-resolution global and cloud-resolving regional climate models. *J. Meteorol. Soc. Japan*, **84**, 199–220.

Yin, J.H., 2005: A consistent poleward shift of the storm tracks in simulations of 21st century climate. *Geophys. Res. Lett*., **32**, L18701, doi:10.1029/2005GL023684.

Yoshizaki, M., et al., 2005: Changes of Baiu (Mei-yu) frontal activity in the global warming climate simulated by a non-hydrostatic regional model. *Scientific Online Letters on the Atmosphere*, **1**, 25–28.

Yuan, X.J., 2004: ENSO-related impacts on Antarctic sea ice: a synthesis of phenomenon and mechanisms. *Antarct. Sci.*, **16**, 415–425.

Zeng, N., H. Qian, E. Munoz, and R. Iacono, 2004: How strong is carbon cycle-climate feedback under global warming? *Geophys. Res. Lett*., **31**, L20203, doi:10.1029/2004GL020904.

Zhai, P.M., X.B. Zhang, H. Wan, and X.H. Pan, 2005: Trends in total precipitation and frequency of daily precipitation extremes over China. *J. Clim*., **18**, 1096–1108.

Zhang, D.F., X.J. Gao, and Z.C. Zhao, 2005a: Simulation of climate in China by RegCM3. *Adv. Clim. Change Res.*, **1**(3), 119–121.

Zhang, D.F., X.J. Gao, H.Z. Bai, and D.L. Li, 2005b: Simulation of climate over Qinghai-Xizang Plateau utilizing RegCM3. *Plateau Meteorol.*, **24**, 714–720.

Zhao, Z.C., X.J. Gao, M.C. Tang, and Y. Xu, 2002: Climate change projections. In: *Assessment for Evolution of Environment in Western China, Vol. 2* [Qin, D.H., and Y.D. Ding (eds.)]. Science Press, Beijing, pp.16–46.

Zhou, J., and K.-M. Lau, 2002: Intercomparison of model simulations of the impact of 1997/98 El Niño on South American Summer Monsoon. *Meteorologica*, **27**(1–2), 99–116.

Zhou, T.J., and Z.X. Li, 2002: Simulation of the East Asian summer monsoon by using a variable resolution atmospheric GCM. *Clim. Dyn*., **19**, 167–180.

Zhou, T.J., and R.C. Yu, 2006: 20th century surface air temperature over China and the globe simulated by coupled climate models. *J. Clim.*, **19**, 5843–5858.

Zou, C.-Z., M.L. van Woert, C. Xu, and K. Syed, 2004: Assessment of the NCEP–DOE Reanalysis-2 and TOVS pathfinder a moisture fields and their use in Antarctic net precipitation estimates. *Mon. Weather Rev*., **132**, 2463–2476.

Zwiers, F.W., and V.V. Kharin, 1998: Changes in the extremes of the climate simulated by CCC GCM2 under CO_2 doubling. *J. Clim*., **11**, 2200–2222.

Annex I

Glossary

Editor: A.P.M. Baede (Netherlands)

Notes: This glossary defines some specific terms as the lead authors intend them to be interpreted in the context of this report. Red, italicised words indicate that the term is defined in the Glossary.

8.2ka event Following the last post-glacial warming, a rapid *climate* oscillation with a cooling lasting about 400 years occurred about 8.2 ka. This event is also referred to as the *8.2kyr event*.

Abrupt climate change The *nonlinearity* of the *climate system* may lead to abrupt climate change, sometimes called *rapid climate change*, *abrupt events or even surprises*. The term *abrupt* often refers to time scales faster than the typical time scale of the responsible forcing. However, not all abrupt climate changes need be *externally forced*. Some possible abrupt events that have been proposed include a dramatic reorganisation of the *thermohaline circulation*, rapid deglaciation and massive melting of *permafrost* or increases in soil *respiration* leading to fast changes in the *carbon cycle*. Others may be truly unexpected, resulting from a strong, rapidly changing forcing of a nonlinear system.

Active layer The layer of ground that is subject to annual thawing and freezing in areas underlain by *permafrost* (Van Everdingen, 1998).

Adiabatic process An adiabatic process is a process in which no external heat is gained or lost by the system. The opposite is called a *diabatic process*.

Adjustment time See *Lifetime*; see also *Response time*.

Advection Transport of water or air along with its properties (e.g., temperature, chemical tracers) by the motion of the fluid. Regarding the general distinction between advection and *convection*, the former describes the predominantly horizontal, large-scale motions of the *atmosphere* or ocean, while convection describes the predominantly vertical, locally induced motions.

Aerosols A collection of airborne solid or liquid particles, with a typical size between 0.01 and 10 µm that reside in the *atmosphere* for at least several hours. Aerosols may be of either natural or *anthropogenic* origin. Aerosols may influence *climate* in several ways: directly through scattering and absorbing radiation, and indirectly by acting as *cloud condensation nuclei* or modifying the optical properties and lifetime of clouds (see *Indirect aerosol effect*).

Afforestation Planting of new forests on lands that historically have not contained forests. For a discussion of the term *forest* and related terms such as afforestation, *reforestation* and *deforestation*, see the IPCC Special Report on Land Use, Land-Use Change and Forestry (IPCC, 2000). See also the report on Definitions and Methodological Options to Inventory Emissions from Direct Human-induced Degradation of Forests and Devegetation of Other Vegetation Types (IPCC, 2003).

Air mass A widespread body of air, the approximately homogeneous properties of which (1) have been established while that air was situated over a particular *region* of the Earth's surface, and (2) undergo specific modifications while in transit away from the source region (AMS, 2000).

Albedo The fraction of *solar radiation* reflected by a surface or object, often expressed as a percentage. Snow-covered surfaces have a high albedo, the surface albedo of soils ranges from high to low, and vegetation-covered surfaces and oceans have a low albedo. The Earth's planetary albedo varies mainly through varying cloudiness, snow, ice, leaf area and land cover changes.

Albedo feedback A *climate feedback* involving changes in the Earth's *albedo*. It usually refers to changes in the *cryosphere*, which has an albedo much larger (~0.8) than the average planetary albedo (~0.3). In a warming *climate*, it is anticipated that the cryosphere would shrink, the Earth's overall albedo would decrease and more *solar radiation* would be absorbed to warm the Earth still further.

Alkalinity A measure of the capacity of a solution to neutralize acids.

Altimetry A technique for measuring the height of the sea, lake or river, land or ice surface with respect to the centre of the Earth within a defined terrestrial reference frame. More conventionally, the height is with respect to a standard *reference ellipsoid* approximating the Earth's oblateness, and can be measured from space by using radar or laser with centimetric precision at present. Altimetry has the advantages of being a geocentric measurement, rather than a measurement relative to the Earth's crust as for a *tide gauge*, and of affording quasi-global coverage.

Annular modes Preferred patterns of change in atmospheric circulation corresponding to changes in the zonally averaged mid-latitude westerlies. The *Northern Annular Mode* has a bias to the North Atlantic and has a large correlation with the *North Atlantic Oscillation*. The *Southern Annular Mode* occurs in the Southern Hemisphere. The variability of the mid-latitude westerlies has also been known as *zonal flow* (or *wind*) vacillation, and defined through a *zonal index*. For the corresponding circulation indices, see Box 3.4.

Anthropogenic Resulting from or produced by human beings.

Atlantic Multi-decadal Oscillation (AMO) A multi-decadal (65 to 75 year) fluctuation in the North Atlantic, in which *sea surface temperatures* showed warm phases during roughly 1860 to 1880 and 1930 to 1960 and cool phases during 1905 to 1925 and 1970 to 1990 with a range of order 0.4°C.

Atmosphere The gaseous envelope surrounding the Earth. The dry atmosphere consists almost entirely of nitrogen (78.1% *volume mixing ratio*) and oxygen (20.9% volume mixing ratio), together with a number of trace gases, such as argon (0.93% volume mixing ratio), helium and radiatively active *greenhouse gases* such as *carbon dioxide* (0.035% volume mixing ratio) and *ozone*. In addition, the atmosphere contains the greenhouse gas water vapour, whose amounts are highly variable but typically around 1% volume mixing ratio. The atmosphere also contains clouds and *aerosols*.

Atmospheric boundary layer The atmospheric layer adjacent to the Earth's surface that is affected by friction against that boundary

surface, and possibly by transport of heat and other variables across that surface (AMS, 2000). The lowest 10 metres or so of the boundary layer, where mechanical generation of turbulence is dominant, is called the *surface boundary layer* or *surface layer*.

Atmospheric lifetime See *Lifetime*.

Attribution See *Detection and attribution*.

Autotrophic respiration *Respiration* by *photosynthetic* organisms (plants).

Bayesian method A Bayesian method is a method by which a statistical analysis of an unknown or uncertain quantity is carried out in two steps. First, a prior probability distribution is formulated on the basis of existing knowledge (either by eliciting expert opinion or by using existing data and studies). At this first stage, an element of subjectivity may influence the choice, but in many cases, the prior probability distribution is chosen as neutrally as possible, in order not to influence the final outcome of the analysis. In the second step, newly acquired data are introduced, using a theorem formulated by and named after the British mathematician Bayes (1702–1761), to update the prior distribution into a posterior distribution.

Biomass The total mass of living organisms in a given area or volume; dead plant material can be included as dead biomass.

Biome A biome is a major and distinct regional element of the *biosphere*, typically consisting of several *ecosystems* (e.g. *forests*, rivers, ponds, swamps within a *region*). Biomes are characterised by typical communities of plants and animals.

Biosphere (terrestrial and marine) The part of the Earth system comprising all *ecosystems* and living organisms, in the *atmosphere*, on land (*terrestrial biosphere*) or in the oceans (*marine biosphere*), including derived dead organic matter, such as litter, soil organic matter and oceanic detritus.

Black carbon (BC) Operationally defined *aerosol* species based on measurement of light absorption and chemical reactivity and/or thermal stability; consists of *soot*, *charcoal* and/or possible light-absorbing refractory organic matter (Charlson and Heintzenberg, 1995, p. 401).

Blocking anticyclone An anticyclone that remains nearly stationary for a week or more at middle to high latitudes, so that it blocks the normal eastward progression of high- and low-pressure systems.

Bowen ratio The ratio of *sensible* to *latent heat fluxes* from the Earth's surface up into the *atmosphere*. Values are low (order 0.1) for wet surfaces like the ocean, and greater than 2 for deserts and *drought* regions.

Burden The total mass of a gaseous substance of concern in the *atmosphere*.

^{13}C Stable isotope of carbon having an atomic weight of approximately 13. Measurements of the ratio of $^{13}C/^{12}C$ in *carbon dioxide* molecules are used to infer the importance of different *carbon cycle* and *climate* processes and the size of the terrestrial carbon *reservoir*.

^{14}C Unstable isotope of carbon having an atomic weight of approximately 14, and a half-life of about 5,700 years. It is often used for dating purposes going back some 40 kyr. Its variation in time is affected by the magnetic fields of the Sun and Earth, which influence its production from cosmic rays (see *Cosmogenic isotopes*).

C3 plants Plants that produce a three-carbon compound during *photosynthesis*, including most trees and agricultural crops such as rice, wheat, soybeans, potatoes and vegetables.

C4 plants Plants that produce a four-carbon compound during *photosynthesis*, mainly of tropical origin, including grasses and the agriculturally important crops maize, sugar cane, millet and sorghum.

Carbonaceous aerosol *Aerosol* consisting predominantly of organic substances and various forms of *black carbon* (Charlson and Heintzenberg, 1995, p. 401).

Carbon cycle The term used to describe the flow of carbon (in various forms, e.g., as *carbon dioxide*) through the *atmosphere*, ocean, terrestrial *biosphere* and *lithosphere*.

Carbon dioxide (CO_2) A naturally occurring gas, also a by-product of burning fossil fuels from fossil carbon deposits, such as oil, gas and coal, of burning *biomass* and of *land use* changes and other industrial processes. It is the principal *anthropogenic greenhouse gas* that affects the Earth's radiative balance. It is the reference gas against which other greenhouse gases are measured and therefore has a *Global Warming Potential* of 1.

Carbon dioxide (CO_2) fertilization The enhancement of the growth of plants as a result of increased atmospheric *carbon dioxide* (CO_2) concentration. Depending on their mechanism of *photosynthesis*, certain types of plants are more sensitive to changes in atmospheric CO_2 concentration. In particular, *C3 plants* generally show a larger response to CO_2 than *C4 plants*.

CFC See *Halocarbons*.

Chaos A *dynamical system* such as the *climate system*, governed by nonlinear deterministic equations (see *Nonlinearity*), may exhibit erratic or chaotic behaviour in the sense that very small changes in the initial state of the system in time lead to large and apparently unpredictable changes in its temporal evolution. Such chaotic behaviour may limit the *predictability* of nonlinear dynamical systems.

Charcoal Material resulting from charring of *biomass*, usually retaining some of the microscopic texture typical of plant tissues; chemically it consists mainly of carbon with a disturbed graphitic structure, with lesser amounts of oxygen and hydrogen (Charlson and Heintzenberg, 1995, p. 402). See *Black carbon*; *Soot*.

Chronology Arrangement of events according to dates or times of occurrence.

Clathrate (methane) A partly frozen slushy mix of methane gas and ice, usually found in sediments.

Climate Climate in a narrow sense is usually defined as the average weather, or more rigorously, as the statistical description in terms of the mean and variability of relevant quantities over a period of time ranging from months to thousands or millions of years. The classical period for averaging these variables is 30 years, as defined by the World Meteorological Organization. The relevant quantities are most often surface variables such as temperature, precipitation and wind. Climate in a wider sense is the state, including a statistical description, of the *climate system*. In various chapters in this report different averaging periods, such as a period of 20 years, are also used.

Climate change Climate change refers to a change in the state of the *climate* that can be identified (e.g., by using statistical tests) by changes in the mean and/or the variability of its properties, and that persists for an extended period, typically decades or longer. Climate change may be due to natural internal processes or *external forcings*, or to persistent *anthropogenic* changes in the composition of the *atmosphere* or in *land use*. Note that the *Framework Convention on Climate Change* (UNFCCC), in its Article 1, defines *climate change* as: 'a change of climate which is attributed directly or indirectly to human activity that alters the composition of the global atmosphere and which is in addition to natural climate variability observed over comparable time periods'. The UNFCCC thus makes a distinction between climate change attributable to human activities altering the atmospheric composition, and *climate variability* attributable to natural causes. See also *Climate variability; Detection and Attribution*.

Climate change commitment Due to the thermal inertia of the ocean and slow processes in the *biosphere*, the *cryosphere* and land surfaces, the *climate* would continue to change even if the atmospheric composition were held fixed at today's values. Past change in atmospheric composition leads to a *committed climate change*, which continues for as long as a radiative imbalance persists and until all components of the *climate system* have adjusted to a new state. The further change in temperature after the composition of the *atmosphere* is held constant is referred to as the *constant composition temperature commitment* or simply *committed warming* or *warming commitment*. Climate change commitment includes other future changes, for example in the hydrological cycle, in *extreme weather* and climate events, and in *sea level change*.

Climate feedback An interaction mechanism between processes in the *climate system* is called a climate feedback when the result of an initial process triggers changes in a second process that in turn influences the initial one. A positive feedback intensifies the original process, and a negative feedback reduces it.

Climate Feedback Parameter A way to quantify the radiative response of the *climate system* to a *global surface temperature* change induced by a *radiative forcing* (units: $W\ m^{-2}\ °C^{-1}$). It varies as the inverse of the effective *climate sensitivity*. Formally, the Climate Feedback Parameter (Λ) is defined as: $\Lambda = (\Delta Q - \Delta F) / \Delta T$, where Q is the global mean radiative forcing, T is the global mean air surface temperature, F is the heat flux into the ocean and Δ represents a change with respect to an unperturbed *climate*.

Climate model (spectrum or hierarchy) A numerical representation of the *climate system* based on the physical, chemical and biological properties of its components, their interactions and *feedback* processes, and accounting for all or some of its known properties. The climate system can be represented by models of varying complexity, that is, for any one component or combination of components a *spectrum* or *hierarchy* of models can be identified, differing in such aspects as the number of spatial dimensions, the extent to which physical, chemical or biological processes are explicitly represented, or the level at which empirical *parametrizations* are involved. Coupled Atmosphere-Ocean General Circulation Models (AOGCMs) provide a representation of the climate system that is near the most comprehensive end of the spectrum currently available. There is an evolution towards more complex models with interactive chemistry and biology (see Chapter 8). Climate models are applied as a research tool to study and simulate the climate, and for operational purposes, including monthly, seasonal and interannual *climate predictions*.

Climate prediction A climate prediction or *climate forecast* is the result of an attempt to produce an estimate of the actual evolution of the *climate* in the future, for example, at seasonal, interannual or long-term time scales. Since the future evolution of the *climate system* may be highly sensitive to initial conditions, such predictions are usually probabilistic in nature. See also *Climate projection*; *Climate scenario*; *Predictability*.

Climate projection A *projection* of the response of the *climate system* to *emission or concentration scenarios* of *greenhouse gases* and *aerosols*, or *radiative forcing* scenarios, often based upon simulations by *climate models*. Climate projections are distinguished from *climate predictions* in order to emphasize that climate projections depend upon the emission/concentration/radiative forcing scenario used, which are based on assumptions concerning, for example, future socioeconomic and technological developments that may or may not be realised and are therefore subject to substantial *uncertainty*.

Climate response
See *Climate sensitivity*.

Climate scenario A plausible and often simplified representation of the future *climate*, based on an internally consistent set of climatological relationships that has been constructed for explicit use in investigating the potential consequences of *anthropogenic climate change*, often serving as input to impact models. *Climate projections* often serve as the raw material for constructing climate scenarios, but climate scenarios usually require additional information such as about the observed current climate. A *climate change scenario* is the difference between a climate scenario and the current climate.

Climate sensitivity In IPCC reports, *equilibrium climate sensitivity* refers to the equilibrium change in the annual mean *global surface temperature* following a doubling of the atmospheric *equivalent carbon dioxide concentration*. Due to computational constraints, the equilibrium climate sensitivity in a *climate model* is usually estimated by running an atmospheric general circulation model coupled to a mixed-layer ocean model, because equilibrium climate sensitivity is largely determined by atmospheric processes. Efficient models can be run to equilibrium with a dynamic ocean.

The *effective climate sensitivity* is a related measure that circumvents the requirement of equilibrium. It is evaluated from model output for evolving non-equilibrium conditions. It is a measure of the strengths of the *climate feedbacks* at a particular time and may vary with forcing history and *climate* state. The climate sensitivity parameter (units: $°C\ (W\ m^{-2})^{-1}$) refers to the equilibrium change in the annual mean *global surface temperature* following a unit change in *radiative forcing*.

The *transient climate response* is the change in the global surface temperature, averaged over a 20-year period, centred at the time of atmospheric carbon dioxide doubling, that is, at year 70 in a 1% yr^{-1} compound carbon dioxide increase experiment with a global coupled climate model. It is a measure of the strength and rapidity of the surface temperature response to *greenhouse gas* forcing.

Climate shift or climate regime shift An abrupt shift or jump in mean values signalling a change in *regime*. Most widely used in conjunction with the 1976/1977 climate shift that seems to correspond to a change in *El Niño-Southern Oscillation* behavior.

Climate system The climate system is the highly complex system consisting of five major components: the *atmosphere*, the *hydrosphere*, the *cryosphere*, the land surface and the *biosphere*, and the interactions between them. The climate system evolves in time under the influence of its own internal dynamics and because of *external forcings* such as volcanic eruptions, solar variations and

anthropogenic forcings such as the changing composition of the atmosphere and *land use change*.

Climate variability Climate variability refers to variations in the mean state and other statistics (such as standard deviations, the occurrence of extremes, etc.) of the *climate* on all *spatial and temporal scales* beyond that of individual weather events. Variability may be due to natural internal processes within the *climate system* (*internal variability*), or to variations in natural or *anthropogenic external forcing* (*external variability*). See also *Climate change*.

Cloud condensation nuclei (CCN) Airborne particles that serve as an initial site for the condensation of liquid water, which can lead to the formation of cloud droplets. See also *Aerosols*.

Cloud feedback A *climate feedback* involving changes in any of the properties of clouds as a response to other atmospheric changes. Understanding cloud feedbacks and determining their magnitude and sign require an understanding of how a change in *climate* may affect the spectrum of cloud types, the cloud fraction and height, and the radiative properties of clouds, and an estimate of the impact of these changes on the Earth's radiation budget. At present, cloud feedbacks remain the largest source of *uncertainty* in *climate sensitivity* estimates. See also *Cloud radiative forcing*; *Radiative forcing*.

Cloud radiative forcing Cloud radiative forcing is the difference between the all-sky Earth's radiation budget and the clear-sky Earth's radiation budget (units: W m^{-2}).

CO_2-equivalent See *Equivalent carbon dioxide*.

Confidence The *level of confidence* in the correctness of a result is expressed in this report, using a standard terminology defined in Box 1.1. See also *Likelihood*; *Uncertainty*.

Convection Vertical motion driven by buoyancy forces arising from static instability, usually caused by near-surface cooling or increases in salinity in the case of the ocean and near-surface warming in the case of the *atmosphere*. At the location of convection, the horizontal scale is approximately the same as the vertical scale, as opposed to the large contrast between these scales in the *general circulation*. The net vertical mass transport is usually much smaller than the upward and downward exchange.

Cosmogenic isotopes Rare isotopes that are created when a high-energy cosmic ray interacts with the nucleus of an *in situ* atom. They are often used as indications of solar magnetic activity (which can shield cosmic rays) or as tracers of atmospheric transport, and are also called *cosmogenic nuclides*.

Cryosphere The component of the *climate system* consisting of all snow, ice and *frozen ground* (including *permafrost*) on and beneath the surface of the Earth and ocean. See also *Glacier*; *Ice sheet*.

Dansgaard-Oeschger events Abrupt warming events followed by gradual cooling. The abrupt warming and gradual cooling is primarily seen in Greenland *ice cores* and in *palaeoclimate* records from the nearby North Atlantic, while a more general warming followed by a gradual cooling has been observed in other areas as well, at intervals of 1.5 to 7 kyr during glacial times.

Deforestation Conversion of forest to non-forest. For a discussion of the term *forest* and related terms such as *afforestation*, *reforestation*, and deforestation see the IPCC Special Report on Land Use, Land-Use Change and Forestry (IPCC, 2000). See also the report on Definitions and Methodological Options to Inventory Emissions from Direct Human-induced Degradation of Forests and Devegetation of Other Vegetation Types (IPCC, 2003).

Desertification Land degradation in arid, semi-arid, and dry sub-humid areas resulting from various factors, including climatic variations and human activities. The United Nations Convention to Combat Desertification defines land degradation as a reduction or loss in arid, semi-arid, and dry sub-humid areas, of the biological or economic productivity and complexity of rain-fed cropland, irrigated cropland, or range, pasture, *forest*, and woodlands resulting from *land uses* or from a process or combination of processes, including processes arising from human activities and habitation patterns, such as (i) soil erosion caused by wind and/or water; (ii) deterioration of the physical, chemical and biological or economic properties of soil; and (iii) long-term loss of natural vegetation.

Detection and attribution *Climate* varies continually on all time scales. *Detection* of *climate change* is the process of demonstrating that climate has changed in some defined statistical sense, without providing a reason for that change. *Attribution* of causes of climate change is the process of establishing the most likely causes for the detected change with some defined level of *confidence*.

Diatoms Silt-sized algae that live in surface waters of lakes, rivers and oceans and form shells of opal. Their species distribution in ocean cores is often related to past *sea surface temperatures*.

Diurnal temperature range The difference between the maximum and minimum temperature during a 24-hour period.

Dobson unit (DU) A unit to measure the total amount of *ozone* in a vertical column above the Earth's surface (*total column ozone*). The number of Dobson units is the thickness in units of 10^{-5} m that the ozone column would occupy if compressed into a layer of uniform density at a pressure of 1,013 hPa and a temperature of 0°C. One DU corresponds to a column of ozone containing $2.69 \times 1{,}020$ molecules per square metre. A typical value for the amount of ozone in a column of the Earth's atmosphere, although very variable, is 300 DU.

Downscaling Downscaling is a method that derives local- to regional-scale (10 to 100 km) information from larger-scale models or data analyses. Two main methods are distinguished: *dynamical downscaling* and *empirical/statistical downscaling*. The dynamical method uses the output of regional *climate models*, global models with variable spatial resolution or high-resolution global models. The empirical/statistical methods develop statistical relationships that link the large-scale atmospheric variables with local/regional climate variables. In all cases, the quality of the downscaled product depends on the quality of the driving model.

Drought In general terms, drought is a 'prolonged absence or marked deficiency of precipitation', a 'deficiency that results in water shortage for some activity or for some group', or a 'period of abnormally dry weather sufficiently prolonged for the lack of precipitation to cause a serious hydrological imbalance' (Heim, 2002). Drought has been defined in a number of ways. *Agricultural drought* relates to moisture deficits in the topmost 1 metre or so of soil (the root zone) that affect crops, *meteorological drought* is mainly a prolonged deficit of precipitation, and *hydrologic drought* is related to below-normal streamflow, lake and groundwater levels. A *megadrought* is a long-drawn out and pervasive drought, lasting much longer than normal, usually a decade or more. For further information, see Box 3.1.

Dynamical system A process or set of processes whose evolution in time is governed by a set of deterministic physical laws. The *climate system* is a dynamical system. See *Abrupt climate change*; *Chaos*; *Nonlinearity*; *Predictability*.

Ecosystem A system of living organisms interacting with each other and their physical environment. The boundaries of what could be called an ecosystem are somewhat arbitrary, depending on the focus of interest or study. Thus, the extent of an ecosystem may range from very small spatial scales to, ultimately, the entire Earth.

Efficacy A measure of how effective a *radiative forcing* from a given *anthropogenic* or natural mechanism is at changing the equilibrium *global surface temperature* compared to an equivalent *radiative forcing* from *carbon dioxide*. A carbon dioxide increase by definition has an efficacy of 1.0.

Ekman pumping Frictional stress at the surface between two fluids (*atmosphere* and ocean) or between a fluid and the adjacent solid surface (Earth's surface) forces a circulation. When the resulting mass transport is converging, mass conservation requires a vertical flow away from the surface. This is called Ekman pumping. The opposite effect, in case of divergence, is called *Ekman suction*. The effect is important in both the *atmosphere* and the ocean.

Ekman transport The total transport resulting from a balance between the Coriolis force and the frictional stress due to the action of the wind on the ocean surface. See also *Ekman pumping*.

El Niño-Southern Oscillation (ENSO) The term *El Niño* was initially used to describe a warm-water current that periodically flows along the coast of Ecuador and Perú, disrupting the local fishery. It has since become identified with a basin-wide warming of the tropical Pacific Ocean east of the dateline. This oceanic event is associated with a fluctuation of a global-scale tropical and subtropical surface pressure pattern called the Southern Oscillation. This coupled *atmosphere*-ocean phenomenon, with preferred time scales of two to about seven years, is collectively known as the El Niño-Southern Oscillation (ENSO). It is often measured by the surface pressure anomaly difference between Darwin and Tahiti and the *sea surface temperatures* in the central and eastern equatorial Pacific. During an ENSO event, the prevailing trade winds weaken, reducing upwelling and altering ocean currents such that the sea surface temperatures warm, further weakening the trade winds. This event has a great impact on the wind, sea surface temperature and precipitation patterns in the tropical Pacific. It has climatic effects throughout the Pacific *region* and in many other parts of the world, through global *teleconnections*. The cold phase of ENSO is called *La Niña*.

Emission scenario A plausible representation of the future development of emissions of substances that are potentially radiatively active (e.g., *greenhouse gases*, *aerosols*), based on a coherent and internally consistent set of assumptions about driving forces (such as demographic and socioeconomic development, technological change) and their key relationships. *Concentration scenarios*, derived from emission scenarios, are used as input to a *climate model* to compute *climate projections*. In IPCC (1992) a set of emission scenarios was presented which were used as a basis for the climate projections in IPCC (1996). These emission scenarios are referred to as the IS92 scenarios. In the IPCC Special Report on Emission Scenarios (Nakićenović and Swart, 2000) new emission scenarios, the so-called SRES scenarios, were published, some of which were used, among others, as a basis for the climate projections presented in Chapters 9 to 11 of IPCC (2001) and Chapters 10 and 11 of this report. For the meaning of some terms related to these scenarios, see *SRES scenarios*.

Energy balance The difference between the total incoming and total outgoing energy. If this balance is positive, warming occurs; if it is negative, cooling occurs. Averaged over the globe and over long time periods, this balance must be zero. Because the *climate system* derives virtually all its energy from the Sun, zero balance implies that, globally, the amount of incoming *solar radiation* on average must be equal to the sum of the outgoing reflected solar radiation and the outgoing *thermal infrared radiation* emitted by the climate system. A perturbation of this global radiation balance, be it *anthropogenic* or natural, is called *radiative forcing*.

Ensemble A group of parallel model simulations used for *climate projections*. Variation of the results across the ensemble members gives an estimate of *uncertainty*. Ensembles made with the same model but different initial conditions only characterise the uncertainty associated with internal *climate variability*, whereas multi-model ensembles including simulations by several models also include the impact of model differences. Perturbed-parameter ensembles, in which model parameters are varied in a systematic manner, aim to produce a more objective estimate of modelling uncertainty than is possible with traditional multi-model ensembles.

Equilibrium and transient climate experiment An *equilibrium climate experiment* is an experiment in which a *climate model* is allowed to fully adjust to a change in *radiative forcing*. Such experiments provide information on the difference between the initial and final states of the model, but not on the time-dependent response. If the forcing is allowed to evolve gradually according to a prescribed *emission scenario*, the time-dependent response of a climate model may be analysed. Such an experiment is called a *transient climate experiment*. See *Climate projection*.

Equilibrium line The boundary between the region on a *glacier* where there is a net annual loss of ice mass (ablation area) and that where there is a net annual gain (accumulation area). The altitude of this boundary is referred to as *equilibrium line altitude*.

Equivalent carbon dioxide (CO_2) concentration The concentration of *carbon dioxide* that would cause the same amount of *radiative forcing* as a given mixture of carbon dioxide and other *greenhouse gases.*

Equivalent carbon dioxide (CO_2) emission The amount of *carbon dioxide* emission that would cause the same integrated *radiative forcing*, over a given time horizon, as an emitted amount of a well mixed *greenhouse gas* or a mixture of well mixed greenhouse gases. The equivalent carbon dioxide emission is obtained by multiplying the emission of a well mixed greenhouse gas by its *Global Warming Potential* for the given time horizon. For a mix of greenhouse gases it is obtained by summing the equivalent carbon dioxide emissions of each gas. Equivalent carbon dioxide emission is a standard and useful *metric* for comparing emissions of different greenhouse gases but does not imply exact equivalence of the corresponding *climate change* responses (see Section 2.10).

Evapotranspiration The combined process of evaporation from the Earth's surface and transpiration from vegetation.

External forcing External forcing refers to a forcing agent outside the *climate system* causing a change in the climate system. Volcanic eruptions, solar variations and *anthropogenic* changes in the composition of the *atmosphere* and *land use change* are external forcings.

Extreme weather event An extreme weather event is an event that is rare at a particular place and time of year. Definitions of *rare* vary, but an extreme weather event would normally be as rare as or rarer than the 10th or 90th *percentile* of the observed *probability density function*. By definition, the characteristics of what is called *extreme weather* may vary from place to place in an absolute sense. Single extreme events cannot be simply and directly attributed to

anthropogenic climate change, as there is always a finite chance the event in question might have occurred naturally. When a pattern of extreme weather persists for some time, such as a season, it may be classed as an *extreme climate event*, especially if it yields an average or total that is itself extreme (e.g., *drought* or heavy rainfall over a season).

Faculae Bright patches on the Sun. The area covered by faculae is greater during periods of high *solar activity*.

Feedback See *Climate feedback*.

Fingerprint The *climate* response pattern in space and/or time to a specific forcing is commonly referred to as a fingerprint. Fingerprints are used to detect the presence of this response in observations and are typically estimated using forced *climate model* simulations.

Flux adjustment To avoid the problem of coupled *Atmosphere*-Ocean General Circulation Models (AOGCMs) drifting into some unrealistic *climate* state, adjustment terms can be applied to the atmosphere-ocean fluxes of heat and moisture (and sometimes the surface stresses resulting from the effect of the wind on the ocean surface) before these fluxes are imposed on the model ocean and atmosphere. Because these adjustments are pre-computed and therefore independent of the coupled model integration, they are uncorrelated with the anomalies that develop during the integration. Chapter 8 of this report concludes that most models used in this report (Fourth Assessment Report AOGCMs) do not use flux adjustments, and that in general, fewer models use them.

Forest A vegetation type dominated by trees. Many definitions of the term *forest* are in use throughout the world, reflecting wide differences in biogeophysical conditions, social structure and economics. For a discussion of the term *forest* and related terms such as *afforestation*, *reforestation* and *deforestation* see the IPCC Report on Land Use, Land-Use Change and Forestry (IPCC, 2000). See also the Report on Definitions and Methodological Options to Inventory Emissions from Direct Human-induced Degradation of Forests and Devegetation of Other Vegetation Types (IPCC, 2003).

Fossil fuel emissions Emissions of *greenhouse gases* (in particular *carbon dioxide*) resulting from the combustion of fuels from fossil carbon deposits such as oil, gas and coal.

Framework Convention on Climate Change See *United Nations Framework Convention on Climate Change* (UNFCCC).

Free atmosphere
The atmospheric layer that is negligibly affected by friction against the Earth's surface, and which is above the *atmospheric boundary layer*.

Frozen ground Soil or rock in which part or all of the *pore water* is frozen (Van Everdingen, 1998). Frozen ground includes *permafrost.* Ground that freezes and thaws annually is called *seasonally frozen ground*.

General circulation The large-scale motions of the *atmosphere* and the ocean as a consequence of differential heating on a rotating Earth, which tend to restore the *energy balance* of the system through transport of heat and momentum.

General Circulation Model (GCM) See *Climate model*.

Geoid The equipotential surface (i.e., having the same gravity potential at each point) that best fits the mean sea level (see *relative sea level*) in the absence of astronomical tides; ocean circulations; hydrological, cryospheric and atmospheric effects; Earth rotation variations and polar motion; nutation and precession; tectonics and other effects such as *post-glacial rebound*. The geoid is global and extends over continents, oceans and *ice sheets*, and at present includes the effect of the permanent tides (zero-frequency gravitational effect from the Sun and the Moon). It is the surface of reference for astronomical observations, geodetic levelling, and for ocean, hydrological, glaciological and climate modelling. In practice, there exist various operational definitions of the geoid, depending on the way the time-variable effects mentioned above are modelled.

Geostrophic winds or currents A wind or current that is in balance with the horizontal pressure gradient and the Coriolis force, and thus is outside of the influence of friction. Thus, the wind or current is directly parallel to isobars and its speed is inversely proportional to the spacing of the isobaric contours.

Glacial isostatic adjustment See *Post-glacial rebound*.

Glacier A mass of land ice that flows downhill under gravity (through internal deformation and/or sliding at the base) and is constrained by internal stress and friction at the base and sides. A glacier is maintained by accumulation of snow at high altitudes, balanced by melting at low altitudes or discharge into the sea. See *Equilibrium line*; *Mass balance*.

Global dimming Global dimming refers to perceived widespread reduction of *solar radiation* received at the surface of the Earth from about the year 1961 to around 1990.

Global surface temperature The global surface temperature is an estimate of the global mean surface air temperature. However, for changes over time, only anomalies, as departures from a climatology, are used, most commonly based on the area-weighted global average of the *sea surface temperature* anomaly and *land surface air temperature* anomaly.

Global Warming Potential (GWP) An index, based upon radiative properties of well-mixed *greenhouse gases*, measuring the *radiative forcing* of a unit mass of a given well-mixed greenhouse gas in the present-day *atmosphere* integrated over a chosen time horizon, relative to that of *carbon dioxide*. The GWP represents the combined effect of the differing times these gases remain in the atmosphere and their relative effectiveness in absorbing outgoing *thermal infrared radiation*. The *Kyoto Protocol* is based on GWPs from pulse emissions over a 100-year time frame.

Greenhouse effect *Greenhouse gases* effectively absorb *thermal infrared radiation*, emitted by the Earth's surface, by the *atmosphere* itself due to the same gases, and by clouds. Atmospheric radiation is emitted to all sides, including downward to the Earth's surface. Thus, greenhouse gases trap heat within the surface-*troposphere* system. This is called the *greenhouse effect*. Thermal infrared radiation in the troposphere is strongly coupled to the temperature of the atmosphere at the altitude at which it is emitted. In the troposphere, the temperature generally decreases with height. Effectively, infrared radiation emitted to space originates from an altitude with a temperature of, on average, –19°C, in balance with the net incoming *solar radiation*, whereas the Earth's surface is kept at a much higher temperature of, on average, +14°C. An increase in the concentration of greenhouse gases leads to an increased infrared opacity of the atmosphere, and therefore to an effective radiation into space from a higher altitude at a lower temperature. This causes a *radiative forcing* that leads to an enhancement of the greenhouse effect, the so-called *enhanced greenhouse effect*.

Greenhouse gas (GHG) Greenhouse gases are those gaseous constituents of the *atmosphere*, both natural and *anthropogenic*, that absorb and emit radiation at specific wavelengths within the spectrum of *thermal infrared radiation* emitted by the Earth's surface, the atmosphere itself, and by clouds. This property causes the *greenhouse effect*. Water vapour (H_2O), *carbon dioxide* (CO_2), nitrous oxide (N_2O), methane (CH_4) and *ozone* (O_3) are the primary greenhouse gases in the Earth's atmosphere. Moreover, there are a number of entirely human-made greenhouse gases in the atmosphere, such as the *halocarbons* and other chlorine- and bromine-containing substances, dealt with under the *Montreal Protocol*. Beside CO_2, N_2O and CH_4, the *Kyoto Protocol* deals with the greenhouse gases sulphur hexafluoride (SF6), hydrofluorocarbons (HFCs) and perfluorocarbons (PFCs).

Gross Primary Production (GPP) The amount of energy fixed from the *atmosphere* through *photosynthesis*.

Ground ice A general term referring to all types of ice contained in freezing and seasonally *frozen ground* and *permafrost* (Van Everdingen, 1998).

Ground temperature The temperature of the ground near the surface (often within the first 10 cm). It is often called *soil temperature*.

Grounding line/zone The junction between a *glacier* or *ice sheet* and *ice shelf*; the place where ice starts to float.

Gyre Basin-scale ocean horizontal circulation pattern with slow flow circulating around the ocean basin, closed by a strong and narrow (100–200 km wide) boundary current on the western side. The subtropical gyres in each ocean are associated with high pressure in the centre of the gyres; the subpolar gyres are associated with low pressure.

Hadley Circulation A direct, thermally driven overturning cell in the *atmosphere* consisting of poleward flow in the upper *troposphere*, subsiding air into the subtropical anticyclones, return flow as part of the trade winds near the surface, and with rising air near the equator in the so-called *Inter-Tropical Convergence Zone*.

Halocarbons A collective term for the group of partially halogenated organic species, including the chlorofluorocarbons (CFCs), hydrochlorofluorocarbons (HCFCs), hydrofluorocarbons (HFCs), halons, methyl chloride, methyl bromide, etc. Many of the halocarbons have large *Global Warming Potentials*. The chlorine- and bromine-containing halocarbons are also involved in the depletion of the *ozone layer*.

Halosteric See *Sea level change*.

HCFC See *Halocarbons*.

HFC See *Halocarbons*.

Heterotrophic respiration The conversion of organic matter to *carbon dioxide* by organisms other than plants.

Holocene The Holocene geological epoch is the latter of two *Quaternary* epochs, extending from about 11.6 ka to and including the present.

Hydrosphere The component of the *climate system* comprising liquid surface and subterranean water, such as oceans, seas, rivers, fresh water lakes, underground water, etc.

Ice age An ice age or *glacial period* is characterised by a long-term reduction in the temperature of the Earth's *climate*, resulting in growth of continental *ice sheets* and mountain *glaciers* (*glaciation*).

Ice cap A dome shaped ice mass, usually covering a highland area, which is considerably smaller in extent than an *ice sheet*.

Ice core A cylinder of ice drilled out of a *glacier* or *ice sheet*.

Ice sheet A mass of land ice that is sufficiently deep to cover most of the underlying bedrock topography, so that its shape is mainly determined by its dynamics (the flow of the ice as it deforms internally and/or slides at its base). An ice sheet flows outward from a high central ice plateau with a small average surface slope. The margins usually slope more steeply, and most ice is discharged through fast-flowing *ice streams* or outlet *glaciers*, in some cases into the sea or into *ice shelves* floating on the sea. There are only three large ice sheets in the modern world, one on Greenland and two on Antarctica, the East and West Antarctic Ice Sheets, divided by the Transantarctic Mountains. During glacial periods there were others.

Ice shelf A floating slab of ice of considerable thickness extending from the coast (usually of great horizontal extent with a level or gently sloping surface), often filling embayments in the coastline of the *ice sheets*. Nearly all ice shelves are in Antarctica, where most of the ice discharged seaward flows into ice shelves.

Ice stream A stream of ice flowing faster than the surrounding *ice sheet*. It can be thought of as a *glacier* flowing between walls of slower-moving ice instead of rock.

Indirect aerosol effect *Aerosols* may lead to an indirect *radiative forcing* of the *climate system* through acting as *cloud condensation nuclei* or modifying the optical properties and lifetime of clouds. Two indirect effects are distinguished:

Cloud albedo effect A radiative forcing induced by an increase in *anthropogenic* aerosols that cause an initial increase in droplet concentration and a decrease in droplet size for fixed liquid water content, leading to an increase in cloud *albedo*. This effect is also known as the *first indirect effect* or *Twomey effect*.

Cloud lifetime effect A forcing induced by an increase in anthropogenic aerosols that cause a decrease in droplet size, reducing the precipitation efficiency, thereby modifying the liquid water content, cloud thickness and cloud life time. This effect is also known as the *second indirect effect* or *Albrecht effect*.

Apart from these indirect effects, aerosols may have a *semi-direct effect*. This refers to the absorption of *solar radiation* by absorbing aerosol, which heats the air and tends to increase the static stability relative to the surface. It may also cause evaporation of cloud droplets.

Industrial revolution A period of rapid industrial growth with far-reaching social and economic consequences, beginning in Britain during the second half of the eighteenth century and spreading to Europe and later to other countries including the United States. The invention of the steam engine was an important trigger of this development. The industrial revolution marks the beginning of a strong increase in the use of fossil fuels and emission of, in particular, fossil *carbon dioxide*. In this report the terms *pre-industrial* and *industrial* refer, somewhat arbitrarily, to the periods before and after 1750, respectively.

Infrared radiation See *Thermal infrared radiation*.

Insolation The amount of *solar radiation* reaching the Earth by latitude and by season. Usually *insolation* refers to the radiation arriving at the top of the *atmosphere*. Sometimes it is specified as referring to the radiation arriving at the Earth's surface. See also: *Total Solar Irradiance*.

Interglacials The warm periods between *ice age* glaciations. The previous interglacial, dated approximately from 129 to 116 ka, is referred to as the *Last Interglacial* (AMS, 2000)

Internal variability See *Climate variability*.

Inter-Tropical Convergence Zone (ITCZ) The Inter-Tropical Convergence Zone is an equatorial zonal belt of low pressure near the equator where the northeast trade winds meet the southeast trade winds. As these winds converge, moist air is forced upward, resulting in a band of heavy precipitation. This band moves seasonally.

Isostatic or Isostasy Isostasy refers to the way in which the *lithosphere* and mantle respond visco-elastically to changes in surface loads. When the loading of the lithosphere and/or the mantle is changed by alterations in land ice mass, ocean mass, sedimentation, erosion or mountain building, vertical isostatic adjustment results, in order to balance the new load.

Kyoto Protocol The Kyoto Protocol to the *United Nations Framework Convention on Climate Change* (UNFCCC) was adopted in 1997 in Kyoto, Japan, at the Third Session of the Conference of the Parties (COP) to the UNFCCC. It contains legally binding commitments, in addition to those included in the UNFCCC. Countries included in Annex B of the Protocol (most Organisation for Economic Cooperation and Development countries and countries with economies in transition) agreed to reduce their *anthropogenic greenhouse gas* emissions (*carbon dioxide*, methane, nitrous oxide, hydrofluorocarbons, perfluorocarbons, and sulphur hexafluoride) by at least 5% below 1990 levels in the commitment period 2008 to 2012. The Kyoto Protocol entered into force on 16 February 2005.

Land use and Land use change *Land use* refers to the total of arrangements, activities and inputs undertaken in a certain land cover type (a set of human actions). The term land use is also used in the sense of the social and economic purposes for which land is managed (e.g., grazing, timber extraction and conservation). *Land use change* refers to a change in the use or management of land by humans, which may lead to a change in land cover. Land cover and land use change may have an impact on the surface *albedo*, *evapotranspiration*, *sources* and *sinks* of *greenhouse gases*, or other properties of the *climate system* and may thus have a *radiative forcing* and/or other impacts on *climate*, locally or globally. See also the IPCC Report on Land Use, Land-Use Change, and Forestry (IPCC, 2000).

La Niña See *El Niño-Southern Oscillation*.

Land surface air temperature The surface air temperature as measured in well-ventilated screens over land at 1.5 m above the ground.

Lapse rate The rate of change of an atmospheric variable, usually temperature, with height. The lapse rate is considered positive when the variable decreases with height.

Last Glacial Maximum (LGM) The Last Glacial Maximum refers to the time of maximum extent of the *ice sheets* during the last glaciation, approximately 21 ka. This period has been widely studied because the *radiative forcings* and boundary conditions are relatively well known and because the global cooling during that period is comparable with the projected warming over the 21st century.

Last Interglacial (LIG) See *Interglacial*.

Latent heat flux The flux of heat from the Earth's surface to the *atmosphere* that is associated with evaporation or condensation of water vapour at the surface; a component of the surface energy budget.

Level of Scientific Understanding (LOSU) This is an index on a 5-step scale (high, medium, medium-low, low and very low) designed to characterise the degree of scientific understanding of the *radiative forcing* agents that affect *climate change*. For each agent, the index represents a subjective judgement about the evidence for the physical/chemical mechanisms determining the forcing and the consensus surrounding the quantitative estimate and its *uncertainty*.

Lifetime Lifetime is a general term used for various time scales characterising the rate of processes affecting the concentration of trace gases. The following lifetimes may be distinguished:

Turnover time (T) (also called *global atmospheric lifetime*) is the ratio of the mass M of a *reservoir* (e.g., a gaseous compound in the *atmosphere*) and the total rate of removal S from the reservoir: T = M / S. For each removal process, separate turnover times can be defined. In soil carbon biology, this is referred to as *Mean Residence Time*.

Adjustment time or *response time* (T_a) is the time scale characterising the decay of an instantaneous pulse input into the reservoir. The term adjustment time is also used to characterise the adjustment of the mass of a reservoir following a step change in the *source* strength. *Half-life* or *decay constant* is used to quantify a first-order exponential decay process. See *response time* for a different definition pertinent to *climate* variations.

The term *lifetime* is sometimes used, for simplicity, as a surrogate for *adjustment time*.

In simple cases, where the global removal of the compound is directly proportional to the total mass of the reservoir, the adjustment time equals the turnover time: $T = T_a$. An example is *CFC*-11, which is removed from the *atmosphere* only by photochemical processes in the *stratosphere*. In more complicated cases, where several reservoirs are involved or where the removal is not proportional to the total mass, the equality $T = T_a$ no longer holds. *Carbon dioxide* (CO_2) is an extreme example. Its turnover time is only about four years because of the rapid exchange between the atmosphere and the ocean and terrestrial biota. However, a large part of that CO_2 is returned to the atmosphere within a few years. Thus, the adjustment time of CO_2 in the atmosphere is actually determined by the rate of removal of carbon from the surface layer of the oceans into its deeper layers. Although an approximate value of 100 years may be given for the adjustment time of CO_2 in the atmosphere, the actual adjustment is faster initially and slower later on. In the case of methane (CH_4), the adjustment time is different from the turnover time because the removal is mainly through a chemical reaction with the hydroxyl radical OH, the concentration of which itself depends on the CH_4 concentration. Therefore, the CH_4 removal rate S is not proportional to its total mass M.

Likelihood The likelihood of an occurrence, an outcome or a result, where this can be estimated probabilistically, is expressed in this report using a standard terminology, defined in Box 1.1. See also *Uncertainty*; *Confidence*.

Lithosphere The upper layer of the solid Earth, both continental and oceanic, which comprises all crustal rocks and the cold, mainly elastic part of the uppermost mantle. Volcanic activity, although part of the lithosphere, is not considered as part of the *climate system*, but acts as an *external forcing* factor. See *Isostatic*.

Little Ice Age (LIA) An interval between approximately AD 1400 and 1900 when temperatures in the Northern Hemisphere were generally colder than today's, especially in Europe.

Mass balance (of glaciers, ice caps or ice sheets) The balance between the mass input to the ice body (accumulation) and the mass loss (ablation, iceberg calving). Mass balance terms include the following:

Specific mass balance: net mass loss or gain over a hydrological cycle at a point on the surface of a *glacier*.

Total mass balance (of the glacier): The specific mass balance spatially integrated over the entire glacier area; the total mass a glacier gains or loses over a hydrological cycle.

Mean specific mass balance: The total mass balance per unit area of the glacier. If *surface* is specified (*specific surface mass balance*, etc.) then ice flow contributions are not considered; otherwise, mass balance includes contributions from ice flow and iceberg calving. The specific surface mass balance is positive in the accumulation area and negative in the ablation area.

Mean sea level See *Relative sea level*.

Medieval Warm Period (MWP) An interval between AD 1000 and 1300 in which some Northern Hemisphere *regions* were warmer than during the *Little Ice Age* that followed.

Meridional Overturning Circulation (MOC) Meridional (north-south) overturning circulation in the ocean quantified by zonal (east-west) sums of mass transports in depth or density layers. In the North Atlantic, away from the subpolar *regions*, the MOC (which is in principle an observable quantity) is often identified with the *Thermohaline Circulation* (THC), which is a conceptual interpretation. However, it must be borne in mind that the MOC can also include shallower, wind-driven overturning cells such as occur in the upper ocean in the tropics and subtropics, in which warm (light) waters moving poleward are transformed to slightly denser waters and *subducted* equatorward at deeper levels.

Metadata Information about meteorological and climatological data concerning how and when they were measured, their quality, known problems and other characteristics.

Metric A consistent measurement of a characteristic of an object or activity that is otherwise difficult to quantify.

Mitigation A human intervention to reduce the *sources* or enhance the *sinks* of *greenhouse gases*.

Mixing ratio See *Mole fraction*.

Model hierarchy See *Climate model* (spectrum or hierarchy).

Modes of climate variability Natural variability of the *climate system*, in particular on seasonal and longer time scales, predominantly occurs with preferred spatial patterns and time scales, through the dynamical characteristics of the atmospheric circulation and through interactions with the land and ocean surfaces. Such patterns are often called *regimes*, *modes* or *teleconnections*. Examples are the *North Atlantic Oscillation* (NAO), the *Pacific-North American pattern* (PNA), the *El Niño-Southern Oscillation* (ENSO), the *Northern Annular Mode* (NAM; previously called Arctic Oscillation, AO) and the *Southern Annular Mode* (SAM; previously called the Antarctic Oscillation, AAO). Many of the prominent modes of climate variability are discussed in section 3.6. See also *Patterns of climate variability*.

Mole fraction Mole fraction, or *mixing ratio*, is the ratio of the number of moles of a constituent in a given volume to the total number of moles of all constituents in that volume. It is usually reported for dry air. Typical values for long-lived *greenhouse gases* are in the order of µmol mol^{-1} (parts per million: *ppm*), nmol mol^{-1} (parts per billion: *ppb*), and fmol mol^{-1} (parts per trillion: *ppt*). Mole fraction differs from *volume mixing ratio*, often expressed in ppmv etc., by the corrections for non-ideality of gases. This correction is significant relative to measurement precision for many greenhouse gases. (Schwartz and Warneck, 1995).

Monsoon A monsoon is a tropical and subtropical seasonal reversal in both the surface winds and associated precipitation, caused by differential heating between a continental-scale land mass and the adjacent ocean. Monsoon rains occur mainly over land in summer.

Montreal Protocol The Montreal Protocol on Substances that Deplete the Ozone Layer was adopted in Montreal in 1987, and subsequently adjusted and amended in London (1990), Copenhagen (1992), Vienna (1995), Montreal (1997) and Beijing (1999). It controls the consumption and production of chlorine- and bromine-containing chemicals that destroy stratospheric *ozone*, such as chlorofluorocarbons, methyl chloroform, carbon tetrachloride and many others.

Microwave Sounding Unit (MSU) A satellite-borne microwave sounder that estimates the temperature of thick layers of the *atmosphere* by measuring the thermal emission of oxygen molecules from a complex of emission lines near 60 GHz. A series of nine MSUs began making this kind of measurement in late 1978. Beginning in mid 1998, a follow-on series of instruments, the Advanced Microwave Sounding Units (AMSUs), began operation.

MSU See *Microwave Sounding Unit*.

Nonlinearity A process is called *nonlinear* when there is no simple proportional relation between cause and effect. The *climate system* contains many such nonlinear processes, resulting in a system with a potentially very complex behaviour. Such complexity may lead to *abrupt climate change*. See also *Chaos*; *Predictability*.

North Atlantic Oscillation (NAO) The North Atlantic Oscillation consists of opposing variations of barometric pressure near Iceland and near the Azores. It therefore corresponds to fluctuations in the strength of the main westerly winds across the Atlantic into Europe, and thus to fluctuations in the embedded cyclones with their associated frontal systems. See NAO Index, Box 3.4.

Northern Annular Mode (NAM) A winter fluctuation in the amplitude of a pattern characterised by low surface pressure in the Arctic and strong mid-latitude westerlies. The NAM has links with the northern polar vortex into the *stratosphere*. Its pattern has a bias to the North Atlantic and has a large correlation with the *North Atlantic Oscillation*. See NAM Index, Box 3.4.

Ocean acidification A decrease in the *pH* of sea water due to the *uptake* of *anthropogenic carbon dioxide*.

Ocean heat uptake efficiency This is a measure (W m^{-2} °C^{-1}) of the rate at which heat storage by the global ocean increases as global surface temperature rises. It is a useful parameter for *climate change* experiments in which the *radiative forcing* is changing monotonically, when it can be compared with the climate sensitivity parameter to gauge the relative importance of climate response and ocean heat uptake in determining the rate of climate change. It can be estimated from a 1% yr^{-1} atmospheric *carbon dioxide* increase experiment as the ratio of the global average top-of-*atmosphere* net downward radiative flux to the *transient climate response* (see *climate sensitivity*).

Organic aerosol *Aerosol* particles consisting predominantly of organic compounds, mainly carbon, hydrogen, oxygen and lesser amounts of other elements. (Charlson and Heintzenberg, 1995, p. 405). See *Carbonaceous aerosol.*

Ozone Ozone, the triatomic form of oxygen (O_3), is a gaseous atmospheric constituent. In the *troposphere*, it is created both naturally and by photochemical reactions involving gases resulting from human activities (*smog*). Tropospheric ozone acts as a *greenhouse gas*. In the *stratosphere*, it is created by the interaction between solar ultraviolet radiation and molecular oxygen (O_2). Stratospheric ozone plays a dominant role in the stratospheric radiative balance. Its concentration is highest in the *ozone layer*.

Ozone hole See *Ozone layer*.

Ozone layer The *stratosphere* contains a layer in which the concentration of *ozone* is greatest, the so-called ozone layer. The layer extends from about 12 to 40 km above the Earth's surface. The ozone concentration reaches a maximum between about 20 and 25 km. This layer is being depleted by human emissions of chlorine and bromine compounds. Every year, during the Southern Hemisphere spring, a very strong depletion of the ozone layer takes place over the antarctic *region*, caused by *anthropogenic* chlorine and bromine compounds in combination with the specific meteorological conditions of that region. This phenomenon is called the *ozone hole*. See *Montreal Protocol*.

Pacific decadal variability Coupled decadal-to-inter-decadal variability of the atmospheric circulation and underlying ocean in the Pacific Basin. It is most prominent in the North Pacific, where fluctuations in the strength of the winter Aleutian Low pressure system co-vary with North Pacific *sea surface temperatures*, and are linked to decadal variations in atmospheric circulation, sea surface temperatures and ocean circulation throughout the whole Pacific Basin. Such fluctuations have the effect of modulating the *El Niño-Southern Oscillation* cycle. Key measures of Pacific decadal variability are the *North Pacific Index (NPI)*, the *Pacific Decadal Oscillation (PDO)* index and the *Inter-decadal Pacific Oscillation (IPO)* index, all defined in Box 3.4.

Pacific-North American (PNA) pattern An atmospheric large-scale wave pattern featuring a sequence of tropospheric high- and low-pressure anomalies stretching from the subtropical west Pacific to the east coast of North America. See PNA pattern index, Box 3.4.

Palaeoclimate *Climate* during periods prior to the development of measuring instruments, including historic and geologic time, for which only *proxy* climate records are available.

Parametrization In *climate models*, this term refers to the technique of representing processes that cannot be explicitly resolved at the spatial or temporal resolution of the model (sub-grid scale processes) by relationships between model-resolved larger-scale flow and the area- or time-averaged effect of such sub-grid scale processes.

Patterns of climate variability See *Modes of climate variability*.

Percentile A percentile is a value on a scale of one hundred that indicates the percentage of the data set values that is equal to or below it. The percentile is often used to estimate the extremes of a distribution. For example, the 90th (10th) percentile may be used to refer to the threshold for the upper (lower) extremes.

Permafrost Ground (soil or rock and included ice and organic material) that remains at or below 0°C for at least two consecutive years (Van Everdingen, 1998).

pH pH is a dimensionless measure of the acidity of water (or any solution) given by its concentration of hydrogen ions (H^+). pH is measured on a logarithmic scale where $pH = -\log_{10}(H^+)$. Thus, a pH decrease of 1 unit corresponds to a 10-fold increase in the concentration of H^+, or acidity.

Photosynthesis The process by which plants take carbon dioxide from the air (or bicarbonate in water) to build carbohydrates, releasing oxygen in the process. There are several pathways of photosynthesis with different responses to atmospheric carbon dioxide concentrations. See Carbon dioxide fertilization; C3 plants; C4 plants.

Plankton Microorganisms living in the upper layers of aquatic systems. A distinction is made between *phytoplankton*, which depend on *photosynthesis* for their energy supply, and *zooplankton*, which feed on phytoplankton.

Pleistocene The earlier of two *Quaternary* epochs, extending from the end of the Pliocene, about 1.8 Ma, until the beginning of the *Holocene* about 11.6 ka.

Pollen analysis A technique of both relative dating and environmental *reconstruction*, consisting of the identification and counting of pollen types preserved in peat, lake sediments and other deposits. See *Proxy*.

Post-glacial rebound The vertical movement of the land and sea floor following the reduction of the load of an ice mass, for example, since the *Last Glacial Maximum* (21 ka). The rebound is an *isostatic* land movement.

Precipitable water The total amount of atmospheric water vapour in a vertical column of unit cross-sectional area. It is commonly expressed in terms of the height of the water if completely condensed and collected in a vessel of the same unit cross section.

Precursors Atmospheric compounds that are not *greenhouse gases* or *aerosols*, but that have an effect on greenhouse gas or aerosol concentrations by taking part in physical or chemical processes regulating their production or destruction rates.

Predictability The extent to which future states of a system may be predicted based on knowledge of current and past states of the system.

Since knowledge of the *climate system*'s past and current states is generally imperfect, as are the models that utilise this knowledge to produce a *climate prediction*, and since the climate system is inherently *nonlinear* and *chaotic*, predictability of the climate system is inherently limited. Even with arbitrarily accurate models and observations, there may still be limits to the predictability of such a nonlinear system (AMS, 2000)

Pre-industrial See *Industrial revolution*.

Probability Density Function (PDF) A probability density function is a function that indicates the relative chances of occurrence of different outcomes of a variable. The function integrates to unity over the domain for which it is defined and has the property that the integral over a sub-domain equals the probability that the outcome of the variable lies within that sub-domain. For example, the probability that a temperature anomaly defined in a particular way is greater than zero is obtained from its PDF by integrating the PDF over all possible temperature anomalies greater than zero. Probability density functions that describe two or more variables simultaneously are similarly defined.

Projection A projection is a potential future evolution of a quantity or set of quantities, often computed with the aid of a model.

Projections are distinguished from *predictions* in order to emphasize that projections involve assumptions concerning, for example, future socioeconomic and technological developments that may or may not be realised, and are therefore subject to substantial *uncertainty*. See also *Climate projection*; *Climate prediction*.

Proxy A proxy *climate* indicator is a local record that is interpreted, using physical and biophysical principles, to represent some combination of climate-related variations back in time. Climate-related data derived in this way are referred to as proxy data. Examples of proxies include *pollen analysis*, *tree ring* records, characteristics of corals and various data derived from *ice cores*.

Quaternary The period of geological time following the *Tertiary* (65 Ma to 1.8 Ma). Following the current definition (which is under revision at present) the Quaternary extends from 1.8 Ma until the present. It is formed of two epochs, the *Pleistocene* and the *Holocene*.

Radiative forcing Radiative forcing is the change in the net, downward minus upward, irradiance (expressed in W m^{-2}) at the *tropopause* due to a change in an external driver of *climate change*, such as, for example, a change in the concentration of *carbon dioxide* or the output of the Sun. Radiative forcing is computed with all tropospheric properties held fixed at their unperturbed values, and after allowing for stratospheric temperatures, if perturbed, to readjust to radiative-dynamical equilibrium. Radiative forcing is called *instantaneous* if no change in stratospheric temperature is accounted for. For the purposes of this report, radiative forcing is further defined as the change relative to the year 1750 and, unless otherwise noted, refers to a global and annual average value. Radiative forcing is not to be confused with *cloud radiative forcing*, a similar terminology for describing an unrelated measure of the impact of clouds on the irradiance at the top of the *atmosphere*.

Radiative forcing scenario A plausible representation of the future development of *radiative forcing* associated, for example, with changes in atmospheric composition or *land use change*, or with external factors such as variations in *solar activity*. Radiative forcing scenarios can be used as input into simplified *climate models* to compute *climate projections*.

Rapid climate change See *Abrupt climate change*.

Reanalysis Reanalyses are atmospheric and oceanic analyses of temperature, wind, current, and other meteorological and oceanographic quantities, created by processing past meteorological and oceanographic data using fixed state-of-the-art weather forecasting models and data assimilation techniques. Using fixed data assimilation avoids effects from the changing analysis system that occurs in operational analyses. Although continuity is improved, global reanalyses still suffer from changing coverage and biases in the observing systems.

Reconstruction The use of *climate* indicators to help determine (generally past) climates.

Reforestation Planting of forests on lands that have previously contained forests but that have been converted to some other use. For a discussion of the term *forest* and related terms such as *afforestation*, reforestation and *deforestation*, see the IPCC Report on Land Use, Land-Use Change and Forestry (IPCC, 2000). See also the Report on Definitions and Methodological Options to Inventory Emissions from Direct Human-induced Degradation of Forests and Devegetation of Other Vegetation Types (IPCC, 2003)

Regime A regime is preferred states of the *climate system*, often representing one phase of dominant patterns or *modes of climate variability*.

Region A region is a territory characterised by specific geographical and climatological features. The *climate* of a region is affected by regional and local scale forcings like topography, *land use* characteristics, lakes, etc., as well as remote influences from other regions. See *Teleconnection*.

Relative sea level Sea level measured by a *tide gauge* with respect to the land upon which it is situated. *Mean sea level* is normally defined as the average relative sea level over a period, such as a month or a year, long enough to average out transients such as waves and tides. See *Sea level change*.

Reservoir A component of the *climate system*, other than the *atmosphere*, which has the capacity to store, accumulate or release a substance of concern, for example, carbon, a *greenhouse gas* or a *precursor*. Oceans, soils and *forests* are examples of reservoirs of carbon. *Pool* is an equivalent term (note that the definition of pool often includes the atmosphere). The absolute quantity of the substance of concern held within a reservoir at a specified time is called the *stock*.

Respiration The process whereby living organisms convert organic matter to *carbon dioxide*, releasing energy and consuming molecular oxygen.

Response time The response time or *adjustment time* is the time needed for the *climate system* or its components to re-equilibrate to a new state, following a forcing resulting from external and internal processes or *feedbacks*. It is very different for various components of the climate system. The response time of the *troposphere* is relatively short, from days to weeks, whereas the *stratosphere* reaches equilibrium on a time scale of typically a few months. Due to their large heat capacity, the oceans have a much longer response time: typically decades, but up to centuries or millennia. The response time of the strongly coupled surface-troposphere system is, therefore, slow compared to that of the stratosphere, and mainly determined by the oceans. The *biosphere* may respond quickly (e.g., to *droughts*), but also very slowly to imposed changes. See *lifetime* for a different definition of response time pertinent to the rate of processes affecting the concentration of trace gases.

Return period The average time between occurrences of a defined event (AMS, 2000).

Return value The highest (or, alternatively, lowest) value of a given variable, on average occurring once in a given period of time (e.g., in 10 years).

Scenario A plausible and often simplified description of how the future may develop, based on a coherent and internally consistent set of assumptions about driving forces and key relationships. Scenarios may be derived from *projections*, but are often based on additional information from other sources, sometimes combined with a *narrative storyline*. See also *SRES scenarios*; *Climate scenario*; *Emission scenario*.

Sea ice Any form of ice found at sea that has originated from the freezing of seawater. Sea ice may be discontinuous pieces (ice floes) moved on the ocean surface by wind and currents (pack ice), or a motionless sheet attached to the coast (land-fast ice). Sea ice less than one year old is called *first-year ice*. *Multi-year ice* is sea ice that has survived at least one summer melt season.

Sea level change Sea level can change, both globally and locally, due to (i) changes in the shape of the ocean basins, (ii) changes in the total mass of water and (iii) changes in water density. Sea level changes induced by changes in water density are called *steric*. Density changes induced by temperature changes only are called *thermosteric*, while density changes induced by salinity changes are called *halosteric*. See also *Relative Sea Level*; *Thermal expansion*.

Sea level equivalent (SLE) The change in global average sea level that would occur if a given amount of water or ice were added to or removed from the oceans.

Seasonally frozen ground See *Frozen ground*.

Sea surface temperature (SST) The sea surface temperature is the temperature of the subsurface bulk temperature in the top few metres of the ocean, measured by ships, buoys and drifters. From ships, measurements of water samples in buckets were mostly switched in the 1940s to samples from engine intake water. Satellite measurements of *skin temperature* (uppermost layer; a fraction of a millimetre thick) in the infrared or the top centimetre or so in the microwave are also used, but must be adjusted to be compatible with the bulk temperature.

Sensible heat flux The flux of heat from the Earth's surface to the *atmosphere* that is not associated with phase changes of water; a component of the surface energy budget.

Sequestration See *Uptake*.

Significant wave height The average height of the highest one-third of the wave heights (sea and swell) occurring in a particular time period.

Sink Any process, activity or mechanism that removes a *greenhouse gas*, an *aerosol* or a *precursor* of a greenhouse gas or aerosol from the *atmosphere*.

Slab-ocean model A simplified presentation in a *climate model* of the ocean as a motionless layer of water with a depth of 50 to 100 m. Climate models with a slab ocean can only be used for estimating the equilibrium response of climate to a given forcing, not the transient evolution of climate. See *Equilibrium and transient climate experiment*.

Snow line The lower limit of permanent snow cover, below which snow does not accumulate.

Soil moisture Water stored in or at the land surface and available for evaporation.

Soil temperature See *Ground temperature*.

Solar activity The Sun exhibits periods of high activity observed in numbers of *sunspots*, as well as radiative output, magnetic activity and emission of high-energy particles. These variations take place on a range of time scales from millions of years to minutes. See *Solar cycle*.

Solar ('11 year') cycle A quasi-regular modulation of *solar activity* with varying amplitude and a period of between 9 and 13 years.

Solar radiation Electromagnetic radiation emitted by the Sun. It is also referred to as *shortwave radiation*. Solar radiation has a distinctive range of wavelengths (spectrum) determined by the temperature of the Sun, peaking in visible wavelengths. See also: *Thermal infrared radiation*, *Insolation*.

Soot Particles formed during the quenching of gases at the outer edge of flames of organic vapours, consisting predominantly of carbon, with lesser amounts of oxygen and hydrogen present as carboxyl and phenolic groups and exhibiting an imperfect graphitic structure. See *Black carbon*; *Charcoal* (Charlson and Heintzenberg, 1995, p. 406).

Source Any process, activity or mechanism that releases a *greenhouse gas*, an *aerosol* or a *precursor* of a greenhouse gas or aerosol into the *atmosphere.*

Southern Annular Mode (SAM) The fluctuation of a pattern like the *Northern Annular Mode*, but in the Southern Hemisphere. See SAM Index, Box 3.4.

Southern Oscillation See *El Niño-Southern Oscillation* (ENSO).

Spatial and temporal scales *Climate* may vary on a large range of spatial and temporal scales. Spatial scales may range from local (less than 100,000 km^2), through regional (100,000 to 10 million km^2) to continental (10 to 100 million km^2). Temporal scales may range from seasonal to geological (up to hundreds of millions of years).

SRES scenarios SRES scenarios are *emission scenarios* developed by Nakićenović and Swart (2000) and used, among others, as a basis for some of the *climate projections* shown in Chapter 10 of this report. The following terms are relevant for a better understanding of the structure and use of the set of SRES scenarios:

Scenario family Scenarios that have a similar demographic, societal, economic and technical change storyline. Four scenario families comprise the SRES scenario set: A1, A2, B1 and B2.

Illustrative Scenario A scenario that is illustrative for each of the six scenario groups reflected in the Summary for Policymakers of Nakićenović and Swart (2000). They include four revised *scenario markers* for the scenario groups A1B, A2, B1, B2, and two additional scenarios for the A1FI and A1T groups. All scenario groups are equally sound.

Marker Scenario A scenario that was originally posted in draft form on the SRES website to represent a given scenario family. The choice of markers was based on which of the initial quantifications best reflected the storyline, and the features of specific models. Markers are no more likely than other scenarios, but are considered by the SRES writing team as illustrative of a particular storyline. They are included in revised form in Nakićenović and Swart (2000). These scenarios received the closest scrutiny of the entire writing team and via the SRES open process. Scenarios were also selected to illustrate the other two scenario groups.

Storyline A narrative description of a scenario (or family of scenarios), highlighting the main scenario characteristics, relationships between key driving forces and the dynamics of their evolution.

Steric See *Sea level change*.

Stock See *Reservoir*.

Storm surge The temporary increase, at a particular locality, in the height of the sea due to extreme meteorological conditions (low atmospheric pressure and/or strong winds). The storm surge is defined as being the excess above the level expected from the tidal variation alone at that time and place.

Storm tracks Originally, a term referring to the tracks of individual cyclonic weather systems, but now often generalised to refer to the *regions* where the main tracks of extratropical disturbances occur as sequences of low (cyclonic) and high (anticyclonic) pressure systems.

Stratosphere The highly stratified region of the *atmosphere* above the *troposphere* extending from about 10 km (ranging from 9 km at high latitudes to 16 km in the tropics on average) to about 50 km altitude.

Subduction Ocean process in which surface waters enter the ocean interior from the surface mixed layer through *Ekman pumping* and lateral *advection*. The latter occurs when surface waters are advected to a region where the local surface layer is less dense and therefore must slide below the surface layer, usually with no change in density.

Sunspots Small dark areas on the Sun. The number of sunspots is higher during periods of high *solar activity*, and varies in particular with the *solar cycle.*

Surface layer See *Atmospheric boundary layer*.

Surface temperature See *Global surface temperature*; *Ground temperature*; *Land surface air temperature*; *Sea surface temperature*.

Teleconnection A connection between *climate variations* over widely separated parts of the world. In physical terms, teleconnections are often a consequence of large-scale wave motions, whereby energy is transferred from source regions along preferred paths in the *atmosphere*.

Thermal expansion In connection with sea level, this refers to the increase in volume (and decrease in density) that results from warming water. A warming of the ocean leads to an expansion of the ocean volume and hence an increase in sea level. See *Sea level change*.

Thermal infrared radiation Radiation emitted by the Earth's surface, the *atmosphere* and the clouds. It is also known as *terrestrial* or *longwave radiation*, and is to be distinguished from the near-infrared radiation that is part of the solar spectrum. Infrared radiation, in general, has a distinctive range of wavelengths (*spectrum*) longer than the wavelength of the red colour in the visible part of the spectrum. The spectrum of thermal infrared radiation is practically distinct from that of shortwave or *solar radiation* because of the difference in temperature between the Sun and the Earth-atmosphere system.

Thermocline The layer of maximum vertical temperature gradient in the ocean, lying between the surface ocean and the abyssal ocean. In subtropical regions, its source waters are typically surface waters at higher latitudes that have *subducted* and moved equatorward. At high latitudes, it is sometimes absent, replaced by a *halocline*, which is a layer of maximum vertical salinity gradient.

Thermohaline circulation (THC) Large-scale circulation in the ocean that transforms low-density upper ocean waters to higher-density intermediate and deep waters and returns those waters back to the upper ocean. The circulation is asymmetric, with conversion to dense waters in restricted regions at high latitudes and the return to the surface involving slow upwelling and diffusive processes over much larger geographic regions. The THC is driven by high densities at or near the surface, caused by cold temperatures and/or high salinities, but despite its suggestive though common name, is also driven by mechanical forces such as wind and tides. Frequently, the name THC has been used synonymously with *Meridional Overturning Circulation*.

Thermokarst The process by which characteristic landforms result from the thawing of ice-rich *permafrost* or the melting of massive *ground ice* (Van Everdingen, 1998).

Thermosteric See *Sea level change*.

Tide gauge A device at a coastal location (and some deep-sea locations) that continuously measures the level of the sea with respect to the adjacent land. Time averaging of the sea level so recorded gives the observed secular changes of the *relative sea level*.

Total solar irradiance (TSI) The amount of *solar radiation* received outside the Earth's *atmosphere* on a surface normal to the incident radiation, and at the Earth's mean distance from the Sun.

Reliable measurements of solar radiation can only be made from space and the precise record extends back only to 1978. The generally accepted value is 1,368 W m^{-2} with an accuracy of about 0.2%. Variations of a few tenths of a percent are common, usually associated with the passage of *sunspots* across the solar disk. The *solar cycle* variation of TSI is of the order of 0.1% (AMS, 2000). See also *Insolation*.

Transient climate response See *Climate sensitivity*.

Tree rings Concentric rings of secondary wood evident in a cross-section of the stem of a woody plant. The difference between the dense, small-celled late wood of one season and the wide-celled early wood of the following spring enables the age of a tree to be estimated, and the ring widths or density can be related to *climate* parameters such as temperature and precipitation. See *Proxy*.

Trend In this report, the word *trend* designates a change, generally monotonic in time, in the value of a variable.

Tropopause The boundary between the *troposphere* and the *stratosphere*.

Troposphere The lowest part of the *atmosphere*, from the surface to about 10 km in altitude at mid-latitudes (ranging from 9 km at high latitudes to 16 km in the tropics on average), where clouds and weather phenomena occur. In the troposphere, temperatures generally decrease with height.

Turnover time See *Lifetime*.

Uncertainty An expression of the degree to which a value (e.g., the future state of the *climate system*) is unknown. Uncertainty can result from lack of information or from disagreement about what is known or even knowable. It may have many types of sources, from quantifiable errors in the data to ambiguously defined concepts or terminology, or uncertain *projections* of human behaviour. Uncertainty can therefore be represented by quantitative measures, for example, a range of values calculated by various models, or by qualitative statements, for example, reflecting the judgement of a team of experts (see Moss and Schneider, 2000; Manning et al., 2004). See also *Likelihood*; *Confidence*.

United Nations Framework Convention on Climate Change (UNFCCC) The Convention was adopted on 9 May 1992 in New York and signed at the 1992 Earth Summit in Rio de Janeiro by more than 150 countries and the European Community. Its ultimate objective is the 'stabilisation of greenhouse gas concentrations in the atmosphere at a level that would prevent dangerous anthropogenic interference with the climate system'. It contains commitments for all Parties. Under the Convention, Parties included in Annex I (all OECD

countries and countries with economies in transition) aim to return *greenhouse gas* emissions not controlled by the *Montreal Protocol* to 1990 levels by the year 2000. The convention entered in force in March 1994. See *Kyoto Protocol*.

Uptake The addition of a substance of concern to a *reservoir*. The uptake of carbon containing substances, in particular *carbon dioxide*, is often called (carbon) *sequestration*.

Urban heat island (UHI) The relative warmth of a city compared with surrounding rural areas, associated with changes in runoff, the *concrete jungle* effects on heat retention, changes in surface *albedo*, changes in pollution and *aerosols*, and so on.

Ventilation The exchange of ocean properties with the *atmospheric surface layer* such that property concentrations are brought closer to equilibrium values with the *atmosphere* (AMS, 2000).

Volume mixing ratio See *Mole fraction*.

Walker Circulation Direct thermally driven zonal overturning circulation in the *atmosphere* over the tropical Pacific Ocean, with rising air in the western and sinking air in the eastern Pacific.

Water mass A volume of ocean water with identifiable properties (temperature, salinity, density, chemical tracers) resulting from its unique formation process. Water masses are often identified through a vertical or horizontal extremum of a property such as salinity.

Younger Dryas A period 12.9 to 11.6 kya, during the deglaciation, characterised by a temporary return to colder conditions in many locations, especially around the North Atlantic.

REFERENCES

AMS, 2000: *AMS Glossary of Meteorology*, 2nd Ed. American Meteorological Society, Boston, MA,http://amsglossary.allenpress.com/glossary/browse.

Charlson, R.J., and J. Heintzenberg (eds.), 1995: *Aerosol Forcing of Climate*. John Wiley and Sons Limited, pp. 91–108. Copyright 1995 ©John Wiley and Sons Limited. Reproduced with permission.

Heim, R.R., 2002: *A Review of Twentieth-Century Drought Indices Used in the United States*. *Bull. Am. Meteorol. Soc.*, **83**, 1149–1165

IPCC, 1992: *Climate Change 1992: The Supplementary Report to the IPCC Scientific Assessment* [Houghton, J.T., B.A. Callander, and S.K. Varney (eds.)]. Cambridge University Press, Cambridge, United Kingdom and New York, NY, USA, 116 pp.

IPCC, 1996: *Climate Change 1995: The Science of Climate Change. Contribution of Working Group I to the Second Assessment Report of the Intergovernmental Panel on Climate Change* [Houghton., J.T., et al. (eds.)]. Cambridge University Press, Cambridge, United Kingdom and New York, NY, USA, 572 pp.

IPCC, 2000: *Land Use, Land-Use Change, and Forestry. Special Report of the Intergovernmental Panel on Climate Change* [Watson, R.T., et al. (eds.)]. Cambridge University Press, Cambridge, United Kingdom and New York, NY, USA, 377 pp.

IPCC, 2001: *Climate Change 2001: The Scientific Basis. Contribution of Working Group I to the Third Assessment Report of the Intergovernmental Panel on Climate Change* [Houghton, J.T., et al. (eds.)]. Cambridge University Press, Cambridge, United Kingdom and New York, NY, USA, 881 pp.

IPCC, 2003: *Definitions and Methodological Options to Inventory Emissions from Direct Human-Induced Degradation of Forests and Devegetation of Other Vegetation Types* [Penman, J., et al. (eds.)]. The Institute for Global Environmental Strategies (IGES), Japan , 32 pp.

Manning, M., et al., 2004: *IPCC Workshop on Describing Scientific Uncertainties in Climate Change to Support Analysis of Risk of Options*. Workshop Report. Intergovernmental Panel on Climate Change, Geneva.

Moss, R., and S. Schneider, 2000: *Uncertainties in the IPCC TAR: Recommendations to Lead Authors for More Consistent Assessment and Reporting*. In: IPCC Supporting Material: Guidance Papers on Cross Cutting Issues in the Third Assessment Report of the IPCC. [Pachauri, R., T. Taniguchi, and K. Tanaka (eds.)]. Intergovernmental Panel on Climate Change, Geneva, pp. 33–51.

Nakićenović, N., and R. Swart (eds.), 2000: *Special Report on Emissions Scenarios*. *A Special Report of Working Group III of the Intergovernmental Panel on Climate Change.* Cambridge University Press, Cambridge, United Kingdom and New York, NY, USA, 599 pp.

Schwartz, S.E., and P. Warneck, 1995: Units for use in atmospheric chemistry. *Pure Appl. Chem.*, 67, 1377–1406.

Van Everdingen, R. (ed.): 1998. *Multi-Language Glossary of Permafrost and Related Ground-Ice Terms*, revised May 2005. National Snow and Ice Data Center/World Data Center for Glaciology, Boulder, CO, http://nsidc.org/fgdc/glossary/.

Annex II

Contributors to the IPCC WGI Fourth Assessment Report

ACHUTARAO, Krishna
Lawrence Livermore National Laboratory
USA

ADLER, Robert
National Aeronautics and
Space Administration
USA

ALEXANDER, Lisa
Hadley Centre for Climate Prediction
and Research, Met Office
UK, Australia, Ireland

ALEXANDERSSON, Hans
Swedish Meteorological and
Hydrological Institute
Sweden

ALLAN, Richard
Environmental Systems Science
Centre, University of Reading
UK

ALLEN, Myles
Climate Dynamics Group, Atmospheric,
Oceanic and Planetary Physics, Department
of Physics, University of Oxford
UK

ALLEY, Richard B.
Department of Geosciences,
Pennsylvania State University
USA

ALLISON, Ian
Australian Antarctic Division and
Antarctic Climate and Ecosystems
Cooperative Research Centre
Australia

AMBENJE, Peter
Kenya Meteorological Department
Kenya

AMMANN, Caspar
Climate and Global Dynamics Division,
National Center for Atmospheric Research
USA

ANDRONOVA, Natalia
University of Michigan
USA

ANNAN, James
Frontier Research Center for Global
Change, Japan Agency for Marine-
Earth Science and Technology
Japan, UK

ANTONOV, John
National Oceanic and
Atmospheric Administration
USA, Russian Federation

ARBLASTER, Julie
National Center for Atmospheric Research
and Bureau of Meteotology Research Center
USA, Australia

ARCHER, David
University of Chicago
USA

ARORA, Vivek
Canadian Centre for Climate Modelling
and Analysis, Environment Canada
Canada

ARRITT, Raymond
Iowa State University
USA

ARTALE, Vincenzo
Italian National Agency for
New Technologies, Energy and
the Environment (ENEA)
Italy

ARTAXO, Paulo
Instituto de Fisica, Universidade
de Sao Paulo
Brazil

AUER, Ingeborg
Central Institute for Meteorology
and Geodynamics
Austria

AUSTIN, John
National Oceanic and Atmospheric
Administration, Geophysical
Fluid Dynamics Laboratory
USA

BAEDE, Alphonsus
Royal Netherlands Meteorological
Institute (KNMI) and Ministry of Housing,
Spatial Planning and the Environment
Netherlands

BAKER, David
National Center for Atmospheric Research
USA

BALDWIN, Mark P.
Northwest Research Associates
USA

BARNOLA, Jean-Marc
Laboratoire de Glaciologie et
Géophysique de l'Environnement
France

BARRY, Roger
National Snow and Ice Data
Center, University of Colorado
USA

BATES, Nicholas Robert
Bermuda Institute of Ocean Sciences
Bermuda

BAUER, Eva
Potsdam Institute for Climate
Impact Research
Germany

BENESTAD, Rasmus
Norwegian Meteorological Institute
Norway

BENISTON, Martin
University of Geneva
Switzerland

BERGER, André
Université catholique de Louvain,
Institut d'Astronomie et de
Géophysique G. Lemaitre
Belgium

BERNTSEN, Terje
Centre for International Climate and
Environmantal Research (CICERO)
Norway

BERRY, Joseph A.
Carnegie Institute of Washington,
Department of Global Ecology
USA

BETTS, Richard A.
Hadley Centre for Climate Prediction
and Research, Met Office
UK

BIERCAMP, Joachim
Deutsches Klimarechenzentrum GmbH
Germany

BINDOFF, Nathaniel L.
Antarctic Climate and Ecosystems
Cooperative Research Centre and CSIRO
Marine and Atmospheric Research
Australia

BITZ, Cecilia
University of Washington
USA

BLATTER, Heinz
Institute for Atmospheric and
Climate Science, ETH Zurich
Switzerland

BODEKER, Greg
National Institute of Water and
Atmospheric Research
New Zealand

BOJARIU, Roxana
National Institute of Meteorology
and Hydrology (NIMH)
Romania

BONAN, Gordon
National Center for Atmospheric Research
USA

Coordinating lead authors, lead authors, and contributing authors are listed alphabetically by surname.

BONFILS, Cèline
School of Natural Sciences,
Univerity of California, Merced
USA, France

BONY, Sandrine
Laboratoire de Météorologie Dynamique,
Institut Pierre Simon Laplace
France

BOONE, Aaron
CNRS CNRM at Meteo France
France, USA

BOONPRAGOB, Kansri
Department of Biology, Faculty of
Science, Ramkhamhaeng University
Thailand

BOUCHER, Olivier
Hadley Centre for Climate Prediction
and Research, Met Office
UK, France

BOUSQUET, Philippe
Institut Pierre Simon Laplace,
Laboratoire des Sciences du
Climat et de l'Environnement
France

BOX, Jason
Ohio State University
USA

BOYER, Tim
National Oceanic and
Atmospheric Administration
USA

BRACONNOT, Pascale
Pascale Braconnot Institu Pierre Simon
Laplace, Laboratoire des Sciences
du Climat et de l'Environnement
France

BRADY, Esther
National Center for Atmospheric Research
USA

BRASSEUR, Guy
Earth and Sun Systems Laboratory,
National Center for Atmospheric Research
USA, Germany

BRETHERTON, Christopher
Department of Atmospheric Sciences,
University of Washington
USA

BRIFFA, Keith R.
Climatic Research Unit, School
of Environmental Sciences,
University of East Anglia
UK

BROCCOLI, Anthony J.
Rutgers University
USA

BROCKMANN, Patrick
Laboratoire des Sciences du
Climat et de l'Environnement
France

BROMWICH, David
Byrd Polar Research Center,
The Ohio State University
USA

BROVKIN, Victor
Potsdam Institute for Climate
Impact Research
Germany, Russian Federation

BROWN, Ross
Environment Canada
Canada

BUJA, Lawrence
National Center for Atmospheric Research
USA

BUSUIOC, Aristita
National Meteorological Administration
Romania

CADULE, Patricia
Institut Pierre Simon Laplace
France

CAI, Wenju
CSIRO Marine and Atmospheric Research
Australia

CAMILLONI, Inés
Universidad de Buenos Aires, Cwentro de
Investigaciones del Mar y la Atmósfera
Argentina

CANADELL, Josep
Global Carbon Project, CSIRO
Australia

CARRASCO, Jorge
Direccion Meteorologica de Chile
and Centro de Estudios Cientificos
Chile

CASSOU, Christophe
Centre National de Recherche Scientifique,
Centre Europeen de Recherche et de
Formation Avancee en Calcul Scientifique
France

CAYA, Daniel
Consortium Ouranos
Canada

CAYAN, Daniel R.
Scripps Institution of Oceanography,
University of California, San Diego
USA

CAZENAVE, Anny
Laboratoire d'Etudes en Géophysique et
Océanographie Spatiale (LEGOS), CNES
France

CHAMBERS, Don
Center for Space Research, The
University of Texas at Austin
USA

CHANDLER, Mark
Columbia University and NASA
Goddard Institute for Space Studies
USA

CHANG, Edmund K.M.
Stony Brook University, State
University of New York
USA

CHAO, Ben
NASA Goddard Institute for Space Studies
USA

CHEN, Anthony
Department of Physics, University
of the West Indies
Jamaica

CHEN, Zhenlin
Dept of International Cooperation,
China Meteorological Administration
China

CHIDTHAISONG, Amnat
The Joint Graduate School of Energy
and Environment, King Mongkut's
University of Technology Thonburi
Thailand

CHRISTENSEN, Jens Hesselbjerg
Danish Meteorological Institute
Denmark

CHRISTIAN, James
Fisheries and Oceans, canada, Candian
Centre for Climate Modelling and Analysis
Canada

CHRISTY, John
University of Alabama in Huntsville
USA

CHURCH, John
CSIRO Marine and Atmospheric
Research and Ecosystems
Cooperative Research Centre
Australia

CIAIS, Philippe
Laboratoire des Sciences du
Climat et de l'Environnement
France

CLARK, Deborah A.
University of Missouri, St. Louis
USA

CLARKE, Garry
Earth and Ocean Sciences,
University of British Columbia
Canada

CLAUSSEN, Martin
Potsdam Institute for Climate
Impact Research
Germany

CLEMENT, Amy
University of Miami, Rosenstiel School
of Marine and Atmospheric Science
USA

COGLEY, J. Graham
Department of Geography, Trent University
Canada

COLE, Julia
University of Arizona
USA

COLLIER, Mark
CSIRO Marine and Atmospheric Research
Australia

COLLINS, Matthew
Hadley Centre for Climate Prediction and Research, Met Office
UK

COLLINS, William D.
Climate and Global Dynamics Division, National Center for Atmospheric Research
USA

COLMAN, Robert
Bureau of Meteorology Research Centre
Australia

COMISO, Josefino
National Aeronautics and Space Administration, Goddard Space Flight Center
USA

CONWAY, Thomas J.
National Oceanic and Atmospheric Administration, Earth System Research Laboratory
USA

COOK, Edward
Lamont-Doherty Earth Observatory
USA

CORTIJO, Elsa
Laboratoire des Sciences du Climat et de l'Environnement, CNRS-CEA-UVSQ
France

COVEY, Curt
Lawrence Livermore National Laboratory
USA

COX, Peter M.
School of Engineering, Computer Science and Mathematics, University of Exeter
UK

CROOKS, Simon
University of Oxford
UK

CUBASCH, Ulrich
Institut für Meteorologie, Freie Universität Berlin
Germany

CURRY, Ruth
Woods Hole Oceanographic Institution
USA

DAI, Aiguo
National Center for Atmospheric Research
USA

DAMERIS, Martin
German Aerospace Center
Germany

DE ELÍA, Ramón
Ouranos Consortium
Canada, Argentina

DELWORTH, Thomas L.
Geophysical Fluid Dynamics Laboratory, National Oceanic and Atmospheric Administration
USA

DENMAN, Kenneth L.
Canadian Centre for Climate Modelling and Analysis, Environment Canada and Department of Fisheries and Oceans
Canada

DENTENER, Frank
European Commission Joint Research Centre; Institute of Environment and Sustainability Climate Change Unit
EU

DESER, Clara
National Center for Atmospheric Research
USA

DETHLOFF, Klaus
Alfred Wegener Institute for Polar and Marine Research, Research Unit Potsdam
Germany

DIANSKY, Nikolay A.
Institute of Numerical Mathematics, Russian Academy of Sciences
Russian Federation

DICKINSON, Robert E.
School of Earth and Atmospheric Sciences, Georgia Institute of Technology
USA

DING, Yihui
National Climate Centre, China Meteorological Administration
China

DIRMEYER, Paul
Center for Ocean-Land-Atmosphere Studies
USA

DIX, Martin
CSIRO
Australia

DIXON, Keith
National Oceanic and Atmospheric Administration
USA

DLUGOKENCKY, Ed
National Oceanic and Atmospheric Administration, Earth System Research Laboratory
USA

DOKKEN, Trond
Bjerknes Centre for Climate Research
Norway

DOTZEK, Nikolai
Deutsches Zentrum für Luft und Raumfahrt, Institut für Physik der Atmosphäre
Germany

DOUTRIAUX, Charles
Program for Climate Model Diagnosis and Intercomparison
USA, France

DRANGE, Helge
Nansen Environmental and Remote Sensing Center, Bjerknes Centre for Climate Research
Norway

DRIESSCHAERT, Emmanuelle
Université catholique de Louvain, Institut d'Astronomie et de Géophysique G. Lemaitre
Belgium

DUFRESNE, Jean-Louis
Laboratoire de Météorologie Dynamique, Institut Pierre Simon Laplace
France

DUPLESSY, Jean-Claude
Centre National dela Recerche Scientifique, Laboratoire des Sciences du Climat et de l'Environnement
France

DYURGEROV, Mark
Institute of Arctic and Alpine Research, University of Colorado at Boulder & Department of Geograpy and Quaternary Geology at Stockholm
Sweden, USA

EASTERLING, David
National Oceanic and Atmospheric Administration, Earth System Research Laboratory
USA

EBY, Michael
University of Victoria
Canada

EDWARDS, Neil R.
The Open University
UK

ELKINS, James W.
National Oceanic and Atmospheric Administration, Earth System Research Laboratory
USA

EMERSON, Steven
School of Oceanography, University of Washington
USA

EMORI, Seita
National Institute for Environmental Studies and Frontier Research Center for Global Change, Japan Agency for Marine-Earth Science and Technology
Japan

ETHERIDGE, David
CSIRO Marine and Atmospheric Research
Australia

EYRING, Veronika
Deutsches Zentrum für Luft und Raumfahrt, Institut für Physik der Atmosphäre
Germany

FAHEY, David W.
National Oceanic and Atmospheric Administration, Earth System Research Laboratory
USA

FASULLO, John
National Center for Atmospheric Research
USA

FEDDEMA, Johannes
University of Kansas
USA

FEELY, Richard
National Oceanic and Atmospheric Administration, Pacific Marine Environmental Laboratory
USA

FEICHTER, Johann
Max Planck Institute for Meteorology
Germany

FICHEFET, Thierry
Université catholique de Louvain, Institut d'Astronomie et de Géophysique G. Lemaitre
Belgium

FITZHARRIS, Blair
Department of Geography, University of Otago
New Zealand

FLATO, Gregory
Canadian Centre for Climate Modelling and Analysis, Environment Canada
Canada

FLEITMANN, Dominik
Institute of Geological Sciences, Uniersity of Bern
Switzerland, Germany

FLEMING, James Rodger
Colby College
USA

FOGT, Ryan
Polar Meteorology Group, Byrd Polar Research Center and Atmospheric Sciences Program, Department of geography, The Ohio State University
USA

FOLLAND, Christopher
Hadley Centre for Climate Prediction and Research, Met Office
UK

FOREST, Chris
Massachusetts Institute of Technology
USA

FORSTER, Piers
School of Earth and Environment, University of Leeds
UK

FOUKAL, Peter
Heliophysics, Inc.
USA

FRASER, Paul
CSIRO Marine and Atmospheric Research
Australia

FRAUENFELD, Oliver
National Snow and Ice Data Center, University of Colorado at Boulder
USA, Austria

FREE, Melissa
Air Resources Laboratory, National Oceanic and Atmospheric Administration
USA

FREI, Allan
Hunter College, City University of New York
USA

FREI, Christoph
Federal Office of Meteorology and Climatology MeteoSwiss
Switzerland

FRICKER, Helen
Scripps Institution of Oceanography, University of California, San Diego
USA

FRIEDLINGSTEIN, Pierre
Institut Pierre Simon Laplace, Laboratoire des Sciences du Climat et de l'Environnement
France, Belgium

FU, Congbin
Start Regional Center for Temperate East Asia, Institute of Atmospheric Physics, Chinese Academy of Science
China

FUJII, Yoshiyuki
Arctic Environment Research Center, National Institute of Polar Research
Japan

FUNG, Inez
University of California, Berkeley
USA

FURRER, Reinhard
Colorado School of Mines
USA, Switzerland

FUZZI, Sandro
National Research Council, Institute of Atmospheric Sciences and Climate
Italy

FYFE, John
Canadian Centre for Climate Modelling and Analysis, Environment Canada
Canada

GANOPOLSKI, Andrey
Potsdam Institute for Climate Impact Research
Germany

GAO, Xuejie
Laboratory for Climate Change, National Climate Centre, China Meteorological Administration
China

GARCIA, Hernan
National Oceanic and Atmospheric Administration, National Oceanographic Data Center
USA

GARCÍA-HERRERA, Ricardo
Universidad Complutense de Madrid
Spain

GAYE, Amadou Thierno
Laboratory of Atmospheric Physics, ESP/CAD, Dakar University
Senegal

GELLER, Marvin
Stony Brook University
USA

GENT, Peter
National Center for Atmospheric Research
USA

GERDES, Rüdiger
Alfred-Wegener-Institute für Polar und Meeresforschung
Germany

GILLETT, Nathan P.
Climatic Research Unit, School of Environmental Sciences, University of East Anglia
UK

GIORGI, Filippo
Abdus Salam International Centre for Theoretical Physics
Italy

GLEASON, Byron
National Climatic Data Center, National Oceanic and Atmospheric Administration
USA

GLECKLER, Peter
Lawrence Livermore National Laboratory
USA

GONG, Sunling
Air Quality Researcch Division, Science & Technology Branch, Environment Canada
Canada

GONZÁLEZ-DAVÍLA, Melchor
University of Las Palmas de Gran Canaria
Spain

GONZÁLEZ-ROUCO, Jesus Fidel
Universidad Complutense de Madrid
Spain

GOOSSE, Hugues
Université catholique de Louvain
Belgium

GRAHAM, Richard
Hadley Centre, Met Office
UK

GREGORY, Jonathan M.
Department of Meteorology, University of Reading and Hadley Centre for Climate Prediction and Research, Met Office
UK

GRIESER, Jürgen
Deutscher Wetterdienst, Global Precipitatioin Climatology Centre
Germany

GRIGGS, David
Hadley Centre for Climate Prediction and Research, Met Office
UK

GROISMAN, Pavel
University Corporation for Atmospheric Research at the National Climatic Data Center, National Oceanic and Atmospheric Administration
USA, Russian Federation

GRUBER, Nicolas
Institute of Geophysics and Planetary Physics, University of California, Los Angeles and Department of Environmental Sciences, ETH Zurich
USA, Switzerland

GUDGEL, Richard
National Oceanic and Atmospheric Administration
USA

GUDMUNDSSON, G. Hilmar
British Antarctic Survey
UK, Iceland

GUENTHER, Alex
National Center for Atmospheric Research
USA

GULEV, Sergey
P. P. Shirshov Institute of Oceanography
Russian Federation

GURNEY, Kevin
Department of Earth and Atmospheric Science, Purdue University
USA

GUTOWSKI, William
Iowa State University
USA

HAAS, Christian
Alfred Wegener Institute
Germany

HABIBI NOKHANDAN, Majid
National Center for Climatology
Iran

HAGEN, Jon Ove
University of Oslo
Norway

HAIGH, Joanna
Imperial College London
UK

HALL, Alex
Department of Atmospheric and Oceanic Sciences, University of California, Los Angeles
USA

HALLEGATTE, Stéphane
Centre International de Recherche sur l'Environnement et le Developpement, Ecole Nationale des Ponts-et-Chaussées and Centre National de Recherches Meteorologique, Meteo-France
USA, France

HANAWA, Kimio
Physical Oceanography Laboratry, Department of Geophysics, Graduate School of Science, Tohoku University
Japan

HANSEN, James
Goddard Institute for Space Studies
USA

HANSSEN-BAUER, Inger
Norwegian Meteorological Institute
Norway

HARRIS, Charles
School of Earth, Ocean and Planetary Science, Cardiff University
UK

HARRIS, Glen
Hadley Centre for Climate Prediction and Research, Met Office
UK, New Zealand

HARVEY, Danny
University of Toronto
Canada

HASUMI, Hiroyasu
Center for Climate System Research, University of Tokyo
Japan

HAUGLUSTAINE, Didier
Institut Pierre Simon Laplace, Laboratoire des Sciences du Climat et de l'Environnement, CEA-CNRS-UVSQ
France

HAYWOOD, James
Hadley Centre for Climate Prediction and Research, Met Office
UK

HEGERL, Gabriele C.
Division of Earth and Ocean Sciences, Nicholas School for the Environment and Earth Sciences, Duke University
USA, Germany

HEIMANN, Martin
Max-Planck-Institut für Biogeochemie
Germany, Switzerland

HEINZE, Christoph
University of Bergen, Geophysical Institute and Bjerknes Centre for Climate Research
Norway, Germany

HELD, Isaac
National Oceanic and Atmospheric Administration, Geophysical Fluid Dynamics Laboratory
USA

HENDERSON-SELLERS, Ann
World Meteorological Organization
Switzerland

HENDON, Henry
Bureau of Meteorology Research Centre
Australia

HEWITSON, Bruce
Department of Environmental and Geographical Sciences, University of Cape Town
South Africa

HINZMAN, Larry
University of Alaska, Fairbanks
USA

HOCK, Regine
Stockholm University
Sweden

HODGES, Kevin
Environmental Systems Science Centre
UK

HOELZLE, Martin
University of Zürich, Department of Geography
Switzerland

HOLLAND, Elisabeth
Atmospheric Chemistry Division, National Center for Atmospheric Research (NCAR)
USA

HOLLAND, Marika
National Center for Atmospheric Research
USA

HOLTSLAG, Albert A. M.
Wageningen University
Netherlands

HOSKINS, Brian J.
Department of Meteorology, University of Reading
UK

HOUSE, Joanna
Quantifying and Understanding the Earth System Programme, University of Bristol
UK

HU, Aixue
National Center for Atmospheric Research
USA, China

HUNKE, Elizabeth
Los Alamos National Laboratory
USA

HURRELL, James
National Center for Atmospheric Research
USA

HUYBRECHTS, Philippe
Departement Geografie, Vrije Universiteir Brussel
Belgium

INGRAM, William
Hadley Centre for Climate Prediction and Research, Met Office
UK

ISAKSEN, Ketil
Norwegian Meteorological Institute
Norway

ISHII, Masayoshi
Fronteir Research Center for Global Change, Japan Agency for Marine-Earth Science and Technology
Japan

JACOB, Daniel
Department of Earth and Planetary Sciences, Harvard University
USA, France

JALLOW, Bubu
Department of Water Resources
The Gambia

JANSEN, Eystein
University of Bergen, Department of Earth Sciences and Bjerknes Centre for Climate Research
Norway

JANSSON, Peter
Department of Physical Geography and Quaternary Geology, Stockholm University
Sweden

JENKINS, Adrian
British Antarctic Survey, Natural Environment Research Council
UK

JONES, Andy
Hadley Centre for Climate Prediction and Research, Met Office
UK

JONES, Christopher
Hadley Centre for Climate Prediction and Research, Met Office
UK

JONES, Colin
Universite du Quebec a Montreal, Canadian Regional Climate Modelling Network
Canada

JONES, Gareth S.
Hadley Centre for Climate Prediction and Research, Met Office
UK

JONES, Julie
GKSS Research Centre
Germany, UK

JONES, Philip D.
Climatic Research Unit, School of Environmental Sciences, University of East Anglia
UK

JONES, Richard
Hadley Centre for Climate Prediction and Research, Met Office
UK

JOOS, Fortunat
Climate and Environmental Physics, Physics Institute, University of Bern
Switzerland

JOSEY, Simon
National Oceanography Centre, University of Southampton
UK

JOUGHIN, Ian
Applied Physics Laboratory, University of Washington
USA

JOUZEL, Jean
Institut Pierre Simon Laplace, Laboratoire des Sciences du Climat et de l'Environnement, CEA-CNRS-UVSQ
France

JOYCE, Terrence
Woods Hole Oceanographic Institution
USA

JUNGCLAUS, Johann H.
Max Planck Institute for Meteorology
Germany

KAGEYAMA, Masa
Laboratoire des Sciences du Climat et de l'Environnement
France

KÅLLBERG, Per
European Centre for Medium-Range Weather Forecasts
ECMWF

KÄRCHER, Bernd
Deutsches Zentrum für Luft und Raumfahrt, Institut für Physik der Atmosphäre
Germany

KARL, Thomas R.
National Oceanic and Atmospheric Administration, National Climatic Data Center
USA

KAROLY, David J.
University of Oklahoma
USA, Australia

KASER, Georg
Institut für Geographie, University of Innsbruck
Austria, Italy

KATTSOV, Vladimir
Voeikov Main Geophysical Observatory
Russian Federation

KATZ, Robert
National Center for Atmospheric Research
USA

KAWAMIYA, Michio
Frontier Research Center for Global Change, Japan Agency for Marine-Earth Science and Technology
Japan

KEELING, C. David
Scripps Institution of Oceanography
USA

KEELING, Ralph
Scripps Institution of Oceanography
USA

KENNEDY, John
Hadley Centre, Met Office
UK

KENYON, Jesse
Duke University
USA

KETTLEBOROUGH, Jamie
British Atmospheric Data Centre, Space Science and Technology Department, Council for the Central Laboratory of the Research Councils
UK

KHARIN, Viatcheslar
Canadian Centre for Climate Modelling and Analysis, Environment Canada
Canada

KHODRI, Myriam
Institut de Recherche Pour le Developpement
France

KILADIS, George
National Oceanic and Atmospheric Administration
USA

KIM, Kuh
Seoul National University
Republic of Korea

KIMOTO, Masahide
Center for Climate System Research, University of Tokyo
Japan

KING, Brian
National Oceanography Centre, Southampton
UK

KINNE, Stefan
Max-Planck Institute for Meteorology
Germany

KIRTMAN, Ben
Center for Ocean-Land-Atmosphere Studies, George Mason University
USA

KITOH, Akio
First Research Laboratory, Climate Research Department, Meteorological Research Institute, Japan Meteorological Agency
Japan

KLEIN, Stephen A.
Lawrence Livermore National Laboratory
USA

KLEIN TANK, Albert
Royal Netherlands Meteorological Institute (KNMI)
Netherlands

KNUTSON, Thomas
Geophysical Fluid Dynamics Laboratory, National Oceanic and Atmospheric Administration
USA

KNUTTI, Reto
Climate and Global Dynamics Division, National Center for Atmospheric Research
Switzerland

KOERTZINGER, Arne
Leibniz Institut für Meereswissenschaften an der Universitat Kiel and Institut fur Ostseeforschung Warnemunde
Germany

KOIKE, Toshio
Department of Civil Engineering, University of Tokyo
Japan

KOLLI, Rupa Kumar
Climatology and Hydrometeorology Division, Indian Institute of Tropical Meteorology
India

KOSTER, Randal
National Aeronautics and Space Administration
USA

KOTTMEIER, Christoph
Institut für Meteorologie, und Klimaforschung, Universitat Karlsruhe/ Forschungszentrum Karlsruhe
Germany

KRIPALANI, Ramesh
Indian Institute of Tropical Meteorology
India

KRYNYTZKY, Marta
University of Washington
USA

KUNKEL, Kenneth
Illinois State Water Survey
USA

KUSHNER, Paul J.
Department of Physics, University of Toronto
Canada

KWOK, Ron
Jet Propulsion Laboratory, California Institute of Technology
USA

KWON, Won-Tae
Climate Research Laboratory, Meteorological Research Institute (METRI), Korean Meteorological Administration
Republic of Korea

LABEYRIE, Laurent
Laboratoire des Sciences du Climat et de l'Environnement
France

LAINE, Alexandre
Laboratoire des Sciences du Climat et de l'Environnement
France

LAM, Chiu-Ying
Hong Kong Observatory
China

LAMBECK, Kurt
Australia National University
Australia

LAMBERT, F. Hugo
Atmospheric, Oceanic and Planetary Physics, University of Oxford
UK

LANZANTE, John
National Oceanic and Atmospheric Administration
USA

LAPRISE, René
Deprtement des Sciences de la Terra et de l'Atmosphere, University of Quebec at Montreal
Canada

LASSEY, Keith
National Institute of Water and Atmospheric Research
New Zealand

LATIF, Mojib
Leibniz Institut für Meereswissenschaften, IFM-GEOMAR
Germany

LAU, Ngar-Cheung
Geophysical Fluid Dynamics Laboratory, National Oceanic and Atmospheric Administration
USA

LAVAL, Katia
Laboratoire de Météorologie Dynamique du CNRS
France

LAVINE, Michael
Duke University
USA

LAWRENCE, David
National Center for Atmospheric Research
USA

LAWRIMORE, Jay
National Oceanic and Atmospheric Administration, National Climatic Data Center
USA

LAXON, Seymour
Centre for Polar Observation and Modelling, University College London
UK

LE BROCQ, Anne
Centre for Polar Observation and Modelling, University of Bristol
UK

LE QUÉRÉ, Corrine
University of East Anglia and British Antarctic Survey
UK, France, Canada

LE TREUT, Hervé
Laboratoire de Météorologie Dynamique du CNRS
France

LEAN, Judith
Naval Research Laboratory
USA

LECK, Caroline
Department of Metorology, Stockholm University
Sweden

LEE, Terry C.K.
University of Victoria
Canada

LEE-TAYLOR, Julia
National Center for Atmospheric Research
USA, UK

LEFEVRE, Nathalie
Institut de Recherche Pour le Developpement, Laboratoire d'Oceanographie et de Climatologie
France

LEMKE, Peter
Alfred Wegener Institute for Polar and Marine Research
Germany

LEULIETTE, Eric
University of Colorado, Boulder
USA

LEUNG, Ruby
Pacific Northwest National Laboratory, National Oceanic and Atmospheric Administration
USA

LEVERMANN, Anders
Potsdam Institute for Climate Impact Research
Germany

LEVINSON, David
National Oceanic and Atmospheric Administration, National Climatic Data Center
USA

LEVITUS, Sydney
National Oceanic and Atmospheric Administration
USA

LIE, Øyvind
Bjerknes Centre for Climate Research
Norway

LIEPERT, Beate
Lamont-Doherty Earth Observatory, Columbia University
USA

LIU, Shiyin
Cold and Arid Regions Environmental and Engineering Research Institute, Chinese Academy of Sciences
China

LOHMANN, Ulrike
ETH Zürich, Institute for Atmospheric and Climate Science
Switzerland

LOUTRE, Marie-France
Université catholique de Louvain, Institut d'Astronomie et de Géophysique G. Lemaitre
Belgium

LOWE, David C.
National Institute of Water and Atmospheric Research
New Zealand

LOWE, Jason
Hadley Centre for Climate Prediction and Research, Met Office
UK

LUO, Yong
Laboratory for Climate Change, National Climate Centre, China Meteorological Administration
China

LUTERBACHER, Jürg
Institute of Geography, Climatology and Meteorology, and National Centre of Competence in Research on Climate, University of Bern
Switzerland

LYNCH, Amanda H.
School of Geography and Environmental Science, Monash University
Australia

MACAYEAL, Douglas
University of Chicago
USA

MACCRACKEN, Michael
Climate Institute
USA

MAGAÑA RUEDA, Victor
Centro de Ciencias de la Atmósfera, Ciudad Universitaria, Universidad Nacional Autonomia de Mexico
Mexico

MALHI, Yadvinder
University of Oxford
UK

MALANOTTE-RIZZOLI, Paola
Massachusetts Institute of Technology
USA, Italy

MANNING, Andrew C.
University of East Anglia
UK, New Zealand

MANNING, Martin
IPCC WGI TSU, National Oceanic and Atmospheric Administration, Earth System Research Laboratory
USA, New Zealand

MANZINI, Elisa
National Institute for Geophysics and Volcanology
Italy

MARENGO ORSINI, Jose Antonio
CPTEC/INPE
Brazil, Peru

MARSH, Robert
National Oceanography Centre, University of Southampton
UK

MARSHALL, Gareth
British Antarctic Survey
UK

MARTELO, Maria
Ministerio del Ambiente y los Rcursos Naturales, Dir. de Hidrologia y Meteorologia
Venezuela

MASARIE , Ken
National Oceanic and Atmospheric Administration, Earth System Research Laboratory, Global Monitoring Division
USA

MASSON-DELMOTTE, Valérie
Laboratoire des Sciences du Climat et de l'Environnement
France

MATSUMOTO, Katsumi
University of Minnesota, Twin Cities
USA

MATSUNO, Taroh
Frontier Research Center for Global Change, Japan Agency for Marine-Earth Science and Technology
Japan

MATTHEWS, H. Damon
University of Calgary and Concordia University
Canada

MATULLA, Christoph
Environment Canada
Canada, Austria

MAURITZEN, Cecilie
Norwegian Meteorological Institute
Norway

MCAVANEY, Bryant
Bureau of Meteorology Research Centre
Australia

MCFIGGANS, Gordon
University of Manchester
UK

MCINNES, Kathleen
CSIRO, Marine and Atmospheric Chemistry Research
Australia

MCPHADEN, Michael
National Oceanic and Atmospheric Administration
USA

MEARNS, Linda
National Center for Atmospheric Research
USA

MEARS, Carl
Remote Sensing Systems
USA

MEEHL, Gerald A.
Climate and Global Dynamics Division, National Center for Atmospheric Research
USA

MEINSHAUSEN, Malte
Potsdam Institute for Climate Impact Research
Germany

MELLING, Humphrey
Fisheries and Oceans Canada
Canada

MENÉNDEZ, Claudio Guillermo
Centro de Investigaciones del Mar y de la Atmósfera, (CONICET-UBA)
Argentina

MENON, Surabi
Lawrence Berkeley National Laboratory
USA

MESCHERSKAYA, Anna V.
Russian Federation

MILLER, John B.
National Oceanic and Atmospheric Administration
USA

MILLOT, Claude
Centre National dela Recherche Scientifique
France

MILLY, Chris
United States Geological Survey
USA

MITCHELL, John
Hadley Centre for Climate Prediction and Research, Met Office
UK

MOKSSIT, Abdalah
Direction de la météorologie Nationale
Morocco

MOLINA, Mario
Scripps Institution of Oceanography, Dept. of Chemistry and Biochemistry, University of California, San Diego
USA, Mexico

MOLINARI, Robert
National Oceanic and Atmospheric Administration, Atlantic Oceanographic and Meteorological Laboratory
USA

MONAHAN, Adam H.
School of Earth and Ocean Sciences, University of Victoria
Canada

MONNIN, Eric
Climate and Environmental Physics, Physics Institute, University of Bern
Switzerland

MONTZKA, Steve
National Oceanic and Atmospheric Administration
USA

MOSLEY-THOMPSON, Ellen
Ohio State University
USA

MOTE, Philip
Climate Impacts Group, Joint Institute for the Study of the Atmosphere and Oceans (JIASO), University of Washington
USA

MUHS, Daniel
United States Geological Survey
USA

MULLAN, A. Brett
National Institute of Water and Atmospheric Research
New Zealand

MÜLLER, Simon A.
Climate and Environmental Physics, Physics Institute, University of Bern
Switzerland

MURPHY, James M.
Hadley Centre for Climate Prediction and Research, Met Office
UK

MUSCHELER, Raimund
Goddard Earth Sciences and Technology Center, University of Maryland & NASA/Goddard Space Flight Center, Climate & Radiation Branch
USA

MYHRE, Gunnar
Department of Geosciences, University of Oslo
Norway

NAKAJIMA, Teruyuki
Center for Climate System Research, University of Tokyo
Japan

NAKAMURA, Hisashi
Department of Earth, Planetary Science, University of Tokyo
Japan

NAWRATH, Susanne
Potsdam Institute for Climate Impact Research
Germany

NEREM, R. Steven
University of Colorado at Boulder
USA

NEW, Mark
Centre for the Environment, University of Oxford
UK

NGANGA, John
University of Nairobi
Kenya

NICHOLLS, Neville
Monash University
Australia

NODA, Akira
Meteorological Research Institute, Japan Meteorological Agency
Japan

NOJIRI, Yukihiro
Secretariat of Council for Science and Technology Policy, Cabinet Office
Japan

NOKHANDAN, Majid Habibi
Iranian Meteorological Organization
Iran

NORRIS, Joel
Scripps Institution of Oceanography
USA

NOZAWA, Toru
National Institute for Environmental Studies
Japan

OERLEMANS, Johannes
Institute for Marine and Atmospheric Research, Utrecht University
Netherlands

OGALLO, Laban
IGAD Climate Prediction and Application Centre
Kenya

OHMURA, Atsumu
Swiss Federal Institute of Technology
Switzerland

OKI, Taikan
Institute of Industrial Science, The University of Tokyo
Japan

OLAGO, Daniel
Department of Geology, University of Nairobi
Kenya

ONO, Tsuneo
Hokkaido National Fisheries Research Institute, Fisheries Research Agency
Japan

OPPENHEIMER, Michael
Princeton University
USA

ORAM, David
University of East Anglia
UK

ORR, James C.
Marine Environment Laboratories, International Atomic Energy Agency
Monaco, USA

OSBORN, Tim
University of East Anglia
UK

O'SHAUGHNESSY, Kath
National Institute of Water and Atmospheric Research
New Zealand

OTTO-BLIESNER, Bette
Climate and Global Dynamics Division, National Center for Atmospheric Research
USA

OVERPECK, Jonathan
Institute for the Study of Planet Earth, University of Arizona
USA

PAASCHE, Øyvind
Bjerknes Centre for Climate Research
Norway

PAHLOW, Markus
Dalhousie University, Bedford Institute of Oceanography
Canada

PAL, Jeremy S.
Loyola Marymount University, The Abdus Salam International Centre for Theoretical Physics
USA, Italy

PALMER, Timothy
European Centre for Medium-Range Weather Forecasting
ECMWF, UK

PANT, Govind Ballabh
Indian Institute of Tropical Meteorology
India

PARKER, David
Hadley Centre for Climate Prediction and Research, Met Office
UK

PARRENIN, Frédéric
Laboratoire de Glaciologie et Géophysique de l'Environnement
France

PAVLOVA, Tatyana
Voeikov Main Geophysical Observatory
Russian Federation

PAYNE, Antony
University of Bristol
UK

PELTIER, W. Richard
Department of Physics, University of Toronto
Canada

PENG, Tsung-Hung
Atlantic Oceanographic and Meteorological Laboratory, National Oceanic and Atmospheric Administration
USA

PENNER, Joyce E.
Department of Atmospheric, Oceanic, and Space Sciences, University of Michigan
USA

PETERSON, Thomas
National Oceanic and Atmospheric Administration, National Climatic Data Center
USA

PETOUKHOV, Vladimir
Potsdam Institute for Climate Impact Research
Germany

PEYLIN, Philippe
Laboratoire des Modélisation du Climat et de l'Environnement
France

PFISTER, Christian
University of Bern
Switzerland

PHILLIPS, Thomas
Program for Climate Model Diagnosis and Intercomparison, Lawrence Livermore National Laboratory
USA

PIERCE, David
Scripps Institution of Oceanography
USA

PIPER, Stephen
Scripps Institution of Oceanography
USA

PITMAN, Andrew
Department of Physical Geography, Macquarie University
Australia

PLANTON, Serge
Météo-France
France

PLATTNER, Gian-Kasper
Climate and Environmental Physics, Physics Institute, University of Bern
Switzerland

PLUMMER, David
Environment Canada
Canada

POLLACK, Henry
University of Michigan
USA

PONATER, Michael
Deutsches Zentrum für Luft und Raumfahrt, Institut für Physik der Atmosphäre
Germany

POWER, Scott
Bureau of Meteorology Research Centre
Australia

PRATHER, Michael
Earth System Science Department, University of California at Irvine
USA

PRINN, Ronald
Department of Earth, Atmospheric and Planetary Sciences, Massachusetts Institute of Technology
USA, New Zealand

PROSHUTINSKY, Andrey
Woods Hole Oceanographic Institution
USA

PROWSE, Terry
Environment Canada, University of Victoria
Canada

QIN, Dahe
Co-Chair, IPCC WGI, China Meteorological Administration
China

QIU, Bo
University of Hawaii
USA

QUAAS, Johannes
Max Planck Institute for Meteorology
Germany

QUADFASEL, Detlef
Institut für Meereskunde, Centre for Marine and Atmospheric Sciences Hamburg
Germany

RAGA, Graciela
Centro de Ciencias de la Atmósfera, Universidad Nacional Autonoma de Mexico
Mexico, Argentina

RAHIMZADEH, Fatemeh
Atmospheric Science & Meteorological Research Center (ASMERC), I.R. of Iran Meteorological Organization (IRIMO)
Iran

RAHMSTORF, Stefan
Potsdam Institute for Climate Impact Research
Germany

RÄISÄNEN, Jouni
Department of Physical Sciences, University of Helsinki
Finland

RAMACHANDRAN, Srikanthan
Space & Atmospheric Sciences Division, Physical Research Laboratory
India

RAMANATHAN, Veerabhadran
Scripps Institution of Oceanography
USA

RAMANKUTTY, Navin
University of Wisconsin, Madison
USA, India

RAMASWAMY, Venkatachalam
National Oceanic and Atmospheric Administration, Geophysical Fluid Dynamics Laboratory
USA

RAMESH, Rengaswamy
Physical Research Laboratory
India

RANDALL, David A.
Department of Atmospheric Science, Colorado State University
USA

RAPER, Sarah C.B.
Manchester Metropolitan University
UK

RAUP, Bruce H.
National Snow and Ice Data Center, University of Colorado
USA

RAUPACH, Michael
CSIRO
Australia

RAYMOND, Charles
University of Washington, Department of Earth and Space Sciences
USA

RAYNAUD, Dominique
Laboratoire de Glaciologie et Géophysique de l'Environnement
France

RAYNER, Peter
Institut Pierre Simon Laplace, Laboratoire des Sciences du Climat et de l'Environnement
France

REHDER, Gregor
Leibniz Institut für Meereswissenschaften an der Universitat Kiel and Institut fur Ostseeforschung Warnemunde
Germany

REID, George
National Oceanic and Atmospheric Administration
USA

REN, Jiawen
Cold and Arid Regions Environmental and Engineering Research Institute, Chinese Academy of Sciences
China

RENSSEN, Hans
Faculty of Earth and Life Sciences, Vrije Universiteit Amsterdam
Netherlands

RENWICK, James A.
National Institute of Water and Atmospheric Research
New Zealand

RIEBESELL, Ulf
Leibniz Institute for Marine Sciences, IFM-GEOMAR
Germany

RIGNOT, Eric
Jet Propulsion Laboratory
USA

RIGOR, Ignatius
Polar Science Center, Applied Physics Laboratory, University of Washington
USA

RIND, David
National Aeronautics and Space Administration, Goddard Institute for Space Studies
USA

RINKE, Annette
Alfred Wegener Institute for Polar and Marine Research
Germany

RINTOUL, Stephen
CSIRO, Marine and Atmospheric Research and Antarctic Climate and Ecosystems Cooperative Research Centre
Australia

RIXEN, Michel
University of Liege and NATO Undersea Research Center
NATO, Belgium

RIZZOLI, Paola
Massachusetts Institute of Technology
USA, Italy

ROBERTS, Malcolm
Hadley Centre for Climate Prediction and Research, Met Office
UK

ROBERTSON, Franklin R.
National Aeronautics and Space Administration
USA

ROBINSON, David
Rutgers University
USA

RÖDENBECK, Christian
Max Planck Institute for Biogeochemistry Jena
Germany

ROECKNER, Erich
Max Planck Institute for Meteorology
Germany

ROSATI, Anthony
National Oceanic and
Atmospheric Administration
USA

ROSENLOF, Karen
National Oceanic and
Atmospheric Administration
USA

ROTHROCK, David
University of Washington
USA

ROTSTAYN, Leon
CSIRO Marine and Atmospheric Research
Australia

ROULET, Nigel
McGill University
Canada

RUMMUKAINEN, Markku
Rossby Centre, Swedish Meteorological
and Hydrological Institute
Sweden, Finland

RUSSELL, Gary L.
National Aeronautics and Space
Administration, Goddard
Institute for Space Studies
USA

RUSTICUCCI, Matilde
Departamento de Ciencias de la
Atmósfera y los Océanos, FCEN,
Universidad de Buenos Aires
Argentina

SABINE, Christopher
National Oceanic and Atmospheric
Administration, Pacific Marine
Environmental Laboratory
USA

SAHAGIAN, Dork
Lehigh University
USA

SALAS Y MÉLIA, David
Météo-France, Centre National de
Recherches Météorologiques
France

SANTER, Ben D.
Program for Climate Model Diagnosis
and Intercomparison, Lawrence
Livermore National Laboratory
USA

SARR, Abdoulaye
Service Météorologique, DMN Sénégal
Senegal

SAUSEN, Robert
Deutsches Zentrum für Luft und Raumfahrt,
Institut für Physik der Atmosphäre
Germany

SCHÄR, Christoph
ETH Zürich, Institute for Atmospheric
and Climate Science
Switzerland

SCHERRER, Simon Christian
Federal Office of Meteorology
and Climatology MeteoSwiss
Switzerland

SCHMIDT, Gavin
National Aeronautics and Space
Administration, Goddard
Institute for Space Studies
USA, UK

SCHMITTNER, Andreas
College of Oceanic and Atmospheric
Sciences, Oregon State University
USA, Germany

SCHNEIDER, Birgit
Leibniz Institut für Meereswissenschaften
Germany

SCHOTT, Friedrich
Leibniz Institut für Meereswissenschaften,
IFM-GEOMAR
Germany

SCHULTZ , Martin G.
Max Planck Institute for Meteorology
Germany

SCHULZ, Michael
Institut Pierre Simon Laplace,
Laboratoire des Sciences du Climat et de
l'Environnement, CEA-CNRS-UVSQ
France, Germany

SCHWARTZ, Stephen E.
Brookhaven National Laboratory
USA

SCHWARZKOPF, Dan
National Oceanic and
Atmospheric Administration
USA

SCINOCCA, John
Canadian Centre for Climate Modelling
and Analysis, Environment Canada
Canada

SEIDOV, Dan
Pennsylvania State University
USA

SEMAZZI, Fred H.
North Carolina State University
USA

SENIOR, Catherine
Hadley Centre for Climate Prediction
and Research, Met Office
UK

SEXTON, David
Hadley Centre for Climate Prediction
and Research, Met Office
UK

SHEA, Dennis
National Center for Atmospheric Research
USA

SHEPHERD, Andrew
School of Geosciences, The
University of Ediburgh
UK

SHEPHERD, J. Marshall
University of Georgia,
Department of Geography
USA

SHEPHERD, Theodore G.
University of Toronto
Canada

SHERWOOD, Steven
Yale University
USA

SHUKLA, Jagadish
Center for Ocean-Land-Atmosphere
Studies, George Mason University
USA

SHUM, C.K.
Geodetic Science, School of Earth
Sciences, The Ohio State University
USA

SIEGMUND, Peter
Royal Netherlands Meteorological
Institute (KNMI)
Netherlands

SILVA DIAS, Pedro Leite da
Universidade de Sao Paulo
Brazil

SIMMONDS, Ian
University of Melbourne
Australia

SIMMONS, Adrian
European Centre for Medium-
Range Weather Forecasts
ECMWF, UK

SIROCKO, Frank
University of Mainz
Germany

SLATER, Andrew G.
Cooperative Institute for Research
in Environmental Sciences,
University of Colorado, Boulder
USA, Australia

SLINGO, Julia
National Centre for Atmospheric
Science, University of Reading
UK

SMITH, Doug
Hadley Centre for Climate Prediction
and Research, Met Office
UK

SMITH, Sharon
Geological Survey of Canada,
Natural Resources Canada
Canada

SODEN, Brian
University of Miami, Rosentiel School
for Marine and Atmospheric Science
USA

SOKOLOV, Andrei
Massachusetts Institute of Technology
USA, Russian Federation

SOLANKI, Sami K.
Max Planck Institute for
Solar System Research
Germany, Switzerland

SOLOMINA, Olga
Institute of Geography RAS
Russian Federation

SOLOMON, Susan
Co-Chair, IPCC WGI, National Oceanic
and Atmospheric Administration,
Earth System Research Laboratory
USA

SOMERVILLE, Richard
Scripps Institution of Oceanography,
University of California, San Diego
USA

SOMOT, Samuel
Météo-France, Centre National de
Recherches Météorologiques
France

SONG, Yuhe
Jet Propulsion Laboratory
USA

SPAHNI, Renato
Climate and Environmental Physics,
Physics Institute, University of Bern
Switzerland

SRINIVASAN, Jayaraman
Centre for Atmospheric and Oceanic
Sciences, Indian Institute of Science
India

STAINFORTH, David
Atmospheric, Oceanic and
Planetary Physics, Department of
Physics, University of Oxford
UK

STAMMER, Detlef
Institut fuer Meereskunde Zentrum
fuer Meeres und Klimaforschung
Universitaet Hamburg
Germany

STANIFORTH, Andrew
Hadley Centre for Climate Prediction
and Research, Met Office
UK

STARK, Sheila
Hadley Centre for Climate Prediction
and Research, Met Office
UK

STEFFEN, Will
Australian National University
Australia

STENCHIKOV, Georgiy
Rutgers, The State University of New Jersey
USA

STERN, William
National Oceanic and
Atmospheric Administration
USA

STEVENSON, David
University of Edinburgh
UK

STOCKER, Thomas F.
Climate and Environmental Physics,
Physics Institute, University of Bern
Switzerland

STONE, Daithí A.
University of Oxford
UK, Canada

STOTT, Lowell D.
Department of Earth Sciences,
University of Southern California
USA

STOTT, Peter A.
Hadley Centre for Climate Prediction
and Research, Met Office
UK

STOUFFER, Ronald J.
National Oceanic and Atmospheric
Administration, Geophysical
Fluid Dynamics Laboratory
USA

STUBER, Nicola
Department of Meteorology,
University of Reading
UK, Germany

SUDO, Kengo
Nagoya University
Japan

SUGA, Toshio
Tohoku University
Japan

SUMI, Akimasa
Center for Climate System
Research, University of Tokyo
Japan

SUPPIAH, Ramasamy
CSIRO
Australia

SWEENEY, Colm
Princeton University
USA

TADROSS, Mark
Climate Systems Analysis Group,
University of Cape Town
South Africa

TAKEMURA, Toshihiko
Research Institute for Applied
Mechanics, Kyushu University
Japan

TALLEY, Lynne D.
Scripps Institution of Oceanography,
University of California, San Diego
USA

TAMISIEA, Mark
Harvard-Smithsonian Center
for Astrophysics
USA

TAYLOR, Karl E.
Program for Climate Model Diagnosis
and Intercomparison, Lawrence
Livermore National Laboratory
USA

TEBALDI, Claudia
National Center for Atmospheric Research
USA

TENG, Haiyan
National Center for Atmospheric Research
USA, China

TENNANT, Warren
South African Weather Service
South Africa

TERRAY, Laurent
Eoropean Centre for Research and Advanced
Training in Scientific Computation
France

TETT, Simon
Hadley Centre for Climate Prediction
and Research, Met Office
UK

TEXTOR, Christiane
Laboratoire des Sciences du
Climat et de l'Environnement
France, Germany

THOMAS, Robert H.
EG&G Technical Services, Inc. and
Centro de Estudios Cientificos (CECS)
USA, Chile

THOMPSON, Lonnie
Ohio State University
USA

THORNCROFT, Chris
Department of Earth and Atmospheric
Science, University at Albany, SUNY
USA, UK

THORNE, Peter
Hadley Centre for Climate Prediction
and Research, Met Office
UK

TIAN, Yuhong
Georgia Institute of Technology
USA, China

TRENBERTH, Kevin E.
Climate Analysis Section, National
Center for Atmospheric Research
USA

TSELIOUDIS, George
National Aeronautics and Space
Administration, Goddard Institute for
Space Studies, Columbia University
USA, Greece

TSIMPLIS, Michael
National Oceanography Centre,
University of Southampton
UK, Greece

UNNIKRISHNAN, Alakkat S.
National Institute of Oceanography
India

UPPALA, Sakari
European Centre for Medium-
Range Weather Forecasts
ECMWF

VAN DE WAL, Roderik Sylvester Willo
Institute for Marine and Atmospheric Research, Utrecht University
Netherlands

VAN DORLAND, Robert
Royal Netherlands Meteorological Institute (KNMI)
Netherlands

VAN NOIJE, Twan
Royal Netherlands Meteorological Institute (KNMI)
Netherlands

VAUGHAN, David
British Antarctic Survey
UK

VILLALBA, Ricardo
Departmento de Dendrocronología e Historia Ambiental, Instituto Argentino de Novologia, Glaciologia y Ciencias Ambientales (IANIGLA - CRICYT)
Argentina

VOLODIN, Evgeny M.
Institute of Numerical Mathematics of Russian Academy of Sciences
Russian Federation

VOSE, Russell
National Oceanic and Atmospheric Administration, National Climatic Data Center
USA

WAELBROECK, Claire
Institut Pierre Simon Laplace, Laboratoire des Sciences du Climat et de l'Environnement, CNRS
France

WALSH, John
University of Alaska
USA

WANG, Bin
National Key Laboratory of Numerical Modeling for Atmospheric Sciences and Geophysical Fluid Dynamics, institute of Atmospheric Physics, Chinese Academy of Sciences
China

WANG, Bin
University of Hawaii
USA

WANG, Minghuai
Department of Atmospheric, Oceanic, and Space Sciences, University of Michigan
USA

WANG, Ray
Georgia Institute of Technology
USA

WANNINKHOF, Rik
Atlantic Oceanographic and Meteorological Laboratory, National Oceanic and Atmospheric Administration
USA

WARREN, Stephen
University of Washington
USA

WASHINGTON, Richard
UK, South Africa

WATTERSON, Ian G.
CSIRO Marine and Atmospheric Research
Australia

WEAVER, Andrew J.
School of Earth and Ocean Sciences, University of Victoria
Canada

WEBB, Mark
Hadley Centre for Climate Prediction and Research, Met Office
UK

WEISHEIMER, Antje
European Centre for Medium-Range Weather Forecasting and Free University, Berlin
ECMWF, Germany

WEISS, Ray
Scripps Institution of Oceanography, University of California, San Diego
USA

WHEELER, Matthew
Bureau of Meteorology Research Centre
Australia

WHETTON, Penny
CSIRO Marine and Atmospheric Research
Australia

WHORF, Tim
Scripps Institution of Oceanography, University of California, San Diego
USA

WIDMANN, Martin
GKSS Research Centre, Geesthacht and School of Geography, Earth and Envrionmental Sciences, University of Birmingham
Germany, UK

WIELICKI, Bruce
National Aeronautics and Space Administration, Langley Research Center
USA

WIGLEY, Tom M.L.
National Center for Atmospheric Research
USA

WILBY, Rob
Environment Agency of England and Wales
UK

WILD, Martin
ETH Zürich, Institute for Atmospheric and Climate Sciencce
Switzerland

WILD, Oliver
Frontier Research Center for Global Change, Japan Agency for Marine-Earth Science and Technology
Japan, UK

WILES, Gregory
The College of Wooster
USA

WILLEBRAND, Jürgen
Leibniz Institut für Meereswissenschaften an der Universität Kiel
Germany

WILLIS, Josh
Jet Propulsion Laboratory
USA

WOFSY, Steven C.
Division of Engineering and Applied Science, Harvard University
USA

WONG, A.P.S.
School of Oceanography, University of Washington
USA, Australia

WONG, Takmeng
National Aeronautics and Space Administration, Langley Research Center
USA

WOOD, Richard A.
Hadley Centre for Climate Prediction and Research, Met Office
UK

WOODWORTH, Philip
Proudman Oceanographic Laboratory
UK

WORBY, Anthony
Australian Antarctic Division and Antarctic Climate and Ecosystems Cooperative Research Centre
Australia

WRATT, David
National Climate Centre, National Institute of Water and Atmospheric Research
New Zealand

WUERTZ, David
National Oceanic and Atmospheric Administration, National Climatic Data Center
USA

WYMAN, Bruce L.
Geophysical Fluid Dynamics Laboratory, National Oceanic and Atmospheric Administration
USA

XU, Li
Department of Atmospheric, Oceanic, and Space Sciences, University of Michigan
USA, China

YAMADA, Tomomi
Japanese Society of Snow and Ice
Japan

YASHAYAEV, Igor
Maritimes Region of the Department of Fisheries and Oceans
Canada

YASUDA, Ichiro
University of Tokyo
Japan

YOSHIMURA, Jun
Meteorological Research Institute
Japan

YU, Rucong
China Meteorological Administration
China

YUKIMOTO, Seiji
Meteorological Research Institute
Japan

ZACHOS, James
University of California, Santa Cruz
USA

ZHAI, Panmao
National Climate Center, China
Meteorological Administration
China

ZHANG, De'er
National Climate Center, China
Meteorological Administration
China

ZHANG, Tingjun
National Snow and Ice Data Center, CIRES,
University of Colorado at Boulder
USA, China

ZHANG, Xiaoye
Chinese Academy of Meteorological
Sciences, Centre for Atmophere
Watch & Services
China

ZHANG, Xuebin
Climate Research Division,
Environment Canada
Canada

ZHAO, Lin
Cold and Arid Regions Environmental
and Engineering Research Institute,
Chinese Academy of Science
China

ZHAO, Zong-Ci
National Climate Center, China
Meteorological Administration
China

ZHENGTENG, Guo
Institute of Geology and Geophysics,
Chinese Academy of Science
China

ZHOU, Liming
Georgia Institute of Technology
USA, China

ZORITA, Eduardo
Helmholtz Zentrum Geesthacht
Germany, Spain

ZWIERS, Francis
Canadian Centre for Climate Modelling
and Analysis, Environment Canada
Canada

Annex III

Reviewers of the IPCC WGI Fourth Assessment Report

Algeria

AMAR, Matari
IHFR, Oran

MATARI, Amar
IHFR, Oran

Australia

CAI, Wenju
CSIRO Marine and Atmospheric Research

CHURCH, John
CSIRO Marine and Atmospheric Research and Ecosystems Cooperative Research Centre

COLMAN, Robert
Bureau of Meteorology Research Centre

ENTING, Ian
University of Melbourne

GIFFORD, Roger
CSIRO Plant Industry

HIRST, Anthony
CSIRO Marine and Atmospheric Research

HOBBINS, Michael
Australian National University

HOWARD, William
Antarctic Climate and Ecosystems Cooperative Research Centre

HUNTER, John
Antarctic Climate and Ecosystems Cooperative Research Centre

JONES, Roger
CSIRO Marine and Atmospheric Research

KININMONTH, William

LYNCH, Amanda H.
School of Geography and Environmental Science, Monash University

MANTON, Michael
Bureau of Meteorology Research Centre

MCAVANEY, Bryant
Bureau of Meteorology Research Centre

MCDOUGALL, Trevor
CSIRO Marine and Atmospheric Research

MCGREGOR, John
CSIRO Marine and Atmospheric Research

MCNEIL, Ben
University of New South Wales

MOISE, Aurel
Bureau of Meteorology Research Centre

NICHOLLS, Neville
Monash University

PITMAN, Andrew
Department of Physical Geography, Macquarie University

RAUPACH, Michael
CSIRO

RINTOUL, Stephen
CSIRO, Marine and Atmospheric Research and Antarctic Climate and Ecosystems Cooperative Research Centre

RODERICK, Michael
Australian National University

ROTSTAYN, Leon
CSIRO Marine and Atmospheric Research

SIEMS, Steven
Monash University

SIMMONDS, Ian
University of Melbourne

TREWIN, Blair
National Climate Centre, Bureau of Meteorology

VAN OMMEN, Tas
Australian Antarctic Division

WALSH, Kevin
School of Earth Sciences, University of Melbourne

WATKINS, Andrew
National Cliamte Centre, Bureau of Meteorology

WHEELER, Matthew
Bureau of Meteorology Research Centre

WHITE, Neil
CSIRO Marine and Atmospheric Research

Austria

BÖHM, Reinhard
Central Institute for Meteorology and Geodynamics

KIRCHENGAST, Gottfried
University of Graz

O'NEILL, Brian
IIASA and Brown University

RADUNSKY, Klaus
Umweltbundesamt

Belgium

BERGER, André
Université catholique de Louvain, Institut d'Astronomie et de Géophysique G. Lemaitre

DE BACKER, Hugo
Royal Meteorological Institute

GOOSSE, Hugues
Université catholique de Louvain

JANSSENS, Ivan A.
University of Antwerp

LOUTRE, Marie-France
Université catholique de Louvain, Institut d'Astronomie et de Géophysique G. Lemaitre

VAN LIPZIG, Nicole
Katholieke Universiteit Leuven

Benin

BOKO, Michel
Universite de Bourgogne

GUENDEHOU, G. H. Sabin
Benin Centre for Scientific and Technical Review

VISSIN, Expédit Wilfrid
LECREDE/DGAT/FLASH/ Université d'Abomey-Calavi

YABI, Ibouraïma
Laboratoire de Climatologie/DGAT/UAC

Brazil

CARDIA SIMÕES, Jefferson
Departamento de Geografia, Instituto de Geociências, Universidade Federal do Rio Grande do Sul

GOMES, Marcos S.P.
Department of Mechanical Research, Pontifical Catholic University of Rio de Janeiro

MARENGO ORSINI, Jose Antonio
CPTEC/INPE

Canada

BELTRAMI, Hugo
St. Francis Xavier University

BROWN, Ross
Environment Canada

Expert reviewers are listed by country. Experts from international organizations are listed at the end.

CAYA, Daniel
Consortium Ouranos

CHYLEK, Petr
Dalhousie University, Departments of Physics and Oceanography

CLARKE, Garry
Earth and Ocean Sciences, University of British Columbia

CLARKE, R. Allyn
Bedford Institute of Oceanography

CULLEN, John
Dalhousie University

DERKSEN, Chris
Climate Research Branch, Meteorological Service of Canada

FERNANDES, Richard
Canada Centre for Remote Sensing, Natural Resources Canada

FORBES, Donald L.
Natural Resources Canada, Geological Survey of Canada

FREELAND, Howard
Department of Fisheries and Oceans

GARRETT, Chris
University of Victoria

HARVEY, Danny
University of Toronto

ISAAC, George
Environment Canada

JAMES, Thomas
Geological Survey of Canada, Natural Resources Canada

LEWIS, C.F. Michael
Geological Survey of Canada, Natural Resources Canada

MACDONALD, Robie
Department of Fisheries and Oceans

MATTHEWS, H. Damon
University of Calgary and Concordia University

MCINTYRE, Stephen
University of Toronto

MCKITRICK, Ross
University of Guelph

PELTIER, Wm. Richard
Department of Physics, University of Toronto

SAVARD, Martine M.
Geological Survey of Canada, Natural Resources Canada

SMITH, Sharon
Geological Survey of Canada, Natural Resources Canada

TRISHCHENKO, Alexander P.
Canada Centre for Remote Sensing, Natural Resources Canada

WANG, Shusen
Canada Centre for Remote Sensing, Natural Resources Canada

WANG, Xiaolan L.
Climate Research Branch, Meteorological Service of Canada

ZWIERS, Francis
Canadian Centre for Climate Modelling and Analysis, Environment Canada

Chile

ACEITUNO, Patricio
Department Geophysics, Universidad de Chile

China

CAI, Zucong
Institute of Soil Science, Chinese Academy of Sciences

CHAN, Johnny
City University of Hong Kong

DONG, Zhaoqian
Polar Research Institute of China

GONG, Dao-Yi
College of Resources Science and Technology, Beijing Normal University

GUO, Xueliang
Institute of Atmospheric Physics, Chinese Academy of Sciences

LAM, Chiu-Ying
Hong Kong Observatory

REN, Guoyu
National Climate Center, China Meteorological Administration

SHI, Guang-yu
Institute of Atmospheric Physics, Chinese Academy of Sciences

SU, Jilan
Lab of Ocean Dynamic Processes and Satellite Oceanography,Second Institute of Oceanography, State Oceanic Administration

SUN, Junying
Centre for Atmosphere Watch and Services, Chinese Academy of Meteorological Sciences, CMA

WANG, Dongxiao
South China Sea Institute of Oceanology, Chinese Academy of Sciences

WANG, Mingxing
Institute of Atmospheric Physics, Chinese Academy of Sciences

XIE, Zhenghui
Institute of Atmospheric Physics, Chinese Academy of Sciences

XU, Xiaobin
Chinese Academy of Meteorological Sciences

YU, Rucong
China Meteorological Administration

ZHAO, Zong-Ci
National Climate Center, China Meteorological Administration

ZHOU, Tianjun
Institute of Atmospheric Physics, Chinese Academy of Sciences

Denmark

GLEISNER, Hans
Atmosphere Space Research Division, Danish Met. Institute

STENDEL, Martin
Danish Meteorological Institute

Egypt

EL-SHAHAWY, Mohamed
Cairo University, Egyptian Environmemntal Affairs Agency

Estonia

JAAGUS, Jaak
University of Tartu

Fiji

LAL, Murari
University of the South Pacific

Finland

CARTER, Timothy
Finnish Environment Institute

KORTELAINEN , Pirkko
Finnish Environment Institute

KULMALA, Markku
University of Helsinki

LAAKSONEN, Ari
University of Kuopio

MÄKIPÄÄ, Raisa
Finnish Forest Research Institute

RÄISÄNEN, Jouni
Department of Physical Sciences, University of Helsinki

SAVOLAINEN, Ilkka
Technical Research Centre of Finland

France

BONY, Sandrine
Laboratoire de Météorologie Dynamique, Institut Pierre Simon Laplace

BOUSQUET, Philippe
Institut Pierre Simon Laplace, Laboratoire des Sciences du Climat et de l'Environnement

BRACONNOT, Pascale
Pascale Braconnot Institu Pierre Simon Laplace, Laboratoire des Sciences du Climat et de l'Environnement

CAZENAVE, Anny
Laboratoire d'Etudes en Géophysique et Océanographie Spatiale (LEGOS), CNES

CLERBAUX, Cathy
Centre National de Recherche Scientifique

CORTIJO, Elsa
Laboratoire des Sciences du Climat et de l'Environnement, CNRS-CEA-UVSQ

DELECLUSE, Pascale
CEA, CNRS

DÉQUÉ, Michel
Météo-France

DUFRESNE, Jean-Louis
Laboratoire de Météorologie Dynamique, Institut Pierre Simon Laplace

FRIEDLINGSTEIN, Pierre
Institut Pierre Simon Laplace, Laboratoire des Sciences du Climat et de l'Environnement

GENTHON, Christophe
Centre National de Recherche Scientifique, Laboratoire de Glaciologie et Géophysique de l'Environnement

GUILYARDI, Eric
Laboratoire des Sciences du Climat et de l'Environnement

GUIOT, Joel
CEREGE, Centre National de Recherche Scientifique

HAUGLUSTAINE, Didier
Institut Pierre Simon Laplace, Laboratoire des Sciences du Climat et de l'Environnement, CEA-CNRS-UVSQ

JOUSSAUME, Sylvie
Centre National de Recherche Scientifique

KANDEL, Robert
Laboratoire de Météorologie Dynamique, Ecole Polytechnique

KHODRI, Myriam
Institut de Recherche Pour le Developpement

LABEYRIE, Laurent
Laboratoire des Sciences du Climat et de l'Environnement

MARTIN, Eric
Météo-France

MOISSELIN, Jean-Marc
Météo-France

PAILLARD, Didier
Laboratoire des Sciences du Climat et de l'Environnement

PETIT, Michel
CGTI

PLANTON, Serge
Météo-France

RAMSTEIN, Gilles
Laboratoire des Sciences du Climat et de l'Environnement

SCHULZ, Michael
Institut Pierre Simon Laplace, Laboratoire des Sciences du Climat et de l'Environnement, CEA-CNRS-UVSQ

SEGUIN, Bernard
INRA

TEXTOR, Christiane
Laboratoire des Sciences du Climat et de l'Environnement

WAELBROECK, Claire
Institut Pierre Simon Laplace, Laboratoire des Sciences du Climat et de l'Environnement, CNRS

Germany

BANGE, Hermann W.
Leibniz Institut für Meereswissenschaften, IFM-GEOMAR

BAUER, Eva
Potsdam Institute for Climate Impact Research

BECK, Christoph
Global Precipitation Climatology Centre

BROVKIN, Victor
Potsdam Institute for Climate Impact Research

CHURKINA, Galina
Max Planck Institute for Biogeochemistry

COTRIM DA CUNHA, Leticia
Max-Planck-Institut für Biogeochemie

DOTZEK, Nikolai
Deutsches Zentrum für Luft und Raumfahrt, Institut für Physik der Atmosphäre

FEICHTER, Johann
Max Planck Institute for Meteorology

GANOPOLSKI, Andrey
Potsdam Institute for Climate Impact Research

GIORGETTA, Marco A.
Max Planck Institute for Meteorology

GRASSL, Hartmut
Max Planck Institute for Meteorology

GREWE, Volker
Deutsches Zentrum für Luft und Raumfahrt, Institut für Physik der Atmosphäre

GRIESER, Jürgen
Deutscher Wetterdienst, Global Precipitatioin Climatology Centre

HARE, William
Potsdam Institute for Climate Impact Research

HELD, Hermann
Potsdam Institute for Climate Impact Research

HOFZUMAHAUS, Andreas
Forschungszentrum Jülich, Institut für Chemie und Dynamik der Geosphäre II: Troposphäre

KOPPMANN, Ralf
Institut für Chemie und Dynamik der Geosphaere, Institut II: Troposphaere, Forschungszentrum Juelich, Juelich, Germany

LATIF, Mojib
Leibniz Institut für Meereswissenschaften, IFM-GEOMAR

LAWRENCE, Mark
Max Planck Institute for Chemistry

LELIEVELD, Jos
Max Planck Institute for Chemistry

LEVERMANN, Anders
Potsdam Institute for Climate Impact Research

LINGNER, Stephan
Europäische Akademie Bad Neuenahr-Ahrweiler GmbH

LUCHT, Wolfgang
Potsdam Institute for Climate Impact Research

MAROTZKE, Jochem
Max Planck Institute for Meteorology

MATA, Louis Jose
Center for Development Research, University of Bonn

MEINSHAUSEN, Malte
Potsdam Institute for Climate Impact Research

MICHAELOWA, Axel
Hamburg Institute of International Economics

MÜLLER, Rolf
Research Centre Jülich

RAHMSTORF, Stefan
Potsdam Institute for Climate Impact Research

RHEIN, Monika
Institute for Environmental Physics, University Bremen

SAUSEN, Robert
Deutsches Zentrum für Luft und Raumfahrt, Institut für Physik der Atmosphäre

SCHOENWIESE, Christian-D.
University Frankfurt a.M., Institute for Atmosphere and Environment

SCHOTT, Friedrich
Leibniz Institut für Meereswissenschaften, IFM-GEOMAR

SCHULZ, Michael
University of Bremen

SCHÜTZENMEISTER, Falk
Technische Universität Dresden, Institut für Soziologie

STAMMER, Detlef
Institut fuer Meereskunde Zentrum fuer Meeres und Klimaforschung Universitaet Hamburg

TEGEN, Ina
Institute for Tropospheric Research

VÖLKER, Christoph
Alfred Wegener Institute for Polar and Marine Research

WEFER, Gerold
University of Bremen, Research Center Ocean Margins

WURZLER, Sabine
North Rhine-Westphalia State Environment Agency

ZENK, Walter
Leibniz Institut für Meereswissenschaften, IFM-GEOMAR

ZOLINA, Olga
Meteorologisches Institut der Universität Bonn

ZORITA, Eduardo
Helmholtz Zentrum Geesthacht

Hungary

ZAGONI, Miklos
Budapest University

India

SRIKANTHAN, Ramachandran
Physical Research Laboratory

TULKENS, Philippe
The Energy and Research Institute (TERI)

Iran

RAHIMZADEH, Fatemeh
Atmospheric Science & Meteorological Research Center (ASMERC), I.R. of Iran Meteorological Organization (IRIMO)

Ireland

FEALY, Rowan
National University of Ireland, Maynooth

SWEENEY, John
National University of Ireland, Maynooth

Italy

ARTALE, Vincenzo
Italian National Agency for New Technologies, Energy and the Environment (ENEA)

BALDI, Marina
Consiglio Nazionale delle Ricerche (CNR), Inst of Biometeorology

BERGAMASCHI, Peter
European Commission, Joint Research Centre, Institute for Environment and Sustainability

BRUNETTI, Michele
Istituto di Scienze dell'atmosfera e del Clima (ISAC) Consiglio Nazionale delle Ricerche (CNR)

CAMPOSTRINI, Pierpaolo
CORILA

COLOMBO, Tiziano
Italian Met Service

CORTI, Susanna
Istituto di Scienze dell'atmosfera e del Clima (ISAC) Consiglio Nazionale delle Ricerche (CNR)

DESIATO, Franco
Agenzia per la protezione dell'ambiente e per i servizi tecnici (APAT)

DI SARRA, Alcide
Italian National Agency for New Technologies, Energy and the Environment (ENEA)

DRAGONI, Walter
Perugia University

ETIOPE, Giuseppe
Istituto Nazionale di Geofisica e Vulcanologia

FACCHINI, Maria Cristina
Consiglio Nazionale delle Ricerche (CNR)

GIORGI, Filippo
Abdus Salam International Centre for Theoretical Physics

LIONELLO, Piero
Univ. of Lecce, Dept."Scienza dei materiali"

MARIOTTI, Annarita
Italian National Agency for New Technologies, Energy and the Environment (ENEA) and Earth System Science Interdisciplinary Center (ESSIC-USA)

MOSETTI, Renzo
OGS

NANNI, Teresa
Istituto di Scienze dell'atmosfera e del Clima (ISAC) Consiglio Nazionale delle Ricerche (CNR)

RUTI, Paolo Michele
Italian National Agency for New Technologies, Energy and the Environment

SANTINELLI, Chiara
Consiglio Nazionale delle Ricerche (CNR)

VAN DINGENEN, Rita
European Commission, Joint Research Centre, Institute for Environment and Sustainability

VIGNUDELLI, Stefano
Consiglio Nazionale delle Ricerche (CNR), Istituto di Biofisica

Japan

ALEXANDROV, Georgii
National Institute for Environmental Studies

ANNAN, James
Frontier Research Center for Global Change, Japan Agency for Marine-Earth Science and Technology

AOKI, Teruo
Meteorological Research Institute, Japan Meteorological Agency

AWAJI, Toshiyuki
Kyoto University

EMORI, Seita
National Institute for Environmental Studies and Frontier Research Center for Global Change, Japan Agency for Marine-Earth Science and Technology

HARGREAVES, Julia
Frontier Research Center for Global Change, Japan Agency for Marine-Earth Science and Technology

HAYASAKA, Tadahiro
Research Institute for Humanity and Nature

IKEDA, Motoyoshi
Hokkaido University

ITOH, Kiminori
Yokohama National University

KAWAMIYA, Michio
Frontier Research Center for Global Change, Japan Agency for Marine-Earth Science and Technology

KIMOTO, Masahide
Center for Climate System Research, University of Tokyo

KITOH, Akio
First Research Laboratory, Climate Research Department, Meteorological Research Institute, Japan Meteorological Agency

KOBAYASHI, Shigeki
TRDL

KONDO, Hiroki
Frontier Research Center for Global Change, Japan Agency for Marine-Earth Science and Technology

MAKI, Takashi
Meteorological Research Institute, Japan Meteorological Agency

MAKSYUTOV, Shamil
National Institute for Environmental Studies

MARUYAMA, Koki
CRIEPI

MATSUNO, Taroh
Frontier Research Center for Global Change, Japan Agency for Marine-Earth Science and Technology

MIKAMI, Masao
Meteorological Research Institute, Japan Meteorological Agency

MIKAMI, Takehiko
Tokyo Metropolitan University

NAKAJIMA, Teruyuki
Center for Climate System Research, University of Tokyo

NAKAWO, Masayoshi
Research Institute for Humanity and Nature

NODA, Akira
Meteorological Research Institute, Japan Meteorological Agency

OHATO, Tetsuo
JAMSTEC

ONO, Tsuneo
Hokkaido National Fisheries Research Institute, Fisheries Research Agency

SASAKI, Hidetaka
Meteorological Research Institute, Japan Meteorological Agency

SATO, Yasuo
Meteorological Research Institute, Japan Meteorological Agency

SEKIYA, Akira
National Institute of Advanced Industrial Science and Technology (AIST)

SHINODA, Masato
Tottori University, Arid Land Research Center

SUGA, Toshio
Tohoku University

SUGI, Masato
Meteorological Research Institute, Japan Meteorological Agency

TOKIOKA, Tatsushi
Frontier Research Center for Global Change, Japan Agency for Marine-Earth Science and Technology

TOKUHASHI, Kazuaki
National Institute of Advanced Industrial Science and Technology (AIST)

TSUSHIMA, Yoko
Japan Agency for Marine-Earth Science and Technology

UCHIYAMA, Akihiro
Meteorological Research Institute, Japan Meteorological Agency

YAMAMOTO, Susumu
Graduate School of Environmental Science, Okayama University

YAMANOUCHI, Takashi
National Institute of Polar Research

YAMASAKI, Masanori
Japan Agency for Marine-Earth Science and Technology

YAMAZAKI, Koji
Graduate School of Environmental Science, Hokkaido University

YOKOYAMA, Yusuke
Department of Earth and Planetary Sciences, University of Tokyo

TSUTSUMI, Yukitomo
Meteorological Research Institute, Japan Meteorological Agency

Republic of Korea

KIM, Kyung-Ryul
Seoul National University, School of Earth and Environmental Services

Mexico

LLUCH-BELDA, Daniel
Centro Interdisciplinario de Ciencias Marinas del IPN

Mozambique

QUEFACE, Antonio Joaquim
Physics Department, Eduardo Mondlane University

Netherlands, Antilles and Aruba

MARTIS, Albert
Climate Research Center, Meteorological Service Netherlands, Antilles & Aruba

Netherlands

BAEDE, Alphonsus
Royal Netherlands Meteorological Institute (KNMI) and Ministry of Housing, Spatial Planning and the Environment

BURGERS, Gerrit
Royal Netherlands Meteorological Institute (KNMI)

DE BRUIN, Henk
Meteorology and Air Quality Group, Wageningen University

DE WIT, Florens

DILLINGH, Douwe
National Institute for Coastal and Marine Management / RIKZ

HAARSMA, Reindert
Royal Netherlands Meteorological Institute (KNMI)

HAZELEGER, Wilco
Royal Netherlands Meteorological Institute (KNMI)

HOLTSLAG, Albert A. M.
Wageningen University

KROON, Dick
Vrije Universiteit, Amsterdam

SIEGMUND, Peter
Royal Netherlands Meteorological Institute (KNMI)

STERL, Andreas
Royal Netherlands Meteorological Institute (KNMI)

VAN AKEN, Hendrik M.
Royal Netherlands Institute for Sea Research (NIOZ)

VAN DE WAL, Roderik Sylvester Willo
Institute for Marine and Atmospheric Research, Utrecht University

VAN DEN HURK, Bart
Royal Netherlands Meteorological Institute (KNMI)

VAN NOIJE, Twan
Royal Netherlands Meteorological Institute (KNMI)

VAN VELTHOVEN, Peter
Royal Netherlands Meteorological Institute (KNMI)

VANDENBERGHE, Jef
Vrije Universiteit, Inst. of Earth Sciences

VEEFKIND, Pepijn
Royal Netherlands Meteorological Institute (KNMI)

VELDERS, Guus J.M.
Netherlands Environmental Assessment Agency (MNP)

New Zealand

ALLOWAY, Brent
Institute of Geological and Nuclear Sciences

BARRETT, Peter
Antarctic Research Centre, Victoria University of Wellington

BODEKER, Greg
National Institute of Water and Atmospheric Research

BOWEN, Melissa
National Institute of Water and Atmospheric Research

CRAMPTON, James
Institute of Geological and Nuclear Sciences

GRAY, Vincent
Climate Consultant

LASSEY, Keith
National Institute of Water and Atmospheric Research

LAW, Cliff
National Institute of Water and Atmospheric Research

MACLAREN, Piers
NZ Forest Research Institute

MULLAN, A. Brett
National Institute of Water and Atmospheric Research

NODDER, Scott
National Institute of Water and Atmospheric Research

RENWICK, James A.
National Institute of Water and Atmospheric Research

SALINGER, M. James
National Institute of Water and Atmospheric Research

SHULMEISTER, James
University of Canterbury

WILLIAMS, Paul W.
Auckland University

WRATT, David
National Climate Centre, National Institute of Water and Atmospheric Research

Norway

BENESTAD, Rasmus
Norwegian Meteorological Institute

FUGLESTVEDT, Jan
Centre for International Climate and Environmantal Research (CICERO)

GODAL, Odd
Department of Economics, University of Bergen

HANSSEN-BAUER, Inger
Norwegian Meteorological Institute

ISAKSEN, Ketil
Norwegian Meteorological Institute

JOHANNESSEN, Ola M.
Nansen Environmental and Remote Sensing Center

KRISTJÁNSSON , Jón Egill
University of Oslo

NESJE, Atle
Department of Earth Science, University of Bergen

PAASCHE, Øyvind
Bjerknes Centre for Climate Research

Peru

GAMBOA, Nadia
Pontificia Universidad Carolica del Pero

Romania

BOJARIU, Roxana
National Institute of Meteorology and Hydrology (NIMH)

BORONEANT, Constanta-Emilia
National Meteorological Administration

BUSUIOC, Aristita
National Meteorological Administration

MARES, Constantin
Romanian Academy, Geodynamics Institute

MARES, Ileana
Romanian Academy of Technical Studies

Russian Federation

MELESHKO, Valentin
Voeykov Main Geophysical Observatory

Slovakia

LAPIN, Milan
Slovak National Climate Program

Spain

AGUILAR, Enric
Climate Change Research Group, Universitat Rovira i Virgili de Tarragona

BLADÉ, Ileana
Department of Astronomy and Meteorology. University of Barcelona

BRUNET, Manola
University Rovira i Virgili

CALVO COSTA , Eva
Institut de Ciències del Mar

GARCÍA-HERRERA, Ricardo
Universidad Complutense de Madrid

GONZÁLEZ-ROUCO, Jesus Fidel
Universidad Complutense de Madrid

LAVIN, Alicia M.
Instituto Espanol de Oceanografia

MARTIN-VIDE, Javier
Physical Geography of the University of Barcelona

MONTOYA, Marisa
Dpto. Astrofisica y Fisica de la Atmosfera, Facultad de Ciencias Fisicas, Universidad Complutense de Madrid

PELEJERO, Carles
Institut de Ciències del Mar, CMIMA-CSIC

RIBERA, Pedro
Universidad Pablo de Olavide

Sweden

HOLMLUND, Per
Stockholm University

KJELLSTRÖM, Erik
Swedish Meteorological and Hydrological Institute

LECK, Caroline
Department of Metorology, Stockholm University

RUMM AINEN, Markku
Rossby Centre, Swedish Meteorological and Hydrological Institute

Switzerland

APPENZELLER, Christof
Federal Office of Meteorology and Climatology MeteoSwiss

BLUNIER, Thomas
Climate and Environmental Physics, University of Bern

BRÖNNIMANN, Stefan
ETH Zürich

CASTY, Carlo
Climate and Environmental Physics

CHERUBINI, Paolo
Swiss Federal Research Institute WSL

ESPER, Jan
Swiss Federal Research Institute WSL

FREI, Christoph
Federal Office of Meteorology and Climatology MeteoSwiss

GHOSH, Sucharita
Swiss Federal Research Institute WSL

HAEBERLI, Wilfried
Geography Department, University of Zürich

JOOS, Fortunat
Climate and Environmental Physics, Physics Institute, University of Bern

KNUTTI, Reto
Climate and Global Dynamics Division, National Center for Atmospheric Research

LUTERBACHER, Jürg
Institute of Geography, Climatology and Meteorology, and National Centre of Competence in Research on Climate, University of Bern

MARCOLLI, Claudia
ETH Zürich, Institute for Atmosphere and Climate

PETER, Thomas
ETH Zürich

PHILIPONA, Rolf
Observatory Davos

PLATTNER, Gian-Kasper
Climate and Environmental Physics, Physics Institute, University of Bern

RAIBLE, C. Christoph
Climate and Environmental Physics, University of Bern

REBETEZ, Martine
Swiss Federal Research Institute WSL

ROSSI, Michel J.
Ecole Polytechnique Fédérale de Lausanne, Laboratoire de Pollution Atmosphérique et Sol

ROZANOV, Eugene
IAC ETHZ and PMOD/WRC

SCHÄR, Christoph
ETH Zürich, Institute for Atmospheric and Climate Science

SIDDALL, Mark
Climate and Environmental Physics, University of Bern

SPAHNI, Renato
Climate and Environmental Physics, Physics Institute, University of Bern

STAEHELIN, Johannes
ETH Zürich

STOCKER, Thomas F.
Climate and Environmental Physics, Physics Institute, University of Bern

WANNER, Heinz
National Centre of Competence in Research on Climate, University of Bern

WILD, Martin
ETH Zürich, Institute for Atmospheric and Climate Sciencce

Thailand

GARIVAIT, Savitri
The Joint Graduate School of Energy and Environment, King Mongkut's University of Technology Thonburi

LIMMEECHOKCHAI, Bundit
Sirindhorn International Institute of Technology, Thammasat Univ.

Togo

AJAVON, Ayite-Lo N.
Atmospheric Chemistry Laboratory

UK

ALEXANDER, Lisa
Hadley Centre for Climate Prediction and Research, Met Office

ALLAN, Richard
Environmental Systems Science Centre, University of Reading

BANKS, Helene
Hadley Centre for Climate Prediction and Research, Met Office

BETTS, Richard A.
Hadley Centre for Climate Prediction and Research, Met Office

BODAS-SALCEDO, Alejandro
Hadley Centre for Climate Prediction and Research, Met Office

BOUCHER, Olivier
Hadley Centre for Climate Prediction and Research, Met Office

BROWN, Simon
Hadley Centre for Climate Prediction and Research, Met Office

BRYDEN, Harry
University of Southampton

CAESAR, John
Hadley Centre for Climate Prediction and Research, Met Office

CARSLAW, Kenneth
University of Leeds

COLLINS, Matthew
Hadley Centre for Climate Prediction and Research, Met Office

COLLINS, William
Hadley Centre for Climate Prediction and Research, Met Office

CONNOLLEY, William
British Antarctic Survey

COURTNEY, Richard S.
European Science and Environment Forum

CRUCIFIX, Michel
Hadley Centre for Climate Prediction and Research, Met Office

FALLOON, Pete
Hadley Centre for Climate Prediction and Research, Met Office

FOLLAND, Christopher
Hadley Centre for Climate Prediction and Research, Met Office

FORSTER, Piers
School of Earth and Environment, University of Leeds

FOWLER, Hayley
Newcastle University

GEDNEY, Nicola
Hadley Centre for Climate Prediction and Research, Met Office

GILLETT, Nathan P.
Climatic Research Unit, School of Environmental Sciences, University of East Anglia

GRAY, Lesley
Reading University

GREGORY, Jonathan M.
Department of Meteorology, University of Reading and Hadley Centre for Climate Prediction and Research, Met Office

GRIGGS, David
Hadley Centre for Climate Prediction and Research, Met Office

HAIGH, Joanna
Imperial College London

HARANGOZO, Steve
British Antarctic Survey

HAWKINS, Stephen J.
The Marine Biological Association of the UK

HIGHWOOD, Eleanor
University of Reading

HINDMARSH, Richard
British Antarctic Survey

HOSKINS, Brian J.
Department of Meteorology, University of Reading

HOUSE, Joanna
Quantifying and Understanding the Earth System Programme, University of Bristol

INGRAM, William
Hadley Centre for Climate Prediction and Research, Met Office

JOHNS, Timothy
Hadley Centre for Climate Prediction and Research, Met Office

JONES, Christopher
Hadley Centre for Climate Prediction and Research, Met Office

JONES, Gareth S.
Hadley Centre for Climate Prediction and Research, Met Office

JONES, Philip D.
Climatic Research Unit, School of Environmental Sciences, University of East Anglia

JOSEY, Simon
National Oceanography Centre, University of Southampton

KING, John
British Antarctic Survey

LE QUÉRÉ, Corrine
University of East Anglia and British Antarctic Survey

LEE, David
Manchester Metropolitan University

LOWE, Jason
Hadley Centre for Climate Prediction and Research, Met Office

MARSH, Robert
National Oceanography Centre, University of Southampton

MARTIN, Gill
Hadley Centre for Climate Prediction and Research, Met Office

MCCARTHY, Mark
Hadley Centre for Climate Prediction and Research, Met Office

MCDONALD, Ruth
Hadley Centre for Climate Prediction and Research, Met Office

MITCHELL, John
Hadley Centre for Climate Prediction and Research, Met Office

MURPHY, James
Hadley Centre for Climate Prediction and Research, Met Office

NICHOLLS, Robert
School of Civil Engineering and the Environment, University of Southampton

PARKER, David
Hadley Centre for Climate Prediction and Research, Met Office

PRENTICE, Iain Colin
Quantifying and Understanding the Earth System Programme, Department of Earth Sciences, University of Bristol

RAPER, Sarah
Manchester Metropolitan University

RAYNER, Nick
Hadley Centre for Climate Prediction and Research, Met Office

REISINGER, Andy
IPCC Synthesis Report TSU

RIDLEY, Jeff
Hadley Centre for Climate Prediction and Research, Met Office

ROBERTS, C. Neil
University of Plymouth, School of Geography

RODGER, Alan
British Antarctic Survey

ROSCOE, Howard
British Antarctic Survey

ROUGIER, Jonathan
Durham University

ROWELL, Dave
Hadley Centre for Climate Prediction and Research, Met Office

SENIOR, Catherine
Hadley Centre for Climate Prediction and Research, Met Office

SEXTON, David
Hadley Centre for Climate Prediction and Research, Met Office

SHINE, Keith
University of Reading

SLINGO, Julia
National Centre for Atmospheric Science, University of Reading

SMITH, Leonard A.
London School of Economics

SROKOSZ, Meric
National Oceanography Centre

STARK, Sheila
Hadley Centre for Climate Prediction and Research, Met Office

STEPHENSON, David
Department of Meteorology, University of Reading

STONE, Daíthí A.
University of Oxford

STOTT, Peter A.
Hadley Centre for Climate Prediction and Research, Met Office

THORNE, Peter
Hadley Centre for Climate Prediction and Research, Met Office

TSIMPLIS, Michael
National Oceanography Centre, University of Southampton

TURNER, John
British Antarctic Survey

VAUGHAN, David
British Antarctic Survey

VELLINGA, Michael
Hadley Centre for Climate Prediction and Research, Met Office

WASDELL, David
Meridian Programme

WILLIAMS, Keith
Hadley Centre for Climate Prediction and Research, Met Office

WOLFF, Eric
British Antarctic Survey

WOOD, Richard A.
Hadley Centre for Climate Prediction and Research, Met Office

WOODWORTH, Philip
Proudman Oceanographic Laboratory

WU, Peili
Hadley Centre for Climate Prediction and Research, Met Office

Uruguay

BIDEGAIN, Mario
Universidad de la Republica

USA

ALEXANDER, Becky
University of Washington

ALEXANDER, Michael
National Oceanic and Atmospheric Administration, Climate Diagnostics Brach, Pysical Science Division, Earth System Research Lab

ALLEY, Richard B.
Department of Geosciences, Pennsylvania State University

ANDERSON, David M.
National Center for Atmospheric Research, Paleoclimatology

ANDERSON, Theodore
University of Washington

ANDERSON, Wilmer
University of Wisconsin, Madison, Physics Department

ANTHES, Richard
University Corporation for Atmospheric Research

ARRITT, Raymond
Iowa State University

AVERYT, Kristen
IPCC WGI TSU, National Oceanic and Atmospheric Administration, Earth System Research Laboratory

BAER, Paul
Stanford University, Center for Environmental Science and Policy

BAKER, Marcia
University of Washington

BARRY, Roger
National Snow and Ice Data Center, University of Colorado

BATES, Timothy
National Oceanic and Atmospheric Administration

BAUGHCUM, Steven
Boeing Company

BENTLEY, Charles R.
University of Wisconsin, Madison

BERNSTEIN, Lenny
International Petroleum Industry Envirionmental Conservation Association & L.S. Bernstein & Associates, LLC

BOND, Tami
University of Illinois at Urbana-Champaign

BROCCOLI, Anthony J.
Rutgers University

BROMWICH, David
Byrd Polar Research Center, The Ohio State University

BROOKS, Harold
National Oceanic and Atmospheric Administration, National Severe Storms Laboratory

BRYAN, Frank
National Center for Atmospheric Research

CAMERON-SMITH, Philip
Lawrence Livermore National Laboratory

CHIN, Mian
National Aeronautics and Space Administration, Goddard Space Flight Center

CHRISTY, John
University of Alabama in Huntsville

CLEMENS, Steven
Brown University

COFFEY, Michael
National Center for Atmospheric Research

COLLINS, William D.
Climate and Global Dynamics Division, National Center for Atmospheric Research

CROWLEY, Thomas
Duke University

CUNNOLD, Derek
School of Earth and Atmospheric Sciences, Georgia Institute of Technology

DAI, Aiguo
National Center for Atmospheric Research

DANIEL, John S.
National Oceanic and Atmospheric Administration, Earth System Research Laboratory

DANILIN, Mikhail
The Boeing Company

D'ARRIGO, Rosanne
Lamont Doherty Earth Observatory

DAVIES, Roger
Jet Propulsion Laboratory, California Institute of Technology

DEL GENIO, Anthony
National Aeronautics and Space Administration, Goddard Institute for Space Studies

DIAZ, Henry
National Oceanic and Atmospheric Administration, Climate Diagnostics Brach, Pysical Science Division, Earth System Research Lab

DICKINSON, Robert E.
School of Earth and Atmospheric Sciences, Georgia Institute of Technology

DIXON, Keith
National Oceanic and Atmospheric Administration

DONNER, Leo
Geophysical Fluid Dynamics Laboratory, National Oceanic and Atmospheric Administration

DOUGLAS, Bruce
International Hurricane Research Center

DOUGLASS, Anne
National Aeronautics and Space Administration, Goddard Space Flight Center

DUTTON, Ellsworth
National Oceanic and Atmospheric Administration, Earth System Research Laboratory, Global Monitoring Division

EASTERLING, David
National Oceanic and Atmospheric Administration, Earth System Research Laboratory

EMANUEL, Kerry A.
Massachusetts Institute of Technology

EVANS, Wayne F.J.
North West Research Associates

FAHEY, David W.
National Oceanic and Atmospheric Administration, Earth System Research Laboratory

FEELY, Richard
National Oceanic and Atmospheric Administration, Pacific Marine Environmental Laboratory

FEINGOLD, Graham
National Oceanic and Atmospheric Administration

FELDMAN, Howard
American Petroleum Institute

FEYNMAN, Joan
Jet Propulsion Laboratory, California Institute of Technology

FITZPATRICK, Melanie
University of Washington

FOGT, Ryan
Polar Meteorology Group, Byrd Polar Research Center and Atmospheric Sciences Program, Department of geography, The Ohio State University

FREE, Melissa
Air Resources Laboratory, National Oceanic and Atmospheric Administration

FU, Qiang
Department of Atmospheric Sciences, University of Washington

GALLO, Kevin
National Oceanic and Atmospheric Administration, NESDIS

GARCIA, Hernan
National Oceanic and Atmospheric Administration, National Oceanographic Data Center

GASSÓ, Santiago
University of Maryland, Baltimore County and NASA

GENT, Peter
National Center for Atmospheric Research

GERHARD, Lee C.
Thomasson Partner Associates

GHAN, Steven
Pacific Northwest National Laboratory

GNANADESIKAN, Anand
National Oceanic and Atmospheric Administration, Geophysical Fluid Dynamics Laboratory

GORNITZ, Vivien
National Aeronautics and Space Administration, Goddard Institute for Space Studies, Columbia University

GROISMAN, Pavel
University Corporation for Atmospheric Research at the National Climatic Data Center, National Oceanic and Atmospheric Administration

GRUBER, Nicolas
Institute of Geophysics and Planetary Physics, University of California, Los Angeles and Department of Environmental Sciences, ETH Zurich

GURWICK, Noel
Carnegie Institution of Washington, Department of Global Ecology

HAKKARINEN, Chuck
Electric Power Research Institute, retired

HALLEGATTE, Stéphane
Centre International de Recherche sur l'Environnement et le Developpement, Ecole Nationale des Ponts-et-Chaussées and Centre National de Recherches Meteorologique, Meteo-France

HALLETT, John
Desert Research Institute

HAMILL, Patrick
San Jose State University

HARTMANN, Dennis
University of Washington

HAYHOE, Katharine
Texas Tech University

HEGERL, Gabriele
Division of Earth and Ocean Sciences, Nicholas School for the Environment and Earth Sciences, Duke University

HELD, Isaac
National Oceanic and Atmospheric Administration, Geophysical Fluid Dynamics Laboratory

HEMMING, Sidney
Lamont Doherty Earth Observatory, Columbia University

HOULTON, Benjamin
Stanford Unviersity, Dept. of Biological Sciences; Carnegie Institution of Washington, Dept. of Global Ecology

HU, Aixue
National Center for Atmospheric Research

HUGHES, Dan
Hughes and Associates

ICHOKU, Charles
Science Systems & Applications, Inc. (SSAI), NASA-GSFC

JACOB, Daniel
Department of Earth and Planetary Sciences, Harvard University

JACOBSON, Mark
Stanford University

JIN, Menglin
Department of Atmospheric and Oceanic Sciences, University of Maryland, College Park

JOYCE, Terrence
Woods Hole Oceanographic Institution

KARL, Thomas R.
National Oceanic and Atmospheric Administration, National Climatic Data Center

KAROLY, David J.
University of Oklahoma

KAUFMAN, Yoram
National Aeronautics and Space Administration, Goddard Space Flight Center

KELLER, Klaus
Pennsylvania State University

KHESHGI, Haroon
ExxonMobil Research and Engineering Company

KNUTSON, Thomas
Geophysical Fluid Dynamics Laboratory, National Oceanic and Atmospheric Administration

KO, Malcolm
National Aeronautics and Space Administration, Langley Research Center

KOUTNIK, Michelle
University of Washington

KUETER, Jeffrey
Marshall Institue

LACIS, Andrew
National Aeronautics and Space Administration, Goddard Institute for Space Studies

LASZLO, Istvan
National Oceanic and Atmospheric Administration

LEULIETTE, Eric
University of Colorado, Boulder

LEVY, Robert
Science Systems & Applications, Inc. (SSAI), NASA-GSFC

LEWITT, Martin

LI, Zhanqing
University of Maryland, Department of Atmospheric and Oceanic Science and ESSIC

LIU, Yangang
Brookhaven National Laboratory

LOVEJOY, Edward R.
National Oceanic and Atmospheric Administration

LUNCH, Claire
Stanford University, Carnegie Institution of Washington

LUPO, Anthony
University of Missouri, Columbia

MACCRACKEN, Michael
Climate Institute

MAGI, Brian
University of Washington

MAHLMAN, Jerry
National Center for Atmospheric Research

MAHOWALD, Natalie
National Center for Atmospheric Research

MANN, Michael
Pennsylvania State University

MANNING, Martin
IPCC WGI TSU, National Oceanic and Atmospheric Administration, Earth System Research Laboratory

MARQUIS, Melinda
IPCC WGI TSU, National Oceanic and Atmospheric Administration, Earth System Research Laboratory

MARTIN, Scot
Harvard University

MASSIE, Steven
National Center for Atmospheric Research

MASTRANDREA, Michael
Stanford University

MATSUMOTO, Katsumi
University of Minnesota, Twin Cities

MATSUOKA, Kenichi
University of Washington

MAURICE, Lourdes
Federal Aviation Administration

MICHAELS, Patrick
University of Virginia

MILLER, Charles
Jet Propulsion Laboratory, California Institute of Technology

MILLER, Laury
National Oceanic and Atmospheric Administration, Lab for Satellite Altimetry

MILLER, Ron
National Aeronautics and Space Administration, Goddard Institute for Space Studies

MILLET, Dylan
Harvard University

MILLY, Chris
United States Geological Survey

MINNIS, Patrick
National Aeronautics and Space Administration, Langley Research Center

MOLINARI, Robert
National Oceanic and Atmospheric Administration, Atlantic Oceanographic and Meteorological Laboratory

MOTE, Philip
Climate Impacts Group, Joint Institute for the Study of the Atmosphere and Oceans (JIASO), University of Washington

MURPHY, Daniel
National Oceanic and Atmospheric Administration, Earth System Research Laboratory

MUSCHELER, Raimund
Goddard Earth Sciences and Technology Center, University of Maryland & NASA/Goddard Space Flight Center, Climate & Radiation Branch

NEELIN, J. David
University of California, Los Angeles

NELSON, Frederick
Department of Geography, University of Delaware

NEREM, R. Steven
University of Colorado at Boulder

NOLIN, Anne
Oregon State University

NORRIS, Joel
Scripps Institution of Oceanography

OPPENHEIMER, Michael
Princeton University

OTTO-BLIESNER, Bette
Climate and Global Dynamics Division, National Center for Atmospheric Research

OVERPECK, Jonathan
Institute for the Study of Planet Earth, University of Arizona

OWENS, John
3M

PATT, Anthony
Boston University

PENNER, Joyce E.
Department of Atmospheric, Oceanic, and Space Sciences, University of Michigan

PETERS, Halton
Carnegie Institution of Washington, Department of Global Ecology

PRINN, Ronald
Department of Earth, Atmospheric and Planetary Sciences, Massachusetts Institute of Technology

PROFETA, Timothy H.
Nicholas Institute of Environmental Policy Solutions, D e University

RAMANATHAN, Veerabhadran
Scripps Institution of Oceanography

RAMASWAMY, Venkatachalam
National Oceanic and Atmospheric Administration, Geophysical Fluid Dynamics Laboratory

RANDERSON, James
University of California, Irvine

RAVISHANKARA, A. R.
National Oceanic and Atmospheric Administration

RIGNOT, Eric
Jet Propulsion Laboratory

RIND, David
National Aeronautics and Space Administration, Goddard Institute for Space Studies

RITSON, David
Stanford University

ROBOCK, Alan
Rutgers University

RUSSO, Felicita
UMBC/JCET

SABINE, Christopher
National Oceanic and Atmospheric Administration, Pacific Marine Environmental Laboratory

SCHIMEL, David
National Center for Atmospheric Research

SCHMIDT, Gavin
National Aeronautics and Space Administration, Goddard Institute for Space Studies

SCHWARTZ, Stephen E.
Brookhaven National Laboratory

SCHWING, Franklin
National Oceanic and Atmospheric Administration Fisheries Service, SWFSC/ERD

SEIDEL, Dian
National Oceanic and Atmospheric Administration, Air Resources Laboratory

SEINFELD, John
California Institute of Technology

SETH, Anji
University of Connecticut, Department of Geography

SEVERINGHAUS, Jeffrey
Scripps Institution of Oceanography, University of California, San Diego

SHERWOOD, Steven
Yale University

SHINDELL, Drew
National Aeronautics and Space Administration, Goddard Institute for Space Studies

SHUKLA, Jagadish
Center for Ocean-Land-Atmosphere Studies, George Mason University

SIEVERING, Herman
University of Colorado - Boulder and Denver

SODEN, Brian
University of Miami, Rosentiel School for Marine and Atmospheric Science

SOLOMON, Susan
Co-Chair, IPCC WGI, National Oceanic and Atmospheric Administration, Earth System Research Laboratory

SOULEN, Richard

STEFFAN, Konrad
University of Colorado

STEIG, Eric
University of Washington

STEVENS, Bjorn
UCLA Department of Atmospheric & Oceanic Sciences

STONE, Peter
Massachusetts Institute of Technology

STOUFFER, Ronald J.
National Oceanic and Atmospheric Administration, Geophysical Fluid Dynamics Laboratory

TAKLE, Eugene
Iowa State University

TAMISIEA, Mark
Harvard-Smithsonian Center for Astrophysics

TERRY, Joyce
Woods Hole Oceanographic Institution

THOMPSON, Anne
Pennsylvania State University, Department of Meteorology

THOMPSON, David
Department of Atmospheric Science, Colorado State University

THOMPSON, LuAnne
University of Washington

THOMPSON, Robert
United States Geological Survey

TRENBERTH, Kevin E.
Climate Analysis Section, National Center for Atmospheric Research

VINNIKOV, Konstantin
University of Maryland

VONDER HAAR, Thomas
Colorado State University

WAITZ, Ian
Massachusetts Institute of Technology

WANG, James S.
Environmental Defense

WEBB, Robert
National Oceanic and Atmospheric Administration, Earth System Research Laboratory

WEISS, Ray
Scripps Institution of Oceanography, University of California, San Diego

WELTON, Ellsworth
National Aeronautics and Space Administration, Goddard Space Flight Center

WIELICKI, Bruce
National Aeronautics and Space Administration, Langley Research Center

WILES, Gregory
The College of Wooster

WINTON, Michael
Geophysical Fluid Dynamics Laboratory, National Oceanic and Atmospheric Administration

WOODHOUSE, Connie
National Climatic Data Center

YU, Hongbin
National Aeronautics and Space Administration, Goddard Space Flight Center

YU, Jin-Yi
University of California, Irvine

ZENDER, Charles
University of California, Irvine

ZHAO, Xuepeng
ESSIC/UMCP & National Oceanic and Atmospheric Administration

International Organizations

PALMER, Timothy
European Centre for Medium-Range Weather Forecasting

RIXEN, Michel
University of Liege and NATO Undersea Research Center

SIMMONS, Adrian
European Centre for Medium-Range Weather Forecasts

Annex IV

Acronyms & Regional Abbreviations

Acronyms

µmol	micromole
20C3M	20th Century Climate in Coupled Models
AABW	Antarctic Bottom Water
AAIW	Antarctic Intermediate Water
AAO	Antarctic Oscillation
AATSR	Advanced Along Track Scanning Radiometer
ACC	Antarctic Circumpolar Current
ACCENT	Atmospheric Composition Change: a European Network
ACE	Accumulated Cyclone Energy or Aerosol Characterization Experiment
ACRIM	Active Cavity Radiometer Irradiance Monitor
ACRIMSAT	Active Cavity Radiometer Irradiance Monitor Satellite
ACW	Antarctic circumpolar wave
ADEC	Aeolian Dust Experiment on Climate
ADNET	Asian Dust Network
AeroCom	Aerosol Model Intercomparison
AERONET	Aerosol RObotic NETwork
AGAGE	Advanced Global Atmospheric Gases Experiment
AGCM	Atmospheric General Circulation Model
AGWP	Absolute Global Warming Potential
AIACC	Assessments of Impacts and Adaptations to Climate Change in Multiple Regions and Sectors
AIC	aviation-induced cloudiness
ALAS	Autonomous LAgrangian Current Explorer
ALE	Atmospheric Lifetime Experiment
AMIP	Atmospheric Model Intercomparison Project
AMO	Atlantic Multi-decadal Oscillation
AMSU	Advanced Microwave Sounding Unit
AO	Arctic Oscillation
AOGCM	Atmosphere-Ocean General Circulation Model
APEX	Atmospheric Particulate Environment Change Studies
AR4	Fourth Assessment Report
ARM	Atmospheric Radiation Measurement
ASOS	Automated Surface Observation Systems
ASTEX	Atlantic Stratocumulus Transition Experiment
ATCM	Atmospheric Transport and Chemical Model
ATSR	Along Track Scanning Radiometer
AVHRR	Advanced Very High Resolution Radiometer
BATS	Bermuda Atlantic Time-series Study
BC	black carbon
BCC	Beijing Climate Center
BCCR	Bjerknes Centre for Climate Research
BIOME 6000	Global Palaeovegetation Mapping project
BMRC	Bureau of Meteorology Research Centre
C^4MIP	Coupled Carbon Cycle Climate Model Intercomparison Project
$CaCO_3$	calcium carbonate
CAMS	Climate Anomaly Monitoring System (NOAA)
CAPE	Convective Available Potential Energy
CCl_4	carbon tetrachloride
CCM	Chemistry-Climate Model
CCCma	Canadian Centre for Climate Modelling and Analysis
CCN	cloud condensation nuclei
CCSR	Centre for Climate System Research
CDIAC	Carbon Dioxide Information Analysis Center
CDW	Circumpolar Deep Water
CERES	Clouds and the Earth's Radiant Energy System
CERFACS	Centre Europeen de Recherche et de Formation Avancee en Calcul Scientific
CF_4	perfluoromethane
CFC	chlorofluorocarbon
$CFCl_3$	CFC-11
CH_2I_2	di-iodomethane (methylene iodide)
CH_2O	formaldehyde
CH_3CCl_3	methyl chloroform
CH_3COOH	acetic acid
CH_4	methane

CLAMS	Chesapeake Lighthouse and Aircraft Measurements for Satellites
CLARIS	Europe-South America Network for Climate Change Assessment and Impact Studies
CLIMAP	Climate: Long-range Investigation, Mapping, and Prediction
CLIVAR	Climate Variability and Predictability Programme
CMAP	CPC Merged Analysis of Precipitation
CMDL	Climate Monitoring and Diagnostics Laboratory (NOAA)
CMIP	Coupled Model Intercomparison Project
CNRM	Centre National de Recherches Météorologiques
CO	carbon monoxide
CO_2	carbon dioxide
CO_3^{2-}	carbonate
COADS	Comprehensive Ocean-Atmosphere Data Set
COARE	Coupled Ocean-Atmosphere Response Experiment
COBE-SST	Centennial in-situ Observation-Based Estimates of SSTs
COWL	Cold Ocean-Warm Land
CPC	Climate Prediction Center (NOAA)
CREAS	Regional Climate Change Scenarios for South America
CRIEPI	Central Research Institute of Electric Power Industry
CRUTEM2v	CRU/Hadley Centre gridded land-surface air temperature version 2v
CRUTEM3	CRU/Hadley Centre gridded land-surface air temperature version 3
CSIRO	Commonwealth Scientific and Industrial Research Organization
CTM	Chemical Transport Model
DEMETER	Development of a European Multimodel Ensemble System for Seasonal to Interannual Prediction
DIC	dissolved inorganic carbon
DJF	December, January, February
DLR	Deutsches Zentrum für Luft- und Raumfahrt
DMS	dimethyl sulphide
D-O	Dansgaard-Oeschger
DOC	dissolved organic carbon
DORIS	Determination d'Orbite et Radiopositionnement Intégrés par Satellite
DSOW	Denmark Strait Overflow Water
DSP	Dynamical Seasonal Prediction
DTR	diurnal temperature range
DU	Dobson unit
EARLINET	European Aerosol Research Lidar Network
EBM	Energy Balance Model
ECMWF	European Centre for Medium Range Weather Forecasts
ECS	equilibrium climate sensitivity
EDGAR	Emission Database for Global Atmospheric Research
EMIC	Earth System Model of Intermediate Complexity
ENSO	El Niño-Southern Oscillation
EOF	Empirical Orthogonal Function
EOS	Earth Observing System
EPICA	European Programme for Ice Coring in Antarctica
ERA-15	ECMWF 15-year reanalysis
ERA-40	ECMWF 40-year reanalysis
ERBE	Earth Radiation Budget Experiment
ERBS	Earth Radiation Budget Satellite
ERS	European Remote Sensing satellite
ESRL	Earth System Research Library (NOAA)
ESTOC	European Station for Time-series in the Ocean
EUROCS	EUROpean Cloud Systems
FACE	Free Air CO_2 Enrichment
FAO	Food and Agriculture Organization (UN)
FAR	First Assessment Report
FRCGC	Frontier Research Center for Global Change
FRSGC	Frontier Research System for Global Change
GAGE	Global Atmospheric Gases Experiment
GARP	Global Atmospheric Research Program
GATE	GARP Atlantic Tropical Experiment
GAW	Global Atmosphere Watch
GCM	General Circulation Model
GCOS	Global Climate Observing System
GCSS	GEWEX Cloud System Study
GEIA	Global Emissions Inventory Activity
GEOS	Goddard Earth Observing System
GEWEX	Global Energy and Water Cycle Experiment
GFDL	Geophysical Fluid Dynamics Laboratory

GHCN	Global Historical Climatology Network
GHG	greenhouse gas
GIA	glacial isostatic adjustment
GIN Sea	Greenland-Iceland-Norwegian Sea
GISP2	Greenland Ice Sheet Project 2
GISS	Goddard Institute for Space Studies
GLACE	Global Land Atmosphere Coupling Experiment
GLAMAP	Glacial Ocean Mapping
GLAS	Geoscience Laser Altimeter System
GLODAP	Global Ocean Data Analysis Project
GLOSS	Global Sea Level Observing System
GMD	Global Monitoring Division (NOAA)
GOME	Global Ozone Monitoring Experiment
GPCC	Global Precipitation Climatology Centre
GPCP	Global Precipitation Climatology Project
GPS	Global Positioning System
GRACE	Gravity Recovery and Climate Experiment
GRIP	Greenland Ice Core Project
GSA	Great Salinity Anomaly
Gt	gigatonne (10^9 tonnes)
GWE	Global Weather Experiment
GWP	Global Warming Potential
H_2	molecular hydrogen
HadAT	Hadley Centre Atmospheric Temperature data set
HadAT2	Hadley Centre Atmospheric Temperature data set Version 2
HadCRUT2v	Hadley Centre/CRU gridded surface temperature data set version 2v
HadCRUT3	Hadley Centre/CRU gridded surface temperature data set version 3
HadISST	Hadley Centre Sea Ice and Sea Surface Temperature data set
HadMAT	Hadley Centre Marine Air Temperature data set
HadRT	Hadley Centre Radiosonde Temperature data set
HadRT2	Hadley Centre Radiosonde Temperature data set
HadSLP2	Hadley Centre MSLP data set version 2
HadSST2	Hadley Centre SST data set version 2
HALOE	Halogen Occultation Experiment
HCFC	hydrochlorofluorocarbon
HCO_3^-	bicarbonate
HFC	hydrofluorocarbon
HIRS	High Resolution Infrared Radiation Sounder
HLM	High Latitude Mode
HNO_3	nitric acid
HO_2	hydroperoxyl radical
HONO	nitrous acid
HOT	Hawaii Ocean Time-Series
hPa	hectopascal
HYDE	HistorY Database of the Environment
IABP	International Arctic Buoy Programme
ICESat	Ice, Cloud and land Elevation Satellite
ICOADS	International Comprehensive Ocean-Atmosphere Data Set
ICSTM	Imperial College of Science, Technology and Medicine
IGBP	International Geosphere-Biosphere Programme
IGBP-DIS	IGBP Data and Information System
IGRA	Integrated Global Radiosonde Archive
IMO	International Meteorological Organization
INDOEX	Indian Ocean Experiment
InSAR	Interferometric Synthetic Aperture Radar
IO	iodine monoxide
IOCI	Indian Ocean Climate Initiative
IOD	Indian Ocean Dipole
IOZM	Indian Ocean Zonal Mode
IPAB	International Programme for Antarctic Buoys
IPO	Inter-decadal Pacific Oscillation
IPSL	Institut Pierre Simon Laplace
IS92	IPCC Scenarios 1992
ISCCP	International Satellite Cloud Climatology Project
ITCZ	Inter-Tropical Convergence Zone
JAMSTEC	Japan Marine Science and Technology Center
JJA	June, July, August
JMA	Japan Meteorological Agency
ka	thousand years ago
KMA	Korea Meteorological Administration
KNMI	Royal Netherlands Meteorological Institute
kyr	thousand years

LASG	National Key Laboratory of Numerical Modeling for Atmospheric Sciences and Geophysical Fluid Dynamics
LBA	Large-Scale Biosphere-Atmosphere Experiment in Amazonia
LBC	lateral boundary condition
LBL	line-by-line
LGM	Last Glacial Maximum
LIG	Last Interglacial
LKS	Lanzante-Klein-Seidel
LLGHG	long-lived greenhouse gas
LLJ	Low-Level Jet
LLNL	Lawrence Livermore National Laboratory
LMD	Laboratoire de Météorologie Dynamique
LOA	Laboratoire d'Optique Atmospherique
LOSU	level of scientific understanding
LSCE	Laboratoire des Sciences du Climat et de l'Environnement
LSM	land surface model
LSW	Labrador Sea Water
LW	longwave
LWP	liquid water path
Ma	million years ago
MAM	March, April, May
MARGO	Multiproxy Approach for the Reconstruction of the Glacial Ocean surface
mb	millibar
MDI	Michelson Doppler Imager
Meteosat	European geostationary meteorological satellite
MFR	Maximum Feasible Reduction
MHT	meridional heat transport
MINOS	Mediterranean Intensive Oxidants Study
MIP	Model Intercomparison Project
MIRAGE	Megacity Impacts on Regional and Global Environments
MISO	Monsoon Intra-Seasonal Oscillation
MISR	Multi-angle Imaging Spectro-Radiometer
MJO	Madden-Julian Oscillation
MLS	Microwave Limb Sounder
MMD	Multi-Model Data set (at PCMDI)
MOC	Meridional Overturning Circulation
MODIS	Moderate Resolution Imaging Spectrometer
mol	mole
MONEX	Monsoon Experiment
MOPITT	Measurements of Pollution in the Troposphere
MOZAIC	Measurement of Ozone by Airbus In-service Aircraft
MPI	Max Planck Institute
MPIC	Max Planck Institute for Chemistry
MPLNET	Micro-Pulse Lidar Network
MRI	Meteorological Research Institute of JMA
MSLP	mean sea level pressure
MSU	Microwave Sounding Unit
Myr	million years
N_2	molecular nitrogen
N_2O	nitrous oxide
N_2O_5	dinitrogen pentoxide
NADW	North Atlantic Deep Water
NAH	North Atlantic subtropical high
NAM	Northern Annular Mode
NAMS	North American Monsoon System
NAO	North Atlantic Oscillation
NARCCAP	North American Regional Climate Change Assessment Program
NASA	National Aeronautics and Space Administration
NCAR	National Center for Atmospheric Research
NCDC	National Climatic Data Center
NCEP	National Centers for Environmental Prediction
NEAQS	New England Air Quality Study
NEP	net ecosystem production
NESDIS	National Environmental Satellite, Data and Information Service
NGRIP	North Greenland Ice Core Project
NH	Northern Hemisphere
NH_3	ammonia
NH_4^+	ammonium ion
NIES	National Institute for Environmental Studies
NIWA	National Institute of Water and Atmospheric Research
NMAT	Nighttime Marine Air Temperature

NMHC	non-methane hydrocarbon
NMVOC	non-methane volatile organic compound
NO	nitric oxide
NO_2	nitrogen dioxide
NO_3	nitrate radical
NOAA	National Oceanic and Atmospheric Administration
NO_x	reactive nitrogen oxides (the sum of NO and NO_2)
NPI	North Pacific Index
NPIW	North Pacific Intermediate Water
NPP	net primary productivity
NRA	NCEP/NCAR reanalysis
NVAP	NASA Water Vapor Project
$O(^1D)$	oxygen radical in the 1D excited state
O_2	molecular oxygen
O_3	ozone
OASIS	Ocean Atmosphere Sea Ice Soil
OCTS	Ocean Colour and Temperature Scanner
ODS	ozone-depleting substances
OECD	Organisation for Economic Co-operation and Development
OGCM	Ocean General Circulation Model
OH	hydroxyl radical
OIO	iodine dioxide
OLR	outgoing longwave radiation
OMI	Ozone Monitoring Instrument
OPAC	Optical Parameters of Aerosols and Clouds
PCMDI	Program for Climate Model Diagnosis and Intercomparison
pCO_2	partial pressure of CO_2
PDF	probability density function
PDI	Power Dissipation Index
PDO	Pacific Decadal Oscillation
PDSI	Palmer Drought Severity Index
PET	potential evapotranspiration
PETM	Palaeocene-Eocene Thermal Maximum
PFC	perfluorocarbon
Pg	petagram (10^{15} grams)
PMIP	Paleoclimate Modelling Intercomparison Project
PMOD	Physikalisch-Meteorologisches Observatorium Davos
PNA	Pacific-North American pattern
PNNL	Pacific Northwest National Laboratory
PNV	potential natural vegetation
POA	primary organic aerosol
POC	particulate organic carbon
POLDER	Polarization and Directionality of the Earth's Reflectance
POM	particulate organic matter
ppb	parts per billion
ppm	parts per million
PR	Precipitation Radar
PREC/L	Precipitation Reconstruction over Land (PREC/L)
PROVOST	Prediction of Climate Variations on Seasonal to Interannual Time Scales
PRP	Partial Radiative Perturbation
PSA	Pacific-South American pattern
PSC	polar stratospheric cloud
PSMSL	Permanent Service for Mean Sea Level
PSU	Pennsylvania State University
psu	Practical Salinity Unit
QBO	Quasi-Biennial Oscillation
RATPAC	Radiosonde Atmospheric Temperature Products for Assessing Climate
RCM	Regional Climate Model
REA	Reliability Ensemble Average
REML	restricted maximum likelihood
RF	radiative forcing
RFI	Radiative Forcing Index
RH	relative humidity
RMS	root-mean square
RSL	relative sea level
RSS	Remote Sensing Systems
RTMIP	Radiative-Transfer Model Intercomparison Project
SACZ	South Atlantic Convergence Zone
SAFARI	Southern African Regional Science Initiative
SAGE	Stratospheric Aerosol and Gas Experiment or Centre for Sustainability and the Global Environment
SAM	Southern Annular Mode or Stratospheric Aerosol Measurement

SAMS	South American Monsoon System
SAMW	Subantarctic Mode Water
SAR	Second Assessment Report or Synthetic Aperture Radar
SARB	Surface and Atmosphere Radiation Budget
SARR	Space Absolute Radiometric Reference
SAT	surface air temperature
SCA	snow-covered area
SCIAMACHY	SCanning Imaging Absorption SpectroMeter for Atmospheric CHartographY
SCM	Simple Climate Model
SeaWiFs	Sea-Viewing Wide Field-of-View Sensor
SF_6	sulphur hexafluoride
SH	Southern Hemisphere
SIO	Scripps Institution of Oceanography
SIS	Small Island States
SLE	sea level equivalent
SLP	sea level pressure
SMB	surface mass balance
SMM	Solar Maximum Mission
SMMR	Scanning Multichannel Microwave Radiometer
SO	Southern Oscillation
SO_2	sulphur dioxide
SO_4	sulphate
SOA	secondary organic aerosol
SOHO	Solar Heliospheric Observatory
SOI	Southern Oscillation Index
SOM	soil organic matter
SON	September, October, November
SORCE	Solar Radiation and Climate Experiment
SPARC	Stratospheric Processes and their Role in Climate
SPCZ	South Pacific Convergence Zone
SPM	Summary for Policymakers
SRALT	Satellite radar altimetry
SRES	Special Report on Emission Scenarios
SSM/I	Special Sensor Microwave/Imager
SST	sea surface temperature
STARDEX	STAtistical and Regional dynamical Downscaling of EXtremes for European regions
STE	stratosphere-troposphere exchange
STMW	Subtropical Mode Water
SUNY	State University of New York
Sv	Sverdrup (10^6 m^3 s^{-1})
SW	shortwave
SWE	snow water equivalent
SWH	significant wave height
T/P	TOPEX/Poseidon
T12	HIRS channel 12
T2	MSU channel 2
$T2_{LT}$	MSU lower-troposphere channel
T3	MSU channel 3
T4	MSU channel 4
TAR	Third Assessment Report
TARFOX	Tropospheric Aerosol Radiative Forcing Experiment
TBO	Tropospheric Biennial Oscillation
TCR	transient climate response
TEAP	Technology and Economic Assessment Panel
TGBM	Tide Gauge Bench Mark
TGICA	Task Group on Data and Scenario Support for Impact and Climate Analysis (IPCC)
THC	Thermohaline Circulation
THIR	Temperature Humidity Infrared Radiometer
TIM	Total Solar Irradiance Monitor
TIROS	Television InfraRed Observation Satellite
TMI	TRMM microwave imager
TOA	top of the atmosphere
TOGA	Tropical Ocean Global Atmosphere
TOM	top of the model
TOMS	Total Ozone Mapping Spectrometer
TOPEX	TOPography EXperiment
TOVS	TIROS Operational Vertical Sounder
TransCom 3	Atmospheric Tracer Transport Model Intercomparison Project
TRMM	Tropical Rainfall Measuring Mission
TSI	total solar irradiance
UAH	University of Alabama in Huntsville

UARS	Upper Atmosphere Research Satellite
UCDW	Upper Circumpolar Deep Water
UCI	University of California at Irvine
UEA	University of East Anglia
UHI	Urban Heat Island
UIO	University of Oslo
UKMO	United Kingdom Meteorological Office
ULAQ	University of L'Aquila
UMD	University of Maryland
UMI	University of Michigan
UNEP	United Nations Environment Programme
UNFCCC	United Nations Framework Convention on Climate Change
USHCN	US Historical Climatology Network
UTC	Coordinated Universal Time
UTRH	upper-tropospheric relative humidity
UV	ultraviolet
UVic	University of Victoria
VIRGO	Variability of Irradiance and Gravity Oscillations
VIRS	Visible Infrared Scanner
VOC	volatile organic compound
VOS	Voluntary Observing Ships
VRGCM	Variable-Resolution General Circulation Model
W	watt
WAIS	West Antarctic Ice Sheet
WCRP	World Climate Research Programme
WDCGG	World Data Centre for Greenhouse Gases
WGI	IPCC Working Group I
WGII	IPCC Working Group II
WGIII	IPCC Working Group III
WGMS	World Glacier Monitoring Service
WMDW	Western Mediterranean Deep Water
WMO	World Meteorological Organization
WOCE	World Ocean Circulation Experiment
WRE	Wigley, Richels and Edmonds (1996)
WWR	World Weather Records
ZIA	0°C isotherm altitude
τ_{aer}	aerosol optical depth

Regional Abbreviations used in Chapter 11

ALA	Alaska
AMZ	Amazonia
ANT	Antarctic
ARC	Arctic
CAM	Central America
CAR	Caribbean
CAS	Central Asia
CGI	East Canada, Greenland and Iceland
CNA	Central North America
EAF	East Africa
EAS	East Asia
ENA	Eastern North America
IND	Indian Ocean
MED	Mediterrranean Basin
NAS	Northern Asia
NAU	North Australia
NEU	Northern Europe
NPA	North Pacific Ocean
SAF	South Africa
SAH	Sahara
SAS	South Asia
SAU	South Australia
SEA	Southeast Asia
SEM	Southern Europe and Mediterranean
SPA	South Pacific Ocean
SSA	Southern South America
TIB	Tibetan Plateau
TNE	Tropical Northeast Atlantic
WAF	West Africa
WNA	Western North America

Index

Note: * indicates the term also appears in the Glossary (Annex I). Page numbers in italics denote tables, figures and boxed material; page numbers for boxed material are followed by B. Page numbers in bold indicate page spans for entire chapters.

8.2 ka event*, 455, 456, 463-464

A

Abrupt climate change*, 57, 106-107, 435-436, 454-457, 463-464
- defined, *775B*, 818
- modelling, 640-643
- projections, *775-777B*, 818-819

ACE index, 304, *305B*, *312B*
Advection*, 355, *356*, 528
Aerosols, 29-30, 106, 131-132, 135-136, 153-180
- aviation aerosols, 188, 561
- climatic factors, 557-558
- couplings and feedbacks, 78-79, 504, 555-566
- direct effect, 153, *154*, 159-160, 168-171, *201*, *203-204*
- direct radiative effect, 157-158
- glaciation effect, *558*, 559, 560-561
- indirect effects*, 30, 153-154, 504, *558*, 559-563, 565-566
- modelling, 159-160, 562-563, *564*, 565, 607
- natural, 555-558, *559*
- precipitation effects, 254, 560, 563, *564*
- projections, 78-79, 755-757, 760, 796-797
- radiative forcing, 29-30, 153-180, 198-200, 559
- satellite and surface-based observations, 154-159
- semi-direct effect, *154*, 555, *558*, 559, 565
- thermodynamic effect, *558*, 559
- total aerosol optical depth, *29*
- total anthropogenic effect, 562-563, *564-565*
- volcanic aerosols, 193-195, *201*, 478
- *See also specific aerosols*

Afforestation*, 528
Africa. *See* Climate projections
Air quality, 28, 79, 502, *540B*, 566-567
Aircraft/aviation, 30, 186-188
- aviation aerosols, 188, 561
- contrails/induced cloudiness, 30, 132, 186-188, *201*, *203-205*

Albedo*, 30, 110, 180-186, 508
- cloud albedo effect, 30, 132, 153-154, 171-180, *201*, *203-205*, *558*, 559-563
- cryospheric-albedo feedback, 110
- ice-albedo feedback, 97
- snow, 30, 184-185, *205*, 343
- snow-albedo feedback, 343, 638-639, 640
- surface albedo, 30, 132, 180-186, *201*, *203-205*
- surface albedo feedback, 593, 638-639

Albrecht effect. *See* Cloud lifetime effect, under Clouds
Altimetry*, 49, 361, 408, 410, 411-412, 431
Ammonia (NH_3), 544-546
Annular modes*, 38-40, 64, 112, 238-239, 286-295, *287B*, 620-621, 780-782
Antarctic Circumpolar Current (ACC), 401-402, 765
Antarctic Circumpolar Wave (ACW), 294-295
Antarctic Oscillation (AAO), *777B*, 782
Antarctic region
- climate projections, *904*, 907-909
- ice sheet (*see* Ice sheets)
- oceans, 401-402, 420
- sea ice, 342, 351, 352, 353, 355

Arctic Ocean, 398, 906
Arctic Oscillation (AO), *777B*, 780
Arctic region
- climate projections, 902-907
- sea ice, 44, *45*, 60, 317, 339, 342, 351-356, 716, *776B*, 851

Asia. *See* Climate projections
Atlantic Multi-decadal Oscillation (AMO)*, 245-246, 293-294
Atlantic Multi-decadal Variability, 623
Atlantic Ocean, 394-399
- hurricanes, 306-312
- past variability, 482
- salinity, 387, 393, 394-399, 420
- sea level change, 413
- temperature, 237, *247*, 387, *392*, 395, 398-399, 420

Atmospheric climate change, 35-43, 82, **235-336**
- circulation, 38, 280-295, *287B*, 318, 709-712, 770
- free atmosphere*, 265-280, 317, 699-701, *730*
- teleconnections, 38-40, 238, 286-295
- temperature of upper air, 36, *37*, 237, 265-271, 699-701
- *See also* Surface climate change

Atmospheric constituents, 129-234
- aerosols, 29-30, 131-132, 153-180
- chemically and radiatively important gases, 24-28, 131, 137-153, 539-555
- contrails and aircraft-induced cloudiness, 30, 132, 186-187, 186-188, *201*, *203-205*
- couplings and feedbacks, 504, 539-555
- modelling, 603
- *See also specific constituents*

Atmospheric modelling, *597-599*, 602-603, 608-613, 623, *646-647*
Attribution of climate change. *See* Detection and attribution of climate change
Australia. *See* Climate projections
Aviation. *See* Aircraft/aviation

B

Bayesian methods*, 726, 744-745, 810
Biogeochemistry, 108-110
- couplings and feedbacks (*see* Climate system couplings)
- modelling, 642-643
- oceanic, 48, 387, 389, 403-408
- projections, 789-811

Biomass burning, 29, 132, *164*, 165-167, *204*, 501-502
Black carbon*, 30, 132, 163-165, 184-185, *205*, 565, 566
- aviation-associated, 561
- projections, 760, 796

Blocking, 282, 285, 623

C

Carbon
- dissolved inorganic carbon (DIC), 387, 403-405, 408, 514, 529-530, 532
- global budget, *26*, *516*, 517-526, *522-523*, *525*
- isotopes, 139, 439, *446B*, 452, 460, 476, 519
- modelling, 618
- oceanic, 387, 403-406, 420, 528-533, *529B*
- organic, fossil fuel, 29, 132, 161-163, *204-205*
- organic, natural, 556-557
- *See also* Black carbon

Carbon cycle*, 26-27, 501, 511-539
- biological pumps, 528-530
- couplings and feedbacks, 77-80, 501, 511-539, *534*, 566
- interannual changes, 523-524, *525*
- marine, 403-406, 408, 437, 528-533, *529B*, *534*, 793
- modelling, 481, 533-539, 591, 604-605, 618
- overview, 511-517
- palaeoclimate, 437, 442, *443*, *446B*, 452, 460
- projections, 750, *777B*, 789-793, 823-825

regional fluxes, 521-523
sources and sinks, *513*, 519-521, 527-531, 604-605, *777B*
terrestrial processes and feedbacks, 526-528
top-down/bottom-up views, 521-522
Carbon dioxide (CO_2)*, 24-27, 77-80, 115, 135, 137-140, 511-515
air-sea fluxes, 403, *404*
atmospheric concentration, 24-27, 131, 137-140, *141*, *146*, 511, 515, *516*, 517
buffering (Revelle factor), 531
in carbon cycle, 501, 511-517
couplings and feedbacks, 77-80, 501, 511-539
dissolved in oceans, 387, 402-406, 408
fertilization*, 185-186, 526-527, 605
global warming potential, 211, *212*
growth rate, 26, 523-526, 790
increase in industrial era, 97, 100, 105-106, 512
palaeoclimate, 54-57, 435-437, 440-450, *446B*, 452-453, 455-456, 459-460, 465, 481
projections, 77-80, 789-811, 822-828
radiative forcing, 25, 131, 136, 137-140, *141*, 185-186, *205*, *207*, *212*
Carbon monoxide (CO), *205*, *207*, 214, 549, 793-794
Carbon tetrachloride (CCl_4), *141*, 145, 146, *212*
Carbonate (CO_3^{2-}), 77, 387, 406, *421*, 442, *443*, *446B*, 460, 530, *532*
buffer system, *529B*, 530
projections, 77, 793, *794*
Caribbean region, 909-917
Central and South America. *See* Climate projections
Chlorofluorocarbons (CFCs), 28, 100, 105-106, *141*, 145, *146*
CFC-11, 28, 100, 145, 420
industrial era increase, 512, *513*
as oceanic tracers, 100, 404, 406, 420
radiative forcing, 131, *141*, *207*, *212*
Circulation
atmospheric, 38, 64, 238-239, 280-295, 318, 565-566, 709-712, *731*, 770
indices, *287B*, 294-295
modelling, 615-616
oceanic, 48, 111-112, 387, 394-402, 417, 420
projections, 770, *777B*, 780-782
Climate*
defined, 104
factors determining, 96-97
human and natural drivers, summarized, 21-35, 81
weather and, 104-105
Climate change*, 35-58, 663-746
atmospheric (*see* Atmospheric climate change)
commitment (*see* Climate change commitment)
concept, 667-670, 678
consistency across observations, 51-54, 239, 317-318
cryospheric (*see* Snow, ice and frozen ground)
current, compared to palaeoclimate changes, 436-437, 465
defined, 667
detection and attribution (*see* Detection and attribution of climate change)
irreversible, *775-777B*
last 1,000 years, 680-683
last 2,000 years, 436, 466-483, *468-469B*
long-term, 822-831
mechanisms, 96, 449
observations, summarized, 35-58
oceanic (*see* Oceanic climate change)
relationship to weather, 104-105
robust findings and key uncertainties, 81-91
surface (*see* Surface climate change)
variability (*see* Climate variability)
See also Climate change science
Climate change commitment*, 68-69, *68B*, *78*, 79-80, 749, 753, 761, 822-831
commitment to year 2300, 822-827
commitment to year 3000 and beyond, 823-827
constant composition commitment scenarios, 753, 822-823
constant emission commitment scenarios, 822
overshoot scenarios, 753, 827-828
sea level, 68, 80, 752, 822, 828-831
stabilisation scenarios, 753, 791-793
temperature, 79, 752, 822-828
zero emission commitment scenarios, 753, 822, 825
Climate change science, 93-127
IPCC history and assessments, 95, 118-121
nature of earth science, 95-99
progress in climate modelling, 112-118
progress in detection and attribution, 100-103
progress in understanding climate processes, 103-112
Climate feedbacks*. *See* Feedbacks
Climate forcing. *See* Radiative forcing
Climate models*, 589-662, 669-670
abrupt climate change, 640-643
advances in, 112-118, 591-593, 596-608
Atmosphere-Ocean General Circulation Models (AOGCMs), *59-60B*, 66-67, 591-592, 596-608, *761*, 797-831, 852-861, 918
Atmosphere-only GCMs (AGCMs), 918-919
C^4MIP, 533-539, 618, 789-790
changes in performance, 618-619
climate sensitivity and feedbacks, 592, 629-640
climate variability, 591, 592, 620-627
confidence in, 591, 600-601, 639-640, 668
construction of, 596
contemporary climate, 608-619
coupled models, 117-118, 481, 532-539, 607, 608-627
downscaling*, *74*, 601, 865, 919-921, 925
Earth System Models of Intermediate Complexity (EMICs), 67, 77, *78*, 591-592, 643-645, *646-647*, 797, 801-802, 823-827, 828
evaluation, 87, 591, 594-596
evolution, 98, *99*, 112-114
extremes, 627-629
flux adjustments*, 117, 591, *597-599*, 607-608, *646-647*
General Circulation Models (GCMs), 114-116, 208, 629-633, 925
hierarchies, *67*, 112-114, 797-800
initialisation, 607-608
intercomparison, 510
large-scale variability, 591-592, 620-627
multi-model data set (MMD), *597-599*, 753-754, *858-860B*
nested regional climate models, 919
resolution, 113-114, 591, 797-800
shorter-term predictions, 626-627
simple climate models, 643-647, 797, 802-804, 844
thresholds, 640-643
See also specific topics and processes
Climate predictions*, 626-627, 643
See also Climate projections
Climate projections*, 66-80, 87-91, **747-940**
about, 753-754, 852-865
Africa, 850, *854*, 866-872
Asia, 850, *855*, 879-887
Australia and New Zealand, 850, *856*, 896-902, *916B*
biogeochemical feedbacks, 77-79, 789-811
Central and South America, 850, *856*, 892-896
change in the 21st century, 69-76, 764-766
emissions, concentrations and radiative forcing, *25*, 755-760
ensemble projections*, 754, 755-760, 766-767, 805-811, 852-861
Europe and the Mediterranean, 850, *854*, 872-879, *917B*
extremes, 782-789, *854-857*, *862-864*, *916-917B*
global projections, 69-74, 89, **747-845**
greenhouse gases, *25*, 755-760
hierarchy of models, 797-800
islands, small, 850, *857*, 909-915

long term change and commitment, 79-80, 749, 822-831
methods, 844-845, 917-925
North America, 850, *855-856*, 887-892
ocean acidification, 793, *794-795*
physical climate system, 760-789
polar regions, 850, *857*, 902-909
probabilistic projections, 807-809, 810-811, 921-925
quantifying, 797-811, 921-925
range of projections, 797-811
regional projections, 74-76, 91, **847-940**
sea level, 68, 70-71, 73, 90, 774, 812-822, *823*, 828-831, 844-845, 909, 914-915, *916-917B*
summary, 749-752, 849-851, *858-860B*
temperature, 69-72, 74-76, 762, *763*, 764-766
uncertainty, 797-800, 805-811

Climate scenarios*, 753, 791-793, 802-804, 822-831
See also SRES scenarios

Climate sensitivity*, 64-66, 88, 114-116, 754, 825-827
climate models, 593, 629-640, *632B*
cumulative distributions, *65*
defined, 629-630
equilibrium climate sensitivity (ECS), 64-65, 88, 718-727, 754, *798-799B*, 825-827
estimation methods, 718-719
instrumental observations, 719-723
key physical processes, 633-637
observational constraints, 718-727, 807-808
palaeoclimate data, 481, 724-725
probability density functions (PDFs), 65, 719-721, 724-725, *798-799B*, 808-809, 923-924
transient climate response (TCR), 66, 88, 691, 718, 723, *724*, 725, 754, *798B*, 800-801, 807

'Climate surprises', *775-777B*

Climate system*, 96-97

Climate system couplings, 77-80, **499-587**, 789-811
aerosols, 78-79, 502, 555-566
atmosphere dynamics, 504, 555
carbon cycle, 77, 501, 511-539, 566
land climate system, 504-511, *505B*
land surface, 501
modelling, *597-599*, 629-640, *646-647*, 754, 765
projections, 77-80, 789-811
reactive gases, 501-502, 539-555, *540B*
scales, 505-507, 566

Climate variability*, 667, 668-669, 702-703, 864
modelling, 591-592, 620-627, 686
modes of*, 286-295, *287B*, 463, 667-668, 778-782, *867B*
patterns of*, 38-40, *39B*, *867B*

Clouds, 40-41, 97, 238, 275-277
aerosol effects, 30, 153-154, *558*, 559-564, 565, 566, 676-677
aviation-induced cloudiness, 30, 132, 186-188, *201*, *203-205*
cloud albedo effect, 30, 153-154, 171-180, *201*, *203-205*, *558*, 559-563
cloud condensation nuclei (CCN)*, *154*, 171, 504, 555, 559
cloud lifetime effect, 153, *154*, 171, 555, *558*, 559-560, 563
couplings and feedbacks, 502, *558*, 559-563, 635-638, 640
modelling, 114-116, 593, 635-638, 640
projections, 766-768
radiative forcing (CRF)*, 173-178, 180, 502, 635, 637-638, 767-768

Coastal zone climate change, *916-917B*

Cold Ocean-Warm Land (COWL) pattern, 622-623

Commitment. *See* Climate change commitment

Confidence*, *22-23B*, 81-91, *120-121B*

Contrails, 30, 132, 186-187, *201*, *203-205*

Cosmic rays, 31, 132, *202*, 476

Coupled models, 117-118, 481, 532-539, 607, 608-627

Couplings. *See* Climate system couplings

Cryosphere*, 43-46, 110, **337-383**, 716-717, *732*
area, volume, and sea level equivalents, 340, *342*, 361, *374*
components, 341-343
feedbacks, 110, 593, 638-639
modelling, 111, 593, 606-607, 638-639
See also Snow, ice and frozen ground

Cyclones
extratropical, 312-313, 316, 712, 788-789
modelling, 591, 613, 628
projections, 74, 751, 786-788, *864*, 915
tropical, 41-43, 239, 304-307, *305B*, *314*, 316, 711-712, 751, 786-788, *864*, 915

D

Dansgaard-Oeschger (DO) events*, 106-107, 111, 455, 456-457

Deforestation*, 512, 517-518, 520-521, 527-528

Detection and attribution of climate change*, *52*, 58-66, 81-86, 135-136, **663-746**
carbon cycle perturbations, 512-515
greenhouse gas increase, 60, 501-502, 512-513
industrial era, air temperature, 683-705, 727, *729-730*
industrial era, other variables, 705-718, *730-732*
introduction/concepts, 667-670
observational constraints, 718-727
observations, summarized, 35-58
pre-industrial, 673, 679-683
progress in, 100-103
radiative forcing and climate response, 31, 131, 670-679
robust findings and key uncertainties, 81-91
statistical methods, 744-745
variability, 667, 668-669, 702-703
See also Palaeoclimate

Dimethyl sulphide (DMS), 78, 557

Dimethylether (CH_3OCH_3), *213*

Dimming. *See* 'Global dimming'

Diurnal temperature range (DTR). *See* Temperature

Downscaling*, *74*, 601, 865, 919-921, 925

Droughts*, 254, 260-265, *261B*, 308, *310-311B*, *315*, 715-716
defined, *314*
palaeoclimate, 435, 437, 482-483
projections, *732*, 750, 783, *859B*, *863*
summary, 43, 54, 238, 317, 318, 435

Dust, 29, 78, 159, 502, 555-556, 797
mineral dust aerosol, 29, 132, 167-168, *204-205*

E

El Niño. *See* El Niño Southern Oscillation

El Niño Southern Oscillation (ENSO)*, 111-112, 245-246, 287-288, 295, 709
cyclones and, 305-306, *305B*, 308
modelling, 592, 601, 623-625
monsoons and, 296-297, *305B*, 780
palaeoclimate, 437, 464, 481-482
projections, 751, 779-780
summary, 38, *39B*, 238

Emissions scenarios*. *See* SRES scenarios

Energy balance*
changes, 392-393, 727-728
mean, 96-97
modelling, 608
radiation, 277-280
surface energy and water balance, 35, *505B*
surface energy budget, 180-186

Equilibrium climate sensitivity (ECS), 64-65, 88, 718-727, 754, *798-799B*, 825-827

Europe and the Mediterranean. *See* Climate projections

Evapotranspiration*, 238, 260, *261B*, *279B*, 507, 769

Extreme events*, 299-316, 696
extratropical storms, 312-313, *314-315*, 316
modelling, 300-303, 627-629
precipitation, 41, 301-303, 308, *314-315*, 316, 714, 782-784, *785*
projections, *52*, 73, 750, 782-789, 849-851, *854-857*, *862-864*, *916-917B*
recent events, *310-311B*

regional (*see* Climate projections)
sea level, 51, 414, *916-917B*
severe local weather, 316
summary, 40, 41, 51, *52*, *53B*, 237, 591
temperature, 40, 237, 300-301, *302*, 308-309, *311-312B*, *314-315*, 316, 698-699, 750, 785-786, *787*
tropical storms, 304-312, *305B*, *314-315*, 316

F

Faculae*, 107, 108, 188, 189, *190*
FAQs
Are extreme events, like heat waves, droughts or floods, expected to change as the Earth's climate changes?, 783
Are the increases in atmospheric carbon dioxide and other greenhouse gases during the industrial era caused by human activities?, 512-513
Can individual extreme events be explained by greenhouse warming?, 696
Can the warming of the 20th century be explained by natural variability?, 702-703
Do projected changes in climate vary from region to region?, 865
Has there been a change in extreme events like heat waves, droughts, floods and hurricanes?, 308-309
How are temperatures on Earth changing?, 252-253
How do human activities contribute to climate change?, 135-136
How is precipitation changing?, 262-263
How likely are major or abrupt climate changes, such as loss of ice sheets or changes in global ocean circulation?, 818-819
How reliable are the models used to make projections of future climate change?, 600-601
If emissions of greenhouse gases are reduced, how quickly do their concentrations in the atmosphere decrease?, 824-825
Is sea level rising?, 409
Is the amount of snow and ice on the Earth decreasing?, 376-377
Is the current climate change unusual compared to earlier changes in Earth's history?, 465
What caused the ice ages and pre-industrial climate changes?, 449-450
What factors determine Earth's climate?, 96-97
What is radiative forcing?, 136
What is the greenhouse effect?, 115-116
What is the relationship between climate change and weather?, 104-105
Feedbacks*, 77-80, 97, **499-587**
carbon cycle, 501, 511-539, *534*, 566, 789-793, 823-825
climate-vegetation, 452, 789-793
cryospheric, 110, 593, 638-639
modelling, 593, 605-606, 629-640, *632B*
permafrost-climate, 110
projections, 77-80, 789-811
snow-albedo, 343, 593, 638-639, 640
water vapour, 593, 630-633, *632B*
water vapour-lapse rate, 633-635, 640
See also Climate system couplings
Fingerprints*, 100, 668
Fires, 501, 527
Floods, *311B*, 783, 784
Fluorinated ethers (HFEs), *213*
Forcing. *See* Radiative forcing
Forests*, 517-518, 520-521, 527-528
Fossil fuel emissions*, 25-29, 138-140, 145, 160-165, *204-205*, 511-518, *546*
Frequently Asked Questions. *See* FAQs
Frozen ground*, 43-44, 340, *341*, 342-343, 369-374, *375*, 376, 772

G

General Circulation Models (GCMs). *See* Climate models
Geopotential height, 280-281, 285
Glacial-interglacial cycles. *See* Palaeoclimate
Glacial isostatic adjustment (GIA)*, 408, 411, 417, 457
Glaciers*, *341*, 342, 356-360, 368, 717
mass balance*, 357-359, 814-816, 844
monitoring, 110
palaeoclimate, 57, 436, *461B*
projections, *776B*, 814-816, 844-845
sea level rise and, 44, *358*, 359, 375, 418, *419*, 814-816, 829
summary, 44, 57, 339, 375, 376, 436
'Global dimming'*, 41, 238, 278-280, *279B*, 317
Global temperature potential (GTP), 215-216
Global warming potentials (GWPs)*, 31, *33-34*, 137, 210-216
Greenhouse effect, 103-106, 115-116, 696
Greenhouse gases (GHGs)*, 23-35, 100, 131, 135-153, 200-206, 512-513
couplings and feedbacks, 501-502, 539-555, *540B*
lifetimes, *212-213*, 824-825
long-lived (LLGHGs), 31-35, 133, 137-153, 198, *201*, *203-204*
palaeoclimate, 435, 436, 440-450, *446B*, 455, 459-460, 481
projections, *753*, 755-760, 789-811, 822-828
radiative forcing, 31-35, 131, 135-136, 153, *203-204*, *212-213*
See also specific gases
Greenland ice sheet. *See* Ice sheets

H

Hadley Circulation*, 295-296, 299, 318
Halocarbons*, 28, 100, 135, *141*, *145*, *205*, 214-215, 512, *513*
Halons, 100, 145, *207*
Heat balance. *See* Energy balance
Heat waves, 40, 73, 308, *311-312B*, *314*, 783
Heinrich events, 455, 456
Holocene. *See* Palaeoclimate
Human influence on climate. *See* Detection and attribution of climate change
Hurricanes, 239, 304, *305B*, 306-312, *312B*, *314*, 316
projections, 750, *864*
See also Cyclones
Hydrochlorofluorocarbons (HCFCs), 28
industrial era increase, 512, *513*
radiative forcing, 131, *141*, 145, 146, *205*, *207*, *212*
Hydrofluorocarbons (HFCs), 100, *141*, 144-145, *146*, *205*
industrial era increase, 512, *513*
summary, 28, 131, *212*
Hydrogen (H_2), 215, 547, *548*
Hydrology. *See* Water
Hydroxyl radical (OH), 131, 147-149, *205*, 502, 550-553, 795, 796

I

Ice, 44-46, 339-343, 346-369, 374-377
flow, 44-45, 342, *367B*, 368
land ice, 354, 418, 419
mass balance*, 357-359, 374-375
pack ice, 342, 353, 355, *356*
river and lake ice, 44, 339, *341*, 342, 346-349, *375*
sea ice (*see* Sea ice)
See also Glaciers; Ice caps; Ice sheets; Ice shelves; Ice streams
Ice ages*, *56B*, 449-450, 453, 641, *776B*
Ice-albedo feedback, 97
Ice caps*, 44, *341*, 356-360, *776B*, 814-816
projection methods, 844-845
sea level change and, 342, *374*, 829
summary, 339, 375-376
Ice cores*, *24*, 54-57, 106, 439, 444, *446B*, 476
Ice nuclei, 171, 188, 502, 555, 559
Ice sheets*, 341-342, 361-369, 717
Antarctic, 46, 341, 342, 361, 364-366, *374*, 375, 376, *776-777B*, 816-820, *821*, 830-831
causes of changes, 366-369, *367B*
dynamics and stability, *44B*, 46, *367B*, 845

Greenland, 46, 70, 341, 342, 361, 363-364, 365-366, *374*, 375, 376, 418, *419*, 772, *776-777B*, 816-820, *821*, 829-830
mass balance*, 80, 361-366, 772, 816-817, 845
modelling, 592, 641-642, *646-647*
palaeoclimate, *367B*, 456-457, 459
projections, 70-71, 80, 772, *776-777B*, 816-820, *821*, 829-831, 845
sea level equivalents, 342, *342*, 361, *374*
sea level rise and, 46, 339, 361, 366, *367B*, 375, 418, 419, 457, 459
summary, 44-46, 339, 340, 374-375
Ice shelves*, *341-342*, 361-362, 366, 369, 717
Larsen B Ice Shelf, 45, 317, 366, 374, *776B*, 819
projections, *776-777B*, 819-820
summary, *341-342*, 374, *375*
Ice streams*, 361, 362, 366, *367B*, 368, 374
Indian Ocean, 400-401
Indian Ocean Dipole (IOD), 295
projections, 910, 911, *914*
salinity, 393, *394*
temperature, 237, 246, 295, 400-401, 420
Insolation*, 436, *445B*, 453, 460, 462, 464, 673
Inter-Tropical Convergence Zone (ITCZ)*, 295, 566, 624
Iodine compounds, 557
Islands, small. *See* Climate projections

J

Jet streams, 280-281, 285

K

Kyoto Protocol gases, 28, 131, *141*, 143-145, 512

L

La Niña. *See* El Niño Southern Oscillation
Labrador Sea, 285, 393, 396, *397B*, 416-417, *776B*
Lake ice, 44, 339, *341*, 342, 346-349, *375*
Land climate system, 504-511, *505B*
modelling, *597-599*, 617-618, *646-647*
Land ice, 354, 418, 419
Land surface air temperature*. *See* Temperature
Land use change*, 180-184, *205*, 243-245, 512, *513*, 526-528, *897-898B*
carbon budget, *516*, 517-518, 527-528
climate projections, 792-793
emissions from, 518
land cover, 30, 136-137, 180-182, *183*, 509, 682-683, 792-793, *897-898B*
land water storage, 126-127, 317, *413*, 418-419
urban effects, 30, 36, 243-245, 259, *506B*
Last Glacial Maximum (LGM)*, 58, 435, 447-451, 673, 679-680, 725, *798-799B*
Latent heat, 97, *393*, 399
Likelihood*. *See* Uncertainties
LOSU (level of scientific understanding)*, *22B*, *201-202*
Low-pass filters, 336

M

Madden-Julian Oscillation (MJO), 592, 601, 625
'Medieval Warm Period'*, 466, *468-469B*
Mediterranean Sea, 399
Meridional heat transport (MHT), 394, 429-430
Meridional Overturning Circulation (MOC)*, 48, 111, 395-397, *397B*, 421, 514, 707
modelling, 603-604, 615-616, 640-642
projections, 72, 80, 752, 772-774, *775-776B*, 801-802, 818, *823*
Methane (CH_4), 27, 77-78, 100, 135, 140-143, 513
atmospheric concentration, *24-25*, 27, 131, 140-143, 146, 501-502, 511-514
atmospheric growth rate, 135, 142-143, 502
couplings and feedbacks, 77-78, 539-544
modelling, 642
palaeoclimate, 435, *444*, 447, *448*, 455, 459-460
permafrost, 642
projections, 502, 793-795, 796
radiative forcing, *25*, 27, 131, 140-143, *205*, *207*, *212*, 214
Methane hydrate, 642
Methyl chloroform (CH_3CCl_3), *141*, 145-146, 147-149, *212*
Methylene chloride (CH_2CH_2), *141*, 145, *213*
Microwave Sounding Unit. *See* MSU (Microwave Sounding Unit)
Mid-latitude circulation, 780-782
Mid-latitude storms, 751
See also Cyclones, extratropical
Milankovitch cycles, *56B*, *445B*, 449
Mineral dust aerosol, 29, 132, 167-168, *204-205*
Mitigation, 753, 827-828
Models. *See* Climate models
Monsoons*, 295-299, 318, 711, 716
modelling, 626
palaeoclimate, 435, 462-463, 464, 482
projections, 751, 778-779, 780
Montreal Protocol gases, 28, 131, *141*, 145-146, 512
Mountain regions, *886B*
MSU (Microwave Sounding Unit)*, 36, 237, *266*, 267-268
Mt. Pinatubo, 98, 109, 142, 193-194, 723
Multi-model data set (MMD), *597-599*, 753-754, *858-860B*

N

Natural climate forcing. *See* Radiative forcing
New Zealand. *See* Climate projections
Nitrate aerosol, 132, 167, *204-205*
Nitric oxides (NO_x), 214, *215*, 544-546, 793-795
Nitrogen compounds, 502, 544-546, *547*
Nitrous oxide (N_2O), 100, 105-106, 115, 135, 143-144, 513
atmospheric concentration, *24-25*, 27, 131, *141*, 143-144, 146, 544
couplings and feedbacks, 544-546, *547*
global budget, 544-546
palaeoclimate, *444*, 447, *448*, 455, 460
radiative forcing, *25*, 27, 131, *141*, *205*, *212*, 214
Non-methane volatile organic compounds (NMVOCs), 214, *215*, 549
Nordic Seas, 396-398
North America. *See* Climate projections
North Atlantic Deep Water (NADW), *395*, 396-398, *421*, 437, 456, 642
North Atlantic Ocean, 394-399, *395*, *397B*, 402, 413, 482
North Atlantic Oscillation (NAO)*, 290-292, 395-399, 402, 408
changes, 238-239, 248, 290-292, 709-710
modelling, 620
past variability, 482
projections, *777B*, 780-781, 806
summary, 38, *39B*, 238-239
teleconnections, *286*, 290-292, 295
North Pacific Index (NPI), *287B*, 289, *290*
Northern Annular Mode (NAM)*, 248, *287B*, 389, 397, 709-710
modelling, 620-621
projections, 780-782
summary, 38, *39B*, 238-239
teleconnections, 290-292, 295

O

Ocean-climate couplings, 501, 503, 519, 521-523, 528-533, *529B*
Ocean precipitation, 259-260
Ocean processes, modelling, 535-538, *597-599*, 603-604, 613-616, 622-623, *646-647*
Oceanic climate change, 385-433, 705-707, *731*
acidification*, 77, 387, 403, 405-406, 408, *529B*, 531, 750, 793, *794-795*
air-sea fluxes, 283-285, 393-394, 403, 408
biogeochemistry, 48, 387, 389, 403-408, 503

biological activity (productivity), 408
carbon/carbon dioxide, 387, 403-406, 408, 420, 793
circulation, 48, 111-112, 387, 394-402, *397B*, 417, 420
coupled ocean-atmospheric dynamics, 111-112, 286-295, 318
decadal variability, 389, 412-413
density, 414-416, 812-814
heat content, 47-48, 387, 389, 390-393, 420, 705-706
heat transports, 393-394, 429-430
nutrients, 406-407
oxygen, 48, 403, 406, *407*, 408, 430
projections, 750-751, 765, 793, *794-795*, 801, 812-822, 822
salinity, 48, *49*, 318, 387, 389-390, 393, 394-402
salinity measurement, 390, 420, 429
sea level, 48-50, *51B*, 387, 408-421, 431, *432*, 707-708, 750-751, 812-822
summary, 47-51, 84, 387-388, 420-421
techniques, error estimation and measurement systems, 429-432
temperature, 61, *62*, 387, 389-393, 394-402, *420*
temperature measurement, 389-390, 429, *430*
thermal expansion*, 387, 408, *412-413*, 414-417, 419-420, 801, 812, 820-821
water masses, 387, 394-402, 417-419, 706-707
See also specific oceans

OH. *See* Hydroxyl radical (OH)
Optimal fingerprinting, 744
Orbital forcing, *56B*, 437, *445B*, 453, 462-463
Oxygen (O_2)
atmospheric, 139
dissolved in oceans, 48, 403, 406, *407*, 408, 430
Ozone*, 115, 135, 149-152, *540B*, 547-550
global budgets, 547-549
precursors, 547-550, 795
projections, 554, 759-760, 793-796
radiative forcing, 28, 132, 149-152, *203-204*, 759
stratospheric, 28, 73, 149-150, 198, *201*, *203-205*, 553-555
tropospheric, 28, 108-110, 150-152, *201*, *203-205*, 513, 547-550

P

Pacific Decadal Oscillation (PDO), 246, 289-290, 295, 389, 408, 709
index, *287B*
modelling, 621
summary, 38, *39B*, 238
Pacific Decadal Variability*, 289-290, 621
Pacific-North American (PNA) pattern*, 286, *286*, *287B*, 288-289, 295
modelling, 622
summary, 38-40, *39B*
Pacific Ocean, 399-400
cyclones, 306, 307
projections, 399-400, 910-911, *915*
salinity, 387, 394-395, 399-400, 402, 420
sea level change, 413-414, 420
temperature, 237, *247*, 399-400, 402, 420
Pacific-South American (PSA) pattern, 288-289, 295
Palaeoclimate*, 54-58, 85, 106-107, **433-497**, 679-683
attribution studies, 64, *446B*, 460
current interglacial (Holocene), 57, 435-436, 453-454, 459-464, *461B*, 679-680
glacial-interglacial variability, 435, 444-459
ice sheets, *367B*, 456-457, 459
last 2,000 years, 436, 466-483, *468-469B*
Last Glacial Maximum (LGM)*, 58, 435, 447-451, 673, 679-680, 725, *798-799B*
Last Interglaciation (LIG), 453, *454*, 458-459
'Medieval Warm Period'*, 466, *468-469B*
methods, 438-440
modelling, 435, 436-437, 439-440, 476-481
orbital forcing, 437, *445B*, 453, 462-463
pre-quaternary climates, 440-444, *441*
sea level, 58, 435, 457-459
uncertainties, 483
Perfluorocarbons (PFCs), 28, 100, 131, *141*, 144, 145, *207*, *212-213*
Permafrost*, *341*, 342-343, 369-372, *373*, 376
permafrost-climate feedback, 110
projections, 772
summary, 43-44, 317, 339, *375*
pH* of oceans, 77, 387, 403, 405-406, 408, *529B*, 531
projections, 750, 793, *794-795*
Photosynthesis*, 186, 514, 527
Plankton*, 439, 504, 514, *529B*, 567
Plant physiology, 185-186
Pleistocene*, 447, 457
PNA. *See* Pacific-North American (PNA) pattern
Polar regions. *See* Climate projections
Pollen analysis*, 439, 455, 471
Pre-quaternary climates*, 440-444, *441*
Precipitation, 254-265, 712-716, *731-732*
aerosol effects, 254, 502, 560, 563, *564*
couplings and feedbacks, 507, 508, 509-510
extreme events, 41, 301-303, 308, *314-315*, 316, 714, 750, 782-784, *785*, *863*
modelling, 611-612, 628
monsoons (*see* Monsoons)
projections, 74, 75-77, 750, 762-763, 768-770, 782-784, *785*, 806, 849-851, *854-857*, *859B*, *863*
regional (*see* Climate projections)
summary, 41-43, 53-54, 238, 317-318
Predictions. *See* Climate predictions
Pressure. *See* Sea level pressure
Probability density functions (PDFs)*, 65, 719-721, 724-725, *798-799B*, 808-809, 923-924
Projections. *See* Climate projections
Proxy methods*, 438-439, 466-475, 481
PRUDENCE project, *873B*, 925

Q

Quasi-Biennial Oscillation (QBO), 266, 283, 625-626

R

Radiation, 277-280, *279B*, 317
couplings and feedbacks, 502, *505B*, 508, 563-564, *565*, 631
modelling, 610-611, 631
Radiative forcing (RF)*, 108-110, **129-234**
aerosols, 29-30, 131-132, 153-180, 559
calculation methodologies, 134, 196-197, 199
chemically and radiatively important gases, 24-28, 131, 137-153
climate response, 64-66, 670-679
concept, 133-137, *136-137B*, 826
contrails and aircraft-induced cloudiness, 132, 186-188
defined, 133
efficacies*, 197-199, *212-213*
external*, 96, 133-134, 152, 667
future impact of current emissions, 77, 206-207
global mean, 31-35, 132, 200-206
global warming potentials and emission metrics, 31, *33-34*, 137, 210-216
modelling, 173-180, 594-596, 607-608, 629-633, 643, 671-673
natural forcings, 96, 137, 188-195, *445B*, 666
orbital forcing, *56B*, 437, *445B*, 453, 462-463
palaeoclimate, 438-439, 444-454, *445B*, 476-481
projections, 752, 755-760, 795, 797
spatial and temporal patterns, 35, 132, 196, 209-210, 674-678
summary, 24-35, 131-132, 199-210
surface albedo and surface energy budget, 132, 180-186, *201*, *203-205*
surface forcing, 35, 133, 153, *170*, 196, 208-210
time evolution, 208-209

uncertainties, 199-200, *201-202*
utility of, 195-199
vertical forcing, 196
See also specific gases and components
Radiosondes, 36, 82, 265-267, 719
Rapid climate change. *See* Abrupt climate change
Regional changes
ocean circulation and water masses, 394-402
projections (*see* Climate projections)
sea level, 413-414
Revelle factor, 531
River and lake ice, 44, 339, *341*, 342, 346-349, *375*
River flow (streamflow), 261-264
River ice, 44, 339, *341*, 342, 346-349, *375*

S

Salinity (of oceans), 48, *49*, 318, 387, 393, 394-402, 420, *421*
measurement, 390, 420, 429
modelling, 613-615
sea level/ocean mass and, 416-417, 417-418
Satellite methods
altimetry, 49, 408, 410, 411-412, *411*, 431
Microwave Sounding Unit (MSU), 36, 237, *266*, 267-268
Scenarios. *See* Climate scenarios; SRES scenarios
Science, climate. *See* Climate change science
Scientific method, 95
Scientific understanding. *See* LOSU (level of scientific understanding)
Sea ice*, *341*, 342, 350-356, 376, 716
Antarctic, 342, 351, 352, 353, 355
Arctic, 44, *45*, 60, 317, 339, 342, 351-356, 716, *776B*, 851
feedbacks, 639
modelling, 592, *597-599*, 606-607, 616-617, 639, *646-647*
projections, 770, *771*, *776B*
summary, 317, 339, 374, *375*
Sea level, 48-50, *51B*, 408-421
attribution for changes, 60-61
budget (global mean sea level change), 48-50, 419-420, 457
change in 20th century (rise), 317, 389, 410-414, *415*, 418-419, *420*, 707-708
change in previous millenia, 58, 409, 435, 457-459
changes projected (*see* projections, below)
commitment, 68, 80, 752, 822, 828-831
contributions to, 44-46, *50*, 60-61, 366, *374*, 375, 408, *413*, 414-420, 751, 812-822
estimation/measurement techniques, 408, 410-412, 431, *432*
extremes, 50, 414, *916-917B*
interannual/decadal variability, *410*, 412-414, 707-708
long-term changes, 412-413
methods of projections, 844-845
palaeoclimate, 58, 409, 435, 457-459
projections, 68, 70-71, 73, 90, 409, 750-751, 812-822, *823*, 909, 914-915, *916-917B*
relative (RSL)*, 413, 457-458
sea level equivalents (SLEs)*, 340, *342*, 361, *374*
summary, 48-50, *51B*, 52-53, 84, 90, 374-375, 387, 420-421
Sea level pressure (SLP), 63, 280, 711
projections, 73, 751, 770, 780-781
Sea salt, 556
Sea surface temperature (SST)*, *101*, 102, 245-247, *312B*, 391
palaeoclimate, *451*, 460
projections, 73, 786-788, 861
rates of warming, 318
summary, 51, 64, 237, 318
tropical cyclones and, 239
Severe weather. *See* Extreme events
Snow, ice and frozen ground, 337-383, 716-717
area, volume, and sea level equivalents, *342*, *374*
frozen ground, 340, *341*, 342-343, 369-374, 376
glaciers and ice caps, 339, *341*, 342, 356-360, *374*, 375, 376, 717
ice sheets and ice shelves, 339-341, *342*, 361-369, *367B*, 374-375, 376, 717
modelling, 592, 593, *599-601*, 606-607, 616-617, 617
projections, 70-71, 73, 80, 750, 770-772, *776B*, 814-816, *859B*, 861
regional projections (*see* Climate projections)
river and lake ice, 339, *341*, 342, 346-349, *375*
sea ice, *341*, 342, 350-356, 374, *375*, 376, 716
snow albedo, 30, 132, 184-185, *205*, 343, 638-639, 640
snow cover, 317, *341*, 342, 343-346, *375*, 376-377, 593, 716-717
snowfall, 258-259
summary, 43-46, 83, 339-340, 374-375
Soil moisture*, 260-265, 509, *510*, 605-606, *769*, 770
Solar forcing, 30-31, 476-478, *479*
Solar irradiance, 30-31, 681-682
'global dimming'*, 238, 278-280, 317
palaeoclimate, 476-478, *479*
total (TSI), 30, 107-108, 132, 188-189, *190*, 198, *201*, *203-205*
Solar variability, 107-108, 188-193
Soot*, 30, 172-173, 184, 559
See also Black carbon
South Atlantic Convergence Zone (SACZ), 295
South Pacific Convergence Zone (SPCZ), 295
Southern Annular Mode (SAM)*, *287B*, 292-293, 295, 389, 710-711
modelling, 620-621
projections, 782
summary, 38, *39B*, 238-239
Southern Ocean, 387, 401-402, 420
modelling, 591, 592, 616
Southern Oscillation. *See* El Niño Southern Oscillation
Southern Oscillation Index (SOI), *287B*
SRES scenarios*, 24-31, 761, 802, 806, 822-827, 852-861, *858-860B*
sea level rise, 68, 70-71, 409, 419, 750-751, 820-822
subset for projections, 753, 761
surface warming, 68-73, 74-77, *79*
Storm tracks*, 281-282, 285, *305B*, 318
Stratosphere*, 265-266, 283
aerosols, 132
ozone, 28, 73, 149-150, 198, *201*, *203-205*, 553-555
stratosphere-troposphere exchange (STE), 795-796
stratospheric-tropospheric relations, *284B*, 795-796
temperature, 36, 62, 237-238, 265-271, 285
water vapour, 274-275
Streamflow. *See* River flow
Sulphate aerosols, 160-161, 193, *194*
couplings and feedbacks, 78-79, 502, 566-567
palaeoclimate, 436, 478, *480*
radiative forcing, 31, 108-110, 160-161, *162*, *204-205*
summary, 31, 132
Sulphur hexafluoride (SF_6), *141*, 144, 145, *146*, *207*
summary, 28, 131, *212*
Sunspots*, 107, 108, 189, *191*, 476
Surface climate change, 82, **235-336**
extreme events, 237, 299-316
modelling, 604-606, *646-647*
precipitation, drought and surface hydrology, 238, 254-265, 301-303, 308, 317, 318
surface fluxes, 283-285, 393-394, 403, 408
temperature, 237, 239, 241-253, 300-301, 308-309, 317, 318
tropics, subtropics, and monsoons, 295-299, 304-315
See also Atmospheric climate change
Surface/surface air temperature*. *See* Temperature

T

Teleconnections*, 38-40, 238, 281, 286-295, *287B*
Temperature, 100-102, 241-253, 683-705
attribution of changes, 58-63
continental temperature change, *61*, 62-63, 74-76, 693-698, 852-862
diurnal temperature range (DTR)*, 36, 237, 243-244, 251, 766-768, 786
extremes, 40, 237, 300-301, *302*, 308-309, *311-312B*, *314-315*, 627-628, 698-699, 750, 785-786, *787*, *862*
free atmosphere, 699-701
global ground surface temperature (GST), 474
global mean surface temperature, 36, *37*, *62*, 237, 247-248, *249*, 252-253, 318, 683-693, *703*, 749
global temperature potential, 215-216
global warming potentials, 31, *33-34*, 137, 210-216
industrial era change, 683-705, 727, *729-730*
last 2,000 years, 435-436, 466-483, *468-469B*
measurement, 100-102, 102, 389-390, 429, *430*
modelling, *600*, 608-610, 613-615, 627-628
nighttime marine air temperature (NMAT), *243*
oceans, 60, *61*, 387, 389-393, 394-402, *420*
palaeoclimate, 435-436, 440-457, *449-450B*, 460-476, *462*, *467-470*, *475*, *477*, 478-481
projections, 69-72, 74-76, 762, *763*, 764-766
relationship with precipitation, 264-265
sea surface temperature (SST), *42*, 51, 64, 73, *101*, 102, 237, 245-247, *312B*, 318, 391
spatial distribution of changes, 37-40, 62-63, 250-251
spatial trend patterns, 250-251
summary, 36-40, 51-52, 60-61, 237, 239, 317-318
surface*, *61*, 62-63, 100-102, 237, 239, 241-253, 317, 318, 683-693
surface air temperature (SAT), 51-52, 339, 474, 749, 845
upper air, 237, 265-271
See also Temperature projections
Temperature projections, 762, *763*, 764-766, 785-786, *787*, 806, 807-811
commitment, climate change, 79, 752, 822-828
extremes, *862*
global temperature at year 2100, 809-810, *858B*
long-term projections, 822-828
regional projections, summarized, 21-23, *854-857*, *858-859B*
summary, 66, 69-72, 74-75, 749-750
See also Climate projections
Terrestrial biosphere*, 504-505, 527-528, 606, *646-647*
Terrestrial ecosystems, 503, 520
Terrestrial processes, modelling, 604-606
Thermal expansion*, 387, 408, *412-413*, 414-417, 419-420
projections, 801, 812, 820-821, *823*, 828-829
Thermohaline Circulation (THC)*, 246-247
See also Meridional Overturning Circulation
Thresholds, 640-643
Tide gauges*, 48-49, 408, 410, 411-412, 431, *432*
Tipping point, *775B*
Top-of-atmosphere (TOA) radiation, 277-278, 317
Total solar irradiance (TSI)*, 107-108, 188-189, *190*, 198, *202-205*
summary, 30, 132
Transient climate response (TCR), 691, 718, 723, *724*, 725, 754, *798B*, 800-801, 807
summary, 66, 88
Tree rings*, 438, 439, 459, 471, 472-473, 475, 476
Tropics, 295-299
climate projections, 751, 779, 786-788, *864*, 915
tropical cyclones, 41-43, 239, 304-307, *305B*, *314*, 316, 711-712, 751, 786-788, *864*, 915
tropical storms, 239, 304-312, *314-315*, 316
Tropopause*, *266*, 270, 699-700
Troposphere*, 265-267, *266*, *730*
nitrous oxide (N_2O), 545, *547*
ozone, 28, 108-110, 150-152, *201*, *203-205*, 513, 547-550
stratospheric-tropospheric relations, *284B*, 795-796
temperature, 36, *37*, 62, 237, *253*, 265-271, *268-269*
water vapour, 40, 238, 272-274, 318, *632B*
Twomey effect. *See* Cloud albedo effect, under Clouds
Typhoons. *See* Cyclones, tropical

U

Uncertainties*, *22-23B*, 81-91, 119-121, 669
quantification, 921-925
Urban effects on climate, 30, 36, 243-245, 259, *506B*
See also Land use change
Urban heat islands*, 102, 185, 237, 243-245
Urban precipitation patterns, 259

V

Vegetation, *505B*, 507, 508-510, 566
modelling, 509-510
projections, *777B*, 789-793
Volatile organic compounds (VOCs), 78, 150, 206, *207*, 214, 547-549, 556-557, 796
Volcanic eruptions, 31, 96-97, 137, 193-195, *201*, 681-682
modelling, 641, 723
Mt. Pinatubo, 98, 109, 142, 193-194, 723
projections, 797
volcanic forcing, 459, *477*, 478, *479*, 673, 678, *731*

W

Walker Circulation*, 112, 295-296, 299, 318
Warming. *See* Temperature
Water, 40-43
land water storage, 318, 418-419
projections, 768-770, 860-861
surface hydrology, 35, 64, 254, 260-265, *261B*, 618, 768-770, *886B*
surface water balance, *505B*
Water vapour, 115, 135, 152, 185, 271-275, 712
feedback, 593, 630-633, *632B*
modelling, 593, 630-633
projections, 796, 860-861
radiative forcing, 28, 131, 152, 185, *201-204*
stratospheric, 274-275
summary, 28, 40, 53-54, 131, 135, 238, 318
surface, 238, 272-274, 318
tropospheric, 40, 238, 272-274, 318
water vapour-lapse rate feedback, 633-635, 640
Waves, ocean, 283-285, 799, 806
Winds, 38, 159, 280-281, 283-285, *864*, 877-878, 902
mid-latitude westerlies, 238-239, 280, 283, 290
See also Cyclones

Y

Younger Dryas*, 455, 456

Sea Level Trends

PRODUCTS
(/products.html)
Data, Analyses, and Publications

PROGRAMS
(/programs.html)
Serving the Nation

EDUCATION
(/education.html)
Tides, Currents, and Predictions

HELP & ABOUT
(/about.html)
Info and how to reach us

Search

SEA LEVEL TRENDS

Home/Map (/sltrends/sltrends.html)

U.S. Stations (/sltrends/sltrends_us.html)

Global Stations (/sltrends/sltrends_global.html)

Data Tables

Mean Sea Level Trend | Interannual Variation

Average Seasonal Cycle (seasonal.htm;jsessionid=0BC559B084EA3FD83F77E799D1492C22?stnid=9414290)

Variation Of 50-Year MSL Trends (50yr.htm;jsessionid=0BC559B084EA3FD83F77E799D1492C22?stnid=9414290)

Previous MSL Trends (sltrends_update.htm;jsessionid=0BC559B084EA3FD83F77E799D1492C22?stnid=9414290)

Mean Sea Level Trend
9414290 San Francisco, California

Sel

U.S. Trends Map (/sltrends/slrmap

U.S. Regional Trends

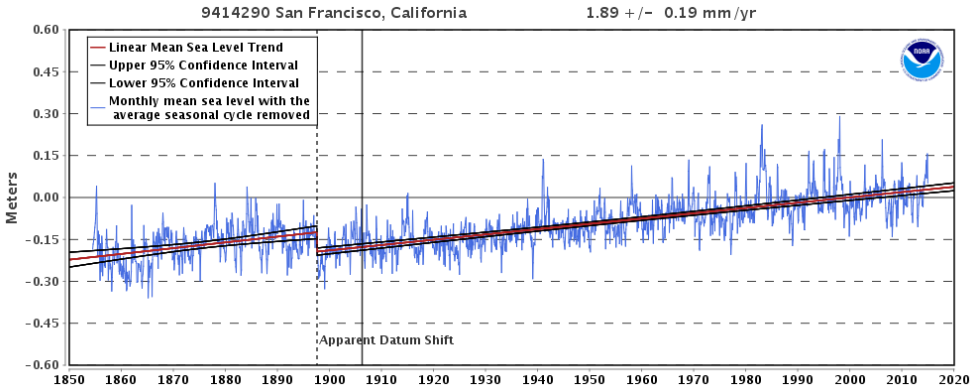
Sel

Global Regional Trends (/sltrends/globalregional.htm)

Anomalies

Sel

Get Adobe Reader (http://tidesandcurrents.noaa.gov/sltrends.html?url=14)



EXPORT TO TEXT (DOWNLOADMEANSEALEVELTRENDSTEXT.HTM;JSESSIONID=0BC559B084EA3FD83F77E799D1492C22?STNID=9414290)

| EXPORT TO CSV (DOWNLOADMEANSEALEVELTRENDSCSV.HTM;JSESSIONID=0BC559B084EA3FD83F77E799D1492C22?STNID=9414290)

| SAVE IMAGE

The mean sea level trend is 1.89 millimeters/year with a 95% confidence interval of +/- 0.19 mm/yr based on monthly mean sea level data from 1897 to 2013 which is equivalent to a change of 0.62 feet in 100 years.
[Metadata: Apparent Datum Shift]

The plot shows the monthly mean sea level without the regular seasonal fluctuations due to coastal ocean temperatures, salinities, winds, atmospheric pressures, and ocean currents. The long-term linear trend is also shown, including its 95% confidence interval. The plotted values are relative to the most recent Mean Sea Level datum established by CO-OPS (http://tidesandcurrents.noaa.gov/datum_options.html). The calculated trends for all stations are available as a table in millimeters/year and in feet/century (mslUSTrendsTable.htm) (0.3 meters = 1 foot).

If present, solid vertical lines indicate times of any major earthquakes in the vicinity of the station and dashed vertical lines bracket any periods of questionable data or datum shift.

Products available at 9414290 San Francisco, California

TIDES/WATER LEVELS

Water Levels (/waterlevels.html?id=9414290)

NOAA Tide Predictions (/noaatidepredictions/NOAATidesFacade.jsp?Stationid=9414290)

Harmonic Constituents (/harcon.html?id=9414290)

Sea Level Trends (/sltrends/sltrends_station.shtml?stnid=9414290)

METEOROLOGICAL/OTHER

Meteorological Observations (/met.html?id=9414290)

Water Temp/Conductivity

PORTS®

San Francisco Bay PORTS® (/ports/index.html?port=sf)

PORTS® product page for San Francisco (/ports/ports.html?id=9414290)

OPERATIONAL FORECAST SYSTEMS

This station is not a member of OFS

INFORMATION

Station Home Page (/stationhome.html?id=9414290)

Data Inventory (/inventory.html?id=9414290)

Datums (/datums.html?id=9414290)

Bench Mark Sheets (/benchmarks.html?id=9414290)

Extreme Water Levels (/est/est_station.shtml?stnid=9414290)

Reports (/reports.html?id=9414290)

Measurement Specifications (/measure.html)

San Francisco Bay Conservation and Development Commission

Climate Change

Climate Change Planning Program

The Bay Area is already working to reduce greenhouse gas emissions, but mitigation alone will not do enough to address sea level rise and other climate change impacts. The region must consider adaptation actions that will reduce the vulnerability of the built and natural environment to the effects of climate change.

The Bay is rising and this is projected to continue. In fact, today's flood is expected to be the future's high tide. Areas that currently flood every ten to twenty years during extreme weather and tides will begin to flood regularly. These areas are home to over 160,000 residents, critical infrastructure, diverse habitats, and valuable community resources. BCDC's Climate Change Program has the following goals:

- RESEARCH: Promote research to improve our understanding of climate change impacts, mitigation and adaptation.
- POLICY: Develop and implement climate change adaptation policies in coordination with regional partners and stakeholders.
- CAPACITY: Build the region's institutional capacity to effectively adapt to climate change in a coordinated and collaborative way.

New Sea Level Rise Policies Fact Sheet
Climate Change Program Summary (November 24, 2010)
Briefing to the Commission on the Local Government Adaptation Assistance Program [1.2MB](March 3, 2011)
Status Report on BCDC Climate Science [172KB] (January 28, 2011)

Projects

Currently, BCDC is advancing the above goals with the following projects

- California King Tides Initiative Report
- Adopted Climate Change Bay Plan Amendment
- Areas Vulnerable to Sea Level Rise in San Francisco Bay
- Adapting to Rising Tides
- Local Government Adaptation Assistance Program (AAP)
- Climate Ready Estuaries San Francisco Estuary Pilot
- Delta Alliance Partnership
- Rising Tides Design Competition
- Innovative Wetland Adaptation Strategies Study
- Regional Sediment Management
- Regional Climate Change Impacts Assessment

Resources

- News and Video
  Find the latest news coverage and recent publications on sea level rise adaptation in California and the Bay Area.
- Resources for Adaptation Planning

Contact

Steve Goldbeck
steveg@bcdc.ca.gov
415.352.3611

Conditions of Use | Privacy Policy
Copyright © 2007 State of California

2007 Buildings Energy Data Book





U.S. Department of Energy

Energy Efficiency and Renewable Energy

Bringing you a prosperous future where energy is clean, abundant, reliable, and affordable

This version is dated: September 2007

D I S C L A I M E R

This document was designed for the internal use of the United States Department of Energy. This document will be occasionally updated and, therefore, this copy may not reflect the most current version.

This document was prepared as account of work sponsored by an agency of the United States Government. Neither the United States Government nor any agency thereof, nor any of their employees, makes any warranty, express or implied, or assumes any legal liability or responsibility for the accuracy, completeness, or usefulness of any information, apparatus, product, or process disclosed, or represents that its use would not infringe privately owned rights. Reference herein to any specific commercial product, process, or service by trade name, trademark, manufacturer, or otherwise, does not necessarily constitute or imply its endorsement, recommendation, or favoring by the United States Government or any agency, contractor or subcontractor thereof. The views and opinions of authors expressed herein do not necessarily state or reflect those of the United States Government or any agency, contractor or subcontractor thereof.

2007 Buildings Energy Data Book

September 2007

Prepared for the
Buildings Technologies Program and
Office of Planning, Budget, and Analysis
Energy Efficiency and Renewable Energy
U.S. Department of Energy

by
D&R International, Ltd.

under contract to
Oak Ridge National Laboratory

Table of Contents

Foreword v
Acknowledgements vii
Introduction viii

Directory

List of Tables ix
Key Terminology xx

Data Summary Sheets

1.0 Energy Consumption Data

1.1 Buildings Sector Energy Consumption 1-1
1.2 Residential Sector Energy Consumption 1-5
1.3 Commercial Sector Energy Consumption 1-9
1.4 Federal Buildings and Facilities Energy Consumption 1-13
1.5 Electric Utility Energy Consumption 1-15

2.0 Characteristics Data

2.1 Residential Sector Characteristics 2-1
2.2 Commercial Sector Characteristics 2-5
2.3 Federal Buildings and Facilities Characteristics 2-9

3.0 Environmental Data

3.1 Carbon Emissions 3-1
3.2 Halocarbons (CFCs, HCFCs, Halons, and HFCs) 3-6
3.3 EPA Criteria Pollutants 3-9
3.4 Construction Waste 3-10

4.0 Economic Data

4.1 Energy Prices and Aggregate Expenditures 4-1
4.2 Residential Sector Expenditures 4-4
4.3 Commercial Sector Expenditures 4-7
4.4 Federal Buildings and Facilities Expenditures 4-9
4.5 Value of Building Construction and Research 4-10
4.6 Employment 4-12

5.0 Market Data

5.1 New Buildings Construction 5-1
5.2 Industrialized Housing (IH) 5-3
5.3 Existing Buildings Retrofits 5-5
5.4 Building Materials/Insulation 5-6
5.5 Windows 5-7

Table of Contents

5.6 Heating, Cooling, and Ventilation Equipment 5-10
5.7 Thermal Distribution Systems 5-16
5.8 Active Solar Systems 5-18
5.9 Lighting 5-20
5.10 Appliances 5-23

6.0 Quad Equivalents
6.1 Quad Definitions and Comparisons 6-1
6.2 Electricity Generation, Transmission, and Distribution 6-3
6.3 Buildings Sector Generic Fuel Quad 6-6
6.4 Electric and Generic Quad Carbon Emissions 6-7

7.0 Buildings Profiles
7.1 Low-Income Housing 7-1
7.2 Typical Appliance Usage 7-5
7.3 Typical/Average Household 7-7
7.4 Typical Commercial Buildings 7-9
7.5 Educational Facilities 7-14

Foreword

The U.S. Department of Energy's (DOE) Office of Energy Efficiency and Renewable Energy has developed this *Buildings Energy Data Book* to provide a current and accurate set of comprehensive buildings-related data, and to promote the use of such data for consistency throughout DOE programs. The following factoids provide some interesting perspective on the energy that powers our nation's buildings.

- Buildings now use 72 percent of all electricity and account for 80 percent of all electric expenditures.
- "Internal gains" account for as much as 27 percent of a home's cooling load.
- There are now 113 million households.
- One-third of all households rent their homes.
- The average new single-family home has increased in size by about 700 square feet since 1980.
- In 2006, 50 percent of all new homes completed were completed in the South. Cooling load management emerges as a priority.
- U.S. buildings carbon dioxide emissions (630 million metric tons of carbon) approximately equal the combined emissions of Japan, France, and the United Kingdom.
- China's projected annual growth rate in carbon dioxide emissions through 2010 is 6.5 times that of the U.S. (5.2 percent vs. 0.8 percent).
- Lighting uses more energy than cooling in the residential sector. This underscores the importance of breakthrough lighting technologies.
- The homebuilding industry shows signs of consolidating. As of 2006, the top five homebuilders hold 20 percent of the total market, the top 20 hold 35 percent, and the top 100 hold 47 percent.
- In 2001, per the *U.S. Lighting Market Characterization Report 2002*, lighting consumed 756 Billion kWh. In 2001, per the *Annual Energy Review 2003*, America's 104 nuclear generating units produced 769 billion kWh, while operating at a capacity factor of 89 percent. It therefore takes our entire nuclear fleet to illuminate America.
- In 2006, 31 percent of all refrigerator sales and 38 percent of all clothes washer sales were ENERGY STAR compliant.

We hope you find the *2007 Buildings Energy Data Book* useful. You are encouraged to comment on errors, omissions, emphases, and organization of this report to one of the persons listed below. Requests for additional copies of this report, additional data, or information on an existing table should be referred to D&R International.

Jordan D. Kelso, PE
D&R International, Ltd.
1300 Spring Street
Suite 500
Silver Spring, Maryland 20910
Telephone: (301) 588-9387
Fax: (301) 588-0854
E-mail: jkelso@drintl.com

The *2007 Buildings Energy Data Book* can be found on the web at:

http://buildingsdatabook.eere.energy.gov/

Acknowledgements

The authors would like to express their thanks to the many individuals who assisted in the preparation of this document. We thank Jerry Dion and the Building Technologies Program along with the Energy Efficiency and Renewable Energy staff for their continued support of the *Buildings Energy Data Book*. We greatly appreciate the input and guidance received over the years from Andrew Nicholls of Pacific Northwest National Laboratory.

Introduction

The *2007 Buildings Energy Data Book* is a statistical compendium prepared and published under contract with the National Energy Technology Laboratory (NETL) with the U.S. Department of Energy's (DOE) Office of Energy Efficiency and Renewable Energy (EERE). Pacific Northwest National Laboratory (PNNL) first published the predecessor to the annual *Buildings Energy Data Book* in 1986. PNNL published these through September 2004. The NETL began support of the *Buildings Energy Data Book* this year.

EERE has developed this *2007 Buildings Energy Data Book* to provide a current and accurate set of comprehensive buildings-related data and to promote the use of such data for consistency throughout DOE programs. Additional data (e.g., more current, widely accepted, and/or better-documented data) and suggested changes should be submitted to D&R International, Ltd. Please provide full source references along with all data.

The *Buildings Energy Data Book* is a compilation of data and does not provide original data. Much of the data gathered is from government documents, models, and analyses. All data sources are included with each data table. Tables are organized into seven chapters: 1: Energy Consumption Data; 2: Characteristics Data; 3: Environmental Data; 4: Economic Data; 5: Market Data; 6: Quad Equivalents; and 7: Buildings Profiles.

List of Tables

Buildings Energy Data Summary Sheets

1 U.S. Residential and Commercial Buildings Primary Energy Consumption 1
2 U.S. Buildings Primary Energy Consumption 1
3 U.S. Buildings Generic Quad 1
4 Buildings Share of U.S. Primary Energy Consumption 1
5 Buildings Share of U.S. Electricity Consumption 1
6 U.S. Electricity Net Generation, by Plant Type 1
7 U.S. Buildings Primary Energy and Expenditure End-Use Splits 2005 1
8 Buildings Energy Prices and Expenditures 1
9 Energy Consumption Intensities, by Year 1
10 Residential (2001) and Commercial (2003) Vintages 2
11 Stock Energy Expenditures 2
12 Carbon Dioxide Emissions for U.S. Buildings 2
13 EPA Emissions for U.S. Buildings, 2002 2
14 Value of New, Improvement & Repair and Building Construction 2
15 1998 Cost Breakdown of a 2,150-Square Foot New Single-Family Home 2
16 Residential New Single-Family Homes Completed 2
17 Design and Construction Employment 2
18 FY 2005 Energy Burdens 2
19 Construction Waste 2
20 Weatherization Facts 2
21 2003 U.S. Private Investment into Construction R&D 2
22 2006 Five Largest Residential Homebuilders 2

1.0 Buildings Sector Energy Consumption 1-1

1.1 Buildings Sector Energy Consumption 1-1
1.1.1 U.S. Residential and Commercial Buildings Total Primary Energy Consumption (Quadrillion Btu and Percent of Total) 1-1
1.1.2 U.S. Buildings *Site* Renewable Energy Consumption (Quadrillion Btu) 1-1
1.1.3 Buildings Share of U.S. Primary Energy Consumption (Percent) 1-1
1.1.4 2005 U.S. Buildings Energy End-Use Splits, by Fuel Type (Quadrillion Btu) 1-2
1.1.5 Shares of U.S. Buildings Generic Quad (Percent) 1-2
1.1.6 Buildings Share of U.S. Electricity Consumption (Percent) 1-3
1.1.7 Buildings Share of U.S. Natural Gas Consumption (Percent) 1-3
1.1.8 Buildings Share of U.S. Petroleum Consumption (Percent) 1-3
1.1.9 Buildings Share of U.S. Petroleum Consumption (Million Barrels per Day) 1-4
1.1.10 World Primary Energy Consumption and Population, by Country/Region 1-4

1.2 Residential Sector Energy Consumption 1-5
1.2.1 Residential Primary Energy Consumption, by Year and Fuel Type (Quadrillion Btu and Percent of Total) 1-5
1.2.2 Residential *Site* Renewable Energy Consumption (Quadrillion Btu) 1-5
1.2.3 2005 Residential Energy End-Use Splits, by Fuel Type (Quadrillion Btu) 1-6

List of Tables

1.2.4 Residential *Delivered* and Primary Energy Consumption Intensities, by Year 1-6
1.2.5 2001 Residential *Delivered* Energy Consumption Intensities, by Vintage 1-7
1.2.6 2001 Residential *Delivered* Energy Consumption Intensities, by Housing Type 1-7
1.2.7 2001 Residential *Delivered* Energy Consumption Intensities, by Census Region 1-7
1.2.8 1997 Residential *Delivered* Energy Consumption Intensities, by Ownership of Unit 1-7
1.2.9 Aggregate Residential Building Component Loads as of 1998 1-8
1.2.10 1997 Residential *Delivered* Energy Consumption Intensities, by Principal Building Type and Vintage 1-8

1.3 Commercial Sector Energy Consumption 1-9
1.3.1 Commercial Primary Energy Consumption, by Year and Fuel Type (Quadrillion Btu and Percent of Total) 1-9
1.3.2 Commercial *Site* Renewable Energy Consumption (Quadrillion Btu) 1-9
1.3.3 2005 Commercial Energy End-Use Splits, by Fuel Type (Quadrillion Btu) 1-10
1.3.4 Commercial *Delivered* and Primary Energy Consumption Intensities, by Year 1-10
1.3.5 Commercial *Delivered* Energy Consumption Intensities, by Vintage 1-11
1.3.6 2003 Commercial *Delivered* Energy Consumption Intensities, by Principal Building Type and Vintage 1-11
1.3.7 2003 Commercial Primary Energy Consumption Intensities, by Principal Building Type 1-11
1.3.8 2003 Commercial *Delivered* Energy Consumption Intensities, by Ownership of Unit 1-11
1.3.9 Aggregate Commercial Building Component Loads as of 1998 1-12
1.3.10 1995 Commercial *Delivered* End-Use Energy Consumption Intensities, by Principal Building Type 1-12

1.4 Federal Buildings and Facilities Energy Consumption 1-13
1.4.1 FY 2005 Federal Primary Energy Consumption (Quadrillion Btu) 1-13
1.4.2 FY 2005 Federal Building Energy Use Shares, by Fuel Type and Agency 1-13
1.4.3 Federal Building *Delivered* Energy Consumption Intensities, by Year 1-13
1.4.4 Federal Agency Progress Toward the Renewable Energy Goal (Trillion Btu) 1-14

1.5 Electric Utility Energy Consumption 1-15
1.5.1 Buildings Share of U.S. Electricity Consumption/Sales (Percent) 1-15
1.5.2 U.S. Electricity Generation Input Fuel Shares (Percent) 1-15
1.5.3 U.S. Electricity Generation Input Fuel Consumption (Quadrillion Btu) 1-15
1.5.4 U.S. Electricity Net Generation, by Plant Type (Billion kWh) 1-16
1.5.5 U.S. Electric Utility and Nonutility Net Summer Electricity Generation Capacity (GW) 1-16
1.5.6 U.S. Electric Power Sector Cumulative Power Plant Additions Needed to Meet Future Electricity Demand 1-17

List of Tables

1.5.7 2005 Existing Capacity, by Energy Source (GW) 1-17
1.5.8 Electric Capacity Factors, by Year and Fuel Type 1-17

2.0 Characteristics Data 2-1

2.1 Residential Sector Characteristics 2-1
2.1.1 Total Number of Households and Buildings, Floorspace, and Household Size, by Year 2-1
2.1.2 Share of Households, by Housing Type and Type of Ownership, as of 2001 (Percent) 2-1
2.1.3 Share of Households, by Census Region and Vintage, as of 2001 (Percent) 2-1
2.1.4 Residential Floorspace (heated square feet), as of 2001 (Percent of Total Households) 2-2
2.1.5 Housing Vintage, as of 2001 2-2
2.1.6 Construction Statistics of New Homes Completed/Placed 2-3
2.1.7 Materials Used in the Construction of a 2,272-Square-Foot Single-Family Home, 2000 2-3
2.1.8 2006 New Homes Completed/Placed, by Census Region (Thousand Units and Percent of Total Units by Housing Type) 2-4
2.1.9 2006 Construction Method of Single-Family Homes, by Region (Thousand Units and Percent of Total Units by Construction Method) 2-4
2.1.10 Market Indices for 2006 ENERGY STAR Qualified New Single-Family Homes, by Selected State (1000s) 2-4

2.2 Commercial Sector Characteristics 2-5
2.2.1 Total Commercial Floorspace and Number of Buildings, by Year 2-5
2.2.2 Principal Commercial Building Types, as of 2003 (Percent of Total Floorspace) 2-5
2.2.3 Number of Floors and Type of Ownership, as of 2003 (Percent of Total Floorspace) 2-6
2.2.4 Share of Commercial Floorspace, by Census Region and Vintage, as of 2003 (Percent) 2-6
2.2.5 Commercial Building Size, as of 2003 (Number of Buildings and Percent of Total Floorspace) 2-6
2.2.6 Commercial Building Vintage, as of 2003 2-6
2.2.7 Commercial Building Median Lifetimes (Years) 2-7
2.2.8 2003 Average Commercial Building Floorspace, by Principal Building Type and Vintage 2-7
2.2.9 U.S. LEED Certified Projects, by Certification Type and State 2-8
2.2.10 U.S. LEED Registered Projects, by Ownership Category 2-8

2.3 Federal Buildings and Facilities Characteristics 2-9
2.3.1 Federal Building Gross Floorspace, by Year and Agency 2-9

List of Tables

3.0 Environmental Data 3-1

3.1 Carbon Emissions 3-1
3.1.1 Carbon Dioxide Emissions for U.S. Buildings, by Year (10^6 metric tons of carbon) 3-1
3.1.2 2005 Buildings Energy End-Use Carbon Dioxide Emissions Splits, by Fuel Type (Million Metric Tons of Carbon Equivalent (MMTCE)) 3-2
3.1.3 2005 Residential Energy End-Use Carbon Dioxide Emissions Splits, by Fuel Type (MMTCE) 3-3
3.1.4 2005 Commercial Energy End-Use Carbon Dioxide Emissions Splits, by Fuel Type (MMTCE) 3-4
3.1.5 World Carbon Dioxide Emissions 3-4
3.1.6 2005 Methane Emissions for U.S. Buildings Energy Production, by Fuel Type (MMTCE) 3-5
3.1.7 2005 Carbon Dioxide Emission Coefficients for Buildings (MMTCE per Quadrillion Btu) 3-5

3.2 Halocarbons (CFCs, HCFCs, Halons, and HFCs) 3-6
3.2.1 Halocarbon Environmental Coefficients and Principal Uses 3-6
3.2.2 Phase-Out Schedule of Halocarbons in the U.S. 3-7
3.2.3 Conversion and Replacements of Centrifugal CFC Chillers 3-7
3.2.4 Estimated U.S. Emissions of Halocarbons, 1987-2001 (MMTCE) 3-8

3.3 EPA Criteria Pollutants 3-9
3.3.1 2002 EPA Emissions Summary Table for U.S. Buildings Energy Consumption (Thousand Short Tons) 3-9
3.3.2 2002 EPA Criteria Pollutant Emissions Coefficients (Million Short Tons/*Delivered* Quadrillion Btu, unless otherwise noted) 3-9

3.4 Construction Waste 3-10
3.4.1 Characteristics of U.S. Construction Waste 3-10
3.4.2 "Typical" Construction Waste Estimated for a 2,000-Square-Foot Home 3-10
3.4.3 1996 Construction and Demolition Debris Generated from Construction Activities and Debris Generation Rates 3-10

4.0 Economic Data 4-1

4.1 Energy Prices and Aggregate Expenditures 4-1
4.1.1 Building Energy Prices, by Year and Major Fuel Type ($2005 per Million Btu) 4-1
4.1.2 Building Energy Prices, by Year and Fuel Type ($2005) 4-1
4.1.3 Buildings Aggregate Energy Expenditures, by Year and Major Fuel Type ($2005 Billion) 4-1
4.1.4 FY 2005 Federal Buildings Energy Prices and Expenditures, by Fuel Type ($2005) 4-2

List of Tables

4.1.5 2005 Buildings Energy End-Use Expenditure Splits, by Fuel Type ($2005 Billion) 4-2
4.1.6 Implicit Price Deflators (2000 = 1.00) 4-3

4.2 Residential Sector Expenditures 4-4
4.2.1 2005 Residential Energy End-Use Expenditure Splits, by Fuel Type ($2005 Billion) 4-4
4.2.2 Average Annual Energy Expenditures per Household, by Year ($2005) 4-4
4.2.3 2001 Energy Expenditures per Household, by Housing Type and Square Footage ($2005) 4-4
4.2.4 2001 Energy Expenditures per Household, by Census Region ($2005) 4-5
4.2.5 2001 Household Energy Expenditures, by Vintage ($2005) 4-5
4.2.6 2001 Households and Energy Expenditures, by Income Level ($2005) 4-5
4.2.7 Energy Burden Definitions and Residential Energy Burdens, by Weatherization Eligibility and Year 4-6
4.2.8 1998 Cost Breakdown of a 2,150-Square-Foot, New Single-Family Home ($2005) 4-6

4.3 Commercial Sector Expenditures 4-7
4.3.1 2005 Commercial Energy End-Use Expenditure Splits, by Fuel Type ($2005 Billion) 4-7
4.3.2 Average Annual Energy Expenditures per Square Foot of Commercial Floorspace, by Year ($2005) 4-7
4.3.3 2003 Energy Expenditures per Square Foot of Commercial Floorspace and per Building, by Building Type ($2005) 4-8
4.3.4 2003 Energy Expenditures per Square Foot of Commercial Floorspace, by Vintage ($2005) 4-8

4.4 Federal Buildings and Facilities Expenditures 4-9
4.4.1 Annual Energy Expenditures per Gross Square Foot of Federal Floorspace Stock, by Year ($2005) 4-9
4.4.2 Direct Appropriations on Federal Buildings Energy Conservation Retrofits and Capital Equipment ($2005 Million) 4-9

4.5 Value of Building Construction and Research 4-10
4.5.1 Estimated Value of All U.S. Construction Relative to the GDP ($2005) 4-10
4.5.2 Value of New Building Construction Relative to GDP, by Year ($2005 Billion) 4-10
4.5.3 Value of Building Improvements and Repairs Relative to GDP, by Year ($2005 Billion) 4-10
4.5.4 2003 U.S. Private Investment into Construction R&D 4-11
4.5.5 1997/1998 International Investment into Construction and Energy R&D 4-11
4.5.6 FY2003-2005 Green Building R&D, as Share of Federal Budget and by Organization 4-11

List of Tables

4.6 Employment 4-12
4.6.1 Buildings Design and Construction Trades, by Year 4-12
4.6.2 Heating, Cooling, and Ventilation Equipment Trades, by Year (1000 Employees) 4-12

5.0 Market Data 5-1

5.1 New Buildings Construction 5-1
5.1.1 2006 Five Largest Residential Homebuilders 5-1
5.1.2 Value of New Building Construction, by Year ($2005 Billion) 5-1
5.1.3 Market Indices for 2006 ENERGY STAR Qualified New Single-Family Homes, by Selected States (1000s) 5-2

5.2 Industrialized Housing (IH) 5-3
5.2.1 2007 Top Five Manufacturers of Factory-Built Housing Units 5-3
5.2.2 2007 Top Five Manufacturers of Modular/3D Housing Units 5-3
5.2.3 2007 Top Five Manufacturers of HUD-Code (Mobile) Homes 5-3
5.2.4 2004 Top Five Manufacturers of Factory-Fabricated Components (Trusses, Wall Panels, Doors) 5-3
5.2.5 2004 Number of Industrialized Housing Manufacturers versus Production Companies (Stick-Builders) 5-4
5.2.6 2006 HUD-Code (Mobile) Home Placements, by Census Region and Top Five States (Percent of National Total) 5-4

5.3 Existing Buildings Retrofits 5-5
5.3.1 Value of Building Improvements and Repairs, by Sector ($2005 Billion) 5-5
5.3.2 2005 Professional and Do-It-Yourself Improvements, by Project ($2005) 5-5
5.3.3 Single-Family Residential Renovations, by Project and Vintage 5-5

5.4 Building Materials/Insulation 5-6
5.4.1 U.S. Insulation Demand, by Type (Million Pounds) 5-6
5.4.2 Industry Use Shares of Mineral Fiber (Glass/Wool) Insulation 5-6
5.4.3 Thermal Performance of Insulation 5-6

5.5 Windows 5-7
5.5.1 Residential Prime Window Sales, by Type (Million Units) 5-7
5.5.2 Residential Storm Window and Door Shipments, by Type (Million Units) 5-7
5.5.3 Nonresidential Window Usage, by Type and Census Region (Million SF of Vision Area) 5-7
5.5.4 Insulating Glass Historical Penetration, by Sector (Percent of Total U.S. Usage) 5-8
5.5.5 Residential Prime Window Sales, by Type (Million Units) 5-8
5.5.6 2005 Residential Prime Window Stock, by Type 5-8
5.5.7 Nonresidential Window Stock and Usage, by Type 5-9
5.5.8 Typical Thermal Performance of Residential Windows, by Type 5-9

List of Tables

5.6 Heating, Cooling, and Ventilation Equipment 5-10

5.6.1 U.S. Heating and Air Conditioning System Manufacturer Shipments, by Type (Including Exports) 5-10
5.6.2 Minimum Efficiency Standards and Maximum Energy Use for Typical Single-Family Residential Heating and Cooling Equipment 5-11
5.6.3 Residential Furnace Efficiencies (Percent of Units Shipped) 5-11
5.6.4 Residential Boiler Efficiencies 5-11
5.6.5 Residential Air Conditioner and Heat Pump Cooling Efficiencies 5-12
5.6.6 Commercial Equipment Efficiencies 5-12
5.6.7 2005 Air-Conditioner/Heat Pump Manufacturer Market Shares (Percent of Products Produced) 5-12
5.6.8 2005 Gas Furnace Manufacturer Market Shares (Percent of Products Produced) 5-13
5.6.9 Major Residential HVAC Equipment Lifetimes, Ages, and Replacement Picture 5-13
5.6.10 Major Commercial HVAC Equipment Lifetimes and Ages 5-13
5.6.11 Main Residential Heating Fuel, by Vintage, as of 2001 (Percent of Total Households) 5-14
5.6.12 Main Residential Heating Equipment, as of 1987, 1993, 1997, and 2001 (Percent of Total Households) 5-14
5.6.13 Main Commercial Heating and Cooling Equipment, as of 1995, 1999, and 2003 (Percent of Total Floorspace) 5-14
5.6.14 Main Commercial Primary Energy Use of Heating and Cooling Equipment, as of 1995 5-15

5.7 Thermal Distribution Systems 5-16

5.7.1 U.S. Commercial Buildings Conditioned Floorspace, Building Type, and System Type (Million SF) 5-16
5.7.2 Thermal Distribution Design Load and Electricity Intensities, by Building Activity 5-16
5.7.3 Thermal Distribution Equipment Design Load and Electricity Intensities, by System Type 5-16
5.7.4 Typical Commercial Building Thermal Energy Distribution Design Load Intensities (Watts per SF) 5-17
5.7.5 Market Share of Major HVAC Equipment Manufacturers ($2005 Million) 5-17
5.7.6 1999 Energy Efficient Motors, Replacements, and Sales, by Horsepower Class 5-17
5.7.7 1999 AC Adjustable Speed Drive Population 5-17

5.8 Active Solar Systems 5-18

5.8.1 Solar Collector Shipments, by Type and Market (Thousand SF, unless noted) 5-18
5.8.2 Thermal Solar Collector Shipments, by End Use (Including Imports and Exports) (Thousand SF) 5-18
5.8.3 2005 Top Five Destinations of Thermal Solar Collector Shipments 5-18

List of Tables

5.8.4 Thermal Solar Collector Manufacturer Statistics 5-18
5.8.5 Shipments of Photovoltaic Cells and Modules, by Market (Peak Kilowatts) 5-19
5.8.6 Annual Shipments of Photovoltaic Cells and Modules (Peak Kilowatts) 5-19
5.8.7 2005 Top 5 Destinations of U.S. Photovoltaic Cell and Module Export Shipments, by Country 5-19

5.9 Lighting 5-20
5.9.1 2001 Total Lighting Technology Electricity Consumption, by Sector (Billion kWh per Year) 5-20
5.9.2 2001 Total Lighting Technology Light Output, by Sector (Trillion Lumen-hour per Year) 5-20
5.9.3 2001 Lamp Wattage, Number of Lamps, and Hours of Usage (Weighted Average) 5-21
5.9.4 1995 Lighting Energy Intensities, by Commercial Building Type 5-21
5.9.5 2003 Lighted Floorspace for the Stock of Commercial Buildings, by Type of Lamp 5-21
5.9.6 Value of Electric Lighting Fixture Shipments ($Million) 5-22
5.9.7 Shipments of Fluorescent Lamp Ballasts 5-22
5.9.8 Typical Efficacies and Lifetimes of Lamps 5-22

5.10 Appliances 5-23
5.10.1 Refrigeration System Shipments, by Type (Including Exports) 5-23
5.10.2 Other Major Appliance Shipments, by Type (Including Exports) 5-23
5.10.3 Minimum Efficiency Standards for Appliances and Equipment 5-24
5.10.4 Refrigerator-Freezer Sizes and Energy Factors (Shipment-Weighted Averages) 5-25
5.10.5 Room Air Conditioner Capacities and Energy Efficiencies (Shipment-Weighted Averages) 5-25
5.10.6 Water Heater Efficiencies 5-26
5.10.7 Other Major Appliance Efficiencies 5-26
5.10.8 2005 Room Air Conditioner Manufacturer Market Shares (Percent of Products Produced) 5-27
5.10.9 2005 Refrigerator Manufacturer Market Shares (Percent of Products Produced) 5-27
5.10.10 2005 Range Manufacturer Market Shares (Percent of Products Produced) 5-27
5.10.11 2005 Microwave Oven Manufacturer Market Shares (Percent of Products Produced) 5-27
5.10.12 2005 Clothes Washer Manufacturer Market Shares (Percent of Products Produced) 5-28
5.10.13 Sales of ENERGY STAR Labeled Appliances, by Year (1000s) and Percent of Total Sales 5-28
5.10.14 2005 Clothes Dryer Manufacturer Market Shares (Percent of Products Produced) 5-28
5.10.15 2005 Water Heater Manufacturer Market Shares (Percent of Products Produced) 5-28

List of Tables

5.10.16 2005 Facsimile and Copier Machine Manufacturer Market Shares (Percent of Products Produced) 5-29
5.10.17 2005 Personal Computer Manufacturer Market Shares (Percent of Products Produced) 5-29
5.10.18 2005 Printer Manufacturer Market Shares (Percent of Products Produced) 5-29
5.10.19 Major Residential and Small Commercial Appliance Lifetimes, Ages, and Replacement Picture 5-30
5.10.20 Major Appliance Ownership (Millions of Households and Percent of U.S. Households) 5-30

6.0 Quad Equivalents 6-1

6.1 Quad Definitions and Comparisons 6-1
6.1.1 Key Definitions 6-1
6.1.2 Consumption Comparisons in 2004 6-1
6.1.3 Carbon Emission Comparisons 6-2
6.1.4 Average Annual Carbon Dioxide Emissions for Various Functions 6-2

6.2 Electricity Generation, Transmission, and Distribution 6-3
6.2.1 2005 Impacts of Saving an Electric Quad 6-3
6.2.2 2005 Existing Capacity, by Energy Source (GW) 6-3
6.2.3 Electric Capacity Factors, by Year and Fuel Type 6-3
6.2.4 Electric Conversion Factors and Transmission and Distribution (T&D) Losses 6-4
6.2.5 Characteristics of New and Stock Generating Capacities, by Plant Type 6-4
6.2.6 Characteristics of New Commercial Distributed Generating Technologies, by Plant Type 6-4
6.2.7 Cost of an Electric Quad Used in the Buildings Sector ($2005 Billion) 6-5

6.3 Buildings Sector Generic Fuel Quad 6-6
6.3.1 Cost of a Generic Quad Used in the Buildings Sector ($2005 Billion) 6-6
6.3.2 Shares of U.S. Buildings Generic Quad (Percent) 6-6
6.3.3 Shares of U.S. Residential Buildings Generic Quad (Percent) 6-6
6.3.4 Shares of U.S. Commercial Buildings Generic Quad (Percent) 6-6

6.4 Electric and Generic Quad Carbon Emissions 6-7
6.4.1 Electric Quad Average Carbon Emissions with Average Stock Utility Fuel Mix and Projected New Marginal Capacity Fuel Mix (Million Metric Tons) 6-7
6.4.2 Average Carbon Emissions from a Generic Quad in the Buildings Sector with Stock Fuel Mix and Projected Fuel Mix of New Marginal Utility Capacity and Site Energy Consumption (Million Metric Tons) 6-7

List of Tables

7.0 Buildings Profiles 7-1

7.1 Low-Income Housing 7-1
7.1.1 Program Definitions 7-1
7.1.2 Energy Burden Definitions 7-1
7.1.3 Households, by Weatherization Eligibility and Year (Million) 7-2
7.1.4 Weatherization Population Facts 7-2
7.1.5 Weatherization Program Facts 7-3
7.1.6 Weatherization Costs and Savings 7-3
7.1.7 Residential Energy Burdens, by Weatherization Eligibility and Year 7-3
7.1.8 FY 2005 Residential Energy Burdens, by Region 7-4
7.1.9 2001 Housing Unit Ownership, by Income Level and Weatherization Eligibility (in Millions) 7-4
7.1.10 2001 Average Energy Expenditures per Household Member and per Square Foot, by Weatherization Eligibility ($2005) 7-4

7.2 Typical Appliance Usage 7-5
7.2.1 Operating Characteristics of Electric Appliances in the Residential Sector 7-5
7.2.2 Operating Characteristics of Natural Gas Appliances in the Residential Sector 7-6
7.2.3 Operating Characteristics of Electric Equipment in the Commercial Sector 7-6

7.3 Typical/Average Household 7-7
7.3.1 2001 *Delivered* Energy End-Uses for an Average Household, by Region (Million Btu per Household) 7-7
7.3.2 2001 End-Use Carbon Dioxide Emissions Splits for an Average Household, by Region (Pounds of CO2) 7-7
7.3.3 2001 Energy End-Use Expenditures for an Average Household, by Region ($2005) 7-7
7.3.4 Materials Used in the Construction of a 2,272-Square-Foot Single-Family Home, 2000 7-7
7.3.5 Characteristics of a Typical Single-Family Home 7-8

7.4 Typical Commercial Buildings 7-9
7.4.1 1995 Commercial Buildings *Delivered* Energy End-Use Intensities, by Building Activity (Thousand Btu per SF) 7-9
7.4.2 Typical Office Building 7-10
7.4.3 Typical School Building 7-11
7.4.4 Typical Mercantile & Service (Retail) Building 7-12
7.4.5 Typical Hospital Building 7-13

7.5 Educational Facilities 7-14
7.5.1 1995 Energy End-Use Intensities and Consumption of Educational Facilities, by Building Activity 7-14
7.5.2 2003-2004 Number of Public K-12 Schools in the United States and Students per School 7-14

List of Tables

7.5.3 National Enrollment and Expenditures for Public K-12 Facilities ($2005) 7-14
7.5.4 Total Expenditures for K-12 Plant Operations and Maintenance, by Function ($2005 Billion) 7-15
7.5.5 New Construction and Renovations Expenditures for Public K-12 Schools ($2006 Billion) 7-15
7.5.6 Percentage of Public K-12 Schools with Inadequate Building Features 7-15

Key Terminology

AAMA	American Architectural Manufacturers Association
ACEEE	American Council for an Energy Efficient Economy
AEO	EIA's Annual Energy Outlook
AFEAS	Alternative Fluorocarbons Environmental Acceptability Study
AFUE	Annual Fuel Utilization Efficiency
AHAM	Association of Home Appliance Manufacturers
ARI	Air-Conditioning and Refrigeration Institute
ASHRAE	American Society of Heating, Refrigerating and Air-Conditioning Engineers
BTS	DOE's Office of Building Technology, State and Community Programs
CBECS	EIA's Commercial Building Energy Consumption Survey
CDD	Cooling Degree Days
CF	Cubic feet
CFC	Chlorofluorocarbon
CHP	Combined Heat and Power
CO	Carbon monoxide
CO2	Carbon dioxide (CO_2)
COP	Coefficient of Performance (dimensionless, heating/cooling capacity: (Btu) over electric input (Btu))
CPS	Bureau of the Census' Current Population Survey
Delivered	Refers to energy used on site (including purchased electricity)
DG	Distributed Generation
DOC	U.S. Department of Commerce
DOE	U.S. Department of Energy
EER	Energy Efficiency Ratio (Btu/watt-hour)
EERE	DOE’s Energy Efficiency and Renewable Energy Office
EF	Energy Factor
EIA	DOE's Energy Information Administration
EPA	U.S. Environmental Protection Agency
FEMP	DOE's Federal Energy Management Program
FT2	Square Feet
FY	Fiscal Year
GAMA	Gas Appliance Manufacturers Association

Key Terminology

GDP	Gross Domestic Product
GWP	Global Warming Potential
HCFC	Hydrochlorofluorocarbon
HFC	Hydrofluorocarbon
HHS	U.S. Department of Health and Human Services
HSPF	Heating Season Performance Factor (Btu/watt-hour)
HUD	U.S. Department of Housing and Urban Development
HVAC/R	Heating, ventilating, and air-conditioning/refrigeration
IEA	International Energy Agency
LBNL	Lawrence Berkeley National Laboratory
LIHEAP	HHS' Low Income Home Energy Assistance Program
LPG	Liquid Petroleum Gas
MEF	Modified Energy Factor
MMTCE	Million metric tons of carbon equivalent (includes only energy consumption effects, unless otherwise noted)
NAHB	National Association of Home Builders
NCES	National Center for Educational Statistics
NEMS	National Energy Modeling System
NIST	National Institute of Standards and Technology
NWWDA	National Wood Window and Door Association
NOx	Nitrogen oxide (NO_x)
OBE	BTS's Office of Building Equipment
OBT	DOE's Office of Building Technology, State and Community Programs (formerly the Office of Building Technologies)
ODP	Ozone Depletion Potential
ORNL	Oak Ridge National Laboratory
OWIP	Office of Weatherization and Intergovernmental Program
PM-2.5	Particulate matter of aerodynamic diameter less than 2.5 microns
PM-10	Particulate matter of aerodynamic diameter less than 10 microns
PNNL	Pacific Northwest National Laboratory
Primary	Refers to energy used at the source (including fuel input to electric power plants)
PV	Photovoltaic

Key Terminology

PY	Program Year
Quad	Quadrillion Btu (10^15 Btu)
R-value	Thermal resistance measured in (Btu/Hr-SF-^{o}F)$^{-1}$
RECS	EIA's Residential Energy Consumption Survey
SEDS	State Energy Data System
SEER	Seasonal Energy Efficiency Ratio (Btu/watt-hour)
SEF	Solar Energy Factor
SF	Square feet
SHGC	Solar heat gain coefficient
SIC	Standard Industrial Classification
Site	Refers to energy used on site (i.e., delivered)
SO2	Sulfur dioxide (SO_2)
SRCC	Solar Rating and Certification Corporation
U-Factor	Thermal conductance measured in (Btu/Hr-SF-^{o}F)
VOC	Volatile organic compounds

1. U.S. Residential and Commercial Buildings Primary Energy Consumption (Quads and % of Totals)

Residential Consumption

	Elec		NGas		Oil		Coal		Renew		**Total**
1990	10.5	61%	4.5	27%	1.4	8%	0.0	0%	0.64	4%	**17.0**
2000	13.3	65%	5.1	25%	1.6	8%	0.0	0%	0.50	2%	**20.5**
2005	**14.8**	**68%**	**5.0**	**23%**	**1.5**	**7%**	**0.0**	**0%**	**0.44**	**2%**	**21.8**
2010	16.0	69%	5.2	22%	1.5	7%	0.0	0%	0.47	2%	**23.1**
2020	17.9	71%	5.4	21%	1.5	6%	0.0	0%	0.46	2%	**25.3**
2030	19.4	72%	5.5	20%	1.5	5%	0.0	0%	0.47	2%	**26.8**

Commercial Consumption

	Elec		NGas		Oil		Coal		Renew		**Total**
1990	9.5	71%	2.7	20%	1.0	7%	0.1	1%	0.10	1%	**13.4**
2000	13.0	75%	3.3	19%	0.8	4%	0.1	1%	0.13	1%	**17.2**
2005	**13.7**	**77%**	**3.1**	**18%**	**0.8**	**4%**	**0.1**	**1%**	**0.15**	**1%**	**17.9**
2010	15.0	78%	3.3	17%	0.8	4%	0.1	1%	0.15	1%	**19.4**
2020	17.8	78%	3.9	17%	0.8	3%	0.1	0%	0.15	1%	**22.7**
2030	21.0	79%	4.4	16%	0.8	3%	0.1	0%	0.16	1%	**26.5**

2. U.S. Buildings Primary Energy Consumption (Quads and % of Total)

	Elec		NGas		Oil		Coal		Renew		**Total**
1990	19.9	66%	7.2	24%	2.4	8%	0.2	1%	0.74	2%	**30.4**
2000	26.3	70%	8.4	22%	2.3	6%	0.1	0%	0.62	2%	**37.7**
2005	**28.6**	**72%**	**8.1**	**20%**	**2.3**	**6%**	**0.1**	**0%**	**0.58**	**1%**	**39.7**
2010	31.0	73%	8.5	20%	2.3	5%	0.1	0%	0.62	1%	**42.5**
2020	35.7	74%	9.3	19%	2.3	5%	0.1	0%	0.62	1%	**48.0**
2030	40.4	76%	9.8	18%	2.3	4%	0.1	0%	0.64	1%	**53.3**

3. U.S. Buildings Generic Quad (% of Total)

	Gas	Oil	Coal	Renew	Nuclear
1990	31%	11%	35%	10%	13%
2000	32%	8%	37%	8%	14%
2005	**31%**	**8%**	**38%**	**8%**	**15%**
2010	31%	7%	38%	9%	14%
2020	31%	6%	39%	9%	14%
2030	27%	6%	45%	9%	13%

4. Buildings Share of U.S. Primary Energy Consumption

	Res	Com	**Bldgs**	Indtry	Trans
1990	20%	16%	**36%**	38%	26%
2000	21%	17%	**38%**	35%	27%
2005	**22%**	**18%**	**40%**	**32%**	**28%**
2010	22%	18%	**40%**	32%	28%
2020	21%	19%	**41%**	30%	29%
2030	20%	20%	**41%**	29%	30%

5. Buildings Share of U.S. Electricity Consumption

	Res	Com	**Bldgs**	Indtry	Trans
1990	34%	31%	**65%**	35%	0%
2000	35%	34%	**69%**	31%	0%
2005	**37%**	**35%**	**72%**	**28%**	**0%**
2010	38%	35%	**73%**	27%	0%
2020	38%	37%	**75%**	25%	0%
2030	40%	40%	**80%**	23%	0%

6. U.S. Electricity Net Generation, by Plant Type (Billion Kilowatthours)

	NGas	Petro	Coal	Renew	Nucl.	Total
1990	265	118	1560	324	577	**2901**
2000	399	98	1911	316	754	**3638**
2005	**546**	**111**	**1956**	**323**	**780**	**3883**
2010	658	82	2090	370	789	**4209**
2020	776	89	2418	416	885	**4781**
2030	609	92	3191	434	896	**5402**

7. U.S. Buildings Primary Energy and Expenditure End-Use Splits, 2005

Energy (Quads and % of Totals)

End Use	Residential		Commercial		**Buildings**	
Space Heating	6.7	31%	2.5	14%	**9.2**	**23%**
Lighting	2.4	11%	4.6	26%	**7.0**	**18%**
Space Cooling	2.7	12%	2.3	13%	**5.0**	**13%**
Water Heating	2.7	12%	1.2	7%	**3.9**	**10%**
Electronics	1.6	7%	1.1	6%	**2.7**	**7%**
Refrigeration	1.6	8%	0.7	4%	**2.4**	**6%**
Cooking	1.0	5%	0.4	2%	**1.3**	**3%**
Wet Clean	1.0	5%			**1.0**	**3%**
Ventilation			1.1	6%	**1.1**	**3%**
Computers	0.2	1%	0.6	3%	**0.8**	**2%**
Other	0.8	4%	2.4	13%	**3.2**	**8%**
Adjust to SEDS	1.0	5%	1.0	5%	**2.0**	**5%**
Total	**21.8**	100%	**17.9**	100%	**39.7**	**100%**

Expenditures ($2005 and % of Totals)

End Use	Residential		Commercial		**Buildings**	
Space Heating	76	35%	27	16%	**101**	**27%**
Lighting	21	10%	36	23%	**57**	**15%**
Space Cooling	23	11%	12	8%	**42**	**11%**
Water Heating	28	13%	19	12%	**40**	**11%**
Electronics	14	6%	9	4%	**23**	**6%**
Refrigeration	14	7%	6	6%	**20**	**5%**
Cooking	10	4%	4	2%	**13**	**4%**
Wet Clean	9	4%			**9**	**3%**
Ventilation			9	6%	**9**	**2%**
Computers	2	1%	5	3%	**7**	**2%**
Other	9	4%	20	13%	**29**	**8%**
Adjust to SEDS	9	4%	11	7%	**20**	**6%**
Total	**215**	100%	**155**	100%	**370**	**100%**

8. Buildings Energy Prices and Expenditures

Prices ($2005/10^6 Btu)

	Residential Buildings				Commercial Buildings				Bldgs
	Elec	NGas	Petro	Avg	Elec	NGas	Petro	Avg	Avg
1990	31.72	7.78	12.09	**16.76**	29.29	6.49	8.22	**16.76**	**16.76**
2000	24.49	8.61	13.02	**14.31**	21.86	6.64	5.68	**16.14**	**15.08**
2005	**27.59**	**12.43**	**16.14**	**19.03**	**25.25**	**11.20**	**12.87**	**21.37**	**20.01**
2010	26.91	10.98	17.70	**18.23**	24.50	9.34	12.71	**20.31**	**19.10**
2020	26.37	10.54	16.79	**18.01**	23.95	8.67	11.67	**19.43**	**18.64**
2030	26.76	11.43	18.11	**19.08**	24.27	9.30	12.61	**19.98**	**19.50**

Petroleum includes distillate and residual fuel oils, LPG, kerosene, and motor gasoline.
2005 average electricity cost: resid. $0.094/kWh, comm. $0.086/kWh, and Bldgs. $0.090/kWh.

Expenditures ($2005 Billion)

	Residential Buildings				Commercial Buildings				Bldgs
	Elec	NGas	Petro	Total	Elec	NGas	Petro	Total	Total
1990	100.0	35.2	17.0	**152.2**	83.8	17.5	7.8	**109.1**	**261.3**
2000	110.7	43.9	20.4	**175.0**	96.0	24.1	6.9	**126.9**	**301.9**
2005	**128.5**	**61.9**	**24.8**	**215.2**	**109.1**	**35.2**	**9.9**	**154.3**	**369.5**
2010	136.2	56.9	27.0	**220.1**	116.9	30.9	9.5	**157.4**	**377.5**
2020	153.0	57.2	25.6	**235.9**	138.4	33.5	9.3	**181.2**	**417.1**
2030	173.1	62.5	26.5	**262.1**	170.7	40.6	10.3	**221.6**	**483.7**

Expenditures exclude wood and coal costs. 2005 U.S. energy expenditures were $1.04 trillion

9. Energy Consumption Intensities, by Year

Residential

	Number of Hhold (10^6)	% Post-00 Hholds	Bldgs (10^6)	*Delivered* Energy Use (10^6Btu/Hhold)	Primary Energy Use (10^6Btu/Hhold)
1980	79.6	N.A.	65.5	124.7	198.8
1990	94.2	N.A.	74.2	103.5	181.0
2000	105.7	N.A.	82.6	106.3	193.9
2005	**113.3**	**9%**	**N.A.**	**102.6**	**192.2**
2010	120.7	16%	N.A.	101.5	191.8
2020	134.7	29%	N.A.	98.3	188.0
2030	147.5	39%	N.A.	94.1	181.5

2000 number of buildings actually from 1997.
2001 households 69% single-family, 25% multi-family, and 6% mobile homes.
2001 *delivered* energy use: 80% single-family, 15% multi-family, and 5% mobile homes.

Commercial

	Floorspace (10^9 SF)	% Post-00 SF	Bldgs (10^6)	*Delivered* Energy Use (10^3Btu/SF)	Primary Energy Use (10^3Btu/SF)
1980	50.9	N.A.	3.1	117.8	208.2
1990	64.3	N.A.	4.5	104.7	207.7
2000	68.5	N.A.	4.7	119.4	250.8
2005	**74.3**	**N.A.**	**N/A**	**114.3**	**241.1**
2010	80.4	16%	N/A	113.0	240.8
2020	92.9	29%	N/A	115.1	244.6
2030	108.0	39%	N/A	115.5	245.2

2000 number of buildings actually from 1999.
2003 floorspace: 22% mercantile & service, 17% office, 14% warehouse, and 14% education. 2003*delivered* energy use: 22% mercantile & service, 19% office, 11% education, and 8% health care.

10. Residential (2001) and Commercial (2003) Vintages

Residential	% of Hholds	Commercial	% of SF
1949 or Before	25%	Prior to 1960	25%
1950 to 1959	13%	1960 to 1979	27%
1960 to 1969	13%	1980 to 1989	15%
1970 to 1979	18%	1990 to 1999	25%
1980 to 1989	17%	2000 to 2003	8%
1990 to 2001	14%		

11. Stock Energy Expenditures ($2005)

	Residential ($/Hhold)	Commercial ($/SF)
1980	1,798	1.92
1990	1,615	1.70
2000	1,617	1.85
2005	**1,899**	**2.09**
2010	1,824	1.97
2015	1,729	1.89
2020	1,751	1.96

12. Carbon Dioxide Emissions for U.S. Buildings

(10^6 Metric Tons of Carbon/Year)

	Buildings			Bldgs % of	Bldgs % of
	Elec	*Site* Fossil	Total	U.S. Emiss	Global Emiss
1990	317.2	153.7	470.9	35%	8%
2000	426.2	167.4	593.5	38%	9%
2005	**466.0**	**164.3**	**630.3**	**39%**	**9%**
2010	498.4	168.7	667.1	39%	9%
2020	579.5	180.9	760.4	40%	8%
2030	697.7	187.7	885.4	41%	8%

Buildings emissions equal emissions of Japan, France, and the U. K. combined.
2005 U.S. emissions = 1,623 MMTCE. 2004 Global emissions = 7,348 MMTCE.

13. EPA Emissions for U.S. Buildings, 2002

(10^6 Short Tons)

	Buildings			Bldgs % of
	Wood/*Site* Fossil	Elec	Total	U.S. Emiss
SO2	0.58	7.34	7.919	52%
NOx	0.73	3.35	4.078	19%
CO	2.50	0.36	2.856	3%
VOCs	0.79	0.04	0.828	5%
PM-2.5	0.38	0.42	0.8	12%
PM-10	0.41	0.50	0.901	4%

14. Value of New, Improvement & Repair Building Construction ($2005 Billion)

	Value of New Construction			Bldgs % of	Value of Improvement & Repair			Bldgs % of
	Resid	Comm	Bldgs	U.S. GDP	Resid	Comm	Bldgs	U.S. GDP
1980	149.4	143.9	293.2	5.0%	96.7	N.A.	N.A.	N.A.
1985	192.1	203.7	395.7	5.8%	132.8	126.2	259.0	3.8%
1990	187.8	204.8	392.7	4.9%	159.5	128.3	287.8	3.6%
1995	214.7	185.8	400.6	4.4%	153.0	111.2	264.2	2.9%
2000	303.5	291.1	594.6	5.4%	172.5	180.6	353.1	3.2%
2005	**490.0**	**285.9**	**775.8**	**6.2%**	**215.0**	**177.4**	**392.4**	**3.2%**

2005 U.S. GDP = $12.46 trillion

15. 1998 Cost Breakdown of a 2,150-Square-Foot, New Single-Family Home ($2005)

	Cost	
Finished Lot	62,539	24%
Construction Cost	4,087	2%
Financing	4,985	2%
Overhead & General Expenses	15,139	6%
Marketing	3,716	1%
Sales Commission	8,940	3%
Profit	24,350	9%

16. Residential New Single-Family Homes Completed

	# of Units	Average SF
1980	957,000	1,730
1990	966,000	2,080
2000	1,241,800	2,266
2006	**1,654,000**	**2,469**

1980 SF extrapolated from 1978 and 1981 data.

17. Design and Construction Employment

	Employees (thousands)		Builders	
	Architects	Construction (1)	(companies)	
1980	N.A.	3,065	93,600	
1990	N.A.	3,861	119,300	
2000	215	5,183	134,079	(2)
2005	**235**	**7,277**	**N.A.**	

1) Excludes industrial building and heavy construction.
2) Builders is for 1997. Builders exclude homebuilding establishments without payrolls, estimated by NAHB at an additional 210,000 in 1992.

18. FY 2005 Energy Burdens

	Mean Individual	Median Individual	Mean Group
All Hholds	6.8%	3.7%	2.9%
Fed Elgble Hhold	14.6%	8.6%	9.1%
Fed Ineligible Hhold	3.2%	2.8%	2.3%

Average income of a Federally eligible household was $16,264 in 2004.

19. Construction Waste

2 to 7 tons for each new single-family detached house.
Average of 4 pounds per square foot for new single-family detached house.
30 to 35 million tons of building construction, renovation, and demolition waste each year.
Construction of typical 2,000 sq.ft. home results in 4 tons of waste (wood/paper: 46%, drywall: 25%, masonry: 13%, other: 17%, hazardous material: 1%)

20. Weatherization Facts

5.8 million homes have been weatherized since 1976.
DOE creates an average energy savings of $358 a year with a cost-benefit ratio of 1.53.
DOE Weatherization program requires that states spend no more than an average of $2,885 per household in PY 2007. All states use energy audits to determine the most cost-effective weatherization measures.

21. 2003 U.S. Private Investment into Construction R&D

Sector	Percent of Sales
Average Construction R&D (1)	0.6
Heavy Construction	2.0
Lumber and Wood Products	0.3
Special Trade Construction	0.2
Fans Blowers and Air Cleaning Equip.	1.6
Commercial Buildings Operations	2.2
Building Technology	
Appliances	2.0
Lighting	1.2
HVAC	1.5
U.S. Industry Average	3.6

1) Includes bridges, roads, buildings, dams, etc.

22. 2006 Five Largest Residential Homebuilders

Homebuilder	Home Closings	% of Closings
D.R. Horton	53,410	5.0%
Pulte Homes	49,568	4.7%
Lennar Homes	41,487	3.9%
Centex Corporation	37,539	3.5%
KB Home	32,124	3.0%
Total of Top Five	**214,128**	**20.2%**
Habitat for Humanity	4,862	0.46%

2006 total U.S. new home closings was 1.06 million. 2006 total share of top 100 builders was 47.0%.

The summary tables correspond to the following tables in Chapters 1 through 7 of the Buildings Energy Data Book

1.	1.2.1, 1.3.1	**5.**	1.1.6	**8.**	4.1.1, 4.1.3	**11.**	4.2.2, 4.3.2	**15.**	4.2.8	**19.**	3.4.1, 3.4.2
2.	1.1.1	**6.**	1.5.4	**9.**	1.2.4, 1.2.6, 1.3.4, 1.3.6,	**12.**	3.1.1	**16.**	2.1.6	**20.**	7.1.1, 7.1.4, 7.1.7
3.	1.1.5	**7.**	1.1.4, 1.2.3, 1.3.3,		2.1.1, 2.1.2, 2.2.1, 2.2.2	**13.**	3.3.1	**17.**	4.6.1	**21.**	4.5.4
4.	1.1.3		4.1.4, 4.2.1, & 4.3.1	**10.**	2.1.5, 2.2.6	**14.**	4.5.2, 4.5.3, 5.1.2	**18.**	4.2.7, 7.1.1	**22.**	5.1.1

1.1.1 U.S. Residential and Commercial Buildings Total Primary Energy Consumption (Quadrillion Btu and Percent of Total)

	Natural Gas		Petroleum (1)		Coal		Renewable(2)		Electricity Sales	Electricity Losses	Electricity Total		TOTAL (2)		Growth Rate 2005-Year
1980	7.52	28%	3.04	11%	0.15	1%	0.87	3%	4.35	10.51	14.86	56%	26.43	100%	-
1990	7.22	24%	2.36	8%	0.16	1%	0.74	2%	6.01	13.92	19.93	66%	30.40	100%	-
2000	8.35	22%	2.32	6%	0.10	0%	0.62	2%	8.03	18.26	26.28	70%	37.67	100%	-
2005	**8.13**	**20%**	**2.31**	**6%**	**0.11**	**0%**	**0.58**	**1%**	**8.98**	**19.58** (3)	**28.55**	**72%**	**39.69**	**100%**	-
2010	8.50	20%	2.28	5%	0.11	0%	0.62	1%	9.83	21.17	31.00	73%	42.50	100%	1.4%
2015	8.98	20%	2.34	5%	0.11	0%	0.61	1%	10.71	22.57	33.28	73%	45.33	100%	1.3%
2020	9.29	19%	2.32	5%	0.11	0%	0.62	1%	11.58	24.12	35.70	74%	48.04	100%	1.3%
2025	9.55	19%	2.30	5%	0.11	0%	0.62	1%	12.49	25.47	37.96	75%	50.53	100%	1.2%
2030	9.83	18%	2.28	4%	0.11	0%	0.64	1%	13.51	26.91	40.41	76%	53.26	100%	1.2%

Note(s): 1) Petroleum includes distillate and residual fuels, liquefied petroleum gas, kerosene, and motor gasoline. 2) Includes *site*-marketed and non-marketed renewable energy in Table 1.1.4. 3) 2005 *site*-to-source electricity conversion = 3.18.

Source(s): EIA, State Energy Data 2004: Consumption, June 2007, Tables 8-12, p. 18-22 for 1980-2000; and EIA, Annual Energy Outlook 2007, Feb. 2007, Table A2, p. 137-139 for 2005-2030 and Table A17, p. 163 for non-marketed renewable energy.

1.1.2 U.S. Buildings *Site* Renewable Energy Consumption (Quadrillion Btu) (1)

	Wood (2)	Solar Thermal (3)	Solar PV (3)	GHP (4)	Total	Growth Rate 2005-Year
1980	0.8670	0.0000	N.A.	0.0000	0.8670	-
1990	0.6760	0.0560	N.A.	0.0090	0.7410	-
2000	0.5490	0.0610	N.A.	0.0170	0.6270	-
2005	**0.5286**	**0.0513**	**0.0011**	**0.0031**	**0.5840**	-
2010	0.5456	0.0604	0.0041	0.0064	0.6165	1.1%
2015	0.5258	0.0691	0.0045	0.0089	0.6083	0.4%
2020	0.5228	0.0769	0.0052	0.0114	0.6162	0.4%
2025	0.5163	0.0841	0.0079	0.0137	0.6220	0.3%
2030	0.5119	0.0916	0.0163	0.0158	0.6357	0.3%

Note(s): 1) Does not include renewable energy consumed by electric utilities (including hydroelectric). 2) Includes wood and wood waste, municipal solid waste, and other biomass used by the commercial sector to cogenerate electricity. 3) Includes only solar energy. 4) GHP = Ground-coupled heat pumps.

Source(s): EIA, State Energy Data 2004: Consumption, June 2007, Tables 8-12, p. 18-22 for 1980-2000; and EIA, AEO 2007, Feb. 2007, Table A17, p. 163 for 2005-2030.

1.1.3 Buildings Share of U.S. Primary Energy Consumption (Percent)

	Buildings Residential	Buildings Commercial	**Buildings Total**	Industry	Transportation	Total	Total Consumption (quads)
1980 (1)	20%	14%	34%	41%	25%	100%	78.3
1990	20%	16%	36%	38%	26%	100%	84.7
2000	21%	17%	38%	35%	27%	100%	98.9
2005	**22%**	**18%**	**40%**	**32%**	**28%**	**100%**	**100.2**
2010	22%	18%	40%	32%	28%	100%	106.6
2015	22%	19%	40%	31%	29%	100%	112.4
2020	21%	19%	41%	30%	29%	100%	118.3
2025	21%	20%	41%	30%	29%	100%	124.5
2030	20%	20%	41%	29%	30%	100%	131.3

Note(s): 1) Renewables are not included in the 1980 data.

Source(s): EIA, State Energy Data 2004: Consumption, June 2007, Tables 8-12, p. 18-22 for 1980-2000; and EIA, AEO 2007, Feb. 2007, Table A2, p. 137-139 for 2005-2030 data and Table A17, p. 163 for non-marketed renewable energy.

1.1.4 2005 U.S. Buildings Energy End-Use Splits, by Fuel Type (Quadrillion Btu)

	Natural Gas	Fuel Oil (1)	LPG	Other Fuel(2)	Renw. En.(3)	*Site* Electric	*Site* Total	*Site* Percent	Primary Electric (4)	Primary Total	Primary Percent
Space Heating (5)	4.86	1.15	0.26	0.23	0.41	0.73	7.65	38.0%	2.32	9.24	23.3%
Lighting						2.19	2.19	10.9%	6.97	6.97	17.6%
Space Cooling	0.02					1.57	1.59	7.9%	4.99	5.02	12.6%
Water Heating	1.71	0.18	0.05		0.05	0.59	2.59	12.9%	1.89	3.88	9.8%
Electronics (6)						0.86	0.86	4.3%	2.73	2.73	6.9%
Refrigeration (7)						0.75	0.75	3.7%	2.38	2.38	6.0%
Cooking	0.45		0.03			0.27	0.75	3.7%	0.86	1.34	3.4%
Ventilation (8)						0.34	0.34	1.7%	1.08	1.08	2.7%
Wet Clean (9)	0.07					0.31	0.38	1.9%	0.98	1.05	2.6%
Computers						0.26	0.26	1.3%	0.83	0.83	2.1%
Other (10)	0.31	0.02	0.26	0.05	0.12	0.77	1.52	7.6%	2.43	3.19	8.0%
Adjust to SEDS (11)	0.71	0.18				0.35	1.24	6.2%	1.10	2.00	5.0%
Total	**8.13**	**1.54**	**0.60**	**0.28**	**0.58**	**8.98**	**20.11**	100%	**28.55**	**39.69**	100%

Note(s): 1) Includes distillate fuel oil (1.45 quad) and residual fuel oil (0.12 quad). 2) Kerosene (0.11 quad) and coal (0.10 quad) are assumed attributable to space heating. Motor gasoline (0.05 quad) assumed attributable to other end-uses. 3) Comprised of wood space heating (0.53 quad), biomass (0.09 quad), solar water heating (0.05 quad), geothermal space heating (less than 0.01 quad), and solar photovoltaics (PV) less than 0.01 quad). 4) *Site* -to-source electricity conversion (due to generation and transmission losses) = 3.18. 5) Includes furnace fans (0.27 quad). 6) Includes color television (0.96 quad) and other office equipment (0.65 quad). 7) Includes refrigerators (1.24 quad) and freezers (0.40 quad). Includes commercial refrigeration. 8) Commercial only; residential fan and pump energy use included proportionately in space heating and cooling. 9) Includes clothes washers (0.11 quad), natural gas clothes dryers (0.07 quad), electric clothes dryers (0.79 quad) and dishwashers (0.08 quad). Does not include water heating energy. 10) Includes residential small electric devices, heating elements, motors, swimming pool heaters, hot tub heaters, outdoor grills, and natural gas outdoor lighting. Includes commercial service station equipment, ATMs, telecommunications equipment, medical equipment, pumps, emergency electric generators, combined heat and power in commercial buildings, and manufacturing performed in commercial buildings. 11) Energy adjustment EIA uses to relieve discrepancies between data sources. Energy attributable to the residential and commercial buildings sector, but not directly to specific end-uses.

Source(s): EIA, Annual Energy Outlook (AEO) 2007, Feb. 2007, Tables A2, p. 137-139, Table A4, p. 142-143, Table A5, p. 144-145, and Table A17, p. 163; EIA, National Energy Modeling System (NEMS) for AEO 2007, Feb. 2007; BTS/A.D. Little, Electricity Consumption by Small End-Uses in Residential Buildings, Aug. 1998, Appendix A for residential electric end-uses; BTS/A.D. Little, Energy Consumption Characteristics of Commercial Building HVAC Systems, Volume II: Thermal Distribution, Auxiliary Equipment, and Ventilation, Oct. 1999, p. 1-2 and 5-25 - 5-26; EIA, AEO 1998, Dec. 1997, Table A5, p. 108-109 for 1995 ventilation; and BTP/Navigant Consulting, U.S. Lighting Market Characterization, Volume I, Sept. 2002, Table 8-2, p. 63;

1.1.5 Shares of U.S. Buildings Generic Quad (Percent) (1)

				Renewables (2)				
	Natural Gas	Petroleum	Coal	Hydroelectric	Other	Total	Nuclear	Total
1980	37%	18%	30%	7%	4%	10%	6%	100%
1990	31%	11%	35%	5%	4%	10%	13%	100%
2000	32%	8%	37%	5%	3%	8%	14%	100%
2005	**31%**	**8%**	**38%**	**5%**	**3%**	**8%**	**15%**	**100%**
2010	31%	7%	38%	5%	4%	9%	14%	100%
2015	32%	7%	38%	5%	4%	9%	14%	100%
2020	31%	6%	39%	5%	4%	9%	14%	100%
2025	29%	6%	42%	5%	4%	9%	14%	100%
2030	27%	6%	45%	4%	4%	9%	13%	100%

Note(s): 1) A generic quad is primary energy apportioned between the various primary fuels according to their relative consumption. See Table 6.1.1 for further explanation. 2) Electric imports included in renewables.

Source(s): EIA, State Energy Data 2004: Consumption, June 2007, Tables 8-12, p. 18-22 for 1980-2000; and EIA, Annual Energy Outlook 2007, Feb. 2007, Table A2, p. 137-139 for 2005-2030 consumption and Table A17, p. 163 for non-marketed renewable energy.

1.1.6 Buildings Share of U.S. Electricity Consumption (Percent)

	Buildings						*Delivered Total*
	Residential	Commercial	**Total**	Industry	Transportation	Total	(quads)
1980	34%	27%	**61%**	39%	0%	100%	7.1
1990	34%	31%	**65%**	35%	0%	100%	9.3
2000	35%	34%	**69%**	31%	0%	100%	11.7
2005 (1)	**37%**	**35%**	**72%**	**28%**	**0%**	**100%**	**12.5**
2010	38%	35%	**73%**	27%	0%	100%	13.5
2015	37%	36%	**74%**	26%	0%	100%	14.5
2020	38%	37%	**75%**	25%	0%	100%	15.4
2025	37%	39%	**76%**	24%	0%	100%	16.5
2030	40%	40%	**80%**	23%	0%	100%	17.6

Note(s): 1) Buildings accounted for 80% (or $238 billion) of total U.S. electricity expenditures.

Source(s): EIA, State Energy Data 2004: Consumption, June 2007, Tables 8-12, p. 18-22 for 1980-2000; and EIA, Annual Energy Outlook 2007, Feb. 2007, Table A2, p. 137-139 for 2005-2030 consumption, Table A3, p. 140-141 for 2005 expenditures.

1.1.7 Buildings Share of U.S. Natural Gas Consumption (Percent)

	Site Consumption				Primary Consumption			U.S. Natural Gas Total
	Buildings	Industry	Electric Gen.	Transportation	**Buildings**	Industry	Transportation	(quads)
1980	**37%**	41%	19%	3%	**50%**	47%	3%	20.4
1990	**37%**	43%	17%	3%	**49%**	47%	3%	19.8
2000	**35%**	40%	22%	3%	**53%**	45%	3%	23.8
2005 (1)	**36%**	**35%**	**26%**	**3%**	**55%**	**42%**	**3%**	**22.6**
2010	**34%**	36%	27%	3%	**54%**	43%	3%	24.7
2015	**34%**	35%	28%	3%	**55%**	42%	3%	26.1
2020	**34%**	35%	27%	3%	**55%**	42%	3%	27.0
2025	**35%**	36%	25%	3%	**54%**	42%	3%	27.1
2030	**37%**	37%	23%	3%	**54%**	43%	3%	26.9

Note(s): 1) Buildings accounted for 62% (or $102 billion) of total U.S. natural gas expenditures.

Source(s): EIA, State Energy Data 2004: Consumption, June 2007, Tables 8-12, p. 18-22 for 1980-2000; and EIA, Annual Energy Outlook 2007, Feb. 2007, Table A2, p. 137-139 for 2005-2030 consumption, Table A3, p. 140-141 for 2005 expenditures.

1.1.8 Buildings Share of U.S. Petroleum Consumption (Percent)

	Site Consumption				Primary Consumption			U.S. Petroleum Total
	Buildings	Industry	Electric Gen.	Transportation	**Buildings**	Industry	Transportation	(quads)
1980	**9%**	28%	8%	56%	**14%**	30%	56%	34.2
1990	**7%**	25%	4%	64%	**10%**	26%	64%	33.6
2000	**6%**	24%	3%	67%	**8%**	24%	67%	38.4
2005	**6%**	**24%**	**3%**	**68%**	**8%**	**25%**	**67%**	**40.6**
2010	**5%**	23%	2%	70%	**7%**	23%	70%	41.8
2015	**5%**	22%	2%	71%	**7%**	22%	71%	44.3
2020	**5%**	21%	2%	72%	**7%**	22%	72%	46.5
2025	**5%**	21%	2%	73%	**6%**	21%	73%	49.0
2030	**4%**	20%	2%	73%	**6%**	21%	73%	52.2

Note(s): 1) Buildings accounted for an estimated 7.5% (or $31 billion) of total U.S. petroleum expenditures.

Source(s): EIA, State Energy Data 2004: Consumption, June 2007, Tables 8-12, p. 18-22 for 1980-2000; and EIA, Annual Energy Outlook 2007, Feb. 2007, Table A2, p. 137-139 for 2005-2030 consumption, Table A3, p. 137-138 for 2005 expenditures.

1.1.9 Buildings Share of U.S. Petroleum Consumption (Million Barrels per Day)

	Buildings					
	Residential	Commercial	**Total**	Industry	Transportation	Total
1980	1.20	1.14	**2.34**	5.17	9.55	17.06
1990	0.90	0.75	**1.66**	4.44	10.89	16.99
2000	1.02	0.65	**1.67**	5.01	13.01	19.70
2005	**0.93**	**0.55**	**1.48**	**4.75**	**12.95**	**19.18**
2010	0.88	0.51	**1.39**	4.59	13.75	19.73
2015	0.90	0.54	**1.45**	4.69	14.77	20.91
2020	0.89	0.55	**1.44**	4.75	15.78	21.97
2025	0.88	0.56	**1.44**	4.87	16.86	23.17
2030	0.87	0.57	**1.44**	5.09	18.11	24.65

Source(s): EIA, Annual Energy Review 2006, June 2007, Table 5.13a for 1980-2000 buildings, Table 5.13b for 1980 to 2000 industry, Table 5.13c for 1980-2000 transportation, and Table 5.13d for 1980-2000 electricity generators; and EIA, Annual Energy Outlook 2007, Feb. 2007, Table A2, p. 137-139 for 2005-2030 consumption; EIA, State Energy Data 2004: Consumption, June 2007, Tables 8-12, p. 18-22 for 1980-2000.

1.1.10 World Primary Energy Consumption and Population, by Country/Region

	Energy Consumption (Quad)				Population (million)				Annual Growth Rate 1990-2004		Annual Growth Rate 2004-2010	
Region/Country	1990	2004		2010	1990	2004		2010	Energy	Pop.	Energy	Pop.
United States	84.7	100.7	22.5%	106.5	254	294	4.6%	310	1.2%	1.1%	0.9%	0.9%
OECD Europe	69.9	81.1	18.2%	84.1	497	532	8.3%	543	1.1%	0.5%	0.6%	0.3%
China	27.0	59.6	13.3%	82.6	1,155	1,307	20.5%	1,355	5.8%	0.9%	5.6%	0.6%
Russia	39.0	30.1	6.7%	32.9	148	144	2.3%	140	-1.8%	-0.2%	1.5%	-0.5%
Other Non-OECD Asia	12.5	24.9	5.6%	30.3	743	962	15.1%	1,054	5.0%	1.9%	3.3%	1.5%
Japan	18.4	22.6	5.1%	23.5	124	128	2.0%	128	1.5%	0.2%	0.7%	0.0%
Central & S. America	14.5	22.5	5.0%	27.7	360	448	7.0%	486	3.2%	1.6%	3.5%	1.4%
Middle East	11.3	21.1	4.7%	26.3	137	191	3.0%	216	4.6%	2.4%	3.7%	2.1%
Oth. Non-OECD Europe	28.3	19.6	4.4%	21.9	200	198	3.1%	198	-2.6%	-0.1%	1.9%	0.0%
India	8.0	15.4	3.4%	18.2	849	1,087	17.0%	1,183	4.8%	1.8%	2.8%	1.4%
Africa	9.5	13.7	3.1%	16.9	636	887	13.9%	1,007	2.6%	2.4%	3.6%	2.1%
Canada	11.1	13.6	3.0%	15.5	28	32	0.5%	34	1.5%	1.0%	2.2%	1.0%
South Korea	3.8	9.0	2.0%	9.6	43	48	0.8%	49	6.4%	0.8%	1.1%	0.3%
Mexico	5.0	6.6	1.5%	8.3	84	106	1.7%	113	2.0%	1.7%	3.9%	1.1%
Australia & N. Zealand	4.4	6.2	1.4%	6.8	20	24	0.4%	25	2.5%	1.3%	1.6%	0.7%
Total World	**347.3**	**446.7**	100%	**511.1**	**5,278**	**6,388**	100%	**6,841**	1.8%	1.4%	2.3%	1.1%

Source(s): EIA, International Energy Outlook 2007, May 2007, Table A1, p. 83 and Table A14, p. 97.

1.2.1 Residential Primary Energy Consumption, by Year and Fuel Type (Quadrillion Btu and Percent of Total)

	Natural Gas		Petroleum (1)		Coal		Renewable(2)		Electricity Sales	Electricity Losses	Electricity Total		TOTAL (2)		Growth Rate 2005-Year
1980	4.86	31%	1.75	11%	0.03	0%	0.85	5%	2.45	5.91	8.36	53%	15.84	100%	-
1990	4.52	27%	1.41	8%	0.03	0%	0.64	4%	3.15	7.30	10.45	61%	17.05	100%	-
2000	5.10	25%	1.56	8%	0.01	0%	0.50	2%	4.07	9.26	13.33	65%	20.50	100%	-
2005	**4.98**	**23%**	**1.54**	**7%**	**0.01**	**0%**	**0.44**	**2%**	**4.66**	**10.15** (3)	**14.81**	**68%**	**21.78**	**100%**	-
2010	5.18	22%	1.53	7%	0.01	0%	0.47	2%	5.06	10.90	15.96	69%	23.15	100%	1.2%
2015	5.35	22%	1.55	6%	0.01	0%	0.46	2%	5.43	11.44	16.87	70%	24.23	100%	1.1%
2020	5.43	21%	1.53	6%	0.01	0%	0.46	2%	5.80	12.08	17.89	71%	25.32	100%	1.0%
2025	5.45	21%	1.49	6%	0.01	0%	0.47	2%	6.13	12.50	18.63	72%	26.05	100%	0.9%
2030	5.47	20%	1.46	5%	0.01	0%	0.47	2%	6.47	12.89	19.36	72%	26.78	100%	0.8%

Note(s): 1) Petroleum includes distillate oil, liquefied petroleum gas, and kerosene. 2) Includes *site*-marketed and non-marketed renewable energy. 3) 2005 *site*-to-source electricity conversion = 3.18.

Source(s): EIA, State Energy Data 2004: Consumption, June 2007, Tables 8-12, p. 18-22 for 1980-2000; and EIA, Annual Energy Outlook 2007, Feb. 2007, Table A2, p.137-139 for 2005-2030 consumption and Table A17, p. 163 for non-marketed renewable energy.

1.2.2 Residential *Site* Renewable Energy Consumption (Quadrillion Btu) (1)

	Wood	Solar Thermal	Solar PV	GHP	Total	Growth Rate 2005-Year
1980	0.8460	0.0000	N.A.	0.0000	0.8460	-
1990	0.5820	0.0560	N.A.	0.0060	0.6440	-
2000	0.4300	0.0610	N.A.	0.0090	0.5000	-
2005	**0.4084**	**0.0267**	**0.0001**	**0.0031**	**0.4382**	-
2010	0.4254	0.0342	0.0010	0.0064	0.4670	1.3%
2015	0.4056	0.0415	0.0011	0.0089	0.4571	0.4%
2020	0.4026	0.0489	0.0012	0.0114	0.4641	0.4%
2025	0.3962	0.0558	0.0013	0.0137	0.4670	0.3%
2030	0.3918	0.0630	0.0015	0.0158	0.4721	0.3%

Note(s): 1) Does not include renewable energy consumed by electric utilities (including hydroelectric).

Source(s): EIA, State Energy Data 2004: Consumption, June 2007, Tables 8-12, p. 18-22 for 1980-2000; and EIA, Annual Energy Outlook 2007, Feb. 2007, Table A17, p. 163 for 2005-2030.

1.2.3 2005 Residential Energy End-Use Splits, by Fuel Type (Quadrillion Btu)

	Natural Gas	Fuel Oil	LPG	Other Fuel(1)	Renw. En.(2)	*Site* Electric	*Site* Total	*Site* Percent	Primary Electric (3)	Primary Total	Primary Percent
Space Heating (4)	3.52	0.82	0.26	0.11	0.41	0.49	5.61	48.2%	1.57	6.69	30.7%
Space Cooling	0.00					0.84	0.84	7.2%	2.67	2.67	12.3%
Water Heating	1.14	0.12	0.05		0.03	0.42	1.75	15.0%	1.33	2.66	12.2%
Lighting						0.75	0.75	6.5%	2.40	2.40	11.0%
Refrigeration (5)						0.52	0.52	4.4%	1.64	1.64	7.5%
Electronics (6)						0.50	0.50	4.3%	1.61	1.61	7.4%
Wet Clean (7)	0.07					0.31	0.38	3.2%	0.98	1.05	4.8%
Cooking	0.22		0.03			0.23	0.48	4.1%	0.74	0.98	4.5%
Computers						0.08	0.08	0.7%	0.25	0.25	1.1%
Other (8)	0.04		0.17		0.00	0.19	0.41	3.5%	0.61	0.83	3.8%
Adjust to SEDS (9)						0.32	0.32	2.8%	1.02	1.02	4.7%
Total	**4.98**	**0.93**	**0.51**	**0.11**	**0.44**	**4.66**	**11.63**	100%	**14.81**	**21.78**	100%

Note(s): 1) Kerosene (0.10 quad) and coal (0.01 quad) are assumed attributable to space heating. 2) Comprised of wood space heating (0.41 quad), solar water heating (0.03 quad), geothermal space heating (less than 0.01 quad), and solar PV (less than 0.01 quad). 3)*Site*-to-source electricity conversion (due to generation and transmission losses) = 3.18. 4) Includes furnace fans (0.27 quad). 5) Includes biomass, (0.02 quad) solar water heating, and (less than 0.01 quad) solar pv. 4)*Site*-to-source electricity conversion (due to 7) Includes clothes washers (0.11 quad), natural gas clothes dryers (0.07 quad), electric clothes dryers (0.79 quad), and dishwashers (0.08 quad). Does not include water heating energy. 8) Includes small electric devices, heating elements, motors, swimming pool heaters, hot tub heaters, outdoor grills, and natural gas outdoor lighting. 9) Energy adjustment EIA uses to relieve discrepancies between data sources. Energy attributable to the residential buildings sector, but not directly to specific end-uses.

Source(s): EIA, Annual Energy Outlook (AEO) 1999, Jan., 1999, Tables A2, p.113-114; EIA, AEO 2007, Feb. 2007, Tables A2, p. 137-139, Table A4, p. 142-143 and Table A17, p. 163; and BTS/A.D. Little, Electricity Consumption by Small End-Uses in Residential Buildings, Aug. 1998, Appendix A for residential electric end-uses.

1.2.4 Residential Delivered and Primary Energy Consumption Intensities, by Year

	Number of Households (10^6)	Percent Post-2000 Households (1)	*Delivered Energy Consumption* Total (10^15 Btu)	*Delivered Energy Consumption* Per Household (10^6 Btu/Hhold)	Primary Energy Consumption Total (10^15 Btu)	Primary Energy Consumption Per Household (10^6 Btu/Hhold)
1980	79.6	N.A.	9.9	124.7	15.8	198.8
1990	94.2	N.A.	9.8	103.5	17.1	181.0
2000	105.7	N.A.	11.2	106.3	20.5	193.9
2005	**113.3**	**9%**	**11.6**	**102.6**	**21.8**	**192.2**
2010	120.7	16%	12.3	101.5	23.1	191.8
2015	127.8	23%	12.8	100.1	24.2	189.7
2020	134.7	29%	13.2	98.3	25.3	188.0
2025	141.2	34%	13.5	95.9	26.0	184.5
2030	147.5	39%	13.9	94.1	26.8	181.5

Note(s): 1) Percent of houses built after Dec. 31, 2000.

Source(s): EIA, State Energy Data 2004: Consumption, June 2007, Tables 8-12, p. 18-22 for 1980-2000; EIA, Annual Energy Outlook 2007, Feb. 2007, Table A2, p. 137-139, Table A4, p. 142-143, and Table A17, p. 163 for 2005-2030, and Table A19, p. 165 for households; and DOC, Statistical Abstract of the United States 2006, Jan. 2006, Table No. 945, p. 626 for 1980-2000 households.

1.2.5 2001 Residential *Delivered* Energy Consumption Intensities, by Vintage

Year	Per Square Foot (10^3 Btu)	Per Household (10^6 Btu)	Per Household Member (10^6 Btu)	Percent of Total Consumption
Prior to 1970	51.6	100.7	40.3	56%
1970 to 1979	45.5	79.0	31.6	15%
1980 to 1989	41.4	79.7	31.9	15%
1990 to 1999	38.5	91.3	31.2	13%
2000 to 2001	36.6	111.1	32.9	1%
Average	46.7	92.2	36.0	

Source(s): EIA, A Look at Residential Energy Consumption in 2001, Apr. 2004, Table CE1-6.1u and Table CE1-6.2u.

1.2.6 2001 Residential *Delivered* Energy Consumption Intensities, by Housing Type

Type	Per Square Foot (10^3 Btu)	Per Household (10^6 Btu)	Per Household Members (10^6 Btu)	Percent of Total Consumption
Single-Family:	**44.8**	**107.3**	**39.8**	**80.1%**
Detached	44.7	108.5	39.6	69.4%
Attached	45.6	100.4	37.5	10.7%
Multi-Family:	**52.1**	**54.3**	**25.8**	**14.6%**
2 to 4 units	56.1	78.1	34.3	7.5%
5 or more units	48.5	41.0	20.5	7.1%
Mobile Homes	**72.0**	**75.9**	**29.4**	**5.3%**
				100%

Source(s): EIA, A Look at Residential Energy Consumption in 2001, Apr. 2004, Table CE1-6.1u and Table CE1-6.2u.

1.2.7 2001 Residential *Delivered* Energy Consumption Intensities, by Census Region

Region	Per Square Foot (10^3 Btu)	Per Household (10^6 Btu)	Per Household Members (10^6 Btu)	Percent of Total Consumption
Northeast	50.4	106.6	42.3	22%
Midwest	53.6	116.7	46.0	29%
South	44.8	82.5	32.1	33%
West	42.5	70.1	24.7	17%
				100%

Source(s): EIA, A Look at Residential Energy Consumption in 2001, Apr. 2004, Table CE1-9c, Table CE1-10c, Table CE1-11c, Table CE1-12c, Table HC1-9a, Table HC1-10a, Table HC1-11a, Table HC1-12a, Table HC2-9a, Table HC2-10a, Table HC2-11a, and Table HC2-12a.

1.2.8 1997 Residential *Delivered* Energy Consumption Intensities, by Ownership of Unit

Ownership	Per Square Foot (10^3 Btu)	Per Household (10^6 Btu)	Per Household Members (10^6 Btu)	Percent of Total Consumption
Owned	**58.3**	**114.7**	**43.3**	**77%**
Rented	**70.3**	**72.5**	**29.4**	**23%**
Public Housing	62.7	51.0	25.3	2%
Not Public Housing	70.9	74.8	29.8	22%
				100%

Source(s): EIA, 1997 Residential Energy Consumption Survey, Nov. 1999.

1.2.9 Aggregate Residential Building Component Loads as of 1998 (1)

	Loads (quads) and Percent of Total Loads			
Component	Heating		Cooling	
Roof	-0.65	12%	0.16	14%
Walls	-1.00	19%	0.11	10%
Foundation	-0.76	15%	-0.07	-
Infiltration	-1.47	28%	0.19	16%
Windows (conduction)	-1.34	26%	0.01	1%
Windows (solar gain)	0.43	-	0.37	32%
Internal Gains	0.79	-	0.31	27%
NET Load	**-3.99**	100%	**1.08**	100%

Note(s): 1) "Loads" represents the thermal energy losses/gains that when combined will be offset by a building's heating/cooling system to maintain a set interior temperature (which then equals *site* energy).

Source(s): LBNL, Residential Heating and Cooling Loads Component Analysis, Nov. 1998, Figure P-1, P-1 and Appendix C: Component Loads Data Tables.

1.2.10 1997 Residential *Delivered* Energy Consumption Intensities, by Principal Building Type and Vintage

	Consumption (10^3 Btu/SF)		Consumption (10^6 Btu/Hhold)		Consumption (10^6 Btu/Member)	
Building Type	Pre-1990	1990-1997	Pre-1990	1990-1997	Pre-1990	1990-1997
Single-Family	**60.9**	**45.1**	**115.4**	**108.4**	**42.6**	**36.8**
Detached	60.2	44.8	118.5	112.8	42.9	36.8
Attached	66.0	48.0	96.1	76.0	40.7	37.3
Multi-Family	**69.0**	**42.6**	**61.1**	**40.8**	**28.8**	**22.4**
2 to 4 units	94.4	50.4	92.8	46.0	41.3	20.1
5 or more units	58.0	41.5	49.3	40.0	23.7	22.8
Mobile Homes	**92.2**	**50.6**	**81.7**	**70.9**	**50.5**	**45.2**

Source(s): EIA, 1997 Residential Energy Consumption Survey, Nov. 1999.

1.3.1 Commercial Primary Energy Consumption, by Year and Fuel Type (Quadrillion Btu and Percent of Total)

	Natural Gas		Petroleum (1)		Coal		Renewable(2)		Electricity Sales	Electricity Losses		Electricity Total		TOTAL (2)		Growth Rate 2005-Year
1980	2.67	25%	1.29	12%	0.12	1%	0.02	**0%**	1.91	4.60		6.51	61%	10.60	100%	-
1990	2.70	20%	0.95	7%	0.12	1%	0.10	**1%**	2.86	6.62		9.48	71%	13.35	100%	-
2000	3.25	19%	0.76	4%	0.09	1%	0.13	**1%**	3.96	9.00		12.96	75%	17.18	100%	-
2004	**3.15**	**18%**	**0.77**	**4%**	**0.10**	**1%**	**0.15**	**1%**	**4.32**	**9.42**	(3)	**13.74**	**77%**	**17.91**	**100%**	-
2010	3.31	17%	0.75	4%	0.10	1%	0.15	1%	4.77	10.27		15.04	78%	19.36	100%	1.3%
2015	3.64	17%	0.79	4%	0.10	0%	0.15	1%	5.28	11.13		16.41	78%	21.09	100%	1.5%
2020	3.86	17%	0.80	3%	0.10	0%	0.15	1%	5.78	12.03		17.81	78%	22.72	100%	1.5%
2025	4.10	17%	0.81	3%	0.10	0%	0.16	1%	6.36	12.97		19.33	79%	24.48	100%	1.5%
2030	4.36	16%	0.81	3%	0.10	0%	0.16	1%	7.03	14.01		21.05	79%	26.49	100%	1.5%

Note(s): 1) Petroleum includes distillate and residual fuels, liquefied petroleum gas, kerosene, and motor gasoline. 2) Includes *site*-marketed and non-marketed renewable energy. 3) 2005 *site*-to-source electricity conversion = 3.18.

Source(s): EIA, State Energy Data 2004: Consumption, June 2007, Tables 8-12, p. 18-22 for 1980-2000; and EIA, Annual Energy Outlook 2007, Feb. 2007, Table A2, p. 137-139 for 2005-2030 and Table A17, p. 163 for non-marketed renewable energy.

1.3.2 Commercial *Site* Renewable Energy Consumption (Quadrillion Btu) (1)

	Wood (2)	Solar Thermal (3)	Solar PV(3)	GHP	Total	Growth Rate 2005-Year
1980	0.0210	N.A.	N.A.	N.A.	0.0210	-
1990	0.0940	N.A.	N.A.	0.0030	0.0970	-
2000	0.1190	N.A.	N.A.	0.0080	0.1270	-
2005	**0.1202**	**0.0246**	**0.0010**	**N.A.**	**0.1458**	-
2010	0.1202	0.0261	0.0032	N.A.	0.1495	0.5%
2015	0.1202	0.0276	0.0035	N.A.	0.1512	0.4%
2020	0.1202	0.0279	0.0040	N.A.	0.1521	0.3%
2025	0.1202	0.0283	0.0066	N.A.	0.1550	0.3%
2030	0.1202	0.0286	0.0148	N.A.	0.1635	0.5%

Note(s): 1) Does not include renewable energy consumed by electric utilities (including hydroelectric). 2) Includes wood and wood waste, municipal solid waste, and other biomass used by the commercial sector to cogenerate electricity. 3) Includes only solar energy.

Source(s): EIA, State Energy Data 2004: Consumption, June 2007, Tables 8-12, p. 18-22 for 1980-2000; and EIA, Annual Energy Outlook 2007, Feb. 2007, Table A17, p. 163 for 2005-2030.

1.3.3 2005 Commercial Energy End-Use Splits, by Fuel Type (Quadrillion Btu)

	Natural Gas	Fuel Oil (1)	LPG	Other Fuel(2)	Renw. En.(3)	*Site* Electric	*Site* Total	*Site* Percent	Primary Electric (4)	Primary Total	Primary Percent
Lighting						1.44	1.44	16.9%	4.57	4.57	25.5%
Space Heating	1.35	0.33		0.13		0.23	2.04	24.0%	0.75	2.55	14.2%
Space Cooling	0.02					0.73	0.75	8.9%	2.32	2.34	13.1%
Water Heating	0.57	0.07			0.02	0.18	0.84	9.9%	0.56	1.23	6.8%
Ventilation						0.34	0.34	4.0%	1.08	1.08	6.0%
Electronics						0.35	0.35	4.2%	1.12	1.12	6.3%
Refrigeration						0.23	0.23	2.7%	0.74	0.74	4.1%
Computers						0.18	0.18	2.2%	0.58	0.58	3.2%
Cooking	0.23					0.04	0.27	3.2%	0.12	0.35	2.0%
Other (5)	0.26	0.02	0.09	0.05	0.12	0.57	1.12	13.2%	1.82	2.37	13.2%
Adjust to SEDS (6)	0.71	0.18				0.03	0.92	10.9%	0.08	0.98	5.5%
Total	**3.15**	**0.61**	**0.09**	**0.17**	**0.15**	**4.32**	**8.49**	100%	**13.74**	**17.91**	100%

Note(s): 1) Includes (0.48 quad) distillate fuel oil and (0.14 quad) residual fuel oil. 2) Kerosene (0.02 quad) and coal (0.10 quad) are assumed attributable to space heating. Motor gasoline (0.05 quad) assumed attributable to other end-uses. 3) Comprised of (0.12 quad) biomass, (0.02 quad) solar water heating, and (less than 0.01 quad) solar pv. 4) *Site* -to-source electricity conversion (due to generation and transmission losses) = 3.18. 5) Includes service station equipment, ATMs, telecommunications equipment, medical equipment, pumps, emergency electric generators, combined heat and power in commercial buildings, and manufacturing performed in commercial buildings. 6) Energy adjustment EIA uses to relieve discrepancies between data sources. Energy attributable to the commercial buildings sector, but not directly to specific end-uses.

Source(s): EIA, Annual Energy Outlook 2007, Feb. 2007, Tables A2, p. 137-139, Table A5, p. 144-145, and Table A17, p. 163; EIA, National Energy Modeling System for AEO 2007, Feb. 2007; BTS/A.D. Little, Energy Consumption Characteristics of Commercial Building HVAC Systems, Volume II: Thermal Distribution, Auxiliary Equipment, and Ventilation, Oct. 1999, p. 1-2 and 5-25 - 5-26; EIA, AEO 1998, Dec. 1997, Table A5, p. 108-109 for 1995 ventilation; and BTP/Navigant Consulting, U.S. Lighting Market Characterization, Volume I, Sept. 2002, Table 8-2, p. 63;

1.3.4 Commercial *Delivered* and Primary Energy Consumption Intensities, by Year

		Floorspace (10^9 SF)	Percent Post-2000 Floorspace (1)	*Delivered Energy Consumption* Total (10^15 Btu)	*Delivered Energy Consumption* Consumption per SF (10^3 Btu/SF)	Primary Energy Consumption Total (10^15 Btu)	Primary Energy Consumption Consumption per SF (10^3 Btu/SF)
1980		50.9	N.A.	6.00	117.8	10.60	208.2
1990		64.3	N.A.	6.73	104.7	13.36	207.7
2000	(2)	68.5	N.A.	8.18	119.4	17.18	250.8
2005	**(2)**	**74.3**	**15%**	**8.49**	**114.3**	**17.91**	**241.1**
2010	(2)	80.4	25%	9.08	113.0	19.36	240.8
2015	(2)	86.5	35%	9.96	115.1	21.09	243.7
2020	(2)	92.9	43%	10.69	115.1	22.72	244.6
2025	(2)	100.1	52%	11.52	115.0	24.48	244.5
2030	(2)	108.0	59%	12.47	115.5	26.49	245.2

Note(s): 1) Percent built after Dec. 31, 2000. 2) Excludes parking garages and commercial buildings on multi-building manufacturing facilities.

Source(s): EIA, State Energy Data 2004: Consumption, June 2007, Tables 8-12, p. 18-22 for 1980-2000; DOE for 1980 floorspace; EIA, Annual Energy Outlook (AEO) 1994, Jan. 1994, Table A5, p. 62 for 1990 floorspace; EIA, AEO 2003, Jan. 2003, Table A5, p. 127 for 2000 floorspace; and EIA, AEO 2007, Feb. 2007, Table A2, p. 137-139, Table A5, p. 144-145, and Table A17, p.163 for 2005-2030.

1.3.5 Commercial *Delivered* Energy Consumption Intensities, by Vintage (1)

Year Constructed	Consumption per Square Foot (10^3 Btu/SF)	
Prior to 1960	84.4	23.3%
1960 to 1969	91.5	12.1%
1970 to 1979	97.0	18.3%
1980 to 1989	100.0	19.1%
1990 to 1999	90.3	19.3%
2000 to 2003	81.6	7.8%
Average	91.0	

Source(s): EIA, 2003 Commercial Buildings Energy Consumption and Expenditures: Consumption and Expenditures Tables, Oct. 2006, Table C1a.

1.3.6 2003 Commercial *Delivered* Energy Consumption Intensities, by Principal Building Type and Vintage (1)

Building Type	Consumption (10^3 Btu/SF) Pre-1959	1960-1989	1990-2003	Building Type	Consumption (10^3 Btu/SF) Pre-1959	1960-1989	1990-2003
Health Care	178.1	216.0	135.7	Education	77.7	88.3	80.6
Inpatient	230.3	255.3	253.8	Service	62.4	86.0	74.8
Outpatient	91.6	110.4	84.4	Food Service	145.2	290.1	361.2
Food Sales	205.8	197.6	198.3	Religious Worship	46.6	39.9	43.3
Lodging	88.2	111.5	88.1	Public Order & Safety	N.A.	101.3	110.6
Office	93.6	94.4	88.0	Warehouse & Storage	N.A.	38.9	33.3
Mercantile	80.4	91.8	94.4	Public Assembly	61.9	107.6	119.7
Retail (Non-Malls)	74.1	63.7	86.4	Vacant	21.4	23.1	N.A.
Retail (Malls)	N.A.	103.9	99.5	Other	161.3	204.9	125.3

Note(s): 1) See Table 1.3.4 for primary versus *delivered* energy consumption.
Source(s): EIA, 2003 Commercial Buildings Energy Consumption and Expenditures: Consumption and Expenditures Tables, Oct. 2006, Table C12a.

1.3.7 2003 Commercial Primary Energy Consumption Intensities, by Principal Building Type (1)

Building Type	Consumption (10^3 Btu/SF)	Percent of Total Consumption	Building Type	Consumption (10^3 Btu/SF)	Percent of Total Consumption
Health Care	345.9	8%	Education	159.0	11%
Inpatient	438.8	6%	Service	151.6	4%
Outpatient	205.9	2%	Food Service	522.4	6%
Food Sales	535.5	5%	Religious Worship	77.0	2%
Lodging	193.1	7%	Public Order and Safety	221.1	2%
Office	211.7	19%	Warehouse and Storage	94.3	7%
Mercantile	223.6	18%	Public Assembly	180.0	5%
Retail (Non-Malls)	172.6	5%	Vacant	33.1	1%
Enclosed & Strip Malls	255.6	13%	Other	318.8	4%

Source(s): EIA, 2003 Commercial Buildings Energy Consumption and Expenditures: Consumption and Expenditures Tables, Oct. 2006, Table C1a.

1.3.8 2003 Commercial *Delivered* Energy Consumption Intensities, by Ownership of Unit (1)

Ownership	Consumption (10^3 Btu/SF)	
Nongovernment Owned	**85.1**	**72%**
Owner-Occupied	87.3	35%
Nonowner-Occupied	88.4	36%
Government Owned	**105.3**	**28%**
		100%

Note(s): 1) Mall buildings are no longer included in most CBECs tables; therefore, some data is not directly comparable to past CBECs.
Source(s): EIA, 2003 Commercial Buildings Energy Consumption and Expenditures: Consumption and Expenditures Tables, June 2006, Table C3.

1.3.9 Aggregate Commercial Building Component Loads as of 1998 (1)

	Loads (quads) and Percent of Total Loads			
	Heating		Cooling	
Component				
Roof	-0.103	12%	0.014	1%
Walls (2)	-0.174	21%	-0.008	-
Foundation	-0.093	11%	-0.058	-
Infiltration	-0.152	18%	-0.041	-
Ventilation	-0.129	15%	-0.045	-
Windows (conduction)	-0.188	22%	-0.085	-
Windows (solar gain)	0.114	-	0.386	32%
Internal Gains				
Lights	0.196	-	0.505	42%
Equipment (electrical)	0.048	-	0.207	17%
Equip. (non-electrical)	0.001	-	0.006	1%
People	0.038	-	0.082	7%
NET Load	**-0.442**	100%	**0.963**	100%

Note(s): 1) "Loads" represents the thermal energy losses/gains that, when combined, will be offset by a building's heating/cooling system to maintain a set interior temperature (which then equals *site* energy). 2) Includes common interior walls between buildings.

Source(s): LBNL, Commercial Heating and Cooling Loads Component Analysis, June 1998, Table 24, p. 45 and Figure 3, p. 61.

1.3.10 1995 Commercial *Delivered* End-Use Energy Consumption Intensities, by Principal Building Type (1)

	Consumption (10^3 Btu/SF)					
Building Type	Space Heating	Space Cooling	Water Heating	Lighting	Total (2)	Percent of Total Consumption
Office	24.3	9.1	8.7	28.1	90.5	21%
Mercantile and Service	30.6	5.8	5.1	23.4	69.6	14%
Education	32.8	4.8	17.4	15.8	75.0	12%
Health Care	55.2	9.9	63.0	39.3	176.4	10%
Lodging	22.7	8.1	51.4	23.2	99.5	8%
Public Assembly	53.6	6.3	17.5	21.9	81.7	7%
Food Service	30.9	19.5	27.5	37.0	241.2	8%
Warehouse and Storage	15.7	0.9	2.0	9.8	44.0	9%
Food Sales	27.5	13.4	9.1	33.9	202.2	4%
Vacant (3)	36.0	1.4	5.2	4.7	26.4	3%
Public Order and Safety	27.8	6.1	23.4	16.4	86.9	2%
Other (4)	59.6	9.3	15.3	26.7	144.0	3%
All Buildings	29.0	6.0	13.8	20.4	90.5	100%

Note(s): 1) Further detail can be found in Table 7.4.1. Parking garages and commercial buildings on multibuilding manufacturing facilities are excluded from CBECS 1995. 2) Includes all end-uses. 3) Includes vacant and religious worship. 4) Includes mixed uses, hangars, crematoriums, laboratories, and other.

Source(s): EIA, Commercial Building Energy Consumption and Expenditures 1995, Apr. 1998, Table EU-2, p. 311.

1.4.1 FY 2005 Federal Primary Energy Consumption (Quadrillion Btu)

Buildings and Facilities	**0.65**	
Vehicles/Equipment/Energy-Intensive Operations	0.97	(mostly jet fuel and diesel)
Total Federal Government Consumption	1.62	

Source(s): DOE/FEMP, Annual Report to Congress on FEMP, Sept. 2006, Table A-1, p. 148 for total consumption and Table A-3, p. 150 for buildings consumption.

1.4.2 FY 2005 Federal Building Energy Use Shares, by Fuel Type and Agency

Fuel Type	*Site* Percent	Primary Percent	Agency	Primary Percent		FY 2005 (10^15 Btu)
Electricity	46.1%	74.7%	DOD	62.9%	Total *Delivered*	
Natural Gas	33.2%	15.6%	USPS	10.0%	Energy Consumption =	0.30
Fuel Oil	9.4%	4.4%	DOE	5.3%	Total Primary	
Coal	4.3%	2.0%	VA	8.5%	Energy Consumption =	0.65
Other	6.9%	3.3%	GSA	4.8%		
Total	100%	100%	Other	8.5%		
			Total	100%		

Note(s): See Table 2.3.1 for floorspace.

Source(s): DOE/FEMP, Annual Report to Congress on FEMP, Sept. 26, 2006, Table A-5, p. 152 for fuel types and Table A-3, p. 150 for agency consumption.

1.4.3 Federal Building *Delivered* Energy Consumption Intensities, by Year (1)

Year	Consumption per Gross Square Foot (10^3 Btu/SF)	Year	Consumption per Gross Square Foot (10^3 Btu/SF)
FY 1985	123.0	FY 1996	115.0
FY 1986	131.3	FY 1997	111.9
FY 1987	136.9	FY 1998	107.7
FY 1988	136.3	FY 1999	106.7
FY 1989	132.6	FY 2000	104.8
FY 1990	128.6	FY 2001	105.9
FY 1991	122.9	FY 2002	104.6
FY 1992	125.5	FY 2003	105.2
FY 1993	122.3	FY 2004	104.9
FY 1994	120.2	FY 2005 (3)	98.2
FY 1995 (2)	117.3	FY 2010 (4)	80.0

Note(s): 1) See Table 2.3.1 for floorspace. 2) Exceeds the National Energy Conservation Policy Act goal of 125,700 Btu/SF. 3) Misses the goal of Executive Order 13123 for FY 2005 of 97,600 Btu/SF. 4) Executive Order 13123 goal.

Source(s): DOE/FEMP, Annual Report to Congress on FEMP, Sept. 29, 2004, Table 5-B, p. 57 for 1990-2002 energy consumption and Table 8-A, p. 65 for 2002 floorspace; DOE/FEMP, Annual Report to Congress on FEMP, Aug. 9, 2005, Table 6-A, p. A-10 for 2003; DOE/FEMP, Annual Report to Congress on FEMP, Feb. 24, 2006, Table 6-A, p. A-10 for 2004; DOE/FEMP, Annual Report to Congress on FEMP, Sept. 26, 2006, Table 2, p. 13 for 1985 and 2005; and DOE/FEMP for remaining data.

1.4.4 Federal Agency Progress Toward the Renewable Energy Goal (Trillion Btu) (1)

	Purchased Renewable Energy	Total Renewable Energy Usage			Total Facility Electricity Use
DOD	5.33	8.35	8%		101.0
GSA	2.25	2.25	23%		9.9
DOE	0.53	0.55	3%		16.7
EPA	0.52	0.53	113%	(2)	0.5
NASA	0.46	0.46	8%		5.5
DOC	0.30	0.30	27%		1.9
Others	0.46	0.56	1%		52.3
All Agencies	**9.85**	**13.00**	7%		**187.8**

Note(s): 1) In July 2000, in accordance with Section 503 of Executive Order 13123, the Secretary of Energy approved a goal that the equivalent of 2.5 percent of electricity consumption from Federal facilities should come from new renewable energy sources by 2005. 2) EPA's renewable energy use is 112.6% of its electricity use due to its purchases and generation of non-electric renewable energy.

Source(s): DOE/FEMP, Annual Report to Congress on FEMP, Sept. 26, 2006, Table 5, p. 21, and p. 20 for note 1.

1.5.1 Buildings Share of U.S. Electricity Consumption/Sales (Percent)

	Buildings					*Delivered* Total
	Residential	Commercial	**Total**	Industry	Transportation	Total	(10^15 Btu)
1980	34%	27%	**61%**	39%	0%	100%	7.1
1990	34%	31%	**65%**	35%	0%	100%	9.3
2000	35%	34%	**69%**	31%	0%	100%	11.7
2005 (1)	**37%**	**35%**	**72%**	**28%**	**0%**	**100%**	**12.5**
2010	38%	35%	**73%**	27%	0%	100%	13.5
2015	37%	36%	**74%**	26%	0%	100%	14.5
2020	38%	37%	**75%**	25%	0%	100%	15.4
2025	37%	39%	**76%**	24%	0%	100%	16.5
2030	37%	40%	**77%**	23%	0%	100%	17.6

Note(s): 1) Buildings accounted for 80% (or $238 billion) of total U.S. electricity expenditures.

Source(s): EIA, State Energy Data 2004: Consumption, June 2007, Tables 8-12, p. 18-22 for 1980-2000; and EIA, Annual Energy Outlook 2007, Feb. 2007, Table A2, p. 137-139 for 2005-2030 consumption, and Table A3, p. 140-141 expenditures.

1.5.2 U.S. Electricity Generation Input Fuel Shares (Percent)

				Renewables				Net Electric	
	Natural Gas	Petroleum	Coal	Hydro.	Oth(2)	Total	Nuclear	Imports	Total
1980	16%	11%	50%	12%	0%	12%	11%	(1)	100%
1990	11%	4%	53%	10%	2%	12%	20%	(1)	100%
2000	14%	3%	53%	7%	2%	9%	21%	(1)	100%
2005	**15%**	**3%**	**52%**	**7%**	**2%**	**9%**	**20%**	**0%**	**100%**
2010	15%	2%	52%	7%	4%	11%	19%	0%	100%
2015	16%	2%	52%	7%	4%	11%	19%	0%	100%
2020	16%	2%	53%	6%	4%	10%	19%	0%	100%
2025	14%	2%	56%	6%	4%	10%	18%	0%	100%
2030	12%	2%	59%	6%	4%	10%	18%	0%	100%

Note(s): 1) Electric imports included in renewables. 2) Includes geothermal, municipal solid waste, biomass, solar thermal, solar PV, and wind.

Source(s): EIA, State Energy Data 2004: Consumption, June 2007, Tables 8-12, p. 18-22 for 1980-2000; and EIA, Annual Energy Outlook 2007, Feb. 2007, Table A2, p. 137-139 for 2005-2030 consumption and Table A17, p. 163 for renewables.

1.5.3 U.S. Electricity Generation Input Fuel Consumption (Quadrillion Btu)

				Renewables				Net Electric		Growth Rate
	Natural Gas	Petroleum	Coal	Hydro.	Oth(2)	Total	Nuclear	Imports	Total	2005-Year
1980	3.80	2.63	12.16	2.87	0.11	2.98	2.74	(1)	24.32	-
1990	3.33	1.29	16.26	3.01	0.64	3.66	6.10	(1)	30.64	-
2000	5.32	1.14	20.22	2.77	0.75	3.52	7.86	(1)	38.06	-
2005	**5.95**	**1.16**	**20.75**	**2.68**	**0.96**	**3.64**	**8.13**	**0.08**	**39.71**	-
2010	6.56	0.90	22.13	2.99	1.68	4.67	8.23	0.04	42.53	1.4%
2015	7.31	0.97	23.45	3.04	1.79	4.83	8.47	0.03	45.07	1.3%
2020	7.40	0.97	25.05	3.05	1.88	4.93	9.23	0.04	47.62	1.2%
2025	6.78	0.99	27.9	3.06	2.04	5.09	9.23	0.04	50.04	1.2%
2030	6.09	1.01	31.14	3.06	2.09	5.15	9.33	0.04	52.77	1.1%

Note(s): 1) Electric imports included in renewables. 2) Includes geothermal, municipal solid waste, biomass, solar thermal, solar PV, and wind.

Source(s): EIA, State Energy Data 2004: Consumption, June 2007, Tables 8-12, p. 18-22 for 1980-2000; and EIA, Annual Energy Outlook 2007, Feb. 2007, Table A2, p. 137-139 for 2005-2030 consumption, and Table A17, p. 163 for renewables.

1.5.4 U.S. Electricity Net Generation, by Plant Type (Billion kWh)

				Renewables						Growth Rate
	Natural Gas	Petroleum	Coal	Hydr(1)	Oth(2)	Total	Nuclear	CHP(3)	Tot.(4)	2005-year
1980	346	246	1,162	276	6	282	251	N.A.	2,286	-
1990	265	118	1,560	286	35	324	577	61	2,901	-
2000	399	98	1,911	266	45	316	754	165	3,638	-
2005	**546**	**111**	**1,956**	**269**	**54**	**323**	**780**	**178**	**3,883**	**-**
2010	658	82	2,090	288	81	370	789	172	4,209	1.6%
2015	756	89	2,233	300	93	416	812	179	4,501	1.5%
2020	776	89	2,418	301	115	416	885	176	4,781	1.4%
2025	702	91	2,766	301	133	434	886	166	5,063	1.3%
2030	609	92	3,191	301	133	434	896	157	5,402	1.3%

Note(s): 1) Electricity used for hydroelectric pumped storage is subtracted from this conventional hydroelectric generation. 2) Includes geothermal, municipal solid waste, wood, biomass, solar thermal, solar photovoltaic, and wind. 3) CHP = Combined heat and Power. Includes CHP plants whose primary business is to sell electricity and heat to the public. 4) Includes batteries, chemicals, hydrogen, pitch, purchased steam, sulfur, distributed generation, and other miscellaneous technologies that are not listed individually.

Source(s): EIA, Annual Energy Outlook 2007, Feb. 2007, Table A8, p. 151-152; EIA, Annual Energy Review 2005, July 2006, Table 8.2c, p. 230 for 1990-2000; and EIA, Annual Energy Review 2002, Oct. 2003, Table 8.2b, p. 149 for 1980.

1.5.5 U.S. Electric Utility and Nonutility Net Summer Electricity Generation Capacity (GW)

Electric Generator	1990	2000	2005	2010	2015	2020	2025	2030
Coal Steam	300	305	306	316	319	343	389	446
Other Fossil Steam	144	135	121	119	89	89	88	87
Combined Cycle	7	29	144	161	163	171	178	179
Comb. Turbine/Diesel	46	79	130	134	118	124	133	152
Nuclear Power	100	98	100	101	102	112	112	113
Pumped Storage	18	20	21	21	21	21	21	21
Fuel Cells	0	0	0	0	0	0	0	0
Conv. Hydropower	75	78	80	80	80	80	80	80
Geothermal	3	3	2	2	3	3	3	3
Municipal Solid Waste	2	3	3	3	4	4	4	4
Biomass	7	2	2	2	2	2	3	4
Solar Thermal	0	0	0	1	1	1	1	1
Solar Photovoltaic	0	0	0	0	0	0	0	0
Wind	2	2	10	17	18	18	18	18
Distributed Generation	N.A.	0	0	0	1	2	5	11
Total	**703**	**754**	**919**	**957**	**920**	**970**	**1,035**	**1,119**

Note(s): 1) Nuclear capacity includes 3 GW of uprates from 2005 to 2030. New nuclear plants are expected to come online 2013-2019.

Source(s): EIA, Annual Energy Outlook (AEO) 1994, Jan. 1994, Table A9, p. 66 and Table A16, p. 73 for 1990; EIA, AEO 2003, Jan. 2003, Table A9, Table 133-134, and Table A17, p.142 for 2000; and EIA, AEO 2007, Feb. 2007, Table A9, p. 153-154 and Table A16, p. 162 for 2005-2030.

1.5.6 U.S. Electric Power Sector Cumulative Power Plant Additions Needed to Meet Future Electricity Demand (1)

Electric Generator	Typical New Plant Capacity (MW)	Number of New Power Plants to Meet Demand 2010	2015	2020	2025	2030
Coal Steam	600	19	30	70	148	242
Combined Cycle	400	42	47	68	85	88
Combustion Turbine/Diesel	160	28	47	87	141	261
Nuclear Power (2)	1,000	-	1	9	9	12
Pumped Storage	142 (3)	-	-	-	-	-
Fuel Cells	10	-	-	-	-	-
Conventional Hydropower	5	4	4	30	42	42
Geothermal	50	4	5	10	13	17
Municipal Solid Waste	30	7	19	19	19	21
Wood and Other Biomass	80	2	2	4	10	22
Solar Thermal	100	1	2	2	2	2
Solar Photovoltaic	5	9	21	37	55	72
Wind	50	147	162	165	165	167
Total		**262**	**340**	**501**	**691**	**947**
Distributed Generation	160 (4)	1	3	13	34	71

Note(s): 1) Cumulative additions after Dec. 31, 2005. 2) Nuclear capacity includes 3 GW of uprates from 2004 to 2030. New nuclear plants are expected to come online 2013-2019. 3) Based on current stock average capacity. 4) Combustion Turbine/Diesel data used.

Source(s): EIA, Annual Energy Outlook (AEO) 2007, Feb. 2007, Table A9, p. 153-154 and Table A16, p. 162; EIA, Assumption to the AEO 2007, Feb. 2007, Table 39, p. 77; and EIA, Electric Power Annual 2005, Sept. 2006, Table 2.2, p. 19 for pumped storage plant capacity and Table 2.6, p. 21 for hydroelectric plant capacity

1.5.7 2005 Existing Capacity, by Energy Source (GW)

	Number of Generators	Generator Nameplate Capacity	Net Summer Capacity	Net Winter Capacity
Coal	1,522	336	313	316
Petroleum	3,753	65	59	63
Natural Gas	5,467	437	383	412
Other Gases	102	2	2	2
Nuclear	104	106	100	102
Hydroelectric Conventional	3,993	77	78	77
Other Renewables	1,671	24	21	21
Pumped Storage	150	20	21	21
Other	45	1	1	1
Total	**16,807**	**1,067**	**978**	**1,015**

Source(s): EIA, Electric Power Annual 2005, Oct. 2006, Table 2.2, pg. 19.

1.5.8 Electric Capacity Factors, by Year and Fuel Type

	Coal	Petroleum	Natural Gas	Nuclear	Conventional Hydroelectric	Solar PV	Wind
1990	59%	29%	25%	66%	45%	13%	18%
1995	63%	19%	29%	77%	45%	17%	21%
2000	71%	21%	31%	88%	40%	15%	27%
2001	69%	22%	29%	89%	31%	16%	20%
2002	70%	18%	25%	90%	38%	16%	27%
2003	72%	22%	21%	88%	40%	15%	21%
2004	72%	23%	22%	90%	39%	17%	25%
2005	73%	24%	23%	89%	40%	15%	23%
2006 (1)	72%	12%	24%	90%	42%	14%	26%

Note(s): 1) Preliminary

Source(s) EIA, Annual Energy Review 2006, June 2007, 8.2a, pg. 226, Table 8.11a, p. 260.

2.1.1 Total Number of Households and Buildings, Floorspace, and Household Size, by Year

	Households (Millions)	Percent Post-2000 Households (1)	Buildings (Millions)	Floorspace (Billion SF)	U.S. Population (Millions)	Average Household Size (2)
1980	80	N.A.	65.5	142.5	227	2.9
1990	94	N.A.	74.2	169.2	250	2.6
2000	106	N.A.	82.6 (3)	168.8 (3)	282	2.7
2005	**113**	**9%**	**N.A.**	**N.A.**	**296**	**2.6**
2010	121	16%	N.A.	N.A.	309	2.6
2015	128	23%	N.A.	N.A.	322	2.5
2020	135	29%	N.A.	N.A.	336	2.5
2025	141	34%	N.A.	N.A.	349	2.5
2030	147	39%	N.A.	N.A.	364	2.5

Note(s): 1) Percent built after Dec. 31, 2000. 2) Number of residents. 3) Number of buildings and floorspace in 1997; for comparison, 1997 households = 101.5 million; percentage of floorspace: 85% single-family, 11% multi-family, and 4% manufactured housing. 2001 households = 107.2 million; percentage of floorspace: 83% single-family, 13% multi-family, and 4% manufactured housing.

Source(s): DOC, Statistical Abstract of the U.S. 2007, Oct. 2006, No. 948, p. 626 1980-2000 households, No. 2-3, p. 7-8 for population; EIA, Annual Energy Outlook 2007, Feb. 2007, Table A4, p. 142-143 for 2005-2030 households and Table A19, p. 165 for housing starts; EIA, Buildings and Energy in the 1980's, June 1995, Table 2.1, p. 23 for residential buildings and floorspace in 1980 and 1990; EIA, RECS 1997 for 1997 buildings and floorspace; and EIA RECS 2001 for 2001 households and floorspace.

2.1.2 Share of Households, by Housing Type and Type of Ownership, as of 2001 (Percent)

Housing Type	Owned	Rented	Total
Single-Family:	**59.1%**	**9.8%**	**68.9%**
Detached	52.1%	6.9%	59.0%
Attached	7.0%	2.9%	9.9%
Multi-Family:	**3.6%**	**21.1%**	**24.8%**
2 to 4 units	2.0%	6.9%	8.9%
5 or more units	1.7%	14.2%	15.9%
Mobile Homes	**5.3%**	**1.0%**	**6.4%**
Total	**68.0%**	**32.0%**	**100%**

Source(s): EIA, A Look at Residential Energy Consumption in 2001, Oct. 2003, Table HC1-2a.

2.1.3 Share of Households, by Census Region and Vintage, as of 2001 (Percent)

Region	Prior to 1970	1970 to 1979	1980 to 1989	1990 to 2001	Total
Northeast	13.3%	2.0%	2.2%	1.4%	18.9%
Midwest	13.5%	3.4%	3.4%	2.6%	22.9%
South	13.8%	7.2%	8.3%	7.1%	36.3%
West	10.3%	5.0%	3.2%	3.4%	21.8%
					100%

Source(s): EIA, A Look at Residential Energy Consumption in 2001, Oct. 2003, Table HC1-2a.

2.1.4 Residential Floorspace (heated square feet), as of 2001 (Percent of Total Households)

Floorspace	
Fewer than 500	4%
500 to 999	20%
1,000 to 1,499	21%
1,500 to 1,999	16%
2,000 to 2,499	13%
2,500 to 2,999	9%
3,000 to 3,499	6%
3,500 to 4,000	4%
4,000 or more	8%
Total	100%

Note(s): The 2001 average new single-family housing floorspace was 2,324 square feet.
Source(s): EIA, A Look at Residential Energy Consumption in 2001, Oct. 2003, Table CE11-6.1u.

2.1.5 Housing Vintage, as of 2001

Vintage	
1949 or Before	25%
1950 to 1959	13%
1960 to 1969	13%
1970 to 1979	18%
1980 to 1989	17%
1990 to 2001	14%
Total	100%

Source(s): EIA, A Look at Residential Energy Consumption in 2001, Oct. 2003, Table HC1-2a.

2.1.6 Construction Statistics of New Homes Completed/Placed

	Single-Family		Multi-Family		Mobile Homes	Total
	1000 Units	Average SF	1000 Units	Average SF	1000 Units	1000 Units
1975	875	1,645	430	1,000	229	1,534
1980	957	1,740	545	979	234	1,736
1981	819	1,720	447	980	229	1,495
1985	1,072	1,785	631	922	283	1,986
1986	1,120	1,825	636	911	256	2,012
1990	966	2,080	342	1,005	195	1,503
1991	838	2,075	253	1,020	174	1,265
1992	964	2,095	194	1,040	212	1,370
1993	1,039	2,095	153	1,065	243	1,435
1994	1,160	2,100	187	1,035	291	1,638
1995	1,066	2,095	247	1,080	319	1,632
1996	1,129	2,120	284	1,070	338	1,751
1997	1,116	2,150	284	1,095	336	1,736
1998	1,160	2,190	314	1,065	374	1,848
1999	1,270	2,223	334	1,104	338	1,942
2000	1,242	2,266	332	1,114	281	1,855
2001	1,256	2,324	315	1,171	196	1,767
2002	1,325	2,320	323	1,166	174	1,822
2003	1,386	2,330	292	1,173	140	1,818
2004	1,532	2,349	310	1,173	124	1,966
2005	1,636	2,434	296	1,247	123	2,055
2006	1,654	2,469	325	1,277	111	2,090

Source(s): DOC, 2006 Characteristics of New Housing, June 2007, p. 4 for single-family completions, p. 260 for single-family average SF; NAHB, Housing Economics, Mar. 1995; NAHB, Facts, Figures and Trends, 1997, Characteristics of New Multi-family Homes, 1971-1995, p. 7; DOC, Current Construction Reports, Characteristics of New Housing, C25/98-A, Table 18, p. 44; DOC, Placements of New Manufactured Homes by Region and Size of Home, 1974-1988; and DOC, Placements of New Manufactured Homes by Region and Size of Home, 1980-2006.

2.1.7 Materials Used in the Construction of a 2,272-Square-Foot Single-Family Home, 2000

13,837 board-feet of lumber
13,118 square feet of sheathing
19 tons of concrete
3,206 square feet of exterior siding material
3,103 square feet of roofing material
3,061 square feet of insulation
6,050 square feet of interior wall material
2,335 square feet of interior ceiling material
226 linear feet of ducting
19 windows
4 exterior doors (3 hinged, 1 sliding)
2,269 square feet of flooring material
12 interior doors
6 closet doors
2 garage doors
1 fireplace
3 toilets; 2 bathtubs; 1 shower stall
3 bathroom sinks
15 kitchen cabinets; 5 other cabinets
1 kitchen sink
1 range; 1 refrigerator; 1 dishwasher; 1 garbage disposal; 1 range hood
1 washer; 1 dryer
1 heating and cooling system

Source(s): NAHB, 2004 Housing Facts, Figures and Trends, Feb. 2004, p. 7; D&R International for appliances and HVAC.

2.1.8 2006 New Homes Completed/Placed, by Census Region
(Thousand Units and Percent of Total Units by Housing Type) (1)

Region	Single-Family Units		Multi-Family Units		Mobile Homes Units		Total
Northeast	128	8%	51	13%	8	7%	187
Midwest	286	19%	40	15%	15	14%	340
South	826	46%	161	49%	65	55%	1,052
West	415	27%	74	23%	24	23%	513
Total	**1,655**	100%	**325**	100%	**111**	100%	**2,091**

Note(s) 1) Preliminary.
Source(s): DOC, Manufacturing, Mining and Construction Statistics: New Residential Construction: New Privately Owned Housing Units Completed, for single- and multi-family; and DOC, Manufacturing, Mining and Construction Statistics: Manufactured Homes Placements by Region and Size of Home, Mar. 2006 for mobile home placements.

2.1.9 2006 Construction Method of Single-Family Homes, by Region
(Thousand Units and Percent of Total Units by Construction Method)

Region	Stick Built Units		Modular Units		Panelized/Precut Units		Total
Northeast	112	7%	11	28%	5	14%	128
Midwest	260	16%	14	35%	11	31%	285
South	797	50%	13	33%	16	46%	826
West	410	26%	2	5%	3	9%	415
Total	**1,579**	100%	**40**	100%	**35**	100%	**1,654**

Source(s): DOC, Manufacturing, Mining and Construction Statistics, New Residential Construction: Type of Construction Method of New One-Family Houses Completed, Mar. 2006.

2.1.10 Market Indices for 2006 ENERGY STAR Qualified New Single-Family Homes, by Selected State (1000s)

	ENERGY STAR Qualified New Homes	New Single-Family Housing Permits	Market Penetration
Nevada	18.9	26.7	71%
Alaska	1.0	1.6	64%
Iowa	5.9	10.3	57%
Texas	60.8	162.8	37%
Hawaii	2.1	5.6	37%
Arizona	20.1	55.6	36%
New Jersey	5.4	17.1	31%
Delaware	1.2	5.0	24%
Vermont	0.5	2.1	24%
Connecticut	1.6	7.1	23%
California	18.1	107.7	17%
New Hampshire	0.8	4.8	17%
Utah	3.6	22.6	16%
Ohio	3.5	27.5	13%
New York	2.6	20.0	13%
Florida	3.3	146.2	2%
United States	**169.8**	**1,378.2**	**12%**

Source(s): EPA, ENERGY STAR Qualified New Homes Market Indices for States, http://www.energystar.gov/index.cfm?fuseaction=qhmi.showHomesMarketIndex for top states; E-mail correspondence with EPA ENERGY STAR program for complete data set.

2.2.1 Total Commercial Floorspace and Number of Buildings, by Year

	Commercial Sector Floorspace (10^9 square feet)	Percent Post-2000 Floorspace (2)	Buildings (10^6)
1980	50.9 (1)	N.A.	3.1 (3)
1990	64.3	N.A.	4.5 (3)
2000 (4)	68.5	N.A.	4.7 (5)
2005 (4)	**74.3**	**15%**	N.A.
2010 (4)	80.4	25%	N.A.
2015 (4)	86.5	35%	N.A.
2020 (4)	92.9	43%	N.A.
2025 (4)	100.1	52%	N.A.
2030 (4)	108.0	59%	N.A.

Note(s): 1) Based on PNNL calculations. 2) Percent built after Dec. 31, 2000. 3) Actually for previous year. 4) EIA now excludes parking garages and commercial buildings on multi-building manufacturing facilities from the commercial building sector. 5) Data is from 1999. In 1999, commercial building floorspace = 64.6 billion square feet.

Source(s): EIA, Annual Energy Outlook (AEO) 1994, Jan. 1994, Table A5, p. 62 for 1990 floorspace; EIA, AEO 2003, Jan. 2003, Table A5, p. 127-128 for 2000 floorspace; EIA, AEO 2007, Feb. 2007, Table A5, p. 144-145 for 2005-2030 floorspace; EIA, Commercial Building Characteristics 1989, June 1991, Table A4, p. 17 for 1990 number of buildings; EIA, Commercial Building Characteristics 1999, Aug. 2002, Table 3 for 1999 number of buildings and floorspace; and EIA, Buildings and Energy in the 1980s, June 1995, Table 2.1, p. 23 for number of buildings in 1980.

2.2.2 Principal Commercial Building Types, as of 2003 (Percent of Total Floorspace) (1)

	Total Floorspace	Total Buildings	Primary Energy Consumption
Office	17%	17%	19%
Mercantile	16%	14%	18%
Retail	6%	9%	5%
Enclosed & Strip Malls	10%	4%	13%
Education	14%	8%	11%
Warehouse and Storage	14%	12%	7%
Lodging	7%	3%	7%
Service	6%	13%	4%
Public Assembly	5%	6%	5%
Religious Worship	5%	8%	2%
Health Care	4%	3%	8%
Inpatient	3%	0%	6%
Outpatient	2%	2%	2%
Food Sales	2%	5%	5%
Food Service	2%	6%	6%
Public Order and Safety	2%	1%	2%
Other	2%	2%	4%
Vacant	4%	4%	1%
Total	100%	100%	100%

Note(s): 1) For primary energy intensities by building type, see Table 1.3.7. Total CBECS 1999 commercial building floorspace is 71.7 billion SF.

Source(s): EIA, 2003 Commercial Buildings Energy Consumption Survey: Consumption and Expenditures Tables, Oct. 2006, Table C1A.

2.2.3 Number of Floors and Type of Ownership, as of 2003 (Percent of Total Floorspace)

Floors	
One	40%
Two	25%
Three	12%
Four to Nine	16%
Ten or More	8%
Total	100%

Ownership	
Nongovernment Owned	**76%**
Owner-Occupied	36%
Nonowner-Occupied	37%
Unoccupied	3%
Government Owned	**24%**
Federal	3%
State	5%
Local	15%
Total	100%

Source(s): EIA, Commercial Building Characteristics 2003, June 2006, Table C1.

2.2.4 Share of Commercial Floorspace, by Census Region and Vintage, as of 2003 (Percent)

Region	Prior to 1960	1960 to 1989	1990 to 2003	Total
Northeast	9%	8%	3%	20%
Midwest	8%	11%	6%	25%
South	5%	18%	14%	37%
West	3%	9%	5%	18%
				100%

Source(s): EIA, 2003 Commercial Buildings Energy Consumption Survey: Building Characteristics Tables, Oct. 2006, Table A2, p. 3-4.

2.2.5 Commercial Building Size, as of 2003 (Number of Buildings and Percent of Total Floorspace)

Square Foot Range	Number of Buildings (1000s)	
1,001 to 5,000	2,586	10%
5,001 to 10,000	948	10%
10,001 to 25,000	810	18%
25,001 to 50,000	261	13%
50,001 to 100,000	147	14%
100,001 to 200,000 (2)	74	14%
200,001 to 500,000 (2)	26	10%
Over 500,000 (2)	8	11%
Total	**4,859**	100%

Note(s): 1) 35% of commercial floorspace is found in 2.2% of commercial buildings that are larger than 100,000 square feet.
Source(s): EIA, 2003 Commercial Buildings Energy Consumption Survey: Building Characteristics Tables, Oct. 2006, Table A1, p. 1-2.

2.2.6 Commercial Building Vintage, as of 2003

	Percent of Total Floorspace
1919 or Before	5%
1920 to 1945	10%
1946 to 1959	10%
1960 to 1969	12%
1970 to 1979	17%
1980 to 1989	17%
1990 to 1999	20%
2000 to 2003	9%
Total	100%

Source(s): EIA, 2003 Commercial Buildings Energy Consumption Survey: Building Characteristics Tables, Oct. 2006, Table A1, p. 1-2.

2.2.7 Commercial Building Median Lifetimes (Years)

Building Type	Median (1)	66% Survival (2)	33% Survival (2)
Health Care	65	48	88
Food Sales	65	49	86
Food Service	65	49	86
Lodging	69	49	98
Mercantile & Service	65	44	96
Assembly	80	54	118
Large Office	73	52	103
Small Office	73	52	103
Education	80	61	104
Warehouse	80	52	123
Other	75	57	99

Note(s): 1) PNNL estimates the median lifetime of commercial buildings is 70-75 years. 2) Number of years after which the building survives. For example, a third of the office buildings constructed today will survive 103 years later.

Source(s): EIA, Assumptions for the Annual Energy Outlook 2007, Feb. 2007, Table 12, p. 28; EIA, Model Documentation Report: Commercial Sector Demand Module of the National Energy Modeling System, Apr. 2007, p. 30-35; and PNNL, Memorandum: New Construction in the Annual Energy Outlook 2003, Apr. 24, 2003 for Note 2.

2.2.8 2003 Average Commercial Building Floorspace, by Principal Building Type and Vintage

	Average Floorspace/Building (1000 SF)			
Building Type	1959 or Prior	1960 to 1989	1990 to 2003	All
Education	27.5	26.9	21.7	25.6
Food Sales	N.A.	N.A.	N.A.	5.6
Food Service	6.4	4.4	5.0	5.6
Health Care	18.5	37.1	N.A.	24.5
Inpatient	N.A.	243.6	N.A.	238.1
Outpatient	N.A.	11.3	11.6	10.4
Lodging	9.9	36.1	36.0	35.9
Retail (Other Than Mall)	6.2	9.3	17.5	9.7
Office	12.4	16.4	14.2	14.8
Public Assembly	13.0	13.8	17.3	14.2
Public Order and Safety	N.A.	N.A.	N.A.	15.4
Religious Worship	8.7	9.6	15.6	10.1
Service	6.1	6.5	6.8	6.5
Warehouse and Storage	19.7	17.2	15.4	16.9
Other	N.A.	N.A.	N.A.	22.0
Vacant	N.A.	N.A.	N.A.	14.1

Source(s): EIA, 2003 Commercial Buildings Energy Consumption Survey: Building Characteristics Tables, June 2006, Table B8, p. 63-69 and Table B9, p. 70-76.

2.2.9 U.S. LEED Certified Projects, by Certification Type and Selected State (1)

	Platinum	Gold	Silver	Bronze	Certified (2)		Platinum	Gold	Silver	Bronze	Certified (2)
Arizona	1	7	4	1	21	New York	3	10	7	0	32
California	12	37	31	0	120	Ohio	0	4	8	0	22
Colorado	2	11	15	0	41	Oregon	2	32	13	1	60
Georgia	2	10	19	0	41	Pennsylvania	3	28	31	0	78
Illinois	4	8	14	0	40	Texas	0	7	13	0	36
Maryland	1	6	5	0	20	Virginia	0	4	9	0	23
Massachusetts	3	6	9	0	41	Washington	1	20	23	0	70
Michigan	0	13	11	0	34	Wisconsin	0	5	6	0	20
New Jersey	0	7	7	0	21						
United States	**43**	**266**	**293**	**3**	**933**						

Note(s): 1) Project types include new construction, major renovations, existing building operations, interior design, homes, neighborhood development, development multi-building complexes, schools, and retail spaces. 2) Certified projects do not constitute the sum total of the other four categories, but rather designate an entirely separate category in and of itself.

Source(s): United States Green Building Council Web site, accessed Aug. 2007.

2.2.10 U.S. LEED Registered Projects, by Ownership Category

Private-Sector Corporations	33%
Local Governments	25%
Nonprofit Corporations	14%
State Governments	13%
Federal Government	10%
Other	5%
Total	100%

Source(s): Building Design & Construction, White Paper on Sustainability, Nov. 2003.

2.3.1 Federal Building Gross Floorspace, by Year and Agency

Fiscal Year	Floorspace (10^9 SF)
FY 1985	3.37
FY 1986	3.38
FY 1987	3.40
FY 1988	3.23
FY 1989	3.30
FY 1990	3.40
FY 1991	3.21
FY 1992	3.20
FY 1993	3.20
FY 1994	3.11
FY 1995	3.04
FY 1996	3.03
FY 1997	3.02
FY 1998	3.07
FY 1999	3.07
FY 2000	3.06
FY 2001	3.07
FY 2002	3.03
FY 2003	3.04
FY 2004	2.97
FY 2005	2.96

Agency	2005 Percent of Total Floorspace
DOD	66%
USPS	12%
GSA	6%
VA	5%
DOE	2%
Other	8%
Total	100%

Note(s): The Federal Government owns/operates over 500,000 buildings, including 422,000 housing structures (for the military) and 51,000 nonresidential buildings.

Source(s): DOE/FEMP for FY 1986-1998; DOE/FEMP, Annual Report to Congress on FEMP, May 10, 2001, Table 7-A, p. 56 for FY 1999; DOE/FEMP, Annual Report to Congress on FEMP, Dec. 11, 2002, Table 8-A, p. 83 for FY 1985 and FY 2000; DOE/FEMP, Annual Report to Congress on FEMP, Feb. 4, 2004, Table 8-A, p. 66 for 2001; DOE/FEMP, Annual Report to Congress on FEMP, Sept. 29, 2004, Table 8-A, p. 65 for 2002; DOE/FEMP, Annual Report to Congress on FEMP, Aug. 9, 2005, Table 6-A, p. 65 for 2003; DOE/FEMP, Annual Report to Congress on FEMP, February 24, 2006, Table 6-A, p. A-10 for 2004; and DOE/FEMP, Annual Report to Congress on FEMP, Sept. 26, 2006, Table 2, p. 13 for 2005 .

3.1.1 Carbon Dioxide Emissions for U.S. Buildings, by Year (10^6 metric tons of carbon) (1)

	Buildings				U.S.			
	Site Fossil	Electricity	Total	Growth Rate 2005-Year	Total	Growth Rate 2005-Year	Buildings % of Total U.S.	Buildings % of Total Global
1980	172.0	255.2	427.1	-	1,281.7	-	33%	8.5%
1990	153.7	317.2	470.9	-	1,359.7	-	35%	8.1%
2000	167.4	426.2	593.5	-	1,581.3	-	38%	9.1%
2005	**164.3** (2)	**466.0** (2)	**630.3**	-	**1,622.6**	-	**39%**	**9.1%** (3)
2010	168.7	498.4	667.1	1.1%	1,695.9	0.9%	39%	8.5%
2015	177.0	539.4	716.4	1.3%	1,798.3	1.0%	40%	7.7%
2020	180.9	579.5	760.4	1.3%	1,895.3	1.0%	40%	7.6%
2025	184.0	635.4	819.4	1.3%	2,026.3	1.1%	40%	7.5%
2030	187.7	697.7	885.4	1.4%	2,169.8	1.2%	41%	7.6%

Note(s): 1) Excludes emissions of buildings-related energy consumption in the industrial sector. Emissions assume complete combustion from energy consumption and exclude energy production activities such as gas flaring, coal mining, and cement production. 2) Carbon emissions calculated from EIA, Assumptions to the AEO 2007 and differs from EIA, AEO 2007, Table A18. Buildings sector total varies by 0.2% from EIA, AEO 2007. 3) U.S. buildings emissions approximately equal the combined carbon emissions of Japan, France, and the United Kingdom.

Source(s): EIA, Emissions of Greenhouse Gases in the U.S. 1985-1990, Sept. 1993, Appendix B, Tables B1-B5, p. 73-74 for 1980; EIA, Emissions of Greenhouse Gases in the U.S. 2003, Dec. 2004, Tables 7-11, p. 29-31 for 1990 and 2000; EIA, Assumptions to the Annual Energy Outlook (AEO) 2007, Mar. 2007, Table 2, p. 9 for carbon coefficients; EIA, AEO 2007, Feb. 2007, Table A2, p. 137-139 for 2005-2030 energy consumption and Table A18, p. 164 for 2005-2030 emissions; EIA, International Energy Outlook 2007, May 2007, Table A10, p. 93 for 2004-2030 global emissions; and EIA, International Energy Annual 2006, July 2006, Table H1, www.eia.doe.gov for 1980-2000 global emission.

3.1.2 2005 Buildings Energy End-Use Carbon Dioxide Emissions Splits, by Fuel Type (Million Metric Tons of Carbon Equivalent (MMTCE)) (1)

	Natural	Petroleum								
	Gas	Distil.	Resid.	LPG	Oth(2)	Total	Coal	Electricity (3)	Total	Percent
Space Heating (4)	70.1	20.0	2.9	4.5	2.3	29.7	2.9	37.8	140.6	22.3%
Lighting								113.7	113.7	18.0%
Space Cooling	0.4							81.5	81.8	13.0%
Water Heating	24.6	3.7		0.8		4.5		30.8	59.9	9.5%
Refrigeration (5)								38.8	38.8	7.4%
Electronics (6)								44.5	44.5	7.1%
Cooking	6.4			0.5		0.5		14.1	21.0	3.3%
Ventilation (7)								17.6	17.6	2.8%
Wet Clean (8)	1.0							15.9	16.9	2.7%
Computers								13.5	13.5	2.1%
Other (9)	4.4	0.5		4.5	0.9	5.9		39.7	50.0	3.2%
Adjust to SEDS (10)	10.3	3.6				3.6		18.0	31.9	3.9%
Total	**117.1**	**27.8**	**2.9**	**10.2**	**3.2**	**44.2**	**2.9**	**466.0**	**630.3**	100%

Note(s): 1) Emissions assume complete combustion from energy consumption, excluding gas flaring, coal mining, and cement production. Emissions exclude wood since it is assumed that the carbon released from combustion is reabsorbed in a future carbon cycle. Carbon emissions calculated from EIA, Assumptions to the AEO 2007 and differs from EIA, AEO 2007, Table A18. Buildings sector total varies by 0.2% from EIA, AEO 2007. 2) Includes kerosene space heating (1.9 MMTCE) and motor gasoline other uses (0.9 MMTCE). 3) Excludes electric imports by utilities. 4) Includes residential furnace fans (4.4 MMTCE). 5) Includes refrigerators (20.3 MMTCE) and freezers (6.5 MMTCE). 6) Includes color television (15.7 MMTCE) and other office equipment. 7) Commercial only; residential fan and pump energy use included proportionately in space heating and cooling. 8) Includes clothes washers (1.8 MMTCE), natural gas clothes dryers (1.0 MMTCE), electric clothes dryers (12.9 MMTCE), and dishwashers (1.3 MMTCE). Does not include water heating energy. 9) Includes residential small electric devices, heating elements, motors, swimming pool heaters, hot tub heaters, outdoor grills, and natural gas outdoor lighting. Includes commercial service station equipment, ATMs, telecommunications equipment, medical equipment, pumps, emergency electric generators, and manufacturing performed in commercial buildings. 10) Emissions related to a discrepancy between data sources. Energy attributable to the buildings sector, but not directly to specific end-uses.

Source(s): EIA, Annual Energy Outlook (AEO) 2007, Feb. 2007, Table A2, p. 137-139, Table A4, p. 142-143 and Table A5, p. 144-145 for energy consumption, and Table A18, p. 164 for emissions; EIA, National Energy Modeling System for AEO 2007, Feb. 2007; EIA, Assumptions to the AEO 2007, Mar. 2007, Table 2, p. 9 for emission coefficients; BTS/A.D. Little, Electricity Consumption by Small End-Uses in Residential Buildings, Aug. 1998, Appendix A for residential electric end-uses; BTS/A.D. Little, Energy Consumption Characteristics of Commercial Building HVAC Systems, Volume II: Thermal Distribution, Auxiliary Equipment, and Ventilation, Oct. 1999, p. 1-2; BTP/Navigant Consulting, U.S. Lighting Market Characterization, Volume I, Sept. 2002, Table 8-2, p.63; and EIA, AEO 1999, Dec. 1998, Table A4, p. 118-119 and Table A5, p. 120-121 for 1996 data.

3.1.3 2005 Residential Energy End-Use Carbon Dioxide Emissions Splits, by Fuel Type (MMTCE) (1)

	Natural	Petroleum							
	Gas	Distil.	LPG	Kerosene	Total	Coal	Electricity (2)	Total	Percent
Space Heating (3)	50.7	16.1	4.5	1.9	22.5	0.3	25.7	99.1	28.9%
Water Heating	16.4	2.3	0.8		3.1		21.7	41.2	12.0%
Space Cooling	0.0						43.6	43.6	12.7%
Lighting							39.2	39.2	11.4%
Refrigeration (4)							26.7	26.7	7.8%
Electronics (5)							26.2	26.2	7.6%
Wet Clean (6)	1.0						15.9	16.9	4.9%
Cooking	3.1		0.5		0.5		12.1	15.6	4.6%
Computers							4.0	4.0	1.2%
Other (7)	0.6		2.9		2.9		10.0	13.6	4.0%
Adjust to SEDS (8)							16.6	16.6	4.9%
Total	**71.8**	**18.4**	**8.7**	**1.9**	**29.0**	**0.3**	**241.7**	**342.8**	100%

Note(s): 1) Emissions assume complete combustion from energy consumption, excluding gas flaring, coal mining, and cement production. Emissions exclude wood since it is assumed that the carbon released from combustion is reabsorbed in a future carbon cycle. Carbon emissions calculated from EIA, Assumptions to the AEO 2007 and differs from EIA, AEO 2007, Table A18. Sector total varies from EIA, AEO 2007. 2) Excludes electric imports by utilities. 3) Includes furnace fans (4.4 MMTCE). 4) Includes refrigerators (20.3 MMTCE) and freezers (6.5 MMTCE). 5) Includes color television (15.7 MMTCE) and other office equipment (10.5 MMTCE). 6) Includes clothes washers (1.8 MMTCE), natural gas clothes dryers (1.0 MMTCE), electric clothes dryers (12.9 MMTCE), and dishwashers (1.3 MMTCE). Does not include water heating energy. 7) Includes small electric devices, heating elements, motors, swimming pool heaters, hot tub heaters, outdoor grills, and natural gas outdoor lighting. 8) Emissions related to a discrepancy between data sources. Energy attributable to the sector, but not directly to specific end-uses.

Source(s): EIA, Annual Energy Outlook (AEO) 2007, Feb. 2007, Table A2, p. 137-139, Table A4, p. 142-143 for energy consumption, and Table A18, p. 164 for emissions; EIA, Assumptions to the AEO 2007, Mar. 2007, Table 2, p. 9 for emission coefficients; BTS/A.D. Little, Electricity Consumption by Small End-Uses in Residential Buildings, Aug. 1998, Appendix A for residential electric end-uses; and EIA, AEO 1999, Dec. 1998, Table A4, p. 118-119 for 1996 electric end-use data.

3.1.4 2005 Commercial Energy End-Use Carbon Dioxide Emissions Splits, by Fuel Type (MMTCE) (1)

	Natural	Petroleum								
	Gas	Distil.	Resid.	LPG	Oth(2)	Total	Coal	Electricity (3)	Total	Percent
Lighting								74.6	74.6	25.9%
Space Heating	19.4	3.9	2.9		0.5	7.3	2.6	12.2	41.4	14.4%
Space Cooling	0.4							37.8	38.2	13.3%
Water Heating	8.2	1.4				1.4		9.2	18.7	6.5%
Electronics								18.3	18.3	6.4%
Ventilation								17.6	17.6	6.1%
Refrigeration								12.1	12.1	4.2%
Computers								9.5	9.5	3.3%
Cooking	3.3							2.0	5.3	1.9%
Other (4)	3.8	0.5		1.5	0.9	2.9		29.8	36.4	12.7%
Adjust to SEDS (5)	10.3	3.6				3.6		1.4	15.3	5.3%
Total	**45.3**	**9.4**	**2.9**	**1.5**	**1.4**	**15.2**	**2.6**	**224.3**	**287.5**	100%

Note(s): 1) Emissions assume complete combustion from energy consumption, excluding gas flaring, coal mining, and cement production. Emissions exclude wood since it is assumed that the carbon released from combustion is reabsorbed in a future carbon cycle. Carbon emissions calculated from EIA, Assumptions to the AEO 2007 and differs from EIA, AEO 2007, Table A18. Sector total varies by less than 0.2% from EIA, AEO 2007. 2) Includes kerosene space heating (0.5 MMTCE) and motor gasoline other uses (0.9 MMTCE). 3) Excludes electric imports by utilities. 4) Includes service station equipment, ATMs, telecommunications equipment, medical equipment, pumps, emergency electric generators, and manufacturing performed in commercial buildings. 5) Emissions related to a discrepancy between data sources. Energy attributable to the sector, but not directly to specific end-uses.

Source(s): EIA, Annual Energy Outlook (AEO) 2007, Feb. 2007, Table A2, p. 137-139, Table A5, p. 144-145 for energy consumption, and Table A18, p. 164 for emissions; EIA, National Energy Modeling System for AEO 2007, Feb. 2007; EIA, Assumptions to the AEO 2007, Mar. 2007, Table 2, p. 9 for emission coefficients; BTS/A.D. Little, Energy Consumption Characteristics of Commercial Building HVAC Systems, Volume II: Thermal Distribution, Auxiliary Equipment, and Ventilation, Oct. 1999, p. 1-2; BTP/Navigant Consulting, U.S. Lighting Market Characterization, Volume I, Sept. 2002, Table 8-2, p.63; and EIA, AEO 1998, Dec. 1997, Table A5, p. 108-109 for 1995 data.

3.1.5 World Carbon Dioxide Emissions (1)

	Emissions (10^6 metric tons of carbon equivalent)				Annual Growth Rate	
Nation/Region	1990	2004		2010	1990-2004	2004-2010
United States	1,362	1,617	22.0%	1,696	1.2%	0.8%
China	612	1,305	17.8%	1,773	5.6%	5.2%
OECD Europe	1,117	1,196	16.3%	1,226	0.5%	0.4%
Russia	637	459	6.2%	494	-2.3%	1.2%
Other Non-OECD Asia	220	435	5.9%	527	5.0%	3.3%
Middle East	192	352	4.8%	437	4.4%	3.7%
Japan	276	344	4.7%	348	1.6%	0.2%
Other Non-OECD Eurasia	507	309	4.2%	343	-3.5%	1.7%
India	158	303	4.1%	350	4.8%	2.4%
Central & S. America	184	280	3.8%	337	3.1%	3.1%
Africa	177	244	3.3%	311	2.3%	4.2%
Canada	129	159	2.2%	177	0.0%	0.0%
South Korea	64	136	1.8%	143	5.5%	0.9%
Australia & New Zealand	79	116	1.6%	129	2.7%	1.8%
Mexico	82	105	1.4%	131	1.8%	3.8%
Total World	**5,792**	**7,348**	100%	**9,249**	**1.7%**	**3.9%**

Source(s): EIA, International Energy Outlook 2007, May 2007, Table A10, p. 93.

3.1.6 2005 Methane Emissions for U.S. Buildings Energy Production, by Fuel Type (MMTCE) (1)

Fuel Type	Residential	Commercial	Buildings Total
Petroleum	0.2	0.1	0.4
Natural Gas	9.8	6.2	15.9
Coal	0.0	0.1	0.1
Wood	2.3	0.0	2.3
Electricity (2)	10.5	9.7	20.2
Total	**22.8**	**16.1**	**38.9**

Note(s): 1) Sources of emissions include oil and gas production, processing, and distribution; coal mining; and utility and site combustion. Carbon equivalent units are calculated by converting methane emissions to carbon dioxide emissions (methane's global warming potential is 23 times that of carbon dioxide) and carbon dioxide to carbon equivalent. 2) Emissions of electricity generators attributable to the buildings sector.

Source(s): EIA, Emissions of Greenhouse Gases in the U.S. 2005, Nov. 2006, Table 15, p. 38 for energy production emissions, and Table 19, p. 42 for stationary combustion emissions; and EIA, Annual Energy Outlook 2007, Feb. 2007, Table A2, p. 137-139 for energy consumption.

3.1.7 2005 Carbon Dioxide Emission Coefficients for Buildings (MMTCE per Quadrillion Btu) (1)

	All Buildings	Residential Buildings	Commercial Buildings
Coal			
Average (2)	25.80	25.80	25.80
Natural Gas			
Average (2)	14.41	14.41	14.41
Petroleum Products			
Distillate Fuel Oil/Diesel	19.76	-	-
Kerosene	19.54	-	-
Motor Gasoline	19.15	-	-
Liquefied Petroleum Gas	17.13	-	-
Residual Fuel Oil	21.29	-	-
Average (2)	19.15	18.88	19.68
Electricity Consumption (3)			
Average - Primary (4)	16.36	16.36	16.36
Average - *Site* (5)	52.01	52.01	52.01
New Generation			
Gas Combined Cycle - *Site* (6)	31.35	31.35	31.35
Gas Combustion Turbine - *Site* (6)	47.23	47.23	47.23
Stock Gas Generator - *Site* (7)	38.40	38.40	38.40
All Fuels (3)			
Average - Primary	15.90	15.76	16.08
Average - *Site*	31.45	29.51	33.91

Note(s): 1) Emissions assume complete combustion from energy consumption, excluding gas flaring, coal mining, and cement production. The combustion of fossil fuels produces carbon in the form of carbon dioxide and carbon monoxide; however, carbon monoxide emissions oxidize in a relatively short time to form carbon dioxide. 2) Coefficients do not match total emissions reported in the AEO 2007 and were adjusted using Assumptions to the AEO 2007. 3) Excludes electricity imports from utility consumption. Includes nuclear and renewable (including hydroelectric) generated electricity. 4) Use this coefficient to estimate carbon emissions resulting from the consumption of energy by electric generators. 5) Use this coefficient to estimate carbon emissions resulting from the consumption of electricity by end-users. 6) Use this coefficient to estimate emissions of the next-built (2005) natural gas-fired, electric generator resulting from the consumption of electricity by end-users. 7) Use this coefficient to estimate emissions of existing natural gas-fired, electric generators resulting from the consumption of electricity by end-users.

Source(s): EIA, Annual Energy Outlook (AEO) 2007, Feb. 2007, Table A2, p. 137-139, Table A8, p. 151-152, Table A17, p. 163 for consumption and Table A18, p. 164 for emissions; EIA, Assumptions to the AEO 2007, Mar. 2007, Table 2, p. 9 for coefficients and Table 38, p. 76 for generator efficiencies; EIA, Annual Energy Review 2006, June 2007, Diagram 5, p. 221 for Transmission and Distribution (T&D) losses.

3.2.1 Halocarbon Environmental Coefficients and Principal Uses

Compound	100-Year Global Warming Potential (CO2 = 1)	Ozone Depletion Potential (ODP) (Relative to CFC-11)	Principal Uses
Chlorofluorocarbons			
CFC-11	4,600	1.00	Blowing Agent, Chillers
CFC-12 (1)	10,600	1.00	Auto A/C, Chillers, & Blowing Agent
CFC-113	6,000	0.80	Solvent
CFC-114	9,800	1.00	Solvent
CFC-115 (2)	7,200	0.60	Solvent, Refrigerant
Hydrochlorofluorocarbons			
HCFC-22 (2)	1,700	0.06	Residential A/C
HCFC-123	120	0.02	Refrigerant
HCFC-124	620	0.02	Sterilant
HCFC-141b	700	0.11	CFC Replacement
HCFC-142b	2,400	0.07	CFC Replacement
Bromofluorocarbons			
Halon-1211	1,300	3.00	Fire Extinguishers
Halon-1301	6,900	10.00	Fire Extinguishers
Hydrofluorocarbons			
HFC-23	12,000	0.00	HCFC Byproduct
HFC-125	3,400	0.00	CFC/HCFC Replacement
HFC-134a	1,300	0.00	Auto A/C, Refrigeration
HFC-152a (1)	140	0.00	Aerosol Propellant
HFC-227ea	2,900	0.00	CFC Replacement

Note(s): 1) R-500: 74% CFC-12 and 26% HFC-152a. 2) R-502: 49% HCFC-22 and 51% CFC-115.

Source(s): Intergovernmental Panel for Climate Change, Climate Change 2001: The Scientific Basis, Jan. 2001, Table 3, p. 47 for global warming potentials and uses; EPA for halon ODPs; AFEAS Internet Homepage, Atmospheric Chlorine: CFCs and Alternative Fluorocarbons, Feb. 1997 for remaining ODPs; and ASHRAE, 1993 ASHRAE Handbook: Fundamental, p. 16.3 for Notes 1 and 2; EPA, Emissions of Greenhouse Gases in the U.S. 2005, Table ES-1, p ES-3 for GWP of HFCs.

3.2.2 Phase-Out Schedule of Halocarbons in the U.S. (1)

Gas	Manufacturing Base Level (2)	Manufacturing Freeze (3)	Montreal Protocol Reduction %	Montreal Protocol Reduction By	U.S. Clean Air Act Reduction %	U.S. Clean Air Act Reduction By
Chlorofluorocarbons (CFCs)	1996	1989	75%	1994	75%	1994
			100%	1996 (4)	100%	1996
Bromofluorocarbons (Halons)	1996	1992	100%	1994 (4)	100%	1994
Hydrochlorofluorocarbons (HCFCs)	1989 HCFC consumption + 2.8 %	1996	35%	2004	35%	2003
			65%	2010	65%	2010
			90%	2015	90%	2015
					99.5%	2020
			100%	2030 (4)	100%	2030
Hydrofluorocarbons (HFCs)	N.A.	N.A.	N.A.	N.A.	N.A.	N.A.

Note(s): (1) The phase-out of halocarbons is consistent with Title VI of the Clean Air Act and is in accordance with the Montreal Protocol and Amendments. (2) The amount of gas produced and consumed in this year is established and defined as the base level. In order to meet basic domestic needs, levels of production are allowed to exceed the base level by up to 10%. (3) After this year, levels of production are no longer permitted to exceed the base year level. (4) With possible essential use exemptions.

Source(s): Federal Register, Vol. 72, No. 123, June 2007, p. 35230, http://www.epa.gov/ozone/title6/phaseout; United Nations Ozone Environmental Programme, Ozone Secretariat, 2005, http://www.unep.ch/ozone/index.shtml; and Title VI, The Clean Air Act of 1990, S.1630, 101st Congress., 2nd Session.

3.2.3 Conversion and Replacements of Centrifugal CFC Chillers

	Conversions	Replacements	Total	Cumulative Percent of 1992 Chillers (1)
Pre-1995	2,304	7,208	9,512	12%
1995	1,198	3,915	5,113	18%
1996	1,311	3,045	4,356	24%
1997	815	3,913	4,728	30%
1998	905	3,326	4,231	35%
1999	491	3,085	3,576	39%
2000	913	3,235	4,148	45%
2001	452	3,324	3,776	49%
2002	360	3,433	3,793	54%
2003	334	2,549	2,883	55%
2004	165	2,883	3,048	59%
2005 (2)	155	2,674	2,829	62%
2006 (2)	130	2,860	2,990	66%
2007 (2)	108	3,002	3,110	70%
Total	**9,641**	**48,452**	**58,093**	

Note(s): 1) In 1992, approximately 80,000 centrifugal CFC chillers were in service, 82% of which used CFC-11, 12% CFC-12, and 6% CFC-113, CFC-114, or R-500. 2) Projected.

Source(s): ARI, Replacement and Conversion of CFC for a Decade Chillers Slower Than Expected Assuring Steady Demand for Non-CFC Units, Apr. 25, 2005; ARI, New Legislation Would Spur Replacement of CFC Chillers, Mar. 31, 2004; ARI, Economy Affects CFC Chiller Phase-out, Apr. 2, 2003; ARI, Half-way Mark in Sight for Replacement and Conversion of CFC Chiller Used for Air Conditioning of Buildings, Apr. 11, 2001; ARI, Replacement and Conversion of CFC Chillers Dipped in 1999 Assuring Steady Demand for Non-CFC Units for a Decade, Mar. 29, 2000; ARI, Survey Estimates Long Use of CFC Chillers Nearly Two-Thirds of Units Still in Place, Apr. 15, 1999; ARI, CFCs Widely Used to Cool Buildings Despite 28-Month Ban on Production, Apr. 8, 1998; ARI, 1997 Chiller Survey, Apr. 9, 1997; Air Conditioning, Heating and Refrigeration News, Apr. 1996, p. 1; and ARI's web site, www.ari.org, Chiller Manufacturer Survey Confirms Slow Pace of Conversion and Replacements of CFC Chillers, Apr. 12, 1995.

3.2.4 Estimated U.S. Emissions of Halocarbons, 1987-2001 (MMTCE)

Gas	1987	1990	1992	1995	1998	2000	2001
Chlorofluorocarbons							
CFC-11	107	67	57	45	31	29	29
CFC-12	318	326	233	150	61	50	62
CFC-113	136	43	28	14	0	0	0
CFC-114	N.A.	13	8	4	0	N.A.	N.A.
CFC-115	N.A.	8	7	6	5	N.A.	N.A.
Bromofluorocarbons							
Halon-1211	N.A.	0	0	0	0	N.A.	N.A.
Halon-1301	N.A.	3	3	3	4	N.A.	N.A.
Hydrochlorofluorocarbons							
HCFC-22	32	37	37	34	35	37	37
HCFC-123	N.A.	0	0	0	0	N.A.	N.A.
HCFC-124	0	0	0	1	1	N.A.	N.A.
HCFC-141b	N.A.	0	0	4	5	1	1
HCFC-142b	N.A.	0	0	5	6	7	7
Hydrofluorocarbons							
HFC-23	13	10	10	8	11	9	6
HFC-125	N.A.	0	0	0	1	1	2
HFC-134a	N.A.	0	0	5	10	12	11
Total	**605**	**508**	**384**	**279**	**170**	**145**	**154**

Source(s): Intergovernmental Panel for Climate Change, Climate Change 2001: The Scientific Basis, Jan. 2001, Table 3, p. 47 for GWPs; EIA, Emissions of Greenhouse Gases in the U.S. 2001, Dec. 2002, Table 29, p. 71 and Table D2, p. D-5 for 1990-2001 emissions; EPA, Inventory of U.S. Greenhouse Gas Emissions and Sinks: 1990–1998, Table ES-6, p. ES-9 for HFCs and Annex L, Table L-1, p. L-2 for 1990-1998 ozone depleting refrigerants; and EIA, Emissions of Greenhouse Gases in the U.S. 1985-1994, Oct. 1995, Table 34, p. 54 for 1987.

3.3.1 2002 EPA Emissions Summary Table for U.S. Buildings Energy Consumption (Thousand Short Tons) (1)

	Buildings				Buildings Percent
	Wood/Site Fossil	Electricity	Total	U.S. Total	of U.S. Total
SO2	575	7,343 (2)	7,918	15,353	52%
NOx	725	3,353	4,078	21,102	19%
CO	2,498	356	2,854	112,049	3%
VOCs	790	37	827	16,544	5%
PM-2.5	384	415	799	6,803	12%
PM-10	405	496	901	22,154	4%

Note(s): 1) VOCs = volatile organic compounds; PM-10 = particulate matter less than 10 micrometers in aerodynamic diameter. PM-2.5 = particulate matter less than 2.5 micrometers in aerodynamic diameter. CO and VOCs site fossil emissions mostly from wood burning. 2) Emissions of SO2 are 28% lower for 2002 than 1994 estimates since Phase II of the 1990 Clean Air Act Amendments began in 2000. Buildings Energy Consumption related to SO2 emissions dropped 27% from 1994 to 2002.

Source(s): EIA, Annual Energy Outlook 2005, Feb. 2005, Table A2, p. 140-142; and EPA, 2002 Average Annual Emissions, All Criteria Pollutants, Aug. 2005, Tables A-2 to A-8.

3.3.2 2002 EPA Criteria Pollutant Emissions Coefficients
(Million Short Tons/*Delivered* Quadrillion Btu, unless otherwise noted)

Residential

	Electricity (1)	Gas	Oil(3)	Coal	Electricity (per primary quad) (1)
SO2	0.870	(2)	0.086	(2)	0.270
NOx	0.397	0.047	0.036	(2)	0.123
CO	0.042	(2)	(2)	(2)	0.013

Commercial

	Electricity (1)	Gas	Oil(3)	Coal	Electricity (per primary quad) (1)
SO2	0.870	(2)	0.351	(2)	0.270
NOx	0.397	0.072	0.102	(2)	0.123
CO	0.042	(2)	(2)	(2)	0.013

All Buildings

	Electricity (1)	Gas	Oil(3)	Coal	Electricity (per primary quad) (1)
SO2	0.870	(2)	0.171	(2)	0.270
NOx	0.397	0.056	0.058	(2)	0.123
CO	0.042	(2)	(2)	(2)	0.013

Note(s): 1) Emissions of SO2 are 28% lower for 2002 than 1994 estimates since Phase II of the 1990 Clean Air Act Amendments began in 2000. Buildings energy consumption related SO2 emissions dropped 27% from 1994 to 2002. 2) Data not available, significant enough, or reliable. 3) Oil includes distillate and residual fuel oils, LPG, motor gasoline, and kerosene.

Source(s): EPA, 2002 Average Annual Emissions, All Criteria Pollutants, Aug. 2005, Tables A-2 to A-8 for emissions; and EIA, AEO 2005, Feb. 2005, Table A2, p. 140-142 for energy consumption.

3.4.1 Characteristics of U.S. Construction Waste

- Two to seven tons of waste (a rough average of 4 pounds of waste per square foot) are generated during the construction of a new single-family detached house.
- 15 to 70 pounds of hazardous waste are generated during the construction of a detached, single-family house. Hazardous wastes include paint, caulk, roofing cement, aerosols, solvents, adhesives, oils, and greases.
- Each year, U.S. builders produce between 30 and 35 million tons of construction, renovation, and demolition (C&D) waste.
- Annual C&D debris accounts for roughly 24% of the municipal solid waste stream.
- Wastes include wood (27% of total) and other (73% of total, including cardboard and paper; drywall/plaster; insulation; siding; roofing; metal; concrete, asphalt, masonry, bricks, and dirt rubble; waterproofing materials; and landscaping material).
- As much as 95% of buildings-related construction waste is recyclable, and most materials are clean and unmixed.

Source(s): First International Sustainable Construction Conference Proceedings, Construction Waste Management and Recycling Strategies in the U.S., Nov. 1994, p. 689; Fine Homebuilding, Construction Waste, Feb./Mar. 1995, p. 70-75; NAHB, Housing Economics, Mar. 1995, p. 12-13; and Cost Engineering, Cost-Effective Waste Minimization for Construction Managers, Vol. 37/No. 1, Jan. 1995, p. 31-39.

3.4.2 "Typical" Construction Waste Estimated for a 2,000-Square-Foot Home (1)

Material	Weight (pounds)		Volume (cu. yd.) (2)
Solid Sawn Wood	1,600	20%	6
Engineered Wood	1,400	18%	5
Drywall	2,000	25%	6
Cardboard (OCC)	600	8%	20
Metals	150	2%	1
Vinyl (PVC) (3)	150	2%	1
Masonry (4)	1,000	13%	1
Hazardous Materials	50	1%	-
Other	1,050	13%	11
Total (5)	**8,000**	100%	**50**

Note(s): 1) See Table 2.1.7 for materials used in the construction of a new single-family home. 2) Volumes are highly variable due to compressibility and captured air space in waste materials. 3) Assuming 3 sides of exterior clad in vinyl siding. 4) Assuming a brick veneer on home's front facade. 5) Due to rounding, sum does not add up to total.

Source(s): NAHB's Internet web site, www.nahb.org, Residential Construction Waste: From Disposal to Management, Oct. 1996.

3.4.3 1996 Construction and Demolition Debris Generated from Construction Activities and Debris Generation Rates

	Debris (million tons)			Debris Generation Rates (lbs/ sq. ft.)	
	Residential	Commercial	Buildings	Residential	Commercial
New Construction	6.6	4.3	10.8	4.38	3.89
Demolition	19.7	45.1	64.8	115	155
Renovation	31.9	28.0	59.9	N.A.	N.A.
Total	**58.2**	**77.4**	**135.5**		

Source(s): EPA/OSW, Characterization of Buildings-Related Construction and Demolition Debris in the United States, June 1998, Tables 3-6, p. 2-3 - 2-8, and Table 8, p. 2-11.

4.1.1 Building Energy Prices, by Year and Major Fuel Type ($2005 per Million Btu)

	Residential Buildings				Commercial Buildings				Building
	Electricity	Natural Gas	Petroleum (1)	Avg.	Electricity	Natural Gas	Petroleum (2)	Avg.	Avg. (3)
1980	32.77	7.51	15.14	15.82	33.50	6.93	11.77	16.63	16.14
1990	31.72	7.78	12.09	16.76	29.29	6.49	8.22	16.76	16.76
2000	24.49	8.61	13.02	14.31	21.86	6.64	5.68	16.14	15.08
2005	**27.59**	**12.43**	**16.14**	**19.03**	**25.25**	**11.20**	**12.87**	**21.37**	**20.01**
2010	26.91	10.98	17.70	18.23	24.50	9.34	12.71	20.31	19.10
2015	25.99	10.24	16.11	17.44	23.33	8.48	11.07	18.94	18.09
2020	26.37	10.54	16.79	18.01	23.95	8.67	11.67	19.43	18.64
2025	26.61	10.97	17.40	18.56	24.23	8.96	12.10	19.77	19.11
2030	26.76	11.43	18.11	19.08	24.27	9.30	12.61	19.98	19.50

Note(s): 1) Residential petroleum products include distillate fuel, LPG, and kerosene. 2) Commercial petroleum products include distillate fuel, LPG, kerosene, motor gasoline, and residual fuel. 3) In 2005, buildings average electricity price was $26.46/10^6 Btu or ($0.090/kWh), average natural gas price was $11.95/10^6 Btu ($12.31/1000 CF), and petroleum was $23.62/10^6 Btu ($2.55/gal.). Averages do not include wood or coal prices.

Source(s): EIA, State Energy Data 2004: Prices and Expenditures, June 2007, Tables 2-3, p. 24-25 for 1980-2000 and prices for note, Tables 8-9, p. 18-19 for 1980-2000 consumption; EIA, Annual Energy Outlook 2007 Feb. 2007, Table A2, p. 137-139, Table A3, p. 140-141, Table A12, p. 158, and Table A13, p. 159 for 2005-2030 consumption and prices; and EIA, Annual Energy Review 2006, June 2007, Appendix D, p. 377 for price deflators.

4.1.2 Building Energy Prices, by Year and Fuel Type ($2005)

	Residential Buildings				Commercial Buildings			
	Electricity (¢/kWh)	Natural Gas (¢/therm)	Distillate Oil ($/gal)	LPG ($/gal)	Electricity (¢/kWh)	Natural Gas (¢/therm)	Distillate Oil ($/gal)	Residual Oil ($/gal)
1980	11.18	75.10	2.03	1.42	11.43	69.26	1.87	1.29
1990	10.82	77.79	1.54	1.30	9.99	64.94	1.14	0.71
2000	9.29	86.13	1.56	1.40	8.28	73.96	1.17	0.76
2005	**9.41**	**124.28**	**2.04**	**1.66**	**8.62**	**112.03**	**1.76**	**1.26**
2010	9.18	109.76	2.06	2.03	8.36	93.36	1.76	1.13
2015	8.87	102.42	1.75	1.96	7.96	84.77	1.49	0.97
2020	9.00	105.40	1.82	1.99	8.17	86.74	1.57	1.06
2025	9.08	109.74	1.88	2.02	8.27	89.60	1.64	1.07
2030	9.13	114.26	1.96	2.05	8.28	93.03	1.73	1.09

Source(s): EIA, State Energy Data 2004: Prices and Expenditures, June 2007, Tables 2-3, p. 24-25 for 1980-2000; EIA, Annual Energy Outlook 2007, Feb. 2007, Table A3, p. 140-141 for 2005-2030 and Table H1, p. 233 for fuels' heat content; and EIA, Annual Energy Review 2006, June 2007, Appendix D, p. 377 for price deflators.

4.1.3 Buildings Aggregate Energy Expenditures, by Year and Major Fuel Type ($2005 Billion) (1)

	Residential Buildings				Commercial Buildings				Total Building
	Electricity	Natural Gas	Petroleum (2)	Total	Electricity	Natural Gas	Petroleum (3)	Total	Expenditures
1980	80.2	36.5	26.5	143.2	63.9	18.5	15.2	97.5	240.7
1990	100.0	35.2	17.0	152.2	83.8	17.5	7.8	109.1	261.3
2000	110.7	43.9	20.4	175.0	96.0	24.1	6.9	126.9	301.9
2005	**128.5**	**61.9**	**24.8**	**215.2**	**109.1**	**35.2**	**9.9**	**154.3**	**369.5**
2010	136.2	56.9	27.0	220.1	116.9	30.9	9.5	157.4	377.5
2015	141.1	54.8	25.0	220.8	123.2	30.8	8.8	162.8	383.7
2020	153.0	57.2	25.6	235.9	138.4	33.5	9.3	181.2	417.1
2025	163.1	59.8	25.9	248.9	154.1	36.7	9.8	200.6	449.5
2030	173.1	62.5	26.5	262.1	170.7	40.6	10.3	221.6	483.7

Note(s): 1) Expenditures exclude wood and coal. 2005 U.S. energy expenditures were $1.04 trillion. 2) Residential petroleum products include distillate fuel oil, LPG, and kerosene. 3) Commercial petroleum products include distillate fuel oil, LPG, kerosene, motor gasoline, and residual fuel.

Source(s): EIA, State Energy Data 2004: Prices and Expenditures, June 2006, p. 24-25 for 1980-2000; EIA, Annual Energy Outlook 2007, Feb. 2007, Table A2, p. 137-139 and Table A3, p. 140-141 for 2005-2030; and EIA, Annual Energy Review 2006, June 2007, Appendix D, p. 377 for price deflators.

4.1.4 FY 2005 Federal Buildings Energy Prices and Expenditures, by Fuel Type ($2005)

Fuel Type	Average Fuel Prices ($/million Btu)	Total Expenditures ($million) (2)
Electricity	20.86 (1)	2,887.8
Natural Gas	8.27	823.7
Fuel Oil	9.34	263.9
Coal	3.01	38.9
Purchased Steam	10.52	130.1
LPG/Propane	12.06	36.7
Other	14.19	77.1
Average	**14.19**	**Total** **4,258.3**

Note(s): 1) $0.071/kWh. 2) Energy used in buildings in FY 2005 accounted for 29.5% of the total Federal energy bill.
Source(s): DOE, Annual Report to Congress on FEMP, Sept. 2006, Table 5, p 152 for prices and expenditures, and p. E-2 for Federal buildings energy expenditures.

4.1.5 2005 Buildings Energy End-Use Expenditure Splits, by Fuel Type ($2005 Billion) (1)

	Natural Gas	Petroleum					Coal	Electricity	Total	Percent
		Distil.	Resid.	LPG	Oth(2)	Total				
Space Heating (3)	58.8	14.5	1.1	5.0	1.6	22.3	0.2	19.6	100.9	27.3%
Lighting								57.1	57.1	15.5%
Space Cooling	0.3							41.6	41.9	11.3%
Water Heating (4)	20.5	2.6		0.9		3.5		16.0	40.0	10.8%
Refrigeration (5)								23.0	23.0	6.2%
Electronics (6)								22.8	22.8	6.2%
Cooking	5.3			0.5		0.5		7.4	13.2	3.6%
Wet Clean (7)	0.9							8.5	9.3	2.5%
Ventilation (8)								8.6	8.6	2.3%
Computers								6.7	6.7	1.8%
Other (9)	2.9	0.3		4.9	0.9	6.1		19.8	28.8	7.8%
Adjust to SEDS (10)	8.5	2.3				2.3		5.9	16.8	4.6%
Total	**97.2**	**19.8**	**1.1**	**11.4**	**2.5**	**34.7**	**0.2**	**237.0**	**369.1**	100%

Note(s): 1) Expenditures include coal and exclude wood (unlike Table 4.1.3). 2) Includes kerosene space heating ($1.3 billion) and motor gasoline other uses ($0.9 billion). 3) Includes furnace fans ($2.3 billion). 4) Includes residential recreation water heating ($1.2 billion). 5) Includes refrigerators ($10.8 billion) and freezers ($9.6 billion). 6) Includes color televisions ($8.3 billion) and other electronics ($5.6 billion). 7) Includes clothes washers ($0.9 billion), natural gas clothes dryers ($0.9 billion), electric clothes dryers ($6.9 billion) and dishwashers ($0.7 billion). 8) Commercial only; residential fan and pump energy use included proportionately in space heating and cooling ($0.5 billion). 9) Includes residential small electric devices, heating elements, motors, swimming pool heaters, hot tub heaters, outdoor grills, and natural gas outdoor lighting. Includes commercial services station equipment, ATMs, telecommunications equipment, medical equipment, pumps, lighting, emergency electric generators, manufacturing performed in commercial buildings. 10) Expenditures related to an energy adjustment EIA uses to relieve discrepancies between data sources. Energy attributable to the residential and commercial buildings sectors, but not directly to specific end-uses.

Source(s): EIA, Annual Energy Outlook 2007, Feb. 2007, Table A2, p. 137-139, Table A3, p. 140-141 for prices, Table A4, p. 142-143 for residential energy consumption, and Table A5, p. 144-145 for commercial energy consumption; EIA, National Energy Modeling System for AEO 2007, Feb. 2007; EIA, State Energy Data 2004: Prices and Expenditures, June 2007, p. 24-25 for coal prices; EIA, Annual Energy Review 2006, June 2007, Appendix D, p. 377 for price deflators; BTS/A.D. Little, Electricity Consumption by Small End-Uses in Residential Buildings, Aug. 1998, Appendix A for residential electric end-uses; BTS/A.D. Little, Energy Consumption Characteristics of Commercial Building HVAC Systems, Volume II: Thermal Distribution, Auxiliary Equipment, and Ventilation, Oct. 1999, p. 1-2, 5-25 and 5-26 for commercial ventilation; BTP/Navigant Consulting, U.S. Lighting Market Characterization, Volume I, Sept. 2002, Table 8-2, p. 63 for commercial lighting; OBT/A.D. Little, Energy Savings Potential for Commercial Refrigeration Equipment, June 1996, Figure 1-1-, p. 1-1; and EIA, AEO 1999, Dec. 1998, Table A5, p. 120 for 1996 commercial refrigeration.

4.1.6 Implicit Price Deflators (2000 = 1.00)

Year	Implicit Price Deflator	Year	Implicit Price Deflator	Year	Implicit Price Deflator
1980	0.54	1990	0.82	2000	1.00
1981	0.59	1991	0.84	2001	1.02
1982	0.63	1992	0.86	2002	1.04
1983	0.65	1993	0.88	2003	1.06
1984	0.68	1994	0.90	2004	1.09
1985	0.70	1995	0.92	2005	1.13
1986	0.71	1996	0.94		
1987	0.73	1997	0.95		
1988	0.76	1998	0.96		
1989	0.79	1999	0.98		

Source(s): EIA, Annual Energy Review 2006, June 2007, Appendix D, p. 377.

4.2.1 2005 Residential Energy End-Use Expenditure Splits, by Fuel Type ($2005 Billion) (1)

	Natural	Petroleum							
	Gas	Distil.	LPG	Kerosene	Total	Coal	Electricity	Total	Percent
Space Heating (2)	43.7	12.0	5.0	1.3	18.3	0.04	13.6	75.7	35.2%
Water Heating (3)	14.1	1.7	0.9		2.6		11.5	28.3	13.1%
Space Cooling (4)	0.0						23.2	23.2	10.8%
Lighting							20.8	20.8	9.7%
Refrigeration (5)							14.2	14.2	6.6%
Electronics (6)							13.9	13.9	6.5%
Cooking	2.7		0.5		0.5		6.4	9.6	4.5%
Wet Clean (7)	0.9						8.5	9.3	4.3%
Computers							2.1	2.1	1.0%
Other (8)	0.5		3.3		3.3		5.3	9.2	4.3%
Adjust to SEDS (9)							8.8	8.8	4.1%
Total	**61.9**	**13.7**	**9.8**	**1.3**	**24.8**	**0.04**	**128.5**	**215.2**	100%

Note(s): 1) Expenditures include coal and exclude wood (unlike Table 4.1.3). 2) Includes furnace fans ($2.3 billion). 3) Includes residential recreation water heating ($1.2 billion). 4) Fan energy use included. 5) Includes refrigerators ($10.8 billion) and freezers ($3.5 billion). 6) Includes color televisions ($8.3 billion) and other electronics ($5.6 billion). 7) Includes clothes washers ($0.9 billion), natural gas clothes dryers ($0.7 billion), electric clothes dryers ($6.4 billion), and dishwashers ($0.9 billion). 8) Includes small electric devices, heating elements, motors, swimming pool heaters, hot tub heaters, outdoor grills, and natural gas outdoor lighting. 9) Expenditures related to an energy adjustment EIA uses to relieve discrepancies between data sources. Energy attributable to the residential building sector, but not directly to specific end-uses.

Source(s): EIA, Annual Energy Outlook 2007, Feb. 2007, Table A2, p. 137-139 and Table A4, p. 142-143 for energy, Table A3, p. 140-141 for prices; EIA, State Energy Data 2004: Prices and Expenditures, June 2007, p. 24 for coal price; EIA, Annual Energy Review 2006, June 2007, Appendix D, p. 377 for price deflators; and BTS/A.D. Little, Electricity Consumption by Small End-Uses in Residential Buildings, Aug. 1998, Appendix A for residential electric end-uses.

4.2.2 Average Annual Energy Expenditures per Household, by Year ($2005)

Year	
1980	1,798
1990	1,615
2000	1,617
2005	**1,899**
2010	1,824
2015	1,729
2020	1,751
2025	1,762
2030	1,777

Source(s): EIA, State Energy Data 2004: Prices and Expenditures, June 2007, p. 24 for 1980-2000; EIA, Annual Energy Outlook 2007, Feb. 2007, Table A2, p. 137-139, Table A4, p. 142-143 for consumption, Table A3, p. 140-141 for prices 2005-2030; EIA, Annual Energy Review 2006, June 2007, Appendix D, p. 377 for price deflators; and DOC, Statistical Abstract of the United States 2007, Feb. 2007, Table No. 949, p. 606 for 1980-2000 occupied units.

4.2.3 2001 Energy Expenditures per Household, by Housing Type and Square Footage ($2005)

	Per Household	Per Square Foot
Single-Family	**1,868**	**0.78**
-Detached	1,899	0.78
-Attached	1,686	0.77
Multi-Family	**1,065**	**1.02**
-2 to 4 units	1,389	1.00
-5 or more units	884	1.05
Mobile Home	**1,471**	**1.40**

Source(s): EIA, A Look at Residential Energy Consumption in 2001, Oct. 2003, Table CE1-6.2u; and EIA, Annual Energy Review 2006, June 2007, Appendix D, p. 377 for price inflators.

4.2.4 2001 Energy Expenditures per Household, by Census Region ($2005)

Region	
Northeast	1,917
Midwest	1,697
South	1,684
West	1,286

Source(s): EIA, A Look at Residential Energy Consumption in 2001, Oct. 2003, Tables CE1-9c, CE1-10c, CE1-11c and CE1-12c; and EIA, Annual Energy Review 2006, June 2007, Appendix D, p. 377 for price inflators.

4.2.5 2001 Household Energy Expenditures, by Vintage ($2005)

Year	Per Household	Per Square Foot	Per Household Member	Percent of Residential Sector Expenditures
Prior to 1970	1,672	0.86	655	52%
1970 to 1979	1,529	0.88	611	16%
1980 to 1989	1,584	0.82	633	16%
1990 to 1999	1,734	0.73	594	14%
2000 to 2001	2,032	0.67	602	1%
				Total 100%
Average	**1,644**	**0.83**	**635**	

Source(s): EIA, A Look at Residential Energy Consumption in 2001, Oct. 2003, Tables CE1-6.1u and CE1-6.2u; and EIA, Annual Energy Review 2006, June 2007, Appendix D, p. 377 for price inflators.

4.2.6 2001 Households and Energy Expenditures, by Income Level ($2005)

Household Income	Households (10^6)		Energy Expenditures by Household	Energy Expenditures by Household Member	Mean Individual Energy Burden (1)
Less than $9,999	11.0	10%	1,039	554	16%
$10,000 to $14,999	7.7	7%	1,124	528	9%
$15,000 to $19,999	8.9	8%	1,290	565	7%
$20,000 to $29,999	14.0	13%	1,315	561	5%
$30,000 to $39,999	13.9	13%	1,398	547	4%
$40,000 to $49,999	13.2	12%	1,518	562	3%
$50,000 to $74,999	21.7	20%	1,683	577	3%
$75,000 to $99,999	8.1	8%	1,825	624	2%
$100,000 or more	8.6	8%	2,231	732	2%
Total	**107.1**	100%			**3%**

Note(s): 1) See Tables 4.2.7 and 7.1.10 for more on energy burdens. 2) A household is defined as a family, an individual, or a group of up to nine unrelated individuals occupying the same housing unit.

Source(s): EIA, A Look at Residential Energy Consumption in 2001, Oct. 2003, Tables CE1-5.1u.; and EIA, Annual Energy Review 2006, June 2007, Appendix D, p. 377 for price inflators.

4.2.7 Energy Burden Definitions and Residential Energy Burdens, by Weatherization Eligibility and Year (1)

Energy burden is an important statistic for policy makers who are considering the need for energy assistance. Energy burden can be defined broadly as the burden placed on household incomes by the cost of energy, or more simply the ratio of energy expenditures to income for a household. However, there are different ways to compute energy burden, and different interpretations and uses of the energy burden statistics. DOE Weatherization primarily uses mean individual burden and mean group burden since these statistics provide data on how an "average" individual household fares against an "average" group of households (that is, how burdens are distributed for the population). DOE Weatherization (and HHS) also uses the median individual burden which shows the burden of a "typical" individual.

	1987	1990		FY 2000 (2)			FY 2005 (3)		
	Mean Group	Mean Indvdl	Mean Group	Mean Indvdl	Mdn Indvdl	Mean Group	Mean Indvdl	Mdn Indvdl	Mean Group
Total U.S. Households	4.0%	6.8%	3.2%	6.1%	3.5%	2.4%	6.8%	3.7%	2.9%
Federally Eligible	**13.0%**	**14.4%**	**10.1%**	**12.1%**	**7.9%**	**7.7%**	**14.6%**	**8.6%**	**9.1%**
Federally Ineligible	4.0%	3.5%	N.A.	3.0%	2.6%	2.0%	3.2%	2.8%	2.3%
Below 125% Poverty Line	13.0%	N.A.	N.A.	N.A.	N.A.	N.A.	20.2%	13.7%	12.8%

Note(s): 1) See Section 7.1 for more on low-income housing. 2) Data are derived from RECS 1997, adjusted to reflect FY 2000, HDD, CDD, 3) Data are derived from RECS 2001, adjusted to reflect FY 2005, HDD, CDD, and fuel prices.

Source(s): HHS, LIHEAP Home Energy Notebook for Fiscal Year 2005, May 2007, Tables A-2a, A-2b, and A-2c, p. 59-61 for FY 2005; HHS, LIHEAP Home Energy Notebook for FY 2000, April 2002, Tables A-2a, A-2b, and A-2c, p. 48-50 for FY 2000; HHS, LIHEAP Report to Congress FY 1995, Aug. 1997, p. 55 for energy burden definitions; HHS, Characterizing the Impact of Energy Expenditures on Low-Income Households: An Analysis of Alternative National Energy Burden Statistics, November 1994, p. vii-ix for burdens; ORNL, Scope of the of the Weatherization Assistance Program: Profile of the Population in Need, Mar. 1994, p. xii for mean individual and mean group burdens and p. xi for 1990 Federally ineligible mean individual burden; and EIA, Household Energy Consumption and Expenditures 1987, Oct. 1989, Table 13, p. 48-50 for 1987 mean group burdens.

4.2.8 1998 Cost Breakdown of a 2,150-Square-Foot, New Single-Family Home ($2005) (1)

	Cost	
Finished Lot	**62,539**	**24%**
Construction Cost		
Inspection/Fees	4,087	2%
Shell/Frame		
Framing	29,928	11%
Windows/Doors	9,940	4%
Exterior Finish	10,939	4%
Foundation	15,610	6%
Wall/Finish Trim	27,301	10%
Flooring	6,978	3%
Equipment		
Plumbing	8,552	3%
Electrical Wiring	5,456	2%
Lighting Fixtures	1,510	1%
HVAC	5,972	2%
Appliances	2,095	1%
Property Features	17,000	6%
Financing	**4,985**	**2%**
Overhead & General Expenses	**15,139**	**6%**
Marketing	**3,716**	**1%**
Sales Commission	**8,940**	**3%**
Profit	**24,350**	**9%**
Total	**265,036**	100%

Note(s): 1) Based on a NAHB survey asking builders to provide a detailed breakdown of the cost of constructing a 2,150SF house with 3 or 4 bedrooms on a 7,500- to 10,000SF lot. Average sales price of a new home in 42 surveyed markets was $226,680 (in $1998).

Source(s): NAHB, The Truth About Regulatory Barriers to Housing Affordability, 1999, p. 4; and EIA, Annual Energy Review 2006, June 2007, Appendix D, p. 377 for price inflators.

4.3.1 2005 Commercial Energy End-Use Expenditure Splits, by Fuel Type ($2005 Billion) (1)

	Natural	Petroleum								
	Gas	Distil.	Resid.	LPG	Oth(2)	Total	Coal (3)	Electricity	Total	Percent
Lighting								36.3	36.3	23.5%
Space Heating	15.1	2.5	1.1		0.3	4.0	0.2	5.9	25.2	16.3%
Space Cooling	0.3							18.4	18.7	12.1%
Water Heating	6.4	0.9				0.9		4.5	11.7	7.6%
Electronics								8.9	8.9	5.8%
Ventilation								8.6	8.6	5.5%
Refrigeration								5.9	5.9	3.8%
Computers								4.6	4.6	3.0%
Cooking	2.6					-		1.0	3.6	2.3%
Other (4)	2.9	0.3		1.6	0.9	2.8		14.5	20.2	13.0%
Adjust to SEDS (5)	8.0	2.3				2.3		0.7	11.0	7.1%
Total	**35.2**	**6.0**	**1.1**	**1.6**	**1.2**	**9.9**	**0.2**	**109.1**	**154.5**	100%

Note(s): 1) Expenditures include coal and exclude wood (unlike Table 4.1.3). 2) Includes kerosene space heating ($0.2 billion) and motor gasoline other uses ($0.7 billion). 3) Coal average price is from 2004. 4) Includes service station equipment, ATMs, medical equipment, telecommunications equipment, pumps, lighting, emergency electric generators, and manufacturing performed in commercial buildings. 5) Expenditures related to an energy adjustment EIA uses to relieve discrepancies between data sources. Energy attributable to the commercial buildings sector, but not directly to specific end-uses.

Source(s): EIA, Annual Energy Outlook (AEO) 2007, Feb. 2007, Table A2, p. 137-139, Table A3, p. 140-141 for prices, and Table A5, p. 144-145 for energy consumption; EIA, National Energy Modeling System for AEO 2006, April 2006; EIA, State Energy Data 2004: Prices and Expenditures, June 2007, p. 25 for coal price; EIA, Annual Energy Review 2006, June 2007, Appendix D, p. 377 for price deflators; BTS/A.D. Little, Energy Consumption Characteristics of Commercial Building HVAC Systems, Volume II: Thermal Distribution, Auxiliary Equipment, and Ventilation, Oct. 1999, p. 1-2, 5-25 and 5-26 for ventilation; BTP/Navigant Consulting, U.S. Lighting Market Characterization, Volume I, Sept. 2002, Table 8-2, p. 63; OBT/A.D. Little, Energy Savings Potential for Commercial Refrigeration Equipment, June 1996, Figure 1-1-, p. 1-1; and EIA, AEO 1999, Dec. 1998, Table A5, p. 120 for 1996 refrigeration.

4.3.2 Average Annual Energy Expenditures per Square Foot of Commercial Floorspace, by Year ($2005)

Year	
1980	1.92
1990	1.70
2000	1.85
2005	**2.31**
2010	2.17
2015	2.08
2020	2.13
2025	2.18
2030	2.21

Source(s): EIA, State Energy Data 2004: Prices and Expenditures, June 2007, p. 25 for 1980-2000; EIA, Annual Energy Outlook (AEO) 2007, Feb. 2007, Table A2, p. 137-139 and Table A5, p. 144-145 for consumption, Table A3, p. 140-141 for prices for 2005-2030; EIA, Annual Energy Review 2006, June 2007, Appendix D, p. 377 for price deflators; EIA, AEO 1994, Jan. 1994, Table A5, p. 62 for 1990 floorspace; and PNNL for 1980 floorspace.

4.3.3 2003 Energy Expenditures per Square Foot of Commercial Floorspace and per Building, by Building Type ($2005) (1)

	Per Square Foot	Per Building (10^3)		Per Square Foot	Per Building (10^3)
Food Service	4.40	24.5	Mercantile	2.01	34.3
Food Sales	4.22	23.4	Education	1.29	33.0
Health Care	2.49	61.2	Service	1.25	8.2
Public Order and Safety	1.86	28.8	Warehouse and Storage	0.72	12.2
Office	1.81	26.8	Religious Worship	0.69	7.0
Public Assembly	1.56	22.1	Vacant	0.31	4.3
Lodging	1.55	55.4	Other	2.69	59.0

Note(s): 1) Mall buildings are no longer included in most CBECs tables; therefore, some data is not directly comparable to past CBECs.

Source(s): EIA, 2003 Commercial Buildings Energy Consumption and Expenditures: Consumption and Expenditures Tables, Oct. 2006, Table 4; and EIA, Annual Energy Review 2006, June 2007, Appendix D, p. 377 for price deflators.

4.3.4 2003 Energy Expenditures per Square Foot of Commercial Floorspace, by Vintage ($2005)

Prior to 1960	1.30
1960 to 1969	1.53
1970 to 1979	1.69
1980 to 1989	1.88
1990 to 1999	1.69
2000 to 2003	1.55
Average	**1.60**

Source(s): EIA, 2003 Commercial Buildings Energy Consumption and Expenditures: Consumption and Expenditures Tables, Table C4; and EIA, Annual Energy Review 2006, June 2007, Appendix D, p. 377 for price inflators.

4.4.1 Annual Energy Expenditures per Gross Square Foot of Federal Floorspace Stock, by Year ($2005)

FY 1985	2.18
FY 2000	1.24
FY 2002	1.35
FY 2003	1.35
FY 2004	1.39
FY 2005	1.44

Note(s): Total Federal buildings and facilities energy expenditures in FY 2005 were $4.26 billion (in $2005).

Source(s): DOE/FEMP, Annual Report to Congress on FEMP, Sept. 26, 2006, Table 7-B, p. 62 for energy costs, and Table 2, p. 13 for floorspace; DOE/FEMP, Annual Report to Congress on FEMP, Feb. 24, 2006, Table 5, p. A-9 for energy costs and Table 6-A, p. A-10 for floorspace; DOE/FEMP, Annual Report to Congress on FEMP, Aug. 9, 2005, Table 5, p. A-9 for energy costs and Table 6-A, p. A-10 for floorspace; DOE/FEMP, Annual Report to Congress on FEMP, Sept. 29, 2004, Table C, p. C-2 for energy costs and Table 8-A, p. 65 for floorspace; and DOE/FEMP, Annual Report to Congress on FEMP, Dec. 2002, Table 8-A, p. 61 for floorspace.

4.4.2 Direct Appropriations on Federal Buildings Energy Conservation Retrofits and Capital Equipment ($2005 Million)

FY 1985	475.92	FY 1991	152.25	FY 1997	256.31	FY 2003	182.64
FY 1986	307.18	FY 1992	189.33	FY 1998	232.97	FY 2004	179.93
FY 1987	88.73	FY 1993	154.18	FY 1999	242.28	FY 2005	290.56
FY 1988	97.70	FY 1994	150.17	FY 2000	137.29		
FY 1989	74.93	FY 1995	399.93	FY 2001	147.70		
FY 1990	92.92	FY 1996	239.61	FY 2002	134.49		

Source(s): DOE/FEMP, Annual Report to Congress on FEMP, Sept. 26, 2006, Table 10-B, p. 32; DOE/FEMP, Annual Report to Congress on FEMP, Dec. 11, 2002, Table 4-A, p. 32; and EIA, Annual Energy Review 2006, June 2007, Appendix D, p. 377 for price deflators.

4.5.1 Estimated Value of All U.S. Construction Relative to the GDP ($2005)

- 2005 estimated value of all U.S. construction is $1.72 trillion (including renovation; heavy construction; public works; residential, commercial, and industrial new construction; and non-contract work).
- Compared to the $12.5 trillion U.S. gross domestic product (GDP), all construction holds a 13.8% share.
- In 2005, residential and commercial building renovation (valued at $392 billion) and new building construction (valued at $776 billion) is estimated to account for over 71% (approximately $1.21 trillion) of the $1.72 trillion.

Source(s): National Science and Technology Council, Construction & Building: Interagency Program for Technical Advancement in Construction and Building, 1999, p. 5; DOC, 1997 Census of Construction Industries: Industry Summary, Jan. 2000, Table 7, p. 15; DOC, Annual Value of Construction Put in Place 2006, June 2007; and EIA, Annual Energy Review 2006, June 2007, Appendix D, p. 377 for price deflators and GDP.

4.5.2 Value of New Building Construction Relative to GDP, by Year ($2005 Billion)

	Value of New Construction Put in Place				Bldgs. Percent of
	Residential	Commercial (1)	All Bldgs. (1)	GDP	Total U.S. GDP
1980	149.4	143.9	293.2	5,819	5.0%
1985	192.1	203.7	395.7	6,825	5.8%
1990	187.8	204.8	392.7	8,018	4.9%
1995	214.7	185.8	400.6	9,055	4.4%
2000	303.5	291.1	594.6	11,067	5.4%
2004	437.8	278.7	716.6	12,223	5.9%
2005	490.0	285.9	775.8	12,456	6.2%

Note(s): 1) New buildings construction differs from Table 4.5.1 by excluding industrial building construction.

Source(s): DOC, Current Construction Reports: Value of New Construction Put in Place, C30, Aug. 2003, Table 1 for 1980-1990; DOC, Annual Value of Private Construction Put in Place, July 2007 for 1995-2006; DOC, Annual Value of Public Construction Put in Place, July 2007 for 1995-2006; and EIA, Annual Energy Review 2006, June 2007, Appendix D, p. 377 for GDP and price deflators; Historic Expenditures for Residential Properties by Property Type: Quarterly 2003-2006 (New structural purposes).

4.5.3 Value of Building Improvements and Repairs Relative to GDP, by Year ($2005 Billion) (1)

	Value of Improvements and Repairs				Bldgs. Percent of
	Residential	Commercial	All Bldgs.	GDP	Total U.S. GDP
1980	96.7	N.A.	N.A.	5,819	N.A.
1985	132.8	126.2 (2)	259.0	6,825	3.8%
1990	159.5	128.3 (3)	287.8	8,018	3.6%
1995	153.0	111.2	264.2	9,055	2.9%
2000	172.5	180.6	353.1	11,067	3.2%
2004	204.5	172.9	377.4	11,067	3.1%
2005	215.0	177.4	392.4	12,456	3.2%

Note(s): 1) Improvements includes additions, alterations, reconstruction, and major replacements. Repairs include maintenance.
2) 1986. 3) 1989.

Source(s): DOC, Expenditures for Residential Improvements and Repairs by Property Type, Quarterly, May 2005 for 1980-1990; DOC, Current Construction Reports: Expenditures for Nonresidential Improvements and Repairs: 1992, CSS/92, Sept. 1994, Table A, p. 2 for 1986-1990 expenditures; DOC, 1997 Census of Construction Industries: Industry Summary, Jan. 2000, Table 7, p. 15; DOC, Annual Value of Private Construction Put in Place, July 2007 for 1995-2005; and EIA, Annual Energy Review 2006, June 2007, Appendix D, p. 377 for GDP and price deflators;

4.5.4 2003 U.S. Private Investment into Construction R&D

Sector	Percent of Sales	Building Technology	Percent of Sales
Average Construction R&D (1)	**1.2**	Building Technology	
Heavy Construction	2.0	Appliances	2.0
Special Trade Construction	0.2	Lighting	1.2
		HVAC	1.5
U.S. Average of All Private R&D (2)	**3.2**	Fans, Blowers, & Air Cleaning Equipment	1.6
Manufacturing Average	3.1	Lumber and Wood Products	0.3
Service Industry Average	3.3	Commercial Building Operations	2.2

Note(s): 1) Includes all construction (e.g., bridges, roads, dams, buildings, etc.).

Source(s): National Science Foundation, Research and Development in Industry: 2003, Table 27, p. 76-77; and Schonfeld & Associates, R&D Ratios & Budgets, June 2003, p. 219-222.

4.5.5 1997/1998 International Investment into Construction and Energy R&D

	Construction Percent of Private R&D to Total Private R&D	Gas, & Water Percent of Private R&D to Total Private R&D	Mining Percent of Private R&D to Total Private R&D
United States	0.2	0.2	0.1
Canada	0.3	2.7	2.9
Germany	0.3	0.3	0.5
France	1.0	3.0	1.8
Italy	0.3	1.7	0.0
Japan	2.1	0.9	0.0
United Kingdom	0.4	1.4	1.4
Russian Federation	0.9	0.5	3.3
Sweden	0.6	0.8	1.1
Finland	0.8	1.6	0.7

Source(s): National Science Foundation, Science & Engineering Indicators -- 2002, Volume 1, Jan. 2002, Table 4-16, p. 4-53.

4.5.6 FY2003-2005 Green Building R&D, as Share of Federal Budget and by Organization

Budget Function	Percent of U.S. Federal Budget	Organization	Average Annual Funding ($1000s)
National Defense	57.2%	DOE	123,170
Health	23.1%	EPA	25,317
Other energy, general science, natural resources, and environment	8.0%	NSF	22,940
Space research and technology	6.3%	PIER (1)	11,100
Transportation	1.5%	DOC-NIST	7,500
Agriculture	1.5%	NYSERDA	5,800
Veterans' benefits and services research	0.7%	HUD	5,000
Green building	**0.2%**	GSA	3,000
Other functions (2)	1.6%	ASHRAE	2,400
Total	100%		

Note(s): 1) PIER = Public Interest Energy Research 1) Other functions include education, training, employment, and social services; income security; and commerce.

Source(s): U.S. Green Building Council, Green Building Research Funding: An Assessment of Current Activity in the United States, 2006, Chart 1, p. 3, Chart 2, p. 3.

4.6.1 Buildings Design and Construction Trades, by Year

		Employees, in thousands			Number of Residential Builder Establishments with Payrolls, in thousands (2)			
		Architects	Construction (1)		New Construction	Remodeling	Both	Total (3)
1980		N.A.	3,065	1982	14.4	21.7	57.5	93.6
1990		N.A.	3,861	1987	38.4	32.8	48.1	119.3
2000	(4)	215	5,183	1992	36.3	43.3	51.0	130.6
2003		180	6,735	1997	46.6	33.6	52.1	134.1
2004		207	6,964	2002	95.4	28.0	47.7	167.4
2005		235	7,277					

Note(s): 1) Does not include industrial building or heavy construction (e.g., dam and bridge building). In 1999, 76% of the employment shown is considered for "production." The entire U.S. construction industry employs an estimated 10 million people, including manufacturing. 2) In 2000, NAHB report having 200,000 members, one-third of which were builders. 3) Excludes homebuilding establishments without payrolls, estimated by NAHB at an additional 210,000 in 1992. 4) NAHB reports that 2,448 full-time jobs in construction and related industries are generated from the construction of every 1,000 single-family homes and 1,030 jobs are created from the construction of every 1,000 multi-family units.

Source(s): DOC, Statistical Abstract of the U.S. 2001, May 2002, Table 593, p. 380 for 2000 architect employment, Table 609, p. 393; Statistical Abstract of the U.S. 2004-2005, December 2004, Table 597, p. 385 for 2003 architect employment, Table 602 for 2005 architect employment, Table 613, p. 400; DOC, 1992 Census of Construction Activities: U.S. Summary, CC92-I-27, Jan. 1996, p. 27-5 for construction employees; DOC, 1997 Economic Census: Construction - Industry Summary, EC97C23IS, Jan. 2000, Table 2, p. 8 for industrial builders; DOC, 1997 Economic Census: Construction - Single-Family Housing Construction, EC97C-2332A, Nov. 1999, Table 10, p. 14 for 1997 builder establishments; DOC, 2002 Economic Census: Construction - New Single-Family Housing Construction, EC02-231-236115, Dec. 2004, New Housing Operatives, ECO2-231-236118, Dec. 2004, Residential Remodelers, EC02-231-236119, Dec. 2004, Industrial Building Construction, 231-236210, Dec. 2004; NAHB, Housing Economics, May 1995, Table 2, p. 14 for 1982-1992 builder establishments; National Science and Technology Council, Construction & Building: Federal Research and Development in Support of the U.S. Construction industry for construction employees in Note 1; NAHB, Housing at the Millennium: Facts, Figures, and Trends, May 2000, p. 21 for Note 2; and NAHB, 1997 Housing Facts, Figures and Trends, 1997, p. 35 for Note 3, and p. 13 for Note 4.

4.6.2 Heating, Cooling, and Ventilation Equipment Trades, by Year (1000 Employees)

Industry	1980	1985	1990	1995	2000	2003
Air Conditioning and Refrigeration Equipment (incl. warm-air furnaces): SIC 3585						
- Total Employment	118.4	122.8	126.9	136.3	150.2	109.1
- Production Workers	81.6	87.2	92.4	102.4	111.6	76.7
Plumbing, Heating, and Air-Conditioning Contractors: SIC 171						
- Total Employment	532.8	605.1	649.2	736.5	928.5	844.9
- Construction Workers	400.4	447.3	476.7	542.4	687.2	630.4
Wholesalers of Hardware, Plumbing and Heating Equipment: SIC 507						
- Total Employment	242.7	254.1	283.8	288.2	318.3	230.5

Source(s): ARI, Statistical Profile of the Air-Conditioning, Refrigeration, and Heating Industry (from U.S. Bureau of Labor Statistics), April 2001, Table 3, p. 10, Table 4, p. 11, Table 5, p. 13, Table 6, p. 14, and Table 8, p. 16 for 1980 to 1990 data; ARI, Statistical Profile of the Air-Conditioning, Refrigeration and Heating Industry, October 2004, Table 3, p. 9, Table 4, p. 10, Table 5, p. 12, Table 6, p. 13 and Table 8, p. 15 for 1995 to 2003 data.

5.1.1 2006 Five Largest Residential Homebuilders

Homebuilder	Number of Home Closings (1)	Gross Revenue ($million)	Market Share of Total New Home Closings (%) (2)
D.R. Horton	53,410	15,016	5.0%
Pulte Homes	49,568	16,267	4.7%
Lennar Homes	41,487	14,274	3.9%
Centex Corporation	37,539	14,400	3.5%
KB Home	32,124	11,004	3.0%
Total of Top Five	**214,128**	**70,961**	**20.2%**
Habitat for Humanity (3)	4,862	357	0.5%

Note(s): 1) 2006 total U.S. new home closings were 1.06 million (only single-family). 2) Total share of closings of top 20 builders was 35%. Total share of the top 100 builders was 47%. 3) Habitat for Humanity built more than 400 homes during the week of May 31, 2007. Habitat for Humanity has built over 1,000 homes in the New Orleans area since Hurricane Katrina. Habitat for Humanity's 2,100 worldwide affiliates have completed more than 200,000 homes since 1976, providing more than 1,000,000 with housing.

Source(s): Builder Magazine, May 2007, Builder 100; e-mail correspondence with Habitat for Humanity for relevant data, Aug. 2007; and Habitat for Humanity, http://www.habitat.org/, for note 3.

5.1.2 Value of New Building Construction, by Year ($2005 Billion)

	Residential	Commercial	All Bldgs.
1980	149.4	143.9	293.2
1985	192.1	203.7	395.7
1990	187.8	204.8	392.7
1995	214.7	185.8	400.6
2000	303.5	291.1	594.6
2003	376.2	270.5	646.7
2004	437.8	278.7	716.6
2005	490.0	285.9	775.8

Note(s): 1) In 2005, new building construction accounted for 6.2% of the $12.5 trillion U.S. GDP. Refer to Chapter 2 for more new buildings statistics.

Source(s): DOC, Current Construction Reports: Value of New Construction Put in Place, C30, Aug. 2003, Table 1 for 1980-1990; DOC, Annual Value of Construction Put in Place, July 2006 for 1995-2005; and EIA, Annual Energy Review 2006, June 2007, Appendix D, p. 377 for price deflators.

5.1.3 Market Indices for 2006 ENERGY STAR Qualified New Single-Family Homes, by Selected State (1000s)

	ENERGY STAR Qualified New Homes	New Single-Family Housing Permits	Market Penetration
Nevada	18.9	26.7	71%
Alaska	1.0	1.6	64%
Iowa	5.9	10.3	57%
Texas	60.8	162.8	37%
Hawaii	2.1	5.6	37%
Arizona	20.1	55.6	36%
New Jersey	5.4	17.1	31%
Delaware	1.2	5.0	24%
Vermont	0.5	2.1	24%
Connecticut	1.6	7.1	23%
California	18.1	107.7	17%
New Hampshire	0.8	4.8	17%
Utah	3.6	22.6	16%
Ohio	3.5	27.5	13%
New York	2.6	20.0	13%
Florida	3.3	146.2	2%
United States	**169.8**	**1,378.2**	**12%**

Source(s): EPA, ENERGY STAR Qualified New Homes Market Indices for States, http://www.energystar.gov/index.cfm?fuseaction=qhmi.showHomesMarketIndex for top states; E-mail correspondence with EPA ENERGY STAR program for complete data set.

5.2.1 2007 Top Five Manufacturers of Factory-Built Housing Units (1)

Company	Units Produced	Gross Sales Volume ($million)	Market Share of Top 25 Company Sales (2)
CMH Manufacturing	31,100	1,327.8	20%
Champion Enterprises, Inc.	21,126	1,286.6	19%
Palm Harbor Homes, Inc.	8,911	679.1	10%
Fleetwood Enterprises, Inc.	15,137	600.0	9%
Skyline Corporation	8,207	376.4	6%

Note(s): 1) Data based on mail-in surveys from manufacturers which may not be entirely complete. 2) Market shares based on total gross sales volume of the factory-built home producers included in the list of the top 25 factory-built producers responding to the survey. In 2007, surveyed factory-built home sales were estimated at $6.6 billion and 133,361 units.

Source(s): HousingZone.com, 2007 Factory Built Housing Results, http://www.housingzone.com/factory.html.

5.2.2 2007 Top Five Manufacturers of Modular/3D Housing Units (1)

Company	Units Produced	Gross Sales Volume ($million)	Market Share of Top 25 Company Sales (2)
Champion Enterprises, Inc.	4,653	438.7	27%
CMH Manufacturing	3,200	228.8	14%
All American Homes, LLC	1,689	165.4	10%
Palm Harbor Homes, Inc.	1,614	162.9	10%
Excel Homes LLC	1,200	110.6	7%

Note(s): 1) Data based on mail-in surveys from manufacturers, which may not be entirely complete. 2) Market shares based on total gross sales volume of the Modular/3D home producers included in the list of the top 25 factory-built producers responding to the survey. In 2007, surveyed modular/3D home sales were estimated at $1.6 billion and 20,601 units.

Source(s): HousingZone.com, 2007 Factory Built Housing Results, http://www.housingzone.com/factory.html.

5.2.3 2007 Top Five Manufacturers of HUD-Code (Mobile) Homes (1)

Company	Units Produced	Gross Sales Volume ($million)	Market Share of Top 25 Company Sales (2)
CMH Manufacturing	27,900	1,099	23%
Champion Enterprises, Inc.	16,473	848	18%
Fleetwood Enterprises, Inc.	15,137	600	12%
Palm Harbor Homes	7,297	516	11%
Skyline Corporation	8,207	376	8%

Note(s): 1) Data based on mail-in surveys from manufacturers, which may not be entirely complete. 2) Market shares based on total gross sales volume of the HUD-Code home producers included in the list of the top 25 factory-built producers responding to the survey. In 2007, surveyed HUD-Code home sales were estimated at $4.83 billion and 109,320 units.

Source(s): HousingZone.com, 2007 Factory Built Housing Results, http://www.housingzone.com/factory.html.

5.2.4 2004 Top Five Manufacturers of Factory-Fabricated Components (Trusses, Wall Panels, Doors) (1)

Company	Gross Sales Volume ($million)	Market Share of Top 26 Company Sales (2)	Number of Employees (3)
Carpenter Contractors	175.0	26%	1,130
Automated Building Company	102.5	15%	702
Landmark Truss	45.0	7%	425
Southern Building Products	25.9	4%	180
Dolan Lumber & Truss	25.1	4%	260

Note(s): 1) Data based on mail-in surveys from manufacturers, which may not be entirely complete. 2) Market shares based on total gross sales volume of producers of only components included in the list of the top 26 IH producers responding to the survey. In 2004, surveyed component sales was estimated at $665.1 million. 3) The top 26 companies employ over 4,970 people at their plants.

Source(s): Automated Builder Magazine, Sept. 2005, p. 40-41.

5.2.5 2004 Number of Industrialized Housing Manufacturers versus Production Companies (Stick-Builders)

Type	Number of Companies
Panelized	3,500
Modular (1)	200
HUD-Code	90
Production Builders	7,000
Component Manufacturers	2,200
Special (Commercial) Units	170

Note(s): 1) 170 of these companies also produce panelized homes.
Source(s): Automated Builder Magazine, Mar. 2005, p. 34-35; Automated Builder Magazine, Jan. 2004, p. 16 for Note 1.

5.2.6 2006 HUD-Code (Mobile) Home Placements, by Census Region and Top Five States (Percent of National Total)

Region		Top Five States	
Northeast	7%	Florida	11%
Midwest	13%	California	8%
South	59%	Texas	8%
West	22%	Arizona	6%
Total	100%	Lousiana	5%

Source(s): DOC, Manufactured Housing Statistics, 2006 New Manufactured Homes Placed by Size of Home, by State, Apr. 2007.

5.3.1 Value of Building Improvements and Repairs, by Sector ($2005 Billion) (1)

	Value of Improvements and Repairs		
	Residential	Commercial	All Bldgs.
1980	96.7	N.A.	N.A.
1985	132.8	126.2 (2)	259.0
1990	159.5	128.3 (3)	287.8
1995	153.0	136.1	289.1
2000	172.5	180.6	353.1
2003	188.7	167.9	356.6
2004	204.5	172.9	377.4
2005	215.0 (4)	177.4 (5)	392.4

Note(s): 1) Improvements includes additions, alterations, reconstruction, and major replacements. Repairs include maintenance. 2) 1986. 3) 1989. 4) Includes 75% improvements and 25% maintenance and repairs. 5) Includes 76% improvements and 24% maintenance and repairs.

Source(s): DOC, Expenditures for Residential Improvements and Repairs by Property Type, Quarterly, May 2005 for 1980-1990; DOC, Current Construction Reports: Expenditures for Nonresidential Improvements and Repairs: 1992, CSS/92, Sept. 1994, Table A, p. 2 for 1986-1990 expenditures; DOC, 1997 Census of Construction Industries: Industry Summary, Jan. 2000, Table 7, p. 15; DOC, Annual Value of Private Construction Put in Place, July 2007 for 1995-2005; and EIA, Annual Energy Review 2006, June 2007, Appendix D, p. 377 for GDP and price deflators;

5.3.2 2005 Professional and Do-It-Yourself Improvements, by Project ($2005)

	Professional Installation			Do-It-Yourself Installation		
Repair/Improvement	Homeowners (10^6)	Total Expenditures ($10^9)	Mean Expenditures ($)	Homeowners (1000)	Total Expenditures ($10^9)	Mean Expenditures ($)
Disaster Repairs	0.61	8.7	14,398	0.20	1.3	6,698
Kitchen Remodeled	1.13	13.0	11,550	1.05	5.7	5,411
Additions Built	1.27	29.5	23,212	1.38	9.3	6,767
Bathroom Remodeled or Added	1.13	8.5	7,527	1.34	3.8	2,852
Exterior Improvements	3.85	23.0	5,983	3.11	7.9	2,527
Siding Replaced or Added	0.82	5.2	6,322	0.39	1.0	2,583
Roof Replacement	2.67	14.1	5,281	0.81	1.9	2,366
HVAC Replacement	2.44	7.1	2,895	0.51	1.5	2,909
Windows/Doors Installed	2.53	7.6	2,995	1.72	2.6	1,501
Flooring/Paneling/Ceiling Replacement	4.65	12.4	2,661	3.48	4.2	1,221
Electric System Replacement	1.35	1.5	1,144	0.89	0.4	451
Plumbing Replacement	0.84	1.4	1,726	2.08	1.0	467
Insulation Added	0.59	1.4	2,361	0.72	1.1	1,513
Appliance/Major Equipment Replacement	3.59	2.4	657	2.49	1.0	385

Note(s): Expenditures are $36.7 billion higher in Table 4.5.3 and 5.3.1. This discrepancy is due to sampling methods used by HUD for the American Housing Survey and DOC in the Survey of Expenditures for Residential Improvements and Repairs.

Source(s): Joint Center for Housing Studies of Harvard University, Improving America's Housing 2007, Feb. 2007, Table A-2, p. 28.

5.3.3 Single-Family Residential Renovations, by Project and Vintage

	Year Home was Built					
	Pre-1946	1946-60	1961-73	1974-80	1981-98	1999 or later
Kitchen remodeled	60%	57%	54%	60%	44%	8%
Bathroom remodeled	59%	52%	59%	55%	40%	4%
Add room(s)	29%	18%	14%	24%	21%	15%
Exterior improvement	21%	15%	15%	16%	9%	4%
Basement room finished	14%	10%	6%	12%	16%	65%
Redesign/Restructure	14%	8%	11%	10%	5%	4%
Bathroom added	8%	7%	6%	7%	6%	27%
Sun room added	4%	6%	3%	4%	5%	8%

Note(s): Data based on a nationwide study of 819 consumers who have remodeled their homes in the past 12 months or will in the next 12 months..

Source(s): Professional Remodeler, Consumer Research: What Consumers Want, Sept. 2002, p.44-50.

5.4.1 U.S. Insulation Demand, by Type (Million Pounds) (1)

Insulation Type	1992		2001		2006 (1)	
Fiberglass	2,938	55%	3,760	54%	4,085	53%
Foamed Plastic	1,223	23%	1,775	25%	1,955	26%
Cellulose	485	9%	665	9%	730	10%
Mineral Wool	402	8%	445	6%	480	6%
Other	309	6%	370	5%	395	5%
Total	**5,357**	100%	**7,015**	100%	**7,645**	100%

Note(s): 1) Projected.
Source(s): National Insulation Association, www.insulation.org, Aug. 2006.

5.4.2 Industry Use Shares of Mineral Fiber (Glass/Wool) Insulation (1)

	1997	1999	2001	2003	2004	2005
Insulating Buildings (2)	70%	71%	72%	65%	64%	63%
Industrial, Equipment, and Appliance Insulation	27%	26%	25%	28%	30%	31%
Unknown	3%	3%	3%	7%	6%	5%
Total	100%	100%	100%	100%	100%	100%

Note(s): 1) Based on value of shipments. 2) Including industrial.
Source(s): DOC, Annual Survey of Manufacturers: Value of Product Shipments 2005, Nov. 2006, Table 1, p. 54 for 2003-2005; and DOC, 2001 Annual Survey of Manufacturers: Value of Product Shipments, Dec. 2002, p. 65 for 1997-2001.

5.4.3 Thermal Performance of Insulation

	R-Value per Inch (1)			R-Value per Inch (1)
Fiberglass (2)			Perlite/Vermiculite	
Batts	3.1 - 4.3	(3)	Loose-Fill	2.1 - 3.7
Loose-Fill	2.5 - 3.7		Foam Boards	
Spray-Applied	3.7 - 3.9		Expanded Polystyrene	3.9 - 4.4
Rock Wool (2)			Polyisocyanurate/	
Loose-Fill	2.5 - 3.7		Polyurethane	5.6 - 7.0
Cellulose			Phenolic	4.4 - 8.2
Loose-Fill	3.1 - 3.7		Reflective Insulation	2 - 17
Spray-Applied	2.9 - 3.5		Vacuum Powder Insulation	25 - 30
			Vacuum Insulation Panel	20 - 100

Note(s): 1) Hr-SF-F/Btu-in. Does not include the effects of aging and settling. 2) Mineral fiber. 3) System R-value depends on heat-flow direction and number of air spaces.
Source(s): ASHRAE, 1997 ASHRAE Handbook: Fundamentals, p. 24-4, 22-5; DOE, Insulation Fact Sheet, Jan. 1988, p. 6; Journal of Thermal Insulation, 1987, p. 81-95; ORNL, ORNL/SUB/88-SA835/1, 1990; ORNL, Science and Technology for a Sustainable Energy Future, Mar. 1995, p. 17; and ORNL for vacuum insulation panel.

5.5.1 Residential Prime Window Sales, by Type (Million Units) (1)

	New Construction				Remodeling/Replacement				Total Construction			
Type	1990	1995	2000	2005	1990	1995	2000	2005	1990	1995	2000	2005
Aluminum (2)	5.9	4.7	3.7	6.5	3.6	3.9	4.0	2.4	9.5	8.6	7.7	8.9
Wood (3)	9.4	11.6	12.8	9.2	7.6	9.4	10.2	10.0	17.0	21.0	23.0	19.2
Vinyl	1.2	4.8	9.0	17.4	7.1	9.6	14.8	23.2	8.3	14.4	23.8	40.6
Other	0.1	0.3	0.4	1.0	0.1	0.2	0.2	0.9	0.2	0.5	0.6	1.9
Total (4)	**16.6**	**21.4**	**25.8**	**34.1**	**18.4**	**23.1**	**29.2**	**36.4**	**35.0**	**44.5**	**55.0**	**70.5**

Note(s): 1) Average window life span is 35-45 years. 2) In 1993, 65% of aluminum-framed windows were thermally broken. 3) Includes vinyl-clad and metal-clad units. 4) Due to rounding, sums may not add up to totals.

Source(s): AAMA/Ducker Research, Industry Statistical Review and Forecast 1992, 1993 for Note 2; AAMA/NWWDA/Ducker Research, Industry Statistical Review and Forecast 1996, 1997, Table 6, p. 6 for 1990; AAMA/WDMA, 2000 AAMA/WDMA Industry Statistical Review and Forecast, Feb. 2001, p. 6 for 1995; 2003 AAMA/WDMA Industry Statistical Review and Forecast, June 2004, p. 6 for 2000 and 2003; and LBNL, Savings from Energy Efficient Windows, Apr. 1993, p. 6 for window life span; AAMA/WDMA/Ducker, Study of U.S. Market For Windows, Doors, and Skylights, Apr. 2006, p. 41 for 2005.

5.5.2 Residential Storm Window and Door Shipments, by Type (Million Units)

	Windows				Doors				Total			
Type	1990	1995	2000	2005	1990	1995	2000	2005	1990	1995	2000	2005
Aluminum	9.9	9.2	8.0	6.6	1.9	3.8	4.3	4.4	11.8	13.0	12.3	11.0
Wood	0.5	1.8	2.3	2.0	0.4	1.3	1.4	1.7	0.9	3.1	3.7	3.7
Other (1)	0.1	0.3	0.3	0.2	0.1	0.1	0.1	0.1	0.2	0.4	0.4	0.3
Total (2)	**10.5**	**11.3**	**10.6**	**8.8**	**2.4**	**5.2**	**5.8**	**6.4**	**12.9**	**16.5**	**16.4**	**15.2**

Note(s): 1) "Other" includes metal over wood/foam core or vinyl, etc. 2) Due to rounding, sums may not add up to totals.

Source(s): AAMA/NWWDA/Ducker Research, Industry Statistical Review and Forecast 1996, 1997, Table 7, p. 7 for 1990; AAMA/NWWDA, 2000 AAMA/WDMA Industry Statistical Review and Forecast, Feb. 2001, p. 7 for 1995; and 2003 AAMA/WDMA Industry Statistical Review and Forecast, June 2004, p. 6 for 2000 and 2003; and AAMA/WDMA/Ducker, Study of U.S. Market for Windows, Doors, and Skylights, Apr. 2006, p. 101, Exhibit G.2 for 2005.

5.5.3 Nonresidential Window Usage, by Type and Census Region (Million SF of Vision Area) (1)

	Northeast		Midwest		South		West		Total	
Type	1995	2005	1995	2005	1995	2005	1995	2005	1995	2005
New Construction										
Commercial Windows (2)	4	32	16	31	21	52	13	30	54	141
Curtain Wall	3	13	6	12	16	23	8	15	33	64
Store Front	7	19	11	20	14	42	11	24	43	104
Total (3)	**14**	**63**	**33**	**62**	**51**	**117**	**32**	**68**	**130**	**310**
Remodeling/Replacement										
Commercial Windows (2)	18	24	25	24	46	30	27	15	116	45
Curtain Wall	4	3	6	2	8	5	10	3	28	18
Store Front	12	8	18	9	24	19	22	10	76	34
Total (3)	**34**	**35**	**49**	**34**	**78**	**53**	**59**	**29**	**220**	**97**
Total										
Commercial Windows (2)	22	57	41	54	67	82	40	45	170	238
Curtain Wall	7	15	12	14	24	27	18	18	61	75
Store Front	19	27	29	29	38	61	33	34	119	150
Total (3)	**48**	**99**	**82**	**97**	**129**	**171**	**91**	**97**	**350**	**463**

Note(s): 1) "Usage" is a good indication of sales. 2) Formerly referred to as Architectural. Includes both shop fabricated (true architectural) and *site fabricated products. 3) Due to rounding, sums may not add up to totals.*

Source(s): AAMA/Ducker Research, Industry Statistical Review and Forecast 1996, Mar. 1997, p. 17 for 1995; and AAMA/WDMA/Ducker, Study of U.S. Market For Windows, Doors, and Skylights, Apr. 2006, p. 81 for 2005.

5.5.4 Insulating Glass Historical Penetration, by Sector (Percent of Total U.S. Usage) (1)

Sector	1985	1990	1995	2000	2005
Residential	73%	86%	89%	92%	94%
Nonresidential	63%	80%	84%	86%	88%

Note(s): 1) "Usage" is a good indication of sales. Includes double- and triple-pane sealed units.

Source(s): Ducker Research, Industry Statistical Review and Forecast 1992, 1993 for 1985; AAMA/Ducker Research, Industry Statistical Review and Forecast 1993, for 1990; AAMA/WDMA, 2000 AAMA/WDMA Industry Statistical Review and Forecast, Feb. 2001, p. 12 for 1995-1997; and 2003 AAMA/WDMA Industry Statistical Review and Forecast, June 2004, p.12 for 1998-2000; and AAMA/WDMA/Ducker, Study of U.S. Market For Windows, Doors, and Skylights, Apr. 2006, for 2005.

5.5.5 Residential Prime Window Sales, by Type (Million Units)

Type	1980	1990	1995	1999	2001	2003	2005
Single Lite	8.6	4.9	5.5	4.8	3.9	4.7	4.2
Two Lite, Sealed, IG (1)	0.0	12.0	37.8	55.2	50.9	55.9	63.8
Other	16.6	18.7	1.3	2.0	1.5	2.2	2.5
Total	**25.2**	**35.6**	**44.5**	**62.0**	**56.3**	**62.8**	**70.5**

Note(s): 1) IG = Insulated Glazing.

Source(s): AAMA/NWWDA, Study of the U.S. Market for Windows and Doors, 1996, Table 22, p.49; AAMA/WDMA Ducker, Study of U.S. and Canadian Market for Windows and Doors, Apr. 2000, Exhibit E.7, p. 55; AAMA/WDMA, Study of the Market for U.S. Doors, Windows and Skylights, Apr. 2004, Exhibit D.4, p. 46; and, AAMA/WDMA/Ducker, Study of U.S. Market For Windows, Doors, and Skylights, Apr. 2006, Exhibit D.8 Conventional Window Glass Usage, p. 50.

5.5.6 2005 Residential Prime Window Stock, by Type

Type	Existing U.S. Stock (1) (% of households)
Single Lite	49%
Two Lite, Non-Sealed	15%
Two Lite, Sealed, IG (2)	35%
Other	1%
Total	100%

Note(s): 1) Assumes 14 single-pane windows are replaced in housing units receiving replacement or remodeled windows. Windows in demolished housing units are assumed to be single pane. 2) IG = Insulated Glazing.

Source(s): EIA, Housing Characteristics 1993, June 1995, Table 3.29a for existing stock data; AAMA/NWWDA, Study of the U.S. Market for Windows and Doors, 1996, Table 22, p.49; AAMA/WDMA Ducker, Study of U.S. and Canadian Market for Windows and Doors, Apr. 2000, Exhibit E.7, p. 55; AAMA/WDMA, Study of the Market for U.S. Doors, Window and Skylights, Apr. 2004, Exhibit D.4, p. 46; U.S. Census Bureau, Manufacturing, Mining and Construction Statistics, New Residential Construction: New Privately Owned Housing Units Completed for 1999-2004 single and multi-family units; and DOC, Current Construction Reports: Housing Completions - Annual Data, Mar. 2001 for 1993-1998 single- and multi-family units. AAMA/WDMA/Ducker, Study of U.S. Market For Windows, Doors, and Skylights, Apr. 2006, for 2005.

5.5.7 Nonresidential Window Stock and Usage, by Type (1)

Type	Existing U.S. Stock (% of buildings)	Glass Area Usage (million square feet) 1992	1995	2001	2003	2005
Single-Pane	53%	42	56	57	48	56
Insulating Glass (2)	47%	188	294	415	373	407
Total	100%	**230**	**350**	**472**	**421**	**463**
Clear	65%	9%	36%	49%	43%	44%
Tinted	28%	54%	40%	24%	17%	15%
Reflective	7%	20%	7%	8%	6%	4%
Low-e	(3)	17%	17%	19%	34%	37%
Total	100%	100%	100%	100%	100%	100%

Note(s): 1) "Usage" is a good indication of sales. 2) Includes double- and triple-pane sealed units (and stock glazing with storm windows). 3) Included as part of the "Tinted" category.

Source(s): EIA, 2003 Commercial Buildings Energy Consumption and Expenditures: Consumption and Expenditures Tables, June 2006, Table B1 for stock data; AAMA, 1994 Combined Study of the Residential and Nonresidential Markets for Windows and Skylights, Table 5, p. 5, for 1992 usage values; AAMA/NWWDA, 1996 Study of the U.S. Market for Windows and Doors, Table 27, p. 60 for 1995 usage values; 2003 AAMA/WDMA Study of the U.S. Market for Windows, Doors and Skylights, Exhibits D.31 and D.32 for 2001; and AAMA/WDMA/Ducker, Study of U.S. Market For Windows, Doors, and Skylights, Apr. 2006, Exhibit D.31 and Exhibit D.32, p. 73 for 2003 and 2005.

5.5.8 Typical Thermal Performance of Residential Windows, by Type (1)

Type	U-Factor (2)	Solar Heat Gain Coefficient (2)
Single-Pane	0.93 - 1.23	0.69 - 0.84
Single-Pane, Tinted	0.90 - 1.21	0.50 - 0.61
Double-Pane	0.49 - 0.73	0.62 - 0.76
Double-Pane, Tinted	0.48 - 0.73	0.40 - 0.54
Double-Pane, Low-e, Gas-fill	0.34 - 0.42	0.48 - 0.58
Double-Pane, Spectrally Selective Low-e, Gas-fill	0.32	0.35
Triple Pane	0.38 - 0.60	0.54 - 0.68
Triple-Pane, 2 Low-e, Gas-fill	0.24	0.40

Note(s): 1) Residential windows available in 1999 had an average U-Factor of 0.47 and a Solar Heat Gain Coefficient of 0.45. 2) U-Factor and SHGC are whole-window values calculated using Windows 4.0 and standard assumptions about frame and glazing dimensions. Ranges reflect differences in frame materials and design; aluminum-frame windows are on the higher end of the ranges, while wood- and vinyl-framed windows have the lowest values.

Source(s): ACEEE, 1996 ACEEE Proceedings, The National Energy Requirements of Residential Windows in the U.S.: Today and Tomorrow, Summer 1996, p. 10.48-10.50; and NFRC, Directory of Certified Products, Dec. 1999, U-Factor Chart from www.nfrc.org for Note 1.

5.6.1 U.S. Heating and Air Conditioning System Manufacturer Shipments, by Type (Including Exports)

Equipment Type	1990 (1000s)	2000 (1000s)	2005 (1000s)	2005 Value of Shipments ($million) (6)
Air Conditioners (1)	**2,920.0**	**5,346.0**	**6,472.3**	**5,836.6**
Heat Pumps	**808.7**	**1,539.2**	**2,336.0**	**2,226.4**
Air-to-Air Heat Pumps	808.7	1,339.4	2,113.9	1,869.5
Water-Source Heat Pumps (2)	N.A.	199.8	222.0	356.9
Chillers	**N.A.**	**38.1**	**37.3**	**1,092.6**
Reciprocating	N.A.	24.8	24.1	462.1
Centrifugal/Screw	5.0	8.5	5.8	566.3
Absorption	N.A.	4.8	7.4	64.2
Furnaces	**2,368.9**	**3,680.7**	**3,623.7**	**2,143.7**
Gas-Fired (3)	1,950.5	3,104.2	3,512.5	2,081.0
Electric	280.0	455.0	N.A.	N.A.
Oil-Fired (4)	138.5	121.5	111.2	62.8
Boilers (5)	**316.1**	**368.4**	**369.7**	**N.A.**

Note(s): 1) Includes exports and gas air conditioners (gas units <10,000 units/yr) and rooftop equipment. Excludes heat pumps, packaged terminal air conditioner units, and room air conditioners. Approximately 95% of unitary air conditioners shipped are 5.5 tons or less (65,000 Btu/Hr). ~70% residential and ~30% commercial applications. 2) Includes ground-source heat pumps (GSHPs), which numbered around 80,600 units shipped in 2005. 3) Gas-fired furnace value of shipments are based on Census unit shipment data, which is about 873,500 units higher than the industry data shown. 4) Oil-fired furnace value of shipments are based on Census unit shipment data, which is approximately 33,600 units lower than the industry data shown. 5) 61% of shipments were gas-fired and 39% were oil-fired. 96% of shipments are cast iron and 4% are steel. 6) Total 2005 value of shipments for heating, ventilation, and air conditioning (HVAC) and refrigeration was $24.7 billion, including industrial and excluding boilers and electric furnaces.

Source(s): ARI, Statistical Profile, Oct. 7, 2004, Table 17, p. 24, Table 18, p. 25, and Table 22, p.30 for air conditioner, air-to-air heat pump, and 1990 centrifugal/screw chiller shipments; ARI, ARI Koldfax, Feb. 2005, p. 1 for 2004 air conditioner shipments; GAMA, GAMA Statistical Highlights: Ten Year Summary, 1987-1996; GAMA, GAMA Statistical Highlights: Ten Year Summary, 1994-2000 for furnace and boiler shipments; GAMA, GAMA News Release, Jan. 2005 for 2004 boiler shipments; GAMA, Statistical Highlights, Mar. 2005, p. 4 for 2004 furnace shipments; Appliance Manufacturer, Feb. 1998 for electric furnace; DOC, Current Industrial Reports: Refrigeration, Air Conditioning and Warm Air Heating Equipment, MA333M(06)-1, July 2007, Table 2 for water-source heat pumps, chillers, and value of shipments; Appliance Magazine Appliance Statistical Review, 54th Annual Report, May 2007, p. S1 - S4 for 2005 Boiler data; ARI Statistical News Releases 2005, http://ari.org/newsroom/stats/2005/; and GAMA News Release, Jan. 2007 for note 5.

5.6.2 Minimum Efficiency Standards and Maximum Energy Use for Typical Single-Family Residential Heating and Cooling Equipment

			Maximum Energy Use for Space Heating (2)							
			1992				2006			
	Minimum Efficiency (1)		New		Existing		New		Existing	
Heating Equipment	1992	2006	North	South	North	South	North	South	North	South
Natural Gas, Furnace	78 AFUE	78 AFUE	1170	445	1489	771	1170	445	1489	771
Oil, Boiler	80 AFUE	80 AFUE	731	N.A.	930	422	731	N.A.	930	422
Electric, Heat Pump	6.8 HSPF	7.7 HSPF	12923	4685	11232	5546	11412	4137	9919	4898

			Maximum Electricity Use for Space Cooling							
			1992				2006			
	Minimum Efficiency (3)		New		Existing		New		Existing	
Cooling Equipment	1992	2006	North	South	North	South	North	South	North	South
Central Air Conditioner	10 SEER	13 SEER	1113	2543	1000	3743	927	2119	833	3119
Electric, Heat Pump	10 SEER	13 SEER	1100	2414	813	2657	846	1857	625	2044

Note(s): 1) AFUE = Annual Fuel Utilization Efficiency. HSPF = Heating Season Performance Factor. 2) Gas use is in therms. Oil use is in gallons. Electricity use is in kWh. 3) SEER = Seasonal Energy Efficiency Ratio.

Source(s): DOC/GPO, Title 10, Chapter 2, Part 430, Section 430.32, Jan 1, 2001, p. 259 for efficiencies; LBNL, Energy Data Sourcebook for the U.S. Residential Sector, Sept. 1997, Table 3.20, p. 52-53 and Table 3.21, p. 58; and Federal Register, Energy Conservation Program for Consumer Products: Central Air Conditioners and Heat Pumps Energy Conservation Standards, Vol. 66, No. 14, Jan. 22, 2001, p. 7170 for central air conditioner and heat pump.

5.6.3 Residential Furnace Efficiencies (Percent of Units Shipped) (1)

Gas-Fired			
AFUE Range	1985	AFUE Range	2006
Below 65%	15%	75% to 88%	64%
65% to 71%	44%	88% and Over	36%
71% to 80%	10%	Total	100%
80% to 86%	19%		
Over 86%	12%		
Total	100%		

Oil-Fired	
AFUE Range	1985
Below 75%	10%
75% to 80%	56%
Over 80%	35%
Total	100%

Average shipped in 1985 (2):	74% AFUE	Average shipped in 1985 (2):	79% AFUE
Average shipped in 1995:	84% AFUE	Average shipped in 1995:	81% AFUE
Best Available in 1981:	85% AFUE	Best Available in 1981:	85% AFUE
Best Available in 2007:	97% AFUE	Best Available in 2007:	87% AFUE

Note(s): 1) Federal appliance standards effective Jan. 1, 1992, require a minimum of 78% AFUE for furnaces. 3) Includes boilers.

Source(s): GAMA's Internet Home Page for 2006 AFUE ranges; GAMA News, Feb. 24, 1987, for 1985 AFUE ranges; LBNL for average shipped AFUE; GAMA, Consumer's Directory of Certified Efficiency Ratings, May 2004, p. 12 and 72-73 for 2004 best-available AFUEs; GAMA Consumers' Directory of Certified Efficiency Ratings for Heating and Water Heating Equipment, May 2007; GAMA Tax Credit Eligible Equipment: Gas- and Oil-Fired Furnaces 95% AFUE or Greater, May 2007; and GAMA AFUE Press Release 2006: U.S. Shipments of gas warm-air central furnaces

5.6.4 Residential Boiler Efficiencies (1)

Gas-Fired Boilers		Oil-Fired Boilers	
Average shipped in 1985 (2):	74% AFUE	Average shipped in 1985 (2):	79% AFUE
Best Available in 1981:	81% AFUE	Best Available in 1981:	86% AFUE
Best Available in 2007:	96% AFUE	Best Available in 2007:	89% AFUE

Note(s): 1) Federal appliance standards effective Jan. 1, 1992, require a minimum of 80% AFUE (except gas-fired steam boiler, which must have a 75% AFUE or higher). 2) Includes furnaces.

Source(s): GAMA, Consumer's Directory of Certified Efficiency Ratings for Residential Heating and Water Heating Equipment, Aug. 2005, p. 88 and 106 for best-available AFUE; and GAMA for 1985 average AFUEs; GAMA Tax Credit Eligible Equipment: Gas- and Oil-Fired Boilers 95% AFUE or Greater, May 2007; and GAMA Consumers' Directory of Certified Efficiency Ratings for Heating and Water Heating Equipment, May 2007.

5.6.5 Residential Air Conditioner and Heat Pump Cooling Efficiencies (1)

Equipment Type	Efficiency Parameter	2004 U.S. Average New Efficiency	2005 Best-Available New Efficiency
Air Conditioners	SEER	11.2 (2)	18.9
Heat Pump - Cooling			
Air-Source	SEER	11.5 (2)	18.6
Ground-Source	EER	16.0	27.0 (3)
Heat Pump - Heating			
Air-Source	HSPF	6.8	10.6
Ground-Source	COP	3.5	4.9 (3)

Note(s): 1) Federal appliance standards effective Jan. 1, 1992, require a minimum SEER of 10. 2) 2003. 3) 2004.

Source(s): EIA/Navigant Consulting, Technology Forecast Updates - Residential and Commercial Building Technologies - Reference Case, Sept. 2004, p. 22-27; ARI, Statistical Profile of the Air-Conditioning, Refrigeration, and Heating Industry, Oct. 2004, p. 27 for shipment-weighted SEERs; and ACEEE : The Most Energy-Efficient Appliances 2005, Apr. 2005.

5.6.6 Commercial Equipment Efficiencies

Equipment Type	Efficiency Parameter	2003 Stock Efficiency	2004 U.S. Average New Efficiency	2004 Best-Available New Efficiency
Chiller				
Reciprocating	COP	2.6	2.9	3.5
Centrifugal	COP	4.7	5.9	7.3
Gas-Fired Absorption	COP	1.0	1.0	N.A.
Gas-Fired Engine Driven	COP	1.0	2.0	N.A.
Rooftop A/C	COP	2.7	3.0	4.0
Rooftop Heat Pump	EER	9.3	10.3	11.7
Boilers				
Gas-Fired	Thermal Efficiency	76	80	90
Oil-Fired	Thermal Efficiency	79	83	89
Electric	Thermal Efficiency	98	98	98
Gas-Fired Furnace	AFUE	76	80	82 (1)
Water Heater				
Gas-Fired	Thermal Efficiency	76	80	99 (1)
Electric Resistance	Thermal Efficiency	96	98	98
Gas-Fired Instantaneous	Thermal Efficiency	76	80	89 (1)

Note(s): 1) 2007.

Source(s): EIA/Navigant Consulting, EIA - Technology Forecast Updates - Residential and Commercial Buildings Technologies Reference Case, Sept. 2004, p. 38-68; and GAMA Consumers' Directory of Certified Efficiency Ratings for Heating and Water Heating Equipment, May 2007.

5.6.7 2005 Air-Conditioner/Heat Pump Manufacturer Market Shares (Percent of Products Produced)

Company	Market Share (%)
UTC/Carrier	28%
Goodman (Amana)	16%
American Standard (Trane)	15%
Lennox	12%
Rheem	11%
York	10%
Nordyne	7%
Others	2%
Total (2)	100%

Total Units Shipped: 8,607,525 (1)

Note(s): 1) Does not include water-source or ground-source heat pumps.

Source(s): Appliance Magazine, A Portrait of the U.S. Appliance Industry, Sept. 2006, p. P-2.

5.6.8 2005 Gas Furnace Manufacturer Market Shares (Percent of Products Produced)

Company	Market Share (%)
UTC/Carrier	30%
Goodman (Amana)	15%
Lennox	14%
American Standard (Trane)	13%
Rheem	11%
York	9%
Nordyne	6%
Others	2%
Total	100%

Total Units Shipped: 3,512,464

Source(s): Appliance Magazine, A Portrait of the U.S. Appliance Industry, Sept. 2006, p. P-2.

5.6.9 Major Residential HVAC Equipment Lifetimes, Ages, and Replacement Picture

Equipment Type	Typical Service Lifetime Range	Average Lifetime	1990 Average Stock Age	Units to be Replaced During 2007 (1000s)
Central Air Conditioners	**8 - 15**	**12**	**9**	**4,063**
Heat Pumps	**8 - 15**	**12**	**8**	**1,025**
Furnaces				**2,287**
Electric	10 - 20	15	11	N.A.
Gas-Fired	12 - 17	15	12	2,107
Oil-Fired	15 - 20	18	N.A.	180
Steam or Hot-Water Boilers (gas and oil)	**20 - 40**	**N.A.**	**14**	**N.A.**

Note(s): Replacement values include smaller commercial building units. Gas/oil furnaces include wall furnaces.

Source(s): Appliance Magazine, A Portrait of the U.S. Appliance Industry, Sept. 2006, p. P-5 for service and average lifetimes, and units to be replaced; ASHRAE, 1999 ASHRAE Handbook: HVAC Applications, Table 3, p. 35.3 for boilers service lifetimes; and EIA, Housing Characteristics 1990, May 1992, Table 7, p. 24 for 1990 average stock ages.

5.6.10 Major Commercial HVAC Equipment Lifetimes and Ages

Equipment Type	Median Lifetime	
Air Conditioners		
Through-the-Wall	15	
Water-Cooled Package	24	(1)
Roof-Top	15	
Chillers		
Reciprocating	20	
Centrifugal	25	(1)
Absorption	23	
Heat Pumps		
Air-to-Air	15	
Water-to-Air	24	(1)
Furnaces (gas or oil)	18	
Boilers (gas or oil)		
Hot-Water	24 - 35	
Steam	25 - 30	
Unit Heaters		
Gas-Fired or Electric	13	
Hot-Water or Steam	20	
Cooling Towers (metal or wood)		
Metal	22	(1)
Wood	20	

Note(s): 1) Data from 2005. All other data is from 1978.

Source(s): ASHRAE, 2007 ASHRAE Handbook: HVAC Applications, Table 4, p. 36.3 for median service lifetimes.

5.6.11 Main Residential Heating Fuel, by Vintage as of 2001 (Percent of Total Households)

Heating Fuel	1949 or Before	1950 to 1959	1960 to 1969	1970 to 1979	1980 to 1989	1990 to 2001
Natural Gas	68%	67%	63%	42%	41%	56%
Electricity	11%	16%	22%	45%	50%	36%
Fuel Oil	14%	13%	8%	4%	2%	2%
LPG	6%	3%	4%	4%	5%	5%
Other (1)	2%	1%	2%	4%	2%	1%
Total (2)	100%	100%	100%	100%	100%	100%

Note(s): 1) Other includes wood and kerosene.
Source(s): EIA, A Look at Residential Energy Consumption in 2001, Apr. 2004, Table HC3-2a.

5.6.12 Main Residential Heating Equipment as of 1987, 1993, 1997, and 2001 (Percent of Total Households)

Equipment Type	1987	1993	1997	2001
Natural Gas	**55%**	**53%**	**53%**	**55%**
Central Warm-Air Furnace	35%	36%	38%	42%
Steam or Hot-Water System	10%	9%	7%	7%
Floor/Wall/Pipeless Furnace	6%	4%	4%	3%
Room Heater/Other	4%	3%	4%	3%
Electricity	**20%**	**26%**	**29%**	**29%**
Central Warm-Air Furnace	8%	10%	11%	12%
Heat Pump	5%	8%	10%	10%
Built-In Electric Units	6%	7%	7%	6%
Other	1%	1%	2%	2%
Fuel Oil	**12%**	**11%**	**9%**	**7%**
Steam or Hot-Water System	7%	6%	5%	4%
Central Warm-Air Furnace	4%	5%	4%	3%
Other	1%	0%	0%	0%
Other	**13%**	**11%**	**9%**	**8%**
Total	100%	100%	100%	100%

Note(s): Other equipment includes wood, LPG, kerosene, other fuels, and none.
Source(s): EIA, A Look at Residential Energy Consumption in 2001, Apr. 2004, Table HC3-2a; EIA, A Look at Residential Energy Consumption in 1997, Nov. 1999, Table HC3-2a, p. 55; EIA, Housing Characteristics 1993, June 1995, Table 3.7b, p. 63; and EIA, Housing Characteristics 1987, May 1989, Table 14, p. 33.

5.6.13 Main Commercial Heating and Cooling Equipment as of 1995, 1999, and 2003 (Percent of Total Floorspace) (1)

Heating Equipment	1995	1999	2003 (2)
Packaged Heating Units	29%	38%	28%
Boilers	29%	29%	32%
Individual Space Heaters	29%	26%	19%
Furnaces	25%	21%	30%
Heat Pumps	10%	13%	14%
District Heat	10%	8%	8%
Other	11%	6%	5%

Cooling Equipment	1995	1999	2003 (2)
Packaged Air Conditioning Units	45%	54%	46%
Individual Air Conditioners	21%	21%	19%
Central Chillers	19%	19%	18%
Residential Central Air Conditioners	16%	12%	17%
Heat Pumps	12%	14%	14%
District Chilled Water	4%	4%	4%
Swamp Coolers	4%	3%	2%
Other	2%	2%	2%

Note(s): 1) Heating and cooling equipment percentages of floorspace add to over 100% since equipment shares floorspace. 2) Malls are no longer included in most CBECs tables; therefore, some data is not directly comparable to past CBECs.
Source(s): EIA, Commercial Building Characteristics 1995, Oct. 1998, Tables B34 and B36 for 1995, and EIA, Commercial Building Characteristics 1999, Aug. 2002, Tables B33 and B34 for 1999; and, EIA, 2003 Commercial Buildings Energy Consumption and Expenditures: Consumption and Expenditures Tables, June 2006, Tables B39 and B41 for 2003.

5.6.14 Main Commercial Primary Energy Use of Heating and Cooling Equipment as of 1995

Heating Equipment		Cooling Equipment	
Packaged Heating Units	25%	Packaged Air Conditioning Units	54%
Boilers	21%	Room Air Conditioning	5%
Individual Space Heaters	2%	PTAC (2)	3%
Furnaces	20%	Centrifugal Chillers	14%
Heat Pumps	5%	Reciprocating Chillers	12%
District Heat	7%	Rotary Screw Chillers	3%
Unit Heater	18%	Absorption Chillers	2%
PTHP & WLHP (1)	2%	Heat Pumps	7%
	100%		100%

Note(s): 1) PTHP = Packaged Thermal Heat Pump, WLHP = Water Loop Heat Pump. 2) PTAC = Packaged Thermal Air Conditioner

Source(s): BTS/A.D. Little, Energy Consumption Characteristics of Commercial Building HVAC Systems, Volume 1: Chillers, Refrigerant Compressors, and Heating Systems, Apr. 2001, Figure 5-5, p. 5-14 for cooling and Figure 5-10, p. 5-18 for heating.

5.7.1 U.S. Commercial Buildings Conditioned Floorspace, Building Type and System Type (Million SF)

	Individual AC	Packaged	Central VAV	Central FCU	Central CAV	Not Cooled	Total
Education	805	2,204	551	466	212	3,522	7,760
Food Sales	-	534	-	-	-	20	554
Food Service	83	1,100	-	-	-	64	1,247
Health Care	134	557	401	334	802	159	2,387
Lodging	1,669	283	85	707	85	779	3,608
Mercantile and Service	333	5,820	1,081	831	249	2,507	10,821
Office	1,257	4,450	2,322	484	1,161	561	10,235
Public Buildings	371	3,337	847	-	741	2,168	7,464
Warehouse/Storage	119	1,482	-	-	102	2,285	3,988
Total	**4,771**	**19,767**	**5,287**	**2,822**	**3,352**	**12,065**	**48,064**

Source(s): BTS/A.D. Little, Energy Consumption Characteristics of Commercial Building HVAC Systems, Volume II: Thermal Distribution, Auxiliary Equipment, and Ventilation, Oct. 1999, Table A2-12, p. B2-1.

5.7.2 Thermal Distribution Design Load and Electricity Intensities, by Building Activity

	Design Load Intensity (W/SF)	End Use Intensity (kWh/SF)
Education	0.5	1.3
Food Sales	1.1	6.4
Food Service	1.5	6.4
Health Care	1.5	5.6
Lodging	0.5	1.9
Mercantile and Service	0.9	2.7
Office	1.3	3.3
Public Assembly	1.2	3.0
Warehouse	0.4	1.8
All Buildings	**1.0**	**2.8**

Source(s): BTS/A.D. Little, Energy Consumption Characteristics of Commercial Building HVAC Systems, Volume II: Thermal Distribution, Auxiliary Equipment, and Ventilation, Oct. 1999, Table 5-11, p. 5-27.

5.7.3 Thermal Distribution Equipment Design Load and Electricity Intensities, by System Type

	Design Load Intensity (W/SF)			End Use Intensity (kWh/SF)		
	Central VAV	Central CAV	Packaged CAV	Central VAV	Central CAV	Packaged CAV
Condenser Fan			0.3			0.2
Cooling Tower Fan	0.2	0.2		0.1	0.2	
Condenser Water Pump	0.2	0.2		0.3	0.3	
Chilled Water Pump	0.2	0.2		0.1	0.2	
Supply & Return Fans	0.7	0.5	0.6	1.2	1.9	1.9
Chiller/Compressor	1.9	1.8	3.3	1.7	2.3	4.0

Source(s): BTS/A.D. Little, Energy Consumption Characteristics of Commercial Building HVAC Systems, Volume II: Thermal Distribution, Auxiliary Equipment, and Ventilation, Oct. 1999, Table 5-11 p. 5-22.

5.7.4 Typical Commercial Building Thermal Energy Distribution Design Load Intensities (Watts per SF)

Distribution System Fans		**Other**	
Central System Supply Fans	0.3 - 1.0	Cooling Tower Fan	0.1 - 0.3
Central System Return Fans	0.1 - 0.4	Air-Cooled Chiller Condenser Fan	0.6
Terminal Box Fans	0.5	Exhaust Fans (2)	0.05 - 0.3
Fan-Coil Unit Fans (1)	0.1 - 0.3	Condenser Fans	0.6
Packaged or Split System Indoor Blower	0.6		
Pumps			
Chilled Water Pump	0.1 - 0.3		
Condenser Water Pump	0.1 - 0.2		
Heating Water Pump	0.1 - 0.2		

Note(s): 1) Unducted units are lower than those with some ductwork. 2) Strong dependence on building type.

Source(s): BTS/A.D. Little, Energy Consumption Characteristics of Commercial Building HVAC Systems, Volume II: Thermal Distribution, Auxiliary Equipment, and Ventilation, Oct. 1999, Table 3-1, p. 3-6.

5.7.5 Market Share of Major HVAC Equipment Manufacturers ($2005 Million)

	Total Market Size
Air Handling Units	931
Cooling Towers	480
Pumps	300
Central System Terminal Boxes	173
Classroom Unit Ventilator	144
Fan Coil Units	111

Source(s): BTS/A.D. Little, Energy Consumption Characteristics of Commercial Building HVAC Systems, Volume II: Thermal Distribution, Auxiliary Equipment, and Ventilation, Oct. 1999, Table 4-1, p. 4-4; and EIA, Annual Energy Review 2006, June 2007, Appendix D, p. 377 for price deflators.

5.7.6 1999 Energy Efficient Motors, Replacements and Sales, by Horsepower Class

	Existing		Replacements	
	Units in Use	Horsepower		Energy Efficient
Horsepower Range	(1000s)	(10^6)	% Retired	Share of New Motors
1 - 5	20,784	59.6	2.5%	17%
5.1 - 20	6,927	81.8	2.0%	29%
21 - 50	2,376	78.2	1.5%	45%
51 - 100	738	59.6	1.0%	52%
101 - 200	412	56.5	0.8%	65%

Source(s): Electrical Apparatus Service Association, Past Trends and Probably Future Changes in the Electric Motor Industry 1990-1999, 2001, p. 18 for existing stock and retirements and p. 28 for energy efficient motor sales

5.7.7 1999 AC Adjustable Speed Drive Population

Horsepower Range	
1 - 5	70%
5.1 - 20	23%
21 - 50	4%
51 - 100	1%
101 - 200	1%
200 +	1%
Total	100%

Source(s): Electrical Apparatus Service Association, Past Trends and Probably Future Changes in the Electric Motor Industry 1990-1999, 2001, p. 30.

5.8.1 Solar Collector Shipments, by Type and Market (Thousand SF, unless noted) (1)

Type	1980	1990	2000	2005 (2)	2005 Value of Shipments ($million)
Solar Thermal Collectors (3)	19,398	11,409	8,354	16,041	45.9
Residential	N.A.	5,851	7,473	14,681	N.A.
Commercial	N.A.	295	810	1,160	N.A.
Industrial	N.A.	(4)	57	31	N.A.
Utility	N.A.	5,236	5	114	N.A.
Other	N.A.	26	10	56	N.A.
Photovoltaics (kW) (5)	(6) 6,897	13,837	88,221	226,916	701.7

Note(s): 1) Includes imports and exports; 2001 solar thermal collector imports were 3.5 million square feet, and exports were 0.8 million square feet. 2) Preliminary. 3) Solar thermal collectors: receive solar radiation, convert it to thermal energy, and are typically used for space heating, water heating, and heating swimming pools. 4) Industrial is included in Other. 5) Generate electricity by the conversion of solar radiation to electrical energy. 6) 1982.

Source(s): EIA, Solar Thermal and Photovoltaic Collector Manufacturing Activities 2005, Aug. 2006, Table 37 and Table 38, p. 21 and 22 for 2004-2005 collector data, Table 47, p. 31 for 2000-2005 PV shipments, and Table 50, p. 34 for PV value of shipments; EIA, Renewable Energy Annual 2001, Nov. 2002, Table 18, p. 19 for 2000 collector data; EIA, Annual Energy Review 1991, June 1992, Table 111, p. 251 for 1990 collector sector; and EIA, Annual Energy Review 2004, Aug. 2005, Table 10.5, p. 291 for 1980-1990 PV shipments.

5.8.2 Thermal Solar Collector Shipments, by End Use (including imports and exports) (Thousand SF) (1)

Type	2000	2003	2004	2005 (2)
Pool Heating	7,863	10,800	13,634	15,041
Hot Water	367	511	452	640
Space Heating	99	76	13	228
Space Cooling	-	-	-	2
Combined Space/Water Heating	2	23	16	16
Process Heating	20	34	-	-
Electricity Generation	3	-	-	114
Total (3)	**8,354**	**11,444**	**14,114**	**16,041**

Note(s): 1) 5.8% of shipments are exported. 2) Approximately 51,000 systems in 2005.

Source(s): EIA, Renewable Energy Annual 2001, Nov. 2002, Table 18, p. 19 for 2000; EIA, Renewable Energy Annual 2003, June 2005, Table 18, p. 10 for 2003; and EIA, Solar Thermal and Photovoltaic Collector Manufacturing Activities 2005, Aug. 2006, Table 38, p. 22 for 2004-2005, Table 30, p. 14 for Note 1, and Table 39, p. 23 for Note 2.

5.8.3 2005 Top Five Destinations of Thermal Solar Collector Shipments

State	Percent of U.S. Unit Shipments
New Jersey	32%
California	31%
Florida	6%
Tennessee	1%
Arizona	1%

Source(s): EIA, Renewable Energy Annual 2005, July 2007, Table 32, p. 16.

5.8.4 Thermal Solar Collector Manufacturer Statistics (1)

- Number of Manufacturers in 2005: 21
- Percentage of Shipped Solar Collectors Produced by Top 5 Manufacturers: 92%
- Percentage of Shipped Solar Collectors Produced by Top 10 Manufacturers: 98%

Note(s): 1) Preliminary.

Source(s): EIA, Solar Thermal and Photovoltaic Collector Manufacturing Activities 2005, Aug. 2006, Table 41, p. 25.

5.8.5 Shipments of Photovoltaic Cells and Modules, by Market (Peak Kilowatts) (1)

Market	1995	2000	2003	2004	2005 (2)
Industrial	7,198	28,808	27,951	30,493	22,199
Residential	6,272	24,814	23,389	53,928	75,040
Commercial	8,100	13,692	32,604	74,509	89,459
Transportation	2,383	5,502	11,089	1,380	1,621
Utility	3,759	6,298	8,474	3,233	143
Government	2,000	4,417	5,538	3,257	28,683
Other	1,347	4,690	313	14,316	9,772
Total	**31,059**	**88,221**	**109,357** (3)	**181,116**	**226,916**

Note(s): 1) Includes imports and exports. 2) Preliminary. 3) Due to rounding, sum does not equal total.

Source(s): EIA, Solar Thermal and Photovoltaic Collector Manufacturing Activities 2005, Aug. 2006, Table 51, p. 35; EIA, Solar Thermal and Photovoltaic Collector Manufacturing Activities 2003, Sept. 2004, Table 30, p.14; 'EIA, Solar Thermal and Photovoltaic Collector Manufacturing Activities 2001, Nov. 2002, Table 30, p. 23; and EIA, Solar Thermal and Photovoltaic Collector Manufacturing Activities 1997, Feb. 1998, Table 29, p. 31.

5.8.6 Annual Shipments of Photovoltaic Cells and Modules (Peak Kilowatts)

Year	Number of Companies	Domestic	Exports	Total
1995	24	11,188	19,871	31,059
1996	25	13,016	22,448	35,464
1997	21	12,561	33,793	46,354
1998	21	15,069	35,493	50,562
1999	19	21,225	55,562	76,787
2000	21	19,838	68,382	88,220
2001	19	36,310	61,356	97,666
2002	19	45,313	66,778	112,091
2003	20	48,664	60,693	109,357
2004	19	78,346	102,770	181,116
2005 (1)	29	134,465	92,451	226,916

Note(s): 1) Preliminary.

Source(s): EIA, Solar Thermal and Photovoltaic Collector Manufacturing Activities 2004, Nov. 2005, Table 45 and Table 47, p. 23 and p.25 for 1995 data; and EIA, Solar Thermal and Photovoltaic Collector Manufacturing Activities 2005, Aug. 2006, Table 45 and Table 47, p. 29 and p.31 for 1996-2005 data.

5.8.7 2005 Top 5 Destinations of U.S. Photovoltaic Cell and Module Export Shipments, by Country

Country	Peak Kilowatts	Percent of U.S. Exports
Germany	49,250	53%
Netherlands	11,997	13%
Singapore	8,560	9%
Canada	3,227	3%
Hong Kong	2,935	3%
All Countries	**92,451**	100%

Source(s): EIA, Solar Thermal and Photovoltaic Collector Manufacturing Activities 2005, Aug. 2006, Table 53, p. 37.

5.9.1 2001 Total Lighting Technology Electricity Consumption, by Sector (Billion kWh per Year) (1)

	Residential		Commercial		Industrial		Other (2)		Total	
Incandescent										
Standard	176	87%	103	26%	2	2%	5	10%	287	38%
Halogen	6	3%	21	5%	0	0%	1	2%	28	4%
Fluorescent										
T5	N.A.		0	0%	0	0%	N.A.		0	0%
T8	N.A.		50	13%	23	21%	0	0%	72	10%
T12	N.A.		157	40%	49	45%	0	0%	206	27%
Compact	1	1%	13	3%	1	1%	N.A.		14	2%
Miscellaneous	18	9%	0	0%	0	0%	1	1%	19	3%
HID										
Mercury Vapor	1	0%	7	2%	3	3%	12	21%	22	3%
Metal Halide	N.A.		34	9%	25	23%	4	7%	62	8%
HP Sodium	0	0%	6	1%	5	5%	30	54%	41	5%
LP Sodium	N.A.		0	0%	0	0%	3	5%	3	0%
Total (3)	**202**	100%	**391**	100%	**108**	100%	**56**	100%	**756**	100%

Note(s): 1) Lumens-hour is a measure of lighting output; Watt-hour is a measure of electrical input for lighting. A value of zero indicates less than 0.5 billion kWh/year. 2) Includes stationary aviation, billboard, and traffic and street lighting. 3) Lighting consumed 756 10^9 kWh of energy in 2001. This amount is equivalent to 99% of the energy generated by all 104 nuclear power plants in the same year.

Source(s): BTS/Navigant Consulting, U.S. Lighting Market Characterization Phase I National Lighting Inventory and Energy Consumption Estimate, July 2002; EIA, Annual Energy Review 2003, Table 9.2 Nuclear Power Plant Operations, p. 271, for note 3.

5.9.2 2001 Total Lighting Technology Light Output, by Sector (Trillion Lumen-hour per Year)(1)

	Residential		Commercial		Industrial		Other (2)		Total	
Incandescent										
Standard	2,504	66%	1,384	6%	22	0%	87	2%	3,997	10%
Halogen	102	3%	392	2%	13	0%	23	0%	530	1%
Fluorescent										
T5	N.A.		13	0%	0	0%	N.A.		13	0%
T8	N.A.		4,208	20%	1,925	24%	1	0%	6,134	16%
T12	N.A.		11,752	54%	3,781	47%	2	0%	15,535	41%
Compact	57	1%	735	3%	35	0%	N.A.		827	2%
Miscellaneous	1,103	29%	24	0%	3	0%	39	1%	1,169	3%
HID										
Mercury Vapo	23	1%	261	1%	149	2%	532	11%	965	3%
Metal Halide	N.A.		2,202	10%	1,605	20%	249	5%	4,055	11%
HP Sodium	8	0%	587	3%	562	7%	3,381	72%	4,539	12%
LP Sodium	N.A.		18	0%	4	0%	408	9%	430	1%
Total	**3,797**	100%	**21,574**	100%	**8,100**	100%	**4,722**	100%	**38,194**	100%

Note(s): 1) Lumens-hour is a measure of lighting output; Watt-hour is a measure of electrical input for lighting. A value of zero indicates less than 0.5 billion kWh/year. 2) Includes stationary aviation, billboard, and traffic and street lighting.

Source(s): BTS/Navigant Consulting, U.S. Lighting Market Characterization Phase I National Lighting Inventory and Energy Consumption Estimate, July 2002.

5.9.3 2001 Lamp Wattage, Number of Lamps, and Hours of Usage (Weighted Average)

	Lamp Wattage (Watts per lamp)				Number of Lamps per Building				Hours of Usage per Day			
	Res	Com	Ind	Other (1)	Res	Com	Ind		Res	Com	Ind	Other
Incandescent												
Standard	66	88	115	115	37	70	12		2	9	14	8
Halogen	202	102	447	167	0	12	1		2	10	14	8
Fluorescent												
T5	N.A.	8	10	N.A.	N.A.	1	0	(2)	N.A.	13	18	N.A.
T8	N.A.	32	30	105	N.A.	93	671		N.A.	10	13	7
T12	N.A.	51	66	190	N.A.	191	646		N.A.	10	13	7
CFL	17	19	27	N.A.	1	32	13		2	11	14	N.A.
Miscellaneous	41	18	34	83	6	1	2		2	10	11	11
HID												
Mercury Vapor	179	331	409	239	0	1	8		3	10	12	11
Metal Halide	N.A.	472	438	23	N.A.	4	47		N.A.	10	14	10
HP Sodium	79	260	394	216	0	1	12		3	10	13	11
LP Sodium	N.A.	104	90	180	N.A.	0	0		N.A.	10	12	12

Note(s): 1) Other includes stationary aviation, billboard, and traffic and street lighting. 2) A value of zero indicates less than 0.5.
Source(s): BTS/Navigant Consulting, U.S. Lighting Market Characterization Phase I National Lighting Inventory and Energy Consumption Estimate, July 2002.

5.9.4 1995 Lighting Energy Intensities, by Commercial Building Type

Building Type	Percent of Total Lighted Floorspace	Percent of Total Annual Lighting Energy	Annual Lighting End-Use Intensity per Total Lighted Floorspace (kWh/SF)
Education	13.6%	10.1%	4.6
Food Sales	1.1%	1.8%	9.9
Food Service	2.4%	4.2%	10.8
Health Care	4.1%	7.7%	11.5
Lodging	6.4%	7.0%	6.8
Mercantile and Service	22.4%	24.8%	6.9
Office	18.6%	24.5%	8.2
Public Assembly	7.0%	7.2%	6.4
Public Order and Safety	2.3%	1.7%	4.8
Warehouse and Storage	14.0%	6.9%	2.9
Other	1.8%	2.2%	7.8
Vacant	6.2%	1.9%	1.3
Total	100%	100%	

Note(s): Total lighted floorspace in 1995 was 56.3 billion square feet. Total lighted floorspace for 1999 was 67.3 billion square feet.
Source(s): EIA, A Look at Commercial Buildings in 1995: Characteristics, Energy Consumption, and Energy Expenditures, Oct. 1998, Table BC-40, p. 187, Table EU-1, p. 306-310, and Table EU-2, p. 311-315.

5.9.5 2003 Lighted Floorspace for the Stock of Commercial Buildings, by Type of Lamp (1)

Total Lighted Floorspace: 62.06 Billion SF

Type of Lamp	Lighted Floorspace (Billion SF) (2)	Percent of Lighted Floorspace
Standard Fluorescent	59.7	96%
Incandescent	38.5	62%
Compact Fluorescent	27.6	44%
High-Intensity-Discharge	20.6	33%
Halogen	17.7	29%

Note(s): 1) Mall buildings are no longer included in most CBECs tables; therefore, some data are not directly comparable to past CBECs.
2) The percentages of lighted floorspace total more than 100% since most floorspace is lighted by more than one type of lamp.
Source(s): EIA, 2003 Commercial Buildings Energy Consumption Survey: Building Characteristics Tables, June 2006, Table B44, p. 220.

5.9.6 Value of Electric Lighting Fixture Shipments ($Million)

Lighting Fixture Type	1985	1990	1995	2000	2001
Residential	786.8	827.6	983.8	1,296.5	983.9
Commercial/Institutional (except spotlight)	1,832.3	2,379.7	2,797.3	3,506.7	3,239.1
Industrial	389.2	529.4	676.3	718.3	628.1
Vehicular (1)	1,001.2	1,620.7	N.A.	N.A.	N.A.
Outdoor	905.5	1,061.5	1,473.0	1,957.4	1,923.2

Note(s): 1) Data for vehicular lighting fixtures was discontinued in 1992.

Source(s): DOC, Electric Lighting Fixtures MA 335L(01)-1, Jan. 2003 for 2000 and 2001; DOC, Current Industrial Reports: Electric Lighting Fixtures, MA335L(99)-1, Dec. 2000, Table 1 for 1990-1999; and DOC, Current Industrial Reports: Electric Lighting Fixtures, MA36L, Oct. 1995, Table 1 for 1985.

5.9.7 Shipments of Fluorescent Lamp Ballasts

	Standard Magnetic Type (1)		Electronic Type		Total		
Year	Quantity (million)	Value ($million)	Quantity (million)	Value ($million)	Quantity (million)	Value ($million)	Electronic Type as a % of Total Units Shipped
1985	70.1	398.9	N.A	N.A.	70.1	398.9	N.A.
1986	69.4	396.1	0.4	11.8	69.8	407.9	1%
1988	74.6	450.9	1.1	25.5	75.7	476.4	1%
1990	78.4	546.3	3.0	69.3	81.4	615.6	4%
1992	83.7	537.7	13.3	274.6	97.0	812.3	14%
1994	83.5	550.0	24.6	390.8	108.1	940.7	23%
1996	67.0	457.8	30.3	451.4	97.3	909.2	31%
1998	63.9	401.4	39.8	512.8	103.7	914.3	38%
2000	55.4	343.0	49.3	555.5	104.8	898.5	47%
2001	46.9	297.1	52.5	580.3	99.4	877.4	53%
2002	40.7	263.3	53.8	573.1	94.5	836.4	57%
2003	35.2	231.8	54.4	557.2	89.7	789.0	61%
2004	30.5	218.4	59.2	579.4	89.7	797.8	66%
2005	22.2	175.1	61.3	594.6	83.5	769.8	73%

Note(s): 1) Standard magnetic type includes uncorrected and corrected power-factor type ballasts.

Source(s): DOC Current Industrial Reports: Fluorescent Lamp Ballasts, MQ335C(05)-5, July 2006 for 2000-2005; DOC, Current Industrial Reports: Fluorescent Lamp Ballasts MQ36C(99)-5, July 2000, Table 1 for 1990-1999; and DOC, Current Industrial Reports: Fluorescent Lamp Ballasts, MQ36C(95), 1996, Table 1 for 1985-1989.

5.9.8 Typical Efficacies and Lifetimes of Lamps (1)

Current Technology	Efficacy (lumens/Watt)	Typical Rated Lifetime (hours)	CRI (2)
Incandescent	10 - 19	750 - 2,500	97
Halogen	14 - 20	2,000 - 3,500	99
Fluorescent - T5	25 - 55	6,000 - 7,500	52 - 75
Fluorescent - T8	35 - 87	7,500 - 20,000	52 - 90
Fluorescent - T12	35 - 92	7,500 - 20,000	50 - 92
Compact Fluorescent	40 - 70	10,000	82
Mercury Vapor	25 - 50	29,000	15 - 50
Metal Halide	50 - 115	30,00 - 20,000	65 - 70
High Pressure Sodium	50 - 124	29,000	22
Low Pressure Sodium	18 - 180	18,000	0
Solid State Lighting	(3)	(4)	70-80

Note(s): 1) Theoretical maximum luminous efficacy of white light is 220 lumens/Watt. 2) CRI = Color Rendition Index, which indicates a lamp's ability to show natural colors. 3) The DOE Solid State Lighting program has set an efficacy goal twice that of fluorescent lights (160 lumen per Watt). 4) Has not been determined.

Source(s): DOE, EERE, Building Technology Program/Navigant Consulting, U.S. Lighting Market Characterization, Volume I: National Lighting Inventory and Energy Consumption Estimate, Sept. 2002, Appendix A, p. 74; DOE/Navigant Consulting, Solid State Lighting Research and Development Portfolio, Mar. 2006, p 55.

5.10.1 Refrigeration System Shipments, by Type (Including Exports)

Appliance Type	1990 (1000s)	2000 (1000s)	2005 (1000s)	2005 Value of Shipments ($million)
Refrigerator-Freezers (1)	7,317	9,462	10,665	5,405
Freezers (chest and upright)	1,328	2,007	2,274	N.A.
Refrigerated Display Cases	359	347	177	N.A.
Unit Coolers	178	207	209	155
Ice-Making Machines	171	385	373	648
Water Cooler	253	348	300 (2)	N.A.
Beverage Vending Machine	229	353	N.A.	N.A.

Note(s): 1) Does not include commercial products value. 2) 2004.

Source(s): Appliance Magazine, 54th Annual Statistical Review, May 2007, p. S1-S4 for refrigerator, freezer, refrigerated display cases, water cooler, and beverage vending machines shipments; The Air Conditioning, Heating and Refrigeration News, Nov. 11, 1995, p. 19 for 1990 unit cooler and ice-making machine shipments; DOC, Current Industrial Reports: Refrigeration, Air Conditioning, and Warm Air Heating Equipment, MA333M(06)-1, July 2007, for 2005 refrigerator-freezer, unit cooler, and ice-making machine data and value of shipments; and AHAM Factbook 2005: A Statistical Overview of the Home Appliance Industry, Table 7, p. 223; and DOC, Current Industrial Reports: Major Household Appliances, MA335f(06)-1, June 2007, Table 2 for 2005 refrigerator-freezer and water cooler data and value of shipments.

5.10.2 Other Major Appliance Shipments, by Type (Including Exports)

Appliance Type	1990 (1000)	2000 (1000)	2005 (1000)	2005 Value of Shipments (5) ($million)
Room Air Conditioners	**3,799**	**6,496**	**8,024**	**1,050**
Ranges (total)	**5,873**	**8,202**	**9,963**	**4,491**
Electric Ranges	3,350	5,026	6,201	2,753
Gas Ranges	2,354	3,176	3,762	1,738
Microwave Ovens/Ranges	**7,693**	**12,644**	**13,862**	**1,377**
Clothes Washers	**5,591**	**7,495**	**9,394**	**3,373**
Clothes Dryers (total)	**4,160**	**6,575**	**8,114**	**2,486**
Electric Dryers	3,190	5,095	6,408	N.A.
Gas Dryers	970	1,480	1,706	N.A.
Water Heaters (total)	**7,252**	**9,329**	**9,455**	**1,609**
Electric (1,2)	3,246	4,299	4,572	638
Gas and Oil (2)	4,005	5,006	4,884	970
Solar (3)	N.A.	24	N.A.	N.A.
Office Equipment				
Personal Computers (4)	N.A.	47,168	59,259	33,028
Copiers	N.A.	1,989	2,013	N.A.
Printers	N.A.	27,945	19,232	1,614
Scanners	N.A.	9,400	N.A.	238

Note(s): 1) Sales of heat pump water heaters were less than 2,000 units in 1994, down from its peak of 8,000 in 1985. 2) Includes residential and small commercial units. 3) Shipments and value of shipments of entire systems. 4) Includes workstations, laptops, and notebooks. 5) Value of shipments are based on Census unit shipment data, which is about 31 million units lower than industry data shown.

Source(s): AHAM, AHAM Fact Book 2000, 2000, Tables 7 and 8, for 1990 data except water heaters; AHAM, AHAM 2005 Fact Book, 2006, Table 7 for 2000-2005 shipments and Table 6, p. 19 for value of shipments of ranges, microwave ovens, laundry equipment, and room air conditioners; GAMA, Statistical Highlights: Ten Year Summary, 1987-1996; GAMA, Statistical Highlights: Ten Year Summary, 1994- 2003 for water heater shipments; GAMA, Statistical Highlights, Dec. 2006 for 2005 water heater shipments; DOC, Current Industrial Reports: Major Household Appliances, MA335F(02)-1, July 2003, Table 2 for value of water heater shipments; EIA, 2000 Solar Thermal and Photovoltaic Collector Manufacturing Activities, July 2001, Table 17, p. 20 for solar water heater data; BTS/OBE, Market Disposition of High-Efficiency Water Heating Equipment, Nov. 1996, p. I-8 for HPWH note; DOC, Current Industrial Reports: Computers and Office and Accounting Machines, MA334R(05)-1, Aug. 2006, Table 2 for value of computer shipments; Appliance, 52nd Annual Statistical Review, May 2005, p. S1-S4 for office equipment shipments; and DOC, Current Industrial Reports: Major Household Appliances, MA335f(06)-1, June 2007, Table 2 for 2005 water heater value of shipments.

5.10.3 Minimum Efficiency Standards for Appliances and Equipment

Refrigerator-Freezers (Auto Defrost) (1)	Adjusted Volume (2) (Cu. Ft.)	Rated Maximum Electricity Use (kWh) 1990	1993	2001
Top freezer w/o through-the-door ice service and all-refrigerators—auto defrost	21	955	685	478
Side freezer w/o through-the-door ice service	25	1,183	797	631
Bottom freezer w/o through-the-door ice service	25	1,183	781	574
Top freezer w/ through-the-door ice service	18	1,015	711	542
Side freezer w/ through-the-door ice service	29	1,428	992	694

Freezers (1)	Adjusted Volume (2) (Cu. Ft.)	Rated Maximum Electricity Use (kWh) 1990	1993	2001
Upright Freezers w/ Manual Defrost	25.7	702	529	452
Upright Freezers w/ Automatic Defrost	30.0	1,103	838	699
Chest Freezers and all other Freezers except Compact Freezers	24.8	590	433	389

Room Air-Conditioners (3)	Minimum EER	Typical Maximum Electricity Use (kWh) (4)
Less than 6,000 Btu/h	9.7	464
6,000 to 7,999 Btu/h	9.7	541
8,000 to 13,999 Btu/h	9.8	842
14,000 to 19,999 Btu/h	9.7	1,314
20,000 Btu/h or more	8.5	1,765

Clothes Dryers (3)	Minimum EF (lbs./kWh)	Typical Maximum Energy Use
Electric, Standard	3.01	835 kWh
Gas	2.67	32 therms

Clothes Washers (3)	Minimum EF (cu. Ft./kWh per cycle) 1994	Minimum Modified EF (cu. Ft./kWh per cycle) 2004	2007	Typical Maximum Electricity Use (kWh) (5)
Top Loading, Standard	1.18	1.04	1.26	1,265
Horizontal-Axis	N.A.	1.04	1.26	731

Dishwashers (3)	Minimum EF (cycles/kWh)	Typical Maximum Electricity Use (kWh)
Standard Dishwasher	0.46	498

Water Heaters (6)	Minimum EF (7) 1990	1991	2004	Typical Maximum Energy Use 1990	1991	2004
Gas-Fired	0.54	0.54	0.59	208 therms	208 therms	191 therms
Oil-Fired	0.51	0.51	0.51	155 gallons	155 gallons	155 gallons
Electric Resistance	0.90	0.88	0.92	3456 kWh	3534 kWh	3380 kWh

Note(s): 1) DOE regulations mandate maximum electrical consumption for appliance based on its size. 2) AV = Adjusted Volume = Refrigerator Compartment + 1.63 * Freezer Compartment. 3) DOE regulations mandate minimum efficiency for appliance. 4) Electric use based on 750 hours of operation. 5) Includes electricity for water heater and clothes dryer. 6) DOE regulations mandate minimum efficiency for appliance based on its size. 7) Based on a 40-gallon tank.

Source(s): DOC/GPO, 2001 CFR, Title 10, Chapter 2, Part 430, Section 430.32, Jan. 1, 2001, p. 258-264 for minimum efficiencies; AHAM, 2000 Major Home Appliance Industry Factbook, Nov. 2000, Table 21, p. 28, for refrigerator and freezer sizes; DOE/EE, Final Rule Technical Support Document: Energy Efficiency Standards for Consumer Products: Clothes Washers, Dec. 2000, p. 10-8; LBNL, Energy Data Sourcebook for U.S. Residential Sector, May 1997, p. 102-103 for clothes dryers, p. 94 for dishwashers; DOE/EE, Technical Support Document: Energy Efficiency Standards for Consumer Products: Water Heaters, Apr. 2000, p. 9-14.

5.10.4 Refrigerator-Freezer Sizes and Energy Factors (Shipment-Weighted Averages)

	Average Volume (cu. ft.)	Consumption/Unit (kWh/yr)	Best-Available (kWh/yr)
1972	18.2	1,726	N.A.
1980	19.6	1,278	N.A.
1985	19.5	1,058	N.A.
1990	20.5	916	N.A.
1991	19.8	857	761
1992	19.8	821	N.A.
1993	20.1	660	631
1994	20.0	653	592
1995	20.0	649	555
1996	20.3	661	524
1997	20.4	669	524
1998	N.A.	N.A.	524
1999	20.6	690	559
2000	21.9	704	523
2001	21.9	565	438
2002	22.2	520	428
2003	22.3	514	428
2004	21.5	500	402

Note(s): The average stock energy uses for refrigerator-freezers was 1,220 kWh/yr in 1990, 1,319 kWh/yr in 1997, and 1,462 kWh/yr in 2001.

Source(s): AHAM, 2000 Major Home Appliance Industry Fact Book, 2000, Table 25, p. 30 for 1972-1985; AHAM, 2005 AHAM Fact Book, 2006, Table 17, p. 40 for 1990-2004; AHAM, 1991, 1993-1999 Directory of Certified Refrigerators and Freezers for 1993-1999 best-available data (at 19.6 or more cu. ft.); LBNL, Center for Building Science News, Summer 1995, p. 6 for 1990 portion of note; EIA, A Look at Residential Energy Consumption in 2001; Apr. 2004, Table CE5-1c for 2001 portion of note; EIA, A Look at Residential Energy Consumption in 1997, Nov. 1999, Table CE5-2c, p. 205 for 1997 portion of note; and ENERGY STAR certified products lists for 2001-2004 best available, http://www.energystar.gov/ia/products/prod_lists/appliances_prod_list.xls.

5.10.5 Room Air Conditioner Capacities and Energy Efficiencies (Shipment-Weighted Averages)

	Average Capacity (Btu/hr)	EER	Best-Available (EER)
1972	10,227	5.98	N.A.
1980	10,607	7.02	N.A.
1985	10,287	7.70	N.A.
1990	10,034	8.73	N.A.
1991	10,846	8.80	N.A.
1992	10,100	8.88	N.A.
1993	10,264	9.05	N.A.
1994	10,087	8.97	12.0
1995	10,099	9.03	12.0
1996	9,928	9.08	12.0
1997	10,015	9.09	12.0
1998	N.A.	N.A.	11.7
1999	9,596	9.07	11.7
2000	9,739	9.30	11.7
2001	9,874	9.63	11.7
2002	9,800	9.75	11.7
2003	9,203	9.75	11.7
2004	9,735	9.71	11.7

Source(s): AHAM, 1997 Major Appliance Industry Fact Book, Oct. 1997, Table 27, p. 32 for 1972; AHAM, AHAM 2003 Fact Book, 2003, Table 25, p. 45 for 1980-1985 average capacity and EER; AHAM, AHAM 2005 Fact Book, 2006, Table 19, p. 42 for 1990-2004 average capacity and EER; AHAM, 1994-1999 Directory of Certified Room Air Conditioners, Mar. 2000 for 1994-2000 best available; and ENERGY STAR certified products lists for 2001-2004 best available, http://www.energystar.gov/ia/products/prod_lists/appliances_prod_list.xls.

5.10.6 Water Heater Efficiencies

Residential Type	Efficiency Parameter (1)	2005 Stock Efficiency	Minimum New Efficiency (2)	2005 Best-Available New Efficiency
Electric Storage	EF	0.88	0.92	0.95
Electric Instantaneous	EF	(3)	0.93	0.99
Electric Heat Pump	EF	(3)	0.92	2.28
Gas-Fired Storage	EF	0.56	0.59	0.65
Gas-Fired Instantaneous	EF	(3)	0.54	0.85
Oil-Fired Storage	EF	0.55	0.51	0.68
Solar	SEF	N.A.	0.80	4.80
Commercial Type				
Electric Storage	Thermal Efficiency	98%	98%	98%
Gas-Fired Storage	Thermal Efficiency	82%	80%	94%
Oil-Fired Storage	Thermal Efficiency	77%	78%	82%

Note(s): 1) EF = energy factor and SEF = solar energy factor, which is the hot water energy delivered by the solar system divided by the electric or gas energy input to the system. 2) Based on a 40-gallon residential type tank. 3) Included in storage stock efficiency.

Source(s): EIA, Supplement to the AEO 2007, Feb. 2007, Table 21 and Table 22 for stock efficiencies; GAMA, Consumer's Directory of Certified Efficiency Ratings for the Residential and Water Heating Equipment, Aug. 2005 for best-available efficiencies and minimum efficiencies; and SRCC, Summary of SRCC Certified Solar Collector and Water Heating System Ratings, Apr. 2000, p. S16 - S20 for SEFs, Table 2.2, p. 4.

5.10.7 Other Major Appliance Efficiencies

Residential Appliance Type	Efficiency Parameter (1)	2003 Stock Efficiency	2004 U.S. Average New Efficiency	2005 Best Available New Efficiency
Dishwashers	EF	0.40	0.60	1.50
Clothes Washers (2)	MEF	0.92	1.35	2.66

Commercial Appliance Type	Efficiency Parameter (1)	2005 Stock Efficiency	U.S. Average New Efficiency	2001 Best Available New Efficiency	
Cooking Equipment:					
Electric Appliances	EF	0.71			
Gas Appliances	EF	0.51			
Laundry Equipment:					
Electric Drying	EF/COP			0.98	(3)
Gas Drying	EF			0.36	(3)
Motors	EF			0.65	(3)
Office Equipment:					
Linear Power Supplies	EF			0.30 - 0.60	(3)
Switching Power Supplies	EF			0.80 - 0.95	(3)
Motors	EF			0.60 - 0.70	(3)

Note(s): 1) EF = Energy Factor. MEF = Modified Energy Factor. COP = Coefficient of Performance. 2) EF does not include remaining moisture content (RMC) of clothes. MEF includes RMC which shows how much the clothes dryer will be needed. 3) 1992.

Source(s): AHAM, AHAM 2005 Fact Book, 2006, Tables 21, p. 44 and Table 22, p. 45 for residential efficiencies; DOE/EPA, Energy Star Appliances, www.energystar.gov, Aug. 2005 for best-available dishwashers and clothes washers; EIA/Navigant Consulting, EIA - Technology Forecast Updates - Residential and Commercial Building Technologies - Reference Case, Sept. 2004, p. 34-37 for residential stock; EIA, Supplement to the AEO 2006, Feb. 2006, Table 22 for average cooking efficiency; and BTS/OBE, Characterization of Commercial Building Appliances, Aug. 1993 for commercial efficiencies.

5.10.8 2005 Room Air Conditioner Manufacturer Market Shares (Percent of Products Produced)

Company	Market Share (%)
LG Electronics (Goldstar)	30%
Fedders	14%
Electrolux (Frigidaire)	14%
Whirlpool	14%
Haier	5%
Samsung	5%
Sharp	4%
Matsushita	2%
Friedrich	4%
Others	8%
Total	100%

Total Units Shipped: 8,032,000

Source(s): Appliance Magazine, A Portrait of the U.S. Appliance Industry, Sept. 2006, p. P-2.

5.10.9 2005 Refrigerator Manufacturer Market Shares (Percent of Products Produced)

Company	Market Share (%)
GE	29%
Electrolux (Frigidaire)	25%
Whirlpool	25%
Maytag (Admiral)	11%
Haier	2%
W.C. Wood	1%
Others	7%
Total	100%

Total Units Shipped: 11,134,000

Source(s): Appliance Magazine, A Portrait of the U.S. Appliance Industry, Sept. 2006, p. P-3.

5.10.10 2005 Range Manufacturer Market Shares (Percent of Products Produced)

Company	Electric Market Share (%)	Gas Market Share (%)
GE	49%	37%
Whirlpool	23%	11%
Maytag	10%	17%
Electrolux (Frigidaire)	10%	25%
Peerless Premier	4%	6%
Others	4%	4%
Total	100%	100%

Total Electric Units Shipped: 6,194,000

Total Gas Units Shipped: 3,756,000

Source(s): Appliance Magazine, A Portrait of the U.S. Appliance Industry, Sept. 2006, p. P-2.

5.10.11 2005 Microwave Oven Manufacturer Market Shares (Percent of Products Produced)

Company	Market Share (%)
LG Electronics (Goldstar)	35%
Sharp	20%
Samsung	12%
Daewoo	9%
Matsushita	8%
Whirlpool	4%
Galanz	3%
Midea	2%
Others	7%
Total	100%

Total Units Shipped: 14,081,000

Source(s): Appliance Magazine, A Portrait of the U.S. Appliance Industry, Sept. 2006, p. P-3.

5.10.12 2005 Clothes Washer Manufacturer Market Shares (Percent of Products Produced)

Company	Market Share (%)
Whirlpool	51%
Maytag	19%
GE	17%
Electrolux (Frigidaire)	9%
Others	4%
Total	100%

Total Units Shipped: 9,225,000

Source(s): Appliance Magazine, A Portrait of the U.S. Appliance Industry, Sept. 2006, p. P-3.

5.10.13 Sales of ENERGY STAR Labeled Appliances, by Year (1000s) and Percent of Total Sales

	Room Air Conditioners		Refrigerators		Clothes Washer		Dishwashers	
	ENERGY STAR	% of Total	ENERGY STAR	% of Total	ENERGY STAR	% of Total	ENERGY STAR	% of Total
1997	474	12%	2,008	25%	226	4%	265	6%
1998	589	13%	1,705	19%	392	6%	955	19%
1999	835	13%	2,218	24%	624	9%	664	12%
2000	1,230	19%	2,489	27%	697	9%	595	11%
2001	642 (1)	12%	1,610 (2)	17%	758	10%	1,119	20%
2002	2,195	36%	1,956	20%	1,262	16%	2,262	36%
2003	2,369	29%	2,570	26%	1,879	23%	1,290	20%
2004	2,859	35%	3,625	33%	2,405	27%	5,437	78%
2005	4,186	52%	3,667	33%	3,362	36%	5,980	82%
2006	3,634	36%	3,452	31%	3,603	38%	6,571	92%

Note(s): 1) On Oct. 1, 2000, ENERGY STAR room air conditioner criteria changed to 10% more efficient than the 2000 federal standard.
2) On Jan. 1, 2001, ENERGY STAR refrigerator criteria changed to 10% more efficient than the 2001 federal standard.

Source(s): Appliance Magazine, US Appliance Industry Shipment Statistics: Factory Unit Shipments for Dec. 2004, May 2005, May 2007, p.S-1 to S-4 for 2004 sales data; and D&R International, Resources for Appliance Manufacturers and Retailers, www.energystar.gov, Mar. 2005, June 2006, May 2007.

5.10.14 2005 Clothes Dryer Manufacturer Market Shares (Percent of Products Produced)

Company	Electric Market Share (%)	Gas Market Share (%)
Whirlpool	56%	55%
Maytag	18%	25%
GE	14%	11%
Electrolux (Frigidaire)	10%	7%
Others	2%	3%
Total	100%	100%

Total Electric Units Shipped: 6,451,000

Total Gas Units Shipped: 1,707,000

Source(s): Appliance Magazine, A Portrait of the U.S. Appliance Industry, Sept. 2006, p. P-3.

5.10.15 2005 Water Heater Manufacturer Market Shares (Percent of Products Produced)

Company	Market Share (%)
Rheem Manufacturing	39%
A.O. Smith/State Industries	26%
American Water Heater	19%
Bradford-White	15%
Others	1%
Total	100%

Total Units Shipped: 9,319,786

Source(s): Appliance Magazine, A Portrait of the U.S. Appliance Industry, Sept. 2006, p. P-3.

5.10.16 2005 Facsimile and Copier Machine Manufacturer Market Shares (Percent of Products Produced)

Company	Facsimile Machine Market Share (%)	Copier Market Share (%)
Hewlett-Packard	33%	10%
Brother	22%	-
Panasonic Panafax	17%	-
Sharp	11%	9%
Lexmark	8%	-
Canon	4%	26%
Xerox	1%	9%
Ricoh	-	8%
Others	4%	38%
Total	100%	100%

Total Facsimile Machine Units Shipped: 3,838,000

Total Copier Units Shipped: 2,013,000

Note(s): In 2004, 95% of facsimile machines sales were ENERGY STAR compliant and 90% are estimated to remain ENERGY STAR enabled.
In 2004, 90% of copier machine sales were ENERGY STAR compliant and 34% are estimated to remain ENERGY STAR enabled.

Source(s): Appliance Magazine, A Portrait of the U.S. Appliance Industry, Sept. 2006, p. P-2; and EIA/Navigant Consulting, EIA - Technology Forecast Updates - Residential and Commercial Building Technologies - Reference Case, Sept. 2004, p. 70 for note.

5.10.17 2005 Personal Computer Manufacturer Market Shares (Percent of Products Produced)

Company	Desktop Computer Market Share (%)	Portable Computer Market Share (%)
Dell	35%	31%
Hewlett-Packard	20%	18%
Gateway	7%	-
Levono (IBM)	2%	5%
Apple	3%	6%
Toshiba	-	11%
Others	33%	29%
Total	100%	100%

Total Desktop Computer Units Shipped: 39,698,000

Total Portable Computer Units Shipped: 19,551,000

Note(s): In 2004, 80% of desktop computer sales were ENERGY STAR compliant and 25% are estimated to remain ENERGY STAR enabled.

Source(s): Appliance Magazine, A Portrait of the U.S. Appliance Industry, Sept. 2006, p. P-2; and EIA/Navigant Consulting, EIA - Technology Forecast Updates - Residential and Commercial Building Technologies - Reference Case, Sept. 2004, p. 70 for note.

5.10.18 2005 Printer Manufacturer Market Shares (Percent of Products Produced)

Company	Ink Jet Printer Market Share (%)	Laser Printer Market Share (%)	Dot Matrix Market Share (%)
Hewlett-Packard	39%	56%	-
Lexmark	18%	7%	10%
Epson	12%	-	23%
Canon	14%	-	-
Dell	18%	12%	
Samsung	-	4%	-
Brother	-	6%	-
Konica-Minolta	-	5%	-
Okidata	-	-	49%
Panasonic	-	-	6%
Genicom (Tally)	-	-	6%
Others	-	10%	6%
Total	100%	100%	100%

Total Ink Jet Units Shipped: 14,463,000

Total Laser Units Shipped: 4,477,000

Total Dot Matrix Units Shipped: 292,000

Note(s): In 2004, 99% of laser printer sales were ENERGY STAR compliant and 47% are estimated to remain ENERGY STAR enabled.

Source(s): Appliance Magazine, A Portrait of the U.S. Appliance Industry, Sept. 2006, p. P-2; and EIA/Navigant Consulting, EIA - Technology Forecast Updates - Residential and Commercial Building Technologies - Reference Case, Sept. 2004, p. 70 for note.

5.10.19 Major Residential and Small Commercial Appliance Lifetimes, Ages, and Replacement Picture

Appliance Type	Typical Service Lifetime Range (years)	Average Lifetime (years)	2001 Average Stock Age (years)	Units to be Replaced During 2007 (1000s)
Refrigerators (1)	10 - 18	14	8	8,109
Freezers	8 - 16	12	12	1,691
Room Air Conditioners	7 - 13	10	8	3,836
Microwave Ovens	7 - 10	9	N.A.	10,895
Ranges (2)				
Electric	12 - 19	16	N.A.	3,459
Gas	14 - 22	18	N.A.	2,414
Clothes Washers	7 - 14	11	N.A.	7,279
Clothes Dryers				
Electric	8 - 15	12	N.A.	4,020
Gas	8 - 15	12	N.A.	1,205
Water Heaters				
Electric	4 - 20	12	9	3,917
Gas	3 - 15	9	9	4,671
Facsimile Machines	3 - 6	4	N.A.	4,541
Portable Computers	2 - 4	3	N.A.	14,887

Note(s): 1) Excluding compact refrigerators. 2) Ranges include free-standing, built-in, high-oven and cooktop/oven combination units.

Source(s): Appliance Magazine, A Portrait of the U.S. Appliance Industry, Sep. 2006, p. P5 - P6 for service and average lifetimes and units to be replaced; EIA, A Look at Residential Energy Consumption in 2001, Apr. 2004, Table HC4-1a and Table HC5-1a for average stock ages.

5.10.20 Major Appliance Ownership (Millions of Households and Percent of U.S. Households)

Appliance Type	1982 Households		1990 Households		1996 Households		2001 Households		2005 Households	
Room Air Conditioners	22.6	27%	30.2	32%	30.4	31%	26.9	26%	27.4	25%
Refrigerators	83.4	100%	91.2	98%	96.8	98%	100.0	96%	104.7	96%
Freezers	35.7	43%	42.4	45%	41.9	42%	42.8	41%	36.1	33%
Electric Ranges/Cooktops	48.4	58%	58.4	63%	65.3	66%	69.2	66%	71.0	65%
Gas Ranges/Cooktops	35.7	43%	36.1	39%	38.3	39%	39.4	38%	42.2	39%
Microwave Ovens	21.4	26%	77.2	83%	89.5	91%	94.6	91%	97.2	89%
Clothes Washers	61.5	74%	86.4	93%	94.3	95%	96.9	93%	90.1	83%
Electric Clothes Dryers	42.3	51%	56.1	60%	60.4	61%	61.8	59%	67.6	62%
Gas Clothes Dryers	12.3	15%	19.1	21%	21.1	21%	19.8	19%	20.7	19%
Personal Computers	N.A.	N.A.	N.A.	N.A.	43.5	44%	N.A.	N.A.	N.A.	N.A.
Number of U.S. Households	**83.6**		**94.0**		**98.9**		**107.0**		**108.8**	

Source(s): AHAM, AHAM 2005 Fact Book, 2006, Table 93, p. 28 for 1982, 1990, 2001 and 2005; AHAM, 2000 Major Home Appliance Industry Fact Book, Nov. 2000, Table 13, p. 21 for 1996; Consumer Electronic Manufacturers Association's Home Page, 1999 for 1997 personal computers; EIA, AEO 1995, Jan. 1995, Table B4, p. 104 for 1990 households; EIA, AEO 2004, Jan. 2004, Table A4 for 2001 households.

6.1.1 Key Definitions

Quad: Quadrillion Btu (10^15 or 1,000,000,000,000,000 Btu)

Generic Quad for the Buildings Sector: One quad of primary energy consumed in the buildings sector (includes the residential and commercial sectors), apportioned between the various primary fuels used in the sector according to their relative consumption in a given year. To obtain this value, electricity is converted into its primary energy forms according to relative fuel contributions (or shares) used to produce electricity in the given year.

Electric Quad (Generic Quad for the Electric Utility Sector): One quad of primary energy consumed at electric utility power plants to supply electricity to end-users, shared among various fuels according to their relative contribution in a given year. (Note: The consumption of an electric quad results in the delivery of just under 1/3 the electric quad due to generation and transmission losses.)

Primary Energy: The total energy consumed by an end-user, including the energy used in the generation and transmission of electricity. Also referred to as "source" energy.

Delivered Energy: The energy consumed by an end-user on site, not including electricity generation and transmission losses.

6.1.2 Consumption Comparisons in 2004

One quad equals:

- 49 million short tons of coal
  - = enough coal to fill a train of railroad cars 4,450 miles long (about one and a half times across the U.S.)
- 971 billion cubic feet natural gas
- 8 billion gallons of gasoline = 21 days of U.S. gasoline use
  - = 19.8 million passenger cars each driven 12,500 miles
  - = 17.0 million light-duty vehicles each driven 12,200 miles
  - = all new passenger cars and light-duty trucks sold, each driven 11,500 miles
  - = 12.7 million stock passenger cars, each driven 11,500 miles = 9% of all passenger cars, each driven 11,500 miles
  - = all new passenger cars each making 6 round-trips from New York to Los Angeles
- 172 million barrels of crude oil = 15 days of U.S. imports = 177 days of oil flow in the Alaska pipeline at full capacity
  - = the amount of crude oil transported by 483 supertankers
- 21 hours of world energy use
- the electricity delivered from 235 coal-fired power plants (200-MW each) in one year
- the electricity delivered from 37 nuclear power plants (1000-MW each) in one year
- average annual per capita consumption of 2.9 million people in the U.S.
- the approximate annual primary consumption of any one of the following states: Arkansas, Connecticut, Iowa, Kansas, Mississippi, Oregon, or West Virginia

Source(s): EIA, Annual Energy Outlook 2007, Feb. 2007, Table A2, p. 137-139, Table A7, p. 149-150, Table A8, p. 151-152, Table A9, p. 153-154, Table A11, p. 156-157 for consumption, Table G1, p. 229 for heat rates; EIA, State Energy Data 2004: Consumption, June 2007, Table S3, p. 5, Table R1, p. 13, and Table R2, p. 14; EIA, Electric Power Annual 2005, September 2006, Table 2.2, p. 19; EIA, International Energy Outlook 2007, May 2007, Table A1, p. 83; DOC, Statistical Abstract of the United States 2007, Oct. 2006, No. 1031, p. 658, No. 1074, p. 686, and No. 1080, p. 690; and Newport News Shipbuilding Web site.

6.1.3 Carbon Emission Comparisons

One million metric ton of carbon-equivalent emissions equals:

- the combustion of 1.92 million short tons of coal
- the coal input to 3 coal plants (200-MW) in one year
- the combustion of 67 billion cubic feet of natural gas
- the combustion of 430 million gallons of gasoline = the combustion of gasoline for 26 hours in the U.S.
  - = 1.0 million new cars, each driven 12,500 miles
  - = 889 thousand new light-duty vehicles, each driven 12,200 miles
  - = 853 thousand new light trucks, each driven 11,000 miles
  - = 0.5 million new passenger cars, each making 5 round trips from New York to Los Angeles
- the combustion of 694 million gallons of LPG
- the combustion of 388 million gallons of kerosene
- the combustion of 375 million gallons of distillate fuel
- the combustion of 321 million gallons of residual fuel
- 72 minutes of world energy emissions
- 5 hours of U.S energy emissions
- 14 hours of U.S. buildings energy emissions
- 26 hours of U.S. residential energy emissions
- 31 hours of U.S. commercial energy emissions
- 3 days of U.S. buildings lighting energy emissions
- average annual per capita emissions of 181,000 people in the U.S.

Source(s): EIA, Annual Energy Outlook (AEO) 2007, Feb. 2007, Table A2, p. 137-139, Table A7, p. 149-150 for consumption, Table A18, p. 167 for emissions, and Table G1, p. 229 for heat rates; EIA, Electric Power Annual 2005, September 2006, Table 2.2, page 19; EIA, International Energy Outlook 2007, May 2007, Table A10, p. 93; EIA, Assumptions to the AEO 2007, Mar. 2007, Table 2, p. 9 for carbon coefficients; and DOC, Statistical Abstract of the United States 2006, Jan. 2006, No. 2, p. 8 and No. 1084, p. 715.

6.1.4 Average Annual Carbon Dioxide Emissions for Various Functions

	Annual Unit Energy Consumption		Carbon Emissions (MTCE)	Carbon Emissions (lb CO2)
Stock Refrigerator	1,249	kWh - Electricity	0.22	1,800
Stock Electric Water Heater	2,549	kWh - Electricity	0.45	3,600
Stock Gas Water Heater	20	million Btu - Natural Gas	0.29	2,300
Stock Oil Water Heater	28	million Btu - Fuel Oil	0.56	4,500
Single-Family Home	107	million Btu	3.09	25,000
Mobile Home	76	million Btu	2.18	17,700
Multi-Family Unit in Large Building	41	million Btu	1.18	9,500
Multi-Family Unit in Small Building	78	million Btu	2.25	18,200
School Building	2,125	million Btu	71.54	578,400
Office Building	1,376	million Btu	46.32	374,500
Hospital, In-Patient	60,152	million Btu	2,025	16,372,500
Stock Vehicles				
Passenger Car	541	gallons - Gasoline	1.3	10,400
Van, Pickup Truck, or SUV	686	gallons - Gasoline	1.6	13,200
Heavy Truck	1,414	gallons - Diesel Fuel	3.5	28,100
Tractor Trailer Truck	11,697	gallons - Diesel Fuel	28.7	232,200

Source(s): EIA, Annual Energy Outlook (AEO) 2007, Feb. 2007, Table A2, p. 137-139 for consumption and Table A18, p. 164 for emissions, and Table G1, p. 229 for gasoline heat rate; EIA, A Look at Residential Energy Consumption in 2001, May 2004, Table CE4-1c for water heater energy consumption, Table HC5-1a for refrigerators and Table CE5-1c for refrigerator energy, and Table CE1-4c for household consumption; EIA, 2003 Commercial Buildings Energy Consumption Survey, June 2006, Table C3, p. 247 for commercial buildings; ORNL, Transportation Energy Data Book: Edition 26, 2007, Table 4.1, p. 4-2, Table 4.2, p. 4-3, Table 5.1, p. 5-2 and Table 5.2, p. 5-3 for vehicles; and EIA, Assumptions to the AEO 2007, Mar. 2007, Table 2, p. 9 for carbon coefficients.

6.2.1 2005 Impacts of Saving an Electric Quad (1)

Plant Fuel Type	Utility Fuel Input Shares (%)	Average-Sized Utility Unit (MW) in 2005	Aggregate Number of Units to Provide the Fuel's Share of the Electric Quad (2)
Natural Gas	15%	79	141
Petroleum	3%	17	95
Coal	52%	221	38
Nuclear	21%	1,015	3
Renewable (3)	9%	21	148
Total	100%		**424**

Note(s): 1) This table displays the breakdown of electric power plants that could be eliminated by saving an electric quad, in exact proportion to the actual primary fuel shares for electricity produced nationwide in 2005. Use this table to estimate the avoided capacity implied by saving one electric quad. 2) Based on the fact that typical U.S. power plants operate less than fully loaded throughout the year. 3) Includes pumped storage.

Source(s): EIA, Electric Power Annual 2005, Sept. 2006, Table 2.2, p. 19; and EIA, Annual Energy Outlook 2007, Feb. 2007, Table A2, p. 137-139 for consumption and Table A8, p. 151-152 for electricity supply.

6.2.2 2005 Existing Capacity by Energy Source (GW)

Plant Fuel Type	Number of Generators	Generator Nameplate Capacity	Net Summer Capacity	Net Winter Capacity
Coal	1,522	336	313	316
Petroleum	3,753	65	59	63
Natural Gas	5,467	437	383	412
Other Gases	102	2	2	2
Nuclear	104	106	100	102
Hydroelectric Conventional	3,993	77	78	77
Other Renewables	1,671	24	21	21
Pumped Storage	150	20	21	21
Other	45	1	1	1
Total	**16,807**	**1,067**	**978**	**1,015**

Source(s): EIA, Electric Power Annual 2005, Oct. 2006, Table 2.2, pg. 19.

6.2.3 Electric Capacity Factors, by Year and Fuel Type

	Coal	Petroleum	Natural Gas	Nuclear	Conventional Hydroelectric	Solar/PV	Wind
1990	59%	29%	25%	66%	45%	13%	18%
1995	63%	19%	29%	77%	45%	17%	21%
2000	71%	21%	31%	88%	40%	15%	27%
2001	69%	22%	29%	89%	31%	16%	20%
2002	70%	18%	25%	90%	38%	16%	27%
2003	72%	22%	21%	88%	40%	15%	21%
2004	72%	23%	22%	90%	39%	17%	25%
2005	73%	24%	23%	89%	40%	15%	23%
2006 (1)	72%	12%	24%	90%	42%	14%	26%

Note(s): 1) Preliminary.

Source(s) EIA, Annual Energy Review 2006, June 2007, 8.2a, pg. 226, Table 8.11a, pg. 260.

6.2.4 Electric Conversion Factors and Transmission and Distribution (T&D) Losses

	2005	2010	2015	2020	2025	2030
Average Utility Delivery Efficiency (1, 2)	31.4%	31.7%	32.2%	32.4%	32.9%	33.4%
Average Utility Delivery Ratio (Btu/kWh) (2, 3)	10,851	10,757	10,601	10,516	10,368	10,210

Transmission and Distribution (T&D) losses as a:

Percent of Electric Generator Fuel Input	3.1%
Percent of Net Electricity Generated (4)	9.5%

Note(s): 1) Use these values to convert primary energy of electric generator fuel input to*delivered* energy. 2) Accounts for fuel conversion losses, plant use of electricity, and T&D losses. 3) Use these values to convert*delivered* electric energy to primary energy. 4) After fuel conversion losses and plant use of electricity.

Source(s): EIA, Annual Energy Outlook 2007, Feb. 2007, Table A2, p. 137-139 for generator consumption and Table A8, p. 151-152 for electricity sales; and EIA, Annual Energy Review 2005, July 2006, Diagram 5, p. 223 for T&D losses.

6.2.5 Characteristics of New and Stock Generating Capacities, by Plant Type

	2006 Heat Rate	2015 Heat Rate	2006 Installed Capital Costs of a Typical Power Plant		
			Price	Size	Cost
New Plant Type	(Btu/kWh)	(Btu/kWh)	($2005 thousand per MW)	(MW)	($2005 million)
Pulverized Coal	8,844	8,661	1,290	600	774
Coal-Gasification Comb. Cycle	8,309	7,477	1,491	550	820
Combined Cycle	7,163	6,866	603	250	151
Advanced Combined-Cycle	6,717	6,403	594	400	238
Combustion Turbine	10,807	10,486	420	160	67
Advanced Combustion Turbine	9,166	8,612	398	230	92
Fuel Cell	7,873	6,960	4,520	10	45
Wind	10,280	10,280	1,206	50	60
Advanced Nuclear	10,400	10,400	2,081	1,350	2,809

Stock Plant Type	2005	2010	2015	2020	2025	2030
Fossil Fuel Steam Heat Rate (Btu/kWh)	10,662	10,455	10,311	10,181	10,024	9,825
Nuclear Energy Heat Rate (Btu/kWh)	10,421	10,421	10,421	10,421	10,421	10,421

Note(s): This table provides comparisons of electric generating plants. Plant use of electricity is included; however, transmission and distribution losses of the electric grid are excluded.

Source(s): EIA, Annual Energy Outlook (AEO) 2007, Feb. 2007, Table A2, p. 137-139, and Table A8, p. 151-152; EIA, Assumptions to the AEO 2007, March 2007, Table 48, p. 89 for fossil fuel heat rates, Table 39, p. 77 for other generator data.

6.2.6 Characteristics of New Commercial Distributed Generating Technologies, by Plant Type

	Efficiency (HHV)		2005 Installed Capital Costs of Typical DG Technologies			Service
		Electrical	Price	Size	Cost	Life
New Plant Type	Electrical	+ Thermal	($2005 per kW)	(kW)	($2005 thousand)	(years)
Solar Photovoltaic	0.16	N.A.	6,329	25	158	30
Fuel Cell	0.36	0.72	5,485	200	1,097	20
Natural Gas Engine	0.32	0.77	1,192	200	238	20
Oil-Fired Engine	0.31	0.82	1,308	200	262	20
Natural Gas Turbine	0.23	0.66	1,908	1000	1,908	20
Natural Gas Microturbine	0.30	0.63	1,709	200	342	20

Source(s): Discovery Insights, Final Report: Commercial and Industrial CHP Technology Cost and Performance Data Analysis for EIA's NEMS, Jan. 2006, Table 7, p. 12; and EIA, Annual Energy Review 2005, July 2006, Appendix D, p. 373.

6.2.7 Cost of an Electric Quad Used in the Buildings Sector ($2005 Billion)

	2005	2010	2015	2020	2025	2030
Residential	8.67	8.54	8.37	8.56	8.76	8.94
Commercial	7.94	7.77	7.51	7.77	7.97	8.11
Buildings Sector	**8.32**	**8.16**	**7.94**	**8.16**	**8.36**	**8.51**

Note(s): This table provides the consumer cost of an electric quad. Use this table to estimate the savings to consumers when a primary quad is saved in the form of delivered electricity.

Source(s): EIA, Annual Energy Outlook 2007, Feb. 2007, Table A2, p. 137-139 and Table A3, p. 140-141.

6.3.1 Cost of a Generic Quad Used in the Buildings Sector ($2005 Billion) (1)

	2005	2010	2015	2020	2025	2030
Residential	9.89	9.53	9.13	9.34	9.58	9.82
Commercial	8.64	8.15	7.74	7.99	8.21	8.38
Buildings Sector	**9.31**	**8.89**	**8.47**	**8.69**	**8.90**	**9.08**

Note(s): 1) See Table 6.1.1 for generic quad definition. This table provides the consumer cost of a generic quad in the buildings sector. Use this table to estimate the average consumer cost savings resulting from the savings of a generic (primary) quad in the buildings sector.
Source(s): EIA, Annual Energy Outlook 2007, Feb. 2007, Table A2, p. 137-139 and Table A17, p. 163 for energy consumption and Table A3, p. 140-141 for energy prices.

6.3.2 Shares of U.S. Buildings Generic Quad (Percent) (1)

					Renewables				
		Natural Gas	Petroleum	Coal	Hydro.	Other	Total	Nuclear	Total
2005	(2)	**31%**	**8%**	**38%**	**5%**	**3%**	**8%**	**15%**	**100%**
2010		31%	7%	38%	5%	4%	9%	14%	100%
2015		32%	7%	38%	5%	4%	9%	14%	100%
2020		31%	6%	39%	5%	4%	9%	14%	100%
2025		29%	6%	42%	5%	4%	9%	14%	100%
2030		27%	6%	45%	4%	4%	8%	13%	100%

Note(s): 1) See Table 6.1.1 for generic quad definition. 2) The total 2005 Buildings sector primary energy consumption was 39.69 quads.
Source(s): EIA, Annual Energy Outlook 2007, Feb. 2007, Table A2, p. 137-139 and Table A17, p. 163 for energy consumption.

6.3.3 Shares of U.S. Residential Buildings Generic Quad (Percent) (1)

					Renewables				
		Natural Gas	Petroleum	Coal	Hydro.	Other	Total	Nuclear	Total (3)
2005	(2)	**33%**	**9%**	**36%**	**5%**	**4%**	**8%**	**14%**	**100%**
2010		33%	8%	36%	5%	5%	10%	13%	100%
2015		33%	8%	36%	5%	5%	9%	13%	100%
2020		32%	7%	37%	5%	5%	9%	14%	100%
2025		31%	7%	40%	4%	4%	9%	13%	100%
2030		29%	7%	43%	4%	4%	9%	13%	100%

Note(s): 1) See Table 6.1.1 for generic quad definition. 2) The total 2005 Residential buildings sector primary energy consumption was 21.78 quads.
Source(s): EIA, Annual Energy Outlook 2007, Feb. 2007, Table A2, p. 137-139 and Table A17, p. 163 for energy consumption.

6.3.4 Shares of U.S. Commercial Buildings Generic Quad (Percent) (1)

					Renewables				
		Natural Gas	Petroleum	Coal	Hydro.	Other	Total	Nuclear	Total (3)
2005	(2)	**29%**	**7%**	**41%**	**5%**	**3%**	**8%**	**16%**	**100%**
2010		29%	6%	41%	5%	4%	9%	15%	100%
2015		30%	5%	41%	5%	4%	9%	15%	100%
2020		29%	5%	42%	5%	4%	9%	15%	100%
2025		27%	5%	44%	5%	4%	9%	15%	100%
2030		26%	5%	47%	5%	4%	8%	14%	100%

Note(s): 1) See Table 6.1.1 for generic quad definition. 2) The total 2005 Commercial buildings sector primary energy consumption was 17.91 quads.
Source(s): EIA, Annual Energy Outlook 2007, Feb. 2007, Table A2, p. 137-139 and Table A17, p. 163 for energy consumption.

6.4.1 Electric Quad Average Carbon Emissions with Average Stock Utility Fuel Mix and Projected New Marginal Capacity Fuel Mix (Million Metric Tons) (1)

	Stock	Projected New Marginal Capacity				
	2005	2010	2015	2020	2025	2030
Petroleum	0.69	0.00	0.00	0.00	0.00	0.00
Natural Gas	2.20	2.34	3.24	2.38	0.99	0.03
Coal	13.39	11.73	12.63	13.75	17.58	20.24
Nuclear	0.00	0.00	0.00	0.00	0.00	0.00
Renewable Energy (2)	0.08	0.06	0.11	0.07	0.06	0.05
Total	**16.36**	**14.13**	**15.97**	**16.20**	**18.63**	**20.33**

Note(s): 1) This table provides estimates of the carbon emissions resulting from consumption of a primary quad at electric utilities. Projected (2010-2030) new marginal capacity emissions will result from natural gas- and coal-fired power plants. Electric generation capacity is projected to increase for biomass, wind, and nuclear power. Biomass and wind power electric generation will increase 2007-2010. Nuclear electric generation capacity will increase 2016-2019. Electricity imports from utility consumption were ignored since this energy was produced outside of the U.S. "Average" means the weighted average of different fuels (e.g., petroleum is the average of residual and distillate fuel oils). The combustion of fossil fuels produces carbon in the form of carbon dioxide and carbon monoxide; however, carbon monoxide emissions oxidize in a relatively short time to form carbon dioxide. 2) Emissions from renewable energy include emissions released from geothermal power and non-biogenic emissions from municipal solid waste.

Source(s): EIA, Annual Energy Outlook 2007, Feb. 2007, Table A2, p. 137-139 and Table A18, p. 164.

6.4.2 Average Carbon Emissions from a Generic Quad in the Buildings Sector with Stock Fuel Mix and Projected Fuel Mix of New Marginal Utility Capacity and Site Energy Consumption (Million Metric Tons) (1)

	Stock			Projected Fuel Mix of New Marginal Utility Capacity and Site Consumption								
	2005			2010			2020			2030		
	Resid.	Comm.	Bldgs.	Resid.	Comm.	Bldgs.	Resid.	Comm.	Bldgs.	Resid.	Comm.	Bldgs.
Electricity (2)	11.11	12.55	11.76	12.58	13.55	13.08	14.01	13.75	13.86	18.32	16.26	17.04
Petroleum	1.33	0.85	1.11	0.32	0.07	0.20	0.33	0.09	0.20	0.36	0.09	0.19
Natural Gas	3.30	2.54	2.96	2.04	1.62	1.83	1.77	2.14	1.98	1.35	2.04	1.78
Renew. En. (3)	0.00	0.00	0.00	0.00	0.00	0.00	0.00	0.00	0.00	0.00	0.00	0.00
Coal	0.02	0.15	0.07	0.00	0.00	0.00	0.00	0.00	0.00	0.00	0.00	0.00
Total	**15.76**	**16.08**	**15.90**	**14.94**	**15.25**	**15.10**	**16.12**	**15.98**	**16.04**	**20.03**	**18.40**	**19.01**

Note(s): 1) This table provides estimates of the carbon emissions resulting from consumption of a generic quad in the buildings sector, at current and projected fuel shares. Projected increases in *site* energy will be primarily met by electricity and natural gas. Projected new marginal emissions will result from natural gas- and coal-fired power plants. Electricity imports from utility consumption were not included since this energy was produced outside of the U.S. "Average" means the weighted average of different fuels (e.g., petroleum is the average of residual and distillate fuel oils, LPG, kerosene, and motor gasoline). The combustion of fossil fuels produces carbon in the form of carbon dioxide and carbon monoxide; however, carbon monoxide emissions oxidize in a relatively short time to form carbon dioxide. 2) Includes renewables. 3) Emissions exclude wood since it is assumed that the carbon released from combustion is reabsorbed in a future carbon cycle.

Source(s): EIA, Annual Energy Outlook (AEO) 2007, Feb. 2007, Table A2, p. 137-139 and Table A17, p. 163 for energy consumption and Table A18, p. 164 for carbon emissions; and EIA, Assumptions to the AEO 2007, March 2007, Table 2, p. 9.

7.1.1 Program Definitions

DOE Weatherization: Department of Energy's Weatherization Assistance Program

DOE Weatherization Eligible Households: Households with incomes at or below 125% of the Federal poverty level, which varies by family size; however, a State may instead elect to use the LIHEAP income standard if its state LIHEAP income standard is at least 125% of the Federal poverty level. Data listed in this chapter include previously weatherized units. DOE Weatherization Eligible Households are a subset of Federally Eligible Households.

DOE Weatherization Recipient Households: Households that have received weatherization under DOE Weatherization funding.

Federally Eligible Households: Households with incomes below the Federal maximum standard of 150% of the poverty line or 60% of the state median income, whichever is higher.

HHS: Department of Health and Human Services

LIHEAP: HHS's Low Income Home Energy Assistance Program

LIHEAP Eligible Households: Households with incomes below the Federal maximum poverty income level, i.e., 150% of the Federal poverty guidelines or 60% of state median income, whichever is higher.

LIHEAP Recipient Households: Households that received fuel subsidies for home heating, cooling, or energy crisis benefits in the year previous to a particular household survey.

Source(s): ORNL, Scope of the Weatherization Assistance Program: Profile of the Population in Need, Mar. 1994, p. 1.2 for Weatherization eligible, Weatherization recipient, and LIHEAP eligible households; EIA, Housing Characteristics 1993, June 1995, p. 336 for Federally eligible for weatherization; and HHS, LIHEAP Report to Congress FY 2001, Feb. 2003, Table E-1, p. 105 and Figure 1, p. iii for LIHEAP recipient household.

7.1.2 Energy Burden Definitions

Energy burden is an important statistic for policy makers who are considering the need for energy assistance. Energy burden can be defined broadly as the burden placed on household incomes by the cost of energy, or more simply the ratio of energy expenditures to household income. However, there are different ways to compute energy burden, and different interpretations and uses of the energy burden statistics. DOE Weatherization primarily uses mean individual burden and mean group burden since these statistics provide data on how an "average" individual household fares against an "average" group of households (that is, how burdens are distributed for the population). DOE Weatherization (and HHS) also uses the median individual burden which shows the burden of a "typical" individual.

Mean Individual Burden: This statistic is calculated by first computing the energy burden for each household using RECS data and then taking a mean of the household-level energy burden estimates. It furnishes the most complete information about how a burden is distributed for the population.

Mean Group Burden: This statistic calculates energy expenditures for all households in the group and divides by the average of all incomes for the group. This statistic is calculated as the ratio between aggregate energy expenditures of a group (from RECS and CPS) and aggregate group income (from CPS).

Median Individual Burden: This statistic is computed by taking a median of the RECS household-level energy burden estimates (the point at which 50% of households have a higher burden value and 50% have a lower value).

Source(s): HHS, LIHEAP Report to Congress FY 2000, Apr. 2002, p. 45 for energy burden definition; HHS, Characterizing the Impact of Energy Expenditures on Low-Income Households: An Analysis of Alternative National Energy Burden Statistics, Nov. 1994, p. vii and ix for burdens; and ORNL, Scope of the Weatherization Assistance Program: Profile of the Population in Need, Mar. 1994, p. xii for mean individual and mean group burdens.

7.1.3 Households, by Weatherization Eligibility and Year (Million) (1)

	Weatherization Recipient			Federally	Federally	Below 125%	Total
	DOE	Other	Total	Eligible (2)	Ineligible	Poverty Line	Households
1977	0.03	-	0.03	N.A.	N.A.	N.A.	74.8
1980	0.18	-	0.18	N.A.	N.A.	N.A.	79.6
1985	0.13	0.17	0.30	N.A.	N.A.	N.A.	87.9
1987	0.10	0.21	0.31	N.A.	N.A.	18.2	90.5
1990	0.09	0.16	0.25	27.9	66.1	18.2	94.2
1991	0.11	0.13	0.23	N.A.	N.A.	N.A.	95.3
1992	0.11	0.12	0.22	N.A.	N.A.	N.A.	96.4
1993	0.09	0.12	0.21	30.7	65.9	19.4	96.6
1994	0.10	0.15	0.25	N.A.	N.A.	N.A.	98.7
1995	0.10	0.13	0.23	N.A.	N.A.	N.A.	100.0
1996	0.06	0.09	0.15	N.A.	N.A.	N.A.	101.0
1997	0.07	0.08	0.15	34.1	67.4	19.7	101.5
1998	0.07	0.09	0.16	N.A.	N.A.	N.A.	102.8
1999	0.07	0.09	0.16	N.A.	73.2	N.A.	104.1
2000	0.08	0.11	0.19	N.A.	N.A.	N.A.	105.2
2001	0.08	0.13	0.20	33.8	73.2	20.1	107.0
2002	0.10	0.10	0.20	N.A.	N.A.	N.A.	110.5
2003	0.10	0.09	0.19	N.A.	N.A.	N.A.	112.0
2004	0.10	0.07	0.17	N.A.	N.A.	N.A.	113.6
2005	0.09	0.08	0.17	N.A.	N.A.	N.A.	115.4
1977-2005	**2.91**	**2.93**	**5.84**	**N.A.**	**N.A.**	**N.A.**	**N.A.**

Note(s): 1) Year of receiving funding follows DOE Weatherization's Program Year of Apr. 1-Mar. 31. 2) Federally eligible for DOE and HHS (LIHEAP) Weatherization. Includes previously weatherized units.

Source(s): DOE for weatherization recipients; EIA, Housing Characteristics 1987, May 1989, Table 9, p. 20 for 1987 data; EIA, Housing Characteristics 1990, May 1992, Table 17, p. 54-55 for 1990 data; EIA, Housing Characteristics 1993, June 1995, Table 3.3a, p. 38-42 for 1993 data; EIA, Annual Energy Outlook (AEO) 1996, Jan. 1996,Table A4, p. 82-83 for 1992 and 1994 households; EIA, AEO 1998, Dec. 1997, Table A4, p. 106-107 for 1995-1996 households; EIA, AEO 2001, Dec.2000, Table A4, p. 133-134 for 1998-2000 households; EIA, AEO 2005, Feb. 2005, Table A4, p. 125-126 for 2002 households; EIA, AEO 2006, Feb. 2006, Table A4, p. 139-140 for 2003-2004 households; EIA, A Look at Residential Energy Consumption in 1997, Nov. 1999, Table HC1-3a, p. 38-39; EIA, RECS 1997 for eligible households; EIA, Residential Energy Consumption 2001, Apr. 2004, Table HC2-3a for 2001 eligible households; National Association for State Community Services programs: Weatherization Assistance Program PY 2005 Funding Survey for 2005 data; EIA, RECS 2001 for eligible households; and DOC, Income, Poverty, and Valuation of Noncash Benefits: 1994, Apr. 1996, Table B-1, for 1991 households.

7.1.4 Weatherization Population Facts

- Roughly 25% of Federally eligible households move in and out of poverty "classification" each year.
- The average income of Federally eligible households in FY 2005 was $16,264, based on RECS and Bureau of the Census' Current Population Survey (CPS) data.
- States target the neediest, especially the elderly, persons with disabilities, and families with children.
- Since the inception of the Weatherization Assistance Program in 1976, over 5.8 million households have received weatherization services.
- In FY 2005, the energy burden on Federally eligible households was over four and a half times the burden on Federally ineligible households (14.6% versus 3.2%).
- DOE weatherization saves an average of 13-34% on home energy bills (depending on main heating fuel). This equates to $1.54 in energy benefits being produced for every $1.00 invested. These services reduce average annual energy costs by $358 per household.

Note(s): For weatherization eligibility terminology, see Table 7.1.10. For acronyms, see Key Terminology.

Source(s): ORNL, Weatherization Works: Final Report on the National Weatherization Evaluation, Sept. 1994, p. 1 for migrating poor; ORNL, 1996 for targeting; HHS, LIHEAP Home Energy Notebook for FY 2005, May 2007, Table A-2a, p. 59 for Federally eligible average income and Table A-2b, p. 60 for energy burdens; ORNL, Progress Report of the National Weatherization Assistance Program, Sept. 1997, DOE, Weatherization Works, Progress Report of the National Weatherization Assistance Program, Feb. 1998; and EERE/OWIP, Weatherization Assistance Program Briefing Book, May 2006 for weatherization savings.

7.1.5 Weatherization Program Facts

- PY 2005 weatherization funding breakdown: DOE 36%, LIHEAP 36%, others 28%. (1)
- The Federal Government's outlay for fuel subsidies runs from $4.0 to 4.4 billion per year. The major two agencies dispensing fuel subsidies are HUD and HHS (through LIHEAP).
- HUD spends over $1.48 billion annually to pay all or part of the total utility bills (including water/sewer) for 1.2 million low-income households. Approximately 22% of public housing authorities' expenditures are for utilities (including water). In addition, HUD estimates tenant expenditures on utilities (excluding water) at about $278 million in 1997.
- LIHEAP spends 85% of its funding for direct fuel subsidies and weatherization. Up to 15% can be spent for weatherization activities and the remainder is spent on fuel subsidies. A maximum of 25% of funding is available for weatherization activities if HHS approves a waiver. LIHEAP weatherization funding has ranged from 8-19% of total LIHEAP funds. Since 2002, LIHEAP weatherization funding has been about 12% of total funds.

Note(s): 1) Program year is Apr. 1 - Mar. 31.

Source(s): National Association for State Community Services programs: Weatherization Assistance Program PY 2005 Funding Survey for spending; HHS, LIHEAP Report to Congress FY 1995, Aug. 1997, p. vii for LIHEAP weatherized households and Table 5, p. 15 for LIHEAP cost splits; HUD, Public Housing Operating Cost Study, June 2003, p. 67-68 for public housing utility costs; and HUD, Congressional Justifications for 2007 Estimates: Public Housing Operating Fund, Mar. 2006 for HUD spending.

7.1.6 Weatherization Costs and Savings

- DOE Weatherization program requires that States spend no more than an average of $2,885 per household in PY 2007. All States are using energy audits to determine the most cost-effective weatherization measures.
- In spite of funding reductions that reduced production, technical advances have produced 80% higher energy savings on a per-dwelling basis. Increases in energy savings were achieved through improvements in: diagnostic technology and techniques, weatherization materials and installation techniques, training, and audit tools.
- DOE weatherization creates an average energy savings of $358 per household, reduces household annual gas heating consumption 31% with a benefit-cost ratio of 1.53.

Source(s): EERE/OWIP, Weatherization Program Notice 07-1, Dec. 1, 2006 for average expenditures; ORNL, Weatherization Plus Progress Report: Poised to Move Forward, June 2001; and EERE/OWIP, Weatherization Assistance Program Briefing Book, May 2007 for savings.

7.1.7 Residential Energy Burdens, by Weatherization Eligibility and Year

	1987	1990		FY 2000 (1)			FY 2005 (2)		
	Mean Group	Mean Indvdl	Mean Group	Mean Indvdl	Mdn Indvdl	Mean Group	Mean Indvdl	Mdn Indvdl	Mean Group
Total U.S. Households	4.0%	6.8%	3.2%	6.1%	3.5%	2.4%	6.8%	3.7%	2.9%
Federally Eligible	**13.0%**	**14.4%**	**10.1%**	**12.1%**	**7.9%**	**7.7%**	**14.6%**	**8.6%**	**9.1%**
Federally Ineligible	4.0%	3.5%	N.A.	3.0%	2.6%	2.0%	3.2%	2.8%	2.3%
Below 125% Poverty Line	13.0%	N.A.	N.A.	N.A.	N.A.	N.A.	N.A.	N.A.	N.A.

Note(s): 1) Data are derived from RECS 1997, adjusted to reflect FY 2000 HDD, CDD, and fuel prices. 2) Data are derived from RECS 2001, adjusted to reflect FY 2004 HDD, CDD, and fuel prices.

Source(s): EIA, Household Energy Consumption and Expenditures 1987, Oct. 1989, Table 13, p. 48-50 for 1987 mean group burdens; ORNL, The Scope of the Weatherization Program: Profile of the Population in Need, Mar. 1994, p. xi. for 1990 Federally ineligible mean individual burden; HHS, Characterizing the Impact of Energy Expenditures on Low-Income Households: An Analysis of Alternative National Energy Burden Statistics, Nov. 1994, p. viii for 1990 total U.S. Households and Federally eligible burdens; HHS, LIHEAP Home Energy Notebook for FY 2000, Apr. 2000, Tables A-2a, A-2b, and A-2c, p. 48-50 for FY 2000; and HHS, LIHEAP Home Energy Notebook for FY 2005, May 2007, Tables A-2a, A-2b, and A-2c, p. 59-61.

7.1.8 FY 2005 Residential Energy Burdens, by Region (1)

	Northeast			South			Midwest			West		
	Mean Indvdl	Mdn Indvdl	Mean Group	Mean Indvdl	Mdn Indvdl	Mean Group	Mean Indvdl	Mdn Indvdl	Mean Group	Mean Indvdl	Mdn Indvdl	Mean Group
Total U.S. Households	8.9%	4.6%	3.3%	7.1%	3.9%	3.0%	6.6%	3.8%	3.1%	4.7%	2.8%	2.0%
Federally Eligible	**18.9%**	**10.2%**	**10.6%**	**15.7%**	**9.6%**	**9.9%**	**14.3%**	**8.9%**	**10.0%**	**9.4%**	**5.4%**	**6.0%**
Federally Ineligible	3.8%	3.4%	2.6%	3.2%	2.9%	2.5%	3.3%	3.0%	2.4%	2.5%	2.2%	1.7%

Note(s): 1) Data are derived from RECS 2001, adjusted to reflect FY 2004 HDD, CDD, and fuel prices. See Table 7.1.4 for totals and Table 7.1.10 for definitions.

Source(s): HHS, LIHEAP Home Energy Notebook for FY 2005, May 2007, Tables A-2a, A-2b, and A-2c, p. 59-61.

7.1.9 2001 Housing Unit Ownership, by Income Level and Weatherization Eligibility (in Millions)

	Single-Family		Multi-Family Unit		Mobile Home	
2001 Household Income	Own	Rent	Own	Rent	Own	Rent
Less than $15,000	5.7	2.9	0.3	8.0	1.2	0.4
$15,000 to $30,000	10.9	2.5	1.0	5.7	2.3	0.4
$30,000 to $49,999	16.4	2.8	1.2	5.2	1.3	0.2
All Households	63.2	10.5	3.9	22.6	5.7	1.1
Federally Eligible	**12.8**	**5.0**	**0.9**	**11.8**	**2.6**	**0.7**
Federally Ineligible	50.4	5.5	3.0	10.8	3.1	0.4
Below 100% Poverty Line	3.8	2.8	0.3	6.5	1.1	0.5

Source(s): EIA, 2001 Residential Energy Consumption Survey: Housing Characteristics Tables, Apr. 2004, Table HC1-3a.

7.1.10 2001 Average Energy Expenditures per Household Member and per Square Foot, by Weatherization Eligibility ($2005)

	Per Household Member	Members/ Hhold	Per Square Foot	Square Feet/ Hhold
Total U.S. Households	642	2.6	0.84	1,975
Federally Eligible	**527**	**2.7**	**0.98**	**1,435**
Federally Ineligible	697	2.5	0.79	2,225
Below 100% Poverty Line	489	2.6	1.02	1,227

Source(s): EIA, 2001 Residential Energy Consumption Survey: Household Energy Consumption and Expenditures Tables, Apr. 2004, Table CE1-5.1u and Table CE1-5.2u; and EIA, Annual Energy Review 2006, June 2007, Appendix D, p. 377 for implicit price deflators.

7.2.1 Operating Characteristics of Electric Appliances in the Residential Sector

	Power Draw (W) (1)			Annual Usage (hours/year)			Annual Consumption (kWh/year)	Annual Cost ($) (2)
	Active	Idle	Off	Active	Idle	Off		
Kitchen								
Coffee Maker	1,000	70	0	38	229	8,493	58	5
Dishwasher	(3) 0	0		(4) 365	0		120	11
Microwave Oven	1,500	0	3	70	0	8,690	131	12
Refrigerator-Freezer							730	69
Freezer							540	51
Lighting								
18-W Compact Fluorescent	18	0	0	1,189	0	0	20	2
60-W Incandescent Lamp	60	0	0	672	0	0	40	4
100-W Incandescent Lamp	100	0	0	672	0	0	70	7
Torchiere Lamp-Halogen	300	0	0	1,460	0	0	440	41
Bedroom and Bathroom								
Hair Dryer	710	0	0	50	0	0	40	4
Waterbed Heater	350	0	0	3,051	0	0	1,070	101
Laundry Room								
Clothes Dryer				(4) 359			1,000	94
Clothes Washer	(3) 0	0	0	(4) 392	0	0	(3) 110	10
Home Electronics								
CPU & Monitor	182/30	0	1337/632		0		260	24
Stereo Systems	33	30	3	1,510	1,810	5,440	119	11
Television	113		4	1,460		7,300	193	18
Analog, <40"	86			(5) 1,095			184	17
Analog, >40"	156			(5) 1,825			312	29
Digital, ED/HD TV, <40"	150			(5) 1,095			301	28
Digital, ED/HD TV, >40"	234			(5) 1,825			455	43
Set-top box	20	0	20	6,450	0	2,310	178	17
DVD/VCR	17	13	3	170	5,150	3,430	78	7
Heating and Cooling								
Dehumidifier	600	0		1,620	0		970	91
Furnace Fan	295	0		1,350	0		400	38
Ceiling Fan (only fan motor)	35			2,310			81	8
Water Heating								
Water Heater-Family of 4	4,500			(6) 64	N.A.	0	4,770	448
Water Heater-Family of 2	4,500			(6) 32	N.A.	0	2,340	220
Portable Spa	4,350	275	0	25	8,735	0	2,525	237
Miscellaneous								
Pool Pump	1,000	0		792	0		790	74
Well Pump	725	0		115	0		80	8
Total Standby	0	57		0	8,760		500	47

Note(s): 1) Power draw will vary due to appliance components and modes of operation. 2) $0.094/kWh. 3) Excludes electricity for water heating and drying. 4) Cycles/year. 5) TVs <40" are estimated on 3 hours/day and TVs >40" are estimated on 5 hours/day. 6) Gallons/day.

Source(s): BTS/A.D. Little, Electricity Consumption by Small End Uses in Residential Buildings, Aug. 1998, Exhibit 6-8, p. 6-10 for clothes washer, computer, dehumidifier, dishwasher, furnace fan, pool pump, torchiere lamp-halogen, waterbed heater, and well pump; LBNL, Energy Data Sourcebook for the U.S. Residential Sector, LBNL-40297, Sept. 1997, p. 100-102 for clothes dryers, Table 10.2, p. 108 for lighting, and p. 62-67 for water heaters; LBNL, Miscellaneous Electricity Use in the U.S. Residential Sector, LBNL-40295, Apr. 1998, Appendix D for hair dryer; EIA, Supplement to AEO 2007, Feb. 2007, Table 21 for refrigerator and freezer; GAMA, Consumer's Directory of Certified Efficiency Ratings for Heating and Water Heating Equipment, Apr. 2000 for water heater power draw; EIA/TIAX, Commercial and Residential Sector Miscellaneous Electricity Consumption: Y2005 and Projections to 2030, Sept. 2006, p. 41-60 for coffee maker, microwave oven, stereo systems, TVs, set-top box, DVD/VCR, ceiling fan, and portable spa; and LBNL for total standby.

7.2.2 Operating Characteristics of Natural Gas Appliances in the Residential Sector

	Average Capacity (10^3 Btu/hr)	Appliance Usage		Annual Consumption (10^6 Btu/year)	Annual Cost ($) (1)
Range	10			4	52
Clothes Dryer		359	(2)	4	53
Water Heating					
Water Heater-Family of 4	40	64	(3)	26	320
Water Heater-Family of 2	40	32	(3)	12	152

Note(s): 1) $1.24/therm. 2) Cycles/year. 3) Gallons/day.

Source(s): A.D. Little, EIA-Technology Forecast Updates - Residential and Commercial Building Technologies - Reference Case, Sept. 2, 1998, p. 30 for range and clothes dryer; LBNL, Energy Data Sourcebook for the U.S. Residential Sector, LBNL-40297, Sept. 1997, p. 62-67 for water heating; GAMA, Consumer's Directory of Certified Efficiency Ratings for Heating and Water Heating Equipment, Apr. 2002, for water heater capacity; and AGA, Gas Facts 1998, Dec. 1999, www.aga.org for range and clothes dryer consumption.

7.2.3 Operating Characteristics of Electric Equipment in the Commercial Sector

	Power Draw (kW) (1)			Annual Usage (hours/year)			Annual Consumption	
	Active	Standby	Off	Active	Standby	Off	(kWh/year)	($) (2)
Medical Imaging Equipment								
MRI	25.0	11.0	7.0	340	3,310	5,110	81,000	6,966
CT	21.0	N.A.	1.7	3,000	N.A.	5,760	73,000	6,278
X-ray	4.0	N.A.	1.6	4,380	N.A.	4,380	24,800	2,133
Vertical Transport								
Elevator	10.0	0.5	0.3	300	8,460	0	7,400	636
Escalator	4.7	N.A.	0.0	4,380	N.A.	4,380	20,500	1,763
Distribution Transformer (3)								
Dry	10.3 W/kVA			8,760	N/A	N/A		
Liquid	4.2 W/kVA			8,760	N/A	N/A		
Water Systems								
Distribution				17,700	billion gallons per year		2,230 kWh/10^6 gal	178
Purification				16,500	billion gallons per year		65 kWh/10^6 gal	5.2
Treatment				14,280	billion gallons per year		1,649 kWh/10^6 gal	132

Note(s): 1) Power draw will vary due to modes of operation. 2) $0.086/kWh. 3) Losses from stepping down power distributed at higher voltages to lower voltages.

Source(s): EIA/TIAX, Commercial and Residential Sector Miscellaneous Electricity Consumption: Y2005 and Projections to 2030, Sept. 2006, p. 16-37; and EIA, Annual Energy Outlook 2007, Feb. 2007, Table A3, p. 140-141 for electricity price.

7.3.1 2001 *Delivered* Energy End-Uses for an Average Household, by Region (Million Btu per Household)

	Northeast	Midwest	South	West	National
Space Heating	63.1	66.8	27.7	29.7	43.9
Space Cooling	3.3	5.1	11.5	5.4	7.7
Water Heating	18.0	17.4	13.9	15.1	15.8
Refrigerator	4.2	4.9	6.0	4.0	5.0
Other Appliances & Lighting	20.1	23.7	24.3	20.2	22.5
Total (1)	**106.6**	**116.7**	**82.5**	**70.1**	**92.2**

Note(s): 1) Due to rounding, sums do not add up to totals.
Source(s): EIA, A Look at Residential Energy Consumption in 2001, Apr. 2004, Table CE1-9c, Table CE1-10c, Table CE1-11c, and Table CE1-12c.

7.3.2 2001 End-Use Carbon Dioxide Emissions Splits for an Average Household, by Region (Pounds of CO2)

	Northeast	Midwest	South	West	National
Space Heating	9,083	8,690	4,890	4,467	6,475
Space Cooling	1,467	2,063	4,742	2,170	3,197
Water Heating	2,936	2,625	3,135	2,530	2,914
Refrigerator	1,444	2,041	2,463	1,796	2,068
Other Appliances & Lighting	6,957	8,694	9,224	7,125	8,177
Total	**21,888**	**24,113**	**24,455**	**18,089**	**22,830**

Source(s): EIA, A Look at Residential Energy Consumption in 2001, Apr. 2004, Tables CE(2-5)-(9-12)c; EIA, Annual Energy Outlook 2007, Feb. 2007, Table A2, p. 137-139, Table A17, p. 163 for consumption data, and Table A18, p. 164 for emissions data; and EIA, Assumptions to the AEO 2007, Feb. 2007, Table 2, p. 9 for coefficients.

7.3.3 2001 Energy End-Use Expenditures for an Average Household, by Region ($2005)

	Northeast	Midwest	South	West	National
Space Heating	777	681	402	358	529
Space Cooling	122	135	311	173	217
Water Heating	248	203	237	202	224
Refrigerator	165	134	159	131	149
Other Appliances & Lighting	654	570	596	542	589
Total (1)	**1,917**	**1,697**	**1,684**	**1,286**	**1,644**

Note(s): 1) Due to rounding, end-uses do not sum to totals.
Source(s): EIA, A Look at Residential Energy Consumption in 2001, Apr. 2004, Table CE1-9e, Table CE1-10e, Table CE1-11e, and Table CE1-12e; EIA, Annual Energy Review 2006, June 2007, Appendix D, p. 377 for price deflators.

7.3.4 Materials Used in the Construction of a 2,272-Square-Foot Single-Family Home, 2000

13,837 board-feet of lumber
13,118 square feet of sheathing
19 tons of concrete
3,206 square feet of exterior siding material
3,103 square feet of roofing material
3,061 square feet of insulation
6,050 square feet of interior wall material
2,335 square feet of interior ceiling material
226 linear feet of ducting
19 windows
4 exterior doors (3 hinged, 1 sliding)
2,269 square feet of flooring material
12 interior doors
6 closet doors
2 garage doors
1 fireplace
3 toilets; 2 bathtubs; 1 shower stall
3 bathroom sinks
15 kitchen cabinets; 5 other cabinets
1 kitchen sink
1 range; 1 refrigerator; 1 dishwasher; 1 garbage disposer; 1 range hood
1 washer; 1 dryer
1 heating and cooling system

Source(s): NAHB, 2004 Housing Facts, Figures and Trends, Feb. 2004, p. 7; D&R International for appliances and HVAC.

7.3.5 Characteristics of a Typical Single-Family Home (1)

Year Built	late 1960s		Building Equipment	Type	Fuel	Age (5)
Occupants	3		Space Heating	Central Warm-Air Furnace	Natural Gas	12
Floorspace			Water Heating	50 Gallons	Natural Gas	9
Heated Floorspace	2047		Space Cooling	Central Air Conditioner		9
Cooled Floorspace	2061					
Garage	2-Car					
Stories	1		Appliances	Type / Fuel / Number	Size	Age (5)
Foundation	Basement		Refrigerator	2-Door	19 Cubic Feet	8
Total Rooms (2)	6		Clothes Dryer	Electric		
Bedrooms	3		Clothes Washer	Top Loading		
Other Rooms	3		Range/Oven	Electric		
Full Bathroom	2		Microwave Oven			
Half Bathroom	0		Dishwasher			
Windows			Color Televisions	3		
Area (3)	235		Ceiling Fans	3		
Number (4)	16		Computer			
Type	Single-Pane		Printer			
Frame	Nonmetal					
Insulation: Well or Adequate						

Note(s): 1) This is a weighted-average house that has combined characteristics of the Nation's stock homes. Although the population of homes with similar traits may be few, these are likely to be the most common. 2) Excludes bathrooms. 3) 11.5% of floorspace. 4) Based on a nominal 3' X 5' window. 5) Years.

Source(s): EIA, A Look at Residential Energy Consumption in 2001, Apr. 2004, Table HC1-4a, HC2-4a, Table HC3-4a, Table HC4-4a, Table HC5-4a, Table HC6-4a, Table HC7-4a, Table CE2-4c, and Table CE3-4c; and EIA, Housing Characteristics 1993, June 1995, Table 3.29a, p. 168-173 for windows area.

7.4.1 1995 Commercial Buildings *Delivered* Energy End-Use Intensities, by Building Activity (Thousand Btu per SF) (1)

	Education	Food Sales	Food Service	Health Care	Lodging	Mercantile & Service	Office
Space Heating	32.8	27.5	30.9	55.2	22.7	30.6	24.3
Space Cooling	4.8	13.4	19.5	9.9	8.1	5.8	9.1
Ventilation	1.6	4.4	5.3	7.2	1.7	2.5	5.2
Water Heating	17.4	9.1	27.5	63.0	51.4	5.1	8.7
Lighting	15.8	33.9	37.0	39.3	23.2	23.4	28.1
Cooking	1.4	5.6	77.5	11.2	6.6	1.5	1.1
Refrigeration	1.0	110.9	31.6	4.7	2.3	0.9	0.4
Office Equipment	1.5	1.3	2.6	15.5	3.8	2.9	15.1
Other	2.9	7.4	13.7	34.4	7.5	3.7	5.2
Total	**79.3**	**213.5**	**245.5**	**240.4**	**127.3**	**76.4**	**97.2**

	Public Assembly	Public Order & Safety	Religious Worship	Warehouse & Storage	Other	Vacant	All Buildings
Space Heating	53.6	27.8	23.7	15.7	59.6	11.9	29.0
Space Cooling	6.3	6.1	1.9	0.9	9.3	0.6	6.0
Ventilation	3.5	2.3	0.9	0.3	8.3	0.3	2.8
Water Heating	17.5	23.4	3.2	2.0	15.3	2.4	13.8
Lighting	21.9	16.4	5.0	9.8	26.7	3.6	20.4
Cooking	2.8	N.A.	0.5	-	N.A.	N.A.	3.7
Refrigeration	1.8	0.2	0.6	1.7	0.7	0.2	3.1
Office Equipment	2.4	5.8	0.4	4.4	15.2	0.5	5.7
Other	3.8	12.7	1.1	3.4	35.9	1.9	6.1
Total	**113.7**	**97.2**	**37.4**	**38.3**	**172.2**	**21.5**	**90.5**

Note(s): 1) Due to rounding, end-uses do not sum to total.

Source(s): EIA, A Look at Commercial Buildings in 1995: Characteristics, Energy Consumption, and Energy Expenditures, Oct. 1998, Table EU-2, p. 311.

7.4.2 Typical Office Building (1)

	Large (>= 25,000 SF)	Small (<25,000 SF)
Stock Floor Area (billion SF)	**8.22**	**4.29**
Floor-Area Weighted Averages		
Building Area (thousand SF)	90 - 137	5.5 - 6.6
Floors	39,240	39,084
Shell		
Percent Glass	40 - 50	15 - 20
Window R-Value	1.39 - 1.71	1.34 - 1.99
Window Shading Coefficient	0.69 - 0.8	0.71 - 0.82
Wall R-Value	2.5 - 6.0	3.9 - 6.3
Roof R-Value	9.1 - 12.6	10.5 - 13.3
Wall Material	masonry	masonry
Roof Material	built-up	built-up
Occupancy		
Average Occupancy (SF/person)	390 - 460	420 - 470
Weekday Hours (hrs/day)	12	11
Weekend Hours (hrs/day)	5	4
Equipment		
Average Power Density (W/SF)	1	1
Full Lighting Hours (hrs/year)	3,580	3,360
Lighting		
Average Power Density (W/SF)	1.3 - 1.8	1.7 - 2.2
Full Lighting Hours (hrs/year)	4,190	3,340
System and Plant		
System and Distribution Type	Constant Volume w/ Reheat VAV w/ Economizer	Packaged Single-Zone Packaged Single-Zone w/ Economizer
Heating Plant	Gas Boiler	Gas Furnace
Cooling Plant	Hermetic Centrifugal Chiller	Direct Expansion
Service Hot Water	Gas Boiler	Gas Water Heater

Note(s): 1) The prototypes are synthetic buildings compiled from statistical data from building surveys or conclusions from previous studies. The physical characteristics, system characteristics, and usage patterns are based upon various surveys, studies, engineering estimates, or engineering judgment.

Source(s): LBNL, Commercial Heating and Cooling Loads Component Analysis, Nov. 1999, Table 10, p. 31.

7.4.3 Typical School Building (1) (2)

	Pre-1980	Post-1980
Stock Floor Area (billion SF)	7.5	0.6
Floor-Area Weighted Averages		
Building Area (thousand SF)	22 - 47	16 - 26
Floors	2	2
Shell		
Percent Glass	27.0	18.0
Window R-Value	1.39 - 1.6	1.67 - 1.71
Window Shading Coefficient	0.80 - 0.83	0.71 - 0.73
Wall R-Value	2.7 - 3.4	5.3 - 5.7
Roof R-Value	10.1 - 10.9	12.6 - 13.3
Wall Material	masonry	masonry
Roof Material	built-up	built-up
Occupancy		
Average Occupancy (SF/person)	105	105
Weekday Hours (hrs/day)	8.0	8.0
Weekend Hours (hrs/day)	2.0	2.0
Equipment		
Average Power Density (W/SF)	0.8	0.8
Full Equipment Hours (hrs/year)	1,136	1,136
Lighting		
Average Power Density (W/SF)	1.8	1.7
Full Lighting Hours (hrs/year)	2,436	2,436
System and Plant		
System and Distribution Type	6 (Classrooms, Gym, Auditorium, Dining, Kitchen) Unit Ventilators	1 Central System Packaged Multi-Zone w/ Economizer
Heating Plant	Gas Boiler	Gas Boiler
Cooling Plant	Hermetic Centrifugal Chiller	Hermetic Centrifugal Chiller
Service Hot Water	Gas Boiler	Gas Boiler

Note(s): 1) The prototypes are synthetic buildings compiled from statistical data from building surveys or conclusions from previous studies. The physical characteristics, system characteristics, and usage patterns are based upon various surveys, studies, engineering estimates, or engineering judgment. 2) For additional data on Educational Facilities, see Section 7.5.

Source(s): LBNL, Commercial Heating and Cooling Loads Component Analysis, June 1998, Table 15, p. 36; and D&R for hours of occupancy.

7.4.4 Typical Mercantile & Service (Retail) Building (1)

	Retail (>= 25,000 SF)	Retail (<25,000 SF)
Stock Floor Area (billion SF)	5.88	6.53
Floor-Area Weighted Averages		
Building Area (thousand SF)	80	5.3 - 6.4
Floors	2	1
Shell		
Percent Glass	15	15
Window R-Value	1.39 - 1.71	1.24 - 1.71
Window Shading Coefficient	0.74 - 0.79	0.85
Wall R-Value	3.1 - 6.4	2.5 - 6.6
Roof R-Value	10.6 - 14.0	9.5 - 13.2
Wall Material	masonry	masonry
Roof Material	built-up	built-up
Occupancy		
Average Occupancy (SF/person)	390 - 460	1,635 - 2,085
Weekday Hours (hrs/day)	12	12
Weekend Hours (hrs/day)	5	4
Equipment		
Average Power Density (W/SF)	0.40	0.50
Full Equipment Hours (hrs/year)	4,750 - 5,850	3,480
Lighting		
Average Power Density (W/SF)	1.6 - 2.1	1.7 - 2.2
Full Lighting Hours (hrs/year)	4,500 - 5,245	3,786 - 4,412
System and Plant		
System and Distribution Type	Constant Volume w/ Reheat VAV w/ Economizer	Packaged Single-Zone Packaged Single-Zone w/ Economizer
Heating Plant	Gas Boiler	Gas Furnace
Cooling Plant	Hermetic Centrifugal Chiller	Direct Expansion
Service Hot Water	Gas Boiler	Gas Water Heater

Note(s): 1) The prototypes are synthetic buildings compiled from statistical data from building surveys or conclusions from previous studies. The physical characteristics, system characteristics, and usage patterns are based upon various surveys, studies, engineering estimates, or engineering judgment.

Source(s): LBNL, Commercial Heating and Cooling Loads Component Analysis, June 1998, Table 11, p. 32.

7.4.5 Typical Hospital Building (1)

	Pre-1980	Post-1980
Stock Floor Area (billion SF)	1.43	0.21
Floor-Area Weighted Averages		
Building Area (thousand SF)	66.2	156
Floors	6	12
Shell		
Percent Glass	25	25
Window R-Value	1.79	1.96
Window Shading Coefficient	0.71	0.66
Wall R-Value	0.3	6.9
Roof R-Value	12.3	11.5
Wall Material	masonry	masonry
Roof Material	built-up	built-up
Occupancy		
Average Occupancy (SF/person)	190	190
Weekday Hours (hrs/day)	24	24
Weekend Hours (hrs/day)	24	24
Equipment		
Average Power Density (W/SF)	2.20	2.20
Full Equipment Hours (hrs/year)	6,962	6,962
Lighting		
Average Power Density (W/SF)	2.1	2.1
Full Lighting Hours (hrs/year)	6,752	6,752
System and Plant		
System and Distribution Type	4-Pipe Fan-Coil in Rooms Reheat in Lobby & Core Single-Zone Reheat in Kitchen Dual-Duct in Kitchen	4-Pipe Fan-Coil in Rooms VAV in Lobby & Core Single-Zone Reheat in Kitchen Dual-Duct in Kitchen
Heating Plant	Gas Boiler	Gas Boiler
Cooling Plant	Hermetic Centrifugal Chiller	Direct Expansion
Service Hot Water	Gas Boiler	Gas Boiler

Note(s): 1) The prototypes are synthetic buildings compiled from statistical data from building surveys or conclusions from previous studies. The physical characteristics, system characteristics, and usage patterns are based upon various surveys, studies, engineering estimates, or engineering judgment.

Source(s): LBNL, Commercial Heating and Cooling Loads Component Analysis, June 1998, Table 14, p. 35.

7.5.1 1995 Energy End-Use Intensities and Consumption of Educational Facilities, by Building Activity (1)

	(10^12 Btu)		(1000 Btu/SF)
Space Heating	254	41%	32.8
Space Cooling	37	6%	4.8
Ventilation	13	2%	1.6
Water Heating	134	22%	17.4
Lighting	122	20%	15.8
Cooking	11	2%	1.4
Refrigeration	8	1%	1.0
Office Equipment	11	2%	1.5
Other	22	4%	2.9
Total (2)	**614**	100%	**79.3**

Note(s): 1) Educational facilities include K-12 as well as higher education facilities. 2) Due to rounding, sum does not add up to total.
Source(s): EIA, Commercial Building Energy Consumption and Expenditures 1995, Apr. 1998, Table 1 for total energy consumption, Table 2 for energy intensities, and Table 4 for expenditures.

7.5.2 2003-2004 Number of Public K-12 Schools in the United States and Students per School

Number of Schools (2004-2005)		Average Number of Students per School (2003-2004)(3)	
Regular (1)	86,487	Elementary	438
Special	1,635	Middle	616
Vocational	326	High	758
Alternative	4,847	Other	266
Total (2)	**93,295**		

Note(s): 1) Regular schools are those responsible for providing free public education for school age children residing within their jurisdiction. 2) Data is based on total number of schools reporting current student enrollment, which varies from the actual number of schools, 96,296. "Special" focuses primarily on special education with materials and instructional approaches to meet the needs of the students. A "vocational" school focuses on technical or career skills and training. An "alternative" school addresses the needs of students that typically cannot be met in a traditional school setting. 3) Averages are for "regular" schools.
Source(s): U.S. Department of Education/National Center for Educational Statistics (NCES), Public Elementary and Secondary Students, Staff, Schools, and School Districts: School Year 2003-04, Feb. 2006, Table 1, p. 3 and Table 8, p. 19.

7.5.3 National Enrollment and Expenditures for Public K-12 Facilities ($2005)

	Enrollment (millions)	Expenditures ($ billion)	Expenditures per Pupil
1986	39.42	277.7	7,045
1990	40.54	330.4	8,149
1995	44.11	361.3	8,191
2000	46.86	426.3	9,098
2003	48.18	474.1	9,840
2005	48.56	496.9	10,293
2010	49.27	555.8	11,403
2015	50.74	653.3	12,878

Source(s): NCES, Projections of Educational Statistics to 2016, Sept. 2006, Table 33, p. 82 for 1990-2014; NCES, Projections of Educational Statistics to 2011, Oct. 2001, Table 33, p. 88 for 1986; and EIA, Annual Energy Review 2006, June 2007, Appendix D, p. 377 for price inflators.

7.5.4 Total Expenditures for K-12 Plant Operations and Maintenance, by Function ($2005 Billion)

	1990		1995		2000		2002	
Salaries and Benefits	15.9	54%	16.6	53%	19.4	51%	20.6	52%
Purchased Services	7.9	27%	9.4	30%	10.9	28%	10.7	27%
Supplies	5.2	18%	5.2	16%	7.7	20%	8.2	20%
Other	0.4	2%	0.3	1%	0.3	1%	0.4	1%
Total	**29.4**	100%	**31.5**	100%	**38.4**	100%	**39.8**	100%

Note(s): 1) Operation and maintenance services include salaries, benefits, supplies, and contractual fees for supervision of operations and maintenance, operating buildings (heating, lighting, ventilating, repair and replacement), care and upkeep of grounds and equipment, vehicle operation and maintenance (other than student transportation), security and other operations and maintenance services.

Source(s): NCES, Digest of Educational Statistics 2005, July 2006, Table 160, p. 263-264; EIA, Annual Energy Review 2006, June 2007, Appendix D, p. 377 for price inflators.

7.5.5 New Construction and Renovations Expenditures for Public K-12 Schools ($2006 Billion)

	New Schools	Additions	Modernizations	Total
1996	6.08	4.12	3.35	13.55
1997	7.43	4.34	3.29	15.06
1998	9.49	6.18	4.88	20.55
1999	7.08	6.01	5.93	19.01
2000	13.36	4.73	6.93	25.02
2001	12.68	4.79	12.87	30.34
2002	13.01	6.34	7.81	27.17
2003	19.15	5.80	6.48	31.44
2004	14.02	5.91	10.89	30.82
2005	12.64	6.33	4.65	23.63
2006	13.70	3.29	8.34	25.33

Source(s): American School and University, 23rd Annual Official Education Report, May 1997 for 1996; American School and University, 24th Annual Official Education Report, May 1998 for 1997; American School and University, 25th Annual Official Education Report, May 1999 for 1998; American School and University, 26th Annual Official Education Report, May 2000 for 1999; American School and University, 27th Annual Official Education Report, May 2001, Table 1, p. 26 for 2000; American School and University, 28th Annual Official Education Report, May 2002, Table 1, p. 24 for 2001; American School and University, 29th Annual Official Education Report, May 2003, Table 1, p. 29 for 2002; American School and University, 30th Annual Official Education Report, May 2004, Table 1, p. 24 for 2003; American School and University, 31st Annual Official Education Report, May 2005, Table 1, p. 29 for 2004; American School and University, 32nd Annual Official Education Report, May 2006, Table 1, p. 24 for 2005; American School and University, 33rd Annual Official Education Report, May 2007, Table 1, p. 30 for 2006; and EIA, Annual Energy Review 2006, June 2007, Appendix D, p. 377.

7.5.6 Percentage of Public K-12 Schools with Inadequate Building Features (1)

	Small		Medium		Large	
	1995	1999	1995	1999	1995	1999
Roofs	26%	24%	25%	22%	32%	22%
Framing, floors, and foundations	18%	19%	18%	12%	17%	14%
Exterior walls, finishes, windows, and doors	26%	31%	26%	21%	28%	23%
Interior finishes	23%	20%	23%	16%	27%	18%
Plumbing	33%	28%	28%	27%	30%	20%
HVAC	36%	29%	35%	32%	39%	26%
Electrical power	28%	23%	25%	21%	27%	22%
Electrical lighting	25%	19%	24%	17%	26%	16%

Note(s): 1) Small school is defined as having 1-299 students, medium 300-599 students, and a large school has 600 or more students.

Source(s): National Center for Education Statistics, Digest of Educational Statistics 2005, July 2006, Table 100, p. 176-177 for 1999; and U.S. GAO, Health, Education, and Human Services Division, America's Schools Report Differing Conditions, GAO/HEHS-96-103, June 1996, Table II.9, p. 45 for 1995.

Thermal Conversion Factors

Fuel	Units	Approximate Heat Content
Coal		
Production	million Btu per short	20.363
Consumption	million Btu per short	20.231
Coke Plants	million Btu per short	26.291
Industrial	million Btu per short	22.178
Residential and Commercial	million Btu per short	22.264
Electric Power Sector	million Btu per short	19.970
Imports	million Btu per short	25.009
Exports	million Btu per short	25.431
Coal Coke	million Btu per short	24.800
Crude Oil		
Production	million Btu per barrel	5.800
Imports	million Btu per barrel	5.977
Petroleum Products		
Consumption	million Btu per barrel	5.373
Motor Gasoline	million Btu per barrel	5.218
Jet Fuel	million Btu per barrel	5.670
Distillate Fuel Oil	million Btu per barrel	5.799
Residual Fuel Oil	million Btu per barrel	6.287
Liquefied Petroleum Gas	million Btu per barrel	3.620
Kerosene	million Btu per barrel	5.670
Petrochemical Feedstocks	million Btu per barrel	5.523
Unfinished Oils	million Btu per barrel	5.825
Imports	million Btu per barrel	5.496
Exports	million Btu per barrel	5.741
Natural Gas Plant Liquids		
Production	million Btu per barrel	3.724
Natural Gas		
Production, Dry	Btu per cubic foot	1,030
Consumption	Btu per cubic foot	1,030
End-Use Sectors	Btu per cubic foot	1,030
Electric Power Sector	Btu per cubic foot	1,029
Imports	Btu per cubic foot	1,024
Exports	Btu per cubic foot	1,009
Electricity Consumption	Btu per kilowatthour	3,412

Note(s): Conversion factors vary from year to year.

Source(s): DOE, EIA, Annual Energy Outlook 2007, Feb. 2007, Table G1, p. 229.



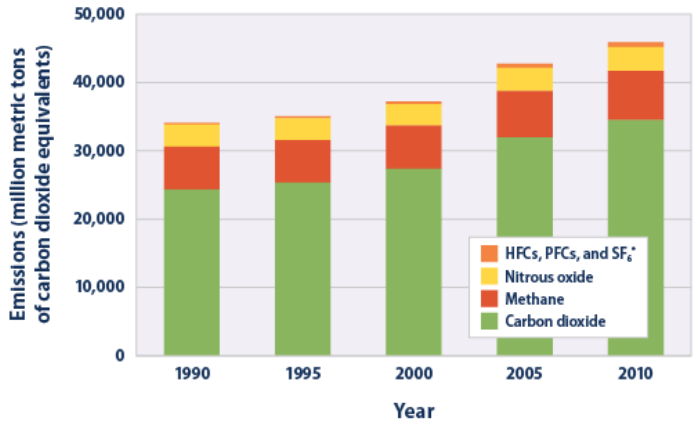
buildingsdatabook.eere.energy.gov

Climate Change

Climate Change Indicators in the United States



Figure 1. Global Greenhouse Gas Emissions by Gas, 1990–2010



Share this indicator:

Web update: May 2014

This figure shows worldwide emissions of carbon dioxide, methane, nitrous oxide, and several fluorinated gases from 1990 to 2010. For consistency, emissions are expressed in million metric tons of carbon dioxide equivalents. These totals include emissions and sinks due to land-use change and forestry.

* HFCs are hydrofluorocarbons, PFCs are perfluorocarbons, and SF_6 is sulfur hexafluoride.

Data source: WRI, 2014;[2] FAO, 2014[3]

Larger image to save or print

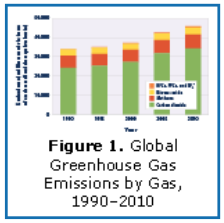


Figure 1. Global Greenhouse Gas Emissions by Gas, 1990–2010

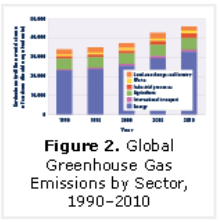


Figure 2. Global Greenhouse Gas Emissions by Sector, 1990–2010

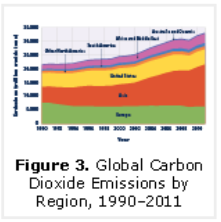


Figure 3. Global Carbon Dioxide Emissions by Region, 1990–2011

Printer-friendly PDF of all text and figures (6 pp, 218K, About PDF)

WCMS

Last updated on Wednesday, July 02, 2014

Key Points

In 2010, estimated worldwide emissions from human activities totaled nearly 46 billion metric tons of greenhouse gases, expressed as carbon dioxide equivalents. This represents a 35 percent increase from 1990 (see Figures 1 and 2). These numbers represent net emissions, which include the effects of land use and forestry.

Between 1990 and 2010, global emissions of all major greenhouse gases

Background

About the Indicator

Indicator Notes

Data Sources

Technical Documentation